Construction of One-Dimensional Multicomponent Molecular Arrays: Control of Electronic and Molecular Motions☆

Jean-Paul Collin, Pablo Gaviña, Valérie Heitz and Jean-Pierre Sauvage*

Laboratoire de Chimie Organo-Minérale, UA 422 au CNRS, Institut de Chimie, Université Louis Pasteur, 4 rue Blaise Pascal, F-67070 Strasbourg, France

Received July 11, 1997

Keywords: One-dimensional multicomponent arrays / Energy- and electron transfer / Molecular motions / Ruthenium / Osmium / Terpyridines / Bis-terpyridines / Bis-cyclometallating ligands / Porphyrins / Copper(I) rotaxane

Transition metals are powerful three-dimensional templates, which can gather various functionalized ligands and orient them in a precise fashion so that complex multicomponent molecular systems can be obtained without constructing covalently-assembled edifices. The compounds thus prepared exhibit precise chemical or physical functions, which are governed by the design of the system. The construction of one-dimensional molecules around ruthenium(II) or osmium(II), using rigid ligands attached to the desired electroactive species, leads to systems that are able to undergo charge separation after photonic excitation. In other related compounds, a ruthenium(II)-based chromophore is, for example, connected to an osmium(II) complex by means of rod-like bridging ligand, thereby ensuring strict control over the Ru···Os distance. By tuning the length and the electronic properties of the bridge, one can control the efficiency of the electronic energy transfer between the two chromophores. In particular, the use of a bis-cyclometallating ligand is very conducive to energy transfer and allows the observation of this process up to a Ru..Os distance of ≈20 Å. By combining the building blocks of these inorganic systems with appropriate porphyrins, long-range (centre-to-centre distance between the donor and the acceptor porphyrins ≈30 Å) and relatively long-lived photoinduced charge separation has been demonstrated. Finally, with copper(I) as the template, compounds of the rotaxane family are obtained, which consist of a coordinating ring threaded by a string-like component. If this acyclic fragment is end-functionalized by two bulky stoppering groups and if it incorporates two different coordination sites (a bi- and a terdentate chelate site), novel dynamic properties are observed. The movement of a given fragment of the molecule is triggered by changing the metal oxidation state. This one-dimensional motion of the ring along the string on which it is threaded is controlled by redox manipulation, resulting in a primitive molecular machine.

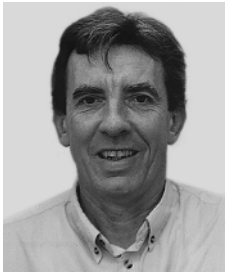

Pablo Gaviña (top left) was born in Valencia, Spain, in 1966. He studied chemistry at the Universidad de Valencia, where he received his Ph. D. in 1994 with Professor R. Mestres, on dienediolates of unsaturated carboxylic acids and on the protection and controlled release of aldehydic pheromones. He then spent two years as postdoctoral fellow with Dr. J.-P. Sauvage, working on chemical topology and on electrochemically induced molecular motions. He is currently working with Professor G. Asensio in the Department of Organic Chemistry of the Universidad de Valencia on enantioselective protonation of prochiral enolates.

Valérie Heitz (bottom left) was born in Strasbourg, France, in 1966. After completing a Ph. D. with Dr. J.-P. Sauvage in 1992 on multiporphyrin systems performing photoinduced electron transfer, she did postdoctoral work with Dr A. Harriman at the Center for Fast Kinetic Research at the University of Texas at Austin. She obtained a position as "Maître de Conférences" at the University of Strasbourg in 1993 and carries out research work in the laboratory of J.-P. Sauvage. Her current interest concerns the synthesis of functional models of photosynthetic reaction centres.

Jean-Paul Collin (top right) was born in 1945 in Metz. After his Ph. D. in electrochemistry with Professor J. P. Schwing at the Louis Pasteur University, Strasbourg, he did postdoctoral work with Professor J.-M. Lehn on water photolysis. He is now a CNRS research director. He joined Dr J.-P. Sauvage's group in 1983 and his present research focuses on photoinduced charge separation in multicomponent molecular systems.

Jean-Pierre Sauvage (bottom right) was born in Paris in 1944. He obtained his Ph. D. from the University of Strasbourg, under the supervision of J.-M. Lehn. After postdoctoral research in Oxford (UK), with M.L.H. Green, he went back to Strasbourg, where the started his own research group in 1980. His interests span from models of the photosynthetic reaction centre to molecular topology.

MICROREVIEWS: This feature introduces the readers to the authors' research through a concise overview of the selected topic. Reference to important work from others in the field is included.

 © WILEY-VCH Verlag GmbH, D-69451 Weinheim, 1998 1434−1948/98/0101−0001 $ 17.50+.50/0

Contents

1. Introduction
2. Complexes of Ruthenium(II) and Osmium(II) Covalently-Linked to Electron Donor and Acceptor Groups
2.1. Synthesis of Terpyridine Ligands
2.2. Synthesis of Diads and Triads Based on $Ru(tpy)_2^{2+}$ -type Photosensitizers
2.3. Synthesis of Diads and Triads Based on $Os(tpy)_2^{2+}$ -type Photosensitizers
2.4. Photoinduced Processes in Diads and Triads Based on $Ru(tpy)_2^{2+}$ and $Os(tpy)_2^{2+}$ - type Photosensitizers
3. Rigid Rod-like Dinuclear Terpyridine-type Complexes
3.1. Synthesis of Bridging Bis-terpyridine Ligands
3.2. Synthesis and Photochemical Behaviour of Rigidly Bridged Heterodinuclear Complexes
3.2.1. Ruthenium-Osmium Complexes
3.2.2. Ruthenium-Rhodium Complexes
4. Rigid Rod-like Dinuclear Complexes with Bis-cyclometallating Terpyridine Analogues
4.1. Synthesis of Cyclometallating and Bridging Bis-cyclometallating Ligands
4.2. Preparation and Properties of Heterodinuclear Cyclometallated Complexes
4.2.1. Ruthenium-Osmium Cyclometallated Complexes
5. Multiporphyrin Linear Systems Assembled by Transition Metal Complexes
5.1. Synthesis of Porphyrin-Metal Bis-terpyridine Diads
5.1.1. Synthesis of the Ligands
5.1.2. Synthesis of the Complexes
5.1.3. Photophysical Properties of the Diads
5.2. Synthesis of a Bis-porphyrin Ruthenium(II) Bis-phenylterpyridine Triad
5.2.1. Synthesis of the Ligands
5.2.2. Synthesis of the Complex
5.2.3. Electron-transfer Properties of the Triad
6. A Copper(I) Rotaxane Incorporating Two Different Sites in a Thread: Molecules in Motion
6.1. Synthesis of the Rotaxane
6.2. Electrochemically-Induced Molecular Motions
7. Conclusion and Prospects

1. Introduction

In complex multicomponent molecular systems, the control of physical properties related to electron- and energy-transfer or displacement of molecular fragments relies, to a large extent, on our mastery of the geometrical properties of the ensemble.

For several years, we have been interested in one-dimensional compounds, for which an axis along the largest dimension of the object can be clearly defined[1][2][3]. If rigidity can also be introduced during the design and synthesis steps, distances and, sometimes, angles between the various components located on the axis can be estimated to a good approximation.

Two distinct aspects of our research are discussed in the present review article: (i) electron- or energy-transfer, and (ii) molecular motions, related to "molecular machines", along an axis.

(i) The aims of the first and main topic are manifold. In the short term, it is important to improve our understanding of electron- and energy-transfer processes and to verify the current theories[4][5][6][7] by modifying at will the distances and orientations between the various chromophores and electrophores of the assembly, and by changing their electronic properties as well as those of the spacer groups used in the construction of the systems. An aspect of this approach is to build and study models[8][9][10][11][12] of photosynthetic reaction centres (RC), which function so efficiently in living organisms, and in particular in photosynthetic bacteria[13][14]. In the long term, it would of course be of great interest to build molecular systems or hybrid devices, containing molecules and organic or inorganic solids, capable of converting light energy into electrochemical or chemical energy[15][16][17]. In other words, the creation of artificial systems able to perform real photosynthesis is a special challenge.

(ii) The second line of research is more recent and is concerned with molecular machines and motors[18][19][20], i.e. molecular ensembles for which a large amplitude and reversible motion can be triggered simply by sending a signal to the molecule from outside. This signal is usually electrochemical (reduction or oxidation of an electroactive component) or photochemical. However, many other types of perturbations can be envisaged: magnetic or electric field, temperature or pressure jump, chemical signal (pH change), etc. In our case, the notion of axis and geometrical control is again essential. Scheme 1 illustrates, in a simplified fashion, the two facets of the work discussed herein.

2. Complexes of Ruthenium(II) and Osmium(II) Covalently Linked to Electron Donor and Acceptor Groups

One of the key features of natural photosynthesis is the efficiency of charge separation. In a multistep procedure, light energy absorbed by a photoactive centre is converted into electrochemical energy with formation of a long-lived charge-separated state. This complex process relies on the subtle arrangement of energy levels for the excited or redox states involving the various chromophores, favouring a cascade-like sequence of electron-transfer steps leading to the charge-separated state.

In the field of transition metal complexes, one can design multicomponent systems for which similar charge separation may occur, provided that the electronic properties of the various chromophores are controlled and selected in a precise fashion, and that there is strict control over the geometrical properties of the set of photo- and electroactive species (Scheme 2).

On the basis of their photochemical, photophysical and electrochemical properties, M(II) polypyridine complexes (M = Ru or Os) are, in principle, suitable photosensitizer components for use in multicomponent systems designed to permit efficient photoinduced charge separation[15][21][22][23][24]. However, with ligands such as 2,2′-bipyridine, the building up of multicomponent molecules

Scheme 1. In a one-dimensional multicomponent system, a photoactive centre (PC) is (a) first excited by a photon. The excited state is subsequently able to transfer an electron to an acceptor (on the right of the PC, not represented). This process induces a series of cascade-like electron-transfer steps the overall effect of which is to create a negative charge on the right-side and a positive hole on the left-side of the array. (b) A redox or photonic signal modifies the coordination requirements of a metal centre (black dot) incorporated in a rotaxane, triggering molecular motions. The shift of the ring and the metal is induced by modification of the metal centre coordination sphere

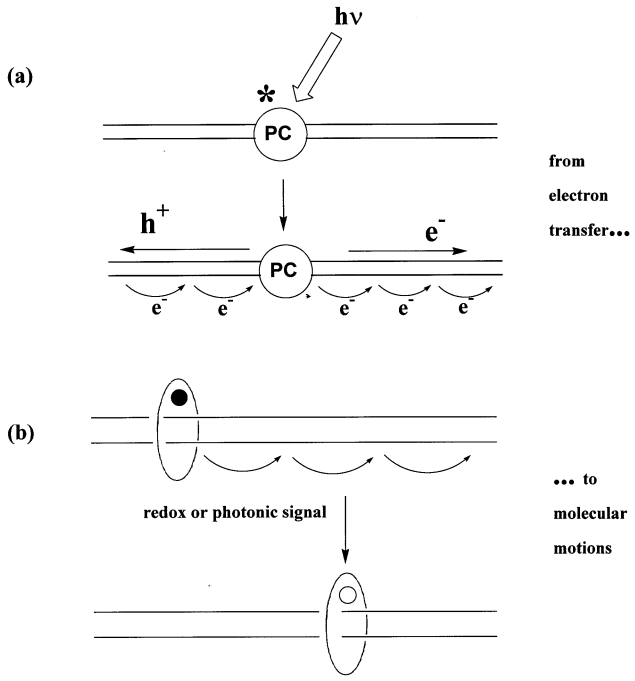

Scheme 2

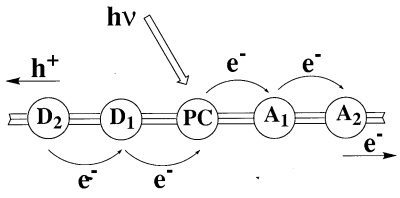

leads to systems in which the acceptor or donor groups linked to the chromophore are relatively close to one another (*cis*-type configuration)[25]. In contrast, the geometry of terpyridine complexes offers the possibility of designing systems in which the D and A components lie in opposite directions with respect to the chromophore (*trans*-type configuration)[1]. In addition, bis-terpyridine complexes bearing substituents at the 4′-position do not lead to isomeric (enantio- and diastereomeric) mixtures, in contrast to the corresponding substituted bipyridine systems. Furthermore, the interposition of aromatic rings (Figure 1) affords a convenient means of increasing the A−D separation[26].

Figure 1. Schematic representation of the photochemically-induced electron-transfer step in an $M(tpy)_2^{2+}$ complex bearing acceptor (A) and donor (D) groups

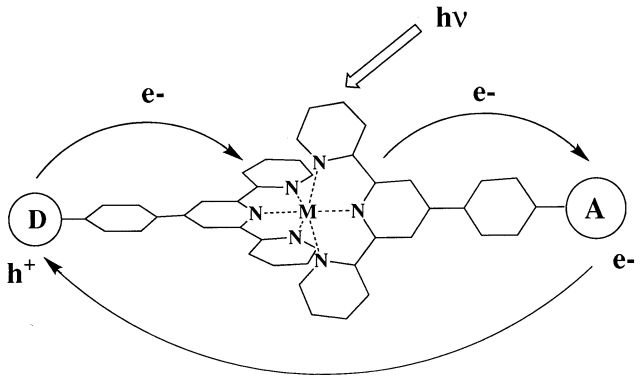

2.1. Synthesis of Terpyridine Ligands

Since the first preparation of the 2,2′:6′,2"-terpyridine ligand 60 years ago by oxidative coupling of pyridine with $FeCl_3$ in an autoclave[27], other strategies involving the coupling of pyridine units (cross-coupling methodology)[28] or the formation of one or two pyridine rings from precursor functions have been developed. Certainly, the most commonly used methodology is the synthesis of the central pyridine ring. The pioneering works of Hantzsch[29], Tschitschibabin[30], Case[31], Kröhnke[32] and others using this principle, have been followed by new developments and improvements. In particular, the works of Constable[33], Potts[34] and Jameson′s group[35] allow the preparation of various substituted terpyridines. In order to obtain large amounts of the 4′-aryl-2,2′:6′,2″-terpyridine, the one-pot Hantzsch synthesis, developed by Case[31] and later by Calzaferri[36], was selected (Figure 2a).

The condensation of the aromatic aldehyde with two equivalents of 2-acetylpyridine gave a 1,5-diketone. Ring closure was achieved using ammonium acetate. In some cases, two terpyridine isomers[37] could be obtained following a 1,2- or 1,4-Michael addition on the unsaturated ketone intermediate (Figure 2b).

The separation of the terdentate ligand, arising from 1,4-addition, from the sterically hindered bidentate ligand was readily achieved by formation of the highly stable $Fe(terpyridine)_2^{2+}$ complex, as described by Constable et al.[33] The iron(II) complex, upon treatment with H_2O_2 in alkaline solution, yielded the free terpyridine in good yield.

The terpyridine-bearing electroactive compounds could be prepared using one of two general strategies. In the first of these, the ligand is synthesized bearing a suitable functionality and the desired electrophore is then introduced in a second step[37][38]. The other possibility involves introduction of the electroactive function into the aromatic aldehyde prior to the terpyridine formation reaction[37]. Both routes have been explored and used, the method of choice being dictated by the chemical stability of the donor or the acceptor groups, since the second ap-

Figure 2. (a) Synthetic route to various substituted terpyridines. (b) Formation of 2,2′:6′,2″-terpyridine and its isomer (2,2′:4′,6″-) via 1,2- or 1,4-Michael addition

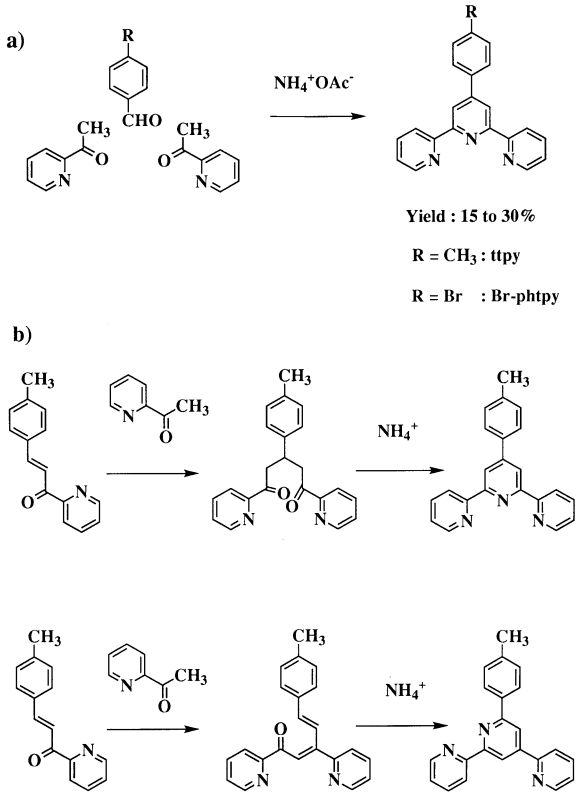

proach implies that the electrophore will have to resist the relatively harsh experimental conditions of the cyclisation reaction. Figure 3 depicts various ligands, containing either D or A units as pendant groups, prepared by these two strategies.

Figure 3. Various tpy derivatives used, with an electrophore rigidly attached to the chelate via a 1,4-phenylene spacer. PTZ = phenothiazine; DPAA = di-*p*-anisylamine; Fc = ferrocene; MV^{2+} = methylviologen

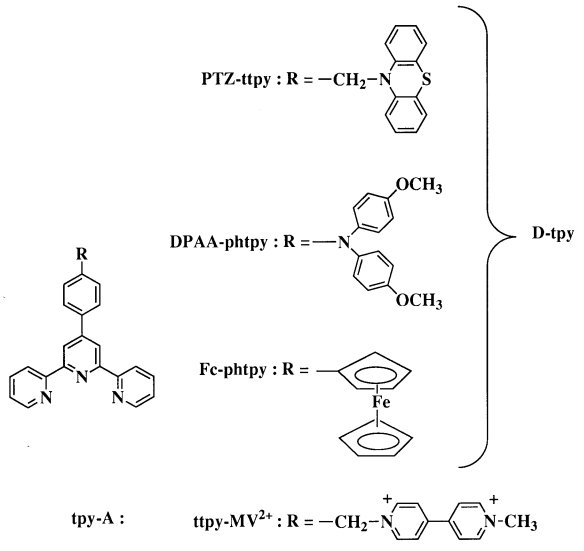

2.2. Synthesis of Diads and Triads Based on $Ru(tpy)_2^{2+}$ -Type Photosensitizers

The various ruthenium(II) complexes prepared and studied are listed in Table 1. The various ligands used are depicted in Figure 3.

Table 1. Preparation of the various ruthenium(II) diad or triad complexes[a] A: sequential method; B: statistical method

Complex	Method[a]	Yield (%)	Reference
(Fc-phtpy)Ru(ttpy)$^{2+}$	A	15	[38]
(Fc-phtpy)Ru(ttpy)$^{2+}$	A	5	[37]
(DPAA-phtpy)Ru(ttpy)$^{2+}$	A	37	[37]
(ttpy)Ru(ttpy-MV^{2+})$^{4+}$	B	8	[26][37]
(PTZ-ttpy)Ru(ttpy-MV^{2+})$^{4+}$	B	5	[26][37]
(DPAA-phtpy)Ru(ttpy-MV^{2+})$^{4+}$	B	8	[26][37]
(Fc-phtpy)Ru(ttpy-MV^{2+})$^{4+}$	B	18	[41]

They have been prepared either in a *sequential manner* (A) or by a *statistical method* (B):

(A): $Ru(ttpy)Cl_3 + tpy{-}D \xrightarrow{(i)} Ru(ttpy)(tpy{-}D)^{2+}$
(i): reflux in ethanol/water/triethylamine for 1 h

(B): "ruthenium blue" + L_1 + $L_2 \xrightarrow{(ii)}$ $Ru(L_1)_2^{2+} + Ru(L_1)(L_2)^{2+} + Ru(L_2)_2^{2+}$
(L_1)(L_2): (ttpy)(ttpy$-MV^{2+}$), (PTZ$-$ttpy)(ttpy$-MV^{2+}$), (DPAA$-$phtpy)(ttpy$-MV^{2+}$)
(ii): reflux in ethanol for 18 h

Method (A) was used for ligands bonded to an electron donor (tpy$-$D). However, it turned out not to be appropriate for the synthesis of complexes containing the ttpy$-MV^{2+}$ ligand. The triads and the electron acceptor diad Ru(ttpy)(ttpy$-MV^{2+})^{4+}$ were thus prepared according to the statistical procedure (B).

2.3. Synthesis of Diads and Triads Based on $Os(tpy)_2^{2+}$ -Type Photosensitizers

Although the coordination sphere of ruthenium is known to be relatively inert vis-à-vis substitution reactions, it is still very labile as compared to osmium. In fact, substituting ligands within the coordination sphere of osmium is notoriously difficult and requires either extremely harsh conditions or multistep procedures involving different metal oxidation states. Using the ligands shown in Figure 3, various osmium(II) complexes could be prepared[26][38][39][40][41]. Due to the chemical fragility of some of the ligands, the very drastic classical conditions, consisting of heating osmium salts and the ligands at very high temperature (typically, refluxing ethylene glycol) for long periods could not be systematically applied. Consequently, more elaborate, specific methods had to be developed. The two general routes used are indicated in Figure 4.

The series of osmium(II) diad and triad complexes prepared and investigated is listed in Table 2.

Importantly, since photophysical measurements are very sensitive to impurities, special care was taken in order to ensure the isolation of very pure samples of the various ruthenium(II) and osmium(II) complexes. For this purpose,

Figure 4. The two general routes to substituted bis(tpy)osmium(II) complexes

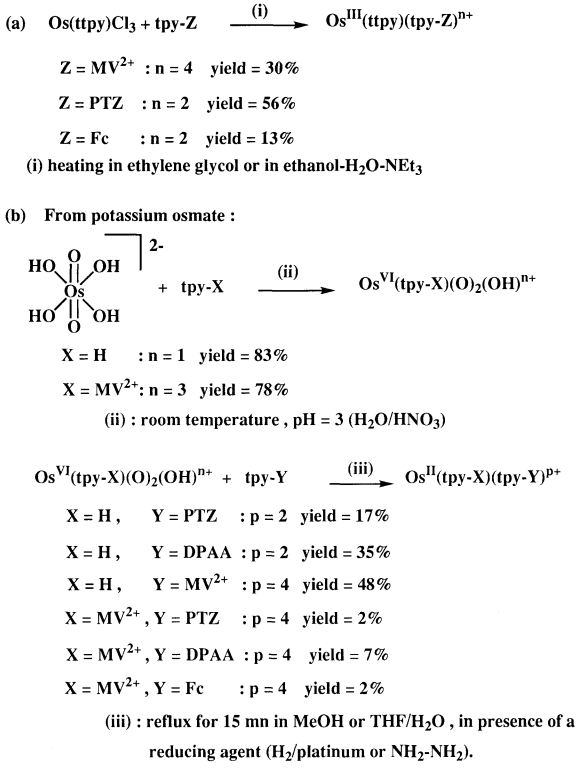

Table 2. The various multicomponent compounds prepared containing a bis-terpyridine osmium(II) central chromophore

Complex	Method (see Figure 4)	Reference
$(ttpy)Os(ttpy\text{-}MV^{2+})^{4+}$	(a) or (b)	[26][40]
$(PTZ\text{-}ttpy)Os(ttpy)^{2+}$	(a)	[26][40]
$(Fc\text{-}phtpy)Os(ttpy)^{2+}$	(a)	[38]
$(DPAA\text{-}phtpy)Os(ttpy)^{2+}$	(b)	[40]
$(PTZ\text{-}ttpy)Os(ttpy\text{-}MV^{2+})^{4+}$	(b)	[39]
$(DPAA\text{-}phtpy)Os(ttpy\text{-}MV^{2+})^{4+}$	(b)	[39]
$(Fc\text{-}phtpy)Os(ttpy\text{-}MV^{2+})^{4+}$	(b)	[41]

all the compounds prepared were subjected to chromatography on silica gel, with a mixture of solvents (usually CH_3CN and H_2O) containing a salt (KNO_3, for instance) as eluent.

2.4. Photoinduced Processes in Diads and Triads Based on $Ru(tpy)_2^{2+}$ and $Os(tpy)_2^{2+}$-Type Photosensitizers

As is normal for ruthenium(II) and osmium(II) polypyridine complexes, light excitation in the spin-allowed MLCT bands eventually leads to population of the lowest energy ^{3}MLCT level[23][42], which is the state responsible for the observed electron-transfer processes. Since $Ru(tpy)_2^{2+}$ is practically non-emitting at room temperature, the experiments on this species and its derivatives were performed at 155 K[43]. For the compounds based on $Os(ttpy)_2^{2+}$, which is luminescent at room temperature, experiments were performed at both 155 K and 298 K[39]. The solvent used was butyronitrile. Detailed mechanisms of the photoinduced processes in these P−A diads and in the D−P−A triads have been given in a previous review article[1]. Photoinduced processes in the D−P−A triads are depicted in Figure 5. At 155 K, the lifetime of the fully charge-separated state D^+-P-A^- (P = Ru) is estimated to be 27 ns. For the Os-based triads, the deactivation via the fully charge-separated state D^+-P-A^- occurs with $k > 10^8\ s^{-1}$. In this case, the transient absorption spectrum of the D^+-P-A^- species is not detected because this species does not accumulate but rapidly reverts to D−P−A.

Figure 5. Photoinduced processes in the $DPAA-P-MV^{2+}$ triads at 155 K, where P is $Ru(ttpy)_2^{2+}$ or $Os(ttpy)_2^{2+}$

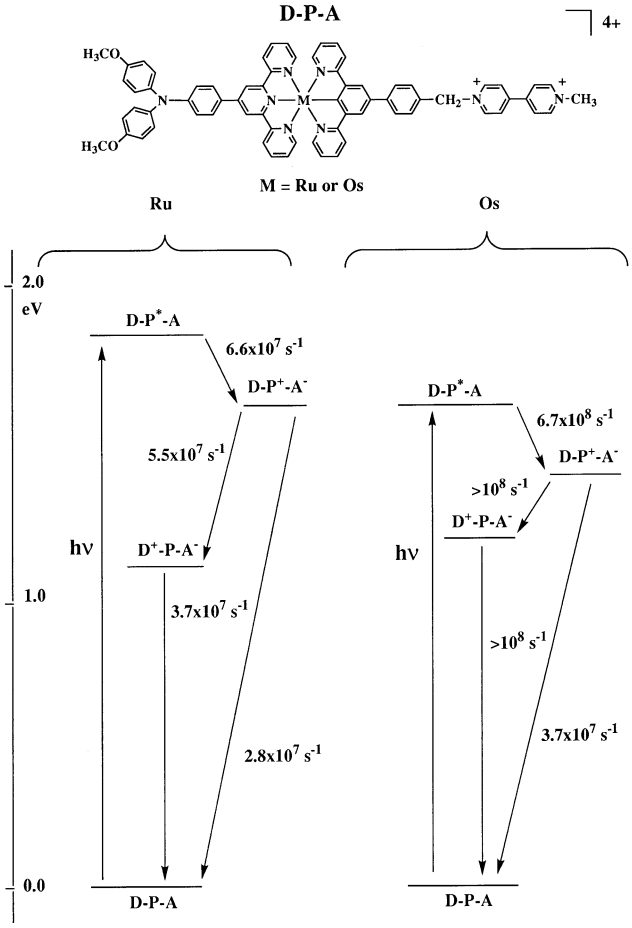

3. Rigid Rod-like Dinuclear Terpyridine-Type Complexes

Symmetrical rigid dinucleating ligands, the syntheses of which are versatile enough to allow modulation of the electronic and geometrical properties, are also promising. The family of compounds discussed in the following section allows us to evaluate the effect of metal-to-metal distance on the rate of energy- or electron-transfer between the donor subunit and the acceptor fragment, and also to assess the influence of the electronic properties of the spacer inserted between the two components.

3.1. Synthesis of Bridging Bis-terpyridine Ligands

By connecting two terpyridine units via a rigid spacer attached to their 4′-positions, bridging ligands displaying axial symmetry can be obtained. The compounds which have been synthesized and used further to make dinuclear complexes are illustrated in Figure 6.

Figure 6. Ligands used in the preparation of the heterodinuclear complexes

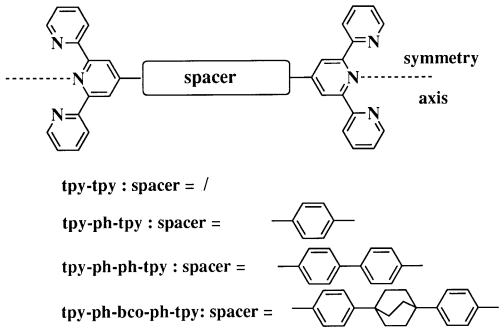

The bis-terpyridine ligand tpy−tpy was synthesized by reductive coupling of 4′-chloro-2,2′:6′,2"-terpyridine, following the methodology recently reported by Constable and Ward[44]. The phenyl-bridged bis-terpyridine ligand tpy−ph−tpy was obtained according to the method developed by Kröhnke et al.[32]. The same reaction has also been used more recently by others[45]. The principle is very general and can allow the preparation of virtually any compound containing several pyridine nuclei attached to aromatic rings. The biphenyl-containing ligand tpy−ph−ph−tpy was obtained by homo-coupling of 4′-*p*-bromophenyl-2,2′:6′,2"-terpyridine in the presence of Ni(0) triphenylphosphane complex and Zn dust in DMF. The yield was 60%, thus allowing preparation of the compound on a gram scale.

It should be noted that the bromo-terpyridine used as starting material is readily available from 2-acetylpyridine and 4-bromobenzaldehyde[36] (Figure 2). This functionalized terpyridine is the ideal precursor to a potentially bridging multi-terpyridine ligand. It should lead to bis-terpyridine systems with various aromatic or saturated spacers, as well as to bridging multi-chelates by connecting several such terpyridine units.

The preparation of the bridging ligand tpy−ph−bco−ph−tpy (bco = 2,2,2-bicyclooctane) was achieved using the multistep procedure shown in Figure 7.

The key intermediate, Br−ph−bco−ph−Br, was prepared following a modification of a procedure previously described by Zimmermann et al.[46]. Treatment of this dibromoarene with 4 equivalents of *t*-butyllithium and 2 equivalents of 2-methoxy-4,4,5,5-tetramethyl-1,3,2-dioxoborolane[47] afforded a diester derivative, which could be purified by crystallization. The successful cross-coupling of the 4′-bromo-2,2′:6′,2"-terpyridine with the diester using $Pd(dppb)Cl_2$ [dppb = 1,4-bis(diphenylphosphane)butane] as catalyst was performed following the methodology developed by Suzuki et al.[48] and recently applied to a water-soluble *p*-phenylene-containing polymer[49].

Figure 7. Reaction used in the synthesis of the bridging ligand tpy−ph−bco−ph−tpy

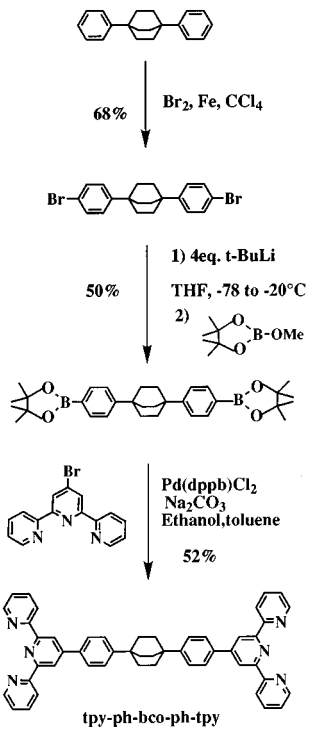

3.2. Synthesis and Photochemical Behaviour of Rigidly Bridged Heterodinuclear Complexes

The rigidly bridged ruthenium(II)-osmium(II)[50][51][52][53] and ruthenium(II)-rhodium(III)[54] complexes are depicted in Figure 8.

The general preparation of the heterodinuclear complexes requires, as a first step, the synthesis of the key complexes $(ttpy)Ru[tpy-(ph)_n-tpy]^{2+}$. These intermediate mononuclear compounds were obtained as follows: $Ru(ttpy)Cl_3$ and $AgBF_4$ were refluxed in acetone in order to remove the chlorine atoms from the metal. The complex obtained was added to a DMF solution of the bridging ligand and the mixture was refluxed for 1 h. After work-up and chromatography on alumina with CH_3CN as eluent, the compounds were isolated as their PF_6^- salts in good yields: $(ttpy)Ru(tpy-tpy)^{2+}$: 85%; $(ttpy)Ru(tpy-ph-tpy)^{2+}$: 77%; $(ttpy)Ru(tpy-ph-ph-tpy)^{2+}$: 76%. All the compounds described were characterized by standard techniques (^{1}H-NMR and FAB-MS). FAB-MS turned out to be particularly useful for these highly positively charged species. In each case, the molecular peak was sufficiently intense to eliminate any ambiguity concerning the structure of the compound.

3.2.1 Ruthenium-Osmium Complexes: The ruthenium complex bearing a free terpyridine site was allowed to react with crude $(ttpy)OsCl_3$ in refluxing *n*BuOH for 7 h. This very insoluble compound was prepared from $OsCl_3.xH_2O$

Figure 8. Mononuclear ruthenium precursors and rigidly bridged ruthenium-osmium and ruthenium-rhodium complexes

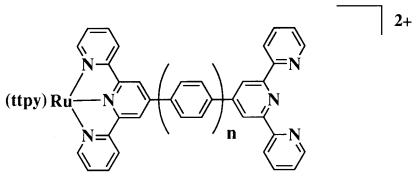

$(ttpy)Ru(tpy\text{-}tpy)^{2+}$: n = 0

$(ttpy)Ru(tpy\text{-}ph\text{-}tpy)^{2+}$: n = 1

$(ttpy)Ru(tpy\text{-}(ph)_2\text{-}tpy)^{2+}$: n = 2

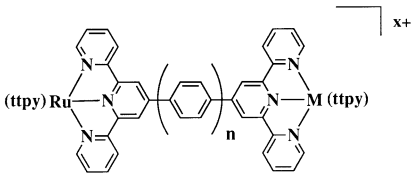

M = Os

$(ttpy)Ru(tpy\text{-}tpy)Os(ttpy)^{4+}$: n = 0

$(ttpy)Ru(tpy\text{-}ph\text{-}tpy)Os(ttpy)^{4+}$: n = 1

$(ttpy)Ru(tpy\text{-}(ph)_2\text{-}tpy)Os(ttpy)^{4+}$: n = 2

$(ttpy)Ru(tpy\text{-}(ph\text{-}bco\text{-}ph\text{-}tpy)Os(ttpy)^{4+}$

M = Rh

$(ttpy)Ru(tpy\text{-}tpy)Rh(ttpy)^{5+}$: n = 0

$(ttpy)Ru(tpy\text{-}ph\text{-}tpy)Rh(ttpy)^{5+}$: n = 1

$(ttpy)Ru(tpy\text{-}(ph)_2\text{-}tpy)Rh(ttpy)^{5+}$: n = 2

and ttpy and used without further purification. In fact, attempts to remove the chloride ions with Ag^+ were of questionable success. Depending upon the starting sample, other ruthenium-osmium complexes could be isolated in low yield[51]. The formation of these by-products seems to reflect the polymeric nature of the poorly-defined starting complex, $(ttpy)OsCl_3$.

Photophysical data (steady-state luminescence spectroscopy and time-resolved spectroscopy methods) indicate a very efficient energy-transfer process from the ruthenium chromophore to the osmium moiety[53][55]. This transfer takes place according to the exchange mechanism of Dexter[4]. Actually, the transfer of energy was found to occur with $k > 10^{10}$ s^{-1}, even for $d_{MM} = 20$ Å (d_{MM} is the intermetal distance). One concludes that the polyphenylene bridge behaves as an extremely good energy transducer. Insertion of a bicyclooctane (bco) unit leads to an internal separation of 24 Å and results in a dramatic decrease in the rate of energy transfer ($k = 4.4 \times 10^6$ s^{-1} as measured at 77 K). This effect is due to the increased internal distance as well as the electronically insulating properties of the saturated bco group. It is nevertheless remarkable that energy transfer still takes place at such a large distance and in spite of the presence of a central insulating group. Studies performed by other groups with systems incorporating ethynyl[56] or other rigid spacers[57][58][59] have led to similar results.

3.2.2. Ruthenium-Rhodium Complexes: The ruthenium complex bearing a free terpyridine site was allowed to react with $(ttpy)RhL_3$ (L = acetone) in refluxing ethanol for 4 h. The latter was obtained similarly to its ruthenium analogue, by replacing the chloride ligands of the complex $(ttpy)RhCl_3$ by solvent molecules using $AgBF_4$ in refluxing acetone. As in the case of ruthenium-osmium complexes, other multinuclear by-products were isolated. Their formation can be explained in terms of reduction of the rhodium(III) centre to rhodium(I) during the complexation reaction, followed by ligand scrambling[54]. Indeed, the coordination sphere of the rhodium(I) metal is labile and the ligand interchange can easily occur.

The photophysics of the binuclear complexes were investigated in 4:1 methanol/ethanol solution at 77 K (rigid glass) and 150 K (fluid solution) and compared with data for the mononuclear $Ru(ttpy)_2^{2+}$and $Rh(ttpy)_2^{3+}$ model compounds[54]. At 77 K, no quenching of the Ru(II)-based excited state was observed, whereas energy transfer from excited state Rh(III) to Ru(II) was observed for all the complexes. At 150 K, energy transfer from excited state Rh(III) to Ru(II) was again observed for all complexes, while quenching of the excited state of Ru(II) by *electron transfer* to Rh(III) was observed, but only in the complex with $n = 0$. The different behaviour between $n = 0$ and $n = 1$, 2 can be rationalized in terms of better suited electronic factors and smaller reorganizational energies for the former species. A number of ruthenium-rhodium diads have also been synthesized and studied in recent years[60][61][62][63]. These display a variety of intercomponent energy- and electron-transfer processes.

4. Rigid Rod-like Dinuclear Complexes with Bis-cyclometallating Terpyridine Analogues

Interestingly, the electronic properties of a multidentate ligand containing pyridine nuclei can be dramatically modified by replacing a nitrogen atom by a carbon atom (phenyl group). This procedure permits us to go from a moderate σ- and π-donating neutral species to a negatively charged ligand, provided that the metal can form a σ-bond to the deprotonated CH group of the phenyl ring. The new ligand would then be negatively charged and would, of course, be expected to behave as a strong donor and be able, for instance, to stabilize high oxidation states or to favour high field complexes. Since $Ru(ttpy)_2^{2+}$ is virtually non-luminescent at room temperature ($\tau = 0.96$ ns in CH_3CN), different approaches have been explored in order to overcome this difficulty. One possibility is to increase the ligand field (LF) or to diminish (to some extent) the metal-to-ligand charge-transfer (MLCT) energy level so that the MLCT and the LF states become well separated. In this context, cyclometallating ligands such as 6-phenyl-2,2′-bipyridine (phbpH) or 1,3-dipyridylbenzene (dpbH) (Figure 9a) have been combined with one terpyridine in heteroleptic complexes.

4.1. Synthesis of Cyclometallating and Bridging Bis-cyclometallating Ligands

Initially, dpbH was prepared according to a synthetic procedure described previously by Bönnemann for 2,2′-(1,4-phenylene)dipyridine[64][65]. A more convenient method employs the mild aromatic cross-coupling reaction originally described by Stille et al.[66]

Figure 9. (a) Cyclometallating and (b) bridging bis-cyclometallating ligands

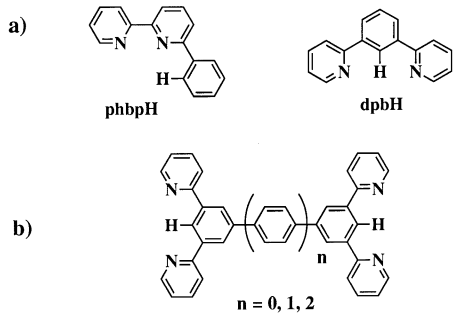

The design of multicomponent systems incorporating these new chromophores and electrophores requires the synthesis of rigid, symmetrical bis-cyclometallating ligands. Mild and efficient aromatic cross-coupling reactions catalysed by various transition metal complexes have recently been used in the synthesis of natural products, large organic receptors[67], dendrimers[68] and one-dimensional polymers[69]. Applied to suitable precursors, these methodologies have permitted the preparation of three bis-cyclometallating ligands (Figure 9b), in which aromatic spacers modulate the separation distance between sites[70]. The universal precursor 5-bromo-1,3-dipyridylbenzene (Figure 10) was obtained by reaction of the 2-trimethylstannylpyridine with 1,3,5-tribromobenzene in the presence of $Pd[P(C_6H_5)_3]_2Cl_2$. It was coupled using nickel(0) to afford a 70% yield of $tpbphH_2$ (tpbph denotes tetrapyridylbiphenyl).

The ligands ($tptphH_2$ and $tpqphH_2$; tph and qph denote terphenyl and quaterphenyl, respectively) with one and two phenylene spacers were prepared using Suzuki ′s cross-coupling procedure as depicted in Figure 10[48].

Figure 10. Synthetic steps leading to bis-cyclometallating ligands

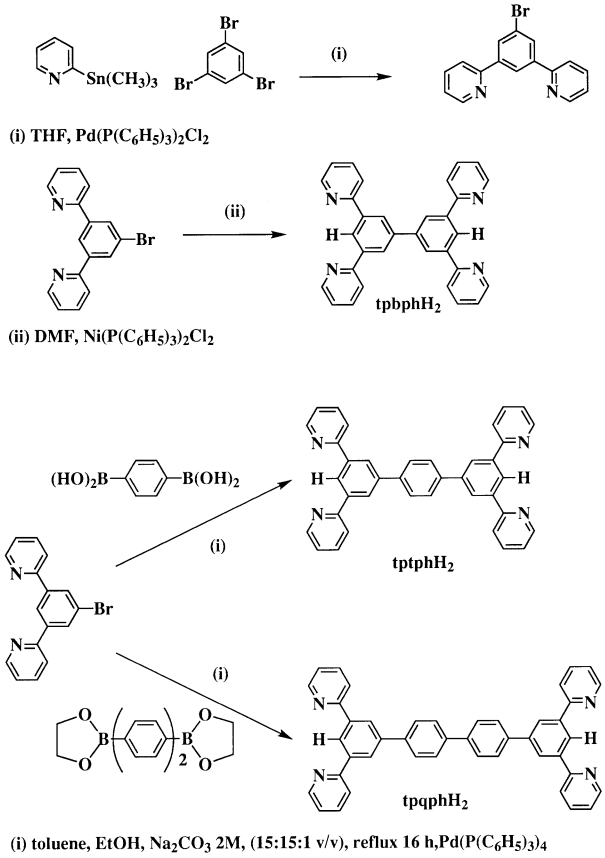

4.2. Preparation and Properties of Rigidly Bridged Ruthenium-Osmium Cyclometallated Complexes

By using the bis-cyclometallating ligands depicted in Figure 10, ruthenium-osmium cyclometallated complexes were prepared with the aim of studying photoinduced energy-transfer processes between the two bridged complex subunits[3][71][72]. The synthetic strategy used was the same as that described for the analogous terpyridine-type complexes (3.2.1.). The mononuclear ruthenium precursors bearing a free cyclometallating site and the corresponding heterodinuclear complexes are represented in Figure 11.

Figure 11. Synthesis of ruthenium-osmium cyclometallated complexes

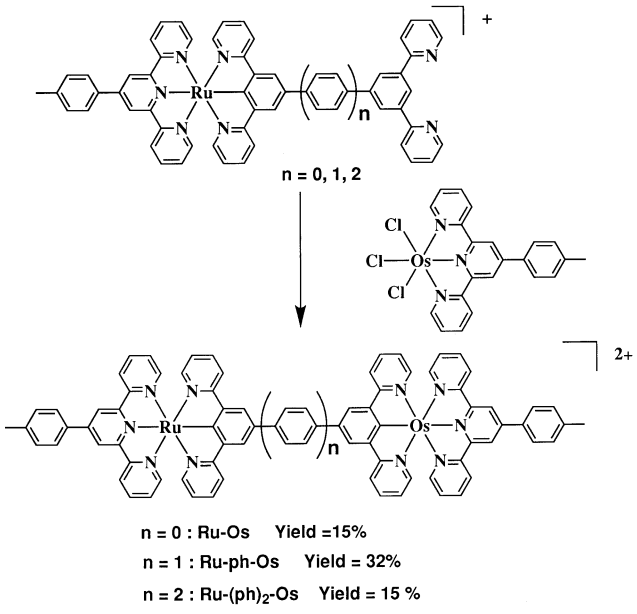

The binuclear complexes containing the dianionic ligands exhibit the same geometrical properties as the previous bis-terpyridine series, with the distance between the metal centres ranging from 11 to 20 Å, depending on the size of the phenylene spacer. For the cyclometallated series, the rate of Ru(II) to Os(II) energy transfer proved to be much slower than for the structurally identical series discussed in the previous section (3.2.1.). Thus, at room temperature, no energy transfer was observed, despite the fact that the ex-

cited state of the chromophore [Ru(ttpy)(dpb)$^+$] exhibits a lifetime of 4.5 ns in acetonitrile. At 77 K, the energy-transfer rate is affected to a large degree by the presence of the phenylene spacer. Energy transfer was found to take place according to a Dexter mechanism[4]. Comparison with analogous complexes containing non-cyclometallating bridging ligands, where the MLCT excited states involved in the energy transfer step are localized on the bridge and very fast energy transfer takes place ($k > 5 \times 10^{10}$ s^{-1}), suggests that the energy-transfer step in the cyclometallated complexes is slower because the involved MLCT excited states are directed toward the terminal ligands[3]. This apparently results in a longer transfer pathway. The main conclusions are that the phenylene spacers are very efficient in transmitting the intermetal electronic communication, but that an important role is also played by the spatial localization of the MLCT excited states involved in the excitation-transfer process (peripheral for the cyclometallated series and bridging for the non-cyclometallating family).

5. Multiporphyrin Linear Systems Assembled by Transition Metal Complexes

Multiporphyrin systems are of considerable interest in the fields of molecular electronics and artificial photosynthesis[15] with regard to converting light signals into high energy separated states. An attractive route to such systems is to use transition metals to assemble ligands, each bearing a porphyrin unit. This strategy, which uses coordination rather than covalent chemistry to interconnect the various components, offers several attractive features: (i) its high flexibility should allow easy preparation of multicomponent systems, and (ii) good geometrical control should be possible. The general concept and the synthetic principle are illustrated in Scheme 3.

Scheme 3. Strategy used to assemble asymmetrical bis-porphyrins around a central transition metal cation (black dot). The basic module consists of a porphyrin (lozenge) covalently attached to a chelate (arc of a circle). Provided the transition metal complex is resistant to ligand-exchange processes, stepwise electron- or energy-transfer can be envisaged after selective illumination of a porphyrin ring

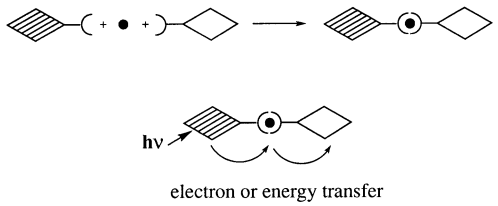

The role of the transition metal is manifold: (i) to gather and orient the system so as to have metallated porphyrins held rigidly at a fixed distance and to have asymmetrical systems able to undergo electron- or energy-transfer; (ii) to modulate the electronic coupling between the donor and acceptor porphyrins, and (iii) to form a complex which could act as a relay in electron transfer or as an antenna in energy transfer.

The ligand to be attached to each porphyrin and the binding mode used to assemble the two modules into the final conjugates are selected so as to facilitate strict stereochemical control, especially with regard to the distance between the porphyrins.

5.1. Synthesis of Porphyrin-Metal Bis-terpyridine Diads

5.1.1. Synthesis of the Ligands: The use of 2,2′:6′,2"-terpyridine as a chelate is indeed very appealing for the strategy outlined in Scheme 3, since substitution at its 4′-position leads to axially symmetric bis-terpyridine complexes. The ligands used in the preparation of the porphyrin-metal bis-terpyridine conjugates are shown in Figure 12a and their syntheses have been described[73].

Figure 12. (a) Structures of the various terpyridine ligands used for the synthesis of the diads. (b) The various terpyridine-porphyrin diads

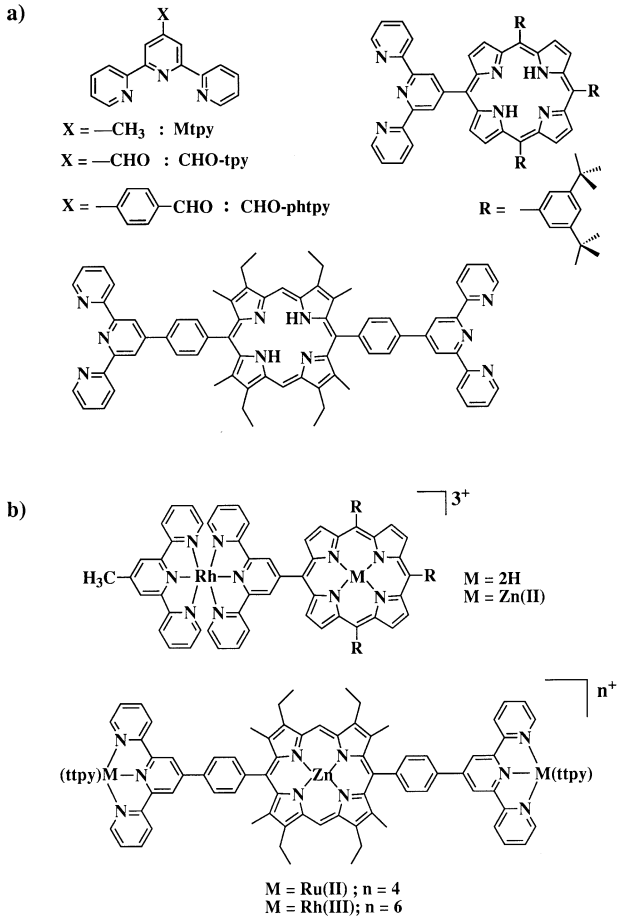

Although the preparation of 4′-methyl-2,2′:6′,2"-terpyridine (Mtpy) is well-documented[74][75][76], we have developed a new route which gives high yields (87%) and allows the preparation of large amounts (10 g scale) of this compound. This alternative route to Mtpy involves the reaction of 4′-trifluoroacetyl-2,2′:6′,2"-terpyridine[74][77] with tetramethyltin, using the general procedure described by Stille[78]. 4′-Formyl-2,2′:6′,2"-terpyridine (CHO−tpy) was prepared from Mtpy by a modification of a procedure developed by Vismara et al.[79], while a Sommelet reaction applied to 4′-tolyl-2,2′:6′,2"-terpyridine led to the corresponding aldehyde (CHO−phtpy)[73] in 40% yield. The

monoterpyridine porphyrin was prepared following Adler's procedure[80] and was isolated in 7% yield. The synthetic strategy for the preparation of bisphenylterpyridine porphyrin is derived from MacDonald's methodology[81], using the improved procedure developed by Lindsey et al.[82] This ligand was obtained pure in 42% yield after two recrystallizations of the crude material.

5.1.2. Synthesis of the Complexes: The complexes synthesized are shown in Figure 12b.

The rhodium(III) and ruthenium(II) complexes were prepared following the same strategy. In the first step, a given substituted terpyridine ligand L was reacted with the metal trichloride according to a literature procedure[37], thereby yielding $MLCl_3$ [M = Ru(III) or Rh(III)]. In the second step, after dechlorination with $AgBF_4$, the solvated complex $ML(acetone)_3^{n+}$ [M = Ru(III) or (RhIII)] was reacted with the appropriate substituted terpyridine in refluxing alcohol (EtOH or *n*BuOH).

Metallation of the free-base porphyrins in the different compounds by zinc acetate is almost quantitative. The purity of each highly-colored complex was checked by thin-layer chromatography, UV/Vis spectroscopy, high resolution ^{1}H-NMR spectrometry and mass spectroscopy.

5.1.3. Photophysical Properties of the Diads: Photophysical properties have been measured for zinc and free-base porphyrins covalently linked to ruthenium(II) or rhodium(III) bis-terpyridine complexes using ultrafast transient absorption spectroscopy and the full study has been reported[73]. In each compound, the appended metal complex quenches porphyrin fluorescence. The quenching is attributed to intramolecular electron transfer from the excited singlet state of the porphyrin to the metal complex. For directly coupled systems, it appears that both forward and reverse electron-transfer steps are extremely fast, and such materials possess little attraction as building blocks. Insertion of a phenyl ring between the components has a profound effect on the dynamics of electron transfer, especially with regard to charge recombination. In particular, the relatively long lifetime (2 ns) of the charge-separated state of the zinc-porphyrin phenyl-bridged ruthenium(II) bis-terpyridine conjugate (Figure 12b) makes the ruthenium(II) complex attractive as a bridge in multicomponent systems. The ruthenium(II) bis-terpyridine-based system has the additional attraction that light absorbed by the complex is transferred to the triplet excited state of the porphyrin by way of an antenna effect.

5.2. Synthesis of a Bis-porphyrin-Ruthenium(II) Bisphenylterpyridine Triad

In order to perform long-range charge separation, the triad represented in Figure 13 was prepared[83][84]. It should be noted that it contains two differently substituted porphyrins, a zinc etioporphyrin-like donor and a gold(III) tetraarylporphyrin acceptor. The $-CH_3$ and $-CH_2CH_3$ substituents located at the periphery of the tetrapyrrolic donor increase the electron-donating ability of the singlet excited state (^{1}*PZn) and thus favour electron transfer to the central $Ru(tpy)_2^{2+}$ unit. On the other hand, the tetraarylporphyrin backbone metallated by a gold(III) centre is a better electron acceptor than the analogous gold(III) etioporphyrin.

Figure 13. The triad

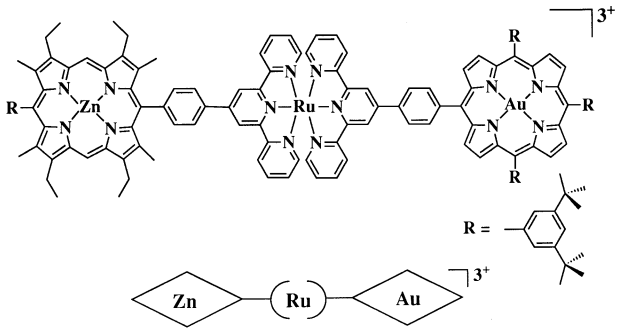

5.2.1. Synthesis of the Ligands: The various precursors leading to the triad are depicted in Figure 14.

Figure 14. The various reagents and ligands used in the preparation of the triad

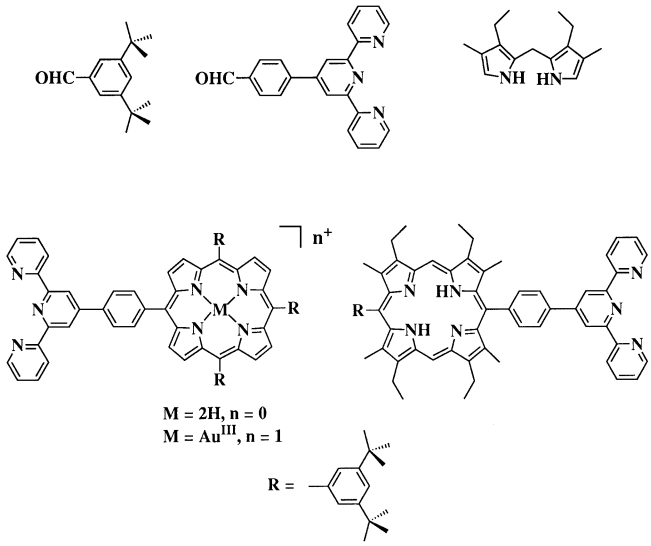

Synthesis of the octaalkyl diaryl porphyrin terpyridine was achieved in 20% yield following MacDonald's methodology[81] using Lindsey's conditions[82]: acid-catalysed condensation of dipyrrylmethane with 3,5-di-*tert*-butylbenzaldehyde and terpyridine benzaldehyde in a molar ratio of 6:5:1 in dichloromethane. The tetraaryl-porphyrin terpyridine was prepared using two different sets of conditions: (i) Using Adler's conditions[80], a mixture of 3,5-di-*tert*-butylbenzaldehyde, terpyridine benzaldehyde and pyrrole in a ratio of 18:1:19 was refluxed in propionic acid giving the desired compound in 13% yield after purification by column chromatography. (ii) Using Lindsey's conditions[82], a mixture of 3,5-di-*tert*-butylbenzaldehyde, terpyridine benzaldehyde and pyrrole in a molar ratio of 15:1:16 in dichloromethane containing trifluoroacetic acid was stirred at room temperature for 12 h. The resulting porphyrinogens were oxidized with tetrachloro-1,4-benzoquinone (chlor-

anil) in refluxing dichloromethane. The crude product was purified by column chromatography, giving pure phenylterpyridine porphyrin in 9% yield. Metallation of the free porphyrin site of this compound with gold(III) was achieved in 85% yield using $KAuCl_4$ and NaOAc in refluxing acetic acid.

5.2.2. Synthesis of the Complex: Stepwise formation of the asymmetrical ruthenium(II) complex from the gold(III) porphyrin phenylterpyridine and free-base porphyrin phenylterpyridine components was realized using a procedure similar to the one described in Section 5.1.2., which is shown schematically in Figure 15.

Figure 15. Stepwise formation of the triad

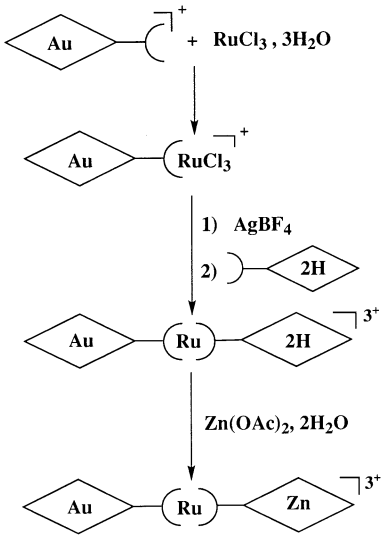

A pure sample of the triad was obtained in 35% yield by successive chromatography on silica gel, eluting with an acetonitrile/water/saturated aq. KNO_3 mixture. Metallation of the free porphyrin site was carried out with $Zn(OAc)_2$ in methanol and afforded the triad as an orange solid in 90% yield.

5.2.3. Electron-Transfer Properties of the Triad: Excitation of the terminal zinc porphyrin in the triad results in electron transfer to the central ruthenium(II) bis-terpyridine complex, which is followed by secondary electron transfer to the appended gold(III) porphyrin (Figure 16). Electron transfer occurs by two consecutive steps over a porphyrin centre-to-centre distance of ca. 30 Å.

Rate constants for the individual steps, as determined from laser photolysis studies[84], are indicated in Figure 16. The primary electron-transfer step leading to reduction of the central Ru(II) complex ($\Delta G° = -0.25$ eV) requires 50 ps and is essentially quantitative. The second electron-transfer process follows, resulting in reduction of the distant gold(III) porphyrin. The rate constant for this second step is found to be 6×10^8 s^{-1}. This process, for which there is a thermodynamic driving force of ca. 0.6 eV, is in competition with reverse electron transfer to restore the ground state. Subsequent charge transfer between the terminal porphyrinic subunits occurs with a rate constant of 3×10^7 s^{-1}

Figure 16. Energy level diagram showing the electron-transfer sequence for the triad

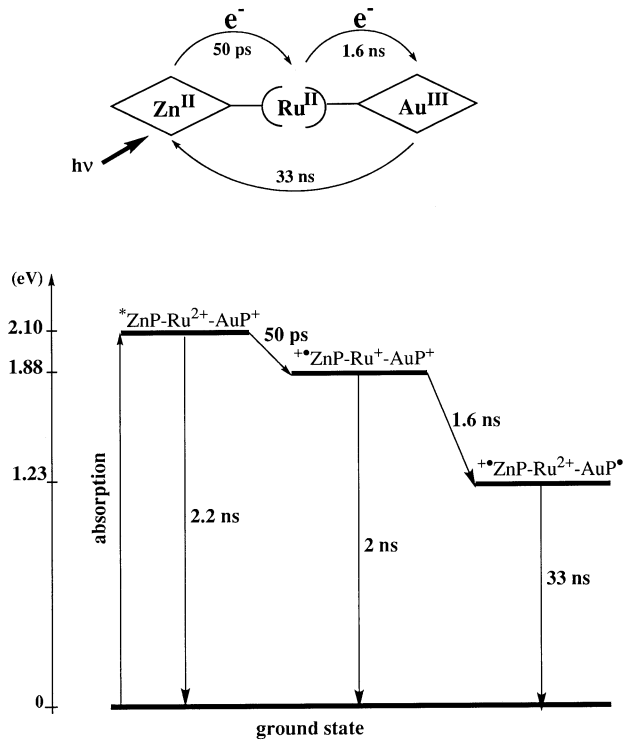

and leads to regeneration of the initial system. It is interesting to compare the lifetime of 33 ns for the ultimate charge-separated state in the triad with the value of 2 ns found for that in the corresponding diad (Section 5.1.3.); this illustrates the advantage of using a multistep electron-transfer pathway.

The salient features of this molecular triad may be summarized as follows: (i) there is rapid interporphyrin electron transfer between linear, fixed-distance subunits, (ii) the ultimate charge-separated state, which has a lifetime of 33 ns, retains almost 60% (1.2 eV) of a photonic input of 2.1 eV and, (iii) the modular synthetic approach is highly versatile, facilitating the preparation of many different $D-A_1-A_2$ triads and higher-order, linear oligomers.

6. A Copper(I) Rotaxane Incorporating Two Different Sites in a Thread: Molecules in Motion

Molecular systems whose motions can be triggered by applying an external signal are currently of special interest, both as mimics of biological systems (redox proteins) and as potential bistable molecular devices[85][86][87][88]. Catenanes and rotaxanes are particularly well-suited in this context since reversible molecular motions using interlocked or threaded rings can be easily performed[18][89][90][91][92]. The use of transition metal-containing systems is also especially favorable since the stereoelectronic requirements of the metal can depend strongly on its oxidation state. This property can be exploited for switching a molecular system from a given geometrical arrangement, corresponding to the most stable coordination for the tran-

sition metal(s) involved, to a different geometry, simply by changing the metal oxidation state by chemical or electrochemical means, ultimately leading to the preferred coordination for the new redox state[93][94][95][96].

6.1 Synthesis of the Rotaxane

A [2]-rotaxane is a molecular system consisting of a ring threaded by a string, with two blocking groups attached at either end of the string in order to prevent dethreading[97]. Such compounds were first prepared long ago[98][99], but were largely considered as mere chemical curiosities. Recently, rotaxanes have undergone a notable revival due to the newly developed efficient procedures which make them relatively easy to make[100][101][102], as well as because of their electro- and photochemical properties[103][104][105] and their aptitude for undergoing controlled molecular motions[18][89][92]. Recently, we reported the synthesis of a copper(I)-assembled rotaxane[106] with a coordinating macrocycle containing a 1,10-phenanthroline (phen) moiety forming the ring, and a threaded fragment incorporating both a phen unit and a 2,2′:6′2″-terpyridine (tpy) coordination site (Figure 17a). The key feature of the system is its potentially dual complexing mode towards a metal, involving the phen or tpy moieties.

Figure 17. (a) Representation of the Cu(I)-rotaxane. (b) Construction principle of the Cu(I)-rotaxane

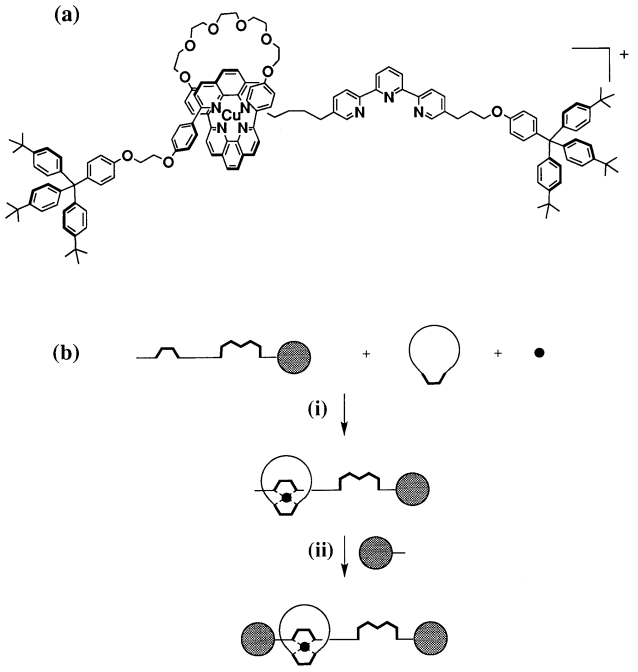

The synthetic strategy is illustrated in Figure 17b. A key step is the metal-directed threading process, often used in the past for making various catenanes and rotaxanes[107]. The bidentate chelate (phen, represented by an inverted U) and the terdentate unit (tpy, represented by a stylized M) are incorporated in an acyclic ligand, already bearing a bulky stopper at one end. The ring contains a phen nucleus. In the threading step (i) of Figure 17, copper(I) (represented by a black circle) forces the string to pass through the ring. Since copper(I) has a pronounced preference for tetracoordination, the threading reaction will selectively lead to the pseudo-rotaxane intermediate. The driving force behind this threading process is the great stability of the pseudotetrahedral bis-chelate complex between copper(I) and the two disubstituted 1,10-phenanthrolines[108]. The blocking reaction is performed by attaching a voluminous group at the other end of the coordinating string.

6.2. Electrochemically-Induced Molecular Motions

The principle of the process is explained in Figure 18. It is based on the difference of preferred coordination number for the two different redox states of the metal: 4 for copper(I) and 5 for copper(II). The electrochemical and chemical steps of the *square scheme* are analysed by a combination of cyclic voltammetry and controlled potential electrolysis experiments. The square scheme of *electron transfer induced* reactions[109] takes place, assuming that the chemical steps (motions of the ring from the phenanthroline to the terpyridine and *vice-versa*) are slow in comparison with the time scale of cyclic voltammetry. The voltammograms obtained demonstrate the perfect reversibility of the system, and also give the orders of magnitude of the rates of the chemical steps.

Figure 18. Square scheme in the copper rotaxane made in Figure 17

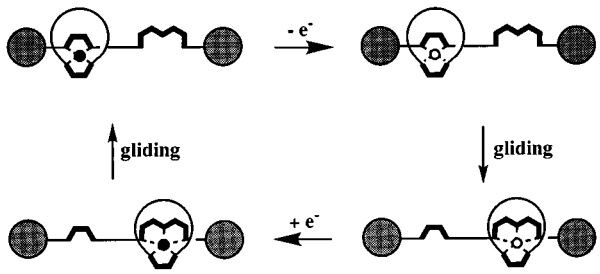

The stable 4-coordinate monovalent complex is oxidized to an intermediate tetrahedral divalent species. Due to the preference of copper(II) for a square-base pyramidal-type geometry, the ring moves to the terpyridine site to give the stable 5-coordinate copper(II) complex. Upon reduction, the 5-coordinate monovalent state is formed as a transient. Finally, the latter undergoes the reorganization process (opposite movement of the ring), thereby regenerating the starting complex [the shaded circle represents copper(I) and the white circle represents copper(II)].

Certainly, rotaxanes are very promising compounds with regard to electrochemically and photochemically induced molecular motions, due to the perfect chemical reversibility of the processes. Interestingly, the rates of the movements in the rotaxane are very different from those measured for related catenanes[19][90][91]. The conversion of copper(II) (4-coordinate state) to copper(II) (5-coodinate state) is much faster in rotaxane than in the interlocking ring systems described previously. This difference could reflect a greater ability of the copper(II) (4-coordinate state) in rotaxane to interact with solvent molecules or anions, the copper(II) centre being perhaps loosely bound to a fifth ligand, which

would thus stabilize intermediate states on the way to copper(II) (5-coordinate state). Interestingly, the sequence of electrochemical and chemical steps involved in the square scheme of Figure 18 is very different from the classical EC mechanism universally encountered in molecular electrochemistry since, in principle, it does not consume electrons.

7. Conclusion and Prospects

Although there may still be a long way to go from the design and synthesis of multifunctional molecules with predicted electrochemical or photochemical properties to the construction of real molecular devices, utilizable as artificial photosynthetic systems, photovoltaic devices or nanoscale components in electronics, the two last decades have nevertheless witnessed substantial progress as far as complex multicomponent molecules and molecular assemblies are concerned. In particular, the use of transition metals has contributed greatly to progress in the field. In this context, the role of the metal is twofold: (i) to gather ligands bearing various functional groups and thus allow the construction of compounds with a defined arrangement, the electro- and photoactive groups incorporated in the molecule being disposed in space with a good geometrical control, and (ii) to provide interesting functions related to electronic molecular motions and thus become operative parts of the system.

In the field of electron- and energy-transfer, in relation to artificial photosynthesis, terpyridine has been used extensively. The coordination geometry and the symmetry of its complexes has been used to good advantage in the construction of several families of compounds incorporating ruthenium(II) or osmium(II) centres connected to various other electro- or photoactive components. Photoinduced charge separation over a long distance (> 20 Å) has been demonstrated in a few instances. If porphyrins are used as building blocks in conjunction with bis-terpyridine ruthenium(II), long-range (30 Å) and long-lived charge separation takes place. Energy transfer between inorganic chromophores [ruthenium(II) and osmium(II) complexes] has also been shown to occur over more than 20 Å, the success of the process being attributable to the inherent rigidity of the bridging spacer used and, above all, to the electronic properties provided by its bis-cyclometallating nature.

Molecular machines constitute an emerging field and, again, strict control over the geometry of the ensemble used and over the trajectory of the fragment(s) set in motion will be essential. It is of course much too early to know whether molecular machines and nanoscopic motors will one day be used in imaging or as molecular information storage devices, but the search for such systems is important and allows the discovery of interesting properties related to molecular dynamics. The rotaxane discussed in the present review article also has a one-dimensional component since the movement observed is that of a ring gliding on a linear fragment on which it is threaded. Presently, the system is close to bistable, but in the future it should be generalized to less primitive molecular machines, with more complex mobility (2 or several fragments in motion) or several possible geometries.

This work was supported by the CNRS (France). Special thanks go to *Balzani*'s, *Barigelletti*'s and *Harriman*'s groups. Thanks are also due to all the members of our team who contributed to the work described in the present review article with so much skill and enthusiasm.

☆ Dedicated to the memory of Professor *M. Momenteau*, a creative porphyrin chemist, who recently passed away untimely.
[1] J.-P. Sauvage, J.-P. Collin, J.-C. Chambron, S. Guillerez, C. Coudret, V. Balzani, F. Barigelletti, L. De Cola, L. Flamigni, *Chem. Rev.* **1994**, *94*, 993.
[2] J.-P. Collin, A. Harriman, V. Heitz, F. Odobel, J.-P. Sauvage, *Coord. Chem. Rev.* **1996**, *148*, 63.
[3] F. Barigelletti, L. Flamigni, J.-P. Collin, J.-P. Sauvage, *J. Chem. Soc., Chem. Comm.* **1997**, 333.
[4] D. L. Dexter, *J. Chem. Phys.* **1953**, *21*, 836.
[5] T. Förster, *Discuss. Faraday Soc.* **1959**, *27*, 7.
[6] R. A. Marcus, *J. Chem. Phys.* **1956**, *24*, 966.
[7] R. A. Marcus, N. Sutin, *Biochim. Biophys. Acta* **1985**, *811*, 265.
[8] J. L. Sessler, M. R. Johnson, S. E. Creager, J. C. Fettinger, J. A. Ibers, *J. Am. Chem. Soc.* **1990**, *112*, **9310**.
[9] D. Gust, T. A. Moore, *Top. Curr. Chem.,* **1991**, *159*, 103.
[10] A. Helms, D. Heiler, G. McLendon, *J. Am. Chem. Soc.* **1992**, *114*, 6227.
[11] D. G. Johnson, M. P. Niemczyk, D. W. Wiederrecht, D. W. Minsek, G. L. Gaines III, W. A. Svec, M. R. Wasielewski, *J. Am. Chem. Soc.* **1993**, *115*, 5692.
[12] A. Osuka, S. Nakajima, K. Maruyama, N. Mataga, T. Asahi, I. Yamazaki, Y. Nishimura, T. Ohno, K. Nozaki, *J. Am. Chem. Soc.* **1993**, *115*, 4577.
[13] J. Deisenhofer, O. Epp, K. Miki, R. Huber, H. Michel, *J. Mol. Biol.* **1984**, *180*, 385.
[14] J.-P. Allen, G. Feher, T. O. Yeates, H. Komiya, D. C. Rees, *Proc. Natl. Acad. Sci. USA* **1987**, *84*, 5730.
[15] V. Balzani, F. Scandola, *Supramolecular Photochemistry*; Ellis Horwood, Chichester, **1990**.
[16] R. Argazzi, C. A. Bignozzi, T. A. Heimer, F. N. Castellano, G. J. Meyer, *Inorg. Chem.* **1994**, *33*, 5741.
[17] M. K. Nazeerudin, A. Kay, I. Rodicio, R. Humphry-Baker, E. Müller, P. Liska, N. Vlachopoulos, M. Grätzel, *J. Am. Chem. Soc.* **1993**, *115*, 6382.
[18] R. A. Bissell, E. Córdova, A. E. Kaifer, J. F. Stoddart, *Nature* **1994**, *369*, 133.
[19] A. Livoreil, C. O. Dietrich-Buchecker, J.-P. Sauvage, *J. Am. Chem. Soc.* **1994**, *116*, 9399.
[20] P. R. Ashton, R. Ballardini, V. Balzani, S. E. Boyd, A. Credi, M. T. Gandolfi, M. Gomez-Lopez, S. Iqbal, D. Philp, J. A. Preece, L. Prodi, H. Ricketts, J. F. Stoddart, M. S. Tolley, M. Venturi, A. J. P. White, D. J. Williams, *Chem. Eur. J.* **1997**, *3*, 152.
[21] T. J. Meyer, *Acc. Chem. Res.* **1989**, *22*, 163.
[22] V. Scandola, M. T. Indelli, C. Choirboli, C. A. Bignozzi, *Top. Curr. Chem.* **1990**, *158*, 73.
[23] A. Juris, V. Balzani, F. Barigelletti, S. Campagna, P. Belser, A. Von Zelewsky, *Coord. Chem. Rev.* **1988**, *84*, 85.
[24] V. Balzani, F. Barigelletti, L. De Cola, *Top. Curr. Chem.* **1990**, *158*, 31.
[25] E. Danielson, C. Elliot, J. W. Merckert, T. J. Meyer, *J. Am. Chem. Soc.* **1987**, *109*, 2519.
[26] J.-P. Collin, S. Guillerez, J.-P. Sauvage, *J. Chem. Soc., Chem. Comm.* **1989**, 776.
[27] G. T. Morgan, F. H. Burstall, *J. Chem. Soc.* **1932**, 20.
[28] T. Kauffmann, J. König, A. Woltermann, *Chem. Ber.* **1976**, *109*, 3864.
[29] A. Hantzsch, *Ann. Chem.* **1882**, *215*, 1.
[30] A. E. Tschitschibabin, *J. Prakt. Chem.* **1924**, *107*, 122.
[31] H. Case, T. J. Kasper, *J. Am. Chem. Soc.* **1956**, *78*, 5842.
[32] F. Kröhnke, *Synthesis* **1976**, 1.
[33] E. C. Constable, M. D. Ward, S. Corr, *Inorg. Chim. Acta* **1988**, *141*, 201.
[34] K. T. Potts, M. J. Cipullo, P. Ralli, G. Theodoridis, *J. Org. Chem.* **1982**, *47*, 3027.
[35] D. L. Jameson, L. E. Guise, *Tetrahedron Lett.* **1991**, *32*, 1999.
[36] W. Spahni, G. Calzaferri, *Helv. Chim. Acta* **1984**, *67*, 450.

[37] J.-P. Collin, S. Guillerez, J.-P. Sauvage, F. Barigelletti, L. De Cola, L. Flamigni, V. Balzani, *Inorg. Chem.* **1991**, *30*, 4230.
[38] J.-C. Chambron, C. Coudret, J.-P. Sauvage, *New J. Chem.* **1992**, *16*, 361.
[39] J.-P. Collin, S. Guillerez, J.-P. Sauvage, F. Barigelletti, L. De Cola, L. Flamigni, V. Balzani, *Inorg. Chem.* **1992**, *31*, 4112.
[40] J.-P. Collin, S. Guillerez, J.-P. Sauvage, *Inorg. Chem.* **1990**, *29*, 5009.
[41] C. Coudret, Thesis, Louis Pasteur University of Strasbourg, **1991**.
[42] T. J. Meyer, *Pure and Appl. Chem.* **1986**, *58*, 1193.
[43] J.-P. Collin, S. Guillerez, J.-P. Sauvage, F. Barigelletti, L. De Cola, L. Flamigni, V. Balzani, *Coord. Chem. Rev.* **1991**, *111*, 291.
[44] E. C. Constable, M. D. Ward, *J. Chem. Soc., Dalton Trans.* **1990**, 1405.
[45] E. C. Constable, J. Lewis, *Polyhedron* **1982**, *1*, 303.
[46] H. E. Zimmermann, R. D. McKelvey, *J. Am. Chem. Soc.* **1971**, *93*, 3638.
[47] R. W. Hoffmann, A. Endesfelder, H.-J. Zeiss, *Carbohydr. Res.* **1983**, *123*, 320.
[48] N. Miyaura, T. Yanagi, A. Suzuki, *Synth. Comm.* **1981**, *11*, 513.
[49] J. M. Tour, J. J. S. Lamba, *J. Am. Chem. Soc.* **1993**, *115*, 4935.
[50] F. Barigelletti, L. Flamigni, V. Balzani, J.-P. Collin, J.-P. Sauvage, A. Sour, E. C. Constable, A. M. W. Cargill-Thompson, *J. Chem. Soc., Chem. Comm.* **1993**, 942.
[51] F. Barigelletti, L. Flamigni, V. Balzani, J.-P. Collin, J.-P. Sauvage, A. Sour, E. C. Constable, A. M. W. Cargill-Thompson *J. Am. Chem. Soc.* **1994**, *116*,7692.
[52] F. Barigelletti, L. Flamigni, V. Balzani, J.-P. Collin, J.-P. Sauvage, A. Sour, *New J. Chem.* **1995**, *19*, 793.
[53] L. Hammarström, F. Barigelletti, L. Flamigni, N. Armaroli, A. Sour, J.-P. Collin, J.-P. Sauvage, *J. Am. Chem. Soc.* **1996**, *118*, 11972.
[54] M. T. Indelli, F. Scandola, J.-P. Collin, J.-P. Sauvage, A. Sour, *Inorg. Chem.* **1996**, *35*, 303.
[55] F. Barigelletti, L. Flamigni, V. Balzani, J.-P. Collin, J.-P. Sauvage, A. Sour, E. C. Constable, A. M. W. Cargill-Thompson, *Coord. Chem. Rev.* **1994**, *132*, 209
[56] V. Grosshenny, A. Harriman, R. Ziessel, *Angew. Chem., Int. Ed. Engl.* **1995**, *34*, 1100.
[57] L. De Cola, V. Balzani, F. Barigelletti, L. Flamigni, P. Belser, A. von Zelewsky, M. Frank, F. Vögtle, *Inorg. Chem.* **1993**, *32*, 5228.
[58] L. De Cola, V. Balzani, F. Barigelletti, L. Flamigni, P. Belser, S. Brenhard, *Recl. Trav. Chim. Pays-Bas* **1995**, *114*, 534.
[59] M. Frank, M. Nieger, F. Vögtle, P. Belser, A. Von Zelewsky, L. De Cola, V. Balzani, F. Barigelletti, L. Flamigni, *Inorg. Chim. Acta* **1996**, *242*, 281.
[60] M. T. Indelli, C. A. Bignozzi, A. Harriman, J. R. Schoonover, F. Scandola, *J. Am. Chem. Soc.* **1994**, *116*, 3768.
[61] M. Furue, M. Hirata, S. Kinoshita, T. Kushida, M. Kamachi, *Chem. Lett.* **1990**, 2065.
[62] K. Nozaki, T. Ohno, M. Haga, *J. Phys. Chem.* **1992**, *96*, 10880.
[63] K. Kalyanasundaram, M. Grätzel, K. Nazeeruddin, *J. Phys. Chem.* **1992**, *96*, 5865.
[64] H. Bönnemann, *Angew. Chem., Int. Ed. Engl.* **1978**, *17*, 505.
[65] M. Beley, J.-P. Collin, R. Louis, B. Metz, J.-P. Sauvage, *J. Am. Chem. Soc.* **1991**, *113*, 8521.
[66] J. K. Stille, *Angew. Chem., Int. Ed. Engl.* **1986**, *25*, 508.
[67] T. R. Kelly, G. J. Bridger, C. Zhao, *J. Am. Chem. Soc.* **1990**, *112*, 8024.
[68] Y. H. Kim, O. W. Webster, *J. Am. Chem. Soc.* **1990**, *112*, 4592.
[69] T. I. Wallow, B. M. Novak, *J. Am. Chem. Soc.* **1991**, *113*, 7411.
[70] M. Beley, S. Chodorowski, J.-P. Collin, J.-P. Sauvage, *Tetrahedron Lett.* **1993**, *34*, 2933.
[71] M. Beley, S. Chodorowski, J.-P. Collin, J.-P. Sauvage, L. Flamigni, F. Barigelletti, *Inorg. Chem.* **1994**, *33*, 2543.
[72] F. Barigelletti, L. Flamigni, M. Guardigli, A. Juris, M. Beley, S. Chodorowski-Kimmes, J.-P. Collin, J.-P. Sauvage, *Inorg. Chem.* **1996**, *35*, 136.
[73] J.-P. Collin, A. Harriman, V. Heitz, F. Odobel, J.-P. Sauvage, *J. Am. Chem. Soc.* **1994**, *116*, 5679.
[74] R. B. Bates, B. Gordon III, P. C. Keller, J. V. Rund, N. S. Mills, *J. Org. Chem.* **1980**, *45*, 168.
[75] T. W. Bell, L. Y. Hu, *Tetrahedron Lett.* **1988**, *29*, 4819.
[76] K. T. Potts, D. A. Usifer, A. Guadalupe, H. D. Abruna, *J. Am. Chem. Soc.* **1987**, *109*, 3961.
[77] K. T. Potts, D. J. Konwar, *J. Org. Chem.* **1991**, *56*, 4815.
[78] A. M. Echavarren, J. K. Stille, *J. Am. Chem. Soc.* **1987**, *109*, 5478.
[79] E. Vismara, F. Fontana, F. Minisci, *Gazz. Chim. Ital.* **1987**, *117*, 135.
[80] A. D. Adler, F. R. Longo, J. D. Finarelli, J. Goldmacher, J. Assour, L. Korsakoff, *J. Org. Chem.* **1967**, *32*, 476.
[81] G. P. Arsenault, E. Bullock, S. F. MacDonald, *J. Am. Chem. Soc.* **1960**, *82*, 4384.
[82] J. S. Lindsey, J. C. Schreiman, H. C. Hsu, P. C. Kearney, A. M. Marguerettaz, *J .Org. Chem.* **1987**, *52*, 827.
[83] F. Odobel, J.-P. Sauvage, *New J. Chem.* **1994**, *18*, 1139.
[84] A. Harriman, F. Odobel, J.-P. Sauvage, *J. Am. Chem. Soc.* **1995**, *117*, 9461.
[85] J. Bixler, G. Bakker, G. McLendon, *J. Am. Chem. Soc.* **1992**, *114*, 6938.
[86] T. Pascher, J. P. Chesick, J. R. Winkler, H. B. Gray, *Science* **1996**, *271*, 1558.
[87] M. Hanazawa, R. Sumiya, Y. Horikawa, M. Irie, *J. Chem. Soc., Chem. Comm.* **1992**, 206.
[88] D. P. Arnold, V. V. Borovkov, G. V. Ponomarev, *Chem. Lett.* **1996**, 485.
[89] R. Ballardini, V. Balzani, M. T. Gandolfi, L. Prodi, M. Venturi, D. Philp, H. G. Ricketts, J. F. Stoddart, *Angew. Chem., Int. Ed. Engl.* **1993**, *32*, 1301.
[90] F. Baumann, A. Livoreil, W. Kaim, J.-P. Sauvage, *J. Chem. Soc., Chem. Comm.* **1997**, 35.
[91] D. J. Cardenas, A. Livoreil, J.-P. Sauvage, *J. Am. Chem. Soc.* **1996**, *118*, 11980.
[92] J.-P. Collin, P. Gavina, J.-P. Sauvage, *J. Chem. Soc., Chem. Comm.* **1996**, 2005.
[93] M. Sano, H. Taube, *J. Am. Chem. Soc.* **1991**, *113*, 2327.
[94] A. Tomita, M. Sano, *Inorg. Chem.* **1994**, *33*, 5825.
[95] L. Zelikovich, J. Libman, A. Shanzer, *Nature* **1995**, *374*, 790.
[96] C. Canevet, J. Libman, A. Shanzer, *Angew. Chem., Int. Ed. Engl.* **1996**, *35*, 2657.
[97] G. Schill, *Catenanes, Rotaxanes and Knots*, Academic Press, New York, **1971**.
[98] G. Schill, H. Zollenkopf, *Liebigs Ann. Chem.* **1969**, *721*, 53.
[99] I. T. Harrison, S. Harrison, *J. Am. Chem. Soc.* **1967**, *89*, 5723.
[100] H. Ogino, *J. Am. Chem. Soc.* **1981**, *103*, 1303.
[101] M. Belohradsky, F. M. Raymo, J. F. Stoddart, *Collect. Czech. Chem. Commun.* **1996**, *61*, 1.
[102] H. W. Gibson, M. C. Bheda, P. T. Egen, *Prog. Polym. Sci.* **1994**, *19*, 843. − D. A. Leigh, A. Murphy, J.P. Smart, A.M.Z. Slawin, *Angew. Chem., Int. Ed. Engl.* **1997**, *36*, 728. − R. J& aumlɛr, F. Vögtle, *Angew. Chem., Int. Ed. Engl.* **1997**, *36*, 930. − A. Harada, J.Li, M. Kamachi, Nature **1994**, *370*, 126. − G. Wenz, B. Keller, *Angew. Chem., Int. Ed. Engl.* **1992**, 31, 197.
[103] J.-C. Chambron, A. Harriman, V. Heitz, J.-P. Sauvage, *J. Am. Chem. Soc.* **1993**, *115*, 6109.
[104] F. Diederich, C. O. Dietrich-Buchecker, J.-F. Nierengarten, J.-P. Sauvage, *J. Chem. Soc., Chem. Comm.* **1995**, 781.
[105] S. S. Zhu, P. J. Carroll, T. M. Swager, *J. Am. Chem. Soc.* **1996**, *118*, 8713.
[106] J.-P. Collin, P. Gavina, J.-P. Sauvage, *New J. Chem.* **1997**, *21*, 525.
[107] J.-C. Chambron, C. O. Dietrich-Buchecker, J.-P. Sauvage in *Comprehensive Supramolecular Chemistry*, Pergamon Press, Oxford, **1996**, 43.
[108] J.-C. Chambron, C. O. Dietrich-Buchecker, J.-F. Nierengarten, J.-P. Sauvage, *J. Chem. Soc., Chem. Comm.* **1993**, 801.
[109] D. H. Evans, *Chem. Rev.* **1990**, *90*, 739.

[97168]

Conformational Flexibility of the Square-Pyramidal Coordination Cap in a Series of Octahedral Nickel(II) Pentaamine Complexes − Magnetochemical Characterization of the Singly μ-Cl-Bridged Nickel(II) Dimer [(pyN_4)Ni-Cl-Ni(pyN_4)](PF_6)$_3$ [pyN_4 = 2,6-Bis(1′,3′-diamino-2′-methylprop-2′-yl)pyridine]

Christian Dietz[a], Frank W. Heinemann[a][+], Jörg Kuhnigk[b][+], Carl Krüger[b][+], Michael Gerdan[c][++], Alfred X. Trautwein[c][++], and Andreas Grohmann*[a]

Institut für Anorganische Chemie, Universität Erlangen-Nürnberg,[a]
Egerlandstraße 1, D-91058 Erlangen, Germany
Fax: +49 (0)9131/857367
E-mail: grohmann@anorganik.chemie.uni-erlangen.de

Max-Planck-Institut für Kohlenforschung,[b]
Kaiser-Wilhelm-Platz 1, D-45470 Mülheim an der Ruhr, Germany

Institut für Physik, Medizinische Universität zu Lübeck,[c]
Ratzeburger Allee 160, D-23538 Lübeck, Germany

Received December 23, 1997

Keywords: Tetrapodal pentadentate ligand / Square pyramidal coordination cap / Pentaamine / Nickel(II) complexes / Magnetochemistry

The architecture of the tetrapodal pentaamine ligand 2,6-bis(1′,3′-diamino-2′-methylprop-2′-yl)pyridine (pyN_4, **1**) allows it to coordinate to nickel(II) as a square pyramidal coordination cap. The pyridine nitrogen atom occupies an apical position of the coordination octahedron, while four equivalent pendent primary amino groups occupy the equatorial positions, with a sixth coordination site remaining for a monodentate ligand. Exchange of this ligand is facile, and a series of complexes [(**1**)NiX]$^{n+}$ (X = OH_2, $OClO_3$, NCS, N_3, {Cl-Ni(pyN_4)}) has been prepared and characterised by elemental analysis, IR and UV/Vis spectroscopies (as applicable), and X-ray structure determination. While the solid state structures show varying degrees of distortion of the ligand cap **1** from C_{2v} symmetry, a polynucleating coordination mode has not been observed. The ligand enables the synthesis of dinuclear nickel(II) complexes containing a single bridging ligand, as exemplified by the singly μ-chloro bridged complex [(**1**)Ni–Cl–Ni(**1**)](PF_6)$_3$. This complex has an antiferromagnetically coupled ground state of total spin $S_T = 0$, as determined from variable-temperature magnetic susceptibility measurements.

Introduction

The objective of our work is to explore the potential of tetrapodal pentadentate ligands as mononucleating head groups in functional transition metal complexes. Ligands of this topology are virtually unknown. Specifically, we aim to create octahedral coordination compounds containing a square-pyramidal coordination cap (a pentadentate ligand) and a substrate (a monodentate ligand), which is bound at the sixth coordination site. Ideally, functional groups appended to the base of the coordination cap will provide an environment for the substrate in which it shows modulated reactivity. Such metal complexes would utilise the principles of simultaneous first- and second-sphere coordination[1][2].

In this context, we recently introduced a tetrapodal pentadentate ligand with an NN_4 donor set, consisting of a central pyridine and four equivalent primary amino nitrogen atoms (pyN_4, **1**)[3]. Structural characterization of a cobalt(III) chloro complex showed that the ligand provides the desired square pyramidal coordination cap. A square-pyramidally coordinating ligand of overall C_{2v} symmetry represents a novel structural motif in coordination chemistry since it has one central donor atom which occupies the apical position of a pyramid, while *four* equivalent pendent donor groups take the basal positions. In the case of octahedral complexes, such a coordination mode leaves a sixth site for the binding of a monodentate substrate. The tetrapodal pentadentate ligand **1** is particularly attractive in that it forces a sixth ligand to coordinate *trans* to a pyridine substituent. While this feature has been suggested to influence the overall reactivity with respect to ligand exchange in certain cases, experimental verification has so far been lacking[4]. A topological relative of **1** has recently been described[5], being virtually identical to a ligand previously used by Canty and co-workers in their studies of the coordination chemistry of palladium(II), where square-pyramidal coordination was not observed[6]. A different type of tetrapodal pentadentate ligand of C_2 symmetry involves a "superstructured"[7][8] porphyrin, *i. e.* the basal donor atoms are incorporated into a macrocyclic ring.[9]

As part of our studies directed toward the synthesis of functional metal complexes with a square-pyramidal coor-

[+] X-ray structure analyses. − [++] Magnetochemical measurements.

 © WILEY-VCH Verlag GmbH, D-69451 Weinheim, 1998 1434−1948/98/0707−1041 $ 17.50+.50/0

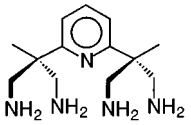

1

dination cap, we have been exploring the coordination behaviour of the pyN_4 ligand **1** and the reactivity of a variety of complex fragments of the type [(**1**)M] (M = Co, Ni, Rh), as well as the further derivatization of this ligand in order to construct a concave ligand periphery and/or an enclosed coordination site. We now wish to report our findings relating to ligand exchange at the fragment $[(\mathbf{1})Ni]^{2+}$, for which we have used the aqua complex $[(\mathbf{1})Ni(H_2O)]Cl_2$ (**2**) as precursor. We were interested in the structural characterization of the aqua complex as well as a series of other complexes $[(\mathbf{1})Ni(X)]^{n+}$ (X = perchlorate, halide, pseudohalide), in order to assess the influence, if any, of monodentate ligands X upon the coordination mode of the pentadentate ligand, and to obtain a quantitative measure of the flexibility of the ligand in those cases where it does provide a square-pyramidal coordination cap.

Exchange reactions have yielded the mono- and dinuclear nickel(II) complexes $[(\mathbf{1})Ni(H_2O)]I_2$ (**4**), $[(\mathbf{1})Ni(OClO_3)](ClO_4)$ (**5**), $[(\mathbf{1})Ni(\mu\text{-}Cl)Ni(\mathbf{1})](PF_6)_3$ (**6**), $[(\mathbf{1})Ni(NCS)](PF_6)$ (**7**), and $[(\mathbf{1})Ni(N_3)](PF_6)$ (**8**). While the solid state structures of these compounds show different degrees of distortion of the ligand cap, the pentaamine ligand **1** does act as a podand in all cases, and a polynucleating coordination mode (which is undesirable in the light of the aims specified above) is not observed. Since the pentadentate ligand effectively blocks five coordination sites in a coordination octahedron, it allows the synthesis of dinuclear complexes containing a single bridging ligand. In view of the interest attached to such complexes, particularly with respect to their magnetic properties[10], we have undertaken the magnetochemical characterization of the dinuclear μ-chloro-bridged nickel(II) complex **6**.

Results and Discussion

Analytical data indicate the nickel(II) aqua complex $[(\mathbf{1})Ni(H_2O)]Cl_2$ (**2**) to be the primary species formed when an ammoniacal aqueous solution of the tetrakis(hydrochloride) salt **1** • 4 HCl (ref.[3]) is treated with one equivalent of $NiCl_2 \bullet 6\ H_2O$. Drying of the purple crystalline material in vacuo results in a colour change to bluish green which indicates removal of the aqua ligand. Addition of $NaClO_4$ to an aqueous solution of **2** and recrystallization of the resulting precipitate from water/methanol (1:1 v/v) gives a crystalline solid (**3**) with no conclusive elemental analysis and IR data. Preliminary X-ray structural data of this solid confirm the pyN_4 ligand to act as a square-pyramidal coordination cap and reveal the presence of at least one uncoordinated perchlorate anion, but do not allow the identification of the monodentate ligand at the sixth coordination site. The residual electron density is compatible with a ligand containing a single "heavy" atom, and both chloride and water are likely candidates, but neither enables further refinement. Hence, the possibility of this substance being a mixture of the chloro and aqua complexes cannot be ruled out.

$[(\mathbf{1})Ni(H_2O)]I_2$ (4)

Exchange of the monodentate ligand is facile in **2** and **3**, and the above results suggest chloride and water compete as ligands for the sixth coordination site. The aqua complex is formed exclusively as the iodide salt $[(\mathbf{1})Ni(H_2O)]I_2$ (**4**) upon recrystallization of **2** from water in the presence of an excess of sodium iodide. These conditions apparently prevent the coordination of chloride, while the large iodide ligand, if accommodated, would induce steric strain as a consequence of van der Waals interactions with the basal amino groups of the complex fragment $[(\mathbf{1})Ni]^{2+}$ (ref.[11]).

The spectroscopic characteristics of **4** resemble those determined for the other complexes in the present series (**5**, **6**, **7**, and **8**). All complexes contain octahedrally coordinated high-spin nickel(II), making ^1H NMR spectra of limited diagnostic value due to paramagnetically shifted and broadened resonances (an assignment is given below for the proton spectrum of **5**, based on approximate integration intensities and chemical shifts). The UV/Vis spectrum of an aqueous solution of **4** is characterized by an absorption attributable to a d-d transition at $\lambda = 543$ nm ($\varepsilon = 3.4\ dm^3\ mol^{-1}\ cm^{-1}$), in keeping with data obtained for other six-coordinate polyamine complexes of Ni(II)[12]. The spectrum is virtually identical to those of complexes **5**, **6**, **7**, and **8**, presumably due to the ease of ligand exchange at the sixth coordination site.

The IR spectrum of **4** shows bands characteristic of N−H, O−H, and skeletal vibrations of the ligand [in particular, the ν(C=C) and ν(C=N) in-plane vibrations of the pyridine ring]. The base peak in the FD mass spectrum is at $m/z = 436$ ($[(\mathbf{1})NiI]^+$), all other peaks having an intensity of less than 10%. In the FAB spectrum, the base peak is again at $m/z = 436$, with a fragment ion at $m/z = 309$ ($[(\mathbf{1})Ni]^+$, 45%). These results indicate that exchange of the aqua ligand for an iodo ligand does occur under the conditions prevailing in the mass spectrometer.

Compound **4** crystallises in the monoclinic space group $P2_1/n$. The molecular structure of the cation, which has no crystallographically imposed symmetry, is shown in Figure 1. The nickel(II) ion is coordinated by the pentaamine ligand **1** in pyramidal fashion, leading to the formation of six six-membered chelate rings, all of which adopt a boat conformation. The aqua ligand completes the Ni(II) coordination octahedron. It forms two weak hydrogen bonds to the two iodide counterions [d(O1···I1) = 3.406(4) A, d(O1···I2) = 3.405(3) A; sum of the van der Waals radii of O and I: 3.50 A[13]]. The arrangement of the equatorial nitrogen atoms around the nickel centre is trapezoidal rather than square planar, with two shorter and two longer $Ni-N_{eq}$ bond distances (Table 1). The angles $N_{eq}-Ni-N_{eq}$ in the NiN_4 plane have average values of 84.9(2)° and 95.2(2)° for diametrically opposite pairs, the smaller value representing the averaged "bite angle" of the 1,3-diaminoprop-2-yl substituents. These groups are displaced slightly

toward the equatorial NiN_4 unit, as indicated by the deviations of the angles at the *ortho* carbon atoms from their ideal values of 120° [N11−C11−C18 116.8(3)°; C12−C11−C18 122.7(4)°; N11−C15−C22 116.7(3)°; C14−C15−C22 122.8(4)°]. Whether this is a consequence of the ligand acting as a podand toward the central nickel ion cannot be said with certainty as similar deviations are observed for the corresponding angles in the tetrakis(hydrobromide) salt **1** • 4 HBr where the *ortho* substituents are not constrained by metal coordination[14]. However, the Ni−N_{ax} bond length at 2.050(3) A is shorter than the average Ni−N_{eq} bond length [2.090(4) A]. By way of comparison, the corresponding Ni−N_{py} bond lengths in the cation $[(H_2O)_5Ni(py)]^{2+}$ and in a Ni(II) cyclam complex with a pendent pyridyl group coordinated *trans* to an aqua ligand are 2.08(1) A[15] and 2.142(4) A[16], respectively, while the averaged Ni−N_{eq} bond length in the latter complex is 1.927(5) A. The nickel−oxygen bond length in **4** [d(Ni−O) = 2.133(3) A] is within the range of values found in both the pentaaqua and the cyclam complexes [*d*(Ni−O) = 2.05(1)···2.18(1) A[15], and *d*(Ni−O) = 2.166(3) A[16], respectively].

Figure 1. Molecular structure of the cation in **4** with thermal ellipsoids drawn at the 50% probability level; hydrogen atoms are omitted for clarity

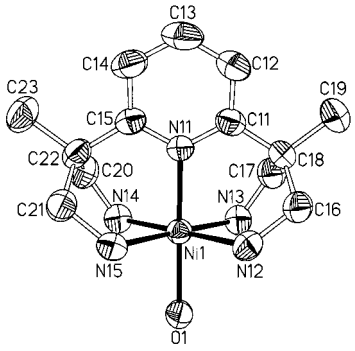

As shown in the side-on view in Figure 2, the $[(pyN_4)Ni]^{2+}$ complex fragment in **4** is distorted from C_{2v} symmetry. The pyridine ring, itself a regular hexagon, is tilted to one side of the (pyN_4)Ni pyramid, inducing a slight bending of the N_{ax}−Ni−O axis relative to the equatorial NiN_4 unit (cf. Table 1 for relevant bond angles N_{ax}−Ni−N_{eq}). This unit shows minor tetrahedral distortion, with diagonally opposite N donor atoms 0.015(4) A above and, respectively, below the plane containing the nickel atom. For the purpose of comparison with the other structures reported in the present publication, the distortion of the ligand cap in **4** from C_{2v} symmetry may be quantified as follows (Table 2): a) The least-squares planes defined by the pyridine ring (N11, C11, C12, C13, C14, C15) on the one hand and the quaternary and methyl carbon atoms C18, C19, C22, C23 on the other do not coincide but form a dihedral angle of 15.4(4)°; b) the least-squares planes defined by the four methylene carbon atoms C16, C17, C20, C21 and the four equatorial amino nitrogen atoms N12, N13, N14, N15 are not parallel but at a dihedral angle of 8.0(1)°; c) one of the distances between pairs of equivalent methylene carbon atoms in the two 1,3-diaminoprop-2-yl groups [*d*(C16···C21)] is widened to a value of 5.399(7) A, while the other [*d*(C17···C20)] is compressed to 4.743(7) A. This distortion (see below for a unifying discussion of possible causes) attests to the flexibility of the ligand backbone. Except for the angles given in Table 1, all other angles in the carbon framework are close to the ideal values expected for sp^2 and sp^3 carbon and nitrogen atoms, respectively.

[(1)Ni(OClO$_3$)](ClO$_4$) (5)

Recrystallization of the ill-defined complex **3** from methanol in the presence of $NaClO_4$ yields single crystalline material whose IR spectrum is characterised by a triply split very intense band between 1088 and 1145 cm^{-1} (ClO_4 str). This is characteristic of unidentate perchlorate coordination (reduction of the local symmetry from T_d to C_{3v})[17] and points to the perchlorato perchlorate complex [(**1**)Ni(OClO$_3$)](ClO$_4$) (**5**). Its ^{1}H NMR spectrum ([D$_6$]DMSO, room temp.) shows paramagnetically shifted resonances over the range 0 to + 140 ppm which can be assigned on the basis of their approximate integration intensities and are in accord with C_{2v} symmetry of the pyN_4 ligand in the complex[18]. As expected, the protons closest to the nickel atom ($-NH_2$, $-CH_2-$) show the most pronounced paramagnetic shifts (128 and 100 ppm, respectively) and the largest line widths. The H^3 (*meta*), H^4 (*para*) and $-CH_3$ protons have signals at 43, 20, and 1 ppm, respectively, with line widths decreasing in this order, which mirrors the increasing remoteness of the proton locations with respect to the nickel center.

The X-ray structural study of **5** shows the cation to have C_1 symmetry in the solid state (Figure 2). The nickel atom is coordinated in distorted octahedral fashion by the pentadentate pyN_4 ligand and an oxygen atom of one of the perchlorate anions. While the diametrically related sets of bond angles N_{eq}−Ni−N_{eq} are comparable to the corresponding values in **4**, the N_{py}−Ni−O unit deviates significantly from linearity [N11−Ni1−O1 166.0(5)°]. However, the coordination cap in **5** is less distorted than in **4**, as is evident from the structural parameters listed in Table 2, which are closer to the ideal values. The Ni−N_{ax} bond is shorter still in **5** [Ni1−N11 2.015(4) A] than in **4** [2.050(3) A], while the average Ni−N_{eq} bond lengths are comparable [**5**: 2.09(1) A; **4**: 2.090(4) A]. The bond length in **5** between nickel and the oxygen atom of the coordinated perchlorate anion has a value of *d*(Ni1−O1) = 2.233(6) A which is shorter than the value found in the nickel(II) perchlorato complex of a pendant-arm macrocyclic ligand which also has an N_5 donor set [*d*(Ni−O) = 2.393(8) A][19]. The bond lengths and angles within both perchlorate anions are in the normal range.

[(1)Ni(μ-Cl)Ni(1)](PF$_6$)$_3$ (6)

Recrystallization of **2** from water in the presence of NH_4PF_6 gives a purple material, and analytical data suggest it is the bridged species [(**1**)Ni(μ-Cl)Ni(**1**)](PF$_6$)$_3$ (**6**). Its formation requires partial dissociation of the monodentate ligand in **2**, in accord with the observation that a vacant coordination site may be created in a complex by NH_4PF_6-induced loss of a labile ligand[20]. Compound **6**, once

Table 1. Selected bond lengths [Å] and angles [°] for **4**, **5**, **6**, **7** and **8** with estimated standard deviations in parentheses

bond or angle	**4**	**5**	**6**	**7**	**8**
Ni1−N11	2.050(3)	2.015(4)	2.05(1)	2.062(4)	2.062(5)
Ni1−N12	2.108(3)	2.01(1)	2.09(1)	2.113(5)	2.119(6)
Ni1−N13	2.068(4)	2.16(1)	2.08(1)	2.110(5)	2.080(6)
Ni1−N14	2.073(4)	2.10(1)	2.07(1)	2.098(6)	2.054(6)
Ni1−N15	2.110(4)	2.08(1)	2.10(1)	2.132(6)	2.106(5)
Ni1−X[a]	2.133(3)	2.233(6)	2.448(2)	2.086(4)	2.156(5)
N11−Ni1−N12	87.2(1)	90.8(4)	89.4(5)	88.8(2)	85.5(2)
N11−Ni1−N15	88.2(1)	91.1(5)	87.5(5)	88.8(2)	85.5(2)
N11−Ni1−N13	92.9(1)	89.0(4)	90.5(5)	90.9(2)	91.3(2)
N11−Ni1−N14	92.3(1)	90.9(4)	90.9(5)	89.8(2)	90.9(2)
N12−Ni1−N13	85.2(2)	88.5(3)	85.8(5)	83.9(2)	85.9(3)
N14−Ni1−N15	84.6(2)	84.7(2)	85.2(5)	84.2(3)	86.6(3)
N13−Ni1−N14	96.3(2)	91.5(5)	94.9(5)	96.6(2)	95.1(3)
N12−Ni1−N15	94.0(2)	95.3(6)	94.1(6)	95.3(3)	92.2(3)
N12−Ni1−N14	178.5(2)	178.3(5)	179.2(5)	178.5(2)	176.3(2)
N13−Ni1−N15	178.6(2)	176.2(5)	177.9(5)	179.1(2)	176.4(3)
N11−Ni1−X[a]	179.32(13)	166.0(5)	178.4(3)	177.1(2)	175.1(2)
Ni1−N12−C16	115.7(3)	118.3(9)	117(1)	116.9(4)	115.9(4)
Ni1−N13−C17	113.6(3)	113.8(8)	116(1)	117.0(3)	114.0(4)
Ni1−N14−C20	114.0(3)	114.8(7)	116(1)	117.0(4)	114.1(4)
Ni1−N15−C21	116.0(3)	116.8(9)	115(1)	115.9(4)	116.0(4)
N12−C16−C18	114.2(4)	115(1)	115(1)	115.4(5)	113.2(5)
N13−C17−C18	113.9(4)	116(1)	113(1)	113.8(5)	115.1(6)
N14−C20−C22	114.5(4)	120(1)	113(1)	114.8(5)	114.5(5)
N15−C21−C22	114.0(3)	112(1)	118(1)	117.3(5)	112.7(5)

[a] **4**: X = O1; **5**: X = O1; **6**: X = Cl1; **7**: X = N1; **8**: X = N21.

formed and isolated, may be recrystallised from water. Whether or not the dinuclear species persists in aqueous solution is uncertain as the UV-Vis spectrum is not significantly different from that of the mononuclear aqua complex **4**. The X-ray structural analysis of **6** confirms the presence of a dinuclear chloro-bridged complex cation in the solid state, making it one of the very few structurally characterised complexes containing a single *unsupported* Ni(II)−X−Ni(II) halide bridge[21]. The compound crystallises in the tetragonal space group $I4_1cd$, and the two halves of the molecule are related by a two-fold rotation axis which bisects the Ni−Cl−Ni′ unit (Figure 3). The bridging chloro substituent (Cl1) and the phosphorus atom of one of the three PF_6^- counterions occupy special positions. The coordination mode of the pentaamine ligand **1** is again pyramidal. The chloro substituent functions as a bridge between two symmetry-equivalent nickel(II) ions, the angle subtended at the μ-chloro ligand by the bonds to Ni1 and Ni1′ being 165.5(3)°. Similar to **4** and **5**, the angles $N_{eq}-Ni-N_{eq}$ in the NiN_4 plane have average values of 85.5(5)° and 94.5(6)° for diametrically opposite pairs, leading to a rectangular rather than a square arrangement of the equatorial amino nitrogen atoms around the nickel centre (Table 1). The C_2 symmetry of the dinuclear ion causes the equatorial NiN_4 unit and its symmetry-related counterpart to adopt an eclipsed conformation. The $Ni-N_{ax}$ bond length (2.049(11) Å) is again shorter than the average $Ni-N_{eq}$ value [2.085(13) pm], but the higher standard deviations in this structure limit the usefulness of this comparison. The Ni−Cl bond length of 2.448(2) Å is appreciably shorter than in two other complexes containing octahedrally coordinated nickel(II) bridged by a single μ-chloro ligand [*d*(Ni−Cl) = 2.941(2) Å[22] and 2.712(4) Å (average)[23], respectively]. The capping pentaamine ligand is again distorted in the sense that the pyridine ring is tilted to one side of the $[NN_4]$Ni pyramid, the degree of distortion being comparable to that observed in **4** (cf. Table 2 for relevant distances and interplanar angles). The hexafluorophosphate counterions show thermal disorder but otherwise have normal structural parameters.

[(1)Ni(NCS)](PF$_6$) (7)

In view of the ready formation of a dinuclear complex from **2** by incorporation of a μ-chloro ligand under suitable conditions, we carried out substitution experiments with potentially bidentate polyatomic anions such as thiocyanate or azide in the anticipation of obtaining dinuclear species containing end-to-end coordinated, μ-(1,3)-pseudohalide bridges. Such complexes are of current interest with respect to their magnetic properties[24][25][26]. So far, however, even in the presence of NH_4PF_6, these reactions have yielded only the mononuclear complexes[27], which X-ray structural analyses have shown to contain terminally coordinated pseudohalide ligands.

The IR spectrum of the complex [(**1**)Ni(NCS)](PF_6) (**7**) is inconclusive with respect to the bonding mode of the SCN^- ligand. The X-ray crystal structure determination shows **7** to be the isothiocyanato complex, its cation having the expected octahedral symmetry. The distortion of the pyN_4 ligand in **7** (Figure 2) is much less severe than in complexes **4** and **6**, and comparable to that in **5**. The least-squares planes defined by the four methylene carbon atoms C16, C17, C20, C21 and the four equatorial amino nitrogen atoms N12, N13, N14, N15 form an angle of only 3.0(2)°, and the distances between pairs of equivalent methylene carbon atoms in the two 1,3-diaminoprop-2-yl groups

Figure 2. Molecular structures of the cations in **4** (top left), **5** (top right), **7** (bottom left), and **8** (bottom right); side-on views are shown in order to illustrate the differing degrees of distortion of the ligand caps; for clarity, ball-and-stick representations have been chosen, and all hydrogen atoms have been omitted; for all structures, the numbering of atoms in the pyridine ring is identical to that shown in Figure 1

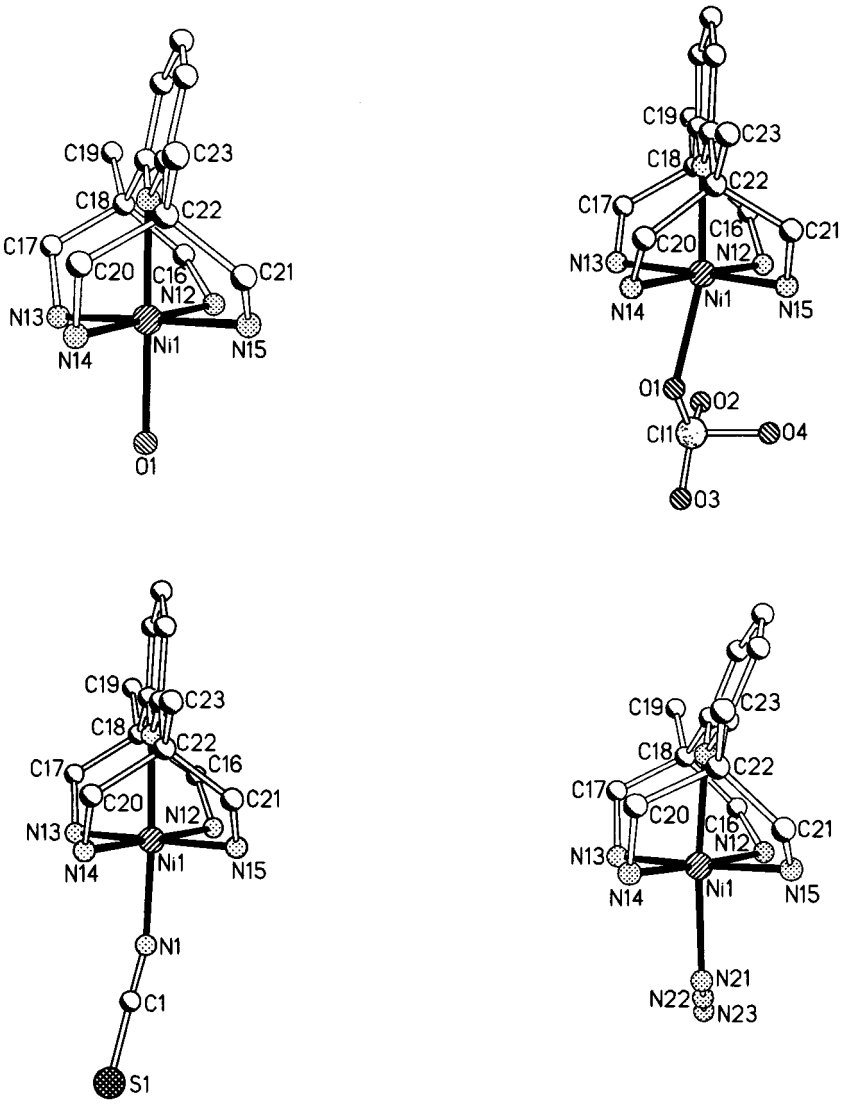

Table 2. Intramolecular angles [°] and distances [Å] illustrating the distortion of the ligand cap in complexes **4**, **5**, **6**, **7** and **8** (with estimated standard deviations in parentheses); see footnote and text for definitions of angles

bond or angle	**4**	**5**	**6**	**7**	**8**
ε[a]	15.4(4)	1(1)	17(1)	5.0(3)	26.8(4)
ζ[b]	8.0(1)	1.3(3)	7.4(4)	3.0(2)	9.8(2)
η[c]	11.6(2)	3.1(6)	13.2(6)	4.0(2)	19.3(2)
d(C16···C21)	5.399(7)	5.18(2)	5.30(3)	5.28(1)	5.44(1)
d(C17···C20)	4.743(7)	5.01(2)	4.80(3)	5.06(1)	4.69(1)

[a] Angle ε between the least-squares planes defined by the pyridine ring (N11, C11, C12, C13, C14, C15) and the quaternary and methyl carbon atoms C18/C19/C22/C23. – [b] Angle ζ between the least-squares planes defined by the equatorial nitrogen atoms N12/N13/N14/N15 and the methylene carbon atoms C16/C17/C20/C21. – [c] Angle η subtended by the lines N11···C13 and N11–Ni1 at N11.

[*d*(C16···C21) and d(C17···C20)] have adjusted to 5.28(1) Å and 5.06(1) Å, respectively. On average, the Ni–N_{eq} bonds in **7** are slightly longer and the Ni–N_{eq}–C angles slightly larger than in the other complexes, and it appears that these differences, and possibly also solid state packing effects, allow the ligand to adopt a conformation closer to C_{2v} symmetry. The isothiocyanato ligand is linear [N1–C1–S1 = 177.8(6)°] and is coordinated to nickel at an angle of

Figure 3. Molecular structure of the cation in **6**; hydrogen atoms have been omitted for clarity; the numbering of atoms in the pyridine ring is identical to that shown in Figure 1

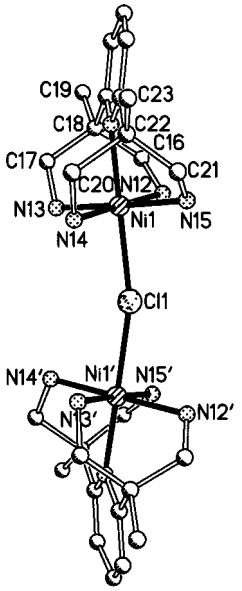

Ni1−N1−C1 = 165.9(5)°, with an Ni1−N1 bond length of 2.086(4) A. Corresponding values for an octahedral nickel(II) complex likewise containing a *trans* py−Ni−NCS unit are 159.0(3)° and 2.022(3) A, respectively[28].

[(1)Ni(N$_3$)](PF$_6$) (8)

The IR spectrum of the azide complex [(**1**)Ni(N$_3$)](PF$_6$) (**8**) shows, in addition to diagnostic bands due to the pyN$_4$ ligand and the hexafluorophosphate counterion, a sharp and very intense band at 2060 cm^{-1} due to the asymmetric stretching vibration of the coordinated azide ligand. Structural analysis reveals a complex cation (Figure 2) in which the distortion of the ligand cap is the most pronounced of all the complexes in the present series. While the Ni−N$_{py}$ bond length *trans* to the azide ligand [*d*(Ni1−N11) = 2.062(5) A] is identical to the corresponding value found in the isothiocyanate complex **7** (Table 1), the pyridine ring (which is planar to within 4 σ) is forced out of coplanarity with the quaternary and the exocyclic methyl carbon atoms of the ligand backbone by 26.8(4)° (Table 2). More significantly than in the other structures, the Ni−N$_{py}$ bond Ni1−N11 is bent from its vertical orientation relative to the NiN$_4$ plane, with relevant angles N$_{ax}$−Ni−N$_{eq}$ ranging from 85.5(2)° to 91.3(2)°. Further distances and angles are given in Table 1, and the complete set of parameters quantifying the ligand distortion in comparison to the other structures is given in Table 2. It is interesting to note that, despite the more serious distortion of the ligand in **8** with respect to the relative orientation of the pyridine ring, the bond angles in the carbon backbone (especially those at the methylene carbon atoms of the 1,3-diaminoprop-2-yl units, cf. Table 1) do not differ significantly from the corresponding values in the other structures. The terminally-coordinated azide ligand is linear [N21−N22−N23 = 177.9(7)°], and is bound to the nickel centre at an angle of Ni1−N21−N22 = 116.4(4)° (an angle approaching 120° is to be expected[29]; corresponding angles in other octahedral Ni(II) complexes containing terminal azide ligands span the range 123···138°[27][30][31][32][33][34]). The bond length *d*(Ni−N$_\alpha$) at 2.156(5) A is somewhat longer than in other terminal nickel(II) azide complexes (2.05···2.12 A)[27][30][31][32][33][34].

The Conformation of the Ligand Cap in 4, 5, 6, 7, and 8

The factors responsible for the varying degrees of distortion of the pentaamine ligand **1** in the solid state structures of **4**, **5**, **6**, **7**, and **8** are difficult to assess. The ligand has the topology of a podand, and hence is inherently more flexible than a macrocyclic or a cage-like arrangement of donor atoms, with their higher degrees of preorganization ("juxtapositional fixedness"[7]). The structures of complexes of **1** in the solid state are therefore expected to be more susceptible to packing effects, the significance of which will vary depending on the nature of the monodentate ligand and of the counterions. On a more subtle level, the *trans* influences ("static *trans* effects"[35][36]) of the monodentate ligands have to be considered. Perchlorate is weakly bound, and its complex has a shorter Ni−N$_{py}$ bond than the other complexes in the series. The tilt of the pyridine ring, however, is obviously unrelated to the length of the bond connecting it to the metal centre (i. e., the *trans* effect of the monodentate ligand). Thus, the isothiocyanato complex **7** and the azide complex **8**, while differing markedly in the degree of distortion of the ligand cap, have Ni−N$_{py}$ bond lengths which are identical within experimental error.

Magnetic Properties of 6

The magnetic behaviour of di- and polynuclear transition metal complexes is being studied extensively. The objective is to define the role played by the bridging ligands in mediating coupling interactions between the paramagnetic metal centers, and in particular to establish magneto-structural correlations[10]. Nickel(II) complexes, especially those containing chain-like one-dimensional arrangements of alternating metal atoms and bridging ligands, feature prominently in this context[29][32][37][38][39]. Bridging groups include carboxylato, nitrito, cyanide, cyanato, thiocyanato and, in particular, azido ligands, and complexes containing single, double, and triple bridges have been characterised[38][39][40]. The scarcity of polynuclear nickel(II) compounds containing an unsupported single halide bridge[21] led us to undertake the magnetochemical characterization of the μ-chloro bridged complex **6**.

The solid-state magnetic susceptibility of **6** was measured at 1.0 T in the temperature range 2 to 295 K using a SQUID magnetometer (MPMS, Quantum Design). Figure 4 shows the variation of both the molar paramagnetic susceptibility χ_M and the effective magnetic moment μ_{eff} (per mol) with temperature. As temperature decreases, χ_M increases slightly, reaching a broad maximum at 225 K, and then decreases to reach a minimum at 30 K. The marked rise of χ_M for T < 20 K is attributed to the presence of a small amount of paramagnetic impurity, presumed to be a monomeric nickel com-

plex. As may be seen from the plot of μ_{eff} versus T, the value of the effective magnetic moment decreases steadily with decreasing temperature from the maximum value of 3.17 μ_B at 295 K ($\chi_M \cdot T = 1.256$ cm^3 K mol^{-1}), reaching a minimum of 0.32 μ_B ($\chi_M \cdot T = 0.013$ cm^3 K mol^{-1}) at temperatures below 25 K. The theoretical spin-only value of the magnetic moment μ_{SO} for two uncoupled Ni(II) spins $S_{Ni} = 1$ is 4 μ_B ($\chi_M \cdot T = 2$ cm^3 K mol^{-1}), which is higher than the experimental value of 3.17 μ_B at 295 K. The data are, however, consistent with strong antiferromagnetic exchange between the two nickel atoms through the bridging chlorine atom, resulting in a diamagnetic ground state with total spin $S_T = 0$. The residual value of μ_{eff} is indicative of the presence of a paramagnetic impurity. The experimental data of **6** have been analysed by a least-squares fit procedure using an isotropic Heisenberg-Dirac-van-Vleck (HDVV) exchange Hamiltonian $H = -2J\,\boldsymbol{S}_1 \cdot \boldsymbol{S}_2$, and taking account of Zeeman splitting as well as corrections for paramagnetic impurity (p) and temperature-independent paramagnetism (TIP)[41]. Diamagnetic correction is based on substracting the sample-holder signal and the contribution $\chi_D = -236 \times 10^{-6}$ cm^3 mol^{-1}, as determined from Pascal's constants[10], from the raw data. A good fit was achieved (solid lines in Figure 4) for isotropic exchange coupling $J = -74$ cm^{-1} between the two paramagnetic sites, average g value $g = 2.18$, paramagnetic impurity with spin $S = 1$ and relative amount $p = 2.7\%$, and TIP = $+171\times10^{-6}$ cm^3 mol^{-1} per nickel atom. It was further assumed that the paramagnetic impurity has about half the molecular weight and half the diamagnetic correction χ_D of **6**. The J value for **6** is considerably larger than the values typically found for antiferromagnetic coupling in Ni(II) chains containing single μ-(1,3)-azido bridges[29,38,42,43] or multiple bridges[44][45][46][47][48][49]. The reason for **6** having such a large J value is that its Ni(II)−X−Ni(II) angle comes closest to 180° of all the Ni(II) chains considered. The g value is as expected for octahedral nickel(II) complexes (cf. the typical value of $g = 2.25$ for $[Ni(H_2O)_6]^{2+}$ [50]). As far as we are aware, **6** is the first complex containing a single halogen bridge between two Ni(II) centres that has been characterised by a magnetochemical method.

Summary

The tetrapodal pentaamine ligand **1** acts as a square-pyramidal coordination cap towards nickel(II) ions in aqueous solution, leaving a sixth site for the binding of a monodentate ligand, which completes the coordination octahedron. Exchange of the monodentate ligand is facile, and the pentadentate ligand shows considerable conformational flexibility, as illustrated by the solid state structures of the aqua, perchlorato, isothiocyanato, and azido complexes. Since the pentaamine ligand effectively blocks five coordination sites in a coordination octahedron, dinuclear Ni(II) complexes containing a single bridging ligand may also be prepared. The ligand thus meets the requirements set out in the Introduction for the construction of coordination caps carrying a functional periphery. Work using the complex fragment $[(\mathbf{1})Ni]^{2+}$ as a template for the derivatization of the tetrapodal pentadentate ligand **1** is currently in progress.

Figure 4. Temperature dependence of the effective magnetic moment μ_{eff} (Bohr magnetons, μ_B) and of the molar magnetic susceptibility χ_M (10^{-3} cm^3 mol^{-1}) of **6**. Squares and dots represent the experimental data, whereas the solid lines are the calculated fits (see text). The scales at left and right have been chosen so as to avoid overlay of the curves.

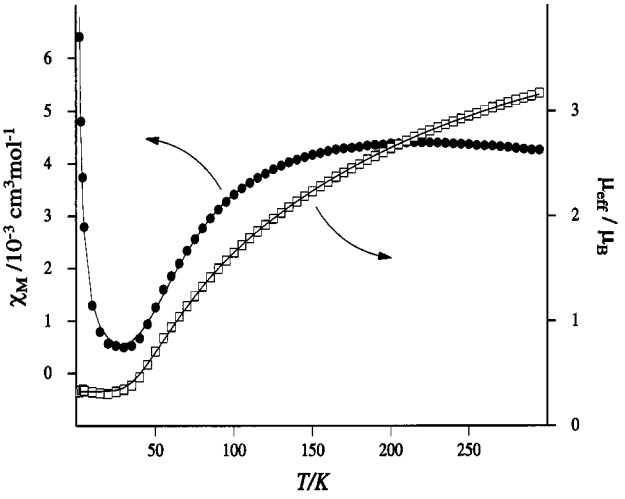

We thank Professor *D. Sellmann* for generous support of this work and Dr. *F. Hampel* for establishing the crystallographic data set of compound **8**. Further, a Liebig-Stipendium from the *Fonds der Chemischen Industrie* (to A. G.) is gratefully acknowledged.

Experimental Section

CAUTION! Although no problems were encountered in this work, transition metal perchlorate and azide complexes with organic ligands are potentially explosive and should be handled with due precautions.

Materials and Instrumentation: 2,6-$C_5H_3N\{CMe(CH_2NH_2)_2\}_2$ (**1**) was prepared as described previously[3]. The aqua complex **2** was prepared by reacting equimolar amounts of **1** • 4 HCl and $NiCl_2$ • 6 H_2O in dilute aqueous ammonia solution and subsequent cation exchange chromatography on Sephadex SPC-25. The chromatography was performed as described in a published procedure[51]. Reagents were AR grade or better and were purchased from Merck, Fluka, and Aldrich. IR (KBr discs) and UV/Vis spectra (solvent: water) were recorded on Perkin-Elmer 16PC FT-IR and Shimadzu UV-3101 PC instruments, respectively. NMR spectra were measured on a JEOL JNM-EX 270 spectrometer, and mass spectra were obtained on a JEOL MSTATION 700 spectrometer. Elemental analyses were performed using a Carlo Erba Elemental Analyzer 1106. Magnetic measurements were carried out on a polycrystalline sample with a SQUID magnetometer (MPMS, Quantum Design).

X-ray Crystallography: Crystal data for compounds **4**, **5**, **6**, **7**, and **8** are given in Table 3, and selected distances and angles are listed in Table 1. The structures of the cations are presented in Figures 1, 2, and 3. Only the cation of **5** shows slight disorder (oxygen atoms of the perchlorato ligand). The structure of **4** was solved by direct methods and refined using the programme package SHELXTL 5.03[52]. An absorption correction (Ψ scans, 10 reflections, $T_{min} = 0.011$, $T_{max} = 0.032$) was carried out. All non-hydrogen atoms were refined anisotropically (full-matrix least-squares). All hydrogen atoms were located in a difference Fourier synthesis, and all hydrogen atoms except H1A and H1B (aqua ligand) were refined isotropically. Both the positional and the isotropic displace-

ment parameters of H1A and H1B were kept constant during refinement. The structure of **5** was solved by direct methods (SHELXS-86) and refined on F^2 using SHELXL 93[53][54]. The structure of **6** was solved by direct methods and refined using the programme package SHELXTL 5.03. For both **5** and **6**, the non-hydrogen atoms were refined anisotropically (full-matrix least-squares), and the hydrogen atoms were positioned geometrically. The structures of **7** and **8** were solved by direct methods and refined using the programme package SHELXTL 5.03. For both structures, all non-hydrogen atoms were refined anisotropically (full-matrix least-squares), and all hydrogen atoms were located in a difference Fourier synthesis and refined isotropically. Crystallographic data (excluding structure factors) for the structures reported in this paper have been deposited with the Cambridge Crystallographic Data Centre as supplementary publication no. CCDC-100 937. Copies of the data can be obtained free of charge on application to CCDC, 12 Union Road, Cambridge CB2 1EZ, UK [Fax: int. code +44 (1223) 336−033; E-mail: deposit@ccdc.cam.ac.uk].

*[(**1**)Ni(H$_2$O)]I$_2$* (**4**): To a solution of **2** (0.94 g, 2.36 mmol) in water (50 ml) was added solid NaI (3.70 g, 24.69 mmol), and the mixture was stirred until all solid had dissolved. The solution was taken to dryness, the remaining solid taken up in as little methanol as possible, and the suspension filtered to remove NaI. Slow evaporation of solvent from the purple filtrate yielded a purple crystalline solid after several days. This was removed by filtration and air-dried. Yield: 0.40 g (0.69 mmol, 29%). Recrystallization from methanol gave single crystals suitable for an X-ray structure analysis. − IR (KBr): ν = 3272 cm^{-1} (br, OH/NH str), 2930 (CH str), 1594 (OH/NH def and C=C/C=N str), 1577 (OH/NH def and C=C/C=N str), 1463 (CH_2 asym def), 1397 (CH_2 sym def), 1024 (C−C skelet), 838 (NH def and CH_{pyr} oop def), 573 (C−C def). − UV/Vis (water): λ_{max} (ε) = 543 nm (3.4 dm^3 mol^{-1} cm^{-1}), 262 (1643). − MS (FD); *m/z* (%): 436 (100) [[(**1**)NiI]$^+$]; (FAB); *m/z* (%): 436 (100) [[(**1**)NiI]$^+$], 309 (45) [[(**1**)Ni]$^+$]. − $C_{13}H_{27}I_2N_5NiO$ (581.91): calcd. C 26.83, H 4.68, N 12.04; found C 26.66, H 4.26, N 11.98.

*[(**1**)Ni(OClO$_3$)](ClO$_4$)* (**5**): To a solution of **2** (0.42 g, 1.00 mmol) in water (5 ml) was added a saturated aqueous solution of $NaClO_4$ (5 ml). The resulting purple precipitate was centrifuged, washed with cold water, and dried in vacuo. Recrystallization from water/methanol (1:1 v/v) gave a crystalline solid (**3**) with no conclusive elemental analysis and IR data. A methanol solution of **3** (5 ml) containing $NaClO_4$ (0.50 g) was heated to reflux and cooled slowly to room temperature to give **5** in the form of single crystals suitable for an X-ray structural analysis. − IR (KBr): ν = 3263 cm^{-1}, 2964, 1576, 1464, 1145 (ClO_4 str), 1116 (ClO_4 str), 1088 (ClO_4 str), 1031, 1020, 822, 626. − ^{1}H NMR ([D$_6$]DMSO, room temp.; all signals paramagnetically broadened) δ = 1 (-CH_3), 20 (H^4), 43 (H^3), 100 (-CH_2-), 128 (-NH_2). − $C_{13}H_{25}Cl_2N_5NiO_8$ (508.99): calcd. C 30.68, H 4.95, N 13.76; found C 30.70, H 5.08, N 13.50.

*[(**1**)Ni(μ-Cl)Ni(**1**)](PF$_6$)$_3$* (**6**): To a solution of **2** (0.42 g, 1.00 mmol) in water (20 ml) was added a saturated aqueous solution of NH_4PF_6 (10 ml). The purple crystalline precipitate that formed was centrifuged, recrystallised from hot water, removed by filtration, washed with water, and air-dried. The resulting crystals were suitable for an X-ray structural analysis. Yield: 0.35 g (0.32 mmol, 64%). − IR (KBr): ν = 3374 cm^{-1}, 2967, 1603, 1579, 1469, 1397, 1084, 1020, 850 (PF_6), 559. − $C_{26}H_{50}ClF_{18}N_{10}Ni_2P_3$ (1090.52): calcd. C 28.64, H 4.62, N 12.84; found C 28.23, H 4.63, N 12.52.

*[(**1**)Ni(NCS)](PF$_6$)* (**7**): A solution of **2** (0.67 g, 1.68 mmol) in water (20 ml) was loaded onto a cation exchange column (Sephadex

Table 3. Crystallographic data for compounds **4**, **5**, **6**, **7** and **8**

	4	**5**	**6**	**7**	**8**
empirical formula	$C_{13}H_{27}I_2N_5NiO$	$C_{13}H_{25}Cl_2N_5NiO_8$	$C_{26}H_{50}ClF_{18}N_{10}Ni_2P_3$	$C_{14}H_{25}F_6N_6NiPS$	$C_{13}H_{25}F_6N_8NiP$
mol. mass	581.91	508.99	1090.54	513.14	497.09
crystal system	monoclinic	orthorhombic	tetragonal	monoclinic	monoclinic
space group (no.)	$P2_1/n$ (no. 14)	$Pna2_1$ (no. 33)	$I4_1cd$ (no. 110)	$P2_1/n$ (no. 14)	$P2_1/c$ (no. 14)
a [A]	9.936(2)	20.705(3)	21.312(3)	11.735(5)	10.703(1)
b [A]	18.804(5)	11.378(1)	21.312(3)	14.447(5)	11.059(1)
c [A]	10.757(3)	8.715(1)	19.010(4)	13.877(6)	17.130(1)
α [°]	90	90	90	90	90
β [°]	92.70(2)	90	90	113.65(3)	94.335(7)
γ [°]	90	90	90	90	90
Z	4	4	8	4	4
V [A^3]	2007.6(9)	2053.1(5)	8635(2)	2155(2)	2021.8(3)
ρ_{calcd} [g cm^{-3}]	1.925	1.647	1.678	1.582	1.633
diffractometer	Nicolet R3m/V	Enraf Nonius CAD4	Siemens P4	Nicolet R3m/V	E. Nonius MACH3
radiation	Mo-K_α	Mo-K_α	Mo-K_α	Mo-K_α	Mo-K_α (rotating anode)
monochromator	graphite	graphite	graphite	graphite	graphite
crystal size [mm^3]	0.60 × 0.40 × 0.40	0.36 × 0.20 × 0.12	0.70 × 0.40 × 0.40	0.45 × 0.30 × 0.25	0.40 × 0.20 × 0.20
T [°C]	293(2)	293(2)	200(2)	293(2)	293(2)
scan	ω	ω-2Θ	ω	ω	ω-Θ
2Θ range	4 ≤ 2Θ ≤ 54	5 ≤ 2Θ ≤ 53	4 ≤ 2Θ ≤ 48	4 ≤ 2Θ ≤ 54	5 ≤ 2Θ ≤ 48
measured reflections	5390	2219	7581	5761	3208
unique reflections	4382	2219	1967	4692	3164
observed reflections[a]	3246	1695	1360	1910	2095
μ(Mo-K_α) [mm^{-1}]	4.050	1.256	1.158	1.135	1.110
refined parameters	300	263	274	362	362
data/parameter ratio	14.6	8.4	7.2	13.0	8.7
*wR*2 (all data)[b]	0.0665	0.1460	0.1996	0.1250	0.1517
*R*1 (obs. data)[c]	0.0289	0.0508	0.0702	0.0518	0.0522
ρ_{fin}(max/min) [e A^{-3}]	0.771/−0.557	0.640/−0.358	1.514/−0.608	0.278/−0.514	0.837/−0.491
weighting scheme[d]	k = 0.0375/l = 0	k = 0.0757/l = 1.6931	k = 0.065/l = 54.317	k = 0.0536/l = 0	k = 0.0794/l = 3.1450

[a] With $F_o \geq 4\,\sigma(F)$; [b] $wR2 = (\{\Sigma[w(F_o^2 - F_c^2)^2]\}/\{\Sigma[w(F_o^2)^2]\})^{0.5}$; [c] $R1 = \Sigma||F_o| - |F_c||/\Sigma|F_o|$ for $F > 4\sigma(F)$; [d] $w = 1/[\sigma^2(F_o^2) + (k \cdot P)^2] + l \cdot P$ and $P = (F_o^2 + 2 \cdot F_c^2)/3$

SPC-25, ∅ 30 mm, length 190 mm), and the column eluted with water (200 ml). Gradient elution with an aqueous solution of NH_4SCN (0.1 M, 150 ml) removed a purple eluate which was concentrated to a volume of 20 ml. To this solution was added a saturated aqueous solution of NH_4PF_6 (10 ml). A single crystalline precipitate formed after several days. – IR (KBr): ν = 3274 cm^{-1}, 2979, 2091 (SCN), 1597, 1465, 1062, 1009, 850 (PF_6), 558. – $C_{14}H_{25}F_6N_6NiPS$ (513.13): calcd. C 32.77, H 4.91, N 16.38; found C 33.03, H 5.24, N 16.44.

*[(**1**)Ni(N$_3$)](PF$_6$)* (**8**): A solution of **2** (0.70 g, 1.75 mmol) in water (25 ml) was loaded onto a cation exchange column (Sephadex SPC-25, ∅ 30 mm, length 190 mm), and the column eluted with water (200 ml). Gradient elution with an aqueous solution of NaN_3 (0.1 M, 200 ml) removed a purple eluate which was taken to dryness. The remaining solid was taken up in methanol (50 ml), the suspension filtered to remove excess NaN_3, and the filtrate again taken to dryness. The residue was dissolved in water (10 ml), and the solution added to a concentrated aqueous solution of NH_4PF_6 (5 ml). The purple precipitate which had formed after several days was removed by filtration, washed quickly with a small amount of cold water, and air-dried. Single crystals suitable for an X-ray structural analysis were obtained by recrystallization from water. – IR (KBr): ν = 3256 cm^{-1}, 2962, 2060 (N_3), 1606, 1467, 1019, 834 (PF_6), 558. – $C_{13}H_{25}F_6N_8NiP$ (497.07): calcd. C 31.41, H 5.07, N 22.54; found C 30.94, H 4.88, N 20.52. Repeated recrystallizations gave samples which analysed consistently too low for N and, to a lesser extent, for C.

[1] H. M. Colquhoun, J. F. Stoddart, D. J. Williams, *Angew. Chem.* **1986**, *98,* 483–503; *Angew. Chem., Int. Ed. Engl.* **1986**, *25*, 487–507.
[2] J. E. Kickham, S. J. Loeb, S. L. Murphy, *Chemistry – A European Journal* **1997**, *3*, 1203–1213.
[3] A. Grohmann, F. Knoch, *Inorg. Chem.* **1996**, *35*, 7932–7934.
[4] E. Ahmed, C. Chatterjee, C. J. Cooksey, M. L. Tobe, G. Williams, M. Humanes, *J. Chem. Soc., Dalton Trans.* **1989**, 645–654.
[5] M. E. de Vries, R. M. La Crois, G. Roelfes, H. Kooijman, A. L. Spek, R. Hage, B. L. Feringa, *J. Chem. Soc., Chem. Commun.* **1997**, 1549–1550.
[6] A. J. Canty, N. J. Minchin, B. W. Skelton, A. H. White, *J. Chem. Soc., Dalton Trans.* **1986**, 2205–2210.
[7] D. H. Busch, *Chem. Rev.* **1993**, *93*, 847–860.
[8] D. H. Busch in *Proceedings of the First Hanford Separation Science Workshop*; Battelle Memorial Institute, Richland, WA, **1993**, p. II.9– II.14.
[9] C.- H. Lee, B. Garcia, T. C. Bruice, *J. Am. Chem. Soc.* **1990**, *112*, 6434–6435.
[10] O. Kahn, *Molecular Magnetism*; VCH, New York, **1993**, and references therein.
[11] A. E. Martell, R. D. Hancock, *Metal Complexes in Aqueous Solution*; Plenum Press, New York, **1996**, p. 39.
[12] A. McAuley, S. Subramanian, T. W. Whitcombe, *Can. J. Chem.* **1989**, *67*, 1650–1656.
[13] A. Bondi, *J. Phys. Chem.* **1964**, *68*, 441–451.
[14] S. Schmidt, L. Omnes, F. W. Heinemann, J. Kuhnigk, C. Krüger, A. Grohmann, *Z. Naturforsch.* **1998**, *53b*, *submitted*.
[15] J. L. Atwood, G. W. Orr, F. Hamada, R. L. Vincent, S. G. Bott, K. D. Robinson, *J. Am. Chem. Soc.* **1991**, *113*, 2760–2761.
[16] E. Kimura, T. Koike, H. Nada, Y. Iitaka, *Inorg. Chem.* **1988**, *27*, 1036–1040.
[17] G. Socrates, *Infrared Characteristic Group Frequencies;* 2nd edn.; Wiley, Chichester, **1994**, p. 220.
[18] T. C. Higgs, C. J. Carrano, *Inorg. Chem.* **1997**, *36*, 298–306.
[19] N. W. Alcock, K. P. Balakrishnan, P. Moore, H. A. A. Omar, *J. Chem. Soc., Dalton Trans.* **1987**, 545–550.
[20] M. A. Bennett, J. C. Jeffery, G. B. Robertson, *Inorg. Chem.* **1981**, *20*, 323–330.
[21] A recent search of the Cambridge Structural Database gave one example each of a fluoro- and bromo- bridged species:[21a] J. Emsley, M. Arif, P. A. Bates, M. B. Hursthouse, *J. Chem. Soc., Dalton Trans.* **1989**, 1273–1276;[21b] ref.[22].
[22] M. G. B. Drew, D. H. Templeton, A. Zalkin, *Inorg. Chem.* **1968**, *7*, 2618–2624.
[23] T. Kajiwara, T. Yamaguchi, H. Oshio, T. Ito, *Bull. Chem. Soc. Jpn.* **1994**, *67*, 2130–2135.
[24] M. Monfort, C. Bastos, C. Diaz, J. Ribas, X. Solans, *Inorg. Chim. Acta* **1994**, *218*, 185–188.
[25] R. Vicente, A. Escuer, J. Ribas, X. Solans, *J. Chem. Soc., Dalton Trans.* **1994**, 259–262.
[26] M. Taniguchi, A. Ouchi, *Bull. Chem. Soc. Jpn.* **1986**, *59*, 3277–3278.
[27] J. Ribas, M. Monfort, B. Kumar Ghosh, X. Solans, M. Font-Bardıa, *Polyhedron* **1996**, *15*, 1091–1095.
[28] S. Brooker, V. McKee, *J. Chem. Soc., Dalton Trans.* **1990**, 3183–3188.
[29] C. G. Pierpont, D. N. Hendrickson, D. M. Duggan, F. Wagner, E. K. Barefield, *Inorg. Chem.* **1975**, *14*, 604–610.
[30] M. K. Urtiaga, M. I. Arriortua, I. G. De Muro, R. Cortes, *Acta Crystallogr., Sect. C* **1995**, *51*, 62–65.
[31] Panmig Jian, Shuangxi Wang, Jishuan Suo, Liufang Wang, Qiangjin Wu, *Acta Crystallogr., Sect. C* **1995**, *51*, 1071–1073.
[32] P. Chaudhuri, M. Guttmann, D. Ventur, K. Wieghardt, B. Nuber, J. Weiss, *J. Chem. Soc., Chem. Commun.* **1985**, 1618–1620.
[33] F. Paap, W. L. Driessen, J. Reedijk, B. Kojic-Prodic, A. L. Spek, *Inorg. Chim. Acta* **1985**, *104*, 55–62.
[34] F. Wagner, M. T. Mocella, M. J. D′Aniello, Jr., A. H.-J. Wang, E. K. Barefield, *J. Am. Chem. Soc.* **1974**, *96*, 2625–2627.
[35] J. D. Atwood, *Inorganic and organometallic reaction mechanisms;* 2nd ed.; VCH, New York, NY, **1997**, p. 48.
[36] S. F. A. Kettle, *Physical Inorganic Chemistry, A Coordination Chemistry Approach*; Spektrum, Oxford, **1996**, p. 92.
[37] J. Ribas, M. Monfort, B. Kumar Ghosh, R. Cortes, X. Solans, M. Font-Bardıa, *Inorg. Chem.* **1996**, *35*, 864–868.
[38] G. A. McLachlan, G. D. Fallon, R. L. Martin, B. Moubaraki, K. S. Murray, L. Spiccia, *Inorg. Chem.* **1994**, *33*, 4663–4668.
[39] A. Escuer, R. Vicente, J. Ribas, M. S. El Fallah, X. Solans, M. Font-Bardıa, *Inorg. Chem.* **1993**, *32*, 3727–3732.
[40] M. Monfort, J. Ribas, X. Solans, *Inorg. Chem.* **1994**, *33*, 4271–4276.
[41] C. Butzlaff, A. X. Trautwein, H. Winkler in *Methods in Enzymology* (Eds.: J. F. Riordan, B. L. Valee), Academic Press, San Diego, **1993**, vol. 227; p. 412; ref.[10], p. 112.
[42] R. Vicente, A. Escuer, J. Ribas, M. S. El Fallah, X. Solans, M. Font-Bardıa, *Inorg. Chem.* **1995**, *34*, 1278–1281.
[43] A. Escuer, R. Vicente, J. Ribas, M. S. El Fallah, X. Solans, *Inorg. Chem.* **1993**, *32*, 1033–1035.
[44] P. Roman, C. Guzman-Miralles, A. Luque, J. I. Beitia, J. Cano, F. Lloret, M. Julve, S. Alvarez, *Inorg. Chem.* **1996**, *35*, 3741–3751.
[45] J. J. Borras-Almenar, E. Coronado, J. Curely, R. Georges, *Inorg. Chem.* **1995**, *34,* 2699–2704.
[46] B. Cabezon, A. Sastre, T. Torres, W. Schäfer, J. J. Borras-Almenar, E. Coronado, *J. Chem. Soc., Dalton Trans.* **1995**, 2305–2310.
[47] L. Ballester, E. Coronado, A. Gutierrez, A. Monge, M. F. Perpinan, E. Pinilla, T. Rico, *Inorg. Chem.* **1992**, *31,* 2053–2056.
[48] C. J. Gomez-Garcıa, E. Coronado, L. Ouahab, *Angew. Chem.* **1992**, *104,* 660–662; *Angew. Chem., Int. Ed. Engl.* **1992**, *31*, 649–651.
[49] E. Coronado, M. Drillon, A. Fuertes, D. Beltran, A. Mosset, J. Galy, *J. Am. Chem. Soc.* **1986**, *108*, 900–905.
[50] C. J. Ballhausen, *Introduction to Ligand Field Theory*; McGraw-Hill, New York, **1962**, p. 129.
[51] A. McAuley, S. Subramanian, T. W. Whitcombe, *J. Chem. Soc., Dalton Trans.* **1993**, 2209–2214.
[52] SHELXTL 5.03 for Siemens Crystallographic Research Systems, Copyright **1995** by Siemens Analytical X-Ray Instruments Inc., Madison, WI, USA.
[53] G. M. Sheldrick, SHELXS-86, Programme for Crystal Structure Solution, Universität Göttingen, **1986**.
[54] G. M. Sheldrick, SHELXL-93, Programme for Crystal Structure Refinement, Universität Göttingen, **1993**.

[97319]

Homogeneous Chromium Catalysts for Olefin Polymerization

Klaus H. Theopold

Department of Chemistry and Biochemistry, Center for Catalytic Science and Technology,
University of Delaware, Newark, DE 19716-2522, USA
Fax: (internat.) +1(302) 831-6335
E-mail: theopold@udel.edu

Received August 19, 1997

Keywords: Chromium / Organometallics / Homogeneous catalysis / Olefin polymerization / Polyethylene

Chromium-based heterogeneous catalysts are used extensively for the polymerization of olefins. There are few homogeneous model systems that allow investigation of the reaction mechanisms and unique characteristics of chromium catalysts. Coordinatively unsaturated paramagnetic chromium alkyls containing a $Cp^*Cr^{III}R$ fragment ($Cp^* = \eta^5\text{-}C_5Me_5$, pentamethylcyclopentadienyl) catalyze the polymerization of ethylene and α-olefins. Correlations between molecular structure and catalytic activity are reviewed.

Introduction

Polymers produced by homopolymerization and/or copolymerization of small olefins such as ethylene and propene are among the most widely used plastics. In 1996 worldwide consumption of polyethylene and polypropylene stood at 40×10^6 and 21×10^6 tons, respectively.[1] Except for so-called low density polyethylene (LDPE), which is made by a high temperature/high pressure radical process, these materials are the products of metal-catalyzed reactions conducted on an enormous scale. Two different kinds of catalysts are used commercially . One group utilizes group 4 metals (Ti, Zr) and can be traced to the Nobel prize-winning discoveries of Ziegler and Natta.[2] There has been much recent interest in this area, due to the development and application of so-called "metallocene" technology, i.e. catalysts based on sophisticated organometallic molecules that facilitate greater control of polymer structure and properties.[3] The second kind of catalyst is based on chromium and was discovered independently by Hogan and Banks at Phillips Petroleum Co.[4] Roughly one third of all polyethylene is currently produced with it, and it is notable for not requiring any cocatalyst (e.g. AlR_3 or methyl aluminoxane, i.e. MAO). Despite much investigative effort, much less is known about the mechanism and active site(s) of this catalyst, and it has not undergone innovations to match the "metallocene revolution". A large obstacle in this regard has been the lack of homogeneous model systems for chromium-based heterogeneous catalysts. This is now beginning to change, and this review covers the relevant organometallic chemistry of chromium, with particular emphasis on studies carried out in the author′s laboratory.

The Phillips catalyst is prepared by impregnation of silica with an inorganic chromium compound (e.g. CrO_3 or various Cr^{III} salts), followed by calcination in oxygen.[5] This leaves the chromium in the hexavalent state. Upon contact with ethylene, the metal is reduced, ultimately forming the catalytically active species. With carbon monoxide as an alternative reducing agent, the surface-bound chromium

Klaus H. Theopold was born in Berlin, Germany in 1954. With a "Vordiplom" from the University of Hamburg he moved to California where he received his Ph. D. in 1982 from the University of California at Berkeley. After a postdoctoral year at MIT, he began his academic career as asssistant professor at Cornell University in 1983. In 1990 he moved to the University of Delaware, where he is currently Professor of Chemistry. His research in synthetic organometallic and inorganic chemistry is aimed at the rational design of homogeneous catalysts for a variety of chemical transformations.

MICROREVIEWS: This feature introduces the readers to the authors′ research through a concise overview of the selected topic. Reference to important work from others in the field is included.

 © WILEY-VCH Verlag GmbH, D-69451 Weinheim, 1998 1434−1948/98/0101−0015 $ 17.50+.50/0

can be reduced to its divalent state (Cr^{II}), and this species will polymerize ethylene.[6] However, the chemical structure, valence state, and mechanism of formation of the active site, i.e. the chromium alkyl actually producing the polymer by repetitive insertion of ethylene, have been the subject of a longstanding controversy. Especially the valence (i.e. the formal oxidation state) of the catalytically active chromium has inspired much speculation, and almost every stable oxidation state of chromium has been held responsible for catalysis at one time or another. Scheme 1 depicts some of the proposed structures; several of the organometallic derivatives could in principle undergo ethylene insertion. Variations of these structures containing binuclear chromium sites (with and without metal−metal bonds) have also been proposed.

Scheme 1

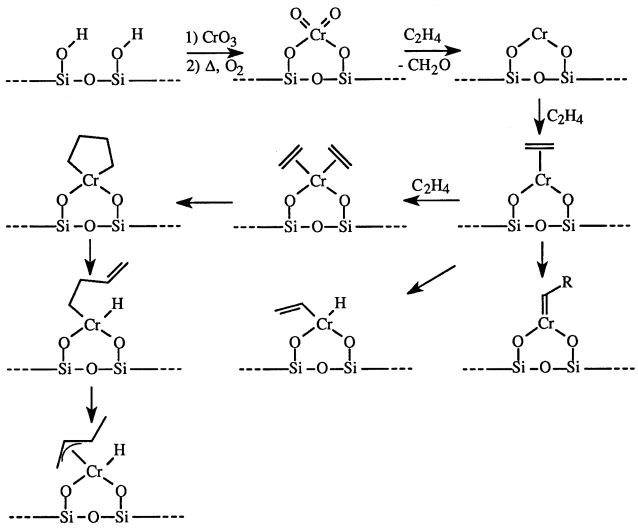

Another chromium catalyst was discovered by Karapinka[7a] and developed by Karol et al.[7b] at Union Carbide in the early 60′s. It is prepared by impregnating dehydroxylated silica with chromocene (Cp_2Cr, Cp = η^5-cyclopentadienyl). While not in use industrially at present, the Union Carbide catalyst shares some of the advantages of the Phillips catalyst, namely high activity and absence of cocatalyst. It is different from the latter, however, in its high selectivity between ethylene and propene (no copolymerization) and its good response to hydrogen (H_2) for molecular weight control. There is little doubt that the reaction of the organometallic molecule with remaining hydroxyl groups on the silica surface results in loss of one cyclopentadienyl ligand and formation of a surface bound CpCr fragment (see Scheme 2). However, it is also clear that the remaining cyclopentadienyl group does not initiate the polymer chain growth; rather it stays coordinated to the chromium during catalysis. Thus there arises the same set of questions about the mechanism of the initiation, and the structure and valence of the active site. Scheme 2 shows some of the commonly proposed candidates for the active site.

Scheme 2

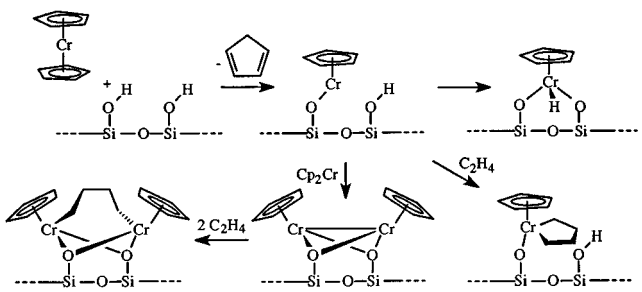

Homogeneous Model Systems

The proposed structures depicted in Schemes 1 and 2 have resulted from many spectroscopic investigations of heterogeneous catalysts combined with extrapolations from the now extensive body of known organometallic structures. However, the relevance of this "deluge of conjecture"[8] is highly questionable. Most of the analytical work utilized IR spectroscopy[9], with some EXAFS[10] and solid state ^1H NMR[11] results added relatively recently. Even for pure substances, most of these techniques can hardly be called definitive structural tools, and synthetic organometallic chemists would not base a detailed molecular structure solely on such results. Furthermore, the most careful studies of this type have come to the conclusion that the catalytically active sites represent only a very small fraction of the surface-bound chromium (< 1%!).[9b] Thus, whatever spectroscopic information is available probably pertains to those chromium species that are inactive. The proposals were further compromised by the fact that until recently the organometallic chemistry of chromium—i.e. the very metal of concern—did not offer realistic model compounds for any of the suggested species. As we have previously noted, "the known organometallic chemistry of said metal concerns low-valent carbonyl derivatives and/or diamagnetic complexes with 18-electron configurations. Such molecules are unlikely candidates for modeling highly reactive (coordinatively unsaturated) and oxide supported alkylchromium compounds".[12] This lacuna in the development of molecular chromium chemistry is largely due to the physical properties of relevant compounds. Chromium alkyls in the intermediate oxidation states of interest (II−IV) are typically "metallaradicals" featuring unpaired electrons. The associated paramagnetism makes characterization by NMR spectroscopy, the most important analytical tool of solution chemistry, more difficult and less informative.[13]

Nevertheless, we are convinced that homogeneous organometallic chemistry is in a position to make an important contribution both to the understanding of present-day heterogeneous catalysts and to the development of the next generation of chromium catalysts. To this end we must create functional models, i.e. well-defined chromium compounds that catalyze the polymerization of olefins in homogeneous solution. The preparation and catalytic activity of molecules incorporating the structural elements of Schemes 1 and 2 will be the best arbiter of their relevance. If a structurally characterized Cr^{IV} metallacycle, to name but one ex-

ample, does not polymerize ethylene in solution (see below), it is unlikely to do so on a silica surface. Conversely, if a class of coordinatively unsaturated $CpCr^{III}$ alkyls consistently exhibits catalytic activity, it must have some claim to being related to the catalytically active site of the Union Carbide catalyst. Let us then review the available homogeneous chemistry.

Cyclopentadienyl Chromium Catalysts

The Union Carbide catalyst is prepared by treatment of silica with chromocene. There have, of course, been attempts to model this reaction with surface hydroxyl groups in homogeneous solution by reaction of chromocene with alcohols or silanols.[14] The products of such reactions are invariably dinuclear Cr^{II} alkoxides (see eq. 1); they do not polymerize or even react with ethylene. One of the obvious advantages of surface-supported organometallics is "site-isolation", i.e. the inability of coordinatively unsaturated species to dimerize and thereby annihilate reaction sites. With respect to the initiation of catalysis, an investigation of the reactivity of a mononuclear complex of the type $CpCr^{II}-OR$ would be desirable; however, such a molecule has not been prepared. The closest we have come is the synthesis of mononuclear $Tp^{tBu,Me}Cr-OPh$ [$Tp^{tBu,Me}$ = hydrotris(3-*tert*-butyl-5-methylpyrazolyl)borato]; the sterically hindered tris(pyrazolyl)borate ligand is isoelectronic to the Cp ring, but its steric bulk prevents dimerization.[15] However, $Tp^{tBu,Me}Cr-OPh$ does not react with ethylene.

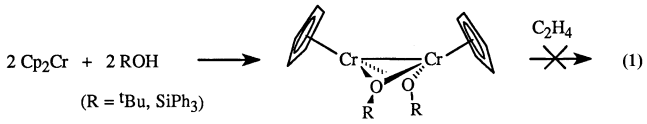

Chromocene by itself does not catalyze the polymerization of ethylene. However, in the presence of an excess of aluminum alkyl and at high ethylene pressure some polymer has been obtained. Under the same conditions, a variety of chromium π-complexes [including bis(arene)chromium$^{0/+}$, CpCr(acac)Br, and $CpCr(NO)_2X$] showed some activity.[16] Wilke et al. found that hexane solutions of tris(allyl)chromium polymerize ethylene under mild conditions[17]; although not a cylopentadienyl derivative, $Cr(\eta^3\text{-}C_3H_5)_3$ is chemically related to Cp_2Cr. The structure of the mixed ligand system $CpCr(\eta^3\text{-}C_3H_5)_2$ has been reported; its reaction with ethylene has not been described in the literature[18], but it is said to be active at modest ethylene pressure.[18c] Bis(indenyl)chromium, a dimeric complex featuring bridging $\mu\text{-}\eta^3$-indenyl ligands, is also a catalyst for ethylene polymerization.[19]

The generally accepted mechanism of polymer chain growth involves coordination of ethylene to a metal atom carrying an alkyl functionality, followed by migratory insertion of the olefin into the metal−carbon bond, thereby increasing the length of the alkyl chain by two carbons (Cossee mechanism).[20] Thus a minimum requirement for the active site is an alkyl group (or hydride) bonded to chromium. Keeping in mind the presence of the ancillary Cp ligand, and maintaining the link to the silica surface via an oxygen atom, one might suggest structure **A** (Scheme 3) as an active site of the Union Carbide catalyst.

Scheme 3

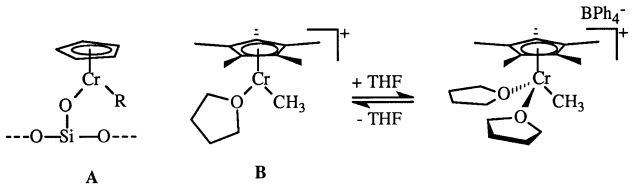

Based on this simple proposal, we began some time ago to explore the synthesis and reactivity of cyclopentadienyl chromium alkyls in the +III oxidation state.[21] For all the familiar reasons (e.g. solubility, stability) we opted for preparing the Cp* derivatives (Cp* = $\eta^5\text{-}C_5Me_5$, i.e. pentamethylcyclopentadienyl), but the qualitative differences caused by this substitution are expected to be minor.[22] Our first success was the synthesis and structural characterization of $[Cp^*Cr(THF)_2Me]BPh_4$ (THF = tetrahydrofuran).[12][23] In solution, this paramagnetic 15-electron cation exists in equilibrium with coordinatively unsaturated $[Cp^*Cr(THF)Me]^+$, via dissociation of a THF ligand (shown by ^1H NMR). Despite their electron deficiency (i.e. three electrons short of the 18-electron configuration), we consider three-legged piano stool complexes of the type Cp^*CrLX_2[24] "coordinatively saturated". If one considers the cyclopentadienyl ring (Cp*), a tridentate chelating ligand, to be occupying one trigonal face of an octahedron, then three additional ligands suffice to complete the octahedral coordination environment of the Cr^{III} ion, one of the most stable entities known to coordination chemists. We suggest that the 13-electron species (**B** in Scheme 3) is a good structural model of the proposed active site of the heterogeneous catalyst (i. e. **A**). Its positive charge may serve to discourage dimerization of the unsaturated species by electrostatic repulsion.

Solutions of $[Cp^*Cr(THF)_2Me]BPh_4$ in dichloromethane catalyzed the polymerization of ethylene at ambient temperature and pressure, without any added cocatalyst. Attempts to polymerize propene with $[Cp^*Cr(THF)_2Me]BPh_4$ were unsuccessful, however. In a typical experiment ca. 10 mg of the chromium compound dissolved in 50 ml CH_2Cl_2 ([cat] = 0.81 mM) produced 1−2 g of polyethylene before activity ceased. Ethylene uptake measurements showed an immediate onset of reaction upon addition of the catalyst. Although no induction period was observed, a slight increase in activity was noted during the initial phase of the reaction. At later times the catalytic activity slowly diminished and effectively ended after ca. one hour. In accord with the dissociation equilibrium depicted in Scheme 3, addition of external THF markedly inhibited the rate of polymerization, presumably by shifting the equilibrium to the coordinatively saturated, unreactive $[Cp^*Cr(THF)_2Me]^+$ cation. This interpretation was also supported by the observation that analogous complexes with more strongly bonded ligands, e.g. $[Cp^*Cr(Py)_2Et]PF_6$ (py = pyridine), were much less effective catalysts. ^1H NMR experiments

and measurements of the rate of polymerization in the presence of various concentrations of THF were used to establish the equilibrium constant for the ligand dissociation [K_{diss} = 1.0(2) M in CH_2Cl_2 at 19°C]. Based on this value, ca 60% of the chromium catalyst exists in the form of the catalytically active 13-electron species $[Cp^*Cr(THF)Me]^+$ under the conditions of the catalytic runs. Taking this into account, the maximum activity measured in these experiments was 1.1 turnover/sec or $>10^5$ g_{PE} $(mol_{Cr}\ h\ atm)^{-1}$, a value that is within an order of magnitude of the quoted activity of commercial catalysts. Measurements of the temperature dependence of the polymerization rate yielded an activation energy (E_a) of 8(1) kcal/mol, which also compares favorably with the value measured for Cp_2Cr/SiO_2 (E_a = 10.1 kcal/mol).[25]

The polymers so obtained were identified as high density polyethylene (HDPE) by IR spectroscopy and melting points (135−140°C). Molecular weight determinations by gel permeation chromatography (GPC) revealed relatively low molecular weights (M_w: 22000−77000; M_n: 14000−20000) and narrow molecular weight distributions (M_w/M_n: 1.9−4.6). The polymers are highly linear, showing no detectable sidebranches by ^{13}C NMR.

The eventual deactivation of the catalysts may be due to several factors. As noted above, the polymerization experiments were carried out without the addition of any cocatalysts. One of the benefits of the latter (typically aluminum alkyls) is their tendency to scrub the ethylene feed of detrimental impurities (e.g. H_2O, O_2), which may react with the catalyst. Without this protection the chromium alkyl will eventually be destroyed. Another possibility may be bimolecular deactivation pathways. β-Hydrogen elimination of a growing polymer chain would yield a Cr^{III} hydride. While such a species might start a new polymer chain (i.e. effect chain transfer) when fixed on a heterogeneous support, we have not been able to prepare a stable mononuclear hydride complex which might model such an intermediate. Attemps to do so have invariably led to reduction to Cr^{II}, presumably accompanied by formation of H_2.[26] Thus β-hydrogen elimination, followed by a binuclear reductive elimination of H_2, may seal the fate of the homogeneous catalyst. A third possibility involves irreversible reactions of the highly electrophilic chromium cation with the solvent or its counterion. In this vein, we have isolated and structurally characterized some unusual chromium complexes resulting from the metal attacking "innocent" anions (see Scheme 4).[12][27] Better noninteracting anions are now available,[28] but only the use of neutral catalysts completely circumvents these problems.

As part of a survey of the factors which are important for the activity of chromium catalysts, it was of interest to ascertain whether the cationic nature of the system described above is essential to the catalysis. After all, its charge is one of the subtle ways model complex **B** differs from the proposed active site **A** (see Scheme 3), which is envisioned as a neutral species. To this end we prepared the neutral dialkyl $Cp^*Cr(CH_2SiMe_3)_2$ (see eq. 2).[29] Although its crystal structure has not been determined yet, the magnetic behavior of the complex in the solid state is consistent with a mononuclear structure devoid of any metal-metal interactions. The effective magnetic moment of $Cp^*Cr(CH_2SiMe_3)_2$ is temperature independent and has a value of μ_{eff} = 3.9(1) μ_B, i.e. the expected spin-only moment for an isolated Cr^{III} ion.

Scheme 4

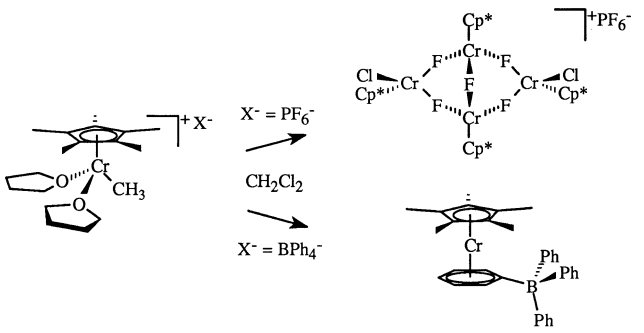

$$CrCl_3(THF)_3 \xrightarrow{Cp^*Li} [Cp^*CrCl_2]_2 \xrightarrow{Me_3SiCH_2Li} Cp^*Cr(CH_2SiMe_3)_2 \quad (2)$$

The steric bulk of the trimethylsilylmethyl groups apparently suffices to prevent dimerization, in contrast to the situation for smaller alkyl groups (see below). There is no spectroscopic evidence for an agostic[30] Cr···H···C interaction, and thus $Cp^*Cr(CH_2SiMe_3)_2$ is best described as a coordinatively unsaturated 13-electron complex. It is also a very good catalyst for the polymerization of ethylene. Hydrocarbon solutions (pentane, toluene) rapidly precipitated polyethylene at reaction temperatures ranging from 0 to −42°C [$Cp^*Cr(CH_2SiMe_3)_2$ slowly decomposes at room temperature]. The polymers had similar physical properties to those produced by $[Cp^*Cr(THF)_2Me]BPh_4$ (M_w: 20000−143000; M_n: 6000−20000; M_w/M_n 3.0−7.0). It is apparent that catalytic activity does not require the chromium alkyl to be positively charged. Indeed, we have found that even an anionic complex can serve as a catalyst precursor. Thus, the ate complex $Li[Cp^*Cr(CH_2Ph)_3]$ (see Scheme 5) polymerized ethylene.[13g] Its rate of polymerization was inhibited by addition of external benzyl lithium, however; presumably dissociation of $LiCH_2Ph$ from the complex generated coordinatively unsaturated $Cp^*Cr(CH_2Ph)_2$, a neutral complex much like $Cp^*Cr(CH_2SiMe_3)_2$. It is probably this intermediate which is responsible for the catalytic activity. Blocking the dissociative pathway, e.g. by sequestering the lithium ion with tetramethylethylenediamine (TMEDA), yielded a coordinatively saturated trialkyl complex, which did not show any polymerization activity. It is not known whether an anionic and yet coordinatively unsaturated Cp^*Cr^{III} alkyl might be active; to test this notion would require the use of a dianionic ligand {e.g. X^{2-} in $[Cp^*Cr^{III}(X)R]^-$}. Even if such a hypothetical 15-electron complex were available, it would still differ in an important way from $[Cp^*Cr(L)R]^+$ and Cp^*CrR_2, both of which exhi-

bit 13-electron configurations. We have not pursued this question.

Scheme 5

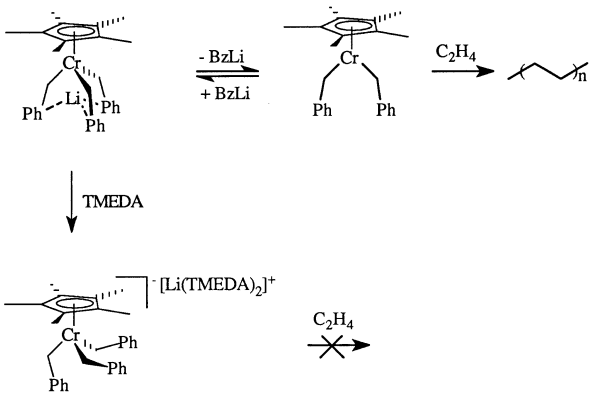

One of the characteristics of the Union Carbide catalyst (Cp_2Cr/SiO_2) distinguishing it from the Phillips catalysts is its pronounced selectivity between ethylene and higher olefins. Basically, it does not react with α-olefins and does not catalyze homopolymerization of the latter or even copolymerization of ethylene with α-olefins. The random incorporation of alkyl branches into the polymer chain gives rise to so-called "linear low density polyethylene" (LLDPE), a material of increasing commercial importance. Our model system seems to behave similarly in this respect as well. It has already been noted that $[Cp^*Cr(THF)_2Me]BPh_4$ failed to polymerize propene under mild conditions. In an attempt to facilitate reaction with α-olefins, and reasoning that the selectivity might be steric in origin, we have prepared chromium complexes with extremely labile ligands. While propene might not be able to compete effectively with THF for the empty coordination site of $[Cp^*Cr(THF)Me]^+$, it might be able to do so if the THF was replaced by a much weaker ligand. With this in mind, we have prepared chromium alkyls stabilized by dialkyl ethers, i.e. $[Cp^*Cr(OR_2)_2CH_2SiMe_3]BAr'_4$ [R = Me, Et, ^{i}Pr; Ar′ = 3,5-bis(trifluoromethyl)phenyl, see Scheme 6].[31] As an indication of the weakness of the chromium−ether bond, structurally characterized $[Cp^*Cr(OEt_2)_2CH_2SiMe_3]BAr'_4$ lost one equivalent of Et_2O when nitrogen gas was passed over the solid. It was also an extremely reactive catalyst, polymerizing ethylene even below its boiling point (b.p. −104°C).

$[Cp^*Cr(OEt_2)_2CH_2SiMe_3]BAr'_4$ also catalyzed the polymerization (or more appropriately, oligomerization) of α-olefins. Reactions of $[Cp^*Cr(OEt_2)_2CH_2SiMe_3]BAr'_4$ with propene and 1-hexene occurred at temperatures close to 0°C and yielded oily residues, which were analyzed by ^{1}H NMR and GC-MS. They were mixtures of oligomers with degrees of polymerization below 20. Finally, copolymerization experiments, in which the same catalyst was exposed to mixtures of ethylene and an α-olefin, yielded pure polyethylene without any indication (^{13}C NMR) of branching.

Because of the great interest in copolymerizations, we have made another attempt to tune the reactivity of chromium catalysts in that direction. So-called "constrained geometry" catalysts containing titanium are known to facilitate incorporation of large amounts of α-olefins into a copolymer.[32] The common structural element of these catalysts is an amido group covalently linked to the cyclopentadienyl ligand via a short bridge (1 or 2 atoms) as shown below.[33]

Scheme 6

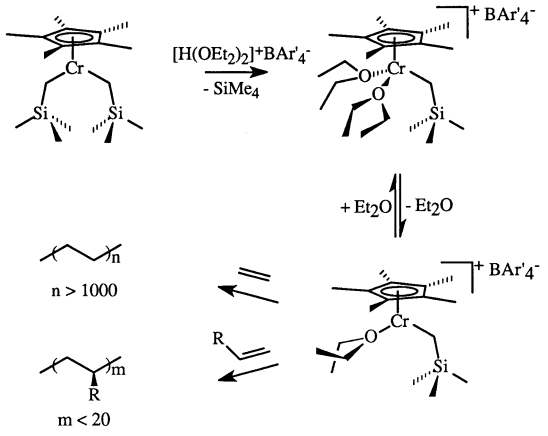

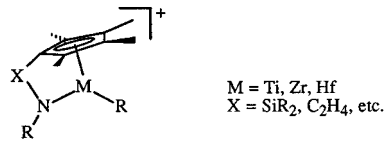

The open access to the metal alkyl is thought to be responsible for the lack of selectivity between different olefins. Hoping to capitalize on this effect, we have prepared isostructural chromium compounds.[34] Scheme 7 shows some of the molecules we have prepared and their reactions with olefins. The sterically demanding trimethylsilylmethyl ligand facilitated the isolation of $[\eta^5\text{-}(Me_4C_5)SiMe_2(N^tBu)]CrCH_2SiMe_3$, i.e. a coordinatively unsaturated Cr^{III} alkyl that has been structurally characterized. True to our expectations, this complex catalyzed the polymerization of ethylene. Remarkably, when the polymerization was carried out in 1-hexene instead of toluene as the solvent, the resulting polymer was still pure polyethylene without any indication of incorporation of the α-olefin. Finally, when the catalyst was presented with pure α-olefin (propene, hexene), a much slower reaction yielded the products of catalytic head-to-tail dimerization and isomerization of the olefin. In this system too, chromium exhibits significant selectivity, favoring ethylene by a wide margin over any other olefin.

We conclude that the Cp^*Cr^{III} model system exhibits considerable selectivity for ethylene, much like Cp_2Cr/SiO_2. While it possesses some activity for the polymerization/oligomerization of α-olefins, the relative rates of polymerization make copolymerizations impractical. Our observations suggest that several factors limit the polymerization of α-olefins. First, the large difference in temperature at which the reactions commence (i.e. differences in rates) suggests that, for example, either the binding or the insertion

Scheme 7

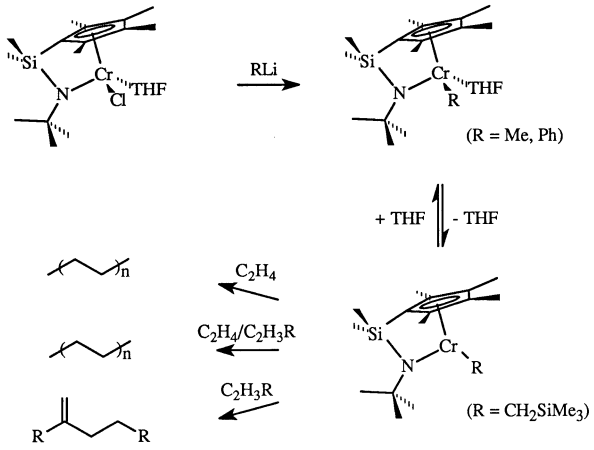

step greatly favors ethylene over propene. On the other hand, the production of α-olefin oligomers of relatively low molecular weight (including dimers for the "constrained geometry" chromium catalyst) indicates that β-hydrogen elimination of a growing chain is much more facile for a Cp*Cr alkyl with tertiary hydrogen atoms. Whatever the underlying reasons for these preferences, they would appear to make cyclopentadienyl chromium systems unsuitable for α-olefin polymerization.

In this context it is appropriate, however, to mention some ambiguity in the available evidence. Jolly has recently reported that amino-substituted cyclopentadienyl chromium derivatives (see eq. 3), in the presence of methylaluminoxane (MAO:Cr = 100:1), polymerize propene (to atactic polypropylene) and copolymerize ethylene and norbornene to an alternating copolymer.[35] MAO is known to confer remarkable enhancements upon the catalytic activity of group 4 metallocene catalysts, and these observations may suggest that chromium systems will show a similar response. In keeping with the noted lack of cocatalyst requirements of heterogeneous chromium catalysts, we have not explored the effects of MAO on the Cp*Cr system. Conversely, based on our work with closely related compounds, a dialkyl or cationic monoalkyl containing the amino-substituted ligand shown in eq. 3 would not by itself be expected to polymerize propene effectively. This apparent ambiguity awaits further study.

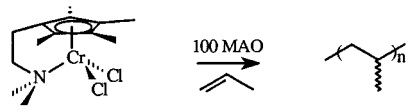

(3)

We conclude that *coordinatively unsaturated Cp*Cr*^{III} alkyls provide a credible structural as well as a functional model for the active site of the Union Carbide catalyst. Their reactivity characteristics parallel those of the heterogeneous catalyst. While the exact origin of the alkyl group in the latter remains unclear, the weight of the available evidence suggests that structure **A** of Scheme 3 is a good approximation of the chromium site in the act of chain propagation. Further support for this notion was provided by a recent theoretical study inspired by [Cp*Cr(THF)$_2$Me]BPh$_4$; its authors noted that the Cr^{III} system "displays many similarities to corresponding group IV systems".[36]

As noted in the introduction (see Scheme 3) many other types of organometallic structures have been proposed to account for the activity of the Union Carbide catalyst. Chief among these are various metallacycles, binuclear catalytic sites, and chromium compounds in formal oxidation states other than +III. During our wide-ranging exploration of the organometallic chemistry of Cp*-ligated chromium we have encountered many molecules which may serve as homogeneous models for such species. For the first time, their catalytic competency can thus be tested directly. If a particular structure does not exhibit any catalytic activity or reactivity with ethylene in homogeneous solution, simply grafting it onto a silica surface will not render it catalytically active. Attachment of a catalyst to a solid support has many advantages, but it is not a license for suspending sound chemical reasoning. Naturally, lack of catalytic activity is merely a negative datapoint, and it can always be argued that a model compound does not capture the actual species in detail. However, since we have described a fully functioning model system (see above), proponents of alternative structures now face the challenge of demonstrating that their candidates can actually do the job.

The proposal of a metallacycle is obviously connected to the desire to create an alkyl ligand via a precedented reaction of a metal site with ethylene. Reductive coupling of two ethylene units to a 1,4-butanediyl ligand is such a transformation, and accordingly metallacyclopentanes and dimetallacyclohexanes have often been considered as initiators of chain growth. Assuming, for the sake of the argument, that the lowest accessible oxidation state of chromium in Cp_2Cr/SiO_2 is +II, then coupling of two ethylene molecules on a mononuclear site would generate a Cr^{IV} metallacycle. This relatively rare oxidation state could be circumvented by considering cooperativity of two chromium sites, resulting in a dinuclear metallacycle with two Cr^{III} centers (see Scheme 2). Other, more complicated sequences of events are conceivable and might lead to any combination of ring size, nuclearity, and oxidation state. In any case, Scheme 8 shows some structurally characterized chromium metallacycles prepared as part of our studies.[37]

Most of these contain four-membered rings; however, it is unlikely that the slight difference in ring size would affect the insertion of ethylene. While the exact mechanism of formation of these molecules has not been determined in all cases, it seems probable that the Cr^{IV} metallacyclopentane with the "constrained geometry" ligand is the product of a reductive coupling of propene, i.e. the very reaction envisioned above for the formation of such structures. Its lack of any further reactivity with ethylene is thus all the more disappointing, if not entirely surprising. Indeed, none of the metallacycles depicted in Scheme 8 catalyzed the polymerization of ethylene. The most likely explanation for this lack or reactivity is the fact that all of the molecules are coordinatively saturated, i.e. in addition to the Cp* ligand they

Scheme 8

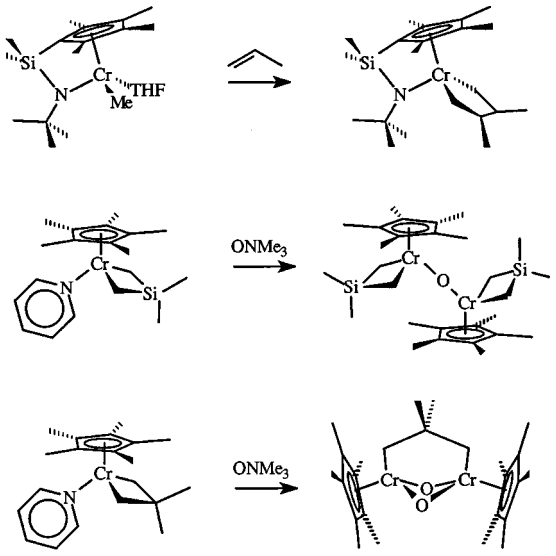

contain three ligands bonded to chromium. Interestingly, this objection was raised, and promptly dismissed, by one of the champions of a metallacycle intermediate.[9e] In any case, these observations certainly do not support the initiation of the catalysis via a metallacycle.

On the same topic, Jolly has reported the preparation of Cr^{III} metallacyclopentanes, inter alia by reductive coupling of ethylene (see eq. 4).[35] These react slowly with ethylene, and the work provides support for the intermediacy of such species in the chromium-catalyzed trimerization of ethylene to hexene.[38] However, activity for the polymerization of ethylene was noted only in the presence of an excess of MAO (100 equiv.). Under these conditions the fate of the metallacycle fragment is unclear.

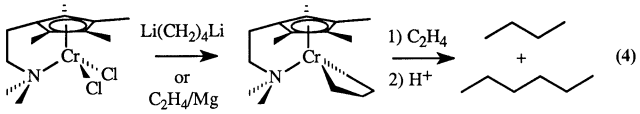

(4)

Dinuclear chromium sites have often been suggested as the locus of catalytic activity. This may seem somewhat counterintuitive, as metal−metal bonding would be possible under these circumstances, which tends to attenuate the reactivity of metal complexes. The latter expectation seemed to be borne out by our experience with dinuclear chromium alkyls. For example, Scheme 9 shows a sequence of transformations of dinuclear complexes beginning with the synthesis of $[Cp^*(CH_3)Cr(\mu\text{-}CH_3)]_2$.[39] This complex is formally analogous to the catalytically active $Cp^*Cr(CH_2SiMe_3)_2$ (see eq. 2), but the lesser steric hindrance of the methyl groups and the electron deficiency of the metal result in dimerization via bridging alkyl groups. We have analyzed the extent of metal−metal bonding between the pseudooctahedral Cr^{III} atoms.[40] Their structures (d_{Cr-Cr}: 2.4−2.6 Å) and magnetic properties were consistent with some metal−metal interactions, which were also supported by EHMO calculations. Metal−metal bonding is rather unusual in Cr^{III} chemistry, and the interactions must certainly be weak. We noted that addition of even weak ligands (e.g. dissolution in THF) rapidly cleaved both $[Cp^*(CH_3)Cr(\mu\text{-}CH_3)]_2$ [to two equiv. of $Cp^*Cr(THF)(CH_3)_2$] and $[Cp^*_2Cr_2(\mu\text{-}CH_3)_3]^+$ {to $Cp^*Cr(THF)(CH_3)_2$ and $[Cp^*Cr(THF)_2CH_3]^+$}. Apparently the interaction with the cyclic ether is stronger than the Cr−Cr bond. However, ethylene binding was apparently not competitive. None of the molecules depicted in Scheme 9 exhibited any activity for the polymerization of ethylene under mild conditions. Thus we see no compelling advantage in postulating binuclear active sites.

Scheme 9

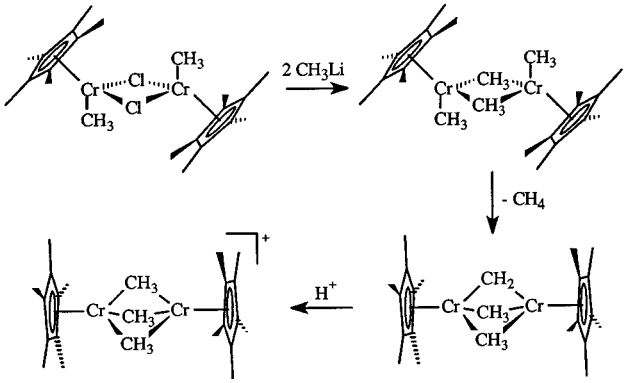

The remaining issue generating some difference of opinion is the valence state of the active chromium species. While even more contentious with regard to the Phillips catalysts, various formal oxidations states have been proposed for the Cp_2Cr/SiO_2 catalyst as well. In the words of its inventors, "it seems reasonable that the active site is an adsorbed, divalent chromium species which is still bonded to one cyclopentadienyl ligand".[7b] Our work points toward Cr^{III} rather than Cr^{II} as the active species, and even higher valence states have been contemplated.

Before describing our relevant observations some remarks of a general nature are perhaps in order. To begin with, we will consider an "active site" only a species which is actually producing polymer chains by repeated insertion of monomer. In general, this will require the presence of an alkyl (or hydride) ligand σ-bonded to chromium. Species that can be transformed into active sites by some reaction, including initiation of a chain via a reaction with ethylene, are merely "catalyst precursors". For example, the Cr^{VI} oxo sites of the calcined Phillips catalysts, or even the Cr^{II} centers resulting from reduction of the former with CO, are precursors rather than active sites. While they have the potential to catalyze the polymerization reaction, and will do so when exposed to ethylene, they are clearly missing an important attribute of the functioning catalyst, namely the growing macromolecule. While this distinction may seem rather restrictive, an unambiguous discussion of the evidence requires it. The initiation event may well change the oxidation state of the chromium (see Schemes 1 and 2), and the chemical situation is complex enough without introducing ambiguity due to ill-defined terminology.

Secondly, any argument about active vs. inactive valence states may be somewhat artificial, inasmuch as the "formal oxidation state" of a metal is a theoretical construct rather than a physical observable. Chromium complexes of the same oxidation state may have widely differing electron densities and partial charges on the metal center; the latter will ultimately determine the reactivity of any compound rather than a number based on willful neglect of any covalent contribution to metal−ligand bonding. As McDaniel put it regarding the Phillips catalysts, " it is ridiculous to speak of a particular valence state as if it were monolithic", and "the environment of the chromium, i.e., its type and arrangement of ligands, may be more important than the formal valence".[5] That said, it is probably overzealous to completely disregard valence as an important factor. There are, after all, good reasons while the concept remains in wide use in inorganic and organometallic chemistry. Furthermore, the coordination environment of the Cp_2Cr/SiO_2 catalyst is delineated fairly well. Thus, it may well be informative to ask which valence state of the metal will render a coordinatively unsaturated CpCr alkyl fragment catalytically active. In any case, in the following we will summarize our experimental observations on this matter.

Our first experiment with respect to oxidation state was a direct comparison of the reaction of isostructural di- and trivalent chromium alkyls with ethylene. Thus, chemical reduction of [Cp*Cr(dmpe)Me]PF_6 [dmpe = bis(dimethylphosphino)ethane] yielded the neutral Cr^{II} alkyl Cp*Cr(dmpe)Me, which has been structurally characterized.[12] Scheme 10 shows the side-by-side comparison of the reactivity of these two compounds.

Scheme 10

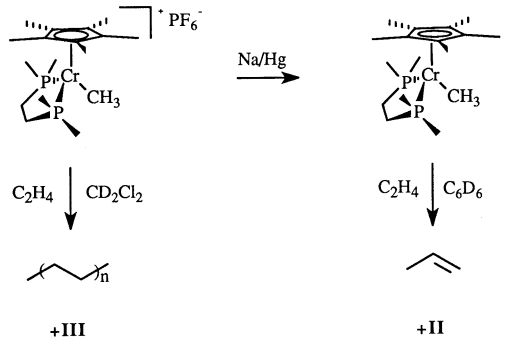

As expected, the Cr^{III} complex catalyzed the polymerization of ethylene; the forcing conditions were presumably due to the presence of the chelating phosphine, which makes the opening up of a coordination site difficult. In contrast, the Cr^{II} alkyl reacted at ambient temperature, reflecting the known substitutional lability of divalent chromium. However, its reaction with ethylene produced propene along with small amounts of other olefins. The likely mechanism of formation of propene consists of insertion of ethylene into the chromium−methyl bond, followed by β-hydrogen elimination of the resulting propyl complex. There appears to be a clear dividing line between the reactivities of these two valence states, at least in this particular system. While the Cr^{III} alkyl repeatedly favors olefin insertion (i.e. chain growth) over β-hydrogen elimination (i.e. chain transfer), the Cr^{II} species exhibits the opposite selectivity. The choice of active oxidation state for polymerization catalysis is obvious.

The set of compounds described above differ from the actual catalyst in that they contain a phosphine ligand. To assess the polymerization activity of a divalent CpCr alkyl, it would be desirable to prepare the simplest such system imaginable, i.e. "CpCrR". We have done just that, however, the resulting species were of course not mononulear compounds with 12-electron configurations. Eq. 5 depicts the synthesis of the dinuclear chromium alkyls of the type [Cr*Cr(μ-R)]$_2$.[41] While of interest as a novel class of organochromium compounds and precursors to chromium hydrides, these complexes did not react with ethylene. This failure is probably due to the strong metal−metal bonding featured by these dimers. The short chromium−chromium distances {e.g. 2.26 Å in [Cr*Cr(μ-CH_3)]$_2$} signal the strength of this interaction, which is a well-precedented feature of Cr^{II} chemistry. Only one of the dinuclear complexes, namely a benzyl complex, catalyzed the polymerization. However, upon closer inspection, we found that isomerization to a mixed valence isomer (Cr^{I},Cr^{III}) was responsible for this activity.[42]

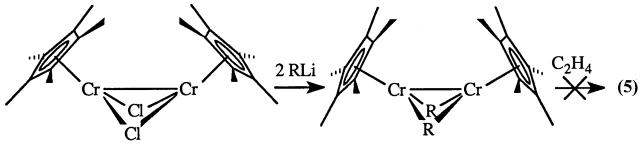

Dimerization of coordinatively unsaturated species has been noted as a "basic dilemma in attempting to model a heterogeneous reaction with compounds in solution".[14a] Thus the chemistry shown in eq. 2 is probably another good argument against the activity of dinuclear chromium sites (see above), but it falls short of ruling out mononuclear, coordinatively unsaturated Cr^{II} alkyls as active sites. However, we have recently obtained a set of compounds that address this question. Utilizing a sterically hindered tris(pyrazolyl)borate ligand, we have prepared divalent chromium alkyls of the type Tp$'^{Bu,Me}$CrR [Tp$'^{Bu,Me}$ = hydrotris(3-*tert*-butyl-3-methylpyrazolyl)borate; R = Et, Ph, CH_2SiMe_3], see Scheme 11.[43] The Tp ligand serves as an isoelectronic, yet sterically more demanding, replacement of the Cp ring. It effectively prevents dimerization, and accordingly the compounds feature mononuclear, four-coordinate Cr^{II}. Remarkably, they adopt an unusual "cis-divacant octahedral" coordination geometry, which leaves two coordination sites on chromium open for binding of the olefin substrate or other ligands.

None of these complexes reacted with ethylene, either at room temperature or upon heating. Indeed, Tp^{tBu,Me}CrEt eventually decomposed via β-hydrogen elimination.

In summary, the available evidence suggests that divalent chromium alkyls are not capable of catalyzing the polymerization of ethylene. They either fail to react with ethylene, or, if they do, the products undergo facile β-hydrogen elim-

Scheme 11

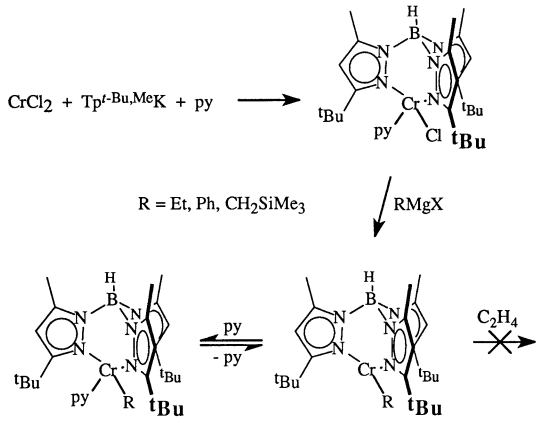

ination. Trivalent cyclopentadienyl chromium alkyls, on the other hand, when coordinatively unsaturated, consistently catalyze the polymerization, and the characteristics of the catalysis faithfully model the Union Carbide catalyst. Much less is known about the reactivity of CpCr alkyls in even higher oxidation states (IV−VI). None of the examples we[44], or others[45], have prepared have proven catalytically active, and it seems likely that the presence of several uninegative ligands beyond the Cp ligand and the polymer chain would render such complexes coordinatively saturated and hence inactive. Thus, based on the extensive available evidence from homogeneous model chemistry, we assert that the active sites of cyclopentadienyl chromium polymerization catalysts, including the Cp_2Cr/SiO_2 catalyst, are coordinatively unsaturated alkyls of trivalent chromium. To suggest otherwise would require experimental evidence in the form of a functioning homogeneous catalyst.

Other Chromium Catalysts

The most significant commercial chromium catalyst is the Phillips catalyst. It is usually prepared by impregnation of silica or silica/alumina with CrO_3, followed by calcination in air. The material resulting from this procedure is commonly thought to contain surface-bound chromate esters, i.e. Cr^{VI} species coordinated only by oxygen atoms (see Scheme 1). The oxidized form of the catalyst can be used for polymerizations. However, an induction period is observed, and products of olefin oxidation (formaldehyde) have been detected. Chromyl derivatives are known to be strong oxidants, which are reduced by olefins.[46]

Attempts to model the activation of the Phillips catalyst in homogeneous solution have met with limited success, although without shedding much light on the detailed nature of the active site (see Scheme 12). Thus, cyclohexane solutions of bis(triphenylsilyl)chromate catalyzed the polymerization of ethylene at high temperatures (T > 130°C) and pressures (P = 350−1500 atm), even in the absence of a cocatalyst.[47] Addition of an aluminum alkyl caused "reduction of the chromium" and onset of ethylene polymerization at room temperature and atmospheric pressure. Similarly, Feher et al. have prepared and structurally characterized a chromate ester of a silasesquioxane, probably the best available structural model of the oxidized Phillips catalyst.[8b] Addition of two equivalents of $AlMe_3$ to benzene solutions of this compound produced dark orange solutions which polymerized ethylene under mild conditions (20°C, 1 atm). However, no further information about the oxidation state or chemical nature of the active catalyst(s) in these systems has been reported.

Scheme 12

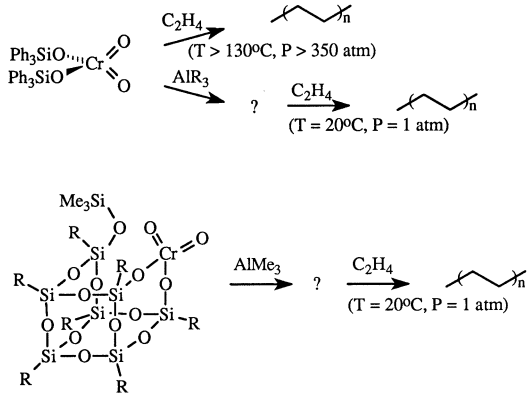

It is apparent that the active site of the Phillips catalyst must contain chromium in a reduced state; however, the exact oxidation state of the metal remains unknown, despite much work and endless debate. Krauss and Stach showed some time ago that under favorable conditions the surface chromium can be reduced with carbon monoxide all the way down to Cr^{II}, and that the resulting coordinatively unsaturated species is indistinguishable in its polymerization behavior from the regular catalyst.[6] Based largely on these observations the catalytic activity of divalent chromium has become the prevailing dogma. However, the nature of the initiation step remains unclear, and the same ambiguities described for the Union Carbide catalyst (see above) exist here too. It is noteworthy that well-characterized Cr^{II} complexes, including coordinatively unsaturated alkyls, have failed to show any polymerization activity.[48]

The most promising recent development in this area has been Gibson's report of highly active homogeneous catalysts derived from bis(imido) chromium(VI) precursors (see eq. 6).[49] While the active species in this system have not yet been structurally characterized, the spectroscopic evidence seems consistent with cationic bis(imido)chromium alkyls featuring hexavalent chromium (Cr^{VI}). Based on the isolobal relationship between Cp- and imido ligands, and its putative d^0 configuration, this system resembles group IV metallocene chemistry (i.e. Cp_2MR^+) much more than any known heterogeneous chromium catalyst.

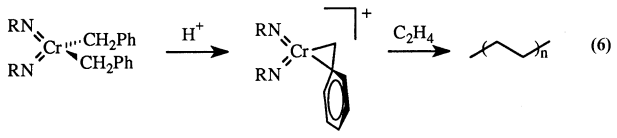

(6)

Conclusions

Coordinatively unsaturated Cp^*Cr^{III} alkyls represent the first well-characterized homogeneous ethylene polymerization catalysts based on chromium. These complexes model the Union Carbide catalyst (Cp_2Cr/SiO_2), and their chemistry may well be related to the Phillips catalyst (CrO_3/SiO_2) as well. Attachment of the compounds to inorganic oxide supports generates heterogeneous catalysts of considerable commercial potential. Looking to the future, this system may serve as the starting point for the design of new single-site catalysts containing chromium, and work toward that end is in progress in several laboratories.

Financial support of this research by the *US National Science Foundation* and *Chevron Chemical Co.* is gratefully acknowledged.

[1] M. S. Reisch, *Chem. Eng. News*, **1997**, (*May 26*), 14.
[2] [2a] K. Ziegler, Belgian Patent 533,362, **1954**. – [2b] K. Ziegler, E. Holzkamp, H. Martin, H. Breil, *Angew. Chem.* **1955**, *67*, 541. – [2c] G. Natta, *J. Polym. Sci.* **1955**, *16*, 143. – [2d] G. Natta, *Angew. Chem.* **1956**, *68*, 393. – [2e] H. Sinn, W. Kaminsky in *Advances in Organometallic Catalysis*, (Eds.: F.G.A. Stone, R. West), Academic Press, New York, **1980**, p. 99.
[3] H. H. Brintzinger, D. Fischer, R. Mülhaupt, B. Rieger, R. M. Waymouth, *Angew. Chem. Int. Ed. Engl.* **1995**, *34*, 1143.
[4] J. P. Hogan, R. L. Banks, U.S. Patent 2,825,721, **1958**.
[5] M. P. McDaniel, *Adv. Catalysis* **1985**, *33*, 47.
[6] [6a] H. L. Krauss, H. Stach, *Inorg. Nucl. Chem. Lett.* **1968**, *4*, 393. – [6b] H. L. Krauss, H. Stach, *Z. Anorg. Allg. Chem.* **1969**, *366*, 280.
[7] [7a] G. L. Karapinka, U.S. Patent 3,709,853, **1973**. – [7b] F. J. Karol, G. L. Karapinka, C. Wu, A. W. Dow, R. N. Johnson, W. L. Carrick, *J. Polym. Sci. , Part A-1* **1972**, *10*, 2621.
[8] [8a] M. P. McDaniel in *Transition Metal Catalyzed Polymerization, Part B,* (Ed.: R. P. Quirk), Harwood Academic Press, New York, **1983**, p. 713. – [8b] F. J. Feher, R. L. Blanski, *J. Chem. Soc., Chem. Commun.* **1990**, 1614.
[9] [9a] S. -L. Fu, J. H. Lunsford, *Langmuir* **1990**, *6*, 1774. – [9b] S. L. Fu, M. P. Rosyneck, J. H. Lunsford, *Langmuir* **1991**, *7*, 1179. – [9c] A. Zecchina, G. Spoto, G. Ghiotti, E. Garrone, *J. Mol. Catal.* **1994**, *86*, 423. – [9d] D. Scarano, G. Spoto, S. Bordiga, L. Carnelli, G. Ricchiardi, A. Zecchina, *Langmuir* **1994**, *10*, 3094. – [9e] A. Zecchina, G. Spoto, S. Bordiga, *Faraday Discuss. Chem. Soc.* **1989**, *87*, 149. – [9f] S. J. Conway, J. W. Falconer, C. H. Rochester, *J. Chem. Soc.,Faraday Trans.* **1989**, *85*, 79. – [9g] B. Rebenstorf, *J. Catal.* **1989**, *117*, 71. – [9h] P. Zielinski, I. G. Dalla Lana, *J. Catal.* **1992**, *137*, 368.
[10] [10a] G. Zhang, P. R. Auburn, D. L. Beach, *Jpn. J. Appl. Phys.* **1993**, *32*, 511. – [10b] P. J. Ellis, R. W. Joyner, T. Maschmeyer, A. F. Masters, D. A. Niles, A. K. Smith, *J. Mol. Cat. A* **1996**, *111*, 297.
[11] M. Schnellbach, F. H. Köhler, J. Blümel, *J. Organomet. Chem.* **1996**, *520*, 227.
[12] B. J. Thomas, S. -K. Noh, G. K. Schulte, S. C. Sendlinger, K. H. Theopold, *J. Am. Chem. Soc.* **1991**, *113*, 893.
[13] [13a] A. Grohmann, F. H. Köhler, G. Müller, H. Zeh, *Chem. Ber.* **1989**, *122*, 897. – [13b] N. Hebendanz, F. H. Köhler, F. Scherbaum, B. Schlesinger, *Magn. Reson. Chem.* **1989**, *27*, 798. – [13c] J. Blümel, P. Hofmann, F. H. Köhler, *Magn. Reson. Chem.* **1993**, *31*, 2. – [13d] F. H. Köhler, B. Metz, W. Strauss, *Inorg. Chem.* **1995**, *34*, 4402. – [13e] J. Blümel, M. Herker, W. Hiller, F. H. Köhler, *Organometallics* **1996**, *15*, 3474. – [13f] R. A. Heintz, T. G. Neiss, K. H. Theopold, *Angew. Chem., Int. Ed. Engl.* **1994**, *33*, 2326. – [13g] G. Bhandari, Y. Kim, J. M. McFarland, A. L. Rheingold, K. H. Theopold, *Organometallics* **1995**, *14*, 738.
[14] [14a] F. J. Karol, C. Wu, W. T. Reichle, N. J. Maraschin, *J. Catal.* **1979**, *60*, 68. – [14b] M. H. Chisholm, F. A. Cotton, M. W. Extine, D. C. Rideout, *Inorg. Chem.* **1979**, *18*, 120.
[15] M. Hörtz, unpublished results.
[16] Y. Tajima, K. Tani, S. Yuguchi, *J. Polym. Sci. B; Polym. Lett.* **1965**, *3*, 529.
[17] G. Wilke, B. Bogdanovic, P. Hardt, P. Heimbach, W. Keim, M. Kröner, W. Oberkirch, K. Tanaka, E. Steinbrücke, D. Walter, H. Zimmermann, *Angew. Chem. Int. Ed. Engl.* **1996**, *5*, 151.
[18] [18a] K. Angermund, A. Döhring, P. W. Jolly, C. Krüger, C. C. Romao, *Organometallics* **1986**, *5*, 1268. – [18b] P. Betz, A. Döhring, R. Emrich, R. Goddard, P. W. Jolly, C. Krüger, C. C. Romao, K. U. Schönfelder, Y. -H. Tsay, *Polyhedron* **1993**, *12*, 22651. – [18c] P. W. Jolly, personal communication.
[19] O.Heinemann, P. W. Jolly, C. Krüger, G. P. J. Verhovnik, *Organometallics*, **1996**, *15*, 5462.
[20] P. Cossee, *J. Catal.* **1964**, *3*, 80.
[21] D. S. Richeson, S. -W. Hsu, N. H. Fredd, G. Van Duyne, K. H. Theopold, *J. Am. Chem. Soc.* **1986**, *108*, 1491.
[22] K. H. Theopold, *Acc. Chem. Res.* **1990**, *23*, 263.
[23] [23a] B. J. Thomas, K. H. Theopold, *J. Am. Chem. Soc.* **1988**, *110*, 5902. – [23b] K.H. Theopold, R.A. Heintz, S.-K. Noh, B.J. Thomas in *Homogeneous Transition Metal Catalyzed Reactions*, (Eds.: W.R. Moser, D.W. Slocum), American Chemical Society, Washington, DC, **1992**, p. 591.
[24] For details on the MLX classification scheme see: M. L. H. Green, *J. Organomet. Chem.* **1995**, *500*, 127.
[25] F. J. Karol, G. L. Brown, J. M. Davison, *J. Polym. Sci.: Polym. Chem. Ed.* **1973**, *11*, 413.
[26] [26a] R. A. Heintz, B. S. Haggerty, H. Wan, A. L. Rheingold, K. H. Theopold, *Angew. Chem. Int. Ed. Engl.* **1993**, *31*, 1077. – [26b] R. A. Heintz, R. L. Ostrander, A. L. Rheingold, K. H. Theopold, *J. Am. Chem. Soc.* **1994**, *116*, 11387.
[27] B. J. Thomas, J. F. Mitchell, J. A. Leary, K. H. Theopold, *J. Organomet. Chem.* **1988**, *348*, 333.
[28] S. H. Strauss, *Chem. Rev.* **1993**, *93*, 927.
[29] R. A. Heintz, Ph. D. thesis, Cornell University, **1994**.
[30] [30a] M. Brookhart, M. L. H. Green, *J. Organomet. Chem.* **1983**, *250*, 395. – [30b] M. Brookhart, M. L. H. Green, L. L. Wong, *Prog. Inorg. Chem.* **1988**, *36*, 1.
[31] P. A. White, J. Calabrese, K. H. Theopold, *Organometallics* **1996**, *15*, 5473.
[32] [32a] J.C. Stevens in *11th International Congress on Catalysis—40th Anniversary*, (Eds.: J.W. Hightower, W.N. Delgass, E. Iglesia, A.T. Bell), Elsevier, Amsterdam, **1996**, p. 11. – [32b] A. A. Montagna, *CHEMTECH* **1995**, (*October*), 44.
[33] [33a] P. J. Shapiro, E. Bunel, W. P. Schaefer, J. E. Bercaw, *Organometallics* **1990**, *9*, 867. – [33b] P. J. Shapiro, W. D. Cotter, W. P. Schaefer, J. A. Labinger, J. E. Bercaw, *J. Am. Chem. Soc.* **1994**, *116*, 4623.
[34] Y. Liang, G. P. A. Yap, A. L. Rheingold, K. H. Theopold, *Organometallics* **1996**, *15*, 5284.
[35] R. Emrich, O. Heinemann, P. W. Jolly, C. Krüger, G. P. J. Verhovnik, *Organometallics* **1997**, *16*, 1511.
[36] V. R. Jensen, K. J. Børve, *Organometallics* **1997**, *16*, 2514.
[37] [37a] Y. Liang, M. S. thesis, University of Delaware, 1996. – [37b] R. Papp, M. S. thesis, University of Delaware, **1997**.
[38] J. R. Briggs, *J. Chem. Soc., Chem. Commun.* **1989**, 674.
[39] [39a] S. -K. Noh, R. A. Heintz, C. Janiak, S. C. Sendlinger, K. H. Theopold, *Angew. Chem. Int. Ed. Engl.* **1990**, *29*, 775. – [39b] S. -K. Noh, S Sendlinger,C., C. Janiak, K. H. Theopold, *J. Am. Chem. Soc.* **1989**, *111*, 9127.
[40] C. Janiak, J. Silvestre, K. H. Theopold, *Chem. Ber.* **1993**, *126*, 631.
[41] R. A. Heintz, R. L. Ostrander, A. L.Rheingold, K. H. Theopold, *J. Am. Chem. Soc.* **1994**, *116*, 11387.
[42] G. Bhandari, A. L. Rheingold, K. H. Theopold, *Chem. Eur. J.* **1995**, *1*, 199.
[43] J. L. Kersten, R. R. Kucharczyk, G. P. A. Yap, A. L. Rheingold, K. H. Theopold, *Chem. Eur. J.* **1997**, *3*, 1668.
[44] S. -K. Noh, R. A. Heintz, B. S. Haggerty, A. L. Rheingold, K. H. Theopold, *J. Am. Chem. Soc.* **1992**, *114*, 1892.
[45] W. A. Herrmann, W. R. Thiel, E. Herdtweck, *J. Organomet. Chem.* **1988**, *353*, 323.
[46] P. Stavropoulos, N. Bryson, M. -T. Youinou, J. A. Osborn, *Inorg. Chem.* **1990**, *29*, 1807.
[47] L. M. Baker, W. L. Carrick, *J. Org. Chem.* **1970**, *35*, 774.
[48] [48a] A. R. Hermes, R. J. Morris, G. S. Girolami, *Organometallics* **1988**, *7*, 2372. – [48b] M. D. Fryzuk, D. B. Leznoff, S. J. Rettig, *Organometallics* **1995**, *14*, 5193.
[49] [49a] M. P. Coles, V. C. Gibson, *Polymer Bulletin* **1994**, *33*, 529. – [49b] M. P. Coles, C. I. Dalby, V. C. Gibson, W. Clegg, M. R. J. Elsegood, *J. Chem. Soc., Chem. Commun.* **1995**, 1709.

[97198]

The Effect of the Bite Angle of Diphosphane Ligands on Activity and Selectivity in Palladium-Catalyzed Allylic Alkylation[+]

Mirko Kranenburg[++], Paul C. J. Kamer*, and Piet W. N. M. van Leeuwen

Van't Hoff Research Institute, Department of Inorganic Chemistry, University of Amsterdam, Nieuwe Achtergracht 166, NL-1018 WV Amsterdam, The Netherlands

Received July 3, 1997

Keywords: Bite angle / Catalysis / P ligands / Palladium / Allylic alkylation

The effect of the natural bite angle (β_n) of diphosphane ligands on catalyst selectivity and activity in the palladium-catalyzed allylic alkylation was investigated. The selectivity and rate of the reaction are mainly determined by steric hindrance induced by the diphosphane ligands. The steric hindrance at the palladium center increases as the natural bite angle of the ligand becomes larger. This results in an increasing selectivity at larger bite angles, but at very large bite angles the rate of the reaction drops. The ligand with the largest calculated bite angle, Xantphos, induced 100% selectivity but the reaction rate became low.

Catalyst selectivity and activity can be influenced by the steric and electronic properties of ligands. Additionally, a third ligand parameter, the bite angle of bidentate ligands,[1] seems to have a crucial effect on reactivity and stability of transition metal complexes. The bite angle can have a tremendous influence on catalyst behavior as shown for the hydroformylation[2][3][4][5] and hydrocyanation[6] reactions.

An intriguing reaction is the palladium-catalyzed allylic substitution reaction. After the discovery by Tsuji[7] further development of this reaction by Trost led to extensive use in organic synthesis.[8] A highly enantioselective palladium diphosphane catalyst was shown to have a large bite angle of 110.5°[9] which indicates that the bite angle can also be of importance in this reaction.

Most studies in this field focused on asymmetric induction and only little attention was paid to regioselectivity. Åkermark and coworkers investigated the influence of the steric bulk of bidentate ligands (substituted phenanthrolines) on the regioselectivity only very recently.[10] A detailed mechanistic and computational study by Bäckvall et al. showed the effect of the electronic properties of ligands on the regioselectivity of the reaction.[11] Steric factors had a large influence on the regioselectivity of this reaction. Recently, both experimental[12][13] and theoretical[14][15] studies were performed on the regioselectivity in the asymmetric allylic substitution, using ligands containing phosphorus and nitrogen donor atoms. Since steric interactions and electronic preferences can induce opposite effects, the involvement of an early or a late transition state remains under debate. All studies mentioned, however, ignored the effect of the bite angle of the ligands, although Trost found that enlarging the bridge of chelating chiral diphosphanes (and consequently increasing the bite angle of the diphosphane) led to higher asymmetric induction.[16]

Here we present a detailed systematic study on the effect of the bite angle of diphosphanes on catalyst activity and selectivity. The catalyst system we employed was prepared in situ using $Pd(DBA)_2$ (DBA = dibenzylidene acetone) and diphosphane in DMF. As a substrate we used 2-hexenylacetate (**1**) and the nucleophile was sodium diethyl methylmalonate (**2**), the same reagent used by Åkermark et al.[10] Only two products were observed: the linear product diethyl 2-(2-hexen-1-yl)-2-methylmalonate (**3**) and the branched product diethyl 2-(1-hexen-2-yl)-2-methylmalonate (**4**). The reaction is depicted in Scheme 1.

Scheme 1

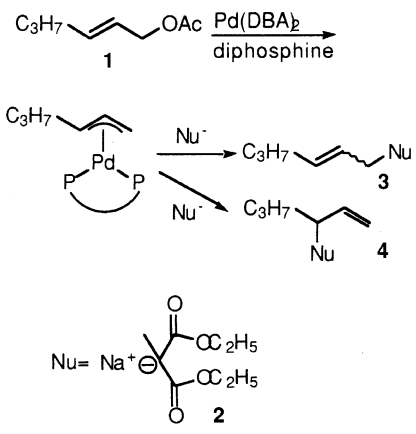

The diphosphane ligands studied as catalyst components were dppe (1,2-bis(diphenylphosphanoethane), dppp (1,3-bis(diphenylphosphanopropane), dppb (1,4-bis(diphenylphosphanobutane), dppf (1,1′-bis(diphenylphosphanoferrocene), DPEphos, Sixantphos, and Xantphos (see Figure 1). The results are summarized in Table 1.

[+] Netherlands Institute for Research in Catalysis (NIOK) Publication UVA 98-6-01.

[++] Present address: DSM Research, P.O. Box. 18, NL-6160 MD Geleen, The Netherlands

 © WILEY-VCH Verlag GmbH, D-69451 Weinheim, 1998 1434–1948/98/0101–0025 $ 17.50+.50/0

Figure 1. Diphosphanes with large bite angles

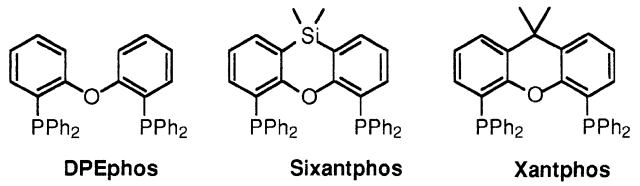

The bite angle of the diphosphane used affects both the activity and the selectivity of the catalyst. A sharp increase in catalyst activity (measured in initial turnover frequency) is observed in going from dppe to dppb. A further increase of the bite angle results in a decrease of the t.o.f.

Table 1. Alkylation of 2-hexenylacetate (**1**) with sodium diethyl methylmalonate (**2**) in DMF[a]

Ligand	Bite angle [°]	t.o.f. [mol/mol Pd/hr][b]	Reaction time [h]	Conversion [%][c]	**3** [%]	**4** [%]
dppe	78.1	82	5	98.5	96.2	3.8
dppp	86.2	111	5	97.9	96.6	3.4
dppb	98.6	393	1	98.0	97.7	2.3
dppf	99.07[d]	118	5	97.6	99.0	1.0
DPEphos	102.7	114	5	98.4	99.7	0.3
Sixantphos	106.5	91	20	97.5	99.6	0.4
Xantphos	110.0	22	20	92.1	100.0	0.0

[a] Conditions: 0.01 mmol $Pd(DBA)_2$, 0.02 mmol ligand, 1.0 mmol of **1**, 2.0 mmol of **2** in 3.0 ml DMF, T = 20°C. The 95% confidence interval of the mean measured values is ±0.1%. – [b] Initial turnover frequency, determined after 5 min. reaction time. – [c] Based on **1**; [d] P–Pd–P angle in X-ray of $(dppf)PdCl_2$.[17]

The selectivity of the reaction towards the linear product **3** increases regularly with an increasing bite angle (see Table 1). Using dppe 3.8% of product **4** is obtained, while dppf leads to 1%. When the Xantphos-type ligands are used, less than 1% of **4** is formed. The differences in amounts of **4** formed using Xantphos-type ligands are within the experimental error and will therefore not be discussed. It is noteworthy that when Xantphos is employed, 100% formation of **3** is observed, i.e. without any trace of **4**, which can prevent laborious purification of the desired product.

The selectivities reported were obtained at maximal conversion, which is nearly quantitative.

The formation of **4** is the result of a nucleophilic attack on the substituted carbon atom of the allyl moiety. In the transition state, the hybridization of this carbon atom changes from sp^2 to sp^3, which results in a bending of the R group towards the phosphane. This causes steric interference of the R group with the diphosphane ligand. A larger diphosphane bite angle results in larger steric interference and consequently less **4** is formed.

The steric interference was investigated by molecular modeling. The data from a P_2Pd[allyl] fragment (obtained from a recent X-ray crystal structure[18]) was superimposed on the structures of [dppe]Pd, the ligand with the smallest bite angle, and that of [Xantphos]Pd, the ligand with the largest bite angle (both taken from the natural bite angle calculations). The results are presented in Figure 2.

Figure 2. View through the P···P axes of [dppe]Pd[allyl] and [Xantphos]Pd[allyl]; H atoms were omitted for clarity

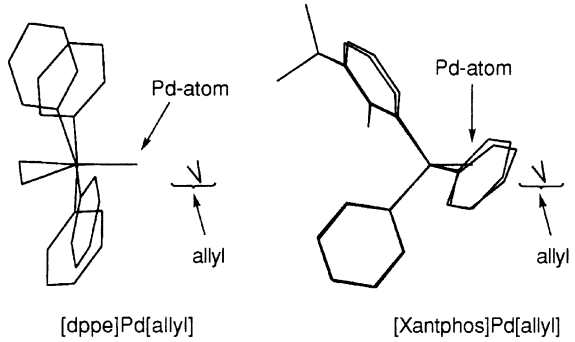

[dppe]Pd[allyl] [Xantphos]Pd[allyl]

In [dppe]Pd[allyl], the allyl fragment experiences no steric interference at all from the diphosphane ligand, while in [Xantphos]Pd[allyl] the allyl fragment interacts with the PPh_2 moieties of the ligand. This can be illustrated by the distances between the terminal allyl carbon atom and the *ipso* carbon atom of the phenyl rings. In [dppe]Pd[allyl] the $C\cdots C_{ipso}$ distances are 3.67 and 4.22 Å, whereas in [Xantphos]Pd[allyl] the $C\cdots C_{ipso}$ distances are 3.12 and 3.55 Å.

The increasing embracement of the allyl fragment at large bite angles not only dictates the regioselectivity, but it also hampers the reaction correspondingly. It is therefore not surprising that the initial turnover frequencies decrease when the natural bite angle of the diphosphane used becomes 100° or larger.

Since the ligand is completely symmetric, the regioselectivity cannot be induced by an electronic effect (trans influence).[12][13] The calculated structure of the complex has an approximate C_s symmetry as supported by crystal structure determinations[19] and solution structures[3] of other complexes. It is therefore unlikely that an electronic difference between the two Pd–C bonds results from steric effects, as suggested by Ward.[15] There is probably not much steric hindrance in the starting Pd allyl complex and the effect of increasing bite angle on the selectivity therefore points to a late transition state for this reaction.

In conclusion, the bite angle of a ligand has been shown to be a parameter of utmost importance for catalyst behavior. In the palladium-catalyzed allylic alkylation of 2-hexenyl acetate, regioselectivity increases with an increasing bite angle. The increased selectivity is induced by the increasing embracing of the allyl fragment by the diphosphane. This purely steric interaction inhibits the formation of the branched side product. The best selectivity with reasonably high reaction rates is obtained with DPEphos.

Experimental Section

Computational Details: All calculations were performed using CAChe WorkSystem software[20] on an Apple Power Macintosh 950 equipped with 2 CAChe CXP coprocessors. The Molecular Mechanics calculations were performed using the MM2 force

field.[21] Block-diagonal Newton-Raphson was used as optimization method. Natural bite angle calculations were performed using a method similar to that described by Casey and Whiteker[1], using a Pd−P bond length of 2.288 Å.[18][19]

For the ligands dppe, dppp and dppb, a starting geometry for the chelate ring resembling the appropriate cycloalkane was used. By this procedure, the global minimum resulting from excessive, stabilizing π-stacking interactions (and a too small a bite angle) was avoided. The geometry obtained this way agrees with geometries observed by X-ray crystallography.[22]

Palladium-Catalyzed Alkylation of Hexenyl Acetate. − General Procedure: To a Schlenk vessel was added $Pd(DBA)_2$, (5.8 mg, 0.01 mmol) and a diphosphane ligand (0.02 mmol), followed by 1 ml of a 1 M solution hexenylactetate (1.0 mmol) and 0.5 M decane (internal standard, 0.5 mmol) in DMF . The Schlenk vessel was kept at 20°C using a water bath and the solution was stirred for 5 min to ensure complete formation of the catalyst. Then 2.0 ml of a 1 M solution of sodium dimethyl malonate in DMF (2.0 mmol) was added. The reaction was monitored with GC at regular time intervals, by working up a small sample in H_2O and ether. The product distribution and the yield were determined using the internal standard.

[1] C. P. Casey, G. T. Whiteker, *Isr. J. Chem.* **1990**, *30*, 299.
[2] W. A. Hermann, C. W. Kohlpainter, H. Bahrmann, W. Konhol, *J. Mol. Cat.* **1992**, *73*, 191.
[3] M. Kranenburg, Y. E. M. van der Burgt, P. C. J. Kamer, P. W. N. M. van Leeuwen, K. Goubitz, J. Fraanje, *Organometallics* **1995**, *14*, 3081.
[4] K. Yamamoto, S. Momose, M. Funahashi, S. Ubata, H. Ohmura, H. Komatsu, M. Miyazawa, *Chem. Lett.* **1994**, 189.
[5] C. P. Casey, G. T. Whiteker, M. G. Melville, L. M. Petrovich, J. A. Gavney Jr., D. R. Powell, *J. Am. Chem. Soc.* **1992**, *114*, 5535.
[6] M. Kranenburg, P. C. J. Kamer, P. W. N. M. van Leeuwen, D. Vogt, W. Keim, *J. Chem. Soc., Chem. Commun.* **1995**, 2177.
[7] J. Tsuji, H. Takahashi, M. Morikawa, *Tetrahedron Lett.* **1965**, 4387.
[8] B. M. Trost, T. R. Verhoeven in *Comprehensive Organometallic Chemistry, Vol. 8* (Ed.: G. Wilkinson), Pergamon, Oxford, U.K. **1982**, p. 799.
[9] B. M. Trost, B. Breit, S. Peukert, J. Zambrano, J. W. Ziller, *Angew. Chem. Int. Ed. Engl.* **1995**, *34*, 2386.
[10] M. P. T. Sjögren, S. Hansson, B. Akermark, A. Vitagliano, *Organometallics* **1994**, *13*, 1963.
[11] A. Aranyos, K. J. Szabo, A. M. Castano, J. E. Bäckvall, *Organometallics*, **1997**, *16*, 1058.
[12] U. Burckhardt, V. Gramlich, P. Hofmann, R. Nesper, P. S. Pregosin, R. Salzmann, A. Togni, *Organometallics* **1996**, *15*, 3496.
[13] A. Togni, U. Burckhardt, V. Gramlich, P. S. Pregosin, R. Salzmann, *J. Am. Chem. Soc.* **1996**, *118*, 1031.
[14] P. E. Blöchl, A. Togni, *Organometallics* **1996**, *15*, 4125.
[15] T. R. Ward, *Organometallics* **1996**, *15*, 2836.
[16] B. M. Trost, D. J. Murphy, *Organometallics* **1985**, *4*, 1143.
[17] T. Hayashi, M. Konishi, Y. Kobori, M. Kumada, T. Higuchi, K. Hirotsu, *J. Am. Chem. Soc.* **1984**, *106*, 158.
[18] H. C. L. Abbenhuis, U. Burckhardt, V. Gramlich, C. Köllner, P. S. Pregosin, R. Salzmann, A. Togni, *Organometallics* **1995**, *14*, 759.
[19] M. Kranenburg, J. G. P. Delis, P. C. J. Kamer, P. W. N. M. van Leeuwen, K. Vrieze, N. Veldman, A. L. Spek, *J. Chem. Soc., Dalton Trans.* **1997**, 1839.
[20] CAChe Scientific Inc., 18700 N.W. Walker Road, Building 92-01, Beaverton, OR 97006, **1994**.
[21] U. Burkert, N. L. Allinger, *Molecular Mechanics*, American Chemical Society, Washington, D.C., **1982**.
[22] A. J. Pavigliani, D. J. Minn, W. C. Fultz, J. L. Burmeister, *Inorg. Chim. Acta* **1989**, *159*, 65.

[97158]

Palladium-Catalyzed Reactions for Fine Chemical Synthesis, 4[◇]

Phosphapalladacycle-Catalyzed Heck Reactions for Efficient Synthesis of Trisubstituted Olefins: Evidence for Palladium(0) Intermediates

Matthias Beller* and Thomas H. Riermeier

Anorganisch-chemisches Institut der Technische Universität München,
Lichtenbergstraße 4, D-85747 Garching, Germany
Fax: (internat.) + 49(0)89/289-13743

Received July 9, 1997

Keywords: Catalysis / Palladium / C−C coupling / Metallacycles / Trisubstituted olefins

The coupling reaction of 1,1-disubstituted olefins (α-methylstyrene, *n*-butyl methacrylate) with various aryl bromides (Heck reaction) has been studied as a new concept to synthesize trisubstituted olefins. Surprisingly, the nature of the base dramatically influences the product distribution. Thus, a systematic investigation on the role of base in Heck reactions of 1,1-disubstituted olefins was performed. Less coordinating bases like NaOAc, NaOBz or Na_2CO_3 yield a statistical distribution of regioisomers with the terminal olefin **10** as the major product. However, by using amines like Bu_3N or diisopropylethylamine (DIPEA) as base internal olefins can be synthesized with high selectivities. With phosphapalladacycle **3** as catalyst precursor, we were able to obtain catalyst turnover numbers up to 1000, while $Pd(OAc)_2/2PPh_3$ was one order of magnitude less active. Analysis of the reaction profile by kinetic investigations led to the postulation of a reduction and subsequent oxidative addition of the catalyst precursor **3** to form **12** as catalytically active intermediate.

Introduction

Trisubstituted, arylated olefins of the type **A** or **B** display interesting pharmacological or physical properties.[2]

Figure 1. Trisubstituted aromatic olefins

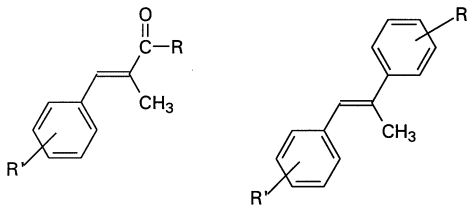

A **B**

In this respect derivatives of α-methylcinnamic acids display hypolipidemic activities.[2a] Further, the substructure is found in active substances such as the antibiotic hygromycin A.[2b] In addition, certain α-methylstilbenes can be used as nematic liquids[2c] with interesting retinoidal properties.[2d] Despite of their broad applications the stereodefined synthesis of trisubstituted alkenes is still a challenge of modern synthetic organic chemistry. Although a number of methodologies have been reported in the literature[3] the problems in synthesizing highly substituted alkenes, e.g. by Wittig reaction are well documented.[4] Thus, the search for alternative methodologies is ongoing.[5]

In this respect, the palladium-catalyzed Heck reaction is a powerful tool for the construction of aryl- and vinyl-substituted carbon−carbon double bonds as it does not interfere with a broad range of functional groups (for reviews see ref.[6]). Recently, we have developed cyclometallated palladium complexes as a new type of efficient catalysts for Heck and related reactions.[7][8] Obviously, olefins **A** or **B** should be available by Heck olefination. However, the low regioselectivity in the formation of the C=C double bond using disubstituted as well as aliphatic olefins is still a major disadvantage for the application of Heck reactions. The low regioselectivity can be explained either by unselective β-hydride elimination during the catalytic cycle, and/or by the tendency of the eliminated HPdX species to undergo readdition and subsequent β-hydride elimination to different hydrogen atoms, thus resulting in isomerization reactions.

As a concept for controlling regioselective olefin formation Tietze et al. have shown that silyl groups in allylsilanes act as terminating group in intramolecular Heck reactions enabling regio- and enantioselective construction of triple-substituted double bonds.[9] More recently, Ricci et al. reported a stereo- and regiocontrolled synthesis of di- and trisubstituted olefins starting from vinylsilanes by a Heck reaction and Pd-catalyzed desilylation reaction sequence.[10] Despite the high selectivities for specific double-bond isomers using silyl-substituted olefins it is obvious that control of the double-bond formation in Heck reactions using simple disubstituted alkenes by other means is a very attractive goal.

Results and Discussion

The interesting properties of α-methylcinnamic acid derivatives[2a][2b][11] prompted us to study regioselective Heck reactions of various aryl bromides **1** with *n*-butyl methacry-

[◇] Part 3: Ref.[1].

 © WILEY-VCH Verlag GmbH, D-69451 Weinheim, 1998 1434−1948/98/0101−0029 $ 17.50+.50/0

late (**2**) as model reaction.[12] Clearly, after insertion of the olefin into the Ar−Pd−Br complex there are two possibilities for β-hydride elimination: it can proceed towards the methyl or the benzylic methylene group. The former reaction leads to α-benzylacrylates **5** with a terminal double bond, the latter to α-methylcinnamic acid esters **4** with an internal double bond. Because of the reactivity of terminal olefins **5** the doubly arylated product **6** can subsequently be formed. In addition, *E* and *Z* isomers of **4** and **6** could be formed. Due to the importance of the β-hydride elimination for determining the double-bond selectivity we anticipitated that the nature of the base will be of major influence for the product distribution. Thus, various bases were examined for the reaction of *n*-butyl methacrylate with 1-bromo-4-fluorobenzene using the phosphapalladacycle catalyst **3** {*trans*-di(μ-acetato)bis[*o*-(di-*o*-tolylphosphanyl)benzyl]dipalladium(II)[13]}. The results are sumarized in Table 1.

Table 1. Heck reaction of *n*-butyl methacrylate with aryl bromides

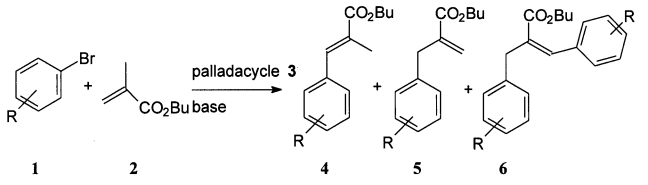

1 **2** **4** **5** **6**

Run	R	Base	Time [h]	Conversion aryl bromide [a] [%]	TON	Internal olefin[b] [%]	Terminal olefin[b] [%]	Double arylated[b] [%]
1	4-F	NaOAc	24	83	8300	39	28	33
2	4-F	Bu_3N	24	36	3600	76	20	4
3	4-F	Bu_3N	24	92	920	79	8	13
4	4-F	DIPEA	24	90	900	82	5	13
5	4-$COCH_3$	NaOAc	18	> 98	980	42	9	49
6	4-$COCH_3$	Bu_3N	4	> 98	980	79	7	14
7	4-OCH_3	NaOAc	18	40	400	45	40	15
8	4-OCH_3	Bu_3N	24	25	250	82	17	1
9	4-Cl	NaOAc	18	> 98	980	38	18	44
10	4-Cl	Bu_3N	4	> 98	980	76	8	16

Reaction: 15 mmol of aryl bromide with 22.5 mmol of butyl methacrylate in the presence of 18 mmol of base and 0.1 or 0.01 mol% of phosphapalladacycle catalyst **3** in 15 ml of DMAc at 135−140°C. − [a] Conversions of the aryl bromides have been determined by GC with internal standard (diethylene glycol dibutyl ether). − [b] Selectivities have been determined by GC on the basis of area percentage.

Indeed, the nature of base significantly influences the regioselectivity of the double bond. Sodium acetate favors the formation of terminal olefin **5**, thus leading to a relatively large extent of doubly arylated products **6** (Table 1, run 1). In contrast, in the presence of 1.2 equiv. of tributylamine the internal olefin **4** is formed as major product (runs 2 and 3). Further improvement of selectivity towards the internal olefin **4** was achieved using the sterically hindered base *N,N*-diisopropylethylamin (DIPEA) which gives so far the best selectivities for this reaction (internal olefin/terminal products, 82:18, run 4). Interestingly, the productivity of the catalyst system is reduced by a factor of 3 in the presence of amines compared to NaOAc (0.01 mol% Pd, runs 1 and 2) which is explained by enhanced stabilization of Pd^{II} intermediates. While the selectivity in the presence of NaOAc is only moderate the catalyst productivity (TON = 8300) is about two orders of magnitude higher compared to previous data of similar reactions.[14]

In order to distinguish between thermodynamic or kinetic control of the double-bond formation the terminal olefin **5** was isolated and treated with NaOAc and Bu_3N under reaction conditions in the presence of the palladium catalyst. Only a negligable amount of isomerization of **5** to the more stable internal olefin **4** was detected. Thus, we assume that the formation of the double bond occurs under kinetic control.

Comparison of the phosphapalladacycle **3** with conventional palladium phosphane complexes which were tested as in situ catalysts shows the superiority of **3**. Significantly lower conversions (16% and < 5%) were obtained in the presence of tributylamine as base and 0.1 mol% $Pd(OAc)_2$/PPh_3 (1:2) or $Pd(OAc)_2$/P(*o*-tolyl)$_3$ (1:2), respectively.

In agreement with previous results[6] the electronic nature of the aryl bromide has dominating effect on the yield of the reaction (runs 5−10). Here, electron-withdrawing substituents enhance the productivity. It is noteworthy that, in all cases where amine is used as base, the ratio of internal olefin to terminal and doubly arylated olefin is approximately 80:20, while with NaOAc as base the ratio is about 40:60. Therefore, we conclude that the electronic nature of the aryl bromide has just a minor effect on the selectivity.

As a suitable candidate for further evaluation of the influence of base on the regioselectivity of Heck reactions with 1,1-disubstituted olefins we considered α-methylstyrene (**8**) which is available on large scale.[15] Here, the olefination of 1-bromo-4-chlorobenzene (**7**) was performed in the presence of 8 different bases. As shown in Scheme 1 five different Heck products can in principle arise from the reaction of **7** and **8** (both *E* and *Z* isomers are possible).

To suppress formation of doubly arylated Heck products an excess of α-methylstyrene **8** (5 equiv.) was used. The results of the model reaction are summarized in Table 2.

Using the phosphapalladacycle *trans*-di(μ-acetato)bis[*o*-(di-*o*-tolylphosphanyl)benzyl]dipalladium(II) (**3**) as catalyst under standard reaction conditions (dimethylacetamide, NaOAc, 0.1 mol% **3**, 135−140°C, 24 h; run 1) the coupling products were isolated in excellent yield (94%). Analogous to the reactions with *n*-butyl methacrylate the highest selectivity for the terminal olefin **10** is observed with NaOAc (**9**/**10**, 35:65). Only a small amount of the doubly arylated product **11** is formed (4% yield). Comparison of the phosphapalladacycle **3** with a classical catalyst system [0.1 mol% $Pd(OAc)_2$/2 PPh_3] gave similar results (run 10). The same regioselectivity (**9**/**10**, 37:63), albeit a lower total yield (66%) was obtained with sodium benzoate as base (run 2). Using inorganic salts such as sodium carbonate (run 3) or sodium hydrogen carbonate (run 4) excellent total yields (97% and 95%) were obtained, but the selectivity towards the terminal product is slightly lower (**9**/**10**, 38:62 and 46:54, respectively). On the other hand high selectivities up to 95:5 towards the internal olefin **9** are observed using tertiary amines as bases. Again, best results were obtained using the sterically hindered amine *N,N*-diisopropylethylamine (DIPEA, run 9, 65% total yield). A slightly lower regiose-

Scheme 1. Heck reaction of 1-bromo-4-chlorobenzene with α-methylstyrene

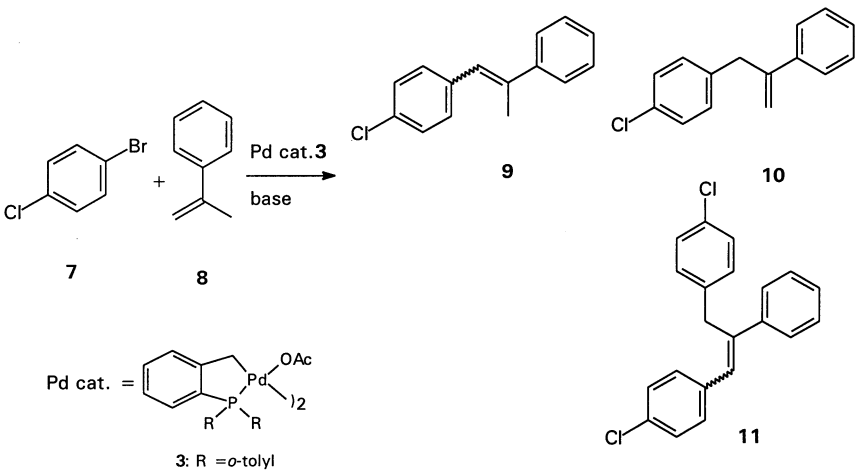

Table 2. Heck reaction of α-methylstyrene with aryl bromides

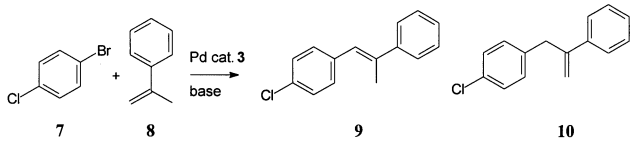

Run	Base	Yield[a] [%]	Internal[b] [%]	Terminal[b] [%]	Double[b] [%]	*E*/*Z*[b]	TON[c]
1	NaOAc	94	35	61	4	17	940
2	PhCOONa	66	37	60	3	18	660
3	Na_2CO_3	97	38	57	5	12	970
4	$NaHCO_3$	95	46	50	4	6.7	950
5	DABCO	69	53	46	1	26	690
6	0.8 NaOAc/0.2 DIPEA	96	61	35	4	4.3	960
7	proton sponge[d]	40	88	12	–	1.6	400
8	Bu_3N	66	89	11	–	2.6	660
9	DIPEA	65	95	5	–	2.5	650
$Pd(OAc_2)/2PPh_3$ (0.1 mol%) as catalyst:							
10	NaOAc	97	37	58	5	11	970
11	DIPEA	14	93	7	–	12	140

Reaction: 15 mmol of 4-bromo-1-chlorobenzene with 75 mmol of α-methylstyrene in the presence of 18 mmol of base and 0.1 mol% of phosphapalladacycle catalyst **3** in 15 ml of DMAc at 135−140°C. After 24 h, the reaction mixture was extracted and the solvent and not converted starting materials were removed in vacuo. The remaining reaction mixture was analyzed by GC, GC/MS, and ^{1}H NMR. − [a] Isolated yields. − [b] Selectivities have been determined by NMR of the isolated products. − [c] TON = mol product/mol catalyst. − [d] 1,8-Bis(dimethylamino)naphthalene.

lectivity (**9**/**10**, 89:11) is observed using tributylamine as base (66% total yield). Other bases or mixtures of bases gave results inbetween sodium acetate and DIPEA. No reaction is observed using chelating amines like TMEDA.

In the presence of amine as base the phosphapalladacycle catalyst **3** was found to be superior in productivity compared to classical catalyst precursors. Thus, the use of 0.1 mol% $Pd(OAc)_2$/2 PPh_3 led to a significantly lower total yields of **9** and **10** (14%, run 11). The selectivity towards the internal olefin is similar to the phosphapalladacycle catalyst **3** (**9**/**10**, 93:7), but there is a clear difference in the *E*/*Z* selectivity (*E*/*Z* = 12).

Scheme 2. Regiochemistry of the β-hydride elimination

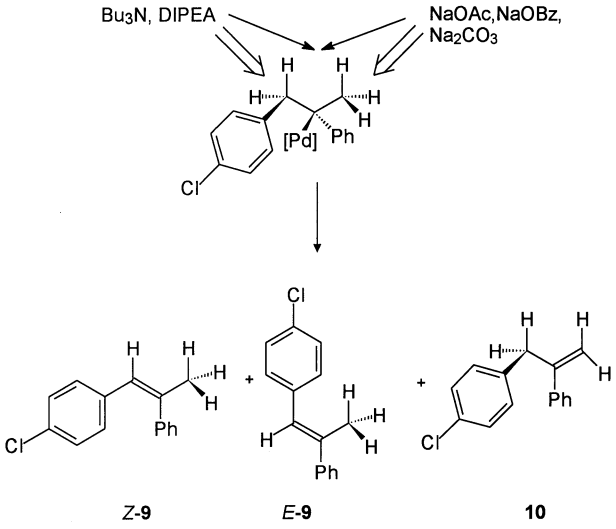

Next we investigated whether an isomerization of the terminal olefin **10** to the internal olefin **9** in the presence of amine is possible. Neither heating of the terminal olefin **10** with catalyst **3** and DIPEA, nor heating of the internal olefin **9** with **3** and sodium acetate results in significant isomerization (< 10%). In addition, a thermodynamic isomerization would not explain the observed amount of the *Z* isomer *Z*-**9**. Thus, we propose a kinetic control for the reaction. In order to explain the different regio- and stereoselectivities (Scheme 2) we propose different mechanism for the proton abstraction (β-hydride elimination) depending on the base. Unfortunately, the β-hydride elimination and reductive elimination of HX from "H−Pd−X" have been scarcely investigated in the literature.[16] Based on simple conformation analysis the stereochemical outcome of the products is explained by β-hydride elimination from the possible intermediates **I1** (leading to **10**), **I2** (leading to *E*-**9** and **10**) and **I3** (leading to *Z*-**9** and **10**) (Scheme 3).

In the presence of less basic salts like NaOAc, NaOBz direct elimination of "H−Pd−X" will occur from inter-

Scheme 3. Conformational analysis of the β-hydride elimination

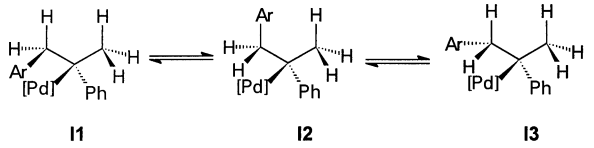

mediates **I1**, **I2** and **I3**. Because of the nearly statistical product ratio (terminal/internal, 3:2) we assume that the less coordinating bases are not involved in the elimination step of "H−Pd−X". However, the amine-assisted elimination takes place towards the most acidic protons (Scheme 2). A direct abstraction of the more acidic benzylic protons would explain for the low selectivity for the *E* isomer ***E*-9** because of a similar acidity of both benzylic protons. Thus, we believe that the base is involved in the β-hydride elimination by proton abstraction. Support for the direct abstraction of the proton may also result from the fact that the amine is blocking coordination sites on the metal centre, which are esssential for β-hydride elimination.

To obtain further mechanistic information about the system concentration vs. time diagrams for the reaction of 1-bromo-4-chlorobenzene (**7**) with α-methylstyrene (**8**) in the presence of NaOAc and DIPEA were compared (Figure 2).

As shown in Figure 2 the base influences the reaction profile dramatically. In the presence of NaOAc the reaction starts immediately leading to the terminal olefin **10** as the major isomer. If the concentration of **10** is high enough (after ca. 5 h) the doubly arylated product **11** (not shown in Figure 2) is produced in small quantities by a consecutive Heck reaction. No initial catalyst activation is observed. However, the reaction with DIPEA as base (Figure 2, lower diagram) shows a sigmoidal concentration vs. time diagram indicating preformation of the active catalyst species. The induction period might be explained by a slowly occurring reduction of the phosphapalladacycle **3**[17] to a monophosphanepalladium(0) compound. Immediately, this species would undergo oxidative addition to 1-bromo-4-chlorobenzene (**7**) to give the palladium complex **12** (Scheme 4). To proof this assumption the oxidative addition product **12** was prepared independently from $Pd[P(o\text{-tolyl})_3]_2Cl_2$ and **7** in a total yield of 66% according to a procedure described by J. F. Hartwig et al.[18]

The concentration vs. time diagrams for the Heck reaction of 1-bromo-4-chlorobenzene (**7**) with α-methylstyrene (**8**) in the presence of 0.1 mol% **12** as catalyst with NaOAc and DIPEA as base are shown in Figure 3.

No induction period is observed in both cases! In the presence of NaOAc as base the reaction catalyzed by **12** starts faster compared to the reaction catalyzed by **3** and a similar product distribution is observed. Also using DIPEA as base the raction starts immediately. The ratio of products initially formed is comparable to the ratio of the different isomers obtained in the phosphapalladacycle-catalyzed reaction. However, after several hours ***E*-9** is formed preferentially with **12** as catalyst yielding in a higher *E*/*Z* ratio.

This findings are rationalized as follows: As shown in Scheme 4 the phosphapalladacycle **3** is reduced to a monophosphanepalladium(0) species. The nature of the reducing agent is not clear in detail. Coordination of amines stabilizes the phosphapalladacycle **3** slowing down the formation of a palladium(0) compound. This results in an induction

Figure 2. Concentration vs. reaction time diagrams; top: NaOAc as base; bottom: DIPEA as base; ● terminal olefin **10**; ■ **Z-9**; ▲ E-**9**[a]

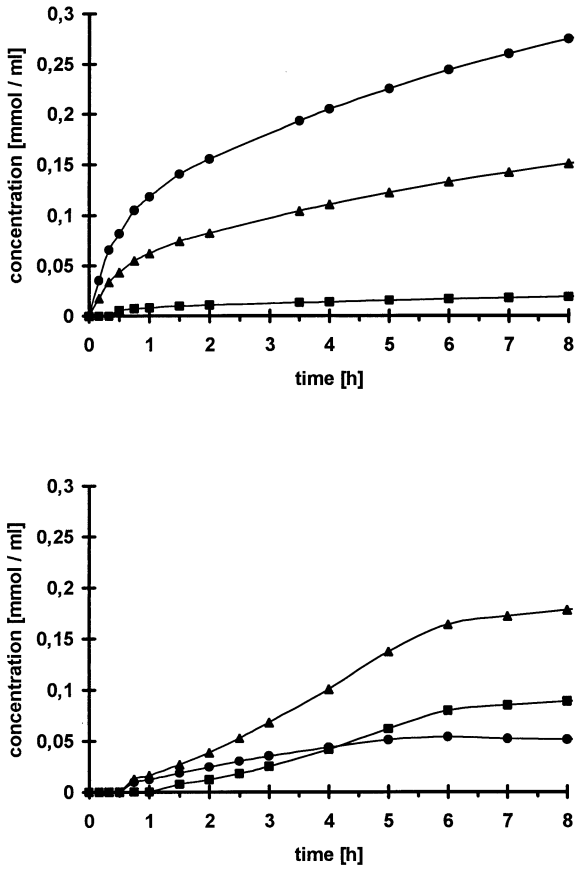

[a] Reaction conditions: 15 mmol of 1-bromo-4-chlorobenzene, 75 mmol of α-methylstyrene, 18 mmol of base and 2 ml of diethylene glycol dibutyl ether were heated in 15 ml of DMAc at 135°C. At $t = 0$ a solution of 0.1 mol% of the phosphapalladacycle **3**, dissolved in 1 ml of DMAc, was added. The course of the reaction was monitored by removing 0.1-ml samples of the reaction mixture. These were washed with 5% HCl solution, then extracted with 1.5 ml of dichloromethane and analyzed by GC.

Scheme 4. Postulated formation of **12** from the phosphapalladacycle **3** (R = *o*-tolyl)

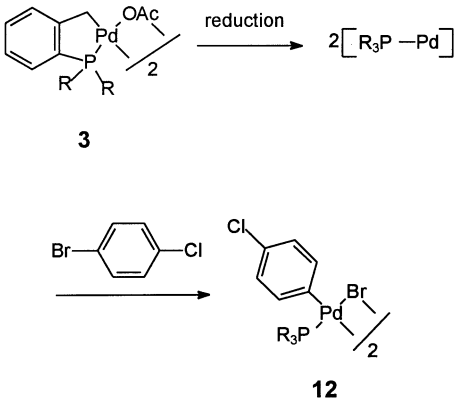

Figure 3. Concentration vs. reaction time diagrams; top: NaOAc as base; bottom: DIPEA as base; ● terminal olefin **10**; ■ Z-**9**; ▲ E-**9**[a]

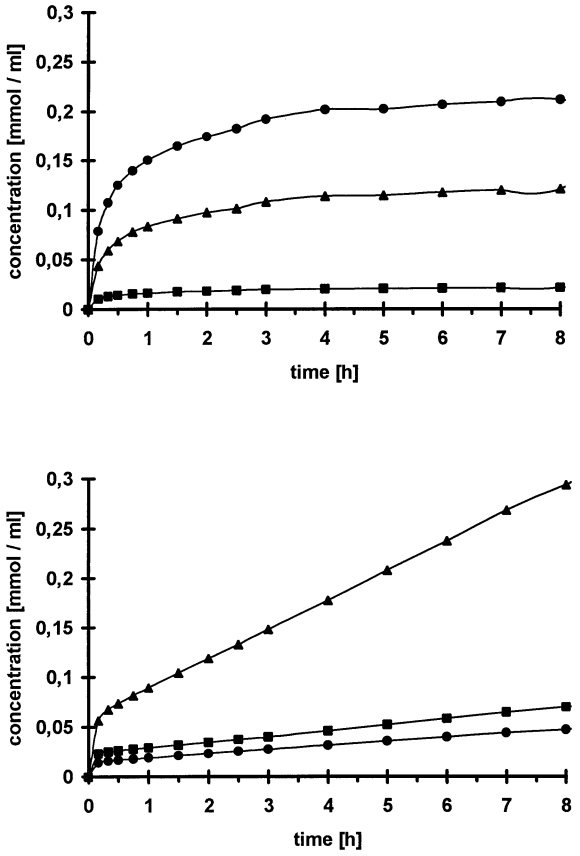

[a] Reaction conditions: 15 mmol of 1-bromo-4-chlorobenzene, 75 mmol of α-methylstyrene, 18 mmol of base and 2 ml of diethylene glycol dibutyl ether were heated in 15 ml of DMAc at 135°C. At $t = 0$ a solution of 0.1 mol% of **12**, dissolved in 1 ml of DMAc, was added. The course of the reaction was monitored by removing 0.1-ml samples of the reaction mixture. These were washed with 5% HCl solution, then extracted with 1.5 ml of dichloromethane and analyzed by GC.

period for the proper catalyst. Furthermore, the rate of oxidative addition is decreased in the presence of amines by blocking of free coordination sites on the Pd^0 species. On the other hand it is known, that the coordination of NaOAc to phosphanepalladium(0) complexes increases the rate of oxidative addition for haloarenes.[19] This explains in general the higher catalyst activity in the presence of NaOAc.

Further evidence for the discussed transformation of the phosphapalladacycle **3** to **12** is obtained by comparing the *E*/*Z* ratio for the different catalysts (**3** and **12**) using DIPEA as base. As a matter of fact the *E*/*Z* ratio produced by **12** in the first hour is identical to that of the phosphapalladacycle **3** during the whole reaction time. Due to side-reactions in the formation of **12** from **3** the productivity of **3** is lower.

In order to demonstrate that the determination of the regiochemistry by the base is a general principle for Heck reactions of 1,1-disubstituted olefins we studied coupling reactions of **2** and **8** with various other aryl bromides (Table 3). As can be seen from Table 3 4-bromotoluene and 1-bromo-4-fluorobenzene behave in a similar manner as described for 1-bromo-4-chlorobenzene. In contrast to Table 1 the coupling reactions with *n*-butyl methacrylate were performed in the presence of five equivalents of the olefin. Thus, the amount doubly arylated products could be minimized.

Table 3: Heck reaction of 1,1-disubstituted olefins with various aryl bromides

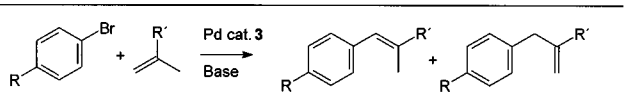

Run	R	R'	Base	Yield[a] [%]	Internal[b] [%]	Terminal[b] [%]	Double[b] [%]	*E*/*Z*[b]	TON[c]
1	CH_3	Ph	NaOAc	62	39	59	2	38	620
2	CH_3	Ph	DIPEA	58	97	3	–	2.2	580
3	F	Ph	NaOAc	96	39	56	5	9	960
4	F	Ph	DIPEA	82	96	4	–	1.6	820
5	Cl	COOBu	NaOAc	99[d]	47[d]	36[d]	17[d]	22[d]	990
6	Cl	COOBu	DIPEA	84[d]	88[d]	7[d]	5[d]	23[d]	840

Reaction: 15 mmol of aryl halide with 75 mmol of olefin in the presence of 18 mmol of base and 0.1 mol% of phosphapalladacycle catalyst **3** in 15 ml of DMAc at 135−140°C (24 h). − [a] Total isolated yields. − [b] Selectivities have been determined by NMR of the isolated products. − [c] TON = mol product/mol catalyst. − [d] Determined by GC analysis.

In conclusion we have demonstrated that the nature of base significantly influences the regiochemistry of the double bond in certain types of Heck reactions. Based on this finding we have developed a new and general valid concept to determine the regiochemistry of Heck reactions of 1,1-disubstituted olefins simply by changing the added base. Moreover, by using phosphapalladacycle **3** as catalyst precursor we have been able to improve the catalyst productivity for Heck coupling reactions of 1,1-disubstituted olefins by at least one order of magnitude. Comparison of the concentration vs. time diagrams for Heck reactions with the phosphapalladacycle **3** and the oxidative addition product **12** as catalysts provides evidence that **3** is a catalyst precursor with **12** as active species.

We gratefully acknowledge support from the *Hoechst AG* and the "*Bayerischer Forschungsverbund Katalyse*" (FORKAT). Prof. *W. A. Herrmann*, *C.-P. Reisinger*, *A. Zapf* (TU München), Prof. *K. Kühlein*, Dr. *H. Geißler* and Dr. *R. W. Fischer* (*Hoechst AG*) are thanked for many stimulating discussions.

Experimental Section

Chemicals were obtained from Aldrich and Fluka. NMR spectra (^1H,^{13}C,^{31}P) were recorded with a Jeol JMX-GX 400 or a Bruker AM 360 instrument. GC-MS spectra were measued with a Hewlett Packard gas chromatograph GC 5890 A equipped with a mass-selective detector MS 5970 B. Elemental analyses were carried out by the Microanalytical Laboratory at the TU München. Quantitative analyses were performed with a Hewlett Packard 6890 instrument using a HP-5 capillary column in conjunction with a flame ionization detector (GC/FID). − Except for the work-up of reaction mixtures, all operations were carried out under nitrogen. Solvents were carefully dried according to standard procedures.

1. *Heck Reactions with n-Butyl Methacrylate:* 15 mmol of aryl halide, 22.5 mmol of *n*-butyl methacrylate (3.58 ml), 18 mmol of tri-*n*-butylamine (4.29 ml), 0.1 mg of 2,6-di-*tert*-butyl-4-methyl-

phenol and 7.0 mg of the phosphapalladacycle **3** were dissolved in 15 ml of *N,N*-dimethylacetamide and stirred at 135−140°C (reaction time as indicated). After cooling, the reaction mixture was extracted with diethyl ether and 5% aqueous HCl for three times. The combined organic phases were neutralized with 10% aqueous $NaHCO_3$ and dried with $MgSO_4$. After removal of the solvent and starting materials in vacuo the products were isolated as colourless oils by distillation or by column chromatography.

n-Butyl 3-(4-Fluorophenyl)-2-methylpropenoate: Isolated by distillation (60%, b.p. 95−100°C/1 mbar). − ^{1}H NMR (360 MHz, 20°C, $CDCl_3$): δ = 7.64 (s, 1 H, C*H*=C), 7.36 (dd, 2 H, $^3J_{HH}$ = 8.6 Hz, $^4J_{FH}$ = 5.5 Hz), 7.06 (dd, $^3J_{HH}$ = 8.6 Hz, $^3J_{FH}$ = 8.6 Hz, 2 H), 4.21 (t, $^3J_{HH}$ = 6.6 Hz, 2 H, COOCH_2), 2.10 (s, 3 H, = C−CH_3), 1.71 (tt, $^3J_{HH}$ = 6.7 Hz, $^3J_{HH}$ = 6.7 Hz, 2 H, COOCH$_2$CH_2) 1.46 (tt, $^3J_{HH}$ = 6.7 Hz, $^3J_{HH}$ = 7.3 Hz, 2 H, COOCH$_2$CH$_2$CH_2), 0.97 (t, $^3J_{HH}$ = 7.3 Hz, 3 H, CH$_2$CH_3). − MS (70 eV); *m/z*: 236 [M$^+$], 180, 134, 109.

n-Butyl 3-(4-Acetylphenyl)-2-methylpropenoate: Isolated by column chromatography (ethyl acetate/hexane, 1:8, 74%). − ^{1}H NMR (360 MHz, 20°C, $CDCl_3$): δ = 7.97 (d, 2 H, $^3J_{HH}$ = 8.3 Hz, 3-Ph-H, 5-Ph-H), 7.67 (s, 1 H, C*H*=C), 7.46 (d, 2 H, $^3J_{HH}$ = 8.3 Hz, 2-Ph-H, 6-Ph-H), 4.23 (t, $^3J_{HH}$ = 6.6 Hz, 2 H, COOCH_2), 2.60 (s, 3 H, COCH_3), 2.12 (s, 3 H, =C−CH_3), 1.73 (tt, $^3J_{HH}$ = 6.6 Hz, $^3J_{HH}$ = 6.6 Hz, 2 H, COOCH$_2$CH_2) 1.47 (tt, $^3J_{HH}$ = 6.7 Hz, $^3J_{HH}$ = 7.4 Hz, 2 H, COOCH$_2$CH$_2$CH_2), 0.98 (t, $^3J_{HH}$ = 7.4 Hz, 3 H, CH$_2$CH_3). − MS (70 eV); *m/z*: 260 [M$^+$], 245, 204, 189, 161, 145, 115.

n-Butyl 3-(4-Methoxyphenyl)-2-methylpropenoate: Isolated by column chromatography (ethyl acetate/hexane, 1:10, 20%). − ^{1}H NMR (360 MHz, 20°C, $CDCl_3$): δ = 7.64 (s, 1 H, C*H*=C), 7.37 (d, 2 H, $^3J_{HH}$ = 8.3 Hz, 2-Ph-H, 6-Ph-H), 6.91 (d, 2 H, $^3J_{HH}$ = 8.3 Hz, 3-Ph-H, 5-Ph-H), 4.18 (t, $^3J_{HH}$ = 6.6 Hz, 2 H, COOCH_2), 3.82 (s, 3 H, OCH_3), 2.13 (s, 3 H, =C−CH_3), 1.65 (tt, $^3J_{HH}$ = 6.6 Hz, $^3J_{HH}$ = 6.6 Hz, 2 H, COOCH$_2$CH_2) 1.44 (tt, $^3J_{HH}$ = 6.7 Hz, $^3J_{HH}$ = 7.4 Hz, 2 H, COOCH$_2$CH$_2$CH_2), 0.97 (t, $^3J_{HH}$ = 7.4 Hz, 3 H, CH$_2$CH_3). − MS (70 eV); *m/z*: 248 [M$^+$], 192, 146, 115, 91.

n-Butyl 3-(4-Chlorophenyl)-2-methylpropenoate: Isolated by distillation (55%, b.p. 120−125°C/1 mbar). − ^{1}H NMR (360 MHz, 20°C, $CDCl_3$): δ = 7.63 (s, 1 H, C*H*=C), 7.38−7.32 (m, 4 H), 4.23 (t, $^3J_{HH}$ = 6.6 Hz, 2 H, COOCH_2), 2.10 (s, 3 H, =C−CH_3), 1.74 (tt, $^3J_{HH}$ = 6.6 Hz, $^3J_{HH}$ = 6.6 Hz, 2 H, COOCH$_2$CH_2) 1.44 (tt, $^3J_{HH}$ = 6.7 Hz, $^3J_{HH}$ = 7.4 Hz, 2 H, COOCH$_2$CH$_2$CH_2), 0.98 (t, $^3J_{HH}$ = 7.4 Hz, 3 H, CH$_2$CH_3). − MS (70 eV); *m/z*: 252 [M$^+$], 196, 179, 150, 115, 89.

n-Butyl 3-(4-Nitrophenyl)-2-methylpropenoate: Isolated by column chromatography (ethyl acetate/hexane, 1:15, 75%). − ^{1}H NMR (360 MHz, 20°C, $CDCl_3$): δ = 8.25 (d, 2 H, $^3J_{HH}$ = 8.9 Hz, 3-Ph-H, 5-Ph-H), 7.70 (s, 1 H, C*H*=C), 7.54 (d, 2 H, $^3J_{HH}$ = 8.9 Hz, 2-Ph-H, 6-Ph-H), 4.25 (t, $^3J_{HH}$ = 6.6 Hz, 2 H, COOCH_2), 2.12 (s, 3 H, =C−CH_3), 1.72 (tt, $^3J_{HH}$ = 6.6 Hz, $^3J_{HH}$ = 6.6 Hz, 2 H, COOCH$_2$CH_2) 1.47 (tt, $^3J_{HH}$ = 6.7 Hz, $^3J_{HH}$ = 7.4 Hz, 2 H, COOCH$_2$CH$_2$CH_2), 0.98 (t, $^3J_{HH}$ = 7.4 Hz, 3 H, CH$_2$CH_3). − MS (70 eV); *m/z*: 263, [M$^+$], 207, 190, 161, 115, 89.

2. *Heck Reactions with α-Methylstyrene:* 15 mmol of the aryl bromide, 75 mmol of α-methylstyrene (8.86 g, **2**), 18 mmol of the base and 7.0 mg of the phosphapalladacycle **3** (0.1 mol% Pd) were dissolved in 15 ml of *N,N*-dimethylacetamide and stirred under a gentle stream of nitrogen at 135−140°C for 24 h. After cooling, the reaction mixture was extracted with dichloromethane and 5% aqueous HCl for three times. The combined organic phases were neutralized with 10% aqueous $NaHCO_3$ and dried with $MgSO_4$. The solvent and starting materials were removed in vacuo. The ratio of the regioisomers was calculated by the relative intensities of the typical signals in the ^{1}H-NMR spectrum ($CDCl_3$, TMS as internal standard). Total yields for different bases are given in Tables 2 and 3.

(E)-4-Chloro-α-methylstilbene (*E*-**4**): ^{1}H NMR (360 MHz, 20°C, $CDCl_3$): δ = 7.5−7.0 (m, 9 H, aromatic protons), 6.76 (s, 1 H, C= C*H*), 2.25 (s, 3 H, −CH_3). − MS (70 eV); *m/z*: 228, [M$^+$], 211, 193, 178.

(Z)-4-Chloro-α-methylstilbene (*Z*-**4**): ^{1}H NMR (360 MHz, 20°C, $CDCl_3$): δ = 7.5−7.0 (m, 9 H, aromatic protons), 6.40 (s, 1 H, C= C*H*), 2.19 (s, 3 H, −CH_3). − MS (70 eV); *m/z*: 228, [M$^+$], 211, 193, 178.

3-(4-Chlorophenyl)-2-phenyl-1-propene (**5**): ^{1}H NMR (360 MHz, 20°C, $CDCl_3$): δ = 7.5−7.0 (m, 9 H, aromatic protons), 5.48 (s, 1 H, C=C*H*), 5.01 (s, 1 H, C=C*H*), 3.79 (s, 2 H, −CH$_2$Ar). − MS (70 eV); *m/z*: 228, [M$^+$], 193, 103.

(E)-4-Fluoro-α-methylstilbene: ^{1}H NMR (360 MHz, 20°C, $CDCl_3$): δ = 7.5−7.0 (m, 9 H, aromatic protons), 6.78 (s, 1 H, C= C*H*), 2.24 (s, 3 H, −CH_3). − MS (70 eV); *m/z*: 212, [M$^+$], 197, 177, 133.

(Z)-4-Fluoro-α-methylstilbene: ^{1}H NMR (360 MHz, 20°C, $CDCl_3$): δ = 7.5−7.0 (m, 10 H, aromatic and olefinic protons), 2.18 (s, 3 H, −CH_3). − MS (70 eV); *m/z*: 212, [M$^+$], 197, 177, 133.

3-(4-Fluorophenyl)-2-phenyl-1-propene: ^{1}H NMR (360 MHz, 20°C, $CDCl_3$): δ = 7.5−7.0 (m, 9 H, aromatic protons), 5.48 (s, 1 H, C=C*H*), 5.01 (s, 1 H, C=C*H*), 3.79 (s, 2 H, −CH_2Ar). − MS (70 eV); *m/z*: 212, [M$^+$],197, 134, 103.

(E)-4-Methyl-α-methylstilbene: ^{1}H NMR (360 MHz, 20°C, $CDCl_3$): δ = 7.5−6.8 (m, 9 H, aromatic protons), 6.43 (s, 1 H, C= C*H*), 2.36 (s, 3 H, Ar-CH_3), 2.28 (s, 3 H, -CH_3). − MS (70 eV); *m/z*: 208, [M$^+$], 193, 178, 115.

(Z)-α,4-Dimethylstilbene: ^{1}H NMR (360 MHz, 20°C, $CDCl_3$): δ = 7.5−6.8 (m, 10 H, aromatic and olefinic protons), 2.18 (s, 3 H, Ar-CH_3), 2.22 (s, 3 H, −CH_3). − MS (70 eV); *m/z*: 208, [M$^+$], 193, 178, 115.

3-(4-Methylphenyl)-2-phenyl-1-propene: ^{1}H NMR (360 MHz, 20°C, $CDCl_3$): δ = 7.5−6.8 (m, 9 H, aromatic protons), 5.44 (s, 1 H, C=C*H*), 4.77 (s, 1 H, C=C*H*), 3.74 (s, 2 H, −CH_2Ar), 2.38 (s, 3 H, Ar-CH_3). − MS (70 eV); *m/z*: 208, [M$^+$], 193, 178, 130, 115, 103.

3. *Synthesis of {Pd[P(o-tolyl)$_3$](p-ClC$_6$H$_4$)(Br)}$_2$* (**12**): 1.21 g (1.54 mmol) of Pd[P(*o*-tolyl)$_3$]$_2$Cl$_2$ and 0.54g (1.78 mmol) of P(*o*-tolyl)$_3$ were suspended in 8 ml of toluene. To this suspension NaOH (0.14 g) in 8 ml of ethanol was added. The reaction mixture was heated at 90°C for 5 h. After cooling, the yellow precipitate was filtered off and washed several times with water, ethanol and diethyl ether. After drying in vacuo, 1.06 g of crude Pd[P(*o*-tolyl)$_3$]$_2$ was obtained. This product was stirred with 1.60 g of 1-bromo-4-chlorobenzene in 20 ml of benzene at room temp. overnight. The suspension was filtered and concentrated. After addition of 20 ml of diethyl ether and cooling to −30°C 0.60 g (66%) of **12** precipitated. − ^{1}H NMR (400 MHz, 80°C, [D$_8$]toluene): δ = 7.03−6.45 (br. m, 32 H), 2,14 (br. s, 18 H). − ^{31}P{^{1}H} NMR (162 MHz, 80°C, [D$_8$]toluene): δ = 26.8. − IR (KBr): $\tilde{\nu}$ = 3054 (m), 2970 (m), 2922 (m), 2861 (m), 1589 (m), 1566 (w), 1467 (vs), 1449 (s), 1200 (w), 1088 (s), 1004 (vs), 807 (vs), 752 (vs), 717 (s), 680 (m), 561 (m), 534 (s), 466 (s). − FAB MS; *m/z*: 520 [M$^+$ − HBr], 430 [M$^+$ − Br−tolyl]. − $C_{54}H_{50}Br_2C_{12}P_2Pd_2 \cdot Et_2O$ (1278.6): calcd. C 54.48, H 4.73, P 4.84; found C 54.66, H 4.44, P 4.88.

[1] M. Beller, T. H. Riermeier, A. Zapf, *Top. Catal.*, in print.
[2] [2a] T. Watanabe, K. Hayashi, S. Yoshimatsu, K. Sakai, *J. Med. Chem.* **1980**, *23*, 50. – [2b] J. G. Buchanan, D. G. Hill, R. H. Wightman, *Tetrahedron* **1995**, *51*, 6033. – [2c] W. R. Young, A. Aviram, R. J. Cox, *J. Am. Chem. Soc.* **1972**, *94*, 3976. – [2d] H. Kagechika, T. Himi, K. Namikawa, E. Kawachi, Y. Hashimoto, K. Shudo, *J. Med. Chem.* **1989**, *32*, 1098.
[3] [3a] H. J. Bestmann, O. Vostrowsky, *Top. Curr. Chem.* **1983**, *109*, 85. – [3b] B. E. Maryanoff, A. B. Reitz, *Chem. Rev.* **1989**, *89*, 863.
[4] D. J. Ager, *Org. React.* **1990**, *38*, 1.
[5] [5a] S. Denmark, J. Amburgery, *J. Am. Chem. Soc.* **1993**, *115*, 10387. – [5b] I. Creton, I. Marek, D. Brasseur, J.-L. Jestin, J.-F. Normant, *Tetrahedron Lett.* **1994**, *35*, 6837. – [5c] S. Sharma, A. C. Oehlschlager, *J. Org. Chem.* **1989**, *54*, 5064. – [5d] I. Flemming, T. W. Newton, *J. Chem. Soc., Perkin Trans. 1* **1984**, 1805. – [5e] B. H. Lipshutz, E. L. Ellsworth, S. H. Dimock, D. C. Reuter, *Tetrahedron Lett.* **1989**, *30*, 2065.
[6] [6a] R. F. Heck, *Palladium Reagents in Organic Synthesis,* Academic Press, London, **1985**. – [6b] R. F. Heck in *Comprehensive Organic Synthesis,* vol. 4 (Eds.: B. M. Trost, I. Flemming), Pergamon Press, Oxford, **1991**, p 833. – [6c] W. Cabri, I. Candiani, *Acc. Chem. Res.* **1995**, *28*, 2. – [6d] J. Tsuji, *Palladium Reagents and Catalysts – Innovations in Organic Synthesis,* Wiley, Chichester, UK, **1995**. – [6e] W. A. Herrmann in *Applied Homogeneous Catalysis* (Eds.: B. Cornils, W. A. Herrmann), VCH, Weinheim, **1996**, p 712. – [6f] A. de Meijere, F. Meyer, *Angew. Chem.* **1994**, *106*, 2437; *Angew. Chem. Int. Ed. Engl. 1994, 33,* 2379.
[7] W. A. Herrmann, C. Broßmer, K. Öfele, C.-P. Reisinger, T. Priermeier, M. Beller, H. Fischer, *Angew. Chem.* **1995**, *107,* 1989; *Angew. Chem. Int. Ed. Engl.* **1995**, *34,* 1844.
[8] M. Beller, H. Fischer, W. A. Herrmann, K. Öfele, C. Broßmer, *Angew. Chem.* **1995**, *107*, **1992;** *Angew. Chem. Int. Ed. Engl.* **1995**, *34*, 1848.
[9] R. Schimpf, L. F. Tietze, *Angew. Chem.* **1994**, *106,* 1138; *Angew. Chem. Int. Ed. Engl.* **1994**, *33*, 1089.
[10] A. Ricci, E. Blart, M. Comes-Franchini, G. Reginato, P. Zani, *Pure Appl. Chem.* **1996**, *68*, 679.
[11] α-Methyl-substituted cinnamic acid derivatives can easily be converted into indanones: M. Beller, T. H. Riermeier, S. Klein, K. Kühlein, unpublished results.
[12] M. Beller, T. H. Riermeier, *Tetrahedron Lett.* **1996**, *37,* 6535.
[13] W. A. Herrmann, C. Brossmer, C.-P. Reisinger, T. H. Riermeier, K. Öfele, M. Beller, *Chem. Eur. J.* **1997**, *3*, 1357.
[14] [14a] B. A. Patel, C. B. Ziegler, N. A. Cortese, J. E. Plevyak, T. C. Zebovitz, M. Terpko, R. F. Heck, *J. Org. Chem.* **1977**, *42*, 3903. – [14b] H. A. Dieck, R. F. Heck, *J. Org. Chem.* **1975**, *40,* 1083. – [14c] A. Kasahara, T. Izumi, M. Maemura, *Bull. Chem. Soc. Jpn.* **1977**, *50*, 1021.
[15] H. A. Dieck, R. F. Heck, *J. Am. Chem. Soc.* **1974**, *96*, 1133.
[16] V. V. Grushin, *Chem. Rev.* **1996**, *96*, 2011.
[17] J. Louie, J. F. Hartwig, *Angew. Chem.* **1996**, *108*, 2531; *Angew. Chem. Int. Ed. Engl.* **1996**, *35*, 2359.
[18] F. Paul, J. Patt, J. F. Hartwig, *Organometallics* **1995**, *14*, 3030.
[19] C. Amatore, E. Carré, A. Jutand, M. A. M′Barki, G. Meyer, *Organometallics* **1995**, *14*, 5605.

[97166]

Water-Soluble Tripodal Phosphane Ligands and Their Rhodium Complexes

Philipp Stößel, Hermann A. Mayer*, and Friedrich Auer

Institut für Anorganische Chemie,
Auf der Morgenstelle 18, D-72076 Tübingen, Germany
Fax: (internat.) +49 (0)7071/295306
E-mail: hermann.mayer@uni-tuebingen.de

Received July 24, 1997

Keywords: Tripodal P ligands / Rhodium / Water-soluble complexes / Immobilization / Biphasic hydroformylation

The synthesis of the water-soluble tripodal phosphane ligand *cis,cis*-1,3,5-$(PPh_2)_3$-1,3,5-$[CH_2(OCH_2CH_2)_xOCH_3]C_6H_6$ (x = 30−160) (**5**) has been achieved in a four-step reaction sequence. The alcohol $Mo(CO)_3$[*cis,cis*-1,3,5-$(PPh_2)_3$-1,3,5-$(CH_2OH)_3C_6H_6$] (**1**) is converted to the corresponding alcoholate **2**, which forms the polyethylene glycol derivative **3** in a polyaddition reaction with oxirane. After methylation of the end groups of **3**, the ligand **5** is obtained by a combined photochemical/oxidative demolybdenation reaction. The water-soluble tripodal phosphane **5** and the methoxymethyl functionalized tripodal ligand **6** react with $Rh(PPh_3)_3(CO)H$ to form the water-soluble and water-insoluble rhodium carbonyl hydrido complexes **5a** and **6a**, respectively. The catalytic activity of the rhodium complex **5a** in the hydroformylation of 1-hexene was found to be comparable in a single-phase system (1-hexene/methanol) with that in the biphasic system (1-hexene/water). Only traces of alcohol were found, which demonstrates that the catalyst **5a** displays higher selectivity in hydroformylation than in hydrogenation.

Simplification of process engineering in the field of biphasic homogeneous catalysts has spurred the successful industrial application of these systems.[1] For example, in aqueous biphasic oxo-catalysis, the reactants and the products stay in the organic phase while the catalyst remains in the aqueous phase.[1][2] Such a two-phase system exhibits low catalytic activity in the hydroformylation of higher olefins because of mass transfer limitations that result from the lower solubility of such longer-chain derivatives in water. Water solubility of transition metal complexes is generally achieved by using phosphane ligands that bear polar substituents such as $-SO_3Na$[1b][1f][3] or $-NR_3^+$.[4] It has been suggested that the problems encountered due to mass transfer limitations may be overcome by using phosphane ligands derivatized with polyalkylene glycol ether groups.[5] The inverse temperature dependence of the solubility of polyalkylene oxide oligomers in water[6] leads to a single-phase system at higher temperatures. In this way, at elevated temperature, the catalyst migrates from the aqueous phase into the organic phase and is available to perform homogeneous catalysis. Upon cooling the system, the catalyst migrates back into the aqueous phase and can be recovered by simple phase separation. Ethylene glycol moieties with various chain lengths have been introduced into several phosphane ligand systems.[5][7][8] Polyethylene glycol has also been used as a hydrophilic film in which water-soluble rhodium complexes were dissolved to act as immobilized homogeneous catalysts.[9]

Herein, we report on the synthesis of water-soluble tripodal phosphanes and their rhodium complexes, and present preliminary results of investigations into the catalytic activity of these complexes in the hydroformylation of 1-hexene. Our goal was to functionalize the cyclohexane backbone of the tripodal phosphane ligand *cis,cis*-1,3,5-$(PPh_2)_3C_6H_9$ (tdppcy)[10] with polyethylene glycol groups, in order to solubilize tdppcy-type ligands and their metal complexes in water.

Results and Discussion

In recent studies, it was demonstrated that the $Mo(CO)_3$ fragment serves as an excellent protecting group when modifying tripodal phosphane ligand systems with a cyclohexane backbone.[11] Thus, the thermally stable tris(hydroxymethyl) complex **1**[11] (Scheme 1) is an ideal starting material for the functionalization of the cyclohexane backbone with polyethylene glycol groups under the rather severe conditions of a base-catalyzed oxirane polyaddition reaction. In the first step, the triol **1** is converted into its corresponding trialcoholate **2** with stoichiometric amounts of NaH in hot THF.

Treatment of a solution of in situ generated **2** with oxirane at 170−185°C leads in a polyaddition reaction to the polymer trisodium alcoholate, which is then converted into the alcohol **3** with anhydrous NH_4Cl. The degree of polymerization can be controlled by adjusting the stoichiometric ratio of oxirane to **1** in the range 90:1 and 500:1. In Table 1, the stoichiometric ratios of oxirane to **1** used in typical polyaddition reactions are listed, together with the properties of the resulting homologous polymers of **3**, the calculated average molecular weights M_p, and degrees of polymerization P.

The parameters M_p and P were calculated independently from the mass balance of the reaction, as well as from the relative integrals of the ethoxy and the phenyl proton sig-

 © WILEY-VCH Verlag GmbH, D-69451 Weinheim, 1998 1434−1948/98/0101−0037 $ 17.50+.50/0

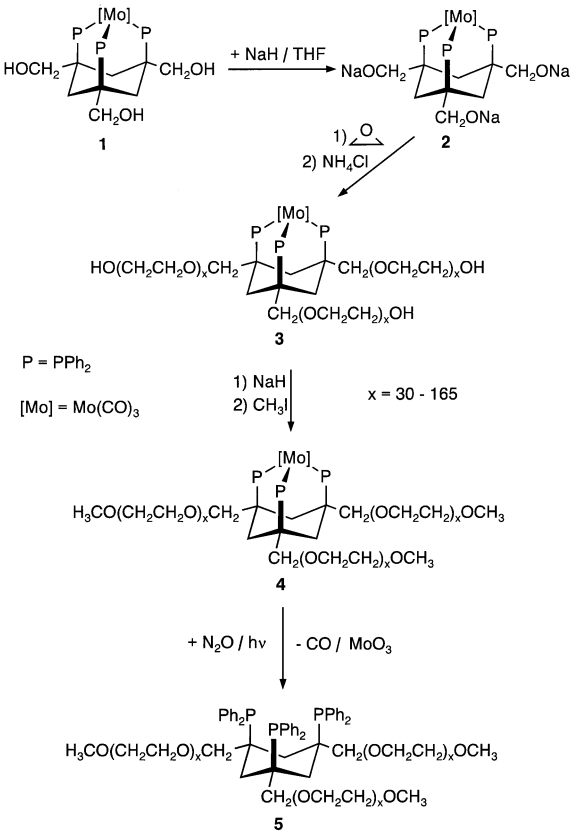

nals in the ^{1}H-NMR spectra.[12] According to Flory, the distribution of the molecular weight of polyethylene glycol ethers follows a Poisson distribution if (i) all the initiating groups are accessible at the beginning of the reaction, (ii) only the reaction of a polymer with a monomer occurs, and (iii) all the reaction steps are kinetically identical.[13] It has been shown that these criteria are met in the case of addition reactions of oxirane to monofunctional alcohols under the conditions of a stoichiometric polyaddition reaction used here.[14] When it is further assumed that the three chains in each molecule grow independently from one another, this leads to a Poisson distribution with an expectation value P for the degree of polymerization of the homologous polymers of **3**. The relation of the degree of polymerization P to the degree of polymerization X of a single chain attached to the cyclohexane backbone is then given by the equation $P = 3\ X$.

The hydroxylic end groups of the homologous polymers of **3** react smoothly with methyl iodide under Williamson ether synthesis conditions to form the corresponding triether complexes **4** (Scheme 1). Polymers **3** and **4** are miscible with water in any ratio when the degree of polymerization is approximately 90 or greater. They are also soluble in polar organic solvents such as THF, CD_2Cl_2, and $CDCl_3$, and swell in diethyl ether. Their properties are comparable with those of polyethylene glycols with similar degrees of polymerization. The local C_{3v} symmetry at the molybdenum centres of **3** and **4** is confirmed by spectroscopic data of the complexes, which are comparable with those of their monomeric counterparts.[11] The IR spectra display two sharp ν(CO) absorptions at 1936 and 1844 cm^{-1} for the $Mo(CO)_3$ fragment besides intense absorptions due to the polyethylene glycol ether chains. The ^{31}P{^{1}H}-NMR spectra show singlets at δ = 46.2 (**3**) and δ = 46.1 (**4**), respectively. In the ^{13}C{^{1}H}-NMR spectra, the ring methylene and the quaternary carbon atoms display complex multiplet patterns as a result of interactions with the phosphorus nuclei. Two multiplets are observed for the axial and equatorial cyclohexane ring protons in the ^{1}H-NMR spectra. Besides the intense absorptions attributable to the ethoxy protons, the hydroxylic end groups of **3** and the methyl end groups of **4** give rise to singlets in the ^{1}H-NMR spectra.

Liberation of the polyethylene glycol functionalized tripodal phosphane ligands **5** can be achieved by irradiating solutions of **4** in the presence of the mild oxidizing agent N_2O (Scheme 2).[11]

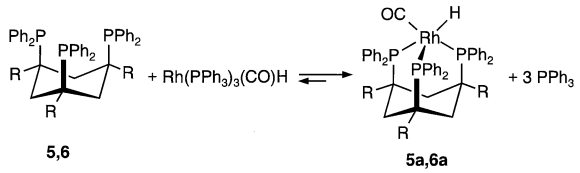

R = $CH_2(OCH_2CH_2)_xOCH_3$ (**5**), CH_2OCH_3 (**6**)

The solubility of **4** allows the reaction to be carried out in a mixture of THF and aqueous K_2CO_3, under which conditions the in-situ generated MoO_3 is converted into soluble molybdate, thereby facilitating easy separation. The homologous tripodal phosphane ligands **5** are obtained in high yields as colorless to off-white waxy materials. Their

Table 1. Average molecular weight (M_P), degree of polymerization (P) and properties of **3**[12]

1:C_2H_4O[a]	T[b] [°]	t[c] [h]	M_P[d]	P[d]	M_P[d]	P[e]	consistency	color	melting range [°C]
1:102.9	180	14	4919	91.2	5078	94.8	highly viscous	pale-yellow, clear	–
1:218.4	170	18	8893	181.5	8985	183.6	waxy	yellow, transparent	52–55
1:223.5	170	18	10255	209.1	10355	211.6	brittle	yellow, transparent	54–57
1:267.6	180	14	12206	256.8	12219	257.1	brittle	yellow, transparent	57–61
1:582.9	175	18	22621	493.5	–[f]	–[f]	brittle	pale-brown, transparent	62–65

[a] Ratio of **1** to oxirane. – [b] Reaction temperature. – [c] Reaction time. – [d] Average molecular weight (M_P), degree of polymerization (P), calculated from the mass balance of the reaction. – [e] Average molecular weight (M_P), degree of polymerization (P), calculated from the relative ^{1}H-NMR integrals of ethoxy and phenyl protons. – [f] Average molecular weight (M_P), degree of polymerization (P) cannot be calculated.

solubilities are comparable to those found for the molybdenum complexes **3** and **4**. The singlets in the $^{31}P\{^1H\}$-NMR spectra of the homologous polymers of **5** are shifted 15.5 ppm further upfield compared to those of the molybdenum complexes. The alkane regions of the $^{13}C\{^1H\}$-NMR spectra display triplets ($\delta = 34.18$, $^2J_{PC} = 18.07$ Hz) and doublets of triplets ($\delta = 42.06$, $^1J_{PC} = 21.57$, $^3J_{PC} = 9.35$ Hz), which result from interaction of the three methylene and the three quaternary carbon atoms with the phosphorus nuclei. In addition, the carbon atoms of the methyl end groups, the ethoxy carbon atoms and the exocyclic methylene carbon atoms attached to the cyclohexane ring are each observed as singlets. In contrast to the spectra of the molybdenum complexes **3** and **4**, the *ipso*, *ortho*, and *meta* carbon atoms of the phenyl rings of **5** are resolved into doublets. The non-equivalent ring methylene hydrogen atoms in the ^{1}H-NMR spectra of **5** give rise to doublets of triplets ($\delta = 1.93$, $^2J_{HH} = 13.61$, $^3J_{PH} = 10.13$ Hz) and broad doublets ($\delta = 2.26$, $^2J_{HH} = 13.61$, $^3J_{PH} < 5.0$ Hz).

When $Rh(PPh_3)_3(CO)H$ is treated with equimolar amounts of the tripodal ligands **5** or **6** at elevated temperatures in DMSO, the solutions become deep-red or orange in color, respectively. ^{31}P-NMR spectroscopic investigations confirm that an equilibrium is set up between the tripod ligands **5**, **6**, the complex $Rh(PPh_3)_3(CO)H$, and free PPh_3, leading to carbonyl hydrido species of the general composition $[Rh(\eta^{n,n+1}\text{tripod})(PPh_3)_{2-n}(CO)H]$, $n = 0-2$. The equilibrium can be shifted in favor of the carbonyl hydrido complexes **5a**, **6a** (Scheme 2) by continuously removing PPh_3 in a liquid-liquid extractor using *n*-hexane as the extracting solvent and DMSO as the reaction medium.[15] However, this reaction procedure has the disadvantage that the high boiling point of DMSO does not allow the complete removal of the solvent from the polyethylene glycol functionalized product **5a**. If, on the other hand, stoichiometric amounts of **5** are treated with $Rh(PPh_3)_3(CO)H$ in a melt at 80°C in vacuo, in the absence of solvent, the PPh_3 is removed by sublimation thereby affording **5a** quantitatively. The red-brown homologous polymers of the carbonyl-hydrido complexes **5a** are obtained as water-soluble waxy solids, while the yellow-orange methoxymethyl functionalized complex **6a** is soluble in polar organic solvents.

Apart from the IR spectroscopic data, which are very sensitive to changes in the functional groups at the *ipso*-position of the cyclohexane ring[16], the spectroscopic data of compound **6a** correspond to those of the polyethylene glycol functionalized complex **5a**. Two absorptions [1973, 1902 cm^{-1} (**5a**) and 1950, 1911 cm^{-1} (**6a**)] are observed in the IR spectra of the carbonyl hydrido complexes **5a**, **6a**, which are characteristic of metal hydride and carbonyl groups, respectively. Doublets in the $^{31}P\{^1H\}$-NMR spectra [$\delta = 40.3$, $^1J_{RhP} = 118.4$ Hz (**5a**), $\delta = 43.3$ $^1J_{RhP} = 117.3$ Hz (**6a**)] and doublets of quartets at $\delta = -8.97$ ($^2J_{PH} = 34.7$, $^1J_{RhH} = 12.9$ Hz) and $\delta = -8.28$ ($^2J_{PH} = 34.5$, $^1J_{RhH} = 12.9$ Hz) in the ^{1}H-NMR spectra of **5a** and **6a**, respectively, are what one would expect for dynamic pentacoordinate rhodium complexes (Scheme 2). Thus, only one set of resonances for the ring methylene and quaternary carbon atoms is observed in the $^{13}C\{^1H\}$-NMR spectra of both complexes. In addition, characteristic signals in the expected regions are found for the polyethylene glycol functions and the methoxymethyl groups.

Preliminary studies aimed at demonstrating the catalytic activity of complex **5a** have been conducted. The results are summarized in Table 2. The hydroformylation of 1-hexene catalyzed by **5a** ($P = 209.1$) was performed either in a single homogeneous phase with methanol as solvent, or in a biphasic system (water/1-hexene).

Table 2. Hydroformylation of 1-hexene with complex **5a** ($P = 91$) as catalyst[a]

product	single phase[b] amount [%]	biphase[c] amount [%]
n-hexane	–	–
1-hexene	4.3	3.5
2- and 3-hexene	26.5	20.5
2-methylhexanal	21.8	29.2
n-heptanal	47.3	46.4
2-methylhexanol	0.1	0.1
n-heptanol	–	0.3

[a] Conditions: 119°C, 2 h, 15 bar of CO, 15 bar of H_2, 1:5000 catalyst to substrate ratio. – [b] 1-Hexene/methanol, 10:3 (v/v). – [c] 1-Hexene/water, 10:3 (v/v).

The pressure of the synthesis gas (15 bar of CO, 15 bar of H_2) and the temperature (119°C) were kept constant during the whole reaction period. The organic products were separated from the catalyst by distillation (single phase) or by decantation of the clear, colorless organic phase from the clear, red-brown aqueous phase (biphase). The hydrocarbon- and aqueous phases were analyzed by $^{31}P\{^1H\}$-NMR spectroscopy. No detectable amounts of **5a** were found in the organic phase, whereas the aqueous phase contained **5a** and decomposition products. Both systems showed high activity, since only minor amounts of 1-hexene remained after a reaction time of 2 h. Catalyst **5a** displayed higher selectivities towards hydroformylation than hydrogenation. In neither medium was any hexane detected, and traces of heptanol were only observed in the biphasic system. The degree of conversion to *n*-heptanal was comparable in both systems, while the extent of hydroformylation of the isomerized hexenes was greater in the biphasic medium.

This work was supported by the *Fonds der Chemischen Industrie*, Frankfurt/Main, Germany, and the *University of Tübingen*. We thank *BASF AG* and *DEGUSSA AG* for loans of $Mo(CO)_6$ and $RhCl_3 \cdot 3\ H_2O$, respectively.

Experimental Section

General: All reactions were carried out under an atmosphere of dry argon using standard Schlenk techniques. Solvents were dried under argon; THF was distilled from Na/Ph_2CO; dichloromethane was distilled from CaH_2; methanol was distilled from Mg; water was degassed by the freeze-pump-thaw technique. Oxirane and N_2O were commercial and medical grade, respectively, and were used without further purification. The molybdenum complex **1**[11], the ligand **6**[11] and $Rh(PPh_3)_3(CO)H$[17] were prepared as described

in the literature. – ^{1}H-, ^{13}C{^{1}H}-, and ^{31}P{^{1}H}-NMR spectra were recorded on a Bruker DRX250 spectrometer operating at 250.13, 62.90, and 101.26 MHz, respectively. ^{1}H chemical shifts were referenced to the residual proton peaks of the solvents and are quoted in ppm downfield from TMS. ^{13}C chemical shifts were calibrated against the deuterated solvent multiplet are referenced to TMS. ^{31}P chemical shifts were measured relative to external 85% H_3PO_4 with downfield values taken as positive. In addition to a ^{13}C{^{1}H}-NMR spectrum, a ^{13}C-DEPT experiment was routinely performed for each compound. Infrared spectra were recorded on a Bruker ISF 48.

Tricarbonyl[cis,cis-1,3,5-tris(diphenylphosphanyl)-1,3,5-tris(hydroxypolyethoxymethyl)cyclohexane]molybdenum (**3**): A steel autoclave fitted with a Teflon inlet was charged with a suspension of 907 mg (1.0 mmol) of **1** and 72 mg (3.0 mmol) of NaH in 120 ml of THF. The suspension was heated to 100°C for 2 h, and then cooled to −20°C, whereupon the desired amount of oxirane was condensed into the autoclave. The reaction mixture was heated at 170°C for 18 h, and was then allowed to cool to room temp. The pale-yellow solution was transferred to a Schlenk tube and the autoclave was rinsed with two 25-ml portions of THF. The combined organic phases were reduced to a volume of 100 ml under reduced pressure so as to remove remaining traces of oxirane. Then, 177 mg (3.3 mmol) of anhydrous NH_4Cl was added. The resulting mixture was heated at 80°C for 2 h, the solvent was removed under reduced pressure at 50−60°C, and the remaining pale-yellow, viscous oil was dissolved in 100 ml of dichloromethane. The salts (NaCl and residual NH_4Cl) were filtered off by passage through a short column of SiO_2 (1 cm) and washed once with 25 ml of dichloromethane. The dichloromethane was removed from the combined solutions under reduced pressure and the pale-yellow residue was dried in vacuo (12 h at 60°C). Yield quantitative. – IR (KBr): $\tilde{\nu}$ = 3487 cm^{-1} ν(OH), 2883 ν(CH_2), 1936, 1844 ν(CO), 1113 ν(OCH_2). – ^{31}P{^{1}H} NMR (CD_3OD): δ = 46.2 (s). – ^{1}H NMR (CD_3OD): δ = 1.77−1.95 (m, 3 H, CHH_e), 2.48−2.81 (m, 3 H, CHH_a), 3.44−3.70 [m, 6 + 4×(*P* − 1) + 12 H, CH_2O(CH_2CH_2O)$_{P-1}$CH_2CH_2OH], 4.56 [br. s, 3 H, $CH_2O(CH_2CH_2O)_{P-1}CH_2CH_2O$*H*], 6.91−7.30 (m, 30 H, C_6H_5). – ^{13}C{^{1}H} NMR (CD_3OD): δ = 30.18−30.82 (m, CH_2), 39.85−40.00 (m, CP), 62.77 [s, $CH_2O(CH_2CH_2O)_{P-1}CH_2$*C*H$_2$OH], 71.29 [s, CH_2O(*C*H$_2$*C*H$_2$O)$_{P-1}$*C*H$_2$CH$_2$OH], 73.45 [s, *C*H$_2$O(CH$_2$CH$_2$O)$_{P-1}$CH$_2$CH$_2$OH], 128.41 (br. s, *meta*-C_6H_5), 129.79 (s, *para*-C_6H_5), 136.85 (br. s, *ortho*-C_6H_5), 138.00−138.51 (m, *ipso*-C_6H_5), 220.66−221.67 (m, CO).

Tricarbonyl[cis,cis-1,3,5-tris(diphenylphosphanyl)-1,3,5-tris(methoxypolyethoxymethyl)cyclohexane]molybdenum (**4**): A mixture of 1.0 mmol of a homologous polymer of **3** and 216 mg (9.0 mmol) of NaH in 150 ml of THF was heated in a sealed Schlenk tube at 80°C for 2 h. After cooling to room temp., 1.1 ml (18.0 mmol) of iodine-free methyl iodide was added dropwise via a syringe. The mixture was heated at 60°C for 16 h under exclusion of light, and was then reduced to a volume of 100 ml under reduced pressure. Subsequently, 481 mg (9.0 mmol) of anhydrous NH_4Cl was added. The resulting mixture was heated at 80°C for 2 h, the solvent was removed under reduced pressure at 50−60°C, and the remaining pale-yellow, viscous oil was dissolved in 100 ml of dichloromethane. The salts (NaCl and residual NH_4Cl) were filtered off by passage through a short column of SiO_2 (1 cm) and washed once with 25 ml of dichloromethane. The dichloromethane was removed from the combined solutions under reduced pressure and the pale-yellow residue was dried in vacuo (16 h at 60°C). Yield 98−100%. – IR (KBr): $\tilde{\nu}$ = 2883 cm^{-1} ν(CH_2), 1936, 1844 ν(CO), 1113 ν(OCH_2). – ^{31}P{^{1}H} NMR (CD_2Cl_2): δ = 46.1 (s). – ^{1}H NMR (CD_2Cl_2): δ = 1.77−1.93 (m, 3 H, CHH_e), 2.48−2.81 (m, 3 H, CHH_a), 3.31 [s, 9 H, $CH_2O(CH_2CH_2O)_{P-1}CH_2CH_2OCH_3$], 3.40−3.66 [m, 6 + 4×(*P* − 1) + 12 H, CH_2O(CH_2CH_2O)$_{P-1}$CH_2-CH_2OCH$_3$], 7.04−7.31 (m, 30 H, C_6H_5). – ^{13}C{^{1}H} NMR (CD_2Cl_2): δ = 29.15−29.73 (m, CH_2), 38.85−39.00 (m, CP), 58.77 [s, $CH_2O(CH_2CH_2O)_{P-1}CH_2CH_2OCH_3$], 69.86 [s, CH_2O(*C*H$_2$-*C*H$_2$O)$_{P-1}$*C*H$_2$*C*H$_2OCH_3$], 71.53 [s, *C*H$_2$O(CH$_2CH_2$O)$_{P-1}CH_2$-CH$_2OCH_3$], 127.34 (br. s, *meta*-C_6H_5), 128.84 (s, *para*-C_6H_5), 135.83 (br. m, *ortho*-C_6H_5), 136.84−137.33 (m, *ipso*-C_6H_5).

cis,cis-1,3,5-Tris(diphenylphosphanyl)-1,3,5-tris(methoxypolyethoxymethyl)cyclohexane (**5**): A solution of 0.5 mmol of **4** in 150 ml of THF and 5 ml of an aqueous solution of K_2CO_3 (2.0 M) were placed in a double-walled Duran Schlenk tube and the mixture was degassed by using the freeze-pump-thaw technique. The vigorously stirred solution was cooled to 15°C (cooling solvent: water) and dinitrogen monoxide (N_2O) was added (1.0−1.3 bar). Then, the reaction mixture was irradiated for 1.5 h with light from a TQ 150 W (Original Hanau) high-pressure mercury lamp, which was positioned 5 cm from the Schlenk tube. After 1.5 h, the progress of the reaction was monitored by ^{31}P{^{1}H}-NMR spectroscopy. If small amounts of the starting material were still present, irradiation was continued. After complete conversion, the brown solution was concentrated to a volume of 10 ml under reduced pressure. The brown, viscous residue was dissolved in 100 ml of dichloromethane, the aqueous layer was removed, and the organic layer was dried over 5 g of CaO (2 h). The CaO was then filtered off and washed with two 25-ml portions of dichloromethane. The solvent was removed under reduced pressure and the colorless to off-white, viscous oil was dried in vacuo (12 h at 60°C). Yield 88−92%. – ^{31}P{^{1}H} NMR (CD_3OD): δ = 30.8 (s). – ^{1}H NMR (CD_3OD): δ = 1.93 (dt, $^2J_{HH}$ = 13.61, $^3J_{PH}$ = 10.13 Hz, 3 H, CHH_a), 2.26 (br. d, $^2J_{HH}$ = 13.61, $^3J_{PH}$ < 5.0 Hz, CHH_e), 3.35−3.80 [m, 6 + 4×(*P* − 1) + 12 H, CH_2O(CH_2CH_2O)$_{P-1}$CH_2CH_2OCH$_3$], 3.41 [s, 9 H, $CH_2O(CH_2CH_2O)_{P-1}CH_2CH_2OCH_3$], 7.37−7.54 (m, 30 H, C_6H_5). – ^{13}C{^{1}H} NMR (CD_3OD): δ = 34.18 (t, $^2J_{PC}$ = 18.07 Hz, CH_2), 42.06 (dt, $^1J_{PC}$ = 21.57, $^3J_{PC}$ = 9.35 Hz, CP), 59.08 [s, $CH_2O(CH_2$-$CH_2O)_{P-1}CH_2CH_2OCH_3$], 71.21 [s, CH_2O(*C*H$_2$*C*H$_2$O)$_{P-1}$*C*H$_2$-*C*H$_2OCH_3$], 72.77 [br. s, *C*H$_2$O(CH$_2CH_2$O)$_{P-1}CH_2CH_2OCH_3$], 129.17 (d, $^3J_{PC}$ = 6.73 Hz, *meta*-C_6H_5), 129.90 (br. s, *para*-C_6H_5), 135.68 (d, $^1J_{PC}$ = 21.57 Hz, *ipso*-C_6H_5), 135.76 (d, $^2J_{PC}$ = 21.57 Hz, *ortho*-C_6H_5).

Carbonylhydrido[cis,cis-1,3,5-tris(diphenylphosphanyl)-1,3,5-tris(methoxypolyethoxymethyl)cyclohexane]rhodium(I) (**5a**): A stirred mixture of a homologous polymer of **5** (0.5 mmol) and 459 mg (0.5 mmol) of $Rh(PPh_3)_3(CO)H$ was heated at 90°C for 24 h under reduced pressure (0.1−0.5 mbar). The PPh_3 sublimed during the course of the reaction. The viscous, deep-red to brown, clear reaction mixture was then allowed to cool to room temp. to furnish a quantitative yield of **5a**. – IR (KBr): $\tilde{\nu}$ = 1973 cm^{-1} ν(RhH), 1902 ν(CO). – ^{31}P{^{1}H }NMR ([D$_8$]THF): δ = 40.3 (d, $^2J_{RhP}$ = 118.4 Hz). – ^{1}H NMR ([D$_8$]THF): δ = −8.97 (dq, $^2J_{PH}$ = 34.69 Hz, $^1J_{RhH}$ = 12.87, 1 H, RhH), 1.82−1.96 (m, 3 H, CHH_e), 2.29−3.18 (m, 3 H, CHH_a), 3.29 [s, 9 H, $CH_2O(CH_2CH_2O)_{P-1}$-$CH_2CH_2OCH_3$], 3.35−3.73 [m, 6 + 4×(*P* − 1) + 12 H, CH_2O-(CH_2CH_2O)$_{P-1}$CH_2CH_2OCH$_3$], 6.96−7.47 (m, 30 H, C_6H_5). – ^{13}C{^{1}H} NMR ([D$_8$]THF): δ = 31.54−31.84 (m, CH_2), 40.68 (d, $^2J_{PC}$ = 13.51 Hz, CP), 58.92 [s, $CH_2O(CH_2CH_2O)_{P-1}CH_2CH_2$-$OCH_3$], 71.17 [s, CH_2O(*C*H$_2$*C*H$_2$O)$_{P-1}$*C*H$_2$*C*H$_2OCH_3$], 72.73 [s, *C*H$_2$O(CH$_2CH_2$O)$_{P-1}CH_2CH_2OCH_3$], 127.59−127.72 (m, *meta*-C_6H_5), 129.81 (br. s, *para*-C_6H_5), 136.12−136.36 (m, *ortho*-C_6H_5), 134.38−140.92 (m, *ipso*-C_6H_5).

Carbonylhydrido[cis,cis-1,3,5-tris(diphenylphosphanyl)-1,3,5-tris(methoxymethyl)cyclohexane]rhodium(I) (**6a**): 385 mg (0.5 mmol)

of **6** and 459 mg (0.5 mmol) of $Rh(PPh_3)_3(CO)H$ were dissolved in 100 ml of DMSO at 100°C. After the reaction mixture had cooled to 60°C, it was extracted with *n*-hexane for 4 h in a liquid-liquid extractor. The reaction mixture was maintained at 60°C throughout the course of the extraction. DMSO was removed from the orange reaction mixture under reduced pressure at 60°C. The remaining orange solid was suspended in 100 ml diethyl ether, the orange solid was filtered off (P3), washed with five 25-ml portions of diethyl ether, and dried in vacuo. Yield 401 mg (89%), m.p. 221°C (dec.). – IR (KBr): $\tilde{\nu}$ = 1950 cm^{-1} ν(RhH), 1911 ν(CO). – $^{31}P\{^1H\}$ NMR ([D$_5$]pyridine): δ = 43.3 (d, $^2J_{RhP}$ = 117.3 Hz). – ^1H NMR ([D$_5$]pyridine): δ = −8.28 (dq, $^2J_{PH}$ = 34.53 Hz, $^1J_{RhH}$ = 12.85, 1 H, RhH), 2.07−2.22 (m, 3 H, CH_eH), 2.47−3.28 (m, 3 H, CH_aH), 3.17 (s, 9 H, CH_2OCH_3), 3.86 (br. s, 6 H, CH_2OCH_3), 7.02−7.76 (m, 30 H, C_6H_5). – $^{13}C\{^1H\}$ NMR ([D$_5$]pyridine): δ = 31.08−31.39 (m, CH_2), 40.08−40.29 (m, CP), 58.44 (s, CH_2OCH_3), 77.32−77.48 (m, CH_2OCH_3), 127.63−127.71 (m, *meta*-C_6H_5), 128.44 (br. s, *para*-C_6H_5), 135.81−135.97 (m, *ortho*-C_6H_5), 139.92−140.43 (m, *ipso*-C_6H_5). – MS (FAB), *m/z*: 899.1 [M^+ − H], 871.2 [M^+ − H − CO]. – $C_{49}H_{52}RhO_4P_3$ (900.77): calcd. C 65.34, H 5.82; found C 65.13, H 5.58.

Hydroformylation: The hydroformylation of 1-hexene with **5a** as catalyst was performed in a 100-ml steel autoclave. During the reaction, the temperature and pressure were monitored electronically and were kept constant. The catalyst and the substrate were transferred into the autoclave under an argon atmosphere. After heating the autoclave to the reaction temperature, the gases CO and H_2 were introduced. After separation, the products were analyzed by gas chromatography and the catalyst residues by $^{31}P\{^1H\}$-NMR spectroscopy.

1-Hexene/Methanol (Single Phase): A mixture of 152.8 mg (0.015 mmol, P = 209.1) of **5a**, 9.4 ml (75 mmol) of 1-hexene, and 2.8 ml of methanol was pressurized with 15 bar of CO and 15 bar of H_2 at 119°C. After 2 h, the autoclave was allowed to cool to room temperature. The organic products were separated by vacuum distillation and analyzed by gas chromatography.

1-Hexene/Water (Biphase): A mixture of 152.8 mg (0.015 mmol, P = 209.1) of **5a**, 2.8 ml of water, and 9.4 ml (75 mmol) of 1-hexene was pressurized with 15 bar of CO and 15 bar of H_2 at 119°C. After 2 h, the autoclave was allowed to cool to room temperature. The clear, colorless organic solution was separated by decantation and distilled prior to gas chromatographic analysis.

[1] [1a] J. A. Moulijin, P. W. N. M. van Leeuwen, R. A. van Santen, in *Catalysis*, Elsevier, Amsterdam, **1993**. – [1b] W. A. Herrmann, C. W. Kohlpaintner, *Angew. Chem.* **1993**, *105*, 1588−1609; *Angew. Chem. Int. Ed. Engl.* **1993**, *32*, 1524−1544. – [1c] B. Cornils, *Angew. Chem.* **1995**, *107*, 1709−1711; *Angew. Chem. Int. Ed. Engl.* **1995**, *34*, 1575−1577. – [1d] G. Papadogianakis, R. A. Sheldon, *New. J. Chem.* **1996**, *20*, 175−185. – [1e] B. Cornils, W. A. Herrmann, R. W. Eckl, *J. Mol. Catal. A.* **1997**, *116*, 27−33. – [1f] F. Joó, A. Kathó, *J. Mol. Catal. A.* **1997**, *116*, 3−26.

[2] M. Beller, B. Cornils, C. D. Frohning, C. W. Kohlpaintner, *J. Mol. Catal. A.* **1995**, *104*, 17−85.

[3] F. Bitterer, O. Herd, A. Heßler, M. Kühnel, K. Rettig, O. Stelzer, W. S. Sheldrick, S. Nagel, N. Rösch, *Inorg. Chem.* **1996**, *35*, 4103−4113.

[4] [4a] A. Heßler, S. Kucken, O. Stelzer, J. Blotevogel-Baltronat, W. S. Sheldrick, *J. Organomet. Chem.* **1995**, *501*, 293−302. – [4b] F. Bitterer, S. Kucken, O. Stelzer, *Chem. Ber.* **1995**, *128*, 275−279.

[5] [5a] Z. Jin, Y. Yan, H. Zuo, B. Fell, *J. Prakt. Chem./Chem. Ztg.* **1996**, *338*, 124−128. – [5b] Z. Jin, X. Zheng, B. Fell, *J. Mol. Catal. A.* **1997**, *116*, 55−58.

[6] H. L. Greenwald, G. L. Brown, *J. Phys. Chem.* **1954**, *58*, 825−828.

[7] [7a] T. Okano, M. Yamamoto, T. Noguchi, H. Konishi, J. Kiji, *Chem. Lett.* **1982**, 977−980. – [7b] Y. Amrani, D. Sinou, *J. Mol. Catal.* **1984**, *24*, 231−233.

[8] T. C. Mitchell, K. Heesche-Wagner, *J. Organomet. Chem.* **1992**, *436*, 43−53.

[9] M. J. Naughton, R. S. Drago, *J. Catal.* **1995**, *155*, 383−389.

[10] H. A. Mayer, H. Otto, H. Kühbauch, R. Fawzi, M. Steimann, *J. Organomet. Chem.* **1994**, *472*, 347−354.

[11] P. Stößel, H. A. Mayer, C. Maichle-Mössmer, R. Fawzi, M. Steimann, *Inorg. Chem.* **1996**, *35*, 5860−5867.

[12] Calculation of M_p and P from: the mass balance of the reaction: $M_p = (W_e \times M_e) / W_e$; $P = M_e \times (W_p - W_e) / M_o \times W_e$ and the relative integrals of the ethoxy and phenyl protons: $M_p = P \times M_o + M_e$; $P = (30\ I_{ethoxy}/4\ I_{phenyl}) - 3/2$; M_p = average of molecular weight [g/mol], P = degree of polymerization, W_e = weight of **1** used [g], W_p = weight of **3** recovered [g], M_e = molecular weight of **1** [g/mol], M_o = molecular weight of oxirane [g/mol], I_{ethoxy} = integral of the ethoxy protons, I_{phenyl} = integral of the phenyl protons.

[13] J. P. Flory, *J. Am. Chem. Soc.* **1940**, *62*, 1561−1565.

[14] J. Gaube, *Chem.-Ing.-Techn.* **1973**, *45*, 979−983.

[15] H. A. Mayer, P. Stößel, R. Fawzi, M. Steimann, *Chem. Ber.* **1995**, *128*, 719−723.

[16] [16a] P. Stößel, W. Heins, H. A. Mayer, R. Fawzi, M. Steimann, *Organometallics* **1996**, *15*, 3393−3403. – [16b] P. Stößel, W. Heins, H. A. Mayer, W. Hörner, T. S. Ertel, H. Bertagnolli, *J. Organomet. Chem.* in press.

[17] N. Ahmad, S. D. Robinson, M. F. Uttley, *J. Chem. Soc., Dalton Trans.* **1972**, 843−847

[97174]

Asymmetric Catalysis, 115[◇]

Enantioselective Palladium-Catalysed Allylation of 1,5-Dimethylbarbituric Acid

Henri Brunner*[a], Irmgard Deml[a], Wolfgang Dirnberger[a], Bernd Nuber[b], and Walter Reißer[a]

Institut für Anorganische Chemie der Universität[a],
D-93040 Regensburg, Germany
Fax: (internat.) +49(0)941/9434439
E-mail: henri.brunner@chemie.uni-regensburg.de

Institut für Anorganische Chemie der Universität[b],
D-69120 Heidelberg, Germany

Received August 4, 1997

Keywords: Asymmetric catalysis / Allylic alkylation / 1,5-Dimethylbarbituric acid / Palladium catalysts / Chiral phosphane imine ligands

Allylation of 1,5-dimethylbarbituric acid (**BS**) with allyl acetate using in situ catalysts of palladium(II) acetylacetonate and chiral phosphane imine ligands results in the enantioselective formation of 5-allyl-1,5-dimethylbarbituric acid (**ABS**) as the main product with up to 34% *ee* and 3,5-diallyl-1,5-dimethylbarbituric acid (**AABS**) as a possible by-product, also with up to 34% *ee*. This reaction is a type of allylic alkylation, the stereoselectivity of which is difficult to control because the new stereocenter is formed in the nucleophile attacking from the side opposite to the metal atom. Classical optically active ligands do not give any enantioselectivity in this palladium-catalysed reaction. Chiral phosphane imine ligands, however, are a successful class of compound, synthesized by Schiff base condensation of 2-formylphenyl(diphenyl)phosphane with optically active primary amines. An optimisation of this ligand type showed that the substituents at the stereogenic center in the imine part should be a hydroxymethyl group and a bulky alkyl group, with the best ligand being the L-*tert*-leucinol derivative. A screening of other types of chiral ligand, e.g. phosphane amines and phosphane trisimines, has also been performed. NMR experiments and a molecular modelling study of the cation $[(\eta^3\text{-allyl})\text{Pd}(\mathbf{2a})_2]^+$ were carried out (tripos force field). The enantioselectivity of the phosphane imine ligands is explained by an interaction of the chiral side arm of one of the ligands, which extends to about 3 Å above the allyl plane, with the incoming nucleophile.

Introduction

The enantioselective palladium-catalysed allylic alkylation is one of the most studied subjects in stereoselective synthesis[2][3][4][5]. Usually the new stereogenic center is formed at one of the carbon atoms of the allylic system. The enantioselectivity of this type of allylic alkylation can be controlled by optically active phosphane ligands bound to the Pd catalyst, which forms an intermediate η^3-allyl complex in the catalytic cycle. High optical inductions have been obtained for systems, in which the new asymmetric center is generated in the allylic moiety[2][3][4][5][6][7][8][9][10][11][12][13][14][15]. However, there is an unsolved problem in the palladium-catalysed allylic alkylation involving the creation of an asymmetric center in the nucleophile, usually a carbanion, which attacks the η^3-allyl system in the C−C bond forming step. Control of the enantioselectivity of this type of allylic alkylation is difficult because the nucleophile approaches the (η^3-allyl)Pd complex from the side opposite to the metal atom (and its optically active ligand). By using special nucleophiles, such as the benzophenoneimine of methyl glycinate[18][19] or 2-acetylcyclohexanone[3], enantioselectivities of 62 and 81% *ee*, respectively, were obtained in the alkylation of allyl acetate.

The enantiomers of chiral barbituric acids show different effects inside the organism[20][21][22][23][24]. These optically active barbituric acids are synthesized by the resolution of racemates[20][25][26] or by regioselective condensation of *N*-methylurea with optically active cyanoacetates[21][22][24]. Although interest in barbituric acids acting as sedative/hypnotic and antiepileptic agents is decreasing, this is not true for barbituric acids which function as short time anesthetics. An important example is Methohexital (Brevimytal®)[20][27][28][29][30][31][32][33][34], an allylated barbituric acid, the synthesis of which in principle could be attempted by stereoselective palladium-catalysed allylic alkylation. An achiral allylation of the unsubstituted barbituric acid has been reported[35].

As a model system for the synthesis of Methohexital by allylic alkylation, we chose the reaction of 1,5-dimethylbarbituric acid with allyl acetate as the allylic component, which we introduced in 1994 together with the pertinent enantiomer analysis[36]. In these previous studies we showed that classical ligands, such as (−)-Diop, (−)-Prophos and (−)-Norphos, only gave the allylated product 5-allyl-1,5-di-

[◇] Part 114: Ref.[1].

 © WILEY-VCH Verlag GmbH, D-69451 Weinheim, 1998 1434−1948/98/0101−0043 $ 17.50+.50/0

methylbarbituric acid in racemic form[36], whereas with the phosphane imine ligands **2a**, **2b**, and **11**, an enantiomeric excess of 10 to 13% was obtained[36].

In this paper we describe our investigations into the enantioselective palladium-catalysed allylation of 1,5-dimethylbarbituric acid with allyl acetate in which we varied the base, solvent, temperature, concentration, Pd/ligand ratio and ligand type[37]. In all, 134 different chiral ligands have been tested[37][38]. We present an explanation for the enantioselectivity of the phosphane imine ligands in the (η^3-allyl)Pd complex[37]. The preparation of new optically active phosphane imine, phosphane amine, and phosphane trisimine ligands is reported[37].

Synthesis of New Optically Active PN Ligands

In the previous studies the phosphane imine ligands **2a**, **2b,** and **11** had given the best results in the Pd-catalysed allylation of 1,5-dimethylbarbituric acid with allyl acetate[36]**.** The synthesis of the new PN ligands described here was carried out bearing in mind information gained from the enantioselectivities obtained in the catalytic model reaction between 1,5-dimethylbarbituric acid/allyl acetate. Schiff base condensation (Scheme 1) of 2-formylphenyl(diphenyl)phosphane **1**[39][40][41] with the optically active primary amines (*R*)-(−)-2-amino-1-butanol, (*S*)-(+)-2-amino-1-butanol, L-alaninol, L-valinol, L-leucinol, (2*S*,3*S*)-(+)-2-amino-3-methyl-1-pentanol (L-isoleucinol), (*S*)-(+)-2-amino-3,3-dimethyl-1-butanol (L-*tert*-leucinol), D-α-phenylglycinol, L-phenylalaninol, L-norephedrine, (1*S*,2*S*)-(+)-2-amino-1-phenyl-1,3-propanediol, L-*tert*-butyl *tert*-leucinate and (+)-dehydroabietylamine in refluxing methanol and dichloromethane, respectively, gave the corresponding phosphane imines **2**−**13** (Scheme 2). Recrystallisation of the dry residues from petroleum ether (boiling range 40−60°C) provided colourless or white-yellow crystals and powders, except in the case of **6**, which is a colourless oil.

Scheme 1. Synthesis of phosphane imines and phosphane amines

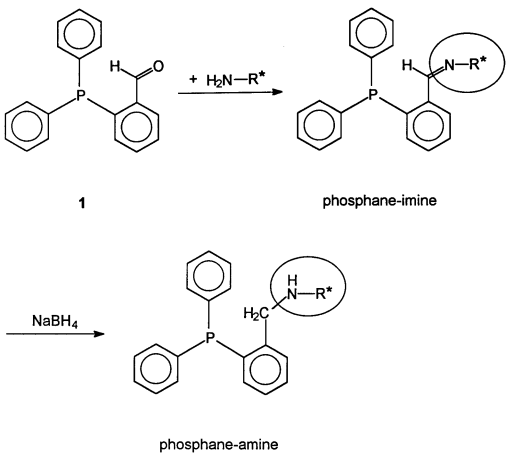

Reduction of the phosphane imines **2a** and **2b** with sodium borohydride at −10°C in methanol (Scheme 1) gave the phosphane amines **14a** and **14b** (Scheme 2).

The phosphane trisimines **15a** and **15b** (Scheme 2) were prepared by Schiff base condensation of tris(2-formylphenyl)phosphane[40][41][42] with an excess of (*R*)-(−)-2-amino-1-butanol and (*S*)-(+)-2-amino-1-butanol, respectively, in refluxing dichloromethane. **15a** and **15b** were isolated as yellow crystalline solids after recrystallisation from petroleum ether (boiling range 40−60°C). The crystals were suitable for X-ray analysis. Figure 1 shows the molecular struc-

Scheme 2. The phosphane imines **2-13**, the phosphane amines **14a**, **14b**, the phosphane trisimines **15a**, **15b**, the osphane octaimine **16**, the deltacyclanephosphane **17** and the osphane oxazolines **18-20**

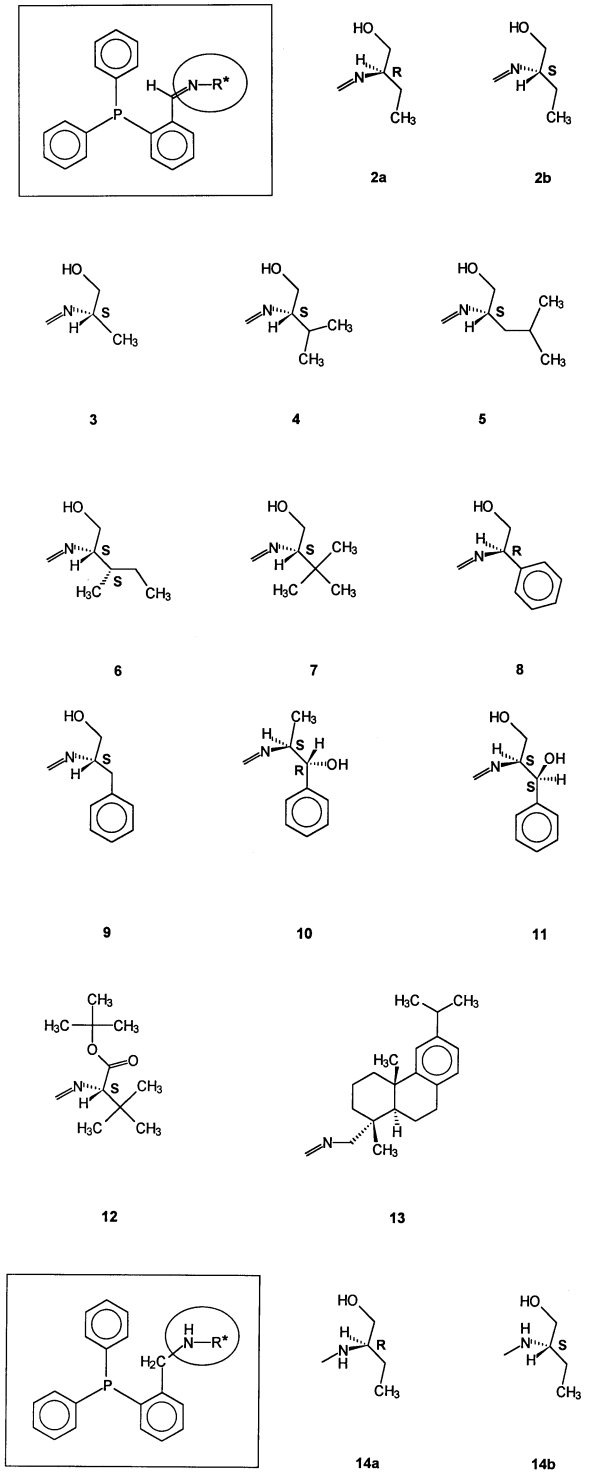

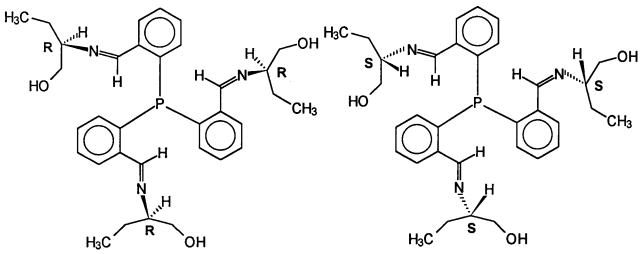

15a **15b**

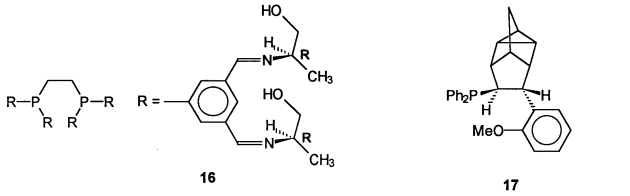

16 **17**

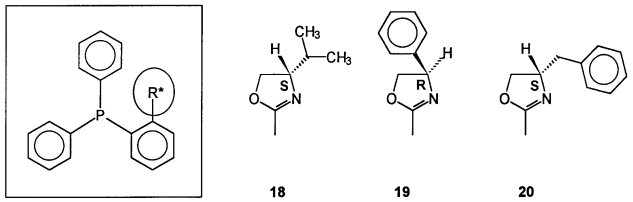

18 **19** **20**

ture of one of the two independent phosphane trisimine molecules **15b** in the unit cell. For details and the CSD number see Experimental Section.

Figure 1. Molecular structure of one of the two independent phosphane trisimine molecules **15b** as ORTEP plot (thermal ellipsoids are depicted with 50% probability)

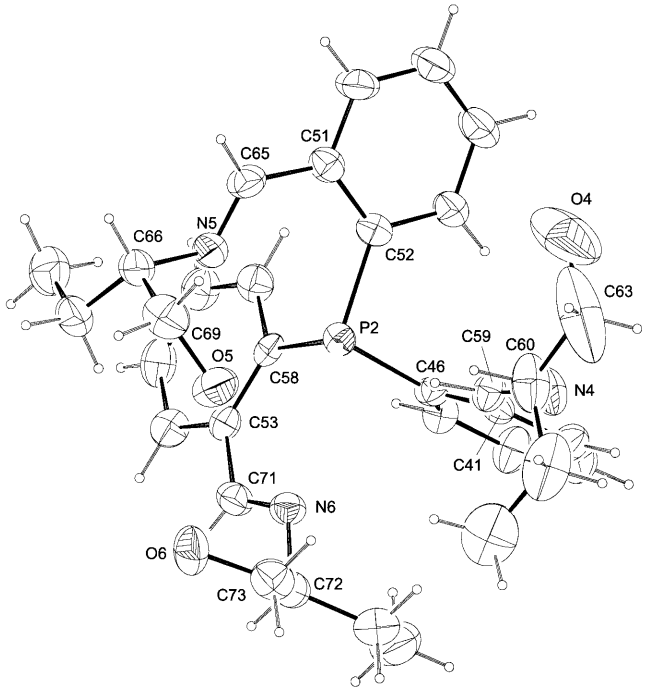

Standard Reaction: The Allylation of 1,5-Dimethylbarbituric Acid

In the catalytic model reaction, 1,5-dimethylbarbituric acid (**BS**) is allylated with allyl acetate to give 5-allyl-1,5-dimethylbarbituric acid (**ABS**) as the main product and 3,5-diallyl-1,5-dimethylbarbituric acid (**AABS**) as a possible by-product (Scheme 3).

Scheme 3. Enantioselective palladium-catalysed allylation of 1,5-dimethylbarbituric acid (**BS**) with allyl acetate

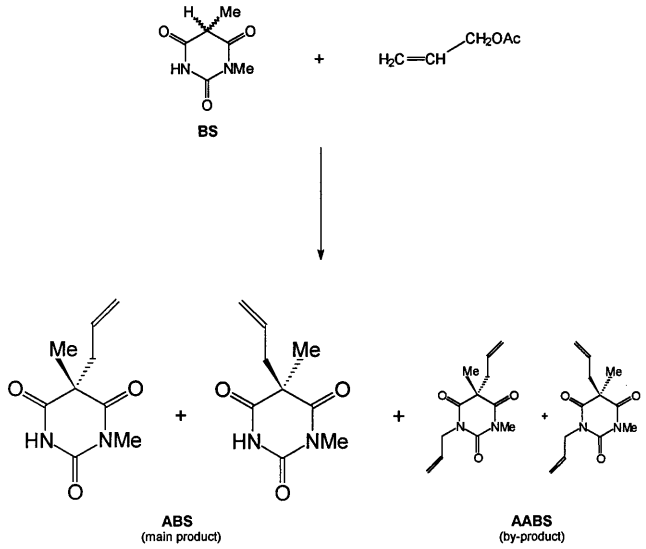

In dichloromethane **BS** is deprotonated with a small excess of a base, such as DBU or NEt_3. To the clear solutionwas added 1 mol% of palladium(II) acetylacetonate, $[Pd(acac)_2]$, 4 mol% of a monodentate optically active phosphane imine ligand and a mixture of dichloromethane and toluene. The addition of allyl acetate starts the reaction. Typically, the clear solution is stirred at 38°C for 24, 48 or 72 hours. A qualitative TLC test (silica 60, Merck; dichloromethane/acetonitrile 25:1) shows how much **ABS**, **AABS** and allyl acetate are present at a specific point of conversion (yellow spots after dipping into a dilute $KMnO_4$ solution). The reaction is stopped with 0.2 M hydrochloric acid. In ordert to remove the excess base, base/acetic acid adduct, and the unreacted **BS**, the organic layer is treated with 0.2 M hydrochloric acid and washed three times with water. Evaporation to dryness removes the excess allyl acetate. Due to the slight water-solubility of **ABS**, about 3% of the yield of **ABS** is lost in the work-up procedure described. This loss, however, cannot be avoided because repeated extraction of the organic layer with hydrochloric acid and water is necessary to remove **BS** quantitatively, as this compound would be detected as a broad peak below the (−)-**ABS** peak in the GC analysis with a Chirasil-Val-L column.

The enantiomeric excess of monoallylated barbituric acid **ABS** and diallylated barbituric acid **AABS** was determined by GC on a Chirasil-Val-L column and on a Lipodex E column, respectively. The first peak detected on the Chirasil-Val-L column was assigned to (−)-**ABS** (configuration unknown) by correlation with an enantiomerically enriched sample (see below). For **AABS**, the symbols (1.) and (2.),

respectively, indicate whether the first or the second detected peak of the two **AABS** enantiomers on the Lipodex E column was in excess. Chemical yields of **ABS** and **AABS** were determined on the same Chirasil-Val-L column using the internal standard benzil. In some cases, e.g. if the chemical yield was below 3%, the by-product 5-chloromethyl-1,5-dimethylbarbituric acid was detected. This compound results from the reaction of the carbanion of **BS** with the solvent dichloromethane[37].

Samples of optically active **ABS** dissolved in dichloromethane did not change their enantiomeric excess after half a year. In a racemisation test under standard catalytic conditions at 25°C, (+)-**ABS** (12.4% *ee*) was dissolved in dichloromethane and then [Pd(acac)$_2$] and PPh_3 were added. After 72 h a sample was examined by GC [12.2% *ee* (+)]. The base DBU was then added. After 48 h, work-up using the usual procedure gave 11.8% *ee* (+) (GC reproducibility about ±0.5% *ee*). Thus, **ABS** is configurationally stable during catalysis.

An enantiomerically enriched sample of (−)-**ABS** was obtained by recrystallisation from water/ethanol (175:1). After this recrystallisation the *ee* in crystals had diminished, whereas it increased in the mother liquor. A crystal of 17.4% *ee* (−)-**ABS** had the optical rotations $[\alpha]_D^{25} = -0.36$ and $[\alpha]_{436}^{25} = -2.4$ (c = 5, CH_2Cl_2). An extrapolation to optical purity gives $[\alpha]_D^{25} = \pm 2.1$ and $[\alpha]_{436}^{25} = \pm 13.8$ for the enantiomers of **ABS**.

The Diallylated 1,5-Dimethylbarbituric Acid AABS

The formation of **AABS** depends on the reaction conditions. When the catalysis is carried out with a 3-fold excess of the base DBU and a 21-fold excess of allyl acetate, **AABS** is produced in 98% yield in refluxing THF after 24 h. After 6 h a yield of 34% **ABS** and 32% **AABS** is obtained in this experiment. The formation of **AABS** depends on the ligand used in the catalyst, although a correlation between the ligand structure and the amount of **AABS** cannot be found. Under standard conditions (25°C or 38°C) the 134 ligands tested give the by-product **AABS** in yields ranging from 0 to 19%[37][38]. Ligands which form 7- to 9-membered chelate rings containing a dioxolane structural element[37][38] (e.g. Diop) give, in all cases, **AABS**, due to the high catalytic activity of their complexes. For example, with the ligand (1*S*,2*S*)-1,2-bis[2′-(diphenylphosphanyl)phenyl]-1,2-dimethoxyethane[43], the reaction was almost complete after 1 h, yielding 78% **ABS** and 8% **AABS**. However, in the case of the the phosphane imine ligand **2a**, formation of **ABS** and **AABS** had not even begun after 1 h[37]. Interestingly, a mixture of the starting material **BS** and the diallylated product **AABS**, in the absence of allyl acetate, under catalytic conditions gave the monoallylated product **ABS**, i.e. the formation of the diallylated product **AABS** is reversible[37].

Catalyses with the Ligand PPh_3

When the catalysis was attempted with [Pd(acac)$_2$] without a ligand, there was no turnover. Addition of triphenylphosphane in dichloromethane at 25°C (base DBU) gave 64% **ABS** and traces of **AABS** (Table 1, entry 1). Thus, the palladium-catalysed allylation of **BS** is an ideal example of a ligand accelerated catalysis[44]. Under the same conditions, but at −17°C, a yield of only 4% **ABS** was obtained after 72 h[37]. The use of [(η^3-allyl)PdCl]$_2$ in place of [Pd(acac)$_2$] afforded 60% **ABS** along with 11% **AABS**, the doubly allylated product (entry 2). Nickel dichlorophosphane complexes (1 mol% of catalyst) gave yields below 2% for **ABS**. With 10 mol%, yields of up to 29% for **ABS** were obtained[38]. Therefore, only Pd-catalysed reactions with 1 mol% of [Pd(acac)$_2$] were investigated further.

Variation of the base, i.e. replacement of DBU by triethylamine, at 38°C in dichloromethane yielded 98% **ABS**, and these conditions are close to those chosen as the standard conditions described later (entry 3). The use of BSA [*N*,*O*-bis(trimethylsilyl)acetamide] as the base in equimolar quantities with respect to **BS**, in dichloromethane at 25°C, gave 63% of **ABS** (entry 4), and this is comparable with the results obtained using DBU (entry 1). When a 1.5 M LDA·THF solution in cyclohexane was added to **BS** dissolved at −72°C in THF (colourless precipitate), low yields of **ABS** and **AABS** were obtained[37]. Stirring a mixture of **BS**, NBu_4OH, the catalyst, and allyl acetate in a two-phase system for 72 h at 25°C gave 59% **ABS** and 6% **AABS** (entry 5). Presynthesis of the tetrabutylammonium salt of **BS** (**NBu_4**BS) makes the addition of a base unnecessary[37]. Thus, **NBu_4**BS in a dichloromethane/toluene mixture (5:1) at 25°C (homogeneous solution) afforded a yield of 44% **ABS** and 1% **AABS** after 24 h (entry 6).

The optically active bases (−)-quinine, (+)-quinidine, (−)-cinchonidine and (+)-cinchonine, in combination with the achiral ligand triphenylphosphane, induced an enantiomeric excess of up to 6% *ee* in **ABS,** with the yields varying from 71 to 90% (entry 7)[37]. 2-Formylphenyldiphenylphosphane (**1**) is the parent compound of the imines **2**−**13**. As this compound could be formed on hydrolysis of these imines, it was tested as a ligand in the catalytic allylation. Indeed, **1** in combination with (−)-quinine as a base induced 6% *ee* (+) for **ABS** (81% yield) and 4% **AABS** (entry 8).

Catalyses with the Phosphane-Imine Ligands 2a and 2b

With a 1:2 ratio of [Pd(acac)$_2$]/**2a** in 10 ml of dichloromethane at 25°C, a yield of 14% and an enantiomeric excess of 8% of (+)-**ABS** was obtained (Table 2, entry 1). Increasing the Pd/ligand ratio to 1:4 and the amount of dichloromethane to 15 ml increased the enantiomeric excess to 10% *ee* and 13% *ee* for (+)-**ABS**, respectively (entries 2, 3). At a reaction temperature of 38°C the yield improved significantly to 63% **ABS** and 9% **AABS** without loss of enantioselectivity (entry 4). With 15 ml of a mixture of dichloromethane/toluene (2:1) as the solvent, the enantiomeric excess rose to 20% *ee* for (+)-**ABS** and 20% *ee* (2.) for **AABS** (entry 5), with the yield being 66% **ABS** and 12% **AABS** (typical standard conditions). The use of triethylamine and (−)-quinine as bases did not improve the enantiomeric excess[37]. Little or no enantioselectivity with ligand **2a** was observed in solvents such as acetonitrile, methanol, tetra-

Table 1. Palladium-catalysed allylation of 1,5-dimethylbarbituric acid (**BS**) with allyl acetate using PPh_3 and **1** as achiral ligands

Entry[a]	Ligand[b]	Base	[ml] Solvent	Temp. [°C]	Time [h]	Yield[c] **ABS** [%]	*ee* [%][d] **ABS** config.	Yield[c] **AABS** [%]
1	PPh_3	DBU	10 CH_2Cl_2	25	24	64	0	0
2[e]	PPh_3	DBU	10 CH_2Cl_2	25	24	60	0	11
3	PPh_3	NEt_3	15 CH_2Cl_2	38	24	98	0	0
4	PPh_3	BSA[f]	6 CH_2Cl_2	25	24	63	0	0
5	PPh_3	NBu_4OH solution in MeOH	5 H_2O + 20 toluene	25	72	59	0	6
6	PPh_3	none; substrate **NBu_4**BS	25 CH_2Cl_2 + 5 toluene	25	24	44	0	1
7	PPh_3	(−)-quinine	10 CH_2Cl_2 + 5 toluene	38	24	73	6 (+)	1
8	**1**	(−)-quinine	10 CH_2Cl_2 + 5 toluene	38	24	81	6 (+)	4

[a] 1 Mol% [$Pd(acac)_2$] was used as procatalyst. − [b] Pd:ligand ratio = 1:4. − [c] Yields were determined by GC on a Chirasil-Val-L column, yields < 0.5% are given as 0%. − [d] The *ee* of **ABS** was measured by GC on a Chirasil-Val-L column. − [e] 0.5 Mol% [(η^3-allyl)PdCl]$_2$ was used as procatalyst. − [f] **BS**:BSA ratio = 1:1 + ≈ 1 mg KOAc.

hydrofuran, chloroform and hexamethylphosphoric triamide (base DBU)[37]. Thus, the best solvent for the allylation of **BS** is a dichloromethane/toluene mixture. As **BS** is only sparingly soluble in toluene, the toluene content is limited in order to keep the reaction mixture homogeneous.

The ligand **2b**, the enantiomer of **2a**, verified with 19% *ee* for (−)-**ABS** and 20% *ee* (1.) for **AABS** the reproducibility of the catalysis and the product analysis under the standard reaction conditions (entry 6). Double stereoselection came into play for the optically active base (−)-quinine in combination with the enantiomeric phosphane imines **2a** and **2b**. Thus, **2a** provided 16% *ee* (+)-**ABS** (78% yield) and **2b** 12% *ee* (−)-**ABS** (entries 7, 8). With (+)-quinidine in combination with **2a**, 3% *ee* was obtained for (+)-**ABS** under the standard conditions[37]. The bases (−)-cinchonidine and (+)-cinchonine, together with ligand **2a**, induced 9% *ee* and 10% *ee* (+)-**ABS** and yields of 87 and 82%, respectively, in a reaction which started as a suspension in a 6:1 mixture of dichloromethane and toluene and which became clear after 41 h under standard conditions. The bases BSA and LDA·THF with ligand **2a** afforded low **ABS** yields[37]. With **NBu_4**BS and the ligands **2a** and **2b**, 12% *ee* (+)- and (−)-**ABS** was obtained, but with a yield of only 20 and 17%, respectively, in a dichloromethane/toluene mixture of 5:1 under the standard reaction conditions[37].

Optimisation of the Lead Structure of 2a

As already mentioned, the phosphane imine ligand **2a** gave an enantioselectivity of 20% *ee* (+)-**ABS** and 20% *ee* (2.) **AABS** using the base DBU in the solvent mixture dichloromethane/toluene (Table 2, entry 5; Table 3, entry 1), and this is superior to all the classical ligands. Therefore, the structure of **2a**, which carries a hydroxymethyl group and an ethyl group at the stereogenic center in its imine substituent in the *ortho* position of one of its phenyl rings, seems to be a lead structure for catalytic allylation in which the new stereocenter is formed at the carbanionic center of the deprotonated nucleophile **BS**. Therefore, we set out to optimize this lead structure.

Ligand **3** is similar to ligand **2b**, having a methyl group instead of an ethyl group and the same hydroxymethyl group in the ligand side arm, and this gives rise to an enantiomeric excess of 9% for (−)-**ABS** with DBU (entry 2) and of 8% for (−)-**ABS** with triethylamine . Thus, a decrease in the size of the alkyl group in the ligand side arm reduces the enantioselectivity. Therefore, we increased the size of the alkyl group in the ligands **4**−**7**, a strategy which turned out to be successful. The phosphane imine **4**, carrying an isopropyl group instead of the ethyl group in **2b**, gave 21% *ee* for (−)-**ABS** and 21% *ee* (1.) for **AABS** with DBU

Table 2. Palladium-catalysed allylation of 1,5-dimethylbarbituric acid (**BS**) with allyl acetate using the phosphane imine ligands **2a** and **2b**

Entry[a]	Ligand	Pd/ligand ratio[a]	Base	[ml] Solvent	Temp. [°C]	Time [h]	Yield[b] **ABS** [%]	*ee* [%][c] **ABS** config.	Yield[b] **AABS** [%]	*ee* [%][c] **AABS** config.
1	**2a**	1:2	DBU	10 CH_2Cl_2	25	72	14	8 (+)	0	−
2	**2a**	1:4	DBU	10 CH_2Cl_2	25	72	26	10 (+)	0	−
3	**2a**	1:4	DBU	15 CH_2Cl_2	25	72	22	13 (+)	0	−
4	**2a**	1:4	DBU	15 CH_2Cl_2	38	72	63	13 (+)	9	12 (2.)
5	**2a**	1:4	DBU	10 CH_2Cl_2 + 5 toluene	38	72	66	20 (+)	12	20 (2.)
6	**2b**	1:4	DBU	10 CH_2Cl_2 + 5 toluene	38	72	66	19 (−)	7	20 (1.)
7	**2a**	1:4	(−)-quinine	10 CH_2Cl_2 + 5 toluene	38	24	78	16 (+)	1	−
8	**2b**	1:4	(−)-quinine	10 CH_2Cl_2 + 5 toluene	38	48	80	12 (−)	3	−

[a] 1 Mol% [$Pd(acac)_2$] was used as procatalyst. − [b] Yields were determined by GC on a Chirasil-Val-L column, yields < 0.5% are given as 0%. − [c] The *ee* of **ABS** was measured by GC on a Chirasil-Val-L column, *ee* of **AABS** was measured by GC on a Lipodex E column.

(entry 3), which is slightly better than the enantioselectivity of **2b** (Table 2, entry 6). Triethylamine and (−)-quinine, respectively, in combination with **4** afforded 18% *ee* for (−)-**ABS** with 89 and 75% yield, respectively[37]. Further enlargement of the alkyl group, i.e. to an isobutyl group in ligand **5**, provided 28% *ee* for (−)-**ABS** and 28% *ee* (1.) for **AABS** with DBU (entry 4). Triethylamine and (−)-quinine, respectively, together with **5** gave 24% *ee* and 23% *ee* for (−)-**ABS**[37]. The ligand **6**, bearing a *sec*-butyl group, gave a similar result for (−)-**ABS** with 26% *ee* with DBU (entry 5) and 20% *ee* with triethylamine (yield 97%)[37]. The best enantiomeric excess in the palladium-catalysed system **BS**/allyl acetate was obtained with the phosphane imine **7**, which contains a *tert*-butyl substituent. **7** induced 34% *ee* for (−)-**ABS** with 77% yield and 1% yield for **AABS** [(34% (1.)] with DBU (entry 6). Ligand **7** with triethylamine as a base afforded 29% *ee* and 89% yield of (−)-**ABS** and 1% yield of **AABS** with 30% *ee* (1.) (entry 7).

nantly (−)-**ABS**, whereas the ligands with the (*R*) configuration (**2a**, **8**) give (+)-**ABS** (bases DBU and triethylamine).

Screening of the Ligands 12−20

Under standard conditions, nitrogen, nitrogen/oxygen and nitrogen/sulfur ligands [e.g. 2,2′-bipyridine, (−)-sparteine, pyridine-oxazolines, etc.] only give yields below 1% for **ABS** in the Pd-catalysed allylation of 1,5-dimethylbarbituric acid[38]. Therefore, the ligand screening concentrated on phosphane ligands[37][38]. Here, we only report representative results.

The phosphane imines **12** and **13**, the phosphane amines **14a** and **14b**, the phosphane trisimines **15a** and **15b**, the phosphane octaimine **16**, the deltacyclanephosphane **17** and the phosphane oxazolines **18**−**20** (Scheme 2) were tested in the standard palladium-catalysed allyllation of 1,5-dimethylbarbituric acid (**BS**) with allyl acetate.

Table 3. Palladium-catalysed allylation of 1,5-dimethylbarbituric acid (**BS**) with allyl acetate using the phosphane imine ligands **2a**−**11**

Entry[a]	Ligand[a]	Base	Solvent	Time [h]	Yield[b] **ABS** [%]	*ee* [%][c] **ABS** config.	Yield[b] **AABS** [%]	*ee* [%][c] **AABS** config.
1	**2a**	DBU	10 CH_2Cl_2 + 5 toluene	72	66	20 (+)	12	20 (2.)
2	**3**	DBU	15 CH_2Cl_2 + 5 toluene	72	74	9 (−)	7	−
3	**4**	DBU	10 CH_2Cl_2 + 5 toluene	48	75	21 (−)	2	21 (1.)
4	**5**	DBU	15 CH_2Cl_2 + 5 toluene	72	71	28 (−)	6	28 (1.)
5	**6**	DBU	15 CH_2Cl_2 + 5 toluene	72	82	26 (−)	4	26 (1.)
6	**7**	DBU	15 CH_2Cl_2 + 5 toluene	72	77	34 (−)	1	34 (1.)
7	**7**	NEt_3	10 CH_2Cl_2 + 5 toluene	72	89	29 (−)	1	30 (1.)
8	**8**	DBU	10 CH_2Cl_2 + 5 toluene	72	40	12 (+)	0	−
9	**9**	DBU	10 CH_2Cl_2 + 5 toluene	48	41	11 (−)	0	−
10	**10**	DBU	15 CH_2Cl_2 + 5 toluene	24	67	2 (−)	4	−
11	**11**	(−)-quinine	10 CH_2Cl_2 + 5 toluene	24	71	6 (+)	1	−

[a] 1 Mol% [$Pd(acac)_2$] was used as procatalyst, Pd : ligand ratio = 1:4 at 38°C. − [b] Yields were determined by GC on a Chirasil-Val-L column, yields < 0.5% are given as 0%; [c] The *ee* of **ABS** was measured by GC on a Chirasil-Val-L column, *ee* of **AABS** was measured by GC on a Lipodex E column.

We subsequently replaced the alkyl group at the stereogenic center with a phenyl and a benzyl group while retaining the hydroxymethyl substituent (ligands **8** and **9**). Phosphane-imine **8** induced 12% *ee* and 13% *ee* for (+)-**ABS** with DBU (entry 8) and triethylamine, respectively. Similar results were obtained with the ligand **9** (entry 9). The results with the ligands **8** and **9** show that phenyl and benzyl substituents in the ligand side arm are not as efficient as alkyl groups. Ligand **10** differs slightly from ligand **3** in that it has a hydroxybenzyl group instead of a hydroxymethyl group, and this gave only 2% *ee* for (−)-**ABS** with DBU (entry 10) and 2% *ee* for (+)-**ABS** with (−)-quinine. Thus, the hydroxymethyl substituent, essential for the optical induction, cannot be replaced by a hydroxybenzyl substituent. With ligand **11**, which compared to **2b** contains a second hydroxy group and an additional phenyl substituent in its chiral side arm, no enantioselectivity was found for **ABS** using DBU[37]. With (−)-quinine and ligand **11**, 6% *ee* (+)-**ABS** was induced (entry 11).

Uniformly, within the phosphane imine ligand family **2**−**11**, the ligands with the (*S*)-configuration of their *N*-bound stereogenic center (**2b**−**7**, **9**−**11**) induce predomi-

Though resembling the phosphane imine ligands **2**−**11**, ligand **12**, a *tert*-butyl *tert*-leucinate, gave only 1% *ee* for (−)-**ABS** with DBU and triethylamine, respectively. Ligand **13** bears the alkylaromatic system of (+)-dehydroabietylamine with no hydroxy group in its side arm, and this afforded racemic **ABS** with DBU and 4% *ee* (+)-**ABS** with (−)-quinine. With 2−3% *ee* for (+)- and (−)-**ABS**, the phosphane amine ligands **14a** and **14b** were much less enantioselective than the corresponding phosphane imine ligands **2a** and **2b**. The change from one-arm phosphane imines **2a** and **2b** to the three-arm phosphane trisimines **15a** and **15b** did not lead to an improvement in the optical induction of **ABS**. With **15a** an enantiomeric excess of 6% *ee* and a yield of only 2% for (−)-**ABS** was found with the base DBU. Interestingly, with **15a** **ABS** was formed with the inverse configuration in comparison to **2a**. Ligand **15b** in combination with (−)-quinine provided (−)-**ABS** with 3% *ee* and in only 1% yield.

With the phosphane octaimine **16**[45], which bears D-alaninol in its eight side arms, an enantiomeric excess of 11% *ee* for (+)-**ABS** was obtained. The incorporation of (*R*)-(−)-2-amino-1-butanol, L-valinol, L-leucinol, L-phenylalan-

inol in the ligand arms and changing the ligand backbone to the 1,2-disubstituted phenylene bridge decreased the enantioselectivity for **ABS**[37]. The deltacyclanephosphane **17**[46] gave 8% *ee* for (+)-**ABS** with DBU. The combination of **17** with (−)-quinine led to an improvement to 11% *ee* for (+)-**ABS** (double stereoselection). The phosphane oxazoline ligands **18**−**20**[47][48] induced up to 99% *ee* in allylations in which the stereogenic center is formed in the allylic system and up to 13% *ee* in allylations in which the stereogenic center is formed in the nucleophile[49][50]. In the catalytic allylation of **BS** with allyl acetate, an enantiomeric excess of only about 1% *ee* for (+)-**ABS** was obtained. Phosphane-oxazoline **20** in combination with (−)-quinine provided 4% *ee* for (+)-**ABS**, probably an effect of (−)-quinine.

A Model for the Catalytically Active Phosphane-Imine Pd Complex

The in situ system consisting of the dimeric (η^3-allyl)palladium chloride and the phosphane imine **2a** was investigated by $^{31}P\{^1H\}$-NMR spectroscopy. In dichloromethane using a Pd/**2a** ratio of 1:1, signals at δ = 36.34 (broad) (0.6 P), 32.81 (0.1 P), 32.63 (0.1 P) and 21.82/21.74 (0.2 P) were observed, the most intense of which could be due to a Pd complex containing **2a** as a P−N chelating ligand similar to the Pd complexes of the phosphane oxazoline ligands[8][9][11][13]. On changing from a Pd/**2a** ratio of 1:1 to a ratio of 1:4, all the signals present in the 1:1 experiment disappeared. Two new doublets of equal intensity arose at δ = 45.86 and 18.67 (coupling constant 341.8 Hz), belonging to the complex [(η^3-allyl)Pd(**2a**)$_2$]Cl. Excess **2a** exhibited a singlet at δ = −9.92 with double the intensity compared to the signals of the coordinated **2a**. In addition there were small signals at δ = 33.28 (oxide of **2a**), 23.27 and 15.20 (broad) (CH_2Cl_2/CD_2Cl_2, external 85% H_3PO_4, 162 MHz, 21°C). After seven days the signal at δ = 15.20 had disappeared and that at δ = 33.28 had increased (increasing oxidation). Thus, using a Pd to ligand ratio of 1:4, a (η^3-allyl)Pd complex formed containing two inequivalent phosphane imine ligands **2a**.

Based on X-ray studies[51][52][53][54][55] and calculations[56] of (η^3-allyl)Pd complexes a molecular modelling study of an (η^3-allyl)Pd complex with two phosphane imine ligands **2a** was carried out using the tripos force field. Figure 2 shows a conformation of this complex obtained on energy minimisation.

The two phosphane imine ligands **2a** turn out to be different. The hydroxy group of one phosphane imine extends to about 3 Å above the allyl plane, whereas the hydroxy group of the other phosphane imine remains below the allyl plane in accord with their NMR inequivalence (Figure 2). Furthermore, a substituted and an unsubstituted phenyl ring, one from each of the two phosphane imines, form a π-stacking pair which participates in the conformational organisation of the two monodentate ligands. Taking into account this phenyl/phenyl interaction, the two monodentate ligands in the (η^3-allyl)Pd complex can be considered a ″chelating″ ligand. The hydroxy group, which is about 3 Å above the allyl plane, can influence the incoming 1,5-dimethylbarbiturate anion (Figure 2), e.g. by forming hydrogen bonds, thus differentiating the N−H and the N−Me side of the **BS** anion (Figure 3), which explains the enantioselectivity of long-arm ligands of the type **2a**.

Figure 2. Conformation of the (η^3-allyl)Pd complex containing two phosphane imine ligands **2a** after energy minimisation

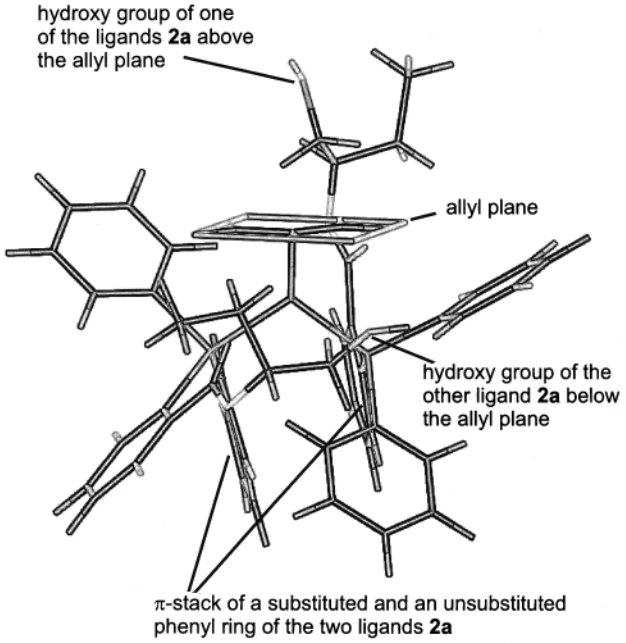

Figure 3. Differentiation between the N−H and the N−Me side of the incoming 1,5-dimethylbarbiturate anion in the formation of the new stereogenic center

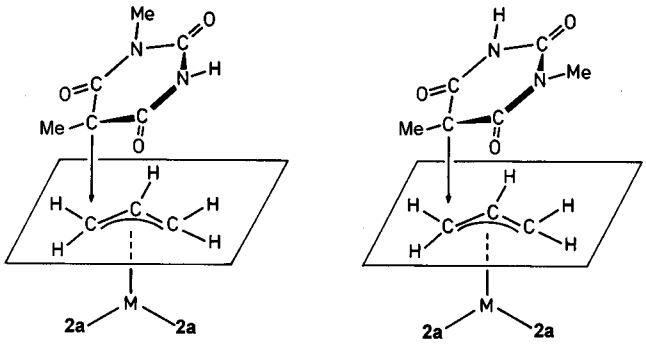

We thank the *Fonds der Chemischen Industrie* and the *BASF*, Ludwigshafen, for support of this work, and PD Dr. *S. Dove* for carrying out the force field calculations.

Experimental Section

NMR spectra were recorded on a Bruker WM 250 or on a Bruker ARX 400 instrument. Chemical shifts (δ) are reported in parts per million (ppm) vs. internal tetramethylsilane (TMS) (^1H) and external 85% H_3PO_4 ($^{31}P\{^1H\}$). − FD mass spectra were obtained on a Finnigan MAT 95, and for EI mass spectra a Varian MAT 311A was used. − Gas chromatography measurements were carried out on a Fisons Instruments GC 8000 series 8130. For integration of gas chromatograms a Spectra-Physics SP 4270 was used. − Infra red spectra were recorded on a Beckman Gitterspektro-

meter IR 4240. − Optical rotations were measured on a Perkin-Elmer polarimeter 241 (1-dm cell). − Melting points were obtained on a Büchi SMP 20 (uncorrected). The X-ray structure analysis was carried out on a AED II diffractometer.

(−)-Quinine, (−)-cinchonidine, and (+)-cinchonine were purchased from Merck, (+)-quinidine from Fluka, (*R*)-(−)-2-amino-1-butanol, (*S*)-(+)-2-amino-1-butanol, (1*S*,2*S*)-(+)-2-amino-1-phenyl-1,3-propanediol, (+)-dehydroabietylamine, L-*tert*-butyl *tert*-leucinate from Merck, L-alaninol, L-valinol, L-leucinol, D-α-phenylglycinol, L-phenylalaninol, L-norephedrine from Fluka, (2*S*,3*S*)-(+)-2-amino-3-methyl-1-pentanol (L-isoleucinol) from Aldrich, (*S*)-(+)-2-amino-3,3-dimethyl-1-butanol (L-*tert*-leucinol) from Sigma or Fluka and used without further purification. 2-Formylphenyl(diphenyl)phosphane (**1**)[39][40][41] and tris(2-formylphenyl)phosphane[40][41][42] were prepared as described in the literature. New analytical data are reported for **1**. The phosphane octaimine **16**[45], the deltacyclanephosphane **17**[46] and the osphane oxazolines **18**−**20**[47][48] were prepared using procedures described in the literature. All the syntheses and catalytic reactions were carried out with dried solvents under a nitrogen atmosphere using standard Schlenk techniques.

2-Formylphenyl(diphenyl)phosphane (**1**): Yellow crystals, m.p. 115−116°C. − IR (KBr): $\tilde{\nu}$ = 1701, 1679 cm^{-1} (C=O). − ^{1}H NMR ($CDCl_3$, 400 MHz): δ = 10.50 (d, ^4J_P = 5.4 Hz, 1 H, aldehyde), 7.97 (ddd, ^4J = 1.8 Hz, ^4J_P = 3.7 Hz, ^3J = 7.2 Hz, 1 H, Ar−H^3), 7.51−7.43 (m, 2 H, Ar−H^4 and Ar−H^5), 7.37−7.25 (m, 10 H, Ar−H), 6.99−6.95 (m, 1 H, Ar−H^6). − ^{31}P{^{1}H} NMR ($CDCl_3$, 162 MHz): δ = −10.99 (s). − $C_{19}H_{15}OP$ (290.30): calcd. C 78.61, H 5.21; found C 78.66, H 5.07.

General Procedure for the Preparation of the Phosphane Imines **2**−**13**. − *Variant A*: 3.45 mmol of the optically active primary amine was dissolved in 10 ml of methanol. 2-Formylphenyl(diphenyl)phosphane (**1**) (3.45 mmol; 1.00 g) and 10 ml of methanol were added to the above solution with stirring and the mixture refluxed for 3 h. After cooling to room temp. the methanol was removed and the resulting residue was dried and recrystallized as described for the individual phosphane imines.

Variant B: 3.45 mmol (or 4.14 mmol) of the optically active primary amine was dissolved in 30 ml of dichloromethane. 2-Formylphenyl(diphenyl)phosphane (**1**) (3.45 mmol; 1.00 g), 1 g of Na_2SO_4, and 10 ml of dichloromethane were added to the above solution with stirring and the mixture refluxed for 3 h. After cooling to room temp. the Na_2SO_4 was filtered off and washed with dichloromethane. The dichloromethane was removed and the resulting residue was treated as in variant A.

(+)-2-[N-(R)-1′-Hydroxybut-2′-ylcarbaldimino]phenyl(diphenyl)phosphane (**2a**): Variant A with 3.45 mmol (307 mg, 325 µl) of (*R*)-(−)-2-amino-1-butanol. Recrystallisation from 50 ml of petroleum ether (boiling range 40−60°C): colourless needles (1.02 g, 82%), m.p. 84.5−85°C. − $[\alpha]_D^{25}$ = +73 (*c* = 1, EtOH). − IR (KBr): $\tilde{\nu}$ = 1639 cm^{-1} (C=N). − ^{1}H NMR ($CDCl_3$, 400 MHz): δ = 8.68 (d, ^4J_P = 4.0 Hz, 1 H, azomethine), 7.80 (ddd, ^4J = 1.5 Hz, ^4J_P = 3.8 Hz, ^3J = 7.7 Hz, 1 H, Ar−H^3), 7.41 (pseudo dt, ^4J = 1.2 Hz, ^3J = 7.6 Hz, 1 H, Ar−H^4 or Ar−H^5), 7.35−7.20 (m, 11 H, Ar−H), 6.88 (ddd, ^4J = 1.2 Hz, ^3J_P = 4.5 Hz, ^3J = 7.6 Hz, 1 H, Ar−H^6), 3.52 (d, ^3J = 5.4 Hz, 2 H, NCH−C*H*$_2$−OH), 3.09 (ddt, ^3J = 4.8 Hz, ^3J = 8.5 Hz, ^3J = 5.4 Hz, 1 H, CHH′−NC*H*−CH$_2$), 1.82 (s br, 1 H, O*H*), 1.42 (dqd, ^3J = 4.8 Hz, ^3J = 7.4 Hz, ^2J = 13.7 Hz, 1 H, NCH−C*H*H′−CH$_3$), 1.30 (qdd, ^3J = 7.4 Hz, ^3J = 8.5 Hz, ^2J = 13.7 Hz, 1 H, NCH−CH*H*′−CH$_3$), 0.62 (pseudo t, ^3J = 7.4 Hz, 3 H, CHH′−C*H*$_3$). − ^{31}P{^{1}H} NMR ($CDCl_3$, 162 MHz): δ = −9.69 (s). − $C_{23}H_{24}NOP$ (361.42): calcd. C 76.44, H 6.69, N 3.87; found C 76.15, H 6.76, N 3.95.

(−)-2-[N-(S)-1′-Hydroxybut-2′-ylcarbaldimino]phenyl(diphenyl)phosphane (**2b**): Variant A with 3.45 mmol (307 mg, 325 µl) of (*S*)-(+)-2-amino-1-butanol. Recrystallisation analogous to **2a** (946 mg, 76%), m.p. 84.5−85°C. − $[\alpha]_D^{25}$ = −73 (*c* = 1, EtOH). − IR, ^{1}H NMR, ^{31}P{^{1}H} NMR analogous to **2a**. − $C_{23}H_{24}NOP$ (361.42): calcd. C 76.44, H 6.69, N 3.87; found C 76.19, H 6.84, N 3.91.

(−)-2-[N-(S)-1′-Hydroxyprop-2′-ylcarbaldimino]phenyl(diphenyl)phosphane (**3**): Variant A with 3.45 mmol (259 mg) of (*S*)-(+)-2-amino-1-propanol (L-alaninol). Recrystallisation from 50 ml of petroleum ether (boiling range 40−60°C): colourless crystals (995 mg, 83%), m.p. 62−63°C. − $[\alpha]_D^{25}$ = −19 (*c* = 1, CH_2Cl_2). − IR (KBr): $\tilde{\nu}$ = 1646 cm^{-1} (C=N). − ^{1}H NMR ($CDCl_3$, 400 MHz): δ = 8.72 (d, ^4J_P = 4.0 Hz, 1 H, azomethine), 7.80 (ddd, ^4J = 1.5 Hz, ^4J_P = 3.8 Hz, ^3J = 7.6 Hz, 1 H, Ar−H^3), 7.40 (pseudo dt, ^4J = 1.3 Hz, ^3J = 7.5 Hz, 1 H, Ar−H), 7.35−7.21 (m, 11 H, Ar−H), 6.89 (ddd, ^4J = 1.2 Hz, ^3J_P = 4.5 Hz, ^3J = 7.7 Hz, 1 H, Ar−H^6), 3.51−3.34 (m, 3 H, NC*H*−C*HH*′−OH), 1.89 (s br, 1 H, OH), 0.96 (d, ^3J = 6.3 Hz, 3 H, NCH−C*H*$_3$). − ^{31}P{^{1}H} NMR ($CDCl_3$, 162 MHz): δ = −9.86 (s). − MS (FD, CH_2Cl_2); *m*/*z* (%): 347.0 (100) [M$^+$]. − $C_{22}H_{22}NOP$ (347.40): calcd. C 76.06, H 6.38, N 4.03; found C 75.74, H 6.28, N 3.98.

(−)-2-[N-(S)-1′-Hydroxy-3′-methylbut-2′-ylcarbaldimino]phenyl(diphenyl)phosphane (**4**): Variant A with 3.45 mmol (356 mg) of (*S*)-(+)-2-amino-3-methyl-1-butanol (L-valinol). Recrystallisation from 50 ml of petroleum ether (boiling range 40−60°C): colourless crystals (795 mg, 61%), m.p. 51−53°C. − $[\alpha]_D^{25}$ = −68 (*c* = 1, CH_2Cl_2). − IR (KBr): $\tilde{\nu}$ = 1643 cm^{-1} (C=N). − ^{1}H NMR ($CDCl_3$, 400 MHz): δ = 8.61 (d, ^4J_P = 3.8 Hz, 1 H, azomethine), 7.78 (ddd, ^4J = 1.5 Hz, ^4J_P = 3.8 Hz, ^3J = 7.6 Hz, 1 H, Ar−H^3), 7.42 (pseudo dt, ^4J = 1.2 Hz, ^3J = 7.5 Hz, 1 H, Ar−H), 7.35−7.20 (m, 11 H, Ar−H), 6.89 (ddd, ^4J = 1.2 Hz, ^3J_P = 4.4 Hz, ^3J = 7.7 Hz, 1 H, Ar−H^6), 3.60 (ddd, ^3J = 5.7 Hz, ^3J = 7.4 Hz, ^2J = 11.1 Hz, 1 H, NCH−C*H*H′−OH), 3.54 (ddd, ^3J = 3.4 Hz, ^3J = 8.2 Hz, ^2J = 11.1 Hz, 1 H, NCH−CH*H*′−OH), 2.87 (pseudo dt, ^3J = 3.4 Hz, ^3J = 7.2 Hz, 1 H, CHH′−NC*H*−CH), 1.80 (ddd, J_P = 3.3 Hz, ^3J = 5.7 Hz, ^3J = 8.2 Hz, 1 H, CHH′−O*H*), 1.68 (pseudo oct., ^3J = 6.8 Hz, 1 H, CH$_3$−C*H*−CH$_3$′), 0.81 (d, ^3J = 6.8 Hz, 3 H, CH−C*H*$_3$), 0.58 (d, ^3J = 6.8 Hz, 3 H, CH−C*H*$_3$′). − ^{31}P{^{1}H} NMR ($CDCl_3$, 162 MHz): δ = −9.33 (s). − MS (FD, CH_2Cl_2); *m*/*z* (%): 375.1 (100) [M$^+$]. − $C_{24}H_{26}NOP$ (375.45): calcd. C 76.78, H 6.98, N 3.73; found C 76.47, H 6.99, N 3.77.

(−)-2-[N-(S)-1′-Hydroxy-4′-methylpent-2′-ylcarbaldimino]phenyl(diphenyl)phosphane (**5**): Variant A with 3.45 mmol (404 mg) of (*S*)-(+)-2-amino-4-methyl-1-pentanol (L-leucinol). Recrystallisation analogous to **4**: colourless needles (962 mg, 72%), m.p. 68−69°C. − $[\alpha]_D^{25}$ = −81 (*c* = 1, CH_2Cl_2). − IR (KBr): $\tilde{\nu}$ = 1637 cm^{-1} (C=N). − ^{1}H NMR ($CDCl_3$, 400 MHz): δ = 8.71 (d, ^4J_P = 4.3 Hz, 1 H, azomethine), 7.81 (ddd, ^4J = 1.3 Hz, ^4J_P = 3.8 Hz, ^3J = 7.6 Hz, 1 H, Ar−H^3), 7.41 (pseudo dt, ^4J = 1.2 Hz, ^3J = 7.5 Hz, 1 H, Ar−H), 7.35−7.20 (m, 11 H, Ar−H), 6.87 (ddd, ^4J = 1.1 Hz, ^3J_P = 4.5 Hz, ^3J = 7.6 Hz, 1 H, Ar−H^6), 3.50 (m, 2 H, NCH−C*H*$_2$−OH), 3.31 (ddt, ^3J = 3.9 Hz, ^3J = 9.4 Hz, ^3J = 5.4 Hz, 1 H, CH$_2$−NC*H*−CH$_2$), 1.85 (s br, 1 H, OH), 1.30 (ddd, ^3J = 4.1 Hz, ^3J = 9.4 Hz, ^2J = 12.8 Hz, 1 H, NCH−C*H*H′−CH), 1.21−1.09 [m, 1 H, CHH′−C*H*(CH$_3$)$_2$], 1.08 (ddd, ^3J = 3.9 Hz, ^3J = 9.1 Hz, ^2J = 12.8 Hz, 1 H, NCH−CH*H*′−CH), 0.72 (pseudo t, ^3J = 6.6 Hz, 6 H, *H*$_3$C−CH−C*H*$_3$′). − ^{31}P{^{1}H} NMR ($CDCl_3$, 162 MHz): δ = −10.05 (s). − MS (FD, CH_2Cl_2); *m*/*z* (%): 389.1

(100) [M$^+$]. − $C_{25}H_{28}NOP$ (389.48): calcd. C 77.10, H 7.25, N 3.60; found C 77.02, H 7.27, N 3.55.

(−)-2-[N-(S)-1′-Hydroxy-(3′S)-methylpent-2′-ylcarbaldimino]phenyl(diphenyl)phosphane (**6**): Variant A with 3.45 mmol (404 mg) of (2*S*,3*S*)-(+)-2-amino-3-methyl-1-pentanol (L-isoleucinol). Recrystallisation analogous to **4**: colourless crystals at −20°C, which form a highly viscous oil at room temp. (798 mg, 59%). − $[\alpha]_D^{25}$ = −72 (*c* = 1, CH_2Cl_2). − IR (film): $\tilde{\nu}$ = 1648 cm^{-1} (C=N). − ^{1}H NMR ($CDCl_3$, 400 MHz): δ = 8.61 (d, ^4J_P = 4.0 Hz, 1 H, azomethine), 7.78 (ddd, ^4J = 1.5 Hz, ^4J_P = 3.8 Hz, ^3J = 7.6 Hz, 1 H, Ar−H^3), 7.42 (pseudo dt, ^4J = 1.2 Hz, ^3J = 7.5 Hz, 1 H, Ar−H), 7.35−7.20 (m, 11 H, Ar−H), 6.89 (ddd, ^4J = 1.2 Hz, ^3J_P = 4.4 Hz, ^3J = 7.7 Hz, 1 H, Ar−H^6), 3.63 (dd, ^3J = 7.3 Hz, ^2J = 11.2 Hz, 1 H, NCH−C*H*H′−OH), 3.54 (dd, ^3J = 3.4 Hz, ^2J = 11.2 Hz, 1 H, NCH−CH*H*′−OH), 2.97 (pseudo dt, ^3J = 3.4 Hz, ^3J = 7.3 Hz, 1 H, CHH′−NC*H*−CH), 1.90 (s br, 1 H, OH), 1.50−1.39 (m, 1 H, CH−C*H*H′−CH_3), 1.10 (dqd, ^3J = 3.8 Hz, ^3J = 7.3 Hz, ^2J = 13.2 Hz, 1 H, CH−CH*H*′−CH_3), 0.83−0.71 (m, 1 H, H_3C−C*H*−CHH′), 0.77 (d, ^3J = 6.9 Hz, 3 H, *H*$_3$C−CH), 0.67 (pseudo t, ^3J = 7.3 Hz, 3 H, CHH′−C*H*$_3$). − $^{31}P\{^1H\}$ NMR ($CDCl_3$, 162 MHz): δ = −9.36 (s). − MS (FD, CH_2Cl_2); *m/z* (%): 389.2 (100) [M$^+$]. − $C_{25}H_{28}NOP$ (389.48): calcd. C 77.10, H 7.25, N 3.60; found C 76.88, H 7.48, N 3.75.

(−)-2-[N-(S)-1′-Hydroxy-3′,3′-dimethylbut-2′-ylcarbaldimino]phenyl(diphenyl)phosphane (**7**): Variant A with 3.45 mmol (404 mg) of (*S*)-(+)-2-amino-3,3-dimethyl-1-butanol (L-*tert*-leucinol). Recrystallisation analogous to **4**: colourless needles (969 mg, 72%), m.p. 85−86°C. − $[\alpha]_D^{25}$ = −66 (*c* = 1, CH_2Cl_2). − IR (KBr): $\tilde{\nu}$ = 1648 cm^{-1} (C=N). − ^{1}H NMR ($CDCl_3$, 400 MHz): δ = 8.59 (d, ^4J_P = 3.8 Hz, 1 H, azomethine), 7.78 (ddd, ^4J = 1.4 Hz, ^4J_P = 3.8 Hz, ^3J = 7.7 Hz, 1 H, Ar−H^3), 7.42 (pseudo dt, ^4J = 1.2 Hz, ^3J = 7.5 Hz, 1 H, Ar−H), 7.35−7.20 (m, 11 H, Ar−H), 6.89 (ddd, ^4J = 1.1 Hz, ^3J_P = 4.3 Hz, ^3J = 7.7 Hz, 1 H, Ar−H^6), 3.64 (ddd, ^3J = 3.2 Hz, ^3J = 10.4 Hz, ^2J = 11.0 Hz, 1 H, NCH−C*H*H′−OH), 3.54 (ddd, ^3J = 3.9 Hz, ^3J = 9.2 Hz, ^2J = 11.0 Hz, 1 H, NCH−CH*H*′−OH), 2.86 (ddd, ^6J_P = 0.8 Hz, ^3J = 3.2 Hz, ^3J = 9.2 Hz, 1 H, NC*H*−CHH′), 1.46 (pseudo td, J_P = 3.9 Hz, ^3J = 3.9 Hz, ^3J = 10.4 Hz, 1 H, CHH′−O*H*), 0.74 [s, 9 H, C(C*H*$_3$)$_3$]. − $^{31}P\{^1H\}$ NMR ($CDCl_3$, 162 MHz): δ = −9.59 (s). − MS (FD, CH_2Cl_2); *m/z* (%): 389.1 (100) [M$^+$]. − $C_{25}H_{28}NOP$ (389.48): calcd. C 77.10, H 7.25, N 3.60; found C 77.12, H 7.25, N 3.52.

(+)-2-[N-(R)-1′-Hydroxy-2′-phenyleth-2′-ylcarbaldimino]phenyl(diphenyl)phosphane (**8**): Variant A with 3.45 mmol (473 mg) of (*R*)-(−)-2-amino-2-phenyl-1-ethanol (D-α-phenylglycinol). Recrystallisation analogous to **4**: yellowish solid (884 mg, 63%), m.p. 47−49°C. − $[\alpha]_D^{25}$ = +141 (*c* = 1, CH_2Cl_2). − IR (KBr): $\tilde{\nu}$ = 1649 cm^{-1} (C=N). − ^{1}H NMR ($CDCl_3$, 400 MHz): δ = 8.65 (d, ^4J_P = 3.5 Hz, 1 H, azomethine), 7.71 (ddd, ^4J = 1.3 Hz, ^4J_P = 3.8 Hz, ^3J = 7.6 Hz, 1 H, Ar−H^3), 7.41 (pseudo dt, ^4J = 1.2 Hz, ^3J = 7.5 Hz, 1 H, Ar−H), 7.38−7.23 (m, 11 H, Ar−H), 7.19−7.15 (m, 3 H, Ar−H), 6.96−6.92 (m, 3 H, Ar−H), 4.41 (dd, ^3J = 5.2 Hz, ^3J = 7.4 Hz, 1 H, NC*H*−CHH′), 3.70−3.62 (m, 2 H, NCH−C*HH*′−OH), 2.46 (s br, 1 H, OH). − $^{31}P\{^1H\}$ NMR ($CDCl_3$, 162 MHz): δ = −8.37 (s). − MS (FD, CH_2Cl_2); *m/z* (%): 409.2 (100) [M$^+$]. − $C_{27}H_{24}NOP$ (409.47): calcd. C 79.20, H 5.91, N 3.42; found C 78.98, H 5.96, N 3.19.

(−)-2-[N-(S)-1′-Hydroxy-3′-phenylprop-2′-ylcarbaldimino]phenyl(diphenyl)phosphane (**9**): Variant B with 3.45 mmol (522 mg) of (*S*)-(−)-2-amino-3-phenyl-1-propanol (L-phenylalaninol). Recrystallisation from 90 ml of pentane: yellowish solid (1.01 g, 69%), m.p. 42−43°C. − $[\alpha]_D^{25}$ = −167 (*c* = 1, CH_2Cl_2). − IR (KBr): $\tilde{\nu}$ = 1652, 1641 cm^{-1} (C=N). − ^{1}H NMR ($CDCl_3$, 400 MHz): δ = 8.29 (d, ^4J_P = 3.8 Hz, 1 H, azomethine), 7.59 (ddd, ^4J = 1.4 Hz, ^4J_P = 3.8 Hz, ^3J = 7.6 Hz, 1 H, Ar−H^3), 7.38 (pseudo dt, ^4J = 1.3 Hz, ^3J = 7.5 Hz, 1 H, Ar−H), 7.35−7.10 (m, 14 H, Ar−H), 6.95−6.92 (m, 2 H, Ar−H), 6.89 (ddd, ^4J = 1.2 Hz, ^3J_P = 4.3 Hz, ^3J = 7.7 Hz, 1 H, Ar−H^6), 3.61−3.51 (m, 2 H, NCH−CH_2−OH), 3.45−3.37 (m, 1 H, CH_2−NC*H*−CHH′), 2.71 (dd, ^3J = 5.3 Hz, ^2J = 13.4 Hz, 1 H, NCH−C*H*H′−Ph), 2.48 (dd, ^3J = 8.3 Hz, ^2J = 13.4 Hz, 1 H, NCH−CH*H*′−Ph), 2.12 (s br, 1 H, OH). − $^{31}P\{^1H\}$ NMR ($CDCl_3$, 162 MHz): δ = −9.14 (s). − MS (FD, CH_2Cl_2); *m/z* (%): 423.2 (100) [M$^+$]. − $C_{28}H_{26}NOP$ (423.49): calcd. C 79.41, H 6.19, N 3.31; found C 79.12, H 6.37, N 3.32.

(+)-2-[N-(1′R,2′S)-1′-Hydroxy-1′-phenylprop-2′-ylcarbaldimino]phenyl(diphenyl)phosphane (**10**): Variant B with 3.45 mmol (522 mg) of (1*R*,2*S*)-(−)-2-amino-1-phenyl-1-propanol (L-norephedrine). Recrystallisation from 18 ml of petroleum ether (boiling range 40−60°C)/THF (5:1): colourless crystals (918 mg, 63%), m.p. 74.5−75°C. − $[\alpha]_D^{25}$ = +8, $[\alpha]_D^{25}$ = +50 (*c* = 1, CH_2Cl_2). − IR (KBr): $\tilde{\nu}$ = 1649 cm^{-1} (C=N). − ^{1}H NMR ($CDCl_3$, 400 MHz): δ = 8.72 (d, ^4J_P = 4.0 Hz, 1 H, azomethine), 7.82 (ddd, ^4J = 1.3 Hz, ^4J_P = 3.8 Hz, ^3J = 7.6 Hz, 1 H, Ar−H^3), 7.41 (pseudo dt, ^4J = 1.2 Hz, ^3J = 7.5 Hz, 1 H, Ar−H), 7.37−7.19 (m, 16 H, Ar−H), 6.89 (ddd, ^4J = 1.1 Hz, ^3J_P = 4.6 Hz, ^3J = 7.8 Hz, 1 H, Ar−H^6), 4.63 (d, ^3J = 3.6 Hz, 1 H, NCH−*H*COH−Ph), 3.49 (dq, ^3J = 3.6 Hz, ^3J = 6.5 Hz, 1 H, H_3C−NC*H*−HCOH), 3.15 (s br, 1 H, OH), 0.77 (d, ^3J = 6.5 Hz, 3 H, *H*$_3$C−NCH). − $^{31}P\{^1H\}$ NMR ($CDCl_3$, 162 MHz): δ = −9.80 (s). − MS (FD, CH_2Cl_2); *m/z* (%): 423.1 (100) [M$^+$]. − $C_{28}H_{26}NOP$ (423.49) · 0.5 THF: calcd. C 78.41, H 6.58, N 3.05; found C 78.16, H 6.73, N 3.30.

(+)-2-[N-(1′S,2′S)-1′,3′-Dihydroxy-1′-phenylprop-2′-ylcarbaldimino]phenyl(diphenyl)phosphane (**11**): Variant A with 3.45 mmol (577 mg) of (1*S*,2*S*)-(+)-2-amino-1-phenyl-1,3-propanediol. Recrystallisation from 150 ml of petroleum ether (boiling range 40−60°C): microcrystalline colourless solid (1.24 g, 82%), m.p. 64−66°C. − $[\alpha]_D^{25}$ = +88 (*c* = 1, EtOH). − IR (KBr): $\tilde{\nu}$ = 1650 cm^{-1} (C=N). − ^{1}H NMR ($CDCl_3$, 400 MHz): δ = 8.30 (d, ^4J_P = 3.2 Hz, 1 H, azomethine), 7.60 (ddd, ^4J = 1.4 Hz, ^4J_P = 3.8 Hz, ^3J = 7.6 Hz, 1 H, Ar−H^3), 7.43 (pseudo dt, ^4J = 1.2 Hz, ^3J = 7.5 Hz, 1 H, Ar−H), 7.38−7.19 (m, 16 H, Ar−H), 6.93 (ddd, ^4J = 1.2 Hz, ^3J_P = 4.5 Hz, ^3J = 7.7 Hz, 1 H, Ar−H^6), 4.66 (d, ^3J = 5.3 Hz, 1 H, NCH−*H*COH−Ph), 3.61−3.34 (m, 3 H, NC*H*−CH_2−OH), 2.76 (s br, 1 H, OH), 1.70 (s br, 1 H, OH). − $^{31}P\{^1H\}$ NMR ($CDCl_3$, 162 MHz): δ = −5.69 (s). − $C_{28}H_{26}NO_2P$ (439.49): calcd. C 76.52, H 5.96, N 3.19; found C 75.70, H 5.96, N 3.38.

(−)-2-[N-(S)-3′,3′-Dimethyl-tert-butyloxy-2′-butyrylcarbaldimino]phenyl(diphenyl)phosphane (**12**): Variant B with 4.14 mmol (775 mg) of (*S*)-(+)-2-amino-3,3-dimethyl-*tert*-butyloxybutyric acid (L-*tert*-butyl *tert*-leucinate). Recrystallisation analogous to **4**: yellowish crystals (1.37 g, 86%), m.p. 94−95°C. − $[\alpha]_D^{25}$ = −99 (*c* = 1, CH_2Cl_2). − IR (KBr): $\tilde{\nu}$ = 1742 cm^{-1} (C=O), 1643 (C=N). − ^{1}H NMR ($CDCl_3$, 400 MHz): δ = 8.88 (pseudo qd, *J* = 0.6 Hz, ^4J_P = 5.4 Hz, 1 H, azomethine), 8.18 (ddd, ^4J = 1.4 Hz, ^4J_P = 4.0 Hz, ^3J = 7.8 Hz, 1 H, Ar−H^3), 7.38 (pseudo ddt, *J* = 0.6 Hz, ^4J = 1.3 Hz, ^3J = 7.5 Hz, 1 H, Ar−H), 7.36−7.23 (m, 11 H, Ar−H), 6.85 (dddd, *J* = 0.6 Hz, ^4J = 1.3 Hz, ^3J_P = 4.7 Hz, ^3J = 7.7 Hz, 1 H, Ar−H^6), 3.43 [d, *J* = 0.6 Hz, 1 H, OOC−NC*H*−C(CH$_3$)$_3$], 1.40 [s, 9 H, COOC(C*H*$_3$)$_3$], 0.87 [s, 9 H, NCH−C(C*H*$_3$)$_3$]. − $^{31}P\{^1H\}$ NMR ($CDCl_3$, 162 MHz): δ = −14.11 (s). − MS (FD, CH_2Cl_2); *m/z* (%): 459.2 (100) [M$^+$]. − $C_{29}H_{34}NO_2P$ (459.60): calcd. C 75.79, H 7.46, N 3.05; found C 75.79, H 7.32, N 3.03.

(+)-2-[N-(1′R,11′R,12′S)-Dehydroabietylcarbaldimino]phenyl(diphenyl)phosphane (**13**): Variant B with 4.14 mmol (1.18 g)

of (+)-dehydroabietylamine. Recrystallisation from 50 ml of ethanol/methanol (3:2): colourless crystals (1.36 g, 71%), m.p. 74−75°C. − $[\alpha]_D^{25}$ = +13 (*c* = 1, CH_2Cl_2). − IR (KBr): $\tilde{\nu}$ = 1638 cm^{-1} (C=N). − ^1H NMR ($CDCl_3$, 400 MHz): δ = 8.87 (d, ^4J_P = 5.1 Hz, 1 H, azomethine), 7.99 (ddd, ^4J = 1.1 Hz, ^4J_P = 3.9 Hz, ^3J = 7.7 Hz, 1 H, Ar−H^3), 7.37−7.20 (m, 12 H, Ar−H), 7.15 (d, ^3J = 8.2 Hz, 1 H, Ar−H), 6.97 (dd, ^4J = 1.7 Hz, ^3J = 8.2 Hz, 1 H, Ar−H), 6.85−6.82 (m, 2 H, Ar−H), 3.38 (d, ^2J = 11.9 Hz, 1 H, N−C*H*H′), 3.26 (dd, *J* = 1.0 Hz, ^2J = 11.9 Hz, 1 H, N−CH*H*′), 2.81 (sept., ^3J = 6.9 Hz, 1 H, $H_3C-CH-CH_3$), 2.77−2.62 (m, 2 H, Ar−CH_2−CH_2), 2.18 (d, $^3J_{axial}$ = 12.8 Hz, 1 H, C_3C-H), 1.83−1.15 (m, 8 H, 4 CH_2), 1.22 (d, ^3J = 6.9 Hz, 6 H, $H_3C-CH-CH_3$), 1.18 (s, 3 H, C_3C-CH_3), 0.92 (s, 3 H, C_3C-CH_3). − $^{31}P\{^1H\}$ NMR ($CDCl_3$, 162 MHz): δ = −13.82 (s). − MS (EI, 70 eV); *m/z* (%): 557.3 (29) [M^+], 542.2 (24) [$M^+ - CH_3$], 303.2 (100) [$Ph_2P(C_6H_4)CHNHCH_2^+$], 302.1 (75) [$Ph_2P(C_6H_4)CHNCH_2^+$], 288.1 (64) [$Ph_2P(C_6H_4)CHN^+$]. − $C_{39}H_{44}NP$ (557.76): calcd. C 83.98, H 7.95, N 2.51; found C 83.62, H 7.99, N 2.58.

Synthesis of the Phosphane amines **14a** *and* **14b**: 750 mg (2.08 mmol) of **2a** (or **2b**) was dissolved in 30 ml of methanol at −10°C followed by the addition of 100 mg (2.64 mmol) of $NaBH_4$. The solution was allowed to come to room temp. within 4 h and heated for 2 h at 50°C. After removal of the methanol, 25 ml of water and 120 ml of dichloromethane were added to the residue. The dichloromethane layer was extracted twice with 25 ml of water and dried with Na_2SO_4. After filtration the dichloromethane was removed and the resulting oil was recrystallized with 20 ml of petroleum ether (boiling range 40−60°C) to give colourless crystals at −20°C. At room temp. the crystals of **14a** (or **14b**) became a highly viscous oil. Yield: 665 mg (88%).

(+)-N-[2-(Diphenylphosphanyl)benzyl]-N-[(R)-1′-hydroxybut-2′-yl]amine (**14a**): $[\alpha]_D^{25}$ = +11, $[\alpha]_{365}^{25}$ = +75 (*c* = 1, CH_2Cl_2). − ^1H NMR ($CDCl_3$, 400 MHz): δ = 7.41 (ddd, ^4J = 1.2 Hz, ^4J_P = 4.5 Hz, ^3J = 7.6 Hz, 1 H, Ar−H^3), 7.36−7.23 (m, 11 H, Ar−H), 7.18 (pseudo dt, ^4J = 1.2 Hz, ^3J = 7.6 Hz, 1 H, Ar−H), 6.92 (ddd, ^4J = 1.2 Hz, ^3J_P = 4.5 Hz, ^3J = 7.6 Hz, 1 H, Ar−H^6), 4.10 (s very br, 2 H, OH and NH), 3.98 (dd, ^4J_P = 1.6 Hz, ^2J = 12.6 Hz, 1 H, Ar−C*H*H′−NH), 3.95 (dd, ^4J_P = 1.2 Hz, ^2J = 12.6 Hz, 1 H, Ar−CH*H*′−NH), 3.60 (dd, ^3J = 3.8 Hz, ^2J = 10.9 Hz, 1 H, NCH−C*H*H′−OH), 3.24 (dd, ^3J = 5.9 Hz, ^2J = 10.9 Hz, 1 H, NCH−CH*H*′−OH), 2.51 (pseudo dq, ^3J = 3.8 Hz, ^3J = 6.3 Hz, 1 H, CHH′−NC*H*−CH_2), 1.36−1.27 (m, 2 H, NCH−CH_2−CH_3), 0.82 (t, ^3J = 7.4 Hz, 3 H, CH_2-CH_3). − $^{31}P\{^1H\}$ NMR ($CDCl_3$, 162 MHz): δ = −15.44 (s). − MS (FD, CH_2Cl_2); *m/z* (%): 363.1 (100) [M^+]. − $C_{23}H_{26}NOP$ (363.44): calcd. C 76.01, H 7.21, N 3.85; found C 74.70, H 7.10, N 3.82.

(−)-N-[2-(Diphenylphosphanyl)benzyl]-N-[(S)-1′-hydroxybut-2′-yl]amine (**14b**): $[\alpha]_D^{25}$ = −11, $[\alpha]_{365}^{25}$ = −75 (*c* = 1, CH_2Cl_2). − ^1H NMR, $^{31}P\{^1H\}$ NMR and MS analogous to **14a**. − $C_{23}H_{26}NOP$ (363.44): calcd. C 76.01, H 7.21, N 3.85; found C 75.72, H 7.28, N 3.82.

Synthesis of the Phosphane trisimines **15a** *and* **15b**: 3.79 ml (40.4 mmol, 3.60 g) of (*R*)-(−)-2-amino-1-butanol [or (*S*)-(+)-2-amino-1-butanol] was dissolved in 10 ml of dichloromethane and 1 g (7 mmol) of Na_2SO_4 was added. A solution of 0.70 g (2.0 mmol) of tris(2-formylphenyl)phosphane[40][41][42] in 10 ml of dichloromethane was added dropwise during 15 min. After 16 h reflux the yellow solution was filtered and the dichloromethane was evaporated. The excess amine was removed by heating under high vacuum at 100°C for 6 h. The resulting yellow oil was dissolved in 50 ml of dichloromethane, stirred for 15 min and filtered. The clear solution was evaporated to dryness. Recrystallisation from 90 ml of petroleum ether (boiling range 40−60°C) afforded yellow crystals of **15a** (or **15b**). Yield 0.90 g (80%).

(+)-Tris[2-(N-(R)-1′-hydroxybut-2′-ylcarbaldimino)-phenyl]phosphane (**15a**): M.p. 106.5−107°C. − $[\alpha]_D^{25}$ = +105 (*c* = 1, EtOH). − IR (KBr): $\tilde{\nu}$ = 1647 cm^{-1} (C=N). − ^1H NMR ($CDCl_3$, 400 MHz): δ = 8.45 (d, ^4J_P = 2.0 Hz, 3 H, azomethine), 7.65−7.59 (m, 3 H, Ar−H^3), 7.38 (pseudo dt, ^4J = 1.2 Hz, ^3J = 7.5 Hz, 3 H, Ar−H), 7.16 (pseudo t, ^3J = 7.4 Hz, 3 H, Ar−H), 6.92 (ddd, ^4J = 1.2 Hz, ^3J_P = 3.8 Hz, ^3J = 7.7 Hz, 3 H, Ar−H^6), 3.76 (s br, 3 H, OH), 3.51−3.37 (m, 6 H, NCH−C*H*H′−OH), 3.02−2.94 (m, 3 H, CHH′−NC*H*−CHH′), 1.25−1.10 (m, 3 H, NCH−C*H*H′−CH_3), 0.92−0.78 (m, 3 H, NCH−CH*H*′−CH_3), 0.41 (pseudo t, ^3J = 7.3 Hz, 9 H, CHH′−CH_3). − $^{31}P\{^1H\}$ NMR ($CDCl_3$, 162 MHz): δ = −10.12 (s). − MS (EI, 70 eV); *m/z* (%): 559.2 (100) [M^+], 486.3 (95) [$M^+ - C_4H_8OH$], 470.3 (39), 459.3 (15) [$M^+ - CHNC_4H_8OH$]. − $C_{33}H_{42}N_3O_3P$ (559.69): calcd. C 70.82, H 7.56, N 7.51; found C 70.38, H 7.64, N 7.45.

(−)-Tris[2-(N-(S)-1′-hydroxybut-2′-ylcarbaldimino)-phenyl]phosphane (**15b**): M.p. 106.5−107°C. − $[\alpha]_D^{25}$ = −105 (*c* = 1, EtOH). − IR, ^1H NMR, $^{31}P\{^1H\}$ NMR and MS analogous to **15a**. − $C_{33}H_{42}N_3O_3P$ (559.69): calcd. C 70.82, H 7.56, N 7.51; found C 70.68, H 7.55, N 7.53.

X-ray Structure Analysis of **15b**: $C_{33}H_{42}N_3O_3P$ (559.69); crystal dimensions 0.30 × 0.45 × 0.50 mm; two independent molecules in the unit cell; crystal system triclinic; space group *C*1/1, *P*1, (1); unit cell dimensions *a* = 10.068(6), *b* = 11.611(7), *c* = 15.125(9) Å, α = 88.08(5), β = 73.55(5), γ = 70.35(5)°, *V* = 1593.3 Å^3; *Z* = 2; density $d_{calcd.}$ = 1.17g/cm^3; μ(Mo-K_α) = 0.12 mm^{-1}; 3.0° < 2θ < 50.5°; total no. of reflections 8224, unique reflections 7653, unique reflections with $I > 2.5\sigma(I)$ 6037; *F*(000) = 600; diffractometer AED II; temp. −70°C. The structure was solved by direct methods using the SHELXTL PLUS version 4.2/800 program system. Hydrogen atoms were calculated by the HFIX program; R = 0.044; R_w = 0.033; residual electron density max. 0.36 e/Å^3, min. −0.39 e/Å^3. Further details of the crystal structure investigation may be obtained from the Fachinformationszentrum Karlsruhe, D-76344 Eggenstein-Leopoldshafen (Germany), on quoting the depository number CSD-407358.

1,5-Dimethylbarbituric Acid (**BS**): Handling of **BS** has been described in the literature[57][58][59][60], but a synthesis and characterisation was not given. 16.6 g (0.722 mol) of sodium was dissolved under reflux in 230 ml of absolute ethanol under a nitrogen atmosphere. After cooling to about 60°C, 25.9 g (0.350 mol) of *N*-methylurea and 20 ml of ethanol and, after 15 min, 59.8 ml (0.350 mol, 61.0 g) of methylmalonic acid diethyl ester were added (colourless precipitate). After 2 h reflux the solvent was removed. The dry residue was dissolved in 400 ml of hot water and, with vigorous stirring, 100 ml of conc. hydrochloric acid was added. After cooling to room temp. the precipitated product was filtered off and washed with 400 ml of cooled diethyl ether. Recrystallisation from 600 ml of absolute ethanol/methanol (3:1) provided colourless crystals, which were washed with petroleum ether (boiling range 40−60°C) and dried under high vacuum at 60°C for several days. Yield 34.7 g (63%), m.p. 170−171°C. − IR (KBr): $\tilde{\nu}$ = 1703 cm^{-1} (C=O). − ^1H NMR ([D$_6$]DMSO, 250 MHz): δ = 11.27 (s, 1 H, NH), 3.72 (q, ^3J = 6.9 Hz, 1 H, *H*CCH$_3$), 3.06 (s, 3 H, N−CH$_3$), 1.34 (d, ^3J = 6.9 Hz, 3 H, HCC*H*$_3$). − $C_6H_8N_2O_3$ (156.14): calcd. C 46.15, H 5.16, N 17.94; found C 46.21, H 5.18, N 17.90.

Enantioselective Palladium-Catalysed Allylation of 1,5-Dimethylbarbituric Acid (**BS**) *with Allyl Acetate:*150 mg (0.961 mmol) of **BS** and 1.01 mmol of base were dissolved in 10 ml of dichlorometh-

ane at 38°C under a nitrogen atmosphere. The following bases were used: DBU (150 µl, 153 mg), triethylamine (140 µl, 102 mg), BSA (247 µl, 205 mg), 1.5 M LDA·THF solution in cyclohexane (673 µl), NBu_4OH solution in methanol (12.5%) (2.59 ml, 2.10 g), (−)-quinine (328 mg), (+)-quinidine (328 mg), (−)-cinchonidine (297 mg) and (+)-cinchonine (297 mg). **BS** and base can be replaced by 382 mg (0.961 mmol) of **NBu_4BS**. After 5 min stirring 2.93 mg (0.0096 mmol) of palladium(II) acetylacetonate, 0.0384 mmol of a monodentate ligand or 0.0192 mmol of a bidentate ligand and 10 ml of a 1:1 mixture of methylene choride/toluene were added to the clear solution. After 2.0 min the reaction was started by the addition of 115 µl (1.07 mmol, 107 mg) of allyl acetate. The solution was stirred for 24, 48 or 72 h at 38°C. For work-up the solution was diluted with 10 ml of dichloromethane and extracted successively with 10 ml and 5 ml of 0.2 M hydrochloric acid and three times with 5 ml of water. The organic layer was dried with Na_2SO_4. The solid was filtered off and washed with 10 ml of dichloromethane. Removal of the solvent from the filtrate left the dry product ready for GC analysis. To the product was added about 25 mg of benzil (GC standard) and 6 ml of dichloromethane. This solution was used to determine the enantiomeric excess of **ABS** and the yield of **ABS** and **AABS** by GC on a Chirasil-Val-L column. Furthermore, a chromatographic analysis of 3 ml of the solution on alumina was carried out in a Pasteur pipette, in which only **AABS** and benzil eluted. The eluate was used for the determination of the enantiomeric excess of **AABS** on a Lipodex E column.

Conditions: 25 m *Chirasil-Val-L* fused silica capillary column (0.25 mm inner diameter, 0.12 µm film thickness, from Chrompack), column temp. 130°C, He pressure 1.2 bar, injector temp. 250°C, detector temp. 230°C [flame ionisation], retention times: (±)-**AABS** 4.24 min, standard benzil 17.10 min, (−)-**ABS** 19.09 min, (+)-**ABS** 20.33 min, separation factor $\alpha_{[(+)\text{-ABS}/(-)\text{-ABS}]} = 1.07$, resolution $R_{[(+)\text{-ABS}/(-)\text{-ABS}]} = 1.80$, mass correlation factors: $f_{\text{benzil/ABS}} = 1.77$ and $f_{\text{benzil/AABS}} = 1.50$; retention times for the enantiomers of 5-chloromethyl-1,5-dimethylbarbituric acid were 34.74 and 35.32 min, respectively. − 50 m *Lipodex E* fused silica capillary column (0.25 mm inner diameter, coated with octakis(2,6-di-*O*-pentyl-3-*O*-butyryl)-γ-cyclodextrine, from Macherey-Nagel), column temp. 110°C (after 45 min the column temp. was raised by 12°C/min to 170°C), H_2 pressure 2.07 bar, injector temp. 250°C, detector temp. 240°C (flame ionisation), retention times: (1.)-**AABS** 42.45 min, (2.)-**AABS** 43.84 min, standard benzil 65.0 min, separation factor $\alpha_{[(2.)\text{-AABS}/(1.)\text{-AABS}]} = 1.03$, resolution $R_{[(2.)\text{-AABS}/(1.)\text{-AABS}]} = 1.74$.

5-Allyl-1,5-dimethylbarbituric Acid (**ABS**): Main product of catalysis under standard reaction conditions. Maximum yield 184 mg (98%) (Table 1, entry 3). Recrystallisation from water/ethanol 175:1 provided colourless crystals, m.p. 131−131.5°C. − IR (KBr): $\tilde{\nu}$ = 1758, 1716, 1680 cm^{-1} (C=O). − ^1H NMR ($CDCl_3$, 400 MHz): δ = 9.03 (s, 1 H, NH), 5.60 (tdd, ^3J = 7.5 Hz, $^3J_{cis}$ = 10.1 Hz, $^3J_{trans}$ = 17.0 Hz, 1 H, $CH_2-CH{=}CHH$), 5.14 (md, $^3J_{trans}$ = 17.0 Hz, 1 H, $CH_2-CH{=}CHH_{trans}$), 5.11 (md, $^3J_{cis}$ = 10.1 Hz, 1 H, $CH_2-CH{=}CH_{cis}H$), 3.28 (s, 3 H, $N-CH_3$), 2.71 (d, ^3J = 7.5 Hz, 2 H, $CH_2-CH{=}CHH$), 1.57 (s, 3 H, $C-CH_3$). − GC-MS (EI, 70 eV); *m/z* (%): 195.9 (6) [M^+], 180.9 (100) [$M^+ - CH_3$], 41.0 (32) [$C_3H_5^+$]. − $C_9H_{12}N_2O_3$ (196.21): calcd. C 55.09, H 6.16, N 14.28; found C 55.09, H 6.23, N 14.09.

3,5-Diallyl-1,5-dimethylbarbituric Acid (**AABS**): By-product of catalysis under standard reaction conditions (yield 0−19%). To produce **AABS**, the standard catalysis was carried out with a 3-fold excess of the base DBU (450 µl) and a 21-fold excess of allyl acetate (2.20 ml) in refluxing THF (10 ml) with a reaction time of 24 h (ligand PPh_3). The THF was removed and 30 ml of dichloromethane was added followed by standard work-up. The resulting liquid was dissolved in dichloromethane and filtered through aluminia to remove traces of **ABS**. For further purification a bulb to bulb distillation was carried out to give a colourless liquid at 130°C and 3 Torr. Yield 222 mg (98%), b.p. ≈ 80°C at 3 Torr. − IR (film): $\tilde{\nu}$ = 1689 cm^{-1} (C=O). − ^1H NMR ($CDCl_3$, 400 MHz): δ = 5.82 (pseudo tdd, ^3J = 6.0 Hz, $^3J_{cis}$ = 10.2 Hz, $^3J_{trans}$ = 17.1 Hz, 1 H, $N-CHH'-CH{=}CHH$), 5.54 (tdd, ^3J = 7.5 Hz, $^3J_{cis}$ = 10.1 Hz, $^3J_{trans}$ = 17.0 Hz, 1 H, $C-CH_2-CH{=}CHH$), 5.28 (pseudo qd, $^{2/4}J$ = 1.3 Hz, $^3J_{trans}$ = 17.1 Hz, 1 H, $N-CHH'-CH{=}CHH_{trans}$), 5.21 (pseudo qd, $^{2/4}J$ = 1.3 Hz, $^3J_{cis}$ = 10.2 Hz, 1 H, $N-CHH'-CH{=}CH_{cis}H$), 5.10 (md, $^3J_{trans}$ = 17.0 Hz, 1 H, $C-CH_2-CH{=}CHH_{trans}$), 5.08 (md, $^3J_{cis}$ = 10.1 Hz, 1 H, $C-CH_2-CH{=}CH_{cis}H$), 4.50 (pseudo tdd, ^4J = 1.3 Hz, ^3J = 6.0 Hz, ^2J = 14.6 Hz, 1 H, $N-CHH'-CH{=}CHH$), 4.44 (pseudo tdd, ^4J = 1.3 Hz, ^3J = 6.0 Hz, ^2J = 14.6 Hz, 1 H, $N-CHH'-CH{=}CHH$), 3.30 (s, 3 H, $N-CH_3$), 2.69 (d, ^3J = 7.5 Hz, 2 H, $C-CH_2-CH{=}CHH$), 1.55 (s, 3 H, $C-CH_3$). − GC-MS (EI, 70 eV); *m/z* (%): 236.0 (100) [M^+], 221.0 (99) [$M^+ - CH_3$], 194.9 (17) [$M^+ - C_3H_5$], 138.0 (90), 41.0 (59) [$C_3H_5^+$]. − $C_{12}H_{16}N_2O_3$ (236.27): calcd. C 61.00, H 6.83, N 11.86; found C 60.95, H 7.04, N 11.63.

5-Chloromethyl-1,5-dimethylbarbituric Acid: Found in catalyses with yields of **ABS** <3%. − $C_7H_9ClN_2O_3$ (204.61). − GC-MS (EI, 70 eV); *m/z* (%): 204.0 (14) [M^+], 189.0 (30) [$M^+ - CH_3$], 169.0 (100) [$M^+ - Cl$], 155.1 (6) [$M^+ - CH_2Cl$], 69.0 (62), 40.9 (27).

Molecular Modelling: The calculations were carried out with the program Sybyl 6.1 using the standard tripos force field on a Silicon Graphics Indigo workstation (tripos metal file with standard geometries and van der Waals parameters of transition metal atoms). After establishment of the geometry of the (η^3-allyl)Pd system and the two P atoms, the P substituents were attached in their standard geometries, the *ortho*-substituent being oriented towards the allyl plane. A conformational analysis with energy minimisation was carried out.

[1] H. Brunner, A. Winter, *J. Organomet. Chem.,* in press.
[2] J.-C. Fiaud in *Metal Promoted Selectivity in Organic Synthesis* (Eds.: A. F. Noels, M. Graziani, A. J. Hubert), Kluwer, Dordrecht, **1991**, p.107.
[3] T. Hayashi in *Catalytic Asymmetric Synthesis* (Ed.: I. Ojima), VCH, New York, **1993**, p. 325.
[4] B. M. Trost, D. L. Van Vranken, *Chem. Rev.* **1996**, *96*, 395.
[5] B. M. Trost, *Acc. Chem. Res.* **1996**, *29*, 355.
[6] U. Leutenegger, G. Umbricht, C. Fahrni, P. v. Matt, A. Pfaltz, *Tetrahedron* **1992**, *48*, 2143.
[7] B. M. Trost, D. L. Van Vranken, C. Bingel, *J. Am. Chem. Soc.* **1992**, *114*, 9327.
[8] P. v. Matt, A. Pfaltz, *Angew. Chem.* **1993**, *105*, 614; *Angew. Chem., Int. Ed. Engl.* **1993**, *32*, 566.
[9] J. Sprinz, G. Helmchen, *Tetrahedron Lett.* **1993**, *34*, 1769.
[10] G. J. Dawson, C. G. Frost, J. M. J. Williams, S. J. Coote, *Tetrahedron Lett.* **1993**, *34*, 3149.
[11] O. Reiser, *Angew. Chem.* **1993**, *105*, 576; *Angew. Chem., Int. Ed. Engl.* **1993**, *105*, 547.
[12] P. v. Matt, O. Loiseleur, G. Koch, A. Pfaltz, C. Lefeber, T. Feucht, G. Helmchen, *Tetrahedron: Asymmetry* **1994**, *5*, 573.
[13] J. V. Allen, S. J. Coote, G. J. Dawson, C. G. Frost, C. J. Martin, J. M. J. Williams, *J. Chem. Soc., Perkin Trans. 1* **1994**, *1*, 2065.
[14] J. M. Brown, D. I. Hulmes, P. J. Guiry, *Tetrahedron* **1994**, *50*, 4493.
[15] B. M. Trost, B. Breit, S. Peukert, J. Zambrano, J. W. Ziller, *Angew. Chem.* **1995**, *107*, 2577; *Angew. Chem., Int. Ed. Engl.* **1995**, *34*, 2386.
[16] P. Wimmer, M. Widhalm, *Chem. Monthly* **1996**, *127*, 669.
[17] A. Pfaltz, *Acta Chem. Scand.* **1996**, *50*, 189.
[18] J.-P. Genêt, D. Ferroud, S. Jugé, J. R. Montès, *Tetrahedron Lett.* **1986**, *27*, 4573.

[19] J. -P. Genêt, S. Jugé, J. R. Montès, J. -M. Gaudin, *J. Chem. Soc., Chem. Commun.* **1988**, 718.
[20] W. J. Doran, *J. Org. Chem*. **1960**, 25, 1737.
[21] J. Knabe, W. Rummel, H. P. Büch, N. Franz, *Arzneim.-Forsch./Drug Res.* **1978**, 28 (II), 7, 1048.
[22] J. Knabe, *Arzneim.-Forsch./Drug Res.* **1989**, 39 (II), 11, 1379.
[23] J. Knabe, H.-D. Höltje, *Lehrbuch der Pharmazeutischen Chemie*, Wissenschaftliche Verlagsgesellschaft, Stuttgart, **1991**.
[24] J. Knabe, *Pharmazie* **1993**, 12, 883.
[25] J. Knabe, R. Kräuter, *Arch. Pharm.* **1965**, 298, 1.
[26] J. Knabe, R. Kräuter, K. Philipson, *Tetrahedron Lett.* **1965**, 571.
[27] United States Patent, *2872448* (Eli Lilly; ert. 3. 2. **1959**; Prior. 4. 4. 1956).
[28] C. Lehmann, *Das Ultrakurznarkotikum Methohexital*, Springer-Verlag, Berlin, **1972**.
[29] S. Ebel, *Synthetische Arzneimittel*, VCH, Weinheim, **1979**, p. 101.
[30] A. Kleemann, J. Engel, *Pharmazeutische Wirkstoffe*, Thieme Verlag, Stuttgart, **1982**, p. 578.
[31] W. Forth, D. Henschler, W. Rummel, *Pharmakologie und Toxikologie*, Bibliographisches Institut & F. A. Brockhaus, Mannheim, **1987**, p. 484.
[32] S. Ebel, H. J. Roth, *Lexikon der Pharmazie*, Thieme Verlag, Stuttgart, **1987**, p. 430.
[33] H.-P. Kuemmerle, G. Hitzenberger, K. H. Spitzy, *Klinische Pharmakologie, Band 6*, ecomed Verlagsgesellschaft, München, **1988**.
[34] Bundesverband der Pharmazeutischen Industrie, *Rote Liste 1996*, Editio Cantor Verlag, Aulendorf, **1996**, Nr. 65010.
[35] M. Prat, M. Moreno-Mañas, J. Ribas, *Tetrahedron* **1988**, 44, 7205.
[36] H. Brunner, J. Fürst, *Inorg. Chim. Acta* **1994**, 220, 63.
[37] W. Reißer, Dissertation, Universität Regensburg, **1997**.
[38] W. Reißer, Diplomarbeit, Universität Regensburg, **1994**.
[39] A. E. Senar, W. Valient, J. Wirth, *J. Org. Chem.* **1960**, *25*, 2001.
[40] G. P. Schiemenz, H. Kaack, *Liebigs Ann. Chem.* **1973**, 1480.
[41] H. Brunner, A. F. M. M. Rahman, *Chem. Ber.* **1984**, 117, 710.
[42] M. R. Whitnall, K. K. (M.) Hii, M. Thornton-Pett, T. P. Kee, *J. Organomet. Chem.* **1997**, *529*, 35.
[43] A. Terfort, H. Brunner, *J. Chem. Soc., Perkin Trans. 1*, **1996**, 1467.
[44] D. J. Berrisford, C. Bolm, K. B. Sharpless, *Angew. Chem.* **1995**, *107*, 1159; *Angew. Chem., Int. Ed. Engl.* **1995**, *34*, 1059.
[45] M. Janura, Dissertation, Universität Regensburg, **1997**.
[46] H. Brunner, A. Reimer, *Chem. Ber.* **1997**, *120*, 1495.
[47] J. V. Allen, G. J. Dawson, C. G. Frost, J. M. J. Williams, S. J. Coote, *Tetrahedron* **1994**, *50*, 799.
[48] M. Peer, J. C. de Jong, M. Kiefer, T. Langer, H. Rieck, H. Schell, P. Sennhenn, J. Sprinz, H. Steinhagen, B. Wiese, G. Helmchen, *Tetrahedron* **1996**, *52*, 7547.
[49] I. C. Baldwin, J. M. J. Williams, R. P. Beckett, *Tetrahedron: Asymmetry* **1995**, *6*, 1515.
[50] I. C. Baldwin, J. M. J. Williams, R. P. Beckett, *Tetrahedron: Asymmetry* **1995**, *6*, 679.
[51] A. E. Smith, *Acta Cryst.* **1965**, *18*, 331.
[52] T. Ohta, T. Hosokawa, S.-I. Murahashi, K. Miki, N. Kasai, *Organometallics* **1985**, *4*, 2080.
[53] J. W. Faller, C. Blankenship, B. Whitmore, S. Sena, *Inorg. Chem.* **1985**, *24*, 4483.
[54] H. Yang, M. A. Khan, K. M. Nicholas, *Organometallics* **1993**, *12*, 3485.
[55] P. Barbaro, P. S. Pregosin, R. Salzmann, A. Albinati, R. W. Kunz, *Organometallics* **1995**, *14*, 5160.
[56] K. J. Szabó, *Organometallics* **1996**, *15*, 1128.
[57] E. Stuckey, *Q. J. Pharm. Pharmacol.* **1942**, *15*, 370.
[58] R. J. Kuffner, M. T. Bush, L. J. Bircher, *J. Am. Chem. Soc.* **1957**, *79*, 1587.
[59] B. H. Bakker, N. P. E. Vermeulen, D. D. Breimer, A. van der Gen, *Recl. Trav. Chim. Pays-Bas* **1979**, *98*, 341.
[60] G. Tóth, S. Makleit, *Acta Chim. Acad. Sci. Hung.* **1981**, *107*, 139.

[97180]

Transition-Metal-Substituted Arsaalkenes, IV[◇]

Metalloarsaalkene [(η^5-C_5Me_5)$(CO)_2$FeAs=C$(NMe_2)_2$] as a Ligand in Carbonylchromium, -iron, and -nickel Complexes☆

Lothar Weber*, Matthias H. Scheffer, Hans-Georg Stammler, and Beate Neumann

Fakultät für Chemie der Universität Bielefeld,
Universitätsstr. 25, D-33615 Bielefeld, Germany

Received August 14, 1997

Keywords: Arsaalkenes / Arsenic ligands / Carbonyl complexes / Chromium / Iron

Reaction of equimolar amounts of the metalloarsaalkene [(η^5-C_5Me_5)$(CO)_2$FeAs=C$(NMe_2)_2$] (**1**) with the carbonyl complexes [$Ni(CO)_4$], [$Fe_2(CO)_9$], and [{(*Z*)-cyclooctene}$Cr(CO)_5$], respectively, affords the adducts [(η^5-C_5Me_5)$(CO)_2$FeAs{$M(CO)_n$}=C$(NMe_2)_2$] with [$M(CO)_n$] = [$Ni(CO)_3$] (**2**); [$Fe(CO)_4$] (**3**), and [$Cr(CO)_5$] (**4**). These feature η^1 coordination of the arsaalkene ligand via the arsenic atom. The molecular structures of the complexes **3** and **4** have been determined by X-ray diffraction analyses.

Introduction

Recently, we reported on the reactivity of the ferriophosphaalkene [(η^5-C_5Me_5)$(CO)_2$FeP=C$(NMe_2)_2$] (**I**) towards [$Ni(CO)_4$], [$Fe_2(CO)_9$], and [{(*Z*)-cyclooctene}$Cr(CO)_5$][2]. The results were surprising in as much as the expected η^1-complex **II** was only obtained with [$Ni(CO)_4$]. Reaction of the metallophosphaalkene with the pentacarbonylchromium complex gave rise to the formation of the thermolabile black [$Cr(CO)_5$] adduct **III**, which in solution underwent an intramolecular condensation to give complex **IV**[2][3]. Upon exposure to [$Fe_2(CO)_9$], compound **I** was converted into the η^2-phosphanylcarbene complex **V** (Scheme 1).

It was intriguing to find out whether the chemistry of the ferrioarsaalkene [(η^5-C_5Me_5)$(CO)_2$FeAs=C$(NMe_2)_2$] (**1**)[4] would mirror that of its phosphorus analogue, i.e. furnishing an arsanylcarbene complex upon treatment with [$Fe_2(CO)_9$] and a condensation product analogous to **III** when treated with [{(*Z*)-cyclooctene}$Cr(CO)_5$].

Results and Discussion

Treatment of **1** with an equimolar amount of tetracarbonylnickel in *n*-pentane in the temperature range −50 to 20°C afforded the tricarbonylnickel adduct **2** as a red-brown air- and moisture-sensitive powder. The dark-red crystalline tetracarbonyliron complex **3** resulted from the reaction of **1** with [$Fe_2(CO)_9$] in *n*-pentane. Product formation was accompanied by effervescence owing to the liberation of carbon monoxide. Black-red **4** precipitated when a mixture of **1** and [{(*Z*)-cyclooctene}$Cr(CO)_5$] in *n*-pentane was allowed to warm from −30°C to ambient temperature. Purification of the obtained carbonylmetal adducts was achieved by recrystallization at −30°C. In the IR spectrum (Nujol) of complex **2**, intense bands at $\tilde{\nu}$ = 2035, 1956, and 1908 cm^{-1} can be assigned to the stretching modes of the terminal carbonyl ligands of the [$Ni(CO)_3$] unit. These absorptions are shifted to lower wavenumbers when compared with the analogous metallophosphaalkene complex [(η^5-C_5Me_5)$(CO)_2$FeP{$Ni(CO)_3$}=C$(NMe_2)_2$] [$\tilde{\nu}$(NiCO) (KBr) = 2034, 1957, 1917 cm^{-1}][2].

The donor strengths of the ferrioarsaalkene **1** and its phosphorus analogue resemble that of the phosphonium ylide $(C_6H_{11})_3P{=}CH_2$ in its [$Ni(CO)_3$] complex [$\tilde{\nu}$(NiCO) (cyclohexane) = 2030, 1955, 1936 cm^{-1}][5]. The terminal carbonyl ligands of the [$Fe(CO)_2$] unit give rise to strong valence absorptions at 1977 and 1936 cm^{-1}. In **1**, the respective υ(CO) bands are observed at $\tilde{\nu}$ = 1970 and 1921 cm^{-1}.

The $^{13}C\{^1H\}$-NMR spectrum of **2** shows a singlet at δ = 215.24 for the methylene carbon atom, which is close to the corresponding resonance in **1** (δ = 214.77). A singlet at δ = 200.96 can be assigned to the carbonyl groups of the [$Ni(CO)_3$] unit in **2**. In the phosphorus analogue this absorption was reported at δ = 199.5. The chemical shifts of the carbonyl signals of the [$Fe(CO)_2$] group in **1** (δ = 221.39) and of its nickel complex **2** (δ = 220.96) also compare well. These data clearly demonstrate that the molecular structure of **2** resembles that of the phosphorus analogue, in which the ferriophosphaalkene is η^1-ligated to the [$Ni(CO)_3$] fragment.

The observance of six intense carbonyl bands in the IR spectrum of the tetracarbonyliron complex **3** ranging from 2000 to 1888 cm^{-1} is consistent with a lowering of the local symmetry of the point group C_{3v} for the [$Fe(CO)_4$] unit with an axial ligand. Comparison with the υ(CO) stretching vibrations in [$Fe(CO)_4$ (PMe_3)] [$\tilde{\nu}$(CO) = 2051, 1977, 1936 cm^{-1}][6] further underlines the pronounced donor capacity of the arsaalkene ligand.

[◇] Part III: Ref.[1].

 © WILEY-VCH Verlag GmbH, D-69451 Weinheim, 1998 1434−1948/98/0101−0055 $ 17.50+.50/0

Scheme 1

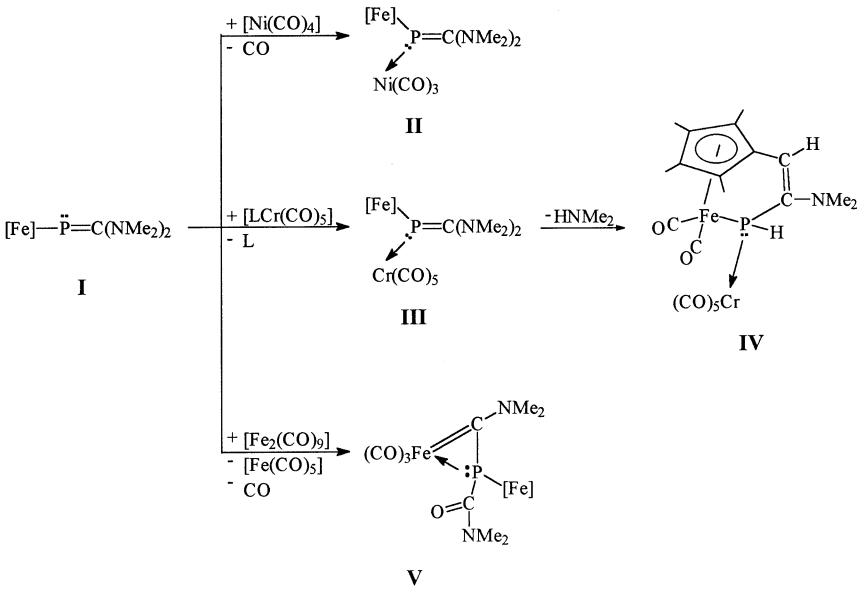

[Fe] = [η^5-(C_5Me_5)$(CO)_2$Fe]; L = (*Z*)-cyclooctene.

Scheme 2

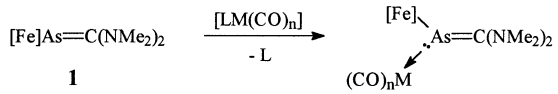

[Fe] = [η^5-(C_5Me_5)$(CO)_2$Fe]

Comp.	[M(CO)n]	L
2	[Ni(CO)3]	CO
3	[Fe(CO)4]	[Fe(CO)5]
4	[Cr(CO)5]	(Z)-C_8H_{14}

The $^{13}C\{^1H\}$-NMR spectrum of **3** shows a singlet at δ = 208.6 for the carbon atom of the As=C unit, while singlets at δ = 219.44 and 219.96 can be attributed to the carbonyl groups of the [Fe(CO)4] and the [$Fe(CO)_2$] fragments. These findings are in marked contrast to the reactivity of [(η^5-C_5Me_5)$(CO)_2$FeP=C$(NMe_2)_2$] towards [$Fe_2(CO)_9$], where phosphanylcarbene complex **V** was obtained as the sole phosphorus-containing product. It is conceivable that the formation of **V** is initiated by a tetracarbonyliron adduct analogous to **3**. A similar situation is encountered with the pentacarbonylchromium complex **4**, the phosphorus analogue of which, compound **III**, undergoes an intramolecular condensation to give **IV**.

Strong carbonyl absorptions at $\tilde{\nu}$ = 2029, 1911, 1891, and 1858 cm^{-1} in the IR spectrum of **4** correspond to the υ(CO) bands in **III** [$\tilde{\nu}$(CO) (KBr) = 2033, 1915, 1897, 1860 cm^{-1}]. In the $^{13}C\{^1H\}$-NMR spectrum of **4**, the carbon atoms of the [$Cr(CO)_5$] unit give rise to singlets at δ = 222.36 (CO_{eq}) and 227.05 (CO_{ax}). A singlet at δ = 220.42 can be attributed to the iron-ligated carbonyl groups. Owing to the removal of electron density from **1** by the [$Cr(CO)_5$] group, this resonance is slightly shifted to higher field (Δδ = 1 ppm). The singlet of the methylene carbon atom of **4** (δ = 214.33) is close to the chemical shift of the free ligand **1** (δ = 214.77).

X-ray Structural Analysis of 3

An ORTEP drawing of **3** is shown in Figure 1; selected bond lengths and angles are given in the caption. The analysis shows that η^1 coordination of the ferrioarsaalkene **1** to the [$Fe(CO)_4$] fragment results in severe distortion of the organoarsenic ligand. In contrast to free **1**, which exhibits a slightly elongated As−C double bond of 1.876(8) Å[4] (theoretical value in $HAs=CH_2$: 1.79 Å[8]), the bond length between the pyramidally configured arsenic atom (sum of angles = 331.53°) and the trigonal-planar atom C(13) (sum of angles = 359.0°) amounts to 1.990(3) Å. This is comparable to the As−C single bonds in the 1,2-dihydroarsete PhAs[−C(Ph)=C(Ph)CH_2−] [1.989(6) and 1.949(4) Å][9].

The iron−arsenic bond lengths Fe(1)−As(1) [2.4559(8) Å] and Fe(2)−As(1) [2.5089(11) Å] differ markedly and are longer than those in precursor **1** [Fe(1)−As(1) = 2.443(2) Å] and in [(η^5-C_5Me_5)$(CO)_2$Fe−As=C(OSiMe_3)(*t*Bu)] [2.407(1) Å].[7] The bond angle Fe(1)−As(1)−C(13) [110.39(8)°] in complex **3** is compressed compared to that in **1** [116.2(3)°]. The presence of an As−C single bond in **3** is consistent with a zwitterionic structure, As^--C^+, which is stabilized by coordination to the [$Fe(CO)_4$] unit and by π conjugation with the lone pairs of electrons on the nitrogen atoms. In keeping with this, relatively short carbon−nitrogen bonds C(13)−N(1) [1.341(3) Å] and C(13)−N(2) [1.345(3) Å] were found in this structure. Both nitrogen atoms are planar [sum of angles at N(1): 359.8°; N(2): 358.5°]. The planes defined by the atoms Fe(1), As(1), C(13) and C(13), N(1), N(2) enclose a dihedral angle of θ = 141.9°. In free **1**, this angle is more obtuse (θ = 155.0°). The arsaalkene ligand occupies an axial position in a distorted

Figure 1. Molecular structure of **3**[a]

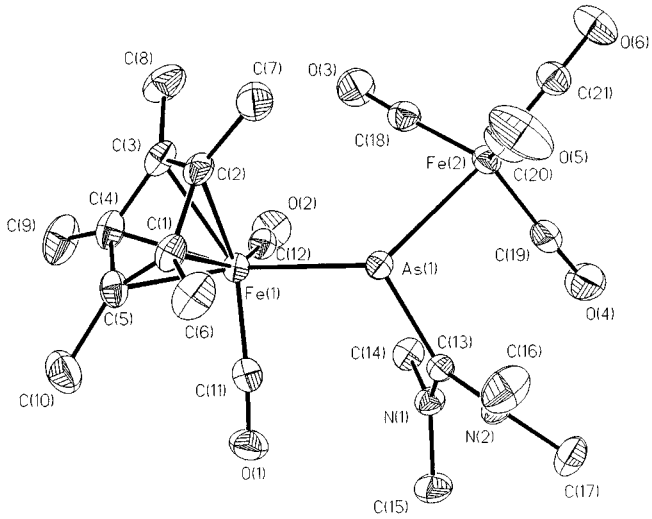

[a] Selected bond lengths [Å] and bond angles [°]: As(1)−C(13) 1.990(3), As(1)−Fe(1) 2.4559(8), As(1)−Fe(2) 2.5089(11), Fe(1)−C(11) 1.757(3), Fe(1)−C(12) 1.754(3), Fe(2)−C(18) 1.775(3), Fe(2)−C(19) 1.784(2), Fe(2)−C(20) 1.793(3), Fe(2)−C(21) 1.762(3), N(1)−C(13) 1.341(3), N(2)−C(13) 1.345(3); C(13)−As(1)−Fe(1) 110.39(8), C(13)−As(1)−Fe(2) 97.65(8), Fe(1)−As(1)−Fe(2) 123.49(3), C(12)−Fe(1)−C(11) 96.48(12), C(11)−Fe(1)−As(1) 87.60(6), C(12)−Fe(1)−As(1) 99.13(9), C(21)−Fe(2)−C(18) 91.40(14), C(21)−Fe(2)−C(19) 93.93(14), C(18)−Fe(2)−C(19) 119.08(14), C(20)−Fe(2)−C(21) 94.17(14), C(18)−Fe(2)−C(20) 123.2(2), C(19)−Fe(2)−C(20) 116.8(2), C(21)−Fe(2)−As(1) 171.93(10), C(18)−Fe(2)−As(1) 86.55(9), C(19)−Fe(2)−As(1) 93.89(10), C(20)−Fe(2)−As(1) 80.50(10), C(13)−N(1)−C(14) 122.3(2), C(13)−N(1)−C(15) 123.5(2), C(14)−N(1)−C(15) 114.0(2), C(13)−N(2)−C(16) 123.2(2), C(13)−N(2)−C(17) 122.2(2), C(16)−N(2)−C(17) 113.1(2), N(1)−C(13)−N(2) 117.3(2), N(1)−C(13)−As(1) 125.8(2), N(2)−C(13)−As(1) 116.9(2).

trigonal bipyramid. Fe(2) deviates by 0.0978 Å from the plane defined by the atoms C(18), C(19), and C(20) towards the opposite side of the arsenic atom. The bond angles between the vector Fe(2)−C(21) and carbon atoms of the equatorial CO groups range from 91.40(14) to 94.17(14)°, and the angle As(1)−Fe(2)−C(21) [171.93(10)°] clearly shows a deviation from linearity. A Newman projection along the vector Fe(2)−As(1) shows an almost eclipsed conformation with torsion angles C(18)−Fe(2)−As(1)−Fe(1) = 5.2° and C(19)−Fe(2)−As(1)−C(13) = 6.9° (Figure 2).

Figure 2. Newman projection of **3** with view along the Fe(2)−As(1) vector (the Cp* ring and the *N*-methyl groups are omitted for clarity)

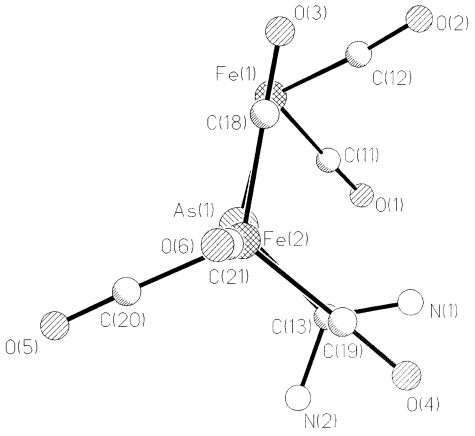

X-ray Structural Analysis of 4

An ORTEP drawing of **4** is shown in Figure 3; selected bond lengths and angles are given in the caption.

The molecule exhibits octahedral geometry. One coordination site is occupied by an η^1-ligated metalloarsaalkene. Again, the complexation of **1** to a carbonylmetal moiety causes a severe distortion of the organoarsenic compound. As in **4**, a single bond of 1.975(2) Å is found between the pyramidal arsenic atom (sum of angles 333.76°) and the planar carbon atom C(13) (sum of angles 359.9°). Both nitrogen atoms are planar (sum of angles 358.8 and 360.0°), and the dihedral angle between the planes defined by the atoms Fe(1), As(1), C(13)and C(13), N(1), N(2) is 142.2°.

Figure 3. Molecular structure of **4**[5]

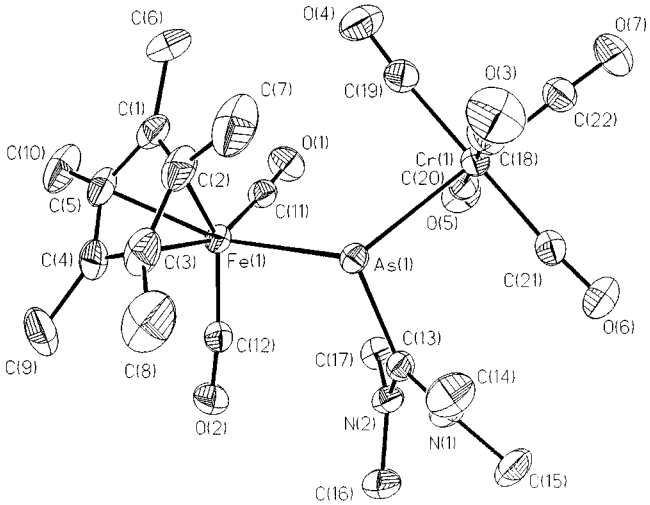

[a] Selected bond lengths [Å] and bond angles [°]: As(1)−C(13) 1.975(2), As(1)−Fe(1) 2.4589(5), As(1)−Cr(1) 2.6277(6), Fe(1)−C(11) 1.753(2), Fe(1)−C(12) 1.747(2), Cr(1)−C(CO)eq = 1.890(2) av., Cr(1)−C(22) 1.828(2), N(1)−C(13) 1.345(3), N(2)−C(13) 1.345(3); C(13)−As(1)−Fe(1) 111.81(6), C(13)−As(1)−Cr(1) 100.39(6), Fe(1)−As(1)−Cr(1) 121.56(2), C(12)−Fe(1)−C(11) 99.06(10), C(12)−Fe(1)−As(1) 91.61(7), C(11)−Fe(1)−As(1) 90.58(7), C(22)−Cr(1)−C(21) 88.72(10), C(22)−Cr(1)−C(20) 88.88(10), C(21)−Cr(1)−C(20) 89.55(10), C(22)−Cr(1)−C(19) 90.55(11), C(22)−Cr(1)−C(18) 91.81(11), C(22)−Cr(1)−As(1) 174.28(8), C(21)−Cr(1)−As(1) 90.52(7), C(20)−Cr(1)−As(1) 96.78(7), C(19)−Cr(1)−As(1) 90.39(7), C(18)−Cr(1)−As(1) 82.53(8), C(13)−N(1)−C(14) 123.2(2), C(13)−N(1)−C(15) 122.5(2), C(14)−N(1)−C(15) 113.1(2), C(13)−N(2)−C(17) 122.2(2), C(13)−N(2)−C(16) 123.7(2), C(17)−N(2)−C(16) 114.1(2), O(1)−C(11)−Fe(1) 176.4(2), O(2)−C(12)−Fe(1) 173.4(2), N(1)−C(13)−N(2) 116.7(2), N(1)−C(13)−As(1) 116.7(2), N(2)−C(13)−As(1) 126.5(2).

The bond length Fe(1)−As(1) [2.4589(5) Å] is comparable with that in **3**. The Cr−As bond [2.6277(6) Å] is shorter than the sum of the Cr^0−As covalent radii of Cr^0 [1.48 Å][10] and As [1.21 Å][11], but is considerably longer than Cr−As single bonds in related carbonylchromium complexes such as $[(\eta^5\text{-}C_5Me_5)(CO)_2FeAs\{Cr(CO)_5\}=C(SSiMe_3)_2]$ [2.524(1) Å][1], $[(\eta^5\text{-}C_5Me_5)(CO)_2\text{-}FeAs\{Cr(CO)_5\}=PMes^*]$ [2.494(1) Å][12], or [Mes*As=

$As\{Cr(CO)_5\}CH(SiMe_3)_2]$ [2.454(1) Å][13]. The As−Cr separation in **4** is similar to the Cr−As π-bond length in the trinuclear complex **5**[14].

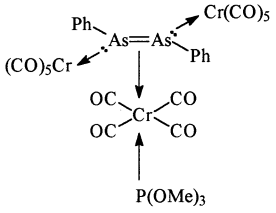

5

A view perpendicular to the $[Cr(CO)_4]$ plane indicates an almost staggered conformation with torsion angles C(19)−Cr(1)−As(1)−Fe(1) = 30.0° and C(21)−Cr(1)−As(1)−C(13) = 24.4° (Figure 4).

Figure 4. Newman projection of **4** with view along the Cr(1)−As(1) vector (the Cp* ring and the *N*-methyl groups are omitted for clarity)

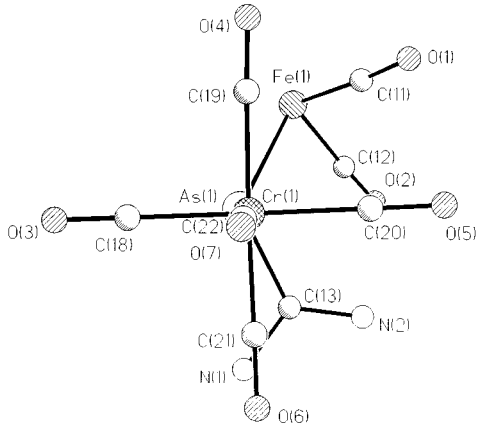

Due to steric hindrance, the ideal C_{4v} symmetry of the $[Cr(CO)_5]$ group is perturbed, as is evident from the angles C(20)−Cr(1)−As(1) [96.78(7)°], C(18)−Cr(1)−As(1) [82.53(8)°] and C(22)−Cr(1)−As(1) [174.28(8)°]. It is also remarkable that the bond length Cr(1)−C(22) [1.828(2) Å] in a *trans* position with respect to the electron-donating ligand is significantly shortened as compared to the other Cr−C(carbonyl) bond lengths [1.881(2)−1.897(3) Å].

To sum up, arsaalkene derivatives are usually thermally less stable and more reactive than their phosphorus analogues[15]. However, here the opposite is encountered. The metalloarsaalkene complexes **3** and **4** are isolable compounds and can be conveniently studied in solution, whereas the corresponding phosphorus compound $[(\eta^5\text{-}C_5Me_5)(CO)_2FeP\{Cr(CO)_5\}=C(NMe_2)_2]$ undergoes a facile condensation with C=C bond formation. The complex $[(\eta^5\text{-}C_5Me_5)(CO)_2FeP\{Fe(CO)_4\}=C(NMe_2)_2]$ could not even be detected spectroscopically in the reaction between the ferriophosphaalkene and $[Fe_2(CO)_9]$.

This work was financially supported by the *Fonds der Chemischen Industrie*, Frankfurt/Main, and the *BASF AG*, Ludwigshafen, which is gratefully acknowledged.

Experimental Section

All manipulations were performed under dry, oxygen-free nitrogen using standard Schlenk techniques. Solvents were dried by standard methods and freshly distilled under argon prior to use. − Infrared spectra were recorded with a Bruker FT-IR IFS 66 spectrometer. − ^1H- and ^{13}C-NMR spectra were recorded in C_6D_6 at 22°C using Bruker AM Advance DRX 500, Bruker AC 250 P, and Bruker AC 100 instruments. Standards: $SiMe_4$ ($^{1\,H,\,13}C$). − Elemental analyses were performed in the microanalytical laboratory of the University of Bielefeld. − The metalloarsaalkene $[(\eta^5\text{-}C_5Me_5)(CO)_2FeAs=C(NMe_2)_2]$ (**1**)[4], $[\{(Z)\text{-cyclooctene}\}Cr(CO)_5]$[16], and $[Fe_2(CO)_9]$[17] were synthesized according to literature procedures. $[Ni(CO)_4]$ was purchased commercially (Strem).

Synthesis of $[(\eta^5\text{-}C_5Me_5)(CO)_2FeAs\{Ni(CO)_3\}=C(NMe_2)_2]$ (**2**): A portion of $[Ni(CO)_4]$ (0.24 g, 1.42 mmol) was added to a chilled solution (−50°C) of $[(\eta^5\text{-}C_5Me_5)(CO)_2FeAs=C(NMe_2)_2]$ (**1**) (0.60 g, 1.42 mmol) in 50 ml of *n*-pentane. The stirred solution was allowed to warm to ambient temperature over a period of 1 h and then the solvent and volatile components were removed. The residue was redissolved in *n*-hexane (30 ml) and the resulting solution was filtered. The filtrate was concentrated to ca. 15 ml and stored overnight at −30°C to afford 0.52 g (65%) of **2** as a red-brown powder. − IR (Nujol, cm^{-1}): $\tilde{\nu}$ = 2035 [s, Ni(CO)], 1977 [s, Fe(CO)], 1956 [s, Ni(CO)], 1935 [s, Fe(CO)], 1908 [s, Ni(CO)]. − ^1H NMR: δ = 1.59 (s, 15 H, C_5Me_5), 2.71 (s, 12 H, NCH_3). − $^{13}C\{^1H\}$ NMR: δ = 9.61 [s, $C_5(CH_3)_5$], 43.99 (s, NCH_3), 95.04 [s, $C_5(CH_3)_5$], 200.96 (s, NiCO), 215.24 (s, As=C), 220.96 (s, FeCO).− $C_{20}H_{27}AsFeNiO_5$ (564.92): calcd. C 42.52, H 4.82, N 4.96; found C 41.89, H 4.85, N 4.64.

Synthesis of $[(\eta^5\text{-}C_5Me_5)(CO)_2FeAs\{Fe(CO)_4\}=C(NMe_2)_2]$ (**3**): Solid $[Fe_2(CO)_9]$ (0.3 g, 0.81 mmol) was added at 20°C to a stirred solution of 0.34 g (0.81 mmol) of **1** in 50 ml of *n*-pentane. The reaction proceeded with effervescence owing to liberation of CO. After stirring for 2 h at room temperature, the ^1H-NMR resonances of **1** had disappeared, and the solvent and volatiles were removed from the solution in vacuo. Drying at 10^{-3} Torr was maintained overnight. The black residue was then redissolved in 10 ml of diethyl ether, and the resulting solution was filtered. Storing at −28°C afforded black-red hexagonal crystals of **3** (0.28 g, 59%). − IR (Nujol, cm^{-1}): $\tilde{\nu}$ = 2000 [s, $Fe(CO)_4$], 1974 [s, $Fe(CO)_2$], 1937 [s, $Fe(CO)_2$], 1927 [m, $Fe(CO)_4$], 1911 [m, $Fe(CO)_4$], 1888 [s, $Fe(CO)_4$]. − ^1H NMR: δ = 1.58 (s, 15 H, C_5Me_5), 2.62 (s, 12 H, NCH_3). − $^{13}C\{^1H\}$ NMR: δ = 9.09 [s, $C_5(CH_3)_5$], 44.63 (s, NCH_3), 96.17 [s, $C_5(CH_3)_5$], 208.6 (s, As=C), 219.44 [s, $Fe(CO)_4$], 219.96 [s, $Fe(CO)_2$]. − $C_{21}H_{27}AsFe_2N_2O_6$ (590.07): calcd. C 42.75, H 4.61, N 4.75; found C 42.56, H 4.50, N 4.37.

Synthesis of $[(\eta^5\text{-}C_5Me_5)(CO)_2FeAs\{Cr(CO)_5\}=C(NMe_2)_2]$ (**4**): A solution of $[\{(Z)\text{-cyclooctene}\}Cr(CO)_5]$ (0.15 g, 0.50 mmol) in 20 ml of *n*-pentane was added dropwise to a cooled solution (−30°C) of **1** (0.21 g, 0.50 mmol) in 30 ml of *n*-pentane. Warming to room temperature led to the formation of a black precipitate. After stirring for 1 h, this was filtered off. The filter cake was washed with *n*-pentane (30 ml), dried in vacuo, and then redissolved in 5 ml of toluene. Upon storing at −30°C, black-red crystals of **4** separated (0.22 g, 71%).− IR (Nujol, cm^{-1}): $\tilde{\nu}$ = 2029 [s, Cr(CO)], 1964 [s, Fe(CO)], 1936 [s, Fe(CO)], 1911 [s, Cr(CO)], 1891 [s, Cr(CO)], 1858 [s, Cr(CO)]. − ^1H NMR: δ = 1.54 (s, 15 H, C_5Me_5), 2.69 (s, 12 H, NCH_3). − $^{13}C\{^1H\}$ NMR: δ = 9.16 [s, $C_5(CH_3)_5$], 44.78 (s, NCH_3), 95.61 [s, $C_5(CH_3)_5$], 214.33 (s, As=C), 220.42 [s, $Fe(CO)_2$], 222.36 [s, $Cr(CO)_{eq}$], 227.05 [s, $Cr(CO)_{ax}$]. − $C_{22}H_{27}AsCrFeN_2O_7$ (614.25): calcd. C 43.02, H 4.43, N 4.56; found C 42.46, H 4.55, N 4.28.

X-ray Structure Determination of [(η^5-C_5Me_5)(CO)$_2$FeAs{Fe(CO)$_4$}=C(NMe$_2$)$_2$} (**3**)[18]: Single crystals of **3** were grown from diethyl ether solution at −28°C. A black crystal of approximate dimensions 1.00 × 0.80 × 0.70 mm was examined on a Siemens P2(1) diffractometer using Mo-K_α radiation at 173 K. Crystal data and refinement details: Cell dimensions: a = 10.240(4), b = 14.922(6), c = 18.190(8) Å, β = 100.93(3)°, V = 2734(2) Å^3, Z = 4, $d_{calcd.}$ = 1.524 g cm^{-3}, μ = 2.302 mm^{-1}, space group $P2_1/n$, semiempirical absorption correction from Ψ scans, 8381 reflections collected, of which 7980 independent (R_{int} = 0.030), 6305 with $I > 2\sigma(I)$. Structure solution and refinement on F^2 with SHELXTL-PLUS and SHELXL-93. 331 parameters, anisotropic refinement for all non-hydrogen atoms, hydrogen atoms treated as riding groups with a 1.2-fold (1.5-fold for methyl groups) isotropic U value of the equivalent U value of the corresponding C atom. $R1$ = 0.059, $wR2$ = 0.097, $GooF(F^2)$ = 1.048, $w^{-1} = \sigma^2(F_o^2) + (0.0386 \cdot P)^2 + 2.32 \cdot P$, where $P = (F_o^2 + 2F_c^2)/3$, max./min. residual electron densities 0.4 and −0.5 eÅ^{-3}.

X-ray Structure Determination of [(η^5-C_5Me_5)(CO)$_2$FeAs{Cr(CO)$_5$}=C(NMe$_2$)$_2$} (**4**)[18]: Single crystals of **4** were grown from benzene at 4°C. A black crystal of approximate dimensions 1.00 × 0.70 × 0.30 mm was examined on a Siemens P2(1) diffractometer using Mo-K_α radiation at 173 K. Crystal data and refinement details: Cell dimensions: a = 9.131(2), b = 11.555(2), c = 14.009(2) Å, α = 100.680(10), β = 107.790(10), γ = 105.920(10)°, V = 1293.6(4) Å^3, Z = 2, $d_{calcd.}$ = 1.577 g cm^{-3}, μ = 2.292 mm^{-1}, space group $P\bar{1}$, semi-empirical absorption correction from Ψ scans, 7978 reflections collected, of which 7541 independent (R_{int} = 0.027), 6431 with $I > 2\sigma(I)$. Structure solution and refinement on F^2 with SHELXTL-PLUS and SHELXL-93. 317 parameters, anisotropic refinement for all non-hydrogen atoms, hydrogen atoms treated as riding groups with a 1.5-fold isotropic U value of the equivalent U value of the corresponding C atom. $R1$ = 0.042, $wR2$ = 0.084, $GooF(F^2)$ = 1.037, $w^{-1} = \sigma^2(F_o^2 + (0.0388 \cdot P)^2 + 0.72 \cdot P$, where $P = (F_o^2 + 2F_c^2)/3$, max./min. residual electron densities 0.5 and −0.4 eÅ^{-3}.

☆ Dedicated to Professor *Manfred Weidenbruch* on the occasion of his 60th birthday.

[1] L. Weber, S. Uthmann, B. Torwiehe, R. Kirchhoff, R. Boese, D. Bläser, *Organometallics* **1997**, *16*, 3188−3193.
[2] L. Weber, O. Kaminski, B. Quasdorff, H.-G. Stammler, B. Neumann, *J. Organomet. Chem.* **1997**, *529*, 329−341.
[3] L. Weber, B. Quasdorff, H.-G. Stammler, B. Neumann, *Chem. Eur. J.*, in press.
[4] L. Weber, O. Kaminski, H.-G. Stammler, B. Neumann, *Chem. Ber.* **1996**, *129*, 223−226.
[5] F. Heydenreich, A. Mollbach, G. Wilke, H. Dreeskamp, E. G. Hoffmann, G. Schroth, K. Seevogel, W. Stempfle, *Isr. J. Chem.* **1972**, *10*, 293−319.
[6] O. Kahn, M. Bigorgne, M. F. Koenig, A. Loutellier, *Spectrochim. Acta, Part A* **1974**, *30*, 1929−1938.
[7] L. Weber, G. Meine, R. Boese, D. Bungardt, *Z. Anorg. Allg. Chem.* **1987**, *549*, 73−86.
[8] K. D. Dobbs, J. E. Boggs, A. H. Cowley, *Chem. Phys. Lett.* **1987**, *141*, 372−375.
[9] W. Tumas, J. A. Suriano, R. L. Harlow, *Angew. Chem.* **1990**, *102*, 89−90; *Angew. Chem. Int. Ed. Engl.* **1990**, *29*, 75.
[10] F. A. Cotton, D. C. Richardson, *Inorg. Chem.* **1966**, *5*, 1851−1854.
[11] L. Pauling, *Grundlagen der Chemie*, Verlag Chemie, Weinheim **1973**, p. 170.
[12] L. Weber, D. Bungardt, R. Boese, *Chem. Ber.* **1988**, *121*, 1535−1539.
[13] A. H. Cowley, J. G. Lasch, N. C. Norman, M. Pakulski, *Angew. Chem.* **1983**, *95*, 1019; *Angew. Chem. Int. Ed. Engl.* **1983**, *22*, 978; *Angew. Chem. Suppl.* **1983**, 1493−1502.
[14] G. Huttner, I. Jibril, *Angew. Chem.* **1984**, *96*, 709−710; *Angew. Chem. Int. Ed. Engl.* **1984**, *23*, 740.
[15] Review: L. Weber, *Chem. Ber.* **1996**, *129*, 367−379.
[16] F.-W. Grevels, V. Skibbe, *J. Chem. Soc., Chem. Commun.* **1984**, 681−683.
[17] G. Brauer (Ed.), *Handbuch der präparativen anorganischen Chemie*, vol. 3, p. 1828f, F. Enke Verlag, Stuttgart, **1981**.
[18] Crystallographic data (excluding structure factors) for the structures reported in this paper have been deposited with the Cambridge Crystallographic Data Centre as supplementary publication no. CCDC-100809. Copies of the data can be obtained free of charge on application to CCDC, 12 Union Road, Cambridge CB2 1EZ, UK [fax (internat.): +44 (0)1223/336033; e-mail: deposit@ccdc.cam.ac.uk].

[97193]

Coordination Chemistry of Lipoic Acid and Related Compounds, 2[◇]

Models for the Inhibition of Dithiol-Containing Enzymes by Organoarsenic Compounds: Synthetic Routes and the Structure of [PhAs(HlipS$_2$)] (HlipS$_2^{2-}$ = Reduced Lipoic Acid)☆

Angelika von Döllen and Henry Strasdeit*

Fachbereich Chemie, Universität Oldenburg
P. O. Box 2503, D-26111 Oldenburg, Germany
Fax: (internat.) +49(0)441/798-3329
E-mail: strasdeit@chemie.uni-oldenburg.de

Received August 15, 1997

Keywords: Arsenic / Bioinorganic chemistry / Dihydrolipoic acid / Lipoic acid / S ligands

The arsenic(III) dithiolate [PhAs(HlipS$_2$)] (**1**, HlipS$_2^{2-}$ = reduced *rac*-lipoic acid) has been obtained via three different routes: (A) from (PhAsO)$_n$ and *rac*-dihydrolipoic acid, (B) from (AsPh)$_6$ and *rac*-lipoic acid, and (C) from PhAsO(OH)$_2$ and *rac*-dihydrolipoic acid. The latter method is also suitable for the preparation of [(4-NH$_2$C$_6$H$_4$)As(HlipS$_2$)] (**2**) from (4-NH$_2$C$_6$H$_4$)AsO(OH)$_2$. *rac*-Dihydrolipoic acid and Me$_2$AsO(OH) react to give [(Me$_2$As)$_2$(HlipS$_2$)] (**3**). These reactions indicate pathways by which mono- and diorganoarsenic compounds of various As oxidation states (I, III, and V) may inhibit enzymes that contain lipoic acid as a cofactor. X-ray structure analysis shows that **1** is a 2,4-disubstituted 1,3,2-dithiarsinane, i. e. a six-membered heterocycle. The phenyl group at the 2-position (As) adopts the axial orientation. (2*RS*,4*RS*)-**1**, which is the isomer found in the crystal, is thermodynamically more stable than the diastereomeric (2*SR*,4*RS*)-**1** by 4.3 ± 0.8 kJ/mol (25°C). In solution, the epimerization by inversion of configuration at the ψ-tetrahedrally coordinated As atom is faster than expected, with acid catalysis (COOH groups!) being a possible cause.

The toxicity of arsenic compounds has been known and used since classical antiquity[2]. In addition to its harmful effects on individuals, arsenic can cause severe public health problems, as a recent case of mass contamination has shown[3]. However, the underlying molecular mechanisms of action are still far from clear. It is assumed that the electronically soft species RAs^{2+} and R$_2$As$^+$ (R = e. g. alkyl, aryl) block biological sulphydryl groups; however, "the inhibition of thiol-enzymes by As^{III}, although widely quoted, is poorly understood"[4].

A probable biological target of arsenic(III) is enzyme-bound lipoic acid (α-lipoic acid, thioctic acid, 5-(1,2-dithiolan-3-yl)pentanoic acid, Hlip)[5][6]. This small biomolecule acts as a cofactor in some multienzyme complexes, namely the pyruvate dehydrogenase (and other α-keto acid dehydrogenases[7][8]) and the glycine cleavage system[9][10]. It has gained attention as a powerful biological antioxidant[11] and is approved in Germany for use as a therapeutic agent[12]. Lipoic acid can be reduced reversibly to dihydrolipoic acid (6,8-dimercaptooctanoic acid, Hlip(SH)$_2$; Scheme 1). This redox equilibrium is part of the enzymatic cycles[13].

It has repeatedly been demonstrated that lipoic acid-containing enzymes are strongly inhibited by As^{III} compounds such as arsenite[14] and organoarsoxanes (RAsO)$_n$[15]. However, only a few relevant low-molecular models have been examined; these were obtained from As^{III} starting materials in all cases[16][17][18]. In the present paper we show that such models are also accessible from compounds of *mono*- and *penta*valent arsenic related to the antimicrobial arsenicals, of which "Salvarsan" is the most prominent example[19]. In addition we report the crystal and molecular structure of [PhAs(HlipS$_2$)] (**1**), which to our knowledge is the first X-ray structure of an organoarsenic complex of a naturally occuring thiolate. A brief report on some of these results has appeared as a conference abstract[20].

Scheme 1

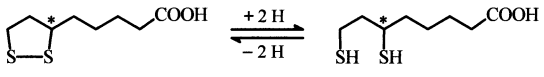

Hlip Hlip(SH)$_2$

Reactions

In the human body, inorganic As^V is partly methylated to MeAsO(OH)$_2$ and Me$_2$AsO(OH), and it has been suggested that the intermediate formation of As^{III} is involved in the biomethylation pathway[21]. The accompanying redox processes are probably coupled to biological thiol/disulphide equilibria. A redox reaction also occurs in the metabolism of the aryl-As^I compound Salvarsan (see below) and results in an As^{III} species, which is thought to be the active form of this formerly used medicinal drug[22]. This

[◇] Part 1: Ref.[1].

 © WILEY-VCH Verlag GmbH, D-69451 Weinheim, 1998 1434−1948/98/0101−0061 $ 17.50+.50/0

prompted us to investigate the redox behaviour of some relevant organoarsenic compounds towards the dithiol dihydrolipoic acid [Hlip$(SH)_2$] and its oxidation product, the cyclic disulphide lipoic acid (Hlip, see Scheme 1).

In tetrahydrofuran (THF), phenylarsonic acid is smoothly reduced by Hlip$(SH)_2$ with the formation of the As^{III} compound [PhAs(HlipS$_2$)] (**1**) and lipoic acid (Eq. 1, method C under Experimental).

$$PhAsO(OH)_2 + 2\ Hlip(SH)_2 \xrightarrow[\text{room temp.}]{\text{THF}} \underset{\mathbf{1}}{[PhAs(HlipS_2)]} + Hlip + 3\ H_2O \quad (1)$$

1 is a disubstituted 1,3,2-dithiarsinane (Scheme 2). Its constitution was deduced from NMR data by Dill et al., who obtained **1** from $PhAsCl_2$ and Hlip$(SH)_2$ in solution but did not isolate the product[18]. The final proof of the structure of **1** comes from our crystal structure determination described below. Eq. 1 includes two reaction steps, namely the reduction of As^V and the subsequent complexation of the As^{III} formed. The second step determines the result of the overall reaction. Therefore, even with the appropriate ratio of phenylarsonic acid to Hlip$(SH)_2$, no phenylarsoxane is obtained (Eq. 2).

$$PhAsO(OH)_2 + Hlip(SH)_2 \not\longrightarrow {}^1/_n\,(PhAsO)_n + Hlip + 2\ H_2O \quad (2)$$

Instead, **1** is formed, and 50% of the $PhAsO(OH)_2$ remains unreacted.

Scheme 2

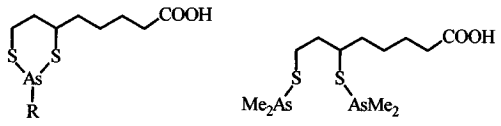

1: R = phenyl
2: R = 4-aminophenyl

3

Starting from phenylarsoxane, there is an alternative and more favourable route to **1** (Eq. 3, method A).

$${}^1/_n\,(PhAsO)_n + Hlip(SH)_2 \xrightarrow[\text{room temp.}]{\text{THF}} \underset{\mathbf{1}}{[PhAs(HlipS_2)]} + H_2O \quad (3)$$

As **1** is the only solid product of this reaction, separation problems, as in the case of method C (Eq. 1; similar solubilities of **1** and Hlip), are avoided. Triphenylarsane was also tested as a starting material. However, no reaction with dihydrolipoic acid was observed. This behaviour distinguishes $AsPh_3$ from $HgPh_2$, which under the same conditions yields the trinuclear complex $[Hg(PhHg)_2(HlipS_2)_2]$[23].

p-Aminophenylarsonic acid [arsanilic acid, (4-$NH_2C_6H_4$)$AsO(OH)_2$] was one of the first arsenicals to be used successfully. Ehrlich has already inferred from biological observations that this compound must be reduced in organisms in order to become active against pathogens[19b]. We have shown that (4-$NH_2C_6H_4$)$AsO(OH)_2$ is reduced by Hlip$(SH)_2$. The reaction, which was carried out in methanol, is analogous to that of $PhAsO(OH)_2$ (Eq. 1) and yields the crystalline As^{III} compound [(4-$NH_2C_6H_4$)As(HlipS$_2$)] (**2**). Spectroscopic data reveal that **2** is *not* zwitterionic, at least in the solid state and in $CDCl_3$, and that it has the same constitution as **1** (Scheme 2). The formation of **2** sheds light on the possible biochemical pathway of arsanilic acid and similar As^V arsenicals. It shows the facile reduction by a biological dithiol as well as the blocking of the coenzyme lipoic acid, which may be the cause or one of the causes of the antimicrobial activity.

The As^I arsenical Salvarsan is an aromatic ring-substituted (3-NH_2, 4-OH) derivative of hexaphenylcyclohexaarsane. While the parent compound is well-defined and forms cyclic $(AsPh)_6$ molecules[24], Salvarsan appears as mixtures of partly oxidized oligomeric and polymeric chains with strongly varying properties[25]. Both compounds contain As−As bonds. In Salvarsan these bonds are oxidatively cleaved under physiological conditions (see above). We used $(AsPh)_6$ as a model for Salvarsan to test whether lipoic acid acts as an oxidizing agent towards aryl-As^I and can accomplish the As−As bond cleavage. No reaction occurred in THF, toluene or diethylene glycol dimethyl ether at temperatures up to the boiling point of the respective solvent. However, when $(AsPh)_6$ and lipoic acid were melted together, compound **1** was formed quantitatively (Eq. 4, method B).

$${}^1/_6\,(AsPh)_6 + Hlip \xrightarrow[130°C]{\text{melt}} \underset{\mathbf{1}}{[PhAs(HlipS_2)]} \quad (4)$$

The need for quite drastic and thus nonphysiological conditions may be rationalized in terms of the different structures of $(AsPh)_6$ and Salvarsan, i.e. cyclic vs. open-chain. Bearing this difference in mind one can expect that in vivo, Salvarsan, after oxidation by a suitable biological disulphide (not necessarily lipoic acid), is able to inhibit lipoic acid dependent enzymes.

Finally, we studied the reaction of dihydrolipoic acid with a *di*organoarsenic(V) compound, namely dimethylarsenic acid [cacodylic acid, $Me_2AsO(OH)$]. Again reduction of As^V to As^{III}, accompanied by As^{III} complexation was observed (Eq. 5).

$$2\ Me_2AsO(OH) + 3\ Hlip(SH)_2 \xrightarrow[\text{room temp.}]{\text{THF}} \underset{\mathbf{3}}{[(Me_2As)_2(HlipS_2)]} + 2\ Hlip + 4\ H_2O \quad (5)$$

Attempted separation of $[(Me_2As)_2(HlipS_2)]$ (**3**, see Scheme 2) from the second nonvolatile product lipoic acid failed, although **3** was unambiguously identified by spectroscopic methods (^{13}C NMR, CI-MS) in the reaction mixture. The 1:2 molar ratio of **3** and Hlip expected from Eq. 5 was confirmed by ^1H-NMR spectroscopy. No unreacted starting material or other products were found. Pure **3** is accessible via reaction of Me_2AsCl with Hlip$(SH)_2$ in the presence of pyridine as a base[16]. Its formation from $Me_2AsO(OH)$ is, however, more relevant to bioinorganic and toxicological questions, because dimethylarsenic acid is a common biomethylation product of arsenate and arsenite[21]. Moreover, this compound is also a herbicide and a chemical weapon ("Agent Blue")[26].

We have shown that mono- and diorganoarsenic(V) compounds of the type $RAsO(OH)_2$ and $R_2AsO(OH)$, respectively, are easily reduced by dihydrolipoic acid. The logical extension of this, the reduction of R_3AsO by $Hlip(SH)_2$, has been studied by others for R = Me[27]. The only products observed were Me_3As and lipoic acid.

Crystal Structure of 1

Crystals of **1** consist of [PhAs(HlipS_2)] molecules (or complexes, to emphasize the semi*metallic* character of arsenic; see Figure 1). The molecules are arranged as symmetric hydrogen-bonded dimers. Each dimer is situated on a crystallographic centre of inversion and has a central eight-membered ring formed by the two carboxylic groups. The O···O distances within the two hydrogen bonds of the ring are 2.657 Å [O(1)···O(2′); 2 − *x*, 2 − *y*, 2 − *z*]. This motif is very common and has been found for the majority of monofunctional carboxylic acids in the crystalline state[28].

Figure 1. View of [PhAs(HlipS_2)] (**1**) in the solid state; non-hydrogen atoms are shown as thermal ellipsoids with 50% probability[a]

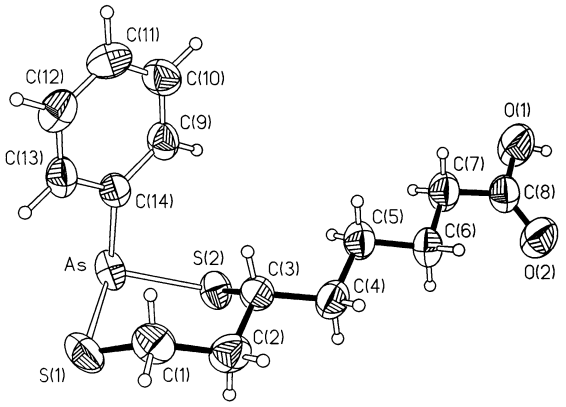

[a] Selected bond lengths [Å] and angles [°]: As−S(1) 2.230(1), As−S(2) 2.227(1), As−C(14) 1.964(4), S(1)−C(1) 1.817(5), S(2)−C(3) 1.848(4), C(1)−C(2) 1.530(6), C(2)−C(3) 1.521(5), C(3)−C(4) 1.529(6), C(4)−C(5) 1.515(6), C(5)−C(6) 1.510(6), C(6)−C(7) 1.509(6), C(7)−C(8) 1.485(6), O(1)−C(8) 1.297(5), O(2)−C(8) 1.208(5), S(1)−As−S(2) 99.41(5), S(1)−As−C(14) 99.49(11), S(2)−As−C(14) 100.51(11), As−S(1)−C(1) 102.55(14), As−S(2)−C(3) 104.56(13), S(1)−C(1)−C(2) 117.1(3), C(1)−C(2)−C(3) 115.9(3), S(2)−C(3)−C(2) 113.0(3), S(2)−C(3)−C(4) 106.5(3), C(2)−C(3)−C(4) 112.2(3), C(3)−C(4)−C(5) 113.9(3), C(4)−C(5)−C(6) 115.9(3), C(5)−C(6)−C(7) 111.1(4), C(6)−C(7)−C(8) 117.0(4), O(1)−C(8)−O(2) 122.0(4), O(1)−C(8)−C(7) 114.2(4), O(2)−C(8)−C(7) 123.8(4).

The [PhAs(HlipS_2)] molecule is a 1,3,2-dithiarsinane disubstituted at the 2-position (As) and the 4-position [C(3)], i.e. it is a 2-arsa-1,3-dithiacyclohexane derivative. The AsS_2C_3 six-membered ring adopts a chair conformation. While the 4-substituent has an equatorial orientation, the phenyl group is axially orientated. This axial conformational preference of a substituent at the As atom is not unexpected. It has been observed before in related molecules such as 2-phenyl-1,3,2-dithiarsinane (solution)[29] and 5-*tert*-butyl-2-phenyl-1,3,2-dithiaphosphinane (solution and solid state)[30] and seems to be a more general phenomenon. The consequences of the alternative equatorial conformation can be easily deduced from Figure 1. Changing the positions of the stereochemically active lone pair and the phenyl group at As [without rotation about the As−C(14) bond!] would cause severe repulsion between the phenyl *ortho*-H atoms and the four lone electron pairs at S(1) and S(2). Rotation about the As−C(14) bond would reduce this unfavourable energy contribution, but on the other hand it would move one of the *ortho*-H atoms towards the lone electron pair at As.

In the conformation of **1** that is actually adopted, *cis*-axial interactions probably occur between the phenyl group and the axial H atoms at C(1) and C(3). As suggested for substituted 1,3,2-dithiaphosphinanes and their dioxo analogues[30b][31], these van der Waals forces may be weakly attractive. In addition, hyperconjugative interactions in the S_2AsPh moiety, similar to those accepted as a basis for the anomeric effect[32], may contribute to the observed axial orientation of the phenyl group in **1**.

There are no intermolecular contacts to As smaller than the sum of the van der Waals radii. Thus the coordination number of As is three, and the geometry around this atom is pyramidal (ψ-tetrahedral). At least one related compound is known, in which, in contrast to **1**, the coordination sphere of the central atom is expanded by secondary As−S bonds. This compound is $[PhAs\{S_2P(OiPr)_2\}_2]$[33]. In **1** the metrical data of the C(14)AsS(1)S(2) part are unexceptional and fall within the ranges found for four other compounds having aryl-$As^{III}S_2$ moieties[34]: As−S 2.23−2.28, As−C 1.95−1.99 Å; S−As−S 92.7−102.1, S−As−C 94.0−101.3°. The As−S bond lengths in **1** lie marginally below the single-bond value calculated from the covalent radii and corrected for the electronegativity difference[35a].

Two chiral centres are present in [PhAs(HlipS_2)]: the one at C(3) belongs to the reduced lipoic acid and a second one at the arsenic atom. According to the numbering scheme for the 1,3,2-dithiarsinane ring, these are the 2- and the 4-position. The structure determination was performed on a crystal of the (2*RS*,4*RS*) racemate. Figure 1 shows the (2*R*,4*R*) enantiomer.

Stereoisomerism of 1

The crystalline products obtained by methods A and C (see Experimental Section) are (2*RS*,4*RS*)-**1** as found by X-ray structure analysis (see above) and spectroscopic comparison. A freshly prepared solution in $CDCl_3$ shows the expected number of 12 signals in the ^{13}C-NMR spectrum. On standing at room temp. for several days, the diastereomer (2*SR*,4*RS*)-**1** gradually forms in the solution. It gives rise to additional, weak signals in the ^1H- and ^{13}C-NMR spectra. Signals at the same positions are observed for the product prepared by method B, i.e. by melting together *rac*-lipoic acid and $(AsPh)_6$ at 130°C. A quantitative evaluation of the NMR spectra of this product gives a content of the minor isomer (2*SR*,4*RS*)-**1** of ca. 16%.

The establishment of equilibrium between the two isomers proceeds much faster in [D_4]methanol than in $CDCl_3$. Starting from pure (2*RS*,4*RS*)-**1**, it is about 90% complete after one day, and after 7 days the final ratio of ca. 85:15 is

attained. This ratio corresponds to $\Delta G = 4.3 \pm 0.8$ kJ/mol at 25°C for the equilibrium shown in Eq. 6.

$$(2RS,4RS)\text{-}\mathbf{1} \rightleftharpoons (2SR,4RS)\text{-}\mathbf{1} \qquad (6)$$

In other words, the (2*RS*,4*RS*) isomer, whose X-ray structure has been determined, is the thermodynamically more stable one. In contrast to **1**, solutions of the compound **2** in $CDCl_3$ exhibit NMR spectra compatible with the pure (2*SR*,4*RS*) isomer. Here further experiments were hampered by the low solubility.

Scheme 3

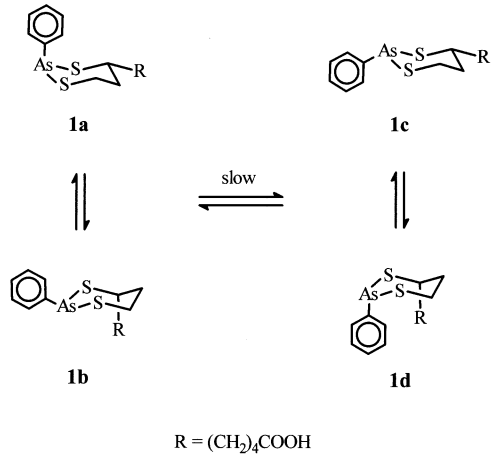

1a **1c** **1b** **1d**

The equilibrium of Eq. 6 is shown in more detail in Scheme 3. **1a** and **1b** are conformational isomers of (2*R*,4*R*)-**1**, while **1c** and **1d** correspond to (2*S*,4*R*)-**1**. The isomer **1a** is shown in Figure 1. (2*S*,4*S*)-**1** and (2*R*,4*S*)-**1** are not considered because they would merely give a mirror image of Scheme 3. In addition to the slow epimerization by inversion of configuration at the arsenic atom, two chair-chair equilibria (**1a/1b** and **1c/1d**) are included. As demonstrated above, (2*R*,4*R*)-**1** is thermodynamically favoured. Under the plausible assumptions that (i) conformations other than chair may be neglected and (ii) the $(CH_2)_4COOH$ substituent prefers the equatorial orientation, it can be concluded that **1a**, together with equal amounts of its enantiomeric form, is the major stereoisomer in solution. Thus, the conjecture that **1c** is most likely the major isomer[18] could not be confirmed.

From the early phase of the transformation of (2*RS*,4*RS*)-**1** into (2*SR*,4*RS*)-**1** in $CDCl_3$ the activation energy can be roughly estimated[35b] at ca. 110 kJ/mol at 25°C if the reaction is assumed to be monomolecular. Mislow and coworkers have found a correlation between the barriers to pyramidal inversion at arsenic and at phosphorus[36]. From this correlation and the activation energy reported for 5-*tert*-butyl-2-phenyl-1,3,2-dithiaphosphinane[30b], a $\Delta G^{\neq}$ value near 180 kJ/mol is expected for **1**. The large discrepancy of ca. 70 kJ/mol can only be accounted for by a mechanism other than a simple pyramidal inversion. Although we did not investigate this problem further, one can hypothesize that acid catalysis by the carboxyl group of **1** may be the determining step. The epimerization would then be self-catalyzed. A possible reaction mechanism involves cleavage of one of the As−S bonds accompanied by protonation of the S atom and $As-O_2C$ bond formation, rotation about the remaining As−S bond, and re-establishment of the first As−S bond by elimination of −COOH. Acid catalysis is consistent with the observed acceleration of the epimerization in [D_4]methanol. While in $CDCl_3$ hydrogen-bonded dimers like those observed in the solid state can be expected, in protic solvents monomers having more easily accessible protons should prevail.

Financial support from the *Deutsche Forschungsgemeinschaft* and the *Fonds der Chemischen Industrie* is gratefully acknowledged. We thank *ASTA Medica AG* for generous donations of *rac*-lipoic acid, Dr. *H. J. Tritschler* for providing us with copies of refs.[11][38a], and Mr. *W. Saak* for helpful discussions and for collecting the diffraction data.

Experimental Section

General: Racemic lipoic acid was obtained as a gift from ASTA Medica AG. Dihydrolipoic acid was prepared by $NaBH_4$ reduction of lipoic acid[37]. The identity of the product and its purity (≥99% based on GC) were checked by high-resolution ^{13}C-NMR spectroscopy (125.8 MHz, $CDCl_3$): δ = 22.03 (C-8), 24.02 (C-3), 26.17 (C-4), 33.67 (C-2), 38.37 (C-5), 39.03 (C-6), 42.48 (C-7), 179.8 (C-1)[38]. Dihydrolipoic acid is a colourless oil which should be stored under nitrogen. Hexaphenylcyclohexaarsane was prepared and purified according to the method described in ref.[39]. All other chemicals were purchased from commercial sources and used without further purification. The solvents were reagent grade. The compounds **1**−**3** were prepared and handled in a glove box under an atmosphere of dry nitrogen. − IR: FT-IR spectrometer Bio-Rad FTS 7PC. − ^{1}H and ^{13}C{^{1}H} NMR: Bruker AM-300, Bruker ARX-500, chemical shifts relative to TMS, solvent signal as internal reference in the ^{13}C-NMR spectra ($CDCl_3$: δ_c = 77.00, [D_4]methanol: δ_c = 49.00). Asterisked signals belong to the minor isomer (2*SR*,4*RS*)-**1**. − MS: Finnigan MAT 212, Finnigan MAT 95. − Elemental analyses: Mikroanalytisches Laboratorium Beller, D-37004 Göttingen, Germany. − *Caution!* Arsenic compounds are highly toxic, and some of them are recognized as human carcinogens. They should therefore be handled with care to avoid exposure.

5-(2-Phenyl-1,3,2-dithiarsinan-4-yl)pentanoic Acid (**1**): *Method A*: 336 mg (2.00 mmol) of phenylarsoxane was added to a solution of 416 mg (2.00 mmol) of *rac*-dihydrolipoic acid in 40 ml of tetrahydrofuran. The solution was stirred for 24 h. Subsequently its volume was reduced in vacuo until an oil remained. From this residue colourless crystals of **1** separated over a two-week period at room temp. The crystals were collected on a glass filter, washed with a small amount of toluene and dried in vacuo. A second crop of crystals was obtained from the filtrate after evaporation. Total yield: 0.43 g (60%), m.p. 97°C. − IR (KBr): $\tilde{\nu}$= 3042 cm^{-1} (w, aryl-CH), 2942 (w, alkyl-CH), 2907 (w, alkyl-CH), 1707 (s, C=O), 1429 (m), 1250 (m), 1206 (m), 745 (m, phenyl group), 370 (m, AsS[40]). − ^{1}H NMR (300 MHz, $CDCl_3$): δ = 1.37−1.66 (m, 6 H), 1.89 (m, 2 H), 2.34 (t, 2 H, CH_2COOH), 2.65 (m, 1 H), 2.83 (m, 2 H), 7.36 (m, 1 H, Ph-*para*), 7.46 ("t", 2 H, Ph-*meta*), 7.87 ("d", 2 H, Ph-*ortho*), 11.5 (br., 1 H, COOH). − ^{1}H NMR (500 MHz, [D_4]methanol; after keeping the solution at room temp. for ca. 7 d): δ = 1.47 (m), 1.58 (m), 1.71 (m)*, 1.82−1.95 (m), 2.21 (m)*, 2.28 (t), 2.66 (m), 2.85 (m), 3.04−3.18 (m)*, 7.40 (m), 7.44 (m)*, 7.50 ("t"), 7.82 (m)*, 7.88 ("d"). − ^{13}C NMR (75.5 MHz, $CDCl_3$): δ = 24.20, 25.07, 27.85, 33.80, 35.73, 38.75, 39.76, 128.7 (Ph-*para*), 129.2, 132.1, 139.2 (Ph-*ipso*), 179.7 (C=O). − ^{13}C NMR (125.8

MHz, [D_4]methanol; after keeping the solution at room temp. for ca. 7 d): δ = 25.58, 25.75*, 26.19, 26.98*, 28.77, 29.85*, 34.77, 36.99, 37.32*, 39.33*, 39.87, 41.01, 46.04*, 129.9, 130.3, 131.4*, 133.1, 133.6*, 140.2*, 140.5, 177.3, 177.4*. − MS (CI, isobutane); *m/z* (%): 359 (100) [MH^+], 341 (14) [$MH^+ - H_2O$], 207 (7) [$MH^+ - C_6H_5As$], 189 (35) [$MH^+ - H_2O - C_6H_5As$]. − $C_{14}H_{19}AsO_2S_2$ (358.4): calcd. C 46.92, H 5.34, As 20.91, S 17.90; found C 47.10, H 5.43, As 20.85, S 18.00.

Method B: An intimate mixture of *rac*-lipoic acid and hexaphenylcyclohexaarsane in a 6:1 molar ratio was heated to 130°C within 1 h. The mixture started melting at ca. 70°C. The clear, initially yellowish melt was kept at 130°C for 3.5 h before it was allowed to cool down to room temp. and to solidify. The reaction was quantitative and yielded a colourless product. − ^{13}C NMR (75.5 MHz, $CDCl_3$): δ = 24.18, 24.28*, 25.04, 25.78*, 27.83, 29.29*, 33.82, 35.71, 36.11*, 38.19*, 38.72, 39.74, 44.84*, 128.7, 128.8*, 129.1, 130.3*, 132.0, 132.6*, 139.2, 179.9.

Method C: *rac*-Dihydrolipoic acid and phenylarsonic acid in a 2:1 molar ratio were dissolved in tetrahydrofuran. The solution turned light yellow due to the formation of lipoic acid. After stirring for 24 h, the solvent was removed in vacuo. Colourless crystals of **1** separated from the remaining oil within 2 weeks. Their IR spectrum was identical with that of the product prepared by method A.

5-[2-(4-Aminophenyl)-1,3,2-dithiarsinan-4-yl]pentanoic Acid (**2**): 434 mg (2.00 mmol) of *p*-aminophenylarsonic acid was added to a stirred solution of 833 mg (4.00 mmol) of *rac*-dihydrolipoic acid in 60 ml of methanol. The arsenic compound slowly dissolved, and after a few hours the yellow colour of lipoic acid emerged. After stirring for 24 h, removal of the solvent in vacuo resulted in the crystallization of small colourless needles of **2**. The product was isolated on a glass filter, washed with a small amount of chloroform and dried in vacuo. Yield 0.53 g (71%), m.p. 122°C. − IR (KBr): $\tilde{\nu}$= 3376 cm^{-1} (m, NH_2), 3302 (w, NH_2), 2932 (w, alkyl-CH), 2868 (w, alkyl-CH), 1707 (s, C=O), 1591 (m), 1495 (m), 1265 (m), 1169 (m), 1074 (m), 818 (m, aryl group), 511 (m), 374 (m, AsS[40]). − ^{1}H NMR (300 MHz, $CDCl_3$): δ = 1.39−1.77 (m, 7 H), 2.12 (m, 1 H), 2.34 (t, 2 H, CH_2COOH), 3.00−3.19 (m, 3 H), 5.6 (br., 3 H, NH_2 and COOH), 6.67 ("d", 2 H, aromatic H), 7.59 ("d", 2 H, aromatic H). − ^{13}C NMR (75.5 MHz, $CDCl_3$): δ = 24.34, 25.71, 30.11, 33.70, 36.54, 38.50, 45.37, 115.1 (H_2NC*C*), 125.5 (AsC), 134.3 (AsC*C*), 148.7 (H_2NC), 178.9 (C=O). − MS (EI, 80 eV); *m/z* (%): 373 (1.4) [M^+], 93 (100) [$C_6H_7N^+$], 66 (50) [$C_5H_6^+$], 65 (37) [$C_5H_5^+$]. − $C_{14}H_{20}AsNO_2S_2$ (373.4): calcd. C 45.04, H 5.40, As 20.07, N 3.75, S 17.18; found C 45.14, H 5.52, As 19.56, N 3.75, S 17.44.

Formation of 6,8-Bis[(dimethylarsanyl)thio]octanoic Acid (**3**) *from Dimethylarsinic Acid and rac-Dihydrolipoic Acid:* 138 mg (1.00 mmol) of $Me_2AsO(OH)$ was added to a stirred solution of 312 mg (1.50 mmol) of *rac*-dihydrolipoic acid in 10 ml of tetrahydrofuran. After stirring overnight, the solvent was evaporated in vacuo. To remove tetrahydrofuran and water completely, the remaining oil was dissolved in dichloromethane, and the solvent was evaporated again. After drying in vacuo, a yellow oil was obtained, which consisted of **3** and lipoic acid in a 1:2 molar ratio. − ^{1}H NMR (500 MHz, $CDCl_3$): The intensities of the signals at δ = 1.24 ($AsCH_3$) and 2.27 (CH_2COOH from **3** and from lipoic acid) were used to determine the product ratio. − ^{13}C NMR (125.8 MHz, $CDCl_3$), **3**: δ = 13.88 ($AsCH_3$), 14.01 ($AsCH_3$), 24.09, 26.10, 28.78, 33.67, 37.04, 40.14, 45.30, 179.7 (C=O). The remaining signals were those of lipoic acid; no signals of unreacted dihydrolipoic acid were found (cf. ref.[38]). − MS (CI, isobutane); *m/z* (%): 416 (32) [M^+], 312 (100) [$MH^+ - As(CH_3)_2$].

X-ray Crystal Structure Analysis of **1**: A suitable single crystal of **1** was obtained from the reaction of *rac*-dihydrolipoic acid with phenylarsonic acid (similar to method C described above). $C_{14}H_{19}AsO_2S_2$, M = 358.36, colourless crystal, crystal size 0.42 × 0.29 × 0.10 mm, triclinic, space group $P\bar{1}$, a = 7.240(1), b = 8.526(1), c = 14.193(2) Å, α = 82.03(1), β = 82.84(1), γ = 67.72(1)°, V = 800.4(2) Å^3, Z = 2, $\rho_{calcd.}$ = 1.487 gcm^{-3}, $F(000)$ = 368, $\mu(MoK_\alpha)$ = 2.38 mm^{-1}. 3983 reflections were measured at 23°C on a Siemens/STOE AED2 diffractometer using graphite-monochromated MoK_α radiation. 5° ≤ 2Θ ≤ 50°, 0 ≤ h ≤ 8, −9 ≤ k ≤ 10, −16 ≤ l ≤ 16, ω/2Θ scans, empirical absorption correction, T_{min} = 0.1803, T_{max} = 0.2880. Structure solution by direct methods[41], refinement on F^2 values (full-matrix least-squares)[42], 2819 independent reflections (R_{int} = 0.0196) of which all were used in the final refinement, 173 parameters, S (on F^2) = 1.097, $R1$ (all data) = 0.0612, $wR2$ (all data) = 0.1079, $R1$ [$I > 2\sigma(I)$] = 0.0438, max. and min. electron density in final difference map: +1.13 and −0.25 eÅ^{-3}. Anisotropic thermal parameters were refined for all non-hydrogen atoms. H atoms were included on idealized positions and were given U values 1.5 (OH) and 1.2 times (CH, CH_2), respectively, the equivalent isotropic displacement factors of the atoms to which they were attached. The H atom of the OH group was allowed to rotate about the C(8)−O(1) bond (AFIX 87 instruction).

Crystallographic data (excluding structure factors) for the structure reported in this paper have been deposited with the Cambridge Crystallographic Data Centre (deposition no. 100410). Copies of the data can be obtained free of charge on application to The Director, CCDC, 12 Union Road, Cambridge CB2 1EZ, UK (fax: int. code +44(0)1223/336-033, e-mail: deposit@chemcrys.cam.ac.uk).

[☆] Dedicated to the memory of our teacher and colleague Prof. Dr. *Siegfried Pohl*, who untimely passed away on December 18, **1996**.

[1] H. Strasdeit, A. von Döllen, A.-K. Duhme, *Z. Naturforsch.* **1997**, *52b*, 17−24.

[2] L. Lewin, *Die Gifte in der Weltgeschichte: toxikologische allgemeinverständliche Untersuchungen der historischen Quellen*, Springer, Berlin, **1920**; reprint, 3rd ed., Gerstenberg, Hildesheim, **1984**, pp. 157−166.

[3] P. Bagla, J. Kaiser, *Science* **1996**, *274*, 174−175. Although being highly toxic in larger amounts, arsenic may be an essential trace element for mammals (see ref.[5]).

[4] Quoted from ref.[5]

[5] O. M. Ni Dhubhghaill, P. J. Sadler, *Struct. Bonding (Berlin)* **1991**, *78*, 129−190.

[6] H. V. Aposhian in *Reviews in Biochemical Toxicology* (Eds.: E. Hodgson, J. R. Bend, R. M. Philpot), Vol. 10, Elsevier, New York, **1989**, pp. 265−299.

[7] T. E. Roche, M. S. Patel (Eds.), *Alpha-Keto Acid Dehydrogenase Complexes: Organization, Regulation, and Biomedical Ramifications*, New York Academy of Sciences, New York, **1989**.

[8] R. N. Perham, *Biochemistry* **1991**, *30*, 8501−8512.

[9] D. Voet, J. G. Voet, *Biochemistry*, 2nd ed., Wiley, New York, **1995**, pp. 541−548, 736−738.

[10] For relevant protein crystallographic studies see: [10a] A. Mattevi, G. Obmolova, E. Schulze, K. H. Kalk, A. H. Westphal, A. de Kok, W. G. J. Hol, *Science* **1992**, *255*, 1544−1550. − [10b] A. Mattevi, G. Obmolova, K. H. Kalk, A. Teplyakov, W. G. J. Hol, *Biochemistry* **1993**, *32*, 3887−3901. − [10c] S. Pares, C. Cohen-Addad, L. Sieker, M. Neuburger, R. Douce, *Proc. Natl. Acad. Sci. USA* **1994**, *91*, 4850−4853. − [10d] C. Cohen-Addad, S. Pares, L. Sieker, M. Neuburger, R. Douce, *Nature Struct. Biol.* **1995**, *2*, 63−68. − [10e] S. Pares, C. Cohen-Addad, L. C. Sieker, M. Neuburger, R. Douce, *Acta Crystallogr. Sect. D* **1995**, *51*, 1041−1051. − [10f] S. S. Mande, S. Sarfaty, M. D. Allen, R. N. Perham, W. G. J. Hol, *Structure* **1996**, *4*, 277−286.

[11] L. Packer, E. H. Witt, H. J. Tritschler, *Free Rad. Biol. Med.* **1995**, *19*, 227−250.
[12] Rote Liste Service GmbH (Ed.), *Rote Liste* **1997**, ECV Editio Cantor, Aulendorf, **1997**, 67001−67016.
[13] For a leading review on the chemical and biological properties of lipoic acid see: L. Teuber, *Sulfur Rep.* **1990**, *9*, 257−349.
[14] D. R. Sanadi, M. Langley, F. White, *J. Biol. Chem.* **1959**, *234*, 183−187.
[15] [15a] K. J. Stevenson, G. Hale, R. N. Perham, *Biochemistry* **1978**, *17*, 2189−2192, and literature cited therein. − [15b] S. R. Adamson, K. J. Stevenson, *Biochemistry* **1981**, *20*, 3418−3424.
[16] C. H. Banks, J. R. Daniel, R. A. Zingaro, *J. Med. Chem.* **1979**, *22*, 572−575.
[17] W. R. Cullen, B. C. McBride, J. Reglinski, *J. Inorg. Biochem.* **1984**, *21*, 179−193.
[18] K. Dill, E. R. Adams, R. J. O'Connor, E. L. McGown, *Chem. Res. Toxicol.* **1989**, *2*, 181−185.
[19] [19a] E. Schröder, C. Rufer, R. Schmiechen, *Pharmazeutische Chemie*, Thieme, Stuttgart, **1982**, pp. 837−840. − [19b] H. Hilmer in *Arzneimittel − Entwicklung, Wirkung, Darstellung* (Eds.: G. Ehrhart, H. Ruschig), Vol. 4, Verlag Chemie, Weinheim, **1972**, pp. 57−76.
[20] H. Strasdeit, A. von Döllen, A.-K. Duhme, *J. Inorg. Biochem.* **1995**, *59*, 228; presented at the 7th International Conference on Bioinorganic Chemistry, Lübeck, Germany, **1995**.
[21] M. Vahter, E. Marafante in *The Biological Alkylation of Heavy Elements* (Eds.: P. J. Craig, F. Glockling), Royal Society of Chemistry, London, **1988**, pp. 105−119.
[22] W. Schunack, K. Mayer, M. Haake, *Arzneistoffe: Lehrbuch der Pharmazeutischen Chemie*, 2nd ed., Vieweg, Braunschweig, **1983**, p. 507.
[23] A. von Döllen, H. Strasdeit, manuscript in preparation.
[24] A. L. Rheingold, P. J. Sullivan, *Organometallics* **1983**, *2*, 327−331.
[25] M. Ya. Kraft, E. N. Sytina, *Proc. Acad. Sci. USSR* **1957**, *116*, 837−840, and literature cited therein.
[26] J. B. Neilands, *Naturwissenschaften* **1973**, *60*, 177−183.
[27] W. R. Cullen, B. C. McBride, J. Reglinski, *J. Inorg. Biochem.* **1984**, *21*, 45−60.
[28] A. Gavezzotti, G. Filippini, *J. Phys. Chem.* **1994**, *98*, 4831−4837; see also: L. Leiserowitz, *Acta Crystallogr. Sect. B* **1976**, *32*, 775−802.
[29] D. W. Aksnes, *Acta Chem. Scand.* **1974**, *A28*, 1175−1179.
[30] [30a] R. O. Hutchins, B. E. Maryanoff, M. J. Castillo, K. D. Hargrave, A. T. McPhail, *J. Am. Chem. Soc.* **1979**, *101*, 1600−1602. − [30b] R. O. Hutchins, B. E. Maryanoff, *J. Am. Chem. Soc.* **1972**, *94*, 3266−3268.
[31] F. G. Riddell, *The Conformational Analysis of Heterocyclic Compounds*, Academic Press, London, **1980**, pp. 123−125.
[32] E. Juaristi, *Introduction to Stereochemistry and Conformational Analysis*, Wiley, New York, **1991**, chapter 17.
[33] R. K. Gupta, A. R. Rai, R. C. Mehrotra, V. K. Jain, B. F. Hoskins, E. R. T. Tiekink, *Inorg. Chem.* **1985**, *24*, 3280−3284.
[34] [34a] E. Adams, D. Jeter, A. W. Cordes, J. W. Kolis, *Inorg. Chem.* **1990**, *29*, 1500−1503 − [34b] A. G. Osborne, R. E. Hollands, R. F. Bryan, S. Lockhart, *J. Organomet. Chem.* **1985**, *288*, 207−217 − [34c] G. Bergerhoff, H. Namgung, *Z. Kristallogr.* **1979**, *150*, 209−213 − [34d] A. W. Cordes, P. D. Gwinup, M. C. Malmstrom, *Inorg. Chem.* **1972**, *11*, 836−838.
[35] [35a] Holleman-Wiberg: *Lehrbuch der Anorganischen Chemie*, 101st ed., de Gruyter, Berlin, **1995**, p.1842. − [35b] *ibid.*, pp. 184, 370.
[36] J. D. Andose, A. Rauk, K. Mislow, *J. Am. Chem. Soc.* **1974**, *96*, 6904−6907, and literature cited therein.
[37] A. F. Wagner, E. Walton, G. E. Boxer, M. P. Pruss, F. W. Holly, K. Folkers, *J. Am. Chem. Soc.* **1956**, *78*, 5079−5081.
[38] For assignments of NMR spectra of dihydrolipoic acid and other lipoic acid derivatives see: [38a] V. Schepkin, T. Kawabata, H. J. Tritschler, L. Packer, *Free Rad. Res.* **1996**, *25*, 195−205. − [38b] J. V. Paukstelis, E. F. Byrne, T. P. O'Connor, T. E. Roche, *J. Org. Chem.* **1977**, *42*, 3941−3944.
[39] S. Samaan in *Methoden der Organischen Chemie (Houben-Weyl)*, 4th ed., vol. XIII/8, Thieme, Stuttgart, **1978**, p. 157.
[40] Tentative assignment. For comparison see: [40a] T. B. Brill, N. C. Campbell, *Inorg. Chem.* **1973**, *12*, 1884−1888 − [40b] K. Volka, P. Adámek, H. Schulze, H. J. Barber, *J. Mol. Struct.* **1974**, *21*, 457−460.
[41] G. M. Sheldrick, *SHELXTL PLUS*, Siemens Analytical X-ray Instruments Inc., Madison, WI, USA, **1990**.
[42] G. M. Sheldrick, *SHELXL-93, Program for Crystal Structure Refinement*, University of Göttingen, Germany, **1993**.

[97195]

Formation and Reactivity of Five-Coordinate Gallium Supported by Salen Ligands

Michael S. Hill and David A. Atwood*

Center for Main Group Chemistry, Department of Chemistry, North Dakota State University, Fargo, North Dakota, 58105-5516, USA

Received May 6, 1997

Keywords: Gallium / Pentacoordination / Salen(*t*Bu)

This work is an exploration into the synthesis and reactivity of five-coordinate gallium complexes of the ligands, Salen(*t*Bu)H_2 [*N,N′*-ethylenebis(3,5-di-*tert*-butylsalicylideneimine), (**1**)], Salpen(*t*Bu)H_2 [*N,N′*-propylenebis(3,5-di-*tert*-butylsalicylideneimine), (**2**)], Salophen(*t*Bu)H_2 [*N,N′*-phenylenebis(3,5-di-*tert*-butylsalicylideneimine), (**3**)], and Salomphen(*t*Bu)H_2 [*N,N′*-(4,5-dimethyl)phenylenebis(3,5-di-*tert*-butylsalicylideneimine), (**4**)]. Fully characterized examples include those of general formula LGaX, where L = **1**, X = Cl (**5**), Et (**6**); **3**, X = Cl (**7**), Et (**10**); **4**, X = Cl (**8**), Me (**9**) Et (**11**). X-ray structural data is presented for **6**, **7**, **9**, **10**, and **11**. The ability of these complexes to undergo either alkane or salt elimination reactions is described. In one reaction the unusual salt: [{Salophen(*t*Bu)Ga(MeOH)}$_2$]$^+$$BPh_4^-$ (**12**) is obtained.

Despite the fact that Salen ligand (Figure 1a) complexes of transition metals[1] have been known for over sixty years,[2] very little has been accomplished with regards to the main group elements. Until recently, monomeric group-13 derivatives of the form, SalenMX (where M = Al, Ga, In and X = halide or alkyl) were uncommon. The first example to be reported was SalpenAlEt.[3] Since that time more have appeared in the literature, including those of aluminum [Salen(*t*Bu)AlX; X = Me, Et, *i*Bu,[4] chloride[5]; SalcenAlEt[6]], indium [Salen(*t*Bu)InX; X = Me, Et, Cl, Br][7] and some aluminum alkoxides[8] and siloxides.[4] The solubilizing influence of the Salen(*t*Bu) ligand (Figure 1b) makes these compounds much more amenable to solution state studies than those of the underivatized Salen ligands (Figure 1a). They provide a unique opportunity to examine the formation and reactivity of the group-13 elements in a five-coordinate geometry. Depending on the nature of the ligand and the substituents on the group-13 element, either a square-pyramidal or trigonal bipyramidal geometry is observed. From these early studies it is clear that there are marked differences in reactivity of the elements in this geometry compared to the more traditional four-coordinate, tetrahedral geometry. The present work will add to this growing base of knowledge on five-coordinate group-13 elements with a description of the first gallium examples. These are of the form LGaX [where L = Salen(*t*Bu)].

Figure 1. General depiction of the Salen (a) and Salen(*t*Bu) (b) classes of ligands

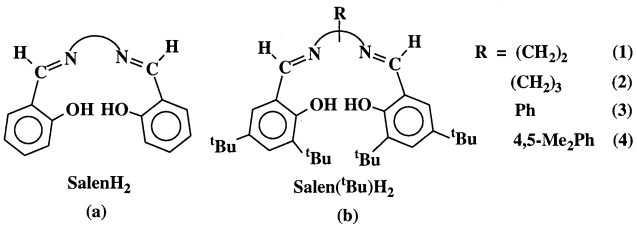

Results and Discussion

Combining one equivalent of Et_2GaCl with **1** or **2** leads to a mixture of predominantly LGaEt with some LGaCl. In the case of the derivatives obtained from **1**, these products (**5** and **6**) can be separated by fractional crystallization. Similar problems were observed in the formation of the analogous aluminum derivatives. In fact, ligands **1** and **2** most readily form open, bimetallic compounds of the sort $L(MR_2)_2$ (where M = Al, Ga and R = alkyl).[9] Use of the the ligands containing an aryl backbone, **3** and **4**, leads to high yields of the chloride derivatives, **7** and **8** without contamination from any LGaEt products. Likewise, the combination of these ligands with $GaEt_3$ leads to isolation of **10** and **11** in high yields.

Scheme 1. The general synthetic pathway for the preparation of **5**−**11**

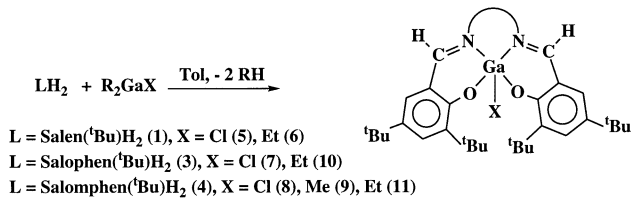

Monomeric species are generally obtained in these types of reactions. For all of the compounds the *t*Bu resonances of the ligands are manifested as a pair of singlets in the region δ = 1.3−1.5. Dimeric derivatives normally show more complexity for these resonances. This is the case, for example with {Salen(*t*Bu)Al}$_2$O.[8] Furthermore, the derivatives of **4** contain only one resonance for the Me−Ph group. The Ga−Et groups are observed as well-defined

 © WILEY-VCH Verlag GmbH, D-69451 Weinheim, 1998 1434−1948/98/0101−0067 $ 17.50+.50/0

triplets and quartets. The aryl derivatives show greater deshielding of these groups with shifts in the range of $\delta = 0.2$ and 0.7. Compound **5** is marginally more shielded with values of $\delta = 0.26$ and 0.83.

The Me resonance of **9** occurs at $\delta = 0.59$. This can be compared to the same shift in the four-coordinate derivatives, $Me_3Ga-thf$ ($\delta = -0.3$)[10], $Me_3Ga-NH(iPr)_2$ ($\delta = 0.33$)[11], $Me_3Ga-PPh_3$ ($\delta = 0.17$)[12], and $(Me_3Ga)_2$-diphos ($\delta = 0.15$). From the limited amount of data that is available it would appear that the five-coordinate shifts occur at lower field than those observed for four-coordinate derivatives.

The five-coordinate environment around the gallium atoms was confirmed structurally for **6**, **7**, **9**, **10**, and **11**. The structure of **7** is the third reported for a group-13 halide bound by a Salen(*t*Bu) ligand (Figure 2).[7] The Ga atom is in a distorted square pyramidal geometry with the ligand occupying the basal plane at a $Ga-N_2O_2$ plane distance of 0.49 Å. The chloride occupies the apical site at a distance of 2.199(3) Å. A similar geometry is observed for the methyl derivative, **9** (Figure 3) which has a $Ga-N_2O_2$ plane distance of 0.63 Å. The Ga−O and Ga−N bond distances shorten by comparison to **7**. Compare, for instance, the Ga−O axial distances (ave = 1.87 Å for **7** and 1.90 Å for **9**). This is a result of the lessened inductive effect of the Me group when compared to Cl. The Ga−Me distance [1.939(5) Å] is fairly standard for four- and five-coordinate compounds.[9][10][11] For example this distance in $[Me_2GaNH(tBu)]_2$ and $Me_3Ga-NH_2(tBu)$ is 1.978(7) Å and 2.01(1) Å, respectively.[13] Compound **9** is actually dimeric in the solid state. The two monomeric units are held together by a relatively close Ga···H (from a Ph−Me group) contact of approximately 3.1 Å.

Figure 2. Molecular structure and atom numbering scheme for Salophen(*t*Bu)GaCl (**7**)

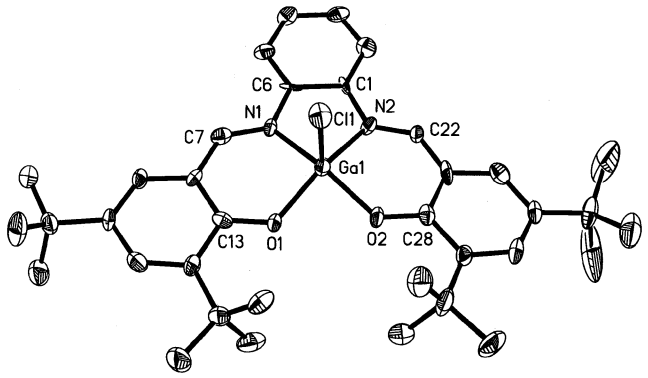

Compound (**6**) adopts a geometry that may best be described as distorted square pyramidal (Figure 4). It contains a fairly obtuse angle [O(2)−Ga(1)−N(1)] of 153.2(4)° that is indicative of a trigonal bipyramidal distortion. Compounds **10** and **11** are more ideally square-pyramidal as a result of the enforced planarity inherent to the aryl backbones of ligands **3** and **4** [a figure (Figure 5) is provided for **10** only]. The $Ga-N_2O_2$ plane distances for **6**, **10**, and **11** are close to one another with values of 0.67 Å, 0.63 Å, and 0.64 Å, respectively. The $Ga-CH_2$ distance does not vary substantially based upon the geometry of the gallium.

Figure 3. Molecular structure and atom numbering scheme for Salomphen(*t*Bu)GaMe (**9**)

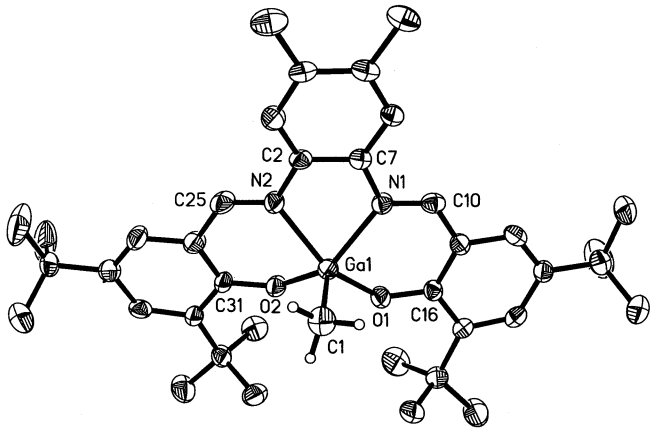

Figure 4. Molecular structure and atom numbering scheme for Salen(*t*Bu)GaEt (**6**)

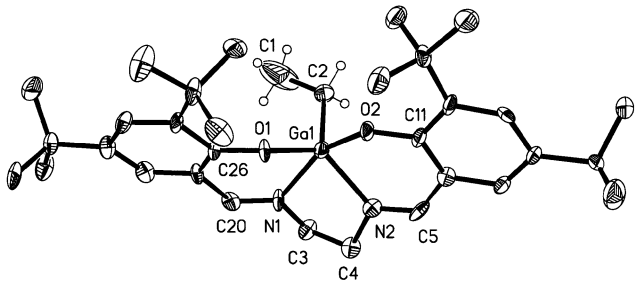

Figure 5. Molecular structure and atom numbering scheme of Salophen(*t*Bu)GaEt (**10**)

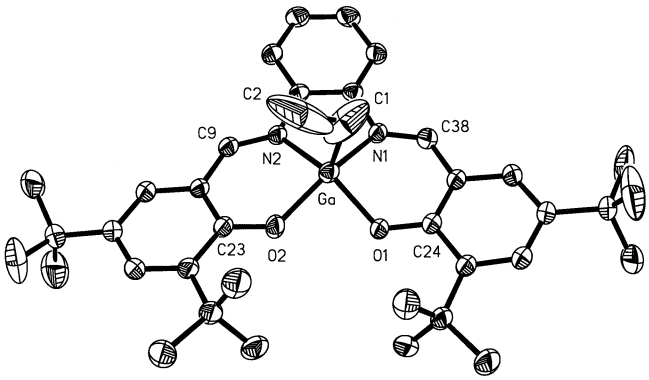

In a manner similar to compound **9**, one of the ethylene hydrogen atoms of **6** is close (3.15 Å) to the gallium atom of a second Salen(*t*Bu)GaEt unit (Figure 6). Dimerization through such close contacts is becoming commonplace in these types of structures.[7] They are also observed in square pyramidal indium derivatives. This may be an indication

that a sixth coordination site may be available, at least to small nucleophiles, in these compounds.

Figure 6. Dimerization of **6** through hydrogen contacts

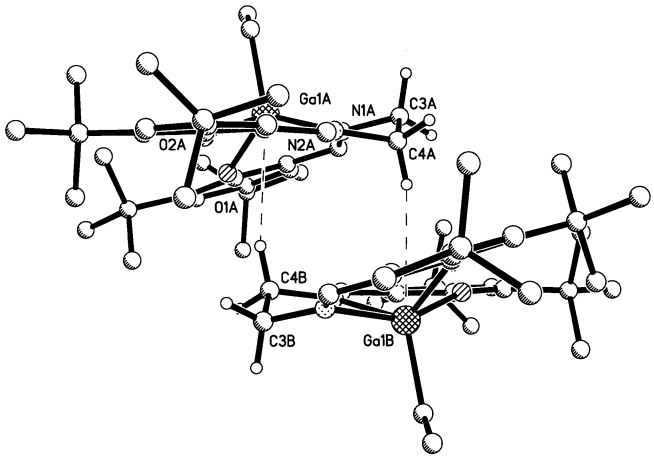

Reactivity Studies

The gallium halide derivative **8** will undergo a salt elimination reaction with MeLi to form the methyl derivative, **9** [Scheme 2(a)]. The same type of product is obtained in the analogous reaction with indium.[7] However, the gallium halide complexes will not undergo halide displacement with Lewis bases such as MeOH [Scheme 2(b)]. This is in contrast to the same reaction for aluminum in which cationic complexes are formed (eg. $[SalenAl(MeOH)_2]^+Cl^-$).[14] Similarly, salt eliminations with the gallium halides and NaOTs (OTs = toluenesulfonic acid) do not occur [Scheme 2(c)] despite the fact that, for aluminum, a wide range of cations ($[SalenAl(base)_2]^+OTs^-$) can be accessed in this manner.[14] For these two reactions [Scheme 2(b) and (c)] gallium and indium behave identically.

Scheme 2. Reactions involving the five-coordinate halide derivatives

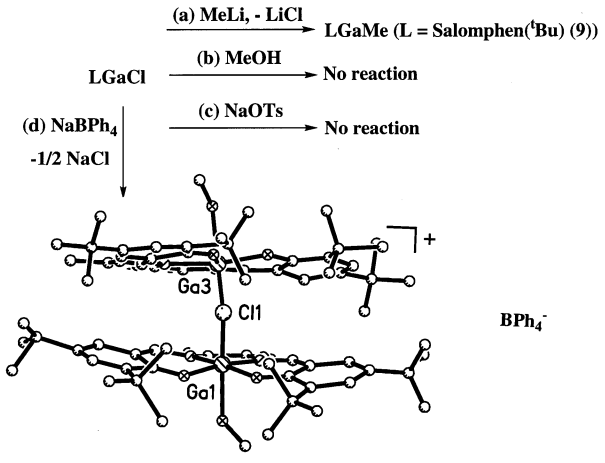

(12)

Cationic aluminum complexes can also be formed containing $[BPh_4]^-$ as the anion. While this reaction was not successful for indium, a new product can be isolated when using gallium. The product is the unusual salt comprised of a cation containing two gallium atoms and the BPh_4 counter-anion [Scheme 2(d)]. The ^{1}H-NMR data is complex and difficult to interpret. However, the results of a partial crystal structure determination and elemental analyses confirms the proposed formulation. Unfortunately, the structure is complicated by the presence of as many as five molecules of MeOH in the independent unit so the structure could not be satisfactorily refined.[15] It can be viewed as being an adduct between the cationic species, $Salen(t\text{Bu})Ga(MeOH)_2]^+$ and a neutral Salen(*t*Bu)GaCl molecule. Within the limits of the quality of the structure, both of the Ga−Cl distances are the same (ca. 2.0 Å) and form a Ga−Cl−Ga′ angle of 149°. That species like **12** may, in fact, represent a new class of bimetallic compounds is evidenced by the Ti^{III} compound, $[\{(acacen)Ti(NO_3)\}_2O]$ (acacen = *N,N′*-ethylenebisacetylacetoneiminato) which has been used to prepare a range of interesting oligomeric metal-chelate derivatives.[16] It will be interesting to see if compound **12** can be utilized similarly.

Gratitude is expressed to the *National Science Foundation* (Grant 9452892) and the donors of the *Petroleum Research Fund* (Grant 31901-AC3), administered by the *American Chemical Society*, for support. The receipt of an *NSF-CAREER Award* (CHE 9625376) is also gratefully acknowledged.

Experimental Section

General Considerations: All manipulations were conducted using Schlenk techniques in conjunction to an inert atmosphere glove box. All solvents were rigorously dried prior to use. − NMR data were obtained on JEOL-GSX-400 and -270 instruments at 270.17 (^{1}H) and are reported relative to $SiMe_4$ and in ppm. − Elemental analyses were obtained on a Perkin-Elmer 2400 Analyzer. − Infrared data were recorded as KBr pellets on a Matheson Instruments 2020 Galaxy Series spectrometer and are reported in cm^{-1}. The reagent 3,5-di-*tert*-butyl-2-hydroxybenzaldehyde was prepared according to the literature.[17] − All of the X-ray data was collected on a Siemens SMART-CCD unit. A complete data set was collected (Θ = 55°) in each case although this number could be reduced to provide a better structure in the final stages of the structure determination. All of the hydrogen atoms were placed into calculated, idealized positions. The structures were solved with the Siemens SHELXTL-Plus suite of programs.

Reaction of Salen(tBu)H$_2$ and Et$_2$GaCl: To a stirred solution of Et_2GaCl, prepared in situ from triethylgallium (0.32 g, 2.03 mmol) and gallium trichloride (0.18 g, 1.02 mmol) in toluene (20 ml), was added Salen(*t*Bu)H_2 (1.50 g, 3.05 mmol). The resultant yellow solution was refluxed for a total of 14 h before removal of solvent in vacuo to yield a yellow solid. NMR analysis of this material indicated a single major product identified as Salen(*t*Bu)GaCl (ca. 60% by integration) and a number of minor products. Attempted fractional cystallisation from methanol solution yielded yellow crystals identified as Salen(*t*Bu)GaEt by single crystal X-ray analysis [0.10 g, 5.5% based on Salen(*t*Bu)H_2, m.p. 223 °C]. Attempts to isolate an analytically pure sample of Salen(*t*Bu)GaCl however were unsuccessful.

Table 1a. Crystal data for Salophen(*t*Bu)GaCl (**7**)and Salomphen-(*t*Bu)GaMe (**9**)

	7	**9**
Formula	$C_{72}H_{92}Cl_2Ga_2N_4O_4$	$C_{39}H_{57}GaN_2O_4$
Formula weight	1287.84	687.59
Crystal system	monoclinic	monoclinic
Space group	$P2_1/c$	$P2_1/c$
a [Å]	10.8756(7)	15.6740(8)
b [Å]	17.029(1)	10.4407(6)
c [Å]	20.584(1)	23.784(1)
α [°]	107.241(1)	90
β [°]	90.021(1)	90.498(1)
γ [°]	107.550(1)	90
V [Å^3]	3454.5(4)	3892.0(4)
Z	2	4
D(calcd) [Mg/m^3]	1.238	1.173
Crystal size [mm^3]	$(0.40)^3$	$(0.5)^3$
Colour, habit	pale yellow cube	pale yellow cube
Temperature [K]	298	298
Abs coeff. [mm^{-1}]	0.906	0.745
θ range solution [°][a]	1.04−18.00	1.55−19.00
Collected refl.	8126	10104
Independent refl.	4643 (r_{int} = 0.0673)	3123 (r_{int} = 0.0559)
Obsd. with $I > 2\sigma(I)$	4606	3115
R_1	0.0591	0.0469
R_1 (all data)	0.0777	0.0558
Goodness of fit on F^2	1.214	1.232
Largest diff. peak and hole	0.358 and −0.341	0.365 and −0.309

[a] All of the data sets were collected to 55°. The range was narrowed during refinement to improve the structure solution.

Salen(tBu)GaCl (**5**): ^{1}H NMR (270 MHz, $CDCl_3$): δ = 1.10 [s, 18 H, C(CH_3)$_3$], 1.40 [s, 18 H, C(CH_3)$_3$], 3.80−4.18 (m, ca. 4 H, CH_2CH_2), 6.72 (s, 2 H, Ar-*H*), 7.47 (s, 2 H, Ar-*H*), 8.50 (s, 2 H, Ar-C*H*).

Salen(tBu)GaEt (**6**): ^{1}H NMR (270 MHz, $CDCl_3$): δ = 0.26 (q, 2 H, CH_2Ga), 0.83 (t, 3 H, CH_2CH_3), 1.27 [s, 18 H, C(CH_3)$_3$], 1.50 [s, 18 H, C(CH_3)$_3$], 3.66−3.68 (m, 2 H, CH_2CH$_2$), 3.83−3.85 (m, 2 H, CH$_2$CH_2) 6.87 (s, 2 H, Ar-*H*), 7.40 (s, 2 H, Ar-C*H*), 8.27 (s, 2 H, Ar-*H*). − IR (KBr, cm^{-1}): $\tilde{\nu}$ = 2953 s, 2903 s, 2864 s, 1649 s, 1618 s, 1535 s, 1440 m, 1411 m, 1303 m, 1253 m, 1199 m, 1168 m, 1055 w, 979 w, 877 w, 831 w, 787 m, 742 m, 700 w, 667 w, 561 w, 462 w. − $C_{34}H_{51}GaN_2O_2$ (589.49): calcd. (found) C 69.30 (69.36), H 8.66 (8.37), N 4.76 (4.63).

Reaction of Salpen(tBu)H$_2$ and Et$_2$GaCl: An identical procedure to that described above, utilizing triethylgallium (0.319 g, 2.03 mmol), gallium trichloride (0.179 g, 1.02 mmol) and Salpen(*t*Bu)H$_2$ (1.544 g, 3.05 mmol) in toluene solution (20 ml), provided a pale green solid upon removal of the solvent. This was demonstrated to be a complex mixture of products by ^{1}H NMR and proved insensitive to further purification by fractional crystallization in a variety of polar and non-polar solvents.

Synthesis of Salophen(tBu)GaCl (**7**): This compound was synthesized utilizing a similar procedure to that described above, employing triethylgallium (0.194 g, 1.23 mmol), gallium trichloride (0.109 g, 0.62 mmol) and Salophen(*t*Bu)H$_2$ (1.00 g, 1.85 mmol) in toluene solution (20 ml). In vacuo removal of solvent afforded the title compound as a pale orange solid in stoichiometric yield which could be crystallized from methanol solution as pale orange crystals suitable for X-ray analysis (0.98 g, 82%) m.p. >260 °C. ^{1}H NMR (270 MHz, $CDCl_3$): δ = 1.33 [s, 18 H, C(CH_3)$_3$], 1.58 [s, 18 H, C(CH_3)$_3$], 7.14 (s, 2 H, Ar-*H*), 7.40 (m, 2 H, Ar-*H*), 7.62 (s, 2 H, Ar-*H*), 7.72 (m, 2 H, Ar-*H*), 8.92 (s, 2 H, Ar-C*H*). − IR (KBr, cm^{-1}): $\tilde{\nu}$ = 2959 s, 2906 m, 2868 m, 1614 s, 1583 s, 1533 s, 1465 m, 1388 m, 1359 m, 1315 w, 1257 m, 1026 w, 835 w, 785 w, 744 m, 540 w. − $C_{72}H_{92}Cl_2Ga_2N_4O_4$ (1287.84): calcd. (found) C 67.16 (67.37), H 7.15 (6.95), N 4.35 (4.17).

Synthesis of Salomphen(tBu)GaCl (**8**): This compound was synthesized by a similar procedure to that outlined above employing triethylgallium (0.276 g, 1.76 mmol), gallium trichloride (0.158 g, 0.88 mmol) and Salomphen(*t*Bu)H$_2$ (1.50 g, 2.64 mmol). In vacuo removal of the solvent produced an orange solid [containing ca.

Table 1b. Crystal data for Salen(*t*Bu)GaEt (**6**), Salophen(*t*Bu)GaEt (**10**), and Salomphen(*t*Bu)GaEt (**11**)

	6	**10**	**11**
Formula	$C_{34}H_{51}GaN_2O_2$	$C_{38}H_{51}GaN_2O_2$	$C_{40}H_{56}GaN_2O_2$
Formula weight	589.49	637.53	666.84
Crystal system	monoclinic	triclinic	monoclinic
Space group	$P2_1/c$	$P\bar{1}$	$P2_1/c$
a [Å]	11.909(1)	9.9771(5)	14.4606(8)
b [Å]	15.593(1)	12.9593(7)	14.6625(8)
c [Å]	18.460(2)	14.7505(8)	19.124(1)
α [°]	90	85.868(1)	90
β [°]	103.340(2)	79.493(1)	106.443(1)
γ [°]	90	71.458(1)	90
V [Å^3]	3321.5(2)	1777.7(2)	3888.9(4)
Z	4	2	4
D(calcd.) [Mg/m^3]	1.179	1.191	1.139
Crystal size [mm^3]	$(0.50)^3$	$(0.4)^3$	$(0.50)^3$
Colour, habit		orange cube	
Temperature [K]	298	298	298
Abs coeff. [mm^{-1}]	0.858	0.807	0.740
θ range solution [°][a]	1.73−20.00	1.40−21.50	1.47−19.99
Collected refl.	9580	6432	11403
Independent refl.	3081 (r_{int} = 0.1732)	3999 (r_{int} = 0.0499)	3608 (r_{int} = 0.0358)
Obsd. with $I > 2\sigma(I)$	3081	3974	3588
R_1	0.1346	0.0493	0.0613
R_1 (all data)	0.1756	0.0527	0.0717
Goodness of fit on F^2	1.710	1.519	1.569
Largest diff. peak and hole	0.931 and −0.388	0.565 and −0.485	1.085 and −0.463

[a] All of the data sets were collected to 55°. The range was narrowed during refinement to improve the structure solution.

Table 2a. Selected bond lengths [Å] and angles [°] for **7** (one molecule only), and **9**

7		**9**	
Ga(1)−O(1)	1.862(6)	Ga(1)−O(1)	1.901(3)
Ga(1)−O(2)	1.881(6)	Ga(1)−O(2)	1.909(3)
Ga(1)−N(1)	2.045(7)	Ga(1)−N(1)	2.064(4)
Ga(1)−N(2)	2.016(7)	Ga(1)−N(2)	2.105(4)
Ga(1)−Cl	2.199(3)	Ga(1)−C(1)	1.939(5)
O(1)−C(13)	1.32(1)	O(1)−C(16)	1.326(5)
O(2)−C(28)	1.30(1)	O(2)−C(31)	1.322(5)
N(1)−C(7)	1.30(1)	N(1)−C(7)	1.404(6)
N(1)−C(6)	1.40(1)	N(1)−C(10)	1.295(6)
N(2)−C(22)	1.30(1)	N(2)−C(2)	1.397(6)
N(2)−C(1)	1.41(1)	N(2)−C(25)	1.270(6)
O(1)−Ga(1)−O(2)	87.4(3)	O(1)−Ga−O(2)	86.4(1)
O(1)−Ga(1)−N(1)	89.5(3)	O(1)−Ga−N(1)	88.5(2)
O(2)−Ga(1)−N(1)	153.8(3)	O(2)−Ga−N(1)	136.8(2)
O(1)−Ga(1)−N(2)	147.2(3)	O(1)−Ga−N(2)	148.8(2)
O(2)−Ga(1)−N(2)	90.1(3)	O(2)−Ga−N(2)	86.8(2)
N(1)−Ga(1)−N(2)	78.6(4)	N(1)−Ga−N(2)	76.0(2)
O(1)−Ga(1)−Cl(1)	109.3(2)	O(1)−Ga−C(1)	109.0(2)
O(2)−Ga(1)−Cl(1)	106.2(2)	O(2)−Ga−C(1)	111.4(2)
N(1)−Ga(1)−Cl(1)	99.4(2)	N(1)−Ga−C(1)	110.8(2)
N(2)−Ga(1)−Cl(1)	102.7(2)	N(2)−Ga−C(1)	101.8(2)

in vacuo removal of solvent produced a red-brown solid which was recrystallized from methanol in air to yield the title compound as a dihydrate as orange crystals suitable for single crystal X-ray analysis (0.15 g, 65%) m.p. >260 °C. − ^{1}H NMR (270 MHz, $CDCl_3$): δ = −0.59 (s, 3 H, Ga-CH_3), 1.3 [s, 18 H, C(CH_3)$_3$], 1.52 [s, 18 H, C(CH_3)$_3$], 2.36 (s, 6 H, Ph-CH_3), 3.48 (br. s, 4 H, H_2O), 7.04 (s, 2 H, Ar-*H*), 7.40 (s, 2 H, Ar-*H*), 7.48 (s, 2 H, Ar-*H*), 8.66 (s, 2 H, Ar-C*H*). − IR (KBr, cm^{-1}): $\tilde{\nu}$ = 2962 s, 2918 m, 2874 m, 1616 s, 1591 s, 1465 w, 1398 m, 1259 m, 1172 m, 1016 m, 808 m, 787 w, 705 w, 491 w. − $C_{39}H_{57}GaN_2O_4$ (687.59): calcd. (found) C 68.35 (68.48), H 8.03 (8.17), N 4.09 (4.67).

Synthesis of Salophen(tBu)GaEt (**10**): A solution of $GaEt_3$ (0.29 g, 1.85 mmol) in toluene (5 ml) was added at room temperature to a stirred solution of Salophen(*t*Bu)H_2 (1.0 g, 1.85 mmol) in toluene (15 ml). The initial golden yellow solution was stirred for 2 h at which point the solvent was removed to yield a pale brown solid. NMR analysis of this material indicated a mixture of products. The solid was redissolved in a further 20 ml of toluene and refluxed for 15 h producing an orange/brown solution. Removal of solvent and subsequent recrystallisation from a hexane/toluene solution yielded the title compound as ruby-red rectangular crystals suitable for X-ray analysis. (1.00 g, 81%). m.p >260 °C. − ^{1}H NMR (270 MHz, $CDCl_3$): δ = 0.23 (q, 2 H, CH_2Ga), 0.73 (t, 3 H, CH_2CH_3), 1.32 [s, 18 H, C(CH_3)$_3$], 1.54 [s, 18 H, C(CH_3)$_3$], 7.02 (d, 2 H, Ar-*H*), 7.34−7.36 (m, 2 H, Ar-*H*), 7.50 (d, 2 H, Ar-*H*), 7.61−7.64 (m, 2 H, Ar-*H*), 8,70 (s, 2 H, Ar-C*H*). − IR (KBr, cm^{-1}): $\tilde{\nu}$ = 2960 s, 2918 m, 2866 m, 1612 s, 1581 s, 1529 s, 1465 w, 1435 w, 1386 m, 1357 w, 1259 m, 1174 m, 1106 m, 1026 m, 866 w, 802 m, 748 m, 528 m. − $C_{38}H_{51}GaN_2O_2$ (637.53): calcd. (found) C 71.62 (71.31), 8.01 (7.75), N 4.40 (4.20).

Table 2b. Selected bond lengths [pm] and angles [°] for **6**, **10**, and **11**

6		**10**		**11**	
Ga(1)−O(1)	1.900(8)	Ga(1)−O(1)	1.905(2)	Ga(1)−O(1)	1.913(4)
Ga(1)−O(2)	1.932(9)	Ga(1)−O(2)	1.907(3)	Ga(1)−O(2)	1.910(4)
Ga(1)−N(1)	2.09(1)	Ga(1)−N(1)	2.107(3)	Ga(1)−N(1)	2.091(5)
Ga(1)−N(2)	2.06(1)	Ga(1)−N(2)	2.072(3)	Ga(1)−N(2)	2.109(5)
Ga(1)−C(2)	1.95(1)	Ga(1)−C(1)	2.019(8)	Ga(1)−C(39)	1.970(9)
O(1)−C(26)	1.31(1)	O(1)−C(24)	1.324(4)	O(1)−C(15)	1.314(7)
O(2)−C(11)	1.32(1)	O(2)−C(23)	1.330(5)	O(2)−C(30)	1.310(7)
N(1)−C(3)	1.45(2)	N(1)−C(38)	1.294(5)	N(1)−C(9)	1.287(7)
N(1)−C(20)	1.27(2)	N(1)−C(3)	1.413(5)	N(1)−C(6)	1.433(7)
N(2)−C(4)	1.50(2)	N(2)−C(9)	1.305(5)	N(2)−C(24)	1.291(7)
N(2)−C(5)	1.29(2)	N(2)−C(8)	1.418(5)	N(2)−C(1)	1.418(7)
O(1)−Ga(1)−O(2)	86.6(4)	O(1)−Ga−O(2)	86.9(1)	O(1)−Ga(1)−O(2)	87.2(2)
O(1)−Ga(1)−N(1)	85.9(4)	O(1)−Ga−N(1)	85.7(1)	O(1)−Ga(1)−N(1)	87.3(2)
O(2)−Ga(1)−N(1)	153.2(4)	O(2)−Ga−N(1)	147.6(1)	O(2)−Ga(1)−N(1)	137.7(2)
O(1)−Ga(1)−N(2)	127.0(4)	O(1)−Ga−N(2)	137.2(1)	O(1)−Ga(1)−N(2)	146.3(2)
O(2)−Ga(1)−N(2)	86.8(4)	O(2)−Ga−N(2)	88.1(1)	O(2)−Ga(1)−N(2)	86.2(2)
N(1)−Ga(1)−N(2)	77.5(5)	N(1)−Ga−N(2)	76.4(1)	N(1)−Ga(1)−N(2)	75.9(2)
O(1)−Ga(1)−C(2)	116.3(5)	O(1)−Ga−C(1)	111.8(2)	O(1)−Ga(1)−C(39)	111.5(3)
O(2)−Ga(1)−C(2)	106.0(5)	O(2)−Ga−C(1)	113.3(3)	O(2)−Ga(1)−C(39)	112.4(3)
N(1)−Ga(1)−C(2)	100.4(6)	N(1)−Ga−C(1)	98.7(2)	N(1)−Ga(1)−C(39)	108.6(3)
N(2)−Ga(1)−C(2)	116.0(5)	N(2)−Ga−C(1)	109.1(2)	N(2)−Ga(1)−C(39)	101.6(3)

5% Salomphen(*t*Bu)GaEt by NMR] which was recrystallized from hexane/toluene solution at −30 °C to yield the title compound as an orange microcrystalline solid (1.35 g, 76%) m.p. >260 °C. − ^{1}H NMR (270 MHz, $CDCl_3$): δ = 1.33 [s, 18 H, C(CH_3)$_3$], 1.58 [s, 18 H, C(CH_3)$_3$], 2.36 (s, 6 H, Ar-CH_3), 7.14 (s, 2 H, Ar-*H*), 7.49 (s, 2 H, Ar-*H*), 7.60 (s, 2 H, Ar-*H*), 8.87 (s, 2 H, Ar-C*H*). − IR (KBr, cm^{-1}): $\tilde{\nu}$ = 2960 s, 2908 m, 2868 m, 1616 s, 1591 s, 1550 s, 1465 m, 1435 m, 1388 m, 1359 m, 1249 m, 1176 s, 1134 w, 1024 w, 839 m, 785 m, 746 w, 653 w, 538 w, 505 w. − calcd. (found) C 67.94 (67.51), H 7.45 (7.63), N 4.17 (3.97).

Synthesis of Salomphen(tBu)GaMe (**9**): Salomphen(*t*Bu)GaCl (0.25 g, 0.37 mmol) was dissolved in diethyl ether (20 ml) and stirred at −78 °C. MeLi (0.27 ml, 1.4 M in diethyl ether, 0.37 mmol) was added producing a deep brown solution. This was allowed to warm to room temperature before evaporation of the solvent to produce a brown solid. Extraction in toluene (15 ml), followed by

Synthesis of Salomphen(tBu)GaEt (**11**): This compound was synthesized by an identical procedure as that outlined for Salophen(*t*Bu)GaEt from $GaEt_3$ (0.28 g, 1.76 mmol) and Salomphen(*t*Bu)H_2 (1.00 g, 1.76 mmol), recrystallisation from a hexane/toluene solution yielding the title compound as an orange rectangular crystals suitable for X-ray analysis. (1.06 g, 87%). m.p. >260 °C. − ^{1}H NMR (270 MHz, $CDCl_3$): δ = 0.19 (q, 2 H, CH_2Ga), 0.71 (t, 3 H, CH_2CH_3), 1.33 [s, 18 H, C(CH_3)$_3$], 1.54 [s,

18 H, C(CH_3)$_3$], 2.35 (s, 6 H, Ar-CH_3), 7.03 (d, 2 H, Ar-*H*), 7.40 (s, 2 H, Ar-*H*), 7.49 (s, 2 H, Ar-*H*), 8.67 (s, 2 H, Ar-C*H*). − IR (KBr, cm^{-1}): $\tilde{\nu}$ = 2962 s, 2910 m, 1618 s, 1593 m, 1548 m, 1410 w, 1261 m, 1174 m, 1089 m, 1018 m, 800 m, 534 w. − $C_{40}H_{56}GaN_2O_2$ (666.84): calcd. (found) C 72.21 (71.94), H 8.27 (8.25), N 4.21 (3.98).

Synthesis of {[Salomphen(tBu)Ga·MeOH]$_2$Cl}BPh$_4$ (**12**): Salomphen(*t*Bu)GaCl (0.30 g, 0.47 mmol) and sodium tetraphenylborate (0.16 g, 0.47 mmol) were stirred as a pale orange solution in methanol (15 ml) for 14 h. At this point the solution was reduced in volume to ca. 5 ml and allowed to crystallise by slow evaporation of the solvent. This produced the title compound as heavily solvated orange needles suitable for X-ray analysis. This material could be converted to a red unsolvated form by storage under vacuum for several hours (total yield, 0.41 g, 52%) m.p. 208−213 °C (dec). − ^{1}H NMR (270 MHz, $CDCl_3$): δ = 0.77−1.56 [complex multiplet, 72 H, C(CH_3)$_3$], 2.46−2.54 (m, 12 H, Ph-CH_3), 3.35 (s, 6 H, HO-CH_3), 6.43−7.60 (m, 32 H, Ar-*H*). − IR (KBr, cm^{-1}): $\tilde{\nu}$ = 2960 s, 2906 m, 2872 m, 1614 s, 1587 m, 1533 s, 1465 m, 1435 m, 1390 m, 1359 m, 1251 m, 1180 m, 1081 m, 806 w, 702 w, 613 w, 540 w, 503 w. − calcd. (found) C 72.62 (73.02), H 7.47 (7.36).

Attempted Reactions:

Salophen(tBu)GaCl and NaOTs (in Dichloromethane): Sodium *p*-toluenesulfonate (0.1 g, 0.51 mmol) was added as a solid to a stirred solution of Salophen(*t*Bu)GaCl (0.25 g, 0.39 mmol) in 15 ml of CH_2Cl_2, thf, or MeO H, dichloromethane (15 ml). The resultant suspension was stirred for 14 h before filtration and evaporation of the solvent to yield an orange solid. This was demonstrated to be unreacted Salophen(*t*Bu)GaCl by ^{1}H NMR.

Crystallographic data (excluding the structure factor tables) for the structures reported in this paper have been deposited with the Cambridge Crystallographic Data Center as supplementary publication CCDC-100614. Copies of the data can be obtained free of charge on application to The Director, CCDC, 12 Union Road, Cambridge CB21EZ, UK [Fax: int. code +44 (0)1223/336-033; E-mail: deposit@chemcrys.cam.ac.uk].

[1] For reviews see: [1a] R. H. Holm, G. W. Everett, Jr., A. Chakravorty, *Prog. Inorg. Chem.* **1966**, *7*, 83. − [1b] M. D. Hobday, T. D. Smith, *Coord. Chem. Rev.* **1972**, *9*, 311.
[2] J. V. Dubsky, A. Sokol, *Collection Czech Chem. Commun.*, **1931**, *3*, 548.
[3] S. J. Dzugan, V. L. Goedken, *Inorg. Chem.* **1986**, *25*, 2858.
[4] D. A. Atwood, M. S. Hill, J. A. Jegier, D. Rutherford, *Organometallics* **1997**, *16*, 2659.
[5] D. Rutherford, D. A. Atwood, *Organometallics*, **1996**, *15*, 4417.
[6] W.-H. Leung, E. Y. Y. Chan, E. K. F. Chow, I. D. Williams, S.-M. Peng, *J. Chem. Soc., Dalton Trans.* **1996**, 1229.
[7] M. S. Hill, D. A. Atwood, *Main Group Chem.*, in press.
[8] P. L. Gurian, L. K. Cheatham, J. W. Ziller, A. R. Barron, *J. Chem. Soc., Dalton Trans.* **1991**, 1449.
[9] K. S. Chong, S. J. Rettig, A. Storr, J. Trotter, *Can. J. Chem.* **1977**, *55*, 2540; M. S. Hill, P. Wei, D. A. Atwood, *Polyhedron*, in press.
[10] A. C. Jones, D. J. Cole-Hamilton, A. K. Holliday, M. M. Ahmad, *J. Chem. Soc., Dalton Trans.* **1983**, 1047.
[11] M. Niemeyer, T. J. Goodwin, S. H. Risbud, P. P. Power, *Chem. Mater.* **1996**, *8*, 2745.
[12] D. C. Bradley, H. Chudzynska, M. C. Faktor, D. M. Frigo, M. B. Hursthouse, B. Hussain, L. M. Smith, *Polyhedron* **1988**, 1289.
[13] D. A. Atwood, R. A. Jones, A. H. Cowley, S. G. Bott, J. L. Atwood, *J. Organomet. Chem.* **1992**, *434*, 143.
[14] [14a] D. A. Atwood, J. A. Jegier, D. Rutherford, *J. Am. Chem. Soc.* **1995**, *117*, 6779. − [14b] M. G. Davidson, C. Lambert, I. Lopez-Solera, P. R. Raithby, R. Snaith, *Inorg. Chem.* **1995**, *34*, 3765. − [14c] D. A. Atwood, J- A. Jegier, D. Rutherford, *Inorg. Chem.* **1996**, *35*, 63.
[15] A reasonable solution could not be obtained despite attempts with 8 crystals and several data sets. The best solution was obtained with: Triclinic, $P\bar{1}$, a = 11.8477(6), b = 16.1054(8), c = 29.481(2) Å, α = 98.628(1), β = 98.826(1), γ = 101.319(1)°, V = 5355.5(5) Å^3, Z = 2, with 25% of the atoms anisotropic the $R1$ value was 11.32% on 11761 data.
[16] F. Franceschi, E. Gallo, E. Solari, C. Floriani, A. Chiesi-Villa, C. Rizzoli, N. Re, A. Sgamellotti, *Chem. Eur. J.* **1996**, *2*, 1466.
[17] G. Casiraghi, G. Casnati, G. Puglia, G. Sartori, G. Terenghi, *J. Chem. Soc., Perkin Trans. 1* **1980**, 1862.

[97109]

Water Soluble Phosphanes, IX[◇]

Nucleophilic Phosphanylation of Fluoroaromatic Compounds with Carboxyl, Carboxymethyl, and Aminomethyl Functionalities – an Efficient Synthetic Route to Amphiphilic Arylphosphanes

Martin Hingst, Michael Tepper, and Othmar Stelzer*

Fachbereich 9, Anorganische Chemie, Bergische Universität-GH Wuppertal,
D-42097 Wuppertal, Germany

Received May 6, 1997

Keywords: Nucleophilic phosphanylation / Phosphanylphthalic acid / Phosphanylphenylacetic acid / Benzylaminophosphanes / Water solubility

Chiral- and multiply-carboxylated phosphanes and phosphanyl derivatives of benzoic and phthalic acids (**1**–**9**) are accessible in high yields by nucleophilic phosphanylation of potassium or lithium salts of commercially available fluorobenzoic and 3-fluorophthalic acids with Ph_2PH, Ph_2PK, $PhPLi_2$, $Ph(K)P-(CH_2)_3-P(K)Ph$ in superbasic media (DMSO/KOH) or in THF and DME. The hitherto unknown phosphanylphenylacetic acids (**10**–**13**) and phosphanylbenzylamines $RR'P-C_6H_4-CH_2-NH_2$ (**14**–**19**, R, R′ = H, Me, Ph) with unsubstituted amino groups were also synthesized by this method. The diphenylphosphanyl derivatives **14**–**16** (R, R′ = Ph) are accessible by an alternative method involving $LiAlH_4$ reduction of the phosphanylbenzonitriles (**20**–**22**), which were obtained in high yields by nucleophilic phosphanylation of the corresponding fluoro- or chlorobenzonitriles. The novel bidentate phosphanylbenzonitrile **23** has also been obtained using this synthetic route. All compounds were completely characterized by elemental analysis, NMR spectroscopy, and mass spectrometry.

Aromatic phosphanes with carboxylated side chains, e.g. $Ph_2P-(CH_2)_n-COOH$, $Ph_2P-C_6H_4-2$-COOH, have been extensively employed as components in catalysts for the oligomerization, polymerization, telomerization and hydroformylation of olefins[2a][2b][2c][2d]. Thus, the catalyst used for the two phase oligomerization of olefins in the "Shell higher olefin process" (SHOP)[2e] is prepared by reaction of bis(cyclooctadiene)nickel(0) with diphenylphosphanylacetic acid. Reduction/substitution reactions performed on pertechnate leads to neutral technetium(III) complexes with carboxylated phosphanes in which the phosphane ligands act as O,P-bidentate systems. The biodistribution of the corresponding ^{99m}Tc labelled species has been studied[2f].

The *o*-, *m*-, and *p*-isomers of diphenylphosphanylbenzoic acid have been reported earlier. These compounds are accessible by multistep[3a][3b][3c] or protective group synthesis[3d], but only in moderate overall yields. Despite the keen interest in these ligands, there are no reports in the literature so far on their higher carboxylated analogs (**A**) or derivatives containing CH_2 spacers between the aromatic ring and the COOH-groups ("phosphanylphenylacetic acids" **B**). Compounds of type **A**, which contain an additional set of hard donor atoms, should show enhanced solubility in water, and both of these factors are important for the application of these ligands in two-phase catalysis[4]. Ligands of type **B** contain activated CH_2 groups and, in addition, the carboxylate substituents are connected in a more flexible manner to the rigid aromatic ring systems. For the sake of comparison we have included phosphanylbenzylamines **C** in our study, and these systems contain aminomethyl groups. These groups can be protonated to give novel cationic water soluble phosphanes **D**. Ligands of this type, bearing quaternary ammonium groups, form palladium complexes with phase transfer properties. They are effective catalysts for the fluorocarbonylation of bromobenzene with CO and KF[4b].

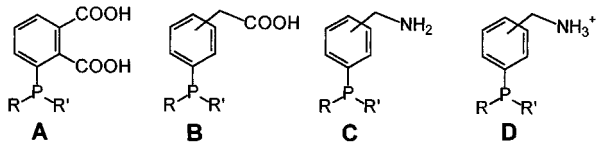

Ligands with functionalized peripheries are of increasing interest[5a] because of their potential for further derivatization, e.g. by esterification with diols to give functionalized linear polymers suitable as insoluble supports for the immobilization of catalysts[5b].

As part of a project aimed at the development of tailor made water soluble phosphanes[6] for two-phase catalysis we have developed new synthetic procedures for these ligands based on nucleophilic phosphanylation of suitable functionalized fluoro-aromatic compounds under different conditions.

[◇] Part VIII: Ref.[1].

 © WILEY-VCH Verlag GmbH, D-69451 Weinheim, 1998 1434–1948/98/0101–0073 $ 17.50+.50/0

Nucleophilic Phosphanylation of Fluorobenzoic and Fluorophthalic Acids

Nucleophilic displacement of the halogen (X) in aromatic compounds X−C_6H_4−Z (X = F, Cl, Br; Z = NO_2, SO_3H, COOH) that contain electron withdrawing substituents (Z), proceeds much faster with the fluoro- than with the chloro- or bromo-compounds. This is well established for the halonitrobenzenes[7a][7b] and a variety of substituted aromatic amines has been obtained by making use of the pronounced reactivity of activated fluorobenzene derivatives towards nitrogen nucleophiles[7c]. The phosphanylation of the commercially available fluorobenzoic or fluorophthalic acids should in an analogous way lead to phosphanylbenzoic or phosphanylphthalic acids. This transformation can be performed in "superbasic" media[8], using secondary or primary phosphanes and solid KOH as the base in aprotic dipolar solvents (e.g. dimethyl sulfoxide). Alternatively, alkali metal phosphides such as Ph_2PK or $PhPLi_2$ can be employed for these nucleophilic aromatic substitution reactions in solvents like 1,2-dimethoxyethane (DME) or tetrahydrofuran (THF).

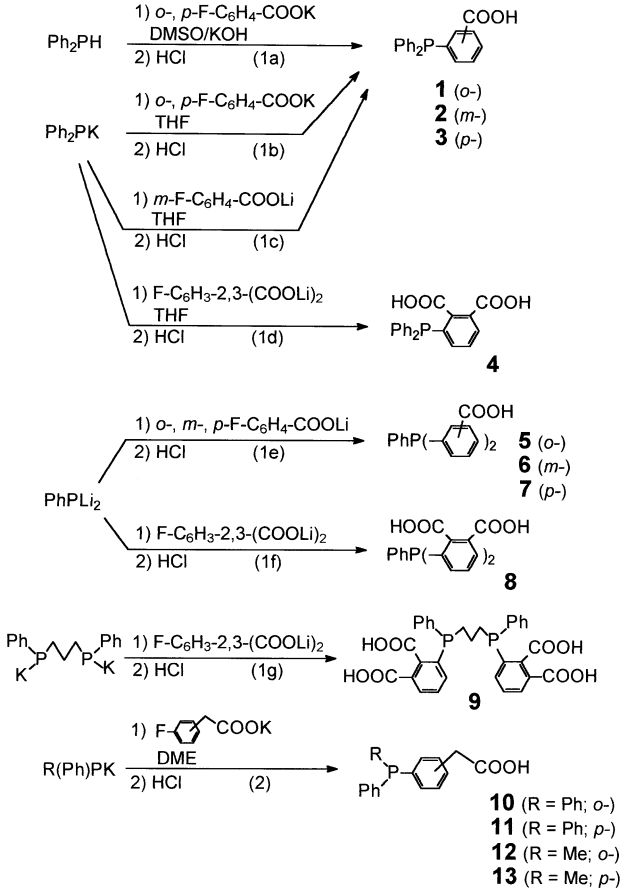

The nucleophilic phosphanylation of *p*-fluorobenzoic acid with Ph_2PH in the superbasic medium at 60 °C afforded the potassium salt of the phosphane **3** in a straightforward manner (eq. 1a). However, the corresponding reaction with the *o*-isomer gave only poor yields of **1**. Diphenylphosphane oxide $Ph_2P(H)O$[9a] and Ph_2PMe[9b] are formed by oxidation of Ph_2PH (Ph_2PK) with DMSO followed by subsequent dealkylation of the intermediate Me_2S with Ph_2PK[10] (eq. 3a,b). The potassium salt of *m*-fluorobenzoic acid did not react with Ph_2PH under these conditions. The COOK substituent in the *m*-position clearly does not activate the fluorine sufficiently for nucleophilic displacement to occur under these conditions.

$$Ph_2PH + Me_2SO \longrightarrow Ph_2P(O)H + Me_2S \quad (3a)$$

$$Me_2S + Ph_2PK \longrightarrow Ph_2PMe + MeSK \quad (3b)$$

If a solution of Ph_2PK in THF is used, then 2-F−C_6H_4−COOK could be phosphanylated to give the phosphane **1** in fair yield (eq. 1b). The *m*-isomer 3-F−C_6H_4−COOK, however, did not react at all even after prolonged reaction times. This might, at least in part, be due to the fact that 3-F−C_6H_4−COOK could not be obtained in a completely anhydrous form. 3-F−C_6H_4−COOK and 2-F−C_6H_4−COOK were prepared by neutralization of the corresponding acids with KOH in aqueous solution and heating the hydrates left after evaporation of water in vacuo at 100−120 °C for a couple of hours. The use of the anhydrous lithium salt 3-F−C_6H_4−COOLi instead of 3-F−C_6H_4−COOK resulted in phosphanylation with Ph_2PK in THF to afford **2** after work up of the reaction mixture (eq. 1c). Anhydrous 3-F−C_6H_4−COOLi can be obtained by deprotonation of the free acid with *n*BuLi or, preferably, $LiN(SiMe_3)_2$[11].

The bis(carboxyphenyl)phosphanes **5**−**7** are accessible, in an analogous way to that described above, by phosphanylation of the lithium salts of the corresponding fluorobenzoic acids with $PhPLi_2$ in THF (eq. 1e). In the case of the *m*-isomer of F-C_6H_4−COOLi, the nucleophilic aromatic substitution proceeds much slower than the corresponding reaction with the *p*- and *o*-isomers. This can be understood in terms of the different stabilization of the Meisenheimer type intermediate **E**[7b] by the COOH/COO^--substituents in the *m*- or *p*- and *o*-position to the fluoro substituent. The synthetic procedure developed for **5**−**7** can be extended to phthalic acid derivatives. Thus, nucleophilic phosphanylation of the Li-salt of 3-fluorophthalic acid with Ph_2PK or $PhPLi_2$ gave **4** or **8** after an acid workup procedure (eq. 1d,f). In the same way, Ph(K)P−$(CH_2)_3$−P(K)Ph was treated with 3-F−C_6H_3−1,2-$(COOLi)_2$ to yield the chiral bidentate tetracarboxylated phosphane **9** (eq. 1g).

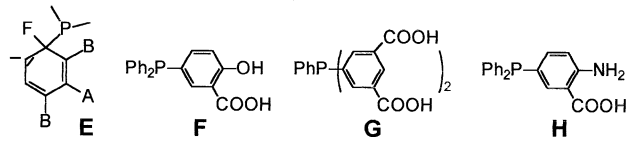

The potassium salts of the phthalic acid derivatives obtained by neutralization of **4**, **8**, and **9** with KOH are highly soluble in water [0.8, 1.3, and 1.0 kg/kg water (20 °C), respectively].

Very recently we have found that carboxylated phosphanes (**1**−**7**) including salicylic, isophthalic, and anthranilic acid derivatives (**F**−**H**) can alternatively be synthesized by Pd-catalyzed P−C coupling reactions between primary

or secondary phosphanes and the corresponding functionalized iodo- or bromo-aromatic compounds[1,12].

The electron impact mass spectra of the phosphane ligands with monocarboxylated phenyl groups (**1**−**3**, **5**−**7**) all show the M^+ peak. Proximity effects[13] in the molecular ions of the *o*-carboxylated phosphanes (**1**, **5**) lead to the loss of CHO from the molecular ion. In the case of the phthalic acid derivatives **4**, **8**, and **9**, the peaks of highest *m*/*z* correspond to ions formed by loss of one or two molecules of H_2O.

Synthesis of Phosphanylphenylacetic Acids

The multiple functionality of the CH_2−COOR(H) group means that phosphanylphenylacetic acids and their esters should show an extended reactivity pattern (e.g. ester condensation) in comparison with benzoic and phthalic acid phosphanes of type **1**−**8**. This can be used for the design of tailor-made ligands with chiral backbones by the modular approach, as reported by Trost, van Vrancken and Bingel[14].

Nucleophilic phosphanylation of fluorophenylacetic acids in dimethoxyethane (DME) was employed for the synthesis of phosphanylphenylacetic acids. The intermediate of type **E**, formed in the rate determining step of these S_N2(Ar) processes, cannot be stabilized by the mesomeric effects of the substituents, and so the nucleophilic replacement is expected to proceed much slower than the analogous reaction of the fluorobenzene derivatives F−C_6H_4−Z [Z = CN (see below), COO^-, SO_3^-] with activating substituents. The weakly electron-withdrawing CH_2COO^- group can only activate the C−F bond in the *ortho* position due to its inductive effect. Thus, the reaction of the potassium salts of *o*- or *p*-fluorophenylacetic acid with Ph_2PK in DME requires 24 h reflux to give the respective isomers of diphenylphosphanylphenylacetic acid (**10**, **11**), after acidification of the reaction mixtures, in satisfactory yields (eq. 2). The P-chiral derivatives (**12**, **13**) can be prepared in an analogous way using Ph(Me)PK instead of Ph_2PK. Potassium fluorophenylacetate (*o*- or *p*-isomer) was obtained by neutralization of the appropriate free acids with a solution of KOH in methanol, followed by heating the solid left after evaporation of the solvent in vacuo (60 °C, 0.01 mbar)[15].

The molecular ion peaks in the mass spectra of the phosphanylphenylacetic acids are of high intensity (**10**) or represent the base peaks (**11**−**13**). The fragmentation pathway leads to the 9-phosphafluorenylium ions[16][17] at *m*/*z* = 183 or 197.

The solubilities of the alkali metal salts of the *p*-diphenylphosphanylphenylacetic acids in water (20 °C) are significantly higher than those of the corresponding *o*-isomers (e.g. Na^+ **10**: 130; Na^+ **11**: 750 g/kg water).

Synthesis of Phosphanylbenzylamines

Phosphanylbenzylamines with a primary amino group are of interest as starting materials for the synthesis of polymerizable phosphanes by acylation with acryl- or methacryloyl chloride[5a]. A new method for preparing water-soluble phosphanes by coupling of the phosphanylbenzylamine $Ph_2P-C_6H_4-CH_2$−4-NH(Me) to polyacrylic acid has very recently been reported[18]. Attempts to prepare phosphanylbenzylamines with a primary amino group by protective group synthesis via their 2,5-dimethylpyrrole derivatives or stabase (cyclic disilazane) adducts have so far been unsuccessful[5a].

We found, however, that phosphanylbenzylamines are accessible in a straightforward manner using a procedure analogous to that employed for the synthesis of the phosphanylphenylacetic acids **10**−**13**. Thus, reaction of *o*-, *m*-, or *p*-fluorobenzylamine with Ph_2PK in DME produced the phosphanes **14**−**16** in good yields. Chiral tertiary (**17** and **18**) and even secondary phosphanylbenzylamines (**19**) are accessible by this synthetic route if Ph(Me)PK or PhPHK are used instead of Ph_2PK (eq. 3a,b)[15].

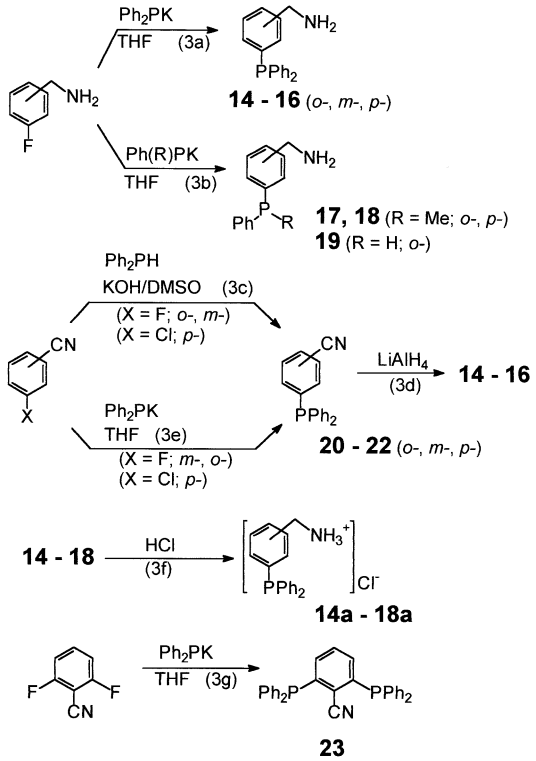

The phosphanylbenzylamines **14** and **15** have been synthesized using an alternative route involving reduction of the cyanophenylphosphanes **20** and **21**[3b][3c][19] with $LiAlH_4$. The cyanophenylphosphanes are attractive starting materials since they can be obtained by a convenient method and in high yields by direct phosphanylation of the corresponding fluoro- or chlorobenzonitriles with Ph_2PH in the superbasic medium DMSO/KOH (eq. 3c,d). The same applies for the *m*-isomer **21**. Somewhat lower yields of the cyanophenylphosphanes (**20**−**22**) are obtained if the phosphanylation of the halobenzonitriles are performed with Ph_2PK in THF (eq. 3e). In both cases the nucleophilic aromatic substitution proceeds almost instantaneously, even at room temperature or below. The synthesis of the cyanophenylphosphanes **20**−**22** according to eq. 3c is therefore

superior to the methods reported in the literature[3b][3c][19].

o-Cyanophenyldiphenylphosphane (**20**) was obtained by nucleophilic phosphanylation of 2-F−C_6H_4−CN according to eq. 3c and 3e in a straightforward manner. However, attempts to synthesize this ligand by reaction of 2-Cl−C_6H_4−CN with Ph_2PM (M = Li, K) gave only very poor yields[19]. This clearly demonstrates the greater reactivity of aromatic C−F bonds towards nucleophiles in comparison with C−Cl bonds[7].The *p*-isomer (**22**) could, however, be obtained from 4-chlorobenzonitrile, indicating that the steric influence of the *o*-substituents may be decisive and override the important electronic effects. In the case of the reactive 2,5-difluorobenzonitrile, both fluoro-substituents in the *o*-positions can be replaced by the bulky Ph_2P-substituents on reaction with Ph_2PK, with the interesting bidentate ligand **23** being formed in high yield (eq. 3g).

Protonation of **14**−**18** at the amino group gives cationic phosphanes (**14a**−**18a**) (eq. 3f), and the water solublities of these compounds range from 5 to 970 g per kg of water at 20 °C. The *p*-isomers have much higher solubilities than the corresponding *ortho*-compounds. At higher temperatures thermal dissociation occurs to give the primary amines and HCl. The mass spectra obtained from **14a**−**18a** therefore show the M^+ peaks of the corresponding phosphanylbenzylamines along with that of HCl.

NMR Spectra of the Phosphane Ligands 1−23

The structural assignments given for **1**−**23** are based mainly on $^{31}P\{^1H\}$- and $^{13}C\{^1H\}$-NMR spectroscopy. ^1H-NMR spectra will only be discussed in certain cases.

Table 1. $^{31}P\{^1H\}$-NMR-spectroscopical data of **1**−**23**; chemical shifts δP relative to 85% H_3PO_4; coupling constants ^1J(PH) in Hz in parentheses[a]

1	−9.6	**10**	−15.0	**17**	−35.3
2	−7.9	**11**	−4.3	**17a**	−35.7
3	−6.9	**12**	−38.0	**18**	−23.0
4	−5.2	**13**	−22.8	**19**	−48.4
5	−1.5	**14**	−14.2		(223.0)
6	−1.4	**15**	−1.7	**20**	−12.8[c], −6.7[d]
7	−1.5	**15a**	−1.7	**21**	−5.6[c], −3.6[d]
8	−5.4	**16**	−4.3	**22**	−5.7[c], −2.5[e]
9[b]	−20.5, −21.2	**16a**	−2.3	**23**	−9.8

[a] Solvents: DMSO (**1**, **3**, **5**−**7**, **20**−**22**), THF (**2**, **4**, **8**), D_2O/KOD (**9**), $CDCl_3$ (**10**, **15a**, **23**), CD_2Cl_2 (**11**−**14**, **16**, **19**, **20**, **21**), [D_6]acetone (**13**, **18**), CD_3OD (**15**, **17**, **16a**, **17a**). − [b] Diastereoisomers. − [c] Solvent DMSO. − [d] Solvent CD_2Cl_2. − [e] Solvent $CDCl_3$.

The ^{31}P-NMR shifts of the triarylphosphane-type ligands (**1**−**8**, **10**, **11**, **14**−**16**, **20**−**22**) are within a narrow range (δP = −1.4 to −15.0), and the δP values of **9**, **12**, **13**, **17**, **18** are typical for alkyl-diaryl phosphanes[20] (Table 1). In both cases the degree of substitution and the nature of the substituents has little influence on the δP values. The resonances of the *o*-isomers are shifted, in most cases, to higher field compared with those of the corresponding *m*- and *p*-isomers (c.f. **10/11**, **14/15/16**, and **20/21/22**). The bidentate carboxylated ligand **9**, containing two asymmetrically substituted phosphorus atoms, is formed as a mixture of two diastereoisomers (meso form and racemate) as indicated by two very close $^{31}P\{^1H\}$-NMR signals. The changes in the $^{31}P\{^1H\}$-NMR shift values of **14**−**17** on protonation with HCl are very small, indicating that the addition of the proton occurs preferentially at the nitrogen atom. The same also applies in the case of the $^{13}C\{^1H\}$-NMR data (c.f. **17/17a**), with the exception of δC(2)(*C*−CH_2−NH_2) (**17**: 147.0, **17a**: 138.6) (Table 2).

The assignment of the $^{13}C\{^1H\}$-NMR signals of **1**−**23** (Table 2; for the numbering scheme of the carbon atoms see Figure 1a) was achieved by comparison of the ^{13}C-shift values with those found in a series of related compounds including Ph_3P[21], Ph_2PH and $PhPH_2$[22]. The assignments were further substantiated by analysis of the proton-coupled spectra, including DEPT spectra[23], and comparison of the relative intensities of the signals. Further support for a correct assignment comes from the relative magnitude of the coupling constants ^nJ(PC), which generally decrease within the series $^2J(PC) > {}^1J(PC)$ and $^2J(PC) > {}^3J(PC) > {}^4J(PC)$[23]. The ^{13}C-NMR spectra could be analyzed using a first order approximation with $^2J(CH) < {}^3J(CH)$ and ^4J(CH) ca. 0 Hz[23]. This is shown for **8** as a representative example in Figure 1c.

The introduction of one COOH, CH_2−COOH, or CH_2−NH_2 substituent into the *o*-, *m*-, or *p*-position of the aromatic ring system causes a shift to lower field of the $^{13}C\{^1H\}$-NMR signals of the corresponding carbon atoms in comparison with those of the unsubstituted carbon atoms in the corresponding isomers and the phenyl rings, the δC values of which may be taken as an internal reference for each compound. On going from the carbonic acids to the respective potassium or sodium salts the $^{13}C\{^1H\}$-NMR spectra do not change very much, as shown for **5** and Na-**5**. The δC values of the resonances assigned to C1 and C3−C6 remain constant within 1 ppm, whereas the signal of C2 is shifted significantly (by about 2 ppm). This is in agreement with the results obtained for benzoic acid and benzoates[23a].

The $^{13}C\{^1H\}$-NMR resonances of the carbon atoms bearing a CN-substituent in **20**−**22** are shifted to higher field by between 10 and 20 ppm in comparison with those of the corresponding unsubstituted carbon atoms in the Ph-groups. This shielding effect of the CN group is well established for mono-, di-, and trisubstituted benzonitrile derivatives[23a][24].

In comparison with the corresponding δC values in phthalic acid (*C*−COOH: δ = 131.4)[25], the $^{13}C\{^1H\}$-NMR resonances of C2 [in **4**: 148.8 (32.0), **8**: 146.5 (34.4) and **9**: 147.3 (34), 147.2 (34)] are shifted drastically to lower field on the introduction of the Ph_2P or PhP(Ar) groups, while those of C4 (δ = 128.8, 129.9 or 130.0 vs. 128.6) are not changed very much. The coupling constants ^2J[PC(2)] in the substituted aromatic ring systems of **4**, **8**, and **9** are significantly greater than those in **1**, **2**, **5**, and **6**. This may be due to the pronounced steric effect of the two COOH groups in *o*- and *m*-positions which favors a conformation of the P−$C_6H_3(COOH)_2$ unit with the phosphorus lone pair in close proximity to C2 (Figure 1b). In general ^2J[PC(2)] in related systems is large when the lone pair is close to the C atom and small when it is remote[23b][23c].

Table 2. $^{13}C\{^1H\}$-NMR data of **1**−**23**[a,b,c]

	C1	C2	C3	C4	C5	C6	C7	C8	C9	C10	C11[d]
1	134.1 (19.2)	139.3 (26.3)	130.1 (3.0)	128.5	132.0	133.6	137.4 (12.1)	133.3 (20.2)	128.5 (7.1)	128.7	167.7
2	137.6 (13.2)	133.5 (19.2)	131.1 (6.1)	129.7	128.9 (7.1)	137.2 (20.2)	136.0 (11.0)	133.2 (20.2)	128.8 (17.0)	129.1	166.8
3	142.9 (14.2)	132.9 (18.7)	129.3 (6.1)	131.0			135.8 (10.1)	133.5 (20.2)	128.9 (7.1)	129.3	167.0
4	133.5 (13)	148.8 (32)	138.4 (10)	128.8	131.5 (4)	137.5 (7)	139.3 (9)	135.2 (19)	130.2 (6)	130.5	177.3[e], 178.7[f] (2)
5	136.0 (20.4)	143.0 (26.5)	131.7 (3.1)	129.2	132.8	135.5	140.4 (12.2)	135.1 (21.4)	129.4 (8.1)	129.5	169.7
6	137.2 (13.1)	133.9 (20.2)	131.5 (6.1)	130.1	129.3 (7.1)	138.0 (19.2)	135.6 (11.1)	133.5 (20.2)	129.1 (7.1)	129.5	166.9
7	142.1 (14.2)	133.3 (19.2)	129.5 (7.1)	131.4			135.1 (10.1)	133.9 (20.2)	129.1 (8.1)	129.7	167.1
8	133.0 (14.3)	146.5 (34.4)	136.3 (7.1)	129.9	128.0 (5.0)	136.2 (7.4)	138.7 (8.1)	134.5 (19.7)	129.4 (6.7)	129.6	177.5[e], 176.0[f] (3.7)
9[h]	133.0[g] (14)[g] 132.8 (14)[g]	147.3 (34) 147.2 (34)	133.5 (8)	130.0	127.3	135.1 (8) 135.2 (8)	139.3 (8) 139.2 (8)	132.4 (17) 132.3 (17)	128.9 (6)	128.6	170.6[e] (4) 167.9[f]
10[i]	137.1 (13.2)	138.5 (27.1)	130.9 (4.4)	129.3	127.8	134.0	136.2 (9.5)	133.9 (19.8)	128.7 (7.3)	129.0	177.8
11[j]	136.2 (4)	134.4 (19.8)	130.6 (7.3)	136.7	–	–	138.2 (11.0)	134.3 (19.8)	129.4 (6.6)	129.5	172.5
12[k]	139.9 (10.3)	138.2 (27.8)	130.4 (5.1)	129.0	127.9	132.0	139.2 (13.9)	131.8 (18.3)	128.3 (5.9)	128.1	177.9
13[l]	138.9 (13.2)	132.5 (18.3)	130.0 (6.6)	132.1	–	–	140.7 (13.2)	132.3 (18.3)	128.9 (6.6)	128.7	175.0
14[m]	136.9 (9.6)	147.7 (24.0)	129.8	127.6	128.5 (5.3)	134.0	135.6 (13.4)	134.3 (19.5)	129.0 (7.1)	129.2	–
15[n]	137.9 (11.2)	133.0 (22.9)	143.9 (7.4)	128.1	129.2 (5.7)	132.5 (16.3)	137.7 (11.2)	134.2 (19.4)	129.0 (6.7)	129.2	
16[o]	136.0 (10.6)	134.5 (19.8)	127.9 (7.1)	143.9	–	–	137.8 (11.1)	134.1 (19.4)	129.0 (7.0)	129.1	
17[p]	140.7 (11.7)	147.0 (22.7)	127.5[s]	129.4[s]	128.2 (5.9)	131.1	137.3 (14.7)	132.1 (18.3)	128.7 (6.6)	128.6	
17a	140.6 (8.8)	138.6 (24.9)	130.4	130.6	131.1 (5.9)	133.3	140.4 (14.7)	133.2 (18.3)	130.2 (6.6)	130.1	
18[q]	141.1 (13.2)	132.7 (18.9)	127.6 (6.9)	144.3	–	–	138.5 (12.2)	132.2 (18.3)	128.8 (6.2)	128.6	
19[r]	135.6 (6.2)	149.5 (15.6)	128.0 (4.0)	129.8	127.0 (2.8)	133.3 (12.6)	134.6 (11.0)	134.4 (17.3)	128.7 (9.2)	128.8	
20	142.7 (19.8)	117.8 (33.0)	132.1 (10.3)	128.5	133.8 (5.1)	133.0 (20.5)	134.5 (10.3)	134.0 (20.5)	128.8 (6.6)	129.4	117.6[s] (3.7)
21	136.6 (17.6)	137.7 (20.5)	112.9 (5.9)	132.1	129.3	140.4 (16.9)	135.9 (11.0)	133.9 (20.2)	129.2 (7.3)	129.5	118.7[s]
22	145.0 (17.6)	133.4 (19.5)	131.7 (6.6)	111.9	–	–	135.6 (11.0)	134.0 (20.5)	128.8 (7.3)	129.4	118.6[s]
23[u]	144.4 (17.9)[t]	122.8 (32.8)	144.4 (17.9)[t]	133.0	131.6	133.0	134.7 (10.5)[t,v]	133.9 (20.6)[t,v]	128.7 (7.2)[t,v]	129.3	115.8[s] (3.5)

[a] Chemical shift δ(C) relative to TMS; coupling constants ^nJ(PC) in Hz in parentheses. – [b] Solvents: CD_2Cl_2 (**10**, **20**, **21**, **23**), D_2O (**8**), $CDCl_3$ (**12**, **14** − **16**, **18**, **22**), [D_6]acetone (**11**, **13**), CD_3OD (**17**, **17**·HCl), C_6H_6 (**19**); [D_6]DMSO (**1**−**4**, **6**, **7**, **9**). – [c] For an indication of the carbon atoms see Figure 1a. – [d] COOH substituent. – [e] Potassium salt; COO^- in the *o*-position. – [f] COO^- in the *m*-position to phosphorus. – [g] Diastereoisomers. – [h] $-CH_2-CH_2-CH_2$: 22.8, 22.2; $CH_2-CH_2-CH_2$: 29.5, 29.4 (13); diasteroisomers. – [i] CH_2-COOH: 39.7 (23.5). – [j] CH_2-COOH: 40.9. – [k] CH_2-COOH: 39.6 (24.1); P−*Me*: 12.4 (13.9). – [l] CH_2-COOH: 41.1; P−*Me*: 12.4 (13.9).– [m] CH_2-NH_2: 45.5 (22.1). – [n] CH_2-NH_2: 46.7. – [o] CH_2-NH_2: 46.3. – [p] CH_2-NH_2: 44.7 (22.7); P−*Me*: 12.2 (13.9). – [q] CH_2-NH_2: 46.3; P−*Me*: 13.0 (14.5). – [r] CH_2-NH_2: 48.2 (15.5). – [s] CN groups.– [t] N = ^nJ(PC) + ^mJ(PC) ; n = 1−3; m = 3−6.– [u] ^4J(PP) = 4.78 ± 0.22 Hz. – [v] C7: ^1J(PC) = 10.26, ^5J(PC) = 0.36 Hz; C8: ^2J(PC) = 20.30, ^{6}(PC) = 0.11 Hz; C9: ^3J(PC) = 7.30 Hz.

Seperate resonances are observed for the two COOH groups in the 2,3-positions in the phthalic acid derivatives. In the case of **4** and **8** the signal at δ ≈ 177.5 shows doublet fine structure [^3J(PC)] and can therefore be assigned to the COOH groups in the *o*-position with respect to the P atom. The bidentate ligand **9** is obtained as a mixture of two diastereoisomers (meso form and racemate, see above) and for this reason a doubling of the $^{13}C\{^1H\}$-NMR resonances of some of the aromatic carbon atoms (C1, C2, C6, C7, C8) is observed. Although the fine structure of the signals assigned to the terminal CH_2 groups of the $(CH_2)_3$ bridge (X-part of an ABX spin system, A and B = ^{31}P, X = ^{13}C) could not be completely resolved, two triplets [^2J(PC)] being observed for the medial CH_2 group.

The presence of two phosphorus atoms in **23** means that the C-atoms C1(3), C4(6), and C7−C9 represent the X-part of ABX spin systems (X = ^{13}C, A and B = ^{31}P; for the numbering scheme for the carbon atoms see Figure 3a). Higher order $^{13}C\{^1H\}$-NMR spectra appearing as doublets of doublets (C1, C3), five line (C9) and six line patterns

Figure 1. (a) Numbering scheme for the carbon atoms in mono- and disubstituted aromatic phosphanes; (b) conformation of the Ph(R)P-group with respect to the plane of the substituted aromatic ring; (c) ^{13}C-NMR spectrum of **8**

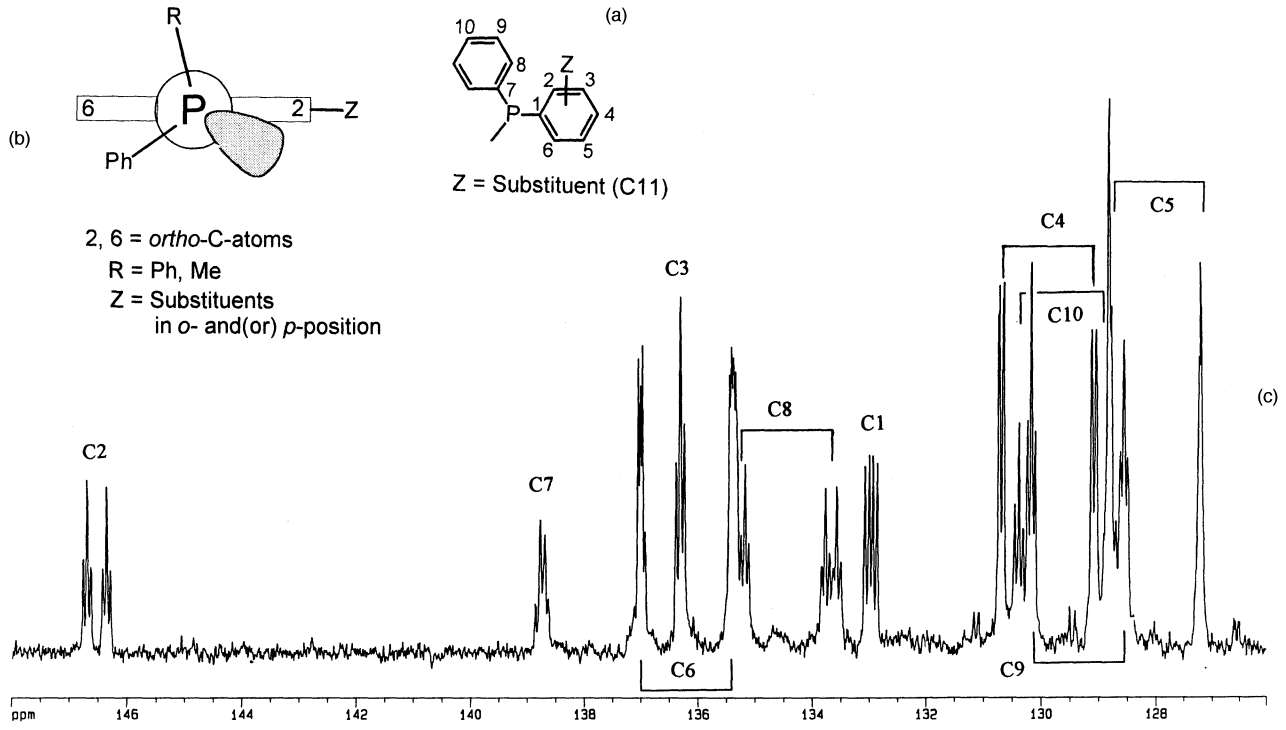

Figure 2. (a) Conformation of the CH_2-X group in **12** and **17**; (b) ^{1}H-NMR spectrum (CH_2-part) of **17**

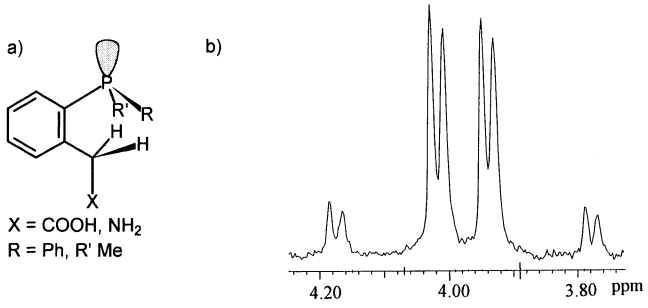

(C7, C8) are observed (Figure 3b). The analysis of the latter gave a value of around 4.8 Hz for the long range P-P coupling constant [^4J(PP)]. The resonances of C2 and C11 (X-parts of XA_2 spin systems) show first order triplet splitting, while singlets are obtained for C4(6) and C5.

The hydrogen atoms of the CH_2 groups in **12**, **17**, **17a**, **19**, and **19**·HCl are diastereotopic due to the asymmetric substitution at the phosphorus atoms (see Figure 2a). The ^{1}H-NMR spectra of these compounds therefore represent the AB part of an ABX spin system (A and B = ^{1}H, X = ^{31}P) and appear as an eight-line pattern in the cases of **17** (Figure 2b), **17a**, and **19**. The coincidence of lines means that a six-line pattern is observed for **19**·HCl and **12**.

This work was supported by the *Bundesministerium für Bildung, Wissenschaft, Forschung und Technologie* and *the Fonds der Chemischen Industrie*. The *Hoechst AG* is thanked for financial support and generous gifts of chemicals.

Experimental Section

Experimental details are given in part VIII of this series[1]. Phenylphosphane, phenylmethyl- and diphenylphosphane were prepared according to literature methods[26]. 2-, 3-, and 4-Fluorobenzoic acid, 3-fluorophthalic acid, 2- and 4-fluorophenylacetic acid, 2-, 3-, and 4-fluorobenzonitrile, and 2- and 4-fluorobenzylamine were purchased from The Aldrich Chemical Company and used without further purification.

Preparation of **1** *by Phosphanylation of 2-F−C_6H_4−COOK with Ph_2PK:* To 20 ml of a 0.5 M solution of Ph_2PK (10.0 mmol) in THF was added 1.8 g (10.0 mmol) of 2-F−C_6H_4−COOK with stirring and the reaction mixture was heated at 60 °C for 20 h. After extraction with 20 ml of conc. KOH solution the aqueous phase was acidified with conc. HCl until a precipitate formed. The mixture was then extracted with 40 ml of diethyl ether and the extracts were dried over Na_2SO_4. Evaporation of the solvent in vacuo gave **1** as a colorless solid. Yield: 1.97 g (64%). − **1**: $C_{19}H_{15}O_2P$ (306.3): calcd. C 74.50, H 4.94; found C 74.20, H 4.96. − MS: (M^+: *m/z* = 306). − IR: ν(COOH): 1695, 1305 cm^{-1}.

Preparation of **2** *and* **4**−**8**: The lithium salts of the fluorobenzoic acids or 3-fluorophthalic acid were added at ambient temperature to either a THF solution of Ph_2PK or to a suspension of $PhPLi_2$ in THF (obtained by metalation of $PhPH_2$ with *n*BuLi in *n*-hexane in the presence of tetramethylethylenediamine at −40 °C), respectively (see Table 4). After the reaction mixtures were refluxed for 2 h the solvents were removed under reduced pressure (30 °C, 1 mbar). The remaining residues were dissolved in 100 ml of water and filtered through a fine porosity fritted funnel. On acidification of the filtrate the phosphanes precipitated as colorless powders which were further purified by recrystallization from methanol/water mixtures. In the cases of compounds **4** and **8** the filtrates

Figure 3. (a) Numbering scheme for the carbon atoms in **23**; (b) $^{13}C\{^1H\}$-NMR spectrum of **23**

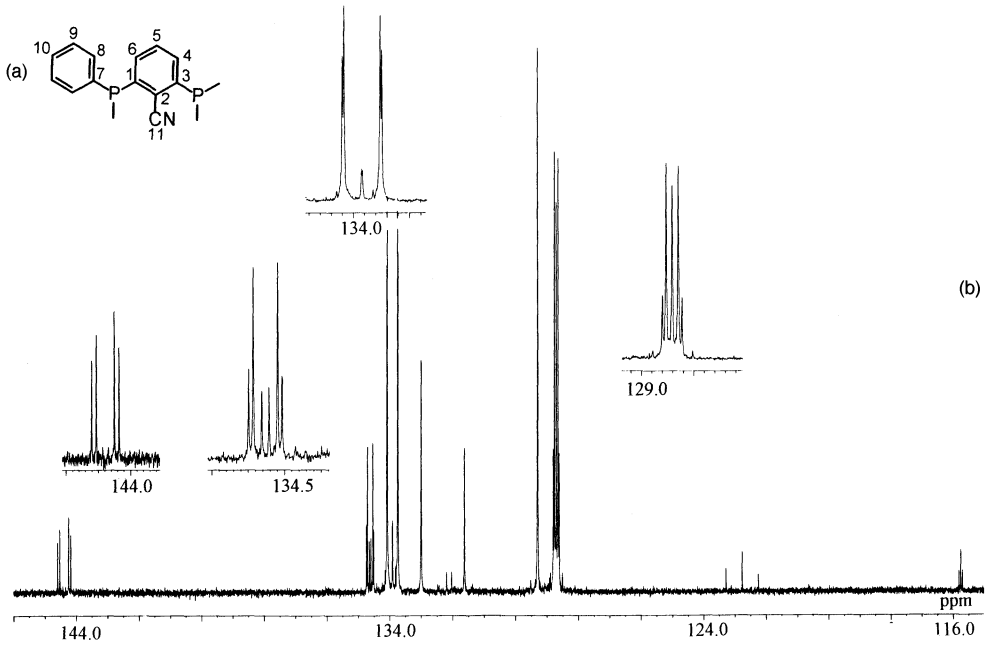

Table 3. Selected ^{1}H-NMR data of **10**−**19**[a]; shifts relative to TMS (int.), coupling constants (in parentheses) in Hz

	P(Me)	CH_2	NH_2	COOH
10		4.12		11.69
11		3.63		
12	1.57 (3.8)[b]	4.10[c] (16.7)[d]		10.74
		3.94[c] (−1.3)[e], −0.2[f]		11.79
13	1.59 (3.1)[b]	3.58		
14		4.05 (1.65)[g]	1.95[h]	
15		3.82	1.61	
16		3.83	2.23	
17	1.59 (4.2)[b]	3.89[c] (14.3)[d]	1.37	
		4.07[c] (−1.73)[e]		
		(−1.94)[f]		
18	1.31 (3.9)[b]	3.55	1.39	
19	5.19[i] (221.3)[j]	3.91[c] (14.4)[d]		
		4.02[c] (0.9)[e,f]		
19·HCl		4.45 (14.1)[d]		
		4.27 (0.3)[e] (−1.9)[f]		

[a] Solvents: $CDCl_3$ (**12**, **14**−**16**, **18**), CD_2Cl_2 (**10**, **13**, **19**), CD_3OD (**17**), [D_6]acetone (**11**). − [b] ^2J(PH). − [c] AB part of ABX spin system. − [d] ^2J(HH) (AB). − [e] ^4J(PH) (AX). − [f] ^4J(PH) (BX). − [g] ^4J(PH). − [h] Broad. − [i] δ (PH). − [j] ^1J(PH).

were extracted with 30 or 50 ml of diethyl ether prior to acidification (reaction conditions and yields are given in Table 4).

2: $C_{19}H_{15}O_2P$ (306.3): calcd. C 74.50, H 4.94; found C 73.81, H 5.19. − MS (M^+: *m/z* = 306). − IR: ν(COOH) = 1695, 1300 cm^{-1}.

4: $C_{20}H_{15}O_4P$ (350.3): calcd. C 68.57, H 4.32; found C 67.83, H 4.64. − MS ($M^+ - H_2O$: *m/z* = 332). − IR: ν(COOH) = 1715, 1280 cm^{-1}.

5: $C_{20}H_{15}O_4P$ (350.3): calcd. C 68.57, H 4.32; found C 66.93, H 4.42. − MS (M^+: *m/z* = 350). − IR: ν(COOH) = 1680, 1300 cm^{-1}.

6: $C_{20}H_{15}O_4P$ (350.3): calcd. C 68.57, H 4.32; found C 68.57, H 4.48. − MS (M^+: *m/z* = 350). − IR: ν(COOH) = 1680, 1300 cm^{-1}.

7: $C_{20}H_{15}O_4P$ (350.3): calcd. C 68.57, H 4.32; found C 68.77, H 4.69. − MS (M^+: *m/z* = 350). − IR: ν(COOH) = 1690, 1295 cm^{-1}.

8: $C_{22}H_{15}O_8P \cdot 4H_2O$ (510.4): calcd. C 51.77, H 4.54; found C 52.24 H 4.33. − MS ($M^+ - 2\,H_2O$: *m/z* = 402). − IR: ν(COOH) = 1715, 1280 cm^{-1}.

Table 4. Syntheses of **2**, **4**−**8**, **10**−**13**

	Ar*F g (mmol)	Phosphide g (mmol)	Solvent ml	Temp. [°C]	Time	Yield g (%)
2	K-3-fluoro-benzoate 1.8 (10)	Ph_2PK 2.24 (10)	THF 30	60	20 h	1.97 (64)
4	Li-3-fluoro-phthalate 2.94 (15)	Ph_2PK 3.36 (15)	THF 30	60	2.5 h	3.7 (70)
5	Li-2-fluoro-benzoate 7.3 (50)	$PhPLi_2$ 3.05 (25)	THF 100	60	5 h	6.3 (72)
6	Li-3-fluoro-benzoate 5.84 (40)	$PhPLi_2$ 2.44 (20)	THF 80	60	6 d	4.3 (61)
7	Li-4-fluoro-benzoate 3.94 (27)	$PhPLi_2$ 1.52 (12.5)	THF 50	20	12 h	3.6 (82)
8	Li-3-fluoro-phthalate 9.8 (50)	$PhPLi_2$ 3.05 (25)	THF 170	60	12 h	8.9 (70)
10	K-2-fluorophenyl-acetate 2.0 (10.4)	Ph_2PK 2.6 (11.4)	DME 30	85	12 h	1.94 (58)
11	K-4-fluorophenyl-acetate 2.0 (10.4)	Ph_2PK 2.6 (11.4)	DME 30	85	12 h	1.8 (54)
12	K-2-fluorophenyl-acetate 2.0 (10.4)	Ph(Me)PK 1.8 (11.4)	DME 30	85	12 h	1.88 (70)
13	K-4-fluorophenyl-acetate 2.18 (11.3)	Ph(Me)PK 2.0 (12.4)	DME 30	85	12 h	1.9 (65)

Preparation of **9**: 1.23 g (32 mmol) of potassium was added to a solution of 3.45 g (31 mmol) of phenylphosphane in 50 ml of THF and the reaction mixture was stirred for 2 h. The reaction mixture was refluxed under nitrogen for an additional 30 min in order to ensure completion of the reaction. Excess potassium was removed by decanting the solution. 3.00 g (15 mmol) of 1,3-dibromopropane was added and the yellow color of the solution disappeared. After

dilution with 30 ml of THF a further equivalent of 1.23 g (32 mmol) of potassium was added and the reaction mixture was again refluxed for 2 h. The lithium salt of 3-fluorophthalic acid was added and the color of the reaction mixture became dark red. After stirring for 12 h at 60−70 °C the color disappeared. All volatile components were then removed under reduced pressure (30 °C, 1 mbar). The residue obtained was dissolved in 200 ml of water and filtered through a fritted funnel. The filtrate was washed with three 50-ml portions of diethyl ether and then acidified with half conc. HCl. The white solid that precipitated was separated by filtration and recystallized from water/methanol. Yield: 4.1 g (41%). − **9**: $C_{31}H_{26}O_8P_2 \cdot 4H_2O$ (660.55): calcd. C 56.37, H 5.19; found C 55.51, H 5.33. − MS ($M^+ - 2\ H_2O$: *m/z* = 552. − IR: ν(COOH) = 1705, 1280 cm^{-1}.

Synthesis of **10**−**13**. − *General Procedure:* To a solution of Ph_2PK or Ph(Me)PK in DME [prepared by metalation of Ph_2PH or Ph(Me)PH with equimolar amounts of potassium] was added potassium 2- or 4-fluorophenyl acetate. The suspensions were refluxed until the yellow color of the potassium phosphides disappeared. The solvent was removed under reduced pressure (20 °C, 0.01 mbar) and, in each case, the solid obtained was dissolved in 50 ml of water. Unreacted phosphane was extracted with dichloromethane. After cooling to about 0 °C, the aqueous phase was acidified with conc. HCl. The phosphanylphenylacetic acids precipitated and were isolated by filtration through a fine porosity fritted funnel. A slurry was obtained by suspending the residue in 50 ml of water and 1 equivalent of KOH was added. The solution formed was filtered, cooled to about 0 °C and acidified with conc. HCl. The precipitate was isolated by filtration and dried in vacuo (20 °C, 0.01 mbar). The amounts of starting materials and yields are given in Table 4.

10: $C_{20}H_{17}O_2P$ (320.3): calcd. C 74.99, H 5.35; found C 74.33, H 5.56. − MS (M^+: *m/z* = 320). − IR: ν(COOH) = 1714 cm^{-1}.

11: $C_{20}H_{17}O_2P$ (320.3): calcd. C 74.99, H 5.35; found C 74.33, H5.49. − MS (M^+: *m/z* = 320). − IR: ν(COOH) = 1736 cm^{-1}.

12: $C_{15}H_{15}O_2P$ (258.3): calcd. C 69.76, H 5.85; found C 68.96, H 5.98. − MS (M^+: *m*/e = 258). − IR ν(COOH) = 1701 cm^{-1}.

13: $C_{15}H_{15}O_2P$ (258.3): calcd. C 69.76, H 5.85; found C 69.08, H 5.89. − MS (M^+: *m/z* = 258). − IR ν(COOH): 1712 cm^{-1}.

Preparation of **14**−**19** *by Phosphanylation of Fluorobenzylamines.* − *General Procedure:* In a typical procedure the fluorobenzylamines were added to a solution of Ph_2PK or Ph(Me)PK in DME with stirring. After heating the reaction mixtures at reflux for 24 h the solvent was evaporated under reduced pressure (20 °C, 0.01 mbar) and the residue obtained was washed with 100 ml of water. The crude products were dried in vacuo and isolated by distillation at 220−240 °C and 10^{-3} mbar. Starting materials, reaction conditions and yields are given in Table 5.

14: $C_{19}H_{18}NP$ (291.4): calcd. C 78.33, H 6.23, N 4.81; found C 77.24, H 6.23, N 4.81. − MS (M^+: *m/z* = 291). − IR: ν_{as}/ν_s-NH_2 = 3376, 3313 cm^{-1}.

15: $C_{19}H_{18}NP$ (291.4): calcd. C 78.33, H 6.23, N 4.81; found C 78.10, H 6.54, N 4.83. − MS (M^+: *m/z* = 291). − IR: ν_{as}/ν_s-NH_2 = 3371, 3298 cm^{-1}.

16: $C_{19}H_{18}NP$ (291.4): calcd. C 78.33, H 6.23, N 4.81; found C 77.33, H 6.46 N 4.51. − MS (M^+: *m/z* = 291). − IR: ν_{as}/ν_s-NH_2 = 3371, 3294 cm^{-1}.

17: $C_{14}H_{16}NP$ (229.3): calcd. C 73.35, H 7.03, N 6.11; found C 72.53, H 7.31, N 6.23. − MS (M^+: *m/z* = 229). − IR: ν_{as}/ν_s-NH_2 = 3356, 3289 cm^{-1}.

18: $C_{14}H_{16}NP$ (229.3): calcd. C 73.35, H 7.03, N 6.11; found C 72.49, H 7.14, N 6.23. − MS (M^+: *m/z* = 229). − IR: ν_{as}/ν_s-NH_2 = 3366, 3304 cm^{-1}.

19: $C_{13}H_{14}NP$ (215.2): calcd. C 72.54, H 6.56, N 6.51; found C 72.38, H 6.67, N 6.29. − MS (M^+: *m/z* = 215). − IR: ν_{as}/ν_s-NH_2 = 3366, 3292 cm^{-1}.

Table 5. Syntheses of **14**−**23** by nucleophilic phosphanylation of Ar*F in DME/THF

	Ar*F(Cl) g (mmol)	Phosphide g (mmol)	Solvent ml	Temp. [°C]	Time	Yield g (%)
14	2-F-benzylamine 3.13 (25)	Ph_2PK[a] 5.6 (25)	DME 50	85	1 d	6.90 (95)
15	3-F-benzylamine 1.25 (10)	Ph_2PK[a] 2.2 (10)	DME 20	85	1 d	1.85 (56)[b]
16	4-F-benzylamine 3.59 (28.7)	Ph_2PK[a] 6.4 (28.7)	DME 30	85	1 d	6.55 (70)[b]
17	2-F-benzylamine 0.98 (7.8)	Ph(Me)PK[a] 1.3 (7.8)	DME 10	85	1 d	1.12 (54)[b]
18	4-F-benzylamine 1.96 (15.7)	Ph(Me)PK[a] 2.5 (15.7)	DME 10	85	1 d	3.02 (84)
19	2-F-benzylamine 9.13 (73)	Ph(H)PK[a] 10.8 (73)	DME 40	85	1 d	7.9 (50)
20	2-F-benzonitrile 1.81 (15)	Ph_2PLi[c] 2.9 (15)	THF 30	−78	15 min	2.65 (62)
21	3-F-benzonitrile 1.39 (11.5)	Ph_2PLi[c] 2.2 (11.5)	THF 30	−78	2 min	2.1 (65)
22	4-Cl-benzonitrile 3.95 (28.7)	Ph_2PK[a] 6.4 (28.7)	DME 30	0	10 h	5.45 (67)
23	2,5-difluoro-benzonitrile 2.83 (20.3)	Ph_2PK[a] 9.13 (40.7)	THF 100	−78	1 min	7.76 (81)

[a] Prepared by reaction of equivalent amounts of Ph_2PH or Ph(Me)PH with potassium (in DME). − [b] Isolated as HCl adducts, for the preparation from the amines see below. − [c] Prepared by reaction of equivalent amounts of Ph_2PH with *n*BuLi (1.6 M solution in *n*-hexane) in stoichiometric ratios in THF.

Synthesis of **20**−**23** *by Phosphanylation of 2- or 3-Fluoro- and 4-Chlorobenzonitrile with Ph_2PM (M = Li, K):* Diphenylphosphane was dissolved in THF and metalated at 0 °C by the addition of the eqivalent amount of *n*BuLi (1.6 M solution in *n*-hexane). The red colored solution of Ph_2PLi was cooled to −78 °C and stoichiometric amounts of 2- or 4-fluorobenzonitrile were added at this temperature. After removal of the solvent in vacuo the oily residue was washed with water and recrystallized from ethanol. For the preparation of **22** and **23**, 4-chlorobenzonitrile or 2,6-difluorobenzonitrile, respectively, were used as starting materials along with Ph_2PK. Ph_2PK was prepared by reaction of equivalent amounts of Ph_2PH and potassium. The workup procedure was the same as that described above. The crude products were recrystallized from methanol. Starting materials, reaction conditions and yields are given in Table 5.

20: $C_{19}H_{14}NP$ (287.3): calcd. C 79.43, H 4.91, N 4.81; found C 79.05, H 4.89, N 4.88. − MS (M^+: *m/z* = 287). − IR: ν(CN) = 2219 cm^{-1}.

21: $C_{19}H_{14}NP$ (287.3): calcd. C 79.43, H 4.91, N 4.81; found C 79.41, H 4.88, N 4.84. − MS (M^+: *m/z* = 287). − IR: ν(CN) = 2225 cm^{-1}.

22: $C_{19}H_{14}NP$ (287.3): calcd. C 79.43, H 4.91, N 4.81; found C 79.02, H 4.84, N 4.86. − MS (M^+: *m/z* = 287). − IR: ν(CN) = 2225 cm^{-1}.

23: $C_{31}H_{23}NP_2$ (471.5): calcd. C 78.97, H 4.92, P 13.14; found C 79.01, H 5.04, P 13.07. − MS (M^+: *m/z* = 471).

Reduction of **20** *and* **21** *with* $LiAlH_4$: To a suspension of 0.38 g (10 mmol) or 0.13 g (3.6 mmol) of $LiAlH_4$ in 80 or 40 ml of THF was added over 15 min a solution of 2.87 g (10 mmol) of **20** or 1.00 g (3.5 mmol) of **21** in 20 or 10 ml of THF. After stirring for 0.5 h at ambient temperature the reaction mixtures were refluxed for 1 h. The precipitate formed on the addition of 20 or 50 ml of water, respectively, was separated by filtration and the solvent was removed in vacuo (20 °C, 0.01 mbar). The remaining crude reaction products were purified by vacuum distillation (220−240 °C, 10^{-3} mbar). Yields: 2.45 g (84%) of **14** and 0.82 g (80%) of **15**.

Protonation of **14** *with HCl:* 0.5 g (1.7 mmol) of diphenylphosphanylbenzylamine (**14**) was dissolved in diethyl ether. An etheral solution of HCl was added until no further precipitate was formed. The solid was filtered off using a coarse porosity fritted funnel and then dried in vacuo (20 °C, 0.1 mbar). Yield: 0.50 g (89%) of **14a**.

14a: $C_{19}H_{19}ClNP$ (327.8): calcd. C 69.62, H 5.84, N 4.27; found C 68.56, H 5.89, N 4.22. − MS (M^+ − HCl: *m*/*z* = 291).

Synthesis of **1**, **3**, **20**−**22** *in the Superbasic Medium. − General Procedure:* Diphenyl- or phenylphosphane were added to a suspension of powdered KOH (88%) in DMSO and the mixtures were stirred for 1 h at ambient temperature. After addition of the appropriate amounts of the fluoroaromatic compounds (see Table 6), the orange to red colored solutions were heated for 70 h at 60−70 °C in the cases of **1** and **3**. The reactions of the fluorobenzonitriles with the phosphanes were complete within a couple of minutes. For the isolation of **1** and **3** the reaction mixtures were first extracted with 200 ml of diethyl ether. After acidification with conc. HCl extraction was repeated with three 75-ml portions of diethyl ether. The organic extracts were washed with 30 ml of water and then dried over $MgSO_4$. The residue obtained after evaporation of the solvents in vacuo was recrystallized from methanol. **20**−**22** were precipitated from the reaction mixtures by addition of 30−40 ml of water and separated by filtration. Further purification was possible by recrystallization from methanol. **1**, **3**, **20**−**22** prepared by this route gave correct analyses. The compounds were identified by NMR spectroscopy (see above). Starting materials, reaction conditions and yields are given in Table 6.

Table 6. Syntheses of **1**, **3**, **20**−**22** by nucleophilic phosphanylation of Ar*F in the superbasic medium DMSO/KOH

	Ar*F(Cl) g (mmol)	Phosphane g (mmol)	DMSO ml	KOH g (mmol)	Temp. [°C]	Time	Yield g (%)
1	2-fluoro-benzoic acid 3.5 (25)	Ph_2PH 4.65 (25)	40	3.83 (60)	20	72 h	3.5 (46)
3	K-4-fluoro-benzoate 4.5 (25)	Ph_2PH 4.80 (25.8)	70	1.9 (30)	55−60	20 h	5.1 (68)
20	2-fluoro-benzonitrile 6.06 (50)	Ph_2PH 9.3 (50)	80	3.83 (60)	20	10 min	11.9 (82)
21	3-fluoro-benzonitrile 1.2 (10)	Ph_2PH 1.86 (10)	40	0.77 (12)	20	10 min	2.4 (82)
22	4-chloro-benzonitrile 1.4 (10)	Ph_2PH 1.86 (10)	50	1.0 (1.5)	20	10 min	2.65 (92)

[1] O. Herd, A. Heßler, M. Hingst, M. Tepper, O. Stelzer, *J. Organomet. Chem.* **1996**, *522*, 69.

[2] [2a] A. E. O'Donell, C. R. Gum, *US Pat*. 4260844, 7. 4. 1981 (Shell Oil Co.); *Chem. Abstr.* **1981**, *95*, 61445g. − [2b] A. T. Kister, E. F. Lutz, *US Pat*. 4020121, 26. 4. 1977 (Shell Oil Co.); *Chem. Abstr.* **1977**, *87*, 6654j. − [2c] M. J. H. Russell, B. A. Murrer, *Fr-Pat*. 2489308, 5. 3. 1982 (Johnson Matthey); *Chem. Abstr.* **1982**, *97*, 55308q. − [2d] W. Richter, R. Kummer, K. Schwirten, *DE* 3126265, 20. 1. 1983 (BASF AG); *Chem. Abstr.* **1983**, *98*, 179637 m; S. D. Burke, J. E. Cobb, *Tetrahedron Lett.* **1986**, *27*, 4237; M. J. H. Russell, *Platinum Met. Rev.* **1988**, *32*, 179; A. Buhling, P. C. Kamer, P. W. N. M. van Leeuwen, *J. Mol. Catal. A: Chem.* **1995**, *98*, 69. − [2e] D. M. Singleton, P. W. Glockner, W. Keim, *DE* 2159370, 8. 6. 1972 (Shell Oil Co.); *Chem. Abstr.* **1972**, *77,* 89124d; M. Peukert, W. Keim, *Organometallics* **1983**, *2*, 594. − [2f] F. Refosco, F. Tisato, G. Bandoli, E. Deutsch, *J. Chem. Soc., Dalton Trans.* **1993**, 2901.

[3] [3a] G. P. Schiemenz, H. U. Siebeneick, *Chem. Ber.* **1969**, *102*, 1883. − [3b] V. Ravindar, H. Hemling, H. Schumann, J. Blum, *Synth. Commun.* **1992**, *22*, 841. − [3c] V. Ravindar, H. Hemling, H. Schumann, J. Blum, *Synth. Commun.* **1992**, *22*, 1453. − [3d] R. Luckenbach, K. Lorenz, *Z. Naturforsch.* **1977**, *32b*, 1038.

[4] [4a] W. A. Herrmann, C. W. Kohlpaintner, H. Bahrmann, W. Konkol, *J. Mol. Catal*. **1992**, *73*, 191. − [4b] T. Okano, N. Harada, J. Kiji, *Chem. Lett.* **1994**, 1057.

[5] [5a] A. Reinholdsson, A. Nikitidis, C. Andersson, *React. Polym.* **1992**, *17*, 187; A. Nikitidis, C. Andersson, *Phosphorus, Sulfur, and Silicon* **1993**, *78*, 141. − [5b] D. E. Bergbreiter, *Soluble Polymer-Bound Reagents and Catalysts*, in Polymeric Reagents and Catalysts (Ed.: W. T. Ford), ACS, Washington, **1986**, ACS Symp. Ser. 308, p. 17; F. R. Hartley, *Supported Metal Complexes*, D. Riedel Publ., Dordrecht, **1985**.

[6] O. Herd, K. P. Langhans, O. Stelzer, N. Weferling, W. S. Sheldrick, *Angew. Chem.* **1993**, *105*, 1097; O. Herd, A. Heßler, K. P. Langhans, O. Stelzer, W. S. Sheldrick, N. Weferling, *J. Organomet. Chem.* **1994**, *475*, 99; F. Bitterer, S. Kucken, O. Stelzer, *Chem. Ber.* **1995**, *128*, 275; A. Heßler, S. Kucken, O. Stelzer, J. Blotevogel-Baltronat, W. S. Sheldrick, *J. Organomet. Chem.* **1995**, *501*, 293.

[7] [7a] C. A. Kingsbury, *J. Org. Chem.* **1964**, *29*, 3262. − [7b] J. March, *Advanced Organic Chemistry*, 3rd edition, p. 576, John Wiley & Sons, New York, **1985**. − [7c] H. Bader, A. R. Hansen, F. J. McCarty, *J. Chem. Soc.* **1966**, 2319.

[8] K. P. Langhans, O. Stelzer, J. Svara, N. Weferling, *Z. Naturforsch.* **1990**, *45b*, 203; E. N. Tsvetkov, N. A. Bondarenko, I. G. Malakhova, M. I. Kabachnik, *Synthesis* **1986**, 198.

[9] [9a] E. Fluck, H. Binder, *Z. Naturforsch.* **1967**, *22b*, 805. − [9b] L. Maier, *Organic Phosphorus Compounds* (Eds.: G. M. Kosolapoff, L. Maier), Vol. 1, p. 1, John Wiley & Sons, New York, London, Sydney, Toronto, **1972**.

[10] K. B. Mallion, F. G. Mann, *J. Chem. Soc*. **1965**, 4115; F. G. Mann, M. J. Pragnell, *J. Chem. Soc*. **1965**, 4120.

[11] U. Wannagat, H. Niederprüm, *Chem. Ber*. **1961**, *94*, 1540.

[12] O. Herd, A. Heßler, M. Hingst, M. Tepper, O. Stelzer, unpublished results.

[13] R. Srinivas, G. K. V. Rao, V. Ravinder, *Org. Mass Spectrometry* **1993**, *28*, 267.

[14] B. M. Trost, D. L. van Vranken, C. Bingel, *J. Am. Chem. Soc.* **1992**, *114*, 9327.

[15] For a preliminary communication see M. Tepper, O. Stelzer, T. Häusler, W. S. Sheldrick, *Tetrahedron Lett.* **1997,** *38*, 2257.

[16] B. Zeeh, J. B. Thomson, *Tetrahedron Lett.* **1969**, 111.

[17] D. H. Williams, R. S. Ward, R. G. Cooks, *J. Am. Chem. Soc.* **1968**, *90*, 966.

[18] T. Malmstroem, H. Weigl, C. Andersson, *Organometallics* **1995**, *14*, 2593.

[19] D. H. Payne, H. Frye, *Inorg. Nucl. Chem. Lett*. **1972**, *8*, 73; J. Erbe, W. Beck, *Chem. Ber.* **1983**, *116*, 3867; W. Wolfsberger, W. Burkart, H. Werner, *Z. Naturforsch.* **1992**, *47b*, 155.

[20] S. Berger, S. Braun, H. O. Kalinowski, *NMR-Spektroskopie von Nichtmetallen*, Bd. 3, ^{31}P-NMR-Spektroskopie, Georg Thieme Verlag, Stuttgart, New York, **1993**.

[21] [21a] T. Bundgaard, H. J. Jakobsen, *Acta Chem. Scand.* **1972**, *26*, 2548. − [21b] G. A. Gray, S. E. Cremer, K. L. Marsi, *J. Am. Chem. Soc.* **1976**, *98*, 2109.

[22] R. Batchelor, T. Birchall, *J. Am. Chem. Soc*. **1982**, *104*, 674.

[23] [23a] H. O. Kalinowski, S. Berger, S. Braun, ^{13}C-NMR-Spektroskopie, Georg Thieme Verlag, Stuttgart, New York, **1984**. − [23b] S. Sorensen, R. S. Hansen, H. J. Jakobsen, *J. Am. Chem. Soc*. **1972**, *94*, 5900; F. Bitterer, O. Herd, A. Heßler, M. Kühnel, K. Rettig, O. Stelzer, W. S. Sheldrick, S. Nagel, N. Rösch, *Inorg. Chem*. **1996**, *35*, 4103. − [23c] L. D. Quin in *Phosphorus-31 NMR Spectroscopy in Stereochemical Analysis* (Eds.: J. G. Verkade,

L. D. Quin), VCH Publishers, Deerfield Beach, Florida, **1987**, p. 391.
[24] F. W. Wehrli, J. W. de Haan, A. I. M. Keulemans, O. Exner, *Helv. Chim. Acta* **1969**, *52*, 103.
[25] M. J. Fifolt, S. A. Sojka, R. A. Wolfe, *J. Org. Chem*. **1982**, *47,* 148.
[26] [26a] M. Baudler, A. Zarkadas, *Chem. Ber.* **1971**, *104*, 1034. – [26b] G. U. Spiegel, O. Stelzer, *Chem. Ber*. **1990**, *123*, 989. – [26c] W. Gee, R. A. Shaw, B. C. Smith, *Inorg. Synth*. **1967**, *9*, 19.
[97111]

Synthesis and Crystal Structures of *P*-Halogeno(imino)methylenephosphoranes X−P(=N*t*Bu$_3$C$_6$H$_2$)=C(SiMe$_3$)$_2$ (X = Cl, Br, I)

Alexander Ruban, Martin Nieger, and Edgar Niecke*

Anorganisch-Chemisches Institut der Universität Bonn,
Gerhard-Domagk-Straße 1, D-53121 Bonn, Germany
Fax: (internat.) +49(0)228/735357

Received July 28, 1997

Keywords: Phosphorus ylides / Bis(ylene)phosphoranes / Halogenophosphoranes / X-ray structure analysis

The iminophosphane (Me$_3$Si)$_3$C−P=N−Mes* (**1**) reacts with iodine to form the imino(methylene)phosphorane I−P(=N−Mes*)=C(SiMe$_3$)$_2$ (**2**). Upon subsequent treatment with AgCl, the corresponding chloro derivative **3** is obtained. Chlorine/bromine exchange in **3** with bromotrimethylsilane affords the bromo analogue **4**. The structures of **2**, **3** and **4** were confirmed by X-ray crystal structure analysis; each of the compounds features a trigonal-planar phosphorus atom.

Introduction

The discovery of the first stable compound containing a trigonal-planar phosphorus(V) center in 1974[1] represents a landmark in organophosphorus chemistry. It opened the door to a rapid development of the chemistry of such compounds and structurally related derivatives[2] . Among these, bis(imino)-[3a] and bis(methylene)phosphoranes[3b] have attracted considerable attention, not only because they are valuable building blocks in organophosphorus and organometallic chemistry[4], but also because they are suitable precursors for monomeric metaphosphate analogues[5] and have found application in the catalysis of olefin polymerization[6]. In contrast, information concerning imino(methylene)phosphoranes, which feature both P−N- and P−C-pπ bonds, is comparatively sparse[3c]. Herein, we report on the synthesis and crystal structure analysis of the first *P*-halogeno(imino)methylenephosphoranes.

Results and Discussion

Treatment of the iminophosphane (Me$_3$Si)$_3$C−P=N−Mes* (**1**)[7], with iodine in THF at −40°C cleanly afforded the *P*-iodo(imino)methylenephosphorane **2**. Further reaction with AgCl in CH_2Cl_2 at 25°C resulted in I/Cl exchange of **2**, yielding the chloro derivative **3**. Subsequent reaction of **3** with Me$_3$SiBr led smoothly to the bromo derivative **4**. By crystallization from small volumes of *n*-hexane, compounds **2**−**4** were isolated as highly air- and moisture-sensitive, red (**2**), light-yellow (**3**), or orange (**4**) crystals (Scheme 1).

Scheme 1

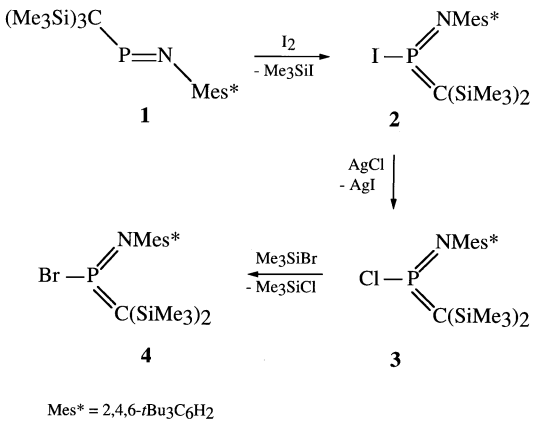

The *P*-halogeno(imino)methylenephosphoranes **2**−**4** have been characterized on the basis of their elemental analyses and ^{1}H-, ^{13}C-, ^{31}P-NMR and mass-spectrometric data. Furthermore, the solid-state structures of compounds **2**−**4** have been determined by X-ray crystallography.

The ^{31}P-NMR chemical shifts of compounds **2**−**4** are observed at relatively low field values, which is typical for bis(ylene)phosphoranes[8]. The deshielding of the phosphorus nuclei on going from the iodo derivative **2** to the chloro analogue **3** [^{31}P: δ = 53.3 (**2**) < 65.2 (**4**) < 72.5 (**3**)] is a characteristic feature of tetracoordinated P^V compounds[9].

The ^{13}C-NMR signals of the methylene carbon atoms, which are observed at lower fields than in "classical" methylenephosphoranes, show the inverse trend. A stronger carbon shielding is found on going from compound **2** to **4** to **3**, i.e. on increasing the electronegativities of the substituents [^{13}C: δ = 68.0 (**2**) > 58.2 (**4**) > 51.7 (**3**)]. At the same time, a significant increase in the magnitude of ^1J(C,P) from 34.1 Hz (**2**) through 50.6 Hz (**4**) to 65.3 Hz (**3**) is observed. An inverse electronegativity effect on both ^{31}P- and ^{13}C-chemical shifts was also observed for substitution at the methylene carbon atom in imino(methylene)phosphoranes and was attributed to a polarization effect[10]. Similar trends in the δ^{31}P, δ^{13}C and ^1J(C,P) values were observed in the corresponding *P*-halogenobis(methylene)-phosphoranes[3a] and *P*-halogenobis(imino)phosphoranes (δ^{31}P)[11]. As compared to compounds **2**−**4**, the ^{31}P nuclei in the former are less shielded by 30 to 65 ppm, while those in the latter appear more shielded by 30 to 70 ppm com-

 © WILEY-VCH Verlag GmbH, D-69451 Weinheim, 1998 1434−1948/98/0101−0083 $ 17.50+.50/0

pared to the corresponding nuclei in the imino(methylene)phosphoranes. Furthermore, a detailed experimental and quantum-chemical study on the influence of phosphorus substituents on ^{15}N-NMR shifts in bis(imino)phosphoranes led to the conclusion that the substituent effects were transmitted by both inductive and mesomeric interactions, and revealed a correlation between increased shielding and higher ylidic character of the ylene bond[12].

Table 1. Representative NMR data of *P*-halogenobis(ylidene)phosphoranes X−P(=A)=B

	δ^{31}P	δ^{13}C(P=C)	$^1J_{PC}$ [Hz]
X = Cl; A = B = N	−18.5	–	–
X = Br; A = B = N	−30.2	–	–
X = I; A = B = N	−42.9	–	–
X = Cl; A = N; B = C	72.5	51.7	65.3
X = Br; A = N; B = C	65.2	58.2	50.6
X = I; A = N; B = C	53.3	68.0	34.1
X = Cl; A = B = C	136.8	83.3	38.6
X = Br; A = B = C	122.5	91.3	30.8
X = I; A = B = C	84.7	102.9	23.5

The constitutions of compounds **2**−**4** were further corroborated by single-crystal X-ray diffraction studies. The phosphorus and carbon atoms of the imino(methylene) moieties exhibit the expected trigonal-planar geometries (Figure 1). The atoms of the CSi_2 and P−N−C_{ipso} moieties are almost coplanar (dihedral angle 4.4−5.6°), while the aryl substituent is approximately orthogonal to the central π-bond system (angle between the plane P−N−C_{ipso} and the aryl plane: 88.8−91.7°). The P−N double bond adopts a (*Z*) configuration, as is observed in *P*-halogeno(imino)-phosphanes[13]. The P−halogen distances [**3**: 206.9(2), **4**: 223.1(1), **2**: 242.9(1) pm] are shortened in comparison with the corresponding bond lengths in bis(imino)phosphoranes[11], but are longer than those in bis(methylene)phosphoranes[14]. The P−N [151.8(3)−153.1(4) pm] and P−C [162.4(4)−164.2(4) pm] distances, as well as the central C−P−N valence angles [129.2(2)−130.5(2)°] represent typical structural features common to both bis(imino)- and bis-(methylene)phosphoranes[3a][3b]. The other bond lengths and angles show no peculiarities.

Figure 1. Crystal structure of the imino(methylene)phosphorane **3**[a]

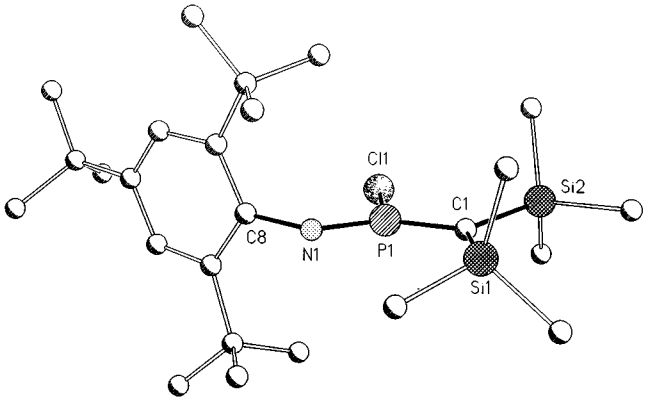

[a] Selected bond lengths [pm] and bond angles [°]: **3**: P(1)−Cl(1) 206.9(2), P(1)−N(1) 152.7(4), P(1)−C(1) 162.4(4), N(1)−C(8) 142.6(5); Cl(1)−P(1)−N(1) 113.1(1), Cl(1)−P(1)−C(1) 116.3(2), N(1)−P(1)−C(1) 130.5(2), P(1)−N(1)−C(8) 127.0(3). − **2**: P(1)−I(1) 242.9(1), P(1)−N(1) 153.1(4), P(1)−C(1) 164.2(4), N(1)−C(8) 142.3(5), I(1)−P(1)−N(1) 112.0(2), I(1)−P(1)−C(1) 118.8(2), N(1)−P(1)−C(1) 129.2(2), P(1)−N(1)−C(8) 125.6(3). − **4**: P(1)−Br(1) 223.1(1), P(1)−N(1) 151.8(3), P(1)−C(1) 162.7(4), N(1)−C(8) 140.8(5); Br(1)−P(1)−N(1) 112.1(1), Br(1)−P(1)−C(1) 117.5(2), N(1)−P(1)−C(1) 130.4(2), P(1)−N(1)−C(8) 127.8(3).

Regarding the potential synthetic utility of these halogeno(imino)methylenephosphoranes, one can expect them to undergo nucleophilic displacement reactions as well as thermally induced β eliminations of silyl halide. Both of these strategies are currently under investigation.

This work was supported by the *Deutsche Forschungsgemeinschaft* and the *Fonds der Chemischen Industrie*.

Experimental Section

All experiments were carried out with the exclusion of air and moisture under argon. Solvents were purified and dried according to standard methods. Compound **1** was prepared according to a literature procedure[7]. − NMR: Bruker AMX 300 (^{31}P: 121.5 MHz, external standard 85% H_3PO_4; ^{1}H: 300.1 MHz, external standard TMS; ^{13}C: 75.5 MHz, external standard TMS). − MS: Kratos Instruments Concept 1 H, Kratos Instruments MS 50, VG Instruments VG 12-250. − Elemental analyses: Analytisches Laboratorium Pascher. − Melting points were determined in sealed glass capillaries and are uncorrected.

Iodo[(2,4,6-tri-tert-butylphenyl)imino][bis(trimethylsilyl)-methylene]phosphorane (**2**): To a solution of iminophosphane **1** (2.61 g, 5 mmol) in 20 ml of THF, an equimolar amount of iodine, dissolved in 20 ml of THF, was added at −40°C. The reaction mixture was then allowed to warm to room temp. under stirring. The solvent and all volatile components were removed in vacuo and the remaining residue was taken up in 30 ml of *n*-hexane. Storage of the resulting solution at 0°C led to the deposition of **2** in the form of red crystals, which were found to be suitable for X-ray structural analysis. − Yield 2.57 g (89.3%), m.p. 111−113°C. − ^{31}P NMR (C_6D_6): δ = 53.3. − ^{1}H NMR (C_6D_6): δ = 0.57 (s, 18 H, $SiMe_3$), 1.47 (s, 9 H, *p*-*t*Bu), 1.72 (s, 18 H, *o*-*t*Bu), 7.61 (d, $^5J_{HP}$ = 5.8 Hz, 2 H, C_6H_2). − ^{13}C NMR (C_6D_6): δ = 5.0 (d, $^3J_{PC}$ = 5.8 Hz, $SiMe_3$), 32.1 (d, J_{PC} = 4.2 Hz, *p*-CCH_3), 32.9 (d, $^5J_{PC}$ = 2.7 Hz, *o*-CCH_3), 35.3 (d, J_{PC} = 4.4 Hz, *p*-CCH_3), 37.2 (d, $^4J_{PC}$ = 4.7 Hz, *o*-CCH_3), 68.0 (d, $^1J_{PC}$ = 34.3 Hz, P=C), 123.0 (d, $^4J_{PC}$ = 11.8 Hz, *m*-Ar), 143.7 (d, $^3J_{PC}$ = 19.1 Hz, *o*-Ar), 145.7 (d, $^5J_{PC}$ = 14.1 Hz, *p*-Ar), 145.8 (d, $^2J_{PC}$ = 24.1 Hz, *ipso*-Ar). − MS (70 eV); *m/z* (%): 574 (49) [M^+], 290 (100) [$tBu_3C_6H_2NP^+$]. − $C_{25}H_{47}INPSi_2$ (594.7): calcd. C 52.15, H 8.22; found C 52.28, H 8.26.

Chloro[(2,4,6-tri-tert-butylphenyl)imino][bis(trimethylsilyl)-methylene]phosphorane (**3**): To a solution of imino(methylene)phosphorane **2** (1.44 g, 2.5 mmol) in 10 ml of CH_2Cl_2, AgCl (0.39 g, 2.7 mmol) was added at room temp. and the suspension was stirred for 12 h. The solvent and the volatiles were then removed in vacuo and the remaining residue was taken up in 20 ml of *n*-hexane. The insoluble silver salt (AgI) was separated by filtration. Storage of the filtrate at 0°C resulted in the deposition of **3** in the form of yellow crystals. − Yield: 1.05 g (86.7%), m.p. 81−82°C. − ^{31}P NMR (C_6D_6): δ = 72.5. − ^{1}H NMR (C_6D_6): δ = 0.40 (s, 9 H, $SiMe_3$), 0.60 (s, 9 H, $SiMe_3$), 1.45 (s, 9 H, *p*-*t*Bu), 1.73 (s, 18 H, *o*-*t*Bu), 7.63 (d, $^5J_{PH}$ = 3.3 Hz, 2 H, C_6H_2). − ^{13}C NMR (C_6D_6): δ = 4.2 (d, $^3J_{PC}$ = 7.0 Hz, $SiMe_3$), 4.6 (d, $^3J_{PC}$ = 2.0 Hz, $SiMe_3$), 32.1 (d, J_{PC} = 3.0, *p*-CCH_3), 32.2 (d, $^5J_{PC}$ = 2.3 Hz, *o*-CCH_3), 35.2 (d, J_{PC} = 3.4 Hz, *p*-CCH_3), 36.9 (d, $^4J_{PC}$ = 3.8 Hz, *o*-CCH_3), 51.7

(d, $^1J_{PC}$ = 65.3 Hz, P=C), 122.7 (d, $^4J_{PC}$ = 8.9 Hz, *m*-Ar), 140.8 (d, $^2J_{PC}$ = 23.3 Hz, *ipso*-Ar), 142.9 (d, $^3J_{PC}$ = 15.7 Hz, *o*-Ar), 145.0 (d, $^5J_{PC}$ = 10.7 Hz, *p*-Ar). − MS (70 eV); *m*/*z* (%): 483 (11) [M^+], 290 (100) [$tBu_3C_6H_2NP^+$]. − $C_{25}H_{47}ClNPSi_2$ (484.2): calcd. C 62.01, H 9.78; found C 62.22, H 9.84.

Bromo[(2,4,6-tri-tert-butylphenyl)imino][bis(trimethylsilyl)-methylene]phosphorane (**4**): To a solution of **3** (1.21 g, 2.5 mmol) in 10 ml of THF was added an equimolar amount of Me_3SiBr and the reaction mixture was stirred for 2 h at room temp. The solvent and the halosilanes were then removed in vacuo and the residue was crystallized from a small volume of *n*-hexane. The product was obtained as an orange, crystalline solid. − Yield 1.16 g (87.5%), m.p. 99−101°C. − ^{31}P NMR (C_6D_6): δ = 65.2. − ^{1}H NMR (C_6D_6): δ = 0.40 (s, 9 H, $SiMe_3$), 0.60 (s, 9 H, $SiMe_3$), 1.45 (s, 9 H, *p*-*t*Bu), 1.73 (s, 18 H, *o*-*t*Bu), 7.62 (d, $^5J_{PH}$ = 3.6 Hz, 2 H, C_6H_2). − ^{13}C NMR (C_6D_6): δ = 4.6 (s, $SiMe_3$), 5.0 (d, $^3J_{PC}$ = 5.7 Hz, $SiMe_3$), 32.1 (d, J_{PC} = 6.1 Hz, *p*-C*C*H$_3$), 32.5 (d, $^5J_{PC}$ = 2.6 Hz, *o*-C*C*H$_3$), 35.2 (d, J_{PC} = 3.8 Hz, *p*-*C*CH$_3$), 37.0 (d, $^4J_{PC}$ = 3.8 Hz, *o*-*C*CH$_3$), 58.2 (d, $^1J_{PC}$ = 50.6 Hz, P=C), 122.8 (d, $^4J_{PC}$ = 10.2 Hz, *m*-Ar), 142.0 (d, $^2J_{PC}$ = 24.4 Hz, *ipso*-Ar), 143.2 (d, $^3J_{PC}$ = 17.1 Hz, *o*-Ar), 145.3 (d, $^5J_{PC}$ = 12.2 Hz, *p*-Ar). − MS (70 eV); *m*/*z* (%): 527 (52) [M^+], 290 (100) [$tBu_3C_6H_2NP^+$]. − $C_{25}H_{47}BrNPSi_2$ (528.7): calcd. C 56.79, H 8.96; found C 56.98, H 9.04.

Crystal-Structure Analyses. − Crystal Data: **2**: $C_{25}H_{47}INPSi_2$, M_r = 575.7, red tablets, 0.60 × 0.50 × 0.35 mm; monoclinic, space group $P2_1/c$ (No. 14), *a* = 8.853(3), *b* = 33.25(1), *c* = 10.666(4) Å, β = 99.75(3)°, *V* = 3094(2) Å^3, *Z* = 4, D_x = 1.24 Mg m^{-3}, μ(Mo-K_α) = 1.18 mm^{-1}, *T* = 293(2) K, *F*(000) = 1200, number of reflections: 7843 (7145 independent, R_{int} = 0.025), *R*(*F*) = 0.054, *wR*(F^2 all data) = 0.153 (266 parameters, 50 restraints). − **3**: $C_{25}H_{47}ClNPSi_2$, M_r = 484.2, yellow blocks, 0.40 × 0.30 × 0.20 mm, monoclinic, space group $P2_1/c$ (No. 14), *a* = 8.902(2), *b* = 32.825(5), *c* = 10.516(1) Å, β = 98.95(1)°, *V* = 3035.4(9) Å^3, *Z* = 4, D_x = 1.06 Mg m^{-3}, μ(Cu-K_α) = 2.44 mm^{-1}, *T* = 293(2) K, *F*(000) = 1056, number of reflections: 4845 (4442 independent, R_{int} = 0.096), *R*(*F*) = 0.075, *wR*(F^2 all data) = 0.232 (266 parameters, 62 restraints). − **4**: $C_{25}H_{47}BrNPSi_2$, M_r = 528.7, orange blocks, 0.80 × 0.70 × 0.50 mm, monoclinic, space group $P2_1/c$ (No. 14), *a* = 8.851(2), *b* = 32.87(1), *c* = 10.556(4) Å, β = 99.15(3)°, *V* = 3032(2) Å^3, *Z* = 4, D_x = 1.16 Mg m^{-3}, μ(Mo-K_α) = 1.50 mm^{-1}, *T* = 293(2) K, *F*(000) = 1128, number of reflections: 5622 (5325 independent, R_{int} = 0.053), *R*(*F*) = 0.055, *wR*(F^2 all data) = 0.151 (266 parameters, 62 restraints). An absorption correction on the basis of Ψ scans was applied.

Structure Solution and Refinement: The structures were solved by direct methods and refined anisotropically on F^2 (program system: SHELXTL-Plus[15], SHELXL-93[16]). Non-hydrogen atoms were refined anisotropically; H atoms were refined using a riding model; the *tert*-butyl groups were found to be disordered. Full details of the crystal structure determinations (except structure factors) have been deposited with the Cambridge Crystallographic Data Centre as supplementary publication no. CCDC-100474 (**2**, **3**, **4**). Copies may be obtained free of charge on application to CCDC, 12 Union Road, Cambridge CB2 1EZ, U.K. [Fax: (internat.) + 44(0)1223/336033; E-mail: deposit@ccdc.cam.ac.uk].

[1] [1a] E. Niecke, W. Flick, *Angew. Chem.* **1974**, *86*, 128; *Angew. Chem. Int. Ed. Engl.* **1974**, *13*, 585. − [1b] O. J. Scherer, N. Kuhn, *Chem. Ber.* **1974**, *107*, 2123. − [1c] S. Pohl, E. Niecke, B. Krebs, *Angew. Chem.* **1975**, 87, 284; *Angew. Chem. Int. Ed. Engl.* **1975**, *14,* 261.

[2] *Multiple Bonds and Low Coordination in Phosphorus Chemistry* (Eds.: M. Regitz, O. J. Scherer), Thieme, Stuttgart, **1990**.

[3] [3a] E. Niecke, D. Gudat in ref.[2], p. 392−404, and cited literature. − [3b] R. Appel in ref.[2], p. 367−374, and cited literature. − [3c] H. Heydt in ref.[2], p. 375−391.

[4] [4a] R. Appel, T. Gaitzsch, F. Knoch, G. Lenz, *Chem. Ber.* **1996**, *119*, 1977. − [4b] E. Niecke, M. Frost, V. von der Gönna, A. Ruban, W. W. Schoeller, *Angew. Chem.* **1994**, *106*, 2170−2172; *Angew. Chem. Int. Ed. Engl.* **1994**, *33,* 2111−2113.

[5] [5a] A. R. Barron, A. H. Cowley, *J. Chem. Soc., Chem. Commun.* **1987**, 1272. − [5b] H. J. Metternich, E. Niecke, *Angew. Chem.* **1991**, *103*, 336−337; *Angew. Chem. Int. Ed. Engl.* **1991**, *30*, 312−313. − [5c] P. Becker, H. Brombach, G. David, M. Leuer, H. J. Metternich, *Chem. Ber.* **1992**, *125,* 771−774.

[6] G. Fink, V. Möhring, *Stud. Surf. Sci. Catal. (Catal. Polym. Olefins)* **1986**, 25, 231.

[7] B. Schinkels, A. Ruban, M. Nieger, E. Niecke, *J. Chem. Soc., Chem. Commun.* **1997**, 293−294.

[8] K. Karaghiosoff in ref.[2], p. 463−471.

[9] S. Berger, S. Braun, H.-W. Kalinowski, *NMR Spectroscopy of Main Group Elements*, vol. III, Thieme Verlag, Stuttgart, **1993**.

[10] E. Niecke, D.-A.Wildbredt, *Chem. Ber.* **1980**, *113*, 1549−1565.

[11] A. Ruban, M. Nieger, E. Niecke, *Angew. Chem.* **1993**, *105*, 1544−1545; *Angew. Chem. Int. Ed. Engl.* **1993**, *32*, 1419−1420.

[12] D. Gudat, E. Niecke, A. Ruban, V. von der Gönna, *Mag. Res. Chem.* **1996**, *34*, 799−806.

[13] [13a] E. Niecke, M. Nieger, F. Reichert, *Angew. Chem.* **1988**, *100,* 1781; *Angew. Chem. Int. Ed. Engl.* **1988**, *27*, 1715. − [13b] V. Romanenko, L. S. Kachkovskaja, M. I. Povolotskii, A. N. Chernega, M. Yu. Antipin, Yu. T. Struchkov, L. N. Markovskii, *Zh. Obshch. Khim.* **1988**, *58*, 958−969. − [13c] M. Nieger, Thesis, Universität Bonn, **1989**. − [13d] E. Niecke, D. Gudat, *Angew. Chem.* **1991**, *103*, 251−270; *Angew. Chem. Int. Ed. Engl.* **1991**, *30*, 217−237.

[14] [14a] R. Appel, A. Westerhaus, *Tetrahedron Lett.* **1982**, *23*, 2017. − [14b] R. Appel, K.-H. Dunken, E. Gaitzsch, T. Gaitzsch, *Z. Chem.* **1984**, *24*, 384−385.

[15] G. M. Sheldrick, *SHELXTL-Plus*, Siemens Analytical X-ray Instruments Inc., Madison, Wisconsin, USA, **1989**.

[16] G. M. Sheldrick, *SHELXL-93*, University of Göttingen, **1993**.

[97177]

Imidotitanium Complexes with Heteroallylic Ligands: Synthesis and Solid-State Structure

Editha Müller[a], Jürgen Müller[a], Falk Olbrich[a], Wolfgang Brüser[a], Wolfram Knapp[b], Dirk Abeln[c], and Frank T. Edelmann*[a]

Chemisches Institut der Otto-von-Guericke-Universität Magdeburg[a],
Universitätsplatz 2, D-39106 Magdeburg, Germany

Institut für Experimentelle Physik der Otto-von-Guericke-Universität Magdeburg[b],
Universitätsplatz 2, D-39106 Magdeburg, Germany

Institut für Anorganische und Analytische Chemie der Universität Hamburg[c],
Martin-Luther-King-Platz 6, D-20146 Hamburg, Germany

Received August 4, 1997

Keywords: Imido complexes / Titanium / Heteroallylic ligands / Benzamidinate ligands / Diiminophosphinate ligands

Treatment of $Ti(NtBu)Cl_2(py)_2$ (**1**, py = pyridine) with bulky heteroallylic ligands in a 1:1 molar ratio affords the monosubstituted derivatives $[PhC(NSiMe_3)_2]Ti(NtBu)Cl(py)_2$ (**2**), $[MeOC_6H_4C(NSiMe_3)_2]Ti(NtBu)Cl(py)$ (**3**), and $[Ph_2P(NSiMe_3)_2]$-$Ti(NtBu)Cl(py)$ (**4**). Similarly, 2:1 reactions afforded the disubstitution products $[PhC(NiPr)_2]_2Ti(NtBu)(py)$ (**6**) and $[Ph_2P(NSiMe_3)_2]_2Ti(NtBu)$ (**7**). The bis(pyridine) adduct $Ph_2P(NSiMe_3)_2Li(py)_2$ (**5**) was isolated as a by-product during the preparation of **4**. The molecular structures of **7** has been established by X-ray crystallography.

The chemistry of transition metal imido complexes continues to be an area of active research.[1−3] Such compounds are of interest as intermediates in organic syntheses as well as catalytically active species.[4−19] Just a few years ago, imidotitanium(IV) complexes were exceedingly rare. The first well characterized monomeric imidotitanium species were reported independently at the same time by Roesky et al. and Rothwell et al. in 1990.[20,21] Following the initial work, various other monomeric and dimeric imido derivatives of titanium have been prepared.[22−30] However, a general route providing straightforward access to a series of Ti=NR species was lacking. The recent preparation of readily accessible precursors such as $Ti(NtBu)Cl_2(py)_2$ (**1**, py = pyridine) and $Ti(NtBu)Cl_2(t\text{Bu-py})_2$ (*t*Bu-py = 4-*tert*-butylpyridine) has greatly facilitated the investigation of these compounds.[31] Various complexes derived from these starting materials have recently been reported by Mountford et al.[31−35] We describe here the synthesis and structural characterization of imidotitanium(IV) complexes containing bulky heteroallylic ligands. Related complexes have so far been reported only for vanadium(V) and niobium(V).[36] The bulky heteroallylic ligands used in this study include the benzamidinate anions $[PhC(NSiMe_3)_2]^-$, $[MeOC_6H_4C(NSiMe_3)_2]^-$, and $[PhC(NiPr)_2]^-$ as well as the diiminophosphinate anion $[Ph_2P(NSiMe_3)_2]^-$.[37−40] Chelating ligands of this type are currently being investigated as alternatives for cyclopentadienyl ligands in the design of novel "metallocene-like" homogeneous catalysts.[41−50]

Syntheses and Structures

Compound **1** is easily made be reacting $TiCl_4$ with *tert*-butylamine in the presence of pyridine.[31−35] Subsequent treatment of **1** with lithium salts of bulky heteroallylic anions in THF solution in a 1:1 molar ratio resulted in formation of the monosubstitution products **2**−**4** (Scheme 1).

Scheme 1. Reaction conditions: *i)* $Li[PhC(NSiMe_3)_2]$, 1 equiv., THF, 20°C; *ii)* $Li[MeOC_6H_4C-(NSiMe_3)_2]$, 1 equiv., THF, 20°C; *iii)* $Li[Ph_2P(NSiMe_3)_2]$, 1 equiv., THF, 20°C

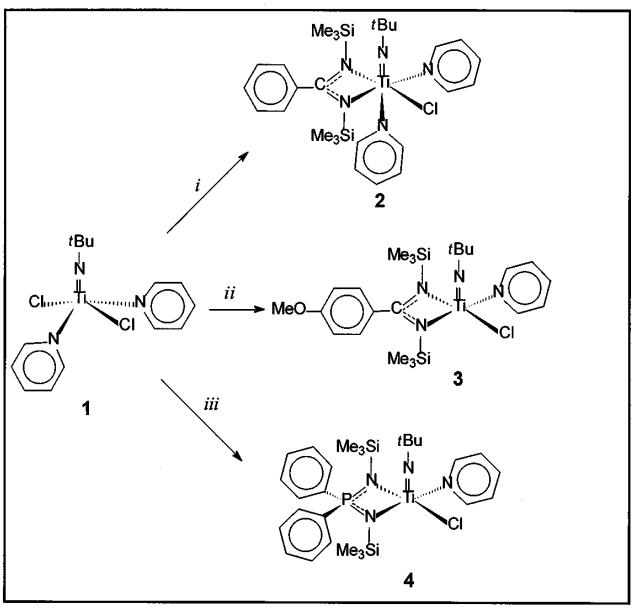

The monosubstituted complexes **2**−**4** form orange crystalline solids, which are soluble in THF or toluene and only marginally soluble in hexane or acetonitrile. All three compounds were fully characterized by elemental analyses and spectroscopic methods. The benzamidinate derivative **2** is

 © WILEY-VCH Verlag GmbH, D-69451 Weinheim, 1998 1434−1948/98/0101−0087 $ 17.50+.50/0

obtained as a bis(pyridine) adduct, while the complexes **3** and **4** contain only one additional pyridine ligand. In addition to the NMR spectroscopic results, the pyridine content of each compound was independently established by GC analysis of hydrolyzed samples. In the case of **2** X-ray quality crystals were grown from a saturated hexane solution. Unfortunately, due to the low quality of all examined crystals, the structure determination was not sufficiently accurate to allow a detailed discussion of bond lengths and angles. However, the crystallographic results confirm the overall structure of **2** as a monomeric *tert*-butylimidotitanium(IV) complex containing one silylated benzamidinate ligand and one chloro function (cf. Scheme 1).

The preparation of **4** from **1** and $Li[Ph_2P(NSiMe_3)_2]$[47–51] in THF solution is generally accompanied by the formation of the by-product $Ph_2P(NSiMe_3)_2Li(THF)_2$ (**5**), which can be isolated by fractional crystallization from hexane, in which it is less soluble than the titanium complex **4**.[51a] Compound **5** forms pale yellow, moisture sensitive crystals. Its molecular structure can be formulated in analogy to the crystallographically characterized THF adduct $Ph_2P(NSiMe_3)_2Li(THF)_2$.[51b] The presence of two pyridine ligands in **5** was further confirmed by a gas chromatographic analysis following hydrolysis of the material.

Similar treatment of **1** with two equivalents of heteroallylic ligands results in clean formation of the disubstituted derivatives **6** and **7** (Scheme 2).

Scheme 2. Reaction conditions: *iv)* $Li[PhC(NiPr)_2]$, 2 equiv., THF, 20°C; *v)* $Li[Ph_2P(NSiMe_3)_2]$, 2 equiv., THF, 20°C

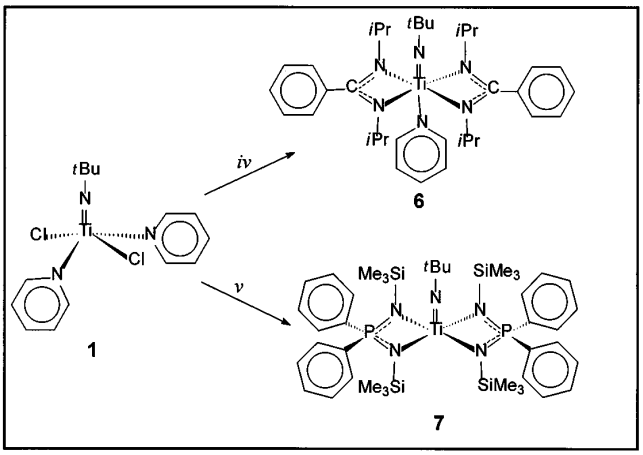

Once again the composition of the products depends on subtle differences in the steric bulk of the heteroallylic ligands. The benzamidinate derivative **6** is obtained as the mono-pyridine solvate, while **7** is an unsolvated, pentacoordinated imidotitanium(IV) species. The complexes are isolated as nicely crystalline, orange or red materials, which are readily susceptible to hydrolysis in the presence of moist air. They exhibit a high solubility in non-polar organic solvents such as toluene or hexane. Both complexes were fully characterized by elemental analyses and spectroscopic methods.

The molecular structure of **7** (Figure 1) was determined by X-ray diffraction. Red single crystals of the compound were grown by slow cooling of a saturated solution in hexane to −20°C. The crystallographic investigation confirms the presence of a monomeric, pentacoordinated imidotitanium complex, in which the central titanium atom is coordinated only to nitrogen. A comparable coordination environment was found for *tert*-butylimidotitanium species containing the aza-macrocyclic ligands tetra- and octamethyldibenzotetraaza[14]annulene (Me4taa and Me8taa, respectively).[31] With 1.680(4) Å the Ti=N bond length falls in the typical range found for other crystallographically characterized imidotitanium complexes (1.672(7)−1.723(4) Å).[35] The Ti−N−C(*t*Bu) angle [175.9(3)°] is much closer to linearity than that in the macrocyclic imidotitanium derivative (Me8taa)Ti(N*t*Bu) [164.3(3)°].[31] The *tert*-butylimido ligand can thus be assumed to act as four-electron donor towards titanium.

Figure 1. Molecular structure of $[Ph_2P(NSiMe_3)_2]Ti(NtBu)$ (**7**)[a]

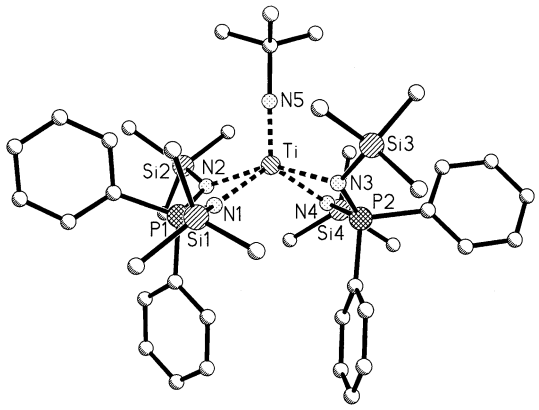

[a] Selected bond lengths [Å] and angles [°]: Ti−N(1) 2.152(5), Ti−N(2) 2.201(4), Ti−N(3) 2.203(5), Ti−N(4) 2.146(5), Ti−N(5) 1.680(4), P(1)−N(1) 1.605(4), P(1)−N(2) 1.596(4), P(2)−N(3) 1.597(4), P(2)−N(4) 1.607(4), N(5)−C(37) 1.481(6), Ti−N(5)−C(37) 175.9(3), N(1)−P(1)−N(2) 103.9(2), N(3)−P(2)−N(4) 104.0(2).

IR Studies

The compounds **2**−**4** and **6**, **7** have also been closely examined by IR and Raman spectroscopy. Assignment of the IR bands was made by spectra comparison as well as by inclusion of the Raman spectra and literature data. The N−C−N chelating units in **2**, **3**, and **6** give rise to a ν_{as} CN_2 band at 1523−1516 cm^{-1} as well as the ν_s CN_2 at 1377−1372 cm^{-1}.[52] The ν_{as} PN_2 vibration in **4** and **7** is assigned to the bands at 1090 and 1095 cm^{-1}, respectively.[53] The $SiMe_3$ groups in **2**−**4** and **7** are characterized by the following bands: δ_{as} CH_3 at 1407−1400 cm^{-1}, δ_s CH_3 at 1249−1245 cm^{-1}, and CH_3 rocking at 770−751 cm^{-1}.[54] Characteristic for the phenyl rings in all compounds are the ring valence vibrations at 1609−1600 cm^{-1} (only **7** shows no absorption in this region), 1592−1572 cm^{-1} and 1485−1477 cm^{-1} as well as the rocking vibrations at 1072−1062 cm^{-1} and at 1034−1028 cm^{-1}. A doublet at 1377−1372 and 1390−1385 cm^{-1} was assigned

to δ_s CH_3 of the *tert*-butyl group in the *tert*-butylimido ligand. In addition, the Raman spectra show at 653−651 cm^{-1} the ν_s (N)−CC_3 vibration of the N−$C(CH_3)_3$ unit.[55] ν Ti−py bands are observed in the spectra of **2**−**4** and **6** at 282−280 cm^{-1}.[56] In addition, the Raman spectra exhibit a ν CH band at 3082−3074 cm^{-1}, which can be assigned to pyridine. In the case of the monosubstituted complexes **2**−**4** the ν TiCl vibrations are observed at 323−321 cm^{-1} (IR) and 328−329 cm^{-1} (Raman), respectively. The isopropyl substituents in **6** give rise to the ν CH band at 1386 cm^{-1} in the IR spectrum as well as bands at 2926 cm^{-1} (ν CH), 2869 cm^{-1} (ν_s CH_3) and 480 cm^{-1} (δ CC_2) in the Raman spectrum.[55] Bands at 2838 cm^{-1} (ν_s CH_3), 1293 and 1040 cm^{-1} (ν CO) in the IR spectrum of **3** are typical for the *p*-methoxy substituent.[53]

Conclusions

In summary, we have shown that monomeric imidotitanium complexes containing bulky heteroallylic ligands can be synthesized starting from the readily accessible precursor Ti(N*t*Bu)Cl_2(py)$_2$ (**1**). Depending on the stoichiometry of the starting materials, 1:1- and 1:2 derivatives can be isolated. Bulky benzamidinate ligands as well as diiminophosphinate anions are equally suited to stabilize monomeric imidotitanium complexes.

We thank the *Deutsche Forschungsgemeinschaft*, the *Fonds der Chemischen Industrie* and the *Otto-von Guericke-Universität Magdeburg* for their continuing financial support.

Experimental Section

All reactions were carried out under purified nitrogen using standard Schlenk-line or dry-box techniques. Solvents were carefully dried over Na/benzophenone and freshly distilled under nitrogen prior to use. − Infrared and Raman spectra were recorded using a Perkin Elmer FTIR-2000 spectrometer equipped with a Raman facility. The IR measurements in the spectral range of 400−200 cm^{-1} were carried out using either Nujol mulls or with the pellet technique using RbBr as embedding medium. KBr pellets were used for spectra in the 4000−400 cm^{-1} range. For this purpose a metal bellow vessel was designed, which greatly facilitates the IR investigation of air-sensitive samples, especially in connection with the dry box technique. A diagram of the vessel is depicted in Figure 2.

The KBr die containing the air- and moisture-sensitive samples was placed under inert atmosphere in the dry-box into the evacuable metal bellow vessel made of steel. The metal bellow serves to level out the height difference of the vessel during power transmission from the hydraulic press onto the KBr die. The vessel is taken out of the dry box and evacuated to ca 10^{-2} mbar. After pressing the pellet the evacuated vessel is taken back into the dry box. The pellet holder containing the pellet is closed air-tight on both sides using IR cell windows and sealing rings, and then taken out of the dry box and inserted into the spectrometer. Very weak bands are not listed in the IR data. − NMR spectra: Bruker AM 250. − X-ray crystallography: Intensities were collected at −100°C on a Nonius CAD4 diffractometer with graphite-monochromated Cu-K_α radiation (λ = 1.54178 Å). The structure was solved by direct methods with SHELXS-86 and refined by full-matrix least-squares procedures using SHELXL-93.[57] A riding model was employed to refine the hydrogen atom positions. − The starting materials Ti(N*t*Bu)Cl_2(py)$_2$ (**1**),[31][35] Li[$RC_6H_4C(NSiMe_3)_2$] (R = H, MeO),[58] Li[PhC(N*i*Pr)$_2$][46] and Li[$Ph_2P(NSiMe_3)_2$][47,48] were prepared according to literature procedures.

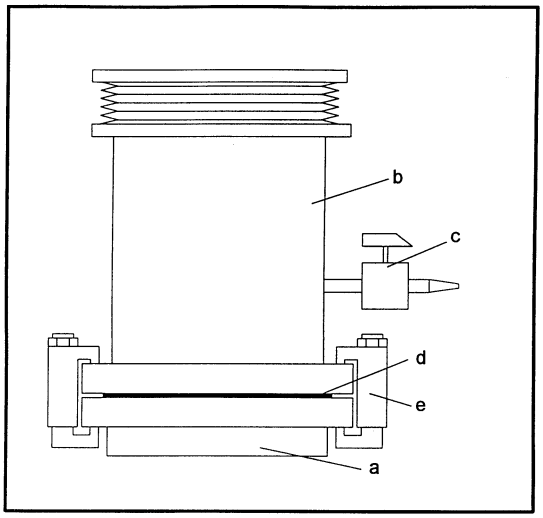

Figure 2. Diagram of the metal bellow vessel. a) base plate, b) cap with metal bellow, c) isolating valve, d) packing ring, e) clamp

*Reactions of Ti(NtBu)Cl_2(py)$_2$ (**1**) with Heteroallylic Ligands (General Procedure):* To a stirred solution of 1.74 g (5.0 mmol) of **1** in 20 ml of THF is added dropwise at room temperature a solution of 5.0 mmol of the ligand in 30 ml of THF (1:1 reactions). For the 1:2 reactions a solution of 10.0 mmol of the ligand in 60 ml of THF is employed. Stirring at room temperature is continued for 8 h and the mixture is evaporated to dryness. The residue is extracted with 40 ml of boiling hexane and filtered while hot through a thin layer of Celite filter aid. Cooling to −20°C for 24 h affords the crude product, which is purified by recrystallization from hexane.

[N,N'-Bis(trimethylsilyl)benzamidinato]-N-tert-butylimidochlorobis(pyridine)titanium(IV) (**2**): Red crystals, m.p. 107−109°C. Yield: 1.36 g (48%). − IR (cm^{-1}): $\tilde{\nu}$ = 2595 s, 2915 m, 2897 m, 1604 m, 1592 w, 1520 m, 1510 w, 1479 m, 1459 m, 1444 m, 1426 m, 1406 m, 1385 (sh) w, 1376 m, 1358 m, 1247 vs, 1027 w, 1042 m, 1029 w, 1013 m, 1002 m, 985 s, 921 s, 840 vs, 785 m, 759 s, 728 m, 700 s, 632 m, 526 m, 508 m, 492 m, 456 w, 392 w, 353 w, 302 w, 280 w. − ^{1}H NMR (C_6D_6): δ = 9.54 (m, 2 H, *p*-C_5H_5N), 8.70 (m, 4 H, *m*-C_5H_5N), 7.01 (m, 4 H, *o*-C_5H_5N), 6.90 (m, 1 H, *p*-C_6H_5), 6.65 (m, 4 H, *o,m*-C_6H_5), 1.35 (s br, 9 H, *t*Bu), 0.35 (s br, 18 H, $SiMe_3$). EI MS (70 eV); *m/z* (%): 567 (1) [M^+], 510 (2) [M^+ − C_4H_9], 263 (49) [$PhC(NSiMe_3)_2^+$], 103 (44) [$PhCN^+$], 73 (100) [$SiMe_3^+$]. − $C_{27}H_{42}ClN_5Si_2Ti$ (567.17): calcd. C 56.29, H 7.35, N 12.16; found C 55.83, H 7.82, N 11.88.

[N,N'-Bis(trimethylsilyl)-p-methoxybenzamidinato]-N-tert-butylimidochloro(pyridine)titanium(IV) (**3**): Red-brown crystals, m.p. 88−90°C. Yield: 1.34 g (51%). − IR (cm^{-1}): $\tilde{\nu}$ = 3069 w, 2954 m, 2897 m, 2838 w, 1609 s, 1583 w, 1516 m, 1489 m, 1477 m, 1459 m, 1443 s, 1425 (sh) s, 1400 m, 1390 (sh) m, 1377 m, 1350 m, 1300 (sh) w, 1293 m, 1249 s, 1171 m, 1108 m, 1071 w, 1040 (sh) m, 1034 m, 1016 s, 993 (sh) s, 983 s, 914 m, 839 vs, 756 s, 720 s, 695 s, 644 s, 633 s, 600 m, 543 m, 519 m, 502 w, 393 w, 389 w. − EI MS (70 eV); *m/z* (%): 527 (4) [M^+], 293 (6) [$MeOC_6H_4C(NSiMe_3)_2^+$], 73 (100) [$SiMe_3^+$]. − $C_{23}H_{39}ClN_4OSi_2Ti$ (527.09): calcd. C 52.41, H 7.46, N 10.63; found C 52.53, H 7.66, N 10.21.

N-tert-Butylimidochloro[P,P-diphenylbis(N-trimethylsilylimino)-phosphinato](pyridine)titanium(IV) (**4**): Orange crystals, m.p. 145−147°C. Yield: 2.61 g (88%). − IR (cm^{-1}): $\tilde{\nu}$ = 2956 m, 2895 m, 1604 w, 1591 w, 1485 w, 1438 m, 1403 w, 1390 w, 1377 w, 1353 w, 1257 s, 1247 s, 1212 m, 1138 s, 1115 vs, 1105 vs, 1090 vs, 1070 s, 1044 m, 1028 w, 1014 w, 999 w, 841 vs, 786 s, 751 s, 724 s, 696 vs, 660 s, 640 m, 626 m, 586 s, 532 vs, 509 s, 428 m, 366 m, 321 s, 297 m, 280 s, 248 m, 214 m. − ^{1}H NMR (C_6D_6): δ = 8,86 (m, 1 H, *p*-C_5H_5N), 8,63 (m, 2 H, m-C_5H_5N), 8,16-7,97 (m, 6 H, *m*,*p*-C_6H_5), 7,06 (m, 2 H, *o*-C_5H_5N), 1,52 (s, 9 H, *t*Bu), 0,33 (s, 9 H, $SiMe_3$), 0,10 (s, 9 H, $SiMe_3$). − EI MS (70 eV); *m*/*z* (%): 593 (2) [M^+], 578 (3) [$M^+ - CH_3$], 345 (100) [$Ph_2PN(SiMe_3)_2^+$], 73 (78) [$SiMe_3^+$]. − $C_{27}H_{42}ClN_4PSi_2Ti$ (593.14): calcd. C 54.68, H 7.14, N 9.45; found C 54.01, H 7.29, N 9.37.

Bis(pyridine)lithium P,P-Diphenylbis(N-trimethylsilylimino)-phosphinate (**5**): This compound was isolated as a by-product during the preparation of **4** and isolated as pale yellow crystals by fractional crystallization from hexane. All spectroscopic data (IR, ^{1}H NMR, ^{31}P NMR) were in good agreement with those of an authentic sample prepared directly by addition of pyridine to a hexane solution of $Li[Ph_2P(NSiMe_3)_2]$.[51] − $C_{28}H_{38}LiN_4PSi_2$ (524.72): calcd. C 64.04, H 7.30, N 10.68; found C 64.11, H 7.44, N 10.03.

N-tert-Butylimidobis[N,N-bis(isopropyl)benzamidinato](pyridine)titanium(IV) (**6**): Ochre, microcrystalline solid, m.p. 138−139°C. Yield: 1.45 g (48%). − IR (cm^{-1}): $\tilde{\nu}$ = 2964 s, 2920 s, 2890 s, 2862 s, 1645 m, 1635 m, 1616 w, 1600 s, 1576 m, 1523 s, 1505 s, 1480 s, 1441 s, 1386 s, 1372 s, 1345 s, 1336 s, 1243 s, 1221 s, 1213 s, 1203 s, 1168 s, 1135 s, 1120 s, 1112 s, 1070 s, 1039 s, 1030 (sh) m, 1007 vs, 949 m, 915 m, 798 m, 782 s, 757 s, 737 m, 701 vs, 631 m, 583 m, 525 s, 432 m, 300 m, 295 (sh) m, 282 m, 277 (sh) m. − ^{1}H NMR (C_6D_6): δ 7.34−7.06 (m, 10 H, C_6H_5), 3.58−3.35 (m, 4 H, *i*Pr-CH), 1.58−1.26 (m, 24 H, *i*Pr-CH_3), 1.01 (s, 9 H, *t*Bu). − $C_{35}H_{52}N_6Ti$ (604.72): calcd. C 69.52, H 8.67, N 13.90; found C 69.58, H 8.79, N 14.12.

N-tert-Butylimidobis[P,P-diphenylbis(N-trimethylsilylimino)-phosphinato]titanium(IV) (**7**): Red crystals, m.p. 130−132°C. Yield: 1.72 g (41%). − IR (cm^{-1}): $\tilde{\nu}$ = 3077 w, 3055 m, 2953 s, 2912 m, 2897 m, 1591 w, 1484 w, 1436 s, 1407 m, 1351 m, 1313 m, 1245 vs, 1209 m, 1181 w, 1153 (sh) m, 1115 vs, 1095 s, 1067 s, 1028 m, 999 w, 933 m, 840 vs, 770 s, 747 s, 731 s, 716 s, 695 s, 663 s, 655 (sh) s, 623 m, 615 m, 595 m, 529 s, 506 m, 489 m, 448 m, 409 m, 261 m, 239 m. − ^{1}H NMR (C_6D_6): δ 8.86 (m, 2 H, *m*-C_5H_5N), 8.65 (m, 1 H, *p*-C_5H_5N), 8.16−7.96 (m, 6 H, *m*,*p*-C_6H_5), 7.07 (m, 4 H, *o*-C_6H_5), 6.56 (m, 2 H, *o*-C_5H_5N), 1.52 (s, 9 H, *t*Bu), 0.33 (s, 9 H, $SiMe_3$), 0.10 (s, 9 H, $SiMe_3$). − $C_{40}H_{65}N_5P_2Si_4Ti$ (838.16): calcd. C 57.32, H 7.82, N 8.36; found C 57.42, H 8.04, N 8.30.

Crystal Structure Determination of **7**: $C_{40}H_{65}N_5P_2Si_4Ti$ (838.17), monoclinic, space group, a = 11.198(15), b = 22.055(26), c = 18.842(23) pm, β = 96.65(10)°, V = 4.6221(10) nm^3, Z = 4, d = 1.204 Mg/m^3, μ = 3.465 mm^{-1}, F(000) = 1792, crystal dimensions: 0.60 × 0.40 × 0.40 mm, 2θ range: 4−60°, number of measured reflexions: 6861 (5533 observed with $F^2 > 2\sigma F^2$), refined parameters: 487, goodness of fit: 1.058, R = 0.0772, wR = 0.1983. Further details of the crystal structure determination may be obtained from the Fachinformationszentrum Karlsruhe, Gesellschaft für wissenschaftlich-technische Information mbH, D-76344 Eggenstein-Leopoldshafen, Germany, on quoting the depository number CSD-380139, the names of the authors, and the journal citation.

[1] W. A. Nugent, B. L. Haymore, *Coord. Chem. Rev.* **1980**, *31*, 123.
[2] W. A. Nugent, J. M. Mayer, *Metal-Ligand Multiple Bonds*, Wiley-Interscience, New York, **1988**.
[3] D. E. Wigley, *Progr. Inorg. Chem.* **1994**, *42*, 239.
[4] P. L. McGrane, T. Livinghouse, *J. Am. Chem. Soc.* **1993**, *115*, 11485.
[5] V. C. Gibson, *Adv. Mater.* **1994**, *6*, 37.
[6] M. P. Coles, V. C. Gibson, *Polym. Bull.* **1994**, *33*, 529.
[7] R. K. Grasselli, J. D. Burrington, *Adv. Catal.* **1981**, 30, 133.
[8] J. D. Burrington, C. T. Katisek, R. K. Grasselli, *J. Catal.* **1984**, *81*, 489.
[9] D. M.-T. Chan, W. A. Nugent, *Inorg. Chem.* **1985**, *24*, 1422.
[10] D. M.-T. Chan, W. C. Fultz, W. A. Nugent, D. C. Roe, T. H. Tulip, *J. Am. Chem. Soc.* **1985**, *107*, 251.
[11] E. A. Maatta, Y. Du, *J. Am. Chem. Soc.* **1988**, *110*, 8249.
[12] E. A. Maatta, Y. Du, A. L. Rheingold, *J. Chem. Soc., Chem. Commun.* **1990**, 756.
[13] M. A. Andrews, H. D. Kaesz, *J. Am. Chem. Soc.* **1979**, *101*, 7238.
[14] M. A. Andrews, G. van Buskirk, C. B. Knobler, H. D. Kaesz, *J. Am. Chem. Soc.* **1979**, *101*, 7245.
[15] L. F. Rhodes, L. M. Venanzi, *Inorg. Chem.* **1987**, *26*, 2692.
[16] S. H. Han, G. L. Geoffroy, *Polyhedron* **1988**, *7*, 2331.
[17] M. Bakir, P. E. Fanwick, R. A. Walton, *Inorg. Chem.* **1988**, *27*, 2016.
[18] S. D. Gray, D. P. Smith, M. A. Bruck, D. E. Wigley, *J. Am. Chem. Soc.* **1992**, *114*, 5462.
[19] G. Perot, *Catal. Today* **1991**, *10*, 447.
[20] H. W. Roesky, H. Voelker, M. Witt, M. Noltemeyer, *Angew. Chem.* **1990**, *102*, 712; *Angew. Chem., Int. Ed. Engl.* **1990**, *29*, 669.
[21] J. E. Hill, R. D. Profilet, P. E. Fanwick, I. P. Rothwell, *Angew. Chem.* **1990**, *102*, 713; *Angew. Chem., Int. Ed. Engl.* **1990**, *29*, 664.
[22] J. E. Hill, P. E. Fanwick, I. P. Rothwell, *Inorg. Chem.* **1991**, *30*, 1143.
[23] C. C. Cummins, C. P. Schaller, G. D. van Duyne, P. T. Wolczanski, A. W. E. Chan, R. Hoffmann, *J. Am. Chem. Soc.* **1991**, *113*, 2985.
[24] R. Duchateau, A. J. Williams, S. Gambarotta, M. Y. Chiang, *Inorg. Chem.* **1991**, *30*, 4863.
[25] Y. Bai, M. Noltemeyer, H. W. Roesky, *Z. Naturforsch.* **1991**, *B46*, 1357.
[26] Y. Bai, H. W. Roesky, H.-G. Schmidt, M. Noltemeyer, *Z. Naturforsch.* **1992**, *B47*, 603.
[27] C. H. Winter, P. H. Sheridan, T. S. Lewkebandara, M. J. Heeg, J. W. Proscia, *J. Am. Chem. Soc.* **1992**, *114*, 1095.
[28] K. M. Doxsee, J. B. Farahi, *J. Chem. Soc., Chem. Commun.* **1990**, 1452.
[29] K. M. Doxsee, J. B. Farahi, H. Hope, *J. Am. Chem. Soc.* **1991**, *113*, 8889.
[30] F.-Q. Liu, A. Herzog, H. W. Roesky, I. Usón, *Inorg. Chem.* **1996**, *35*, 741.
[31] S. C. Dunn, A. S. Batsanov, P. Mountford, *J. Chem. Soc., Chem. Commun.* **1994**, 2007.
[32] S. C. Dunn, P. Mountford, O. V. Shishkin, *Inorg. Chem.* **1996**, *35*, 1006.
[33] S. C. Dunn, P. Mountford, D. A. Robson, *J. Chem. Soc., Dalton Trans.* **1997**, 293.
[34] G. I. Nikonov, A. J. Blake, P. Mountford, *Inorg. Chem.* **1997**, *36*, 1107.
[35] A. J. Blake, P. E. Collier, S. C. Dunn, W.-S. Li, P. Mountford, O. V. Shishkin, *J. Chem. Soc., Dalton Trans.*, **1997**, 1549.
[36] [36a] M. H. Ribeiro da Costa, J. H. Teuben, unpublished results, **1994**. − [36b] P. J. Stewart, A. J. Blake, P. Mountford, *Inorg. Chem.* **1997**, *36*, 1982.
[37] F. T. Edelmann, *Coord. Chem. Rev.* **1994**, *137*, 403.
[38] F. T. Edelmann, *J. Alloys Compd.* **1994**, *207/208*, 182.
[39] R. Duchateau, C. T. van Wee, A. Meetsma, J. H. Teuben, *J. Am. Chem. Soc.* **1993**, *115*, 4931.
[40] D. Herscovics-Korine, M. S. Eisen, *J. Organomet. Chem.* **1995**, *503*, 307.
[41] R. Gómez, R. Duchateau, A. N. Chernega, A. Meetsma, F. T. Edelmann, J. H. Teuben, M. L. H. Green, *J. Chem. Soc., Dalton Trans.* **1995**, 217.
[42] J. R. Hagadorn, J. Arnold, *Organometallics* **1994**, *13*, 4670.
[43] J. C. Flores, J. C. W. Chen, M. D. Rausch, *Organometallics* **1995**, *14*, 1827.

[44] D. Walther, R. Fischer, H. Görls, J. Koch, B. Schweder, *J. Organomet. Chem*. **1996**, *508*, 13.
[45] D. Walther, R. Fischer, M. Friedrich, P. Gebhardt, H. Görls, *Chem. Ber.* **1996**, *129*, 1389.
[46] J. Richter, F. T. Edelmann, M. Noltemeyer, H.-G. Schmidt, M. Shmulinson, M. S. Eisen, *J. Mol. Catal*., in press.
[47] H. Schmidbaur, K. Schwirten, H.-H. Pickel, *Chem. Ber*. **1969**, *102*, 564.
[48] W. Wolfsberger, W. Hager, *Z. Anorg. Allg. Chem.* **1977**, *433*, 247.
[49] A. Recknagel, M. Witt, F. T. Edelmann, *Z. Naturforsch*. **1991**, *B46*, 1328.
[50] [50a] A. Steiner, D. Stalke, *Inorg. Chem.* **1993**, *32*, 1977. – [50b] A. Recknagel, A. Steiner, M. Noltemeyer, S. Brooker, S. Stalke, F. T. Edelmann, *J. Organomet. Chem*. **1991**, *414*, 327.
[51] E. Müller, J. Müller, H.-G. Schmidt, M. Noltemeyer, F. T. Edelmann, *Phosphorus Sulfur Silicon*, **1996**, 121.
[52] K. Dehnicke, *Chem.-Ztg.* **1990**, *114*, 295.
[53] N. B. Colthup, L. H. Daly, S. E. Wiberly, *Introduction to Infrared and Raman Spectroscopy*, 3. Edition, Academic Press, **1990**.
[54] N. P. G. Roeges, *A Guide to the Complete Interpretation of Infrared Spectra of Organic Structures*, John Wiley & Sons, **1994**.
[55] D. Lien-Vien, N. B. Colthup, W. G. Fateley, J. G. Grasselli, *The Handbook of Infrared and Raman Characteristic Frequencies of Organic Molecules*, Academic Press, **1991**.
[56] K. Nakamoto, *Infrared and Raman Spectra of Inorganic and Coordination Compounds*, 4. Edition, John Wiley & Sons, **1986**.
[57] G. M. Sheldrick, *SHELXS-86; SHELXL-93, Programme zur Verfeinerung von Kristallstrukturen*, Göttingen, **1986**, **1993**.
[58] M. Wedler, F. Knösel, M. Noltemeyer, F. T. Edelmann, *J. Organomet. Chem*. **1990**, *388*, 21.

[97184]

The Molecular Structure of Some Transition-Metal Complexes with 1,2,3,4-Tetrazole-5-thiolate Anions☆

Heinrich Nöth*, Wolfgang Beck, and Klaus Burger

Institute of Inorganic Chemistry, University of Munich,
Meiserstraße 1, D-80333 München, Germany

Received August 12, 1997

Keywords: 2-Methyl-1,2,3,4-tetrazole-5-thiolates / 2-Phenyl-1,2,3,4-tetrazole-5-thiolates / Palladium / Platinum / Copper / Silver / Gold / Molecular structures

The molecular structures of nine transition metal tetrazolethiolates have been determined by X-ray structure determinations. The ligand is invariably coordinated through its sulfur atom to the metal center [M = Pd^{II}, Cu^{I}, Ag^{I}, Au^{I}, Au^{III}, and Hg]. The M−S−C bond angles vary considerably, but this cannot be correlated with variations in the C−S bond lengths. Intermolecular association occurs for $Ph_3PAu(SCN_4Me)$ via Au−S contacts, leading to dimeric strands in the solid state. The copper compound $(Ph_3P)_3Cu_4(SCN_4Me)_4$ (**5**), possesses a rather asymmetric structure: one Cu atom is tricoordinated by 3 sulfur atoms, the other three are tetracoordinated by P and N as well as by S atoms.

Introduction

It is well known that mercaptotetrazoles exist as their tetrazinethione tautomers[1]. Deprotonation leads to the tetrazolethiolate anion, which can be considered as a 6π-electron ring system[2]. It binds to metal atoms via its sulfur atom as is evident from IR spectra[3]. However, as shown for organotin complexes of mercaptotetrazoles, one of the nitrogen atoms of the tetrazole ring can also be involved in coordination[4]. This is not necessarily indicated by IR data. Therefore, X-ray structure investigations were necessary to complement other methods of structure analysis that we have performed on neutral and anionic palladium, platinum, copper, silver, and mercury complexes of 2-methyl- and 2-phenyl-1,2,3,4-tetrazole-5-thiolates. These compounds were first reported in 1977[3].

Neutral Complexes

Two types of transition-metal complexes of the mercaptotetrazole ligand have hitherto been described: (i) neutral complexes of the type $L_nM(SCN_4R)_m$ and (ii) anionic complexes $[M(SCN_4R)_m]^{n-}$, while cationic complexes with these ligands are as yet unknown. Neutral mercury, gold, silver, and copper complexes **1**−**5** were available for X-ray structure analyses.

$(Ph_3P)_2Hg(SCN_4Ph)_2$ **1** $(Ph_3P)AuSCN_4Me$ **2** $(Ph_3P)AuSCN_4Ph$ **3**

$(Ph_3P)_2AgSCN_4Ph$ **4** $(Ph_3P)_3Cu_4(SCN_4Me)_4$ **5**

The mercury complex **1** has a tetracoordinated metal center as shown in Figure 1. As has been suggested previously[3], only the sulfur atom of the tetrazolethiolate binds to the metal atom. In the case of compound **1**, the metal atom resides in a distorted tetrahedral environment. The mercury atom lies on a crystallographic twofold rotation axis and imposes C_2 point group symmetry on the molecule. There is a large variation in bond angles: the angle P1−Hg−P1a is rather wide [125.6(1)°] while the S1−Hg−S1a bond angle is compressed [95.7(1)°]. This reflects the larger steric requirement of the triphenylphosphane ligand. The two planes, P−Hg−P and S−Hg−S, are not perpendicular to one another; the twist angle is 78.9°. This is the result of an interaction between one phenyl group of the Ph_3P ligand and the tetrazole ring, which come into close contact and are oriented almost parallel to one another (interplanar angle: 18.4°). Moreover, the CN_4 plane is twisted with respect to the Hg1−S1−C1 plane by 17.8°, while the N-bonded phenyl group C2−C7 is in turn twisted by 125.6° with respect to the CN_4 plane.

Figure 1. ORTEP representation of the molecular structure of the mercury complex **1** in the solid state; hydrogen atoms are omitted for clarity

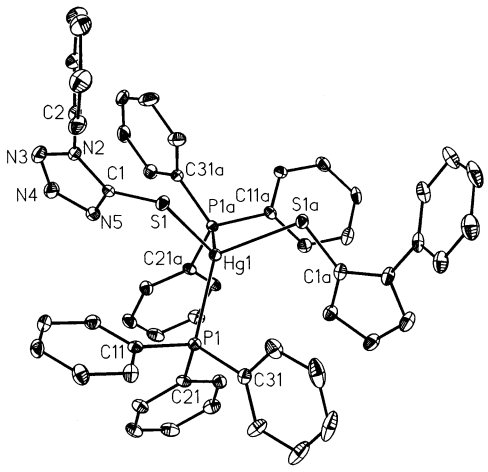

 © WILEY-VCH Verlag GmbH, D-69451 Weinheim, 1998 1434−1948/98/0101−0093 $ 17.50+.50/0

Table 1. Selected bond lengths [Å] and bond angles [°] with estimated standard deviations (in parentheses) for compounds **1**–**9**

Lengths [Å]	$(Ph_3P)_2Hg(SCN_4Ph)_2$ **1**[a]	$(Ph_3P)AuSCN_4Me$ **2**	$(Ph_3P)AuSCN_4Ph$ **3**	$(Ph_3P)_2Ag(SCN_4Ph)$ **4**	$(Ph_3P)_3Cu_4(SCN_4Me)_3$ **5**[a]
M–P1	2.500(3)	2.261(1)	2.265(2)	2.478(1)	2.219(2)
M–P2	–	–	–	2.449(1)	–
M–S1	2.566(3)	2.325(1)	2.304(2)	2.530(1)	2.387(1)
M–S2	–	–	–	–	2.397(2) (S7)
S1–C1	1.716(5)	1.740(4)	1.733(7)	1.698(5)	1.717(7)
C1–N2	1.352(6)	1.342(5)	1.346(9)	1.363(6)	1.357(7)
N2–N3	1.364(6)	1.354(5)	1.378(8)	1.367(7)	1.354(8)
N3–N4	1.297(7)	1.289(5)	1.295(9)	1.291(7)	1.297(7)
N4–N5	1.361(6)	1.354(5)	1.366(8)	1.352(7)	1.376(7)
N5–C1	1.338(7)	1.331(5)	1.346(8)	1.345(7)	1.343(7)
Angles [°]					
P1–M–P2	125.6(1)	–	–	124.55(5)	–
P1–M–S1	100.37(6)	170.11(3)	172.68(5)	115.31(4)	117.26(6)
P2–M–S1	95.7(1)[b]	–	–	120.09(5)	–
M–S1–C1	103.2(2)	97.5(1)	105.3(2)	90.8(2)	106.9(2)
S1–C1–N2	123.5(4)	123.7(3)	123.9(4)	127.7(4)	124.0(5)
S1–C1–N5	128.9(4)	128.2(3)	127.1(5)	125.6(4)	130.1(4)
C1–N2–N3	108.9(4)	108.7(3)	107.8(5)	108.6(5)	110.4(5)
N2–N3–N4	105.9(4)	105.9(3)	106.3(6)	106.3(4)	106.2(5)
N3–N4–N5	111.6(4)	111.8(3)	111.9(5)	111.5(5)	110.4(5)
N4–N5–C1	106.1(4)	105.5(3)	105.0(6)	106.8(4)	107.2(5)
N5–C1–N2	107.6(4)	108.1(4)	109.0(5)	106.7(4)	105.9(6)

Table 1 *(Continued)*

Lengths [Å]	$Hg(SCN_4Me)_4^{2-}$ **6**[a]	$Pd(SCN_4Me)_4^{2-}$ **7**[a]	$Au(SCN_4Ph)_4^-$ **8**[a]	$Au(SCN_4Ph)_2^-$ **9**[a]
M–S1	2.535(3)	2.332(1)	2.356(1)	2.279(2)
M–S2	2.595(3)	2.339(1)	2.358(1)	2.288(2)
M–S3	2.507(2)	–	–	–
M–S4	2.534(3)	–	–	–
S1–C1	1.73(1)	1.727(4)	1.743(6)	1.748(7)
S2–C3	1.73(1)	1.735(4)	1.735(6)	1.725(7)
C1–N2	1.33(1)	1.342(5)	1.334(8)	1.360(8)
N2–N3	1.36(1)	1.363(5)	1.349(7)	1.351(8)
N3–N4	1.30(1)	1.284(5)	1.302(8)	1.299(8)
N4 -N5	1.33(1)	1.336(5)	1.353(7)	1.352(9)
N5–C1	1.33(1)	1.323(5)	1.325(8)	1.327(9)
Angles [°]				
S1–M–S2	106.22(9)	88.61(4)	89.41(5)	175.15(7)
S1–M–S	112.9(1) (S3)	91.39(4) (S2a)	90.59(5) (S2a)	–
M–S1–C1	100.5(4)	108.3(1)	106.8(2)	110.1(2)
M–S2–C2	98.1(3)	106.9(1)	107.2(2)	102.6(2)
S1–C1–N2	123.7(9)	126.0(3)	124.8(5)	128.9(5)
S1–C1–N5	126.4(8)	125.8(3)	126.9(5)	123.0(5)
C1–N2–N3	109.3(9)	108.2(4)	109.3(5)	108.2(5)
N2–N3–N4	104.3(9)	106.5(4)	105.2(5)	106.3(6)
N3–N4–N5	112.7(8)	110.9(4)	111.6(5)	111.4(6)
N4–N5–C1	105.7(9)	106.3(3)	105.5(5)	106.1(5)
N5–C1–N2	108(1)	108.1(4)	108.3(5)	107.9(6)

[a] Bond parameters for only one tetrazolethiolate unit is given. Those of the other tetrazolethiolate groups are similar within esd's. – [b] S1–M–S1a.

Surprisingly, the Hg–P bond is shorter than the Hg–S distance. The opposite might have been expected considering the atomic radii of P and S atoms. Trends in the bonding parameters of the tetrazole thiolate ligand will be discussed later.

Amongst the coinage metal tetrazolethiolates, those of Au^I are the simplest ones. Two closely related compounds, $Ph_3PAuSCN_4R$ [R = Me (**2**); Ph (**3**)], have been investigated, which differ considerably as far as intermolecular interactions are concerned. The methyl compound **2** shows a dicoordinated gold atom and an almost linear array of the core atoms P, Au and S and angle 170.1(3)°, see Figure 2]. There is clearly very little steric strain in the molecule because the C–P–C bond angles lie in the narrow range from 105.5 to 107.2(3)°; the largest deviation from the ideal tetrahedral angle is only 4°. It should also be noted that the Au1–S1–C1 bond angle is rather small for that of a thiolate.

Figure 2. ORTEP representation of the molecular structure of the gold 2-methyltetrazolethiolate **2** in the crystal; hydrogen atoms are omitted for clarity

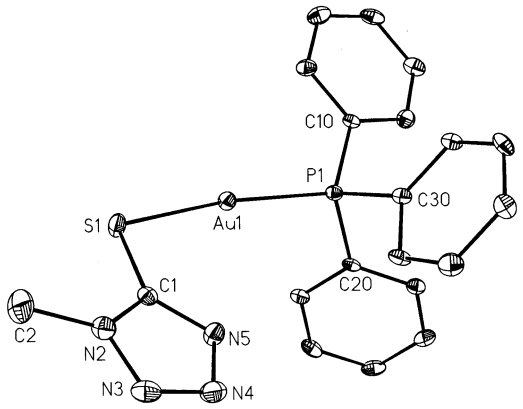

Figure 3. View of two associated molecules of **2** as present in the crystal

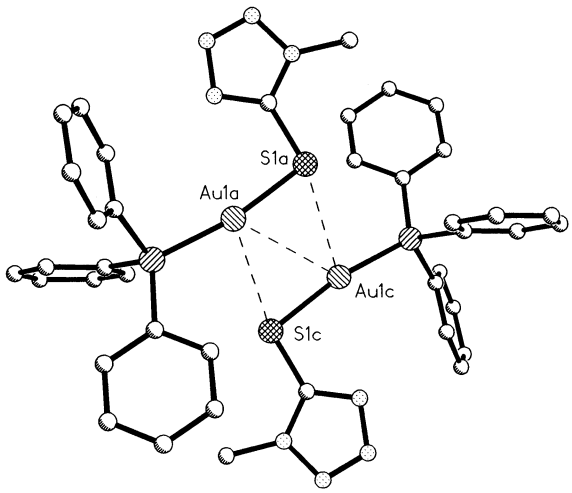

The tetrazole ring forms an angle of 13.2° with the P1–Au1–S1 plane. Interplanar angles between the phenyl groups range from 70.8 to 77.8°, and the C1–C6 plane is almost perpendicularly oriented to the P1–Au1–S1 plane. As in the case of compound **1**, we also observe a longer metal–S bond compared to the metal–P bond for the gold complex **2**, the difference between the bond lengths being

0.037 Å. This is, however, much smaller than that in **1** (0.066 Å).

In the lattice, the molecules of **2** are associated to dimers (see Figure 3) by weak intermolecular gold−sulfur contacts with a distance of 3.423 Å. However, the closest intermolecular Au−Au distance in **2** is 3.946 Å. Therefore, there is no bonding interaction between these atoms as is often found in gold(I) thiolates[5].

Although the overall molecular structure of the gold phenyltetrazolethiolate **3** (see Figure 4) resembles that of compound **2**, considerable differences become apparent upon close inspection. While the P1−Au1−S1 bond angles [172.68(5)°] and the C−P−C bond angles are very similar, the tetrazole ring is twisted out of the P1−Au1−S1 plane by 19.3°. More significant with regard to the packing of the molecules in the lattice is the effect of the phenyl group attached to the tetrazole ring. This group is twisted by 47.7° in relation to the nitrogen-containing ring. Compared with compound **2**, the Au−S bond is not significantly longer but at 105.3(2)° the Au1−S1−C1 bond angle is much wider. However, the most important difference between the two gold thiolates is the packing in the lattice: In compound **3** there are no intermolecular Au−S contacts. In fact, the shortest intermolecular distances between non-hydrogen atoms are between atom C16 of a PPh group and atoms C1, N2 and N3 (3.740, 4.014 and 4.165 Å, respectively).

Figure 4. ORTEP plot of the molecular structure of gold 2-phenyltetrazolethiolate **3**

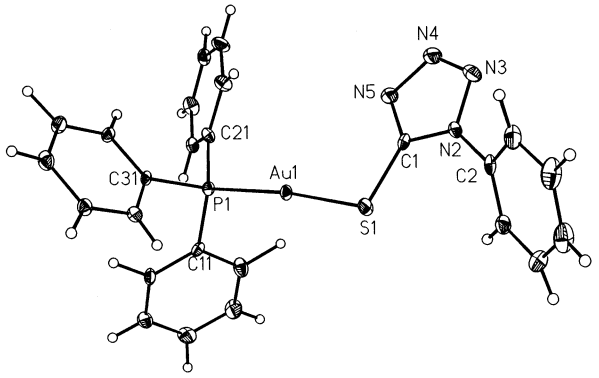

In contrast to the gold complexes **2** and **3**, the silver 2-phenyltetrazolethiolate **4**, which crystallizes as $(Ph_3P)_2AgSCN_4Ph \cdot CH_2Cl_2$, coordinates to two triphenylphosphane ligands. This results in a planar P_2AgS structural unit (see Figure 6, sum of bond angles at Ag: 359.9°) with respect to which the CN_4 ring plane is twisted by 117.5°; the phenyl group bonded to the tetrazole ring forms an interplanar angle of 134.5° with the latter. The interplanar orientations of the phenyl rings of the phosphane ligands range from 88.0 to 97.0° for P1, and are 75.9, 94.4 and 114.0° for those at P2, the latter being much less evenly distributed than the former. Ag−P bond lengths are shorter by 0.08 and 0.05 Å for P2 and P1, respectively, compared to the Ag−S distance. Due to the rather acute Ag1−S1−C1 bond angle of 90.8(2)°, atom N5 comes relatively close to atom Ag1, the distance being 2.897 Å. This seems to be the reason why the two P−Ag1−S1 bond angles differ by 5.2°.

The copper methyltetrazolethiolate $Ph_3PCuSCN_4Me$ proved to be dimeric in solution suggesting a structure akin to type **A**[3]. However, crystals obtained from dichloromethane solution were shown by X-ray structure analysis to have a different composition: $Cu_4(SCN_4Me)_4(PPh_3)_3$ (compound **5**). Thus, one triphenylphosphane ligand is lost out of 4 monomeric units. The molecular structure of the tetranuclear complex **5**, which crystallizes with one molecule of CH_2Cl_2 per molecule of **5**, is depicted in Figure 7.

The assembly of the core atoms of **5** is rather asymmetric. Three copper atoms are tetracoordinated and one (Cu4) is only tricoordinated if Cu−Cu interactions are neglected [Cu4−Cu1: 2.745(1), Cu4−Cu3: 2.850(1) Å]. Atom Cu4 is the only one that has no triphenylphosphane as a coordination partner. It *only* coordinates to sulfur atoms. The S−Cu4−S bond angles range from 87.76(5) to 116.51(6)°. This corresponds to a strongly distorted trigonal-pyramidal array. A similar distortion is found for atom Cu1, where the tetrahedral angles span a range from 96.7(1) to 121.3(1)°. Deviations from tetrahedral symmetry are much smaller for atom Cu3 [103.5−121.5(2)°] and are smallest for atom Cu2 [101.6(1)−113.0(2)°]. Atoms Cu1 and Cu3 have one P, one N, and two S atoms as coordination partners, while atom Cu2 is surrounded by one P, one S, and two N atoms. The Cu−P bond lengths are different in terms of the 3σ criterion although the range (2.22−2.27 Å) does not suggest significant differences. This is not the case for the Cu−S bonds, which vary markedly (2.24−2.40 Å). Much less variation is observed for the Cu−N bond lengths [2.029−2.074(5) Å] and only the N atoms in the 5-position are found to be involved in bonding, as suggested previously (Formula **A**)[2].

Figure 8 gives a better perspective of the core structure of compound **5** than Figure 7. It represents a view almost down the Cu−S axis of the unique CuS_3 unit. One notes 5 six-membered rings and one eight-membered ring. The structure of this compound must be regarded as being rather unique.

Anionic Complexes

The anionic metal tetrazolethiolates **6**−**9** have in common a tetraphenylarsonium cation. Their AsC_4 core has a symmetry close to the point group T_d, which does not hold for the whole cation. In the tetraphenylarsonium salt of **6**, the As atom is located on a crystallographic twofold axis, but for all the other compounds the arsenic atom is found in a general position.

The mercury atom of the anion **6** (see Figure 9) resides in a general position, and out of the four Hg−S−C bond angles only two are equal [100.5(3)°] while the other two are 98.1(3)° and 103.0(4)°. This asymmetry becomes even more evident when one inspects the interplanar angles that the tetrazole rings form with the respective Hg−S−C planes: these range from 73.1° for S1 to 110.3° for S2 and 71.8° for S3, to finally 138.9° for S4. Two of the methyltetrazolethiolate units are mutually oriented in a "*syn*"

Figure 5. Stereoview of the unit cell of compound **3** showing the absence of intermolecular Au···S contacts

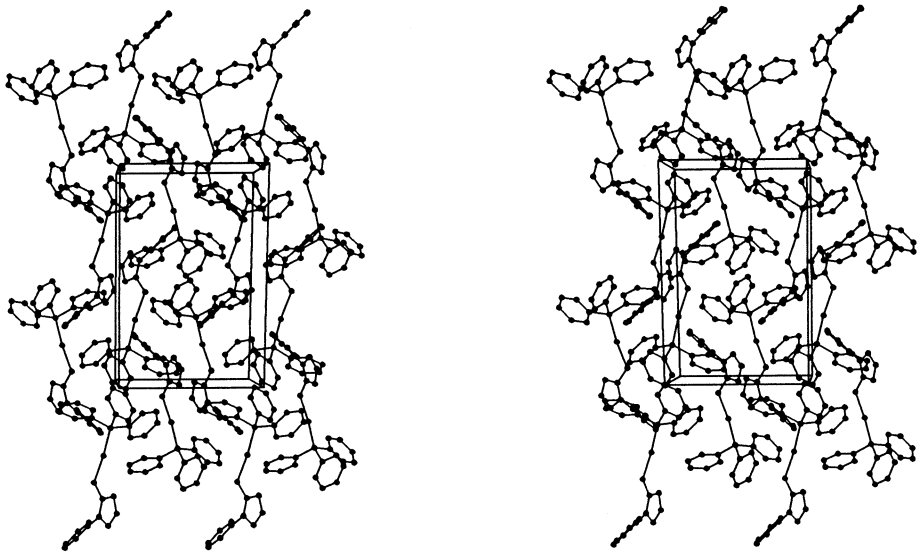

Figure 6. ORTEP representation of the molecular structure of the silver 2-methyltetrazolethiolate **4**; hydrogen atoms omitted for the sake of clarity

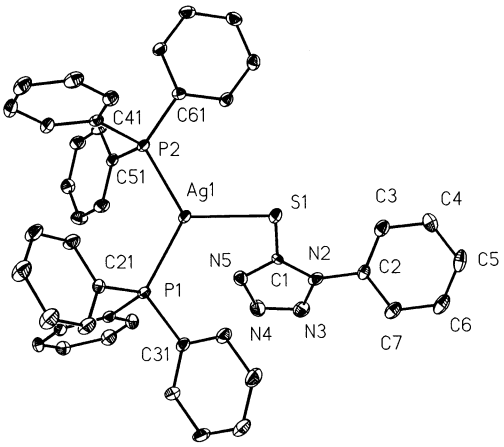

Figure 7. The molecular structure of the copper complex **5**; ORTEP representation of the molecule; hydrogen atoms omitted[a]

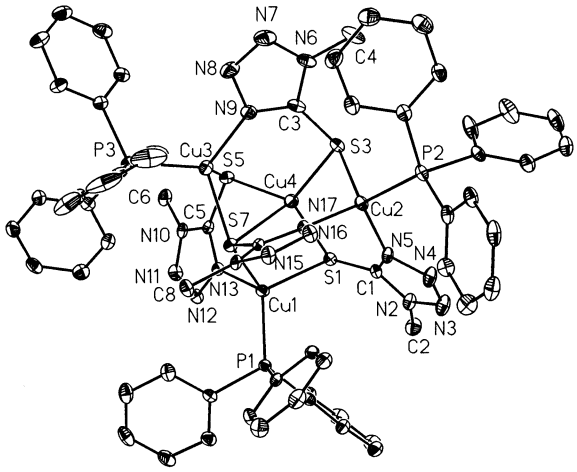

[a] Additional selected bond lengths [Å] and bond angles [°]: Cu2−N5 2.074(5), Cu2−P2 2.270(2), Cu2−N17 2.053(4), Cu2−S4 2.395(2), Cu3−P3 2.242(2), Cu3−S5 2.384(2), Cu3−S7 2.398(2), Cu4−S4 2.250(2), Cu4−S1 2.290(2), Cu4−S5 2.316(2), S4−C3 1.729(6), S5−C5 1.713(6), S4−C3 1.729(6); P1−Cu1−N13 121.3(1), S1−Cu1−N13 98.5(1), S1−Cu1−S7 113.47(5), S7−Cu1−N13 96.7(1), N17−Cu2−N5 112.8(2), N16−Cu2−P2 107.0(1), N5−Cu2−P2 111.4(1), N17−Cu2−S4 113.0(1), N5−Cu2−S4 101.6(2), S5−Cu3−S7 95.89(5), P3−Cu3−S7 104.42(6), P3−Cu3−S5 121.76(7), N9−Cu3−S5 103.5(2), S4−Cu4−S5 117.18(6), S1−Cu4−S7 103.66(5), S5−Cu4−S7 87.76(5), S4−Cu4−S7 112.92(6), S1−Cu4−S5 116.50(6).

fashion (S2 and S4), while the other two (S1 and S3) adopt an "*anti*" orientation. It is, therefore, not surprising that the four Hg−S bond lengths are not equal [range 2.507(2)−2.595(3) Å]. There is no correlation between the Hg−S bond length and the Hg−S−C bond angle.

The Pd atom of the anion **7** (see Figure 10) lies on a center of inversion. Its tetrazole units are twisted with respect to the PdS_4 plane by 71.9 and 75.8° (S1 and S2), respectively. Hence, the point group symmetry for this anion approaches S_4. Bond angles at the sulfur atoms are 108.3(1) and 106.9(1)°, and the corresponding Pd−S bond lengths are 2.332(1) and 2.339(1) Å.

As in the case of the Pd^{II} complex anion **7**, we also find a planar geometry around the gold(III) atom in the complex anion **8** (see Figure 11). This anion also has a symmetry close to point group S_4 since its metal atom resides on an inversion center. In this case, the tetrazole units are oriented almost perfectly orthogonally to the AuS_4 plane, with interplanar angles of 89.4 and 89.7°. However, the Au−S−C planes are not coplanar and the plane Au1−S1−C1 forms an angle of 11.3° with the plane Au1−S2−C2. It is interesting to note that the bond angles Au−S−C are rather wide at 107.2(2) and 106.8(2)°, and that, like the angles, there is no significant difference between the Au−S bond lengths [2.356(1) and 2.358(1) Å].

A rather unusual geometry is observed for the Au^{I} anion **9** (see Figure 12). There is an almost linear arrangement of atoms S1−Au1−S2 [175.15(7)°]. The tetrazole units form grossly different interplanar angles with the S1−Au1−S2

Figure 8. The core structure of molecule **5**

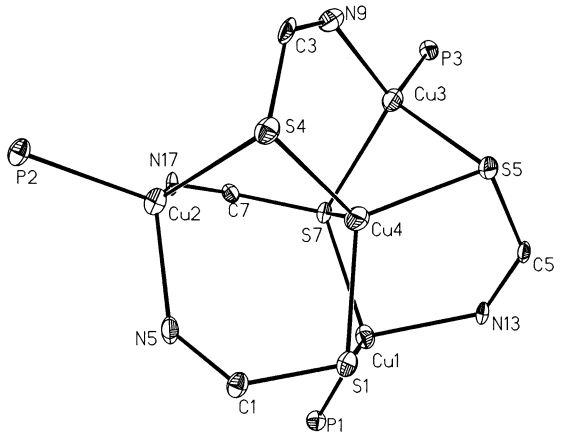

$Hg(SCN_4Ph)_4^{2-}$ **6**

$Pd(SCN_4Me)_4^{2-}$ **7**

$Au(SCN_4Me)_4^-$ **8**

$Au(SCN_4Ph)_2^-$ **9**

Figure 9. ORTEP plot of the 2-methyltetrazolethiolato mercurate **6**; the cation is not depicted; hydrogen atoms are omitted for clarity

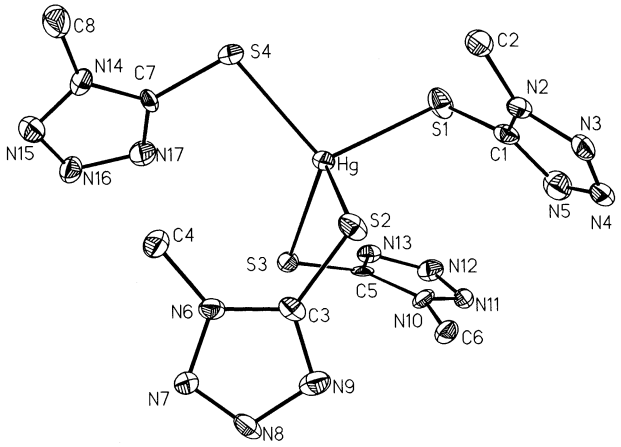

Figure 10. The molecular structure of the palladate anion **7**; hydrogen atoms omitted

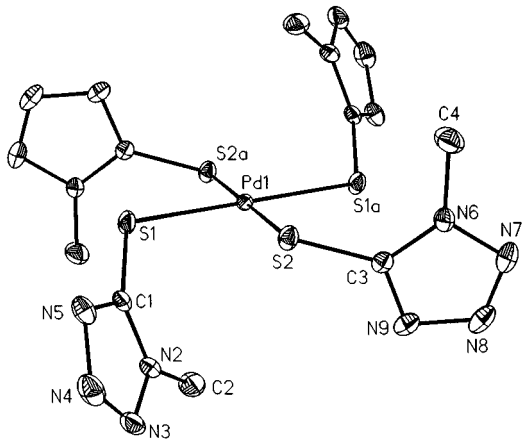

Figure 11. ORTEP representation of the molecular structure of the Au^{III} complex anion **8**; hydrogen atoms omitted for clarity

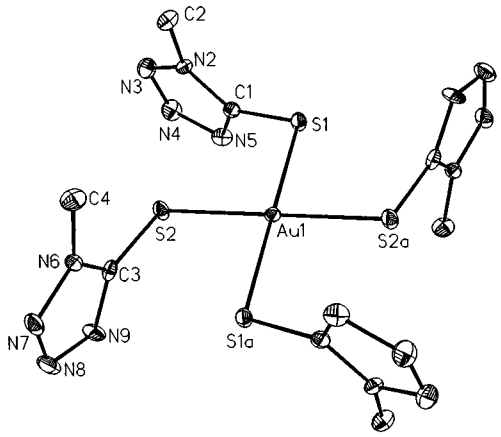

plane: 33° for tetrazole C1, and 114.8° for tetrazole C3. At least as different are the orientations of the planes of the phenyl groups in relation to the respective tetrazole rings. Interplanar angles are 92.2° and 130.8°, respectively. This leads to a molecular arrangement in which one of the two phenyl groups comes close to the gold center. In spite of this orientation, it is apparent that the Au−S1−C bond angle is wider [110.1(2)°] than the comparable angle at atom S2 [102.6(2)°]. If there were an η^6 interaction of a phenyl ring with the gold atom, one would expect that this phenyl group would be that with the more acute bond angle at the sulfur atom. This is obviously not the case.

Figure 12. The molecular structure of the bis(2-phenyltetrazolethiolato) aurate(I) (**9**), depicted in an orientation that shows the steric shielding of the gold atom by one phenyl group

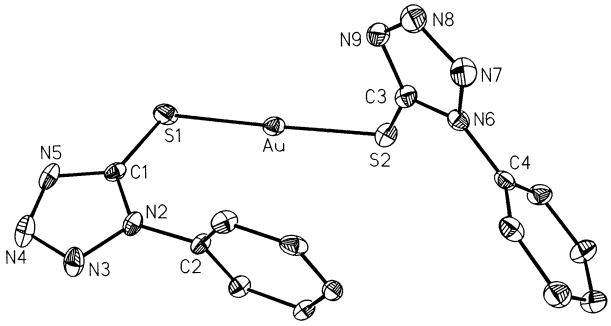

Discussion

The present study on the molecular structures of 2-substituted metal tetrazolethiolates, as determined by X-ray structure analysis, confirm those suggested previously except in the case of the silver and copper compounds. All except the copper compound **5** show that the sulfur atom of the tetrazolethiolate coordinates to the metal center in accord with the hard/soft concept of acids and bases. Within the coinage group, compound **5** is also the only one in which nitrogen atoms are also involved in coordination, and this also fits with theory because the copper atom is the hardest in the coinage metal group. Moreover, the Cu−Cu atom distances calculated for **5** are too long to sug-

Table 2. Crystallographic data and data related to data acquisition and refinement for compounds **1**−**9**

Compound	**1**	**2**	**3**	**4**	**5**	**6**	**7**	**8**	**9**
Chem. formula	$C_{50}H_{40}HgN_8P_2S_2$	$C_{20}H_{18}AuN_4PS$	$C_{25}H_{20}AuN_4PS$	$C_{44}H_{37}AgCl_2N_4P_2S$	$C_{63}H_{59}Cl_2Cu_4N_{16}P_3S_4$	$C_{56}H_{52}As_2HgN_{16}S_4$	$C_{56}H_{52}As_2N_{16}PdS_4$	$C_{32}H_{32}AsAuN_{16}S_4$	$C_{38}H_{30}AsAuN_8S_2$
Form. Wght.	1079.55	574.38	636.45	894.55	1586.47	1427.81	1333.62	1040.86	934.71
Cryst. size [mm]	0.2×0.3×0.42	0.12×0.21×0.35	0.1×0.1×0.5	0.2×0.2×0.3	0.1×0.1× 0.1	0.2×0.22×0.3	0.012×0.2×0.3	0.08×0.15×0.3	0.1×0.15×0.21
Cryst. system	Monoclinic	Monoclinic	Monoclinic	Triclinic	Monoclinic	Monoclinic	Monoclinic	Monoclinic	Monoclinic
Space group	*C*2/*c*	*P*2(1)/*n*	*P*2(1)/*n*	$P\bar{1}$	*P*2(1)/*n*	*P*2(1)	*P*2(1)/*n*	*C*2/*c*	*P*2(1)/*n*
a [Å]	19.561(3)	8.241(1)	13.0159(1)	10.126(2)	12.999(2)	10.4952(7)	7.498(4)	18.5892(7)	12.793(9)
b [Å]	9.996(1)	14.621(4)	10.8504(1)	13.314(3)	15.559(2)	22.762(1)	14.921(7)	6.4765(2)	13.677(1)
c [Å]	25.047(3)	16.895(4)	17.2007(1)	16.550(4)	34.030(1)	13.2473(7)	25.71(1)	33.105(1)	21.154(2)
α [°]	90.00	90.00	90.00	67.345(6)	90.00	90.00	90.00	90.00	90.00
β [°]	108.396(1)	103.848(1)	104.746(1)	84.590(9)	91.023(9)	112.741(1)	90.865(7)	103.103(1)	105.71(1)
γ [°]	90.00	90.00	90.00	80.29(1)	90.00	90.00	90.00	90.00	90.00
V [Å^3]	4647(1)	1976.6(7)	2349.21(3)	2028.3(8)	6881.3(15)	2918.6(3)	2876(2)	3881.9(2)	3563.2(5)
Z	4	4	4	2	4	2	2	4	4
ρ(calcd.) [Mg/m^3]	1.543	1.930	1.799	1.465	1.531	1.625	1.540	1.781	1.742
μ [mm^{-1}]	3.515	7.642	6.440	0.796	1.541	3.958	1.663	4.900	5.208
F(000)	2152	1104	1232	912	3232	1420	1352	2048	1832
Index range	$-25\le h\le 25$	$-9\le h\le 9$	$-16\le h\le 16$	$-13\le h\le 10$	$-11\le h\le 11$	$-11\le h\le 11$	$-9\le h\le 9$	$-23\le h\le 23$	$-14\le h\le 13$
	$-11\le k\le 11$	$-17\le k\le 17$	$-13\le k\le 13$	$-16\le k\le 16$	$-19\le k\le 19$	$-25\le k\le 25$	$-19\le k\le 19$	$-5\le k\le 8$	$-17\le k\le 17$
	$-32\le l\le 31$	$-21\le l\le 21$	$-22\le l\le 11$	$-20\le l\le 20$	$-43\le l\le 43$	$-12\le l\le 14$	$-27\le l\le 27$	$-41\le l\le 40$	$-26\le l\le 26$
2θ [°]	55.02	55.06	57.60	57.82	55.38	46.70	55.16	58.02	55.00
Temp. [K]	293(2)	193	193	183	173	193	173	193	293(2)
Refl. collected	12181	10502	13008	11520	73528	13067	13961	10328	17994
Refl. unique	4496	2848	3760	6205	11158	7488	5345	3537	6645
Refl. obsd. (4σ)	3738	2526	3288	5591	8603	7095	4081	2467	4928
R (int.)	0.0733	0.0524	0.0495	0.0254	0.0584	0.0590	0.0495	0.0766	0.0708
No. variables	353	245	334	487	832	712	360	248	451
Weighting scheme[a] x/y	0.0344/ 20.4391	0.0234/ 3.2786	0.0478/ 7.3801	0.0643/ 8.1945	0.0000/ 33.1493	0.0403/ 14.4528	0.0077/ 4.1949	0.0188/ 34.7310	0.0285/ 17.7889
GOOF	1.083	1.069	1.143	1.063	1.256	1.151	1.197	1.316	1.127
Final *R* (4σ)	0.0380	0.0273	0.0348	0.0469	0.0589	0.0341	0.0421	0.0398	0.0395
Final *wR*2	0.0774	0.0482	0.0855	0.1259	0.1013	0.0965	0.0726	0.0834	0.0842
Larg. res. peak [e/Å^3]	1.488	1.374	2.451	0.907	1.127	0.726	0.460	1.157	1.012

[a] $w^{-1} = \sigma^2F_o^2 + (xP)^2 + yP$; $P = (F_o^2 + 2F_c^2)/3$.

gest metal−metal bonding. Also, there are no close Au−Au contacts in **2**, although significant Au−Au interactions have been found in a related compound, $Ph_3PAuSPh$, which forms pairs in the crystal via Au−Au contacts [Au−Au 3.135(3), Au−S 2.30(1), and Au−P 2.26(1) Å][3].

The structural parameters obtained for complexes **1**−**9** show that there is *no* correlation between the magnitude of the M−S−C bond angle and the C−S bond length. It is, however, interesting to note that the M−S−C bond angle varies considerably. For the neutral complexes, the range covered is 97.5−106.9°, while for the anionic species it is 100.5−110.1°. There is also a range from 1.698(5)−1.740(4) Å for the C−S bond lengths found for the neutral complexes and a somewhat smaller range [1.72(1)−1.746(9) Å] for the anions. These bond lengths correspond to those found for thiourea [1.71(1)][6], thioacetamide [1.713(6)][7] and 3-hydrazino-5-mercapto-1,2,4-triazole [1.74(1)][7], but are definitely longer than the C=S double bond in CS_2 [1.555(1) Å]. Therefore, they are intermediate between the C−S single (1.82 Å) and C=S double bond lengths (see also the discussion in ref.[9]). Consequently, the bonding in this ligand is best described by the canonical formulae **B** to **D**.

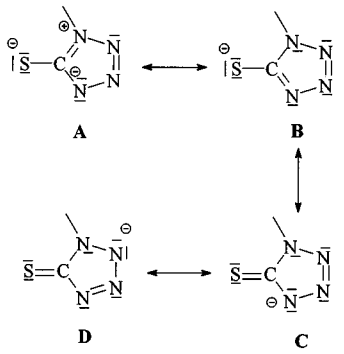

Although the tetrazole ring can be considered as a 6π-electron heterocycle, the electron distribution is obviously not uniform because the N3−N4 bond is significantly shorter than the two other N−N bonds, let alone the C−N bonds[9]. Most notably, the N4−N5 bond is distinctly longer than the N3−N4 bond. This indicates that the canonical formulae **B** and **D** make the largest contributions to the ground state.

A comparison of the M−S bonds to the same metal center in neutral and anionic species reveals that these

bonds are *longer* in the neutral complexes than in the anionic species, e.g. by 0.01 Å for M = Hg and by 0.05 and 0.03 Å, for M = Au^{I}. The longer Au−S bonds for the aurate anion **7** are clearly the consequence of the higher coordination number. However, the Au−S bond lengths for **2**, **3**, **8**, and **9** fall into the range observed for many other complexes with Au−S bonds (2.28−2.79 Å), while the Cu−S bond lengths of **5** are best compared with those in $(Me_4N)_2Cu_5(SPh)_7$ [2.159(3) Å][10].

The copper complex **5** demonstrates that the Cu−S bond lengths to the tetrazolethiolate units are elongated when the N5 atom is involved in coordination to the copper atoms. Thus, the canonical forms **B** and **C** become more significant in this situation. In contrast, the trimeric tetrazolethiolato complex $Me_3Sn(SCN_4Ph)$, where association occurs via the N3 atom, shows a shortening of the N4−N5 bond [1.35(2) Å] and a lengthening of the N3−N4 bond [1.35(2) Å]. This indicates that in this situation formula **D** makes a significant contribution to the ground state. It remains to investigate structures of tetrazolethiolates with truly hard acids in order to find out whether the hard cation will only bind to nitrogen and/or to sulfur as well. The only compound reported to date is the potassium crown compound (12-crown-4)$KSCN_4Me$[9], in which the S and one N atom coordinate to the potassium ion. In addition, there is a fairly short distance between the potassium ion and the ring carbon atom, but this cannot be considered as a potassium−carbon bond.

We are grateful to the *Fonds der Chemischen Industrie* and *Chemetall GmbH* for generous support. Also, we are indebted to Dr. *I. Krossing* for recording the data set of compound **4**.

Experimental Section

The compounds used for the X-ray structure determinations were the original samples[3]. Only the Cu complex **5** had to be crystallized from dichloromethane, and the structure determination showed the loss of a triphenylphosphane ligand.

All compounds were mounted on a glass fibre with a small amount of perfluoroether oil. After optical alignment at 193 K on a Siemens P4 diffractometer equipped with a Siemens CCD area detector, the unit cells were determined from the reflections of four sets of 15 frames each recorded at four different χ settings by changing ϕ by 0.3° between each frame. Data were recorded from a total of 1200 frames with 10-s exposures and changes in φ by 0.3° at two different χ settings. Data reduction was performed with the program SAINT, and an empirical absorption correction was applied using all data with esd′s larger than 20. The structures were solved by the heavy-atom method; the model was complemented by difference Fourier synthesis and refined by using the programs SHELXL-93 and -97[10]. All non-hydrogen atoms were refined with anisotropic temperature parameters. Although many or all hydrogen positions could be located, the positions of hydrogen atoms were calculated and included as a riding model in the final cycles of the calculations. The crystallographic data are compiled in Table 2. Thermal ellipsoids in the figures represent a 25-% probability level. Further information on the crystal-structure determinations has been deposited with the Cambridge Crystallographic Data Centre as supplementary publication no. CCDC-100802 and may be obtained from CCDC, 12 Union Road, Cambridge CB2 1EZ, U.K. [Fax (internat.): + 44 (0)1223/336033; e-mail: deposit@.cam.ac.uk].

☆ Dedicated to Prof. Dr. *G. Huttner* on the occasion of his 60th birthday.

***Note Added in Proof* (December 3, 1997):** There has been a review on the coinage metals: M. D. Jansen, D. M. Grove, G. van Koten, *Prog. Inorg. Chem.* **1997**, *46*, 97−149.

[1] E. Lieber, C. N. R. Rao, C. N. Pillaj, J. Ramachandran, R. D. Hites, *Can. J. Chem*. **1958**, *36*, 801−806; R. Könnecke, E. Lippmann, E. Kleinpeter, *Z. Chem*. **1975**, *15*, 402; B. Ellis, P. J. Griffith, *Spectrochim. Acta* **1966**, *22*, 205−211.
[2] A. I. Power, *Coord. Chem. Rev.* **1969**, *4*, 463; R. N. Butler, *Adv. Heterocycl. Chem.* **1977**, *21*. 323; G. J. Palenik, *Acta Crystallogr.* **1963**, *16*, 596.
[3] W. Beck, K. Burger, M. Keubler, *Z. Anorg. Allg. Chem*. **1977**, *428*, 173−186.
[4] [4a] R. Cea-Olivares, O. Jiménez-Sandoval, G. Espinosa-Pérez, C. Silvestru, *J. Organomet. Chem*. **1994**, *484*, 33−36. − [4b] R. J. Deeth, K. C. Molloy, M. F. Makou, S. Whittaker, *J. Organomet. Chem*. **1992**, *430*, 25.
[5] M. Nakomoto, W. Hiller, H. Schmidbaur, *Chem. Ber*. **1993**, *126*, 605−610; L. G. Kuzmina, T. V. Bankova, V. A. Churakov, G. V. S. Kuzmin, N. V. Dvortsova, *Russ. J. Coord. Chem*. **1997**, *23*, 279−288.
[6] N. R. Kunchur, M. R. Truter, *J. Chem. Soc*. **1958**, 2551.
[7] M. R. Truter, *J. Chem. Soc*. **1960**, 997.
[8] M. E. Senko, D. H. Templeton, *Acta Crystallogr*. **1958**, *11*, 808.
[9] R. Cea-Olivares, O. Jiménez-Sandoval, S. Hernández-Ortega, M. Sandez, R. A. Toscano, I. Haiduc, *Heteroatom Chem.* **1995**, *6*, 89−97.
[10] I. G. Dance, *Aust. J. Chem*. **1978**, *31*, 2195−2206.
[11] G. W. Sheldrick, University of Göttingen, **1997**.

[97192]

Halogenation of Bis(phosphonio)isophosphindolide Salts: Oxidation versus Substitution

Dietrich Gudat*, Andreas W. Holderberg, and Martin Nieger

Anorganisch Chemisches Institut der Universität Bonn,
Gerhard-Domagk-Straße 1, D-53121 Bonn, Germany
Fax: (internat.) + 49(0)228/73-5327
E-mail: dgudat@uni-bonn.de

Received September 11, 1997

Keywords: Phosphorus heterocycles / Halogens / Oxidations / Electrophilic aromatic substitutions

Bis(phosphonio)isophosphindolide iodide **1**[I] reacts with an equimolar amount of I_2 to yield the trihalide **1**[I_3], while treatment of **1**[X] (X = Br, OTf) with excess Br_2 furnishes the dibromophosphonium salt **6c**[X]. The bromo-substituted bis(phosphonio)isophosphindolide cations **5a** and **5b** are identified as intermediates in this reaction; **5b**[Br] is also obtained in pure form by reaction of **6c**[Br] with Zn or NEt_3. Reaction of **1**[OTf] with one equivalent of $PhICl_2$ (**7**) affords the dichlorophosphonium salt **8a**[OTf], which undergoes further substitution reactions in the presence of excess **7** and reacts with Me_3SiI to give a mixture of **1**[OTf] and I_2 rather than a substitution product **9**[OTf]. The results of a crystal-structure determination of **8a**[OTf] are reported and the mechanistic aspects of the different oxidation/substitution reactions are discussed.

In the course of our investigation of the coordination chemistry of bis(phosphonio)isophosphindolide ions, we found that the cation **1**[1] easily undergoes oxidative alcoholysis reactions in the coordination sphere of Hg^{2+} or Pd^{2+} ions to yield dialkoxy-substituted phosphonium ions **2** (Scheme 1)[2]. This reaction is related to the conversion of σ^2,λ^3-phosphinines **3** into 1,1-dialkoxy-σ^4,λ^5-phosphinines **4** (Scheme 1), which takes place under similar conditions[3]. In looking for a way to achieve oxidation of bis(phosphonio)isophosphindolides without the assistance of transition metals, we investigated the behaviour of the salts **1**[X] (X = halide, triflate) towards halogens, anticipating that a similar reaction as the oxidative halogenation of σ^2,λ^3-phosphinines[3] should occur. The results of these studies are presented here. The studies revealed, however, a more complex reactivity pattern which is characterised by competition between the expected oxidation with substitution reactions at the fused ring system.

Scheme 1. (X = Br, OTf)

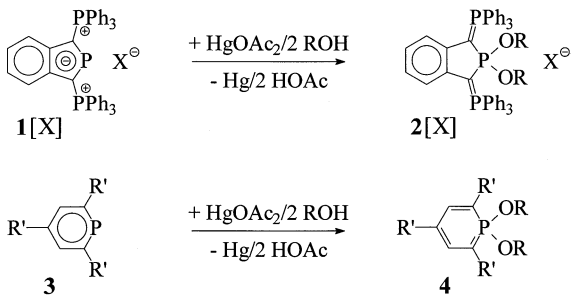

Results

Reactions

Treatment of a CH_2Cl_2 solution of **1**[I] with an equimolar amount of I_2 produced almost instantaneously a brown solution. While ^1H- and ^{31}P-NMR data indicated the presence of the unchanged cation **1**, UV/Vis and Raman spectra showed bands attributable to I_3^- anions [UV/Vis: λ_{max} = 361, 294 nm (ref.[4]: 360, 290 nm); Raman: $\tilde{\nu}$ = 112, 145 cm^{-1} (ref.[5]: 52, 114, 145 cm^{-1})], suggesting the formation of a salt **1**[I_3] by electrophilic attack of iodine on the halide anion of the starting material (Scheme 2). The crude product was isolated as a dark brown, highly moisture-sensitive solid after evaporation of all volatiles, but decomposed during attempts to achieve any further purification by recrystallisation.

Reaction of **1**[Br] or **1**[OTf] with a substoichiometric amount of Br_2 (0.5 to 0.9 equiv.) in CH_2Cl_2 produced, according to a ^{31}P-NMR-spectroscopic assay, a mixture of the unreacted cation **1** with two further products which displayed ABX or A_2X patterns with $\delta^{31}P$ and $^2J_{PP}$ values very similar to those of **1**. Analysis of (+)-FAB mass spectra and two-dimensional $^1H,^{31}P$-HMQC/HMQC-TOCSY NMR spectra of the product mixture allowed the identification of the reaction products as the bromo-substituted bis(phosphonio)isophosphindolide ions **5a** and **5b**. This suggests that a bromination at the fused ring system of **1** with conservation of the two-coordinate phosphorus atom had occurred.

Addition of more Br_2 did not result in further conversion of **1** into **5a** and **5b**, but rather in the formation of two new species whose ^{31}P-NMR signals displayed ABX or A_2X patterns with much smaller values of $^2J_{PP}$ and a marked up-

 © WILEY-VCH Verlag GmbH, D-69451 Weinheim, 1998 1434–1948/98/0101–0101 $ 17.50+.50/0

Scheme 2

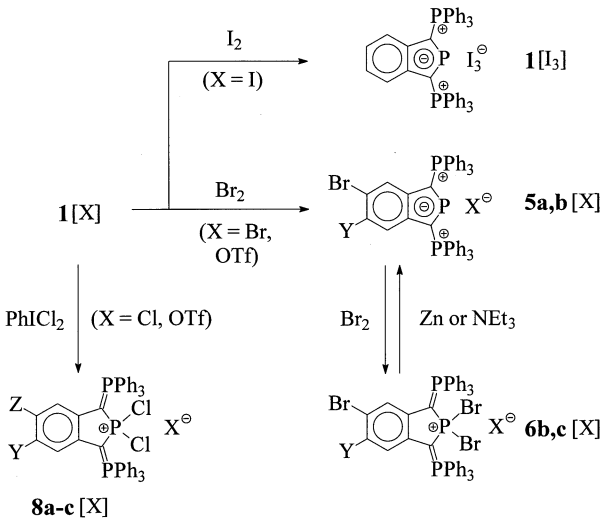

	5a,6b	5b,6c	8a	8b	8c
Y	H	Br	H	Cl	Cl
Z	-	-	H	H	Cl

field shift of the P^X resonance. On this basis the new species were found to be the oxidation products **6b** and **6c**. Complete conversion of all intermediates into **6c** was finally observed after four equivalents of Br_2 had been added. Evaporation of the solution formed gave a brown, highly moisture-sensitive residue of crude **6c**[X] which contained approximately 3−5% of nonphosphorus-containing compounds as impurities. Although attempts towards further purification failed because of decomposition of the highly reactive dihalo-phosphonium moiety, the constitution of the cation was unambiguously confirmed by means of multinuclear NMR investigations.

A further chemical proof of the identity of **6c** was obtained from its reactions with Zn or, alternatively, with excess NEt_3, which afforded the dibromo-substituted bis-(phosphonio)isophosphindolide **5b** by selective reduction of the Br_2P unit. The salt **5b**[Br] was isolated in analytically pure form as a white solid that was fairly stable to both air and moisture and was characterised by NMR spectroscopy. The monobrominated cation **5a**, which was not accessible in preparative amounts by this procedure, was formed as the main product (70% of phosphorus-containing species) in the reaction of a mixture of **6b** and **6c** (prepared in situ from the reaction of **1**[OTf] with 2.5 equiv. of Br_2) with an equimolar amount of **1**[OTf]. Chromatographic workup produced a small quantity of crude **5a**[OTf] which, although still contaminated by small amounts of **1** and **5b**, proved sufficient for an unambiguous NMR-spectroscopic structure elucidation.

Reaction of **1**[X] (X = Cl, OTf) with an equimolar amount of $PhICl_2$ (**7**), which was chosen as a chlorinating agent because of its superior handling as compared to elemental Cl_2, furnished selectively the oxidation products **8a**[X]. The triflate salt **8a**[OTf] was precipitated by addition of ether and isolated after recrystallisation as a light yellow, moisture-sensitive solid which is readily soluble in aprotic dipolar solvents such as CH_2Cl_2 or THF. The product was characterised by means of NMR spectroscopy and an X-ray crystal-structure determination.

Further reaction of **8a**[X] with an excess of **7** in the presence of NEt_3 as an acid scavenger was found to proceed in a more complicated way than the reaction with Br_2 and yielded a mixture of several species rather than a single final product. Attempts towards isolation of single components remained unsuccessful, but inspection of ^{31}P-NMR spectra of the mixtures allowed the identification of two species which displayed ABX and A_2X coupling patterns with very similar values for $\delta^{31}P$ and J_{PP} as **8a** and were tentatively formulated as the chlorinated cations **8b** and **8c**. The additional presence of a singlet resonance attributable to $[ClPPh_3]^+$, together with several unidentified AX-type multiplets, suggested that in addition to the H/Cl exchange, partial decomposition of the molecular skeleton by cleavage of an exocyclic phosphonio substituent had also occurred. Initial formation of **8b** and **8c** as the main products was likewise observed upon treatment of **1**[OTf] with an excess of **7** in pure CH_2Cl_2, but the products were found to decompose completely during the further course of the reaction.

Reaction of **8a**[OTf] with two equivalents of Me_3SiI proceeded with quantitative formation of **1**[OTf] and I_2. No evidence for the formation of a substitution product **9**[OTf] was obtained; this compound is presumably unstable with respect to disproportionation (Scheme 3). A slow, but selective conversion of **8a** into **1** was also observed upon addition of pyridine or NEt_3 to CH_2Cl_2 solutions of **8a**[OTf] and keeping the resulting mixtures for several days; in this case, the nature of the oxidation products was not elucidated.

Scheme 3. (X = Cl, OTf)

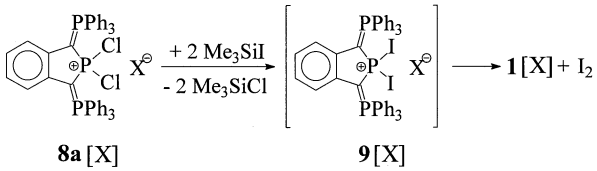

NMR-Spectroscopic Investigations

The $\delta^{31}P$ values for the two-coordinate phosphorus atoms in the cations **1** and **5a** and **5b** are shifted to lower field with increasing number of Br substituents, while the resonances of the nuclei in the phosphonio groups and those of the quaternary C-1/C-3 carbon atoms remain essentially unchanged (Table 1). Likewise, the values of both $^2J P^A P^X$ and $^4J P^A P^B$ are very similar for all three compounds. The position of the bromine atom in **5a** follows immediately from the $^1H\{^{31}P\}$-NMR spectrum; the resonances of the hydrogen atoms at the central ring appear as an AMX-type pattern whose middle proton shows a splitting by a large and a small coupling which is characteristic

of a 1,2,4-substituted benzene moiety. The $^1H\{^{31}P\}$-NMR spectrum of **5b** displays a singlet for the protons adjacent to the bromine atoms which splits into an apparent doublet in an undecoupled spectrum. A correlation peak with the upfield ^{31}P resonance in a $^1H,^{31}P$-HMQC spectrum revealed that the splitting must arise from coupling with the two exocyclic phosphorus nuclei rather than the single endocyclic phosphorus nucleus. The magnitude of the $^nJ_{HP}$ couplings [J = +(−)3.3 and −(+)1.7 Hz] which were determined by iterative analysis suggested attachment of the hydrogen atoms in the 4,7 rather than in the remote 5,6 positions of the fused ring system. This hypothesis was further corroborated by a strong correlation peak connecting the 4-H/7-H and C-1/C-3 signals in a $^1H,^{13}C$-HMBC spectrum which is in accord with the presence of a three-bond coupling pathway.

Table 1. ^{31}P-NMR and selected ^{13}C-NMR data of **1, 5a, 5b, 6b, 6c**, and **8a−c**; chemical shifts are given in ppm, coupling constants in Hz; P^A, P^B, and P^X denote the phosphorus nuclei in ABX- or A_2X-spin systems, respectively

	$\delta^{31}P$				$\delta^{13}C$	J_{PC}	
	P^A, P^B	P^X	$^2J_{P^A,P^BP^X}$	$^4J_{P^AP^B}$	C-1/C-3	$^1J_{PC}$	$^3J_{PC}$
1[a][b]	16.3	241.8	−91.4	+8.6[c]	109.0	+96.6 (P^A) −56.0 (P^X)	+14.0
5a	16.2 16.1	246.9	90.6 90.3	8.5	110.5 110.3	110 56 (P^X) 112 57 (P^X)	1415
5b	16.0	2 52.9	88.4	8.6[c]	112.00	141.3 (P^A) 58.3 (P^X)	13.7
6b	11.83 11.80	−34.7	44.5	4.5	−	−	−
6c	11.9	−33.0	44.5	4.6[c]	49.53	119.3 123.7	8.1
8a	11.3	49.2	44.7	4.6[c]	46.18	142.2 126.2	7.7
8b	11.40 11.43	50.3	43.9	4.5	−	−	−
8c	11.4	51.7	43.2	−	−	−	−

[a] $\delta^{31}P$, $\delta^{13}C$, and $^2J_{PP}$ from ref.[1]. − [b] Signs of coupling constants were determined from a two-dimensional $^{31}P,^{13}C$ shift correlation. − [c] Values of $^4J^{P^AP^{A'}}$ were obtained from analysis of appropriate ^{13}C satellites in the ^{31}P-NMR spectra.

The $\delta^{31}P$ values of the endocyclic phosphorus atoms in the oxidation products **6b** and **6c** range between those of acyclic dichlorophosphonium salts ($\delta^{31}P$ = 66−104[6]) and 1,1-dichloro-λ^5,σ^4-phosphinines ($\delta^{31}P$ = 7−17[7]), while formal replacement of Cl by Br in **8b** and **8c** induces a comparable upfield shift of $d^{31}P$ as in the cyclophosphazene system[8]. The magnitudes of $^2J^{P^AP^X}$ and $^4J^{P^AP^B}$ are about half as large as in **1**, **5a** and **5b**. The ^{13}C-NMR signals of the quaternary C-1/C-3 atoms in **6c** and **8a** reveal similar upfield shifts with respect to **1**, **5b** as were previously found for the 1,1-dialkoxy-substituted cations **2**[2], suggesting a pronounced ylidic character for the exocyclic P−C bonds. As in **5b**, the resonance of the 4-H/7-H atoms of **6c** and **8c** appears as a singlet in the $^1H\{^{31}P\}$-NMR spectrum and splits to a triplet in the undecoupled spectrum due to coupling with the two exocyclic ^{31}P nuclei.

Molecular Structure of 8a

Crystalline **8a**[OTf] consists of discrete anions and cations and contains an additional solvent molecule per formula unit. No contacts closer than van der Waals distances are exhibited by any of the single components. As in **1**[9], the fused ring system in the cation **8a** (Figure 1) is planar, with a standard deviation of the ring atoms and the two exocyclic phosphorus atoms from the mean plane of 0.030 Å. The difference between endocyclic [1.695(4), 1.697(4) Å] and exocyclic P−C bond lengths [1.723(4), 1.729(4) Å] is similar to **1**[9], but both types of bonds are somewhat shorter than there. The two P−Cl bonds [1.991(2), 2.063(2) Å] differ in length. Both exceed the bond length of 1.91 Å in $[PCl_4][FeCl_4]$[10] and lie between the values of equatorial and axial bonds in PCl_5 (2.02, 2.14 Å[10]). The central P(1) atom displays a distorted tetrahedral coordination, with the C(2)−P(1)−C(9) [99.5(2)°] and Cl(1)−P(1)−Cl(2) angles [97.4(1)°] being significantly more acute than the ideal angle of 109.4°. Interestingly, the two chlorine atoms exhibit a slightly asymmetric arrangement with respect to the plane through P(1), C(2), and C(9), with the longer P(1)−Cl(2) bond showing a larger tilt angle with respect to this plane. Regarding, however, the large thermal ellipsoid at Cl(2) (Figure 1), it remains uncertain if this effect indicates a real structural distortion or is merely the consequence of larger librational motion of the chlorine atom.

Figure 1. ORTEP view (50-% probability ellipsoids) of the cation in crystalline **8a** [OTf][a]

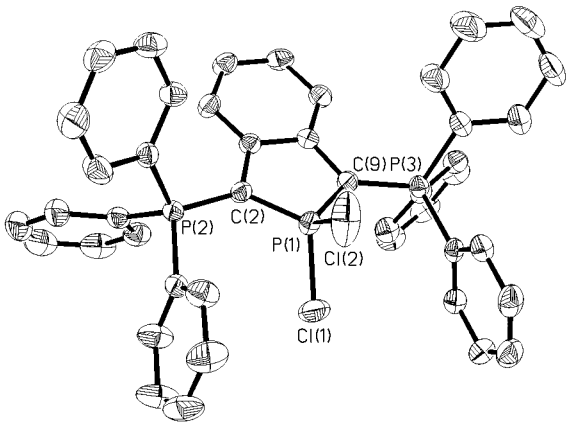

[a] Selected bond lengths [Å] and angles [°]: Cl(1)−P(1) 1.991(2), Cl(2)−P(1) 2.063(2), P(1)−C(2) 1.695(4), P(1)−C(9) 1.697(4), C(2)−P(2) 1.729(4), C(9)−P(3) 1.723(4); Cl(1)−P(1)−Cl(2) 97.4(1), C(2)−P(1)−C(9) 99.5(2), C(2)−P(1)−Cl(1) 116.2(1), C(2)−P(1)−Cl(2) 115.1(2), C(9)−P(1)−Cl(1) 116.9(1), C(9)−P(1)−Cl(2) 112.8(1).

The oxidation of the bis(phosphonio)isophosphindolide cation **1** to the 1,1-dihalogeno derivatives **6b, 6c** and **8a**, as well as the corresponding retro reaction (that is reduction of the formed products to give **1, 5a** and **5b**, respectively) resemble similar reactions of phosphinines[3][7]. The bonding in the products **6** and **8** may be described, as is suggested by the drawings in Scheme 2, in terms of a bis-ylide which receives additional electronic stabilisation by negative

hyperconjugation into the central dihalophosphonium moiety[11]. The instability of the corresponding 1,1-diiodo derivative **9** which becomes evident both in the failure to observe oxidation of **1** with I_2 as well as in the formation of **1** and I_2 after treatment of **8a** with Me_3SiI, reflects the lower oxidative power of the heavier halogen.

The reaction of **1** with Br_2 in which the formation of the substituted bis(phosphonio)isophosphindolides **5a** and **5b** precedes the formation of the oxidation products **6b** and **6c** deserves some further comment. In principle, **5a** and **5b** may be generated by either of two mechanisms: (a) direct electrophilic substitution of **1**, or (b) a multistep pathway (Scheme 4) involving initial oxidation of **1** to **6a**, subsequent substitution of the oxidation product to give **6b** and **6c**, and final reaction of these species with **1** under formation of **5a** and **5b** and regeneration of **6a** (because of the recursive nature of the overall reaction, **6a** needs to be present only in a catalytic quantity).

Scheme 4. Proposed mechanism for the formation of **5a** and **5b** during the reaction of **1** with Br_2 (X = Br, OTf; Y = H, Br)

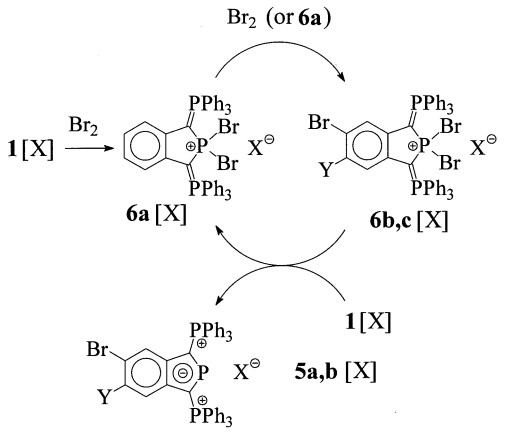

The available experimental results do not allow a definitive determination of the reaction mechanism to be made; however, we favour the second alternative because it allows an explanation of the observed reactions of **1** with Br_2 and $PhICl_2$ in terms of a common mechanism. Moreover, this mechanism is equivalent to the "indirect" electrophilic substitution of λ^3-phosphinines[3], and all crucial steps in the sequence had been verified independently. Thus, reduction of a 1,1-dibromobis(phosphonio)isophosphindolide by **1** is involved in the conproportionation of **6a** and **1** to give **5a** (see above). Furthermore, it was recently shown by Schmidpeter[12] that ylide substituents may activate aromatic ring systems for electrophilic substitution so that a particularly high reactivity for the double ylide substituted benzene moieties in **6a** (and **8a**) is expected. Considering the *o*-/*p*-directing capability of ylide groups[12], exchange of all four hydrogen atoms in **6a** should in principle be possible. The observed regioselectivity indicates a higher reactivity at the 5,6 positions, while tri- and tetrasubstitution are presumably prevented by the deactivating influence (−I effect) of the halide substituents. The failure to observe **6a** in significant concentration beside the substitution products **6b** and **6c** suggests that either electrophilic substitution of **6a** occurs at a much higher rate or that **6a** exhibits a higher tendency for reductive debromination than **6b** and **6c**; both explanations again highlight the importance of deactivation of the aromatic system by halide substituents. The difference in the reactions of **1** with Br_2, where the formation of the substitution products **5a** and **5b** apparently precedes that of the oxidation product, and with **7**, where this is not the case, may be attributable to a higher kinetic lability and/or lower thermodynamic stability of **6a** as compared to **8a**. This is also in accord with the observed different rates of amine-induced reductive elimination reactions, and was predicted by the lower stability of 1,1-dibromo- as compared to 1,1-dichlorophosphinines[4].

Financial support of this work by the *Deutsche Forschungsgemeinschaft* and the *Fonds der Chemischen Industrie* is gratefully acknowledged.

Experimental Section

General: All manipulations were carried out under dry argon. Solvents were dried using standard procedures. − NMR spectra: Bruker AMX 300 (^{1}H: 300.13 MHz, ^{13}C: 75.46 MHz, ^{31}P: 121.5 MHz). ^{1}H,^{31}P(^{13}C)-HMQC- and HMQC-TOCSY spectra were measured using standard pulse sequences from the Bruker Pulse Program library. Spectra of samples in nondeuterated solvents were recorded with suppression of the solvent resonances by presaturation. Chemical shifts were referenced to ext. TMS (^{1}H and ^{13}C) and 85% H_3PO_4 (^{31}P, Ξ = 40.480747 MHz); a positive sign denotes a shift to lower frequencies. Coupling constants are given as absolute values. The atoms in the isophosphindole ring system are denoted by C-1 to C-7a and 4-H to 7-H, and atoms within the C_6H_5 substituents by C(H)^{para}, C(H)^{meta}; the assignment of the resonances was derived from 2D ^{1}H,^{13}C-HMQC/HMBC spectra. For ^{13}C-NMR signals which are the X part of AA′MX- or AA′X-spin systems, ΣJ denotes the absolute value of the sum of the couplings to the exocyclic phosphorus nuclei, and J_M the coupling to the endocyclic phosphorus atom. − UV/Vis: Uvikon 860. − Raman Spectra: Bruker RFS 100. − MS: Kratos Concept 1 H, Xe-FAB, *m*-nitrobenzaldehyde matrix; molecular masses refer to the most abundant isotopes. − Melting points were determined in sealed capillaries. − Elemental analyses: Heraeus CHNO-Rapid or Mikroanalytisches Labor Pascher, Remagen.

Reaction of **1**[I] *with* I_2*:* To a solution of 0.63 g (0.81 mmol) of **1**[I] in 20 ml of CH_2Cl_2 was added 0.21 g (0.81 mmol) of I_2, and the mixture stirred for 30 min at ambient temperature until a clear solution was obtained. Removal of all volatiles in vacuo produced a brown, highly moisture- and air-sensitive solid whose ^{1}H- and ^{31}P-NMR spectra were identical with those of **1**[I]. UV/Vis and Raman spectroscopy (for data see text) indicated the presence of I_3^- ions, suggesting the formation of **1**[I_3^-]. Attempts at recrystallisation of the product from CH_2Cl_2/Et_2O mixtures failed due to the onset of extensive decomposition reactions.

Reaction of **1**[Br] *with* Br_2*:* A solution of 4.86 g (30.4 mmol) of Br_2 in 70 ml of CH_2Cl_2 was added dropwise within 2 h to a solution of 5.60 g (7.60 mmol) of **1**[Br] in 30 ml of CH_2Cl_2. Interrupting the reaction at different stages and subjecting an aliquot of the reaction mixture to ^{1}H- and ^{31}P-NMR-spectroscopic analysis allowed the identification of cations **5a, 5b** and **6b** as reaction intermediates. The red-brown solution resulting at the end of the reac-

tion was concentrated to dryness and the residue redissolved in CH_2Cl_2. Inspection of ^{1}H-, ^{13}C-, and ^{31}P-NMR spectra revealed the presence of **6c** as the only phosphorus-containing component, together with small amounts (3−5% by integration of ^{1}H-NMR spectra) of nonphosphorus-containing impurities which were not analysed further. Attempts to purify the crude product by recrystallisation from different solvent mixtures were unsuccessful and promoted increasing decomposition of **6c**.

6b: ^{1}H NMR (CH_2Cl_2): δ = 7.9−7.7 (m, 30 H, C_6H_5), 6.47 (m, 1 H, 6-H), 6.23 (m, 1 H, 4-H), 6.07 (m, 1 H, 7-H). − ^{1}H{^{31}P} NMR (CH_2Cl_2): δ = 7.9−7.7 (m, 30 H, C_6H_5), 6.47 (dd, J_{HH} = 8.3, 1.9 Hz, 1 H, 6-H), 6.23 (d, J_{HH} = 1.9 Hz, 1 H, 4-H), 6.07 (d, J_{HH} = 8.3 Hz, 1 H, 7-H).

6c: ^{1}H NMR (CH_2Cl_2): δ = 7.88−7.75 (m, 18 H, H^{meta}, H^{para}), 7.71 (m, 12 H, H^{ortho}), 6.30 (t, ΣJ = 3.6 Hz, 2 H, H-4,7). − ^{1}H{^{31}P} NMR (CH_2Cl_2): δ = 7.88−7.75 (m, 18 H, H^{meta}, H^{para}), 7.71 (m, 12 H, H^{ortho}), 6.30 (s, 1 H, 4,7-H). − ^{13}C NMR (CH_2Cl_2): δ = 137.48 (m, ΣJ = 18.7 Hz, J_M = 31.2 Hz, C-3a,7a), 134.74 (m, ΣJ = 2.5 Hz, C^{para}), 134.51 (m, ΣJ = 10.9 Hz, C^{ortho}), 130.03 (m, ΣJ = 13.2 Hz, C^{meta}), 121.49 (m, ΣJ = 3.7 Hz, J_M = 18.3 Hz, C-4,7), 119.69 (m, ΣJ = 95.5 Hz, $^3J_{PC}$ = 3.0 Hz, C^{ipso}), 113.3 (d, J_{PC} = 2.5 Hz, C-5,6), 49.53 (ddd, $^1J_{PC}$ = 119.3, 123.7 Hz,$^3J_{PC}$ = 8.1 Hz, C-1,3).

Reduction of **6b and 6c**: To a stirred solution of crude **6c**[Br], which was prepared as described above, was added 3.64 g (36.0 mmol) of dry NEt_3. After continued stirring for 30 min, the reaction mixture was concentrated to dryness, the remaining solid redissolved in 40 ml CH_2Cl_2, and the resulting solution extracted twice with 25 ml of water. The organic phase was separated and dried with Na_2SO_4. Slow addition of 30 ml of ether produced a yellow precipitate which was collected by filtration and washed twice with 20 ml of ether. Recrystallisation from CH_2Cl_2/Et_2O gave 4.48 g of **5b**[Br]·CH_2Cl_2 (60%) as a light yellow powder, m.p. 186°C. For the preparation of compound **5a**, 1.00 g of **1**[OTf] and 50 mg (3 mmol) of Br_2 were treated as described above. To the resulting solution, which contained according to an ^{31}P-NMR-spectroscopic analysis approx. 70% of **6b**, was added with stirring 1.00 g (1.24 mmol) of **1**[OTf]. Chromatographic workup (silica gel, eluent: CH_2Cl_2) furnished 100 mg of a white solid which consisted of a mixture of **5a** (60%), **5b** (35%), and **1** (5%) according to an NMR-spectroscopic assay. No further separation by fractional crystallisation was achieved, and NMR-spectroscopic characterisation of **6b** was performed with the crude product mixture.

5a[OTf]: ^{1}H NMR ($CDCl_3$): δ = 7.72−7.55 (m, 30 H, C_6H_5), 7.03 (br. d, J_{HH} = 1.8 Hz, 1 H, 4-H), 6.95 (dd, J_{HH} = 1.8, 8.7 Hz, 1 H, 6-H), 6.80 (dd, J_{HH} = 8.7 Hz, ΣJ_{PH} = 2 Hz, 1 H, 7-H). − ^{1}H{^{31}P} NMR ($CDCl_3$): δ = 7.72−7.55 (m, 30 H, C_6H_5), 7.03 (d, J_{HH} = 1.8 Hz, 1 H, 4-H), 6.95 (dd, J_{HH} = 1.8, 8.7 Hz, 1 H, 6-H), 6.80 (d, J_{HH} = 8.7 Hz, 1 H, 7-H). − ^{13}C NMR ($CDCl_3$): δ = 146.6 (m, C-3a), 144.12 (m, C-7a), 134.52 (s, C^{para}), 134.48 (s, C^{para}), 133.9−133.7 (m, C^{ortho}), 130.20−129.9 (m, C^{meta}), 124.49 (br. s, C-4), 124.47 (br. s, C-6), 122.67 (ddd, J_{PC} = 92/3/3 Hz, C^{ipso}), 122.01 (br. m, C-7), 121.90 (ddd, J_{PC} = 92/2/1 Hz, C^{ipso}), 117.85 (s, C-5), 110.5 (ddd, $^1J_{PC}$ = 110/56 Hz,$^3J_{PC}$ = 14 Hz, C-1,3), 110.3 (ddd, $^1J_{PC}$ = 112/57 Hz,$^3J_{PC}$ = 15 Hz, C-1,3).

5b[Br]: $C_{44}H_{32}Br_3P_3$·CH_2Cl_2 (895.39): calcd. C 55.13, H 3.70; found C 55.41, H 3.88. − UV/Vis (CH_2Cl_2): λ_{max} (lg ε_{max}) = 370 (sh), 345 (4.1), 274 (sh), 261 (4.5) nm. − ^{1}H NMR ($CDCl_3$): δ = 7.77−7.57 (m, 30 H, C_6H_5), 7.12 {m, iterative analysis as an $[AX]_2$ spin system gave J_{PH} = +(−)3.4, −(+)1.7 Hz, J_{HH} = 0.9 Hz, 2 H, 4,7-H}. − ^{13}C NMR ($CDCl_3$): δ = 144.49 (m, ΣJ = 24.0 Hz, J_M = 2.7 Hz, C-3a,7a), 135.02 (m, ΣJ = 2.3 Hz, C^{para}), 134.23 (m, ΣJ = 9.9 Hz, C^{ortho}), 130.503 (m, ΣJ = 20.2 Hz, C^{meta}), 124.79 (br. m, C-4,7), 121.90 (m, ΣJ = 92.6 Hz, $^3J_{PC}$ = 2.8 Hz, C^{ipso}), 120.52 (q, J_{FC} = 320.2 Hz, CF_3SO_3), 118.09 (s, C-5,6), 112.00 (ddd, $^1J_{PC}$ = 96.9, 58.2 Hz,$^3J_{PC}$ = 13.7 Hz, C-1,3).

Reaction of **1**[OTf] *with* $PhICl_2$: To a stirred solution of 1.50 g (1.86 mmol) of **1**[OTf] in 20 ml of CH_2Cl_2 was added dropwise a solution of 0.51 g (1.86 mmol) of $PhICl_2$ in 20 ml of CH_2Cl_2. Subsequent dropwise addition of 15 ml of Et_2O to the yellow fluorescing solution produced a yellow precipitate which was collected by filtration, washed with Et_2O and dried in vacuo to give 1.48 g of **8a**[OTf]·CH_2Cl_2 (91%), m.p. 201°C. The same product was obtained when the reaction was conducted in the presence of 0.55 ml of NEt_3. Reaction of **1**[OTf] with an excess of $PhICl_2$ (1.5 to 4 equiv.) under the same conditions produced, according to ^{31}P-NMR-spectroscopic analysis, complex product mixtures which contained beside unreacted **8a** various amounts of the supposed substitution products **8b** and **8c** and several components whose resonances appeared as singlets or AX-type patterns. With the exception of a singlet at δ = 63.4 which was assigned to $[ClPPh_3]^+$ by comparison with an authentic sample, none of these products was identified. Separation of the mixtures and isolation of individual compunds proved not to be feasible.

8a[OTf]: $C_{45}H_{34}Cl_2F_3P_3SO_3$·$CH_2Cl_2$ (960.58): calcd. C 57.52, H 3.78; found C 56.98, H 3.66. − ^{1}H NMR ($CDCl_3$): δ = 7.74−7.57 (m, 30 H, C_6H_5), 6.41 (m, 2 H, 5,6-H), 6.21 (m, 2 H, 4,7-H). − ^{13}C NMR ($CDCl_3$): δ = 135.69 (m, ΣJ = 18.7 Hz, J_M = 33.5 Hz, C-3a,7a), 134.86 (m, ΣJ = 3 Hz, C^{para}), 134.72 (m, ΣJ = 10.7 Hz, C^{ortho}), 130.33 (m, ΣJ = 13.0 Hz, C^{meta}), 121.36 (q, J_{FC} = 320.9 Hz, CF_3SO_3), 119.76 (d, J = 2.5 Hz, C-5,6), 118.66 (m, ΣJ = 4 Hz, J_M = 19.8, C-4,7), 121.38 (m, ΣJ = 92.7 Hz, $^3J_{PC}$ = 3.2 Hz, C^{ipso}), 46.18 (ddd, $^1J_{PC}$ = 142.2, 126.2 Hz,$^3J_{PC}$ = 7.7 Hz, C-1,3).

Crystal-Structure Determination of **8a**[OTf] *at 200(2) K:* $[C_{44}H_{34}Cl_2P_3][CF_3SO_3]$·$CH_2Cl_2$, M = 960.52, yellow plates, crystal size 0.30 × 0.23 × 0.20 mm, monoclinic, space group $P2_1/c$ (no. 14): a = 12.4581(4), b = 22.5518(6), c = 16.5854(6) Å, β = 104.852(4)°, V = 4504.0(2) Å^3, Z = 4, $\rho_{calcd.}$ = 1.416 Mg m^{-3}, F(000) = 1968, μ(Cu-K_α) = 4.28 mm^{-1}. 8443 reflections (8143 independent reflections with R_{int} = 0.032) were collected with an Enraf-Nonius MACH3 diffractometer (Cu-K_α radiation, graphite monochromator, 2θ/ω scans) in the range 3° ≤ θ ≤ 68° (−14 ≤ h ≤ 14, −27 ≤ k ≤ 0, 0 ≤ l ≤ 19). Of these, 8142 were used for structure solution (direct methods) and refinement (full-matrix least squares on F^2, 542 parameters and 82 restraints, nonhydrogen atoms anisotropic, hydrogen atoms with a "riding" model); wR_2 = 0.176 {$R_1[I > 2\sigma(I)]$ = 0.066}. A semiempirical absorption correction on the basis of ψ scans and an extinction correction were applied. Crystallographic data (excluding structure factors) have been deposited at the Cambridge Crystallographic Data Centre under the number CCDC-100692. Copies of the data can be obtained free of charge on application to CCDC, 12 Union Road, Cambridge CB2 1EZ, UK [Fax: internat.+44(1223)336-033, E-mail: deposit@ccdc.cam.ac.uk].

[1] A. Schmidpeter, M. Thiele, *Angew. Chem.* **1991**, *103*, 333; *Angew. Chem. Int. Ed. Engl.* **1991**, *30*, 308.
[2] D. Gudat, M. Nieger, M. Schrott, *Inorg. Chem.* **1997**, *36*, 1476.
[3] G. Märkl, in *Multiple Bonds and Low Coordination in Phosphorus Chemistry* (Eds.: M. Regitz, O. J. Scherer), Georg Thieme Verlag, Stuttgart **1990**, p. 220 ff, and cited refs.
[4] *Gmelin's Handbuch der Anorganischen Chemie*, Iod (Syst. Nr. 8), 8th ed., Verlag Chemie, Berlin, **1933**, 423.
[5] W. Gabes, H. Gerling, *J. Mol. Struct.* **1972**, *14*, 267.
[6] J. C. Tebby in *Phosphorus-31 NMR Spectroscopy in Stereochemical Analysis* (Eds.: J. G. Verkade, L. D. Quin), VCH Publishers, Deerfield Beach, **1987**, p. 26.

[7] H. Kanter, W. Mach, K. Dimroth, *Chem. Ber.* **1977**, *110*, 395.
[8] S. S. Krishnamurthy, M. Woods in *Ann. Rep. NMR Spectrosc.* **1987**, *19*, 175, and cited refs.
[9] D. Gudat, M. Schrott, M. Nieger, *Chem. Ber.* **1995**, *128*, 259.
[10] Data from: A. F. Wells, *Structural Inorganic Chemistry*, 5th ed., Clarendon Press, Oxford **1993**, pp. 846ff.
[11] The extent of stabilisation is large enough to prevent protonation of the ylide functionality by hydrogen bromide which is formed as a coproduct during the substitution reaction.
[12] G. Jochem, A. Schmidpeter, M. Thomann, H. Nöth, *Angew. Chem.* **1994**, *106*, 708; *Angew. Chem. Int. Ed. Engl.* **1994**, 33, 663.

[97206]

The Structural Chemistry of Aziridino- and Azetidinosilanes☆

Gerald Huber, Alexander Jockisch, and Hubert Schmidbaur*

Anorganisch-chemisches Institut der Technischen Universität München,
Lichtenbergstrasse 4, D-85747 Garching, Germany

Received September 19, 1997

Keywords: Silicon / Aminosilanes / Aziridine / Azetidine / Molecular conformation / Configuration determination / Nitrogen

In a continuation of structural investigations of poly(amino)-silanes, a series of silicon derivatives of aziridine and azetidine have been prepared. Analogies with the isoelectronic phosphorus ylide species and the high barrier to inversion at nitrogen in small N heterocycles were suggestive of steeply pyramidal and rather rigid configurations at the N atoms in the title compounds. Tetrakis(*N*-aziridino)silane (**1**) and tetrakis(*N*-azetidino)silane (**2**) have been synthesized from $SiCl_4$ and $LiN(CH_2)_x$ (x = 2, 3). Compound **1** is also formed when $LiN(CH_2)_2$ and $HSiCl_3$ are used as starting materials, but with free aziridine a non-volatile product (**1a**) is obtained. In neither case could any trace of $HSi[N(CH_2)_2]_3$ be detected. In contrast, $RSiCl_3$ (R = Me, Ph) could readily be converted into the corresponding tris(*N*-aziridino)silanes (**3**, **4**) by treatment with excess aziridine. Tris(*N*-azetidino)silane (**5**) was accessible from $HSiCl_3$ and excess azetidine, but the product was found to contain an unknown impurity. In order to determine the local symmetry and the dynamics of the aziridine rings, ^{1}H-NMR spectra were recorded at low temperature (−80°C). No splitting of the signals was observed, indicating that the inversion barriers are extremely low, even in the highly strained three-membered heterocycles. Nevertheless, single-crystal X-ray diffraction studies of the *N*-triphenylsilyl derivatives of aziridine (**6**) and azetidine (**7**) revealed an aziridinyl group with a steeply pyramidal configuration at nitrogen in **6** (sum of the angles at N 313.32°), and an azetidinyl group with a flat geometry in **7** (sum of the angles at N 350.96°). The Si−N bond is significantly shorter in **7** as compared to that in **6**.

Introduction

Aziridine derivatives of *phosphorus* have been extensively studied owing to their widely established application in pharmacology and agriculture.[1][2][3] The most important variants of this usage are based on cyclic phosphazene compounds in which all the phosphorus atoms are exclusively bound to nitrogen. In order to trace the physiological effects to structural parameters, the molecular structures of several representative examples have been investigated.[4][5][6][7][8] *Azetidine* derivatives of *phosphorus* are less well investigated. Only a limited selection of compounds of this family have been described in the literature, for which no comparable chemotherapeutic or agrochemical uses are discernible.[9]

The taxonomy of related *N-silylated aziridines* and *azetidines* is far less developed[10][11] and no systematic investigation has been made of their properties and structural characteristics.[12] This is particularly true for compounds based solely on silicon-nitrogen frameworks, with only one example appearing in the patent literature.[13] Fundamental representatives, such as tetrakis(*N*-aziridino)- or tetrakis(*N*-azetidino)silane (**1**, **2**), have not hitherto been described.

As part of an ongoing investigation of poly(amino)silanes[14][15] we have recently initiated a study of silicon derivatives of aziridine and azetidine, mainly oriented towards a full structural characterization of prototype compounds, and an account of our results is given in the present paper.

Our previous investigations had centered on tetrakis(*N*-pyrrolidino)- and tetrakis(*N*-morpholino)silanes, which are the higher members of the homologous series of *N*-silylated, saturated N-heterocycles, albeit with strain-free five- and six-membered rings, respectively. While these and other standard dialkylaminosilanes typically possess the much debated planar configuration at nitrogen,[14] the aziridine or azetidine substituents are the only analogs where a steeply pyramidal configuration can be expected. This is also suggested by findings for the isoelectronic phosphorus ylide species, which were shown to have pronounced pyramidality at the ylidic carbon atoms of the cyclopropylide and cyclobutylide groups, respectively.[16][17]

In view of the good leaving-group properties of silicon substituents, the silylated heterocycles reported herein are expected to be useful aziridinating/azetidinating agents, which might be employed as substitutes for the rather hazardous free heterocycles.[18][19][20][21]

Results

Preparative Results

Tetrakis(*N*-aziridino)silane (**1**) and tetrakis(*N*-azetidino)-silane (**2**) have been prepared by the reaction of silicon tetrachloride with slightly in excess of four equivalents of the appropriate lithiated heterocycles in diethyl ether at low temperature (−60°C). Compound **1** was obtained as a colorless, distillable liquid, solidifying at 8°C, while the homolog **2** was obtained as a crystalline solid at room temperature, melting at 45°C. All attempts to grow single crystals of **1** and **2** were unsuccessful owing to pertinacious twinning, regardless of the method employed (from the melt, from

 © WILEY-VCH Verlag GmbH, D-69451 Weinheim, 1998 1434−1948/98/0101−0107 $ 17.50+.50/0

solution or by sublimation). Characterization of the compounds is therefore wholly based on the analytical and spectroscopic data (Experimental Section).

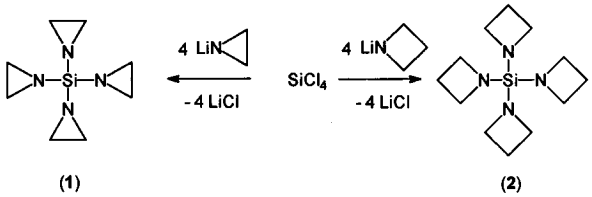

(1) (2)

Compound **1** was also generated in the reaction of *tri*-chlorosilane with lithium aziridinide, probably through an amide-catalyzed redistribution of the substituents [H/Cl/$N(CH_2)_2$] at silicon and/or hydride-induced aziridine ring opening. With $HSiCl_3$ and free aziridine in an organic solvent at −60°C, large amounts of a non-volatile, probably polymeric material were obtained. In neither reaction was any trace of the expected compound $HSi[N(CH_2)_2]_3$ detected.

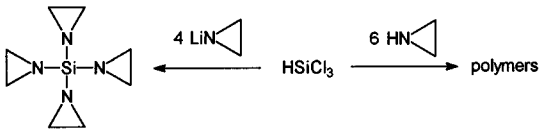

(1) (1a)

Trichloro(*methyl-* and *-phenyl*)silane are readily converted to the corresponding tris(*N*-aziridino)silanes (**3**, **4**) upon treatment with excess aziridine.

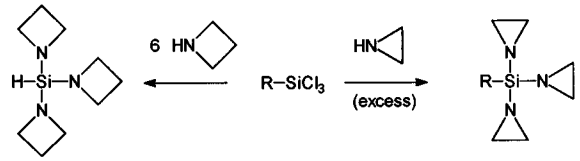

R = H (**5**) R = CH_3 (**3**)

Ph (**4**)

Tris(*N*-azetidino)silane (**5**) could be prepared from $HSiCl_3$ and excess azetidine, but purification of the product was not fully satisfactory. The analytical data seemingly indicate a rather pure product, but the values given in the Experimental Section nevertheless refer to a compound containing an unknown impurity. The MS and NMR data can be interpreted in terms of the presence of two isomers $\{HSi[N(CH_2)_3]_3\}_n$, but the nature of these isomers is not clear. Dimerization by azetidine ring-opening appears to be the most likely possible process.[22]

Because no poly(*N*-aziridino)- or poly(*N*-azetidino)silanes proved amenable to the growth of single crystals for structure determination, the *N-triphenylsilyl derivatives of aziridine* (**6**) and *azetidine* (**7**) were also prepared. Compound **6** has previously been synthesized from triphenylsilane, aziridine and alkali metals as catalysts in a dehydrocondensation reaction.[23] In the present study, **6** and **7** were obtained by the reaction of triphenylsilane with the appropriate lithiated heterocycles.

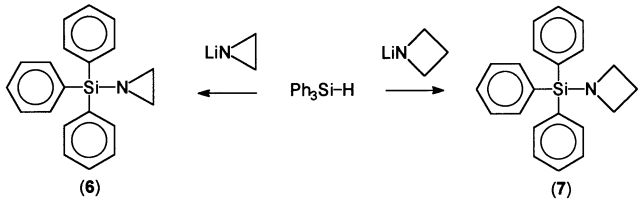

(6) (7)

Both compounds could be obtained in pure form, and single crystals of acceptable quality were readily grown from their solutions [m.p. 104°C (**6**), 86°C (**7**)].

NMR Spectroscopy

Assignment of the general patterns of the $^{29}Si\{^1H\}$- and $^{13}C\{^1H\}$-NMR spectra of the new silanes was largely straightforward. Regarding the ^1H-NMR spectra, however, the aspects of local symmetry of the aziridine rings and their dynamics have to be considered: A flat configuration at nitrogen, or a rapid inversion at this atom, would render the hydrogen atoms above and below the ring equivalent [(virtual) local symmetry with two perpendicular mirror planes, point group C_{2v} (on the NMR time scale)], while a rigid pyramidal configuration or a very slow inversion requires non-equivalent hydrogen atoms at the CH_2 groups (point group C_S). This also applies to the azetidine homologs, where additionally a flexible puckering of the four-membered ring has to be taken into account.

All compounds investigated in the present study exhibit only singlet ^1H resonances for the aziridine rings or show only multiplets characteristic of C_{2v}-symmetrical azetidine rings in solution at room temperature. Because it is implausible to assume a fully planar ground state for the aziridine/azetidine nitrogen atom, this result indicates a low barrier to nitrogen inversion. It is even more surprising that the pseudo-symmetry of the aziridinyl and azetidinyl groups is retained at temperatures as low as −80°C in all cases. This is in contrast to the "rigidity" of other simple organic derivatives of these heterocycles, which were found to have much higher barriers to inversion.[24] It therefore appears that the presence of silicon as the N-substituent atom has a marked effect on the inversion energetics. As found for other pairs of alkyl- and silylamines, even for strained small-ring amines, there is clearly a very significant lowering of the energy of the transition state for inversion.

Unfortunately, the coalescence/splitting temperature of the signals of the hydrogen atoms above and below the ring planes could not be attained, and therefore the energy of activation can only be estimated. Assuming chemical shift differences $\Delta\delta$ of less than 1 ppm, the barrier must be lower than 8.5 (± 2.5) kcal/mol, and is thus less than half of that determined for *N*-alkyl- or *N*-arylaziridines.[24] When evaluating this result it should be kept in mind that for unstrained tri-, di- and monosilylamines, completely flat ground-state geometries were found experimentally, and that state-of-the-art theoretical calculations have confirmed this unusual geometry and predict extremely flat energy profiles for pyramidalization.[14][15] This general pattern is

still reflected in the most strained example of the silylaziridines.

Crystal Structures

Crystals of *N-triphenylsilylaziridine* (**6**) are triclinic, space group $P\bar{1}$ with $Z = 2$ formula units in the unit cell. The molecules have no crystallographically imposed symmetry owing to a propeller-type arrangement of the three phenyl groups at silicon (Figure 1).

Figure 1. Molecular structure of compound **6** (ORTEP drawing with 50% probability ellipsoids, H atoms omitted for clarity)[a]

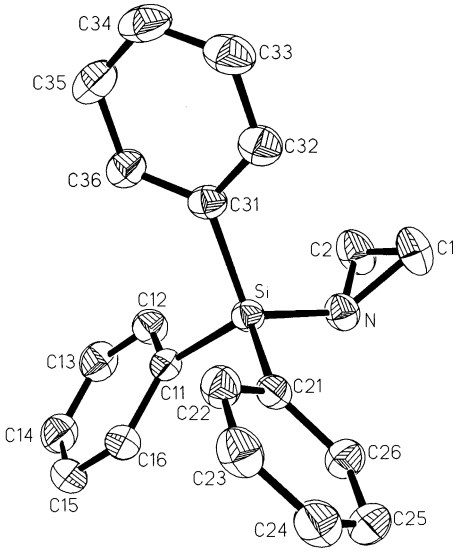

[a]Selected bond lengths [Å] and angles [°]: Si−N 1.7308(11), Si−C11 1.8658(13), Si−C21 1.8655(14), Si−C31 1.8744(13), N−C1 1.462(2), N−C2 1.456(2), C1−C2 1.470(2); N−Si−C11 105.94(6), N−Si−C21 105.81(6), N−Si−C31 114.28(6), C11−Si−C21 111.74(6), C11−Si−C31 109.59(6), C21−Si−C31 109.44(6), Si−N−C1 127.16(10), Si−N−C2 124.63(10), C2−N−C1 60.48(10), N−C1−C2 59.55(9), C1−C2−N 59.97(9).

The most important result of this structure determination is the geometry of the aziridinyl group, with its steeply pyramidal configuration at nitrogen. The plane of the three-membered ring forms an angle of 132.8° with the Si−N vector, and the sum of the angles at nitrogen amounts to only 312.3°. The conformation of the molecule with regard to the relative orientation of the $SiPh_3$ group and the $N(CH_2)_2$ unit, with its lone pair of electrons at the nitrogen atom, is staggered. The phenyl group *trans* to the lone pair at N has the largest N−Si−C angle [N−Si−C31 = 114.28(6)°]. The two remaining N−Si−C angles are almost equal, with individual values of N−Si−C11 = 105.94(6)° and N−Si−C21 = 105.81(6)°. The silicon atoms thus adopt a distorted tetrahedral geometry with bond lengths Si−N and Si−C in the range expected for standard single bonds (captions to Figure 1 and Table 1). The dimensions of the aziridine ring are also not unusual.

Crystals of *N-triphenylsilylazetidine* (**7**) are monoclinic, space group $P2_1/c$, with $Z = 4$ formula units in the unit cell. The molecules have no crystallographically imposed symmetry because of an adverse orientation of the phenyl rings at silicon (Figure 2).

Figure 2. Molecular structure of compound **7** (ORTEP drawing with 50% probability ellipsoids, H-atoms omitted for clarity)[a]

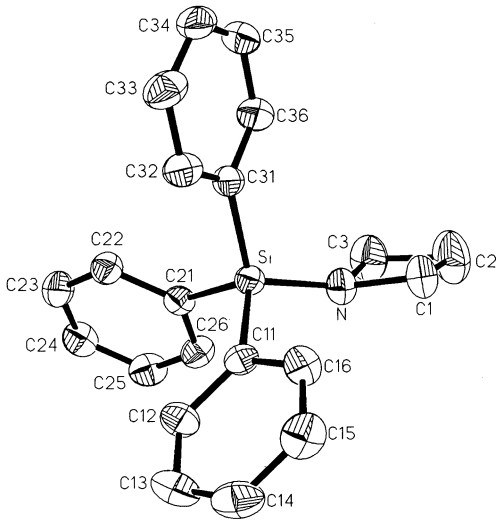

[a]Selected bond lengths [Å] and angles [°]: Si−N 1.7059(14), Si−C11 1.871(2), Si−C21 1.869(2), Si−C31 1.873(2), N−C1 1.481(2), N−C3 1.477(2), C1−C2 1.523(3), C2−C3 1.522(3); N−Si−C11 107.79(7), N−Si−C21 107.03(7), N−Si−C31 113.54(7), C11−Si−C21 109.74(7), C11−Si−C31 107.48(7), C21−Si−C31 111.17(7), Si−N−C1 127.63(11), Si−N−C3 131.76(12), N−C1−C2 89.6(2), C1−C2−C3 88.3(2), C2−C3−N 89.7(2), C3−N−C1 91.60(14).

The nitrogen atom of the azetidinyl group has a rather flattened pyramidal configuration, which can be quantified by the angle between the plane through the atoms N, C1 and C3 and the Si−N vector (156.2°), and by the sum of the angles at nitrogen (351.0°). As expected, the geometry at the nitrogen in **7** is much closer to planar than at that in **6**, but is nevertheless still distinctly non-planar.

The azetidine is folded, with an angle of 170.3° between the planes N−C1−C3 and C1−C2−C3, representing a flat butterfly structure. As in compound **6**, the conformation of the molecule is staggered with a wide angle N−Si−C31 = 113.54(7)° and two very similar angles for N−Si−C11 [107.79(7)°] and N−Si−C21 [107.03(7)°]. The bond lengths at silicon and in the four-membered ring show no anomalies (captions to Figure 2 and Table 1). It should be noted, however, that the Si−N bond is significantly shorter in **7** as compared to that in **6**, while there are no differences in the Si−C bond lengths. This difference may reflect a strengthening of the Si−N bond as the geometry at nitrogen is flattened, in agreement with the traditional concept of (p−d)π bonding, which, although now widely abandoned, is also consistent with the presently accepted (p−σ*)π model.[25]

Discussion and Conclusions

The structural investigations of a silylaziridine and of a silylazetidine have provided valuable reference data for a comparison with the isoelectronic phosphonium ylides.[16][17] From Table 1, it appears that the lattices of neither of the two pairs of compounds are isomorphous, but that the individual molecules share the same structural motifs with regard to the configuration at the functional atom

(nitrogen and ylidic carbanion, respectively) and the conformation. In the staggered rotamers, the lone pair of electrons at N or C is clearly "stereochemically active" and co-determines the overall structure. However, the carbanions show more pronounced pyramidalization than the amine nitrogen atoms and give rise to large deviations of the phosphorus atoms from the plane of the heterocycle. This is strong evidence for the "ylide" model of bonding with a highly polar P−C function, which should definitely be favored over the "ylene" form with P=C multiple bonding. For $Ph_3PC(CH_2)_2$, the non-equivalence of the hydrogen atoms above and below the cyclopropane plane could be demonstrated by a splitting of the ^{1}H-NMR resonances in solution at −80°C. For $Ph_3SiN(CH_2)_2$, this low-temperature limit was not sufficient to observe the same phenomenon, which indicates that the silylamine is more flexible than the phosphonium ylide.

The comparatively flat geometries of the silylaziridine and the silylazetidine are probably a consequence of the much greater difference in electronegativity of silicon and nitrogen (relative to phosphorus and carbon), which makes an Si−N linkage a strongly polar bond. The energy profile of such inherently polar bonds has been correctly predicted to be rather insensitive e.g. to deformations of bond angles,[26] and this is borne out by the present family of silazanes with their enormous flexibility: Although the ground-state geometries are rather steep, the activation energies for inversion at nitrogen are still sufficiently low to make these molecules fluxional on the NMR time-scale (see above).

It has been noted previously in theoretical studies of phosphonium cyclopropylides, as well as of silylamines, that inversion at carbon or nitrogen, respectively, has to be accompanied by P−C/Si−N bond rotation in order to regenerate the ground-state geometry.[27] This should be a minor contribution as compared to inversion, however, because rotation about Si−N and P−C bonds is known to be associated with very low barriers indeed, generally not in excess of 1 kcal/mol.

This work was supported by the *Deutsche Forschungsgemeinschaft* and the *Fonds der Chemischen Industrie*. The authors are grateful to Prof. *N. Rösch* and Ms. *K. Albert* for providing results of theoretical calculations prior to publication and to Mr. *J. Riede* for determining the X-ray data sets.

Experimental Section

All experiments were carried out under dry, pure nitrogen. Solvents and glassware were treated accordingly. Standard equipment was used throughout. Aziridine[28] and azetidine[29] were prepared according to literature procedures. Due to the method of preparation, the sample of azetidine contained benzene, which was quantified by ^{1}H-NMR spectroscopy. All other starting materials were commercially available. − NMR: Jeol GX 400 and Jeol GX 270, solutions in C_6D_6 at 23°C unless otherwise stated. − MS: GC/MS with mass-selective detector HP 5971 A (EI, 70 eV) and MAT 311 A (EI, 70 eV). − IR: Perkin-Elmer 1650 FT-IR.

Lithium Amides: In a typical reaction, *n*-butyllithium (1.7 M in hexane) was added dropwise to a solution of aziridine or azetidine in diethyl ether at −60°C. The reaction mixture was allowed to warm to room temperature and was stirred for 0.5 h. Then, the suspension was cooled to −60°C once more and used immediately in the subsequent reactions.

Tetrakis(N-aziridino)silane (**1**): A solution of silicon tetrachloride (0.86 ml, 7.5 mmol) or trichlorosilane (1.00 ml, 10 mmol) in 20 ml of diethyl ether was added dropwise to a suspension of lithium aziridinide [35 mmol, from 2.00 ml (39 mmol) of aziridine and 20.6 ml (35 mmol) of a 1.7 M solution of *n*-butyllithium in hexane] in 50 ml of diethyl ether at −60°C. After stirring the reaction mixture at room temperature for 15 h, the precipitate was separated, the solvent was removed from the filtrate in vacuo, and the remaining residue was extracted with pentane. **1** was separated from the extract by distillation (30°C, 0.05 mbar). Colorless liquid, 0.93 g (63%), m.p. 8°C. − ^{1}H NMR: δ = 1.77 (s, 24 H, CH_2). − ^{1}H NMR ([D$_8$]toluene, 23°C): δ = 1.73 (s, 24 H, CH_2). − ^{1}H NMR ([D$_8$]toluene, −80°C): δ = 1.77 (s, 24 H, CH_2). − ^{13}C{^{1}H} NMR: δ = 19.8 (CH_2). − ^{13}C NMR ([D$_8$]toluene, 23°C): δ = 19.6 (CH_2). − ^{29}Si{^{1}H} NMR: δ = −24.6. − ^{29}Si NMR: δ = −24.6 (m, $^3J_{Si,H}$ = 5 Hz). − ^{29}Si NMR ([D$_8$]toluene, 23°C): δ = −24.4 (m, $^3J_{Si,H}$ = 5 Hz). − ^{29}Si NMR ([D$_8$]toluene, −80°C): δ = −22.9 (m, br.). − ^{15}N NMR: δ = −390.2 (quint, $^2J_{N,H}$ = 2 Hz). − MS (EI, 70 eV) *m/z*: 196 [M$^+$], 154 [M$^+$ − $N(CH_2)_2$], 112 [154 − $N(CH_2)_2$], 70 [112 − $N(CH_2)_2$]. − IR (film): $\tilde{\nu}$ = 3041 m (ν NC_2H_4), 2983 m, 2900 m, 1276 s, 945 s, 683 s. − $C_{12}H_{24}N_4Si$ (196.32): calcd. C 48.9, H 8.2, N 28.5; found C 49.2, H 7.9, N 29.1.

Reaction of Trichlorosilane with Aziridine as Free Base (**1a**): 6 equiv. of aziridine (3.07 ml, 60 mmol) in 20 ml of diethyl ether was added dropwise to a solution of trichlorosilane (1.00 ml, 10 mmol) in 50 ml of diethyl ether at −60°C over a period of 15 min. After the reaction mixture had warmed to room temperature, stirring was continued for 1 h. The suspension was then filtered, the solvent was removed in vacuo, and a sample was prepared in C_6D_6 for NMR spectroscopy. − ^{1}H NMR: δ = 2.74 (m), 3.04 (m). − ^{13}C{^{1}H} NMR: δ = 42.7, 47.8. − ^{29}Si{^{1}H} NMR: δ = −34.6.

Tetrakis(N-azetidino)silane (**2**): A solution of silicon tetrachloride (0.22 ml, 2.0 mmol) in 10 ml of diethyl ether was added dropwise over a period of 5 min to a suspension of lithium azetidinide [10 mmol, from 2.00 ml (14.6 mmol) of a solution of azetidine, containing 42 mol-% of benzene and 5.9 ml (10 mmol) of a 1.7 M solution of *n*-butyllithium in hexane] in 50 ml of diethyl ether at −60°C. After stirring the reaction mixture at room temperature for 10 h, the precipitate was separated, the solvent was removed from the filtrate in vacuo, and the remaining residue was purified by distillation (40°C, 0.05 mbar). The crude product was crystallized from pentane at −60°C. Colorless crystals, 0.18 g (36%), m.p. 45°C. − ^{1}H NMR: δ = 2.24 (quint, 8 H, $^3J_{H,H}$ = 7 Hz, CCH_2), 3.94 (t, 16 H, $^3J_{H,H}$ = 7 Hz, NCH_2). − ^{13}C{^{1}H} NMR: δ = 21.8 (CCH_2), 49.4 (NCH_2). − ^{29}Si{^{1}H} NMR: not detected. − MS (EI, 70 eV) *m/z*: 252 [M$^+$], 196 [M$^+$ − $N(CH_2)_3$], 140 [196 − $N(CH_2)_3$].

Tris(N-aziridino)methylsilane (**3**): To a solution of trichloro(methyl)silane (1.17 ml, 10 mmol) in 50 ml of diethyl ether, 6 equiv. of aziridine (3.07 ml, 60 mmol) in 20 ml of diethyl ether was added dropwise over a period of 15 min at −60°C. After stirring for 20 h at room temperature, the reaction mixture was filtered and the solvent was removed in vacuo. The remaining oil was purified by distillation (50°C, 0.05 mbar). Colorless liquid, 1.12 g (66%). − ^{1}H NMR: δ = 0.11 (s, 3 H, CH_3), 1.70 (s, 12 H, CH_2). − ^{13}C{^{1}H} NMR: δ = −7.9 ($SiCH_3$), 19.7 (CH_2). − ^{29}Si NMR: δ = −4.5. − MS (EI, 70 eV) *m/z*: 169 [M$^+$], 127 [M$^+$ − $N(CH_2)_2$], 85 [127 − $N(CH_2)_2$]. − $C_7H_{15}N_3Si$ (169.30): calcd. C 49.7, H 8.9, N 24.8; found C 49.0, H 8.8, N 25.5.

Tris(N-aziridino)phenylsilane (**4**): Analogously to the preparation of **3**, **4** was prepared from 1.60 ml (10 mmol) of trichloro(phenyl)silane and 3.58 ml (70 mmol) of aziridine. After purification by distillation (100°C, 0.05 mbar), a colorless liquid was obtained. Yield 1.27 g (55%). − ^{1}H NMR: δ = 1.76 (s, 12 H, CH_2), 7.21 (m, 3 H, 3/4/5-H), 7.79 (m, 2 H, 2/6-H). − ^{13}C{^{1}H} NMR: δ = 20.1 (CH_2), 127.8 (C-2/6), 130.3 (C-4), 132.2 (C-3/5), 134.7 (C-1). − ^{29}Si{^{1}H} NMR: δ = −19.0. − MS (EI, 70 eV) *m/z*: 231 [M^+], 189 [$M^+ - N(CH_2)_2$]. − $C_{12}H_{17}N_3Si$ (231.37): calcd. C 62.3, H 7.4, N 18.2; found C 61.8, H 7.5, N 17.6.

Tris(N-azetidino)silane (**5**): To a solution of 7 equiv. of azetidine (2.00 ml of a solution of azetidine containing 42 mol-% of benzene, 14.6 mmol) in 50 ml of diethyl ether, trichlorosilane (0.20 ml, 2 mmol) in 10 ml of diethyl ether was added dropwise over a period of 15 min at −60°C. After the reaction mixture had warmed to room temperature, stirring was continued for 1 h. After filtration, the solvent was removed in vacuo and the remaining oil was distilled (100°C, 0.05 mbar) to give a colorless liquid. Yield 0.11 g (28%). − ^{1}H NMR: δ = 2.17 (quint, 6 H, $^3J_{H,H}$ = 7 Hz, CCH_2), 3.80 (t, 12 H, $^3J_{H,H}$ = 7 Hz, NCH_2), 4.36 (s, 1 H, SiH). − ^{13}C{^{1}H} NMR: δ = 21.9 (CCH_2), 48.7 (NCH_2). − ^{29}Si NMR: δ = −39.0 (d, $^2J_{Si,H}$ = 148 Hz). − MS (EI, 70 eV) *m/z*: 197 [M^+], 141 [$M^+ - N(CH_2)_3$], 85 [141 − $N(CH_2)_3$].

(N-Aziridino)triphenylsilane (**6**): A solution of triphenylsilane (1.04 g, 4 mmol) in 20 ml of diethyl ether was added dropwise to a suspension of lithium aziridinide [10 mmol, from 0.82 ml (16 mmol) of aziridine and 6.00 ml (10 mmol) of a 1.7 M solution of *n*-butyllithium in hexane] in 50 ml of diethyl ether at −60°C. After stirring the reaction mixture at room temperature for 15 h, the precipitate was separated, the solvent was removed from the filtrate in vacuo, and the remaining solid was extracted with pentane. **6** crystallized from this solution at 0°C. Colorless crystals, 1.48 g (61%), m.p. 104°C. − ^{1}H NMR: δ = 1.69 (s, 4 H, NCH_2), 7.20 (m, 9 H, 3/4/5-H), 7.77 (m, 6 H, 2/6-H). − ^{13}C{^{1}H} NMR: δ = 21.0 (NCH_2), 128.1 (C-2/6), 130.0 (C-4), 134.3 (C-3/5), 136.0 (C-1). − ^{29}Si{^{1}H} NMR: δ = −9.1. − MS (EI, 70 eV) *m/z*: 301 [M^+], 259 [$M^+ - N(CH_2)_2$], 182 [259 − C_6H_5], 105 [182 − C_6H_5]. − $C_{20}H_{19}NSi$ (301.46): calcd. C 79.7, H 6.4, N 4.7; found C 79.5, H 6.5, N 4.5.

(N-Azetidino)triphenylsilane (**7**): To a suspension of lithium azetidinide [5 mmol, from 1.00 ml (8 mmol) of a solution of azetidine containing 28 mol-% of benzene and 3.00 ml (5 mmol) of a 1.7 M solution of *n*-butyllithium in hexane] in 50 ml of diethyl ether, a solution of triphenylsilane (1.04 g, 4 mmol) in 20 ml of diethyl ether was added dropwise at −60°C. After stirring the reaction mixture at room temperature for 15 h, the precipitate was separated, and the filtrate was concentrated in vacuo. From this solution, compound **7** crystallized at −30°C. Colorless crystals, 0.61 g (48%), m.p. 86°C. − ^{1}H NMR: δ = 2.12 (quint, 2 H, $^3J_{H,H}$ = 7 Hz, CCH_2), 3.83 (t, 4 H, $^3J_{H,H}$ = 7 Hz, NCH_2), 7.21 (m, 9 H, 3/4/5-H), 7.71 (m, 6 H, 2/6-H). − ^{13}C{^{1}H} NMR: δ = 21.4 (CCH_2), 49.8 (NCH_2), 128.1 (C-2/6), 129.8 (C-4), 135.4 (C-3/5), 136.0 (C-1). − ^{29}Si{^{1}H} NMR: δ = −17.9. − MS (EI, 70 eV) *m/z*: 315 [M^+], 259 [$M^+ - N(CH_2)_3$], 182 [259 − C_6H_5], 105 [182 − C_6H_5]. − $C_{21}H_{21}NSi$ (315.49): calcd. C 80.0, H 6.7, N 4.4; found C 79.3, H 6.8, N 4.4.

Crystal Structure Determinations: Specimens of compounds **6** and **7** of suitable quality and size were mounted in glass capillaries and used for measurements of precise cell constants and intensity data collection on an Enraf-Nonius CAD4 diffractometer [Mo-K_α radiation, λ(Mo-K_α) = 0.71073 Å]. During data collection, three standard reflections were measured periodically as a general check of crystal and instrument stability. No significant changes were observed. The structures were solved by direct methods (SHELXS-86)[30] and refined by full-matrix least-squares techniques against F^2 (SHELXL-93)[31]. The thermal motion of all non-hydrogen atoms was treated anisotropically. All hydrogen atoms of compounds **6** and **7** were found and refined with isotropic contributions. Further information on crystal data, data collection and structure refinement is summarized in Table 1. Selected interatomic distances and angles are given in the corresponding figure captions. Anisotropic thermal parameters, tables of distances and angles, and atomic coordinates have been deposited at the Fachinformationszentrum Karlsruhe, D-76344 Eggenstein-Leopoldshafen, Germany. The data are available on request on quoting the depository numbers CSD-407949 (**6**) and CSD-407950 (**7**).

Table 1. Crystal data, data collection and structure refinement for compounds **6** and **7**

	6	**7**
crystal data		
formula	$C_{20}H_{19}NSi$	$C_{21}H_{21}NSi$
M_r	301.45	315.48
crystal system	triclinic	monoclinic
space group	$P\bar{1}$ (no. 2)	$P2_1/c$ (no. 14)
a [Å]	8.640(2)	10.923(1)
b [Å]	9.812(2)	8.468(1)
c [Å]	10.858(2)	19.255(3)
α [°]	65.55(3)	90
β [°]	89.01(3)	100.17(1)
γ [°]	83.13(3)	90
V [Å^{-3}]	831.4(3)	1753.0(4)
$D_{calcd.}$ [g cm^{-3}]	1.204	1.195
Z	2	4
F(000) [e]	320	672
μ (Mo-K_a) [cm^{-1}]	1.37	1.33
data collection		
T [°C]	−74	−80
scan mode	ω-θ	ω-θ
hkl ranges	0→+11	−13→+13
	−12→+12	0→+10
	−13→+13	0→+23
$\sin(\theta/\lambda)_{max}$ [Å^{-1}]	0.64	0.64
measured refl.	3612	3524
unique refl.	3612	3428 (R_{int} = 0.0235)
refl. used for refinement	3610	3425
absorption correction	none	none
structure refinement		
refined parameters	275	292
H atoms (found)	19	21
final *R* values [$I > 2\sigma(I)$]:		
*R*1[a]	0.0339	0.0351
*wR*2[b]	0.0907	0.0878
$(\text{shift/esd})_{max}$	< 0.001	< 0.001
$\Delta\rho_{fin}$(max/min) [eÅ^{-3}]	+0.382/−0.228	+0.353/−0.227

[a] $R = \Sigma(\|\|F_o\| - \|F_c\|\|)/\Sigma|F_o|$. − [b] $wR2 = \{[\Sigma w(F_o^2 - F_c^2)^2]/\Sigma[w(F_o^2)^2]\}^{1/2}$; $w = 1/[\sigma^2(F_o^2) + (ap)^2 + bp]$; $p = (F_o^2 + 2F_c^2)/3$; a = 0.0518 (**6**), 0.0466 (**7**); b = 0.2096 (**6**), 0.6142 (**7**).

☆ Dedicated to Professor *M. Weidenbruch* on the occasion of his 60th birthday.

[1] D. E. C. Corbridge, *Studies in Inorganic Chemistry 20, Phosphorus, An Outline of Its Chemistry, Biochemistry and Uses*, 5th ed., Elsevier, Amsterdam, **1995**, p. 452.
[2] *Comprehensive Heterocyclic Chemistry II, A Review of the Literature 1982−1995*, 1st ed., Elsevier, Oxford, New York, Tokyo, vol. 1A, **1996**, pp. 58−60.
[3] *Beilstein, Handbook of Organic Chemistry*, 4th ed., Springer, Berlin, Heidelberg, E V 20/1, **1988**, pp. 94−132.
[4] E. Subramanian, J. Trotter, *J. Chem. Soc. A* **1969**, 2309.

[5] K. C. K. Swamy, M. D. Poojary, S. S. Krishnamurthy, H. Manohar, *J. Chem. Soc., Dalton Trans.* **1985**, 1881.
[6] T. S. Cameron, J.-F. Labarre, F. Sournis, J. C. Van de Gampel, A. A. van der Huizen, *J. Chim. Phys.; Phys.-Chim. Biol.* **1985**, *82*, 941.
[7] T. S. Cameron, B. Borecka, W. Kwiatowski, *J. Am. Chem. Soc.* **1994**, *116*, 1211.
[8] F. Sournies, G. Guerch, J.-F. Labarre, J. Jaud, *J. Mol. Struct.* **1990**, *238*, 383.
[9] *Beilstein, Handbook of Organic Chemistry*, 4th ed., Springer, Berlin, Heidelberg, E V 20/1, **1988**, pp. 148−149.
[10] E. V. Bakhareva, M. G. Voronkov, P. V. Arbuzov, R. G. Mirshov, V. I. Rakhlin, S. B. Seredenin, *Khim. Farm. Zh.* **1995**, *29*, 31; *Chem. Abstr.* **1996**, *124*, 241h.
[11] M. G. Voronkov, L. N. Alekseeva, B. Brizga, A. Zile, V. P. Kozyukov, N. S. Fedotov, L. Kruzmetra, E. Lukevics, I. N. Lyashenko, V. F. Mironov, *Khim. Farm. Zh.* **1967**, *1*, 26; *Chem. Abstr.* **1968**, *68*, 38460s.
[12] O. J. Scherer, M. Schmidt, *Chem. Ber.* **1965**, *98*, 2243.
[13] J. Heyna, A. Bauer, *Ger. Patent* 834990, **1952**; *Chem. Abstr.* **1957**, 14819.
[14] G. Huber, A. Schier, H. Schmidbaur, *Chem. Ber.* **1997**, *130*, 1167.
[15] G. Huber, A. Schier, N. W. Mitzel, H. Schmidbaur, *Chem. Ber.* **1997**, *130*, 1175.
[16] H. Schmidbaur, A. Schier, B. Milewski-Mahrla, U. Schubert, *Chem. Ber.* **1982**, *115*, 722.
[17] H. Schmidbaur, A. Schier, D. Neugebauer, *Chem. Ber.* **1983**, *116*, 2173.
[18] R. W. Millar, S. P. Philbin, *Tetrahedron* **1997**, *53*, 4371, and literature cited therein.
[19] D. Seebach, T. Vettiger, H. M. Müller, D. A. Plattner, W. Petter, *Liebigs Ann. Chem.* **1990**, *7*, 687.
[20] C. Braun, W. Dell, H. E. Sasse, M. L. Ziegler, *Z. Anorg. Allg. Chem.* **1979**, *450*, 139.
[21] N. S. Nametkin, L. E. Ledina, V. N. Perchenko, L. G. Batalova, *Dokl. Akad. Nauk SSSR* **1974**, *219*, 1130.
[22] N. S. Nametkin, V. N. Perchenko, L. G. Batalova, *Dokl. Akad. Nauk SSSR* **1965**, *160*, 1087.
[23] N. S. Nametkin, V. N. Perchenko, L. G. Batalova, *Dokl. Chem.* **1964**, *158*, 660.
[24] W. B. Jennings, D. R. Boyd in *Cyclic Organonitrogen Stereodynamics* (Eds.: J. B. Lambert, Y. Takeuchi), VCH, Weinheim, **1992**, pp. 105−125.
[25] H. Schmidbaur in *Tailor-Made Silicon-Oxygen Compounds, From Molecules to Materials* (Eds.: R. Corriu, P. Jutzi), Vieweg, Braunschweig, Wiesbaden, **1996**, pp. 13−30.
[26] K. Albert, N. Rösch, submitted to *Chem. Ber.*
[27] M. A. Vincent, H. F. Schäfer III, A. Schier, H. Schmidbaur, *J. Am. Chem. Soc.* **1983**, *105*, 3806.
[28] C. F. H. Allen, F. W. Spangler, E. R. Webster, *Org. Synth.* **1963**, *Coll. Vol. 4*, 433.
[29] J. Szmuszkovicz, M. P. Kane, L. G. Laurian, C. G. Chidester, T. A. Scahill, *J. Org. Chem.* **1981**, *46*, 3562.
[30] G. M. Sheldrick, C. Krüger, R. Goddard, Oxford Univ. Press **1985**, 175−189.
[31] G. M. Sheldrick, *Progr. for the Refinement of Structures*, Univ. Göttingen, **1993**.

[97209]

Synthesis, Structure, and Dynamic Behaviour of Transition Metal Chelate Complexes with Atropisomeric Dithioether Ligands

Serafino Gladiali*[a], Davide Fabbri[b], Làszlò Kollàr[c], Carmen Claver*[d], Nuria Ruiz[d], Angel Alvarez-Larena[e], and Joan F. Piniella[e]

Dipartimento di Chimica, Università di Sassari[a],
Via Vienna 2, I-07100 Sassari, Italy
Fax: (internat.) +39(0)79/229559
E-mail: gladiali@ssmain.uniss.it

Istituto C. N. R. per L'Applicazione delle Tecniche Chimiche Avanzate ai Problemi Agrobiologici[b],
Via Vienna 2, I-07100-Sassari, Italy

Department of Inorganic Chemistry, Janus Pannonius University[c],
P.O. Box 266, H-7601 Pécs, Hungary

Departament de Química, Universitat Rovira i Virgili[d],
Plaça Imperial Tarraco 1, E-43005 Tarragona, Spain

Area de Cristallografia i Mineralogia, Universitat Autonoma de Barcelona[e],
E-08193 Bellaterra, Spain

Received July 29, 1997

Keywords: S ligands / Transition metals / Fluxionality

The preparation and characterization of Rh^{I}, Pd^{II}, and Pt^{II} complexes with chiral C_2-symmetrical dithioether ligands derived from 1,1′-binaphthalene-2,2′-dithiol (BINAS) are reported. All complexes are fluxional in solution at room temp. Interconversion between the stereoisomers can take place through conformational equilibration of the chelate ring, and/or inversion of configuration at the stereogenic sulfur. In the solid state the palladium derivative of Me_2BINAS shows a twisted chair conformation of the chelate ring, with both methyl groups in equatorial positions.

Recent investigations by our groups have shown that, in the hydroformylation of styrene[1], rhodium(I) complexes with the atropisomeric dithioethers **1** and **2** (Scheme 1), either preformed or prepared in situ by addition of the appropriate amount of the sulfur donor ligand to a suitable rhodium diolefin precursor $[Rh(cod)(\mu\text{-}X)]_2$ (cod:1,5-cyclooctadiene; X:Cl; MeO), are endowed with a high catalytic activity. Quantitative conversions of the substrate, with complete chemoselectivity in the formation of the aldehydes **3** and **4** (Scheme 1), are easily attained; even at room temp. and for a fairly wide range of carbon monoxide/hydrogen (1:1) pressures.

Scheme 1. Atropisomeric dithioether ligands

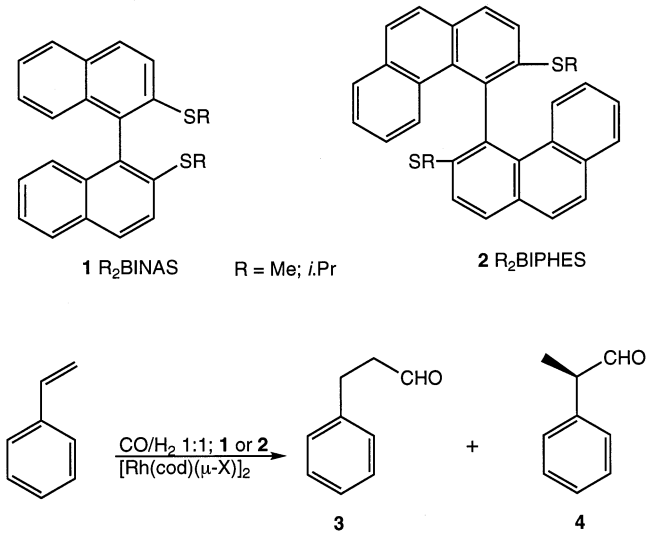

As these catalysts favour carbon monoxide insertion into the more substituted vinylic carbon, the major product is the branched isomer **4**, which, in the most favourable cases, can account for more than 95% of the reaction mixture. This regioselectivity, which is among the highest recorded in the hydroformylation of styrene, prompted us to exploit the potential of the enantiopure derivatives **1** and **2** in enantioselective hydroformylation. Transfer of chirality from the ligand to the product does take place, but the efficiency is quite low and the best enantiomeric excess (e.e.) obtained so far is only slightly greater than 20%. Albeit low, this value is in the range of the e.e.′s normally obtained in this reaction after more than twenty years of experimentation using rhodium catalysts containing diphosphane ligands as chiral modifiers[2].

A notable feature of the dithioether ligands **1** and **2** is that upon coordination to the metal they can give rise to different diastereomeric complexes, since the two sulfur donors become stereogenic centers. This fact is expected to

 © WILEY-VCH Verlag GmbH, D-69451 Weinheim, 1998 1434−1948/98/0101−0113 $ 17.50+.50/0

significantly affect the asymmetric bias of enantioselective hydroformylation, as the possibility of matching or mismatching combinations of the original stereogenic element of the ligand, the chiral biaryl backbone, and the newly established stereocenters, can easily be envisaged.

The formation of an unfavourable mixture of diastereomeric rhodium complexes, each one featuring its own stereodifferentiating ability, may well account for the low e.e. obtained in the hydroformylation of styrene. Alternatively this may be due to the configurational lability of the S-stereocenters under hydroformylation conditions.

In order to direct our research in this field on a more rational basis, we were interested to gain further information on the stability and the stereochemistry of the complexes used as catalysts. For this reason we investigated in more detail the coordination chemistry of the atropisomeric dithioethers **1** and **2** with d^8 transition metal centers.

Here we report on the preparation, structure and dynamic behaviour of the cationic and neutral complexes **5**, **6** and **7** obtained from the binaphthyl derivative **1** (R = Me; Me_2BINAS).

Figure 1. Me_2BINAS complexes

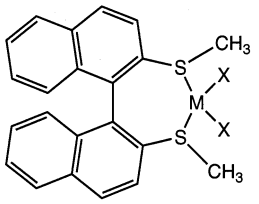

5 M = Rh; 2X = 1,5-cyclooctadiene
6 M = Pd; X = Cl
7 M = Pt; X = Cl

Results and Discussion

Preparation of the Complexes: The reaction of **1** with $[Rh(cod)_2]^+X^-$ (X = ClO_4; BF_4) **8** in CH_2Cl_2 solution proceeded, with the displacement of one 1,5-cyclooctadiene ligand, to afford the cationic complexes $[Rh(cod)(Me_2BINAS)]^+X^-$ **5**, isolated in high yield after the addition of diethyl ether. When the reaction was performed in the presence of a moderate excess of ligand **1**, the occasional formation of a byproduct, apparently a rhodium complex containing two units of dithioether ligand, was noticed. This product has not yet been fully characterized.

The chelate Pd complex **6** was obtained by the reaction of $[PdCl_2(PhCN)_2]$ **9** with an equimolar amount of the dithioether **1** in methylene chloride. The complex separated as a red solid upon the addition of diethyl ether. Under these conditions, the corresponding Pt complex $[PtCl_2(PhCN)_2]$ **10** does not react with the ligand **1** at room temp. However under UV irradiation at 254 nm in $CHCl_3$, chelate complexation of the dithioether ligand to the platinum center, with displacement of the ancillary benzonitrile ligands, takes place and is completed in a few hours. Addition of hexane leads to the precipitation of the complex **7** as a pale yellow solid.

Attempts to prepare complexes of binaphthalene thioethers **1** with a more demanding substituent on the sulfurs, such as isopropyl, have been so far unsuccessful since no reaction occurred at room temp.

Molecular Structure of [$PdCl_2(Me_2BINAS)$], (**6**): The molecular structure of **6** has been determined by X-ray diffraction analysis. A view of the molecule is given in Figure 2 and the most significant bond angles and lengths are listed in Table 1.

Figure 2. PLUTON[16] view of the molecular structure of $[PdCl_2(Me_2BINAS)]$ (**6**)

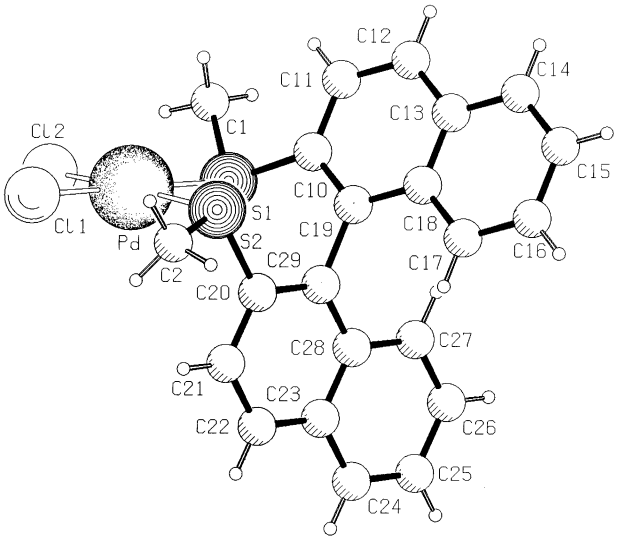

Table 1. Selected bond lenghts (Å) and angles (°) for complex $[PdCl_2(Me_2BINAS]$ (**6**)

Bonds (Å)		Angles (°)	
Pd-S1	2.316(2)	S1-Pd-S2	89.55(6)
Pd-S2	2.297(2)	Cl2-Pd-S2	175.73(6)
Pd-Cl1	2.285(2)	Cl2-Pd-S	187.57(6)
Pd-Cl2	2.305(2)	Cl1-Pd-S2	92.45(6)
C1-S1	1.805(9)	Cl1-Pd-S1	177.76(6)
S2-C2	1.791(7)	Cl1-Pd-Cl	290.38(7)
		Pd-S1-C1	107.29(26)
		Pd-S2-C2	112.19(25)

The crystal contains discrete mononuclear units of **6** in which the dithioether acts as a chelate ligand in a seven-membered ring with a highly distorted twisted chair conformation. Both the methyl groups are located in a pseudo-equatorial position giving the structure an overall C_2-symmetry, where the Pd atom is located on a two-fold axis. Both S-stereocenters display a pyramidal geometry and have the same relative configuration, whereas the binaphthyl moiety has the opposite chiral notation. As expected, the naphthyl rings are significantly bent and with a dihedral angle of 110.9(1)° between their planes, which allows the opposing hydrogens at C17 and C27 to be located at a comfortable distance apart (2.830(6) Å). These data suggest that the chiral diaryl backbone is, basically, free from torsional strain.

On the contrary, fairly short distances have been calculated between the hydrogen at C11 and two hydrogen atoms

of the C1-methyl (2.108(9) and 2.333(9) Å), and between the hydrogen at C21 and one hydrogen atom of the C2-methyl (2.189(9) Å). This may cause some destabilization of the diequatorial structure with respect to those structures with the methyl group(s) in an axial disposition.

The coordination around the Pd atom is essentially square planar. The Pd−S bond distances (2.297(2) and 2.316(2) Å) are comparable with those observed in other Pd complexes with diaryl[3] or aryl alkyl[4] sulfide ligands (2.293 and 2.288 Å, respectively). The Pd−Cl bond lengths (2.285(2) and 2.305(2) Å) are in the normal range for Pd chlorides with a *trans*-thioether donor[5], but are some seventy standard deviations shorter than those in *trans*-phosphane complexes (2.362 and 2.367 Å)[6]. This difference gives a measure of the weaker *trans* influence of the sulfur as compared to the phosphorus donor. The remaining bond distances and angles within the structure of the dithioether ligand are unexceptional.

Of the possible stereoisomers of the complex **6**, which differ either in the conformation of the chelate ring or in the spatial arrangement of the *S*-methyl substituents, this one is expected to be the most stable because both methyl groups are located in equatorial positions of the energetically favoured twisted chair conformation[7]. Although its preferential separation in the crystalline form obtained from the solution does not necessarily depend on a higher inherent stability, but may only reflect small differences in solubility or in crystal packing energy, NMR evidence is in keeping with the view that this isomer corresponds to the main product present in solution at low temperature.

Variable-Temperature NMR Characterization: The proton NMR spectrum of the rhodium complex **5** (X = ClO_4) shows, in the non aromatic region, two multiplets (4 H) at δ = 4.76 and 4.36, two broad signals (2 H) at δ = 2.47 and 2.10 and a singlet (6 H) at δ = 2.42 for the *S*-methyl protons. The first four resonances can be attributed to the *exo*- and *endo*-olefinic protons and to the methylene groups of the coordinated cyclooctadiene, respectively. The aromatic part of the spectrum is characterized by the presence of six peaks in the range δ = 8.21−7.00, roughly four doublets (2 H) and two triplets (2 H), which corresponds to the typical pattern of a C_2-symmetrical 2,2′-disubstituted binaphthalene. The shape of the NMR spectrum is not affected when the sample is cooled down to 193 K. In particular, the methyl resonance at δ = 2.42 does not show any apparent splitting.

The variable-temperature proton NMR spectrum of the palladium complex **6** is shown in Figure 3. At room temp. **6** shows a C_2-symmetrical pattern for the aromatic protons of the binaphtalene backbone and a broad singlet at δ = 2.7 corresponding to both the *S*-methyl substituents.

A less significant, but not negligible line broadening is also apparent in two aromatic peaks in the low field region of the spectrum. At 253 K, the two aromatic and the *S*-methyl resonances resolve into two different signals in an approximate 4:1 ratio, and a new peak appears at about 1.7 ppm. From 233 K down to 193 K this last new signal is quite sharp and shows the same intensity as the lower intensity peak arising from the splitting of the original *S*-methyl resonance (Figure 3).

Figure 3. variable temperature ^{1}H-NMR spectrum of [$PdCl_2$(Me$_2$-BINAS)] (**6**)

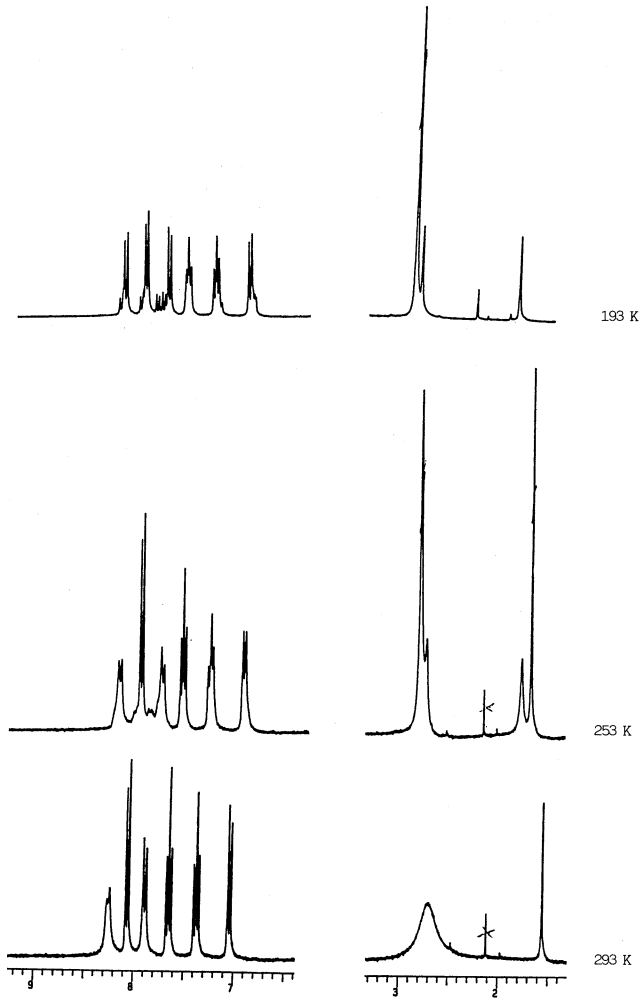

Since several stereoisomers with different spatial arrangements of the *S*-methyl substituents and different conformations of the seven-membered chelate ring are expected for the complex **6**, in principle this temperature dependent NMR spectrum may well reflect the presence of a dynamic equilibrium between two of these. An approximate energy barrier of 55 kJ mol^{-1} can be calculated for this process by line shape analysis of the variable temperature ^{1}H-NMR spectra, applying the coalescence temperature method[8].

The variable temperature ^{1}H-NMR spectra of the aromatic part of the platinum complex **7** is shown in Figure 4. The attributions to the protons have been assigned on the basis of selective decoupling and NOE experiments.

At room temp. the aromatic region shows six resonances with a pattern consistent with a C_2-symmetrical binaphthalene derivative. A significant line broadening is observed for the signals of three protons which apparently are close to the low exchange limit at room temp., while the remaining three protons give fairly sharp peaks. At 253 K all the aromatic protons give partially overlapping, sharp multiplets

Figure 4. Variable-temperature ^{1}H-NMR spectrum of [$PtCl_2(Me_2BINAS)$], (**7**): Aromatic part

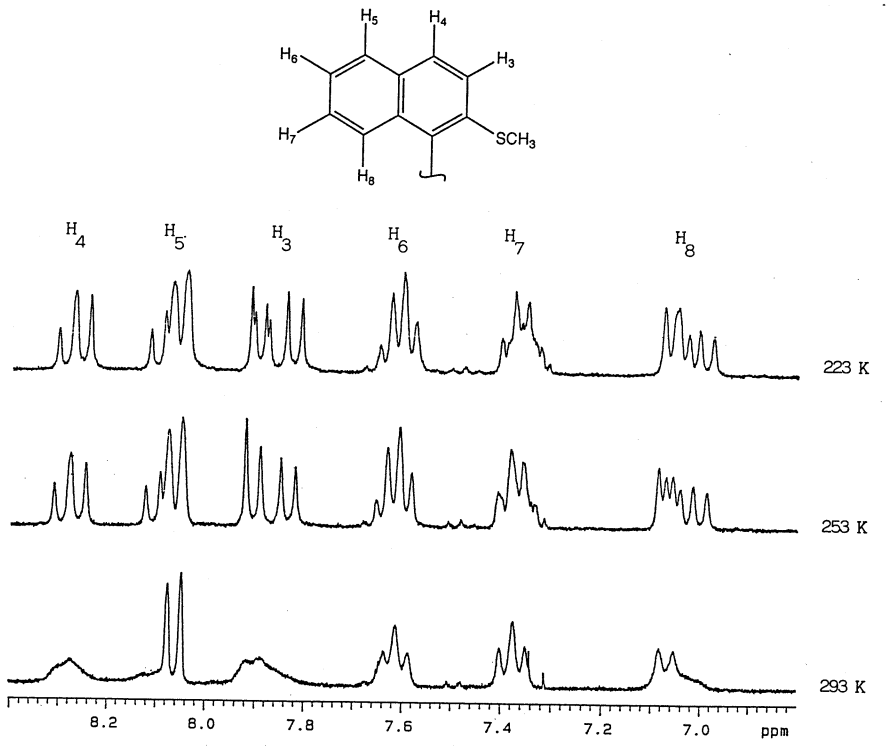

indicative of the presence of a mixture of two C_2-symmetrical species in ratio of about 3:2. At a lower temperature the more abundant of these isomers undergoes a further dynamic process which leads to the formation of an additional product. Some resonances, in particular the one attributed to H_3, are further split into two separate sets of signals. The emerging stereoisomer at 223 K is apparently devoid of C_2-symmetry, as indicated by the number of observable peaks. Unfortunately, due to the poor solubility of the complex, the NMR spectra could not be recorded at temperatures lower than 223 K. These data show that at room temp. two diastereomeric platinum complexes are slowly interconverting and that the major one is involved in a further dynamic process at lower temperatures.

At room temp., the *S*-methyl groups give rise to three broad singlets at δ = 2.82, 2.72 and 1.80, of roughly the same intensity, which do not collapse even at 320 K. These peaks are all accompanied by Pt satellites, confirming the chelate coordination of the sulfur centers to the metal. At 253 K the approximate values of the $^3J_{Pt-H}$ of these couplings, from the most shielded to the most deshielded signal, are 38 Hz, 44 Hz and 41 Hz, respectively. These values are substantially constant in the range of temperature explored.

Correlated spectra indicate that the two resonances at higher field belong to the same product. This suggests that the predominant stereoisomer of **7** has two unequivalent methyl substituents resonating at δ = 2.72 and δ = 1.80, while the less abundant one has a C_2-symmetrical structure with two equivalent methyl groups resonating at δ = 2.82.

Irradiation of this peak causes a significant NOE enhancement of the H_3 proton on the naphthalene ring, which is consistent with an equatorial location for this methyl group. This indicates that the minor isomer has both methyl groups in equatorial position and the seven membered chelate ring in chair or twisted chair conformation, in order to fulfill the condition of C_2 symmetry.

When the methyl signal of the minor isomer at δ = 2.82 is under irradiation, it is apparent that also the resonances of the methyl groups of the major species at δ = 2.72 and 1.80 experience NOE and, vice versa, irradiation of these peaks shows a similar effect on the δ = 2.82 peak. These NOE experiments also indicate that the less shielded methyl resonance of the major isomer belongs to an equatorial methyl group, whereas the more shielded methyl resonance belongs to an axial group. From these data the major isomer of the platinum complex **7** can be assigned to having an ax-eq disposition of the methyl substituents.

The peaks of the aromatic part of the NMR spectrum of the Pt complex are too close together and not appropriately shaped for a reliable determination of the activation energy of the dynamic processes to be achieved. However, the presence of well separated methyl resonances at room temp. indicates that this complex is less fluxional than the Pd counterpart and that the activation energy for the first equilibrium should be higher than the 55 kJ mol^{-1} found for the Pd complex.

Aside from the relative diastereomeric ratio and equilibration rates, the overall pictures emerging from the dynamic NMR investigation of the platinum and the palladium complexes are quite similar, with the basic difference that, unlike the platinum case, in the palladium complex it is the major species which has the eq−eq methyl groups.

Discussion

The dynamic behaviour shown by the Pd and Pt complexes indicates that different species are present in solution and that the interconversion among them is a fast process on the NMR timescale at room temp. Scheme 2 summarizes the interplay among the possible stereoisomers (diaxial species are omitted).

Scheme 2. Possible stereoisomers of Me_2BINAS complexes; the absolute configuration of the stereogenic sulfur centers are indicated; the binaphthalene backbone (R configuration) and the additional ligands at the metal are omitted for clarity

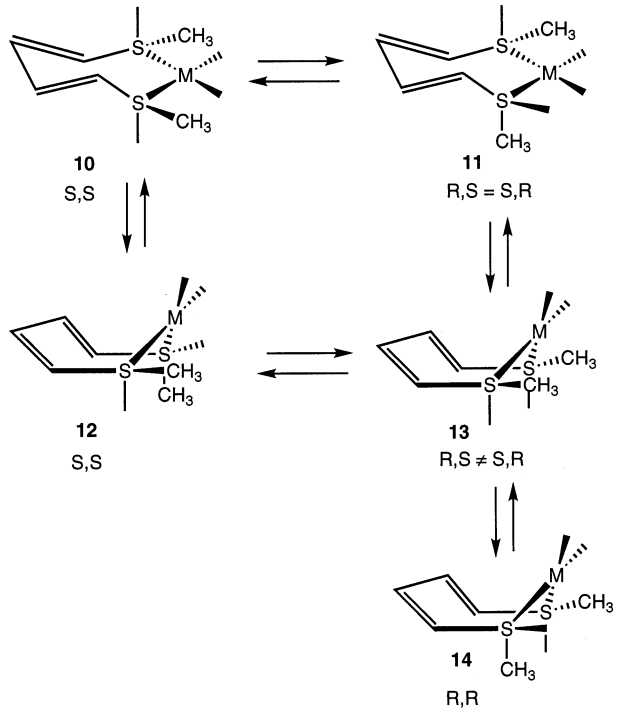

For the interconversion between these species three different hypothesis can be formulated: 1) interconversion between two different conformations of the seven membered chelate ring of comparable stability; 2) epimerization at the stereogenic sulfur through dissociation-recombination; 3) pyramidal inversion at the stereogenic sulfur in the bound state with no dissociation. In the first hypothesis the configurations at both the sulfur atoms are preserved during the dynamic process, while the second and the third transformations are accompanied by a net inversion of configuration at one or both stereogenic sulfur(s).

The fact that the position of the chemical shifts of the methyl substituents and the values of the relevant $^3J(^{195}Pt,^1H)$ coupling constants of the Pt complex are invariant in the temperature range scanned rules out the second hypothesis, and lends better support to the view that dissociation of the S donors is not occurring at any time.

From the NMR spectra of the platinum complex **7** two species can be univocally identified. The minor isomer has two equatorial *S*-methyl substituents and an overall C_2-symmetry. These conditions are met only by compound **10** having the seven membered chelate ring in a twisted chair (or chair) conformation, but not by the corresponding boat conformer **13**. The same chair structure can be attributed to the major isomer of the palladium complex which shows the same NMR pattern. Thus, the structure shown in the solid state by the Pd complex **6** corresponds to the structure of the predominant isomer in solution.

The second species identified by NMR has an equatorial-axial disposition of the methyl groups and is the predominant one in the Pt complex, even at room temp. Three different structures are conceivable for this isomer: one which mantains the twisted chair conformation and the C_2-symmetry (**11**) and two with a twisted boat conformation of comparable stability and C_1 symmetry (**12** and **14**). The ^{1}H-NMR spectra at −20°C suggest a C_2-symmetrical structure for this compound. While this condition is met by the chair conformer **11**, it cannot be overlooked that an apparent C_2 symmetry can result from a fast interconversion of two C_1-symmetrical stereoisomers such as **12** and **14**.

Actually, at −50°C a further dynamic process causes the C_2-symmetrical pattern of the aromatic resonances to be broken down. Notably, chemical shifts and shapes of the signals due to the methyl groups do not show any apparent change at this stage. As the surroundings of the methyl substituents are quite similar in **12** and **14**, both these facts seem to us to lend better support to the second assumption.

We can confidently conclude that in the case of the platinum complex **7**, the eq-eq chair conformer **10** is slowly interconverted at room temp. into the ax-eq boat conformers **12** and **14** which, under the same conditions, are rapidly interconverting. The same is probably true for the palladium derivative **6**, which is more fluxional than the Pt counterpart.

For the equilibration between **10** and **12** (or **14**) to occur, both changes in the chelate ring conformation and inversion of configuration at one stereogenic sulfur are required. The available data do not allow us to envisage which process is occurring first, but it is known that they are both feasible and can even take place simultaneously[9].

The structures having both the methyl groups equatorial are expected to be more stable, but this is not the case for the platinum complex where the predominant species has an axial methyl substituent. Actually, a non-bonding interaction is present between the hydrogen at the aryl carbon 3 (adjacent to that bound to the sulfur) and the equatorial methyl substituent. This is evidenced by a short contact distance in the solid state structure of the Pd complex (ca. 2.1 Å) and should be even more severe in the case of the Pt derivative due to the larger ionic radius. In keeping with this, the equilibrium of the platinum complex is shifted towards the ax-eq isomer.

Nothing can be said about the dynamics of the rhodium complex **5** which is probably highly fluxional over the range of temperatures scanned.

Conclusions

The dithioether complexes reported here are all fluxional at room temp. This dynamic behaviour is extremely pronounced in the case of rhodium(I) derivatives whose dia-

stereoisomers did not show isolated NMR resonances even at −80°C. Due to this property, Rh complexes with Me_2BINAS do not seem well suited for use in enantioselective catalysis where high e.e.'s should not be expected.

This work was carried out within the framework of the COST D2 program of the C.E.C. "Selective synthesis". Financial support from *the Italian Ministero dell' Università e della Ricerca Scientifica e Tecnologica* (MURST 60% and 40%), the *Spanish CICYT* (Ministerio de Educacion y Ciencia) and *CIRIT* (Generalitat de Catalunya), Proj. QFN-95-4725-C03 and the *Hungarian Research Fund* (OTKA 25525) is gratefully acknowledged. L. K. would like to thank dr. *Gabor Szalontai* (NMR Laboratory, University of Veszprem) for many NMR experiments on the Pt complex and for useful discussions. S. G. likes to thank Prof. *Dieter Sellmann* (University of Erlangen-Nürnberg) for reading and commenting on the manuscript.

Experimental Section

Melting points are uncorrected. Infrared spectra were recorded in KBr pellets on a BIO-RAD FTS-7PC spectrophotometer. ^{1}H and ^{13}C spectra were recorded on a Varian VXL 5000 spectrometer at 300 and 75.5 MHz, respectively, in CD_2Cl_2 and $CDCl_3$. Chemical shifts of protons and carbons are reported in ppm referred to TMS as an internal standard. Elemental analyses were performed with a Perkin Elmer Analyser 240 B. Commercial chemical reagents were used as received and solvents were dried by standard procedures and stored over molecular sieves under an inert atmosphere. $[Rh(cod)_2]^+X^-$[10], $PtCl_2(PhCN)_2$[11] and $PtCl_2(PhCN)_2$[12] were prepared according to the literature.

Preparation of [Rh(cod)(Me$_2$BINAS)]ClO$_4$ (**5**): The ligand Me_2BINAS (99.3 mg, 0.29 mmol) was added to a solution of $[Rh(cod)_2]ClO_4$ (100 mg, 0.24 mmol) in dichloromethane (5 ml). After stirring at room temp. for 15 min, diethyl ether was added to give a yellow precipitate of $[Rh(cod)(Me_2binas)]ClO_4$ which was filtered off and dried in vacuo (147.8 mg, 94% yield). − IR (KBr, cm^{-1}): $\tilde{\nu}$ = 1096 s, 625 m. − ^{1}H NMR (300 MHz, $CDCl_3$): δ = 8.21 (d, *J* = 9 Hz, 2 H, ArH); 8.04 (d, *J* = 8.2 Hz, 2 H, ArH); 7.76 (d, *J* = 8.5 Hz, 2 H, ArH); 7.58 (t, *J* = 7.6 Hz, 2 H, ArH); 7.34 (t, *J* = 8.2 Hz, 2 H, ArH); 7.00 (d, *J* = 9 Hz, 2 H, ArH); 4.76 (br. m, 4 H, CH cod); 4.36 (br. m, 4 H CH, cod); 2.42 (s, 3 H, CH_3); 2.10 (d, *J* = 9.3 Hz, 4 H, CH_2 cod); 1.80 (br. m, 4 H, CH_2 cod). No splitting is observed at low temperatures. − ^{13}C NMR ($CDCl_3$): δ = 133.9, 132.6, 130.2, 129.7, 129.1, 127.0, 124.6 (Ar); 82.0 (CH cod); 79.9 (CH, cod); 34.2 (CH_2, cod); 15.9 (SCH_3). − $RhC_{30}H_{30}S_2ClO_4$ (657.0): calcd. C 54.9, H 4.5, S, 9.7; found C 55.0, H 4.5, S 9.7.

Preparation of [PdCl$_2$(Me$_2$BINAS)] (**6**): The ligand Me_2BINAS (50 mg, 0.144 mmol) was added to a solution of $[PdCl_2(PhCN)_2]$ (50 mg, 0.13 mmol) in dichloromethane (5 ml). After stirring at room temp. for 20 min, diethyl ether was added to give a red precipitate of **6** which was filtered off and dried in vacuo (54.1 mg, 73.1% yield). − ^{1}H NMR ($CDCl_3$): see text. − Mass spectrum (FAB); *m/z*: 523 (M^+), 489 (M − Cl), 452 (M − 2 Cl), 346 (Me_2binas). − Conductivity in CH_2Cl_2: 0.041 S·cm^2·eq^{-1}. − $C_{22}H_{18}Cl_2PdS_2$ (523.8): calcd. C 50.4, H 3.4, S 12.2; found C 50.6, H 3.3, S 12.1.

Preparation of [PtCl$_2$(Me$_2$BINAS)] (**7**): The ligand Me_2BINAS (172 mg, 0.5 mmol) was added to a solution of $[PtCl_2(PhCN)_2]$ (235 mg, 0.5 mmol) in chloroform (45 ml) and the solution was irradiated (254 nm) at 35°C for 11 h. The chloroform was evaporated and the yellow residue was taken up with benzene (20 ml). The yellow precipitate was filtered off and dried in vacuo (160 mg, 53% yield). − ^{1}H NMR ($CDCl_3$): see text. − $C_{22}H_{18}Cl_2PtS_2$ (612.5): calcd. C 43.11, H 2.96; found C 43.11, H 2.96.

X-ray Structure Determination and Refinement of [PdCl$_2$(Me$_2$BINAS)] (**6**): X-ray quality crystals of the complex **6** were grown by slow diffusion of diethyl ether into a CH_2Cl_2 solution. $C_{22}H_{18}ClPd_2S_2$, *M* = 523.81. Monoclinic, *a* = 8.144(2), *b* = 27.416(7), *c* = 9.416(2), β = 92.98(2), V = 2099(1) Å^3 (by least-squares refinement on diffractometer angles for 25 automatically centred reflexions, λ = 0.71069 Å), space group $P2_1/c$ (No. 14), *Z* = 4, D_x = 1.657 g cm^{-3}. Yellow, air stable crystals, μ(Mo-K_α) = 13.42 cm^{-1}. CAD4 diffractometer, ω/2θ mode with ω scan width = 0.80 + 0.35 tan θ, ω scan speed 1.3−5.5° min^{-1}, graphite-monochromated Mo-K_α radiation. Reflection ranges for the data collection were 1° < θ < 25° and −9 ≤ *h* ≤ 9, 0 ≤ *k* ≤ 32, 0 ≤ *l* ≤ 11. 3690 unique reflections (Lp and empirical absorption correction from ψ scans[13], minimum/maximum transmission = 0.786:0.999), 2634 observed reflections with $I > 2\sigma(I)$. Direct methods (SHELXS-86 program)[14] and full-matrix least-squares refinement on F^2 for all the reflections (SHELXL-93 program)[15] were applied.

Naphthyl groups were refined as rigid groups because some of their geometrical parameters were not sensible, and at the end of refinement were close to standard values. All non-hydrogen atoms were refined anisotropically. Hydrogen atoms were placed in calculated positions with isotropic temperature factors fixed at 1.2 times (naphthyl H) or 1.5 times (methyl H) U_{eq} for the corresponding carbon atoms. The weighting scheme was $w = 1/[\sigma^2(F_o^2) + (0.1075P)^2]$ where $P = [\max(F_o^2,0) + 2F_c^2)]/3$. Final R(*F*) and $R_w(F^2)$ values were 0.047 and 0.148 for reflections with $I > 2\sigma(I)$. Thermal parameters, a complete list of bond lengths and angles and further details of **6** are available from Fachinformationzentrum Karlsruhe, D-76344 Eggenstein-Leopoldshafen, on quotation of the depository number CSD-407608.

[1] [1a] C. Claver, S. Castillon, N. Ruiz, G. Delogu, D. Fabbri, S. Gladiali, *Chem. Commun.* **1993**, 1833. − [1b] N. Ruiz, A. Aaliti, J. Fornies, A. Ruiz, C. Claver, C. J. Cardin, D. Fabbri, S. Gladiali, *J. Organomet. Chem.*, in press.
[2] Review: S. Gladiali, J. C. Bayón, C. Claver, *Tetrahedron Asymmetry* **1995**, *6*, 1453.
[3] L. R. Gray, D. J. Gulliver, W. Levason, M. Webster, *Acta Crystallogr. C* **1983**, *39*, 877.
[4] G. R. Clark, J. D. Orbell, *J. Organomet. Chem.* **1981**, *215*, 121.
[5] B. de Groot, G. S. Hanan, S. J. Loeb, *Inorg. Chem.* **1991**, *30*, 4644.
[6] [6a] D. S. Payne, J. A. A. Mukuolu, J. C. Speakman, *Chem. Commun.* **1965,** 599; − [6b] R. A. Jacobson, L. L. Martin, *Inorg. Chem.* **1971**, *10*, 1795.
[7] D. F. Bocian, H. L. Strauss, *J. Am. Chem. Soc.* **1977**, *99*, 2876.
[8] A. A. Watson, A. C. Willis, S. B. Wild, *J. Organomet. Chem.* **1993**, *445,* 71.
[9] A. Albinati, J. Eckert, P. Pregosin, H. Rüegger, R. Salzman, C. Stössel, *Organometallics* **1997**, *16*, 579.
[10] R. Usòn, L. A. Oro, M. A. Garralda, C. Claver, P. Lahuerta, *Transition Met. Chem.* **1979**, *9*, 55.
[11] M. S. Karasch, R. C. Seyler, F. R. Mayo, *J. Am. Chem. Soc.* **1938**, *60*, 882.
[12] F.R. Hartley, *Organomet. Chem. Rev. A* **1970**, *6*, 119.
[13] A. C. T. North, P. C. Philips and F. S. Mathews, *Acta Crystallogr., Sect. A* **1968**, *24*, 351.
[14] G. M. Sheldrick, SHELXS 86, in *Crystallographic Computing 3* (Eds.: G. M. Sheldrick, C. Krüger, R. Goddard), Oxford University Press, Oxford, **1985**, pp. 175−178.
[15] G. M. Sheldrick, *SHELXL 93, A Program for the Refinement of Crystal Structures,* University of Göttingen, Göttingen, **1992**.
[16] A. L. Spek, *PLUTON 93, A Program for the Display and Analysis of Crystal and Molecular Structures,* University of Utrecht, The Netherlands, **1993**.

[97178]

[(Arene)(Diene)Fe] and [(Arene)(Diazadiene)Fe] Complexes: Preparation, Reactivity, and Catalytic Properties☆

Pascal Le Floch[a], Falk Knoch[b], Frank Kremer[b], Francois Mathey[a], Joachim Scholz[c], Wolfgang Scholz[b], Karl-Heinz Thiele[c], and Ulrich Zenneck*[b]

Laboratoire "Hétéroéléments et Coordination" URA CNRS 1499 Ecole Polytechnique[a],
F-91128 Palaiseau Cedex, France

Institut für Anorganische Chemie der Universität Erlangen-Nürnberg[b],
Egerlandstraße 1, D-91058 Erlangen, Germany
Fax: (internat.) + 49(0)9131/85-7367
E-mail: Zenneck@anorganik.chemie.uni-erlangen.de

Fachbereich Chemie der Universität Halle-Wittenberg[c],
Geusaer Straße, D-06217 Merseburg, Germany

Received August 5, 1997

Keywords: Arene complexes / Catalysis / Diazadiene complexes / Iron / Metal vapour

Two different routes to novel [(diene)(η^6-2,6-dimethylpyridine)Fe] complexes are reported, both of which utilize metal vapour reactions. The presence of two small substituents on the 2,6-position of pyridine is essential for the η^6-coordination of the heterocycle. Investigations on the reactivity and stability of the [(diene)(η^6-arene)Fe] complexes are presented, including those of the benzene, phosphinine, and pyridine derivatives. These investigations give some hints to the relevant factors for determining the interaction between an iron atom and a π-coordinated neutral arene ligand, and their modification by a nitrogen or a phosphorus atom. Selective substitution of the 1,5-cyclooctadiene (COD) ligand of [(COD)(η^6-arene)Fe] complexes by some 1,4-diaza-1,3-diene (DAD) derivatives is possible in the case of the benzene or phosphinine arene ligands, and [(DAD)(η^6-arene)Fe] complexes are formed, but all DAD derivatives tested so far cause the complete disintegration of [(COD)(η^6-2,6-dimethylpyridine)Fe]. [(DAD)(η^6-arene)Fe] complexes exhibit a catalytic potential, which was evaluated by experiments on the catalytic cyclodimerization of 1,3-butadiene in the presence of [$(Et_2AlOEt)_2$] as a co-catalyst. This reaction yields up to 92% of 1,5-cyclooctadiene, and an almost quantitative butadiene conversion is possible in the presence of less than 0.1% of the catalyst. Structural investigations on [(*N*,*N*′-bis(cyclohexyl)ethylenediimine)(η^6-toluene)Fe] **5a** reveal some details of the Fe-DAD interaction. An effective electron back-donation from occupied iron d-orbitals into the π*-LUMO of the DAD is indicated.

Diazadienes (DAD, **1**) exhibit a rich coordination chemistry[1], as they can formally act as 2-, 4-, 6-, or 8-electron donors. Metal coordination of the heterodiene is possible in different conformations since rotation of the central C−C-bond is only slightly energetically hindered (20−28 kJmol^{-1}). The most frequent case is coordination in the end-on chelate ligating mode, where the σ-lone pairs of the two nitrogen atoms are donated to a metal atom. A high catalytic potential has been found for such σ-diazadiene iron complexes in connection with unsaturated hydrocarbons. For example [$(DAD)_2$Fe] (**2**) derivatives[2] are catalysts for the cyclodimerization of 1,3-dienes in the presence of alkyl aluminium co-catalysts, to form vinylcyclohexene and 1,5-cyclooctadiene derivatives. [(DAD)$FeCl_2$] is activated by Grignard reagents. It allows efficient cyclodimerization, or co-dimerization, reactions of dienes and alkenes under mild conditions, and a Diels-Alder type reaction of 1,3-dienes with alkynes[3].

Both catalytically active species have the 12 valence electron (VE) fragment [(DAD)Fe] in common, which is believed to be part of the true catalyst[4]. With the aim of finding new catalytically active species with complementary properties to the known ones, and as the influence of the leaving ligand of a pro-catalyst may be decisive for such a process, we are interested in (DAD)Fe complexes with labile co-ligands.

On the basis of our own work on arene iron complexes, we have some knowledge about the conditions necessary to replace an arene ligand by other substrates at ambient or slightly elevated temperatures[5], and thus we decided to prepare the novel [(η^6-arene)(DAD)Fe] complexes. Attempts to prepare this class of compounds have been reported, but no full evidence was presented[6]. We found convenient synthetic routes for their preparation, including the iron complexes of heteroarenes. Some initial experiments on their catalytic potential demonstrated the merits of the concept.

Our synthetic approach to these complexes is that of an alkene ligand exchange reaction by diazadiene derivatives, which are allowed to react with [bis(alkene)(η^6-arene)Fe] or the corresponding diene complexes. Such compouds are known for benzene[7] and phosphinine[8] derivatives acting as the η^6-arene ligand, but no report about a pyridine derivative of this type has yet appeared in the literature. As

 © WILEY-VCH Verlag GmbH, D-69451 Weinheim, 1998 1434−1948/98/0101−0119 $ 17.50+.50/0

pyridine derivatives are believed to be decisively different in their π-ligand properties in respect to the other arenes, [(diene)(η^6-pyridine)Fe] complexes were our first synthetic goal. As for the phosphinines, the σ-lone pair of the hetero atom has to be shielded by one, or better two, *o*-substituents attached to the ring ligand in order to prevent the kinetically preferred σ-coordination[9][10]. The most simple pyridine derivative fulfilling this condition is 2,6-dimethylpyridine, which we therefore included in our studies.

The diazadiene derivatives **1a–g** used in this study are shown in Table 1.

Table 1. Diazadiene derivatives used

1a – g 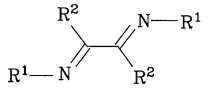

	R^1	R^2
1a	Cyclohexyl	H
1b	*iso*-Propyl	H
1c	*tert*-Butyl	H
1d	*p*-Tolyl	Me
1e	*p*-Tolyl	Ph
1f	*p*-Anisyl	Me
1g	2,6-Dimethylphenyl	Me

[(Diene)(η^6-2,6-Dimethylpyridine)Fe] Complexes and their Reactivity Towards Diazadienes

Highly reactive [(COD)$_2$Fe] was prepared in situ by reacting 1,5-cyclooctadiene (COD) with iron atoms in a metal vapour reaction[11]. Addition of 2,6-dimethylpyridine to the mixture at low temperatures results in the substitution of one COD ligand, and the desired product [(COD)(η^6-2,6-dimethylpyridine)Fe] **3a** is formed in a moderate yield. The same experiments have been performed with [(COD)$_2$Fe] and 2-trimethylsilylpyridine, 2,6-bis(trimethylsilyl)pyridine, or 2,6-bis(chloromethyl)pyridine. According to NMR studies of the crude product, the monosilylated heterocycle gave around a 5% yield of the corresponding [(COD)(η^6-2-trimethylsilylpyridine)Fe]. Due to the small amounts formed, no workup was attempted. The other pyridine derivatives failed completely to produce any observable π-complexes.

[(2,3-Dimethylbutadiene)(η^6-2,6-dimethylpyridine)Fe] **3b** is accessible directly, but only in poor yield, by a three-component reaction of stoichiometric quantities of iron vapour, 2,3-dimethylbutadiene and 2,6-dimethylpyridine. To the best of our knowledge, **3a** and **3b** represent the first examples of (η^6-pyridine)iron complex derivatives.

3a and **3b** are soluble in polar and apolar organic solvents, but strong donor solvents, such as acetonitrile, rapidly destroy the COD complex **3a**. Solutions of **3a** decompose slowly even in apolar solvents at room temp., whereas **3b** is stable under these conditions, probably due to the stabilizing effect of the conjugated diene ligand. Therefore the NMR spectroscopic characterization of **3a** has to be done at −10°C or lower. This problem does not exist for **3b**.

Scheme 1

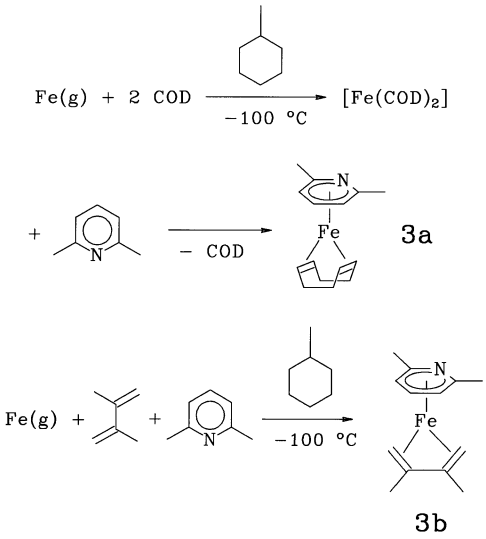

Both compounds exhibit all the characteristics of π-complexes. There is no hint of σ-coordination of the nitrogen atom. For example the NMR data of **3a** and **3b** are closely related to those of their carbacyclic analogues [(COD)(η^6-toluene)Fe] and [(2,3-dimethylbutadiene)(η^6-toluene)Fe], respectively[12]. The observation of high-field coordination shifts for all ring nuclei investigated are a proof for the π-coordination of the heterocycle in both cases. In contrast to the otherwise much more reactive arene iron species [(ethene)$_2$(η^6-toluene)Fe] (**4**) (vide infra), the reaction of 2,6-dimethylpyridine complex **3a** and *N*,*N*′-bis(cyclohexyl)ethylenediimine **1a** results in a complete exchange of ligands and [(*N*,*N*′-bis(cyclohexyl)ethylenediimine)$_2$Fe] (**2a**) is formed as the only isolable species. This a known compound[2][4].

As expected, the reactivity of the η^6-coordinated 2,6-dimethylpyridine ligand of the iron atom is different from that of the carbacycle toluene. As hoped for, it is enhanced, but to such an extent that the replacement of the heterocycle by **1a** occurs parallel with the desired substitution of the diene ligand. [(DAD)(η^6-2,6-dimethylpyridine)Fe] complexes cannot therefore be made in this way.

Scheme 2

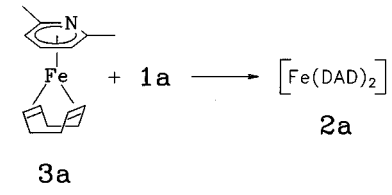

[(DAD)(η^6-Toluene)Fe] Complexes

[(Ethene)$_2$(η^6-toluene)Fe][7] **4** is well known as a highly reactive starting material which gives convenient access to many (η^6-toluene)Fe complexes, or FeL$_n$ species, at low temperatures, depending on the reaction partners[5][13]. In contrast to the significantly more stable pyridine π-complex **3a** only the two ethene ligands of **4** are substituted by **1a**,

b, and **g** around −20°C, and [(DAD)(η⁶-toluene)Fe] derivatives **5a−c** are formed in satisfactory to good yields.

Scheme 3

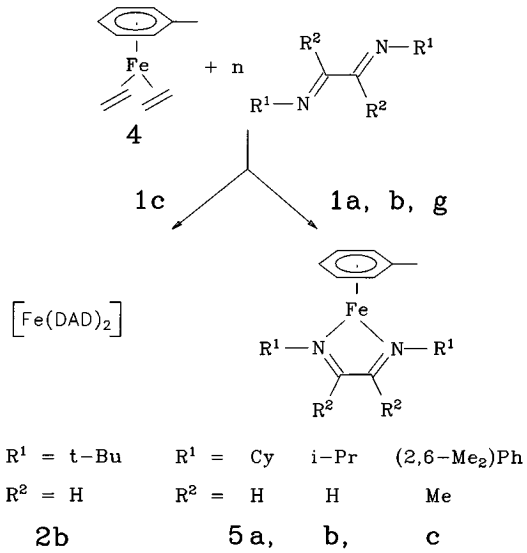

To our surprise, the complete coordination sphere of **4** was substituted under the same reaction conditions by the bis(*tert*-butyl) species **1c**, and the corresponding [(DAD)$_2$Fe] derivative **2b**[4] is the only isolable product of this reaction. Finally, the tolyl compounds **1d**, **e** and the anisyl derivative **1f** produce multicomponent reaction mixtures, which we have not been able to work up yet. Compared to the others, which substitute only the ethene ligands of **4**, **1c** contains bulkier *N*-alkyl substituents, but the increase in bulk is small compared to the cyclohexyl substituents of **1a**, and the 2,6-dimethyl phenyl substituents of **1g.** Therefore, the reason for this selective reactivity of DAD derivatives towards **4** is not yet clear and this point is currently under investigation.

Solid or dissolved **5a−c** are stable at room temp. and the solutions start decomposing around 40°C. Workup by column chromatography, however, requires low temperatures in order to prevent heavy losses. As was the case for **3a** and **b** the interpretation of the spectroscopic data of **5a−c** is straightforward and the desired products are definitely formed.

As **5** represents only the second class of compounds observed where arene iron fragments are combined with N-donor co-ligands in stable complexes, we are interested in more detailed information about the bonding situation between the metal and its ligands. In particular the Fe-DAD interaction is of interest. This fragment should be closely related to the active species of the diene dimerization (DAD)Fe catalysts.

An X-ray structure determination of crystalline [(*N,N′*-bis(cyclohexyl)ethylenediimine)(η⁶-toluene)Fe] **5a** was accomplished. The molecular structure in the solid state is shown in Figure 1 and some selected bond lengths are summarized in Table 2.

There are no unusually short intermolecular distances detectable in the unit cell. As a consequence, the details of the molecular structure have to be discussed mainly on the basis of intramolecular considerations. In full accord with the spectra, the DAD ligand acts as a chelate ligand, donating its N-lone pair electrons to the iron atom, and all ring carbon atoms of the planar toluene ligand are within bonding distance to the metal. The variation of the Fe−C bond lenths is small (208−210 pm), thus the metal is symmetrically bonded to the carbacycle. The Fe-DAD chelate ring is also planar, and both rings are oriented perpendicular to each other (90.4°). The bond distances within the ferradiazacyclobutadiene substructure of **5a** reflect the bonding situation between the iron atom and the DAD ligand, which is our main point of interest in this context. There is only one study dealing with related structural and electronic features of an arene iron complex. The authors who investigated [(2,2′-bipyridyl)(η⁶-toluene)Fe] **6**[14] point out the significant role of back-donation of π-electron density from the iron atom into the π*-orbitals of the bipyridyl ligand which they deduced from C−C- and C−N bond length variations within the bipyridyl ligand. This effect reduces the d-electron density of the occupied orbitals of the metal involved in this interaction.

If we compare the bond lenghts between free[15] and coordinated **1a** within **5a,** the distance C26−C36 is reduced by 7.8 pm, whereas the average of the distances C26−N1 and C36−N2 is increased by 4.3 pm. Exactly the same trends are observed for the corresponding parts of the molecule **6,** but the effect is slightly smaller (−7.3 and +3.9 pm, respectively)[14]. As a consequence the same interpretation seems to be appropriate for both compounds and we have to state that there is a slightly stronger electron back-donation from the iron atom of **5a** into the π*-LUMO of **1a**, which is antibonding in respect to the C=N double bonds, but bonding in respect to the central C26−C3 single bond. This synergetic metal−ligand interaction creates a partial

Figure 1. Molecular structure of **5a** in the solid state

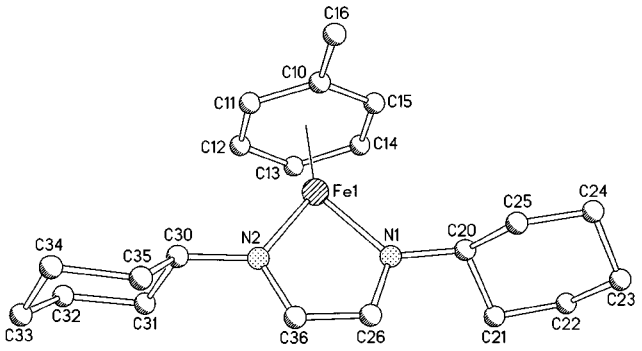

Table 2. Selected bond lenghts (pm) of **5a**

Fe−C10	208.1(3)	Fe−C11	209.4(3)
Fe−C12	208.7(3)	Fe−C13	208.9(3)
Fe−C14	210.0(3)	Fe−C15	210.1(3)
Fe−N1	189.9(2)	Fe−N2	190.1(2)
N1−C20	146.6(3)	N2−C30	146.4(3)
N1−C26	134.4(4)	N2−C36	133.6(4)
C26−C36	137.9(4)		

double bond character of the Fe−N bonds as well, which manifests itself in extremely short Fe−N bonds in the case of **5a** and **6** in relation to other examples of N-donor ligands complexed to iron[14]. We can thus classify the DAD as a very good π-acceptor of Fe d-electrons, and this interpretation is confirmed by independent NDDO calculations[16]. The decisive role of back-bonding for complexes of the type [(arene)(N−N−donor)Fe] is demonstrated by the experiments which aimed to produce [(toluene)(TMEDA)Fe], but which resulted in a completely different chemistry[17]. Being the formal hydrogenation product of a DAD derivative, the saturated N−N donor ligand TMEDA forms a closely related chelate ring with a complexed metal atom, but it completely lacks an appropriate π*-orbital and therefore cannot act as an π-acceptor.

[(DAD)(η⁶-2-Trimethylsilyl-4,5-Dimethylphosphinine)Fe] Complexes

From earlier work we know about the activating role of nitriles in initiating reactions of stable [(COD)(η⁶-2-trimethylsilyl-4,5-dimethylphosphinine)Fe] **7**, which require the dissociation of the Fe−COD π-bond[8]. Because of a close relation between imine and nitrile N-donor ligands, DAD derivatives have first been reacted with **7** in the absence of nitriles. The reaction works, but requires elevated temperatures and the yields, as well as the purity of the products obtained, are not convincing. Running the same reaction with acetonitrile as the solvent, the substitution of COD by the DAD derivatives **1a, d, e, f** takes place at room temp. and moderate yields of the desired products are obtained. The [(DAD)(η⁶-2-trimethylsilyl-4,5 dimethylphosphinine)Fe] derivatives **8a−d** have been prepared in this way.

Scheme 4

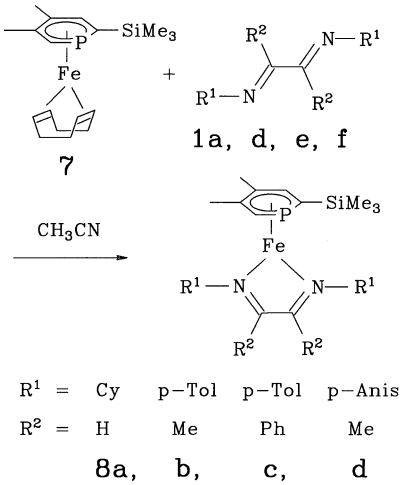

8a−d are much more robust than the other π-complexes reported in this paper. Workup by column chromatography, for example, is possible at room temp. without losses.

Some Considerations on the Stability of Arene Iron Complexes

The preparative results of this study give an improved insight into the relative stability and reactivity of π-arene iron complexes of pyridine, benzene, and phosphinine derivatives. All three allow the preparation of [(arene)(diene)Fe] complexes[18]. Their stability as pure compounds, as solvated complexes in solution, or during workup by chromatography always increases in the sequence: pyridine < benzene < phosphinine.

In reacting such complexes with DAD derivatives, the same order is reproduced. The pyridine complex is disintegrated completely by DADs, even at temperatures below room temp. In spite of the fact that we did not react a diene, but the bis(ethene)Fe complex **4,** with different DADs, we can state that there is a differentiated behaviour, depending on the DAD substituents. However, in several cases the DAD derivative substitutes the ethene ligands in the presence of a π-toluene spectator ligand. The phosphinine complex **7**, however, requires either elevated temperatures, or the presence of nitriles as activating solvents, for the desired substitution reaction. Up to now, we found no indication of a substitution of the P-heterocycle of **7** parallel to the replacement of the COD ligand.

Without thermochemical data it is difficult to differentiate between thermodynamic and kinetic factors of complex stabilization. We believe in the predominance of the first factor, as the accessibility of the iron atom is not very different for the investigated substances.

Details of the electronic structures of the free arenes have been investigated for the unsubstituted rings[19] and these data have been used for comparing the π-ligand properties of benzene and phosphinine. Phosphinine is an equivalent π-donor but is the better π-acceptor ligand for transition metal atoms compared to benzene[20]. The two highest occupied orbitals of phosphinine are energetically close to the degenerate HOMO (e_{1g}) of benzene, but the LUMO (b_1) of phosphinine is significantly stabilized with respect to the LUMO (e_{2u}) of benzene. For pyridine the situation is different. Due to the higher electronegativity of the nitrogen atom combined with good π-orbital overlap, the LUMO (a_2) of pyridine is stabilized, but the HOMO is closer in its energy to the HOMO of benzene[19]. Consequently pyridine can be classified as a weaker π-donor, but a comparable π-acceptor ligand, with respect to benzene. From the combined data, we can rank the donor and acceptor capabilities of the arenes as follows:

π-Donor strength: phosphinine ≅ benzene > pyridine.

π-Acceptor potential: phosphinine > benzene ≅ pyridine.

For electron-rich transition metals such as iron, the combination of both factors determine the bonding energy of the metal to the π-ligand of such complexes. Thus the experimental findings, and this interpretation of the bonding situation of arene iron complexes, are in a good agreement.

Catalytic Properties

The catalytic potential of the [(DAD)(arene)Fe] complexes was tested by experiments on the catalytic cyclodimerization of 1,3-butadiene. For the purpose of comparison analogous reaction conditions to those for the [$(DAD)_2$Fe] catalysts were initially chosen, including the use of the [$(Et_2AlOEt)_2$] co-catalyst[4]. The cyclodimerization of 1,3-buta-

diene yields two main products, and [4 + 2] and [4 + 4] cyclic addition reactions are the favoured processes, which result in the formation of vinyl cyclohexene (VCH) and COD, respectively.

Scheme 5

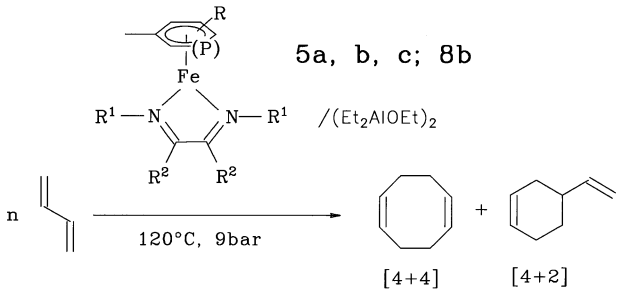

5a−c and **8b** have been tested as catalysts for this reaction and control experiments have been carried out with [(COD)(toluene)Fe][12]; all in the presence, as well as in the absence, of the $[(Et_2AlOEt)_2]$ co-catalyst. To rule out an independent role for $[(Et_2AlOEt)_2]$, this also was used (without an iron complex). Product analysis was done by gas chromatography. Some selected data are summarized in Table 3.

Table 3. Selected data of catalytic cyclodimerization of 1,3-butadiene

Experiment No.	Catalyst / mmol	$[(Et_2AlOEt)_2]$ / mmol	COD TON[a]	VCH TON[a]	Selectivity % COD[c]
1	**5a** / 0.062	0.4	972[b]	240	80.2
2	**5a** / 0.062	0.8	503	159	76.0
3	**5a** / 0.062	0.2	455	166	73.3
4	**5c** / 0.062	0.4	1479[b]	130	91.9
5	**8a** / 0.062	0.4	94	54	63.7

[a] TON = Turnover number, mole product per mole catalyst. − [b] Almost quantitative butadiene conversion. − [c] Percentage of the volatile products COD + VCH.

As hoped for, **5a−c** and **8b**, all in combination with the co-catalyst only, are cyclodimerization catalysts for the formation of COD and smaller amounts of VCH, whereas the combination [(COD)(toluene)Fe]/$[(Et_2AlOEt)_2]$ yields only a little VCH. Product yield and chemoselectivity of the [(arene)(COD)Fe] catalysts are closely related to those of the other (DAD)Fe systems[2][3][4], a first indication of comparable catalytic processes for the complete family of catalysts. The main difference is the lower reactivity of the [(arene)-(DAD)Fe] complexes. The optimal temp. here is 120°C, whereas $[DAD)_2Fe]$ requires less elevated temperatures, and the in situ reduction of $[(DAD)FeCl_2]$ results in the formation of an active species which already transfoms butadiene at room temp. A strong argument for the (DAD)Fe fragment to be part of the catalytically active species is deduced from the control experiments. Neither [(COD)(toluene)Fe] or $[(Et_2AlOEt)_2]$ alone, nor a mixture of both components, are able to induce the formation of COD, the main product of the catalytic reaction. As mentioned above, the presence of the co-catalyst in the reaction mixture is essential. The best results have been obtained with a molar ratio of catalyst/co-catalyst ≅ 2:13. In some experiments the butadiene was almost completely converted into the products, thus the maximal number of turnovers is most probably higher than the greatest number given in Table 3. Complete reaction of butadiene was also found, in some cases, with the other (DAD)Fe catalysts[21].

Toluene complexes **5,** and the phosphinine species **8b,** differ slightly in their selectivity of COD formation. Depending on the reaction conditions, 76−92% COD are formed by the derivatives of **5**, whereas **8b** produces 64% COD, but the difference in their reactivity is much more pronounced. Under the same conditions the catalysts **5** act approximately ten times faster than **8b**. We believe the higher turover frequency of the toluene complexes to be the main reason for their almost quantitative butadiene conversion.

The much higher reactivity of the complexes **5a−c** nicely parallels our findings on the substitution reactions of iron complexes with toluene or phosphinine π-arene ligands (vide supra). Obviously, the stronger Fe−phosphinine interaction hampers the generation of the true (DAD)Fe catalyst from the pro-catalyst **8b**. On the other hand, closed shell 18 valence electron (VE) species like **5a−c** are relatively stable. In contrast to the paramagnetic 16 VE $[(DAD)_2Fe]$ derivatives, for example, hydrolysis does not play a role here. Thus the reactivity of the catalytically active systems follows the stability of the different types of (DAD)Fe complexes, another hint that there are analogous reaction mechanisms in all cases.

We thank the *Fonds der Chemischen Industrie* and the *Deutsche Forschungsgemeinschaft* for financial support, Prof. Dr. *D. Sellmann*, Erlangen for providing X-ray structure facilities, and Dr. *F. Heinemann*, Erlangen for substantial help in evaluating the X-ray data.

Experimental Section

All reactions were carried out under a dry, oxygen free, nitrogen atmosphere. Solvents were purified by conventional methods, distilled and stored under nitrogen. − Unless otherwise stated, NMR spectra were recorded around room temp. on a Jeol FT-JNM-EX 270 spectrometer (269.6 MHz for ^1H, 67.7 MHz for ^{13}C, and 109.4 MHz for ^{31}P NMR), using dimethylpolysiloxane and solvent signals as internal standards for ^1H and ^{13}C, and 85% H_3PO_4/water as an external standard for ^{31}P NMR. The degree of substitution of the C-atoms was determined by DEPT spectra. − Mass spectra were recorded on a varian MAT 212 spectrometer (EI, 70 eV). − Microanalyses were peformed at the analytical department of the institute, using a Carlo Erba Elemental Analysers Mod. 1106. − Gas chromatography was done with a Philips PYE UNICAM PU 4500 chromatograph equipped with a supelcowax 10 capillary column l = 60 m, dia. = 0.75 mm. Column chromatography (15 × 1 cm) was accomplished with neutral degassed alumina or silica (Merck), deactivated with 5% degassed water. − Metal vapour reactions were carried out in a locally constructed rotating metal atom reactor[22], which uses resistively heated alumina crucibles in tungsten baskets as metal evaporators. The reactor allows low temp. reactions of metal vapours with liquid substrates, or solutions of substrates in low melting point solvents, and the transfer of cold solutions with complete exclusion of air and moisture.

The following starting materials have been prepared according to published procedures: DAD derivatives **1a**[23a], **1b**, **c**[23b], **1d**, **e**, **f**[23c], **1g**[23d], [(ethene)$_2$(η^6-toluene)Fe] **4**[7] , and [(COD)(η^6-2-trimethylsilyl-4,5-dimethylphosphinine)Fe] **7**[8]. All other substances have been purchased from commercial sources in synthetic quality and have been purified by distillation and saturation with pure nitrogen gas. Prior to use, 1,3-butadiene was condensed from a gas cylinder in a Schlenck tube at −78°C and stored there for several hours on a molecular sieve (0.5 nm).

[(COD)(η^6-2,6-dimethylpyridine)Fe] (**3a**): 8 g of iron gas (0.14 mol) was distilled into a mixture of 26,4 g of 1,5-*cis*-*cis*-cyclooctadiene (COD) (0.24 mol) and 300 ml of methylcyclohexane. During the course of reaction the gas pressure and the temp. of the liquid phase were held below 10^{-2} Pa and −100°C, respectively. The colour of the reaction mixture turned to dark green, while [(COD)$_2$Fe] was formed[11]. After completion of the metal vapour reaction, the cooling bath was removed. When close to −50°C the mixture was transferred to a round bottom flask and 921 mg 2,6-dimethylpyridine (8.6 mmol) was added at −40°C. It was then stirred and allowed to warm up slowly in air. Around −5°C the colour turned to red and the reaction was completed by stirring for 3 h at room temp.. Solvent and excess of COD were stripped off in vacuum and the residue was diluted in light petroleum ether (PE). Column chromatography (−30°C; alumina/5% water) resulted in two red fractions eluted by PE and toluene/THF (1:2), respectively. The toluene/THF solution contained red **3a**. Removal of the solvents and recrystallization from *n*-pentane yielded 716 mg (30,7%) of the dark red crystalline solid. − ^{1}H NMR ([D$_8$]toluene, −10°C): δ = 5.45 (d, J_{HH} = 10 Hz, 2 H, CH-pyr.), 3.05 (m, 1 H, CH-pyr.), 2.85 (m, 4 H, CH-COD), 2.55 (m, 4 H, CH$_2$-COD/*endo*); 2.35 (s, 6 H, CH$_3$-pyr.), 1.85 (m, 4 H, CH$_2$-COD/*exo*). − ^{13}C{^{1}H} NMR ([D$_8$]toluene, −10°C): δ = 115.8 (C-pyr.), 86.2 (CH-pyr.), 78.2 (s, CH-pyr.), 68.0 (CH-COD), 31.4 (CH$_2$-COD); 20.4 (CH$_3$-pyr.). − MS (70 eV) *m/z*: 271 [M$^+$], 163 [M$^+$ − COD]. − $C_{15}H_{21}FeN$ (271.10): calcd. C 66.44, H 7.81, N 5.17, found: C 66.50, H 7.90, N 5.03.

Reaction of **3a** *with DAD* **1a**: 222 mg of **3a** (0.82 mmol) was added to a solution of 180 mg of *N,N′*-bis(cyclohexyl)ethylenediimine **1a** (0.82 mmol) in 30 ml of toluene at −10°C. The mixture was stirred for 15 h without cooling, thus the temp. increased slowly to room temp.. Then the resulting dark suspension was filtered at −60°C through 3 cm alumina on a frit and a red solution was obtained. After removal of the solvent and recrystallization from *n*-pentane 123 mg (64.1%) of analytically pure, dark crystalline [bis(*N,N′*-bis(cyclohexyl)ethylenediimine)iron] was afforded. Within the experimental limits, all data on this compound are identical with those published in the literature[4].

[(η^4-2,3-Dimethylbutadiene)(η^6-2,6-dimethylpyridine)Fe] (**3b**): 8 g of iron gas (0.14 mol) was distilled into a mixture of 11.7 g of 2,3-dimethylbutadiene (0.14 mol), 15.3 g of 2,6-dimethylpyridine (0.14 mol), and 300 ml of methylcyclohexane as described before. The reaction mixture darkened until it was finally almost black. After completion of the metal vapour reaction, the cooling bath was removed to allow slow warming up. At −25°C the mixture was filtered through 3 cm alumina/5% H_2O on a frit, the alumina was extracted with toluene/THF, the liquid phases united, and the solvent removed in vacuo. Redilution in PE and column chromatography (−30°C; alumina/5% water) resulted in the formation of two red fractions (PE and toluene/THF, 1:4). The second fraction contained the desired product **3b**. Recystallization from *n*-pentane gave 584 mg (1,7%) of red needles. − ^{1}H NMR ([D$_6$]benzene): δ = 5.12 (m, 1 H, CH-pyr.), 4.57 (m, 2 H, CH-pyr.), 2.30 (s, 6 H, CH$_3$), 1.93 (s, 6 H, CH$_3$), 1.04 (s, 2 H, CH$_2$-butad.), −0.53 (s, 2 H, CH$_2$-butad.). − ^{13}C{^{1}H} NMR ([D$_6$]benzene): δ = 113.4 (C-pyr.), 91.2 (CH-pyr.), 84.7 (s, CH-pyr.), 78.9 (C-butad.), 39.8 (CH$_2$-butad.), 23.3 (CH$_3$), 19.3 (CH$_3$). − MS (70 eV) *m/z*: 245 [M$^+$], 163 [M$^+$ − butad.], 138 [M$^+$ − pyr.]. $C_{13}H_{19}FeN$ (245.14): calcd. − C 63.69, H 7.81, N 5.71, found: C 63.76, H 7.75, N 5.52.

[(N,N′-Bis(cyclohexyl)ethylenediimine)(η^6-toluene)Fe] (**5a**): 292 mg of *N,N′*-bis(cyclohexyl)ethylenediimine (**1a**) (1.33 mmol) was suspended by stirring in 50 ml of toluene (1.35 mmol), and a solution of 275 mg of (1.35 mmol) [(ethene)$_2$(η^6-toluene)Fe] **4** in 10 ml of toluene was added, both were at −40°C. A badly isolated cooling bath (three plastic bowls of the same size, one put into the other) containing ca. 200 ml of ethanol at a temp. of , originally, ca. −40°C, allowed a slow increase in the temp. At −20°C the reaction mixture turned dark. The reaction was completed by stirring overnight at room temp.. After removal of the solvent, the residue was dissolved in PE. Column chromatography (−30°C; alumina) yielded two fractions (PE and PE/toluene, 3:1). The second fraction contained the desired red brown product **5a**. It was recrystallized twice, from acetonitrile and *n*-pentane, yielding 234 mg (47.7%) of dark crystals. − ^{1}H NMR ([D$_6$]benzene): δ = 6.76 (s, 2 H, CH-imine), 5.58 (t, *J* = 6 Hz, 1 H, CH-tol.), 5.20 (t, *J* = 6 Hz, 2 H, CH-tol.), 5.11 (d, *J* = 7 Hz, 2 H, CH-tol.), 4.47 (m, 2 H, CH-cy.), 2.30 (s, 3 H, CH$_3$-tol.), 2.24 (s, 4 H, CH$_2$-cy.), 1.55 (m, 14 H, CH$_2$-cy.), 1.10 (m, 2 H, CH$_2$-cy.). − ^{13}C{^{1}H} NMR ([D$_6$]benzene): δ = 133.9 (CH-imine), 92.2 (C-tol.), 80.9 (CH-tol.), 79.4 (CH-tol.) 79.3 (CH-tol.), 70.0 (CH-cy.), 35.5 (CH$_2$-cy.); 27.1 (CH$_2$-cy.), 26. 5 (CH$_2$-cy.), 21.4 (CH$_3$-tol.). − MS (70 eV) *m/z*: 368 [M$^+$], 276 [M$^+$ − **1a**]. − $C_{21}H_{32}FeN_2$ (368.19).

[(N,N′-Bis(2-propyl)ethylenediimine)(η^6-toluol)Fe] (**5b**): Preparation as described for **5a** from 266 mg (1.90 mmol) of **1b** and 387 mg (1.90 mmol)of **4**. Recrystallization from *n*-pentane yielded 315 mg (57.6%) of **5b**. − ^{1}H NMR ([D$_6$]benzene): δ = 6.75 (s, 2 H, CH-imine), 5.55 (t, *J* = 6 Hz, 1 H, CH-tol.), 5.08 (t, *J* = 6 Hz, CH-tol.), 5.01 (d, *J* = 6 Hz, 2 H, CH-tol.), 4.80 (sept, *J* = 6 Hz, 1 H, CH-isopr.), 2.27 (s, 3 H, CH$_3$-tol.), 1.40 (d, *J* = 7 Hz, 12 H, CH$_3$-isopr.). − ^{13}C{^{1}H} NMR ([D$_6$]benzene): δ = 133.4 (CH-imine), 92.8 (C-tol.), 81.1 (CH-tol.), 79.8 (CH-tol.), 79.7 (CH-tol.), 60,4 (CH-isopr.), 24,6 (CH$_3$-isopr.), 21.8 (CH$_3$-tol.). − MS (70 eV) *m/z*: 288 [M$^+$], 196 [M$^+$ − **1b**]. − $C_{15}H_{24}FeN_2$ (288.21).

[(N,N′-Bis(2,6-dimethylphenyl)-2,3-butanediimine)(η^6-toluene)Fe] (**5c**): Preparation as described for **5a** from 316 mg (1.08 mmol) of **1g** and 265 mg (1.30 mmol) of **4**. Recrystallization from *n*-pentane yielded 161 mg (33.9%) of **5c**. − ^{1}H NMR ([D$_6$]benzene): δ = 7.2 (m, 6 H, CH-phenyl), 5.30 (t, *J* = 5 Hz, 1 H, CH-tol.), 4.52 (t, *J* = 5 Hz, 2 H, CH-tol.), 4.46 (d, *J* = 5 Hz, 2 H, CH-tol.), 2.26 (s, 12 H, CH$_3$-phenyl), 1.95 (s, 3 H, CH$_3$-tol.), 1.00 (s, 6 H, CH$_3$-imine). − ^{13}C{^{1}H} NMR ([D$_6$]benzene): δ = 157.1 (C-phenyl), 141.6 (C-phenyl), 131.0 (CH-phenyl), 129.2 (C-imine), 124.5 (CH-phenyl), 94.5 (C-tol.), 82.0 (CH-tol.), 81.3 (CH-tol.), 80.7 (CH-tol.), 20,1 (CH$_3$-tol.), 18,3 (CH$_3$-phenyl); 15,6 (CH$_3$-imine). − MS (70 eV) *m/z*: 277 [**1g**$^+$−CH$_3$]. − $C_{25}H_{32}FeN_2$ (368.19).

[(N,N′-Bis(cyclohexyl)ethylenediimine)(η^6-2-trimethylsilyl-4,5-dimethylphosphinine)Fe] (**8a**): 179 mg (0,81 mmol) of **1a**, 293 mg (0,81 mmol) of [(COD)(η^6-2-trimethylsilyl-4,5-dimethylphosphinine)Fe] **7** and 50 ml of acetonitrile were mixed at room temp. and stirred for 20 h. The orange reaction mixture slowly darkens and finally was nearly black. After removal of the solvent in vacuo the residue was dissolved in PE and subjected to column chromatography on silica/5% water. PE eluted some unreacted **7** and free phosphinine, whereas PE/toluene (1:1) gave a dark red fraction. Removal of the solvent and recrystallization afforded 146 mg (28.1%)

of dark red **8a**. – ^{1}H NMR ([D$_6$]benzene): δ = 6.75 (s, 2 H, CH-imine), 5.43 (d, J_{PH} = 10 Hz, 1 H, CH-phosp.) 4.70 (d, J_{PH} = 36 Hz, 1 H, CH-phosp.), 4.25 (m, 2 H, CH-cy.), 2.55 (m, 5 H, CH-cy. + CH_3 -phosp.), 2.35 (s, 3 H, CH_3 -phosp.), 2.00 (m, 2 H, CH-cy.), 1.52 (m, 14 H, CH-cy.), 1.06 (m, 2 H, CH-cy.), 0.45 [s, 9 H, $Si(CH_3)_3$]. – ^{13}C{^{1}H} NMR ([D$_6$]benzene): δ = 137,8 (CH-imine), 99.0 (d, J_{PC} = 12 Hz, CH-phosp.), 95.2 (d, J_{PC} = 8 Hz, CH-phosp.), 93.6 (d, J_{PC} = 78 Hz, C-phosp.), 90.0 (d, J_{PC} = 8 Hz, C-phosp.), 89.2 (d, J_{PC} = 68 Hz, CH-phosp.), 69.8 (CH-cy.), 43.6 (CH_2-cy.), 34.6 (CH_2-cy.), 27.0 (CH_2-cy.), 26.8 (CH_2-cy.), 26.4 (CH_2-cy.), 23.4 (CH_3-phosp.), 22.4 (CH_3-phosp.), 1,4 [$Si(CH_3)_3$]. – ^{31}P{^{1}H} NMR ([D$_6$]benzene): δ = –17.7. – MS (70 eV) *m/z*: 472 [M$^+$]. – $C_{24}H_{41}FeN_2PSi$ (368.19).

[(N,N′-Bis(4-tolyl)-2,3-butanediimine)(η^6-2-trimethylsilyl-4,5-dimethylphosphinine)Fe] (**8b**): Preparation as described for **8a** from 279 mg (1.06 mmol) of **1d** and 381 mg (1.06 mmol) of **7**. Recrystallization from *n*-pentane, yielded 219 mg (30.4%) of dark red **8b**. – ^{1}H NMR ([D$_6$]benzene): δ = 7.75 (d, J_{HH} = 8 Hz, 2 H, CH-tolyl), 7.10 (d, J_{HH} = 8 Hz, 2 H, CH-tolyl), 7.0 (m, 4 H, CH-tolyl), 5.05 (d, J_{PH} = 9 Hz, 1 H, CH-phosp.), 3.99 (d, J_{PH} = 36 Hz, 1 H, CH-phosp.), 2.50 (s, 3 H, CH_3-phosp.), 2.24 (s, 3 H, CH_3-phosp.), 2.22 (s, 6 H, CH_3-tolyl), 1.00 (s, 6 H, CH_3-imine), 0.36 [s, 9 H, $Si(CH_3)_3$]. – ^{13}C{^{1}H} NMR ([D$_6$]benzene): δ = 157.1 (C-tolyl), 146.1 (C-tolyl), 134.0 (C-imine), 125.6 (CH-tolyl), 124.3 (CH-tolyl), 99.0 (d, J_{PC} = 13.5 Hz, C-phosp.), 97.3 (d, J_{PC} = 6.6 Hz, CH-phosp.), 96.6 (d, J_{PC} = 77.9 Hz, C-phosp.), 91.2 (d, J_{PC} = 67.7 Hz, CH-phosp.), 90.2 (d, J_{PC} = 10.1 Hz, C-phosp.), 23.1 (CH_3-phosph.), 22.6 (CH_3-phosph.), 21.1 (CH_3-tolyl), 17.7 (CH_3-imine), 1.4 [$Si(CH_3)_3$]. – ^{31}P{^{1}H} NMR ([D$_6$]benzene): δ = –12.85 (s). – MS (70 eV) *m/z*: 516 [M$^+$], 320 [M$^+$ – phosp.]. – $C_{28}H_{37}FeN_2PSi$ (516.18).

[(N,N′-Bis(4-tolyl)-1,2-diphenylethylenediimine)(η^6-2-trimethylsilyl-4,5-dimethylphosphinine)Fe] (**8c**): Preparation as described for **8a** from 870 mg (2.23 mmol) of **1e** and 792 mg (2.20 mmol) of **7**. Chromatography was done with PE/toluene (3:1) and toluene. Toluene eluted the product. Recrystallization from PE yielded 270 mg (19.1%) of dark red **8c**. – ^{1}H NMR ([D$_6$]benzene): δ = 8.13 (dd, J_{HH} = 7 / 1 Hz, 2 H, CH-aryl) 7.05 (dd, J_{HH} = 7 / 1 Hz, 2 H, CH-aryl), 6.88 (dd, J_{HH} = 8 / 1 Hz, 2 H, CH-aryl), 6.70 (m, 6 H, CH-aryl), 6.60 (m, 6 H, CH-aryl), 5.48 (d, J_{PH} = 10 Hz, 1 H, CH-phosp.), 4.43 (d, J_{PH} = 34 Hz, 1 H, CH-phosp.), 2.55 (s, 3 H, CH_3-phosp.), 2.15 (s, 3 H, CH_3-phosp.), 2.03 (s, 6 H, CH_3-diimine), 0.25 [s, 9 H, $Si(CH_3)_3$]. – ^{13}C{^{1}H} NMR ([D$_6$]benzene): δ = 157.0 (C-aryl), 152.4 (C-aryl), 138.9 (C-aryl or C-imine), 133.6 (C-aryl or C-imine), 130.4 (C-aryl or C-imine), 127.3 (C-aryl), 126.9 (C-aryl), 126.0 (C-aryl), 125.6 (C-aryl), 103.2 (br., C-phosp.), 99.6 (br., C-phosp.), 99.0 (br., C-phosp.), 94.5 (br., C-phosph.), 90.6 (br., C-phosph.), 22.8 (CH_3-phosph.), 22.7 (CH_3-phosph.), 21.0 (CH_3-tolyl), 1.2 [$Si(CH_3)_3$]. – ^{31}P{^{1}H} NMR ([D$_6$]benzene): δ = –11,7 (s). – MS (70 eV) *m/z*: 641 [M$^+$]. – $C_{38}H_{41}FeN_2PSi$ (640.21): calcd. C 71.24, H 6.45, N 4.37, found C 71.12, H 6.81, N 3.94.

[(N,N′-Bis(4-anisyl)-2,3-butanediimine)(η^6-2-trimethylsilyl-4,5-dimethylphosphinine)Fe] (**8d**): Preparation as described for **8a** from 241 mg (0.81 mmol) of **1f** and 290 mg (0.87 mmol) of **7**. Recrystallization from *n*-pentane yielded 145 mg (32.5%) of dark red **8d**, which was always contaminated with traces of a second uncharacterized product. – ^{1}H NMR ([D$_6$]benzene): δ = 7.75 (d, J_{HH} = 8 Hz, 2 H, CH-anisyl), 7.01 (d, J_{HH} = 8 Hz, 2 H, CH-anisyl), 6.88 (d, J_{HH} = 8 Hz, 2 H, CH-anisyl), 6.79 (d, J_{HH} = 8 Hz, 2 H, CH-anisyl), 5.05 (d, J_{PH} = 9 Hz, 1 H, CH-phosp.), 4.01 (d, J_{PH} = 31 Hz, 1 H, CH-phosp.), 3.40 (s, 6 H, CH_3-anisyl.), 2.50 (s, 3 H, CH_3-phosp.), 2.20 (s, 3 H, CH_3-phosp.), 1.03 (s, 3 H, CH_3-imine), 0.35 [s, 9 H, $Si(CH_3)_3$]. – ^{13}C{^{1}H} NMR ([D$_6$]benzene): δ = 157.3 (C-anisyl), 152,6 (C-anisyl), 146.3 (C-imine), 126.0 (CH-anisyl), 125.1 (CH-anisyl), 99.1 (d, J_{PC} = 12 Hz, C-phosp.), 97.3 (d, J_{PC} = 8 Hz, C-phosp.), 96.5 (d, J_{PC} = 78 Hz, C-phosp.), 91.2 (d, J_{PC} = 68 Hz, C-phosp.), 90.1 (d, J_{PC} = 9 Hz, C-phosp.), 55.0 (CH_3-anisyl), 23.1 (CH_3-phosp.), 22.7 (CH_3-phosp.), 17.7 (CH_3-imine, 1,4 [$Si(CH_3)_3$]. – ^{31}P{^{1}H} NMR ([D$_6$]benzene): δ = –13.4 (s). – MS (70 eV) *m/z*: 546 [M$^+$]. – $C_{28}H_{37}FeN_2O_2PSi$ (548.17).

General Procedure of Catalytic Cyclodimerization and Gas Chromatographic Product Analysis: Ca. 30 ml of purified 1,3-butadiene was condensed at –20°C into a glass tube, and defined solutions of catalyst and co-catalyst in a few ml of toluene are added. In some of the experiments 15 ml of additional solvents (toluene or diethylether) have been used with negligible effects on product formation. The tube was then put into a 250-ml stainless steel autoclave which contained an argon atmosphere. After closing the autoclave, the bottom half of it was placed in an oil bath and heated up to the reaction temp. for 3 h, whilst butadiene built up a gas pressure inside. At 80°C reactor temp. the volatile components of the reaction mixture were transferred in vacuo into a cold (77 K) trap and the content of the trap was analysed by gas chromatography later.

The volatile components butadiene, COD, VCH, and toluene of the product mixture were separated by the capillary down to the base line. For quantitative determinations defined amounts of THF were added. A complete calibration procedure was done for the integrated peaks of COD and THF and the VCH was then related to the COD. In all cases a linear correlation was observed. The data allow us to relate the molar amounts of product formed to the amounts of catalysts used in the experiments. These results are presented as the "turnover number of substrate molecules per molecule catalyst" (TON). The precise ratio of butadiene conversion, however, was undeterminable in our experimental setup, as the exact amounts of butadiene which have had contact with the catalysts remained unknown. In cases where we detected only traces of remaining butadiene in the product mixture, an almost quantitative conversion is assumed. Higher oligomers of butadiene are formed to some extent, but no analysis was attempted. An summary of the experimental data is given in Table 3.

Crystal Structure Determination: Suitable crystals of **5a** were grown in *n*-pentane at –40°C. The data were collected on a Sie-

Table 4. Crystal data of **5a**

Empirical formula	$C_{21}H_{32}FeN_2$
Colour, form	almost black cube
Size [mm]	0.7×0.6×0.6×0.6
Crystal system	monoclinic
Space group	$P\ 2_1/c$
Unit cell dimensions [Å]	a = 10.629(3)
Unit cell dimensions [A]	a = 10.629(3)
	b = 14.181(3)
	c = 13.398(4)
	β = 103.83(3)
Volume [Å^3]	1961(1)
Z	4
Molecular mass	368.19
Density (calcd.)	1.248 gcm^{-3}
Absorption coefficient	0.773 mm^{-1}
Number of refined parameters	217
F(000)	792
Reflections measured	6343
Independent reflections	3217
Goodnesss-of-fit at F^2	1.110
$R1$	0.0389
wR_2	0.1048

mens P4 diffractometer with Mo-K_α radiation (λ = 0.71073 Å) and a graphite monochromator (Table 4.). The crystal structures were solved by direct methods (SHELXS-86[24]) and refined by SHELXL-93[25]. Non-hydrogen atoms were refined anisotropically; the hydrogen atoms were taken from a difference fourier calculation and included as fixed contributions in the final stages of a least squares refinements. Other experimental details are given in Table 4. Crystallographic data (excluding structure factors) for the structure report in this paper have been deposited with the Cambridge Crystallographic Data Centre as supplementary pubilication no. CCDC-100543. Copies of the data can be obtained free of charge on application to The Director, CCDC, 12 Union Road, GB-Cambridge CB12 1EZ [Fax: (internat.) + 44(0)1223/336-033, E-mail: deposit@ccdc.cam.ac.uk].

[☆] Dedicated to Professor *Gottfried Huttner* on the occasion of his 60th birthday.

[1] G. van Koten, K. Vrieze in *Advances in Organometallic Chemistry* (Ed.: F. G. A. Stone, R. West), Academic Press, New York, **1982**, *21*, 152; G. van Koten, K. Vrieze in *Comprehensive Coordination Chemistry* (Ed.: G.Wilkinson, R. D. Gillard, J. A. McCleverty), Pergamon Press, Oxford, **1987**, *2*, 206.

[2] H. tom Dieck, H. Bruder, *J. Chem. Soc. Chem. Commun*. **1977**, 24.

[3] H. tom Dieck in *Organometallics in Organic Synthesis* (Ed.: H. Werner, G. Erker), Springer Verlag, Heidelberg, **1989**, 21.

[4] H. tom Dieck, R. Diercks, L. Stamp, H. Bruder, T. Schuld, *Chem. Ber.* **1987**, *120*, 1943.

[5] D. Böhm, F. Knoch, S. Kummer, U. Schmidt, U. Zenneck, *Angew. Chem.* **1995**, *107*, 251; *Angew. Chem. Int. Ed. Engl.* **1995**, *34*, 198; C. Brodt, S. Niu, H. Pritzkow, M. Stephan, U. Zenneck, *J. Organometal. Chem.* **1993**, *459*, 283; U. Zenneck, *Angew. Chem.* **1990**, *102*, 171; *Angew. Chem. Int. Ed. Engl.* **1990**, *29*, 126.

[6] K. Hellfeld, Dissertation, Univ. Hamburg, **1984**; J. Dietrich, Dissertation, Univ. Hamburg, **1984**.

[7] U. Zenneck, W. Frank, *Angew. Chem.* **1986**, *98*, 806; *Angew. Chem. Int. Ed. Engl.* **1986**, *25*, 831.

[8] F. Knoch, F. Kremer, U. Schmidt, U. Zenneck, P. Le Floch, F. Mathey, *Organometallics* **1996**, *15*, 2713.

[9] H. G. Biedermann, K. Öfele, N. Schuhbauer, J. Tajtelbaum, *Angew. Chem.* **1975**, *87*, 634; *Angew. Chem. Int. Ed. Engl.* **1975**, *14*, 639; H. G. Biedermann, K. Öfele, J. Tajtelbaum, *Z. Naturforsch. 1976*, *31b*, 321; K. Dimroth, R. Thamm, H. Kaletsch, Z. Naturforsch. **1984**, *39b*, 207; R. E. Schmidt, W. Massa, *Z. Naturforsch.* **1984**, *39b*, 213; K. H. Ponnell, B. L. Kalsotra, C. Parkanyi, *J. Heterocycl. Chem.* **1978**, *15*, 1057; S. G. Davies, M. R. Shipton, *J. Chem. Soc. Chem. Commun.* **1989**, 995; *J. Chem. Soc. Chem. Commun. 1990*, 1780.

[10] P. E. Riley, R. E. Davis, *Inorg. Chem.* **1976**, *15,* 2735; L. H. Simons, P. E. Riley, R. E. Davis, J. J. Lagowski, *J. Am. Chem. Soc.***1976**, *98*, 1044; E. J. Wucherer, E. L. Muetterties, *Organometallics* **1987**, *6*, 1691; *ibid.* **1987**, *6*, **1696**; C. Elschenbroich, J. Koch, J. Kroker, M. Wünsch, W. Massa, G. Baum, G. Stork, *Chem. Ber.* **1988**, *121*, 1983.

[11] R. Mackenzie, P. L. Timms, *J. Chem. Soc. Chem. Comm.* **1974**, 650.

[12] S. D. Ittel, C. A. Tolman, *J. Organomet. Chem.* **1979**, *172*, C47; *Organometallics* **1982**, *1*, 1432.

[13] U. Schmidt, U. Zenneck, *J. Organomet. Chem*. **1992**, *440*, 187.

[14] L. J. Radonovich, M. W. Eyring, T. J. Groshens, K. J. Klabunde, *J. Am. Chem. Soc.* **1982**, *104*, 2816.

[15] J. Keijsper, H. van der Poel, L. H. Polm, G. van Koten, P. F. A. B. Seignette, R. Varenhorst, C. Stam, *Polyhedron* **1982**, *2*, 1111.

[16] J. Reinhold, R. Benedix, P. Birner, H. Hennig, *Inorg. Chim. Act.* **1979**, *33*, 209.

[17] J. J. Schneider, U. Specht, R. Goddard, C. Krüger, J. Ensling, P. Gütlich, *Chem. Ber.* **1995**, *128*, 941.

[18] Arene = 2,6-dimethylpyridine: this work; arene = phosphinine: ref.[8]; arene = benzene derivatives: refs.[12][13].

[19] P. D. Burrow, A. J. Ashe III, D. J. Belville, K. B. Jordan, *J. Am. Chem. Soc.* **1982**, *104*, 245.

[20] C. Elschenbroich, M. Nowotny, B. Metz, W. Massa, J. Graulich, *Angew. Chem.* **1991**, *103*, 601; *Angew. Chem. Int. Ed. Engl.*, **1991**, *30*, 547.

[21] H. tom Dieck, J. Dietrich, *Angew. Chem.* **1985**, *97*, 795; *Angew. Chem. Int. Ed. Engl.* **1985**, *24*, 781.

[22] U. Zenneck, *Chem. Unserer Zeit*, **1993**, *27*, 208.

[23] [23a] J. F. Carson, *J. Am. Chem. Soc.* **1953**, *75*, 4337. – [23b] J. M. Kliegman, R. K. Barnes, *Tetrahedron* **1970**, *26*, 2555. – [23c] J. Scholz, B. Richter, R. Goddard, C. Krüger, *Chem. Ber.* **1993**, *126(1)*, 57. – [23d] H. tom Dieck, M. Svoboda, T. Greiser, *Z. Naturforsch.* **1981**, *36B*, 823.

[24] G. M. Sheldrick, *Acta Cryst*. **1990**, *A46*, 467.

[25] G. M Sheldrick, SHELXL-93, Universität Göttingen, **1993**.

[97187]

Photochemical Reactions of Transition Metal Organyl Complexes with Olefins, 20[◇]

Light-Induced Codimerisation of Acetylene and Olefins at a Binuclear Tungsten Complex☆

Cornelius G. Kreiter*, Ulrich Kern, Gotthelf Wolmershäuser, and Gert Heckmann

Fachbereich Chemie der Universität Kaiserslautern,
Erwin-Schrödinger-Straße, D-67663 Kaiserslautern, Germany

Received June 18, 1997

Keywords: Tungsten / Ditungsten complexes / Acetylene complex / Tritungsten complex / W−W single bond / W−W triple bond / Photochemistry / C−C bond formations / Olefins

$[W_2(\eta^5\text{-}C_5H_5)_2(CO)_4(\mu\text{-}\eta^{2:2}\text{-}C_2H_2)]$ (**1**) and ethylene (**A**) react when irradiated with UV light at 253 K predominantly to $[W_2(\eta^5\text{-}C_5H_5)_2(CO)_3(\mu\text{-}\eta^{1:4}\text{-}C_4H_5)(\mu\text{-}H)]$ (**3A**), $[W_2(\eta^5\text{-}C_5H_5)_2(CO)_4(\mu\text{-}\eta^{1:3}\text{-}C_4H_6)]$ (**4A**), and thermolabile $[W_2(\eta^5\text{-}C_5H_5)_2(CO)_3(\eta^4\text{-}C_4H_6)]$ (**5A**). Similarly, propene (**B**), 1-butene (**C**), and (*E*)-2-butene (**D**) yield mixtures of $[W_2(\eta^5\text{-}C_5H_5)_2(CO)_3(\mu\text{-}H)(\mu\text{-}\eta^{1:4}\text{-}1,3\text{-dien-1-yl})]$ (**3B**, **3 C, 3D**), $[W_2(\eta^5\text{-}C_5H_5)_2(CO)_4(\mu\text{-}\eta^{1:3}\text{-}C_4H_5R]$ (**4B**, **4C**), and $[W_2(\eta^5\text{-}C_5H_5)_2(CO)_2(\mu\text{-}\eta^{1:2}\text{-}CO)(\eta^4\text{-}1,3\text{-diene})$ (**5B**, **5 C, 5D**). With **B** and **C** also thermolabile $[W_2(\eta^5\text{-}C_5H_5)_2(CO)_3(\mu\text{-}\eta^{2:2}\text{-}C_2H_2)(\eta^2\text{-}C_2H_3R)]$ (**2B**, **2C**) are formed. A by-product of the reaction of **1** with **D** is $[W(\eta^5\text{-}C_5H_5)(CO)(H)\{\eta^4\text{-}(E)\text{-}C_5H_7CH_3\}]$, which is generated in two diastereomeric forms (**6**, **6′**). In contrast, **1** yields no complexes with (*Z*)-2-butene (**E**) which contain ligands formed from coordinated acetylene and the olefin. From the reaction mixture only trinuclear $[W_3(\eta^5\text{-}C_5H_5)_3(CO)_5(\mu\text{-}\eta^{1:2}\text{-}C_2H_3)]$ (**7**) was isolated, an alicyclic complex with a W−W single and a W−W triple bond. The crystal and molecular structures of **5D** and **7** were determined by X-ray structure analysis. The constitutions of the other complexes were ascertained by IR and ^{1}H-NMR spectroscopy.

Introduction

Unsaturated hydrocarbons like alkenes or alkynes react in different ways with transition metal complexes. Oligomerisation, cyclooligomerisation and polymerisation are well-known reactions catalysed by transition metal complexes. Pre-requisite for a linkage of unsaturated hydrocarbons by C−C bond formation is the coordination of the substrates at one or two adjacent metal centres. Binuclear complexes offer after a suitable activation the possibility for a simultaneous coordination of two alkenes or alkynes followed by a C−C bond formation between the coordinated hydrocarbons. Examples for these types of reactions are the thermal oligomerisations of alkynes[2][3][4] at $[M_2(\eta^5\text{-}L)_2(CO)_4]$ complexes (M = Cr, Mo; L = C_5H_5, C_9H_7)[5][6][7][8], which proceed stepwise via $[M_2(\eta^5\text{-}L)_2(CO)_4(\mu\text{-}\eta^{2:2}\text{-alkyne})]$ as intermediates[9]. We have been able to show, that acetylene reacts photochemically with $[M_2(\eta^5\text{-}C_5H_5)_2(CO)_4(\mu\text{-}\eta^{2:2}\text{-}C_2H_2)]$ (M = Mo, W) predominantly to yield $[M_2(\eta^5\text{-}C_5H_5)_2(CO)_2(\mu\text{-}\eta^{1:3:3:1}\text{-}C_6H_6)]$[10].

By light-induced CO cleavage $[M_2(\eta^5\text{-}C_5H_5)_2(CO)_3(\mu\text{-}\eta^{2:2}\text{-}C_2H_2)]$ complexes are generated at low temperatures with potentially free coordination sites, well suited to coordinate unsaturated hydrocarbons. Not only acetylene, but also alkenes are coordinated and linked with the acetylene ligand when $[Mo_2(\eta^5\text{-}C_5H_5)_2(CO)_3(\mu\text{-}\eta^{2:2}\text{-}C_2H_2)]$ or $[Mo_2(\eta^5\text{-}C_9H_7)_2(CO)_3(\mu\text{-}\eta^{2:2}\text{-}C_2H_2)]$ is reacted with ethylene or alkenes[11][12]. This system allows a specific generation of hydrocarbons by codimerisation of acetylene and alkenes. In order to study the reaction behaviour of simple alkenes at binuclear complexes also the tungsten homologue $[W_2(\eta^5\text{-}C_5H_5)_2(CO)_4(\mu\text{-}\eta^{2:2}\text{-}C_2H_2)]$ was allowed to react with ethylene and some simple alkenes. The results of these investigations will be discussed in the following.

Preparative Results

The photoreaction of (μ-$\eta^{2:2}$-acetylene)tetracarbonylbis(η^5-cyclopentadienyl)ditungsten(*W*−*W*) (**1**) was carried out at 253 K with the olefins ethylene (**A**), propene (**B**), 1-butene (**C**), (*E*)-2-butene (**D**), or (*Z*)-2-butene (**E**) in petroleum ether/THF or ether/THF. The progress of the reaction is monitored by IR spectroscopy using the υCO stretching bands in the region from 2200 to 1700 cm^{-1}. Immediately after the bands of **1** have vanished the irradiation is stopped and the solvent is removed from the reaction mixture. The residue is separated by column chromatography on alumina at 253 K into its components, the isolated compounds are re-crystallised from ether. The complexes were characterised with IR and ^{1}H NMR spectroscopy and by C,H elemental analyses.

The photoreaction of **1** with ethylene (**A**) is conducted in petroleum ether/THF (1:1). By column chromatography of the reaction mixture three binuclear complexes can be isolated: (μ-$\eta^{1:4}$-1,3-butadien-1-yl)tricarbonylbis(η^5-cyclopentadienyl)(μ-hydrido)ditungsten(*W*−*W*) (**3A**) (μ-$\eta^{1:3}$-2-butene-1,1-diyl)tetracarbonylbis(η^5-cyclopentadienyl)-

[◇] Part 19: Ref.[1].

 © WILEY-VCH Verlag GmbH, D-69451 Weinheim, 1998 1434−1948/98/0101−0127 $ 17.50+.50/0

ditungsten(*W*−*W*) (**4A**) and (η^4-1,3-butadiene)tricarbonylbis(η^5-cyclopentadienyl)ditungsten(*W*−*W*) (**5A**).

$$\mathbf{1} + C_2H_4 \xrightarrow[243\ K]{h\cdot\nu} [W_2(\eta^5\text{-}C_5H_5)_2(CO)_3(\mu\text{-}\eta^{1:4}\text{-}C_4H_5)(\mu\text{-}H)]\ (\mathbf{3A})\ (3\%)$$

$$[W_2(\eta^5\text{-}C_5H_5)_2(CO)_4(\mu\text{-}\eta^{1:3}\text{-}C_4H_6)]\ (\mathbf{4A})\ (2\%)$$

$$[W_2(\eta^5\text{-}C_5H_5)_2(CO)_3(\eta^4\text{-}C_4H_6)]\ (\mathbf{5A})\ (2\%)$$

Propene (**B**) and 1-butene (**C**) react with **1** to analogous compounds. In addition to the dienyl bridged hydrido complexes **3B**, **3C** and the related 2-pentene-1,1-diyl and 2-hexene-1,1-diyl complexes **4B**, **4C** the η^4-diene compounds **5B**, **5C** with bridging μ-$\eta^{1:2}$-CO ligands and the very thermolabile substitution products with olefin acetylene ligands **2B**, **2C** were isolated from the reaction mixtures. The olefin complexes **2B**, **2C** rearrange at room temperature readily into the corresponding dienyl hydrido complexes **3B**, **3C**.

$$\mathbf{1} + C_2H_3R \xrightarrow[243\ K]{h\cdot\nu} [W_2(\eta^5\text{-}C_5H_5)_2(CO)_3(\mu\text{-}\eta^{2:2}\text{-}C_2H_2)(\eta^2\text{-}C_2H_3R)]\ (\mathbf{2B}, \mathbf{2C})\ (4\%, 5\%)$$

$$[W_2(\eta^5\text{-}C_5H_5)_2(CO)_3(\mu\text{-}H)(\mu\text{-}\eta^{1:4}\text{-}C_4H_4R)]\ (\mathbf{3B}, \mathbf{3C})\ (4\%, 6\%)$$

$$[W_2(\eta^5\text{-}C_5H_5)_2(CO)_4(\mu\text{-}\eta^{1:3}\text{-}C_4H_5R]\ (\mathbf{4B}, \mathbf{4C})\ (1\%, 1\%)$$

$$[W_2(\eta^5\text{-}C_5H_5)_2(CO)_2(\mu\text{-}\eta^{1:2}\text{-}CO)(\eta^4\text{-}C_4H_5R)]\ (\mathbf{5B}, \mathbf{5C})\ (5\%, 5\%)$$

$$R = CH_3, C_2H_5$$

With (*E*)-2-butene (**D**) one mononuclear and three binuclear complexes are obtained after chromatography. No simple olefin complex has been detected in this case. Again a dienyl-bridged hydrido complex **3D** and a diene complex **5D** are formed. The generation of **4C** must be explained with an isomerisation of the olefin prior to the C−C bond formation. The mononuclear complex **6** contains like **5D** the η^4-(*E*)-3-methyl-1,3-pentadiene ligand. When **3D** is warmed in solution it rearranges into **5D**.

$$\mathbf{1} + C_4H_8 \xrightarrow[243\ K]{h\cdot\nu} [W_2(\eta^5\text{-}C_5H_5)_2(CO)_3(\mu\text{-}H)(\mu\text{-}\eta^{1:4}\text{-}C_5H_6CH_3)]\ (\mathbf{3D})\ (5\%)$$

$$[W_2(\eta^5\text{-}C_5H_5)_2(CO)_4(\mu\text{-}\eta^{1:3}\text{-}C_3H_3C_3H_7]\ (\mathbf{4C})\ (1\%)$$

$$[W_2(\eta^5\text{-}C_5H_5)_2(CO)_2(\mu\text{-}\eta^{1:2}\text{-}CO)(\eta^4\text{-}C_5H_7CH_3)]\ (\mathbf{5D})\ (7\%)$$

$$[W(\eta^5\text{-}C_5H_5)(CO)(H)(\eta^4\text{-}C_5H_7CH_3)]\ (\mathbf{6})\ (1\%)$$

The photolysis of **1** in presence of (*Z*)-2-butene (**E**) yields no products with ligands, formed from acetylene and the olefin. Possibly, the steric demand of the *Z*-standing methyl groups causes this distinct differences of the reactivity. The starting material **1** is consumed only after 300 min and mainly decomposed into insoluble material. By column chromatography a trinuclear vinyl-bridged complex was isolated in addition to traces of other not yet characterised compounds.

$$\mathbf{2} + C_4H_8 \xrightarrow[243\ K]{h\cdot\nu} [W_3(\eta^5\text{-}C_5H_5)_3(CO)_5(\mu\text{-}\eta^{1:2}\text{-}C_2H_3)]\ (\mathbf{7})\ (1\%)$$

^{1}H-NMR Spectra

The ^{1}H-NMR spectroscopic data of the isolated complexes **2B**−**7** are given in the Experimental Section. For the binuclear complexes **2B**−**5D**, two singlets of the chemically different η^5-cyclopentadienyl ligands and additional signals due to ligands formed from acetylene and the olefins **A**−**D** are observed. The chemical shifts and the coupling constants of these signals together with the IR data allow justified suggestions for the constitutions of the complexes.

The photoreactions of **1** with propene (**B**) or 1-butene (**C**) yield the two η^2-olefin compounds **2B** and **2C**. Both are very temperature sensitive and can not be isolated in a pure state therefore. Two doublets in the ^{1}H-NMR spectra at δ = 2.35, 4.02 (**2B**) and δ = 2.33, 4.06 (**2C**) with coupling constants of 2 Hz are assigned to the bridging acetylene ligand. Four resonances in the spectrum of **2B** between δ = 1.03 and 2.30 with the relative intensities of 1:1:3:1 correspond to the η^2-coordinated propene ligand. Analogously, in the spectrum of **2C** a triplet and two multiplets for an ethyl group and three signals of single intensity between δ = 0.96 and 2.29 of the vinyl group were found. In solution **2B** and **2C** rearrange already at 273 K quickly into the μ-$\eta^{1:4}$-dienyl-μ-hydrido complexes **4B** and **4C**. Decomposition under formation of the starting material **1** is also observed.

The ^{1}H-NMR spectra of the μ-$\eta^{1:4}$-dienyl-μ-hydrido complexes show a strongly high-field shifted signal, typical for bridging hydrido ligands. The signals of the binuclear tungsten compounds **3A**, **3B**, **3C** and **3D** are accompanied by two pairs of ^{183}W satellites by which the bridging function of the hydrido ligands is further proved.

Five signals of **3A** with single intensity are related to each other by spin-spin couplings have to be assigned to the μ-$\eta^{1:4}$-1,3-butadien-1-yl ligand. The coupling constant J_{23} = 4.5 Hz is indicative for an *s-cis* conformation.

The ^{1}H-NMR spectra of **3B** and **3C** show two AB-spin systems each. Two doublets represent H1 and H2 with vicinal coupling constants of 6.0 Hz. Two doublets at higher field are due to H4 (*E*) and H4 (*Z*) with geminal coupling constants of 3.0 and 2.0 Hz. A singlet for **3B**, and two double quadruplets and a triplet for **3C** prove a methyl and an ethyl group at C3.

In the ^{1}H-NMR spectra of **3A**−**3D** a second hydrido signal of low intensity is found, which indicates the presence of a second isomer. Spin saturation experiments for **3B** and **3D** prove an exchange process between the two isomers. The increase of temperature causes first broadening of the signals of H1 and H2. At 303 K, they start narrowing again. Simultaneously the conversion to the corresponding η^4-diene complexes **5B** and **5D** is observed.

The tetracarbonyl complexes with μ-$\eta^{1:3}$-2-alkene-1,1-diyl ligands **4A**−**4C** were isolated only in low yields form the reactions of **1** with **A**−**D**. In the case of **D** as olefin component, an isomerisation to **C** has to be assumed prior CC bond formation. The complexes **4A**−**4C** are stable at room temperature.

The characterisation by ^{1}H-NMR spectroscopy is quite simple. Typical for all of these complexes is the resonance

of H1 at low field δ = 9.35 (**4A**, **4B**) and δ = 8.97 (**4C**). In the region of the proton resonances of coordinated olefins two signals for H2 and H3 are obtained. The vicinal coupling constants between H1, H2 and H3 reach from 8.5 to 10 Hz. The complexes differ according to the signals of the alkyl substituents (methyl, ethyl, propyl) in 3*E* position.

The ^{1}H-NMR spectra of the tricarbonyl-η^4-diene complexes **5A**, **5B**, **5C** and **5D** show at 243 K or 253 K the typical signal patterns for η^4-coordinated 1,3-butadiene, 2-methyl-1,3-butadiene, 2-ethyl-1,3-butadiene and (*E*)-3-methyl-1,3-pentadiene ligands. According to the stereochemistry of the complexes with the diene ligand in *ortho* orientation to the adjacent cyclopentadienyl ring, proved for **5D** with an X-ray structure analysis, four different stereoisomers (two pairs of enantiomers) are reasonable for such complexes with unsymmetrically substituted diene ligands. There is no evidence for the presence of a second pair of enantiomers in the spectra of **5B**, **5C** and **5D**. Obviously the energy difference between the pairs of enantiomers is too large to a allow a detectable population of the less favoured isomers.

The ^{1}H-NMR spectra of the complexes **5A**−**5D** were measured at variable temperatures between 223 and 283 K. Like the corresponding η^4-2,3-dimethyl-1,4-butadiene dimolybdenum complex for which an enantiomerisation was proved[13], **5A** shows signal broadening, although the dynamic behaviour could not be studied completely due to its thermal sensitivity. In contrast **5B**−**5D** show no dynamic effects.

The mononuclear complex **6**, **6′** is obtained only in minor amounts as a mixture of stereoisomers. The ^{1}H-NMR spectrum of **6**, **6′** contains two sets of eight signals with a proportion of 85:15. Two signals at δ = −9.65 and −6.13 with ^{183}W satellites of 76 and 74 Hz are assigned to the hydrido ligands. In each case three double doublets, a quadruplet, a singlet, and a doublet, the two latter of threefold intensity correspond with the (*E*)-3-methyl-1,3-pentadiene ligands of the two species. The chemical shifts of the (*E*)-3-methyl-1,3-pentadiene ligands in the two isomers are quite similar, the largest differences are found for H1 *E* and $CH_3$4 *E*. As a consequence of the asymmetric tungsten atom, and the asymmetrically substituted diene, two diastereomeric pairs of enantiomers are possible. When *o*-orientation is assumed on the basis of the observed chemical shifts for both isomers, the hydrido ligand is in one diastereomer in the vicinity of C1, in the other in the vicinity of C4. The large difference of the chemical shifts of the hydrido ligands is well understood on the basis of this assumption.

The trinuclear complex **7** is unexpectedly formed when **1** is irradiated in presence of (*Z*)-2-butene and is isolated in form of red-brown crystals in reasonable yield. Only three cyclopentadienyl singlets and three double doublets of single intensity at δ = 7.04, 4.72, 1.79 are observed in the ^{1}H-NMR spectrum. The double doublets are indicative for a bridging vinyl ligand. The spectrum is in accord with the molecular structure of **7** determined by X-ray structure analysis.

Crystal and Molecular Structures of 5D and 7

Reddish brown crystals of tricarbonylbis(η^5-cyclopentadienyl)[η^4-(*E*)-3-methyl-1,3-pentadiene]ditungsten-(*W*−*W*) (**5D**) are obtained in reasonable yields when **1** is allowed to react with (*E*)-2-butene. The complex crystallises in the monoclinic space group $P2_1/n$ with constants of the unit cell of *a* = 1089.3(2), *b* = 1240.5(3), *c* = 1303.7(2) pm, and ß = 95.914(14)°. The molecular structure of **5D** resembles to that of tricarbonylbis(η^5-methylcyclopentadienyl)(η^4-2,3-dimethyl-1,3-butadiene)dimolybdenum-(*Mo*−*Mo*)[12]. The W1−W2 bond length in the binuclear complex is found with 311.69(8) pm, typical for a W−W single bond[14]. The distances of the cyclopentadienyl ligands from the tungsten centres differ slightly from each other, W1 being somewhat closer with 196.9 pm than W2 with 202.1 pm. The (*E*)-3-methyl-1,3-pentadiene is η^4-coordinated to W1 and adopts *ortho* orientation[15]. The diene is originated by C−C bond formation between the acetylene ligand and the olefin **D**. Remarkably, the methyl groups being in *E* position in **D** are now in *Z* position to each other in **5D**. While W1−C1 = 221.3(10) pm and W1−C4 = 222.8(9) pm are of similar length, W1−C2 = 233.0(9) pm is found distinctly shorter than W1−C3 = 239.4(9) pm. Like in other η^4-diene complexes the C−C bond lengths of the diene entity are equal within experimental error. From the three CO ligands coordinated to W2, one is found in a normal terminal bond situation. The second CO ligand is semibridging to W1 with W1−C6 = 290.8(9) pm and W2−C6−O6 = 166.2(9)°. The third one forms a bridge between the two tungsten centres by a side-on coordination to W1 and shows only a slight bending with W2−C8−O8 = 169.1(11)°. By this type of coordination the CO ligand donates four electrons to the two tungsten centres. Examples for bridging, 4e-donor CO ligands are known for homo binuclear complexes[13][16][17][18] but especially for heteronuclear complexes[19][20][21][22][23][24].

The brown, trinuclear tungsten complex **7** crystallises in the monoclinic space group $P2_1/n$ with constants of the unit cell of *a* = 780.61(7) pm, *b* = 2197.1(3) pm, *c* = 1403.80(11) pm, and ß = 100.753(6)°. It shows noticeably different W−W bond lengths with W1−W2 = 304.65(11) pm and W2−W3 = 254.07(10) pm. They are in accord with W−W single[14] and triple bonds[25][26][27]. The three cyclopentadienyl ligands have similar distances to the pertinent metal centres with 201.0, 204.2, and 202.6 pm. Three of the five CO ligands are normal terminal ones. In contrast the CO ligands 5 and 6 are found in a special stereochemical situation. This kind of bond situation for CO ligands was observed for the first time in tetracarbonylbis(η^5-pentamethylcyclopentadienyl)dichromium[28], a binuclear complex with Cr−Cr triple bond and with four only slightly bent CO ligands, although heavily inclined toward the adjacent metal centres. Similar molecular geometries were also found for tetracarbonylbis(η^5-cyclopentadienyl)dimolybdenum[5], tetracarbonylbis(η^5-cyclopentadienyl)dichromium[29] and tetracarbonylbis(η^5-indenyl)dimolybdenum[8].

Figure 1. SCHAKAL projection of the molecular structure of **5D**; selected bond lengths [pm] and bond angles [°][a]; M(1) centre of C(11)−C(15), M(2) centre of C(21)−C(25)

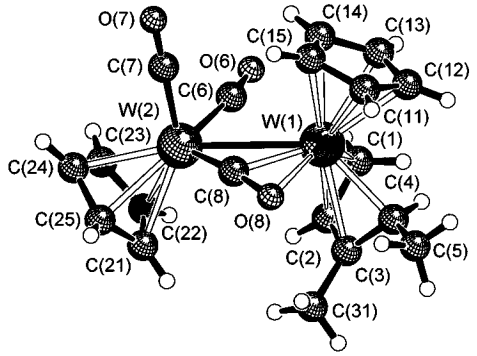

[a]W(1)−W(2) 311.69(8), W(1)−M(1) 196.9, W(2)−M(2) 202.1, W(1)−C(1) 221.3(10), W(1)−C(2) 233.0(9), W(1)−C(3) 239.4(9), W(1)−C(4) 222.8(9), W(1)−C(6) 290.8(9), W(1)−C(8) 212.2(9), W(1)−O(8) 220.3(6), W(2)−C(6) 196.7(11), W(2)−C(7) 193.9(11), W(2)−C(8) 190.3(10), C(6)−O(6) 115.7(12), C(7)−O(7) 115.7(12), C(8)−O(8) 124.5(11); M(1)−W(1)−W(2) 116.1, M(2)−W(2)−W(1) 141.6, W(1)−W(2)−C(6) 65.3(4), W(1)−W(2)−C(7) 94.0(5), W(1)−W(2)−C(8) 41.9(4), W(2)−C(6)−O(6) 166.2(9), W(2)−C(7)−O(7) 178.2(9), W(2)−C(8)−O(8) 169.1(71).

Complex **7** can be considered to contain two subunits. The first one is related to (η^3-allyl)dicarbonyl(η^5-cyclopentadienyl)metal complexes of group 6[30], the second to tetracarbonylbis(η^5-cyclopentadienyl)dichromium[28].

Figure 2. SCHAKAL projection of the molecular structure of **7**; selected bond lengths [pm] and bond angles [°]; M(1) centre of C(11)−C(15), M(2) centre of C(21)−C(25), M(3) centre of C(31)−C(35)[a]

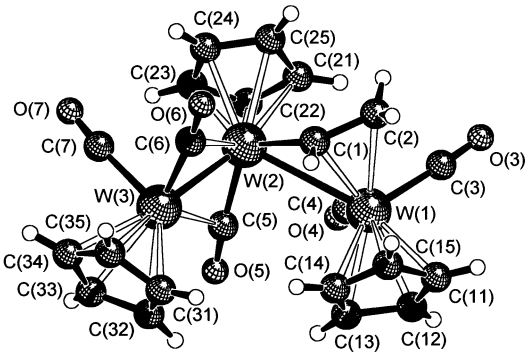

[a]W(1)−W(2) 304.65(11), W(2)−W(3) 254.07(10), W(1)−M(1) 201.0, W(2)−M(2) 204.2, W(3)−M(3) 202.6, W(1)−C(1) 221(2), W(1)−C(2) 230(2), W(2)−C(1) 210(2), W(2)−C(5) 194(2), W(2)−C(6) 253(2), W(3)−C(5) 236(2), W(3)−C(6) 192(2), W(3)−C(7) 202(2); W(1)−W(2)−W(3) 110.47(3), M(1)−W(1)−W(2) 125.5, M(2)−W(2)−W(1) 116.0, M(2)−W(2)−W(3) 132.8, M(3)−W(3)−W(2) 159.2, W(2)−C(5)−O(5) 168(2), W(3)−C(6)−O(6) 168.3(14), W(3)−C(7)−O(7) 175(2).

The bonding situation of the first subunit can be compared with those in the well-known (η^3-allyl)dicarbonyl(η^5-cyclopentadienyl)metal complexes. Formally W2, which is bonded to C1 and W1, replaces a sp^2-methylene group. In the second entity, vice versa, W1 and C1 replace in a formal sense a terminal CO ligand. In contrast to tetracarbonylbis(η^5-cyclopentadienyl)dichromium and the related compounds with all four CO ligands inclined to the adjacent metal centres, in complex **7** only two of them show this special type of coordination. This result is a good evidence for the assumption, that the inclination of only slightly bent CO ligands to a second metal centre and long metal−oxygen bonds is primarily due to steric and not due to electronic reasons. While for the two independent units of tetracarbonylbis(η^5-cyclopentadienyl)dichromium the angle Cr−Cr−M (M centre of the cyclopentadienyl ligand) is found with 158.7 and 165.0°, respectively, and in tetracarbonylbis(η^5-cyclopentadienyl)dimolybdenum close to 180°, the corresponding angles in **7** are W3−W2−M2 = 132.8(9)° and W2−W3−M3 = 159.2(9)°.

In complex **7** the three W atoms show an angular arrangement with W1−W2−W3 = 110.4(1)°. The plane defined by the three tungsten atoms is more or less perpendicular to the planes of the three cyclopentadienyl ligands with dihedral angles of 88.6, 82.2, and 82.9°. Remarkably, the two CO ligands 4 and 7 deviate only slightly from this plane and the C−W bonds penetrate the plane with 4.1 and 6.9°. W2, W3, C5 and C6 form an idealised parallelogram which is folded along the line W2, W3 with 162.4°. The distances W2−C5 and W3−C6 are short and amount 194(2) pm and 192(2) pm. The distances W2−C6 and W3−C5 are distinctly longer with 253(2) pm and 236(2) pm. The angles at C5 and C6 are found with 71.7(9) and 68.1(8)°, at W2 and W3 with 104.9(10) and 112.0(10)°. The sum of this angles is 356.7° as a consequence of the folding.

Complex **7** is also related to dinuclear complexes with μ-$\eta^{2:1}$-vinyl-bridging ligands[31][32]. It is an interesting example for a trinuclear complex with formal electron numbers of 17, 14, and 15 at the three tungsten centres. W−W single and triple bonds have to be considered for this trinuclear, angular 46 electron complex taking into account the 18 electron rule.

Discussion

The photoreaction of (μ-$\eta^{2:2}$-acetylene)tetracarbonylbis(η^5-cyclopentadienyl)ditungsten(*W*−*W*) (**1**) with ethylene yields at 253 K three complexes, [$W_2(\eta^5$-$C_5H_5)_2(CO)_3(H)(\mu$-$\eta^{1:4}$-1,3-butadien-1-yl)] (**3A**), [$W_2(\eta^5$-$C_5H_5)_2(CO)_4(\mu$-$\eta^{1:3}$-2-butene-1,1-diyl)] (**4A**), and [$W_2(\eta^5$-$C_5H_5)_2(CO)_3(\eta^4$-1,3-butadiene)] (**5A**) which are closely related to each other and allow conclusions about the reaction behaviour of unsaturated hydrocarbons in the coordination spheres of two tungsten centres. All products contain C_4 ligands, which result from a C−C bond formation between acetylene and ethylene and successive H shifts.

Binuclear complexes become accessible by photochemically induced formation of C_4 ligands from acetylene and ethylene which are only partially formed when 1,3-butadiene is reacted directly with [$M_2(\eta^5$-$C_5H_4CH_3)_2(CO)_6$] complexes (M = Mo, W)[33]. With [$Mo_2(\eta^5$-$C_5H_4CH_3)_2$-$(CO)_6$] 1,3-butadiene yields [$Mo(\eta^5$-$C_5H_4CH_3)$-$(CO)_2\{\eta^3$-(*E*)-2-butenyl}], [$Mo(\eta^5$-$C_5H_4CH_3)(CO)_2\{\eta^3$-(*Z*)-2-butenyl}], [$Mo_2(\eta^5$-$C_5H_4CH_3)_2(CO)_3(\eta^4$-butadiene)], and [$Mo_2(\eta^5$-$C_5H_4CH_3)_2(CO)_2(\mu$-$\eta^4$-butadiene)][13]. In the case of the photoreaction of [$W_2(\eta^5$-$C_5H_4CH_3)_2(CO)_6$] with 1,3-butadiene the only isolable product is [$W_2(\eta^5$-

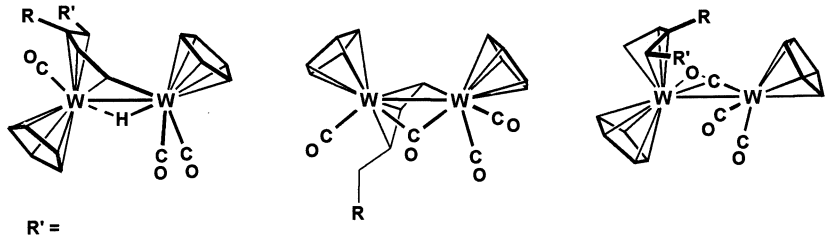

R =	R' =			
H	H	**3A**	**4A**	**5A**
CH_3	H	**3B**	**4B**	**5B**
C_2H_5	H	**3C**	**4C**	**5C**
CH_3	CH_3	**3D**		**5D**

$C_5H_4CH_3)_2(CO)_4\{\mu\text{-}\eta^{1:3}\text{-}(E)\text{-2-butene-1,1-diyl}\}]$,[18] the analogue to **4A**.

Examples of C−C bond formations between small molecules in the coordination sphere of metals have been observed already in the past. $[Ru_2(\eta^5\text{-}C_5H_5)_2(CO)_2(CH_3CN)(\mu\text{-vinyl})]^+$ reacts with ethylene to $[Ru_2(\eta^5\text{-}C_5H_5)_2(CO)_2(\mu\text{-H})(\mu\text{-}\eta^{2:2}\text{-1,3-butadiene})]^+$ and by deprotonation to $[Ru_2(\eta^5\text{-}C_5H_5)_2(CO)_2(\mu\text{-}\eta^{2:2}\text{-1,3-butadiene})]$[34]. Similarly, binuclear complexes with alkylidene bridges like $[M_2(\eta^5\text{-}C_5H_5)_2(CO)_3(\mu\text{-ethylidene})]$ (M = Fe, Ru) react with alkynes to the correspondingly substituted $\mu\text{-}\eta^{1:3}$-alkenediyl complexes[35][36].

Closely related to ($\mu\text{-}\eta^{1:4}$-1,3-butadiene-1-yl)tricarbonylbis(η^5-cyclopentadienyl)(μ-hydrido)ditungsten(*W*−*W*) (**3A**), one of the products of the photoreaction of **1** with **A** is $[Mo_2(\eta^5\text{-}C_5H_4CH_3)_2(CO)_3(H)(\eta^{1:4}\text{-1,3-cycloheptadien-1-yl})]$, which is obtained when $[Mo_2(\eta^5\text{-}C_5H_4CH_3)_2(CO)_4]$ is irradiated in presence of 1,3-cycloheptadiene. The cyclic, $\eta^{1:4}$-coordinated dienyl and the hydrido ligand form bridges between the two metal centres[37]. Comparable bonding situations are also found in $[Rh_2\{(i\text{-}C_3H_7)_2PCH_2CH_2P(i\text{-}C_3H_7)_2\}_2(\mu\text{-H})(\eta^{1:4}\text{-1,3-butadiene-1-yl})]$, a product of the reaction of $[Rh_2\{(i\text{-}C_3H_7)_2PCH_2CH_2P(i\text{-}C_3H_7)_2\}_2(\mu\text{-H})_2]$ with 1,3-butadiene[38]. In both cases the diene is transformed into a dienyl ligand by hydrogen shift to the metal centre.

(η^4-1,3-Butadiene)tricarbonylbis(η^5-cyclopentadienyl)ditungsten(*W*−*W*) (**5A**) belongs to a group of complexes with side-on-coordinated, bridging CO ligands, donating 4 electrons to the metal centres. $[M_2(\eta^5\text{-}C_5H_4CH_3)_2(CO)_3(\eta^4\text{-diene})]$ complexes (M = Mo, W) are generated photochemically from $[M_2(\eta^5\text{-}C_5H_4CH_3)_2(CO)_4]$ with certain dienes[13][18]. They may be considered as derivatives of $[Mo_2(\eta^5\text{-}C_5H_5)_2(CO)_5]$ which is stabile only in matrix[39]. Of special interest is the 4-electron carbonyl bridge with a υCO band around 1600 cm^{-1}[13][18].

($\mu\text{-}\eta^{1:3}$-2-Butene-1,1-diyl)tetracarbonylbis(η^5-cyclopentadienyl)ditungsten(*W*−*W*) (**4A**) contains a 1,3-metalladiene core. Complexes of this type are generated under quite different conditions. $[Mo_2(\eta^5\text{-}C_5H_5)_2(CO)_4]$ reacts thermally with 3,3-dimethylcyclopropene by ring opening to $[Mo_2(\eta^5\text{-}C_5H_5)_2(CO)_4(\mu\text{-}\eta^{1:3}\text{-3-methyl-2-butene-1,1-diyl})]$[40][41]. The photoreaction of $[W_2(\eta^5\text{-}C_5H_4CH_3)_2(CO)_4]$ with 1,3-butadiene yields the analogous 2-butene-1,1-diyl complex[18]. 1,3-Metalladiene complexes may adopt *s-cis*[30][41] or *s-trans* configurations[42][43]. The ^{1}H-NMR-spectroscopic data of **4A** are in accord with the *s-cis* configuration.

Also with propene (**B**), 1-butene (**C**), or (*E*)-2-butene (**D**) hydrido-dienyl, 2-alkene-1,1-diyl and 1,3-diene complexes are formed. With **B** and **C** in addition the thermolabile, simple substitution products ($\mu\text{-}\eta^{2:2}$-acetylene)tricarbonylbis(η^5-cyclopentadienyl)(η^2-propene)ditungsten(*W*−*W*) (**2B**) and the corresponding 1-butene complex (**2C**) can be isolated and characterised by IR and ^{1}H-NMR spectroscopy. At room temperature **2B**, **2C** rearrange readily into the hydrido-dienyl complexes **3B**, **3C**.

The isolated products give good evidence for the route of the photochemical reaction when ($\mu\text{-}\eta^{2:2}$-acetylene)tetracarbonylbis(η^5-cyclopentadienyl)ditungsten(*W*−*W*) (**1**) is irradiated in the presence of olefins. In a primary step one CO ligand is cleaved from **1**. In contrast to mononuclear, electronically and coordinativly unsaturated carbonylmetal complex fragments with 16 electrons, the 32 electron intermediate, ($\mu\text{-}\eta^{2:2}$-acetylene)tricarbonylbis(η^5-cyclopentadienyl)ditungsten(*W*−*W*) (**8**), is probably stabilised by formation of a 4-electron carbonyl bridge like in the diene complexes **5A**−**5D**. This stabilisation would prolong the life time of **8**, but it might also delay the coordination of the olefin.

Addition of an olefin to **8** yields (η^2-acetylene)tricarbonylbis(η^5-cyclopentadienyl)(η^2-olefin)ditungsten(*W*−*W*) (**2**) which is moderately stable with propene or 1-butene as olefin component. In **2** two unsaturated hydrocarbon ligands are coordinated to a metal centre, a pre-requisite for a C−C bond formation. Insertion of the olefin into a W−C bond of the $W_2C_2H_2$ core yields the intermediate ($\mu\text{-}\eta^{1:2:1}$-1-butene-1,4-diyl)tricarbonylbis(η^5-cyclopentadienyl)ditungsten(*W*−*W*) (**9**).

In a formal approach the $W_2C_2H_2$ fragment can be classified as a ditungstatetrahedrane and the WC_2H_4 entity as a tungstacyclopropane. By using this approach, the C−C bond formation is a kind of reductive elimination or reductive rearrangement, because it is accompanied by the cleavage of two W−C bonds. Also the electron deficit in **9** is possibly compensated by a 4-electron carbonyl bridge.

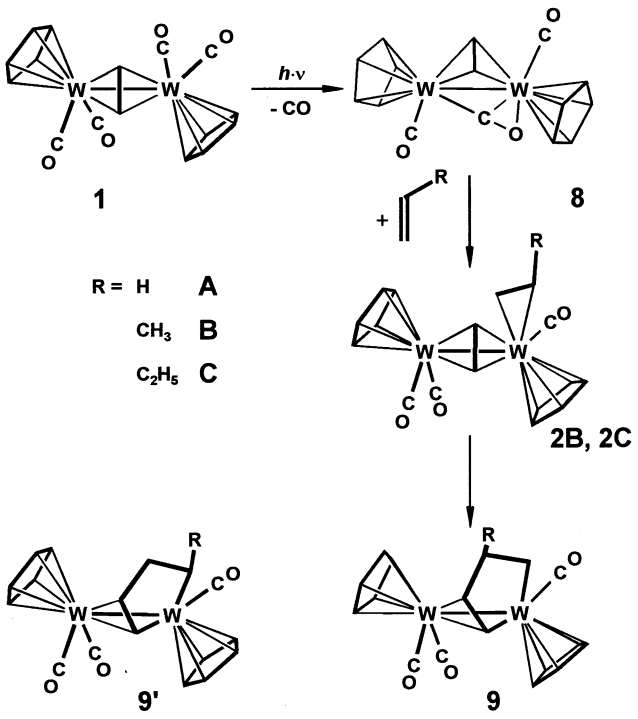

Unsymmetrically substituted olefins like **B** or **C** may form up to four different stereoisomers of **9**.

The 1-alkene-1,4-diyl ligands in **9** contain in β-position methylene or methine groups, which are susceptible to a β-elimination. This elimination leads immediately to the (μ-$\eta^{1:4}$-diene-1-yl)tricarbonylbis(η^5-cyclopentadienyl)-hydridoditungsten(*W*−*W*) complexes **3A**−**3D**.

In general, the complexes **3** rearrange at room temperature by H shift to C1 of the diene-1-yl ligand quickly into the (diene)tricarbonylbis(η^5-cyclopentadienyl)ditungsten complexes **5**. This reaction can also be interpreted as a reductive rearrangement, leading to 32-electron complexes.

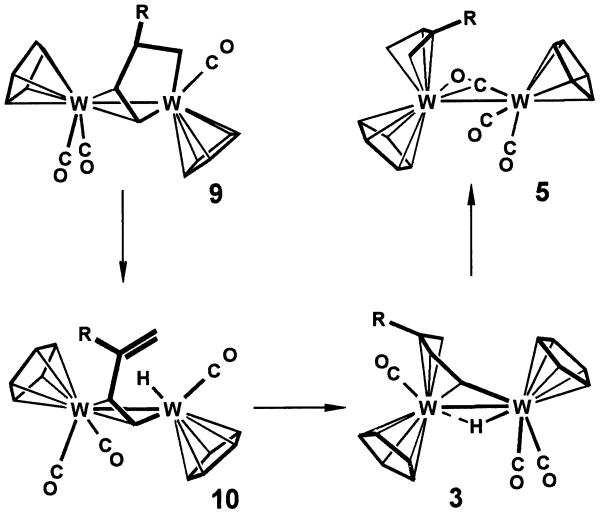

In addition to the hydrogen transfer to C1 also a transfer to C4 of the 1,3-butadiene-1-yl ligand and the coordination of carbon monoxide is possible which generates the (μ-$\eta^{1:3}$-2-alkene-1,1-diyl)tetracarbonylbis(η^5-cyclopentadienyl)-ditungsten(*W*−*W*) complexes **4A**, **4B** and **4C**.

Interestingly, the complexes **3B**−**3D** and **5B**−**5D** contain branched hydrocarbon ligands which are formed from acetylene and the olefins by C−C bond formation between acetylene and C2 of the olefins. Although the methyl groups in **D** are in *E* position, in the products **3D** and **5D** they are found in *Z* position, therefore a rotation around the C3−C4 bond has to be considered while intermediate **9** rearranges into **3**.

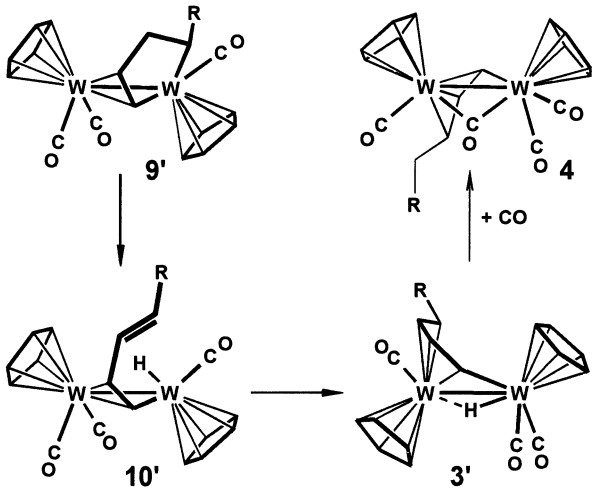

No branched hydrocarbon ligands are found in **4B** and **4C,** so the C−C bond formation involves C1 of the olefins. Furthermore, no corresponding dienyl-hydrido or diene complexes are observed. Obviously, the dienyl-hydrido precursor complexes **9** rearrange faster and are not detectable therefore. Small amounts of **4C** are also isolated from the reaction mixture of **1** and **D**. There are two explanations for this result. Either the olefin **D** contains impurities of **C** or the olefin is isomerised under the reaction conditions prior the C−C bond formation.

The by-product of the reaction of **1** with **D**, carbonyl(η^5-cyclopentadienyl)hydrido{η^4-(*E*)-3-methyl-1,3-pentadiene}-tungsten is generated in the two diastereomeric forms **6**, and **6′**. In addition to the centre of chirality at the tungsten atoms, the unsymmetrically substituted 1,3-diene ligand is planar chiral. Therefor diastereomers have to be expected and are obtained in a ratio of 0.85:0.15.

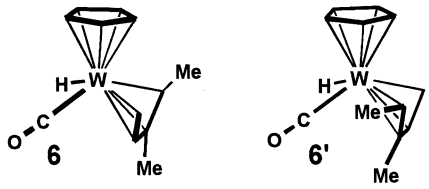

Finally, it should be mentioned, that (*Z*)-2-butene (**E**) does not form hydrocarbon ligands with acetylene at all. The only product obtained is the trinuclear tungsten complex **7** with a W−W single and a W−W triple bond and a vinyl bridge.

This research was supported by the *Volkswagen-Stiftung*, the *Deutsche Forschungsgemeinschaft* and the *Verband der Chemischen Industrie.*

Experimental Section

All treatments and reactions were performed under dry, oxygen-free nitrogen. Solvents were dried with sodium/benzophenone or phosphorus pentoxide and saturated with nitrogen. − For column chromatography neutral alumina (Macherey, Nagel & Co KG, Düren) was heated in vacuum at 423 K and deactivated with 5% of water, saturated with nitrogen. − Photolysis reactions were conducted using a high-pressure mercury lamp (TQ 718, Heraeus Noblelight GmbH, Kleinostheim) operating at 700 W, which was immersed into a 750-ml vessel of Duran® with a cooling jacket. − C,H elemental analyses: Perkin-Elmer microanalyser 240. − IR (2200−1500 cm^{-1}): Perkin-Elmer Model 881. − ^1H NMR: Puls-FT-NMR-Spektrometer AMX 400 (Bruker) at 400.13 MHz. Chemical shifts are given relatively to TMS calculated from the solvent as internal standard. − (μ-$\eta^{2:2}$-Acetylene)tetracarbonylbis(η^5-cyclopentadienyl)ditungsten(*W*−*W*) (**1**) was prepared according to literature procedures[6][9]. All other reagents were commercial products.

1. *Photoreaction of (μ-η²:²-Acetylene)tetracarbonylbis(η⁵-cyclopentadienyl)ditungsten(W−W)* (**1**) *with Ethylene* (**A**): 1.6 g (2.5 mmol) of (μ-$\eta^{2:2}$-acetylene)tetracarbonylbis(η^5-cyclopentadienyl)ditungsten(*W*−*W*) (**1**) was dissolved in 750 ml of petroleum ether/THF (1:1). The solution was cooled to 243 K, and for 10 min ethylene (**A**) was condensed into it. During the photolysis nitrogen was bubbled through the solution and the progress of the reaction was controlled by IR spectroscopy in regular intervals. Irradiation was continued until the υCO bands of **1** had vanished. The solvent was removed in vacuo at 253 K and the residue was separated by column chromatography on alumina into two main fractions. The residue of the first main fraction was dissolved in 10 ml of ether and was subject of a further chromatography.

1st Fraction (pentane/ether 2:1): Starting material **1**.

2nd Fraction (pentane/ether 2:1): Pink solution; after removal of the solvent and crystallisation from ether, thermolabile (η^4-1,3-butadiene)tricarbonylbis(η^5-cyclopentadienyl)ditungsten(*W*−*W*) (**5A**) was obtained as red powder. Due to the thermal sensitivity of **5A** only a spectroscopic characterisation was possible (2%). − IR: $\tilde{\nu}$ = 1905 (s), 1825 (s), 1555 (m) cm^{-1}. − ^1H NMR (CD_2Cl_2, 213 K): δ = 5.41 (ddd, *J* = 7.5, 7.0, 7,0, 1 H, H2), 3.23 (ddd, *J* = 7.5, 7.0, 7.0 Hz, 1 H, H3), 2.92 (dd, *J* = 7.0, 4.0 Hz, 1 H, H4 *E*), 2.15 (d, *J* = 7.0, 2.0 Hz, 1 H, H1 *E*), 1.47 (dd, *J* = 7.0, 2.0 Hz, 1 H, H1 *Z*), 1.43 (dd, *J* = 7.0, 4.0 Hz, 1 H, H4 *Z*); 5.43 (s, 5 H, C_5H_5), 5.07 (s, 5 H, C_5H_5).

3rd Fraction (pentane/ether, 2:1): Orange solution. During the removal of the solvent, orange crystals of (μ-$\eta^{1:4}$-1,3-butadien-1-yl)tricarbonylbis(η^5-cyclopentadienyl)(μ-hydrido)ditungsten(*W*−*W*) (**3A**) started to precipitate. The solid residue was crystallised from ether (3%). − IR: $\tilde{\nu}$ = 1925 (sh), 1910 (s), 1835 (s) cm^{-1}. − ^1H NMR (CD_2Cl_2, 243 K): δ = 4.52 (dd, *J* = 6.5, 1.0 Hz, 1 H, H1), 4.19 (dd, *J* = 6.5, 4.5 Hz, 1 H, H2), 4.00 (dddd, *J* = 9.0, 7.5, 4.5, 1.0 Hz, 1 H, H3), 2.00 (dd, *J* = 7.5, 3.0 Hz, 1 H, H4 *E*), 1.42 (dd, *J* = 9.0, 3.0 Hz, 1 H, H4 *Z*), 5.46 (s, 5 H, C_5H_5), 5.20 (s, 5 H, C_5H_5), 17.62 [s, $^1J(^{183}W-^1H)$ = 46, 54 Hz, 1 H, W−H]. − $C_{17}H_{16}O_3W_2$ (636.01): calcd. C 32.1, H 2.5; found C 31.9, H 2.5.

4th Fraction (ether): Bright green solution, which turned red during removal of the solvent. By crystallisation of the residue from ether (μ-$\eta^{1:3}$-2-butene-1,1-diyl)tetracarbonylbis(η^5-cyclopentadienyl)ditungsten(*W*−*W*) (**4A**) was isolated as red crystalline powder (2%). − IR: $\tilde{\nu}$ = 1945 (vs), 1900 (s), 1840 (s), 1775 (m) cm^{-1}. − ^1H NMR (CD_3COCD_3, 253 K): δ = 9.35 (dd, *J* = 9.0, 1.0 Hz, 1 H, H1), 6.24 (dd, *J* = 9.0, 9.0 Hz, 1 H, H2), 1.47 (dqd, *J* = 9.0, 6.0, 1.0 Hz, 1 H, H3), 1.80 (d, *J* = 6.0 Hz, 3 H, H4), 5.53 (s, 5 H, C_5H_5), 5.46 (s, 5 H, C_5H_5).

2. *Photochemical Reactions of* **1** *with Propene* (**B**): According to Procedure 1, 2.0 g (3.15 mmol) of **1** and propene (**B**) in 750 ml of ether/THF (6:1) were irradiated at 253 K for 85 min. After removal of the solvent, the residue was separated by column chromatography.

1st Fraction (pentane/ether 3:1): Starting material **1**.

2nd Fraction (pentane/ether 3:1): Orange solution, which contains a mixture of **1** and (μ-$\eta^{2:2}$-acetylene)tricarbonylbis(η^5-cyclopentadienyl)(η^2-propene)ditungsten(*W*−*W*) (**2B**) (4%). Even after repeated chromatography complex **2B** could not be obtained in a pure state. − IR: $\tilde{\nu}$ = 1957 (m), 1914 (s), 1826 (s) cm^{-1}. − ^1H NMR (C_7D_8, 233 K): δ = C_3H_6 1.03 (dd, *J* = 9.5, 2.0 Hz, 1 H, H1 *E*), 1.82 (dd, *J* = 11.0, 2.0 Hz, 1 H, H1 *Z*), 2.30 (ddq, *J* = 11.0, 9.5, 6.0 Hz, 1 H, H2), 1.85 (d, *J* = 6.0 Hz, 3 H, H3); C_2H_2 2.35 (d, *J* = 2.0 Hz, 1 H, H1), 4.02 (d, *J* = 2.0 Hz, 1 H, H2); 4.98 (s, 5 H, C_5H_5), 4.95 (s, 5 H, C_5H_5).

3rd Fraction (pentane/ether 2:1): Red solution, which already yielded tricarbonylbis(η^5-cyclopentadienyl)(η^4-2-methyl-1,3-butadiene)ditungsten(*W*−*W*) (**5B**) as red, microcrystalline powder (5%). − IR: $\tilde{\nu}$ = 1899 (s), 1806 (m), 1551 (m) cm^{-1}. − ^1H NMR (C_7D_8, 243 K): δ = 2.71 (dd, *J* = 4.0, 1.5 Hz, 1 H, H1 *E*), 1.36 (dd, *J* = 4.0, 2.0 Hz, 1 H, H1 *Z*), 1.34 (s, 3 H, 2-CH_3), 4.96 (dddd, *J* = 7.0, 7.0, 2.0, 1.5 Hz, 1 H, H3), 2.90 (dd, *J* = 7.0, 2.5 Hz, 1 H, H4 *E*), 1.57 (dd, *J* = 7.0, 2.5 Hz, 1 H, H4 *Z*), 5.07 (s, 5 H, C_5H_5), 4.91 (s, 5 H, C_5H_5). − $C_{18}H_{18}O_3W_2$ (650.04): calcd. C 33.26, H 2.79; found C 33.4, H 2.8.

4th Fraction (pentane/ether 1:1): Yellow-orange zone; after removal of the solvent and crystallisation from ether, tricarbonylbis(η^5-cyclopentadienyl)(μ-hydrido)(μ-$\eta^{1:4}$-3-methyl-1,3-butadien-1-yl)ditungsten(*W*−*W*) (**3B**) was isolated as orange powder (4%). − IR: $\tilde{\nu}$ = 1924 (sh), 1909 (s), 1831 (s) (υCO); 1961 (w) (υMH) cm^{-1}. − ^1H NMR ($CDCl_3$, 243 K): δ = 4.39 (dd, *J* = 6.0, 2.0 Hz, 1 H, H1), 4.03 (d, *J* = 6.0 Hz, 1 H, H2), 2.11 (s, 3 H, 3-CH_3), 1.89 (d, *J* = 3.0 Hz, 1 H, H4 *E*), 1.59 (d, *J* = 3.0 Hz, 1 H, H4 *Z*), 5.45 (s, 5 H, C_5H_5), 5.11 (s, 5 H, C_5H_5), −17.38 (d, *J* = 2.0 Hz, $^1J^{183}W-^1H$ 46, 56 Hz, 1 H, W−H). − $C_{18}H_{18}O_3W_2$ (650.04): calcd. C 33.26, H 2.79; found C 32,2, H 2,6.

5th Fraction (pentane/THF 1:1): The residue of the red-brown solution was crystallised from ether. Tetracarbonylbis(η^5-cyclopentadienyl)(μ-$\eta^{1:3}$-2-penten-1,1-diyl)ditungsten(*W*−*W*) (**4B**) was obtained as red-brown crystals (1%). − IR: $\tilde{\nu}$ = 1948 (vs), 1905 (s), 1848 (s), 1775 (m) cm^{-1}. − ^1H NMR (CD_3COCD_3, 283 K): δ = 9.35 (dd, *J* = 8.5, 1.0 Hz, 1 H, H1), 6.20 (dd, *J* = 10.0, 8.5 Hz, 1 H, H2), 1.50 (dddd, *J* = 10.0, 10.0, 3.5, 1.0 Hz, 1 H, H3), 1.65 (ddq, *J* = 14.0, 10.0, 7.5 Hz, 1 H, H4), 2.10 (dqd, *J* = 14.0, 7.5, 3.5, Hz, 1 H, H4′), 1.01 (t, *J* = 7.5 Hz, 3 H, H5), 5.52 (s, 5 H, C_5H_5), 5.46 (s, 5 H, C_5H_5). − $C_{19}H_{18}O_4W_2$ (678.05): calcd. C 33.66, H 2.68; found C 33.4, H 2.8.

3. *Photochemical Reactions of* **1** *with 1-Butene* (**C**): According to Procedure 1, 1.6 g (2.5 mmol) of **1** and 1-butene (**C**) were irradiated in 750 ml of ether/THF (6:1) for 90 min with UV light. Column chromatography on Al_2O_3 yielded four characterised products.

1st Fraction (pentane/ether 3:1): Yellow zone, very small amount of substance, discarded.

2nd Fraction (pentane/ether 3:1): Starting material **1**.

3rd Fraction (pentane/ether 3:1): Orange solution; after removal of the solvent, a mixture of **1** and (μ-$\eta^{2:2}$-acetylene)(η^2-1-butene)-tricarbonylbis(η^5-cyclopentadienyl)ditungsten(*W*−*W*) (**2C**) was isolated as orange powder (5%). Even by repeated chromatography, **2C** could not be isolated in pure form. − IR: $\tilde{\nu}$ = 1965 (m), 1921 (s), 1834 (m) cm^{-1}. − ^1H NMR (C_7D_8, 233 K): C_4H_8: δ = 0.96 (dd, *J* = 9.5, 2.5 Hz, 1 H, H1 *E*), 1.75 (dd, *J* = 11.0, 2.5 Hz, 1 H, H1 *Z*), 2.29 (m, *J* = 11.0, 9.5, 4.0 Hz, 1 H, H2), 1.20 (m, *J* = 14.0, 7.0 Hz, 1 H, H3), 2.02 (m, *J* = 14.0, 7.0, 4.0 Hz, 1 H, H3′), 1.41 (t, *J* = 7.0 Hz, 3 H, H4); C_2H_2: δ = 2.33 (d, *J* = 2.0 Hz, 1 H, H1), 4.06 (d, *J* = 2.0 Hz,1 H, H2); 4.96 (s, 5 H, C_5H_5), 4.90 (s, 5 H, C_5H_5).

4th Fraction (pentane/ether 2:1): Red solution, after removal of the solvent tricarbonylbis(η^5-cyclopentadienyl)(η^4-3-methylene-1-pentene)ditungsten(*W*−*W*) (**5C**) was obtained as red, crystalline powder (5%). − IR: $\tilde{\nu}$ = 1900 (s), 1806 (m), 1551 (m) cm^{-1}. − ^1H NMR ($CDCl_3$, 253 K): δ = 2.60 (d, *J* = 4.0 Hz, 1 H, H1 *E*), 1.39 (d, *J* = 4.0 Hz, 1 H, H1 *Z*); 2-C_2H_5: δ = 0.89 (m, *J* = 7.0 Hz, 2 H), 0.99 (t, *J* = 7.0 Hz, 3 H); δ = 4.85 (dd, *J* = 7.0, 7.0 Hz, 1 H, H3), 2.42 (dd, *J* = 7.0, 2.5 Hz, 1 H, H4 *E*), 1.58 (dd, *J* = 7.0, 2.5 Hz, 1 H, H4 *Z*), 5.39 (s, 5 H, C_5H_5), 5.08 (s, 5 H, C_5H_5). − $C_{19}H_{20}O_3W_2$ (664.07): calcd. C 34.37, H 3.04; found C 34.5, H 3.2.

5th Fraction (ether): Yellow-orange solution, from which after removal of the solvent tricarbonylbis(η^5-cyclopentadienyl)(μ-hydrido)(μ-$\eta^{1:4}$-3-methylene-1-penten-1-yl)ditungsten(*W*−*W*) (**3C**) results as an orange powder (6%). − IR: $\tilde{\nu}$ = 1924 (sh), 1909 (s), 1830 (s) (υCO); 1961 (w) (υMH) cm^{-1}. − ^1H NMR ($CDCl_3$, 243 K): δ = 4.43 (d, *J* = 6.0 Hz, 1 H, H1), 4.06 (d, *J* = 6.0 Hz, 1 H, H2); 3-C_2H_5: δ = 1.84 (dq, *J* = 16.0, 7.0 Hz, 1 H), 1.72 (dq, *J* = 16.0, 7.0 Hz, 1 H), 1.24 (t, *J* = 7.0 Hz, 3 H); δ = 1.87 (d, *J* = 2.0 Hz, 1 H, H4 *E*), 1.53 (d, *J* = 2.0 Hz, 1 H, H4 *Z*), 5.44 (s, 5 H, C_5H_5), 5.09 (s, 5 H, C_5H_5), −17.37 [s, $^1J(^{183}W-^1H)$ = 47, 53 Hz, 1 H, W−H]. − $C_{19}H_{20}O_3W_2$ (664.07): calcd. C 34.37, H 3.04; found C 34.7, H 3.0.

6th Fraction (pentane/THF 1:1): From the red solution tetracarbonylbis(η^5-cyclopentadienyl)(μ-$\eta^{1:3}$-2-hexene-1,1-diyl)-ditungsten(*W*−*W*) (**4C**) was obtained after recrystallisation in form of red crystals (1%). − IR: $\tilde{\nu}$ = 1945 (vs), 1901 (s), 1842 (s), 1771 (m) cm^{-1}. − ^1H NMR ($CDCl_3$, 253 K): δ = 8.97 (d, *J* = 9.0 Hz, 1 H, H1), 5.90 (dd, *J* = 9.0, 9.0 Hz, 1 H, H2), 1.72 (m, *J* = 9.0, 3.5 Hz, 1 H, H3), 2.12 (m, *J* = 3.5 Hz, 1 H, H4), 1.45 (m, *J* = 7.0 Hz, 3 H, H5), 0.89 (t, *J* = 7.0 Hz, 3 H, H6), 5.35 (s, 5 H, C_5H_5), 5.23 (s, 5 H, C_5H_5).

4. *Photochemical Reactions of* **1** *with (E)-2-Butene* (**D**): According to Procedure 1, 1.6 g (2.5 mmol) of **1** and (*E*)-2-butene (**D**) were irradiated with UV light in 750 ml of ether/THF (6:1) for 85 min. The reaction mixture was separated into its components by column chromatography.

1st Fraction (pentane/ether, 3:1): Yellow zone of small intensity; after crystallisation of the residue from pentane, few yellow crystals of carbonyl(η^5-cyclopentadienyl)hydrido[η^4-(*E*)-3-methyl-1,3-pentadiene]tungsten (**6**, **6′**) were isolated (1%). − IR: $\tilde{\nu}$ = 1927 cm^{-1}. − ^1H NMR (CD_2Cl_2, 253 K): Major isomer (0.85): δ = −0.12 (dd, *J* = 9.0, 4.0 Hz, 1 H, H1 *Z*), 1.49 (ddd, *J* = 8.0, 4.0, 3.0 Hz, 1 H, H1 *E*), 4.07 (dd, *J* = 9.0, 8.0 Hz, 1 H, H2), 2.37 (s, 1 H, 3-CH_3), 0.42 (q, *J* = 6.0 Hz, 1 H, H4 *Z*), 1.91 (dd, *J* = 6.0, 1.0 Hz, 3 H, H5), 4.87 (s, 5 H, C_5H_5), −6.13 [dd, *J* = 3.0, 1.0, Hz, $^1J(^{183}W-^1H)$ = 74 Hz, 1 H, W−H); minor isomer (0.15): δ = −0.04 (dd, *J* = 7.0, 3.5 Hz, 1 H, H1 *Z*), 1.49 (ddd, *J* = 7.0, 3.5, 1.0 Hz, 1 H, H1 *E*), 4.44 (dd, *J* = 7.0, 7.0 Hz, 1 H, H2), 2.46 (s, 1 H, 3-CH_3), 0.70 (q, *J* = 6.0 Hz, 1 H, H4 *Z*), 1.41 (d, *J* = 6.0 Hz, 3 H, H5), 4.87 (s, 5 H, C_5H_5), −9.65 [d, *J* = 1.0, Hz, $^1J(^{183}W-^1H)$ = 76 Hz, 1 H, W−H).

2nd Fraction (pentane/ether 3:1): Starting material **1**.

3rd Fraction (pentane/ether, 2:1): Red-brown solution, already during removal of the solvent red-brown crystals of tricarbonylbis(η^5-cyclopentadienyl)[η^4-(*E*)-3-methyl-1,3-pentadiene]-ditungsten(*W*−*W*) (**5D**) precipitated (7%). − IR: $\tilde{\nu}$ = 1901 (s), 1810 (m), 1548 (m) cm^{-1}. − ^1H NMR (C_7D_8, 253 K): δ = 2.88 (dd, *J* = 7.0, 3.0 Hz, 1 H, H1 *E*), 1.55 (dd, *J* = 7.0, 3.0 Hz, 1 H, H1 *Z*), 4.81 (t, *J* = 7.0, 7.0 Hz, 1 H, H2), 1.23 (s, 3 H, 3-CH_3), 1.66 (q, *J* = 6.0 Hz, 1 H, H4 *Z*), 2.03 (d, *J* = 6.0 Hz, 3 H, H5), 5.08 (s, 5 H, C_5H_5), 4.79 (s, 5 H, C_5H_5). − $C_{19}H_{20}O_3W_2$ (664.07): calcd. C 34.37, H 3.04; found C 34.3, H 2.9.

4th Fraction (pentane/ether 2:1): Orange fraction, which yielded after removal of the solvent an orange mixture of **5D** and tricarbonylbis(η^5-cyclopentadienyl)(μ-hydrido)[μ-$\eta^{1:4}$-(*E*)-3-methyl-1,3-pentadien-1-yl]ditungsten(*W*−*W*) (**3D**) (5%). Even by repeated chromatography **3D** was not obtained in a pure state. − IR: $\tilde{\nu}$ = 1923 (s), 1902 (s), 1834 (s) cm^{-1}. − ^1H NMR ($CDCl_3$, 243 K): δ = 4.54 (dd, *J* = 6.5, 1.5 Hz, 1 H, H1), 3.93 (d, *J* = 6.5 Hz, 1 H, H2), 2.05 (s, 3 H, 3-CH_3), 2.26 (q, *J* = 6.5 Hz, 1 H, H4 *Z*), 1.37 (d, *J* = 6.5 Hz, 3 H, H5), 5.47 (s, 5 H, C_5H_5), 5.12 (s, 5 H, C_5H_5), −18.14 [d, *J* = 1.5 Hz, $^1J(^{183}W-^1H)$ = 47, 56 Hz, 1 H, W−H). − $C_{19}H_{20}O_3W_2$ (664.07): calcd. C 34.4, H 3.0; found C 34,6, H 2,8.

5th Fraction (pentane/THF 4:1): Bright-red zone, after recrystallisation red crystals of **4C** (1%).

5. *Photochemical Reactions of* **1** *with (Z)-2-Butene* (**E**): According to Procedure 1, 1.8 g (2.8 mmol) of **1** and (*Z*)-2-butene (**E**) were irradiated with UV light in 750 ml of ether/THF (6:1) for 300 min. The reaction mixture contained large amounts of insoluble decomposition products. It was filtered through compressed filter flakes and brought to dryness at 253 K.

1st Fraction (pentane/ether 3:1): Starting material **1**.

2nd Fraction (pentane/ether 3:1): Yellow-orange solution, discarded.

3rd Fraction (ether): Red-brown solution; after partial removal of the solvent and cooling to 198 K, red-brown crystals of pentacarbonyltris(η^5-cyclopentadienyl)(μ-$\eta^{1:2}$-vinyl)tritungsten-(*W*−*W*−*W*) (**7**) were formed (1%). − IR: $\tilde{\nu}$ = 1925 (sh), 1910 (vs), 1849 (s), 1840 (sh) cm^{-1}. − ^1H NMR ($CDCl_3$, 253 K): δ = 7.04 (dd, *J* = 11.0, 11.0 Hz, 1 H, H1), 4.72 (dd, *J* = 11.0, 1.0 Hz, 1 H, H2 *E*), 1.79 (dd, *J* = 11.0, 1.0 Hz, 1 H, H2 *Z*), 5.43 (s, 5 H, C_5H_5), 5.37 (s, 5 H, C_5H_5), 4.88 (s, 5 H, C_5H_5). − $C_{22}H_{18}O_5W_3$ (913.93): calcd. C 28.91, H 1.99; found C 30.3, H 2.4.

6. *X-ray Structural Analysis of* **5D**[44]: $C_{19}H_{20}O_3W_2$, *M* = 664.05 $g \cdot mol^{-1}$, monoclinic space group $P2_1/n$, *a* = 1089.3(2), *b* = 1240.5(3), *c* = 1303.7(2) pm, β = 95.914(14)°, *V* = 1.7522(6) nm^3, *Z* = 4, ρ(calcd.) = 2.517 $g \cdot cm^{-3}$. Crystal size 0.40 × 0.25 × 0.05 mm, *T* = 293 K. Using a CAD4 diffractometer (Enraf Nonius), radiation Mo-K_α, wavelength λ = 71.073 pm, scan type ω-$^1/_3$q, 4487 reflections were collected in the θ range 2.27−22.45°. After data reduction, 2267 symmetry-independent reflections (R_{int} = 0.0512) were obtained. The structure was solved by direct methods using SHELXS-86[45] and refined by full-matrix least-squares against F^2 with SHELXL-93[46]. 232 parameters were refined to $R[I > 2\sigma(I)]$ = 0.0281, *wR*2(all data) = 0.0750. The hydrogen atoms of the cyclopentadienyl ligands and the methyl groups were located geometrically. All the other hydrogen atoms were detected. For the refinement the C−H distance was set to 97 pm, and the tempera-

ture factors of the hydrogen atoms were fixed at 1.2 times U_{eq} of the corresponding carbon atoms.

7. *X-ray Structural Analysis of* **7**[44]: $C_{22}H_{18}O_5W_3$, M = 913.91 g·mol^{-1}, monoclinic space group $P2_1/n$, a = 780.61(7), b = 2197.1(3), c = 1403.80(11) pm, β = 100.753(6)°, V = 2.3654(4) nm^3, Z = 4, ρ(calcd.) = 2.566 g·cm^{-3}. Crystal size 0.62 × 0.30 × 0.03 mm, T = 293 K. Using a CAD4 diffractometer (Enraf Nonius), radiation Mo-K_α, wavelength λ = 71.073 pm, scan type ω-θ, 4426 reflections were collected in the θ range 1.74−24.99°. After data reduction, 3880 symmetry-independent reflections (R_{int} = 0.099) were obtained. The structure was solved by direct methods using SHELXS-86[45] and refined by full-matrix least squares against F^2 with SHELXL-93[46]. 280 parameters were refined to $R[I > 2\sigma(I)]$ = 0.0491, $wR2$(all data) = 0.1245. The hydrogen atoms of the cyclopentadienyl ligands were located geometrically. All the other hydrogen atoms were found. For the refinement the temperature factor of the hydrogen atoms was set to the 1.2-fold value of that of the related carbon atom. The data set was modified using PLATON-92[47] to account for a multiply disordered ether molecule on a centre of inversion.

☆ Dedicated to Professor Dr. *Gottfried Huttner* on the occasion of his 60th birthday.

[1] C. G. Kreiter, A. Georg, G. J. Reiß, *Chem. Ber.* **1997**, *130*, 1197.
[2] S. A. R. Knox, R. F. D. Stansfield, F. G. A. Stone, M. J. Winter, P. Woodward, *J. Chem. Soc., Chem. Commun.* **1978**, 221.
[3] S. A. R. Knox, R. F. D. Stansfield, F. G. A. Stone, M. J. Winter, P. Woodward, *J. Chem. Soc., Dalton Trans.* **1982**, 173.
[4] M. Green, P. A. Kale, R. J. Mercer, *J. Chem. Soc., Chem. Commun.* **1987**, 375.
[5] J. Klingler, W. Butler, M. D. Curtis, *J. Am. Chem. Soc. 1975*, *97*, 3535; **1978**, *100*, 5034.
[6] D. S. Ginley, C. R. Bock, M. S. Wrighton, *Inorg. Chim. Acta* **1977**, *23*, 85.
[7] R. Birdwhistell, P. Hackett, A. R. Manning, *J. Organomet. Chem.* **1978**, *157*, 239.
[8] M. A. Greaney, J. S. Merola, T. R. Halbert, *Organometallics* **1985**, *4*, 2057.
[9] W. I. Bailey, Jr., M. H. Chisholm, F. A. Cotton, L. A. Rankel, *J. Am. Chem. Soc.* **1978**, *100*, 5764.
[10] C. G. Kreiter, A. Würtz, P. Bell, *Chem. Ber.* **1992**, *125*, 377.
[11] C. G. Kreiter and U. Kern, *J. Organomet. Chem.* **1993**, *459*, 199.
[12] C. G. Kreiter, R. Meuser, W. Frank, S. Müller-Becker, *Acta Crystallogr., Sect. C* **1996**, *52*, 2701.
[13] C. G. Kreiter, G. Wendt, J. Kaub, *J. Organomet. Chem.* **1988**, *346*, 35.
[14] R. D. Adams, D. M. Colins, F. A. Cotton, *Inorg. Chem.* **1974**, *13*, 1086.
[15] C. G. Kreiter, *Adv. Organomet. Chem.* **1986**, *26*, 297.
[16] R. Colton, C. J. Commons, B. F. Hoskins, *J. Chem. Soc., Chem. Commun.* **1975**, 363.
[17] C. J. Commons, B. F. Hoskins, *Austr. J. Chem.* **1975**, *28*, 1663.
[18] C. G. Kreiter, G. Wendt, J. Kaub, *Chem. Ber.* **1989**, *122*, 215.
[19] A. A. Pasynskii, Yu. V. Skripkin, I. L. Eremenko, V. T. Kalinnikov, G. G. Aleksandrov, V. G. Andrianov, Yu. T. Struchkov, *J. Organomet. Chem.* **1979**, *165*, 49.
[20] P. T. Barger, J. E. Bercaw, *J. Organomet. Chem.* **1980**, *201*, C39.
[21] B. Longato, J. R. Norton, J. C. Huffmann, J. A. Marsella, K. G. Caulton, *J. Am. Chem. Soc.* **1981**, *103*, 209.
[22] G. M. Dawkins, M. Green, K. A. Mead, J.-Y. Salaün, F. G. A. Stone, P. Woodward, *J. Chem. Soc., Dalton Trans.* **1983**, 527.
[23] G. A. Carriedo, D. Hodgson, J. A. K. Howard, K. Marsden, F. G. A. Stone, M. J. Went, P. Woodward, *J. Chem. Soc., Chem. Commun.* **1982**, 1006.
[24] M. R. Awang, R. D. BarrM. Green, J. A. K. Howard, T. B. Marder, F. G. A. Stone, *J. Chem. Soc. Dalton Trans.* **1985**, 2009.
[25] M. H. Chisholm, F. A. Cotton, Extine, and B. R. Stults, *J. Am. Chem. Soc.* **1976**, *98*, 4477; **1976**, *98*, 4486.
[26] M. H. Chisholm, F. A. Cotton, M. Extine, M. Millar, B. R. Stults, *Inorg. Chem.* **1976**, *15*, 2244.
[27] M. H. Chisholm, F. A. Cotton, M. Extine, B. R. Stults, *Inorg. Chem.* **1976**, *15*, 2252; **1977**, *16*, 603.
[28] J. Potenza, P. Giordano, D. Mastropaolo, A. Efraty, *Inorg. Chem.* **1974**, *13*, 2540.
[29] M. D. Curtis, W. M. Butler, *J. Organomet. Chem.* **1978**, *155*, 131.
[30] J. W. Faller, D. F. Chodosh, D. Katahira, *J. Organomet. Chem.* **1980**, *187,* 227.
[31] C. G. Kreiter, K. H. Franzreb, W. Michels, U. Schubert, *Z. Naturforsch., B* **1985**, *40*, 1188.
[32] C. G. Kreiter, K. H. Franzreb, W. S. Sheldrick, *Z. Naturforsch., B* **1986**, *41*, 904.
[33] G. Wendt, Dissertation, Univ. Kaiserslautern, **1986**.
[34] G. C. Bruce, S. A. R. Knox, A. J. Phillips, *J. Chem. Soc., Chem. Commun.* **1990**, 716.
[35] A. F. Dyke, S. A. R. Knox, P. J. Naish, G. E. Taylor, *J. Chem. Soc., Chem. Commun.* **1980**, 803.
[36] P. Q. Adams, D. L. Davies, A. F. Dyke, S. A. R. Knox, K. A. Mead, P. Woodward, *J. Chem. Soc., Chem. Commun.* **1983**, 222.
[37] C. G. Kreiter, G. Wendt, J. Kaub, *J. Organomet. Chem.* **1988**, *352*, 307.
[38] M. D. Fryzuk, T. Jones, F. W. B. Einstein, *J. Chem. Soc., Chem. Commun.* **1984**, 1556.
[39] R. H. Hooker, K. A. Mahmoud, A. J. Rest, *J. Organomet. Chem.* **1983**, *254*, C25.
[40] G. K. Barker, W. E. Carroll, M. Green, A. J. Welch, *J. Chem. Soc., Chem. Commun.* **1980**, 1071.
[41] W. E. Carroll, M. Green, A. G. Orpen, C. J. Schaverien, I. D. Williams, A. J. Welch, *J. Chem. Soc., Dalton Trans.* **1986**, 1021.
[42] M. Green, A. G. Orpen, C. J. Schaverien, I. D. Williams, *J. Chem. Soc., Chem. Commun.* **1983**, 1399.
[43] M. Green, A. G. Orpen, C. J. Schaverien, I. D. Williams, *J. Chem. Soc., Dalton Trans.* **1987**, 1313.
[44] Crystallographic data (excluding structure factors) for the structures reported in this paper have been deposited with the Cambridge Crystallographic Data Centre as supplementary publication no. CCDC-100498. Copies of the data can be obtained free of charge on application to CCDC, 12 Union Road, Cambridge CB2 1EZ, UK (fax: int. code + (1223) 336-033, e-mail: deposit@ccdc.cam.ac.uk).
[45] G. M. Sheldrick, *SHELXS-86, Program for Crystal Structure Solution*, Universität Göttingen, **1986**.
[46] G. M. Sheldrick, *SHELXL-93, Program for Crystal Structure Refinement*, Universität Göttingen, **1993**.
[47] P. van der Sluis, A. L. Spek, *Acta Crystallogr., Sect. A* **1990**, *46*, 194.

[97148]

A Spectro- and Conductometric Study of the Reaction of Imidazoline-2-selone Derivatives with Bromine − Crystal Structure of 1,2-Bis(3-methyl-4-imidazolin-2-ylium dibromoselenanide)ethane

Francesco Bigoli[a], Paola Deplano[b], Francesco A. Devillanova[b], Vito Lippolis*[b], Maria Laura Mercuri*[b], Maria Angela Pellinghelli[a] and Emanuele F. Trogu[b]

Dipartimento di Chimica Generale ed Inorganica, Chimica Analitica, Chimica Fisica, Università degli Studi di Parma[a], Viale delle Scienze 78, I-43100 Parma, Italy

Dipartimento di Chimica e Tecnologie Inorganiche e Metallorganiche, Università degli Studi di Cagliari[b], Via Ospedale 72, I-09124 Cagliari, Italy
E-mail: mercuri@vaxca1.unica.it, lippolis@vaxca1.unica.it

Received June 23, 1997

Keywords: Bromine / Imidazoline-2-selone / Hypervalent Se compounds / Dications

The oxidative addition of Br_2 to the imidazoline-2-selone derivatives **1a**−**c** has been studied by spectrophotometric and conductometric techniques. The experimental results clearly indicate that this reaction involves the dications **2a**−**c**, containing an Se−Se bond, as intermediates in the formation of the hypervalent 10-Se-3 selenium compounds **3a**−**c** containing the Br−Se−Br group. The crystal structure of 1,2-bis(3-methyl-4-imidazolin-2-ylium dibromoselenanide)ethane (**3c**), a new stable hypervalent 10-Se-3 compound, is also reported.

Introduction

In recent years, a great deal of synthetic and structural characterization work has been carried out on the products of the reactions of the donors **1a**−**c**, containing the imidazoline-2-selone ring, with acceptors such as diiodine,[1] interhalogens (IBr and ICl)[2] and unsaturated polynitriles (TCNQ).[3]

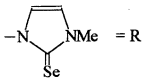

CH_3-R	(**1a**)
R-CH_2-R	(**1b**)
R-$(CH_2)_2$-R	(**1c**)

A variety of products has been obtained including neutral adducts, dications containing the Se−Se bridge, and hypervalent 10-Se-3[4] compounds containing the I−Se−I group.

While addition of I_2 to **1a** and **1c** quantitatively produces the I−Se−I insertion derivatives, the corresponding reaction of Br_2 with **1a** has recently been reported[5] to give the analogous Br−Se−Br insertion derivative **3a** with a 1:1 **1a**/Br_2 molar ratio and an ionic compound with a 1:0.5 **1a**/Br_2 molar ratio. This latter has been hypothesized to be 2,2′-diselenobis(1,3-dimethyl-4-imidazolinium) dibromide (**2a**) on the basis of previous studies carried out by Arduengo and Burgess[6] on the oxidative addition complexes of the sulfur analogue of **1a** with Br_2. However, we have previously obtained **2a** by reacting **1a** with IBr in a 1:1 molar ratio and have reported its structural characterization.[2] In order to ascertain whether **1b** and **1c** show the same behavior as **1a** in the reaction with bromine, and whether dications containing the Se−Se bridge are intermediates in the formation of the hypervalent compounds, a spectrophotometric and a conductometric study of this reaction has been undertaken. The X-ray crystal structure of 1,2-bis-(3-methyl-4-imidazolin-2-ylium dibromoselenanide)ethane (**3c**) is also reported.

Results and Discussion

Upon reaction of **1a**−**c** with 0.5 equiv. of molecular bromine in CH_3CN, ionic compounds consisting of dications containing the Se−Se bridge and Br^- counterions (**2a**−**c**) are obtained. When 1 equiv. of Br_2 per selenium atom is used, hypervalent selenium compounds featuring the Br−Se−Br group (**3a**−**c**) are produced.

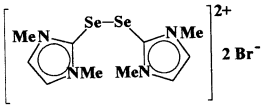

2a

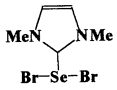

3a

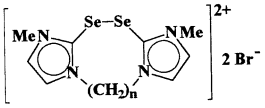

n=1 **2b**

n=2 **2c**

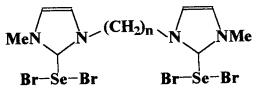

n=1 **3b**

n=2 **3c**

As mentioned above, we have previously obtained compound **2a** by the reaction of **1a** with IBr and have reported its X-ray structural characterization.[2] The crystal structure of **3a** was recently determined by Williams et al.[5] while this study was being carried out. The reported data are consistent with the crystal data of the sample isolated by us.

 © WILEY-VCH Verlag GmbH, D-69451 Weinheim, 1998 1434−1948/98/0101−0137 $ 17.50+.50/0

Single crystals suitable for X-ray studies have also been obtained for **3c**. The crystallographic data are given in Table 1, the geometrical parameters are listed in Table 2. The structural data of **3c** are in good agreement with those of the corresponding iodo derivative.[1][7][8] In fact, the molecule (Figure 1) shows a pseudo two-fold axis and a *gauche* conformation [N(11)−C(41)−C(42)−N(12) 59(1)°]; the Br−Se−Br fragments are asymmetric [Se(11)−Br(11) 2.662(2), Se(11)−Br(21) 2.521(2), Se(12)−Br(12) 2.650(3), Se(12)−Br(22) 2.531(4) Å], essentially linear [Br(11)−Se(11)−Br(21) 175.7(1)°, Br(12)−Se(12)−Br(22) 172.1(1)°], and roughly perpendicular to the corresponding imidazoline ring [the values of the Br−Se−C−N torsion angles are in the −101(1) to 78(1)° range]. The dihedral angle between the two imidazoline rings is 46.6(5)°. The Se atoms show a roughly square-planar coordination due to the very appreciable interactions Se(11)···Br(21) (x, $-y$, $z - 1/2$) 3.344(3) Å and Se(12)···Br(22) (x, $-y$, $1/2 + z$) 3.754(3) Å. These interactions are responsible for the formation of chains in the directions of c through the axial glide plane. The chains are held together by weak interactions of the type Br···C and C···C (Figure 2). The structure shows considerable similarities with those of **2a**[5] and $SeBr_2tmtu$[9].

Figure 1. ORTEP view of **3c**; thermal ellipsoids are drawn at a 30% probability level

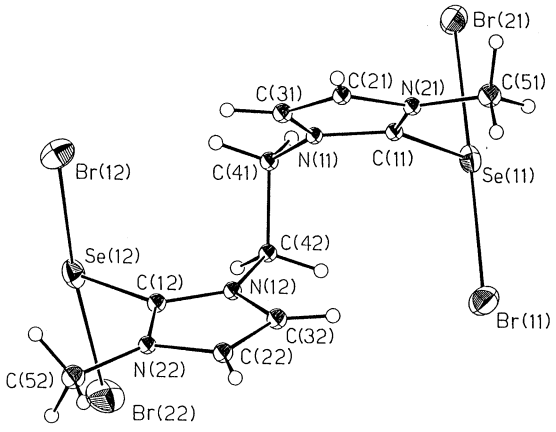

Figure 2. Projection of the structure of **3c** along [001]

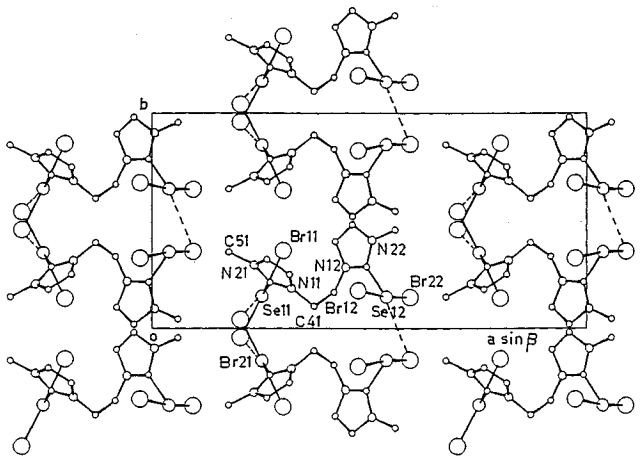

Table 1. Crystallographic data of **3c**: $C_{10}H_{14}Br_4N_4Se_2$

formula	$C_{10}H_{14}Br_4N_4Se_2$
molecular mass [g/mol]	667.78
crystal system	monoclinic
space group	*Cc*
a [Å]	21.399(5)
b [Å]	10.619(6)
c [Å]	8.090(7)
β [°]	90.72(2)
U [Å^3]	1838(2)
Z	4
d_c [g cm^{-3}]	2.413
diffractometer	Philips PW 1100
radiation	graphite-monochromated
wavelength	Mo-K_α (λ = 0.71073 Å)
F(000)	1240
T [K]	295
crystal size [mm]	0.11 × 0.56 × 0.62
μ [cm^{-1}]	127.13
scan mode	θ-2θ
scan speed [° min^{-1}]	3−9.6
scan width [°]	1.20 + 0.345 tan θ
θ range for intensity collection [°]	3−30
data collected	± *h*, *k*, *l*
no. of measured reflections	2844
no. of reflections with $I \geq 2\sigma(I)$	2090
no. of refined parameters	180
min./max. height in final Δρ map [eÅ^{-3}]	−0.51/1.70
$R = \Sigma\|(\Delta F)\|/\|\Sigma F_o\|$	0.0549
$wR = [\Sigma w(\Delta F)^2/\Sigma w F_o^2]^{1/2}$	0.0692
k, $g(w = k/[\sigma^2(F_o) + gF_o^2])$	1.5042, 0.001495

Table 2. Bond lengths [Å] and angles [°], with e.s.d.'s. in parentheses, of **3c**: $C_{10}H_{14}Br_4N_4Se_2$

bond lengths [Å]			
Se(11)−Br(11)	2.662(2)	N(21)−C(51)	1.45(2)
Se(11)−Br(21)	2.521(2)	N(12)−C(12)	1.30(2)
Se(11)−C(11)	1.95(1)	N(12)−C(32)	1.39(2)
Se(12)−Br(12)	2.650(3)	N(12)−C(42)	1.47(2)
Se(12)−Br(22)	2.531(4)	N(22)−C(12)	1.39(2)
Se(12)−C(12)	1.88(1)	N(22)−C(22)	1.40(2)
N(11)−C(11)	1.37(2)	N(22)−C(52)	1.45(2)
N(11)−C(31)	1.37(2)	C(21)−C(31)	1.34(2)
N(11)−C(41)	1.43(2)	C(41)−C(42)	1.56(2)
N(21)−C(11)	1.35(2)	C(22)−C(32)	1.34(2)
N(21)−C(21)	1.39(2)		
bond angles [°]			
Br(21)−Se(11)−C(11)	88.2(4)	C(22)−N(22)−C(52)	127.8(12)
Br(11)−Se(11)−C(11)	88.1(4)	C(12)−N(22)−C(52)	127.0(12)
Br(11)−Se(11)−Br(21)	175.7(1)	C(12)−N(22)−C(22)	105.1(10)
Br(22)−Se(12)−C(12)	88.8(4)	N(11)−C(11)−N(21)	107.2(11)
Br(12)−Se(12)−C(12)	83.3(4)	Se(11)−C(11)−N(21)	126.0(9)
Br(12)−Se(12)−Br(22)	172.1(1)	Se(11)−C(11)−N(11)	126.8(9)
C(31)−N(11)−C(41)	125.1(11)	N(21)−C(21)−C(31)	107.4(12)
C(11)−N(11)−C(41)	126.4(11)	N(11)−C(31)−C(21)	108.4(12)
C(11)−N(11)−C(31)	108.5(10)	N(11)−C(41)−C(42)	111.9(10)
C(21)−N(21)−C(51)	125.7(12)	N(12)−C(12)−N(22)	108.7(11)
C(11)−N(21)−C(51)	125.8(12)	Se(12)−C(12)−N(22)	124.5(8)
C(11)−N(21)−C(21)	108.4(10)	Se(12)−C(12)−N(12)	126.7(11)
C(32)−N(12)−C(42)	124.6(11)	N(22)−C(22)−C(32)	109.8(13)
C(12)−N(12)−C(42)	124.8(11)	N(12)−C(32)−C(22)	105.6(11)
C(12)−N(12)−C(32)	110.6(11)	N(12)−C(42)−C(41)	111.5(10)

In the low-frequency region, the FT-Raman spectra of **3a**−**c** each show two strong peaks at 187 ± 6 and 152 ± 6 cm^{-1}, attributable to υ_{as} and υ_s of the Br−Se−Br three-body system, respectively.[5][9][10] Similarities are also ob-

served in the FT-Raman spectra of **2a** and **2c**; thus, the peaks at 248 and 189 cm^{-1} for **2c** must be in part associated with the υ(Se−Se) vibration, in accordance with the findings for **2a** and other dications.[2] The FT-Raman spectrum of **2b** is more complicated and, in addition to the peaks at 250 and 187 cm^{-1} (the intensities of which are reversed compared to those found for **2a** and **2c**), shows one strong peak at 176 cm^{-1}. This spectrum could be explained by hypothesizing that in **2b** some dication units interact strongly with Br^- ions forming an Se−Se−Br three-body system, which could be vibrationally described as a Br_3^- unit. In fact, for an only slightly asymmetric Br_3^- anion, the symmetric stretching vibration υ_1 is found near 160 cm^{-1} and the antisymmetric υ_3 near 190 cm^{-1}.[10][11] From this, it follows that the peak at 176 cm^{-1} could be assigned to the υ_1 mode of the Se−Se−Br group, while the increased intensity of the peak at 187 cm^{-1} is most likely attributable to the contribution from the υ_3 antisymmetric vibration of the Se−Se−Br group.

In order to ascertain whether the aforementioned dications are intermediates in the formation of the hypervalent selenium compounds, we have investigated the oxidative addition of Br_2 in CH_3CN solution by UV/visible spectroscopy and conductometric measurements.

The addition of increasing amounts of Br_2 to CH_3CN solutions of **1a**, **1b** or **1c** produces a drastic change in the electronic spectra of the free ligands; the main features are similar in the three cases and, as shown in Figure 3a for **1c**, two well-defined isosbestic points are observed at 291 and 301 nm indicating an initial conversion of the free ligand into a new species up to a 1:1 **1c**/Br_2 molar ratio and subsequent transformation of this species once its formation is completed. A spectrum identical to that recorded for the 1:1 **1c**/Br_2 solution is obtained from a CH_3CN solution of **2c**; thus, the formation of the dication is unequivocally proven when working at this molar ratio. The dication undergoes a further transformation upon increasing the amount of bromine to a 1:2 **1c**/Br_2 molar ratio, leading to **3c** as shown by the UV/Visible spectrum of **3c** compared with that recorded on the 1:2 **1c**/Br_2 solution. The spectral features of **3a**−**c** are very similar to those of a tribromide due to the great similarity of the chromophores Br−Se−Br and $[Br-Br-Br]^-$.[12] In Figure 3b, a plot of the absorbance at 260 nm versus the **1c**/Br_2 molar ratio is depicted; it shows that the formation of **2c** and subsequently of **3c** is quantitative. A similar plot is observed for **1b**, whereas for **1a** less evident equivalence points at the 1:0.5 and 1:1 **1a**/Br_2 ratios might suggest that the formation of the dication and of the hypervalent compound are equilibrium reactions. In order to further support the hypothesis that dications **2a**−**c** are intermediates in the formation of the hypervalent compounds **3a**−**c**, another experiment was carried out in which increasing amounts of Br_2 were added to CH_3CN solutions of **2a**−**c**; the resulting UV/visible spectra indeed showed that the hypervalent compounds were formed.

The oxidative addition of bromine to **1a**−**c** has also been investigated by conductometric measurements. The conductivities of CH_3CN solutions of the free ligands were monitored during stepwise Br_2 addition. Figure 4 shows plots of the molar conductivities versus the Br_2/**L** molar ratios; formation of an ionic species is clearly evident from the increase in the conductivity values up to a 1:1 Br_2/**L** (1:0.5 for **1a**) molar ratio. This species disappears upon the addition of further Br_2 and conductivity reaches a minimum value at a 2:1 Br_2/**L** (1:1 for **1a**) molar ratio. The UV/visible spectra of the solutions at the 1:1 and 2:1 Br_2/**L** (**L** = **1b**, **1c**) molar ratios, respectively, showed the corresponding dications and hypervalent compounds to be the only species present. The conductometric titration of **1a**, on the other hand, indicates an equilibrium reaction between the three species **1a**, **2a** and **3a**, in line with the spectrophotometric evidence.

Figure 3. 3a: UV/Vis spectra at 293 K in a 0.1-cm silica cell of CH_3CN solutions containing fixed amounts of **1c** ([**1c**] = 2.5 × 10^{-4} mol l^{-1}) and variable Br_2 concentrations in the ratios: (a) 1:0; (b) 1:0.2; (c) 1:0.4; (d) 1:0.6; (e) 1:0.8; (f) 1:1; (g) 1:1.2; (h) 1:1.4; (i) 1:1.6; (l) 1:2. − 3b: Plot of the absorbances of the same CH_3CN solutions of **1c** and Br_2 as in (3a) versus [**1c**]/[Br_2] molar ratios at λ = 260 nm. The increase in absorbance over the 1:2 **1c**/Br_2 molar ratio could be attributed to the presence of Br_3^- in the Br_2 solution used for the titration. In fact, in Br_2 solutions with concentrations ranging from 1 × 10^{-3} to 2.5 × 10^{-3} mol l^{-1}, about 1−2% of Br_3^- is observed

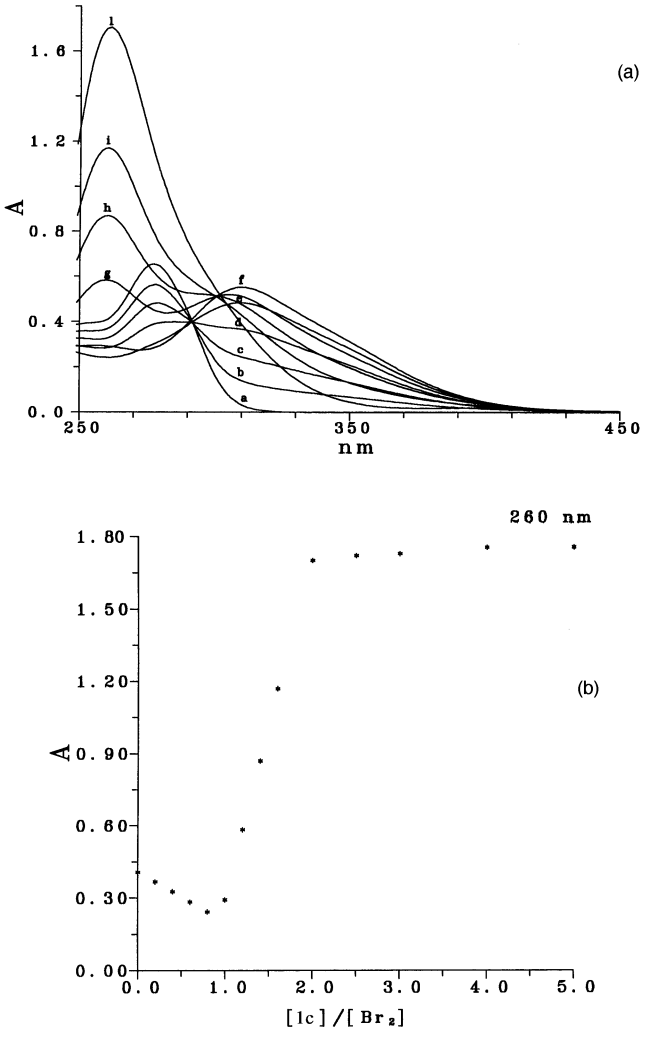

Figure 4. Plots of the molar conductivities recorded during the titrations of **1a**−**c** {[**1a**] = 2.16 × 10^{-3} mol l^{-1} (□); [**1b**] = 1.06 × 10^{-3} mol l^{-1}(○); [**1c**] = 1.99 × 10^{-4} mol l^{-1}(◆)} with Br_2 ([Br_2] = 9.61 × 10^{-3}; 1.04 × 10^{-2} ; 1.93 × 10^{-3} mol l^{-1} for **1a**−**c,** respectively) versus the [Br_2]/[L] molar ratios

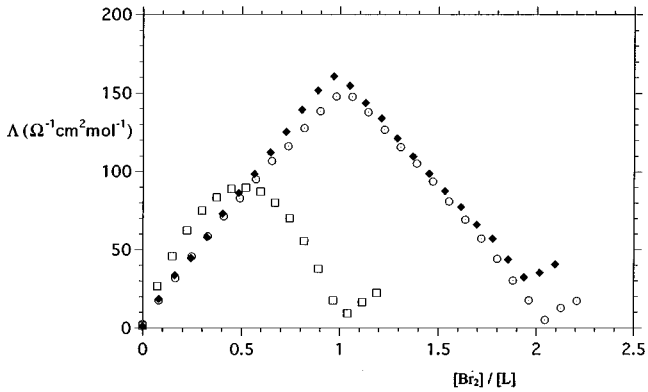

The observed reactions of **1a**−**c** with Br_2 are in good agreement with their electrochemical behavior. To confirm the tendency of the three ligands to undergo oxidation we also carried out an electrochemical study in CH_2Cl_2 solution (**2a**−**c** and **3a**−**c** are also obtained using CH_2Cl_2 as the solvent instead of CH_3CN; the electrochemical measurements were performed in CH_2Cl_2 for solubility reasons). In fact, cyclic voltammograms scanned in the anodic direction and reversed at +1.0 and −0.2 V to the starting potential (0.0 V), show two irreversible oxidations and one irreversible reduction for **1a** and **1c**, while only one broad oxidation peak and one reduction peak are observed for **1b** (see Table 3). When the scans are performed in the cathodic direction, the reduction peak does not appear for all ligands. This peak could therefore be attributed to the reduction of the oxidation products. The two oxidation peaks may be related to a two-step process involving the initial oxidation of one Se atom, which then interacts with either the unoxidized Se atom of the same molecule in the case of **1b** and **1c**, or with the Se atom of a different molecule in the case of **1a**. Subsequently, according to a simplified molecular orbital description for the Se−Se bond formation, this intermediate has one electron in the antibonding molecular orbital, which is removed in the second oxidation step to give the Se−Se dication.

Table 3. Anodic peak (*Epa*) and cathodic peak potentials (*Epc*) determined by cyclic voltammetry in CH_2Cl_2 for **1a**−**c** (1 × 10^{-3} mol l^{-1}). Pt electrode *vs.* SCE (saturated calomel electrode) in the presence of Bu_4NBF_4 (1 × 10^{-1} mol l^{-1}). Scan rate: 100 mV s^{-1}

L	Epa_1 (V)	Epa_2 (V)	*Epc* (V)[a]
1a	+0.57	+0.75	+0.08
1b	+0.60	+0.73	+0.24
1c	+0.50	+0.66	+0.04

[a] These peaks do not appear when scanning is started in the cathodic direction.

Conclusions

In this paper, we have reported the structure of the hypervalent Se compound obtained by oxidative addition of Br_2 to **1c** (**3c**). Hypervalent 10-Se-3 compounds of this type are quite uncommon, **3a**,[5] 1,3-diisopropyl-4,5-dimethyl-4-imidazolin-2-ylium diiodoselenanide[7] and the diiodoselenanides obtained from **1a** and **1c**[1] being the only such compounds structurally characterized to date. We have also demonstrated that the reactions of **1a**−**c** with bromine leading to the hypervalent compounds are two-step oxidation processes involving as intermediates the dications (**2a**−**c**), which contain Se−Se bridges. It is relevant that such dications are not formed in the reaction of **1a**−**c** with diiodine,[1] neither in solution nor in the solid state, whatever the molar ratio of reactants used. Only in the case of the reaction of diiodine with the saturated analogue of **1a**, i.e. *N*,*N*′-dimethylimidazolidine-2-selone, was formation of the corresponding dication observed; the solid product was found to be a mixed-valence compound containing equimolecular amounts of the CT complex and the dication having two triodides as counterions.[13] Finally, while **1a**−**c** show the same behavior in the reaction with bromine, the reaction with diiodine is more selective since different products are obtained from these rather similar donors.

The *Ministero della Università e Ricerca Scientifica e Tecnologica of Italy* (MURST 40%, Reattività e Catalisi) is acknowledged for support in this research.

Experimental Section

Materials: Reagents and solvents of reagent grade purity were used as received from Aldrich. The compounds **1a**−**c** were prepared as described previously.[1]

Compounds **2a**−**c** *and* **3a**−**c***:* The compounds **3a**−**c** were prepared by leaving to stand CH_3CN solutions of the ligands and Br_2 in a 1:1 (for **1a**) or 1:2 (for **1b** and **1c**) molar ratio at room temperature. After several days, well-shaped yellow-orange crystals of **3c** suitable for X-ray diffraction studies and yellow-orange crystals of **3a** and **3b** were obtained. Yields of each compound were typically 70%. The compounds **2a**−**c**, obtained as yellow microcrystals, were prepared analogously using a 1:0.5 (for **1a**, yields 88%) or 1:1 (for **1b** and **1c**, yields 90%) molar ratio. Elemental analysis data and FT-Raman spectra for **2a** and **3a** have been reported previously.[2]

2a: Electronic spectrum (250−550 nm): λ_{max} (ε) = 275 (22280), 312 nm (20480 l mol^{-1} cm^{-1}).

2b: $C_9H_{12}N_4Br_2Se_2$: calcd. C 21.88, H 2.45, N 11.34; found C 22.09, H 2.52, N 11.39. − Raman (500−50 cm^{-1}): $\tilde{\nu}$ = 290 (2.0), 250 (5.2), 218 (1.9), 187 (7.6), 176 (10), 135 (3.0), 128 (5.0), 92 (3.4), 74 (3.4). − Electronic spectrum (250−550 nm): λ_{max} (ε) = 292 nm (28200 l mol^{-1} cm^{-1}).

2c: $C_{10}H_{14}Br_2N_4Se_2$ × 0.5 CH_3CN: calcd. C 25.00, H 2.96, N 11.93; found C 25.19, H 3.15, N 12.06. − Raman (500−50 cm^{-1}): $\tilde{\nu}$ = 282 (1.0), 248 (10.0), 189 (1.3), 87 (1.1). − Electronic spectrum (250−550 nm): λ_{max} (ε) = 310 nm (19900 l mol^{-1} cm^{-1}).

3a: Electronic spectrum (250−550 nm): λ_{max} (ε) = 260 nm (32600 l mol^{-1} cm^{-1}).

3b: $C_9H_{12}Br_4N_4Se_2$: calcd. C 16.54, H 1.85, N 8.57; found C 16.77, H 1.90, N 8.64. − Raman (500−50 cm^{-1}): $\tilde{\nu}$ = 193 (10.0),

153 (7.5), 137 (3.0), 107 (2.8), 85 (2.7). − Electronic spectrum (250−550 nm): λ_{max} (ε) = 262 nm (58000 l mol^{-1} cm^{-1}).

3c: $C_{10}H_{14}Br_4N_4Se_2$: C 17.99, H 2.11, N 8.39; found C 18.11, H 2.17, N 9.26. − Raman (500−50 cm^{-1}): $\tilde{\nu}$ = 184 (10.0), 146 (9.4), 64 (2.5). − Electronic spectrum (250−550 nm): λ_{max} (ε) = 260 nm (56400 l mol^{-1} cm^{-1}).

X-ray Data Collection and Structure Refinement: Crystallographic data are given in Table 1. The diffraction measurements were made on a Philips PW 1100 diffractometer with graphite-monochromated Mo-K_α radiation (see Table 1); the data were collected using the θ−2θ scan technique. During the data reduction, intensities were corrected for Lorentz and polarization effects. A correction for absorption was applied: maximum and minimum values for the transmission factors were 1.000 and 0.514.[14][15] Solution by direct methods (SHELX-86),[16] full-matrix least-squares refinement, and anisotropic thermal parameters for all non-hydrogen atoms were used. The H-atoms were introduced in calculated positions and refined "riding" on the corresponding atoms with unique isotropic thermal parameters [U = 0.0725(166) Å^2]. The weighting scheme $w = k/[\sigma^2(F_o) + gF_o^2]$ was applied, with k = 1.5042 and g = 0.001495. Scattering factors were taken from ref.[17]. The final difference density map showed a minimum peak of −1.40 Å^{-3} and a maximum peak of 1.29 Å^{-3}. Structure refinement and final geometric calculations were carried out with the SHELX-76[18] and PARST[19] programs. The drawing was produced using ORTEP[20] and PLUTO.[21]

Spectroscopic Measurements. − FT-Raman Spectra: FT-Raman spectra (resolution ± 4 cm^{-1}) were recorded on a Bruker RFS100 FTR spectrometer fitted with an indium-gallium arsenide detector (room temp.) and operating with an excitation frequency of 1064 nm (Nd:YAG laser). The power level of the laser source was tuned between 20−40 mW. The solid samples, in the form of powders or crystals, were packed into suitable cells and then fitted into the compartment designed for use with a 180° scattering geometry. No sample decomposition was detected during the experiments. The values given in parentheses represent the intensities of the peaks relative to the strongest, which is given a value of 10.

UV/Visible Measurements: Electronic spectra were recorded of solutions in CH_3CN (freshly distilled from CaH_2) using a Cary 5 spectrophotometer equipped with a temperature probe accessory connected to a thermostatted multi-cell block. The CH_3CN solutions of Br_2 were standardized with a standard aqueous $Na_2S_2O_3$ solution (0.1000 mol l^{-1}) according to traditional methods.

1a: A set of 11 solutions containing a fixed concentration of the ligand (2.50 × 10^{-4} mol l^{-1}) and variable Br_2 concentrations ranging from 2.50 × 10^{-5} to 5.00 × 10^{-4} mol l^{-1} (in the ratios [**1a**]:[Br_2] = 1:0; 1:0.1; 1:0.2; 1:0.3; 1:0.4; 1:0.5; 1:0.6; 1:0.8; 1:1; 1:1.5; 1:2), was prepared. Spectra were recorded at T = 20°C, in the 250−550 nm range, using 0.1-cm path length silica cells.

1b: A set of 15 solutions containing a fixed concentration of the ligand (2.50 × 10^{-4} mol l^{-1}) and variable Br_2 concentrations ranging from 5 × 10^{-5} to 1.25 × 10^{-3} mol l^{-1} (in the ratios [**1b**]:[Br_2] = 1:0; 1:0.2; 1:0.4; 1:0.6; 1:0.8; 1:1; 1:1.2; 1:1.4; 1:1.6; 1:2; 1:2.4; 1:2.6; 1:3; 1:4; 1:5) was prepared. Spectra were recorded at T = 20°C in the 250−550 nm range using 1-cm path length silica cells.

1c: A set of 14 solutions containing a fixed concentration of the ligand (2.50 × 10^{-4} mol l^{-1}) and variable Br_2 concentrations ranging from 5.00 × 10^{-5} to 1.25 × 10^{-3} mol l^{-1} (in the ratios [**1c**]:[Br_2] = 1:0; 1:0.2; 1:0.4; 1:0.6; 1:0.8; 1:1; 1:1.2; 1:1.4; 1:1.6; 1:2; 1:2.5; 1:3; 1:4; 1:5), was prepared. Spectra were recorded at T = 20°C, in the 250−550 nm range, using 1-cm path length silica cells.

Conductiometric Titrations: Conductometric titrations were carried out at T = 25°C in a standard thermostatted cell using solutions in CH_3CN (freshly distilled from CaH_2), with a Model 120 microprocessor conductivity meter "Analytical Control". The k cell (1.23 cm^{-1}) was determined by measuring the conductivity of three solutions of kiln-dried (12 h) KCl (0.1, 0.01 and 0.001 mol l^{-1}, respectively) in doubly-distilled deionized water at T = 25°C. The conductivity values were corrected for the dilution error using the multiplicative factor $f = (V + V_o)/V_o$, where V_o is the starting volume (30 ml) of the **1a**, **1b** and **1c** solutions and V is the volume of the added Br_2 solution. Conductivity was recorded 5 minutes after each Br_2 addition in order to let the temperature equilibrate to 25°C.

Electrochemistry: Cyclic voltammetry experiments were performed using a conventional three-electrode cell, consisting of a Pt counter electrode and a Pt micro-working electrode *vs.* SCE (saturated calomel electrode). The experiments were performed at room temperature in anhydrous CH_2Cl_2. The solution was 1 × 10^{-3} mol l^{-1} in **L** (**1a, 1b, 1c**) with Bu_4NBF_4 (1 × 10^{-1} mol l^{-1}) as the supporting electrolyte. A stream of argon was passed through the solution prior to the scan. Data were recorded on a computer-controlled EG&G (Princeton Applied Research) potentiostat-galvanostat model 273 EG&G, using Model 270 electrochemical analysis software. The scan rate was 100 mV s^{-1}.

[1] F. Bigoli, P. Deplano, F. A. Devillanova, V. Lippolis, M. L. Mercuri, M. A. Pellinghelli, E. F. Trogu, *Gazz. Chim. Ital.* **1994**, *124*, 445−454.
[2] F. Bigoli, F. Demartin, P. Deplano, F. A. Devillanova, F. Isaia, V. Lippolis, M. L. Mercuri, M. A. Pellinghelli, E. F. Trogu, *Inorg. Chem.* **1996**, *35*, 3194−3201.
[3] F. Bigoli, P. Deplano, F. A. Devillanova, A. Girlando, V. Lippolis, M. L. Mercuri, M. A. Pellinghelli, E. F. Trogu, *Inorg. Chem.* **1996**, *35*, 5403−5406.
[4] 10-Se-3 means that 10 electrons are formally associated with Se, to which 3 ligands are bonded: C. W. Perkins, J. C. Martin, A. J. Arduengo, W. Lau, A. Alegrie, J. K. Kochi, *J. Am. Chem. Soc.* **1980**, *102*, 7753−7759.
[5] D. J. Williams, private communications.
[6] A. J. Arduengo, E. M. Burgess, *J. Am. Chem. Soc.* **1977**, *99*, 2376−2378.
[7] N. Kuhn, T. Kratz, G. Henkel, *Chem. Ber.* **1994**, *127*, 849−851.
[8] W.-W. du Mont, *Main Group Chemistry News* **1994**, *2*, 18−26.
[9] K. J. Wynne, P. S. Pearson, M. J. Newton, J. Golen, *Inorg. Chem.* **1976**, *15*, 1449−1451.
[10] M. Bodelsen, G. Borch, P. Klaeboe, P. H. Nielsen, *Acta Chem. Scand.* **1980**, *A34*, 125−139.
[11] W. Gabes, D. J. Stufkens, H. Gerding, *J. Mol. Struct.* **1973**, *17*, 329−340.
[12] A. I. Popov, R. F. Swensen, *J. Am. Chem. Soc.* **1955**, *77*, 3724−2726.
[13] F. Demartin, F. A. Devillanova, F. Isaia, V. Lippolis, G. Verani, *Inorg. Chim. Acta* **1997**, *255*, 203−205.
[14] N. Walker, D. Stuart, *Acta Crystallogr., Sect. A* **1983**, *39*, 158−166.
[15] F. Ugozzoli, *Comput. Chem.* **1987**, *11*, 109−120.
[16] G. M. Sheldrick, *SHELXS-86: Program for the Solution of Crystal Structures*, Universität Göttingen, Germany, **1986**.
[17] *International Tables for X-ray Crystallography*; vol. IV, Kynoch Press, Birmingham, U.K., **1974**, *149*, 99−102.
[18] G. M. Sheldrick, *SHELX-76: Program for Crystal Structure Determination*, University of Cambridge, U.K., **1976**.
[19] M. Nardelli, *Comput. Chem.* **1983**, *7*, 95−98.
[20] C. K. Johnson, *ORTEP, Report ORNL-3794*, revised, Oak Ridge National Laboratory, Tennessee, **1965**.
[21] W. D. S. Motherwell, PLUTO, University of Cambridge, U.K., **1976**.

[97152]

Five- and Six-Coordinate Nitrogen in Azaborane Clusters

Peter Paetzold

Institut für Anorganische Chemie, Technische Hochschule Aachen,
D-52056 Aachen, Germany
Fax: (internat.) + 49(0)241/888-8288
E-mail: peter.paetzold@ac.rwth-aachen.de

Received October 7, 1997

Keywords: Azaboranes / Six-coordinate nitrogen / Deltahedral clusters / Cluster opening / Cluster closure

In the majority of known azaboranes $N_aB_bH_c$ and their derivatives, the coordination number of the nitrogen atoms within the cluster does not exceed the classical values of 3 or 4. In the azaboranes *closo*-NB_9H_{10}, *nido*-$NB_{10}H_{13}$, and *closo*-$NB_{11}H_{12}$ and in their derivatives, however, the nitrogen atoms are 5- or 6-coordinate and thus represent a novel bonding situation. The synthesis, structure, and reactivity of these azaboranes are reviewed in this article.

Introduction

Azaboranes $N_aB_bH_c$ are closed deltahedral borane clusters or fragments thereof, in which at least one BH vertex is replaced by an NH vertex. Azaborates are the corresponding anions $[N_aB_bH_c]^{n-}$. Derivatives of azaboranes are formed by the addition of Lewis bases L to give $N_aB_bH_cL_d$ or by the substitution of hydrogen atoms by anionic groups X to give $N_aB_bH_cX_d$ (X = F, OR, NR_2, R etc.). Heteroazaboranes $S_aN_bC_cB_dH_eM_f$ are those azaboranes in which BH vertices have been replaced by S, CH, M etc.; the symbol M in this context means the fragment of a transition-metal complex with the metal atom being incorporated into the cluster skeleton.

If the bonding within borane clusters is described in terms of localized bonds, then electron deficiency makes it necessary to take skeletal three-centre, two-electron [(3c,2e)] bonds into account in addition to the more usual two-centre, two-electron [(2c,2e)] bonds. The skeletal coordination number, called *connectivity* (c), may exceed the value $c = 3$; this value would allow a skeletal atom to form four traditional (2c,2e) bonds, including one radial (2c,2e) bond between the skeletal atom and its *exo* ligand. Values of $c = 3-5$ are usually encountered in borane clusters, and $c = 6$ is found in a few cases. With $c > 3$, (2c,2e) bonds are no longer sufficient for the description of bonds. It may be de-

Figure 1. Localized bonds for a skeletal atom A with different connectivities of A

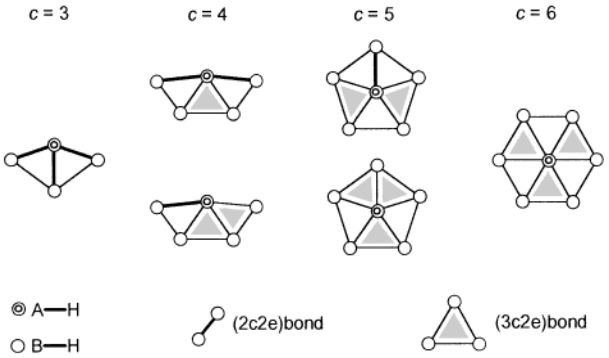

Peter Paetzold, born in 1935, received his doctoral degree on his work with Egon Wiberg at the Ludwig-Maximilians-Universität in Munich in 1961. He became Professor of inorganic chemistry and Director of the Institut für Anorganische Chemie at the Rheinisch-Westfälische Technische Hochschule in Aachen in 1968. He focused his interest on synthetic, structural and mechanistic aspects of boron chemistry. Due to his work, major progress was achieved in the chemistry of azidoboranes (the analogues of carbonic azides), iminoboranes (the analogues of alkynes, presenting a BN triple bond), boron-nitrogen ring compounds (the analogues of cyclobutadiene, benzene, Dewar benzene, and cyclooctatetraene), azadiboriridines (the analogues of cyclopropenyl cations, presenting a BB bond of unexpected basicity), and azaborane clusters (the analogues of dicarbaborane clusters, presenting five- and six-coordinate nitrogen). The analogy of the couples BN and CC, also of the couples BO and CN, is the common thread running through his work.

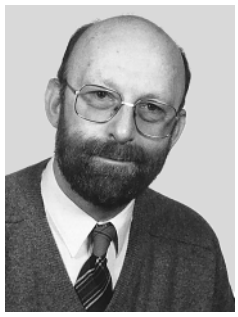

MICROREVIEWS: This feature introduces the readers to the authors' research through a concise overview of the selected topic. Reference to important work from others in the field is included.

 © WILEY-VCH Verlag GmbH, D-69451 Weinheim, 1998 1434–1948/98/0202–0143 $ 17.50+.50/0

Table 1. Formal charge $\delta_F(A)$ of skeletal atoms A = B, C, N, depending on the number t of (3c,2e) and y of (2c,2e) bonds at A (see Figure 1)

c	3	4	4	5	5	6
t/y	0/3	1/2	2/1	2/1	3/0	3/0
$\delta_F(B)$	−3/3	−2/3	−1/3	−1/3	0	0
$\delta_F(C)$	0	+1/3	+2/3	+2/3	+3/3	+3/3
$\delta_F(N)$	+3/3	+4/3	+5/3	+5/3	+6/3	+6/3

duced from Figure 1 that for c = 4−6 at least one, two or three (3c,2e) bonds are necessarily present, respectively, provided the atom A obeys to the octet rule. (Note that connectivities c = 3−6 correspond to overall coordination numbers of 4−7 by inclusion of the *exo* ligand.)

The discovery in 1963 that carbon atoms within the icosahedral C_2B_{10} skeleton of the carbaborane $C_2B_{10}H_{12}$[1] exhibited a connectivity c = 5 (coordination number = 6) changed the traditional view of the bonding situation of

Figure 2. Azaboranes and azaheteroboranes with a nitrogen connectivity of 2 or 3 (read BR instead of BH in **1−6**)

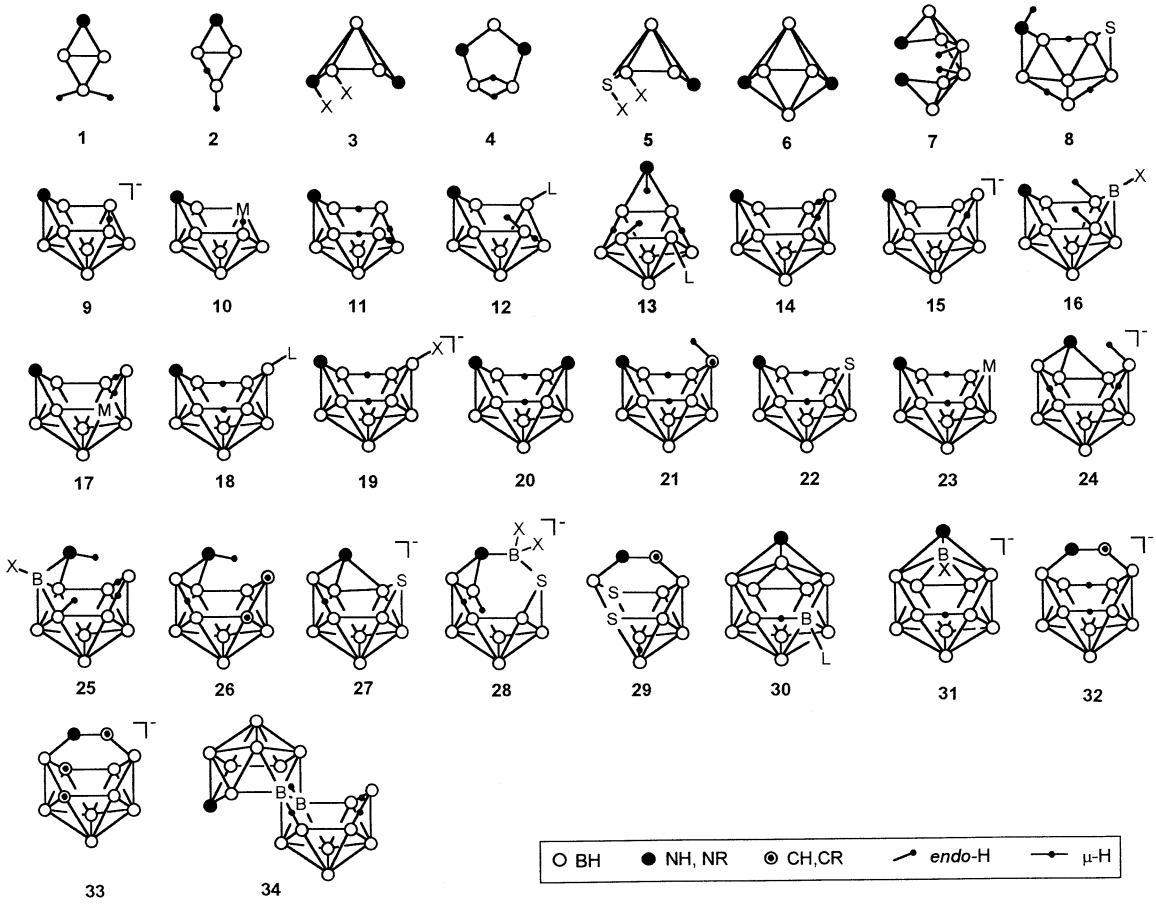

Table 2. Azaboranes and azaheteroboranes with nitrogen connectivity of 2 or 3

Vertices	Type	Skeletal atoms	Number in Figure 2
4	*nido*	NB_3	**1**[5][6] **2**[6]
5	*arachno*	N_2B_3 SNB_3	**3**[6] **4**[7] **5**[8]
6	*nido*	N_2B_4	**6**[9][10]
8	*arachno*	N_2B_6	**7**[11]
8	*hypho*	SNB_6	**8**[12]
9	*nido*	NB_8 NB_7M	**9**[13] **10**[14]
9	*arachno*	NB_8	**11**[15] **12**[13][16]
9	*hypho*	NB_8	**13**[17]
10	*nido*	NB_9 NB_8M	**14**[13][18][19][20][21][22] **15**[23] **16**[23] **17**[24]
10	*arachno*	NB_9 N_2B_8 NCB_8 SNB_8 NB_8M	**18**[21][25][26] **19**[25] **20**[27] **21**[28] **22**[12] **23**[24]
11	*arachno*	NB_{10} NC_2B_8 SNB_9	**24**[20][29][30] **25**[31] **26**[2][32][33] **27**[30]
11	*hypho*	SNB_9 S_2NCB_7	**28**[30] **29**[34]
12	*nido*	NB_{11}	**30**[35] **31**[35][36]
12	*arachno*	NCB_{10} NC_3B_8	**32**[37] **33**[37]
18	*nido*	NB_{17}	**34**[38]

carbon-containing molecules. Whereas the formal charge of boron changes from −1 to the more favourable value of 0 as a result of an increase in its connectivity (Table 1), the formal charge of carbon may become +1 with a connectivity of $c = 6$ or even $c = 5$. Since carbon is more electronegative than boron and its real charge is less positive than that of boron, the B−C skeletal bonds must be highly polarized, and actually the border case $c = 6$ is not observed for carbon. Indeed, there is a strong tendency in the reactions of icosahedral carbaboranes to reduce the connectivity of carbon. The more electronegative nitrogen shows a formal charge of at least +4/3 or +5/3, when incorporated into a cluster skeleton with $c = 4$ or 5, respectively. Hence, a very large bond polarisation must be expected in corresponding azaboranes. Nevertheless, the carbaborane $NC_2B_8H_{11}$ with $c(N) = 4$ was synthesized as early as 1974[2], followed in 1986 by the closed cluster molecule NB_9H_{10}[3], and finally, the icosahedral cluster molecule $NB_{11}H_{12}$ in 1991. The discovery of $NB_{11}H_{12}$, which is isoelectronic with $C_2B_{10}H_{12}$, represented the first observation of the connectivity $c(N) = 5$[4]. Certainly, the reactivity of the highly coordinated azaboranes is governed by their tendency to reduce the connectivity at nitrogen.

A great number of small azaboranes and heteroazaboranes clusters with $c(N) = 2$ and larger ones with $c = 3$ are known. The skeletal nitrogen atoms in these azaboranes are bonded in a way that may be interpreted only in terms of (2c,2e) bonds. A survey is given in Figure 2 and Table 2. In terms of Wade′s rules, *nido*, *arachno*, and *hypho* clusters are present, although no *closo* species are found. Note that the same structural pattern, an icosahedral fragment, holds for all the molecules and anions **11**−**34**. Note also that in cases of $c(N) = 2$ (**1**−**5**, **7, 8, 13**, **29**, **32**, **33**) π bonds need to be taken into account in order to provide the nitrogen atom with an electron octet.

A much smaller number of azaboranes and heteroazaboranes with $c(N) = 4$, 5 have been described; Table 3 and Figure 3 present a synopsis. All these clusters are derived from three parent azaboranes, all of which are well-characterized: *closo*-NB_9H_{10} (**35**), *nido*-$NB_{10}H_{13}$ (**38**), and *closo*-$NB_{11}H_{12}$ (**43**). It is intended here to review the synthesis, structure, and reactivity of these azaboranes with 5- and 6-coordinate nitrogen centres. Part of this chemistry has already been reviewed[50][51][52][53]. We start with a section about synthetic procedures that still includes all of the azaboranes.

Synthesis

The commercially available decaborane, $B_{10}H_{14}$, is the starting material for the synthesis of the azaboranes **8**−**45**, presented in this section. The synthesis of the azaboranes **1**−**7**, which starts from the azadiboriridine NB_2R_3 or from iminoboranes RB(NR′), will not be discussed here. There are three synthetic possibilities that include a change of skeletal atoms: the addition (*insertion*) or the removal (*degradation*) of a skeletal atom or both (*degradative insertion*). In addition, there are two possibilities that involve a change only in the skeletal *arrangement*, and which go hand in hand with a transformation in the direction *arachno* → *nido* → *closo* (*closure*) or vice versa (*opening*). Changes in the ligand sphere or in the hydrogen bridge area (e.g. deprotonations) are not considered in this section.

Figure 3. Azaboranes and azaheteroboranes with nitrogen of connectivity 4 or 5

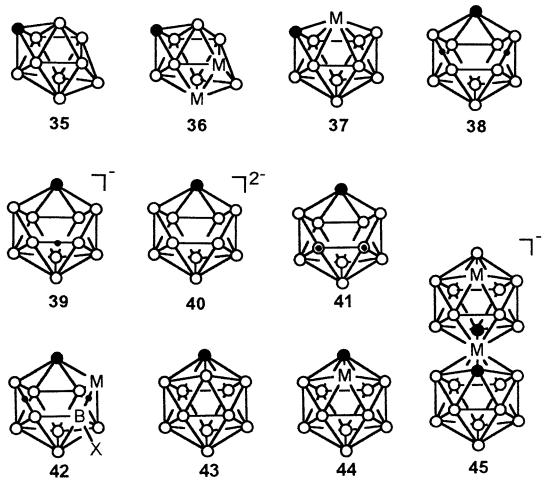

Table 3. Azaboranes and azaheteroboranes with nitrogen connectivity of 4 or 5

Vertices	Type	Skeletal atoms	Number in Figure 3
10	*closo*	NB_9 NB_7M_2	**35**[3][13][39] **36**[40]
11	*closo*	NB_9M	**37**[19][41]
11	*nido*	NB_{10} NC_2B_8 NB_9M	**38**[31][42] **39**[43][44] **40**[43][44] **41**[2][32][33][45] **42**[46]
12	*closo*	NB_{11} $NB_{10}M$	**43**[4][21][36][47][48][49] **44**[43][44] **45**[44]

Insertion

We describe here the insertion of sulphur S (into azaboranes), nitrenes NH or NR (into boranes), metal-complex fragments M (into azaboranes), and borylenes BH (into azaboranes). The insertion of elemental sulphur transforms the *nido* anion **15** into the *arachno* anion **27**, the sulphur atom contributing four electrons to the cluster [Eq. (1)]. The anion **15** is easily available from RNB_9H_{11} (**14**) by applying the base 1,8-bis(dimethylamino)naphthalene (*proton sponge*)[30].

$$[RNB_9H_{10}]^- + 1/8\ S_8 \rightarrow [S(RN)B_9H_{10}]^- \quad (1)$$

The insertion of a nitrene unit NR into a B_9 skeleton can be achieved by first transforming $B_9H_{13}(SMe_2)$ into $B_9H_{13}(NH_2R)$ followed by a dehydrogenation in boiling xylene to give products of type **14** [Eq. (2)][13][21]. [Note the identity of the structures **14** given in Eq. (2) and in Figure 2].

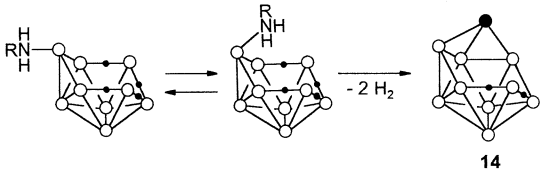

(2)

The insertion of a unit NH (from HN_3) into $B_{10}H_{12}L_2$ (L = SMe_2) to give **25** with a bridging NH_2 group [*c*(N) = 2] is accompanied by an H/N_3 ligand exchange [Eq. (3)][31].

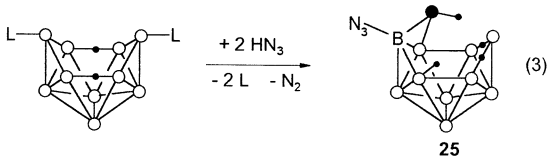

(3)

25

The reaction of CB_8H_{14} first with $NaNO_2$ and then with hydrochloric acid yields NCB_8H_{13} (**21**); the stoichiometry of this insertion of an NH vertex is unknown[28]. The insertion of metal cations into azaboranes, on the other hand, follows a clear cut stoichiometry. The 10-vertex *nido* species NB_9H_{12} (**14**) is transformed into an 11-vertex species either of the *closo* type [**37**; M = CpCo[19], (cymene)Ru[41]; Eq. (4)] or the *nido* type (**42**; X = Cl, M = Cp*Ir[46]). The 11-vertex *nido* species $[NB_{10}H_{12}]^-$ (**39**) and $[NB_{10}H_{11}]^{2-}$ (**40**) are transformed into the 12-vertex *closo* species $NB_{10}H_{11}M$ [**44**; M = $(Ph_3P)_2HRh$[43], $(C_6Me_6)Ru$, $(Ph_3P)_2Ni$[44]; Eqs. (5), (6)] or $[M(NB_{10}H_{11})_2]^-$ (**45**; M = Co[44]). The *arachno* 9-vertex species NB_8H_{13} (**11**), finally, gives the *nido* species $NB_8H_{11}M$ [**23**; M = $(Me_2PhP)_2Pt$[24]; Eq. (7)].

$$NB_9H_{12} + 1/2\ [(C_{10}H_{14})RuCl_2]_2 \rightarrow NB_9H_{10}[Ru(C_{10}H_{14})] + 2\ HCl \quad (4)$$

$$[NB_{10}H_{12}]^- + (Ph_3P)_3RhCl \rightarrow NB_{10}H_{11}[RhH(PPh_3)_2] + PPh_3 + Cl^- \quad (5)$$

$$[NB_{10}H_{11}]^{2-} + 1/2\ [(C_6Me_6)RuCl_2]_2 \rightarrow NB_{10}H_{11}[Ru(C_6Me_6)] + 2\ Cl^- \quad (6)$$

$$NB_8H_{13} + [(PhMe_2P)_2PtCl_2] \rightarrow NB_8H_{11}[Pt(PMe_2Ph)_2] + 2\ HCl \quad (7)$$

The insertion of a BH unit into azaboranes plays an important role in the synthesis of the icosahedral species $NB_{11}H_{12}$ (**43**). It is possible to start from the *nido* clusters $NB_{10}H_{13}$ (**38**) or NB_9H_{12} (**14**) and insert one or two BH units, respectively [Eq. (8)[4] and (9)[48]]. The thermal dehydrogenation (140°C) of **38** or **14** in the presence of BH_3 yields the *closo* anion $[NB_{11}H_{11}]^-$, either directly [Eq. (8)[4]] or via *closo*-$(Me_2SBH_2)NB_{11}H_{11}$ [Eq. (9)[48]; the anion can then easily be protonated to give **43**.

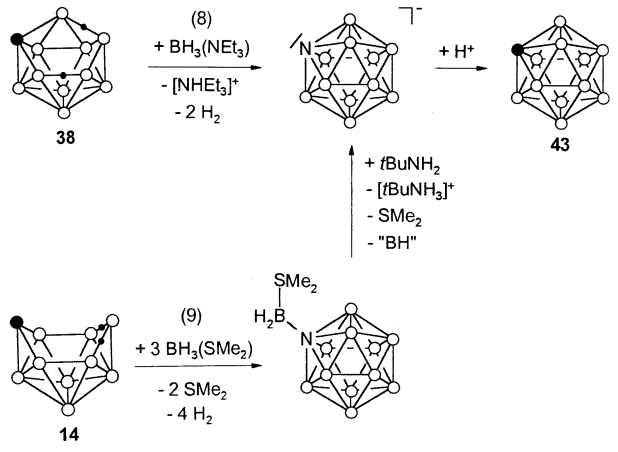

The synthesis of the *N*-organo *closo* 12-vertex derivative $RNB_{11}H_{11}$ can be achieved in one step from RNB_9H_{11} (**14**) [Eq. (10)][21].

$$RNB_9H_{11} + 2\ BH_3(SMe_2) \rightarrow RNB_{11}H_{11} + 2\ SMe_2 + 3\ H_2 \quad (10)$$

The insertion of a molecule BH_3 without loss of H_2 should transform a *nido* into an *arachno* species, exemplified by the formation of the anion **24** from the anion **15** [Eq. (11)][29][30].

$$[RNB_9H_{10}]^- + BH_3(thf) \rightarrow [RNB_{10}H_{13}]^- + thf \quad (11)$$

Both a carbyne unit and a nitrene unit are inserted when nitriles R′CN are added to the anions $[B_{10}H_{13}]^-$ or $[C_2B_8H_{11}]^-$ to give the 12-vertex *arachno* clusters $[N(R'C)B_{10}H_{13}]^-$ (**32**) and $[NC_2(R'C)B_8H_{11}]^-$ (**33**), respectively[37].

Degradation

The *nido* cluster NB_9H_{12} (**14**) is sensitive towards protic agents. One boron atom is removed by the attack of water in the presence of an acid to give *arachno*-NB_8H_{13} (**11**) [Eq. (12)][15].

$$NB_9H_{12} + 3\ H_2O \rightarrow NB_8H_{13} + B(OH)_3 + H_2 \quad (12)$$

One boron vertex is removed from *closo*-RNB_9H_9 and recovered in the borazine $(HBNR')_3$, when primary amines are applied, either according to Eq. (13) in polar THF or according to Eq. (14) in less polar, noncoordinating dichloromethane giving the *nido* anion **9** or the *arachno* species **12**, respectively[13].

$$RNB_9H_9 + 2\ R'NH_2 \rightarrow [R'NH_3][RNB_8H_9] + 1/3\ (HBNR')_3 \quad (13)$$

$$RNB_9H_9 + 2\ R'NH_2 \rightarrow RNB_8H_{10}(NH_2R') + 1/3\ (HBNR')_3 \quad (14)$$

The elimination of a BH_3 unit from the anions $[NB_{10}H_{14}]^-$ and $[NB_{10}H_{13}(N_3)]^-$ (**24**) on protonation may be accompanied by a cluster closure and is therefore mentioned in a later section.

Degradative Insertion

The first production of an azaborane with *c*(N) = 3 dates back to 1967, when two products, including the *arachno* cluster **19** (X = H)[25], were isolated from the reaction of decaborane and a thionitrosyl amine [Eq. (15)]. The fate of the expelled B atom is not known.

$$B_{10}H_{14}/Me_2NNS \rightarrow [SB_{10}H_{11}]^-/[(Me_2N)NB_9H_{12}]^- \quad (15)$$

Going from thionitrosyl to nitrosyl made a series of azaboranes available by the application of $NaNO_2$ in acidic media[54]. The transformation of the carbaborate $[C_2B_9H_{12}]^-$ into a mixture of $NC_2B_8H_{13}$ (**26**) and $NC_2B_8H_{11}$ (**41**) marked the starting point for this method in 1974[2], followed by the synthesis of NB_9H_{12} (**14**) in 1975;

the workup can be done with conc. H_2SO_4 [Eq. (16)][15] or with iodine, giving a 57% yield[19].

$$B_{10}H_{14}/NaNO_2/H_2SO_4 \rightarrow NB_9H_{12} \quad (16)$$

The diazaborane $N_2B_8H_{12}$ (**20**) can be prepared from NB_9H_{12} (**14**) by the same method. More stoichiometric clarity is achieved when the ionic nitrite is replaced by alkylnitrites [Eq. (17)][39]. The expelled boron vertex is then identified as trialkoxyborane.

$$B_{10}H_{14} + 3\ EtONO \rightarrow NB_9H_{12} + B(OEt)_3 + H_2 + NO + NO_2 \quad (17)$$

The thiaborane SB_9H_{11} was transformed by the action of BuONO into a mixture of SNB_6H_{11} (**8**) and SNB_8H_{11} (**22**)[12], and $B_{18}H_{22}$ into $NB_{17}H_{20}$ (**34**)[38].

We formally consider the nitrogen atoms of bridging amino groups to be skeletal atoms with $c = 2$ throughout this review article; the alternative position would be to view such groups as having the same functionality as two skeletal ligands, one of which contributes one and the other two electrons. The very first synthetic route to a larger azaborane was by the degradative insertion of an NHEt vertex by reacting $B_9H_{13}(SEt_2)$ with NH_2Et. The *hypho* cluster **13** (L = NH_2Et) was synthesized by this method in 1962[55] and was structurally identified in 1963[17]. The expelled boron vertex was presumably incorporated into a borazine [Eq. (18)].

$$B_9H_{13}(SEt_2) + 3\ NH_2Et \rightarrow (EtHN)B_8H_{11}(NH_2Et) + SEt_2 + 2\ H_2 + 1/3\ (HBNEt)_3 \quad (18)$$

The 10% yield of NB_7H_9M [**10**; M = $Ir(PMe_3)_3$] from the action of N_2H_4 on $B_8H_{12}M'$ [M′ = $Ir(CO)(PMe_3)_2$] is formally the result of a degradative insertion[14].

A metal rather than a nitrogen vertex may be inserted under expulsion of a boron vertex. For example, $NB_8H_{11}M$ [**17**; M = $(C_6Me_6)Ru$] may be formed from NB_9H_{12} (**14**) and $[MCl_2]_2$[24] and azadirhoda-*closo*-decaborane **36** (M = Cp*Rh) from the *hypho*-borane **13** and $[MCl_2]_2$ [Eq. (19)][40].

$$(EtHN)B_8H_{11}(NH_2Et) + [Cp^*RhCl_2]_2 + 4\ NaH \rightarrow (EtN)B_7H_7(RhCp^*)_2 + BH_3(NH_2Et) + 4\ NaCl + 3\ H_2 \quad (19)$$

Closure

Thermal dehydrogenation of *nido*-NB_9H_{12} at 375−400°C makes *closo*-NB_9H_{10} available [Eq. (20)][3], and the dehydrogenation of RNB_9H_{11} follows the same pattern to give RNB_9H_9[13].

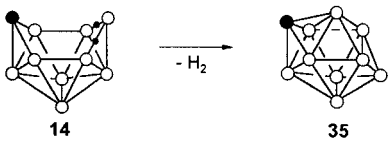

(20)

The *arachno* species $NB_{10}H_{14}(N_3)$ (**25**) undergoes an elimination of HN_3 in boiling xylene to give the *nido* cluster **38** [Eq. (21)]; the degradation product **14**, however, is the predominant product component [Eq. (22)][31]. Upon protolysis, the 11-vertex *arachno* anions of type **24,** $[RNB_{10}H_{13}]^-$ [from **15** by the insertion of BH_3, Eq. (11)] or $[NB_{10}H_{13}(N_3)]^-$ (from **25** by deprotonation[20]), are also predominantly degraded to give products of type **14** [Eq. (23)][20][29][30]; in the case of $[NB_{10}H_{14}]^-$, the *nido* species **38** is the concurrent closure product [Eq. 24)][29]. The deprotonation of **25**, according to Eq. (25)[20], represents a closure process that transforms one *arachno* structure (**25**) into another (**24**). Note that the skeleton of **24** can formally be derived from the corresponding *nido* skeleton of **30** or **31** by the removal of a vertex with $c = 4$, thus increasing the pentagonal aperture of **30** and **31** by one vertex; a vertex of $c = 5$ needs to be removed in order to transform **30** or **31** formally into **25** with a heptagonal aperture.

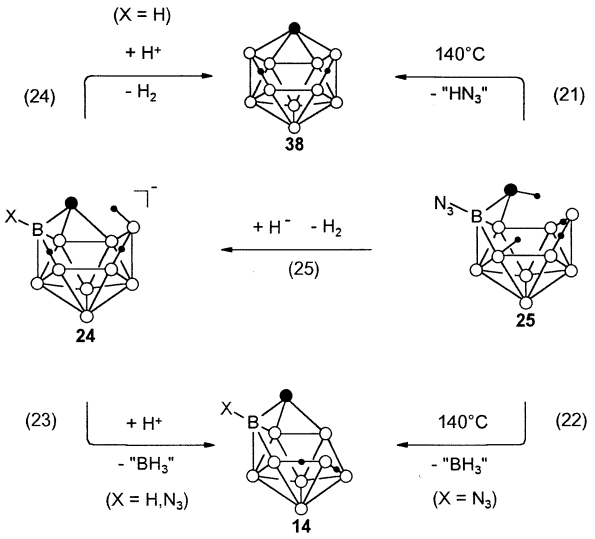

Opening

The opening of the *closo* species RNB_9H_9 (**35**) and $RNB_{11}H_{11}$ (**43**) by protic agents HX, neutral bases L, or anionic bases X^- gives *nido* products of the type $RNB_9H_{10}X$ (**16**), $RNB_{11}H_{11}L$ (**30**), or $[RNB_{11}H_{11}X]^-$ (**31**), respectively, as discussed in a later section. The *nido* clusters RNB_9H_{11} (**14**) are transformed into the *arachno* clusters $RNB_9H_{11}L$ (**18**) by the addition of Lewis bases L; the term "opening" has only an electronic meaning in this case, since the topology of the 10-vertex cluster skeleton is the same for *nido* and *arachno* species.

Structure

The geometry of the parent aza-*closo*-boranes NB_9H_{10} (**35**) and $NB_{11}H_{12}$ (**43**) have been determined from Hartree-Fock SCF calculations with 3-21G an 6-31G* basis sets as well as from X-ray (**35**) and electron diffraction work (**43**) (Table 4). The structures represent a C_{4v} distorted bicapped tetragonal antiprism and a C_{5v} distorted icosahedron, respectively, as expected from Wade′s cluster rules. We denote the three types of symmetrically equivalent boron atoms as *ortho*, *meta*, and *para* with respect to their distance from the nitrogen vertex. Typically, the nitrogen vertex of

NB_9H_{10} is in one of the two capping positions with $c = 4$. The highly symmetric structures, calculated for NB_9H_{10} and $NB_{11}H_{12}$ and observed for $NB_{11}H_{12}$ in the gas phase, are also present in solution, according to NMR data; they are slightly distorted in crystalline NB_9H_{10} and in two crystalline derivatives of $NB_{11}H_{12}$ (Table 4). Although the skeletal distances of the free molecules are in general longer than those in the crystal, the sequence is the same when going through the five zones of equivalent distances for C_{4v} or C_{5v} symmetry. The BN bonds, the shortest in both *closo* clusters, are distinctly shorter in the NB_9 than in the NB_{11} skeleton, a phenomenon that is apparently related to the different connectivity of the nitrogen atom. A smaller effect of the same type and origin is observed for the boron atoms in the *antipodal* position, i.e. the apex opposite to the nitrogen atom.

A typical feature of both polyhedra is the short distance between the nitrogen atom and the polyhedral centre, if compared to the boron atoms. The penetration of the nitrogen atom into the cluster widens the B−B distances in the upper pyramidal basis making them the largest in the skeleton. In addition, the four (five) B−H bonds in the upper pyramidal basis are shifted away from the radial direction towards the nitrogen atom, thereby shielding it considerably.

six-coordinated nitrogen atoms ($c = 5$) into the skeletons of the *closo* 12-vertex species.

Although the formal charge of the nitrogen atom is highly positive, the real atomic charge is expected to be most negative at the electronegative nitrogen atom of NB_9H_{10} or $NB_{11}H_{12}$, whereas the most positive positions should be the nitrogen-bound hydrogen atom and the boron atoms adjacent to the nitrogen atom (*ortho* position, *o*-B). This is confirmed by ab initio calculations of the atomic charges, which are quantitatively different depending on whether calculated according to the methods of either Mulliken or Löwdin (Table 5). Qualitatively, however, the results of the two calculations are in accord and indicate that the boron atoms in the *meta* position (*m*-B) are the most negatively charged ones, the antipodal boron atoms (*para* position, *p*-B) range between *o*-B and *m*-B, and the least positively charged hydrogen atoms are the antipodal ones. The large calculated dipole moments of ca. 5.1 (**35**) and 4.6 D (**43**) are oriented with their positives ends towards the negatively charged nitrogen atoms, demonstrating that all the 20 (24) atoms and particularly the hydrogen atoms on the symmetry axis contribute to the dipole moment.

The sequence $m > p > o$ for the charge densities at the boron atoms (Table 5) does not parallel the ^{11}B-NMR chemical shifts, which form a series $m > o > p$ with decreas-

Table 4. Calculated and experimental distances in *closo*-NB_9 and -NB_{11} skeletons[a]

	NB_9H_{10} calcd.[56][57]	NB_9H_{10} X-ray[39]	$NB_{11}H_{12}$ calcd.[56]	$NB_{11}H_{12}$ GED[47]	$RNB_{11}H_{11}$[b] X-ray[21]	$NB_{11}H_{10}Y$[c] X-ray[48]
Upper pyramid (B−N)	157.7	152	171.0	171.6(9)	171.9	172.2
Upper pyramidal basis	187.4	181	182.1	182.5(6)	179.6	179.7
Antiprismatic zone	180.6	175	176.7	179.1(5)	174.5	175.2
Lower pyramidal basis	186.9	177	180.8	179.1(5)	177.3	178.3
Lower pyramid	171.1	163	179.8	179.1(5)	177.0	178.1

[a]Average of four (five) slightly different values in the four pyramidal zones and of eight (ten) values in the antiprismatic zone in the NB_9 (NB_{11}) skeleton in the case of crystal data − [b] R = $PhCH_2$ − [c] Group Y represents a $-BH_2-NEt-CH_2-CH_2-$ chain, bridging N and B2

The structures of the azametalla-*closo*-boranes $NB_7H_8(RhCp^*)_2$ (**36**)[40], $NB_{10}H_{11}[RhH(PPh_3)_2]$[43], and $NB_{10}H_{11}[Ru(C_6Me_6)]$ (**44**)[44] have also been investigated in the crystalline phase and represent typical 10- or 12-vertex *closo* structures, respectively.

The azametallaboranes **37**, $NB_9H_{10}(CoCp^*)$[19] and $NB_9H_{10}[Ru(cymene)]$[41], represent the rare case of a 11-vertex *closo* species for which the structure has been confirmed. Typically, the metal atom is in the unique position with $c = 6$; this position is unfavourable for boron and impossible for nitrogen.

The *nido* 11-vertex molecules $RNB_{10}H_{12}$ (R = $NB_2Ht Bu_3$; **38**), $NC_2B_8H_{11}$ (**41**), and $NB_9H_{11}Cl(IrCp^*)$ (**42**) can be described as the expected icosahedral fragment structures with a pentagonal aperture, which is confirmed by crystal structure analysis[42][45][46].

There is no doubt that five-coordinated nitrogen atoms ($c = 4$) are incorporated into the borane cluster skeletons of the *closo* 10-, *closo* 11- and *nido* 11-vertex species and

ing field [in CD_2Cl_2, standard $BF_3(OEt_2)$]: −21.7, −5.6, 62.4 (NB_9H_{10})[39] and −11.9, −9.8, 2.7 ($NB_{11}H_{12}$)][4]. The downfield shift of *p*-B, particularly with NB_9H_{10}, is called the *antipodal effect*. It has been compared to the corresponding antipodal effect exhibited by the isoelectronic species XB_9H_9 and $XB_{11}H_{11}$ with X = AlH^{2-}, BH^{2-}, CH^-, S etc. The antipodal effect for NB_9H_{10} has been described as greatly influenced by the paramagnetic part of the chemical shielding; the HOMO−LUMO energy difference is also an important factor, as are the tangential p_x, p_y orbitals at the *p*-B atom, which are called *NMR-active*[57][58][59]. Since precise calculated geometrical data are available, computational methods such as IGLO allow the calculation of ^{11}B-NMR data which are in good accord with experimental results[47].

An analysis of the charge distribution in clusters should provide an understanding of which vertices will be attacked by electrophiles and which by nucleophiles. The products of ligand substitution, opening, and even degradation reac-

Table 5. Mulliken (a) and Löwdin (b) atomic charges of NB_9H_{10} and $NB_{11}H_{12}$[56]

		N	*o*-B	*m*-B	*p*-B	1-H	*o*-H	*m*-H	*p*-H
NB_9H_{10}	(a)	−1.073	0.184	−0.068	0.092	0.434	0.000	0.027	−0.024
	(b)	−0.234	0.062	−0.135	−0.077	0.291	0.030	0.040	0.031
$NB_{11}H_{12}$	(a)	−1.065	0.097	−0.054	0.009	0.443	0.037	0.037	0.029
	(b)	−0.222	0.027	−0.123	−0.078	0.295	0.040	0.048	0.038

tions may be predicted, provided that the first step of the reaction determines the products and that the ground-state polarities determine the transition state of that first step. In the case of NB_9H_{10} and $NB_{11}H_{12}$, one would expect nucleophiles to attack the *ortho* position and electrophiles the *meta* position. Such an expectation is met for nucleophiles, which exclusively attack at the *ortho* belt, whereas electrophiles attack either in the *para* or in the *meta*, but never in the *ortho* position (see following sections).

The binding electrons in closed boranes are delocalized over the whole skeleton in a way that is strongly suggestive of the π electrons in benzene-type molecules, and closed boranes have therefore been denoted as aromatic systems. In this context, azaboranes may be compared to pyridine. In the old-fashioned valence-bond description of benzene, the delocalization of the π electrons is achieved by introducing resonance between structures built up by localized (2c, 2e) π bonds. Such a procedure can also be applied to boranes, where the resonating structures are built up by localized (2c,2e) and (3c,2e) bonds[60]. The icosahedral dodecaborate $[B_{12}H_{12}]^{2-}$ is given as an example. This anion may be built up by y (2c,2e) bonds and t (3c,2e) bonds. The 24 atoms contribute 60 valence orbitals and 50 valence electrons. From the balances $60 = 3t + 2y$ and $50 = 2t + 2y$, we find $y = 15$ and $t = 10$. There are twelve B−H (2c,2e) bonds leaving three (2c,2e) and ten (3c,2e) bonds to build up the cluster skeleton. Four resonance structures of different energy can be constructed (Figure 4). Each of the structures **A** and **B** of C_1 symmetry is related to 120 degenerate resonance structures, the structure **C** (C_3 symmetry) allows 40 and the structure **D** (C_{3v} symmetry) 20 degenerate structures, which altogether sum up to 300 resonating structures. (Note that the number of degenerate structures is equal to the ratio of the order of the group I_h to the order of the corresponding subgroup.) The number of structures would be increased if we allowed those which (a) contain also open instead of only closed (3c,2e) bonds, (b) contain edges without bonding interaction, (c) contain vertices not obeying the octet rule. In going from $[B_{12}H_{12}]^{2-}$ to the isoelectronic $NB_{11}H_{12}$ the degeneracy decreases and structures in which the nitrogen atom adopts one of the (2c,2e) bonds become favourable.

Figure 4. Resonance formulae **A**−**D** of $[B_{12}H_{12}]^{2-}$, front and rear side of the icosahedral structure being shown for each

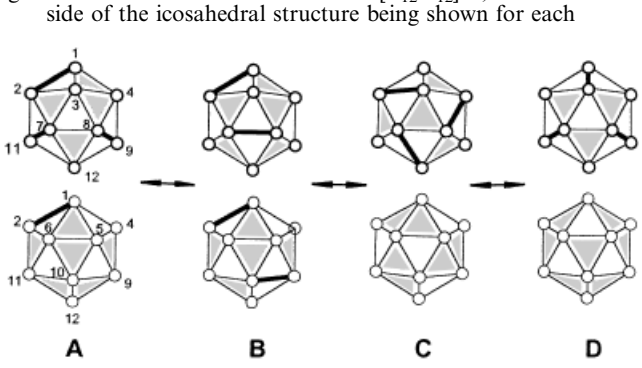

Reactivity

Little is known about the reactivity of the azametalla-*closo*-boranes with either an NB_7M_2 (**36**), NB_9M (**37**), or $NB_{10}M$ skeleton (**44**, **45**). The same is true for the reactivity of the *nido* 11-vertex clusters $NC_2B_8H_{11}$ (**41**) and $NB_9H_{11}ClM$ (**42**). More is known about the reactivity of *closo*-NB_9H_{10} (**35**), *closo*-$NB_{11}H_{12}$ (**43**), and *nido*-$NB_{10}H_{13}$ (**38**).

Redox Reactions

The *N*-alkyl derivatives RNB_9H_9 and $RNB_{11}H_{11}$ are stable towards iodine and bromine, even if dissolved in liquid bromine[49]. A mixture of $RNB_{11}H_{11}$ and liquid chlorine may be kept for a while at low temperature, but can undergo a spontaneous violent reaction. No doubt BN, $BHal_3$ and HHal are the thermodynamically stable products from a mixture of $NB_{11}H_{12}$ and excess Hal_2, but such a mixture is more or less metastable. Strong reduction agents like alkali metals do not react with $RNB_{11}H_{11}$.

Brønsted Acid/Base Reactions

The skeleton of the *closo* species RNB_9H_9 and $RNB_{11}H_{11}$ is stable if dissolved in strong acids such as triflic acid F_3CSO_3H[49]; a proton/proton exchange cannot be excluded, however. The nitrogen-bound protons of the parent molecules NB_9H_{10} and $NB_{11}H_{12}$ can be easily removed by bases, in the case of $NB_{11}H_{12}$ even with the weak base NEt_3, to give the anions $[NB_9H_9]^-$ and $[NB_{11}H_{11}]^-$. These anions can easily be alkylated by RI and RO_3SCF_3, respectively, if R represents an α-unbranched alkyl group[3][21][36]; bulky alkyl and aryl groups R cannot be fixed to the nitrogen atom of the anions, but such derivatives RNB_9H_9 and $RNB_{11}H_{11}$ are available from RNB_9H_{11} by either dehydrogenation [Eq. (20)] or insertion of two BH units [Eq. (10)], respectively.

The *nido* cluster $NB_{10}H_{13}$ (**38**) can be deprotonated once or twice by hydride bases, depending on the stoichiometric amount of base. The protons are removed from the bridging positions, not from the NH group. The corresponding anions $[NB_{10}H_{12}]^-$ (**39**) and $[NB_{10}H_{11}]^{2-}$ (**40**) are isoelectronic with the anions $[C_2B_9H_{12}]^-$ and $[C_2B_9H_{11}]^{2-}$ and, like these, they offer a pentagonal open face which is isolobal with $C_5H_5^-$ and is ready, therefore, to form pentahapto bonds with transition-metal species M^{2+}. A third proton cannot be removed from $[NB_{10}H_{11}]^{2-}$. Interestingly, the *nido*-azadicarbaborane $NC_2B_8H_{11}$ (**41**) which is isoelectronic with $NB_{10}H_{13}$ can be deprotonated at the nitrogen atom, since bridging hydrogen atoms are absent; applying K_2CO_3 and MeI consecutively gives the corresponding *N*-

methyl derivative[32][45]. Nevertheless, the terminal nitrogen atom and not one of the bridging protons becomes active when $NB_{10}H_{13}$ is added to the azadiboriridine NB_2tBu_3 to yield $(NB_2HtBu_3)NB_{10}H_{12}$[42].

Electrophilic Substitution

The *closo* clusters RNB_9H_9 (R = *p*-ClC_6H_4) and $RNB_{11}H_{11}$ (R = Me) react neither with triflic acid (as mentioned above) nor with methyl triflate. A mixture of one of the clusters, with methyl triflate as the solvent and triflic acid as a catalyst, however, results in a five- and six-fold methylation after four hours [Eqs. (26), (27)][49].

$$NB_9H_9 + 5\ MeOTrf \rightarrow RNBH_4Me_5 + 5\ HOTrf \quad (26)$$

$$RNB_{11}H_{11} + 6\ MeOTrf \rightarrow RNB_{11}H_5Me_6 + 6\ HOTrf \quad (27)$$

As expected from the cluster charge distribution, the *ortho* positions remain unattacked by the electrophile, whereas the *meta* and *para* positions are completely substituted. The same procedure transforms the *ortho*-dicarbaborane $C_2B_{10}H_{12}$ into $C_2B_{10}H_2Me_{10}$; all boron vertices in this product carry methyl groups, even those adjacent to carbon[61]. If the methylation of the aza-*closo*-boranes is prolonged by 16 hours, one of the methyl groups in each of the products is replaced by a triflate group [Eqs. (28), (29)].

$$RNB_9H_4Me_5 + HOTrf \rightarrow RNB_9H_4Me_4(OTrf) + CH_4 \quad (28)$$

$$RNB_{11}H_5Me_6 + HOTrf \rightarrow RNB_{11}H_5Me_5(OTrf) + CH_4 \quad (29)$$

The triflate group is fixed to a *meta* position in the 10-vertex product, but to a *para* position in the icosahedral species. An electrocyclic mechanism via a six-membered cyclic transition state has been proposed for the reactions (28) and (29)[49].

Although *ortho*-alkyl derivatives of NB_9H_{10} are not available by electrophilic alkylation, they are available, if one starts from $NB_9H_{11}R$ with the group R in the 9 position. The thermal dehydrogenation yields NB_9H_9R with R in *ortho* position [Eq. (30)]. The starting material can be synthesized from NB_9H_{12} and the corresponding alkenes by hydroboration[22]. As expected, the 9-alkyl derivative $PhNB_9H_{10}R$ gives the *meta*-alkyl derivative $PhNB_{11}H_{10}R$ on ring closure with $BH_3(SMe_2)$ [Eq. (31)][30].

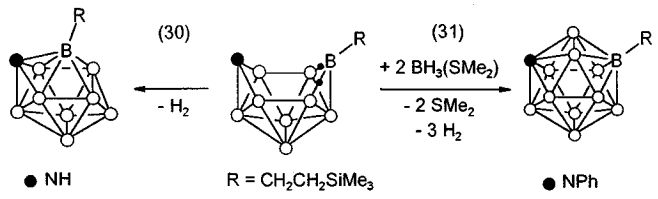

A singular alkylation at the *ortho* belt of the closed NB_{11} skeleton is observed when the synthesis of $NB_{11}H_{12}$ from NB_9H_{12} is performed with $BH_3(NEt_3)$ instead of $BH_3(SMe_2)$, according to Eq. (9). At 200 °C the product, expected from Eq. (9), is apparently not stable, and undergoes a further dehydrogenation; a B−C bond is formed from a CH_3 and a BH moiety [Eq. (32)][48]. An intermolecular dehydrogenation of this type has never been observed; the loss in entropy would be too great.

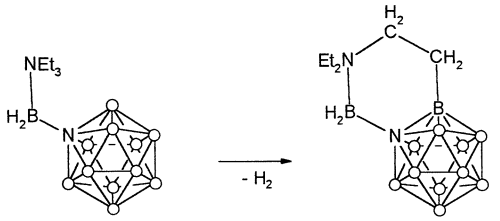

The bromination of the same *closo* species that were used for the methylation, yields either a fivefold-brominated or a monobrominated product when $AlBr_3$ acts as a Friedel−Crafts catalyst [Eqs. (33), (34)][49].

$$RNB_9H_9 + 5\ Br_2 \rightarrow RNB_9H_4Br_5 + 5\ HBr \quad (33)$$

$$RNB_{11}H_{11} + Br_2 \rightarrow RNB_{11}H_{10}Br + HBr \quad (34)$$

As expected, the bromination takes place in the *meta* and *para* position of the NB_9, but exclusively in the *para* position of the NB_{11} skeleton. Iodination in the presence of $AlCl_3$ stops at the diiodination to give $RNB_9H_7I_2$, with iodine in the *meta* and *para* position, or at the moniiodation to give the *para* product $RNB_{11}H_{10}I$.

There is some similarity in the halogenation of the azaboranes RNB_9H_9 and $RNB_{11}H_{11}$ on the one hand and of the isoelectronic thiaboranes SB_9H_9 and $SB_{11}H_{11}$ on the other; these can be halogenated once, twice or three times, preferably in the *meta*, also in the *para*, but not in the *ortho* position[62][63][64]. The isoelectronic carbaborates $[CB_9H_{10}]^-$ and $[CB_{11}H_{12}]^-$ also undergo a similar electrophilic halogenation to give $[CB_9H_9Hal]^-$ (Hal = Cl, Br, I, in the *meta* position) or $[CB_9H_5Hal_5]^-$ (Hal = Cl, Br, in the *meta* and *para* positions)[65][66][67] and to give $[CB_{11}H_{11}Hal]^-$ (Hal = Cl, Br, I, in the *para* position) or $[CB_{11}H_{10}I_2]^-$ (I in the *meta* and *para* position) or $[CB_{11}H_6Hal_6]^-$ (Hal = Cl, Br, in the *meta* and *para* position)[68][69][70].

Cluster Opening by Bases

The 10-vertex aza-*closo*-borane RNB_9H_9 (**35**) can be opened by amines. Whereas simple tertiary amines like NEt_3, N*i*Bu_3 do not react with RNB_9H_9 (R = *p*-ClC_6H_4), the bifunctional tertiary amine $Me_2N-CH_2-CH_2-NMe_2$ (tmen) gives a 1:1 adduct via one of the basic nitrogen atoms, which attacks one of the *ortho* positions. The *closo* species is transformed into a *nido*-NB_9 skeleton that contains an unsymmetric hydrogen bridge without fluxional behaviour, according to NMR data at room temperature [Eq. (35)][23]. The same type of hydrogen bridge is present in the anions $[RNB_9H_{10}]^-$ (**15**; R = Ph, $PhCH_2$), which are formed from RNB_9H_{11} (**14**) by the addition of $R'NH_2$ (R′ = *t*Bu) and subsequent deprotonation of the adduct (**18**) by hydride [Eq. (36)][23]. The difference in reactivity

between ordinary tertiary amines and tmen is not understood.

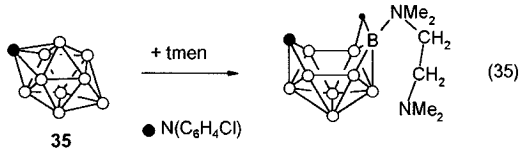

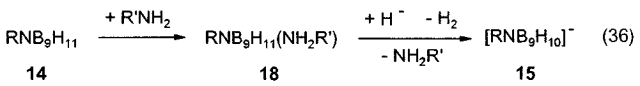

The *closo* species RNB_9H_9 is degraded when an excess of primary or secondary amine is applied. A secondary amine like $NHEt_2$ or $NHiPr_2$ and even a primary amine with a bulky group like NH_2tBu simply opens RNB_9H_9 without degradation, when an excess of amine is avoided. The hydrogen atoms of the reacting moieties BH and NH are found in the open face of the product [Eq. (37)]. Bridging positions B8−B9 and B10−B9 would be expected if the product $RNB_9H_{10}(NR'R'')$ was a *nido* cluster, whereas bridging positions B5−B10 and B7−B8 would indicate an *arachno* cluster. An electron count, according to Wade's rules, predicts a *nido* product $RNB_9H_{10}X$ (**14**) if the ligand X behaved like a hydrogen atom, but would give an *arachno* product if X acted as a three-electron ligand, forming a σ and a dative π bond, due to a lone pair of X. The two non-*exo*-hydrogen atoms of the product, Eq. (37), were found by NMR methods to be predominantly in an *endo* position at B8 and B10, i.e. a position inbetween those typical for *nido* and *arachno* 10-vertex clusters. Such an electronic-hybrid situation was also concluded from the ^{11}B-NMR data[23] apparently because of weak BN π bonding between the amino ligand and the cluster.

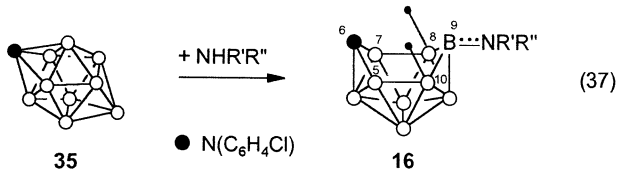

In the case of the *closo*-borane $RNB_{11}H_{11}$ (**43**), simple tertiary amines such as NEt_3 are added to the *ortho* position to give the *nido* cluster **30** by the migration of the former terminal hydrogen atom into a neighbouring bridge position in the open pentagonal face (R = Ph) [Eq. (38)][35].

$$PhNB_{11}H_{11} + NEt_3 \rightarrow PhNB_{11}H_{11}(NEt_3) \quad (38)$$

The similarity of the steric course of reactions (35) and (37) is elucidated by observing the *closo* clusters along the main axes. The reduction of the connectivity at the nitrogen atom to $c = 3$ involves the opening of one B−N bond in reaction (35), but of two B−N bonds in reaction (38). No B−B bond is opened during reaction (38), whereas three B−B bonds are opened and one B−B bond is closed during reaction (35), which can be considered to be the reverse of the dehydrogenation, Eq. (30), with respect to the skeletal changes.

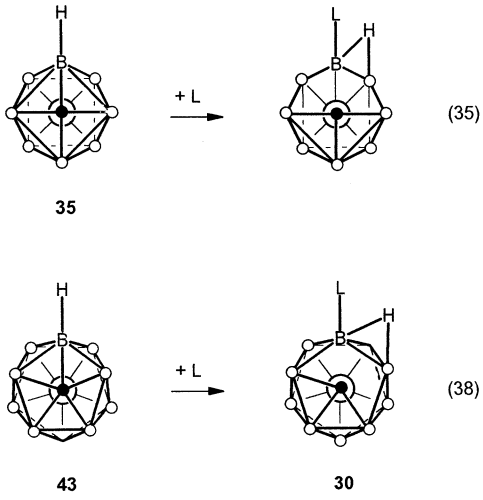

nido products of type **31** are formed when anions X^- are added to *closo*-$RNB_{11}H_{11}$ [Eq. (39)][35]. Substances MX as different as LiMe, LiBu, K[O*t*Bu], $[N(PPh_3)_2]Cl$, $[S(NMe_2)_3][Me_3SiF_2]$ (X = F by elimination of Me_3SiF), and $K[BHEt_3]$ (X = H by elimination of BEt_3) have been allowed to react with $MeNB_{11}H_{11}$.

$$MeNB_{11}H_{11} + MX \rightarrow M[MeNB_{11}H_{11}X] \quad (39)$$

In the case of protic agents such as HOMe, the anion MeO^- is added to $RNB_{11}H_{11}$ (R = H, Me, Et, Ph), and the proton, the corresponding cation, is dissolved in the organic medium, e.g. CH_2Cl_2. Efforts to isolate the free acid $H[RNB_{11}H_{11}(OMe)]$ resulted in a complete degradation of the cluster. The cluster anion can be precipitated, however, from solutions of the free acid by adding salts such as $[N(PPh_3)_2]Cl$, leaving HCl in the solvent[36]. No deuterium is incorporated into the cluster if DOMe instead of HOMe is applied, proving that the bridging hydrogen atom in the anion **31** is one of the hydrogen atoms of the starting material **43** and that there is no hydrogen/deuterium exchange between the anion **31** and DOMe[36]. A secondary amine such as the protic agent $HNEt_2$ yields the salt-type product $[H_2NEt_2][RNB_{11}H_{11}(NEt_2)]$[35].

We assume that the mechanism of the formation of anions **31** from **43** is best described by the reaction sequence (40), which starts with the addition of X^- to **43**, followed by a series of rearrangements of a hydrogen atom from an *endo* into a bridging position and vice versa. The second intermediate in this sequence corresponds to the isolated neutral adduct $RNB_{11}H_{11}(NEt_3)$ (**30**). [Only the 6-vertex upper halves of the 12-vertex polyhedral anions are drawn in sequence (40).]

The anions $[RNB_{11}H_{11}X]^-$ (**31**) are remarkably stable in protic media including aqueous acids and bases. Efforts have failed to deprotonate the anion $[PhNB_{11}H_{11}(OH)]^-$ in order to study the oxo-ligand in the expected dianion $[PhNB_{11}H_{11}O]^{2-}$, even though the strongest bases have

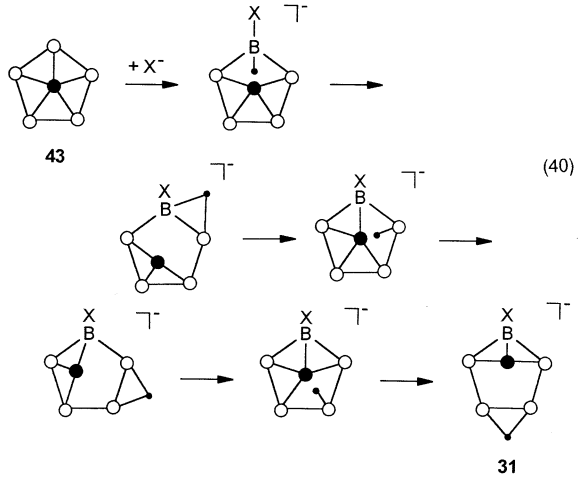

been applied. A degradation of the anions **31** has never been observed.

To summarize the findings on cluster opening: The closed NB_9 and NB_{11} skeletons of **35** and **43** are stable toward oxidation and reduction and toward Brønsted and Lewis acids. The *closo*-NB_{11} skeleton is opened by anionic or neutral bases to give a *nido*-NB_{11} skeleton with a nonplanar pentagonal aperture; this *nido* skeleton is stable towards degradation by bases. This is in striking contrast to the behaviour of the isoelectronic C_2B_{10} skeleton, which undergoes a degradative opening with bases to give the *nido*-C_2B_9 skeleton, whose planar pentagonal aperture is the basis for the synthesis of so many dicarbametalla-*closo*-dodecaboranes. The isoelectronic *nido*-NB_{10} clusters are not available from *closo*-NB_{11} systems and have to be synthesized by an alternative method. The *closo*-NB_9 skeleton can be opened by amines, if no excess is applied, but will be opened and degraded by protic bases in excess.

Degradative Opening of *closo*-RNB_9H_9

The *closo*-NB_9 skeleton is transformed into the *nido*-NB_8 skeleton in a sufficiently polar, aprotic medium such as thf as has been shown for RNB_9H_9 with R = *p*-ClC_6H_4, *p*-MeC_6H_4, $PhCH_2$[13]; the *nido* anion $[RNB_8H_9]^-$ (**9**) is the product. The expelled boron atom is found in a borazine molecule $(HBNiPr)_3$, if *i*$PrNH_2$ is the attacking base [Eq. (13)], but will be detected in the anion BF_4^-, if fluorides such as $[NBu_4]F$ or $[S(NMe_2)_3][Me_3SiF_2]$ are the degrading agents, according to reactions of unknown stoichiometry. The reaction of RNB_9H_9 with *i*$PrNH_2$ or other primary amines in the less polar solvent CH_2Cl_2, on the other hand, yields the *arachno*-NB_8 species $RNB_8H_{10}(NH_2R')$ [**12**; Eq. (14)][13].

Applications of Azaboranes

The nitrogen-bound amino group in the anion $[(Me_2N)NB_9H_{12}]^-$ [**19**; Eq. (15)] can be treated with MeI to form $(Me_3N)NB_9H_{12}$[25]. This product and similar ones are reported to be useful as blowing agents, in electrical resistors, and as reducing agents[71].

[1] [1a] T. L. Heying, J. W. Ager, S. L. Clark, D. J. Mangold, H. L. Goldstein, M. Hillman, R. J. Polak, J. W. Szymanski, *Inorg. Chem.* **1963**, *2*, 1089. – [1b] M. M. Fein, J. Bobinski, N. Mayes, N. Schwartz, M. S. Cohen, *Inorg. Chem.* **1963**, *2*, 1111. – [1c] L. I. Zakharkin, V. I. Stanko, V. A. Brattsev, Y. A. Chapovskii, Y. T. Struchkov, *Izv. Akad. Nauk SSSR, Ser. Khim.* **1963**, 2069.
[2] J. Plešek, B. Štibr, S. Heřmánek, *Chem. Ind. (London)* **1974**, 662.
[3] A. Arafat, J. Baer, J. C. Huffman, L. J. Todd, *Inorg. Chem.* **1986**, *25*, 3757.
[4] J. Müller, J. Runsink, P. Paetzold, *Angew. Chem.* **1991**, *103*, 201; *Angew. Chem., Int. Ed. Engl.* **1991**, *30*, 175.
[5] P. Paetzold, B. Redenz-Stormanns, R. Boese, M. Bühl, P. v. R. Schleyer, *Angew. Chem.* **1990**, *102*, 1059; *Angew. Chem. Int. Ed. Engl.* **1990**, *29*, 1059.
[6] M. Müller, T. Wagner, U. Englert, P. Paetzold, *Chem. Ber.* **1995**, *128*, 1.
[7] S. Küpper, U. Englert, P. Paetzold, *Heteroatom Chem.* **1990**, *1*, 479.
[8] M. Müller, U. Englert, P. Paetzold, *Chem. Ber.* **1995**, *128*, 1105.
[9] R. Boese, B. Kröckert, P. Paetzold, *Chem. Ber.* **1987**, *120*, 1913.
[10] P. Paetzold, B. Redenz-Stormanns, R. Boese, *Chem. Ber.* **1991**, *124*, 2435.
[11] S. Kuepper, P. Paetzold, R. Boese, *Chem. Ber.* **1993**, *126*, 1787.
[12] T. Jelínek, J. D. Kennedy, B. Stibr, *J. Chem. Soc., Chem. Commun.* **1993**, 1628.
[13] M. Roth, P. Paetzold, *Chem. Ber.* **1995**, *128*, 1221.
[14] J. Bould, N. P. Rath, L. Barton, *Organometallics* **1996**, *15*, 4916.
[15] K. Baše, J. Plešek, S. Heřmánek, J. Huffman, P. Ragatz, R. Schaeffer, *J. Chem. Soc., Chem. Commun.* **1975**, 934.
[16] T. Jelínek, B. Stibr, J. D. Kennedy, *Collect. Czech. Chem. Commun.* **1994**, *59*, 2244.
[17] R. Lewin, P. G. Simpson, W. N. Lipscomb, *J. Chem. Phys.* **1963**, *39*, 1532.
[18] K. Baše, F. Hanousek, J. Plešek, B. Štibr, A. Lycka, *J. Chem. Soc., Chem. Commun.* **1981**, 1162.
[19] J. G. Kester, J. C. Huffman, L. J. Todd, *Inorg. Chem.* **1988**, *27*, 4528.
[20] J. Müller, P. Paetzold, U. Englert, J. Runsink, *Chem. Ber.* **1992**, *125*, 97.
[21] F. Meyer, J. Müller, M. U. Schmidt, P. Paetzold, *Inorg. Chem.* **1993**, *32*, 5053.
[22] F. Meyer, M. U. Schmidt, P. Paetzold, *Chem. Ber.* **1995**, *128*, 947.
[23] R. Roth, P. Paetzold, *Coll. Czech. Chem. Commun.* **1997**, *62*, 1299.
[24] J. H. Jones, B. Štibr, J. D. Kennedy, M. Thornton-Pett, *Inorg. Chim. Acta* **1994**, *227*, 163.
[25] W. R. Hertler, F. Klanberg, E. L. Muetterties, *Inorg. Chem.* **1967**, *6*, 1696.
[26] B. Štibr, J. Holub, T. Jelínek, X. L. R. Fontaine, J. Fusek, J. D. Kennedy, M. Thornton-Pett, *J. Chem. Soc., Dalton Trans.* **1996**, 1741.
[27] B. Štibr, J. D. Kennedy, T. Jelínek, *J. Chem. Soc., Chem. Commun.* **1990**, 1309.
[28] J. Holub, T. Jelínek, J. Plešek, B. Štibr, S. Heřmánek, J. D. Kennedy, *J. Chem. Soc., Chem. Commun.* **1991**, 1389.
[29] F. Meyer, Dissertation, Technische Hochschule Aachen, **1993**.
[30] E. Leuschner, Dissertation, Technische Hochschule Aachen, **1997**.
[31] J. Müller, P. Paetzold, R. Boese, *Heteroatom Chem.* **1990**, *1*, 461.
[32] J. Plešek, S. Heřmánek, *Pure Appl. Chem.* **1974**, *39*, 431.
[33] V. A. Brattsev, S. P. Knyazev, G. N. Danilova, V. I. Stanko, *Zh. Obshch. Khim.* **1975**, *45*, 1393.
[34] S. O. Kang, G. T. Furst, L. G. Sneddon, *Inorg. Chem.* **1989**, *28*, 2339.
[35] P. Lomme, F. Meyer, U. Englert, P. Paetzold, *Chem. Ber.* **1995**, *128*, 1225.
[36] F. Meyer, J. Müller, P. Paetzold, R. Boese, *Angew. Chem.* **1992**, *104*, 1221; *Angew. Chem. Int. Ed. Engl.* **1992**, *31*, 1227.
[37] A. E. Wille, K. Su, P. J. Carroll, L. G. Sneddon, *J. Am. Chem. Soc.* **1996**, *118*, 6407.
[38] T. Jelínek, J. D. Kennedy, B. Štibr, *J. Chem. Soc., Chem. Commun.* **1994**, 677.
[39] L. Schneider, U. Englert, P. Paetzold, *Z. Anorg. Allg. Chem.* **1994**, *620*, 1191.
[40] U. Doerfler, J. D, Kennedy, L. Barton, C. M. Collins, N. P. Rath, *J. Chem. Soc., Dalton Trans.* **1997**, 707.
[41] K. Baše, M. Bown, X. L. R. Fontaine, N. N. Greenwood, J.

D. Kennedy, B. Štibr, M. Thornton-Pett, *J. Chem. Soc., Chem. Commun.* **1988**, 1240.
[42] M. Müller, U. Englert, P. Paetzold, *Inorg. Chem.* **1995**, *34*, 5925.
[43] H. P. Hansen, J. Müller, U. Englert, P. Paetzold, *Angew. Chem.* **1991**, *103*, 1357; *Angew. Chem. Int. Ed. Engl.* **1991**, *10*, 1377.
[44] H.-P. Hansen, U. Englert, P. Paetzold, *Z. Anorg. Allg. Chem.* **1995**, *621*, 719.
[45] J. Plešek, S. Heřmánek, J. Huffman, P. Ragatz, R. Schaeffer, *J. Chem. Soc., Chem. Commun.* **1975**, 935.
[46] K. Nestor, X. L. R. Fontaine, J. D. Kennedy, B. Štibr, K. Baše, M. Thornton-Pett, *Collect. Czech. Chem. Commun.* **1991**, *56*, 1607.
[47] D. Hnyk, M. Bühl, P. v. R. Schleyer, H. V. Volden, S. Gundersen, J. Müller, P. Paetzold, *Inorg. Chem.* **1993**, *32*, 2442.
[48] L. Schneider, U. Englert, P. Paetzold, *Chem. Ber.* **1994**, *127*, 87.
[49] P. Lomme, M. Roth, U. Englert, P. Paetzold, *Chem. Ber.* **1996**, *129*, 1227.
[50] L. J. Todd, A. Arafat, J. Baer, J. C. Huffman in *Advances in Boron and the Boranes* (Eds.: J. F. Liebman, A. Greenberg, R. E. Williams), VCH, Weinheim, **1988**, p. 287.
[51] P. Paetzold, *Pure Appl. Chem.* **1991**, *63*, 345.
[52] P. Paetzold, J. Müller, F. Meyer, H.-P. Hansen, L. Schneider, *Pure Appl. Chem.* **1994**, *66*, 255.
[53] W. Dirk, E. Leuschner, P. Lomme, P. Paetzold, M. Roth in *Advances in Boron Chemistry* (Ed.: W. Siebert), The Royal Society of Chemistry, Cambridge, **1997**, p. 399.
[54] K. Baše, *Collect. Czech. Chem. Commun.* **1983**, *48*, 2593.
[55] B. M. Graybill, A. R. Pitochelli, M. F. Hawthorne, *Inorg. Chem.* **1962**, *1*, 626.
[56] R. Zahradník, V. Balaji, J. Michl, *J. Comput. Chem.* **1991**, *12*, 1147.
[57] M. Bühl, P. v. R. Schleyer, Z. Havlas, D. Hnyk, S. Heřmánek, *Inorg. Chem.* **1991**, *30*, 3107.
[58] S. Heřmánek, D. Hnyk, Z. Havlas, *J. Chem. Soc., Chem. Commun.* **1989**, 1859.
[59] T. P. Fehlner, P. T. Czech, R. F. Fenske, *Inorg. Chem.* **1990**, *29*, 3103.
[60] W. N. Lipscomb, *Angew. Chem.* **1977**, *89*, 685.
[61] W. Jian, C. B. Knobler, M. D. Mortimer, M. F. Hawthorne, *Angew. Chem.* **1995**, *107*, 1470; *Angew. Chem., Int. Ed. Engl.* **1995**, *34*, 1332.
[62] W. L. Smith, B. J. Meneghelli, N. McClure, R. W. Rudolph, *J. Am. Chem. Soc.* **1976**, *98*, 624.
[63] W. L. Smith, B. J. Meneghelli, D. A. Thompson, P. Klymko, N. McClure, M. Bower, *Inorg. Chem.* **1977**, *16*, 3008.
[64] J. Plešek, S. Heřmánek, *J. Chem. Soc., Chem. Commun.* **1975**, 127.
[65] R. J. Wiersema, M. F. Hawthorne, *Inorg. Chem.* **1973**, *12*, 785.
[66] Z. Xie, D. Liston, T. Jelínek, V. Mitro, R. Bau, C. A. Reed, *J. Chem. Soc., Chem. Commun.* **1993**, 384.
[67] S. V. Ivanov, J. J. Rockwell, S. M. Miller, O. P. Anderson, K. A. Solntsev, S. H. Strauss, *Inorg. Chem.* **1966**, *35*, 7882.
[68] T. Jelínek, J. Plešek, S. Heřmánek, B. Stibr, *Collect. Czech. Chem. Commun.* **1986**, *51*, 819.
[69] T. Jelínek, P. Baldwin, W. R. Scheidt, C. A. Reed, *Inorg. Chem.* **1993**, *32*, 1982.
[70] Z. Xie, T. Jelínek, R. Bau, C. A. Reed, *J. Am. Chem. Soc.* **1994**, *116*, 1907.
[71] E. I. du Pont de Nemours, and Co. (W. R. Hertler, Inv.), US-Pat. 3,428,439 (February 18, 1969) [*Chem. Abstr.* **1969**, *70*, 96154x].

[97229]

The Effect of the Bite Angle of Diphosphane Ligands on Activity and Selectivity in Palladium-Catalyzed Cross-Coupling[+]

Mirko Kranenburg[++], Paul C. J. Kamer*, and Piet W. N. M. van Leeuwen

Van't Hoff Research Institute, Department of Inorganic Chemistry, University of Amsterdam
Nieuwe Achtergracht 166, NL-1018 WV Amsterdam, The Netherlands

Received July 3, 1997

Keywords: Bite angle / Catalysis / P ligands / Palladium / Cross-coupling

The effect of the natural bite angle (β_n) of diphosphane ligands on catalyst selectivity and activity in the palladium-catalyzed cross-coupling of *sec*-butyl magnesium chloride with bromobenzene was investigated. The calculated natural bite angles range from 78° for dppe (1,2-bisdiphenylphosphanoethane) to 110° for Xantphos. The natural bite angle of diphosphane ligands has a large effect on catalyst selectivity and activity. Both rate and selectivity of the cross-coupling reaction increase with increasing bite angle and reach a maximum value with DPEphos (β_n = 102.7°). Larger bite angles of the diphosphane ligands result in a decreased selectivity and activity.

Transition metal catalyzed carbon−carbon bond formation is an important tool for organic chemists and a challenging area of research in homogeneous catalysis. Nickel and palladium catalysts with tailored phosphane ligands have been applied successfully in the cross-coupling reaction. The influence of the type of (di)phosphane used is very large, although the effect is not yet fully understood.[1][2] One of the steric parameters for diphosphanes is the bite angle induced by the ligand.[3] Hayashi et al. found that dppf [1,1′-bis(diphenylphosphanoferrocene)], a diphosphane with a large P−Pd−P bite angle of 99.1° in [dppf]$PdCl_2$, has the highest activity and selectivity of a range of (di)phosphane ligands. Furthermore, comparison of different diphosphanes revealed an increase of selectivity with an increasing bite angle.[4][5]

We have developed a new group of diphosphanes capable of enforcing large bite angles (see Figure 1).[6] According to our calculations, these ligands have natural bite angles varying from 102° to 110° (for palladium complexes). Recent studies on hydroformylation,[6] hydrocyanation,[7] and allylic alkylation[8] showed that changes in the bite angle of these ligands have a strong influence on catalyst selectivity. Since the steric and electronic properties of these ligands are the same, all effects on selectivity or activity can be attributed to the bite angle. Here we present a study on the effect of the bite angle of chelating diphosphanes on the activity and selectivity in the palladium-catalyzed cross-coupling reaction.

We prepared mononuclear, *cis*-(P-P)$PdCl_2$ (**1−4a**) complexes of the Xantphos-type ligands (see Figure 1) and the analogous (diphosphane)$PtCl_2$ complexes (**1−4b**). The platinum(II) complexes showed large Pt−P coupling constants of 3640−3800 Hz, indicative of square planar *cis* coordination. The palladium complexes were utilized as catalysts in the coupling of *sec*-butylmagnesium chloride with bromobenzene (see eq. 1, Table 1).[4][5]

Figure 1. Diphosphanes with large bite angles

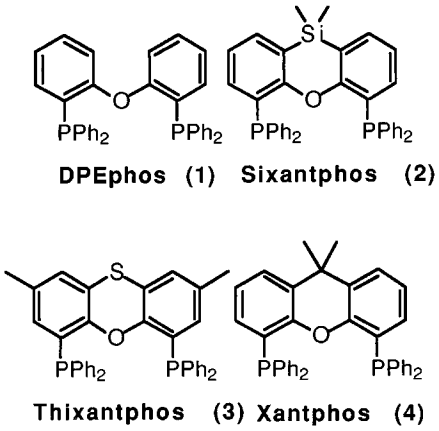

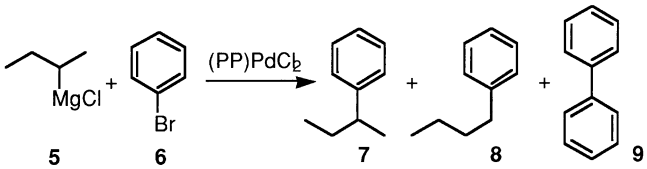

Homocoupling, an important competing reaction in the cross-coupling reaction,[9] was not taken into account in Hayashi's study. We therefore applied their best catalytic system, dppf$PdCl_2$, under identical conditions and analyzed the product mixture for the presence of **9**, the homocoupled product. An amount of 3% was observed, which has a small effect on the overall selectivity of this catalyst system. The initial turnover frequency was 79 mol (mol Pd)$^{-1}$ h^{-1}

[+] Netherlands Institute for Research in Catalysis (NIOK) publication UVA 98-6-02
[++] Present address: DSM Research, P.O. Box. 18, 6160 MD Geleen, The Netherlands

 © WILEY-VCH Verlag GmbH, D-69451 Weinheim, 1998 1434−1948/98/0202−0155 $ 17.50+.50/0

Table 1. Cross-coupling of 2-butylmagnesium chloride with bromobenzene in diethyl ether

Ligand	Bite angle [°]	t.o.f.[a] [mol (mol Pd)$^{-1}$ h^{-1}]	Reaction time [h]	Conversion[b] [%]	**7** [%]	**8** [%]	**9** [%]
dppe [c]	78.1	n.d.	48	4	0	0	n.d.
dppp [c]	86.2	n.d.	24	67	69	31	n.d.
dppb [c]	98.7	n.d.	8	98	51	25	n.d.
dppf	99.07 [d]	79	2	100	95	2	3
DPEphos	102.9	181	2	100	98	1	1
Sixantphos	106.5	36	16	58.8	67	17	16
Thixantphos	107.2	24	16	36.5	51	17	32
Xantphos	110.0	24	16	23.6	41	19	40

Conditions: 0.04 mmol catalyst, 8 mmol **5** and 4 mmol **6** in 20 ml ether, T = 20°C. The 95% confidence interval of the mean measured values is ±1.1%. – n.d.: not determined – [a] Initial turnover frequency, determined after 5 min. of reaction time. – [b] Conversions based on **6**. – [c] Results from reference[5], dppe = 1,2-bis(diphenylphosphano-ethane), dppp = 1,3- bis(diphenylphosphano-propane), dppb = 1,4-bis(diphenylphosphano-butane). – [d] Since we are not able to model the ferrocene-unit accurately, the natural bite angle for dppf is taken as 99.1°, the P–Pd–P angle from the X-ray structure of (dppf)$PdCl_2$[5].

Scheme 1

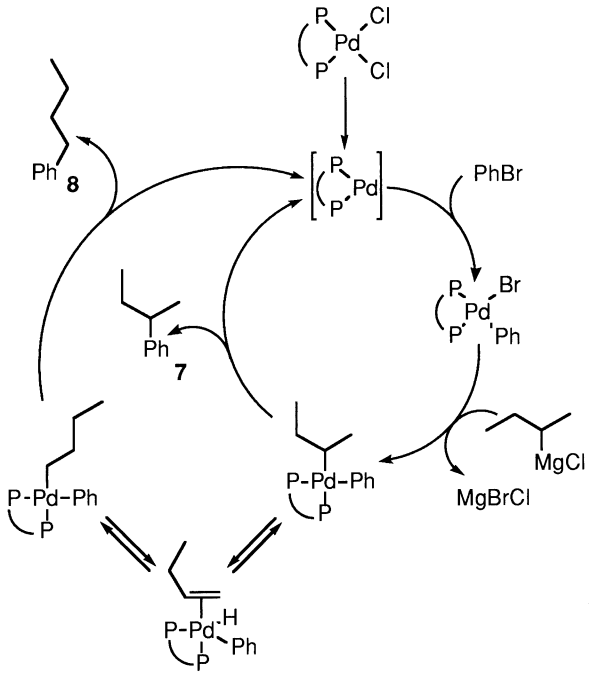

The catalyst containing DPEphos, β_n = 102.7°, was even more active and selective than the one with dppf. The cross-coupling product **7** was obtained in a selectivity of 98% (compared to 95% for dppf), with only 1% of the homocoupled **9**, and 1% of **8**. The observed initial turnover frequency is 181 mol (mol Pd)$^{-1}$h^{-1}, which is 2.3 times as high as the initial t.o.f. we observed for dppf.

Increasing the β_n of the diphosphane resulted in a decrease of both catalyst activity (an initial t.o.f. of 36 mol/mol/h using Sixantphos) and selectivity. The amount of cross-coupling product **7** decreased, whereas the homocoupled **9** and the sideproduct **8** were formed in larger amounts. At still larger bite angles the amount of homocoupling product **9** increased to a level of 40%.

Which step in the catalytic cycle is rate determining, is still under debate. Evidence has been presented that the rate-determining step can be either one of the following steps: the oxidative addition,[10][11] the transmetallation,[12][13] or the reductive elimination step.[14][15]

Brown and Guiry studied the effect of the P–Pd–P bite angle on the rate of reductive elimination. Both experimental work and extended Hückel calculations showed that the P–Pd–P angle increased along the reaction pathway. To investigate this effect they prepared a ruthenium analogue of dppf in order to increase the bite angle to 105–110°. The ruthenium-based ligand exhibited a slightly larger reactivity for reductive elimination than dppf, but the effect was marginal.[16]

An increasing P–Pd–P angle results in a decreasing R–Pd–R′ angle in the intermediate of the catalytic cycle. This smaller R–Pd–R′ angle accelerates reductive elimination. The optimum is reached at a P–Pd–P angle of ca. 102°. The reaction rates of [DPEphos]$PdCl_2$ and [dppf]$PdCl_2$ are similar, which seems to imply that DPEphos still induces a distorted square planar coordination. When the P–Pd–P angle increases further, the Pd(II) species will no longer have a square planar geometry. We propose that this distortion leads to an increasing R–Pd–R′ angle, which results in a decreasing relative rate of reductive elimination. This might explain the decrease of the rate of reaction when going from DPEphos to Xantphos.

An explanation for the formation of *n*-butylbenzene (**8**) can be the increased tendency to form trigonal bipyramidal intermediates with an increasing bite angle. The large bite angle induced by the Xantphos-type diphosphanes stabilize trigonal bipyramidal geometries, and the phosphorus donor atoms will be coordinated in the equatorial plane. This may lead to an increased rate of β-hydride elimination and reinsertion (see Scheme 1). The 1-alkyl palladium intermediate can react further to yield **8**. The ligands that are most suitable for stabilizing trigonal bipyramids, Sixantphos, Thixantphos, and Xantphos give rise to the formation of large amounts of **8**. Additionally, oxidative addition of a second molecule of bromobenzene results in the formation of a trigonal bipyramidal [(diphosphane)$Pd^{IV}(Ph)_2Bu]^+$ Br^- complex.[14] Stabilization of this complex by ligands inducing larger bite angles can explain the increasing amounts of homocoupled product **9** (see Scheme 2). The alternative mechanism of transmetallation between isobutylmagnesium chloride and bromobenzene, however, cannot be excluded.

Scheme 2

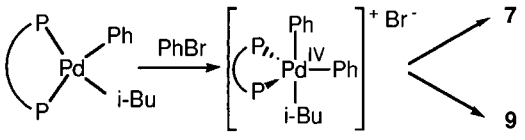

In conclusion it was found that in the (diphosphane)$PdCl_2$-catalyzed cross-coupling of 2-butylmagnesium chloride with bromobenzene, the selectivity reaches the highest value when the natural bite angle of the diphosphane used is ca. 100°. The rate of the reaction is also maximal at this value. The best selectivity and activity are obtained for DPEphos, a diphosphane with a natural bite angle of 102°. We propose that diphosphanes with larger bite angles stabilize trigonal bipyramidal intermediates leading to 1-butyl-benzene and homocoupled biphenyl.

Experimental Section

Computational Details: All calculations were performed using CAChe WorkSystem software[17] on an Apple Power Macintosh 950 equipped with 2 CAChe CXP coprocessors. The Molecular Mechanics calculations were performed using the MM2 force field.[18] Block-diagonal Newton-Raphson was used as optimization method. Natural bite angle calculations were performed using a method similar to that described by Casey and Whiteker[3] using a Pd−P bond length of 2.288 Å.[5][19]

For the ligands dppe, dppp and dppb, a starting geometry for the chelate ring resembling the appropriate cycloalkane was used. By this procedure, the global minimum resulting from excessive, stabilizing π-stacking interactions (and having a too small a bite angle) was avoided. The geometry obtained in this way is in agreement with geometries observed by X-ray crystallography.[20]

Synthesis: The diphosphane ligands were prepared according to literature procedures.[6]

Complex Synthesis: In a typical experiment, ligand (0.121 g, 0.225 mmol) and $(PhCN)_2PdCl_2$ (0.087 g, 0.225 mmol) ware placed in a Schlenk flask, and flushed with N_2. THF (10 ml) was added, and the reaction mixture was stirred overnight at room temp. The solvent was removed in vacuo, the resulting yellow powder was washed 3 times with 10 ml of diethyl ether, then dried in vacuo.

(DPEphos)$PdCl_2$ (**1a**): Yield: 0.198 g (0.251 mmol, 98%) of yellow powder. − $^{31}P\{^1H\}$ NMR ($CDCl_3$) δ = 19.3.

(DPEphos)$PtCl_2$ (**1b**) Yield: 0.162 g (0.201 mmol, 95%) of yellow powder. − $^{31}P\{^1H\}$ NMR ($CDCl_3$) δ = 2.0 ($J_{Pt\text{-}P}$ = 3795 Hz).

(Sixantphos)$PdCl_2$ (**2a**):Yield: 0.150 g (0.251 mmol, 86%) of yellow powder. − $^{31}P\{^1H\}$ NMR ($CDCl_3$) δ = 24.8.

(Sixantphos)$PtCl_2$ (**2b**): Yield: 0.161 g (0.187 mmol, 88%) of yellow powder. − $^{31}P\{^1H\}$ NMR ($CDCl_3$) δ = 7.6 ($J_{Pt\text{-}P}$ = 3663 Hz).

(Thixantphos)$PdCl_2$ (**3a**): Yield: 0.256 g (0.330 mmol, 91%) yellow powder. − $^{31}P\{^1H\}$ NMR ($CDCl_3$) δ = 25.3.

(Thixantphos)$PtCl_2$ (**3b**): Yield: 0.163 g (0.189 mmol, 89%) offwhite powder. − $^{31}P\{^1H\}$ NMR ($CDCl_3$) δ = 8.4 ($J_{Pt\text{-}P}$ = 3641 Hz).

(Xantphos)$PdCl_2$ (**4a**): Yield: 0.140 g (0.185 mmol, 82%) yellow powder. − $^{31}P\{^1H\}$ NMR ($CDCl_3$) δ = 22.7.

(Xantphos)$PtCl_2$ (**4b**): Yield: 0.149 g (0.176 mmol, 83%) pale yellow powder. − $^{31}P\{^1H\}$ NMR ($CDCl_3$) δ = 6.6 ($J_{Pt\text{-}P}$ = 3695 Hz).

Palladium-Catalyzed Cross-Coupling of Bromobenzene with sec-Butylmagnesium Chloride. General Procedure: The catalyst (0.04 mmol) was placed in a 50 ml Schlenk flask equipped with a stirring bar. Diethyl ether (10 ml)was added, and the reaction mixture was kept at the desired temperature using a water bath (20° C). Bromobenzene (0.42 ml, 4 mmol) and *n*-decane as an internal standard (0.8 ml, 4.1 mmol) were added, followed by 10 ml of a solution of *sec*-butylmagnesium chloride (0.8 M in ether). Samples were hydrolyzed with 10% hydrochloric acid, the organic layer was separated, and analyzed by GC.

[1] M. Kumada, *Pure & Appl. Chem.* **1980**, *52*, 669.
[2] E. Negishi, *Acc. Chem. Res.* **1982**, *15*, 340.
[3] C. P. Casey, G. T. Whiteker, *Isr. J. Chem.* **1990**, *30*, 299.
[4] T. Hayashi, M. Konishi, M. Kumada, *Tetrahedron Lett.* **1979**, *21*, 1871.
[5] T. Hayashi, M. Konishi, Y. Kobori, M. Kumada, T. Higuchi, K. Hirotsu, *J. Am. Chem. Soc.* **1984**, *106*, 158.
[6] M. Kranenburg, Y. E. M. van der Burgt, P. C. J. Kamer, P. W. N. M. van Leeuwen, K. Goubitz, J. Fraanje, *Organometallics* **1995**, *14*, 3081.
[7] M. Kranenburg, P. C. J. Kamer, P. W. N. M. van Leeuwen, D. Vogt, W. Keim, *J. Chem. Soc., Chem. Commun.* **1995**, 2177.
[8] M. Kranenburg, P. C. J. Kamer, P. W. N. M. van Leeuwen, *Eur. J. Inorg. Chem.*, **1998**, 25−27.
[9] R. van Asselt, C. J. Elsevier, *Organometallics* **1994**, *13*, 1972.
[10] J. F. Fauvarque, A. Jutand ,*J. Organomet. Chem.* **1981**, *209*, 109.
[11] J. F. Fauvarque, A. Jutand, *J. Organomet. Chem.* **1979**, *177*, 273.
[12] V. Farina, B. Krishnan, *J. Am. Chem. Soc.* **1991**, *113*, 9585.
[13] E. Negishi, T. Takahashi, S. Baba, D. E. van Horn, N. Okukado, *J. Am. Chem. Soc.* **1987**, *109*, 2393.
[14] A. Gillie, J. K. Stille, *J. Am. Chem. Soc.* **1980**, *102*, 4933.
[15] F. Ozawa, T. Ito, Y. Nakamura, A. Yamamoto, *Bull. Chem. Soc. Jpn.* **1981**, *54*, 1868.
[16] J. M. Brown, P. J. Guiry, *Inorg. Chim. Acta* **1994**, *220*, 249.
[17] CAChe Scientific Inc., 18700 N.W. Walker Road, Building 92-01, Beaverton, OR 97006 1994.
[18] U. Burkert, N. L. Allinger, *Molecular Mechanics*, American Chemical Society, Washington, D.C. **1982**.
[19] H. C. L. Abbenhuis, U. Burckhardt, V. Gramlich, C. Köllner, P. S. Pregosin, R. Salzmann, A. Togni, *Organometallics* **1995**, *14*, 759.
[20] A. J. Pavigliani, D. J. Minn, W. C. Fultz, J. L. Burmeister, *Inorg. Chim. Acta* **1989**, *159*, 65.

[97159]

An Unusual Ring Structure of an Oligomeric Oxotitanium Alkoxide Carboxylate

Guido Kickelbick and Ulrich Schubert*

Institut für Anorganische Chemie der Technischen Universität Wien,
Getreidemarkt 9, A-1060 Wien, Austria
Fax: (internat.) + 43(0)1/581-6668
E-mail: uschuber@fbch.tuwien.ac.at

Received September 25, 1997

Keywords: Oxo clusters / Titanium / Metal alkoxides / Sol-gel processes / Carboxylato complexes / Solid-state structures

$Ti_9O_8(OPr)_4(methacrylate)_{16}$ was obtained by the reaction of $Ti(OPr)_4$ with an excess of methacrylic acid and analyzed by X-ray diffraction. The compound consists of a ring of nine $[TiO_6]$ octahedra linked by six μ_2- and only two μ_3-oxide bridges.

When metal alkoxides are treated with carboxylic acids, β-diketones, or related compounds, the alkoxide groups are replaced to some extent by the corresponding bidentate anionic ligands (BL^-).[1] There are three main objectives in using compounds of the type $E(OR)_y(BL)_x$ as precursors in sol-gel chemistry: (i) they have a lower reactivity than the parent alkoxides, (ii) organic functions can be introduced in the derived materials,[2] and (iii) the size of the primarily formed oxo particles can be controlled.[1] The primary hydrolysis products are the building blocks for organically modified non-silicate sol-gel materials. Chemical "nano-engineering" of sol-gel materials is only possible when several fundamental structural issues concerning the oxo clusters are understood and eventually controlled: (i) the coordination number of the central atom, (ii) the kind of linkage of the coordination polyhedra (vertex-, edge-, face-sharing), (iii) the number of shared vertices, edges, or faces, and (iv) the coordination mode of the organic ligands.

Carboxylates are often used as the bidentate ligands. One particular advantage of such compounds is that they allow the easy introduction of functional substituents. We recently succeeded in characterizing a coherent series of oxozirconium carboxylate clusters derived from the corresponding alkoxides.[3] The structures of $Zr_6(OH)_4O_4(OMc)_{12}$ (OMc = methacrylate), $[Zr_6(OH)_4O_4(acrylate)_{12}]_2$ and $Zr_6(OH)_4O_4(OOCR)_{12}(PrOH)$ [R = C(Me)=CH_2, C_6H_5] are highly condensed, with a $Zr_6(\mu_3\text{-}OH)_4(\mu_3\text{-}O)_4$ cluster core and octacoordinate zirconium atoms. When the Zr/bidentate ligand ratio is increased from 1:2 to 1:3, the structures open up, as in $Zr_4O_2(OMc)_{12}$ with a distorted butterfly structure (hepta- and octacoordinate Zr atoms)[3] or polymeric $[Zr(OnPr)(O_3SMe)_3]_\infty$ (heptacoordinate Zr atoms).[4] A high degree of substitution by bidentate ligands is possible because of the high coordination numbers of the zirconium atoms.

In contrast to the compounds discussed above, the maximum coordination number of titanium is 6. This restricts the maximum carboxylate/titanium ratio (x) of oxotitanium carboxylates to 2, i.e. to the composition $TiO(OOCR)_2$ (provided that all carboxylate ligands are bidentate). In oxotitanium carboxylate *alkoxide* derivatives x must be < 2 to accommodate the OR ligands. The maximum value of x found in structurally characterized oxotitanium carboxylate alkoxides to date is 1.33 in $Ti_6O_4(OR)_8(OOCR')_8$ [R′ = Me: R = Et, *n*Bu, *i*Pr;[5] R′ = C(Me)=CH_2: R = Et[6]]. Smaller degrees of substitution were found in $Ti_6O_4(OR)_{12}(OOCR')_4$ [R′ = Me: R = *i*Pr; R′ = μ_3-$CCo_3(CO)_9$: R = Et] and $Ti_4O_4(OR)_4[OOC{-}CCo_3(CO)_9]_4$ (R = *i*Pr, Ph).[7] The titanium atoms are octahedrally coordinated in all derivatives, and the carboxylate ligands are bridging. The linkage of the octahedra shows variations with the main difference between the cluster types being the ratio between shared vertices and edges.

Results

We have isolated a crystalline derivative of composition $Ti_9O_8(OPr)_4(OMc)_{16}$ (**1**) with $x = 1.78$. This compound was obtained by treating $Ti(OPr)_4$ with a 4-fold excess of methacrylic acid. The water for the hydrolysis of the OPr groups was generated in situ by esterification of methacrylic acid with the cleaved alcohol. We do not currently have any information regarding the sequence of the substitution and hydrolysis reactions necessary to convert $Ti(OPr)_4$ to **1**. We would like to emphasize that we did not intend to identify all products formed in this particular reaction. Instead, our goal was to gather additional structural information on carboxylate-substituted oxotitanium compounds as potential building blocks in titania-based inorganic-organic hybrid materials. The unusual structure of **1** is shown in Figure 1.

The compound consists of a ring of nine $[TiO_6]$ octahedra linked by six μ_2- and only two μ_3-oxide bridges. All titanium atoms are octahedrally coordinated and all methacrylate groups are bridging, as in the known oxotitanium carboxylates. However, the higher degree of substitution by

 © WILEY-VCH Verlag GmbH, D-69451 Weinheim, 1998 1434−1948/98/0202−0159 $ 17.50+.50/0

Figure 1. The structure of $Ti_9O_8(OPr)_4(methacrylate)_{16}$ (**1**)[a]

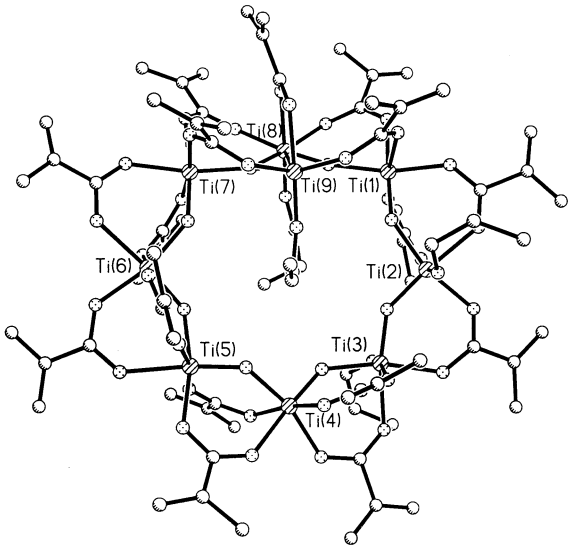

[a] Selected bond lengths [pm] and angles [°]: Ti(1)−O(215) 193.4(11), Ti(1)−O(212) 173.7(10), Ti(2)−O(212) 192.2(11), Ti(2)−O(210) 181.1(12), Ti(3)−O(210) 179.3(11), Ti(3)−O(213) 191.6(11), Ti(4)−O(213) 171.5(11), Ti(4)−O(211) 191.1(12), Ti(5)−O(211) 171.5(11), Ti(5)−O(214) 190.2(11), Ti(6)−O(214) 173.4(11), Ti(6)−O(216) 190.1(12), Ti(7)−O(216) 174.2(11), Ti(7)−O(217) 193.3(12), Ti(8)−O(217) 195.3(11), Ti(8)−O(215) 195.5(11), Ti(9)−O(215) 194.0(10), Ti(9)−O(217) 194.5(11); O(212)−Ti(1)−O(215) 96.6(5), O(210)−Ti(2)−O(212) 100.5(5), O(210)−Ti(3)−O(213) 99.0(5), O(213)−Ti(4)−O(211) 99.6(5), O(211)−Ti(5)−O(214) 97.9(5), O(214)−Ti(6)−O(216) 100.0(5), O(216)−Ti(7)−O(217) 97.6(5), O(215)−Ti(8)−O(217) 78.4(4), O(215)−Ti(9)−O(217) 78.9(5), Ti(3)−O(210)−Ti(2) 142.8(6), Ti(5)−O(211)−Ti(4) 135.4(6), Ti(1)−O(212)−Ti(2) 136.0(6), Ti(4)−O(213)−Ti(3) 136.0(6), Ti(6)−O(214)−Ti(5) 134.8(6), Ti(1)−O(215)−Ti(9) 125.3(6), Ti(1)−O(215)−Ti(8) 134.1(6), Ti(9)−O(215)−Ti(8) 100.5(5), Ti(7)−O(216)−Ti(6) 133.5(6), Ti(7)−O(217)−Ti(9) 126.6(5), Ti(7)−O(217)−Ti(8) 132.2(5), Ti(9)−O(217)−Ti(8) 100.4(5).

the bidentate carboxylate ligands forces the structure to become less condensed, since a coordination number larger than 6 (as in the Zr structures) is not possible. Unlike the less substituted derivatives, which are known, only two of the octahedra [Ti(8) and Ti(9)] share an edge, while the other octahedra [Ti(1)−Ti(7)] share *cis* vertices (Figure 2), i.e. only two oxygen atoms [O(215) and O(217)] are μ_3, while the remaining six oxygen atoms are μ_2.

All but two pairs of neighboring Ti octahedra are bridged by two methacrylate ligands. Ti(8)/Ti(9) and Ti(2)/Ti(3) are connected by only one methacrylate bridge, the second bridge is replaced by two OPr ligands (one at each Ti atom). This makes the macrocycle asymmetric with regard to the OPr substitution. There is a remarkable alternation in the bond distances of the μ_2-O bridges. With the exception of O(210), which bridges the OPr-substituted metal atoms Ti(2) and Ti(3), each μ_2-O bridge exhibits a long (190.1−193.4 pm) and a short (171.5−173.7 pm) Ti−O distance, although the *trans* substituent is the same (carboxylate bridge). The asymmetric Ti−O−Ti distances are compensated for by asymmetric carboxylate bridges, i.e. the Ti−O(carboxylate) distance *trans* to a short Ti−O(bridge) distance is lengthened [208.8−215.5 pm vs. 197.1−210.8 pm for the other Ti−O(carboxylate) distances].

Figure 2. Linkage of the coordination octahedra in $Ti_9O_8(OPr)_4(methacrylate)_{16}$ (**1**)

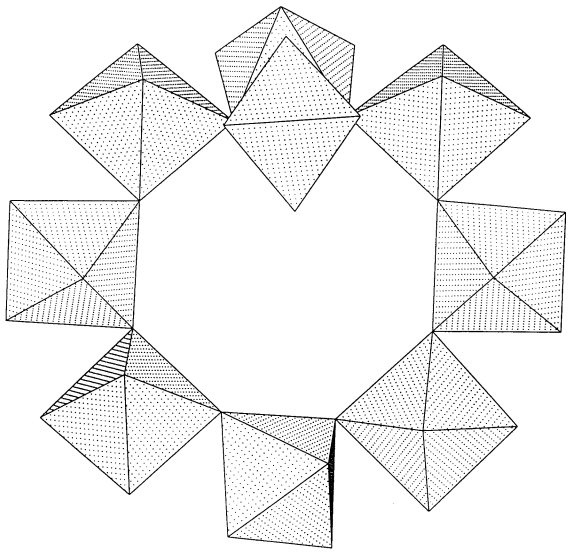

The overall structure is a balance between the sum of all coordination numbers and charges (c.n. 6 and charge +4 per titanium atom). The structural features in **1** can be understood by first considering a hypothetical structure of $[TiO_{2/2}(OOC-R)_2]_n$ with two bridging carboxylate ligands and one μ_2-oxide per formula unit. If two bridging carboxylate ligands are replaced by four monodentate OR groups, the sum of all c.n. is maintained, but there are two additional negative charges. These must be compensated for by the loss of one oxide. This, on the other hand, creates two empty coordination sites, which is compensated for by two other μ_2-oxygen atoms becoming μ_3. $[Ti(\mu_2\text{-}O)(OOCR')_2]_n$ is thus converted into $Ti_n(\mu_2\text{-}O)_{n-3}(\mu_3\text{-}O)_2(OR)_4(OOCR')_{2n-2}$. In all known oxotitanium alkoxide structures,[8] including the carboxylate-substituted derivatives mentioned above,[5][6][7] most $[TiO_6]$ octahedra share edges, and there is a substantial number of μ_3-oxygen atoms, characteristic of the rutile structure. In the structure of **1**, only one pair of octahedra shares an edge and, as a consequence, there are only two μ_3-oxygen atoms. This is an alternative way of expressing the above statement that a high value of x results in more open (= less condensed) structures.

The consequence for sol-gel processing is that for the first-row transition elements the bidentate ligand:metal ratio (x) should not be forced to high values if sufficiently condensed oxo structures are desired. A "natural" limit appears to be $x = 1.33$, as has been found in the structures of the $Ti_6O_4(OR)_8(OOCR')_8$ derivatives. Higher values of x result in polymeric rather than condensed structures. Only if the metal center can increase its coordination number beyond 6 do higher values of x still give condensed oxo clusters.

This work was supported by the *Fonds zur Förderung der wissenschaftlichen Forschung* (FWF).

Experimental Section

Preparation of **1**: 2.5 g (29 mmol) of methacrylic acid (Aldrich, as received) was mixed under Ar with 2.07 g (7.3 mmol) of $Ti(OPr)_4$ (Aldrich, as received) and stored in a closed Schlenk tube at ambient temperature. An orange solid (2.98 g) precipitated during 7 d, consisting of an approximate 1:1 mixture of an amorphous powder and colorless crystals. A suitable crystal was selected for X-ray structure analysis.

X-ray Structure Analysis for **1**: Monoclinic, space group *Ia*, a = 2357.24(5), b = 1855.37(1), c = 2610.62(6) pm, β = 112.933(1)°, $V = 10515.2(3)\cdot10^6$ pm^3, $d_{calcd.}$ = 1.362 g cm^{-3} for Z = 4. $F(000)$ = 4456, μ(Mo-K_α) = 0.727 mm^{-1}, λ = 71.073 pm, T = 203 K, crystal size = 0.14 × 0.10 × 0.08 mm. A crystal was sealed in a glass capillary and mounted on a Siemens SMART diffractometer with a CCD area detector. A hemisphere of data was collected by a combination of three sets of exposures (24943 reflections). Each set had a different ϕ angle for the crystal, and each exposure took 15 s and covered 0.3° in ω (2.8° ≤ 2Θ ≤ 46.0°). The data were corrected for polarization and Lorentz effects, and an empirical absorption correction (SADABS) was applied (10712 unique reflections). The structure was solved by direct methods (SHELS86). Refinement was carried out with the full-matrix least-squares method based on F^2 (SHELXL93) with anisotropic thermal parameters for all non-hydrogen atoms. Hydrogen atoms were inserted in calculated positions and refined riding with the corresponding atom. Refinement converged at R_1 = 0.069 [for 7062 reflections with $I > 2\sigma(I)$], wR_2 = 0.150 $\{w = [\sigma^2(F_o)^2 + (0.0887P)^2 + 17.77P]^{-1}$, where $P = (F_o^2 + 2F_c^2)/3\}$; final GOF = 1.064. The final difference map showed no peak larger than +0.942 e^{-3} and no hole larger than −0.359 e Å^{-3}.[9]

[1] U. Schubert, N. Hüsing, N. Lorenz, *Chem. Mater.* **1995**, *7*, 2010.
[2] C. Sanchez, M. In, *J. Non-Cryst. Solids* **1992**, *147/148*, 1.
[3] G. Kickelbick, U. Schubert, *Chem. Ber.* **1997**, *130*, 473. − G. Kickelbick, P. Wiede, U. Schubert, *Inorg. Chem.*, submitted.
[4] A. Lorenz, G. Kickelbick, U. Schubert, *Chem. Mater.*, in press.
[5] S. Doeuff, Y. Dromzee, F. Taulelle, C. Sanchez, *Inorg. Chem.* **1989**, *28*, 4439. − I. Gautier-Luneau, A. Mosset, J. Galy, *Z. Kristallogr.* **1987**, *180*, 83. − I. Laaziz, A. Larbot, C. Guizard, J. Durand, L. Cot, *Acta Crystallogr.* **1990**, *C46*, 2332.
[6] U. Schubert, E. Arpac, W. Glaubitt, A. Helmerich, C. Chau, *Chem. Mater.* **1992**, *4*, 291.
[7] S. Doeuff, Y. Dromzee, C. Sanchez, *C. R. Acad. Sci., Sect. 2* **1989**, *308*, 1409. − X. Lei, M. Shang, T. P. Fehlner, *Organometallics* **1996**, *15*, 3779.
[8] R. Schmid, A. Mosset, J. Galy, *J. Chem. Soc., Dalton Trans.* **1991**, 1999. − V. W. Day, T. A. Eberspacher, W. G. Klemperer, C. W. Park, F. S. Rosenberg, *J. Am. Chem. Soc.* **1991**, *113*, 8190. − V. W. Day, T. A. Eberspacher, W. G. Klemperer, C. W. Park, *J. Am. Chem. Soc.* **1993**, *115*, 8469. − V. W. Day, T. A. Eberspacher, Y. Chen., J. Hoa, W. G. Klemperer, *Inorg. Chim. Acta* **1995**, *229*, 391. − N. Stenou, F. Robert, C. Sanchez, *Mater. Res. Soc. Symp. Proc.* **1996**, *435*, 487. − C. F. Campana, Y. Chen., V. W. Day, W. G. Klemperer, R. A. Sparks, *J. Chem. Soc., Dalton Trans.* **1996**, 691.
[9] Crystallographic data (excluding structure factors) for the structure reported in this paper have been deposited with the Cambridge Crystallographic Data Centre. Copies of the data can be obtained free of charge on application to CCDC, 12 Union Road, Cambridge C82 1EZ, UK [fax int. code +44(0)1223/336-033, e-mail: deposit@ccdc.cam.ac.uk] quoting the depository number CCDC-100716.

[97219]

Coordination Behaviour of the New Multidentate Ligand 3,5-Bis(dimethylaminomethyl)pyridine with Palladium(II) and Platinum(II) Metal Centres

María-Cristina Lagunas[a], Robert A. Gossage[a], Wilberth J. J. Smeets[b], Anthony L. Spek[b], and Gerard van Koten*[a]

Department of Metal-Mediated Synthesis, Debye Institute, Utrecht University[a],
Crystal and Structural Chemistry, Bijvoet Centre for Biomolecular Research, Utrecht University,[b]
Padualaan 8, NL-3584 CH Utrecht, The Netherlands

Received July 21, 1997

Keywords: Pyridine ligands / Bidentate bridging ligands / Palladium / Platinum / N ligands

The synthesis of the new potentially tridentate ligand 3,5-bis(dimethylaminomethyl)pyridine (**3**) is described. Coordination chemistry of this ligand has been investigated with Pd^{II} and Pt^{II} precursor compounds. Both a bidentate bridging bonding motif and a monodentate bonding mode is observed. The latter compounds incorporate **3** by coordination through the pyridinic N atom only. The former complexes contain ligand **3** bonded to 2 metal centres by bridging through coordination of one trialkyl N donor atom and the pyridinic N atom. The solid-state structure of a ligand bridged Pd dimer has been elucidated by single-crystal X-ray diffraction and corroborates with the solid-state IR data that suggested a *trans*-$PdCl_2$ unit was present.

Introduction

Organometallic and main-group complexes containing the terdentate ligand $[2,6\text{-}(Me_2NCH_2)_2C_6H_3]^-$ (NCN: "pincer" ligand; Scheme 1) have been extensively investigated in this laboratory over the past decade.[1][2] This work has involved a systematic study of the reactivity of these compounds with a concurrent investigation of their catalytic and electronic characteristics. Recently, we have begun to expand this chemistry to include functionalized versions of the NCN ligand containing synthetically useful groups in the *para* position of the arene ring. This has enabled the attachment of organometallic compounds to a variety of polymeric[3] and dendrimeric supports.[4] *para*-Substituted NCN ligands have also provided a convenient gateway into bi- and trimetallic systems,[5][6][7][8][9][10] and to hydrogen-bonded transition-metal networks ("molecular wires").[11][12] The introduction of a heteroatom in the aromatic ring, as in the case of the pyridine compound [2,6-$(Me_2NCH_2)C_5H_3N$] (NN′N; Scheme 1), represents a neutral version of the NCN ligand and results in modified reactivity of the resulting complexes incorporating this so-called "pyridine pincer".[13] Recent work has demonstrated that derivatives of NN′N containing a d^6 Ru^{II} metal centre present interesting structural and catalytic properties.[14]

Scheme 1

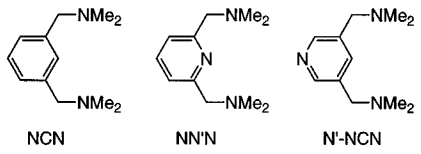

Milstein and co-workers have recently described several rhodium and palladium complexes containing the related monoanionic diphosphanylpyridine ligand [3,5-$(Ph_2PCH_2)_2C_5H_2N]^-$ (N-PCP; Scheme 2). Subsequent coordination of the palladium compound [(N-PCP)PdCl] through the pyridinic nitrogen atom to a second metal center (M_2) was shown to influence the electron density of the coordinated Pd atom.[15a]

The reactivity of structurally similar pyridinium salts (specially of those derived from 3,5-pyridinediamides) towards various nucleophiles to form 1,2- and 1,4-dihydropyridines has also attracted recent attention. These compounds serve as models for NAD/NADH systems.[16] In this respect, the study of a ligand system derived from a 3,5-disubstituted aminopyridine presents an additional reason for investigation.

Scheme 2

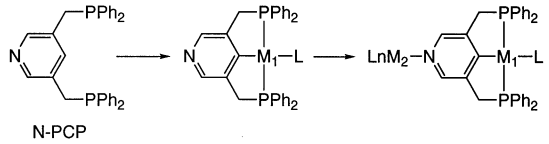

We report herein the synthesis of the neutral pyridine-based ligand $[3,5\text{-}(Me_2NCH_2)_2C_5H_3N]$ (N′-NCN: **3**; Scheme 1), a potentially bridging ligand, and examine its coordination properties towards platinum and palladium in the 2+ oxidation state. Several coordination motifs are possible for this neutral N′-NCN ligand. Here the effect of the different Lewis basicity of the donor atoms (i.e. pyridine N vs. trialkyl amine N) towards various palladium and platinum precursors is investigated. Coordination through the trialkyl N atoms of the pincer "arms" or through the pyridinic N have been achieved depending on the reaction conditions. We have combined different NCN-based ligands in the same molecule, and have studied the reactivity of NCN-N′-metalated species (pyridinium ions) towards other metal precursors.

 © WILEY-VCH Verlag GmbH, D-69451 Weinheim, 1998 1434–1948/98/0202–0163 $ 17.50+.50/0

Results and Discussion

Ligand Synthesis

The starting compound 3,5-$(ClCH_2)_2C_5H_3N$ (**2**) was prepared from 3,5-$[HOC(O)]_2C_5H_3N$ (**1**) by a modified version of a previously published method (see Experimental).[16][17][18] The dimethyl ester of **1** was first reduced with excess of $LiAlH_4$ to the diol 3,5-$(HOCH_2)_2C_5H_3N$, which upon boiling with $SOCl_2$ gave compound **2** in 33% overall yield. The ligand 3,5-$(Me_2NCH_2)_2C_5H_3N$ (**3**) was synthesized in 90% yield by a reaction of **2** and an excess of Me_2NH in benzene (see Scheme 3). After subsequent drying ($MgSO_4$) and solvent evaporation, compounds **2** and **3** were assessed to be of sufficient purity by GC/MS, and ^{1}H- and $^{13}C\{^1H\}$-NMR spectroscopy for further synthetic applications.

Scheme 3

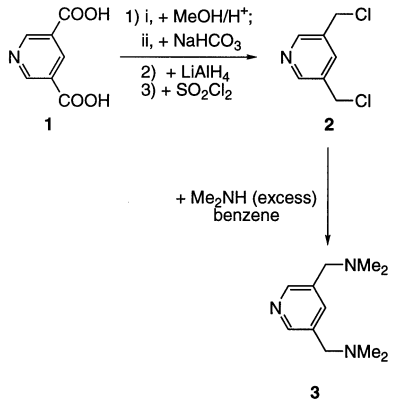

N′-NCN Coordination Compounds

With the aim of synthesizing orthometallated palladium complexes containing ligand **3**, the reaction between equimolar amounts of **3**, Li_2PdCl_4 and NaOAc in MeOH solution was investigated. Deprotonation of ligand **3** did not occur[15b] and immediate precipitation of compound **4** as a yellow solid took place (ca. 60% yield). Compound **4** could also be prepared in slightly higher yield by treating **3** with Li_2PdCl_4 (1:1) in MeOH. Small amounts of a second compound **5** were obtained in both these reactions (Scheme 4). This complex is the N(Py)-coordinated compound *trans*-$[Pd(N'\text{-}NCN)_2Cl_2]$ and was isolated in low yield (10%) from the mother liquor of the reactions. A high-yield synthesis of **5** is possible by using $PdCl_2(cod)$ (cod = cycloocta-1,5-diene) and excess **3**.

The ^{1}H-NMR spectra of compounds **4** and **5** show pronounced downfield shifts for hydrogen atoms assumed to be in close proximity to the metal atom compared with the corresponding values of free ligand **3**.

The ^{1}H-NMR spectrum at room temperature of compound **4** presents four singlets for the CH_2 and CH_3 groups. These are assigned to the non-coordinated arm (δ = 3.45, 2.22) and at lower field to the coordinated one [δ = 3.85 (br.), 2.66]. The signals of the three pyridine protons appear as three singlets at δ = 11.51, 8.47, and 7.58 (2-H, 6-H, and 4-H, respectively). It is assumed that a fast flip of the 12-membered ring that contains the two Pd atoms occurs in solution on the NMR timescale. This would explain the chemical shift equivalence between both diastereotopic protons of the CH_2 and CH_3 groups of the coordinated arm. The pronounced downfield shift observed for pyridine 2-H atoms upon coordination (Δδ = 3.1) contrasts with the small shift of the 6-H protons (Δδ = 0.06; Table 1). Such a high deshielding may be due to the proximity of this proton with respect to both a Cl and a Pd atom, as indicated by the short H···Cl and H···Pd interactions present in the solid-state structure (vide infra). Large downfield shifts of protons situated close to a d^8 metal center and above the bonding plane (pseudoaxial position) have been described in the literature and are attributed to the paramagnetic anisotropy of the metal atom[19] or to the presence of weak CH···M agostic interactions.[20] A deshielding effect is also expected for H atoms involved in short C−H···Cl contacts or in hydrogen bonds. The $^{13}C\{^1H\}$-NMR spectrum of **4** does not present any unusual features, revealing only four singlets for the two inequivalent CH_2 and NCH_3 groups and five singlets for the aromatic C atoms, in support of the above discussion (Table 2). The IR spectrum of **4** contains a band at 343 cm^{-1} that is assigned to the Pd−Cl stretching vibration of *trans*-dichloride ligands.

Scheme 4

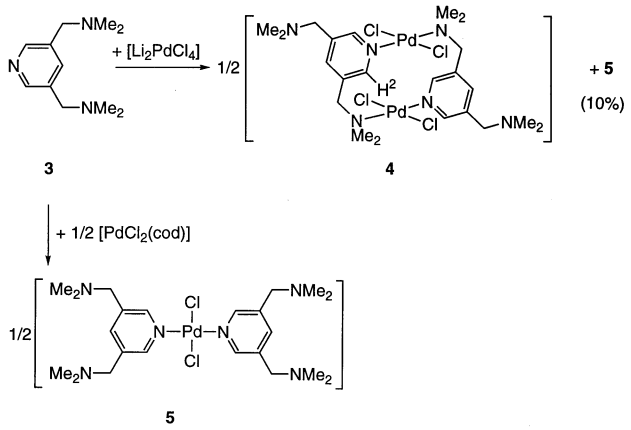

The pyridinic 2,6-H and 4-H in compound **5** resonate as a doublet and a broad singlet at δ = 8.63 and 7.81, respectively in the ^{1}H NMR. The same resonances appear at δ = 8.41 and 7.62 in free **3**. The CH_2 and NCH_3 groups in **5** (singlets at δ = 3.45 and 2.26) have similar chemical shifts to those of **3** (Table 1). The $^{13}C\{^1H\}$-NMR spectrum of **5** presents five singlets of the coordinated ligand (Table 2). The *trans* configuration of compound **5** was supported by the presence of a single IR absorbance at 345 cm^{-1}, assigned to the Pd−Cl stretching vibration as in **4**.

(NCN)Pt(N′-NCN) Complexes

Previous publications have described the synthesis and reactivity of stable Pt complexes containing the monoanionic $[NCN]^-$ ligand. These compounds possess a variety of interesting properties involving the oxidative addition of halogens and alkyl halides (**6** and **7**: Scheme

Table 1. ^{1}H-NMR-spectroscopic data for compounds **3**–**5**, **8**, **9**[a]

	Py	Ph	(Ph)CH_2	(Py)NCH_2	(Ph)NCH_3	(Py)CH_3
3	8.41[b] (d; 2,6-H) 7.62[b] (t; 4-H)			3.42 (s)		2.23 (s)
4	11.51 (s; 2-H) 8.47 (s; 6-H) 7.58 (s; 4-H)			3.85 (br. s) 3.45 (s)		2.66 (s) 2.22 (s)
5	8.63[c] (d; 2,6-H) 7.81 (s[br]; 4-H)			3.45 (s)		2.26 (s)
8[d]	8.96[e] (m; 2,6-H) 8.01 (s [br]; 4-H)	7.05[f] (t; 4-H) 6.93[f] (d; 3,5-H)	4.30[g] (m)	3.63 (s)	2.89[h] (m)	2.25 (s)
9[d,i]	8.97 (s; 2,6-H)	7.20 (s; 2,6-H)	4.38[i] (m)	3.64 (s)	2.93[k] (m)	2.26 (s)

[a] ^{1}H-NMR data recorded at 200 or 300 MHz. Chemical shifts in ppm (δ from external $SiMe_4$ (δ = 0.0). $CDCl_3$ solutions were used except where noted. – [b] $^4J(^1H\text{-}^1H)$ = 3 Hz. – [c] $^4J(^1H\text{-}^1H)$ = 1.4 Hz. – [d] ^{1}H NMR in [D_6]acetone. – [e] $^4J(^1H\text{-}^1H)$ = 1.5 Hz. $^3J(^{195}Pt\text{-}^1H)$ = 13.7 Hz. – [f] $^3J(^1H\text{-}^1H)$ = 7 Hz. – [g] $^3J(^{195}Pt\text{-}^1H)$ = 50 Hz. – [h] $^3J(^{195}Pt\text{-}^1H)$ = 40 Hz. – [i] $^{19}F\{^1H\}$ = −77.9 (s, CF_3SO_3). – [i] $^3J(^{195}Pt\text{-}^1H)$ = 48 Hz. – [k] $^3J(^{195}Pt\text{-}^1H)$ = 39 Hz.

Table 2. $^{13}C\{^1H\}$-NMR-spectroscopic data for compounds **3**–**5**, **8**, **9**[a]

	Py + Ph	(Ph)CH_2	(Py)CH_2	(Ph)NCH_3	(Py)NCH_3
3	149.2 (2,6-Py), 137.3 (4-Py), 133.8 (3,5-Py)		61.3		45.3
4	156.1, 153.7, 141.6, 135.7, 132.1		66.3, 60.5		53.4, 45.3
5	152.0 (2,6-Py), 139.6 (4-Py), 135.9 (3,5-Py)		60.5		45.3
8	149.7, 143.5 (m; 2,6-Ph)[b], 142.8 (1-Ph), 139.7, 138.6, 125.2, 119.7	77.4	65.8	53.9	45.3
9[c]	150.9, 146.2 (m; 2,6-Ph)[d], 143.2 (1-Ph), 140.6, 140.3, 139.4, 119.0	78.0 (m)[e]	61.1	54.1	45.4

[a] $^{13}C\{^1H\}$-NMR data recorded at 50 or 75 MHz. Chemical shifts in ppm (δ) from external $SiMe_4$ (δ = 0.0) except where noted. Aromatic signals not all unequivocally assigned. All signals are singlets unless otherwise noted. – [b] $^2J(^{195}Pt\text{-}^{13}C)$ = 67 Hz. – [c] $^{13}C\{^1H\}$ NMR in [D_6]acetone. – [d] $^2J(^{195}Pt\text{-}^{13}C)$ = 70 Hz. – [e] $^2J(^{195}Pt\text{-}^{13}C)$ = 48 Hz.

5).[1][10] Replacement of the coordinated MeCN ligands in complexes **6** and **7** by ligand **3** was therefore examined.

The starting compound **6** was prepared in situ by the reaction of the known complex PtCl[$(Me_2NCH_2)_2C_6H_3$][25] (**10**) with $Ag(O_3SCF_3)$ in MeCN (see Experimental Section). Compound **3** was then reacted separately with the cationic platinum complexes **6** and **7** in dry acetone to give the corresponding products **8** and **9** (Scheme 5). Displacement of MeCN by **3** takes place only when an excess of the latter is used. The structure proposed for compounds **8** and **9**, in which the ligand **3** coordinates to platinum through the pyridinic nitrogen atom, was confirmed by ^{1}H- and $^{13}C\{^1H\}$-NMR spectroscopy. These spectra show similar features to those of the parent compounds **7** and **10**, in addition to the resonances expected for coordinated **3**. Appropriate downfield shifts of the pyridinic 2,6-H and 4-H atoms with respect to **3** is observed, in addition to the presence of ^{195}Pt satellites associated with the resonance assigned to the 2,6-H of the pyridine ring (Table 1).

The addition of a drop of MeCN to a solution of **8** in [D_6]acetone resulted in partial conversion of **8** into the starting complex **6**, with liberation of free ligand **3**. This was observed in situ by ^{1}H-NMR spectroscopy. Compounds **8** and **9** are moisture-sensitive as slow ligand exchange processes between **3** and H_2O have likewise been observed (^{1}H NMR).

Scheme 5

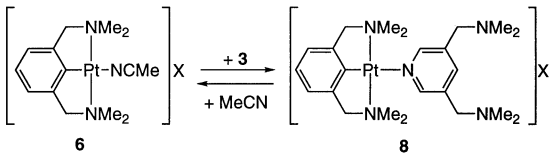

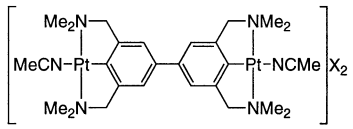

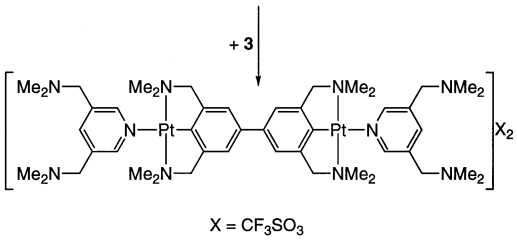

The high lability of ligand **3** in compounds **8** and **9** made it difficult to draw conclusions concerning the subsequent coordination of **3** through the N atoms of the "arms". Thus, reaction of **9** with 2 equivalents of $PtCl_2(SEt_2)_2$ in dry acetone gave, among other non identified compounds, the neutral complex [ClPt(NCN−NCN)PtCl][10] which precipitated from the reaction mixture and was identified by its ^{1}H-NMR spectrum in $CDCl_3$.

In a subsequent reaction, ligand **3** and compound **8** were allowed to react with 1 equiv. of $[Pd(MeCN)_4](BF_4)_2$ in

[D_6]acetone. After 15 min, the ^{1}H-NMR spectrum of the reaction mixture showed the presence of at least three compounds. The most abundant product being complex **6**. Unfortunately, the minor components of the mixture could not be unequivocally assigned.

An ORTEP diagram representing the solid-state molecular structure of compound **4** in the crystal is depicted in Figure 1. Selected bond lengths and angles are listed in Table 3. The molecule of **4** has an inversion center at the center which is also a crystallographic inversion center. A distorted square-planar coordination at the Pd metal centre is observed. The value of the angles N1−Pd1−N3a are smaller than 180° [174.51(4)° and 172.9(1)°, respectively] and N3a is positioned significantly (0.24 Å) out of the plane determined by Pd1, Cl1, Cl2, and N1 (mean plane deviation 0.001 Å). This plane forms an angle of ca. 53° with the pyridine ring. The Pd1−Cl (average) and Pd1−N1 atom distances in complex **4** are 2.298(1) and 2.031(3) Å, respectively, and lie within the range observed in other *trans*-dichloropalladium(II) complexes containing pyridine ligands: 2.289−2.310 Å and 2.024−2.043 Å respectively.[21] The Pd1−N3a atom distance in **4** [2.102(3) Å] is similar to that found in related aryldimethylaminopalladium complexes.[10][22]

Figure 1. An ORTEP diagram (50-% probability level) of the molecular structure of complex **4** showing the adopted numbering scheme

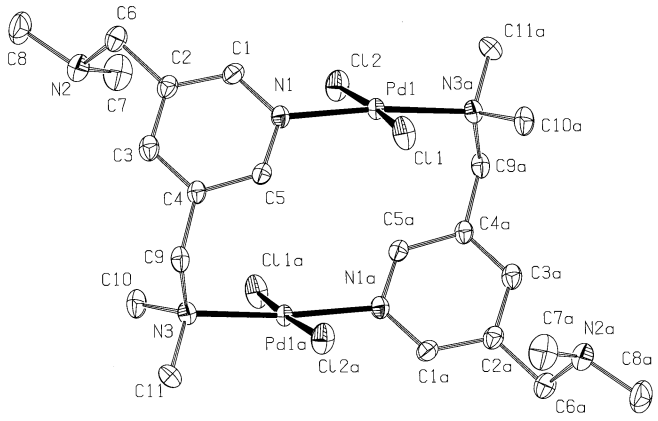

Table 3. Selected bond lenghts [Å] and angles [°] of compound **4**

Pd(1)−Cl(1)	2.2882(11)	Cl(1)−Pd(1)−Cl(2)	174.51(4)
Pd(1)−Cl(2)	2.3086(11)	Cl(1)−Pd(1)−N(1)	87.73(9)
Pd(1)−N(1)	2.031(3)	Cl(1)−Pd(1)−N(3a)	94.74(9)
Pd(1)−N(3)a	2.102(3)	Cl(2)−Pd(1)−N(1)	86.78(9)
		Cl(2)−Pd(1)−N(3a)	90.69(9)
		N(1)−Pd(1)−N(3a)	172.92(14)

The 12-membered ring containing the Pd atoms adopts a strained zigzag "chair"-like conformation which brings H51 close to both the Pd1a and the C11 atoms with H···Cl [2.73(3) Å] and H···Pd [2.69(2) Å] interatomic distances considerably shorter than the sum of the corresponding Van der Waals radii[23] (indicated by dotted lines in the Figure). Similar short Pd···H contacts have been identified in other Pd^{II} complexes.[19a][21b][21c][24] The C5−H51···C11 angle in complex **4** [109.6(19)°] is too far from linearity as to be considered a typical hydrogen bond. The intramolecular Pd···Pd distance [4.5997(8) Å] is virtually identical to the sum of their contact radii (4.6 Å).[23] Some of these features are comparable to those observed in other dipalladium ring systems described by Constable et al., e.g. [Pd_2Cl_4-{$Me_2N(CH_2)_nNMe_2$}$_2$] (n = 5, 7)[25] and [Pd_2Cl_4{Me_2NN=$CH(CH_2)_3CH$=$NNMe_2$}$_2$].[25b] The higher thermodynamic stability of these 16- and 20-membered cyclic systems with respect to their open-chain analogues has been explained in terms of entropy and conformational effects. Such influences can be derived from the presence of bulky NMe_2 groups occupying "corner positions" in the ring, the existence of double bonds in the ligand system, and/or the formation of short H···H and H···Pd attractive transannular interactions (e.g. 2.4 Å and 2.6−2.7 Å, respectively in [Pd_2Cl_4{$N(NMe_2)$=$CH(CH_2)_3CH$=$N(NMe_2)$}$_2$]).[25b] In spite of the obvious similarities between both our ligand system and complexes **3** and **4** and those studied by Constable et al., we suggest that short intramolecular interactions present in complex **4** (a more rigid system) may be due to geometrical contraints within the molecule, and not to forces of attractive nature. However, it is noticeable that although a certain degree of flexibility of the ring at room temperature in solution has been shown by ^{1}H-NMR spectroscopy (vide supra), short H···Cl and/or H···Pd contacts still appear to be important in solution.

Conclusions

It has been demonstrated that the potentially multidentate ligand 3,5-bis(dimethylaminomethyl)pyridine (**3**) can be synthesized in good yield from the corresponding bis(chloromethyl)pyridine. The coordination versatility of **3** has been shown in complex **4**, where N_{py}−Pd and Me_2N−Pd bonds are present, and in complexes **5**, **8**, and **9** in which only bonding through N_{Py} are observed. The three latter complexes represent a linear geometry of the NCN and N′-NCN ligands and thus are a potential starting point for the synthesis of organometallic chains. Our attempts to ligate the free NMe_2 groups of **8** and **9**, and hence to increase the number of metal centres, has not so far been successful. This may be a manifestation of the inherit lability of the N_{py}−M bond in these compounds.

This work was supported in part (A. L. S. and W. J .J. S.) by the *Netherlands Foundation of Chemical Research (SON)* with financial aid form the *Netherlands Organisation for Scientific Research (NWO)*. Mr. *Bert T. G. Lutz*, Department of Analytical Molecular Spectrometry, Faculty of Chemistry, Utrecht University is gratefully acknowledged for the infrared analyses of compounds **4** and **5**. The *European Community* is thanked for the award of a Fellowship (*Human Capital and Mobility Program, cat. 30*) to M. C. L. The authors would like to thank *H. Pruiksma* for assistance in the preparation of this manuscript.

Experimental Section

General: All experiments were conducted under dry nitrogen using standard Schlenk techniques. Solvents were dried over appropriate materials and distilled prior to use. − Elemental analyses were performed by Dornis und Kolbe, Mikroanalytisches Labora-

torium (Mülheim, Germany). – ^{1}H- and ^{13}C{^{1}H}-NMR spectra were recorded at 298 K with a Bruker AC200 or AC300 spectrometers. – Infrared spectra were recorded as Nujol mulls deposited on disposable polyethene substrates (700–100 cm^{-1}) with a Perkin Elmer Model 2000 FT-IR spectrometer equipped with a MIRTGS (for MIR) and FIRTGS (for FIR) detector. The instrument was flushed with nitrogen and connected to a PC under SPECTRUM software. – Melting (decomposition) points were measured using a Büchi melting-point apparatus. The boiling point of compound **3** was determined by the Siwoloboff method. – GC/MS analyses were recorded with a Unicam Automass instrument using electron impact (EI, 70eV). – Starting materials: $[Li_2PdCl_4]$[26] and $[PdCl_2(cod)]$[27] were prepared according to literature procedures. $Ag(O_3SCF_3)$ was purchased from Aldrich and $C_5H_3N(CO_2H)_2$-3,5 (**1**) from Avocado.

Synthesis of 3,5-(ClCH$_2$)$_2$C$_5$H$_3$N (**2**):[28] To a suspension of $LiAlH_4$ (1 g, 26.3 mmol) in Et_2O (25 ml) was added 3,5-$[MeO(O)C]_2C_6H_3N$ (1.7 g, 8.7 mmol).[29] The resulting yellow mixture was stirred for 15 h and MeOH (50 ml) was then added slowly to destroy excess $LiAlH_4$. The solvent was then removed in vacuo and the residue extracted in a Soxhlet apparatus with MeOH (12 h). The solution was subsequently concentrated to to give 3,5-$(HOCH_2)_2C_5H_3N$ as a yellow oil [^{1}H NMR (CD_3OD, 300 MHz), δ = 8.42 (s, 2 H, 2,6-Py*H*), 7.82 (s, 1 H, 4-Py*H*), 4.66 (s, 4 H, C*H*$_2$)]. Thionyl chloride (150 ml) was then added to the oil and the mixture refluxed for 18 h yielding a brown suspension. Excess of $SOCl_2$ was distilled off (vacuo) and the flask placed in an ice bath. Aqueous NaOH (100 ml; 4 M) was added slowly to the residue. The aqueous layer was then extracted with CH_2Cl_2 (4 × 25 ml) and the combined organic layers were dried with $MgSO_4$. The solvent was then removed in vacuo to give **2** as an off-white solid (2.9 g, 47% yield based on the starting ester). Mp: 86°C. – MS (EI, 70 eV); *m/z* (%): 175 (22.1) [M$^+$], 140 (100), 104 (11.0), 77 (25.0), 51 (16.3).

Synthesis of 3,5-(Me$_2$NCH$_2$)$_2$C$_5$H$_3$N (N′-NCN; **3**): A three-necked round-bottom flask was placed in an ice bath and charged with benzene (20 ml) and Me_2NH (17 ml, 255 mmol). A solution of **2** (2.4 g, 13.8 mmol) in 200 ml of benzene was then added via a dropping funnel during 30 min. The reaction mixture was allowed to reach room temperature and then stirred for 1 h yielding a yellow suspension which was concentrated in vacuo to ca. 100 ml and subsequently filtered. The filtrate was concentrated to dryness to give the product **3** as an orange liquid, which was dissolved in pentane and dried with $MgSO_4$ overnight (yield: 2.4 g, 90%). Bp: 178–180°C.[24] – MS (EI, 70 eV); *m/z* (%): 193 (3.8) [M$^+$], 150 (100), 105 (73.1), 77 (40.4), 58 (99.0).

Synthesis of μ-[{η^1-N,N′-3,5-(Me$_2$NCH$_2$)$_2$C$_6$H$_3$N}(PdCl$_2$)]$_2$ (**4**): To a solution of $[Li_2PdCl_4]$ (0.19 mg, 0.724 mmol) in MeOH was added **3** (0.14 mg, 0.724 mmol). The resulting yellow suspension was stirred overnight and then filtered. The solid thus obtained was then washed with MeOH and Et_2O and subsequently dried in vacuo. Compound **4** was isolated as a yellow solid, which was recrystallized from CH_2Cl_2 /Et_2O and dried on P_2O_5 (yield: 0.18 g, 67%). Mp: 179–180 (dec.)°C. – IR [υ(PdCl)]: $\tilde{\nu}$ = 343 cm^{-1}. – $C_{22}H_{38}Cl_4N_6Pd_2$: calcd. C 35.65, H 5.16, N 11.34; found: C 35.31, H 5.23, N 11.08.

Synthesis of trans-[{η^1-3,5-(Me$_2$NCH$_2$)$_2$C$_6$H$_3$N}$_2$PdCl$_2$] (**5**): To a solution of $[PdCl_2(cod)]$ (63 mg, 0.22 mmol) in CH_2Cl_2 was added an excess of **3** (172 mg, 0.891 mmol). After 30 min, the solution was concentrated in vacuo to approximately 2–3 ml and Et_2O was then added to precipitate the product (**5**) as a pale yellow solid. This was washed with Et_2O and dried (yield 70 mg, 60% yield). Mp: 110°C (dec). – IR [υ(PdCl)]: $\tilde{\nu}$ = 345 cm^{-1}. – $C_{22}H_{38}Cl_2N_6Pd$: calcd. C 46.86, H 6.79, N 14.90; found: C 46.53, H 6.92, N 14.47.

Synthesis of [{η^1-3,5-(Me$_2$NCH$_2$)$_2$C$_6$H$_3$N}Pt{η^3-NCN-2,6-(Me$_2$NCH$_2$)$_2$C$_6$H$_3$}](CF$_3$SO$_3$) (**8**): To a solution of [(η^3-NCN-2,6-{Me_2NCH_2}$_2$C$_6$H$_3$)PtCl][18] (96.4 mg, 0.228 mmol) in MeCN was added $Ag(O_3SCF_3)$ (64.4 mg, 0.250 mmol). The resulting suspension was stirred for 10 min and then filtered through a plug of Celite. The filtrate was concentrated to dryness and washed with Et_2O to give compound **6** as a colorless solid. Complex **6** was then dissolved in dry acetone and **3** (74 mg, 0.38 mmol) was added to the solution. Upon addition of Et_2O to the reaction mixture, compound **8** precipitated as a colourless solid, which was filtered, washed with Et_2O, and dried in vacuo (yield: 140 mg, 85%). Mp: 165°C (dec). – $C_{24}H_{38}F_3N_5O_3PtS$: calcd. C 39.56, H 5.26, N 9.61; found C 39.32, H 5.36, N 9.42.

Synthesis of [{η^1-3,5-(Me$_2$NCH$_2$)$_2$C$_6$H$_3$N}Pt{η^3-NCN-2,6-(Me$_2$NCH$_2$)$_2$C$_6$H$_2$}](CF$_3$SO$_3$)$_2$ (**9**): To a solution of **7** (51.9 mg, 0.045 mmol)[10] in dry acetone was added an excess of **3** (80 mg, 0.41 mmol). The resulting yellow solution was stirred at room temperature for 30 min. The solvent was then removed in vacuo and the residue washed with Et_2O (2 × 5 ml) to give **9** as a pale yellow solid (yield: 50 mg, 76%). Mp: 137–140°C (dec). – ^{19}F{^{1}H} NMR [$(CD_3)_2CO$, 200 MHz], δ = –77.9 (s, C*F*$_3$SO$_3$). – $C_{48}H_{74}F_6N_{10}O_6Pt_2S_2$: calcd. C 39.61, H 5.12, N 9.62; found C 39.54, H 5.04, N 9.46.

X-ray Structure Determination of Complex **4**: X-ray data were collected for an orange needle-shaped crystal at 150 K with an Enraf-Nonius CAD4T on rotating anode. Numerical data on the structure determination are collected in Table 4. The unit-cell parameters were derived from the 25 SET4[30] setting angles. The structure was solved with automated Patterson techniques using DIRDIF96[31] and refined on F^2 using the program SHELX96.[32] All other calculations (including the ORTEP illustration) were done with PLATON.[33]

Table 4. Crystal data and details on the structure determination of complex **4**

Empirical formula	$C_{22}H_{38}Cl_4N_6Pd_2$
Formula weight	741.23
Crystal system	Monoclinic
Space group	$P2_1/c$ (no. 14)
a [Å]	10.0020(6)
b [Å]	13.3358(18)
c [Å]	12.5944(14)
β [°]	120.186(7)
V [Å^3]	1452.1(3)
Z	2
$D_{calcd.}$ [g cm^{-3}]	1.695
F (000)	744
μ(Mo-$K_α$) [cm^{-1}]	16.3
Crystal size [mm]	0.10×0.13×0.38
Temperature [K]	150
Radiation, λ [Å] (graphite-monochromated)	Mo-$K_α$, 0.71073
θ (min., max.) [°]	2.4, 27.5
Scan (type and range) [°]	0.75 + 0.35tanθ
Dataset	−12/12; 0/17; −16/16
Tot., uniq. data, *R* (int)	7017, 3324, 0.049
Observed data [$I > 2.0σ(I)$]	2486
N_{ref}, N_{par}	3324, 167
R, *wR*	0.0348, 0.0620[a]
S	1.00
Max. and av. shift/error	0.00, 0.00
Min. and max. resd. electron dens. [e/Å^3]	−0.51, 0.48

[a] $w = 1/[σ^2(F_o^2) + (0.0172\ P)^2]$; where $P = (F_o^2 + 2\ F_c^2)/3$.

Hydrogen atoms were located at calculated positions and refined riding on their carrier atoms. A final difference map did not show any significant residual density. The structure contains no residual solvent-accessible voids as indicated by the PLATON/SOLV option.[33]

Crystallographic data (excluding structure factors) for the structure reported in this paper have been deposited with the Cambridge Data Centre as supplementary publication no. CCDC-100824. Copies of the data can be obtained free of charge on application to CCDC, 12 Union Road, Cambridge CB2 1EZ, UK [Fax: internat. code + 44(0)1223/336-033; E-mail: deposit@ccdc.cam.-co.uk].

[1] G. van Koten, *Pure Appl. Chem.* **1989**, *61*, 1681.
[2] M. H. P. Rietveld, D. M. Grove, G. van Koten, *New J. Chem.* **1997**, *21*, 751.
[3] [3a] L. A. van de Kuil, D. M. Grove, J. W. Zwikker, L. W. Jenneskens, W. Drenth, G. van Koten, *Chem. Mater.* **1994**, *6*, 675. – [3b] D. Pathmamanohan, P. Wijkens, D.M. Grove, A.P. Philipse, *Langmuir* **1996**, *12*, 4372.
[4] J. W. J. Knapen, A. W. van der Made, J. C. de Wilde, P. W. N. M. van Leeuwen, P. Wijkens, D. M. Grove, G. van Koten, *Nature* **1994**, *372*, 659.
[5] J.-P. Sutter, D. M. Grove, M. Beley, J.-P. Collin, N. Veldman, A. L. Spek, J.-P. Sauvage, G. van Koten, *Angew. Chem.* **1994**, *106*, 1359; *Angew. Chem. Int. Ed. Engl.* **1994**, *33*, 1282.
[6] S. L. James, N. Veldman, A. L. Spek, G. van Koten, *Chem. Commun.* **1996**, 253.
[7] P. Steenwinkel, S. L. James, D. M. Grove, N. Veldman, A. L. Spek, G. van Koten, *Chem. Eur. J.* **1996**, *2*, 1440.
[8] P. Steenwinkel, S. L. James, N. Veldman, H. Kooijman, A. L. Spek, D. M. Grove, G. van Koten, *Organometallics*, submitted.
[9] P. Steenwinkel, G. van Koten, A. L. Spek, manuscript in preparation.
[10] M. C. Lagunas, R. A. Gossage, W. J. J. Smeets, A. L. Spek, G. van Koten, *Organometallics*, in press.
[11] P. J. Davies, N. Veldman, D. M. Grove, A. L. Spek, B. T. G. Lutz, G. van Koten, *Angew. Chem.* **1996**, *108*, 2078; *Angew. Chem. Int. Ed. Engl.* **1996**, *35*, 1959.
[12] S. L. James, G. Verspui, A. L. Spek, G. van Koten, *Chem. Commun.* **1996**, 1309.
[13] B. A. Markies, P. Wijkens, J. Boersma, H. Kooijman, N. Veldman, A. L. Spek, G. van Koten, *Organometallics* **1993**, *13*, 3244.
[14] [14a] R. A. T. M Abbenhuis, M. M.Bergshoef, J. Boersma, W. J. Smeets, N. Veldman, D. Kruis, A. L. Spek, G. van Koten, manuscript in preparation. – [14b] Q. Jiang, D. van Plew, S. Murtuza, X. Zhang, *Tetrahedron Lett.* **1996**, *37*, 797 and references therein.
[15] [15a] A. Weisman, M. Gozin, H.-B. Kraatz, D. Milstein, *Inorg. Chem.* **1996**, *35*, 1792. – [15b] M. E. van der Boom, S.-Y. Liou, L. J. W. Shimon, Y. Ben-David, D. Milstein, *Organometallics* **1996**, *15*, 2562.
[16] [16a] U. Eisher, J. Kuthan, *Chem. Rev.* **1972**, *72*, 1. – [16b] F. Rob, J. J. van Ramesdonk, W. van Gerresheim, P. Bosma, J. J. Scheele, J. W. Verhoeven, *J. Am. Chem. Soc.* **1984**, *106*, 3826. – [16c] J. C. Speelman, R. M. Kellogg, *J. Org. Chem.* **1990**, *55*, 647. – [16d] Y.-D. Wu, D. K. W. Lai, K. N. Houk, *J. Am. Chem. Soc.* **1995**, *117*, 4100.
[17] K. Tsuda, N. Ikekawa, R. Takasaki, Y. Yamakawa, *Chem. Pharm. Bull. Jpn.* **1953**, *1*, 142.
[18] K. J. Przybilla, F. Vögtle, *Chem. Ber.* **1989**, *122*, 347.
[19] [19a] A. J. Deeming, I. P. Rothwell, M. B. Hursthouse, L. New, *J. Chem. Soc., Dalton Trans.* **1978**, 1490. – [19b] R. G. Miller, R. D. Stauffer, D.R. Faheu, D. R. Parnell, *J. Am. Chem. Soc.* **1970**, *92*, 1511. – [19c] J. F. van Baar, K. Vrieze, D. J. Stufkens, *J. Organomet. Chem.* **1974**, *81*, 247.
[20] [20a] A. Albinati, P. S. Pregosin, F. Wombacher, *Inorg. Chem.* **1990**, *29*, 1812 and references therein. – [20b] F. Neve, M. Ghedini, A. Crispini, *Organometallics* **1992**, *11*, 3324.
[21] [21a] M. C. Navarro-Ranninger, S. Martinez-Cabrera, S. Garcia-Blanco, *Acta Crystallogr.* **1985**, *C41*, 21. – [21b] G. Vasapollo, C. F. Nobile, M. Latronico, M. Lanfranchi, M. A. Pellinghelli, *J. Organomet. Chem.* **1987**, *336*, 429. – [21c] J. Vicente, M. T. Chicote, M. C. Lagunas, P. G. Jones, E. Bembenek, *Organometallics* **1994**, *13*, 2143. – [21d] P. B. Viossat, N.-H. Dung, F. Robert, *Acta Crystallogr.* **1993**, *C49*, 84.
[22] J. Terheijden, G. van Koten, F. Muller, D. M. Grove, K. Vrieze, E. Nielsen, C.H. Stam, *J. Organomet. Chem.* **1986**, *315*, 401.
[23] A. Bondi, *J. Phys. Chem.* **1964**, *68*, 441.
[24] J.-M. Valk, F. Maassarani, P. van der Sluis, A. L. Spek, J. Boersma, G. van Koten, *Organometallics* **1994**, *13*, 2320.
[25] [25a] A. Constable, W. S. McDonald, B. L. Shaw, *J. Chem. Soc., Dalton Trans.* **1979**, 496. – [25b] A. Constable, W. S. McDonald, B. L. Shaw, *J. Chem. Soc., Dalton Trans.* **1979**, 1109.
[26] P. M. Henry, O. W. Marks, *Inorg. Chem.* **1971**, *10*, 373.
[27] J. Chatt, L. M. Vallarino, L. M. Venanzi, *J. Chem. Soc.* **1957**, 3413.
[28] This procedure is analogous to the modified method of Tsuda et al.[17] described by Przybilla et al.[18]
[29] Prepared from 3,5-$[HOC(O)]_2C_5H_3N$ by esterification with MeOH-H_2SO_4 followed by neutralization with $NaHCO_3$ (see: H. Meyer, H. Tropsch. *Monatsh. Chem.* **1914**, *35*, 207).
[30] J. L. de Boer, A. J. M. Duisenberg, *Acta Crystallogr. Sect. A* **1990**, *40*, C-410.
[31] P. T. Beurskens, G. Beurskens, W. P. Bosman, R. de Gelder, S. Garcia-Grande, R. O. Gould, R. Isreal, J. M. M. Smits *The DIRDIF-96 Program System*, Nijmegen University, The Netherlands, **1996**.
[32] G. M. Sheldrick, *SHELX-96, Program for Crystal Structure Refinement*, University of Göttingen, Germany, **1996**.
[33] A. L. Spek, *Acta Crystallogr., Sect. A* **1990**, C-34.

[97172]

Synthesis, Spectroscopy, and Magnetic Properties of Transition-Metal Complexes with the Diethyl 2-Quinolylmethylphosphonate (2-qmpe) Ligand − Crystal Structures of $[Ni(2\text{-qmpe})_4(H_2O)_2](ClO_4)_2$ and $[Mn(2\text{-qmpe})_4(H_2O)_2](ClO_4)_2$ Showing Unexpected O-Binding of the qmpe Ligands

Justyn Ochocki*[a], Bogumila Zurowska[b], Jerzy Mroziński[b], Huub Kooijman[c], Anthony L. Spek[c], and Jan Reedijk[d]

Institute of Chemistry, Medical University[a],
Muszynskiego 1, PL-90-151 Lodz, Poland
E-mail: Ochocki@lodz.pdi.net

Institute of Chemistry, Wroclaw University[b],
PL-50-383 Wroclaw, Poland

Bijvoet Center for Biomolecular Research, Crystal and Structural Chemistry, Utrecht University[c],
Padualaan 8, NL-3584 CH Utrecht, The Netherlands

Leiden Institute of Chemistry, Gorlaeus Laboratories, Leiden University[d],
P.O. Box 9502, NL-2300 RA Leiden, The Netherlands

Received August 20, 1997

Keywords: Ligand field spectra / Phosphonate complexes / X-ray structures

The synthesis and characterization of transition-metal coordination compounds containing the ligand diethyl 2-quinolylmethylphosphonate (2-qmpe) is described. Complexes of Co^{II}, Mn^{II}, Ni^{II}, Cd^{II}, and Zn^{II} were found to be mutually isomorphous according to their X-ray powder diffraction patterns and IR spectra. The new coordination compounds were identified and characterized by elemental analysis, magnetic measurements, infrared and ligand-field spectra. The crystal structures of the complexes $[M(2\text{-qmpe})_4(H_2O)_2](ClO_4)_2$ (M = Ni, **1**; Mn, **2**) reveal six-coordinate $[M(2\text{-qmpe})_4(H_2O)_2]$ cations with the qmpe ligand coordinating via the oxygen rather than via the nitrogen atom, as well as lattice perchlorate anions. The metal ion is octahedrally surrounded by the four oxygen atoms of the four organic ligands. The non-participation of the pyridine nitrogen atom is unusual. The two water molecules occupy the fifth and the sixth coordination sites in a *trans* configuration. The coordinated water molecules are strongly hydrogen-bonded to the pyridine nitrogen atom of the 2-qmpe, further stabilizing the solid-state structure. The geometry of the metal ion can be described as distorted octahedral. For the Cu^{II} complex, a hydroxo-bridged dinuclear structure of the type $[Cu(2\text{-qmpe})_2(OH)(H_2O)_2]_2(ClO_4)_2$ is proposed, based on its spectroscopic and magnetic properties. Ligand-field spectra of the Co and Ni compounds were found to be in agreement with the tetragonally distorted octahedral geometry.

Introduction

During the last decade there has been a great increase in interest in ligands containing a phosphoryl group and a heterocyclic ring[1]. Organophosphorus derivatives of pyridine and quinoline with the phosphonic chain *ortho* or *para* with respect to the endocyclic nitrogen atom have been shown to possess significant bactericidal and herbicidal activity. Coordination compounds of phosphonic acids and their esters with transition-metal ions have been the subject of several studies due to the fact that complexes of such compounds exhibit biological activity[1][2][3][4][5][6][7][8][9][10][11][12][13][14]. In recent years, platinum(II) complexes of phosphonate ligands have attracted attention as a result of their significant antitumor activity[8]. Phosphonate ligands bearing a heterocyclic ring have some interesting features with regard to their coordination chemistry; they contain two potential donor atoms, the heterocyclic nitrogen and phosphoryl oxygen atoms, in a suitable orientation for chelation. Over the years, we have studied in detail the complex-forming properties of phosphonate ligands towards transition-metal ions. The coordination behaviour of pyridylmethylphosphonate ligands was examined by single-crystal X-ray structure determinations, which showed that various coordination modes are possible[10][28]. In a previous study, the results of spectroscopic and magnetic studies on transition-metal complexes with diethyl 2- and 4-pyridylmethylphosphonate ligands (2-pmpe, 4-pmpe), as well as the structures of high-spin $[Co(4\text{-pmpe})_4(H_2O)_2](ClO_4)_2(H_2O)_2$, where the ligand bridges the cobalt ions with both ends of the molecule coordinating to a different metal ion forming infinite chains, and of $[Co(2\text{-pmpe})_2Cl_2]$, where the 2-pmpe acts as a bidentate N,O-bonded chelate ligand, were reported[10]. As the biological activity of coordination compounds depends on the presence of metal ions[6], we have studied the biological properties of complexes with pyridylmethylphosphonate ligands. Preliminary investigations have shown that 2-pyridylmethylphosphonic acid labelled with technetium (^{99m}Tc) forms a complex, which when administered to rats shows a high re-

 © WILEY-VCH Verlag GmbH, D-69451 Weinheim, 1998 1434−1948/98/0202−0169 $ 17.50+.50/0

nal clearance value[15a]. Recently, we investigated the effect of *cis*-$[PtCl_2(4\text{-pmpe})_2]$ and *cis*-$[PtCl_2(NH_3)_2]$ on murine mast cells[11] and on the aggregation of platelet-rich plasma[12]. Both of the complexes tested were found to activate mast cells so as to secrete histamine by a non-cytotoxic, active secretory process[11]. *cis*-Platinum complexes incorporating diethyl 2-, 3-, or 4-pyridylmethylphosphonate ligands showed in vivo cytostatic activity against mice Sa180 sarcoma solid tumours[13] and were found to exhibit alkylating activity in vitro[14]. In order to broaden the scope of this work and to determine the effects of the additional benzene ring, we have now extended our studies to the diethyl 2-quinolylmethylphosphonate ligand (2-qmpe). The 2-qmpe ligand, which has the desired 2-quinolyl group as well as a phosphonate group, can act either as a monodentate N-bonded, as a monodentate O-bonded, or as a bidentate N,O-bonded chelate ligand in forming coordination compounds with transition-metal ions. In the present work, we report on a modification of a previously[15] reported synthesis of diethyl 2-quinolylmethylphosphonate that simplifies the procedure and results in improved yields. We also report on the synthesis, spectroscopic and magnetic properties of coordination compounds of the 2-qmpe ligand with several transition-metal ions and perchlorate ions. These were investigated with regard to their structural and magnetic properties, which provide a chemical basis for the biological activity. The representative compounds $[Ni(2\text{-qmpe})_4(H_2O)_2](ClO_4)_2$ (**1**) and $Mn(2\text{-qmpe})_4(H_2O)_2](ClO_4)_2$ (**2**) were chosen for X-ray crystallographic studies in an attempt to determine which of the potential binding sites of the 2-qmpe ligand, N or O, is attached to the metal centre, as well as to allow comparison with the previously published crystal stucture of $[Co(4\text{-pmpe})_2(H_2O)_2](ClO_4)_2(H_2O)_2$. The structure of **2** is described in detail.

Results and Discussion

General

The condensation of 2-chloromethylquinoline with triethyl phosphite affords diethyl 2-quinolylmethylphosphonate (2-qmpe). The synthesis of 2-qmpe from 2-chloromethylquinoline by the reaction with diethyl sodium phosphite has been reported previously[15]. In the present investigation, we modified a previously reported[15a] synthesis of 2-qmpe, resulting in a simplified procedure and increased yields. The ligand was synthesized by the phosphorylation of 2-chloromethylquinoline with triethyl phosphite and checked for purity by spectroscopic and analytical methods.

The 2-qmpe system is a powerful ligand able to form coordination compounds of the types $[M(2\text{-qmpe})_4(H_2O)_2]_2(ClO_4)_2$, [M = Co^{II}, Ni^{II}, Mn^{II}, Cd^{II}, or Zn^{II}] and $[Cu(2\text{-qmpe})_2(OH)(H_2O)_2]_2(ClO_4)_2$. The structures of the complexes were unambiguously confirmed by a combination of NMR and IR experiments and by elemental analyses. Analytical data are reported in Table 1. A hydroxo-bridged structure is proposed for the Cu^{II} compound, which is supported by chemical and physical evidence. Dinuclear copper compounds having one or two OH groups as bridging ligands are known[16] and are magnetically interesting.

Table 1. Analytical[a] data for the diethyl 2-quinolylmethylphosphonate complexes

No.	Complex	Analysis (%)					M.p.
		M	H	C	N	P	[°C]
1	$[Co(2\text{-qmpe})_4(H_2O)_2](ClO_4)_2$	4.21 (4.18)	5.35 (5.43)	47.33 (47.67)	3.66 (3.97)	8.85 (8.78)	122−125
2	$[Ni(2\text{-qmpe})_4(H_2O)_2](ClO_4)_2$	4.32 (4.16)	5.28 (5.43)	47.65 (47.68)	3.86 (3.97)	8.63 (8.78)	124−126
3	$[Mn(2\text{-qmpe})_4(H_2O)_2](ClO_4)_2$	3.85 (3.90)	5.34 (5.44)	47.22 (47.81)	3.77 (3.98)	8.75 (8.81)	122−124
4	$[Cu(2\text{-qmpe})_2(OH)(H_2O)_2]_2(ClO_4)$	8.35 (8.21)	5.18 (5.34)	43.56 (43.42)	3.87 (3.62)	8.18 (8.00)	131−134
5	$[Cd(2\text{-qmpe})_4(H_2O)_2](ClO_4)_2$	7.77 (7.68)	5.20 (5.23)	45.78 (45.93)	3.93 (3.83)	8.65 (8.46)	171−172
6	$[Zn(2\text{-qmpe})_4(H_2O)_2](ClO_4)_2$	4.87 (4.61)	5.56 (5.40)	47.24 (47.45)	3.91 (3.95)	8.56 (8.74)	103−105

[a] Calculated values are given in parentheses.

Spectroscopic Studies

Ligand-field spectra (Table 2) of the nickel(II) compound exhibit three spin-allowed bands which, in order of decreasing energy, are assigned to the $^3T_{1g}(P) \leftarrow {}^3A_{2g}$ (υ_3), $^3T_{1g}(F) \leftarrow {}^3A_{2g}$ (υ_2), and $^3T_{2g} \leftarrow {}^3A_{2g}$ (υ_1) transitions[17]. In addition, a shoulder at ca. 21050 cm^{-1} in-forbidden [$^1T_{2g} \leftarrow {}^3A_{2g}$ (υ_5)] and a weak absorption at 15750 cm^{-1} [$^1E_g \leftarrow {}^3A_{2g}$ (υ_4)] are observed. The origin of the υ_4 band has been discussed elsewhere[17][18]. The υ_1 band shows weak signs of a splitting, which can be attributed to the lower, tetragonal symmetry of the nickel(II) compound. A complete assignment of the components in D_{4h} symmetry was not considered as meaningful, in view of the broad bands. The calculated value for D_q is in the lower range for Ni^{II}, reflecting the weak ligand field for phosphoryl ligands. Spectroscopic studies dealing with spectral and magnetic characterization of the nickel compounds have recently been reported[19].

The electronic spectra of the cobalt(II) compound exhibit three spin-allowed bands, corresponding to the $^4T_{2g} \leftarrow {}^4T_{1g}(F)$ (υ_1), $^4A_{2g} \leftarrow {}^4T_{1g}(F)$ (υ_2), and $^4T_{1g}(P) \leftarrow {}^4T_{1g}(F)$ transitions. The υ_2 transition usually appears as a weak peak, so that accurate determination of the band maximum is not possible. A shoulder at ca. 21000 cm^{-1} on the high-energy side of the visible band is assigned to spin-orbit components and to a spin-forbidden transition[20]. The asymmetric near-IR band υ_1 gives evidence for octahedral stereochemistry, albeit tetragonally distorted[17]. The crystal-field parameters B and D_q were calculated using well-known methods[20]. The relatively high values of the ligand-field Racah parameter B might reflect the deviation from octahedral geometry[17].

The copper(II) complex exhibits one broad asymmetric d-d band at 13200 cm^{-1}, associated with the $^2T_{1g} \leftarrow {}^2E$ transition in O_h symmetry. The position and shape of this band indicate tetragonally elongated octahedral geometry[21][22].

The extremely low values of the intensities of the bands for the octahedral manganese(II) complex are not unusual[17]. The spectrum shows bands as shoulders on a high-energy ligand or CT band at ca. 25000 cm^{-1} and ca.

19000 cm^{-1}, which can be assigned to $^4A_{1g}$, $^4E_g(G) \leftarrow {}^6A_{1g}$ and $^4T_{1g}(G) \leftarrow {}^6A_{1g}$ transitions, respectively. The other characteristic bands for d-d transitions are masked by UV absorption and are difficult to recognize in the complex and thus the ligand-field parameters cannot be calculated.

In general, the IR spectra of all the complexes appear complicated and a complete assignment of each spectrum is difficult. Only some observations concerning the major bands will therefore be discussed. The IR spectra of the complexes of Co^{II}, Ni^{II}, Mn^{II}, Cd^{II}, and Zn^{II} are very similar with respect to band positions, shapes, and relative intensities, indicating a similar conformation for the five compounds. X-ray powder patterns also showed these five complexes to be mutually isomorphous. The IR spectrum of the Cu^{II} compound, however, indicates quite different structural features.

Evidence for the presence of ClO_4^- was obtained from the infrared spectra. All of the perchlorate compounds show a strong band near 1100 cm^{-1} (asymmetric stretch), a sharp band at 625 cm^{-1} (asymmetric bend) and a very weak absorption at 930−935 cm^{-1} (symmetric stretch), indicative of uncoordinated perchlorate anions[23][24].

The absorption bands attributed to the C=C and C=N of the quinoline ring, observed in the region 1600−1500 cm^{-1} in the free ligand, remain unchanged upon complex formation, confirming non-involvement of the quinolyl nitrogen atom in the metal coordination. In the far-IR region, no metal−nitrogen stretching vibrations are observed.

The absorption band at 1255 cm^{-1}, which corresponds to the P=O stretching of the ligand, is shifted by ca. 15−20 cm^{-1} towards lower frequencies in the spectra of all the complexes, in agreement with coordination of the phosphoryl group to the metal(II) ion[25].

In all the complexes, coordinating water is present. The δ(H−O−H) bending vibrations of coordinated water are observed at 1600−1650 cm^{-1}, whereas the O−H stretching bands are observed around 3400−3600 cm^{-1}. In the spectrum of the Cu^{II} compound, bands at 884 cm^{-1} and 530 cm^{-1} are assigned to H_2O rocking and wagging modes, respectively. On the other hand, the band observed at 440 cm^{-1} is attributable to Cu−O (for coordinated water) stretching vibrations[23]. A very sharp infrared peak at 3540 cm^{-1} can be assigned as the υ(OH) stretching frequency of the hydroxo bridge[26]. Furthermore, the investigated complex exhibits the bridging (Cu−OH) bending mode at 950 cm^{-1}. Support for the assignment of the bridge between two copper centres comes from the absorption at about 520 cm^{-1}, which appears as a doublet (asymmetric and symmetric modes) due to υ(Cu−O) copper−oxygen stretching OH vibrations[27].

^{1}H-NMR spectroscopy is a useful tool for the investigation of complexes of methylphosphonate ligands with N-heterocyclic rings, since coordination of the metal ion via N gives rise to a characteristic downfield shift of the proton signals of the CH_2−P methylene group[28] and this seems to be a general trend in such complexes[2]. We observed[28] a remarkable downfield shift for *trans*-dichlorobis(diethyl 2-pyridylmethylphosphonato-*N*)palladium(II), [Pd(2-pmpe)$_2$Cl$_2$]. Most notable is the downfield shift of 1.17 ppm for the CH_2 signal, which may be explained by the decrease in electron density in the pyridine ring caused by the coordination to the metal ion. In fact, a crystal-structure determination[28] of *trans*-[Pd(3-pmpe)$_2$Cl$_2$] confirmed that the metal ion is bound in a monodentate fashion to the pyridine-N. Comparison of the chemical shifts of the cadmium(II) (**5**) and zinc(II) (**6**) coordination compounds with those of the free 2-qmpe ligand enables us to make an assignment of the ^{1}H-NMR signals. The ^{1}H-NMR spectra of complexes **5** and **6** show the signals hardly shifted in comparison with those of the free ligand. The signal that appears as a doublet due to ^{31}P-^{1}H coupling is assigned to the CH_2−P protons and is not shifted upon coordination to the transition-metal centre. This clearly implies a lack of electron transfer from the quinoline to the metal centre and indicates that the pyridine nitrogen atom does not participate in coordination.

The effective magnetic moments (Table 2) of the cobalt(II), nickel(II), and manganese(II) complexes are within the usually observed ranges of experimental values for high-spin complexes in octahedral configurations[29]. Cadmium(II) and zinc(II) complexes are diamagnetic. Variable-temperature (4.2−294 K) magnetic susceptibility measurements (Table 2, Figure 1) of the Cu^{II} complex clearly indicate a magnetic interaction between the paramagnetic centres, suggesting a hydroxo-bridged [Cu(2-qmpe)$_2$(OH)(H$_2$O)$_2$]$_2$(ClO$_4$)$_2$ dinuclear structure. The susceptibility curve for this compound increases with decreasing temperature until a maximum is reached at 73 K. Below 73 K, the susceptibility χ_M (and μ_{eff}) decreases markedly with decreasing temperature. The μ_{eff}(Cu) at 294 K is 1.91 B.M., which is in the range expected for an octahedral Cu^{II} ion. In the molecular antiferromagnetics under study, the magnetic interactions are limited to two magnetic centres, the singlet-triplet separation defined as 2*J* being a measure of this effect. This parameter was determined by fitting the results to the modified Bleaney-Bowers expression[30]

$$\chi_{Cu}^{corr} = \frac{Ng_{av}^2\beta^2}{3kT}[1 + 1/3(e^{-2J/kT})]^{-1}(1-x) + (\frac{Ng_{imp}^2\beta^2}{4kT})$$

where $\chi_{Cu}{}^{corr}$ is the molar magnetic susceptibility calculated per copper(II) ion, *J* is the exchange parameter in the Heisenberg-Dirac-van Vleck Hamiltonian ($H = -2JS_1S_2$), *p* is the percentage of monomeric form of the complex, and other symbols have their usual meaning. In the least-squares fitting procedure, two parameters were calculated, the singlet-triplet 2*J* energy gap and *g*; these values amounted to −80 cm^{-1} and 2.34, respectively. The agreement factor *R* was found to be 3.97×10^{-3}, where $R = \Sigma_i[(\chi_i{}^{exptl} - \chi_i{}^{calcd})^2 / (\chi_i{}^{exptl})^2]$

The EPR X-band powder spectrum of the Cu^{II} compound does not exhibit absorption, suggesting a strong

Table 2a. Electronic spectral data for $[M(2\text{-qmpe})_4(H_2O)_2](ClO_4)_2$ and $[Cu(2\text{-qmpe})_2(OH)(H_2O)_2]_2(ClO_4)_2$

Compound	Band position [cm^{-1}]	[cm^{-1}]	[cm^{-1}]	Dq[a] [cm]	B[a] [cm]
$[Co(2\text{-qmpe})_4(H_2O)_2](ClO_4)_2$	20760 (sh) υ_3	19050 υ_3	7270 υ_1	790	855
$[Ni(2\text{-qmpe})_4(H_2O)_2](ClO_4)_2$	24690 υ_3	12990 υ_2	7810 υ_1	780	950
$[Mn(2\text{-qmpe})_4(H_2O)_2](ClO_4)_2$	25000 (sh)	19000 (sh)			
$[Cu(2\text{-qmpe})_2(OH)(H_2O)_2]_2(ClO_4)_2$	13200				

Table 2b. Magnetic data for $[M(2\text{-qmpe})_4(H_2O)_2](ClO_4)_2$ and $[Cu(2\text{-qmpe})_2(OH)(H_2O)_2]_2(ClO_4)_2$

	T [K]	Magnetic susceptibility $10^6 \times c_M$ [cm^3/mol]	μ_{eff} [B.M.]	Curie constant C [cm^3/mol]	Weiss constant [K]	R[b]
$[Co(2\text{-qmpe})_4(H_2O)_2](ClO_4)_2$	77	28300	4.29	2.80	−19.9	$7.37 \cdot 10^{-7}$
	294	8870	4.60			
$[Ni(2\text{-qmpe})_4(H_2O)_2](ClO_4)_2$	77	12900	2.95	1.05	3.0	$2.03 \cdot 10^{-7}$
	294	3610	2.93			
$[Mn(2\text{-qmpe})_4(H_2O)_2](ClO_4)_2$	77	54000	5.94	4.28	3.3	$2.43 \cdot 10^{-7}$
	294	14500	5.92			
$[Cu(2\text{-qmpe})_2(OH)(H_2O)_2]_2(ClO_4)_2$	4.2[d]	2080	0.26		−65.4[c]	$4.89 \cdot 10^{-8}$
	77	3520	1.52			
	294	1540	1.91			

[a] Calculated from refs.[18][20]. – [b] $R = \Sigma_i[(\chi_i^{exptl} - \chi_i^{calcd})^2 / (\chi_i^{exptl})^2]$. – [c] In the range 100 K to room temperature. – [d] All experimental points are presented in Figure 1.

Figure 1. Relation of the magnetic susceptibility (χ_{Cu}): circles, experimental susceptibility; dashed line, calculated and experimental magnetic moment (μ_{eff}) vs. T for $[Cu(2\text{-qmpe})_2(OH)(H_2O)_2]_2(ClO_4)_2$

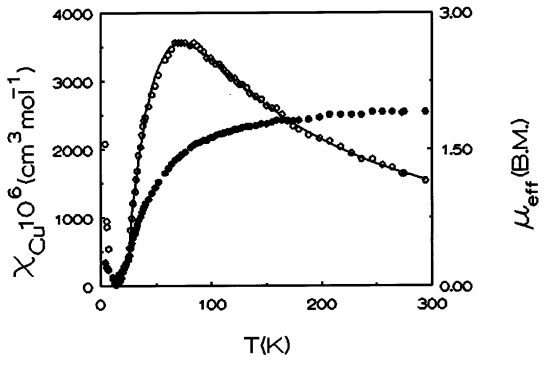

magnetic interaction, e.g. as in a dinuclear unit. Such interactions can be transmitted by hydroxy ligands, resulting in an EPR-silent spectrum[31].

The nickel compound does not exhibit an X-band EPR spectrum. The cobalt compound shows no lines at room temperature, but one line is seen at 77 K at $g = 5.80$. The EPR spectrum of the Mn^{II} complex consists of a single, broad, asymmetric line. A hyperfine structure (6 lines) typical for a $^{55}Mn^{II}$ ion is not resolved, and only some fine-structure due to zero-field splitting is visible, which is not uncommon for Mn^{II}[32].

Crystal Structure Determination

Relevant bond-length and bond-angle information for $[Ni(2\text{-qmpe})_4(H_2O)_2](ClO_4)_2$ (**1**) is given in Table 3. The Ni atom has crystallographically imposed inversion symmetry and is in a distorted octahedral environment, of which the equatorial coordination sphere is formed by the four O-donor atoms of the phosphoryl groups of the 2-qmpe ligands. The axial ligands are two water molecules. The molecular structure is stabilized by hydrogen bonds donated by these water molecules to the quinoline nitrogen atoms (see Table 4). The isomorphous Mn compound **2** displays the same molecular structure and crystal packing. The molecular structure of $[Mn(2\text{-qmpe})_4(H_2O)_2](ClO_4)_2$ is shown in Figure 2. The water molecules bound to the manganese ion are also hydrogen-bonded to the nitrogen atom at a very short distance O−H···N = 2.799 Å. The structure as a whole is stabilized by intramolecular hydrogen-bond interactions.

Conclusions

A number of new coordination compounds with the diethyl 2-quinolylmethylphosphonate ligand have been synthesized. To the best to our knowledge, the results described herein show for the first time that, unexpectedly, the ligand 2-qmpe coordinates to M^{II} through the oxygen atom of the phosphonate group, and not through the pyridine nitrogen atom. This may be attributable to steric factors. Intramolecular O−H···N hydrogen bonds from H_2O toward N seem to stabilize the complexes. The complexes of Co^{II}, Ni^{II}, Mn^{II}, Cd^{II}, and Zn^{II} are six-coordinate, having four 2-qmpe ligands and two *trans* water molecules in a tetragonally elongated octahedral stereochemistry (MO_6 chromophore), as revealed by the crystal-structure determinations. The non-participation of the pyridine group is unusual. A contribution of the pyridine nitrogen atoms was observed in related ligands in an earlier study[10][28], when the reactivity of pyridylmethylphosphonate ligands towards transition-metal ions was studied. For the Cu^{II} compound, a hydroxo-bridged dinuclear structure is proposed, i.e. $[Cu(2\text{-qmpe})_2(OH)(H_2O)_2]_2(ClO_4)_2$; this is supported by chemical analysis and the antiferromagnetic coupling evident from the magnetic susceptibility data.

In summary, we have demonstrated that the P=O donor atom in the 2-qmpe ligand has a very high affinity towards divalent transition-metal ions. These observations may have important consequences, as subsequent studies will deal with platinum pyridyl- and quinolylmethylphosphonate complexes, which can be regarded as antitumour agents.

We gratefully acknowledge support of this work by a grant from the *Tempus Programme – Individual Mobility Grant IMG-96-PL-2154* for J.O. This work has also been partly financed by the *State Committee for Scientific Research* and by the *Netherlands Foundation of Chemical Research (SON)* (*A.L.S.*), with aid from the *Netherlands Organization for Scientific Research (NWO)*.

Table 3. Selected bond lengths [Å] and angles [°] for **1** and **2** with e.s.d.'s in parentheses[a]

Compound	**1**	**2**
Bond Lengths		
M (1)−O(10)	2.019(5)	2.132(3)
M (1)−O(30)	2.046(5)	2.169(4)
M (1)−O(50)	2.079(6)	2.204(4)
P(10)−O(10)	1.500(5)	1.467(4)
P(10)−O(11)	1.550(6)	1.557(4)
P(10)−O(12)	1.555(7)	1.567(4)
P(10)−C(20)	1.781(8)	1.771(5)
P(30)−O(30)	1.470(6)	1.479(4)
P(30)−O(31)	1.580(6)	1.558(5)
P(30)−O(32)	1.519(8)	1.564(5)
P(30)−C(40)	1.803(9)	1.775(6)
Bond Angles		
O(10)−M(1)−O(30)	90.3 (2)	89.37(14)
O(10)−M(1)−O(50)	91.2(2)	92.32(13)
O(10)−M(1)−O(10)a	180.00	180.00
O(10)−M(1)−O(30)a	89.7(2)	90.63(14)
O(10)−M(1)−O(50)a	88.8(2)	87.68(13)
O(30)−M(1)−O(50)	89.0(2)	88.04(14)
O(10)a−M(1)−O(30)	89.7(2)	90.63(14)
O(30)−M(1)−O(30)a	180.00	180.00
O(30)−M(1)−O(50)a	91.0(2)	91.92(14)
O(10)a−M(1)−O(50)	88.8	87.68(13)
O(30)a−M(1)−O(50)	91.0(2)	91.92(14)
O(50)−M(1)−O(50)a	180.00	180.00
O(10)a−M(1)−O(30)a	90.3(2)	89.37(14)
O(10)a−M(1)−O(50)a	91.2(2)	92.32(13)
O(30)a−M(1)−O(50)a	89.0(2)	88.08(14)

[a] Suffix denotes symmetry operation $-x, -y, 1 - z$.

Figure 2. Perspective drawing of **2**; non-hydrogen-bonding hydrogen atoms and the counter ions are omitted for clarity; only the major disorder component is shown

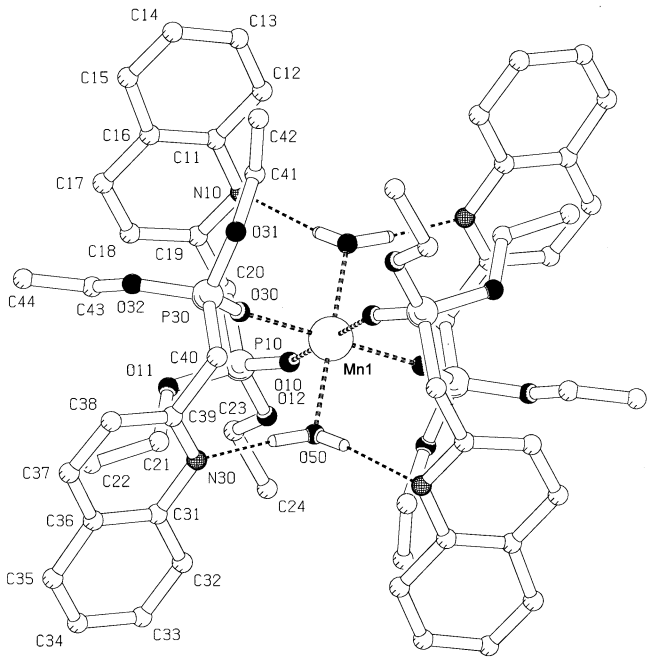

Experimental Section

General: All commercial reagents were ACS reagent grade. − IR spectra (50−4000 cm^{-1}) were recorded with a Perkin-Elmer 180 spectrophotometer using KBr pellets. − Solid-state electronic spectra (28000−50000 cm^{-1}) were measured with a Beckman UV 5240 spectrophotometer fitted with a reflectance attachment, using MgO as a reference. − EPR spectra were recorded with a Radiopan SE/X 2543 spectrometer at X-band frequencies at room temperature

Table 4. Relevant interatomic distances [Å] and angles [°] for the hydrogen-bonding interactions in $[Ni(2\text{-qmpe})_4(H_2O)_2](ClO_4)_2$ (**1**) and in $[Mn(2\text{-qmpe})_4(H_2O)_2](ClO_4)_2$ (**2**) with e.s.d.'s. in parentheses

D−H···A	D−H	H···A	D···A	D−H···A
Compound **1**				
$O_{50}-H_{501}\cdots N_{10}$[a]	0.79(8)	2.14(9)	2.921(9)	174(9)
$O_{50}-H_{502}\cdots N_{30}$	0.87(9)	1.97(9)	2.811(10)	161(8)
Compound **2**				
$O_{50}-H_{502}\cdots N_{10}$[b]	0.72(7)	2.13(6)	2.919(6)	167(7)
$O_{50}-H_{501}\cdots N_{30}$	0.80(6)	2.09(7)	2.799(6)	168(7)

[a] Denotes symmetry operation $-x, -y, 1 - z$. − [b] Denotes symmetry operation $-x, -y, 1 - z$.

Table 5. Crystallographic data for compounds **1** and **2**

Compound	**1**	**2**
Crystal data		
Formula	$C_{55}H_{76}N_4NiO_{14}P_4 \cdot 2\ ClO_4$	$C_{55}H_{76}N_4MnO_{14}P_4 \cdot 2\ ClO_4$
Molecular weight	1410.73	1406.97
Crystal system	triclinic	triclinic
Space group	$P\bar{1}$ (No. 2)	$P\bar{1}$ (No. 2)
a [Å]	11.7164(14)	11.7027(9)
b [Å]	12.623(3)	12.7259(11)
c [Å]	12.784(4)	12.8297(10)
α [°]	66.79(2)	66.956(7)
β [°]	72.91(2)	73.273(7)
γ [°]	85.74(2)	85.969(7)
V [Å^3]	1659.1(8)	1681.9(3)
$D_{calcd.}$ [g cm^{-3}]	1.412	1.389
Z	1	1
F (000)	738	735
μ [$^{-1}$] (Mo-K_α)	5.4	4.3
Crystal size [mm]	0.4 × 0.4 × 0.2	0.4 × 0.4 × 0.2
Data collection		
T [K]	298	293
θ_{min}, θ_{max} [°]	1.76, 27.50	1.74, 27.50
Wavelength (Mo-K_α) [Å]	0.71073 (graphite monochr.)	0.71073 (Zr-filtered)
Scan type	ω/2θ	ω/2θ
Δω [°]	1.61 + 0.35 tan θ	0.90 + 0.35 tan θ
Horiz., vert. aperture [mm]	4.15, 4.00	2.44, 5.00
X-ray exposure time [h]	43	113
Linear decay (%)	3	2
Reference reflections	2 0 3, 2 2 2, $\bar{5}$ 1 $\bar{2}$	2 $\bar{2}$ 1, 0 $\bar{2}$ $\bar{3}$, 4 0 2
Data set	−15/15, −10/16, −15/16	−15/15, −16/16, −16/16
Total data	10240	8770
Total unique data	7594 [R_{int} = 0.067]	7720 [R_{int} = 0.050]
DIFABS corr. range	0.656, 1.468	0.609, 1.157
Refinement		
No. of refined parameters	409	440
Final R[a]	0.120 [2312 $F_o > 4\sigma(F_o)$]	0.073 [2984 $F_o > 4\sigma(F_o)$]
Final $wR2$[b]	0.209	0.185
Goodness of Fit	1.15	0.88
Weighting scheme[c]	$[\sigma^2(F^2) + (0.0400P)^2]^{-1}$	$[\sigma^2(F^2) + (0.0773P)^2]^{-1}$
$(\Delta/\sigma)_{av}$, $(\Delta/\sigma)_{max}$	0.026, −0.363	0.000, 0.004
Min. and max. residual density [e Å^{-3}]	−0.94, 0.58	−0.51, 0.42

[a] $R = \Sigma||F_o| - |F_c||/\Sigma|F_o|$. − [b] $wR2 = \{\Sigma[w(F_o^2 - F_c^2)^2]/\Sigma[w(F_o^2)^2]\}^{1/2}$. − [c] $P = [\max(F_o^2,0) + 2F_c^2]/3$.

and at 77 K (liquid nitrogen). Solid diphenylpicrylhydrazyl (dpph) was used as the reference and magnetic fields were calibrated with proton and lithium NMR probes. − NMR: ^{1}H-NMR spectra were recorded with a Bruker MSL-300 spectrometer employing a frequency of 300 MHz, TMS as internal standard. − ^{31}P-NMR spectra were recorded with a Bruker MSL-300 instrument at 121.496 MHz with 85% phosphoric acid as external standard. − Magnetic susceptibility measurements: See below.

2-Chloromethylquinoline: 1.0 g (5.0 mmol) of 2-chloromethylquinoline hydrochloride was dissolved in 75 ml of water and the solution was brought to pH ≈ 8 by the addition of Na_2CO_3. The yellow product was filtered and dried in vacuo. Yield: 0.7 g (84%), m.p. 43−45°C (petroleum ether). − IR (KBr): $\tilde{\nu}$ = 700−900 cm^{-1} (CH), 1400−1700 (C=N), 3000−3800 (CH). − ^{1}H NMR ($CDCl_3$): δ = 4.82 (s, 2 H, CH_2Cl), 7.52−8.20 (m, 6 H, aromatic H).

Diethyl 2-Quinolylmethylphosphonate: A mixture of 2-chloromethylquinoline (1.77 g, 1·10^{-2} mol) and triethyl phosphite (25 ml, 1.4·10^{-1} mol) was stirred under reflux for 24 h. After this period, TLC analysis indicated complete phosphorylation. The excess triethyl phosphite was then evaporated yielding a yellow oil. Colorless diethyl 2-quinolylmethylphosphonate was obtained by distillation in vacuo. Yield: 2.2 g (78%). − ^{1}H NMR ($CDCl_3$): δ = 1.23 (t, $^3J_{HH}$ = 7 Hz, 6 H, 2 POCH$_2$CH_3), 3.63 (d, $^2J_{HP}$ = 22 Hz, 2 H, CH_2P), 4.13 (dq, $^2J_{POCH}$ = 7 Hz, $^3J_{HH}$ = 7 Hz, 4 H, 2 POCH_2CH$_3$), 7.36−8.23 (m, 6 H, aromatic H). − ^{31}P{^{1}H} NMR ($CHCl_3$): δ = 24.53.

Preparation of the Complexes: The coordination compounds were synthesized by addition of the appropriate hydrated metal perchlorate (1 mmol), dissolved in 10 ml of water, to a solution of 2-qmpe (4 mmol) in 20 ml of ethanol. The resulting solutions were filtered to remove any insoluble material. Following evaporation of the solvent at room temperature, the compounds crystallized after a few days. Crystals of **1** and **2** suitable for single-crystal X-ray diffraction studies were grown from saturated ethanolic solutions of the complexes at room temperature. The Mn, Ni, Co, Cd, and Zn compounds are isomorphous, as shown by X-ray powder diffraction experiments.

Magnetic Measurements: Magnetic susceptibility measurements (80−300 K) were carried out using the Gouy method on a sensitive Cahn RM-2 electronic balance at a magnetic field strength of 9.9 kOe. Over the temperature range 4.2−300 K, measurements were made by the Faraday method, using a Cahn RG-HV electrobalance and a magnetic field of 5.25 kOe. The standard employed for calibration was $HgCo(NCS)_4$, for which the magnetic susceptibility was taken as 16.44·10^{-6} cm^3 g^{-1}. Corrections for diamagnetism of the constituent atoms were made by using Pascal constants. The effective magnetic moments were calculated from μ_{eff} = 2.83 $(\chi^M T)^{1/2}$, after corrections for temperature-independent paramagnetism of 60·10^{-6} (Cu^{II}) and 220·10^{-6} cm^3 mol^{-1} (Ni^{II}).

X-ray Crystallography: Crystals of **1** and **2** (both colorless) suitable for X-ray diffraction were glued to the tip of a Lindemann glass capillary and transferred to an Enraf-Nonius CAD4 diffractometer on a rotating anode (for **1**) or in a sealed tube (for **2**). Crystals of **1** were of limited quality, as indicated by highly structured broad reflection profiles. Accurate unit-cell parameters and an orientation matrix were determined by least-squares refinement of the setting angles of a set of well-centered reflections (SET4)[33] in the range 9.84° < θ < 13.75° and 4.12° < θ < 12.83° for **1** and **2**, respectively. Reduced-cell calculations did not indicate higher lattice symmetry[34]. Crystal data and details of the data collection and refinement are given in Table 5. Data were corrected for Lp effects and for observed linear decay of the reference reflections. An empirical absorption/extinction correction (DIFABS)[35] was applied for both compounds. The structures were solved by automated Patterson methods and subsequent difference Fourier techniques (DIRDIF-92[37] and SHELX-86[36] for **1** and **2**, respectively). Both compounds were refined on F^2 by full-matrix least-squares techniques (SHELXL-93)[38]; no observance criterion was applied during refinement. 14 deviating reflections displaying an unequal background were omitted during the final refinement cycles of compound **1**. Hydrogen atoms were included in the refinement in calculated positions riding on their carrier atoms, except for water hydrogen atoms of both compounds, which were located on a difference Fourier map and subsequently included in the refinement. Two ethyl groups of compound **2** proved to be disordered; a disorder model consisting of two alternative sites and occupation factors was included in the refinement. Weak bond constraints had to be introduced on this moiety in order to obtain a reasonable geometry. Non-hydrogen atoms were refined with anisotropic thermal parameters. The hydrogen atoms were refined with a fixed isotropic thermal parameter related to the value of the equivalent isotropic thermal parameter of their carrier atoms by a factor amounting to 1.5 for the water and methyl hydrogen atoms, and 1.2 for the other hydrogen atoms, respectively. The relatively high R value for **1** is attributed to the rather poor quality of the available crystals. Neutral atom scattering factors and anomalous dispersion corrections were taken from the International Tables for Crystallography[39]. Geometrical calculations and illustrations were performed with the PLATON package[40]; all calculations were performed on a DEC station 5000 cluster. Crystallographic data (excluding structure factors) for the structures reported in this paper have been deposited with the Cambridge Crystallographic Data Centre as supplementary publication no. CCDC-100672. Copies of the data can be obtained free of charge on application to CCDC, 12 Union Road, Cambridge CB2 1EZ, UK [Fax: (internat.) +44 (0)1223/336033; E-mail: deposit@ccdc.cam.ac.uk].

[1] J. Ochocki, A. Erxleben, B. Lippert, *J. Heterocycl. Chem.*, in press.
[2] [2a] L. Tusek-Bozic, I. Matijasic, G. Bocelli, G. Calestani, A. Furlani, V. Scarcia, A. Papaioannou, *J. Chem. Soc., Dalton Trans.* **1991**, 195. − [2b] L. Tusek-Bozic, I. Matijasic, G. Bocelli, P. Sgarabotto, A. Furlani, V. Scarcia, A. Papaioannou, *Inorg. Chim. Acta* **1991**, *185,* 229.
[3] M. Horiguchi, M. Kandatsu, *Nature* **1959**, *184*, 901.
[4] [4a] J. S. Kittredge, E. Roberts, D. G. Simonsen, *Biochemistry* **1962**, *1*, 624. − [4b] J. S. Kittredge, R. R. Hughes, *Biochemistry* **1964**, *3*, 991.− [4c] J. S. Kittredge, E. Roberts, *Science* **1969**, *164*, 37.
[5] R. Engel, *Chem. Rev.* **1977**, *77*, 349.
[6] [6a] J. J. R. Frausto da Silva, R. J. P. Williams, *The Biological Chemistry of the Elements: The Inorganic Chemistry of Life,* Clarendon Press, Oxford, U.K., **1991**. − [6b] B. Lippert, *An Inorganic Perspective of Life,* NATO ASI Series, Kluwer Academic Publishers, Dordrecht, **1995**, *459*, 179. − [6c] M. Sabat, B. Lippert, *Met. Ions Biol. Syst*. **1966**, *33*, 143.
[7] [7a] D. Chen, M. Bastain, F. Gregan, A. Holy, H. Sigel, *J. Chem. Soc., Dalton Trans.* **1993**, 1537. − [7b] H. Sigel, D. Chen, N. A. Corfu, F. Gregan, A. Holy, M. Strasak, *Helv. Chim. Acta* **1992**, *75*, 2634. − [7c] M. Bastian, D. Chen, F. Gregan, G. Liang, H. Sigel, *Z. Naturforsch.* **1993**, *48b*, 1279. − [7d] H. Sigel, S. S. Massoud, N. A. Corfu, *J. Am. Chem. Soc.* **1994**, *116*, 2958. − [7e] H. Sigel, *Chem. Soc. Rev.* **1993**, *22*, 255.
[8] M. J. Bloemink, J. P. Dorenbos, R. J. Heetebrij, B. K. Keppler, J. Reedijk, H. Zahn, *Inorg. Chem.* **1994**, *33*, 1127.
[9] Th. Klenner, P. Valenzuela-Paz, F. Amelung, H. Münch, H. Zahn, B. K. Keppler, H. Blum, *Metal Complexes In Cancer Chemotherapy* (Ed.: B. K. Keppler), VCH, Weinheim, **1993**.
[10] [10a] J. Ochocki, K. Kostka, B. Zurowska, J. Mroziński, E. Galdecka, Z. Galdecki, J. Reedijk, *J. Chem. Soc., Dalton Trans.* **1992**, 2955. − [10b] J. Ochocki, B. Zurowska, J. Mroziński, J.

Reedijk, *IIIrd Symposium on Inorganic Biochemistry and Molecular Biophysics*, VIth International Scientific School on Biological Macromolecules, **1991**, Proceedings, p.212.
[11] E. Brzezinska-Blaszczyk, M. Mincikiewicz, J. Ochocki, *Eur. J. Pharmacol.* **1996**, *298*, 155.
[12] B. Kostka, J. Ochocki, *Pharmazie* **1996**, *51*, 990.
[13] J. Ochocki, J. Graczyk, J. Reedijk, *J. Inorg. Biochem.* **1995**, *59*, 240.
[14] L. Najman-Bronzewska, J. Ochocki, *Pharmazie* **1997**, *52*, 198.
[15] [15a] K. Kostka, J. Ochocki, *Pol. J. Chem.* **1988**, *62*, 595. – [15b] V. Jagodic, B. Bozic, L. Tusek-Bozic, M. J. Herak, *J. Heterocycl. Chem.* **1980**, *17*, 685.
[16] [16a] D. L. Levis, W. E. Hatfield, D. J. Hodgson, *Inorg. Chem.* **1972**, *11*, 2216. – [16b] D. J. Hodgson, *Prog. Inorg. Chem.* **1975**, *19*, 173. – [16c] V. H. Crawford, *Inorg. Chem.* **1976**, *15*, 2107. – [16d] C. Arcus, *J. Inorg. Nucl. Chem.* **1977**, *39*, 285. – [16e] M. S. Haddad, D. N. Hendrickson, *Inorg. Chim. Acta* **1978**, *28*, L121.
[17] A. B. P. Lever, *Inorganic Electronic Spectroscopy*, Elsevier, Amsterdam, **1986**.
[18] J. Reedijk, P. W. N. M. van Leeuwen, W. L. Groeneveld, *Recl. Trav. Chim. Pays-Bas* **1968**, *87*, 129.
[19] [19a] N. de Vries, J. Reedijk, *Inorg. Chem.* **1991**, *30*, 3700. – [19b] E. Bouwman, P. Evans, H. Kooijman, J. Reedijk, A. L. Spek, *J. Chem. Soc., Chem. Commun.* **1993**, 1746.
[20] J. Reedijk, W. L. Driessen, W. L. Groeneveld, *Recl. Trav. Chim. Pays-Bas* **1969**, *88*, 1095.
[21] [21a] B. J. Hathaway, D. E. Billing, *Coord. Chem. Rev.* **1970**, *5*, 143. – [21b] B. J. Hathaway, D. E. Billing, *Coord. Chem. Rev.* **1981**, *35*, 211. – [21c] B. J. Hathaway, *J. Chem. Soc., Dalton Trans.* **1972**, 1196. – [21d] J. Reedijk, D. Knetsch, B. Nieuwenhuijse, *Inorg. Chim. Acta* **1971**, *5*, 568.
[22] [22a] J. Reedijk, *Transition Met. Chem.* **1981**, *6*, 195. – [22b] W. L. Driessen, S. Gorter, W. G. Haanstra, L. K. J. Laarhoven, J. Reedijk, K. Goubitz, F. R. Seljee, *Recl. Trav. Chim. Pays-Bas* **1993**, *112*, 309.
[23] K. Nakamoto, *Infrared and Raman Spectra of Inorganic and Coordination Compounds*, John Wiley and Sons, New York, **1978**.
[24] B. J. Hathaway, A. E. Underhill, *J. Chem. Soc.* **1961**, 3091.
[25] [25a] E. Uhling, M. J. Shafer, *J. Inorg. Nucl. Chem.* **1968**, *30*, 3109. – [25b] N. N. Speca, L. L. Pytlewski, N. M. Karayannis, *J. Inorg. Nucl. Chem.* **1972**, *34*, 3671. – [25c] N. M. Karayannis, C. Owens, L. L. Pytlewski, M. M. Labes, *J. Inorg. Nucl. Chem.* **1970**, *32*, 83. – [25d] N. M. Speca, N. M. Karayannis, L. L. Pytlewski, *Inorg. Chim. Acta* **1972**, *6*, 639. – [25e] F. A. Cotton, R. D. Barnes, E. Bannister, *J. Chem. Soc.* **1960**, 2199.
[26] [26a] I. E. Dickson, R. Robson, *Inorg. Chem.* **1974**, *13*, 1301. – [26b] J. J. Grzybowski, P. M. Merrel, F. L. Urbach, *Inorg. Chem.* **1978**, *17*, 3078.
[27] [27a] J. R. Ferraro, W. R. Walker, *Inorg. Chem.* **1965**, *4*, 1382. – [27b] W. R. McWhinnie, *J. Inorg. Nucl. Chem.* **1965**, *27*, 1063.
[28] J. Ochocki, P. M. van Vliet, W. J. J. Smeets, J. Reedijk, presented at the NATO ASI, *An Inorganic Perspective of Life*, book of abstracts, Rhode Island, **1994**, 163.
[29] F. E. Mabbs, D. J. Machin, *Magnetism and Transition Metal Complexes,* Chapman Hall, London, **1973**.
[30] B. Bleaney, K. D. Bowers, *Proc. Roy. Soc., London* **1952**, *A214*, 451.
[31] [31a] J. Reedijk, D. Knetsch, B. Nieuwenhuijse, *Inorg. Chim. Acta* **1971**, *5*, 568. – [31b] I. Sotofte, K. Nelsen, *Acta Chem. Scand. Sect. A* **1981**, *35*, 733. – [31c] J. Reedijk, A. R. Siedle, R. A. Velapoldi, J. A. M. van Hest, *Inorg. Chim. Acta* **1983**, *74*, 109. – [31d] A. Bencini, D. Gatteschi, *Electron Paramagnetic Resonance of Exchange Coupled Systems*, Springer Verlag, Berlin, **1990**. – [31e] B. B. Goodman, J. B. Raymor, *Adv. Inorg. Chem. Radiochem.* **1970**, *135*, 13. – [31f] V. K. Voronkowa, L. V. Mosima, Yu. V. Yablokov, M. A. Yampolskaya, *Dokl. Akad. Nauk SSSR*, **1979**, *910*, 246.
[32] [32a] R. D. Dowsing, J. F. Gibson, *J. Chem. Phys.* **1969**, *50*, 294. – [32b] R. D. Dowsing, J. F. Gibson, D. M. L. Goodgame, M. Goodgame, P. J. Hayward, *J. Chem. Soc. A* **1969**, 1242. – [32c] R. B. Birdy, G. Brun, D. M. L. Goodgame, M. Goodgame, *J. Chem. Soc., Dalton Trans.* **1979**, 149. – [32d] L. Latos-Grazynski, A. Jezierski, *Inorg. Chim. Acta.* **1985**, *106*, 13.
[33] J. L. de Boer, A. J. M. Duisenberg, *Acta Crystallogr., Sect. A* **1984**, *40*, 410.
[34] A. L. Spek, *J. Appl. Crystallogr.* **1988**, *21*, 578.
[35] N. Walker, D. Stuart, *Acta Crystallogr., Sect. A* **1983**, *39*, 158.
[36] G. M. Sheldrick, *SHELXS-86,* Universität Göttingen, **1986**.
[37] P. T. Beurskens, G. Admiraal, G. Beurskens, W. P. Bosman, S. Garcia-Granda, R. O. Gould, J. M. M., Smits, C. Smykalla, *The DIRDIF program system, Technical report of the Crystallography Laboratory,* University of Nijmegen, The Netherlands, **1992**.
[38] G. M. Sheldrick, *SHELXL-93,* Universität Göttingen, **1993**.
[39] A. J. C. Wilson, *International Tables for Crystallography, Volume C*, Kluwer Academic Publishers, Dordrecht, The Netherlands, **1992**.
[40] A. L. Spek, *Acta Crystallogr., Sect. A* **1990**, *46*, C34.

[97196]

The Acid-Induced Rearrangement of 1-Hydroxyalkyltris(trimethylsilyl)silanes

Katrin Sternberg and Hartmut Oehme*

Fachbereich Chemie der Universität Rostock,
D-18051 Rostock, Germany
Fax: (internat.) +49(0)381/498-1763

Received September 15, 1997

Keywords: Silanes / Rearrangements / Polysilanes / Hypersilylalcohols / 1,2-Trimethylsilyl migration

In the presence of strong acids, such as HCl or H_2SO_4, 1-hydroxyalkyltris(trimethylsilyl)silanes $(Me_3Si)_3Si-C(OH)R^1R^2$ (**1a–f**) isomerize by 1,2-Me_3Si/OH exchange to give the trimethylsilylmethylsilanols $(Me_3Si)_2Si(OH)-C(SiMe_3)R^1R^2$ (**4a–f**) [R^1,R^2: **a**: Me, Me; **b**: H, 4-MeC_6H_4; **c**: H, 4-*i*PrC_6H_4; **d**: H, Mes; **e**: H, 2-$Me_2NC_6H_4$; **f**: H, 2,4,6-$(MeO)_3C_6H_2$]. A mechanism for the isomerization is proposed. In the case of the reaction of **1d** with sulfuric acid, the silylsulfate $(Me_3Si)_2Si(OSO_3H)-C(SiMe_3)HMes$ (**5**) was isolated. **5** is the intermediate in the H_2SO_4-catalyzed isomerization of **1d** and was converted in situ with methanol, acetic anhydride, HF or HCl to give the respective methoxysilane **6**, acetoxysilane **7**, fluorosilane **8**, or chlorosilane **9**. Deprotonation of **4a, d, f** with sodium hydride causes a further rearrangement, a 1,3-C,O-trimethylsilyl migration, to give the siloxanes $(Me_3Si)_2(Me_3SiO)Si-CHR^1R^2$ (**11a, d, f**).

The base-induced elimination of trimethylsilanolate from 1-hydroxyalkyltris(trimethylsilyl)silanes (**1**) proved to be a suitable method for the synthesis of silaethenes. The mechanism of the process is interpreted as a variation of the Peterson reaction, in such a way that a carbon atom in the original Peterson product is replaced by a silicon atom. The polysilanylalcohols **1** are readily available by the addition of tris(trimethylsilyl)silylmagnesium bromide to the carbonyl group of aldehydes or ketones[1], and the isolated polysilanylalcohols are deprotonated with organolithium compounds, initiating the elimination of trimethylsilanolate to give transient silenes, which were characterized by trapping reactions and as different kinds of dimers (Eq. 1)[2]. The generation of silenes by the Peterson mechanism can also be performed in an in situ reaction from $(Me_3Si)_3SiLi$ and carbonyl compounds[3], and recently Apeloig et al. successfully applied this method to the synthesis of new stable silenes[4].

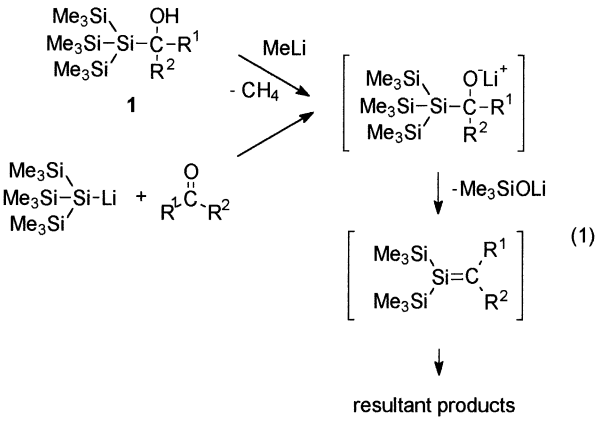

(1)

The Peterson reaction, originally the formation of olefins by a base-induced elimination of trimethylsilanol from 2-trimethylsilyl alcohols, can also be performed under acidic conditions[5]. During the course of our studies on the synthetic utility of 1-hydroxyalkyltris(trimethylsilyl)silanes (**1**) we therefore explored their conversion by strong acids which, in contrast to the base-promoted sila-Peterson reaction, did not give elimination and silene formation but an interesting rearrangement of the hydroxyalkylpolysilanes **1** into 1-trimethylsilylalkylsilanols **4**.

The Reaction of 1-Hydroxyalkyltris(trimethylsilyl)silanes (1) with Acids

Strong acids, such as hydrochloric acid in ether, cause the 1-hypersilylalcohols **1a–f** to rapidly undergo a rearrangement to afford the bis(trimethylsilyl)-1-trimethylsilylalkylsilanols **4a–f**. The silanols **4a–f** are colorless solids. Their structures were elucidated on the basis of their IR, NMR and MS data (see Experimental Section).

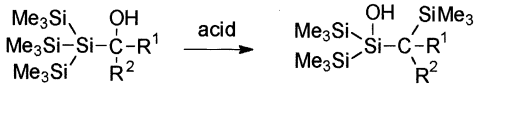

(2)

a: R^1 = R^2 = Me
b: R^1 = H; R^2 = 4-Me-C_6H_4
c: R^1 = H; R^2 = 4-iPr-C_6H_4
d: R^1 = H; R^2 = Mes
e: R^1 = H; R^2 = 2-Me_2N-C_6H_4
f: R^1 = H; R^2 = 2,4,6-$(MeO)_3C_6H_2$

The proposed pathway for the conversion of **1a–f** into **4a–f** is outlined in Eq. 3. The acid-catalyzed elimination of water from the alcohols **1a–f**, affording the carbenium ions **2a–f**, is followed by a migration of one trimethylsilyl group

 © WILEY-VCH Verlag GmbH, D-69451 Weinheim, 1998 1434–1948/98/0202–0177 $ 17.50+.50/0

from the central silicon atom to the neighboring carbon atom and attack of X^-, the conjugate base of the acid used as the catalyst, at the electrophilic silicon. Hydrolysis of the Si−X bond of **3a−f** by the eliminated water gives the silanols **4a−f**.

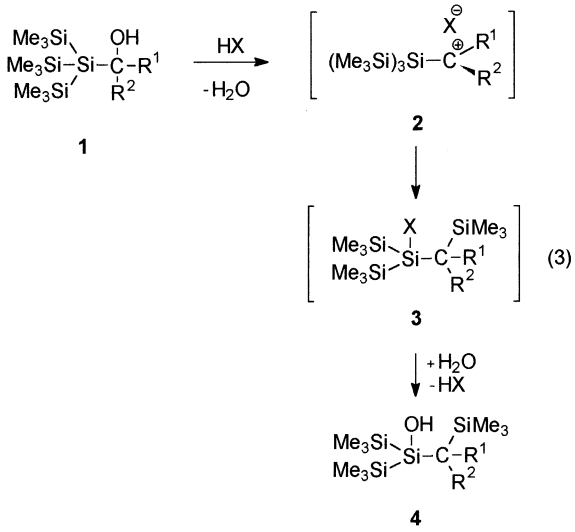

(3)

As the subject of some mechanistic studies we have chosen compound **1d**. The kinetic control of its conversion into **4d** (^{1}H NMR, solvent - [D_6]acetone, equimolar quantities of trifluoroacetic acid) revealed that the consumption of the alcohol **1d**, as well as the generation of the silanol **4d**, is a first-order process. Additional water in the reaction mixture does not increase the rate of formation of **4d**. Thus, a bimolecular reaction, involving a direct attack of water at the central tetracoordinated silicon atom of **2d** facilitating the trimethylsilyl shift and increasing the rate of the silanolate formation, can be excluded − at least in the rate-determining step of the reaction.

1,2-Migrations of alkyl, aryl and also trimethylsilyl groups from a tetracoordinated silicon center to a neighboring carbenium center appear to be common and have been described in the literature. Kumada et al. studied the $AlCl_3$-catalyzed rearrangement of chloromethyldisilanes into chlorosilanes[6]. They suggested a mechanism involving a slow rate-determining step consisting of the ionization of the carbon-chlorine bond, followed by a fast step involving synchronous nucleophilic attack by the halide on silicon and migration of a Me_3Si group from silicon to carbon. A similar mechanism was reported by Brook et al.[7] for the closely related reaction, the boron trifluoride-induced rearrangement of (hydroxymethyl)silicon compounds to give fluorosilanes. The BCl_3-induced conversion of methoxymethyltris(trimethylsilyl)silanes $(Me_3Si)_3Si-CH(OMe)R$ into the chlorosilanes $(Me_3Si)_2Si(Cl)-CH(SiMe_3)R$, described by Märkl et al., is similarly discussed as a synchronous process[8].

Isomerizations of silyl-substituted carbenium ions with the simultaneous generation of a silylium-ion intermediate or transition state have been described more recently[9]. An important contribution to this area was made by Apeloig and Stanger, who provided evidence of a direct, solvent-unassisted 1,2-methyl migration of a solvolytically produced α-trimethylsilyl carbenium ion[10]. These experimental observations confirm expectations deduced from theoretical work, according to which α-silyl carbenium ions should generally be less stable than the isomeric silylium ions[10][11]. In our particular case the 1,2-trimethylsilyl shift is probably favored by the fact that the hyperconjugative stabilization of the silylium-ion transition-states by the $CR^1R^2SiMe_3$ groups is more effective than the stabilization of the carbenium ions **2a−f** by the hypersilyl substituent. Whereas an α-silyl group at a carbenium ion center destabilizes the system relative to a methyl group[11], trimethylsilylmethyl groups cause a small but significant stabilization of a silylium ion[12].

Both mechanisms, the synchronous process involving X^- in the trimethylsilyl shift and that involving a silylium-ion intermediate, fit the experimental results and agree with the proposed reaction path of the conversion of **1a−f** into **4a−f**. However, detailed information on the nature of the intermediates cannot be obtained from the data available and, in particular, the question of the existence of a silylium-ion intermediate remains unanswered.

Recently we became aware of a related rearrangement, the conversion of trimethylsiloxymethyl-chlorosilanes $(Me_3Si)_2Si(Cl)-C(OSiMe_3)R_2$ via chloromethyldisiloxanes $(Me_3Si)_2Si(OSiMe_3)-C(Cl)R_2$ into trimethylsilylmethylchlorodisiloxanes $Me_3Si(Me_3SiO)Si(Cl)-C(SiMe_3)R_2$, and it is very likely that this proceeds along a similar reaction path[13].

The polysilanylalcohols **1e** and **1f** were included in our studies with the aim of stabilizing the intermediate carbenium ion by introducing electron-donating substituents and thus preventing the 1,2-Si,C-trimethylsilyl shift. However, as demonstrated in Eq. 2, **1e** and **1f** follow the same isomerization pattern and give the silanols **4e** and **4f**, respectively.

When concentrated sulfuric acid is used as the catalyst for the rearrangement of **1a−f**, the water eliminated from the alcohols is not available and other nucleophiles present in the mixture can attack the electrophilic silicon center of **3a−f** to give the functionalized silanes **6−9**. For these experiments we have chosen to study **1d**. Thus, the addition of several drops of concentrated H_2SO_4 to a solution of **1d** in methanol results in the formation of the methoxysilane **6**. Under the same conditions **1e** and **1f** give **6e** and **6f**, respectively. The reaction of **1d** with sulfuric acid in acetic anhydride affords the acetoxysilane **7**. Similarly, when a mixture of HF and H_2SO_4 is added to an ethereal solution of **1d**, the fluorosilane **8** is formed almost quantitatively. The chlorosilane **9** is obtained by passing gaseous HCl through a solution of **1d** and H_2SO_4 in ether (Eq. 4).

All these reactions proceed through the silylsulfate **5**, and **6−9** are formed by replacement of the HSO_4 group of **5** by the appropriate nucleophile. This was demonstrated by the reaction of **1b** with sulfuric acid in ether in the absence of further nucleophiles, which allowed the isolation of **5** in the

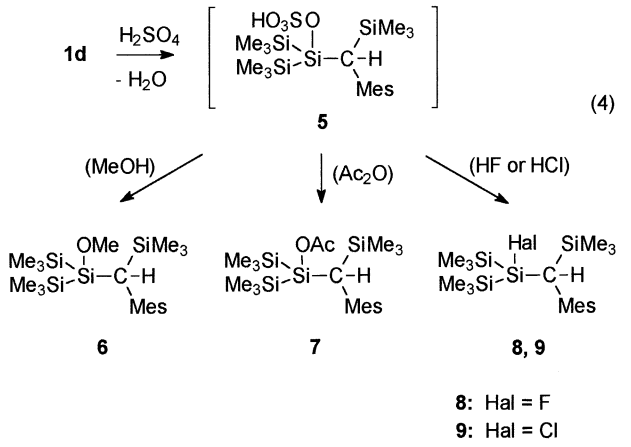

form of a colorless, crystalline, highly moisture-sensitive compound.

The structures of **4**–**9** were elucidated by a full spectral analysis [IR; ^{1}H-, ^{13}C- and ^{29}Si-NMR spectroscopy, MS and elemental analyses (see Experimental Section)].

The Base- Induced Rearrangement of the 1-Trimethylsilylalkylsilanols 4 into the Disiloxanes 11

Deprotonation of the silanols **4** with sodium hydride leads to a further rearrangement, with one trimethylsilyl group migrating from carbon to oxygen. The reaction was performed with **4a**, **4d** and **4f**, producing the disiloxanes **11a**, **11d** and **11f**, respectively (Eq. 5).

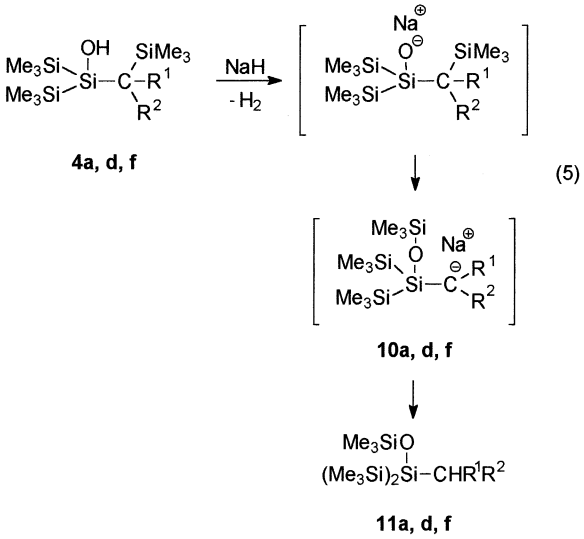

Such 1,3-C,O-trimethylsilyl migrations are well known, e.g. they are probably part of the Peterson olefination process[5]. Interestingly, the conversion of **4a, d, f** into **11a, d, f** is easily achieved by treatment with NaH in THF. In ether the reaction proceeds very slowly, and after deprotonation of **4a, d, f** with organolithium reagents, the silanols were recovered unchanged. This demonstrates the dependence of the nucleophilicity of the silanolate oxygen atom on the counter ion and the solvent. In the course of the Peterson reaction, the 1,3-Si,O-trimethylsilyl migration is followed by a trimethylsilanolate elimination to establish the olefinic double bond. In contrast, in the case of **10a, d, f** the high energy of the silicon oxygen bond, as expected, prevents a silanolate elimination and silaethene formation.

We gratefully acknowledge the support of our research by the *Deutsche Forschungsgemeinschaft* and the *Fonds der Chemischen Industrie.* We thank Dr. *M. Michalik,* Dr. *W. Baumann* and Prof. *N. Stoll* for recording the NMR and mass spectra.

Experimental Section

All reactions involving organometallic reagents were carried out under purified argon. – NMR: Bruker AC 250 or Bruker ARX 300, tetramethylsilane as internal standard. – IR: Nicolet 205 FT-IR. – MS: Intectra AMD 402, chemical ionization with isobutane as the reactant gas. – $(Me_3Si)_3SiLi \cdot 3$ THF[14], **1a**[1], **1c**[15], **1d**[1] and **1e**[2] were prepared as reported in the literature. – All yields given refer to amounts obtained after chromatographic separation and purification. – The syntheses and the spectral data characterizing the structures of **4a**, **4c**, **4d**, **6** and **8** were described previously[15].

Synthesis of the 1-Hydroxyalkyltris(trimethylsilyl)silanes **1b** and **1f**: As described previously[1], **1b** and **1f** were prepared by the reaction of tris(trimethylsilyl)silylmagnesium bromide, made from 14.7 g (0.03 mol) of $(Me_3Si)_3SiLi \cdot 3$ THF and an equimolar quantity of $MgBr_2$ and 3.6 g (0.03 mol) of 4-methylbenzaldehyde or 5.89 g (0.03 mol) of 2,4,6-trimethoxybenzaldehyde, respectively.

1b: The product was purified by column chromatography (silica gel, heptane/ethyl acetate 20/1) and recrystallization from acetonitrile; yield 7.2 g (65%), m.p. 78°C. – IR (nujol): $\tilde{\nu}$ = 3518.5 cm^{-1} (OH). – ^{1}H NMR ([D$_6$]benzene): δ = 0.26 (s, $SiCH_3$, 27 H), 1.12 (d, ^3J = 2.74 Hz, OH, 1 H), 2.12 (s, *p*-CH_3, 3 H), 4.81 (d, ^3J = 2.74 Hz, CH, 1 H), 6.97 (m, ArH, 2 H), 7.16 (m, ArH, 2 H). – ^{13}C NMR ([D$_6$]benzene): δ = 1.8 ($SiCH_3$), 21.0 (*p*-CH_3); 69.2 (CH), 125.8, 129.1 (arom. CH), 135.6, 145.0 (quart. arom. C). – ^{29}Si NMR ([D$_6$]benzene): δ = −13.1 ($SiMe_3$), −67.7 (*Si*$SiMe_3$). – MS: *m/z* (%) = 351 (100) [M^+ − OH], 295 (4) [M^+ − $SiMe_3$], 277 (6) [M^+ − $C_6H_4CH_3$], 247 (16) [$Si(SiMe_3)_3^+$], 121 (15) [M^+ − $Si(SiMe_3)_3$]. – $C_{17}H_{36}OSi_4$ (368.81): calcd. C 55.36, H 9.84; found C 55.13, H 9.81.

1f: Recrystallized from heptane, yield 12.0 g (90%), m.p. 115°C. – IR (nujol): $\tilde{\nu}$ = 3579.8 cm^{-1} (OH free), 3455.0 (OH ass.). – ^{1}H NMR ([D$_6$]benzene): δ = 0.31 (s, $SiCH_3$, 27 H), 3.23 (s, *o*-OCH_3, 6 H), 3.34 (s, *p*-OCH_3, 3 H), 3.45 (d, OH, 1 H, ^3J = 10.98 Hz), 5.93 (d, CH, 1 H, ^3J = 10.98 Hz), 6.0 (s, ArH, 2 H). – ^{13}C NMR ([D$_6$]benzene): δ = 1.7 ($SiCH_3$), 54.7 (*o*-OCH_3), 54.9 (*p*-OCH_3), 59.0 (CH), 127.6 (arom. CH), 115.6, 157.4, 160.1 (quart. arom. C). – ^{29}Si NMR ([D$_6$]benzene): δ = −12.6 ($SiMe_3$), −73.1 (*Si*$SiMe_3$). – MS: *m/z* (%) = 444 (0.6) [M^+]; 371 (3) [M^+ − $SiMe_3$]; 197 (100) [M^+ − $Si(SiMe_3)_3$]. – $C_{19}H_{40}O_4Si_4$ (444.87): calcd. C 51.30, H 9.06; found C 51.14, H 9.22.

Isomerization of **1b**, **1e** *and* **1f** *into the Silanols* **4b**, **4e** *and* **4f**:

4b: To an ethereal solution of 0.5 g (1.35 mmol) of **1b** was added an equimolar quantity of ethereal HCl at room temperature and the mixture was stirred for 5 h. After addition of aqueous $NaHCO_3$ solution, the organic phase was separated, dried and the solvent evaporated. Kugelrohr distillation and chromatographic purification (silica gel, heptane/ethyl acetate 20/1) of the residue gave 0.25 g (50%) of colorless crystals, m.p. 48°C. – IR (nujol): $\tilde{\nu}$ = 3647 and 3676 cm^{-1} (OH), 3427 (OH ass.). – ^{1}H NMR ([D]$_6$benzene): δ = 0.12, 0.14 and 0.18 (3 s, $SiCH_3$, 3 × 9 H), 2.05 (s, CH, 1 H), 2.10 (s, Ar−CH_3, 3 H), 6.93 (m, ArH, 4 H). – ^{13}C NMR

([D$_6$]benzene): δ = −0.4, 0.0 and 0.6 ($SiCH_3$), 20.9 ($ArCH_3$), 30.1 (CH), 129.4, 129.5, 133.3 and 138.6 (arom. C). − ^{29}Si NMR ([D$_6$]benzene): δ = −19.2 and −18.7 (Si*Si*Me$_3$), 1.9 ($CSiMe_3$), 10.4 (SiOH). − MS: *m/z* (%) = 368 (3) [M$^+$], 353 (5) [M$^+$ − CH_3], 295 (40) [M$^+$ − $SiMe_3$], 279 (80) [M$^+$ − Me_3SiOH], 73 (100) [$SiMe_3^+$]. − $C_{17}H_{36}OSi_4$ (368.81): calcd. C 55.36, H 9.84; found C 56.10, H 10.20.

4e: 0.04 ml (0.75 mmol) of conc. H_2SO_4 was added to a solution of 0.3 g (0.75 mmol) of **1e** in heptane and the mixture was stirred for 3 h. Workup as described above and chromatographic purification (silica gel, heptane/ethyl acetate 10/1) gave 0.12 g (40%) of a colorless solid, m.p. 60°C. − IR (nujol): $\tilde{\nu}$ = 3613 and 3655 cm^{-1} (OH), 3400 (OH ass.). − ^{1}H NMR ([D$_6$]benzene): δ = 0.04, 0.23 and 0.24 (3 s, $SiCH_3$, 3 × 9 H), 0.92 (br. s, OH, 1 H), 2.45 (s, NCH_3, 6 H), 3.12 (s, CH, 1 H), 6.92−7.35 (m, ArH, 4 H). − ^{13}C NMR ([D$_6$]benzene): δ = −0.5, −0.3 and 1.3 ($SiCH_3$), 22.8 (CH), 45.3 (NCH_3), 120.6, 124.4, 125.1, 130.5 139.6 and 151.9 (arom. C). − ^{29}Si NMR ([D$_6$]benzene): δ = −19.5 and −19.2 (Si*Si*Me$_3$), 2.3 ($CSiMe_3$), 14.0 (SiOH). − MS: *m/z* (%) = 397 (100) [M$^+$], 353 (3) [M$^+$ − NMe_2], 338 (100) [M$^+$ − NMe_2 − CH_3]. − $C_{18}H_{39}NOSi_4$ (397.86): calcd. C 54.34, H 9.88, N 3.52; found C 54.52, H 9.94, N 3.60.

4f: As described for **4e**, 0.3 g (0.67 mmol) of **1f** and 0.04 ml (0.75 mmol) of H_2SO_4 gave, after chromatographic separation (silica gel, heptane/ethyl acetate 5/1), 0.2 g (66%) of colorless crystals, m.p. 53°C. − IR (nujol): $\tilde{\nu}$ = 3557 and 3675 cm^{-1} (OH), 3390 (OH ass.). − ^{1}H NMR ([D$_6$]benzene): δ = 0.08, 0.24 and 0.33 (3 s, $SiCH_3$, 3 × 9 H), 1.54 (s, OH, 1 H), 2.70 (s, CH, 1 H), 3.24, 3.34 and 3.39 (3 s, OCH_3, 3 × 3 H), 6.06 and 6.10 (2 d, ^4J = 2.45 Hz, ArH, 2 H). − ^{13}C NMR ([D$_6$]benzene): δ = −0.5, −0.3 and 1.6 ($SiCH_3$), 16.1 (CH), 54.5, 54.9 and 55.2 (OCH_3), 90.9, 91.3, 112.8, 157.4, 158.2 and 158.2 (arom. C). − ^{29}Si NMR ([D$_6$]benzene): δ = −19.5 and −19.3 (Si*Si*Me$_3$), 2.3 ($CSiMe_3$), 11.8 (SiOH). − MS: *m/z* (%) = 445 (1) [M$^+$ + H], 429 (5) [M$^+$ − CH_3], 371 (100) [M$^+$ − $SiMe_3$]. − $C_{19}H_{40}O_4Si_4$ (444.87): calcd. C 51.30, H 9.06; found C 51.16, H 9.02.

Reaction of **1d** *with Sulfuric Acid*: 0.1 ml (1.9 mmol) of conc. H_2SO_4 was added to a solution of 0.3 g (0.75 mmol) of **1d** in 30 ml of ether at room temperature. After 3 h the solvent was evaporated and the colorless, slowly crystallizing residue was washed with pentane to give 0.26 g (72%) of **5**; m.p. 84−88°C. − IR (cap.): $\tilde{\nu}$ = 2224 and 2477 cm^{-1} (SOH), 840 (SO_2 symm.), 941 (SO_2 asymm.). − ^{1}H NMR ([D$_6$]benzene): δ = 0.21, 0.24 and 0.36 (3 s, $SiCH_3$, 3 × 9 H), 2.10, 2.31 and 2.39 (3 s, $ArCH_3$, 3 × 3 H), 2.77 (s, CH, 1 H), 6.75 (s, ArH, 2 H). − ^{13}C NMR ([D$_6$]benzene): δ = 0.2, 0.3 and 2.0 ($SiCH_3$), 20.7, 22.6 and 23.2 ($ArCH_3$), 25.0 (CH), 129.7, 130.0, 133.6, 135.7 136.0 and 137.3 (arom. C). − ^{29}Si NMR ([D$_6$]benzene): δ = −15.1 and −14.1 (Si*Si*Me$_3$), 3.6 ($CSiMe_3$), 32.6 ($SiOSO_3H$). − MS: *m/z* (%) = 475 (35) [M$^+$ − H], 379 (100) [M$^+$ − HSO_4], 403 (25) [M$^+$ − $SiMe_3$], 306 (40) [M$^+$ − HSO_4 − $SiMe_3$]. − $C_{19}H_{40}O_4SSi_4$ (476.93): calcd. C 47.85, H 8.45, S 6.72; found C 47.26, H 8.36, S 6.28.

Synthesis of the Methoxysilanes **6e** and **6f**: A 2.5-fold molar excess of H_2SO_4 was added to a solution of **1e** or **1f** in methanol at room temperature. After 5−8 h the solvent was evaporated and the residue was separated by column chromatography.

6e: A solution of 0.3 g (0.75 mmol) of **1e** and 0.1 ml (1.9 mmol) of H_2SO_4 in 30 ml of methanol gave, after evaporation of the solvent and chromatographic purification (silica gel, heptane/ethyl acetate 20/1), 0.2 g (65%) of a colorless solid, m.p. 125−130°C. − ^{1}H NMR ([D$_6$]benzene): δ = 0.05, 0.26 and 0.30 (3 s, $SiCH_3$, 3 × 9 H), 2.47 (s, NCH_3, 6 H), 3.09 (s, CH, 1 H), 3.38 (s, OCH_3, 3 H), 6.93−6.98 and 7.39−7.42 (2 m, ArH, 4 H). − ^{13}C NMR ([D$_6$]benzene): δ = 0.5, 0.6 and 1.1 ($SiCH_3$), 21.9 (CH), 45.2 (NCH_3), 53.7 (OCH_3), 120.5, 124.1, 124.9, 127.5, 139.7 and 150.0 (arom. C). − ^{29}Si NMR ([D$_6$]benzene): δ = −19.8 and −19.5 (Si*Si*Me$_3$), 2.9 ($CSiMe_3$), 18.4 (SiOMe). − MS: *m/z* (%) = 410 (1) [M$^+$ − H], 396 (20) [M$^+$ − CH_3], 338 (100) [M$^+$ − $SiMe_3$]. − $C_{19}H_{41}NOSi_4$ (411.88): calcd. C 55.41, H 10.03, N 3.40; found C 55.07, H 9.85, N 3.35.

6f: 0.3 g (0.67 mmol) of **1f** and 0.01 ml (1.7 mmol) of H_2SO_4 in methanol gave, after chromatographic purification, 0.22 g (70%) of colorless crystals, m.p. 121°C. − ^{1}H NMR ([D$_6$]benzene): δ = 0.20, 0.27 and 0.28 (3 s, $SiCH_3$, 3 × 9 H), 3.00 (s, CH, 1 H), 3.33, 3.35, 3.39 and 3.50 (4 s, OCH_3, 4 × 3 H), 6.08 and 6.10 (2 d, ^4J = 2.4 Hz, ArH, 2 H). − ^{13}C NMR ([D$_6$]benzene): δ = 0.3, 0.8 and 1.3 ($SiCH_3$), 14.0 (CH), 53.8, 54.4, 54.8 and 55.0 (OCH_3), 90.7, 90.8, 110.9, 157.6, 158.3 and 158.4 (arom. C). − ^{29}Si NMR ([D$_6$]benzene): δ = −18.9 and −18.8 (Si*Si*Me$_3$), 2.2 ($CSiMe_3$), 14.9 (SiOMe). − MS: *m/z* (%) = 458 (40) [M$^+$], 443 (10) [M$^+$ − CH_3], 427 (100) [M$^+$ − OMe], 385 (50) [M$^+$ − $SiMe_3$]. − $C_{20}H_{42}O_4Si_4$ (458.89): calcd. C 52.35, H 9.23; found C 52.42, H 9.14.

Reaction of **1d** *with Sulfuric Acid in Acetic Anhydride:* 0.3 g (0.76 mmol) of **1d** and 0.1 ml (1.9 mmol) of conc. H_2SO_4 were dissolved in 30 ml of acetic anhydride and the solution was refluxed for 10 h. After evaporation of the acetic anhydride, chromatographic separation (silica gel, heptane/ethyl acetate 5/1) gave 0.27 g (82%) of **7**, m.p. 125°C. − IR (KBr): $\tilde{\nu}$ = 1712 cm^{-1} (CO). − ^{1}H NMR ([D$_6$]benzene): δ = 0.10, 0.16 and 0.31 (3 s, $SiCH_3$, 3 × 9 H), 1.78 (s, $OCOCH_3$, 3 H), 2.13 and 2.27 (2 s, Ar-*o*-CH_3, 2 × 3 H), 2.36 (s, Ar-*p*-CH_3, 3 H), 2.60 (s, CH, 1 H), 6.77 and 6.78 (2 s, Ar-H, 2 × 1 H). − ^{13}C NMR ([D$_6$]benzene): δ = 0.3, 0.5 and 2.0 ($SiCH_3$), 20.7, 21.2 and 22.2 ($ArCH_3$), 22.8 (CH), 129.6, 130.1, 133.2, 135.5, 135.6 and 138.2 (arom. C), 149.2 (OCO*C*H$_3$), 171.2 (O*C*OCH$_3$). − ^{29}Si NMR ([D$_6$]benzene): δ = −16.0 and −15.2 (Si*Si*Me$_3$), 2.9 ($CSiMe_3$), 12.9 ($SiOCOCH_3$). − MS: *m/z* (%) = 438 (100) [M$^+$], 423 (40) [M$^+$ − CH_3], 365 (100) [M$^+$ − $SiMe_3$], 233 (80) [$(Me_3Si)_2$-$SiOC(O)CH_3^+$]. − $C_{21}H_{42}O_2Si_4$ (438.91): calcd. C 57.47, H 9.65; found C 57.23, H 9.44.

Synthesis of **9**: Gaseous HCl was passed through a solution of 0.3 g (0.76 mmol) of **1d** and 0.1 ml (1.9 mmol) of H_2SO_4 in 30 ml of ether. The reaction was monitored by TLC and continued until all the alcohol **1d** had been consumed. The solvent was evaporated and the ether was replaced by pentane. After the addition of Na_2CO_3 the solution was filtered and the pentane evaporated to give a colorless solid, 0.19 g (60%), m.p. 45°C. − IR (cap.): $\tilde{\nu}$ = 690 cm^{-1} (SiCl). − ^{1}H NMR ([D$_6$]benzene): δ = 0.16 (s, $SiCH_3$, 18 H), 0.19 (s, $SiCH_3$, 9 H), 2.09, 2.20 and 2.33 (3 s, $ArCH_3$, 3 × 3 H), 2.65 (s, CH, 1 H), 6.72 (s, ArH, 2 H). − ^{13}C NMR ([D$_6$]benzene): δ = −0.6, 0.1 and 2.0 ($SiCH_3$), 20.7, 22.6 and 23.6 ($ArCH_3$), 24.0 (CH), 129.7, 130.0, 133.6, 135.2, 135.5 and 137.6 (arom. C). − ^{29}Si NMR ([D$_6$]benzene): δ = −21.8 (Si*Si*Me$_3$), 4.0 ($CSiMe_3$), 13.1 (SiCl). − MS: *m/z* (%) = 414 (10) [M$^+$], 399 (30) [M$^+$ − CH_3], 379 (2) [M$^+$ − Cl], 341 (60) [M$^+$ − $SiMe_3$]. − $C_{19}H_{39}ClSi_4$ (415.31): calcd. C 54.95, H 9.47, Cl 8.54; found C 54.36, H 9.42, Cl 8.20.

Isomerization of the Silanols **4a, d, f** *into the Disiloxanes* **11a, d, f**: A two-fold molar excess of sodium hydride was added to a solution of the appropriate silanol in THF at room temperature. After stirring for 3−8 h (monitored by chromatography) water was added and the product was extracted with ether. After drying with $MgSO_4$ the ether was evaporated and the residue was purified by column chromatography (silica gel, heptane/ethyl acetate 20/1).

11a: 0.3 g (1.0 mmol) of **4a** and 0.05 g (2 mmol) of NaH gave 0.19 g (65%) of a colorless oil. − IR (cap.): $\tilde{\nu}$ = 1050 cm^{-1} (SiOSi). − ^1H NMR ([D_6]benzene): δ = 0.28 (s, $SiSiCH_3$, 18 H), 0.31 (s, $OSiCH_3$, 9 H), 1.15 (d, ^3J = 6.7 Hz, CCH_3, 6 H), 1.31 (sept, ^3J = 6.7 Hz, CH, 1 H). − ^{13}C NMR ([D_6]benzene): δ = 1.3 ($SiSiCH_3$), 2.7 ($OSiCH_3$), 21.0 (CCH_3), 23.0 (CH). − ^{29}Si NMR ([D_6]benzene): δ = −20.4 (Si*Si*Me_3), 6.1 and 6.3 (*Si*$SiMe_3$ and $OSiMe_3$). − MS: *m*/*z* (%) = 306 (42) [M^+], 305 (100) [$M^+ - CH_3$], 263 (15) [$M^+ - C_3H_7$]. − $C_{12}H_{34}OSi_4$ (306.74): calcd. C 46.99, H 11.17; found C 46.76, H 11.12.

11d: 0.3 g (0.75 mmol) of **4d** and 0.04 g (1.7 mmol) of NaH afforded 0.15 g (50%) of a colorless oil. − IR (nujol): $\tilde{\nu}$ = 1054 cm^{-1} (SiOSi). − ^1H NMR ([D_6]benzene): δ = 0.12 (s, $SiSiCH_3$, 18 H), 0.13 (s, $OSiCH_3$, 9 H), 2.18 (s, *p*-$ArCH_3$, 3 H), 2.26 (s, *o*-$ArCH_3$, 6 H), 2.45 (s, CH_2, 2 H), 6.80 (s, ArH, 2 H). − ^{13}C NMR ([D_6]benzene): δ = −1.1 ($SiSiCH_3$), 2.3 ($OSiCH_3$), 20.9 (*p*-$ArCH_3$), 21.6 (CH_2), 22.0 (*o*-$ArCH_3$), 129.1, 133.2, 134.6 and 135.8 (arom. C). − ^{29}Si NMR ([D_6]benzene): δ = −19.5 (Si*Si*Me_3), 3.3 (*Si*SiMe_3), 6.9 ($OSiMe_3$). − MS: *m*/*z* (%) = 396 (40) [M^+ − H], 381 (95) [$M^+ - CH_3$], 323 (75) [$M^+ - SiMe_3$], 307 (20) [M^+ − $OSiMe_3$], 277 (100) [$M^+ - C_6H_2Me_3$]. − $C_{19}H_{40}OSi_4$ (396.87): calcd. C 57.50, H 10.16; found C 57.24, H 10.10.

11f: 0.3 g (0.7 mmol) of **4f** and 0.035 g (1.5 mmol) of NaH gave 0.22 g (75%) of a colorless oil. − IR (cap.): $\tilde{\nu}$ = 1062 (SiOSi). − ^1H NMR ([D_6]benzene): δ = 0.22 (s, $SiSiCH_3$, 18 H), 0.29 (s, $OSiCH_3$, 9 H), 2.73 (s, CH_2, 2 H), 3.39 (s, *o*-OCH_3, 6 H), 3.42 (s, *p*-OCH_3, 3 H), 6.12 (s, ArH, 2 H). − ^{13}C NMR ([D_6]benzene): δ = −1.2 ($SiSiCH_3$), 2.3 ($OSiCH_3$), 12.9 (CH_2), 54.8 (*o*-OCH_3), 54.9 (*p*-OCH_3), 90.6, 109.1, 157.9 and 158.8 (arom. C). − ^{29}Si NMR ([D_6]benzene): δ = −19.6 (Si*Si*Me_3), 0.9 (*Si*Si*Me*$_3$), 6.3 ($OSiMe_3$). − MS: *m*/*z* (%) = 445 (10) [M^+ + H], 429 (35) [$M^+ - CH_3$], 371 (100) [$M^+ - SiMe_3$], 355 (10) [$M^+ - OSiMe_3$]. − $C_{19}H_{40}O_4Si_4$ (444.87): calcd. 51.30, H 9.06; found C 51.22, H. 9.14.

[1] C. Krempner, H. Reinke, H. Oehme, *Chem. Ber*. **1995**, *128*, 143−149.
[2] C. Krempner, D. Hoffmann, R. Kempe, H. Oehme, *Organometallics* **1997**, *16*, 1828−1832 and literature cited therein.
[3] D. Bravo-Zhivotovskii, V. Brande, A. Stanger, M. Kapon, Y. Apeloig, *Organometallics* **1992**, *11*, 2326−2328; J. Ohshita, Y. Masaoka, M. Ishikawa, *Organometallics* **1991**, *10*, 3775−3776; J. Ohshita, Y. Masaoka, M. Ishikawa, T. Takeuchi, *Organometallics* **1993**, *12*, 876−879; H. Oehme, R. Wustrack, A. Heine, G. M. Sheldrick, D. Stalke, *J. Organomet. Chem.* **1993**, *452*, 33−39.
[4] Y. Apeloig, M. Bendikov, M. Yuzefovich, M. Nakash, D. Bravo-Zhivotovskii, D. Bläser, R. Boese, *J. Am. Chem. Soc.* **1996**, *118*, 12228−12229.
[5] I. Fleming in *Comprehensive Organic Chemistry* (Eds.: D. Barton, W. D. Ollis), Pergamon, Oxford, **1979**, vol. 3, p. 640; W. P. Weber, *Silicon Reagents for Organic Synthesis*, Springer-Verlag, Heidelberg, **1983**, p. 58.
[6] K. Tamao, M. Kumada, *J. Organomet. Chem.* **1971**, *30*, 339−347.
[7] A. G. Brook, K. H. Pannell, G. E. LeGrow, J. J. Shuto, *J. Organomet. Chem.* **1964**, *2*, 491−493.
[8] G. Märkl, M. Horn, W. Schlosser, *Tetrahedron Lett*. **1986**, *27*, 4019−4022.
[9] P. D. Lickiss, *J. Chem. Soc., Dalton Trans.* **1992**, 1333−1338; J. Chojnowski, W. Stanczyk, *Main Group Met. Chem.* **1994**, *2*, 6−15; J. B. Lambert, L. Kania, S. Zhang, *Chem. Rev.* **1995**, *95*, 1191−1201; R. Bakhtiar, C. M. Holznagel, D. B. Jacobson, *J. Am. Chem. Soc.* **1992**, *114*, 3227−3235 and literature cited therein.
[10] Y. Apeloig, A. Stanger, *J. Am. Chem. Soc*. **1987**, *109,* 272−273.
[11] Y. Apeloig, A. Stanger, *J. Am. Chem. Soc*. **1985**, *107,* 2806−2807.
[12] N. Basso, S. Görs, E. Popowski, H. Meyr, *J. Am. Chem. Soc.* **1993**, *115,* 6025−6028.
[13] F. Luderer, H. Reinke, H. Oehme, *Z. Anorg. Allg. Chem.,* submitted.
[14] G. Gutekunst, A. G. Brook, *J. Organomet. Chem*. **1982**, *225*, 1−3.
[15] K. Sternberg, M. Michalik, H. Oehme, *J. Organomet. Chem.*, **1997**, *533*, 265− 268.

[97208]

Magnetic Interaction in Dinuclear Triphos−Cobalt Complexes with Co···Co Separations of 8 and 10 Å

Katja Heinze, Gottfried Huttner*, and Peter Schober

University of Heidelberg, Department of Inorganic Chemistry,
Im Neuenheimer Feld 270, D-69120 Heidelberg, Germany
Fax: (internat.) +49(0)6221/545707
E-mail: katja@sun0.urz.uni-heidelberg.de

Received September 23, 1997

Keywords: Tripodal ligands / Cobalt complexes / Bridging ligands / Exchange coupling

Weak antiferromagnetic exchange interactions are observed in two Co^{II} dimers of the general formula $[\{(triphos)Co\}_2(\mu\text{-dicarboxylato})](BF_4)_2$ where the dicarboxylate is the dianion of fumaric acid [**3**·$(BF_4)_2$] or terephthalic acid [**4**·$(BF_4)_2$] and triphos is the tridentate phosphorus ligand 1,1,1-tris(diphenylphosphanomethyl)ethane. In these complexes the metal ions are separated by 8 and 10 Å, as determined by X-ray crystallography. Insight into the interaction pathway is gained through molecular orbital calculations performed on model compounds. The influence of bridging-ligand distortions and the stereochemistry around the two cobalt centres is discussed.

Introduction

Magnetic exchange interactions between two paramagnetic centres have attracted considerable interest from inorganic chemists.[1][2][3] The investigations have mainly been focused on the simplest case where two electrons at two d^9-Cu^{II} centres ($S_1 = S_2 = \frac{1}{2}$) are separated by an organic spacer leading to new good quantum numbers of $S = 0$ (singlet state) and $S = 1$ (triplet state) for these systems.[1][2][3] Factors that govern the nature of the interaction such as orbital topology and orbital overlap are quite well understood and are used to design antiferro- and ferromagnetically coupled systems[4][5] although it is not yet possible to use theory to make quantitative explanations and predictions.[2] In the case of two interacting spins at two copper centres the interaction is mediated through the σ-framework of the bridging unit.[2] Maximum overlap between the bridging-ligand orbitals and the copper orbitals which leads to a stabilisation of the singlet state is obtained for a $d_{x^2-y^2}$ ground state of the copper ion in a square-planar or square-pyramidal geometry as opposed to a trigonal-bipyramidal situation.[2][7] With this favourable electronic configuration, antiferromagnetic exchange interaction is observed even with Cu···Cu separations larger than 10 Å.[6][7][13] The organic spacers employed for obtaining large intramolecular distances are dicarboxylic acids (or the dianions derived from them) with a rigid, usually conjugated, core. However, the coordination mode of carboxylates at metal centres can vary drastically (Scheme 1) and has a large influence on both the coordination geometry around the metal and the magnetic exchange interaction. A relatively large interaction is found if the carboxylate coordinates in a monodentate fashion with an additional hydrogen-bridge system (Scheme 1, iii);[6][7] an interaction is also predicted for the symmetrical bidentate coordination mode (Scheme 1, iv).[8] In other cases the magnetic interaction is small and may instead be *inter*molecular in nature.[8][9][10][11][12] One exception is the complex $[\{(bpy)(H_2O)Cu\}_2(\mu\text{-terephthalato})](ClO_4)_2$, although its structure has not so far been determined.[13]

Scheme 1. Binding modes of carboxylates R−COO^- at metal centres

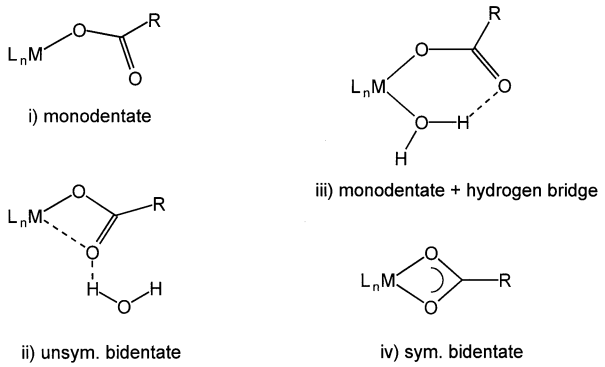

We have focused our attention on a cobalt(II) system with the tridentate ligand triphos [1,1,1-tris(diphenylphosphanomethyl)ethane]. This ligand induces a fivefold coordination around the cobalt centre providing two free *cis*-coordination sites[14][15][16] needed for a bidentate coordination mode of the carboxylate (Scheme 1, iv). The phosphorus donor set usually splits the metal-d orbitals such that a low-spin configuration (d^7) with one unpaired electron is obtained.[14][15] Furthermore the three bulky diphenylphosphano groups insulate the individual complex molecules from each other leaving no *inter*molecular interaction pathway accessible. This often represents a severe problem in the study of *intra*molecular interactions especially over large distances.[2][6]

 © WILEY-VCH Verlag GmbH, D-69451 Weinheim, 1998 1434−1948/98/0202−0183 $ 17.50+.50/0

In order to address the questions concerning magnetic exchange interactions (i) within a d^7/d^7 system and (ii) over distances up to 10 Å we describe here the syntheses, solid-state structures and magnetic behaviour of dinuclear triphos−Co^{II} complexes bridged by the dianions of fumaric and terephthalic acid. In addition, we describe molecular orbital calculations which qualitatively explain the interaction pathway.

Results and Discussion

Preparation of Complexes: The reaction of triphos with $Co(BF_4)_2 \cdot 6\ H_2O$ and the appropriate dicarboxylic acid in THF/ethanol in the ratio 1:1:0.5 yields red-brown solutions from which the complex salts [{(triphos)Co}$_2$(μ-fumarato)]$(BF_4)_2$ [**3**$\cdot(BF_4)_2$] and [{(triphos)Co}$_2$(μ-terephthalato)]$(BF_4)_2$ [**4**$\cdot(BF_4)_2$] were isolated (Scheme 2).

Scheme 2. Dinuclear triphos−Co^{II} complexes

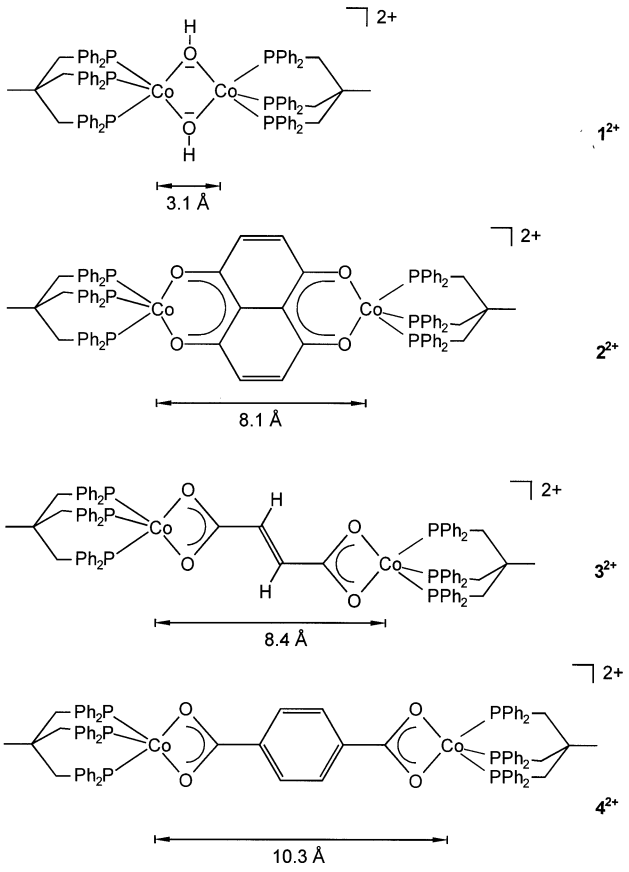

The UV/Vis spectra of the solutions are almost identical and are similar to that of the mononuclear complex [{(triphos)Co}(η^2-acetate)](BPh_4),[17] suggesting an analogous coordination environment and geometry. The absorptions observed can be assigned to d-d transitions of a square-pyramidal d^7-low-spin complex.[18][19] The dinuclear composition of $\mathbf{3}^{2+}$ and $\mathbf{4}^{2+}$ is confirmed by the observed M^+ peaks in the FAB mass spectra with correct isotopic distributions as well as signals for dications M^{2+} at *m*/2*e*. The IR spectra show the typical bands for the triphos ligand,[20] as well as the broad absorption of the tetrafluoroborate counter ions at 1055−1059 cm^{-1}. Unfortunately the $\tilde{\nu}_{as}(CO_2^-)$ and $\tilde{\nu}_s(CO_2^-)$ absorptions could not be identified as they overlap with the $\tilde{\nu}$(C=C) and δ(C−H) absorptions of the aromatic rings of the triphos ligand. For **4**$\cdot(BF_4)_2$ a medium strong band is observed at 1514 cm^{-1} which is tentatively assigned to the $\tilde{\nu}$(C=C) vibration of the aromatic ring of the bridging terephthalato ligand. In the cyclic voltammogram (CH_3CN, vs. SCE) both complexes show only quasi- and irreversible oxidation and reduction waves (see Experimental Section).

Crystal Structures: The complexes **3**$\cdot(BF_4)_2$ and **4**$\cdot(BF_4)_2$ crystallise in the monoclinic, centrosymmetric space groups $P2_1/c$ and $P2_1/n$, respectively. Table 1 summarises selected bond lengths and angles. The crystal structures consist of centrosymmetric discrete dinuclear dications (Figures 1 and 2), BF_4^- counterions and solvent molecules.

Figure 1. View of the dication of **3**$\cdot(BF_4)_2$

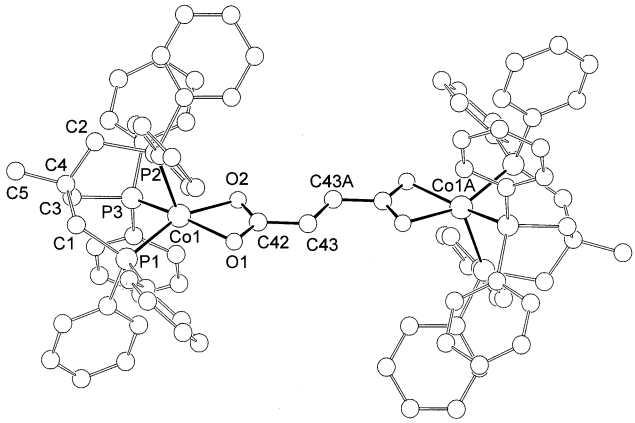

Figure 2. View of the dication of **4**$\cdot(BF_4)_2$

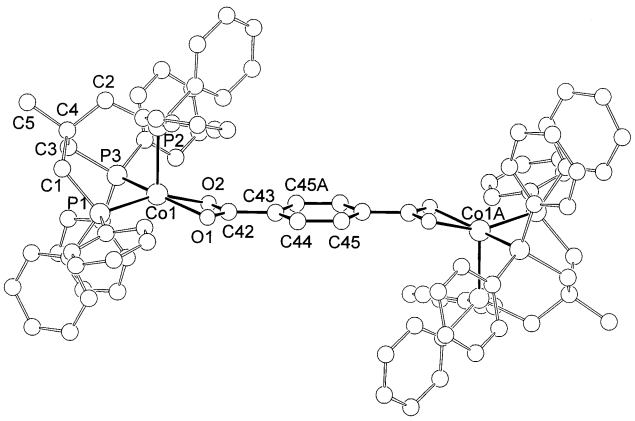

The packing of the molecules is such that no short intermolecular contacts arise: Co···Co(intermolecular) 11.8 Å [**3**···$(BF_4)_2$], 11.6 Å [**4**···$(BF_4)_2$], Co···F 7.6−10 Å [**3**···$(BF_4)_2$], 9−11 Å [**4**···$(BF_4)_2$] which provide perfect magnetic insulation of the dimeric cations. The geometry around the metal centres can be described as distorted square-pyramidal with the P2 atom occupying the axial coordination site (Figures 1 and 2). The carboxylates coordinate in a symmetric bidentate fashion with almost equal

Table 1. Selected bond lengths [Å][a] and angles [°][a] for $\mathbf{3}\cdot(BF_4)_2$ and $\mathbf{4}\cdot(BF_4)_2$

	$\mathbf{3}\cdot(BF_4)_2$	$\mathbf{4}\cdot(BF_4)_2$		$\mathbf{3}\cdot(BF_4)_2$	$\mathbf{4}\cdot(BF_4)_2$
Co1−O1	2.005(3)	2.025(4)	O1−Co1−O2	65.8(1)	66.0(2)
Co1−O2	1.998(3)	1.992(4)	P1−Co1−P2	92.15(4)	84.11(7)
Co1−P1	2.189(1)	2.204(2)	P1−Co1−P3	89.52(4)	88.96(7)
Co1−P2	2.298(1)	2.269(2)	P2−Co1−P3	90.04(4)	91.71(7)
Co1−P3	2.187(1)	2.164(2)	P1−Co1−O1	99.43(9)	106.8(2)
O1−C42	1.272(5)	1.265(8)	P1−Co1−O2	158.12(9)	155.9(1)
O2−C42	1.265(5)	1.280(7)	P2−Co1−O1	108.0(1)	98.2(1)
C42−C43	1.476(5)	1.490(8)	P2−Co1−O2	107.49(9)	109.5(1)
C43−C44	−	1.402(9)	P3−Co1−O1	159.4(1)	160.6(1)
C44−C45	−	1.395(9)	P3−Co1−O2	99.77(8)	95.1(1)
C43−C45A	−	1.39(1)	Co1−O1−C42	87.8(2)	86.5(3)
C43−C43A	1.304(8)	−	Co1−O2−C42	88.3(2)	87.6(4)
Co1···C42	2.332(4)	2.322(6)	O1−C42−C43	121.1(4)	122.9(6)
Co1···Co1A	8.37	10.31	O2−C42−C43	120.8(3)	118.5(6)
			O1−C42−O2	118.1(3)	118.5(5)

[a] Estimated standard deviations of the least significant figures are given in parentheses.

Co−O and C−O bond lengths (Table 1). The small angle O−Co−O is similar to that found in monocarboxylate complexes of the triphos−Co^{II} fragment.[16][17][21] The distance between the carbon atom of the carboxylate fragment and the central -system (double bond in $\mathbf{3}^{2+}$, aromatic ring in $\mathbf{4}^{2+}$) is that of a $C(sp^2)-C(sp^2)$ single bond.[22] The carboxylate groups and the plane of the central π-systems are almost coplanar, the tilting angle being 7.8° ($\mathbf{3}^{2+}$) and 4.2° ($\mathbf{4}^{2+}$). The intramolecular Co···Co separations are 8.37 Å ($\mathbf{3}^{2+}$) and 10.31 Å ($\mathbf{4}^{2+}$).

Magnetic Susceptibility: Variable-temperature magnetic susceptibility data for the two complexes were measured in the temperature range 7−290 K using a Faraday balance (Figures 3 and 4). These data were fitted to the Bleaney−Bowers equation[2] and the result is represented by the solid lines in Figures 3 and 4.[23] From these fits the singlet−triplet splittings are estimated as $2J = -36$ cm^{-1} [$\mathbf{3}\cdots(BF_4)_2$] and -16 cm^{-1} [$\mathbf{4}\cdots(BF_4)_2$]. *Inter*molecular interactions (vide supra) can be safely excluded and the observed antiferromagnetic exchange coupling must therefore be *intra*molecular in nature. The results are compiled in Table 2 along with the results of EPR measurements. Also included are the data of two previously described dinuclear triphos-Co^{II} complexes with oxygen donor coligands, [{(triphos)Co}$_2$(μ-OH)$_2$]$(BPh_4)_2$ [$\mathbf{1}\cdots(BPh_4)_2$][17] and [{(triphos)Co}$_2$(μ-1,4,5,8-tetraoxonaphthaleno)]$(BF_4)_2$ [$\mathbf{2}\cdots BF_4)_2$][24] (Scheme 2).

The EPR spectra in solution at 295 K and in a THF−CH_2Cl_2 glass at 100 K show only broad unresolved signals centred at $g = 2.12$ which is a typical value for low-spin Co^{II} complexes.[24][25][26][27][28]

Molecular Orbital Calculations: To gain insight into the possible interaction pathway, molecular orbital calculations on idealised and simplified model compounds were performed at the SCF level of theory. The frontier molecular orbitals of the complexes are depicted in Figures 5 and 6. The symmetry labels *g* and *u* refer to the inversion centres of the molecules. According to Hoffmann[3] the splitting of the singlet and triplet state is related to the energy difference

Figure 3. Temperature dependence of χ_M and μ_{eff} of a solid sample of $\mathbf{3}\cdot(BF_4)_2$

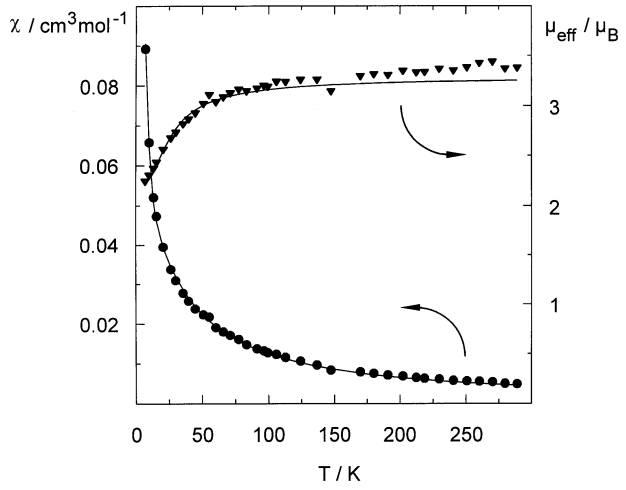

Figure 4. Temperature dependence of χ_M and μ_{eff} of a solid sample of $\mathbf{4}\cdot(BF_4)_2$

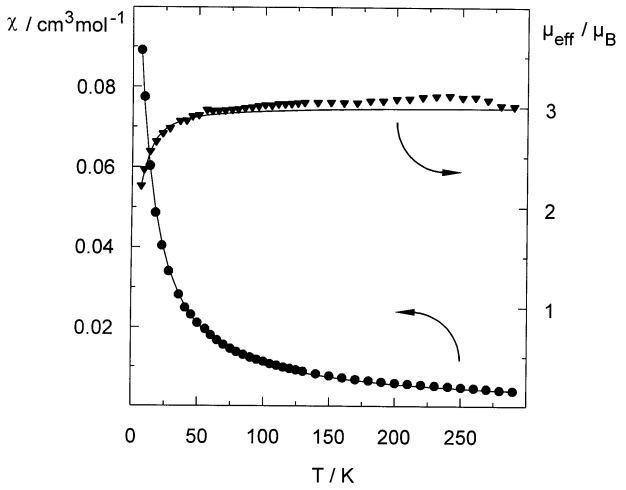

Table 2. Magnetic and EPR data of dinuclear triphos−Co^{II} complexes

compound	$-2J/cm^{-1}$	g_{mag}	g (295 K)	Ref.
$\mathbf{1}^{2+}$	144	2.45	n.d.	[17]
$\mathbf{2}^{2+}$	58	1.99	2.11	[24]
$\mathbf{3}^{2+}$	36	2.03	2.12	this paper
$\mathbf{4}^{2+}$	16	1.82	2.12	this paper

of the two frontier molecular orbitals $\varepsilon_1 - \varepsilon_2$ through $-2J = E_T - E_S = -2K_{ab} + (\varepsilon_1 - \varepsilon_2)^2\cdot(J_{aa} - J_{ab})^{-1}$ where K_{ab} is the two-electron exchange integral and J_{aa}, J_{ab} are the one- and two-centre coulomb repulsion integrals. Assuming that K_{ab}, J_{aa}, and J_{ab} vary only slowly in closely related compounds the energy difference of the *spin states* is proportional to the square of the splitting of one-electron *energy levels*.

As expected from simple ligand-field theory[29] the unpaired electron of each cobalt centre in a square-pyramidal coordination geometry occupies a d_{z^2} orbital (with an ad-

Figure 5. Orbital splitting and orbital symmetry of the model complex of $\mathbf{3}^{2+}$ [a]

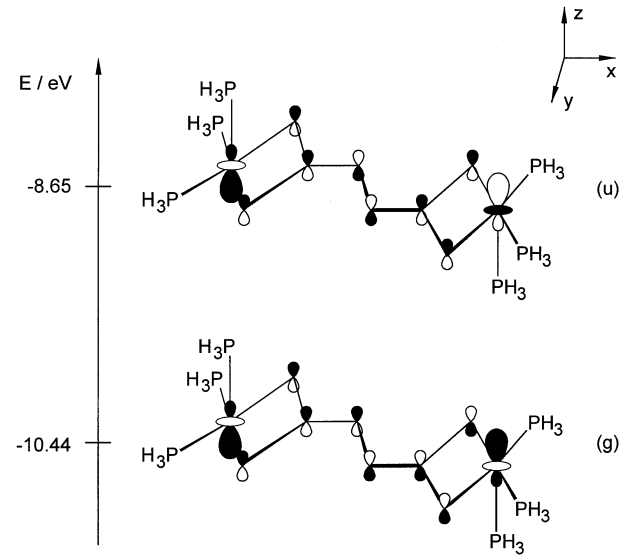

[a] The contribution of ligand orbitals is exaggerated. The composition is approximately 77% metal, 20% PH_3 and 3% bridging ligand.

Figure 6. Orbital splitting and orbital symmetry of the model complex of $\mathbf{4}^{2+}$ [a]

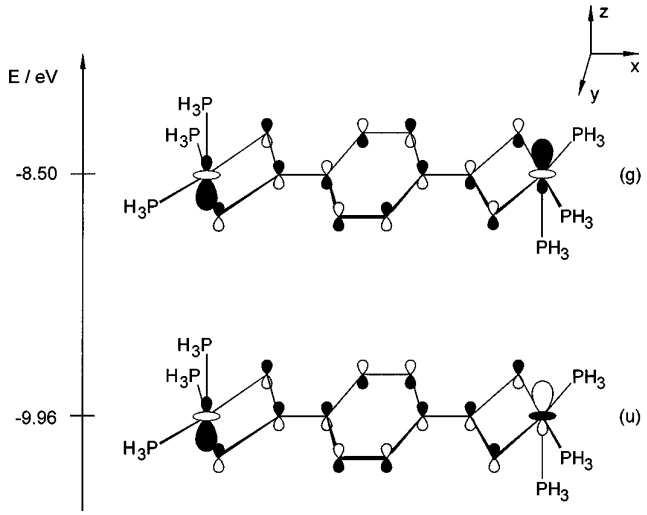

[a] The contribution of ligand orbitals is exaggerated. The composition is approximately 77% metal, 20% PH_3 and 3% bridging ligand.

mixture of 5% s and 9% p_z). The highest occupied orbitals of the dimer are the symmetric and antisymmetric combinations of these monomer orbitals. In the fumarato complex ($\mathbf{3}^{2+}$) the in-phase combination (*g*, Figure 5) is lower in energy than the out-of-phase combination (*u*, Figure 5), while the reverse is true for the terephthalato complex ($\mathbf{4}^{2+}$) (Figure 6). The qualitative level ordering of the ligand orbitals follows the expected trend from nodal structure: one (HOMO) and two (LUMO) nodal planes for the ligand-MOs of $\mathbf{3}^{2+}$ and two (HOMO) and three (LUMO) for $\mathbf{4}^{3+}$ (Figures 5 and 6).

As opposed to the d^9/d^9 case (Cu^{II}/Cu^{II}) the magnetic orbitals of the cobalt centres (d_{z^2} + p_z) are orientated almost perpendicular (*z* axis) to the plane of the carboxylato group (*xy* plane). This orientation precludes any interaction through the σ-framework of the bridging ligand but provides a pathway over the π-system of the bridge. The magnetic exchange coupling mediated by the π-system of the ligand is expected to be much smaller than an interaction through the σ-system (better orbital overlap) and the experimental results (small splitting in the cobalt case and larger splitting in the copper case) seem to support this expectation. However, inspite of the large distances between the metal centres and the poorer overlap between the metal and the ligand orbitals, a weak antiferromagnetic exchange is observed which is more than two orders of magnitude larger than the calculated singlet−triplet energy gap ($2J$ = -0.1 cm^{-1}, d_{M-M} = 10.3 Å) based on a statistical analysis.[2] Thus even switching from the σ-interaction pathway in Cu−Cu dimers to a π-interaction in Co−Co complexes does not prevent a magnetic coupling of the two metal centres separated by 10 Å.

In order to relate the singlet−triplet energy gap to the energy difference between the highest one-electron energy levels the HOMO−LUMO gaps of model compounds of $\mathbf{3}^{2+}$ and $\mathbf{4}^{2+}$ were calculated; also included in the calculation were models of the complexes $\mathbf{1}^{2+}$ and $\mathbf{2}^{2+}$.[17][24] The results are summarised in Table 3. In fact, the simple calculation reflects the correct ordering of decreasing antiferromagnetic interaction $\mathbf{1}^{2+} > \mathbf{2}^{2+} > \mathbf{3}^{2+} > \mathbf{4}^{2+}$ (Tables 2 and 3).

Table 3. Orbital energies and orbital energy splitting values

compound	ε_1/eV	ε_2/eV	$\Delta E^2=(\varepsilon_1-\varepsilon_2)^2$	Co···Co/Å
$\mathbf{1}^{2+}$	−12.232	−8.602	13.18	3.07
$\mathbf{2}^{2+}$	−10.533	−8.459	4.30	8.11
$\mathbf{3}^{2+}$	−10.438	−8.649	3.20	8.37
$\mathbf{4}^{2+}$	−9.958	−8.500	2.13	10.31

Furthermore the square of the calculated energy difference $\Delta E^2 = (\varepsilon_1 - \varepsilon_2)^2$ correlates well with the experimental singlet−triplet splitting $-2J$ ($-2J$ [cm^{-1}] = 11.0 × ΔE^2 [eV^2] + 0.61; r^2 = 0.982) (Figure 7) showing that even this simple and qualitative model can explain the observed antiferromagnetic interaction in d^7/d^7 dinuclear complexes.

Encouraged by these results the influence of distortions within the dinuclear complex on the singlet−triplet energy gap was studied. In the first study the central phenyl ring of the model complex $\mathbf{4}^{2+}$ was rotated around the x-axis (Figures 6 and 8). The dihedral angle between the plane of the phenyl ring and the basal planes of the metal-surrounding square pyramids was varied from 0 to 90°. Qualitatively the overlap between the p-orbitals at the carbon atoms C42 and C43 (Figures 2 and 8) should decrease and at the 90° distortion they should be strictly orthogonal leading to a vanishing HOMO−LUMO gap, ΔE, and thus to a zero antiferromagnetic interaction. With the employed calculation method the highest molecular orbitals become degenerate at a dihedral angle of 70°. However, too much significance should not be ascribed to the computed angle since the value is dependent on the choice of exponents for

Figure 7. Correlation of the experimental S/T gap ($2J$) and the the square of the calculated HOMO−LUMO gap (ΔE^2)

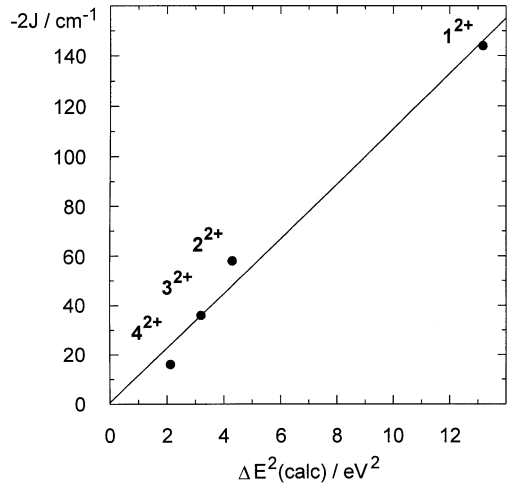

the carbon p-orbital. A similar situation was encountered in the study of the Cu−O−Cu angle variation in di-μ-OH copper dimers.[2][3] Experimentally this distortion could be achieved by attaching large substituents onto the phenyl ring of the bridging ligand; this is currently being attempted.

Figure 8. Distortion of the ligand π-system

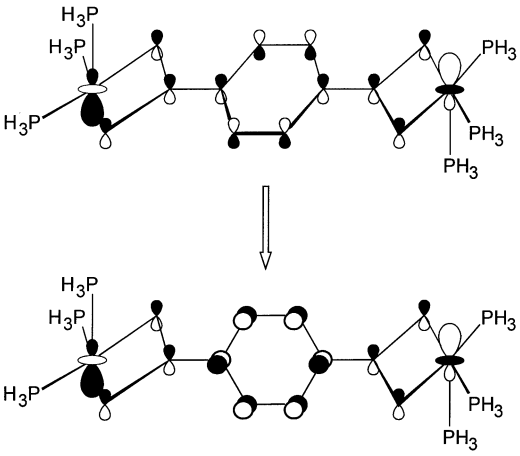

Figure 9. Square pyramid−trigonal bipyramid distortion

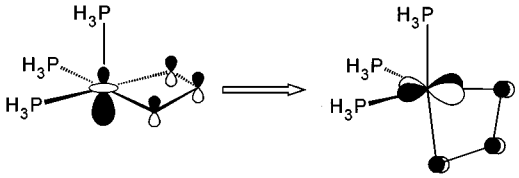

The second distortion possible in five-coordinate complexes is the transformation of the coordination polyhedron from square pyramidal to trigonal bipyramidal. This can be achieved by rotating the carboxylate chelating ligand out of the basal plane (xy plane) into the xz plane while maintaining the geometry of the $(PH_3)_3Co$ fragment (Figure 9). The hybridisation of the cobalt centres changes from d_{z^2} (+s and p_z) to almost pure d_{xy} (+p_y) (in this coordinate system) as has been shown previously.[29] The calculations show than this distortion has only a very small effect on the HOMO−LUMO energy gap; the π-type overlap of the metal d-hybrid orbitals with the oxygen p-orbitals obviously remains almost constant during the distortion. The small energy difference and activation barrier between square-pyramidal and trigonal-bipyramidal distorted triphos−Co complexes has been experimentally shown by EPR[24][25][26][27][28] and NMR spectroscopy[30][31][32] as well as by the fact that in one case both conformational isomers have been isolated in the solid state.[33] This is consistent with the assumption that neither the total energy nor the energy gap of the frontier orbitals change significantly during the distortion. Therefore unlike the Cu−Cu dimers[2][7] the singlet−triplet splitting in Co−Co dimers of the type described in this work appears relatively insensitive towards this geometrical distortion.

In summary, this work has shown that intramolecular antiferromagnetic exchange coupling occurs in dinuclear triphos−Co^{II} complexes up to a metal−metal distance of 10 Å. The interaction is transmitted through the π-system of the bridging ligand. The experimental results can be explained within a simple MO approach at the SCF level of theory. Distortions within the π-system of the bridging ligand are predicted to decrease the HOMO−LUMO gap and thus the antiferromagnetic coupling while distortions from a square-pyramidal to a trigonal-bipyramidal geometry around the metal centre are predicted to have a negligible influence on the HOMO−LUMO gap.

This work received support from the *Deutsche Forschungsgemeinschaft*, the *Fonds der Chemischen Industrie*, and the *Volkswagenstiftung*.

Experimental Section

Computational Details: Calculations were performed on an Apple Macintosh IIfx with the CACHe/ZINDO program Version 3.6 (M. C. Zerner 1990−1994) with INDO/1 parameters. Orbital energies were obtained from an SCF calculation of the singlet state without symmetry constraints. The geometry of the molecules was idealized to a square pyramidal polyhedron around the metal centre and a planar bridging ligand. The triphos ligand was replaced by three isoelectronic PH_3 groups. Distances and angles were as follows: Co−P_{eq} 2.19 Å, Co−P_{ax} 2.26 Å, Co−O 2.00 Å, P−H 1.38 Å, O−Co−O 65.8°, P−Co−P 90.0°, O−C−O 118.0°.

General Methods: Unless noted otherwise all manipulations were carried out under an inert atmosphere by means of standard Schlenk techniques. All solvents were dried by standard methods and distilled under inert gas. − NMR: Bruker AC 200 at 200.13 MHz (^{1}H). − IR: Bruker FTIR IFS-66, as CsI disks. − UV/Vis/NIR: Perkin Elmer Lambda 19. − MS: Finnigan MAT 8230. − EPR: Bruker ESP 300 E, X-band, standard cavity ER 4102, temperature control unit Eurotherm B-VT 2000, external standard diphenylpicrylhydrazyl (DPPH). − Elemental analyses: microanalytical laboratory of the Organisch-Chemisches Institut, University of Heidelberg. − Melting points: Gallenkamp MFB-595 010, melting points are not corrected. − Cyclic voltammetry: Metrohm "Universal Meß- und Titriergefäß", Metrohm GC electrode RDE 628, platinum electrode, SCE electrode, Princeton Applied Re-

search potentiostat Model 273, 10^{-3} M in 0.1 M nBu$_4$NPF$_6$/CH$_3$CN. – Magnetic measurements were carried out on a Faraday type magnetometer in the temperature range 7–290 K. The magnetic field applied was 10 kG. Mercury tetrakis(thiocyanato)cobaltate was used as a susceptibility standard. Corrections for diamagnetism were estimated using Pascal's constants[34] as $915 \cdot 10^{-6}$ [**3**·(BF$_4$)$_2$] and $955 \cdot 10^{-6}$ cm^3 mol^{-1} [**4**·(BF$_4$)$_2$]. Magnetism of the samples was found to be field-independent. The effective magnetic moment was calculated by using the equation $\mu_{eff} = 2.83\ (\chi_M\ T)^{1/2}$, whereas the exchange parameters J and g_{mag} were obtained by a least-squares fitting of the susceptibility data to the Bleaney-Bowers equation for dinuclear complexes with $S_1 = S_2 = 1/2$, where $2J$ is the energy difference between the singlet and the triplet states ($H = -2J \cdot S_1 \cdot S_2$). A further parameter p, representing the percentage of a mononuclear impurity with $S = {}^3/_2$ (high-spin Co^{II}), was introduced although the exact nature of the actual impurity (oligomer, polymer) was unknown: p = 6.7% [**3**·(BF$_4$)$_2$], 5.7% [**4**·(BF$_4$)$_2$]. The variations in g_{mag} values are not significant and result from the fitting method. Magnetic measurements in solution (CD$_2$Cl$_2$) were conducted according to the method of Evans.[35] Diphenylpicrylhydrazyl (DPPH) was used as a susceptibility standard.

Chemicals: 1,1,1-Tris(diphenylphosphanomethyl)ethane, CH$_3$C(CH$_2$PPh$_2$)$_3$[36], Co(BF$_4$)$_2$·6 H$_2$O[37].

Crystallographic Structure Determinations: The measurements were carried out on a Siemens P4 (Nicolet Syntex) R3m/v four-circle diffractometer with graphite-monochromated Mo-K_α radiation. All calculations were performed using the SHELXT PLUS software package. Structures were solved by direct methods with the SHELXS-86 program and refined with the SHELX93 program.[38] Graphics were prepared using XPMA and ZORTEP.[39] An absorption correction (ψ scan, $\Delta\psi = 10°$) was applied to all data. Atomic coordinates and anisotropic thermal parameters of the nonhydrogen atoms were refined by a full-matrix least-squares calculation. Table 4 is a compilation of the data for the structure determinations. Further details of the crystal structure determinations may be obtained from the Fachinformationszentrum Karlsruhe, D-76344 Eggenstein-Leopoldshafen (Germany), on quoting the depository numbers CSD-407616 [**3**·(BF$_4$)$_2$], and CSD-407617 [**4**·(BF$_4$)$_2$].

(μ-Fumarato)bis[{1,1,1-tris(diphenylphosphanomethyl)-ethane}cobalt] Bis(tetrafluoroborate) [**3**·(BF$_4$)$_2$] *and (μ-Terephthalato)bis[{1,1,1-tris(diphenylphosphanomethyl)ethane}-cobalt] Bis(tetrafluoroborate)* [**4**·(BF$_4$)$_2$]: A solution of Co(BF$_4$)$_2$·6 H$_2$O (341 mg, 1 mmol) in EtOH (10 ml) was added to a solution of the triphos ligand (624 mg, 1 mmol) in THF (15 ml). Addition of the dicarboxylic acid [fumaric acid for **3**·(BF$_4$)$_2$; 58 mg, 0.5 mmol; terephthalic acid for **4**·(BF$_4$)$_2$; 83 mg, 0.5 mmol] to the orange-coloured solution caused a slow colour change to red-brown. After the solution had been stirred for two hours it was filtered and the solvents were evaporated. The solid residue was washed with Et$_2$O, dissolved in CH$_2$Cl$_2$ and filtrated over 2 cm of Kieselgur. The clear, red solution was concentrated in vacuo until the complex started to precipitate. Precipitation was completed by adding 10 ml of Et$_2$O. Recrystallisation from CH$_2$Cl$_2$/Et$_2$O yielded 356 mg (43%) of **3**·(BF$_4$)$_2$ and 410 mg (48%) of **4**·(BF$_4$)$_2$, respectively. Vapour diffusion of Et$_2$O into a concentrated solution of the complex [**3**·(BF$_4$)$_2$ in acetone; **4**·BF$_4$)$_2$ in CH$_2$Cl$_2$] afforded red needle-shaped crystals suitable for X-ray crystallographic analysis.

3·(BF$_4$)$_2$: M.p. 250°C (decomp.). – IR (CsI): $\tilde{\nu}$ = 3058 cm^{-1} (m), 1485 (m), 1436 (s), 1283 (m), 1093 (s), 1055 (br), 999 (m), 829 (w), 738 (s), 692 (s), 513 (s). – MS (FAB); *m/z* (%): 1599 (18) [M$^+$ + F], 1480 (11) [M$^+$], 875 (38) [M$^+$ – triphos-Co + Ph + 1], 797 (40) [M$^+$ – triphos-Co], 740 (5) [M^{2+}], 683 (52) [triphos-Co$^+$], 547 (43) [triphos-Ph$^+$]. – UV/Vis (CH$_2$Cl$_2$): λ_{max} (ε) = 489 nm (3550 M^{-1} cm^{-1}), 966 (1030). – CV (CH$_3$CN): $E_{1/2}$ = –0.30 V (qrev.), +0.35 V (qrev.). – μ_{eff}(CD$_2$Cl$_2$): 3.5 μ_B. – C$_{86}$H$_{80}$B$_2$Co$_2$F$_8$O$_4$P$_6$ (1654.9): calcd. for **3**·(BF$_4$)$_2$·3 CH$_2$Cl$_2$: C 55.98, H 4.54; found C 55.11, H 5.04.

4·(BF$_4$)$_2$: M.p. 240°C (decomp.). – IR (CsI): $\tilde{\nu}$ = 3059 cm^{-1} (m), 1514 (m), 1485 (m), 1434 (s), 1409 (m), 1279 (w), 1096 (s), 1059 (br), 998 (m), 854 (s), 833 (w), 738 (s), 694 (s), 514 (s). – MS (FAB); *m/z* (%): 1549 (42) [M$^+$ + F], 1530 (21) [M$^+$], 925 (74) [M$^+$ – triphos-Co + Ph + 1], 847 (71) [M$^+$ – triphosCo], 765 (8) [M^{2+}], 683 (56) [triphosCo$^+$], 547 (72) [triphos-Ph$^+$]. – UV/Vis (CH$_2$Cl$_2$): λ_{max} (ε) = 474 nm (3130 M^{-1} cm^{-1}), 650 (230), 963 (880). – CV (CH$_3$CN): E_p = –0.37 V (irr.), $E_{1/2}$ = +0.27 V (qrev.). – μ_{eff}(CD$_2$Cl$_2$): 3.1 μ_B. – C$_{90}$H$_{82}$B$_2$Co$_2$F$_8$O$_4$P$_6$ (1705.0): calcd. for **4**·(BF$_4$)$_2$·1 CH$_2$Cl$_2$: C 61.07, H 4.73; found C 60.56, H 5.03.

Table 4. Crystallographic data for **3**·(BF$_4$)$_2$ and **4**·BF$_4$)$_2$

	3·BF$_4$)$_2$	**4**·(BF$_4$)$_2$
formula	C$_{86}$H$_{80}$P$_6$O$_4$Co$_2$B$_2$F$_8$ · 3 (CH$_3$)$_2$CO	C$_{90}$H$_{82}$P$_6$O$_4$Co$_2$B$_2$F$_8$ · 4 CH$_2$Cl$_2$
M_r/g mol^{-1} (without solvates)	1654.9	1705.0
crystal size/mm	0.50 × 0.30 × 0.30	0.40 × 0.30 × 0.20
crystal system	monoclinic	monoclinic
Z	2	2
space group (no.)	$P2_1/c$ (14)	$P2_1/n$ (14)
a/Å	15.794(3)	11.676(4)
b/Å	17.424(3)	13.441(3)
c/Å	18.759(6)	30.421(7)
β [°]	70.42(2)	96.44(3)
V/Å^3	4864(2)	4744(2)
ρ (calcd)/g cm^{-3}	1.249	1.426
T/K	200	200
2θ range [°]	4.5–51.1	3.9–52.0
scan speed/° min^{-1}	$\dot{\omega}$ = 10.0	$\dot{\omega}$ = 10.0
no. rflns measured	9385	9577
no. unique rlfns	9045	9113
no. reflns obs.	6782	5196
obs. criterion	$I > 2\sigma(I)$	$I > 2\sigma(I)$
no. of paramenters	628	581
R_1/%	5.6	8.1
R_w/% (refinement on F^2)	18.2	23.6

[1] O. Kahn, *Angew. Chem.* **1985**, *97*, 837–853; *Angew. Chem. Int. Ed. Engl.* **1985**, *24*, 834–850.
[2] O. Kahn, *Molecular Magnetism*, VCH, Weinheim (Germany), **1993**, and references cited therein.
[3] P. J. Hay, J. C. Thibeault, R. Hoffmann, *J. Am. Chem. Soc.* **1975**, *97*, 4884–4899.
[4] O. Kahn, J. Galy, Y. Journaux, J. Jaud, L. Morgenstern-Badarau, *J. Am. Chem. Soc.* **1982**, *104*, 2165–2176.
[5] Y. Journaux, O. Kahn, H. Coudanne, *Angew. Chem.* **1982**, *94*, 647–648; *Angew. Chem., Int. Ed. Engl.* **1982**, *21*, 624–625.
[6] K.-S. Bürger, P. Chaudhuri, K. Wieghardt, B. Nuber, *Chem. Eur. J.* **1995**, *1*, 583–593.
[7] P. Chaudhuri, K. Oder, K. Wieghardt, S. Gehring, W. Haase, B. Nuber, J. Weiss, *J. Am. Chem. Soc.* **1988**, *110*, 3657–3658.
[8] M. Verdaguer, J. Gouteron, S. Jeannin, Y. Jeannin, O. Kahn, *Inorg. Chem.* **1984**, *23*, 4291–4296.
[9] E. G. Bakalbassis, J. Mrozinsky, C. A. Tsipis, *Inorg. Chem.* **1984**, *23*, 4291–4296.
[10] E. G. Bakalbassis, A: P. Bozopoulos, J. Mrozinsky, P. J. Rentzeperis, C. A. Tsipis, *Inorg. Chem.* **1988**, *27*, 529–532.
[11] Ti^{III}/Ti^{III} dimers: L. C. Francesconi, D. R. Corbin, A. W. Clauss, D. N. Hendrickson, G. D. Stucky, *Inorg. Chem.* **1981**, *20*, 2078–2083.
[12] Fe^{III}/Fe^{III} dimer: M. Dusek, V. Petricek, J. Kamenicek, Z. Sindelar, *Acta Cryst.* **1992**, *C48*, 1579–1582.

[13] E. G. Bakalbassis, C. A. Tsipis, *Inorg. Chem.* **1985**, *24*, 4231−4233.
[14] L. Sacconi, F. Mani, *Transition Met. Chem. (N.Y.)* **1982**, *8*, 179−252, and references cited therein.
[15] R. Morassi, I. Bertini, L. Sacconi, *Coord. Chem. Rev.* **1973**, *11*, 343−402, and references cited therein.
[16] S. Beyreuther, J. Hunger, G. Huttner, S. Mann, L. Zsolnai, *Chem. Ber.* **1996**, *129*, 745−757.
[17] C. Mealli, S. Midollini, L. Sacconi, *Inorg. Chem.* **1975**, *14*, 2513−2521.
[18] C. Furlani, *Coord. Chem. Rev.* **1968**, 3, 141−167, and references cited therein.
[19] B. R. Higginson, C. A. McAuliffe, L. M. Venanzi, *Helv. Chim. Acta* **1975**, *58*, 1261−1271.
[20] For assignments see: J. Ellermann, K. Dorn, *Chem. Ber.* **1966**, *99*, 653−657.
[21] V. Sernau, G. Huttner, J. Scherer, O. Walter, *Chem. Ber.* **1996**, *129*, 243−245.
[22] H. A. Bent, *Chem. Rev.* **1961**, *61*, 275−311.
[23] As the nature of the impurity is not known (presumably oligo- or polymeric species consisting of high-spin Co^{II} and dicarboxylates) the obtained fits to the susceptibilty data are not of the same quality as found with analogous copper compounds.
[24] K. Heinze, S. Mann, G. Huttner, L. Zsolnai, *Chem. Ber.* **1996**, *129*, 1115−1122.
[25] V. Körner, A. Asam, G. Huttner, L. Zsolnai, *Z. Naturforsch.* **1994**, *49b*, 1183−1195.
[26] C. A. Ghilardi, F. Laschi, S. Midollini, A. Orlandini, G. Scapacci, P. Zanello, *J. Chem. Soc. Dalton Trans.* **1995**, 531−540.
[27] V. Körner, G. Huttner, L. Zsolnai, M. Büchner, A. Jacobi, D. Günauer, *Chem. Ber.* **1996**, *129*, 1587−1601.
[28] V. Sernau, G. Huttner, M. Fritz, B. Janssen, M. Büchner, C. Emmerich, O. Walter, L. Zsolnai, D. Günauer, T. Seitz, *Z. Naturforsch.* **1995**, *50b*, 1638−1652.
[29] A. R. Rossi, R. Hoffmann, *Inorg. Chem.* **1975**, *14*, 365−374.
[30] C. Bianchini, D. Masi, C. Mealli, A. Meli, G. Martini, F. Laschi, P. Zanello, *Inorg. Chem.* **1987**, *26*, 3683−3693.
[31] S. Vogel, G. Huttner, L. Zsolnai, *Z. Naturforsch.* **1993**, *48b*, 641−652.
[32] V. Körner, S. Vogel, G. Huttner, L. Zsolnai, O. Walter, *Chem. Ber.* **1996**, *129*, 1107−1113.
[33] K. Heinze, G. Huttner, L. Zsolnai, P. Schober, *Inorg. Chem.* **1997**, *36*, 5457−5469.
[34] A. Weiss, H. Witte, *Magnetochemie*, VCH, Weinheim (Germany), **1973**, 77−94.
[35] [35a] D. F. Evans, *J. Chem. Soc.* **1959**, 2003−2005. − [35b] T. H. Crawford, J. Swanson, *J. Chem. Educ.* **1971**, *48*, 382−386.
[36] A. Muth, *Diplomarbeit*, University of Heidelberg, **1989**.
[37] H. Funk, F. Binder, *Z. Anorg. Allg. Chem.* **1926**, *155*, 327.
[38] [38a] G. M. Sheldrick, *SHELXS 86*, *Program for Crystal Structure Solution*, University of Göttingen, **1986**. − [38b] G. M. Sheldrick, *SHELXL 93*, *Program for Crystal Structure Refinement*, University of Göttingen, **1993**.
[39] L. Zsolnai, G. Huttner, *XPMA*, *ZORTEP*, University of Heidelberg, **1997**.

[97217]

Polynuclear Complexes with Propynylidene C_3-Bridges: General Synthetic Route to Bis-, Tris-, and Tetrakis(ethynylcarbene) Complexes☆

Cornelia Hartbaum, Gerhard Roth, and Helmut Fischer*

Fakultät für Chemie, Universität Konstanz, Fach M727,
D-78457 Konstanz, Germany

Received October 7, 1997

Keywords: Polynuclear complexes / Carbene complexes / Bridging ligands / Alkynyl complexes

The sequential reaction of two equivalents of the dimethylamino(ethynyl)carbene complexes [$(CO)_5M{=}C(NMe_2)C{\equiv}CH$] [M = W (**1a**), Cr (**1b**)] with two equivalents of *n*BuLi and one equivalent of a transition metal dichloride, [$Cl_2M'(L_n)$], affords trinuclear biscarbene complexes of the type [$(CO)_5M{=}C(NMe_2)C{\equiv}C{-}M'(L_n){-}C{\equiv}CC(NMe)_2{=}M(CO)_5$] [$M'(L_n)$ = $Ni(PEt_3)_2$ (**2a**, **b**), $Pd(PEt_3)_2$ (**3a**, **b**), $Pt(PEt_3)_2$ (**4a**, **b**), $Fe(dmpe)_2$ (**6a**), Hg (**8a**), $Ti(\eta^5\text{-}C_5H_5)_2$ (**9a**, **b**)] [dmpe = 1,2-bis(dimethylphosphino)ethane]. Treatment of **1a** with equimolar amounts of first *n*BuLi and then [$Cl_2M'(L_n)$] results in the formation of the monosubstitution products [$(CO)_5W{=}C(NMe_2)C{\equiv}CM'(L_n)$] [$M'(L_n)$ = *trans*-$Pd(PEt_3)_2Cl$ (**5a**), *trans*-$Fe(dmpe)_2Cl$ (**7a**)]. Additionally, the synthesis of the heterobimetallic ethynylcarbene complex [$(CO)_5W{=}C(NMe_2)C{\equiv}CPd(PEt_3)_2C{\equiv}CH$] (**10a**), starting from **1a** and [$ClPd(PEt_3)_2C{\equiv}CH$], is described. When three equivalents of **1a** are treated, first with three equivalents of *n*BuLi and then with one equivalent of the trihalides PCl_3 or BBr_3, the novel tris(ethynylcarbene) complexes [$\{(CO)_5W{=}C(NMe_2)C{\equiv}C\}_3E$] [E = B (**11a**), P (**12a**)] are obtained. The reaction of four equivalents of **1a**, **b** with four equivalents of *n*BuLi, followed by addition of one equivalent of a group 14 tetrachloride [$M'Cl_4$], yields the novel tetrakis(ethynylcarbene) complexes [$\{(CO)_5M{=}C(NMe_2)C{\equiv}C\}_4M'$] [M' = Si (**13a**, **b**), Ge (**14a**), Sn (**15a**, **b**)]. The complexes **8a**, **9a**, **12a**, and **15a** were characterized by X-ray structural analyses. All spectroscopic and structural data suggest that the carbene fragments and the central transition metal or heteroatom in these new bis-, tris-, and tetrakis(ethynylcarbene) complexes interact only weakly.

Introduction

Polynuclear transition metal complexes with π-conjugated carbon bridges have recently attracted considerable interest due to their potentially useful chemical and physical properties. An application as materials for nonlinear optics has been proposed[1]. In addition, π systems, such as highly ethynylated organic and organometallic compounds, have been intensively studied since they represent viable monomers for the synthesis of high carbon polymers. Transition metal σ-acetylide complexes[2] and ethynyl-substituted half sandwich complexes can be considered as building blocks in the synthesis of linear[3], star-shaped[3d][4], and spherical[5] structures.

A wide range of π-conjugated acetylide transition metal complexes of the type [$L_nM{-}(C{\equiv}C)_x{-}M'L'_{n'}$] have already been reported[1a]. Examples for conjugated bis(Fischer carbene)complexes of the type [$L_nMC(YR)\mathbf{C}_c(RY)CML_n$] (with $\mathbf{C}_c$ = conjugated carbon bridge, Y = O, NR) are also known. Symmetrical complexes containing phenyl[6][7], biphenyl[8], binaphthyl[7], anthracene[9], 1,6-methano[10]annulene-2,7-diyl[10], alkenyl,[11] or ammonium pentadienide[12] bridges are readily accessible. By contrast, apart from our results on the synthesis of the C_4HgC_4-bridged complex [$(CO)_5W{=}C(NMe_2)C{\equiv}CC{\equiv}CHgC{\equiv}CC{\equiv}CC(NMe_2){=}W(CO)_5$][13], examples of π-conjugated metal-bridged trinuclear biscarbene complexes are unknown[14]. Nevertheless, all these systems may represent suitable substructures for the construction of two- and three-dimensional networks.

Previously, we reported on the efficient preparation of bimetallic ethynylcarbene complexes by nucleophilic substitution of a lithiated ethynyl- or butadiynylcarbene complex for the halide X in metal monohalides [$XM'(L'_m)$][13][15]. In this paper we report on a general synthetic route to a wide range of π-conjugated metal-bridged bis-, tris-, and tetrakis(Fischer carbene) complexes. These carbene complexes can be considered as a new type of monomeric polyacetylenic organometallic building blocks for the synthesis of two and three dimensional structures.

Results and Discussion

Extension of the concept of coupling a L_nMC_3 with a $M'L_m$ fragment to the treatment of the dimethylamino(ethynyl)carbene complexes of tungsten and chromium with different metal dihalides afforded metal-bridged biscarbene complexes of the general type [$(CO)_5M{=}C(NMe_2)C{\equiv}C{-}M'(L_m){-}C{\equiv}CC(NMe_2){=}M(CO)_5$]. The dimethylamino(trimethylsilylethynyl)carbene complexes [$(CO)_5M{=}C(NMe_2)C{\equiv}CSiMe_3$] (M = W, Cr) proved to be suitable precursors for the L_nMC_3 fragment. Desilylation with KF/THF/MeOH[15], followed by deprotonation with *n*BuLi, gave the lithiated acetylide [$(CO)_5M{=}C(NMe_2)C{\equiv}CLi$] (M = W, Cr). Treatment of two equivalents of this tungstate (or chromate) in situ with one equivalent of the metal dichloride [$Cl_2M(PEt_3)_2$] (M = Ni, Pd, Pt) resulted

 © WILEY-VCH Verlag GmbH, D-69451 Weinheim, 1998 1434–1948/98/0202–0191 $ 17.50+.50/0

in formation of the pale yellow *trans*-bis(ethynylcarbene) complexes **2**–**4** in yields, after chromatography, of 66–72% (Scheme 1).

Scheme 1

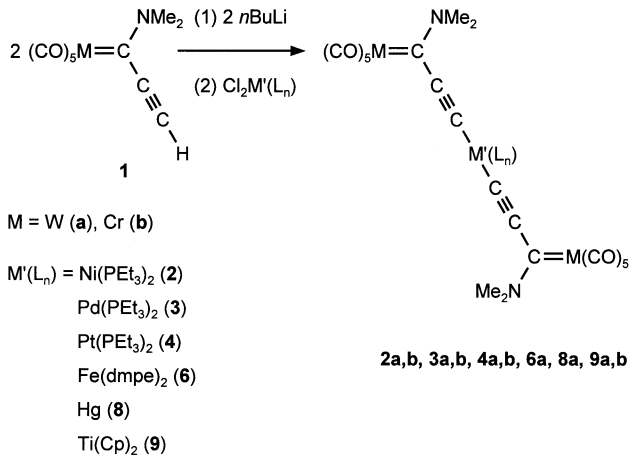

As expected, the reaction of equimolar amounts of the lithiated complex $[(CO)_5W{=}C(NMe_2)C{\equiv}CLi]$ and a metal dichloride under the same conditions led to the formation of a monosubstituted product. Thus, when **1a** was treated at −80°C, first with *n*BuLi and then with the equimolar amount of $[Cl_2Pd(PEt_3)_2]$, chromatographic work up of the reaction mixture afforded the complex **5a** in a yield of 61% (Scheme 2).

Scheme 2

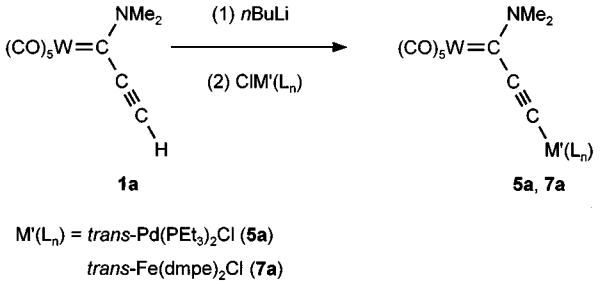

Analogous reaction sequences were carried out with the iron dichloride $[Cl_2Fe(dmpe)_2]$ [dmpe = 1, 2-bis(dimethylphosphino)ethane]. Addition of an equimolar amount of *n*BuLi to two equivalents of **1a**, followed by addition of one equivalent of the metal dichloride, gave the linear *trans*-substituted trinuclear complex **6a** in a yield of 35% (Scheme 1). The reaction of equimolar amounts of the educt complexes resulted in the formation of the bimetallic ethynylcarbene complex **7a** in a yield of 29% (Scheme 2).

Similar to **2**–**4**, and **6**, treatment of two equivalents of deprotonated ethynylcarbene complex **1a** and one equivalent of the dichloride $HgCl_2$ resulted in the formation of a linear biscarbene complex (Scheme 1). Chromatographic work up of the reaction mixture afforded compound **8a** in a yield of 57%. This *trans*-coordinated complex represents the only trinuclear complex without any coligands at the central metal in this series.

A tetrahedrally coordinated trinuclear biscarbene complex was obtained, when two equivalents of the lithiated complexes **1a**, **b** were treated with one equivalent of the dichloride $[Cl_2Ti(\eta^5\text{-}C_5H_5)_2]$ (Scheme 1). The red biscarbene complexes **9a**, **b** were obtained in yields of 67% (**9a**) and 68% (**9b**), respectively. Tweezer compounds such as the bisalkynyl substituted titanocene complexes of the type $[(\eta^5\text{-}C_5H_4R)_2Ti(C{\equiv}CR')_2]$ are well known[16][17][18]. The formation of monoalkynyl substituted titanocenes $[(\eta^5\text{-}C_5H_4R)_2TiCl(C{\equiv}CR')]$ by reaction of equimolar amounts of an acetylide and a metal dihalide could also be observed[16]. Efforts to prepare an analogous monosubstituted ethynylcarbene complex $[(CO)_5W{=}C(NMe_2)C{\equiv}CTiCl(\eta^5\text{-}C_5H_5)_2]$ starting from **1a** failed. Only a small amount of the disubstituted product **9a** was isolated.

Apart from **2**–**4**, and **8a** the synthesis of asymmetrically π-conjugated linear systems was intended. Treatment of the deprotonated complex **1a** with $[ClPd(PEt_3)_2C{\equiv}CH]$ afforded the light yellow ethynyl propynylidene palladium complex $[(CO)_5W{=}C(NMe_2)C{\equiv}CPd(PEt_3)_2C{\equiv}CH]$ **10a** in rather moderate yield (23%) (Scheme 3). The monosubstitution product **5a** was obtained as a by-product in a yield of 19%. Obviously, the ethynyl chloro palladium complex was contaminated with small amounts of $[Cl_2Pd(PEt_3)_2]$, which reacted with deprotonated **1a** to yield **5a**. Further investigations, in order to optimize the synthesis of **10a** and to apply this compound as starting material for polynuclear complexes with longer π-conjugated metal–carbon systems, are presently under way.

Scheme 3

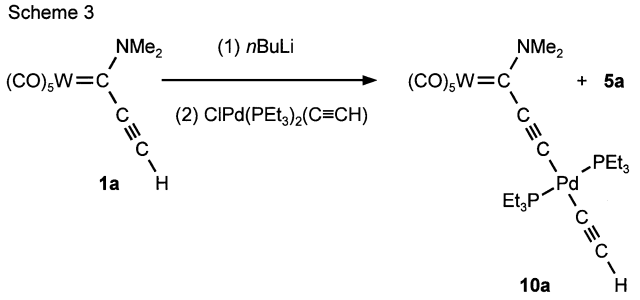

The nucleophilic substitution of complexes **1a** and **1b** is not restricted to transition metal halides, but can also be applied to halides of main group elements. By the reaction of three equivalents of the deprotonated ethynylcarbene complex **1a** with one equivalent of either the group 13 trihalide BBr_3, or the group 15 trihalide PCl_3 tris(ethynylcarbene) complexes of the general type $[\{(CO)_5W{=}C(NMe)_2C{\equiv}C\}_3E]$ were obtained in good to high yield [E = B: 61% (**11a**), P: 81% (**12a**)] (Scheme 4).

Tetrahalides of the main group metals can also be employed for analogous nucleophilic substitution reactions with the lithiated complex **1**. When four equivalents of the deprotonated ethynylcarbene complex **1a** were treated with one equivalent of a group 14 tetrachloride $M'Cl_4$, pentanuclear tetrakiscarbene complexes $\{[(CO)_5W{=}C(NMe)_2C{\equiv}C]_4M'\}$ were obtained in good yield [M′ = Si: 60% (**13a**), Ge: 59% (**14a**), Sn: 76% (**15a**)] (Scheme 5). In the case of silicium and tin the corresponding chromium

Scheme 4

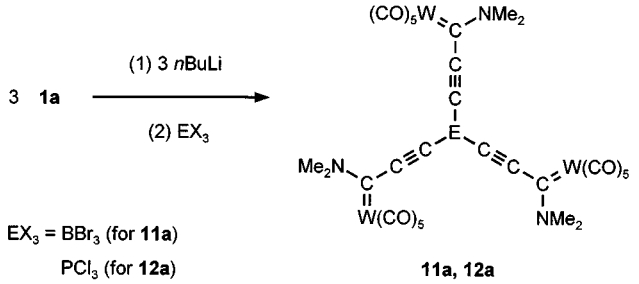

complexes were prepared in a similar manner with yields of 54% (**13b**) and 71% (**15b**), respectively.

All complexes **13**−**15** are stable in the solid state and in solution, when carefully dried solvents are used. In the series Sn → Ge → Si the tin compounds are the most stable. By comparison, the M−C bond of the silicium and germanium derivatives is easily cleaved by hydrolysis or by contact with silica. Therefore, complexes **14a** and **15a**, **b** can only be filtered over cellite, whereas **14a**, **b** can be purified by column chromatography on silica.

Scheme 5

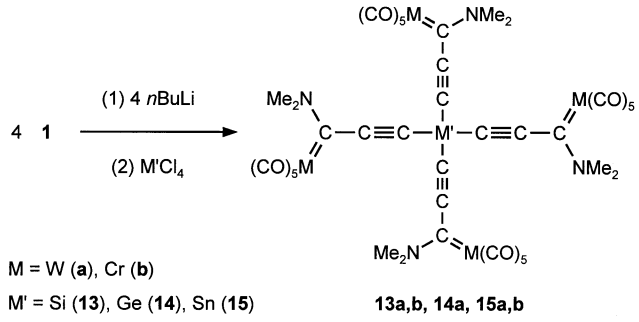

All other new complexes are stable at room temp. Compounds **2**−**15** were characterized by spectroscopic means and elemental analyses. The positions of the ν(CO) absorptions of the pentacarbonyl metal moiety in complexes **2**−**4**, **8a**, and **9** are only slightly influenced by variation of the propynylidene metal substituent M′(L_n). In contrast, the absorptions of the two iron-substituted complexes **6a** and **7a** are found at lower wavenumbers. The unsymmetrically substituted compounds **5a** and **10a** show absorptions similar to those of the *trans*-biscarbene complex **3a**. However, the A^1(*trans*) and the E absorptions of all complexes **2**−**10a** are at significantly smaller wavenumbers than those of the corresponding educt complexes **1**, indicating the π-basic properties of M′(L_n) in [$(CO)_5M{=}C(NMe_2)C{\equiv}C{-}$M′-($L_n$)$-C{\equiv}CC(NMe_2){=}M(CO)_5$] or [$(CO)_5M{=}C(NMe_2)$-$C{\equiv}$CM′($L_n$)], respectively. This tendency is less pronounced for the tris- and tetrakis(ethynylcarbene) complexes **11a**, **12a**, and **13**−**15**.

The two carbene fragments of the linear trinuclear biscarbene complexes **2**−**4**, **6a**, and **8a** can be regarded as π-conjugated. The ethynyl groups can mutually interact through metal d_{xy} and d_{yz} orbitals. For *trans*-coordinated square-planar dialkynyl complexes [$(Et_3P)_2M(C{\equiv}CR)_2$] (M = Ni, Pd, Pt), showing the same D_{2h} symmetry, π-conjugation involving the metal d-orbitals has already been discussed[19].

The stretching frequencies of the carbon−carbon triple bonds in the complexes **2**−**4** are significantly smaller than those of the unsubstituted ethynylcarbene complexes **1** [$\tilde{\nu}$(C≡C) = 2118 cm^{-1}]. This is commonly observed with σ-acetylenic transition metal complexes, and can be considered as evidence for the increase in polarity of the acetylenic bond upon coordination to the metal[17][20]. In the series **2** → **3** → **4** the ν(C≡C) absorptions shift to higher wavenumbers due to the increasing donating capacity of the M′$(PEt_3)_2$ moiety, and thus to the increasing polarity of the C≡C bond. For alkynyl complexes of group 10 metals an analogous order of ν(C≡C) frequencies has been noted[20]. In this case the M←CCR bond polarity, and not the M→CCR π-backbonding[20], was found to exert the dominating influence on the ν(C≡C) frequency.

For the two inequivalent *trans*-ethynyl moieties in **10a** only one ν(C≡C) absorption was observed [$\tilde{\nu}$(C≡C) = 2036 cm^{-1}]. Compared to **3a** and **10a**, complex **5a** shows a ν(C≡C) absorption band at significantly higher energy [$\tilde{\nu}$(C≡C) = 2032 cm^{-1} (**3a**), 2045 cm^{-1}(**5a**)]. The *trans*-position of the chloride ligand is known to cause a decrease in the polarity of the M−C≡ bond[21] thus leading to the observed shift of the ν(C≡C) absorption. The same tendency has already been observed for the disubstituted complex [$PhC{\equiv}CPd(PPh_3)_2C{\equiv}CPh$] [$\tilde{\nu}$(C≡C) = 2110 cm^{-1}][22] and the monosubstituted derivative [$ClPd(PPh_3)_2C{\equiv}CPh$] [$\tilde{\nu}$(C≡C) = 2125 cm^{-1}][23]. Compared to the phenyl substituted ethynyl complexes [$PhC{\equiv}CM(PEt_3)_2C{\equiv}CPh$] (M = Ni, Pd, Pt)[22], [$PhC{\equiv}CFe(dmpe)_2C{\equiv}CPh$][24] and [$ClFe(dmpe)_2C{\equiv}CPh$][25] the ν(C≡C) band of complexes **2**−**4**, **6a**, and **7a** is at lower wavelength, indicating that the $(CO)_5M{=}C(NMe_2)$ fragment acts as a stronger donor than the phenyl group. The IR spectrum of **8a** shows no ν(C≡C) band although a ν(C=C) absorption can be observed for the phenyl substituted complex $[Hg(C{\equiv}CPh)_2]$[26]. Similarly, but in contrast to $[(\eta^5\text{-}C_5H_4R)_2Ti(C{\equiv}CR')_2]$ (R′ = alkyl, aryl, $SiMe_3$)[16c], no ν(C≡C) absorption was observed for the complexes **9**.

Complex **11a** shows a very weak ν(C≡C) absorption at $\tilde{\nu}$ = 2126 cm^{-1}. However, no ν(C≡C) absorption was observed for **12a**, in contrast to $P(C{\equiv}CR)_3$ with R = H, Me, or Ph[27][28][29]. The frequencies of the ν(C≡C) absorption of the tetrakiscarbene complexes **13**−**15** decrease in the series **13** → **14** → **15** [$\tilde{\nu}$(C≡C) = 2132 cm^{-1} (**13a**, **14a**), 2118 cm^{-1} (**15a**)]. A similar tendency is observed for [M′$(C{\equiv}CH)_4$] [$\tilde{\nu}$(C≡C) = 2062 cm^{-1} (M′ = Si, Ge), 2042 cm^{-1} (M′ = Sn)][30], but the opposite trend is observed for the biscarbene complexes **2**−**4**.

The resonance of the carbene carbon atom in the ^{13}C-NMR spectra of the complexes **2**−**15** is at rather high field (δ = 238−250 for M = Cr and δ = 218−231 for M = W). This compares well with the shifts usually observed for simple aminocarbene complexes. As expected from the trend in the IR spectroscopic data of **1** and **2**−**9**, substitution of M′(L_n) for H in compounds of the type [$(CO)_5M{=}C(NMe_2)C{\equiv}CR$] [R = H, M′($L_n$)] results in an upfield shift of the C(carbene) resonance. A similar trend is

observed for the tris- and tetrakis(ethynylcarbene) complexes **11a**, **12a**, and **13**−**15**.

The ethynyl $^{13}C_\alpha$ and $^{13}C_\beta$ resonances of complexes **2**−**4** were unambiguously assigned on the basis of the coupling constants $J_{^{13}C,^{31}P}$ and in the case of **4** additionally on the basis of the coupling constants $J_{^{13}C,^{31}P}$. As a rule, the relationship $|^2J_{^{13}C,^{31}P}| > |^3J_{^{13}C,^{31}P}|$ was used in analogy to the assignment of the C_α and C_β resonances of the corresponding bisalkynyl complexes $[RC_\beta{\equiv}C_\alpha M(PEt_3)_2C_\alpha{\equiv}C_\beta R]$[21].

The shielding of the C_α and the C_β atom increases with increasing radius of the central metal (Ni < Pd < Pt). This observation has already been made for alkyl- or aryl-substituted bisalkynyl complexes of these metals[21] and is consistent with the IR spectroscopic data of **2**−**4**.

The difference $\Delta = \delta(C_\alpha)-\delta(C_\beta)$ in the ethynyl resonances for **3** [Δ = 41.04 ppm (**3a**), 45.0 ppm (**3b**)] and **4** [Δ = 35.01 ppm (**4a**), 38.98 ppm (**4b**)] is much more pronounced than for the phenyl-substituted bisalkynyl complexes $[PhC{\equiv}CM(PEt_3)_2C{\equiv}CPh]$ [M = Pd: Δ = 0.3 ppm, δ = 111.7 (C_α), 111.4 (C_β)[21]; M = Pt: Δ = −1.7 ppm, δ = 108.3 (C_α), 110.0 (C_β)][31] which indicates an increased polarity of the C≡C bond in the biscarbene complexes **2**−**4** when compared to bisalkynyl complexes. This can be explained with the stronger π-basic capacity of the $(CO)_5M{=}C(NMe_2)$ fragment relative to the phenyl group.

As already discussed, the π-backbonding of the central metal to the acetylide ligand is more pronounced in the halide-substituted complex **5a** than in the biscarbene compounds **2**−**4**. This tendency is reflected in the highfield shift of the C_α and C_β resonance of **5a** [δ = 149.51 (C_α), 118.68 (C_β)] when compared to **3a** [δ = 163.88 (C_α), 122.84 (C_β)]. The same trend has been found in the ^{13}C- and ^{31}P-NMR spectra of comparable bisalkynyl complexes $[RC{\equiv}CM(PEt_3)_2C{\equiv}CR]$[21] and alkynyl complexes $[ClM(PEt_3)_2C{\equiv}CR]$[21].

Compared to **2a**−**4a**, the $Fe(dmpe)_2$-substituted complexes **6a** and **7a** show a significant lowfield shift of the ethynyl resonances. Therefore, the $Fe(dmpe)_2$ fragment seems to have a stronger π-backbonding capacity than the $M(PEt_3)_2$ fragment (M = Ni, Pd, Pt). In contrast to **3a** and **5a**, the substitution of $(CO)_5W{=}C(NMe)_2C{\equiv}C$ in **6a** for Cl in **7a** does not result in a significant shift of the ethynyl resonances [**6a**: δ = 195.33 (C_α), 135.10 (C_β); **7a**: δ = 194.81 (C_α), 140.29 (C_β)]. However, the ^{13}C- and ^{31}P-NMR spectra of $[PhC{\equiv}CFe(dmpe)_2C{\equiv}CPh]$[25] and $[ClFe(dmpe)_2C{\equiv}CPh]$[24a][24c] are rather consistent with the results found for **3a**/**5a**.

As expected, the bisethynyl complex $[(CO)_5W{=}C(NMe_2)C_\beta{\equiv}C_\alpha Pd(PEt_3)_2C_{\alpha'}{\equiv}C_{\beta'}H]$ (**10a**) shows two different pairs of resonances for the ethynyl carbons [δ = 166.59 (C_α), 122.86 (C_β), 103.35 ($C_{\alpha'}$), 96.41 ($C_{\beta'}$)]. The assignment of the C_α, $C_{\alpha'}$, C_β, and $C_{\beta'}$ resonances is based on the comparison with $[HC{\equiv}CPd(PEt_3)_2C{\equiv}CH]$[21] and **3a**. As a result, the chemical shifts indicate a stronger π-basicity for the $(CO)_5W{=}C(NMe_2)C{\equiv}C$ than for the C≡CH fragment.

The ^1H- and ^{13}C-NMR spectra of complexes **8a**, **b** exhibit only one singlet for the cyclopentadienyl rings implying that the protons and the carbons of both rings are equivalent. In contrast, free rotation of the cyclopentadienyl rings is hindered for bulky substituents R [R = $CH_2C(Ph)_2H$ or $CH_2C(Ph)_2CN$] in $[(\eta^5\text{-}C_5H_5)_2Ti(C{\equiv}CR)_2]$[17]. Obviously, the carbene fragment in **8a**, **b** is small enough to avoid a similar effect.

Due to the nuclear spin I = 3/2 of boron the ethynyl resonances in the ^{13}C-NMR spectrum of **11a** appear as quartets. The identification of C_α (δ = 147.07) and C_β (δ = 101.39) is based on the decreasing size of the J_{BC} coupling constants ($^1J_{BC}$ = 71.2 Hz, $^2J_{BC}$ = 14.4 Hz). Whereas the ^1H-NMR spectrum of complex **11a** shows two distinct resonances for the NMe_2 group that of **12a** shows a doublet at δ = 3.77 ($^6J_{PH}$ = 1.2 Hz) and a singlet at δ = 3.61. The doublet is assigned to the methyl group in the *cis*-position with respect to the $W(CO)_5$ fragment at the N−C(carbene) bond. A similar homoallyl coupling between $C{-}CH_3$ and *cis*-$N{-}CH_3$ has already been observed for $[(CO)_5Cr{=}C(Me)NMe_2]$ ($^5J_{HH}$ = 0.9 Hz)[32]. Both ethynyl resonances of **12a** appear as doublets. In contrast, $P(C{\equiv}CC_6H_5)_3$ shows a doublet at δ = 109.5 ($^1J_{PC}$ = 18 Hz) and a singlet at δ = 82.3[27]. The C_α and C_β NMR resonances of complex **12a** were unambiguously assigned on the basis of the $^{13}C,^{31}P$ coupling constants. The doublet at higher field (δ = 107.15) with the larger coupling constant $^1J_{PC}$ = 11.4 Hz was therefore attributed to C_α and that at lower field (δ = 115.17), with the smaller coupling constant $^2J_{PC}$ = 8.1 Hz, to C_β. Compared to $P(C{\equiv}CPh)_3$ the C_β resonance of **12a** is downfield suggesting that the $(CO)_5W{=}C(NMe_2)$ fragment acts as a stronger acceptor than the phenyl group. The resonance in the ^{31}P-NMR spectrum of **12a** (δ = −98.92) resembles that of $P(C{\equiv}CPh)_3$ (δ = −85.1)[27] rather than that of $P(C{\equiv}CH)_3$ (δ = +91)[33] or $P(C{\equiv}CMe)_3$ (δ = +87)[28].

The $^{13}C_{(\alpha,\beta)}$ resonances of **15a**, **b** were assigned on the basis of J_{SnC} coupling constants with $^1J_{^{117}SnC,^{119}SnC}$ = 1169.5 Hz, 1118.2 Hz and $^2J_{^{117}SnC,^{119}SnC}$ = 218.9 Hz, 209.5 Hz. In contrast to **2**−**4**, the resonances of the C_α and C_β carbons of **13a**, **b**, **14a**, and **15a**, **b** are almost independent of the central metal atom [C_α, C_β: 118.73, 106.14 (**13a**); 117.66, 105.11 (**14a**); 119.47, 109.59 (**15a**)]. Compared to $[M'(C{\equiv}CPh)_4]$[34] or $[M'(C{\equiv}CMe)_4]$[34][35] the C_α resonances of complexes **13a**, **b**, **14a**, and **15a**, **b** are downfield.

In summary, the C_α resonance in the NMR spectra of the complexes **2**−**16** is at significantly lower field when compared to the corresponding phenyl-substituted ethynyl complexes[18][21][24c][25][31][36] and the difference $\Delta = \delta(C_\alpha)-\delta(C_\beta)$ is much more pronounced. These two trends can be explained by the stronger π-basicity of the $(CO)_5W{=}C(NMe_2)C{\equiv}C$ fragment when compared to that of the phenyl group, which gives rise to an increase in the polarity of the C≡C bond in the direction $M{-}C(\delta+){\equiv}C(\delta-)$.

Structures of 8a, 9a, 12a, and 15a

The structures of the complexes **8a**, **9a**, **12a**, and **15a** were also established by X-ray structural analyses (Figures 1−4). Within error limits the $(CO)_5W{=}C(NMe)_2C{\equiv}C$ unit of the

Figure 1. ORTEP plot of complex **8a** (ellipsoids drawn at 50% level, hydrogens omitted)[a]

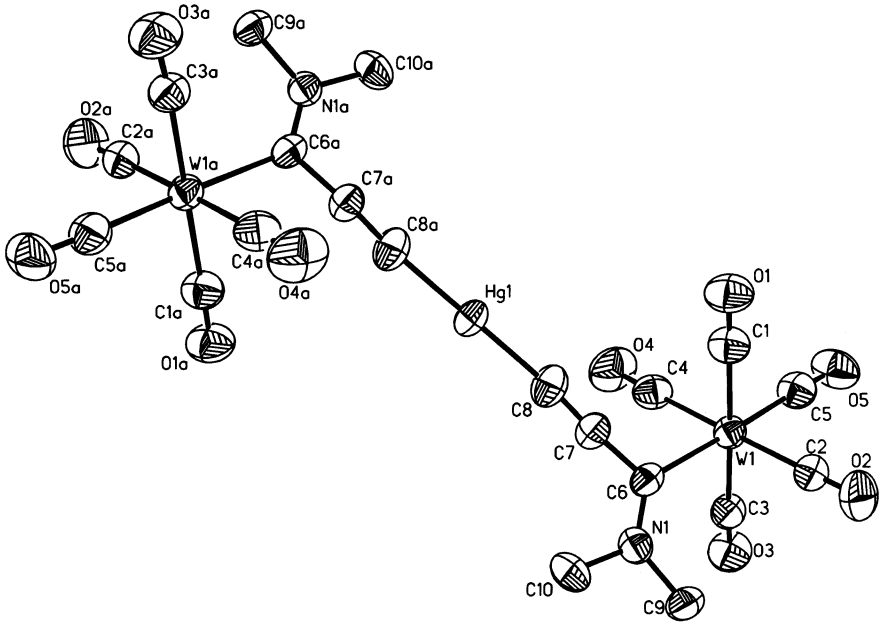

[a] Selected bond lengths [Å] and bond angles [deg]: Hg(1)−C(8) 1.994(9), C(8)−C(7) 1.20(1), C(7)−C(6) 1.43(1), C(8a)−Hg(1)−C(8) 180.0(1), Hg(1)−C(8)−C(7) 175(1), C(8)−C(7)−C(6) 175(1).

complexes **8a**, **9a**, **12a**, and **15a** is identical to that of the heterobimetallic ethynylcarbene complexes $[(CO)_5M{=}C(NMe)_2C{\equiv}CM'L_n]$ discussed previously[15]. The carbene carbon atoms (sum of angles: 359.2°−360.0°) as well as the nitrogen atoms (sum of angles: 359.9°−360.0°) of **8a**, **9a**, **12a**, and **15a** are trigonal planar coordinated. The rather long W−C(carbene) distance of the trinuclear complexes **8a** and **9a** [2.237(9) Å (**8a**), 2.244 and 2.250(7) Å (**9a**)], and the rather short C(carbene)−N bond [1.31(1) Å (**8a**), 1.32 and 1.33(1) Å (**9a**)], indicate a considerable double-bond character for the C(carbene)−N bond, similar to $[(CO)_5M{=}C(NMe)_2C{\equiv}CM'L_n]$ [W−C(carbene): 2.249(6) to 2.266(5) Å, C(carbene)−N: 1.298(6) to 1.323(8) Å][15]. This double-bond character is also reflected in the two distinct ^{1}H- and ^{13}C-NMR NMe resonances.

In the crystal, complex **8a** shows a centrosymmetric geometry with the Hg(1) atom as the center of symmetry, resulting in a *trans*-coordination of Hg(1) [C(8a)−Hg(1)−C(8): 180.0(1)°] (Figure 1) and a *trans*-configuration of the two bulky $W(CO)_5$ fragments. Also the

Figure 2. ORTEP plot of complex **9a** (ellipsoids drawn at 35% level, hydrogens omitted)[a]

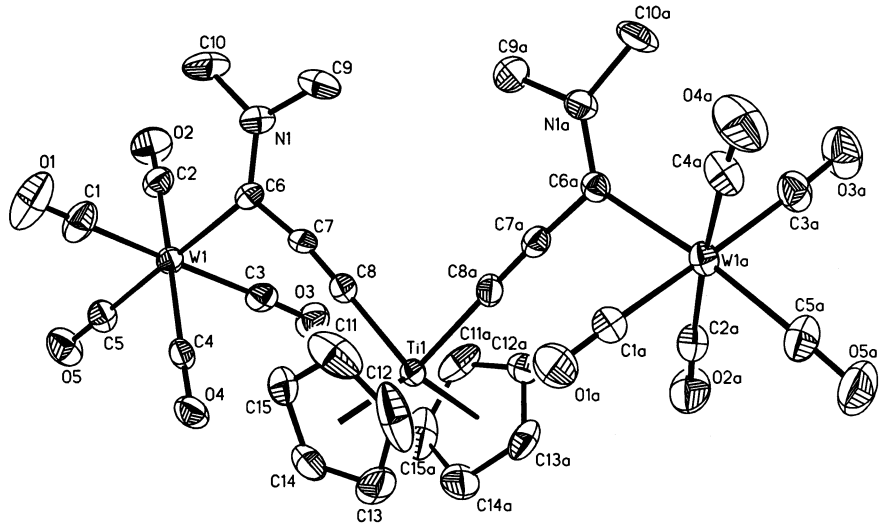

[a] Selected bond lengths [Å] and bond angles [deg]: Ti(1)−C(8a) 2.081(7), Ti(1)−C(8) 2.080(8), C(8a)−C(7a) 1.22(1), C(8)−C(7) 1.22(1), Ti(1)−D(1) 2.029, Ti(1)−D(1a) 2.038, C(7a)−C(6a) 1.41(1), C(7)−C(6) 1.40(1), D(1)−Ti(1)−D(1a) 135.3, Ti(1)−C(8a)−C(7a) 179.1(7), Ti(1)−C(8)−C(7) 178.7(8), C(8a)−C(7a)−C(6a) 176.4(8), C(8)−C(7)−C(6) 172.0(8), C(8a)−Ti(1)−C(8) 97.0(3) [D(1) and D(1a) denote the centroids of the cyclopentadienyl rings].

Hg−C≡C−C(carbene) unit of each σ-ligand is nearly linear [Hg(1)−C(8)−C(7): 175(1)°, C(8)−C(7)−C(6): 175(1)°], similar to the noncentrosymmetric bis(phenylethynyl)mercury-1,10-phenanthroline adduct [$Hg(C{\equiv}CPh)_2{\cdot}C_{12}H_8N_2$] (170, 176° and 173, 176°)[37]. The Hg(1)−C(8) distance and the C≡C distance of **8a** [1.994(9) Å and 1.20(1) Å] resemble those of [$Hg(C{\equiv}CPh)_2{\cdot}C_{12}H_8N_2$) (2.05, 2.03 Å and 1.17, 1.18 Å[37]).

Figure 2 shows that the ethynyl ligands of **9a** are twisted against each other, with the bulky $W(CO)_5$ fragments on the external sides. The two η^5-C_5H_5 ligands are staggered. The CpTiCp angle is typical for many group IV bent metallocene complexes with D(1)−Ti−D(1a) = 135.3°, where D(1)/D(1a) denote the centroids of the cyclopentadienyl rings {for comparison [$(\eta^5$-$C_5H_4SiMe_3)_2Ti(C{\equiv}CSiMe_3)_2$]: 134.7°[38], [$(\eta^5$-$C_5H_4SiMe_3)_2Zr(C{\equiv}CMe)_2$]: 132.6°[39]}. The bite angle C(8)−Ti(1)−C(8a) in **9a** [97.0(3)°] resembles that in [$(\eta^5$-$C_5H_4SiMe_3)_2Ti(C{\equiv}CC{\equiv}CFc)_2$] (Fc = ferrocenyl) [97.2(3)°][40] or in [$([\eta^5$-$C_5H_4]_2SiMe_2)Ti(C{\equiv}CSiMe_3)_2$] [100.8(5)][41]. The atoms W(1), C(6), N(1), C(7), C(8), Ti(1), C(8a), C(7a), C(6a), N(1a), and W(1a) nearly lie within a plane. The deviations from the plane through C(6), Ti(1) and C(6a) are less than ±0.08 Å. The σ-ethynyl ligands exhibit an almost linear carbon framework [C(8)−C(7)−C(6): 172.0(8)°, C(8a)−C(7a)−C(6a): 176.4(8)°]. The C≡C distances in **9a** [C(8)−C(7): 1.22(1) Å, C(8a)−C(7a): 1.22(1) Å] do not significantly deviate from typical C≡C bond lengths in similar titanocene or zirconocene complexes such as [$(\eta^5$-$C_5H_4SiMe_3)_2Ti(C{\equiv}CSiMe_3)_2$] [1.203(9), 1.214(6) Å][38], [$(\eta^5$-$C_5H_4SiMe_3)_2Zr(C{\equiv}CMe)_2$] [1.206(4) Å][39] or [$\{(\eta^5$-$C_5H_4)_2SiMe_2\}Ti(C{\equiv}CSiMe_3)_2$] [1.20(2), 1.21(2) Å][41], or ethynylcarbene complexes such as **1a** (1.196 Å)[42] or [$(CO)_5CrC(OMe)C{\equiv}CPh$] [1.19(3) Å][43]. The Ti(1)−C(8) and Ti(1)−C(8a) distances in **9a** [2.080(8), 2.081(7) Å] are similar to those found in [$(\eta^5$-$C_5H_4SiMe_3)_2Ti(C{\equiv}CSiMe_3)_2$] [2.124(5), 2.103(5) Å][38] or [$(\eta^5$-$C_5H_4SiMe_3)_2Ti(C{\equiv}CC{\equiv}CFc)_2$] (Fc = ferrocenyl) [2.099(7), 2.090(7) Å][40], but are remarkably shorter than those in titanocene complexes with sp^3-hybridized carbon atoms, e.g. such as [$(\eta^5$-$C_5H_5)_2Ti(CH_2Ph)_2$] [2.239(6), 2.210(5) Å][44], [$(\eta^5$-$C_5H_5)_2TiMe_2$] [2.170(2), 2.181(2) Å][45] and [$(\eta^5$-$C_9H_7)_2TiMe_2$] [2.21(2) Å][46]. In the case of [$(\eta^5$-$C_5H_4SiMe_3)_2Ti(C{\equiv}CSiMe_3)_2$] this is regarded as evidence for some π-conjugation between the acetylide ligands and the d^0-configurated 16-valence electron titanocene fragment[38].

The X-ray structural analyses of **12a** and **15a** also unambiguously establish their structure (Figures 3 and 4). The phosphorus atom in **12a** is pyramidally coordinated, similar to $P(C{\equiv}CPh)_3$[47] or $P(C{\equiv}CH)_3$[48], and the three bond angles at the phosphorus atom [C(8)−P(1)−C(8a): 106.2(7)°, C(8a)−P(1)−C(8b): 102.5(7)°, C(8)−P(1)−C(8b): 103.5(6)°] are similar [$P(C{\equiv}CPh)_3$: 100.7(0.5)°[47], $P(C{\equiv}CH)_3$: 102, 102, 99°[48]]. However, in contrast to the propeller like arrangement of the three phenyl rings in the $P(C{\equiv}CPh)_3$, complex **12a** is not C_3-symmetric in the crystal. In **15a** the bond angles of the central Sn atom are between 107.9(6)° and 111.9(7)° and resemble those of $Sn(C{\equiv}CSiMe_3)_4$ [107.9(1)° to 112.4(3)°][49].

Figure 3. Plot of complex **12a** (ellipsoids drawn at 35% level, hydrogens omitted)[a]

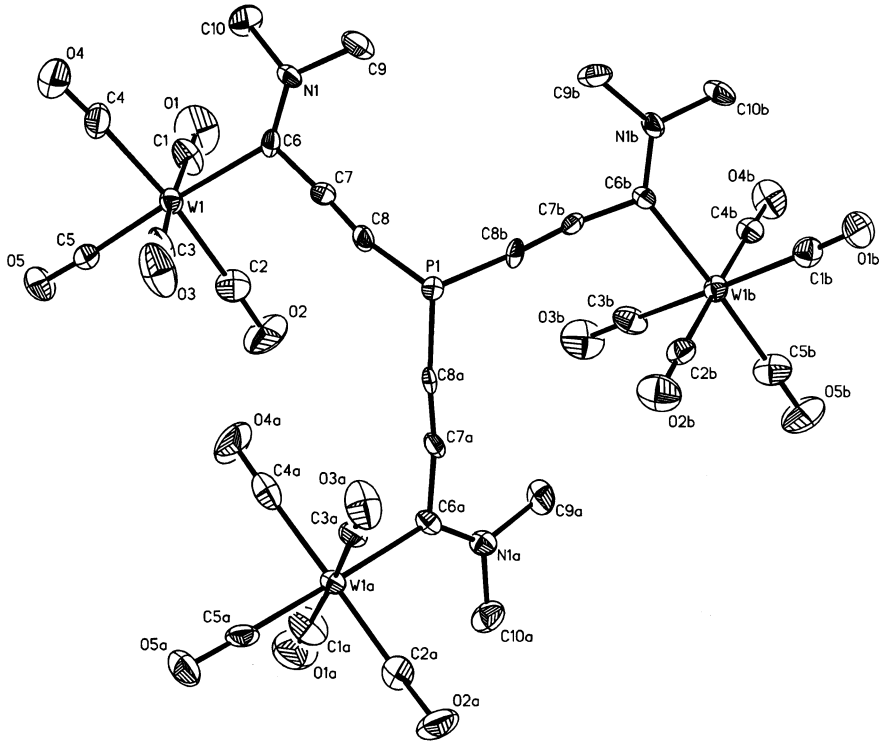

[a] Selected bond angles [deg]: C(8)−P(1)−C(8a) 106.2(7), C(8a)−P(1)−C(8b) 102.5(7), C(8)−P(1)−C(8b) 103.5(6).

Figure 4. Plot of complex **15a** (ellipsoids drawn at 25% level, hydrogens omitted)[a]

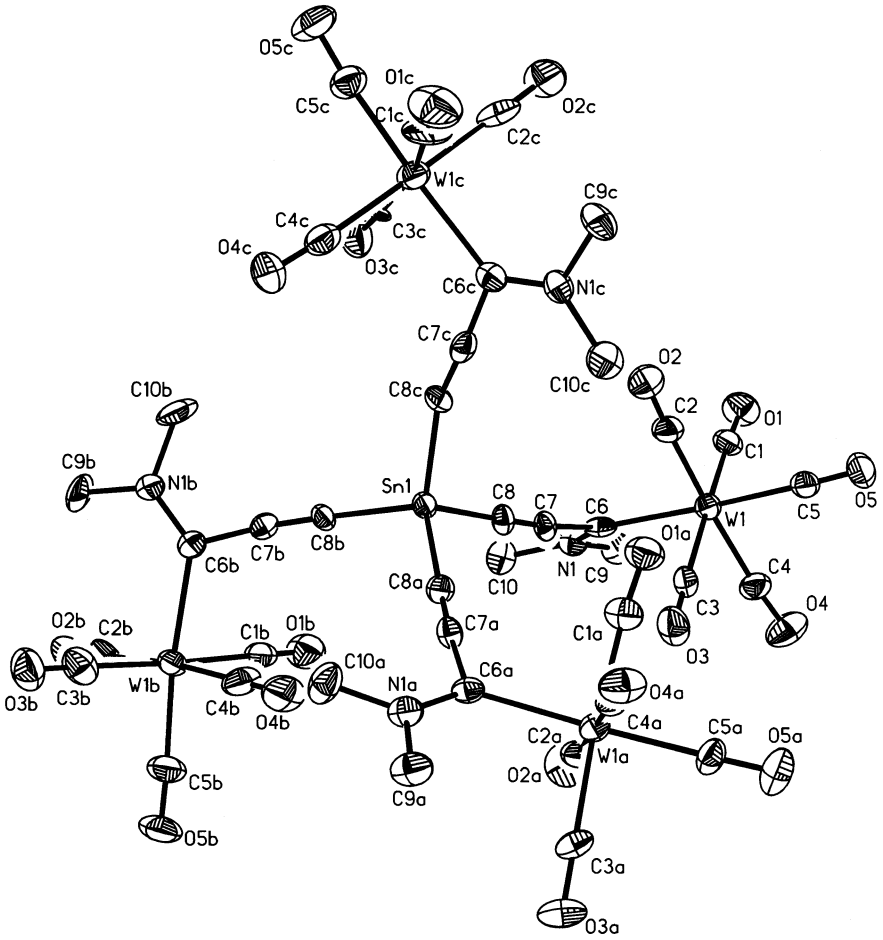

[a] Selected bond angles [deg]: C(8)−Sn(1)−C(8a) 108.7(7), C(8a)−Sn(1)−C(8b) 109.2(6), C(8a)−Sn(1)−C(8c) 107.9(6), C(8)−Sn(1)−C(8b) 109.8(7), C(8)−Sn(1)−C(8c) 109.2(6), C(8b)−Sn(1)−C(8c) 111.9(7).

Due to the poor quality of the data set and consequently the large standard deviations of the bond lengths a detailed discussion of the interatomic distances is not feasible.

Conclusions

The coupling of ethynylcarbene complexes $[(CO)_5M{=}C(NMe)_2C{\equiv}CH]$ (M = W, Cr) with metal halides to form heteronuclear complexes with π-conjugated C_3 propynylidene bridges is not restricted to metal monohalides $[XM'(L_n)]$[15] but can also be applied to metal polyhalides $[X_mM'(L_n)]$ (m = 2−4). Thus, a wide range of novel π-conjugated tri-, tetra-, and pentanuclear complexes $[\{(CO)_5M{=}C(NMe)_2C{\equiv}C\}_mM'(L_n)]$ are readily accessible by nucleophilic substitution of the lithiated ethynylcarbene complex $[(CO)_5M{=}C(NMe)_2C{\equiv}CLi]$ (M = W, Cr) for the chlorides in $[Cl_mM'(L_n)]$. Transition metals, main group metals as well as other main group elements can be employed as the central linking atom M′.

In *trans*-biscarbene complexes interaction of the two carbene fragments through the ethynyl triple bonds and the d_{xy} and d_{yz} orbitals of the central metal is conceivable. However, the IR and NMR spectra indicate that the mesomeric interaction between the carbene fragments and the central metal is rather small. The central metal $M'(L_n)$ fragment acts as a weak π-donor. With increasing π-donor properties of the $M'(L_n)$ fragment the mesomeric interaction also increases. However, in all cases the influence of the $M'(L_n)$ fragment is inferior to that of the strong π-donor substituent NMe_2 at the carbene carbon.

π-Interaction between the central metal and the acetylide ligands in the pyramidally coordinated complex **12a**, the probably trigonal-planar complex **11a**, and the tetrahedrally coordinated tetrakiscarbene complexes **13**−**15**, is even less pronounced than in the biscarbene complexes.

The π-conjugated polymetallic complexes described here can be considered as monomers for the synthesis of organometallic systems with extended two and three dimensional π-conjugated metal-carbon networks.

Support of this work by the *Fonds der Chemischen Industrie* is gratefully acknowledged. We thank *B. Weibert* for collecting the data sets for the X-ray structural analyses.

Experimental Section

All operations were performed under argon by using standard Schlenk techniques. Solvents were dried by refluxing over CaH_2 (CH_2Cl_2) or sodium/benzophenone ketyl (pentane, Et_2O, THF)

and were freshly distilled prior to use. The yields refer to analytically pure substances and were not optimized. Silica gel used for column chromatography (Fa. J. T. Baker, silica gel for flash chromatography) was argon-saturated. For the synthesis of **1a**, **b** by desilylation of $[(CO)_5M{=}C(NMe_2)C{\equiv}CSiMe_3]$[42] (M = W, Cr), KF/THF/MeOH[15] was used instead of Bu_4NF/H_2O[42]. The complexes $[Cl_2Ni(PEt_3)_2]$[50], $[Cl_2Fe(dmpe)_2]$[51], $[Cl_2Ti(\eta^5\text{-}C_5H_5)_2]$[52], and $[ClPd(PEt_3)_2\ C{\equiv}CH]$[53] were prepared according to literature procedures. $[Cl_2Pd(PEt_3)_2]$ and $[Cl_2Pt(PEt_3)_2]$ were purchased from Aldrich. − NMR: Bruker AC 250, Bruker WM 250, Bruker DRX 600, and Jeol JNX 400; chemical shifts are reported relative to internal TMS (^1H and ^{13}C) or external H_3PO_4 (^{31}P). Unless mentioned otherwise, NMR spectra were recorded in $CDCl_3$ at room temperature. Abbreviations: vt = virtual triplet, dvt = double virtual triplet, tvt = triple virtual triplet, vquint = virtual quintet. − IR: Biorad FTS 60. − MS: Finnigan MAT 312. The peaks *m/z* are based on the following isotopes: ^{48}Ti, ^{52}Cr, ^{56}Fe, ^{58}Ni, ^{74}Ge, ^{106}Pd, ^{120}Sn, ^{184}W, ^{195}Pt, ^{202}Hg. − Elemental analyses: Heraeus CHN-O-RAPID.

General Synthetic Route to Compounds **2a**, **b**−**4a**, **b**: 2.00 mmol of *n*BuLi (1.25 ml of a 1.6 M solution in hexane) was added at −80°C to a solution of 2.00 mmol of **1a** (0.81 g) or **1b** (0.55 g) in 20 ml of Et_2O. On stirring for 30 min at −80°C, the yellow solution turned cloudy. Then, 1.00 mmol of $[Cl_2M(PEt_3)_2]$ [M = Ni (0.37 g), Pd (0.41 g), Pt (0.50 g)] and 5 ml of THF were added and the dark yellow solution was stirred for 30 min at room temp. The solvent was evaporated in vacuo, the residue dissolved in 5 ml of THF and chromatographed with pentane/THF [4:1 (**2a**,**b**), 7:2 (**3a**,**b**, **4a**,**b**)] at −40°C on silica. Light yellow bands were eluted, which afforded, after removal of the solvent in vacuo and recrystallization from CH_2Cl_2/pentane [3:1 (**2a**,**b**, **3a**,**b**), 4:1 (**4a**,**b**)], the complexes **2a**,**b**−**4a**,**b** as light yellow crystals.

trans-Bis[pentacarbonyl(1-dimethylaminopropynylidene)tungsten]bis(triethylphosphane)nickel (**2a**) *and trans-Bis[pentacarbonyl(1-dimethylaminopropynylidene)chromium]bis(triethylphosphane)nickel* (**2b**): **2a**: Yield: 0.74 g (67%, based on **1a**), m.p. 122°C (dec.). − IR (THF): $\tilde{\nu}$(CO) = 2058 cm^{-1} w, 1965 w, 1920 vs, 1900 m, $\tilde{\nu}$(C≡C) = 2008 cm^{-1} w. − ^1H NMR: δ = 1.15 (tvt, $^{3/5}J_{PH} = {}^3J_{HH}$ = 8.0 Hz, 18 H, CH_2CH_3), 1.77−1.89 (m, 12 H, CH_2), 3.50 (s, 6 H, NCH_3), 3.67 (s, 6 H, NCH_3). − ^{13}C NMR: δ = 8.31 (CH_2CH_3), 16.52 (vt, $^{1/3}J_{PC}$ = 14.6 Hz, CH_2), 44.08 (NCH_3), 51.00 (NCH_3), 131.88 (C_β), 168.40 (t, $^2J_{PC}$ = 38.8 Hz, C_α), 199.45 (s and d, $^1J_{WC}$ = 127.1 Hz, *cis*-CO), 203.88 (*trans*-CO), 223.54 (W=C). − ^{31}P NMR: δ = 22.71. − MS (FAB, NBOH); *m/z* (%): 1102 (7) [M^+], 962 (6), 906 (7) [$M^+ - n$ CO, *n* = 5, 7]. − $C_{32}H_{42}N_2NiO_{10}P_2W_2$ (1103.0): calcd. C 34.85, H 3.84, N 2.54; found C 35.09, H 3.78, N 2.42.

2b: Yield: 0.55 g (66%, based on **1b**), m.p. 99°C (dec.). − IR (THF): $\tilde{\nu}$(CO) = 2049 cm^{-1} w, 1966 w, 1925 vs, 1903 m, $\tilde{\nu}$(C≡C) = 2007 cm^{-1} w. − ^1H NMR: δ = 1.14 (tvt, $^{3/5}J_{PH} = {}^3J_{HH}$ = 8.0 Hz, 18 H, CH_2CH_3), 1.76−1.88 (m, 12 H, CH_2), 3.52 (s, 6 H, NCH_3), 3.72 (s, 6 H, NCH_3). − ^{13}C NMR: δ = 8.31 (CH_2CH_3), 16.55 (vt, $^{1/3}J_{PC}$ = 14.5 Hz, CH_2), 45.64 (NCH_3), 48.78 (NCH_3), 130.27 (C_β), 170.75 (t, $^2J_{PC}$ = 39.4 Hz, C_α), 218.43 (*cis*-CO), 224.00 (*trans*-CO), 241.71 (Cr=C). − ^{31}P NMR: δ = 23.19. − $C_{32}H_{42}Cr_2N_2NiO_{10}P_2$ (839.3): calcd. C 45.79, H 5.04, N 3.34; found C 46.00, H 5.09, N 3.25.

trans-Bis[pentacarbonyl(1-dimethylaminopropynylidene)tungsten]bis(triethylphosphane)palladium (**3a**) *and trans-Bis[pentacarbonyl(1-dimethylaminopropynylidene)chromium]bis(triethylphosphane)palladium* (**3b**): **3a**: Yield: 0.81 g (70%, based on **1a**), m.p. 146°C (dec.). − IR (THF): $\tilde{\nu}$(CO) = 2058 cm^{-1} w, 1966 w, 1920 vs, 1901 m, $\tilde{\nu}$(C≡C) = 2032 cm^{-1} w. − ^1H NMR: δ = 1.13 (tvt, $^{3/5}J_{PH} = {}^3J_{HH}$ = 8.1 Hz, 18 H, CH_2CH_3), 1.84−1.96 (m, 12 H, CH_2), 3.53 (s, 6 H, NCH_3), 3.69 (s, 6 H, NCH_3). − ^{13}C NMR: δ = 8.31 (CH_2CH_3), 16.80 (vt, $^{1/3}J_{PC}$ = 14.8 Hz, CH_2), 44.19 (NCH_3), 51.16 (NCH_3), 122.84 (C_β), 163.88 (t, $^2J_{PC}$ = 16.1 Hz, C_α), 199.48 (s and d, $^1J_{WC}$ = 128.5 Hz, *cis*-CO), 204.12 (*trans*-CO), 226.59 (W=C). − ^{31}P NMR: δ = 19.79. − MS (FAB, NBOH); *m/z* (%): 1150 (4) [M^+], 982 (8), 854 (20), 926 (9) [$M^+ - n$ CO, *n* = 6−8]. − $C_{32}H_{42}N_2O_{10}P_2PdW_2$ (1150.8): calcd. C 33.40, H 3.68, N 2.43; found C 33.76, H 3.60, N 2.17.

3b: Yield: 0.62 g (70%, based on **1b**), m.p. 124°C (dec.). − IR (THF): $\tilde{\nu}$(CO) = 2050 cm^{-1} w, 1967 w, 1923 vs, 1904 m, $\tilde{\nu}$(C≡C) = 2032 cm^{-1} w. − ^1H NMR: δ = 1.12 (tvt, $^{3/5}J_{PH} = {}^3J_{HH}$ = 8.1 Hz, 18 H, CH_2CH_3), 1.83−1.95 (m, 12 H, CH_2), 3.55 (s, 6 H, NCH_3), 3.76 (s, 6 H, NCH_3). − ^{13}C NMR: δ = 8.31 (CH_2CH_3), 16.80 (vt, $^{1/3}J_{PC}$ = 15.0 Hz, CH_2), 45.72 (NCH_3), 48.91 (NCH_3), 121.38 (C_β), 166.38 (t, $^2J_{PC}$ = 16.9 Hz, C_α), 218.38 (*cis*-CO), 224.12 (*trans*-CO), 244.96 (Cr=C). − ^{31}P NMR: δ = 20.19. − $C_{32}H_{42}Cr_2N_2O_{10}P_2Pd \cdot 1/4\ CH_2Cl_2$ (887.1 + 21.2): calcd. C 42.65, H 4.72, N 3.08; found C 42.71, H 4.75, N 3.11.

trans-Bis[pentacarbonyl(1-dimethylaminopropynylidene)tungsten]bis(triethylphosphane)platinum (**4a**) *and trans-Bis[pentacarbonyl(1-dimethylaminopropynylidene)chromium]bis(triethylphosphane)platinum* (**4b**): **4a**: Yield: 0.89 g (72%, based on **1a**), m.p. 169°C (dec.). − IR (THF): $\tilde{\nu}$(CO) = 2059 cm^{-1} w, 1965 w, 1920 vs, 1902 m, $\tilde{\nu}$(C≡C) = 2034 cm^{-1} w. − ^1H NMR: δ = 1.11 (tvt, $^{3/5}J_{PH} = {}^3J_{HH}$ = 8.1 Hz, 18 H, CH_2CH_3), 1.98−2.03 (m, 12 H, CH_2), 3.51 (s, 6 H, NCH_3), 3.69 (s, 6 H, NCH_3). − ^{13}C NMR: δ = 8.09 (s and d, $^3J_{PtC}$ = 24.7 Hz, CH_2CH_3), 16.14 (vt and dvt, $^2J_{PtC}$ = 35.5 Hz, $^{1/3}J_{PC}$ = 17.8 Hz, CH_2), 44.16 (NCH_3), 51.15 (NCH_3), 123.04 (s and d, $^2J_{PtC}$ = 269.7 Hz, C_β), 159.22 (t and dt, J_{PtC} = 977.8 Hz, $^2J_{PC}$ = 14.6 Hz, C_α), 199.43 (s and d, $^1J_{WC}$ = 127.9 Hz, *cis*-CO), 204.17 (s and d, $^1J_{WC}$ = 130.0 Hz, *trans*-CO), 227.32 (W=C). − ^{13}C NMR ([D$_8$]THF): δ = 8.45 (s and d, $^3J_{PtC}$ = 24.7 Hz, CH_2CH_3), 17.04 (vt and dvt, $^2J_{PtC}$ = 36.6 Hz, $^{1/3}J_{PC}$ = 18.3 Hz, CH_2), 44.54 (NCH_3), 51.49 (NCH_3), 124.06 (s and d, $^2J_{PtC}$ = 270.8 Hz, C_β), 159.07 (t and dt, $^1J_{PtC}$ = 980.0 Hz, $^2J_{PC}$ = 14.6 Hz, C_α), 200.39 (s and d, $^1J_{WC}$ = 127.9 Hz, *cis*-CO), 204.25 (*trans*-CO), 226.03 (W=C). − ^{31}P NMR: δ = 10.57 (s and d, $^1J_{PtP}$ = 2318.9 Hz). − MS (FAB, NBOH); *m/z* (%): 1239 (9) [M^+], 1211 (5), 1183 (10), 1071 (9) [$M^+ - n$ CO, *n* = 1, 2, 6]. − $C_{32}H_{42}N_2O_{10}P_2PtW_2$ (1239.4): calcd. C 31.01, H 3.42, N 2.26; found C 31.20, H 3.43, N 2.42.

4b: Yield: 0.67 g (69%, based on **1b**), m.p. 142°C (dec.). − IR (THF): $\tilde{\nu}$(CO) = 2051 cm^{-1} w, 1967 w, 1923 vs, 1902 m, $\tilde{\nu}$(C≡C) = 2032 cm^{-1} w. − ^1H NMR: δ = 1.10 (tvt, $^{3/5}J_{PH} = {}^3J_{HH}$ = 8.1 Hz, 18 H, CH_2CH_3), 1.96−2.05 (m, 12 H, CH_2), 3.54 (s, 6 H, NCH_3), 3.73 (s, 6 H, NCH_3). − ^{13}C NMR: δ = 8.10 (s and d, $^3J_{PtC}$ = 25.6 Hz, CH_2CH_3), 16.15 (vt and dvt, $^2J_{PtC}$ = 35.5 Hz, $^{1/3}J_{PC}$ = 17.7 Hz, CH_2), 45.67 (NCH_3), 48.91 (NCH_3), 121.65 (s and d, $^2J_{PtC}$ = 270.8 Hz, C_β), 161.78 (t and dt, $^1J_{PtC}$ = n. f., $^2J_{PC}$ = 14.6 Hz, C_α), 218.33 (*cis*-CO), 224.14 (*trans*-CO), 245.68 (Cr=C). − ^{13}C NMR ([D$_8$]THF): δ = 8.46 (s and d, $^3J_{PtC}$ = 24.7 Hz, CH_2CH_3), 16.99 (vt and dvt, $^2J_{PtC}$ = 35.5 Hz, $^{1/3}J_{PC}$ = 17.8 Hz, CH_2), 46.11 (NCH_3), 49.25 (NCH_3), 122.66 (s and d, $^2J_{PtC}$ = 270.8 Hz, C_β), 161.64 (t and dt, $^1J_{PtC}$ = 978.9 Hz, $^2J_{PC}$ = 14.5 Hz, C_α), 219.43 (*cis*-CO), 224.62 (*trans*-CO), 243.93 (Cr=C). − ^{31}P NMR: δ = 10.85 (s and d, $^1J_{PtP}$ = 2323.9 Hz). − MS (FAB, NBOH); *m/z* (%): 975 (6) [M^+], 919 (16), 891 (8), 835 (31), 807 (15), 779 (89), 751 (11), 723 (37), 695 (100) [$M^+ - n$ CO, *n* = 2, 3, 5−10], 577 (55) [$M^+ - PEt_3 - 10$ CO]. − $C_{32}H_{42}Cr_2N_2O_{10}P_2Pt$ (975.7): calcd. C 39.39, H 4.34, N 2.87; found C 39.44, H 4.42, N 2.74.

Pentacarbonyl{3-[chloro-trans-bis(triethylphosphane)palladio]-1-dimethylaminopropynylidene)}tungsten (**5a**): 2.00 mmol of *n*BuLi (1.25 ml of a 1.6 M solution in hexane) was added at −80°C to a solution of 2.00 mmol (0.81 g) of **1a** in 20 ml of Et_2O. On stirring the solution for 30 min at −80°C, a white precipitate was formed. Then, 2.00 mmol (0.83 g) of $[Cl_2Pd(PEt_3)_2]$ and 5 ml of THF were added and the dark yellow solution was stirred for 30 min at room temp. After removal of the solvent in vacuo, the residue was dissolved in 5 ml of THF and chromatographed with pentane/THF (7:2) at −40°C on silica. The light yellow band contained **5a**. Yield: 0.95 g (61%, based on **1a**), m.p. 127°C (dec.). − IR (THF): $\tilde{\nu}$(CO) = 2060 cm^{-1} w, 1965 w, 1921 vs, 1901 m, $\tilde{\nu}$(C≡C) = 2045 cm^{-1} w. − ^{1}H NMR: δ = 1.16 (tvt, $^{3/5}J_{PH}$ = $^3J_{HH}$ = 8.1 Hz, 18 H, CH_2CH_3), 1.85−1.97 (m, 12 H, CH_2), 3.53 (s, 3 H, NCH_3), 3.69 (s, 3 H, NCH_3). − ^{13}C NMR: δ = 8.10 (CH_2CH_3), 15.07 (vt, $^{1/3}J_{PC}$ = 14.2 Hz, CH_2), 44.28 (NCH_3), 51.13 (NCH_3), 118.68 (t, $^3J_{PC}$ = 4.7 Hz, C_β), 149.51 (t, $^2J_{PC}$ = 15.2 Hz, C_α), 199.27 (s and d, $^1J_{WC}$ = 127.0 Hz, *cis*-CO), 203.84 (s and d, $^1J_{WC}$ = 129.9 Hz, *trans*-CO), 226.61 (s and d, $^1J_{WC}$ = 86.5 Hz, W=C). − ^{31}P NMR: δ = 19.31. − MS (FAB, NBOH); *m/z* (%): 781 (5) [M^+], 753 (4), 725 (6), 669 (18), 641 (44) [$M^+ - n$ CO, n = 1, 2, 4, 5]. − $C_{22}H_{36}ClNO_5P_2PdW$ (782.2): calcd. C 33.78, H 4.64, N 1.79; found C 33.73, H 4.53, N 1.72.

trans-Bis[1',2'-bis(dimethylphosphino)ethane]bis[pentacarbonyl(1-dimethylaminopropynylidene)tungsten]iron (**6a**): 2.00 mmol of *n*BuLi (1.25 ml of a 1.6 M solution in hexane) was added at −80°C to a solution of 2.00 mmol (0.81 g) of **1a** in 20 ml of Et_2O. On stirring for 30 min at −80°C, the yellow solution turned cloudy. After 1.00 mmol (0.43 g) of $[Cl_2Fe(dmpe)_2]$ and 5 ml of THF were added, the dark red solution was stirred for 30 min at room temp. The solvent was evaporated in vacuo, the residue was dissolved in 5 ml of CH_2Cl_2 and chromatographed with pentane/CH_2Cl_2 (4:1) at −40°C on silica. An orange band was eluted. After removal of the solvent in vacuo, complex **6a** was obtained as an analytically pure orange solid. Yield: 0.41 g (35%, based on **1a**), m.p. 173°C (dec.). − IR (THF): $\tilde{\nu}$(CO) = 2054 cm^{-1} w, 1914 vs, 1895 sh, $\tilde{\nu}$(C≡C) = 1941 cm^{-1} m. − ^{1}H NMR: δ = 1.52 (br. s, 24 H, PCH_3), 1.89 (br. s, 8 H, CH_2), 3.44 (s, 6 H, NCH_3), 3.64 (s, 6 H, NCH_3). − ^{13}C NMR: δ = 17.66 (vquint, $^{1/3}J_{PC}$ = 5.9 Hz, PCH_3), 30.79 (vquint, $^{1/2/3}J_{PC}$ = 12.9 Hz, CH_2), 43.77 (NCH_3), 51.53 (NCH_3), 135.10 (C_β), 195.33 (m_c, C_α), 200.14 (s and d, $^1J_{WC}$ = 126.8 Hz, *cis*-CO), 203.04 (*trans*-CO), 221.59 (W=C). − ^{31}P NMR: δ = 65.66. − MS (FAB, NBOH); *m/z* (%): 1164 (25) [M^+], 1108 (5), 996 (7), 968 (11), 940 (11), 912 (10), 884 (11), [$M^+ - n$ CO, n = 2, 6−10]. − $C_{32}H_{44}FeN_2O_{10}P_4W_2$ (1164.2): calcd. C 33.02, H 3.81, N 2.41; found C 32.84, H 3.71, N 2.38.

3-{trans-Bis[1',2'-bis(dimethylphosphino)ethane]chloroferrio}-1-dimethylaminopropynylidene(pentacarbonyl)tungsten (**7a**): 2.00 mmol of *n*BuLi (1.25 ml of a 1.6 M solution in hexane) was added at −80°C to a solution of 2.00 mmol (0.81 g) of **1a** in 20 ml of Et_2O. On stirring the yellow solution for 30 min at −80°C, a white precipitate was formed. After 2.00 mmol (0.85 g) of $[Cl_2Fe(dmpe)_2]$ and 10 ml of THF were added, the dark red solution was stirred for 30 min at room temp. and then the solvent was removed in vacuo. The residue was dissolved in 5 ml of CH_2Cl_2 and chromatographed at −40°C on silica. With pentane/CH_2Cl_2 (7:2) an orange band was eluted, which afforded the complex **7a** as an analytically pure orange solid, after evaporation of the solvent in vacuo. Yield: 0.46 g (29%, based on **1a**), m.p. 135°C (dec.). − IR (THF): $\tilde{\nu}$(CO) = 2053 cm^{-1} w, 1913 vs, 1891 sh, $\tilde{\nu}$(C≡C) = 1942 cm^{-1} m. − ^{1}H NMR: δ = 1.43 (br. s, 12 H, PCH_3), 1.52 (br. s, 12 H, PCH_3), 1.94 (br. s, 8 H, CH_2), 3.29 (s, 3 H, NCH_3), 3.53 (s, 3 H, NCH_3). − ^{13}C NMR: δ = 13.91 (vquint, $^{1/3}J_{PC}$ = 5.4 Hz, PCH_3), 16.63 (vquint, $^{1/3}J_{PC}$ = 6.5 Hz, PCH_3), 30.13 (vquint, $^{1/2/3}J_{PC}$ = 12.6 Hz, CH_2), 43.08 (NCH_3), 51.11 (NCH_3), 140.29 (C_β), 194.81 (m_c, C_α), 200.19 (s and d, $^1J_{WC}$ = 127.9 Hz, *cis*-CO), 203.10 (s and d, $^1J_{WC}$ = 128.9 Hz, *trans*-CO), 217.82 (W=C). − ^{31}P NMR: δ = 63.79. − MS (FAB, NBOH); *m/z* (%): 795 (36) [M^+], 760 (10) [M^+ − Cl], 739 (8), 711 (19), 683 (81), 655 (22) [$M^+ - n$ CO, n = 2−5]. − $C_{22}H_{38}ClFeNO_5P_4W$ (795.6): calcd. C 33.21, H 4.81, N 1.76; found C 33.23, H 4.91, N 1.80.

Bis[pentacarbonyl(1-dimethylaminopropynylidene)tungsten]mercury (**8a**): 4.00 mmol of *n*BuLi (2.50 ml of a 1.6 M solution in hexane) was added at −80°C to a solution of 2.00 mmol (1.62 g) of **1a** in 40 ml of Et_2O. On stirring the yellow solution for 30 min at −80°C, the formation of a white precipitate was observed. 2.00 mmol (0.54 g) of $HgCl_2$ and 10 ml of THF were then added and the dark yellow solution was stirred for 30 min at room temp. The solvent was evaporated in vacuo and the residue was dissolved in 8 ml of CH_2Cl_2 and chromatographed at −40°C on silica. With pentane/CH_2Cl_2 (3:1) a yellow band was eluted. Evaporation of the solvent in vacuo and recrystallization from 30 ml of Et_2O/pentane (5:2) afforded yellow crystals. Yield: 1.15 g (57%, based on **1a**), m.p. 109°C (dec.). − IR (THF): $\tilde{\nu}$(CO) = 2062 cm^{-1} w, 1972 w, 1926 vs, 1909 sh. − ^{1}H NMR: δ = 3.62 (s, 6 H, CH_3), 3.76 (s, 6 H, CH_3). − ^{13}C NMR: δ = 46.69 (CH_3), 51.72 (CH_3), 106.42 (C_β), 158.67 (C_α), 198.56 (s and d, $^1J_{WC}$ = 128.3 Hz, *cis*-CO), 203.93 (s and d, $^1J_{WC}$ = 88.3 Hz, *trans*-CO), 230.77 (s and d, $^1J_{WC}$ = 130.1 Hz, W=C). − MS (FAB, NBOH); *m/z* (%): 1010 (57) [M^+], 982 (10), 954 (15), 898 (24) [$M^+ - n$ CO, n = 1, 2, 4], 642 (100), 614 (32), 586 (26), 558 (15) [$M^+ - n$ CO − Hg, n = 6−9]. − $C_{20}H_{12}HgN_2O_{10}W_2$ (1008.6): calcd. C 23.82, H 1.20, N 2.78; found C 23.90, H 1.23, N 2.87.

Dicyclopentadienyl{bis[pentacarbonyl(1-dimethylaminopropynylidene)tungsten]}titanium (**9a**) *and Dicyclopentadienyl-{bis[pentacarbonyl(1-dimethylaminopropynylidene)chromium]}-titanium* (**9b**): 4.00 mmol of *n*BuLi (2.50 ml of a 1.6 M solution in hexane) was added at −80°C to a solution of 4.00 mmol of **1a** (1.62 g) or **1b** (1.10 g) in 40 ml of Et_2O. On stirring the yellow solution for 30 min at −80°C, a white solid precipitated. After 2.00 mmol (0.50 g) of $[Cl_2Ti(Cp)_2]$ and 10 ml of THF were added, the dark red solution was stirred for 30 min at room temp. The solvent was evaporated in vacuo. The residue was dissolved in 8 ml of CH_2Cl_2 and chromatographed with pentane/CH_2Cl_2 [4:1(**9a**), 7:2 (**9b**)] at −40°C on silica. A red band was eluted, which gave red crystals after removal of the solvent in vacuo and recrystallization from 50 ml of Et_2O/pentane [4:1(**9a**), 5:2 (**9b**)].

9a: Yield: 1.32 g (67%, based on **1a**), m.p. 142°C (dec.). − IR (THF): $\tilde{\nu}$(CO) = 2058 cm^{-1} w, 1969 w, 1924 vs, 1906 sh. − ^{1}H NMR: δ = 3.40 (s, 6 H, CH_3), 3.65 (s, 6 H, CH_3), 6.33 (s, 10 H, C_5H_5). − ^{13}C NMR: δ = 45.64 (CH_3), 50.60 (CH_3), 112.27 (C_5H_5), 134.87 (C_β), 199.03 (s and d, $^1J_{WC}$ = 127.1 Hz, *cis*-CO), 203.95, 204.05 (*trans*-CO, C_α), 220.06 (W=C). − MS (FAB, NBOH); *m/z* (%): 986 (32) [M^+], 958 (4), 930 (20), 902 (10), 874 (15), 846 (25), 818 (100), 790 (18), 762 (41), 734 (25), 706 (21) [$M^+ - n$ CO, n = 1−10]. − $C_{30}H_{22}N_2O_{10}TiW_2$ (986.1): calcd. C 36.54, H 2.25, N 2.84; found C 36.38, H 2.43, N 2.69.

9b: Yield: 0.98 g (68%, based on **1b**), m.p. 131°C (dec.). − IR (THF): $\tilde{\nu}$(CO) = 2049 cm^{-1} w, 1969 w, 1927 vs, 1908 sh. − ^{1}H NMR: δ = 3.43 (s, 6 H, CH_3), 3.73 (s, 6 H, CH_3), 6.34 (s, 10 H, C_5H_5). − ^{13}C NMR: δ = 46.99 (CH_3), 48.40 (CH_3), 112.09 (C_5H_5), 132.85 (C_β), 207.19 (C_α), 217.84 (*cis*-CO), 223.94 (*trans*-CO), 238.34 (Cr=C). − $C_{30}H_{22}Cr_2N_2O_{10}Ti$ (722.4): calcd. C 49.88, H 3.07, N 3.88; found C 49.96, H 3.03, N 3.87.

Pentacarbonyl{1-dimethylamino-3-[ethynyl-trans-bis(triethylphosphane)palladio]propynylidene}tungsten (**10a**): 3.00 mmol of *n*BuLi (1.88 ml of a 1.6 M solution in hexane) was added at −80°C to a solution of 3.00 mmol of **1a** (1.22 g) in 30 ml of Et_2O. On stirring the yellow solution for 30 min at −80°C, the formation of a white solid was observed. 3.00 mmol (1.21 g) of $[ClPd(PEt_3)_2C{\equiv}CH]$ {contaminated with small amounts of $[Cl_2Pd(PEt_3)_2]$} and 10 ml of THF were then added. The dark yellow solution was stirred for 30 min at room temp. and then the solvent was evaporated in vacuo. The residue was dissolved in 6 ml of THF and chromatographed at −40°C on silica. With pentane/THF (4:1) first a light yellow band containing **10a** was eluted. With pentane/THF (7:2) a further light yellow band containing **5a** was eluted. Evaporation of the solvent in vacuo gave complexes **5a** and **10a** as light yellow solids. **5a**: Yield 0.44 g (19%, based on **1a**). − **10a**: Yield: 0.52 g (23%, based on 1**a**), m.p. 87°C (dec.). − IR (THF): $\tilde{\nu}$(CO) = 2059 cm^{-1} w, 1966 w, 1920 vs, 1898 m, $\tilde{\nu}$(C≡C) = 2034 cm^{-1} w. − ^1H NMR: δ = 1.08−1.21 (m, 18 H, CH_2CH_3), 1.90−2.02 (m, 12 H, CH_2), 2.19 (t, $^4J_{PH}$ = 1.8 Hz, 1 H, ≡CH), 3.51 (s, 3 H, NCH_3), 3.67 (s, 3 H, NCH_3). − ^{13}C NMR: δ = 8.38 (CH_2CH_3), 16.76 (vt, $^{1/3}J_{PC}$ = 14.5 Hz, CH_2), 44.01 (NCH_3), 51.05 (NCH_3), 96.41 ($C_{\beta'}$), 103.35 (t, $^2J_{PC}$ = 17.4 Hz, $C_{\alpha'}$), 122.86 (C_β), 166.59 (t, $^2J_{PC}$ = 16.6 Hz, C_α), 199.52 (s and d, $^1J_{WC}$ = 126.9 Hz, *cis*-CO), 204.23 (*trans*-CO), 226.32 (W=C). − ^{31}P NMR: δ = 19.29. − MS (70 eV); *m/z* (%): 771 (9) [M^+], 743 (4), 715 (5), 687 (7), 659 (16), 631 (14) [$M^+ - n$ CO, n = 1−5]. − $C_{24}H_{37}NO_5P_2PdW$ (771.8): calcd. C 37.35, H 4.83, N 1.81; found C 37.47, H 4.87, N 1.93.

Tris[pentacarbonyl(1-dimethylaminopropynylidene)tungsten]boron (**11a**): 3.00 mmol of *n*BuLi (1.88 ml of a 1.6 M solution in hexane) was added at −80°C to a solution of 3.00 mmol (1.22 g) of **1a** in 30 ml of Et_2O. On stirring the yellow solution for 30 min at −80°C, the yellow solution turned cloudy. After 1.00 mmol of BBr_3 (1.00 ml of a 1.0 M solution in hexane) was added, the solution was stirred for 30 min at room temp. The solvent of the brown solution was evaporated in vacuo, and the residue was dissolved in 6 ml of CH_2Cl_2 and chromatographed at −40°C on silica. With pentane/CH_2Cl_2 (3:1) a yellow band was eluted, which afforded, after removal of the solvent in vacuo, the complex **11a** as an analytically pure beige solid. Yield: 0.75 g (61%, based on **1a**), m.p. 126°C (dec.). − IR (Et_2O): $\tilde{\nu}$(CO) = 2062 cm^{-1} w, 1980 w, 1925 vs, 1900 sh, $\tilde{\nu}$(C≡C) = 2126 cm^{-1} vw. − ^1H NMR ([D_6]acetone): δ = 3.64 (s, 9 H, CH_3), 3.77 (s, 9 H, CH_3). − ^{13}C NMR ([D_6]acetone): δ = 45.42 (CH_3), 51.55 (CH_3), 101.39 (q, $^2J_{BC}$ = 14.4 Hz, C_β), 147.07 (q, $^1J_{BC}$ = 71.2 Hz, C_α), 199.59 (s and d, $^1J_{WC}$ = 128.2 Hz, *cis*-CO), 205.54 (*trans*-CO), 227.86 (W=C). − $C_{30}H_{18}BN_3O_{15}W_3$ (1222.8): calcd. C 29.47, H 1.48, N 3.44; found C 29.30, H 1.57, N 3.31.

Tris[pentacarbonyl(1-dimethylaminopropynylidene)tungsten]phosphorus (**12a**): 3.00 mmol of *n*BuLi (1.88 ml of a 1.6 M solution in hexane) was added at −80°C to a solution of 3.00 mmol (1.22 g) of **1a** in 30 ml of Et_2O. On stirring the yellow solution for 30 min at −80°C, a white precipitate was formed. 1.00 mmol (0.14 g) of PCl_3 was then added and the solution stirred for 30 min at room temp. After the solvent of the orange solution was evaporated in vacuo, the residue was dissolved in 6 ml of CH_2Cl_2 and chromatographed with pentane/CH_2Cl_2 (4:1) at −40°C on silica. An orange band containing **12a** was eluted. After removal of the solvent in vacuo and recrystallization from 30 ml of Et_2O/pentane (3:1) the complex **12a** was obtained as orange crystals. Yield: 1.01 g (81%, based on **1a**), m.p. 135°C (dec.). − IR (Et_2O): $\tilde{\nu}$(CO) = 2064 cm^{-1} w, 1977 w, 1934 vs. − ^1H NMR : δ = 3.61 (s, 9 H, CH_3), 3.77 (d, 9 H, $^6J_{PH}$ = 1.19 Hz, CH_3). − ^{13}C NMR: δ = 47.66 (CH_3), 51.60 (CH_3), 107.15 (d, $^1J_{PC}$ = 11.4 Hz, C_α), 115.17 (d, $^2J_{PC}$ = 8.1 Hz, C_β), 197.86 (s and d, $^1J_{WC}$ = 127.2 Hz, *cis*-CO), 203.46 (s and d, $^1J_{WC}$ = 128.9 Hz, *trans*-CO), 226.32 (s and d, $^1J_{WC}$ = 87.0 Hz, W=C). − ^{31}P NMR: δ = −98.92. − MS (FAB, NBOH); *m/z* (%): 1243 (17) [M^+], 1103 (5), 1047 (8), 1019 (11), 991 (11), 963 (10), 935 (9), 907 (17), 879 (18), 851 (10), 823 (13) [$M^+ - n$ CO, n = 5, 7−15]. − $C_{30}H_{18}N_3O_{15}PW_3$ (1243.0): calcd. C 28.99, H 1.46, N 3.38; found C 29.03, H 1.38, N 3.36.

Tetrakis[pentacarbonyl(1-dimethylaminopropynylidene)tungsten]silicon (**13a**) *and Tetrakis[pentacarbonyl(1-dimethylaminopropynylidene)chromium]silicon* (**13b**): 4.00 mmol of *n*BuLi (2.50 ml of a 1.6 M solution in hexane) was added at −80°C to a solution of 4.00 mmol of **1a** (1.62 g) or **1b** (1.10 g) in 40 ml of Et_2O. On stirring the yellow solution for 30 min at −80°C, a white solid precipitated. 1.00 mmol (0.17 g) of $SiCl_4$ was then added, and the solution stirred for 30 min at room temp. The orange solution was filtered over 10 cm of cellite with 200 ml of Et_2O. After evaporation of the solvent in vacuo and recrystallization from 60 ml of Et_2O/pentane (4:1) complexes **13a**, **b** were obtained as orange crystals. **13a**: Yield: 0.99 g (60%, based on **1a**), m.p. 135°C (dec.). − IR (Et_2O): $\tilde{\nu}$(CO) = 2064 cm^{-1} w, 1979 w, 1935 vs, $\tilde{\nu}$(C≡C) = 2132 cm^{-1} vw. − ^1H NMR : δ = 3.58 (s, 12 H, CH_3), 3.76 (s, 12 H, CH_3). − ^{13}C NMR: δ = 47.51 (CH_3), 51.77 (CH_3), 106.14 (C_β), 118.73 (C_α), 197.89 (s and d, $^1J_{WC}$ = 128.4 Hz, *cis*-CO), 203.82 (s and d, $^1J_{WC}$ = 128.5 Hz, *trans*-CO), 229.28 (s and d, $^1J_{WC}$ = 88.2 Hz, W=C). − MS (FAB, NBOH); *m/z* (%): 1644 (3) [M^+], 1532 (4), 1392 (4), 1364 (4), 1336 (5), 1308 (5), 1224 (4), 1140 (6), 1112 (6), 1084 (7) [$M^+ - n$ CO, n = 4, 9−12, 15, 18−20]. − $C_{40}H_{24}N_4O_{20}SiW_4$ (1644.1): calcd. C 29.22, H 1.47, N 3.41; found C 29.30, H 1.69, N 3.27.

13b: Yield: 0.60 g (54%, based on **1b**), m.p. 115°C (dec.). − IR (Et_2O): $\tilde{\nu}$(CO) = 2056 cm^{-1} w, 1981 w, 1938 vs, $\tilde{\nu}$(C≡C) = 2130 cm^{-1} vw. − ^1H NMR : δ = 3.64 (s, 12 H, CH_3), 3.89 (s, 12 H, CH_3). − ^{13}C NMR: δ = 48.81 (CH_3), 49.60 (CH_3), 104.12 (C_β), 122.28 (C_α), 216.64 (*cis*-CO), 223.94 (*trans*-CO), 249.88 (Cr=C). − $C_{40}H_{24}Cr_4N_4O_{20}Si$ (1116.7): A correct analysis of **13b** has not yet been obtained.

Tetrakis[pentacarbonyl(1-dimethylaminopropynylidene)tungsten]germanium (**14a**): 4.00 mmol of *n*BuLi (2.50 ml of a 1.6 M solution in hexane) was added at −80°C to a solution of 4.00 mmol (1.62 g) of **1a** in 40 ml of Et_2O. On stirring the yellow solution for 30 min at −80°C, the yellow solution turned cloudy. After 1.00 mmol (0.21 g) of $GeCl_4$ was added, the solution was stirred for 30 min at room temp. Then the orange solution was filtered over 10 cm of cellite with 200 ml of Et_2O. Removal of the solvent in vacuo afforded the complex **14a** as an orange solid, which gave orange crystals after recrystallization from 60 ml of Et_2O/pentane (9:2). Yield: 1.00 g (59%, based on **1a**), m.p. 138°C (dec.). − IR (Et_2O): $\tilde{\nu}$(CO) = 2064 cm^{-1} w, 1980 w, 1935 vs, $\tilde{\nu}$(C≡C) = 2132 cm^{-1} vw. − ^1H NMR : δ = 3.58 (s, 12 H, CH_3), 3.77 (s, 12 H, CH_3). − ^{13}C NMR: δ = 47.40 (CH_3), 51.80 (CH_3), 105.11 (C_β), 117.66 (C_α), 197.95 (s and d, $^1J_{WC}$ = 127.2 Hz, *cis*-CO), 203.82 (s and d, $^1J_{WC}$ = 128.6 Hz, *trans*-CO), 229.23 (W=C). − MS (FAB, NBOH); *m/z* (%): 1690 (10) [M^+], 1578 (8), 1438 (21), 1298 (16), 1270 (13), 1214 (14), 1158 (24) [$M^+ - n$ CO, n = 4, 9, 14, 15, 17, 19]. − $C_{40}H_{24}GeN_4O_{20}W_4$ (1688.6): calcd. C 28.45, H 1.43, N 3.32; found C 28.51, H 1.51, N 3.26.

Tetrakis[pentacarbonyl(1-dimethylaminopropynylidene)tungsten]tin (**15a**) *and Tetrakis[pentacarbonyl(1-dimethylaminopropynylidene)chromium]tin* (**15b**): 4.00 mmol of *n*BuLi (2.50 ml of a 1.6 M solution in hexane) was added at −80°C to a solution of 4.00 mmol of **1a** (1.62 g) or **1b** (1.10 g) in 40 ml of Et_2O. On stirring

Table 1. Crystallographic data of **8a**, **9a**, **12a**, and **15a**

	8a	**9a**	**12a**	**15a**
Empirical formula	$C_{10}H_6Hg_{0.5}NO_5W \cdot 0.4\ CH_2Cl_2$	$C_{30}H_{22}N_2O_{10}TiW_2$	$C_{30}H_{18}N_3O_{15}PW_3 \cdot 0.25\ CH_2Cl_2$	$C_{40}H_{24}N_4O_{20}SnW_4 \cdot CHCl_3$
Crystal size [mm^3]	0.3 × 0.3 × 0.3	0.3 × 0.3 × 0.4	0.3 × 0.3 × 0.3	0.4 × 0.4 × 0.4
Formula mass	538.3	986.1	1264.2	1854.1
Crystal system	monoclinic	monoclinic	monoclinic	monoclinic
Space group	$P2_1/n$	$P2_1/c$	$C2/c$	$P2_1/c$
a [Å]	9.752(2)	12.233(3)	14.791(1)	13.099(2)
b [Å]	8.844(2)	15.806(3)	23.191(2)	30.388(3)
c [Å]	17.033(2)	16.916(3)	25.275(2)	14.398(1)
β [deg]	93.88(1)	98.91(1)	102.31(1)	98.43(1)
V [Å^3]	1466.0(5)	3232(1)	8470(1)	5669(1)
Z	4	4	8	4
Density [g·cm^{-3}]	2.439	2.027	1.983	2.172
Temperature [K]	232	234	244	245
Absorption [mm^{-1}]	13.418	7.551	8.436	8.911
Min/max transm	0.0080/0.0334	0.0613/0.1386	0.0977/0.1630	0.0151/0.0465
Indepdt reflns	3199	7053	8615	12366
Obsd reflns [$F > x\sigma(F)$]	2568 (x = 3)	5394 (x = 4)	6029 (x = 4)	7183 (x = 4)
F(000)	975.20	1864	4692	3424
Index range	+12, +11, ±21	+15, +20, ±21	+18, +29, ±32	+16, +38, ±18
Params refined	180	406	481	638
Final R	0.0386	0.0449	0.0604	0.0627
Final R_w	0.0442	0.0446	0.0644	0.0615
Largest diff peak/hole [e·Å^{-3}]	+1.82/−1.36	+1.07/−1.04	+2.23/−1.65	+2.28/−1.58

the yellow solution for 30 min at −80°C, the formation of a white precipitate was observed. 1.00 mmol (0.26 g) of $SnCl_4$ was then added and the solution stirred for 30 min at room temp. The solvent of the orange solution was evaporated in vacuo, and the residue was dissolved in 8 ml of CH_2Cl_2 and chromatographed at −40°C on silica. With pentane/CH_2Cl_2 [4:1(**15a**), 7:2 (**15b**)] an orange band was eluted, which afforded after removal of the solvent in vacuo complexes **15a**, **b** as analytically pure orange solids. Recrystallization from 30 ml of Et_2O/pentane [3:1(**15a**), 5:2 (**15b**)] gave orange crystals**. 15a**: Yield: 1.32 g (76%, based on **1a**), m.p. 136°C (dec.). − IR (Et_2O): $\tilde{\nu}$(CO) = 2064 cm^{-1} w, 1979 w, 1933 vs, $\tilde{\nu}$(C≡C) = 2118 cm^{-1} vw. − ^{1}H NMR : δ = 3.59 (s, 12 H, CH_3), 3.76 (s, 12 H, CH_3). − ^{13}C NMR: δ = 47.32 (CH_3), 51.74 (CH_3), 109.59 (s and 2 d, $^2J_{^{117}Sn C,^{119}Sn C}$ = 218.9 Hz, 209.5 Hz, C_β), 119.47 (s and 2 d, $^1J_{^{117}Sn C,^{119}Sn C}$ = 1169.5 Hz, 1118.2 Hz, C_α), 198.07 (s and d, $^1J_{WC}$ = 128.4 Hz, *cis*-CO), 203.89 (s and d, $^1J_{WC}$ = 128.7 Hz, *trans*-CO), 229.41 (s and d, $^1J_{WC}$ = 88.2 Hz, W=C). − MS (FAB, NBOH); *m/z* (%): 1736 (10) [M$^+$], 1512 (3), 1484 (6), 1456 (7), 1428 (8), 1400 (12), 1372 (14), 1344 (17), 1316 (13), 1288 (17), 1260 (12), 1232 (13), 1204 (13), 1176 (13) [M$^+$ − n CO, n = 8−20]. − $C_{40}H_{24}N_4O_{20}SnW_4$ (1734.7): calcd. C 27.70, H 1.39, N 3.23; found C 27.80, H 1.43, N 3.15.

15b: Yield: 0.86 g (71%, based on **1b**), m.p. 112°C (dec.). − IR (Et_2O): $\tilde{\nu}$(CO) = 2057 cm^{-1} w, 1982 w, 1937 vs, $\tilde{\nu}$(C≡C) = 2115 cm^{-1} vw. − ^{1}H NMR : δ = 3.65 (s, 12 H, CH_3), 3.88 (s, 12 H, CH_3). − ^{13}C NMR: δ = 48.65 (CH_3), 49.56 (CH_3), 107.68 (s and 2 d, $^2J_{^{117}Sn C,^{119}Sn C}$ = 219.9 Hz, 210.3 Hz, C_β), 123.05 (s and 2 d, $^1J_{^{117}Sn C,^{119}Sn C}$ = 1167.5 Hz, 1115.7 Hz, C_α), 216.84 (*cis*-CO), 223.97 (*trans*-CO), 250.09 (Cr=C). − $C_{40}H_{24}Cr_4N_4O_{20}Sn$ (1207.3): calcd. C 39.79, H 2.00, N 4.64; found C 39.67, H 2.19, N 4.64.

X-ray Structural Analyses of **8a**, **9a**, **12a**, *and* **15a**: Single crystals were grown from pentane/Et_2O [2:5 (**8a**), 1:4 (**9a**), 1:3 (**12a**, **15a**)], respectively, and mounted in a glass capillary. All crystal data were collected on a Siemens P4 diffractometer (Wyckoff scan, scan range 4° < 2θ < 54°, scan speed variable: 4 to 30° min^{-1} in ω) with a graphite monochromator (Mo-$K\alpha$, λ = 0.71073 Å). Semi-empirical absorption corrections were employed (ψ-scans with 10 reflections). The structures were solved with Patterson methods using the Siemens SHELXTL PLUS program package. The positions of the hydrogen atoms were calculated by assuming ideal geometry (d_{C-H} = 0.96 Å), and their coordinates were refined together with the attached carbon atoms as a "riding model". The positions of all other atoms were refined anisotropically by full-matrix least-squares techniques. Complete lists of atom coordinates and thermal parameters were deposited[54].

☆ Dedicated to Professor *Warren Roper* on the occasion of his 60th birthday.

[1] Recent reviews: [1a] W. Beck, B. Niemer, M. Wieser, *Angew. Chem.* **1993**, *105*, 969−996; *Angew. Chem. Int. Ed. Engl.* **1993**, *32*, 923−949. − [1b] H. Lang, *Angew. Chem.* **1994**, *106*, 569−572; *Angew. Chem. Int. Ed. Engl.* **1994**, *33*, 547−550. − [1c] U. H. F. Bunz, **1996**, *108*, 1047−1049; *Angew. Chem. Int. Ed. Engl.* **1996**, *35*, 969−971. − [1d] J. S. Schumm, D. L. Pearson, J. M. Tour, *Angew. Chem.* **1994**, *106*, 1445−1448; *Angew. Chem. Int. Ed. Engl.* **1994**, *33*, 1360−1363. − [1e] W. Weng, T. Bartik, J. A. Gladysz, *Angew. Chem.* **1994**, *106*, 2269−2272; *Angew. Chem. Int. Ed. Engl.* **1994**, *33*, 2199−2202. − [1f] T. Bartik, B. Bartik, M. Brady, R. Dembinski, J. A. Gladysz, *Angew. Chem.* **1996**, *108*, 467−469; *Angew. Chem. Int. Ed. Engl.* **1996**, *35*, 414−417.

[2] F. Diederich, R. Faust, V. Gramlich, P. Seiler, *J. Chem. Soc., Chem. Commun.* **1994**, 2045−2046 and literature cited therein.

[3] [3a] J. E. C. Wiegelmann, U. H. F. Bunz, P. Schiel, *Organometallics* **1994**, *13*, 4649−4651. − [3b] M. Altmann, U. H. F. Bunz, *Makromol. Rapid. Commun.* **1994**, *15*, 785−789. − [3c] J. E. C. Wiegelmann, U. H. F. Bunz, *Organometallics* **1993**, *12*, 3792−3794. − [3d] U. H. F. Bunz, J. C. Wiegelmann-Kreiter, *Chem. Ber.* **1996**, *129*, 785−797.

[4] [4a] J. E. C. Wiegelmann-Kreiter, U. H. F. Bunz, *Organometallics* **1995**, *14*, 4449−4451. − [4b] U. H. F. Bunz, V. Enkelmann, *Organometallics* **1994**, *13*, 3823−3833. − [4c] U. H. F. Bunz, V. Enkelmann, *Angew. Chem.* **1993**, *105*, 1712−1714; *Angew. Chem. Int. Ed. Engl.* **1993**, *32*, 1653−1655.

[5] [5a] U. H. F. Bunz, V. Enkelmann, F. Beer, *Organometallics* **1995**, *14*, 2490−2495. − [5b] U. H. F. Bunz, V. Enkelmann, J. Räder, *Organometallics* **1993**, *12*, 4745−4747.

[6] E. O. Fischer, W. Röll, N. H. T. Huy, K. Ackermann, *Chem. Ber.* **1982**, *115*, 2951−3212.

[7] M. Havránek, M. Hušák, D. Dvorák, *Organometallics* **1995**, *14*, 5024−5029.
[8] N. H. T. Huy, P. Lefloch, F. Robert, Y. Jeannin, *J. Organomet. Chem.* **1987**, *327*, 211−221.
[9] T. Albrecht, J. Sauer, *Tetrahedron Lett.* **1994**, *35*, 561−564.
[10] R. Neidlein, S. Gürtler, *Helv. Chim. Acta* **1994**, *77*, 2303−2322.
[11] [11a] V. Péron, E. Porhiel, V. Ferrand, H. Le Bozec, *J. Organomet. Chem.* **1997**, *539*, 201−203. − [11b] A. Geisbauer, S. Mihan, W. Beck, *J. Organomet. Chem.* **1995**, *501*, 61−66. − [11c] R. Aumann, H. Heinen, *Chem. Ber.* **1987**, *120*, 537−540.
[12] R. Aumann, B. Jasper, R. Fröhlich, S. Kolita, *J. Organomet. Chem.* **1995**, *502*, 137−141.
[13] C. Hartbaum, H. Fischer, *Chem. Ber./Recl.* **1997**, *130*, 1063−1067.
[14] To our knowledge $[(CO)_5CrC(OMe)(CH_2)_4Zn(CH_2)_4C(OMe)Cr(CO)_5]$ represents the only biscarbene complex of this type, however whithout a conjugated carbon bridge: H. Stadtmüller, P. Knochel, *Organometallics* **1995**, *14*, 3163−3166.
[15] C. Hartbaum, G. Roth, H. Fischer, *Chem. Ber./Recl.* **1997**, *130*, 479−488.
[16] [16a] H. Lang, C. Weber, *Organometallics* **1995**, *14*, 4415−4417. − [16b] H. Lang, S. Blau, H. Pritzkow, L. Zsolnai, *Organometallics* **1995**, *14*, 1850−1854. − [16c] H. Lang, D. Seyferth, *Z. Naturforsch.* **1990**, *45b*, 212−220.
[17] R. Jimenez, M. C. Barral, V. Moreno, A. Santos, *J. Organomet. Chem.* **1979**, *174*, 281−287.
[18] A. Sebald, P. Fritz, B. Wrackmeyer, *Spectrochim. Acta* **1985**, *41a*, 1405−1407.
[19] H. Masai, K. Sonogashira, N. Hagihara, *Bull. Chem. Soc. Jpn.* **1971**, *44*, 2226−2230.
[20] J. Manna, K. D. John, M. D. Hopkins, *Adv. Organomet. Chem.* **1995**, *38*, 79−154.
[21] A. Sebald, B. Wrackmeyer, W. Beck, *Z. Naturforsch.* **1983**, *38b*, 45−56.
[22] H. Masai, K. Sonogashira, N. Hagihara, *J. Organomet. Chem.* **1971**, *26*, 271−276.
[23] J. Burgess, M. E. Howden, R. D. W. Kemmitt, N. S. Sridhara, *J. Chem. Soc., Dalton Trans.* **1978**, 1577−1581.
[24] [24a] L. D. Field, A. V. George, T. W. Hambley, *Inorg. Chem.* **1990**, *29*, 4565−4569. − [24b] A. Hills, D. L. Hughes, M. Jimenez-Tenorio, G. J. Leigh, *J. Organomet. Chem.* **1990**, 3*91*, C41−C44. − [24c] D. L. Hughes, G. J. Leigh, M. Jimeneztenorio, A. T. Rowley, *J. Chem. Soc., Dalton Trans.* **1993**, 75−82.
[25] L. D. Field, A. V. George, E. Y. Malouf, I. H. M. Slip, T. W. Hambley, *Organometallics* **1991**, *10*, 3842−3848.
[26] C. Cauletti, C. Furlani, M. N. Piancatelli, A. Sebald, B. Wrackmeyer, *Inorg. Chem.* **1984**, *23*, 1113−1119.
[27] H. Lang, L. Zsolnai, *J. Organomet. Chem.* **1989**, *369*, 131−135.
[28] F. A. Miller, D. H. Lemmon, *Spectrochim. Acta* **1967**, *23a*, 1099−1109.
[29] W. M. A. Smit, G. Dijkstra, *J. Mol. Structure* **1971**, *7*, 223−239.
[30] R. E. Sacher, D. H. Lemmon, F. A. Miller, *Spectrochim. Acta* **1967**, *23a*, 1169−1176.
[31] A. Sebald, C. Stader, B. Wrackmeyer, *J. Organomet. Chem.* **1986**, *311*, 233−242.
[32] F. Moser, E. O. Fischer, *J. Organomet. Chem.* **1968**, *13*, 387−398.
[33] D. Rosenberg, W. Drenth, *Tetrahedron* **1971**, *27*, 3893−3907.
[34] R. Köster, G. Seidel, I. Klopp, C. Krüger, G. Kehr, J. Süß, B. Wrackmeyer, *Chem. Ber.* **1993**, *126*, 1385−1396.
[35] B. Wrackmeyer, G. Kehr, A. Sebald, J. Kümmerlen, *Chem. Ber.* **1992**, *125*, 1597−1603.
[36] A. Sebald, B. Wrackmeyer, *Spectrochim. Acta* **1982**, *38a*, 163−173.
[37] E. Gutiérrez−Puebla, A. Vegas, *Acta Cryst*. **1978**, *34b*, 3382−3384.
[38] H. Lang, M. Herres, L. Zsolnai, *Organometallics* **1993**, *12*, 5008−5011.
[39] G. Erker, W. Frömberg, R. Benn, R. Mynott, K. Angermund, C. Krüger, *Organometallics* **1989**, *8*, 911−920.
[40] Y. Hayashi, M. Osawa, K. Kobayashi, Y. Wakatsuki, *Chem. Commun*. **1996**, 1617−1618.
[41] H. Lang, S. Blau, B. Nuber, L. Zsolnai, *Organometallics* **1995**, *14*, 3216−3223.
[42] A. Rahm, W. D. Wulff, A. L. Rheingold, *Organometallics* **1993**, *12*, 597−599.
[43] G. Huttner, H. Lorenz, *Chem. Ber.* **1975**, *108*, 1864−1870.
[44] J. Scholz, F. Rehbaum, K.-H. Thiele, R. Goddard, P. Betz, C. Krüger, *J. Organomet. Chem.* **1993**, *443*, 93−99.
[45] U. Thewalt, T. Wöhrle, *J. Organomet. Chem.* **1994**, *464*, C17−C19.
[46] J. L. Atwood, W. E. Hunter, D. C. Hrncir, E. Samuel, H. Alt, M. D. Rausch, *Inorg. Chem.* **1975**, *14*, 1757−1762.
[47] J. Kroon, J. B. Hulscher, F. Peerdeman, *J. Mol. Structure* **1971**, *7*, 217−221.
[48] D. Mootz, G. Sassmannshausen, *Z. Anorg. Allg. Chem.* **1967**, *355*, 200−208.
[49] C. Dallaire, M. A. Brook, A. D. Bain, C. S. Frampton, J. E. Britten, *Can. J. Chem.* **1993**, *71*, 1676−1683.
[50] K. A. Jensen, P. H. Nielsen, C. Th. Pedersen, *Acta Chem. Scand.* **1963**, *17*, 1115−1125.
[51] J. Chatt, R. G. Hayter, *J. Chem. Soc.* **1961**, 5507−5510.
[52] W. P. Fehlhammer, W. A. Herrmann, K. Öfele in *Handbuch der Präparativen Anorganischen Chemie* (Ed.: G. Brauer), vol. 3, 3rd ed., Ferdinand Enke Verlag, Stuttgart **1981**, chapter 3.
[53] K. Onitsuka, T. Joh, S. Takahashi, *Bull. Chem. Soc. Jpn.* **1992**, *65*, 1179−1181.
[54] Further details of the crystal structure investigations are available on request from the Fachinformationszentrum Karlsruhe, Gesellschaft für wissenschaftlich-technische Information mbH, D-76344 Eggenstein-Leopoldshafen, on quoting the depository numbers CSD-407744 (**8a**), CSD-407745 (**9a**), CSD-407746 (**12a**), CSD-407747 (**15a**), the names of authors, and the journal citation.

[97227]

Contributions to the Coordination and Structural Chemistry of Gallium(III) and Indium(III) Halides: Complexes with Bi- and Tridentate Tertiary Phosphanes

Marcus Sigl, Annette Schier, and Hubert Schmidbaur*

Anorganisch-chemisches Institut der Technischen Universität München,
Lichtenbergstrasse 4, D-85747 Garching, Germany

Received September 15, 1997

Keywords: Gallium(III) halides / Indium(III) halides / Phosphanes, polydentate / Complexes / Crystallography / Lewis acid catalysis

The reactions of gallium and indium trihalides with 1,2-bis-(diphenylphosphanyl)benzene (DP) and bis[(2-diphenylphosphanyl)phenyl]phenylphosphane (TP) lead to a variety of molecular and ionic complexes. Treatment of $InCl_3$ with DP results in $[(DP)_2InCl_2]^+[InCl_4]^-$ (**1**). With $InBr_3$ or InI_3 molecular 1:1 complexes $(DP)InX_3$ (**2**: X = Br, **3**: X = I) and ionic 1:2 complexes $[(DP)InX_2]^+[InX_4]^-$ (**4**: X = Br, **5**: X = I) are obtained. With $GaBr_3$ and GaI_3 only the ionic complexes $[(DP)GaX_2]^+[GaX_4]^-$ (**6**: X = Br, **7**: X = I) are generated. According to single-crystal X-ray analyses the environment of the metal center is octahedral in the cation of **1**, square pyramidal in **3**, and tetrahedral in the cations of **5** and **7**. The reactions of TP with GaI_3 or InI_3 afford ionic complexes $[(TP)MI_2]^+[MI_4]^-$ (**8**: M = Ga, **9**: M = In). As shown by ^{31}P-NMR studies and X-ray analyses, TP acts as a bidentate ligand in both complexes. The central phosphorus atom is not engaged in coordinative bonding. The ^{31}P resonances of all compounds appear at higher field as compared to the free ligand. This phenomenon calls for further investigations and a detailed theoretical treatment.

Introduction

Traditional Lewis acid catalysis has been dominated for a long time by the use of boron and aluminium halides.[1] It is only very recently that the analogous compounds of the heavier congeners in group 13, gallium and indium, have also been employed for this purpose.[2] Prominent examples are the $InCl_3$ catalysis of the Mukayama aldol reaction or special variations of the Diels-Alder reaction,[3] but also the $GaBr_3$-mediated methyl transfer of alkylsilanes and -siloxanes.[4] In most of these reactions the anhydrous binary halides EX_3 are employed, but there is growing interest in a mediation of the catalytic effect by the introduction of neutral or cationic donor/acceptor complexes, X_3E-L_n and $[X_2EL_n]^+$, respectively. The soft donor ligand L is expected to be reversibly displaced by the substrate of the reaction. It can also serve as a component which enhances the solubility and stability of the Lewis acid catalyst EX_3.

The formation of donor/acceptor complexes of gallium and indium halides is known for a wide variety of neutral donor ligands L.[5] Among these the cationic species are of special interest, because analogous cationic complexes of boron and aluminium are already well established as active catalysts in the living polymerization of propylene oxide and in Diels-Alder reactions.[6] Structurally characterized ionic species derived from gallium or indium trihalides in previous work are limited to O or N donors like pyridine, bipyridyl, methylpyrazole, or a crown ether, but also dimethyl sulfoxide, triphenylphosphane oxide, dimethylglycol, or hexamethyl phosphoric triamide etc.[7]

Complexes of gallium and indium halides with tertiary phosphanes have been considered only sporadically, and very little information is available on the stoichiometry and structure of such coordination compounds.[8] This is true in particular for complexes with polydentate phosphanes, for which a large variety of structural concepts can be conceived.[8a][8b][8c]

We have therefore initiated a systematic investigation of this chemistry, and in the present paper we report a first set of results obtained for ligands based on a phenylenebis(diphenylphosphane) skeleton.

Preparative Results

In order to secure chelation of the metal trihalides, a bidentate ligand was chosen in which the two donor centers are fixed in a *cis* position at a rigid backbone. 1,2-Bis-(diphenylphosphanyl)benzene (DP) is the most common prototype for this kind of ligands, and in bis[(2-diphenylphosphanyl)phenyl]phenylphosphane (TP) the same structural principle is extended to give a tripodal tertiary phosphane.

Anhydrous $InCl_3$ reacts with equimolar quantities of DP to give almost quantitative yields of an air-stable but moisture-sensitive crystalline product (**1**, 91% yield, m.p. 243°C), soluble in di- and trichloromethane [Eq. (1)]. Solvation in THF causes decomposition indicated by the release of phosphane ligand. The crystal structure analysis has shown that this compound is not a molecular 1:1 complex (below). Instead the reaction is associated with a halide redistribution between two indium atoms to give an ionic product

 © WILEY-VCH Verlag GmbH, D-69451 Weinheim, 1998 1434–1948/98/0202–0203 $ 17.50+.50/0

containing an $[InCl_4]^-$ anion and a bis-chelated cation $[(DP)_2InCl_2]^+$ with hexacoordinated indium atoms. Addition of excess $InCl_3$ has no effect regarding the nature of the product, and no complexes of the stoichiometry $(DP)(InCl_3)_2$ or $[(DP)InCl_2]^+$ $[InCl_4]^-$ can be isolated. The NMR spectra of solutions of $[(DP)_2InCl_2]^+[InCl_4]^-$ in $CDCl_3$ are consistent with fully symmetrically bound ligand molecules as suggested by only one set of phenyl and phenylene resonances (^1H,^{13}C). The singlet ^{31}P resonance also supports the proposed molecular symmetry, but the phosphorus nuclei are strongly shielded ($\delta P = -26.6$ in $CDCl_3$) which is very unexpected for tetracoordinated phosphorus atoms.

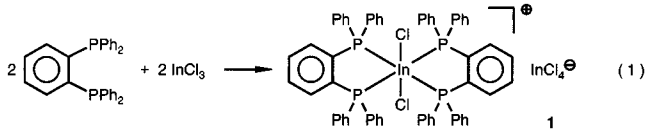

Unlike the results obtained with $InCl_3$, the nature of the product of the reaction of DP with $InBr_3$ and InI_3 depends on the molar ratio between the phosphane and the indium halide [Eq. (2) and (3)]. The 1:1 addition compound of DP with $InBr_3$ is assigned a molecular, non-ionic structure (**2**, 89% yield, m.p. 268°C, $\delta P = -26.9$) with a pentacoordinated indium atom. The compound is stable towards THF and its ^{13}C-NMR spectrum resembles that of $(DP)InI_3$, for which the non-ionic structure was confirmed by a crystal structure analysis (below, **3**, 75% yield, m.p. 239°C, $\delta P = -31.7$). The redistribution of halide anions as observed for **1** is excluded in both cases, because of serious steric congestion of the larger halogen atoms at a hexacoordinated metal center.

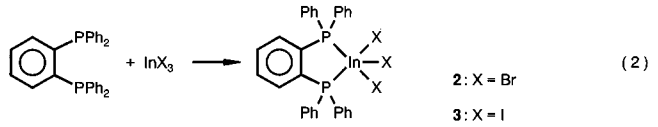

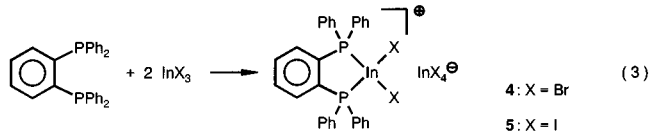

If the same components are allowed to react in the molar ratio of 1:2, ionic products are obtained, in which the $[InX_4]^-$ anion is accompanied by a cation $[(DP)InX_2]^+$ with tetracoordinated indium atoms (**4**, X = Br, 95% yield, m.p. 251°C, $\delta P = -20.0$; **5**, X = I, 87% yield, m.p. 199°C, $\delta P = -27.9$). The structure of **5** has also been determined by X-ray crystallography. The ^{13}C-NMR data of **5** show a distinct similarity with those of the bromo analog **4**.

In order to investigate whether an addition of nucleophiles to the tetracoordinated cationic indium complexes **4** and **5** is possible, reactions with THF, acetone and $OPPh_3$ were carried out. The reaction was found to transform the cationic complexes into the corresponding molecular 1:1 complexes [Eq. (4)].

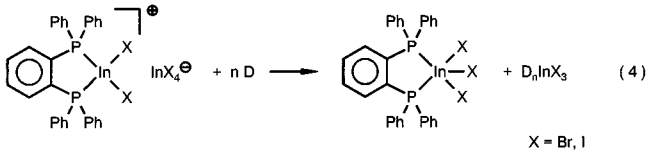

Cationic complexes of the type $[(DP)GaX_2]^+[GaX_4]^-$ with X = Br, I were also obtained with the lighter congener gallium [**6**, X = Br, 81% yield, m.p. 259°C, $\delta P = -22.1$; **7**, X = I, 95% yield, m.p. 219°C, $\delta P = -29.3$; Eq. (5)]. The ionic structure of the iodo compound with tetracoordinated gallium atoms in both the cation and the anion was confirmed in X-ray structure analysis (below).

Attempts to synthesize molecular gallium complexes analogous to **2** or **3** have failed.

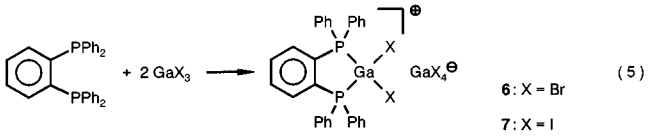

Treatment of GaI_3 with TP in the molar ratio of 2:1 gives the ionic complex $[(TP)GaI_2]^+[GaI_4]^-$ in 83% yield [**8**, m.p. 267°C; Eq. (6)]. Earlier work with boron halides and a number of transition-metal salts has shown, that TP represents a potent tripodal ligand.[9] As derived from ^{31}P-NMR studies and X-ray analysis (below), in the present case TP acts only as a bidentate ligand, however, and the central phosphorus atom remains uncoordinated.

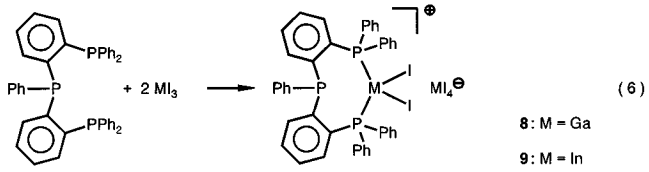

The reaction with InI_3 produces the indium analog of **8** in 88% yield (**9**, m.p. 259°C), for which the analytical and structural data (^{31}P NMR, X-ray diffraction) prove tetracoordinated metal centers. No molecular complex $(TP)InI_3$ could be obtained from equimolar quantities of TP and InI_3. The ionic complex **9** was again formed and half of the TP ligand applied (2:1 molar ratio!) remained unaffected.

NMR-Spectroscopic Investigations

The ^1H- and ^{13}C-NMR spectra of the complexes are characterized by complex multiplets and by a large number of phenyl/phenylene resonances, respectively, which were not analyzed any further because the δ and J data are not expected to be relevant to the discussion of structure and bonding in the individual species.

The ^{31}P-NMR spectra of the *DP complexes* show only one resonance with a large half width (ca. 80 Hz) owing to quadrupole broadening originating from interactions with the ^{115}In and $^{71/69}Ga$ nuclei which all have high quadrupole

moments. This line broadening is of course proof for the coordinative bonding of the phosphorus donors to the metal acceptors. It is very surprising, however, that the chemical shifts δP of the complexes are all in the range from −20 to −35 and hence upfield from the resonance of the free DP ligand (δP = −13.1 in $CDCl_3$). It is generally true for most phosphane complexes of main-group as well as transition metals that there is a downfield "coordination shift" between the free ligand and the corresponding complex. In the present cases this "coordination shift" is inverted. There is no straightforward explanation for this phenomenon, although it is tempting to ascribe the effect to the very low electronegativity of the heavy group 13 elements. Further experimental work and − more importantly − theoretical studies are required to clarify this point.

In the two *TP complexes* the resonances of the phosphorus atoms show marked differences: While the signals of the two terminal phosphorus atoms have a severe line broadening with poorly resolved (if any) splitting, the resonance of the central phosphorus atom is rather sharp and has the expected splitting for the A part of an AB_2 spin system (Figures 1 and 2). The implications of the two spectra are threefold:

1) The lack of quadrupole broadening of the signal of the central phosphorus atoms is proof that this atom is not strongly coordinated to indium or gallium, respectively. For the Ga compound this is clearly ruled out completely by the narrow line width, while for In there is discernible broadening, but still much less than for the terminal phosphorus atoms. (The same conclusions can be drawn from the crystal structure studies below.)

2) The *J*(P,P) coupling constants of the complexes are larger than in the free ligand, indicative of the change of hybridization at phosphorus upon complexation (from p to sp^3) as suggested by the Fermi contact mechanism.

3) There is no downfield shift of the resonance of the terminal or central phosphorus atoms upon complexation. On the contrary, all resonances are again (as for DP, above) shifted strongly *upfield* as compared to free TP.

Figure 1. $^{31}P\{^1H\}$-NMR spectrum of **8** in CD_2Cl_2 at 20°C; chemical shifts (δ values)

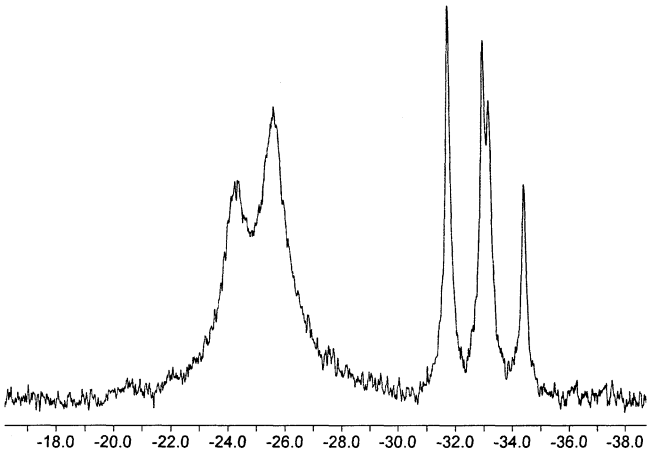

Figure 2. $^{31}P\{^1H\}$-NMR spectrum of **9** in CD_2Cl_2 at 20°C; chemical shifts (δ values)

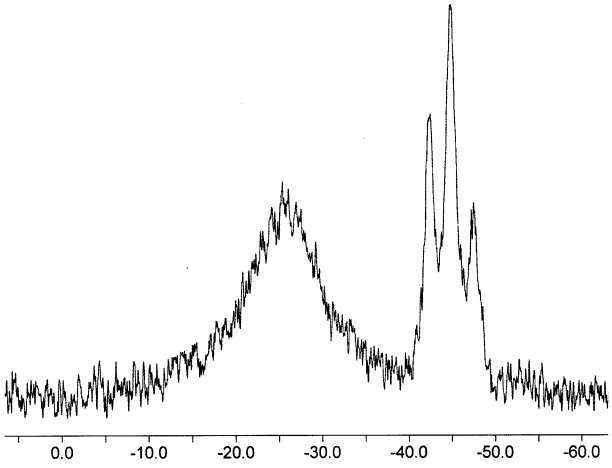

Structural Investigations

Complexes of 1,2-Bis(diphenylphosphanyl)benzene (DP): The compound with the net formula $(DP)InCl_3$ (**1**) was found to have the ionic structure $[(DP)_2InCl_2]^+[InCl_4]^-$. The complex crystallizes in the triclinic space group $P\bar{1}$ with two formula units in the unit cell. The asymmetric unit contains two crystallographically independent halves of the cation and one anion. The *anion* with In3 as the central atom has a standard tetrahedral structure with bond lengths and angles in the ranges documented in the literature. The two *cation* halves are complemented by their second halves which are related by crystallographic centers of inversion (Figure 3). As shown by a schematic superposition (Figure 4), the two cations are structurally very similar, and in a discussion of the details both cations can be treated together.

Figure 3. Molecular structure of the cation in **1** with atomic numbering (ORTEP drawing, 50% probability ellipsoids, only one of the two crystallographically independent cations is shown, hydrogen atoms omitted for clarity)[a]

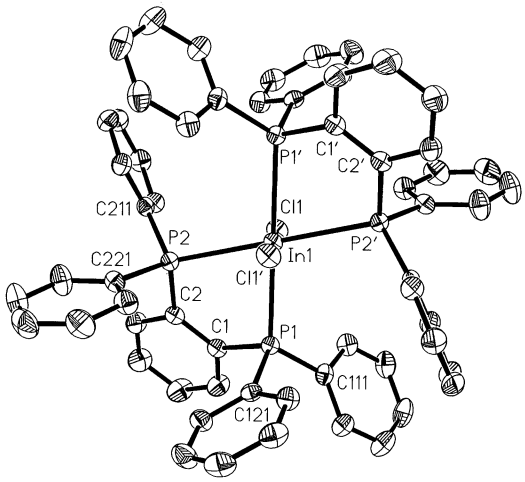

[a] Selected bond lengths [Å] and angles [°]: In1−Cl1 2.4822(5) [2.4838(6)], In1−P1 2.6648(6) [2.6849(6)], In1−P2 2.7133(6) [2.7374(6)]; Cl1−In1−Cl1′ 180.0 [180.0], Cl1−In1−P1 85.35(2) [85.50(2)], Cl1−In1−P2 82.77(2) [85.39(2)], P1−In1−P2 76.14(2) [73.29(2)]. The data in brackets refer to the second independent cation accordingly.

Figure 4. Superposition of the two crystallographically independent cations in **1**

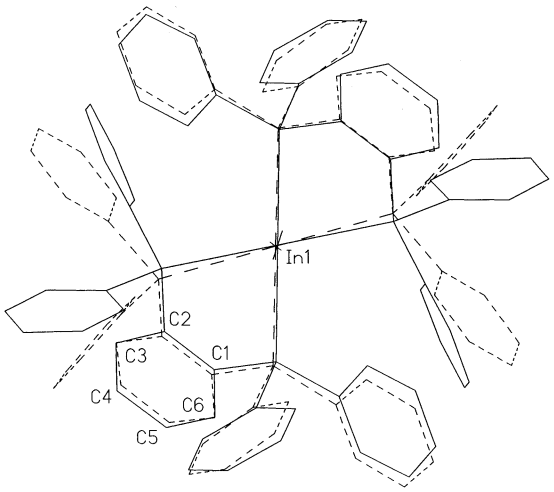

Figure 5. Molecular structure of **3** with atomic numbering (ORTEP drawing, 50% probability ellipsoids, hydrogen atoms omitted for clarity)[a]

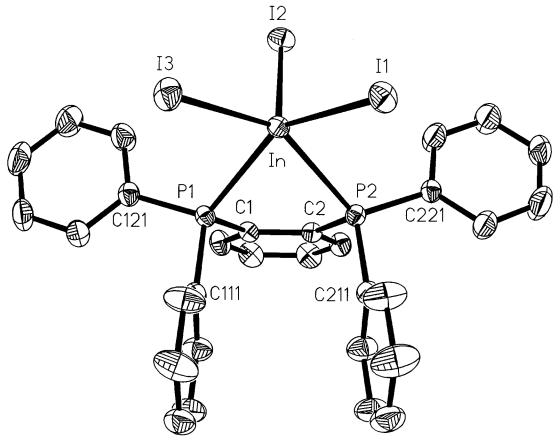

[a] Selected bond lengths [Å] and angles [°]: In−I2 2.7134(4), In−I1 2.7729(4), In−I3 2.7875(5), In−P1 2.7140(9), In−P2 2.7569(9); I3−In−I1 95.306(13), I1−In−I2 109.336(14), I2−In−I3 108.045(14), I1−In−P2 89.66(2), I3−In−P1 89.37(2), I2−In−P1 99.82(2), I2−In−P2 97.99(2), P1−In−P2 71.44(3).

The indium atoms in the cations are in an octahedral environment with two chloride ligands in the apical positions and two chelate ligands spanning equatorial edges. The angles at In1 and In2 are all close to 90 or 180°. The In1/In2−Cl bond lengths in the octahedra [average 2.4830 Å] are significantly longer than the In3−Cl bond lengths [average 2.3487 Å] in the tetrahedral anion. This result is in agreement with previous observations for two different polyhedra with a common central element having the same ligands.

The four chelate rings are in envelope conformations with the metal atoms out of the plane containing the phenylene rings and the phosphorus atoms. In both cases the geometry of the rings and their substituents is very close to mirror symmetry, the individual mirror planes passing through Cl1−In1−Cl1′/Cl2−In2−Cl2′ and bisecting the phenylene rings (Figures 3 and 4).

The compound with the net formula $(DP)InI_3$ (**3**) was found to be a molecular, non-ionic species. It crystallizes in the triclinic space group $P\bar{1}$ with two formula units in the unit cell. The individual molecules have no crystallographically imposed symmetry, but the molecular geometry follows very closely mirror symmetry as related to a plane passing through the In−I2 unit and bisecting the phenylene ring (Figure 5).

The indium atom is pentacoordinated in a quasi square-pyramidal environment, where I2 occupies the apical position and the ligand spans one edge of the basal square plane and with the other two iodine atoms at the remaining basal vertices. The chelate ring has an envelope conformation as already noted for $[(DP)_2InCl_2]^+$. The In−I2 distance (apical) is significantly shorter [2.7134(4) Å] than the In−I1/I3 distances [basal, average 2.7802 Å]. This deviation corresponds to two different sets of I−In−I angles, a smaller one for I1−In−I3 [95.306(13)°] and two larger ones for I1−In−I2 [109.336(14)°] and I2−In−I3 [108.045(14)°].

The compound of the stoichiometry $(DP)(InI_3)_2$ (**5**) has an ionic structure $[(DP)InI_2]^+[InI_4]^-$. It crystallizes in the triclinic space group $P\bar{1}$ with two formula units in the unit cell. The anion has a slightly distorted tetrahedral geometry at the central indium atom (In2) with standard bond lengths. The geometry of the cation (Figure 6) deviates only slightly from mirror symmetry. The indium atom In1 is in a tetrahedral environment and part of a chelate ring with an envelope conformation. Following a very general rule, the In−I distances are significantly shorter in the cation [average 2.6570 Å] than in the anion [average 2.6993 Å]. Both distances are shorter, however, than the bond lengths for pentacoordinate indium (above), and this reduction also applies to the In−P bonds in the tetra- as compared to the pentacoordinate species (see captions to figures).

The gallium analog of the composition $(DP)GaI_3$ (**7**) has the same structure $[(DP)GaI_2]^+[GaI_4]^-$ like its indium counterpart (Figure 7). The crystals are also triclinic, space group $P\bar{1}$, $Z = 2$, but are not isomorphous with the indium compound. The general description can be adopted from $[(DP)InI_2]^+$ $[InI_4]^-$. Where variations appear, these are only associated with the difference in the covalent radii of gallium and indium.

Complexes of Bis[(2-diphenylphosphanyl)phenyl]phenylphosphane (TP): The complexes $(TP)(InI_3)_2$ (**9**) and $(TP)(GaI_3)_2$ (**8**) have ionic structures $[(TP)MI_2]^+[MI_4]^-$ with M = In, Ga. The crystals are isomorphous (space group $P\bar{1}$, $Z = 2$) with very similar cell dimensions (Table 2). The anions are tetrahedral tetraiodometallate moieties with structural details closely comparable to those of the DP complexes (above).

The metal atoms of the cations are also tetracoordinated with bond angles I−M−I and P−M−P at 103.02(2)/

Figure 6. Molecular structure of the cation in **5** with atomic numbering (ORTEP drawing, 50% probability ellipsoids, hydrogen atoms omitted for clarity)[a]

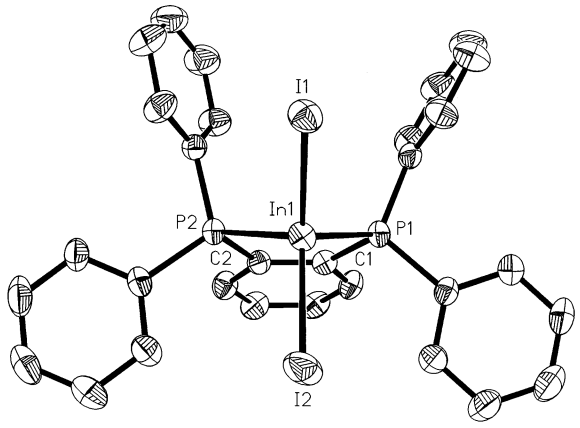

[a] Selected bond lengths [Å] and angles [°]: In1−I1 2.6644(6), In1−I2 2.6497(5), In1−P1 2.5862(11), In1−P2 2.5635(11); I1−In1−I2 118.12(2), I1−In1−P1 116.22(3), I1−In1−P2 113.78(3), I2−In1−P1 111.02(3), I2−In1−P2 110.47(3), P1−In1−P2 81.61(4).

Figure 7. Molecular structure of the cation in **7** with atomic numbering (ORTEP drawing, 50% probability ellipsoids, hydrogen atoms omitted for clarity)[a]

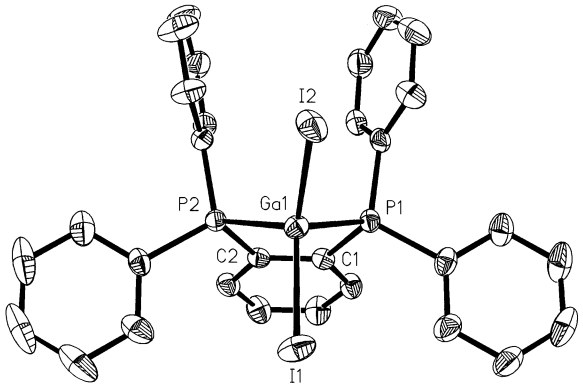

[a] Selected bond lengths [Å] and angles [°]: Ga1−I1 2.4904(6), Ga1−I2 2.4912(7), Ga1−P1 2.3976(13), Ga1−P2 2.4085(12); I1−Ga1−I2 115.02(2), I1−Ga1−P1 110.84(4), I1−Ga1−P2 110.05(4), I2−Ga1−P1 112.64(4), I2−Ga1−P2 119.90(4), P1−Ga1−P2 84.49(4).

113.11(3)° for In and 103.43(3)/113.71(5)° for Ga, respectively (Figures 8 and 9). Deviations from the regular tetrahedral angle are thus very small and not indicative of *tri*-podal action of the ligand. Bond lengths M−I and M−P are also similar to those in the DP complexes (above).

Closer inspection of the structural diagrams shows, however, that the distance In1−P3 [2.8933(10) Å] in the indium compound is not that much larger (about 10%) than the distances In−P1 [2.6239(10) Å] and In1−P2 [2.5982(10) Å]. This observation suggests that coordinative bonding of the middle phosphorus atom (P3) of the TP ligand to In1 cannot a priori be ruled out. In fact, the rather rigid geometry of the ligand leaves no choice and virtually forces the third phosphorus atom into the bonding region of the metal atom.

Figure 8. Molecular structure of the cation in **8** with atomic numbering (ORTEP drawing, 50% probability ellipsoids, hydrogen atoms omitted for clarity)[a]

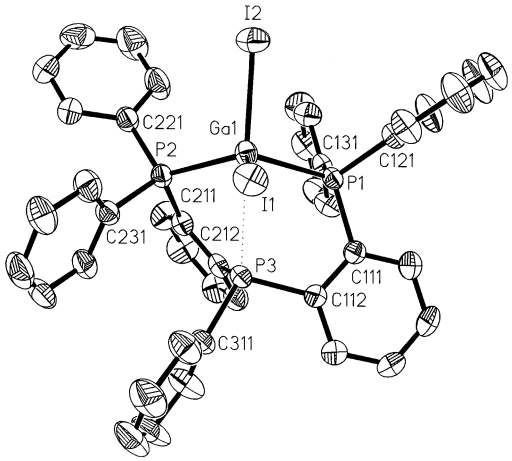

[a] Selected bond lengths [Å] and angles [°]: Ga1−I1 2.5473(8), Ga1−I2 2.5818(8), Ga1−P1 2.435(2), Ga1−P2 2.420(2), Ga1−P3 2.905(2); I1−Ga1−I2 103.43(3), I1−Ga1−P1 113.05(4), I1−Ga1−P2 118.84(4), I2−Ga1−P1 100.36(4), I2−Ga1−P2 104.55(4), P1−Ga1−P2 113.71(5), Ga1−P3−C112 103.3(3), Ga1−P3−C212 96.6(2), Ga1−P3−C311 137.2(3).

Figure 9. Molecular structure of the cation in **9** with atomic numbering (ORTEP drawing, 50% probability ellipsoids, hydrogen atoms omitted for clarity)[a]

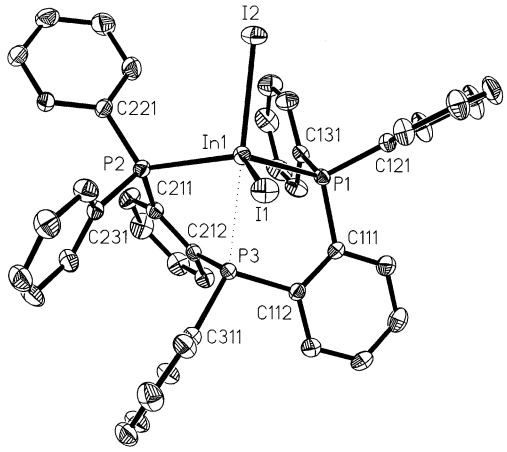

[a] Selected bond lengths [Å] and angles [°]: In1−I1 2.7092(5), In1−I2 2.7376(5), In1−P1 2.6239(10), In1−P2 2.5982(10), In1−P3 2.8933(10); I1−In1−I2 103.02(2), I1−In1−P1 115.35(2), I1−In1−P2 119.96(2), I2−In1−P1 98.19(2), I2−In1−P2 102.94(2), P1−In1−P2 113.11(3), In1−P3−C112 106.13(12), In1−P3−C212 98.36(12), In1−P3−C311 132.91(13).

A simple geometrical calculation of the orientation of the lone pair of electrons at P3 (taking this atom as a pseudo-tetrahedral center) leads to the conclusion, however, that this vector is not pointing towards the metal atom, but into a direction where In1−P3 interaction is rather poor. This is e.g. borne out by the large spread of the angles from In1−P3−C212 = 98.36(12)° and In1−P3−C112 = 106.13(12)° to In1−P3−C311 = 132.91(13)°. The difference of the In−I distances in the cation and the anion of **9** are surprisingly small (only a few percent).

Table 1. Crystal data, data collection, and structure refinement for compounds **1**, **3**·2 $CHCl_3$, and **5**·CH_2Cl_2

	1	**3**·2 $CHCl_3$	**5**·CH_2Cl_2
crystal data			
formula	$C_{60}H_{48}Cl_6In_2P_4$	$C_{32}H_{26}Cl_6I_3InP_2$	$C_{31}H_{26}Cl_2I_6In_2P_2$
M_r	1335.20	1180.69	1522.40
crystal system	triclinic	triclinic	triclinic
space group	$P\bar{1}$	$P\bar{1}$	$P\bar{1}$
a [Å]	11.146(1)	9.651(1)	10.611(1)
b [Å]	13.514(1)	12.455(1)	13.103(1)
c [Å]	20.782(1)	17.311(1)	17.522(1)
α [°]	77.48(1)	107.97(1)	68.94(1)
β [°]	81.98(1)	90.35(1)	75.58(1)
γ [°]	70.99(1)	99.00(1)	69.76(1)
V [Å^3]	2881.2(4)	1951.7(3)	2121.3(3)
$\rho_{calcd.}$ [gcm^{-3}]	1.539	2.009	2.383
Z	2	2	2
$F(000)$	1336	1116	1384
μ(Mo-K_α) [cm^{-1}]	12.28	34.94	56.75
absorption corr.	ψ scans	ψ scans	ψ scans
T_{min}/T_{max}	0.96/0.99	0.74/0.99	0.70/0.99
data collection			
T [°C]	−74	−74	−74
scan mode	ω	ω-Θ	ω
hkl range	−13→14, −17→15, −25→26	−12→12, −15→15, 0→22	−12→13, 0→16, −20→22
$\sin(\theta/\lambda)_{max}$ [Å^{-1}]	0.64	0.64	0.64
measured refl.	16992	8232	8800
refls. used for refinement	12467	8199	8766
solution	direct methods	Patterson	Patterson
refinement			
refined parameters	652	397	388
H atoms (found/calcd.)	0/48	0/26	0/26
final R values [$I > 2\sigma(I)$]			
$R1$[a]	0.0249	0.0277	0.0305
$wR2$[b]	0.0571	0.0689	0.0717
$GOOF$	1.073	1.092	1.131
$(\text{shift/error})_{max}$	<0.001	<0.001	<0.001
ρ_{fin}(max/min) [eÅ^{-3}]	0.865/−0.610	2.738/−1.809[c]	1.294/−1.782

[a] $R1 = \Sigma(||F_o|-|F_c||)/\Sigma|F_o|$. − [b] $wR2 = \{[\Sigma w(F_o^2-F_c^2)^2]/\Sigma[w(F_o^2)^2]\}^{1/2}$; $w = 1/[\sigma^2(F_o^2)+(ap)^2+bp]$; $p = (F_o^2+2F_c^2)/3$; a = 0.0210 (**1**), 0.0322 (**3**·2 $CHCl_3$), 0.0303 (**5**·CH_2Cl_2); b = 2.62 (**1**), 5.04 (**3**·2 $CHCl_3$), 6.60 (**5**·CH_2Cl_2). − [c] Residual electron densities located around solvent $CHCl_3$.

Table 2. Crystal data, data collection, and structure refinement for compounds **7**, **8**, and **9**

	7	**8**	**9**
crystal data			
formula	$C_{30}H_{24}Ga_2I_6P_2$	$C_{42}H_{33}Ga_2I_6P_3$	$C_{42}H_{33}I_6In_2P_3$
M_r	1347.27	1531.43	1621.63
crystal system	triclinic	triclinic	triclinic
space group	$P\bar{1}$	$P\bar{1}$	$P\bar{1}$
a [Å]	10.832(1)	10.432(1)	10.435(1)
b [Å]	11.107(1)	14.676(1)	14.583(1)
c [Å]	16.929(1)	16.260(2)	16.394(2)
α [°]	89.93(1)	82.04(1)	80.96(1)
β [°]	72.36(1)	79.48(1)	79.17(1)
γ [°]	88.24(1)	81.35(1)	82.02(1)
V [Å^3]	1940.0(3)	2403.9(4)	2404.5(4)
$\rho_{calcd.}$ [gcm^{-3}]	2.306	2.116	2.240
Z	2	2	2
$F(000)$	1228	1420	1492
μ(Mo-K_α) [cm^{-1}]	62.64	51.01	49.39
absorption correction	ψ-scans	ψ-scans	ψ-scans
T_{min}/T_{max}	0.52/0.99	0.70/0.99	0.63/0.99
data collection			
T [°C]	−74	+23	−74
scan mode	ω	ω-Θ	ω-Θ
hkl range	−13→12, −13→13, −17→0	0→12, −17→18, −19→19	−12→13, −18→18, 0→20
$\sin(\theta/\lambda)_{max}$ [Å^{-1}]	0.62	0.62	0.64
measured reflections	6984	8648	10144
refls. used for refinement	6973	8624	10089
solution	direct methods	solution of **9** was used	Patterson
refinement			
refined parameters	361	478	478
H atoms (found/calcd.)	0/24	0/33	0/33
final R values [$I > 2\sigma(I)$]			
$R1$[a]	0.0304	0.0433	0.0279
$wR2$[b]	0.0739	0.1072	0.0671
$GOOF$	1.089	1.083	1.203
$(\text{shift/error})_{max}$	< 0.001	< 0.001	< 0.001
ρ_{fin}(max/min) [eÅ^{-3}]	3.368/−1.927[c]	3.125/−2.012[c]	1.082/−1.585[c]

[a] $R1 = \Sigma(||F_o|-|F_c||)/\Sigma|F_o|$. − [b] $wR2 = \{[\Sigma w(F_o^2-F_c^2)^2]/\Sigma[w(F_o^2)^2]\}^{1/2}$; $w = 1/[\sigma^2(F_o^2)+(ap)^2+bp]$; $p = (F_o^2+2F_c^2)/3$; a = 0.0316 (**7**), 0.0600 (**8**), 0.0296 (**9**); b = 8.92 (**7**), 7.93 (**8**), 5.43 (**9**). − [c] Residual electron densities located around iodine atoms.

The situation is very similar in the structure of the gallium analog **8**, where the distance Ga1−P3 is 2.905(2) Å and thus almost equal to In1−P3 (above), but much larger as compared to Ga1−P1 [2.435(2) Å] and Ga1−P2 [2.420(2) Å]. The angles Ga1−P3−C112/ C212/C311 vary over a range of 40°, with individual values of 103.3(3)/ 96.6(2)/137.2(3)°, respectively, and are not in agreement with tetrahedral coordination of the phosphorus atom P3.

From the structural data it thus appears that neither the indium nor the gallium atom in the $[(TP)MI_2]^+$ cations of **8** and **9** (M = In, Ga) is pentacoordinated by the two halogen atoms and the potentially tripodal ligand. Although the inflexibility of the TP ligand holds the central phosphorus atom in close proximity of the metal atom, the bonding interaction is poor in spite of the sub-van-der-Waals distance of only ca. 2.90 Å. It is gratifying that this result is in full agreement with the essence of the NMR data regarding in particular the line widths and the coupling pattern of the ^{31}P-NMR resonances, although the chemical-shift parameters are much more difficult to evaluate. More comprehensive data sets are clearly needed in order to allow a deeper understanding of the chemical-shift increments responsible for non-classical signal displacements in the NMR spectra of main-group metal complexes.

This work was supported by the *Deutsche Forschungsgemeinschaft* and the *Fonds der Chemischen Industrie*. The authors are grateful to Mr. *J. Riede* for establishing the X-ray data sets.

Experimental Section

General: All experiments were carried out routinely in purified dry nitrogen. Solvents were dried and kept under nitrogen, and glassware was oven-dried and filled with nitrogen. 1,2-Bis(diphenylphosphanyl)benzene[10] and bis[(2-diphenylphosphanyl)phenyl]-phenylphosphane[9a] were prepared according to literature procedures, all other starting materials were commercially available. Gallium and indium trihalides were stored and handled in a glove box.

[1,2-Bis(diphenylphosphanyl)benzene]$_2$InCl$_2^+$ InCl$_4^-$ (**1**): Indium trichloride (99 mg, 0.45 mmol) is added to a solution of 1,2-bis(diphenylphosphanyl)benzene (202 mg, 0.45 mmol) in 10 ml of toluene and stirred for 2 h at 80°C. The white precipitate is collected and recrystallized from chloroform/pentane. Yield 273 mg (91%), colorless crystals, m.p. 243°C. – ^{1}H NMR ($CDCl_3$, 20°C): δ = 7.78–7.11 (m, Ph). – ^{13}C{^{1}H} NMR (v. s.): δ = 128.8, 132.1, 135.3 (AXX′, phenylene); 125.8, 129.2, 131.6, 134.2 (AXX′, Ph). – ^{31}P{^{1}H} NMR (v. s.): δ = −26.6 (br. s). – $C_{60}H_{48}Cl_6In_2P_4$ (1335.30): calcd. C 53.97, H 3.62; found C 53.31, H 3.65.

[1,2-Bis(diphenylphosphanyl)benzene]InBr$_3$ (**2**): As described for compound **1**, with indium tribromide (95 mg, 0.268 mmol) and 1,2-bis(diphenylphosphanyl)benzene (120 mg, 0.268 mmol). Yield 191 mg (89%), colorless crystals, m.p. 268°C. – ^{1}H NMR ($CDCl_3$, 20°C): δ = 7.74–7.09 (m, Ph). – ^{13}C{^{1}H} NMR (v. s.): δ = 131.9, 135.2, 135.4 (AXX′, phenylene); 126.3, 129.1, 131.4, 134.3 (AXX′, Ph). – ^{31}P{^{1}H} NMR (v. s.): δ = −26.9 (br. s). – $C_{30}H_{24}Br_3InP_2$ (801.00): calcd. C 44.99, H 3.02; found C 44.53, H 3.05.

[1,2-Bis(diphenylphosphanyl)benzene]InI$_3$ (**3**): As described for compound **1**, with indium triiodide (126 mg, 0.255 mmol) and 1,2-bis(diphenylphosphanyl)benzene (114 mg, 0.255 mmol). Yield 180 mg (75%), colorless crystals, m.p. 239°C. – ^{1}H NMR ($CDCl_3$, 20°C): δ = 7.65–7.12 (m, Ph). – ^{13}C{^{1}H} NMR (v. s.): δ = 131.7, 135.4, 135.8 (AXX′, phenylene); 127.1, 129.0, 131.1, 134.2 (AXX′, Ph). – ^{31}P{^{1}H} NMR (v. s.): δ = −31.7 (br. s). – $C_{30}H_{24}I_3InP_2$ (942.00): calcd. C 38.25, H 2.57; found C 37.63, H 2.81.

[1,2-Bis(diphenylphosphanyl)benzene]InBr$_2^+$ InBr$_4^-$ (**4**): As described for compound **1**, with indium tribromide (190 mg, 0.536 mmol) and 1,2-bis(diphenylphosphanyl)benzene (120 mg, 0.268 mmol). Yield 293 mg (95%), colorless crystals, m.p. 251°C. – ^{1}H NMR ($CDCl_3$, 20°C): δ = 7.94–7.30 (m, Ph). – ^{13}C{^{1}H} NMR (v. s.): δ = 131.6, 134.9, 136.8 (AXX′, phenylene); 121.3, 130.5, 133.9, 134.2 (AXX′, Ph). – ^{31}P{^{1}H} NMR (v. s.): δ = −20.0 (br. s). – $C_{30}H_{24}Br_6In_2P_2$ (1155.53): calcd. C 31.18, H 2.09; found C 30.89, H 2.02.

[1,2-Bis(diphenylphosphanyl)benzene]InI$_2^+$ InI$_4^-$ (**5**): As described for compound **1**, with indium triiodide (394 mg, 0.795 mmol) and 1,2-bis(diphenylphosphanyl)benzene (178 mg, 0.40 mmol). Yield 495 mg (87%), colorless crystals, m.p. 199°C. – ^{1}H NMR ($CDCl_3$, 20°C): δ = 8.02–7.28 (m, Ph). – ^{13}C{^{1}H} NMR (v. s.): δ = 131.2, 135.2, 136.9 (AXX′, phenylene); 120.9, 130.4, 133.8, 134.1 (AXX′, Ph). – ^{31}P{^{1}H} NMR (v. s.): δ = −27.9 (br. s). – $C_{30}H_{24}I_6In_2P_2$ (1437.53): calcd. C 25.07, H 1.68; found C 25.20, H 1.73.

[1,2-Bis(diphenylphosphanyl)benzene]GaBr$_2^+$ GaBr$_4^-$ (**6**): As described for compound **1**, with gallium tribromide (151 mg, 0.448 mmol) and 1,2-bis(diphenylphosphanyl)benzene (109 mg, 0.224 mmol). Yield 210 mg (81%), colorless crystals, m.p. 259°C. – ^{1}H NMR ($CDCl_3$, 20°C): δ = 7.76–7.14 (m, Ph). – ^{13}C{^{1}H} NMR (v. s.): δ = 133.9, 135.9, 136.9 (AXX′, phenylene); 119.0, 130.6, 134.2, 134.5 (AXX′, Ph). – ^{31}P{^{1}H} NMR (v. s.): δ = −22.1 (br. s). – $C_{30}H_{24}Br_6Ga_2P_2$ (1065.33): calcd. C 33.82, H 2.27; found C 33.48, H 2.14.

[1,2-Bis(diphenylphosphanyl)benzene]GaI$_2^+$ GaI$_4^-$ (**7**): As described for compound **1**, with gallium triiodide (201 mg, 0.446 mmol) and 1,2-bis(diphenylphosphanyl)benzene (100 mg, 0.223 mmol). Yield 285 mg (95%), colorless crystals, m.p. 219°C. – ^{1}H NMR ($CDCl_3$, 20°C): δ = 8.02–7.28 (m, Ph). – ^{13}C{^{1}H} NMR (v. s.): δ = 131.2, 135.2, 136.9 (AXX′, phenylene); 120.9, 130.4, 133.8, 134.1 (AXX′, Ph). – ^{31}P{^{1}H} NMR (v. s.): δ = −29.3 (br. s). – $C_{30}H_{24}I_6Ga_2P_2$ (1347.33): calcd. C 26.74, H 1.80; found C 26.48, H 1.75.

{Bis[(2-diphenylphosphanyl)phenyl]phenylphosphane}GaI$_2^+$-GaI$_4^-$ (**8**): As described for compound **1**, with gallium triiodide (219 mg, 0.485 mmol) and bis[(2-diphenylphosphanyl)phenyl]phenylphosphane (153 mg, 0.243 mmol). Recrystallization of the white precipitate from methylene chloride/pentane yielded 309 mg (83%) of colorless crystals, m.p. 267°C. – ^{31}P{^{1}H} NMR (CD_2Cl_2, 20°C): δ = −33 (A_2B, J = 213 Hz, $P^{cent.}$), −25 (A_2B, $P^{term.}$). – $C_{42}H_{33}Ga_2I_6P_3$ (1531.51): calcd. C 32.94, H 2.17; found C 32.58, H 2.09.

{Bis[(2-diphenylphosphanyl)phenyl]phenylphosphane}InI$_2^+$-InI$_4^-$ (**9**): As described for compound **8**, with indium triiodide (253 mg, 0.511 mmol) and bis[(2-diphenylphosphanyl)phenyl]phenylphosphane (161 mg, 0.255 mmol). Yield 364 mg (88%), colorless crystals, m.p. 259°C. – ^{31}P{^{1}H} NMR (CD_2Cl_2, 20°C): δ = −45 (A_2B, J = 282 Hz, $P^{cent.}$), −26 (A_2B, $P^{term.}$). – $C_{42}H_{33}Ga_2I_6P_3$ (1621.71): calcd. C 31.11, H 2.05; found C 30.78, H 2.04.

Reactions of **4** *and* **5** *with Oxygen Donors:* [(DP)$InBr_2$]$^+$ [$InBr_4$]$^-$ (**4**, 100 mg, 0.086 mmol) is dissolved in 5 ml of THF and layered with pentane. The colorless crystals obtained show the same analytical data (mp, EA, NMR) as compound **2**. [(DP)InI_2]$^+$[InI_4]$^-$ (**5**, 100 mg, 0.069 mmol) is dissolved in 10 ml of $CHCl_3$ and 0.1 ml of acetone is added. After heating to reflux, a colorless solid is precipitated with pentane. The product shows the same analytical data as compound **3**. Similar results are obtained with $OPPh_3$ (50 mg, 0.18 mmol).

Crystal Structure Determinations: Specimens of suitable quality and size of compounds **1**, **3**·2 $CHCl_3$, **5**·CH_2Cl_2, **7**, **8**, and **9** were mounted in glass capillaries and used for measurements of precise cell constants and intensity-data collection on an Enraf Nonius CAD4 diffractometer [Mo-K_α radiation, λ(Mo-K_α) = 0.71073 Å]. During data collection, three standard reflections were measured periodically as a general check of crystal and instrument stability. No significant changes were observed for either compound. Lp correction was applied and intensity data were corrected for absorption effects. The structures were solved by direct and Patterson methods (SHELXS-86), respectively, and completed by full-matrix least-squares techniques against F^2 (SHELXL-93). The thermal motion of all non-hydrogen atoms was treated anisotropically. All hydrogen atoms were placed in idealized calculated positions and allowed to ride on their corresponding carbon atoms with fixed isotropic contributions ($U_{iso(fix)}$ = 1.5 × U_{eq} of the attached C atom). Further information on crystal data, data collection, and structure refinement are summarized in Tables 1 and 2. Important interatomic distances and angles are shown in the corresponding figure captions. Anisotropic thermal parameters, tables of distances and angles, and atomic coordinates have been deposited with Fachinformationszentrum Karlsruhe, Gesellschaft für wissenschaftlich-technische Information mbH, D-76344 Eggenstein-Leopoldshafen. The data are available on request on quoting CSD-407907 (**1**), -407908 (**3**), -407905 (**5**), -407906 (**7**), -407904 (**8**), -407903 (**9**).

[1] [1a] L. A. Paquette in *Encyclopedia of Reagents for Organic Synthesis*, Wiley & Sons, New York, **1995**, 153−160 and 645−674. − [1b] W. Carruthers in *Cycloaddition Reactions in Organic Synthesis*, Pergamon Press, Oxford, **1990**, 50−54. − [1c] G. A. Olah in *Friedel-Crafts Chemistry*, Wiley & Sons, New York, **1972**, 215−392.

[2] J. A. Miller in *Chemistry of Aluminium, Gallium, Indium and Thallium*, A. J. Downs (Ed.), Chapman & Hall, London, **1993**, 372−429.

[3] [3a] T.-P. Loh, J. Pei, G.-Q. Cao, *J. Chem. Soc., Chem. Commun*. **1996**, 1819−1820. − [3b] T.-P. Loh, J. Pei, M. Lin, *J. Chem. Soc., Chem. Commun*. **1996**, 2315−2316.

[4] [4a] H. Schmidbaur, W. Findeiß, *Chem. Ber.* **1966**, *99*, 2187−2191. − [4b] M. G. Woronkow, S. V. Basenko, M. V. Ustinov, *Zh. Obshch. Khim.* **1995**, *65*, 1482−1486.

[5] [5a] D. G. Tuck in *Chemistry of Aluminium, Gallium, Indium, and Thallium*, A. J. Downs (Ed.), Chapman & Hall, London, **1993**, 430−473. − [5b] D. G. Tuck in *Comprehensive Coordination Chemistry*, G. Wilkinson, R. D. Gillard, J. A. McCleverty (Eds.), Pergamon Press, Oxford, **1987**, vol. 3, 126−167. − [5c] D. G. Tuck in *Comprehensive Organometallic Chemistry*, G. Wilkinson, F. G. A. Stone, E. W. Abel (Eds.), Pergamon Press, Oxford, **1982**, vol. 1, 683−723. − [5d] A. J. Carty, D. G. Tuck in *Progress in Inorganic Chemistry*, S. J. Lippard (Ed.), Wiley & Sons, New York, **1975**, vol. 19, 243−337.

[6] [6a] J. A. Jegier, D. A. Atwood, *Inorg. Chem*. **1997**, *36*, 2034−2039. − [6b] J. A. Jegier, D. A. Atwood, *Inorg. Chem*. **1996**, *35*, 4277−4282. − [6c] T. Aida, S. Inoue, *Acc. Chem. Res.* **1996**, *29*, 39−48. − [6d] Y. Hayashi, J. J. Rohde, E. J. Corey, *J. Am. Chem. Soc*. **1996**, *118*, 5502−5503.

[7] [7a] W. T. Robinson, C. J. Wilkins, Z. Zeying, *J. Chem. Soc., Dalton Trans.* **1990**, 219−227. − [7b] M. A. Malyarick, A. B. Ilyuhin, S. P. Petrosyants, *Polyhedron* **1993**, *12*, 2403−2409. − [7c] F. B. W. Einstein, D. G. Tuck, *J. Chem. Soc., Chem. Commun*. **1970**, 1182−1183. − [7d] J. A. C. Clyburne, R. D. Culp, S. Kamepalli, A. H. Cowley, A. Decken, *Inorg. Chem*. **1996**, *35*, 6651−6655. − [7e] L. A. Kloo, M. J. Taylor, *J. Chem. Soc., Dalton Trans.* **1997**, 2693−2696. − [7f] R. Restivo, G. J. Palenik, *J. Chem. Soc., Dalton Trans.* **1972**, 341−344. − [7g] I. Sinclair, R. W. H. Small, I. J. Worrall, *Acta Crystallogr.* **1981**, *B37*, 1290−1292. − [7h] F. Kratz, B. Nuber, J. Weiss, B. K. Keppler, *Polyhedron* **1992**, *11*, 487−498. − [7i] S. Bock, H. Noth, A. Wietelmann, *Z. Naturforsch*. **1990**, *B45*, 979−984.

[8] [8a] M. A. Brown, J. A. Castro, D. G. Tuck, *Can. J. Chem*. **1997**, *75*, 333−341. − [8b] M. A. Brown, E. J. Wells, D. G. Tuck, *Can. J. Chem*. **1996**, *74*, 1535−1549. − [8c] I. A. Degnan, N. W. Alcock, S. M. Roe, M. G. H. Wallbridge, *Acta Crystallogr.* **1992**, *C48*, 995−999. − [8d] A. J. Carty, *Can. J. Chem*. **1967**, *45*, 345−351. − [8e] A. J. Carty, *Can. J. Chem*. **1967**, *45*, 3187−3192. − [8f] U. Flörke, H.-J. Haupt, *Z. Kristallogr.* **1991**, *196*, 299−301. − [8g] R. L. Wells, S. R. Aubuchon, S. S. Kher, M. S. Lube, P. S. White, *Chem. Mater*. **1995**, *7*, 793−800. − [8h] M. V. Veidis, G. J. Palenik, *J. Chem. Soc., Chem. Commun*. **1969**, 586−587. − [8i] W. Clegg, N. C. Norman, N. L. Pickett, *Acta Crystallogr.* **1994**, *C50*, 36−38. − [8j] N. W. Alcock, I. A. Degnan, O. W. Howarth, M. G. H. Wallbridge, *J. Chem. Soc., Dalton Trans.* **1992**, 2775−2780.

[9] [9a] J. G. Hartley, L. M. Venanzi, D. C. Goodall, *J. Chem. Soc*. **1963**, 3930−3936. − [9b] B. Chiswell, L. M. Venanzi, *J. Chem. Soc. (A)* **1966**, 417−419. − [9c] R. J. Mynott, P. S. Pregosin, L. M. Venanzi, *J. Coord. Chem*. **1973**, *3*, 145−148. − [9d] M. Sigl, A. Schier, H. Schmidbaur, *Chem. Ber*. **1997**, *130*, 1411−1416.

[10] G. A. Bowmaker, R. Herr, H. Schmidbaur, *Chem. Ber*. **1983**, *116*, 3567−3579.

[97207]

2-Oxacyclopentylidene, 2-Oxacyclohexylidene, and 2-Oxacycloheptylidene Rhenium Complexes by Reaction of ω-Alkynols with the $[\{MeC(CH_2PPh_2)_3\}Re(CO)_2]^+$ Auxiliary

Claudio Bianchini*[a], Andrea Marchi[b], Nicoletta Mantovani[b], Lorenza Marvelli[b], Dante Masi[a], Maurizio Peruzzini*[a], and Roberto Rossi*[b]

Istituto per lo Studio della Stereochimica ed Energetica dei Composti di Coordinazione, CNR[a], Via J. Nardi 39, 50132 Firenze, Italy

Laboratorio di Chimica Nucleare ed Inorganica, Dipartimento di Chimica, Università di Ferrara[b], Via Borsari 46, 44100 Ferrara, Italy

Received September 29, 1997

Keywords: Rhenium / Oxacyclocarbene complexes / Vinylidene complexes / Alkynols / Tripodal ligands

Various β-, γ-, and δ-alkynols have been reacted with the 16e$^-$ fragment $[(triphos)Re(CO)_2]^+$ generated in situ by H_2 elimination from $[(triphos)Re(CO)_2(\eta^2\text{-}H_2)]BF_4$ [triphos = $MeC(CH_2PPh_2)_3$]. Irrespective of the length of the alkyl chain between the C≡C and OH functional groups in the ω-alkynol, 2-oxacyclocarbene complexes are obtained. These include the 2-oxacyclopentylidene derivatives $[(triphos)Re(CO)_2\{=CCH_2CH_2CH_2O\}]BF_4$ and $[(triphos)Re(CO)_2\{=CCH_2CH_2CH(Me)O\}]BF_4$, the 2-oxacyclohexylidene derivatives $[(triphos)Re(CO)_2\{=CCH_2CH_2CH_2CH_2O\}]BF_4$ and $[(triphos)Re(CO)_2\{=CCH_2CH_2CH_2CH(Me)O\}]BF_4$, and the 2-oxacycloheptylidene complex $[(triphos)Re(CO)_2\{=CCH_2CH_2CH_2CH_2CH_2O\}]BF_4$. The latter compound contains a unprecedented seven-membered oxacarbene ring. The rhenium-assisted δ-alkynol to 2-oxacyloheptylidene rearrangement proceeds via the hydroxybutylvinylidene kinetic intermediate $[(triphos)Re(CO)_2\{C=C(H)CH_2CH_2CH_2CH_2OH\}]BF_4$, which has been characterized in both the solid state and solution. An X-ray analysis has been carried out on a single crystal of $[(triphos)Re(CO)_2\{=CCH_2CH_2CH(Me)O\}]BF_4$. The structure of this complex consists of $[(triphos)Re(CO)_2\{=CCH_2CH_2CH(Me)O\}]^+$ cations and tetrafluoroborate anions with no interspersed solvent molecules. A *facial* triphos ligand, two *cis*-disposed carbonyl groups and a 2-oxacyclopentylidene ligand coordinate the Re centre in a slightly distorted octahedral environment.

Introduction

The reaction of alkynols with unsaturated metal fragments provides a convenient synthetic route to 2-oxacyclocarbene complexes,[1] that are receiving increasing attention as organometallic synthons in several catalytic and stoichiometric elaborations.[2][3] The most widely studied of these, are the reactions of β-alkynols to give 2-oxacyclopentylidene derivatives, and various complexes with ruthenium,[4][5][6][7] osmium,[8] manganese,[9] rhenium,[9a] and metals of the chromium group[1][10] have recently been described. The β-alkynol to oxacyclocarbene rearrangement has been shown to proceed via preliminary metal-assisted 1-alkyne to vinylidene tautomerization.[1][10b][11] For β-alkynols, the formation of cyclic Fischer carbene implies the generation of hydroxyethylvinylidene derivatives (**I**), which have been intercepted spectroscopically in a few cases (Scheme 1).[5] Vinylidenes are highly polarized C_2 ligands and both experimental[12][13] and theoretical studies[14] show the C_α atom to be an electrophilic centre susceptible to attack by almost any sort of nucleophile (alcohols, water, amines, thiols, phosphanes, etc.).[12] In case of β-hydroxyethylvinylidene ligands, the oxacarbene ring forms via intramolecular attack by the OH group of the dangling hydroxyalkyl substituent at the C_α atom. When this happens it is implicit that the ring-closure reaction affording the Fischer carbene (**II**) is favored over the equally possible elimination of water to give the vinylvinylidene derivative (**III**).[15]

Scheme 1. Reactions of 3-butyn-1-ol with metal-ligand systems

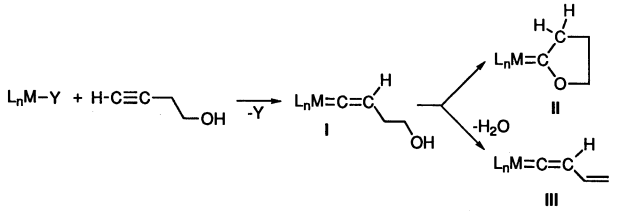

It has been observed experimentally that the intramolecular attack by the hydroxy group is increasingly disfavored as the number of CH_2 spacers between the triple bond and the OH group in the alkynol increases. Indeed, 2-oxacyclohexylidene complexes derived from metal-assisted rearrangements of γ-alkynols are quite rare compounds,[1][8a][10b] while no example involving δ-alkynols has yet been reported.[16][17] In actuality, δ-alkynols are still reactive substrates towards transition metal fragments. Due to the length of the pendant hydroxyalkyl tail, however, their activation results in the preferential formation of stable hydroxybutylvinylidene complexes.[8][18] In no case was the hydroxybutylvinylidene intermediate seen to convert to the 2-oxacycloheptylidene isomer.

 © WILEY-VCH Verlag GmbH, D-69451 Weinheim, 1998 1434–1948/98/0202–0211 $ 17.50+.50/0

Stimulated by the idea that a comparative study involving the reaction of a unique metal fragment with different ω-alkynols could have provided additional information on the mechanism of formation of 2-oxacarbene complexes as well as their chemistry, we decided to examine the reactions of various β-, γ-, and δ-alkynols with the kinetically inert organometallic support $[\{MeC(CH_2PPh_2)_3\}Re(CO)_2]^+$.[19] We were gratified to find that Fischer carbene complexes are selectively formed, via kinetic hydroxyvinylidene intermediates, irrespective of the number of CH_2 spacers. The hydroxyvinylidene complex has exclusively been intercepted with the δ-alkynol 5-hexyn-1-ol and its conversion to the thermodynamic 2-oxacycloheptylidene product has been studied.

Results and Discussion

The preparations and principal reactions reported in this article are summarized in Scheme 2. Selected spectroscopic data (IR and NMR) are collected in Table 1, or are provided in the Experimental Section. The total and unambiguous assignment of all the hydrogen and carbon resonances for all rhenium complexes was obtained by a combination of 1D- and 2D-NMR spectroscopy including $^1H\{^{31}P\}$, DEPT-135, $^1H,^1H$-COSY, $^1H,^1H$-NOESY, and $^1H,^{13}C$-HETCOR experiments.

Scheme 2. Reactions of $[(triphos)Re(CO)_2]^+$ auxiliary with ω-alkynols

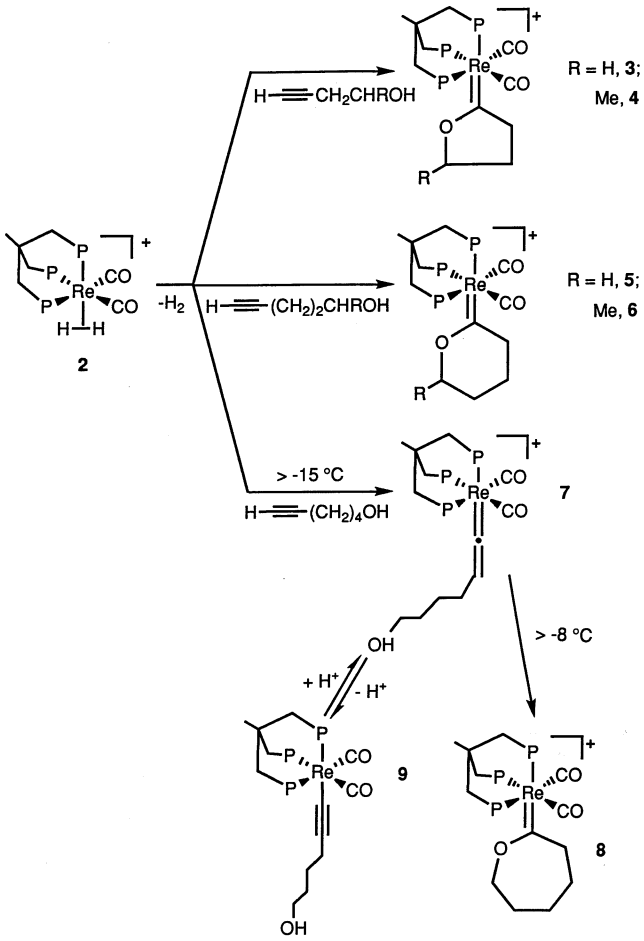

Synthesis and Characterization of 2-Oxacycloalkylidene Complexes: In earlier work,[19] we have shown that [(triphos)Re(CO)$_2$H] (**1**) reacts with $HBF_4\cdot OMe_2$ in CH_2Cl_2 to give $[(triphos)Re(CO)_2(\eta^2\text{-}H_2)]BF_4$ (**2**) which contains a weakly bound dihydrogen ligand.[19] We have now found that **2** in CH_2Cl_2 reacts with 3-butyn-1-ol yielding the 2-oxacyclopentylidene complex $[(triphos)Re(CO)_2\{=CCH_2\text{-}CH_2CH_2O\}]BF_4$ (**3**). The selective formation of this Fischer carbene complex takes place already at −10°C, and proceeds with no detectable intermediate on the NMR timescale. The room-temperature $^{31}P\{^1H\}$-NMR spectrum consists of an AM_2 pattern with chemical shifts and coupling constants in line with those reported for other cationic carbene complexes of the general formula $[(triphos)Re(CO)_2\{CRR'\}]Y$.[20] The magnetic equivalence of the two phosphorus atoms lying *trans* to the two carbonyl ligands is consistent with a rapid rotation of the oxacyclopentylidene group about the Re=C bond. The oxacarbene ligand continues to rotate freely even at −80°C. A very low-energy barrier to rotation is typical of carbene and vinylidene groups bonded to the $[(triphos)Re(CO)_2]^+$ fragment,[19][20] and it is also commonly encountered in carbene complexes with other transition metals.[9b][21] The most direct spectroscopic evidence of the presence of a carbene ligand in **3** is provided by the $^{13}C\{^1H\}$-NMR spectrum which contains a doublet of triplets centred at δ = 293.4 ($J_{CPtrans}$ = 35.0 Hz, J_{CPcis} = 8.9 Hz).[12][13] The other oxacyclopentylidene carbon atoms resonate at δ = 85.3, 62.7, and 22.8, consistent with this type of ligand, while the two carbonyl carbon atoms appear as a second-order multiplet at δ = 197.0. This may properly be computed using an AXX′Y spin system (A: carbonyl C atom, X and X′: P atoms *trans* to the CO ligands, Y: P atom *trans* to the carbene ligand; see Table 1).[19][20][22] The proton NMR spectrum correlates well with the spectra of various 2-oxacyclocarbene metal complexes containing three methylene groups in the ring.[4] A cyclic oxacarbene ligand in **3** is finally supported by the IR spectrum displaying a medium intensity ν(COC) band at 1194 cm^{-1} and two strong ν(CO) absorptions at wavenumbers (1962 and 1912 cm^{-1}) that are typical of $[(triphos)Re(CO)_2\{=CRR'\}]Y$ carbene compounds.[20]

Replacing 3-butyn-1-ol with (±)-4-pentyn-2-ol in the reaction with **2** affords the substituted 2-oxa-3-methyl-cyclopentylidene complex $[(triphos)Re(CO)_2\{=CCH_2CH_2CH\text{-}(Me)O\}]BF_4$ (**4**) as air-stable orange crystals. As expected, the presence of a stereogenic carbon atom in the oxacarbene ring differentiates the spectroscopic characteristics of **4** from those of **3**. For example, the $^{31}P\{^1H\}$-NMR spectrum of **4** consists of an AMQ spin system, while the carbonyl carbons appear in the $^{13}C\{^1H\}$-NMR spectrum as a well-resolved doublet of triplets (δ = 198.6, $J_{CPtrans}$ = 45.5 Hz, J_{CPcis} = 5.7 Hz). The stereocenter in the 2-oxacyclopentylidene ring also leads to the chemical and magnetic nonequivalence of the methylene protons. For this reason, the resonances of the oxacarbene-ring protons could only be unambiguously assigned by means of 2D-COSY and 2D-phase sensitive NOESY NMR spectra. In particular, the

Table 1. Selected ^{1}H-, ^{13}C{^{1}H}-, and ^{31}P{^{1}H}-NMR spectral data and IR absorptions for the complexes

Complex	^{1}H δ (mult, *J*, assignt)[b,c]	^{13}C{^{1}H} δ (mult, *J*, assignt)[b,c]	^{31}P {^{1}H} δ[c,d] IR (KBr) cm^{-1}
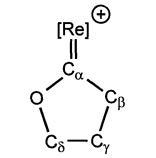 **3**	1.73 (qu, J_{HH} 7.8, H_γ, 2H) 3.28 (td, J_{HH} 7.7, J_{HP} 0.6, H_β, 2H) 4.06 (t, J_{HH} 7.6, H_δ, 2H)	293.4 (dt, $J_{CPtrans}$ 35.0, J_{CPcis} 8.9, C_α) 197.0 (m, CO) 85.3 (d, J_{CP} 3.2, C_δ) 62.7 (d, J_{CP} 5.7, C_β) 22.8 (s, C_γ)	δ_A -15.90, J_{AM} 22.1 δ_M -11.86 ν(CO) 1962; 1912 ν(COC) 1194
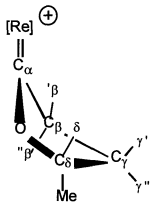 **4**	1.15 (d, $J_{MeH\delta}$ 6.3Hz, CH_3 carbene, 3H) 1.35 (dddd, $J_{H\gamma'H\gamma''}$ 12.8, $J_{H\gamma''H\beta'}$ 9.2, $J_{H\gamma''H\delta}$ 6.3, $J_{H\gamma''H\beta''}$ 3.6, $H_{\gamma''}$, 1H) 2.05 (dddd, $J_{H\gamma'H\gamma''}$ 12.8, $J_{H\gamma'H\beta''}$ 8.8, $J_{H\gamma'H\delta}$ 6.7, $J_{H\gamma'H\beta'}$ 3.6, $H_{\gamma'}$, 1H) 3.10 (ddd, $J_{H\beta''H\beta'}$ 19.8, $J_{H\beta'H\gamma''}$ 9.2, $J_{H\beta'H\gamma'}$ 3.6, $H_{\beta'}$, 1H) 3.68 (ddd, $J_{H\beta'H\beta''}$ 19.8, $J_{H\beta''H\gamma'}$ 8.8, $J_{H\beta''H\gamma''}$ 3.6, $H_{\beta''}$, 1H) 4.77 (dpsqu, $J_{H\delta H\gamma'}$ 6.7, $J_{H\delta Me} \cong J_{H\delta H\gamma''}$ 6.3, H_δ, 1H)	294.5 (dt, $J_{CPtrans}$ 35.6, J_{CPcis} 9.2, C_α) 198.6 (dt, $J_{CPtrans}$ 45.5, J_{CPcis} 5.7, CO) 98.5 (d, J_{CP} 3.2, C_δ) 65.5 (d, J_{CP} 5.0, C_β) 32.5 (s, C_γ) 22.4 (s, CH_3 carbene)	δ_A -13.10, J_{AM} 26.7 δ_M -14.73, δ_Q -16.63, $J_{AQ} \approx J_{MQ}$ 21.3 ν(CO) 1958, 1906 ν(COC) 1223
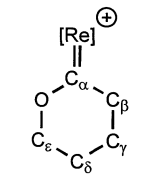 **5**	1.50 (m, H_γ+ H_δ, 4H) 3.28 (t, $J_{H\beta H\gamma}$ 6.8, H_β, 2H) 3.44 (t, $J_{H\varepsilon H\delta}$ 6.0, H_ε, 2H)	303.0 (dt, $J_{CPtrans}$ 36.8, J_{CPcis} 9.5, Cα) 198.0 (m, CO) 75.0 (d, J_{CP} 2.5, C_ε) 55.6 (d, J_{CP} 3.8, C_β) 21.1 (s, C_δ) 16.7 (s, C_γ)	δ_A -16.71, J_{AM} 21.4 δ_M -10.70 ν(CO) 1956, 1902 ν(COC) 1273
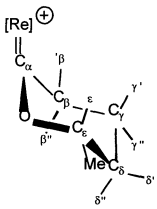 **6**	1.01 (d, $J_{MeH\varepsilon}$ 6.3, CH_3 carbene, 3H) 1.35 (m, $H_{\beta'}$ + $H_{\beta''}$, 2H) 1.60 (m, $H_{\gamma'}$+CH_3 triphos, 4H) 1.96 (m, $H_{\delta'}$,1H) 2.40-2.70 (m, $H\gamma''$+ CH_2 triphos , 7H) 3.92 (ddd, $J_{H\beta''H\beta'}$ 17.1, $J_{H\beta''H\gamma'}$ 5.8, $J_{H\beta''H\gamma''}$ 3.6, $H_{\beta''}$, 1H) 4.14 (m, H_ε, 1H)	305.3 (dt, $J_{CPtrans}$ 36.9, J_{CPcis} 8.6, C_α) 197.1 (dt, $J_{CPtrans}$ 44.5, J_{CPcis} 7.6, CO) 83.9 (d, J_{CP} 2.2, C_ε) 55.8 (dt, $J_{CPaxial}$ 4.5, J_{CPeq} 1.3, C_β) 28.7 (s, C_δ) 20.3 (s, CH_3 carbene) 16.9 (s, C_γ)	δ_A -12.80, J_{AM} 20.1 δ_M -14.00, J_{AQ} 23.5 δ_Q -16.56, J_{MQ} 20.7 ν(CO) 1962, 1896 ν(COC) 1252
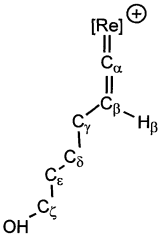 **7**	1.43 (psqu, $J_{H\delta H\gamma} \approx J_{H\delta H\varepsilon}$ 7.4 H_δ 2H) 1.61 (m, H_ε, 2H) 2.38 (psq, $J_{H\gamma H\beta}$ 8.3, $J_{H\gamma H\delta}$ 7.4, H_γ 2H) 3.53 (tpsq $J_{H\beta H\gamma}$ 8.3,$J_{HPA} \approx J_{HPM}$ 2.8, H_β vinylidene, 1H) 3.64 (br t, $J_{H\zeta H\varepsilon}$ 6.1, H_ζ, 2H)	343.9 (dt, $J_{CPtrans}$ 32.1, J_{CPcis} 11.6, C_α) 191.7 (m, CO) 111.0 (dt, $J_{CPtrans}$ 12.7, J_{CPcis} 2.5, C_β) 52.1 (s, C_ζ) 31.5 (s), 27.6 (s) (C_δ e C_ε) 19.8 (s, Cγ)	δ_A -19.41, J_{AM} 23.2 δ_M -15.82 ν(CO) 2008, 1946 ν(C=C) 1663 ν(OH) 3550
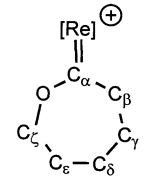 **8**	1.41 (m, H_ε, 2H) 1.70 (m, H_γ+ Hδ, 4H) 3.57 (m, H_β, 2H) 3.91 (t, $J_{H\zeta H\varepsilon}$ 4.6, H_ζ, 2H)	310.8 (dt, $J_{CPtrans}$ 38.4, J_{CPcis} 8.6, C_α) 198.1 (AXX'Y spin sistem, J_{AX} 7.0, J_{AY} 5.8, $J_{AX'}$ -8.2, $J_{XX'}$ 26.8, CO) 78.6 (d, J_{CP} 2.9 C_ζ) 60.1 (d, J_{CP} 5.2, C_β) 29.1, 28.2, 21.5 (all s, C_γ, C_δ, C_ε)	δ_A -17.14, J_{AM} 20.9 δ_M -11.49 ν(CO) 1956, 1890

latter experiment allowed us to establish the spatial relationships between the H_δ proton at $\delta = 4.77$ (which correlates with the CH carbon at $\delta = 98.5$ in the 2D-^{1}H,^{13}C-HMQC NMR experiment) and the signal at $\delta = 2.05$ of the opposite $H_{\gamma'}$ proton. Following this assignment, the remaining proton and carbon resonances were readily and reliably identified. Significant sections of the NOESY and COSY spectra are presented in Figure 1.

Figure 1. (**A**) Section ($\delta = 5.00 - 0.90$) of the phase-sensitive 2D-^{1}H NOESY spectrum of **4** (500.13 MHz, CD_2Cl_2, 25°C, τ_{mix} 800 ms) showing the negative cross-peaks between the protons of the 2-oxa-3-methyl-cyclopentylidene ring. (**B**) Contour plot of a section ($\delta = 5.00-0.90$) of the 2D-^{1}H COSY spectrum of **4** (500.13 MHz, CD_2Cl_2, 25°C) showing the scalar couplings for the protons of the 2-oxa-3-methyl-cyclopentylidene ring

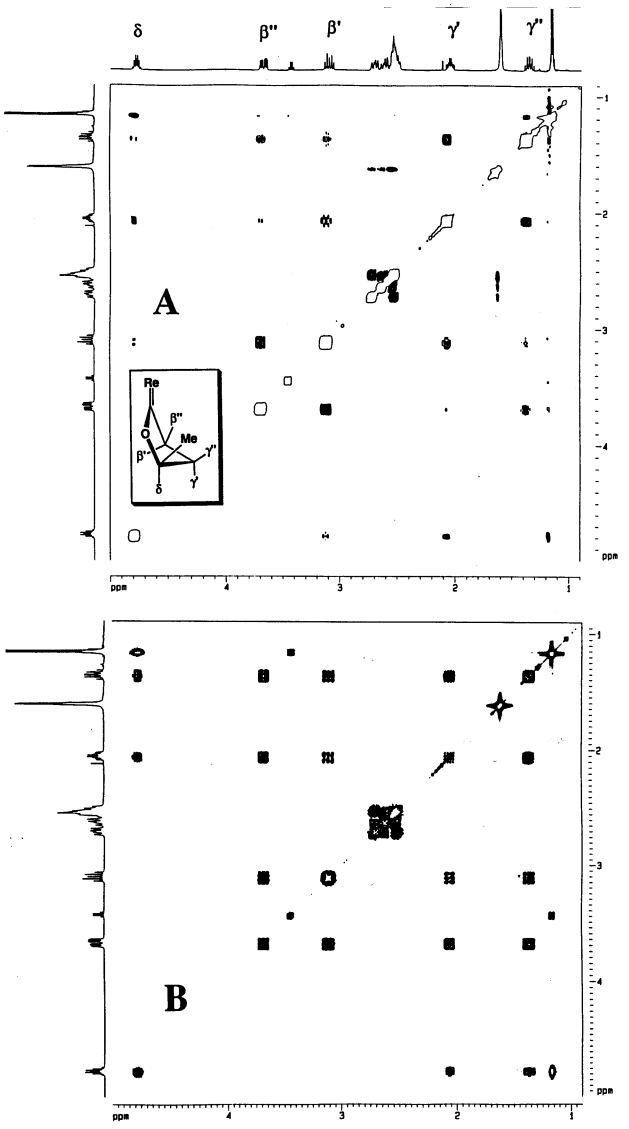

The solid-state structure of the 2-oxa-3-methyl-cyclopentylidene complex (**4**) has been determined by a single-crystal X-ray analysis. A view of the complex cation is shown in Figure 2, while selected bond lengths and angles are given in Table 2.

The structure of **4** consists of $[(triphos)Re(CO)_2\{=CCH_2CH_2CH(Me)O\}]^+$ cations and tetrafluoroborate anions with no interspersed solvent molecules. A *facial* triphos ligand, two *cis* disposed carbonyl groups and an oxacyclopentylidene ligand co-ordinate the Re center in a slightly distorted octahedral environment. The $Re-C_{carbene}$ bond length [$d_{Re=C} = 2.02(2)$ Å] is shorter than that found in the alkoxycarbene complex $[(triphos)Re(CO)_2\{=C(OEt)CH_3\}]BF_4$ [$d_{Re=C} = 2.071(8)$ Å],[20] but longer than that reported for the vinylidene complex $[(triphos)Re(CO)_2\{=C=C(H)Ph\}]BPh_4$ [$d_{Re=C} = 1.925(6)$ Å].[20] Noticeably, the present $Re-C_{carbene}$ distance is also shorter than that found in $(CO)_5Re=CCH_2CH_2CH_2O$ [$d_{Re=C} = 2.125$ Å][9a] and in $Br(CO)_4Re=COCH_2CH_2O$ [$d_{Re=C} = 2.135$ Å].[23] The oxacyclopentylidene ring adopts an "envelope" conformation with small deviations from the mean plane defined by the rhenium atom, and by the O3 and C8 to C12 atoms. The largest deviation affects the C10 atom (−0.0201 Å) in β-position with respect to O3. Deviations from planarity are often encountered in this class of oxacyclocarbene complexes and deformations ranging from

Figure 2. ORTEP Drawing of the complex cation $[(triphos)Re(CO)_2\{=CCH_2CH_2CH(Me)O\}]^+$ in **4-BF$_4$**. Only the *ipso* carbons of the phenyl rings of the triphos ligand are shown for the sake of clarity

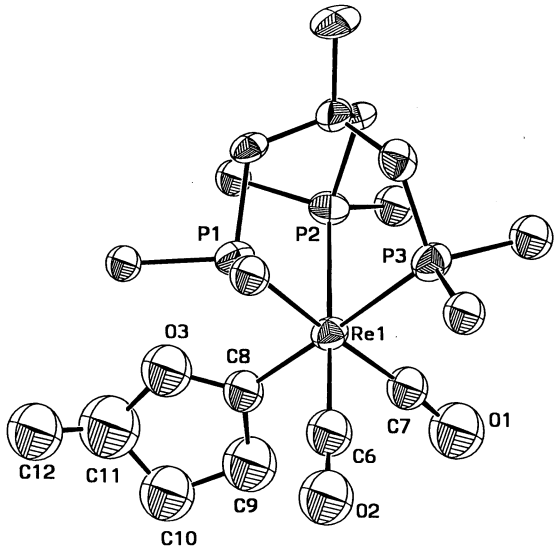

Table 2. Selected bond distances and angles for **4-BF$_4$**

Re−P1	2.488(4)	C7−O1	1.21(2)
Re−P2	2.490(4)	C8−O3	1.31(2)
Re−P3	2.466(4)	C8−C9	1.51(2)
Re−C6	1.89(2)	C9−C10	1.47(2)
Re−C7	1.85(2)	C10−C11	1.47(2)
Re−C8	2.02(2)	C11−C12	1.36(2)
C6−O2	1.16(2)	C11−O3	1.56(2)
C8−Re−C6	87.7(3)	C8−Re−C7	85.1(3)
C6−Re−C7	87.8(3)	C8−Re−P1	91.2(2)
C6−Re−P1	172.0(2)	C7−Re−P1	99.9(2)
C8−Re−P2	96.9(2)	C6−Re−P2	87.1(2)
C7−Re-P2	174.5(2)	P1−Re−P2	85.15(6)
C8−Re−P3	174.1(2)	C6−Re−P3	97.6(2)
C7−Re-P3	92.3(2)	P1−Re−P3	84.03(7)
P2−Re−P3	86.16(6)	O2−C7−Re	174.1(6)
C9−C8−Re	173.0(6)	C8−C9−C10	122.3(7)

practically planar systems to significantly distorted rings have been reported.[24][25] A comparable distortion has been reported for the molybdenum complex $[MoI(CO)_2\{=COCH_2CH_2CH_2\}(\eta^5\text{-}C_5H_5)]$.[26] The C8−O3 distance and the other metrical parameters pertaining to the carbene ligand fall into the range determined for related complexes.[5][9][23][24][25][26]

Reactions of **2** *with γ- and δ-Alkynols:* When either 4-pentyn-1-ol or (±)-5-hexyn-2-ol are allowed to react with a CH_2Cl_2 solution of **2** at room temperature, the Fischer carbene complexes $[(triphos)Re(CO)_2\{=CCH_2CH_2CH_2\text{-}CH(R)O\}]BF_4$ (R = H, **5**; R = Me, **6**) are obtained in good yields (Scheme 2). To the best of our knowledge, known examples of oxacyclohexylidene metal complexes are limited to the chromium complex $(CO)_5Cr\{=CCH_2\text{-}CH_2CH_2CH_2O\}$ described by Dötz,[1] the manganese compound $Cp(CO)(PPh_3)Mn=C\{OCH_2C(Me)_2CH_2CH(Me)\}$ synthesized by Geoffroy and coworkers,[9b] the molybdenum derivative $[Mo\{=CH_2(CH_2)_2CH_2O\}(dppe)(\eta\text{-}C_7H_7)]PF_6$ (dppe = $Ph_2PCH_2CH_2PPh_2$) reported by Whiteley and co-workers,[10b] and the indenyl osmium complex $[(\eta^5\text{-}C_9H_7)Os\{=CCH_2CH_2CH_2CH_2O\}(PPh_3)_2]$ described by Gimeno.[8a]

The presence of oxacyclohexylidene rings in **5** and **6** is shown by the $^{13}C\{^1H\}$-NMR spectra which exhibit four different methylene resonances (singlets at δ = 16.7, 21.6, 55.6, and 75.0), while the carbene carbon atoms resonate at δ = 303.0 (**5**: dt, $J_{CPtrans}$ = 36.8 Hz, J_{CPcis} = 9.5 Hz) and at δ = 305.3 (**6**: dt, $J_{CPtrans}$ = 36.9 Hz, J_{CPcis} = 8.6 Hz). As expected the NMR properties of **6** are similar to those of **4**, which analogously contains a stereogenic carbon atom in the ring.[27]

Monitoring the reactions between **2** and 4-pentyn-1-ol [or (±)-5-hexyn-2-ol] by multinuclear NMR spectroscopy in the temperature range from −50 to +20°C showed no intermediate species in the course of the conversion of **2** to **5** (or **6**). In contrast, V. T. NMR spectroscopy has revealed that the hydroxybutylvinylidene complex $[(triphos)Re(CO)_2\{=C=C(H)CH_2CH_2CH_2CH_2OH\}]BF_4$ (**7**) is an intermediate to the oxacarbene thermodynamic product $[(triphos)Re(CO)_2\{=CCH_2CH_2CH_2CH_2CH_2O\}]\text{-}BF_4$ (**8**) when **2** is reacted with a δ-alkynol such as $HC\equiv CCH_2(CH_2)_2CH_2OH$. The hydroxyvinylidene complex is stable in solution below −10°C. Above this temperature it slowly but selectively transforms into the 2-oxacycloheptylidene isomer **8** (Scheme 2). The conversion is fast at room temperature. Nonetheless, the stability at low temperature allows **7** to be unambiguously characterized in solution and isolated in the solid state as well.

Bands in the IR spectrum of **7** at 1663 (C=C) and ca. 3550 cm^{-1} (OH), diagnose the presence of a hydroxyvinylidene ligand. These absorptions are not present in the IR spectrum of **8**, in which the stretching frequencies of the two CO′s are at lower energy (1960 and 1900 cm^{-1}) compared to those of **7** (2008 and 1946 cm^{-1}) due to the greater π-acceptor character of the hydroxyvinylidene ligand.[14][20] In keeping with this electronic effect, the phosphorus resonances of **8** (δ_A = −17.14, δ_M = −11.49, J_{AM} = 20.9 Hz) are shifted to low field with respect to those of **7** (δ_A = −19.41, δ_M = −15.82, J_{AM} = 23.2 Hz). The $^{13}C\{^1H\}$-NMR spectrum of **7** displays the characteristic low-field resonance of the vinylidene C_α atom (δ = 343.9), while the resonance of the C_β atom appears at higher field (doublet of triplets at δ = 111.0).[12][13][21] Four signals, spanning from δ = 52.1 (C_ζ) to δ = 19.8 (C_γ) are assigned to the CH_2 carbon atoms of the δ-hydroxybutyl substituent in the vinylidene ligand. In the proton NMR spectrum of **7**, the vinylidene hydrogen resonance appears as a well-resolved triplet of pseudoquartets at δ = 3.53 which collapses into a triplet of 8.3 Hz in the broad-band phosphorus-decoupled spectrum.

Further experimental evidence of the vinylidene nature of the organyl ligand in **7** is provided by the reaction of the latter compound with Brønsted bases, such as NEt_3, which remove the vinylidene hydrogen atom, leading to the clean formation of the σ-alkynyl complex $[(triphos)Re(CO)_2\text{-}\{C\equiv CCH_2CH_2CH_2CH_2OH\}]$ (**9**).[12][20] This reaction is reversible and **9** re-generates **7** by treatment with protic acids. The alkynyl derivative **9** has been isolated and authenticated spectroscopically by comparison with several Re^I alkynyls of the formula $[(triphos)Re(CO)_2(C\equiv CR)]$.[20]

A careful and complete analysis of the $^{13}C\{^1H\}$-NMR spectrum was carried out for the unambiguous identification of **8**. Key features are a doublet of triplets at δ = 310.8, assigned to the carbene carbon atom, and five methylene resonances assigned to the five CH_2 groups of the 2-oxacycloheptylidene ring. The presence of five methylene resonances was of crucial importance for ruling out a vinyl-vinylidene structure which might have been formed via the alternative water-elimination pathway (Scheme 1). Of the five methylene resonances, only those of the C_ζ (δ = 78.6) and C_β (δ = 60.1) carbons, proximal to the oxygen and to the carbene carbon atoms, respectively, appear as doublets with small phosphorus-carbon couplings. The remaining CH_2 resonances (between δ = 29.1 and 21.5) are singlets with no discernible coupling.

Fischer carbene complexes containing oxacycloheptylidene rings are extremely rare. To the best of our knowledge, the only example reported in the literature is the dinuclear dimanganese complex $[(CO)_5Mn-Mn(CO)_4\{=CO\text{-}CH_2CH_2CH_2CH_2CH_2\}]$.[16] This, however, was prepared by the alternative reaction of the bistriflate $TfOCH_2CH_2CH_2CH_2CH_2OTf$ with the carbonyl metalate salt $K[Mn(CO)_5]$ in THF, and not by δ-alkynol activation.[16][17]

Conclusions

Our study of the reactions of the $16e^-$ $[(triphos)Re(CO)_2]^+$ support with different β-, γ-, and δ-alkynols has shown that cyclic carbenes are formed irrespective of the separation between the triple bond and the hydroxy functional group. We have also demonstrated that this cyclization reaction occurs via the hydroxyalkylvinylidene complexes. For the particular case of the δ-alkynol 5-hexyn-1-ol the kinetic hydroxybutylvinylidene intermediate has been intercepted in solution and isolated in the solid state. Its thermal rearrange-

ment to the thermodynamic 2-oxacycloheptylidene product has been observed, showing that the intramolecular nucleophilic attack by the OH group at the vinylidene C_α atom may still be favored over H_2O elimination to give vinylvinylidene products. The same should be true for long-chain ω-alkynols. Studies are currently in progress to scrutiny the chemistry of this new family of rhenium 2-oxacarbenes.

Thanks are due to Prof. *A. Medici* (University of Ferrara, Italy) for a gift of (±)-5-hexyn-2-ol and to Prof. *J. Gimeno* (University of Oviedo, Spain) for communicating some preliminary results prior to publication.

Experimental Section

General Procedure: Tetrahydrofuran (THF), *n*-hexane, and diethyl ether were purified by distillation over sodium/benzophenone under a nitrogen atmosphere. Dichloromethane and ethanol were purified by distillation under nitrogen over calcium hydride. The ligand $CH_3C(CH_2PPh_2)_3$ (triphos)[28] and the complexes [(triphos)-$Re(CO)_2H$] (**1**)[19] and [(triphos)$Re(CO)_2(\eta^2\text{-}H_2)]BF_4$ (**2**)[20] were prepared as described in the literature. All the alkynols were purchased from Aldrich except for (±)-5-hexyn-2-ol which was provided by Prof. A. Medici (Department of Chemistry, University of Ferrara). The purity of all alkynols was checked by ^{1}H-NMR spectroscopy, and, when necessary, they were distilled under inert atmosphere prior to use. All the other reagents and chemicals were reagent grade and, unless otherwise stated, were used as received from commercial suppliers. All reactions and manipulations were routinely performed under a dry nitrogen atmosphere by using standard Schlenk-tube techniques. CD_2Cl_2 for NMR measurements (Merck and Aldrich) was dried over molecular sieves (4 Å). – ^{1}H- and $^{13}C\{^1H\}$-NMR spectra were recorded on Varian VXR 300, Bruker AC200, or Bruker AVANCE DRX 500 spectrometers operating at 299.94, 200.13, or 500.13 MHz (^{1}H) and 75.42, 50.32, or 125.80 MHz (^{13}C), respectively. Peak positions are relative to tetramethylsilane and were calibrated against the residual solvent resonance (^{1}H) or the deuterated solvent multiplet (^{13}C). ^{13}C-DEPT, and gated $^{13}C\{^1H\}$-decoupled NMR experiments were run on the Bruker AC200 spectrometer. ^{1}H,^{13}C-2D HETCOR NMR experiments were recorded on either the Bruker AC200 spectrometer using the XHCORR pulse program or the Bruker AVANCE DRX 500 spectrometer equipped with a 5-mm triple-resonance probe-head for ^{1}H detection and inverse detection of the heteronucleus (inverse correlation mode, HMQC experiment) with no sample spinning. The ^{1}H,^{1}H-2D COSY NMR experiments were routinely conducted on the Bruker AC200 instrument in the absolute magnitude mode using a 45° or 90° pulse after the incremental delay. The ^{1}H,^{1}H-2D COSY NMR experiments on the racemate complexes **4** and **6** were acquired on the AVANCE DRX 500 Bruker spectrometer using the phase-sensitive TPPI mode with double quantum filter. ^{1}H,^{1}H-2D NOESY NMR experiments were conducted on the same instrument in the phase-sensitive TPPI mode in order to discriminate between positive and negative cross peaks. – $^{31}P\{^1H\}$ NMR spectra were recorded on either the Varian VXR 300 or Bruker AC200 instruments operating at 121.42 and 81.01 MHz, respectively. Chemical shifts were measured relative to external 85% H_3PO_4 with downfield values taken as positive. The proton NMR spectra with broad-band phosphorus decoupling were recorded on the Bruker AC200 instrument equipped with a 5-mm inverse probe and a BFX-5 amplifier device using the wideband phosphorus decoupling sequence GARP.[29] – Computer simulations of NMR spectra were carried out with a locally developed package containing the programs LAOCN3[30] and DAVINS.[31] The initial choices of shifts and coupling constants were refined by iterative least-squares calculations using the experimental digitized spectrum. The final parameters gave a satisfactory fit between experimental and calculated spectra, the agreement factor *R* being less than 1% in all cases. – Infrared spectra were recorded in KBr pellets on a Nicolet 510 P spectrometer operating in the FT mode, or as Nujol mulls on a Perkin–Elmer 1600 series FT-IR spectrometer between KBr plates. – Conductivities were measured with an ORION model 990101 conductance cell connected to a model 101 conductivity meter. The conductivity data were obtained at sample concentrations of ca. $1\cdot10^{-3}$ M in nitroethane solutions at room temperature (21°C). – Elemental analyses were performed with a Carlo Erba model 1106 elemental analyzer.

Synthesis of [(triphos)Re(CO)$_2${=CCH$_2$CH$_2$CH$_2$O}]BF$_4$ (**3**): A dichloromethane (5 ml) solution of the complex [(triphos)-$Re(CO)_2(\eta^2\text{-}H_2)]BF_4$ (**2**) was prepared in a 25-ml Schlenk-flask by treating [(triphos)$Re(CO)_2H$] (**1**) (0.25 g, 0.26 mmol) with $HBF_4.OMe_2$ (33 µl, 0.27 mmol) at −20°C under nitrogen.[19] To this solution, a slight excess of 3-butyn-1-ol (23 µl, 0.30 mmol) was added with stirring, and the solution was slowly brought to room temperature. During this time, the color of the resulting solution changed from pale yellow to orange. After the reaction mixture was allowed to reach room temperature, stirring was continued for additional 30 min. The solvent was removed under reduced pressure and the solid residue washed with 2 × 2 ml of ethanol and 2 × 3 ml of diethyl ether. The crude reaction product was recrystallized from dichloromethane/diethyl ether (1:1, v/v) to yield orange crystals of [(triphos)Re(CO)$_2${=CCH$_2$CH$_2$CH$_2$O}]BF$_4$ (**3**). Yield 80%. – $C_{47}H_{45}BF_4O_3P_3Re$: calcd. C 55.14, H 4.45; found C 55.20, H 4.55.– ^{1}H NMR (CD_2Cl_2, 22°C, 200.13 MHz): (the numbering scheme for the hydrogen and carbon resonances of this complex as well as all the other new complexes described in this paper is given in Table 1) δ = 1.62 (q, J_{HP} = 3.1 Hz, $CH_{3(triphos)}$, 3 H), 1.73 (quint, J_{HH} = 7.8 Hz, H_γ, 2 H), 2.54 (d, $J_{HP\,axial}$ = 8.8 Hz, CH_2P_{axial}, 2 H), 2.70 (m, CH_2P_{equat}, 4 H), 3.28 (td, J_{HH} = 7.7 Hz, J_{HP} = 0.6 Hz, H_β, 2 H), 4.06 (t, J_{HH} = 7.6 Hz, H_δ, 2 H). $^{13}C\{^1H\}$ NMR (CD_2Cl_2, 22°C, 50.32 MHz): δ = 293.4 (dt, $J_{CP\,trans}$ = 35.0 Hz, $J_{CP\,cis}$ = 8.9 Hz, C_α), 197.0 (m, CO), 85.3 (d, J_{CP} = 3.2 Hz, C_δ), 62.7 (d, J_{CP} = 5.7 Hz, C_β), 40.3 (q, J_{CP} = 9.9 Hz, $CH_{3(triphos)}$), 39.7 (q, J_{CP} = 3.5 Hz, $MeC_{(triphos)}$), 35.1 (td, N = $J_{CP\,equat'}$ + $J_{CP\,equat''}$ = 14.0 Hz, $J_{CP\,axial}$ = 4.5 Hz, CH_2P_{equat}), 32.4 (dt, $J_{CP\,axial}$ = 23.5 Hz, $J_{CP\,equat}$ = 4.4 Hz, CH_2P_{axial}), 22.8 (s, C_γ).– $^{31}P\{^1H\}$ NMR (CD_2Cl_2, 22°C, 81.01 MHz): AM_2 spin system, δ_A = −15.90, δ_M = −11.86, J_{AM} = 22.1 Hz. $-\Lambda_{M(nitroethane)}$ = 80 Ω^{-1} cm^2 mol^{-1}.

Recrystallization of **3** from dichloromethane/ethanol in the presence of 2 equiv of $NaBPh_4$, yielded the corresponding tetraphenylborate salt (**3′**) in ca. 90% yield. – [(triphos)Re(CO)$_2$-{=CCH$_2$CH$_2$CH$_2$O}]BPh$_4$ (**3′**, $C_{71}H_{65}BO_3P_3Re$): calcd. C 67.89, H 5.21; found C 67.19, H 5.01. – $\Lambda_{M(nitroethane)}$ = 53 Ω^{-1} cm^2 mol^{-1}.

Synthesis of [(triphos)Re(CO)$_2${=CCH$_2$CH$_2$CH(Me)O}]BF$_4$ (**4**): The methyl-substituted oxycarbene complex **4**, was obtained as described above for **3** using (±)-4-pentyn-2-ol (24 µl, 0.26 mmol) instead of 3-butyn-1-ol. The reaction was complete after stirring the mixture at room temperature for 1 h. Work-up as above gave [(triphos)Re(CO)$_2${=CCH$_2$CH$_2$CH(Me)O}]BF$_4$ (**4**) as orange microcrystals. Yield 85%. – $C_{48}H_{47}BF_4O_3P_3Re$: calcd. C 55.55, H, 4.56; found C 54.99, H 4.38. – ^{1}H NMR (CD_2Cl_2, 25°C, 500.13 MHz): δ = 1.15 (d, $J_{MeH\delta}$ = 6.3 Hz, $CH_{3(carbene)}$, 3 H), 1.35 (dddd, $J_{H\gamma''H\gamma'}$ = 12.8 Hz, $J_{H\gamma''H\beta'}$ = 9.2 Hz, $J_{H\gamma''H\delta}$ = 6.3 Hz, $J_{H\gamma''H\beta''}$ = 3.6 Hz, $H_{\gamma''}$, 1H), 1.62 (q, J_{HP} = 3.0 Hz, $CH_{3(triphos)}$, 3 H), 2.05 (dddd, $J_{H\gamma'H\gamma''}$ = 12.8 Hz, $J_{H\gamma'H\beta''}$ = 8.8 Hz, $J_{H\gamma'H\delta}$ = 6.7 Hz,

$J_{H\gamma'H\beta'}$ = 3.6 Hz, $H_{\gamma'}$, 1 H), 2.60 (m, $CH_{2(triphos)}$, 6 H), 3.10 (ddd, $J_{H\beta''H\beta'}$ = 19.8 Hz, $J_{H\beta'H\gamma''}$ = 9.2 Hz, $J_{H\beta'H\gamma'}$ = 3.6 Hz, $H_{\beta'}$, 1 H), 3.68 (ddd, $J_{H\beta'H\beta''}$ = 19.8 Hz, $J_{H\beta''H\gamma'}$ = 8.8 Hz, $J_{H\beta''H\gamma''}$ = 3.6 Hz, $H_{\beta''}$, 1 H), 4.77 (dpsquint, $J_{H\delta H\gamma'}$ = 6.7 Hz, $J_{H\delta Me} \approx J_{H\delta H\gamma''}$ = 6.3 Hz, H_δ, 1 H). – $^{13}C\{^1H\}$ NMR (CD_2Cl_2, 22°C, 50.32 MHz): δ = 294.5 (dt, $J_{CPtrans}$ = 35.6 Hz, J_{CPcis} = 9.2 Hz, C_α), 198.6 (dt, $J_{CPtrans}$ = 45.5 Hz, J_{CPcis} = 5.7 Hz, CO), 98.5 (d, J_{CP} = 3.2 Hz, C_δ), 65.5 (d, J_{CP} = 5.0 Hz, C_β), 42.1 (q, J_{CP} = 10.1 Hz, $CH_{3(triphos)}$), 41.6 (q, J_{CP} = 3.6 Hz, $MeC_{(triphos)}$), 37.3 (d, $J_{CPequat}$ = 25.7 Hz, CH_2P_{equat}), 36.6 (dt, $J_{CPaxial}$ = 22.2 Hz, $J_{CPequat}$ = 4.7 Hz, CH_2P_{axial}), 32.5 (s, C_γ), 22.5 (s, $CH_{3(carbene)}$). – $^{31}P\{^1H\}$ NMR (CD_2Cl_2, 22°C, 81.01 MHz): AMQ spin system, δ_A = –13.10, δ_M = –14.73, δ_Q = –16.63, J_{AM} = 26.7 Hz, J_{AQ} = 21.3 Hz, J_{MQ} = 21.3 Hz. – $\Lambda_{M(nitroethane)}$ = 81 Ω^{-1} cm^2 mol^{-1}.

Synthesis of [(triphos)Re(CO)$_2${=CCH$_2$CH$_2$CH$_2$CH$_2$O}]BF$_4$ (**5**): A slight excess of 4-pentyn-1-ol (40 µl, 0.37 mmol) was added with stirring to a solution of **2** (0.26 mmol) prepared as described above. Usual work-up gave pale orange crystals of [(triphos)Re(CO)$_2${=CCH$_2$CH$_2$CH$_2$CH$_2$O}]BF$_4$ (**5**). Yield 80%. – $C_{48}H_{47}BF_4O_3P_3Re$: calcd. C 55.55, H 4.56; found C 55.49, H 4.50. – ^1H NMR (CD_2Cl_2, 25°C, 500.13 MHz): δ = 1.50 (m, H_γ + H_δ, 4 H), 1.68 (q, J_{HP} = 3.0 Hz, $CH_{3(triphos)}$, 3 H), 2.48 (d, $J_{HPaxial}$ = 8.8 Hz, CH_2P_{axial}, 2 H), 2.70 (m, CH_2P_{equat}, 4 H), 3.28 (t, $J_{H\beta H\gamma}$ = 6.8 Hz, H_β, 2 H), 3.44 (t, $J_{H\varepsilon H\delta}$ = 6.0 Hz, H_ε, 2 H). – $^{13}C\{^1H\}$ NMR (CD_2Cl_2, 22°C, 50.32 MHz): δ = 303.0 (dt, $J_{CPtrans}$ = 36.8 Hz, J_{CPcis} = 9.5 Hz, C_α), 198.0 (m, CO), 75.0 (d, J_{CP} = 2.5 Hz, C_ε), 55.6 (d, J_{CP} = 3.8 Hz, C_β), 40.3 (q, J_{CP} = 10.4 Hz, $CH_{3(triphos)}$), 39.7 (q, J_{CP} = 3.8 Hz, $MeC_{(triphos)}$), 32.5 (td, N = $J_{CPequat'}$ + $J_{CPequat''}$ = 14.0 Hz, $J_{CPaxial}$ = 4.4 Hz, CH_2P_{equat}), 32.5 (dt, $J_{CPaxial}$ = 22.9 Hz, $J_{CPequat}$ = 4.3 Hz, CH_2P_{axial}), 21.1 (s, C_δ), 16.7 (s, C_γ). – $^{31}P\{^1H\}$ NMR (CD_2Cl_2, 22°C, 81.01 MHz): AM_2 spin system, δ_A = –16.71, δ_M = –10.70, J_{AM} = 21.4 Hz. – $\Lambda_{M(nitroethane)}$ = 82 Ω^{-1} cm^2 mol^{-1}.

Synthesis of [(triphos)Re(CO)$_2${=CCH$_2$CH$_2$CH$_2$CH(Me)O}]BF$_4$ (**6**): A two-fold excess of (±)-5-hexyn-2-ol (54 µl, 0.55 mmol) was syringed into a dichloromethane solution of **2** (0.026 mmol) prepared as described above. Orange microcrystals of [(triphos)Re(CO)$_2${=CCH$_2$CH$_2$CH$_2$CH(Me)O}]BF$_4$ (**6**) were obtained in ca. 65% yield after usual work up. – $C_{49}H_{49}BF_4O_3P_3Re$: calcd. C 55.88, H 4.69; found C 55.90, H 4.72. – ^1H NMR (CD_2Cl_2, 25°C, 200.13 MHz): δ = 1.01 (d, $J_{MeH\varepsilon}$ = 6.3 Hz, $CH_{3(carbene)}$, 3 H), 1.35 (m, $H_{\beta'}$ + $H_{\delta'}$, 2 H), 1.60 (m, $H_{\gamma'}$ + $CH_{3(triphos)}$, 4 H), 1.96 (m, $H_{\delta'}$, 1H), 2.40 – 2.70 (m, $H_{\gamma''}$ + $CH_{2(triphos)}$, 7H), 3.92 (ddd, $J_{H\beta''H\beta'}$ = 17.1 Hz, $J_{H\beta''H\gamma'}$ = 5.8 Hz, $J_{H\beta''H\gamma''}$ = 3.6 Hz, $H_{\beta''}$, 1 H), 4.14 (m, H_ε, 1H). – $^{13}C\{^1H\}$ NMR (CD_2Cl_2, 20°C, 50.32 MHz): δ = 305.3 (dt, $J_{CPtrans}$ = 36.9 Hz, J_{CPcis} = 8.6 Hz, C_α), 197.1 (dt, $J_{CPtrans}$ = 44.5 Hz, J_{CPcis} = 7.6 Hz, CO), 83.9 (d, J_{CP} = 2.2 Hz, C_ε), 55.8 (dt, $J_{CPaxial}$ = 4.5 Hz, $J_{CPequat}$ = 1.3 Hz, C_β), 39.7 (q, J_{CP} = 10.1 Hz, $CH_{3(triphos)}$), 39.5 (q, J_{CP} = 3.2 Hz, $MeC_{(triphos)}$), 35.7 (td, N = $J_{CPequat'}$ + $J_{CPequat''}$ = 5.0 Hz, $J_{CPaxial}$ = 2.5 Hz, CH_2P_{equat}), 35.1 (td, N = $J_{CPequat'}$ + $J_{CPequat''}$ = 5.0 Hz, $J_{CPaxial}$ = 2.4 Hz, CH_2P_{equat}), 32.8 (dt, $J_{CPaxial}$ = 22.2 Hz, $J_{CPequat}$ = 4.8 Hz, CH_2P_{axial}), 28.7 (s, C_δ), 20.3 (s, $CH_{3(carbene)}$), 16.9 (s, C_γ). – $^{31}P\{^1H\}$ NMR (CD_2Cl_2, 22°C, 81.01 MHz): AMQ spin system, δ_A = –12.80, δ_M = –14.00, δ_Q = –16.56, J_{AM} = 20.1 Hz, J_{AQ} = 23.5 Hz, J_{MQ} = 20.7 Hz. – $\Lambda_{M(nitroethane)}$ = 85 Ω^{-1} cm^2 mol^{-1}.

In Situ NMR Studies: Reactions of [(triphos)Re(CO)$_2$(η^2-H$_2$)]BF$_4$ (**2**) *with 3-Butyn-1-ol, (±)-4-Pentyn-2-ol, or 4-Pentyn-1-ol:* Deoxygenated CD_2Cl_2 (0.8 ml) was transferred under nitrogen into a 5-mm NMR tube previously charged with **1** (0.025 g, 0.028 mmol). The addition of 3.3 µl of HBF4·OMe2 dissolved the monohydride **1** within a few minutes to give a solution of **2** which was cooled down to –78°C. After 2.3 µl (0.030 mmol) of 3-butyn-1-ol was syringed into the tube, this was flame-sealed under nitrogen at –78°C and then introduced into the NMR probe of the spectrometer precooled to –50°C. The progress of the reaction was followed by variable-temperature (V.T.) $^{31}P\{^1H\}$- and ^1H-NMR spectroscopy. No reaction occurred until the temperature was raised to about –10°C. At this temperature, the molecular hydrogen complex started converting to the oxycarbene derivative **3.** Within 1 h at –10°C, **3** was the only product detectable by ^{31}P-NMR spectroscopy.

In analogous experiments, (±)-4-pentyn-2-ol or 4-pentyn-1-ol were substituted for 3-butyn-1-ol. Monitoring the reaction by V.T.-NMR spectroscopy showed no intermediate species for the transformation of **2** into **4** or **5**.

In Situ NMR Studies: Reaction of [(triphos)Re(CO)$_2$(η^2-H$_2$)]BF$_4$ (**2**) *with 5-Hexyn-1-ol:* To a dry-ice/acetone cooled solution of **2** (0.050 mmol) in CD_2Cl_2 (0.8 ml), prepared in a 5-mm NMR tube from **1** and $HBF_4 \cdot OMe_2$, was added 6.3 µl (0.055 mmol) of 5-hexyn-1-ol. The tube was flame-sealed and the reaction progress was monitored by V.T.-NMR spectroscopy. A reaction between **2** and the alkynol already occurred at –15°C to give the vinylidene complex [(triphos)Re(CO)$_2${=C=C(H)CH$_2$CH$_2$CH$_2$CH$_2$OH}]BF$_4$ (**7**) as the only new rhenium-containing product. A complete transformation of **2** into **7** was observed after 6 h at –15°C. Heating the NMR tube to room temperature caused the transformation of **7** into the carbene [(triphos)Re(CO)$_2${=CCH$_2$CH$_2$CH$_2$CH$_2$CH$_2$O}]BF$_4$ (**8**) at ca. –8°C. The formation of **8** was complete after the sample was heated to 20°C for 1 h.

NMR Data for **7**: ^1H NMR (CD_2Cl_2, –16°C, 500.13 MHz): δ = 1.43 (psquint, $J_{H\delta H\gamma} \approx J_{H\delta H\varepsilon}$ = 7.4 Hz, H_δ, 2 H), 1.61 (m, H_ε, 2 H), 1.67 (q, J_{HP} = 3.0 Hz, $CH_{3(triphos)}$, 3 H), 2.38 (psq, $J_{H\gamma H\beta}$ = 8.3 Hz, $J_{H\gamma H\delta}$ = 7.4 Hz, H_γ, 2 H), 2.46 (d, $J_{HPaxial}$ = 9.3 Hz, CH_2P_{axial}, 2 H), 2.54 (m, CH_2P_{equat}, 2 H), 2.73 (m, CH_2P_{equat}, 2 H), 3.53 (tpsq, transforms into a triplet in the $^1H\{^{31}P\}$-NMR spectrum, $J_{H\beta H\gamma}$ = 8.3 Hz, $J_{HPA} \approx J_{HPM}$ = 2.8 Hz, $H_{\beta(vinylidene)}$, 1 H), 3.64 (br t, $J_{H\zeta H\varepsilon}$ = 6.1 Hz, H_ζ, 2 H); the resonance of the OH proton was not observed. – $^{13}C\{^1H\}$ NMR (CD_2Cl_2, –16°C, 50.32 MHz): δ = 343.9 (dt, $J_{CPtrans}$ = 32.1 Hz, J_{CPcis} = 11.6 Hz, C_α), 191.7 (m, CO), 111.0 (dt, $J_{CPtrans}$ = 12.7 Hz, J_{CPcis} = 2.5 Hz, C_β), 52.1 (s, C_ζ), 39.7 (q, J_{CP} = 10.2 Hz, $CH_{3(triphos)}$), 39.2 (br s, $MeC_{(triphos)}$), 36.9 (m, CH_2P_{axial}), 32.4 (m, CH_2P_{equat}), 31.5 (s) and 27.6 (s) (C_δ and C_ε), 19.8 (s, C_γ). – $^{31}P\{^1H\}$ NMR (CD_2Cl_2, –16°C, 81.01 MHz): AM_2 spin system, δ_A = –19.41, δ_M = –15.82, J_{AM} = 23.2 Hz.

NMR Data for **8**: ^1H NMR (CD_2Cl_2, 22°C, 200.13 MHz): δ = 1.41 (m, H_ε, 2 H), 1.66 (q, J_{HP} = 2.9 Hz, $CH_{3(triphos)}$, 3 H), 1.7 (m, partially masked by triphos CH_3 resonance, assigned by 2D-^1H,^1H-COSY NMR experiment, H_γ + H_δ, 4 H), 2.53 (d, $J_{HPaxial}$ = 8.7 Hz, CH_2P_{axial}, 2 H), 3.57 (m, H_β, 2 H), 3.91 (t, $J_{H\zeta H\varepsilon}$ = 4.6 Hz, H_ζ, 2 H). – $^{13}C\{^1H\}$ NMR (CD_2Cl_2, 22°C, 75.42 MHz): δ = 310.8 (dt, $J_{CPtrans}$ = 38.4 Hz, J_{CPcis} = 8.6 Hz, C_α), 198.1 (AXX′Y spin system, J_{AX} = 7.0 Hz, J_{AY} = 5.8 Hz, $J_{AX'}$ = –8.2 Hz, $J_{XX'}$ = 26.8 Hz, CO), 78.6 (d, J_{CP} = 2.9 Hz, C_ζ), 60.1 (d, J_{CP} = 5.2 Hz, C_β), 40.2 (q, J_{CP} = 10.1 Hz, $CH_{3(triphos)}$), 39.7 (q, J_{CP} = 4.1 Hz, $MeC_{(triphos)}$), 35.6 (td, N = $J_{CPequat}$ + $J_{CPequat'}$ = 14.0 Hz, $J_{CPaxial}$ = 4.4 Hz, CH_2P_{equat}), 32.7 (dt, $J_{CPaxial}$ = 22.3 Hz, $J_{CPequat}$ = 4.8 Hz, CH_2P_{axial}), 29.1 (s), 28.2 (s), and 21.5 (s), (C_γ, C_δ and C_ε). – $^{31}P\{^1H\}$ NMR (CD_2Cl_2, 25°C, 81.01 MHz): AM_2 spin system, δ_A = –17.14, δ_M = –11.49, J_{AM} = 20.9 Hz. – $\Lambda_{M(nitroethane)}$ = 80 Ω^{-1} cm^2 mol^{-1}.

Synthesis of [(triphos)Re(CO)$_2${=C=C(H)CH$_2$CH$_2$CH$_2$CH$_2$-OH}]BF$_4$ (**7**): A slight excess of 5-hexyn-1-ol (60 µl, 0.55 mmol) was added to a stirred solution of **2** (0.26 mmol) prepared as described above and maintained at −15°C. The resulting solution was stirred for 15 min, then the solvent was removed under reduced pressure to give a raspberry-colored powder. The solid residue was washed with diethyl ether before being dried under vacuum. NMR spectroscopy showed it to contain **7**, occasionally contaminated by some **8** (usually less than 10%). − $C_{49}H_{49}BF_4O_3P_3Re$: calcd. C 55.88, H 4.69; found C 55.70, H 4.74.

Synthesis of [(triphos)Re(CO)$_2${=CCH$_2$CH$_2$CH$_2$CH$_2$-CH$_2$O}]BF$_4$ (**8**): A solution of **7** obtained by reacting **2** with 5-hexyn-1-ol as described above, was slowly warmed to room temperature with stirring. Within 30 min, the reaction mixture became pale yellow. Evaporation of the solvent under reduced pressure gave **8** as yellow microcrystals. Yield 90%. − $C_{49}H_{49}BF_4O_3P_3Re$: calcd. C 55.88, H 4.69; found C 55.92, H 4.75.

Synthesis of [(triphos)Re(CO)$_2${C≡CCH$_2$CH$_2$CH$_2$CH$_2$OH}] (**9**): To a Schlenk-tube charged with the vinylidene complex **7** (0.19 g, 0.20 mmol) in CH_2Cl_2 (5 ml) at −15°C, a three-fold excess of neat NEt_3 (85 µl, 0.60 mmol) was added with stirring. An immediate reaction took place to give a pale yellow solution. The reaction mixture was stirred for 1 h at room temperature. After the solvent was removed in vacuo, the pale yellow residue was washed with water (2 × 1 ml), ethanol (2 × 1 ml) and diethyl ether (2 × 2 ml) before being dried under vacuum. Yield 80%. − $C_{49}H_{48}O_3P_3Re$: calcd. C 60.98, H 5.02; found C 60.70, H 5.1. − ^{1}H NMR (CD_2Cl_2, 25°C, 200.13 MHz): δ = 1.3 − 1.6 (m, H_δ+ H_γ, 4 H), 1.77 (q, J_{HP} = 3.4 Hz, $CH_{3(triphos)}$, 3 H), 2.3 − 2.7 (m, $CH_{2(triphos)}$ + H_γ, 8 H), 3.60 (t, $J_{H\zeta H\varepsilon}$ = 6.5 Hz, 2 H); the resonance of the OH proton was not observed. − ^{31}P{^{1}H} NMR (CD_2Cl_2, 22°C, 81.01 MHz): AM_2 spin system, δ_A = −6.55, δ_M = −20.30, J_{AM} = 17.2 Hz.

Reaction of **9** *with HBF·OMe$_2$:* A 5-mm NMR tube was charged with a CD_2Cl_2 solution (0.8 ml) of **9** (0.020 g, 0.02 mmol), and cooled to −78°C. Addition of one equiv of HBF4·OMe2 (25 µl, 0.20 mmol) selectively regenerated **7** as shown by ^{31}P{^{1}H}-NMR analysis at −20°C.

X-ray Diffraction Study of [(triphos)Re(CO)$_2${=CCH$_2$-CH$_2$CH(Me)O}]BF$_4$ (**4**): A summary of crystal and intensity data is presented in Table 3. Experimental data were recorded at room temperature (20°C) on an Enraf-Nonius CAD4. A set of 25 carefully centered reflections in the range 6.5° < θ < 8.5° was used for determining the lattice constants. As a general procedure, the intensity of three standard reflections were measured periodically every 200 reflections for orientation and intensity control. This procedure did not reveal an appreciable decay of intensities. The data were corrected for Lorentz and polarization effects. Atomic scattering factors were those tabulated by Cromer and Waber,[32] with anomalous dispersion corrections taken from ref.[33]. An empirical absorptions correction was applied by using the program XABS2[34] with transmission factors in the range 0.631−1.425. The computational work was carried out by intensively using the program SHELX93.[35] Final atomic co-ordinates of all atoms and structure factors are available on request from the authors and are provided as supplementary material.

Pale orange crystals of **4** were grown in air from a dilute dichloromethane/ethanol solution. A parallelepiped crystal with dimension 0.25 × 0.20 × 0.11 mm was used for the data collection. The structure was solved by direct methods using the SIR92 program.[36] Refinement was done by full-matrix least-squares calculations, initially with isotropic thermal parameters then with anisotropic thermal parameters for Re, P, and C atoms of the triphos skeleton. The phenyl rings were treated as rigid bodies with D_{6h} symmetry, and the hydrogen atoms were allowed to ride on the attached carbon atoms. Crystallographic disorder was detected in the region of the tetrafluoroborate anion resulting in a double image of the four fluorine atoms. The two sets of fluorines were assigned a population factor of 0.6 and 0.4 respectively.

Table 3. Summary of crystal data and structure refinement for **4-BF$_4$**

Formula	$C_{48}H_{47}BF_4O_3P_3Re$		
Formula weight	1038.23	Crystal size [mm]	0.20×0.15×0.25
Crystal System	monoclinic	Space group	*P* 21/*n* (No. 14)
a [Å]	10.689(2)	*α* [deg]	90
b [Å]	17.921(4)	*β* [deg]	94.54(2)
c [Å]	23.175(5)	*γ* [deg]	90
V [Å^3]	4425(2)	*Z*	4
ρ(calcd) [gcm^{-3}]	1.558	Abs. coeff. [mm^{-1}]	2.912
F(000)	2080		
θ range [deg]	2.74−22.47		
Index ranges		$-11 \le h \le 11$, $0 \le k \le 19$, $0 \le l \le 24$	
Reflections collected		5763	
Independent reflections		5763 [*R*(int) = 0.0000]	
Refinement method		Full-matrix least squares on F^2	
Data/constraints/parameters		5763/0/234	
Goodness-of-fit on F^2		1.016	
Final *R* indices [$I > 2\sigma(I)$]		*R*1 = 0.0611; *wR*2 = 0.1226	
R indices (all data)		*R*1 = 0.1577; *wR*2 = 0.1564	
Largest difference peak [eÅ^3]		0.861 and −0.796	

Crystallographic data (excluding structure factors) for the structure reported in this paper have been deposited with the Cambridge Crystallographic Data Centre (deposition number 100775). Copies of the data can be obtained free of charge on application to CCDC, 12 Union Road, Cambridge CB2 1EZ, UK [fax (internat): +44(0)123/336-033, e-mail: deposit@chemcrys.cam.ac.uk].

[1] K. H. Dötz, W. Sturm, H. G. Alt, *Organometallics* **1987**, *6*, 1424.
[2] N. Ruiz, D. Péron, P. H. Dixneuf, *Organometallics* **1995**, *14*, 1095 and references therein.
[3] K. H. Dötz, H. Fischer, P. Hofmann, F. R. Kreissl, U. Schubert, K. Weiss, *Transition Metal Carbene Complexes;* Verlag Chemie: Weinheim, Germany, **1983**.
[4] H. Le Bozec, K. Ouzzine, P. H. Dixneuf, *Organometallics* **1991**, *10*, 2768.
[5] L. P. Barthel-Rosa, K. Maitra, J. Fischer, J. H. Nelson, *Organometallics* **1997**, *16*, 1714.
[6] H. Werner, A. Stark, P. Steinert, C. Grünwald, J. Wolf, *Chem. Ber.* **1995**, *128*, 49.
[7] W.-H. Leung, E. Y. Y. Chan, I. D. Williams, W.-T. Wong, *Organometallics* **1997**, *16*, 3234.
[8] [8a] M. P. Gamasa, J. Gimeno, M. Gonzalez-Cueva, E. Lastra, *J. Chem. Soc. Dalton Trans.* **1996**, 2547. − [8b] H. Werner, W. Knaup, M. Schulz, *Chem. Ber.* **1991**, *124*, 1121.
[9] [9a] E. Fritsch, T. Kerscher, K. Polborn, W. Beck, *J. Organomet. Chem.* **1993**, *460*, C25. − [9b] C. Kelley, N. Lugan, M. R. Terry, G. L. Geoffroy, B. S. Haggerty, A. L. Rheingold, *J. Am. Chem. Soc.* **1992**, *114*, 6735.
[10] [10a] P. Quayle, S. Rahman, L. M. Ward, J. Herbert, *Tetrahedron Lett.* **1994**, *35*, 3801. − [10b] R. L. Beddoes, R. W. Grime, Z. I. Hussain, M. W. Whiteley, *J. Chem. Soc. Dalton Trans.* **1996**, 3893.
[11] S. G. Davies, J. P. McNally, A. J. Smallridge, *Adv. Organomet. Chem.* **1990**, *30*, 1.
[12] The literature of vinylidene complexes is extensive. Some comprehensive reviews are: [12a] M. I. Bruce, *Chem. Rev.* **1991**, *91*, 197. − [12b] A. B. Antonova, A. A. Ioganson, *Russ. Chem. Rev.* **1989**, *58*, 593. − [12c] M. I. Bruce, A. G. Swincer, *Adv. Organomet. Chem.* **1983**, *22*, 59.
[13] Recent leading references of transition metal vinylidene complexes: [13a] I. Ara, J. R. Berenguer, J. Forniés, E. Lalinde, M.

Tomas, *Organometallics* **1996**, *15*, 1014. – [13b] R. L. Beddoes, C. Bitcon, R. W. Grime, A. Ricalton, M. W. Whiteley, *J. Chem. Soc. Dalton Trans.* **1995**, 2873. – [13c] J. M. O'Connor, K. Hübner, R. Merwin, L. Pu, *J. Am. Chem. Soc.* **1995**, *117*, 8861. – [13d] C. Bianchini, P. Innocenti, M. Peruzzini, A. Romerosa, F. Zanobini, *Organometallics* **1996**, *15*, 272. – [13e] M. A. Esteruelas, F. J. Lahoz, E. Oñate, L. A. Oro, C. Valero, B. Zeier, *J. Am. Chem. Soc.* **1995**, *117*, 7935. – [13f] R. Wiedemann, J. Wolf, H. Werner, *Angew. Chem. Int. Ed. Engl.* **1995**, *34,* 1244. – [13g] H. Werner, *J. Organomet. Chem.* **1994**, *475*, 45. – [13h] D. Touchard, P. Haquette, N. Pirio, L. Toupet, P. H. Dixneuf, *Organometallics* **1993**, *12*, 3132. – [13i] C. Bianchini, M. Peruzzini, A. Romerosa, F. Zanobini, *Organometallics* **1995**, *14*, 3152. – [13j] C. Bianchini, L. Glendenning, M. Peruzzini, A. Romerosa, F. Zanobini, *J. Chem. Soc. Chem. Commun.* **1994**, 2219. – [13k] C. Bianchini, J. A. Casares, M. Peruzzini, A. Romerosa, F. Zanobini, *J. Am. Chem. Soc.* **1996**, *118*, 6415. 4585. – [13l] I. de los Rios, M. Jimenez Tenorio, M. C. Puerta, P. Valerga, *J. Am. Chem. Soc.* **1997**, *119*, 6529.

[14] N. M. Kostic′, R. F. Fenske, R. F. *Organometallics* **1982**, *1*, 974.

[15] [15a] J. P. Selegue, B. A. Young, S. L. Logan, *Organometallics* **1991**, *10*, 1972. – [15b] V. Cadierno, M. P. Gamasa, J. Gimeno, J. Borge, S. Garcia-Granda, *Organometallics* **1997**, *16*, 3178 and references therein.

[16] E. Lindner, M. Pabel, R. Fawzi, H. A. Mayer, K. Wurst, *J. Organomet. Chem.* **1992**, *435*, 109.

[17] The ruthenium carbenes [Ru(=$COCH_2CH_2CH_2CH_2$)(η^5-C_9H_7)LL′] (L, L′ = tertiary phosphane) have recently been synthesized by Gimeno and coworkers by reaction of 5-hexyn-1-ol with [RuCl(η^5-C_9H_7)LL′] in the presence of $NaPF_6$. The X-ray analysis of the compound when L = L′ = PPh_3 has been determined: J. Gimeno, personal communication.

[18] H. Werner, T. Rappert, *Chem. Ber.* **1993**, *126*, 669.

[19] C. Bianchini, A. Marchi, L. Marvelli, M. Peruzzini, A. Romerosa, R. Rossi, A. Vacca, *Organometallics* **1995**, *14*, 3203.

[20] C. Bianchini, A. Marchi, L. Marvelli, M. Peruzzini, A. Romerosa, R. Rossi, *Organometallics* **1996**, *15*, 3804.

[21] M. P. Gamasa, J. Gimeno, B. M. Martin-Vaca, J. Borge, S. Garcia-Granda, E. Perez-Carreño, *Organometallics* **1994**, *13*, 4045.

[22] S. I. Hommeltoft, A. D. Cameron, T. A. Shackleton, M. E. Fraser, S. Fortier, M. C. Baird, *Organometallics* **1986**, *5*, 1380.

[23] G. L. Miessler, S. Kim, R. A. Jacobson, R. J. Angelici, *Inorg. Chem.* **1987**, *26*, 1690.

[24] M. Berry, J. Martin-Gil, J. A. K. Howard, F. G. A. Stone, *J. Chem. Soc., Dalton Trans.* **1980**, 1625.

[25] [25a] P. Nombel, N. Lugan, R. Mathieu, *J. Organomet. Chem.* **1995**, *503*, C22. – [25b] R. F. Stepanick, N. C. Payne, *J. Organomet. Chem.* **1974**, *72*, 453.

[26] N. A. Bailey, P. L. Chell, C. P. Manuel, A. Mukhopadhyay, D. Rogers, H. E. Tabbron, M. J. Winter, *J. Chem. Soc. Dalton Trans.* **1983**, 2397.

[27] A single-crystal X-ray diffraction study on **5** has fully confirmed the structural formulation determined in solution by multinuclear NMR spectroscopy. Details of this structure will be provided elsewhere.

[28] W. Hewertson, R. Watson, *J. Chem. Soc.* **1962**, 1490.

[29] B. E. Mann, *Adv. Organomet. Chem.* **1988**, *28*, 397.

[30] S. Castellano, A. A. Bothner-By, *J. Chem. Phys.* **1964**, *41*, 3863.

[31] [31a] D. S. Stephenson, G. A. Binsch, *J. Magn. Res.* **1980**, *37*, 395. – [31b] D. S. Stephenson, G. A. Binsch, *J. Magn. Res.* **1980**, *37*, 409.

[32] D. T. Cromer, J. T. Waber, *Acta Crystallogr.* **1965**, *18*, 104.

[33] *International Tables of Crystallography*, Vol. IV, Kynoch Press: Birmingham, UK, **1974**.

[34] S. Parkin, B. Moetzi, H. Hope, *J. Appl. Crystallogr.* **1995**, *28*, 53.

[35] G. M. Sheldrick, *SHELX-93. Program for Structure Refinement,* University of Göttingen, Germany, **1993**.

[36] A. Altomare, G. Cascarano, C. Giacovazzo, A. Guagliardi, M. C. Burla, G. Polidori, M. Camalli, *J. Appl. Crystallogr.* **1994**, *27*, 435.

[97211]

A New and Easy Route to Polysilanylpotassium Compounds☆[1]

Christoph Marschner

Institut für Anorganische Chemie, Technische Universität Graz
Stremayrgasse 16, 8010 Graz, Austria
Fax: (internat.) +43(0)316/873-8701
E-Mail: marschner@anorg.tu-graz.ac.at

Received August 20, 1997

Keywords: Polysilanes / Polysilyl anions / Silylpotassium / Silicon

A method is presented for the synthesis of tertiary, secondary, and primary polysilylpotassium compounds. Reaction of potassium *tert*-butoxide, in either DME or THF, with a suitable precursor molecule, proceeds by cleavage of a trimethylsilyl–polysilanyl bond, and formation of trimethylsilyl *tert*-butyl ether and a polysilanylpotassium compound. This route allows easy and flexible access to a number of novel polysilanylpotassium compounds, avoiding the hitherto common use of poisonous mercury compounds.

As is known from the pioneering work of Gilman and coworkers tetrakis(trimethylsilyl)silane can react with methyllithium to form tetramethylsilane and tris(trimethylsilyl)-silyllithium.[2]

$$(Me_3Si)_4Si + MeLi \rightarrow (Me_3Si)Me + \underset{\mathbf{1}}{(Me_3Si)_3SiLi} \quad (1)$$

The latter compound has been rapidly accepted as a prototype of a bulky nucleophilic polysilyl anion and, only recently, has been referred to as "hypersilyl" group.[3] It has been used for the synthesis of transition metal silyl compounds,[4] for the generation of silenes by means of sila-Peterson reaction,[5] and for a number of other purposes.[6] However, it is noticeable that this reagent, although so widely accepted, has rarely been the subject of variation. Only very recently have Klinkhammer[7] and Oehme[8] reported on the synthesis of the potassium and magnesium analogs, however the isotetrasilanyl moiety has almost never been varied. Nevertheless, Apeloig et al. have recently shown that variation of this moiety can be of some advantage. They have been able to show that an increase in the size of ligand gives rise to the formation of stable silenes.[9][5g]

Although it would be interesting to have a set of bulky polysilyl groups differing in reactivity and, especially, in size,[10] in order to achieve different degrees of steric hindrance, this problem has not so far been systematically addressed. The reason for this becomes obvious if one looks at a fact that was first pointed out by Gilman,[11] and then recently studied in more detail by Apeloig et al.,[12] namely that if polysilanes with "inner" Si–Si bonds react with methyllithium there is a pronounced tendency for these "inner" Si–Si bonds to undergo scission. This means that, for example, hexakis(trimethylsilyl)disilane yields **1** and tris(trimethylsilyl)methylsilane in the reaction with methyllithium (Eq. 2).

$$(Me_3Si)_6Si_2 + MeLi \rightarrow \underset{\mathbf{1}}{(Me_3Si)_3SiLi} + MeSi(SiMe_3)_3 \quad (2)$$

The results described in this paper show that this is not a primary limitation, and that it can be easily overcome by the correct choice of the transmetalating agent.

Results and Discussion

Our studies on the synthesis of dendritic and branched polysilanes[13] led to the investigation of some aspects of the chemistry of polysilyl anions. In reactions directed towards the formation of polysilanes with monosilyl anions and silyl halides we often found that the use of the potassium compound was superior to the use of lithium anions. So it was reasonable to also address the use of lithium vs. potassium in the case of the "hypersilyl" anion. Although this compound was already known from the work of Klinkhammer,[7] transmetalation from the corresponding bis-"hypersilyl" mercury, zinc, or cadmium compounds with potassium did not seem to be a real alternative to the use of the readily available "hypersilyllithium" **1**.[2] We felt that a really competitive synthesis must introduce the potassium in as easy a fashion as the lithium. So the obvious reagent of choice was potassium *tert*-butylate, which very effectively transforms dodecamethylcyclohexasilane into the corresponding undecamethylcyclohexasilanylpotassium.[14]

Indeed initial experiments showed that the conversion of tetrakis(trimethylsilyl)silane with *tert*-butylate in DME or THF, in a clean and almost quantitative reaction, gives "hypersilylpotassium" **1a** accompanied by the formation of trimethylsilyl *tert*-butyl ether (Eq. 3).

$$(Me_3Si)_4Si + KO\mathit{t}Bu \rightarrow \underset{\mathbf{1a}}{(Me_3Si)_3SiK} + (Me_3Si)O\mathit{t}Bu \quad (3)$$

Changing the solvent to toluene or pentane gives **1a** as a crystalline compound, with one or two molecules of the

 © WILEY-VCH Verlag GmbH, D-69451 Weinheim, 1998 1434–1948/98/0202–0221 $ 17.50+.50/0

etheral solvent still present, as can be seen from ^{1}H- and ^{13}C-NMR data. This synthesis of **1a** can be regarded as a significant improvement, avoiding the use of poisonous heavy metal compounds which are in turn prepared from **1** or tris(trimethylsilyl)silane.[7] It is an interesting alternative to use **1a** instead of **1** because the reactivities are comparable, the potassium compound being slightly more reactive. We found that the stoichiometry of the potassium reaction is easier to control dealing with potassium *tert*-butylate, which is a weightable solid, compared to methyllithium solutions which may have more or less well defined concentrations.

Treatment of **1a** with a variety of electrophiles proceeded as smoothly as expected (Scheme 1). Reaction with aqueous sulfuric acid gives the hydrosilane **2**, reaction with ethyl bromide yielded the ethylated product **3**, and silylation with a number of phenylated silyl chlorides was easily achieved (**4a,b,c**). Syntheses of an acylsilane (**5**),[15] and of the known zirconocene hypersilyl chloride (**6**),[16] can be achieved in a straightforward manner. The reaction of **1a** with 1,2-dibromoethane at −78°C proceeds in an analogous manner to that of the corresponding lithium compound **1**, and yields the dimerisation product **7**.

Scheme 1

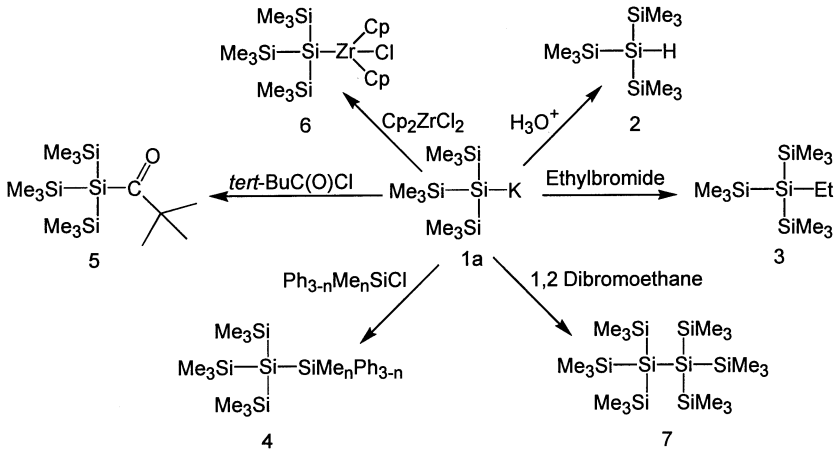

4a can be converted quantitatively to the corresponding bromosilane **8** by a protodesilylation reaction in neat hydrogen bromide at −78°C. The reaction of **8** with another equivalent of **1a** gives bis-"hypersilyl"-dimethylsilane **9** (Eq. 4). The latter compound was found first by Sakurai et al. as one of the products in the aluminum trichloride catalyzed isomerisation of linear permethylnonasilane,[17] and was recently synthesized by Apeloig et al.[12][18]

$$\underset{\mathbf{4a}}{(Me_3Si)_3SiSiMe_2Ph} + HBr \rightarrow \underset{\mathbf{8}}{(Me_3Si)_3SiSiMe_2Br} \rightarrow \underset{\mathbf{9}}{[(Me_3Si)_3Si]_2SiMe_2} \quad (4)$$

Compounds **7** and **9** were chosen to test the reaction with potassium *tert*-butylate for its ability to differentiate between "inner" and "outer" Si−Si bonds. From Gilmans work it is known that the reaction of **7** with methyllithium leads to the formation of **1** and tris(trimethylsilyl)methylsilane.[11] Similarly Apeloig et al. also found, in the reaction of **9** with methyllithium, exclusive cleavage of one of the "inner" Si−Si bonds.[12]

In contrast to these findings the reaction to give the potassium polysilanyl, using potassium *tert*-butylate, exhibits the opposite selectivity, splitting exclusively one of the "outer" Si−$SiMe_3$ bonds (**10**, **11**).

$$RSi(SiMe_3)_3 + KO\mathit{t}Bu \rightarrow RSi(SiMe_3)_2K + (Me_3Si)O\mathit{t}Bu \quad (5)$$

R = $(Me_3Si)_3Si$ **7** **10**
R = $(Me_3Si)_3SiSiMe_2$ **9** **11**

These results open the door for the synthesis of higher polysilyl anions. Both of the anions **10** and **11** are already known as lithium analogs. The lithium analog of **10** was observed by Gilman in the reaction of **7** with **1**.[11] The lithium derivative of **11** was found by Apeloig et al. in a reaction that they describe as the addition of methyllithium to a disilene.[12]

The polysilyl anions **10** and **11** are candidates for experiments in which the polysilyl moiety is required to be of increased size compared to the "hypersilyl" unit in order to fulfill its stabilizing function. It also should be mentioned that in both cases we attempted to obtain the dianionic species by the addition of another equivalent of potassium *tert*-butylate, but failed under normal reaction conditions. However, experiments to obtain such compounds are still in progress in our laboratory. The results reported so far have demonstrated that the potassium polysilanyls are serious competitors to their lithium analogs when higher polysilyl anions are required. The following section will show that this chemistry is also able to yield smaller polysilyl anions.

When ethylated **3** was subjected to standard treatment with potassium *tert*-butylate the reaction proceeded as expected and secondary potassium trisilane **12** was formed.

$$\underset{\mathbf{3}}{(Me_3Si)_3SiEt} + KO\mathit{t}Bu \rightarrow \underset{\mathbf{12}}{(Me_3Si)_2Si(Et)K} + (Me_3Si)O\mathit{t}Bu \quad (6)$$

As **12** can as easily be treated with electrophiles, as was demonstrated for **1a**, the sequence: tetrakis(trimethylsilyl)si-

lane → $(Me_3Si)_3SiK$ (**1a**) → $(Me_3Si)_3SiE$ (**3**) → $(Me_3Si)_2Si(E)K$ (**12**) → $(Me_3Si)_2Si(E)E'$ offers an interesting method of access to 2,2′-disubstituted trisilanes.[19]

Even more interesting, but unfortunately less selective, is the conversion of **2**. Under analogous conditions a secondary potassium trisilane **13** was formed with hydrogen and potassium attached to the same silicon atom. The reaction is accompanied by the formation of **1a**, which seems to be the result of a deprotonation reaction. The ratio of these two products is about 7:3 in favor of **13**.

$$\underset{\mathbf{2}}{(Me_3Si)_3SiH} + KO\mathit{t}Bu \rightarrow 0.7\ \underset{\mathbf{13}}{(Me_3Si)_2Si(H)K} + 0.3\ \underset{\mathbf{1a}}{(Me_3Si)_3SiK} + 0.7\ (Me_3Si)O\mathit{t}Bu + 0.3\ HO\mathit{t}Bu \quad (7)$$

While it has been shown so far that tertiary and secondary potassium silanyls are easily available from the reaction of suitable precursors with potassium *tert*-butylate, and it is also known that monosilyl potassium compounds are accessible from disilanes by reaction with C_8K,[20] primary potassium silanyls are not so easy to obtain.

The reaction of octamethyltrisilane with potassium *tert*-butylate in DME shows some rather complex chemistry, which we are currently studying in more detail, but which does not provide a suitable route to pentamethyldisilanylpotassium. Since 1,1-diphenyltrimethyldisilanyl alkali compounds are known to form from the reaction of 2,2-diphenylhexamethyltrisilane with methyllithium or sodium potassium alloy,[21] it was decided to test our reaction conditions on 2-phenylheptamethyltrisilane. However addition of one equivalent of potassium *tert*-butylate to the latter gave not only the desired disilanylpotassium compound **14**, but also a substantial amount of trimethylsilylpotassium, which was detected by ^{29}Si NMR. Changing the solvent to THF slowed down the reaction rate and did improve the ratio, but only slightly. It was finally found that optimum reaction conditions could be achieved by gradual addition of potassium *tert*-butylate to a THF solution of the starting material.

Analysis of ^{29}Si-NMR data from the experiments described and from the literature (see Table 1) shows some interesting details. Comparison of the shift values of the silicon atom with a trimethylsilyl substituent and the analog bearing a negative charge shows a high field shift of about 60 ppm, for tertiary alkali silanyls (entries 1−3), and of 33 ppm for the generation of a secondary potassium silanyl compound with one alkyl group (entry 4). Interestingly the substitution of a trimethylsilyl group by hydrogen (cf. entry 5) also gives a $\Delta\delta_{Si}$ value similar to the tertiary alkali silanyl (entry 1). Comparison of the known ^{29}Si-NMR value of H_3SiK (entry 10) with that of the respective trimethylsilylated compound shows that even a trihydrogenated silicon atom shifts some 60 ppm to higher field when the trimethylsilyl substituent is replaced by potassium.

While the change from secondary alkali silanyls to primary ones (entry 4 vs. 6) is not so pronounced, the influence of a phenyl group on the silicon atom bearing the negative charge is indicative, as can be seen by comparison of entries 6 and 7. In the case of the permethylated molecule (entry 6) a 26 ppm higher field shift is observed, while the molecule with one phenyl group shows only a 16 ppm shift. Obviously some of the negative charge can be transferred onto the phenyl group, resulting in a weaker deshielding effect. A very similar case is that of the monosilyl alkali compounds. While trimethylsilylpotassium shows an even weaker shift (only 14 ppm) compared to hexamethyldisilane (entry 8), dimethylphenylsilyllithium (entry 9) shows the weakest shift in the entire series (about 6 ppm) compared to the trimethylsilylated compound.

Table 1. Comparison of ^{29}Si-NMR shift values of polysilyl alkali compounds with the respective trimethylsilylated molecules

Entry	Oligosilane	$\delta_{Si-SiMe_3}$	Alkali silanyl	δ_{Si-M}	$\Delta\delta_{Si}$
1	$(Me_3Si)_4Si$[a]	−135.6	$(Me_3Si)_3SiK$[a]	−195.8	60.2
2	$(Me_3Si)_3SiSi(SiMe_3)_3$[a]	−129.5	$(Me_3Si)_3SiSi(SiMe_3)_2K$[a]	−192.7	63.2
3	$(Me_3Si)_3SiSiMe_2Si(SiMe_3)_3$[a]	−117.8	$(Me_3Si)_3SiSiMe_2Si(SiMe_3)_2K$[a]	−187.0	69.2
4	$(Me_3Si)_3SiEt$[a]	−78.6	$(Me_3Si)_2EtSiK$[a]	−111.7	33.1
5	$(Me_3Si)_3SiH$[a]	−115.4	$(Me_3Si)_2HSiK$[a]	−181.1	65.7
6	$Me_3SiSiMe_2SiMe_3$[b]	−48.7	$Me_3SiSiMe_2Li$[c]	−74.9	26.2
7	$Me_3SiSiMePhSiMe_3$[d]	−46.0	$Me_3SiSiMePhK$[d]	−62.9	16.9
8	$Me_3SiSiMe_3$[b]	−20.5	Me_3SiK[e]	−34.4	13.9
9	$PhMe_2SiSiMe_3$[b]	−21.7	$PhMe_2SiLi$[b]	−27.3	5.6
10	Me_3SiSiH_3[f]	−97.7	H_3SiK[b]	−165.0	67.3

[a] Measured in DME. − [b] Value taken from ref.[26]. − [c] Value taken from ref.[27]. − [d] measured in THF. − [e] Value taken from ref.[22]. − [f] A sample of Me_3SiSiH_3 was kindly provided by Dr. Robert Zink.

From the comparison of these data it is evident that the silicon atom bearing the negative charge can gain a release of charge which depends on the kind of substituents attached. While hydrogen and silyl groups, in accordance with their respective electropositive characters, do not take a great deal of the charge, charge can be transferred to methyl and, to an even greater extent, to phenyl groups,[22] which in turn leads to smaller values of $\Delta\delta_{Si}$.

One should mention here that analysis of these NMR data has to be undertaken with some caution with respect to the solvents used in the measurement. While the shifts of the uncharged compounds are relatively independent of solvent effects the silyl potassium compounds show a rather pronounced dependence on the solvent. Compared to the reported ^{29}Si-NMR data of $\delta = -185$ for **1a** in deuterobenzene, we found that a complexing solvent such as DME causes an additional upfield shift of 11 ppm, indicating a less covalent character for the Si−K bond. Formation of **1a** in THF results in a signal at −194 ppm. Subsequent crystallization from pentane shows the presence of two molecules of THF in the ^{1}H-NMR spectrum, and a value of $\delta = -189.5$ in the ^{29}Si-NMR spectrum. So we can observe, for one compound, a difference in the shift value of some 10 ppm depending on the solvent. However, it was considered that, as the data compared in Table 1 always refer to compounds in etheral solvents, this comparison was valid. Also the tendencies discussed are so pronounced that the solvent effects are relatively small.

The author wants to express his gratitude to the late Prof. *Hengge* for his encouragement and support, and for stimulating discussions. The *Wacker AG*, Burghausen, kindly provided chlorosilanes as starting materials. CHM is the recipient of an APART (Austrian Program for Advanced Research and Technology) scholarship of the *Austrian Academy of Science*, Vienna which is gratefully acknowledged.

Experimental Section

All reactions were carried out in flame-dried glassware under an inert atmosphere of dry argon or nitrogen. Solvents were distilled prior to use from either sodium or sodium potassium alloy. Starting materials tetrakis(trimethylsilyl)silane[23] and 2-phenylheptamethyltrisilane[24] were prepared according to literature procedures. $PhMe_2SiCl$, $Ph_2MeSiCl$, Ph_3SiCl, potassium *tert*-butylate, 1,2-dibromoethane, and ethyl bromide were used without further purification.

^1H-, ^{13}C-, and ^{29}Si-NMR spectra were recorded on a Bruker MSL 300 at the indicated frequencies. ^{29}Si-NMR spectra were measured either in C_6D_6 or directly from the reaction mixture using a D_2O capillary providing an external lock signal. In all cases, except for **2** and **13**, the INEPT pulse sequence was employed. − GC/MS was performed on an HP 5890/II gas chromatgraph with an HP 5971/A MSD, an HP1 (Cross-linked methyl silicone) column and helium as a carrier gas. − Elemental analyses of the branched polysilanes were done using a Heraeus elementar vario EL apparatus. For some reason the carbon values found in the elemental analyses are too low when certain compounds were analyzed with quarternary silicon atoms. While the hydrogen values correspond nicely to the calculated numbers we attribute the low carbon values to the formation of silicon carbide, which seems to be very favorable in the cases of the compounds mentioned.

General Procedure: Starting material and one equivalent of potassium *tert*-butylate were mixed together in a flask and either DME or THF added. Almost immediately the solution turned yellow and, after some time, sometimes orange. Completion of the reaction was detected either by ^{29}Si-NMR spectroscopy (D_2O capillary as external lock) and/or by obtaining a derivative and subsequent GC/MS or GC analysis. The derivative was obtained by adding a 20-µl sample of the reaction mixture into a solution of 100 µl of ethyl bromide in 2 ml of ether, or by addition of the sample into the etheral phase of a 2 ml ether/2 ml 2 M H_2SO_4 mixture followed by mixing of the layers.

Tris(trimethylsilyl)silylpotassium (**1a**): In a typical experiment tetrakis(trimethylsilyl)silane (3.10 g, 9.66 mmol) was treated with *tert*-BuOK (1.14 g, 10.14 mmol) in 5 ml of either DME or THF following the general procedure. While the conversion in DME was usually complete within 10 min the use of THF sometimes required reaction times up to 60 min. − ^{29}Si NMR (59.6 MHz, DME, D_2O lock): δ = −3.93, −195.83, (59.6 MHz, THF, D_2O lock): δ = −4.55, −194.10.

A sample of **1a** prepared in THF on the same scale as described above, which was isolated by removal of solvent in vacuo and crystallization from toluene and pentane (3.20 g, 7.71 mmol, 80%), was identified by ^1H NMR and ^{13}C NMR as a complex containing two molecules of THF. − ^1H NMR (300 MHz, C_6D_6): δ = 3.42 (m, 8 H), 1.47 (m, 8 H), 0.47 (s, 27 H). − ^{13}C NMR (75.4 MHz, C_6D_6): δ = 68.33, 25.93, 7.67. − ^{29}Si NMR (59.6 MHz, C_6D_6): δ = −5.35, −189.56.

Tris(trimethylsilyl)silane (**2**): **1a** was generated in THF from tetrakis(trimethylsilyl)silane (1.00 g, 3.11 mmol) following the general procedure. After complete conversion the solution of **1a** in THF was slowly poured into a mixture of ethyl ether (30 ml), aqueous H_2SO_4 (1 M solution, 50 ml), and ice. The organic layer was dried over Na_2SO_4 and evaporated in vacuo. The remaining oil (720 mg, 2.90 mmol, 93%) was pure by GC/MS. − ^{29}Si NMR (59.6 MHz, pentane, D_2O lock): δ −10.92, −115.36 (d, J = 156 Hz). − MS (70 eV): *m/z* (%): 248 (33) [M^+], 233 (27) [M^+ − Me], 174 (82) [M^+ − $HSiMe_3$], 160 (100) [M^+ − $SiMe_4$], 159 (88) [MH − $SiMe_4$], 73 (80) [$SiMe_3$]. − IR, ^1H and ^{13}C NMR data in accordance to the literature.[25]

Tris(trimethylsilyl)ethylsilane (**3**): Compund **3** was prepared from tetrakis(trimethylsilyl)silane (2.00 g, 6.22 mmol) by essentially the same method as for **2** with the difference that the solution of **1a** was poured into a mixture of ethyl ether (30 ml) and ethyl bromide (5 ml). After complete addition the solution was stirred for 5 min at room temp. and aqueous H_2SO_4 (1 M solution, 50 ml) was added. The workup was the same as for **2**. The remaining white solid (1.43 g, 5.17 mmol, 83%) was found, using GC/MS and NMR, to be pure. An analytical sample was recrystallized from ethanol (mp: 136−138°C). − ^1H NMR (300 MHz, $CDCl_3$): δ = 1.10 (t, J = 8.0 Hz, 3 H), 0.82 (q, J = 7.9 Hz, 2 H), 0.17 (s, 27 H). − ^{13}C NMR (75.4 MHz, $CDCl_3$): δ = 13.11, 1.39, 0.00. − ^{29}Si NMR (59.6 MHz, pentane, D_2O lock): δ −12.35, −78.81. − MS (70 eV): *m/z* (%): 276 (20) [M^+], 261 (4) [M^+ − Me], 203 (19) [M^+ − $SiMe_3$], 188 (30) [M^+ − $SiMe_4$], 175 (27) [M^+ − $EtSiMe_3$], 73 (100) [$SiMe_3$]. − $C_{11}H_{32}Si_4$ (276.72) calcd. C 47.75, H 11.66; found C 47.46, H 11.71.

1,1,1-Tris(trimethylsilyl)dimethylphenyldisilane (**4a**): **1a** was prepared from tetrakis(trimethylsilyl)silane (3.10 g, 9.66 mmol) and *tert*-BuOK (1.14 g, 10.1 mmol) in THF by the general procedure. After complete reaction the solvent was removed in vacuo and toluene (15 ml) was added. The mixture was cooled to −78°C and chlorodimethylphenylsilane (1.81 g, 10.6 mmol) was added in toluene (10 ml) gradually over 5 min. The reaction was stirred for further 12 h at room temp.. The workup was done by the addition of aqueous H_2SO_4 (1 M solution, 20 ml), extraction of the aqueous phase with two portions of ether, and drying of the combined organic phases over Na_2SO_4. After removal of the solvent by evaporation the white residue was crystallized from ethanol to give **4a** (3.00 g, 7.83 mmol, 81%) as white crystals (mp: 156−157°C). − ^1H NMR (300 MHz, $CDCl_3$): δ = 7.56 (m, 2 H), 7.36 (m, 3 H), 0.54 (s, 6 H), 0.18 (s, 27 H). − ^{13}C NMR (75.4 MHz, $CDCl_3$): δ = 141.46, 134.32, 128.68, 127.86, 3.02, 1.42. − ^{29}Si NMR (59.6 MHz, pentane, D_2O lock): δ = −8.92, −12.48, −133.23. − MS (70 eV): *m/z* (%): 382 (14) [M^+], 367 (7) [M^+ − Me], 294 (4) [M^+ − $SiMe_4$], 232 (93) [$Me_2Si_2(SiMe_3)_2$], 135 (79) [$SiMe_2Ph$], 73 (100) [$SiMe_3$]. − $C_{17}H_{38}Si_5$ (382.92) calcd. C 53.32, H 10.00; found C, 53.04 H 9.93.

1,1,1-Tris(trimethylsilyl)methyldiphenyldisilane (**4b**): **4b** was prepared following the procedure for the synthesis of **4a**, and on the same scale, using methyldiphenylchlorosilane (2.47 g, 10.6 mmol) as an electrophile. White crystals of **4b** (3.06 g, 6.88 mmol, 71%) were isolated after crystallization from ethanol (mp: 161−164°C). − ^1H NMR (300 MHz, $CDCl_3$): δ = 7.56 (m, 4 H), 7.33 (m, 6 H), 0.79 (s, 3 H), 0.14 (s, 27 H). − ^{13}C NMR (75.4 MHz, $CDCl_3$): δ = 138.90, 135.41, 128.97, 127.86, 3.10, 0.58. − ^{29}Si NMR (59.6 MHz, pentane, D_2O lock): δ = −8.95, −11.95, −132.84. − MS (70 eV): *m/z* (%): 444 (4) [M^+], 429 (2) [M^+ − Me], 294 (4) [M^+ − $PhSiMe_3$], 232 (100) [$Me_2Si_2(SiMe_3)_2$], 197 (75) [$SiMePh_2$], 135 (34) [$SiMe_2Ph$], 73 (47) [$SiMe_3$]. − $C_{22}H_{40}Si_5$ (444.99) calcd. C 59.38, H 9.09; found C 59.32, H 9.01.

1,1,1-Tris(trimethylsilyl)triphenyldisilane (**4c**): **4c** was prepared following the procedure for the synthesis of **4a**, and on the same

scale, using triphenylchlorosilane (3.13 g, 10.5 mmol) as an electrophile. White crystals of **4c** (3.74 g, 7.37 mmol, 76%) were yielded after crystallization from ethanol (mp: 263−266°C). − ^{1}H NMR (300 MHz, $CDCl_3$): δ = 7.52 (m, 6 H), 7.37 (m, 9 H), 0.18 (s, 27 H). − ^{13}C NMR (75.4 MHz, $CDCl_3$): δ = 137.71, 136.71, 129.26, 127.99, 3.19. − ^{29}Si NMR (59.6 MHz, pentane, D_2O lock): δ = −9.17, −10.22, −130.84. − MS (70 eV): *m/z* (%): 297 (1) [M^+ − $SiPhMe_2$ − $HSiMe_3$], 282 (8) [M^+ − $SiPhMe_2$ − $SiMe_4$], 259 (93) [$SiPh_3$)], 232 (100) [$Me_2Si_2(SiMe_3)_2$], 135 (28) [$SiMe_2Ph$], 73 (47) [$SiMe_3$]. − $C_{27}H_{42}Si_5$ (507.06) calcd. C 63.96, H 8.35; found C 63.81, H 8.39.

Tris(trimethylsilyl)silylpivaloate (**5**): **1a** was generated following the general procedure from tetrakis(trimethylsilyl)silane (3.00 g, 9.35 mmol) in THF. After removal of the solvent toluene (10 ml) was added and the solution was added slowly to an ice cold solution of pivaloyl chloride (1.16 g, 9.63 mmol) in toluene (10 ml). After complete conversion, which was checked by GC/MS, the reaction mixture was poured into an ice/sulfuric acid mixture (10%). The aqueous layer was extracted with ether (2 × 20 ml) and the combined organic layer dried over Na_2SO_4. After removal of the solvent final purification was achieved by chromatography on silica with toluene/heptane, 10:1. Spectral data of the compound (2.17 g, 6.52 mmol, 70%) were in accordance with the literature.[15]

Tris(trimethylsilyl)silylchlorozirconocene (**6**): **1a** was generated following the general procedure from tetrakis(trimethylsilyl)silane (2.00 g, 6.23 mmol) in DME. After complete conversion the solution was added, using a syringe pump, over a period of 40 min to a suspension of Cp_2ZrCl_2 (1.82 g, 6.22 mmol) in pentane (10 ml). Complete conversion was detected by ^{29}Si NMR after another 60 min stirring at room temp. Crystallization was achieved by removal of the solvent, addition of 20 ml of pentane and storage at −75°C. Extremely air-sensitive red crystals (3.12 g, 5.78 mmol, 93%) were obtained. − Spectral data in accordance to literature values.[16]

Hexakis(trimethylsilyl)disilane (**7**): **1a** was generated following the general procedure from tetrakis(trimethylsilyl)silane (5.00 g, 15.6 mmol) in THF. After complete conversion the solution was cooled to −78°C and 1,2-dibromoethane (1.63 g, 8.67 mmol) in ethyl ether (30 ml) was added dropwise over a period of 30 min. The solution then was allowed to come to room temp. and was poured into an ice/aqueous H_2SO_4 mixture. The organic layer was dried over Na_2SO_4 and the solvent removed in vacuo. The remaining white crystals (3.80 g) were shown by ^{29}Si NMR to be 90% pure **7**, with tetrakis(trimethylsilyl)silane being the only impurity. Sublimation (120°C, 1 mbar) removed about 300 mg of tetrakis(trimethylsilyl)silane. Finally pure **7** was obtained by recrystallization from acetone and ethanol which gave **7** (3.16 g 6.38 mmol, 82%) as white crystals. − ^{1}H NMR (300 MHz, $CDCl_3$): δ = 0.20 (s). − ^{13}C NMR (75.4 MHz, $CDCl_3$): δ = 4.60. − ^{29}Si NMR (59.6 MHz, pentane, D_2O lock): δ = −9.04, −129.49. − MS (70 eV): *m/z* (%): 406 (0.2) [M^+ − $SiMe_4$], 247 (6) [M^+ − $Si(SiMe_3)_3$], 232 (29) [M^+ − $MeSi(SiMe_3)_3$], 73 (100) [$SiMe_3$].

1,1,1-Tris(trimethylsilyl)dimethylbromodisilane (**8**): A flask equipped with a reflux condenser cooled to −80°C and charged with a sample of **4a** (2.40 g, 6.27 mmol) was cooled to −80°C and approx. 10 ml of hydrogen bromide was condensed on under a pressure of 200−500 mbar. After 30 min the cooling bath was removed and the solution of **4a** in hydrogen bromide was refluxed for 90 min. Then hydrogen bromide was removed in vacuo and pentane was distilled onto the residue (10 ml). The solution was filtered over a plug of glass wool and the solvent of the filtrate was removed in vacuo. The remaining white powder of **8** (2.40 g, 6.22 mmol, 99%) was pure by GC and NMR. − ^{1}H NMR (300 MHz, C_6D_6): δ = 0.71 (s, 6 H), 0.26 (s, 27 H). − ^{13}C NMR (75.4 MHz, C_6D_6): δ = 8.08, 2.90. − ^{29}Si NMR (59.6 MHz, C_6D_6): δ = 25.81, −9.61, −127.92; MS (70 eV): *m/z* (%): 369/371 (4/5) [M^+ − Me], 311/313 (1/2) [M^+ − $SiMe_3$], 232 (45) [M^+ − $BrSiMe_3$], 73 (100) [$SiMe_3$]. − $C_{11}H_{33}BrSi_5$ (385.71) calcd. C 34.25, H 8.62; found C 33.97, H 8.57.

1,1,1,3,3,3-Hexakis(trimethylsilyl)dimethyltrisilane (**9**): A solution of **1a** [prepared from tetrakis(trimethylsilyl)silane (1.66 g, 5.17 mmol) in DME] in toluene (5 ml) was added slowly at −50°C to a solution of **8** (1.81 g, 4.70 mmol) in toluene (5 ml). The reaction was allowed to reach room temp. and was followed by ^{29}Si NMR. After complete conversion a workup was performed by the addition of aqueous H_2SO_4 (1 M solution, 20 ml), extraction of the aqueous layer with two portions of ether, and drying of the combined organic layers over Na_2SO_4. Solvent was removed in vacuo and the residue was subjected to Kugelrohr distillation (1 mbar, 250°C) to remove volatile components. Finally crystallization of the remaining solid was achieved from ethanol/ethyl acetate to yield **9** (1.62 g, 2.92 mmol, 62%) as white crystals (mp: 168−171; ref.[17] 170−172°C). − ^{1}H NMR (300 MHz, $CDCl_3$): δ = 0.50 (s, 6 H), 0.23 (s, 54 H). − ^{13}C NMR (75.4 MHz, $CDCl_3$): δ = 5.81, 4.10. − ^{29}Si NMR (59.6 MHz, pentane, D_2O lock): δ = −8.64, −25.19, −117.70. − MS (70 eV): *m/z* (%): 537 (1) [M^+ − Me], 305 (97) [M^+ − $Si(SiMe_3)_3$], 232 (100) [$Me_2Si_2(SiMe_3)_2$], 73 (95) [$SiMe_3$]. − $C_{20}H_{60}Si_9$ (553.47) calcd. C 43.40, H 10.93; found C 41.94, H 10.92.

Pentakis(trimethylsilyl)disilanylpotassium (**10**): Compound **10** was prepared from **7** (200 mg, 0.40 mmol) and *tert*-BuOK (44 mg, 0.40mmol) in DME following the general procedure. The only product after complete consumption of **7**, as detected by NMR and GC/MS of derivatives of the samples, was **10**. − ^{29}Si NMR (59.6 MHz, DME, D_2O lock): δ = −5.58, −10.68, −128.92, −192.62. − H_3O^+ quench: ^{1}H NMR (300 MHz, $CDCl_3$): δ = 2.81 (s, 1 H), 0.33 (s, 18 H), 0.32 (s, 27 H). − ^{13}C NMR (75.4 MHz, $CDCl_3$): δ = 3.74, 3.54. − ^{29}Si NMR (59.6 MHz, pentane, D_2O lock): δ = −11.84, −13.38, −118.02, −135.04. − MS (70 eV): *m/z* (%): 407 (3) [M^+ − Me], 348 (18) [M^+ − $HSiMe_3$], 333 (2) [M^+ − $HSiMe_4$], 259 (4) [M^+ − $H_2Si_2Me_7$], 73 (100) [$SiMe_3$]. − Ethyl bromide quench: ^{1}H NMR (300 MHz, $CDCl_3$): δ = 1.13 (t, *J* = 7.0 Hz, 3 H), 0.97 (q, *J* = 7.0 Hz, 2 H), 0.26 (s, 27 H), 0.24 (s, 18 H). − ^{13}C NMR (75.4 MHz, $CDCl_3$): δ = 13.52, 5.11, 4.18, 3.01. − ^{29}Si NMR (59.6 MHz, pentane, D_2O lock): δ = −8.94, −11.73, −68.92, −130.43. − MS (70 eV): *m/z* (%): 377 (6) [M^+ − $SiMe_3$], 275 (4), [M^+ − 2 $SiMe_3$, − Et], 232 (26) [$Me_2Si_2(SiMe_3)_2$], 73 (100) [$SiMe_3$]. The experiment was repeated in THF with essentially the same results. Removal of solvent and crystallization from pentane gave white crystals solvated with two molecules of THF in an almost quantitative yield (220 mg, 0.37 mmol, 93%). − ^{1}H NMR (300 MHz, C_6D_6): δ = 3.41 (m, 8 H), 1.46 (m, 8 H), 0.51 (s, 18 H), 0.46 (s, 27 H). − ^{13}C NMR (75.4 MHz, C_6D_6): δ = 68.28, 25.94, 8.82, 4.78.

1,1,3,3,3-Pentakis(trimethylsilyl)-2,2-dimethyltrisilanylpotassium (**11**): Compound **11** was prepared from **9** (95 mg, 0.17 mmol) and *tert*-BuOK (19 mg, 0.17 mmol) in DME following the general procedure. The reaction was followed directly by ^{29}Si NMR and GC/MS of the quenched samples. Conversion was complete after 60 min. Addition of another equivalent of *tert*-BuOK (19 mg, 0.17 mmol) did not result in a second splitting reaction but led to the slow decomposition of the product after two days. − ^{29}Si NMR (59.6 MHz, DME, D_2O lock): δ = −3.21, −8.80, −16.12, −127.09, −186.99. − H_3O^+ quench: MS (70 eV): *m/z* (%): 480 (0.1) [M^+], 406 (3) [M^+ − $HSiMe_3$], 305 (63) [M^+ − $HSi(SiMe_3)_3$], 231 (25) [$Me_2Si_2(SiMe_3)_2$ − H], 73 (100) [$SiMe_3$]. − Ethyl bromide quench:

MS (70 eV): *m/z* (%): 493 (0.2) [M^+ − Me], 305 [M^+ − EtSi(SiMe$_3$)$_2$], 232 (30) [$Me_2Si_2(SiMe_3)_2$], 188 (24) [EtSi(SiMe$_3$) − Me], 73 (100) [SiMe$_3$)].

Bis(trimethylsilyl)ethylsilylpotassium (**12**): Compound **12** was prepared from **3** (89 mg, 0.36 mmol) and *tert*-BuOK (40 mg, 0.36 mmol) in DME following the general procedure. The reaction was followed directly by ^{29}Si NMR and GC/MS of the quenched samples. It was found to be complete after 25 min. − ^{29}Si NMR (59.6 MHz, DME, D_2O lock): δ = −6.82, −111.68. − H_3O^+ quench: MS (70 eV): *m/z* (%): 204 (14) [M^+], 189 (7) [M^+ − Me], 161 (8) [M^+ − SiMe$_3$], 130 (29) [M^+ − HSiMe$_3$], 102 (65) [M^+ − EtSiMe$_3$)], 73 (100) [SiMe$_3$]. − Ethyl bromide quench: MS (70 eV): *m/z* (%): 232 (12) [M^+], 159 (16) [M^+ − SiMe$_3$], 131 (27) [MH^+ − EtSiMe$_3$], 73 (100) [SiMe$_3$]. Repeating the experiment the same scale in THF led to the same results with some increased reaction time. Removals of solvent and crystallization from pentane gave white crystals (56 mg, 0.20 mmol, 56%), which were shown by NMR to contain half a molecule of THF coordinated to the silyl potassium compound. − ^{1}H NMR (300 MHz, C_6D_6): δ = 3.37 (m, 2 H), 1.37 (m, 2 H), 1.24 (t, *J* = 7.8 Hz, 3 H), 0.86 (q, *J* = 7.8 Hz, 2 H), 0.32 (s, 18 H). − ^{13}C NMR (75.4 MHz, C_6D_6): δ = 68.42, 25.82, 19.57, 5.03, 3.69.

Bis(trimethylsilyl)silylpotassium (**13**): Compound **13** was prepared from **2** (775 mg, 3.11 mmol) and *tert*-BuOK (385 mg, 3.43 mmol) in DME following the general procedure. The reaction was followed directly by ^{29}Si NMR and GC/MS of the quenched samples. Complete conversion was reached after 2 h and gave **13** and **1a** in a ratio of about 7:3. − IR $\tilde{\nu}$: 1891 cm^{-1} (Si−H). − ^{29}Si NMR (59.6 MHz, DME, D_2O lock): δ = −4.02, −181.14 (d, *J* = 82 Hz). − H_3O^+ quench: MS (70 eV): *m/z* (%):, 176 (11) [M^+], 161 (16) [M^+ − Me], 101 (9) [M^+ − H_2SiMe_3], 88 (21) [M^+ − SiMe$_4$], 73 (100) [SiMe$_3$]. − Ethyl bromide quench: MS: vide supra. The experiment was repeated in THF on larger scale and gave essentially the same results. Removal of the solvent and crystallization from pentane gave a mixture of **13** and **1a** with THF coordinated to the alkali silanyl compounds. − ^{1}H NMR (300 MHz, C_6D_6): δ = 3.51 (m), 1.38 (m), 1.29 (s, 1 H), 0.47 (s, 18 H), 0.43 (s, 27 H).

1-Phenyltetramethyldisilanylpotassium (**14**): Compound **14** (200 mg, 0.75 mmol) was prepared from 2-phenylheptamethyltrisilane in THF following the general procedure, with the variation that *tert*-BuOK (85 mg, 0.75 mmol) was added in several portions over two hours. − ^{29}Si NMR (59.6 MHz, THF, D_2O lock): δ = −12.33, −62.96. − H_3O^+ quench: MS (70 eV): *m/z* (%): 194 (21) [M^+], 179 (15) [M^+ − Me], 135(83) [M^+ − HSiMe$_2$], 121 (21) [M^+ − SiMe$_3$], 105 (28) [M^+ − HSiMe$_4$], 73 (100) [SiMe$_3$]. − Ethyl bromide quench: MS (70 eV): *m/z* (%): 222 (20) [M^+], 207 (4) [M^+ − Me], 193 (14) [M^+ − Et], 149 (39) [M^+ − SiMe$_3$], 135 (44) [SiPhEt], 121 (100) [HSiPhMe], 105 (17) [SiPh], 73 (27) [SiMe$_3$].

☆ In memoriam Prof. *Edwin Hengge*.

[1] Presented in part at the *XIth International Symposium on Organosilicon Chemistry*, 1.−6. Sept. **1996**, Montpellier, France.

[2] [2a] H. Gilman, J. M. Holmes, C. L. Smith, *Chem. Ind. (London)* **1965**, 848. − [2b] G. Gutekunst, A. G. Brook, *J. Organomet. Chem.* **1982**, *225,* 1.

[3] Using the term "hypersilyl" we follow the proposal of N. Wiberg, made at the *Xth International Symposium on Organosilicon Chemistry* in Posnan, Poland, *1993*.

[4] [4a] T. D. Tilley in *The Chemistry of Organic Silicon Compounds,* Chapter 24, (Eds.: S. Patai, Z. Rappoport), Wiley, Chichester, **1989**, p. 1415. − [4b] T. D. Tilley in *The Silicon Heteroatom Bond,* (Eds.: S. Patai, Z. Rappoport), Wiley, Chichester, **1991**, p. 309.

[5] [5a] D. Hoffmann, H. Reincke, H. Oehme, *Z. Naturforsch.* **1996**, *51b*, 370. − [5b] F. Luderer, H. Reincke, H. Oehme, *Chem. Ber.* **1996**, *129*, 15. − [5c] Ch. Wendler, H. Oehme, *Z. Anorg. Allg. Chem.* **1996**, *622*, 801. − [5d] C. Krempner, H. Reincke, H. Oehme, *Chem. Ber.* **1995**, *128*, 1083. − [5e] F. Luderer, H. Reincke, H. Oehme, *J. Organomet. Chem.* **1996**, *510,* 181. − [5f] C. Krempner, H. Reincke, H. Oehme, *Chem. Ber.* **1995**, *128*, 143. − [5g] D. Bravo-Zhivotovskii, V. Braude, A. Stanger, M. Kapon, Y. Apeloig, *Organometallics* **1992**, *11*, 2326.

[6] [6a] E. Jeschke, T. Gross, H. Reincke, H. Oehme, *Chem. Ber.* **1996**, *129*, 841. − [6b] Y. Apeloig, I. Zharov, D. Bravo-Zhivotovskii, Y. Ochvinnikov, Y. Struchkov, *J. Organomet. Chem.* **1995**, *499,* 73. − [6c] D. Bravo-Zhivotovskii, Y. Apeloig, Y. Ochvinnikov, V. Igonin, Y. T. Struchkov, *J. Organomet. Chem.* **1993**, *446,* 123. − [6d] H. Oehme, R. Wustrack, A. Heine, G. M. Sheldrick, D. Stalke, *J. Organomet. Chem.* **1993**, *452,* 33.

[7] K. W. Klinkhammer, W. Schwarz, *Z. Anorg. Allg. Chem.* **1993**, *619*, 1777.

[8] C. Krempner, H. Oehme, *J. Organomet. Chem.* **1994**, *464*, C7.

[9] For the synthesis of (*tert*-BuMe$_2$Si)(Me$_3$Si)$_2$SiLi and (*tert*-BuMe$_2$Si)$_2$(Me$_3$Si)SiLi see: Y. Apeloig, M. Bendikov, M. Yuzefovich, M. Nakash, D. Bravo-Zhivotovskii, D. Bläser, R. Boese, *J. Am. Chem. Soc.* **1996**, *118*, 12228.

[10] For an interesting comparison of the size of ligands see: J. Frey, E. Schottland, Z. Rappoport, D. Bravo-Zhivotovskii, M. Nakash, M. Botoshansky, M. Kaftory, Y. Apeloig, *J. Chem. Soc. Perkin Trans. 2* **1994**, 2555.

[11] H. Gilman, R. L. Harrel, *J. Organomet. Chem.* 1967, *9*, 67.

[12] Y. Apeloig, M. Yuzefovich, M. Bendikov, D. Bravo-Zhivotovskii, K. Klinkhammer, *Organometallics* **1997**, *16*, 1265.

[13] Ch. Marschner, E. Hengge in: *Organosilicon Chemistry III,* N. Auner, J. Weis , Eds., VCH, Weinheim, in press.

[14] F. Uhlig, P. Gspaltl, M. Trabi, E. Hengge, *J. Organomet. Chem.* **1995**, *493*, 33.

[15] [15a] A. G. Brook, J. W. Harris, J. Lennon, M. El Sheik, *J. Am. Chem. Soc.* **1979**, *101*, 83. − [15b] A. G. Brook, F. Abdesajken, G. Gutekunst, N. Plavac, *Organometallics* **1982**, *1*, 994.

[16] B. K. Campion, J. Falk, T. D. Tilley, *J. Am. Chem. Soc.* **1987**, *109*, 2049.

[17] M. Ishikawa, J. Iyoda, H. Ikeda, K. Kotake, T. Hashimoto, M. Kumada, *J. Am. Chem. Soc.* **1981**, *103*, 4845.

[18] An X-ray structure of **9** reveals a bond angle between the two hypersilyl groups and the central silicon atom of 125.7°. Ch. Marschner, Ch. Kayser, P. Felde, to be published elsewhere.

[19] The only other convenient access to 2-metallated trisilanes which is known to the author employs transmetallation from the respective mercury substituted compounds: A. Sekiguchi, M. Nanjo, C. Kabuto, H. Sakurai, *J. Am. Chem. Soc.* **1995**, *117,* 4195.

[20] A. Fürstner, H. Weidmann, *J. Organomet. Chem.* **1988**, *354,* 15.

[21] A. G. Brook, A. Baumegger, A. J. Lough, *Organometallics* **1992**, *11,* 310.

[22] G. A. Olah, R. J. Hunadi, *J. Am. Chem. Soc.* **1980**, *102,* 6989

[23] H. Gilman, C. L. Smith, *J. Organomet. Chem.* **1967**, *8,* 245.

[24] M. Kumada, M. Ishikawa, S. Maeda, *J. Organomet. Chem.* **1964**, *2,* 478.

[25] [25a] H. Bürger, W. Killian, *J. Organomet. Chem.* **1971**, *26,* 47. − [25b] H. C. Marsmann, W. Raml, E. Hengge, *Z. Naturforsch.* **1981**, *35b*, 1541.

[26] H. C. Marsmann in *NMR Basic Principles and Progress 17,* ^{29}Si-NMR Spectroscopic Results, (Eds.: P. Diehl, E. Fluck, R. Kosfeld), Springer-Verlag Berlin Heidelberg, 1981.

[27] K. Krohn, K. Khanbabaee, *Angew. Chem.* **1994**, *106*, 100; *Angew. Chem., Int. Ed. Engl.* **1994**, *33*, 99.

[97197]

Organophosphorus Compounds, 125[◇]

Hydrostannylation of Phosphaalkynes☆

Marion Schmitz, Rudolf Göller, Uwe Bergsträßer, Stefan Leininger, and Manfred Regitz*

Fachbereich Chemie der Universität Kaiserslautern,
Erwin-Schrödinger-Strasse, D-67663 Kaiserslautern, Germany
Fax: (internat.) + 49(0)631/205-3921

Received September 22, 1997

Keywords: Hydrostannylation / Phosphaalkynes / 1,2-Dihydro-1,3-diphosphetes / Homocubanes / Carbonyl complexes

The hydrostannylation of phosphaalkynes **8** with tin hydrides **1** depends on the stoichiometry employed: Thus, the 1,2-dihydro-1,3-diphosphetes **10** are isolated when an excess of phosphaalkyne **8** is used. On the other hand, an increase in the tin hydride concentration favors the formation of the phosphanes **11** and **12**. Synthesis of the 1,2-dihydro-1,3-diphosphetes **14** and **16** was achieved by the use of diorganotin hydrides **13** or chloro(organo)tin hydrides **4**, respectively. An isolated and characterized by-product of the latter reaction was the phosphorus-carbon-tin cage **17**. Furthermore, the following reactions of the 1,2-dihydro-1,3-diphosphetes **10** were performed: isomerization reactions, complexation reactions with transition-metal complexes, and substitution of the hydrogen atom by iodine.

Introduction

Addition reactions of organotin compounds to unsaturated systems have been known for a long time[2]. Following the hydrostannylation of alkenes which, as a consequence of the mild reaction conditions and high selectivity, has found wide-ranging applications, the first 1,2-addition of triorganotin hydrides to acetylenes was achieved in 1959[3][4]. In comparison to the hydrostannylation reactions of the corresponding olefins, the additions to C−C triple-bond systems proceed more readily. The vinyltin compounds **2** are the primary products of these reactions which then undergo, albeit somewhat delayed, addition of a second equivalent of the triorganotin hydride **1** to furnish the ditin compounds **3**. Modification of the organotin hydride by the introduction of a halogen atom to give the diorgano(halo)tin hydrides **4**[5] provides further new possibilities for the synthesis of numerous mixed substituted organotin compounds **5**[6].

We recently reported on hydrostannylation reactions in the chemistry of low-coordinated phosphorus, namely the selective 1,2-addition of organotin compounds to Becker-type phosphaalkenes **6** to furnish the stannylphosphanes **7**[7].

The central theme of the present work is the reactivity of organotin hydrides and organo(halo)tin hydrides towards kinetically stabilized $\lambda^3\sigma^1$-phosphaalkynes and the related question of whether the primary products of the 1,2-addition of tin hydrides to the P−C triple-bond system will be sufficiently stable to permit their isolation.

Reactions with Triorganotin Hydrides 1

Reactions of the tin hydrides **1** with an excess of the phosphaalkynes **8a−c** in *n*-pentane at room temperature for 2 weeks gave rise to the 2-stannyl-substituted 1,2-dihydro-1,3-diphosphetes **10** in good yields. The reaction of tributyltin hydride (**1a**) with 1-adamantylphosphaalkyne (**8b**) required heating at 60°C for 4 hours for completion.

The natures of the 1,2-dihydro-1,3-diphosphetes **10a−f** were deduced from their analytical and spectroscopic data. The valency vibrations at 2160−2340 cm^{-1} in the IR spectra provided the first evidence for the presence of the PH function. A doublet of doublets at $\delta = 6.78-7.8$ with $^1J_{H,P}$ coupling constants of between 163 and 168 Hz was found in the ^{1}H-NMR spectra for these protons, which were originally bonded to the tin atoms. The splitting into a doublet of doublets and the integration values of the signals clearly demonstrate that compounds **10** are 1:2 adducts formed from one equivalent of the tin hydride **1** and two equiva-

[◇] Part 124: Ref.[1].

 © WILEY-VCH Verlag GmbH, D-69451 Weinheim, 1998 1434−1948/98/0202−0227 $ 17.50+.50/0

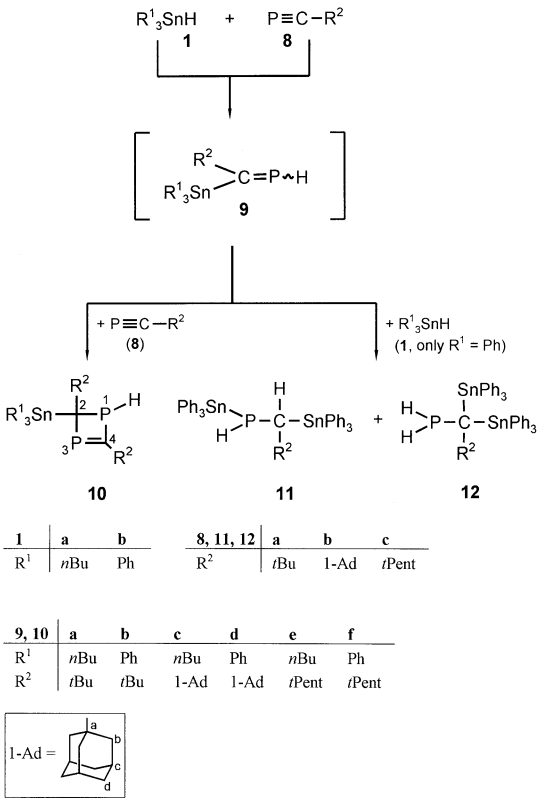

1	a	b
R^1	*n*Bu	Ph

8, 11, 12	a	b	c
R^2	*t*Bu	1-Ad	*t*Pent

9, 10	a	b	c	d	e	f
R^1	*n*Bu	Ph	*n*Bu	Ph	*n*Bu	Ph
R^2	*t*Bu	*t*Bu	1-Ad	1-Ad	*t*Pent	*t*Pent

lents of the phosphaalkyne **8**. The proposed compositions of the products were further supported by elemental analyses or high-resolution mass spectrometry. The ^{31}P-NMR spectra each reveal the typical AX spin system for 1,2-dihydro-1,3-diphosphetes[8][9]. The signals for the $\lambda^3\sigma^2$-phosphorus atoms occur in the expected low-field positions (δ = 369−376) while those of the $\lambda^3\sigma^3$-phosphorus atoms are found at $\delta = -5$ to +3. Both signals experience $^2J_{P,P}$ couplings of 35 to 44 Hz and appear as doublets. Thus, the existence of the structurally isomeric 1,4-dihydro-1,2-diphosphetes can be excluded on the basis of the small P,P couplings[10]. In the proton-undecoupled ^{31}P-NMR spectra the signals for the $\lambda^3\sigma^3$-phosphorus atom are further split by $^1J_{P,H}$ couplings and those of the $\lambda^3\sigma^2$-phosphorus atoms by $^3J_{P,H}$ couplings to give a doublet of doublets. A comparison of the measured values with those of previously known 1,2-dihydro-1,3-diphosphetes[8][11][12] supports the proposed constitutions. The ^{13}C-NMR spectra provide further diagnostic evidence. The doublet of doublets with large (ca. 50 Hz) and small (ca. 20 Hz) $^1J_{C,P}$ coupling constants observed at low field is characteristic for the skeletal sp^2 carbon atoms[13]. The second skeletal carbon atoms give rise to signals in the typical sp^3 region with appreciably smaller $^1J_{C,P}$ coupling constants. The varying chemical shifts of the tin atoms in the ^{119}Sn-NMR spectra can be rationalized in terms of the differing substitution: The tin atoms of the tributyl-substituted derivatives give rise to signals in the region typical for tetraalkyl-substituted tin compounds[14] while increasing phenyl substitution results in a stepwise shift to higher field[15].

A more careful consideration of the structures of compounds **10** reveals the presence of two centers of chirality: In addition to the asymmetric carbon atom C2 the phosphorus atom P1 should be chiral and configurationally stable . However, only one set of signals was observed in all of the NMR spectra and therefore it must be assumed that only one diastereomer is formed in each case. An exact assignment to one of the possible isomers is not possible on the basis of the spectroscopic data.

An increase in the tin hydride concentration favors the increased formation of the phosphanes **11** and **12**. When triphenyltin hydride (**1b**) was used in excess the phosphanes **11** were formed in yields exceeding 75%, while the isomeric compounds **12** were only observed as by-products (yields: < 5%). In comparison to triphenyltin hydride (**1b**), the lower hydrostannylation activity of tributyltin hydride (**1a**)[17] was not sufficient to alter the reaction course decisively in the direction of the phosphanes **11** and **12**; accordingly, the reaction mixtures contained appreciable amounts (60%) of the dihydrodiphosphetes **10** and a separation of the individual components was not possible.

The ^{31}P-NMR and ^{1}H-NMR spectra are of particular diagnostic value for the structural elucidation of the distannyl-substituted phosphanes **11**. The ^{31}P-NMR spectra of **11** each contain a singlet in the region typical for stannyl-substituted phosphanes[7] with $^1J_{P,^{117,119}Sn}$ coupling constants of ca. 720 Hz. In the proton-coupled ^{31}P-NMR spectra these signals are split into doublets by $^1J_{P,H}$ couplings of ca. 200 Hz. In the ^{1}H-NMR spectra doublet signals at δ = 3.03−3.32 with appropriate $^1J_{H,P}$ coupling constants are observed for the PH function while the protons added to carbon atoms give rise to signals at δ = 2.86−2.94. The $^2J_{H,P}$ coupling constants of about 4 Hz are very small. Integration of the individual signal groups clearly shows the 1:2 ratio of phosphaalkyne **8** to tin hydride **1b**. The presence of the PH function is further supported by a valency vibration at 2240 cm^{-1} in the IR spectra. The presence of two nonequivalent tin atoms is also apparent from the ^{119}Sn-NMR spectra. The triphenylstannyl groups directly bonded to phosphorus give doublet signals at $\delta = -73/-75$ with $^1J_{Sn,P}$ coupling constants of ca. 730 Hz, while the signals of *C*-bonded tin atoms appear as singlets at $\delta = -104$. Identification of the phosphanes **12a−c**, which were not isolated, was based on direct ^{31}P-NMR-spectroscopic investigation of the reaction solutions. The chemical shifts of $\delta = -136.4$ (**12a**), −143.7 (**12b**), and −138.1 (**12c**), as well as the $^1J_{P,H}$ coupling constants [198.1 Hz (**12a**), 198.8 Hz (**12b**), 216.6 Hz (**12c**)], support the proposed structures.

The phosphaalkenes **9** may be postulated as reactive intermediates in these stoichiometry-dependent reactions. These species then undergo stabilization either in a formal [2 + 2] cycloaddition to give the 1,2-dihydro-1,3-diphosphetes **10** or by renewed 1,2-addition of a further equivalent of tin hydride **1** to furnish the phosphanes **11** and **12**. The preferential formation of the phosphanes **11** over **12** can be rationalized in terms of both steric and electronic factors.

Reactions with Diorganotin Dihydrides

When the diorganotin dihydrides **13a**, **b** are allowed to react with an appreciable excess of the phosphaalkyne **8a** the primary products are the 1,2-dihydro-1,3-diphosphetes **14a**, **b**. However, these species undergo an unspecific decomposition so that their isolation is not possible. Even so, they can be characterized by ^{31}P-NMR and IR spectroscopy through termination of the reaction after 24 hours and removal of the volatile tin hydrides **13a**, **b** together with the excess phosphaalkyne **8a** under vacuum (oil pump).

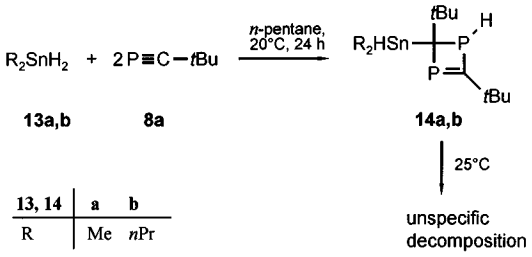

The spectroscopic data of these compounds are in good agreement with those of the 1,2-dihydro-1,3-diphosphetes **10** discussed above. Therefore the constitutions of these hydrostannylation products may be considered as certain. One special feature resulting from the presence of the tin hydride function should be mentioned: The IR spectra contain SnH valency vibrations at 1790/1800 cm^{-1} in addition to the PH valency vibrations. This tin hydride function is presumably the cause of the unspecific decomposition reactions.

Reactions with Chlorodiorganotin Hydrides

Reactions of the chlorodiorganotin hydrides **4** with the phosphaalkyne **8a** proceed much less selectively than those with the triorganotin hydrides **1**. In addition to the 1,2-dihydro-1,3-diphosphetes **16b**, **c** formed as main products, numerous by-products are observed by ^{31}P-NMR-spectroscopic monitoring of the reaction solutions. One of these by-products is the cage compound **17**. Product **17b** cannot be isolated, while **17c** has been isolated in pure form by crystallization from pentane at −20°C and completely characterized. Complete separation of the reaction mixtures into their components by either column chromatography or bulb-to-bulb distillation was not possible.

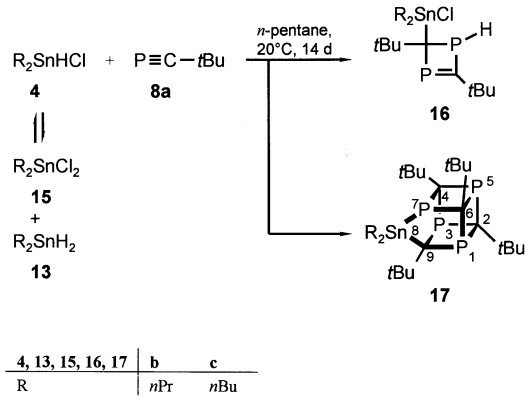

The ^{1}H-, ^{13}C-, ^{31}P-NMR, and IR data for the 1,2-dihydro-1,3-diphosphetes **16b**, **c** were taken from the crude reaction solutions and are in good agreement with those of the 1,2-dihydro-1,3-diphosphetes **10**. Thus, a detailed discussion of these data and the mechanism of the formation of the products is unnecessary in the light of the information given in the previous section.

The constitution of the cage compound **17c** was supported by mass spectrometry and elemental analysis. Linkage of the four phosphaalkyne units gives rise to an A_2MX spin system in the ^{31}P-NMR spectrum. As a consequence of the C_S symmetry, the phosphorus atoms P1 and P3 are magnetically equivalent (δ = 221). The signals for P5 and P7 appear at δ = 184 and δ = −72. The unusually low-field signals for the $\lambda^3\sigma^3$-phosphorus atoms P1, P3, and P5 are, in fact, not surprising when one considers that the pentacyclic compound **17c** is formally derived from tetraphosphacubane, which gives a ^{31}P-NMR signal at δ = 257[18]. These values can be explained on the basis of the bonding model derived for tetraphosphacubane, which reveals a strong interaction between the lone elctron pairs of the phosphorus atoms and the phosphorus-carbon σ bonds of the cubane skeleton. This effect is responsible for the dramatic low-field shifts of the phosphorus signals as well as the extreme high-field shifts of the signals for the skeletal carbon atoms in the ^{13}C-NMR spectrum[19]. A further indication in favor of the proposed structure is given by the tin satellite lines in the ^{31}P-NMR spectrum: P7 exhibits a characteristic $^1J_{P,Sn}$ coupling of 744 Hz, clearly demonstrating that P7 and tin are directly adjacent[20]. Tin satellites with $^3J_{P,Sn}$ coupling constants of 109 Hz are observed for the signal of P5. Accordingly, the ^{119}Sn-NMR signal for the tin atom (δ = 328) is split into a doublet of doublets ($^1J_{P,^{119}Sn}$ = 784 Hz, $^3J_{P,^{119}Sn}$ = 113 Hz). As a consequence of the C_S symmetry the ^{1}H-NMR spectrum contains only three signals for the four *tert*-butyl groups, with an intensity ratio of 1:2:1. For the same reason the skeletal carbon atoms C4 and C6 are magnetically equivalent in the ^{13}C-NMR spectrum (pt, δ = 37.6, $^1J_{C,P}$ = 13.5 Hz). Carbon atom C2 gives, as required by the discussed bonding model, a signal at extremely high field (δ = −17.2) (cf. skeletal carbon atom signals of tetraphosphacubane: δ = −29.1)[18][19]. Finally, the skeletal carbon atom C9 produces a ^{13}C-NMR signal at δ = 22.7.

From a mechanistic point of view, the formation of the cage compounds **17** may be considered as a cyclooligomerization of the phosphaalkyne **8a** in the coordination sphere of tin. Since the reaction of the 1,2-dihydro-1,3-diphosphete **16c** with an excess of the phosphaalkyne **8a** does not lead to the formation of the homocubane **17c**, the existence of the 1,2-dihydro-1,3-diphosphete **16c** as an intermediate can be discounted. Similarly, subsequent attempts to introduce the stannyl unit into a skeletal bond of tetraphosphacubane[18] by reaction of the latter with dibutyl(chloro)tin hydride (**4b**) were unsuccessful. Thus, a plausible mechanism involves the stepwise construction of the P/C skeleton by oligomerization of the phosphaalkyne units at tin.

Thermal Isomerization of the 1,2-Dihydro-1,3-diphosphetes 10

After heating of the 1,2-dihydro-1,3-diphosphetes **10a−d** in toluene at 90°C for 6 hours, quantitative isomerization of the original 2-stannyl-substituted 1,2-dihydro-1,3-diphosphetes into the 1-stannyl-substituted derivatives **18a−d** is observed.

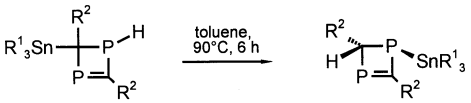

10 **18**

10, 18	a	b	c	d
R^1	*n*Bu	Ph	*n*Bu	Ph
R^2	*t*Bu	*t*Bu	1-Ad	1-Ad

The natures of the 1,2-dihydro-1,3-diphosphetes **18** obtained were unequivocally demonstrated by mass spectrometry and elemental analysis. Evidence for the arrangement of the substituents was provided by analysis of the NMR spectra in comparison with the data for the starting compounds **10a−d**. Thus, the ^{31}P-NMR signals of the $\lambda^3\sigma^2$-phosphorus atoms experienced high-field shifts of almost 20 ppm, while the signals of the $\lambda^3\sigma^3$-phosphorus atoms changed only slightly (δ = 2−3). The direct adjacency of tin to phosphorus is apparent from the tin satellites at the signal of P1 with $^1J_{P,^{117,119}Sn}$ coupling constants of more than 1000 Hz and the markedly smaller $^3J_{P,^{117,119}Sn}$ coupling constants of 170 Hz at P3. The same couplings also appear in the ^{119}Sn-NMR spectra. Because of the migration of the hydrogen atom from phosphorus to carbon the ^{1}H-NMR signal of this proton experiences a pronounced diamagnetic shift from δ = 7.5 to 2.6 and, instead of the original splitting into a doublet of doublets, appears merely as a doublet with a small $^2J_{H,P}$ coupling of 1.4 Hz. The magnitude of this $^2J_{H,P}$ coupling can be interpreted as evidence for the *trans* arrangement of **18**[21]. In the ^{13}C-NMR spectra the skeletal carbon atoms C4 give the expected doublet of doublet signals at low field (δ = 238.1−240.4; $^2J_{C,P}$ = 53/40 Hz) while the signals of the second skeletal carbon atom appear as doublets ($^1J_{C,P}$ = 22 to 24 Hz) at δ = 36.4−39.1 in the typical sp^3 region. An X-ray crystallographic analysis of product **18d** (Figure 1) supplied final confirmation of the *trans* orientation of the adamantyl group and the triphenylstannyl group. Since only one isomer was obtained from each experiment and since the $\lambda^3\sigma^3$-phosphorus atoms should be configurationally stable[16], the same arrangement of the substituents can also safely be assumed for the compounds **18a−c**.

The four-membered diphosphacyclobutene ring deviates slightly from planarity (sum of internal angles: 358.9°). The dihedral angle between the planes C(1)−P(1)−C(2) and C(1)−P(2)−C(2) amounts to 10.7°. The P(2)−C(2) bond length of 169.7 pm is in the typical range for P−C double bonds[22], whereas the P(1)−C(2) single bond is somewhat shortened to 181.5 pm. The tin atom exists in a distorted tetrahedral environment.

Figure 1. Molecular structure of **18d**[a]

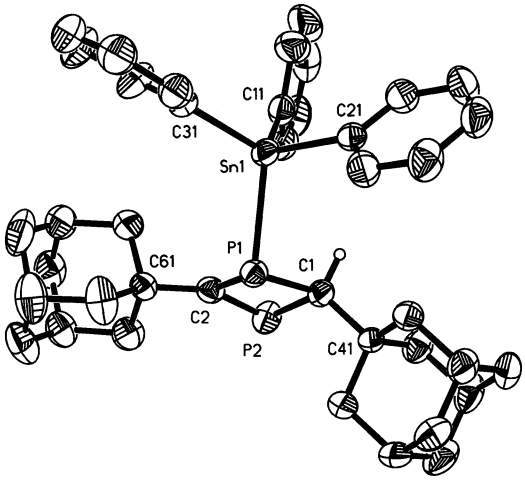

[a] Selected bond lengths [pm] and angles [°]: P(1)-C(2) 181.5(4), P(1)-C(1) 188.7(4), P(2)-C(2) 169.7(4), P(2)-C(1) 187.1(4), Sn(1)-C(21) 214.5(4), Sn(1)-C(31) 214.2(4), Sn(1)-C(11) 215.1(4), Sn(1)-P(1) 252.84(12); C(2)-P(1)-C(1) 82.2(2), C(2)-P(2)-C(1) 85.9(2), P(2)-C(1)-P(1) 91.2(2), P(2)-C(2)-P(1) 99.7(2), C(41)-C(1)-P(1) 118.1(3), C(41)-C(1)-P(2) 118.7(3), C(61)-C(2)-P(1) 130.0(3), C(61)-C(2)-P(2) 130.0(3), C(11)-Sn(1)-P(1) 115.27(12), C(21)-Sn(1)-P(1) 103.33(10), C(31)-Sn(1)-P(1) 113.14(10).

Complexation Behavior of 10

Phosphane ligands have found a wide range of applications in organometallic chemistry[23][24]. A common method for the preparation of phosphorus-containing transition-metal complexes comprises of a ligand-exchange reaction between phosphorus compounds and carbonyl transition-metal complexes.

In the case of the 1,2-dihydro-1,3-diphosphetes **10**, both complexation of one phosphorus atom (→ **19**) and complete complexation of both phosphorus atoms (→ **20**) are possible using $W(CO)_5$·THF. Reactions of the 1,2-dihydro-1,3-diphosphetes **10a, b** with excess $Fe_2(CO)_9$ furnish the doubly complexed derivatives **21a**, **b**.

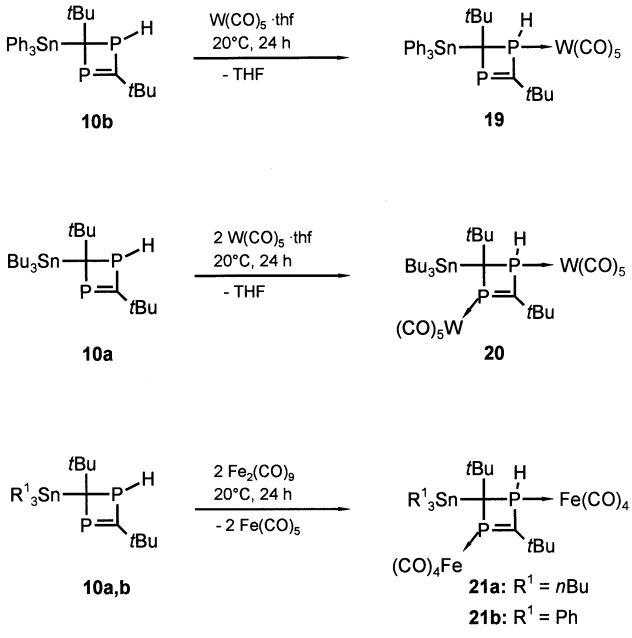

The spectroscopic characterization of the complexes **19**, **20**, and **21** is relatively simple. For the pentacarbonyltungsten complexes **19** and **20** the η^1 coordination of the metal fragment at P1 (for compound **19**) or at P1 and P3 (for compound **20**) is impressively demonstrated by the characteristic P-W couplings[25] in the ^{31}P-NMR spectra. The complexation has only a minor influence on the ^{13}C-NMR data of the starting materials with additional characteristic signals being observed at low field for the carbonyl groups (see Experimental Section). Furthermore, CO valency vibrations appear in the IR spectra of compounds **19**, **20**, and **21**. The compositions of the products were further substantiated by mass spectrometry and elemental analysis.

Reaction of 10 with Iodine

Conversion of the PH function of the 1,2-dihydro-1,3-diphosphete **10b** into a PI function can be achieved by treatment of **10b** with a solution of iodine in diethyl ether at room temperature.

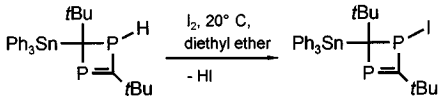

10b **22**

The degradation of the PH function is immediately demonstrated by the absence of the corresponding signal in the ^{1}H-NMR spectrum. Also, no P,H couplings can be seen in the proton-coupled ^{31}P-NMR spectrum. In comparison to that of the starting material the ^{13}C-NMR signal for C2 experiences a shift of almost 20 ppm to lower field. Finally, the increases in the $^1J_{C,P}$ coupling constants are noteworthy. The composition of the 1,2-dihydro-1,3-diphosphete **22** was substantiated by mass spectrometry and elemental analysis.

We thank the *Fonds der Chemischen Industrie* for generous financial support. We are also grateful to the *Deutsche Forschungsgemeinschaft* (Graduate College *Phosphorus as Connecting Link Between Various Chemical Disciplines*) for generous financial support and a post-graduate grant (to M. S.).

Experimental Section

General: All experiments were carried out under argon (purity: > 99.998%) in previously evacuated and oven-dried Schlenk vessels. The solvents were anhydrous and stored under argon. – Melting points: Mettler FP 61 (heating rate: 3°C/min), uncorrected. – Elemental analyses: Perkin-Elmer EA 240. – ^{1}H NMR: Varian EM 360 (60 MHz), Bruker AC 200 and AMX 400; chemical shifts are relative to the solvent signals, and converted to TMS. – ^{13}C NMR: Bruker AC 200 and AMX 400; chemical shifts are relative to the solvent signals. – ^{31}P NMR: Bruker AC 200, external standard H_3PO_4. – MS: Finnigan MAT 90 (70 eV). – IR: Perkin-Elmer 16 PC FT-IR and Perkin-Elmer 1310. – Chemicals: Triphenyltin hydride (**1b**) was prepared from triphenyltin chloride[26], dimethyltin dihydride (**13a**)[27], dipropyltin dihydride (**13b**)[28], dibutyltin dihydride (**13c**)[29], dipropyltin dichloride (**15b**)[30], and the phosphaacetylenes **8a**[31], **b**[32], **c**[31] were prepared as described in the literature. All other starting materials were purchased from commercial suppliers.

1,2-Dihydro-1,3-diphosphetes **10**. – *General Procedure:* To a solution of phosphaalkyne **8** in pentane was added the tin hydride **1**. The mixture was stirred for two weeks at room temperature and the solvent removed under vacuum. The residue was purified by chromatography or crystallization.

2,4-Di-tert-butyl-2-tributylstannyl-1,2-dihydro-1λ³,3λ³-diphosphete (**10a**): From **8a** (800 mg, 8 mmol) in pentane (3 ml) and **1a** (873 mg, 3 mmol); chromatography on aluminum oxide (5% H_2O) with pentane yielded **10a** (413 mg, 28%) as a yellow, non-distillable oil. – ^{1}H NMR (C_6D_6): δ = 0.65–1.94 (m, 45 H, Bu-H and *t*Bu-H), 6.73 (dd, $^1J_{H,P}$ = 164.7 Hz, $^3J_{H,P}$ = 21.5 Hz, 1 H, P–H). – ^{13}C{^{1}H} NMR (C_6D_6): δ = 13.5 (s, $^1J_{C,^{117/119}Sn}$ = 315.7 Hz, Sn–*C*H$_2$), 13.9 (s, Sn–[CH$_2$]$_3$–*C*H$_3$), 28.0 (s, SnCH$_2$*C*H$_2$), 29.7 [dd, $^3J_{C,P}$ = 10.1/5.8 Hz, C(*C*H$_3$)$_3$], 30.0 (s, *C*H$_2$CH$_3$), 30.8 [d, $^3J_{C,P}$ = 5 Hz, C(*C*H$_3$)$_3$], 36.4 (dd, $^1J_{C,P}$ = 39.2/5.5 Hz, C2), 37.1 [d, $^2J_{C,P}$ = 7.7 Hz, *C*(CH$_3$)$_3$], 39.8 [d, $^2J_{C,P}$ = 6.3 Hz, *C*(CH$_3$)$_3$], 222.56 (dd, $^1J_{C,P}$ = 52.1/23.2 Hz, C4). – ^{31}P{^{1}H} NMR (C_6D_6): δ = 0.7 (d, $^2J_{P,P}$ = 39.1 Hz, P-1), 375.6 (d, $^2J_{P,P}$ = 39.1 Hz, P-3). – ^{119}Sn{^{1}H} NMR (C_6D_6): δ = 3.85 (s). – IR (film): $\tilde{\nu}$ = 2940, 2910, 2860, 2200 (P–H), 1455, 1355, 1210, 1110, 840 cm^{-1}. – MS; *m/z* (%): 492 (13) [M$^+$], 291 (39) [SnBu$_3^+$], 235 (76) [HSnBu$_2^+$], 179 (100) [H$_2$SnBu$^+$], 57 (38) [C$_4$H$_9^+$]. – $C_{22}H_{46}P_2Sn$ (491.26): calcd. C 53.8, H 9.4; found C 53.6, H 9.3.

2,4-Di-tert-butyl-2-triphenylstannyl-1,2-dihydro-1λ³,3λ³-diphosphete (**10b**): From **8a** (4 g, 40 mmol) in pentane (5 ml) and **1b** (3.43 g, 9.8 mmol); crystallization from 3 ml of pentane at –20°C yielded **10b** (2.6 g, 48% based on **1b**) as a yellow solid with m.p. 68°C. – ^{1}H NMR (C_6D_6): δ = 1.16 (s, 9 H, *t*Bu-H), 1.65 (s, 9 H, *t*Bu-H), 7.42–7.48 (m, 9 H, *m*-, *p*-C$_6$H$_5$), 7.57 (dd, $^1J_{H,P}$ = 166 Hz, $^3J_{H,P}$ = 18.6 Hz, 1 H, P–H), 8.05–8.08 (m, 6 H, *o*-C$_6$H$_5$). – ^{13}C{^{1}H} NMR (C_6D_6): δ = 29.9 [d, $^3J_{C,P}$ = 3.6 Hz, C(*C*H$_3$)$_3$], 30.3 [d, $^3J_{C,P}$ = 9.0 Hz, C(*C*H$_3$)$_3$], 37.4 [d, $^2J_{C,P}$ = 7.2 Hz, *C*(CH$_3$)$_3$], 39.2 (dd, $^1J_{C,P}$ = 38.2/4 Hz, C2), 39.6 [d, $^2J_{C,P}$ = 5.4 Hz, *C*(CH$_3$)$_3$], 128.7 (s, $^2J_{C,^{117/119}Sn}$ = 49.4 Hz, *o*-C), 129.2 (s, *p*-C), 138.0 (s, $^3J_{C,^{117/119}Sn}$ = 35.0 Hz, *m*-C), 141.6 (s, $^1J_{C,^{117/119}Sn}$ = 471.2/492.8 Hz, *ipso*-C), 224.4 (dd, $^1J_{C,P}$ = 51.6/22.9 Hz, C4). – ^{31}P{^{1}H} NMR (C_6D_6): δ = 2.5 (d, $^2J_{P,P}$ = 35.8 Hz, P-1), 372.1 (d, $^2J_{P,P}$ = 35.8 Hz, P-3). – ^{119}Sn{^{1}H} NMR (C_6D_6): δ = –99.75 (pt, $^2J_{^{119}Sn,P}$ = 24.4 Hz). – IR (KBr): $\tilde{\nu}$ = 3040, 2920, 2180 (P–H), 1450, 1410, 1350, 1100, 840 cm^{-1}. – MS; *m/z* (%): 552 (5) [M$^+$], 351 (100) [SnPh$_3^+$], 197 (24) [SnPh$^+$], 57 (18) [C$_4$H$_9^+$]. – $C_{28}H_{34}P_2Sn$ (551.23): calcd. C 61.0, H 6.2; found C 61.3, H 6.2.

2,4-(Diadamant-1-yl)-2-tributylstannyl-1,2-dihydro-1λ³,3λ³-diphosphete (**10c**): From **8b** (360 mg, 2 mmol) in pentane (2 ml) and **1a** (291 mg, 1 mmol); after stirring the reaction mixture for two weeks at room temperature the solution was heated to 60°C for 4 h; chromatography on aluminum oxide (5% H_2O) with pentane yielded **10c** (150 mg, 23%) as a yellow, non-distillable oil. – ^{1}H NMR (C_6D_6): δ = 1.10–2.62 (m, 57 H, Ad-H and Bu-H), 6.81 (dd, $^1J_{H,P}$ = 164 Hz, $^3J_{H,P}$ = 22 Hz, 1 H, P–H). – ^{13}C{^{1}H} NMR (C_6D_6): δ = 13.8 (s, $^1J_{C,^{117/119}Sn}$ = 313.8 Hz, Sn–*C*H$_2$), 13.9 (s, Sn–[CH$_2$]$_3$–*C*H$_3$), 28.1 (s, $^2J_{C,^{117/119}Sn}$ = 63.0 Hz, SnCH$_2$*C*H$_2$), 29.2 (s, C-c), 29.5 (s, C-c), 30.2 (s, $^3J_{C,^{117/119}Sn}$ = 35.3 Hz, *C*H$_2$CH$_3$), 37.0 (s, 2 × C-d), 37.4 (d, $^1J_{C,P}$ = 30.5 Hz, C-2), 38.9 (d, $^2J_{C,P}$ = 6.3 Hz, C-a), 41.2 (br. d, $^3J_{C,P}$ = 7.6 Hz, C-b), 42.1 (d, $^2J_{C,P}$ = 5.7 Hz, C-a), 43.5 (d, $^3J_{C,P}$ = 3.8 Hz, C-b), 222.6 (dd, $^1J_{C,P}$ = 51/22.4 Hz, C-4). – ^{31}P{^{1}H} NMR (C_6D_6): δ = –5.2 (d, $^2J_{P,P}$ = 43.6 Hz, P-1), 373.3 (d, $^2J_{P,P}$ = 43.6 Hz, P-3). – IR (film): $\tilde{\nu}$ = 2920–2800, 2160 (P–H), 1440, 1320, 1270, 1140 cm^{-1}. – MS; *m/z* (%): 649 (36) [M$^+$], 291 (46) [SnBu$_3^+$], 135 (100) [Ad$^+$]. – $C_{34}H_{58}P_2Sn$ (647.49): calcd. C 63.1, H 9.0; found C 63.4, H 8.9.

2,4-(Diadamant-1-yl)-2-triphenylstannyl-1,2-dihydro-1λ³,3λ³-diphosphete (**10d**): From **8b** (300 mg, 1.7 mmol) in pentane (5 ml)

and **1b** (296 mg, 0.8 mmol); evaporation of the solvent and washing of the residue with pentane yielded **10d** (198 mg, 35%) as a yellow solid with m.p. 92°C. – ^{1}H NMR (C_6D_6): δ = 1.38–2.63 (m, 30 H, Ad-H), 7.20–7.41 (m, 9 H, *m*-, *p*-C_6H_5), 7.44 (dd, $^1J_{H,P}$ = 168 Hz, $^3J_{H,P}$ = 21 Hz, 1 H, P–H), 7.87–8.09 (m, 6 H, *o*-C_6H_5). – ^{13}C{^{1}H} NMR (C_6D_6): δ = 28.9 (s, C-c), 29.2 (s, C-c), 36.5 (s, C-d), 36.7 (s, C-d), 39.1 (d, $^2J_{C,P}$ = 6.5 Hz, C-a), 41.6 (br. d, $^3J_{C,P}$ = 10.0 Hz, C-b), 41.9 (d, $^2J_{C,P}$ = 5.6 Hz, C-a), 42.1 (d, $^3J_{C,P}$ = 5.6 Hz, C-b), 128.7 (s, $^2J_{C,^{117/119}Sn}$ = 49.0 Hz, *o*-C), 129.0 (s, *p*-C), 138.2 (s, $^3J_{C,^{117/119}Sn}$ = 35.3 Hz, *m*-C), 142.2 (s, $^1J_{C,^{117/119}Sn}$ = 467.4/489.1 Hz, *ipso*-C), 223.9 (dd, $^1J_{C,P}$ = 50.2/21.3 Hz, C-4), the C-2 signal could not be detected because of signal overlap. – ^{31}P{^{1}H} NMR (C_6D_6): δ = –4.1 (d, $^2J_{P,P}$ = 43 Hz, P-1), 369.2 (d, $^2J_{P,P}$ = 43 Hz, P-3). – ^{119}Sn{^{1}H} NMR (C_6D_6): δ = –101.43 (s). – IR (KBr): $\tilde{\nu}$ = 3030, 2940, 2865, 2818, 2180 (P–H), 1432, 1413, 1330, 1295, 1249, 715, 685 cm^{-1}. – MS; *m/z* (%): 708 (6) [M^+], 351 (100) [$SnPh_3^+$], 135 (47) [Ad^+]. – $C_{40}H_{46}P_2Sn$ (707.5): calcd. C 67.9, H 6.6; found C 67.6, H 6.5.

2,4-Di-tert-pentyl-2-tributylstannyl-1,2-dihydro-1λ³,3λ³-diphosphete (**10e**): From **8c** (357 mg, 3.13 mmol) in pentane (5 ml) and **1a** (407 mg, 1.4 mmol); chromatography on aluminum oxide (5% H_2O) with pentane yielded **10e** (540 mg, 74%) as a yellow, non-distillable oil. – ^{1}H NMR (C_6D_6): δ = 0.86–1.59 (m, 45 H, *t*Pent-H and Bu-H), 6.78 (dd, $^1J_{H,P}$ = 163.04 Hz, $^3J_{H,P}$ = 20.27 Hz, 1 H, P–H). – ^{13}C{^{1}H} NMR (C_6D_6): δ = 8.0 (s, $^1J_{C,^{117/119}Sn}$ = 341.3 Hz, Sn–*C*H_2), 9.2 (s, CH_2CH_3), 9.6 (s, CH_2CH_3), 13.5 (s, Sn–[CH_2]$_3$–*C*H_3), 24.7 [br. d, $^3J_{C,P}$ = 6.4 Hz, C(*C*H_3)$_2$], 25.8 [br. d, $^3J_{C,P}$ = 8.0 Hz, C(*C*H_3)$_2$], 27.1 (s, $SnCH_2CH_2$), 29.9 [s, $^3J_{C,^{117/119}Sn}$ = 21.7 Hz, Sn(CH_2)$_2$*C*H_2CH$_3$], 34.7 (dd, $^3J_{C,P}$ = 9.2/4.4 Hz, *C*H_2CH$_3$), 35.4 [d, $^2J_{C,P}$ = 7.2 Hz, *C*(CH$_3$)$_2$CH$_2$CH$_3$], 36.1 (dd, $^3J_{C,P}$ = 7.2/4.0 Hz, *C*H_2CH$_3$), 38.4 (d, $^1J_{C,P}$ = 40.2 Hz, *C*2), 39.2 [d, $^2J_{C,P}$ = 6.4 Hz, *C*(CH$_3$)$_2$CH$_2$CH$_3$], 221.0 (dd, $^1J_{C,P}$ = 52.2, 24.1 Hz, C-4). – ^{31}P{^{1}H} NMR (C_6D_6): δ = 1 (d, $^2J_{P,P}$ = 41 Hz, P-1), 379 (d, $^2J_{P,P}$ = 41 Hz, P-3). – IR (pentane): $\tilde{\nu}$ = 2942, 2912, 2880, 2340 (P–H), 1644, 1456 cm^{-1}. – MS; *m/z* (%): 520 (5) [M^+], 291 (100) [$SnBu_3^+$], 235 (59) [$HSnBu_2^+$], 177 (60) [$SnBu^+$], 71 (44) [$C(CH)_3CH_2CH_3^+$], 57 (16) [$C_4H_9^+$]. – HR-MS: $C_{24}H_{50}P_2Sn$: calcd. 520.2409; found 520.2385.

2,4-Di-tert-pentyl-2-triphenylstannyl-1,2-dihydro-1λ³,3λ³-diphosphete (**10f**): From **8c** (422 mg, 3.7 mmol) in pentane (5 ml) and **1b** (123 mg, 0.35 mmol); evaporation of the solvent and washing of the residue with pentane yielded **10f** (70 mg, 34%) as a yellow solid with m.p. 86°C. – ^{1}H NMR (C_6D_6): δ = 0.70 (t, $^3J_{H,H}$ = 7.24 Hz, 3 H, CH_2CH_3), 0.82 (t, $^3J_{H,H}$ = 7.87 Hz, 3 H, CH_2CH_3), 0.86 [s, 3 H, C(CH$_3$)$_2$], 0.88 [s, 3 H, C(CH$_3$)$_2$], 1.27 [s, 3 H, C(CH$_3$)$_2$], 1.29 [s, 3 H, C(CH$_3$)$_2$], 7.10–7.18 (m, 9 H, *m*, *p*-C_6H_5), 7.27 (dd, $^1J_{H,P}$ = 166.59 Hz, $^3J_{H,P}$ = 19.98 Hz, 1 H, P–H), 7.73–7.82 (m, 6 H, *o*-C_6H_5). – ^{13}C{^{1}H} NMR (C_6D_6): δ = 9.1 (s, CH_2CH_3), 9.5 (s, CH_2CH_3), 24.8 [br. s, C(*C*H$_3$)$_2$], 25.1 [br. s, C(*C*H$_3$)$_2$], 35.2 (br. s, *C*H_2CH$_3$), 35.8 (br. s, *C*H_2CH$_3$), 39.7 (d, $^1J_{C,P}$ = 6.7 Hz, C2) , 41.3 [s, *C*(CH$_3$)$_2$CH$_2$CH$_3$], 42.5 [s, *C*(CH$_3$)$_2$CH$_2$CH$_3$], 128.4 (s, *o*-C), 128.8 (s, *p*-C), 137.8 (s, $^3J_{C,^{117/119}Sn}$ = 34.4 Hz, *m*-C), 141.6 (s, *ipso*-C), 222.7 (dd, $^1J_{C,P}$ = 52.0, 22.4 Hz, C-4). – ^{31}P{^{1}H} NMR (C_6D_6): δ = 3 (d, $^2J_{P,P}$ = 40 Hz, P-1), 376 (d, $^2J_{P,P}$ = 40 Hz, P-3). – IR (pentane): $\tilde{\nu}$ = 2990, 2199 (P–H), 1468, 1429, 1261, 1072, 1021, 807, 726 cm^{-1}. – MS; *m/z* (%): 580 (1) [M^+], 351 (100) [$SnPh_3^+$], 274 (20) [$SnPh_2^+$], 197 (62) [$SnPh^+$], 77 (20) [$C_6H_5^+$], 71 (13) [$C(CH_3)_2CH_2CH_3^+$]. – HR-MS: $C_{30}H_{38}P_2Sn$: calcd. 580.1470; found 580.1465.

1,2-Bis(triphenylstannyl)phosphanes **11a**, **b**. – *General Procedure:* To a solution of phosphaacetylene **8** in pentane was added triphenyltin hydride (**1b**). The mixture was stirred for one week at 20°C, the solvent removed under vacuum, and the residue washed several times with pentane.

[tert-Butyl(triphenylstannyl)methyl]triphenylstannylphosphane (**11a**): From **8a** (0.4 g, 4 mmol) in pentane (5 ml) and **1b** (6.32 g, 18 mmol) to furnish **11a** (2.6 g, 81%) as a pale yellow powder with m.p. 154°C. – ^{1}H NMR (C_6D_6): δ = 1.04 (s, 9 H, *t*Bu), 2.94 (d, $^2J_{H,P}$ = 4.5 Hz, 1 H, PC–H), 3.32 (d, $^1J_{H,P}$ = 196.2 Hz, 1 H, P–H), 7.05–7.13 (m, 18 H, *m*-, *p*-C_6H_5), 7.47–7.49 (m, 6 H, *o*-C_6H_5), 7.62–7.66 (m, 6 H, *o*-C_6H_5). – ^{13}C{^{1}H} NMR (C_6D_6): δ = 28.8 (d, $^1J_{C,P}$ = 36.1 Hz, P*C*H, ^{1}H coupl.: $^1J_{C,H}$ = 129.3 Hz), 32.4 [d, $^3J_{C,P}$ = 10.4 Hz, C(*C*H$_3$)$_3$], 35.4 [d, $^2J_{C,P}$ = 17.7 Hz, *C*(CH$_3$)$_3$], 129.26 (s, *o*-C), 129.30 (s, *o*-C), 129.4 (s, *p*-C), 129.6 (s, *p*-C), 137.9 (s, *m*-C), 138.1 (s, *m*-C), 139.1 (d, $^2J_{C,P}$ = 4 Hz, *ipso*-C), 140.2 (s, *ipso*-C). – ^{31}P{^{1}H} NMR (C_6D_6): δ = –170 (s, $^1J_{P,^{117,119}Sn}$ = 716 Hz). – ^{119}Sn{^{1}H} NMR (C_6D_6): δ = –73 (d, $^1J_{^{119}Sn,P}$ = 732 Hz, P–Sn), –104 (s, PC–Sn). – IR (KBr): $\tilde{\nu}$ = 3030, 2920, 2240 (P–H), 1460, 1410, 1350, 1320, 1285, 1250, 1210, 1180, 1060, 1010, 985, 855, 750, 715, 685 cm^{-1}. – MS; *m/z* (%): 802 (0.2) [M^+], 451 (2) [M^+ – $SnPh_3$], 351 (100) [$SnPh_3^+$], 197 (18) [$SnPh^+$], 57 (9) [$C_4H_9^+$]. – $C_{41}H_{41}PSn_2$ (802.14): calcd. C 61.4, H 5.2; found C 61.4, H 5.2.

[Adamant-1-yl(triphenylstannyl)methyl]triphenylstannylphosphane (**11b**): From **8b** (0.3 g, 1.66 mmol) in pentane (5 ml) and **1b** (3.16 g, 9 mmol) to furnish **11b** (1.01 g, 75%) as a colorless powder with m.p. 185°C (dec.). – ^{1}H NMR (C_6D_6): δ = 1.2–1.9 (m, 15 H, Ad-H), 2.86 (d, $^2J_{H,P}$ = 3.7 Hz, 1 H, PC–H), 3.03 (d, $^1J_{H,P}$ = 198.4 Hz, 1 H, P–H), 6.9–7.25 (m, 18 H, *m*-, *p*-C_6H_5), 7.3–7.8 (m, 12 H, *o*-C_6H_5). – ^{13}C{^{1}H} NMR (C_6D_6): δ = 31.3 (s, C-c), 31.4 (d, $^1J_{C,P}$ = 39.4 Hz, P*C*H, ^{1}H coupl.: $^1J_{C,H}$ = 127.7 Hz), 38.2 (d, $^2J_{C,P}$ = 15.2 Hz, C-a), 38.6 (s, C-d), 46.7 (d, $^3J_{C,P}$ = 11.1 Hz, C-b), 130.7 (s, *o*-C), 130.9 (s, *o*-C), 131.0 (s, *p*-C), 131.2 (s, *p*-C), 139.4 (s, *m*-C), 139.7 (s, *m*-C), 140.9 (d, $^2J_{C,P}$ = 3.3 Hz, *ipso*-C), 142.8 (s, *ipso*-C). – ^{31}P{^{1}H} NMR (C_6D_6): δ = –175 (s, $^1J_{P,^{117,119}Sn}$ = 724 Hz). – ^{119}Sn{^{1}H} NMR (C_6D_6): δ = –75 (d, $^1J_{^{119}Sn,P}$ = 731 Hz, P–Sn), –104 (s, PC–Sn). – IR (KBr): $\tilde{\nu}$ = 3030, 2910, 2840, 2240 (P–H), 1480, 1425, 1310, 1100, 1070, 1020, 1000, 890, 730, 700 cm^{-1}. – $C_{47}H_{47}PSn_2$ (880.25): calcd. C 64.1, H 5.4; found C 64.0, H 5.3.

1,2-Dihydro-1,3-diphosphetes **14a**, **b**. – *General Procedure:* To a solution of phosphaalkyne **8** in pentane was added the diorganotin dihydride **13** and the mixture stirred at room temperature for 24 h. The solvent, unreacted phosphaalkyne **8**, and tin hydride **13** were removed under vacuum. Further purification by distillation, chromatography, or crystallization was not possible.

2,4-Di-tert-butyl-2-hydridodimethylstannyl-1,2-dihydro-1λ³,3λ³-diphosphete (**14a**): From **8a** (800 mg, 8 mmol) in pentane and **13a** (452 mg, 3 mmol) to furnish **14a** (70 mg, 7%) as a yellow oil. – ^{31}P{^{1}H} NMR (C_6D_6): δ = 1.9 (dd, $^1J_{P,H}$ = 161.5 Hz, $^2J_{P,P}$ = 40.9 Hz, P-1), 371.5 (dd, $^2J_{P,P}$ = 40.9 Hz, $^3J_{P,H}$ = 18.5 Hz, P-3). – IR (film): $\tilde{\nu}$ = 2930, 2910, 2170 (P–H), 1790 (Sn–H), 1450, 1350, 1250, 1240, 1050, 1010, 860, 830, 760, 620 cm^{-1}.

2,4-Di-tert-butyl-2-hydridodipropylstannyl-1,2-dihydro-1λ³,3λ³-diphosphete (**14b**): From **8a** (800 mg, 8 mmol) in pentane and **13b** (620 mg, 3 mmol) to furnish **14b** (110 mg, 9%) as a yellow oil. – ^{31}P{^{1}H} NMR (C_6D_6): δ = –0.4 (dd, $^1J_{P,H}$ = 163 Hz, $^2J_{P,P}$ = 41 Hz, P-1), 369.7 (dd, $^2J_{P,P}$ = 41 Hz, $^3J_{P,H}$ = 21 Hz, P-3). – IR (film): $\tilde{\nu}$ = 3000, 2980, 2920, 2900, 2160 (P–H), 1800 (Sn–H), 1350, 1250, 1240, 1050, 1010, 860, 830, 770, 750 cm^{-1}.

1,2-Dihydro-1,3-diphosphetes **16** *and Homocubane* **17**. – *General Procedure:* Diorganotin dichloride **15** was dissolved in toluene (3 ml) and pentane (3 ml) and cooled to 0°C. Diorganotin dihydride

13 was added and the reaction solution was stirred for 15 min. Phosphaalkyne **8** was added. After a few hours the color of the reaction solution changed to red-brown and after 14 d the solvent was removed under vacuum. The residue was taken up in pentane (10 ml). Unreacted diorganotin dihydride **13** was crystallized at −20°C, further crystallization at −20°C yielded the homocubane **17**. Compound **17b** could not be isolated. It was not possible to purify the oils which contained the 1,2-dihydro-1,3-diphosphetes **16** as main products.

2,4-Di-tert-butyl-2-chlorodipropylstannyl-1,2-dihydro-1λ³,3λ³-diphosphete (**16b**): From **15b** (690 mg, 2.5 mmol), **13b** (520 mg, 2.5 mmol), and **8a** (1600 mg, 16 mmol) to furnish **16b** (ca. 85%). − ^{1}H NMR (C_6D_6): δ = 0.85−1.9 (m, 32 H, Pr-H and *t*Bu-H), 6.82 (dd, $^1J_{H,P}$ = 166 Hz, $^3J_{H,P}$ = 20 Hz, 1 H, P−H). − ^{13}C{^{1}H} NMR (C_6D_6): δ = 18.8 (s, CH_2CH_3), 20.4 (s, $SnCH_2CH_2$), 23.1 (s, $SnCH_2$), 29.7 [dd, $^3J_{C,P}$ = 9.6/4.8 Hz, C(*C*H$_3$)$_3$], 30.6 [br. d, $^3J_{C,P}$ = 4.8 Hz, C(*C*H$_3$)$_3$], 37.1 [br. d, $^2J_{C,P}$ = 8.0 Hz, *C*(CH$_3$)$_3$], 40.2 [br. s, *C*(CH$_3$)$_3$], 43.2 (dd, $^1J_{C,P}$ = 39.0/6.0 Hz, C-2), 227.6 (dd, $^1J_{C,P}$ = 53.8/24.1 Hz, C-4). − ^{31}P{^{1}H} NMR (C_6D_6): δ = −5.5 (d, $^2J_{P,P}$ = 43.1 Hz, P-1), 365.7 (d, $^2J_{P,P}$ = 43.1 Hz, P-3). − IR (film): ṽ = 2930, 2842, 2200 (P−H), 1450, 1380, 1350, 1208, 1103, 1055 cm^{-1}.

2,4-Di-tert-butyl-2-dibutylchlorostannyl-1,2-dihydro-1λ³,3λ³-diphosphete (**16c**): From **15c** (900 mg, 2.96 mmol), **14c** (696 mg, 2.96 mmol) and **8a** (2000 mg, 20 mmol) to furnish **16c** (ca. 85%). − ^{1}H NMR (C_6D_6): δ = 0.8−1.9 (m, 36 H, Bu-H and *t*Bu-H), 6.77 (dd, $^1J_{H,P}$ = 166.5 Hz, $^3J_{H,P}$ = 19.5 Hz, 1 H, P−H). − ^{13}C{^{1}H} NMR (C_6D_6): δ = 14.0 [s, Sn(CH$_2$)$_3$*C*H$_3$], 20.3 (s, Sn*C*H$_2$), 27.2 (s, CH_2CH_2), 28.8 (s, CH_2CH_2), 29.7 [br. d, $^3J_{C,P}$ = 10 Hz, C(*C*H$_3$)$_3$], 30.7 [br. d, $^3J_{C,P}$ = 4.0 Hz, C(*C*H$_3$)$_3$], 37.1 [d, $^2J_{C,P}$ = 7.2 Hz, *C*(CH$_3$)$_3$], 40.2 [d, $^2J_{C,P}$ = 2.4 Hz, *C*(CH$_3$)$_3$], 43.2 (br. d, $^1J_{C,P}$ = 33.7 Hz, C-2), 227.6 (dd, $^1J_{C,P}$ = 53.0/23.3 Hz, C-4). − ^{31}P{^{1}H} NMR (C_6D_6): δ = −5.3 (d, $^2J_{P,P}$ = 43 Hz, P-1), 366.1 (d, $^2J_{P,P}$ = 43 Hz, P-3). − IR (film): ṽ = 2930, 2900, 2880, 2210 (P−H), 1450, 1380, 1370, 1349, 1209, 1104, 1070, 1015 cm^{-1}.

2,4,6,9-Tetra-tert-butyl-8-dibutylstanna-1,3,5,7-tetraphospha-pentacyclo[4.3.0.0^{2,5}.0^{3,9}.0^{4,7}]nonane (**17c**): From **15c** (900 mg, 2.96 mmol), **13c** (696 mg, 2.96 mmol) and **8a** (2000 mg, 20 mmol) to furnish **17c** (210 mg, 6%) as yellow crystals with m.p. 145°C. − ^{1}H NMR (C_6D_6): δ = 0.87 (t, $^3J_{H,H}$ = 7.2 Hz, 6 H, CH$_2$−C*H*$_3$), 1.08 (s, 9 H, *t*Bu-H), 1.22−1.47 (m, 8 H, CH$_2$−CH$_2$), 1.27 (s, 18 H, *t*Bu-H), 1.5−1.61 (m, 4 H, CH$_2$−CH$_2$), 1.72 (s, 9 H, *t*Bu-H). − ^{13}C{^{1}H} NMR (C_6D_6): δ = −17.2 (m, C-2), 13.6 [s, Sn(CH$_2$)$_3$*C*H$_3$], 18.7 (s, Sn*C*H$_2$), 22.7 (m, C-9), 26.0 [m, 2 × C(*C*H$_3$)$_3$], 27.1 [m, 2 × C(*C*H$_3$)$_3$], 27.7 (s, CH_2CH_2), 30.2 (s, CH_2CH_2), 34.4 [m, 2 × *C*(CH$_3$)$_3$], 35.1 [pt, $^2J_{C,P}$ = 7.2 Hz, 2 × *C*(CH$_3$)$_3$], 37.6 (pt, $^1J_{C,P}$ = 13.5 Hz, C-4/C-6). − ^{31}P{^{1}H} NMR (C_6D_6): δ = −72.1 (dt, $^2J_{P,P}$ = 21.0/7.6 Hz, $^1J_{P,Sn}$ = 743.9 Hz, 1 P, P-7), 183.8 (dt, $^2J_{P,P}$ = 21.0/15.3 Hz, $^3J_{P,Sn}$ = 109 Hz, 1 P, P-5), 221.4 (dd, $^2J_{P,P}$ = 15.3/7.6 Hz, 2 P, P-1/P-3). − ^{119}Sn NMR (C_6D_6): δ = 328 (dd, $^1J_{^{119}Sn,P}$ = 784 Hz, $^3J_{^{119}Sn,P}$ = 113 Hz). − IR (KBr): ṽ = 2925, 2890, 2830, 1450, 1372, 1343, 1213, 760, 734, 696, 670 cm^{-1}. − MS; *m/z* (%): 634 (15) [M$^+$], 521 (31) [M$^+$ − 2Bu + H], 400 (14) [Cubane$^+$]. − $C_{28}H_{54}P_4Sn$ (633.3): calcd. C 53.1, H 8.6; found C 53.2, H 8.4.

Thermolysis of **10a−d**. − *General Procedure:* The 1,2-dihydro-1,3-diphosphete **10** was dissolved in toluene (5 ml) and heated at 90°C for 6 h. Removal of the solvent yielded the 1-stannyl-substituted 1,2-dihydro-1,3-diphosphetes **18**.

trans-2,4-Di-tert-butyl-1-tributylstannyl-1,2-dihydro-1λ³,3λ³-diphosphete (**18a**): From **10a** (413 mg, 0.84 mmol) to furnish **18a** (413 mg, 100%) as a yellow oil with b.p. 170°C/5 × 10^{-3} mbar. − ^{1}H NMR (C_6D_6): δ = 0.9−1.9 (m, 45 H, Bu-H and *t*Bu-H), 2.05 (s, 1 H, PC−H). − ^{13}C{^{1}H} NMR (C_6D_6): δ = 10.8 (d, $^2J_{C,P}$ = 1.2 Hz, $^1J_{C,^{117/119}Sn}$ = 266.1 Hz, Sn−*C*H$_2$), 14.1 [s, Sn−(CH$_2$)$_3$−*C*H$_3$], 27.8 (s, SnCH$_2$*C*H$_2$), 28.1 [dd, $^3J_{C,P}$ = 14.0/9.4 Hz, C(*C*H$_3$)$_3$], 29.9 (s, *C*H$_2$CH$_3$), 31.0 [dd, $^3J_{C,P}$ = 9.3/3.9 Hz, C(*C*H$_3$)$_3$], 33.6 [d, $^2J_{C,P}$ = 6.2 Hz, *C*(CH$_3$)$_3$], 36.4 (d, $^1J_{C,P}$ = 23.1 Hz, C-2), 40.7 [pt, $^2J_{C,P}$ = 7.0 Hz, *C*(CH$_3$)$_3$], 239.8 (dd, $^1J_{C,P}$ = 51.8/39.9 Hz, C-4). − ^{31}P{^{1}H} NMR (C_6D_6): δ = 6.9 (d, $^2J_{P,P}$ = 39.1 Hz, $^1J_{P,^{117,119}Sn}$ = 869.9 Hz, P-1), 349.4 (d, $^2J_{P,P}$ = 39.1 Hz, P-3). − ^{119}Sn NMR (C_6D_6): δ = −36 (dd, $^1J_{^{119}Sn,P}$ = 916 Hz, $^3J_{^{119}Sn,P}$ = 147 Hz). − IR (film): ṽ = 2950, 2925, 2870, 1470, 1380, 1220, 1125, 860 cm^{-1}. − MS; *m/z* (%): 492 (9) [M$^+$], 57 (77) [C$_4$H$_9^+$]. − $C_{22}H_{46}P_2Sn$ (491.26): calcd. C 53.8, H 9.4; found C 54.0, H 9.3.

trans-2,4-Di-tert-butyl-1-triphenylstannyl-1,2-dihydro-1λ³,3λ³-diphosphete (**18b**): From **10b** (940 mg, 1.8 mmol) to furnish **18b** (940 mg, 100%) as a yellow powder with m.p. 78°C. − ^{1}H NMR (C_6D_6): δ = 1.17 (s, 9 H, *t*Bu-H), 1.28 (s, 9 H, *t*Bu-H), 2.83 (d, $^2J_{H,P}$ = 1.4 Hz, 1 H, PC−H), 7.21−7.31 (m, 9 H, *m*-, *p*-C$_6$H$_5$), 7.76−7.79 (dd, $^3J_{H,H}$ = 7.7 Hz, $^4J_{H,H}$ = 1 Hz, $^3J_{H,Sn}$ = 45.8 Hz, 6 H, *o*-C$_6$H$_5$). − ^{13}C{^{1}H} NMR (C_6D_6): δ = 27.8 [dd, $^3J_{C,P}$ = 7.6/4.9 Hz, C(*C*H$_3$)$_3$], 30.9 [dd, $^3J_{C,P}$ = 9.4/4.0 Hz, C(*C*H$_3$)$_3$], 33.6 [d, $^2J_{C,P}$ = 6.3 Hz, *C*(CH$_3$)$_3$], 36.7 (d, $^1J_{C,P}$ = 23.2 Hz, C2, ^{1}H coupl.: $^1J_{C,H}$ = 135.7 Hz), 40.9 [dd, $^2J_{C,P}$ = 7.2/5.4 Hz, *C*(CH$_3$)$_3$], 129.1 (s, $^2J_{C,^{117/119}Sn}$ = 62.8 Hz, *o*-C), 129.5 (s, $^4J_{C^{117,119}Sn}$ = 11.7 Hz, *p*-C), 138.0 (s, $^3J_{C,^{117/119}Sn}$ = 35.0 Hz, *m*-C), 139.6 (d, $^2J_{C,P}$ = 2.7 Hz, *ipso*-C), 238.1 (dd, $^1J_{C,P}$ = 53.0/39.5 Hz, C-4). − ^{31}P{^{1}H} NMR (C_6D_6): δ = 2.8 (d, $^2J_{P,P}$ = 45.8 Hz, $^1J_{P,^{119}Sn}$ = 1060.5 Hz, $^1J_{P,117Sn}$ = 1014.7 Hz, P-1), 353.3 (d, $^2J_{P,P}$ = 45.8 Hz, $^3J_{P,^{117,119}Sn}$ = 167.9 Hz, P-3). − ^{119}Sn{^{1}H} NMR (C_6D_6): δ = −157 (dd, $^1J_{^{119}Sn,P}$ = 1056 Hz, $^3J_{^{119}Sn,P}$ = 177 Hz). − IR (KBr): ṽ = 3060, 2960, 1430, 1360, 1075, 1025, 1000, 730, 700 cm^{-1}. − MS: *m/z* (%) = 551 (3) [M$^+$], 351 (81) [SnPh$_3^+$], 131 (100) [P$_2$C$_5$H$_9^+$], 57 (20) [C$_4$H$_9^+$]. − $C_{28}H_{34}P_2Sn$ (551.23): calcd. C 61.0, H 6.2; found C 61.3, H 6.2.

trans-2,4-(Diadamant-1-yl)-1-tributylstannyl-1,2-dihydro-1λ³,3λ³-diphosphete (**18c**): From **10c** (200 mg, 0.31 mmol) to furnish **18c** (200 mg, 100%) as a yellow, non-distillable oil. − ^{1}H NMR (C_6D_6): δ = 0.9−2.3 (m, 57 H, Ad-H and Bu-H), 2.65 (s, 1 H, P−CH). − ^{13}C{^{1}H} NMR (C_6D_6): δ = 11.0 (s, Sn−*C*H$_2$), 13.9 (s, Sn−[CH$_2$]$_3$−*C*H$_3$), 27.8 (s, SnCH$_2$*C*H$_2$), 29.1 (s, C-c), 29.2 (s, C-c), 30.0 (s, *C*H$_2$CH$_3$), 35.6 (d, $^2J_{C,P}$ = 5.7 Hz, C-a), 36.9 (s, *C*d), 37.1 (s, C-d), 38.5 (d, $^1J_{C,P}$ = 22.9 Hz, C-2), 40.3 (dd, $^3J_{C,P}$ = 8.6/4.8 Hz, C-b), 42.9 (dd, $^2J_{C,P}$ = 6.7/3.8 Hz, C-a), 43.2 (dd, $^3J_{C,P}$ = 9.1/4.3 Hz, C-b), 240.4 (dd, $^1J_{C,P}$ = 50.6/40.1 Hz, C-4). − ^{31}P{^{1}H} NMR (C_6D_6): δ = 0.3 (d, $^2J_{P,P}$ = 44.0 Hz, $^1J_{P,^{117,119}Sn}$ = 907.2 Hz, P-1), 340.1 (d, $^2J_{P,P}$ = 44.0 Hz, $^3J_{P,^{117,119}Sn}$ = 149 Hz, P-3). − IR (film): ṽ = 2985, 2870, 2850, 1455, 1350, 1250, 1070, 875, 840 cm^{-1}. − $C_{34}H_{58}P_2Sn$ (647.49): calcd. C 63.1, H 9.0; found C 62.0, H 8.9.

trans-2,4-(Diadamant-1-yl)-1-triphenylstannyl-1,2-dihydro-1λ³,3λ³-diphosphete (**18d**): From **10d** (198 mg, 0.28 mmol) to furnish **18d** (198 mg, 100%) as a yellow, crystalline solid with m.p. 165°C. − ^{1}H NMR (C_6D_6): δ = 1.2−2.15 (m, 30 H, Ad-H), 2.43 (br., 1 H, PC−H), 6.9−7.35 (m, 9 H, *m*-, *p*-C$_6$H$_5$), 7.5−7.8 (m, 6 H, *o*-C$_6$H$_5$). − ^{13}C{^{1}H} NMR (C_6D_6): δ = 28.89 (s, C-c), 28.92 (s, C-c), 35.6 (d, $^2J_{C,P}$ = 5.6 Hz, C-a), 36.5 (s, C-d), 36.9, (s, C-d), 39.1 (d, $^1J_{C,P}$ = 24.1 Hz, C-2), 40.1 (dd, $^3J_{C,P}$ = 8.0/4.1 Hz, C-b), 43.1 (dd, $^2J_{C,P}$ = 8.8/4.0 Hz, C-b), 43.4 (dd, $^2J_{C,P}$ = 6.8/3.5 Hz, C-a), 129.0 (s, *o*-C), 129.4 (s, $^4J_{C,^{117/119}Sn}$ = 11.2 Hz, *p*-C), 137.7 (s, $^3J_{C,^{117/119}Sn}$ = 34.5 Hz, *m*-C), 139.9 (d, $^2J_{C,P}$ = 2.4 Hz, *ipso*-C), 238.4 (dd, $^1J_{C,P}$ = 51.4/39.4 Hz, C-4). − ^{31}P{^{1}H} NMR (C_6D_6): δ = −5.0 (d, $^2J_{P,P}$ = 45.8 Hz, $^1J_{P,^{117,119}Sn}$ = 1050.5 Hz, P-1), 349.4 (d, $^2J_{P,P}$ = 45.8 Hz, $^3J_{P,^{117,119}Sn}$ = 175 Hz, P-3). − ^{119}Sn{^{1}H} NMR (C_6D_6): δ = −159 (dd, $^1J_{^{119}Sn,P}$ = 1099 Hz, $^3J_{^{119}Sn,P}$ = 177 Hz). − IR (KBr): ṽ = 3030, 2870, 2820, 1460, 1430, 1410, 1330, 1300,

1250, 1090, 985, 715, 685 cm^{-1}. – MS; *m/z* (%): 708 (2) [M^+], 700 (3) [$(SnPh_3)_2^+$], 357 (15) [$M^+ - SnPh_3$], 351 (100) [$SnPh_3^+$], 135 (73) [Ad^+]. – $C_{40}H_{46}P_2Sn$ (707.5): calcd. C 67.9, H 6.6; found C 67.7, H 6.7.

Complexations of **10a**,**b** *with Pentacarbonyltungsten·Tetrahydrofuran. – General Procedure:* A solution of pentacarbonyltungsten·THF was prepared by irradiation of a solution of hexacarbonyltungsten in THF (HPK, 125 W, Phillips) for 35 min. To this solution was added **10** in THF (10 ml) and the mixture was stirred at room temperature for 24 h. The solvent was then removed under vacuum and excess hexacarbonyltungsten was sublimed at 40°C under vacuum. The residue was taken up in pentane and yielded compounds **19**, **20** on crystallization at −20°C.

(2,4-Di-tert-butyl-2-triphenylstannyl-1,2-dihydro-η¹-1λ³,3λ³-diphosphete)pentacarbonyltungsten (**19**): From hexacarbonyltungsten (1.75 g, 5 mmol) and 1,2-dihydro-1,3-diphosphete **10b** (2.05 g, 3.72 mmol) to furnish **19** (1.46 g, 45%) as a yellow-orange, crystalline powder with m.p. 153.2°C (dec.). – ^{1}H NMR (C_6D_6): δ = 1.18 (s, 9 H, *t*Bu-H), 1.69 (s, 9 H, *t*Bu-H), 7.39−7.45 (m, 9 H, *m*-, *p*-C_6H_5), 7.9−8.0 (m, 6 H, *o*-C_6H_5), 9.08 (dd, $^1J_{H,P}$ = 280 Hz, $^3J_{H,P}$ = 13.8 Hz, 1 H, P-H). – $^{13}C\{^1H\}$ NMR (C_6D_6): δ = 29.5 [d, $^3J_{C,P}$ = 5.0 Hz, C(*C*H_3)$_3$], 31.3 [d, $^3J_{C,P}$ = 7.0 Hz, C(*C*H_3)$_3$], 37.5 [s, *C*(CH_3)$_3$], 39.9 [s, *C*(CH_3)$_3$], 45.6 (dd, $^1J_{C,P}$ = 40/13 Hz, C-2), 129.1 (s, *o*-C), 129.7 (s, *p*-C), 137.8 (s, *m*-C), 140.1 (s, *ipso*-C), 198.1 (d, $^2J_{C,P}$ = 6.4 Hz, $CO_{equatorial}$), 198.7 (d, $^2J_{C,P}$ = 18.5 Hz, CO_{axial}), 209.5 (dd, $^1J_{C,P}$ = 52/11 Hz, C-4). – $^{31}P\{^1H\}$ NMR (C_6D_6): δ = 15.3 (s, $^1J_{P,W}$ = 209 Hz, P-1), 399.2 (s, P-3). – $^{119}Sn\{^1H\}$ NMR (C_6D_6): δ = −98.6 (m). – IR (KBr): $\tilde{\nu}$ = 3020, 2920, 2200 (P−H), 2020 (CO), 1960 (CO), 1900 (CO), 1450, 1400, 1050, 820 cm^{-1}. – MS: *m/z* (%) = 875 (24) [M^+], 797 (100) [M^+ − Ph], 553 (24) [M^+ − $W(CO)_5$], 351 (96) [$SnPh_3^+$]. – $C_{33}H_{34}O_5P_2SnW$ (875.12): calcd. C 45.3, H 3.9; found C 45.3, H 4.0.

μ-(2,4-Di-tert-butyl-2-tributylstannyl-1,2-dihydro-η¹-1λ³,η¹-3λ³-diphosphete)bis(pentacarbonyltungsten) (**20**): From hexacarbonyltungsten (600 mg, 1.7 mmol) and 1,2-dihydro-1,3-diphosphete **10a** (260 mg, 0.53 mmol) to furnish **20** (360 mg, 60%) as a yellow powder with m.p. 118°C (dec.). – ^{1}H NMR (C_6D_6): δ = 0.91−1.67 (m, 36 H, CH_2 and *t*Bu-H), 0.97 (t, $^3J_{H,H}$ = 7.24 Hz, 9 H, CH_2CH_3), 7.71 (dd, $^1J_{H,P}$ = 295.09 Hz, $^3J_{H,P}$ = 31.81 Hz, 1 H, P-H). – $^{13}C\{^1H\}$ NMR (C_6D_6): δ = 13.6 (s, Sn−*C*H_2), 15.1 (s, Sn−[CH_2]$_3$−*C*H_3), 27.7 (s, $^2J_{C,^{117/119}Sn}$ = 69.1/72.3 Hz, $SnCH_2CH_2$), 29.8 (s, $^3J_{C,^{117/119}Sn}$ = 18.5 Hz, *C*H_2CH$_3$), 31.4 [d, $^3J_{C,P}$ = 4.8 Hz, C(*C*H_3)$_3$], 31.5 [d, $^3J_{C,P}$ = 5.6 Hz, C(*C*H_3)$_3$], 36.9 [s, *C*(CH_3)$_3$], 39.5 [s, *C*(CH_3)$_3$], 51.9 (dd, $^1J_{C,P}$ = 16/8 Hz, C-2), 194.9 (dd, $^1J_{C,P}$ = 39.8/7.7 Hz, C-4), 195.8 (d, $^2J_{C,P}$ = 7.2 Hz, $CO_{equatorial}$), 196.5 (d, $^2J_{C,P}$ = 31.3 Hz, CO_{axial}), 197.9 (d, $^2J_{C,P}$ = 5.6 Hz, $CO_{equatorial}$), 198.5 (d, $^2J_{C,P}$ = 28.9 Hz, CO_{axial}). – $^{31}P\{^1H\}$ NMR (C_6D_6): δ = 6 (d, $^2J_{P,P}$ = 26 Hz, $^1J_{P,W}$ = 222 Hz, P-1), 294 (d, $^2J_{P,P}$ = 26 Hz, $^1J_{P,W}$ = 244 Hz, P-3). – IR (pentane): $\tilde{\nu}$ = 2972, 2929, 2079 (P−H), 2070 (CO), 1982 (CO), 1964 (CO), 1464, 1378, 893 cm^{-1}. – MS; *m/z* (%): 1138 (2) [M^+], 847 (39) [M^+ − $SnBu_3$], 813 (17) [M^+ − $W(CO)_5$ − H], 679 (53) [M^+ − $SnBu_3$ − 6 CO], 291 (100) [$SnBu_3^+$], 235 (72) [$HSnBu_2^+$], 57 (32) [$C_4H_9^+$]. – $C_{32}H_{46}O_{10}P_2SnW_2$ (1139.04): calcd. C 33.74, H 4.07; found C 32.86, H 3.90.

Complexations of **10a**,**b** *with Enneacarbonyldiiron. – General Procedure:* To a solution of **10** in pentane (10 ml) was added enneacarbonyldiiron and the mixture stirred at room temperature for 24 h. The solution was then filtered through Celite and compounds **21** were crystallized from pentane at −78°C.

μ-(2,4-Di-tert-butyl-2-tributylstannyl-1,2-dihydro-η¹-1λ³,η¹-3λ³-diphosphete)bis(tetracarbonyliron) (**21a**): From enneacarbonyldiiron (1.5 g, 4 mmol) and 1,2-dihydro-1,3-diphosphete **10a** (920 mg, 1.87 mmol) to furnish **21a** (420 g, 27%) as a red-brown solid with m.p. 184°C. – ^{1}H NMR (CD_2Cl_2): δ = 0.95 (t, $^3J_{H,H}$ = 7.21 Hz, 9 H, CH_2CH_3), 1.21−1.66 (m, 18 H, CH_2), 1.44 (s, 9 H, *t*Bu-H), 1.45 (s, 9 H, *t*Bu-H), 7.20 (dd, $^1J_{H,P}$ = 307.25 Hz, $^3J_{H,P}$ = 30.52 Hz, 1 H, P-H). – $^{13}C\{^1H\}$ NMR (C_6D_6): δ = 13.7 (s, Sn−*C*H_2), 15.2 (s, Sn−[CH_2]$_3$−*C*H_3), 27.8 (s, $^2J_{C,^{117/119}Sn}$ = 71.5 Hz, $SnCH_2CH_2$), 29.8 (s, $^3J_{C,^{117/119}Sn}$ = 17.8 Hz, *C*H_2CH$_3$), 30.6 [dd, $^3J_{C,P}$ = 11.2/10.4 Hz, C(*C*H_3)$_3$], 31.1 [s, C(*C*H_3)$_3$], 38.2 [s, *C*(CH_3)$_3$], 39.8 [s, *C*(CH_3)$_3$], 61.9 (d, $^1J_{C,P}$ = 14.8 Hz, C-2), 195.1 (pt, $^1J_{C,P}$ = 14.4 Hz, C-4), 214.6 (d, $^2J_{C,P}$ = 11.2 Hz, CO), 217.3 (d, $^2J_{C,P}$ = 10.4 Hz, CO). – $^{31}P\{^1H\}$ NMR (C_6D_6): δ = 48 (d, $^2J_{P,P}$ = 27 Hz, P-1), 315 (d, $^2J_{P,P}$ = 26 Hz, P-3). – IR (pentane): $\tilde{\nu}$ = 2986−2843, 2068 (P-H), 2054 (CO), 1971 (CO), 1472, 1453, 1362, 1261, 1022, 907, 730 cm^{-1}. – MS; *m/z* (%): 828 (0.2) [M^+], 660 (1) [M^+ − $Fe(CO)_4$], 492 (16) [M^+ − 2 $Fe(CO)_4$], 291 (70) [$SnBu_3^+$], 235 (96) [$HSnBu_2^+$], 179 (100) [H_2SnBu^+], 57 (33) [$C_4H_9^+$], – $C_{30}H_{46}Fe_2O_8P_2Sn$ (827.02): calcd. C 43.57, H 5.61; found C 43.13, H 5.61.

μ-(2,4-Di-tert-butyl-2-triphenylstannyl-1,2-dihydro-η¹-1λ³,η¹-3λ³-diphosphete)bis(tetracarbonyliron) (**21b**): From enneacarbonyldiiron (400 mg, 1.1 mmol) and 1,2-dihydro-1,3-diphosphete **10b** (200 mg, 0.36 mmol) to furnish **21b** (220 mg, 69%) as a red-brown solid with m.p. 124°C. – ^{1}H NMR (CD_2Cl_2): δ = 1.05 (s, 9 H, *t*Bu-H), 1.60 (s, 9 H, *t*Bu-H), 7.39−7.79 (m, 15 H, C_6H_5), 7.67 (dd, $^1J_{H,P}$ = 308.18 Hz, $^3J_{H,P}$ = 28.82 Hz, 1 H, P−H). – $^{13}C\{^1H\}$ NMR (C_6D_6): δ = 29.7 [dd, $^3J_{C,P}$ = 11.2 Hz, C(*C*H_3)$_3$], 31.7 [s, C(*C*H_3)$_3$], 38.5 [s, *C*(CH_3)$_3$], 39.5 [s, *C*(CH_3)$_3$], 65.3 (dd, $^1J_{C,P}$ = 20.5/5.6 Hz, C-2), 129.3 (s, $^2J_{C,^{117/119}Sn}$ = 53.0 Hz, *o*-C), 130.1 (s, *p*-C), 137.9 (s, $^3J_{C,^{117/119}Sn}$ = 37.0 Hz, *m*-C), 139.8 (s, *ipso*-C), 196.3 (pt, $^1J_{C,P}$ = 15 Hz, C-4), 213.8 (d, $^2J_{C,P}$ = 10.4 Hz, CO), 216.6 (d, $^2J_{C,P}$ = 10.4 Hz, CO). – $^{31}P\{^1H\}$ NMR (C_6D_6): δ = 47 (d, $^2J_{P,P}$ = 34 Hz, P-1), 313 (d, $^2J_{P,P}$ = 33 Hz, P-3). – IR (KBr): $\tilde{\nu}$ = 3449, 2959, 2236 (P−H), 2072 (CO), 2057 (CO), 2007 (CO), 1981 (CO), 1945 (CO), 1450, 1428, 1360, 1211, 843 cm^{-1}. – MS; *m/z* (%): 887 (0.2) [M^+ − H], 748 (1) [M^+ − 5 CO], 351 (100) [$SnPh_3^+$], 169 (51) [$HFe(CO)_4^+$], 57 (55) [$C_4H_9^+$].

2,4-Di-tert-butyl-1-iodo-2-triphenylstannyl-1,2-dihydro-1λ³,3λ³-diphosphete (**22**): A solution of iodine (280 mg, 1.1 mmol) in diethyl ether was added dropwise to a suspension of 1,2-dihydro-1,3-diphosphete **10b** (600 mg, 1.1 mmol) in diethyl ether (5 ml). The reaction mixture was stirred 15 min at room temperature and then the solvent and all volatile compounds were removed under vacuum to furnish **22** as a yellow, non-distillable oil. Yield: about 90%. – ^{1}H NMR (C_6D_6): δ = 1.05 (s, 9 H, *t*Bu-H), 1.22 (s, 9 H, *t*Bu-H), 7.0−7.29 (m, 9 H, *m*-, *p*-C_6H_5), 7.87−8.12 (m, 6 H, *o*-C_6H_5). – $^{13}C\{^1H\}$ NMR (C_6D_6): δ = 30.2 [d, $^3J_{C,P}$ = 4.5 Hz, C(*C*H_3)$_3$], 30.6 [dd, $^3J_{C,P}$ = 11.7/3.6 Hz, C(*C*H_3)$_3$], 38.8 [d, $^2J_{C,P}$ = 8.1 Hz, *C*(CH_3)$_3$], 41.5 [dd, $^2J_{C,P}$ = 7.2/2.7 Hz, *C*(CH_3)$_3$], 58.1 (pt, $^1J_{C,P}$ = 42.6 Hz, C-2), 130.4 (s, $^4J_{C,^{117/119}Sn}$ = 13.5 Hz, *p*-C), 136.6 (s, $^2J_{C,^{117/119}Sn}$ = 48.5 Hz, *o*-C), 138.8 (s, $^3J_{C,^{117/119}Sn}$ = 36.8 Hz, *m*-C), 142.6 (s, *ipso*-C), 230.3 (pt, $^1J_{C,P}$ = 56.6 Hz, C-4). – $^{31}P\{^1H\}$ NMR (C_6D_6): δ = 5.5 (d, $^2J_{P,P}$ = 126.4 Hz, P-1), 324.9 (d, $^2J_{P,P}$ = 126.4 Hz, P-3). – IR (film): $\tilde{\nu}$ = 3035, 2930, 1460, 1420, 1355, 1065, 1015, 990, 720, 690 cm^{-1}. – MS; *m/z* (%): 677 (10) [M^+], 351 (71) [$SnPh_3^+$], 77 (51) [Ph^+], 57 (21) [$C_4H_9^+$].

X-ray Structural Analysis of **18d**[33]: Siemens P-4 diffractometer, graphite monochromator, Mo-K_α (λ = 0.71073 Å), structure solution by direct methods (SHELXTL-PLUS[34]) and structure refinement by SHELXL-93[35]. Semi-empirical absorption correction by

use of Ψ scans. Hydrogen atoms were placed in geometrically calculated positions (d_{C-H} = 0.960 Å). $C_{40}H_{46}P_2Sn$; M = 707.4 g·mol^{-1}; monoclinic; space group $C2/c$; a = 33.813(7), b = 9.565(2), c = 21.797(4) Å, β = 101.33(3)°, V = 6912(2) Å^3; Z = 8; $D_{calcd.}$ = 1.360 Mg/m^3; μ = 8.59 cm^{-1}; crystal size 0.30 × 0.25 × 0.20 mm; ω scan: 1.23° ≤ Θ ≤ 26.00°. 7998 reflections collected, 6750 independent reflections ($R_{int.}$ = 0.0254); max./min. transmission: 0.880/0.761; 392 parameters; $w^{-1} = [\sigma^2(F_o^2) + (0.0466P)^2 + 8.3105P]$ and $P = [(F_o^2)+2F_c^2]/3$; R = 0.0386, R_w = 0.0905 for 6750 reflections with $I > 2\sigma(I)$ and R = 0.0651, R_w = 0.1039 for all data; residual electron density 483 e·nm^{-3} and −433 e·nm^{-3}, *GOF* (on F^2) = 1.007.

☆ Dedicated to Professor *Manfred Weidenbruch* on the occasion of his 60th birthday.

[1] A. Nachbauer, U. Bergsträßer, S. Leininger, M. Regitz, *Synthesis* **1997**, in press.

[2] G. J. M. van der Kerk, J. G. A. Luijten, J. G. Noltes, *Chem. Ind.* **1956**, 352.

[3] G. J. M. van der Kerk, J. G. A. Luijten, J. G. Noltes, *J. Appl. Chem.* **1959**, *9*, 106−113.

[4] [4a] J. G. Noltes, G. J. M. van der Kerk, *Chimia* **1962**, *16*, 122−127. − [4b] J. G. Noltes, G. J. M. van der Kerk, *Recl. Trav. Chim. Pays-Bas* **1962**, *81*, 41−48.

[5] A. K. Sawyer, H. G. Kuivila, *Chem. Ind.* **1961**, 260.

[6] W. P. Neumann, J. Pedain, *Tetrahedron Lett.* **1964**, 2461−2465.

[7] M. Schmitz, R. Göller, M. Regitz, *Synthesis* **1997**, 455−460.

[8] R. Appel, V. Barth, F. Knoch, *Chem. Ber.* **1983**, *116*, 938−950.

[9] B. Breit, M. Regitz, *Chem. Ber.* **1993**, *126*, 1945−1950.

[10] S. Lochschmidt, A. Schmidpeter, *Phosphorus Sulfur* **1988**, *29*, 73−109.

[11] [11a] G. Becker, W. Becker, R. Knebl, H. Schmidt, M. Mildenbrand, M. Westerhausen, *Phosphorus Sulfur* **1987**, *30*, 349−352. − [11b] R. Knebl, Ph.D. Thesis, University of Stuttgart, **1988**.

[12] R. Schneider, Ph.D. Thesis, University of Kaiserslautern, **1991**.

[13] K. Karaghiosoff in *Multiple Bonds and Low Coordination in Phosphorus Chemistry* (Eds.: M. Regitz, O. J. Scherer), 1st ed., Thieme, Stuttgart **1990**, p. 463ff.

[14] A. P. Tupciauskas, N. M. Sergeev, Yu. A. Ustynyk, *Org. Magn. Resonance*, **1971**, *3*, 655−659.

[15] W. McFarlane, J. C. Maire, M. Delmas, *J. Chem. Soc., Dalton Trans.* **1972**, 1862−1865.

[16] Appel and coworkers reported only one isomer of a 1,2-dihydro-1,3-diphosphete in temperature-dependent ^{31}P-NMR measurements, see also ref.[8].

[17] G. Bähr, S. Pawlenko in Houben-Weyl: *Methoden der Organischen Chemie, Metallorganische Verbindungen, Vol. 13/6 Germanium, Zinn,* 4th ed., Thieme, Stuttgart, **1978**, p. 239.

[18] T. Wettling, J. Schneider, O. Wagner, C. G. Kreiter, M. Regitz, *Angew. Chem.* **1989**, *101*, 1035−1037; *Angew. Chem. Int. Ed. Engl.* **1989**, *28*, 1013−1015.

[19] R. Gleiter, K. H. Pfeifer, M. Baudler, G. Scholz, T. Wettling, M. Regitz, *Chem. Ber.* **1990**, *123*, 757−760.

[20] W. McFarlane, N. H. Rees, *Polyhedron* **1989**, *8*, 2047−2050.

[21] J. P. Albrand, D. Gagnaire, J. B. Robert, *J. Chem. Soc., Chem. Commun.* **1968**, 1469−1470.

[22] R. Appel: "*Phosphaalkenes, Phosphacarbaoligoenes and Phosphaallenes*" in *Multiple Bonds and Low Coordination in Phosphorus Chemistry* (Eds.: M. Regitz, O. J. Scherer), 1st ed., Thieme, Stuttgart **1990**, p. 160.

[23] J. Emsley, D. Hall, *The Chemistry of Phosphorus*, Harper & Row Ltd., London **1976**, p. 177−207.

[24] O. Stelzer, *Topics in Phosphorus Chemistry*, Wiley & Sons, New York, **1977**, vol. 9, p. 1−229.

[25] [25a] E. O. Fischer, L. Knauss, R. L. Keiter, J. G. Verkade, *J. Organomet. Chem.* **1972**, *37*, C7−C10. − [25b] H. C. E. Mc Farlane, W. Mc Farlane, D. S. Rycroft, *J. Chem. Soc. Dalton Trans.* **1976**, 1616−1622.

[26] See ref.[17], p. 257 and references cited therein.

[27] A. E. Finholt, A. C. Bord Jr., K. E. Wilzbach, H. E. Schlesinger, *J. Am. Chem. Soc.* **1947**, *69*, 2692−2696.

[28] A. K. Sawyer, J. E. Brown, G. S. May, *J. Organomet. Chem.* **1968**, *11*, 192−194.

[29] G. J. M. van der Kerk, J. G. Noltes, J. G. A. Luijten, *J. Appl. Chem.* **1957**, *7*, 366−369.

[30] K. A. Kocheshkov, *Ber. Dtsch. Chem. Ges.* **1933**, *66*, 1661−1665.

[31] W. Rösch, U. Hees, M. Regitz, *Chem. Ber.* **1987**, *120*, 1645−1652.

[32] T. Allspach, M. Regitz, G. Becker, W. Becker, *Synthesis* **1986**, 31−36.

[33] Further details of the crystal structure determination are available on request from the Fachinformationszentrum Karlsruhe, Gesellschaft für wissenschaftlich-technische Information mbH, D-76344 Eggenstein-Leopoldshafen, on quoting the depository number CSD-407748, the names of the authors, and the journal citation.

[34] *SHELXTL-PLUS*, Siemens Analytical X.-ray Instruments, Madison, Wisconsin, USA **1991**.

[35] G. M. Sheldrick, *SHELXL-93*, a program for structure refinement, Göttingen, Germany, **1993**.

[97215]

Titanium Complexes with a Linked Amido−Cyclopentadienyl Ligand and a Bidentate Organyl Group: Synthesis, Structure, and Ethene Polymerization Activity☆

Thomas Eberle, Thomas P. Spaniol, and Jun Okuda*

Institut für Anorganische Chemie und Analytische Chemie, Universität Mainz,
Johann-Joachim-Becher-Weg 24, D-55099 Mainz, Germany

Received October 10, 1997

Keywords: Titanium complexes / Amido−cyclopentadienyl ligand / Titanium alkyl / Intramolecular coordination / Ethene polymerization

Titanium complexes containing a linked isopropyl- or benzylamido(tetramethylcyclopentadienyl) ligand $C_5Me_4SiMe_2NR$ (R = *i*Pr, CH_2Ph,) and one bidentate organyl group $C_6H_4(CH_2NMe_2)$-2, $CH_2C_6H_4(NMe_2)$-2, and {η^5-$C_5H_3(CH_2NMe_2)$-2}Fe(η^5-C_5H_5) were prepared by salt metathesis of the corresponding dichloro complex Ti(η^5:η^1-$C_5Me_4SiMe_2NR)Cl_2$ with the lithium organyl. Single crystal X-ray structural analysis of Ti(η^5:η^1-$C_5Me_4SiMe_2NCH_2Ph$)-{$C_6H_4(CH_2NMe_2)$-2}Cl and of Ti(η^5:η^1-$C_5Me_4SiMe_2N$*i*Pr)-{$CH_2C_6H_4(NMe_2)$-2}Cl revealed the presence of intramolecular coordination with square pyramidal geometry around titanium. In the ferrocenyl derivative Ti(η^5:η^1-C_5Me_4-$SiMe_2NCH_2Ph$)[{η^5-$C_5H_3(CH_2NMe_2)$-2}Fe(η^5-C_5H_5)]Cl the NMe_2 group is not bonded at the titanium atom. Ethene polymerization catalyzed by these complexes upon activation with methylaluminoxane was examined.

Introduction

Homogeneous polymerization catalysts based on titanium complexes with the linked amido−cyclopentadienyl ligand $C_5Me_4SiMe_2N$*t*Bu[1a][1b][1c] have recently gained enormous technological importance for the efficient synthesis of novel copolymers of ethene with α-olefins such as 1-octene and styrene[2]. The initial design of this ligand system by Bercaw and Shapiro[1a][1b][1c] was guided by the increased Lewis acidity of the metal complexes that would accommodate the bulkier comonomers more easily, compared to *ansa*-metallocenes containing a linked bis(cyclopentadienyl) ligand. Because of the great industrial interest not many detailed studies on structure−activity relationships of this class of complexes have so far appeared in the open literature[3]. In particular the influence of each of the ligand moieties on the polymerization performance remains unknown. We have synthesized and characterized several titanium complexes containing a linked amido−cyclopentadienyl ligand with different amido and cyclopentadienyl substituents[1d][1h][1i][1j][4a]. More recently, the influence of a donor-functionalized amido side chain on the Lewis acidity of the titanium center has been investigated in some detail[4]. In continuation of these studies we describe here the synthesis and characterization of some new titanium complexes with this ligand system and assess their activity towards ethene polymerization. In particular we focus on those systems that contain a bidentate organyl group, since they may give a clue to the possible polymerization of functionalized monomers.

Results and Discussion

The established synthetic route to titanium dichloro complexes containing a linked amido−cyclopentadienyl ligand $C_5Me_4SiMe_2NR$ is the metathesis of $TiCl_3(THF)_3$ with the dimetallated ligand $[C_5Me_4SiMe_2NR]^{2-}$, followed by chlorination with $PbCl_2$[1h][1i][1j]. However, in the case of the prototypical ligand system $C_5Me_4SiMe_2N$*t*Bu, the yield of the isolated crystalline product Ti(η^5:η^1-$C_5Me_4SiMe_2N$*t*Bu)Cl_2 (**1**)[5] was invariably low in our hands, never exceeding 40%. Obviously, the nature of the amido substituent R in the ligand $C_5Me_4SiMe_2NR$ critically influences the yield of Ti(η^5:η^1-$C_5Me_4SiMe_2NR)Cl_2$ and we suspected that a tertiary amido substituent causes significant steric hindrance during coordination of the bidentate ligand to the titanium center. Thus, the reaction of the doubly deprotonated ligand $Li_2[C_5Me_4SiMe_2NAd]$ (Ad = 1-adamantyl) resulted only in a yield of 30% for the titanium dichloro complex Ti(η^5:η^1-$C_5Me_4SiMe_2NAd)Cl_2$ (**2**). Low yield was also encountered during the preparation of Ti(η^5:η^1-$C_5Me_4SiMe_2NCMe_2$-CH_2*t*Bu)Cl_2 (**3**), derived from the inexpensive 1,1,3,3,-tetramethylbutylamine. However, the analogous reaction with $Li_2[C_5Me_4SiMe_2N$*i*Pr] gave the yellow crystalline isopropylamido derivative Ti(η^5:η^1-$C_5Me_4SiMe_2N$*i*Pr)Cl_2 (**4**) in excess of 70% yield (Scheme 1). Analytical and spectroscopic characterizations of **1**−**4** are straightforward. In the ^{1}H-NMR spectrum of **4**, a low field shift of the methine proton (δ = 5.55) is observed which is typical for all related complexes with secondary amido groups [Ti(η^5:η^1-$C_5H_4SiMe_2N$-*i*Pr)Cl_2: δ = 5.69[1j]; Ti{η^5:η^1-$C_5Me_4(CH_2)_nSiMe_2N$*i*Pr}Cl_2: δ = 5.92 (*n* = 2), δ = 6.57 (*n* = 3)[6]].

 © WILEY-VCH Verlag GmbH, D-69451 Weinheim, 1998 1434−1948/98/0202−0237 $ 17.50+.50/0

Scheme 1

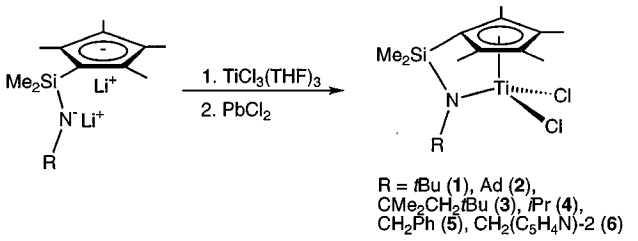

R = *t*Bu (**1**), Ad (**2**), CMe_2CH_2tBu (**3**), *i*Pr (**4**), CH_2Ph (**5**), $CH_2(C_5H_4N)$-2 (**6**)

Yet another limitation to the complexation of the $C_5Me_4SiMe_2NR$ ligand was noted, when (2-pyridyl)methyl-amido as a "hetero-benzylamido" ligand was introduced. Previously we had synthesized the benzylamido complex $Ti(\eta^5{:}\eta^1\text{-}C_5Me_4SiMe_2NCH_2Ph)Cl_2$ (**5**) without any difficulty[1j]. However, after tedious workup, $Ti\{\eta^5{:}\eta^1\text{-}C_5Me_4SiMe_2NCH_2(C_5H_4N)\text{-}2\}Cl_2$ (**6**) was recovered only in 30% yield as orange crystals. The NMR data indicate the existence of a mirror plane and do not allow the distinction between a rigid intramolecular interaction of the pyridyl group at the titanium center and a fluxional complexation. However, in the the ^{1}H-NMR spectrum of **6** the *ortho* proton of the pyridyl group at $\delta = 9.40$ is remarkably shifted to low field compared to that in the ligand precursor $(C_5Me_4H)SiMe_2NHCH_2(C_5H_4N)$-2 ($\delta = 8.59$).

We successfully introduced each of the organyl ligands with an appended *N*,*N*-dimethylamino donor group 2-(*N*,*N*-dimethylaminomethyl)phenyl, 2-(*N*,*N*-dimethylamino)benzyl and {2-(*N*,*N*-dimethylamino)methyl}ferrocenyl by substituting one chloro ligand in **4** and **5** through salt metathesis. This type of bidentate organyl ligands were reported to be capable of stabilizing extremely sensitive monomeric, paramagnetic bis(cyclopentadienyl)titanium(III) derivatives[7]. Attempts to obtain compounds with two organyl groups failed so far, presumably due to the steric repulsion ot these bulky groups. As summarized in Scheme 2, the complexes **7**−**10** were obtained in good yields by the reaction in toluene of the dichloro precursors **4** and **5** with one equivalent of lithium{2-(*N*,*N*-dimethylaminomethyl)-phenyl} and lithium{2-(*N*,*N*-dimethylamino)benzyl}, respectively. The complexes **7** and **8** were isolated as yellow, **9** and **10** as red crystals, sensitive to air and moisture. They were fully characterized by NMR spectroscopy, mass spectral and elemental analysis.

Complexes **7**−**10** are soluble in toluene and THF, but only slightly soluble in aliphatic hydrocarbons. In contrast to the dichloro complexes **4** and **5**, the ^{1}H-NMR spectra reveal four signals for the methyl groups at the cyclopentadienyl ring as well as two for the methyl groups at the silicon due to the asymmetric titanium metal center. All methylene protons of the various CH_2 groups in **7**−**10** are diastereotopic, each giving rise to an AB spin pattern. The chemical shift differences between the two doublets for the CH_2NMe_2 group in **7** and **8** with $\Delta\delta > 1.1$ ppm are unusually large[8]. In **9** and **10**, the resonances due to the CH_2 group at titanium are centered around $\delta = 2.3$.

At room temperature, a single resonance is observed for the methyl groups of the *N*,*N*-dimethylamino group for

Scheme 2

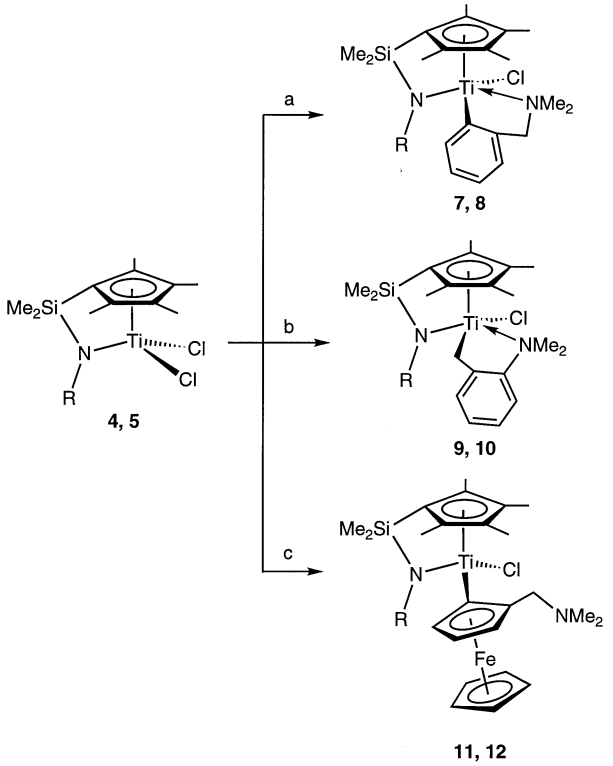

a) $Li\{C_6H_4(CH_2NMe_2)\text{-}2\}$; b) $Li\{CH_2C_6H_4NMe_2)\text{-}2\}$; c) $Li[\{\eta^5\text{-}C_5H_3(CH_2NMe_2)\text{-}2\}Fe(\eta^5\text{-}C_5H_5)]$

7−**10** in both the ^{1}H- and ^{13}C-NMR spectra. The diastereotopic methyl groups are rendered equivalent through the fast inversion at the nitrogen atom. This finding suggests that the *N*,*N*-dimethylamino function in these complexes is either not coordinated at the titanium or undergoes a rapid association−dissociation equilibration process on the NMR time scale. Temperature dependent ^{1}H-NMR measurements of **9** down to −50°C in $CDCl_3$ only resulted in slight changes in the chemical shifts and no decoalescence of the NMe_2 signal was observed. Based on what we have learned from the titanium complexes with the potentially tridentate ligand system $[C_5R'_4SiMe_2NCH_2CH_2NMe_2]^{2-}$ ($C_5R'_4 = C_5H_4$, C_5H_3tBu, C_5Me_4)[4a][4b], the latter scenario appears to be more probable, in particular in view of the crystal structures of **8** and **9** (vide infra). Likewise, a similar bonding situation can be found for the trichloro complexes of the type $Ti(\eta^5\text{-}C_5H_4CH_2CH_2NRR')Cl_3$[9a][9b].

According to single crystal X-ray structural analysis, the structures of **8** and **9** in the solid state unequivocally reveal the presence of a Ti−NMe_2 interaction (Figure 1 and 2). In the 2-(*N*,*N*-dimethylaminomethyl)phenyl derivative **8** the titanium−amino nitrogen bond length is 240.1(3) pm, whereas in the benzyl derivative **9** the corresponding bond distance is 254.0(1) pm. Nitrogen−titanium bond lengths in tetravalent titanium complexes range from 226 to 245 pm[9], estimated titanium−amine distances are in the range of 196 to 197 pm[10]. The bond distances observed in **8** and

9 are clearly longer than average. In Ti(η^5:η^1:η^1-$C_5H_4SiMe_2NCH_2CH_2NMe_2$)$Cl_2$ a bond length of 241.8(7) pm was observed[4b]. Interestingly, the titanium(III) complex (η^5-C_5H_5)Ti{($C_6H_4(CH_2NMe_2)$-2} shows Ti−N bond distances of 298.9(4) pm[11]. The coordination geometry for each complex **8** and **9** can be best described as square pyramidal, where the atoms N1, N2, Cl, and C15(C19) define a plane and the cyclopentadienyl ring resides perpendicular to this plane. In both **8** and **9**, the *N*,*N*-dimethylamino group adopts the coordination site trans to the amido ligand. This coordination avoids the amido and the benzyl/phenyl ligand from competing for the same metal-derived orbitals. The amido nitrogen atoms have almost planar geometry in agreement with all structurally characterized Ti(IV) complexes containing the linked amido−cyclopentadienyl ligand[12]. There is no α-agostic interaction for the benzyl group in **9**, as was observed in the crystal structure of Ti(η^5:η^1-$C_5Me_4SiMe_2NCH_2Ph$)$(CH_2Ph)_2$[1j]. Both the Ti−C15 of 217.1(2) pm and Ti−C15−C16 of 112.83(9)° are within the expected range.

Figure 1. ORTEP diagram of the molecular structure of Ti(η^5:η^1-$C_5Me_4SiMe_2NCH_2Ph$){$C_6H_4(CH_2NMe_2)$-2}Cl (**8**); thermal ellipsoids are drawn at 50% probability level; hydrogen atoms are omitted for the sake of clarity[a]

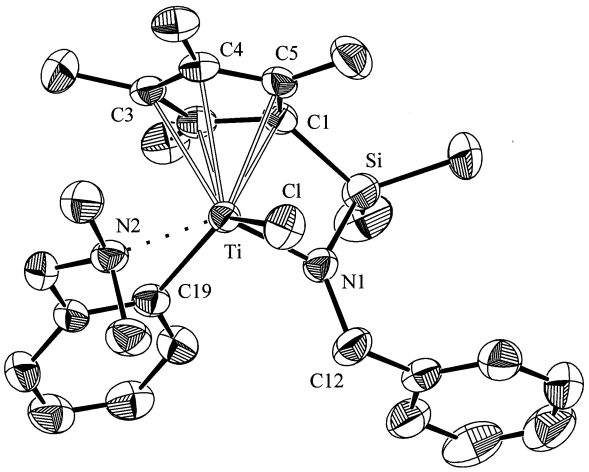

[a] Selected bond distances [pm] and angle [°]; Cp denotes the cyclopentadienyl centroid: Ti−N1 194.1(3), Ti−Cl 238.40(11), Ti−N2 240.1(3), Ti−Cp 209.9(4), Ti−C1 229.9(4), Ti−C2 239.5(4), Ti−C3 253.1(4), Ti−C4 250.4(4), Ti−C5 237.3(4), Ti−C19 219.5(4), Cp−Ti−N1 105.5, Ti−N1−Si 106.3(2), Ti−N1−C12 123.5(3), Si−N1−C12 130.1(3), Cl−Ti−N1 90.3(1), Cl−Ti−N2 79.42(9), N1−Ti−N2 139.7(1).

The reaction of the dichloro complexes **4** and **5** with Li[{η^5-$C_5H_3(CH_2NMe_2)$-2}Fe(η^5-C_5H_5)], generated in situ by lithiation of {2-(*N*,*N*-dimethylamino)methyl}ferrocene with *n*-butyllithium, gave the mono(ferrocenyl) derivative **11** and **12** as hydrocarbon-soluble, violet crystals in yields of 43 and 48%, respectively (Scheme 2). In the ^{1}H- and ^{13}C-NMR spectra of **11** and **12**, the asymmetry of the molecule can be easily detected by the occurence of diastereotopic resonances. The presence of the ferrocenyl moiety is obvious from the sharp singlet due to the η^5-C_5H_5 group at δ = 4.46 and 4.39 for **11** and **12**, respectively, as well as a set of three resonances around δ = 4.0 for the η^5-$C_5H_3(CH_2NMe_2)$-2 part. As in the case of **7**−**10**, only one

Figure 2. ORTEP diagram of the molecular structure of Ti(η^5:η^1-$C_5Me_4SiMe_2NiPr$){$CH_2C_6H_4(NMe_2)$-2}Cl (**9**); thermal ellipsoids are drawn at 50% probability level; hydrogen atoms are omitted for the sake of clarity[a]

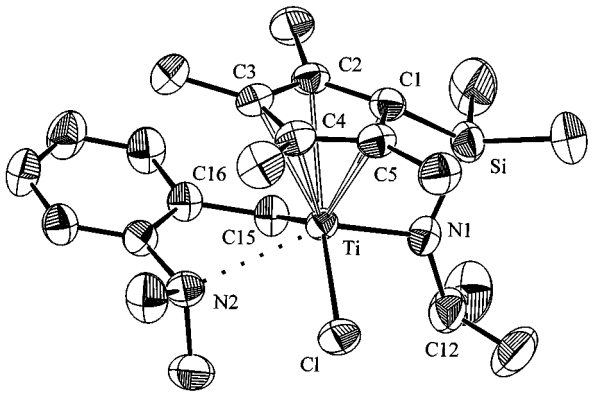

[a] Selected bond distances (pm) and angle (°); Cp denotes the cyclopentadienyl centroid: Ti−N1 192.57(12), Ti−Cl 237.27(7), Ti−N2 254.03(13), Ti−Cp 208.4(2), Ti−C1 229.5(2), Ti−C2 241.4(2), Ti−C3 251.9(2), Ti−C4 247.5(2), Ti−C5 233.8(2), Ti−C15 217.2(2), Cp−Ti−N1 105.6, Ti−N1−Si 105.81(6), Ti−N1−C12 122.2(1), Si−N1−C12 131.3(1), Cl−Ti−N1 93.66(4), Cl−Ti−N2 78.39(3), N1−Ti−N2 139.35(5), Ti−C15−C16 112.83(9).

signal for the *N*,*N*-dimethylamino group is recorded in the ^{1}H- and ^{13}C-NMR spectra, excluding a rigid coordination of the *N*,*N*-dimethylamino group at the titanium center in solution.

The single crystal X-ray structure analysis of **12** (Figure 3) reveals a monodentate 2-(*N*,*N*-dimethylamino)ferrocenyl ligand in which the *N*,*N*-dimethylamino group is directed away from the titanium atom. Somewhat shorter Ti−N1, Ti−Cp and Ti−Cl distances as compared to **8** were found. The Ti−C19 distance of 210.5(3) pm is shorter. The bonding mode of **12** does not differ from that found in the titanocenes Ti(η^5-$C_5H_5)_2Cl_{(2-n)}$[{η^5-$C_5H_3(CH_2NMe_2)$-2}Fe(η^5-C_5H_5)]$_n$ (n = 1, 2)[13], whereas in the half-sandwich complex Ti(η^5-C_5H_5)Cl_2[{η^5-$C_5H_3(CH_2NMe_2)$-2}Fe(η^5-C_5H_5)][9c] a bidentate ferrocenyl ligand was observed. The well-known significantly stronger inductive effect of the ferrocenyl group in comparison to the phenyl group may be responsible for the bonding mode observed in **12**[14].

The intense color the ferrocenyl derivatives **11** and **12** exhibit are due to the presence of low-energy charge-transfer bands. For instance, the UV/Vis spectrum of a hexane solution of **12** exhibits absorptions at λ = 525 nm (ε = 340) and 406 nm (ε = 1270) besides a strong band at 225 nm (ε = $2.9 \cdot 10^4$). According to cyclovoltammetric studies in 1,2-dimethoxyethane solutions, these complexes show a rather complicated electrochemical behavior: One reversible oxidation wave at an electrode potential (E_p = 0.485 V for **11**, 0.524 V for **12**) can be attributed to the oxidation of the ferrocenyl moiety. Other oxidation waves observed are irreversible. Furthermore, the complexes **11** and **12** exhibited only irreversible reduction waves, with no reversible reduction of the titanium(IV) center being detectable.

Ethene polymerizations catalyzed by the complexes using methylaluminoxane (MAO) as cocatalyst were examined in

Figure 3. ORTEP diagram of the molecular structure of Ti(η^5:η^1-$C_5Me_4SiMe_2NCH_2Ph$)[{η^5-$C_5H_3(CH_2NMe_2)$-2}Fe(η^5-C_5H_5)]Cl (**12**); thermal ellipsoids are drawn at 50% probability level; hydrogen atoms are omitted for the sake of clarity[a]

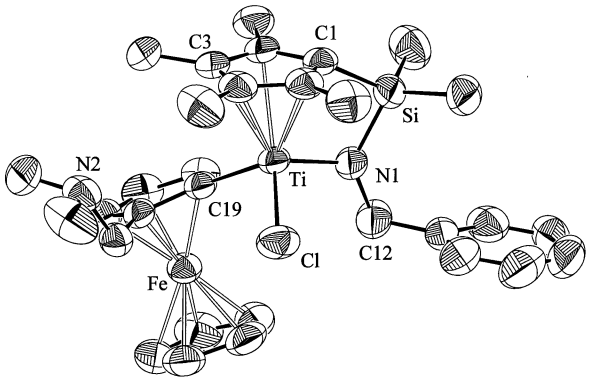

[a] Selected bond distances [pm] and angle [°]; Cp denotes the cyclopentadienyl centroid: Ti−N1 191.3(3), Ti−Cl 227.61(11), Ti−Cp 204.4(3), Ti−C1 230.8(3), Ti−C2 236.9(3), Ti−C3 243.7(3), Ti−C4 240.6(3), Ti−C5 234.0(3), Ti−C19 210.5(3), Cp−Ti−N1 105.5, Ti−N1−Si 107.2(1), Ti−N1−C12 124.1(2), Si−N1−C12 128.7(2), Cl−Ti−N1 105.7(9).

a preliminary manner, as summarized in Table 1. Compared to the activity of the prototypical catalyst **1** with a *tert*-butylamido or **2** with the adamantyl, the isopropylamido substituent complex **4** is less active, whereas the benzylamido complex **5** exhibits the highest activity. The substitution of one chloro ligand by a bidentate organyl group influenced the activity in a different manner. **8** shows only moderately decreased activity, suggesting that the cationic active species formed by the action of MAO from both **5** and **8** are identical. However, the introduction of the ferrocenyl group as in **12** results in a catalyst that produces low yields of polyethene under the same conditions. The melting temperatures of the isolated polyethenes, as determined by DSC, range between 134 and 142°C.

Table 1[a]

Complex	Yield[g]	Activity[b]	T_m[°C][c]	ΔH[J/g][c]
Ti(η^5:η^1-$C_5Me_4SiMe_2NtBu$)Cl_2 (**1**)	4.11	950	141.6	128.4
Ti(η^5:η^1-$C_5Me_4SiMe_2NAd$)Cl_2 (**2**)	2.01	460	133.5	108.5
Ti(η^5:η^1-$C_5Me_4SiMe_2NiPr$)Cl_2 (**4**)	0.43	100	142.2	103.9
Ti(η^5:η^1-$C_5Me_4SiMe_2NCH_2Ph$)Cl_2 (**5**)	13.34	3090	135.6	138.2
Ti(η^5:η^1-$C_5Me_4SiMe_2NCH_2Ph$)-{$C_6H_4(CH_2NMe_2)$-2}Cl (**8**)	8 .89	2060	140.0	151.5
Ti(η^5:η^1-$C_5Me_4SiMe_2NCH_2Ph$)-[{η^5-$C_5H_3(CH_2NMe_2)$-2}Fe(η^5-C_5H_5)]Cl (**12**)	0.35	80	138.6	121.9

[a] Polymerization conditions: titanium complex 5 μmol, methylaluminoxane 2500 μmol in toluene at 23°C, constant ethene pressure 3 bar, reaction time 2 h. − [b] Activity in kg(PE)/molTi·h·c_{ethene}. − [c] Determined by DSC.

Financial support of this work by the *Fonds der Chemischen Industrie*, the *Bundesministerium für Bildung, Wissenschaft, Forschung und Technologie*, and *BASF AG* (Kunststofflaboratorium) is gratefully acknowledged. We thank the *Freiburger Materialforschungszentrum* (Prof. *R. Mülhaupt*) for DSC measurements and Mr. *O. Schiemann* and Prof. *C. Elschenbroich*, Marburg, for helping us with cyclovoltammetry. *WITCO GmbH*, Bergkamen, kindly supplied us with MAO solutions.

Experimental Section

General: All manipulations were performed under argon using standard Schlenk techniques. Solvents were purified, dried, and distilled under argon. − ^{1}H and ^{13}C NMR: Bruker AC 200 or Bruker AM 400. − Mass spectra: Finnigan 8230. − UV/Vis: Zeiss spectrophotometer DM4. − Elemental analyses: Microanalytical laboratory of the university. − The following reagents were synthesized using literature procedures: $C_5Me_4H(SiMe_2Cl)$[1c], $TiCl_3(THF)_3$[15], Ti(η^5:η^1-$C_5Me_4SiMe_2NCH_2Ph$)Cl_2[7], {2-[(*N*,*N*-dimethylamino)-methyl]phenyl}lithium[16], [2-(*N*,*N*-dimethylamino)benzyl]lithium[17], {2-[(*N*,*N*-dimethylamino)methyl)]ferrocenyl}lithium[17].

N-[Dimethyl(tetramethylcyclopentadienyl)silyl](1-adamantyl)-amine: (C_5Me_4H)$SiMe_2Cl$ (2.38 g, 11.1 mmol) was added to a suspension of Li(NHAd) (1.74 g, 11.1 mmol) in 70 ml of hexane at −78°C. The reaction mixture was allowed to warm to room temp. and stirred for 14 h. Filtration of the resulting suspension and removal of all volatiles in vacuo gave (C_5Me_4H)$SiMe_2NHAd$ as a yellow oil, yield 2.01 g (55%). − ^{1}H NMR (C_6D_6): δ = 0.27 (s, 6 H, $SiCH_3$), 1.06 (s, 1 H, NH), 1.66 (s, 6H, CCH_3), 1.74 (br d, 3 H, CH_2, Ad), 1.83 (s, 6H, CCH_3), 1.99 (br s, 3 H, CH, Ad), 2.04 (br d, 6 H, CH_2, Ad), 2.17 (br s, 3 H, CH, Ad), 2.92 (s, 1 H, C_5Me_4H). − ^{13}C{^{1}H} NMR (C_6D_6): δ = 4.0 ($SiCH_3$), 11.4, 15.0 (CCH_3), 30.5 (3-Ad), 36.7 (4-Ad), 47.6 (2-Ad), 53.9, 57.2 (*ipso*-Ad, C_5Me_4H at Si), 133.3, 135.4 (C_5Me_4).

Dichloro{η^5:η^1-N-dimethyl(tetramethylcyclopentadienyl)silyl](1-adamantyl)amido}titanium (**2**)**:** Crude $Li_2(C_5Me_4SiMe_2NAd)$ (1.41 g, 4.1 mmol), obtained by deprotonation of (C_5Me_4H)$SiMe_2NHAd$ with 2 equiv. of Li*n*Bu in hexane, was dissolved in 20 ml of THF and added dropwise to a suspension of $TiCl_3(THF)_3$ (1.53 g, 4.1 mmol) in 40 ml of toluene at −60°C. After warming to room temp., the green reaction mixture was stirred for 2 h and treated with $PbCl_2$ (1.15 g, 4.1 mmol). After stirring for 12 h, the solvent was removed under vacuum and the residue was extracted with 50 ml of a toluene/hexane mixture (2:1). Filtration of the extracts, followed by concentrating the filtrate and cooling to −20°C afforded in several crops Ti(η^5:η^1-$C_5Me_4SiMe_2NAd$)Cl_2 as yellow crystals, yield 0.57 g (31%); by-product: Ti(η^5:η^1-C_5Me_4H)Cl_3. − ^{1}H NMR (C_6D_6): δ = 0.61 (s, 6 H, $SiCH_3$), 1.64 (br dd, 6 H, CH_2, 4-Ad), 2.09 (br s, 3 H, CH, 3-Ad), 2.14, 2.16 (s, 6H, CCH_3), 2.22 (br d, 6 H, CH_2, 2-Ad). − ^{13}C{^{1}H} NMR (C_6D_6): δ = 5.9 ($SiCH_3$), 13.1, 16.2 (CCH_3), 30.7 (3-Ad), 36.3 (4-Ad), 45.6 (2-Ad), 63.8 (*ipso*-Ad), 104.1 (C_5Me_4 at Si), 137.9, 140.6 (CCH_3). − EI MS; *m*/*z* (%): 445 (88) [M^+], 414 (31) [M^+ − Me], 390 (33) [M^+ − C_4H_7], 356 (100) [M^+ − C_4H_9Cl], 324 (27) [M^+ − $C_6H_6Cl_2$], 297 (21) [$C_{11}H_{19}Cl_2SiTi^+$], 237 (27) [$C_5H_{17}Cl_2Ti^+$], 197 (35) [$C_{11}H_{23}NSi^+$], 159 (33) [$C_{10}H_{11}Si^+$], 149 [$C_9H_{13}Si^+$]. − $C_{21}H_{33}Cl_2NSiTi$ (446.4): calcd. C 56.51, H 7.45, N 3.14; found C 55.29, H 7.55, N 4.38.

N-[Dimethyl(tetramethylcyclopentadienyl)silyl](1,1,3,3-tetramethylbutyl)amine: (C_5Me_4H)$SiMe_2Cl$ (3.00 g, 14.0 mmol) was added to a suspension of Li($NHCMe_2CH_2tBu$) (1.89 g, 14.0 mmol) in 60 ml of hexane at −78°C. The reaction mixture was allowed to warm to room temp. and stirred for 14 h. Filtration of the resulting suspension and removal of all volatiles in vacuo gave crude (C_5Me_4H)$SiMe_2NHCMe_2CH_2tBu$ which was distilled at 95°C and $8\cdot10^{-3}$ mbar to give a yellow oil, yield 2.15 g (50%). − ^{1}H NMR (C_6D_6): δ = 0.34 (s, 6 H, $SiCH_3$), 0.51 (s, 1 H, NH), 1.08 [s, 9 H, $C(CH_3)_3$], 1.24 [s, 6 H, $C(CH_3)_2$], 1.42 (s, 2 H, CH_2), 1.81 (s, 6 H, CCH_3), 1.94 (s, 6 H, CCH_3), 2.80 (s, 1 H, C_5Me_4H). − ^{13}C{^{1}H} NMR (C_6D_6): δ = 2.9 ($SiCH_3$), 11.4, 14.9 (CCH_3), 31.9 [$C(CH_3)_3$,

$C(CH_3)_3$], 33.6 [$C(CH_3)_2$], 53.2, 56.8 [$C(CH_3)_2$, C_5Me_4H at Si], 58.9 (CH_2), 133.4, 135.3 (CCH_3). − EI MS; *m/z* (%): 307 (27) [M^+], 236 (15) [$C_{14}H_{26}NSi^+$], 186 (100) [$C_{10}H_{24}NSi^+$], 121 (10) [$C_9H_{13}^+$], 114 (13) [$C_8H_{18}^+$], 105 (11) [$C_6H_9^+$], 74 (42) [$C_2H_8NSi^+$], 59 (10) [$C_2H_7Si^+$], 55 (5) [$C_2H_3Si^+$]. − $C_{19}H_{37}NSi$ (307.6): calcd. C 74.19, H 12.12, N 4.55; found C 73.72, H 12.12, N 5.03.

Dichloro {η⁵:η¹-N-dimethyl(tetramethylcyclopentadienyl)-silyl](1,1,3,3-tetramethylbutyl)amido}titanium (**3**): Crude $Li_2(C_5Me_4SiMe_2NCMe_2CH_2tBu)$ (1.86 g, 5.8 mmol), obtained by deprotonation of $(C_5Me_4H)SiMe_2NHCMe_2CH_2tBu$ with 2 equiv. of Li*n*Bu in hexane, was dissolved in 40 ml of THF and added dropwise to a suspension of $TiCl_3(THF)_3$ (2.16 g, 5.8 mmol) in 30 ml of toluene at −60°C. After warming to room temp., the green reaction mixture was stirred for 2 h and treated with $PbCl_2$ (1.61 g, 5.8 mmol). After stirring for 12 h, the solvent was removed under vacuum and the residue was extracted with 80 ml of a toluene/hexane mixture (2:1). Filtration of the extracts, followed by concentrating the filtrate and cooling to −20°C afforded $Ti(\eta^5{:}\eta^1\text{-}C_5Me_4SiMe_2NCMe_2CH_2tBu)Cl_2$ as yellow crystals; yield 0.47 g (19%). − ^{1}H NMR (C_6D_6): δ = 0.62 (s, 6 H, $SiCH_3$), 1.10 [s, 9 H, $C(CH_3)_3$], 1.75 [s, 6 H, $C(CH_3)_2$], 1.87 (s , 2 H, CH_2), 2.13 (s, 6 H, CCH_3), 2.14 (s, 6 H, CCH_3). − $^{13}C\{^1H\}$ NMR (C_6D_6): δ = 6.0 ($SiCH_3$), 13.0, 16.2 (CCH_3), 31.7 [$C(CH_3)_3$], 31.7 [$C(CH_3)_2$], 31.8 [$C(CH_3)_3$], 57.3 (CH_2), 67.0 [$C(CH_3)_2$], 104.1 (C_5Me_4 at Si), 138.2, 140.5 (CCH_3). − EI MS; *m/z* (%): 408 (7) [M^+ − Me], 352 (100) [M^+ − CH_2CMe_3], 296 (17) [M^+ − $NCMe_2CH_2CMe_3$], 261 (4) [M^+ − $NCMe_2CH_2CMe_3$, − Cl], 243 (3) [$C_{15}H_{21}NSi^+$], 203 (2) [$C_{12}H_{17}NSi^+$], 177 (9) [$C_{11}H_{17}Si^+$], 161 (6) [$C_{10}H_{13}Si^+$], 148 (4) [$C_8H_{12}Si^+$], 119 (2) [$C_9H_{11}^+$], 57 (16) [$C_2H_5Si^+$]. − $C_{19}H_{35}Cl_2NSiTi$ (424.4): calcd. C 53.78, H 8.31, N 3.30; found C 52.76, H 8.40, N 5.06.

N-[Dimethyl(tetramethylcyclopentadienyl)silyl]isopropylamine: $(C_5Me_4H)SiMe_2Cl$ (4.83 g, 22.5 mmol) was added to a suspension of Li(NH*i*Pr) (1.46 g, 22.5 mmol) in 60 ml of hexane at −78°C. The reaction mixture was allowed to warm to room temp. and stirred for 14 h. Filtration of the resulting suspension and removal of all volatiles in vacuo gave crude $(C_5Me_4H)SiMe_2NHiPr$ which was distilled at 70°C and $8\cdot10^{-3}$ mbar to give a yellow oil; yield 4.30 g (80%). − ^{1}H NMR ($CDCl_3$): δ = 0.01 (s, 6 H, $SiCH_3$), 0.30 (s, 1 H, NH), 1.05 (d, $^3J_{HH}$ = 7 Hz, 6 H, $CHCH_3$), 1.83 (s, 6 H, CCH_3), 1.98 (s, 6 H, CCH_3), 2.88 (s, 1 H, C_5Me_4H), 3.04 (sept, $^3J_{HH}$ = 7 Hz, 1 H, $CHCH_3$). − $^{13}C\{^1H\}$ NMR ($CDCl_3$): δ = -1.6 ($SiCH_3$), 11.1, 14.5 (CCH_3), 27.9 ($CHCH_3$), 43.2 ($CHCH_3$), 56.9 (C_5Me_4H at Si), 133.0, 135.5, (CCH_3). − EI MS; *m/z* (%): 237 (16) [M^+], 196 (3) [MH_2^+ − C_3H_7], 179 (2) [$C_{11}H_{20}Si^+$], 164 (100) [$C_5H_{15}NSi^+$], 73 (9) [$C_2H_7NSi^+$]. − $C_{14}H_{27}NSi$ (237.5): calcd C 70.81, H 11.46, N 5.90; found C 70.77, H 11.33, N 6.04.

Dichloro {η⁵:η¹-N-dimethyl(tetamethylcyclopentadienyl)silyl]-isopropylamido}titanium (**4**): Crude $Li_2(C_5Me_4SiMe_2NiPr)$ (3.75 g, 15.0 mmol), obtained by deprotonation of $(C_5Me_4H)SiMe_2NHiPr$ with 2 equiv. of Li*n*Bu in hexane, was dissolved in 40 ml of THF and added dropwise to a suspension of $TiCl_3(THF)_3$ (5.57 g, 15.0 mmol) in 80 ml of toluene at −60°C. After warming to room temp., the green reaction mixture was stirred for 2 h and treated with $PbCl_2$ (4.18 g, 15.0 mmol). After stirring for 12 h, the solvent was removed under vacuum and the residue was extracted with 100 ml of a toluene/hexane mixture (2:1). Filtration of the extracts, followed by concentrating the filtrate and cooling to −20°C afforded $Ti(\eta^5{:}\eta^1\text{-}C_5Me_4SiMe_2NiPr)Cl_2$ as yellow crystals, yield 3.75 g (70%). − ^{1}H NMR (C_6D_6): δ = 0.47 (s, 6 H, $SiCH_3$), 1.13 (d, $^3J_{HH}$ = 6 Hz, 6 H, $CHCH_3$), 2.09 (s, 6 H, CCH_3), 2.10 (s, 6 H, CCH_3), 5.45 (sept, $^3J_{HH}$ = 6 Hz, 1 H , $CHCH_3$). − $^{13}C\{^1H\}$ NMR (C_6D_6): δ = 4.7 ($SiCH_3$), 12.9, 16.0 (CCH_3), 24.0 ($CHCH_3$), 55.6 ($CHCH_3$), 102.0 (C_5Me_4 at Si), 135.8, 140.1 (CCH_3). − EI MS; *m/z* (%): 353 (10) [M^+], 338 (100) [M^+ − Me], 318 (2) [M^+ − Cl], 296 (36) [M^+ − N*i*Pr], 283 (5) [M^+ − 2Cl], 204 (4) [$C_{12}H_{18}NSi^+$], 177 (10) [$C_{11}H_{17}Si^+$], 163 (4) [$C_{10}H_{15}Si^+$], 119 (3) [$C_9H_{11}^+$], 97 (2) [$C_4H_7NSi^+$], 73 (2) [$C_2H_7NSi^+$]. − $C_{14}H_{25}Cl_2NSiTi$ (354.2): calcd. C 47.47, H 7.11, N 3.95; found C 47.67, H 7.20, N 3.85.

N-[Dimethyl(tetramethylcyclopentadienyl)silyl](2-pyridyl)-methylamine: $(C_5Me_4H)SiMe_2Cl$ (2.82 g, 13.2 mmol) was added to a suspension of $Li\{NHCH_2(C_5H_4N)\text{-}2\}$ (1.50 g, 13.2 mmol) in 60 ml of hexane at −78°C. The reaction mixture was allowed to warm to room temp. and stirred for 14 h. Filtration of the resulting solution and removal of the solvent in vacuo gave crude $(C_5Me_4H)SiMe_2NHCH_2(C_5H_4N)\text{-}2$ which was distilled at 135°C and $8\cdot10^{-3}$ mbar to give a yellow oil, yield 2.56 g (68%). − ^{1}H NMR (C_6D_6): δ = 0.14 (s, 6 H, $SiCH_3$), 1.46 (s, 1 H, NH), 1.94 (s, 6 H, CCH_3), 2.19 (s, 6 H, CCH_3), 2.98 (s, 1 H, C_5Me_4H), 4.17 (d, $^3J_{HH}$ = 8 Hz, 2 H, CH_2), 6.76 (m, 1 H, 4-C_5H_4N), 7.11 (d, $^3J_{HH}$ = 8 Hz, 1 H, 6-C_5H_4N), 7.23 (m, 1 H, 5-C_5H_4N), 8.59 (d, $^3J_{HH}$ = 5 Hz, 1 H, 3-C_5H_4N). − $^{13}C\{^1H\}$ NMR ($CDCl_3$): δ = -2.6 ($SiCH_3$), 11.1, 14.3 (CCH_3), 47.7 (CH_2), 56.6 (C_5Me_4H at Si), 120.8 (5-C_5H_4N), 121.3 (6-C_5H_4N), 132.7, 135.6 (C_5Me_4), 136.3 (5-C_5H_4N), 148.8 (3-C_5H_4N), 162.9 (*ipso*-C_5H_4N). − EI MS; *m/z* (%): 252 (8) [M^+ − C_2H_{10}], 196 (100) [MH^+ − C_6H_5N], 181 (12) [$C_{11}H_{21}Si^+$], 163 (6) [$C_8H_{11}N_2Si^+$], 131 (13) [$C_6H_3N_2Si^+$], 120 (39) [$C_9H_{12}^+$], 105 (25) [$C_6H_5N_2^+$], 91 (6) [$C_6H_5N^+$], 75 (39) [$C_2H_9NSi^+$], 58 (2) [$C_2H_6Si^+$]. − $C_{17}H_{26}N_2Si$ (286.5): calcd. C 71.27, H 9.15, N 9.78; found C 68.16, H 9.88, N 11.44.

Dichloro {η⁵:η¹-N-dimethyl(tetamethylcyclopentadienyl)silyl](2-pyridylmethyl)amido}titanium (**6**): $Ti(\eta^5{:}\eta^1\text{-}C_5Me_4SiMe_2NCH_2\text{-}2\text{-}C_5H_4N)Cl_2$ was obtained from the reaction of $Li_2(C_5Me_4SiMe_2NCH_2\text{-}2\text{-}C_5H_4N)$ (2.02 g, 6.78 mmol) with $TiCl_3(THF)_3$ (2.51 g, 6.78 mmol) and $PbCl_2$ (1.89 g, 6.78 mmol) in THF as an orange solid in a manner analogous to that described for the synthesis of **4**; yield 0.85 g (31%). − ^{1}H NMR (C_6D_6): δ = 0.46 (s, 6 H, $SiCH_3$), 2.31 (s, 6 H, CCH_3), 2.45 (s, 6 H, CCH_3), 4.46 (s, 2 H, CH_2), 6.57 (d, $^3J_{HH}$ = 8 Hz, 1 H, 6-C_5H_4N), 6.68 (t, $^3J_{HH}$ = 6 Hz, 1 H, 4-C_5H_4N), 6.94 (dt, $^3J_{HH}$ = 8 Hz, $^4J_{HH}$ = 2 Hz, 1 H, 5-C_5H_4N), 9.40 (d, $^3J_{HH}$ = 6 Hz, 1 H, 3-C_5H_4N). − $^{13}C\{^1H\}$ NMR (C_6D_6): δ = 1.8 ($SiCH_3$), 13.4, 15.9 (CCH_3), 63.5 (CH_2), 102.6 (C_5Me_4 at Si), 119.0 (4-C_5H_4N), 121.1 (6-C_5H_4N), 134.8, 136.2 (CCH_3), 138.7 (5-C_5H_4N), 152.7 (3-C_5H_4N), 161.9 (*ipso*-C_5H_4N). − EI MS; *m/z* (%): 402 (5) [M^+], 387 (7) [M^+ − Me), 372 (14) [M^+ − C_2H_6], 238 (7) [M^+ − $C_6H_8NCl_2$], 178 (14) [$C_{11}H_{18}Si^+$], 163 (100) [$C_8H_{11}N_2Si^+$], 133 (7) [$C_6H_5N_2Si^+$], 121 (27) [$C_9H_{13}^+$], 105 (27) [$C_6H_5N_2^+$], 93 (30) [$C_6H_7N^+$], 79 (17) [$C_5H_5N^+$], 73 (27) [$C_2H_7NSi^+$], 59 (32) [$C_2H_7Si^+$], 52 (11) [C_2Si^+]. − $C_{17}H_{24}Cl_2N_2SiTi$ (403.3): calcd. 50.63 H, 6.00 N, 6.95; found C 49.61, H 6.16, N 7.10.

Ti(η⁵:η¹-C₅Me₄SiMe₂NiPr){C₆H₄(CH₂NMe₂)-2}Cl (**7**): A mixture of **4** (0.60 g, 1.69 mmol) and $Li\{C_6H_4(CH_2NMe_2)\text{-}2\}$ (0.24 g, 1.69 mmol) was treated dropwise with 65 ml of toluene at −60°C and stirred for 12 h at room temp. After removal of the solvent, the residue was extracted with 60 ml of CH_2Cl_2. Removal of CH_2Cl_2 and crystallization from toluene at −50°C afforded yellow crystals, yield 0.55 g (72%). − ^{1}H NMR (C_6D_6): δ = 0.75 (s, 3 H, $SiCH_3$), 0.81 (s, 3 H, $SiCH_3$), 1,46 (d, $^3J_{HH}$ = 6 Hz, 3 H, $CHCH_3$), 1.58 (d, $^3J_{HH}$ = 6 Hz, 3 H, $CHCH_3$), 1.63 (s, 3 H, CCH_3), 1.80 (s, 3 H, CCH_3), 1.91 (s, 3 H, CCH_3), 2.47 (s, 6 H, NCH_3), 2.57 (s, 3 H, CCH_3), 2.84 (d, $^2J_{HH}$ = 14 Hz, 1 H, NCH_2), 3.95 (d, $^2J_{HH}$ = 14 Hz, 1 H, NCH_2), 4.87 (sept, $^3J_{HH}$ = 6 Hz, 1 H, $CHCH_3$), 6.92 (m, 1 H, C_6H_4), 7.17 (m, 2 H, C_6H_4), 7.83 (m, 1 H, C_6H_4). −

$^{13}C\{^1H\}$ NMR (C_6D_6): δ = 5.3, 5.8 ($SiCH_3$), 12,8, 17.1, 18.0 (CCH_3), 24.1, 25,8 ($CHCH_3$), 49.3 (NCH_3), 55.9 ($CHCH_3$), 70.8 (CH_2NMe_2), 103.0 (C_5Me_4 at Si), 122.5, 125.6, 126.3 (C_6H_4), 131.4, 131.1, 134.0, 138.2, 144.27 (CCH_3, C_6H_4), 145.5 (2-C_6H_4), 195.1 (1-C_6H_4). – EI MS; *m/z* (%): 452 (5) [M^+], 437 (6) [M^+ – Me], 410 (3) [M^+ – C_3H_6], 318 (19) [M^+ – $C_6H_4CH_2NMe_2$, – C_3H_6], 134 (100) [$C_6H_4CH_2NMe_2^+$]. – $C_{23}H_{37}ClNSiTi$ (453.0): calcd. C 60.99, H 8.23, N 6.18; found C 60.88, H 8.16, N 6.30.

Ti(η⁵:η¹-C₅Me₄SiMe₂NCH₂Ph){C₆H₄(CH₂NMe₂)-2}Cl (**8**): A mixture of **5** (1.27 g, 3.16 mmol) and Li{$C_6H_4(CH_2NMe_2)$-2} (0.45 g, 3.19 mmol) was treated dropwise with 65 ml of toluene at −60°C and stirred for 12 h at room temp. After removal of the solvent, the residue was extracted with 60 ml of CH_2Cl_2. Removal of CH_2Cl_2 and crystallization from toluene at −50°C afforded yellow crystals, yield 1.08 g (68%). – ^1H NMR (C_6D_6): δ = 0.18 (s, 3 H, $SiCH_3$), 0.44 (s, 3 H, $SiCH_3$), 1.51 (s, 3 H, CCH_3), 1.70 (s, 3 H, CCH_3), 1.78 (s, 3 H, CCH_3), 2.38 (s, 6 H, NCH_3), 2.49 (s, 3 H, CCH_3), 2.73 (d, $^2J_{HH}$ = 14 Hz, 1 H, C_6H_4-2-CH_2), 3.85 (d, $^2J_{HH}$ = 14 Hz, 1 H, C_6H_4-2-CH_2), 5.12 (d, $^2J_{HH}$ = 14 Hz, 1 H, NCH_2Ph), 5.70 (d, $^2J_{HH}$ = 14 Hz, 1 H, NCH_2Ph), 6.83 (d, $^3J_{HH}$ = 7 Hz, 1 H, C_6H_4), 7.14 (m, 5 H, C_6H_5), 7.54 (m, 2 H, C_6H_4), 7.67 (d, $^3J_{HH}$ = 7 Hz, 1 H, C_6H_4). – $^{13}C\{^1H\}$ NMR (C_6D_6): δ = 3.4, 3.7 ($SiCH_3$), 12.6, 12.7, 17.1, 17.9 (CCH_3), 49.4 (NCH_2Ph), 59.91 ($SiMe_2NCH_2$), 70.9 (CH_2NMe_2), 104.0 (C_5Me_4 at Si), 122.6, 126.5, 127.1, 127.4, 128.6, 129.1, 129.3, 130.4, 130.8, 142.3, 143.0, 145.7 (C_6H_5, C_6H_4, CCH_3, *ipso*-C_6H_5), 195.94 (1-C_6H_4). – EI MS; *m/z* (%): 500 (8) [M^+], 485 (6) [M^+ – Me], 410 (11) [M^+ – $C_6H_4CH_2$], 134 (100) [$Me_2NCH_2C_6H_4^+$], 106 (23) [$PhCH_2NH^+$], 91 (59) [$PhCH_2^+$], 78 (8) [$C_6H_6^+$]. – $C_{27}H_{37}ClN_2SiTi$ (501.0): calcd. C 64.78, H 7.46, N 5.60; found C 65.05, H 7.83, N 6.22.

Ti(η⁵:η¹-C₅Me₄SiMe₂NiPr){CH₂C₆H₄(NMe₂)-2}Cl (**9**): A mixture of **4** (0.62 g, 1.74 mmol) and $LiCH_2C_6H_4(NMe_2)$-2 (0.25 g, 1.74 mmol) was treated with 50 ml of toluene at −50°C and stirred for 14 h at room temp. After removal of the solvent, the residue was extracted with 50 ml of a toluene/hexane mixture (1:1). Filtration and cooling to −50°C afforded red crystals, yield 0.51 g (65%). – ^1H NMR (C_6D_6): δ = 0.58 (s, 3 H, $SiCH_3$), 0.64 (s, 3 H, $SiCH_3$), 1.14 (s, 3 H, CCH_3), 1.16 (d, $^3J_{HH}$ = 7 Hz, 3 H, CHCH_3), 1.44 (d, $^3J_{HH}$ = 6 Hz, 3 H, CHCH_3), 1.99 (s, 3 H, CCH_3), 2.14 (s, 3 H, CCH_3), 2.29 (d, $^2J_{HH}$ = 12 Hz, 1 H, $TiCH_2$), 2.39 (overlap. d, $^2J_{HH}$ = 10 Hz, 1 H, $TiCH_2$), 2.40 (s, 3 H, CCH_3), 2.69 (s, 6 H, NCH_3), 5.19 (sept, $^3J_{HH}$ = 6 Hz, 1 H, CHCH$_3$), 6.86 (d, $^3J_{HH}$ = 8 Hz, 1 H, 3-C_6H_4), 6.93 (m, 1 H, 4-C_6H_4,), 7.05 (dt, $^3J_{HH}$ = 8 Hz, $^4J_{HH}$ = 1 Hz, 1 H, 5-C_6H_4), 7.12 (d, $^3J_{HH}$ = 7.5 Hz, 1 H, 6-C_6H_4). – $^{13}C\{^1H\}$ NMR (C_6D_6): δ = 4.5, 6.1 ($SiCH_3$), 10.4, 12.5, 14.5, 16.8 (CCH_3), 24.2, 24.5 ($CHCH_3$), 46.9 (NCH_3), 55.0 ($CHCH_3$), 72.2 ($TiCH_2$), 102.7 (C_5Me_4 at Si), 118.7, 123.4, 124.9 (C_6H_4), 130.3, 130.9, 132.0, 135.8 (CCH_3), 144.7 (1-C_6H_4), 152.5 (2-C_6H_4). – EI MS; *m/z* (%): 318 (100) [M^+ – $CH_2C_6H_4NMe_2$], 274 (5) [M^+ – $CH_2C_6H_4NMe_2$, – C_3H_8], 260 (53) [M^+ – $CH_2C_6H_4NMe_2$, – C_3H_8N], 243 (11) [M^+ – $CH_2C_6H_4NMe_2$, – $C_4H_{13}N$], 230 (3) [M^+ – $CH_2C_6H_4NMe_2$, – $C_5H_{14}N$], 224 (6) [M^+ – $CH_2C_6H_4NMe_2$, – C_3H_9N, – Cl], 202 (4) [$C_{12}H_{16}NSi^+$], 166 (4) [$C_{10}H_{18}Si^+$], 118 (16) [$C_9H_{10}^+$]. – $C_{23}H_{37}ClNSiTi$ (453.0): calcd. C 60.99, H 8.23, N 6.18; found C 60.83, H 8.43, N 6.22.

Ti(η⁵:η¹-C₅Me₄SiMe₂NCH₂Ph){CH₂C₆H₄(NMe₂)-2}Cl (**10**): A mixture of **5** (0.85 g, 2.11 mmol) and $LiCH_2C_6H_4(NMe_2)$-2 (0.30 g 2.11 mmol) was treated with 50 ml of toluene at −50°C and stirred for 14 h at room temp. After removal of the solvent, the residue was extracted with 50 ml of a toluene/hexane mixture (1:1). Filtration and cooling to −50°C afforded red crystals; yield 0.65 g (61%). – ^1H NMR (C_6D_6): δ = 0.13 (s, 3 H, $SiCH_3$), 0.41 (s, 3 H, $SiCH_3$), 1.06 (s, 3 H, CCH_3), 1.99 (s, 3 H, CCH_3), 2.11 (s, 3 H, CCH_3), 2.23 (d, $^2J_{HH}$ = 12 Hz, 1 H, $TiCH_2$), 2.34 (d, $^2J_{HH}$ = 12 Hz, 1 H, $TiCH_2$), 2.49 (s, 3 H, CCH_3), 2.73 (s, 6 H, NCH_3), 4.69 (d, $^2J_{HH}$ = 14 Hz, 1 H, NCH_2), 5.88 (d, $^2J_{HH}$ = 14 Hz, 1 H, NCH_2), 7.08 (m, 7 H, Ph, C_6H_4), 7.62 (m, 2 H, Ph, C_6H_4). – $^{13}C\{^1H\}$ NMR (C_6D_6): δ = 1.0, 3.6 ($SiCH_3$), 10.3, 12.4, 14.3, 17.1 (CCH_3), 47.7 (NCH_3), 59.3 (NCH_2), 73.7 ($TiCH_2$), 104.7 (C_5Me_4 at Si), 118.4, 123.4, 125.3 (C_6H_4), 127.3, 128.3, 128.6 (C_6H_5), 129.5, 130.5, 131.5, 135.5, 143.0 (CCH_3, *ipso*-C_6H_5), 144.9 (1-C_6H_4), 153.1 (2-C_6H_4). – EI MS; *m/z* (%): 500 (9) [M^+], 366 (45) [M^+ – $CH_2C_6H_4NMe_2$], 261 (13) [M^+ – $CH_2C_6H_4NMe_2$, – NCH_2Ph], 163 (8) [$C_9H_{13}NSi^+$], 134 (100) [$CH_2C_6H_4NMe_2^+$], 118 (6) [$C_9H_{10}^+$], 91 (3) [$PhCH_2^+$], 58 (4) [$SiMe_2^+$]. – $C_{27}H_{37}ClN_2SiTi$ (501.0): calcd. C 64.73, H 7.44, N 5.59; found C 64.49, H 7.49, N 5.83.

Ti(η⁵:η¹-C₅Me₄SiMe₂NiPr)[{η⁵-C₅H₃(CH₂NMe₂)-2}Fe(η⁵-C₅H₅)]Cl (**11**): To a solution of **4** (0.97 g, 2.74 mmol) in 90 ml of toluene cooled to −78°C was slowly added Li[{η^5-$C_5H_3(CH_2NMe_2)$-2}Fe(η^5-C_5H_5)] (0.68 g, 2.74 mmol), dissolved in 5 ml of diethyl ether. The mixture was allowed to warm up to room temperature and stirred for additional 17 h. The solvent was evaporated and the residue was extracted with 70 ml of hexane. Concentrating and cooling of the solution to −20°C afforded of violet crystals, yield 0.66 g (43%). – ^1H NMR (C_6D_6): δ = 0.64 (s, 3 H, $SiCH_3$), 0.74 (s, 3 H, $SiCH_3$), 1.36 (d, $^3J_{HH}$ = 7 Hz, 3 H, CHCH_3), 1.56 (d, $^3J_{HH}$ = 7 Hz, 3 H, CHCH_3), 1.81 (s, 3 H, CCH_3), 2.19 (s, 3 H, CCH_3), 2.21 (s, 3 H, CCH_3), 2.23 (s, 6 H, NCH_3), 2.26 (s, 3 H, CCH_3), 3.13 (d, $^2J_{HH}$ = 12 Hz, 1 H, NCH_2), 3.43 (d, $^2J_{HH}$ = 12 Hz, 1 H, NCH_2), 3.85 (m, 1 H, C_5H_3), 4.28 (m, 1 H, C_5H_3), 4.38 (m, 1 H, C_5H_3), 4.46 (s, 5 H, C_5H_5), 5.91 (sept, $^3J_{HH}$ = 7 Hz, 1 H, CHCH$_3$). – $^{13}C\{^1H\}$ NMR (C_6D_6): δ = 5.6, 5.8 ($SiCH_3$), 12.8, 13.3, 15.6, 15.9 (CCH_3), 25.8, 26.8 ($CHCH_3$), 45.7 (NCH_3), 52.9 ($CHCH_3$), 62.2 (NCH_2), 68.8 (4-C_5H_3), 71.4 (C_5H_5), 71.9, 74.2, (C_5H_3), 89.6 (2-C_5H_3), 100.0 (C_5Me_4 at Si), 127.2, 133.1, 136.6, 137.2, 138.4 (CCH_3, 1-C_5H_3). – EI MS; *m/z* (%): 560 (100) [M^+], 516 (5) [M^+ – C_3H_8], 360 (10) [M^+ – $C_{11}H_{12}Fe$], 317 (11) [$C_{14}H_{24}NClSiTi^+$], 281 (5) [$C_{14}H_{23}NSiTi^+$], 242 (35) [$C_{13}H_{16}NFe^+$], 199 (13) [$C_{11}H_{11}Fe^+$], 186 (2) [$C_{11}H_{26}Si^+$], 121 (4) [$C_5H_4Fe^+$]. – $C_{27}H_{41}N_2ClFeSiTi$ (560.9): calcd. C 57.82, H 7.37, N 4.99; found C 57.61, H 7.24, N 5.10.

Ti(η⁵:η¹-C₅Me₄SiMe₂NCH₂Ph)[{η⁵-C₅H₃(CH₂NMe₂)-2}Fe(η⁵-C₅H₅)]Cl (**12**): To a solution of **5** (1.27 g, 3.16 mmol) in 90 ml of toluene cooled to −78°C was slowly added 0.78 g (3.16 mmol) of Li[{η^5-$C_5H_3(CH_2NMe_2)$-2}Fe(η^5-C_5H_5)], dissolved in 5 ml of diethyl ether. The mixture was allowed to warm up to room temperature and stirred for additional 17 h. The solvent was evaporated and the residue was extracted with 70 ml of hexane. Concentrating and cooling of the solution to −20°C afforded violet crystals, yield 0.92 g (48%). – ^1H NMR (C_6D_6): δ = 0.28 (s, 3 H, $SiCH_3$), 0.30 (s, 3 H, $SiCH_3$), 1.98 (s, 3 H, CCH_3), 2.07 (s, 3 H, CCH_3), 2.27 (s, 3 H, CCH_3), 2.34 (s, 6 H, NCH_3), 2.39 (s, 3 H, CCH_3), 3.05 (d, $^2J_{HH}$ = 13 Hz, 1 H, CH_2NCH$_3$), 3.87 (d, $^3J_{HH}$ = 1 Hz, 1 H, C_5H_3), 4.08 (d. $^2J_{HH}$ = 13 Hz, 1 H, CH_2NCH$_3$), 4.21 (m, 1 H, C_5H_3), 4.36 (d, $^3J_{HH}$ = 1 Hz, 1 H, C_5H_3), 4.39 (s, 5 H, C_5H_5), 5.80 (d, $^2J_{HH}$ = 15 Hz, 1 H, NCH_2Ph), 5.98 (d, $^2J_{HH}$ = 15 Hz, 1 H, NCH_2Ph), 7.26 (m, 3 H, C_6H_5), 7.55 (d, $^3J_{HH}$ = 7 Hz, 2 H, *o*-C_6H_5). – $^{13}C\{^1H\}$ NMR (C_6D_6): δ = 2.2, 3.5 ($SiCH_3$), 12.3, 12.6, 16.0, 16.4 (CCH_3), 46.0 (NCH_3), 58.4 (CH_2Ph), 62.4 (CH_2NCH_3), 68.6 (4-C_5H_3), 71.1 (C_5H_5), 72.5 (3-C_5H_3), 75.2 (5-C_5H_3), 88.2 (2-C_5H_3), 102.0 (C_5Me_4 at Si), 127.5, 127.9, 128.9, 129.1, 133.1, 134.3, 136.5, 138.4, 139.6 (CCH_3, C_5H_3, C_6H_5), 142.8 (*ipso*-C_6H_5). – EI MS; *m/z* (%): 608 (100) [M^+], 452 (22) [$C_{22}H_{28}N_2FeSiTi^+$], 407 (7) [$C_{20}H_{21}NFeSiTi^+$], 365 (50)

Table 2. Crystallographic data and parameters of the crystal structure determinations

Compound	**8**	**9**	**12**
Chem. formula	$C_{27}H_{37}ClN_2SiTi$	$C_{23}H_{37}ClN_2SiTi$	$C_{31}H_{41}ClFeN_2SiTi$
Form wght	501.03	452.99	608.95
Cryst size [mm]	0.8 × 0.2 × 0.2	0.3 × 0.4 × 0.8	0.40 × 0.45 × 0.7
Cryst system	orthorhombic	triclinic	monoclinic
Space group	$P2_12_12_1$	$P\bar{1}$	$P2_1/n$
a [Å]	7.912(2)	8.545(2)	9.955(3)
b [Å]	11.233(1)	11.925(2)	14.297(3)
c [Å]	28.881(4)	12.755(4)	21.438(3)
α [°]		106.70(2)	
β [°]		100.47(2)	92.79(2)
γ [°]		92.51(1)	
V [Å^3]	2566.8(8)	1217.8(5)	3047(1)
Z	4	2	4
ρ_{calcd} [g cm^{-3}]	1.297	1.235	1.327
μ[mm^{-1}]	0.502	0.521	0.887
F(000)	1064	484	1280
T [K]	296(2)	296(2)	296(2)
$2\theta_{max}$ [°]	60.0	60.0	56.0
Index ranges	$-7 \le h \le 11$, $-10 \le k \le 15$, $-27 \le l \le 40$	$0 \le h \le 12$, $-16 \le k \le 16$, $-17 \le l \le 17$	$0 \le h \le 13$, $0 \le k \le 18$, $-28 \le l \le 28$
Absorption correction	empirical (ψ-scans)	none	empirical (ψ-scans)
Transmission (min/max)	95.57/99.97	98.66/99.98	91.91/99.91
Reflections			
Collected/independent	5612/5178 [R_{int} = 0.016]	7493/7054 [R_{int} = 0.008]	7715/7310 [R_{int} = 0.010]
Independent with $I>2\sigma(I)$	3916	5960	4950
No. of parameters	437	402	393
*R*1/*wR2*/*s* (all data)	0.0791/0.1222/1.171	0.0436/0.0965/1.127	0.0826/0.1305/1.138
*R*1/*wR2*/*s* [$I>2\sigma(I)$]	0.0515/0.1020/1.138	0.0325/0.0857/1.094	0.0435/0.1011/1.083
Resid. electron density [e Å^{-3}]	0.474/−0.610	0.390/−0.349	0.489/−0.367

$[C_{18}H_{24}ClNSiTi^+]$, 329 (3) $[C_{18}H_{23}NSiTi^+]$, 298 (5) $[C_{16}H_{16}NSiTi^+]$, 261 (12) $[M^+ - FcN, - NCH_2Ph]$, 243 (29) $[C_{13}H_{17}NFe^+]$, 199 (47) $[C_{11}H_{11}Fe^+]$, 186 (3) $[C_{11}H_{26}Si^+]$, 177 (8) $[C_{11}H_{17}Si^+]$, 121 (49) $[C_5H_5Fe^+]$, 91 (54) $[PhCH_2^+]$, 77 (2) $[Ph^+]$, 58 (10) $[C_2H_6Si^+]$. – $C_{31}H_{41}N_2ClFeSiTi$ (609.0): calcd. C 61.15, H 6.79, N 4.60; found C 60.99, H 6.76, N 4.66.

Crystal Structure Determination of **8**, **9 and 12**: X-ray data were collected with an Enraf-Nonius CAD4 diffractometer at room temperature by using Mo-K_α radiation and ω scans. The structures were solved by direct methods (SHELXS-86) and refined by full-matrix least squares (SHELXL-93) against F^2. Non-hydrogen atoms were refined anisotropically. The hydrogen atoms were located in difference Fourier maps and refined isotropically, except for **12** where the hydrogen atoms of the methyl groups are included in calculated positions. For **8** and **9**, isotropic temperature factors were refined. Crystallographic data are summarized in Table 2[18].

Polymerization: A 0.5 l Büchi reactor was charged with 200 ml of toluene and at constant ethene pressure of 3 bar (c = 0.432 mol/l) a mixture of 1.25 ml of catalyst (c = 4 mmol/l) and 1.5 ml of MAO ($c \approx$ 1.658 mol/l) was added at the pressure of 3.5 bar and stirred for 2 h at 23°C. After the reaction mixture was drained into 0.5 l of methanol acidified with 10 ml of concentrated aqueous HCl, the polymer was collected by filtration, washed with methanol, and dried to constant weight. Melting points were determined by DSC.

☆ Dedicated to Professor *Pascual Royo* on the occasion of his 60th birthday.

[1] [1a] P. J. Shapiro, E. Bunel, W. P. Schaefer, J. E. Bercaw, *Organometallics* **1990**, *9*, 867. – [1b] W. E. Piers, P. J. Shapiro, E. E. Bunel, J. E. Bercaw, *Synlett* **1990**, *2*, 74. – [1c] P. J. Shapiro, W. D. Cotter, W. P. Schaefer, J. A. Labinger, J. E. Bercaw, *J. Am. Chem. Soc.* **1994**, *116*, 4623. – [1d] J. Okuda, *Chem. Ber.* **1990**, *123*, 1649. – [1e] W. A. Herrmann, M. J. A. Morawietz, *J. Organomet. Chem.* **1994**, *482*, 169. – [1f] S. Circuelos, T. Cuenca, P. Gómez-Sal, A. Manzanero, P. Royo, *Organometallics* **1995**, *14*, 177. – [1g] S. Ciruelos, T. Cuenca, R. Gómez, P. Gómez-Sal, A. Manzanero, P. Royo, *Organometallics* **1996**, *15*, 5577. – [1h] F. Amor, J. Okuda, *J. Organomet. Chem.* **1996**, *520*, 245. – [1i] J. Okuda, S. Verch, T. P. Spaniol, R. Stürmer, *Chem. Ber.* **1996**, *129*, 1429. – [1j] J. Okuda, T. Eberle, T. P. Spaniol, *Chem. Ber.* **1997**, *130*, 209.

[2] [2a] J. A. Canich, (Exxon Chemical Co.), U.S. Patent 5,026,798, **1991**. – [2b] J. C. Stevens, F. J. Timmers, G. W. Rosen, G. W. Knight, S. Y. Lai (Dow Chemical Co.), European Patent Application, EP 0416815 A2, **1991**. – [2c] D. D. Devore, F. J. Timmers, D. L. Hasha, R. K. Rosen, T. J. Marks, P. A. Deck, C. L. Stern, *Organometallics* **1995**, *14*, 3132. – [2d] K. Soga, T. Uozumi, S. Nakamura, T. Toneri, T. Teranishi, T. Sano, T. Arai, *Macromol. Chem. Phys.* **1996**, *197*, 4237. – [2e] F. G. Sernetz, R. Mülhaupt, R. M. Waymouth, *Macromol. Chem. Phys.* **1996**, *197*, 1071. – [2f] T. Shiomura, T. Asanuma, N. Inoue, *Macromol. Rapid Commun.* **1996**, *17*, 9.

[3] [3a] J. C. Stevens, *Metcon 93*, Houston, Mai 26–28, **1993**, p. 157; J. C. Stevens, *Stud. Surface Sci. Cat.* **1994**, *89*, 277. – [3b] F. G. Sernetz, R. Mülhaupt, F. Amor, T. Eberle, J. Okuda, *J. Polym. Sc., Part A* **1997**, *35*,1571. – [3c] P.-J. Sinnema, K. Liekelema, O. K. B. Staal, B. Hessen, J. H. Teuben, *J. Mol. Catal.*, in press. – [3d] A. L. McKnight, M. A. Masood, R. M. Waymouth, *Organometallics* **1997**, *16*, 2879.

[4] [4a] K. E. du Plooy, U. Moll, S. Wocadlo, W. Massa, J. Okuda, *Organometallics* **1995**, *14*, 3129. – [4b] J. Okuda, K. E. du Plooy, W. Massa, H.-C. Kang, U. Rose, *Chem. Ber.* **1996**, *129*, 275. – [4c] F. Amor, T. P. Spaniol, J. Okuda *Organometallics* **1997**, *16*, 4765. For related ligand systems, see: Y. Mu, W. E. Piers, D. C. MacQuarrie, M. J. Zaworotko, V. G. Young, Jr., *Organometallics* **1996**, *15*, 2720.

[5] T. Eberle, J. Okuda, unpublished results.

[6] P.-J. Sinnema, L. van der Veen, A. L. Spek, N. Veldman, J. H. Teuben, *Organometallics* **1997**, *16*, 4245.

[7] L. Manzer, *J. Am. Chem. Soc.* **1978**, *100*, 8068.

[8] C. Floriani, F. Corazza, W. Lesueur, A. Chiesi-Villa, C. Guastini, *Angew. Chem.* **1989**, *101*, 93; *Angew. Chem. Int. Ed. Engl.* **1989**, *28*, 66.

[9] [9a] J. C. Flores, J. C. W. Chien, M. D. Rausch, *Organometallics* **1994**, *13*, 4140. – [9b] W. A. Herrmann, M. J. Morawietz, T. Priermeier, K. Mashima, *J. Organomet. Chem.* **1995**, *486*, 291. – [9c] P. B. Hitchock, D. L. Hughes, G. J. Leigh, J. R. Sanders, J. S. de Souza, *J. Chem. Soc. Chem.* **1996**, 1985. – [9d] S. Fokken, T. P. Spaniol, H.-C. Kang, W. Massa, J. Okuda, *Organometallics* **1996**, *15*, 5069. – [9e] M. Enders, R. Rudolph, H. Pritzkow, *Chem. Ber.* **1996**, *129*, 459.
[10] H. Bürger, K. Wiegel, U. Thewalt, D. Schomburg, *J. Organomet. Chem.* **1975**, *87*, 301.
[11] L. E. Manzer, R. C. Gearhart, L. J. Guggenberger, J. F. Whitney, *J. Chem. Soc. Chem. Comm.* **1976**, 942.
[12] M. F. Lappert, P. P. Power, R. R. Sanger, R. C. Sribastava, *Metal and Metalloid Amides*, Wiley, New York, **1980**.
[13] K.-H. Thiele, C. Krüger, T. Bartik, M. Dargatz, *J. Organomet. Chem.* **1988**, *352*, 115.
[14] M. Wedler, H. W. Roesky, F. T. Edelmann, *Z. Naturforsch.* **1988**, *43b*, 1461.
[15] L. E. Manzer, *Inorg. Synth.* **1982**, *21*, 135.
[16] J. T. B. H. Jastrzebski, G. van Koten, *Inorg. Synth.* **1989**, *26*, 152.
[17] D. W. Slocum, B. W. Rockett, C. R. Hauser, *J. Am. Chem. Soc.* **1965**, *87*, 1241.
[18] Further details of the crystal structure investigation are available on request from the Fachinformationszentrum Karlsruhe, Gesellschaft für wissenschaftlich-technische Information mbH, D-76344 Eggenstein-Leopoldshafen, Germany, on quoting the depository number CSD-407857 for **8**, -407855 for **9**, and -407856 for **12**, the names of the authors and the journal citation.

[97230]

Homoleptic Organometallic Compounds of Zinc, Cadmium, and Mercury, Intramolecularly Stabilized by Amine Ligands

Herbert Schumann*, Silke Freitag, Frank Girgsdies, Holger Hemling, and Gabriele Kociok-Köhn

Institut für Anorganische und Analytische Chemie der Technischen Universität Berlin,
Straße des 17. Juni 135, D-10623 Berlin, Germany
Fax: (internat.) +49 (0)30/314-22168
E-mail: schumann@mailszrz.zrz.tu-berlin.de

Received June 4, 1997

Keywords: Alkylamines / Arylamines / Zinc / Cadmium / Mercury / X-ray diffraction

Homoleptic intramolecularly stabilized organozinc, -cadmium, and -mercury compounds MR_2, with R bearing an amino function, have been synthesized from the corresponding metal dichlorides MCl_2 and the lithium salts $LiC_6H_4CH_2NEt_2$-2 (**1**), $LiC_6H_3(CH_2NMe_2)_2$-2,6 (**2**), $LiC_6H_3(CH_2NEt_2)_2$-2,6 (**3**), $(LiCH_2CH_2CH_2)_2NMe$ (**4**), and $LiCH_2CH_2CH_2NC_5H_{10}$ (**5**). The crystal structures of $Hg(C_6H_4CH_2NEt_2\text{-}2)_2$ (**1c**), $[M(CH_2CH_2CH_2)_2NMe]_2$ [M = Zn (**4a**), Hg (**4c**)], and of $M(CH_2CH_2CH_2NC_5H_{10})_2$ [M = Zn (**5a**), Cd (**5b**)] have been determined by X-ray diffraction. **4a** and **4c** form dimers with an unusual coordination number (three) of the central metal.

Introduction

Diorganometal compounds of the group 12 elements are of increasing interest in connection with the development of MOVPE techniques (**M**etal **O**rganic **V**apor **P**hase **E**pitaxy) for the generation of type II-VI semiconductors. In particular, the dimethyl or diethyl derivatives of zinc, cadmium, and mercury have been used as precursors[1a][1b][1c]. Unfortunately, these compounds are highly water sensitive and, with the exception of the zinc compounds, extremely toxic. It was to be expected that the use of *N*-donor functionalized ligands, which are able to coordinate intramolecularly with the metal center by formation of chelate rings, should result in a considerable increase in the stability of such organometallic derivatives. Although numerous dialkyl-metal compounds of the group 12 elements are known which are intermolecularly stabilized by mono-, bi-, and tridentate amines, e.g. by NMe_3, NEt_3, py[2], 2,2′-bipy[2][3][4][5][6][7][8][9][10], 1,10-phen[2][3][4][10], tmeda[6][7][11], *N*,*N*,*N*′,*N*′-tetraethylethylenediamine (teeda)[2][4], (−)-sparteine[12], and triazines $(RNCH_2)_3$ (R = Me, Et, *i*Pr)[13], only a few intramolecularly *N*-stabilized species are known. $Zn(CH_2CH_2CH_2NMe_2)_2$, synthesized by Boersma et al. in 1978, was the first and, to date, the best investigated compound of this type[14][15][16]. The corresponding cadmium species and the corresponding diethylamino derivative of zinc were prepared by Thiele et al.[16], the diorganozinc, -cadmium, and -mercury compounds bearing 2-$Me_2NC_6H_4CH_2$- and/or 2-$Me_2NCH_2C_6H_4$- as arylamino ligands by Atwood et al.[17], van Koten et al.[18], and O′Brien et al.[19]. Deacon et al. succeeded in synthesizing bis[2-(pyridin-2′-yl)phenyl]mercury and bis[2-(pyrazol-1′-yl)phenyl]-mercury[20]. A comprehensive paper concerning the structure of organomercury compounds and their secondary interactions has been published by Kuz′mina and Struchkov[21].

In this paper we present some interesting new homoleptic compounds of the group 12 elements with alkyl- and arylamine ligands.

Results and Discussion

1. Intramolecularly Stabilized Arylamino Compounds

The reaction of two equivalents of $LiC_6H_4CH_2NEt_2$-2 (**1**)[22][23][24][25], $LiC_6H_3(CH_2NMe_2)_2$-2,6 (**2**), or $LiC_6H_3(CH_2NEt_2)_2$-2,6 (**3**)[22][26] with one equivalent of MCl_2 (M = Zn, Cd, or Hg) gave the corresponding diorganozinc compounds **1a**, **2a**, **3a**, the diorganocadmium compounds **1b, 3b**, and the diorganomercury compounds **1c**, **2c**, **3c** in yields of 64 to 85% (Scheme 1). The lower yields obtained for **1b**, **3b**, and **2c** were caused by some decomposition accompanied by precipitation of metallic cadmium or mercury. With the exception of **3c**, which is a highly viscous liquid, all other derivatives are colorless solids at room temperature.

Scheme 1

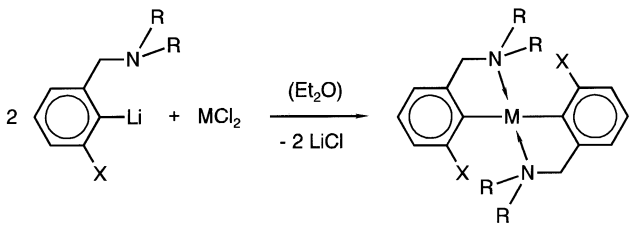

1 X = H, R = Et
2 X = CH_2NMe_2, R = Me
3 X = CH_2NEt_2, R = Et

M = Zn **1a**, Cd **1b**, Hg **1c**
M = Zn **2a**, Hg **2c**
M = Zn **3a**, Cd **3b**, Hg **3c**

 © WILEY-VCH Verlag GmbH, D-69451 Weinheim, 1998 1434−1948/98/0202−0245 $ 17.50+.50/0

Table 1. ^{1}H- and ^{13}C-NMR data of the arylamino compounds **1a**−**3c**

	^{1}H-NMR δ [ppm]				^{13}C-NMR δ [ppm]			
	CH_3	CH_3CH_2	CH_2C_{aryl}	$C_{aryl}H$	CH_3	CH_3CH_2	CH_2C_{aryl}	C_{aryl}−1
1a	0.64	2.52	3.52	7.10···8.02	8.75	45.25	61.79	157.75
1b	0.77	2.43	3.44	7.09···7.40	10.33	45.90	62.07	160.72
1c	1.09	2.69	3.68	7.24···7.97	11.21	46.39	61.60	171.10
2a	2.16	–	3.36	6.96···7.27	45.60	–	65.00	159.10
2c	2.19	–	3.41	7.02···7.18	48.25	–	71.58	176.00
3a	0.85	2.63	3.74	7.29···7.43	10.35	46.09	63.42	158.44
3b	0.86	2.61	3.49	7.08···7.33	10.27	45.81	63.52	163.69
3c	0.92	2.58	3.70	7.16···7.36	10.13	45.41	61.17	171.74

Within each group of compounds, the ^{1}H-NMR signal of the methyl protons and the ^{13}C-NMR signal of the phenyl carbon atom bound to the metal center shift to lower fields on going from the zinc to the mercury species. In the spectra of the cadmium and mercury derivatives **1b**, **2c**, and **3c**, ^{1}H- and ^{13}C-metal coupling was observed. The coupling constants of **1b** [$^3J(^1H,^{111/113}Cd)$ = 26, 19 Hz and $^{2,3}J(^{13}C,^{113}Cd)$ = 20, 12 Hz] are in the expected range[27][28]. The coupling constants of **3c** [$^{1,2,3}J(^{13}C,^{199}Hg)$ = 714, 22, 42 Hz] demonstrate that the usual relationship $^1J > {}^3J > {}^2J$ is also valid for the spin pair ^{13}C,^{199}Hg[29], while the absolute values ^2J and ^3J of **3c** and ^3J of **2c** (40.5 Hz) are somewhat smaller than those given in the literature[26][27]. The appearance of one NMR signal for both of the amino functions of each ligand in **2a**−**2c** and **3a**−**3c** indicates a dynamic behaviour of these complexes in solution. Selected NMR data of the arylamino compounds are summarized in Table 1.

The mass spectra of **1a**, **1b**, **1c**, **2c**, **3a**, and **3c** show the peak for the corresponding molecular ion, whereas the spectra of the zinc and cadmium species **2a** and **3b** show only ligand fragments.

Crystallization of **1c** from Et_2O/*n*-pentane afforded crystals suitable for X-ray structure determination. The molecular structure of **1c** is depicted in Figure 1a, and selected bond lengths and bond angles are listed in Table 2. The structure may be compared with that of the corresponding methylamine derivatives $M(C_6H_4CH_2NMe_2\text{-}2)_2$ (M = Cd[19] and Hg[17]). The angle C1−M−C1′ becomes larger with increasing radius of the central metal. This angle is 174° in $Cd(C_6H_4CH_2NMe_2)_2$, exactly 180° in $Hg(C_6H_4CH_2NMe_2)_2$ and nearly 180° in **1c** [176.7(1)°]. The same trend is observed for the angle N−M−N′ {$M(C_6H_4CH_2NMe_2)_2$: M = Cd (116.12°), Hg (180°); **1c** [151.2(2)°]}. Accordingly, the geometric arrangement of the ligands around the metal atom changes from a distorted trigonal bipyramid with one vacancy in the equatorial plane for $Cd(C_6H_4CH_2NMe_2)_2$, to a square planar system in **1c** and $Hg(C_6H_4CH_2NMe_2)_2$. The bond distance Hg−C1 in **1c** [206.9(4) pm] is similar to that in $Hg(C_6H_4CH_2NMe_2)_2$ (210 pm) and other mercury diaryl compounds[20][21][30][31]. The Hg−N distance [294.2(3) pm] is only slightly longer than that in the *N*-methyl derivative (289 pm), but it is still in the same range as other comparable Hg−N interactions[20][21][32]. The Hg···Hg distance [349.3(3) pm] in **1c** is remarkably short at just over twice the van der Waals radius of mercury (173 pm[32]). Figure 1b shows that two molecules of **1c** are situated very close to one another, resulting in a slight bend of the phenyl groups out of the phenylmercury plane away from the Hg···Hg axis. One of the two ethyl substituents at each nitrogen atom avoids close contact by being situated in the same direction, whereas the second ethyl group remains in the plane. A similar effect

Figure 1a. ORTEP plot of the molecular structure of **1c**

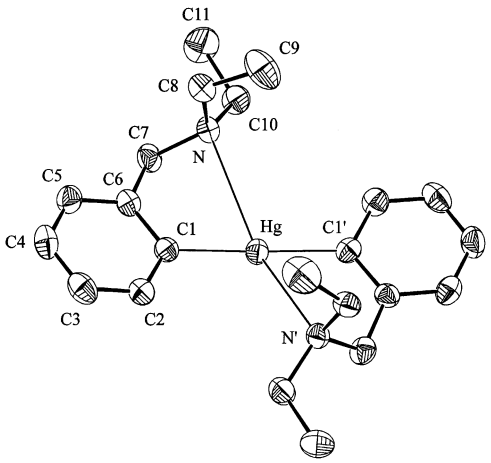

Figure 1b. PLUTON plot of two molecules of **1c** in the crystal

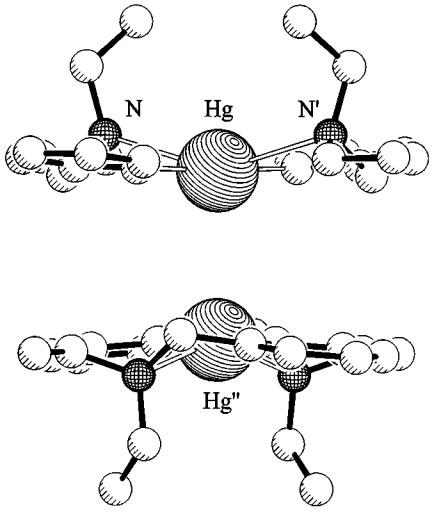

Table 2. Selected bond lengths [pm] and angles [°] of **1c**. E.s.d.s are given in parentheses

atoms	bond lenghts	atoms	bond angles
Hg···Hg′′	349.3(3)	N−Hg−N′	151.2(2)
Hg−N	294.2(3)	C1−Hg−C1′	176.7(1)
Hg−C1	206.9(4)	N−Hg−C1	71.3(1)
C1−C2	139.8(5)	C2−C1−Hg	121.5(3)
C1−C6	140.4(5)	C6−C1−Hg	121.2(3)

Symmetry transformations used to generate equivalent atoms: ′: $-x$, $1/2-y$, z. − ″: $1/4-y$, $1/4+x$, $5/4-z$.

was observed in the analogous compound $Cd(C_6H_4CH_2NMe_2)_2$ with a Cd···Cd distance of 317.6 pm and this is probably caused by weak crystal packing forces[19]. The arrangement of the molecules in terms of the metal···metal axis differs: it is staggered for **1c** with an angle of 90° and eclipsed for the cadmium derivative. Surprisingly, this phenomenon of crystal packing with short metal···metal contacts was not detected in $Hg(C_6H_4CH_2NMe_2)_2$[17].

Unfortunately, it was not possible to obtain crystals suitable for X-ray investigations of **2a**, **2c**, **3a**, **3b**, and **3c** in which the appropriate metal is bonded to tridentate amino ligands. However, we also solved the crystal and molecular structure of the starting material $LiC_6H_3(CH_2NEt_2)_2$-2,6 (**3**)[33] which has recently been published by Hey-Hawkins et al.[34].

2. Intramolecularly Stabilized Alkylamino Compounds

We used tridentate bis(3-lithiopropyl)methylamine, $(LiCH_2CH_2CH_2)_2NMe$[35] (**4**), and bidentate 3-(*N*-piperidino)propyllithium, $LiCH_2CH_2CH_2NC_5H_{10}$[36] (**5**), for the synthesis of compounds **4a** to **4c**, and **5a** to **5c**.

The 5,13-diaza-5,13-dimethyl-1,9-dimetallacyclohexadecanes **4a**−**c** were prepared by treating equimolar amounts of MCl_2 (M = Zn, Cd, Hg) with $(LiCH_2CH_2CH_2)_2NMe$ in Et_2O at ambient temperatures (Scheme 2). The colorless and moisture sensitive compounds were isolated with yields of 75% for the Zn compound **4a** and 72% for the Hg derivative **4c**. The yield of the Cd species **4b** was only 49% due to decomposition during the reaction and precipitation of metallic cadmium. As indicated by the mass spectra of **4b** and **4c**, and as proved by X-ray structural analysis of **4a** and **4c**, the compounds **4a** to **4c** form dimers consisting of sixteen-membered rings.

Scheme 2

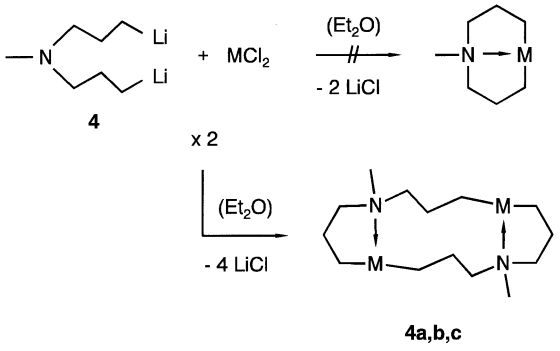

M = Zn **4a**, Cd **4b**, Hg **4c**

Treating MCl_2 (M = Zn, Cd, Hg) with a twofold amount of $Li(CH_2)_3NC_5H_{10}$ in Et_2O produced the bis(3-*N*-piperidino)propylmetal compounds **5a** to **5c** (Scheme 3) with yields of 76%, 65%, and 58%, respectively. The reaction with $HgCl_2$ was accompanied by the elimination of some metallic mercury. **5a** and **5b** are colorless crystalline solids which melt at 80°C or decompose above 90°C, respectively. **5b** changes color to yellow on exposure to light. **5c** forms colorless prisms at −20°C, but is a liquid at room temperature. The mass spectra of the three compounds show the molecular ion peak, but only with very low intensity. The first step in the fragmentation of **5b** and **5c** is the separation of the ligand as a whole, a process which could not be observed for **5a**.

Scheme 3

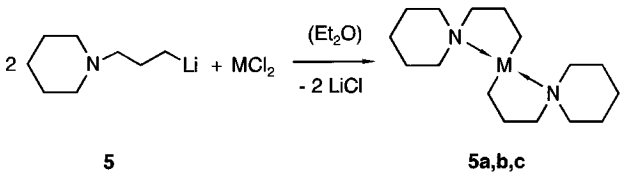

M = Zn **5a**, Cd **5b**, Hg **5c**

Table 3. ^1H- and ^{13}C-NMR data of the alkylamino compounds **4a**−**5c**

no.	^1H NMR δ [ppm]				^{13}C NMR δ [ppm]			
	MCH_2	CH_2	CH_2N	NCH_3	MCH_2	CH_2	CH_2N	NCH_3
4a	0.32[a]	1.85[a]	2.23[a]	1.86[a]	8.46	25.87	61.17	41.87
4b	0.67	2.01	2.25	1.89	12.14	32.56	61.89	41.93
4c	0.99	2.06	2.25	1.91	27.58	37.56	62.20	41.95
5a	0.48	1.29	2.19	–	8.22	24.82	64.06	–
5b	0.59	1.31	2.14...19	–	13.29	26.31	64.30	–
5c	1.08	1.34	2.21	–	25.08	36.72	63.36	–

[a] $T = 65$°C.

Table 4. Selected bond lengths [pm] and angles [°] of **4a** and **4c**. E.s.d.s are given in parentheses

atoms	bond lengths		atoms	bond angles	
	4a (M = Zn) [a]	**4c** (M = Hg) [b]		**4a** (M = Zn) [a]	**4c** (M = Hg) [b]
M−C1	197.9(3)	209(2)	C1−M−C7	156.38(13)	176.7(5)
M−C7	198.3(3)	209(2)	C1−M−N	87.38(11)	76.3(6)
M−N	221.6(2)	277.4(11)	C7−M−N	112.51(11)	102.7(5)
C1−C2	152.9(4)	156(2)	C4−N−M	103.8(2)	102.4(7)
C2−C3	152.1(4)	148(2)	C5−N−M	118.7(2)	120.6(8)
C5−C6′	152.2(4)	149(2)	C3−N−M	102.9(2)	97.6(7)
C6′−C7′	152.7(4)	156(2)	C2−C1−M	105.4(2)	110.1(11)

Symmetry transformations used to generate equivalent atoms: [a] ′: $-x + 1, -y + 2, -z + 2$. − [b] ′: $-x + 1, -y + 1, -z$.

Figure 2. ORTEP plot of the molecular structure of **4a**

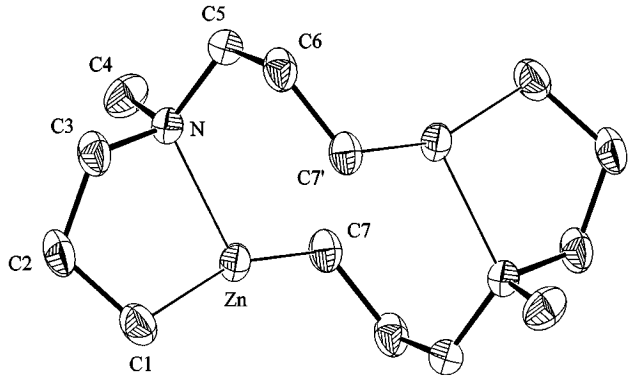

Figure 3. ORTEP plot of the molecular structure of **4c**

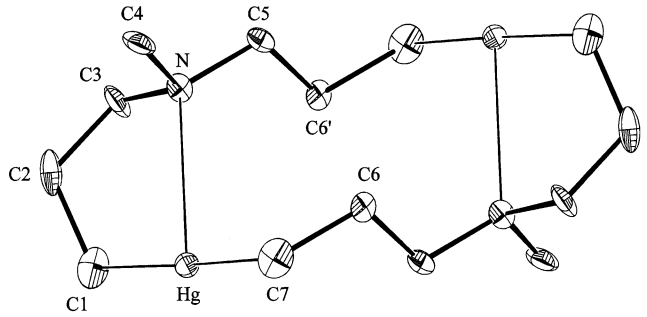

In a similar way to other homoleptic dialkyl complexes of the group 12 elements[13][37], comparison of the ^{1}H- and ^{13}C-NMR spectra of the alkylamino compounds shows a shift in the signals due to the metal-bonded CH_2 groups to lower fields on going from the zinc to the appropriate mercury derivative (Table 3).The NMR spectra of **4a, 4b** and **4c** show only one signal for the two different methylene groups bonded to the metal centers indicating a dynamic behaviour in solution. X-ray structure determinations performed on the metallacyclohexadecanes **4a** and **4c** (suitable crystals were obtained from *n*-pentane) prove the dimeric nature of the molecules in the solid state (Figures 2 and 3, Table 4). Each of the two metal atoms is coordinated to two carbon atoms belonging to different ligand molecules and one nitrogen atom. The sum of the angles C1−M−C7, C1−M−N, and C7−M−N is 356° for **4a** and **4c**, and this indicates that the four atoms essentially lie in a plane with a

Figure 4. ORTEP plot of the molecular structure of **5a**

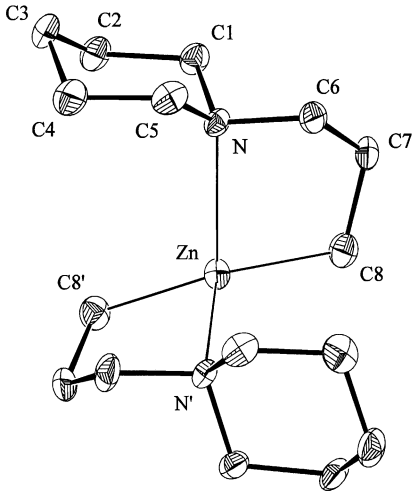

Table 5. Selected bond lengths [pm] and angles [°] of **5a** and **5b**. E.s.d.s are given in parentheses

atoms	bond lengths		atoms	bond angles	
	5a (M = Zn)	**5b** (M = Cd)		**5a** (M = Zn)	**5b** (M = Cd)
M−C8	199.2(3)	216.4(2)	C8−M−C8′	155.5(2)	166.2(2)
M−N	240.4(2)	264.2(2)	C8−M−N′	110.04(11)	109.62(8)
N−C5	146.9(4)	146.7(3)	C8−M−N	84.75(11)	78.84(8)
N−C1	147.2(4)	146.6(2)	N−M−N′	107.47(12)	107.42(7)
C3−C4	151.5(5)	151.1(4)	C1−N−M	110.0(2)	110.03(12)
C4−C5	151.9(5)	151.0(4)	C5−N−M	121.8(2)	119.29(14)
C6−C7	151.1(5)	151.7(4)	C6−N−M	96.1(2)	96.90(12)
			C7−C8−M	110.2(2)	110.7(2)

Symmetry transformation used to generate equivalent atoms: ′: $-x, y, -z + 1/2$.

Figure 5. PLUTON plot of the molecular structure of **5b**

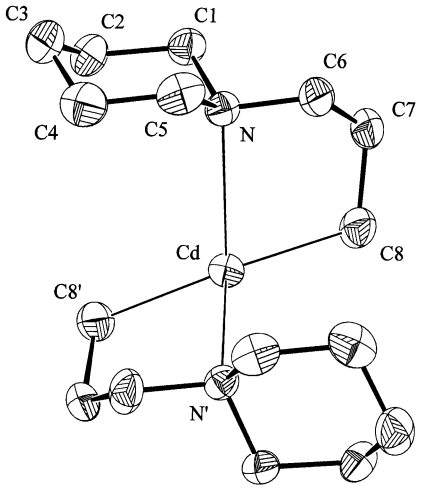

more or less T-shaped ligand arrangement around the metal atoms. Thus, the linear arrangement of the ligands usually found in dialkylzinc and -mercury compounds is not changed to a significant extent by the additional coordination of the nitrogen atom, indicating only a weak interaction [C1−Zn−C7 156.38(13)°; C1−Hg−C7 176.7(5)°]. This agrees with the relatively long M−N distances [Zn−N 221.6(2) pm; Hg−N 277.4(11) pm]. The M−C1 distances [Zn−C1 197.9(3) pm; Hg−C1 209(2) pm] are in the normal range for comparable complexes[9][11][12][15][31][38][39]. The triple coordination of the metal atoms is extremely unusual for group-12 elements.

The molecular structures of **5a** and **5b** (crystals suitable for X-ray structural analysis were obtained by crystallization from *n*-pentane) show the metal atom to be tetracoordinated by the binding methylene carbon and the nitrogen atom of each of the two ligands (Figures 4 and 5, Table 5). The intramolecular stabilization of the metal center by the nitrogen atom seems to be as weak in **5a** and **5b** as it was in the case of the metallacyclohexadecanes **4a** and **4c** because the distances Zn−N [240.4(2) pm] and Cd−N [264.2(2) pm] are also quite long. Furthermore, as in **4a** and **4c** and also in the comparable tetracoordinated $Zn(CH_2CH_2CH_2NMe_2)_2$[15], the C8−M−C8′ angle is closer to 180° [**5a** Zn: 155.5(2)°; **5b** Cd: 166.2(2)°] than to a tetrahedral angle. Similar long M−N distances and large C8−M−C8′angles are known in some intermolecular amine-stabilized dialkylmetal species, e.g. $[M(CH_2CMe_3)_2{\cdot}tmeda]$ (M = Zn: 241.1 pm, 148°; M = Cd: 264.2 pm, 157°)[11]. In a similar way to $Cd(C_6H_4CH_2NMe_2)_2$[19], comparable donor stabilized cadmium[11][40] and zinc complexes $Zn(CH_2CH_2CH_2X)_2$ (X = NMe_2, PPh_2, OMe, SMe)[15][38][41], the coordination sphere around the metal center is more accurately described as a distorted trigonal bipyramid with one vacancy in the equatorial plane than as a tetrahedron. The piperidyl rings in **5a** and **5b** have a chair conformation turning away from the metal center.

Conclusion

Aryl- and alkylamino metal compounds of the group-12 elements have been synthesized and the molecular structure of some representative examples investigated. In comparison to the linear structure of pure diaryl or dialkyl compounds of group-12 elements, the intramolecular metal−nitrogen coordination through chelate ring formation has only a weak influence on the geometry of the molecules, a situation which is similar to that in intermolecularly *N*-stabilized diorgano metal derivatives of these elements.

We are grateful to the *Deutsche Forschungsgemeinschaft* and the *Fonds der Chemischen Industrie* for financial support.

Experimental Section

1. General: The starting anhydrous metal chlorides (Merck) were dried under vacuum and stored under an argon atmosphere. The aryl- and alkylamine ligand systems and their lithium compounds (**1** to **5**) were prepared using known procedures. All reactions yielding organometallic species were performed using standard Schlenk techniques under dry argon and in dry solvents distilled from sodium/benzophenone. − Melting points and thermal decomposition temperatures were determined in sealed capillaries under argon with an HWG-SG 2000, HWS Mainz, and are uncorrected. − NMR (Bruker ARX 200): ^1H NMR (200 MHz): ext. TMS; $^{13}C\{^1H\}$ NMR (50.26 MHz): ext. TMS; ^{113}Cd NMR (400 MHz): ext. $Cd(CH_3)_2$. − MS (Varian MAT 311 A) analyses were carried out using electron impact ionisation with 70 eV. − Elemental analyses: Perkin-Elmer Series II CHNS/O analyser 2400.

2. Crystal Structure Determinations: Crystals of **1c**, **4a**, **4c**, **5a**, and **5b** were mounted on glass fibers and transferred to an Enraf-Nonius CAD4 four circle diffractometer (Mo-K_α radiation) equipped with a low temperature device. Data for all compounds were collected with ω-2θ scans. Intensity data were monitored after every 200 reflections through the measurement of three standard reflections. Raw data were corrected for Lorentz, polarization, and for absorption effects (DIFABS)[42]. The structures were solved using Direct Methods (SHELXS-86)[43] and the refinement of the molecules was performed using difference-Fourier methods (SHELXL-93)[44]. The older program, SHELX-76[45], was also used to prepare the data for DIFABS. All non-hydrogen atoms were refined anisotropically, whereas hydrogen atoms were placed at calculated positions with d_{CH} = 98 pm and U_{iso} = 8 pm^2. Molecular plots were obtained using the programs ZORTEP[46] and PLUTON[47]. Further details on crystals, data collection, and refinement are listed in Table 6.

Crystallographic data (excluding structure factors) for the structures reported in this paper have been deposited with the Cambridge Crystallographic Data Centre as supplementary communication no. CCDC-100487. Copies of the data can be obtained free of charge on application to The Director, CCDC, 12 Union Road, Cambridge CB2 1EZ, UK (fax: int code +44(0)1223/336-033, e-mail: deposit@chemcrys.cam.ac.uk).

3. Synthesis of the Complexes

Bis(2-diethylaminomethylphenyl)zinc (**1a**): 2-Diethylaminomethylphenyllithium (**1**) (4.06 g, 24.0 mmol) was dissolved in Et_2O (100 ml) and a solution of $ZnCl_2$ (1.64 g, 12.0 mmol) in Et_2O (40 ml) was added dropwise. The mixture became pale orange, was warmed up slightly, and a white precipitate formed. After stirring for 14 h at room temperature the Et_2O was removed in vacuo. The remain-

Table 6. Crystal data and details of the structure analysis for compounds **1c**, **4a**, **4c**, **5a**, and **5b**

	1c	**4a**	**4c**	**5a**	**5b**
Formula	$C_{22}H_{32}HgN_2$	$C_{14}H_{30}N_2Zn_2$	$C_{14}H_{30}Hg_2N_2$	$C_{16}H_{32}N_2Zn$	$C_{16}H_{32}CdN_2$
Mol. mass [g mol^{-1}]	525.10	357.14	627.58	317.81	364.84
Temperature [K]	160(2)	199(2)	178(2)	165(2)	199(2)
Wavelength [Å]	0.71069	0.71069	0.71069	0.71069	0.71069
Crystal system	tetragonal	triclinic	triclinic	monoclinic	monoclinic
Space group	$I\,4_1/a$ (No. 88)	$P\,-1$ (No.2)	$P\,-1$ (No.2)	$C\,2/c$ (No.15)	$C\,2/c$ (No.15)
a [Å]	19.956(3)	7.0440(9)	7.164(2)	17.368(3)	18.089(5)
b [Å]	19.956(3)	7.1367(14)	7.879(5)	6.074(2)	6.1133(10)
c [Å]	10.566(3)	8.511(2)	8.052(2)	15.388(3)	15.399(4)
α [°]	90	99.08(2)	89.38(4)	90	90
β [°]	90	91.975(14)	75.90(2)	92.27(2)	90.87(2)
γ [°]	90	106.760(14)	73.24(4)	90	90
V [Å^3]	4208(2)	403.11(12)	421.2(3)	1622.1(8)	1702.7(7)
Z	8	1	1	4	4
$D_{calcd.}$ [g cm^{-3}]	1.66	1.471	2.474	1.301	1.423
μ(Mo-K_α) [mm^{-1}]	14.066	2.962	18.191	1.505	1.274
F(000)	2624	188	288	688	760
Crystal size [mm^3]	0.48×0.36×0.24	0.27×0.15×0.12	1.00×0.65×0.40	0.50×0.25×0.20	0.70×0.45×0.25
θ range for data collection [°]	1, 24	2.43, 25.02	2.61, 25.90	2.35, 24.93	2.25, 24.97
Index ranges	$0\le h\le 22$ $0\le k\le 22$ $0\le l\le 12$	$0\le h\le 8$ $-8\le k\le 8$ $-10\le l\le 10$	$-8\le h\le 8$ $-9\le k\le 9$ $0\le l\le 9$	$0\le h\le 20$ $-18\le l\le 18$ $0\le k\le 7$	$-21\le h\le 21$ $0\le l\le 18$ $0\le k\le 7$
Refl. collected	2078	1547	1748	1462	1569
Independent refl.	1533 (R_{int} = 0.02)	1420 (R_{int} = 0.0120)	1587 (R_{int} = 0.2613)	1411 (R_{int} = 0.1057)	1503 (R_{int} = 0.0289)
Absorption corr.	DIFABS	None	DIFABS	None	ψ-scan 1.00 and 0.91
Refinement method	Full-Matrix-Least-Squares on F	Full-Matrix-Least-Squares on F^2	Full-Matrix-Least-Squares on F^2	Full-Matrix-Least-Squares on F^2	Full-Matrix-Least-Squares on F^2
Data / restraints / parameters	1533 / 0 /122	1420 / 0 / 83	1484 / 0 / 83	1408 / 0 / 87	1499 / 0 / 87
Goodness-of-fit on F^2	–	1.120	1.089	1.073	1.053
Final R indices [$I>2\sigma(I)$]	$R1$ = 0.0204 $wR1$ = 0.0142	$R1$ = 0.0278 $wR2$ = 0.0724	$R1$ = 0.0570 $wR2$ = 0.1485	$R1$ = 0.0469 $wR2$ = 0.1212	$R1$ = 0.0192 $wR2$ = 0.0545
R indices (all data)	–	$R1$ = 0.0301 $wR2$ = 0.0740	$R1$ = 0.0725 $wR2$ = 0.2115	$R1$ = 0.0514 $wR2$ = 0.1293	$R1$ = 0.0205 $wR2$ = 0.0650
Largest diff. peak and hole; min./max. [eA^{-3}]	0.39 / −0.38	0.560 / −0.834	30.227 / −40.557	10.504 / −10.212	0.496 / −0.345

ing pale yellow solid was suspended in *n*-hexane. The reaction mixture was filtered through a fine glass frit and the filtrate volume was reduced to about 50 ml. Storing at −20°C yielded 3.98 g (85%) of colorless crystalline **1a**, m.p. 40°C. – ^{1}H NMR (C_6D_6): δ = 0.64 (t, ^3J = 7.2 Hz, CH_3), 2.52 (q, ^3J = 7.2 Hz, CH_3CH_2), 3.52 (s, CH_2C_{aryl}), 7.10-8.02 (m, $C_{aryl}H$). – ^{13}C NMR (C_6D_6): δ = 8.75 (CH_3), 45.25 (CH_3CH_2), 61.79 (CH_2C_{aryl}), 125.1 (*C*-3), 126.16 (*C*-5), 126.22 (*C*-4), 139.38 (*C*-6), 146.73 (*C*-2), 157.75 (*C*-1). – MS; *m/z* (%): 388 (5) [M(^{64}Zn)$^+$], 316 (8) [M$^+$ − NEt_2], 226 (8) [$ZnC_6H_4CH_2NEt_2^+$], 162 (89) [$C_6H_4CH_2NEt_2^+$], 148 (58) [$C_6H_4CH_2NEtMe^+$], 91 (100) [$C_7H_7^+$], and others. – $C_{22}H_{32}N_2Zn$ (389.90): calcd. C 67.77, H 8.27, N 7.18; found C 67.60, H 8.06, N 7.41.

Bis(2-diethylaminomethylphenyl)cadmium (**1b**): In a similar way to **1a**, $CdCl_2$ (2.93 g, 16 mmol) and **1** (5.41 g, 32 mmol) yielded 4.12 g (59%) of colorless crystalline **1b**, m.p. 62°C. Although the mixture was protected from light during the reaction, the formation of cadmium metal was observed. – ^{1}H NMR (C_6D_6): δ = 0.77 (t, ^3J = 7.2 Hz, CH_3), 2.43 (q, ^3J = 7.2 Hz, CH_3CH_2), 3.44 (s, CH_2C_{aryl}), 7.09-7.40 (m, $C_{aryl}H$), 7.94 [dd, sat.,^3J = 6.6 Hz, ^4J = 1.3 Hz, ^3J(^{1}H,$^{111/113}$Cd) = 26/19 Hz, C-6*H*]. – ^{13}C NMR (C_6D_6): δ = 10.33 (CH_3), 45.90 (CH_3CH_2), 62.07 [sat., ^3J(^{13}C,^{113}Cd) = 12 Hz, CH_2C_{aryl}], 126.31 (*C*-3), 126.40 (*C*-5), 126.91 (*C*-4), 140.30 [sat.,^2J(^{13}C,^{113}Cd) = 20 Hz, *C*-6], 147.21 (*C*-2), 160.72 (*C*-1). – ^{113}Cd NMR (C_6D_6): δ = −163.10. – MS; *m/z* (%): 439 (3) [M(^{114}Cd)$^+$], 365 (7) [M$^+$ − NEt_2], 274 (8) [$CdC_6H_4NEt_2^+$], 114 (5) [Cd$^+$], and others, as for **1a**. – $C_{22}H_{32}CdN_2$ (436.91): calcd. C 60.48, H 7.38, N 6.41; found C 60.89, H 7.59, N 7.12.

Bis(2-diethylaminomethylphenyl)mercury (**1c**): In a similar way to **1a**, $HgCl_2$ (2.71 g, 10 mmol) and **1** (3.38 g, 20 mmol) yielded 4.37 g (83%) of colorless crystalline **1c**, m.p. 74°C. – ^{1}H NMR (C_6D_6): δ = 1.09 (t, CH_3), 2.69 (q, CH_3CH_2), 3.68 (s, CH_2C_{aryl}), 7.24−7.97 (m, $C_{aryl}H$). – ^{13}C NMR (C_6D_6): δ = 11.21 (CH_3), 46.39 (CH_3CH_2), 61.60 (sat., CH_2C_{aryl}), 126.79 (*C*-3), 127.09 (*C*-5), 129.19 (*C*-4), 138.86 (sat., *C*-6), 148.03 (sat., *C*-2), 171.10 (*C*-1). – MS; *m/z* (%): 526 (6) [M(^{202}Hg)$^+$], 497 (5) [M$^+$ − Et], 453 (2) [M$^+$ − NEt_2], 202 (<1) [Hg$^+$], and others as for **1a**. – $C_{22}H_{32}HgN_2$ (525.10): calcd. C 50.32, H 6.14, N 5.33; found C 50.80, H 6.38, N 5.35.

Bis[2,6-bis(dimethylaminomethyl)phenyl]zinc (**2a**): A solution of 2,6-bis(dimethylaminomethyl)phenyllithium (**2**) (0.23 g, 1.16 mmol) in Et_2O (30 ml) was mixed in portions with $ZnCl_2$ (0.079 g, 0.58 mmol). The mixture was stirred for 12 h and during this time a white precipitate formed. The suspension was chilled and filtered through a fine glass frit. The pale yellow filtrate was stored at −20°C and gave 0.19 g (73%) of colorless crystalline **2a**, m.p. 94°C. – ^{1}H NMR ([D$_8$]THF): δ = 2.16 (s, CH_3), 3.36 (s, CH_2), 6.96−7.27 (m, $C_{aryl}H$). – ^{13}C NMR ([D$_8$]THF): δ = 45.60 (CH_3), 65.00 (CH_2), 128.10 (*C*-3,5), 130.00 (*C*-4), 140.30 (*C*-2,6), 159.10 (*C*-1). – MS; *m/z* (%): 192 (33) [$C_6H_4(CH_2NMe_2)_2^+$], 149 (100) [$C_6H_4(CH_3)CH_2NMe_2^+$], and others. – $C_{24}H_{38}N_4Zn$ (447.99): calcd. C 64.35, H 8.55, N 12.51; found C 64.19, H 8.44, N 12.62.

Bis[2,6-bis(dimethylaminomethyl)phenyl]mercury (**2c**): In a similar way to **2a**, $HgCl_2$ (0.25 g, 0.93 mmol) and **2** (0.37 g, 1.87 mmol) yielded 0.31 g (57%) of colorless fine crystalline **2c**, m.p. 139°C. The mixture was protected from light; although during the reaction, the formation of mercury metal was observed. – ^{1}H NMR ([D$_8$]THF): δ = 2.19 (s, CH_3), 3.41 (CH_2), 7.02-7.18 (m, C$_{aryl}H$). – ^{13}C NMR ([D$_8$]THF): δ = 48.25 (*C*H$_3$), 71.58 [sat., $^3J(^{13}C,^{199}Hg)$ = 40.5 Hz, *C*H$_2$], 129.20 (*C*-3,5), 130.60 (*C*-4), 150.80 (sat., *C*-2,6), 176.00 (sat., *C*-1). – MS; *m/z* (%): 584 (<1) [M(^{202}Hg)$^+$], 202 (1) [Hg$^+$], and others as for **2a**. – $C_{24}H_{38}HgN_4$ (583.19): calcd. C 49.43, H 6.57, N 9.61; found C 49.21, H 6.33, N 9.48.

Bis[2,6-bis(diethylaminomethyl)phenyl]zinc (**3a**): A solution of **3** (1.07 g, 4.2 mmol) in Et_2O (40 ml) was mixed in portions with $ZnCl_2$ (0.29 g, 2.1 mmol). The reaction mixture warmed up slightly. After stirring for 16 h at room temperature the solvent was removed in vacuo. The remaining solid was suspended in *n*-pentane. The mixture was filtered through a fine glass frit, and the filtrate volume was reduced to about 20 ml. Storing at −20°C yielded 0.82 g (70%) of colorless fine crystalline **3a**, m.p. 102°C. – ^{1}H NMR (C_6D_6): δ = 0.85 (t, ^3J = 7.1 Hz, CH_3), 2.63 (q, ^3J = 7.1 Hz, CH$_3$CH_2), 3.74 (s, CH_2C$_{aryl}$), 7.29-7.43 (m, CH_{aryl}). – ^{13}C NMR (C_6D_6): δ = 10.35 (*C*H$_3$), 46.09 (CH$_3$*C*H$_2$), 63.42 (*C*H$_2$C$_{aryl}$), 124.85 (*C*-3,5), 126.68 (*C*-4), 147.54 (*C*-2,6), 158.44 (*C*-1). – MS; *m/z* (%): 558 (15) [M(^{64}Zn)$^+$], 529 (3) [M$^+$ – C_2H_5], 310 (17) [ZnC$_6$H$_3$(CH$_2$NEt$_2$)$_2^+$], 247 (100) [C$_6$H$_3$(CH$_2$NEt$_2$)$_2^+$], and others. – $C_{32}H_{54}N_4Zn$ (560.20): calcd. C 68.61, H 9.72, N 10.00; found C 68.40, H 9.69, N 10.11.

Bis[2,6-bis(diethylaminomethyl)phenyl]cadmium (**3b**): In a similar way to **3a**, $CdCl_2$ (0.21 g, 1.14 mmol) was mixed with **3** (0.58 g, 2.28 mmol) and yielded 0.43 g (62%) of colorless crystals of **3b**, m.p. 137°C. Although the mixture was protected from light during the reaction, the formation of cadmium metal was observed. – ^{1}H NMR (C_6D_6): δ = 0.86 (t, ^3J = 7.2 Hz, CH_3), 2.61 (q, ^3J = 7.1 Hz, CH$_3$CH_2), 3.49 (s, CH_2C$_{aryl}$), 7.08-7.33 (m, C$_{aryl}H$). – ^{13}C NMR (C_6D_6): δ = 10.27 (*C*H$_3$), 45.81 (CH$_3$*C*H$_2$), 63.52 (sat., *C*H$_2$C$_{aryl}$), 124.51 (*C*-3,5), 126.01 (*C*-4), 147.54 (sat., *C*-2,6), 163.69 (*C*-1). – ^{113}Cd NMR (C_6D_6): δ = −182.58. – MS; *m/z* (%): 246 (2) [C$_6$H$_3$(CH$_2$NEt$_2$)$_2^+$ – H], and others as for **3a**. – $C_{32}H_{54}CdN_4$ (607.21): calcd. C 63.30, H 8.96, N 9.23; found C 63.08, H 8.94, N 9.51.

Bis[2,6-bis(diethylaminomethyl)phenyl]mercury (**3c**): In a similar way to **3a**, $HgCl_2$ (0.86 g, 3.17 mmol) and **3** (1.61 g, 6.33 mmol) yielded 1.41 g (64%) of colorless crystals of **3c** which melt below room temperature. – ^{1}H NMR (C_6D_6): δ = 0.92 (t, ^3J = 7.1 Hz, CH_3), 2.58 (q, ^3J = 7.1 Hz, CH$_3$CH_2), 3.70 (s, CH_2C$_{aryl}$), 7.16 (t, ^3J = 7.4 Hz, C-3,5*H*), 7.36 (d, ^3J = 7.2 Hz, C-4*H*). – ^{13}C NMR (C_6D_6): δ = 10.13 (*C*H$_3$), 45.41 (CH$_3$*C*H$_2$), 61.17 [sat., $^3J(^{13}C,^{199}Hg)$ = 42 Hz, *C*H$_2$C$_{aryl}$], 125.57 (*C*-3,5), 126.56 (*C*-4), 146.60 [sat., $^2J(^{13}C,^{199}Hg)$ = 22 Hz, *C*-2,6], 171.74 [sat., $^1J(^{13}C,^{199}Hg)$ = 714 Hz, *C*-1]. – MS; *m/z* (%): 696 (<1) [M(^{202}Hg)$^+$], 623 (2) [M$^+$ – NEt_2], 247 (100) [C$_6$H$_3$(CH$_2$NEt$_2$)$_2^+$], 202 (1) [Hg$^+$], and others as for **3a**. – $C_{32}H_{54}HgN_4$ (695.40): calcd. C 55.27, H 7.83, N 8.06; found C 54.84, H 8.00, N 8.07.

(5,13-Diaza)-5,13-dimethyl-1,9-dizincacyclohexadecane (**4a**): **4** (2.04 g, 16.05 mmol) was dissolved in Et_2O (150 ml) and mixed in portions with $ZnCl_2$ (2.19 g, 16.05 mmol). The reaction mixture warmed up slightly and a white precipitate formed. After stirring at room temperature for 12 h the solvent was removed in vacuo. The remaining solid was suspended in *n*-pentane and filtered through a fine glass frit. The filtrate volume was reduced to about 50 ml. Storing at −20°C yielded 2.15 g (75%) of large colorless crystals of **4a**, m.p. 71°C. – ^{1}H NMR (C_6D_6, *T* = 338 K): δ = 0.32 (t, ^3J = 7.1 Hz, ZnCH_2), 1.85 (quint, ^3J = 6.9/6.6 Hz, CH_2), 1.86 (s, CH_3), 2.23 (t, ^3J = 6.4 Hz, CH_2N). – ^{13}C NMR (C_6D_6): δ = 8.46 (Zn*C*H$_2$), 25.87 (*C*H$_2$), 41.87 (*C*H$_3$), 61.17 (*C*H$_2$N). – MS; *m/z* (%): 177 (6) [1/2 M(^{64}Zn)$^+$], 149 (13) [1/2 M$^+$ – CH_2CH_2], 84 (100) [$C_5H_{10}N^+$], and others. – $C_{14}H_{30}N_2Zn_2$ (357.19): calcd. C 47.08, H 8.47, N 7.84; found C 46.93, H 8.42, N 7.89.

(5,13-Diaza)-5,13-dimethyl-1,9-dicadmacyclohexadecane (**4b**): In a similar way to **4a**, $CdCl_2$ (1.20 g, 6.53 mmol) and **4** (0.83 g, 6.53 mmol) yielded 0.72 g (49%) of colorless fine crystalline **4b**, m.p. 89°C. Although the mixture was protected from light during the reaction, the formation of cadmium metal was observed. – ^{1}H NMR (C_6D_6): δ = 0.67 (t, ^3J = 7.0 Hz, CdCH_2), 1.89 (s, CH_3), 2.01 (quint, ^3J = 6.9/6.6 Hz, CH_2), 2.25 (t, ^3J = 6.5 Hz, CH_2N). – ^{13}C NMR (C_6D_6): δ = 12.14 (Cd*C*H$_2$), 32.56 (*C*H$_2$), 41.93 (*C*H$_3$), 61.89 (*C*H$_2$N). – MS; *m/z* (%): 454 (<1) [M(^{114}Cd)$^+$], 227 (3) [1/2 M(^{114}Cd)$^+$], 114 (3) [Cd$^+$], and others as for **4a**. – $C_{14}H_{30}Cd_2N_2$ (451.21): calcd. C 37.27, H 6.70, N 6.21; found C 37.01, H 6.58, N 6.34.

(5,13-Diaza)-5,13-dimethyl-1,9-dimercuracyclohexadecane (**4c**): In a similar way to **4a**, $HgCl_2$ (0.14 g, 0.51 mmol) and **4** (0.065 g, 0.51 mmol) yielded 0.23 g (72%) of colorless crystalline **4c**, m.p. 97°C. – ^{1}H NMR (C_6D_6): δ = 0.99 (t, ^3J = 6.9 Hz, HgCH_2), 1.91 (s, CH_3), 2.06 (quint, ^3J = 6.9/6.5 Hz, CH_2), 2.25 (t, ^3J = 6.5 Hz, CH_2N). – ^{13}C NMR (C_6D_6): δ = 27.58 (Hg*C*H$_2$), 37.56 (*C*H$_2$), 41.95 (*C*H$_3$), 62.20 (*C*H$_2$N). – MS; *m/z* (%): 627 (<1) [M$^+$], 315 (<1) [1/2 M(^{202}Hg)$^+$], 202 (4) [Hg$^+$], and others as for **4a**. – $C_{14}H_{30}Hg_2N_2$ (627.59): calcd. C 26.79, H 4.82 N, 4.46; found C 26.68, H 4.80, N 4.73.

Bis[3-(N-piperidino)propyl]zinc (**5a**): $ZnCl_2$ (0.43g, 3.19 mmol) was added portionwise to a suspension of **5** (0.85g, 6.38 mmol) in Et_2O (50 ml). The cloudy reaction mixture was stirred at room temperature for 18 h. After removing the solvent and addition of *n*-pentane, the mixture was filtered through a fine glass frit. The pale yellow filtrate was concentrated to a volume of about 30 ml and yielded, after storing at −20°C, 0.77 g (76%) of colorless crystalline **5a**, m.p. 80°C. – ^{1}H NMR (C_6D_6): δ = 0.48 (t. ^3J = 7.1 Hz, ZnCH_2), 1.29 (m, ^3J = 5.5 Hz, ZnCH$_2$CH_2), 1.52 [quint, ^3J = 5.6 Hz, N(CH$_2$CH_2)$_2$CH$_2$], 2.01 [m, ^3J = 6.2 Hz, N(CH$_2$CH$_2$)$_2$CH_2], 2.19 (t, ^3J = 5.6 Hz, CH_2N), 2.27 [t, ^3J = 5.4 Hz, N(CH_2CH$_2$)$_2$CH$_2$]. – ^{13}C NMR (C_6D_6): δ = 8.22 (Zn*C*H$_2$), 24.82 [*C*H$_2$CH$_2$N(CH$_2$*C*H$_2$)$_2$CH$_2$], 25.37 [N(CH$_2$CH$_2$)$_2$*C*H$_2$], 55.05 [N(*C*H$_2$CH$_2$)$_2$CH$_2$], 64.06 (*C*H$_2$N). – MS; *m/z* (%): 316 (<1) [M(^{64}Zn)$^+$], 127 (8) [$C_5H_{10}N(CH_2)_2CH_3^+$], 98 (100) [C$_5$H$_{10}$NCH$_2^+$], and others. – $C_{16}H_{32}N_2Zn$ (317.84): calcd. C 60.46, H 10.15, N 8.81; found C 60.37, H 9.97, N 9.24.

Bis[3-(N-piperidino)propyl]cadmium (**5b**): In a similar way to **5a**, $CdCl_2$ (0.805 g, 4.39 mmol) and **5** (1.17 g, 8.79 mmol) yielded 1.04 g (65%) of large colorless crystals of **5b**, m.p. > 90°C (dec.). – ^{1}H NMR (C_6D_6): δ = 0.59 (t, ^3J = 6.9 Hz, CdCH_2), 1.31 (m, ^3J = 5.1 Hz, CdCH$_2$CH_2), 1.56 [quint, ^3J = 5.6 Hz, N(CH$_2$CH_2)$_2$CH$_2$], 2.04 [m, N(CH$_2$CH$_2$)$_2$CH_2], 2.14-2.19 [m, CH_2N(CH_2CH$_2$)$_2$CH$_2$]. – ^{13}C NMR (C_6D_6): δ = 13.29 [sat., $^1J(^{13}C,^{111/113}Cd)$ = 307/294 Hz, Cd*C*H$_2$], 24.94 [N(CH$_2$CH$_2$)$_2$*C*H$_2$], 25.88 [N(CH$_2$*C*H$_2$)$_2$CH$_2$], 26.31 [sat., $^2J(^{13}C,^{113}Cd)$ = 15.4 Hz, CdCH$_2$*C*H$_2$), 55.38 [N(*C*H$_2$CH$_2$)$_2$CH$_2$], 64.30 [sat., $^3J(^{13}C,^{113}Cd)$ = 14.7 Hz, *C*H$_2$N]. – MS; *m/z* (%): 366 (<1) [M(^{114}Cd)$^+$], 240 (5) [$C_5H_{10}N(CH_2)_3Cd^+$], and others as for **5a**. – $C_{16}H_{32}CdN_2$ (364.85): calcd. C 52.67, H 8.84, N 7.68; found C 53.28, H 8.51, N 8.36.

Bis[3-(N-piperidino)propyl]mercury (**5c**): In a similar way to **5a**, $HgCl_2$ (1.09 g, 4.01 mmol) and **5** (1.07 g, 8.03 mmol) yielded 1.06

g (58%) of colorless crystalline **5c**, which melts below room temperature. Because of the formation of fine mercury metal in the mixture, the reaction time was shortened to 4 h. – ^{1}H NMR (C_6D_6): δ = 1.08 (t, ^3J = 6.7 Hz, $HgCH_2$), 1.34 (m, br., $HgCH_2CH_2$), 1.55 [quint, ^3J = 5.7 Hz, $N(CH_2CH_2)_2CH_2$], 2.12 [m, ^3J = 6.3 Hz, $N(CH_2CH_2)_2CH_2$], 2.21 (t, ^3J = 6.0 Hz, CH_2N), 2.25 [m, br., $N(CH_2CH_2)_2CH_2$]. – ^{13}C NMR (C_6D_6): δ = 25.08 ($HgCH_2$), 26.36 [$N(CH_2CH_2)_2CH_2$], 27.03 [$N(CH_2CH_2)_2CH_2$], 36.72 ($HgCH_2CH_2$), 55.16 [$N(CH_2CH_2)_2CH_2$], 63.36 (NCH_2). – MS; *m/z* (%): 454 (2) [$M(^{202}Hg)^+$], 327 (2) [$C_5H_{10}N(CH_2)_3Hg^+$], 202 (20) [Hg^+], and others as for **5a**. – $C_{16}H_{32}HgN_2$ (453.04): calcd. C 42.42, H 7.12, N 6.18; found C 42.17, H 7.05, N 6.38.

[1] [1a] G. B. Stringfellow, *Organometallic Vapor-Phase Epitaxy: Theory and Practice,* Academic Press, London, **1989**, chapter 6.5. – [1b] U. W. Pohl in *Current Topics in Crystal Growth Research, Research Trends* (Ed.: J. Menon), Trivandrum, India **1995**. – [1c] A. C. Jones, P. O′Brien, *CVD of Compound Semiconductors*, VCH, Weinheim, **1997**.
[2] K.-H. Thiele, *Z. Anorg. Allg. Chem.* **1963**, *325*, 156–168.
[3] G. E. Coates, S. J. Green, *J. Chem. Soc.* **1962**, 3340–3348.
[4] K.-H. Thiele, *Z. Anorg. Allg. Chem.* **1964**, *330*, 8–17.
[5] H. Rau, K.-H. Thiele, *Z. Anorg. Allg. Chem.* **1967**, *355*, 253–264.
[6] J. G. Noltes, J. Boersma, *J. Organomet. Chem.* **1967**, *9,* 1–4.
[7] J. G. Noltes, J. W. G. van den Hurk, *J. Organomet. Chem.* **1964**, *1*, 377–383.
[8] P. O′Brien, J. R. Walsh, A. C. Jones, S. A. Rushworth, *Polyhedron* **1990**, *9,* 1483–1485.
[9] E. Wissing, M. Kaupp, J. Boersma, A. L. Spek, G. van Koten, *Organometallics* **1994**, *13*, 2349–2356.
[10] J. G. Noltes, J. W. G. van den Hurk, *J. Organomet. Chem.* **1965**, *3*, 222–228.
[11] P. O′Brien, M. B. Hursthouse, M. Motevalli, J. R. Walsh, A. C. Jones, *J. Organomet. Chem.* **1993**, *449*, 1–8.
[12] M. Motevalli, P. O′Brien, A. J. Robinson, J. R. Walsh, P. B. Watt, *J. Organomet. Chem.* **1993**, *461,* 5–7.
[13] M. B. Hursthouse, M. Motevalli, P. O′Brien, J. R. Walsh, A. C. Jones, *Organometallics* **1991**, *10*, 3196–3200.
[14] H. K. Hofstee, J. Boersma, J. D. van der Meulen, G. J. M. van der Kerk, *J. Organomet. Chem.* **1978**, *153*, 245–252.
[15] J. Dekker, J. Boersma, L. Fernholt, A. Haaland, A. L. Spek, *Organometallics* **1987**, *6*, 1202–1206.
[16] K.-H. Thiele, E. Langguth, G. E. Müller, *Z. Anorg. Allg. Chem.* **1980**, *462*, 152–158.
[17] J. L. Atwood, D. E. Berry, S. R. Stobart, M. J. Zaworotko, *Inorg. Chem.* **1983**, *22*, 3480–3482.
[18] A. F. M. J. van der Ploeg, C. E. M. van der Kolk, G. van Koten, *J. Organomet. Chem.* **1981**, *212,* 283–290.
[19] O. F. Z. Khan, D. M. Frigo, P. O′Brien, A. Howes, M. B. Hursthouse, *J. Organomet. Chem.* **1987**, *334,* C27–C30.
[20] D. S. C. Black, G. B. Deacon, G. L. Edwards, B. M. Gatehouse, *Aust. J. Chem.* **1993**, *46*, 1323–1336.
[21] L. G. Kuz′mina, Y. T. Struchkov, *Croat. Chem. Acta* **1984**, *57,* 701–724.
[22] W. Wassermann, Ph. D. Thesis, Technical University of Berlin, **1990**.
[23] A. C. Cope, R. N. Gourley, *J. Organomet. Chem.* **1967**, *8*, 527–533.
[24] L. E. Manzer, *J. Organomet. Chem.* **1977**, *135*, C6–C9.
[25] A. Osman, R. G. Steevensz, D. G. Tuck, H. A. Meinema, J. G. Noltes, *Can. J. Chem.* **1984**, *62*, 1698–1700.
[26] G. van Koten, J. T. B. H. Jastrzebski, J. G. Noltes, A. L. Spek, J. C. Schoone, *J. Organomet. Chem.* **1978**, *148*, 233–245.
[27] R. G. Kidd, R. J. Goodfellow in *NMR and the Periodic Table* (Ed.: Harris, Mann), Academic Press, London, **1978**, chapter 8K.
[28] R. J. Goodfellow in *Multinuclear NMR* (Ed.: J. Mason), Plenum Press, New York, **1987**, chapter 21.
[29] T. Fäcke, S. Berger, *J. Organomet. Chem.* **1994**, *471*, 35–38.
[30] J. Vicente, M.-D. Bermudez, F.-J. Carrion, P. G. Jones, *Chem. Ber.* **1996**, *129*, 1395–1399.
[31] C. E. Holloway, M. Melnik, *J. Organomet. Chem.* **1995**, *495*, 1–31.
[32] A. J. Canty, G. B. Deacon, *Inorg. Chim. Acta* **1980**, *45*, L225–L227.
[33] S. Freitag, Ph. D. Thesis, Technical University of Berlin, **1995**.
[34] R. Schlengermann, J. Sieler, S. Jelonek, E. Hey-Hawkins, *Chem. Commun.* **1997**, 197–198.
[35] U. Hartmann, Ph. D. Thesis, Technical University of Berlin, **1989**.
[36] T. Seuß, Ph. D. Thesis, Technical University of Berlin, **1992**.
[37] D. M. Heinekey, S. R. Stobart, *Inorg. Chem.* **1978**, *17*, 1463–1466.
[38] J. Dekker, Ph. D. Thesis, University of Utrecht, **1986**.
[39] M. Westerhausen, M. Wieneke, W. Schwarz, *J. Organomet. Chem.* **1996**, *522*, 137–146.
[40] C. E. Holloway, M. Melnik, *J. Organomet. Chem.* **1996**, *522*, 167–175.
[41] J. Boersma, L. Fernholt, A. Haaland, *Acta Chem. Scand.* **1984**, *A38*, 523–527.
[42] N. Walker, D. Stewart, *Acta Crystallogr.* **1983**, *A39*, 158.
[43] G. M. Sheldrick, SHELXS-86, *Program for Crystal Structure Determination*, Universität Göttingen, Germany, **1986**.
[44] G. M. Sheldrick, SHELXL-93, *Program for Crystal Structure Determination*, Universität Göttingen, Germany, **1993**.
[45] G. M. Sheldrick, SHELX-76, *Program for Structure Determination*, University of Cambridge, UK, **1976**.
[46] L. Zsolnai, H. Pritzkow, *ORTEP-Program for Personal Computer*, Universität Heidelberg, Germany, **1994**.
[47] A. L. Spek, *PLUTON*, University of Utrecht, Holland, **1992**.

[97134]

Synthesis and Structural Characterization of Azatitanacyclobutane Derivatives

Rüdiger Beckhaus*, Martin Wagner, and Ruimin Wang

Institut für Anorganische Chemie der Rheinisch-Westfälischen Technischen Hochschule Aachen,
D-52056 Aachen, Germany

Received August 5, 1997

Keywords: Titanium / Vinylidene complexes / [2+2] Cycloaddition / Metallacycles / Azatitanacyclobutanes / Clathrates

The titanocene vinylidene intermediate [$Cp^*_2Ti{=}C{=}CH_2$] (**9**) reacted with the carbodiimides R−N=C=N−R [R = *p*-$CH_3C_6H_4$ (**19a**), C_6H_{11} (**19b**)] to give the N=C-cycloaddition products [$Cp^*_2Ti\{-NR-C(=NR)-(C=CH_2)-\}$] [(R = *p*-$CH_3C_6H_4$ (**20a**), C_6H_{11} (**20b**)]. The X-ray structure of **20a** in form of a surprisingly stable *n*-hexane clathrate is presented. The azatitanacyclobutane [$Cp^*_2Ti\{-NPh-C(Ph)(H)-(C=CH_2)-\}$] (**22**) was formed from the reaction between **9** and benzylidene aniline [PhN=C(Ph)H (**21**)]. Reactivity studies showed that azatitanacyclobutanes are unreactive upon typical ring-enlargement reactions as observed for other four-membered titanacycles.

Oxatitanacyclobutanes (**1**) and azatitanacyclobutenes (**3**) are under discussion as intermediates in reactions of Ti=CR_2 with carbonyl compounds or nitriles. The high electrophilicity of the metal centre has generally prevented the isolation and characterization of oxa- and azatitanacyclobutenes: spontaneous ring opening reactions afford carbonyl olefination (**1**→**2**), or products of vinylimido intermediates (**3**→**4**).[1] The present paper deals with the formation of azatitanacyclobutane complexes (**5**) prepared by [2+2] cycloaddition of a Ti=C and N=C units.

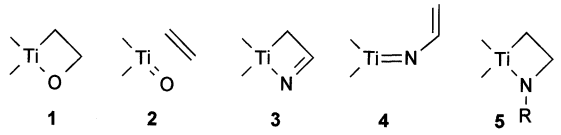

1 **2** **3** **4** **5**

From the thermally generated titana-allene intermediate $Cp^*_2Ti{=}C{=}CH_2$ (**9**), formed by ethane or methane elimination from $Cp^*_2Ti[-CH_2CH_2(C=CH_2)-]$ (**10**) or $Cp^*_2Ti(CH{=}CH_2)(CH_3)$ (**8**), a wide range of four-membered titanacycles (**11**−**18**) can be produced.[2][3][4][5][6][7][8] The high thermal stability of these titanacycles is the major advantage of using **9** instead of titanium methylene intermediates.[2a]

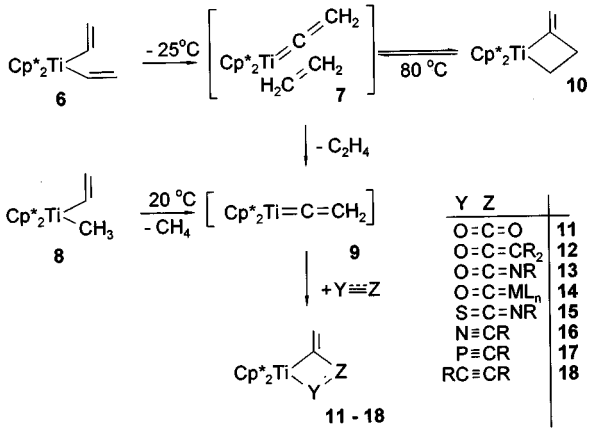

Results and Discussion

The vinylmethyl derivative **8** reacts with one equivalent of the carbodiimide RN=C=NR (R = *p*-$CH_3C_6H_5$ **19a**, R = C_6H_{11} **19b**) at room temperature in *n*-hexane as solvent with evolution of methane to give a dark green solution, from which the azatitanacyclobutane complexes **20** are obtained as green crystals (**20a**) or as a green oil (**20b**). These compounds are formed nearly quantitatively (NMR) and can be isolated in 92% (**20a**) and 88% (**20b**) yield. The mass spectra show the expected molecular peaks. For **20b**, a cycloreversion with formation of **9** can be detected from the fragmentation pattern, whereas for **20a**, the liberation of a C_5Me_5 ligand is the main fragmentation step, indicating a higher stability of the azatitanacyclobutane unit.

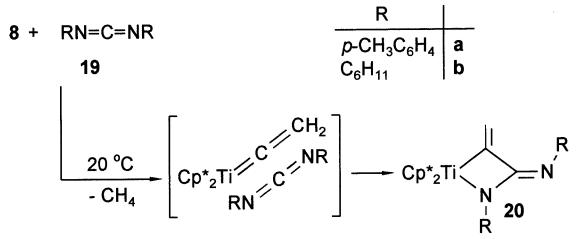

The two chemical shift signals in the ^{1}H-NMR spectra for the protons of the *exo*-methylene group in **20** (**20a** δ = 4.13, 5.87; **20b** δ = 4.52, 6.32) appear to be a distinguishing feature of the new complexes and similar metallacycles. In addition, the chemical shifts of the ring carbon atoms in the ^{13}C-NMR spectra are in accordance with a σ titanium-bonded sp^2 carbon atom (**20a** δ = 202.5; **20b** δ = 202.0). The eight ring proton signals of the two *p*-tolyl substituents in **20a** are detectable upon cooling to −80°C [ring A: (C11−C16, assignment according to Figure 1) δ = 4.63 (d, 1 H), 9.81 (d, 1 H), 6.68 (d, 1 H), 7.10 (d, 1 H); ring B: (C21−C26) 7.26 (m, 4 H)]. The low field shift of one proton signal in ring A (δ = 9.81) is attributed to a hydrogen bridge between the N2 and the H atom at C12, as concluded from

 © WILEY-VCH Verlag GmbH, D-69451 Weinheim, 1998 1434−1948/98/0202−0253 $ 17.50+.50/0

comparison of δ values in NH compounds.[9] Indeed, in the X-ray structure the distance C12−N2 (2.875 Å) was found to be short. The rotation of ring A is probably blocked in solution at lower temperatures, as indicated by ^{13}C NMR: three *ortho* C signals (δ = 120.1, 121.6, 123.3) of the two aromatic rings are detectable, whereas at room temperature, only two ortho carbon resonances (δ = 121.6, 122.1) are present. Surprisingly, only six of the eight expected protons are detectable at room temperature [δ = 7.09 (m, 4 H), 6.85 (d, 2 H)], similar to the observation of other *N*-phenyl ligands in samarium complexes.[10]

The structure of **20a** was confirmed by X-ray structure determination. The PLATON plot[11a] is shown in Figure 1, and relevant bond lengths and angles are given in Table 1. The azatitanacyclobutane is obtained as a surprisingly stable clathrate $2[Cp^*_2Ti\{-N(p\text{-}CH_3C_6H_4)C(=N-p\text{-}CH_3C_6H_4)(C=CH_2)-\}] \cdot n\text{-}C_6H_{14}$. It crystallizes in space group $P\bar{1}$ with complex molecules in general position (2*i*) and *n*-hexane on the crystallographic inversion centers (1*e*) (s. Figure 2). The atoms of the aliphatic chain exhibit small displacement parameters, and all hydrogen atoms of the *n*-hexane molecule could be located in a Fourier difference synthesis. Bond length and angles are in good agreement with a previous report.[11c] The cocrystallization of the *n*-hexane molecule illustrates in an excellent manner the highly organophilic character of permethylated metallocene complexes of the type $Cp^*_2TiX_2$.

Figure 1. PLATON drawing[11a] of 2 $[Cp^*_2Ti\{-N(p\text{-}CH_3C_6H_4)C(=N-p\text{-}CH_3C_6H_4)C(=CH_2)-\}\cdot n\text{-}C_6H_{14}]$ (**20a** · 0.5 C_6H_{14}) (30% ellipsoids) (two titanocene molecules and one molecule *n*-hexane are present in the unit cell)

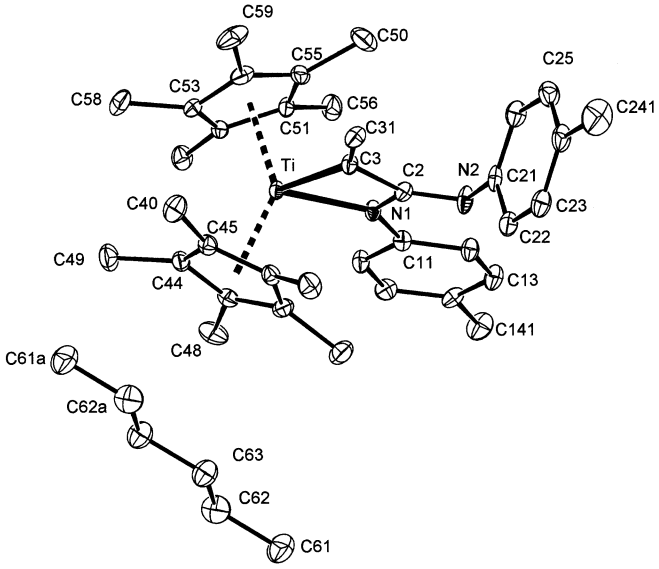

The azatitanacyclobutane ring is planar. The *p*-tolyl ring A (C11−C16) is localized in the plane of the four-membered ring, whereas ring B (C21−C26) is orientated perpendicular to the equatorial plane. The sum of the angles at N1 is approximately 358°, which means that the nitrogen ring atom must be sp^2 hybridized with the lone pair located in a vacant p-orbital perpendicular to the ring plane.

Figure 2. SCHAKAL drawing[11b] of molecular packing of 2 $[Cp^*_2Ti\{-N(p\text{-}CH_3C_6H_4)C(=N-p\text{-}CH_3C_6H_4)C(=CH_2)-\}\cdot C_6H_{14}]$ (**20a**· 0.5 C_6H_{14}) view on *ab*-plane; hydrogen atoms of **20a** omitted, hexane molecules shaded

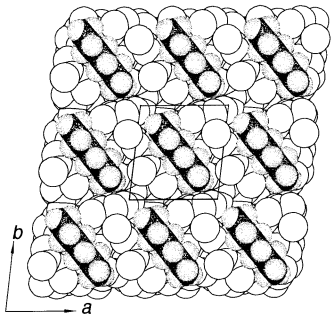

Compared to the azatitanacyclobutene **16** (R = *t*Bu) the Ti−N1 distance in **20a** was found to be significantly longer, resulting from the hybridization of the nitrogen atom. In contrast with **16**, in **20** a pϕ−dϕ interaction is no longer possible, due to the perpendicular orientation of the lone pair at the titanium-bonded nitrogen to the Cp^*_2Ti-acceptor orbitals in **20**.[12] This behaviour is in accordance with the general observation that reactivity of bent titanocene complexes is determined by the electron-deficient character of the metal centre, in combination with the orientation of the acceptor orbitals in the equatorial plane of the metallocene fragment.[13] The N1−C2 distance in **20** is in accordance with a N−C single bond, as expected.[12] To summarize, the structural data suggest that the reactivity of **20a** should differ from that of **16**. The short C3−C2 distance in **16** [1.485(3) Å] indicates a stronger C−C bond than that found in **20a** [1.505(4) Å]. Electrocyclic ring-opening reactions are indeed observed for **16**, whereas cycloreversion reactions are expected for azametallacyclobutanes, and are observed in the mass spectrometric fragmentation behaviour of **20b**, and the dynamic properties of other azametallacyclobutanes derived from $[Cp_2Zr{=}NR]$[15] or $[(tBu_3SiO)_2Ti{=}NR]$[16] intermediates and olefins.

Table 1. Selected bond lenghts [Å] and angles [deg] in 2 $[Cp^*_2Ti\{-N(p\text{-}CH_3C_6H_4)C(=N-p\text{-}CH_3C_6H_4)C(=CH_2)-\}\cdot n\ C_6H_{14}]$ (**20a**·0.5 *n* C_6H_{14}) and the azatitanacyclobutene $[Cp^*_2TiN{=}C(tBu)C{=}CH_2]$ (**16**)[6], assignment according the figure

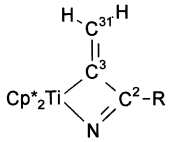

distances [Å]			angles [°]		
	20a	**16**		**20a**	**16.00**
Ti−C3	2.129(3)	2.134(2)	C3−Ti−N1	65.8(1)	67.8(1)
Ti−N1	2.084(2)	2.017(2)	Ti−N1−C2	97.4(2)	94.5(1)
Ti−C2	2.64	2.48	Ti−C3−C31	140.6(2)	145.4(2)
N1−C2	1.374(4)	1.290(3)	Ti−N1−C11	135.5(2)	−
C2−N2	1.287(4)	−	C11−N1−C2	124.6(3)	−
C2−C3	1.505(4)	1.485(3)	N1−C2−C3	105.1(2)	113.2(2)
C3−C31	1.329(4)	1.337(3)	C2−C3−Ti	91.5(2)	84.4(1)

When **8** reacts with *N*-benzylidene aniline, the azatitanacyclobutane derivative **22** is formed by cycloaddition of **9** with **21**. Compound **22** was isolated in 30% yield as thermally stable (mp 158°C, dec.) red crystals. The expected molecular peak is found in the mass spectrum, and fragmentation occurs mainly with formation of a $Cp^*_2Ti{=}NR$ fragment (40.7%). Attempts to use this reactivity pattern for preparative purposes, e. g. in reaction with acetone, have until now been unsuccessful.

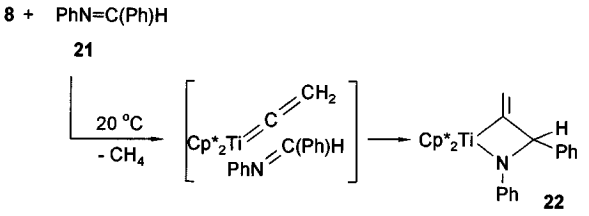

Proton transfer reactions leading to azavinylidene derivatives $Cp^*_2Ti(N{=}CPh_2)CH{=}CH_2$ occur when Schiff bases with nitrogen bearing an acidic hydrogen atom are used.[17] In the case of *N*-benzylidenemethylamine, the fulvene complex $Cp^*(\eta^5{:}\eta^1\text{-}C_5Me_4CH_2)TiCH{=}CH_2$ is formed instead of the metallacyclic cycloaddition product.

To compare the reactivity of **20** to that of the other four-membered titanacycles **10**−**18**, different reactions were carried out. With isonitriles, a fast and selective insertion into the Ti−C σ-bond is observed for **10**[18] and **18**[7a] (Ti−C bond opposite to the *exo*-CH_2 group) as well as for the oxetanes **11**−**14**,[8a][19]. The azatitanacyclobutanes **20** are however inert to ring enlargements with small molecules (RNC, R = *t*Bu, C_6H_{11}). Especially fast reactions take place between **16** and nitriles to form six-membered rings.[6] However, in the case of **20** no reactions are detectable. These reactions are summarized in Scheme 1. The azatitanacyclobutane **20** also appears to be inert in the presence of protic agents (PhC≡CH, PhOH, MeOH). Only with HCl/Et_2O the formation of $Cp^*_2TiCl_2$ is observed.

Scheme 1. Ring enlargement reactions of small titanacycles

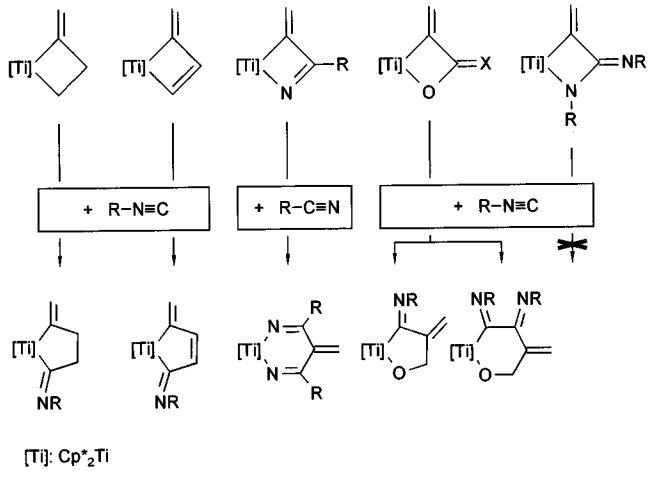

This work was supported by the *Deutsche Forschungsgemeinschaft* and the *Fonds der Chemischen Industrie.*

Experimental Section

General: The preparation and handling of compounds were performed with rigorous exclusion of air and moisture under a nitrogen atmosphere, using a standard vacuum line and Schlenk techniques. All solvents were dried with the appropriate drying agents and distilled under a nitrogen atmosphere. Deuterated solvents were degassed by freeze-pump-thaw cycles and dried over molecular sieves (3 or 4 Å) prior to use. − ^{1}H- and ^{13}C-NMR spectra were recorded on a Varian Unity 500 spectrometer. Chemical shifts are reported in ppm with reference to residual protons in deuterated solvents ([D_6]benzene, δ = 7.15 for ^{1}H-NMR spectroscopy; [D_6]benzene, δ = 127.96 for ^{13}C-NMR spectroscopy). − Mass spectroscopic analyses were performed on a Finnigan MAT 95 mass spectrometer. − Infrared spectra were recorded as KBr pellets on a Perkin−Elmer 1720X FT-IR spectrometer. − Elemental analyses were carried out at the Analytische Laboratorien in Lindlar, Germany. − The titanocene complex $[Cp^*_2Ti(CH{=}CH_2)CH_3]$ (**8**) was prepared by literature procedures.[4] The Schiff bases were purchased from Aldrich.

Preparation of **20a**: To a solution of **8** (200 mg, 0.55 mmol) in 30 ml of *n*-hexane was added di-*p*-tolylcarbodiimide (**19a**) (0.12 g, 0.55 mmol) at −20°C. The mixture was stirred and warmed to 25°C over 4 h, forming a dark green solution, from which **20a** precipitates. Recrystallization from *n*-hexane at −20°C, yields **20a** as dark green crystals (210 mg, 67%) − mp 150−153°C (dec.) − ^{1}H NMR (C_7D_8, 500 MHz, −80°C): δ = 1.56 [s, 30 H, $C_5(CH_3)_5$], 2.19 (s, 3 H, CH_3), 2.32 (s, 3 H, CH_3), 4.06 (s, 1 H, =CH*H*), 5.79 (s, 1 H, =C*H*H), 4.63 (d, 1 H, *J* = 7.9 Hz), 6.68 (d, 1 H, *J* = 7.6 Hz), 7.10 (d, 1 H, *J* = 7.3 Hz), 7.26 (m, 4 H), 9.81 (d, 1 H, *J* = 7.9 Hz). − ^{1}H NMR (C_7D_8, 500 MHz, 25°C): δ = 1.68 [s, 30 H, $C_5(CH_3)_5$], 2.19 (s, 3 H, CH_3), 2.30 (s, 3 H, CH_3), 4.08 (s, 1 H, = CH*H*), 5.76 (s, 1 H, =C*H*H), 6.85 (d, 2 H, *J* = 6.4 Hz), 7.09 (m, 4 H). − ^{13}C{^{1}H} NMR (C_7D_8, 125 MHz, −80°C) δ = 12.7 [$C_5(CH_3)_5$], 21.2 (CH_3), 21.2 (CH_3), 118.7 (=CH_2), 120.1, 121.6, 123.3, 128.6, 128.7, 130.2, 146.0, 152.1 (Ph, 2 signals hidden), 140.5 (N-C=N). 201.5 (TiC), 125.4 [$C_5(CH_3)_5$]. − ^{13}C{^{1}H} NMR (C_7D_8, 125 MHz, 25°C) δ = 12.7 [$C_5(CH_3)_5$], 21.0 (CH_3), 21.1 (CH_3), 118.4 (=CH_2), 121.6, 122.1, 128.3, 128.4, 129.9, 146.1, 151.8 (Ph, 1 signal hidden), 140.3 (N-C=N), 202.5 (TiC), 125.7 [$C_5(CH_3)_5$]. − IR (KBr): $\tilde{\nu}$ = 2909 (m), 2854 (m), 1608 (w), 1590 (w), 1541 (s), 1504 (s), 1497 (s), 1453 (m), 1434 (m), 1335 (s), 1303 (s), 819 (s) cm^{-1}. − EI-MS (70 eV) *m/e* (*I*rel) 566 (57) [M^+], 459 (19), 461 (2), 432 (60), 384 (19), 318 (26). − $C_{37}H_{46}N_2Ti$ (566.67): calcd. C 78.42, H 8.18, N 4.94; found C 78.69, H 8.10, N 4.89.

Preparation of **20b**: To a solution of **8** (200 mg, 0.55 mmol) in 30 ml of *n*-hexane was added dicyclohexylcarbodiimid (**19b**) (110 mg, 0.55 mmol) at −20°C. The mixture was stirred and warmed to 25°C over 12 h. The solvent was removed to dryness, yielding **20b** as a dark green oil. (220 mg, 73%) − ^{1}H NMR (300 MHz, C_6D_6) δ = 0.88−2.14 (m, 20 H, C_6H_{11}), 1.75 [s, 30 H, $C_5(CH_3)_5$], 4.04 (tt, J_{HH} = 4.0 and 5.4 Hz, 1 H, N−CH), 4.44 (tt, J_{HH} = 3.4 and 11.4 Hz, 1 H, N−CH), 4.52 (s, 1 H, =CH_2), 6.32 (s, 1 H, = CH_2). − ^{13}C NMR (C_6D_6, 75 MHz): δ = 12.7 [$C_5(CH_3)_5$], 25.9, 26.9, 27.3, 27.5, 33.6, 37.7, 55.7, 56.2 (C_6H_{11}), 112.0 (=CH_2), 124.3 [$C_5(CH_3)_5$], 139.6 (N−*C*=N), 202.0 (Ti−C). − EI-MS (70 eV) *m/e* (%): 550 (10) [M^+], 453 (5) [M^+ − N − C_6H_{11}], 416 (14) [M^+ + H − $C_5(CH_3)_5$], 344 (91) [M^+ − $C_{13}H_{22}N_2$], 318 (100) [M^+ − $C_{15}H_{24}N_2$]. − $C_{35}H_{54}N_2Ti$ (550.8): calcd. C 76.32, H 9.90, N 5,09; found C 73.65, H 10.22, N 5.09.

Preparation of **22**: To a solution of **8** (300 mg, 0.83 mmol) in 30 ml of *n*-hexane was added N-benzylideneaniline (**21**) (150 mg) at −20°C. The mixture was stirred and warmed to 25°C over 12 h.

After filtration, the solvent was concentrated to 50%. After cooling to −78°C **22** was formed as red crystals (130 mg, 30%): − mp 158°C, dec. − ^{1}H NMR (300 MHz, C_6D_6, TMS): δ = 1.67, 1.80 [each 15 H, $C_5(CH_3)_5$], 3.89 (1 H, C*H*Ph), 4.69 (d, 1 H, =CH_2, *J* = 3.0 Hz); 6.05 (d, 1 H, =CH_2, *J* = 2.4 Hz); 5.84, 6.15, 6.58, 6.86 (each 1 H, PhH); 7.09, 7.26, 7.37 (each 2 H, PhH). − $^{13}C\{^1H\}$ NMR (75 MHz, C_6D_6, TMS): δ = 12.7, 13.0 [$C_5(CH_3)_5$]; 47.9 (CHPh); 107.7 (=CH_2); 114.8, 116.5, 118.7 (arom. C); 123.9, 124.2 [$C_5(CH_3)_5$]; 125.8, 128.2, 129.1 (arom. C); 139.2 (C−*C*ipso); 154.1 (N−Cipso); 217.8 (Ti−C). MS: *m/z* (%): 525.5 (9.5) [M^+], 343.3 (5.8) [$M^+ - C_{13}H_{12}N$], 318.2 (9.1) [$M^+ - C_{15}H_{13}N$], 274.3 (40.7) [$M^+ - C_{19}H_{23}$], 115.0 (100). − $C_{35}H_{43}NTi$ (525.67): C 79.96, H 8.26, N 2.67; found: C 79.58, H 8.17, N 2.70.

Structure Determination and Refinement of **20a**: Geometry and intensity data were collected on a ENRAF-Nonius CAD4 diffractometer with graphite-monochromated Mo-K_α radiation. Crystal data, data collection parameters, and convergence results are compiled in Table 2. After Lorentz and polarization corrections, an empirical absorption correction based on azimuthal scans[20] was applied, before averaging symmetry related intensity data. **20a** was crystallized from *n*-hexane in the composition 2 [Cp*$_2$Ti{−N(*p*-$CH_3C_6H_4$)−C(=N−*p*-$CH_3C_6H_4$)−C(=CH_2)−}]·*n*-C_6H_{14}. The structure was solved by direct methods,[21] refined with the SDP program system.[22] In the final refinement cycles, hydrogen atoms were included in riding geometry with fixed isotropic displacement parameters [d_{C-H} = 0.98 Å, U_{iso}(H) = 1.30 U_{eq}(C)]. Further details of the crystal structure investigations are available on request from the Cambridge Crystallographic Data Centre, on quoting the depository number CCDC-100571.

Table 2. Crystal data, data collection parameters, and convergence results of **20a**

Formula	$C_{40}H_{53}N_2Ti$	*Data collection*	
Formula weight	609.78	Wavelength λ [Å]	0.71073
Crystal size [mm^3]	0.28×0.32×0.36	Temperature [K]	203
Space group (no)	$P\bar{1}$(2)	Scan range θ [°]	3.0−26.0
		Scan type	ω-2θ
Crystal data		Absorption correction (min./max)	empirical (0.851/0.996)
a [Å]	9.756(5)	Reflection measured	12085
b [Å]	10.445(1)	Independent reflections	6709
c [Å]	17.604(2)		
α [deg]	79.57(1)	*Refinement results*	
β [deg]	79.53(2)	Obeserved reflections	4453, $I>1.0\sigma(I)$
γ [deg]	81.14(2)	Variables refined	388
V (Å^3)	1721(1)	*R*, R_W[a]	0.059, 0.061
Z	2	*GOF*	1.339
μ [cm^{-1}]	2.73	Max. residual electron density [eÅ^{-3}]	0.547
*D*calc [gcm^{-3}]	1.177		

[a] $R = \Sigma||F_o| - |F_c||/\Sigma|F_o|$; $R_W = [\Sigma w(|F_o| - |F_c|)^2/\Sigma w|F_o|^2]^{1/2}$; $w^{-1} = \sigma^2(F_o)$; GOF = $[\Sigma w(|F_o| - |F_c|)^2/n_{obs} - n_{var}]^{1/2}$; n_{obs}: no of observations; n_{var}: no of varibales refined.

[1] Review: [1a] R. Beckhaus, *Angew. Chem.* **1997**, *109*, 694; *Angew. Chem. Int. Ed. Engl.* **1997**, *36*, 686. − Carbonylolefination **1**→**2**: [1b] R. H. Grubbs, R. H. Pine, *Alkene Metathesis and Related Reactions* in *Comprehensive Organic Synthesis* (Ed.: B. M. Trost), Pergamon, New York, **1991**, vol. 5, chapter 9.3, p. 1115. − [1c] S. H. Pine, *Carbonyl Methylenation and Alkylidation using Titanium-Based Reagents* in *Organic Reactions* (Ed.: L. A. Paquette), John Wiley & Sons, **1993**, vol. 43, p. 1. − [1d] N. A. Petasis, S.-P. Lu, *Tetrahedron Lett.* **1995**, *36*, 2393. − [1e] D. L. Hughes, J. F. Payack, D. Cai, T. R. Verhoeven, P. J. Reider, *Organometallics* **1996**, *15*, 663. − vinylimido derivatives **3**→**4**: [1f] K. M. Doxsee, L. C. Garner, J. J. J. Juliette, J. K. M. Mouser, T. J. R. Weakley, *Tetrahedron* **1995**, *51*, 4321. − [1g] K. M. Doxsee, J. J. J. Juliette, K. Zientara, G. Nieckarz, *J. Am. Chem. Soc.* **1994**, *116*, 2147. − [1h] K. M. Doxsee, J. K. M. Mouser, J. B. Farahi, *Synlett* **1992**, 13. − [1i] K. M. Doxsee, J. B. Farahi, H. Hope, *J. Am. Chem. Soc.* **1991**, *113*, 8889. − [1j] K. M. Doxsee, J. B. Farahi, *J. Chem. Soc., Chem. Commun.* **1990**, 1452. − [1k] K. M. Doxsee, J. B. Farahi, *J. Am. Chem. Soc.* **1988**, *110*, 7239.

[2] **10**[2a][2b], **11**−**13**[3a][3b], **14**[4], **15**[5], **16**, **17**[6], **18**[7a][7b] − [2a] R. Beckhaus, S. Flatau, S. I. Troyanov, P. Hofmann, *Chem. Ber.* **1992**, *125*, 291. − [2b] R. Beckhaus, *Alkenyl-, Allyl- and Dienyl-Complexes of main Group Elements and Transition Metals* in *Synthetic Methods of Inorganic and Organometallic Chemistry* (Ed.: W. A. Herrmann), Georg-Thieme-Verlag, Stuttgart, in print, **1997**.

[3] [3a] R. Beckhaus, I. Strauß, T. Wagner, P. Kiprof, *Angew. Chem.* **1993**, *105*, 281; *Angew. Chem. Int. Ed. Engl.* **1993**, *32*, 264. − [3b] R. Beckhaus, I. Strauß, T. Wagner, *Z. Anorg. Allg. Chem.* **1997**, *623*, 654.

[4] R. Beckhaus, J. Oster, T. Wagner, *Chem. Ber.* **1994**, *127*, 1003.

[5] R. Beckhaus, J. Sang, T. Wagner, U. Böhme, *J. Chem. Soc., Dalton Trans.* **1997**, 2249.

[6] R. Beckhaus, I. Strauß, T. Wagner, *Angew. Chem.* **1995**, *107*, 738; *Angew. Chem. Int. Ed. Engl.* **1995**, *34*, 688.

[7] [7a] R. Beckhaus, J. Sang, T. Wagner, B. Ganter, *Organometallics* **1996**, *15*, 1176. − [7b] R. Beckhaus, J. Sang, U. Englert, U. Böhme, *Organometallics* **1996**, *15*, 4731.

[8] [8a] R. Beckhaus, J. Oster, J. Sang, I. Strauß, M. Wagner, *Synlett* **1997**, 241. − [8b] R. Beckhaus, *J. Chem. Soc., Dalton Trans.* **1997**, 1991.

[9] M. Hesse, H. Meier, B. Zeeh, *Spektroskopische Methoden in der organischen Chemie*, Georg Thieme Verlag, Stuttgart, New York, **1987**, 3. ed.

[10] W. J. Evans, D. K. Drummond, L. R. Chamberlain, R. J. Doedens, S. G. Bott, H. Zhang, J. L. Atwood, *J. Am. Chem. Soc.* **1988**, *110*, 4983.

[11] [11a] A. L. Spek, *Acta Crystallo.* **1990**, *A46*, C34. − [11b] Keller, E.; Schakal 88, Program for the Graphical Representation of Crystallographie and Melcular Models, University of Freiburg, Germany, **1988**. − [11c] M. Müller, T. Wagner, U. Englert, P. Paetzold, *Chem. Ber.* **1995**, *128*, 1.

[12] F. H. Allen, O. Kennrad, D. G. Watson, L. Brammer, A. G. Orpen, R. Taylor, *J. Chem. Soc., Perkin Trans. 2* **1987**, S1-S19.

[13] Differences in Ti−N bond distances, depending on the orbital orientation are illustrated in Cp*$_2$TiNR^{1}R^2 complexes: if there is no steric hindrance, the substituents on the nitrogen atom R^1 = R^2 = H[14a], R^1 = H , R^2 = Me[14b] will be rotated out of the equatorial plane of the Cp*$_2$Ti fragment to maximise dπ−pπ overlapping and short Ti−N distances are found [1.944(2) A, 1.955(2) A]. In the case of larger substituents R^1 = Me, R^2 = Ph the R groups are now located in the equatoraial plane, and consequently dπ-pπ-interaction is no longer possible so that longer Ti−N distances are found [2.054(2) A].[14c] − R. Beckhaus, *Titanocenes* in *Metallocenes* (Eds.: R. L. Halterman, A. Togni), VCH , Weinheim, **1997**.

[14] [14a] E. Brady, W. Lukens, J. Telford, G. Mitchell, *Acta Crystallo.* **1994**, *C51*, 558. − [14b] Lukens Jr., W. W., M. R. Smith III, R. A. Andersen, *J. Am. Chem. Soc.* **1996**, *118*, 1719. − [14c] J. Feldman, J. C. Calabrese, *J. Chem. Soc., Chem. Commun.* **1991**, 1042.

[15] P. J. Walsh, F. J. Hollander, R. G. Bergman, *Organometallics* **1993**, *12*, 3705.

[16] J. L. Bennett, P. T. Wolczanski, *J. Am. Chem. Soc.* **1994**, *116*, 2179.

[17] R. Beckhaus, M. Wagner, R. Wang, *Z. Anorg. Allg. Chem.*, in print.

[18] R. Beckhaus, C. Zimmermann, T. Wagner, E. Herdtweck, *J. Organomet. Chem.* **1993**, *460*, 181.

[19] R. Beckhaus, J. Oster, *Z. Anorg. Allg. Chem.* **1995**, *621*, 359.

[20] A. C. T. North, D. C. Phillips, F. S. Mathews, *Acta Cryst.* **1968**, *A24*, 351.

[21] G. M. Sheldrick, *SHELXS86, Programm for Structure Solutions*, University of Göttingen, **1986**.

[22] ENRAF-Nonius, *SDP Version 5.0*, Delft, The Netherlands, **1989**.

[97186]

Chemistry of 2*H*-Azaphosphirene Complexes, 8[◇]

Synthesis and Spectroscopic Data of *para*-Substituted (3-Phenyl-2*H*-azaphosphirene)tungsten Complexes☆

Rainer Streubel*, Annette Ostrowski, Siegfried Priemer, Udo Rohde, Jörg Jeske, and Peter G. Jones

Institut für Anorganische und Analytische Chemie der Technischen Universität Braunschweig,
Postfach 3329, D-38023, Braunschweig, Germany
Fax: (internat.) +49(0)531/391-5387
E-mail: r.streubel@tu-bs.de

Received September 8, 1997

Keywords: Phosphorus heterocycles / 2*H*-Azaphosphirene complexes / Carbene complexes / Tungsten / Cyclizations

High-yield synthesis of *para*-substituted pentacarbonyl(3-phenyl-2*H*-azaphosphirene)tungsten complexes is reported, using a multi-step rearrangement reaction. Spectroscopic and mass-spectrometric data of these heterocyclic complexes are discussed; the ^{31}P-NMR-chemical shifts clearly reflect the electronic influence of the *para*-phenyl substituents and the correlation with Hammett σ^{p}-constants is almost linear.

2*H*-azirenes and their heterocyclic analogs (**I**), containing a ring system with a C=N moiety and a further heteroatom, are of current theoretical and synthetic interest.[2] The latter heterocycles are expected to suffer from destabilizing effects due to interaction of the lone pair(s) of the E fragment with the π electrons of the C=N double bond. Such is the case with 1*H*-diazirenes (E = NR)[3] and 1*H*-thiazirenes (E = S).[4] The former rearranges, if it is transiently formed, even at low temperatures to give 3*H*-diazirenes[5] or ring-expanded products[6] and the latter yields nitrile sulfides[7] (**II**: E = S, Scheme 1). Recently, a marked increase in stability of a 1-phosphonio-substituted 1*H*-diazirene derivative was observed[8] and a negative hyperconjugation was proposed to explain this phenomenon.[8][9] Interestingly, neither 2*H*-azaphosphirenes nor 1*H*-oxazirenes exist, even in matrices at low temperatures. The latter have been subjected to a theoretical study, in which an asymmetric bonding of the oxygen with respect to the geometric center of the imine bond was predicted, thus minimizing the electronic destabilization.[10] The former has only been mentioned as plausible intermediate.[11] Because of the relationship of the isolobal fragments RP and S, 2*H*-azaphosphirenes should be of particular interest. Moreover, to the best of our knowledge as yet uninvestigated is the influence of coordinating such heteroazirenes and their acyclic zwitterionic isomers, the 1,3-dipoles, to a metal-complex fragment via the "apical"- (**III**) and "terminal"-bonded atom E (**IV**, E = O, S, NR, PR; Scheme 1).

Recently, we reported the first synthesis of coordinated 2*H*-azaphosphirenes (**III**: E = PR), which was also the first access to heteroazirene complexes in general. We explained the product formation by a multi-step rearrangement reaction of transiently formed metal carbene complexes involving metallaheterobutadienes (**V**), which are isomeric to **III**, as key intermediates.[12] Even more recently, we obtained the first evidence for a nitrilium phosphane ylide complex (**IV**: E = PR). The transient formation of such a complex was achieved by thermal ring opening of a 2*H*-azaphosphirene complex.[13]

Scheme 1. Unsaturated three-membered heterocycles containing nitrogen and a second heteroatom and their zwitterionic acyclic isomers, the 1,3-dipoles (propargylic resonance structure). − **I**, **II**: E = CR_2, NR, PR, O, S. − R, R′ = alkyl, aryl. − **III**, **IV**, **V**: E = NR, PR, O, S. − R, R′ = alkyl, aryl. − [M] = metal complex fragment

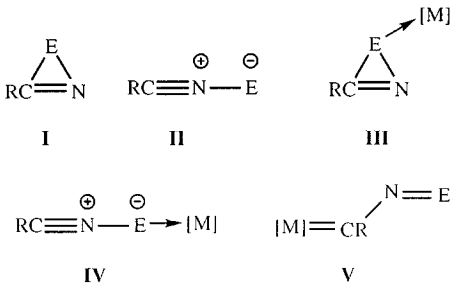

In order to exploit this synthetic route to 2*H*-azaphosphirene complexes and to study the rearrangement cascade, we have now reacted a variety of *para*-phenyl-substituted (aminocarbene)tungsten complexes **1a**−**c**, **d**,[14] **e**−**h** with [bis(trimethylsilyl)methylene]chlorophosphane (**2**)[15] in the presence of triethylamine (Scheme 2). The reaction proceeded smoothly to the (2*H*-azaphosphirene)tungsten complexes **3a**−**h**, and, as in our first approach, we observed neither long-lived intermediates nor side products. Complexes **3a**−**g** were obtained in good yields, after low-temperature column chromatography, whereas complex **3h** showed some decomposition upon chromatography.

[◇] Part 7: See ref.[1].

 © WILEY-VCH Verlag GmbH, D-69451 Weinheim, 1998 1434−1948/98/0202−0257 $ 17.50+.50/0

Scheme 2. Synthesis of (2*H*-azaphosphirene)tungsten complexes **3a−h**

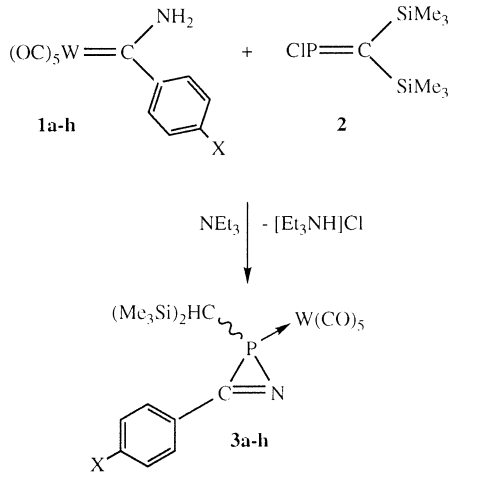

X	1a,3a	1b,3b	1c,3c	1d,3d	1e,3e	1f,3f	1g,3g	1h,3h
	CF_3	Br	Cl	H	F	Me	OMe	NMe_2

With respect to the ring formation reaction, all carbene complexes employed in this study behave approximately equivalently. Nevertheless, longer reaction times were observed for **3e−h**, which bear more electron-releasing *para* substituents. Doubling the reaction time led to the formation of small amounts of [{$(Me_3Si)_2HCP(H)Cl$}$W(CO)_5$]. This product resulted, at least formally, from the ring-cleavage reaction of the (2*H*-azaphosphirene)tungsten complexes **3a−h** with triethylammonium chloride. This has been verified for complex **3d**, which was treated in pure form with triethylammonium chloride under similar reaction conditions.[16]

From the spectroscopic data of these complexes, the phosphorus and carbon nuclear magnetic resonances are the most significant. The phosphorus and carbon resonances as well as the phosphorus-tungsten coupling constants clearly reflect the electronic influence of the *para* substituent of the phenyl group on the three-membered ring. Moreover, the correlation of $\delta^{31}P$ with the Hammett σ^p-constants[17] (Table 1) is almost linear. This should be useful for extrapolations of ^{31}P-NMR chemical-shift values of unknown (2*H*-azaphosphirene)tungsten complexes. EI mass-spectrometric experiments have shown that the (2*H*-azaphosphirene)tungsten complexes **3a−h** undergo predominantly ring cleavage subsequent to the ionization process, yielding aryl nitriles and the terminal (phosphanediyl)-tungsten complex radical cation.

The molecular structure of complex **3d** was confirmed by X-ray crystallography (Figure 1).[18] One very characteristic feature is the three-membered ring with a short C−N distance [1.272(7) Å] and a very acute endocyclic angle at the phosphorus atom [41.9(2)°]. The observation that the endocyclic P−C and P−N bond lengths of **3d** are similar [1.759(5) and 1.795(4) Å], is remarkable. This becomes even more obvious, if the structural data of **3d** are compared to

Table 1. ^{13}C- and ^{31}P-NMR data of the ring atoms of the 2*H*-azaphosphirene ringsystem of **3a−h** (in $CDCl_3$, [*] in C_6D_6) and Hammett σ^p-constants

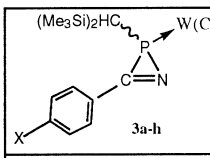		$\delta^{31}P$ [ppm]	$^1J_{W,P}$ [Hz]	$\delta^{13}C$ [ppm]	σ^p
X = CF_3	**3a**	- 102.0	297.5	193.1	0.54
Br	**3b**	- 105.2	296.8	192.2	0.23
Cl	**3c**	- 105.4	296.1	192.0	0.23
H	**3d**	- 108.8	294.7	192.3	0.00
F[*]	**3e**	- 109.1	295.6	190.8	0.06
Me	**3f**	- 111.2	293.1	191.4	-0.17
OMe	**3g**	- 115.1	292.5	190.2	-0.27
NMe_2	**3h**	- 117.6	291.5	187.8	-0.83

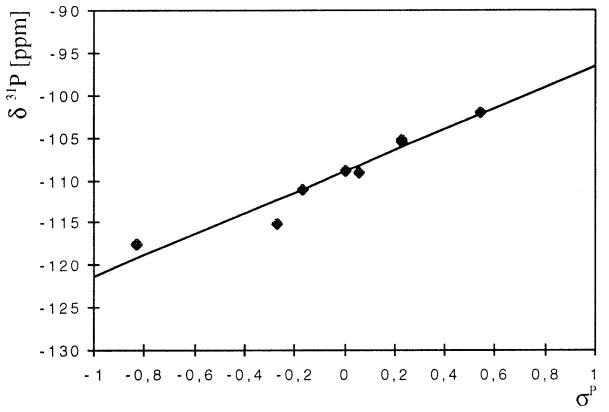

Figure 1. Molecular structure of **3d** in the crystal (ellipsoids represent 50-% probability levels, hydrogen atoms are omitted for clarity)[a]

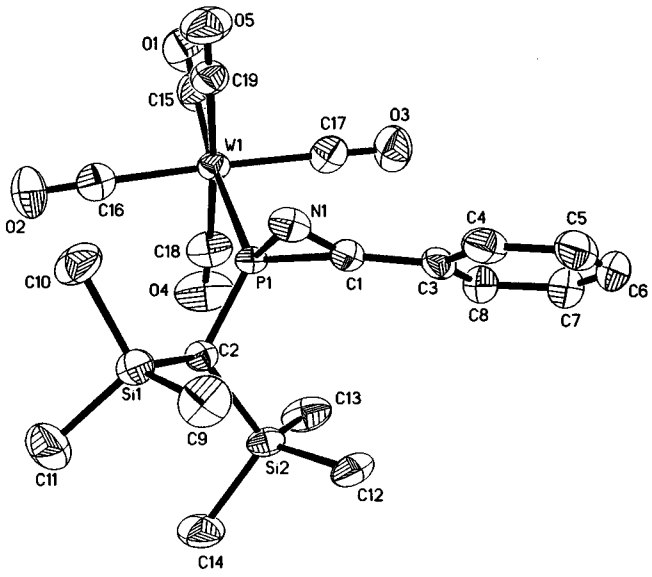

[a] Selected bond lengths [Å] and angles [°]: P(1)−C(1) 1.759(5), P(1)−C(2) 1.808(5), P(1)−N(1) 1.795(4), W(1)−P(1) 2.470(2), N(1)−C(1) 1.272(7), C(19−C(3) 1.457(7); C(2)−P(1)−W(1) 1.243(2), C(1)−P(1)−N(1) 41.9(2), N(1)−C(1)−P(1) 70.6(3), C(1)−N(1)−P(1) 67.5(3), N(1)−C(1)−C(3) 134.2(5)

those of a related (azaphosphiridine)tungsten complex[19] in which the bond lengths of the saturated three-membered P−C−N ring were determined to P−C 1.835(4), C−N 1.478(5) and P−N 1.728(3) Å. As in the molecular structure of **3g**,[12] **3d** reveals a coplanar arrangement of the two ring moieties (interplanar angle 2°), thus enabling an effective p_π-p_π-electron interaction.

Support by the *Deutsche Forschungsgemeinschaft* and the *Fonds der Chemischen Industrie* is gratefully acknowledged.

Experimental Section

General: All operations were carried out under deoxygenated dry nitrogen as inert gas, solvents were dried according to standard procedures. − NMR spectra were recorded on a Bruker AC-200 spectrometer (200 MHz for ^{1}H; 50.3 MHz for ^{13}C; 188.3 MHz for ^{19}F; 81 MHz for ^{31}P) using [D$_6$]chloroform and [D$_6$]benzene as solvent and internal standard; shifts are given relative to tetramethylsilane (^{1}H,^{13}C), $CFCl_3$ (^{19}F), and 85% H_3PO_4 (^{31}P). − MS: Finnigan Mat 8430 (70 eV). − Elemental analyses: Carlo Erba analytical gaschromatograph. − IR: Biorad FT-IR 165.

General Procedure for the Preparation of {[Amino(aryl)carbene]pentacarbonyltungsten} Complexes: The ethoxy(aryl)carbenetungsten complexes were prepared according to ref.[20] and reacted, without purification, with ammonia. A gentle flow of ammonia was bubbled through a solution of 5 mmol of the ethoxy(aryl)carbenetungsten complexes in 60 ml of diethyl ether until a yellow color persisted and thin-layer liquid chromatography (SiO_2) indicated that all starting material had reacted. All volatile compounds were removed under reduced pressure (0.1 mbar) and the yellow residue was washed twice with a little pentane and subsequently dried in vacuo or, if necessary, purified by column chromatography.

[{Amino(4-trifluoromethylphenyl)carbene}pentacarbonyltungsten(0)] (**1a**): 2.1 g of **1a** (84%) was obtained as a yellow powder after low-temperature chromatography (SiO_2, −10°C; hexane/diethyl ether 10:1). M.p. 106°C (decomp.). − IR (KBr): $\tilde{\nu}$ = 3441 (w) cm^{-1}, 3343 (w), 3288 (w) (NH), 2067 (s), 1963 (m), 1947 (vs), 1893 (vs), 1878 (s) (CO). − ^{1}H NMR ($CDCl_3$): δ = 7.31 (d, $^2J_{HH}$ = 7.38 Hz, 2 H, Ar-*H*), 7.70 (d, $^2J_{HH}$ = 7.38 Hz, 2 H, Ar-*H*), 8.66 (br, 2 H, N*H*$_2$). − ^{13}C{^{1}H} NMR ($CDCl_3$): δ = 122.7 (s, *o*-*C*), 123.7 (q,$^1J_{CF}$ = 272.2 Hz, *C*F$_3$), 127.8 (q,$^3J_{CF}$ = 4.0 Hz, *m*-*C*), 131.3 (q, $^2J_{CF}$ = 32.9 Hz, *p*-*C*), 156.1 (s, *i*-*C*), 197.7 (s, $^1J_{CW}$ = 127.1 Hz, *cis*-*C*O), 203.4 (s, $^1J_{CW}$ = 125.6 Hz, *trans*-*C*O), 266.6 (d, $^1J_{CW}$ = 89.1 Hz, W=*C*R$_2$). − ^{19}F{^{1}H} NMR: δ = −63.2 (s, C*F*$_3$). − MS (70 eV, ^{184}W); *m*/*z* (%): 497 (26) [M$^+$], 469 (22) [M$^+$− CO], 413 (22) [M$^+$− 3 CO], 385 (28) [M$^+$− 4 CO], 357 (100) [M$^+$− 5 CO]. − $C_{13}H_6F_3NO_5W$ (497.0): calcd. C 31.39, H 1.21, N 2.82; found C 31.38, H 1.25, N 2.75.

[{Amino(4-bromophenyl)carbene}pentacarbonyltungsten(0)] (**1b**): 2.4 g of **1b** (93%) was obtained as a yellow orange powder. M.p. 135°C (decomp.). − IR (KBr): $\tilde{\nu}$ = 3425 (w) cm^{-1}, 3342 (w), 3284 (w) (NH), 2064 (s), 1982 (s), 1930 (vs), 1904 (vs), 1882 (s) (CO). − ^{1}H NMR ($CDCl_3$): δ = 7.14 (d, $^2J_{HH}$ = 8.53 Hz, 2 H, Ar-*H*), 7.56 (d, $^2J_{HH}$ = 8.53 Hz, 2 H, Ar-*H*), 8.63 (br, 2 H, N*H*$_2$). − ^{13}C{^{1}H} NMR ($CDCl_3$): δ = 124.5 (s, *p*-*C*), 124.8 (s, *o*-*C*), 131.9 (s, *m*-*C*), 151.6 (s, *i*-*C*), 198.0 (s, $^1J_{CW}$ = 127.6 Hz, *cis*-*C*O), 203.2 (d, $^1J_{CW}$ = 125.3, *trans*-*C*O), 265.2 (s, $^1J_{CW}$ = 89.4 Hz, W=*C*R$_2$). − MS (70 eV, ^{81}Br, ^{184}W); *m*/*z* (%): 509 (20) [M$^+$], 481 (24) [M$^+$− CO], 425 (68) [M$^+$− 3 CO], 296 (34) [W(CO)$_4^+$], 268 (100) [W(CO)$_3^+$]. − $C_{12}H_6BrNO_5W$ (507.8): calcd. 508.8946; found 508.8946 ± 2 ppm.

[{Amino(4-chlorophenyl)carbene}pentacarbonyltungsten(0)] (**1c**): 1.9 g of **1c** (84%) was obtained as a yellow powder after low-temperature chromatography (SiO_2, −10°C; hexane/diethyl ether 10:1). M.p. 116°C (decomp.). − IR (KBr): $\tilde{\nu}$ = 3447 (w) cm^{-1}, 3329 (w), 3271 (w) (NH), 2060 (s), 1983 (s), 1975 (s), 1898 (s) (CO). − ^{1}H NMR ($CDCl_3$): δ = 7.22 (d, $^3J_{HH}$ = 8.50 Hz, 2 H, Ar-*H*), 7.41 (d, $^3J_{HH}$ = 8.50 Hz, 2 H, Ar-*H*), 8.59 (br, 2 H, N*H*$_2$). − ^{13}C{^{1}H} NMR ($CDCl_3$): δ = 124.7 (s, *m*/*o*-*C*), 124.8 (s, m/*o*-*C*), 129.0 (s, *m*-*C*), 131.4 (s, *p*-*C*), 151.0 (s, *i*-*C*), 197.9 (s, *cis*-*C*O), 203.3 (s, *trans*-*C*O), 265.4 (s, W=*C*R$_2$). − MS (70 eV, ^{35}Cl, ^{184}W); *m*/*z* (%): 463 (36) [M$^+$], 435 (32) [M$^+$− CO], 379 (100) [M$^+$− 3 CO], 351 (40) [M$^+$− 4 CO], 323 (80) [M$^+$− 5 CO], 139 (39) [M$^+$− W(CO)$_5^+$]. − $C_{12}H_6ClNO_5W$ (463.0): calcd. C 31.07, H 1.30, N 3.02; found C 31.31, H 1.45, N 3.00.

[{Amino(phenyl)carbene}pentacarbonyltungsten(0)][10] (**1d**): 1.9 g of **1d** (90%) was obtained as a yellow powder. M.p. 83°C (decomp.). − IR (KBr): $\tilde{\nu}$ = 3441 (w) cm^{-1}, 3342 (w), 3288 (w) (NH), 2067 (s), 1963 (m), 1947 (vs), 1893 (vs), 1878 (m) (CO). − ^{1}H NMR ($CDCl_3$): δ = 7.31 (mc, 2 H, m-Ar-*H*), 7.41 (mc, 3 H, *o*-, *p*-Ar-*H*), 8.56 (br, 2 H, N*H*$_2$). − ^{13}C{^{1}H} NMR ($CDCl_3$): δ = 123.3 (s, *m*-*C*), 128.7 (s, *o*-*C*), 130.3 (s, *p*-C), 152.8 (s, *i*-*C*), 198.2 (s, $^1J_{CW}$ = 126.6 Hz, *cis*-*C*O), 202.4 (s, $^1J_{CW}$ = 126.6 Hz, *trans*-*C*O), 266.4 (d, $^1J_{CW}$ = 89.3 Hz, W=*C*R$_2$). − MS (70 eV, ^{184}W); *m*/*z* (%): 429 (32) [M$^+$], 401 (39) [M$^+$− CO], 345 (100) [M$^+$− 3 CO]. − $C_{12}H_7NO_5W$ (429.0): calcd. C 33.59, H 1.64, N 3.26; found C 33.54, H 1.65, N 3.15.

[{Amino(4-fluorophenyl)carbene}pentacarbonyltungsten(0)] (**1e**): 2.0 g of **1e** (90%) was obtained as a yellow powder. M.p. 147°C. - IR (KBr): $\tilde{\nu}$ = 3438 (m) cm^{-1}, 3331 (m), 3271 (m) (NH), 2064 (s), 1968 (s), 1949 (s), 1910 (s), 1881 (s) (CO). − ^{1}H NMR ($CDCl_3$): δ = 7.15 (m$_c$, 2 H, *o*-C), 7.36 (m$_c$, 2 H, *m*-C), 8.66 (s, br, 2 H, NH_2). − ^{13}C{^{1}H} NMR ($CDCl_3$): δ = 115.5 (d, $^2J_{CF}$ = 21.9 Hz, *m*-*C*), 125.8 (d, $^3J_{CF}$ = 8.8 Hz, *o*-*C*), 148.7 (s, *i*-*C*), 163.6 (d, $^1J_{CF}$ = 250.9 Hz, *p*-*C*), 198.0 (s, $^1J_{CW}$ = 127.1 Hz, *cis*-*C*O), 203.2 (s, *trans*-*C*O), 263.6 (s, W=*C*R$_2$). − ^{19}F{^{1}H} NMR ($CDCl_3$): δ = −110.2 (s). − MS (70 eV, ^{184}W); *m*/*z* (%): 447 (43) [M$^+$], 419 (31) [M$^+$− CO], 363 (100) [M$^+$− 3 CO]. − $C_{12}H_6FNO_5W$ (447.0): calcd. C 32.24, H 1.35, N 3.13; found C 32.05, H 1.34, N 3.05.

[{Amino(4-methylphenyl)carbene}pentacarbonyltungsten(0)] (**1f**): 1.7 g of **1f** (75%) was obtained as a yellow powder. M.p. 79°C (decomp.). − IR (KBr): $\tilde{\nu}$ = 3440 (w) cm^{-1}, 3327 (w), 3270 (w) (NH), 2067 (s), 1982 (m), 1934 (vs), 1908 (vs), 1884 (vs) (CO). − ^{1}H NMR ($CDCl_3$): δ = 2.39 (s, 3 H, Me), 7.24 (mc, 5 H, Ar-*H*), 8.55 (br, 2 H, N*H*$_2$). − ^{13}C{^{1}H} NMR ($CDCl_3$): δ = 21.3 (s, Me), 124.1 (s, *m*-*C*), 129.4 (s, *o*-*C*), 141.2 (s, *p*-*C*), 149.8 (s, *i*-*C*), 198.3 (s, $^1J_{CW}$ = 126.6 Hz, *cis*-*C*O), 202.4 (s, *trans*-*C*O), 264.8 (s, W=*C*R$_2$). − MS (70 eV, ^{184}W); *m*/*z* (%): 443 (32) [M$^+$], 415 (38) [M$^+$− CO], 359 (100) [M$^+$− 3 CO]. − $C_{13}H_9NO_5W$ (443.1): calcd. C 35.24, H 2.05, N 3.16; found C 35.43, H 2.00, N 3.19.

[{Amino(4-methoxyphenyl)carbene}pentacarbonyltungsten(0)] (**1g**): 1.6 g of **1g** (68%) was obtained as a yellow powder. M.p. 85°C (decomp.). − IR (KBr): $\tilde{\nu}$ = 3440 (m) cm^{-1}, 3327 (w), 3270 (m) (NH), 2067 (s), 1982 (m), 1934 (vs), 1908 (vs), 1884 (vs) (CO). − ^{1}H NMR ($CDCl_3$): δ = 3.86 (s, 3 H, OMe), 6.95 (m$_c$, 2 H, Ar-*H*), 7.41 (m$_c$, 2 H, Ar-*H*), 8.56 (br, 2 H, N*H*$_2$). − ^{13}C{^{1}H} NMR ($CDCl_3$): δ = 55.7 (s, OMe), 113.0 (s, *m*-*C*), 132.5 (s, *o*-*C*), 142.7 (s, *p*-*C*), 150.6 (s, *i*-*C*), 198.1 (s, *cis*-*C*O), 203.8 (s, *trans*-*C*O), 264.0 (s, W=*C*R$_2$). − MS (70 eV, ^{184}W); *m*/*z* (%): 459 (26) [M$^+$], 431 (36) [M$^+$− CO], 375 (100) [M$^+$− 3 CO]. − $C_{13}H_9NO_6W$ (459.1): calcd. C 33.59, H 1.64, N 3.26; found C 33.54, H 1.65, N 3.15.

[{Amino(4-dimethylaminophenyl)carbene}pentacarbonyltungsten(0)] (**1h**): 1.4 g of **1h** (58%) was obtained as a

yellow powder after low-temperature chromatography (SiO_2, −10°C; hexane/diethyl ether, 2:1). M.p. 135°C (decomp.). − IR (KBr): $\tilde{\nu}$ = 3459 (w) cm^{-1}, 3340 (w), 3261 (w) (NH), 2059 (s), 1966 (m), 1923 (vs), 1893 (vs), 1878 (m) (CO). − ^1H NMR ($CDCl_3$): δ = 3.06 [s, 6 H, N(CH_3)$_2$], 6.68 (d, $^2J_{HH}$ = 9.06 Hz, 2 H, Ar-*H*), 7.51 (d, $^2J_{HH}$ = 9.06 Hz, 2 H, Ar-*H*), 8.01 (s, br, 1 H, N*H*), 8.49 (s, br, 1 H, N*H*). − $^{13}C\{^1H\}$ NMR ($CDCl_3$): δ = 40.1 [s, N(CH_3)$_2$], 110.7 (s, Ph), 129.2 (s, Ph), 137.2 (s, Ph), 152.0 (s, *i-C*), 199.0 (s, $^1J_{CW}$ = 127.0 Hz, *cis-C*O), 203.3 (s, $^1J_{CW}$ = 126.9 Hz, *trans-C*O), 254.9 (d, $^1J_{CW}$ = 89.4 Hz, W=*C*R$_2$). − MS (70 eV, ^{184}W); *m/z* (%): 472 (22) [M^+], 444 (36) [M^+ − CO], 388 (66) [M^+ − 3 CO], 360 (44) [M^+ − 4 CO], 332 (40) [M^+ − 5 CO], 240 (100) [$W(CO)_2^+$]. − $C_{14}H_{12}N_2O_5W$ (472.1): calcd. 472.0256; found 472.0256 ± 2 ppm.

General Procedure for the Preparation of Pentacarbonyl(2H-azaphosphirene)tungsten Complexes: To a solution of 1.5 mmol of amino(aryl)carbenetungsten complexes **1a−h** in 15 ml of diethyl ether 0.34 g (1.5 mmol) of **2** and 5 ml of NEt_3 was added at 0°C. The reaction mixture was stirred at ambient temp. until **2** was consumed (^{31}P-NMR control). The yellow-orange reaction mixture was evaporated to dryness under reduced pressure (0.1 mbar). The residue was extracted with 30 ml of pentane and filtered. The filtration residue was washed twice with 5 ml of pentane, the organic phases combined and the solvent removed under reduced pressure. The residue was purified, if necessary, by low-temperature column chromatography on silica gel.

[{2-Bis(trimethylsilyl)methyl-3-(4-trifluoromethylphenyl)-2H-azaphosphirene-κP}pentacarbonyltungsten(0)] (**3a**): After 24 hours stirring, 0.64 g of **3a** (62%) was obtained as a yellow powder, m.p. 112−114°C (decomp.). − IR (KBr): $\tilde{\nu}$ = 2077 (m) cm^{-1}, 1977 (m, br), 1977 (s), 1949 (vs), 1931 (s), 1923 (vs), 1909 (s) (CO), 1616 (w) (CN). − ^1H NMR ($CDCl_3$): δ = 0.11 (s, 9 H, $SiMe_3$), 0.31 (s, 9 H, $SiMe_3$), 0.73 (d, $^2J_{HP}$ = 3.18 Hz, 1 H, PC*H*), 7.90 (d, $^3J_{HH}$ = 8.22 Hz, 2 H, Ar-*H*), 8.14 (d, $^3J_{HH}$ = 8.22 Hz, 2 H, Ar-*H*). − $^{13}C\{^1H\}$ NMR ($CDCl_3$): δ = 1.4 (d, $^3J_{CP}$ = 3.4 Hz, $SiMe_3$), 2.1 (d, $^3J_{CP}$ = 3.0 Hz, $SiMe_3$), 27.8 (d, $^1J_{CP}$ = 23.9 Hz, P*C*H), 123.4 (q, $^1J_{CF}$ = 273.1 Hz, *C*F$_3$), 126.8 (q, $^3J_{CF}$ = 11.1 Hz, *m-C*) 129.6 (s, *o-C*), 129.9 (d, $^2J_{CP}$ = 14.3 Hz, *i-C*), 135.4 (q, $^2J_{CF}$ = 33.0 Hz, *p-C*), 193.1 (d, Σ J_{PC} = 1.5 Hz, P*C*N), 195.7 (d, $^1J_{CW}$ = 126.3 Hz, $^2J_{CP}$ = 8.7 Hz, *cis-C*O), 197.4 (d, $^2J_{CP}$ = 37.0 Hz, *trans-C*O). − $^{31}P\{^1H\}$ NMR ($CDCl_3$): δ = −102.0 (s, $^1J_{PW}$ = 297.5 Hz). − $^{19}F\{^1H\}$ NMR ($CDCl_3$): δ = −63.7 (s, CF_3). − MS (70 eV, ^{184}W); *m/z* (%): 685 (0.5) [M^+], 514 (28) [$(OC)_5WPCH(SiMe_3)_2^+$], 486 (100) [$(OC)_4WPCH(SiMe_3)_2^+$], 458 (30) [$(OC)_3WPCH(SiMe_3)_2^+$], 430 (41) [$(OC)_2WPCH(SiMe_3)_2^+$], 402 (32) [$(OC)WPCH(SiMe_3)_2^+$], 374 (30) [$WPCH(SiMe_3)_2^+$], 171 (44) [$(CF_3C_6H_4)CN^+$], 73 (77) [$SiMe_3^+$]. − $C_{20}H_{23}F_3NO_5PSi_2W$ (685.4): calcd. C 35.04, H 3.36, N 2.04; found C 34.74, H 3.43, N 1.95.

[{2-Bis(trimethylsilyl)methyl-3-(4-bromophenyl)-2H-azaphosphirene-κP}pentacarbonyltungsten(0)] (**3b**): After 26 hours stirring and purifying by low-temperature chromatography (SiO_2, −10°C; hexane/diethyl ether 50:1) 0.53 g of **3b** (51%) was obtained as a yellow powder, m.p. 117°C. − IR (KBr): $\tilde{\nu}$ = 2075 (m) cm^{-1}, 1946 (m), 1946 (vs), 1930 (s), 1919 (vs), 1907 (m) (CO), 1582 (CN). − ^1H NMR ($CDCl_3$): δ = 0.10 (s, 9 H, $SiMe_3$), 0.29 (s, 9 H, $SiMe_3$), 0.68 (d, $^2J_{HP}$ = 3.10 Hz, 1 H, PC*H*), 7.77 (d, $^3J_{HH}$ = 8.57 Hz, 2 H, Ar-*H*), 7.87 (d, $^3J_{HH}$ = 8.57 Hz, 2 H, Ar-*H*). − $^{13}C\{^1H\}$ NMR ($CDCl_3$): δ = 1.4 (d, $^3J_{CP}$ = 3.4 Hz, $SiMe_3$), 2.1 (d, $^3J_{CP}$ = 3.2 Hz, $SiMe_3$), 27.7 (d, $^1J_{CP}$ = 24.0 Hz, P*C*H), 125.5 (d, $^2J_{CP}$ = 15.1 Hz, *i-C*), 129.3 (s, *o-C*), 130.6 (s, *p-C*), 133.2 (s, *m-C*), 192.2 (d, Σ J_{PC} = 1.9 Hz, P*C*N), 195.7 (d, $^1J_{CW}$ = 125.6 Hz, $^2J_{CP}$ = 8.7 Hz, *cis-C*O), 197.5 (d, $^2J_{CP}$ = 36.7 Hz, *trans-C*O). − $^{31}P\{^1H\}$ NMR ($CDCl_3$): δ = −105.2 (s, $^1J_{PW}$ = 296.8 Hz). − MS (70 eV, ^{81}Br, ^{184}W); *m/z* (%): 697 (0.5) [M^+], 514 (28) [$(OC)_5WPCH(SiMe_3)_2^+$], 486 (100) [$(OC)_4WPCH(SiMe_3)_2^+$], 458 (40) [$(OC)_3WPCH(SiMe_3)_2^+$], 430 (44) [$(OC)_2WPCH(SiMe_3)_2^+$], 402 (30) [$(OC)WPCH(SiMe_3)_2^+$], 374 (36) [$WPCH(SiMe_3)_2^+$], 181 (46) [$(^{79}BrC_6H_4)CN^+$], 102 (42) [$(C_6H_4)CN^+$], 73 (81) [$SiMe_3^+$]. − $C_{19}H_{23}BrNO_5PSi_2W$ (696.3): calcd. C 32.81, H 3.31, N 2.01; found C 33.29, H 3.54, N 2.04.

[{2-Bis(trimethylsilyl)methyl-3-(4-chlorophenyl)-2H-azaphosphirene-κP}pentacarbonyltungsten(0)] (**3c**): After 21 hours stirring, 0.65 g of **3c** (66%) was obtained as a yellow powder, m.p. 108°C. − IR (KBr): $\tilde{\nu}$ = 2073 (s) cm $^{-1}$, 1985 (s), 1967 (vs), 1938 (vs), 1918 (vs) (CO), 1618 (CN). − ^1H NMR ($CDCl_3$): δ = 0.07 (s, 9 H, $SiMe_3$), 0.26 (s, 9 H, $SiMe_3$), 0.65 (d, $^2J_{HP}$ = 3.1 Hz, 1 H, PC*H*), 7.58 (d, 2 H, $^3J_{HH}$ = 8.53 Hz, *o*-C*H*), 7.74 (d, 2 H, $^3J_{HH}$ = 8.53 Hz, *m*-C*H*). − $^{13}C\{^1H\}$ NMR ($CDCl_3$): δ = 1.4 (d, $^3J_{CP}$ = 3.0 Hz, $SiMe_3$), 2.1 (d, $^3J_{CP}$ = 3.3 Hz, $SiMe_3$), 27.7 (d, $^1J_{CP}$ = 24.2 Hz, P*C*H), 125.1 (d, $^2J_{CP}$ = 15.1 Hz, *i-C*), 130.2, 130.6 (s, *m-C*, *o-C*), 140.6 (d, *p-C*), 192.0 (d, Σ J_{CP} = 2.0 Hz, P*C*N), 195.7 (d, $^2J_{CP}$ = 8.9 Hz, *cis-C*O), 197.6 (d, $^2J_{CP}$ = 36.6 Hz, *trans-C*O). − $^{31}P\{^1H\}$ NMR ($CDCl_3$): δ = −105.4 (s, $^1J_{PW}$ = 296.1 Hz). − MS (CI, *iso*-C_4H_9, pos., $^{35}Cl^{184}W$); *m/z* (%): 652 (16) [M+H$^+$], 515 (12) [M+H$^+$ − ClC_6H_4CN], 193 (100) [$H_3PCH(SiMe_3)_2^+$]. − $C_{19}H_{23}ClNO_5PSi_2W$ (651.8): calcd. C 35.01, H 3.56, N 2.15; found C 34.92, H 3.46, N 2.25.

[{2-Bis(trimethylsilyl)methyl-3-phenyl-2H-azaphosphirene-κP}pentacarbonyltungsten(0)] (**3d**): After 26 hours stirring 0.68 g of **3d** (73%) was obtained as a yellow powder, m.p. 109−110°C (decomp.). − IR (hexane): $\tilde{\nu}$ = 2076 (s) cm^{-1}, 1989 (s), 1957-1941 (vs, br), 1925 (sh) (CO), 1619 (vw) (CN). − IR (KBr): $\tilde{\nu}$ = 2072 (s) cm^{-1}, 1987 (m), 1967 (s), 1938 (vs), 1922 (vs) (CO), 1619 (vw) (CN). − ^1H NMR ($CDCl_3$): δ = 0.11 (s, 9 H, $SiMe_3$), 0.30 (s, 9 H, $SiMe_3$), 0.68 (d, $^2J_{HP}$ = 2.9 Hz, 1 H, PC*H*), 7.00 (m_c, 3 H, Ar-*H*), 8.03 (m_c, 2 H, Ar-*H*). − $^{13}C\{^1H\}$ NMR ($CDCl_3$): δ = 1.3 (d, $^3J_{CP}$ = 3.3 Hz, $SiMe_3$), 2.1 (d, $^3J_{CP}$ = 3.1 Hz, $SiMe_3$), 27.6 (d, $^1J_{CP}$ = 24.0 Hz, P*C*H), 126.6 (d, $^2J_{CP}$ = 14.9 Hz, *i-C*), 129.5 (s, *m-C*), 129.7 (s, *o-C*), 134.1 (s, *p-C*), 192.3 (d, Σ J_{PC} = 1.3 Hz, P*C*N), 195.9 (d, $^1J_{CW}$ = 125.8 Hz, $^2J_{CP}$ = 8.8 Hz, *cis-C*O), 197.7 (d, $^2J_{CP}$ = 36.4 Hz, *trans-C*O). − $^{31}P\{^1H\}$ NMR ($CDCl_3$): δ = −108.8 (s, $^1J_{PW}$ = 294.7 Hz). − MS (70 eV, ^{184}W); *m/z* (%): 617 (1) [M^+], 514 (30) [M^+ − PhCN], 486 (100) [M^+ − PhCN − CO], 103 (52) [$PhCN^+$], 73 (80) [$SiMe_3^+$]. − $C_{19}H_{24}NO_5PSi_2W$ (617.4): calcd. C 36.96, H 3.93, N 2.27; found C 36.74, H 3.88, N 2.23.

[{2-Bis(trimethylsilyl)methyl-3-(4-fluorophenyl)-2H-azaphosphirene-κP}pentacarbonyltungsten(0)] (**3e**): After 20 hours stirring 0.68 g of **3e** (71%) was obtained as a yellow powder, m.p. 115°C. − IR (KBr): $\tilde{\nu}$ = 2074 (s) cm $^{-1}$, 1988 (s), 1974 (s), 1938 (s), 1917 (s) (CO), 1598 (CN). − ^1H NMR (C_6D_6): δ = 0.01 (s, 9 H, $SiMe_3$), 0.26 (s, 9 H, $SiMe_3$), 0.68 (d, $^2J_{HP}$ = 3 Hz, 1 H, PC*H*), 6.63 (m_c, 2 H, *o*-C*H*), 7.74 (m_c, 2 H, *m*-C*H*). − $^{13}C\{^1H\}$ NMR (C_6D_6): δ = 1.2 (d, $^3J_{CP}$ = 3.1 Hz, $SiMe_3$), 2.1 (d, $^3J_{CP}$ = 3 Hz, $SiMe_3$), 27.7 (d, $^1J_{CP}$ = 24 Hz, P*C*H), 117.2 (d, $^2J_{CF}$ = 22.5 Hz, *m-C*), 123.1 (dd, $^2J_{CP}$ = 15 Hz, $^4J_{CF}$ = 2.6 Hz, *i-C*), 132 (d, $^3J_{CF}$ = 9.3 Hz, *o-C*), 166.2 (d, $^1J_{CF}$ = 256.5 Hz, *p-C*), 190.8 (d, Σ J_{CP} = 1.7 Hz, P*C*N), 196.3 (d, $^1J_{CW}$ = 135.2 Hz, $^2J_{CP}$ = 8.8 Hz, *cis-C*O), 197.8 (dd, $^1J_{CW}$ = 146.6 Hz, $^2J_{CP}$ = 36 Hz, *trans-C*O). − $^{31}P\{^1H\}$ NMR (C_6D_6): δ = −109.1 (s, $^1J_{PW}$ = 296.1 Hz). − $^{19}F\{^1H\}$ NMR (C_6D_6): δ = −102.6 (s). − MS (CI, NH_3, pos., ^{184}W); *m/z* (%): 636 (100) [M^+], 515 (18) [M^+ − FC_6H_4CN]. − $C_{19}H_{23}FNO_5PSi_2W$ (635.4): calcd. C 35.92, H 3.65, N 2.2; found C 35.93, H 3.59, N 2.12.

[{2-Bis(trimethylsilyl)methyl-3-(4-methylphenyl)-2H-azaphosphirene-κP}pentacarbonyltungsten(0)] (**3f**): Stirring for 48 hours

afforded 0.46 g of **3f** (49%) as a yellow powder, m.p. 104−105°C (decomp.). − For ^{1}H-, ^{13}C- and ^{31}P-NMR data see ref.[8] − MS (CI, isobutane, pos., ^{184}W); *m/z* (%): 632 (6) [(M+H)$^+$·], 604 (5) [(M$^+$ − CO)·], 515 (10) [(M+H)$^+$ − C_8H_7N], 442 (22) [(M+H)$^+$ − C_8H_7N − Me_3Si], 117 (100) [$C_8H_7N^+$]. − $C_{20}H_{26}NO_5PSi_2W$ (631.7): calcd. C 38.02, H 4.20, N 2.22; found C 38.30, H 4.20, N 2.20.

[{2-Bis(trimethylsilyl)methyl-3-(4-methoxyphenyl)-2H-azaphosphirene-κP}pentacarbonyltungsten(0)] (**3g**): Stirring for 48 hours afforded 0.44 g of **3g** (45%) as a yellow powder, m.p. 103−104°C (decomp.). − For ^{1}H-, ^{13}C- and ^{31}P-NMR data see ref.[8]. − MS (70 eV, ^{184}W); *m/z* (%): 647 (1) [M$^+$], 604 (3) [M$^+$ − CO − Me], 486 (6) [M$^+$ − C_8H_7NO − CO], 133 (90) [$C_8H_7NO^+$], 104 (100) [$C_7H_4O^+$]. − $C_{20}H_{26}NO_6PSi_2W$ (647.4): calcd. C 37.08, H 4.05, N 2.16; found C 37.06, H 4.13, N 2.16.

[{2-Bis(trimethylsilyl)methyl-3-(4-dimethylaminophenyl)-2H-azaphosphirene-κP}pentacarbonyltungsten(0)] (**3h**): Stirring for 56 hours and low-temperature column chromatography (two times) of the residue (SiO_2, −10°C; hexane/diethyl ether, 9:1) afforded 0.24 g of **3h** (24%) as a yellow powder, m.p. 110°C (decomp). − IR (KBr): $\tilde{\nu}$ = 2072 (m) cm^{-1}, 2062 (s), 1979 (m), 1945 (vs), 1908 (s), 1885 (s) (CO), 1593 (m) (CN). − ^{1}H NMR ($CDCl_3$): δ = 0.12 (s, 9 H, $SiMe_3$), 0.28 (s, 9 H, $SiMe_3$), 0.61 (d, $^2J_{HP}$ = 2.43 Hz, 1 H, PC*H*), 3.11 (s, 6 H, NCH_3), 6.81 (d, $^3J_{HH}$ = 8.98 Hz, 2 H, Ar-*H*), 7.86 (d, $^3J_{HH}$ = 8.98 Hz, 2 H, Ar-*H*). − ^{13}C{^{1}H} NMR ($CDCl_3$): δ = 1.4 (d, $^3J_{CP}$ = 3.2 Hz, $SiMe_3$), 2.2 (d, $^3J_{CP}$ = 3.2 Hz, $SiMe_3$), 26.5 (d, $^1J_{CP}$ = 24.4 Hz, P*C*H), 40.1 [s, N(CH_3)$_2$], 111.8 (s, *m-C*), 112.6 (d, $^2J_{CP}$ = 15.0 Hz, *i-C*), 131.8 (s, *o-C*), 154.0 (s, *p-C*), 187.8 (d, Σ J_{PC} = 3.1 Hz, P*C*N), 196.2 (d, $^1J_{CW}$ = 127.5 Hz, $^2J_{CP}$ = 8.8 Hz, *cis-C*O), 198.3 (d, $^2J_{CP}$ = 24.0 Hz, *trans-C*O). − ^{31}P{^{1}H} NMR ($CDCl_3$): δ = −117.6 (s, $^1J_{PW}$ = 291.5 Hz). − MS (70 eV): M$^+$ could not be detected by EI MS; using CI MS [($Me_2NC_6H_4$)CN^+] was found to be the basic peak.

Crystal-Structure Determination of **3d**[18]: $C_{19}H_{24}NO_5PSi_2W$, *M* = 617.39, *P*$\bar{1}$, *a* = 9.167(4), *b* = 10.793(4), *c* = 13.775(5) Å, α = 89.27(2)°, β = 85.92(3)°, γ = 64.88(3)°, *V* = 1230.6(8) Å^3, *Z* = 2, d_{calc} = 1.666 Mg/m^3, μ = 4.883 mm^{-1}, *T* = 143 K. A yellow prism (0.7 × 0.7 × 0.4 mm) was mounted in inert oil. 6565 intensities were measured (2Θ 6−50°) using Mo-K_α radiation on a Stoe STADI-4 diffractometer. After absorption correction (ψ scans) 4319 were unique (R_{int} = 0.0251) and 4318 used for all calculations (program SHELXL-93). All hydrogen atoms (except rigid methyl groups) were refined with a riding model. The final *wR(F*^{2}*)* was 0.0883 with conventional *R(F)* 0.0324 for 268 parameters and 129 restraints. Highest peak 1996, hole −1835 e/nm^3.

☆ Dedicated to Professor *Manfred Weidenbruch* on the occasion of his 60th birthday.

[1] H. Wilkens, J. Jeske, P. G. Jones, R. Streubel, *J. Chem. Soc., Chem. Commun.*, in press.

[2] A. Pawda, A. D. Woolhouse in A. R. Katritzky, C. W. Rees (Eds.) *Comprehensive Heterocyclic Chemistry*, vol. 7, Pergamon Press, Oxford, **1984**, p. 47.

[3] G. Bertrand, C. Wentrup, *Angew. Chem.* **1994**, *106*, 549−568; *Angew. Chem. Int. Ed. Engl.* **1994**, *33*, 527−546.

[4] R. M. Paton, *Chem. Soc. Rev.* **1989**, *18*, 33−52.

[5] [5a] S. Fischer, C. Wentrup, *J. Chem. Soc., Chem. Commun.* **1980**, 502−503. − [5b] R. A. Moss, J. Terpinski, D. P. Cox, D. Z. Denney, K. J. Krogh-Jespersen, *J. Am. Chem. Soc.* **1985**, *107*, 2743−2748.

[6] N. Dubau-Assibat, A. Baceiredo, G. Bertrand, *J. Am. Chem. Soc.* **1996**, *118*, 5216−5220.

[7] [7a] A. Holm, N. Harrit, I. Trabjerg, *J. Chem. Soc., Perkin Trans. I* **1978**, 746−750. − [7b] A. Holm, J. J. Christiansen, C. Lohse, *J. Chem. Soc. Perkin Trans. I* **1979**, *1*, 960−962.

[8] G. Alcaraz, V. Piquet, A. Baceiredo, F. Dahan, W. W. Schoeller, G. Bertrand, *J. Am. Chem. Soc.* **1996**, *118*, 1060−1065.

[9] [9a] A. E. Reed, P. v. R. Schleyer, *J. Am. Chem. Soc.* **1990**, *112*, 1434−1445. − [9b] D. G. Gilheany, *Chem. Rev.* **1994**, *94*, 1339−1374.

[10] W. A. Lathan, L. Radom, P. C. Hariharan, W. J. Hehre, J. A. Pople, *Top. Curr. Chem.* **1973**, *40*, 1−45.

[11] [11a] M. Rahmoune, Y. Y. C. Yeung Lam Ko, F. Tonnard, R. Carrie, PSI−BLOCS Conference, Palaiseau, France, **1988**, poster abstract. − [11b] M. Rahmoune, Y. Y. C. Yeung Lam Ko, R. Carrie, F. Tonnard, *New J. Chem.* **1989**, *13*, 891−898; comment: This paper neither describes nor mentions non-coordinated 2*H*-azaphosphirenes.

[12] R. Streubel, J. Jeske, P. G. Jones, R. Herbst-Irmer, *Angew. Chem.* **1994**, *106*, 115−117; *Angew. Chem. Int. Ed. Engl.* **1994**, *33*, 80−82.

[13] R. Streubel, H. Wilkens, A. Ostrowski, C. Neumann, F. Ruthe, P. G. Jones, *Angew. Chem.* **1997**, *109*, 1549−1550; *Angew. Chem. Int. Ed. Eng.* **1997**, *36*, 1492−1493.

[14] G. M. Bodner, S. B. Kahl, K. Bork, B. N. Storhoff, J. E. Wuller, L. J. Todd, *Inorg. Chem.* **1973**, *12*, 1071−1074.

[15] R. Appel, A. Westerhaus, *Tetrahedron Lett.* **1981**, *22*, 2159−2160.

[16] R. Streubel, unpublished results.

[17] C. Hansch, A. Leo, S. H. Unger, K. H. Kim, D. Nikaitani, E. J. Lien, *J. Med. Chem.* **1973**, *16*, 1207−1216.

[18] Crystallographic data (excluding structure factors) for the structure reported in this paper have been deposited with the Cambridge Crystallographic Data Centre as supplementary publication no. CCDC-100687. Copies of the data can be obtained free of charge on application to The Director, CCDC, 12 Union Road, UK-Cambridge CB2 1EZ [fax: int. code +44(1223)336-033; E-mail: deposit@chemcrys.cam.ac.uk].

[19] R. Streubel, A. Ostrowski, H. Wilkens, F. Ruthe, J. Jeske, P. G. Jones, *Angew. Chem.* **1997**, *109*, 409−413; *Angew. Chem. Int. Ed. Engl.* **1997**, *36*, 378−381.

[20] [20a] E. O. Fischer, H. J. Kollmeier, *Chem. Ber.* **1971**, *104*, 1339−1346. − [20b] E. O. Fischer, M. Leupold, *Chem. Ber.* **1972**, *105*, 599−608.

[97204]

(Pyrazolylborate)zinc Organophosphate Complexes Resulting from Hydrolytic Cleavage of Phosphate Esters☆

Karl Weis, Michael Rombach, Michael Ruf, and Heinrich Vahrenkamp*

Institut für Anorganische und Analytische Chemie der Universität Freiburg,
Albertstrasse 21, D-79104 Freiburg, Germany

Received September 27, 1997

Keywords: Zinc complexes / Pyrazolylborate ligands / Phosphate ligands / Hydrolytic cleavage / Condensation

Five different (pyrazolylborate)zinc hydroxide complexes Tp*Zn−OH (**1**) were used as hydrolytic reagents towards esters of various acids of phosphorus. Trimethyl phosphate and trimethyl phosphite could not be cleaved. Dimethyl and diphenyl phosphite yielded $Tp^{tBu,Me}Zn-OPHO(OR)$ (**2**, **3**). Triphenyl phosphate reacted slowly producing moderate yields of $Tp^*Zn-OPO(OPh)_2$ (**4**). Tris(*p*-nitrophenyl) phosphate was cleaved rapidly, forming $Tp^*Zn-OPO(OC_6H_4NO_2)_2$ (**5**) and $Tp^*Zn-OC_6H_4NO_2$ (**6**). Alkylbis(*p*-nitrophenyl) phosphates showed intermediate reactivity, losing *p*-nitrophenolate upon hydrolysis and producing $Tp^*Zn-OPO(OR)(OC_6H_4NO_2)$ (**7**, **8**). When phosphorus acid diesters were employed, condensation between the Zn−OH and P−OH functions occurred. This proved to be the convenient way of preparing the organophosphate complexes $Tp^*Zn-OPO(Ph)_2$ (**9**), $Tp^*Zn-OPO(OPh)_2$ (**4**), and $Tp^*Zn-OPO(OC_6H_4NO_2)_2$ (**5**). Six structure determinations showed the structural variability of the resulting complexes.

One of the largest group of enzymes are those which catalyze phosphate transfer[1]. Many of them are metalloenzymes[2], quite often having two or three metal ions in the active center[3]. Of the metals involved (Mg, Fe, Mn, and Zn) zinc plays an important role, being present for instance in alkaline[4] and acid[5] phosphatases, nucleases[6][7], phospholipases[8], phosphotriesterases[9], and DNA and RNA polymerases[10]. All these latter enzymes are involved in the making and breaking of phosphate ester (P−OR) linkages in their various biological occurrencies.

The importance of the subject and the ease of modelling the biological substrates by simple phosphoric acid esters like tris(*p*-nitrophenyl) phosphate has attracted organic chemists and coordination chemists early on. Research groups which have investigated the metal (specifically zinc) ion or complex catalyzed phosphate ester hydrolysis are, among others, those of Breslow[11], Chin[12], Brown[13], Kimura[14], Bianchi[15], and Yashiro[16]. Stoichiometric reactions and structural models for zinc complexes were provided, among others, by Krebs[17], Kitajima[18], Fenton[19], Lippard[20], and ourselves[21]. A typical characteristic of the model mechanisms or structures is the involvement of bidentate phosphate, being coordinated via two of its oxygen atoms to either one or two metal ions. Monodentate coordination is the exception, and to date just one structure of a mononuclear zinc complex bearing a phosphate only as a monodentate ligand has been published[21].

We are interested in exploiting the hydrolytic activity of zinc-bound water molecules or hydroxide groups in an isolated situation, i.e. one where the kind and number of other ligands on zinc leaves just one coordination site for H_2O or OH^-, thereby encapsulating it in an enzyme-like manner. The purpose is to make the reacting zinc complexes strictly monofunctional and allowing only monodentate coordination for the substrate too. We have so far tested it for zinc model complexes of tripodal N,N,N [e.g. tris(benzimidazolylmethyl)amine][22] and N,N,O (e.g. dipicolylglycine)[23] ligands. In our hands the substituted (pyrazolylborate)zinc hydroxides Tp*Zn−OH turned out to be the best nucleophiles, being active in the hydrolysis of esters[24], amides[24], CO_2[25][26] and similar systems with cumulated double bonds[27]. We have also briefly communicated the hydrolytic cleavage of phosphate esters and diphosphates by them[28].

This paper starts a series of publications on the cleavage of phosphate-containing materials by Zn−OH and $Zn-OH_2$ complexes. In order to lay a preparative and structural basis for further work, simple esters of various acids of phosphorus were treated with the five Tp*Zn−OH complexes **1a**−**e**. The reaction conditions were chosen such that one ester group each could be cleaved off, and due to the insolubility of the Tp*Zn−OH complexes in water the reactions were meant to be stoichiometric rather than catalytic.

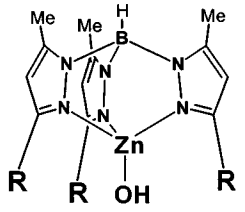

1a (R = a): $Tp^{tBu,Me}Zn-OH$
1b (R = b): $Tp^{Ph,Me}Zn-OH$
1c (R = c): $Tp^{Cum,Me}Zn-OH$
1d (R = d): $Tp^{Py,Me}Zn-OH$
1e (R = e): $Tp^{Pic,Me}Zn-OH$

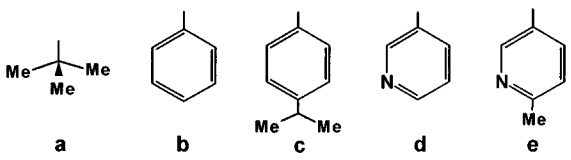

 © WILEY-VCH Verlag GmbH, D-69451 Weinheim, 1998 1434−1948/98/0202−263 $ 17.50+.50/0

"Small" Phosphates and Phosphites

The first attempts at ester cleavage were made with trimethyl phosphite and trimethyl phosphate. Both turned out to be unreactive toward the Tp*Zn−OH reagents. Although, being small molecules, they allow easy access of a nucleophile to phosphorus, their alkyl ester functions seem to be too inert. Making them even smaller led to success, however. Dimethyl phosphite [$HPO(OMe)_2$] reacted with **1a** and **1c**, diphenyl phosphite [$HPO(OPh)_2$] reacted with **1a** producing in very good yields the zinc-phosphate complexes **2a**, **2c**, and **3a** as the products of the hydrolytic removal of one OR group. Both the liberated methanol and phenol did not show up in the form of zinc complexes, in accord with our experience that they don't react with Tp*Zn−OH[29]. One attempt at using an ester of methylphosphonic acid, namely $MePO(OMe)_2$, was also met with failure.

$Tp^{R,Me}Zn-OPHO(OMe)$
2a: R = *t*Bu
2c: R = Cum

$Tp^{tBu,Me}Zn-OPHO(OPh)$
3a

The spectroscopic identification of complexes **2a**, **2c**, and **3a** was easy due to their simple ^{1}H-NMR spectra containing the very typical P-H doublet. Confirmation of their constitutional assignment was obtained by a structure determination of **2c** (see Figure 1). The structure shows the expected pseudotetrahedral coordination of zinc with a symmetrical attachment of the $Tp^{Cum,Me}$ ligand and the Zn−O bond very close to the trigonal axis of the Tp*Zn unit. As such it provides no unusual features for a Tp*Zn−OX complex. The bonding situation of its phosphite ligand is discussed below.

Figure 1. Molecular structure of **2c**[a]

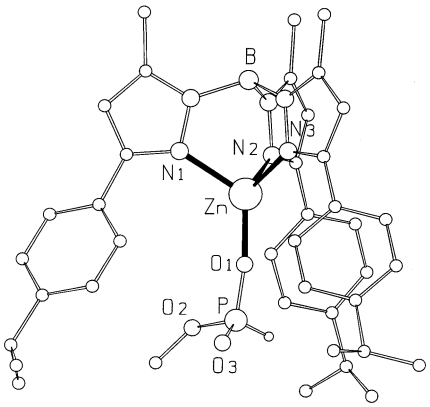

[a] Coordination environment of zinc: Zn−O1 1,825(5), Zn−N1 2.016(5), Zn−N2 2.026(5), Zn−N3 2.016(5) A; O1−Zn−N1 123.0(2), O1−Zn−N2 122.0(2), O1−Zn−N3 122.3(2)°. − In the crystal one methanol molecule is attached to O3 by a hydrogen bond.

Triphenyl Phosphate

Aryl phosphates are more amenable to hydrolytic cleavage than trialkyl phosphates, yet they are not typically used for model studies for which *p*-nitrophenyl phosphates are the favourites. It turned out that our Tp*Zn−OH reagents are aggressive enough to remove one phenolate ligand from them, especially when applied in large excess for kinetic studies[30]. Stoichiometric reactions were relatively slow and led to product mixtures containing some starting material and side products which were not easy to separate. Thus **1d** and $PO(OPh)_3$ gave only traces of **4d**. Both **1b** and **1c** underwent relatively clean reactions with $PO(OPh)_3$ as evidenced by ^{31}P-NMR spectroscopy. After isolation, the products **4b** and **4c** were of moderate yield. Samples were also obtained of **4b** by condensation (see below) and of **4c** by hydrolytic cleavage of tetraphenyl diphosphate[31].

$Tp^{R,Me}Zn-OPO(OPh)_2$
4a: R = *t*Bu
4b: R = Ph
4c: R = Cum
4d: R = Py

The spectroscopic identification of complexes **4** rests mainly on the ^{1}H-NMR data of their Tp* ligands and the ^{31}P-NMR and υ(P=O) IR data of their phosphate ligands. The assignment was rounded off by a structure determination of **4b** (see Figure 2). It shows a less symmetrical arrangement around the zinc ion as evidenced by the Zn−N bond lengths and the O−Zn−N angles.

Figure 2. Molecular structure of **4b**[a]

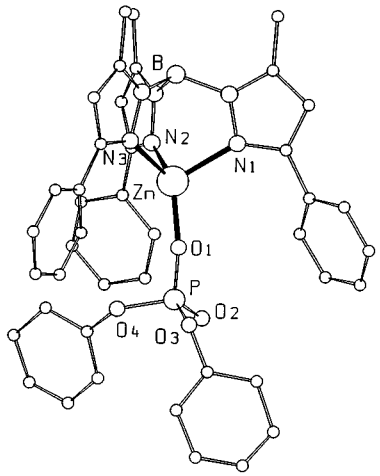

[a] Coordination environment of zinc : Zn−O1 1,854(2), Zn−N1 2.009(3), Zn−N2 2.019(2), Zn−N3 2.060(2) A; O1−Zn−N1 114.6(1), O1−Zn−N2 130.8(1), O1−Zn−N3 119.5(1)°.

Tris(*p*-nitrophenyl) Phosphate

As expected, tris(*p*-nitrophenyl) phosphate reacted fast and cleanly with the Tp*Zn−OH reagents. It was, in our hands[30] like in others, the substrate of choice for kinetic measurements. We used it for stoichiometric reactions with **1b** and **1c**. In order to achieve complete consumption of the phosphate, two equivalents of the zinc complex had to be used. The reason for this is fast reaction of the liberated *p*-nitrophenol with the zinc−hydroxide unit in terms of a condensation reaction leading to the *p*-nitrophenolate complexes **6**, as we have described before[29]. Thus the hydrolytic cleavages of the phosphate yielded equimolar mixtures of

the phosphate complexes **5b**, **c** and the phenolate complexes **6b**, **c** which were separated.

$Tp^{R,Me}Zn-OPO(OC_6H_4-p\text{-}NO_2)_2$
5a: R = *t*Bu
5b: R = Ph
5c: R = Cum
5e: R = Pic

$Tp^{R,Me}Zn-OC_6H_4-p\text{-}NO_2$
6b: R = Ph
6c: R = Cum
6e: R = Pic

The spectroscopic identification of **5b** and **5c** rests on the ^{1}H-NMR data for the Tp* ligands and the υ(P=O) and δ(^{31}P) values again. Compounds **6b** and **6c** which we have described before[29] were identified spectroscopically. Crystals suitable for a structure determination were obtained of **5e** (see below). They turned out to contain hydrated **5e** with five-coordinate zinc (see Figure 3). Five-coordination of zinc seems to be the rule rather than the exception in zinc complexes of tris(3-pyridyl-3′-pyrazolyl)borato ligands[31][32][33]. In **5e** the geometry at zinc is that of a distorted trigonal bipyramid [angle O2−Zn−N3 170.8(1)°, angles between apical and equatorial ligands 85−96°, angles between equatorial ligands 97−139°]. The zinc-bound water molecule is connected via a hydrogen bond to the P=O oxygen (2.69 Å). The phosphate attachment is discussed below.

Figure 3. Molecular structure of **5e** · H_2O[a]

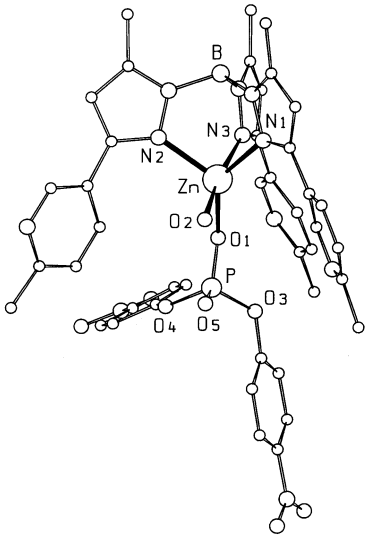

[a] Coordination environment of zinc: Zn−O1 1.996(2), Zn−O2 2.082(2), Zn−N1 2.070(3), Zn−N2 2.072(3), Zn−N3 2.202(3) Å.

Alkylbis(*p*-nitrophenyl) Phosphates

The alkylbis(*p*-nitrophenyl) phosphates contain two ester functions of quite different lability. It could therefore be predicted that they would lose only one *p*-nitrophenolate unit upon hydrolysis by Tp*Zn−OH. This was verified for ethylbis(*p*-nitrophenyl) phosphate with **1b**, **1c**, and **1e** as well as for cyclohexylbis(*p*-nitrophenyl) phosphate with **1e**. Reaction products were the zinc phosphate complexes **7b**, **7c**, **7e**, and **8e** together with the *p*-nitrophenolate complexes **6b**, **6c**, and **6e**, some of which were again difficult to separate. The various steps of the workup procedure resulted in partial hydrolytic destruction in case of **7b** and **7e**, liberating the free pyrazole which was then coordinated to zinc giving the addition products **7b′** and **7e′**. The presence of the additional pyrazole ligands in these complexes was found by ^{1}H-NMR spectroscopy. Otherwise the spectroscopic data of complexes **7** and **8** are in accord with their constitutions and quite similar to those of the related complexes with other phosphate ligands.

$Tp^{R,Me}Zn-OPO(OEt)(OC_6H_4-p\text{-}NO_2)$
7b: R = Ph
7c: R = Cum
7e: R = Pic

7b · 3-methyl-5-phenylpyrazole **7b′**

7e · 3-methyl-5-picolylpyrazole **7e′**

$Tp^{Pic,Me}Zn-OPO(OCy)(OC_6H_4-p\text{-}NO_2)$
8e

Of these complexes, one each with fourfold (**8e**) and fivefold (**7b′**) coordination at zinc was chosen for a structure determination. An unusual feature of all complexes **7** and **8** is the presence of phosphorus atoms with four different substituents. The crystals of **8e** and **7b′** are, however, not enantiomerically pure but belong to the centrosymmetric space group P−1.

Complex **8e** (see Figure 4) shares with complex **2c** the symmetrical attachment of the Tp* ligand to zinc. However, unlike the situation in **2c** the Zn−O bond is bent away significantly from the trigonal axis of the Tp* ligand, making the phosphate attachment in **8e** more like that in **4b**.

Figure 4. Molecular structure of **8e**[a]

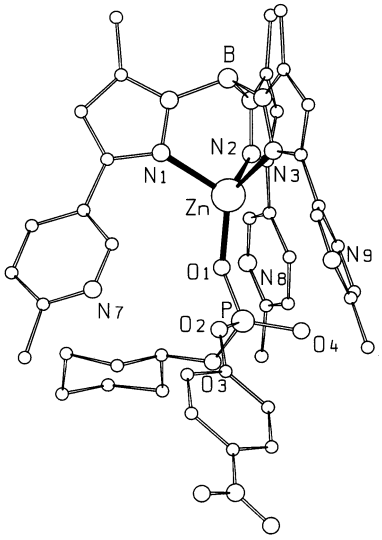

[a] Coordination environment of zinc: Zn−O1 1,854(2), Zn−N1 2.028(3), Zn−N2 2.030(2), Zn−N3 2.033(2) Å; O1−Zn−N1 118.8(1), O1−Zn−N2 116.4(1), O1−Zn−N3 131.8(1)°.

The coordination of zinc in complex **7b′** (see Figure 5) is quite unusual. The attachment of the free pyrazole molecule exerts a kind of a trans effect, pushing one of the Tp* pyrazole donors away on the opposite side of the zinc ion. The result is a very unsymmetrical coordination of the Tp* ligand to zinc, with the Zn−N1 distance (2.90 Å) practically outside a bonding range. The symmetry about the zinc ion can, however, best be described as trigonal-bipyramidal

with N7 and N1 in the apical positions (angle 172°). The angles between the axial and equatorial donors range from 77 to 105°, those between the equatorial donors between 101 and 125°. On the other hand all angles between N7 and the equatorial donors are much larger than 90° (maximum N7−Zn−O1 with 105°), indicating that the four donors O1, N2, N3, and N7 also define a flattened tetrahedron. It seems that electronic preferences favour tetrahedral coordination for **7b′** but the geometrical restraints of the Tp* ligand don′t allow to completely remove the fifth donor, resulting in the observed intermediate type of coordination.

Figure 5. Molecular structure of **7b′**[a]

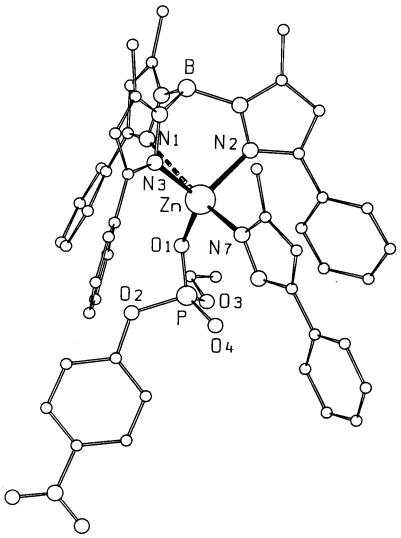

[a] Coordination environment of zinc: Zn−O1 1.912(3), Zn−N1 2.897(4), Zn−N2 2.022(3), Zn−N3 2.003(3), Zn−N7 2.082(4) Å.

Condensation Reactions

In addition to the phosphoric acid triesters we also tried to find out about the hydrolytic cleavage of phosphoric acid diesters. These are of course acids themselves and as such capable of destroying the pyrazolylborate ligands hydrolytically. To our surprise, however, their main reactivity towards the Tp*Zn−OH complexes consisted in a condensation reaction producing the corresponding diesterphosphate complexes. We then learnt that every $X_2P(O)OH$ compound undergoes this reaction yielding Tp*Zn−O-$P(O)X_2$.

In the context of this paper we applied the condensation reaction to **1a** and diphenylphosphinic acid, giving a good yield of **9a**. Similarly, **1a** with diphenyl phosphate and bis(*p*-nitrophenyl) phosphate yielded **4a** and **5a**, **1b** with both reagents yielded **4b**, **5b**, and **1e** with bis(*p*-nitrophenyl) phosphate yielded **5e** (which was used for the structure determination, see above).

$Tp^{tBu,Me}Zn-OP(O)Ph_2$
9a

The destructive power of the acidic phosphoric acid diesters came to effect in only one case, the reaction between **1d** and bis(*p*-nitrophenyl) phosphate. In the course of this reaction one of three Tp*Zn units was lost liberating zinc ions in a way which is unclear as yet. The combination of two Tp*Zn units, one zinc ion, four phosphate anions, and two water molecules then resulted in the formation of complex **10d**, the constitution of which became only clear by a structure determination. The schematic drawing of **10d** (see Figure 6) shows a octahedral zinc ion in the center and two five-coordinate zinc ions in the periphery. On both sides one phosphate each is bridging the zinc ions while the other is terminal. One pyridyl substituent of each $Tp^{Py,Me}$ ligand is used as a donor toward the central zinc ion as observed before in $[(Tp^{Py,Me}Zn)_2(\mu\text{-}H_3O_2)]^+$ [32]. Hydrogen bridging stabilizes the structure which is unique as a whole but comprised of established structural units.

Figure 6. Schematic drawing of complex **10d**[a]

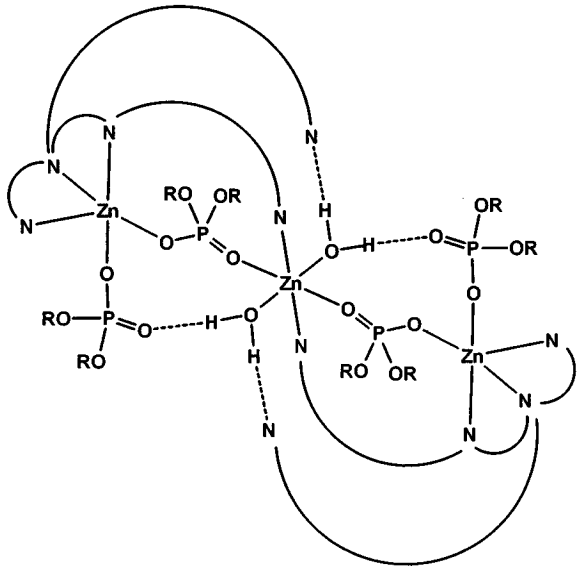

[a] R = *p*-nitrophenyl, the three interconnected N atoms bound to the outer Zn ions represent $Tp^{Py,Me}$ ligands, the four long curves represent one pyridyl substituent each of $Tp^{Py,Me}$.

Figure 7 displays the molecular structure of **10d**, with all atoms except the α-C of the *p*-nitrophenolate units omitted for clarity. The molecule is centrosymmetric. The central zinc ion is in a nearly ideal octahedral ZnN_2O_4 environment with Zn−O and Zn−N distances (2.12−2.14 Å) typically longer than those in all other zinc complexes of this paper. The peripheral zinc ions have a distorted trigonal-bipyramidal ZnN_3O_2 environment comparable to that in **5e** (*trans* angle O1−Zn1−N3 168°, *cis* angles 81−100°, equatorial angles 98−141°). The double-bridged linkage between Zn1 and Zn2 via one phosphate and one pyridylpyrazole unit represents a 10-membered heterocyclic ring.

Discussion of the Zinc−Phosphate Interactions

All the phosphite and phosphate complexes obtained here are molecular compounds soluble in nonpolar organic solvents. This implies that their zinc−phosphate interactions are covalent, as is also evidenced by the structure determinations. We became aware that this may be a questionable statement when observing that the Zn−O−P angles

Figure 7. Molecular structure of **10d**[a]

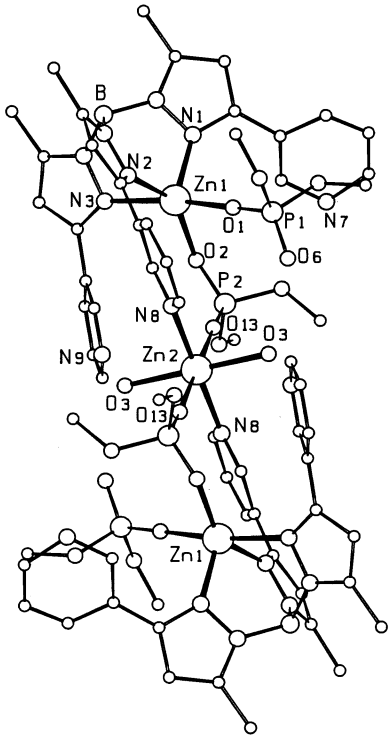

[a] Coordination environments of the zinc ions: Zn1−N1 2.034(5), Zn1−N2 2.070(5), Zn1−N3 2.224(5), Zn1−O1 2.067(4), Zn1−O2 1.960(4), Å Zn2−N8 2.140(7), Zn2−O3 2.125(6), Zn2−O13 2.128(5) Å.

are never close to the tetrahedral angle to be expected for covalent oxygen and that the formal single bonds P−O(Zn) are almost as short as the formal double bonds P=O. The data related to this are assembled in Table 1 which also includes values from two complexes in the accompanying paper[31].

Table 1 Bonding parameters for the zinc−phosphate interactions

complex	Zn−O	O−P	P=O	Zn−O−P	O−P=O
complexes with four-coordinate zinc					
2c	1.83	1.46	1.45	172	115
4b	1.85	1.48	1.46	155	121
8e	1.85	1.50	1.46	149	119
complexes with intermediate coordination					
7b′	1.91	1.49	1.47	142	120
4c′[a]	1.91	1.49	1.47	147	120
complexes with five-coordinate zinc					
5e·H_2O	2.00	1.50	1.47	136	121
10d[b]	2.07	1.46	1.46	178	123
4e·H_2O[a]	1.95	1.50	1.46	139	118

[a] Structures described in ref.[31]. − [b] Only the terminal phosphate is considered.

The table shows that in all cases there is an almost complete equalization of the formal single and double P−O bonds. Although the "double" bonds are shorter throughout, their shortening amounts to a maximum of 0.04 Å. When referenced against the P−O(R) bond lengths of truely single bonds in the same compounds (1.57−1.60 Å) or the standard value for a true P=O double bond (ca. 1.45 Å[34]) it becomes clear that both P−O bonds in the phosphate complexes described here have close to double bond character as is also observed in various ionic phosphates[34]. This relation to ionic phosphate is underlined by the quite constant and normal values of the O−P=O angles.

The Zn−O bond lengths cannot be used as a measure of the zinc−phosphate interactions. They simply reflect the coordination number of zinc, as made visible by the grouping of compounds in the table. For each of the three groups the range of Zn−O bond lengths is typical, increasing with the coordination number, and all of them are shorter than the value for octahedral zinc (2.15−2.20 Å). Conversely the bond lengths and angles of the P−O entities under consideration do not reflect the coordination number of zinc.

The most variable structural detail in this context is the Zn−O−P angle, showing a spread from 136 to 178°. As the individual values of this angle cannot be related to other bond lengths or angles in the corresponding complexes, they cannot reflect electronic situations, i.e. they must be determined by geometric constraints. This is, however, only obvious for **2c** where the phosphite ligand is "compressed" by the *tert*-butyl substituents of the Tp* ligand. In the other cases it must reflect a combination of intramolecular forces. Altogether the softness of the Zn−O−P angle is the second strong indicater for the rather polar nature of the zinc−phosphate interactions. As such it is reminiscent of the Si−O−Si linkage in silicates and siloxanes which has been discussed in similar terms in the light of modern MO theory[35].

Conclusions

The nucleophilic strength of the "enzyme models" Tp* Zn−OH has been demonstrated for a wide range of esters of phosphorus acids as well as for Tp* ligands of varying polarity and steric bulk. In a favourable case even an alkyl ester could be cleaved. Phenyl esters were of moderate, *p*-nitrophenyl esters of high reactivity. This work has lain the preparative basis for kinetic studies aimed at elucidating mechanistic details of the cleavage reactions.

In terms of enzyme modelling the reactions of the alkyl esters are the only ones of relevance. Phosphate transfer from mononucleotides or phospholipids involves the cleavage of aliphatic phosphate esters, i.e. those which are most difficult to hydrolyze. We have shown that this is in principle possible with Tp*Zn−OH. When an alkyl and a *p*-nitrophenyl ester group are present in a phosphoric acid ester, it is exclusively the latter which is cleaved off. Cleavage reactions of this kind have led here to the new class of metal phosphate complexes containing chiral phosphorus centers.

All cleavage reactions by Tp*Zn−OH have shown that a single zinc ion (or Zn−OH, or Zn−OH_2 unit) is sufficient to perform the hydrolysis. The rates of the cleavage reactions observed here are also not smaller than those reported for some dinuclear model complexes, irrespective of the fact that our reactions are stoichiometric rather than catalytic. All reactions end with the formation of phosphate complexes, allowing the mechanistic conclusion that the metal

ion and the phosphate are in contact during the ester cleavage.

The structure determinations of the zinc phosphate complexes have yielded two important pieces of information. Firstly they indicate that the bonding between zinc and phosphate is quite polar in nature. Secondly they show a variety of coordination geometries and ligand arrangements around zinc which is puzzling at first glance. We are optimistic, however, that a systematic analysis of the structures of all odd-shaped Tp*Zn(X)(Y) complexes will allow a superposition yielding a reaction trajectory for the nucleophilic transformation of substrates by Tp*Zn−OH. We are in the course of further structural and basic kinetic work with the aim of finding this trajectory.

This work was supported by the *Deutsche Forschungsgemeinschaft* and the *Fonds der Chemischen Industrie*. We thank Dr. *W. Deck* and Mr. *B. Müller* for help with the NMR and X-ray work.

Experimental Section

General experimental methods and measuring techniques see ref.[36]. The Tp*Zn−OH complexes[25][27][33][37] and the alkylbis(*p*-nitrophenyl) phosphates[38] were prepared according to published procedures. All other reagents were obtained commercially. Solvents were air- and water-free. − IR data (cm^{-1}) were recorded from KBr pellets. − ^{1}H- and ^{31}P-NMR data (δ in ppm, int. TMS, ext. H_3PO_4) were recorded from $CDCl_3$ solutions. All compounds are characterized in Table 2.

2a: 200 mg (0.395 mmol) of **1a** and 43.5 mg (0.395 mmol) of dimethylphosphite in 20 ml of dichloromethane were stirred for 16 h. The solvent was removed in vacuo and the residue crystallized from methanol. Yield 210 mg (90%) of **2a**. − IR: 2554m (BH), 1252vs (P=O). − ^{1}H NMR: 1.41 [s, 27 H, *t*Bu], 2.39 [s, 9 H, Me(pz)], 3.72 [d, J = 12.1 Hz, 3 H, OMe], 5.84 [s, 3 H, H(pz)], 7.10 [d, J = 647 Hz, 1 H, PH]. − ^{31}P NMR: −0.6.

2c: 1.00g (1.44 mmol) of **1c** and 1.20 g (10.9 mmol) of dimethyl phosphite in 30 ml of toluene were stirred for 2 h. The solvent was removed in vacuo, the residue washed with 2 ml of cold methanol and then crystallized from methanol. Yield 0.92 g (81%) of **2c**. − IR: 2537m (BH), 1246s (P=O). − ^{1}H NMR: 1.23 [d, J = 6.9 Hz, 18 H, Me(*i*Pr)], 2.50 [s, 9 H, Me], 2.94 [sept, J = 6.9 Hz, 3 H, CH(*i*Pr)], 3.19 [d, J = 11.8 Hz, 3 H, OMe], 6.21 [s, 3 H, CH(pz)], 6.27 [d, J = 654 Hz, 1 H, PH], 7.31 [d, J = 8.2 Hz, 6 H, Ph(3,5)], 7.60 [d, J = 8.2 Hz, 6 H, Ph(2,6)]. − ^{31}P NMR: 1.0.

3a: As before from 500 mg (0.988 mmol) of **1a** and 231 mg (0.988 mmol) of diphenylphosphite. Repeated crystallization from acetonitrile yielded 430 mg (67%) **3a**. − IR: 2558m (BH), 1259s (P=O). − ^{1}H NMR: 1.41 [s, 27 H, *t*Bu], 2.40 [s, 9 H, Me(pz)], 5.86 [s, 3 H, H(pz)], 7.09 [m, 1 H, Ph], 7.30 [m, 4 H, Ph], 7.38 [d, J = 664 Hz, 1 H, PH]. − ^{31}P NMR: −5.0.

General Procedure for the Cleavage of Aryl Phosphates: Two equivalents of the Tp*Zn−OH complex and one equivalent of the aryl phosphate were stirred in a solvent at room temp. All volatiles were removed in vacuo. Treatment of the residue with acetonitrile or ethanol yielded a solution of the phosphate complex and a residue of the phenolate complex. When already known, the phenolate complex was discarded. Otherwise it was recrystallized and characterized (see below). The solution of the phosphate complex was evaporated to dryness in vacuo and the product recrystallized.

4b: From 300 mg (0.530 mmol) of **1b** and 86.5 mg (0.265 mmol) of triphenyl phosphate in 20 ml of CH_2Cl_2 for 3 d. Crystallization from acetonitrile yielded 73.5 mg (36%) of **4b**. − IR: 2549m (BH), 1230s (P=O). − ^{1}H NMR: 2.52 [s, 9 H, Me(pz)], 6.25 [s, 3 H, H(pz)], 6.86 [d, J = 7.3 Hz, 4 H, Ph(phos(2,6))], 6.89−7.27 [m, 9 H, Ph], 7.24 [m, 6 H, Ph(3,5)], 7.64 [d, J = 7.4 Hz, 6 H, Ph(2,6)]. − ^{31}P NMR: −16.6.

4c: From 300 mg (0.433 mmol) of **1c** and 70.7 mg (0.217 mmol) of triphenyl phosphate in 20 ml of CH_2Cl_2 for 4 d. Crystallization from acetonitrile yielded 91 mg (45%) of **4c**. − IR: 2552m (BH), 1282s (P=O). − ^{1}H NMR: 1.04 [d, ^3J = 6.9 Hz, 18 H, Me(*i*Pr)], 2.53 [s, 9 H, Me(pz)], 2.70 [sept, ^3J = 6.9 Hz, 3 H, H(*i*Pr)], 6.26 [s, 3 H, H(pz)], 6.68 [d, ^3J = 7.5 Hz, 4 H, Ph(phos(2,6))], 6.95 [m, ^3J = 7.5 Hz, 6 H, Ph(phos(3,4,5))], 7.13 [d, ^3J = 8.1 Hz, 6 H, Ph(3,5)], 7.62 [d, ^3J = 8.1 Hz, 6 H, Ph(2,6)]. − ^{31}P NMR: −16.6.

4d: From 500 mg (0.879 mmol) of **1d** and 143 mg (0.438 mmol) of triphenyl phosphate in 40 ml of CH_2Cl_2 for 16 h. Several recrystallizations from acetonitrile were necessary to yield 35 mg (5%) of **4d**. − IR: 2553m (BH), 1261s (P=O). − ^{1}H NMR: 2.57 [s, 9 H, Me(pz)], 6.27 [s, 3 H, H(pz)], 6.56 [d, ^3J = 8.1 Hz, 4 H, Ph(2,6)], 7.05 [m, 6 H, Ph(3,4,5)], 7.05 [dd, ^3J = 7.9 Hz, ^3J = 4.6 Hz, 3 H, Py(5)], 8.11 [d, ^3J = 7.9 Hz, 3 H, Py(6)], 8.21 [d, ^3J = 4.6 Hz, 3 H, Py(4)], 8.67 [s, 3 H, Py(2)]. − ^{31}P NMR: −14.9.

5b: From 300 mg (0.530 mmol) of **1b** and 122 mg (0.265 mmol) of tris(*p*-nitrophenyl)phosphate in 5 ml of CH_2Cl_2 for 24 h. Two recrystallizations from acetonitrile yielded 37.3 mg (16%) of **5b**. − IR: 2554m (BH), 1548s, 1344s (NO), 1256s (P=O). − ^{1}H NMR: 2.56 [s, 9 H, Me(pz)], 6.27 [s, 3 H, H(pz)], 6.71 [d, ^3J = 7.3 Hz, 4 H, Nitr(2,6)], 7.20 [m, 3 H, Ph(4)], 7.35 [m, 6 H, Ph(3,5)], 7.63 [d,

Table 2 Characterization of the new complexes

no.	m.p. [°C]	formula mol. mass	analyses calcd./found C	H	N
2a	142	$C_{25}H_{45}BN_6O_3PZn$ 584.9	51.43 51.92	7.60 7.50	14.40 13.73
2c7	182	$C_{40}H_{50}BN_6O_3PZn$ 770.1	62.39 61.93	6.54 6.51	10.91 10.58
3a	235	$C_{30}H_{46}BN_6O_3PZn \cdot H_2O$ 663.9	54.27 54.32	7.29 7.16	12.66 12.71
4a	256	$C_{36}H_{50}BN_6O_4PZn$ 738.0	58.59 58.36	6.83 6.76	11.39 11.34
4b	166	$C_{42}H_{38}BN_6O_4PZn$ 798.0	63.22 63.99	4.80 4.86	10.53 11.16
4c	197	$C_{51}H_{56}BN_6O_4PZn$ 924.2	66.28 65.55	6.11 6.07	9.10 8.93
4d	179	$C_{39}H_{35}BN_9O_4PZn$ 801.0	47.83 47.26	3.38 3.28	14.22 14.79
5a	246	$C_{36}H_{48}BN_8O_8PZn$ 828.0	52.22 51.62	5.84 5.87	13.59 13.47
5b	179	$C_{42}H_{36}BN_8O_8PZn \cdot CH_3CN$ 888.0 + 41.1	56.89 56.76	4.23 4.18	13.57 13.62
5c	199	$C_{51}H_{54}BN_8O_6PZn \cdot H_2O$ 1014.2 + 18.0	59.34 58.46	5.47 5.56	10.86 10.91
5e	159	$C_{42}H_{41}BN_{11}O_9PZn$ $\cdot 1/2\,CH_2Cl_2$ ($\cdot H_2O$) 951.1 + 42.5	51.38 51.69	4.26 4.10	15.51 15.83
6e	239	$C_{36}H_{35}BN_{10}O_3Zn \cdot CH_2Cl_2$ 731.9 + 84.9	56.51 56.08	4.69 4.78	18.09 18.03
7b′	153	$C_{48}H_{47}BN_9O_6PZn$ 953.1	60.49 60.88	4.97 4.95	13.23 13.32
7c	181	$C_{47}H_{55}BN_7O_6PZn$ 921.2	61.28 61.12	6.02 5.94	10.64 10.54
7e′	178	$C_{48}H_{51}BN_{13}O_6PZn$ 1013.2	56.90 55.14	5.07 4.92	17.97 17.38
8e	171	$C_{42}H_{46}BN_{10}O_6PZn \cdot CH_2Cl_2$ 894.1 + 84.9	52.76 52.50	4.94 5.01	14.31 14.59
10d	120	$C_{102}H_{86}B_2N_{26}O_{34}P_4Zn_3$ 2561.6	47.83 47.26	3.38 3.28	14.22 14.79

^3J = 7.3 Hz, 6 H, Ph(2,6)], 7.89 [d, ^3J = 7.3 Hz, 4 H, Nitr(3,5)]. − ^{31}P NMR: −18.9.

5c: From 300 mg (0.433 mmol) of **1c** and 70.7 mg (0.217 mmol) of tris(*p*-nitrophenyl)phosphate in 10 ml of CH_2Cl_2 for 2 d. Two recrystallizations from acetonitrile yielded 22 mg (10%) of **5c**. − IR: 3130w (H_2O), 2561m (BH), 1553m, 1344s (NO), 1258m (P=O). − ^{1}H NMR: 1.06 [d, ^3J = 6.8 Hz, 18 H, Me(*i*Pr)], 2.55 [s, 9 H, Me(pz)], 2.73 [sept, ^3J = 6.9 Hz, 3 H, H(*i*Pr)], 6.24 [s, 3 H, H(pz)], 6.69 [d, ^3J = 8.2 Hz, 4 H, Nitr(3,5)], 7.21 [d, ^3J = 8.2 Hz, 6 H, Ph(3,5)], 7.57 [d, ^3J = 8.2 Hz, 6 H, Ph(2,6)], 7.87 [d, ^3J = 8.2 Hz, 4 H, Nitr(2,6)]. − ^{31}P NMR: −19.4.

7b′: From 500 mg (0.884 mmol) of **1b** and 168 mg (0.442 mmol) of ethylbis(*p*-nitrophenyl) phosphate in 10 ml of $CHCl_3$ for 24 h. Recrystallization from methanol/acetonitrile (1:1). Yield 129 mg (31%) of **7b′**. − IR: 2551m (BH), 1544s, 1343s (NO), 1251s (P=O). − ^{1}H NMR: 0.99 [t, ^3J = 7.1 Hz, 3 H, Me(OEt)], 2.49 [s, 12 H, Me(py), Me(pz(a))], 3.65 [dq, ^3J = 7.1 Hz, ^3J = 7.1 Hz, 2 H, CH_2(OEt)], 5.82 [s, 1 H, H(pz(a))], 6.26 [s, 3 H, H(pz)], 7.04−7.57 [m, 16 H, Ph], 7.59 [d, ^3J = 7.3 Hz, 6 H, Ph(2,6)], 8.00 [d, ^3J = 7.2 Hz, 2 H, Nitr(3,5)]. − ^{31}P NMR: −8.2.

7c: From 233 mg (0.336 mmol) of **1c** and 62.0 mg (0.168 mmol) of ethylbis(*p*-nitrophenyl) phosphate in 5 ml of $CHCl_3$ for 48 h. Crystallization from acetonitrile yielded two crystal fractions which had to be sorted manually (**6c** and **7c**). Yield 43 mg (28%) of **7c**. − IR: 2551m (BH), 1550m, 1344s (NO), 1256s (P=O). − ^{1}H NMR: 0.84 [t, ^3J = 7.1 Hz, 3 H, Me(OEt)], 1.15 [d, ^3J = 6.9 Hz, 18 H, Me(*i*Pr)], 2.55 [s, 9 H, Me(pz)], 2.79 [sept, ^3J = 6.9 Hz, 3 H, H (*i*Pr)], 3.46 [dq, ^3J = 7.1 Hz, ^3J = 7.1 Hz, 2 H, CH_2(OEt)], 6.23 [s, 3 H, H(pz)], 6.74 [d, ^3J = 7.2 Hz, 2 H, Nitr(2,6)], 7.29 [d, ^3J = 8.2 Hz, 6 H, Ph(3,5)], 7.61 [d, ^3J = 8.2 Hz, 6 H, Ph(2,6)], 7.84 [d, ^3J = 7.2 Hz, 2 H, Nitr(3,5)]. − ^{31}P NMR: −12.0.

7e′: From 312 mg (0.550 mmol) of **1e** and 101 mg (0.275 mmol) of ethylbis(*p*-nitrophenyl) phosphate in 5 ml of $CHCl_3$ for 48 h. Recrystallization from acetonitrile. Yield 107 mg (46%) of **7e′**. − IR: 2537m (BH), 1545m, 1342s (NO), 1248s (P=O). − ^{1}H NMR: 1.02 [t, ^3J = 7.1 Hz, 3 H, Me(OEt)], 2.34 [s, 12 H, Me(py), Me-(py(a))], 2.55 [s, 12 H, Me(pz)], 3.67 [dq, ^3J = 7.1 Hz, ^3J = 7.1 Hz, 2 H, CH_2(OEt)], 5.91 [s, 1 H, H(pz(a))], 6.29 [s, 3 H, H(pz)], 7.08 [d, ^3J = 8.0 Hz, 3 H, Py(5)], 7.12 [d, 1 H, Py(5(a))], 7.25 [d, ^3J = 7.2 Hz, 2 H, Nitr(2,6)], 7.64 [dd, ^3J = 8.0 Hz, ^4J = 2.2 Hz, 1 H, Py(6(a))], 7.93 [dd, ^3J = 8.0 Hz, ^4J = 2.1 Hz, 3 H, Py(6)], 8.13 [d, ^3J = 7.2 Hz, 2 H, Nitr(3,5)], 8.55 [d, ^4J = 2.1 Hz, 1 H, Py(2(a))], 8.59 [d, ^4J = 2.1 Hz, 3 H, Py(2)]. − ^{31}P NMR: −8.3.

8e: From 500 mg (0.818 mmol) of **1e** and 175 mg (0.414 mmol) of cyclohexylbis(*p*-nitrophenyl) phosphate in 20 ml of CH_2Cl_2 for 16 h. Recrystallization from acetonitrile/dichloromethane (4:1). Yield 278 mg (75%) of **8e**. − IR: 2570m (BH), 1544m, 1340s (NO), 1251s (P=O). − ^{1}H NMR: 0.91 [m, 2 H, Cy(4)], 1.28 [m, 4 H, Cy(3), C(5)], 1.36 [m, 4 H, Cy(2), Cy(6)], 2.44 [s, 9 H, Me(py)], 2.56 [s, 9 H, Me(pz)], 3.61 [m, ^3J = 7.6 Hz, 1 H, Cy(1)], 6.31 [s, 3 H, H(pz)], 7.09 [d, ^3J = 9.1 Hz, 2 H, Nitr(2,6)], 7.27 [d, ^3J = 8.0 Hz, 3 H, Py(5)], 8.03 [dd, ^3J = 8.0 Hz, ^4J = 2.1 Hz, 3 H, Py(6)], 8.09 [d, ^3J = 9.1 Hz, 2 H, Nitr(3,5)], 8.63 [d, ^4J = 2.1 Hz, 3 H, Py(2)]. − ^{31}P NMR: −11.3.

General Procedure for the Condensation Reactions: The reagents were combined in 20 ml of dichloromethane and stirred for one day. The solvent was removed in vacuo and the residue crystallized from acetonitrile.

Table 3 Crystallographic details

	2c	**4b**	**5e**·H_2O	**7b′**	**8e**	**10d**
formula	$C_{40}H_{50}BN_6O_3PZn$ · CH_3OH	$C_{42}H_{38}BN_6O_4PZn$	$C_{42}H_{41}BN_{11}O_9PZn$ · CH_3CN · CH_3CN	$C_{48}H_{47}BN_9O_6PZn$ · H_2O	$C_{42}H_{46}BN_{10}O_6PZn$ · 1/2 CH_2Cl_2	$C_{51}H_{43}BN_{13}O_{17}P_2$-$Zn_{1.5}$ · CH_3CN · 5 · 1/2 CH_3CN
mol. mass	802.1	797.9	1012.6	971.1	936.5	1424.5
cryst. from	methanol	acetonitrile	acetonitrile	dichloromethane/ benzene	dichloromethane/ acetonitrile	acetonitrile
crystal size [mm]	0.6 × 0.4 × 0.2	1.20 × 1.10 × 0.60	0.6 × 0.6 × 0.4	0.80 × 0.60 × 0.60	0.5 × 0.4 × 0.2	0.5 × 0.4 × 0.2
space group	$P2_1/n$	$P\bar{1}$	$P\bar{1}$	$P\bar{1}$	$P\bar{1}$	$P\bar{1}$
Z	4	2	2	2	2	2
a [Å]	17.685(2)	10.988(4)	10.5440(4)	12.8873(6)	12.0108(6)	12.328(2)
b [Å]	14.015(1)	11.324(7)	13.9212(8)	13.4892(12)	12.8637(10)	14.050(6)
c [Å]	18.795(3)	16.255(14)	18.299(3)	17.4426(11)	15.489(2)	20.417(4)
α [°]	90	103.81(5)	101.970(7)	95.04(3)	71.162(7)	108.37(2)
β [°]	114.80(1)	91.51(5)	102.873(6)	91.95(3)	89.353(6)	97.38(2)
γ [°]	90	90.50(4)	101.036(4)	118.44(3)	80.276(5)	104.43(3)
V [Å^3]	4228.8(9)	1963.2(22)	2480.8(4)	2646.0(3)	2230.0(3)	3166.8(16)
d (calc.) [g·cm^{-3}]	1.23	1.35	1.36	1.22	1.40	1.49
d (obs.) [g·cm^{-3}]	1.21	1.31	1.30	1.18	1.35	1.44
temp. (K)	293(2)	293(2)	293(2)	293(2)	293(2)	200(2)
μ (Mo-$K\alpha$) [mm^{-1}]	0.662	0.716	0.593	0.549	0.705	0.707
Θ range [°]	2.5−26.3	3.1−26.0	2.5−26.0	2.8−26.0	2.3−26.0	3.1−26.0
hkl range	$-22\le h\le 19$ $-17\le k\le 0$ $0\le l\le 23$	$-13\le h\le 0$ $-13\le k\le 13$ $-20\le l\le 20$	$0\le h\le 13$ $-17\le k\le 16$ $-22\le l\le 21$	$-15\le h\le 15$ $-16\le k\le 16$ $-21\le l\le 0$	$-14\le h\le 0$ $-15\le k\le 15$ $-19\le l\le 19$	$0\le h\le 14$ $-17\le k\le 16$ $-24\le l\le 24$
refl. measd.	8828	8079	10277	10698	9168	12308
indep. refl.	8564	7663	9726	10342	8726	11729
obs. refl. (I>2σ(I))	4550	6922	6894	7855	6798	7581
parameters	478	496	640	622	578	998
refl. refined	8534	7662	9715	10337	8718	11702
R (obs. refl.): $R1$, $wR2$	0.079, 0.196	0.044, 0.122	0.046, 0.124	0.061, 0.203	0.046, 0.116	0.075, 0.163
R (all refl.): $R1$, $wR2$	0.176, 0.280	0.050, 0.131	0.088, 0.152	0.087, 0.237	0.073, 0.137	0.142, 0.215
residual el. density e/ Å^3	+1.1 −0.7	+0.8 −0.7	+0.6 −0.3	+1.1 −0.3	+0.9 −0.5	+1.2 −2.1

9a: From 500 mg (0.988 mmol) of **1a** and 215 mg (0.988 mmol) of diphenylphosphinic acid. Yield 620 mg (88%) of **9a** which was not analytically pure and could not be purified by repeated crystallizations. − IR: 2547m (BH), 1218vs (P=O). − ^{1}H NMR: 1.26 [s, 27 H, *t*Bu], 2.37 [s, 9 H, Me(pz)], 5.81 [s, 3 H, H(pz)], 7.32 [m, 6 H, Ph], 8.05 [m, 4 H, Ph]. − ^{31}P NMR: +17.8.

4a: From 200 mg (0.395 mmol) of **1a** and 98.7 mg (0.395 mmol) of diphenyl phosphate. Yield 260 mg (88%) of **4a**. − IR: 2552m (BH), 1290vs (P=O). − ^{1}H NMR: 1.41 [s, 27 H, *t*Bu], 2.39 [s, 9 H, Me(pz)], 5.84 [s, 3 H, H(pz)], 7.03 [m, 2 H, Ph], 7.19 [m, 8 H, Ph]. − ^{31}P NMR: −17.3.

5a: From 200 mg (0.395 mmol) of **1a** and 134 mg (0.395 mmol) of bis(*p*-nitrophenyl) phosphate. Yield 290 mg (75%) of **5a**. − IR: 252m (BH), 1537s, 1345s (NO), 1302vs (P=O). − ^{1}H NMR: 1.38 [s, 72 H, *t*Bu], 2.41 [s, 9 H, Me(pz)], 5.88 [s, 3 H, H(pz)], 7.42 [d, J = 8.9 Hz, 4 H, Ph], 8.17 [d, J = 8.9 Hz, 4 H, Ph].

4b: From 300 mg (0.530 mmol) of **1b** and 133 mg (0.530 mmol) of diphenyl phosphate. Yield 368 mg (87%).

5b: From 250 mg (0.442 mmol) of **1b** and 150 mg (0.442 mmol) of bis(*p*-nitrophenyl) phosphate. Yield 310 mg (79%).

5e: From 500 mg (0.818 mmol) of **1e** and 278 mg (0.817 mmol) of bis(*p*-nitrophenyl) phosphate. Yield 694 mg (91%) of **5e**. − IR: 3378w (H_2O), 2554m (BH), 1518s, 1344s (NO), 1258m (P=O). − ^{1}H NMR: 2.36 [s, 9 H, Me(py)], 2.58 [s, 9 H, Me(pz)], 6.31 [s, 3 H, H(pz)], 6.92 [d, ^3J = 9.1 Hz, 4 H, Nitr(2,6)], 7.13 [d, ^3J = 8.0 Hz, 3 H, Py(5)], 7.89 [dd, ^3J = 8.0 Hz, ^4J = 2.3 Hz, 3 H, Py(6)], 8.02 [d, ^3J = 9.1 Hz, 4 H, Nitr(3,5)], 8.66 [d, ^4J = 2.3 Hz, 3 H, Py(2)]. − ^{31}P NMR: −17.2.

Preparation of **10d**: 500 mg (0.879 mmol) of **1d** and 299 mg (0.879 mmol) of bis(*p*-nitrophenyl) phosphate in 40 ml of CH_2Cl_2 were stirred for 16 h. The solvent was removed in vacuo, the residue picked up in 50 ml of hot acetonitrile, filtered hot and left to crystallize at room temp.. After 3 days 330 mg (44%) of **10d** had precipitated. − IR: 2551m (BH), 1517s, 1345s (NO), 1257m (P=O). − ^{1}H NMR: 2.55 [s, 18 H, Me(pz)], 6.56 [s, 6 H, H(pz)], 7.35 [d, ^3J = 9.3 Hz, 16 H, Nitr(3,5)], 7.54 [dd, ^3J = 7.9 Hz, ^3J = 4.8 Hz, 6 H, Py(5)], 7.97 [ddd, ^3J = 7.9 Hz, ^4J = 2.2 Hz, ^4J = 1.6 Hz, Py(6)], 8.15 [d, ^3J = 9.3 Hz, 16 H, Nitr(2,6)], 8.64 [dd, ^3J = 4.8 Hz, ^4J = 1.6 Hz, 6 H, Py(4)], 8.79 [d, ^4J = 2.2 Hz, 6 H, Py(2)]. − ^{31}P NMR: −13.4.

Structure Determinations[39]: Diffraction data were recorded with the ω/2θ technique on a Nonius CAD4 diffractometer fitted with a molybdenum tube (K_α, λ = 0.7107 Å) and a graphite monochromator. No absorption corrections were applied. The structures were solved with direct methods and refined anisotropically with the SHELX program suite.[40] Hydrogen atoms were included with fixed distances and isotropic temperature factors 1.2 times those of their attached atoms. Parameters were refined against F^2. The R values are defined as $R_1 = \Sigma F_o - F_c/\Sigma F_o$ and $wR_2 = \{\Sigma[w(F_o^2 - F_c^2)^2/\Sigma[w(F_o^2)^2]\}^{1/2}$. Drawings were produced with SCHAKAL.[41] Table 3 lists the crystallographic data.

☆ Dedicated to Professor *Achim Müller* on the occasion of his 60th birthday.

[1] D. Voet, J. Voet, *Biochemistry*, Wiley, New York, **1990**.
[2] See volumes no. 5, 8, 15, and 32 in *Metal Ions in Biological Systems* (Ed.: H. Sigel), Marcel Dekker, New York, **1973−1997**.
[3] N. Sträter, W. N. Lipscomb, T. Klabunde, B. Krebs, *Angew. Chem.* **1996**, *108*, 2158−2191; *Angew. Chem. Int. Ed. Engl.* **1996**, *35*, 2024−2055.
[4] E. E. Kim, H. W. Wyckoff, *Clin. Chim. Acta* **1990**, *186*, 175−187.
[5] N. Sträter, T. Klabunde, P. Tucker, H. Witzel, B. Krebs, *Science* **1995**, *268*, 1489−1492.
[6] A. Volbeda, A. Lahm, F. Sakiyama, D. Suck, *EMBO J.* **1991**, *10*, 1607−1618.
[7] L. A. Kohlstaedt, J. Wang, J. M. Friedman, P. A. Rice, T. A. Steitz, *Science* **1992**, *256*, 1783−1790.
[8] S. Hansen, L. K. Hansen, E. Hough, *J. Mol. Biol.* **1993**, *231*, 870−876.
[9] M. M. Benning, J. M. Kuo, F. M. Raushel, M. M. Holden, *Biochemistry* **1994**, *33*, 15001−15007.
[10] C. M. Joyce, T. A. Steitz, *Annu. Rev. Biochem.* **1994**, *63*, 777−822.
[11] W. H. Chapman, R. Breslow, *J. Am. Chem. Soc.* **1995**, *117*, 5462−5469.
[12] B. Linkletter, J. Chin, *Angew. Chem.* **1995**, *107*, 529−531; *Angew. Chem. Int. Ed. Engl.* **1995**, *34*, 472−474.
[13] R. S. Brown, M. Zamkanei, J. L. Cocho, *J. Am. Chem. Soc.* **1984**, *106*, 5222−5228.
[14] T. Koike, S. Kajitani, I. Nakamura, E. Kimura, M. Shiro, *J. Am. Chem. Soc.* **1995**, *117*, 1210−1219.
[15] C. Bazzicalupi, A. Bencini, A. Bianchi, V. Fusi, C. Giorgi, P. Paoletti, B. Valtancoli, D. Zanchi, *Inorg. Chem.* **1997**, *36*, 2784−2790.
[16] M. Yashiro, A. Ishikubo, M. Komiyama, *J. Chem. Soc. Chem. Commun.* **1997**, 83−84.
[17] K. Schepers, B. Bremer, B. Krebs, G. Henkel, E. Althaus, B. Mosel, W. Müller-Wermuth, *Angew. Chem.* **1990**, *102*, 582−584; *Angew. Chem. Int. Ed. Engl.* **1990**, *29*, 531−533.
[18] S. Hikichi, M. Tanaka, Y. Moro-oka, N. Kitajima, *J. Chem. Soc. Chem. Commun.* **1992**, 814−815.
[19] H. Adams, N. A. Bailey, D. E. Fenton, Q.-Y. He, *J. Chem. Soc. Dalton Trans.* **1997**, 1533−1539.
[20] J. J. Wilker, S. J. Lippard, *Inorg. Chem.* **1997**, *36*, 969−978.
[21] A. Abufarag, H. Vahrenkamp, *Inorg. Chem.* **1995**, *34*, 2204−2216.
[22] T. Brandsch, F. A. Schell, K. Weis, M. Ruf, B. Müller, H. Vahrenkamp, *Chem. Ber.* **1997**, *130*, 283−289.
[23] A. Abufarag, H. Vahrenkamp, *Inorg. Chem.* **1995**, *34*, 2207−2216.
[24] M. Ruf, H. Vahrenkamp, *Chem. Ber.* **1996**, *129*, 1025−1028.
[25] R. Alsfasser, M. Ruf, S. Trofimenko, H. Vahrenkamp, *Chem. Ber.* **1993**, *126*, 703−710.
[26] M. Ruf, F. A. Schell, R. Walz, H. Vahrenkamp, *Chem. Ber.* **1997**, *130*, 101−104.
[27] M. Ruf, H. Vahrenkamp, *Inorg. Chem.* **1996**, *35*, 6571−6578.
[28] M. Ruf, K. Weis, H. Vahrenkamp, *J. Chem. Soc. Chem. Commun.* **1994**, 135−136.
[29] R. Walz, K. Weis, M. Ruf, H. Vahrenkamp, *Chem. Ber.* **1997**, *130*, 975−980.
[30] K. Weis, M. Rombach, H. Vahrenkamp, unpublished.
[31] K. Weis, H. Vahrenkamp, *Eur. J. Inorg. Chem.* **1998**, 271−274, succeeding paper.
[32] M. Ruf, K. Weis, H. Vahrenkamp, *J. Am. Chem. Soc.* **1996**, *118*, 9288−9294.
[33] K. Weis, H. Vahrenkamp, *Inorg. Chem.*, in print.
[34] A. F. Wells, *Structural Inorganic Chemistry*, Clarendon Press, Oxford, **1975**.
[35] H. Bock, *Angew. Chem.* **1989**, *101*, 1659−1682; *Angew. Chem. Int. Ed. Engl.* **1989**, *28*, 1627−1650.
[36] M. Förster, R. Burth, A. K. Powell, T. Eiche, H. Vahrenkamp, *Chem. Ber.* **1993**, *126*, 2643−2648.
[37] M. Ruf, R. Burth, K. Weis, H. Vahrenkamp, *Chem. Ber.* **1996**, *129*, 1251−1257.
[38] R. Charubala, W. Pfleiderer, *Heterocycles* **1981**, *15*, 761−776. F. Eckstein, V. Kutzke, *Tetrahedron Lett.* **1986**, *27*, 1657−1660.
[39] The crystallographic data of the structures described in this paper were deposited with the Cambridge Crystallographic Data Centre as "supplementary publication no. CCDC-100723". Copies of these data are available free of charge from the following address: The Director, CCDC, 12 Union Road, GB-Cambridge CB2 1EZ (Telefax: Int. +12 23/3 36 0 33; E-mail: teched@chemcrys.cam.ac.uk).
[40] G. M. Sheldrick, *SHELX-86* and *SHELXL-93*, Programms for Crystal Structure Determination, Universität Göttingen, **1986** and **1993**.
[41] E. Keller, Program *SCHAKAL*, Universität Freiburg, **1993**.

[97222]

Hydrolytic Cleavage of Diphosphates, Sulfonatophosphates, and Disulfonates by (Pyrazolylborate)zinc Hydroxide Complexes☆

Karl Weis and Heinrich Vahrenkamp*

Institut für Anorganische und Analytische Chemie der Universität Freiburg,
Albertstrasse 21, D-79104 Freiburg, Germany

Received September 27, 1997

Keywords: Zinc complexes / Pyrazolylborate ligands / Hydrolytic cleavage / Diphosphate / Sulfonatophosphate / Disulfonate

Three (pyrazolylborate)zinc hydroxide complexes Tp*Zn−OH were used as hydrolytic reagents to cleave the P−O−P, P−O−S, and S−O−S linkages of organic diphosphates, sulfonatophosphates, and disulfonates. The resulting complexes of the types Tp*Zn−OPO(OR)$_2$ and Tp*Zn−O-SO$_2$R could also be obtained by condensation reactions between Tp*Zn−OH and HO−PO(OR)$_2$ or HO−SO$_2$R. Two of them were characterized by structure determinations.

Among the many phosphate transferring enzymes, an important class are those which cleave the P−O−P linkages of oligophosphates, e.g. ADP, ATP, or inorganic pyrophosphate[1][2][3]. As a rule these are metalloenzymes, quite often containing two or three metal ions in the active center, typically magnesium, manganese or zinc[4]. In all cases the labile coordination positions on the metal ions are occupied by water molecules in the resting enzymes and by the reacting phosphate entities in the working enzymes. Here like in other hydrolytic metalloenzymes the essential nucleophile is likely to be a M−OH unit[5].

While the modelling of enzymes cleaving phosphate esters by metal coordination compounds is very well established (see preceding paper[6] and references cited therein), we are not aware of related studies concerning the cleavage of P−O−P or related systems[7]. We therefore started such a study using our established "enzyme model" in the form of the highly nucleophilic pyrazolylborate zinc hydroxide complexes Tp*Zn−OH[8][9][10][11][12][13]. Following our preliminary communication on a P−O−P system, i.e. an anhydride of a phosphoric acid[14], we extended the studies to a S−O−S system, i.e. an anhydride of a sulfonic acid, and a P−O−S system, i.e. a mixed anhydride. The latter bears relevance in relation to adenosine-3′-phosphate-5′-phosphosulfate (PAPS), a sulfate resource of various organisms[15]. Our main interest was to find out how efficient our Tp*Zn−OH complexes would be for the cleavage of these anhydride systems.

As the "enzyme models" we used the three Tp*Zn complexes **1a**−**c**. Their "substrates" were chosen to be molecular rather than ionic species, i.e. containing fully esterified phosphate units [(RO)$_2$P(O)O] or sulfate units (RSO$_2$O). The purpose of this was to locate the reactivity in the anhydride linkages rather than the acidic P−OH or S−OH functions and to ease reaction with the Tp*Zn−OH complexes which are not water-soluble. As a result the reactions were predetermined to be stoichiometric rather than catalytic.

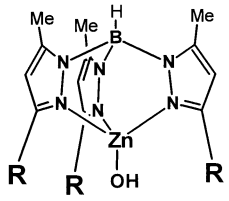

1a (Tp^{tBu,Me}Zn-OH) : R = t-butyl

1b (Tp^{Cum,Me}Zn-OH): R = p-cumenyl

1c (Tp^{Pic,Me}Zn-OH) : R = 5′-picolyl

Reactions and Products

It was found that of the three Tp*Zn−OH complexes **1a** does not react with diphosphates. The steric bulk of the *tert*-butyl groups seems to be too high. The other attempts at diphosphate cleavage went smoothly and produced the cleavage products in high yields. Tetraethyl diphosphate and **1b** yielded **2b**, tetraphenyl diphosphate upon reaction with **1b** and **1c** yielded **3b** and **3c** of which **3b** was obtained before by cleavage of PO(OPh)$_3$ with **1b**[6]. Upon recrystallization from acetonitrile which was not fully dried both **3b** and **3c** were converted to adducts, as found out by the subsequent structure determinations. Of these **3b′** results from partial hydrolytic destruction of the Tp^{Cum,Me} ligand while **3c′** simply involves addition of a water molecule.

Tp^{Cum,Me}Zn−OPO(OEt)$_2$ **2b**

Tp^{R,Me}Zn−OPO(OPh)$_2$
3a: R = *t*Bu
3b: R = Cum
3c: R = Pic

(Tp^{Cum,Me})(3-methyl-5-cumenyl-pyrazole)Zn−OPO(OPh)$_2$ **3b′**

(Tp^{Pic,Me})(H$_2$O)Zn−OPO(OPh)$_2$ **3c′**

The S−O−S system employed was the anhydride of *p*-toluenesulfonic acid (SOS). It reacted easily with **1c**, forming **4c** in good yields which was crystallized as a hydrate again. As the mixed anhydride we used that of diphenylphosphate and *p*-toluenesulfonic acid (POS). Its reaction with **1c** at room temperature was complete within about half a day. The product mixture consisted of an equimolar

 © WILEY-VCH Verlag GmbH, D-69451 Weinheim, 1998 1434−1948/98/0202−0271 $ 17.50+.50/0

mixture of **3c** and **4c** as evidenced by IR and ^{1}H- as well as ^{13}C-NMR spectroscopy. The separation of this mixture proved to be too cumbersome, however.

$Tol-SO_2-O-SO_2-Tol$ (SOS) $(PhO)_2PO-O-SO-Tol$ (POS)

$Tp^{R,Me}Zn-OSO_2-Tol$

4a: R = *t*Bu
4b: R = Cum
4c: R = Pic

The first step of the hydrolytic cleavages of the anhydrides by Tp*Zn−OH must result in the liberation of one equivalent of the corresponding acid while the other half of the anhydride becomes attached to zinc as in complexes **2**−**4**. Following the reactions spectroscopically gave no evidence, however, for the free acids $(RO)_2POOH$ or TosOH. Instead only the complexes **2**, **3**, or **4** were observed. This means that the free acids react quickly with excessive Tp*Zn−OH by means of a condensation reaction. Accordingly, employing a 1:1 stoichiometry for Tp*Zn−OH and anhydride resulted in only half-consumption of the anhydride. Therefore a 2:1 stoichiometry was applied for the preparations.

It could then be shown that the formation of the zinc phosphate and sulfonate complexes by condensation is indeed a fast reaction. It worked for the diorganophosphates yielding **3a** and **c** (see preceding paper[6]). It worked for all three Tp*Zn−OH complexes with *p*-toluenesulfonic acid, resulting in complexes **4a**−**c** of which **4a** has already been described by us[16]. For preparative purposes this condensation reaction is the method of choice to obtain complexes like **3** and **4**.

The identification of the Tp*Zn phosphate and sulfonate complexes consisted mainly in the structure determinations described here and in previous papers. The spectral data (see Experimental Section) are in agreement. Specifically the IR bands of the BH, P=O, and S=O functions, the ^{1}H-NMR resonances of the Tp* ligands, and the ^{31}P-NMR resonances are of diagnostic value.

Structure Determinations

The basic structural information on the complex types **2**, **3**, and **4** was already available due to the structure determinations of **4a** and various $Tp^*Zn-OPOX_2$ compounds[6][16][17]. In addition to this, the X-ray analyses of **3b′** and **3c′** were worthwhile because they yielded coordination patterns of zinc which differ from the usual tetrahedral Tp*Zn−X arrangement. In both cases, despite the steric bulk of the pyrazoles′ 3-substituents (Cum, Pic) and despite the presence of the voluminous phosphate ligand, a further ligand (the pyrazole in **3b′** and the water molecule in **3c′**) can exist in the ligand sphere of zinc. This finally breaks the rule that the sterically demanding Tp* ligands are "tetrahedral enforcers". In a later paper we will discuss the mechanistic implications arising from a comparison of the very variable geometry at the five-coordinated zinc ion in Tp*Zn(X)(Y) complexes.

Complex **3b′** (see Figure 1) contains the two coligands (phosphate and pyrazole) close to each other [angle O1−Zn−N8 103.1(2)°] and connected by a hydrogen bond between O4 and N7 (2.78 Å). The coordination of the Tp* ligand to zinc is very unusual. While the pyrazole nitrogen atoms N1 and N2 are attached at normal distances, N3 is practically nonbonding. Thus the geometry of **3b′** is intermediate between a flattened tetrahedron with N8 at the apex and an elongated trigonal bipyramid with N8 at the "short" and N3 at the "long" apex. In terms of a S_N2 substitution at a tetrahedral center this represents a situation close to the final state, i.e. with the entering group (N8) almost firmly bound and the leaving group (N3) almost completely removed. Complex **3b′** is, after $Tp^{Ph,Me}$(3-methyl-5-phenylpyrazole)Zn−OPO(OEt)(OC_6H_4−*p*-NO_2)[6], the second example of this kind of Tp*Zn complexes with a coordination intermediate between four- and fivefold.

Figure 1. Molecular structure of **3b′**[a]

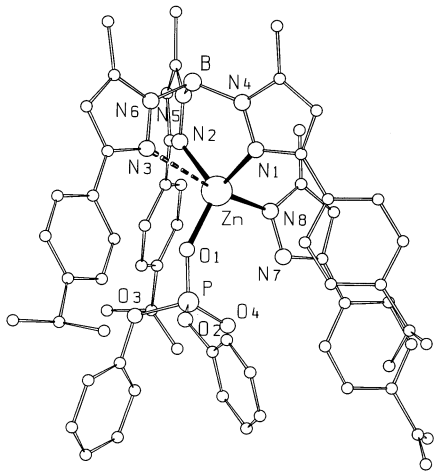

[a] Selected bond lengths [Å] and angles [°]: Zn−O1 1.905(4), Zn−N1 1.983(5), Zn−N2 2.004(5), Zn−N3 3.090(5), Zn−N8 2.080(5), P−O1 1.486(4), P−O4 1.467(4), N8−Zn−N3 171.9(2), Zn−O1−P 147.3(3).

The pyrazole ligand and the phosphate ligand in **3b′** display no unusual features. The Zn−O bond is relatively short, but typical for Tp*Zn−O compounds[6][8][9][10][11][12][13][14]. The phosphate ligand shows the typical equalization of the "single" and "double" P−O bonds P−O1 and P−O4 that we have observed previously[6][18]. Together with the rather large P−O−Zn angle it must reflect a partly ionic nature of the Zn−O bond. Similar observations hold for the Zn−O, P−O, and P−O−Zn interactions in complex **3c′** (see Figure 2). Zinc phosphate complexes not bearing Tp* ligands normally have longer Zn−O bonds, as evidenced by the two examples bearing diphenylphosphate ligands[19][20].

Like in **3b′**, the two coligands in **3c′** (water and phosphate) are linked by a hydrogen bond (O2−O5 2.77 Å). Otherwise there is no similarity between **3b′** and **3c′**. However, **3c′** is a close analogue of the complex $Tp^{Pic,Me}(H_2O)$-Zn−OPO(OC_6H_4−*p*-NO_2)$_2$ which was obtained by phosphate ester hydrolysis[6]. The Tp* ligand in **3c′** is bound in a symmetrical fashion, and the coordination geometry about the zinc ion is strictly trigonal-bipyramidal with one pyrazole nitrogen and the water oxygen on the apical posi-

Figure 2. Molecular structure of **3c′**[a]

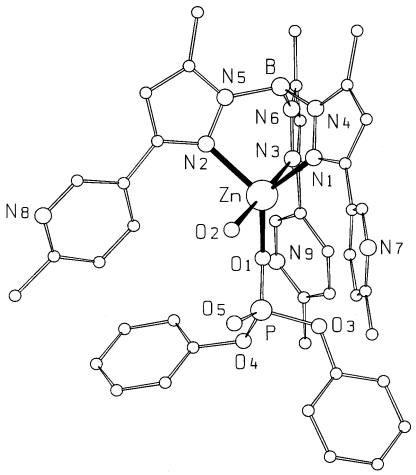

[a] Selected bond lengths [Å] and angles [°]: Zn−O1 1.947(3), Zn−N1 2.065(4), Zn−N2 2.069(4), Zn−N3 2.200(4), Zn−O2 2.102(3), P−O1 1.496(3), P−O5 1.464(4), N3−Zn−O2 178.9(1), Zn−O1−P 138.6(2).

tions. The bond lengths at zinc are larger than in tetrahedral Tp*Zn−O complexes[6][8][9][10][11][12][13][14], reflecting the increase in coordination number, and typically the bonds holding the two apical atoms are elongated. A comparison of **3b′** and **3c′** in terms of bond lengths shows that all comparable ligand donor atoms except N3 are closer to zinc in **3b′**, thus qualifying **3b′** as tetrahedral rather than trigonal-bipyramidal.

Conclusions

The work in this paper has shown that the hydrolytic prowess of the Tp*Zn−OH "enzyme models" extends to the cleavage of the E−O−E links in inorganic polyacids. Part of the driving force of the hydrolytic cleavages seems to be the capturing of the resulting anionic fragments as O-bound ligands. These are not replaceable by water or other donor ligands. Instead these can be bound as additional ligands in five-coordinate Tp*(L)Zn−OPO(OR)$_2$ complexes.

This work was supported by the *Deutsche Forschungsgemeinschaft* and by the Fonds der Chemischen Industrie. We thank Dr. *W. Deck* and Mr. *B. Müller* for help with the NMR and X-ray work.

Experimental Section

General experimental methods and measuring techniques see ref.[21]. The Tp*Zn−OH complexes[8][10][22], the diphosphate[23] and the sulfonatophosphate[24] were prepared according to the published procedures. All other reagents were obtained commercially. Solvents were degassed but not dried. IR data (cm^{-1}) were recorded from KBr pellets, ^{1}H- and ^{31}P-NMR data (δ in ppm, int. TMS, ext. H_3PO_4) were recorded from $CDCl_3$ solutions.

Hydrolytic Cleavages: *Tetraethyl Diphosphate and* **1b**: 138 mg (0.200 mmol) of **1b** and 29.0 mg (0.100 mmol) of tetraethyl diphosphate in 20 ml of dichloromethane were stirred at room temp. for 16 h. The solvent was removed in vacuo. Recrystallization from acetonitrile at −25°C yielded 110 mg (66%) of **2b**, m. p. 184°C. − $C_{43}H_{56}BN_6O_4PZn$ (828.1): calcd. C 62.36, H 6.82, N 10.15; found C 61.55, H 6.68, N 9.96. − IR: 2550m (BH), 1252s (P=O). − ^{1}H NMR: 0.85 [t, J = 7.0 Hz, 6 H, Me(OEt)], 1.24 [d, J = 6.9 Hz, 18 H, Me(*i*Pr)], 2.52 [s, 9 H, Me(pz)], 2.92 [sept, J = 6.9 Hz, 3 H, CH(*i*Pr)], 3.44 [dt, J = 7.0 Hz, 7.0 Hz, 4 H, CH_2(OEt)], 6.22 [s, 3 H, CH(pz)], 7.35 [d, J = 8.2 Hz, 6 H, Ph(3,5)], 7.66 [d, J = 8.2 Hz, 6 H, Ph(2,6)]. − ^{31}P NMR: −2.0.

Tetraphenyl Diphosphate and **1b**: As before with 500 mg (0.722 mmol) of **1b** and 174 mg (0.361 mmol) of tetraphenyl diphosphate in 40 ml of CH_2Cl_2. When the reaction and workup were performed under strictly anhydrous conditions, they resulted in 620 mg (93%) of **3b**[6].

Recrystallization of 300 mg (0.325 mmol) of **3b** from hot undried acetonitrile resulted in the formation of 237 mg (86%) **3b′**, m. p. 191°C. − $C_{64}H_{72}BN_8O_4PZn$ (1124.5). calcd. C 68.36, H 6.45, N 9.97; found C 68.11, H 6.43, N 9.95. − IR: 2545 (BH), 1242s (P=O). − ^{1}H NMR: 0.97 [d, ^3J = 6.9 Hz, 18 H, Me(*i*Pr)], 1.24 [d, ^3J = 6.9 Hz, 6 H, Me(*i*Pr(a))], 2.49 [s, 9 H, Me(pz)], 2.49 [s, 3 H, Me(pz(a))], 2.62 [sept, ^3J = 6.9 Hz, 3 H, H(*i*Pr)], 2.89 [sept, ^3J = 6.9 Hz, 1 H, H(*i*Pr(a))], 5.98 [s, 1 H, H(pz(a))], 6.21 [s, 3 H, H(pz)], 6.91 [d, ^3J = 8.2 Hz, 2 H, Ph(3,5(a))], 7.02 [d, ^3J = 8.1 Hz, 6 H, Ph(3,5)], 7.07 [m, 10 H, Ph(phos(2,3,4,5,6))], 7.45 [d, ^3J = 8.2 Hz, 2 H, Ph(2,6(a))], 7.54 [d, ^3J = 8.1 Hz, 6 H, Ph(2,6)]. − ^{31}P NMR: −13.9.

Tetraphenyl Diphosphate and **1c**: As before with 500 mg (0.818 mmol) of **1c** and 200 mg (0.415 mmol) of tetraphenyl diphosphate in 40 ml of CH_2Cl_2 Recrystallization from undried acetonitrile yielded 645 mg (92%) of **3c′**, m. p. 148°C. − $C_{42}H_{43}BN_9O_5PZn$ (861.0): calcd. C 58.54, H 5.03, N 14.64; found C 58.43, H 5.01, N 14.71. − IR: 3300m,br (H_2O), 2557m (BH), 1231s (P=O). − ^{1}H NMR: 2.30 [s, 9 H, Me(py)], 2.56 [s, 9 H, Me(pz)], 6.30 [s, 3 H, H(pz)], 6.76 [d, ^3J = 8.1 Hz, 4 H, Ph(phos(2,6))], 7.06 [m, ^3J = 8.1 Hz, 6 H, Ph(phos(3,4,5))], 7.06 [d, ^3J = 8.0 Hz, 3 H, Py(5)], 8.04 [dd, ^3J = 8.0 Hz, ^4J = 2.1 Hz, 3 H, Py(6)], 8.57 [d, ^4J = 2.1 Hz, 3 H, Py(2)]. − ^{31}P NMR: −15.0.

p-Toluenesulfonic Acid Anhydride (SOS) and **1c**: As before with 500 mg (0.818 mmol) of **1c** and 136 mg (0.413 mmol) of SOS in 40 ml of CH_2Cl_2. Recrystallization from undried acetonitrile/dichloromethane (5:1) yielded 506 mg (79%) of **4c**·H_2O·1/2 CH_2Cl_2, m. p. 132°C. − $C_{37}H_{40}BN_9O_4SZn$·1/2 CH_2Cl_2 (783.0 + 42.5): calcd. C 54.56, H 5.01, N 15.27; found C 54.37, H 4.80, N 15.26. − IR: 3400m,br (H_2O), 2544m (BH), 1378s (S=O). − ^{1}H NMR: 2.21 [s, 9 H, Me(py)], 2.36 [s, 3 H, Me(Tos)], 2.55 [s, 9 H, Me(pz)], 3.25 [s, 2 H, H_2O, (broad)], 6.24 [s, 3 H, H(pz)], 7.00 [d, ^3J = 8.1 Hz, 3 H, Py(5)], 7.06 [d, ^3J = 8.2 Hz, 2 H, Tos(3,5)], 7.24 [d, ^3J = 8.2 Hz, 2 H, Tos(2,6)], 7.98 [dd, ^3J = 8.1 Hz, ^4J = 2.3 Hz, 3 H, Py(6)], 8.51 [d, ^4J = 2.3 Hz, 3 H, Py(2)].

Diphenylphosphato-p-toluenesulfonate (POS) and **1c**: 500 mg (0.818 mmol) of **1c** and 167 mg of POS in 40 ml of CH_2Cl_2 were stirred under anhydrous conditions for 16 h at room temp. The solvent was removed in vacuo and the residue picked up in $CDCl_3$. ^{1}H- and ^{31}P-NMR spectra showed that the starting materials had disappeared and the solution contained an equimolar mixture of **3c** and **4c**.

Condensation Reactions (for **3a** and **c** see preceding paper[6]): **4b**: 276 mg (0.400 mmol) of **1b** and 76.0 mg (0.400 mmol) of *p*-toluenesulfonic acid hydrate in 20 ml of dichloromethane were stirred at room temp. for 8 h under strictly anhydrous conditions. Removal of the solvent in vacuo and recrystallization from carefully dried acetonitrile yielded 265 mg (78%) of **4b**, m. p. 158°C. − $C_{46}H_{53}BN_6O_3SZn$ (846.2): calcd. C 65.29, H 6.31, N 9.93; found

C 64.42, H 6.07, N 9.46. – IR: 2552m (BH), 1292s (S=O). – ^{1}H NMR: 1.12 [d, J = 6.9 Hz, 18 H, Me(*i*Pr)], 2.53 [s, 9 H, Me(pz)], 2.78 [sept, J = 6.9 Hz, 3 H, CH(*i*Pr)], 6.21 [s, 3 H, CH(pz)], 6.86 [d, J = 7.9 Hz, 2 H, CH(Tos)], 7.02 [d, J = 7.9 Hz, 2 H, CH(Tos)], 7.12 [d, J = 8.1 Hz, 6 H, Ph(3,5)], 7.56 [d, J = 8.1 Hz, 6 H, Ph(2,6)].

4c: 500 mg (0.818 mmol) of **1c** and 141 mg (0.819 mmol) of *p*-toluenesulfonic acid hydrate in 40 ml of CH_2Cl_2 were stirred at room temp. for 16 h. Removal of the solvent and recrystallization from acetonitrile/dichloromethane (5:1) under non-anhydrous conditions yielded 583 mg (91%) of **4c**·H_2O·1/2 CH_2Cl_2.

Structure Determinations[25]: Crystals of **3b′** and **3c′** were obtained from undried acetonitrile. Diffraction data were recorded at room temperature with the ω/2θ technique on a Nonius CAD4 diffractometer fitted with a molybdenum tube (K_α, λ = 0.7107 Å) and a graphite monochromator. Semiempirical absorption corrections based on ψ scans were applied. The structures were solved with direct methods and refined anisotropically with the SHELX program suite.[26] Hydrogen atoms were included with fixed distances and isotropic temperature factors 1.2 times those of their attached atoms. Parameters were refined against F^2. The R values are defined as $R_1 = \Sigma F_o - F_c / \Sigma F_o$ and $wR_2 = \{\Sigma[w(F_o^2 - F_c^2)^2 / \Sigma[w(F_o^2)^2]\}^{1/2}$. Drawings were produced with SCHAKAL.[27] Table 1 lists the crystallographic data.

Table 1. Crystallographic data for complexes **3b′** and **3c′**

	3b′	**3c′**
formula	$C_{64}H_{72}BN_8O_4PZn$	$C_{42}H_{43}BN_9O_5PZn$
mol. mass	1124.5	861.0
cryst. size [mm]	0.5 × 0.5 × 0.4	0.6 × 0.5 × 0.4
space group	*P*2(1)/*c*	*P*2(1)/*n*
Z	4	4
a [Å]	18.240(2)	12.9610(11)
b [Å]	13.618(4)	16.832(2)
c [Å]	25.104(4)	19.708(4)
β [°]	102.590(15)	105.79(1)
V [Å^3]	6085.7(21)	4137.2(10)
^{d}calcd.[g·cm^{-3}]	1.23	1.38
^{d}obsd. [g·cm^{-3}]	1.19	1.31
μ (Mo-K_α) [mm^{-1}]	0.483	0.689
Θ-range [°]	2.2–23.7	2.4–26.0
hkl range	$-20 \le h \le 20$	$-15 \le h \le 15$
	$0 \le k \le 15$	$-20 \le k \le 0$
	$0 \le l \le 28$	$-24 \le l \le 0$
refl. measd.	9491	8332
indep. refl.	9246	8093
obs. refl. [$I > 2\sigma(I)$]	4006	4396
parameters	732	532
R (obs.. refl.)	$R1$ = 0.058, $wR2$ = 0.105	$R1$ = 0.054, $wR2$ = 0.113
R (all refl.)	$R1$ = 0.241, $wR2$ = 0.166	$R1$ = 0.168, $wR2$ = 0.160
res. el. dens. [e/A^{-3}]	+0.5 / −0.5	+0.5 / −0.4

☆ Dedicated to Professor *Manfred Weidenbruch* on the occasion of his 60th birthday.

[1] For ATP ases and related enzymes see J. B. Lingrel, T. Kuntzweiler, *J. Biol. Chem.* **1994**, *31*, 19659–19662.

[2] For kinases see H. J. Müller-Dieckmann, G. E. Schulz, *J. Mol. Biol.* **1994**, *236*, 361–367.

[3] For inorganic pyrophosphatases see J. Kankare, T. Salminen, R. Lahti, B. S. Cooperman, A. A. Baykov, A. Goldman, *Biochemistry* **1996**, *35*, 4670–4677.

[4] N. Sträter, W. N. Lipscomb, T. Klabunde, B. Krebs, *Angew. Chem.* **1996**, *108*, 2158–2191; *Angew. Chem. Int. Ed. Engl.* **1996**, *35*, 2024–2055.

[5] D. W. Christianson, *Adv. Protein Chem.* **1991**, *42*, 281–355.

[6] K. Weis, M. Ruf, M. Rombach, H. Vahrenkamp, *Eur. J. Inorg. Chem.* **1998**, 263–270, preceding paper.

[7] For a review on interactions of metal ions with nucleoside oligophosphates see H. Sigel, *Chem. Soc. Rev.* **1993**, *22*, 255–267.

[8] R. Alsfasser, M. Ruf. S. Trofimenko, H. Vahrenkamp, *Chem. Ber.* **1993**, *126*, 703–710.

[9] M. Ruf, K. Weis, H. Vahrenkamp, *J. Am. Chem. Soc.* **1996**, *118*, 9288–9294.

[10] M. Ruf, H. Vahrenkamp, *Inorg. Chem.* **1996**, *35*, 6571–6578.

[11] M. Ruf, H. Vahrenkamp, *Chem. Ber.* **1996**, *129*, 1025–1028.

[12] M. Ruf, F. A. Schell, R. Walz, H. Vahrenkamp, *Chem. Ber.* **1997**, *130*, 101–104.

[13] M. Ruf, K. Weis, H. Vahrenkamp, *Inorg. Chem.* **1997**, *36*, 2130–2137.

[14] M. Ruf, K. Weis, H. Vahrenkamp, *J. Chem. Soc. Chem. Commun.* **1994**, 135–136.

[15] S. Lyle, D. H. Geller, K. Ng, J. Westley, N. B. Schwartz, *Biochem. J.* **1994**, *301*, 349–354.

[16] T. Brandsch, F. A. Schell, K. Weis, M. Ruf, B. Müller, H. Vahrenkamp, *Chem. Ber.* **1997**, *130*, 283–289.

[17] S. Hikichi, M. Tanaka, Y. Moro-oka, N. Kitajima, *J. Chem. Soc. Chem. Commun.* **1992**, 814–815.

[18] A. Abufarag, H. Vahrenkamp, *Inorg. Chem.* **1995**, *34*, 2207–2216.

[19] T. Tanase, S. P. Watton, S. J. Lippard, *J. Am. Chem. Soc.* **1994**, *116*, 9401–9402.

[20] K. Schepers, B. Bremer, B. Krebs, G. Henkel, E. Althaus, B. Mosel, W. Müller-Warmuth, *Angew. Chem.* **1990**, *102*, 582–584; *Angew. Chem. Int. Ed. Engl.* **1990**, *29*, 531–533.

[21] M. Förster, R. Burth, A. K. Powell, T. Eiche, H. Vahrenkamp, *Chem. Ber.* **1993**, *126*, 2643–2648.

[22] M. Ruf, R. Burth, K. Weis, H. Vahrenkamp, *Chem. Ber.* **1996**, *129*, 1251–1257.

[23] S. Corby, G. W. Kenner, A. R. Todd, *J. Am. Chem. Soc.* **1958**, *80*, 1234–1243.

[24] W. Dabkowski, Z. Skrzypczynski, J. Michalski, N. Piel, L. W. McLaughlin, F. Cramer, *Nucl. Acids Res.* **1984**, *12*, 9123–9135.

[25] The crystallographic data of the structures described in this paper were deposited with the Cambridge Crystallographic Data Centre as "supplementary publication no. CCDC-100726". Copies of these data are available free of charge from the following address: The Director, CCDC, 12 Union Road, GB-Cambridge CB2 1EZ (Telefax: Int. +44(00)12 23/3 36 0 33; E-mail: teched@chemcrys.cam.ac.uk).

[26] G. M. Sheldrick, *SHELX-86* and *SHELXL-93*, Programms for Crystal Structure Determination, Universität Göttingen, **1986** and **1993**.

[27] E. Keller, Program *SCHAKAL*, Universität Freiburg, **1993**.

[97223]

Transition-Metal-Catalyzed Oxidations, 7[◇]

Spectroscopic Evidence for Intramolecular $Mo^{VI}(O_2)\cdots HO-C$ Hydrogen Bonding in Solution

Holger Glas, Michael Spiegler, and Werner R. Thiel*

Anorganisch-chemisches Institut, Technische Universität München
Lichtenbergstr. 4, D-85747 Garching
Fax: (internat.) + 49(0)89/289-13473
E-mail: thiel@arthur.anorg.chemie.tu-muenchen.de

Received July 10, 1997

Keywords: Molybdenum / Peroxo complexes / Hydrogen bonds / Catalysis

The ring-opening reaction of epoxycyclohexane with 2-[3(5)-pyrazolyl]pyridine results in the formation of racemic *trans*-2-[3-(2-pyridyl)-1-pyrazolyl]cyclohexanol (**1**). Kinetic resolution with lipase B from *candida antarctica* gives the (1*S*,2*S*) enantiomer of **1**, the solid-state structure of which was determined by X-ray crystallography, as an enantiomerically pure tridentate ligand. Investigation by NMR spectroscopy of the corresponding oxodiperoxomolybdenum complex **2**, where **1** acts as a bidentate chelate, proves the formation of a weak intramolecular $Mo^{VI}(O_2)\cdots HO-C$ bridge in $CHCl_3$ solution. This H bonding is broken by solvents such as acetone, THF or DMF, which are capable of forming hydrogen bonds to alcohols. Intermolecular hydrogen bonds between the OH groups and molybdenum peroxo moieties are also found in the solid-state structure of **2**, leading to a helical arrangement of the peroxo complexes.

Peroxo complexes of high-valent transition metals are used as catalysts or stoichiometric reagents for the oxidation of organic and inorganic substrates[2]. We have investigated the role of seven-coordinate oxodiperoxomolybdenum complexes in the catalytic epoxidation of olefins[1] and have focused on bidentate *N*-alkylated 2-[3(5)-pyrazolyl]pyridine ligands, first described by H. Brunner et al.[3]. This ligand system allows the introduction of long alkyl side chains, leading to excellent solubility of the derived molybdenum catalysts in organic solvents, and a variation of the donor strength by the inclusion of electron donating and withdrawing groups attached to the heteroaromatic rings. The latter feature enables a correlation of electronic ligand properties with epoxidation activities of the catalysts[1]. From spectroscopic and kinetic investigations on peroxo complexes bearing olefinic side chains, we postulated a new reaction mechanism for the catalytic olefin epoxidation with seven-coordinate peroxomolybdenum complexes. In this mechanism the oxidizing agent (e.g. *tert*-butyl hydroperoxide) is activated by the Lewis acidic transition-metal center, resulting in an oxygen transfer from the hydroperoxide, and not from the η^2-coordinated peroxo ligands, to the olefin[4].

One crucial point of this mechanism is a proton transfer from the hydroperoxide to one of the peroxo ligands. NMR investigations (^1H,^{13}C,^{17}O NMR) on the reactivity of peroxomolybdenum complexes in the presence of strong Lewis and Brønsted acids, showed that the peroxo ligands are preferentially protonated while the oxo ligand is a poor proton acceptor[5]. These spectroscopic findings are in agreement with the results of Extended Hückel calculations on the model complex $(NH_3)_2MoO(O_2)_2$, which proved that the three highest occupied molecular orbitals of such compounds possess mainly π^* character at the peroxo ligands and only low σ^* and π^* character at the oxo ligand. From a mechanistic point of view, this proton transfer should start with the formation of a hydrogen bond between the hydroperoxide and an η^2-peroxo ligand. Since we were never able to prove such interactions between the weak Brønsted base η^2-O_2 and weak Brønsted acids like hydroperoxides or alcohols by means of spectroscopy, the energies of these bonds should be low. To overcome this problem, we synthesized new *N*,*N*-donor ligands of the pyrazolylpyridine type bearing OH functions in the side chain, which should lead to the formation of an intramolecular hydrogen bond. In the present paper, we describe the synthesis of such ligands and the corresponding peroxomolybdenum complexes, along with the NMR- and IR-spectroscopic evidence for a weak intramolecular $Mo^{VI}(O_2)\cdots H-OR$ interaction in solution.

Results and Discussion

The *N*-alkylation of 2-[3(5)-pyrazolyl]pyridines is usually carried out by a deprotonation (NaH) alkylation (RX, X = Br, I) sequence with THF as the solvent[6]. According to this procedure, primary linear alkyl substituents can be introduced with high regioselectivities and high yields. From geometric considerations, intramolecular hydrogen bonding would require a 2-hydroxyethyl or a 3-hydroxypropyl group, which can easily be attached to the pyrazole moiety of the

[◇] Part 6: Ref.[1].

 © WILEY-VCH Verlag GmbH, D-69451 Weinheim, 1998 1434–1948/98/0202–0275 $ 17.50+.50/0

chelate ligand by nucleophilic ring opening of oxiranes or oxetanes. For synthetic reasons we focused on the ring opening of epoxycyclohexane with pyrazolylpyridine, generating a 1,2-disubstituted cyclohexane ring, which would also be expected to increase solubility of the desired peroxo complexes.

Heating a 1:1.5 mixture of 2-[3(5)-pyrazolyl]pyridine and epoxycyclohexane for 4 h at 170°C in a pressure tube[7] gives *rac-trans*-2-[3-(2-pyridyl)-1-pyrazolyl]cyclohexanol (**1**) in more than 90% yield (Scheme 1).

Scheme 1. i. 160°C, 4 h, pressure tube; ii. isopropenyl acetate, molecular sieve 4 A, lipase B from *candida antarcica*, 37°C, 4 h

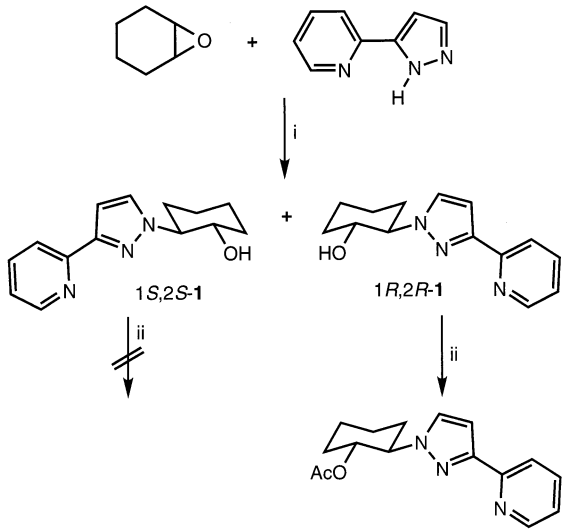

As the resonances of the two protons connected to the substituted cyclohexane carbon atoms are observed at almost identical δ values, the conformation of the aliphatic ring system cannot be determined by means of NMR spectroscopy. However, we expect the cyclohexane ring to occupy the thermodynamically favored chair conformation with both substituents oriented in an equatorial position, as found in similar compounds[8].

Since we are interested in such compounds as enantiomerically pure ligands for enantioselective catalysis and as starting material for the synthesis of chiral ligands[9], we investigated the kinetic resolution of **1**[10]. Acylation of **1** with isopropenyl acetate in the presence of lipase B from *candida antarctica*[11] selectively leads to the formation of the acetate with the (1*R*,2*R*) configuration (Scheme 1), which can be separated from (1*S*,2*S*)-**1** by preparative MPLC. The absolute configuration of the non-acylated derivative was determined by X-ray-crystallographic methods (see below). For the corresponding 2-pyrazolylcyclohexanol, an identical stereoselectivitiy of the enzymatic esterification was found[10]. Figure 1 shows the molecular structure of (1*S*,2*S*)-**1** in the solid state, along with characteristic bond lengths and angles. Further crystallographic and experimental details are given in Table 1 in the Experimental Section.

(1*S*,2*S*)-**1** crystallizes from diethyl ether at 4°C in the monoclinic space group $P2_1$ with one additional molecule

Figure 1. PLATON plot[12] of (1*S*,2*S*)-**1** (the additional water molecule has been omitted); thermal ellipsoids are at the 50-% level[a]

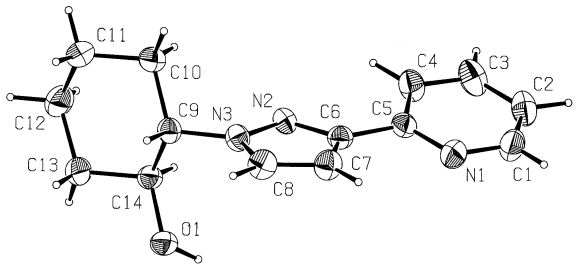

[a] Bond lengths [Å] angles [°] and dihedral angles [°]: N(1)−C(1) 1.332(3), N(1)−C(5) 1.339(2), N(2)−N(3) 1.357(2), N(2)−C(6) 1.342(2), N(3)−C(8) 1.350(2), N(3)−C(9) 1.464(2), C(1)−C(2) 1.386(3), C(2)−C(3) 1.376(3), C(3)−C(4) 1.384(3), C(4)−C(5) 1.386(2), C(5)−C(6) 1.478(2), C(6)−C(7) 1.405(3), C(7)−C(8) 1.359(3), C(9)−C(10) 1.534(3), C(9)−C(14) 1.526(3), C(10)−C(11) 1.523(3), C(11)−C(12) 1.524(3), C(12)−C(13) 1.528(3), C(13)−C(14) 1.516(3), O(1)−C(14) 1.431(2), O(1)−H(1A) 0.91(3), O(1)−H(2B) 1.87(3), O(2)−H(1A) 1.82(3), O(2)−H(2A) 0.87(3), N(2)−H(2A) 2.10(3), O(2)−H(2B) 0.94(3); C(14)−O(1)−H(1A) 110.7(19), H(2A)−O(2)−H(2B) 96.48(11), O(1)−H(1A)−O(2) 172(3), O(2)−H(2A)−N(2) 160(3), O(2)−H(2B)−O(1) 180(3); N(1)−C(5)−C(6)−N(2) −168.96(17).

of water per formula unit. In the solid state structure of enantiomerically pure 2-pyrazolylcyclohexanol[10], the molecules are linked by hydrogen bonds between the hydroxy groups and the pyrazole moieties, resulting in a helical arrangement. In the case of (1*S*,2*S*)-**1**, this kind of molecular organization is hampered by the bulky pyridyl ring. Therefore, an additional molecule of water is incorporated, forming a new system of hydrogen bonds, which includes the OH group of the cyclohexanolyl fragment as proton donor and acceptor and the pyrazolyl moiety (N2) of (1*S*,2*S*)-**1** as an acceptor site (Figure 2).

Figure 2. PLUTON plot[12] showing the hydrogen-bonding system, which builds the solid-state structure of (1*S*,2*S*)-**1**

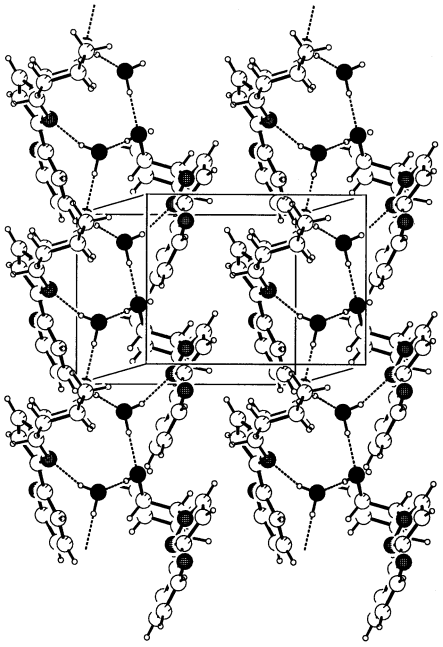

The structure is best described by an arrangement of water molecules around the crystallographic 2_1 axis, linking the (pyridyl)pyrazolylcyclohexanol molecules to form infinite columns. For reasons of optimization of electronic interaction between the pyridine and the pyrazole ring and steric repulsion between the protons at C4/C7 and the lone pairs at N1/N2, the heteroaromatic rings are twisted by about 10° from coplanarity. All intra- and intermolecular bond lengths and angles were observed as expected. The absolute structure was determined by refinement of the Flack parameter $\chi = -0.061(0.2)$[13]. The refinement of the enantiomorphic structure model with (1*R*,2*R*)-**1** resulted in higher *R* values ($R_1 = 0.035$, $\omega R_2 = 0.098$) and a Flack parameter $\chi = 1.003(0.2)$.

The treatment of *rac*-**1** and (1*S*,2*S*)-**1** with an excess of molybdic acid (hydrated MoO_3), dissolved in H_2O_2, results in the formation of the seven-coordinate peroxo complexes *rac*-**2** and (1*S*,2*S*)-**2** (Scheme 2).

Scheme 2. i. $MoO_3 \cdot (H_2O)_x$, H_2O_2, room temp., 4 h

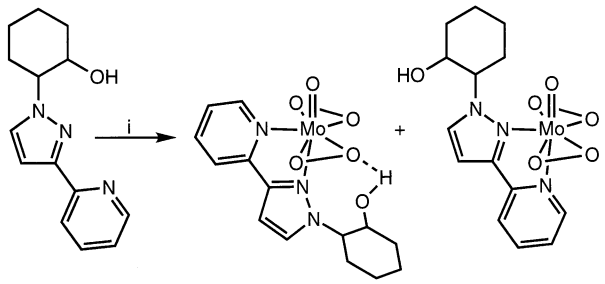

1 **2A** **2B**

Owing to the two different donor centers of the pyrazolylpyridine ligands, the seven-coordinate peroxomolybdenum complexes can exist in two isomeric forms (**A** and **B**). By means of NMR spectroscopy it was found that these isomers are in equilibrium in solution[14]. In a detailed study, we recently showed that the isomer ratios correlate with the individual donor properties of the heterocyclic ring systems[1].

Solutions of *rac*-**2** and (1*S*,2*S*)-**2** show the same behavior, which does not depend on the electronic properties of the ligand, but on the nature of the solvent. In chloroform, only isomer **A** can be detected, whereas in donor solvents capable of forming hydrogen bonds with alcohols, like acetone, the isomers **A** and **B** can be observed as expected in a 2:1 ratio. Thus, the electronic characteristics of the chelate ligand cannot be the reason for the special structural feature of **2** in solution in $CHCl_3$. We therefore believe an intramolecular hydrogen bond to be responsible for this behavior.

From investigations on the isomer ratios (**A**:**B**) of peroxomolybdenum complexes bearing pyrazolylpyridine ligands with electron-withdrawing and -donating substituents[1], we can estimate the enthalpy of the intramolecular hydrogen-bond formation to be at least −8 kJ/mol, which corresponds to data from the literature on the thermodynamics of hydrogen bonds between alcohols and ketones ($\Delta G \approx -12$ to −24 kJ/mol)[15].

Infrared-spectroscopic investigations at low concentrations (3 mM) in solution support the formation of an intramolecular hydrogen bond: cyclohexanol gives a sharp O−H absorption at 3611 cm^{-1} in chloroform, but a shift of about 100 cm^{-1} towards lower wave numbers is observed in acetone solution, leading to a broad band at 3514 cm^{-1}, typical for associated O−H groups. In contrast to these findings, the IR spectra of **2** in solution, which again show broad O−H absorptions, differ only slightly on a change in the nature of the solvent [chloroform: ν(O−H) = 3491 cm^{-1}; acetone: ν(O−H) = 3509 cm^{-1}]. This fact provides strong evidence for the formation of hydrogen bonds in both cases: intramolecular in chloroform and intermolecular [OH···O=C$(CH_3)_2$] in acetone solution. The intramolecular hydrogen bond could alternatively be formed between the OH group of the chelate-ligand side chain and the oxo or one of the η^2-O_2 ligands coordinated to molybdenum. In acetone solution, **2** shows two Mo=O stretching vibrations: one at 956 cm^{-1} and an intense shoulder at 950 cm^{-1}, which can be assigned to the two isomers **A** and **B**. The asymmetric and symmetric O−O stretching vibrations are observed at 877 and 868 cm^{-1} for both isomers. In $CHCl_3$, the M=O absorption at 950 cm^{-1} almost vanishes, while the other M=O vibration is shifted to 962 cm^{-1}, indicating an almost selective formation of one isomer. The two O−O absorptions are shifted to lower wave numbers (875 and 865 cm^{-1}), indicating slightly weakened O−O bonds, which would agree with hydrogen bonding to a η^2-O_2 ligand. A reduction in the donor capability of the peroxo ligands can be compensated by increased π-backbonding from the oxo ligand to the molybdenum center, as confirmed by the shift of the Mo=O stretching frequency to higher wave numbers. However, hydrogen bonding to the oxo ligand would weaken the Mo=O bond and therefore shift the Mo=O absorption to lower wave numbers. The Mo=O and O−O absorptions of peroxomolybdenum complexes bearing pyrazolylpyridine ligands with unfunctionalized alkyl side chains, like [2-(3-butylpyrazol-1-yl)pyridine]oxodiperoxomolybdenum(VI)[6], which cannot participate in any intramolecular hydrogen bonding, show only weak solvent dependences [acetone: 962, 957 cm^{-1} ($2 \times \nu_{Mo=O}$), 877, 868 cm^{-1} ($2 \times \nu_{O=O}$); $CHCl_3$: 963, 956 cm^{-1} ($2 \times \nu_{Mo=O}$), 878, 866 cm^{-1} ($2 \times \nu_{O=O}$)].

From these results, it is clear that the intramolecular hydrogen bond should be formed between the OH group (H^+ donor) and one η^2-O_2 ligand (H^+ acceptor) in $CHCl_3$ solution, and this is in agreement with spectroscopic investigations of peroxomolybdenum complexes in the presence of strong Lewis and Brønsted acids[5]. This interaction would favor an orientation of the pyrazole moiety *trans* to the oxo ligand (isomer **A**, Scheme 2). However, this geometry is not in accordance with the assignments of the spectra of these complexes, which we published in previous papers[1][4][5][6], a contradiction which had to be clarified.

Crystallization of *rac*-**2** from chloroform gives yellow needles and a small amount of yellow plates (< 5%). Investigations of the needle-like material by X-ray crystallography indicated the solid-state structure of *rac*-**2**, which

crystallizes in the orthorhombic and acentric space group $Pca2_1$. Figure 3 shows the molecular structure of *rac*-**2** along with bond lengths and angles. Further crystallographic and experimental details are given in Table 1 in the Experimental Section.

Figure 3. PLATON plot[12] of the asymmetric unit of *rac*-**2**; thermal ellipsoids are at the 50-% level[a]

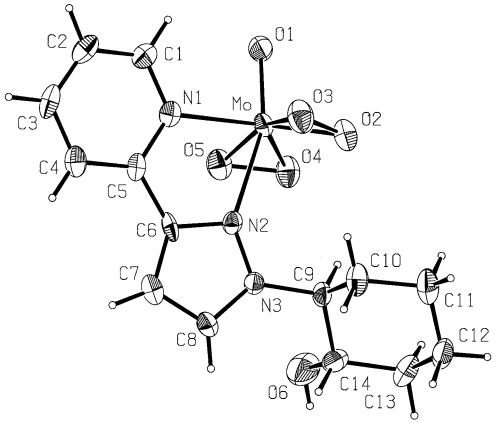

[a] Bond lengths [Å] angles [°] and dihedral angles [°]: Mo−O(1) 1.675(5), Mo−O(2) 1.898(3), Mo−O(3) 1.951(5), Mo−O(4) 1.899(4), Mo−O(5) 1.955(4), Mo−N(1) 2.224(3), Mo−N(2) 2.347(4), O(2)−O(3) 1.457(5), O(4)−O(5) 1.467(5), O(6)−H(6A) 0.820, O(6)−C(14) 1.419(7), O(4)−H(6A) 2.532, O(5)−H(6A) 2.010; O(1)−Mo−O(2) 105.1(2), O(1)−Mo−O(3) 102.0(2), O(1)−Mo−O(4) 104.9(2), O(1)−Mo−O(5) 98.9(2), O(1)−Mo−N(1) 90.2(2), O(1)−Mo−N(2) 160.3(2), O(2)−Mo−O(3) 44.5(2), O(4)−Mo−O(5) 44.7(2), N(1)−Mo−N(2) 70.3(2), O(6)−H(6A)−O(4) 139.0, O(6)−H(6A)−O(5) 171.4; C(6)−N(2)−N(3)−C(8) 0.5(5).

Only isomer **A** is found in the solid-state structure, with pyrazole *trans* to the oxo ligand, like it is observed in $CHCl_3$ solution. However, in the solid state the hydrogen bond is not *intra*- but *inter*molecular between the OH group and an η^2-O_2 ligand, linking two peroxomolybdenum complexes and finally leading to the formation of a helical arrangement (Figure 4). The crystals include helices of opposite chirality.

Figure 4. PLUTON plot[12] of the helical arrangement formed by hydrogen bonding in the solid-state structure of *rac*-**2**

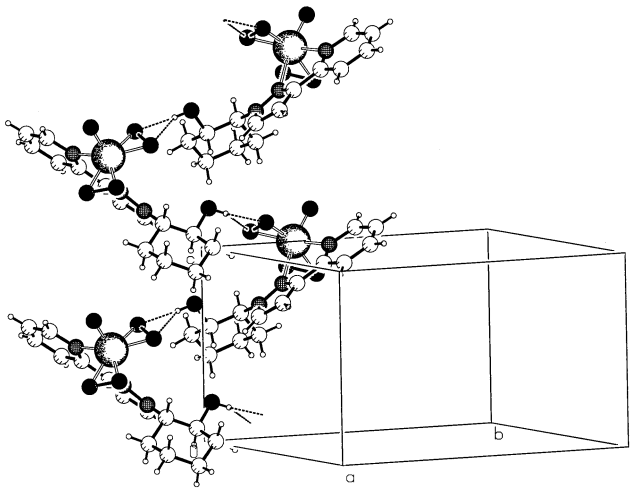

Clearly, intermolecular hydrogen bonding is energetically favored in the solid state with respect to the intramolecular mode observed in solution. Besides the OH···O_2 bond, which has previously been observed in the solid-state structure of only one other high-valent transition-metal peroxo compound[16], *rac*-**2** shows the typical structure of a molybdenum oxodiperoxo fragment coordinated to a bidentate *N*,*N*′-ligand[4][6][17]. Owing to the *trans* influence of the oxo ligand, the distance Mo−N2 is about 12 pm larger than Mo−N1. The peroxo ligands are bent with respect to the oxo ligand, leading to a distorted pentagonal-bipyramidal coordination geometry.

An analogous structure was found for the second type of crystalline material (yellow plates) in which pyrazole is *trans* to the oxo ligand. Owing to the poor crystal quality and a severe problem of disorder concerning the orientation of the OH group at the cyclohexane ring relative to the mirror plane of the $MoO(O_2)_2$ fragment, it was not possible to finish the structure refinement with acceptable *R* values (R_1 = 0.0993, $\omega R2$ = 0.2780)[18].

For the final assignment of the spectroscopic data of **2**, we carried out powder-diffraction and solid-state NMR experiments. Powder diffraction of the solid material, either crystalline or microcrystalline, can be correlated with the crystal data of the single-crystal diffraction experiment (space group $Pca2_1$) and, in addition, ^{13}C CPMAS experiments gave only one set of resonances. Therefore, the NMR spectra of the peroxo complexes in solution can now be assigned correctly (see Experimental Section). As shown in Scheme 2 the pyrazole fragment in isomer **A** is oriented *trans* to the oxo ligand.

The peroxo complexes **2** catalyze the epoxidation of olefins in the presence of *tert*-butyl hydroperoxide. Detailed investigations on the epoxidation of prochiral olefins with (1*S*,2*S*)-**2** unequivocally showed that racemic epoxides are formed under standard conditions (50 °C, $CHCl_3$). The hydroxy group of the ligand remains unaffected during these reactions, which is in agreement with findings in the literature that neutral peroxomolybdenum complexes do not catalyze the oxidation of alcohols. In contrast, alcohols are preferentially oxidized to the corresponding ketones in the presence of anionic peroxomolybdenum complexes[19]. However, conversion of the OH function of **1** into a carbonyl group can be achieved quantitatively by Swern oxidation[20]. Oxidation of enantiomerically pure (1*S*,2*S*)-**1** yields a racemic mixture of **3** under these conditions. We are interested in such compounds as building blocks for chiral multidentate ligands and are therefore currently working on the resolution of *rac*-**3**. The corresponding peroxomolybdenum complex **4** is available in a similar way to **2** by simply stirring a peroxidic solution of molybdic acid with a solution of **3** in dichloromethane (Scheme 3).

NMR spectroscopy shows that the peroxo complex **4** exists in chloroform solution as a 4.5:1 mixture of the two isomers **A** and **B**. This gives an indication of the slightly stronger electron-withdrawing properties of the β-oxo group compared to the β-hydroxy group of **1**, favoring the population of isomer **A**. The corresponding peroxo complex

Scheme 3. i. $(CH_3)_2SO$, $(COCl)_2$, NEt_3, −72°C, CH_2Cl_2; ii. $MoO_3{\cdot}(H_2O)_x$, H_2O_2, room temp., 4 h

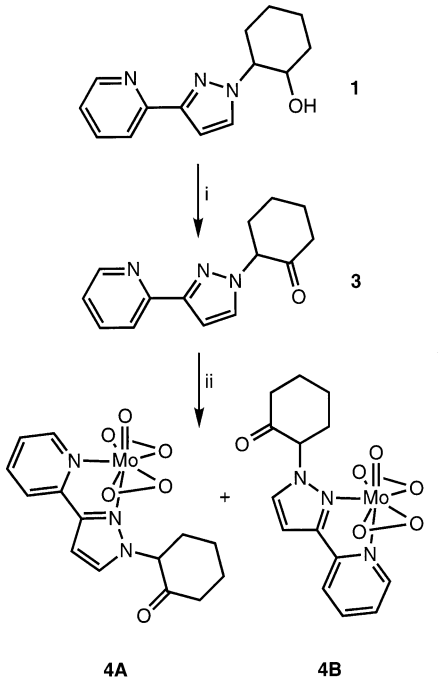

4 catalyzes the epoxidation of olefins in the presence of *tert*-butyl hydroperoxide, showing an activity comparable to that of other peroxomolybdenum complexes[6].

Conclusion

Proton-transfer reactions play an important role in many organic transformations catalyzed by high-valent transition-metal centers. From a mechanistic point of view, hydrogen-bond formation can be considered as the primary step in such reactions. With the synthesis of *trans*-2-[3-(2-pyridyl)-1-pyrazolyl]cyclohexanol (**1**), we succeeded not only in establishing a new chiral polydentate ligand system with potential applications in enantioselective catalysis, but were also able to obtain thermodynamic information on the strength of an $Mo^{VI}(\eta^2\text{-}O_2)\cdots HO{-}C$ interaction. Such an interaction in solution has never been described in detail before. Owing to the low Lewis basicity of the peroxo ligand coordinated to a high-valent transition-metal center this interaction is weak and can therefore be broken by Lewis-basic solvents. In the solid state, this hydrogen bond is no longer intramolecular but intermolecular. The formation of the intramolecular hydrogen bond in solution allowed a new assignment of the NMR data of pyrazolylpyridine peroxomolybdenum complexes. A simple and high-yield transformation of the secondary alcohol **1** into the ketone **3** led to a new chiral building block for multidentate ligand systems. The potential of such a system as a metal-complexing agent was proved by the formation of the corresponding peroxo complex **4**.

The authors wish to thank Prof. *W. A. Herrmann,* the *Deutsche Forschungsgemeinschaft* and the *Fonds der Chemischen Industrie* for support of this work, and *Henricke Heise* for performing the CPMAS experiments.

Experimental Section

2-[3(5)-Pyrazolyl]pyridine was synthesized according to a published procedure[3]. Immobilized lipase B from *candida antarctica* was a generous gift from Novo Nordisk. All other starting materials were purchased from Aldrich. Isopropenyl acetate was distilled from K_2CO_3 before use. The NMR (Bruker DPX 400), infrared (Perkin-Elmer 1600 Series FTIR) and mass spectra (GC MS: Hewlett-Packard gas chromatograph HP 5890 and mass selective detector HP 5970), and all elemental analyses were carried out at the *Anorganisch-chemisches Institut der TU München*. The numbering of the NMR spectra is carried out according to Scheme 4.

Scheme 4. Labeling scheme for the assignment of NMR data

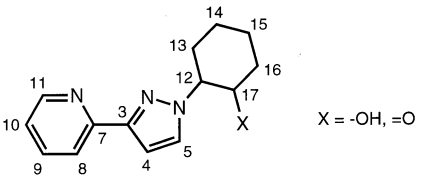

rac-[3-(2-Pyridyl)-1-pyrazolyl]cyclohexanol (*rac*-**1**): A mixture of 2-[3(5)-pyrazolyl]pyridine (2.0 g, 13.9 mmol) and epoxycyclohexane (2.0 g, 2.1 ml, 20.8 mmol) was heated for 4 h at 170°C in a pressure tube (Aldrich Z18,108-0). The dark-colored product was dissolved in dichloromethane and treated with 5.0 g of silica gel. The solvent was removed in vacuo and the powdery product transferred to a Soxhlet extractor. Extraction with diethyl ether and removal of the solvent yielded **1** (3.1 g, 92%) as a pale yellow oil. − IR (KBr, cm^{-1}): $\tilde{\nu}$ = 3382 s, br. (OH), 2935 vs, 2857 s, 1595 vs, 1567 m, 1490 s, 1459 s, 1432 m, 1410 m, 1365 m, 1278 m, 1264 w, 1229 s, 1149 w, 1074 s, 1000 w, 954 m, 870 w, 797 m, 765 vs, 708 w, 644 w, 621 w. − ^{1}H NMR (400 MHz, 25°C, $CDCl_3$): δ = 8.55 (d, $^3J_{10,11}$ = 5.0 Hz, 11-H), 7.88 (d, $^3J_{8,9}$ = 8.0 Hz, 8-H), 7.65 (dt, $^3J_{9,10}$ = 7.5 Hz, $^4J_{9,11}$ = 2.0 Hz, 9-H), 7.47 (d, $^3J_{4,5}$ = 2.5 Hz, 5-H), 7.13 (dd, 10-H), 6.85 (d, 4-H), 3.91 (m, 12-H, 13-H), 2.14 (m, $-CH_2-$, 2 H), 1.87−1.18 (m, $-CH_2-$, 6 H), not observed (OH). − $^{13}C\{^1H\}$ NMR (100.6 MHz, 25°C, $CDCl_3$): δ = 152.1 (C-7), 151.4 (C-3), 149.2 (C-11), 136.5 (C-9), 129.7 (C-5), 122.3 (C-10), 120.0 (C-8), 104.0 (C-4), 72.9 (C-17), 67.2 (C-12), 33.3 (C-16), 31.0 (C-13), 24.8 (C-14), 23.9 (C-15). − MS (EI); *m/z* (%): 243 (25) [M^+], 226 (2) [M^+ − OH], 215 (25) [$M^+ - C_2H_4$], 200 (6) [$M^+ - C_3H_7$], 187 (13) [$M^+ - C_4H_8$], 172 (100) [$M^+ - C_4H_7O$], 158 (51) [$M^+ - C_5H_9O$], 146 (46) [$C_5H_4N{-}C_3H_3N_2^+$], 145 (25) [$C_5H_4N{-}C_3H_2N_2^+$], 117 (14) [$C_5H_4N{-}C_3H_2^+$], 78 (22) [$C_5H_4N^+$].

(1S,2S)-[3-(2-Pyridyl)-1-pyrazolyl]cyclohexanol Hydrate [(1*S*,2*S*)-**1**·H_2O]: *rac*-**1** (0.50 g, 2.06 mmol) was dissolved in isopropenyl acetate (1.36 ml, 1.24 g, 12.36 mmol). Molecular sieves (4 Å, 0.5 g) and immobilized lipase B from *candida antarctica* (16 mg) were added and the mixture stirred for 4 h at 37°C. The reaction was quenched by the addition of dichloromethane (15 ml) and the enzyme filtered off. All volatile material was removed in vacuo and the ester separated from the alcohol by MPLC (SiO_2:YMC SL06S21, 30 μm; ethyl acetate/hexane 4:1). Yield: 0.22 g (44%, > 95% ee by NMR) of (1*S*,2*S*)-**1**. Recrystallization from diethyl ether gave colorless plates of the monohydrate. − $C_{14}H_{17}N_3O{\cdot}H_2O$ (261.33): calcd. C 64.35, H 7.33, N 16.08; found C 63.29, H 7.20, N 15.55.

rac- and (1S,2S)-Oxodiperoxo{[3-(2-pyridyl)-1-pyrazolyl]-cyclohexanol}molybdenum(VI) [*rac*- and (1*S*,2*S*)-**2**]: A solution of

molybdic acid ($MoO_3 \cdot H_2O$, 0.41 g, 2.56 mmol) in 30% H_2O_2 (5 ml) was treated with a solution of *rac*-**1** or (1*S*,2*S*)-**1** (0.31 g, 1.28 mmol) in dichloromethane (10 ml) and several drops of glacial acetic acid. After 4 h of stirring at room temperature, the phases were separated, the aqueous phase was extracted twice with dichloromethane (10 ml) and the combined organic phases were washed twice with water (15 ml). After removal of the solvent in vacuo, the peroxo complexes were obtained as yellow, microcrystalline solids in almost quantitative yields, and were rinsed with diethyl ether. Recrystallization of *rac*-**2** from acetonitrile gave a crystalline material (0.37 g, 69%). – IR (KBr, cm^{-1}): $\tilde{\nu}$ = 3489 vs br. (OH), 3138 w, 3084 w, 2926 m, 2854 w, 1612 m, 1559 w, 1540 w, 1506 w, 1457 w, 1437 m, 1376 w, 1224 w, 1083 w, 1062 w, 956 s (Mo=O), 871 m, 859 s (2 × O–O), 770 m, 662 w, 587 m, 540 w. – ^{1}H NMR (400 MHz, 25°C, $CDCl_3$): δ = 9.30 (d, $^3J_{10,11}$ = 5.5 Hz, 11-H), 8.23 (dt, $^3J_{8,9}$ = $^3J_{9,10}$ = 8.0 Hz, $^4J_{9,11}$ = 1.5 Hz, 9-H), 7.92 (d, 8-H), 7.65 (t, 10-H), 7.42 (d, $^3J_{4,5}$ = 2.5 Hz, 5-H), 6.77 (d, 4-H), 4.33 (dt, $^3J_{12,13ax}$ = $^3J_{12,17}$ = 10.5 Hz, $^4J_{12,13eq}$ = 2.5 Hz, 12-H), 3.37 (dt, $^3J_{16,17ax}$ = 10.5 Hz, $^4J_{16,17eq}$ = 2.5 Hz, 17-H), 2.78–1.20 (m, $-CH_2-$, 8 H). – ^{1}H NMR (400 MHz, 25°C, [D_6]acetone): isomer **A**: δ = 9.27 (d, $^3J_{10,11}$ = 5.0 Hz, 11-H), 8.53 (dt, $^3J_{8,9}$ = $^3J_{9,10}$ = 8.0 Hz, $^4J_{9,11}$ = 1.5 Hz, 9-H), 8.38 (d, 8-H), 7.92 (t, 10-H, 5-H), 7.13 (d, $^3J_{4,5}$ = 2.5 Hz, 4-H), 4.26 (dt, $^3J_{12,13ax}$ = $^3J_{12,17}$ = 12.0 Hz, $^4J_{12,13eq}$ = 4.0 Hz, 12-H), 3.70 (m, 17-H), 2.80–1.20 (m, $-CH_2-$, 8 H); isomer **B**: δ = 8.66 (d, $^3J_{10,11}$ = 5.0 Hz, 11-H), 8.17 (d, $^3J_{8,9}$ = 7.5 Hz, 8-H), 8.05 (m, 9-H, 5-H), 7.48 (d, $^3J_{4,5}$ = 2.5 Hz, 4-H), 7.42 (ddd, $^3J_{9,10}$ = 7.0 Hz, $^4J_{8,10}$ = 2.0 Hz, 10-H), 5.13 (dt, $^3J_{12,13ax}$ = $^3J_{12,17}$ = 12.5 Hz, $^4J_{12,13eq}$ = 4.0 Hz, 12-H), 3.35 (m, 17-H), 2.80–1.20 (m, $-CH_2-$, 8 H). – ^{13}C{^{1}H} NMR (100.6 MHz, 25°C, $CDCl_3$): δ = 154.7 (C-11), 149.4 (C-7), 143.8 (C-3), 142.8 (C-9), 129.2 (C-5), 125.0 (C-10), 122.5 (C-8), 105.0 (C-4), 75.1 (C-17), 67.7 (C-12), 35.8 (C-16), 31.9 (C-13), 24.9 (C-14), 24.8 (C-15). – ^{13}C CPMAS (75.468 MHz, 25°C): δ = 155.9 (C-11), 150.2 (C-7), 145.7 (C-3, C-9), 130.7 (C-5), 124.0 (C-10), 122.6 (C-8), 104.5 (C-4), 67.8 (C-17, C-12), 35.7 (C-16, C-13), 25.2 (C-14, C-15). – $C_{14}H_{17}N_3O_6Mo$ (419.25): calcd. C 40.11, H 4.09, N 10.02; found C 40.16, H 4.13, N 10.09.

rac-[3-(2-Pyridyl)-1-pyrazolyl]cyclohexanone (*rac*-**3**): Dimethyl sulfoxide (0.75 ml, 0.88 g, 11.3 mmol) was added to a solution of **1** (1.15 g, 4.73 mmol) in dichloromethane (30 ml) at −72°C. After 30 min, oxalyl chloride (1.33 ml, 1.93 g, 15.2 mmol) was added dropwise and, after a further 60 min, triethylamine (2.92 ml, 2.22 g, 21.9 mmol) was added. The reaction mixture was stirred for a further 60 min at −60°C and the reaction was quenched with water (1 ml). The mixture was extracted twice with dichloromethane (30 ml), the combined organic phases washed with brine, dried with $MgSO_4$ and the solvent was removed in vacuo. Recrystallization from diethyl ether gave **3** (1.11 g, 97%) as colorless needles. – IR (KBr, cm^{-1}): $\tilde{\nu}$ = 3131 w, 2940 s, 2864 m, 1725 vs (CO), 1593 s, 1567 w, 1490 m, 1458 m, 1430 w, 1366 m, 1278 w, 1222 m, 1128 w, 1051 w, 992 w, 956 w, 767 s, 710 w, 622 w. – ^{1}H NMR (400 MHz, 25°C, $CDCl_3$): δ = 8.59 (d, $^3J_{10,11}$ = 54.5 Hz, 11-H), 7.85 (d, $^3J_{8,9}$ = 8.0 Hz, 8-H), 7.66 (dt, $^3J_{9,10}$ = 7.5 Hz, $^4J_{9,11}$ = 2.0 Hz, 9-H), 7.47 (d, $^3J_{4,5}$ = 2.0 Hz, 5-H), 7.15 (dd, 10-H), 6.92 (d, 4-H), 5.13 (dd, $^3J_{12,13ax}$ = 13.0 Hz, $^3J_{12,13eq}$ = 4.5 Hz, 12-H), 2.63–1.70 (m, $-CH_2-$, 8 H). – ^{13}C{^{1}H} NMR (100.6 MHz, 25°C, $CDCl_3$): δ = 204.7 (C-17), 152.1 (C-7), 151.1 (C-3), 149.4 (C-11), 136.4 (C-9), 130.3 (C-5), 122.3 (C-10), 120.1 (C-8), 104.7 (C-4), 69.6 (C-12), 41.3 (C-16), 34.6 (C-13), 27.2 (C-14), 24.7 (C-15). – MS (EI); *m/z* (%): 241 (37) [M^+], 213 (8) [$M^+ - CO$], 198 (5) [$M^+ - C_3H_7$], 185 (6) [$M^+ - C_4H_8$], 184 (9) [$M^+ - C_3H_5O$], 172 (63) [$M^+ - C_5H_9$], 170 (4) [$M^+ - C_4H_7O$], 158 (20) [$C_5H_4N-C_3H_2N_2-CH_3^+$], 145 (100) [$C_5H_4N-C_3H_2N_2^+$], 117 (13) [$C_5H_4N-C_3H_2^+$], 78 (25)[$C_5H_4N^+$]. – $C_{14}H_{15}N_3O \cdot 0.25H_2O$ (245.79): calcd. C 68.41, H 6.36, N 17.09; found C 68.65, H 6.02, N 16.93.

rac-Oxodiperoxo{[3-(2-pyridyl)-1-pyrazolyl]cyclohexanone}-molybdenum(VI) (*rac*-**4**): A solution of molybdic acid ($MoO_3 \cdot H_2O$, 0.34 g, 1.90 mmol) in 30% H_2O_2 (5 ml) was treated with a solution of *rac*-**3** (0.25 g, 0.95 mmol) in dichloromethane (10 ml) and several drops of glacial acetic acid. After 4 h of stirring at room temperature, the phases were separated, the aqueous phase was extracted twice with dichloromethane (10 ml) and the combined organic phases were washed twice with water (15 ml). After removal of the solvent in vacuo followed by washing with diethyl ether, the product was obtained as a yellow, microcrystalline solid in almost quantitative yield. – IR (KBr, cm^{-1}): $\tilde{\nu}$ = 3124 m, 2934 m, 2869 w, 1732 s (CO), 1616 s, 1567 w, 1532 w, 1504 w, 1442 m, 1395 m, 1383 w, 1297 w, 1241 m, 1165 w, 1127 w, 1103 m, 1081 w, 1029 w, 977 w, 955 vs (Mo=O), 876 m, 865 vs (2 × O–O), 777 s, 665 m, 585 m, 540 w. – ^{1}H NMR (400 MHz, 25°C, [D_6]acetone): isomer **A**: δ = 9.23 (d, $^3J_{10,11}$ = 5.5 Hz, 11-H), 8.20 (dt, $^3J_{8,9}$ = $^3J_{9,10}$ = 8.0 Hz, $^4J_{9,11}$ = 1.2 Hz, 9-H), 7.91 (d, 8-H), 7.62 (dd, 10-H), 7.40 (d, $^3J_{4,5}$ = 2.5 Hz, 5-H), 6.72 (d, 4-H), 5.41 (dd, $^3J_{12,13ax}$ = 13.6 Hz, $^3J_{12,13eq}$ = 5.5 Hz, 12-H), 2.80–1.55 (m,– CH_2-, 8 H); isomer **B**: δ = 8.60 (br, 11-H), 8.05 (d, $^3J_{4,5}$ = 3.0 Hz, 5-H), 7.83 (d, $^3J_{8,9}$ = 8.0 Hz, 8-H), 7.77 (dt, $^3J_{9,10}$ = 7.5 Hz, $^4J_{9,11}$ = 1.5 Hz, 9-H), 7.19 (dd, 10-H), 7.04 (d, 4-H), 6.17 (dd, $^3J_{12,13ax}$ = 13.6 Hz, $^3J_{12,13eq}$ = 5.5 Hz, 12-H), 2.80–1.55 (m, $-CH_2-$, 8 H); isomer ratio **A**:**B** = 4.5:1. – ^{13}C{^{1}H} NMR (100.6 MHz, 25°C, [D_6]acetone): isomer **A**: δ = 203.2 (C=O), 154.5 (C-11), 150.9 (C-7), 144.5 (C-3), 142.9 (C-9), 132.1 (C-5), 125.1 (C-10), 122.8 (C-8), 104.3 (C-4), 68.9 (C-12), 41.2 (C-16), 34.9 (C-13), 27.6 (C-14), 24.6 (C-15); isomer **B**: δ = 202.7 (C=O), 147.2 (C-11), 139.2 (C-9), 136.9 (C-5), 125.1 (C-10), 120.7 (C-8), 105.1 (C-4), not detected (C-3, C-7), 68.5 (C-12), 40.8 (C-16), 34.6 (C-13), 27.1 (C-14), 24.4 (C-15). – $C_{14}H_{15}N_3O_6Mo$ (417.23): calcd. C 40.30, H 3.62, N 10.07; found C 40.35, H 3.83, N 9.88.

Crystallographic Structure Determination and Structure Refinement of (1*S*,2*S*)-**1** · H_2O *and rac*-**2**: The crystals were fixed inside a Lindemann glass capillary. The intensity data were obtained at 293 K with graphite-monochromated Mo-K_α radiation using a STOE IPDS[21] in the case of *rac*-**2** and at 193 K with graphite-monochromated Cu-K_α radiation using an Enraf Nonius CAD4[22] diffractometer in the case of (1*S*,2*S*)-**1**. A combined absorption and decay correction, using the program DECAY[21] (smooth factor 8) was applied on the data set of *rac*-**2**. During the data collection for (1*S*,2*S*)-**1**, three standard reflections lost 12% of intensity, which was corrected with the program MolEN[22]. Preliminary positions of heavy atoms were found by direct methods (SIR92[23]), while positions of the other non-hydrogen atoms were determined from successive Fourier difference maps coupled with an initial isotropic least-squares refinement (SHELXL93[24]). The hydrogen atoms of (1*S*,2*S*)-**1** were all located in the difference Fourier maps and refined with isotropic temperature parameters. In the case of *rac*-**2** all hydrogen atoms were placed in calculated positions, included in the structure-factor calculation, but were not refined. Additional crystal data, data collection and refinement parameters are presented in Table 1.

Crystallographic data (excluding structure factors) for the structures reported in this paper have been deposited with the Cambridge Crystallographic Data Centre (CCDC-100572). Copies of the data may be obtained free of charge on application to CCDC, 12 Union Road, Cambridge CB2 1EZ, UK [fax: int. code +(1223)336-033; e-mail: deposit@ccdc.cam.ac.uk].

X-ray Powder Diffraction: The X-ray diffraction pattern was recorded with a Huber Guinier diffractometer 642 with Ge mono-

Table 1. Crystal data and collection parameters for compounds (1*S*,2*S*)-**1** and *rac*-**2**

	(1*S*,2*S*)-**1**	*rac*-**2**
empirical formula	$C_{14}H_{19}N_3O_2$	$C_{14}H_{17}MoN_3O_6$
formula weight [a.m.u]	261.32	419.25
color, habit	colorless plates	yellow needles
crystal system	monoclinic	orthorhombic
space group	$P2_1$ (no. 4)	$Pca2_1$ (no. 29)
a [Å]	9.4298(11)	13.4166(11)
b [Å]	7.2854(4)	13.8384(9)
c [Å]	10.5036(12)	8.3365(5)
β [°]	106.692(6)	90.00
V [Å^3]	691.19(12)	1547.8(2)
Z	2	4
calcd. density [g cm^{-1}]	1.256	1.799
μ [mm^{-1}]	0.694	0.885
F(000)	280	848
T [°C]	193(2)	293(2)
radiation type	Cu-K_α	Mo-K_α
diffractometer	CAD4	STOE IPDS
data collection range	$2 < \Theta < 68$	$1.6 < \Theta < 26.0$
number of reflections collected	4886	12686
number of unique reflections	2491	2472
number of refl. used for refinem.	2491	2472
observation criteria	$I > \sigma(I)$	$I > \sigma(I)$
refined parameters	224	217
reflections/parameter	10.22	10.01
Flack parameters	−0.06(21)	−0.01(5)
final *R*1	0.0401	0.0309
final ω*R*2	0.0872	0.0714
GOF	1.065	1.176
largest remaining feature in electron density map	0.163/−0.272	0.538/−0.503

chromator (λ = 154.056 pm) at 293 K with a 5-s scan time and 0.01° step width (step-scanning method). Selected data: space group: orthorhombic, $Pca2_1$ (no. 29); *a* = 13.4682, *b* = 13.8860, *c* = 8.1370 Å; *V* = 1521.78 Å^3; most intense reflections (*hkl*/Θ value/rel. intensity): 010/3.18°/9.1%, 110/4.57°/5.4%, 020/6.35°/25.2%, 200/6.58°/37.4%, 111/6.97°/100%, 121/8.89°/76.1%, 221/10.55°/12.6%, 230/11.67°/23.8%.

[1] W. R. Thiel, J. Eppinger, *Chem. Eur. J.* **1997**, *3*, 696−705.
[2] [2a] *Organic Synthesis by Oxidation with Metal Compounds* (Eds.: W. J. Mijs, C. H. R. T. de Jonge), Plenum Press, New York, **1986**. − [2b] R. A. Sheldon in *The Chemistry of Peroxides* (Ed.: S. Patai), Wiley, New York, **1983**.
[3] H. Brunner, T. Scheck, *Chem. Ber.* **1992**, *125*, 701−709.
[4] W. R. Thiel, T. Priermeier, *Angew. Chem.* **1995**, *107*, 1870−1871; *Angew. Chem. Int. Ed. Engl.* **1995**, *34*, 1737−1738.
[5] W. R. Thiel, *Chem. Ber.* **1996**, *129*, 575−580.
[6] W. R. Thiel, M. Angstl, T. Priermeier, *Chem. Ber.* **1994**, *127*, 2373−2379.
[7] [7a] H. Kotsuki, H. Hayakawa, M. Wakao, T. Shimanouchi, M. Ochi, *Tetrahedron Asymm.* **1995,** *6*, 2665−2668. − [7b] H. Kotsuki, K. Hayashida, T. Shimanouchi, H. Nishizawa, *J. Org. Chem.* **1996,** *61*, 984−990. − [7c] P. Barbaro, C. Bianchini, V. Sernau, *Tetrahedron Asymm.* **1996,** *7*, 843−850.
[8] [8a] P. Barbaro, C. Bianchini, V. Sernau, *Tetrahedron Asymm.* **1996**, *7*, 843−850. − [8b] C. L. Thurner, M. Barz, M. Spiegler, W. R. Thiel, *J. Organomet. Chem.* **1997**, *541*, 39−49. − [8c] C. L. Thurner, M. Barz, M. Spiegler, W. R. Thiel, *Acta Crystallogr. C,* in press.
[9] M. Barz, M. U. Rauch, W. R. Thiel, *J. Chem. Soc., Dalton Trans.* **1997**, 2155−2161.
[10] M. Barz, E. Herdtweck, W. R. Thiel, *Tetrahedron Asymm*. **1996**, *7*, 1717−1722.
[11] [11a] T. V. Hansen, V. Waagen, V. Partali, H. W. Anthonsen, T. Anthonsen, *Tetrahedron Asymm.* **1995,** *6*, 499−504. − [11b] H. Frykman, N. Öhrner, T. Norin, K. Hult, *Tetrahedron Lett.* **1993,** *34*, 1367−1370. − [11c] G. Nicolosi, A. Patti, M. Piattelli, C. Sanfilippo, *Tetrahedron Asymm*. **1995,** *6*, 519−524. − [11d] H. Sundram, A. Golebbiowski, C. R. Johnson, *Tetrahedron Lett*. **1994,** *35*, 6975−6976.
[12] A. L. Spek, *Acta Crystallogr. C* **1990**, *A46*, C34−C34.
[13] H. D. Flack, *Acta Crystallogr. C* **1983**, *A39*, 876−881.
[14] M. Mattner, PhD Thesis, TU München, **1995**.
[15] S. N. Vinogradov, R. H. Linnell, *Hydrogen Bonding*, Van Nostrand Reinhold Company, New York, **1971**.
[16] W. Winter, C. Mark, V. Schurig, *Inorg.Chem.* **1980**, *19*, 2045−2049.
[17] [17a] E. O. Schlemper, G. N. Schrauzer, L. A. Hughes, *Polyhedron* **1984**, *3*, 377−380. − [17b] W. A. Herrmann, W. R. Thiel, J. G. Kuchler, J. Behm, E. Herdtweck, *Chem. Ber.* **1990**, *123*, 1963−1970.
[18] Data for the plate-like crystals: crystal system, monoclinic; space group, $P2_1/c$ (int. table no. 14); *a* = 13.4460(8); *b* = 8.4082(3); *c* = 15.1809(8) A; β = 115.328(5)°; *V* = 1551.32(15) A^3; *Z* = 4; $D_{calcd.}$ = 1.778 g cm^{-3}; *F*(000) = 832; μ = 8.8 cm^{-1}; *T* = 193 K; Mo-K_α radiation; STOE IPDS; oscillation mode; *h*, *k*, *l*: −16/16, −10/10, −18/18; total no. of refl.: 17095; no. of unique refl.: 2934; no. of observed refl.: 2357; no. of parameters: 221, *R* = 0.0993, ω*R*2 = 0.2780; GOF = 1.23; res. electr. densities: −1.38/+2.57; additional material is available from the authors.
[19] *Catalytic Oxidations with Hydrogen Peroxide as Oxidant* (Ed.: G. Strukul), Kluwer Academic Publishers, Rotterdam, **1992**.
[20] J. A. Mancuso, S.-L. Huang, D. Swern, *J. Org. Chem.* **1978**, *43*, 2480−2482.
[21] STOE & CIE GmbH, *IPDS Operating System, Version 2.6*, Darmstadt, **1995**.
[22] Enraf-Nonius, *CAD4 Software, Version 5*, Delft, **1989**.
[23] A. Altomare, G. Cascarano, C. Giacovazzo, A. Guagliardi, *J. Appl. Crystallogr. C* **1993**, *26*, 343−350.
[24] G. Sheldrick, *SHELXL 93*, Universität Göttingen, **1993**.

[97167]

K_2AuPS_4, Tl_2AuPS_4, K_2AuAsS_4, and $KAu_5P_2S_8$: Syntheses, Structures, and Properties of Quaternary Gold Thiophosphate and Thioarsenate Compounds

Sandra Löken and Wolfgang Tremel*

Institut für Anorganische Chemie und Analytische Chemie der Johannes-Gutenberg-Universität, Becherweg 24, D-55099 Mainz, Germany

Received July 16, 1997

Keywords: Gold / Chalcogenide / Flux reaction / Structure determination / Metal-metal bonding

The novel compounds K_2AuPS_4 (**1**), Tl_2AuPS_4 (**2**), K_2AuAsS_4 (**3**), and $KAu_5P_2S_8$ (**4**) have been synthesized by direct reaction of the elements with a molten alkaline polythiophosphate(arsenate) flux at 550°C. The crystal structures of these compounds have been determined by single-crystal X-ray diffraction techniques. **1**, **2**, and **3** crystallize in the monoclinic space group $P2_1/m$. The structures of **1**, **2**, and **3** consist of infinite, one-dimensional anionic chains running along the crystallographic *b* axis. The chains are separated by potassium or thallium ions. Neighbouring Au atoms are bridged by MS_4^{3-} tetrahedra (M = P, As) in a *trans* orientation. Compound **4** crystallizes in the space group $P2_1/c$. The anionic chains of **4** are built up from linear AuS_2 dumbbell units and PS_4^{3-} tetrahedra. The chains extend along the $[1\bar{1}0]$ and $[1\bar{1}0]$ direction and are separated by charge balancing K^+ cations. Each of the compounds was investigated by differential thermal analysis, FT-IR, and solid-state UV/Vis diffuse reflectance spectroscopy.

Introduction

Most transition metals react with chalcogen or chalcogen-containing compounds to give transition-metal chalcogenides. These compounds have been the subject of numerous studies during the past decades because of their intriguing electronic and chemical properties such as superconductivity[1], charge-density wave behavior[2] and intercalation chemistry[3], which are imparted by the low-dimensional character of the early transition-metal compounds. On the right-hand side of the Periodic Table, transition-metal chalcogenides prefer three-dimensional structures akin to those of pyrites or marcasite. Several papers on this matter have recently been published[4], while a general explanation for these observations was advanced long ago by Hoffmann and Zheng[5]. When we move across the transition series, the d bands decrease in energy and become narrower. At the same time, the band filling increases. These two competing factors determine the trend in the Fermi level: It falls as one moves to electron-rich transition metals. If bands of Q−Q (Q = chalcogen) σ and σ* character are superimposed on these transition-metal d bands, the Fermi level will be above the bands with Te−Te σ* character for the early transition metals, i.e. on the left-hand side of the Periodic Table, but below for the late transition metals, i.e. on the right-hand side. The result is a gradual increase of Q−Q bonding in metal chalcogenides as we move across the transition-metal series from left to right. Compounds at the crossover point are most interesting from a theoretical point of view, because in these cases a straightforward prediction of their electronic properties by a formal assignment of oxidation states becomes impossible. In the simple binary compounds, one can reach the crossover point by varying the metal or the chalcogen components. As far as the metals are concerned, chalcogenides of the coinage metals are definitely such borderline cases. For gold tellurides such as $AuTe_2$, a compound with a very distorted CdI_2 structure, even more ambiguities arise, as now the metal (Pauling elec-

Figure 1. Unit cell view down the a) [010] axis, b) [100] axis for K_2AuAsS_4 (**2**) (medium grey spheres: As, black spheres: Au, open spheres: S, large grey spheres: K)

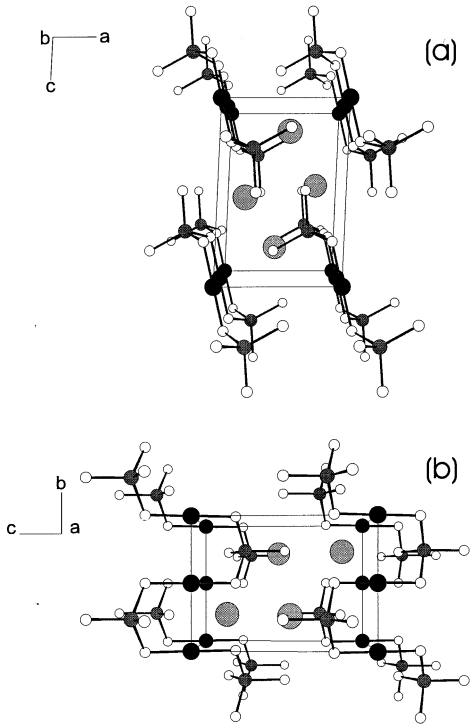

 © WILEY-VCH Verlag GmbH, D-69451 Weinheim, 1998 1434−1948/98/0202−0283 $ 17.50+.50/0

Table 1. Selected bond lengths [Å] and angles [°] for K_2AuPS_4 (**1**), Tl_2AuPS_4 (**2**), and K_2AuAsS_4 (**3**) (with standard deviations in parentheses)

Atoms	K_2AuPS_4	Tl_2AuPS_4	K_2AuAsS_4
	Distances		
Au−Au	3.364(0) × 2	3.335(0) × 2	3.430(0) × 2
Au−S1	2.298(2) × 2	2.300(3) × 2	2.292(4) × 2
Au−A2	3.810(4) × 2	3.430(1) × 2	3.823(6) × 2
P−S1	2.082(4) × 2	2.079(5) × 2	2.185(5) × 2
P−S2	2.013(5)	2.026(7)	2.139(7)
P−S3	2.018(5)	2.020(7)	2.142(7)
mean P(As)−S	2.049	2.051	2.163
A1−S1	3.413(4) × 2	3.368(3) × 2	3.497(7) × 2
A1−S1	3.307(4) × 2	3.356(4) × 2	3.334(7) × 2
A1−S2	3.176(5)	3.244(5)	3.178(9)
A1−S3	3.456(1) × 2	3.415(1) × 2	3.511(2) × 2
A1−S3	3.319(5)	3.340(5)	3.342(8)
A1−S3	3.202(5)	3.143(5)	3.254(8)
A2−S1	3.446(4) × 2	3.401(4) × 2	3.489(7) × 2
A2−S2	3.366(0) × 2	3.336(0) × 2	3.431(0) × 2
A2−S2	3.212(6)	3.027(5)	3.22(1)
A2−S3	3.314(5)	3.429(5)	3.270(9)
mean A−S	3.347	3.329	3.386
	Angles		
S1−Au−S1	180.00(7)	180.0(1)	180.0(1)
P(As)−S1−Au	107.0(1)	110.4(2)	106.2(2)
S1−P(As)−S1	111.2(2)	112.1(2)	111.0(2)
S2−P(As)−S1	111.3(1) × 2	111.0(2) × 2	111.6(2) × 2
S3−P(As)−S1	103.6(1) × 2	103.9(2) × 2	103.3(2) × 2
S3−P(As)−S2	115.2(2)	114.6(3)	115.4(3) × 2

Figure 2. $KAu_5P_2S_8$ (**4**) viewed down the [110] axis (medium grey spheres: K, open spheres: Au, PS_4 tetrahedra), Au−Au short contacts are shown by dashed lines

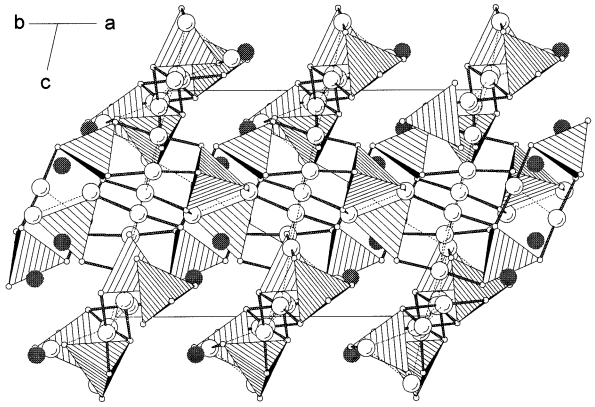

Figure 3. Anionic structure of $KAu_5P_2S_8$ (**4**, open spheres: Au, PS_4 tetrahedra)

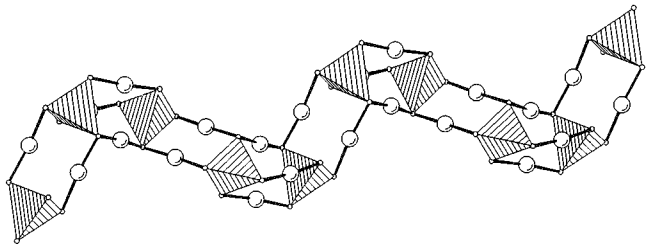

Table 2. Selected bond lengths [Å] and angles [°] for $KAu_5P_2S_8$ (**4**) (with standard deviations in parentheses)

Atoms	Distance	Atoms	Distance
Au1−Au2	3.393(3)	Au5−S7	2.31(1)
Au1−Au3	2.962(3)	mean Au−S	2.31
Au1−Au3	3.033(3)	K1−S1	3.43(2)
Au1−Au4	3.138(3)	K1−S2	3.21(2)
Au1−Au5	3.204(3)	K1−S4	3.24(2)
Au2−Au2	3.148(3)	K1−S6	3.47(2)
Au2−Au3	3.043(3)	K1−S7	3.29(2)
Au3−Au4	3.121(3)	K1−S8	3.71(2)
Au5−Au5	3.193(3)	K1−S8	3.42(2)
mean Au−Au	3.137	mean K−S	3.40
Au2−K1	3.71(1)	S1−P1	1.98(2)
Au1−S4	2.31(1)	S2−P1	2.03(2)
Au1−S7	2.31(2)	S4−P1	2.16(2)
Au2−S4	2.32(1)	S5−P1	2.06(2)
Au2−S5	2.30(1)	S3−P2	1.99(2)
Au3−S1	2.34(1)	S6−P2	2.06(2)
Au3−S3	2.30(1)	S7−P2	2.12(2)
Au4−S2	2.30(1)	S8−P2	2.07(2)
Au4−S8	2.32(1)	mean S−P	2.06
Au5−S6	2.30(2)		
Atoms	**Angle**	**Atoms**	**Angle**
S7−Au1−S4	174.6(4)	S5−P1−S2	110.3(8)
S5−Au2−S4	174.1(5)	S5−P1−S4	105.8(7)
S3−Au3−S1	174.5(4)	S6−P2−S3	112.1(8)
S8−Au4−S2	172.3(5)	S7−P2−S3	113.4(7)
S7−Au5−S6	175.4(4)	S7−P2−S6	106.8(7)
P1−S1−Au3	101.3(6)	S8−P2−S3	115.6(8)
P1−S2−Au4	102.7(6)	S8−P2−S6	104.4(8)
P1−S4−Au1	96.1(6)	S8−P2−S7	103.6(8)
P1−S4−Au2	104.5(6)	P2−S3−Au3	102.3(7)
P1−S5−Au2	99.4(7)	P2−S6−Au5	94.5(7)
S2−P1−S1	120.5(8)	P2−S7−Au1	102.7(7)
S4−P1−S1	105.6(7)	P2−S7−Au5	58.3(6)
S4−P1−S2	108.8(7)	P2−S8−Au4	99.8(7)
S5−P1−S1	104.9(8)		

tronegativities: Au 2.2, Te 2.1) is the more electronegative partner compared to the chalcogen atom.

Metal−metal bonding is an additional point of interest in many coinage metal systems (M = Cu, Ag, Au)[6]. If the geometrical constraints of the ligand or the structure allow, many compounds show a tendency to cluster or polymerize. Such behaviour has been observed in many binary cluster compounds of the general types $[Au_m(PR)_{3m}]^{x+}$ and $[Au_{m+1}(PR_3)_m]^{y+}$[7], molecular alkylcopper compounds[8a], pentaazenidocopper complexes[8b], Hartl's iodocuprates[9], and in multinuclear copper chalcogenide clusters of the $Cu_{2n}Q_n(PR_3)_x$-type reported by Fenske and co-workers[10]. In many of these compounds, the metal−metal distances are comparable to, or are sometimes considerably shorter than, the M−M separations in the elemental metals. Thus, the obvious question arises[11] as to the nature of the interactions between metal centers at such short distances.

We have been intrigued by these questions and have studied the ternary and quaternary systems A/Au/Q (A = alkali metal; Q = S, Se, Te) and A/Au/B/Q (B = group 14 or 15 element). The use of electropositive cations such as alkali metal ions permits the stabilization of gold compounds with the relatively electronegative elements sulfur[12] and

Table 3. Crystal data, details of the data collection, and structure analysis of K_2AuPS_4 (**1**), Tl_2AuPS_4 (**2**), K_2AuAsS_4 (**3**), and $KAu_5P_2S_8$ (**4**)

Empirical formula	K_2AuPS_4	Tl_2AuPS_4	K_2AuAsS_4	$KAu_5P_2S_8$
Formula weight	434.4	764.9	478.3	1342.3
Diffractometer	Siemens P4	Siemens P4	Siemens P4	Nicolet P21
Radiation	Mo-K_α	Mo-K_α	Mo-K_α	Mo-K_α
Monochromator	graphite	graphite	graphite	graphite
Data-collection mode	θ-2θ scan	θ-2θ scan	θ-2θ scan	ω scan
Crystal size [mm]	0.2×0.12×0.06	0.3×0.1×0.06	0.15×0.08×0.04	0.3×0.04×0.04
T [K]	203	198	198	293
Wavelength	λ = 0.71073	λ = 0.71073	λ = 0.71073	λ = 0.71073
Crystal system	monoclinic	monoclinic	monoclinic	monoclinic
Space group	$P2_1/m$	$P2_1/m$	$P2_1/m$	$P2_1/c$
a [Å]	6.497(1)	6.459(1)	6.555(1)	10.054(2)
b [Å]	6.727(1)	6.669(1)	6.859(1)	13.464(3)
c [Å]	9.434(2)	9.193(2)	9.533(2)	11.968(2)
β [°]	92.69(3)	93.84(3)	92.64(3)	106.16(3)
V [Å^3]	411.9(2)	395.1(2)	428.1(2)	1556.2(5)
Z	2	2	2	4
$D_{calcd.}$ [g/cm^3]	3.502	6.43	3.711	5.729
μ(Mo-K_α)[mm^{-1}]	19.975	60.358	22.868	48.485
Absorption correction	semiempirical, Ψ scan, laminar (001)	semiempirical, Ψ scan, ellipsoid	semiempirical, Ψ scan, ellipsoid	semiempirical, Ψ scan, pseudoellipsoid
Min./max. transmission	0.3752, 0.9311	0.290, 0.735	0.4841,0.5423	0.5546, 0.9825
F(000) [e]	392	640	428	2882
θ range for data collection[°]	4.0−54.0	4.0−54.0	4.0−54.0	4.0−54.0
Index ranges	$-1 \le h \le 8$ $-8 \le k \le 8$ $-12 \le l \le 12$	$-7 \le h \le 7$ $-8 \le k \le 8$ $-11 \le l \le 11$	$-7 \le h \le 8$ $-1 \le k \le 8$ $-11 \le l \le 7$	$0 \le h \le 12$ $-17 \le k \le 17$ $-15 \le l \le 14$
Data collected	2148	1969	1040	6147
Unique data	964 (R_{int} = 0.046)	924 (R_{int} = 0.042)	767(R_{int} = 0.054)	3424 (R_{int} = 0.126)
Observed data	696 [$I > 2\sigma(I)$]	784 [$I > 2\sigma(I)$]	550 [$I > 2\sigma(I)$]	1433 [$I > 3\sigma(I)$]
Refinement method	Full-matrix least squares on F	Full-matrix least squares on F	Full-matrix least squares on F	Full-matrix least squares on F
Parameters	47	47	47	146
Final R indices [$I > 2\sigma(I)$]	R = 0.0291	R = 0.0380	R = 0.0448	R = 0.0784
	Rw = 0.0627	Rw = 0.0959	Rw = 0.0923	Rw = 0.1028
Goodness-of-Fit	1.069	1.100	1.103	1.311
Extinction coefficient	0.0016(4)	0.0124(8)	0.0015(5)	0.00038(4)
Largest diff. peak and hole [eÅ^{-3}]	1.00; −1.40	2.66; −4.02	1.84; −1.61	3.25; −3.19

phosphorus. Thus, no ternary thiophosphates of Au exist. In contrast, for the lighter metals numerous compounds belonging to the ternary Ag−P−S[13] family have been reported in the literature, and some compounds of the type Cu−P−S[14] are known. Being itself rather electronegative, the usual, preferred chemistry for gold is through "soft" interactions with metalloids such as Te[15] and Bi[16].

In this paper, we report on two new thiophosphates of gold and an isostructural thioarsenate. A short account of this work has appeared elsewhere[17]. The compounds are K_2AuPS_4 (**1**), Tl_2AuPS_4 (**2**), K_2AuAsS_4 (**3**), and $KAu_5P_2S_8$ (**4**). During the preparation of this manuscript, one of the compounds presented here, K_2AuPS_4, was reported in the literature[18]. The compounds were prepared from Au, A_2S, S, and P_2S_5 or As_2S_3. The alkaline polythiophosphate or polythioarsenate forms a flux in situ. Kanatzidis and coworkers have used this feature to good advantage in the synthesis of metal thiophosphates such as $A_2AuP_2Se_6$ (A = K, Rb)[19], $A_2MP_2Se_6$ (A = K, Rb; M = Mn, Fe)[21], $A_2M_2P_2Se_6$ (A = K, Cs; M = Cu, Ag)[20], $A_3M(PS_4)_2$ (A = Rb, Cs; M = Sb, Bi)[20], as well as several main-group derivatives[21][22][23][24].

The structures of the title compounds have been determined by single-crystal X-ray diffraction techniques. Thermal and optical properties have also been investigated. One possible application of such compounds of the late transition metals stems from the fact that they have direct optical band gaps. Thus, they may be of interest in infra-red sensing. Also of interest is the observation of short Au−Au contacts in one of the compounds reported here.

Results and Discussion

Crystal Structures of K_2AuPS_4, K_2AuAsS_4, and Tl_2AuPS_4

Compounds **1**, **2**, and **3** are isostructural. Their structures consist of anionic columns separated by potassium cations, as shown in Figure 1. Selected distances and angles are compiled in Table 1. The $[AuPS_4]^{2-}$ columns run parallel to and are centered about the b axis. In these chains, neighbouring Au^I atoms are linked by PS_4^{3-} tetrahedra in a *trans* orientation. The distances in **1** are as follows: The Au−S distance is 2.298(2) Å, comparable to that in KAuS [2.305(6) Å][12a], Na_3AuS_2 [2.301(7) Å][12b], and $K_4Au_6S_5$ [2.295(6) Å][12c]. The PS_4 tetrahedra are slightly distorted.

The average P−S distance is 2.047 Å, with the individual P−S distances ranging from 2.014 to 2.080 Å. The S−P−S angles fall in a narrow range between 103.7 and 115.7°. Two crystallographically distinct K^+ cations K(1) and K(2) are situated between the anionic fragments and are surrounded by 6 and 9 S atoms, respectively, with an average K−S distance of 3.347 Å.

In **2**, the mean As−S distance is 2.165 Å. The AsS_4 units are slightly distorted with S−As−S bond angles ranging from 103.3 to 115.7°. The Au−Au distance (3.43 Å) is slightly longer than that in the thiophosphate. All other distances and angles are in the same range as those in the thiophosphate.

$KAu_5P_2S_8$

Compound **4** crystallizes with a structure that is characterized by infinite anionic $[Au_5P_2S_8]^-$ chains and isolated K^+ cations. The angular chains extend along the [110] and [1$\bar{1}$0] direction, as shown in Figure 2. The anionic framework is built up from linear AuS_2 dumbbell units and PS_4^{3-} tetrahedra, as shown in Figure 3. The edges of two PS_4^{3-} tetrahedra are alternately connected by two and three Au^+ ions, to form eight-membered $P(SAuS)_2P$ rings. Each PS_4^{3-} tetrahedron is linked to neighbouring tetrahedra by 5 Au atoms, so that S(4) and S(7) are coordinated by two Au atoms. These anionic chains interact with each other through close Au−Au d^{10}−d^{10} contacts [Au(1)−Au(3) 2.961 Å, Au(2)−Au(3) 3.043 Å]. This is not the case in **1**, which has Au−Au contacts of 3.364 Å. The short Au−Au distances are remarkable, since no sulfide bridging ligands or other steric effects are present that might account for this behaviour. The Au−Au short contacts are classical d^{10}−d^{10} interactions, which are also observed in KAuS[12d]. The intra-chain Au−Au distances are short, ranging from 3.035(2) [Au(1)−Au(3)] to 3.204(2) Å. A theoretical interpretation of the Au−Au bonding in terms of the electron localization function (ELF)[26] will be presented in a separate communication[27]. The Au atoms have a different number of homoatomic contacts. Au is almost linearly coordinated (∡ S−Au−S: 174.1−175.5°); the mean Au−S bond length is 2.31 Å, which is normal for linear AuS_2 fragments[12].

The structure contains two crystallographically distinct P sites. The PS_4^{3-} tetrahedra have a slightly distorted geometry, with bond lengths varying from 2.0−2.15 Å [P(1)−S] and 2.0−2.12 Å [P(2)−S]; bond angles range from 104−116° for [∡ S−P(2)−S] and from 105−120° for [∡ S−P(1)−S]. The distortion arises because one edge of the PS_4^{3-} tetrahedra has two Au neighbours, resulting in a longer P−S distance. The K^+ ions fill the voids in the structure. They are highly coordinated by seven K−S contacts in the range between 3.2 and 3.7 Å. Selected bond lengths and angles for **4** are given in Table 2.

Properties − Thermal Analysis

Differential thermal analysis (DTA) showed that **1**, **2**, and **4** melt congruently at 386, 412, and 394°C, respectively. Figure 4(a) shows the DSC trace obtained upon heating and cooling of the starting materials (polysulfide, As_2S_3, elements). The sharp exotherm near 100°C corresponds to the reaction leading to the clean product K_2AuAsS_4. The sharp exotherm at 386°C obtained upon cooling thus corresponds to the crystallization of molten K_2AuAsS_4. For comparison, Figure 4(b) shows the DSC trace (heating and cooling) of pure K_2AuAsS_4. Figure 4(c) shows the powder diffractogram of the products obtained from the in situ reaction in the DSC cell. The vertical lines mark expected peak positions of the K_2AuAsS_4 structure obtained from the single-crystal study.

Figure 4. a) DSC diagram of the starting compounds of K_2AuAsS_4 (**2**), b) DSC diagram of K_2AuAsS_4 (**2**), c) powder pattern after the DSC experiments

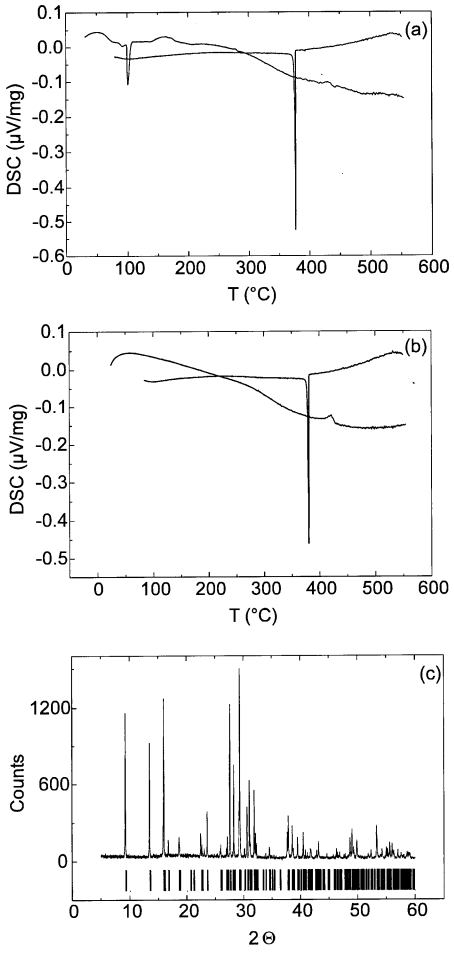

The optical absorption properties of the compounds **1**, **3**, and **4** were assessed by studying their UV/vis-near IR reflectance spectra. The spectra confirm the semiconducting nature of the materials by revealing the presence of abrupt optical gaps, as can be seen in Figure 5. The band gaps of **1** and **2** are 2.63 and 2.20 eV, respectively. Higher energy absorptions are readily resolved in these spectra and are assigned to electronic S→Au charge-transfer transitions. The band gap of **4** is found to be 2.14 eV.

The infrared spectra of the compounds are shown in Figure 6. The spectrum of **1** displays absorptions at ca. 613, ca. 557, ca. 521, ca. 471, ca. 397, ca. 370, ca. 272, ca. 245,

Figure 5. Plots of absorbance (arbitrary units) vs. energy (eV) for a) K_2AuPS_4 (**1**), b) K_2AuAsS_4 (**2**), and c) $KAu_5P_2S_8$ (**4**)

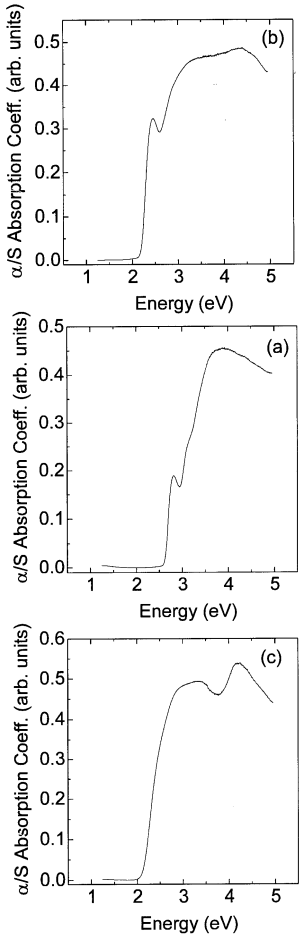

and ca. 228 cm^{-1}. The vibrations can mainly be assigned to PS_4 stretching modes by analogy with $Na_3PS_4 \cdot 8\ H_2O$[28]. The far-IR spectrum of **2** displays absorptions at ca. 459, ca. 430, ca. 401, ca. 392, ca. 353, ca. 314, ca. 293, and ca. 216 cm^{-1}. These values are shifted to lower energies in comparison with those of the thiophosphate because of the greater mass of As. Compound **4** exhibits absorptions at ca. 660, ca. 552, ca. 459, ca. 395, ca. 326, and ca. 236 cm^{-1}.

This research was supported by the *Fonds der Chemischen Industrie.* The donation of quartz tubes from *Heraeus Quarzschmelze* Hanau (Dr. *Höfer*) and of gold from *Degussa AG* is gratefully acknowledged. We are indebted to Dr. *Ram Seshadri* for fruitful discussions and a critical reading of the manuscript.

Experimental Section

Synthesis: Starting materials were gold metal powder, P_2S_5 (Fluka, 99.99% purity, Alfa), As_2S_3 (Alfa, 99.998%), K_2S and S powder (Riedel, 99.999%).

Potassium Gold Thiophosphate, K_2AuPS_4 (**1**): A mixture of Au powder (0.164 g, 0.833 mmol), K_2S (0.092 g, 0.833 mmol), P_2S_5 (0.093 g, 0.417 mmol), and S (0.013 g, 0.417 mmol) was loaded into a silica tube in a glovebox. The tube was evacuated and sealed in vacuo. The mixture was heated to 550°C over a period of 12 h and maintained at this temperature for 4 d. It was then allowed to cool slowly to room temperature at a rate of 4°C/h. The yellow, plate-like crystals thus obtained were found to be stable in air and insoluble both in water and in common organic solvents. The collected material was washed with water and then dried by rinsing with diethyl ether.

Figure 6. Far-IR spectra of a) K_2AuPS_4 (**1**), b) K_2AuAsS_4 (**2**), and c) $KAu_5P_2S_8$ (**4**)

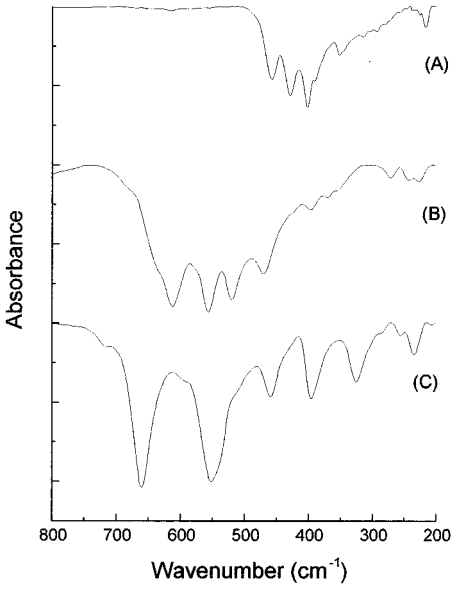

Table 4. Atomic coordinates and equivalent isotropic displacement parameters for K_2AuPS_4 (**1**) (with standard deviations in parentheses)

Atom	*X*	*Y*	*Z*	*U*(eq)[a]
Au	0	1/2	0	0.0197(1)
P	0.2669(5)	1/4	0.2804(4)	0.0153(9)
K1	0.7959(5)	1/4	0.4641(3)	0.0221(8)
K2	0.4570(6)	1/4	0.8346(4)	0.032(1)
S1	0.9061(3)	0.0054(6)	0.7622(2)	0.0223(5)
S2	0.5280(6)	1/4	0.1738(4)	0.023(1)
S3	0.3070(6)	1/4	0.4939(3)	0.0200(9)

[a] The isotropic equivalent displacement parameter is defined as one-third of the trace of the orthogonalized U_{ij} tensor.

Table 5. Atomic coordinates and equivalent isotropic displacement parameters for Tl_2AuPS_4 (**2**) (with standard deviations in parentheses)

Atom	*X*	*Y*	*Z*	*U*(eq)[a]
Au	0	1/2	0	0.0119(2)
P	0.2843(8)	1/4	0.7296(5)	0.008(1)
Tl1	0.7896(1)	1/4	0.54139(9)	0.0162(3)
Tl2	0.4242(2)	1/4	0.15382(9)	0.0218(3)
S1	0.8824(6)	0.4914(5)	0.2306(4)	0.0128(10)
S2	0.5623(9)	1/4	0.8456(5)	0.014(2)
S3	0.3020(8)	1/4	0.5111(5)	0.011(1)

[a] The isotropic equivalent displacement parameter is defined as one-third of the trace of the orthogonalized U_{ij} tensor.

Table 6. Atomic coordinates and equivalent isotropic displacement parameters for K_2AuAsS_4 (**3**) (with standard deviations in parentheses)

Atom	*X*	*Y*	*Z*	*U*(eq)[a]
Au	0	1/2	0	0.0190(3)
As	0.2721(4)	1/4	0.2802(3)	0.0145(8)
K1	0.7977(8)	1/4	0.4662(6)	0.021(2)
K2	0.4537(10)	1/4	0.8373(7)	0.030(2)
S1	0.9079(6)	0.0125(8)	0.7653(5)	0.025(1)
S2	0.550(1)	1/4	0.1715(8)	0.026(3)
S3	0.3071(10)	1/4	0.5047(7)	0.019(2)

[a] The isotropic equivalent displacement parameter is defined as one-third of the trace of the orthogonalized U_{ij} tensor.

Table 7. Atomic coordinates and equivalent isotropic displacement parameters for $KAu_5P_2S_8$ (**4**) (with standard deviations in parentheses)

Atom	*X*	*Y*	*Z*	*U*(eq)[a]
Au1	0.2324(2)	0.2618(1)	0.0457(2)	0.0226(7)
Au2	0.4382(2)	0.4042(1)	−0.0710(2)	0.0231(8)
Au3	0.2395(2)	0.2447(2)	−0.1994(1)	0.0194(7)
Au4	0.0586(2)	0.0830(2)	−0.3585(2)	0.0310(8)
Au5	0.1170(3)	0.0473(2)	−0.0505(2)	0.0360(9)
K1	0.309(1)	0.7480(10)	0.170(1)	0.047(5)
S1	0.411(1)	0.1233(9)	−0.1367(10)	0.023(5)
S2	0.236(1)	−0.0171(9)	−0.378(1)	0.027(5)
S3	0.079(2)	0.3711(9)	−0.244(1)	0.028(5)
S4	0.454(1)	0.3266(9)	0.105(1)	0.025(5)
S5	0.423(2)	0.465(1)	−0.254(1)	0.041(6)
S6	0.236(1)	−0.095(1)	−0.069(1)	0.041(5)
S7	0.013(2)	0.197(1)	−0.032(1)	0.037(5)
S8	−0.136(1)	0.177(1)	−0.364(1)	0.038(6)
P1	0.408(2)	0.0577(9)	−0.286(1)	0.020(5)
P2	0.939(1)	0.183(1)	0.1170(9)	0.027(5)

[a] The isotropic equivalent displacement parameter is defined as one-third of the trace of the orthogonalized U_{ij} tensor.

Thallium Gold Thiophosphate, Tl_2AuPS_4 (**2**): Au powder (35 mg, 0.178 mmol), Tl_2S (79 mg, 0.355 mmol), P_2S_5 (78 mg, 0.178 mmol), and S (57 mg, 1.778 mmol) were heated to 700°C over a period of 12 h and maintained at this temperature for 4 d. The mixture was then slowly cooled to room temperature at a rate of 4°C/h. The long, red plates thus obtained were found to be both air- and water-stable.

Potassium Gold Thioarsenate, K_2AuAsS_4 (**3**): Pure material was obtained by heating a mixture of Au powder (0.123 g, 0.625 mmol), K_2S (0.069 g, 0.625 mmol), As_2S_3 (0.077 g, 0.312 mmol), and S (0.03 g, 0.937 mmol) in analogy to the procedure described for **1**. Orange, plate-like crystals were formed, which were found to be slightly air-sensitive and which decomposed in water.

Potassium Gold Thiophosphate, $KAu_5P_2S_8$ (**4**): 0.123 g (0.62 mmol) of Au, 0.034 g (0.31 mmol) of K_2S, 0.069 g (0.31 mmol) of P_2S_5, and 0.04 g (1.25 mmol) of S were heated as described above. Red, needle-shaped crystals were collected from the charge under inert atmosphere and were washed with anhydrous diethyl ether. The crystals were found to disintegrate in water or after exposure to air for 1 d.

Structure Determination: Crystal structures were determined from single-crystal X-ray diffraction data at 294 K for **4** and at 200 K for the other two compounds. A Siemens P4 diffractometer was used for the data collection. After Lorentz and polarization corrections, absorption corrections were made by acquiring Ψ scans and using the program XEMP in the SHELXTL package[29]. The structures were solved in the different space groups using direct methods with the package SHELXTL. Refinements were performed against F_o^2.using SHELXL-93[30]. Final refinement cycles included anisotropic thermal parameters on all atoms. Details of the data collection and refinement are given in Table 3. The final atomic and equivalent thermal parameters are listed in Tables 4−7. Further details of the crystal structure determinations may be obtained from the Fachinformatioszentrum Karlsruhe, D-76344 Eggenstein-Leopoldshafen (Germany), on quoting the depository numbers CSD-407912 (K_2AuPS_4), -407910 (Tl_2AuPS_4), -407913 (K_2AuAsS_4), and -407911 ($KAu_5P_2S_8$).

Physical Measurements − Thermal Analysis: Differential thermal analyses were performed with a Netzsch STA 429 thermal analyzer. Typically, samples of 30 mg of ground crystalline material were heated in quartz ampoules in vacuo. An empty quartz ampoule of equal mass was used as a reference. The samples were heated to the 600°C at a rate of 3°C/min and were then cooled to 50°C at the same rate. The DTA samples were examined by powder X-ray diffraction (D5000, Siemens) after the experiments.

Optical Spectra: UV/Vis/NIR spectra were acquired with a CARY 5 G (Varian) in the reflectance mode using a diffuse reflectance integrating sphere. The samples were diluted with $BaSO_4$.

Infrared Spectra: FT-IR spectra of samples pressed into KBr pellets were recorded with a Galaxy-2030 FT-IR spectrometer (Mattson Instruments).

[1] *Topics in Current Physics, Superconductivity in Ternary Compounds*, (Eds.: Ø. Fischer, M. B. Maple), Springer, Berlin, **1982**.
[2] J. A. Wilson, F. J. DiSalvo, S. Mahajan, *Adv. Phys.* **1975**, *24*, 117.
[3] [3a] M. S. Whittingham, A. J. Jacobson, *Intercalation Chemistry*, Academic Press, New York, **1982**. − [3b] R. H. Friend, A. D. Yoffe, *Adv. Phys.* **1987**, *36*, 1.
[4] [4a] J. Rouxel, *Chem. Eur. J.* **1996**, *2*, 1053. − [4b] M. Evain, *Eur. J. Solid State Inorg. Chem.* **1994**, *31*, 683. − [4c] S. Jobic, R. Brec, J. Rouxel, *J. Solid State Chem.* **1992**, *96*, 169. − [4d] S. Jobic, J. Rouxel, *J. Alloys Compd.* **1992**, *178*, 233. − [4e] S. Jobic, P. Deniard, R. Brec, J. Rouxel, A. Jouanneaux, A. Fitch, *Z. Anorg. Allg. Chem.* **1991**, *199*, 598.
[5] R. Hoffmann, C. Zheng, *J. Phys. Chem.* **1985**, *89*, 4175.
[6] *Unkonventionelle Wechselwirkungen in der Chemie metallischer Elemente* (Ed.: B. Krebs), VCH Publishers, Weinheim, **1992**.
[7] K. P. Hall, D. M. P. Mingos, *Prog. Inorg. Chem.* **1983**, *32*, 239.
[8] [8a] S. Gambarotta, C. Floriani, A. Chiesa-Villa, C. Guastini, *J. Chem. Soc., Chem. Commun.* **1983**, 1156. − [8b] J. Beck, J. Strähle, *Angew. Chem.* **1985**, *97*, 419; *Angew. Chem. Int. Ed. Engl.* **1985**, *24*, 409.
[9] H. Hartl, F. Mahdjour-Hassan-Abadi, *Angew. Chem.* **1984**, *96*, 359; *Angew. Chem. Int. Ed. Engl.* **1984**, *23*, 378; H. Hartl, F. Mahdjour-Hassan-Abadi, F. Fuchs, *Angew. Chem.* **1984**, *96*, 497; *Angew. Chem. Int. Ed. Engl.* **1984**, *23*, 514.
[10] D. Fenske in *Clusters and Colloids* (Ed.: G. Schmid), VCH Publishers, Weinheim, **1994**, pp. 212.
[11] [11a] P. K. Mehrotra, R. Hoffmann, *Inorg. Chem.* **1978**,*17*, 2187. − [11b] A. Dedieu, R. Hoffmann, *J. Am. Chem. Soc.* **1978**, *100*, 2074.
[12] See for example:
[12a] KAuS: K. O. Klepp, W. Bronger, *J. Less-Common Metals* **1987**, *127*, 65. − [12b] Na_3AuS_2: K. O. Klepp, W. Bronger, *J. Less-Common Metals* **1987**, *132*, 173. − [12c] $K_4Au_6S_5$: K. O. Klepp, W. Bronger, *J. Less-Common Metals* **1988**, *137*, 13. − [12d] $KAuS_5$: M. G. Kanatzidis, *Chem. Mater.* **1990**, *2*, 353. − [12e] AAuX (with A = Na, K, Rb, Cs; X = S, Se, Te): W. Bronger, H. U. Karthage, *J. Alloys Compd.* **1992**, *184*, 87.
[13] [13a] $AgPS_3$: P. Toffoli, P. Khodadad, N. Rodier, *Acta Crystallogr.* **1978**, *B34*, 3561. − [13b] $Ag_4P_2S_6$: P. Toffoli, P. Khodadad, N. Rodier, *Acta Crystallogr.* **1983**, *C39*, 1485; P. Toffoli, P.

Khodadad, N. Rodier, *Acta Crystallogr.* **1982**, *B38*, 2374. – [13c] $Ag_4P_2S_7$: P. Toffoli, P. Khodadad, N. Rodier, *Acta Crystallogr.* **1977**, *B33*, 1492. – [13d] Ag_7PS_6: R. Blachnik, U. Wickel, *Z. Naturforsch.* **1980**, *B35*, 1268. – [13e] $Ag_7P_3S_{11}$: P. Toffoli, P. Khodadad, N. Rodier, *Acta Crystallogr.* **1982**, *B38*, 2374.

[14] [14a] $CuPS_2$: J. K. Kom, J. Flahaut, L. Domange, *C. R. Seances Acad. Sci. Paris* **1963**, *257*, 3919. – [14b] Cu_3PS_4: R. Nitsche, P. Wild, *Mat. Res. Bull.* **1970**, *4*, 419; *J. Solid State Chem*. **1983**, *49*, 43.

[15] G. Tunell, L. Pauling, *Acta Crystallogr.* **1952**, *5*, 375.

[16] T. H. Geballe, V. B. Compton, *Rev. Mod. Phys.* **1963**, *35*, 1.

[17] S. Löken, W. Tremel, *12th International Conference on Solid Compounds of Transition Elements*, St. Malo, April 22−25, **1997**, Abstract P-D 49.

[18] K. Chondroudis, J. A. Hanko, M. G. Kanatzidis, *Inorg. Chem.* **1997**, *36*, 2623.

[19] K. Chondroudis, T. J. McCarthy, M. G. Kanatzidis, *Inorg. Chem.* **1996**, *35*, 3451.

[20] T. J. McCarthy, M. G. Kanatzidis, *J. Alloys Compd.* **1996**, *236*, 70.

[21] T. J. McCarthy, M. G. Kanatzidis, *Inorg. Chem.* **1995**, *34*, 1257; A. Sutorik, M. G. Kanatzidis, *Progr. Inorg. Chem.* **1995**, *43*, 151.

[22] T. J. McCarthy, M. G. Kanatzidis, *J. Chem. Soc., Chem. Commun.* **1994**, 1089.

[23] T. J. McCarthy, M. G. Kanatzidis, *Chem. Mater.* **1993**, *5*, 1061.

[24] K. Chondroudis, T. J. McCarthy, M. G. Kanatzidis, *Inorg. Chem.* **1996**, *35*, 840.

[25] K. Chondroudis, M. G. Kanatzidis, *Inorg. Chem.* **1995**, *34*, 5401.

[26] C. Felser, S. Löken, Y. Grin, W. Tremel, unpublished results.

[27] [27a] A. D. Becke, K. E. Edgecomb, *J. Chem. Phys.* **1990**, *92*, 5397. – [27b] B. Silvi, A. Savin. *Nature* **1994**, *371*, 683.

[28] A. Feltz, G. Pfaff, *Z. Anorg. Allg. Chem.* **1978**, *442*, 41.

[29] G. M. Sheldrick, Siemens Analytical X-ray Instruments Inc., Madison, WI, USA, **1991**.

[30] G. M. Sheldrick, *SHELXL 93, Program for the refinement of Crystal Structures*, Univerity of Göttingen, Germany, **1993**.

[97169]

Synthesis and Structure of the First η^1-Borazine Complexes

Holger Braunschweig*[a], Carsten Kollann[a], and Matthias Müller[b]

Institut für Anorganische Chemie der Technischen Hochschule[a]
Templergraben 55, D-52056 Aachen
E-mail: holger.braunschweig@ac.rwth-aachen.de

Chemical Crystallography Laboratory, University of Oxford[b]
9 Parks Road, Oxford OX1 3PD, UK

Received August 21, 1997

Keywords: Boron / Iron / Boryl complexes / η^1-Coordinated borazine

A series of η^1-borazine complexes were obtained by the reaction of trichloroborazine with $Na[(\eta^5\text{-}C_5R_5)Fe(CO)_2]$. The compounds $[\{(C_5R_5)(CO)_2Fe\}_nCl_{3-n}B_3N_3H_3]$ (**1a**, n = 1, R = Me; **1b**, n = 2, C_5R_5 = C_5H_4Me; **1c**, n = 3, R = H) have one to three iron−boron σ bonds and Fe−B π-interactions can be ruled out from the spectroscopic and structural results. All new borazine complexes were isolated as orange crystalline solids and characterized by multinuclear NMR methods and IR spectroscopy. The structure of **1b** in the crystalline state was also determined by a single-crystal X-ray study.

Introduction

The chemistry of borazine and its derivatives, in terms of their role as ligands in transition-metal complexes, is restricted to a few examples, such as $[(EtBNEt)_3Cr(CO)_3]$[1a][1b]. In these compounds, which are mostly derived from peralkylated borazines, the $(RBNR)_3$ ligand always shows η^6 coordination similar to the corresponding benzene complexes[2][3]. η^1-Coordinated borazines with a boron−transition metal bond are believed to play an important role in the $[RhH(CO)(PPh_3)_3]$-catalyzed hydroboration of acetylenes with $(HBNH)_3$. This reaction yields a variety of alkenyl-substituted borazines which are suitable precursors for conversion into ceramic materials[4]. The similarity between this reaction and the rhodium-catalyzed hydroboration with boranes[5] suggests the oxidative addition of a borazine B−H bond to the metal center with formation of a boryl complex. However, there is no spectroscopic evidence for the formation of such a compound. Structurally characterized boryl complexes have, in most cases, been obtained from catecholborane and its derivatives[6a][6b][6c][6d][6e][6f][6g]. As a consequence of our investigations of alternative transition metal complexes of boron[7a][7b], we report here the synthesis and structure of the first η^1-coordinated borazine complexes having boron−transition metal σ bonds.

Results and Discussion

The reaction of $(ClBNH)_3$ with two equivalents of $Na[(C_5H_4Me)Fe(CO)_2]$, as shown in Eq. 1, gives a borazine derivative with two boron−iron bonds, $[\{(C_5H_4Me)Fe(CO)_2\}_2ClB_3N_3H_3]$ (**1b**) as orange needles in 29% yield. The structure of **1b** in solution can be elucidated from the NMR and IR spectra. The compound shows two broad resonances at δ = 5.53 and δ = 6.20 (2:1 ratio) in the ^{1}H-NMR spectrum, corresponding to the nitrogen-bound hydrogen atoms, along with characteristic ^{11}B-NMR signals in a 1:2 ratio for the Cl- and Fe-substituted boron atoms, respectively, at δ = 27.2 and δ = 53.1. The relative high field shift of 68 ppm for the second signal compared to that of $[CpFe(CO)_2BPh_2]$[6c] is largely due to the B−N multiple bond character in the borazinyl ring. There is no evidence for an Fe−B π-interaction, which has been established for $[CpFe(CO)_2BCat]$ (Cat = OC_6H_4O)[6c] in solution, and evidence for this is provided by the CO stretching frequencies of **1b** (1996 and 1937 cm^{-1}) that match the IR data of the methyl complex $[(C_5H_4Me)Fe(CO)_2Me]$ (1995 and 1935 cm^{-1})[8].

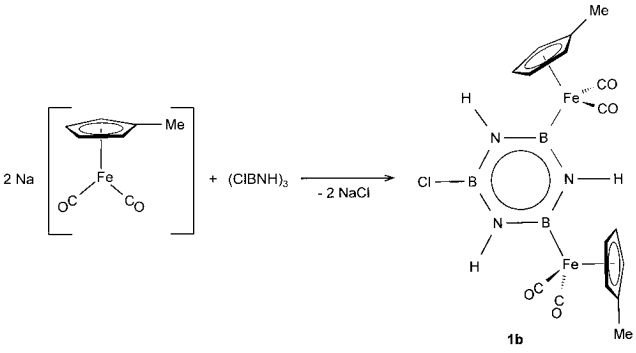

In the crystal (Figure 1) **1b** adopts C_1 symmetry. Fe-B π-interactions in the solid state can be excluded because of the orthogonal arrangement of the N−B−N planes with respect to the Cp centroid−Fe−B planes (90.6° and 94.5°)[6c][9]. The Fe−B distances of 2.041(1) and 2.045(1) Å, respectively, can be compared with the value of 2.034(3) Å found for $[CpFe(CO)_2BPh_2]$, which shows a similar geometry in the crystal in terms of the dihedral angle between the Cp centroid−Fe−B and C−B−C planes (75°)[6c]. The replacement of two Cl atoms by the more bulky $[(C_5H_4Me)Fe(CO)_2]$ moieties has no significant influence on the geometry of the central six-membered B−N core, as shown

 © WILEY-VCH Verlag GmbH, D-69451 Weinheim, 1998 1434−1948/98/0202−0291 $ 17.50+.50/0

by the B−N bond distances [1.414(2)−1.442(2) Å] and N−B−N angles [115.3(1)−120.5(1)°] which resemble the corresponding values in the parent compound $(ClBNH)_3$; the planarity of the $(B-N)_3$ ring of **1b** is also preserved[10].

Figure 1. Structure of **1b** in the crystal (ellipsoids at 50% probability, drawing package CAMERON[14]).

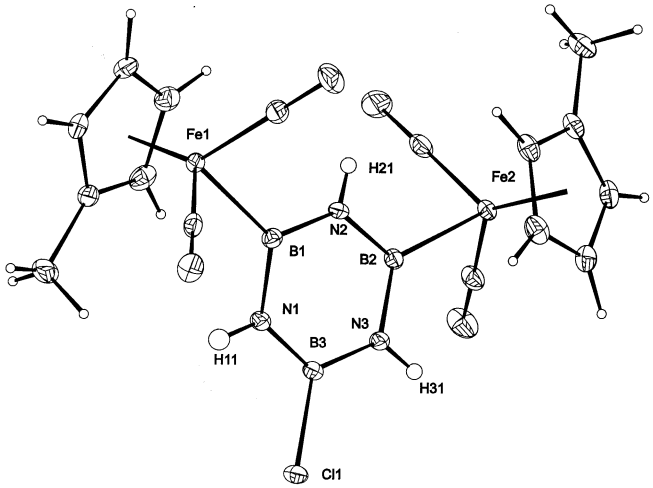

Selected distances (Å) and angles (°): Fe1−B1 2.041(1); Fe2−B2 2.045(1); B1−N1 1.441(2); B3−N1 1.410(2); Fe1−centroid 1 1.721; Fe2−centroid 2 1.716; Fe1−B1−N1 123.10(9); Fe2−B2−N2 120.64(9); N1−B1−N2 115.3(1), N2−B2−N3 115.4(1)

Apart from **1b**, the corresponding borazine complexes containing one or three boron−iron bonds, respectively, were obtained by similar methods. In the case of the monosubstituted derivative $[\{(C_5Me_5)Fe(CO)_2\}Cl_2B_3N_3H_3]$ (**1a**) the best results were obtained from the reaction of $(ClBNH)_3$ with one equivalent $Na[(C_5Me_5)Fe(CO)_2]$, while $[\{CpFe(CO)_2\}_3B_3N_3H_3]$ (**1c**) is obtained with three equivalents of $Na[CpFe(CO)_2]$. In order to obtain the crystalline compounds **1a,b** it was necessary to employ the alkylated Cp derivatives, whereas the parent compound, $Na[CpFe(CO)_2]$, always led to oily products containing impurities. The structures of **1a**,**c** in solution can be deduced from the similarity between the IR- and NMR-spectroscopic data and the results obtained for **1b**. All compounds proved to be extremely air-sensitive and showed signs of decomposition after storage at room temperature under a nitrogen atmosphere for a few days.

Conclusion

The first η^1-borazine complexes have been obtained by the reaction of trichloroborazine with $Na[(\eta^5\text{-}C_5R_5)Fe(CO)_2]$, extending the scope of borazine in transition-metal chemistry. Depending on the borazine-to-iron ratio employed, the mono-, di- and trisubstituted compounds $[\{(C_5R_5)(CO)_2Fe\}_nCl_{3-n}BNH_3]$ (**1a**, n = 1, R = Me; **1b**, n = 2, $C_5R_5 = C_5H_4Me$; **1c**, n = 3, R = H) were obtained as crystalline solids. These complexes show, both in solution and in the crystal, iron−boron σ bonds with no further π stabilization, which was proved by NMR and IR spectroscopy as well as by X-ray studies.

This work was supported by the *Deutsche Forschungsgemeinschaft* and the *Fonds der Chemischen Industrie*.

Experimental Section

All manipulations were carried out under a dry nitrogen atmosphere in Schlenk glassware. Solvents and reagents were dried by standard procedures, distilled, and stored under nitrogen and over molecular sieves. $Na[(\eta^5\text{-}C_5R_5)Fe(CO)_2]$[11] and $(ClBNH)_3$[12] were synthesized according to the literature procedures. − NMR: Varian Unity 500 at 499.843 (^{1}H, internal standard TMS), 150.364 (^{11}B, external standard $BF_3\cdot OEt_2$ in C_6D_6), 125.639 MHz (^{13}C{^{1}H}, APT, internal standard TMS); all NMR spectra were recorded in C_6D_6 as solvent. − Elemental analyses (C, H, N): Carlo-Erba elemental analyzer, model 1106. − IR: Perkin-Elmer FT-IR 1720x.

[2,4-Dichloro-6-{(η^5-pentamethylcyclopentadienyl)dicarbonyliron}borazine] (**1a**): 0.86 g (3.18 mmol) of $Na[(C_5Me_5)Fe(CO)_2]$ was suspended in 20 ml of benzene and a solution of 0.58 g (3.18 mmol) of $(ClBNH)_3$ in 15 ml of benzene was added dropwise at ambient temperature. After stirring for 45 min all volatile materials were removed under high vacuum (25°C/0.001 torr) and the solid residue was treated with 40 ml of hexane and filtered. 0.25 g (20%) of **1a** was recovered from the filtrate at −30°C as yellow needles. − ^{1}H NMR δ = 1.33 (s, 15 H, Me), 4.68 (s, 1 H, ClBNHBCl), 5.52 (s, 2 H, ClBNHBFe). − ^{11}B NMR: δ = 28.44 (s, 2 B, BCl), 58.99 (s, 1 B, BFe). − ^{13}C NMR: δ = 9.55 (Me), 94.66 (C1−C5, C_5Me_5), 217.55 (CO). − IR (hexane): $\tilde{\nu}$ = 1995, 1935 cm^{-1} (CO). − $C_{16}H_{17}B_3ClFe_2N_3O_4$ (494.91): calcd. C 38.83, H 3.46, N 8.49; found C 38.48, H 3.51, N 8.53.

[Chloro-4,6-bis{(η^5-methylcyclopentadienyl)dicarbonyliron}borazine] (**1b**): As described for **1a**, $Na[(C_5H_4Me)Fe(CO)_2]$ (0.90 g, 4.20 mmol) was reacted with $(ClBNH)_3$ (0.39 g, 2.10 mmol) and 0.30 g (29%) of $[\{(C_5H_4Me)Fe(CO)_2\}_2ClB_3N_3H_3]$ (**1b**) was recovered from the filtrate at −30°C as orange crystals. − ^{1}H NMR: δ = 1.51 (s, 6 H, Me), 3.92−4.05 (broad, 8 H, C_5H_4), 5.53 (s, 2 H, ClBNHBFe), 6.20 (s, 1 H, FeBNHBFe). − ^{11}B NMR: δ = 27.15 (s, 1 B, BCl), 53.05 (s, 2 B, BFe). − ^{13}C NMR: δ = 12.97 (Me), 81.50, 84.31 (C2−C4, C_5H_4), 99.86 (C1, C_5H_4), 217.19 (CO). − IR (hexane): $\tilde{\nu}$ = 1996, 1937 cm^{-1} (CO). − $C_{12}H_{18}B_3Cl_2FeN_3O_2$ (395.48): calcd. C 36.45, H 4.59, N 10.56; found C 36.33, H 4.60, N 10.56.

[2,4,6-Tris{(η^5-cyclopentadienyl)dicarbonyliron}borazine] (**1c**): As described for **1a**, 1.29 g (6.45 mmol) of $Na[CpFe(CO)_2]$ suspended in 30 ml of benzene was reacted with 0.40 g (2.15 mmol) of $(ClBNH)_3$ and 0.37 g (28%) of **1c** was obtained as orange needles. − ^{1}H NMR: δ = 4.28 (s, 15 H, C_5H_5), 6.03 (s, 3 H, NH). − ^{11}B NMR: δ = 49.69 (s). − ^{13}C NMR: δ = 83.10 (C_5H_5), 217.46 (CO). − IR (hexane): $\tilde{\nu}$ = 1988, 1928 cm^{-1} (CO). − $C_{21}H_{18}B_3Fe_2N_3O_6$ (606.36): calcd. C 41.46, H 2.98, N 6.91; found C 41.08, H 3.02, N 6.86.

Crystal Data for **1b**: $C_{16}H_{17}B_3ClFe_2N_3O_4$, M = 494.91 g mol^{-1}, unit cell dimensions: a = 13.682(1) Å, b = 7.163(1) Å, c = 20.504 Å, V = 2009.3 Å^3, β = 90.864(1)°, $P2_1/n$, Z = 4, D_{calcd} = 1.636 cm^{-3}, μ = 16.05 cm^{-1}. The data were collected using an Enraf-Nonius DIP2020 image plate diffractometer at 150 K with Mo-K_α radiation, λ = 0.71069 Å. 26825 reflections were measured giving 3954 reflections with $I > 3\,\sigma(I)$. The images were processed with DENZO and SCALEPACK programs[14]. All non-hydrogen atoms were refined in anisotropic and all nitrogen-bound hydrogen atoms in isotropic approximation. The carbon-bound hydrogen atoms were placed geometrically and included in the final refinement with fixed positional and thermal parameters. A correction for second-

ary extinction was applied and refinement completed using a Chebyshev weighting scheme with parameters 4.09, 3.54, and 3.18[15]. Refinement on F converged at $R = 0.032$, $R_w = 0.048$, and GOF = 0.86. A final difference Fourier synthesis showed minimum and maximum residual electron densities of -0.71 and 0.63 e Å^{-3}. Further details of the crystal-structure investigations can be obtained from the Cambridge Crystallographic Data Centre (CCDC, 12 Union Road, GB-Cambridge CB2 1EZ; Tel.: Int. +7247/808-205, Telefax: Int. +44(0)1223/336-033; E-mail: deposit@chemcrys.-cam.ac.uk; World Wide Web: http://www.ccdc.cam.ac.uk) on quoting the depository number 100374.

[1] [1a] H. Werner, R. Prinz, E. Deckelmann, *Chem. Ber.* **1969**, *102*, 95−103. − [1b] G. Huttner, B. Krieg, *Angew. Chem.* **1971**, *83*, 541−542; *Angew. Chem. Int. Ed. Engl.* **1971**, *10*, 499−500.

[2] G. E. Herberich, *Comprehensive Organometallic Chemistry: Boron Ring Systems as Ligands to Metals*; Pergamon, Oxford, **1984**; vol. 1, chapter 5.

[3] M. F. Bailey, L. F. Dahl, *Inorg. Chem*. **1965**, *4*, 1298−1306.

[4] [4a] A. T. Lynch, L. G. Sneddon, *J. Am. Chem. Soc.* **1987**, *109*, 5867−5868. − [4b] A. T. Lynch, L. G. Sneddon, *J. Am. Chem. Soc.* **1989**, *111*, 6201−6209.

[5] A. D. Dorigo, P. von Ragué Schleyer, *Angew. Chem.* **1995**, *107*, 108−111; *Angew. Chem. Int. Ed. Engl.* **1995**, *34*, 107−110.

[6] [6a] J. R. Knorr, J. S. Merola, *Organometallics* **1990**, *9*, 3008−3012. − [6b] S. A. Westcott, N. J. Taylor, T. B. Marder, R. T. Baker, N. J. Jones, J. C. Calabrese, *J. Chem. Soc., Chem. Commun.* **1991**, 304−305. − [6c] J. F. Hartwig, S. Huber, *J. Am. Chem. Soc.* **1993**, *115*, 4908−4909. − [6d] P. Nguyen, H. P. Blom, S. A. Westcott, N. J. Taylor, T. B. Marder, *J. Am. Chem. Soc.* **1993**, *115*, 9329−9330. − [6e] J. F. Hartwig, S. R. de Gala, *J. Am. Chem. Soc.* **1994**, *116*, 3661−3662. − [6f] D. R. Lantero, D. H. Motry, D. L. Ward, M. R. Smith, *J. Am. Chem. Soc.* **1994**, *116*, 10811−10812. − [6g] C. Dai, G. Stringer, F. F. Corrigan, N. J. Taylor, T. B. Marder, N. C. Norman, *J. Organomet. Chem*. **1996**, *513*, 273−275.

[7] [7a] H. Braunschweig, T. Wagner, *Angew. Chem.* **1995**, *107*, 904−905; *Angew. Chem. Int. Ed. Engl.* **1995**, *34*, 825−826. − [7b] H. Braunschweig, B. Ganter, M. Koster, T. Wagner, *Chem. Ber.* **1996**, *129*, 1099−1101.

[8] P. Eilbracht, P. Dahler, *Chem. Ber.* **1980**, *113*, 542−554.

[9] B. E. R. Schilling, R. Hoffmann, J. W. Faller, *J. Am. Chem. Soc.* **1979**, *101*, 592−598.

[10] K. Anzenhofer, *Mol. Phys.* **1966**, *11*, 495−498.

[11] D. L. Reger, V. Fauth, M. D. Dukes, *Syn. React. Inorg. Metal-Org. Chem.* **1977**, *7*, 151−154.

[12] C. A. Brown, A. W. Laubengayer, *J. Am. Chem. Soc.* **1955**, *77*, 3699−3700.

[13] L. J. Pearce, K. C. Prout, D. J. Watkin, *CAMERON*, Chemical Crystallography Laboratory, Oxford, **1996**.

[14] D. Gewirth, *The HKL Manual*, written with the cooperation of the program authors Z. Otwinowski and W. Minor, Yale University, **1995**.

[15] E. Prince, *Mathematical Techniques in Crystallography and Material Sciences*, Springer: New York, **1982**.

[97200]

Nickel-Catalysed 1,4-Addition of Aryl Groups to Enones Using Aryldialkylaluminum Compounds

Jürgen Westermann*, Ute Imbery, Anh Thu Nguyen, and Klaus Nickisch

Schering AG Berlin,
Müllerstraße 178, D-13342 Berlin, Germany
Fax: (internat.) + 49(0)30/468-18008
E-mail: juergen.westermann@schering.de

Received November 5, 1996

Keywords: Conjugate addition / Enones / Steroids

The transmetallation of arylmagnesium halides or aryllithium with Me_2AlCl results in the formation of aryldimethylaluminum compounds. These arylaluminum compounds are useful reagents for conjugate additions to enones in the presence of $Ni(acac)_2$ as a catalyst. 3-Aryl ketones are obtained in good yields in these catalytic reactions. Starting from the 3-oxo-$\Delta^{1,4}$-steroids this method gives access to 1α-arylsteroids.

The addition of organometallic compounds to enones is one of the most important reactions in organic synthesis for C−C bond formation, and various synthetic methods which focus on this problem have been developed[1]. Organocuprates are widely explored in stochiometric as well as in catalytic reactions[2]. In connection with the conjugate addition reactions of organoaluminum compounds to enones we have reported the following: (a) the 1,4-addition reaction can be catalysed by copper salts for the transfer of alkyl groups[3a]; (b) under the catalysis of nickel the method is efficient for the transfer of a methyl group, even in the case of highly sterically hindered enones[3b]. To investigate the transition metal catalysed transfer of an aryl group we have studied the possibility of using mixed aryldialkylaluminum compounds in the conjugate addition of an aryl group to α,β-unsaturated enones.

Organoaluminum compounds are useful reagents for organic syntheses[4a] in both catalysed and non-catalysed reactions. Amongst these the triarylaluminum compounds are reported to react in a conjugate addition with nitroalkenes[4b][4c], diarylaluminum chlorides exhibit conjugate addition to acrylamides when irradiated[4c], and arylaluminum halides add to enones in the absence of a catalyst[4d]. Triarylaluminum compounds react with aryl iodides in the presence of a palladium catalyst to produce unsymmetrical diaryl ketones[5a], and are also useful for the synthesis of aryl-substituted *o*-allylphenols[5b]. Arylaluminum complexes are helpful in the oxirane ring opening of *trans*-2,3-epoxy alcohols as described by K. H. Ahn[5c][5d].

The conjugate addition of aryl groups to enones can be achieved in general by molar and catalytic copper reactions[1][2], or by arylzinc compounds in sonication reactions[6a][6b]. In a recent paper we studied the nickel-catalysed 1,4-arylation of enones by aryltitanate complexes[7].

Nickel salts catalyse not only the addition of trimethylaluminum to enones[8a][8b], but also, as reported by J. Schwartz[8c], the transfer of an alkinyl group from dialkyl(alkynyl)aluminum to enones in good yields. The conjugate addition of an aryl group of mixed dialkyl(aryl)alanes has not so far been reported.

Results

In 1,4-addition reactions the use of molar organocopper reagents is often necessary, or the assistance of Lewis acids is required to give good results[9]. Cuprates are "softer" reagents than aryllithium or arylmagnesium halides, which are the reagents in transition metal catalysed reactions in the Kharasch procedure. The latter reagents lead mainly to a carbonyl attack when the enones are sterical hindered or when the cross-conjugated dienone **12** is the substrate, which results in undesired 1,2-adducts.

The authors were looking for a general catalytic method for the transfer of an aryl group to an enone in a simple manner, and therefore tested mixed aryldimethylaluminum compounds. Dialkyl(aryl)aluminum compounds are prepared by transmetallation of organolithium compounds with dimethylaluminum chloride in tetrahydrofuran[5a][5c].

Surprisingly it was found that the dialkyl(aryl)alanes **1a−e** are suitable reagents for the transfer of an aryl group to enones.

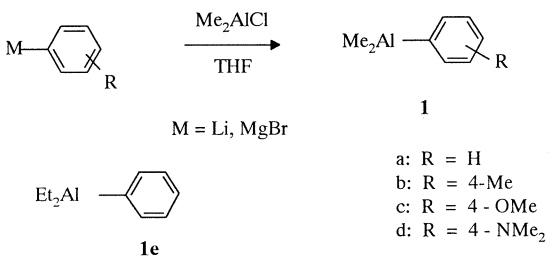

In the presence of 5 mol-% of the catalyst $Ni(acac)_2$ a clean conversion of the alane **1a** with the enone **2** was ob-

 © WILEY-VCH Verlag GmbH, D-69451 Weinheim, 1998 1434−1948/98/0202−0295 $ 17.50+.50/0

served. After workup, the β-aryl ketone **3** could be isolated in 88% yield.

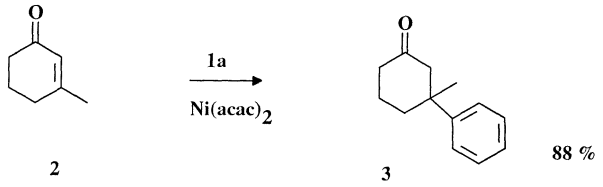

2 3

Furthermore, in the addition of the alane **1a** to 3,5,5-trimethylcyclohex-1-en-3-one (**4**) the yield of the product **5a** was 83%. The alanes **1c** and **1d**, with different substituents at the aryl group, were used in the addition to carvone **4**. It is promising that the addition to sterically hindered enones is possible. Also the conversion of 4-methylpent-2-ene-3-one (**6**) gave high yields of the products **7a−b**. In general, the aryl group is selectively transferred and no alkyl transfer has been observed[10].

The alanes **1a** and **1b** were prepared from commercially available aryllithium compounds. **1c** was prepared from 4-methoxyphenylmagnesium bromide. **1d** was prepared from 4-dimethylaminophenyllithium which was prepared from 4-dimethylaminophenyl bromide and *sec*-butyllithium by halogen/metal exchange. The reaction of the alanes **1d** with **4** gave **5d** in a yield of 65%. This shows that the method is sucessful for the addition to sterically hindered enones. The addition of an aryl group to the less hindered enone **6** gave the products **7** in high yields. The conversion of pulegone **8** with **1a** resulted in the formation of the ketone **9a** in a 85:15 ratio of two diastereomers. When **1e** (prepared from Et_2-AlCl and PhLi) was tested in the reaction with **4** the formation of **5a** was observed in a yield of 85%. Further examples are given in Table 1.

In testing the nucleophilic properties of mixed aryldimethylaluminum compounds versus a carbonyl group it was found that the alane **1a** gave, in the reaction with isophorone (**4**) under typical conditions (4 h, 0°C) without a catalyst, less than 1% of the 1,2-addition product **4a**. This indicates that the solvent THF has a reduced tendency for a 1,2-addition of a methyl or a phenyl group to the carbonyl group. This low 1,2-addition rate is a good assumption to make for a catalytic process. In comparison with the $Ni(acac)_2$-catalysed reaction the conversion was low, the main compound identified (98%) was the starting material **4**.

J. Y. Satoh et. al. report the introduction of a 1-phenyl group to a Δ^1-steroid by a copper-catalysed reaction in a yield of only 49%[11]. In our experiments the steroidal enone **10** reacted with the alane **1a** to give the product **11**, in a yield of 81%, without cleavage of the 17-acetate group. This is an example of the selective reaction conditions.

Less is known in the literature about conjugate additions of arylmetals to 3-oxo-$\Delta^{1,4}$-steroids of type **12,** in either stochiometric or catalytic reactions[3a]. The introduction of a phenyl group to position 1 of the steroid **12** was attempted in our laboratory using common catalytic methods. The result was a simple carbonyl attack; phenylmagnesium bromide in the presence of catalytic copper bromide yielded

Table 1. $Ni(acac)_2$-catalysed 1,4-arylations of enones with $ArAlMe_2$

Enone	$ArAlMe_2$	Cond.	Product	Yield	Ref.
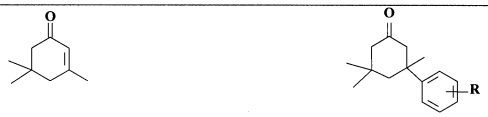					
	1a	4 h, 0 °C	**5a**: R = H	83 %	[7]
4	**1c**	2 h, 0 °C	**5c**: R = 4-MeO	79 %	[12a]
	1d	4 h, 0 °C	**5d**: R = 4-Me_2N	65 %	–
	1e	4 h, 0 °C	**5a**: R = H	85 %	[7]
6	**1a**	1 h, 0 °C	**7a**: R = H	95 %	[12b]
	1b	1 h, 0 °C	**7b**: R = 4-Me	96 %	[12c]
8	**1a**	1 h, 0 °C	**9a**: R = H	95 %	[12d]
10	**1a**	2 h, 0 °C	**11**	81 %	–
12	**1a**	4 h, 0 °C	**13a**: R = H	90 %	–
	1b	4 h, 0 °C	**13b**: R = Me	77 %	–
	1c	3 h, 0 °C	**13c**: R = 4-MeO	89 %	–
	1d	3 h, 0 °C	**13d**: R = 4-Me_2N	78 %	–

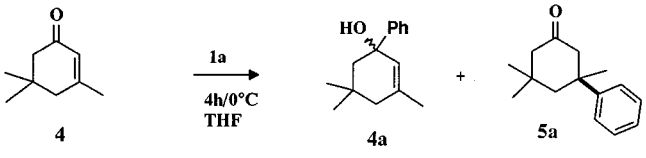

4 4a 5a

	4a	5a	4
no catalyst	< 1%	-	98 %
5 mol-% $Ni(acac)_2$	<1 %	83 %	<2%

only the 1,2-addition product. In contrast to this the reaction of **12** with two equivalents of high-order cuprate ArThCuCNLi[9] was sucessful with molar copper reagent, and gave the 1,4-adduct **13a** in a yield of 65%.

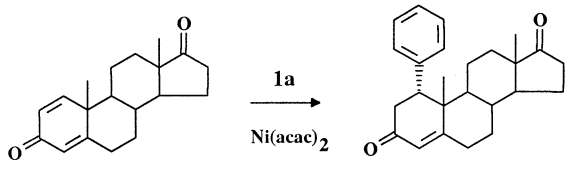

12 13a

The experiments using the enone **12** and the alanes **1a−d** in the nickel-catalysed reaction gave the products **13a−d** in good to excellent yields. This is similar to the PhLi/Me_2-AlCl system in the nickel-catalysed reaction, and shows that Et_2AlCl is also useful. In the reaction of **1a** with **12** only 3% of 5β-methylandrost-4-ene-3,17-dione, which originates in the methylation of **12** in a side reaction, were produced. In the reactions of the alane **1d**, prepared from the Grignard reagent (*p*-Me_2N-ArMgBr), the yield was somewhat lower than in the experiment where **1d** was derived from 4-dimethylaminophenyllithium. This was prepared from the bromo compound by metal exchange with *n*-butyllithium in THF (see Experimental Section).

In the absence of the catalyst $Ni(acac)_2$ no reaction was observed. Optimal yields of conjugate addition product were obtained when 1.2−1.3 equivalents of aryldimethylaluminum was used. A small excess of arylalane was necessary to produce optimal yields, otherwise the unreacted starting material is methylated in a side reaction. When the aryl groups in the reagent are consumed, it seems that the starting compound is methylated by the dimethylaluminum enolates as methyl source under the catalysis of a nickel salt.

In the experiments the catalyst [$Ni(acac)_2$] was used in the commercial form without initial activation, similar to the use of DIBAH[8c]. It was found that the alane **1d** from phenylmagnesium bromide reacts faster with the enones **4** and **12** than the alane **1d** prepared from aryllithium, and that it also gives a better yield. A small amount of biaryl is usually isolated in the reactions. This comes from the biaryls in the aryllithium or arylmagnesium solutions.

5 mol-% of the catalyst gave a satisfactory yield, the optimal amount of the catalyst is in the range 2−5%. There were no advantages in the use of [$Ni(PPh_3)_4$] and [$Ni(PPh_3)_2Cl_2$] over the less expensive catalyst [$Ni(acac)_2$]. The alane **1a** and the enone **4** did not show a selective aryl transfer with the catalysts CuBr, CuCN and CuCl. The result was a statistical mixture of methylated and arylated product in the copper-catalysed reactions.

Conclusion

These experiments have demonstrated that dimethylaluminum chloride is a versatile carrier for aryl groups in transmetallation reactions, from arylmagnesium or -lithium compounds to arylalanes. This can be exploited for a chemoselective 1,4-aryl transfer to enones and cross-conjugated steroidal dienones catalysed by Ni^{II} salts.

Experimental Section

All reactions were carried out in capped vials under nitrogen. The products were isolated from the reaction mixture by preparative chromatography on silica gel (Merck F 254s) with ethyl acetate/hexane as eluent. The analysis of the products was carried out on a gas chromatograph, fitted with a 25 m × 0.2 mm CP Sil 19 CB fused capillary column. The detector signal was integrated. The column temp. was programmed to rise from 150 to 250°C at 10°C/min. Phenyllithium, *p*-tolyllithium, $Ni(acac)_2$ (95%), and the ketones **2**, **4**, **6**, **8**, were purchased from Aldrich. Dimethylaluminum chloride was used as a 1 M solution in hexane from Aldrich. 4-Dimethylaminophenyllithium was prepared from *p*-dimethylaminophenyl bromide by transmetallation with a *n*-butyllithium solution (1.6 M in hexane) in THF at 0°C/30 min, *p*-methoxyphenylmagnesium bromide was prepared from *p*-bromoanisol and magnesium in THF in a standard procedure[5c]. All solvents were used in commercial grade without any further purification.

General Procedure: 13 mmol [6.5 ml of a 2 M solution of phenylmagnesium bromide (or phenyllithium)] was added to 12 mmol of dimethylaluminum chloride (12 ml of a 1 M solution in hexane) at −20°C. The mixture was stirred for 10 min at −20°C. Then 10 mmol of the enone in 15 ml of THF was added at −20°C, followed by 0.5 mmol (0.128 g) of [$Ni(acac)_2$]. The reaction mixture was then stirred for 1−4 h at 0°C, during this time the solution was allowed to warm up to the temp. shown in Table 1. The reaction mixture was quenched with aqueous NH_4Cl solution and stirred for 15 min. The product was then extracted using ethyl acetate and dried with Na_2SO_4. Chromatography of the reaction product on silica gel and elution of the product with ethyl acetate/hexane gave the 3-aryl ketones in the yields shown in Table 1. All reactions described in the text and in Table 1 were performed on a 10-mmol scale.

3-Methyl-3-phenylcyclohexan-1-one (**3**)[12e]: From 1.3 ml (1.1 g, 10 mmol) of **2**, yield 1.65 g (88%) of **3**. − ^{1}H NMR (300 MHz, $CDCl_3$, 25°C, TMS): δ = 1.33 (s, 3 H, 3-CH_3), 1.55−2.24 (m, 4 H), 2.34 (t, *J* = 3.25 Hz, 2 H), 2.45 (d, *J* = 7.5 Hz, 2 H), 7.19−7.33 (m, 5 H).

3,5,5-Trimethyl-3-phenylcyclohexan-1-one (**5a**)[7]: From 1.54 ml [97%, 1.38 g (10 mmol)] of isophorone (**4**), yield 1.79 g (83%) of **5a**. − ^{1}H NMR (300 MHz, $CDCl_3$, 25°C, TMS): δ = 0.4 (s, 3 H, 3-CH_3), 1.03 (s, 3 H), 1.04 (s, 3 H), 1.88−2.45 (m, 5 H), 3.0−3.1 (m, 1 H), 7.1−7.4 (m, 5 H).

3,5,5-Trimethyl-3-(4-methoxyphenyl)cyclohexan-1-one (**5c**)[12a]: From 1.54 ml [97%, 1.42 g (10 mmol)] of isophorone (**4**), yield 1.86 g (79%) of **5c,** colourless oil. **5c**. − ^{1}H NMR (300 MHz, $CDCl_3$, 25°C, TMS): δ = 0.39 (s, 3 H, 3-CH_3), 1.02 (s, 3 H), 1.33 (s, 3 H), 1.5−2.5(m, 5 H), 3.0−3.1 (d, 1 H), 3.77 (s, 3 H), 6.8−7.3 (m, 4 H).

3,5,5-Trimethyl-3-(4-dimethylaminophenyl)cyclohexan-1-one (**5d**): From 1.54 ml [97%, 1.42 g (10 mmol)] of **4**, yield 1.68 g (65%) of **5d**: colourless crystals, m.p. 113.6°C. − $C_{17}H_{25}NO$ (259.4): calcd. C 78.8, N 5.39, H 8.88; found C 78.45, N 5.6, H 9.53. − MS CI (70 eV): *m/z* = 260 $[M - H]^+$ (98%). − ^{1}H NMR (300 MHz, $CDCl_3$, 25°C, TMS): δ = 0.45 (s, 3 H, 3-CH_3), 1.042 (s, 3 H), 1.35 (s, 3 H), 1.65−2.4 (m, 5 H), 2.9 (t, 3 H), 2.95−3.05 (m, 1 H), 6.65−7.2 (m, 4 H). − ^{13}C NMR (100 MHz, $CDCl_3$): δ = 28.36, 33.08, 35.07, 36.01, 42.05, 51.50, 51,60, 54.43, 55.15, 113.52, 126.88, 139.88, 157.63, 211.63.

4-Methyl-4-phenylpentan-2-one (**7a**)[12b]: From 0.99 g (10 mmol) of **6**, yield 1.63 g (95%) of **9a**. − ^{1}H NMR (300 MHz, $CDCl_3$, 25°C, TMS): δ = 1.32 (s, 6 H, 4-CH_3), 1.8 (s, 3 H), 2.75 (s, 2 H), 7.15−7.5 (m, 5 H).

4-Methyl-4-(4-methylphenyl)pentan-2-one (**7b**)[12c]: From 0.99 g (10 mmol) of **6**, yield 1.78 g (96%) of **9b**. − ^{1}H NMR (300 MHz, $CDCl_3$, 25°C, TMS): δ = 1.4 (s, 6 H, 4-CH_3), 1.82 (s, 3 H), 2.33 (s, 3 H, Ar-CH_3), 2.72 (s, 2 H), 7.1−7.3 (m, 4 H).

2-(1-Methyl-1-phenylethyl)-5-methylcyclohexanone (**9a**)[12c]: From 1.52 g (10 mmol) of **8**, yield 2.18 g (95%) of **9a**. − ^{1}H NMR (300 MHz, $CDCl_3$, 25°C, TMS): δ = 0.91/0.98 (d, 3 H, 5-CH_3), 1.42 (d, 6 H), 1.0−2.75 (m, 8 H), 7.15−7.4 (m, 5 H).

17β-Acetoxy-1α-phenylandrostan-3-one (**11**): From 3.3 g (10 mmol) of **10**, yield 3.3 g (81%) of **11**, colourless crystals, m.p. 197°C. − $C_{27}H_{36}O_3$ (408.6): calcd. C 79.36, H 8.88; found C 79.45,

H 8.71. − MS CI/NH_3 (70 eV): *m/z* = 409 $[M - H]^+$ (10%), 426 $[M - NH_4]^+$ (90%). − ^{1}H NMR (300 MHz, $CDCl_3$, 25°C, TMS): δ = 0.82 (s, 3 H, 18-CH_3), 1.25 (s, 3 H, 19-CH_3), 0.4−2.5 (m, 16 H), 2.05 (s, 3 H), 2.8−2.9 (m, 1 H), 3.3 (d, 1 H), 4.5−4.6 (m, 1 H, 17-H), 7.02−7.35 (m, 5 H). − ^{13}C NMR (100 MHz, $CDCl_3$): δ = 11.68, 14.32, 20.34, 20.73, 22.51, 26.59, 27.96, 29.39, 35.09, 35.71, 37.15, 38.48, 42.07, 43.36, 43.97, 47.78, 49.43, 49.76, 81.64, 125.78, 127.26, 128.15, 141.26, 170.24, 211.25.

1α-Phenylandrost-4-ene-3,17-dione (**13a**): From 2.84 g (10 mmol) of **12**, yield 3.25 g (90%) of **13a,** colourless crystals, m.p. 189.6°C. − $C_{25}H_{30}O_2$ (362.5): calcd. C 82.82, H 8.34; found C 83.05, H 8.26. − MS CI/NH_3 (70 eV): *m/z* = 363 $[M - H]^+$ (97%). − ^{1}H NMR (300 MHz, $CDCl_3$, 25°C, TMS): δ = 0.91 (s, 3 H, 18-CH_3), 1.47 (s, 3 H, 19-CH_3), 0.8−2.1 (m, 16 H), 2.35−2.6 (m, 1 H), 2.95−3.1 (m, 1 H), 5.98 (s, 1 H, 4-H), 7.1−7.3 (m, 5 H, Ar-H). − ^{13}C NMR (100 MHz, $CDCl_3$): δ = 13.70, 20.02, 21.02, 21.72, 21.96, 29.27, 30.89, 33.20, 35.51, 35.59, 41.97, 42.21, 47.20, 47.41, 50.64, 125.51, 126.81, 128.61, 128.76, 142.69, 168.90, 197.68, 220.049. The less polar fraction (90 mg, 2.7% yield) is *5β-methylandrost-1-ene-3,17-dione*[12f].

1α-(4-Methylphenyl)androst-4-ene-3,17-dione (**13b**): From 2.84 g (10 mmol) of **12**, yield 2.90 g (77%) of **13b,** colourless crystals, m.p. 212°C. − $C_{26}H_{32}O_2$ (376.5): calcd. C 83.55, H 8.56; found C 83.7, H 8.4. − MS CI/NH_3 (70 eV): *m/z* = 377 $[M - H]^+$ (99%).− ^{1}H NMR (300 MHz, $CDCl_3$, 25°C, TMS): δ = 0.9 (s, 3 H, 18-CH_3), 1.4 (s, 3 H, 19-CH_3), 0.8−2.1 (m), 2.3 (s, 3 H, Ar-CH_3), 2.35−2.60 (m, 4 H), 2.95 (d, *J* = 7.5 Hz, 1 H), 3.05 (d, *J* = 9 Hz, 1 H), 5.95 (s, 1 H, 4-H), 6.9−7.15 (m, 4 H, Ar-H). − ^{13}C NMR (100 MHz, $CDCl_3$): δ = 12.98, 19.20, 20.11, 20.78, 21.14, 28.47, 30.05, 32.40, 34.69, 34.79, 41.27, 41.38, 46.88, 46.62, 49.46, 49.78, 124.61, 127.75, 128.42, 135.36, 138.71, 168.08, 197.00, 219.31.

1α-(4-Methoxyphenyl)androst-4-ene-3,17-dione (**13c**): From 2.84 g (10 mmol) of **12**, yield 3.4 g (89%) of **13c,** colourless crystals, m.p. 196°C. − $C_{26}H_{32}O_3$ (392.5): calcd. C 79.55 H 7.94; found C 79.82, H 8.17. − MS CI/NH_3 (70 eV): *m/z* = 393 $[M - H]^+$ (90%), 410 $[M - NH_4]^+$ (98%). − ^{1}H NMR (300 MHz, $CDCl_3$, 25°C, TMS): δ = 0.89 (s, 3 H, 18-CH_3), 1.48 (s, 3 H, 19-CH_3), 0.8−2.1 (m, 12 H), 2.35−2.6 (m, 3 H), 2.95−3.06 (m, 1 H), 3.2−3.25 (m, 1 H), 3.75 (s, 3 H), 5.5 (s, 1 H, 4-H), 6.7−7.2 (m, 4 H, Ar-H). − ^{13}C NMR (100 MHz, $CDCl_3$) δ = 12.99, 19.21, 20.81, 21.16, 28.48, 30.09, 32.42, 34.74, 34.80, 41.34, 41.49, 46.36, 46.64, 49.02, 49.85, 54.28, 113.08, 124.63, 133.82, 157.35, 167.97, 197.08, 219.25.

1α-(4-Dimethylaminophenyl)androst-4-ene-3,17-dione (**13d**): From 2.84 g (10 mmol) of **12**, yield 3.145 g (78%) of **13d,** colourless crystals, m.p. 202°C. − $C_{27}H_{35}NO_2$ (405.6): calcd. C 79.55, H 7.94, N 3.45; found C 79.82, H 8.17, N 3.56. − MS CI/NH_3 (70 eV): *m/z* = 406 $[M - H]^+$ (95%). −^{1}H NMR (300 MHz, $CDCl_3$, 25°C, TMS): δ = 0.91 (s, 3 H, 18-CH_3), 1.46 (s, 3 H, 19-CH_3), 0.8−2.1 (m, 12 H), 2.35−2.55 (m, 3 H), 2.89 (s, 6 H), 2.95−3.06 (m, 1 H), 3.15 (m, 1 H), 5.95 (s, 1 H, 4-H), 6.55−7.1 (m, 4 H, Ar-H). − ^{13}C NMR (100 MHz, $CDCl_3$): δ = 13.77, 20.33, 21.58, 21.58, 21.96, 29.25, 30.88, 33.24, 35.56, 40.43, 42.19, 42.36, 47.11, 49.63, 50.61, 112.59, 125.35.

[1] P. Perlmutter in *Conjugate Addition Reactions in Organic Synthesis*, Pergamon Press, Oxford, **1992**.
[2] B. H. Lipshutz, *Synthesis* **1987**, 325−341.
[3] [3a] J. Westermann, K. Nickisch, *Angew. Chem.* **1993**, *105*, 1429; *Angew. Chem. Int. Ed. Engl.* **1993**, *32*, 1368. − [3b] J. Westermann, S. Flemming, J. Kabbara, K. Nickisch, H. Neh, *Synthesis* **1995**, 317−320.
[4] [4a] K. Maruoka, H. Yamamoto, *Tetrahedron* **1988**, *44*, 5001. − [4b] I. Fleming, R. C. Moses, M. Tercel, J. Ziv, *J. Chem. Soc., Perkin Trans. 1* **1991**, 617. − [4c] A. Pecunioso, R. Menicagli, *J. Org. Chem.* **1988**, *53*, 45−49. − [4d] K. Rück, H. Kunz, *Synlett* **1992**, 343. − [4e] E. C. Ashby, S. A. Noding, *J. Org. Chem.* **1979**, *44*, 4792−4797.
[5] [5a] N. A. Bumagin, A. B. Ponomaryov, I. P. Beletskaya, *Tetrahedron Lett*. **1985**, *26*, 4819−4822. − [5b] A. Alberola et al., *Synthesis* **1984**, 238−240. − [5c] K. H. Ahn, J. S. Kim, C. S. Jin, D. H. Kang, D. S. Han, Y. S. Shin, D. H. Kim, *Synlett* **1992**, 306. − [5d] K. H. Kim et al., *J. Heterocycl. Chem.* **1993**, *90*, 825−827.
[6] [6a] C. Petrier, J. C. de Souza Barbosa, C. Dupuy, J.-P. Luche, *J. Org. Chem.* **1985**, *50*, 5761−5765. − [6b] J. L. Luche, C. Petrier, J.-P. Lansard, A. E. Greene, *J. Org. Chem*. **1983**, *48*, 3837−3839.
[7] S. Flemming, J. Kabbara, K. Nickisch, H. Neh, J. Westermann, *Tetrahedron Lett*. **1994**, *35*, 6075−6078.
[8] [8a] J. A. Jeffery, A. Meisters, T. Mole, *J. Organomet. Chem*. **1974**, *74*, 365. − [8b] E. C. Ashby, G. Heinsohn, *J. Org. Chem*. **1974**, *39*, 3297−3299. − [8c] J. Schwartz, D. B. Carr, R. T. Hansen, F. M. Dayrit, *J. Org.Chem*. **1980**, *45*, 3053−3061.
[9] B. H. Lippshutz, D. A. Parker, J. A. Kozlowski, S. L. Nguyen, *Tetrahedron Lett.* **1984**, *25*, 5959.
[10] The aryl group from mixed alkylarylzinc compounds seems also to be faster transferred than an alkyl group, see ref.[6a], see also: W. Tückmantel, K. Oshima, H.Nozaki, *Chem. Ber.* **1986**, *119*, 1581.
[11] T. T. Takahashi, J. Y. Satoh, *Bull. Chem. Soc. Jpn*. **1976**, *49*, 1089−1072.
[12] [12a] B. L. Shapiro, M. D. Johnston, M. J. Shapiro, *Org. Magn. Reson.* **1973**, *5*, 21−27. − [12b] M. Suzuki, T. Suzuki, T. Kawagashi, R. Noyori, *Tetrahedron Lett*. **1980**, *21*, 1247. − [12c] C. Pichat, *Bull. Soc. Chim. Fr*. **1949**, *177*, 183−184. − [12d] D. Pottin, J. Maddaluno, F. Dumas, *Synth. Commun*. **1990**, *20*, 2805−2813. − [12e] H. O. House, J. M. Wilkins, *J. Org. Chem.* **1978**, *43*, 2443−2454; G. Cahiez, M. Alami, *Tetrahedron Lett.* **1989**, *27*, 3541−3544. − [12f] J. Westermann, H. Neh, K. Nickisch, *Chem. Ber.* **1996**, *129*, 963−966.

[97260]

Dinuclear Molybdenum(III) and Tungsten(III) Calix[4]arene Complexes – Metal-Metal Triple Bonds Supported by Bridging Calix[4]arene Ligands☆

Udo Radius* and Juri Attner

Institut für Anorganische Chemie
Engesserstr. Geb. 30.45, D-76128 Karlsruhe, Germany
Fax: (internat.) +49 (0)721/661921
E-mail: uradius@achibm6.chemie.uni-karlsruhe.de

Received October 22, 1997

Keywords: Calix[4]arenes / Calix[4]arene complexes / Molybdenum / Tungsten / Metal-metal bonding

Addition of *p-tert*-butylcalix[4]arene LH_4 to the dinuclear compounds $M_2(NMe_2)_6$ (M = Mo, W) results in the formation of $[NH_2Me_2]_2[L_2M_2]$ **1** (M = Mo) and **2** (M = W). Both compounds have been characterized by spectroscopic methods and single-crystal X-ray diffraction. The metal–metal distances of **1** and **2**, of 2.194(1) Å and 2.293(1) Å, respectively, are consistent with the retention of the M≡M triple bond. Both "ate" complexes contain a $[M{\equiv}M]^{6+}$ dimetal core, supported by two bridging μ_2-κ^2O,κ^2O-calix[4]arene ligands in the solid state. These compounds are the first examples of a formally fourfold deprotonated calix[4]arene acting as a μ_2-κ^2O,κ^2O bridging ligand for two transition metal centres. The calix[4]arenes in **1** and **2** are distorted from a *cone* conformation in the uncomplexed ligand, to an *elliptical cone* section. ^{1}H-NMR data at variable temperatures suggest fluxional behaviour of **1** and **2** in solution.

Introduction

Calixarenes and related macrocycles have received considerable attention for their host–guest chemistry, and their ability to bind metals.[1] There is currently much interest in the synthesis and structural characterization of new metallocalixarenes.[2][3][4][5] The simplest of the calixarenes, the calix[4]arene system, usually binds in an tetradentate fashion, and retains its *cone*-like appearance. In recent examples, it has been found that the calix[4]arene is capable of adopting alternative conformations in binding to metal centres, for example in an alkali-metal constrained *elliptical cone* conformation, in which the calixarene oxygen atoms adopt mutually *cis*- and *trans* sites in an octahedral geometry.[2h] There has also been an example of an *elliptical* calixarene arrangement in the absence of alkali-metal ions for mononuclear complexes.[2c]

These terminal ligating forms of the *p-tert*-butylcalix[4]arene ligand (L) have also been reported for dinuclear complexes, strongly dependant on alkali metal binding sites. C. Floriani and co-workers have recently published studies on the reduction of $LWCl_2$ in the absence of σ-donor/π-acceptor ligands.[2g] Two dinuclear species, $[Na(py)(thf)]_2[L_2W_2(\mu\text{-}Cl)_2]$ **A** and $[\mu\text{-}Na(py)_3][\mu\text{-}Na(py)_2][L_2W_2]$ **B** were structurally characterized in the course of this investigation (see Scheme).

In the former molecule (**A**), the calix[4]arene ligand adopts an *elliptical cone* arrangement, in which the sodium ions are ligated within the calixarene cavity. Each alkali-metal ion of this dinuclear ditungsten(IV) complex interacts with two oxygen atoms and two arene entities of the phenoxide groups of the calix[4]arene ligand.

The X-ray structure analysis of the ditungsten(III) species (**B**) reveals a tetragonal prismatic environment for the

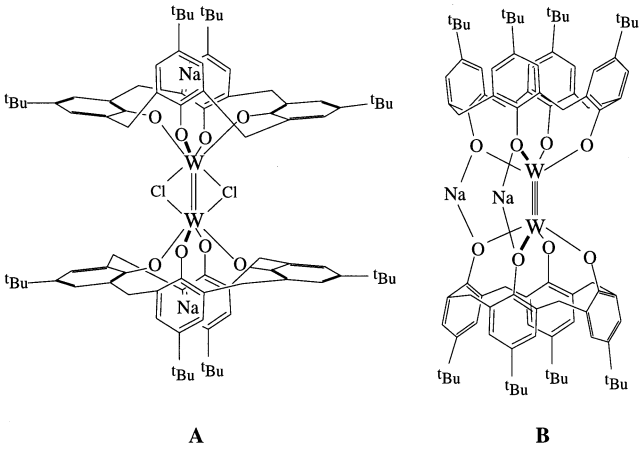

$[W{\equiv}W]^{6+}$ metal core, spanned by two terminal calix[4]arene ligands in their *cone* conformations. Each sodium atom bridges two oxygen atoms of the calix[4]arene ligands. The reported tungsten–tungsten bond length at 2.313(1) Å is in range for tungsten–tungsten triple bonds.

We herein report our preliminary findings concerning the reaction of *p-tert*-butylcalix[4]arene LH_4 with dimolybdenum- and ditungstenhexamid $M_2(NMe_2)_6$ (M = Mo, W), which resulted in the isolation and characterization of two complexes $[NH_2Me_2]_2[L_2M_2]$ **1** (M = Mo) and **2** (M = W). The central $[L_2M_2]$ moieties in **1** and **2** are isoelectronic but not isostructural to the formally double negatively charged $[L_2W_2]^{2-}$ entity of **B**. Whereas in **A** and **B**, the macrocycles are terminally coordinated to each tungsten centre, the metal-metal multiple bonds in **1** and **2** are supported by bridging calix[4]arene ligands.

 © WILEY-VCH Verlag GmbH, D-69451 Weinheim, 1998 1434–1948/98/0303–0299 $ 17.50+.50/0

Results and Discussion

The reactions of *p-tert*-butylcalix[4]arene LH_4 with the dimetallahexamides $M_2(NMe_2)_6$ in toluene at 100°C gave $[NH_2Me_2]_2[L_2M_2]$ (M = Mo, **1**; M = W, **2**) after work-up in good to excellent yields, although the formation of small quantities of side products was observed. Some of these minor products have been structurally characterized.[6] Dissolution of the main products in acetonitrile on warming up to 80°C, and then cooling to room temperature afforded a crop of dark green crystals suitable for X-ray analysis. Each compound crystallizes in the monoclinic space group $P2_1/c$, with six non-coordinated molecules of acetonitrile. Figure 1 and Figure 2 show SCHAKAL plots of the solid state structure of the dianions of **1** (Figure 1) and **2** (Figure 2). Selected bond lengths and bond angles are given in the captions.

Figure 1. SCHAKAL drawing of the solid state structure of **1** (only the anion is depicted), showing the atom labeling scheme. Hydrogen atoms are omitted for clarity[a]

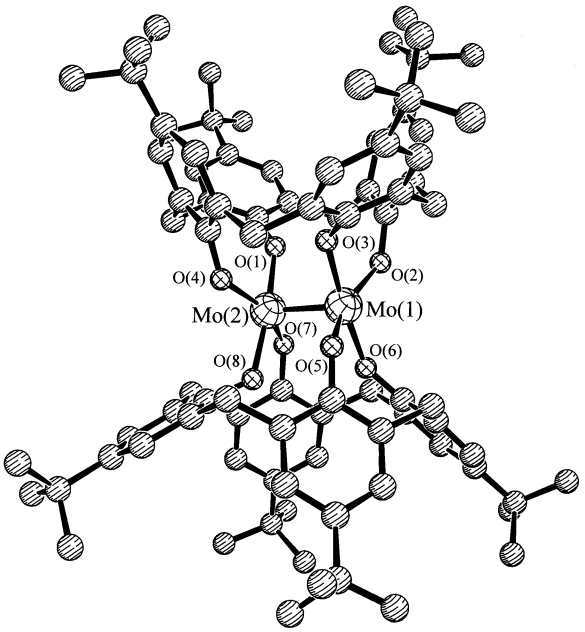

[a] Selected bond lengths [Å] and angles [°]: Mo(1)−Mo(2): 2.1938(7), Mo(1)−O(2): 2.011(2), Mo(1)−O(3): 1.970(2), Mo(1)−O(5): 2.022(2), Mo(1)−O(6): 1.938(2), Mo(2)−O(1): 1.942(2), Mo(2)−O(7): 2.016(2), Mo(2)−O(4): 1.991(2), Mo(2)−O(8): 1.979(2), O(2)−Mo(1)−O(3): 86.42(9), O(2)−Mo(1)−O(5): 155.91(10), O(2)−Mo(1)−O(6): 93.53(10), O(3)−Mo(1)−O(5): 87.53(10), O(3)−Mo(1)−O(6): 173.76(10), O(5)−Mo(1)−O(6): 90.02(10), O(1)−Mo(2)−O(4): 89.75(10), O(1)−Mo(2)−O(7): 91.81(10), O(1)−Mo(2)−O(8): 173.15(10), O(4)−Mo(2)−O(7): 155.39(10), O(4)−Mo(2)−O(8): 89.39(9), O(7)−Mo(2)−O(8): 86.16(9), O(2)−Mo(1)−Mo(2): 102.42(8), O(3)−Mo(1)−Mo(2): 92.53(7), O(5)−Mo(1)−Mo(2): 101.13(7), O(6)−Mo(1)−Mo(2): 93.57(8), O(1)−Mo(2)−Mo(1): 93.60(8), O(4)−Mo(2)−Mo(1): 102.37(8), O(7)−Mo(2)−Mo(1): 102.03(7), O(8)−Mo(2)−Mo(1): 93.23(7).

Both dimethyl ammonium counterions of the molybdenum compound **1** are located inside the calix[4]arene cavities. In the tungsten compound **2**, one cation is replaced by an acetonitrile molecule, thus leaving one dimethylammonium counterion in the cavity of one of the calix[4]arene

Figure 2. SCHAKAL drawing of the solid state structure of **2** (only the anion is depicted), showing the atom labeling scheme. Hydrogen atoms are omitted for clarity[a]

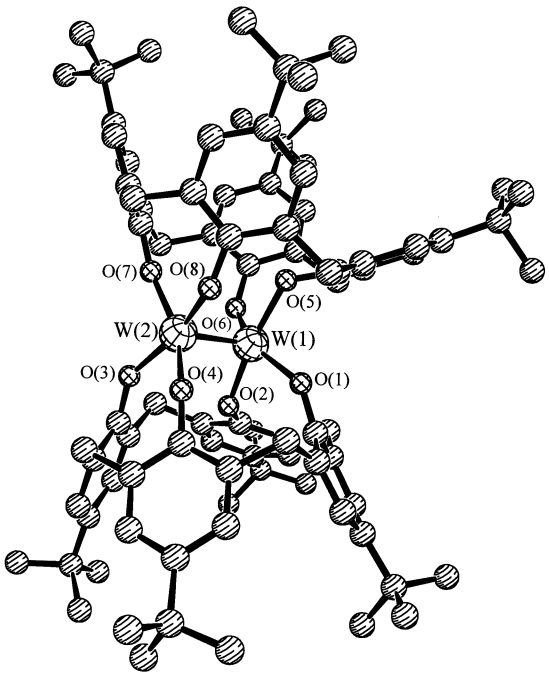

[a] Selected bond lengths [Å] and angles [°]: W(1)−W(2): 2.2926(9), W(1)−O(1): 1.976(5), W(1)−O(2): 1.958(4), W(1)−O(5): 1.998(4), W(1)−O(6): 1.985(5), W(2)−O(3): 1.973(4), W(2)−O(4): 1.989(5), W(2)−O(7): 1.949(5), W(2)−O(8): 2.051(4), O(1)−W(1)−O(2): 88.57(18), O(1)−W(1)−O(6): 149.09(19), O(1)−W(1)−O(5): 87.64(18), O(2)−W(1)−O(5): 169.56(18), O(2)−W(1)−O(6): 91.93(18), O(5)−W(1)−O(6): 86.36(18), O(3)−W(2)−O(4): 89.74(18), O(3)−W(2)−O(7): 91.53(19), O(3)−W(2)−O(8): 158.82(19), O(4)−W(2)−O(7): 153.3(2), O(4)−W(2)−O(8): 79.71(17), O(7)−W(2)−O(8): 89.92(18), O(1)−W(1)−W(2): 106.31(13), O(2)−W(1)−W(2): 94.65(14), O(5)−W(1)−W(2): 95.76(13), O(6)−W(1)−W(2): 104.46(14), O(3)−W(2)−W(1): 101.58(14), O(4)−W(2)−W(1): 105.02(13), O(7)−W(2)−W(1): 100.85(15), O(8)−W(2)−W(1): 98.89(13).

ligands [O(1)−O(4)] and leaving the other one uncoordinated (not shown in Figure 1 and 2). The C−N vector of the acetonitrile molecule is pointing out of the calix[4]arene pocket [O(5)−O(8)]. This orientation is similar to that of a previously studied inclusion complex of acetonitrile by a calix[4]arene macrocycle, tetraethyl *p-tert*-butylcalix[4]arenetetracarbonate]·MeCN.[7] The C−N−C planes of the dimethylammonium ions inside the calix[4]arene cavities of **1** are almost parallel to the planes defined by the oxygen and C_{ipso} carbon atoms of the O(3),O(1) [3.4(5)°], and O(6),O(8) [2.4(5)°] phenoxide moieties. The acute angle between the C−N−C plane, and the corresponding planes of the O(5),O(7) phenoxide entities of **2** is 14.7(9)°. The smallest (calculated) distances of a calix[4]arene oxygen atom to a hydrogen atom of the ammonium counterion are 2.67 Å to O(8) in **1**, and 2.34 Å to O(3) in **2**.[8]

The metal-metal bond lengths of 2.194(1) Å (Mo−Mo) in **1**, and of 2.293 (1) Å (W−W) in **2** are in the range expected for molybdenum−molybdenum or tungsten−tungsten triple bonds.[9] The coordination sphere of the [M≡M]

unit is a distorted tetragonal prismatic (partly staggered). The smallest angles of intersection between the planes defined by O−M(1)−M(2) and O−M(2)−M(1) come to approximately 30° in **1**, and 20° to 30° in **2**. A similar $[M_2O_8]$ structural type was reported for d^3-d^3 dimers in the "ate" complexes $K_2[M_2(OCH_2tBu)_8]$ (M = Mo, W) by M. H. Chisholm and co-workers.[10]

The X-ray single crystal structure determinations show that **1** and **2** contain a $[M{\equiv}M]^{6+}$ dimetal core, supported by two bridging μ_2-κ^2O,κ^2O-calix[4]arene ligands. The complexes **1** and **2** are, to the best of our knowledge, the first examples of a formally fourfold deprotonated calix[4]arene acting as a μ_2-κ^2O,κ^2O bridging ligand for two transition metal centres. These compounds are probably best compared to $LH_2Mo_2(OAc)_2$[3b], where a similar bridging mode was reported for the doubly deprotonated calix[4]arene ligand. In this compound, the hydrogen atoms form bonds to the phenoxide oxygen atoms of the calix[4]arene ligand, which retains the *cone* conformation and bridges two metal-metal quadruple bonded molybdenum atoms.

Both macrocyclic ligands of the molybdenum complex (**1**) are symmetrically distorted from the *cone* conformation. Each bridging calix[4]arene shows two opposing phenoxide rings − those of the oxygen atoms O_{inside} [O(1), O(3), O(6), and O(8)] − pushed away from the macrocycle and two − those of the oxygen atoms $O_{outside}$ [O(2), O(4), O(5), and O(7)] − towards the macrocycle. Thus, they define an *elliptical cone* section, along the O(1)−O(3) and O(6)−O(8) axis. As a result of this distortion, the bond distances $M{-}O_{inside}$ are slightly shorter, e. g. 1.942(2) Å for Mo(2)−O(1) vs. 2.016(2) Å for Mo(2)−O(7), and the bond angles $O_{inside}{-}M{-}M'$ are close to 90°. Consequently, the $O_{inside}{-}M{-}O_{inside}$ angles of approximately 175.5° are much larger than the corresponding $O_{outside}{-}M{-}O_{outside}$ angles of approximately 155.5°.

The angle of intersection between the least square planes through the carbon atoms of the methylene bridges and the least square planes through a phenoxide moiety, defined by the oxygen atom and the C_{ipso} and C_{ortho} carbon atoms, can serve as a good measurement for the tilting of the phenoxide entities of the calix[4]arene ligand. We calculated these angles for the $O_{outside}$ phenoxide moieties to be in a range between 74.3(2)° and 76.5(2)°, and for the O_{inside} phenoxide entities between 26.9(2)° and 37.9(2)°. The appropriate angles of the mononuclear calix[4]arene complex LMoNMes (Mes = mesityl),[11] in which the calix[4]arene ligand retains the *cone*-like shape might be a good reference. We calculated for this compound an angle of 59.0(1)° on average, with values ranging from 56.7(1)° to 61.4(1)°.

The bridging calix[4]arene ligands of the tungsten compound **2** are also heavily distorted from the *cone* conformation of the parent calix[4]arene LH_4. In contrast to the symmetrical tilting in **1**, only one phenoxide group per ligand − those of O(2) and O(5) − is pushed away from the macrocycle. The angles between the planes of these moieties and the corresponding reference plane through the methylene carbon atoms are 27.0(3)° and 28.8(3)°, respectively. We attribute this difference between the ligand systems in **1** and **2** in the solid state structure to steric reasons, resulting from the slightly longer bonding distance of the tungsten−tungsten triple bond. However, in solution we could observe signals due to two different types of phenoxide groups in the low temperature ^{1}H-NMR spectrum for **1** and **2**. Both compounds show a splitting of the signals of the *tert*-butyl hydrogen atoms and aromatic protons of the *p-tert*-butylcalix[4]arene ligand at low temperatures. At room temperature, we observe, for example, a sharp signal for the *tert*-butyl protons of **2**, and a broadened singlett in the case of **1**. These signals split on cooling to two sharp singletts at low temperatures. The coalescence temperature for this process is 252 K for the ditungsten compound **2**, and 282 K for the dimolybdenum compound **1**. These NMR data suggest fluxional behaviour of the μ_2-κ^2O,κ^2O bridging calix[4]arene ligand in solution, i.e. an interconversion of the O_{inside} and $O_{outside}$ phenoxide rings of the dinuclear compounds **1** and **2**. We calculated free activation enthalpies of 59.0 kJ/mol (**1**) and 52.2 kJ/mol (**2**) for this process. Details on the ^{1}H-NMR investigations at variable temperatures, on the characterization of side products, and on the reactivity of **1** and **2** will be given elsewhere.[6]

This work was supported by the *Deutsche Forschungsgemeinschaft* and the *Fonds der Chemischen Industrie* (Liebig fellowship for U. R.). Generous support from *Prof. Dr. D. Fenske* is gratefully acknowledged. We would like to thank *Dr. G. Baum* and *Dr. A. Eichhöfer* for helpful discussions as well as *Fa. H. C. Starck GmbH*, Goslar, for a gift of metal chlorides.

Experimental Section

General: All reactions and subsequent manipulations involving organometallic reagents were performed under argon atmosphere using standard Schlenk techniques. The preparation of samples for spectroscopy was accomplished by using a glove box Braun MB 150 BG-I. Solvents were dried according to standard procedures, stored over activated 4 Å molecular sieve and degassed prior use. Deuterated solvents were obtained from Aldrich Inc. (all 99 atom% D), dried according to standard procedures and stored over activated 4 Å molecular sieves. − NMR spectra were recorded on a Bruker AC 250. ^{13}C-NMR spectra are broad-band proton decoupled (^{13}C{^{1}H}). Standard DEPT-135 experiments were recorded to distinguish -CH_3 and -CH type carbons from -C or -CH_2 type carbons in the ^{13}C-NMR spectrum. NMR data are listed in parts per million (ppm) and are reported relative to tetramethylsilane. Coupling constants are quoted in Hertz. Residual solvent peaks used as internal standards were as follows: $CDCl_3$, δ = 7.24 (^{1}H) or natural-abundance carbon signal at δ = 77.0; C_7D_8, δ = 2.09 (^{1}H). − EI-MS spectra were recorded on a Varian MAT 3830 (70 eV). − Elemental analyses were performed by the microanalytical laboratory of the author's department. − Infrared spectra were recorded as KBr pellets on a Bruker IFS 28 and are reported in cm^{-1}. − *p-tert*-butyl-calix[4]arene,[12] $Mo_2(NMe_2)_6$,[13] and $W_2(NMe_2)_6$,[14] were prepared as described in the literature. All other reagents were purchased from commercial sources and purified by standard techniques.

Preparation of Bis(dimethylammonium) Di-μ_2-κ^2O,κ^2O-p-tert-butylcalix[4]arenedimolybdate(III) (**1**): A solution of 250 mg (0.55 mmol) of $Mo_2(NMe)_6$ and 812 mg (1.10 mmol) of *p-tert*-butylcalix[4]arene−toluene adduct in 40 ml of toluene, was stirred for 8 h at

100°C. All volatiles were removed in vacuo, the yellow-greenish residue was washed with 20 ml of hexane and collected. Yield: 737 mg, 85%. Crystals suitable for X-ray analysis were grown in a saturated acetonitrile solution. m.p. 368°C (dec.). – IR (KBr): $\tilde{\nu}$ = 3129 vs, 2959 vs, 1743 w, 1597 m, 1552 m, 1449 vs, 1391 m, 1361 m, 1290 vs, 1206 s, 1121 m, 910 s, 873 m, 828 s, 801 m, 763 m, 745 s, 730 m, 694 m, 542 vs, 467 m, 430 m, 404 m. – ^{1}H NMR ($CDCl_3$, 298 K) δ = 7.15 (s, br, 4 H, aromatic *H*), 6.87 (s, 4 H, aromatic *H*), 5.85 (d, 2 H, $^2J_{HH}$ = 12.2 Hz, C*H*$_2$), 3.37 (d, 2 H, $^2J_{HH}$ = 12.2 Hz, C*H*$_2$), 2.94 (s, 4 H, C*H*$_2$), 2.57 [br, 2 H, *H*$_2$N(CH$_3$)$_2^+$], 1.19 [s, br, 36 H, C(C*H*$_3$)$_3$], 0.75 [t, 6 H, $^3J_{HH}$ = 5.2 Hz, H$_2$N(C*H*$_3$)$_2^+$]. – ^{1}H NMR (C_7D_8, 333 K): δ = 7.26 (d, 4 H, $^4J_{HH}$ = 2.6 Hz, aromatic *H*), 6.94 (d, 4 H, $^4J_{HH}$ = 2.6 Hz, aromatic *H*), 6.30 (d, 2 H, $^2J_{HH}$ = 12.2 Hz, C*H*$_2$), 3.51 (d, 2 H, $^2J_{HH}$ = 12.2 Hz, C*H*$_2$), 3.17 (d, 2 H, $^2J_{HH}$ = 13.4 Hz, C*H*$_2$), 2.90 [br, 2 H, *H*$_2$N(CH$_3$)$_2^+$], 2.88 (d, 2 H, $^2J_{HH}$ = 13.4 Hz, C*H*$_2$), 1.20 [s, 36 H, C(C*H*$_3$)$_3$], 0.86 [t, 6 H, $^3J_{HH}$ = 5.5 Hz, H$_2$N(C*H*$_3$)$_2^+$]. – ^{1}H NMR (C_7D_8, 233K): δ = 7.36 (d, 2 H, $^4J_{HH}$ = 2.0 Hz, aromatic *H*), 7.23 (d, 2 H, $^4J_{HH}$ = 2.3 Hz, aromatic *H*), 6.94 (d, 2 H, $^4J_{HH}$ = 2.0 Hz, aromatic *H*), 6.91 (d, 2 H, $^4J_{HH}$ = 2.3 Hz, aromatic *H*), 6.44 (d, 2 H, $^2J_{HH}$ = 12.4 Hz, C*H*$_2$), 3.63 (d, 2 H, $^2J_{HH}$ = 12.4 Hz, C*H*$_2$), 3.24 (d, 2 H, $^2J_{HH}$ = 13.9 Hz, C*H*$_2$), 2.88 (d, 2 H, $^2J_{HH}$ = 13.9 Hz, C*H*$_2$), 2.70 [br, 2 H, *H*$_2$N(CH$_3$)$_2^+$], 1.29 [s, 18 H, C(C*H*$_3$)$_3$], 1.17 [s, 18 H, C(C*H*$_3$)$_3$], 0.76 [br, 6 H, H$_2$N(C*H*$_3$)$_2^+$]. – ^{13}C NMR ($CDCl_3$, 298 K): δ = 31.79 [s, C(*C*H$_3$)$_3$], 33.31 (s, *C*H$_2$), 33.87 [s, *C*(CH$_3$)$_3$], 34.84 (s, *C*H$_2$), 37.99 [s, N(*C*H$_3$)$_2$], 123.85, 125.12 (s, aromatic *C*H), 128.97, 131.66 (s, aromatic *C*), 139.46 (s, aromatic *C*^{t}Bu), 164.55 (s, aromatic *C*O). – EI/MS (70 eV) *m/z* (%): 1481(63) ([L_2Mo_2 – H]$^+$), 1426(36) ([L_2Mo_2 – C_4H_8]$^+$). – $C_{92}H_{120}O_8Mo_2N_2$ (1576.7) calcd.: C 70.02, H 7.67, N 1.78; found: C 69,55, H 7.92, N 1.80.

Preparation of Bis(dimethylammonium) Di-μ$_2$-κ^{2}O,κ^{2}O-p-tert-butylcalix[4]areneditungstate(III) (**2**): A solution of 250 mg (0.40 mmol) of $W_2(NMe)_6$ and 590 mg (0.80 mmol) of *p-tert*-butylcalix[4]arene–toluene adduct in 40 ml of toluene was stirred for 8 h at 100°C. All volatiles were removed in vacuo, the green residue was washed with 20 ml of hexane and collected. Yield: 630 mg, 90%. Crystals suitable for X-ray analysis were grown from a saturated acetonitrile solution. m.p. 446°C (dec.). – IR (KBr): $\tilde{\nu}$ = 3132 vs, 2967 vs, 1742 w, 1598 s, 1553 s, 1480 vs, 1361 vs, 1312 s, 1210 s, 1120 s, 1026 m, 1008 w, 912 vs, 874 s, 829 vs, 800 s, 763 s, 729 s, 694 m, 538 vs, 463 m, 425 m, 396 m. – ^{1}H NMR ($CDCl_3$, 298 K) δ = 7.21 (d, 4 H, $^4J_{HH}$ = 2.2 Hz, aromatic *H*), 6.95 (d, 4 H, $^4J_{HH}$ = 2.2 Hz, aromatic *H*), 5.95 (d, 2 H, $^2J_{HH}$ = 12.2 Hz, C*H*$_2$), 3.40 (d, 2 H, $^2J_{HH}$ = 12.2 Hz, C*H*$_2$), 3.27 (d, 2 H, $^2J_{HH}$ = 13.4 Hz, C*H*$_2$), 3.08 (d, 2 H, $^2J_{HH}$ = 13.4 Hz, C*H*$_2$), 2.33 [s, br, 2 H, *H*$_2$N(CH$_3$)$_2^+$], 1.23 [s, 36 H, C(C*H*$_3$)$_3$], 0.66 [t, 6 H, $^3J_{HH}$ = 5.3 Hz, HN(C*H*$_3$)$_2^+$]. – ^{1}H NMR (C_7D_8, 298 K): δ = 7.28 (d, 4 H, $^4J_{HH}$ = 2.5 Hz, aromatic *H*), 6.95 (d, 4 H, $^4J_{HH}$ = 2.5 Hz, aromatic *H*), 6.41 (d, 2 H, $^2J_{HH}$ = 12.1 Hz, C*H*$_2$), 3.56 (d, 2 H, $^2J_{HH}$ = 12.1 Hz, C*H*$_2$), 3.48 (d, 2 H, $^2J_{HH}$ = 13.5 Hz, C*H*$_2$), 3.03 (d, 2 H, $^2J_{HH}$ = 13.5 Hz, C*H*$_2$), 2.58 [br, 2 H, *H*$_2$N(CH$_3$)$_2^+$], 1.21 [s, 36 H, C(C*H*$_3$)$_3$], 0.69 [t, 6 H, $^3J_{HH}$ = 5.2 Hz, H$_2$N(C*H*$_3$)$_2^+$]. – ^{1}H NMR (C_7D_8, 213 K): δ = 7.36 (s, 2 H, aromatic *H*), 7.23 (s, 2 H, aromatic *H*), 6.96 (s, 2 H, aromatic *H*), 6.93 (s, 2 H, aromatic *H*), 6.53 (d, 2 H, $^2J_{HH}$ = 12.2 Hz, C*H*$_2$), 3.67 (d, 2 H, $^2J_{HH}$ = 12.2 Hz, C*H*$_2$), 3.54 (d, 2 H, $^2J_{HH}$ = 13.1 Hz, C*H*$_2$), 3.02 (d, 2 H, $^2J_{HH}$ = 13.1 Hz, C*H*$_2$), 2.45 [br, 2 H, *H*$_2$N(CH$_3$)$_2^+$], 1.31 [s, 18 H, C(C*H*$_3$)$_3$], 1.17 [s, 18 H, C(C*H*$_3$)$_3$], 0.62 [br, 6 H, H$_2$N(C*H*$_3$)$_2^+$]. – ^{13}C NMR ($CDCl_3$, 298 K): δ = 31.60 [s, C(*C*H$_3$)$_3$], 32.77 (s, *C*H$_2$), 33.63 [s, *C*(CH$_3$)$_3$], 35.44 (s, *C*H$_2$), 37.65 [s, N(CH$_3$)$_2$], 123.65, 125.13 (s, aromatic *C*H), 129.14, 131,77 (s, aromatic *C*), 138,95 (s, aromatic *C*^{t}Bu), 162.39 (s, aromatic *C*O). – $C_{92}H_{120}O_8N_2W_2$ (1748.8) calcd.: C 63.16, H 6.91, N 1.60, found: C 62.98, H 7.01, N 1.42.

Crystal Structure Analysis of **1**: Stoe-IPDS diffractometer (Mo-K_a radiation), T = 200(2) K; data collection and refinement: SHELXS-90[15] and SHELXL-96[16]; monoclinic, space group $P2_1/c$; lattice constants a = 26.393(5), b = 17.607(4), c = 23.468(5) Å, β = 114.59(3), V = 9917(3) Å^3, Z = 4, μ(Mo-K_α) = 0.31 mm^{-1}, $2\Theta_{max}$ = 52°; 18104 independent reflections measured, of which 14857 were considered observed with $I > 2\sigma(I)$; max./min. residual electronic density 2.172 and –1.439 e/Å^3. 1088 parameters (C, O, N, Mo anisotropic, the positions of the H atoms were calculated for idealized positions); R_1 = 0.0659, wR_2 = 0.1798.

Crystal Structure Analysis of **2**: Stoe-STADI IV diffractometer (Mo-K_a radiation), T = 203(2) K; data collection and refinement: SHELXS-90[15] and SHELXL-96[16]; monoclinic, space group $P2_1/c$; lattice constants a = 23.840(8), b = 15.500(7), c = 21.935(8) Å, β = 100.85(3), V = 10015(6) Å^3, Z = 4, μ(Mo-K_α) = 2.35 mm^{-1}, $2\Theta_{max}$ = 50°; 17236 independent reflections measured, of which 13273 were considered observed with $I > 2\sigma(I)$; max./min. residual electronic density 3.046 and –2.061 e/Å^3. 1118 parameters (C, O, N, W anisotropic, the positions of the H atoms were calculated for idealized positions); R_1 = 0.048; wR_2 = 0.1203. – Further details of the crystal structure investigation are available from the Fachinformationszentrum Karlsruhe, D-76344 Eggenstein-Leopoldshafen (Germany) on quoting the depository number CSD-407859 and CSD-407860, the names of the authors and the journal citation.

☆ Dedicated to Professor *Hartmut Bärnighausen* on the occasion of his 65th birthday.

[1] For reviews on calixarenes see for example: – [1a] C. D. Gutsche, *Calixarenes*, The Royal Society of Chemistry, Cambridge **1989**. – [1b] J. Vincens, V. Böhmer (ed.), *Calixarenes: A versatile Class of Macrocyclic Compounds*, Kluwer, Dordrecht **1991**. – [1c] C. D. Gutsche, *Prog. Macrocycl. Chem.* **1987**, *3*, 93–165. – [1d] V. Böhmer, *Angew. Chem.* **1995**, *107*, 785–818; *Angew. Chem. Int. Ed. Engl.* **1995**, *34*, 713–745. – [1e] D. M. Roundhill, *Prog. Inorg. Chem.* **1995**, *43*, 533–565.

[2] [2a] F. Corazza, C. Floriani, A. Chiesi-Villa, C. Guastini, *J. Chem. Soc., Chem. Commun.* **1990**, 640–641. – [2b] F. Corazza, C. Floriani, A. Chiesi-Villa, C. Guastini, *J. Chem. Soc., Chem. Commun.* **1990**, 1083–1084. – [2c] F. Corazza, C. Floriani, A. Chiesi-Villa, C. Rizzoli, *Inorg.Chem.* **1991**, *30*, 4465–4468. – [2d] A. Zanotti-Gerosa, E. Solari, L. Giannini, C. Floriani, A. Chiesi-Villa, C. Rizzoli, *J. Chem. Soc., Chem. Commun.* **1996**, 119–120. – [2e] L. Giannini, E. Solari, A. Zanotti-Gerosa, C. Floriani, A. Chiesi-Villa, C. Rizzoli, *Angew. Chem.* **1996**, *108*, 3051–3053; *Angew. Chem. Int. Ed. Engl.* **1996**, *35*, 2825–2827. – [2f] B. Castellano, A. Zanotti-Gerosa, E. Solari, C. Floriani, A. Chiesi-Villa, C. Rizzoli, *Organometallics* **1996**, *15*, 4894–4896. – [2g] L. Giannini, E. Solari, A. Zanotti-Gerosa, C. Floriani, A. Chiesi-Villa, C. Rizzoli, *Angew. Chem.* **1997**, *109*, 763–765; *Angew. Chem. Int. Ed. Engl.* **1997**, *36*, 763–765. – [2h] A. Zanotti-Gerosa, E. Solari, L. Giannini, C. Floriani, A. Chiesi-Villa, C. Rizzoli, *J. Chem. Commun.* **1997**, 183–184.

[3] [3a] J. A. Acho, L. H. Doerrer, S. J. Lippard, *Inorg. Chem.* **1995**, *34*, 2542–2556. – [3b] J. A. Acho, S. J. Lippard, *Inorg. Chim. Acta* **1995**, *229*, 5–8.

[4] [4a] V. C. Gibson, C. Redshaw, W. Clegg, M. R. J. Elsegood, *J. Chem. Soc., Chem. Commun.* **1995**, 2371–2372. – [4b] V. C. Gibson, C. Redshaw, W. Clegg, M. R. J. Elsegood, *J. Chem. Soc., Chem. Commun.* **1997**, 1605–1606.

[5] [5a] J. L. Atwood, M. G. Gardiner, C. Jones, C. L. Raston, B. W. Skelton, A. H. White, *J. Chem. Soc., Chem. Commun.* **1996**, 2487–2488. – [5b] M. G. Gardiner, S. M. Lawrence, C. L. Raston, B. W. Skelton, A. H. White, *J. Chem. Soc., Chem. Commun.* **1996**, 2491–2492.

[6] U. Radius, J. Attner, manuscript in preparation.

[7] M. A. McKervey, E. M. Seward, G. Ferguson, B. L. Ruhl, *J. Org. Chem.* **1986**, *51*, 3581–3584.

[8] The hydrogen oxygen distances in water are assumed to be 0.99 Å for the O–H bond and 1.76 Å for the hydrogen bridge to the next water molecule, see: A. F. Hollemann, E. Wiberg,

Lehrbuch der Anorganischen Chemie, 33rd edition, deGruyter, Berlin **1985**, p. 285.
[9] F. A. Cotton, R. A. Walton, *Multiple Bonds Between Metal Atoms*, 2nd edition, Clarendon Press, Oxford **1993**, chapter 5.
[10] T. A. Budzichowski, M. H. Chisholm, K. Folting, J. C. Huffman, W. E. Streib, *J. Am. Chem. Soc.* **1995**, *117*, 7428−7440.
[11] U. Radius, J. Attner, *unpublished results.*
[12] C. D. Gutsche, M. Iqbal, A. T. Watson, C. H. Heathcock, *Org. Synth.* **1989**, *68*, 234−237.
[13] M. H. Chisholm, D. A. Haitko, C. A. Murillo, F. A. Cotton, S. Han, *Inorg. Synth.* **1982**, *21*, 53−56.
[14] M. H. Chisholm, J. D. Martin, J. E. Hill, I. P. Rothwell, *Inorg. Synth.* **1992**, *29*, 137−140.
[15] G. M. Sheldrick, *SHELXS-90. Program for Crystal Structure Refinement*, Universität Göttingen, **1990**.
[16] G. M. Sheldrick, *SHELXS-96. Program for Crystal Structure Solution*, Universiät Göttingen, **1996**.

[97248]

Isoelectronic Arduengo-Type Carbene Analogues with the Group IIIa Elements Boron, Aluminum, Gallium, and Indium

Andreas Sundermann, Markus Reiher, and Wolfgang W. Schoeller*

Fakultät für Chemie, Universität Bielefeld,
Postfach 10 01 31, D-33501 Bielefeld, Germany

Received September 22, 1997

Keywords: Ab initio calculations / Carbene homologues / Boron / Isoelectronic analogues / Heterocycles

While Arduengo-type carbenes are now well established for the Group IVa elements carbon, silicon and germanium, they are experimentally unknown for the isoelectronic anions with the Group IIIa elements boron, aluminum, gallium, and indium. In the present quantum chemical investigations, the bonding features of this class of compounds are explored. As a result, they are predicted to be stable species with sizeable singlet-triplet energy separations and electron affinities. Hence, they may be considered as valid targets for experimental investigations. An analysis of the electron density distribution in the case of boron and aluminum reveals a strongly polar B−N bond for the former, and a half Al−N bond with positive charge at the aluminum, emphasizing the donor-acceptor formulation for the latter.

Introduction

Since the pioneering studies of Wanzlick on nucleophilic carbenes[1], their successful isolation as stable species became prominent in the reports of Arduengo et al.[2][3] on the imidazo-2-ylidene, **1** (E = C).

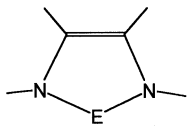

1

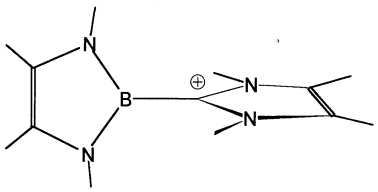

2

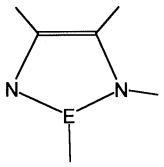

3

Subsequent experimental studies included the preparation of the analogous silylene[4], **1** (E = Si), and germylene[5], **1** (E = Ge), derivatives. In order to gain insight into the peculiar stability of the Arduengo-type carbenes, various quantum chemical calculations have been performed on **1**[6][7][8][9][10][11][12][13][14]. Furthermore, investigations of their photoelectron spectra[9] and a detailed analysis of their chemical shielding tensors have been reported[10].

Meanwhile, the enormous stability of the valence isoelectronic diaminophosphenium cation is a well established matter in phosphorus chemistry[15][16], in particular in ring systems analogous to **1**[17][18][19][20]. The halogen precursors of the latter dissociate spontaneously into the cyclic cation and a halide anion[17]. In contrast, Arduengo-type carbenes with Group IIIa elements are as yet unknown. If these compounds are considered as being isoelectronic with the Arduengo-type carbenes, they would bear a negative charge at the Group IIIa element. The capability of Group IIIa elements to stabilize a negative charge has nevertheless been demonstrated by experimental and theoretical studies on B−B and Al−Al bonded systems[21][22][23][24][25][26][27][28][29]. For boron, one-electron [24][25][26] as well as two-electron[21][22] reductions have been observed. In contrast, for the Al−Al bond, only one-electron reduction has been found[27][28][29]. These findings indicate that it might be feasible to prepare Arduengo-type carbenes in which E (= C, Si, Ge) is replaced by a valence isoelectronic Group IIIa element bearing a negative charge.

We report herein on an exploration of the bonding properties of Arduengo-type carbenes, **1**, with E = $B^{(-)}$, $Al^{(-)}$, $Ga^{(-)}$, $In^{(-)}$. A first experimental approach to this class of compounds has recently been undertaken in the synthesis and structural elucidation of **2**[30]. This structure is found to contain the diazaborolyl unit. In addition, we include in our investigations the 1,2-shifted structural isomers **3**.

Methodology

The geometries of the various molecular structures were energy optimized at the density functional theory level[31][32], utilizing Becke's three-parameter functional[33] with local and non-local electron correlation contributions. For the optimization of the geometries, the 6-31++g(d,p) basis set was used for carbon and hydrogen, as well as for boron, aluminum, and gallium[34]. One set of diffuse s,p-functions[35] and polarization functions[36] were added. Alterna-

 © WILEY-VCH Verlag GmbH, D-69451 Weinheim, 1998 1434−1948/98/0303−0305 $ 17.50+.50/0

tively, the relativistic pseudopotentials of Basch and Krauss[37], with a double-ζ description for the valence space, were employed for the evaluation of structures in the homologous series containing boron to indium. For these cases, the basis sets were again augmented by one set of polarization functions (at all atoms) and one set of diffuse sp-functions (at all atoms). The coefficients for the supplementary functions were chosen according to the recommendations made for the utilization of the Gamess program[38]. Single point calculations were additionally performed (for the cases of boron and aluminum) at a triple-ζ level, with the 6-311++g(d,p) basis set[39] and with the MP4SDTQ(fc) approximation[40] for the electron correlation correction treatment. For the evaluation of the energies in the open-shell cases (doublets), the spin-projection technique of Schlegel[41] was applied. Zero-point vibrational energies were included in the relative energies, unless noted otherwise. All stationary points were verified by calculation of the corresponding Hessian matrices. For the calculations, we used the Gaussian-94[42] and Gamess[43] programs. The electron distributions in the various molecular structures were examined within the natural bond orbital (NBO) partitioning scheme[44].

Results and Discussion

Qualitative Considerations: The stabilities of the carbene structures are determined by (a) the singlet-triplet energy separations, and (b) the electron affinities in **1** (E = $B^{(-)}$, $Al^{(-)}$, $Ga^{(-)}$, $In^{(-)}$). If the singlet-triplet energy separations are small, the carbene-type structures will not be stable and will be capable of facile radical reactions (with solvents, etc.). The electron affinities, on the other hand, give a quantitative measure of the anion stabilities. If the electron affinities are large, then the possibility of preparing the anion can be considered as being realistic. In practice, however, the anions are surrounded by cations (e.g. as lithium salts). Hence, their stabilities will be mediated by crystal effects[45].

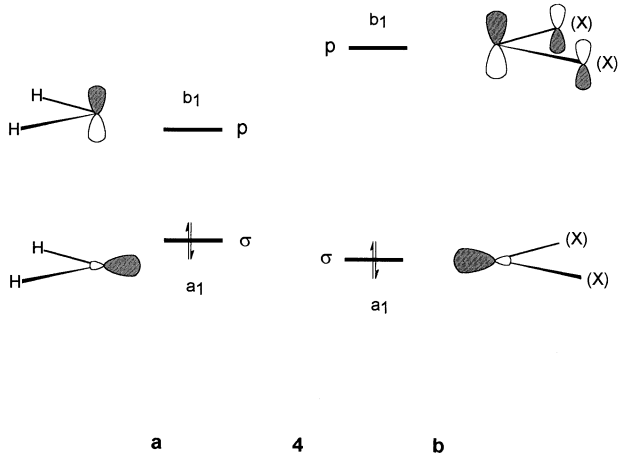

a **4** **b**

The frontier orbitals of methylene, **4a**, are given by the lone pair orbital at the central atom, σ, and the p-orbital[46]. Within C_{2v} symmetry they are confined to a_1 and b_1 representations. Both orbitals are energetically in close proximity to each other, hence a triplet ground state $^3B_1$ is preferred[47]. In a stabilized carbene, **4b** (X = NH_2, halogens), a similar sequence of orbitals is present[48]. Since the energy splitting between HOMO (σ) and LUMO (p) becomes larger for these structures, a singlet ground state results[49].

The frontier orbital system of **1** can be viewed in a similar manner, as a mutual interaction between the orbitals of the diene unit (A) and the orbitals at E (B). The composition of the orbital system is given in (C) [= (A)−(B), Figure 1].

Figure 1. Diagram showing schematic interaction between a diene unit (A) and E (B), resulting in the cyclic compound (C) [= (A)−(B)]

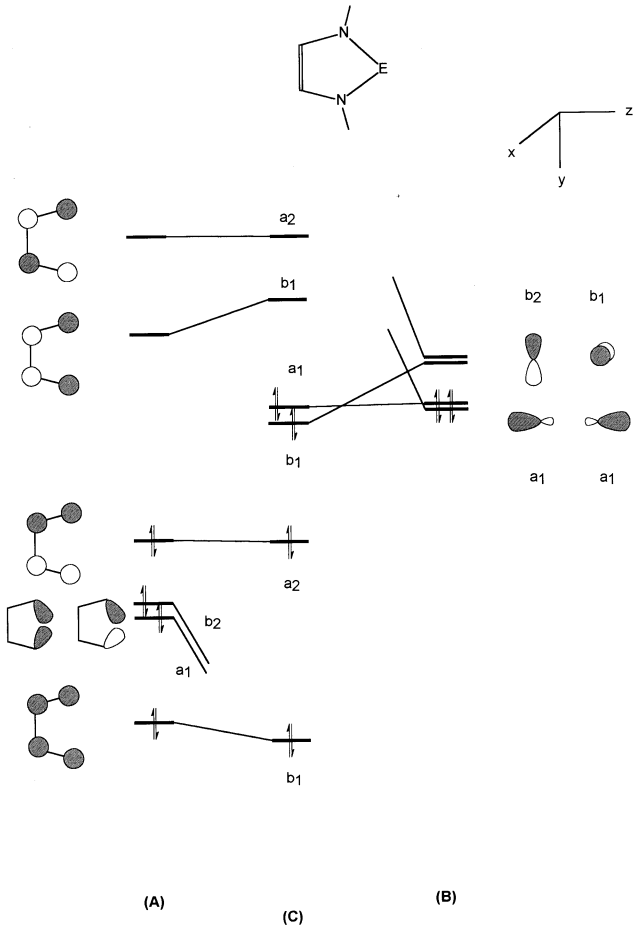

The p_y-orbital forms two linear combinations with the s-orbital ($s \pm p_y$), of which one ($s + p_y$) remains non-bonding upon interaction with the corresponding orbitals at (A). On the other hand, the other combination ($s - p_y$) can strongly overlap with the a_1 orbitals at fragment (A). Similarly, the b_2 orbital at (B) strongly interacts with the antibonding lone pair combination b_2 at (A). In addition, π-type interaction occurs among the b_1 orbitals, between (A) and (B). Consequently, the relevant occupied frontier orbitals at (C) can be depicted as in formula **5**.

As mentioned above, the stabilities of the anions are determined by their electron affinities, i.e. the tendency to retain their negative charge. Consequently, it is necessary to examine the anions, the corresponding neutral doublet

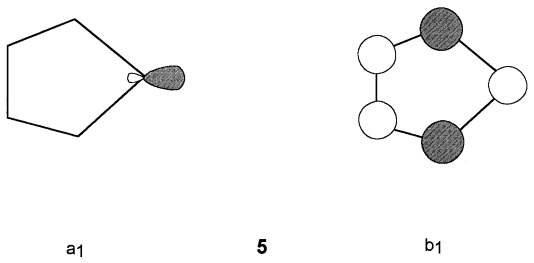

states, and the energy differences between the two species. The resulting Slater determinants for the singlet ground state of the anion and the two relevant doublet states are given as follows:

$\Psi\ (^1A_1) = ...(b_1)^2(a_1)^2 >$

$\Psi\ (^2A_1) = ...(b_1)^2(a_1)^1 >$

$\Psi\ (^2B_1) = ...(a_1)^2(b_1)^1 >$

The relevant triplet states for **1** are described by the following Slater determinants:

$\Psi\ (^3B_1) = ...(a_1)^1(b_1)^1 >$

$\Psi\ (^3A_1) = ...(b_1)^1(b_1)^1 >$

The first of these ($^3B_1$) refers to the lowest-energy triplet state, as has been evaluated for the classical Arduengo carbene[7]. All the states in question were examined by the quantum chemical calculations.

It should be noted that **1** is not the only feasible molecular structure. It might well be possible that it undergoes a 1,2-hydrogen shift with formation of species **3**. Consequently, we also included these possible structural isomers for the species in question in our evaluations.

Equilibrium Geometries: The equilibrium geometries of all these structures, **1** and **3**, (bond lengths in Å, bond angles in degrees) are collected in Figure 2.

Minimum-energy structures were established by (3N − 6) positive vibrations of each species. The geometries were obtained with (a) all-valence basis sets, or alternatively with (b) effective core potential methods (ECP's, values in parentheses) (for details, see the Methodology section). All structures were obtained at the DFT level.

The anions of **1** invariably adopt C_{2v} symmetry. The valence angle at E ranges from 97.8° [X = $B^{(-)}$] to 77° [X = $In^{(-)}$]. This indicates that the equilibrium geometries of these ring systems are largely determined by the angle strain due to the first-row atoms C and N.

The bonding situation is somewhat more complicated in the doublet states. Interestingly, the doublet states undergo a change in their electronic (ground) state in the sequence E = B to In. In the case E = B, a $^2A_1$ ground state is observed, while for E = In it becomes $^2B_1$. An intermediate case is **1**, E = Al. Here, both states, $^2A_1$ and $^2B_1$, mingle with each other with concomitant Jahn-Teller interactions[50]. Symmetry breaking occurs to give C_s symmetry, through induction of b_1 vibration within C_{2v} symmetry. For this case (E = Al), the five-membered ring is tilted out of the plane (∡ CNNAl = 14.2° for $^2A'$). We acknowledge

Figure 2. Equilibrium geometries of lowest-energy singlets (first entry) and doublets (second entry) of **1** (E = B, Al, Ga, In) and **3** (E = B, Al, Ga), at all-valence electron (ECP) level

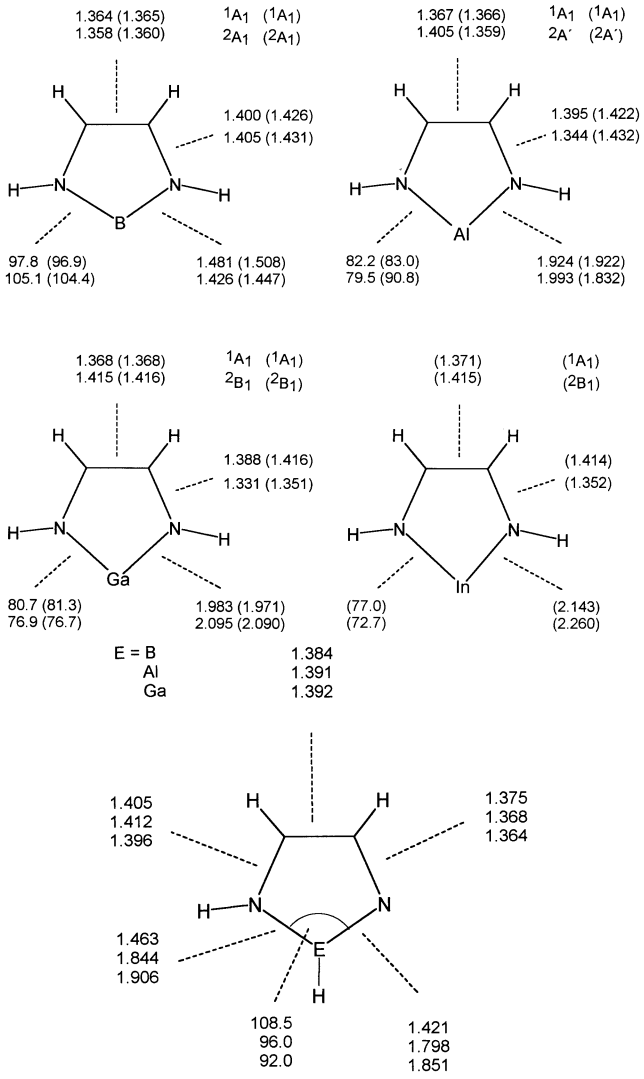

that a more rigorous approach for the study of the Jahn-Teller phenomena in the (neutral) doublet states would require elaborate MCSCF calculations with subsequent multi-reference CI calculations. For the case at hand, a detailed study of the crossing of the electronic hypersurfaces of the various doublet states was not attempted.

The rearranged structures **3** invariably adopt C_s symmetry. Again, all species possess (3N − 6) positive vibrations in their equilibrium geometries. Thus, they correspond to energy minima on the electronic hypersurfaces. In general, the E−N bonds in **3** are shorter than those in the structures **1**. Notably, the E−N bond to the twofold coordinated nitrogen atom is always shorter than that to the substituted nitrogen. This can be rationalized in terms of two prominent resonance structures, which contribute to bonding in the ground states.

In canonical structure **a**, the negative charge is localized at the nitrogen atom, while in **b** it is shifted towards E (= B, Al, Ga) with formation of a (partial) double bond. The

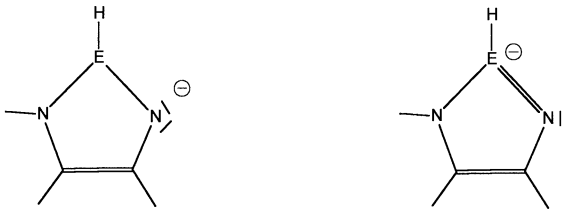

a b

predominance of canonical structure **b** over **a** is determined by the electronegativity of E and the gain in π-energy. Although it is difficult to assess both factors quantitatively, one would expect that **3** becomes increasingly stabilized over (the singlet ground state) **1** in the order X = In < Ga < Al < B. As will be shown in the following section, this is indeed the case.

Energy Considerations: The electron affinities and singlet-triplet energy separations are the specific properties that determine the stabilities of the various species **1**. These are presented in Table 1.

Table 1. Electron affinities (in kcal/mol) [first entries] and singlet-triplet energy separations [second entries] for structure **1** (E = B to In); values in parentheses are derived from ECP calculations

Atom E		DZP[a]	DZP/ZPE[b]	TZP[c]	MP4[d]
B	($^1A_1 \rightarrow {}^2A_1$)	7.0 (9.3)[e]	8.4	7.2	3.3 (2.8)
	($^1A_1 \rightarrow {}^3A_1$)	20.2 (22.6)	20.9	20.4	23.1 (23.5)
Al	($^1A_1 \rightarrow {}^2A'$)	32.5 (34.3)	33.1	33.4	34.5
	($^1A_1 \rightarrow {}^3B_1$)	41.3 (50.5)	41.5	42.4	45.3
Ga	($^1A_1 \rightarrow {}^2B_1$)	27.0 (32.1)	28.1	26.7	39.3
	($^1A_1 \rightarrow {}^3A_1$)	52.0 (47.9)			
In	($^1A_1 \rightarrow {}^2B_1$)	(27.0)			
	($^1A_1 \rightarrow {}^3A_1$)	(38.8)			

[a] b3lyp/6-31++g(d,p). – [b] Method [a] plus zero-point vibrational energy correction (unscaled). – [c] b3lyp/6-311++g(d,p)//b3lyp(6-31++g(d,p). – [d] MP4SDTQ(fc)/6-31++g(d,p)//b3lyp/6-31++g(d,p). – [e] b3lyp/ECP-31++g(d,p).

For the cases X = B to Ga, they were explored with the all-valence electron basis set methods, and also with the ECP's (at times within the DFT procedure). For E = In, our considerations rely solely on the results of the ECP calculations. For the structures where the results of both quantum chemical procedures are available (all-valence electron basis sets and ECP's), the different approaches are seen to yield similar energy quantities. On closer inspection of the data, it can be seen that for E = B the electron affinity is found to be rather small. The value is only marginally changed by zero-point vibrational energy corrections or at an improved triplet-ζ basis set level. On the other hand, for all cases the singlet-triplet energy separations are sizeable. Thus, a singlet ground state of all structures is ensured. The electron affinity, and hence the stability of the anion, is increased for the higher element homologues. In essence, for all higher element homologues, the electron affinities are larger than those for the first-row element boron. Again, zero-point energy vibrational correction as well as explicit CI methods, such as the MP4SDTQ approach, yield comparable energy quantities.

To evaluate the feasibility of the synthesis of **1**, it is necessary to have knowledge of the relative energetic ordering of **1** and **3**, given the same element E. Corresponding energy quantities were evaluated at various levels of sophistication for the cases E = B, Al and Ga, and are listed in Table 2.

Table 2. Energy differences (in kcal/mol) between **1** and **3**, at various levels of sophistication

Atom E	DZP[a]	DZP/ZPE[b]	TZP[c]
B	−40.8	−42.4	−40.7
Al	17.6	13.9	17.9
Ga	23.9		

[a] b3lyp/6-31++g(d,p). – [b] Method [a] plus zero-point vibrational energy correction. – [c] b3lyp/6-311++g(d,p)//b3lyp/6-31++g(d,p).

The trends in the energies are obvious. For E = B, the 1,2-hydrogen shifted structure is the lowest-energy alternative. In the other cases, **1** is more stable than **3**. It should be noted, however, that in the case of carbenes it has been recently demonstrated that although 1,2-hydrogen migrations are very exothermic, their occurrence is highly unlikely from a kinetic point of view[51].

Improvement of the basis set (level C) or the inclusion of zero-point vibrational energy contributions (level B) does not significantly alter the situation. There is a clear-cut tendency of enhanced stability of **1** over **3**, with increasing atomic number of E. The case E = In was not further explored, but it seems reasonable to assume that it is at least as stable as the case E = Ga (**1** in relation to **3**).

Electron Density Distributions: It is informative to analyze the electron distributions in **1** and **3**. The relevant values were computed within the natural bond orbital (NBO) scheme[44]. For the cases E = B and Al, these are displayed in Figure 3.

The electron distributions in E = B and E = Al reveal fundamental differences. For **1**, E = B, the E−N bond is almost a single bond, while it is almost a half bond for E = Al. Simultaneously, E releases electron density towards the neighbouring, more electronegative nitrogen atoms, with a concomitant strengthening of the E−N bonds. Similar trends are also observed in the Ga and In analogues, although detailed populations are not given here. Considering the data in more detail, the s/p ratio (atomic populations for the valence electrons) for the lone pair amounts to 1.378/0.918 for E = B and 1.660/0.536 for E = Al. (The corresponding π-populations of valence electrons are given in brackets in Figure 3).

Evidently, a fundamental change in the bonding is observed on going from E = B to E = Al. The Laplacians of the electron density for these two cases (as determined by the method of "atoms in molecules"[52], are shown in Figure 3b. For E = B, a non-bonding lone pair orbital (at E) is present. It is diminished in the case E = Al, in favour of an increased p-electron density at the neighbouring nitrogens. Furthermore, in the latter case (E = Al), the electron

Figure 3. (a) NBO analysis (natural atomic charges with π-occupancies in curly brackets), in parentheses Wiberg bond indices (in the NAO basis) and (b) Laplacians of the electron densities for **1**, E = B and Al

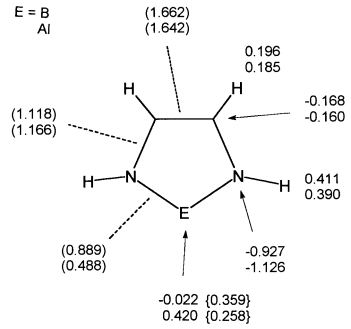

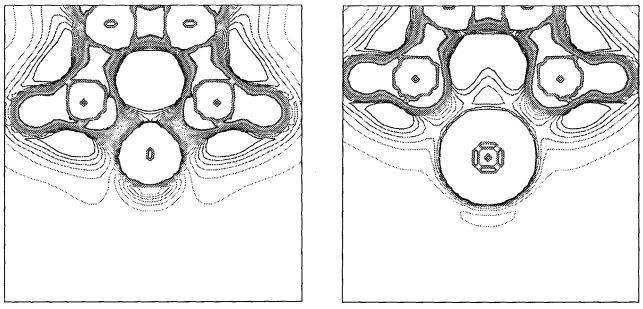

E = B E = Al

density is more concentrated at the nitrogens compared with the former (E = B). All these findings are in accord with the predominance of canonical structure **c** for E = B, and a donor-acceptor formulation **d** for E = Al. For the higher element homologue E = Al, a cyclic delocalization of electrons does not occur.

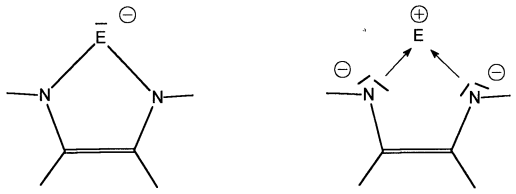

c **d**

The structure **d** is dominant if E represents an electropositive element (as compared with nitrogen) and becomes increasingly so in the order X = Al < Ga < In.

Conclusions

The results of our quantum chemical study can be summarized as follows:

1. Arduengo-type carbene structures in which an isovalent electronic species E = $B^{(-)}$, $Al^{(-)}$, $Ga^{(-)}$, $In^{(-)}$ constitutes the divalent center are stable species. They possess singlet ground states and adopt C_{2v} symmetrical structures.

2. Although the central atom is relatively electropositive as compared with its neighbouring nitrogen atoms, the species possess bound states; i.e. they have a strong tendency to retain the negative charge. In other words, the corresponding doublet states have a strong electron affinity.

3. This is due to the enhancement of a chelate-type structure, in which the electropositive element E (In > Ga > Al) can release its formal negative charge to the more electronegative neighbouring nitrogen atoms.

4. Furthermore, with increasing atomic number of E, a possible 1,2-hydrogen rearrangement, which results in the formation of a "classical" structure becomes disfavored.

On the basis of our quantum chemical considerations, cyclic carbene structures of the Arduengo-type containing the Group IIIa elements should be interesting targets for synthetic verifications.

We thank the *Fonds der Chemischen Industrie* for financial support and a dissertation grant for one of us (M.R.). Support of this work by the *Deutsche Forschungsgemeinschaft* is also acknowledged. We also thank Prof. *L. Weber* and Dipl.-Chem. *E. Dobbert* for useful discussions.

[1] H. W. Wanzlick, *Angew. Chem.* **1960**, *72*, 494.
[2] 1,3-Adamantyl derivative: A. J. Arduengo, III, R. L. Harlow, M. Kline, *J. Am. Chem. Soc.* **1991**, *113*, 361.
[3] 1,3-Dimethyl derivative: A. J. Arduengo, III, H. V. R. Dias, R. L. Harlow, M. Kline, *J. Am. Chem. Soc.* **1992**, *114*, 5530.
[4] M. Denk, R. Lennon, R. Hayashi, R. West, A. V. Belyakov, H. P. Verne, A. Haaland, M. Wagner, N. Metzler, *J. Am. Chem. Soc.* **1994**, *116*, 2691.
[5] W. A. Herrmann, M. Denk, J. Behm, W. Scherer, F.-R. Klingan, H. Bock, B. Solouki, M. Wagner, *Angew. Chem.* **1992**, *104*, 1489; *Angew. Chem. Int. Ed. Engl.* **1992**, *31*, 1485.
[6] D. A. Dixon, A. J. Arduengo, III, *J. Phys. Chem.* **1991**, *95*, 4180.
[7] J. Cioslowski, *Int. J. Quantum Chem. Symp.* **1993**, *27*, 309.
[8] A. J. Arduengo, III, H. V. R. Dias, D. A. Dixon, R. L. Harlow, W. T. Klooster, T. F. Koetzle, *J. Am. Chem. Soc.* **1994**, *116*, 6812.
[9] A. J. Arduengo, H. Bock, H. Chen, M. Denk, D. A. Dixon, J. C. Green, W. A. Herrmann, N. L. Jones, M. Wagner, R. West, *J. Am. Chem. Soc.* **1994**, *116*, 6641.
[10] A. J. Arduengo, III, D. A. Dixon, K. K. Kumashiro, C. Lee, W. P. Power, K. W. Zilm, *J. Am. Chem. Soc.* **1994**, *116*, 6361.
[11] C. Heinemann, W. Thiel, *Chem. Phys. Lett.* **1994**, *217*, 11.
[12] C. Heinemann, W. A. Herrmann, W. Thiel, *J. Organomet. Chem.* **1994**, *475*, 73.
[13] C. Heinemann, T. Müller, Y. Apeloig, H. Schwarz, *J. Am. Chem. Soc.* **1996**, *118*, 2023.
[14] C. Boehme, G. Frenking, *J. Am. Chem. Soc.* **1996**, *118*, 2039.
[15] A. H. Cowley, R. Kemp, *Chem. Rev.* **1985**, *85*, 367.
[16] M. Sanchez, M. R. Mazieres, L. Lamande, R. Wolf, *Multiple Bonds and Low Coordination Chemistry in Phosphorus Chemistry* (Eds.: M. Regitz, O. Scherer), Georg Thieme Verlag, Stuttgart, **1990**.
[17] M. K. Denk, S. Gupta, R. Ramachandran, *Tetrahedron Lett.* **1996**, *37*, 9025.
[18] D. Gudat, *Coord. Chem. Rev.*, in press.
[19] I. A. Litvinov, V. A. Naumov, T. V. Gryazna, A. N. Pudovik, A. M. Kibardin, *Dokl. Akad. Nauk SSSR* **1990**, *312*, 623.
[20] For the analogous saturated system, see N. Burford, P. Losier, C. Macdonald, V. Kyrimis, P. K. Bakshi, T. S. Cameron, *Inorg. Chem.* **1994**, *33*, 1434.
[21] A. Moezzi, R. A. Bartlett, P. P. Power, *Angew. Chem.* **1992**, *104*, 1075; *Angew. Chem. Int. Ed. Engl.* **1992**, *31*, 1082.
[22] A. Moezzi, M. M. Olmstead, P. P. Power, *J. Am. Chem. Soc.* **1992**, *114*, 2715.
[23] M. A. Petrie, P. P. Power, H. V. R. Diaz, K. Ruhlandt-Senge, K. M. Waggoner, R. J. Wehmschulte, *Organometallics* **1993**, *12*, 1086.
[24] E. Kaufmann, P. v. R. Schleyer, *Inorg. Chem.* **1988**, *27*, 3987.
[25] J. E. Leffler. G. B. Watts, T. Tanigaki, E. Dolan, D. S. Miller, *J. Am. Chem. Soc.* **1970**, *92*, 6825.
[26] H. Klusik, A. Berndt, *Angew. Chem.* **1981**, *93*, 903; *Angew. Chem. Int. Ed. Engl.* **1981**, *20*, 870.

[27] A. Berndt, H. Klusik, K. Schlüter, *J. Organomet. Chem.* **1981**, *C25*, 222.
[28] C. Pluta, K.-R. Pörschke, C. Krüger, K. Hildenbrand, *Angew. Chem.* **1993**, *105*, 451; *Angew. Chem. Int. Ed. Engl.* **1993**, *32*, 388.
[29] W. Uhl, A. Vester, W. Kaim, J. Poppe, *J. Organomet. Chem.* **1993**, *454*, 9.
[30] L. Weber, E. Dobbert, H.-G. Stammler, B. Neumann, R. Boese, D. Bläser, *Chem. Ber./Recueil* **1997**, *130*, 705.
[31] P. Hohenberg, W. Kohn, *Phys. Rev.* **1964**, *136*, B864; W. Kohn, L. J. Sham, *Phys. Rev.* **1965**, *140*, A1133.
[32] R. G. Parr, W. Yang, *Density-Functional Theory of Atoms and Molecules*, Oxford University Press, Oxford, **1989**.
[33] A. D. Becke, *Phys. Rev.* **1988**, *A38*, 3098; A. D. Becke, *J. Chem. Phys.* **1993**, *98*, 5648.
[34] R. Ditchfield, W. J. Hehre, J. A. Pople, *J. Chem. Phys.* **1971**, *54*, 724; W. J. Hehre, R. Ditchfield, J. A. Pople, *J. Chem. Phys.* **1972**, *56*, 2257; P. C. Hariharan, J. A. Pople, *Theor. Chim. Acta* **1973**, *28*, 213. See also *Gaussian 94 User's Reference Manual*, M. J. Frisch, A. Frisch, J. B. Foresman, Gaussian, Inc., Pittsburgh, PA 15106, and references cited therein.
[35] T. Clark, J. Chandrasekhar, G. W. Spitznagel, P. v. R. Schleyer, *J. Comput. Chem.* **1983**, *4*, 294.
[36] M. J. Frisch, J. A. Pople, J. S. Binkley, *J. Chem. Phys.* **1984**, *80*, 3265.
[37] W. J. Stevens, H. Basch, M. Krauss, *J. Chem. Phys.* **1984**, *81*, 6026; W. J. Stevens, H. Basch, M. Krauss, P. Jasien, *Can. J. Chem.* **1992**, *70*, 612; T. Cundari, W. J. Stevens, *J. Chem. Phys.* **1993**, *98*, 5555.
[38] M. W. Schmidt, K. K. Baldridge, J. A. Boatz, J. H. Jensen, S. Koseki, M. S. Gordon, K. A. Nguyen, T. L. Windus, S. T. Elbert, *QCPE Bull.* **1990**, *10*, 52.
[39] R. Krishnan, J. S. Binkley, R. Seeger, J. A. Pople, *J. Chem. Phys.* **1980**, *72*, 650; A. D. McLean, G. S. Chandler, *J. Chem. Phys.* **1980**, *92*, 5639.
[40] C. Møller, M. S. Plesset, *Phys. Rev.* **1934**, *46*, 618; R. Krishnan, J. A. Pople, *Int. J. Quantum Chem.* **1978**, *14*, 91.
[41] H. B. Schlegel, *J. Chem. Phys.* **1986**, *84*, 4530.
[42] M. J. Frisch, G. W. Trucks, H. B. Schlegel, P. M. W. Gill, B. G. Johnson, M. A. Robb, J. R. Cheeseman, T. A. Keith, G. A. Peterson, J. A. Montgomery, K. Raghavachari, M. A. Al-Laham, V. G. Zakrzewski, J. V. Ortiz, J. B. Foresman, J. Cioslowski, B. B. Stefanov, A. Nanayakkara, M. Challacombe, C. Y. Peng, P. Y. Ayala, W. Chen, M. W. Wong, J. L. Andres, E. S. Replogle, R. Gomperts, R. L. Martin, D. J. Fox, J. S. Binkley, D. J. Defrees, J. Baker, J. P. Stewart, M. Head-Gordon, C. Gonzalez, J. A. Pople, *Gaussian 94 (Revision A.1)*, Gaussian, Inc., Pittsburgh, PA, **1995**.
[43] M. W. Schmidt, K. K. Baldridge, J. A. Boatz, S. T. Elbert, M. S. Gordon, J. H. Jensen, S. Koseki, N. Matsunaga, K. A. Nguyen, S. J. Su, T. L. Windus, M. Dupuis, J. A. Montgomery, *J. Comput. Chem.* **1993**, *14*, 1347.
[44] A. Reed, L. A. Curtiss, F. Weinhold, *Chem. Rev.* **1988**, *88*, 899.
[45] W. W. Schoeller, T. Busch, *J. Mol. Struct. (THEOCHEM)* **1994**, *313*, 27. For the importance of solvation in determining carbenoid structures, see W. W. Schoeller, *Chem. Phys. Lett.* **1995**, *241*, 21.
[46] B. M. Gimarc, *Molecular Structure and Bonding*, Academic Press, New York, **1979**.
[47] E. R. Davidson, in *Diradicals* (Ed.: W. T. Bordon), Wiley-Interscience, New York, **1982**.
[48] G. Trinquier, *J. Am. Chem. Soc.* **1990**, *112*, 2130; for further references see therein.
[49] W. W. Schoeller, *J. Mol. Struct. (THEOCHEM)*, in press.
[50] F. L. Pilar, *Elementary Quantum Chemistry*, McGraw-Hill, New York, **1968**.
[51] G. Maier, J. Endres, H. P. Reisenauer, *Angew. Chem.* **1997**, *109*, 1788; *Angew. Chem. Int. Ed. Engl.* **1997**, *36*, 1709.
[52] R. F. W. Bader, *Atoms in Molecules*, Clarendon Press, Oxford, **1994**.

[97214]

Group-13 Metal-Induced Coordination Variation of the Bis(2-pyridyl)amide Ligand in Solution and in the Solid State

Heinz Gornitzka and Dietmar Stalke*

Institut für Anorganische Chemie der Universität Würzburg,
Am Hubland, D-97074 Würzburg, Germany
E-mail: dstalke@chemie.uni-wuerzburg.de

Received October 22, 1997

Keywords: Molecular recognition / Amides / Aluminium / Thallium / Structure elucidation

Ligands containing aromatic nitrogen heterocycles play a leading role in the molecular self assembling processes that lead to macromolecular architectures. The inductive effect of various metal fragments on those building blocks has not yet been studied systematically. To evaluate this effect we synthesized the homologous series of Group-13 metal complexes $[Me_2AlPy_2N]$ (**1**), $[Me_2GaPy_2N]$ (**2**), $[Me_2InNPy_2]_2$ (**3**), and $[Me_2TlNPy_2]_\infty$ (**4**) (Py = 2-NC_5H_4), and characterized them by low-temperature X-ray structure analysis and ^{15}N-NMR spectroscopy in solution. The electronic equivalence of the central and the ring nitrogen atoms leaves the energetic hyperface of the anion quite flat, and the electron density is polarized according to the requirements of the metal. In the aluminum and the gallium complexes **1** and **2** the metal center is coordinated exclusively through the nitrogen atoms within the pyridyl rings. The complexes with these hard metals are close-contact ion pairs. In the indium complex **3** the *cis-cis* orientation gives rise to a dimeric structure, while the unprecedented *cis-trans* arrangement in the thallium compound **4** leads to a polymeric structure. The complexes **3** and **4** have to be regarded as separated ion pairs of Me_2M^+ cations and Py_2N^- anions without any covalent bonds between the anionic moiety and the dimethylmetal cations, even in the solid state. The series of complexes proves the bis(2-pyridyl)amide to be an excellent self-adapting ligand. These findings are substantiated by NMR-spectroscopic studies in solution. Not only do the steric requirements of N heteroaromatic ligands have to be considered in molecular self-assembling processes but also the inductive effect of the different metal fragments.

Introduction

The use of aromatic nitrogen heterocycles has given a great impetus to metal coordination chemistry.[1] Due to the low-energy π* orbitals pyridine and its derivatives are valuable σ donors and π acceptors in the bonding synergism of transition-metal complexes.[2] Classical N-heteroaromatic donor ligands are pyridine, 2,2′-bipyridine and 1,10-phenanthroline.

Scheme 1

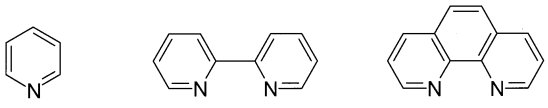

pyridine 2,2'-bipyridine 1,10-phenanthroline

In metal-induced molecular recognition processes various linkages of the simple building blocks yield polydentate macromolecular ligands tailored to the steric requirements of the nanomolecular architectures present. Helical arrangements with transition-metal centers are one focus of interest.[3] A spheric palladium polymacrocycle containing triazine bridgeheads has also been synthesized,[4] and metallo carotenate molecular wires containing pyridyl or bipyridyl ends coordinated to metal centers combine the electronic or photochemical properties of a metal fragment and the conjugated electron system of the carotenes.[5]

Over the last years our work has been concerned with the design and fine tuning of monoanionic ligands, containing N-heteroaromatic rings, which show a different coordination behavior towards soft and hard metals.[6] In these systems a single p block element in a low oxidation state links two or three pyridyl (Py) or pyrazolyl (Pz) rings. Metal coordination is achieved by the ring nitrogen atoms but never by the bridgehead atom. Anionic systems studied so far are the pyridyldiphenylmethyl,[7] dipyridylmethyl,[8] dipyridylphosphide and -arsenide,[9] tripyrazolylgermanate and -stannate.[10] These ligands are formally carbanions, phosphides and arsenides but in metal coordination they behave as amides. For instance the phosphorus or arsenic(III) center is only two-coordinate to both *ipso*-carbon atoms and the structures do not comprise any short M−P or M−As bonds. The negative charge in the anions is located almost entirely on the nitrogen atoms of the pyridyl substituents.

Scheme 2. Dipyridylmethyl, -phosphide and -arsenide coodination to metal centers

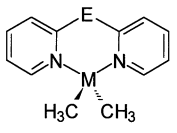

E = CH, P, As

M = Al, Ga

To counterbalance the electron-withdrawing effect of the ring nitrogen atoms we isoelectronically replaced the CH

 © WILEY-VCH Verlag GmbH, D-69451 Weinheim, 1998 1434−1948/98/0303−0311 $ 17.50+.50/0

group, the P or the As bridgeheads by a nitrogen atom. In this paper a systematic study of the coordination behavior of the Py_2N^- anion, in both the solid state and solution, towards Group-13 metals is presented. The relationship between the geometry of a coordinated and an uncoordinated ligand system in solution and in the solid state is of special interest in the study of self-assembling systems.[11] The dipyridylamide ligand is anticipated to permit a *transoid* orientation in the uncoordinated form in solution, as found in 2,2′-bypiridine[12] and shown in Scheme 3.

Scheme 3. The *transoid* versus *cisoid* coordination of 2,2′-bipyridine

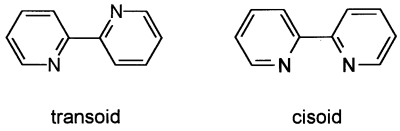

Because of electrostatic repulsion between the N lone pairs and the weak attraction between N and CH sites in antiparallel orientation of the N sites, they should favor the *transoid* over *cisoid* arrangement. A priori one can think of three different coordination modes.

Scheme 4. Feasible coordination modes of the dipyridylamide ligand

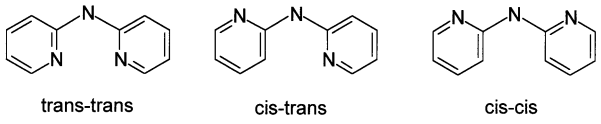

In the known complexes of neutral bis(2-pyridyl)amine the *trans-trans* coordination mode to both ring nitrogen atoms is observed [$(HNPy_2)CuHal_2$ (Hal = Br[13a], Cl[13b])], [$(HNPy_2)_2Cd-(ONO)_2$[13c], $(HNPy_2)M(CO)_4$ (M = Cr, Mo, W)].[13d] In the monomeric $M(Py_2N)_2$ (M = Cu[14a], Ru, Pd[14b][14c]) complexes *trans-trans* arrangements of both ring nitrogen atoms coordinated to the metal center are found, while in $(Py_2N)W(CO)_5$,[15] the tungsten atom apparently is exclusively coordinated to the central nitrogen atom. A *cis-cis* arrangement and coordination to all three nitrogen atoms is found in the dimer of $[(Py_2N)Tl(C_6F_5)_2]_2$.[16] This coordination is emulated in the polymeric complexes of $[Cu(Py_2N)]_n$[17], $[M_3(Py_2N)_4Hal_2]_n$ (M = Cu[18a], Ni[18b]). It seems worthy to note that until now a *cis-trans* coordination of the dipyridylamide ligand has not been observed.

To study the coordination behavior of the bis(2-pyridyl)-amide anion systematically in both the solid state and in solution the Group-13 metal complexes $[Me_2AlPy_2N]$ (**1**), $[Me_2GaPy_2N]$ (**2**), $[Me_2InNPy_2]_2$ (**3**), and $[Me_2TlNPy_2]_\infty$ (**4**) have been synthesized and characterized by low-temperature X-ray structures as well as by ^{15}N-NMR spectroscopy in solution.

Results and Discussion

Preparation of 1−4

Compounds **1**−**3** were synthesized by adding trimethylmetal compounds to a solution of bis(2-pyridyl)amine (eq 1).

$$n\,HNPy_2 + n\,Me_3M \longrightarrow [Me_2MPy_2N]_n + n\,MeH \quad (1)$$

1: M = Al; –10 °C in diethyl ether; $n = 1$

2: M = Ga; –78 °C in toluene; $n = 1$

3: M = In; 1 h reflux in toluene; $n = 2$

To obtain the compound **4** trimethylthallium has to be synthesized first in situ by adding methyllithium to a solution of dimethylthallium iodide in ether.[19] The second step is the addition of one equivalent of bis(2-pyridyl)amine (eq. 2).

$$n\,Me_2TlI \xrightarrow[2.\ +\ n\ HNPy_2\ ,\ -\ MeH]{1.\ +\ n\ MeLi,\ -\ n\ LiI} [Me_2TlNPy_2]_n \quad (2)$$

4 $n = \infty$

^{15}N-NMR-Spectroscopic Experiments

To gain information about the coordination behavior of the bis(2-pyridyl)amide ligand in the complexes **1**−**4** in solution we recorded NMR spectra. Particularly informative are the results of the ^{15}N-NMR-spectroscopic experiments. The spin of the ^{15}N nucleus is 1/2 and this gives sharp signals in the NMR experiments. Therefore, this method is particularly suitable to compare non-equivalent nitrogen atoms in solution. The chemical shift of the nucleus is correlated to its electronic shielding.

The neutral bis(2-pyridyl)amine gives rise to two signals which differ considerably with respect to their chemical shifts (assignment in analogy to similar systems[20]) because of the magnetically non-equivalent nitrogen sites (Table 1). In the aluminum and the gallium complexes **1** and **2** the signals of both nitrogen atoms display very similar chemical shifts, demonstrating the electron density to be shifted from the central nitrogen atom (the signal is more than 80 ppm downfield relative to that of the starting material) to the ring nitrogen atoms (where there is more than a 70 ppm upfield shift). These findings are further substantiated by the ^{1}H- and ^{13}C-NMR experiments. The two ^{15}N-NMR-spectroscopic shifts of both nitrogen sites in **3** and **4** differ by about 100 ppm and show a similar deviation of the signals as does the neutral system. Furthermore, in the ^{1}H- and the ^{13}C-NMR spectra of **4** the coupling of the related nuclei with the thallium nucleus are resolved ($^2J_{H-Tl}$ = 396.7, $^1J_{C-Tl}$ = 2574.7 Hz). There has no Tl−N coupling been detected. The coupling constants are in good agreement with separated linear dimethylthallium cations in solution.[21] Thus, the indium and the thallium compounds **3** and **4** are solvent-separated ion pairs in THF solution, while the aluminum and gallium complexes **1** and **2** are stable contact ion pairs, even in THF solution. To investi-

Table 1. δ ^{15}N-NMR-spectroscopic shift (THF/C_6D_6) of **1**−**4**

	Py_2NH	**1**	**2**	**3**	**4**
NC_5H_4	−107	−181	−182	−121	−117
N_{center}	−266	−184	−190	−230	−216

gate the nature of these complexes in the solid state, the crystal structures were determined.[22]

Crystal Structure of Me_2AlPy_2N (1) and Me_2GaPy_2N (2)

As in in the structures of Me_2AlPy_2CH,[8] Me_2GaPy_2CH,[8] Me_2AlPy_2P,[9] Me_2GaPy_2P[9] and Me_2AlPy_2As[9] **1** and **2** form monomers in the solid state (Figure 1). Despite the electronic competition between the deprotonated central nitrogen atom and the ring nitrogen atoms in **1** and **2** the metal center is chelated by the two ring nitrogen atoms without any contact with the central nitrogen atom (Figure 1). The anion shows *trans-trans* coordination (Scheme 4).

The Al−N distances of 191.5 pm in **1** are in good agreement with the literature values for aluminum amides,[23] but are about 15 pm shorter than the Al−N donor bonds to neutral 2,2′-bipyridyl[24a] or pyridine.[24b] The Al−C bond lengths (195.0 pm) are comparable with the distances in Me_3Al.[25] The N−Al−N angle (93.5°) is more acute than in the related bis(2-pyridyl)methyl derivative[8] (97.1°), and the aluminum atom is not in the plane of the ligand but is 28.3 pm out of the mean plane of the Py_2N^- ligand. These phenomena are due to the different "bite" of the amide ligand compared to that of the methyl ligand. The N···N distance (279.1 pm) is 7 pm shorter than in the bis(2-pyridyl)-methyl ligand. In contrast to the bis(2-pyridyl)methyl ligand the amide is not strictly planar, but the pyridyl rings are twisted by 10.4° with respect to each other. The basic structural parameters of the central nitrogen atom N1 (av. N−C 134.3 pm and C−N−C 125.5°) show that this atom is sp^2-hybridized. The expected C−N−C bond angle of 120° for an unstrained system is widened by the coordinated aluminum atom. Obviously, no electron density is accumulated at the central nitrogen atom.

The gallium atom in **2**, like the aluminum atom in **1**, is coordinated to the ring nitrogen atoms (Figure 1b). It is 32.1 pm out of the plane of the anion. The two pyridyl rings are twisted by 12.1°. The slightly longer Ga−N bonds of 197.5 (N2) and 196.9 (N3) pm reflect the decrease in the covalent contribution to the metal−nitrogen bonds from aluminum to gallium, but are in good agreement with the literature values for gallium amides.[23] The Ga−C distances (Ga1−C11 194.2 and Ga1−C12 195.6 pm) are similar to the distances found for Me_3Ga in the gas phase.[26]

Crystal Structure of 3

To study the change in coordination behavior of the bis(2-pyridyl)amide anion to larger and softer cations, the bis(2-pyridyl)amine was treated with 1 equiv. of freshly prepared Me_3In.[27] The dimethylindium bis(2-pyridyl)amide (**3**) forms a dimeric structure in the solid state (Figure 2).

Figure 1. Solid-state structure of Me_2AlPy_2N (**1**) (a) and Me_2GaPy_2N (**2**) (b); anisotropic displacement parameters are depicted at a probability level of 50%

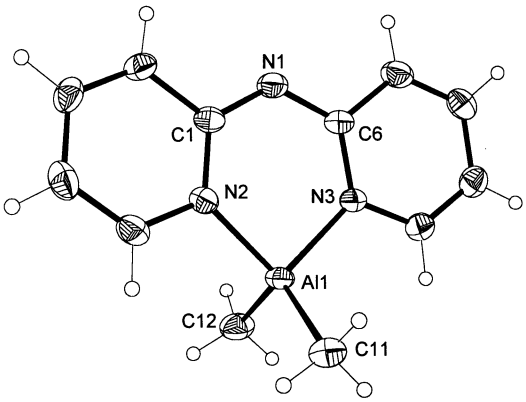

a

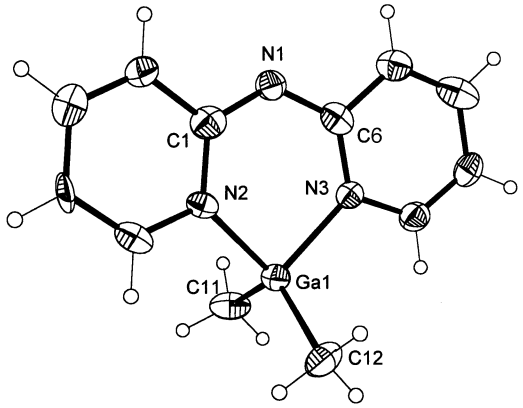

b

Figure 2. Solid-state structure of $[Me_2InNPy_2]_2$ (**3**); anisotropic displacement parameters are depicted at a probability level of 50%

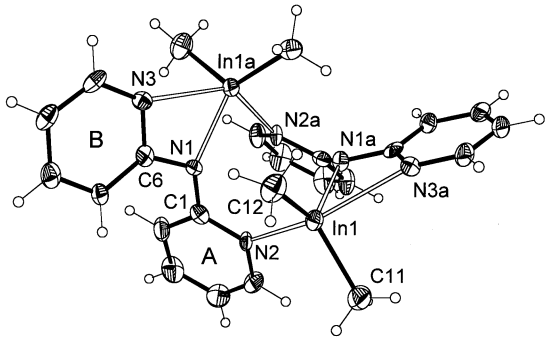

The dimer shows C_2 symmetry with the two-fold axis in the center of the molecule. The metal atom is coordinated by the pyridyl nitrogen atoms, but they are coordinated to different metal centers, providing the links in the dimer. Additionally each indium atom is coordinated by the depro-

tonated central nitrogen atom. All three nitrogen atoms of the ligand are pointing in the same direction, hence, the ligand coordinates in the *cis-cis* fashion (Scheme 4). The five atoms at each metal center form a distorted trigonal-bipyramidal coordination polyhedron. C11, C12, and N1A occupy the equatorial positions (sum of the angles 355.5°) while N2 and N3A reside in the axial positions (N2−In1−N3a 138.1°). The distance of the indium atom to the central nitrogen atom (220.4 pm) is considerably shorter than that to the ring nitrogen atoms (In1−N2 236.6 and In1−N3A 261.1 pm). These distances are found in $Me_3In \cdot$N-donorbase adducts like $Me_3In \cdot$tetramethylpiperidine (250.2 pm) and have to be regarded as dative bonds[28]. Only the In1−N1 distance is in good agreement with In−N bond lengths in indium amides (av. 223.3 pm in [Me_2InN-methylpiperazinyl]$_2$[29]). The indium−carbon distances (213.3 and 215.1 pm) are in good agreement with the literature values of trimethylindium adducts[28] and of dimethylindium complexes[29]. In **3** the distribution of the electron density must be notably different to that in the molecules of **1** and **2**. The anionic system is less planar than in **1** and **2**. The pyridyl rings are twisted by 58.3° with respect to each other to prevent full conjugation. The bond lengths of the central nitrogen atom differ (N1−C1 138.5 and N1−C6 135.9 pm) and are longer than in **1** and **2**.

Crystal Structure of 4

In the solid-state structures of **1**−**3** the tendency to greater isolation of the dimethylmetal cation moieties Me_2M^+, (M=Al, Ga, In) in the complexes can be ascertained. These phenomena should be even more pronounced in the dimethylthallium bis(2-pyridyl)amide complex. The dimethylthallium cation is known to be a very stable fragment that often forms separated linear cations.[21] To see whether this is valid with the dipyridyl amide ligand as well, we synthesized the thallium derivative **4** from freshly synthesized trimethylthallium[19] and bis(2-pyridyl)amine. **4** crystallizes as a polymer (Figure 3).

Figure 3. Solid-state structure of [Me_2TlNPy_2]$_\infty$ (**4**); anisotropic displacement parameters are depicted at a probability level of 50%

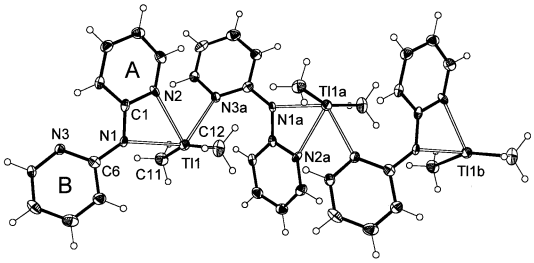

The helical polymer is made up by a crystallographic 2_1-screw axis. The thallium atoms are coordinated by the two methyl carbon atoms and three nitrogen atoms of the anionic ligand, but it seems arbitrary to assign any coordination polyhedron to the metal atom. It seems worth noting that in **4** the *cis-trans* arrangement (Scheme 4) of the bis(2-pyridyl)amide ligand is observed for the first time. The central, as well as one ring nitrogen atom (N1 and N2 in Figure 3), coordinate to the same metal center (Tl1), while the second ring (B in Figure 3) turns about the central N−C bond and coordinates to a second metal center (Tl1a) providing the polymeric link. The pyridyl rings are twisted by 38.2° with respect to each other to prevent full conjugation of the Py_2N^- anion. In contrast to **3** the shortest M−N distance is not found to be to the central nitrogen but to one ring nitrogen atom (Tl1−N2 248.1 pm). The other two are considerably longer (Tl1−N1 259.2; Tl2−N3a 268.9 pm). However, all three Tl−N contacts have to be regarded as weak donor bonds, since Tl−N bonds in thallium amides are normally shorter.[30] The Tl−C bonds are similar in length to those determined for the Me_2M^+ cations[21], but about 8 pm shorter than the shortest Tl−C contact in Me_3Tl.[31] The Me_2M^+ cation is almost linear (C11−Tl1−C12 158.3°), only bent slightly by the additional weak coordination of the three nitrogen atoms to the open side.

Structural Comparison

As mentioned above, the MMe_2 fragment in the complexes approaches linearity as the Group-13 metal gets heavier. The C−M−C angle widens from 116.9 (M = Al) to 120.8 (M = Ga), 126.1 (M = In) and finally to 158.3° (M = Tl). Hence the Me_2M^+ cationic character is most pronounced in the In and Tl complexes. The contacts to the Py_2N^- anion in the aggregates of **3** and **4** are only weak, while the hard metals, aluminum in **1** and gallium in **2**, induce metal amide bond lengths on the molecular level.

Table 2. Bond lengths [pm] of the Py_2N^- anion in **1**−**4** compared to the starting material

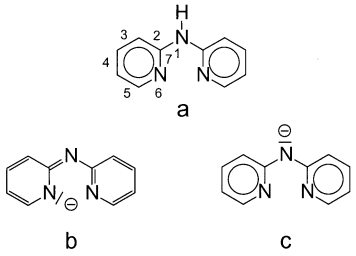

Compound	1	2	3	4	5	6	7
Py_2NH (a)	138.0	139.5	137.0	137.0	136.5	134.0	133.5
1 and **2**	134.5	141.7	136.0	139.4	135.6	136.3	136.4
3 A[a]	138.5	140.6	137.3	137.5	135.8	135.9	134.0
3 B[a]	135.9	140.4	137.2	137.9	136.9	134.1	136.1
4 A[a]	136.2	143.0	137.5	139.2	137.1	132.3	135.1
4 B[a]	134.8	140.6	133.7	140.3	135.8	134.5	137.1

[a] A and B refer to the ring labeling in Figures 2 and 3.

The bis(2-pyridyl)amide ligand itself reveals different coordination behavior toward small hard and large soft cations in solution and in the solid state. In the compounds with the hard aluminum and gallium cations the anion exclusively coordinates the metal centers through the two ring nitrogen atoms. This coordination mode has previously

been observed in aluminum and gallium complexes of the bis(2-pyridyl)methyl anion.[8] Coordination of the ring nitrogen atoms and the ^{15}N-NMR-specroscopic shift lead the negative charge in **1** and **2** to be accumulated at the ring hetero atoms. In **3** and **4** the NMR experiments in solution, and the coordination through the central nitrogen atom in the solid state, indicate an accumulation of negative charge at this position. This different electronic situation has to induce structural differences in the Py_2N^- anion. Close inspection of the solid-state structures should be decisive in determining whether the resonance form **b**, with the charge at the ring nitrogen atom and localized double bonds in the rings, or the mesomeric form **c**, with the charge at the central nitrogen atom and delocalized rings, contributes most to the description of the structures (Table 2).

All experiments prove that **b** is the form which contributes most for **1** and **2**. Unlike the neutral system[32] described in **a** the double bonds are localized in positions 1, 3, and 5. The bonds 6 and 7 of the pyridyl nitrogen atom are lengthened significantly, also indicating as well an accumulation of the negative charge on these nitrogen atoms. In **3** and **4** the bonding situation is more complex. The pyridyl rings are not coplanar and both are involved in a different coordination. The notation A and B refers to the two different rings in Figures 2 and 3, respectively. Ring A in **3** is similar to the delocalized rings of bis(2-pyridyl)amide. Ring B, however, exhibits significant deviations from the neutral molecule. The bond in position 1 is shortened by 2.1 pm, and that in position 7 is lengthened by 2.6 pm, relative to the amine. Coupling of the central nitrogen atom to ring B and the marginal shift of electron density from the original place of deprotonation to the pyridyl ring B are established in this structure. Both nitrogen atoms are members of the azaallyl system coordinated to the same indium atom to give an InN_2C four-membered ring. In **4** significant shift of electron density to ring B can be detected. The bond in position 1 is shortened by 3.2 pm and there is partial localization of double bonds in the positions 3 and 5. As a consequence the $Tl-N_{ring}$ bond is more than 11 pm shorter than the $Tl-N_{central}$ bond. The nitrogen atom of the delocalized ring A provides the longest metal donor bond (about 21 pm longer).

Conclusion

The bis(2-pyridyl)methyl and the bis(2-pyridyl)phosphide anions coordinate metal atoms exclusively through the nitrogen atoms within the pyridyl rings. Due to the electropositive bridgehead atoms these ligands behave like amides with the electron density accumulated at the ring nitrogen atoms. The bis(2-pyridyl)amides discussed here show a higher coordination flexibility towards metals. The electronic equivalence of the central and the ring nitrogen atoms leaves the energetic hyperface of the anion quite flat and the electron density is polarized according to the requirements of the metal. In the complexes with the hard metal aluminum (**1**) and gallium (**2**) the coordination is the same as that observed in the bis(2-pyridyl)methyl and -phosphide ligands. With the soft metals indium and thallium the system changes its coordination behavior to suit the larger, and easier to polarize, cations. In these complexes the deprotonated nitrogen atom participates in the coordination and the ligand forms a bridging group. In the indium complex **3** the *cis-cis* orientation gives rise to a dimeric structure, while the unprecedented *cis-trans* arrangement in the thallium compound **4** leads to a polymeric structure in the solid state. In the aluminum and the gallium complexes **1** and **2** the metal−nitrogen bond lengths are in good agreement with literature values for metal amides. In the indium and thallium complexes most metal−nitrogen distances are too long for metal amides, partly due to their higher aggregation. They approach separated Me_2M^+ and Py_2N^- residues, even in the solid state. In solution the Al and Ga complexes are close contact ion pairs while the In and Tl complexes dissolve as solvent-separated ion pairs. Hence, not only the steric requirements of N-heteroaromatic ligands have to be considered in molecular self-assembling processes, but also the inductive effect of different metal fragments (like in any complexation).

Funding was kindly provided by the *Deutsche Forschungsgemeinschaft*, the *Fonds der Chemischen Industrie*, and the *Stiftung Volkswagenwerk*. Support by *Bruker axs-Analytical X-Ray Systems*, Karlsruhe, is greatly acknowledged.

Experimental Section

All manipulations were performed under dry nitrogen with Schlenk techniques or in an argon drybox. Solvents were dried over Na/K alloy and distilled prior to use. NMR spectra were obtained with a Bruker MSL 400 or AM 250 instrument. All NMR spectra were recorded in C_6D_6 or [D_8]THF with $SiMe_4$ (^{1}H, ^{13}C), CH_3NO_2 (^{15}N) and $AlCl_3$ (^{27}Al) as external standards. EI mass spectra were measured with Finnigan MAT 8230 or Varian MAT CH 5 instruments.

1: 1.00 g (5.8 mmol) of $HN(2\text{-}NC_5H_4)_2$ in 25 ml of Et_2O was treated with an equimolar amount of Me_3Al (2.90 ml of a 2.0 M solution) at −10°C. Stirring for 12 h at room temp. gave a yellow solution with a little of a yellow precipitate. Addition of 5 ml of THF gave a clear solution. Crystallization from this solution at −35°C yielded crystals suitable for X-ray diffraction. Yield 0.78 g (80%), m.p. 146°C. − ^{1}H NMR ([D_8]THF, room temp.): δ = −0.66 (s, CH_3), 6.68 (ddd, $^3J_{5,4}$ 6.8 Hz, $^3J_{5,6}$ = 6.1 Hz, $^4J_{5,3}$ = 1.2 Hz, 5-H), 6.93 (ddd, $^3J_{3,4}$ = 8.8 Hz, $^4J_{3,5}$ = 1.2 Hz, $^5J_{3,6}$ = 0.9 Hz, 3-H), 7.54 (ddd, $^3J_{4,3}$ = 8.8 Hz, $^3J_{4,5}$ = 6.8 Hz, $^4J_{4,6}$ = 1.9 Hz, 4-H), 7.74 (ddd, $^3J_{6,5}$ = 6.1 Hz, $^4J_{6,4}$ = 1.9 Hz, $^5J_{6,3}$ = 0.9 Hz, 6-H). − ^{13}C NMR (THF/C_6D_6, room temp.): δ = −10.5 (s, CH_3), 112.9 (s, C-5), 124.8 (s, C-3), 139.2 (s, C-4), 140.5 (s, C-6), 158.6 (s, C-2). − ^{15}N NMR (THF/C_6D_6, room temp.): δ = −181.1 (s, NC_5H_4), −184.5 (s, N_{center}). − ^{27}Al NMR (THF/C_6D_6, room temp.): δ = 150. − MS (70 eV); *m/z* (%): 227 (14) [$Me_2Al(NC_5H_4)_2N$], 212 (100) [$MeAl(NC_5H_4)_2N$], 197 (10) [$Al(NC_5H_4)_2N$], 120 (10) [$Al(NC_5H_4)N$], 106 (14) [$Al(NC_5H_4)$].

2: 4.00 g (34.8 mmol) of Me_3Ga in 50 ml toluene was treated with 5.96 g (34.8 mmol) of $HN(2\text{-}NC_5H_4)_2$, dissolved in 20 ml of toluene, at −78°C. Stirring for 12 h at room temp. gave a yellow solution. Crystallization from this solution at −35°C for 3 d yielded crystals in the form of pale yellow needles suitable for X-ray diffraction. Yield 7.48 g (80%), m.p. 134°C. − ^{1}H NMR ([D_8]THF, room temp.): δ = −0.10 (s, CH_3), 5.97 (ddd, $^3J_{4,5}$ = 6.8 Hz, $^3J_{4,3}$ = 6.0 Hz, $^4J_{4,6}$ = 1.3 Hz, 4-H), 6.83 (ddd, $^3J_{5,6}$ = 8.8 Hz,

$^3J_{5,4}$ = 6.8 Hz, $^4J_{5,3}$ = 2.0 Hz, 5-H), 7.05 (ddd, $^3J_{3,4}$ = 6.0 Hz, $^4J_{3,5}$ = 2.0 Hz, $^5J_{3,6}$ = 0.8 Hz, 3-H), 7.09 (ddd, $^3J_{6,5}$ = 8.8 Hz, $^4J_{6,4}$ = 1.3 Hz, $^5J_{6,3}$ = 0.8 Hz, 6-H). – ^{13}C NMR (THF/C_6D_6, room temp.): δ = −7.5 (s, CH_3), 112.4 (s, C-5), 124.7 (s, C-3), 138.2 (s, C-4), 141.1 (s, C-6), 158.6 (s, C-2). – ^{15}N NMR (THF/C_6D_6, room temp.): δ = −181.5 (s, *N*C_5H_4), −189.8 (s, N_{center}). – MS (70 eV); *m/z* (%): 269 (14) [$Me_2Ga(NC_5H_4)_2N$], 254 (100) [$MeGa(NC_5H_4)_2N$], 238 (24) [$Ga(NC_5H_4)_2N$].

3: 1.80 g (11.3 mmol) of Me_3In in 10 ml of toluene was treated with 1.93 g (11.3 mmol) of HN(2-$NC_5H_4)_2$, dissolved in 10 ml of toluene at room temp. Stirring for 24 h at room temp. gave a colorless precipitate. Heating under reflux for 1 h gave a clear solution. Colorless needles crystallized upon cooling the solution slowly to room temp. These crystals were suitable for X-ray diffraction. Yield 3.10 g (89%), m.p. 208°C. – ^{1}H NMR (C_6D_6, room temp.): δ = 0.24 (s, CH_3), 6.11 (dd, $^3J_{5,4}$ = 7.2 Hz, $^3J_{5,6}$ = 5.0 Hz, 5-H), 6.68 (d, $^3J_{3,4}$ = 8.2 Hz, 3-H), 6.92 (dd, $^3J_{4,3}$ = 8.2 Hz, $^3J_{4,5}$ = 7.2 Hz, 4-H), 7.77 (d, $^3J_{6,5}$ = 5.0 Hz, 6-H). – ^{13}C NMR (C_6D_6, room temp.): δ = −5.3 (s, CH_3), 113.5 (s, C-5), 114.0 (s, C-3), 138.7 (s, C-4), 147.1 (s, C-6), 163.2 (s, C-2). – ^{15}N NMR (THF/C_6D_6, room temp.): δ = −120.7 (s, *N*C_5H_4), −230.2 (s, N_{center}). – MS (70 eV); *m/z* (%): 315 (20) [$Me_2InN(NC_5H_4)_2$], 300 (100) [$MeInN(NC_5H_4)_2$], 285 (68) [$InN(NC_5H_4)_2$], 170 (78) [$N(NC_5H_4)_2$], 145 (24) [Me_2In].

4: 2.00 g (5.5 mmol) of Me_2TlI in 30 ml of *n*-hexane was treated with 3.44 ml (5.5 mmol) of a 1.6 M solution of MeLi in Et_2O at room temp. After stirring for 2 h, a solution of 0.95 g (5.5 mmol) of HN(2-$NC_5H_4)_2$ in 20 ml of Et_2O was added. This reaction mixture was stirred for 24 h at room temp. The solvent was removed under vacuum and the precipitate was suspended in toluene and the LiI was removed by filtration. Colorless needles crystallized from the clear solution at room temp. These crystals were suitable for X-ray diffraction. Yield 1.12 g (50%), m.p. 179°C. – ^{1}H NMR (C_6D_6, room temp.): δ = 0.82 (d, $^2J_{Me-Tl}$ = 396.7 Hz, CH_3), 6.35 (ddd, $^3J_{5,4}$ = 7.0 Hz, $^3J_{5,6}$ = 5.1 Hz, $^4J_{5,3}$ = 1.0 Hz, 5-H), 7.10 (ddd, $^3J_{3,4}$ = 8.5 Hz, $^4J_{3,5}$ = 1.1 Hz, $^5J_{3,6}$ = 0.9 Hz, 3-H), 7.22 (ddd, $^3J_{4,3}$ = 8.5 Hz, $^3J_{4,5}$ = 7.0 Hz, $^4J_{4,6}$ = 2.0 Hz, 4-H), 8.06 (ddd, $^3J_{6,5}$ = 5.1 Hz, $^4J_{6,4}$ = 2.0 Hz, $^5J_{6,3}$ = 0.9 Hz, 6-H). – ^{13}C NMR (THF/C_6D_6, room temp.): δ = 8.7 (d, $^1J_{Me-Tl}$ = 2574.7 Hz, CH_3), 112.1 (s, C-5), 112.9 (s, C-3), 137.4 (s, C-4), 147.3 (s, C-6), 161.1 (s, C-2). – ^{15}N NMR (THF/C_6D_6, room temp.): δ = −117.3 (s, *N*C_5H_4), −215.8 (s, N_{center}). – MS (70 eV); *m/z* (%): 405 (26) [$Me_2TlN(NC_5H_4)_2$], 390 (36) [$MeTlN(NC_5H_4)_2$], 375 (90) [$TlN(NC_5H_4)_2$], 235 (18) [Me_2Tl], 205 (100) [Tl], 170 (20) [$N(NC_5H_4)_2$].

X-ray Measurements of **1**–**4**: All data were collected at low temperatures using an oil-coated shock-cooled crystal[33] on a Stoe-

Table 3. Selected bond lengths [pm] and angles [°] of **1**–**4**

1		**2**		**3**		**4**	
N1–C1	134.3(2)	N1–C1	133.9(13)	N1–C1	138.5(7)	N1–C1	136.2(9)
N1–C6	134.2(2)	N1–C6	135.4(12)	N1–C6	135.9(7)	N1–C6	134.8(10)
				In1–N1A	220.4(5)	Tl1–N1	259.2(7)
Al1–N2	191.6(2)	Ga1–N2	197.5(7)	In1–N2	236.6(5)	Tl1–N2	248.1(7)
Al1–N3	191.4(2)	Ga1–N3	196.9(7)	In1 N3A	261.1(5)	Tl1 N3A	268.9(6)
Al1–C(av)	195.0	Ga1–C(av)	194.9	In1–C (av)	214.2	Tl1–C (av)	213.4
C1–N1–C6	125.5(2)	C1–N1–C6	127.6(8)	C1–N1–C6	121.1(5)	C1–N1–C6	124.5(7)
C11–Al1–C12	116.9(1)	C11–Ga1–C12	120.8(4)	C11–In1–C12	126.1(3)	C11–Tl1–C12	158.3(4)

Table 4. Crystal data for **1**–**4** at 153 K

	1	**2**	**3**	**4**
Formula	$C_{12}H_{14}AlN_3$	$C_{12}H_{14}GaN_3$	$C_{12}H_{14}InN_3$	$C_{12}H_{14}TlN_3$
Mol. mass	227.2	270.0	315.1	404.6
Cryst. size [mm]	0.5 × 0.3 × 0.3	0.3 × 0.2 × 0.2	0.4 × 0.2 × 0.2	0.2 × 0.2 × 0.2
Space group	*Pbca*	*Pbca*	$P2_12_12$	$P2_12_12_1$
a [pm]	692.5(1)	692.5(1)	1633.7(3)	710.5(1)
b [pm]	1233.4(2)	1238.5(2)	789.3(2)	1099.7(2)
c [pm]	2779.9(4)	2775.0(6)	974.9(2)	1555.6(3)
V [nm^3]	2.374(1)	2.380(1)	1.257(1)	1.215(1)
Z	8	8	4	4
T [K]	153(2)	153(2)	153(2)	153(2)
ρ_c [Mgm^{-3}]	1.271	1.507	1.665	2.211
μ [mm^{-1}]	0.146	2.288	1.857	13.264
F(000)	960	1104	624	752
2Θ range [°]	8–50	8–45	8–45	8–55
No. of refln measd.	3749	3505	3045	1630
No. of unique reflns.	2103	1548	1654	1625
No. of restraints	28	0	0	0
Refined param.	181	147	147	147
$R1$[a] [$I > 2\sigma(I)$]	0.040	0.061	0.028	0.029
$wR2$[b] (all data)	0.115	0.183	0.066	0.071
$g1$; $g2$[c]	0.072; 0.423	0.075; 17.187	0.031; 0.010	0.045; 0.436
Flack *x* param.			−0.008(61)	0.003(22)
Highest diff peak (10^{-6} e pm^{-3})	0.25	0.89	0.76	0.72
Absorbt. corr.		semi-empirical	semi-empirical	semi-empirical
Trans. min; max		0.499; 0.993	0.562; 0.870	0.617; 1.000

[a] $R1 = \Sigma\|F_o| - |F_c\|/\Sigma|F_o|$. – [b] $wR2 = \{\Sigma[w(F_o^2 - F_c^2)^2]/\Sigma[w(F_o^2)^2]\}^{1/2}$. – [c] $w = 1/[\sigma^2(F_o^2) + (g1 \cdot P)^2 + g2 \cdot P]$; $P = (F_o^2 + 2F_c^2)/3$.

Siemens AED diffractometer with Mo-K_α (λ = 71.073 pm) radiation. A semiempirical absorption correction[34] was employed for structures **2**−**4**. The structures were solved by direct methods using SHELXS-90[35] and refined with all data on F^2 with a weighting scheme using SHELXL-93.[36] All non-hydrogen atoms were refined anisotropically. The hydrogen atoms of the molecules were geometrically idealized and refined using a riding model. Refinement of an inversion twin parameter[37] [x = −0.008(61) (**3**), 0.003(22) (**4**) where x = 0 for the correct absolute structure and +1 for the inverted structure] confirmed the absolute structures of **3** and **4**. Selected bond lengths and angles of **1**−**4** can be found in Table 3, relevant crystallographic data for **1**−**4** are presented in Table 4. Crystallographic data (excluding structure factors) for the structures reported in this paper have been deposited with the Cambridge Crystallographic Data Centre as supplementary publication no. CCDC-100792. Copies of the data can be obtained free of charge on application to CCDC, 12 Union Road, Cambridge CB2 1EZ, UK [fax: (internat.) + 44(1223)336-033; e-mail: deposit@ccdc.cam.ac.uk].

[1] [1a] A. R. Katritzky, J. M. Lagowski, *The Principles of Heterocyclic Chemistry*, Methuen, London, **1967**. – [1b] J. A. Joule, G. F. Smith, *Heterocyclic Chemistry*, Van Nostrand Reinhold, London, **1978**. – [1c] G. R. Newkome, W. W. Paudler, *Contemporary Heterocyclic Chemistry*, Wiley, New York, **1982**. – [1d] A. R. Katritzky, C. W. Rees, *Comprehensive Heterocyclic Chemistry*, Pergamon, Oxford, **1984**. – [1e] J. Reedijk, in *Comprehensive Coordination Chemistry* (Eds.: G. Wilkinson, R. D. Gillard, J. A. McCleverty), vol. 2, Pergamon, Oxford, **1987**, p. 73. – [1f] T. Eicher, S. Hauptmann, *Chemie der Heterocyclen*, Georg Thieme Verlag, Stuttgart, New York, **1994**. – [1g] A. Togni, L. M. Venanzi, *Angew. Chem.* **1994**, *106*, 517; *Angew. Chem. Int. Ed. Engl.* **1994**, *33*, 497. – [1h] D. T. Davies, *Aromatische Heterocyclen*, VCH, Weinheim, **1995**.

[2] [2a] F. Blau, *Ber. Dtsch. Chem. Ges.* **1888**, *84*, 85. – [2b] E. C. Constable, P. J. Steel, *Coord. Chem. Rev.* **1989**, *93*, 205. – [2c] P. J. Steel, *Coord. Chem. Rev.* **1990**, *106*, 227. – [2d] C. E. Kriley, P. E. Faucrick, I. P. Rothwell, *J. Am. Chem. Soc.* **1994**, *116*, 5225.

[3] [3a] J.-M. Lehn, *Science* **1985**, *227*, 849. – [3b] J.-M. Lehn, *Angew. Chem*. **1990**, *102*, 1347; *Angew. Chem. Int. Ed. Eng*. **1990**, *29*, 1304. – [3c] E. C. Constable, *Angew. Chem.* **1991**, *103*, 1482; *Angew. Chem. Int. Ed. Engl.* **1991**, *30*, 1450. – [3d] J.-M. Lehn, *J. Coord. Chem*. **1992**, *27*, 3. – [3e] E. C. Constable, M. J. Hannon, D. A. Tocher, *Angew. Chem.* **1992**, *104*, 218, *Angew. Chem. Int. Ed. Engl.* **1992**, *31*, 230. – [3f] E. C. Constable, A. J. Edwards, P. R. Raithby, J. V. Walker, *Angew. Chem.* **1993**, *105*, 1486; *Angew. Chem. Int. Ed. Engl.* **1993**, *32*, 1465. – [3g] A. Williams, *Chem. Eur. J.* **1997**, *3*, 15. – [3h] H. Plenio, *Angew. Chem.* **1997**, *109*, 358; *Angew. Chem. Int. Ed. Engl.* **1997**, *36*, 348.

[4] M. Fujita, D. Oguro, M. Miyazawa, H. Oka, K. Yamaguchi, K. Ogura, *Nature* **1995**, *378*, 469.

[5] [5a] H.-J. Schneider, H. Dürr, *Frontiers in Supramolecular Organic Chemistry and Photochemistry*, VCH, Weinheim, **1991**, 12. – [5b] A. Harriman, R. Ziessel, *J. Chem. Soc., Chem. Commun*. **1996**, 1707.

[6] For recent review: T. Kottke, D. Stalke, *Chem. Ber.* **1997**, 130, 1365.

[7] U. Pieper, D. Stalke, *Organometallics* **1993**, *12*, 1201.

[8] [8a] H. Gornitzka, D. Stalke, *Angew. Chem.* **1994**, *106*, 695; *Angew. Chem., Int. Ed. Engl.* **1994**, *33*, 693. – [8b] H. Gornitzka, D. Stalke, *Organometallics* **1994**, *13*, 4398.

[9] [9a] A. Steiner, D. Stalke, *J. Chem. Soc., Chem. Commun.* **1993**, 444. – [9b] A. Steiner, D. Stalke, *Organometallics* **1995**, *14*, 2422.

[10] [10a] A. Steiner, D. Stalke, *J. Chem. Soc., Chem. Commun.* **1993**, 1702. – [10b] A. Steiner, D. Stalke, *Inorg. Chem.* **1995**, *34*, 4846.

[11] D. S. Lawrence, T. Jiang, M. Levett, *Chem. Rev.* **1995**, *95*, 2229.

[12] G. S. Hanan, J.−M. Lehn, N. Kyritsakas, J. Fischer, *J. Chem. Soc., Chem. Commun.* **1995**, 765.

[13] [13a] N. Ray, S. Tyagi, B. Hathaway , *J. Chem. Soc., Dalton Trans.* **1982**, 143. – [13b] E. Spodine, A. M. Atria, R. Baggio, M. T. Garland, *Acta Crystallogr., Sect. C* **1996**, *52*, 1407. – [13c] E. A. Griffith, H.−Y. Li, E. L. Amma, *Inorg. Chim. Acta* **1988**, *148*, 203. – [13d] R. A. Howie, G. Izquierdo, G. P. McQuillian, *Inorg. Chim. Acta* **1983**, *72*, 165.

[14] [14a] O. R. Rodig, T. Brückner, B. K. Hurlburt, R. K. Schlatzer, T. L. Venable, E. Sinn, *J. Chem. Soc., Dalton Trans.* **1981**, 196. – [14b] J. F. Geldard, F. Lions, *J. Am. Chem. Soc.* **1962**, *84*, 2262. – [14c] H. C. Freeman, M. R. Snow, *Acta Crystallogr., Sect. C* **1965**, *18*, 843.

[15] B. S. Creavav, G. V. Gallagher, R. A. Howle, C. Long, G. P. Mcquillian, unpublished results, quoted as ref. [17] in ref.[14c].

[16] G. B. Deacon, S. J. Faulks, B. M. Gatehouse, A. Jozsa, J. *Inorg. Chim. Acta* **1977**, *21*, L1.

[17] P. Akhter, J. Hathaway, unpublished results, quoted as ref. [22] in ref.[14c].

[18] [18a] L.-P. Wu, P. Field, T. Morrissey, C. Murphy, P. Nagle, B. Hathaway, C. Simmons, P. Thornton, *J. Chem. Soc., Dalton Trans.* **1990**, 3835. – [18b] S. Aduldecha, B. Hathaway, *J. Chem. Soc., Dalton Trans.* **1991**, 993.

[19] H. Gilman, R. G. Jones, *J. Am. Chem. Soc.* **1946**, *68*, 517.

[20] [20a] C. Gatti, A. Ponti, A. Gamba, G. Pagani, *J. Am. Chem. Soc.* **1992**, *114*, 8634. – [20b] G. C. Levi, R. L. Lichter, *Nitrogen-15 Nuclear Magnetic Resonance Spectroscopy*, Wiley, New York, **1979**. – [20c] G. J. Martin, L. M. Maryvonne, J.-P. Gonesnard, ^{15}N-*NMR Spectroscopy*, Springer, Berlin, **1981**.

[21] [21a] G. D. Shier, R. S. Drago, *J. Organomet. Chem.* **1966**, *5*, 330. – [21b] A. G. Lee, "The Chemistry of Thallium" in *Topics in Inorganic and General Chemistry* (Ed.: P. L. Robinson), Elsevier, Amsterdam, **1971**.

[22] The structure-determining factors of the cations towards "carbanions" have been investigated by i. e.: C. Lambert, P. v. R. Schleyer, *Angew. Chem.* **1994**, *106*, 1187; *Angew. Chem. Int. Ed. Engl.* **1994**, *33*, 1129.

[23] [23a] K. M. Waggoner, P. P. Power, *J. Am. Chem. Soc.* **1991**, *113*, 3385. – [23b] M. Veith, A. Spaniol, J. Pöhlmann, F. Gross, V. Huch, *Chem. Ber.* **1993**, *126*, 2625.

[24] [24a] P. L. Bellavance, E. R. Corey, J. Y. Corey, G. W. Hey, *Inorg. Chem*. **1977**, *16*, 462. – [24b] P. Pullmann, K. Hensen, J.W. Bats, *Z. Naturforsch., B* **1982**, *37*, 1312.

[25] [25a] R. G. Vranka, E. L. Amma, *J. Am. Chem. Soc.* **1967**, *89*, 3121. – [25b] S. K. Byram, J. K. Fawcett, S. C. Nyburg, R. J. O′Brien, *J. Chem. Soc., Chem. Commun.* **1970**, 16. – [25c] J. C. Huffmann, W. E. Streib, *J. Chem. Soc., Chem. Commun.* **1971**, 911.

[26] B. Beagley, D. G. Schmidling, I. A. Steer, *J. Mol. Struct.* **1974**, *21*, 437.

[27] H. C. Clark, A. L. Pickard, *J. Organomet. Chem.* **1967**, *8*, 427.

[28] D. C. Bradley, H. Dawes, D. M. Frigo, M. B. Hursthouse, B. Hussain, *J. Organomet. Chem.* **1987**, *325*, 55.

[29] [29a] A. M. Arif, D. C. Bradley, H. Dawes, D. M. Frigo, M. B. Hursthouse, B. Hussain, *J. Chem. Soc., Dalton Trans.* **1987**, 2159. – [29b] M. A. Petrie, K. Ruhlandt-Senge, H. Hope, P. P. Power, *Bull. Soc. Chim. Fr.* **1993**, *130*, 851.

[30] [30a] K. W. Hellmann, L. H. Gade, A. Steiner, D. Stalke, F. Möller, *Angew. Chem*. **1997**, *109*, 99; *Angew. Chem. Int. Ed. Engl*. **1997**, *36*, 160. – [30b] K. W. Hellmann, L. H. Gade, R. Fleischer, D. Stalke, *J. Chem. Soc., Chem. Commun.* **1997**, 527. – [30c] K. W. Hellmann, L. H. Gade, R. Fleischer, T. Kottke, *Chem. Eur. J.* **1997**, *3*, 1801.

[31] G. M. Sheldrick, W. S. Sheldrick, *J. Chem. Soc*. **1970**, 128.

[32] [32a] J. E. Johnson, R. A. Jacobson, *Acta. Crystallogr., Sect. B* **1973**, *29*, 1669. – [32b] G. I. Pyrka, A. A. Pinkerton, *Acta. Crystallogr., Sect.C* **1992**, *48*, 91.

[33] [33a] T. Kottke, D. Stalke, *J. Appl. Crystallogr.* **1993**, *26*, 615. – [33b] T. Kottke; R. J. Lagow, D. Stalke, *J. Appl. Crystallogr.* **1996**, *29*, 465.

[34] A. C. T. North, D. C. Phillips, F. S. Mathews, *Acta Crystallogr., Sect. A* **1968**, *24*, 351.

[35] G. M. Sheldrick, *Acta Crystallogr., Sect. A* **1990**, *46*, 467.

[36] G. M. Sheldrick, *SHELXL-93, Program for Crystal Structure Refinement*, University of Göttingen, **1993**.

[37] [37a] H. D. Flack, *Acta Crystallogr., Sect. A* **1983**, 39, 876. – [37b] G. Bernardinelli, H. D. Flack, *Acta Crystallogr., Sect. A* **1985**, *41*, 500.

[97243]

Rigid Bidentate Nitrogen Ligands in Organometallic Chemistry and Homogeneous Catalysis, 14[◇]

Monodentate and Bridging Coordination of 3,3′-Annelated 2,2′-Bipyridines in Zerovalent Palladium- and Platinum-*p*-quinone Complexes

René A. Klein[a], Peter Witte[a], Ruud van Belzen[a], Jan Fraanje[b], Kees Goubitz[b], Milco Numan[b], Henk Schenk[b], Jan M. Ernsting[a], and Cornelis J. Elsevier*[a]

J. H. van′t Hoff Research Institute[a], Universiteit van Amsterdam,
Nieuwe Achtergracht 166, NL-1018 WV Amsterdam, The Netherlands
Fax: (internat.) +31(0)20/5256456
E-mail: else4@anorg.chem.uva.nl

Amsterdam Institute of Molecular Studies[b], Universiteit van Amsterdam,
Nieuwe Achtergracht 166, NL-1018 WV Amsterdam, The Netherlands

Received October 31, 1997

Keywords: Palladium / Platinum / Bidentate nitrogen ligands / *p*-Quinone / Alkenes

Compounds of the type M(N∩N-κ*N*)(nq)$_2$ and M$_2$(μ^2-N∩N)-(μ^2-pbq)$_2$, in which nq = 1,4-naphthoquinone, pbq = 1,4-benzoquinone, and N∩N is a monodentate or bridging ligand of the α-diimine type, were obtained from reactions of Pd(dba)$_2$ in toluene with the 3,3′-annelated-2,2′-bipyridines: 4,5-diazafluoren-9-one (dafo) and 4,5-diazafluorene (dafe) in the presence of the appropriate *p*-quinone. In the corresponding reactions with 2,2′-bipyridine (bpy), 1,10-phenanthroline (phen), 2,2′-bipyrimidine (bpym), *N*,*N*′-dicyclohexyl-1,4-diaza-1,3-butadiene (chex-dab), bis[*N*-(*o*,*o*′-diisopropyl)phenylimino]acenaphthene (*o*,*o*′-*i*Pr$_2$-bian) and 5,6-dihydro-1,10-phenanthroline (dh-phen) only complexes of the type M(N∩N-κ^2*N*)(Q) were formed (Q = nq, pbq). The structures of the complexes have been established by NMR in solution and by X-ray diffraction in the solid state; crystal structures of Pd(bpy-κ^2*N*)(η^2-pbq) (**1**) Pd(dafo-κ*N*)(η^2-nq)$_2$ (**14**) and Pd$_2$(μ^2-dafo)(μ^2,η^2:η^2-pbq)$_2$ (**16**) have been determined. Of the ligands, dafo and dafe are the only ones apt to form complexes containing a monodentate or bridging N∩N ligand. This behaviour is ascribed to the geometrical constraints of dafo and dafe; the annelation by one carbon atom at the 3,3′-positions in these ligands causes an increase in bite angle from approximately 77° to 82°.

Introduction

The chemistry of complexes containing an alkene coordinated to a low-valent metal from the platinum group has received considerable attention and studies have been particularly aimed at trigonal planar zerovalent platinum and nickel complexes of general formula ML$_2$(alkene) where L is a phosphane[1][2][3]. Zerovalent palladium complexes containing nitrogen ligands have received relatively little attention.[4][5][6] We have previously reported about compounds consisting of organopalladium or -platinum fragments (where the metal has the formal oxidation state II or IV) and a rigid bidentate nitrogen ligand (RBN), such as bis(*N*-arylimino)acenaphthene (Ar-bian)[7], bis(*N*-phenylimino)camphane (Ar-bic), bis(*N*-arylimino)phenanthrene (Ar-bip)[8], see Figure 1, as well as those containing zerovalent palladium and an electron-deficient alkene[6].

These and similar compounds are versatile catalysts in e.g., catalytic (multicomponent) C-C coupling reactions[9][10][11], in homogeneous catalyzed hydrogenation of alkenes[12] and as models for copolymerization and as active catalysts in polymerizations of alkenes[13][14]. The rigid bidentate ligands employed sofar by us have bite-angles of about 77°.

Figure 1. Rigid bidentate nitrogen ligands

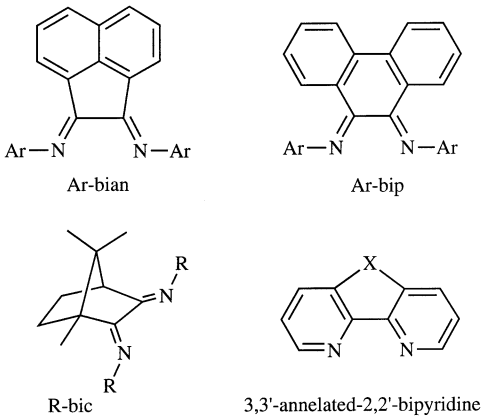

In many cases, bidentate ligands may dissociate one ligating atom (if only temporarily) during a reaction sequence, or undergo elongation of one of the metal-to-ligand bonds, as has been shown for an increasing number of cases, not only those involving hemi-labile ligands[15]. Monodentate coordination has e.g. been observed for phenanthrolines[16]

[◇] For part 13, see ref.[18], part 12, see ref.[11]. Netherlands Institute for Research in Catalysis (NIOK) publication uva 98-3-01.

 © WILEY-VCH Verlag GmbH, D-69451 Weinheim, 1998 1434−1948/98/0303−0319 $ 17.50+.50/0

and for an Ar-bian ligand in the case of an(η^3-allyl)Pd^{II} compound[17], but not for complexes of Pd^0. Despite these observations, there is a clear tendency of the Ar-bian and similar rigid ligands to remain bidentate coordinated to the metal centre, which is partly caused by the favourable bite-angle of about 77°.

It was anticipated that a slight increase of the bite-angle, while maintaining rigidity, would lead to reduced overlap between relevant metal and ligand orbitals and hence to an enhanced aptitude for dissociation of one of the donor atoms. To this end we have turned to members of the series of 3,3′-annelated-2,2′-bipyridines, for which the bite angle as well as the planarity of the ligand system varies with the number of methylene groups in the bridge[18] especially 4,5-diazafluoren-9-one (dafo)[19] and 4,5-diazafluorene (dafe)[20], see Figures 2 and 3.

Figure 2. Ligands and abbreviations

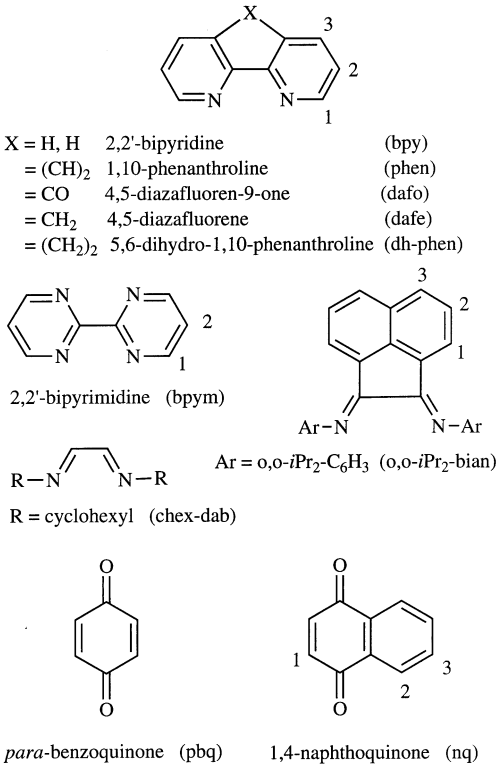

Figure 3. Decreasing orbital overlap between the metal atom (M = Pd, Pt) and a bidentate coordinating α-diimine ligand going from bipyridine (α = 77°) to dafo (X = CO) and dafe (X = CH2; β = 82°)

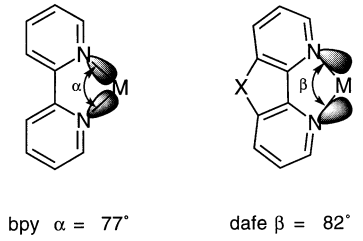

For dafo and dafe the bite-angle is 82°[18]. Consequently, one may expect that the altered lone-pair orientation on the nitrogen donor atoms of dafo and dafe, as illustrated in Figure 3, would facilitate the monodentate or bridging coordination mode for these ligands. In order to substantiate our expectations, we have decided to undertake a study of coordination compounds of zero-valent Pd and Pt containing the bidentate nitrogen ligands mentioned and suitable alkenes. For comparison, we employed a series of other rigid and flexible α-diimine ligands, such as 2,2′-bipyridine, 1,10-phenanthroline, 2,2′-bipyrimidine, 1,4-diaza-1,3-butadiene, and Ar-bian (Figure 2). In keeping with previous studies[21][22][23][24][25][26][27][28][29][30][31][32][33][34][35][36][37], stabilization of the zerovalent metal center by employing the strong π-acceptor *p*-quinone (Q) ligands *para*-benzoquinone (pbq) and 1,4-naphthoquinone (nq) was anticipated. Since *p*-quinones are potentially bidentate ligands, the ML_2Q complexes could be tetrahedral although it is well known that Pd^0 shows a tendency to be trigonal planar[38]. Furthermore because of the bisalkenic function of the *p*-quinones, it was foreseen that these might also support the formation of dinuclear complexes with bridging ligands[25][31][32][34].

In this paper the propensity of the 3,3′-annelated-2,2′-bipyridine ligands to stabilize compounds in which the bisnitrogen ligand coordinates in a monodentate way, i.e., $M(N\cap N\text{-}\kappa N)(\eta^2\text{-nq})_2$, or in which both the bisnitrogen ligand as well as *p*-benzoquinone are bridging between two metal centers, i.e., $M_2(\mu^2\text{-}N\cap N)(\mu^2,\eta^2\text{:}\eta^2\text{-pbq})_2$, is demonstrated. The structural and bonding features of these unique complexes have been elucidated, both in the solid state and in solution.

Results and Discussion

Synthesis of Zerovalent Palladium and Platinum Complexes (1−24)

At first, attempts were made to synthesize zerovalent Pd(N∩N)(alkene) complexes with electron poor alkenes such as dimethylfumarate, fumaronitrile or maleic anhydride. Unfortunately, for the bisnitrogen ligands, dafo, dafe or dh-phen (Figure 2), no isolable zerovalent palladium complexes could be obtained with any of these alkenes. However, employing the more electron-accepting *p*-quinones, relatively stable zerovalent palladium and platinum complexes have been obtained (Scheme 1).

Independent of the relative amount of starting materials, i.e. $Pd(dba)_2$, alkene and bidentate nitrogen ligand (Figure 2), zerovalent palladium complexes **1**−**11** with the general formula Pd(N∩N)(alkene) were formed [Scheme 1, type I; N∩N= bpy, phen, dh-phen, chex-DAB, *o,o′*-iPr_2-bian or bpym, and alkene = 1,4-benzoquinone (pbq) or 1,4-naphthoquinone (nq)]. Compounds **1**, **2**, **7**, and **8** have been reported previously[27]. The analytical data together with the crystal structure of Pd(bpy)(η^2-pbq) (**1**)[39] confirmed the 1:1:1 ratio of the metal, bisnitrogen ligand and *p*-quinone. These complexes are well soluble and stable in polar solvents such as chloroform, dichloromethane and tetrahydrofuran. Complexes containing bpym, *o,o′*-iPr_2-bian, cyclohexyl-DAB are even slightly soluble in ether and therefore they had to be synthesized in a slightly different way.

Scheme 1. Synthesis of zerovalent palladium and platinum complexes. bpy = 2,2′-bipyridine, phen = 1,10-phenanthroline, chex-dab = N,N′-dicyclohexyl-1,4-diaza- 1,3-butadiene, *o,o′*-*i*Pr2-bian = bis{*N*-(*o,o′*-diisopropyl)-phenylimino}acenaphthene, bpym = 2,2′-bipyrimidine, dafo = 4,5-diazafluoren-9-one), dafe = 4,5-diazafluorene, dh-phen = 5,6-dihydro-1,10-phenanthroline; pbq = 1,4-benzoquinone, nq = 1,4-naphthoquinone.

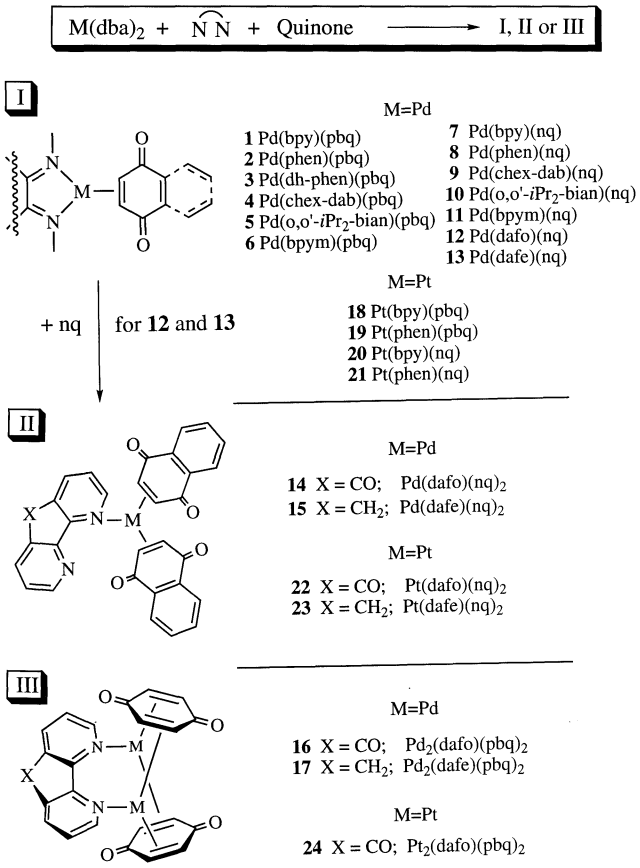

The Pd(N∩N-κ^2*N*)(*p*-quinone) complexes (**12**, **13**) were obtained using dafe or dafo and nq in a ratio 1:1:1 with respect to the starting material Pd(dba)$_2$. When using two equivalents of nq with respect to the starting material Pd(dba)$_2$ in the presence of dafo or dafe, the reaction resulted in complexes with the formula Pd(N∩N-κ*N*)(η^2-nq)$_2$ (**14**, **15**), as appeared from the ^{1}H NMR, analytical data, and an X-ray crystal structure for **14** (Scheme 1, type II). In these complexes a feature *uniquely* observed for these ligands occurs: dafo and dafe coordinate in a *monodentate* fashion and both nq ligands are η^2-coordinated. These complexes could also be prepared by adding one equivalent of nq to the complexes Pd(N∩N-κ^2*N*)(η^2-nq) (**12**, **13**) by substitution of one nitrogen atom. The compounds are soluble in polar solvents, but not very stable, decomposition takes place even at low temperatures.

When dafo or dafe was employed in combination with pbq, instead of nq, in attempts to synthesize zerovalent palladium complexes of the types mentioned above, yet another type of complex was obtained. Analytical and ^{1}H-NMR data revealed that, independent of the applied stoichiometry, always a complex of type Pd$_2$(μ^2-N∩N)(μ^2,η^2:η^2-pbq)$_2$ (**16**, **17**) was formed (Scheme 1, type III). Their molecular structure was confirmed by a single-crystal X-ray structure determination for **16** (vide infra). When using substoichiometric amounts of dafo or dafe and pbq with respect to the palladium metal, again complexes **16** and **17** were formed and part of the Pd(dba)$_2$ was recovered. The structure of a related dinuclear zerovalent palladium compound containing a bridging DAB moiety, [Pd(dmfu)$_2$]$_2$-μ-DAB, (DAB = *t*BuN=CH−CH=N*t*Bu), has been postulated but not isolated[40]. The complexes **16** and **17** are poorly soluble in polar solvents, in which slow decomposition takes place.

Several platinum analogues (**18**−**24**) could be synthesized in a similar way starting from Pt(dba)$_2$ (Scheme 1), albeit that, due to the slower substitution at platinum compared to palladium, distinctly longer reaction times were required.

p-Quinone Substitution Reactions

In order to determine (i) the relative thermodynamic stability of the various complexes and (ii) the coordination behaviour of the respective N∩N-ligands in these cases, several *p*-quinone exchange reactions were carried out. The 1,4-naphthoquinone (nq) in the complex of type Pd(N∩N-κ^{2}N)(nq) (**7**−**11**) can be readily substituted for *p*-benzoquinone (pbq), adding one equivalent of the latter to these complexes yielded the Pd(N∩N−κ^2*N*)(pbq) analogues (**1**, **2**, **4**−**6**). Interestingly, when adding one equivalent of pbq to Pd(N∩N-κ^2*N*)(η^2-nq) (**12**, **13**), the novel bridged compounds Pd$_2$(μ^2-N∩N)(μ^2,η^2:η^2-pbq)$_2$ (**16**, **17**) were formed with the concomitant release of one molecule of bidentate nitrogen ligand and nq, instead of Pd(N∩N-κ*N*)(η^2-nq)(η^2-pbq). Adding an excess of nq to the Pd(N∩N-κ^2*N*)(η^2-nq) complexes (**7**−**11**) did not result in substitution of a nitrogen donor in these complexes, which would have resulted in the formation of complexes similar to Pd(N∩N−κ*N*)(η^2-nq)$_2$ (**14**, **15**). The formation of the latter type of complex is thus an exclusive property of the dafo and dafe within this series of bidentate nitrogen ligands. Adding one equivalent of pbq to the complex Pd(N∩N-κN)(η^2-nq)$_2$ (**14**, **15**) did not yield the mixed *p*-quinone complexes either; complete conversion to Pd$_2$(μ^2-N∩N)(μ^2,η^2:η^2-pbq)$_2$ (**16**, **17**) took place. Adding substoichiometric quantities of pbq to Pd(N∩N−κN)(η^2-nq)$_2$ (**14**, **15**) yielded only a mixture of Pd$_2$(μ^2-N∩N)(μ^2-pbq)$_2$ (**16**, **17**) and Pd(N∩N-κN)(η^2-nq)$_2$ (**14**, **15**), no mixed *p*-quinone complexes were observed. Adding nq to any of the complexes containing pbq did not result in substitution, the starting compounds were recovered. Hence, the complexes containing pbq are thermodynamically more stable than the complexes containing nq, which order is consistent with the relative electron-accepting properties of the *p*-quinones[35][35][37].

Alkene Substitution Reaction

The mechanism of alkene substitution in zerovalent palladium and platinum complexes has been described either by dissociative [via 14e Pd(N∩N-κ^2*N*)] or associative [via Pd(N∩N-κ^2*N*)(alkene)$_2$] pathways[6][41][42][43][44]. Clearly,

Scheme 2. Possible mechanism of alkene substitution in which the complexes **14**, **15**, **22**, and **23** are representative for the Pd(N∩N-κ*N*)(alkene)$_2$ intermediate

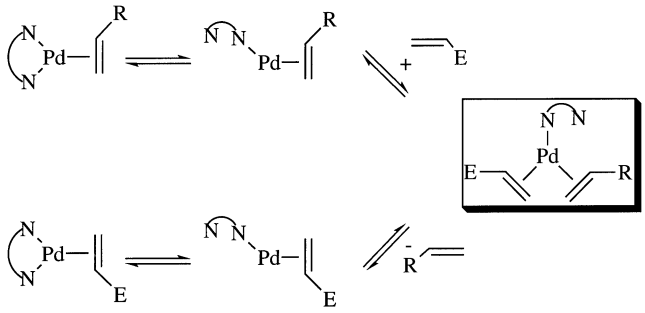

one of the donor atoms of the N∩N-ligand dafo or dafe can be non-coordinating, as has been unequivocally demonstrated by the isolation of the complexes **14**, **15**, **22**, and **23** and the X-ray crystal structure of **14**. These are 16-electron, Pd(N∩N-κ*N*)(η^2-alkene)$_2$ species. Hence, in addition to the mechanisms for alkene exchange mentioned above, the pathway as outlined in Scheme 2, in which dissociation of one of the N donor atoms of plays a key role, should be taken into account[45].

X-ray Crystal Structures of 1, 14, and 16

The molecular structures of **1, 14**, and **16** and the adopted numbering schemes are given in Figures 4−6. Selected bond distances and angles have been compiled in Tables 1 and 2. In all three complexes the palladium atom adopts a trigonal coordination geometry (taking the mid-point of the η^2-bond of the quinone as the point of attachment). In complex **1**, the palladium atom is bonded to two nitrogen atoms of the bpy ligand and one alkenic moiety of the *p*-quinone molecule. In complexes **14** and **16**, palladium is bonded to one nitrogen atom and to two alkenic moieties. In the latter complex, dafo bridges between two Pd^0 centers. In complexes **1** and **14** the *p*-quinone acts as a mono-, and in complex **16** as a bis-alkenic ligand.

The average Pd−N distances in **14** and **16** are comparable to those in several other Pd−α-diimine complexes, e.g. in PdCl(Me)(9,10-Me_2Phen)(ma)[46], PdCl(Me)(*o,o'*-*i*Pr_2-bian)[7], Pd(*o,o'*-*i*Pr_2-bian)(ma)[6] and in Pd(bpy)(dba)[47], but in **1** it is significantly shorter and similar to Pd(*p*-Tolbian)(ma)[48]. The average Pd−C distances are shorter than those in most other Pd(N∩N)(η^2-alkene) complexes, i.e. in PdCl(Me)(9,10-Me_2Phen)(ma)[46], Pd(bpy)(dba)[47], $Pd(dba)_3$[49], $Pd_2(dba)_3\cdot CH_2Cl_2$[50], $Pd_2(dba)_3\cdot CHCl_3$[27], and $Pd(Cy_2PCH_2CH_2PCy_2)(\eta^2\text{-}CH_2{=}CH{-}CH{=}CH_2)$[51]. Complexes **1** and **14** display a slight distortion from the trigonal planar situation, as reflected by the twist around the metal-alken bond of 9.49(0.46)° for complex **1** and 9.84(0.13) and 5.99(0.13)° for complex **14**. Such a "tetrahedral" distortion is a known phenomenon in d^{10} metal-alkene complexes[1c]. The plane of best fit through the *p*-quinone residues and the coordination plane intersect at 78.57(0.49)° for **1** and at 94.29(0.23) and 99.91(0.21)° for **14**, indicating that the metal-alkene bond is approximately perpendicular to the plane of the *p*-quinone. The perpendicular coordination of the pbq moiety is depicted in Figure 4b by a side-on view of the coordination plane of **1**.

Figure 4a. Ortep drawing (30% probability level) of **1**

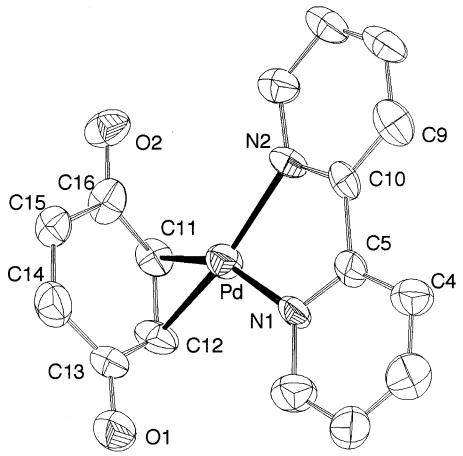

Figure 4b. Molecular plot of **1** viewed through the coordination plane

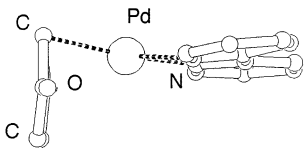

Table 1. Selected (bond) distances [Å] for the complexes **1**, **14**, and **16** (e.s.d.'s in parentheses)

Pd(bpy)(pbq) (**1**)		Pd(dafo)(nq)$_2$ (**14**)		Pd_2(dafo)(pbq)$_2$ (**16**)	
				Pd(1)−Pd(2)	2.7747(4)
Pd−N(1)	2.121(12)	Pd(1)−N(1A)	2.1646(6)	Pd(1)−N(1)	2.166(4)
Pd−N(2)	2.101(11)	Pd(1)−N(2A)	3.070(5)	Pd(2)−N(2)	2.191(3)
Pd−C(11)	2.162(17)	Pd(1)−C(12A)	2.1764(7)	Pd(1)−C(12)	2.153(4)
Pd−C(12)	2.167(13)	Pd(1)−C(21A)	2.1558(7)	Pd(1)−C(13)	2.197(4)
O(1)−C(13)	1.27(2)	O(2A)−C(20A)	1.2137(9)	O(2)−C(14)	1.221(5)
O(2)−C(16)	1.255(19)	O(3A)−C(13A)	1.2188(10)	O(3)−C(20)	1.223(4)
N(1)−C(5)	1.340(17)	N(1A)−C(11A)	1.3286(10)	N(1)−C(5)	1.330(5)
N(2)−C(10)	1.299(19)	N(2A)−C(10A)	1.3188(10)	N(2)−C(10)	1.337(5)
C(5)−C(10)	1.53(2)	C(10A)−C(11A)	1.4709(11)	C(5)−C(10)	1.502(5)
C(11)−C(12)	1.43(2)	C(22A)−C(31A)	1.4293(13)	C(12)−C(13)	1.390(7)
C(14)−C(15)	1.38(2)	C(12A)−C(21A)	1.3937(11)	C(15)−C(16)	1.387(7)

Table 2. Selected bond angles [°] for the complexes **1**, **14**, and **16** (e.s.d.'s in parentheses)

Pd(bpy)(pbq) (**1**)		Pd(dafo)$(nq)_2$ (**14**)		Pd_2(dafo)$(pbq)_2$ (**16**)	
N(1)−Pd−N(2)	77.0(4)				
		N(1A)−Pd(1)−C(21A)	92.11(3)	N(1)−Pd(1)−C(12)	89.16(15)
		N(1A)−Pd(1)−C(31A)	95.46(3)	N(1)−Pd(1)−C(18)	97.13(13)
C(11)−Pd−C(12)	38.4(5)	C(12A)−Pd(1)−C(21A)	37.53(3)	C(15)−Pd(2)−C(16)	37.48(17)
		C(22A)−Pd(1)−C(31A)	38.54(3)	C(21)−Pd(2)−C(22)	37.33(14)
N(1)−Pd−C(12)	123.4(4)				
N(1)−C(5)−C(10)	115.6(12)	N(1A)−C(11A)−C(10A)	126.88(7)	N(1)−C(5)−C(10)	130.6(3)
N(2)−C(10)−C(5)	113.3(13)	N(2A)−C(10A)−C(11A)	126.36(7)	N(2)−C(10)−C(5)	130.3(3)
		C(12A)−Pd(1)−C(22A)	96.28(3)	C(13)−Pd(1)−C(19)	98.74(16)

The alkenic and the carbonyl bonds in the *p*-quinone molecules in each of the three complexes are longer than in the free *p*-quinones[52], but the elongation of the coordinated C=C bond in **14** and **16** is less than in complex **1**, in which there are two nitrogen donor atoms instead of one. The carbonyl groups are bent away from the plane through the alkenic carbon atoms by 5.17(1.59) and 6.93(1.47)° for **1**, by 1.89(0.71), 0.43(0.42), 9.43(0.86), and 5.04 (0.83)° for **14**, and by 5.82(0.41), 0.74(0.41), 10.68(0.41), and 12.88(0.40)° for **16**.

Figure 5. Ortep drawing (30% probability level) of **14**

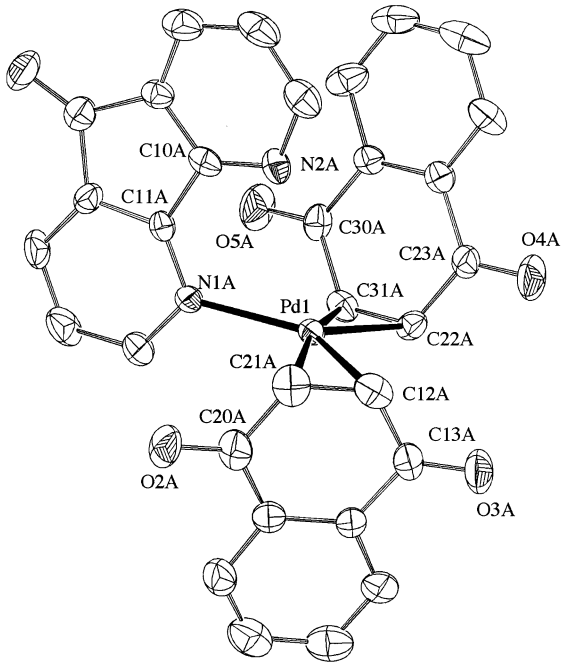

These angular distortions as well as elongations of the C=O double bonds in the *p*-quinone residue are comparable to those in $Pt(PPh_3)_2$(pbq)[30] and is also present in each of the previously reported structures with nickel−[53] and cobalt−*p*-quinone complexes[54]. In the case of **16**, the relatively large angular distortion of the carbonyl carbon atoms (vide supra) is mainly due to a steric interaction between the carbonyl groups of the two coordinated pbq moieties as is revealed by the view along the palladium palladium axis (Figure 6b). The distortion in the nitrogen ligands depends on the type of complex. Since dafo is monodentate coordinated in **14**, it shows no significant changes in bond angles and distances upon coordination compared with the free ligand[55]. However, in **16** the nitrogen ligand is distorted due to bridging coordination to two metal centers. The palladium atoms are not in the plane of the ligand; one palladium is positioned above and the other below the plane defined by N(1)C(5)C(10)N(2). The Pd(1)−Pd(2) vector intersects this plane by 7.72(0.35)°. This feature is nicely demonstrated in Figure 6c. The N(1)C(5)C(10) angle is 130.0° (free ligand 127.5°)[55] and the torsion angle N(1)C(5)C(10)N(2) is 11.3° (free ligand 0.0°). In complex **1**, due to the tetrahedral distortion, a torsion angle in the contiguous atoms N(1)C(5)C(10)N(2) of 7.43° is observed. The imine bonds in **1** and **16** are slightly elongated upon coordination in comparison with the free ligands.

Figure 6a. Ortep drawing (30% probability level) of **16**

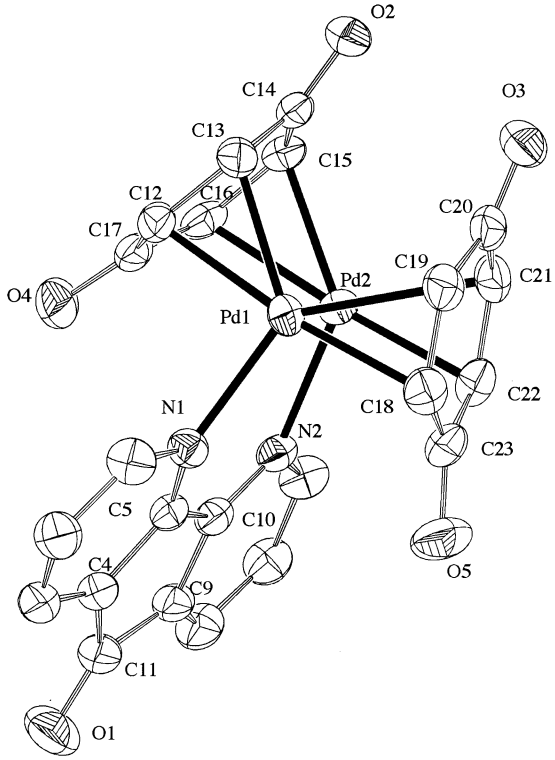

The structure of the Pd(dafo)$(nq)_2$ complex (**14**) is unique, no similar complexes are known. An interesting feature of **14** is the non-bonding Pd(1A)−N(2A) distance of

Figure 6b. Plot of **16** viewed along the Pd(1)−Pd(2) axis

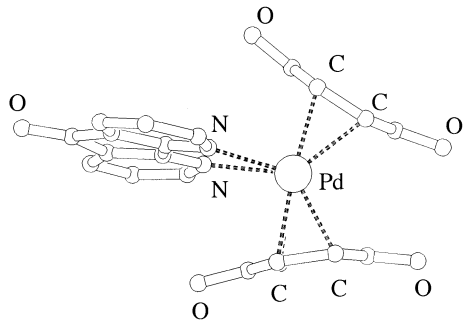

Figure 6c. Plot of **16** viewed through the Pd(1)−N(1)−N(2)−Pd(2) plane

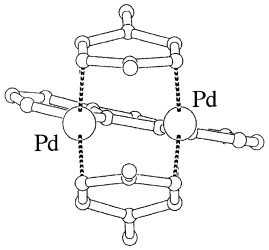

3.070(5) Å, which is too long for any significant bonding interaction between these two atoms. This non-bonding Pd−N distance is longer than the similar Pt−N distance in $PtCl_2(Me_2\text{-phen})(PPh_3)_2$ [2.673(6) Å][56]. The N(2A) atom is approaching an apical position at palladium and does not intermolecularly coordinate towards another palladium. There is no tendency for **14** to form a dimeric palladium complex such as **16**, which is probably due to the steric bulk of the *p*-naphthoquinone compared to *p*-benzoquinone.

The solid-state structure of complex **16** is unprecedented but resembles that of $Pd_2(dba)_3$[50], however, in the latter the two palladium centers are bridged by three dienes instead of two as in **16**. The Pd(1)−Pd(2) distance in complex **16** [2.7747(4) Å] is significantly shorter than in $Pd_2(dba)_3\cdot CHCl_3$ [3.245(2) Å][27] and $Pd_2(dba)_3\cdot CH_2Cl_2$ [3.237(5) Å][50]. The short Pd-Pd distance in **16** is due to the smaller span and conformational restriction of the dafo ligand as compared to dba and is close to a Pd^I-Pd^I bond, which usually range from 2.53 to 2.75 Å[57][58][59][60][61][62].

IR Spectroscopy

The infrared spectra of the complexes all show a bathochromic shift of the stretching frequency ν(C=O) of the *p*-quinones as compared to the free *p*-quinone[63], the magnitude of which depends on the type of complex. In the M(N∩N-κ*N*)(η^2-nq)$_2$ complexes, ν(C=O) is only slightly shifted ($\Delta\nu$ = 5 cm^{-1}), wheras in the type $M_2(\mu^2$-N∩N)(μ^2,η^2:η^2-pbq)$_2$ this shift is approximately 30 cm^{-1} and in the type M(N∩N-κ^2*N*)(η^2-Q) it amounts to $\Delta\nu$ = 60 cm^{-1}. The latter shift is larger than for comparable structures reported, $\Delta\nu$(CO) = 44, 25, and 18 cm^{-1} in $PdL_2(\eta^2$-pbq) for L = *n*Bu_3P, Ph_3P, and PhO_3P, respectively[24] and 43 and 47 cm^{-1} in Pd(COD)(η^2-Q) for Q = pbq and nq, respectively[30]. In structures of the type $Pt(PPh_3)_2(\eta^2$-Q) in which the *p*-quinone represents a series of substituted derivatives[30], this shift is usually 30−60 cm^{-1}. These low-frequency shifts underscore the importance of the back donation from palladium to the *p*-quinone and is an indicative tool to determine the type of complex obtained, as ν(C=O) decreases with an increasing number of nitrogen donor atoms coordinated to the palladium relative to thenumber of *p*-quinone double bonds. The relative small shifts reported for complexes **1**−**24** indicate only a relatively minor perturbation of the C=O stretching mode, hence coordination is apparently only through the double bonds of the *p*-quinone moiety, as has been confirmed by the X-ray crystal structures determined for **1**, **14**, and **16**. For compounds in which the C=O function participates in the bonding, ν(C=O) decreases much more (150−200 cm^{-1})[22].

NMR Spectroscopy

The ^{1}H- and ^{13}C-NMR data for the complexes **1**−**24** show the expected high-frequency shift for the protons of the nitrogen ligands upon coordination. Compared to the free *p*-quinones[64], the alkenic protons of the coordinated *p*-quinone show a shift of 0.96−1.75 ppm to lower frequency, which is comparable to the shift for complexes Pd(COD)(η^2-pbq) ($\Delta\delta$ = 1.03 ppm) and Pd(COD)(η^2-nq) ($\Delta\delta$ = 1.94 ppm)[30]. However, these shifts are considerably smaller than the shifts reported for the complexes of the type M(L)$_2$(η^2-alkene) (M = Pd, Pt, alkene = dmfu, ma, fn) where they amount to 3−3.5 ppm[6]. The alkenic carbon atoms show for the complexes of the type Pd(N∩N-κ^2*N*)(η^2-Q) a shift of ca. 30 ppm to lower frequency in their ^{13}C-NMR spectra, and of ca. 60 ppm for the complexes of the type M(N∩N-κ*N*)(η^2-nq)$_2$ and $Pd_2(\mu^2$-N∩N)(μ^2,η^2:η^2-pbq)$_2$, in keeping with the considerable amount of back-donation from palladium to the *p*-quinone caused by the combination of an electron rich d^{10} metal center with a σ-donating α-diimine ligand. The low frequency shifts of the alkenic protons in the analogous platinum complexes are more pronounced than in the palladium complexes, which is due to the higher Lewis basicity of platinum.

The ^{1}H-NMR spectra of the complexes Pt(N∩N-κ^2*N*)(η^2-pbq), **18** and **19** show fluxional behaviour; at ambient temperature and 300.13 MHz the protons assigned to the pbq appear as a slightly broadened singlet (the platinum satellites are not observed) which broadens upon lowering the temperature. At 213 K two broadened singlets belonging to the pbq ligand are present. We ascribe this feature to a degenerate rearrangement in which the Pt(N∩N-κ^2*N*) moiety is alternatingly η^2-bonded to either of the two equivalent alkenic sites of *p*-benzoquinone. The free energy of activation ($\Delta G^{\neq}$) for this process was calculated[65] to be 50.3±1.0 kJmol^{-1} (241 K) for **18** and 52.1±1.0 kJmol^{-1} (238 K) for **19**. The slow exchange regime could be reached, in contrast to the observation for Pt(COD)(η^2-pbq) in which it could not be reached even at 183 K[25]. For **1**−**6**, the palladium analogues of **18** and **19**, slow exchange could not be reached at 180 K (300.13 MHz), only a slight broad-

ening of the pbq-signal is observed. The ^{1}H-NMR data of the Pd(N∩N-κ^2*N*)(pbq) complexes (**1**−**6**) imply for the complexes in solution, either a rigid structure with the pbq η^4-bonded to the metal, or a low-energy degenerate rearrangement of a ground state η^2-bonded ligand. In view of the other results in solution and solid state, we prefer to assume the latter. For the platinum complexes it has been proven that in solution the latter assumption is true while clearly the rearrangement is in slow exchange at 213 K. Evidently, the rearrangement proceeds on the NMR time scale via an *intra*molecular process, since variation of the concentration had no effect on the free energy of activation of this rearrangement.

The complexes containing bpym, **6** and **11**, show dynamic behaviour resembling a previously described internal rotation of the two rings in bpym relative to each other in Pd(bpym)(η^3-allyl) compounds[66]. The exchange requires a cleavage of a Pd−N bond, i.e. a mechanism is involved in which two-coordinate intermediate complexes[67] exist in which the bidentate nitrogen ligand is coordinated in a monodentate way. The observed free energies of activation for this internal rotation are similar to those reported[66], $\Delta G^{\neq}$ = 53.7±1.0 kJmol^{-1} (243 K) for **6** and $\Delta G^{\neq}$ = 52.1±1.0 kJmol^{-1} (251 K) for **11**.

In complexes Pd(N∩N-κ*N*)(η^2-nq)$_2$ (**14**, **15**), both halves of the nitrogen ligand, which coordinates in a monodentate way, show identical chemical shifts in the ^{1}H- as well as in the ^{13}C-NMR spectra down to 160 K. We assign this behaviour to fast exchange between alternatingly coordinating N atoms of the ligand towards the palladium atom, representing a ligand flipping process analogous to that described by Natile[56]. These authors observed that, for Pt(2,9-dimethyl-1,10-phen)(PPh_3)Cl_2, in which the phenanthroline ligand coordinates in a monodentate way, the ligand flipping could be stopped at 150 K and splitting of the ligand signals is observed. The alternative, which is in agreement with the ^{1}H-NMR spectra, is the existence of the complexes **14** and **15** as tetrahedral 18e complexes in which the nitrogen ligand coordinates in a bidentate mode. However, in view of the solid state structure of **14** and the exchange experiments with *p*-quinones, which showed that complexes of type Pd(N∩Nκ^2*N*)(η^2-nq)$_2$ could be obtained for dafo and dafe ligands, but *not* in the cases utilizing bpy, phen etc., we reject this possibility. Adopting the view that the structure in solution is the same as the one in the solid state, i.e. a 16e complex with monodentate coordinating nitrogen ligand, the observations are easily explained on the basis of the different geometrical constraints of dafo and dafe (i.e. the larger bite angle) as compared to bpy and phen (see the introduction). In the case of **14**, and **15**, concomitantly with the ligand flipping another dynamic process takes place, as witnessed by a broadened singlet for the nq signals, indicating that the *p*-quinones are rotating. For this process, the slow exchange limit could not be reached (170 K at 300 MHz).

A peculiar dependence of the ^{1}H-NMR spectra of the complexes $Pt_2(\mu^2$-dafo)$(\mu^2,\eta^2{:}\eta^2$-pbq)$_2$ (**24**), $Pd_2(\mu^2$-dafo)$(\mu^2,\eta^2{:}\eta^2$-pbq)$_2$ (**16**) and $Pd_2(\mu^2$-dafe)$(\mu^2,\eta^2{:}\eta^2$-pbq)$_2$ (**17**) on the temperature has been observed. In the ^{1}H-NMR spectrum of the Pt compound **24**, the protons of pbq appear at 300.13 MHz as an A_2B_2 pattern with Δν(A−B) = 177 Hz, *J*(Pt,H) = 87.7 and 29.7 Hz. Cooling down the sample in $CDCl_3$ to 218 K showed a temperature dependence of the shifts for A and B as Δν(A−B) decreased by 30 Hz. The protons of pbq in the $Pd_2(\mu^2$-N∩N$)(\mu^2$-pbq$)_2$ complexes appear, in agreement with the solid state structure, at 293 K as an AA′BB′ pattern as is shown by the bottom spectrum in Figure 7. Simulation of the spectra (300.13 MHz) showed that for **16** Δν(A−B) = 9 Hz and the coupling constants are 8.3, 2.2, and 0.2 Hz. For **17** these values are Δν = 27 Hz and *J* = 8.2, 2.1, and 0.2 Hz. When cooling the sample to 253 K, the signal reverts into a singlet, upon further cooling to 213 K the pbq signal appears again as an AA′BB′ pattern albeit rather broadened (top spectrum, Figure 7; the latter broadening is probably due to the viscosity of the solvent at this temperature). We ascribe this process, on the basis of the observations made for the analogous platinum complex **24**, vide supra, to a temperature dependence of the chemical shift of the protons involved.

Figure 7. Variable-temperature ^{1}H-NMR of CH protons of pbq in **16**

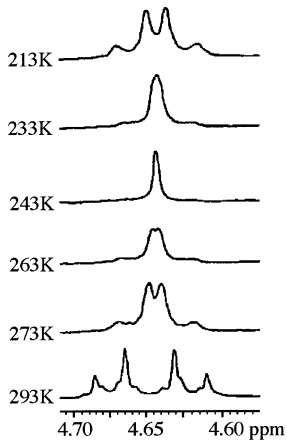

Conclusion

A remarkable difference in coordination behaviour is observed between bidentate nitrogen ligands dafo and dafe and the other nitrogen ligands used in this study. In the case of dafo and dafe, exceptional Pd(N∩N-κ*N*)(η^2-nq)$_2$ and $Pd_2(\mu^2$-N∩N$)(\mu^2,\eta^2{:}\eta^2$-pbq$)_2$ complexes are formed. The monodenate or bridging coordination of the N∩N ligand in these instances is mainly a consequence of the annelation on the 3,3′-position of 2,2′-bipyridine by one carbon atom, by virtue of which the bite-angle of the ligands dafo and dafe is slightly but significantly larger compared to those of 2,2′-bipyridyl, phenanthroline, Ar-bian, and open-chain diazabutadienes. The stoichiometry in the Pd_x(N∩N)$(Q)_2$ complexes where N∩N = dafo or dafe depends on the nature of the *p*-quinone.

We thank the *Organization for the Advancement of Pure Research* (SON/NWO) and the *Stichting John van Geuns Fonds* for financial support for obtaining NMR instruments.

Experimental Section

General: All experiments were carried out using standard Schlenk techniques, under an atmosphere of dry nitrogen. The solvents were dried according to standard procedures and distilled before use. − ^{1}H- and ^{13}C-NMR spectra were recorded on a Bruker AMX 300 NMR spectrometer at 300.13 and 75.48 MHz, respectively. Chemical shift values are in ppm relative to TMS as external standard with high frequency shifts signed positive (protons are numbered according to Figure 2). Abbreviations used are s = singlet, d = doublet, t = triplet, pst = pseudo triplet, q = quartet, sep = septet, m = multiplet, br = broad; multiplicity, coupling constants (Hz) and number of protons in parenthesis. − IR spectra (KBr) were recorded on a Biorad FTS-7 IR spectrometer; abbreviations used: s = strong, m = medium, w = weak, br = broad, sh = shoulder. − Elemental analysis were carried out by Dornis and Kolbe, Mikroanalytisches Laboratorium, Mülheim a.d. Ruhr, Germany. − Mass spectra (FAB) were recorded by the Institute of Mass spectroscopy of the University of Amsterdam. − Dibenzylideneacetone (dba)[68], $Pd(dba)_2$[69], $Pt(dba)_2$[70], 4,5-diazafluoren-9-one (dafo)[19], 4,5-diazafluorene (dafe)[20], 5,6-dihydro-1,10-phenanthroline (dh-phen)[20], *N,N′*-dicyclohexyl-1,4-diaza-1,3-butadiene (chex-dab)[71][72] and bis[*N*-(*o,o′*-diisopropyl)phenylimino]-acenaphthene (*o,o′*-*i*Pr2-bian)[7] were synthesized according to published procedures. The *p*-quinones (Q) 1,4-benzoquinone (pbq) and 1,4-naphthoquinone (nq) and the *N*-ligands 2,2′-bipyridine (bpy), 2,2′-bipyrimidine (bpym), and 1,10-phenanthroline (phen) are commercially available and were used as received. Compounds **1**[39], **2**, **7** and **8** are known[27].

Synthesis of Palladium Complexes Pd(N∩N)(Q) (**1**−**3**, **7**, **8**, **12**, **13**): A typical procedure for the synthesis of [*(2,3-η)-1,4-benzoquinone](2,2′-bipyridine-k²N,N′)palladium(0)* (**1**), is given. $Pd(dba)_2$ (124.3 mg = 0.22 mmol), bpy (35.8 mg = 0.23 mmol), and pbq (26.8 mg = 0.25 mmol) were dissolved in toluene (60 ml) and stirred for thirty minutes at 20°C. The colour of the solution changed from dark purple to yellow and a dark compound precipitated. A solid was separated, which was dissolved in dichloromethane (50 ml) and this solution was filtered through Celite to remove metallic palladium. The solution was concentrated to ca. 5 ml and the product was precipitated with hexane (30 ml). The precipitate was filtered off and washed twice with toluene (30 ml), twice with ether (30 ml), and with hexane (30 ml) and dried under vacuum which gave a red brown solid (85%). The analogous complexes were synthesized in a similar way. The yields ranged from 84 to 93%. Dark red crystals of suitable for an X-ray crystal structure determination were obtained by slow diffusion of hexane in a solution of **1** in dichloromethane at 4°C.

(2,2′-Bipyridine-k²N,N′)[(2,3-η)-1,4-Benzoquinone]-palladium(0) (**1**): ^{1}H NMR ($CDCl_3$, 293 K): 8.55 (d, 4.7, H1), 8.09 [d, 7.9, H(X)], 8.01 (dd, 7.9, 7.9, H2), 7.53 (dd, 7.9, 4.7, H3), 5.71 [s, H(pbq)]. − ^{13}C NMR ($CDCl_3$, 213 K): 178.3 (s, *C*=O), 153.8 (s), 150.7 (d), 140.1 (d), 127.7 (s), 122.5 (d), 103.5 (d). − IR: 1602 (s, br). − Mass found *m/z* = 371 (calcd. = 370.7).

(1,10-Phenanthroline-k²N,N′)[(2,3-η)-1,4-benzoquinone]-palladium(0) (**2**): ^{1}H NMR ($CDCl_3$, 293 K): 8.90 (d, 4.7, H1), 8.47 (d, 8.2, H3), 7.83 (dd, 8.2, 4.7, H2), 7.95 [s, H(X)], 5.79 [s, H(pbq)]. − ^{13}C NMR ($CDCl_3$, 213 K): 179.0 (s, *C*=O), 150.7 (d), 145.8 (s), 138.8 (d), 129.8 (s), 127.8 (d) 126.4 (d), 103.3 (d). − IR: 1585 (s, br). − Mass found *m/z* = 397 (calcd. 396.4).

(5,6-Dihydro-1,10-phenanthroline-k²N,N′)[(2,3-η)-1,4-benzoquinone]palladium(0) (**3**): ^{1}H NMR ($CDCl_3$, 293 K): 8.32 (d, 5.0, H1), 7.72 (d, 7.7, H3), 7.40 (dd, 7.7, 5.0, H2), 5.79 [s, br, H(pbq)], 3.13 [s, H(X)]. − ^{13}C NMR ($CDCl_3$, 273 K): 189.6 (s, *C*=O), 151.4 (s), 148.8 (d), 138.6 (d), 135.3 (s), 127.1 (d), 102.4 (d), 26.7 (t). − IR: 1588 (s, br). − Mass found *m/z* = 397 (calcd. = 396.7).

(2,2′-Bipyridine-k²N,N′)[(2,3-η)-1,4-naphthoquinone]-palladium(0) (**7**): ^{1}H NMR ($CDCl_3$, 293 K): 8.58 [d, 5.1, H1(NN)], 8.06 [m, H3(NN) + H2(nq)], 7.92 [m, H2(NN)], 7.46 [m, H(X) + HH3(nq)], 4.97 [s, br, H1(nq)]. − ^{13}C NMR ($CDCl_3$, 293 K): (*C*=O not observed), 153.9 (s), 151.2 (d), 139.2 (d), 133.2 (s), 129.6 (d), 127.2 (d), 125.7 (d), 121.8 (d), 105.0 (d). − IR: 1617 (s, br). − Mass found *m/z* = 421 (calcd. 420.7).

(1,10-Phenanthroline-k²N,N′)[(2,3-η)-1,4-naphthoquinone]-palladium(0) (**8**): ^{1}H NMR ($CDCl_3$, 293 K): 8.94 [d, 4.7, H1(NN)], 8.37 [d, 8.2, H2(nq)], 8.07 [m, H3(nq)], 7.82 [s, H(X)], 7.79 [dd, 8.2, 4.7, H2(NN)], 7.42 [m, H3(NN)], 5.01 [s, H1(nq)]. − ^{13}C NMR not recorded due to low solubility and instability. − IR: 1617 (s, br). − Mass found *m/z* = 447 (calcd. 446.9).

(4,5-Diazafluoren-9-one-k²N,N′)[(2,3-η)-1,4-naphthoquinone]-palladium(0) (**12**): ^{1}H NMR ($CDCl_3$, 293 K): 8.02 [d, 7.6, H1(NN)], 7.93 [m, H3(NN) + H2(nq)], 7.58 [m, H3(nq)], 7.38 [dd, 7.6, 5.4, H2(NN)], 5.66 [s, br, H1(nq)]. − ^{13}C NMR not recorded due to low solubility and instability. − IR: 1629 (s), 1727 (s, dafo). − Mass found *m/z* = 447 (calcd. 446.7).

(4,5-Diazafluorene-k²N,N′)[(2,3-η)-1,4-naphthoquinone]-palladium(0) (**13**): ^{1}H NMR ($CDCl_3$, 293 K): 8.33 [m, br, H1(NN)], 7.94 [m, H3(NN) + H2(nq)], 7.48 [m, H3(nq)], 7.40 [m, H2(NN)], 5.12 [s, H1(nq)], 4.03 [s, H(X)]. − ^{13}C NMR not recorded due to low solubility and instability. − IR: 1626 (s). − Mass found *m/z* = 433 (calcd. 432.8).

Synthesis of Palladium Complexes Pd(N∩N)(Q) (**4**−**6** and **9**−**11**): A typical procedure for the synthesis of *[(2,3-η)-1,4-benzoquinone](o,o′-iPr₂-bian-k²N,N′)palladium(0)* (**5**) is given. $Pd(dba)_2$ (124.3 mg = 0.22 mmol), *o,o′*-*i*Pr_2-bian (115.1 mg = 0.23 mmol), and pbq (26.8 mg = 0.25 mmol) were dissolved in acetone (50 ml) and stirred for thirty minutes at 20°C. It was difficult to see a clear colour change although the colour of the solution slightly changed from dark purple to dark red. The solution was filtered to remove the metallic palladium and the solution was concentrated to a fraction of its original amount. The product was precipitated with hexane (30 ml) and washed twice with ether (30 ml) and with hexane (30 ml) and dried under vacuum which gave a red brown solid (87%). The other complexes were synthesized in a similar way. The yields ranged from 87 to 95%.

(N,N′-Dichexyl-1,4-diaza-1,3-butadiene-k²N,N′)[(2,3-η)-1,4-benzoquinone]palladium(0) (**4**): ^{1}H NMR ($CDCl_3$, 293 K): 8.06 (s, NN), 5.47 [s, H(pbq)], 3.45 [m, NC*H*(*c*hex)], 1.90−1.28 [m, (*c*hex)]. − ^{13}C NMR ($CDCl_3$, 293 K): 186.6 (s, *C*=O), 156.6 (d), 98.9 (d), 71.0 (d), 32.8 (t), 24.3 (t), 24.2 (t). − IR: 1615, 1634. − Mass found *m/z* = 435 (calcd. 435.4).

Bis(o,o′-diisopropylphenylimino)-acenaphtene-k²N,N′)[(2,3-η)-1,4-benzoquinone]palladium(0) (**5**): ^{1}H NMR ($CDCl_3$, 293 K): 8.03 (d, 8.3, H3), 7.16 (pst, H2), 7.36 [m, H(Ph)], 6.73 (d, 11.7, H1), 5.28 [s, H(pbq)], 3.29 [sept, 6.8, (C*H*, *i*Pr)], 1.43 [d, 6.8, (CH_3, *i*Pr)], 0.96 [d, 6.9, (CH_3, *i*Pr)]. − ^{13}C NMR ($CDCl_3$, 293 K): 185.2 (s, *C*=O), 167.1 (s), 143.4 (s), 142.9 (s), 137.2 (s), 131.1 (s), 130.6 (d), 128.6 (d), 127.0 (s), 126.9 (s), 124.14 (d), 123.7 (d), 99.0 (d), 28.7 (d), 23.3 (q), 22.9 (q). − IR: 1623. − Mass found *m/z* = 715 (calcd. = 715.8).

(2,2′-Bipyrimidine-k²N,N′)[(2,3-η)-1,4-benzoquinone]-palladium(0) (**6**): ^{1}H NMR ($CDCl_3$, 293 K): 8.95 (s, br, H1), 7.66 (pst, H2), 5.82 [s, br, H(pbq)]. − ^{13}C NMR ($CDCl_3$, 293 K): 189.2 (s, *C*=O), 159.8 (s), 158.1 (d), 121.6(d), 10.2 (d). − IR: 1645 (s).

(N,N'-Dichexyl-1,4-diaza-1,3-butadiene-k²N,N')[(2,3-η)-1,4-naphthoquinone]palladium(0) (**9**): ^{1}H NMR ($CDCl_3$, 293 K): 7.98 [m, H2(nq)], 7.96 (s, NN), 7.48 [m, H3(nq)], 4.59 [s, H1(nq)], 3.40 [m, NC*H*(*c*hex)], 1.88-1.28 [m, (*c*hex)]. − ^{13}C NMR ($CDCl_3$, 293 K): 184.7 (s, *C*=O), 156.3 (d), 136.1 (s), 131.0 (d), 124.9 (d), 71.1 (d), 32.9 (t), 32.4 (t), 24.2 (t), =*C*H (nq) not observed. − IR: 1622 (s), 1633 (sh). − Mass found *m/z* = 485.15 (calcd. 484.88). − $C_{24}H_{30}N_2O_2Pd$: found (calcd.): C, 59.28 (59.44), H, 6.256 (6.24), N, 5.65 (5.77).

(o,o'-iPr₂-bian-k²N,N')[(2,3-η)-1,4-Naphthoquinone]palladium(0) (**10**): ^{1}H NMR ($CDCl_3$, 293 K): 7.99 [d, 8.3, H3(NN)], 7.83 [dd, 7.0, 3.6, H2(NN)], 7.51−7.28 [m, 10 H (NN + nq)], 6.64 [d, 7.23, H1(NN)], 4.46 [s, H1(nq)], 3.50 [sept, 6.7, (C*H*, *i*Pr)], 2.78 [sept, 6.7, (C*H*, *i*Pr)], 1.54 [d, 6.4, (C*H*$_3$, *i*Pr)], 1.02 [d, 6.4, (C*H*$_3$, *i*Pr)], 1.01 [d, 6.7, (C*H*$_3$, *i*Pr)], 0.76 [d, 6.7, (C*H*$_3$, *i*Pr)]. − ^{13}C NMR ($CDCl_3$, 293 K): 183.3 (s, *C*=O), 166.9 (s), 143.2 (s), 139.8 (s), 137.5 (s), 137.1 (s), 135.7 (s), 131.1 (s), 130.4 (d), 128.5 (d), 126.9 (d), 126.9 (s), 125.2 (d), 124.1 (d), 123.8 (d), 123.5 (d), 58.7 (d), 28.7 (d), 28.6 (d), 23.6 (q), 23.1 (q), 22.8 (q), 22.7 (q). − IR: 1639 (s). − Mass found *m/z* = 765.27 (calcd. 765.23). − $C_{46}H_{46}N_2O_2Pd$: found (calcd.): C, 71.11 (71.29), H, 6.16 (6.26), N, 3.66 (3.78).

(2,2'-Bipyrimidine-k²N,N')[(2,3-η)-1,4-naphthoquinone]palladium(0) (**11**): ^{1}H NMR ($CDCl_3$, 293 K): 8.97 [s, br, H1(NN)], 8.05 [m, H2(nq)], 7.63 [pst, H2(NN)], 7.45 [m, H3(nq)], 4.89 [s, H1(nq)]. − ^{13}C NMR ($CDCl_3$, 293 K): 180.5 (s, *C*=O), 158.9 (s), 157.9 (d), 136.1 (s), 131.3 (d), 125.1 (d), 123.7 (d), =*C*H (nq) not observed. − IR: 1620 (s, br). − Mass found *m/z* = 423.01 (calcd. 422.68).

Synthesis of Platinum Complexes Pt(N∩N)(Q) (**18−21**): The platinum complexes **18−21** were synthesized in a similar way as **1**, but distinctly longer reaction times were needed (14 h at 20°C) and the yields ranged from 73 to 85%.

[(2,3-η)-1,4-Benzoquinone](2,2'-bipyridine-k²N,N')platinum(0) (**18**): ^{1}H NMR ($CDCl_3$, 293 K): 9.00 (d, 5.1, J_{Pt-H}: 33.4, H1), 8.10 (m, H2), 8.09 (m, H3), 7.55 [d, 5.1, H(X)], 5.49 [s, br, H(pbq)]. − ^{13}C NMR not recorded due to low solubility and instability. − IR: 1617 (s, br). − Mass found *m/z* = 460 (calcd. 459.4).

(1,10-Phenanthroline-k²N,N')[(2,3-η)-1,4-benzoquinone]platinum(0) (**19**): ^{1}H NMR ($CDCl_3$, 293 K): 9.32 (d, 5.0, J_{Pt-H}: 31.1, H1), 8.59 (d, 8.2, H3), 7.79 [s, H(X)], 7.87 (dd, 8.2, 5.0, H2), 5.56 [s, br, H(pbq)]. − ^{13}C NMR not recorded due to low solubility and instability. − IR: 1617 (s, br). − Mass found *m/z* = 484 (calcd. 483.4).

(2,2'-Bipyridine-k²N,N')[(2,3-η)-1,4-naphthoquinone]platinum(0) (**20**): ^{1}H NMR ($CDCl_3$, 293 K): 9.01 [d, 5.0, J_{Pt-H}: 31.5, H1(NN)], 8.10 [m, H2(nq)], 8.04 [d, 8.0, H(X)], 7.79 [d, 8.0, H2(NN)], 7.52 [dd, 8.0, 5.0, H3(NN)], 7.48 [m, H3(nq)], 4.60 [s, J_{Pt-H}: 75.9, H1(nq)]. − ^{13}C NMR not recorded due to low solubility and instability. − IR: 1625 (s). − Mass found *m/z* = 510 (calcd. 509.4).

(1,10-Phenanthroline-k²N,N')[(2,3-η)-1,4-naphthoquinone]platinum(0) (**21**): ^{1}H NMR ($CDCl_3$, 293 K): 9.33 [d, 4.9, J_{Pt-H}: 31.1, H1(NN)], 8.50 [d, 8.2, H3(NN)], 8.11 [m, H2(nq)], 7.87 [s, H(X)], 7.84 [dd, 8.2, 4.9, H2(NN)], 7.44 [m, H3(nq)], 4.74 [s, J_{Pt-H}: 76.1, H1(nq)]. − ^{13}C NMR not recorded due to low solubility and instability. − IR: 1625 (s). − Mass found *m/z* = 534.078 (calcd. 533.4).

Synthesis of Palladium Complexes Pd(N∩N)(Q)₂ (**14**, **15**): These compounds can be synthesized in two ways, either in one or in two steps, and both methods will be described here.

Method A: (4,5-Diazafluoren-9-one-κN)bis[(2,3-η²)-1,4-naphthoquinone]palladium(0) (**14**): To a brown/red solution of Pd(dafo)(nq) **12** (44.8 mg = 0.1 mmol) in dichloromethane (50 ml) was added naphtoquinone (nq) (15.9 mg = 0.1 mmol), and the solution turned green/yellow after several minutes at 20°C. The same work-up procedure as for the Pd(N∩N)(Q) complexes was followed and this gave a green/yellow solid (83%).

Method B: Pd(dafo)(nq)₂ (**14**) *and Pd(dafe)(nq)₂* (**15**): $Pd(dba)_2$ (140.5 mg = 0.24 mmol), dafo (0.25 mmol), and nq (79.1 mg = 0.50 mmol) were dissolved in 40 ml of toluene and stirred for two hours at 20°C. The colour of the solution changed from dark purple to yellow and a dark compound precipitated. The same work-up procedure as for the Pd(N∩N)(Q) complexes was followed and this gave a green/yellow solid (yield: 93% for **14** and 87% for **15**). Orange crystals suitable for X-ray diffraction were obtained by slow diffusion of hexane in a solution of **14** in dichloromethane/methanol (1:1, v/v) at 4°C.

(4,5-Diazafluoren-9-one-κN)bis[(2,3-η²)-1,4-naphthoquinone]palladium(0) (**14**): ^{1}H NMR ($CDCl_3$, 293 K): 8.01 [d, 7.4, H1(NN)], 7.78 [m, H3(NN) + H2(nq)], 7.49 [m, H3(nq)], 7.28 [dd, 7.4, 5.4, H2(NN)], 5.19 [s, H1(nq)]. − ^{13}C NMR ($CDCl_3$, 223 K): 188.5 (s, *C*=O), 185.4 (s, *C*=O), 161.4 (s), 154.7 (d), 133.8 (d), 133.7 (s), 133.5 (d), 130.6 (s), 127.1 (d), 126.5 (d), 80.9 (d). − IR: 1653 (s, br), 1730 (s, dafo). − Mass found *m/z* = 628 ([M+Na]$^{+\cdot}$) (calcd. 627.9). − $C_{31}H_{18}N_2O_5Pd$: found (calcd.): C, 58.74 (58.15), H, 2.76 (2.83), N, 4.28 (4.37).

(4,5-Diazafluorene-κN)bis[(2,3-η²)-1,4-naphthoquinone]palladium(0) (**15**): ^{1}H NMR ($CDCl_3$, 293 K): 8.02 [d, 7.7, H1(NN)], 7.89 [m, H3(NN) + H2(nq)], 7.52 [m, H3(nq)], 7.32 [dd, 7.7, 5.1, H2(NN)], 5.47 [s, H1(nq)], 3.98 [s, H(X)]. − ^{13}C NMR ($CDCl_3$, 223 K): 185.4 (s, *C*=O), 157.1 (s), 149.3 (d), 134.7 (d), 133.8 (s), 133.5 (d), 139.3 (s), 126.3 (d), 125.0 (d), 33.3 (t), =*C*H (nq) not observed. − IR: 1657 (s, br). − Mass found *m/z* = 433 (calcd. 591.0), the found mass corresponds to [Pd(dafe)(nq)]$^+$.

Synthesis of Platinum Complexes Pt(N∩N)(Q)₂ (**22**, **23**): The analogous platinum complexes **22**, **23** were synthesized in a similar way according to method B as described above but again longer reaction times were needed (14 hrs at 20°C). The yields were 75 and 78% respectively.

(4,5-Diazafluoren-9-one-κN)bis[(2,3-η²)-1,4-naphthoquinone]platinum(0) (**22**): ^{1}H NMR ($CDCl_3$, 293 K): 8.05 [d, 7.6, H1(NN)], 7.78 [m, H3(NN) + H2(nq)], 7.47 [m, H3(nq)], 7.30 [dd, 7.6, 5.4, H2(NN)], 4.77 [s, br, H1(nq)]. − ^{13}C NMR ($CDCl_3$, 223 K): 188.7 (s, *C*=O), 187.9 (s, *C*=O), 134.3 (d), 134.0 (s), 133.8 (d), 133.4 (d), 130.6 (s), 125.9 (d), 67.9 (d), *C*=N (s) and *C*=N (d) not observed. − IR: 1654 (s), 1731 (s, dafo). − Mass found *m/z* = 716 ([M+Na]$^+$) (calcd. 716.6). − $C_{31}H_{18}N_2O_5Pt$: found (calcd.): C, 49.65 (49.09), H, 2.79 (2.39), N, 3.91 (3.69).

(4,5-Diazafluorene-κN)bis[(2,3-η²)-1,4-naphthoquinone]platinum(0) (**23**): ^{1}H NMR ($CDCl_3$, 293 K): 7.92 [d, 7.9, H1(NN)], 7.73 [m, H3(NN) + H2(nq)], 7.43 [m, H3(nq)], 7.23 [m, H2(NN)], 4.75 [s, br, H1(nq)], 3.98 [s, H(X)]. − ^{13}C NMR ($CDCl_3$, 223 K): 189.1 (s, *C*=O), 134.5 (s), 134.1 (s), 133.6 (d), 133.3 (d), 127.2 (d), 125.8 (d), 67.8 (d), 33.3 (t), *C*=N (s) and *C*=N (d) not observed. − IR: 1666 (s, br). − Mass found *m/z* = 702 ([M+Na]$^+$) (calcd. 702.6).

Synthesis of Palladium Complexes Pd₂(N∩N)(Q)₂ (**16**, **17**): A typical procedure for the synthesis of *bis{[μ-(2,3-η²:5,6-η²)]-1,4-benzoquinone}-μ-(4,5-diazafluoren-9-one-k²N,N')bis-[palladium(0)]* (**16**) is given. $Pd(dba)_2$ (140.5 mg = 0.24 mmol), dafo (0.12 mmol) and pbq (25.9 mg = 0.24 mmol) were dissolved

in toluene (50 ml) and stirred for fifteen minutes at 20°C. The colour of the solvent changed from dark purple to yellow and a dark green compound precipitated. This solid was washed with toluene (2 × 20 ml) and with diethylether (2 × 20 ml). In order to remove the metallic palladium the compound was dissolved in dichloromethane and filtered through Celite. The solution was evaporated to a fraction of its original amount and the product was precipitated with hexane. The remaining yellow green solid was dried in vacuum (yield: 90% for **16** and 88% for **17**). Dark green crystals suitable for X-ray diffraction were obtained by slow diffusion of hexane in a solution of **16** in dichloromethane/methanol (1:1, v/v) at 4°C.

Bis{[μ-(2,3-η²:5,6-η²)]-1,4-benzoquinone}-μ-(4,5-diazafluoren-9-one-k²N,N′)bis[palladium(0)] (**16**): ^{1}H NMR ($CDCl_3$, 293 K): 8.79 (d, 5.5, H1), 8.31 (d, 7.6, H3), 7.48 (dd, 7.6, 5.5, H2), 4.45 [ddd, 8.3, 2.2, 0.2, H(pbq)], 4.48 [ddd, 4.0, 1.0, 0.1, H(pbq)]. − ^{13}C NMR not recorded due to low solubility. − IR: 1629 (s, br), 1726 (s, dafo). − Mass found *m/z* = 634 ([M+Na]$^+$) (calcd. = 634.2). − $C_{23}H_{14}N_2O_5Pd_2$: found (calcd.): C, 44.57 (45.20), H, 2.65 (2.31), N, 4.38 (4.58).

Bis{[μ-(2,3-η²:5,6-η²)]-1,4-benzoquinone}-μ-(4,5-diazafluorene-k²N,N′)bis[palladium(0)] (**17**): ^{1}H NMR ($CDCl_3$, 293 K): 8.75 (d, 4.5, H1), 8.16 (d, 7.6, H3), 7.40 (dd, 7.6, 4.5, H2), 4.65 [ddd, 8.2, 2.1, 0.2, H(pbq)], 4.56 [ddd, 8.2, 2.1, 0.2, H(pbq)], 4.07 (s). − ^{13}C NMR (CD_2Cl_2, 293 K): 189.1 (s, *C*=O), 154.2 (d), 146.7 (s), 138.0 (d), 125.6 (d), 83.0 (d), 79.6 (d), 34.3 (t), *C*=CH (s, dafe) not observed. − IR: 1634 (s, br). − Mass found *m/z* = 597 (calcd. 597.2).

Synthesis of Platinum Complexe $Pt_2(N\cap N)(Q)_2$ (**24**): The analogous platinum complex **24** was synthesized similarly, but a reaction time of 14 hrs was required; the yield was 71%.

Bis{[μ-(2,3-η²:5,6-η²)]-1,4-benzoquinone}-μ-(4,5-diazafluoren-9-one-k²N,N′)bis[platinum(0)] (**24**): ^{1}H NMR ($CDCl_3$, 293 K): 8.83 (d, 5.5, J_{Pt-H}: 29.7, H1), 8.39 (d, 7.6, H3), 7.49 (dd, 7.6, 5.7, H2), 4.45 [d, 7.5, J_{Pt-H}: 87.7, H(pbq)], 3.86 [d, 7.5, J_{Pt-H}: 44.6, H(pbq)]. − ^{13}C NMR not recorded due to low solubility. − IR: 1640 (s, br), 1733 (s, dafo).

p-Quinone Substitution Reactions: *p*-Quinone substitution reactions were carried out for several combinations of complexes and *p*-quinones in varying stoichiometries. A typical experiment has been described below and the other substitution reactions proceeded in a similar way. *p*-Benzoquinone (11.2 mg = 0.1 mmol) was added to a solution of **7** (37.1 mg = 0.1 mmol) in dichloromethane (30 ml), which solution was then stirred for one hour at 20°C. After evaporation of the solvent the remaining solid was washed with diethylether (3 × 10 ml) and dried in vacuum. The residue as well as the organic products were analyzed with ^{1}H NMR spectroscopy.

X-ray Crystal Structure Determination: The crystal, collection, and refinement data of complexes **1**, **14**, and **16** have been compiled

Table 3. Crystallographic data for Pd(bpy)(pbq) **1**, Pd(dafo)(nq)$_2$ **14**, and Pd_2(dafo)(pbq)$_2$ **16**

Complex	**1**	**14**	**16**
Crystal data			
Formula	$C_{16}H_{12}N_2O_2Pd \cdot 2\ H_2O$	$C_{31}H_{14}N_2O_5Pd$	$C_{23}H_{14}N_2O_5Pd_2 \cdot CH_3OH$
Mol. weight	406.7	600.9	643.2
Cryst. system	monoclinic	orthorhombic	monoclinic
Space group	*C*2/*c*	*Pbn*2$_1$	*P*2$_1$/*c*
a [Å]	18.980(1)	10.909(4)	11.791(4)
b [Å]	7.627(7)	14.434(8)	12.470(3)
c [Å]	22.948(1)	30.391(2)	14.275(4)
α [°]	90	90	90
β [°]	108.572(4)	90	91.57(4)
γ [°]	90	90	90
V [Å^3]	3148.93(4)	4785.3(18)	2098.12(1)
Z	8	8	4
D_{calc} [g cm^{-3}]	1.72	1.682	2.03
μ [cm^{-1}]	99.3	67.9	17.4
F(000)	1632	2400	1264
crystal size [mm^3]	0.03 × 0.40 × 0.70	0.50 × 0.40 × 0.40	0.30 × 0.50 × 0.70
Collection			
T [K]	293	293	293
θ_{min}, θ_{max} [°]	4.1, 64.9	2.9, 69.9	1.7, 29.9
Radiation [Å]	1.5418 (Cu-*Kα*)	1.54180 (Cu-*Kα*)	0.71069 (Mo-*Kα*)
Scan type	ω/2θ	ω/2θ	ω/2θ
Acq. time [h]	60	57	80
Linear decay [%]	0	6	0
Ref. reflections	O(−,1) O(−,1) 1, 0 0 6	1 O(−,2) 4, 2 0 0	O(−,2) 2 3, 2 2 1
Data set (*h, k, l*)	21:20; −8:0; 0:26	0:13; −17:0; 0:36	−16:16; 0:17; 0:20
Total unique data	2576	4608	6067
Total obs. data	2216 [$I > 2.5\sigma(I)$]	4359 [$F_o > 4\sigma(F_o)$]	4950 [$I > 2.5\sigma(I)$]
DIFABS corr. range	0.55−1.91	0.668−1.509	0.91−1.34
Refinement			
Refined params	255	705	379
Final *R* [a]	0.102	0.0422	0.030
Final R_w [b]	0.163	−	0.049
Final *wR2* [c]	−	0.112	−
w^{-1} [d]	$6.6+F_o+0.0071F_o^2$	$\sigma F^2+0.831P^2+3.20P$	$9.5+F_o+0.0063F_o^2$
$(\Delta/\sigma)_{max}$	0.16	0.01	0.66
ρ_{min}, ρ_{max} (e Å^{-3})	−2.5, 6.1	−1.13, 2.99	−0.9, 0.6

[a] $R1 = \Sigma(||F_o| - |F_c||)/\Sigma|F_o|$, − [b] $R_w = \{\Sigma[w(||F_o| - |F_c||)^2]/\Sigma[w(F_o^2)]\}^{0.5}$. − [c] $wR2 = \{\Sigma[w(F_o^2 - F_c^2)^2]/\Sigma[wF_o^2]^2\}^{0.5}$. − [d] $P = [\mathrm{Max}(F^2_{obs},0) + 2F^2_{calc}]/3$.

in Table 3. Data collection for these crystals was performed on an Enraf-Nonius CAD-4 diffractometer with graphite-monochromated Cu-*Kα* radiation for **1** and **14** and Mo-*Kα* radiation for **16** and ω-2θ scan. Two reference reflections were measured hourly and showed no decrease during the course of the data collection for the complexes **1** and **16** and 6% decrease for complex **14**, which was corrected for. Unit-cell parameters were refined by a least-squares fitting procedure using 23 reflections with 80<2θ<84° for **1**, 80.1<2θ<84.9° for **14**, and 40<2θ<42° for complex **16**. Corrections for Lorentz and polarization effects were applied. The structure of the complexes **1** and **16** was solved by Direct Methods while the structure of **14** was solved by the PATTY option of the DIRDIF91 program system[73]. After isotropic refinements on **1** and **16**, peaks were found in a ΔF synthesis which were interpreted as water and methanol respectively which were used as solvents during crystallization. The hydrogen atoms were calculated. Full-matrix least-squares refinement on *F*, anisotropic for the non-hydrogen atoms and isotropic for the hydrogen atoms, restraining the latter in such a way that the distance to their carrier remained constant at approximately 1.09 Å, converged to the R -values mentioned in Table 3. An empirical absorption correction, DIFABS[74] was applied. Scattering factors were taken from the literature[75][76][77]. Since the space group of complex **14** is polar, it was necessary to use the Flack absolute structure parameter[78], which refined to $x = 0.032(11)$. In case of the crystals of complex **14**, the matching of the two independent molecules for all non-hydrogen atoms resulted in a rms-value of 0.13 Å and a non-crystallographic center of symmetry is present (located at $x = 0.50$, $y = 0.37$, $z = 0.38$). The anomalous scattering of Pd was taken into account. For **1** and **16** calculations were performed with XTAL[79] and for **14** with SHELXL[80]. Thermal ellipsoid and molecular plots were made using the PLUTON and PLATON programs[81]. Atomic coordinates, thermal parameters and bond lengths and angles have been deposited ar the Cambridge Crystallographic Data Centre, see instructions to authors. Any request to the CCDC for this material should quote the full literature citation and the reference number 100791.

[1] G. K. Anderson, *Chemistry of the Platinum Group Metals, Recent Developments*; Hartley, F. R. Ed.; Elsevier: Amsterdam, **1991**, pp 338-406.
[2] R. Ugo, *Coord. Chem. Rev.* **1990**, *3*, 319.
[3] S. D. Ittel, J. A. Ibers, *Adv. Organomet. Chem.* **1976**, *14*, 33.
[4] Ts. Ito, S. Hasegawa, Y. Takahashi, Y. Ishii, *J. Organomet. Chem.* **1974**, *73*, 401.
[5] C. G. Pierpont, R. M. Buchanan, H. H. Downs, *J. Organomet. Chem.* **1977**, *124*, 103.
[6] R. van Asselt, C. J. Elsevier, W. J. J. Smeets, A. L. Spek, *Inorg. Chem.* **1994**, *33*, 1521 and references cited herein.
[7] R. van Asselt, C. J. Elsevier, W. J. J. Smeets, A. L. Spek, R. Benedix, *Recl. Trav. Chim. Pays-Bas* **1994**, *113*, 88.
[8] R. van Belzen, R. A. Klein, W. J. J. Smeets, A. L. Spek, R. Benedix, C. J. Elsevier, *Recl. Trav. Chim. Pay-Bas* **1996**, *115*, 275.
[9] R. van Asselt, C. J. Elsevier, *Organometallics* **1992**, *11*, 1999.
[10] R. van Asselt, C. J. Elsevier, *Tetrahedron* **1994**, *50*, 323.
[11] R. van Belzen, H. Hoffmann, C. J. Elsevier, *Angew. Chemie* **1997**, *109,* 1833; *Angew. Chemie, Int. Ed. Engl.* **1997**, *36,* 1743.
[12] R. van Asselt, C. J. Elsevier, *J. Mol. Catal.* **1991**, *65*, L13.
[13] R. van Asselt, E. E. C. G. Gielens, R. E. Rülke, K.Vrieze, C. J. Elsevier, *J. Am. Chem. Soc.* **1994**, *116,* 977.
[14] L. K. Johnson, C. M. Kilian, M. Brookhart, *J. Am. Chem. Soc.* **1995**, *117,* 6414.
[15] E. Lindner, S. Pautz, M. Haustein, *Coord. Chem. Rev.* **1996**, *155,* 145.
[16] F. P. Fanizzi, L. Maresca, G. Natile, M. Lanfranchi, A. Tiripicchio, G. Pacchioni, *J. Chem. Soc., Chem. Commun.* **1992**, 333.
[17] J. H. Groen, C. J. Elsevier, K. Vrieze, W. J. J. Smeets, A. L. Spek, *Organometallics* **1996**, *15,* 3445.
[18] R. A. Klein, R. van Belzen, K. Vrieze, C. J. Elsevier, R. P. Thummel, J. Fraanje, K. Goubitz, *Coll. Czech. Chem. Commun.* **1997**, *62*, 238-256.
[19] R. P. Thummel, F. Lefoulon, R. Mahadevan, *J. Org. Chem.* **1985**, *50*, 3824.
[20] L. J. Henderson, F. R. Fronczek, W. R. Cherry, *J. Am. Chem. Soc.* **1984**, *106*, 5876.
[21] G. N. Schrauzer, K. C. Dewhirst, *J. Am. Chem. Soc.* **1964**, *86*, 3265.
[22] M. D. Glick, L. F. Dahl, *J. Organomet. Chem.* **1965**, *3*, 200.
[23] F. Calderazzo, R. Henzi, *J. Organomet. Chem.* **1967**, *10*, 483,
[24] A. A. Vlček, J. Hanzlik, *Inorg. Chem.* **1967**, *6*, 2053.
[25] S. Cenini, R. Ugo, G. La Monica, *J. Chem. Soc. A* **1971**, 416.
[26] G. La Monica, G. Navazio, P. Sandrini, S. Cenini, *J. Organomet. Chem.* **1971**, *31*, 89.
[27] T. Ukai, H. Kawazura, Y. Ishii, J. J. Bonnet, J. A. Ibers, *J. Organomet. Chem.* **1974**, *65*, 253.
[28] H. Minematsu, S. Takahashi, N. Hagiwara, *J. Organomet. Chem.* **1975**, *91*, 389.
[29] H. Minematsu, S. Takahashi, N. Hagiwara, *J. Chem. Soc., Chem. Commun.* **1975**, 466.
[30] R. S. Vagg, *Acta Cryst.* **1977**, *B33*, 3708.
[31] M .J. Chetcuti, J. A. K. Howard, M. Pfeffer, J. L. Spencer, F. G. A. Stone, *J. Chem. Soc., Dalton Trans.* **1981**, 276.
[32] M. J. Chetcuti, J. A. Herbert, J. A. K. Howard, M. Pfeffer, J. L. Spencer, F. G. A. Stone, *J. Chem. Soc., Dalton Trans.* **1981**, 284.
[33] M. Hiramatsu, T. Fujinami, S. Sakai, *J. Organomet. Chem.* **1981**, *218*, 409.
[34] E. Uhlig, R. Fischer, R. Kirmse, *J. Organomet. Chem.* **1982**, *239*, 385.
[35] M. Hiramatsu, H. Nakano, T. Fujinami, S. Sakai, *J. Organomet. Chem.* **1982**, *236*, 131.
[36] M. Hiramatsu, K. Shiozaki, T. Fujinami, S. Sakai, *J. Organomet. Chem.* **1983**, *246*, 203.
[37] L.S. Liebeskind, S.W. Riesinger, *Tetrahedron Lett.* **1991**, *32*, 5681.
[38] L. Malatesta, R. Ugo, S. Cenini, *Adv. Chem. Series*, E. F. Gould (Ed.), **1976**, *62*, 318.
[39] After submission of our manuscript, a paper containing the X-ray molecular structure of **1** appeared: B. Milani, A. Anzilutti, L. Vicentini, A. Sessanta o Santi, E. Zangrando, S. Geremia, G. Mestroni, *Organometallics,* **1997**, *16*, 5064.
[40] K. J. Cavell, D. J. Stufkens, K. Vrieze, *Inorg. Chim. Acta* **1980**, *47*, 67.
[41] P. T. Cheng, C. D. Cook, S. C. Nyburg, K. Y. Wan, *Inorg. Chem.* **1971**, *10*, 2210.
[42] C. D. Cook, K. Y. Wan, *Inorg. Chem.* **1971**, *10*, 2696.
[43] J. Halpern, T. A. Weil, *J. Chem. Soc. Chem.Commun*. **1973**, 631.
[44] F. Ozawa, T. Ito, Y. Nakamura, A. Yamamoto, *J. Organomet. Chem.* **1979**, *168*, 375.
[45] Recently, an X-ray crystal structure of a divalent palladium complex [PdCl(η^3-allyl)(Ar-bian-κ*N*) authenticated the possibility of monodentate coordination of sterically demanding *rigid* α-diimine ligands[17]. This finding indicates that dissociation of one N atom is retarded for RBN ligands such as Ar-bian, but that also in these cases it may be a vital process in insertion reactions of CO and unsaturated organic compounds into Pd−C bonds.
[46] V. G. Albano, C. Castellari, M. E. Cucciolito, A. Panunzi, A. Vitagliano, *Organometallics* **1990**, *9*, 1269.
[47] C. G. Pierpont, R. M. Buchanan, H. H. Downs, *J. Organomet. Chem.* **1977**, *124*, 103.
[48] H. Kooijman, A. L. Spek, R. van Belzen, C. J. Elsevier, *Acta Cryst. C*, **1997**, *C53*, 1593.
[49] M. C. Mazza, C. G. Pierpont, *Inorg. Chem.* **1973**, *12*, 2955.
[50] Pierpont. C. G.; Mazza, M. C. *Inorg. Chem.* **1974**, *13*, 1891.
[51] R. Benn, P. Betz, R. Goddard, P. W. Jolly, N. Kokoel. C. Krüger, I. Topalovic, *Z. Naturforsch*. **1991**, *46B*, 1395.
[52] J. Trotter, *Acta Cryst.* **1960**, *13*, 86.
[53] M. D. Glick, L. F. Dahl, *J. Organomet. Chem.* **1965**, *3*, 200.
[54] V. A. Uchtman, L. F. Dahl, *J. Organomet. Chem.* **1972**, *40*, 403.
[55] R. A. Klein, R. van Belzen, C. J. Elsevier, J. Fraanje, K. Goubitz, to be published.
[56] F. P. Fanizzi, M. Lanfranchi, G. Natile, *Inorg. Chem*. **1994**, *33*, 3331 and references cited herein.
[57] Y. Yamamoto, H. Yamazaki, *Bull. Chem. Soc. Jpn*. **1985**, *58*, 1843.
[58] S. Z. Goldberg, R. Eisenberg, *Inorg. Chem.* **1976**, *15*, 535.

[59] M. L. Kullberg, F. R. Lemke, D. R. Powell, C. P. Kubiak, *Inorg. Chem.* **1985**, *24*, 3589.
[60] N. M. Rutherford, M. M. Olmstead, A. L. Balch, *Inorg. Chem.* **1984**, *23,* 2833.
[61] T. E. Krafft, C. I. Hejna, J. S. Smith, *Inorg. Chem.* **1990**, *29*, 2682.
[62] W. L. Wilson, J. H. Nelson, N. W. Alcock, *Organometallics* **1990**, *9*, 1699.
[63] IR stretching frequencies of free *p*-quinones: pbq($\nu_{C=O}$) = 1662 cm^{-1}, nq($\nu_{C=O}$) = 1660 cm^{-1}.
[64] ^{1}H-NMR data of the free quinones: $\delta(H_{(pbq)})$ = 6.72 (s), $\delta(H_{(nq)})$ = 8.07 (m, H2), 7.75 (m, H3), 6.97 (s, H1).
[65] $\Delta G^{\neq} = 2.303 \cdot R T_c$ (10.319 − log k' + log T_c) where T_c= coalescence temperature and $k' = \pi\Delta\nu/2^{1/2}$, see: I. C. Calder, P. J. Garrat, *J. Chem. Soc. B* **1967**, 660.
[66] A. Gogoll, J. Örnebro, H. Grennberg, J. Bäckvall, *J. Am. Chem. Soc.* **1994**, *116*, 3631.
[67] D. L. Thorn, R. Hoffmann, *J. Am. Chem. Soc.* **1978**, *100*, 2079.
[68] C. R. Conard, M. A. Doliver, *Organic Synthesis;* Wiley, New York, **1943**; Collect. Vol. II, p 167.
[69] M. F. Rettig, P. M. Maitlis, *Inorg. Synth*. **1977**, *17*, 134.
[70] K. Moseley, P. M. Maitlis, *J. Chem.Soc., Dalton Trans.* **1974**, 169.
[71] H. Bock, H. tom Dieck, *Chem. Ber*. **1967**, *100*, 228.
[72] H. tom Dieck, I.W. Renk, *Chem. Ber*. **1971**, *104*, 92.
[73] J. M. M. Smits, H. Behm, W. P. Bosman, J. Beurskens, *Crystallogr. Spectrosc. Res.* **1991**, *18*, 447.
[74] N. Walker, D. Stuart, *Acta Cryst.* **1983**, *A39*, 158.
[75] D. T. Cromer, J. B. Mann, *Acta Cryst.* **1969**, *A24*, 321.
[76] *International Tables for X-ray crystallography* **1974**, Kynoch Press, Birmingham, Vol. IV, p 55.
[77] A. J. C. Wilson, *The International Tables for X-ray Crystallography* , **1992**, Vol. C, A.J.C. Wilson, Ed., Kluwer, Dordrecht.
[78] H. D. Flack, *Acta Cryst.* **1983**, *A39*, 876.
[79] *XTAL3.2*, S. R. Hall, H. D. Flack, J. M. Stewart (Eds.), **1992**, Reference Manual, Universities of Western Australia, Geneva and Maryland.
[80] *SHELXL-93, Program for the Refinement of Crystal Structures,* **1993**, G. M. Sheldrick, Univ. of Göttingen, Germany.
[81] A. L. Spek, *Acta Cryst.* **1990**, *A46*, C34.

[97247]

Bis(pentamethylcyclopentadienyl)-Substituted Phosphanes: Synthesis and Structure

Jörg Ebels[a], Rudolf Pietschnig[a], Sirpa Kotila[b], André Dombrowski[a], Edgar Niecke*[a], Martin Nieger[a], and Hans Michael Schiffner[a]

Anorganisch-Chemisches Institut der Universität Bonn,[a]
Gerhard-Domagk-Straße 1, D-53121 Bonn, Germany

University of Jyväskylä,[b]
P.O. Box 35, FIN-40101 Jyväskylä, Finland

Received October 16, 1997

Keywords: Bis(pentamethylcyclopentadienyl)phosphanes / Aminobis(pentamethylcyclopentadienyl)phosphanes

The bis(1,2,3,4,5-pentamethyl-1,3-cyclopentadien-1-yl)phosphanes **3**−**7** are formed in good yields by the reaction of the halogenophosphanes **2a** or **2b** with the appropriate nucleophile. Following another route, the dialkylaminobis(pentamethylcyclopentadienyl)phosphanes **11a**−**c** have been synthesized by the treatment of dichloro(dialkylamino)phosphanes with two equivalents of (pentamethylcyclopentadienyl)lithium. The compounds **3**−**11** have been characterized by multinuclear NMR spectroscopy and **3**, **5**, **6**, and **11a** have also been characterized by single-crystal X-ray diffraction studies. The molecular structure of **11a** is governed by steric congestion, which typically would lead to a parallel arrangement of the two pentamethylcyclopentadienyl ligands at the phosphorus atom. However, surprisingly, the crystal structure of the (dimethylamino)phosphane **11a**, exhibits a tilted, rather than a parallel, conformation of the pentamethylcyclopentadienyl groups [tilt angle: 130.6(1)°].

Previous comprehensive investigations of the main-group cyclopentadienyl (Cp) compounds[1][2][3] have revealed a variety of unusual structures and bonding modes analogous to those observed for the cyclopentadienyl transition-metal compounds[4]. Depending on the availability of the valence orbitals and the geometric parameters of the central atom, mono-, di-, tri-, and pentahapto complexation has been achieved[5][6][7][8]. Moreover, by replacing Cp with the permethylated Cp* substituent, a significantly increased kinetic stability of the resulting complexes could be achieved, which made the isolation of several new types of compounds possible[3][4].

In the course of studies dealing with the dynamic behaviour of such systems (1,5-sigmatropic rearrangements) several pentamethylcyclopentadienyl-(Cp*-)substituted phosphanes have been synthesized[9][10]. On heating these Cp*-substituted phosphanes were shown to be thermally stable, which is not the case for the corresponding Cp compounds[11][12]. Recently, in the case of Cp*-substituted phosphenium cations and iminophosphanes, the haptotropic rearrangement has been proven to occur[13].

Results

Halogeno-Substituted Bis(Cp*)phosphanes

The synthesis of the chloro- and bromobis(Cp*)phosphanes[10] has been optimized, to enable characterisation by X-ray crystallography[23]. Treatment of PCl_3/PBr_3 with 2.5 equivalents of Cp*Li[10][14] at 0°C in pentane and after stirring for 10 h affords the desired halogenobis(Cp*)phosphanes **2a** and **2b**. Both compounds are obtained as yellow, thermally stable solids, that can be distilled in vacuo.

Scheme 1. Synthesis of new bis(Cp*)phosphanes by nucleophilic displacement

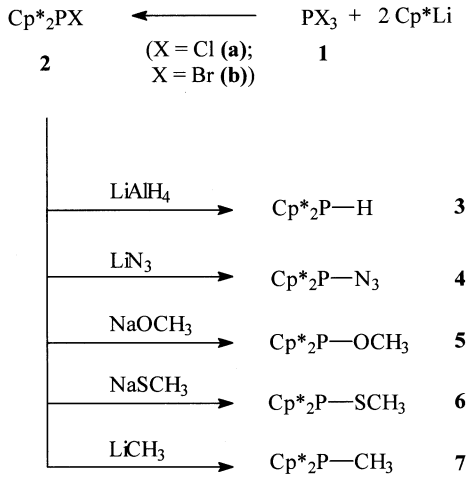

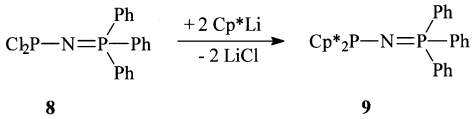

Starting from these halogenophosphanes **2a** and **2b** a variety of previously unknown bis(Cp*)phosphanes could be obtained by a nucleophilic displacement reaction. There-

 © WILEY-VCH Verlag GmbH, D-69451 Weinheim, 1998 1434−1948/98/0303−0331 $ 17.50+.50/0

fore, the reduction to the phosphane **3**, on reaction of **2a**, **b** with lithium tetrahydridoaluminate in ether, proceeds in the usual manner. Due to the coupling with the directly bonded proton ($^1J_{PH} = {}_1$90.0 Hz) and the six methyl protons ($^3J_{PH} = {}_1$6.5 Hz) the ^{31}P-NMR spectrum of compound **3** exhibits a characteristic pattern of a doublet of septuplets.

The reaction of the halogenophosphanes with lithium azide in pyridine produces the azidophosphane **4** in good yield. The reaction time depends strongly on the nature of the halogen atom. While the reaction takes several days for **2a**, in the case of **2b** the exchange is completed after 1−2 h, which may be due to the weaker P−Br bond compared to the P−Cl bond.

In general, owing to the high steric congestion of the two Cp* substituents, a prolonged reaction time is necessary. However, in the case of the thermally stable compounds the reaction rate can be increased by heating the reaction mixture. Since the displacement of the Cp* moiety is a common side reaction of the nucleophilic attack at **2a**, **b**, a detailed balance of the reaction parameters is necessary. Reaction of **2a**, **b** with sodium methoxide at 40−50°C in methanol readily furnishes **5** as a crystalline compound. However, the corresponding (methylthio)phosphane **6** could be obtained at lower temperatures (0°), if a highly polar solvent such as DMF is used. With respect to this conversion the bromo derivative **2b** is seen to be more reactive than the chloro congener **2a**. Since sodium thiomethoxide is unsoluble in pure toluene or other unpolar solvents, a mixture of toluene/DMF is used as solvent in order to achieve a good solubility of the nucleophile. Methyllithium also reacts with **2a** and **2b** by displacement of the halide group at low temperature, despite the transition state of this reaction being more strained than in the previous cases. The conversion of **2a**,**b** into compound **7** is optimized in ether.

The identity of the compounds **3**−**7** was confirmed by NMR spectroscopy and elemental analysis. In addition, crystals suitable for an X-ray structure determination have been obtained for **3**, **5** and **6**.

NMR Spectra: In contrast to the compounds Cp*PR_2, which exhibit a mirror plane perpendicular to the ring, molecules of the type Cp*$_2$PR show diastereotopic methyl groups, which is similar to the situation in the phosphanes Cp*PRR′. All methyl groups are anisochronous, which corresponds to the observation of five sets of signals in the proton-NMR spectra.[10] However, these signals sometimes do not appear resolved, as, for instance, in the case of the compounds **3** and **4**, where the chemical shift of the methyl groups in positions 3 and 4 are almost the same.[15]

Figure 1. The NMR data were assigned according to the depicted numbering

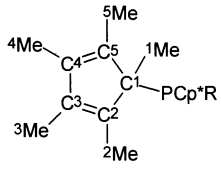

Table 1. ^{1}H-NMR data of **3**−**7** (C_6D_6)

	3	**4**	**5**	**6**	**7**
2,5-Me_2	1.72	1.89 1.81	1.90 1.78	2.07 1.94	1.85 1.69
3,4-Me_2	1.61	1.70	1.71 1.64	1.78 1.74	1.41 1.29
1-Me	0.95 d ($^3J_{HP}$ = 16.3 Hz)	1.33 d ($^3J_{HP}$ = 16.5 Hz)	1.26 d ($^3J_{HP}$ = 15.2 Hz)	1.42 d ($^3J_{HP}$ = 16.8 Hz)	1.35 d ($^3J_{HP}$ = 11.2 Hz)
R	R = H 3.48 d ($^1J_{HP}$ = 190.0 Hz)	R = N_3 −	R = OMe 3.50 d ($^3J_{HP}$ = 12.9 Hz)	R = SMe 2.29 d ($^3J_{HP}$ = 13.7 Hz)	R = Me 1.3 d ($^2J_{HP}$ = 10.4 Hz)

Table 2. ^{13}C-NMR data of **3**−**7** (C_6D_6)

	3	**4**	**5**	**6**	**7**
C-2−5	139.5 d (J_{CP} = 1.5 Hz) 137.4 d (J_{CP} = 8.8 Hz) 134.9 d (J_{CP} = 4.6 Hz) 134.0 (s)	138.9 d (J_{CP} = 2.0 Hz) 136.5 d (J_{CP} = 5.9 Hz) 135.3 d (J_{CP} = 2.8 Hz 134.6 (s)	139.4 d (J_{CP} = 1.2 Hz) 135.3 d (J_{CP} = 2.4 Hz) 134.9 d (J_{CP} = 9.1 Hz) 134.2 d (J_{CP} = 15.0 Hz)	140.0 d (J_{CP} = 2.3 Hz) 137.3 d (J_{CP} = 14.1 Hz) 135.5 d (J_{CP} = 4.1 Hz) 134.6 d ($^1J_{CP}$ = 18.9 Hz)	137.9 d (J_{CP} = 10.4 Hz) 136.3 d (J_{CP} = 12.9 Hz 134.4 d (J_{CP} = 11.9 Hz) 133.3 d (J_{CP} = 12.6 Hz)
C-1	56.3 d ($^1J_{CP}$ = 27.0 Hz)	60.7 d ($^1J_{CP}$ = 35.4 Hz)	62.3 d ($^1J_{CP}$ = 26.3 Hz)	60.1 d ($^1J_{CP}$ = 38.5 Hz)	58.6 d ($^1J_{CP}$ = 27.7 Hz)
2−5-Me	11.8 11.4 11.2	12.5 11.6 11.3 11.0	12.3 11.5 11.3 11.2	13.1 11.7 11.6 11.4	11.9 11.7 11.1 11.0
1-Me	20.4 d ($^2J_{CP}$ = 22.0 Hz)	19.4 d ($^2J_{CP}$ = 18.8 Hz)	19.4 d ($^2J_{CP}$ = 18.6 Hz)	21.5 d ($^2J_{CP}$ = 19.6 Hz)	22.5 d ($^2J_{CP}$ = 10.4 Hz)
R	R = H −	R = N_3 −	R = OMe 61.2 (s)	R = SMe 22.3 d ($^2J_{CP}$ = 27.2 Hz)	R = Me 21.6 d ($^1J_{CP}$ = 60.6 Hz)

An incidental isochrony of the methyl groups 3 and 4, not only in the ^{1}H- but also in ^{13}C{^{1}H}-NMR spectra, can be observed in compound **2**. A borderline case of this situation may be ascribed to compounds **5** and **7**, in which the ^{13}C-NMR signals of the carbon atoms appear very close to each other but are still distinguishable. Owing to the greater dispersion of ^{13}C-NMR shifts, the influence of the substituents attached to the phosphorus atom on the shielding of the methyl groups 3 and 4 is more significant in ^{13}C-NMR than ^{1}H-NMR spectroscopy.

X-ray Structures of 3, 5, and 6: The molecular structures of **3**, **5**, and **6** in the crystal show significant similarities. The X-ray structures agree well with the results from multinuclear NMR spectroscopy and confirm the presence of

two η^1-bounded Cp* rings in all three cases. These rings are planar (deviation < 1 pm) and exhibit an almost parallel relative arrangement. However, these rings adopt no ecliptic conformation but are slightly twisted, probably in order to minimize repulsive interactions of the methyl groups. The planarity of these rings causes a deviation from ideal tetrahedral angles at the saturated, sp^3-hybridised carbon atoms (angles: C5−C1−C2 and. C12−C11−C15). These findings correspond well with the results for other bis(η^1-Cp*)-substituted congeners, for which X-ray structures are available, e.g. Cp^*_2S[16] or $Cp^*_2SiCl_2$[17]. The proton in the secondary phosphane **3** can not be localized in the differential Fourier-analysis, due to the proximity of the phosphorus atom. The P−C bond lengths in all the three molecules are in the range of 187.7−190.6 pm, as expected for such compounds, but are slightly elongated with respect to the standard bond length of 185 pm.[18]

The largest P−C value in this series has been found for compound **6**. However, the P−S distance (211.7 pm) in this compound, as well as the P−O distance (164.1 pm) in **5** are completely normal and in the range for regular P−chalkogene single bonds.[18]

Figure 2. Molecular structure of Cp^*_2PH **3**[a]

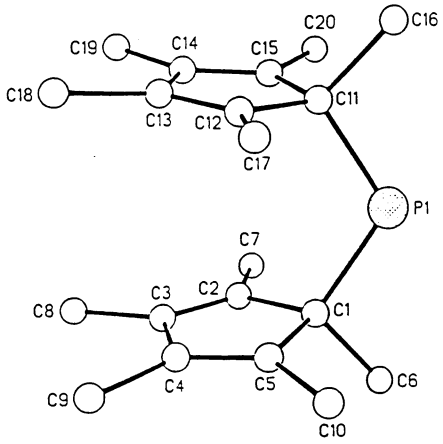

[a] Selected bond lengths [pm] and angles [°]: P1−C1 187.7 (4), P1−C11 188.9 (5); C1−P1−C11 112.6 (2), P1−C1−C6 104.1 (3), P1−C11−C16 103.4 (3); interplanar angle between Cp* planes: 9.6(3)°.

Amino-Substituted Bis(Cp*)phosphanes

The formation of amino-functionalized bis(Cp*)phosphanes can be accomplished by an inverse strategy, connecting the P−N bond prior to the P−C bonds. Therefore the corresponding aminodichlorophosphane was treated with 2.2 equivalents of Cp*Li in pentane as solvent.

For convenience an exess of Cp*Li was used, which reduces the reaction time significantly. The presence of two Cp* moieties at the same phosphorus atom limits, due to steric hindrance, the variety of possible substituents at the nitrogen atom. An imino group should be a suitable nitrogen-containing substituent because it has a small steric bulk. Following this concept the phosphoraneimino-substituted bis(Cp*)phosphane **9**, was readily obtained as pale

Figure 3. Molecular structure of Cp^*_2POMe **5**[a]

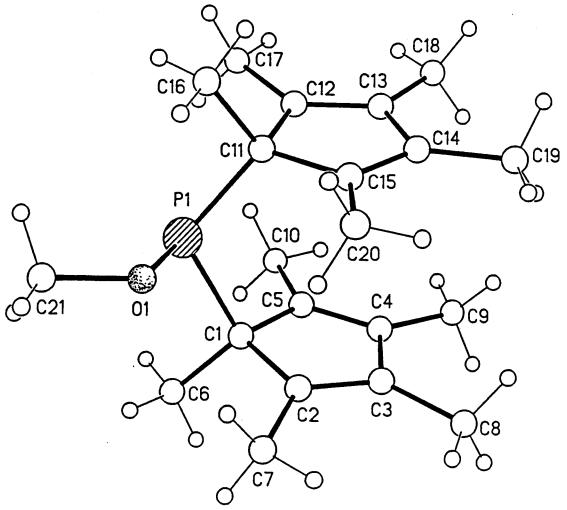

[a] Selected bond lengths [pm] and angles [°]: P1−O1 164.1 (3), P1−C1 188.0 (4), P1−C11 187.8 (4); C1−P1−C11 110.5 (2), P1−C1−C6 104.0 (2), P1−C11−C16 105.0 (2), O1−P1−C1 100.2 (2), O1−P1−C11 100.2 (2), P1−O1−C21 118.7 (3); interplanar angle between Cp* planes: 7.0(2)°.

Figure 4. Molecular structure of Cp^*_2PSMe **6**[a]

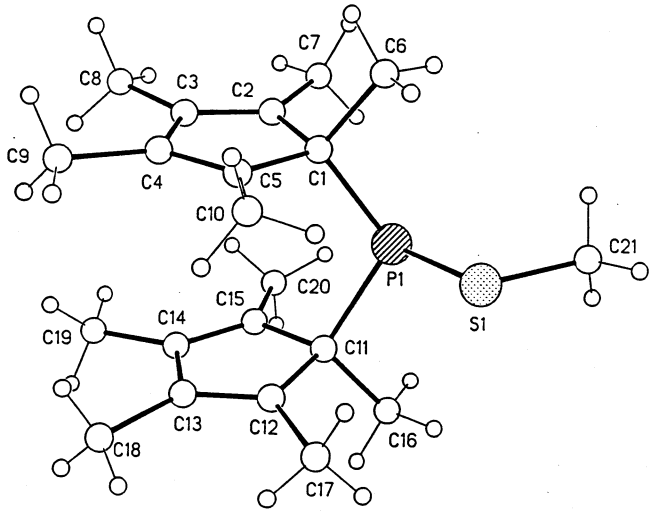

[a] Selected bond lengths [pm] and angles [°]: P1−S1 211.7 (1), P1−C1 190.6 (3), P1−C11 189.7 (3); C1−P1−C11 110.3 (1), P1−C1−C6 106.3 (2), P1−C11−C16 104.8 (2), S1−P1−C1 104.1 (1), S1−P1−C11 102.6 (1), P1−S1−C21 101.3 (1); interplanar angle between Cp* planes: 7.5(2)°.

Scheme 2. Synthesis of the aminobis(Cp*)phosphanes **11**

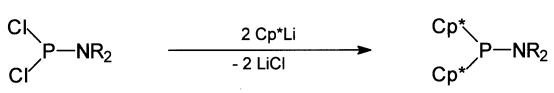

10 **11**

(R= CH_3, **a**; C_2H_5, **b**; $(CH_2)_5$, **c**)

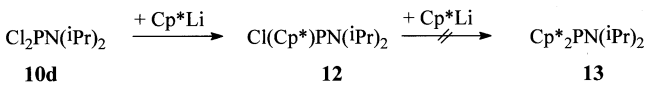

10d **12** **13**

yellow solid starting from the corresponding dichlorophosphane **8** and two equivalents of Cp*Li[15].

Moreover, the syntheses of the dimethylamino (**11a**) and diethylamino (**11b**) derivatives were also sucessful by this method, while in contrast the introduction of an diisopropylamino group failed. In the latter case the reaction of dichloro(diisopropylamino)phosphane (**10d**)[19] with excess Cp*Li produces the monosubstituted phosphane **12**[20].

NMR Spectra: Similar to the ^{1}H-NMR spectra of the compounds **3**−**7**, the anisochrony of all methyl groups in the bis(Cp*)aminophosphanes **11a**−**c** can be observed as well. However, the signals for the latter compounds appear clearly separated and do not overlap as in the previously described case.

Figure 5. The NMR data were assigned according to the depicted numbering

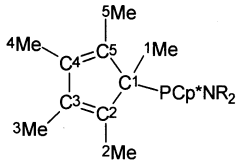

Table 3. ^{1}H-NMR data of **11a**−**c** (C_6D_6)

	11a	**11b**	**11c**
2,5-Me	1.85 1.76	1.87 1.81	1.87 1.80
3,4-Me	1.74 1.69	1.75 1.69	1.76 1.70
1-Me	0.96 d ($^3J_{HP}$ = 15.5 Hz)	0.90 d ($^3J_{HP}$ = 15.2 Hz)	0.91 d ($^3J_{HP}$ = 15.3 Hz)
R	R = NMe_2 2.63 d ($^3J_{HP}$ = 7.9 Hz)	R = $N(CH_2CH_3)_2$ CH_2: 2.94 (m) CH_3: 0.87 d ($^3J_{HH}$ = 7.1 Hz)	R = N[−$C^1H_2C^2$- $H_2C^3H_2CH_2CH_2$−] C^1H_2: 2.93 (m) $C^{2,3}H_2$: 0.87 (m)

X-ray Structure of **11a**: The dimethylamino-substituted bis(Cp*)phosphane **11a** crystallizes as colourless prisms and in the space group $P\bar{1}$. Similarly to the previously described structures both rings are bonded in an η^1 manner and are perfectly planar. However, a significantly different feature of this molecule is the surprisingly nonparallel orientation of the Cp* rings, which are tilted by 130.6(1)°. This compound represents the first example of a bis(Cp*)-phosphane with a nonparallel arrangement of the Cp* rings.

It is unlikely that this unusual geometry is due to a direct interaction of the nitrogen atom and its lone pair with the twisted Cp* ring, since the almost planar environment at this center [$\measuredangle$ N: 358.8(1)°] is a common feature of aminophosphanes[21][22]. Any influence of the phosphorus atom, which is pyramidalized to the same extent [$\Sigma\measuredangle$ P: 325.3(1)°]

Table 4. ^{13}C-NMR data of **11a**−**c** (C_6D_6)

	11a	**11b**	**11c**
C-2−5	140.1 d (J_{CP} = 1.9 Hz) 140.0 d (J_{CP} = 11.4 Hz) 135.1 d (J_{CP} = 1.5 Hz) 134.6 d (J_{CP} = 3.8 Hz)	141.1 d (J_{CP} = 3.4 Hz) 141.0 d (J_{CP} = 10.7 Hz) 135.2 d (J_{CP} = 1.9 Hz) 134.7 d (J_{CP} = 3.4 Hz)	141.0 d (J_{CP} = 3.4 Hz 140.6 d (J_{CP} = 9.5 Hz) 134.8 d (J_{CP} = 1.9 Hz) 134.3 d (J_{CP} = 3.4 Hz)
C-1	65.3 d ($^1J_{CP}$ = 43.1 Hz)	65.6 d ($^1J_{CP}$ = 46.1 Hz)	65.5 d ($^1J_{CP}$ = 45.4 Hz)
2−5-Me	13.0 d (J_{CP} = 6.9 Hz) 12.3 d (J_{CP} = 11.4 Hz) 11.7 d (J_{CP} = 5.3 Hz)	13.3 d (J_{CP} = 8.4 Hz) 12.5 d (J_{CP} = 12.6 Hz) 11.7 d (J_{CP} = 5.0 Hz)	13.1 d (J_{CP} = 8.8 Hz) 12.2 d (J_{CP} = 11.4 Hz) 11.6 d (J_{CP} = 8.8 Hz)
1-Me	19.7 d ($^2J_{CP}$ = 21.0 Hz)	19.1 d ($^2J_{CP}$ = 19.1 Hz)	19.4 d ($^2J_{CP}$ = 21.0 Hz)
R	R = NMe_2 46.9 d ($^2J_{CP}$ = 18.8 Hz)	R = $N(CH_2CH_3)_2$ CH_2 : 34.7 (s) CH_3 : 15.4 d ($^3J_{CP}$ = 1.9 Hz)	R = N[−$C^1H_2C^2$- $H_2C^3H_2CH_2CH_2$−] C^1H_2 : 34.5 (s) C^2H_2 : 27.9 d ($^3J_{CP}$ = 5.0 Hz) C^3H_2 : 24.9 (s)

as in other bis(Cp*)phosphanes, on the arrangement of the rings can also be discounted.

The most probable reason for this unusual geometric feature arises from the packing of the molecules within the crystal. There is an orientation of one proton of the methyl group in the 4-position towards the twisted Cp* ring of another molecule, generated by symmetry transformation $-x$, $2 - y$, $2 - z$, and vice versa.

Figure 6. Intermolecular interactions of the aminophosphane **11a** in the crystal

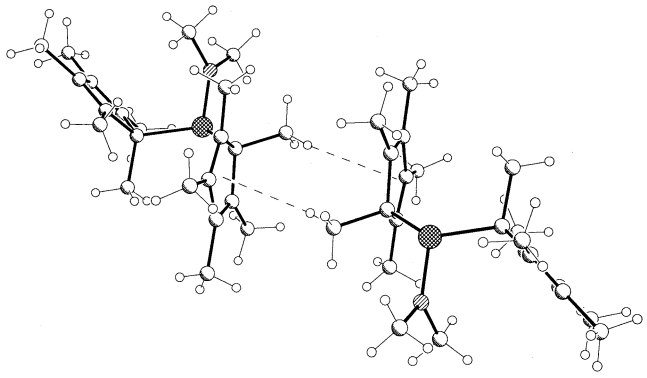

The P−C bond lengths in **11a** [191.1(3) pm] are even longer than in the previously mentioned compounds. Additionally, the P−N bond appears slightly shortened [168.0(3) pm]. These findings may be ascribed to tendency towards partial ionic character in **11a**.

Figure 7. Molecular structure of Cp_2PNMe_2 **11a**[a]

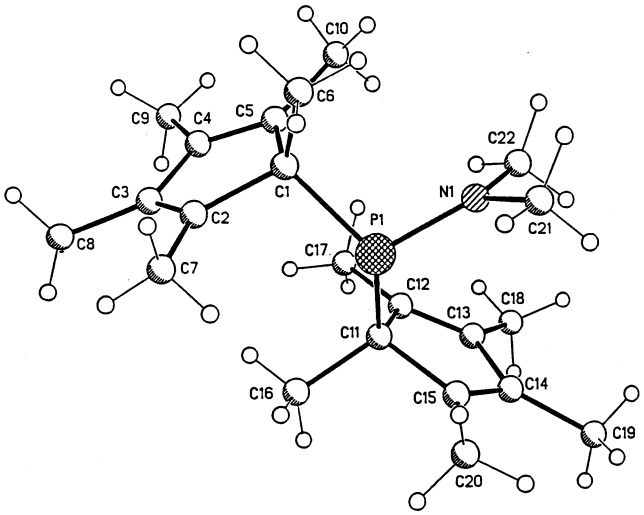

[a] Selected bond lengths [pm] and angles [°]: P1−N1 168.0 (3), P1−C1 191.1 (3), P1−C11 191.0 (3), N1−C21 145.7 (5), N1−C22 144.6 (5); C1−P1−C11 112.7 (1), N1−P1−C1 106.8 (1), N1−P1−C11 105.8 (1), P1−N1−C21 116.5 (3), P1−N1−C22 128.8 (3), C21−N1−C22 113.5 (3); interplanar angle between Cp* planes: 130.6(1)°.

We thank the *Deutsche Forschungs-Gemeinschaft* and the *Fonds der Chemischen Industrie* for continued financial support. S. K. thanks the *Finnish Academy of Science* for a grant.

Experimental Section

All reaction steps were carried out under dried argon in order to exclude air and moisture; glassware, reagents and solvents were similarly prepared. − ^{31}P NMR: Bruker AMX 300 (121.5 MHz); external standard 85% H_3PO_4. − ^{13}C NMR: Bruker AMX 300 (75.5 MHz); external standard tetramethylsilane. − ^{1}H NMR: Bruker AMX 300 (300 MHz); external standard tetramethylsilane. ^{31}P- and ^{13}C-NMR spectra were recorded with ^{1}H decoupling. A positive sign means low field with respect to the standard. − MS: Kratos MS 50 and VG Instruments VG 12-250 (EI, direct inlet). The given *m/z* values refer to the isotope of highest abundance for each element. − M.p.: Measured without correction in sealed capillaries in a melting point apparatus supplied by Firma Büchi, Flawil/Switzerland. − Elemental analyses: Heraeus CHN-O-Rapid. − The literature procedure for the syntheses of the bis(Cp*)halogenophosphanes **2a** and **2b** has been slighly modified[10].

Chlorobis(1,2,3,4,5-pentamethyl-2,4-cyclopentadien-1-yl)phosphane (**2a**) *and Bromobis(1,2,3,4,5-pentamethyl-2,4-cyclopentadien-1-yl)phosphane* (**2b**): 1.8 ml (20 mmol) of PCl_3 or 19 ml (20 mmol) of PBr_3 was added slowly at 0°C to a suspension of 3.4 g (24 mmol) of Cp*Li in 50 ml of pentane. The mixture was cooled to room temp. and stirred vigorously for a further 10 h. The insoluble precipitate was removed by filtration and washed several times with pentane. The volume of the combined filtrate was reduced to approximately 10 ml, the product crystallised on cooling to −35°C. − **2a**: Yield: 5.5 g (87%, rel. PCl_3). − ^{31}P{^{1}H} NMR (C_6D_6): δ = 165.5 (s). − **2b**: Yield: 6.4 g (82%, rel. PBr_3). − ^{31}P{^{1}H} NMR (C_6D_6): δ = 167.8 (s).

Bis(1,2,3,4,5-pentamethyl-2,4-cyclopentadien-1-yl)phosphane (**3**): A solution of 1.5 g (4.5 mmol) of **2a** in 3 ml of diethyl ether was added, at 0°C, to a suspension of 70 mg of $LiAlH_4$ in 5 ml of diethyl ether. After warming to room temp. and further stirring, the solvent was removed. The residue was extracted with pentane and, after separation from the unsoluble precipitate, the filtrate was concentrated. On cooling to −35°C, the product was obtained as colorless crystals. Yield: 0.8g (59%), m.p. 108°C. − ^{31}P{^{1}H} NMR (C_6D_6): δ = −42.2 (s). − MS (180°C/70 eV); *m/z* (%): 302 (8) [M^+], 167 (100) [M^+ − Cp*], 135 (13) [Cp*$^+$] and further fragments. − $C_{20}H_{31}P$ (302.2): calcd. C 79.43, H 10.33; found C 77.71, H 10.33.

Azidobis(1,2,3,4,5-pentamethyl-2,4-cyclopentadien-1-yl)phosphane (**4**): 3.5 g (9.2 mmol) of **1b** was dissolved in 5 ml of pyridine. While cooling with ice, 0.47 g (9.5 mmol) of LiN_3 was added as pure solid. Under continuous stirring, the mixture was warmed to room temp. within 0.5 h and the pyridine was removed in vacuo. The residue was extracted with pentane and, after separation from the unsoluble precipitate, the filtrate was concentrated. On cooling to −35°C the product was obtained as colorless solid, which was then recrystallised several times to remove impurities. Yield: 2.3 g (73%), m.p.. 70°C (dec.). − ^{31}P{^{1}H} NMR (C_6D_6): δ = 138.2 (s) − MS (100°C/70 eV), *m/z* (%): 343 (8) [M^+], 315 (6) [$M^+ - N_2$], 301 (4) [$M^+ - N_3$], 270 (29) [Cp*$_2^+$], 208 (39) [M^+ − Cp*], 135 (13) [Cp*$^+$] and further fragments. − UV/Vis (pentane): λ_{max} (lgε) = 215 nm, 230, 265. − $C_{20}H_{30}N_3P$ (343.5): calcd. C 69.94, H 8.80, N 12.23; found C 68.69, H 8.67, N 12.02.

Methoxybis(1,2,3,4,5-pentamethyl-2,4-cyclopentadien-1-yl)phosphane (**5**): 0.64 g (1.9 mmol) of **1a** was dissolved in 10 ml of pentane and added, under continuous stirring, to 0.05 g (2.1 mmol) of sodium in 20 ml of methanol at room temp. After the addition was completed, the mixture was stirred for a further 3 h at 40°C. The volatile components were removed in vacuo, and the residue extracted with pentane. After filtration and on cooling to −70°C, the product was obtained as white needles. Yield: 0.46 g (73%), m.p. 84−88°C. − ^{31}P{^{1}H} NMR (C_6D_6): δ = 184.8 (s) − MS (100°C/40 eV); *m/z* (%): 332 (3) [M^+], 301 (0.5) [$M^+ - OCH_3$], 197 (100) [M^+ − Cp*], 135 (70) [Cp*$^+$] and further fragments. − An analysis was not performed.

Methylthiobis(1,2,3,4,5-pentamethyl-2,4-cyclopentadien-1-yl)phosphane (**6**): 0.54 g (1.5 mmol) of **1b**, dissolved in 3 ml of toluene/DMF (2:1), was added to an equivalent amount of $NaSCH_3$ (0.1 g) in 2 ml of DMF at 0°C. The solution was stirred for 1 h at ambient temp. The solvents were evaporated under reduced pressure and the residue extracted with pentane. After separation of the solid precipitate, the filtrate was concentrated and the product crystallised at −35°C. Recrystalisation at the same temp. yielded the product as pale yellow crystals. Yield 0.46 g (88%), m.p. 95−100°C. − ^{31}P{^{1}H} NMR (C_6D_6): δ = 85.1 (s) − MS (100°C/35 eV); *m/z* (%): 348 (15) [M^+], 301 (15) [$M^+ - SCH_3$], 270 (3) [Cp*$_2^+$], 213 (100) [M^+ − Cp*], 166 (30) [Cp*P$^+$], 135 (50) [Cp*$^+$] and further fragments. − $C_{21}H_{33}PS$ (348.5): calcd. 348.2041; found 348.2046 (MS).

Methylbis(1,2,3,4,5-pentamethyl-2,4-cyclopentadien-1-yl)phosphane (**7**): 3.5 ml (2.2 mmol) of CH_3Li (1.6 M in diethyl ether) was added slowly to 0.67 g (2 mmol) of **1a** in 5 ml of diethyl ether at −78°C. After warming to room temp., the volatile parts of the mixture were removed in vacuo. The residue was extracted with pentane and, after separation from the unsoluble precipitate, the filtrate was concentrated. On cooling to −35°C, the product was obtained as a solid which was recrystallised several times, finally at 0°C to yield 0.5 g (79%) of white crystals. m.p. 138−140°C. − ^{31}P{^{1}H} NMR (C_6D_6): δ = 72.9 (s) − MS (100°C/35 eV); *m/z* (%): 316 (15) [M^+], 301 (5) [$M^+ - CH_3$], 270 (1) [Cp*$_2^+$], 181 (100)

[M^+ − Cp*], 166 (20) [Cp*P^+], 135 (60) [Cp*$^+$] and further fragments. − $C_{21}H_{33}P$ (316.5): calcd. 316.2322; found 316.2327 (MS).

Bis(1,2,3,4,5-pentamethyl-2,4-cyclopentadien-1-yl)-(triphenylphosphoranylimino)phosphane (**9**): A suspension of 0.6 g (4.0 mmol) of Cp*Li in pentane (10 ml) was treated dropwise with 0.8 g (2 mmol) of dichloro(triphenylphosphoranylimino)phosphane[15] at −40°C. The solution was stirred for a further 12 h and warmed to room temp. After filtration, the solution was concentrated and the product isolated after crystallisation from ether/THF at 5°C. The product **8** was obtained as yellow crystals. Yield 0.8 g (70%), m.p. 170°C (dec.). − $^{31}P\{^1H\}$ NMR (ether/C_6D_6): δ = 93.0 (d, $^2J_{PP}$ = 109 Hz), 17.8 (d, J_{PP} = 109 Hz). − ^1H NMR ([D_8]THF): δ = 7.9−7.6 (m, 2 H), 7.5−7.4 (m, 3 H) H arom., 2.0 (s, 3 H), 1.7 (s, 6 H), 0.7 (d, 3 H, $^3J_{PH}$ = 14.1 Hz) C_5Me_5. − $^{13}C\{^1H\}$ NMR ([D_8]THF): δ = 141.7 (d, 2.1 Hz), 138.7 (s), 138.0 (s), 136.6 (d, 1.5 Hz), 63.0 (dd, $^1J_{PC}$ = 39.5 Hz, $^3J_{PC}$ = 9.6 Hz) C_5 ring; 133.7 (d, 2.6 Hz), 133.1 (dd, $^1J_{PC}$ = 45.2 Hz, $^3J_{PC}$ = 2.7 Hz), 129.1 (s), 128.5 (s) C_{arom}; 22.1 (d, $^2J_{PC}$ = 11.6 Hz), 13.7 (d, 2.7 Hz), 12.5 (s), 11.5 (s), 11.4 (s) C_5Me_5. − MS (300°C/40 eV); *m/z* (%): 577 (6) [M^+], 576 (13) [M^+ − H], 443 (60 [M^+ − Cp*], 308 (100) [M^+ − 2Cp*], 262 (65) [PPh_3^+], 135 (44) [Cp*$^+$] and further fragments. − $C_{38}H_{45}NP_2$ (577): calcd. C 79.00, H 7.85, N 2.42; found C 78.91, H 8.05, N 2.39.

(Dialkylamino)bis(1,2,3,4,5-pentamethyl-2,4-cyclopentadien-1-yl)-phosphanes (**11a**−**c**): A suspension of 0.68 g (4.8 mmol) of Cp*Li in pentane was treated dropwise with 2 mmol of **10a**−**c** at room temp. The solution was stirred for a further 12 h and filtered afterwards. The solution was concentrated and the product isolated after crystallisation at −35°C. In all three cases yellow crystals were obtained.

(Dimethylamino)bis(1,2,3,4,5-pentamethyl-2,4-cyclopentadien-1-yl)-phosphane (**11a**): Yield: 0.59 g (86%), m.p. 103−105°C. − $^{31}P\{^1H\}$ NMR (C_6D_6): δ = 117.3 (s). − MS (25°C/70 eV); *m/z* (%): 345 (0.2) [M^+], 301 (0.4) [M^+ − $N(CH_3)_2$], 270 (0.7) [Cp*$_2^+$], 213 (100) [M^+ − Cp*], 166 (20) [Cp*P^+], 135 (20) [Cp*$^+$] and further fragments. − An analysis was not performed.

(Diethylamino)bis(1,2,3,4,5-pentamethyl-2,4-cyclopentadien-1-yl)-phosphane (**11b**): Yield: 0.61 g (81%), m.p. 53−55°C. − $^{31}P\{^1H\}$ NMR (C_6D_6): δ = 116.5 (s). − MS (200°C/25 eV); *m/z* (%): 373 (2) [M^+], 301 (1) [M^+ − $N(C_2H_5)_2$], 270 (15) [Cp*$_2^+$], 238 (90) [M^+ − Cp*], 166 (20) [Cp*P^+], 135 (100) [Cp*$^+$] and further fragments. − $C_{24}H_{40}NP$ (373.6): calcd. C 77.17, H 10.79, N 3.75; found C 76.91, H 10.85, N 3.53.

Bis(1,2,3,4,5-pentamethyl-2,4-cyclopentadien-1-yl)piperidinophosphane (**11c**): Yield: 0.58 g (75%), m.p. 83−85°C. − $^{31}P\{^1H\}$ NMR (C_6D_6): δ = 116.8 (s). − MS (200°C/25 eV); *m/z* (%): 385 (4) [M^+], 301 (1) [M^+ − $N(CH_2)_5$], 250 (90) [M^+ − Cp*], 166 (35) [Cp*P^+], 135 (100) [Cp*$^+$] and further fragments. − $C_{25}H_{40}NP$ (385.6): calcd. C 77.88, H 10.46, N 3.63; found C 77.41, H 10.02, N 3.48.

X-ray Structure Determination of **3**, **5**, **6**, *and* **11a**: The structures were solved by direct methods (SHELXTL-Plus[24]). The non-hydrogen atoms were refined anisotropically, H atoms were refined using a riding model [full-matrix least-squares refinement on F (**3**, **5**: SHELXTL-plus[24]) and F^2 (**6**, **11a**: SHELXL-93[25]), respec-

Table 5. Crystallographic data and summary of data collection and refinement

	3	**5**	**6**	**11a**
formula	$C_{20}H_{31}P$	$C_{21}H_{33}OP$	$C_{21}H_{33}PS$	$C_{22}H_{36}NP$
M_r	302.4	332.4	348.5	345.5
dimensions [mm]	0.90×0.90×0.90	0.30×0.50×0.90	0.45×0.40×0.25	0.40×0.35×0.20
crystal system	monoclinic	monoclinic	monoclinic	triclinic
space group	$P2_1/c$ (No. 14)	$P2_1/n$ (No. 14)	$P2_1/c$ (No. 14)	$P\bar{1}$ (No. 2)
a [Å]	10.374(2)	13.491(4)	8.664(1)	8.837(2)
b [Å]	11.237(2)	10.497(2)	14.509(3)	11.531(3)
c [Å]	16.529(3)	14.435(5)	16.805(3)	11.928(3)
α [°]	90	90	90	72.99(2)
β [°]	91.08(1)	99.34(3)	97.22(1)	72.61(2)
γ [°]	90	90	90	78.59(2)
V [Å^3]	1931(1)	2017(1)	2095.7(6)	1101.0(5)
Z	4	4	4	2
ρ [g cm^{-3}]	1.04	1.10	1.11	1.04
μ [mm^{-1}]	0.132	0.135	0.230	0.128
F(000)	664	728	760	380
diffractometer	Nicolet R3m	Enraf-Nonius CAD4	Nicolet R3m	Nicolet R3m
radiation	Mo-K_α	Mo-K_α	Mo-K_α	Mo-K_α
λ [Å]	0.71073	0.71073	0.71073	0.71073
T [K]	298(2)	193(2)	293(2)	293(2)
$2\theta_{max.}$ [°]	50	48	50	50
	$-12 \le h \le 12$	$-15 \le h \le 15$	$-10 \le h \le 10$	$-10 \le h \le 10$
	$0 \le k \le 13$	$0 \le h \le 12$	$0 \le h \le 17$	$-13 \le h \le 13$
	$0 \le h \le 19$	$0 \le h \le 16$	$0 \le h \le 20$	$0 \le h \le 14$
no. of measured data	3747	3493	3815	4106
no. of unique data	3417	3148	3680	3901
no. of obs. data/s for [$F > s\sigma(F)$]	2550/4	2209/3	2419/4	2505/4
R_{int}	0.146	0.012	0.020	0.046
refinement on	F	F	F^2	F^2
no. of parameters	191	208	219	229
R [for $F > \sigma(F)$]	0.101	0.062	0.053	0.063
wR	0.123	0.073		
$wR2$ (all data)			0.146	0.180
max./min. difference peak [e/Å^3]	0.42/−0.43	0.81/−0.27	0.44/−0.17	0.32/−0.25

tively]. In **3** an extinction correction was applied and the H(P) could not be localized. Further details are given in Table 5. Additional information on the crystal-structure investigations may be obtained from the Fachinformationszentrum Karlsruhe, D-76344 Eggenstein-Leopoldshafen (FRG) on quoting the depository number CSD-407789 (**3**), -407790 (**5**), -407791 (**6**), -407792 (**11a**), the names of the authors, and the journal citation.

[1] P. Jutzi, *Nachr. Chem. Techn. Lab.* **1978**, *26*, 422−424.
[2] P. Jutzi, *Adv. Organomet. Chem.* **1986**, *26*, 217−295.
[3] P. Jutzi, *Comments Inorg. Chem.* **1987**, *6*, 123−144.
[4] Ch. Elschenbroich, A. Salzer, *Organometallchemie*, B.G. Teubner, Stuttgart, **1990**.
[5] S. G. Baxter, A. H. Cowley, S. K. Mehrotra, *J. Am. Chem. Soc.* **1981**, *103*, 5572−5573.
[6] P. Jutzi, B. Hampel, M. B. Hursthouse, I. A. Howes, *Organometallics* **1986**, *5*, 1944−1948.
[7] P. R. Schonberg, R. T. Paine, C. F. Campana, *J. Am. Chem. Soc.* **1979**, *101*, 7726−7728.
[8] P. Jutzi, T. Wippermann, C. Krüger, H. J. Kraus, *Angew. Chem.* **1983**, *95*, 244; *Angew. Chem. Int. Ed. Engl.* **1983**, *22*, 250.
[9] H. Saleske, Ph. D. Thesis, Universität Würzburg **1983**.
[10] P. Jutzi, H. Saleske, *Chem. Ber.* **1984**, *117*, 222−233.
[11] J. E. Bentham, E. V. A. Ebsworth, H. Moretto, D. W. H. Rankin, *Angew. Chem.* **1972**, *84*, 683; *Angew. Chem. Int. Ed. Engl.* **1972**, *11*, 640.
[12] F. Mathey, J. P. Lampin, *Tetrahedron* **1975**, *31*, 2885.
[13] D. Gudat, H. M. Schiffner, M. Nieger, D. Stalke, A. J. Blake, H. Gondey, E. Niecke, *J. Am. Chem. Soc* **1992**, *114*, 8857.
[14] F. X. Kohl, P. Jutzi, *J. Organomet. Chem.* **1983**, *243*, 119.
[15] H. M. Schiffner, Ph. D. Thesis, Universität Bonn **1991**.
[16] A. J. Bard, A. H. Cowley, J. K. Leland, G. J. N. Thomas, N. C. Norman, P. Jutzi, Ch. P. Morley, F. Schlüter, *J. Chem. Soc., Dalton Trans.* **1985**, 1303−1307.
[17] P. Jutzi, D. Kanne, M. Hursthouse, A. J. Jones, *Chem. Ber.* **1988**, *121*, 1299−1305.
[18] R. Rademacher, *Strukturen organischer Moleküle*, vol. 2, VCH Verlagsgesellschaft mbH, Weinheim, **1987**.
[19] W. Albers, W. Krüger, W. Storzer, R. Schmutzler, *Synth. React. Inorg. Met.-Org. Chem.* **1985**, *15*, 187−195.
[20] Characterisation: A. Loew, Ph. D. Thesis, Universität Bonn **1995**.
[21] L. V. Velkow, L. S. Khalkin, V. V. Evdokimov, *J. Struct. Chem.* **1982**, *3*, 495−497.
[22] G. Schick, A. Loew, M. Nieger, K. Airola, E. Niecke, *Chem. Ber.* **1996**, *129*, 211−217.
[23] J. Ebels, E. Niecke, M. Nieger, R. Pietschnig, *Bull. Chem. Soc. Fr.*, submitted for publication.
[24] G.M. Sheldrick, *SHELXTL-Plus*, Siemens Analytical X-ray Instruments Inc. Madison, WI, USA, **1989**.
[25] G.M. Sheldrick, *SHELXL-93*, University of Göttingen, **1993**.

[97234]

Diastereoselective Substitution of PR_3 for CO in Carbene(dicarbonyl)-cyclopentadienyl Complexes of Manganese − Synthesis of (S_{Mn})- and (R_{Mn})-[Cp(CO)(PR_3)Mn=C(OR*)R′] Complexes

Helmut Fischer*, Kerstin Weißenbach, Christoph Karl, and Armin Geyer

Fakultät für Chemie, Universität Konstanz, Fach M727,
D-78457 Konstanz, Germany
E-mail: hfischer@dg6.chemie.uni-konstanz.de

Received October 20, 1997

Keywords: Carbene complexes / Carbyne complexes / Asymmetric synthesis / Carbohydrates / Chiral auxiliaries

Chiral carbene complexes [Cp(CO)$_2$Mn=C(OR*)Ph] (**4a**−**e**) were prepared by reaction of [Cp(CO)$_2$Mn=C(OAc)Ph] (**2**) with HOR* [HOR* = 1,2:3,4-di-*O*-isopropylidene-D-galactopyranose (**3a**), 2,3,4,6-tetra-*O*-acetyl-D-galactopyranose (**3b**), 2,3,4,6-tetra-*O*-acetyl-D-glucopyranose (**3c**), (*S*)- (**3d**) and (*R*)-1,2-*O*-isopropylideneglycerol (**3e**)]. The replacement of a CO ligand with $PTol_3$ in **4a**−**e** proceeded diastereoselectively to give [Cp(CO)($PTol_3$)Mn=C(OR*)Ph] (**5a**−**e**). The diastereoselectivity increased in the order **a**, **b**, **c**, **d**: de = 8% (**5a**), 33% (**5b**), 70% (**5c**), > 96% (**5d**). For (*R*)-**5d** the isomer with the (*S*) configuration at manganese (S_{Mn}) was formed predominantly. For (*S*)-**5d**, only (R_{Mn},*S*)-**5d** was detected (de > 96%). Photolysis of (*R*)-**4d** in the presence of phosphites or phosphanes afforded (S_{Mn})-[Cp(CO)(PR_3)Mn=C(OR*)Ph] [PR_3 = $P(OPh)_3$ (**8**), $P(OMe)_3$ (**9**), $P(OMe)_2Ph$ (**10**), $P(OMe)Ph_2$ (**11**), PPh_3 (**12**), $P(C_6H_4Cl\text{-}p)_3$ (**13**)] with a de > 96%. Photolysis of (*S*)-**4d** in the presence of $P(OMe)_3$ gave (R_{Mn},*S*)-**9**. Complex (*R*)-**14** [related to (*R*)-**4d**] was obtained from [Cp(CO)$_2$Mn=C(OAc)Tol-*p*] and **3d**. Replacement of CO by PR_3 in (*R*)-**14** gave (S_{Mn},*R*)-[Cp(CO)(PR_3)Mn=C(OR*)Tol-*p*] [R = Tol-*p* (**15**), OMe (**16**), C_6H_4Cl-*p* (**17**)] with a de > 96%. In solution, the $PTol_3$-substituted complex **5d** is configurationally stable whereas the $P(OMe)_3$ complex **9** epimerizes slowly at room temperature in CH_2Cl_2, Et_2O, and THF within about one week.

Introduction

Chiral transition-metal complexes play a prominent role in enantioselective synthesis and catalysis. In these complexes either the metal[1] or one or more ligands carry the chiral information. Although a wide variety of carbohydrates are available from the chiral pool, the number of reports on their use as chiral auxiliaries in transition-metal chemistry is rather restricted.[2] The preparation of new carbohydrates via organometallic compounds was recently described by Dötz et al.[3]

Recently, we reported the synthesis of chiral complexes of manganese and rhenium. These complexes, of the type [Cp(CO)$_2$M=C(OR*)R′] (M = Mn, Re, OR* = mannofuranosyl, glucofuranosyl, fructopyranosyl, R′ = Ph, Tol), were obtained by addition of the monoanion of the corresponding protected carbohydrate to the cationic carbyne complexes [Cp(CO)$_2$M≡CR′]$^+$.[4]

Another route to chiral carbene complexes involves nucleophilic substitution by chiral alcoholates, such as (−)-mentholate and borneolate, of the acetoxy substituent in acetoxycarbene complexes of manganese [Cp(CO)$_2$Mn=C(OAc)R′].[5][6]

Photolysis of the chiral carbohydratocarbene complexes in the presence of phosphanes or phosphites (L) afforded chiral-at-metal carbene complexes of the type [Cp(CO)(L)M=C(OR*)R′]. The diastereomeric excess (de) ranged from 0 to 80% and depended on the nature of the carbohydrate and the entering phosphorus ligand. The diastereoselectivity increased with increasing nucleophilicity of L. The highest diastereoselectivity was obtained with OR* = 2,3:5,6-di-*O*-isopropylidene-β-D-mannofuranosyl and L = tritolylphosphane.

In this paper we report (a) on the synthesis of chiral dicarbonyl(carbohydratocarbene) complexes by alcoholysis of [acetoxy(aryl)carbene]dicarbonyl(cyclopentadienyl)manganese with protected carbohydrates and chiral alcohols, (b) on the synthesis of diastereomerically pure carbene(carbonyl)phosphane complexes, and (c) on the ready access to pure compounds of both configurations at the chiral metal center.

Results and Discussion

Successive reaction of the lithium benzoylmanganate **1** with TMEDA and acetyl bromide gave the thermolabile acetoxy carbene complex **2** as described previously.[5] The reaction of **2** with partially protected carbohydrates that are unprotected either in the 6-position [1,2:3,4-di-*O*-isopropylidene-D-galactopyranose (**3a**)] or in the 1-position [2,3,4,6-tetra-*O*-acetyl-D-galactopyranose (**3b**) and 2,3,4,6-tetra-*O*-acetyl-D-glucopyranose (**3c**)] afforded the chiral-at-ligand dicarbonyl(cyclopentadienyl)[alkoxy(phenyl)carbene] complexes **4a**−**c** in 40−66% yield (Scheme 1). The complexes (*R*)- and (*S*)-**4d** were obtained from the reaction of **2** with the enantiomerically pure alcohols (*S*)- and (*R*)-1,2-*O*-isopropylideneglycerol, (*S*)- and (*R*)-**3d**.[7]

 © WILEY-VCH Verlag GmbH, D-69451 Weinheim, 1998 1434−1948/98/0303−0339 $ 17.50+.50/0

Scheme 1

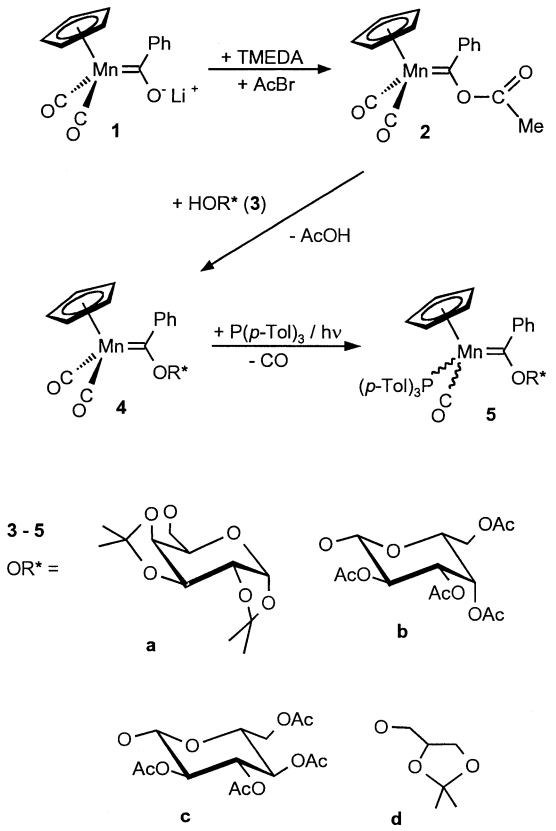

The NMR spectra of **4a**−**c** unambiguously show that the carbohydrato residue is bonded to the carbene carbon atom by the oxygen atom at C-6 (**4a**) or at C-1 (**4b**, **c**). The absence of a low-field resonance for the 1-H atom at the anomeric center in **4b** and **4c** indicates an β-configuration of the glucosyl and the galactosyl groups. This configuration was confirmed by the X-ray structural analysis of **4c** (Figure 1).

Complex **4c** exhibits a pseudo-octahedral geometry (Figure 1). The Mn−C(carbene) distance [1.857(7) Å] is comparable to that usually observed in CpL_2Mn(carbene) complexes.[4][8] The carbene ligand adopts the sterically least congested conformation. The carbene plane [C(8), Mn(1), C(9), O(8)] is slightly twisted with respect to the plane formed by the atoms C(7), Mn(1), and C(8) [torsion angle C(7)−Mn(1)−C(8)−O(8) −27.9(8)°] and strongly twisted with respect to the phenyl plane [torsion angle Mn(1)−C(8)−C(9)−C(10) 64.0(9)°].

In our earlier studies on the selectivity of the CO/PR_3 exchange in carbohydratocarbene complexes, the highest diastereoselectivity was observed for PR_3 = tri(*p*-tolyl)phosphane. Therefore, tri(*p*-tolyl)phosphane was also used in the initial studies with **4a**−**d**. Photolysis of the complexes **4a**−**d** in toluene at −30°C for several minutes in the presence of tritolylphosphane afforded the carbene complexes **5a**−**d** in moderate to high yield (Scheme 1). The compounds **5b** and **5c** are slightly photolabile. Partial decomposition had already occurred during irradiation, thus reducing the yield. Total transformation of the dicarbonyl complexes led to a low yield. Since the starting materials, complexes **4b** and **4c**, can be easily separated from the product complexes **5b** and **5c**, irradiation was terminated before **4b** and **4c** were completely consumed.

Figure 1. Structure of complex **4c** in the crystal (without H atoms)[a]

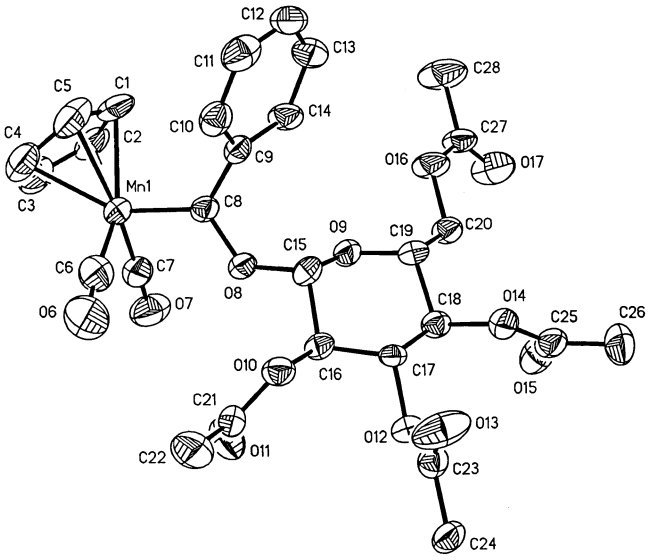

[a] Selected distances [Å] and angles [°] (standard deviations in parentheses): Mn(1)−C(6) 1.773(10), Mn(1)−C(7) 1.747(9), Mn(1)−C(8) 1.857(7), C(6)−O(6) 1.156(12), C(7)−O(7) 1.168(11), C(8)−O(8) 1.375(8); C(6)−Mn(1)−C(7) 89.4(4), C(6)−Mn(1)−C(8) 88.4(4), Mn(1)−C(8)−C(9) 124.8(5), Mn(1)−C(8)−O(8) 119.2(5), C(9)−C(8)−O(8) 116.0(6).

The ^{1}H-NMR signals of the cyclopentadienyl protons were easily detected and appeared as doublets due to coupling with the phosphorus atom. For **5a**−**c** two doublets were observed in each case: δ = 4.49, 4.53 ($^3J_{PH}$ = 1.82 Hz, 1.80 Hz; **5a**), 4.60, 4.63 ($^3J_{PH}$ = 1.79 Hz, 1.55 Hz; **5b**), and 4.64, 4.71 ($^3J_{PH}$ = 1.71 Hz, 1.45 Hz; **5c**). Therefore, the complexes **5a**−**c** were obtained as mixtures of diastereomers. The diastereomeric excess varied considerably. The diastereomeric excess, as determined by integration of the Cp resonances in the reaction mixtures, was 8% (**5a**), 33% (**5b**), and 70% (**5c**). In contrast to **5a**−**c**, each of the two glycerol derivatives (*R*)-**5d** and (*S*)-**5d** exhibit only one doublet for the cyclopentadienyl ring (δ = 4.45, $^3J_{PH}$ = 1.6 Hz). Similarly, only one ^{13}C-resonance signal for the Cp carbon atoms, and one ^{31}P signal for the tritolylphosphane ligand were detected for (*R*)-**5d** and (*S*)-**5d**. From these results a de of > 96% was deduced.

Complex (*R*)-**5d** was assigned the (S_{Mn}) configuration [(S_{Mn},*R*)-**5d**].[9] In order to corroborate the assignment, the complex was transformed into the known β-mannofuranosylcarbene complex (S_{Mn})-**7β**.[5] The structure of (S_{Mn})-**7β** has already been established by X-ray analysis.[5] Treatment of (S_{Mn},*R*)-**5d** with BCl_3 gave the chiral cationic carbyne complex (S_{Mn})-**6** by abstraction of [OR*]$^-$. Subsequent reaction with the sodium salt of an α,β mixture of 2,3:5,6-di-*O*-isopropylidene-D-mannofuranose Na[OR^1] afforded the α-mannofuranosylcarbene complex (S_{Mn})-**7α** (Scheme 2).

The identity of (S_{Mn})-**7α** was confirmed by comparison of its ^{1}H-NMR spectrum with that of an authentic sample.

Scheme 2

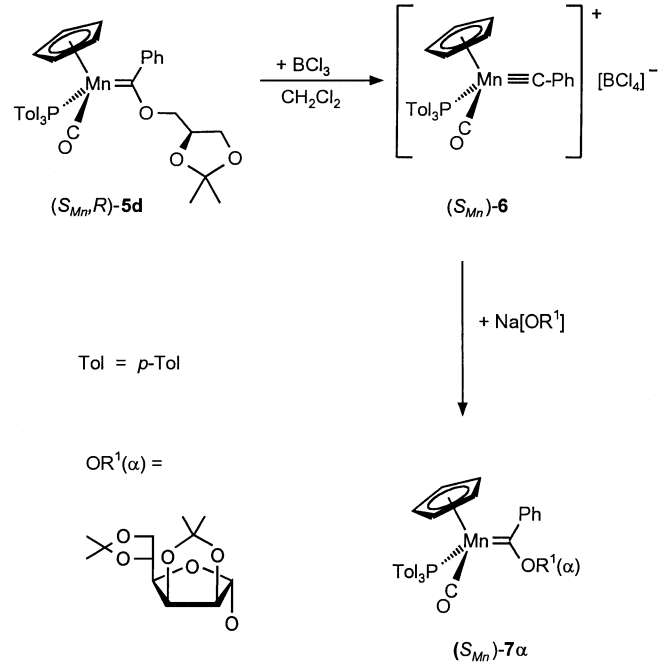

When the same reaction sequence was applied to (*S*)-**5d** the diastereomer (R_{Mn})-**7α** was obtained. Therefore, (*S*)-**5d** was assigned the (R_{Mn}) configuration.

The carbohydrate substituent clearly exerts considerable influence on the diastereoselectivity of the CO exchange reaction. From earlier experiments it followed that the photo-induced Mn−CO dissociation is the initiating and rate-limiting step of the substitution reaction. The range of diastereoselectivities observed can be rationalized by the different abilities of the OR* groups to intramolecularly stabilize the diastereomeric intermediates. It is very likely that an oxygen atom of the OR* substituent coordinates to the vacant coordination site of the intermediate resulting from loss of a CO ligand.

In the synthesis of complex **5a** the coordinating oxygen atom in the intermediate is presumably the pyranosyl oxygen atom, giving rise to the formation of a six-membered metallaheterocycle. However, due to the anomeric effect the pyranosyl oxygen atom is relatively electron-poor. Therefore, the coordination is weak and, consequently, the diastereomeric excess is only 8%.

The intermediate in the synthesis of **5b** and **5c** can be stabilized by interaction with either the carbonyl oxygen atom of the acetate group at C-2 (formation of an eight-membered metallacycle) or with the pyranosyl oxygen atom (formation of a five-membered metallacycle). The reactions of tri(*p*-tolyl)phosphane with tetramethyl- and tetrabenzyl-protected gluco- and galactopyranosylcarbene complexes instead of **4b** and **4c** gave diastereoselectivities similar to those of **4b** and **4c**.[10] Therefore, the formation of an eight-membered metallacycle by interaction of manganese with the carbonyl oxygen atom of the acetate group at C-2 in the intermediate is unlikely. The difference in the de values is probably caused by steric interaction of the acetoxy substituent at C-4 with the cyclopentadienyl ring.

The significantly higher diastereoselectivity in the reaction of (*R*)-**4d** and (*S*)-**4d** with $PTol_3$, as compared to that of **4a**−**c**, is probably due to the higher flexibility of the isopropylideneglycerol substituent in forming the most stable metallacyclic intermediate.

In contrast to furanosyl- and pyranosylcarbene complexes, the high diastereoselectivity of the PR_3/CO exchange is not confined to tritolylphosphane as the entering nucleophile. Within the limits of error, the replacement of CO by $P(OPh)_3$, $P(OMe)_3$, $P(OMe)_2Ph$, $P(OMe)Ph_2$, PPh_3, and $P(C_6H_4Cl\text{-}p)_3$ in (*R*)-**4d** also proceeded diastereospecifically (de > 96%) to afford (S_{Mn},*R*)-**8**−**13** (Scheme 3).

Scheme 3

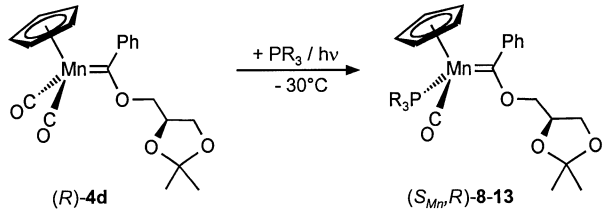

PR_3	$P(OPh)_3$	$P(OMe)_3$	$P(OMe)_2Ph$	$P(OMe)Ph_2$	PPh_3	$P(C_6H_4Cl\text{-}p)_3$
	8	**9**	**10**	**11**	**12**	**13**

Analogously, the photolysis of (*S*)-**4d** in the presence of $P(OMe)_3$ gave (R_{Mn},*S*)-**9** (Scheme 4).

Scheme 4

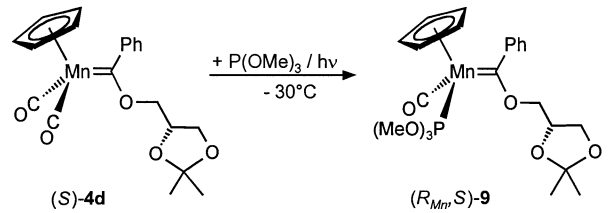

The reaction of (*R*)-**14** with PR_3 afforded the complexes (S_{Mn},*R*)-**15**−**17** (Scheme 5) with a de > 96%. Complex (*R*)-**14** was prepared from [$Cp(CO)_2Mn$=C(OAc)Tol-*p*] and (*S*)-**3d**[7] in an analogous way to (*R*)-**4d**.

Scheme 5

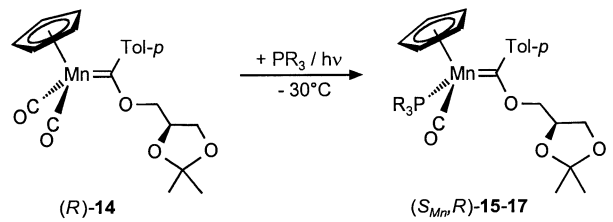

R = Tol-*p* (**15**), OMe (**16**), C_6H_4Cl-*p* (**17**)

In contrast, photolysis of [Cp(CO)$_2$Mn=C(β-*O*-mannofuranosyl)Tol-*p*] in the presence of phosphites or phosphanes gave much lower de values [PR_3 = $P(OPh)_3$ (0%), $P(OMe)_3$ (12%), $P(C_6H_4Cl\text{-}p)_3$ (56%)].

All NMR spectra of the complexes **8**−**17** showed the expected resonances to confirm the formation of only one diastereomer in each case. However, the 600-MHz NMR spectra of these complexes indicated the presence of two isomers in solution. Most of the complexes exhibited two sets of ^{1}H- and ^{13}C-resonance signals for the diastereotopic methyl groups of the isopropylidene function [$\Delta\delta(^1H)$ = 0.01−0.03 ppm, $\Delta\delta(^{13}C)$ = 0.1 ppm; see Experimental Section]. For complex **8** two doublets for the carbonyl and the carbene carbon atom [$\Delta\delta(^{13}C)$ = 0.2 ppm] were observed, and for the complexes **8** and **10**−**12** two ^{31}P signals [$\Delta\delta(^{31}P)$ = 0.2 ppm] were detected.

Both isomers are in equilibrium, as shown by variable-temperature NMR spectroscopy. Complex (S_{Mn},*R*)-**5d** exhibits two sets of resonance signals for the diastereotopic methyl groups. The ratio of the two sets at room temperature was 1:1. When the solution was cooled the ratio was 5:1 (at −23°C) and > 20:1 (at −43°C). Warming the solution to ambient temperature restored the original 1:1 ratio.

In order to determine whether or not the splitting of the signals indicated the presence of a mixture of diastereomers, a diastereomeric mixture of (S_{Mn},*R*)-**5d** and (S_{Mn},*S*)-**5d** was prepared from (S_{Mn})-**6** and a mixture of the sodium salts of 1,2-(*S*)- and 1,2-(*R*)-*O*-isoproylidene gycerol [(*S*)- and (*R*)-**3d**]. For (S_{Mn},*R*)-/(S_{Mn},*S*)-**5d** the shift difference between the ^{31}P signals was $\Delta\delta(^{31}P)$ = 1.9 ppm, and this value is approximately 10 times larger than that observed with **8** and **10**−**12**. Therefore, the splitting of the signals cannot be due to a mixture of diastereomers.

Hindered rotation around (a) the C(carbene)−aryl bond, (b) the Mn=C(carbene) bond, and (c) the C(carbene)−O bond may account for the splitting of signals. Complex (S_{Mn},*R*)-**15** exhibits a simple A_2B_2 pattern for the C(carbene)−C_6H_4Me hydrogen atoms. Therefore, option (a) can be ruled out. Barriers to rotation around the C(carbene)−C(aryl) bonds in neutral aryl-substituted, heteroatom-stabilized carbene complexes are usually very low.[11] However, substantial barriers were observed in cationic benzylidene complexes of iron and ruthenium, [Cp(CO)$_2$M=C(C_6H_4R)H]$^+$ and [Cp(CO)(PPh_3)M=C(C_6H_4R)H]$^+$ (M = Fe, Ru; R = H, F, Me, OMe: $\Delta G^{\neq}$ = 9.0−14.5 kcal/mol).[12]

The two remaining possibilities, (b) and (c), have been observed in various carbene complexes.[13][14] The bonding situation in [Cp(CO)$_2$Mn=C(OMe)Ph] and [Cp(CO)$_2$Mn=CMe_2] has also been analyzed theoretically.[15] The splitting of the Cp resonance signal in [Cp(CO)(PPh_3)Mn=C(OMe)-Ph] at low temperature (below −90°C) was attributed by Geoffroy et al. to a hindered rotation around the Mn=C(carbene) bond. An activation barrier of $\Delta G^{\neq}$ = 9.8 kcal/mol was calculated.[8a] However, for the complexes (S_{Mn},*R*)-/(R_{Mn},*S*)-**5d** and (S_{Mn},*R*)-**8**−**17** we consider hindered rotation around the C(carbene)−O bond [(*E*)/(*Z*) isomerization with respect to the C−O partial double bond, see Scheme 6] to be a preferable explanation for the NMR-spectroscopic observations since a splitting of signals was not observed with either the corresponding mannofuranosylcarbene or the gluco- and galactopyranosylcarbene complexes. The bulkiness of the OR* substituents in these complexes presumably disfavors the (*Z*) conformation. The strong temperature dependence of the equilibrium constant also agrees well with (*E*)/(*Z*) isomerism.

Scheme 6

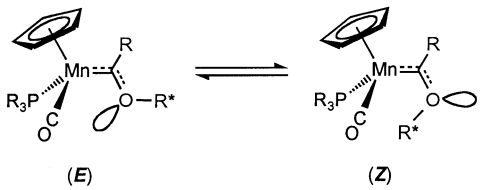

Similarly, two sets of ^{13}C- and ^{31}P-NMR signals were reported for the alkoxy(amino)carbene complexes of platinum *cis*-[$Cl_2(PPh_3)$Pt=C(NHR′)OR″] (R′ = Me, Et; R″ = 1,2,3,4-tetra-*O*-deoxy-β-D-glucosyl) and these were explained in terms of hindered rotation around the carbene carbon−heteroatom bond.[2c]

Epimerization studies were carried out with the $PTol_3$- and the $P(OMe)_3$-substituted complexes (S_{Mn},*R*)-**5d** and (S_{Mn},*R*)-**9**. In pentane and CH_2Cl_2, (S_{Mn},*R*)-**5d** was configurationally stable for at least 96 hours at room temperature. However, in neat $P(OMe)_3$ substitution of the coordinated $PTol_3$ by $P(OMe)_3$ was observed. The substitution presumably proceeds by an associative mechanism. An associative mechanism has also been suggested for the substitution of PPh_3 by $PTol_3$ in the related complex [Cp(CO)(PPh_3)Mn=C(OMe)Et]. The reaction rate was observed to increase with increasing $PTol_3$ concentration.[8a]

The $P(OMe)_3$-substituted complex (S_{Mn},*R*)-**9** was stable in pentane or acetone, but slowly epimerized in dichloromethane, diethyl ether, and tetrahydrofuran. The (S_{Mn},*R*)-/(R_{Mn},*R*)-**9** ratio after 96 hours at room temperature was 4.4 (CH_2Cl_2), 2.76 (Et_2O), and 4.8 (THF). The epimerization rate was enhanced by exposure to daylight. After 96 hours at room temperature in the dark, the (S_{Mn},*R*)-/(R_{Mn},*R*)-**9** ratio was only 6.5 as opposed to 2.76 when exposed to light. The epimerization is very likely to proceed by dissociation and readdition of $P(OMe)_3$. Consequently, when $P(OCD_3)_3$ was added to a solution of (S_{Mn},*R*)-**9** in Et_2O the (S_{Mn},*R*)-/(R_{Mn},*R*)-**9** ratio after 96 hours was within the limits of error, and was the same as that in the absence of uncoordinated phosphite. In addition, $P(OCD_3)_3$ was incorporated into the complex.

In contrast to our results with carbene complexes, the phosphite-substituted benzoyl complex [Cp(NO){$P(OEt)_3$}-Mn−C(O)Ph] is configurationally stable[16] whereas the PPh_3-substituted acyl complexes [Cp(NO)(PPh_3)-Mn−C(O)C_6H_4R] racemize in toluene (half-life for R = H: 21 minutes at 25°C). A dissociative mechanism was deduced from kinetic studies.[17][18] A linear relationship between the Hammett σ constants of the *para* substituents and the rates of racemization was observed. However, the

steric effect seemed to be the most important factor in determining the configurational stability of the complexes.[1b] The higher configurational stability of (S_{Mn},*R*)-**5d** as compared to phosphite-substituted complex (S_{Mn},*R*)-**9** is probably due to the stronger Mn−P bond in the phosphane complex.

Our results demonstrate that diastereomerically pure carbene(phosphane) and -(phosphite) complexes of manganese are readily available through PR_3/CO exchange in chiral [Cp(CO)$_2$Mn=C(OR*)R′] complexes. Both configurations at manganese [(R_{Mn}) and (S_{Mn})] are accessible by choosing either an (*S*)- or an (*R*)-glycerol derivative as the chiral auxiliary. The carbene(phosphane) complexes are configurationally stable. Reaction of these complexes with Lewis acids gives a convenient method for the preparation of enantiomerically pure chiral-at-metal [Cp(CO)LMn(carbyne)]$^+$ complexes (see Scheme 2). The configuration at the manganese atom does not change on addition of nucleophiles to the carbyne carbon atom in these complexes [e. g. (S_{Mn})-**6**], meaning that a large number of enantiomerically pure carbene complexes is readily accessible. Finally, oxidative decomplexation of the carbene ligand and addition of other nucleophiles (L′) should now offer a simple route to other chiral complexes of manganese [Cp(CO)(PR_3)MnL′].

Support of this work by the *Fonds der Chemischen Industrie* is gratefully ackowledged.

Experimental Section

All operations were carried out under either nitrogen or argon by using conventional Schlenk techniques. Solvents were dried by refluxing over sodium/benzophenone ketyl or CaH_2 and were freshly distilled prior to use. The silica gel used for chromatography (J. T. Baker, silica gel for flash chromatography) was saturated with argon. The yields refer to analytically pure compounds and were not optimized. The complexes **1**[19] and **2**,[5] the carbohydrates 2,3,4,6-tetra-*O*-acetyl-D-glucopyranose and 2,3,4,6-tetra-*O*-acetyl-D-galactopyranose,[20][21] 1,2:3,4-di-*O*-isopropylidene-D-galactopyranose[22] as well as $PTol_3$ and tris(*p*-chlorophenyl)phosphane[23] were prepared according to literature procedures. $PPh(OMe)_2$ and $PPh_2(OMe)$ were purchased from Strem Chemicals, Inc. $P(OPh)_3$ was obtained from Janssen, TMEDA from Merck. $P(OMe)_3$ and acetyl bromide were purchased from Fluka. − IR: FT-IR spectrophotometer, Bio.-Rad. − ^{1}H NMR, ^{31}P NMR, and ^{13}C NMR: Bruker WM 250, Bruker AC 250, Bruker DRX 600, Jeol JNX 400. Unless specifically mentioned, ^{1}H-NMR spectra were recorded at 250 MHz and ^{13}C- and ^{31}P-NMR spectra at 400 MHz. All spectra were recorded in [D$_6$]acetone at room temp. Chemical shifts are reported relative to the residual solvent peaks [^{1}H: δ(H) = 2.05 and ^{13}C: δ(*C*H$_3$) = 29.8] or to external H_3PO_4 (^{31}P). − MS: Finnigan MAT 312 (EI) or Finnigan MAT 312/AMD5000 (FAB).

General Procedure for the Synthesis of the Complexes **4a**−**c**, (*R*)-**4d**, (*S*)-**4d** *and* (*R*)-**14**: 4.5 mmol of the corresponding carbohydrate or glycerol derivative was added at −50°C to a solution of **2** or its tolylcarbene analogue, prepared from 3.0 mmol of acetyl bromide and 3.0 mmol of **1** or Li[Cp(CO)$_2$Mn−C(=O)Tol-*p*], respectively, in 50 ml of CH_2Cl_2. The resulting solution was stirred for 0.5 h at −50°C, warmed to 0°C and stirred for a further 4.5 h at 0°C. The solvent was removed in vacuo at room temp. The dark brown residue was dissolved in CH_2Cl_2/pentane {6:1 (**4a**), 2:1 (**4b**), 8:3 (**4c**), 2:1 [(*R*)- and (*S*)-**4d**, (*R*)-**14**]} and chromatographed at −20°C on silica gel with mixtures of CH_2Cl_2, pentane and ether (see below for ratios).

General Procedure for the Synthesis of the Complexes **5a**−**d**, **8**−**13**, *and* **15**−**17**: A solution of 0.6 mmol of **4a**−**d** or **14**, and 0.9 mmol of the corresponding PR_3 in 30 ml of toluene was irradiated (see below for duration) at −30°C while passing a slow stream of argon through the solution. The solvent was removed in vacuo at room temp. The residue was dissolved in CH_2Cl_2/pentane (see below for ratio) and chromatographed at −20°C on silia gel.

Dicarbonyl(cyclopentadienyl)[(1:2,3:4-di-O-isopropylidene-D-galactopyranos-6-yloxy)phenylcarbene]manganese (**4a**): Chromatography with CH_2Cl_2/pentane (6:1) afforded a yellow band (30 mg) and then elution with CH_2Cl_2/pentane/Et_2O (6:1:0.5) gave a dark red band. Removal of the solvent from the dark red fraction afforded complex **4a** as a sticky brown oil. Yield: 1.47 g (66%, based on **2**). − IR (CH_2Cl_2): ν(CO) = 1959 cm^{-1} vs, 1888 s. − ^{1}H NMR: δ = 1.30, 1.32, 1.34, 1.52 (4 × s, 3 H each, Me), 4.10−4.69 (m, 6 H, 2-H, 3-H, 4-H, 5-H, CH_2), 4.78 (s, 5 H, Cp), 5.46−5.53 (m, 1 H, 1-H), 7.02−7.06 (m, 2 H, Ph), 7.27−7.39 (m, 3 H, Ph). − ^{13}C NMR: δ = 24.7, 25.1, 26.3, 26.4 (Me), 67.8 (C-6), 71.3 (C-4), 71.6 (C-2), 71.8 (C-5), 75.5 (C-3), 87.9 (Cp), 97.1 (C-1), 109.2, 109.9 (*C*Me$_2$), 123.7, 128.2, 154.9 (Ph), 232.7, 232.9 (2 × CO), 334.3 (Mn=C). − MS (EI, 70 eV): *m*/*z* (%) = 524 (8) [M$^+$], 509 (5) [M$^+$ − Me], 468 (100) [M$^+$ − 2 CO], 120 (26) [CpMn$^+$]. − $C_{26}H_{29}MnO_8$·1/5 pentane (538.6): calcd. C 60.18, H 5.87; found C 60.21, H 5.77.

Dicarbonyl(cyclopentadienyl)[(2,3,4,6-tetra-O-acetyl-β-D-galactopyranosyloxy)phenylcarbene]manganese (**4b**): Chromatography with CH_2Cl_2/pentane (7:3) gave a yellow band (60 mg). Subsequent elution with CH_2Cl_2/pentane/Et_2O (7:3:1) first gave a dark red and then an orange band. Removal of the solvent of the orange fraction afforded complex **4b** as an orange oil. Crystallization from 75 ml of CH_2Cl_2/pentane (2:1) gave an orange powder. Yield: 730 mg (40%, based on **2**), m.p. 68°C (dec.). − IR (CH_2Cl_2): ν(CO) = 1971 cm^{-1} vs, 1903 s. − ^{1}H NMR: δ = 1.92, 2.03, 2.08, 2.16 (4 × s, 3 H each, Me), 4.05−4.18 (m, 3 H, H-5, CH_2), 4.83 (s, 5 H, Cp), 5.19−5.24 (m, 1 H, 3-H), 5.37−5.38 (m, 1 H, H-4), 5.43−5.46 (m, 1 H, 1-H), 5.52−5.63 (m, 1 H, 2-H), 7.04−7.07 (m, 2 H, Ph), 7.30−7.39 (m, 3 H, Ph). − ^{13}C NMR: δ = 20.4, 20.5, 20.6 (Me), 62.3 (C-6), 68.0 (C-4), 69.4 (C-2), 71.3 (C-5), 72.3 (C-3), 88.5 (Cp), 99.1 (C-1), 124.2, 128.2, 129.6, 153.9 (Ph), 169.7, 170.0, 170.4, 170.6 (*C*OMe), 231.3, 232.5 (2 CO), 334.2 (Mn=C). − MS (EI, 70 eV): *m*/*z* (%) = 612 (0.5) [M$^+$], 556 (0.4) [M$^+$ − 2 CO], 331 (40) [OR*$^+$ − OH], 225 (9) [CpMnC(Ph)O$^+$], 55 (58) [Mn$^+$]. − $C_{28}H_{29}MnO_{12}$ (612.1): calcd. C 54.91, H 4.77; found C 55.02, H 4.99.

Dicarbonyl(cyclopentadienyl)[(2,3,4,6-tetra-O-acetyl-β-D-glucopyranosyloxy)phenylcarbene]manganese (**4c**): Chromatography with CH_2Cl_2/pentane (8:3) gave a yellow band (200 mg), and then elution with CH_2Cl_2/pentane/Et_2O (8:3:1) gave first a brown and then an orange band. The orange band afforded **4c** as an orange powder. Recrystallization from 7 ml of CH_2Cl_2 gave **4c** as light orange plates. Yield: 910 mg (46%, based on **2**), m.p. 130°C (dec.). − IR (CH_2Cl_2): ν(CO) = 1972 cm^{-1} vs, 1905 s. − ^{1}H NMR: δ = 1.95, 1.97, 2.03, 2.07 (4 × s, 3 H each, Me), 3.71−3.78 (m, 1 H, 5-H), 4.05−4.24 (m, 2 H, CH_2), 4.83 (s, 5 H, Cp), 5.08−5.39 (m, 4 H, 1-H, 2-H, 3-H, 4-H), 7.32−7.35 (m, 2 H, Ph), 7.38−7.44 (m, 3 H, Ph). − ^{13}C NMR: δ = 20.4 (4 Me), 62.5 (C-6), 68.9 (C-4), 71.8 (C-2), 72.9 (C-5), 73.1 (C-3), 88.6 (Cp), 98.8 (C-1), 124.2, 128.1, 128.5, 153.5 (Ph), 169.6, 169.9, 170.2, 170.6 (4 *C*OMe), 231.4, 232.3 (2 CO), 333.8 (Mn=C). − MS (70 eV): *m*/*z* (%) = 612 (2) [M$^+$], 556 (0.4) [M$^+$ − 2 CO], 331 (66) [OR*$^+$ − OH], 271 (6) [OR*$^+$ − OH

− HOAc], 225 (15) [CpMnC(Ph)O$^+$]. − $C_{28}H_{29}MnO_{12}$·4/3 CH_2Cl_2 (725.3): calcd. C 48.54, H 4.40; found C 48.76, H 4.51.

Dicarbonyl(cyclopentadienyl)[(2R)-2,3-(isopropylidenedioxy)-prop-1-yloxy)phenylcarbene]manganese [(*R*)-**4d**]: Chromatography with CH_2Cl_2/pentane (2:1) gave first a yellow band (20 mg) and then a red band (80 mg). Elution with CH_2Cl_2/pentane/Et_2O (2:1:0.5) gave a brown/red band which contained (*R*)-**4d**. Evaporation of the solvent afforded (*R*)-**4d** as a sticky brown oil. Yield: 690 mg (41%, based on **2**). − IR (pentane): ν(CO) = 1975 cm^{-1} sh, 1964 vs, 1918 sh, 1905 s. − ^{1}H NMR: δ = 1.30, 1.34 (2 × s, 3 H each, Me), 3.87−3.93 (m, 1 H, 2-H), 4.12−4.18 (m, 1 H, 3-H), 4.43−4.53 (m, 3 H, CH_2-1, 3-H), 4.74 (s, 5 H, Cp), 7.00−7.03 (m, 2 H, Ph), 7.27−7.39 (m, 3 H, Ph). − ^{13}C NMR: δ = 25.6, 27.0 (Me), 66.9 (C-3), 74.9 (C-2), 77.0 (C-1), 88.1 (Cp), 110.1 (CMe_2), 123.7, 128.1, 128.3, 155.5 (Ph), 232.9 (2 CO), 334.5 (Mn=C). − MS (EI, 70 eV): *m/z* (%) = 396 (24) [M$^+$], 381 (6) [M$^+$ − Me], 340 (77) [M$^+$ − 2 CO], 120 (52) [MnCp$^+$], 55 (100) [Mn$^+$]. − $C_{20}H_{21}MnO_5$·1/4 pentane (414.1): calcd. C 61.60, H 5.84; found C 61.79, H 5.50.

Dicarbonyl(cyclopentadienyl)[(2S)-2,3-(isopropylidenedioxy)-prop-1-yloxy)phenylcarbene]manganese [(*S*)-**4d**]: Chromatography with CH_2Cl_2/pentane (2:1) gave first a yellow band (20 mg) and then a red band (80 mg). Elution with CH_2Cl_2/pentane/Et_2O (2:1:0.5) gave a brown/red band which contained (*S*)-**4d**. Evaporation of the solvent afforded (*S*)-**4d** as a sticky brown oil. Yield: 750 mg (45%, based on **2**). − The spectroscopic data are identical to those of (*R*)-**4d**. − MS (EI, 70 eV): *m/z* (%) = 396 (9) [M$^+$], 381 (2) [M$^+$ − Me], 340 (35) [M$^+$ − 2 CO], 120 (61) [MnCp$^+$], 55 (100) [Mn$^+$]. − $C_{20}H_{21}MnO_5$ (396.1): calcd. C 60.61, H 5.34; found 61.14, H 5.41.

Carbonyl(cyclopentadienyl)[(α-1:2,3:4-di-O-isopropylidene-D-galactopyranos-6-yloxy)phenylcarbene](tritolylphosphane)-manganese (**5a**). Irradiation time: 11 min. Chromatography with CH_2Cl_2/pentane (6:1) gave a yellow band. Further elution with CH_2Cl_2/pentane/Et_2O (12:2:1) gave two red bands which gave **5a** as a mixture of diastereomers in a ratio of 54:46 (determined by ^{1}H-NMR spectroscopy). Removal of the solvent and crystallization from 8 ml of pentane afforded **5a** as an orange powder. Yield: 290 mg (45%, based on **4a**), m.p. 45°C (dec.). − IR (pentane): ν(CO) = 1849 cm^{-1} s. − ^{1}H NMR: δ = 1.26, 1.28, 1.31, 1.32, 1.34, 1.38, 1.42, 1.52 (8 × s, total 12 H, Me), 2.33, 2.34 (2 × s, total 9 H, $C_6H_4CH_3$), 3.85−4.09 (m, 1 H, H-5), 4.10−4.35 (m, 3 H, 4-H, CH_2), 4.36−4.42 (m, 1 H, 3-H), 4.49, 4.53 (2 d, $^3J_{PH}$ = 1.8 Hz each, total 5 H, Cp), 4.58−4.62 (m, 1 H, 2-H), 4.47−5.53 (m, 1 H, 1-H), 6.62−6.66 (m, 2 H, Ph), 7.00−7.56 (m, 15 H, arom.). − ^{13}C NMR: δ = 21.2 ($C_6H_4CH_3$), 24.5, 24.6, 24.7, 25.1, 25.2, 26.3, 26.6, 26.7 (Me), 68.0, 68.4 (C-6), 71.3, 71.4 (C-4), 71.4, 71.6 (C-2), 71.8, 72.0 (C-5), 72.2, 72.7 (C-3), 87.7, 88.0 (Cp), 97.3 (C-1), 125.9, 126.1, 126.8, 127.2, 127.6, 128.3, 129.1, 129.2, 129.3, 130.0, 130.1, 130.2, 133.7, 133.8, 133.9, 134.2, 135.8, 135.9, 136.2, 136.3, 139.6, 139.7, 153.4, 153.9 ($C_6H_4CH_3$, Ph), 237.7, 237.9 ($^2J_{PC}$ = 33.0 Hz each, CO), 326.0 (Mn=C). − MS (FAB, NBOH, NaI): *m/z* (%) = 823 (35) [MNa$^+$], 800 (4) [M$^+$], 772 (7) [M$^+$ − CO], 468 (100) [M$^+$ − CO − $PTol_3$]. − $C_{46}H_{50}MnO_7P$ (800.3): calcd. C 68.98, H 6.30; found C 68.14, H 6.54.

Carbonyl(cyclopentadienyl)[(2,3,4,6-tetra-O-acetyl-β-D-galacto-pyranosyloxy)phenylcarbene](tritolylphosphane)manganese (**5b**): Irradiation time: 9 min. Chromatography with CH_2Cl_2/pentane (7:3) first gave a yellow band (20 mg). Further elution with CH_2Cl_2/pentane/Et_2O (7:3:1) gave a red band which, after removal of the solvent, gave **5b** as an orange oil in a 66:34 ratio of diastereomers (determined by ^{1}H-NMR spectroscopy). Yield: 130 mg (19%, based on **4b**). − IR (CH_2Cl_2): ν(CO) = 1848 cm^{-1} s. − ^{1}H NMR: δ = 1.91, 1.94, 1.97, 1.98, 2.01, 2.04, 2.07, 2.08 (8 × s, total 12 H, COMe), 2.31 (s, 9 H, $C_6H_4CH_3$), 3.97−4.10 (m, 3 H, 5-H, CH_2), 4.60 (d, $^3J_{PH}$ = 1.8 Hz), 4.63 (d, $^3J_{PH}$ = 1.6 Hz, total 5 H, Cp), 4.80−4.98 (m, 1 H, 3-H), 5.15−5.19 (m, 1 H, 4-H), 5.24−5.73 (m, 2 H, 1-H, 2-H), 6.87−7.44 (m, 17 H, arom.). − ^{13}C NMR (600 MHz): δ = 20.4, 20.5, 20.6 (Me), 21.1, 21.2 ($C_6H_4CH_3$), 61.9 (CH_2), 68.2 (C-4), 69.1 (C-2), 71.6 (C-5), 71.7 (C-3), 87.5, 87.6 (Cp), 95.0 (C-1), 126.9, 127.0, 129.2, 129.3, 129.4, 129.5, 130.0, 133.5, 133.6, 133.7, 133.8, 133.9, 139.9, 152.6 (C_6H_4, Ph), 169.9, 170.0, 170.4, 170.6 (*C*OMe), *C*O and Mn=*C* not detected. − MS (FAB, NBOH, NaI): *m/z* (%) = 911 (2) [MNa$^+$], 888 (3) [M$^+$], 860 (10) [M$^+$ − CO], 556 (18) [M$^+$ − CO − $PTol_3^+$], 513 (34) [M$^+$ − CO − $PTol_3$ − Ac], 424 (39) [CpMnPTol_3^+]. − $C_{48}H_{50}MnO_{11}P$·1/4 CH_2Cl_2 (910.1): calcd. C 63.68, H 5.59; found C 63.47, H 5.50.

Carbonyl(cyclopentadienyl)[(2,3,4,6-tetra-O-acetyl-β-D-gluco-pyranosyloxy)phenylcarbene](tritolylphosphane)manganese (**5c**): Irradiation time: 13 min. Chromatography with CH_2Cl_2/pentane (8:3) gave a yellow band and subsequent elution with CH_2Cl_2/pentane/Et_2O (8:3:1) gave an orange band. Removal of the solvent of the orange fraction in vacuo at room temp. afforded complex **5c** as an orange oil in a 85:15 ratio of diastereomers (determined by ^{1}H-NMR spectroscopy). Yield: 120 mg (24%, based on **4c**). − IR (CH_2Cl_2): ν(CO) = 1848 cm^{-1} s. − ^{1}H NMR: δ = 2.00, 2.01, 2.08, 2.09 (4 × s, 3 H each, COMe), 2.36 (s, 9 H, $C_6H_4CH_3$), 4.15−4.28 (m, 2 H, CH_2), 4.44−4.50 (m, 1 H, 5-H), 4.64 (d, $^3J_{PH}$ = 1.7 Hz), 4.71 (d, $^3J_{PH}$ = 1.5 Hz, total 5 H, Cp), 4.86−5.41 (m, 4 H, 1-H, 2-H, 3-H, 4-H), 6.90−7.36 (m, 17 H, arom.). − ^{13}C NMR (600 MHz): δ = 20.4, 20.5, 20.6, 20.7, 20.8, 20.9 (COCH_3), 21.2 ($C_6H_4CH_3$), 63.0 (CH_2), 68.9 (C-4), 70.5 (C-2), 71.1 (C-5), 72.9 (C-3), 87.5, 87.8 (Cp), 94.1 (C-1), 124.2, 126.7, 127.0, 128.1, 128.8, 129.4, 129.5, 133.7, 133.8, 139.9 (C_6H_4, Ph), 152.7, 153.6 (Ph), 169.8, 169.9, 170.0, 170.1, 170.4, 170.5 (*C*OMe), 236.4 (d, $^2J_{PC}$ = 30.2 Hz, CO), 323.5 (d, $^2J_{PC}$ = 33.3 Hz, Mn=C). − ^{31}P NMR: δ = 79.8, 81.7. − MS (FAB, NBOH, NaI): *m/z* (%) = 911 (2) [MNa$^+$], 886 (5) [M$^+$ − 2 H], 860 (9) [M$^+$ − CO], 513 (51) [M$^+$ − CO − $PTol_3$ − Ac], 424 (65) [CpMnPTol_3^+]. − $C_{48}H_{50}MnO_{11}P$·1/5 pentane (903.7): calcd. C 65.13, H 5.89; found C 65.58, H 5.80.

Carbonyl(cyclopentadienyl){[(2R)-2,3-(isopropylidenedioxy)-prop-1-yloxy]phenylcarbene}(tritolylphosphane)manganese [(S_{Mn},*R*)-**5d**]: Irradiation time: 9 min. Chromatography with pentane/CH_2Cl_2 (2:1) gave a yellow band and subsequent elution with CH_2Cl_2/pentane/Et_2O (4:2:1) gave a red band. The red fraction contained (S_{Mn},*R*)-**5d**. Removal of the solvent and crystallization from 10 ml of pentane gave (S_{Mn},*R*)-**5d** as an orange powder. Yield: 220 mg [51%, based on (*R*)-**4d**], m.p. 56°C (dec.). − $[\alpha]_D^{20}$ = +11 (*c* = 1, CH_2Cl_2). − IR (pentane): ν(CO) = 1875 cm^{-1} sh, 1859 s. − ^{1}H NMR: δ = 1.28, 1.29, 1.32, 1.34 (4 × s, total 6 H, Me), 2.35 (s, 9 H, $C_6H_4CH_3$), 3.62−3.65 (m, 1 H, 2-H), 3.71−4.77 (m, 2 H, CH_2), 4.04−4.07 (m, 1 H, 1-H), 4.28−4.37 (m, 1 H, 1-H), 4.45 (d, $^3J_{PH}$ = 1.6 Hz, 5 H, Cp), 6.65−6.70 (m, 2 H, Ph), 7.00−7.33 (m, 15 H, arom.). − ^{13}C NMR (600 MHz): δ = 21.2 ($C_6H_4CH_3$), 25.6, 27.1 (Me), 67.2 (C-3), 73.5 (C-2), 75.5 (C-1), 87.5 (Cp), 109.6 (CMe_2), 127.2, 129.3, 129.4 (Ph), 133.8, 133.9, 134.2, 134.4, 135.9, 136.3, 139.4, 139.8 (C_6H_4), 154.7 (Ph), 238.0 (d, $^2J_{PC}$ = 34.1 Hz, CO), 335.2 (d, $^2J_{PC}$ = 28.0 Hz, Mn=C). − ^{31}P NMR (600 MHz): δ = 84.1. − MS (EI, 70 eV): *m/z* (%) = 672 (0.02) [M$^+$], 644 (0.06) [M$^+$ − CO], 480 (0.13) [CpPTol_3(CO)$_2$Mn$^+$], 424 (2.2) [MnCpPTol_3^+], 340 (1.3) [M$^+$ − CO − $PTol_3$], 304 (100) [PTol_3^+]. − $C_{40}H_{42}MnO_4P$ (672.2): calcd. C 71.41, H 6.30; found C 70.00, H 6.54.

Carbonyl(cyclopentadienyl){[(2S)-2,3-(isopropylidenedioxy)-prop-1-yloxy]phenylcarbene}(tritolylphosphane)manganese [(R_{Mn},*S*)-**5d**]: Irradiation time: 9 min. Chromatography with pentane/CH_2Cl_2 (2:1) gave a yellow band and subsequent elution with CH_2Cl_2/pentane/Et_2O (4:2:1) gave a red band. The red fraction contained (R_{Mn},*S*)-**5d**. Removal of the solvent and crystallization from 10 ml of pentane gave (R_{Mn},*S*)-**5d** as an orange powder. Yield: 230 mg [53%, based on (*S*)-**4d**], m.p. 56°C (dec.). − $[\alpha]_D^{20}$ = −12 (*c* = 1, CH_2Cl_2). − The IR and NMR spectra were identical with those of (S_{Mn},*R*)-**5d**. − MS (EI, 70 eV): *m/z* (%) = 672 (0.04) [M^+], 644 (0.13) [M^+ − CO], 480 (0.5) [$CpPTol_3(CO)_2Mn^+$], 424 (8) [$MnCpPTol_3^+$], 340 (8) [M^+ − CO − $PTol_3$], 304 (100) [$PTol_3^+$]. − $C_{40}H_{42}MnO_4P$ (672.2): calcd. C 71.41, H 6.30; found C 70.54, H 6.51.

Carbonyl(cyclopentadienyl)[(2,3:5,6-di-O-isopropylidene-α-D-mannofuranosyloxy)phenylcarbene](tritolylphosphane)manganese [(S_{Mn})-**7α**]: 0.25 ml (0.4 mmol) of a solution of BCl_3 in hexane was added to 130 mg (0.2 mmol) of [S_{Mn},*R*]-**5d** in 6 ml of CH_2Cl_2 at −70°C. 50 ml of pentane precooled to −70°C was then added to the above solution. The carbyne complex (S_{Mn})-**6** precipitated as a brown powder. After decanting, the residue was washed with 7 ml of Et_2O and several times with 10 ml portions of pentane, both precooled to −70°C. Complex (S_{Mn})-**6** was dried in vacuo at −40°C to give an orange powder. The complex was identified by comparison of its IR spectrum [ν(CO) = 2012 cm^{-1} s, in CH_2Cl_2] with that reported in ref.[5] The residue was dissolved in 10 ml of CH_2Cl_2, precooled to −70°C, and a solution of 140 mg (0.5 mmol) of the sodium salt of 2,3:5,6-di-*O*-isopropylidenemannofuranose in 5 ml of CH_2Cl_2 was added at −70°C. The solution was warmed to room temp. and the solvent removed in vacuo. The workup and the purification were carried out analogously to those reported in ref.[5] Complex (S_{Mn})-**7α** was identified by a comparison of its IR [ν(CO) = 1862 cm^{-1} s, in pentane] and its ^{1}H-NMR spectrum with those reported in ref.[5]

Carbonyl(cyclopentadienyl){[(2R)-2,3-(isopropylidenedioxy)-prop-1-yloxy]phenylcarbene}(triphenyl phosphite)manganese [(S_{Mn},*R*)-**8**]: Irradiation time: 9 min. The purification of the reaction products was carried out analogously to that of (S_{Mn},*R*)-**5d**. Red oil. Yield: 250 mg [61%, based on (*R*)-**4d**]. − IR (pentane): ν(CO) = 1899 cm^{-1} sh, 1888 sh, 1868 s. − ^{1}H NMR (600 MHz): δ = 1.24, 1.28, 1.32 (3 × s, total 6 H, Me), 3.74−3.84, 3.93−4.08, 4.28−4.49 (3 × m, total 5 H, CH_2-1, 2-H, CH_2-3), 4.12 (d, $^3J_{PH}$ = 1.9 Hz, 5 H, Cp), 7.05−7.53 (m, 20 H, Ph, OPh). − ^{13}C NMR (600 MHz): δ = 25.6, 27.1 (Me), 67.2 (C-3), 67.3 (C-2), 75.2 (C-1), 86.6 (Cp), 109.8 (*C*Me_2), 122.6, 124.8, 124.9, 125.1, 127.5, 127.7, 128.2, 128.7, 128.9, 129.0, 129.4, 129.6, 130.2, 130.7, 153.0, 154.9, 155.2 (Ph, OPh), 235.6 (d, $^2J_{PC}$ = 44.0 Hz, CO) 235.8 (d, $^2J_{PC}$ = 47.9 Hz, CO), 327.2 (d, $^2J_{PC}$ = 41.5 Hz, Mn=C), 327.4 (d, $^2J_{PC}$ = 42.7 Hz, Mn=C). − ^{31}P NMR (600 MHz): δ = 194.9, 195.2. − MS (EI, 70 eV): *m/z* (%) = 678 (1.4) [M^+], 585 (0.4) [M^+ − OPh], 547 (0.4) [M^+ − OR*], 430 (5.7) [$CpMn(P(OPh)_3)^+$], 340 (56) [M^+ − CO − $P(OPh)_3$], 310 (36) [$P(OPh)_3^+$], 217 (100) [$P(OPh)_2^+$]. − $C_{37}H_{36}MnO_7P\cdot 1/3$ pentane (702.6): calcd. C 66.10, H 5.74; found C 66.41, H 5.69.

Carbonyl(cyclopentadienyl){[(2R)-2,3-(isopropylidenedioxy)-prop-1-yloxy]phenylcarbene}(trimethyl phosphite)manganese [(S_{Mn},*R*)-**9**]: Irradiation time: 8 min. The purification of the reaction products was carried out analogously to that of (S_{Mn},*R*)-**5d**. Red oil. Yield: 180 mg [60%, based on (*R*)-**4d**]. − IR (pentane): ν(CO) = 1867 cm^{-1} s. − ^{1}H NMR (600 MHz): δ = 1.30, 1.33, 1.34 (3 × s, total 6 H, Me), 3.61, 3.62 (d, $^3J_{PH}$ = 11.0 Hz, total 9 H, OMe), 3.85−3.98, 4.11−4.43 (both m, total 5 H, CH_2-1, 2-H, CH_2-3), 4.45, 4.46 (d, $^3J_{PH}$ = 1.7 Hz, total 5 H, Cp), 7.11−7.32 (m, 5 H, Ph). − ^{13}C NMR (600 MHz): δ = 25.6, 25.7, 27.0, 27.1 (Me), 52.2 (OMe), 67.4, 67.5, 75.3, 75.4, 75.5, 75.6 (C-1, C-2, C-3), 86.6 (Cp), 109.8 (*C*Me_2), 125.1, 125.2, 127.0, 127.1, 127.4, 128.7, 128.9, 129.3, 130.1, 130.2, 156.9, 157.2 (Ph), 237.0 (m, CO), 324.8 (m, Mn=C). − ^{31}P NMR: δ = 204.6. − MS (EI, 70 eV): *m/z* (%) = 492 (11) [M^+], 477 (0.6) [M^+ − Me], 461 (3) [M^+ − OMe], 340 (100) [M^+ − $P(OMe)_3$ − CO], 93 (66) [$P(OMe)_2^+$]. − $C_{22}H_{30}MnO_7P$ (492.4): calcd. C 53.65, H 6.14. A correct elemental analysis could not be obtained.

Carbonyl(cyclopentadienyl){[(2S)-2,3-(isopropylidenedioxy)-prop-1-yloxy]phenylcarbene}(trimethyl phosphite)manganese [(R_{Mn},*S*)-**9**]: Irradiation time: 8 min. The purification of the reaction products was carried out analogously to that of (S_{Mn},*R*)-**5d**. Red oil. Yield 170 mg [58%, based on (*S*)-**4d**]. − All spectroscopic data were identical to those of (S_{Mn},*R*)-**9**. − MS (EI, 70 eV): *m/z* (%) = 492 (11) [M^+], 477 (0.6) [M^+ − Me], 461 (3) [M^+ − OMe], 340 (100) [M^+ − $P(OMe)_3$ − CO], 93 (66) [$P(OMe)_2^+$]. − $C_{22}H_{30}MnO_7P$ (492.4). A correct elemental analysis could not be obtained.

Carbonyl(cyclopentadienyl){[(2R)-2,3-(isopropylidenedioxy)-prop-yloxy]phenylcarbene}dimethoxy(phenyl)phosphane]-manganese [(S_{Mn},*R*)-**10**]: Irradiation time: 11 min. The workup and the purification of the reaction products were carried out analogously to those of (S_{Mn},*R*)-**5d**. Red oil. Yield: 210 mg [65%, based on (*R*)-**4d**]. − IR (pentane): ν(CO) = 1884 cm^{-1} sh, 1866 s. − ^{1}H NMR (600 MHz): δ = 1.25, 1.28, 1.29 (3 × s, total 6 H, Me), 3.55 (d, $^3J_{PH}$ = 11.3 Hz), 3.63 (d, $^3J_{PH}$ = 11.7 Hz, total 6 H, OCH_3), 3.75−4.14 (m, 5 H, CH_2-1, 2-H, CH_2-3), 4.42 (s, 5 H, Cp), 6.99−7.05, 7.13−7.17, 7.38−7.41, 7.48−7.49 (all m, total 10 H, arom.). − ^{13}C NMR (600 MHz): δ = 25.6, 25.7, 27.1 (Me), 52.5, 52.6, 53.1 (OMe), 67.2, 67.4, 74.9, 75.1, 75.2, 75.5 (C-1, C-2, C-3), 87.1 (Cp), 109.8 (*C*Me_2), 125.4, 125.5, 127.1, 127.2, 127.3, 128.7, 128.8, 130.0, 130.07, 130.11, 130.14, 130.4, 141.9, 142.0, 142.3, 157.1, 157.3 (Ph), 236.7 (d, $^2J_{PC}$ = 30.1 Hz, CO), 322.7 (m, Mn=C). − ^{31}P NMR (600 MHz): δ = 226.0, 226.1 − MS (EI, 70 eV): *m/z* (%) = 538 (11) [M^+], 510 (5) [M^+ − CO], 407 (1.4) [M^+ − OR*], 340 (100) [M^+ − CO − L]. − $C_{27}H_{32}MnO_6P\cdot 1/3$ pentane (562.3): calcd. C 61.21, H 6.45; found C 61.12, H 6.58.

Carbonyl(cyclopentadienyl){[(2R)-2,3-(isopropylidenedioxy)-prop-1-yloxy]phenylcarbene}(methoxydiphenylphosphane)-manganese [(S_{Mn},*R*)-**11**]: Irradiation time: 8 min. The purification of the reaction products was carried out analogously to that of (S_{Mn},*R*)-**5d**. Red oil. Yield: 190 mg [54%, based on (*R*)-**4d**]. − IR (pentane): ν(CO) = 1861 cm^{-1} s. − ^{1}H NMR (600 MHz): δ = 1.23, 1.24, 1.25, 1.28 (4 × s, total 6 H, Me), 3.56 (d, $^3J_{PH}$ = 12.0 Hz), 3.58 (d, $^3J_{PH}$ = 12.1 Hz, total 3 H, OMe), 3.50−3.52, 3.62−3.63, 3.71−3.75, 3.87−3.90, 4.04, 4.11−4.13 (total 5 H, CH_2-1, 2-H, CH_2-3), 4.47 (d, $^3J_{PH}$ = 1.6 Hz, 5 H, Cp), 6.93−6.96, 7.12−7.17, 7.30−7.32, 7.30−7.32, 7.43, 7.60, 7.61 (all m, total 15 H, Ph) − ^{13}C NMR (600 MHz): δ = 25.5, 25.6, 27.0 (Me), 53.3 (OMe), 67.1, 67.4, 74.4, 74.9, 75.0, 75.2 (C-1, C-2, C-3), 87.2, 87.3 (Cp), 109.4, 109.5 (*C*Me_2), 125.3, 125.4, 127.1, 127.4, 127.5, 128.4, 128.5, 128.7, 128.8, 130.5, 131.0, 131.1, 131.7, 131.8, 142.3, 142.5, 156.0, 156.2 (Ph), CO and Mn=C not detected. − ^{31}P NMR: δ = 193.4, 193.7 − MS (EI, 70 eV): *m/z* (%) = 584 (6) [M^+], 556 (4) [M^+ − CO], 340 (100) [M^+ − CO − L], 336 (31) [$CpMnL^+$], 216 (33) [L^+], 55 (64) [Mn^+]. − $C_{32}H_{34}MnO_5P$ (584.5): calcd. C 65.75, H 5.86; found C 65.90, H 5.78.

Carbonyl(cyclopentadienyl){[(2R)-2,3-(isopropylidenedioxy)-prop-1-yloxy]phenylcarbene}(triphenylphosphane)manganese [(S_{Mn},*R*)-**12**]: Irradiation time: 11 min. The workup and the purifi-

cation of the reaction products were carried out as desribed for the reaction of (*R*)-**4d** with tritolylphosphane. Recrystallization from pentane/CH_2Cl_2 (10:1) afforded dark red crystals. Yield: 290 mg [48%, based on (*R*)-**4d**], m.p. 110°C. − IR (pentane): ν(CO) = 1877 cm^{-1}sh, 1862 s. − ^{1}H NMR: δ = 1.29, 1.32, 1.35, 1.38 (4 × s, total 6 H, Me), 3.63−4.43 (m, 5 H, CH_2-1, 2-H, CH_2-3), 4.47 (d, $^3J_{PH}$ = 1.7 Hz, 5 H, Cp), 6.67−6.71 (m, 2 H, Ph), 7.00−7.07, 7.31−6.65 (m, total 18 H, arom.). − ^{13}C NMR: δ = 25.6, 25.7, 27.2 (Me), 67.2, 67.5, 73.6, 74.4, 75.5 (C-1, C-2, C-3), 87.6 (Cp), 109.6, 109.7 (*C*Me_2), 125.7, 125.8, 127.1, 127.3, 127.4, 127.6, 128.2, 128.5, 128.6, 128.7, 129.0, 129.2, 129.4, 129.5, 129.6, 130.0, 130.2, 133.9, 134.0, 134.3, 138.9, 139.2, 154.5, 154.6 (Ph), 237.7 (d, $^2J_{PC}$ = 30.5 Hz, CO), 326.0 (d, $^2J_{PC}$ = 30.5 Hz, Mn=C), 325.9 (d, $^2J_{PC}$ = 29.3 Hz, Mn=C). − ^{31}P NMR: δ = 87.16, 87.30. − MS (EI, 70 eV): *m/z* (%) = 630 (0.1) [M^+], 602 (0.07) [M^+ − CO], 340 (19) [M^+ − CO − L], 262 (100) [L^+]. $C_{37}H_{36}MnO_4P$ (630.6): calcd. C 70.47, 5.75; found C 70.66, H 5.90.

Carbonyl(cyclopentadienyl){[(2R)-2,3-(isopropylidenedioxy)-prop-1-yloxy]phenylcarbene}[tris(p-chlorophenyl)phosphane]-manganese [(S_{Mn},*R*)-**13**]: Irradiation time: 10 min. Workup and purification of the reaction products were carried out analogously to those of (S_{Mn},*R*)-**5d**. Red oil. Yield 310 mg [70%, based on (*R*)-**4d**]. − IR (pentane): ν(CO) = 1860 cm^{-1} s. − ^{1}H NMR: δ = 1.31, 1.35, 1.38 (3 × s, total 6 H, Me), 3.54−3.57, 3.73−3.78, 3.82−3.93, 4.06−4.14, 4.38−4.46 (5 × m, 5 H, CH_2-1, 2-H, CH_2-3), 4.55 (d, $^3J_{PH}$ = 1.6 Hz, 5 H, Cp), 6.68−6.72, 7.04−7.13, 7.31−7.49 (3 × m, 17 H, arom.). − ^{13}C NMR: δ = 25.5, 25.6, 27.1, 27.2 (Me), 66.9, 67.2, 73.6 (C-1, C-2, C-3), 87.7 (Cp), 109.7, 109.8 (*C*Me_2), 125.8, 125.9 (Ph), 127.4 (C_6H_4), 128.3 (Ph), 129.0, 129.1 (C_6H_4), 129.2, 129.4, 129.8 (Ph), 135.3, 135.4, 136.2 (C_6H_4), 137.0, 137.4, 153.4 (Ph), 237.1 (d, $^2J_{PC}$ = 30.2 Hz, CO), 327.2 (d, $^2J_{PC}$ = 31.7 Hz, Mn=C). − ^{31}P NMR: δ = 87.9, 88.0. − MS (FAB, NBOH): *m/z* (%) = 732 (100) [M^+, ^{35}Cl], 484 (10) [CpMnL$^+$]. − $C_{37}H_{33}Cl_3MnO_4P$ (733.9): calcd. C 60.65, 4.54; found C 60.27, H 4.88.

[Acetoxy(tolyl)carbene]dicarbonyl(cyclopentadienyl)manganese: The preparation was carried out analogously to **2**.[5] The complex was identified by comparison of its IR data [ν(CO) = 1983 cm^{-1} s, 1917 s, in CH_2Cl_2] with those of the corresponding phenylcarbene complex **2**.[5]

Dicarbonyl(cyclopentadienyl)[{(2R)-2,3-(isopropylidenedioxy)-prop-1-yloxy}tolylcarbene]manganese [(*R*)-**14**]: The preparation and workup were carried out analogously to those of (*R*)-**4d**. Evaporation of the solvent afforded (*R*)-**14** as a brown oil. Yield: 1.05 g [53%, based on the acetoxy(tolyl)carbene complex]. − IR (pentane): ν(CO) = 1976 cm^{-1} sh, 1964 vs, 1917 sh, 1903 s. − ^{1}H NMR: δ = 1.30, 1.35 (2 × s, 3 H each, Me), 2.33 (s, 3 H, $C_6H_4CH_3$), 3.87−3.93 (m, 1 H, 2-H), 4.12−4.18 (m, 1 H, 3-H), 4.44−4.51 (m, 3 H, CH_2-1, 3-H), 4.72 (s, 5 H, Cp), 6.95−6.98 (m, 2 H, C_6H_4), 7.15−7.18 (m, 3 H, C_6H_4). − ^{13}C NMR: δ = 21.1 ($C_6H_4CH_3$) 25.6, 27.0 (Me), 66.9 (C-3), 74.9 (C-2), 77.0 (C-1), 87.8 (Cp), 110.0 (*C*Me_2), 124.0, 128.7, 130.0, 138.1, 152.9 (Ph), 232.8 (2 × CO), 335.2 (Mn=C). − MS (EI, 70 eV): *m/z* (%) = 410 (10) [M^+], 395 (2) [M^+ − Me], 354 (50) [M^+ − 2 CO], 280 (5) [M^+ − OR*], 120 (40) [MnCp$^+$], 55 (100) [Mn^+]. − $C_{21}H_{23}MnO_5$·1/3 pentane (434.4): calcd. C 62.67, H 6.62; found C 62.55, H 5.98.

Carbonyl(cyclopentadienyl){[(2R)-2,3-(isopropylidenedioxy)-prop-1-yloxy]tolylcarbene}(tritolylphosphane)manganese [(S_{Mn},*R*)-**15**]: The irradiation and the workup were carried out analogously to those of (S_{Mn},*R*)-**5d**. Red powder. Yield: 230 mg [46%, based on (*R*)-**14**], m.p. 52°C (dec.). − IR (pentane): ν(CO) = 1874 cm^{-1} sh, 1857 s. − ^{1}H NMR: δ = 1.29, 1.31, 1.34, 1.37 (4 × s, total 6 H, CH_3), 2.24 (s, 9 H, $C_6H_4CH_3$), 2.34 (s, 9 H, $PC_6H_4CH_3$), 3.58−3.87, 3.98−4.12, 4.28−4.35 (all m, total 5 H, CH_2-1, 2-H, CH_2-3), 4.44 (d, $^3J_{PH}$ = 1.6 Hz, 5 H, Cp), 6.60 (d, *J* = 7.8 Hz, 2 H, C_6H_4), 6.80 (d, *J* = 7.9 Hz, 2 H, C_6H_4), 7.13−7.30 (m, 12 H, C_6H_4). − ^{13}C NMR: δ = 21.1 ($C_6H_4CH_3$), 25.4, 25.5 (Me), 66.9, 67.2, 75.4 (C-1, C-2, C-3), 87.5, 87.7 (Cp), 109.7, 109.8 (*C*Me_2), 124.1, 125.9, 126.0 (C_6H_4), 128.0 (PC_6H_4), 128.7 (C_6H_4), 128.9, 128.0 (PC_6H_4), 129.5, 129.8, 130.0, 130.2 (C_6H_4), 135.2, 135.3, 136.1 (PC_6H_4), 137.2, 137.4, 151.1 (C_6H_4), 154.7 (Ph), 237.5 ($^2J_{PC}$ = 31.6 Hz, CO), 328.1 ($^2J_{PC}$ = 30.2 Hz, Mn=C). − ^{31}P NMR: δ = 89.0. − MS (EI, 70 eV): *m/z* (%) = 686 (0.05) [M^+], 658 (0.1) [M^+ − CO], 304 (100) [$PTol_3^+$], 120 (22) [CpMn]. − $C_{41}H_{35}MnO_4P$ (672.2): calcd. C 72.67, H 5.21; found C 72.17, H 6.46.

Carbonyl(cyclopentadienyl){[(2R)-2,3-(isopropylidenedioxy)-prop-1-yloxy]tolylcarbene}(trimethyl phosphite)manganese [(S_{Mn}, *R*)-**16**]: Irradiation time: 8 min. The purification of the reaction products was carried out analogously to that of (S_{Mn},*R*)-**5d**. Red oil. Yield: 170 mg [56%, based on (*R*)-**14**]. − IR (pentane): ν(CO) = 1882 cm^{-1} sh, 1870 sh, 1862 s. − ^{1}H NMR: δ = 1.30, 1.33, 1.34 (3 × s, total 6 H, Me), 2.29 (s, 9 H, $C_6H_4CH_3$), 3.60 (d, $^3J_{PH}$ = 11.0 Hz, 9 H, OMe), 3.80−3.89, 4.07−4.14, 4.24−4.41 (all m, total 5 H, CH_2-1, 2-H, CH_2-3), 4.45 (s, 5 H, Cp), 7.04−7.17 (m, 4 H, Tol). − ^{13}C NMR: δ = 21.1 ($C_6H_4CH_3$), 25.7, 25.8 (Me), 52.1 (OCH_3), 67.5, 67.6, 74.9, 75.2, 75.5 (C-1, C-2, C-3), 86.5 (Cp), 109.8, 109.8 (*C*Me_2), 125.3, 125.4, 128.0, 130.0, 136.6, 136.7, 154.6, 154.9 (C_6H_4), 236.8 (d, $^2J_{PC}$ = 46.4 Hz, CO), 325.5, 325.6 (d, both $^2J_{PC}$ = 41.5 Hz, Mn=C). ^{31}P NMR: δ = 204.8. − MS (EI, 70 eV): *m/z* (%) = 506 (12) [M^+], 475 (3) [M^+ − OMe], 375 (2) [M^+ − OR*], 254 (100) [M^+ − $P(OMe)_3$ − CO], 120 (34) [$CpMn^+$], 55 (56) [Mn^+]. − $C_{23}H_{32}MnO_7P$·1/3 pentane (530.2): calcd. C 55.85, H 6.84; found C 56.57, H 6.69.

Carbonyl(cyclopentadienyl){[(2R)-2,3-(isopropylidenedioxy)-prop-1-yloxy]tolylcarbene}[tris(p-chlorophenyl)phosphane]-manganese [(S_{Mn},*R*)-**17**]: Irradiation time: 12 min. The workup and the purification of the reaction products were carried out analogously to those of (S_{Mn},*R*)-**5d**. Red powder. Yield 280 mg [60%, based on (*R*)-**14**], m.p. 72−75°C. − IR (pentane): ν(CO) = 1868 cm^{-1} sh, 1961 s. − ^{1}H NMR: δ = 1.31, 1.34, 1.38 (3 × s, total 6 H, Me), 2.27 (s, 3 H, $C_6H_4CH_3$), 3.55−3.60, 3.74−3.92, 4.07−4.15, 4.44−4.47 (all m, total 5 H, CH_2-1, 2-H, CH_2-3), 4.55 (s, 5 H, Cp), 6.58−6.70, 6.79−6.90, 7.12−7.40 (m, total 16 H, arom.). − ^{13}C NMR: δ = 21.1 ($C_6H_4CH_3$), 25.5, 27.0 (Me), 67.1, 72.2, 75.7 (C-1, C-2, C-3), 87.4, 87.9 (Cp), 109.7, 109.8 (*C*Me_2), 125.9, 127.9, 128.9, 129.0, 130.0, 135.2, 135.3, 136.1, 136.9, 137.2, 137.3, 151.1 (C_6H_5, C_6H_4), 237.5 (d, $^2J_{PC}$ = 31.6 Hz, CO), 328.0 ($^2J_{PC}$ = 28.9 Hz, Mn=C). − ^{31}P NMR: δ = 88.2. − MS (FAB, NBOH): *m/z* (%) = 748 (85) [M^+, ^{35}Cl], 484 (100) [CpMnL$^+$]. − $C_{38}H_{35}Cl_3MnO_4P$ (772.1): calcd. C 61.72, 5.09; found C 62.12, H 4.89.

X-ray Structural Analysis of **4c**: $C_{28}H_{31}MnO_{12}·CH_2Cl_2·CH_4O$, molecular mass 731.4, crystal size 0.3 × 0.3 × 0.3 mm (obtained by slow diffusion of pentane into a solution of **4c** in CH_2Cl_2/methanol); monoclinic crystal system, space group C_2, *a* = 16.793(4), *b* = 12.929(3), *c* = 16.992(4) Å, β = 109.63(1)°; *V* = 3476.6(14) Å^3, *Z* = 4, $d_{calcd.}$ = 1.397 g cm^{-3}; μ (Mo-K_α) = 0.577 mm^{-1}, *F*(000) = 1520. Wyckoff scan, 2θ range 4−54°, scan speed variable 2.0−30.0° min^{-1} in ω. 4117 independent reflections with 3978 [$F > 3\sigma(F)$]. Data were collected at −31°C with the crystal mounted in a glass capillary on a Siemens P4 diffractometer (graphite monochromator, Mo-K_α radiation, λ = 0.71073 Å). The structure was solved (Patterson methods) and refined by using the SHELXTL

PLUS (VMS) program package. 397 parameters refined, $R = 0.068$, $Rw = 0.065$. Largest difference peak (hole) +0.60 eÅ^{-3} (−0.50 eÅ^{-3}). The positions of the hydrogen atoms were calculated by assuming ideal geometry ($d_{C-H} = 0.96$ Å) and their coordinates were refined together with the attached C atoms as a "riding model". The dichloromethane was disordered and was isotropically refined in two different positions assuming equal occupation. Methanol was also isotropically refined. The positions of all other atoms were refined anisotropically by full-matrix least-squares methods. Complete lists of atomic coordinates and thermal parameters were deposited.[24]

[1] For leading references on chiral-at-metal transition metal complexes see: [1a] H. Brunner, *Angew. Chem.* **1971**, *83*, 274; *Angew. Chem. Int. Ed. Engl.* **1971**, *10*, 249. – [1b] H. Brunner, *Adv. Organomet. Chem.* **1980**, *18*, 151.

[2] [2a] K. H. Dötz, W. Straub, R. Ehlenz, K. Peseke, R. Meisel, *Angew. Chem.* **1995,** *107,* 2023−2024; *Angew. Chem. Int. Ed. Engl.* **1995**, *34*, 1856−1858. – [2b] R. Aumann, *Chem. Ber.* **1992**, *125*, 2773−2778. – [2c] T. Pill, K. Polborn, W. Beck, *Chem. Ber.* **1990**, *123*, 11−17. – [2d] J. M. Dalla Riva Toma, D. E. Bergstrom, *J. Org. Chem.* **1994**, *59*, 2418−2422. – [2e] J. Burger, P. Klüfers, *Chem. Ber.* **1995**, *128*, 75−79.

[3] [3a] K.-H. Dötz, O. Neuß, M. Nieger, *Synlett* **1996**, 995−996. – [3b] K. H. Dötz, W.-C. Haase, M. Klumpe, M. Nieger, *J. Chem. Soc., Chem. Commun.* **1997**, 1217−1218. – [3c] R. Ehlenz, O. Neuß, M. Teckenbrock, K. H. Dötz, *Tetrahedron* **1997**, *53*, 5143−5158.

[4] H. Fischer, J. Schleu, G. Roth, *Chem. Ber.* **1995**, *128*, 373−378.

[5] H. Fischer, J. Schleu, *Chem. Ber.* **1996**, *129*, 385−390.

[6] J. Schleu, Thesis, Universität Konstanz, **1996**.

[7] Although the stereogenic center is not involved in the substitution of the alcoholates in **3d** and **3e** for the acetoxy group in **2** its designation changes. That is because the reaction of the (*S*)-glycerol **3d** gives the (2*R*)-2,3-dihydroxypropyloxycarbene complex **4d**. This is due to a change in the priority of the different groups at the stereogenic center.

[8] [8a] C. Kelley, N. Lugan, M. R. Terry, G. L. Geoffroy, B. S. Haggerty, A. L. Rheingold, *J. Am. Chem. Soc.* **1992**, *114*, 6735−6749. – [8b] U. Schubert, *Organometallics* **1982**, *1*, 1085−1088. – [8c] A. D. Redhouse, *J. Organomet. Chem.* **1975**, *99*, C29−C30. – [8d] W. A. Herrmann, J. L. Hubbard, I. Bernal, J. D. Korp, B. L. Haymore, G. L. Hillhouse, *Inorg. Chem.* **1984**, *23*, 2978−2983. – [8e] P. Friedrich, G. Besl, E. O. Fischer, G. Huttner, *J. Organomet. Chem.* **1977**, *139*, C68−C72. – [8f] C. Barbeau, K. S. Dichmann, L. Ricard, *Can. J. Chem.* **1973**, *51*, 3027−3031. – [8g] G. Le Borgne, E. Gentric, D. Grandjean, *Acta Crystallogr., Sect. B* **1975**, *31*, 2824−2829.

[9] The absolute configuration is assigned according to the modification of the Cahn-Ingold-Prelog priority rules proposed by Tirouflet et al. The η^5-C_5H_5 ligand is considered to be a pseudo-atom of atomic number 30, which gives the following sequence: η^5-C_5H_5 > PR_3 > CO > C(OR*)Ph. – [9a] C. Lecomte, Y. Dusausoy, J. Protas, J. Tirouflet, A. Dormond, *J. Organomet. Chem.* **1974**, *73*, 67−76. – [9b] T. E. Sloan, *Top. Stereochem.* **1981**, *12*, 1−36.

[10] K. Weissenbach, H. Fischer, unpublished results.

[11] [11a] C. G. Kreiter, E. O. Fischer, *XXIIIrd International Congress of Pure and Applied Chemistry*, Butterworths, London, vol. 6, **1971**, 151−168. – [11b] H. Brunner, J. Doppelberger, E. O. Fischer, M. Lappus, *J. Organomet. Chem.*, **1976**, *112*, 65−78.

[12] [12a] M. Brookhart, J. R. Tucker, G. R. Husk, *J. Organomet. Chem.* **1980**, *193*, C23−C26. – [12b] M. Brookhart, W. B. Studabaker, M. B. Humphrey, G. R. Husk, *Organometallics* **1989**, *8*, 132−140. – [12c] M. Brookhart, Y. Liu in *Advances in Metal Carbene Chemistry* (Ed.: U. Schubert), Kluwer Acadenic Publishers, Dordrecht, **1989**, 251−270.

[13] Examples for rotation around the Mn=C(carbene) bond: M. J. McGeary, T. L. Tonker, J. L. Templeton, *Organometallics* **1985**, *4*, 2102−2106 and ref.[8a]

[14] For hindered rotation around the C(carbene)−OR bond see e.g.: [14a] C. G. Kreiter, E. O.Fischer, *Angew. Chem.* **1969**, *81*, 780−781; *Angew. Chem. Int. Ed. Engl.* **1969**, *8*, 761. – [14b] E. O. Fischer, C. G. Kreiter, H. J. Kollmeier, J. Müller, R. D. Fischer, *J. Organomet. Chem.* **1971**, *28*, 237−258. – [14c] E. O. Fischer, H.-J. Beck, C. G. Kreiter, J. Lynch, J. Müller, E. Winkler, *Chem. Ber.* **1972**, *105*, 162−172. – [14d] V. Guerchais, C. Lapinte, J.-Y. Thépot, L. Toupet, *Organometallics* **1988**, *7*, 604−612.

[15] [15a] N. M. Kostic, R. F. Fenske, *J. Am. Chem. Soc.* **1982**, *104*, 3879−3884. – [15b] D. S. Marynick, C. M. Kirkpatrick, *J. Am. Chem. Soc.* **1985**, *107*, 1993−1994.

[16] H. Brunner, W. Steger, *J. Organomet. Chem.* **1976**, *120*, 239−256.

[17] H. Brunner, M. Langer, *J. Organomet. Chem.* **1975**, *87*, 223−240.

[18] H. Brunner, J. A. Aclasis, *J. Organomet. Chem.* **1976**, *104*, 347−362.

[19] E. O. Fischer, A. Maasböl, *Chem. Ber.* **1967**, *100*, 2445−2456.

[20] M. L. Wolfrom, A. Thompson, *Meth. Carbohydr. Chem.* **1962**, vol. I/II, p. 334.

[21] M. Mikamo, *Carbohydr. Res.* **1989**, *191*, 150−153.

[22] C. E. Ballou, H. O. L. Fischer, *J. Am. Chem. Soc.* **1954**, *76*, 3188−3193.

[23] K. Sasse in *Methoden Org. Chem. (Houben-Weyl) 4th ed.*, **1963**, vol. XII/1, p. 32ff.

[24] Crystallographic data (excluding structure factors) for the structure reported in this paper have been deposited with the Cambridge Crystallographic Data Centre. Copies of the data can be obtained free of charge on application to CCDC, 12 Union Road, Cambridge CB2 1EZ, UK [fax: int. code +44(1223)336-033, e-mail: deposit@ccdc.cam.ac.uk].

[97237]

Activation of Dichloromethane by (Phosphane)$_n$rhodium(I) Complexes − X-ray Structure of [{(PEt$_3$)$_2$RhCl}$_2$(μ-Cl)$_2$(μ-CH$_2$)]

Jean-Jacques Brunet*, Xavier Couillens, Jean-Claude Daran, Ousmane Diallo, Christine Lepetit, and Denis Neibecker

Laboratoire de Chimie de Coordination du CNRS, UPR 8241,
205 route de Narbonne, F-31077 Toulouse Cedex 4, France
Fax: (internat.) +33 (0) 561 553 003
E-mail: brunet@lcctoul.lcc-toulouse.fr

Received November 11, 1997

Keywords: Rhodium / Phosphanes / Ligand redistribution / Dichloromethane activation / Oxidative addition

Dichloromethane reacts with dinuclear rhodium complexes [{(PR$_3$)$_2$Rh}$_2$(μ-Cl)$_2$] to give the bridging-methylene complexes [{(PR$_3$)$_2$RhCl}$_2$(μ-Cl)$_2$(μ-CH$_2$)] (PR$_3$ = PEt$_3$, PPh$_2$Me). The structure of the PEt$_3$ complex has been established by X-ray diffraction study. The early stages of the reaction of [{(C$_8$H$_{14}$)$_2$Rh}$_2$(μ-Cl)$_2$] with monophosphanes have been monitored by ^{31}P NMR, evidencing chloride bridges cleavage and phosphane redistribution processes.

Activation of dihalomethanes by low oxidation state transition metal complexes has attracted a great deal of interest as a means of generating haloalkyl transition metal derivatives which are versatile precursors for a wide range of useful compounds[1]. Oxidative addition of diiodo and dibromomethane is well documented, and, although less common, the case of dichloromethane is now well recognized.

Several examples of simple oxidative addition of dichloromethane (CH_2Cl_2) to electron-rich Rh^I complexes of mono or polydentate phosphorus[2][3], nitrogen[4][5][6], sulfur[7], and phosphorus/nitrogen[8][9] ligands have been reported. They usually afford chloromethylrhodium(III) complexes.

However, we found only two examples of double oxidative addition of CH_2Cl_2 on binuclear Rh^I complexes[10][11]. The chloride-bridged rhodium(I) dimer [{(dppe)Rh}$_2$(μ-Cl)$_2$] [dppe = 1,2-bis(diphenylphosphanyl)ethane] has been reported to react with CH_2Cl_2 to generate a bridging-methylene rhodium(III) complex (eq. 1)[10].

$$[\{(dppe)Rh\}_2(\mu\text{-}Cl)_2] + CH_2Cl_2 \xrightarrow{25°C,\ 36h} [\{(dppe)RhCl\}_2(\mu\text{-}Cl)_2(\mu\text{-}CH_2)] \quad (1)$$

The other example concerns the oxidative addition of *gem*-dichlorocarbons on the binuclear basic complex [{Rh(μ-pz)(CN*t*Bu)$_2$}$_2$] (pz = pyrazolate) to give [{Rh(μ-pz)Cl(CN*t*Bu)$_2$}$_2$(μ-CHR)][11].

In this paper, we report that activation of CH_2Cl_2 to generate methylene-bridged dimers is not limited to dinuclear Rh^I complexes and to Rh^I complexes bearing chelating diphosphanes, and can be obtained from both mononuclear and dinuclear monophosphane rhodium(I) complexes. Furthermore, some insight is given on the intermediates involved in the reaction of monophosphanes with the chloro-bridged dimer [{(C$_8$H$_{14}$)$_2$Rh}$_2$(μ-Cl)$_2$], **1** (C$_8$H$_{14}$ = cyclooctene).

As part of our work on the synthesis of amidorhodium complexes, we have been led to prepare the dimer [{(PEt$_3$)$_2$Rh}$_2$(μ-Cl)$_2$], **2**[12][13]. Compound **2** is prepared in pure form [^{31}P{^{1}H} NMR, δ (THF) = 44.3, $J_{P\text{-}Rh}$ = 194 Hz] by treating 4 equivalents of PEt$_3$ with **1** in THF. It can also be prepared in CH_2Cl_2 by reacting the starting materials for 10 min, followed by immediate evaporation of the solvent. Incidentally, we observed that if the reaction time in CH_2Cl_2 is longer than 10 min, a second complex is formed [^{31}P{^{1}H} NMR, δ (CH_2Cl_2) = 31.1, $J_{P\text{-}Rh}$ = 147 Hz] which becomes the only reaction product after 2 h. This new complex was isolated by precipitation with THF. Apart from the expected signals for the triethylphosphane ligands, the ^{1}H-NMR spectrum exhibits a broad signal at δ = 3.7, which becomes sharper on phosphorus decoupling, and the ^{13}C{^{1}H,^{31}P} NMR spectrum shows a triplet at δ = 38.9 ($J_{C\text{-}Rh}$ = 22 Hz, see Experimental Section). These signals could correspond to the methylene bridge of a dinuclear Rh^{III} complex, as suggested by the relatively small $J_{P\text{-}Rh}$ coupling constant. This complex was definitely identified as the methylene-bridged dinuclear complex [{(PEt$_3$)$_2$RhCl}$_2$(μ-Cl)$_2$(μ-CH$_2$)] **3** by single crystal X-ray diffraction analysis.

The molecular structure, which has a 2-fold symmetry, is shown in Figure 1. The binuclear structure is built up by two rhodium centers joined by two chloride ligands and a bridging methylene unit the carbon of which is located on the 2-fold axis. This structure is very similar to that of the recently reported [{(dppe)RhCl}$_2$(μ-Cl)$_2$(μ-CH$_2$)] complex[10]. As in the dppe compound, each rhodium center has a symmetrical, quasi-octahedral environment and formally can be considered as Rh^{III}. A comparison of important bond distances and bond angles within the

 © WILEY-VCH Verlag GmbH, D-69451 Weinheim, 1998 1434−1948/98/0303−0349 $ 17.50+.50/0

Figure 1. Molecular structure and numbering scheme for $[\{(PEt_3)_2RhCl\}_2(\mu\text{-}Cl)_2(\mu\text{-}CH_2)]$.

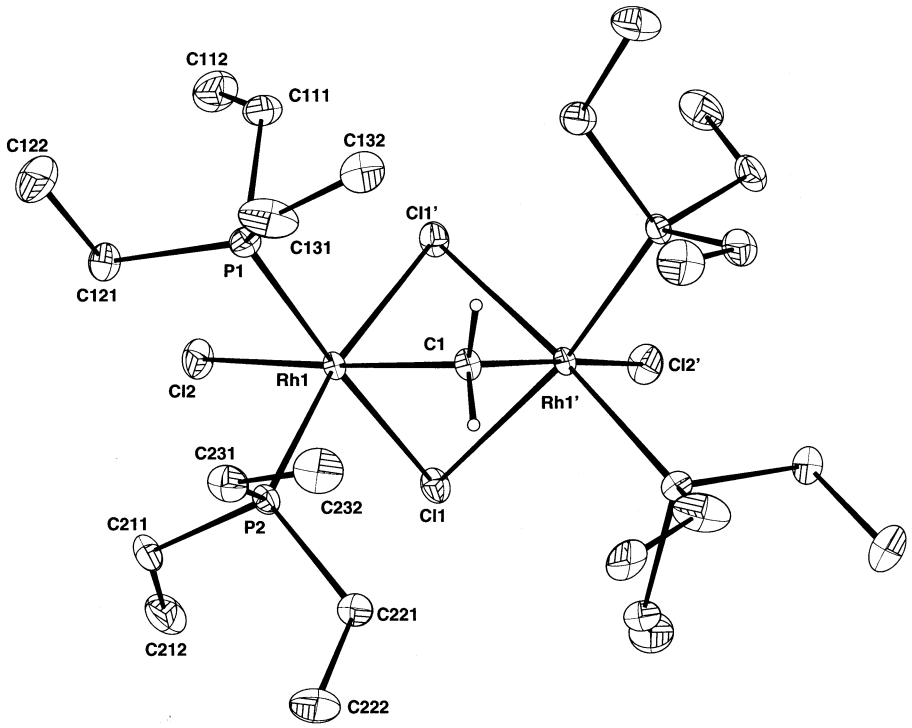

$Rh_2Cl_4P_4CH_2$ framework for the two complexes is given in Table 1.

Table 1. Comparison of interatomic distances [Å] and bond angles [°] within the $Rh_2Cl_4P_4CH_2$ framework of $[\{L_2RhCl\}_2(\mu\text{-}Cl)_2(\mu\text{-}CH_2)]$. E.s.d.s. in parentheses refers to the last significant digit

	L = PEt_3	L = dppe
Rh(1)−Cl(1)	2.4458(4)	2.4532(7)
Rh(1)−Cl(1′)	2.4618(4)	2.4700(8)
Rh(1)−Cl(2)	2.5310(4)	2.5071(7)
Rh(1)−P(1)	2.2851(4)	2.2587(8)
Rh(1)−P(2)	2.2605(4)	2.2394(8)
Rh(1)−C(1)	2.060(2)	2.057(3)
Cl(1)−Rh(1)−Cl(1′)	81.64(2)	82.35(3)
Cl(1)−Rh(1)−Cl(2)	89.69(1)	94.15(3)
Cl(1′)−Rh(1)−Cl(2)	87.41(1)	93.07(3)
Cl(1)−Rh(1)−P(1)	174.87(2)	176.65(3)
Cl(1′)−Rh(1)−P(1)	93.28(1)	99.23(3)
Cl(2)−Rh(1)−P(1)	89.40(1)	88.72(3)
Cl(1)−Rh(1)−P(2)	89.61(1)	93.74(3)
Cl(1′)−Rh(1)−P(2)	169.97(1)	175.99(3)
Cl(2)−Rh(1)−P(2)	97.49(1)	86.30(3)
P(1)−Rh(1)−P(2)	95.51(2)	84.72(3)
Cl(1)−Rh(1)−C(1)	81.95(4)	80.70(7)
Cl(1′)−Rh(1)−C(1)	81.55(4)	80.29(7)
Cl(2)−Rh(1)−C(1)	166.99(5)	172.0(1)
P(1)−Rh(1)−C(1)	98.04(4)	96.62(8)
P(2)−Rh(1)−C(1)	92.42(3)	100.02(7)
Rh(1)−Cl(1)−Rh(1′)	75.58(1)	76.20(2)
Rh(1)−C(1) −Rh(1′)	93.7(1)	95.2(2)

The main differences are observed for the angles around the metal atom. They are certainly related to the larger strain resulting from the chelating coordination of the dppe ligand, as is clearly shown by the P(1)−Rh(1)−P(2) angle which varies from 95.51° in the triethylphosphane complex to 84.72° in the dppe one.

This results (eq. 2) shows that the activation of CH_2Cl_2 by a chloride-bridged rhodium(I) dimer discovered by Fryzuk et al. (eq. 1) is not limited to the case of rhodium(I) complexes with chelating diphosphanes[10].

$$[\{(PEt_3)_2Rh\}_2(\mu\text{-}Cl)_2] \;\xrightarrow[\text{RT, 2h}]{CH_2Cl_2}\; [\{(PEt_3)_2RhCl\}_2(\mu\text{-}Cl)_2(\mu\text{-}CH_2)] \quad (2)$$

2 → **3**

More surprisingly, the same methylene-bridged dinuclear rhodium complex **3** is formed as the major product by reaction of the mononuclear complex $[(Et_3P)_3RhCl]$ with CH_2Cl_2 for 24 h at room temperature. On the basis of ^{31}P-NMR analysis, some others unidentified (phosphane)rhodium complexes are also formed in small amounts.

$$[(PEt_3)_3RhCl] \;\xrightarrow[\text{RT, 24 h}]{CH_2Cl_2}\; [\{(PEt_3)_2RhCl\}_2(\mu\text{-}Cl)_2(\mu\text{-}CH_2)] + \ldots \quad (3)$$

3

This result (eq. 3) is somewhat surprising in view of the reaction described by Milstein et al. in the case of PMe_3 (eq. 4)[2].

$$[(PMe_3)_3RhCl] + CH_2Cl_2 \xrightarrow{C_6H_6} \begin{matrix}[(PMe_3)_3RhCl_2(CH_2Cl)] \\ + \\ [(PMe_3)_2RhCl_3(CH_2PMe_3)]\end{matrix} \xrightarrow{\Delta} X \quad (4)$$

Indeed PEt_3 and PMe_3 have similar electronic properties (pK_a 8.69 vs 8.65) and differ by their cone angles, only (132° vs 118°)[14]. Nevertheless, this reaction may occur via displacement of an equilibrium between $[(PEt_3)_3RhCl]$ and $[\{(PEt_3)_2Rh\}_2(\mu\text{-}Cl)_2]$, a well-known process in the case of $[(PPh_3)_3RhCl]$[15]. The different behaviour of $[(PMe_3)_3RhCl]$ may be merely ascribed to the unfavorable dissociation of the smaller phosphane.

In the course of our study of the reaction of PEt_3 (4 equiv.) with $[\{(C_8H_{14})_2Rh\}_2(\mu\text{-}Cl)_2]$ **1**, we made another interesting observation. Indeed, according to literature data[16][17][18], e.g. in the case of Ph_2PMe[18], this reaction was believed to occur by stepwise replacement of the cyclooctene ligands, without cleavage of the chloride bridges, to ultimately yield $[\{(PEt_3)_2Rh\}_2(\mu\text{-}Cl)_2]$ (**2**). We surprisingly observed that, after a few min at room temp. in dichloromethane, the very major phosphane complex is $[(PEt_3)_3RhCl]$. The reaction rapidly evolves to generate the chloride-bridged dimer **2**, together with the bridging-methylene one **3** which is the only product after 1 h. The observation of $[(PEt_3)_3RhCl]$ as the only phosphane complex (no free PEt_3) at the early stage of the reaction implies the presence of unreacted **1** and suggests a subsequent redistribution of the phosphane ligands. This was demonstrated independently by reacting $[(PEt_3)_3RhCl]$ (4 equiv.) with **1** (1 equiv.) in THF, affording quantitatively $[\{(PEt_3)_2Rh\}_2(\mu\text{-}Cl)_2]$ (^{31}P NMR) (eq. 5).

$$4[(PEt_3)_3RhCl] + \underset{\mathbf{1}}{[\{(C_8H_{14})_2Rh\}_2(\mu\text{-}Cl)_2]} \xrightarrow[10\ min]{THF} 3\underset{\mathbf{2}}{[\{(PEt_3)_2Rh\}_2(\mu\text{-}Cl)_2]} \quad (5)$$

The above results led us to reinvestigate the previously reported reaction of PPh_2Me (4 equiv.) with **1**[18] by ^{31}P-NMR monitoring at the early stage of the reaction at room temperature. In THF, the reaction is very fast. Within 5 min the main reaction product is $[\{(PPh_2Me)_2Rh\}_2(\mu\text{-}Cl)_2]$ and only traces of other complexes {among which $[(PPh_2Me)_3RhCl]$} are observable. In CH_2Cl_2, however, a mixture of 5 complexes is observed after 5−10 min. The major product is $[(PPh_2Me)_3RhCl]$ (^{31}P NMR: δ = 31.8, dt, $J_{P\text{-}Rh}$ = 187 Hz, $J_{P\text{-}P}$ = 42 Hz and δ = 16.5, dd, $J_{P\text{-}Rh}$ = 139 Hz, $J_{P\text{-}P}$ = 42 Hz). Among the four others complexes, only two could be identified. On the basis of literature data[18], one is $[\{(PPh_2Me)(C_8H_{14})Rh\}_2(\mu\text{-}Cl)_2]$ (^{31}P NMR δ = 40.4, $J_{P\text{-}Rh}$ = 187 Hz) while the other is the expected $[\{(PPh_2Me)_2Rh\}_2(\mu\text{-}Cl)_2]$ (^{31}P NMR: δ = 34.0, $J_{P\text{-}Rh}$ = 196 Hz). Among the two other minor complexes, one gives a broad doublet (^{31}P NMR: δ = 32.8, $J_{P\text{-}Rh}$ = 194.5 Hz) and the second a spin figure which resembles that of a tris(phosphane)rhodium(I) complex (^{31}P NMR: δ = 22.8, dt, $J_{P\text{-}Rh}$ = 150 Hz, $J_{P\text{-}P}$ = 24 Hz anf δ = 10.6, dd, $J_{P\text{-}Rh}$ = 96 Hz, $J_{P\text{-}P}$ = 24 Hz). After 20 min, all the above signals have evolved to leave those of the dinuclear complex $[\{(PPh_2Me)_2Rh\}_2(\mu\text{-}Cl)_2]$, exclusively. Then this signal progressively vanishes to cleanly leave a doublet (^{31}P NMR: δ = 17.7, $J_{P\text{-}Rh}$ = 148 Hz) attributed to the methylene-bridged $[\{(PPh_2Me)_2RhCl\}_2(\mu\text{-}Cl)_2(\mu\text{-}CH_2)]$ (**4**) which can be readily isolated. This CH_2Cl_2 activation appears to be slower than in the case of $[\{(PEt_3)_2Rh\}_2(\mu\text{-}Cl)_2]$, probably as a consequence of the lower electron-donating ability of PPh_2Me (pK_a = 4.57) as compared to that of PEt_3[14].

It is thus clear that when $[\{(C_8H_{14})_2Rh\}_2(\mu\text{-}Cl)_2]$ **1** is treated with 4 equivalents of PR_3 (either PEt_3 or PPh_2Me), cleavage of chloride bridges occurs, followed by phosphane redistribution, affording the dinuclear complexes $[\{(PR_3)_2Rh\}_2(\mu\text{-}Cl)_2]$. In both cases, these complexes activate CH_2Cl_2 to give the methylene-bridged complexes $[\{(PR_3)_2RhCl\}_2(\mu\text{-}Cl)_2(\mu\text{-}CH_2)]$.

As a complement, we also studied the reaction of **1** with only 2 equivalents of either PEt_3 or PPh_2Me, again by ^{31}P-NMR monitoring at the early stage of the reaction at room temperature. Indeed, the authors who previously reported on the reaction with PPh_2Me indicated that the NMR spectra were recorded several hours after mixing the reactants[18].

In both cases, after 5−10 min mixing the reactants in THF at room temperature, the tetrasubstituted $[\{(PR_3)_2Rh\}_2(\mu\text{-}Cl)_2]$ and the disubstituted $[\{(C_8H_{14})(PR_3)Rh\}_2(\mu\text{-}Cl)_2]$ complexes are present as the two major products. In the case of PPh_2Me, three others complexes are also observable, two of them giving rise to doublets (^{31}P NMR: δ = 40.0, $J_{P\text{-}Rh}$ = 187 Hz and δ = 33.2, $J_{P\text{-}Rh}$ = 195 Hz) and the third one (minor) giving a spin figure corresponding to a tris(phosphane)rhodium complex, as previouly observed with 4 equivalents of PPh_2Me (vide supra). After 2 h, only the doublet corresponding to the expected $[\{(C_8H_{14})(PR_3)Rh\}_2(\mu\text{-}Cl)_2]$ is present.

Thus, although the cleavage of the chloride bridges could not be clearly evidenced in the case of two equivalents of phosphane, these results indicate that reaction of monophosphanes with $[\{(C_8H_{14})_2Rh\}_2(\mu\text{-}Cl)_2]$ always involves substitution of the four cyclooctene ligands, followed by redistribution of the phosphane with unreacted starting complex.

It must be noted that a *related* ligand redistribution process has been recently evidenced by NMR in the special case of terdentate nitrogen ligands[5].

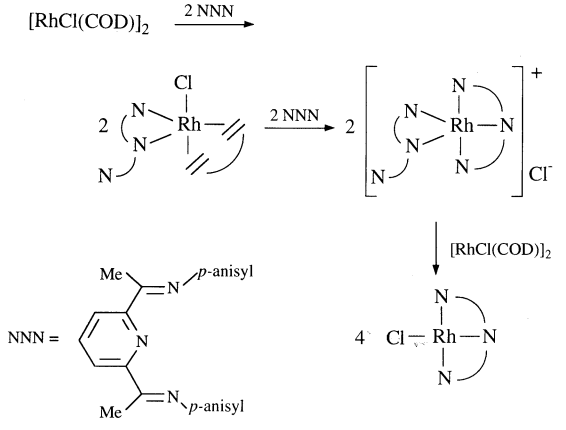

The resulting complex has also been shown to react with CD_2Cl_2 at 298 K to yield the corresponding chloro-

methyl complex $[RhCl_2(CD_2Cl)(\{2,6\text{-}C(Me)=N\text{-}p\text{-}anisyl\}_2C_5H_3N)]$[5].

This research was supported by the *Centre National de la Recherche Scientifique* and by the *Région Midi-Pyrénées* (France) which are gratefully acknowledged. The authors also wish to thank *B. Donnadieu* for collection of the X-ray data and *F. Lacassin* for NMR experiments.

Experimental Section

General: All reactions were performed under argon using standard Schlenk techniques. $[\{(C_8H_{14})_2Rh\}_2(\mu\text{-}Cl)_2]$ **1** was prepared according to the literature procedure[19]. − C, H analyses: Perkin-Elmer 2400 apparatus. − NMR: Bruker AC 200 (monitoring of reactions), AMX 400 (isolated complexes) (400.1, 162.0, 100.6, and 12.6 MHz, for ^1H, ^{31}P, ^{13}C, and ^{103}Rh, respectively). For ^1H NMR, CD_2Cl_2 as solvent, $\delta_H = 5.33$; for ^{31}P NMR, H_3PO_4 as external standard; for ^{13}C NMR, CD_2Cl_2 as solvent, $\delta_C = 52.9$; for ^{103}Rh NMR, CD_2Cl_2 as solvent, rhodium metal as external standard.

[{(PEt$_3$)$_2$RhCl}$_2$(μ-Cl)$_2$(μ-CH$_2$)] (**3**): Triethylphosphane (0.37 ml, 2.51 mmol) was added to a solution of $[\{(C_8H_{14})_2Rh\}_2(\mu\text{-}Cl)_2]$ (0.450 g, 0.63 mmol) in CH_2Cl_2 (20 ml). After 2 h stirring at room temp., the solvent was evaporated under reduced pressure. The resulting powder was washed with THF (20 ml) and dried in vacuo (0.401 g, 77%). − ^1H NMR: δ = 1.25 (m, 36 H, C*H*$_3$CH$_2$P), 2.00 (m, 12 H, CH$_3$C*H*$_2$P), 2.15 (m, 12 H, CH$_3$C*H*$_2$P), 3.69 (bs, 2 H, CH$_2$).−$^{31}P\{^1H\}$ NMR: δ = 34.4, d, $J_{P\text{-}Rh}$ = 147 Hz. − $^{13}C\{^1H,^{31}P\}$ NMR: δ = 8.12 (s, *C*H$_3$CH$_2$), 18.20 (s, CH$_3$*C*H$_2$), 38.88 (t, $J_{C\text{-}Rh}$ = 22 Hz, *C*H$_2$). − $^{103}Rh\{^1H\}$ NMR: δ = 1696 (t). − $C_{25}H_{62}Cl_4P_4Rh_2$ (834.3): calcd. C 35.99, H 7.49; found C 35.32, H 7.43.

[{(PPh$_2$Me)$_2$RhCl}$_2$(μ-Cl)$_2$(μ-CH$_2$)] (**4**): The same procedure as above was followed using PPh_2Me (41 µl; 0.217 mmol) and $[\{(C_8H_{14})_2Rh\}_2(\mu\text{-}Cl)_2]$ (0.039 g; 0.054 mmol) in CH_2Cl_2 (0.7 ml) and 6 h stirring at room temp. (0.045 g; 71%). − ^1H NMR: δ = 1.53 ($A_3XMX'A'_3$ spin system with a broad line symmetrically flanked by two sharp lines separated by 10.8 Hz, 12 H, C*H*$_3$P), 4.25 (bs, 2 H, C*H*$_2$), 6.9−7.6 (m, 40 H, aromatic H). − $^{31}P\{^1H\}$ NMR: δ = 20.31, d, $J_{P\text{-}Rh}$ = 148.7 Hz. − $^{13}C\{^{31}P\}$ NMR: δ = 14.90 (q, $J_{C\text{-}H}$ = 133 Hz, *C*H$_3$P), 56.78 (tt, $J_{C\text{-}H}$ = 143 Hz, $J_{C\text{-}Rh}$ = 18 Hz, *C*H$_2$), 127−133 (aromatic C). − $^{103}Rh\{^1H\}$ NMR: δ = 1847 (t). − $C_{53}H_{54}Cl_4P_4Rh_2$ (1162.5): calcd. C 54.76, H 4.68; found C 54.25, H 4.49.

X-ray Crystallographic Analysis of [{(PEt$_3$)$_2$RhCl}$_2$(μ-Cl)$_2$(μ-CH$_2$)] (**3**): X-ray quality crystals were obtained by slow diffusion of THF vapors into a concentrated CH_2Cl_2 solution of the complex. The data were collected on a Stoe Imaging Plate Diffraction System (IPDS) equipped with an Oxford Cryosystems cooler device. The crystal-to-detector distance was 80 mm. 115 exposures (2 min per exposure) were obtained with $0 < \varphi < 149.5°$ and with the crystals rotated through 2° in φ. Coverage of the unique set was over 99% complete to at least 24°. Crystal decay was monitored by measuring 200 reflexions per image. The Final unit cell parameters were obtained by the least-squares refinement of 5000 reflections. Only statistical fluctuations were observed in the intensity monitors over the course of the data collection.

The structure was solved by direct methods (SIR92)[20] and refined by least-squares procedures on F_o. One of the methyl of an ethyl group attached to P(1) is distributed statistically over two positions. The coordinates for these disordered carbon atoms were refined applying geometrical restraints to maintain reasonable C−C distances and C−C−C bond angles. H atoms were located on difference Fouriers maps, but they were introduced in calculation in idealized positions [d(CH) = 0.96 Å] and their atomic coordinates were recalculated after each cycle. They were given isotropic thermal parameters 20% higher than those of the carbon to which they are attached. Only the H atoms attached to the C methylene carbon were refined with an isotropic thermal parameter. Least-squares refinements were carried out by minimizing the function $\Sigma w(|F_o| - |F_c|)^2$, where F_o and F_c are the observed and calculated structure factors. The weighting scheme used in the last refinement cycles was $w = w'\{1 - [\Delta F/6\sigma(F_o)]^2\}^2$ where $w' = 1/\Sigma_1{}^nA_rT_r(x)$ with 3 coefficients Ar for the Chebyshev polynomial $A_rT_r(x)$ where x was $F_c/F_c(max)$[21]. Models reached convergence with $R = \Sigma(||F_o| - |F_c||)/\Sigma(|F_o|)$ and $R_w = [\Sigma w(|F_o| - |F_c|)^2/\Sigma w(F_o)^2]^{1/2}$, having values listed in Table 1. Criteria for a satisfactory complete analysis were the ratios of rms shift to standard deviation less than 0.1 and no significant features in final difference maps. Details of data collection and refinement are given in Table 2.

Table 2. Crystal and collection data for compound **3**·2 CH_2Cl_2

Crystal Parameters	
formula	$C_{25}H_{62}Cl_4P_4Rh_2 \cdot 2\ CH_2Cl_2$
fw [g]	1004.15
shape (color)	box (yellow)
size [mm]	0.50 × 0.40 × 0.30
crystal system	orthorhombic
space group	*Pnan*
a [Å]	13.1328(9)
b [Å]	17.479(2)
c [Å]	18.734(2)
V [Å^3]	4300.5(6)
Z	4
F(000)	2052
ρ (calcd) [g·cm^{-3}]	1.551
µ (Mo-K_α) [cm^{-1}]	14.238
Data collection	
Diffractometer	IPDS Stoe
monochromator	graphite
radiation	Mo-K_α (λ = 0.71073)
detector distance [mm]	80
Scan mode	
φ range [°]	$0 < \varphi < 149.5$
φ incr. [°]	1.3
exposure time [min]	2
2θ range [°]	$4.9 < 2\theta < 47.9$
no. of rflns collected	19755
no. of unique rflns	3308
merging factor R(int)	0.0353
reflections used [$I > 2\sigma(I)$]	2737
Refinement	
R	0.0186
R_w	0.0213
Weighting scheme	Chebyshev
Coefficient .Ar	1.39, −0.222, 1.22
$(\Delta/s)_{max}$	0.009
Δr_{max}	0.39
Δr_{min}	−0.35
GOF	1.102

The calculations were carried out with the CRYSTALS package programs[22] running on a PC. The drawing of the molecule was realized with the help of CAMERON[23]. The atomic scattering factors were taken from International Tables for X-ray Crystallography[24]. Crystallographic data (excluding structure factors) for the structure reported in this paper have been deposited at the Cambridge Crystallographic Data Centre as supplementary publication no. CCDC-100808. Copies of the data can be obtained free of charge on application to CCDC, 12 Union Road, Cambridge CB2 1EZ, UK [Fax: int. code + 44(1223)336-033; E-mail: deposit@ccdc.cam.ac.uk].

[1] H. B. Friedrich, J. R. Moss, *Adv. Organomet. Chem.* **1991**, *33*, 235−290.
[2] T. B. Marder, W. C. Fultz, J. C. Calabrese, R. L. Harlow, D. Milstein, *J. Chem. Soc.*, *Chem. Commun.* **1987**, 1543−1545.
[3] P. J. Fennis, P. H. M. Budzelaar, J. H. G. Frijns, A. G. Orpen, *J. Organomet. Chem.* **1990**, *393*, 287−298.
[4] H. Nishiyama, M. Horihata, T. Hirai, S. Wakamatsu, K. Itoh, *Organometallics* **1991**, *10*, 2706−2708.
[5] H. F. Haarman, F. R. Bregman, J. M. Ernsting, N. Veldman, A. L. Spek, K. Vrieze, *Organometallics* **1997**, *16*, 54−67.
[6] H. F. Haarman, J. M. Ernsting, M. Kranenburg, H. Kooijman, N. Veldman, A. L. Spek, P.W.N.M. van Leeuwen, K. Vrieze, *Organometallics* **1997**, *16*, 887−900.
[7] T. Yoshida, T. Ueda, T. Adachi, K. Yamamoto, T. Higuchi, *J. Chem. Soc.*, *Chem. Commun.* **1985**, 1137−1138.
[8] E. G. Burns, S. S. C. Chu, P. de Meester, M. Lattman, *Organometallics* **1986**, *5*, 2383−2384.
[9] K. Kashiwabara, A. Morikawa, T. Suzuki, K. Isobe, K. Tatsumi, *J. Chem. Soc., Dalton Trans.* **1997**, 1075−1081.
[10] G. E. Ball, W. R. Cullen, M. D. Fryzuk, B. R. James, S. J. Rettig, *Organometallics* **1991**, *10*, 3767−3769.
[11] M. A. Ciriano, M. A. Tena, L. A. Oro, *J. Chem. Soc., Dalton Trans.* **1992**, 2123−2124.
[12] J-J. Brunet, G. Commenges, D. Neibecker, K. Philippot, L. Rosenberg, *Inorg. Chem.* **1994**, *33*, 6373−6379.
[13] J-J. Brunet, J.-C. Daran, D. Neibecker, L. Rosenberg, *J. Organomet. Chem.* **1997**, *538*, 251−256.
[14] M. M. Rahman, H. Y. Liu, W. P. Giering, *Organometallics* **1987**, *6*, 650−658.
[15] J. A. Osborn, F. H. Jardine, J. F. Young, G. Wilkinson, *J. Chem. Soc.* **1966**, *(A)*, 1711−1732.
[16] H. L. M. Van Gaal, F. L. A. van den Bekerom, *J. Organomet. Chem.* **1977**, *134*, 237−248.
[17] H. Werner, L. Hofmann, R. Feser, W. Paul, *J. Organomet. Chem.* **1985**, *281*, 317−347.
[18] V. V. S. Reddy, A. Varshney, G. M. Gray, *J. Organomet. Chem.* **1990**, *391*, 259−266.
[19] A. van der Ent, A. L. Onderdelinden, *Inorg. Synth.* **1973**, *14*, 92−95.
[20] A. Altomare, G. Cascarano, G. Giacovazzo, A. Guagliardi, M.C. Burla, G. Polidori , M. Camalli, *SIR92* − a program for automatic solution of crystal structures by direct methods, *J. Appl. Cryst.* **1994**, *27*, 435.
[21] E. Prince, *Mathematical Techniques in Crystallography*, Berlin, Springer-Verlag, **1982**.
[22] D. J. Watkin, C. K. Prout, J. R. Carruthers, P.W. Betteridge, *CRYSTALS Issue 10*, Chemical Crystallography Laboratory, University of Oxford, Oxford, **1996**.
[23] D. J. Watkin, C. K. Prout, L.J. Pearce, *CAMERON*, Chemical Crystallography Laboratory, University of Oxford, Oxford, **1996**.
[24] *International Tables for X-ray Crystallography*, Vol. C, Kynoch Press, Birmingham, UK, **1992**.

[97264]

The Reactions of $R_2Ga-GaR_2$ and $R_2In-InR_2$ [R = $CH(SiMe_3)_2$] with Protic Reagents: Substituent Exchange versus Cleavage of the Element−Element Bond

Werner Uhl*[a], Rene Graupner[a], Ingo Hahn[a], Thomas Spies[a], and Walter Frank[b]

Fachbereich Chemie der Universität Oldenburg[a],
Postfach 2503, D-26111 Oldenburg, Germany
Fax: (internat.) + 49(0)441/798-3352

Fachbereich Chemie der Universität Kaiserslautern[b],
Erwin-Schrödinger-Straße 52, D-67663 Kaiserslautern, Germany
Fax: (internat.) + 49(0)631/2052-187

Received August 14, 1997

Keywords: Gallium / Indium / Low-valent compounds

Tetrakis[bis(trimethylsilyl)methyl]digallane(4) (**1**) with a Ga−Ga single bond and the corresponding diindane(4) **2** with an In−In single bond were treated with different protic reagents: *tert*-Butyl alcohol did not react with **1** at all, while phenol gave a mixture of unknown products, which could not be separated. The more acidic pentafluorophenol did not react as an acid, but C−F bonds were cleaved to form almost quantitatively the dimer $(R_2GaF)_2$ **5**, which was characterized by a crystal-structure determination. Water and **1** yielded the dimeric dialkylgallium hydroxide **6**. The Ga−Ga bond was also cleaved by the reaction of **1** with durylthiophenol (duryl = 2,3,5,6-tetramethylphenyl), which gave two main products: $R_2Ga(SDuryl)$ **7** and $RGa(SDuryl)_2$ **8**. In contrast, the chelating acid dibenzoylmethane reacted by means of a substituent exchange, with the release of two equiv. of bis(trimethylsilyl)methane for each formula unit of **1**, to form **9**, in which the Ga−Ga bond is retained and each chelating 1,3-diphenyl-1,3-propanedionato ligand is in a terminal position bonded to only one Ga atom, in more than 80% yield. The Ga−Ga bond is shortened [244.1(1) pm] compared to that in the starting compound tetraalkyldigallane(4) **1**. The In−In bond of diindane(4) **2** is, however, cleaved in a similar reaction with dibenzoylmethane, and only the fragmentation product dialkyl(1,3-diphenyl-1,3-propanedionato)indium **10** could be isolated.

Tetrakis[bis(trimethylsilyl)methyl]dielement(4) compounds with the elements aluminium[1], gallium (**1**)[2], and indium (**2**)[3] in an unusually low oxidation state of +II and an element−element single bond, showed a remarkable reactivity towards carboxylic acids: Dialane(4) reacted on treatment with benzoic acid by the insertion of the Al atoms into the O−H bond, the cleavage of the Al−Al bond and the reduction of the proton by two electrons to give a hydride anion[4]. Both dialkylaluminium fragments of the product are unsymmetrically bridged by an O,O′-benzoato group and an hydride ion to form the six-membered heterocycle **3**. A similar product could not be obtained with diindane(4) **2**, which may be due to the inherently low thermal stability of In−H bonds. Instead, two monoindium compounds, monomeric R_2InO_2CR and dimeric $RIn(O_2CR)_2$, were formed[4], probably by fragmentation, the precipitation of indium metal and the release of elemental hydrogen. The most interesting products, **4**, were isolated from the reactions of digallane(4) **1** with aromatic and aliphatic carboxylic acids[5]. Two bis(trimethylsilyl)methyl groups are replaced by carboxylato groups, which occupy a bridging position above the considerably shortened Ga−Ga bond. Remarkably, the C−Ga−Ga−C group is almost linear and the angle between the normals of the planes of the carboxylato ligands approaches 90°. The reaction of **1** with less acidic diphenyltriazene led to a partial fragmentation and oxidation of digallane(4) **1**. Two main products are formed: by cleavage of the Ga−Ga bond the monogallane $R_2Ga(N_3Ph_2)$ and by substituent exchange, the digallane $R_2Ga_2(N_3Ph_2)_2$, in which, in contrast to **4**, the chelating substituents are terminally bonded[6]. The substituent exchange thus opened up an easy route for the synthesis of novel organodigallium compounds, and we systematically employed further protic reagents like alcohol or acetylacetone derivatives.

Reactions of Digallane(4) 1 with Alcohols and Water

tert-Butyl alcohol did not react with **1** at all, even when a large molar excess of 4 equiv. of the alcohol for each formula unit of **1** was used, and the mixture was refluxed in hexane for several days. The reaction of the more acidic phenol in a molar ratio of 2 to 1 in boiling hexane resulted in the complete consumption of **1** after a period of four days, but a mixture of unknown products was formed, which could not be separated by recrystallization; only trace amounts of a colorless solid, which was not further characterized, crystallized out of solution in pentane. Pentafluorophenol reacted with **1** not as an acid, but by the cleavage of

 © WILEY-VCH Verlag GmbH, D-69451 Weinheim, 1998 1434−1948/98/0303−0355 $ 17.50+.50/0

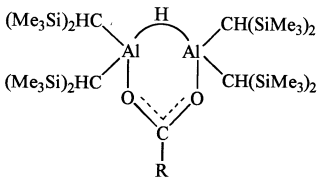

3

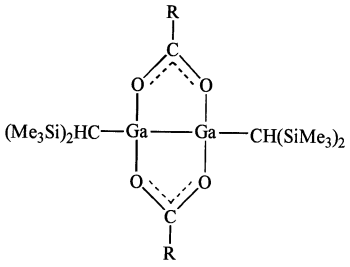

4

C−F bonds. The reaction required more than 48 h in boiling hexane, and only one product could be isolated after recrystallization from pentane in a yield of more than 80%. A dialkylgallium fluoride **5**, which is a dimer in the solid state (see below) and in solution, as cryoscopically determined in benzene, was formed by the cleavage of the Ga−Ga bond (eq. 1). **5** thus differs from the recently published analogous compound $Br-Ga[CH(SiMe_3)_2]_2$[7] and the corresponding chloroaluminium derivative $Cl-AlR_2$[1], which are both monomeric in solution, with coordinatively unsaturated central atoms, probably due to strong steric interactions between the bulky bis(trimethylsilyl)methyl substituents. A dimer was, however, also observed in the corresponding hydroxide[8], so that, interestingly, the smallest donor atoms are able to form the most stable dimers. Because OH and F are the most electronegative of the employed substituents, this observation may be explained as resulting from a more effective ionic interaction and a high electrostatic contribution to the bonding in these molecules. The monomeric bromide $BrGaR_2$ and the dimeric fluoride **5** differ significantly in their ^{13}C-NMR spectra. The C atoms bonded to gallium show a chemical shift of $\delta = 25.6$ in the bromo derivative, which is within the range usually observed with bis(trimethylsilyl)methyl compounds of tricoordinated Ga atoms[2][7]. In **5**, however, the corresponding resonance is shifted to higher field ($\delta = 16.6$), characteristic for compounds with tetracoordinated Ga atoms. Absorptions in the IR spectra at 525 and 490 cm^{-1} could be assigned to the stretching vibrations of the Ga_2F_2 unit[9]. Dimesityl- and diisopropylgallium fluoride, as recently published by Neumüller et al.[10], are also dimeric in solution, and the IR absorptions at 473 and 450 cm^{-1} (R = mesityl) and 496 cm^{-1} (R = benzyl) were assigned to the Ga_2F_2 molecular center. In comparison to these gallium fluorides ($\delta = -152.7$ and -169.7) the ^{19}F-NMR resonance of **5** is shifted downfield to $\delta = -109.5$. The similar cleavage of a C−F bond of a fluorinated aromatic compound accompanied by the formation of an Al−F bond has recently been reported[11].

Water also does not react with **1** by the release of bis(trimethylsilyl)methane, but by the oxidation of the gallium

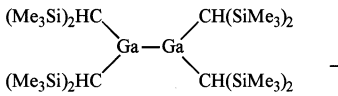

1

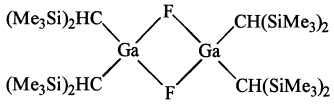

5

(1)

atoms and cleavage of the Ga−Ga bond. Dimeric dialkylgallium hydroxide **6** is formed (eq. 2), which is isolated after recrystallization from *n*-pentane in a yield of about 50%. Elemental hydrogen is probably formed as a byproduct, which could, however, not be detected due to its small amount. **6** has been obtained in our group before by another route and was characterized by a crystal-structure determination[8].

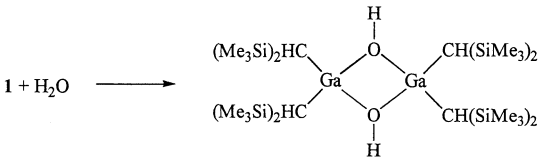

6

(2)

The behavior of thioalcohols was investigated in a reaction of **1** with the sterically shielded durylthiol (duryl = 2,3,5,6-tetramethylphenyl). After 72 h in boiling hexane, 70% of **1** was consumed. Two new products were formed, which could be separated with difficulty by repeated recrystallization to yield a small amount of an enriched sample of **8**, while the second component **7**, could only be detected in mixtures with **8**. Both products were identified spectroscopically as $R_2GaSDuryl$ **7** and $RGa(SDuryl)_2$ **8**. The pure compounds **7** and **8** could not be obtained by the reaction of $Ga[CH(SiMe_3)_2]_3$[2] with one or two equiv. of durylthiol in solution or in a melt at 120°C; in all reactions, **7** was only formed as a minor component, while reactions in the molar ratio of 1:2 gave impure samples of **8**, which could not be purified by recrystallization. The spectroscopic information obtained for the impure monothiolato product is not sufficient enough to discuss the degree of oligomerization, but the dithiolato product seems to be at least a dimer with a tetracoordinated Ga atom, as can be seen from the chemical shift of the carbon atom bonded to Ga ($\delta = 15.5$).

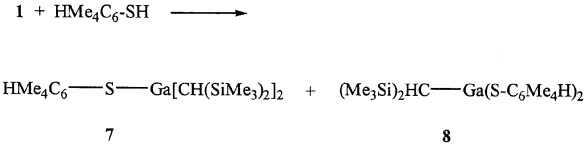

7 8

(3)

Reaction of Digallane(4) 1 and Diindane(4) 2 with Dibenzoylmethane

As shown before, non-chelating acidic compounds such as alcohols or thioalcohols reacted exclusively by the cleavage of the Ga−Ga bond. We hoped to realize the substituent exchange by retaining the Ga−Ga bond, when we treated **1** with a chelating protic acetylacetone derivative. This reaction was of particular interest because, up to now, we had observed either a bridging or a terminal coordination by the chelating ligand in the products of both successful substituent exchange reactions. The reason for this different behavior is not well understood, but it possibly depends on the distance between the coordinating atoms (bite) with the N−N distance in the triazenido ligand too short to facilitate the bridging of the Ga−Ga bond.

When we treated a yellow solution of the digallane(4) **1** in pentane with two equiv. of dibenzoylmethane at −50°C (eq. 4), the color changed at about −10°C to give an orange solution, from which orange-red crystals of **9** were obtained at −50°C in a yield of 79%. In contrast to the reactions described above, two equiv. of $CH_2(SiMe_3)_2$ are formed for each formula unit of **1**, as shown by NMR spectroscopy. Elemental analysis, mass spectrometry, the cryoscopic molar-mass determination in benzene and the integration of the ^{1}H-NMR spectrum confirm the structure of a digallium compound with two bis(trimethylsilyl)methyl and two 1,3-diphenyl-1,3-propanedionato substituents. In the NMR spectra, the resonances of the methine protons and the α-carbon atoms of the $CH(SiMe_3)_2$ groups are strongly shifted upfield (^{1}H: δ = −0.09; ^{13}C: δ = 10.4) compared to those of the starting compound **1** (δ = 1.09 and 25.9, respectively)[2], clearly indicating a coordination number of four at the Ga atoms. The atoms of the electronically delocalized π system of the 1,3-diphenyl-1,3-propanedionato group show the usual chemical shifts: δ = 185.7 [*C*(O)], 93.9 [*C*(H)] and δ = 6.52 (*H*). In contrast to the colorless triazenido or carboxylato digallium compounds mentioned above, **9** is deeply orange with absorptions at 420 and 340 nm in the UV/Vis spectrum; the color, however, is mainly a function of the chelating group and is often observed in its reaction products.

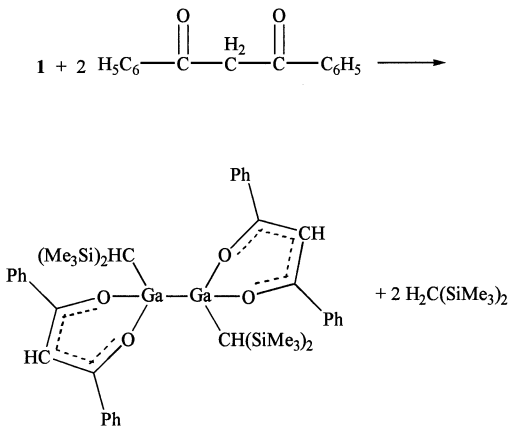

9 (4)

Until now, all reactions of protic reagents with diindane(4) **2** resulted in the cleavage of the In−In bond and precipitation of elemental indium. Because of the formation of the digallium compound **9** in a high yield with only minor byproducts, we treated **2** with dibenzoylmethane under similar conditions to those described above for **1** in a molar ratio of 1:2. As originally intended, the formation of bis(trimethylsilyl)methane could be detected by NMR spectroscopy, but only as a minor component, and a black precipitate of elemental indium indicated a disproportionation reaction and the fragmentation of the starting compound **2**. A crystalline product was isolated from *n*-pentane at −30°C, which was identified by its NMR spectra and its molar mass as the dialkylindium compound **10** (eq. 5). The yield of **10** based on dibenzoylmethane amounted to only 43%, and an excess of the diketone crystallized as a second fraction. Reactions in an equimolar ratio gave **10** in a yield of 86% based on dibenzoylmethane, but a small part of the starting compound **2** was recovered. The course of these reactions may give some insight into the reaction mechanism: Similar to the reactions with carboxylic acids[4] described in the introduction, the In atoms are probably oxidized by the OH proton of the enol form of the diketone, accompanied by insertion into the O−H bond. The intermediate with an In−H bond similar to the Al compound **3** is unstable, and decomposes by the release of elemental hydrogen, which may lead to the formation of the isolated product dialkyl(1,3-diphenyl-1,3-propanedionato)indium **10** and an InR_2 radical, which could disproportionate via an alkylindium(I) derivative, stable only with bulkier $C(SiMe_3)_3$ substituents[12], to form elemental indium and the corresponding trialkylindane. The highly soluble indane[3] could indeed be identified as the main component of the mother liquor after isolation of **10** and the unreacted diindane(4) **2**. Product **10** was synthesized by the treatment of the corresponding trialkylindane with one equiv. of dibenzoylmethane in a yield of almost 90%. Due to its molar mass in benzene, **10** is monomeric in solution. The resonances of the methine groups bonded to indium are shifted upfield [^{1}H: δ = −0.18 (*H*CIn); ^{13}C: δ = 11.9 (*C*In)], which is characteristic of a coordination number of four at the indium atom and verifies the chelating coordination by the 1,3-diphenyl-1,3-propanedionato ligand.

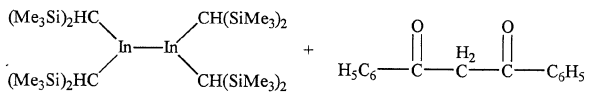

2 (5)

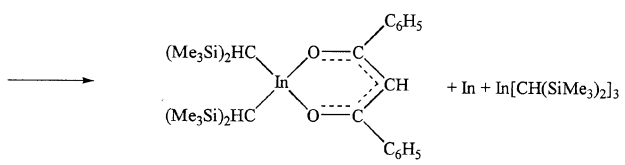

10

Crystal Structures of Compounds 5 and 9

Figure 1 shows the molecular structure of the dimeric compound $(R_2GaF)_2$ **5** [R = $CH(SiMe_3)_2$], which crystallizes in the centrosymmetric triclinic space group $P\bar{1}$ with two dimers in each unit cell. The four $CH(SiMe_3)_2$ substituents are arranged in a terminal position and the dialkylgallium fragments are bridged by both fluorine atoms. A four-membered Ga_2F_2 heterocycle results; this is almost ideally planar with a maximum deviation of an atom of 2.9 pm. The GaC_2 planes with the methine carbon atoms of the bis(trimethylsilyl)methyl groups are almost exactly perpendicular to this plane, and the normals of the planes include angles of 90.6° (Ga1C1C2) and 89.6° (Ga2C3C4). The bond angles in the heterocycle are most acute at the Ga atoms (76.9°) and much enlarged at the F atoms (103.0°); almost identical angles were observed in the recently published corresponding di(μ-hydroxo)digallium derivative[8]. Dialkylgallium fluorides have been known for a long time. They usually form trimers (R = Me, Et[13], *i*Pr[10]), and it was only recently that a dimer, which was sterically highly shielded by four bulky mesityl substituents, was characterized by a crystal-structure determination[10]. A tetrameric modification was observed by Schmidbaur et al. with R = Me[13]. The Ga−F bonds in **5** and $(Mes_2GaF)_2$ [194.7(2) pm] are quite similar; for **5** they deviate only slightly from the average value of 196.6 pm. The $CH(SiMe_3)_2$ substituents of comparable dialuminium or digallium compounds usually show a conformation in which the methine hydrogen atom of one substituent points between both $SiMe_3$ groups of the second $CH(SiMe_3)_2$ substituent[1][2][3]. This conformation is only observed at the atom Ga1 in **5**, while at Ga2 the four trimethylsilyl groups are neighbored and can be transferred onto each other by non-crystallographic mirror planes. Thus, the molecule is not centrosymmetric in the solid state, although only one singlet of the $SiMe_3$ groups was observed in the NMR spectra in solution. The molecule shows a disorder (54−46%), and the bis(trimethylsilyl)methyl group of C2 occupies a second position, which gives the same conformation as observed at Ga2. The point group of the second molecule is thus approximately D_{2h}.

The molecular structure of **9** is depicted in Figure 2. The molecule is located on a crystallographic center of symmetry, which intersects the Ga−Ga bond. Two bis(trimethylsilyl)methyl groups are replaced by chelating 1,3-diphenyl-1,3-propanedionato ligands, which in contrast to the corresponding carboxylato derivative **4**[5], but similarly to the product obtained with diphenyltriazene[6], occupy terminal positions and are bonded to only one Ga atom. Due to its crystallographic symmetry, the molecule has an ideal *trans* conformation. The Ga−Ga bond length is 244.0 pm, which is slightly shorter than in the triazenide compound [245.79(6) pm] with a synclinal molecular conformation[6], but longer than in **4** [238.5(2) pm][5]. Compared to the starting compound **1** [254.1(1) pm][2] a significant shortening is observed; all Ga−Ga distances lie in the range characteristic of Ga−Ga bonds in organoelement or inorganic derivatives[14]. The Ga−C bond length is lengthened [199.5(5) pm] compared to the carboxylato-bridged compound **4** [195.7(8) pm], but the Ga−O distances are significantly reduced [**9**: 195.9(3) pm; **4**: 201.1(6) pm], which might be caused by the bridging of the Ga−Ga bond and the resulting larger steric stress in **4**. The distance between the coordinating atoms in the chelate ring of **9** (278.9 pm) is much larger than in the carboxylato-bridged derivative **4** (224.0 pm)[5]. A shorter bite is observed with the triazenido ligand (209.2 pm)[6], which occupies a terminal position.

Figure 1. Molecular structure of **5**; the ellipsoids are drawn at the 40% probability level; methyl groups are omitted for clarity; only one position of the disordered $CH(SiMe_3)_2$ group at C2 is drawn[a]

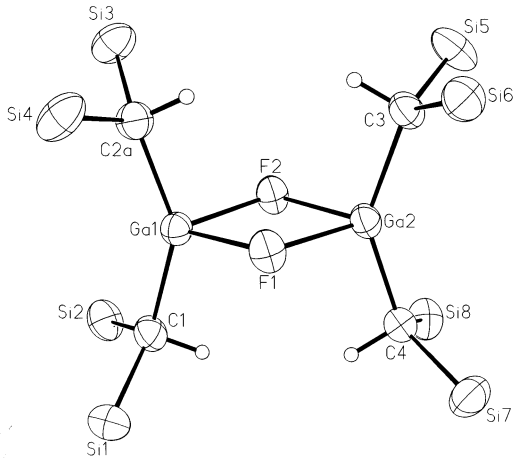

[a] Selected bond lengths [pm] and angles [°]: Ga1−F1 196.3(3), Ga1−F2 195.4(3), Ga2−F1 197.4(3), Ga2−F2 197.3(3), Ga1···Ga2 307.7, Ga1−C1 197.1(5), Ga1−C2 199.7(9), Ga1−C2A 194(1), Ga2−C3 196.5(5), Ga2−C4 196.4(5); F1−Ga1−F2 77.2(1), F1−Ga2−F2 76.5(1), Ga1−F1−Ga2 102.8(1), Ga1−F2−Ga2 103.2(1), C1−Ga1−C2 126.8(3), C1−Ga1−C2A 147.1(4), C3−Ga2−C4 143.8(2).

Figure 2. Molecular structure of **9**; the ellipsoids are drawn at the 40% probability level; methyl and phenyl groups are omitted for clarity; only one position of the disordered $CH(SiMe_3)_2$ group at C1 is drawn[a]

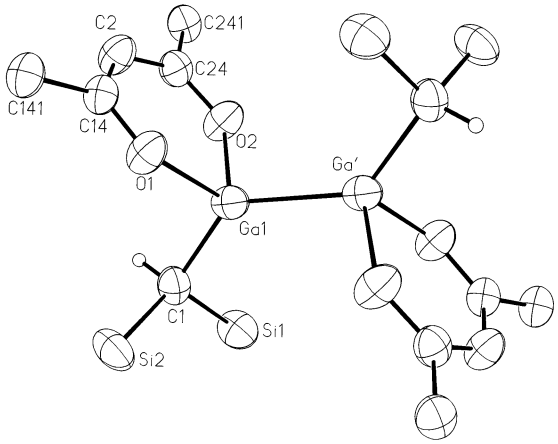

[a] Selected bond lengths [pm] and angles [°]: Ga1−Ga1′ 244.0(1), Ga1−C1 199.5(5), Ga1−O1 195.9(3), Ga1−O2 194.8(3); O1−Ga1−O2 91.1(1), O1−Ga1−C1 102.8(2), O2−Ga1−C1 103.6(2), Ga1′−Ga1−C1 133.9, Ga1′−Ga1−O1 110.0(1), Ga1′−Ga1−O2 107.2(1) (symmetry operation to generate Ga1′: $-x$, $-y$, $1-z$).

The kind of the coordination, terminal or bridging, seems therefore not to be determined by the magnitude of the distance between the coordinating atoms, and remains an open question, in which case a particular coordination is adopted. The (1,3-diphenyl-1,3-propanedionato)gallium heterocycle is almost planar, with the maximum deviation from the plane of 8.1 pm by the oxygen atom O1; its bond lengths and angles resemble that of comparable derivatives of gallium in an oxidation state of +III[15].

We are grateful to the *Deutsche Forschungsgemeinschaft* and the *Fonds der Chemischen Industrie* for generous financial support.

Experimental Section

General: All procedures were carried out under purified argon in dried solvents (*n*-pentane, cyclopentane, and *n*-hexane with $LiAlH_4$, benzene with Na/benzophenone). Compounds **1** and **2** were synthesized as described in ref.[2][3], durylthiol was obtained by the reduction of $ClSO_2-C_6Me_4H$ with $LiAlH_4$[16], dibenzoylmethane and pentafluorophenol (Aldrich) were sublimed in vacuo, *tert*-butyl alcohol was treated with Na and distilled, phenol (99+%, Aldrich) was used without further purification.

Synthesis of $(R_2GaF)_2$ **5**: 0.91 g (1.17 mmol) of digallane(4) **1** was dissolved in 50 ml of *n*-hexane and treated with 0.43 g (2.34 mmol) of solid pentafluorophenol. The mixture was heated under reflux for 48 h, and the color changed from yellow to colorless. The solvent was evaporated and the residue recrystallized from *n*-pentane (20/−30°C). Yield: 0.83 g (87%); colorless, slightly air-sensitive crystals; m.p. (argon; closed capillary) 157°C. − ^{1}H NMR (C_6D_6, 300 MHz): δ = 0.17 (1 H, GaCH), 0.16 (18 H, $SiMe_3$). − ^{13}C NMR (C_6D_6, 75.5 MHz): δ = 16.6 (GaC), 3.5 ($SiMe_3$). − ^{19}F NMR (C_6D_6, 282 MHz): δ = −109.5. − IR (CsBr, paraffin): $\tilde{\nu}$ = 1314 cm^{-1} (w), 1262 (sh), 1252 (vs, δCH_3), 1171 (w), 1018 (vs), 995 (sh, δCH), 843 (vs), 777 (s), 762 (s), 723 [s, ρCH_3(Si)], 673 (m, ν_{as}SiC), 646 (w), 613 (w, ν_sSiC), 573 (vw), 527 (w, νGa_2F_2), 509 (w, νGaC_2), 490 (w, νGa_2F_2), 463 (vw, νGaC_2), 421 (vw), 376 (vw, δSiC). − $C_{28}H_{76}F_2Ga_2Si_8$ (815.0): calcd. F 4.7, Ga 17.1; found F 4.5, Ga 16.9. − Mol. mass: 745 (cryoscopically in benzene).

Reaction of Digallane(4) **1** *with Water:* Digallane(4) **1** (0.19 g, 0.25 mmol) was dissolved in 20 ml of *n*-hexane and treated with 8.8 µl of water. The mixture was stirred vigorously for 6 h until the water phase was completely consumed. The solvent was evaporated, and the residue recrystallized from *n*-hexane (20/−50°C). Yield: 0.103 mg (51%) colorless crystals of compound **6**; characterization see ref.[8].

Reaction of Digallane(4) **1** *with Durylthiol:* Digallane(4) **1** (0.695 g, 0.896 mmol) was dissolved in 40 ml of *n*-hexane and cooled to −30°C. 23.3 ml of a 0.077 M solution of durylthiol (1.79 mmol) in *n*-hexane was added. The mixture was warmed to room temperature and stirred for 72 h. The pale yellow solution was concentrated and the residue recrystallized from *n*-pentane. A mixture of both products **7** and **8** was obtained with the dithiol derivative **8** enriched as the less soluble component. − ^{1}H NMR of $R_2GaSCMe_4H$ **7** (C_6D_6, 300 MHz): δ = 6.76 (1 H, phenyl), 2.55 and 2.10 (each 6 H, methyl of duryl), 0.22 (36 H, $SiMe_3$); methine proton signal not detected. − Characterization of **8**: colorless, slightly air-sensitive crystals; m.p. (argon; closed capillary) 146°C. − ^{1}H NMR (C_6D_6, 300 MHz): δ = 6.71 (2 H, phenyl), 2.48 and 2.05 (each 12 H, methyl of duryl), 0.18 (18 H, $SiMe_3$); methine proton signal not detected. − ^{13}C NMR (C_6D_6, 75.5 MHz): δ = 137.3, 134.0, 132.3, 130.9 (all phenyl), 21.0 and 20.2 (methyl of duryl), 15.5 (GaC), 3.2 ($SiMe_3$). − IR (CsBr, paraffin): $\tilde{\nu}$ = 1553 cm^{-1} (w, phenyl); 1462 (vs), 1377 (vs, paraffin); 1302 (w), 1260 (m), 1250 (s, δCH_3), 1155 (vw), 1020 (m), 1003 (m, δCH), 964 (m), 862 (s), 839 (vs), 775 (s), 762 (s), 721 [s, ρCH_3(Si)], 675 (m, ν_{as}SiC), 629 (w), 613 (vw, ν_sSiC), 546 (w), 517 (w, νGaC), 461 (m), 430 (w), 397 (w), 378 (w, νGaS, δSiC). − $C_{27}H_{45}GaS_2Si_2$ (559.7): calcd. Ga 12.5; found Ga 12.2.

Synthesis of Dialkylbis(µ-1,3-diphenyl-1,3-propanedionato-O,O′)digallium **9**: A solution of 0.314 g (1.40 mmol) of dibenzoylmethane in 50 ml of *n*-pentane was added dropwise to a cooled solution (−50°C) of digallane(4) **1** (0.518 g, 0.67 mmol) in 75 ml of *n*-pentane. The mixture was slowly warmed to room temperature, and the color changed at about −10°C from yellow to orange. The solvent was evaporated, the residue thoroughly dried in vacuo to completely remove bis(trimethylsilyl)methane and recrystallized from 60 ml of *n*-pentane (20/−50°C). Yield: 0.478 g (79%); orange-red, slightly air-sensitive crystals; m.p. (argon; closed capillary) 168−169°C. − ^{1}H NMR (C_6D_6, 300 MHz): δ = 7.81 (4 H, pseudo-d, *o*-H of phenyl), 7.09 (2 H, pseudo-t, *p*-H of phenyl), 7.01 (4 H, pseudo-t, *m*-H of phenyl), 6.52 [1 H, s, $HC(CO)_2$], 0.40 (18 H, s, $SiMe_3$), −0.09 (1 H, s, GaCH). − ^{13}C NMR (C_6D_6, 75.5 MHz): δ = 185.7 (CO), 138.3, 132.2, 128.4 (all phenyl), 93.9 [$C(CO)_2$], 10.4 (GaC), 3.8 ($SiMe_3$). − IR (CsBr, paraffin): $\tilde{\nu}$ = 1973 cm^{-1} (vw), 1954 (vw), 1912 (vw), 1892 (vw), 1852 (vw), 1804 (vw), 1765 (vw, phenyl), 1591 (m), 1535 (s), 1524 (s, chelate), 1466 (vs), 1362 (vs, paraffin), 1316 (s), 1304 (s), 1252 (sh), 1244 (s), 1229 (sh, δCH_3), 1182 (m), 1157 (m), 1127 (m), 1092 (m), 1063 (s, νCC, νCO), 1022 (vs), 999 (w, δCH), 970 (vw), 953 (vw), 939 (s), 914 (s), 862 (sh), 841 (vs), 787 (m), 756 (vs), 716 νr, ρCH_3(Si)], 694 (sh), 681 (s), 669 (sh, ν_{as}SiC), 629 (s), 617 (s, ν_sSiC), 556 (s), 527 (s), 509 (vs), 494 (m), 455 (w, νGaC, νGaO), 436 (w), 395 (w), 338 (vw, δSiC). − UV (*n*-hexane): λ_{max} (lg ε) = 200 nm (5.0), 260 (4.6), 340 (4.7), 421 (3.8). − FD MS; *m/z*: 903.3, 904.7, 906.7 [all M^+, in agreement with a calculated isotope pattern]. − $C_{44}H_{60}Ga_2O_4Si_4$ (904.7): calcd. Ga 15.4; found Ga 15.4. − Mol. mass: 855 (cryoscopically in benzene).

Reaction of Diindane(4) **2** *with Dibenzoylmethane:* A solution of 0.086 g (0.38 mmol) of dibenzoylmethane in 20 ml of *n*-pentane was added to a cooled (−90°C) solution of 0.323 g (0.37 mmol) of diindane(4) **2** in 20 ml of *n*-pentane. The mixture was slowly warmed to room temperature, the color changed from orange to brown and elemental indium precipitated. After filtration and concentration, compound **10** crystallized as a yellow solid on cooling to −50°C. A quarter of the starting compound **2** was isolated as a second fraction. The mother liquor contained the readily soluble $In[CH(SiMe_3)_2]_3$ as a main component. Yield of **10**: 0.210 g (86% based on dibenzoylmethane); characterization of **10**: see below.

Synthesis of Dialkyl(1,3-diphenyl-1,3-propanedionato-O,O′)indium **10**: A solution of 0.348 g (1.55 mmol) of dibenzoylmethane in 30 ml of *n*-pentane was added to a cooled (−80°C) solution of 0.943 (1.59 mmol) of $In[CH(SiMe_3)_2]_3$ in 20 ml of *n*-pentane. The mixture was slowly warmed to room temperature, filtered and concentrated in vacuo. **10** crystallized on cooling to −30°C. Yield: 0.931 g (89%); yellow, slightly air-sensitive crystals; m.p. (argon; closed capillary) 121°C. − ^{1}H NMR (C_6D_6, 300 MHz): δ = 7.98 (4 H, pseudo-d, *o*-H of phenyl), 7.13 (6 H, m, phenyl), 6.83 [1 H, s, $HC(CO)_2$], 0.29 (36 H, s, $SiMe_3$), −0.18 (2 H, s, GaCH). − ^{13}C NMR (C_6D_6, 75.5 MHz): δ = 186.6 (CO), 139.8, 132.0, 128.7, 127.8 (all phenyl), 95.2 [$C(CO)_2$]; 11.9 (GaC), 3.9 ($SiMe_3$). − IR (CsBr, paraffin): $\tilde{\nu}$ = 1971 cm^{-1} vw, 1954 (vw), 1912 (vw), 1892 (vw), 1802 (vw), 1718 (vw, phenyl), 1591 (s, phenyl), 1541 (s), 1516 (vs, νCO, νCC of the chelate), 1476 (vs), 1364 (vs, paraffin), 1312 (m), 1259 (m), 1258 (s), 1246 (s), 1227 (m, δCH_3), 1184 (w), 1157 (w), 1125 (w), 1092 (w), 1057 (w, νCC,νCO), 1020 (s), 1011 (s,

δCH), 968 (vw), 936 (m), 926 (m), 914 (m), 843 (vs), 785 (m), 772 (m), 754 (m), 743 (s), 708 [s, ρCH_3(Si)], 677 (s), 665 (s, ν_{as}SiC), 625 (m), 610 (w, ν_sSiC), 542 (w), 521 (w), 484 (m, νInC, νInO), 394 (vw, δSiC). − $C_{29}H_{49}InO_2Si_4$ (656.9): calcd. In 17.5; found In 17.2. − Mol. mass: 605 (cryoscopically in benzene).

Crystal-Structure Determinations: Single crystals of compounds **5** and **9** were obtained by recrystallization from hexane and cyclopentane, respectively. Crystal data and structure refinement parameters are given in Table 1[19]. Both compounds show a disorder of one bis(trimethylsilyl)methyl group, which is best described as a different orientation of the methine hydrogen atoms. Although the carbon atoms occupy different positions in each disordered group, the Si atoms coincide in compound **5**; in **9** all atoms of the $CH(SiMe_3)_2$ group are disordered. The disordered atoms were isotropically refined under restrictions of bond lengths and angles (exception: the higher occupied position in **9**); the occupancy factors are 0.54 and 0.46 in **5** and 0.87 and 0.13 in **9**.

Table 1. Crystal data and data-collection parameters for **5** and **9**

	5	**9**
Formula	$C_{28}H_{76}F_2Ga_2Si_8$	$C_{44}H_{60}Ga_2O_4Si_4$
Crystal system	triclinic	triclinic
Space group	$P\bar{1}$; no. 2[17]	$P\bar{1}$; no. 2[17]
Z	2	1
T [K]	293(2)	293(2)
$d_{calcd.}$ [g/cm^3]	1.138	1.252
a [pm]	952.3(1)	1058.3(2)
b [pm]	1250.1(2)	1130.6(2)
c [pm]	2185.7(2)	1208.2(2)
α [°]	79.568(9)	67.93(3)
β [°]	88.652(9)	64.60(3)
γ [°]	68.54(1)	74.41(3)
V [10^{-30} m^3]	2379.0(6)	1200.2(4)
μ [mm^{-1}]	1.358	1.259[a]
Crystal size [mm]	0.14 × 0.15 × 0.34	0.39 × 0.44 × 0.46
Diffractometer	Siemens P4	Siemens P4
Radiation	Mo-K_α (graphite monochromator)	
Range	3.6° ≤ 2Θ ≤ 50°	4° ≤ 2Θ ≤ 50°
Reciprocal space	$-1 \le h \le 11$	$-1 \le h \le 12$
	$-14 \le k \le 14$	$-12 \le k \le 12$
	$-25 \le l \le 25$	$-13 \le l \le 14$
Scan mode	ω	ω
Independent reflections	8241	4181
Number of reflections [with $F^2 > 2\,\sigma(F^2)$]	5133	3284
Program	SHELXTL, SHELXL-93[b][18]	
Parameters	384	292
$R = \Sigma\|\|F_o\| - \|F_c\|\|/\Sigma\|F_o\|$ $[F^2 > 2\,\sigma(F^2)]$	0.0474	0.0559
$wR^2 = [\Sigma w(F_o^2-F_c^2)^2/\Sigma w(F_o^2)^2]^{1/2}$ (all data)	0.1560	0.1158
Max. residual [10^{30} e/m^3]	0.469	0.863
Min. residual [10^{30} e/m^3]	−0.341	−0.514

[a] Empirical absorption correction. − [b] Solutions by direct methods; full-matrix refinement with all independent structure factors.

[1] W. Uhl, *Z. Naturforsch., B: Chem. Sci.* **1988**, *43*, 1113−1118.
[2] W. Uhl, M. Layh, T. Hildenbrand, *J. Organomet. Chem.* **1989**, *364*, 289−300.
[3] W. Uhl, M. Layh, W. Hiller, *J. Organomet. Chem.* **1989**, *368*, 139−154.
[4] W. Uhl, R. Graupner, S. Pohl, W. Saak, W. Hiller, M. Neumayer, *Z. Anorg. Allg. Chem.* **1997**, *623*, 883−891.
[5] W. Uhl, I. Hahn, H. Reuter, *Chem. Ber.* **1996**, *129*, 1425−1428.
[6] W. Uhl, I. Hahn, R. Wartchow, *Chem. Ber.* **1997**, *130*, 417−420.
[7] W. Uhl, M. Layh, G. Becker, K. W. Klinkhammer, T. Hildenbrand, *Chem. Ber.* **1992**, *125*, 1547−1551. A similarly different behavior has recently been observed between bis[tetramethylpiperidino]aluminium fluoride and the analogous compounds of the heavier halogens: J. Krossing, H. Nöth, C. Tacke, M. Schmidt, H. Schwenk, *Chem. Ber.* **1997**, *130*, 1047−1052.
[8] W. Uhl, I. Hahn, M. Koch, M. Layh, *Inorg. Chim. Acta* **1996**, *249*, 33−39.
[9] J. Weidlein, U. Müller, K. Dehnicke, *Schwingungsfrequenzen I − Hauptgruppenelemente*, Georg Thieme Verlag, Stuttgart, **1981**.
[10] B. Neumüller, F. Gahlmann, *Z. Anorg. Allg. Chem.* **1992**, *612*, 123−129. B. Neumüller, F. Gahlmann, *Angew. Chem.* **1993**, *105*, 1770−1771; *Angew. Chem. Int. Ed. Engl.* **1993**, *32*, 1701−1702. − Further organoelement Ga−F derivatives in: B. Werner, T. Kräuter, B. Neumüller, *Inorg. Chem.* **1996**, *35*, 2977−2980; T. Kräuter, B. Neumüller, *Z. Anorg. Allg. Chem.* **1995**, *621*, 597−606; B. Werner, T. Kräuter, B. Neumüller, *Organometallics* **1996**, *15*, 3746−3751; B. Neumüller, F. Gahlmann, *Z. Anorg. Allg. Chem.* **1993**, *619*, 1897−1904; B. Werner, B. Neumüller, *Chem. Ber.* **1996**, *129*, 355−359; F.−Q. Liu, A. Künzel, A. Herzog, H. W. Roesky, M. Noltemeyer, R. Fleischer, D. Stalke, *Polyhedron* **1997**, *16*, 61−65. − Review: B. Neumüller, *Coord. Chem. Rev.* **1997**, *158*, 69−101.
[11] Y.-X. Chen, C. L. Stern, T. J. Marks, *J. Am. Chem. Soc.* **1997**, *119*, 2582−2583.
[12] W. Uhl, R. Graupner, M. Layh, U. Schütz, *J. Organomet. Chem.* **1995**, *493*, C1−C5; R. D. Schluter, A. H. Cowley, D. A. Atwood, R. A. Jones, J. L. Atwood, *J. Coord. Chem.* **1993**, *30*, 25−28.
[13] H. Schmidbaur, J. Weidlein, H.-F. Klein, K. Eiglmeier, *Chem. Ber.* **1968**, *101*, 2268−2277; H. Schmidbaur, H.-F. Klein, *ibid.* **1968**, *101*, 2278−2279; H. Schmidbaur, H.-F. Klein, K. Eiglmeier, *Angew. Chem.* **1967**, *79*, 821−822; *Angew. Chem. Int. Ed. Engl.* **1967**, *6*, 806−807. J. J. Eisch, *J. Am. Chem. Soc.* **1962**, *84*, 3830−3836.
[14] X. He, R. A. Bartlett, M. M. Olmstead, K. Ruhlandt-Senge, B. E. Sturgeon, P. P. Power, *Angew. Chem.* **1993**, *105*, 761−762; *Angew. Chem. Int. Ed. Engl.* **1993**, *32*, 717−718; D. Loos, H. Schnöckel, D. Fenske, *Angew. Chem.* **1993**, *105*, 1124−1125; *Angew. Chem. Int. Ed. Engl.* **1993**, *32*, 1059−1060; W. Hönle, G. Gerlach, W. Weppner, A. Simon, *J. Solid State Chem.* **1986**, *61*, 171−180; G. Linti, W. Köstler, *Angew. Chem.* **1996**, *108*, 593−595; *Angew. Chem. Int. Ed. Engl.* **1996**, *35*, 550−552; G. Linti, R. Frey, M. Schmidt, *Z. Naturforsch., B: Chem. Sci.* **1994**, *49*, 958−962; M. Julien-Pouzol, S. Jaulmes, M. Guittard, F. Alapini, *Acta Crystallogr. B* **1979**, *35*, 2848−2851; A. Kuhn, A. Chevy, R. Chevalier, *Acta Crystallogr. B* **1976**, *32*, 983−984; S. Paashaus, R. Kniep, *Z. Naturforsch., B: Chem. Sci.* **1990**, *45*, 667−678; D. S. Brown, A. Decken, A. H. Cowley, *J. Am. Chem. Soc.* **1995**, *117*, 5421−5422; A. K. Saxena, H. Zhang, J. A. Maguire, N. S. Hosmane, A. H. Cowley, *Angew. Chem.* **1995**, *107*, 378−380; *Angew. Chem. Int. Ed. Engl.* **1995**, *34*, 332−334; X.-W. Li, W. T. Pennington, G. H. Robinson, *J. Am. Chem. Soc.* **1995**, *117*, 7578−7579; X.-W. Li, Y. Xie, P. R. Schreiner, K. D. Gripper, R. C. Crittendon, C. F. Campana, H. F. Schaefer, G. H. Robinson, *Organometallics* **1996**, *15*, 3798−3803; B. Beagley, S. M. Godfrey, K. J. Kelly, S. Kungwankunakorn, C. M. McAuliffe, R. G. Pritchard, *J. Chem. Soc., Chem. Commun.* **1996**, 2179−2180; M. C. Kuchta, J. B. Bonanno, G. Parkin, *J. Am. Chem. Soc.* **1996**, *118*, 10914−10915; A. H. Cowley, A. Decken, C. A. Olazabal, *J. Organomet. Chem.* **1996**, *524*, 271−273.
[15] K. Dymock, G. J. Palenik, *Acta Crystallogr. B* **1974**, *30*, 1364−1366; B. Ballarin, G. A. Battiston, F. Benetollo, R. Gerbasi, M. Porchia, D. Favretto, P. Traldi, *Inorg. Chim. Acta* **1994**, *217*, 71−78.
[16] S. Pohl, M. Harmjanz, private communication.
[17] T. Hahn (Ed.), *International Tables for Crystallography, Space Group Symmetry*, Kluwer Academic Publishers, Dordrecht−Boston−London, **1989**, vol. A.
[18] *SHELXTL-Plus REL. 4.1*, Siemens Analytical X-RAY Instruments Inc., Madison, USA, **1990**; G. M. Sheldrick *SHELXL-93, Program for the Refinement of Structures*, Universität Göttingen, **1993**.
[19] Further details of the crystal-structure determinations are available from the Fachinformationszentrum Karlsruhe, D-76344 Eggenstein-Leopoldshafen (Germany), on quoting the depository numbers CSD−407196 (**5**) and −407197 (**9**).

[97194]

A Convenient Synthesis of Phosphonic Anhydrides − Trimers $[RPO_2]_3$ (R = *tert*-Butyl, 2-Methylphenyl, 2,4,6-Trimethylphenyl): Their Structures and Reaction Products

Klaus Diemert, Wilhelm Kuchen*, Wolfgang Poll, and Frank Sandt

Institut für Anorganische Chemie und Strukturchemie der Heinrich-Heine-Universität, Universitätsstraße 1, D-40225 Düsseldorf, Germany

Received August 27, 1997

Keywords: Phosphorus / Phosphonic anhydrides / Oligophosphonic acids / Peptide synthesis / Solid-state structures

By reaction of $RP(O)Cl_2$ with $RP(O)(OSiMe_3)_2$, phosphonic anhydrides $(RPO_2)_3$ (R = *t*Bu, 2-methylphenyl, 2,4,6-trimethylphenyl) **1a−c** are conveniently obtained. In contrast to **1b** and **1c**, compound **1a** is remarkably stable against protolysis. Intermediates of hydrolysis of **1a**, namely tris(*tert*-butyl)triphosphonic acid (**2**) and bis(*tert*-butyl)diphosphonic acid (**3**), can also be isolated in good yield. The structures of **1−3** were determined mainly by NMR spectroscopy (^1H, ^{13}C, ^{31}P). Assuming an energetic preference for the chair conformations in solution, and considering the steric requirements of the bulky substituents R, configurations Ia (point group C_s, two R in equatorial positions) for **1a** and **b**, and IIa (point group C_{3v}, all R equatorial) for **1c** are suggested. − Reaction of **1a** with *N*-benzyloxycarbonylglycine (**4**) in methanol affords strong evidence that in the first step of peptide synthesis with $(RPO_2)_3$, a mixed anhydride of triphosphonic acid and the *N*-protected amino acid is formed. − The crystal structure of **1a** (monoclinic, space group $P2_1/n$) widely corresponds to the suggested configuration Ia, but reveals an envelope conformation for the six-membered ring with a P_3O_2 plane in the crystal. In the crystal structure of the octahydrate of the disodium salt of **2** (monoclinic, space group $P2_1/c$), it can be seen that the polar end groups of the anions $[tBu_3P_3O_7]^{2-}$ together with the water molecules and the Na^+ cations form hydrogen-bonded double-layers, strictly separated from each other by the non-polar *tert*-butyl groups of the anions.

Introduction

A variety of methods have been reported in the literature for the preparation of phosphonic anhydrides $(RPO_2)_n$. These methods usually result in mixtures of oligomers which are difficult to separate[1][2][3].

Compounds of this composition were also obtained when the corresponding cyclophosphanes were oxidized with dry oxygen (R = CF_3, average number $\bar{n}$ = 3−4[4], R = Ph, $\bar{n}$ = 5[5]).

Thermolysis and flash vacuum pyrolysis of tBuP(O)(OSiMe_3)X (X = Cl, Br) afforded the trimer $(t\text{BuPO}_2)_3$[6].

Among other alkylphosphonic anhydrides, compound $(\text{PrPO}_2)_3$, which is commercially available, is recommended as a condensation reagent in the synthesis of peptides[7].

As phosphinic anhydrides $R_2P(O)-O-P(O)R_2$ are readily accessible by treating $R_2P(O)Cl$ and silyl esters $R_2P(O)(OSiMe_3)$ with elimination of Me_3SiCl[8], we now used the analogous reaction between phosphonoyl chlorides $RP(O)Cl_2$ and silyl phosphonates $RP(O)(OSiMe_3)_2$ for the synthesis of the title compounds. By this method we obtained, in excellent yield and purity, alkyl compounds $(RPO_2)_n$ as highly viscous, colorless oils that are readily hydrolyzable. They can be distilled under vacuum, and some of them gradually crystallize after standing at room temperature. According to cryoscopic measurements in benzene, $\bar{n}$ varied from 11 (R = Pr) to 6 (R = Bu, Pentyl) within a wide range of concentrations[9].

In case of bulky substituents R, we isolated well-defined trimers **1a−1c**. Their configurations and some of their reactions are discussed in the following sections[10].

Trimeric Phosphonic Anhydrides 1a−1c

On heating equimolar quantities of $RP(O)Cl_2$ and $RP(O)(OSiMe_3)_2$, **1a−1c** are obtained as colorless crystals with sharp melting points. While **1a** and **1b** are readily soluble in toluene, benzene, $CHCl_3$, or CH_2Cl_2, **1c** is fairly soluble only in the latter two solvents. **1b** and **1c** are rapidly dissolved by methanol or H_2O, with the formation of phosphonic acid esters RP(O)(OMe)OH or phosphonic acids $RP(O)(OH)_2$.

$(RPO_2)_3$

1

a: R = *t* Bu
b: R = 2-methylphenyl
c: R = 2,4,6-trimethylphenyl

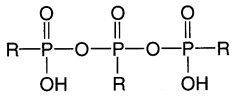

2

R = *t* Bu
2a: Disodium salt · 2 H_2O
2b: Disodium salt · 8 H_2O

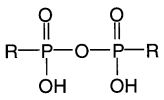

3

R = *t* Bu
3a: Disodium salt · 3 H_2O

1a, however, is remarkably stable in this respect. As shown by NMR spectroscopy, solutions of **1a** in methanol

 © WILEY-VCH Verlag GmbH, D-69451 Weinheim, 1998 1434−1948/98/0303−0361 $ 17.50+.50/0

or ethanol remain unchanged even after boiling for several hours. Hydrolysis is so slow that it is possible (as is shown later) to isolate intermediates of this reaction.

While in the mass spectra of **1b** and **1c**, abundant peaks for the molecular ions are observed, the signal for $M^{+\cdot}$ in the spectrum of **1a** is of low intensity. The spectrum of the latter compound is characterized by a successive loss of C_4H_8 from the molecular ion. A peak m/z = 192 (19%) corresponding to $[HPO_2]_3^{+\cdot}$ indicates that this process can occur without fragmentation of the six-membered ring.

NMR Spectra

Assuming a six-membered ring structure for **1**, and an energetic preference for the chair conformations, structures I and II, both with conformations a and b, have to be considered (Figure 1).

Figure 1. Possible structures of cyclic trimers **1** (chair conformations), point groups, and $^{31}P\{^1H\}$ spin systems

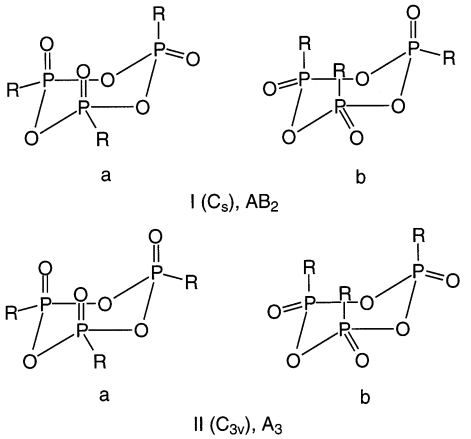

These should give rise to AB_2 or A_3 spin systems in their $^{31}P\{^1H\}$-NMR spectra, and we did in fact observe AB_2 systems for **1a** and **1b** and an A_3 system for **1c**. The correspondence of the observed spectra given in the Experimental Section with spectra simulated with parameters ν_A = 1912.3 Hz, ν_B = 1824.1 Hz, J_{AB} = 50.9 Hz (**1a**) and ν_A = 163.5 Hz, ν_B = −33.1 Hz, J_{AB} = 42.6 Hz (**1b**) is excellent. Considering the steric requirements of the bulky substituents R, structure Ia is therefore suggested for **1a** and **1b**, while structure IIa appears to be the most probable one for **1c**. In the crystal, **1a** adopts an envelope conformation with point group C_s and a P_3O_2 plane.

The ^{1}H-NMR spectra are in accordance with the suggested structures for **1a** and **1b**. The spectrum of the *tert*-butyl compound shows two doublets of relative intensity 1:2, a ratio that has also been found for the methyl protons in the spectrum of the 2-methylphenyl compound **1b**. The spectrum of **1c**, however, is more complex as several broad resonance signals for methyl groups and aromatic protons are observed.

Tris(*tert*-butyl)triphosphonic Acid (2), Bis(*tert*-butyl)diphosphonic Acid (3), and Their Disodium Salts 2a, 2b, and 3a

By reaction of equimolar quantities of **1a** and H_2O in ethanol at 50−60°C for 3.5 h, **2** is obtained as colorless crystals that are soluble in $CHCl_3$, methanol, or ethanol, and melt at 152°C. **2** is a strong dibasic acid (in water at room temperature: pK_{a1} not determinable, pK_{a2} = 2.29). Aqueous solutions of **2** were found to be stable for at least 10 h at room temperature. The $^{31}P\{^1H\}$-NMR spectrum corresponds to an AB_2 spin system (with close approximation to AX_2), and the $^1H\{^{31}P\}$-NMR spectrum shows two resonance signals (intensity ratio 2:1) for the *tert*-butyl groups, as well as one signal in the range of acidic protons. Neutralisation of **2** by NaOH affords **2a**, the dihydrate of its disodium salt. The octahydrate **2b** is obtained by diffusion-controlled precipitation from aqueous solutions of **2a** with acetone. **2b** forms large transparent leaflets, the crystal structure of which is reported.

Bis(*tert*-butyl)diphosphonic acid (**3**) is formed together with *tert*-butylphosphonic acid when the triphosphonic acid (**2**) is heated with concentrated hydrochloric acid for 1 h. After 4 h, tBuP(O)$(OH)_2$ is the sole reaction product. Reaction of **1a** with EtONa (molar ratio 1:4) in refluxing ethanol for 1 h affords the disodium salt of acid **3**. Both compounds were isolated as hydrates of composition **3**·1.5 H_2O and **3a**. They form colorless needles, which loose their water of crystallization on heating at 80−100°C. Compound **3**, m.p. 198−200°C, is soluble in water or acetone, **3a** readily dissolves only in water.

Reaction of (tBuP$O_2)_3$ (1a) with an *N*-Protected Amino Acid

Considering the general methods for peptide synthesis with other phosphorus compounds[11] it can be assumed that with $(PrPO_2)_3$ for example, the first step of the reaction is ring opening and formation of a mixed anhydride of the corresponding triphosphonic acid, and an *N*-protected amino acid. In a subsequent step, the mixed anhydride is thought to react with a carboxyl-protected amino acid, affording triphosphonic acid and the peptide.

Since **1a**, as well as the triphosphonic acid **2**, have been found to be stable against methanolysis, we tried to substantiate the opening step of this peptide synthesis by treating equimolar amounts of **1a** and the *N*-protected amino acid *N*-benzyloxycarbonylglycine (**4**) in methanol. After 3 h at 65°C, the reaction was complete. The reaction product, a colorless, highly viscous oil, was investigated by NMR spectroscopy and GC-MS. The conclusions drawn from the results are shown in Scheme 1, and may be summarized as follows:

The $^{31}P\{^1H\}$-NMR spectrum ($CDCl_3$) of the reaction mixture reveals the presence of one AX_2 system and several strongly overlapping multiplets at δ = 21−23, 30−31, and 32−34. The parameters of the AX_2 system (δ_A = 21.30 (t); δ_X = 31.30 (d); J_{AX} = 49.3 Hz) correspond well with those of the triphosphonic acid **2**. Moreover, a precipitate obtained by adding hexane to the methanolic solution of the reaction product was clearly identified as **2**.

P,P-COSY reveals the presence of 2 AMX spin systems with the following parameters: δ_A = 22.10 (t); δ_M = 30.40 (d); δ_X = 33.70 (d); J_{AM} = 48.3 Hz; J_{AX} = 46.9 Hz and δ_A = 21.80 (t); δ_M = 30.60 (d); δ_X = 33.10 (d); J_{AM} = 47.7 Hz; J_{AX} = 47.2 Hz. The AMX systems possibly result from

Scheme 1. Suggested reaction of **1a** with *N*-benzyloxycarbonylglycine (**4**) (methanol, 65°C, 3 h), R = *t*Bu

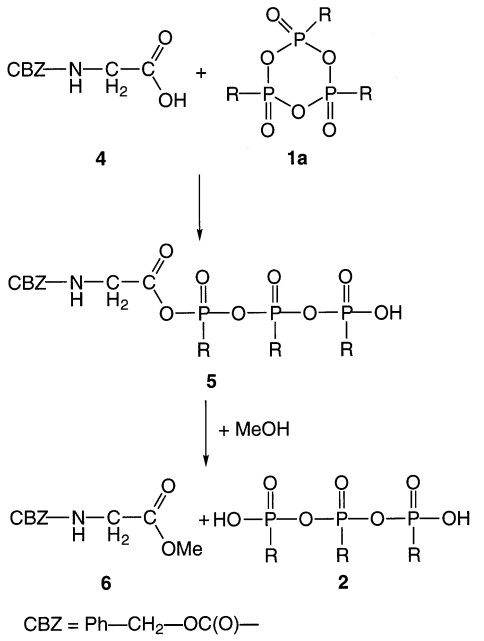

the two pairs of diastereomers expected for the mixed anhydride **5** in Scheme 1. According to this scheme, acid **2** and the methyl ester **6**, detected by GC-MS, are formed by methanolysis of **5**. Alternatively, reaction of **4** with **5**, with formation of the anhydride of **4** followed by methanolysis, may be regarded as the source of **6** and **2**.

The ^{1}H-NMR spectrum ($CDCl_3$) of the reaction product shows groups of resonance signals that correspond to protons of the compounds in Scheme 1. They can be assigned as follows:

$\delta(PCCH_3)$ = 1.06−1.56; $\delta(CH_2COOH)$ = 3.51−3.80; $\delta(COCH_3)$ = 4.00−4.06; $\delta(C_6H_5CH_2)$ = 5.17; $\delta(C_6H_5CH_2)$ = 7.24−7.53; $\delta(OH)$ = 9.50−9.70 (s, br.).

Thus, there is strong evidence that mixed anhydrides of phosphonic acids and *N*-protected amino acids (in Scheme 1 represented by **5**) are intermediates in peptide synthesis with $(RPO_2)_n$.

Crystal Structures

In the molecular structure of **1a** in the crystal, trimeric units of tBuPO$_2$ form six-membered rings of P_3O_3, with two *tert*-butyl groups directed to one side of the ring and one group to the other (Figure 2). In slight contrast to the assumed chair conformation used for the interpretation of the NMR data in solution, the P_3O_3 ring takes on an envelope conformation in the crystal, with the oxygen atom O23 as an apex with a deviation of 0.43 Å from the least-squares plane defined by the other five ring atoms. Although the observed deviations from the furthermore assumed symmetry (C_S) of the molecule are small (C_S asymmetry parameters for atoms P1 and O23 are only 2°), their significance is supported by the molecule lying in general position 4e of space group $P2_1/n$.

All bond lengths and angles are in good agreement with common values, and no intermolecular contacts less than the sum of the corresponding van der Waals radii occur. Remarkable geometrical parameters are the angles P1−O12−P2 and P1−O13−P3 with 136.2 and 136.0° respectively, in contrast to the more common value of 130.3° for P2−O23−P3. Also, a distortion of the tetrahedral coordination of the phosphorus atoms is observed, insofar as all bond angles involving the P=O bonds are widened [On−Pn−Cn 116.0−116.5°, On−Pn−O(ring) 111.6−114.6°], and the remaining angles reduced [O(ring)−Pn−O(ring) 101.0−102.8°, O(ring)−Pn−Cn 105.1−106.3° with n = 1, 2, or 3, respectively].

The molecular structure of **2b** consists of one anion $[t\mathrm{Bu_3P_3O_7}]^{2-}$, two Na^+ cations, and eight water molecules, with all atoms in general positions 4e of space group $P2_1/c$. While most geometrical parameters of the anion (Figure 3) agree well with usual values, the oxygen atoms of the two configurations P1−O21−P2 and P2−O23−P3 are significantly shifted towards the central phosphorus atom P2 [mean bond lengths 1.574(3) Å for P2(central)−O and 1.641(2) Å for P1/P3(terminal)−O]. These discrepancies in the four formally equivalent single P−O bonds may be in correlation with the fact that the double bonded O22 at the central P atom is the only atom of the anion coordinating

Figure 2. Molecular structure of **1a** in the crystal[14], thermal ellipsoids represented on a 25% probability scale, hydrogen atoms with fixed radii of 0.15 Å

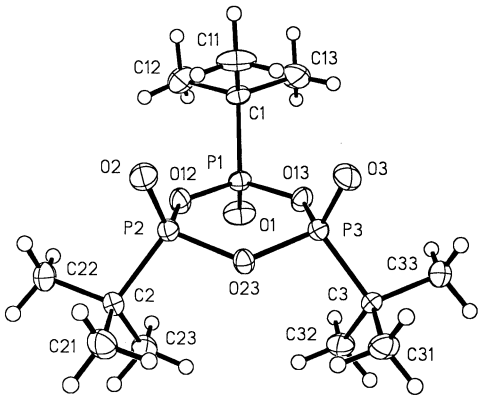

Figure 3. Anion $[t\mathrm{Bu_3P_3O_7}]^{2-}$ of **2b** in the crystal[14], thermal ellipsoids represented on a 40% probability scale, hydrogen atoms with fixed radii of 0.17 Å

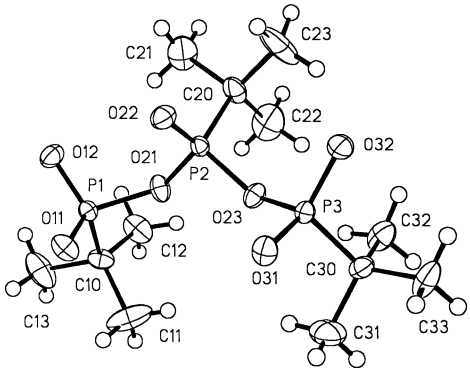

one of the sodium atoms. The other oxygen atoms O11, O12, O31, and O32 accept two or three hydrogen bonds donated by seven of the eight water molecules.

Atom Na1 is hexacoordinated by five water molecules and atom O22 in the form of a distorted octahedron. The coordination of Na2 is made up by five water molecules only, best described as a highly distorted square-based pyramid, sharing one edge with the octahedron of Na1. These two concatenated polyhedra are expanded to a unit of four edge-connected polyhedra by a crystallographic inversion center lying on another edge of the Na1 octahedron.

The complete connectivity of cations, anions, and water molecules making up the crystal structure is very complex (if only because of 16 different hydrogen bonds). In summary it can be said that the anions and seven of the eight water molecules form a hydrogen-bonded layer parallel to the *ac* plane. Two of these layers are concatenated by the eighth water molecule and the two Na^+ cations to form a double layer with all polar parts of the crystal structure (water, Na^+, end groups PO_2^-) on the inside and the non-polar *tert*-butyl groups on the outside of such a double layer. By this arrangement of the anions, any further connectivity between those layers to form a three-dimensional framework is prevented, and only van der Waals contacts between methyl groups of neighbouring layers are observed.

Experimental Section

The silyl esters, and compounds **1** were prepared and handled under inert conditions. − Melting points (uncorrected) were determined in sealed tubes with a melting-point apparatus 510 H (Büchi, Switzerland). − ^{1}H-, ^{13}C-, and ^{31}P-NMR spectroscopy: Bruker AM 200, TMS (^{1}H), sodium salt of 3(trimethylsilyl)propionic acid (^{1}H, ^{13}C) as internal and 85% H_3PO_4 (^{31}P) as external reference. Downfield shifts are positive and given in parts per million, and coupling constants are expressed in Hz. − EI-MS: Varian Mat 311 A (IE 70 eV). − GC-MS: GC 5890−MSD 5970 (Hewlett Packard). Only the main peaks are listed. − Cryoscopy: Cryoscopic unit A 0284 (Knaur, Berlin). − Osmometry: Osmometric unit 11.00, T = 37°C (Knaur, Berlin). − Thermogravimetry: Mettler TA 1. − pK_a values: Potentiometric titration with NaOH using hardware of Schott, Hofheim and the program system MINI T401 and ITERAX[12]. − Elemental analysis: C,H,N: Analyzer 2400 (Perkin−Elmer). P: Photometrically[13] after decomposition with conc. HNO_3 in a stainless steel bomb, type DAB II (Berghof, D-72800 Emingen).

X-ray Crystallographic Study of **1a**: $C_{12}H_{27}O_6P_3$; formula mass 360.25 g mol^{-1}; monoclinic space group $P2_1/n$ (no. 14); a = 7.590(3), b = 27.06(1), c = 8.926(3) Å; β = 95.16(3)°; V = 1826(1) Å^3; Z = 4; $d_{calcd.}$ = 1.310 Mg m^{-3}; μ(Mo-K_α) = 0.346 mm^{-1}; F(000) = 768. Siemens P3 (upgraded Syntex P2$_1$) diffractometer, Mo-K_α radiation (λ = 0.71073 Å), graphite monochromator. Data collection at room temperature in ω/2Θ mode (4° ≤ 2Θ ≤ 55°) on a colorless crystal of about 0.5 × 0.6 × 0.9 mm yielded 4460 reflections, which after merging the symmetry equivalents, gave 4169 independant reflections with 3150 observations with $I > 2\sigma(I)$[14]. After solving the structure by direct methods[15] a final full-matrix least-squares refinement against F^2 [16] of all 4169 reflections resulted in $wR2$ = 0.1773 and $R1$ (obs. refl. only) = 0.0526 for 199 variables, using a "riding" model for the hydrogen atoms with U(H) = 1.3U_{eq}(C). A final difference Fourier map gave min./max. residual electron densities of −0.72/0.50 e Å^{-3}[17].

X-ray Crystallographic Study of **2b**: $C_{12}H_{43}Na_2O_{15}P_3$; formula mass 566.35 g mol^{-1}; monoclinic space group $P2_1/c$ (no. 14); a = 10.869(1), b = 31.139(4), c = 9.123(1) Å; β = 114.59(1)°; V = 2807.7(5) Å^3; Z = 4; $d_{calcd.}$ = 1.340 Mg m^{-3}; μ(Mo-K_α) = 0.301 mm^{-1}; F(000) = 1208. Siemens P3 (upgraded Syntex P2$_1$) diffractometer, Mo-K_α radiation (λ = 0.71073 Å), graphite monochromator. Data collection at room temperature in ω/2Θ mode (4° ≤ 2Θ ≤ 55°) on a colorless crystal of about 0.2 × 0.5 × 0.6 mm yielded 6791 reflections which after merging the symmetry equivalents gave 6405 independant reflections with 4930 observations with $I > 2\sigma(I)$[14]. After solving the structure by direct methods[15] a final full-matrix least-squares refinement against F^2 [18] of all 6405 reflections resulted in $wR2$ = 0.1190 and $R1$ (obs. refl. only) = 0.0404 for 362 variables. For the H atoms of the methyl groups, a riding model with U(H) = 1.3U_{eq}(C) was used, while the H atoms of the water molecules, all being involved in hydrogen bonds, were refined independently with isotropic temperature factors. A final difference Fourier map gave min./max. residual electron densities of −0.67/1.50 e Å^{-3}[17].

Starting materials were mostly prepared according to methods reported in the literature: $(Me_3SiO)_3P$[19], *t*BuP(O)Cl$_2$[20][21], 2-MeC$_6$H$_4$P(O)Cl$_2$[22][23][24], 2,4,6-Me$_3$C$_6$H$_2$P(O)Cl$_2$[24][25], *t*BuP(O)(OSiMe$_3$)$_2$[26], *N*-benzyloxycarbonylglycine[27].

Bis(trimethylsilyl) 2-Methylphenylphosphonate: Following the procedure of Issleib et al.[28] 16 mmol of $(Me_3SiO)_3P$ was added dropwise with stirring to a mixture of 16 mmol of 2-bromotoluene and 0.8 mmol of anhydrous $NiCl_2$ at 160°C. The Me_3SiBr formed in the reaction was continuously distilled off and the residue distilled in vacuo. Colorless, hydrolyzable liquid, b.p. 94°C/0.2 Torr; yield 57%. − $C_{13}H_{25}O_3PSi_2$ (316.5): calcd. C 49.34, H 7.96; found: C 48.95, H 7.86. − EI-MS; *m/z* (%): 316 (30). − ^{31}P{^{1}H} NMR (neat): δ = 0.52 (s). − ^{1}H NMR (C_6D_6): δ = −0.63 (d, $^4J_{PH}$ = 1.16, OSi*Me*$_3$), 1.79 (s, C$_6$H$_4$*Me*), 6.24 (m, C$_6$*H*$_4$Me), 7.37 (m).

Bis(trimethylsilyl) 2,4,6-Trimethylphenylphosphonate: Preparation as before from 21 mmol of $(Me_3SiO)_3P$, 21 mmol of 2,4,6-Me$_3$C$_6$H$_2$Br, and 1 mmol of $NiCl_2$; yield 41%. Colorless, hydrolyzable liquid, b.p. 91°C/0.15 Torr, m.p. 39°C. − $C_{15}H_{29}O_3PSi_2$ (344.5): calcd. C 52.29, H 8.48; found C 52.08, H 7.51. − EI-MS; *m/z* (%): 344 (34). − ^{31}P{^{1}H} NMR (toluene): δ = 4.5 (s). − ^{1}H NMR (C_6D_6): δ = 0.45 (s, OSi*Me*$_3$), 2.24 (s, C$_6$H$_2$*Me*$_3$), 3.06 (s) (intensity ratio 1:2), 6.98 (d, C$_6$H$_2$).

tert-Butylphosphonic Anhydride **1a**: A mixture of 50 mmol of *t*BuP(O)Cl$_2$ and 50 mmol of *t*BuP(O)(OSiMe$_3$)$_2$ was heated for 8 h at 170−180°C and the Me_3SiCl formed was continually distilled off. Subsequently, the reaction product was heated for another 3 h at 110°C in vacuo in order to remove unreacted starting materials, and crystallized from toluene/pentane; yield 46%. Colorless crystals, m.p. 166°C, 150−152°C[6]; 194−195°C[3]. − $C_{12}H_{27}O_6P_3$ (360.3): calcd. C 40.01, H 7.55, P 25.79; found C 39.89, H 7.56, P 25.71. − Mol. mass (cryoscopic in benzene): 358 (0.031 molal), 375 (0.089 molal). − EI-MS; *m/z* (%): 360 (3), 304 (80), 248 (67), 192 (19), 57 (100). − ^{31}P{^{1}H} NMR ($CDCl_3$): AB$_2$ spin system, δ$_A$ = 24.23, δ$_B$ = 23.83, J_{AB} = $^2J_{PP}$ = 50.6, δ = 24.12 (s, $CDCl_3$)[6], 31.16 (s, C_6D_6)[3]. − ^{1}H{^{31}P} NMR (C_6D_6): δ = 1.43 (s), 1.32 (s), intensity ratio 1:2.

2-Methylphenylphosphonic Anhydride (**1b**): 13 mmol of 2-MeC$_6$H$_4$P(O)(OSiMe$_3$)$_2$ and 13 mmol of 2-MeC$_6$H$_4$P(O)Cl$_2$ in 40 ml of toluene were heated so that the Me_3SiCl which formed and small amounts of toluene were continually distilled off. At the end of the reaction the distillate consisted solely of toluene. After concentrating the solution, **1b** was precipitated by slow addition of ligroin (100−140°C); yield 97%. Colorless, very hydrolyzable crystals, m.p.

123−125°C. − $C_{21}H_{21}O_6P_3$ (462.3): calcd. C 54.65, H 4.58, P 20.10; found C 54.34, H 4.38, P 19.90. − Mol. mass (cryoscopic in benzene): 458 (0.085 molal), 462 (0.112 molal). − EI-MS; *m/z* (%): 462 (100), 309 (19), 155 (28). − $^{31}P\{^1H\}$ NMR (C_6D_6): AB_2 spin system, $\delta_A = 1.99$, $\delta_B = -0.46$; $J_{AB} = {}^2J_{PP} = 42.6$. − ^1H NMR (C_6D_6): δ = 2.72 (s, CH_3), 3.01 (s), intensity ratio 2:1; 7.04 (m, C_6H_4), 8.25 (m), 8.65 (m).

2,4,6-Trimethylphenylphosphonic Anhydride (**1c**): Preparation as mentioned before from 20 mmol of 2,4,6-$Me_3C_6H_2P(O)(OSiMe_3)_2$ and 20 mmol of 2,4,6-$Me_3C_6H_2P(O)Cl_2$ in 70 ml of toluene. The anhydride formed is only sparingly soluble in toluene, and was thus precipitated in the course of the reaction as colorless hydrolyzable crystals that could be used without further purification; yield 58%, m.p. 250°C. − $C_{27}H_{33}O_6P_3$ (546.5): calcd. C 59.34, H 6.09, P 17.00; found C 59.02, H 5.83, P 17.00. − EI-MS; *m/z* (%): 546 (100), 364 (38), 183 (40). − $^{31}P\{^1H\}$ NMR ($CDCl_3$): δ = 1.48 (s). − ^1H NMR ($CDCl_3$): δ = 2.34, 2.59, 2.81 (intensity ratio 2:4:3, CH_3); 6.97, 7.04 (C_6H_2), (in all cases broad signals).

Tris(tert-butyl)triphosphonic Acid (**2**): A solution of 40 mmol of **1a** in 150 ml of ethanol, containing 40 mmol of H_2O, was heated at 60°C for 3 h. After evaporation of the solvent, the residue is washed with ligroin (100−140°C) and dried in vacuo; yield 54%. Colorless, crystalline powder, soluble in $CHCl_3$, MeOH, EtOH, or water, m.p. 152°C. − $C_{12}H_{29}O_7P_3$ (378.3): calcd. C 38.01, H 7.73, P 24.56; found C 38.02, H 7.87, P 24.30. − The acid is associated via hydrogen bonds. − IR (KBr): $\tilde{\nu}$ = 2663 cm^{-1}, 2298 cm^{-1}, 1654 cm^{-1}. − Mol. mass (osmometric in $CHCl_3$, 37°C): 609 (0.063 molal, 672 (0.123 molal). − $^{31}P\{^1H\}$ NMR (C_6D_6): AB_2 spin system, $\delta_A = 20.31$, $\delta_B = 31.05$; $J_{AB} = {}^2J_{PP} = 49.3$. − ^1H NMR ($CDCl_3$): δ = 1.30 (d, $^3J_{PH}$ = 18.2, PCMe), 1.36 (d, $^3J_{PH}$ = 19.6), intensity ratio 2:1, 11.84 (s, OH).

Disodium Salts of Tris(tert-butyl)triphosphonic Acid, Dihydrate (**2a**) *and Octahydrate* (**2b**): After neutralization of 5 mmol of **2** in 10 ml of H_2O with 1 M NaOH, the resulting sodium salt was precipitated by adding acetone. Crystallization from acetone/water and drying at 20°C in vacuo afforded **2a** as shiny small leaflets that are readily soluble in water; yield practically quantitative. **2b** was obtained as transparent plates, m.p. > 300°C, from a concentrated solution of the disodium salt in H_2O by diffusion-controlled precipitation with acetone, and drying in vacuo at 20°C. − $C_{12}H_{27}Na_2O_7P_3 \cdot 2\ H_2O$ (458.3): calcd. C, 31.45; H, 6.82; P, 20.28; found C, 31.17; H, 6.63; P, 20.05. − $C_{12}H_{27}Na_2O_7P_3 \cdot 8\ H_2O$ (566.4): calcd. C, 25.45; H, 7.65; found C, 25.60; H, 7.58. − According to the results of thermogravimetric measurements, both hydrates loose their water of crystallization completely between 80−100°C. − $^{31}P\{^1H\}$ NMR (D_2O): AB_2 spin system, $\delta_A = 19.80$, $\delta_B = 29.50$; $J_{AB} = {}^2J_{PP} = 49.7$. − ^1H NMR (D_2O): δ = 1.16 (d, $^3J_{PH}$ = 16.9, PC*Me*), 1.27 (d, $^3J_{PH}$ = 18.91), intensity ratio 2:1.

Bis(tert-butyl)diphosphonic Acid (**3**): After heating 2.6 mmol of **2** with 10 ml of conc. hydrochloric acid for 1 h, the clear solution was cooled to room temperature. The resulting precipitate was filtered off and dried in vacuo at 20°C. Crystallization from toluene afforded colorless needles, m.p. 198−200°C that are soluble in acetone and sparingly soluble in H_2O; yield 23%. − $C_8H_{20}O_5P_2 \cdot 1.5\ H_2O$ (285.2): calcd. C 33.68, H 8.07, P 21.73; found C 33.28, H 8.16, P 21.45. − EI-MS; *m/z* (%): 459 (11), 259 (22), 202 (100), 146 (33), 138 (51), 123 (12), 83 (20), 57 (83). − $^{31}P\{^1H\}$ NMR ([D_6]acetone): δ = 32 (s). − ^1H NMR ([D_6]acetone): δ = 1.40 (m, PCMe); 4.55 (s, br., POH).

tert-Butylphosphonic Acid can be isolated from the filtrate by concentration and crystallization of the residue from toluene; yield 72%; colorless needles, m.p. 188−190°C (see ref.[30] 191°C), soluble in H_2O or acetone. − $^{31}P\{^1H\}$ NMR ([D_6]acetone): δ = 39.50 (see ref.[30] 37.00, [D_6]acetone).

Disodium Salt **3a**: A solution of EtONa from 28.4 mmol of Na in 20 ml of EtOH was added dropwise to 7.1 mmol of **1a** in 20 ml of EtOH. After heating for 1 h, the sodium salt formed was filtered off and dried in vacuo at 20°C; yield 57%. Colorless needles from water/acetone, m.p. > 320°C. Loss of weight between 80−110°C: 15.5% (TG), calcd.: 15.16%. − $C_8H_{18}Na_2O_5P_2 \cdot 3\ H_2O$ (356.2): calcd. C 26.98, H 6.79, P 17.39; found C 26.78, H 6.82, P 17.39. − $^{31}P\{^1H\}$ NMR (D_2O): 26.30 (s). − ^1H NMR (D_2O): $[AX_9]_2$ spin system centered at δ = 1.13. − ^{13}C NMR (D_2O): X-part of an AA′X spin system centered at δ = 33.91, coupling constants obtained according to ref.[29]: $^2J_{PP}$ = 48.6; $^1J_{PC}$ = 144.5; $^3J_{PC'}$ = 2.0.

Reaction of **1a** *with N-Benzyloxycarbonylglycine* (**4**): 10 mmol of **4** in 20 ml of methanol was added to a heated solution of 10 mmol of **1a** in 10 ml of methanol. After boiling the mixture for 3 h, the solvent was removed in vacuo at room temperature. The residue was a highly viscous, colorless liquid. − $^{31}P\{^1H\}$ NMR ($CDCl_3$): AX_2 spin system $\delta_A = 21.30$ (t); $\delta_X = 31.30$ (d); $J_{AX} = 49.3$; two AMX spin systems $\delta_A = 22.10$ (t); $\delta_M = 30.40$ (d); $\delta_X = 33.70$ (d); $J_{AM} = 48.3$; $J_{AX} = 46.9$ and $\delta_A = 21.80$ (t); $\delta_M = 30.60$ (d); δ_X = 33.10 (d); $J_{AM} = 47.7$; $J_{AX} = 47.2$ Hz. − ^1H NMR ($CDCl_3$): δ = 1.06−1.56 ($PCCH_3$); 3.51−3.80 (CH_2COOH); 4.00−4.06 ($COCH_3$); 5.17 ($C_6H_5CH_2$); 7.24−7.53 ($C_6H_5CH_2$); 9.50−9.70 (s, br., OH). − GC-MS of **6**; *m/z* (%): 223(9), 108(80), 91(100).

[1] K. Sasse, *Methoden Org. Chem. (Houben-Weyl), 4th ed.*, **1963**, vol. 12/1, p. 612−613.
[2] K. H. Worms, M. Schmidt-Dunker in *Organic Phosphorus Compounds* (Eds.: G. M. Kosolapoff, L. Maier), John Wiley & Sons, New York, **1976**, Vol. 7, 75.
[3] S. Fuchs, H. Schmidbaur, *Z. Naturforsch., B* **1995**, *50*, 855−858.
[4] W. Mahler, A. B. Burg, *J. Am. Chem. Soc.* **1958**, *80*, 6161−6167.
[5] W. Kuchen, H. Buchwald, *Chem. Ber.* **1958**, *91*, 2296−2304.
[6] O. I. Kolodiazhnyi, E. V. Grishkun, *Phosphorus Sulfur Silicon* **1995**, *103*, 191−197.
[7] [7a] H. Wissmann, H. J. Kleiner, *Angew. Chem.* **1980**, *92*, 129−130; *Angew. Chem. Int. Ed. Engl.* **1980**, *19*, 133. − [7b] H. Wissmann, *Phosphorus Sulfur* **1987**, *30*, 645−648. − [7c] E. Buschmann, Th. Zierke, Ger. Offen. DE 19,527,574; *Cem. Abstr.* **1997**, *126*, 186376a.
[8] [8a] H. Steinberger, Dissertation, University of Düsseldorf, **1973**. − [8b] G. Hägele, W. Kuchen, H. Steinberger, *Z. Naturforsch., B* **1974**, *29*, 349−357. − [8c] W. Kuchen, H. Steinberger, *Z. Anorg. Allg. Chem.* **1975**, *413*, 266−278.
[9] F. Sandt, Diploma thesis, University of Düsseldorf, **1990**.
[10] [10a] F. Sandt, Dissertation, University of Düsseldorf, **1996**. − [10b] K. Diemert, W. Kuchen, D. Mootz, W. Poll, F. Sandt, *Phosphorus Sulfur Silicon* **1996**, *111*, 100.
[11] P. Stelzel, *Methoden Org. Chem. (Houben-Weyl), 4th ed.*, **1974**, vol. 15/2, p. 226−253.
[12] A. Bier, Dissertation, University of Düsseldorf, **1993**.
[13] G. Wünsch, *Optische Analysenmethoden zur Bestimmung anorganischer Stoffe*, 1st ed., de Gruyter, Berlin, **1983**.
[14] *SHELXTL PLUS, Structure Determination System, Revision 4.21/V*, Siemens Analytical X-Ray Instruments, Inc., Madison, WI, **1990**.
[15] G. M. Sheldrick, "SHELXS-86", *Acta Crystallogr.* **1990**, *A46*, 467−473.
[16] G. M. Sheldrick, *SHELXL-97, Program for the Refinement of Crystal Structures*, Universität Göttingen, **1997**.
[17] Crystallographic data (excluding structure factors) for the structures reported in this paper have been deposited with the Cambridge Crystallographic Data Centre as supplementary publication no. CCDC-100660. Copies of the data can be obtained free of charge on application to CCDC, 12 Union Road, Cambridge CB2 1EZ, UK [fax: int. code + 44(1223)336-033, e-mail: deposit@ccdc.cam.ac.uk).
[18] G. M. Sheldrick, *SHELXL-93, Program for the Refinement of Crystal Structures*, Universität Göttingen, **1993**.
[19] P. W. Deroo, A. F. Rosenthal, Y. A. Isaacson, L. A. Vargas, R. Bittmann, *Chem. Phys. Lipids* **1976**, *16*, 60−70.

[20] J. P. Clay, *J. Org. Chem.* **1951**, *16*, 892−894.
[21] A. M. Kinnear, E. A. Perren, *J. Chem. Soc.* **1952**, 3437−3445.
[22] A. Michaelis, *Justus Liebigs Ann. Chem.* **1896**, *293*, 261−325.
[23] R. C. Grabiak, J. A. Miles, G. M. Schwenzer, *Phosphorus Sulfur* **1980**, *9*, 197−202.
[24] S. Freeman, M. J. P. Harger, *J. Chem. Soc., Perkin Trans. 1* **1987**, 1399−1406.
[25] N. G. Bentrude, W. N. Setzer, A. E. Sopchic, *J. Am. Chem. Soc.* **1988**, *110*, 7119−7127.
[26] K. Diemert, U. Englert, W. Kuchen, F. Sandt, *Angew. Chem.* **1997**, *109*, 251−253; *Angew. Chem. Int. Ed. Engl.* **1997**, *36*, 241.
[27] M. Bergmann, C. Zervas, *Ber. Dtsch. Chem. Ges.* **1932**, *65*, 1192−1201.
[28] R. Issleib, A. Balszuweit, J. Kötz, St. Richter, R. Leutloff, *Z. Anorg. Allg. Chem.* **1985**, *529*, 151−156.
[29] G. Hägele, W. Kückelhaus, H. Quast, *Chem.-Ztg.* **1985**, *109*, 405−408.
[30] R. Schmutzler, G. S. Reddy, *Z. Naturforsch., B* **1965**, *20*, 832−835.

[97202]

Soluble Chloro- and Aryl(phthalocyaninato)indium(III) Complexes: Synthesis and Characterization

Michael Hanack* and Heino Heckmann

Institut für Organische Chemie, Universität Tübingen,
Auf der Morgenstelle 18, D-72076 Tübingen, Germany
Fax: (internat.) +49(0)7071/295244
E-mail: hanack@uni-tuebingen.de
http://www.uni-tuebingen.de/hanack/index.html

Received September 19, 1997

Keywords: Phthalocyanines / Indium / Indium−carbon bond

The synthesis of highly soluble chloro(phthalocyaninato)indium(III) complexes R_xPcInCl (**3a**: R^1 = *tert*-butyl, R^2 = H, x = 4 and **4a**: $R^1 = R^2$ = *n*-pentyl, x = 8), and their reactions with R′MgBr [R′ = *p*-trifluoromethylphenyl- (**b**), *m*-trifluoromethylphenyl- (**c**), *p*-fluorophenyl- (**d**), perfluorophenyl- (**e**)] leading to the stable σ-bonded aryl(phthalocyaninato)indium(III) complexes **3b−e**, **4b−e** are described. All compounds were characterized by IR, UV/Vis, MS, ^{1}H, ^{13}C and ^{19}F NMR as well as elemental analyses. Phenyl(phthalocyaninato)indium(III) (**4f**) was prepared by the reaction of $(n\text{-}C_5H_{11})_8$PcInCl (**4a**) with PhLi. The high solubility of the complexes **3a−e** and **4a−f** is, aside from the influence of the peripheral substituents, considered to be derived from the large dipole moments present which are due to the strongly electron withdrawing axial ligands, and from the lower tendency of axially substituted phthalocyaninato metal complexes to form aggregates.

Phthalocyanines and phthalocyaninato metal complexes have been investigated in detail for many years[1], particularly with regard to their properties as dyes[2]. More recently their widespread potential in material sciences[3] has been discovered. Besides numerous other applications these "functional dyes" have also attracted considerable interest in the field of non-linear optics[4]. It is the extensively delocalized π-system in phthalocyanines which gives rise to large optical non-linearities. Furthermore, due to the diversity of the structural features[5] of phthalocyanines, tuning of the optical properties can be achieved by synthetic variations. For example, about 70 different elements have been incorporated into the phthalocyanine core, some of them with different oxidation states, and in addition there are one or two sites which coordinate a variety of axial ligands. The introduction of a diversity of peripheral substituents, with many possibilities to alter the substitution pattern with respect to the number and position of the substituents, has a strong influence[6] on the electronic absorption spectra and optical non-linearities. Other factors[4] which affect optical non-linearities are the length of π-electron conjugation, the crystal structure, and the thin film fabrication techniques employed. The aim of our current research is a systematic study of the effect of axial substitution on non-linear optical (NLO) properties, and specifically on the optical limiting properties of phthalocyanines. Axial substitution will have several effects: it can alter the electronic structure of the phthalocyanine, it can introduce a dipole moment perpendicular to the macrocycle, and, via steric effects, it can also alter the spatial relationships between neighbouring molecules and thus the magnitude of the intermolecular interactions. Large axial substituents can alter the packing of the molecules in the solid state and the tendency to aggregate in solution. Each of these effects can influence the NLO properties. In fact a correlation between the magnitude of the third-order non-linear optical susceptibility tensor $\chi^{(3)}$ for third harmonic generation (THG) experiments[4] and axial substitution has been noted. The reason for this effect may be associated with the fact that there is a permanent dipole moment in these materials.

Several axially substituted phthalocyanines have been reported[4][7] to be good non-linear absorbers for optical limiting, but there has been no study of the effect of different axial substitution patterns on the relevant optical properties of these materials.

Our approach here is to investigate the influence of different axial substituents on the reverse saturable absorption, and optical limiting properties, of soluble peripherally alkylsubstituted phthalocyaninatoindium(III) complexes. Among the axially substituted phthalocyanines, $(t\text{Bu})_4$PcInCl[7] has one of the largest positive non-linear absorption coefficients. It has been used to manufacture optical limiting devices.

A comparative study of the optical properties of $(t\text{Bu})_4$PcInCl with several aryl substituted phthalocyaninatoindium(III) complexes (see Scheme 1) is in progress. The aryl ligands are chosen so as to alter both the spatial and electronic properties of the materials. Compared with the chloro ligand, aryl substituents will introduce steric crowding and should reduce the tendency, which is common in phthalocyanines, to form aggregates . Due to the increasing electron withdrawing properties of the aryl ligands, these

 © WILEY-VCH Verlag GmbH, D-69451 Weinheim, 1998 1434−1948/98/0303−0367 $ 17.50+.50/0

materials should possess an increasing ground state dipole moment.

Scheme 1. Synthesis of the chloro- and aryl(phthalocyaninato)indium(III) complexes

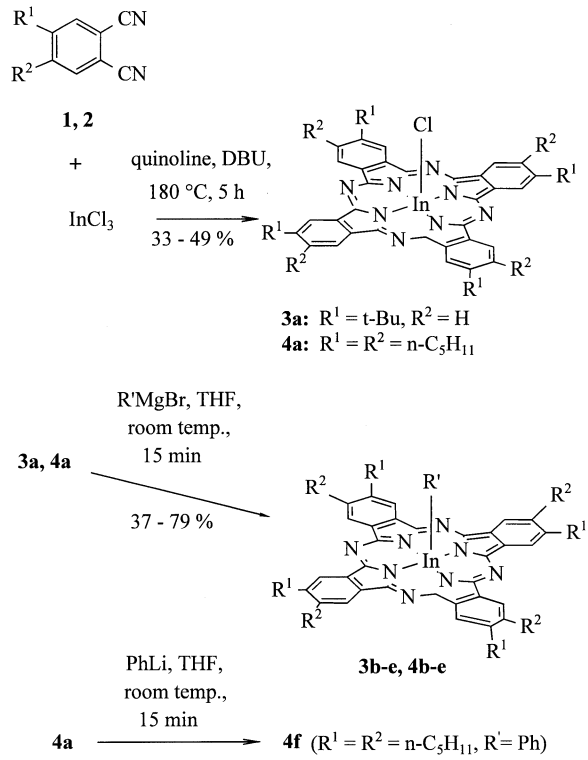

No.	R^1	R^2
1	t-Bu	H
2	n-C_5H_{11}	n-C_5H_{11}
3	t-Bu	H
4	n-C_5H_{11}	n-C_5H_{11}

No.	R'	abbreviation
a	-Cl	
b	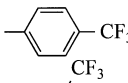	p-TMP
c	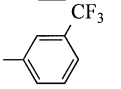	m-TMP
d	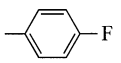	p-FP
e	-C_6F_5	PFP
f	-Ph	

We have therefore synthesized a series of monoaxially chloro and aryl substituted phthalocyaninatoindium(III) complexes R_xPcIn(R′) [**3**: R^1 = *tert*-butyl, R^2 = H, x = 4 and **4**: R^1 = R^2 = *n*-pentyl, x = 8; R′ = chloro- (**a**), *p*-trifluoromethylphenyl- (**b**), *m*-trifluoromethylphenyl- (**c**), *p*-fluorophenyl- (**d**), perfluorophenyl- (**e**), phenyl- (**f**); see Scheme 1], which we expect to have similar steric, but different electronic, properties.

Although there are some reports on the preparation of phthalocyaninato[8] as well as porphyrinato[9] metal complexes with metal−alkyl or metal−aryl σ-bonds, to our knowledge nothing is known about complexes of the type PcIn(R′). From studies of alkyl- and aryl(porphyrinato)indium(III) complexes[10] it is known that their stability depends largely on the electron withdrawing properties of the axial ligands. Organometallic complexes containing strongly electron withdrawing perfluoroaryl groups generally show quite different properties than derivatives of the same containing a simple phenyl group[11]. In many cases it was shown that the carbon−metal bond in perfluorophenyl metal complexes is extraordinarily robust for a σ-bond[12].

Coincidentally, the electron withdrawing properties of the ligands which were attached to the indium atom in order to obtain complexes with substantial axial dipole moments are, at the same time, responsible for the stability of these compounds.

Results and Discussion

The complexes (*t*Bu)$_4$PcInCl (**3a**)[7] and (C_5H_{11})$_8$PcInCl (**4a**) were prepared starting from stoichiometric amounts of 4-*tert*-butylphthalonitrile (**1**)[13] or 4,5-bis(*n*-pentyl)-phthalonitrile (**2**)[14] and $InCl_3$ in quinoline in the presence of catalytic amounts of DBU. The aryl(phthalocyaninato)-indium(III) complexes **3b−e** and **4b−e** were synthesized by the reaction of freshly prepared aryl Grignard compounds with the respective R_xPcInCl complexes **3a** or **4a** (see Scheme 1). The complexes **3a−e** and **4a−e** were characterized by IR, UV/Vis, MS, ^{1}H, ^{13}C, and ^{19}F NMR as well as elemental analyses.

In an attempt to synthesize the parent phenyl(phthalocyaninato)indium(III) complexes **3f** and **4f** starting from PhLi and **3a** or **4a,** it became clear that these compounds are less stable than the fluorinated derivatives. Only a few milligrams of **4f** could be isolated by extraction with *n*-hexane from the crude product. The decomposition product R_8PcH_2 showed poor solubility in this solvent. The small amount obtained limited the characterization of **4f** to MS, IR and UV/Vis. However, a satisfactory elemental analysis could be obtained for this complex. Phenyl(phthalocyaninato)indium(III) **3f** could not be separated from (*t*Bu)$_4$PcH$_2$ in the same way due to the high solubility of the latter in *n*-hexane.

The complexes are highly soluble in various organic solvents such as toluene, dichloromethane, and chloroform. The tetrasubstituted compounds **3a−e** exhibit a much higher solubility in acetone than the corresponding octa-substituted compounds, **4a−f**. (*t*Bu)$_4$PcIn(PFP) (**3e**) is even slightly soluble in methanol. In general, the aryl substituted complexes **3b−e** and **4b−f** are more soluble in solvents of medium polarity, such as dichloromethane, than the corresponding chloroindium(III) complexes **3a** and **4a**. The peripherally tetrasubstituted phthalocyanines **3a−e** consist of a mixture of four structural isomers[15], as regards the fact, that the *tert*-butyl groups can occupy either two positions R^1 or R^2 in each of the isoindoline units of the macrocycles. They are more soluble[3a][16] than their structural counterparts that have eight substituents, assuming the same substitution pattern (herein: 2,3). The high solubility of the aryl substituted phthalocyanines **3b−e** and **4b−f** indicates that they possess quite large axial dipole moments. The enhanced solubility of the complexes **3b−e** and **4b−f**, com-

pared to the chloro analogues **3a** and **4a**, shows that the usual tendency of phthalocyanines to form aggregates[17] can be effectively suppressed by axial substitution. The more sterically demanding the axial ligands are, the lower will be the degree of aggregation.

Elemental analyses and mass spectral data of all the investigated phthalocyaninatoindium(III) complexes suggest the molecular formulas $R_xPcInCl$ and $R_xPcIn(R')$ for the compounds **3a**, **4a** and **3b−e**, **4b−f**, respectively. For each complex a cluster of peaks, almost identical in intensity to that calculated for its respective isotopic composition, was observed in the field desorption mode. Fragmentation was not observed under these conditions.

In Table 1 the IR data of the aryl(phthalocyaninato)indium(III) complexes are reported. Only the additional absorptions, which do not appear in the spectra of the respective chloro substituted phthalocyanines **3a** or **4a**, are listed in Table 1. Characteristic vibrations for aryl groups bound to a metal atom[18] are found in the range 190−1650 cm^{-1}. In the 670−830 cm^{-1} range vibrational frequencies associated with the C−H out of plane deformation modes of the axial aryl groups appear. The intense absorption bands of the C−F stretching mode are found between 900−1460 cm^{-1}. The vibrational frequencies between 1500−1640 cm^{-1} are associated with the ring vibrations of the axial ligands. The weak absorption band of the In−Cl stretching mode at 336 and 327 cm^{-1} appears in the spectra of the chloro derivatives **3a** and **4a**, respectively. The In−C stretching mode can not be unambiguously assigned due to coupling with C−C modes and vibrations of the phthalocyaninic macrocycle.

Table 1. IR data of the investigated $R_xPcIn(R')$ complexes (KBr pellets)

Axial ligand R′	Phthalocyanine Pc	$\tilde{\nu}$ [cm^{-1}]												
p-TMP	**3b**		1599			1388		1164	1128		1016	819	678	
	4b		1598			1388		1163	1127	1047	1015	825	677	
m-TMP	**3c**				1466	1315		1165	1127	1060		794	683	
	4c					1316		1164	1126	1060		795	682	
p-FP	**3d**		1578				1228	1164				814		505
	4d		1577			1358	1226	1164				812		506
PFP	**3e**	1635	1531	1506	1463						959			
	4e	1636		1506	1464	1357				1054	958			
Ph	**4f**					1359								

The electronic absorption data of the complexes investigated are summarized in Table 2. The spectra of **3a−e** and **4a−f** show the typical pattern[17a] of phthalocyaninato metal complexes, with an intense Q band absorption and its vibrational satellites Q(1,0) and Q(2,0), as well as lower intensity π-π* transitions within the heteroaromatic π-system [B(0,0), B(1,0)]. Introduction of electron-donating alkyl groups in the periphery of the macrocycle leads to a bathochromic shift of the Q band maximum[6b][6c]. The octasubstituted complexes **4a−e** have their Q band shifted to the red by $\Delta\lambda$ = 16.0−17.3 nm, and the tetrasubstituted complexes **3a−e** by $\Delta\lambda$ = 7.1−7.8 nm (see Table 2), with respect to the unsubstituted PcInCl[19]. In contrast, the axial ligands introduced have little influence on the wavelength of the Q band maximum. The observed red shifts are only of the order of 1 nm.

Table 2. UV/Vis data of the investigated $R_xPcInCl$ and $R_xPcIn(R')$ complexes in chloroform

Phthalocyanine Pc	Axial ligand R′	λ_{max} [nm]				
		B(1.0)[a]	B(0.0)	Q(2.0)	Q(1.0)[a]	Q(0.0)
PcInCl (unsubst.)	Cl	337.9	358.2	622.5	656.8	690.2
3a	Cl	339.7	359.5	628.2	667.1	697.3
3b	*p*-TMP	340.9	369.3	628.6	667.3	698.0
3c	*m*-TMP	341.4	368.6	628.5	666.5	697.8
3d	*p*-FP	341.0	368.5	628.2	666.0	697.4
3e	PFP	341.9	365.6	628.7	665.7	697.8
4a	Cl	342.2	361.3	635.4	675.4	706.2
4b	*p*-TMP	353.7	375.3	636.4	675.6	707.2
4c	*m*-TMP	354.0	374.9	636.2	675.9	707.3
4d	*p*-FP	354.6	375.0	635.8	674.9	706.7
4e	PFP	349.3	370.1	636.3	675.7	707.5
4f	Ph	353.6	375.9	635.8	676.2	706.6

[a] All of these bands appear as shoulders.

The ^{1}H-NMR spectrum of $(t\text{Bu})_4$PcInCl (**3a**) shows three multiplets in the aromatic region centred at δ = 8.30, 9.30 and 9.45 for the 1-H, 2-H and the 2′-H protons, respectively (see Figure 1). The values for the corresponding protons of all of the aryl substituted complexes **3b−e** are close to those of **3a**, despite the different axial ligands. ^{1}H-NMR data of protons of the macrocycle and peripheral substituents are listed in the experimental section for each compound. The downfield shifts of $\Delta\delta \approx$ 0.4, 0.18 and 0.13 for the 1-H, 2-H and 2′-H protons in these compounds point to the fact that the σ-bonded aryl groups lead to stronger deshielding of the aromatic protons, especially of those closer to the heteroaromatic ring system (2-H, 2′-H), than does the chloro ligand. The same can be seen by comparison of $(C_5H_{11})_8$PcInCl (**4a**) and $(C_5H_{11})_8PcIn(R')$ (**4b−e**). In the ^{1}H-NMR spectrum of **4a** the aromatic protons give rise to a singlet at δ = 9.10. The signals of the corresponding protons 2,2′-H of **4b−e** are shifted downfield by $\Delta\delta$ = 0.16−0.18.

In contrast, the signals of the axial ligands are considerably shielded by the influence of the large diamagnetic ring-current[20] of the heteroaromatic π-electron system of the phthalocyanine. The shorter the distance between these protons and the centre of the macrocycle, the larger the upfield shift (see Table 3). This is in agreement with the

Figure 1. Notation of the atoms of the macrocycles and axial ligands

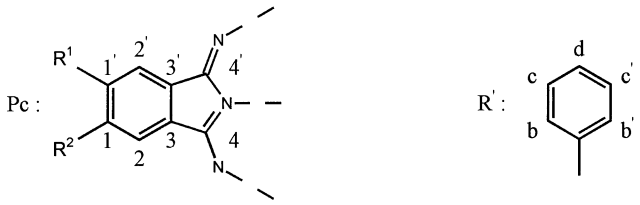

proposed structures for the aryl(phthalocyaninato)indium(III) complexes **3b–e** and **4b–e**. The absolute upfield shifts were explicitly calculated by comparing the shifts of corresponding protons for the $R_xPcIn(R')$ complexes and for R′Br, where no influence of a macrocyclic diamagnetic ring-current exists.

Table 3. ^{1}H-NMR data[a] of the protons for the axial ligands in the $R_xPcIn(R')$ complexes and for R′Br[a]

Axial ligand R′	Phthalocyanine Pc		Protons of R′ δ	multi/ intens	Protons of R′Br δ	Upfield shift Δδ
p-TMP	**3b**	H-b,b′	4.17	d/2	7.61	−3.44
		H-c,c′	6.17	d/2	7.47	−1.30
	4b	H-b,b′	4.18	d/2	7.61	−3.43
		H-c,c′	6.15	d/2	7.47	−1.32
m-TMP	**3c**	H-b′	4.10	d/1	7.66	−3.56
		H-b	4.41	s/1	7.76	−3.35
		H-c′	6.03−6.09	m/1	7.31−7.37	−1.28
		H-d	6.46	d/1	7.54	−1.08
	4c	H-b′	4.12	d/1	7.66	−3.54
		H-b	4.42	s/1	7.76	−3.34
		H-c′	6.01−6.07	m/1	7.31−7.37	−1.30
		H-d	6.45	d/1	7.54	−1.09
p-FP	**3d**	H-b,b′	3.98−4.04	m/2	7.40−7.45	−3.41
		H-c,c′	5.64−5.71	m/2	6.90-6.97	−1.25
	4d	H-b,b′	4.00−4.06	m/2	7.40−7.45	−3.39
		H-c,c′	5.62−5.70	m/2	6.90−6.97	

[a] Spectra were recorded in $CDCl_3$ at 300K (250.131MHz).

In the ^{13}C-NMR spectra of the compounds synthesized a slight deshielding effect is observed for the carbon atoms close to the indium atom. Again the signals for those carbon atoms in the aryl(phthalocyaninato)indium complexes **3b–e** and **4b–e**, being closer to the phthalocyanine core (C-4 and C-4′), are shifted further downfield than those for C-3 and C-3′ (see Figure 1). Only some of the carbon atom resonances of the axial ligands could be detected. This is due to the C–F coupling leading to split signals of low intensity, the low number of atoms in each set of magnetically equivalent carbon atoms in the ligand compared to the macrocycle, and to the fact that the solubility of the complexes is still too low with regard to the factors limiting the signal intensity which were mentioned previously.

The ^{19}F-NMR data of eight $R_xPcIn(R')$ complexes are given in Table 4. $CDCl_3$ was used as internal standard with $CFCl_3$ as a reference. One narrow singlet was observed for the complexes PcIn(*p*-TMP) (**3b**, **4b**) and PcIn(*m*-TMP) (**3c**, **4c**), all with similar chemical shifts and close to the fluorine signal in α,α,α-trifluorotoluene at −63.9[21]. Due to H–F coupling, multiplets centred at −113.4 and −113.8 are observed for the complexes PcIn(*p*-FP) (**3d**) and (**4d**), respectively. These values are close to that of fluorine in fluorobenzene: −113.1[21]. Three signals are found in the spectra of the perfluorophenyl complexes **3e** (**4e**) at −122.1 (−122.0), −160.9 (−161.2) and −153.3 (−153.7) for the *o*-, *m*-, and *p*-fluorine atoms, respectively. In relation to pentafluorobenzene, whose signals for the same nucleus are at −139.2, −162.7 and −154.5[22a], the *o*-fluorine atoms close to the indium(III) metal are remarkably deshielded. The deshielding of aromatic fluorine atoms in complexes where they are in the *ortho* position of a metal–carbon bond has already been observed and discussed[22]. The spin systems of fluorine in the PcIn(PFP) complexes **3e** and **4e** have typical AA′MM′X patterns[23], which is in agreement with their proposed structures.

Table 4. ^{19}F-NMR data[a] for the $R_xPcIn(R')$ complexes in chloroform

Axial ligand R′	Phthalocyanine Pc		Fluorine atoms multi/intens	δ
p-TMP	**3b**	*p*-CF_3	s	−64.1
	4b	*p*-CF_3	s	−64.1
m-TMP	**3c**	*m*-CF_3	s	−63.7
	4c	*m*-CF_3	s	−63.6
p-FP	**3d**	*p*-F	m	−113.4[b]
	4d	*p*-F	m	−113.8[b]
PFP	**3e**	*o*-F	m/2	−122.0 − (−122.2)
		m-F	m/2	−160.8 − (−161.1)
		p-F	m/1	−153.2 − (−153.3)
	4e	*o*-F	m/2	−121.8 − (−122.1)
		m-F	m/2	−161.0 − (−161.3)
		p-F	m/1	−153.6 − (−153.8)

[a] Spectra were recorded in $CDCl_3$ at 300K (235.334 MHz). Chemical shifts (δ) upfield from the reference $CFCl_3$ are defined as negative. – [b] With broad-band proton decoupling.

In conclusion stable aryl(phthalocyaninato)indium(III) complexes have been prepared starting from chloro(phthalocyaninato)indium(III) and aryl Grignard reagents or aryl lithium compounds, respectively. Electron withdrawing substituents at the aryl ligands are essential to increase the stability of the complexes obtained. All aryl(phthalocyaninato)indium(III) compounds prepared are highly soluble in common organic solvents. Studies on the non-linear optical properties of these new phthalocyaninato complexes, particularly with regard to their optical limiting properties, are in progress.

We would like to thank Dr. *J. S. Shirk* of the *Naval Research Laboratory* in Washington, DC for many helpful discussions and Mrs. *Heike Dorn* for recording the ^{19}F-NMR spectra. We thank the *Fonds der Chemischen Industrie* for the financial support of this work.

Experimental Section

All reactions were carried out under a dry nitrogen atmosphere. THF was distilled from sodium benzophenone ketyl prior to use, quinoline from calcium hydride. *p*-Trifluoromethylbromobenzene, *m*-trifluoromethylbromobenzene, *p*-fluorobromobenzene, perfluorobromobenzene were obtained from commercial sources. 4-*tert*-Butylphthalonitrile (**1**)[13] and 4,5-bis(*n*-pentyl)phthalonitrile (**2**)[14] were prepared according to literature procedures. – FT-IR:

Perkin Elmer Spectrum 1000. − UV/Vis: Shimadzu UV-365. − MS: Varian Mat 711 (FD, temperature of the ion source: 30°C). − ^{1}H, ^{13}C NMR: Bruker AC 250 (^{1}H: 250.131 MHz, ^{13}C: 62.902 MHz). − ^{19}F NMR: Bruker Avance DRX 250 (235.334 MHz). − Elemental Analyses: Carlo-Erba Elemental Analyser 1104, 1106.

General Procedures: The Grignard compounds R′MgBr [R′ = *p*-trifluoromethylphenyl- (**b**), *m*-trifluoromethylphenyl- (**c**), *p*-fluorophenyl- (**d**), perfluorophenyl- (**e**)] were prepared by stirring a mixture of the corresponding substituted bromobenzenes [338 mg (**b**, **c**), 263 mg (**d**), 371 mg (**e**); 1.5 mmol] and Mg turnings (38.9 mg, 1.6 mmol), previously activated by means of an ultrasonic bath, in freshly dried THF (3 ml) at room temp. After most of the magnesium had been consumed, the solution was diluted to a volume of 10 ml by addition of THF. The solution was transferred into a pressure equalizing addition funnel containing a small quantity of glass wool to hold back excess solid magnesium.

Chloro-(tetra-(tert-butyl)phthalocyaninato)indium(III) and Chloro-(octa-(n-pentyl)phthalocyaninato)indium(III) (**3a**, **4a**): A mixture of $InCl_3$ (1.52 g, 6.88 mmol), 4-*tert*-butylphthalonitrile [(**1**), 5.07 g, 27.52 mmol] or 4,5-bis(*n*-pentyl)phthalonitrile [(**2**), 7.38 g, 27.52 mmol], dry quinoline (12 ml), and DBU (1 ml) were stirred at 180°C for 5 h. The solvent was removed by distillation under reduced pressure, leaving a dark green residue, which was chromatographed on silica gel using chloroform as the eluent in order to remove large amounts of the impurities. Then the crude compounds **3a** and **4a** were recrystallized from mixtures of CH_2Cl_2/MeOH (v/v 4:3) or $CHCl_3$/EtOH (v/v 15:7), respectively, by slowly evaporating the more volatile chloromethanes in a rotary evaporator at 40−60°C under slightly reduced pressure. To complete crystallization, the mixtures were kept in a refrigerator overnight. The complexes were collected by filtration, washed twice with methanol and dried at 80°C in vacuo. − (tBu)$_4$PcInCl (**3a**): Yield 2.98 g (49%), blue-green microcrystals. − IR (KBr): $\tilde{\nu}$ = 3075 cm^{-1} vw, 2957 vs, 2903 m, 2866 m, 1613 vw, 1485 s, 1393 m, 1364 m, 1330 vs, 1280 m, 1256 s, 1199 w, 1147 w, 1087 vs, 1047 m, 922 s, 896 w, 831 m, 761 w, 746 m, 693 w, 671 w, 602 vw, 568 vw, 524 vw, 444 vw, 336 w. − UV/Vis ($CHCl_3$): λ_{max} = 697.3 nm, 667.1 (sh), 628.2, 359.5, 339.7 (sh). − ^{1}H NMR ($CDCl_3$): δ = 1.82−1.84 (m, 36 H, tBu), 8.27−8.33 (m, 4 H, 1-H), 9.27−9.33 (m, 4 H, 2-H), 9.42−9.47 (m, 4 H, 2′-H). − ^{13}C NMR ($CDCl_3$): δ = 32.01−32.04 (CH_3), 36.16 (CMe_3), 119.71−119.80 (C-2′), 123.09−123.21 (C-2), 128.48−128.56 (C-1), 135.07−135.23 (C-3), 137.49−137.72 (C-3′), 152.74−153.50 (C-4,4′), 154.55−154.72 (C-1′). − MS (FD); *m*/*z*: 886.2 [M$^+$]. − $C_{48}H_{48}ClInN_8$ (887.2): calcd. C 64.98; H 5.45; Cl 4.00; N 12.63; found C 65.16; H 5.36; Cl 4.13; N 12.30. − (C_5H_{11})$_8$PcInCl (**4a**): Yield 2.75 g (33%), bluish green needles. − IR (KBr): $\tilde{\nu}$ = 2959 cm^{-1} vs, 2927 vs, 2858 s, 1618 vw, 1483 m, 1465 m, 1460 m, 1451 m, 1401 m, 1377 w, 1335 vs, 1100 vs, 1080 s, 1011 w, 892 w, 873 vw, 744 m, 733 w, 724 w, 327 vw. − UV/Vis ($CHCl_3$): λ_{max} = 706.2 nm, 675.4 (sh), 635.4, 361.3, 342.2 (sh). − ^{1}H NMR ($CDCl_3$): δ = 1.04 (t, J = 7.0 Hz, 24 H, CH_3), 1.47−1.71 (m, 32 H, γ,δ-CH_2), 1.93−2.05 (m, 16 H, β-CH_2), 3.12−3.18 (m, 16 H, α-CH_2), 9.10 (s, 8 H, 2,2′-H). − ^{13}C NMR ($CDCl_3$): δ = 14.22 (CH_3), 22.79 (δ-CH_2), 31.58, 32.38, 34.05 (α,β,γ-CH_2), 123.41 (C-2), 135.62 (C-3), 144.30 (C-1), 152.93 (C-4). − MS (FD); *m*/*z*: 1222.3 [M$^+$]. − $C_{72}H_{96}ClInN_8$ (1223.9): calcd. C 70.66; H 7.91; Cl 2.90; N 9.16; found C 70.57; H 8.01; Cl 2.94; N 9.23.

Aryl(tetra-(tert-butyl)phthalocyaninato)indium(III) and Aryl-(octa-(n-pentyl)-phthalocyaninato)indium(III) (**3b−e**, **4b−e**): In a typical reaction, a freshly prepared solution of R′MgBr [R′ = *p*-trifluoromethylphenyl- (**b**), *m*-trifluoromethylphenyl- (**c**), *p*-fluorophenyl- (**d**), perfluorophenyl- (**e**)] in THF (10 ml; 0.15 M R′MgBr), was added dropwise to a stirred solution of **3a** or **4a** (0.3 mmol) in dry THF (25 ml). The reaction was monitored by TLC (silica gel/toluene) and stopped when all of the R_xPcInCl (**3a**, **4a**) had been consumed. The deep green mixture was poured on ice and was extracted several times with diethyl ether. The combined organic layers were washed with water and dried with $MgSO_4$. After evaporation of the solvent, the residue was subjected to column chromatography (silica gel/toluene). Light was strictly excluded during this step. Further purification of the complex was achieved by recrystallization from mixtures of CH_2Cl_2 and methanol, as described above. The pure phthalocyanine was dried in vacuo at 70°C for 3 h. − (tBu)$_4$PcIn(*p*-TMP) (**3b**): Yield 134.4 mg (45%), bluish green powder. − IR (KBr): $\tilde{\nu}$ = 3076 cm^{-1} vw, 2959 s, 2903 m, 2867 w, 1614 w, 1599 vw, 1487 s, 1388 m, 1365 m, 1327 vs, 1280 m, 1257 s, 1200 w, 1164 m, 1152 m, 1128 s, 1086 vs, 1047 s, 1016 w, 954, 922 m, 897 vw, 831 m, 819 w, 760 w, 747 m, 694 w, 678 w, 671 w, 603 vw, 566 vw, 525 vw, 446 vw. − UV/Vis ($CHCl_3$): λ_{max} = 698.0 nm, 667.3 (sh), 628.6, 369.3, 340.9 (sh). − ^{1}H NMR ($CDCl_3$): δ = 1.80 (m, 36 H, tBu), 4.17 (d, J = 7.6 Hz, 2 H, H-b,b′), 6.17 (d, J = 7.6 Hz, 2 H, H-c,c′), 8.32−8.36 (m, 4 H, 1-H), 9.44−9.52 (m, 4 H, 2-H), 9.57−9.59 (m, 4 H, 2′-H). − ^{13}C NMR ($CDCl_3$): δ = 32.00−32.04 (CH_3), 36.12−36.15 (CMe_3), 119.68 (C-2′), 122.54 (q, J = 3.7 Hz, C-c,c′) 123.04 (C-2), 128.29−128.36 (C-1), 134.26 (C-a), 135.40−135.48 (C-3), 137.84−137.92 (C-3′), 153.69−154.24 (C-4,4′), 154.38−154.48 (C-1′). − ^{19}F NMR ($CDCl_3$): δ = −64.1. − MS (FD); *m*/*z*: 995.9 [M$^+$]. − $C_{55}H_{52}F_3InN_8$ (996.9): calcd. C 66.27; H 5.26; N 11.24; found C 66.43; H 5.29; N 10.95. − (tBu)$_4$PcIn(*m*-TMP) (**3c**): Yield 132.2 mg (44%), bluish green powder. − IR (KBr): $\tilde{\nu}$ = 3079 cm^{-1} vw, 2959 s, 2905 m, 2868 w, 1613 w, 1487 s, 1466 w, 1394 m, 1365 m, 1327 vs, 1315 vs, 1280 m, 1257 s, 1199 w, 1165 m, 1150 w, 1127 s, 1085 vs, 1060 m, 1047 m, 922 m, 896 vw, 831 m, 794 vw, 760 w, 747 m, 693 w, 683 vw, 671 w, 603 vw, 567 vw, 525 vw, 446 vw. − UV/Vis ($CHCl_3$): λ_{max} = 697.8 nm, 666.5 (sh), 628.5, 368.6, 341.4 (sh). − ^{1}H NMR ($CDCl_3$): δ = 1.78−1.80 (m, 36 H, tBu), 4.10 (d, J = 7.6 Hz, 1 H, H-b′), 4.41 (s, 1 H, H-b), 6.03−6.09 (m, 1 H, H-c′), 6.46 (d, J = 7.6 Hz, 1 H, H-d), 8.32−8.35 (m, 4 H, 1-H), 9.44−9.53 (m, 4 H, 2-H), 9.57−9.60 (m, 4 H, 2′-H). − ^{13}C NMR ($CDCl_3$): δ = 32.00−32.03 (CH_3), 36.12−36.15 (CMe_3), 119.68 (C-2′), 123.05 (C-2), 123.90 (q, 3.7 Hz, C-d), 126.38 (C-b′), 128.31−128.37 (C-1), 130.21 (q, J = 3.7 Hz, C-b), 135.39−135.45 (C-3), 137.39−137.41 (C-a), 137.81−137.89 (C-3′), 153.77−154.32 (C-4,4′), 154.44−154.52 (C-1′). − ^{19}F NMR ($CDCl_3$): δ = −63.7. − MS (FD); *m*/*z*: 995.9 [M$^+$]. − $C_{55}H_{52}F_3InN_8$ (996.9): calcd. C 66.27; H 5.26; N 11.24; found C 66.59; H 5.34; N 11.40. − (tBu)$_4$PcIn(*p*-FP) (**3d**): Yield 136.3 mg (48%), bluish green powder. − IR (KBr): $\tilde{\nu}$ = 3077 cm^{-1} vw, 2958 vs, 2903 m, 2866 m, 1613 m, 1578 m, 1488 vs, 1393 s, 1364 m, 1329 vs, 1280 s, 1256 s, 1228 m, 1200 w, 1164 m, 1151 m, 1085 vs, 1047 s, 922 s, 896 w, 831 m, 814 m, 760 m, 747 s, 693 w, 672 w, 603 vw, 567 vw, 525 w, 505 vw, 445 vw. − UV/Vis ($CHCl_3$): λ_{max} = 697.4 nm, 666.0 (sh), 628.2, 368.5, 341.0 (sh). − ^{1}H NMR ($CDCl_3$): δ = 1.79−1.80 (m, 36 H, tBu), 3.98−4.04 (m, 2 H, H-b,b′), 5.64−5.71 (m, 2 H, H-c,c′), 8.31−8.35 (m, 4 H, 1-H), 9.43−9.51 (m, 4 H, 2-H), 9.57−9.59 (m, 4 H, 2′-H). − ^{13}C NMR ($CDCl_3$): δ = 32.00−32.04 (CH_3), 36.10−36.13 (CMe_3), 113.53 (d, J = 19.0 Hz, C-c,c′), 119.63 (C-2′), 123.01 (C-2), 128.20−128.27 (C-1), 135.44−135.53 (C-3), 137.86−137.95 (C-3′), 153.72−154.19 (C-4,4′), 154.27−154.41 (C-1′), 162.05 (d, J = 246.9 Hz, C-d). − ^{19}F{^{1}H} NMR ($CDCl_3$): δ = −113.4. − MS (FD); *m*/*z*: 946.2 [M$^+$]. − $C_{54}H_{52}FInN_8$ (946.9): calcd. C 68.50; H 5.54; N 11.83; found C 67.43; H 5.55; N 11.35. − (tBu)$_4$PcIn(PFP) (**3e**): Yield 118.5 mg (39%), bluish green powder. − IR (KBr): $\tilde{\nu}$ = 3076 cm^{-1} vw, 2958 s, 2904 m, 2865 m, 1635 vw, 1613 w, 1531 w, 1506 s, 1487 s, 1463 vs, 1394 m, 1364 m, 1330 vs, 1280 m, 1256 s, 1200 w, 1151

w, 1086 vs, 1047 m, 959 m, 922 m, 896 w, 831 m, 761 w, 747 m, 693 w, 672 w, 602 vw, 567 vw, 525 vw, 446 vw. – UV/Vis ($CHCl_3$): λ_{max} = 697.8 nm, 665.7 (sh), 628.7, 365.6, 341.9 (sh). – ^{1}H NMR ($CDCl_3$): δ = 1.79–1.81 (m, 36 H, *t*Bu), 8.33–8.37 (m, 4 H, 1-H), 9.44–9.51 (m, 4 H, 2-H), 9.58 (m, 4 H, 2′-H). – ^{13}C NMR ($CDCl_3$): δ = 32.00–32.04 (CH_3), 36.15–36.18 (CMe_3), 119.74 (C-2′), 123.12–123.15 (C-2), 128.42–128.49 (C-1), 135.31–135.39 (C-3), 137.73–137.86 (C-3′), 153.37–154.08 (C-4,4′), 154.52–154.64 (C-1′). – ^{19}F NMR ($CDCl_3$): δ = −122.0 – (−122.2) (F-b,b′), −160.8 – (−161.1) (F-c,c′), −153.2 – (−153.3) (F-d). – MS (FD); *m/z*: 1018.0 [M^+]. – $C_{54}H_{48}F_5InN_8$ (1018.8): calcd. C 63.66; H 4.75; N 11.00; found C 64.20; H 4.95; N 10.45. – $(C_5H_{11})_8$PcIn(*p*-TMP) (**4b**): Yield 251.0 mg (63%), dark green powder. – IR (KBr): $\tilde{\nu}$ = 2956 cm^{-1} vs, 2928 vs, 2859 s, 1618 vw, 1598 vw, 1484 m, 1465 m, 1400 w, 1388 w, 1378 w, 1325 vs, 1163 m, 1127 m, 1098 vs, 1081 s, 1047 m, 1015 w, 894 w, 868 vw, 825 vw, 744 m, 732 w, 677 w. – UV/Vis ($CHCl_3$): λ_{max} = 707.2 nm, 675.6 (sh), 636.4, 375.3, 353.7 (sh). – ^{1}H NMR ($CDCl_3$): δ = 1.03 (t, *J* = 7.0 Hz, 24 H, CH_3), 1.46–1.70 (m, 32 H, γ,δ-CH_2), 1.95–2.07 (m, 16 H, β-CH_2), 3.15–3.22 (m, 16 H, α-CH_2), 4.18 (d, *J* = 7.6 Hz, 2 H, H-b,b′), 6.15 (d, *J* = 7.6 Hz, 2 H, H-c,c′), 9.26 (s, 8 H, 2,2′-H). – ^{13}C NMR ($CDCl_3$): δ = 14.19 (CH_3), 22.77 (δ-CH_2), 31.63, 32.35, 34.06 (α,β,γ-CH_2), 122.43 (q, *J* = 3.4 Hz, C-c,c′), 123.41 (C-2), 134.36 (C-a), 135.85 (C-3), 144.14 (C-1), 153.84 (C-4). – ^{19}F NMR ($CDCl_3$): δ = −64.1. – MS (FD); *m/z*: 1332.5 [M^+]. – $C_{79}H_{100}F_3InN_8$ (1333.5): calcd. C 71.15; H 7.56; N 8.40; found C 70.92; H 7.45; N 8.29. – $(C_5H_{11})_8$PcIn(*m*-TMP) (**4c**): Yield 317.5 mg (79%), green powder. – IR (KBr): $\tilde{\nu}$ = 2956 cm^{-1} vs, 2928 vs, 2860 s, 1618 vw, 1484 m, 1466 m, 1452 m, 1401 w, 1378 w, 1334 s, 1316 s, 1164 m, 1126 m, 1099 vs, 1081 s, 1060 w, 1012 w, 894 w, 869 vw, 795 vw, 744 m, 732 w, 682 vw. – UV/Vis ($CHCl_3$): λ_{max} = 707.3 nm, 675.9 (sh), 636.2, 374.9, 354.0 (sh). – ^{1}H NMR ($CDCl_3$): δ = 1.03 (t, *J* = 7.0 Hz, 24 H, CH_3), 1.46–1.70 (m, 32 H, γ,δ-CH_2), 1.96–2.08 (m, 16 H, β-CH_2), 3.16–3.22 (m, 16 H, α-CH_2), 4.12 (d, *J* = 7.0 Hz, 1 H, H-b′), 4.42 (s, 1 H, H-b), 6.01–6.07 (m, 1 H, H-c′), 6.45 (d, *J* = 7.7 Hz, 1 H, H-d), 9.28 (s, 8 H, 2,2′-H). – ^{13}C NMR ($CDCl_3$): δ = 14.19 (CH_3), 22.76 (δ-CH_2), 31.62, 32.35, 34.06 (α,β,γ-CH_2), 123.40 (C-2), 123.73 (q, *J* = 3.7 Hz, C-d), 126.26 (C-b′), 130.28 (q, *J* = 3.7 Hz, C-b), 135.84 (C-3), 137.51 (C-a), 144.12 (C-1), 153.89 (C-4). – ^{19}F NMR ($CDCl_3$): δ = −63.6. – MS (FD); *m/z*: 1332.3 [M^+]. – $C_{79}H_{100}F_3InN_8$ (1333.5): calcd. C 71.15; H 7.56; N 8.40; found C 71.12; H 7.53; N 8.62. – $(C_5H_{11})_8$PcIn(*p*-FP) (**4d**): Yield 142.4 mg (37%), green powder. – IR (KBr): $\tilde{\nu}$ = 2955 cm^{-1} vs, 2927 vs, 2858 s, 1617 vw, 1577 w, 1485 s, 1465 m, 1456 m, 1400 w, 1378 w, 1358 m, 1333 vs, 1226 w, 1164 w, 1098 vs, 1012 w, 894 w, 868 w, 812 w, 745 m, 732 w, 506 vw. – UV/Vis ($CHCl_3$): λ_{max} = 706.7 nm, 674.9 (sh), 635.8, 375.0, 354.6 (sh). – ^{1}H NMR ($CDCl_3$): δ = 1.03 (t, *J* = 7.0 Hz, 24 H, CH_3), 1.47–1.70 (m, 32 H, γ,δ-CH_2), 1.96–2.08 (m, 16 H, β-CH_2), 3.17–3.23 (m, 16 H, α-CH_2), 4.00–4.06 (m, 2 H, H-b,b′), 5.62–5.70 (m, 2 H, H-c,c′), 9.28 (s, 8 H, 2,2′-H). – ^{13}C NMR ($CDCl_3$): δ = 14.19 (CH_3), 22.77 (δ-CH_2), 31.64, 32.35, 34.06 (α,β,γ-CH_2), 113.42 (d, *J* = 18.5 Hz, C-c,c′), 123.40 (C-2), 135.58 (d, *J* = 6.5 Hz, C-b,b′), 135.91 (C-3), 144.07 (C-1), 153.91 (C-4). – ^{19}F{^{1}H} NMR ($CDCl_3$): δ = −113.8. – MS (FD); *m/z*: 1282.5 [M^+]. – $C_{78}H_{100}FInN_8$ (1283.5): calcd. C 72.99; H 7.85; N 8.73; found C 72.71; H 7.66; N 8.71. – $(C_5H_{11})_8$PcIn(PFP) (**4e**): Yield 233.1 mg (57%), green powder. – IR (KBr): $\tilde{\nu}$ = 2955 cm^{-1} vs, 2927 vs, 2859 vs, 1636 vw, 1617 w, 1506 s, 1483 s, 1464 vs, 1401 m, 1357 vs, 1333 vs, 1098 vs, 1074 vs, 1054 m, 1010 w, 958 vs, 895 m, 871 w, 744 s, 733 m, 725 m. – UV/Vis ($CHCl_3$): λ_{max} = 707.5 nm, 675.7 (sh), 636.3, 370.1, 349.3 (sh). – ^{1}H NMR ($CDCl_3$): δ = 1.04 (t, *J* = 7.1 Hz, 24 H, CH_3), 1.48–1.71 (m, 32 H, γ,δ-CH_2), 1.97–2.09 (m, 16 H, β-CH_2), 3.17–3.23 (m, 16 H, α-CH_2), 9.27 (s, 8 H, 2,2′-H). – ^{13}C NMR ($CDCl_3$): δ = 14.20 (CH_3), 22.78 (δ-CH_2), 31.61, 32.40, 34.09 (α,β,γ-CH_2), 123.40 (C-2), 135.75 (C-3), 144.19 (C-1), 153.39 (C-4). – ^{19}F NMR ($CDCl_3$): δ = −121.8 – (−122.1) (F-b,b′), −161.0 – (−161.3) (F-c,c′), −153.6 – (−153.8) (F-d). – MS (FD); *m/z*: 1353.9 [M^+]. – $C_{78}H_{96}F_5InN_8$ (1355.5): calcd. C 69.12; H 7.14; N 8.27; found C 69.10; H 6.83; N 8.21.

First Results in the Preparation of Phenyl(octa-(n-pentyl)phthalocyaninato)indium(III) (**4f**): Phenyllithium in cyclohexane/diethyl ether (0.5 M) at room temp. was added dropwise to a solution of **4a** (122.4 mg, 0.1 mmol) in dry THF (25 ml). The reaction was monitored by TLC (silica gel/toluene) and stopped when all of the R_8PcInCl (**4a**) had been consumed. The deep green mixture obtained was worked up as described above. The complex **4f** was separated from the crude mixture by stirring it in *n*-hexane. Due to the insolubility of the metal free phthalocyanine (formed during the reaction) in this solvent, pure phenyl(phthalocyaninato)indium(III) was obtained after filtration and evaporation of the solvent. – $(C_5H_{11})_8$PcIn(Ph) (**4f**): Green powder. – IR (KBr): $\tilde{\nu}$ = 2955 cm^{-1} vs, 2926 vs, 2858 s, 1618 vw, 1483 m, 1466 m, 1400 w, 1378 w, 1359 m, 1333 s, 1098 vs, 1079 m, 1011 w, 893 w, 868 vw, 745 m, 732 w, 724 m. – UV/Vis ($CHCl_3$): λ_{max} = 706.6 nm, 676.2 (sh), 635.8, 375.9, 353.6 (sh). – MS (FD); *m/z*: 1263.7 [M^+]. – $C_{78}H_{101}InN_8$ (1265.5): calcd. C 74.03; H 8.04; N 8.85; found C 73.97; H 7.91; N 8.96.

[1] *Phthalocyanines: Properties and Applications* (Eds.: C. C. Leznoff, A. B. P. Lever), VCH Publishers, Inc., New York, **1989–1996**, vol. 1–4.

[2] F. H. Moser, A. L. Thomas, *The Phthalocyanines* CRC Press: Boca Raton, FL, **1983**.

[3] For reviews: [3a] M. Hanack, M. Lang, *Adv. Mater.* **1994**, *6*, 819. – [3b] H. Schulz, H. Lehmann, M. Rein, M. Hanack, *Struct. Bonding* **1991**, *74*, 41.

[4] H. S. Nalwa, J. S. Shirk in *Phthalocyanines: Properties and Applications* (Eds.: C. C. Leznoff, A. B. P. Lever), VCH Publishers, Inc., New York, **1996**, vol. 4, p. 79.

[5] M. Hanack, R. Polley, H. Heckmann, *Methods of Organic Chemistry (Houben-Weyl),* 4th ed. **1997**, vol. E9d, p. 717–842.

[6] [6a] N. Kobayashi, N. Sasaki, Y. Higashi and T. Osa, *Inorg. Chem.* **1995**, *34*, 1636. – [6b] H. Konami and M. Hatano, *Chem. Lett.* **1988**, 1359. – [6c] G. Schmid, E. Witke, U. Schlick, S. Knecht, M. Hanack, *J. Mater. Chem.* **1995**, *5*, 855.

[7] Optical limiting properties of $(t\text{Bu})_4$PcInCl were measured by J.W. Perry et. al., *Science* **1996**, *273*, 1533. No synthesis of this material was given.

[8] M. Hanack, K. Mitulla, G. Pawlowski, L. R. Subramanian, *J. Organomet. Chem.* **1981**, *204*, 315; and references therein.

[9] K. M. Kadish, *Prog. Inorg. Chem.* **1986**, *34*, 435.

[10] [10a] A. Tabard, R. Guilard, K. M. Kadish, *Inorg. Chem.* **1986**, *25*, 4277. – [10b] R. Guilard, P. Cocolios, P. Fournari, *J. Organomet. Chem.* **1977**, *129*, C11. – [10c] R. Guilard, P. Cocolios, P. Fournari, *J. Organomet. Chem.* **1979**, *179*, 311.

[11] P. M. Treichel, F. G. A. Stone, *Adv. Organomet. Chem.* **1964**, *1*, 143.

[12] [12a] P. M. Treichel, M. A. Chaudhari, F. G. A. Stone, *J. Organomet. Chem.* **1963**, *1*, 98. – [12b] R. D. Chambers and T. Chivers, *Proc. Chem. Soc.* **1963**, 208.

[13] [13a] S. A. Mikhalenko, S. V. Barkanova, O. L. Lebedev, E. A. Luk'yanets, *Zh. Obshch. Khim.* **1971**, *41*, 2735; *J. Gen. Chem. USSR* **1971**, *41*, 2770. – [13b] M. Hanack, J. Metz, G. Pawlowski, *Chem. Ber.* **1982**, *115*, 2836.

[14] M. Hanack, P. Haisch, H. Lehmann, L. R. Subramanian, *Synthesis* **1993**, 387.

[15] [15a] M. Sommerauer, C. Rager, M. Hanack, *J. Am. Chem. Soc.* **1996**, *118*, 10085. – [15b] M. Hanack, G. Schmid, M. Sommerauer, *Angew. Chem.* **1993**, *105*, 1540; *Angew. Chem. Int. Ed. Engl.* **1993**, *32*, 1422. – [15c] G. Schmid, M. Sommerauer, M. Geyer, M. Hanack in *Phthalocyanines: Properties and Applications* (Eds.: C. C. Leznoff, A. B. P. Lever), VCH Publishers, Inc., New York, **1996**, vol. 4, p. 1.

[16] A. Beck, K.-M. Mangold, M. Hanack, *Chem. Ber.* **1991**, *124*, 2315.

[17] [17a] M. J. Stillman, T. Nyokong in *Phthalocyanines: Properties and Applications* (Eds.: C. C. Leznoff, A. B. P. Lever), VCH Publishers, Inc., New York, **1989**, vol. 1, p. 133. – [17b] A. W. Snow and N. L. Jarvis, *J. Am. Chem. Soc.* **1984**, *106*, 4706. – [17c] A. R. Monahan, J. A. Brado and A. F. Deluca, *J. Phys. Chem.* **1972**, *76*, 446.

[18] [18a] E. Maslowsky, Jr. in *Vibrational Spectra of Organometallic Compounds* 2nd ed., Wiley, New York, **1978**. – [18b] G. Socrates in *Infrared Characteristic Group Frequencies* 2nd ed., John Wiley, Chichester, New York, Brisbane, Toronto, **1994**.

[19] Unsubstituted PcInCl was prepared according to a literature procedure: J. P. Linsky, T. R. Paul, R. S. Nohr, M. E. Kenney, *Inorg. Chem.* **1980**, *19*, 3131. The UV/Vis spectrum was recorded in $CHCl_3$.

[20] [20a] T. R. Janson, A. R. Kone, J. F. Sullivan, K. Knox, M. E. Kenney, *J. Am. Chem. Soc.* **1969**, *91*, 5210. – [20b] T. Koyama, T. Suzuki, K. Hanabusa, H. Shirai, N. Kobayashi, *Inorg. Chim. Acta* **1994**, *218*, 41. – [20c] J. E. Maskasky, J. R. Mooney, M. E. Kenney, *J. Am. Chem. Soc.* **1972**, *94*, 2132. – [20d] U. Keppeler, W. Kobel, H.-U. Siehl, M. Hanack, *Chem. Ber.* **1985**, *118*, 2095.

[21] [21a] V. Wray, *Ann. Rep. NMR Spectrosc.* **1980**, *10B*, 1. – [21b] V. Wray, *Ann. Rep. NMR Spectrosc.* **1983, 14**, 1.

[22] [22a] M. I. Bruce, *J. Chem. Soc. A* **1968**, 1459. – [22b] J. W. Emsley, L. Phillips, *Prog. Nucl. Magn. Reson. Spectrosc.* **1971**, *7*, 1.

[23] P. Bladon, D. W. A. Sharp and J. M. Winfield, *Spectrochim. Acta* **1964**, *20*, 1033.

[97201]

Metal Complexes of Biologically Important Ligands, 101[◇]

Oxidative Addition of α-Bromoglycine to Palladium(0) and Platinum(0) Complexes: α-Metallated Amino Acids as Models for Intermediates in the Metal-Catalyzed Hydrogenation of Dehydroamino Acids☆

Bernd Kayser, Christopher Missling, Jörg Knizek[2], Heinrich Nöth[2], Wolfgang Beck*

Institut für Anorganische Chemie der Ludwig-Maximilians-Universität,
Meiserstraße 1, D-80333 München, Germany

Received September 22, 1997

Keywords: α-Metallated amino acids / Palladium / Platinum / Oxidative addition / α-Bromoglycinate

Oxidative addition of methyl *N*-benzoyl-2-bromoglycinate to bis(dibenzylideneacetone)palladium, in the presence of 2,2′-bipyridyl, and to $(Ph_3P)_2Pt(\eta^2\text{-}C_2H_4)$ gives the α-metallated glycine esters **1a** and **2a**. Abstraction of bromide from **1a**, **2a**, using $AgSbF_6$ or $AgBF_4$, affords the cationic C,O-chelate complexes $[(bpy)Pd{-}CH(CO_2Me)NHC(Ph)O]^+$ (**1b**,**c**) and $[(Ph_3P)_2Pt{-}CH(CO_2Me)NHC(Ph)O]^+$ (**2b**), respectively, featuring coordination of the amide O atom. The complexes **1b** and **2b** have been characterized by X-ray diffraction.

α-Haloglycine esters are valuable synthons for the synthesis of modified α-amino acids[3]. Recently, we used these compounds for the introduction of α-amino acid residues into organometallic systems[4], giving products that may find application in the labelling of amino acids and peptides, a growing field in bioinorganic chemistry[5]. α-Metallated amino acids are intermediates in the asymmetric hydrogenation of dehydroamino acids and have been detected as such by Halpern et al.[6] and Brown et al.[7] by means of NMR spectroscopy.

Structures of α-metallated amino acids have been reported by Vahrenkamp et al.[8] and by ourselves[4b]. Recently, Bergens et al.[9] characterized a C,O-bound intermediate in the hydrogenation of methyl α-acetamidocinnamate, derived from a $(BINAP)(H)Ru^{II}$ catalyst.

The easy access to α-metallated amino acids by oxidative addition of methyl *N*-benzoyl-2-bromoglycinate to $Me_2Pt(bpy)$ (bpy = 2,2′-bipyridyl)[4b] prompted us to search for square-planar complexes with the halide and the *C*-bound α-amino acid in a *cis* configuration. Abstraction of halide from these should yield simple models for intermediates in the hydrogenation of dehydroamino acids, with coordination of the amide O atom.

The oxidative addition of organic halides to zerovalent palladium and platinum complexes[10], e.g. to $(Ph_3P)_2Pt(\eta^2\text{-}C_2H_4)$[11] or to $(dba)_2Pd$ (dba = dibenzylideneacetone)[12] is a general method for the synthesis of σ-bonded organometallic complexes.

Results and Discussion

The reactions of methyl *N*-benzoyl-2-bromoglycinate with $(dba)_2Pd$ in the presence of bpy, and with $(Ph_3P)_2Pt(\eta^2\text{-}C_2H_4)$ yielded the α-metallated complexes **1a** and **2a**, respectively, in good yields. The compounds were found to be light-sensitive and relatively unstable in air and towards organic solvents. Abstraction of bromide from **1a**, **2a**, using $AgSbF_6$ or $AgBF_4$, led to coordination of the amide group, thereby affording the stable C,O-chelate complexes **1b**,**c** and **2b**.

The IR spectra of **1a** and **2a** show typical ester and amide absorptions at 1715 and 1640 cm^{-1}. The shift of the carbonyl ester band to lower wavenumbers ($\tilde{\nu} \approx 30\ cm^{-1}$) compared with the corresponding band in α-amino acid esters has been observed previously[4b]. The lower wavenumber of the amide absorption in **1b**,**c** and **2b** (1600 cm^{-1}) is characteristic of a coordinated amide group. The ^{1}H-NMR spectrum of **1a** exhibits a doublet due to the CH proton, as expected, while that of complex **1c** features a broad singlet.

The signal of the Pt−CH proton in **2a** appears as a pseudo-quadruplet with satellites due to ^{195}Pt−C−H coupling. In the ^{1}H-NMR spectrum of **2b**, a doublet of triplets is observed for the α-CH proton due to *cis* and *trans* ^{31}P−Pt−C−H coupling.

The ^{13}C-NMR spectra of **1c** and **2b** show the expected resonances. Two ^{31}P-NMR signals for the two non-equivalent P atoms are observed for **2b**. Their ^1J(Pt−P) values differ significantly because of the different *trans* influence of the strong C and weak O donors, similar to the situation in $(Ph_3P)_2Pt{-}C(H)(CO_2R)C(O)O$[13].

Cationic alkyl- or acyl$(bpy)Pd^{II}$ complexes readily react with CO, isonitriles, alkenes or allenes[14]. Surprisingly, **1a** does not undergo insertion of CO, ethylene or allene at atmospheric pressure. Treatment with *tert*-butylisonitrile leads only to coordination of the isonitrile {$\tilde{\nu} = 2222\ cm^{-1}$ [ν(CN)]} and no insertion product could be detected.

[◇] Part 100: Ref.[1].

 © WILEY-VCH Verlag GmbH, D-69451 Weinheim, 1998 1434−1948/98/0303−0375 $ 17.50+.50/0

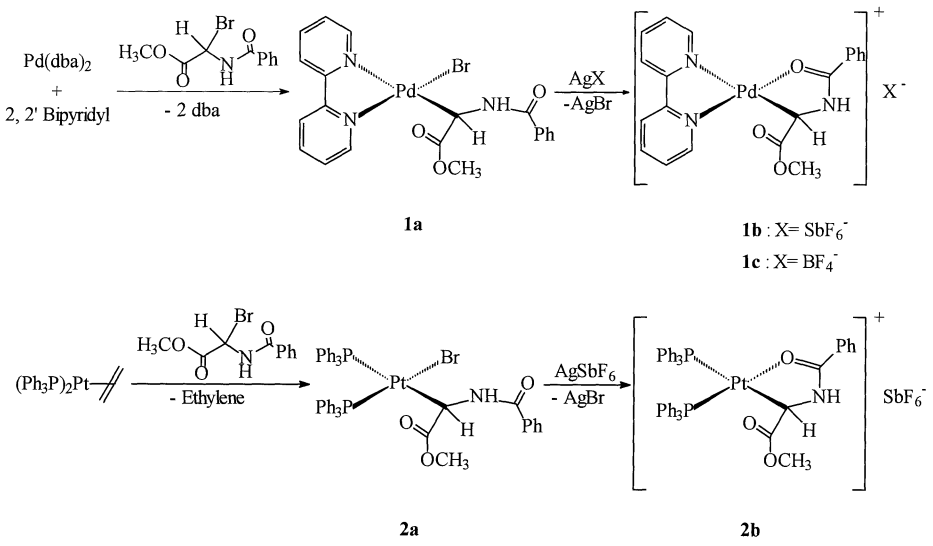

Figure 1. Molecular structure of **1b**[a]

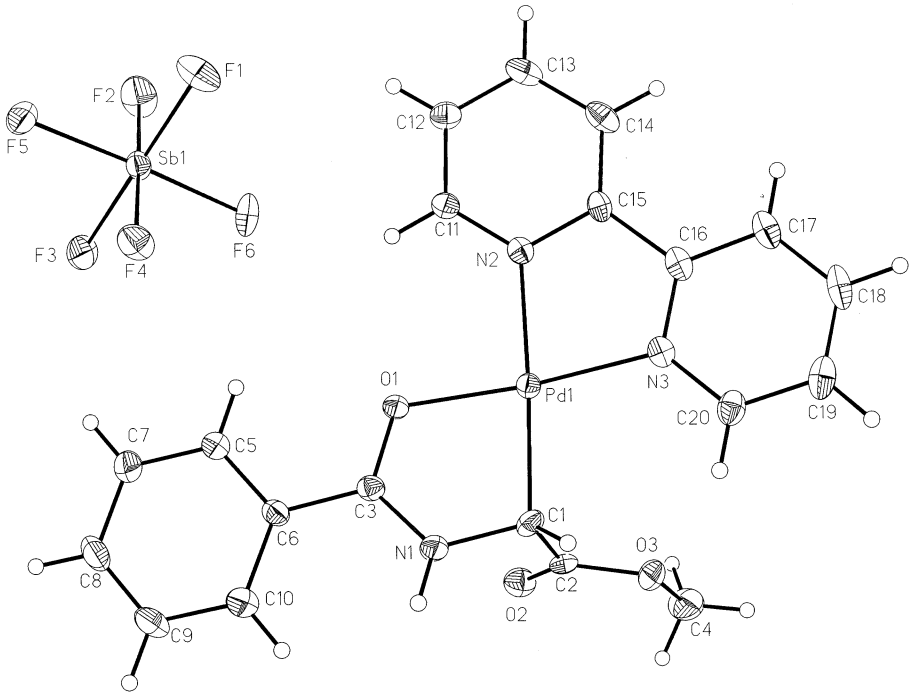

[a] Selected bond lengths [pm] and angles [°]: Pd1−N2 205.2(5), Pd1−N3 201.9(5), Pd1−O1 201.3(4), Pd1−C1 203.3(6), O1−C3 127.5(7), C3−N1 132.2(8), N1−C1 146.0(8); N2−Pd−N3 80.0(2), O1−Pd1−C1 82.4(2), Pd1−C1−N1 104.2(4), Pd1−O1−C3 113.4(4).

Crystal Structure Determinations of 1b and 2b

Crystals suitable for structure determination by X-ray diffraction were obtained by liquid-liquid diffusion of diethyl ether into an acetone solution of **1b** at room temperature and from a dichloromethane solution of **2b** layered with *n*-pentane. The unit cell of **1b** was found to contain the α*S* and α*R* enantiomers (at C1), with a parallel arrangement of the molecules and pairs of enantiomers (with a center of symmetry, Pd···Pd 427 pm) in the lattice. As expected on the basis of the spectroscopic data, the amino acid is coordinated to the Pd atom through the α-carbon atom and the amide group (Figure 1).

The palladium center in **1b** has a square-planar environment with Pd−N distances (203−205 pm) similar to those reported for related complexes[12][15]. The Pd−C distance [203.3(6) pm] compares well with values found for other sp^3 carbon atoms *trans* to an sp^2 nitrogen atom[15]. The acyl CO bond length [127.5(7) pm] is typical for a carbonyl group, although the CO absorption in the IR spectrum (1602 cm^{-1}) is suggestive of more single-bond character. The α-carbon atom is approximately tetrahedrally coordinated, with the largest deviation from ideal geometry being manifested in the N−C−Pd angle (104°). The chelate ring is almost planar and has a (small) O−C−N−C torsion angle of 11.7°.

Figure 2. Structure of **2b**[a]

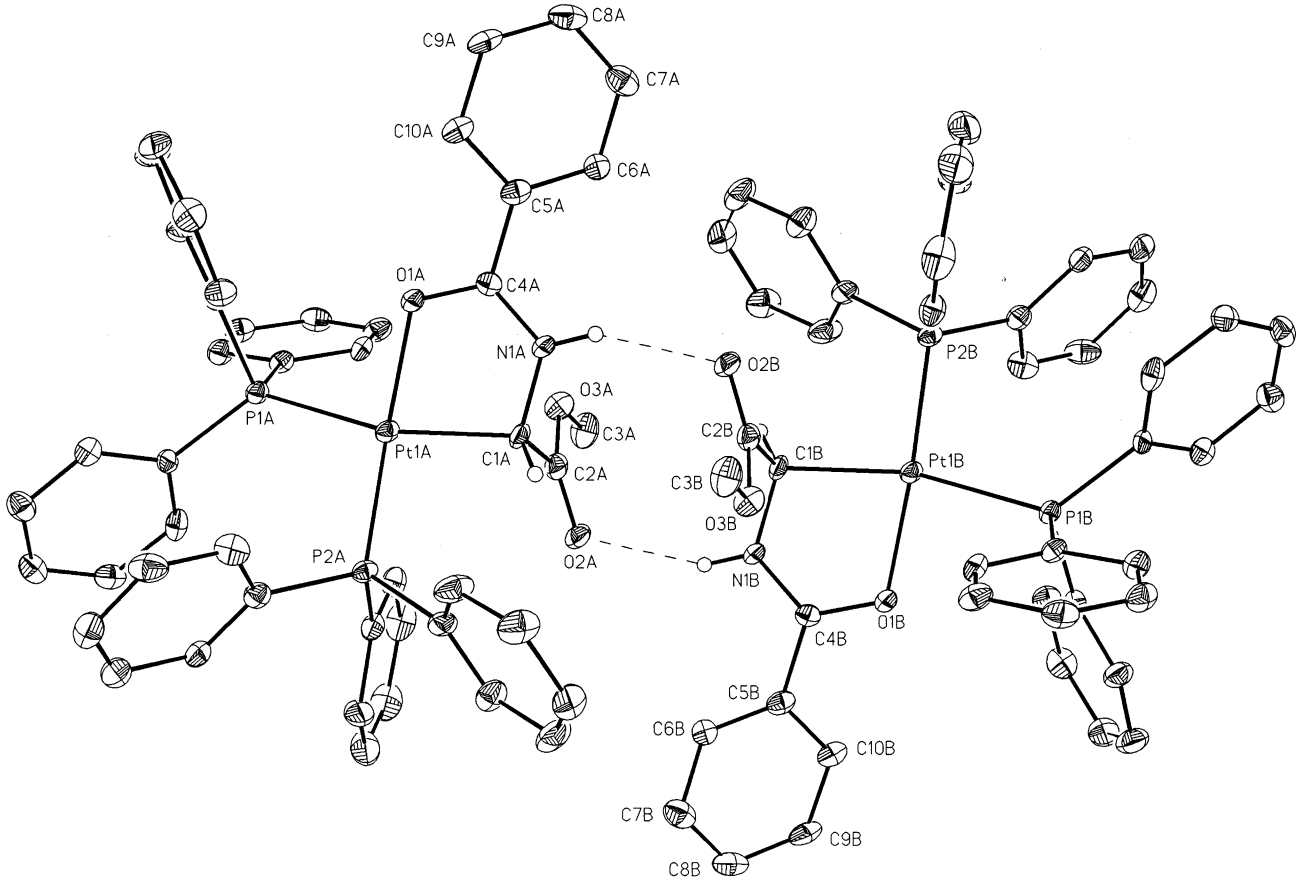

[a] Selected bond lengths [pm] and angles [°]: Pt1−P1 232.8(2), Pt1−P2 223.3(2), Pt1−O1 208.9(4), Pt1−C1 210.0(6), O1−C4 128.1(7), C4−N1 130.9(8), N1−C1 146.0(8); P1−Pt1−P2 99.91(6), C1−Pt1−O1 80.8(2), Pt1−C1−N1 104.4(4), Pt1−O1−C4 112.1(4).

A similar structure is found for **2b**. The two P atoms in **2b** are seen to deviate from the coordination plane by 18° and 3.4°, respectively. The Pt−α-C bond length [210.0(6) pm] is comparable to that found in other platinum(II) complexes with Pt−α-alkyl bonds[16].

Interestingly, pairs of enantiomers α*S* and α*R* are found in the crystal (Figure 2), which are linked through two hydrogen bonds between the amino and the carbonyl groups of the methyl ester (N−H···O 286 pm).

Support by the *Deutsche Forschungsgemeinschaft* and the *Fonds der Chemischen Industrie* is gratefully acknowledged. We thank Professor Dr. *W. Steglich*, München, for valuable discussions.

Experimental Section

General: All reactions were carried out in dry solvents under argon. − NMR: Jeol GSX 270 (^{1}H 270.0; ^{13}C 100.4; ^{31}P 109.3 MHz) with tetramethylsilane as internal standard; H_3PO_4 (85%) as external standard. − IR: 5ZDX FT-IR. − $(dba)_2Pd$[18], (η^2-ethylene)$(Ph_3P)_2Pt$[19] and methyl *N*-benzoyl-2-bromoglycinate[3b] were prepared according to literature procedures. $AgBF_4$ and $AgSbF_6$ were purchased from Aldrich and stored in the dark under argon.

(bpy)[CH(NHCOPh)(CO$_2$Me)]PdBr (**1a**): To a solution of 173 mg (0.3 mmol) of $(dba)_2Pd$ in 10 ml of benzene, 47 mg (0.3 mmol) of 2,2′-bipyridyl and 82 mg (0.3 mmol) of methyl *N*-benzoyl-2-bromoglycinate were added. The mixture was stirred for 1 h

Table 1. Details of the crystal structure determinations[17]

	1b	**2b**
Formula	$C_{20}H_{18}F_6N_3O_3PdSb$	$C_{46}H_{40}F_6NO_3P_2PtSb$
M_r	690.52	1147.57
Crystal system	monoclinic	triclinic
Space group	*P*2(1)/*c*	*P*$\bar{1}$
a [Å]	8.422(2)	11.9029(1)
b [Å]	18.357(4)	12.4852(1)
c [Å]	14.958(3)	16.3340(1)
α [°]	90°	94.012(1)
β [°]	105.643(9)	92.620(1)
γ [°]	90°	114.292(1)
V [Å^3]	2227.0(9)	2199.64(3)
Z	4	2
$\rho_{calcd.}$ [gcm^{-3}]	2.060	1.733
μ [mm^{-1}]	2.099	3.930
Crystal size	0.2 × 0.15 × 0.12	0.3 × 0.3 × 0.2
2θ range [°]	3.6−58.8	3.6−58.8
Index range	±*h*, ±*k*, ±*l*	±*h*, ±*k*, ±*l*
Collected reflns.	6146	13135
Independent reflns. [R_{int} (%)]	4281 [2.45]	7027 [3.21]
Max./min. transmissions	0.727/0.606	0.710/0.497
Parameters	307	596
*R*1/*wR*2 [*F* > 4σ(*F*)]	0.0488/0.0914	0.0424/0.1039
GoF	1.368	1.139
Largest diff. peak and hole [eÅ^{-3}]	0.445/−0.502	1.685/−2.364

at room temp., during the course of which a yellow-green powder precipitated. The precipitate was separated by centrifugation, washed with diethyl ether (2 × 10 ml), and dried in vacuo. Yield 128 mg (80%), yellow-green powder, m.p. 164°C. – IR (KBr): $\tilde{\nu}$ = 3407 cm^{-1} m (NH), 1716 s (CO_2), 1633 s (NCO). – ^1H NMR ($CDCl_3$): δ = 3.74 (s, 3 H, CH_3), 5.32 (d, ^3J = 9.2 Hz, 1 H, CH), 7.36–7.49 (m, 4 H, NH, C_6H_5), 7.57–7.74 (m, 2 H, bpy), 7.86–8.21 (m, 6 H, bpy, C_6H_5), 9.25 (d, ^3J = 3.94 Hz, 1 H, *o*-bpy), 9.35 (d, ^3J = 5.4 Hz, 1 H, *o*-bpy). – $C_{20}H_{18}N_3O_3BrPd \cdot 0.5C_6H_6$ (573.8): calcd. C 48.15, H 3.69, N 7.32; found C 47.97, H 3.71, N 7.26.

[CH(NHCOPh)(CO$_2$Me)](PPh$_3$)$_2$PtBr (**2a**): To a solution of 224 mg (0.3 mmol) of (η^2-ethylene)($Ph_3P)_2Pt$ in 10 ml of benzene, 82 mg (0.3 mmol) of methyl *N*-benzoyl-2-bromoglycinate was added. Gas evolution was observed and the yellow solution was stirred for 1 h. A white residue was separated by centrifugation, the volatiles were evaporated from the supernatant solution, and the residue was washed with pentane (3 × 15 ml). Yield 268 mg (90%), white powder, m.p. 104°C (decomp.). – IR (KBr): $\tilde{\nu}$ = 3413 cm^{-1} m (NH), 1713 s (CO_2), 1647 s (NCO), 280 m (PtBr). – ^1H NMR (C_6D_6): δ = 3.78 (s, 3 H, CH_3), 5.44 (pseudo-q, $^3J_{PH}$ = 9.7 Hz, $^2J_{PtH}$ = 93.6 Hz, 1 H, CH), 6.94–8.74 (m, 36 H, NH, C_6H_5, PPh_3). – ^{31}P NMR (C_6D_6): δ = 17.90 (d, $^2J_{PP}$ = 16.5 Hz, $^1J_{PtP}$ = 1902.9 Hz), 20.45 (d, $^2J_{PP}$ = 16.5 Hz, $^1J_{PtP}$ = 4481.5 Hz). – $C_{46}H_{40}NO_3BrP_2Pt$ (991.8): calcd. C 55.71, H 4.07, N 1.41; found C 55.51, H 4.76, N 1.75.

General Procedure for the Abstraction of Bromide from **1a** and **2a**: To a solution of 160 mg (0.3 mmol) of **1a** [or 297 mg (0.3 mmol) of **2a**] in 10 ml of acetone, a solution of 58 mg (0.3 mmol) of $AgBF_4$ or 103 mg (0.3 mmol) of $AgSbF_6$ in 5 ml of acetone was added. Reaction was indicated by the rapid precipitation of AgBr; the suspension was stirred for 1 h in the dark at room temp. and then the precipitate was separated by centrifugation. The colorless/yellow solution was concentrated in vacuo and the residue was washed with diethyl ether (**1b**,**c**) or pentane (**2b**) (2 × 15 ml) and dried in vacuo.

[(bpy)Pd–CH(CO$_2$Me)NHC(Ph)O]$^+$ BF$_4^-$ (**1c**): Yield 154 mg (95%), colorless powder, m.p. 193°C (decomp.). – IR (KBr): $\tilde{\nu}$ = 3410 cm^{-1} m (NH), 1707 s (CO_2), 1602 s (NCO), 1083 (BF_4^-). – ^1H NMR ($CDCl_3$ + DMSO): δ = 3.33 (s, 3 H, CH_3), 4.57 (s, 1 H, CH), 7.14–7.43 (m, 5 H, Ph, bpy), 7.71 (d, ^3J = 7.6 Hz, 2 H, Ph), 7.92 (pseudo-q, ^3J = 7.7 Hz, 2 H, bpy), 8.01–8.11 (m, 2 H, bpy), 8.43 (d, ^3J = 5.5 Hz, 1 H, bpy), 8.71 (d, ^3J = 5.2 Hz, 1 H, bpy), 9.77 (s, 1 H, NH). – ^{13}C NMR ($CDCl_3$ + DMSO): δ = 50.86, 51.25 (CH, CH_3), 122.30, 122.98, 126.64, 126.71, 126.73, 127.77, 128.07, 132.89, 140.07, 140.44, 147.62, 152.66, 152.71, 155.72 (bpy, Ph), 173.90, 178.63 (CO_2, NCO). – $C_{20}H_{18}BF_4N_3O_3Pd$ (541.6): calcd. C 44.35, H 3.35, N 7.76; found C 43.89, H 3.17, N 7.61.

[(Ph$_3$P)$_2$Pt–CH(CO$_2$Me)NHC(Ph)O]$^+$ SbF$_6^-$ (**2b**): Yield 309 mg (90%), colorless powder, m.p. 158°C (decomp.). – IR (KBr): $\tilde{\nu}$ = 3437 cm^{-1} m (NH), 1709 m (CO_2), 1607 m (NCO), 1098 (SbF_6^-). – ^1H NMR ($CDCl_3$): δ = 3.27 (s, 3 H, CH_3), 5.44 (dt, $^3J_{(PH)trans}$ = 9.9 Hz, $^3J_{(PH)cis}$ = 2.1 Hz, $^3J_{HH}$ = 2.1 Hz, $^2J_{PtH}$ = 46.8 Hz, 1 H, CH), 7.00–7.71 (m, 35 H, PPh_3, Ph), 8.24 (pd, $^4J_{PH}$ = 6.5 Hz, $^3J_{HH}$ = 2.1 Hz, 1 H, NH). – ^{13}C NMR ($CDCl_3$): δ = 50.62 (CH_3), 62.82 (dd, $^2J_{(PC)trans}$ = 81.8 Hz, $^2J_{(PC)cis}$ = 3.6 Hz, CH), 127.57–134.87 (m, 42 C, PPh_3, Ph), 173.64 (d, $^3J_{(PC)trans}$ = 4.7 Hz, CO_2), 180.78 (dd, $^3J_{(PC)trans}$ = 10.6 Hz, $^3J_{(PC)cis}$ = 3.4 Hz, NCO). – ^{31}P NMR ($CDCl_3$): δ = 8.33 (d, $^2J_{PP}$ = 19.8 Hz, $^1J_{PtP}$ = 4223.1 Hz), 22.87 (d, $^2J_{PP}$ = 19.8 Hz, $^1J_{PtP}$ = 2243.5 Hz). – $C_{46}H_{40}F_6NO_3P_2PtSb$ (1147.6): calcd. C 48.14, H 3.51, N 1.22; found C 48.53, H 3.89, N 1.24.

Crystal Structure Determinations: A suitable single crystal of **1b** or **2b** was mounted on a glass fibre with perfluoroether oil. After cooling to –80°C, the crystal was optically centered on a Siemens P4 four-circle diffractometer equipped with a CCD area detector. The dimensions of the unit cell were determined from the observed reflections (> 10 σ) in 4 × 15 frames with different ψ and χ orientations. Data collection was performed with 10-s exposures at two different χ settings with Δψ intervals of 0.3° (altogether 1296 frames). Data reduction was performed with the program SAINT of Siemens Analytical Instruments, and a semiempirical absorption correction was applied. The structures were solved by the heavy-atom method and successive Fourier synthesis using the SHELX-93 program (G.W. Sheldrick, University of Göttingen). All non-hydrogen atoms were refined anisotropically. H atoms bound to carbon atoms were placed in calculated positions and refined with a riding model. *N*-bonded H atoms were located in the difference Fourier synthesis and were freely refined with a fixed isotropic N. Selected crystallographic data and data relating to the structure solutions and refinement are summarized in Table 1.

☆ Dedicated to Professor *Wolfgang Herrmann*, as a mark of friendship and respect, on the occasion of his 50th birthday.

[1] K. Severin, R. Bergs, W. Beck, *Angew. Chem.*, in press.

[2] X-ray diffraction measurements.

[3] [3a] R. Kober, W. Steglich, *Liebigs Ann. Chem.* **1983**, 599–609. – [3b] R. Kober, K. Papadopoulos, W. Miltz, D. Enders, W. Steglich, *Tetrahedron* **1985**, *41*, 1693–1701. – [3c] P. Münster, W. Steglich, *Synthesis* **1987**, 223–225. – [3d] G. Apitz, M. Jäger, S. Jaroch, S. Kratzel, L. Schäffeler, W. Steglich, *Tetrahedron* **1993**, *49*, 8223–8232. – [3e] Th. Bretschneider, W. Miltz, P. Münster, W. Steglich, *Tetrahedron* **1988**, *44*, 5403–5414. – [3f] V. A. Burgess, C. J. Easton, M. P. Hay, P. J. Steel, *Aust. J. Chem.* **1988**, *41*, 701–710. – [3g] S. Jaroch, T. Schwarz, W. Steglich, P. Zistler, *Angew. Chem.* **1993**, *105*, 1803–1805; *Angew. Chem. Int. Ed. Engl.* **1993**, *32*, 1771.

[4] [4a] B. Kayser, K. Polborn, W. Steglich. W. Beck, *Chem. Ber.* **1997**, *130*, 171–177. – [[4b] B. Kayser, H. Nöth, M. Schmidt, W. Steglich, W. Beck, *Chem. Ber.* **1996**, *129*, 1617–1620.

[5] [5a] G. Jaouen, A. Vessiéres, I. S. Butler, *Acc. Chem. Res.* **1993**, *26*, 361–369. – [5b] M. Salmain, M. Gunn, A. Gorfti, S. Top, G. Jaouen, *Bioconjugate Chem.* **1993**, *4*, 425–433. – [5c] A. Gorfti, M. Salmain, G. Jaouen, M. J. McGlinchey, A. Bennouna, A. Mousser, *Organometallics* **1996**, *15*, 142–151. – [5d] A. J. Gleichmann, J. M. Wolff, W. S. Sheldrick, *J. Chem. Soc., Dalton Trans.* **1995**, 1549–1554. – [5e] J. M. Wolff, A. J. Gleichmann, W. S. Sheldrick, *J. Inorg. Biochem.* **1995**, *59*, 219. – [5f] J. M. Wolff, W. S. Sheldrick, *Chem. Ber.* **1997**, *130*, 981–988; *J. Organomet. Chem.* **1997**, *531*, 141–149. – [5g] R. Krämer, *Angew. Chem.* **1996**, *108*, 1287–1289; *Angew. Chem. Int. Ed. Engl.* **1996**, *35*, 1197–1199. – [5h] M. Schweiger, T. Ederer, K. Sünkel, W. Beck, *J. Organomet. Chem.*, in press.

[6] [6a] A. S. C. Chan, J. J. Pluth, J. Halpern, *Inorg. Chim. Acta* **1979**, *37*, L477–L479. – [6b] A. S. C. Chan, J. Halpern, *J. Am. Chem. Soc.* **1980**, *102*, 838–840. – [6c] J. Halpern, *Pure Appl. Chem.* **1983**, *55*, 99–196.

[7] [7a] J. M. Brown, P. A. Chaloner, *J. Chem. Soc., Chem. Commun.* **1980**, 344–346. – [7b] J. M. Brown, P. J. Maddox, *J. Chem. Soc., Chem. Commun.* **1987**, 1276–1278. – [7c] J. M. Brown, *Chem. Soc. Rev.* **1993**, *22*, 25–41. – [7d] J. A. Ramsden, T. D. W. Claridge, J. M. Brown, *J. Chem. Soc., Chem. Commun.* **1995**, 2469–2471.

[8] [8a] D. Mani, H.-T. Schacht, A. Powell, H. Vahrenkamp, *Organometallics* **1987**, *6*, 1360–1361. – [8b] D. Mani, H.-T. Schacht, A. K. Powell, H. Vahrenkamp, *Chem. Ber.* **1989**, *122*, 2245–2251.

[9] J. A. Wiles, S. H. Bergens, *J. Am. Chem. Soc.* **1997**, *119*, 2940–2941.

[10] A. J. Canty, G. K. Anderson, in *Comprehensive Organometallic Chemistry II* (Eds.: E. W. Abel, F. G. A. Stone, G. Wilkinson), Pergamon Press, **1995**, *9*, 225, 431.

[11] J. P. Birk, J. Halpern, A. L. Pickard, *J. Am. Chem. Soc.* **1968**, *90*, 4491−4492; A. R. Siedle, R. A. Newmark, W. B. Gleason, *J. Am. Chem. Soc.* **1986**, *108*, 767−773.
[12] B. A. Markies, A. J. Canty, W. de Graaf, J. Boersma, M. D. Janssen, M. P. Hogerheide, W. J. J. Smeets, A. L. Spek, G. van Koten, *J. Organomet. Chem.* **1994**, *482*, 191−199; P. K. Byers, A. J. Canty, *Organometallics* **1990**, *9*, 210−220.
[13] W. Henderson, R. D. W. Kemmitt, A. L. Davis, *J. Chem. Soc., Dalton Trans.* **1993**, 2247−2250.
[14] R. van Asselt, E. E. C. G. Gielens, R. E. Rülke, K. Vrieze, C. J. Elsevier, *J. Am. Chem. Soc.* **1994**, *116*, 977−985; J. G. P. Delis, P. G. Aubel, K. Vrieze, P. W. N. M. van Leeuwen, *Organometallics* **1997**, *16*, 2948−2957; R. E. Rülke, D. Kliphuis, C. J. Elsevier, J. Fraanje, K. Goubitz, P. W. N. M. van Leeuwen, K. Vrieze, *J. Chem. Soc., Chem. Commun.* **1994**, 1817−1819.
[15] P. K. Byers, A. J. Canty, B. W. Skelton, A. H. White, *J. Organomet. Chem.* **1987**, *336*, C55−C60; V. De Felice, V. G. Albano, C. Castellari, M. E. Cucciolito, A. De Renzi, *J. Organomet. Chem.* **1991**, *403*, 269−277; B. A. Markies, M. H. P. Rietveld, J. Boersma, A. L. Spek, G. van Koten, *J. Organomet. Chem.* **1992**, *424*, C12−C16.
[16] I. Zahn, K. Polborn, B. Wagner, W. Beck, *Chem. Ber.* **1991**, *124*, 1065−1073; A. G. Thayer, N. C. Payne, *Acta Crystallogr., Sect. C* **1986**, *42*, 1305−1310.
[17] Crystallographic data (excluding structure factors) for the structures reported in this paper have been deposited with the Cambridge Crystallographic Data Centre as supplementary publication no. CCDC-100822. Copies of the data can be obtained free of charge on application to CCDC, 12 Union Road, Cambrige CB2 1EZ, U.K. [Fax: (internat.) + 44 (0)1223 336033; e-mail: deposit@ccdc.cam.ac.uk].
[18] M. F. Rettig, P. M. Maitlis, *Inorg. Synth.* **1990**, *28*, 110−113.
[19] U. Nagel, *Chem. Ber.* **1982**, *115*, 1998−1999.

[97213]

Ylidylphosphanes and -diphosphanes

Florian Breitsameter[a], Alfred Schmidpeter*[a], and Annette Schier[b]

Institut für Anorganische Chemie, Ludwig-Maximilians-Universität[a]
Meiserstrasse 1, D-80333 München, Germany
Fax: +49 (0)89/5902-578
E-mail: alf@anorg.chemie.uni-muenchen.de

Anorganisch-chemisches Institut, Technische Universität München[b]
Lichtenbergstrasse 4, D-85747 Garching, Germany

Received September 29, 1997

Keywords: Phosphanes / Phosphorus ylides / Nucleophilic addition / Structure elucidation / NMR spectroscopy

Chlorophosphanyl and dichlorophosphanyl alkylidene- and benzylidenephosphoranes **6** and **8** are converted by reaction with $LiAlH_4$ to the respective phosphanes **7** and **9**. The former can be isolated, but decompose on heating or on protonation to give the ylidyl diphosphane **11** and the phosphonium ylide or phosphonium salt, respectively. The final products are the cyclooligophosphanes **15**–**17**. Only the *C-tert*-butyl derivative **7c** is stable in both regards. The conformation of the RPH group in **7** as compared to that of the RPCl group in **6** clearly reflects their different interaction with the ylide moiety.

The most notable feature of ylide-substituted halophosphanes **1** (X = Cl, Br) is the elongated P–X bond and the ease of dissociation of this bond[1][2][3].

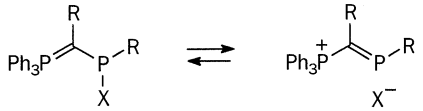

1

In these compounds, the electron-accepting halophosphane moiety matches the electron-donating ylide moiety. As a consequence, the system is stabilized and in particular the $C-P^{III}$ bond is strengthened. The exchange of the halogen for hydrogen will, in contrast result in a mismatch of the two moieties and consequently in labile P–C bonds. With the exception of **7e**[4] (see below), no primary or secondary phosphanes with an ylide substituent are known. Special examples of secondary ylidylphosphanes **4** with Ar = 2,4,6-$tBu_3C_6H_2$ are proposed as intermediates from the 2:1 reaction of triphenylphosphonium ylide **2** and the monochlorophosphane **3**. The final products of this reaction are triphenylphosphane and the phosphaalkenes **5** [mixtures of (*E*/*Z*) isomers][5].

We report here the synthesis of ylidylphosphanes by a Cl/H-substitution and on their thermal decomposition, which is different to the one described for **4**.

Synthesis of Ylidylphosphanes

By reaction with $LiAlH_4$ at −40°C in THF solution, the chlorophosphanyl benzylidenephosphoranes **6** are converted to the phosphanyl derivatives **7**, which are stable at room temperature and can be isolated as orange (R = alkyl) or yellow (R = Ph) crystals. The compounds are readily

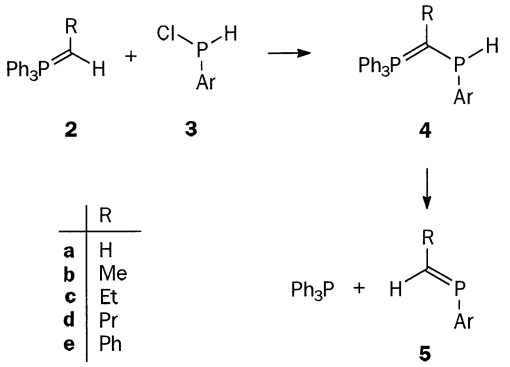

	R
a	H
b	Me
c	Et
d	Pr
e	Ph

soluble in THF and benzene but hardly soluble in pentane, and, except for **7c**, they are unstable in dichloromethane. This synthesis could not be extended, however, to examples with Me in place of Ph as the substituent at the ylidic carbon atom. In this case, from the analogous reaction, no ylidylphosphanes could be identified. A further example of type **7**, with two ylide substituents (**7e**, R = Ph_3PCPh) is formed as stable red crystals from the reaction of the bis(ylidyl)phosphenium chloride $(Ph_3PCPh)_2P^+Cl^-$ with $LiAlH_4$[4].

Under the same conditions, dichlorophosphanyl benzylidenephosphoranes **8a**, **b** and dichlorophosphanyl trimethylsilylmethylenephosphorane **8c** are converted by $LiAlH_4$ to the respective ylidylphosphanes **9**. They can be identified in solution at −40°C by their NMR spectra and can be observed for a short time at room temperature, but due to their thermal instability they cannot be isolated. In the reaction of **8c**, the bis(ylidyl)diphosphane **10c** is observed as a second, slightly more thermally-stable product.

Of particular interest among the ^{31}P-NMR data (Table 1) are the coupling constants $^2J_{PP}$ of the ylidylphosphanes

 © WILEY-VCH Verlag GmbH, D-69451 Weinheim, 1998 1434–1948/98/0303–0381 $ 17.50+.50/0

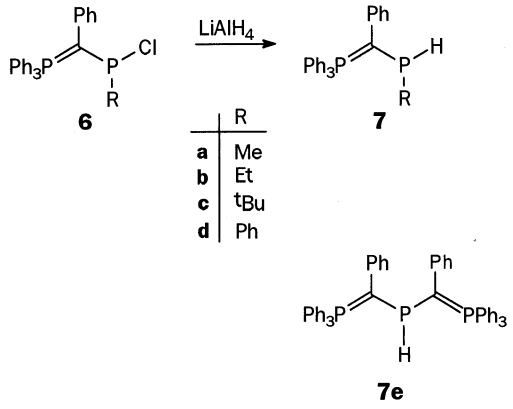

9 and **7**. They are considerably smaller than those of the dichlorophosphanes **8** (around 227 Hz) and the chlorophosphanes **6** (around 179 Hz). A value around 159 Hz as found for most compounds **9** and **7** still corresponds, however, to a synperiplanar orientation of the electron lone pair at P^{III} and the phosphonio group (as it is also observed in the crystal, see below). The much smaller constants of **9c** and **7e**, however, indicate that the antiperiplanar conformer has a large predominance in these cases.

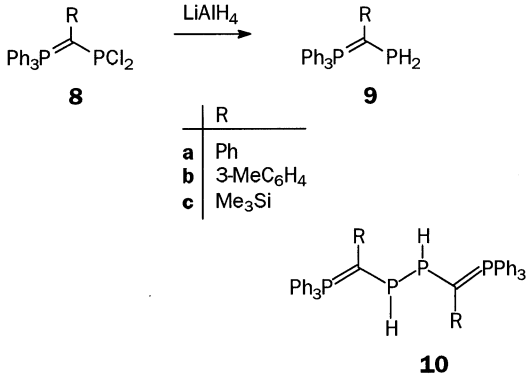

The ^{13}C-NMR spectra of compounds **7** as compared to those of compounds **6** reflect the Cl/H exchange by a high-field chemical shift of the ylidic carbon signal as well as by a slight increase in $^1J_{P(V)C}$ and a sharp decrease in $^1J_{P(III)C}$. These changes correspond well to a reduced electron transfer from the ylide to the P^{III} moiety.

Like other secondary phosphanes, the ylidylphosphane **7d** can be converted to the corresponding lithium phosphide by reaction with butyllithium in tetrahydrofuran.

Molecular Structures of Ylidylphosphanes

Crystals of **7a**·THF and **7d**·0.5 THF, suitable for X-ray structure analyses were obtained from THF solutions saturated at ambient temperature, to which pentane was added. The results of the structure determinations are shown in Figure 1 and Table 2. In both cases, the ylidic carbon atom C1 has a planar coordination sphere and the electron lone pair at P2 shows a roughly synperiplanar orientation with respect to the phosphonio center P1. This conformation has been found, in general, for ylidylphosphanes[1]. The bond lengths and angles of the two structures do not differ significantly and are in agreement with standard values.

For comparison, Table 2 also shows the structural data of the chlorophosphane **6a**. While the pyramidal P^{III}-coordination (sum of angles 302±1°) and the average of the two dihedral angles (130±2°) is essentially the same in all three cases, the conformation and the individual dihedral angles P1−C1−P2−C2 and P1−C1−P2−H/Cl in the hydrogen derivatives **7** are quite different from those in the chloro compound **6**. The angle P−C−P−Cl in **6** is, in fact, much smaller than the average, resulting in a near-ecliptic alignment of the P−Cl bond and the ylidic electron pair and allowing an effective charge transfer into the P−Cl bond. The corresponding dihedral angles P−C−P−H in **7** are, in contrast, larger than the average value and the P−H bond seems to avoid the described alignment. The dihedral angles are thus inversely ordered to the substituent's electronegativity Cl > C and C > H. The different charge transfer connected to the different conformation can also be monitored from the bond P2−C1 which is much shorter in the chloro derivative **6** than in the hydrogen derivatives **7**. Finally the

Table 1. ^{31}P-NMR data of ylidylphosphanes **9** and **7** (in THF) and the protonation products **19** (Cl^-) and **20** (BF_4^-) of **7c**, **d** (in CH_2Cl_2) as well as ^{13}C-NMR data of the ylidic carbon atom of **7** (in C_6D_6, coupling constants J in Hz)

	C−R	*P*−R	$\delta^{31}P^V$	$\delta^{31}P^{III}$	$^2J_{PP}$	$^1J_{PH}$	$d^{13}C$	$^1J(P^VC)$	$^1J(P^{III}C)$
9a	Ph	H	21.5	−133.4	159.6	194.8			
9b	3-MeC_6H_4	H	21.7	−133.0	159.6	194.1			
9c	$SiMe_3$	H	28.1	−129.0	91.5				
7a	Ph	Me	20.7	−88.0	160.9	203.5	26.6	115.2	22.9
7b	Ph	Et	20.9	−67.5	152.6	201.9	25.9	114.4	24.4
7c	Ph	*t*Bu	21.5	−33.2	154.9	207.1	27.7	111.0	31.3
7d	Ph	Ph	22.5	−51.8	167.7	219.1	26.2	114.5	19.2
7e	Ph	Ph_3PCPh	17.2	−55.8	87.4	236.6			
19c	Ph	*t*Bu	26.7	−19.9	24.9	203.0			
			26.2	−0.2	76.6	216.4			
19d	Ph	Ph	25.0	−47.4	42.5				
			24.9	−19.7	51.9				
20c	Ph	*t*Bu	26.8	−21.0	26.0	216.9			
			26.4	−1.3	76.8	222.9			
20d	Ph	Ph	24.7	−46.1	42.4				
			24.2	−22.0	58.8				

Figure 1. Molecular structures of **7a** (top) and **7d** (bottom) in the crystal (thermal ellipsoids with 50% probability). The hydrogen atoms, except the *P*-bonded one are omitted for clarity

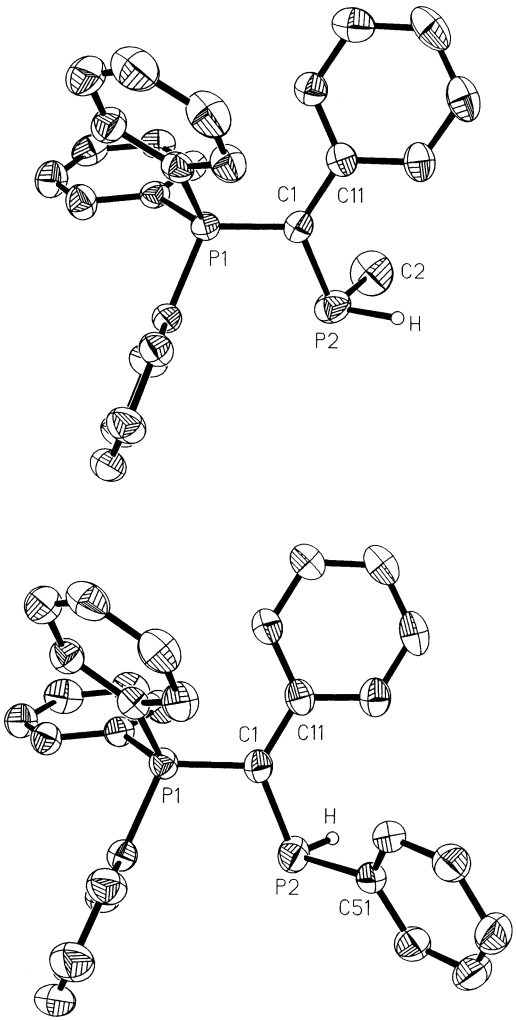

difference in bonding is also of significant influence on the P−C−P-angles.

Table 2. Relevant bond lengths [pm], bond and dihedral angles [°] of **7a** and **7d** and of **6a** for comparison

	6a	**7a**	**7d**
P1−C1	173.0(2)	171.2(3)	172.2(3)
C1−C11	149.8(2)	146.6(4)	146.6(4)
P2−C1	172.5(2)	178.6(3)	177.6(3)
P2−C2	183.6(2)	183.7(4)	183.5(3)[b]
P2−H	−	137(4)	116
P1−C1−C11	116.8(1)	120.4(2)	119.5(2)
P2−C1−C11	122.7(1)	123.5(2)	125.3(2)
P1−C1−P2	118.7(1)	115.2(2)	114.5(1)
C1−P2−C2	101.3(1)	103.9(2)	107.7(1)[b]
C1−P2−H	107.2(1)[a]	101(2)	101
C2−P2−H	92.2(1)[a]	96(2)	93[b]
P1−C1−P2−C2	163.8	121.8	126.5[b]
P1−C1−P2−H	100.8[a]	139.0	137.2

[a] Cl in place of H. − [b] C51 in place of C2.

Thermolysis of Ylidylphosphanes

If the ylidylphosphanes **7a**, **b**, **d** are heated in solution to 60 °C for several hours, they completely decompose to the ylide **2e** and a mixture of the cyclotri-, cyclotetra-, and cyclopentaphosphanes **15**, **16**, and **17**. The formation of this mixture seems to be kinetically determined and requires a pathway consistent with the formation of small cyclophosphanes off the thermodynamic equilibrium. Such a pathway is proposed in Scheme 1. If the heating is interrupted after a few minutes, besides unreacted ylidylphosphanes **7**, the ylidyldiphosphanes **11** can in fact be clearly identified by their ^{31}P-NMR spectra and, somewhat less clearly, also the ylidyltriphosphanes **12**.

Scheme 1

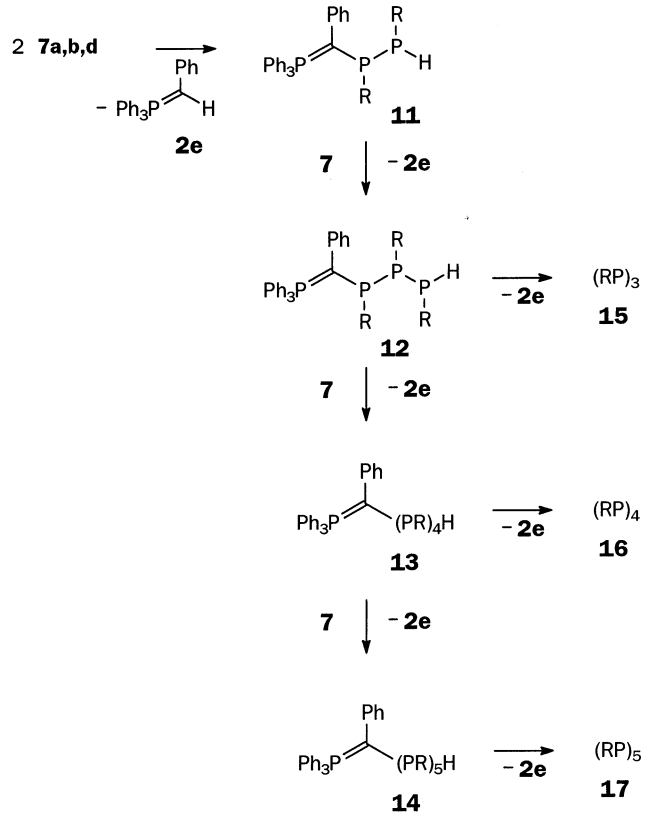

A condensation of the general type shown below, as it is observed here for the case of X = Ph_3PCPh (e.g. in the reaction 2 × **7** → **2e** + **11**) is unknown in the case of other organo substituents X, but is well known in case of amino substituents X[6] and phosphino substituents X. The latter reaction has been described as a disproportionation of a diphosphane[7]. All these reactions may be understood by a four-centred mechanism involving a proton transfer and a nucleophilic/electrophilic interaction of the two tervalent phosphorus atoms.

The bis(ylidyl)phosphane **7e** (R = Ph_3PCPh) also decomposes rapidly at 60 °C. As a primary product, the respective diphosphane **18e** can be detected in the ^{31}P-NMR spectrum. In addition, however, the primary ylidylphosphane **9a** and the bis(ylidyl)diphosphane **10a** are observed. As ylidyl-

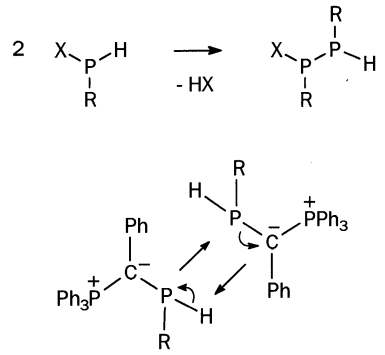

substituted cyclophosphanes seem not to be stable, the thermolysis finally yields a complex mixture which cannot be analyzed. If an equimolar mixture of **7e** and **7d** is heated, only the 1,2-bis(ylidyl)diphosphane **18d** is observed as product and not its 1,1-isomer. This suggests that the course of the reaction is determined by the proton transfer step; in the case under discussion the course is thus decided by the higher basicity of the ylidic carbon atoms of **7e** as compared to that of **7d**. In contrast to **7a**,**b**, and **d**, the *tert*-butyl derivative **7c** is thermally stable and remains unchanged in refluxing benzene for at least one week.

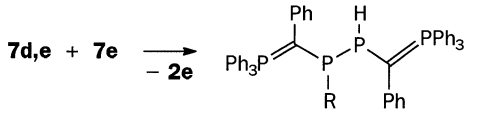

18d R = Ph
18e R = CPhPPh$_3$

Protonation and Alkylation of Ylidylphosphanes

Instead of warming, the formation of ylidyldiphosphanes from **7** can also be initiated by adding half an equivalent of HCl. From a 2:1 reaction of **7d** with HCl in ether, the benzylphosphonium chloride precipitates and the ylidyldiphosphane **11d** remains in solution. With more HCl added, the ylidyldiphosphane is converted to more phosphonium chloride and a mixture of cyclophosphanes. In addition, a minor amount of $PhPH_2$ is observed as a product of further reduction.

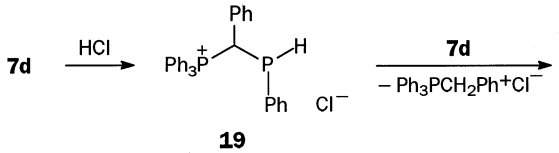

19

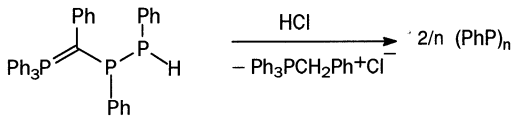

11d

The ylidyldiphosphane obviously results from the condensation of the primary product of protonation **17** with more ylidylphosphane **7d**. Consequently, the protonation of an ylidylphosphane **7** without a concomitant condensation can be achieved, if any temporary excess of **7** is avoided, i.e. if **7d** is added to HBF_4. In this way the phosphanyl benzylphosphonium tetrafluoroborate **20** precipitates from THF and is isolated as a mixture of two diastereomers. Followed with a second molecule of **7**, the cation of **20** enters the expected condensation and this way an access to mixed substituted ylidyldiphosphanes is provided. With **7b**, **c** the ylidyldiphosphanes **11f**, **g** are obtained. Their formation can be understood to result from a nucleophilic attack of the ylidylphosphane **7** on the cation of **20**.

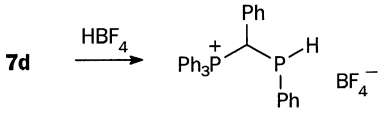

20

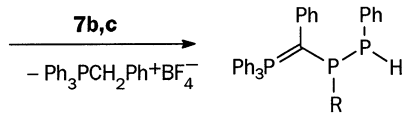

11f R = Et
11g R = ^{t}Bu

The *tert*-butylsubstituted ylidylphosphane **7c**, which resists the thermal condensation (see above), does not undergo an HCl-initiated condensation either. Its hydrochloride **19c** and hydrotetrafluoroborate **20c** therefore are stable even in presence of excess **7c**.

Methyl iodide alkylates **7d** at the phosphorus atom with a concomitant shift of the proton to the carbon atom to give the phosphonium iodide **21** which corresponds to the product **17** from the initial protonation step. With a chlorophosphane such as $MePCl_2$ **7d** reacts in a way analogous to HCl yielding the phosphonium chloride **22** and a mixture of phenyl cyclophosphanes.

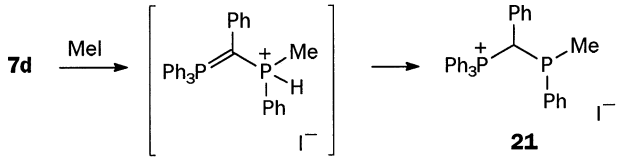

21

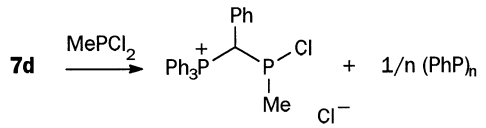

22

NMR Spectra of Ylidyl Di- and Triphosphanes

For most of the diphosphanes **10**, **11**, and **18**, two diastereomers are observed in the ^{31}P-NMR spectrum with slightly different coupling constants $^1J_{PP}$ (Table 3). For the phenyl derivative **11d**, this difference is quite large and allows a tentative assignment of the signals to the individual diastereomers. Due primarily to the steric interaction of the ylidyl substituent at the one phosphorus atom with the

phenyl substituent at the other phosphorus atom, the share of the *trans* conformation should be smaller for the (*R*,*R*)- than for the (*R*,*S*)-isomer and consequently $^1J_{PP}$ should be larger for the (*R*,*R*)- than for the (*R*,*S*)-isomer. In all cases a $^3J_{PP}$ coupling is observed for only one of the two diastereomers. In agreement with the phenyl derivative **11d**, this is assigned to the (*R*,*S*)-isomer for all the other derivatives too. For the ylidyltriphosphane **12b** all four diastereomers can be identified in the ^{31}P-NMR spectrum (Table 3).

The ylidylphosphane **7c** adds in a 2:1 ratio to platinum dichloride. The complex **25** contains the unchanged ligand in a *trans*-coordination and is formed as a roughly equimolar mixture of two diastereomers. Their ^{31}P-NMR data are almost identical and result, therefore, in overlapping spectra which could, however, be analyzed by calculation[8]. The coordination to platinum is demonstrated by the coordination shift from $\delta^{31}P^{III} = -33.2$ to 6.0, by the increase in P−H-coupling from $^1J_{PH} = 207.1$ to 379.0 Hz, and the decrease of P−P-coupling from $^2J_{PP} = 154.9$ to 14.5 and

Table 3. ^{31}P-NMR data of ylidyldiphosphanes **10**, **11,** and **18** and ylidyltriphosphanes **12** (in C_6H_6 or THF, coupling constants *J* in Hz)

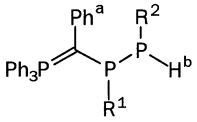

Fraction [%]		R^1	R^2		δ_A	δ_B	δ_C	δ_D	$^2J_{AB}$	$^3J_{AC}$	$^1J_{BC,\ BB'}$ $^3J_{BD}$		$^{1,2}J_{CD}$	$^1J_{PCH}$
10a		H	$CPhPPh_3$	AA′BB′	20.1[a]	−82.0	−							
10c[b]	74	H	$CSiMe_3$-PPh_3	AA′BB′	26.6	−70.0	−		114.1		−128.0			
	26			AA′BB′	25.6	−71.9	−		−					
11a	51	Me	Me	ABC	20.0	−44.8	−95.8		187.8	−	206.6			201.3
	49			ABC	20.8	−45.1	−89.8		187.8	11.7	199.5			183.1
11b	49	Et	Et	ABC	19.8	−30.1	−66.7		186.7	−	208.4			209.1
	51			ABC	20.8	−33.0	−65.2		185.4	11.4	222.5			202.3
11d	68	Ph	Ph	ABC	21.6	−13.9	−60.5		204.0	−	301.0			194.6
	32			ABC	22.5	−19.1	−52.4		208.9	9.6	223.4			203.5
711f	52	Et	Ph	ABC	20.5	−15.4	−60.5		186.9	−	222.1			
	48			ABC	21.1	−18.2	−49.1		187.9	7.8	251.2			
11g	57	*t*Bu	Ph	ABC	21.1	12.1	−64.0		200.3	−	253.3			
	43			ABC	22.0	6.6	−69.8		202.4	10.4	272.9			
18d		Ph	$CPhP^DPh_3$	ABCD	20.7	−27.6	−62.4	20.5	191.0	−	227.3		177.5	205.5
18e[c]		$CPhP^EPh_3$	$CPhPPh_3$	ABCDE	15.2	−36.7	−76.7	25.2	200.9	16.1	125.6		172.3	
12b	24	Et	P^DHEt[d]	ABCD		−26.6	−48.1	−79.5	187.8	5.3	200.7	80.4	241.2	
	18			ABCD		−21.2	−39.9	−80.7	187.8	5.9	218.9	70.4	209.5	
	22			ABCD		−15.9	−43.5	−83.4	187.8	4.7	228.9	29.1	194.3	
	36			ABCD		−16.4	−47.3	−78.2	185.8	2.4	195.4	65.7	216.6	

[a] Superimposed. − [b] For **10c** $SiMe_3$ in place of Ph. − [c] $\delta_E = 19.3$, $J_{BE} = 220.1$, $J_{CE} = 16.1$, $^1J_PE_H = 189.9$, $^2J_PE_H = 38.4$. − [d] For **12b** Et in place of H.

Adduct and Complex Formation of Ylidylphosphanes

As it is well known of other phosphanes, the ylidylphosphanes **7** also add to carbon disulfide. The adduct undergoes a proton shift to the ylidic carbon atom to give the betaine **23** which can be deprotonated, yielding the ylidylphosphanyl dithioformate **24**.

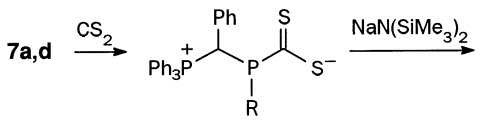

23a R = Me
23b R = Ph

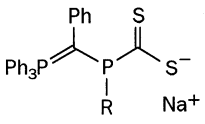

24

16.6 Hz as well as by the satellite signals originating from the ^{195}Pt-containing isotopomer with $^1J_{PtP} = 2331.4$ Hz. The coupling constant $^2J_{PP} = 513.6$ Hz between the coordinated phosphorus atoms of the two ligand molecules is characteristic of a *trans* coordination[9].

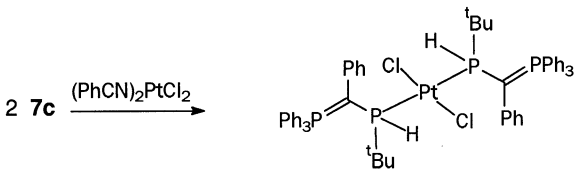

25

Complex formation in which an ylidylphosphane makes use not only of its phosphane site is exemplified by the complex of **7c** with the 16-electron fragment $CpMn(NO)CO^+$. Through an additional nucleophilic interaction of the ylidic carbon atom with the carbonyl group, a four-membered ring is formed in this case[10].

Experimental Section

All manipulations were carried out in flame-dried glassware under argon using Schlenk tube techniques. Dry dichloromethane and benzene were used as obtained (Fluka). Pentane was dried over molecular sieves (4 Å). Tetrahydrofuran was dried by refluxing with sodium/benzophenone and subsequent distillation. Melting points were determined in sealed capillaries. – NMR: JEOL GSX 270 (^{7}Li, ^{31}P), JEOL EX 400 (^{1}H, ^{13}C) with Me_4Si (int.), 85% H_3PO_4 (ext.), and aqueous LiCl (ext.) as standards. The aromatic hydrogen atoms in *ortho*, *meta*, and *para* positions of C-Ph are identified as 2-, 3-, 4-H, those of P^{III}-Ph as 6-, 7-, 8-H and those of Ph_3P as *o*-, *m*-, *p*-H. – The ylidyl chlorophosphanes **6**[2] and **8**[1] were prepared as described.

[α-(Methylphosphanyl)benzylidene]triphenylphosphorane (**7a**): To a stirred suspension of $LiAlH_4$ (0.76 g, 20.0 mmol) in 20 ml of THF, a solution of **6a** (8.65 g, 20.0 mmol) in 175 ml of THF was added dropwise at −40°C over 2 h. After cooling the grey suspension for an additional 6 h, it was warmed up to ambient temperature over 2 h. The precipitate was filtered off, and the orange filtrate was concentrated to 50% of its original volume. After standing at room temperature for 12 h, orange crystals were filtered off, washed with THF, and dried in vacuo. By concentration of the filtrate to about 20% of its original volume a second crop could be obtained. Yield 6.78 g (78%) of **7a**·0.5 THF, dec. > 60−63°C. – ^{1}H NMR (C_6D_6): δ = 1.35 (t, $^2J_{PH}$ = 6.0 Hz, $^3J_{HH}$ = 6.0 Hz, CH_3), 5.04 (ddq, $^1J_{PH}$ = 205.8 Hz, $^3J_{PH}$ = 24.3 Hz, $^3J_{HH}$ = 6.6 Hz, 1 H, P-H), 6.75 (tm, *J* = 7.3 Hz, *J* = 0.7 Hz, 1 H, 4-H), 6.93−7.09 (m, 11 H, arom. H), 7.42 (d, $^4J_{PH}$ = 7.9 Hz, 2 H, 2-H), 7.62−7.69 (m, 6 H, *o*-H). – ^{13}C{^{1}H} NMR (C_6D_6): δ = 8.6 (dd, $^1J_{PC}$ = 15.3 Hz, $^3J_{PC}$ = 3.8 Hz, CH_3), 26.6 (dd, $^1J_{PC}$ = 115.2, 22.9 Hz, C=PPh_3), 118.5 (s, 4-C), 126.7 (d, $^4J_{PC}$ = 10.7 Hz, 3-C), 128.5 (d, $^3J_{PC}$ = 11.4 Hz, *m*-C), 130.1 (dd, $^1J_{PC}$ = 86.2 Hz, $^3J_{PC}$ = 5.0 Hz, *i*-C), 131.4 (d, $^4J_{PC}$ = 3.1 Hz, *p*-C), 133.2 (d, $^3J_{PC}$ = 9.2 Hz, 2-C), 134.5 (dd, $^2J_{PC}$ = 9.2 Hz, $^4J_{PC}$ = 2.3 Hz, *o*-C), 145.5 (d, $^2J_{PC}$ = 11.5 Hz, 1-C). – $C_{26}H_{24}P_2 \cdot 1/2\ C_4H_8O$ (434.48): calcd. C 77.41, H 6.50; found C 77.12, H 6.35.

[α-(Ethylphosphanyl)benzylidene]triphenylphosphorane (**7b**): Prepared as described above from (0.53 g, 14.0 mmol) of $LiAlH_4$ and **6b** (6.19 g, 13.9 mmol). Yield 4.97 g (80%) of **7b**·0.5 THF, dec. > 66°C. – ^{1}H NMR (C_6D_6): δ = 1.06 (dt, $^3J_{PH}$ = 17.1 Hz, $^3J_{HH}$ = 7.8 Hz, 3 H, CH_3), 1.42 (m, 2 H, THF), 1.78−1.96 (m, 2 H, CH_2), 3.56 (m, 2 H, THF), 4.91 (dddd, $^1J_{PH}$ = 204.6 Hz, $^3J_{PH}$ = 20.0 Hz, $^3J_{HH}$ = 7.8, $^3J_{HH}$ = 3.4 Hz, 1 H, P-H), 6.72 (tt, *J* = 7.3 Hz, *J* = 1.0 Hz, 1 H, 4-H), 6.95−7.07 (m, 11 H, arom. H), 7.42 (d, $^4J_{PH}$ = 8.3 Hz, 2 H, 2-H), 7.63−7.69 (m, 6 H, *o*-H). – ^{13}C{^{1}H} NMR (C_6D_6): δ = 11.8 (d, $^2J_{PC}$ = 16.8 Hz, CH_3), 16.7 (dd, $^1J_{PC}$ = 10.6 Hz, $^3J_{PC}$ = 3.0 Hz, CH_2), 25.8 (s, THF), 25.9 (dd, $^1J_{PC}$ = 114.4 HZ, $^1J_{PC}$ = 24.4 Hz, C=PPh_3), 67.8 (s, THF), 118.5 (s, 4-C), 126.6 (d, $^4J_{PC}$ = 10.2 Hz, 3-C), 128.5 (d, $^3J_{PC}$ = 10.7 Hz, *m*-C), 130.1 (dd, $^1J_{PC}$ = 87.0 Hz, $^3J_{PC}$ = 6.1 Hz, *i*-C), 131.4 (s, *p*-C), 133.2 (d, $^3J_{PC}$ = 10.7 Hz, 2-C), 134.6 (d, $^2J_{PC}$ = 9.2 Hz, *o*-C), 146.0 (d, $^2J_{PC}$ = 10.7 Hz, 1-C). – $C_{27}H_{26}P_2.1/2\ C_4H_8O$ (448.50): calcd. C 77.66, H 6.74; found C 76.84, H 7.07.

[α-(tert-Butylphosphanyl)benzylidene]triphenylphosphorane (**7c**): Prepared as described above from (0.84 g, 22.1 mmol) of $LiAlH_4$ and **6c** (10.56 g, 22.2 mmol). Yield 6.53 g (67%) of **7c**, m.p. 124−126°C. – ^{1}H NMR (C_6D_6): δ = 1.53 (d, $^3J_{PH}$ = 12.5 Hz, CH_3), 5.27 (dd, $^1J_{PH}$ = 210.7 Hz, $^3J_{PH}$ = 25.6 Hz, P-H), 7.01 (t, *J* = 7.1 Hz, 1 H, 4-H), 7.26−7.37 (m, 11 H, arom. H), 7.85 (d, $^4J_{PH}$ = 8.6 Hz, 2 H, 2-H), 7.95−8.01 (m, 6 H, *o*-H). – ^{13}C{^{1}H} NMR (C_6D_6): δ = 27.7 (dd, $^1J_{PC}$ = 111.0 Hz, $^1J_{PC}$ = 31.3 Hz, C=PPh_3), 30.9 (d, $^2J_{PC}$ = 15.6 Hz, CH_3), 32.6 [dd, $^1J_{PC}$ = 15.6 Hz, $^3J_{PC}$ = 4.2 Hz, C-$(CH_3)_3$], 119.3 (s, 4-C), 127.6 (s, 3-C), 128.4 (d, $^3J_{PC}$ = 11.8 Hz, *m*-C), 130.4 (dd, $^1J_{PC}$ = 85.8 Hz, $^3J_{PC}$ = 4.6 Hz, *i*-C), 131.4 (d, $^4J_{PC}$ = 3.1 Hz, *p*-C), 134.1 (d, $^3J_{PC}$ = 19.8 Hz, 2-C), 134.8 (dd, $^2J_{PC}$ = 8.8 Hz, $^4J_{PC}$ = 1.9 Hz, *o*-C), 146.4 (dd, $^2J_{PC}$ = 11.1, 1.1 Hz, 1-C). – $C_{29}H_{30}P_2$ (440.50): calcd. C 79.07, H 6.86; found C 78.40, H 6.99.

[α-(Phenylphosphanyl)benzylidene]triphenylphosphorane (**7d**): Prepared as described above from (0.82 g, 21.6 mmol) of $LiAlH_4$ and **6d** (10.75 g, 21.7 mmol). Yield 9.53 g (89%) of **7d**·0.5 THF, dec. > 84°C. – ^{1}H NMR (C_6D_6): δ = 1.42 (m, 2 H, THF), 3.56 (m, 2 H, THF), 5.86 (dd, $^1J_{PH}$ = 220.6 Hz, $^3J_{PH}$ = 21.4 Hz, P-H), 6.69 (tt, *J* = 7.3 Hz, *J* = 1.0 Hz, 1 H, 4-H), 6.91−7.21 (m, 14 H, arom. H), 7.45 (d, $^3J_{PH}$ = 8.1 Hz, 2 H, 2-H), 7.68−7.74 (m, 8 H, *o*-H/6-H). – ^{13}C{^{1}H} NMR (C_6D_6): δ = 25.6 (s, THF), 26.2 (dd, $^1J_{PC}$ = 114.5 Hz, $^1J_{PC}$ = 19.2 Hz, C=PPh_3), 67.6 (s, THF), 118.4 (s, 4-C), 125.8 (d, $^4J_{PC}$ = 11.5 Hz, 3-C), 126.0 (s, 8-C), 127.8 (C_6D_6), 128.1 (superimposed, *i*-C), 128.2 (d, superimposed, 7-C), 128.4 (d, $^3J_{PC}$ = 11.5 Hz, *m*-C), 129.8 (d, $^2J_{PC}$ = 15.4 Hz, 6-C), 131.4 (d, $^4J_{PC}$ = 3.1 Hz, *p*-C), 132.2 (d, $^3J_{PC}$ = 10.0 Hz, 2-C), 134.3 (dd, $^2J_{PC}$ = 9.2 Hz, $^4J_{PC}$ = 1.5 Hz, *o*-C), 143.9 (dd, $^1J_{PC}$ = 20.0 Hz, $^3J_{PC}$ = 6.9 Hz, 5-C), 146.2 (d, $^2J_{PC}$ = 12.3 Hz, 1-C). – $C_{31}H_{26}P_2 \cdot 1/2\ C_4H_8O$ (496.55): calcd, C 79.82, H 6.09; found C 79.57, H 5.57.

[α-(Phosphanyl)benzylidene]triphenylphosphorane (**9a**): To a stirred suspension of $LiAlH_4$ (0.73 g, 19.2 mmol) in 20 ml of THF, a solution of **8a** (3.47 g, 7.7 mmol) in 20 ml of THF was added dropwise at −40°C over 30 min. The brown suspension was stirred for an additional 30 min. The precipitate was filtered off, and the orange filtrate was concentrated to 50% of its original volume. Compound **9a** is stable in solution below −40°C.

[(3-Methylphenyl)phosphanylmethylidene]triphenylphosphorane (**9b**): Prepared as described above from (112 mg, 2.9 mmol) of $LiAlH_4$ and **8b** (0.55 g, 1.2 mmol). **9b** is stable in solution below −40°C.

[(3-Methylphenyl)phosphanylmethylidene]triphenylphosphorane (**9c**): Prepared as described above from $LiAlH_4$ (0.12 mg, 3.2 mmol) and **8c** (0.71 g, 3.2 mmol). Compound **10c** is observed as a by-product. After standing at ambient temperature for 10 h, **9c** and **10c** can no longer be detected by ^{31}P NMR.

Deprotonation of **7d**: In an NMR tube, **7d** (105 mg, 0.2 mmol) was dissolved in 0.5 ml of THF. A 1.56 mol/l solution of *n*BuLi (0.13 ml, 0.2 mmol) in hexane was added. After 10 min, a ^{31}P-NMR spectrum of the deep red solution was recorded at room temp. ^{31}P{^{1}H} NMR (THF, hexane): AB (40%), δ_A = 21.6 δ_B = −54.9 (broad, superimposed), J_{AB} = 57.1 Hz, AB (21%), δ_A = 20.8, δ_B = −54.9 (broad, superimposed), J_{AB} = 57.6 Hz, δ = 8.6 (s, 7%), 4.5 (s, 11%), −6.5 (d, *J* = 187.9.5 Hz, 5%), −32.7 (d, *J* = 188.4 Hz, 4%). In the ^{1}H-coupled ^{31}P-NMR spectrum no $^1J_{PH}$ could be detected. – ^{7}Li{^{1}H} NMR (THF, hexane): δ = 2.3 (s).

Thermolysis of Ylidylphosphanes **7a**, **b**, **d**, **e**: In an NMR tube a solution of **7a**, **b**, **d**, **e** (0.3 mmol) in 0.05 ml of THF was warmed to 60°C for 120 seconds. After 5 min a ^{31}P-NMR spectrum of the red (**7d** orange) solution was recorded at room temp. (For results see text and Table 3). Further heating of **7a**, **b**, **d** to 60°C for an additional 5 h yielded a mixture of the cyclophosphanes **15**, **16**, and **17** and the ylide **2e**. A solution of **7c** in C_6H_6 remains unchanged after refluxing for 7 d.

Cothermolysis of **7d** *and* **7e**: In an NMR tube, a solution of **7d** (91 mg, 0.2 mmol) and **7e** (146 mg, 0.2 mmol) in 0.7 ml of THF was warmed at 60°C for 240 seconds. After 5 min, a ^{31}P-NMR

spectrum of the red solution showed a mixture of **2e**, **18d**, and starting materials.

Ylidyl Diphosphane **11d**: To a stirred solution of **7d** (3.75 g, 7.6 mmol) in 60 ml of THF, a solution of 1.0 mol/l HCl (3.78 ml, 3.8 mmol) in diethyl ether and 20 ml of THF was added dropwise at 0°C over 30 min. The white precipitate of $Ph_3P-CH_2Ph^+Cl^-$ was filtered off, and 80 ml of pentane was added to the yellow solution. After cooling to −20°C for 12 h, the yellow precipitate was filtered off, washed twice with THF/pentane (1:1) and dried in vacuo. The ^{31}P NMR of the precipitate showed the signals for **11d** and for small residues of **7d**.

Reaction of **7d** *with HCl:* To a fresh solution of **7d** (210 mg, 04 mmol) in 5 ml of dichloromethane 1.0 mol/l HCl (0.47 ml, 0.5 mmol) in diethyl ether was added. After 5 min, a ^{31}P-NMR spectrum was recorded. It showed the signals of **19d**, $Ph_3P-CH_2Ph^+Cl^-$, **16d**, **17d**, and $PhPH_2$.

Preparation of **20d**: A solution of **7d** (2.10 g, 4.2 mmol) in 20 ml of THF was added dropwise to a solution of 54% HBF_4 (0.82 ml, 4.2 mmol) in diethyl ether and 8 ml of THF at −60°C over 10 min. After additional stirring for 10 min, the white precipitate was filtered off, washed twice with pentane and dried in vacuo. Yield: 2.09 g (91%) of **20d** (2 diastereomers), m.p. 162−165°C. − ^1H NMR ($CDCl_3$): δ = 4.41 (ddd, $^1J_{PH}$ = 222.9 Hz, $^3J_{PH}$ = 8.8 Hz, $^3J_{HH}$ = 7.8 Hz, PH), 4.89 (ddd, $^1J_{PH}$ = 216.9 Hz, $^3J_{HH}$ = 5.0 Hz, J = 1.2 Hz, PH), 4.98 (dd, $^2J_{PH}$ = 17.3 Hz, $^3J_{HH}$ = 7.7 Hz, CH), 5.42 (dd, $^2J_{PH}$ = 14.5 Hz, $^3J_{HH}$ = 4.9 Hz, CH), 6.69−7.74 (m, 50 H, arom. H). − $C_{31}H_{27}BP_2F_4$ (548.31): calcd. C 67.91, H 4.96; found C 67.38, H 4.82.

Reaction of **7c** *with HCl:* In an NMR tube, 1.0 mol/l HCl (0.25 ml, 0.3 mmol) in diethyl ether was added to a solution of **7c** (213 mg, 0.5 mmol) in 0.5 ml of THF. After 30 min, a ^{31}P-NMR spectrum was recorded and showed signals of equal amounts for **7c** and **20c**.

Ylidyldiphosphane **11f**: In an NMR tube, **20d** (158 mg, 0.3 mmol) and **7b** (126 mg, 0.3 mmol) were suspended in 0.5 ml of THF. After 10 min, a ^{31}P-NMR spectrum was recorded and showed the signals for **11f**, **3d**, $Ph_3P-CH_2Ph^+Cl^-$, and **2e**.

Ylidyldiphosphane **11g**: As described above from **20d** (103 mg, 0.2 mmol) and **7c** (81 mg, 0.2 mmol). A ^{31}P NMR showed the signals for **7c**, **11g**, and **20c**.

Reaction of **7d** *with MeI:* To a stirred solution of **7d** (0.16 g, 0.3 mmol) in 7 ml of THF, a solution of MeI (0.02 ml, 0.4 mmol) in 5 ml of THF was added dropwise. After 1 h, a white precipitate had formed. $^{31}P\{^1H\}$ NMR (THF, CH_2Cl_2): **7d**, AB (**21**), δ_A = 21.2, δ_B = 13.7, J_{AB} = 59.9 Hz, $(PhP)_3$.

Reaction of **7d** *with* $MePCl_2$*:* As described earlier from **7d** (0.20 g, 0.4 mmol) and methyldichlorophosphane (0.039 ml, 0.4 mmol). 5 ml of dichloromethane were added to the suspension to yield a colourless solution. $^{31}P\{^1H\}$ NMR (THF, CH_2Cl_2): AB (**22**), δ_A = 97.6, δ_B = 24.9, J_{AB} = 62.2 Hz, **16d**, **17d**.

Reaction of **7a** *with* CS_2*:* To a stirred suspension of **7a** (1.48 g, 3.4 mmol) in 25 ml of THF, a solution of carbon disulfide (0.21 ml, 3.5 mmol) in 10 ml of THF was added at 0°C over 15 min. After 10 min the pale red precipitate was filtered off, washed twice with THF/pentane (1:1) and dried in vacuo. − $^{31}P\{^1H\}$ NMR (CH_2Cl_2): AB (**23a**), δ_A = 25.1, δ_B = 13.4, J_{AB} = 89.3 Hz, δ = 23.6 (s). In an NMR tube, 110 mg of the precipitate and $NaN(SiMe_3)_2$ (45 mg) were dissolved in 0.5 ml of THF, to yield a red solution. − $^{31}P\{^1H\}$ NMR (THF): AB (**24**), δ_A = 28.9, δ_B = 19.1, J_{AB} = 191.0 Hz, δ = 8.4 (s).

Reaction of **7d** *with* CS_2*:* As described above from **7d** (0.90 g, 1.8 mmol) and carbon disulfide (0.11 ml, 1.8 mmol). − $^{31}P\{^1H\}$ NMR (CH_2Cl_2): AB (**23b**), δ_A = 25.7, δ_B = 18.2, J_{AB} = 98.1 Hz, δ = 23.1 (s). The product was recrystallized from dichloromethane/pentane (2:1). − ^1H NMR ($CDCl_3$): δ = 5.32 (m, broad, 1 H, CH), 6.69−6.91 (m, 4 H, arom. H), 6.96 (t, J = 7.81 Hz, arom. H), 7.21−7.50 (m, 9 H, arom. H, *m*-H), 7.57−7.74 (m, 10 H, arom. H, *o*-H). − $^{13}C\{^1H\}$-NMR ($CDCl_3$): δ = 47.8 (dd, $^1J_{PC}$ = 54.2 Hz, 50.4 Hz, CH).

PtCl₂ Complex of **7c**: In an NMR tube, $PtCl_2(PhCN)_2$ (53 mg, 0.1 mmol) was added to a solution of **7c** (104 mg, 0.2 mmol) in 0.5 ml of THF. After 30 min, a ^{31}P-NMR spectrum of the yellow solution was recorded. − $^{31}P\{^1H\}$ NMR (THF): AB (**7c**, 57%), $[AB]_2$ (**25**, diastereomer I, 16%), $[AB]_2X$ (**25**, X = Pt, 7%), δ_A = 18.8, δ_B = 6.0 (superimposed), $^2J_{AB}$ = 16.6 Hz, $^1J_{BX}$ = 2331.4 Hz, $[AB]_2$ (**25**, diastereomer II, 10%), $[AB]_2X$ (**25**, X = Pt, 5%), δ_A = 18.6, δ_B = 6.0 (superimposed), $^2J_{AB}$ = 14.5 Hz, $^1J_{BX}$ = 2331.4 Hz.

Crystal Structure Determinations: Specimens of suitable quality and size were mounted in glass capillaries and used for measurements of precise cell constants and intensity data collection on an Enraf Nonius CAD4 diffractometer [Mo-K_α radiation, λ(Mo-K_α) = 0.71073 Å]. During data collection, three standard reflections were measured periodically as a general check of crystal and instrument stability. No significant changes were observed for either compound. Lp correction was applied, but intensity data were not corrected for absorption effects. The structures were solved by direct methods (SHELXS-86) and completed by full-ma-

Table 4 Crystallographic data and details of data collection and structure refinement of compounds **7a**, **d**

	7a·THF	**7d**·0.5 THF
Crystal data		
Formula	$C_{30}H_{32}OP_2$	$C_{33}H_{30}O_{0.5}P_2$
M_r	470.54	496.51
Crystal system	monoclinic	monoclinic
Space group	$P2_1/c$	$P2_1/n$
Crystal dimensions [mm]	0.4 × 0.45 × 0.45	0.15 × 0.45 × 0.45
a [Å]	9.057(1)	9.969(1)
b [Å]	14.423(2)	14.426(1)
c [Å]	19.788(2)	19.040(1)
β	94.34(1)	104.10(1)
V [Å^3]	2577.6(6)	2655.7(4)
r [g cm^{-3}]	1.212	1.242
Z	4	4
F (000) [e]	1000	1048
μ (Mo-K_α) [cm^{-1}]	1.83	1.86
Data collection		
T [°C]	− 62	− 68
Scan Mode	Θ-Θ	ω
h, k, l range	0/10, 0/17, −23/23	0/11, 0/17, −23/22
$\sin(\theta/\lambda)_{max}$ [Å^{-1}]	0.59	0.62
Measured refl.	4848	4754
Unique refl.	3989	4495
Observed refl.	4629	4489
Refinement		
Refined parameters	329	314
H atoms (found/calcd.)	1/23	1/29
$R1$[a]	0.0513	0.0492
$wR2$[b]	0.0652	0.1217
(shift/error)$_{max}$	<0.001	<0.001
ρ_{fin} (max/min) [eÅ^{-3}]	0.30/−0.26	0.93/−0.33

[a] $R1 = \Sigma(||F_o| - |F_c||)/\Sigma|F_o|$. − [b] $wR2 = \{[\Sigma w(F_o^2 - F_c^2)^2]/\Sigma[w(F_o^2)^2]\}^{1/2}$; $w = 1[\sigma^2(F_o^2) + (ap)^2 + bp]$; $p = (F_o^2 + 2F_c^2)/3$; a = 0.0592 (**7a**·THF), 0.0627 (**7d**·0.5 THF); b = 2.91 (**7a**·THF), 2.02 (**7d**·0.5 THF).

trix-least squares techniques against F^2 (SHELXL-93). The thermal motion of all non-hydrogen atoms was treated anisotropically, except for those of the solvent THF molecules, which were disordered in both compounds. C−*H* atoms were placed in idealized calculated positions and allowed to ride on their corresponding carbon atoms with fixed isotropic contributions ($U_{iso(fix)} = 1.5 \times U_{eq}$ of the attached C atom). The P−*H* atoms were found and included with isotropic (**7a**·THF) and fixed isotropic contributions (**7d**·0.5 THF, $U_{iso(fix)} = 0.08$ Å^2). Further information on crystal data, data collection and structure refinement are summarized in Table 4. Important interatomic distances and angles are shown in Table 2. Anisotropic thermal parameters, tables of distances and angles, and atomic coordinates have been deposited with Fachinformationszentrum Karlsruhe, Gesellschaft für wissenschaftlich-technische Information mbH, D-76344 Eggenstein-Leopoldshafen. The data are available on request on quoting CSD-407613 (**7a**·THF), -407614 (**7d**·0.5 THF).

[1] A. Schmidpeter, H. Nöth, G. Jochem, H.-P. Schrödel, K. Karaghiosoff, *Chem. Ber.* **1995**, *128*, 379−393.
[2] G. Jochem, F. Breitsameter, A. Schier, A. Schmidpeter, *Heteroatom Chem.* **1996**, *7*, 239−247.
[3] A. Schmidpeter, G. Jochem, C. Klinger, C. Robl, H. Nöth, *J. Organomet. Chem.* **1997**, *529*, 87−102.
[4] G. Jochem, A. Schmidpeter, H. Nöth, *Z. Naturforsch. B* **1996**, *51*, 267−276.
[5] G. Märkl, W. Bauer, *Angew. Chem.* **1989**, *101*, 1698−1699; *Angew. Chem. Int. Ed. Engl.* **1989**, *28*, 1695−1696.
[6] E. Niecke, W. Güth, M. Lysek, *Z. Naturforsch. B* **1985**, *40*, 331−334.
[7] M. Baudler, B. Carlsohn, D. Koch, P.K. Medda, *Chem. Ber.* **1978**, *111*, 1210−1216.
[8] DAVINX: D.S. Stephenson, in *Encyclopedia of Nuclear Magnetic Resonance* (Eds. D.M. Grant, R.K. Harris), Wiley, Chichester **1995**.
[9] *cis*- and *trans*-$PtCl_2(PMe_2H)_2$: $^2J_{PP} = 0$ and 515 Hz, respectively: J.G. Verkade, *Coord. Chem. Rev.* **1972/1973**, *9*, 1−106.
[10] I.-P. Lorenz, J. Geicke, unpublished; Dissertation J. Geicke, Universität München **1997**, 71−73.

[97220]

Specific Chelate Tuning of the Substitution Kinetics of Platinum(II) Complexes in Aqueous Solution

Ulrich Fekl and Rudi van Eldik*

Institute for Inorganic Chemistry, University of Erlangen-Nürnberg,
Egerlandstr. 1, D-91058 Erlangen, Germany
Fax: (internat.) +49(0)9131/857387
E-mail: vaneldik@anorganik.chemie.uni-erlangen.de

Received October 2, 1997

Keywords: Substitution mechanism / Platinum / Pressure dependence / Kinetics / Dinuclear complex

Both reaction steps observed for the substitution of water by thiourea in the complexes $[Pt(en)(OH_2)_2]^{2+}$ and $[Pt(phen)(OH_2)_2]^{2+}$ (en = ethylenediamine, phen = 1,10-phenanthroline) were investigated under pseudo-first-order conditions using the stopped-flow technique. The substitution of the second water molecule in each complex was also studied under high pressure. The observed pseudo-first-order rate constants k_{obs} (s^{-1}) obeyed the equation $k^{1,2}{}_{obs} = k^{1,2}[tu]$ (tu = thiourea), where "1" and "2" refer to the first and the second substitution reactions, respectively. Kinetic parameters associated with the substitution process are: $k^1{}_{en}$ (25.0°C, pH = 3.0, I = 0.1 M) = 25.6 M^{-1} s^{-1}, $\Delta H^{\#}$ = 51 kJ mol^{-1}, $\Delta S^{\#}$ = −48 J K^{-1} mol^{-1}; $k^2{}_{en}$ (same conditions) = 12.1 M^{-1} s^{-1}, $\Delta H^{\#}$ = 30 kJ mol^{-1}, $\Delta S^{\#}$ = −124 J K^{-1} mol^{-1}, $\Delta V^{\#}$ = −7 cm^3 mol^{-1}; $k^1{}_{phen}$ (25.0°C, pH = 1.0, I = 0.1 M) = 2900 M^{-1} s^{-1}, $\Delta H^{\#}$ = 41 kJ mol^{-1}, $\Delta S^{\#}$ = −41 J K^{-1} mol^{-1}; $k^2{}_{phen}$ (same conditions) = 1170 M^{-1} s^{-1}, $\Delta H^{\#}$ = 37 kJ mol^{-1}, $\Delta S^{\#}$ = −61 J K^{-1} mol^{-1}, $\Delta V^{\#}$ = −5 cm^3 mol^{-1}. The temperature and pressure dependence of all the processes studied suggest an associative substitution mechanism. The hydroxo-bridged dinuclear complex $[\{Pt(phen)(\mu\text{-}OH)\}_2]^{2+}$ is formed from $[Pt(phen)(OH_2)_2]^{2+}$ in aqueous solution unless the solution is very dilute and highly acidic. The X-ray structure of $[\{Pt(phen)(\mu\text{-}OH)\}_2](F_3CSO_3)_2 \cdot 2\ H_2O$ was determined. It belongs to the triclinic space group $P\bar{1}$ and has one formula unit in the unit cell. The unit cell dimensions are a = 7.126(5), b = 9.665(5), c = 12.774(7) Å; α = 71.85(5) , β = 85.52(5), γ = 73.12(5) deg; V = 799.9(8) $Å^3$. The structure was solved with the Patterson method and refined to R = 0.061. A square planar coordination of the platinum centers is observed, with no deviations from planarity but distortions due to the small bite angle of phen and the four-membered ring. No significant lengthening of the Pt−O bond [mean value: 2.03(1) Å] is observed in comparison with $[\{Pt(NH_3)_2(\mu\text{-}OH)\}_2]^{2+}$.

Introduction

The substitution kinetics of d^8 transition metal complexes are both of fundamental[1][2][3][4][5] and practical importance, the latter stemming from applications in catalysis[6][7] and cancer chemotherapy[8][9][10][11][12]. In particular the influence of spectator ligands has found considerable attention. For example, a recent study showed that the rate of DMSO-exchange on *cis*-$[Pt('N_2')(CH_3)(DMSO)]^+$ ($'N_2'$ = *N,N*-chelating ligand) can vary by ten orders of magnitude depending on the nature of the non-leaving $'N_2'$ spectator group[13]. The more labile complexes of platinum and palladium often contain electron-withdrawing groups such as phenanthroline, bipyridine or terpyridine[13][14][15][16][17].

We are mainly interested in complexes which offer two labile substitution sites and two non-leaving N-donors in the *cis*-position, since similar systems are used in tumor therapy. Complexes of the structure *cis*-$[Pt^{II}am_2x_2]$ (am = am(m)ine, x = leaving group) have been investigated systematically since the discovery by Rosenberg, that *cis*-$[Pt(NH_3)_2Cl_2]$ (Cisplatin) exhibits anti-tumor activity[18]. Since then, Cisplatin has been very succesfully used against testicular cancer and with good results against ovarian tumors, cancer of the head, neck, and bladder. Unfortunately, the anti-tumor activity of Cisplatin and structurally related compounds does not extend to the most common tumors like lung tumors or adenotumors of the gastrointestinal tract[10]. Promising results were recently obtained with platinum complexes containing α-diimine ligands instead of amine ligands[19][20][21][22]. This prompted us to investigate the substitution behaviour of complexes with two *cis*-bound labile ligands and an electron-withdrawing non-leaving α-diimine group in aqueous solution.

In the present study we have chosen to investigate the substitution of water by thiourea, a strong nucleophile, in $[Pt(phen)(OH_2)_2]^{2+}$. For comparison, we have investigated the corresponding reactions with $[Pt(en)(OH_2)_2]^{2+}$. The complex $[Pt(phen)(OH_2)_2]^{2+}$ was generated by cleaving the hydroxo-bridged dimer $[\{Pt(phen)(\mu\text{-}OH)\}_2]^{2+}$ with perchloric acid. X-ray structural data for the dimer were obtained.

Results and Discussion

Structure of $[\{Pt(phen)(\mu\text{-}OH)\}_2](F_3CSO_3)_2 \cdot 2\ H_2O$

An ORTEP view of the molecular structure of $[\{Pt(phen)(\mu\text{-}OH)\}_2](F_3CSO_3)_2 \cdot 2\ H_2O$ together with the atom numbering scheme of the most important unique atoms is shown in Figure 1, whereas the crystallographic

 © WILEY-VCH Verlag GmbH, D-69451 Weinheim, 1998 1434−1948/98/0303−0389 $ 17.50+.50/0

data are summarized in Table 1 and the relevant intramolecular distances and angles in Table 2. Some intermolecular distances and angles are also shown in Table 2, which suggest that the structure is stabilized by the water molecule of crystallization. The latter apparently forms hydrogen bonds to both the oxygen atoms of the $F_3CSO_3^-$ ion and the hydrogen atom of the μ-hydroxo groups. There is a crystallographic center of inversion between the two platinum atoms. The $N_2PtO_2PtN_2$ moiety is planar, and deviations from the best plane calculated through the eight atoms are within the error limits. The mean deviation from the best plane is smaller than 0.01 Å. The phen ligand is nearly planar, but slightly twisted. A torsion of 7.2° N(1)−C(12)−C(11)−N(2) is found. The chelate ligand forces a bite angle N(1)−Pt−N(2) of 81.3(4)°. The geometric features of the phen ligand are in good agreement with values reported in the literature for other phen containing complexes of platinum or palladium[23][24][25]. Pt−O distances of 2.02(1) and 2.03(1) Å are found together with Pt−N distances of 1.99(1) and 2.01(1) Å. It is noteworthy, that the Pt−O distances are within the experimental error limits the same as found in the cations[26][27][28] $[\{Pt(NH_3)_2(\mu\text{-}OH)\}_2]^{2+}$ and $[\{Pt(N,N\text{-dimethylethylenediamine})(\mu\text{-}OH)\}_2]^{2+}$. Since the phen ligand causes an increase (with respect to the amine derivative) in the rate of substitution of the *trans* ligands by a factor of 10^2 (see below), it is quite remarkable, that this enhanced reactivity is not mirrored in the Pt−O bond distance of the dimer. A strong kinetic *trans*-effect without a corresponding static *trans*-influence is an effect caused by π-acceptor ligands[29]. This clearly shows that the increase in lability in this case does not result from bond weakening to the leaving group. Therefore, the structural data support the interpretation of the kinetic data in terms of an associatively activated substitution mechanism (see below).

Figure 1. View of $[\{Pt(phen)(\mu\text{-}OH)\}_2](F_3CSO_3)_2 \cdot 2\ H_2O$ showing the atomic numbering scheme. For clarity's sake only one counterion and water molecule are shown. The thermal ellipsoids are 50% equiprobability envelopes, with hydrogens as spheres of arbitrary diameter.

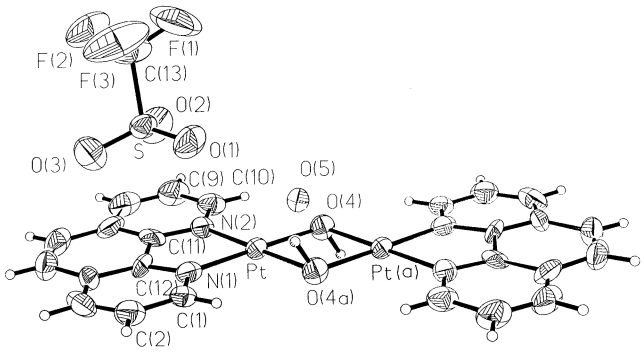

Reaction of $[Pt(en)(OH_2)_2]^{2+}$ with Thiourea

The reaction of $[Pt(en)(OH_2)_2]^{2+}$ with thiourea (tu) was studied at a pH of 3.0 in order to prevent formation of hydroxo-bridged oligomers (see above). Preliminary studies were performed by ^{1}H-NMR. A 0.1 M solution of $[Pt(en)(OD_2)_2]^{2+}$ (300 μl) was prepared and reacted in an NMR tube with 200 μl of 0.4 M tu. DNO_3 was used to preadjust the pH* to 3.00. Before mixing, the signal of $[Pt(en)(OD_2)_2]^{2+}$ (singlett at δ = 2.51 with satellites, $^3J_{H\text{-}Pt}$ = 24 Hz) was observed, while after mixing a signal due to $[Pt(en)tu_2]^{2+}$ δ = 2.83 ($^3J_{H\text{-}Pt}$ = 24 Hz) was seen. After 48 h a product indicative of a very slow reaction was observed: the appearence of a signal due to uncoordinated en (δ = 3.06, no satellites) was accompanied by an increase in pH* to 8.1. These observations point to a substitution of en by tu, which is thought to be due to the strong *trans*-effect of the already coordinated tu. The initial substitution of water by tu, however, was too fast to be measured by NMR and was therefore followed by UV-Vis spectroscopy. Two reactions were observed in accord with reactions (1) and (2).

A clear separation of two reaction rates which differ only by a small factor (approximately 2 in the present case, as

Table 1. Crystallographic data[62] for $[\{Pt(phen)(\mu\text{-}OH)\}_2](F_3CSO_3)_2 \cdot 2\ H_2O$

formula	$C_{26}H_{18}N_4O_8F_6S_2Pt_2 \cdot 2\ H_2O$
fw	1118.0
cryst. dimensions [mm]	0.6 × 0.18 × 0.05
cryst. system	triclinic
space group	$P\bar{1}$
a [Å]	7.126(5)
b [Å]	9.665(7)
c [Å]	12.774(5)
α [deg]	71.85(5)
β [deg]	85.52(5)
γ [deg]	73.12(5)
V [Å^3]	799.9(8)
Z	1
T [K]	293(2)
d_{calc} [g cm^{-3}]	2.321
μ [mm^{-1}]	8.95
Index ranges	$-8 \le h \le 8$, $-11 \le k \le 11$, $-14 \le l \le 14$
F(000)	508.0
θ range [deg]	$2.99 \le \theta \le 23.97$
radiation (Mo-K_α) [Å]	0.71069 (graphite monochromator)
R_1[a] (all data)	0.061
wR_2[b] (all data)	0.141
GooF[c]	1.356

[a] $R_1 = \Sigma(\|F_0| - |F_c\|)/\Sigma(|F_0|)$. − [b] $wR_2 = [\Sigma w(F_0^2 - F_c^2)^2/\Sigma(wF_0^2)^2]^{1/2}$; $w = 1/[\sigma^2(F_0^2) + (aP)^2 + bP]$; $P = (\max(F_0^2) + 2F_c^2)/3$; − [c] $GooF = [\Sigma[w(F_0^2 - F_c^2)^2]/(n-p)]^{1/2}$; n = number of reflexes measured; p = number of parameters used.

Table 2. Selected distances [Å] and angles [deg] for $[\{Pt(phen)(\mu\text{-}OH)\}_2](F_3CSO_3)_2 \cdot 2\ H_2O$

Pt−N(1)	1.986(10)	O(5)−O(1)	2.87(1)
Pt−N(2)	2.007(10)	O(5)−O(4a)[a]	2.66(1)
Pt−O(4)	2.024(9)	O(4)−Pt−O(4a)[a]	81.0(4)
Pt−O(4a)[a]	2.032(8)	N(1)−Pt−N(2)	81.3(4)
Pt−Pt(a)[a]	3.0837(14)	Pt−O(4)−Pt(a)[a]	99.0(4)
N(1)−C(1)	1.329(14)	O(1)−O(5)−O(3*)[b]	118(1)
N(1)−C(12)	1.364(14)	Pt−O(4)−H(11)	103(1)
N(2)−C(10)	1.32(2)	Pt−N(1)−C(12)	114.2(7)
N(2)−C(11)	1.34(2)	Pt−N(2)−C(11)	112.8(8)
C(11)−C(12)	1.43 (2)	N(1)−C(12)−C(11)	113(1)
O(5)−O(3*)[b]	2.86(1)	(2)−C(11)−C(12)	118(1)

[a] Coordinates for atoms labelled 'a': $1-x$, $1-y$, $1-z$. − [b] Coordinates of O(3*) are obtained from the coordinates of O(3) by the symmetry operations: $2-x$, $-y$, $1-z$.

$$[Pt(en)(OH_2)_2]^{2+} + tu \xrightarrow{k_1} [Pt(en)tu(OH_2)]^{2+} + H_2O \quad (1)$$

$$[Pt(en)tu(OH_2)]^{2+} + tu \xrightarrow{k_2} [Pt(en)(tu)_2]^{2+} + H_2O \quad (2)$$

will be shown below) by UV-Vis spectroscopy depends on the changes in absorbance associated with the two reactions. A favourable situation is the case where the absorbance change for the first reaction is much smaller than the absorbance change for the second reaction. This enables the observation of a typical induction curve, from which both rates can be obtained with a rather low error. A series of measurements at different wavelengths demonstrated that the reaction can be followed at 276 nm, where this condition is best fulfilled. It can be seen from the spectra shown in Figure 2, that the absorbance change for the second substitution step at 276 nm is more than five times larger than the absorbance change for the first substitution step. Under these conditions an induction behaviour is observed (Figure 3). The observed time trace was fitted to a two exponential model. The fitted curve is shown in the lower part of Figure 3, whereas the deviation from the fit (residuals) is indicated in the upper part of Figure 3. The two exponential model is confirmed by the fact that the residuals are statistically scattered. A linear dependence of the observed rate constants on the tu concentration was found (Figure 4). The absence of an intercept suggests that both steps are irreversible in nature.

The two observed reactions were assigned to the substitution steps (1) and (2) by pre-mixing the complex solution with sub-stoichiometric amounts of thiourea. The absorbance change associated with the fast reaction decreases to a much larger extent than the absorbance change associated with the slower reaction with increasing amount of pre-added thiourea, which provides evidence that the first reaction is the faster one. The temperature dependence results in the activation parameters quoted in Table 3.

The effect of high pressure on the reaction could not be followed at 276 nm due to the absorption properties of the pressure medium employed (*n*-heptane). Therefore the absorbance change at 330 nm was used, which, however, did not allow the evaluation of the first substitution step, since the absorbance changes for the two steps are too similar (see Figure 2) to allow separation. Following the arguments outlined for the very similar spectral situation of the Pt(phen) system below, the second (slower) reaction can be followed at 330 nm. For this step (Figure 5) the dependence of ln(k) on the applied pressure was linear within the experimental error limits. From this dependence an activation volume of -7.1 ± 0.9 cm^{3}mol^{-1} was obtained. These activation parameters are in accord with those generally observed for associative substitution reactions of d^8 complexes[4][30]. The more negative entropy of activation for the second step might be due to the steric hindrance caused by the thiourea ligand already coordinated during the first step. The $\Delta H^{\#}$ values are discussed below.

Figure 2. UV-Vis spectra of the reactants, intermediate and product for the two-step substitution reaction obtained using a 0.88 cm tandem cuvette. Conditions: [Complex] = 0.1 mM, pH = 3.0, I = 0.1 M, T = 25°C. The spectrum of $[Pt(en)(OH_2)tu]^{2+}$ was obtained from an equilibrated solution containing a fourfold platinum excess over thiourea and was corrected for the excess platinum background. The spectrum of an equimolar amount of uncoordinated tu was then added arithmetically in order to show the overall absorbance change observed for the formation of the 1:1 complex.

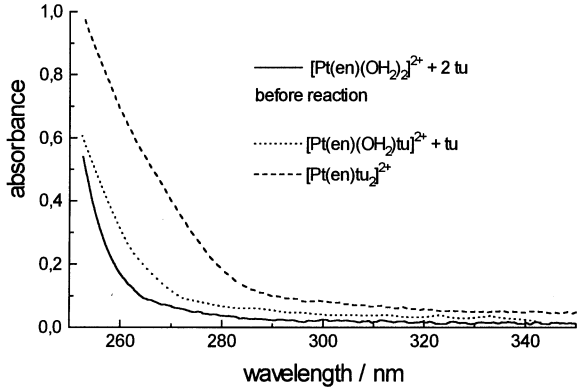

Figure 3. Fit of two exponentials and residuals (upper part) for the reaction of $[Pt(en)(OH_2)_2]^{2+}$ (0.1 mM) with thiourea (5 mM) followed at 276 nm. pH = 3.0, I = 0.1 M ($NaClO_4$), T = 25.0°C.

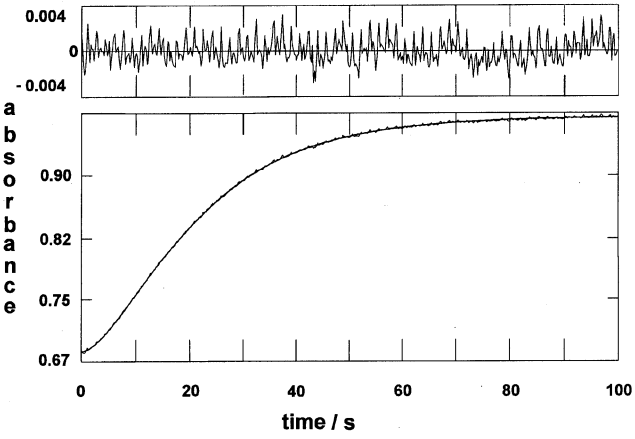

The Equilibrium Between $[Pt(phen)(OH_2)_2]^{2+}$ and $[\{Pt(phen)(\mu\text{-}OH)\}_2]^{2+}$

During the investigation of the hydrolysis behaviour of Cisplatin the property of complexes of the type $[Pt('N_2')(OH_2)_2]^{2+}$ ('N_2' = am(m)ine$_2$ or bidentate amine) to form dimeric[26][27][28][31], trimeric[32][33][34] and (rarely) tetrameric[35] species of the general formula $[\{Pt('N_2')(\mu\text{-}OH)\}_n]^{n+}$ was discovered. In dilute solutions the higher oligomers are not formed, but dimeric species must be taken into account in the appropriate pH range. Preparation of the monomeric diaqua complexes is possible at a pH of 2 or 3. Attempts to synthesize the diaqua complex in the case where 'N_2' is an aromatic α-diimine, the central atom being platinum or palladium, has led to studies[36][37][38][39] that were criticized later by Wimmer and Castan[31][40], who showed that under the selected conditions reported for synthesis and reaction, the dimeric species is the main species present in solution. In the present study attempts were made to apply the synthetic route for the preparation of

Figure 4. Reaction of $[Pt(en)(OH_2)_2]^{2+}$ (0.1 mM) with thiourea; k_{obs} as a function of thiourea concentration, followed at 276 nm. pH = 3.0, I = 0.1 M ($NaClO_4$), T = 25.0°C.

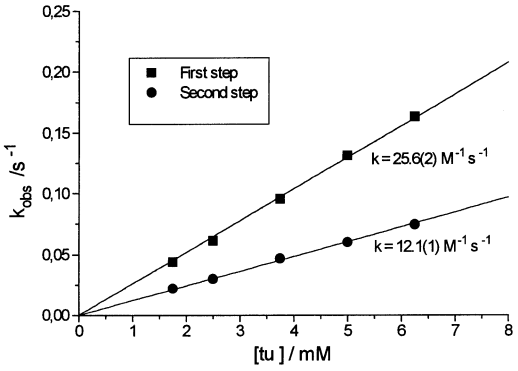

Table 3. Temperature dependence and activation parameters for the first (k_1) and second (k_2) step in the irreversible substitution of water by thiourea (6.25 mM) in $[Pt(en)(OH_2)_2]^{2+}$ (0.1 mM) at pH = 3.0, I = 0.1 M, reaction followed at λ = 276 nm

T /°C	k_1 / M^{-1} s^{-1}	k_2 / M^{-1} s^{-1}
10.0	10.1 ± 0.5	6.0 ± 0.1
15.0	12.2 ± 1.3	7.7 ± 0.6
20.0	19.8 ± 1.6	9.1 ± 0.5
25.0	26.1 ± 1.6	11.8 ± 0.2
30.0	38.2 ± 3.2	14.8 ± 0.2
35.0	62.2 ± 4.3	18.2 ± 0.5
activation parameter	1st step	2nd step
$\Delta H^{\#}$ / kJ mol^{-1}	50.6 ± 3.5	29.9 ± 0.9
$\Delta S^{\#}$ / J K^{-1} mol^{-1}	−48 ± 12	−124 ± 3

Figure 5. Determination of the volume of activation for the substitution of the remaining water molecule in $[Pt(en)(OH_2)tu]^{2+}$ by thiourea. This is done by plotting the logarithm of the ratio k/k_0 (where k and k_0 denote the rate constant for elevated and ambient pressure, respectively) according to: $\delta(\ln k)/\delta p = -\Delta V^{\#}/RT$. The measured values are shown together with the linear regression results; $\Delta V^{\#} = -7.1 \pm 0.9$ cm^3 mol^{-1}. Experimental conditions: [Pt] = 0.8 mM, [tu] = 25 mM, pH = 3.0, I = 0.1 M, T = 25.0°C, reaction followed at 330 nm.

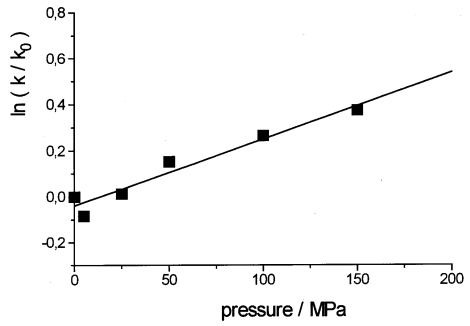

$[Pt('N_2')(OH_2)_2]^{2+}$ to the phen complex. Even at pH 2, the formation of a precipitate was observed, which was yellow or orange red, depending on whether silver trifluormethanesulfonate or silver perchlorate was used. UV-Vis spectroscopy, IR spectroscopy and elemental analysis showed this to be identical with the dimer reported in the literature[31][40]. During our investigations we found that the dimer does react with strong nucleophiles, which is in accord with the well known reactivity of analogous halo-bridged dimers[41][42][43]. Its reaction with thiourea is currently being investigated in more detail. In contrast to the behaviour observed for terminal hydroxo ligands bound to platinum or palladium[44][45][46], which cannot easily be substituted, bridging hydroxo-groups are relatively labile, which could be responsible for the high and unspecific toxicity[47][48][49] of these compounds. Preliminary studies on the reactivity of $[\{Pt(phen)(\mu\text{-}OH)\}_2]^{2+}$ with thiourea, however, have shown that the dimeric complex reacts ca. 100 times slower than the monomeric one. This allowed us to distinguish between the reactions of the dimer and the monomer species and conditions suitable for complete cleavage of the dimer were found (see next section).

Reaction of $[Pt(phen)(OH_2)_2]^{2+}$ with Thiourea

The cleavage of the hydroxo-bridged dimer to give the monomeric diaquacomplex is complete following hydrolyses of a 0.05 mM (with respect to platinum) solution of the dimer in 0.1 M perchloric acid for 40 min at 100°C. The reaction of $[Pt(phen)(OH_2)_2]^{2+}$ with thiourea had to be studied at very low thiourea concentrations, since the separation of both substitution steps was only possible at a wavelength of 260 nm, where the reactant and the intermediate (1:1 complex) have almost identical absorptivities which lead to the favourable observation of an induction curve. The observation at 260 nm is made impossible by the absorption of thiourea itself (broad and intense band with a maximum at 238 nm), if a concentration higher than 0.5 mM is used. First the reaction of 2.5×10^{-5} M $[Pt(phen)(OH_2)_2]^{2+}$ with 0.5 mM thiourea was followed over a spectral range from 250 to 370 nm for 10 s and a Global Analysis evaluation was performed. This revealed that two first-order reactions occurred and gave preliminary k_{obs} values of 1.3 s^{-1} and 0.6 s^{-1}. The residuals of the fit were smaller than 2% of the absorbance change and statistically scattered. The spectra of $[Pt(phen)(OH_2)_2]^{2+}$, $[Pt(phen)(OH_2)tu]^{2+}$ (calculated using the Global Analysis software) and $[Pt(phen)(tu)_2]^{2+}$ are shown in Figure 6. The spectral changes do not show very characteristic features, since the bands observed are due to intraligand π-π^* transitions of the phen ligand. These are known to show a relatively weak dependence on the nature of the coordination sphere of the metal centre[31][40][50]. The aim of the Global Analysis treatment was to confirm the two-step mechanism and to provide a spectrum of the intermediate 1:1-complex. For the determination of the exact rate constants the kinetics were followed at a single wavelength, 260 nm, using complex concentrations of 2.5×10^{-5} and 1.0×10^{-5} M for the temperature and concentration dependence, respectively. Each k_{obs} value reported is the mean value of at least five measurements. From the concentration dependence (Figure 7) bimolecular rate constants of 2900±40 M^{-1} s^{-1} and 1170±10 M^{-1} s^{-1} were obtained. The assignment of the two reactions was done by pre-mixing (see above), showing that also in this case the first reaction step is the faster one. Activation parameters are derived from the temperature de-

pendence and summarized in Table 4. In the case of the $[Pt(phen)(OH_2)_2]^{2+}$ complex the $\Delta H^{\#}$ values for the first and the second substitution step do not differ significantly. The fact that the second reaction is slower seems to be completely due to the more negative entropy of activation, resulting from steric hindrance due to the thiourea molecule already coordinated. This contrasts with the observations for the $[Pt(en)(OH_2)_2]^{2+}$ complex, where an even more negative $\Delta S^{\#}$ for the second step in comparison to the first one is accompanied by a decrease in $\Delta H^{\#}$ by 20 kJ mol^{-1} (Table 3). We believe that this anomaly of the en complex is caused by hydrogen bonding of the amine protons to thiourea in the transition state. It could be argued, that the fact that we observe the second step to be slower by a factor of roughly two (at room temperature) for the en- as well as for the phen-system is due to a statistical factor in the sense that the first entering tu can substitute two water positions, whereas the second one only one. This probability consideration would be valid for a dissociative mechanism, where the probability of dissociation is proportional to the number of coordinated water molecules. It would not be valid for the case of a limiting associative mechanism, where the bond to the leaving group is not weakened during formation of a five-coordinate intermediate. The nucleophilic attack governs the rate and will not be influenced by the number of possible leaving groups. For an interchange mechanism, where bond-making and bond-breaking take place simultaneously, certainly a statistical factor will contribute, which however will be difficult to estimate. In the present system all observations point to a mechanism which is associative in nature: thus either a limiting associative (A) or an associative interchange (I_a) mechanism.

It is generally accepted that the determination of the volume of activation can elucidate the nature of the intimate mechanism. If no charge is neutralized or created during the reaction, a significantly negative volume of activation points to an associative (A) or associatve interchange (I_a) mechanism. For the system under investigation, the pressure dependence of the reaction could not be followed at 260 nm because of the absorption of the pressure medium (*n*-heptane). This made the simultaneous observation of both steps under high pressure impossible. However, the observation of the second step was possible due to the spectral properties of the species involved and the ratio of the reaction rates. This effect is described in the literature[51]. For a biphasic first-order process, the absorption changes in the following way as function of time (R, I, and P denoting reactant, intermediate and product, respectively):

$$Abs = d[R]_0\{e^{-k_1 t}\left(\varepsilon_R + \frac{e^{-k_1 t}}{e^{-k_2 t}-e^{-k_1 t}}\varepsilon_I - \frac{e^{-k_2 t}}{e^{-k_2 t}-e^{-k_1 t}}\varepsilon_P\right) + \varepsilon_P + e^{-k_2 t}\left(-\frac{e^{-k_1 t}}{e^{-k_2 t}-e^{-k_1 t}}\varepsilon_I + \frac{e^{-k_1 t}}{e^{-k_2 t}-e^{-k_1 t}}\varepsilon_P\right)\} \quad (3)$$

For the system under investigation, it was found experimentally that $k_1 \approx 5/2\ k_2$. Insertion of $k_1 \approx 5/2\ k_2$ into equation (3) leads to a monophasic time-dependence of the absorbance $Abs_{(t)}$, if $\varepsilon_I - \varepsilon_R \approx 2/3\ (\varepsilon_P - \varepsilon_I)$.

This condition is fulfilled at 350 nm (compare Figure 6), such that the second reaction step can be followed at this wavelength under the assumption that the ratio k_1/k_2 remains approximately constant. This assumption was confirmed by the fact that even under high pressure, single exponential kinetics were always observed at this wavelength. From the pressure dependence of the rate constants (Figure 8) a volume of activation of -5.0 ± 0.8 cm^3/mol was calculated. This confirms the assignment of an associative or associative interchange mechanism. The activation volumes found in the present study compare well with available data on the substitution of water by uncharged sulfur donor nucleophiles in related complexes (Table 5).

Figure 6. UV-Vis spectra of reactant, intermediate (calculated using Global Analysis) and product. pH = 1.0, I = 0.1M, T = 25.0°C, [Pt] = 0.025 mM. Background absorption of thiourea (0.5 mM) was subtracted.

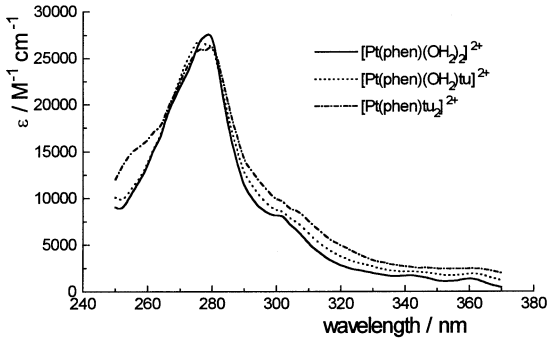

Figure 7. Reaction of $[Pt(phen)(OH_2)_2]^{2+}$ (0.01 mM) with thiourea; k_{obs} as a function of thiourea concentration . pH = 1.0, I = 0.1 M, T = 25.0°C. The reaction was followed at 260 nm.

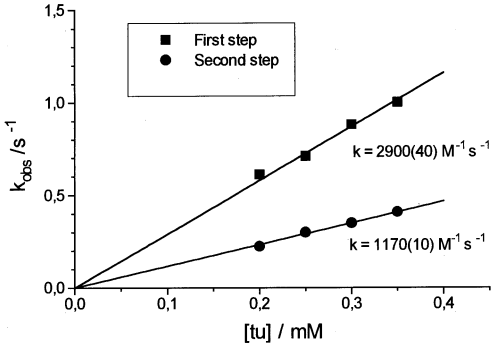

Table 4. Temperature dependence for the first (k_1) and second (k_2) step in the irreversible substitution of water by thiourea (0.5 mM) in $[Pt(phen)(OH_2)_2]^{2+}$ (0.025 mM) at pH = 1.0, I = 0.1 M. The reaction was followed at 260 nm (isosbestic for the first step)

T /°C	k_1 / M^{-1} s^{-1}	k_2 / M^{-1} s^{-1}
15.0	1500 ± 40	686 ± 10
25.0	2560 ± 160	1240 ± 20
35.0	4540 ± 80	2040 ± 20
45.0	8400 ± 200	3300 ± 40
activation parameter	1st step	2nd step
$\Delta H^{\#}$ / kJ mol^{-1}	41 ± 2	37.3 ± 0.7
$\Delta S^{\#}$ / J K^{-1} mol^{-1}	−41 ± 6	−61 ± 2

Figure 8. Determination of the volume of activation for the substitution of the remaining water molecule in $[Pt(phen)(OH_2)tu]^{2+}$ by thiourea (compare Figure 5). $\Delta V^{\#} = -5.0 \pm 0.8$ cm^{3}mol^{-1}). Experimental conditions: [Pt] = 0.1 mM, [tu] = 2.0 mM, pH = 1.0, I = 0.1 M, T = 25.0°C, reaction followed at 350 nm.

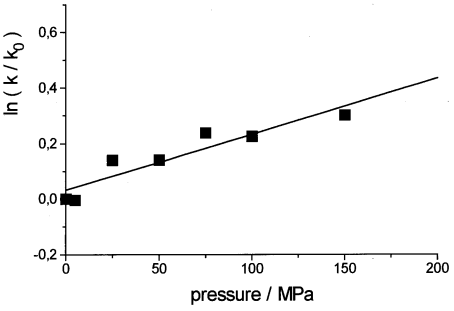

Table 5. Summary of rate constants (298.1 K) and $\Delta V^{\#}$ data for the substitution of H_2O by uncharged sulfur donor nucleophiles in Pt^{II} and Pd^{II} complexes

complex	nucleophile	k / M^{-1} s^{-1}	$\Delta V^{\#}$/ cm^3 mol^{-1}	ref.
$[Pd(Me_5dien)(OH_2)]^{2+}$	$SC(NH_2)_2$	1583 ± 46	−9.4 ± 0.4	[a]
	$SC(NHMe)_2$	718 ± 28	−9.1 ± 0.6	[a]
	$SC(NMe_2)_2$	195 ± 5	−13.4 ± 0.7	[a]
$[Pd(Et_5dien)(OH_2)]^{2+}$	$SC(NH_2)_2$	1.12 ± 0.04	−8.4 ± 0.3	[a]
	$SC(NHMe)_2$	0.54 ± 0.01	−10.2 ± 0.6	[a]
	$SC(NMe_2)_2$	0.117 ± 0.002	−12.7 ± 0.6	[a]
$[Pt(OH_2)_4]^{2+}$	$SC(NH_2)_2$	13.9		[b]
	Me_2S	0.90 ± 0.02	−15.3 ± 0.4	[b]
	Et_2S	0.48 ± 0.02	−17.0 ±0.3	[b]
$[Pt(en)(OH_2)_2]^{2+}$	$SC(NH_2)_2$	25.6 ± 0.2		[c]
$[Pt(en)(OH_2)tu]^{2+}$	$SC(NH_2)_2$	12.1 ± 0.1	−7.1 ± 0.9	[c]
$[Pt(phen)(OH_2)_2]^{2+}$	$SC(NH_2)_2$	2900 ± 40		[c]
$[Pt(phen)(OH_2)tu]^{2+}$	$SC(NH_2)_2$	1170 ± 10	−5.0 ± 0.8	[c]

[a] Ref.[57] — [b] Ref.[58] — [c] This work.

Conclusion

We conclude that the results of this study have shown that the use of phenanthroline instead of ethylenediamine increases the substitution rates of diaqua complexes by a factor of 10^2, during which the associative way of substitution is retained. This effect was investigated in aqueous media for a platinum complex exhibiting two labile positions. As far as we know, we are the first to have generated the complex $[Pt(phen)(OH_2)_2]^{2+}$ (and not the dimer) in solution and have investigated its reactivity. The observations are in good agreement with earlier studies on monophasic substitution reactions by sulfur-containing nucleophiles performed in non-aqueous media on complexes of Pt or Pd bearing aliphatic amines and aromatic imines by way of comparison. A factor of approximately 10^2 (the factors range between 41 and 64) was found in the latter studies[14][16]. The factor of 2×10^4 reported by Romeo et al.[13] for DMSO exchange on the complexes $[Pt(phen)Me(DMSO)]^+$ and $[Pt(en)Me(DMSO)]^+$, obviously calls for a further explanation beyond the electron-withdrawing effect of phen alone. The electronic effects of the *cis* Pt−C bond and of the *trans* phen ligand seem to act cooperatively.

As far as possible anti-tumor activity is concerned, it seems a reasonable assumption, that platinum complexes of α-diimines exhibiting two labile positions can bind to DNA in a fashion similar to the well-established binding mode of Cisplatin[52][53], using both substitution sites for the covalent binding of purine bases. The enhanced reactivity for both substitution steps is a feature which adds to the unique properties of such ligands as DNA intercalators[54][55][56].

The authors gratefully acknowledge financial support from the *Deutsche Forschungsgemeinschaft* and *Fonds der Chemischen Industrie*. They also wish to acknowledge the work of Dr. *Günter Liehr*, who solved the X-ray structure.

Experimental Section

Materials: All chemicals were used as received. $[Pt(phen)Cl_2]$ and AgF_3CSO_3 were purchased from Aldrich in the highest quality available. Thiourea and $HClO_4$ were p.a. quality from Merck. $NaClO_4$ was p.a. quality from Fluka. Non-aqueous solvents were purchased from Roth in p.a. quality (ROTIPURAN®). Ultra pure water was used for the kinetic measurements.

Syntheses

$[Pt(en)Cl_2]$ and $[Pt(en)(OH_2)_2]^{2+}$: The $[Pt(en)Cl_2]$ complex was prepared in 76% yield using a procedure from the literature[59]. Calc. for $[Pt(en)Cl_2]$: C 7.37, H 2.47, N 8.59%; found: C 7.19, H 2.41, N 8.37%. The IR spectrum was in excellent agreement with that reported in the literature[60]. A stock solution of the diaqua complex was prepared according to literature methods[61] by treating the dichloro complex with $AgNO_3$ in acidic solution, followed by filtration of the AgCl precipitate. A MILLIPORE filter (0.2 μm) was used for this purpose.

$[\{Pt(phen)(\mu\text{-}OH)\}_2](F_3CSO_3)_2 \cdot 2\ H_2O$: The title complex was prepared in the following way: 335 mg of $[Pt(phen)Cl_2]$ (0.75 mmol) was stirred together with 580 mg of AgF_3CSO_3 (2.25 mmol) in 50 ml of EtOH/H_2O (9:1) at 75°C in the dark for 4 h. The fine bright yellow precipitate, which formed was filtered off with a MILLIPORE-filter (0.2 μm). The product was extracted from the wet precipitate by stirring in 100 ml of an acetone/H_2O mixture (1:1) at 50°C. AgCl was removed from this suspension by filtering the yellow solution with a MILLIPORE-filter (0.2 μm). On cooling to room temperature, yellow crystals (ca. 0.5 mm in diameter) formed within 24 h. These were washed with H_2O, EtOH, and Et_2O and dried under vacuum for 2 h. Yield: 200 mg (48%). The experimental analysis was in excellent agreement with the theoretically expected values for the dihydrate. Calc. for $[\{Pt(phen)(\mu\text{-}OH)\}_2](F_3CSO_3)_2 \cdot 2\ H_2O$: C 27.91, H 1.98, N 5.01%; found: C 28.05, H 1.88, N 4.94%. − ^{1}H-NMR ([D$_7$]DMF, 300.13 MHz, assignment based on coupling pattern and constants): δ = 9.05 [d, 4 H, $^3J_{H\text{-}H}$ = 8.1 Hz, aromat. CH *para* to N]; 9.00 [d, 4 H, $^3J_{H\text{-}H}$ = 5.3 Hz, aromat. CH *ortho* to N]; 8.27 [dd, 4 H, $^3J_{H\text{-}H}$ = 8.1, 5.3, aromat. CH *meta* to N]; 8.16 [s, 4 H, aromat. CH, middle ring of phen]. ^{13}C-NMR ([D$_6$]acetone/D_2O (1:1), 100.62 MHz, tentative assignment according to similar complexes): δ = 151.4 [*ortho* to N]; 147.4 [*ipso, ortho* to N]; 142.0 [*para* to N]; 131.6; 129.9; 127.9.

$[Pt(phen)(OH_2)_2](ClO_4)_2$: The diaqua complex was prepared as a 0.05 mM solution by cleavage of the hydroxo-bridged dimer according to the following procedure: 5 ml of a 0.5 mM stock solution of $[\{Pt(phen)(\mu\text{-}OH)\}_2](F_3CSO_3)_2$ in water was diluted to 80 ml. This solution was then heated to boiling. To this solution 0.01 mol $HClO_4$ in the form of a 60% solution was added. An orange coloured precipitate of $[\{Pt(phen)(\mu\text{-}OH)\}_2](ClO_4)_2$ appeared and

dissolved after some minutes. After boiling for 40 min. the volume was adjusted to 100 ml. This solution was prepared freshly for each measurement.

Instrumentation: UV-Vis spectra were recorded on a Shimadzu UV-2101-PC spectrophotometer. − IR spectra were recorded on a Mattson Polaris FT-IR-spectrophotometer using KBr pellets. − NMR spectra were measured on an Avance DPX 300 (Bruker) with TSP as internal standard. − The pH values measured in D_2O are referred to as "pH*" and reported without any correction for the isotope effect. − Chemical analyses were performed on a Carlo Erba Elemental Analyser 1106. − Kinetic measurements on the en complexes were performed on a Biologic SFM-3/S (Claix, France) stopped-flow instrument coupled to an on-line data aquisition system. The syringe control device MPS-51 and the BIOKINE-Software V3.0 from the same supplier were used. The kinetic traces were converted into olis-format with BIOKOLIS (1990) and evaluated using the OLIS KINFIT (Bogart, GA) program. Measurements on the phen complexes were performed using SX-18MV hardware and software from APPLIED PHOTOPHYSICS. The Global Analysis evaluation of the data was done with the Pro-Kineticist software, which is part of the SX-18MV software. Rapid scan spectra were recorded with a J&M-Tidas 16-416 diode-array detector connected to the SX-18MV stopped-flow apparatus. Measurements under high pressure were performed on a home-made high-pressure stopped-flow instrument[62]. Kinetic measurements, unless otherwise stated, were performed at a temperature of 25.0±0.1 °C and an ionic stength of 0.1 M, which was adjusted with $NaClO_4$ if necessary. The pH of the solution was 1.0 and 3.0 for the phen and the en complexes, respectively. All kinetic measurements were performed under pseudo-first-order conditions and a pseudo-first-order behaviour was found.

X-ray Crystallography: Crystals of $[\{Pt(phen)(\mu\text{-}OH)\}_2](F_3CSO_3)_2 \cdot 2\,H_2O$ suitable for X-ray crystallography were obtained by slow evaporation of the solvent from a saturated solution of the complex in acetone/H_2O (20:1). The scattering data were collected using a CAD-4 (Enraf-Nonius) diffractometer. All reflections with $I > 2\sigma(I)$ were used in the analysis. Details on data collection and the crystal data are given in Table 1[63]. Standard software and literature was used[64][65][66][67]. The structure was solved using the Patterson method and refined anisotropically (non-hydrogens) by the full-matrix least-squares method. The hydrogen atom of the hydroxo-bridge was found in the Fourier map. As a refinement of the O(4)−H(11) distance was not possible, this distance was fixed using the option DFIX of the SHELX software (distance = 0.99 Å, σ = 0.03) and the orientation refined.

[1] F. Basolo, R. G. Pearson, *Mechanisms of Inorganic Reactions*, John Wiley and Sons Inc., New York, **1967.**
[2] A. Peloso, *Coord. Chem. Rev.* **1973**, *10*, 123.
[3] R. G. Wilkins, *Kinetics and Mechanism of Reactions of Transition Metal Complexes*, VCH, Weinheim, **1991.**
[4] R. van Eldik in *Inorganic High Pressure Chemistry, Vol. 7* (Ed: R. van Eldik), Elsevier, Amsterdam, **1986**, p. 395.
[5] F. Basolo, *Coord. Chem. Rev.* **1996**, *154*, 151.
[6] G. W. Parshall, *Homogeneous Catalysis*, Wiley, New York, **1980**.
[7] K. I. Zamaraev, *Topics in Catalysis* **1996**, *3*, 1.
[8] M. Hartmann, B. K. Keppler, *Comments Inorg. Chem.* **1995**, *16*, 339.
[9] J. Reedijk, A. M. Fichtinger-Schepman, A. T. van Oosterom, P. van de Putte, *Structure and Bonding* **1987**, *67*, 53.
[10] B. K. Keppler in *Metal Complexes in Cancer Chemotherapy* (Ed.: B. K. Keppler), VCH, Weinheim, **1993**, p. 1.
[11] J. Arpalahti, in *Metal Ions in Biological Systems, Vol. 32* (Ed.: A. Sigel, H. Sigel), Marcel Dekker, New York, **1996**, p. 379.
[12] I. Bertini, H. B. Gray, S. J. Lippard, J. S. Valentine, *Bioinorganic Chemistry*, University Science Books, Mill Valley, CA, **1994**.
[13] R. Romeo, L. M. Scolaro, N. Nastasi, G. Arena, *Inorg. Chem.* **1996**, *35*, 5087.
[14] P. C. Haake and P. A. Cronin, *Inorg. Chem. 2* **1963**, 879.
[15] R. C. Conrad, J. V. Rund, *Inorg. Chem.* **1972**, *11*, 129.
[16] M. Cusumano, G. Gugliemo, V. Ricevuto, *Inorg. Chim. Acta* **1978**, *27*, 197.
[17] R. Romeo, G. Arena, L. M. Scolaro, M. R. Plutino, *Inorg. Chim. Acta* **1995**, *240*, 81.
[18] B. Rosenberg, L. van Camp, J. E. Trosko, V. H. Monsour, *Nature* **1969**, *222*, 385.
[19] R. Mital, N. Jain, T. S. Srivastata, *Inorg. Chim. Acta* **1989**, *166*, 135.
[20] R. Mital, T. S. Srivastata, H. K. Parekh, M. P. Chitnis, *J. Inorg. Biochem.* **1991**, *41*, 93.
[21] H. M. Mansuri-Torshizi, T. S. Srivastata, H. K. Parekh, M. P. Chitnis, *J. Inorg. Biochem.* **1992**, *45*, 135.
[22] A. Gund, B. K. Keppler, *Angew. Chem.* **1994**, *106*, 198*; Angew. Chem. Int. Ed. Engl.* **1994**, *33*, 186.
[23] S. Geremia, L. Randaccio, G. Mestroni, B. Milani, *J. Chem. Soc. Dalton Trans.* **1992**, 2117.
[24] B. Milani, E. Alessio, G. Mestroni, A. Sommazzi, F. Garbassi, E. Zangrando, N. Bresciani-Pahor, L. Randaccio, *J. Chem. Soc. Dalton Trans.* **1994**, 1903.
[25] G. Bruno, F. Nicolò, R. Scopelleti, G. Arena, *Acta Crystallogr. Sect. C* **1996**, *52*, 827.
[26] R. Faggiani, B. Lippert, C. J. L. Lock, B. Rosenberg, *J. Am. Chem. Soc.* **1977**, *99*, 777.
[27] B. Lippert, C. J. L. Lock, B. Rosenberg, M. Zvagulis, *Inorg. Chem.* **1978**, *17*, 2971.
[28] F. D. Rochon, R. Melanson, A. Morneau, *Magn. Reson. Chem.* **1992**, *30*, 697.
[29] T. G. Appleton, H. C. Clark, L. E. Manzer, *Coord. Chem. Rev.* **1973**, *10*, 335.
[30] R. van Eldik, T. Asano, B. le Noble, *Chem. Rev.* **1989**, *89*, 549.
[31] S. Wimmer, P. Castan, F. L. Wimmer, N. P. Johnson, *J. Chem. Soc. Dalton Trans.* **1989**, 403.
[32] R. Faggiani, B. Lippert, C. J. L. Lock, B. Rosenberg, *Inorg. Chem.* **1977**, *16*, 1192.
[33] R. Faggiani, B. Lippert, C. J. L. Lock, B. Rosenberg, *Inorg. Chem.* **1978**, *17*, 1941.
[34] F. D. Rochon, R. Melanson, *Acta Crystallogr. Sect. C* **1988**, *44*, 474.
[35] F. D. Rochon, A. Morneau, R. Melanson, *Inorg. Chem.* **1988**, *27*, 10.
[36] L. Rasmussen, C. K. Joergensen, *Inorg. Chim. Acta* **1969**, *3*, 547.
[37] G. Anderegg, H. Wanner, *Inorg. Chim. Acta* **1986**, *113*, 101.
[38] Y. H. Chao, A. Holtzer, S. H. Mastin, *J. Am. Chem. Soc.* **1977**, 8024.
[39] B. Norden, *FEBS lett.* **1978**, *94*, 204.
[40] S. Wimmer, P. Castan, F. L. Wimmer, N. P. Johnson, *Inorg. Chim. Acta* **1988**, *142*, 13.
[41] R. G. Pearson, M. M. Muir, *J. Am. Chem. Soc.* **1966**, *88*, 2163.
[42] M. Cusumano, A. Giannetto, P. Ficarra, R. Ficarra, S. Tommasini, *J. Chem. Soc. Dalton Trans.* **1991**, 1581.
[43] A. D. Ryabov, L. G. Kuz′mina, V. A. Polyakov, G. M. Kazankov, E. S. Ryabova, M. Pfeffer, R. van Eldik, *J. Chem. Soc. Dalton Trans.* **1995**, 999.
[44] J. J. Pienaar, E. L. J. Breet, R. van Eldik, *Inorg. Chim. Acta* **1989**, *155*, 249.
[45] J. Arpalahti and P. Lehikoinen, *Inorg. Chem.* **1990**, *29*, 2564.
[46] J. Arpalahti, *Inorg. Chem.* **1990**, *29*, 4598.
[47] S. K. Aggarwal, J. A. Broomhead, D. P. Fairlie, M. W. Whitehouse, *Cancer Chemother. Pharmacol.* **1980**, *4*, 249.
[48] I. A. Ross, D. P. Fairlie, M. W. Whitehouse, *Chem. Biol. Interact.* **1980**, *31*, 111.
[49] J. A. Broomhead, D. P. Fairlie,M. W. Whitehouse, *Chem. Biol. Interact.* **1980**, *31*, 113.
[50] O. Wernberg, A. Hazell, *J. Chem. Soc. Dalton Trans.* **1980**, 973.
[51] J. H. Espenson, *Chemical Kinetics and Reaction Mechanism*, 2nd ed., McGraw-Hill, New York, **1995**, p. 76.
[52] P. M. Takahara, A. C. Rosenzweig, C. A. Frederick, S. J. Lippard, *Nature* **1995**, *377*, 649.
[53] P. M. Takahara, C. A. Frederick, S. J. Lippard, *J. Am. Chem. Soc.* **1996**, *118*, 12309.
[54] C. S. Peyratout, T. K. Aldridge, D. K. Crites, D. R. McMillin, *Inorg. Chem.* **1995**, *34*, 4484.
[55] O. Yamauchi, A. Odani, H. Masuda, H. Sigel, in *Metal Ions in*

Biological Systems, Vol. 32 (Eds.: A. Sigel, H. Sigel), Marcel Dekker, New York, **1996**, p. 207.
[56] M. Howe-Grant, K. C. Wu, W. R. Bauer, S. J. Lippard, *Biochem.* **1976**, *15*, 4339.
[57] J. Berger, M. Kotowski, R. van Eldik, U. Frey, L. Helm, A. E. Merbach, *Inorg. Chem.* **1989**, *28*, 3759.
[58] S. Elmroth, Z. Bugarcic, L. I. Elding, *Inorg. Chem.* **1992**, *31*, 3551.
[59] S. Al-Baker, J. C. Dabrowiak, *Inorg. Chem.* **1987**, *26*, 613.
[60] A. F. M. Siebert, *Dissertation*, Fakultät für Chemie, Ruhr-Universität, Bochum, **1995**.
[61] J. Arpalahti, B. Lippert, *Inorg. Chem.* **1990**, *29*, 104.
[62] R. van Eldik, D. A. Palmer, R. Schmidt, H. Kelm, *Inorg. Chim. Acta* **1981**, *50*, 131.
[63] Tables giving further information about the crystal structure (23 pages, including structure factor tables) can be obtained from the authors on request. Details on the crystal structure determination (excluding structure factors) can also be obtained from the Fachinformationszentrum Karlsruhe, 76344 Eggenstein-Leopoldshafen (e-mail: crysdata@fiz-karlsruhe.de) on quoting the CSD number 406492.
[64] S. R. Hall, J. M. Stewart, *Xtal3.2. Crystallographic Program System*, Univ. of Western Australia, Australia und Maryland (USA), **1992**.
[65] G. M. Sheldrick, *SHELXL-93. A System for Crystal Structure Refinement*, Göttingen, **1993**.
[66] ENRAF-NONIUS Inc., *ARGUS. Cad4-Mach3 diffractometer software.*
[67] T. H. Hahn, *International Tables for Crystallography, Vol. A*, D. Reidel Publishing Company, Dordrecht (NL), Boston (USA), **1984**.

[97226]

Organometallic Selenolates, 8[◇]

The Reaction of Potassium Polyselenides with [CpW(CO)$_3$Cl] in DMF Formation and Crystal Structure of [CpW(CO)$_3$SeC(O)NMe$_2$] and {[CpW(CO)$_3$]$_2$Se$_4$}

Peter G. Jones, Jörg Laube, and Carsten Thöne*

Institut für Anorganische und Analytische Chemie der Technischen Universität,
Postfach 3329, D-38023 Braunschweig, Germany

Received October 20, 1997

Keywords: Polychalcogenides / Selenium / Selenocarbamato complexes / ^{77}Se NMR / Crystal structure

The reactions of the potassium polyselenides "K_2Se_6" and "K_2Se_8" with [CpW(CO)$_3$Cl] and 18-crown-6 in DMF lead to a mixture of the selenido complexes {[CpW(CO)$_3$]$_2$Se$_4$} **1** and [(18-crown-6)K]$^+$[CpW(Se$_4$)$_2$]$^-$ **3** and the Se−bonded selenocarbamato complex [CpW(CO)$_3$SeC(O)NMe$_2$] **2** in yields depending on the selenium content of the used potassium polyselenides ("K_2Se_6" or "K_2Se_8"). A similar reaction in THF produces {[CpW(CO)$_3$]$_2$Se$_4$} as the main product. X-ray structures of **1** and **2** were determined. In **1** the Se$_4$-chain is bonded in a μ^2-η^1 fashion, with corresponding W−Se bond lengths of 264.0(1) and 264.3(1) pm. The Se−Se bond lengths lie in the range 232 to 237 pm. The first example of an η^1 Se-bonded selenocarbamato ligand is observed in the crystal structure of **2**, with a W−Se bond length of 263.1(1) pm. The ^{77}Se-NMR data are compared with the corresponding data of related complexes.

The synthesis of oligoselenido complexes via reactions of alkali-metal polyselenides with appropriate transition metal complexes is widely applicable and the resulting oligoselenido complexes are of particular interest because of their potential use as solid state precursors and the versatile binding modes of Se_n^{2-} [1]. However, the synthesis of organoselenolato complexes using the same route is restricted to accessible organic selenolates or diselenides[2]. For this reason, there is still a need for new synthetic methods that can avoid this difficulty. Recently, we described the formation of organometallic selenolates via selenium insertion into the alkali-metal−transition-metal bonds of appropriate carbonylates such as MM′Cp(CO)$_3$ (M = Li, Na, K; M′ = Mo, W) and MMn(CO)$_5$[3]. The resulting selenolates react with a variety of organic electrophiles to form the corresponding organoselenolato complexes, whereas oxidation with O_2 in the presence of SiO_2 leads to oligoselenido complexes[4]. Here we report on the reaction of the potassium polyselenides "K_2Se_6" and "K_2Se_8" with CpW(CO)$_3$Cl in DMF, producing the organoselenolato complex [CpW(CO)$_3$SeC(O)NMe$_2$] and the tetraselenido complexes {[CpW(CO)$_3$]$_2$Se$_4$} and [(18-crown-6)K]$^+$[CpW(Se$_4$)$_2$]$^-$.

Results and Discussion

Potassium polyselenides can be easily prepared by reducing elemental selenium with KBEt$_3$H in DMF at 150°. The resulting nearly black solutions contain formally "K_2Se_6" or "K_2Se_8", if an appropriate Se/KBEt$_3$H ratio is used[5]. The exact composition of such polyselenides is very difficult to predict, since complicated equilibria can be observed in solution[6]. Thus a reaction of such polyselenides with metal halide complexes can lead to various products depending on the metal center, the solvent and the temperature.

When [CpW(CO)$_3$Cl] is stirred overnight with a DMF solution of "K_2Se_6" in the presence of 18-crown-6, three products can be separated: {[CpW(CO)$_3$]$_2$Se$_4$} **1** (10%), [CpW(CO)$_3$SeC(O)NMe$_2$] **2** (40%), and the salt [(18-crown-6)K]$^+$[CpW(Se$_4$)$_2$]$^-$ **3** (9%).

The reaction mechanism is not clear, since the formyl group of DMF must be deprotonated in the initial step of the formation of **2**. A few reports concerning the synthesis of η^1-bonded selenocarbamato complexes have been published in which [Me$_2$NH$_2$][SeC(O)NMe$_2$] or CSe_2 in the presence of Me$_2$NH are required as the starting materials[7]. However, these alternative routes are not widely applicable and can lead also to the chelated η^2-derivatives.

If "K_2Se_8" is employed instead of "K_2Se_6", **3** is the main product and only traces of **1** and **2** are produced. The reason for this difference seems to be the high stability of $M(Se_4)_n^{2-}$ complexes (M = Zn, Cd, Hg, Ag, Au, Mo, W, Pd, Rh, Ir, Ru, Ni, Pt, Mn) that contain five-membered MSe_4 rings[8]. However, if THF is used as the solvent in the reaction of "K_2Se_6" with [CpW(CO)$_3$Cl], **1** is formed as the main separable product (35%) together with some decomposition products. A more straightforward synthesis of **1** has been developed recently in our laboratory. It comprises the insertion of three seleniums into the Li−W bond of LiWCp(CO)$_3$ and subsequent oxidation with O_2 in the presence of SiO_2[4].

[◇] Part 7: Ref.[1]

 © WILEY-VCH Verlag GmbH, D-69451 Weinheim, 1998 1434−1948/98/0303−0397 $ 17.50+.50/0

Scheme 1. The reaction of "K_2Se_6" with $[CpW(CO)_3Cl]$ and 18-crown-6 in DMF

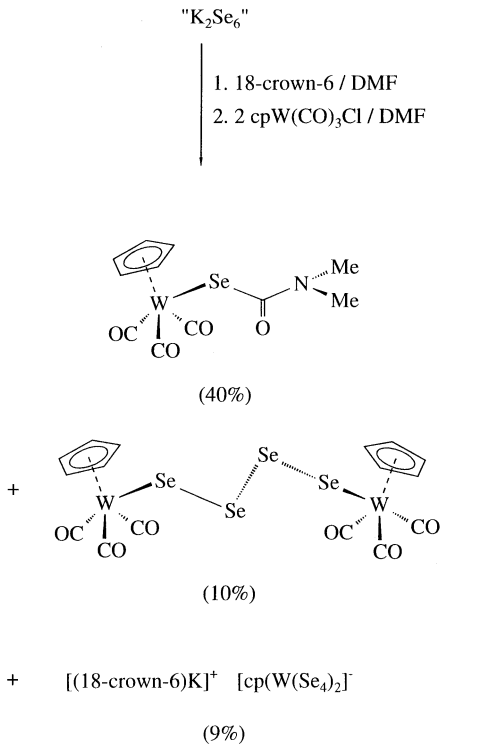

The ^{77}Se-NMR data of **1**, **2**, and **3** are consistent with their structures and comparable with related complexes. The ^{77}Se-NMR spectrum of **1** has been already described and seems to be typical of oligoselenido complexes with μ^2-η^1 bonded selenium chains in which the metal-bonded selenium atom is usually shifted highfield[4]. The chemical shifts in the ^{77}Se-NMR spectra are strongly influenced by electronic and steric effects and cannot always be interpreted by simple means. Thus, the spectrum of **3** shows a completely different pattern. The metal-bonded selenium atoms are deshielded; ^{183}W satellites and a corresponding ^{77}Se-^{183}W coupling constant of 80 Hz are observed. There are only few reported $^1J(^{77}Se\text{-}^{183}W)$ coupling constants and the values range from 35 Hz in $[CpW(CO)_3SeC(O)Ph]$[9] to 112 Hz in the $W_3Se_9^{2-}$ anion[8b]. Recently the cp* derivative $[(\sigma\text{-}C_5Me_5)(CO)_5WSeMe]$ has been published with a $^1J(^{77}Se\text{-}^{183}W)$ value of 49 Hz[10]. Unfortunately, for **2**, no ^{183}W satellites could be observed because of the broadness of the signal, but the chemical shift of −136.1 ppm is in good accordance with the data of related complexes[3a][3b][3c][3d][3e][3f].

Crystal Structures of $\{[CpW(CO)_3]_2Se_4\}$ (1) and $[CpW(CO)_3SeC(O)NMe_2]$ (2)

The crystal structure of **1** is presented in Figure 1. It consists of two $cpW(CO)_3$ moieties, which are bridged by an Se_4 chain in a μ^2-η^1 fashion. This structural motif is rare and the only reported examples are $[Cp_2Hf(\mu\text{-}O)(\mu\text{-}Se_4)HfCp_2]$ and $[Au_2(\mu\text{-}Se_2)(\mu\text{-}Se_4)]^-$[11].The conformation of the Se_4 group in **1** can be described by its torsion angles [W1−Se1−Se2−Se3: 75.51(6)°; Se1−Se2−Se3−Se4: 51.81(7)°, Se2−Se3−Se4−W2: 78.70(6)°] as a helical chain with corresponding bond angles at selenium ranging from 104.53(6) to 110.69(5)°. In the triselenido complex $\{[CpW(CO)_3]_2Se_3\}$, comparable absolute values of the torsion angles were observed [W1−Se1−Se3−Se2: 83.12(7)°; Se1−Se3−Se2−W2: 88.31(7)°][4]. The W−Se bond lengths, W1−Se1 263.99(11) pm and W2−Se4 264.29(10) pm, are comparable with the W−Se bond lengths in $\{[CpW(CO)_3]_2Se_3\}$ (263.2(1), 265.1(1) pm). Similar bond lengths were also found in a series of organoselenolato tungsten complexes and they are attributable to W−Se single bonds (vide infra). The W-bonded Se_2 moieties display Se−Se bond lengths of 232.1(2) and 232.2(2) pm, whereas the central Se−Se bond Se2−Se3 [236.7(2) pm] is 4.5 pm longer, indicating that this bond should display a more pronounced reactivity.

The crystal structure of **2** is presented in Figure 2. The atoms W, C4, O4, N, C5, and C6 are approximately coplanar (mean deviation 1.3 pm); the selenium atom lies 20

Figure 1. Molecular structure of $\{[CpW(CO)_3]_2Se_4\}$ (**1**) (50% probability ellipsoids, H atoms omitted for clarity)[a]

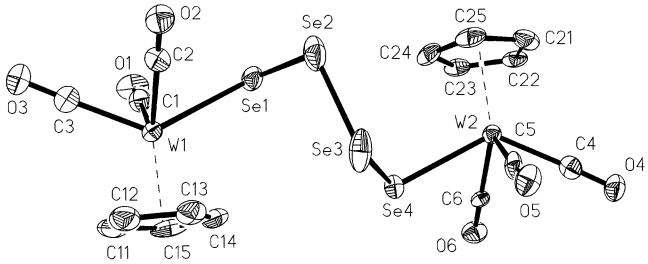

[a] Selected bond lengths [pm] and angles [°]: W1−Cp (ring center) 201.0, W1−Se1 263.99(11), Se1−Se2 232.1(2), Se2−Se3 236.7(2), Se3−Se4 232.2(2), Se4−W2 264.29(10), W2−Cp (ring center) 200.6; C1−W1−Se1 75.1(3), C2−W1−Se1 75.9(3), C3−W1−Se1 130.2(3), W1−Se1−Se2 110.69(5), Se1−Se2−Se3 104.53(6), Se2−Se3−Se4 105.49(6), Se3−Se4−W2 109.65(5), C4−W2−Se4 129.3(3), C5−W2−Se4 75.3(2), C6−W2−Se4 74.7(3).

Figure 2. Molecular structure of $[CpW(CO)_3SeC(O)NMe_2]$ (**2**) (50% probability ellipsoids, cp hydrogens omitted for clarity)[a]

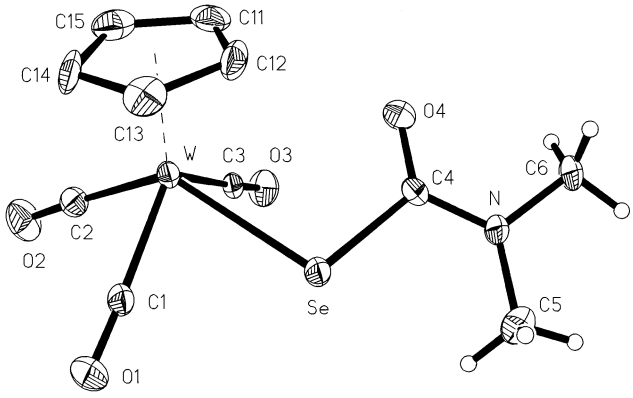

[a] Selected bond lengths [pm] and angles [°]: W−Cp (ring center) 200.6, W−Se 263.08(8), Se−C4 196.1(6), C4−N 133.6(8), N−C5 146.3(8), N−C6 146.7(8); C1−W−Se 74.3(2), C2−W−Se 129.4(2), C3−W−Se 75.6(2), W−Se−C4 103.8(2), Se−C4−N 114.5(4), O4−C4−N 123.8(6), Se−C4−O4 121.7(5), C4−N−C5 124.4(5), C4−N−C6 118.0(5), C5−N−C6 117.3(5).

pm out of this plane. The W−Se bond length of 263.08(8) pm is comparable with other W−Se bond lengths in organoselenolato tungsten complexes with terminal selenolato ligands {e.g. 258.8(2) pm in $[(\eta^7\text{-}C_7H_7)(CO)_2WSePh]$[12]; 263(2) pm in $[CpW(CO)_3SeCH_2CHCH_2]$[3d] and 262.3(1) pm in $[CpW(CO)_3SeCH_2Ph]$[3a]}, whereas complexes with bridging selenolato groups display considerably shorter W−Se bond lengths {e.g. 251.3(5) pm in $[W_2Cl_4(\mu\text{-}SePh)(\mu\text{-}Cl)(dppm)_2]$[13] and 254.9(1) pm in $[PPh_4]_2[Cl_3W(\mu\text{-}SeCl)(\mu\text{-}SePh)_2WCl_3]$[14]}. The selenium atom displays a slightly distorted tetrahedral angle of 103.8(2)°.

Experimental Section

All manipulations were carried out under a dry nitrogen atmosphere using conventional Schlenk techniques. − NMR: Bruker AC 200 (^{1}H 200 MHz, ^{13}C 50.3 MHz, ^{77}Se 38.2 MHz). The spectra were recorded using $CDCl_3$ or C_6D_6 as solvents. Standards: ^{1}H, ^{13}C TMS internal; ^{77}Se Me_2Se external. − IR: Biorad FTS 165. − MS: Finnigan MAT 8430. − *N,N*-Dimethylformamide (DMF) was distilled under nitrogen prior to use. Tetrahydrofuran (THF) was dried over sodium in nitrogen atmosphere. $KBEt_3H$ (1 M in THF), Se, and 18-crown-6 were purchased from Aldrich and used as received. $[CpW(CO)_3Cl]$ was prepared according to the literature method[15].

Reaction of "K_2Se_6"/18-Crown-6 with $[CpW(CO)_3Cl]$ in DMF: 2.7 ml of a solution of $KBEt_3H$ (1 M in THF, 2.7 mmol) were added to 20 ml of DMF. After 10 min of stirring, 0.64 g of Se (8.1 mmol) were added, and the mixture was refluxed for 2 h. After cooling to room temperature, 0.71 g of 18-crown-6 (2.7 mmol) were added to the deep green solution, which was then combined with a solution of 1 g of $[CpW(CO)_3Cl]$ in 20 ml of DMF over a period of 10 min via a syringe. Stirring for 18 h afforded a dark green reaction mixture, which was evaporated to dryness. The residue was extracted three times with 50-ml portions of diethyl ether, leaving a black residue. The work-up procedure of the red organic extract comprised removal of the solvent in vacuo and column chromatography (SiO_2, 20 × 4 cm, CH_2Cl_2/acetone, 95:5, as eluent). The first red band was characterized as $\{[CpW(CO)_3]_2Se_4\}$ **1**[4]. The second orange band corresponds to $[CpW(CO)_3SeC(O)NMe_2]$ **2**. The black precipitate was treated with 10 ml of CH_2Cl_2/acetone, 9:1. The crude mixture was then filtered and column chromatography in the same solvent mixture (SiO_2, 20 × 4 cm) afforded $[(18\text{-crown-}6)K]^+[CpW(Se_4)_2]^-$ **3** in the deep green band accompanied by a small amount of immobile brown impurities.

1: Yield 0.122 g (10%), m.p. 126°C. The spectroscopic data were consistent with those previously described[4].

2: Yield: 0.520 g (40%), m.p. 138°C. − ^{1}H NMR (C_6D_6): δ = 2.65 (s, 3 H, CH_3), 2.87 (s, 3 H, CH_3), 4.9 (s, 5 H, C_5H_5). − ^{13}C NMR (C_6D_6) δ = 36.4 (s, CH_3), 39.8 (s, CH_3), 93.1 (s, C_5H_5), 164.8 (s, μ-CO), 213.9, 226.2 (s, CO). − ^{77}Se NMR (C_6D_6): δ = −136.1 (s). − IR (CH_2Cl_2): $\tilde{\nu}$ = 2029, 1951, 1925 (CO), 1626 (μ−CO). − MS (70 ev); *m/z* (%): 457 (88) [M^+ − CO], 429 (43) [M^+ − 2 CO], 401 (100) [M^+ − 3 CO]. − $C_{11}H_{11}NO_4SeW$ (484.0): calcd. C 27.30, H 2.29, N 2.89; found C 27.31, H 2.38, N 2.84.

3: Yield: 0.140 g (9% on Se), m.p. 153°C. − ^{1}H NMR ($CDCl_3$): δ = 3.47 (s, 24 H, CH_2), 5.02 (s, 5 H, C_5H_5). − ^{13}C NMR ($CDCl_3$): δ = 70.1 (s, CH_2), 94.6 (s, C_5H_5). − ^{77}Se NMR ($CDCl_3$): δ = 486.1 (s, Se-*Se*-*Se*-Se), 866.3 [s, ^{183}W satellites, $J(^{77}Se\text{-}^{183}W)$ 80 Hz, W-*Se*). − MS (70 ev); *m/z* (%): 303 (100) [M^+]. − $C_{17}H_{29}KO_6Se_8W$ (1184.0): calcd. C 17.25, H 2.47; found C 17.41, H 2.46.

Reaction of "K_2Se_6"/18-Crown-6 with $[CpW(CO)_3Cl]$ in THF: A similar reaction in THF employing the same quantities of Se, 18-crown-6, and $[CpW(CO)_3Cl]$ led to the formation of **1** as the main product in 40% yield, together with insoluble inorganic tungsten selenides.

Reaction of "K_2Se_8"/18-Crown-6 with $[CpW(CO)_3Cl]$ in DMF: The reaction was performed as described above using 0.85 g of Se (10.8 mmol). After evaporating to dryness, the black residue was washed three times with 25 ml portions of diethyl ether. In contrast to the reaction with "K_2Se_6", the organic extract contained only traces of **1** and **2**. The remaining black precipitate was treated as described above, yielding 0.48 g **3** (30%), accompanied by immobile brown impurities.

Crystal Structure Determinations[16]: Suitable crystals of **1** and **2** were obtained by layering CH_2Cl_2 solutions with hexanes (ambient temperature), mounted on glass fibers in inert oil and transferred to the cold gas stream of the diffractometer (Siemens P4, −100°C) equipped with an LT-2 low-temperature attachment. Mo-K_α radiation (λ = 0.71073 Å, graphite monochromator) was used to collect the intensity data in the ω-scan mode. Cell constants were refined from setting angles of 62 reflections in the 2 Θ range 8−23°. Absorption corrections based on ψ-scans were applied. The crystallographic program system used was SHELXL-93[17]. Both structures were solved by direct methods and refined by full-matrix least-squares procedures on F^2. All non-H atoms were refined anisotropically; hydrogen atoms were included using a riding model or as rigid methyls. The final difference Fourier maps were featureless; in the case of **1**, the highest peak of 1.95 e Å^{-3} is located near the

Table 1. X-ray structure analyses, details of solution and refinement

Compound	**1**	**2**
Empirical formula	$C_{16}H_{10}O_6Se_4W_2$	$C_{11}H_{11}NO_4SeW$
Formula weight [g mol^{-1}]	981.78	484.02
Crystal system	triclinic	monoclinic
Space group (No.)	$P\bar{1}$ (2)	$P2_1/n$ (14)
a [pm]	654.96(6)	653.4(2)
b [pm]	1266.46(12)	3272.9(5)
c [pm]	1299.99(10)	668.4(1)
α [°]	86.198(6)	
β [°]	79.570(6)	112.75(2)
γ [°]	84.402(8)	
V [Å^3]	1054.1(2)	1318.2(5)
$\rho_{calc.}$ [g cm^{-3}]	3.09	2.44
Z	2	4
F (000) [e]	876	896
μ [cm^{-1}]	178.4	115.3
Crystal size [mm]	0.50 × 0.15 × 0.10	0.32 × 0.30 × 0.08
2 Θ_{max} [°]	50	50
T [°C]	−100	−100
Measured reflections	3929	2879
Unique reflections	3707	2315
R_{int}	0.0244	0.0324
No. of parameters	253	165
No. of restraints	122	86
min/max Transmission	0.38/1.00	0.37/0.96
R (*F*), F > 4σ (*F*)[a]	0.0346	0.0254
R_w (F^2), all refl.[b]	0.0846	0.0564
Weighting parameters (*a,b*)	0.0921, 0	0.031, 0
S [c]	0.97	0.99
max. Δ/σ	< 0.001	< 0.001
ρ_{fin} (max/min) [e Å^{-3}]	1.95/−1.83	0.98/−1.02

[a] $R(F) = \Sigma\|F_o| - |F_c\|/\Sigma|F_o|$. − [b] $wR(F^2) = [\Sigma\{w(F_o^2-F_c^2)^2\}/\Sigma\{w(F_o^2)^2\}]^{0.5}$; $w^{-1} = (F_o^2) + (aP)^2 + bP$, where $P = [F_o^2 + 2F_c^2]/3$ and *a* and *b* are constants adjusted by the program. − [c] $S = [\Sigma\{w(F_o^2-F_c^2)^2\}/(n-p)]^{0.5}$, where *n* is the number of data and *p* the number of parameters.

W atom. Additional crystallographic data are presented in Table 1. Selected bond lengths and angles are listed in the Figure captions.

[1] [1a] M. A. Ansari, J. A. Ibers, *Coord. Chem. Rev.* **1990**, *100*, 223−266. − [1b] D. Coucouvanis, *Acc. Chem. Res.* **1991**, *24*, 1−8. − [1c] L. C. Roof, J. W. Kolis, *Chem. Rev.* **1993**, *93*, 1037−1080. − [1d] M. G. Kanatzidis, S. P. Huang, *Coord. Chem. Rev.* **1994**, *130*, 509−621.

[2] J. Arnold, *Progr. Inorg. Chem.* **1995**, *43*, 353−417.

[3] [3a] W. Eikens, P. G. Jones, C. Kienitz, C. Thöne, *J. Chem. Soc., Dalton Trans.* **1994**, 3329−3330. − [3b] W. Eikens, S. Jäger, P. G. Jones, C. Thöne, *J. Organomet. Chem.* **1996**, *511*, 67−75. − [3c] W. Eikens, S. Jäger, P. G. Jones, J. Laube, C. Thöne, *Chem. Ber.* **1996**, *129*, 1275−1279. − [3d] P. G. Jones, J. Laube, C. Thöne, *Inorg. Chem.* **1997**, *36*, 2097−2102. − [3e] P. G. Jones, J. Laube, C. Thöne, *Acta Crystallogr.* **1997**, *C53* 1539−1542. − [3f] T. M. Klapötke, M. Broschag, *Compilation of reported ^{77}Se NMR Chemical Shifts − up to the year 1994*, John Wiley & Sons, Chichester, **1996**, pp. 12−13.

[4] P. G. Jones, C. Thöne, *Inorg. Chem.* **1996**, *35*, 6625−6626.

[5] J. A. Gladysz, J. L. Hornby, J. E. Garbe, *J. Org. Chem.* **1978**, *43*, 1204−1208.

[6] F. Weller, J. Adel, K. Dehnicke, *Z. Allg. Anorg. Chem.* **1987**, *548*, 125−132.

[7] [7a] G. Nagao, K. Tanaka, T. Tanaka, *Inorg. Chim. Acta* **1980**, *42*, 43−48. − [7b] K. Tanaka, K. Ueda, T. Tanaka, *Inorg. Nucl. Chem.* **1981**, *43*, 2029−2032. − [7c] E. Román, D. Catheline, D. Astruc, *J. Organomet. Chem.* **1982**, *236*, 229−236.

[8] [8a] 69 crystal structures of $M(Se_4)_n$ derivatives are included in the CCDC data base (April 1997); F. H. Allen, O. Kennard, *Chem. Des. Autom. News* **1993**, *8*, 31 − 37. − [8b] For $W(Se_4)_n$ derivatives see: R. W. M. Wardle, S. Bhaduri, C.-N. Chau, J. A. Ibers, *Inorg. Chem.* **1988**, *27*, 1747−1755.

[9] S. Jäger, P. G. Jones, C. Thöne, unpublished work.

[10] C. M. Bates, C. P. Morley, *J. Organomet. Chem.* **1997**, *533*, 197−200.

[11] [11a] N. Albrecht, E. Weiss, *J. Organomet. Chem.* **1988**, *355*, 89−98. − [11b] S.-P. Huang, M. G. Kanatzidis, *Inorg. Chem.* **1991**, *30*, 3572−3575.

[12] A. Rettenmaier, K. Weidenhammer, M. L. Ziegler, *Z. Anorg. Allg. Chem.* **1981**, *478*, 91−100.

[13] J. A. M. Canich, F. A. Cotton, K. R. Dunbar, L. R. Falvello, *Inorg. Chem.* **1988**, *27*, 804−811.

[14] J. M. Ball, P. M. Boorman, J. F. Fait, H. B. Kraatz, J. F. Richardson, D. Collison, F. E. Mabbs, *Inorg. Chem.* **1990**, *29*, 3290−3293.

[15] [15a] T. S. Piper, G. Wilkinson, *J. Inorg. Nucl. Chem.* **1956**, *3*, 104−124. − [15b] C. E. Coffey, *J. Inorg. Nucl. Chem.* **1963**, *25*, 179−185.

[16] Crystallographic data (excluding structure factors) for the structures reported in this paper have been deposited with the Cambridge Crystallographic Data Centre. Copies of the data can be obtained free of charge on application to The Director, CCDC, 12 Union Road, Cambridge CB2 1EZ, UK (fax: int. code +44 (1223) 336-033, e-mail: deposit@chemcrys.cam.ac.uk) on quoting the deposition number 100769.

[17] G. M. Sheldrick, *SHELXL-93*, *Program for Crystal Structure Refinement*, University of Göttingen, F. R. G., **1993**.

[97238]

Mono- and Dinuclear Carbonyl Complexes of (1,4,7-Trimethyl-1,4,7-triazacyclononane)rhodium(I): Facile Migration of a C(O)OMe Ligand at a Dinuclear Rh(μ-CO)$_2$Rh Core

Bas de Bruin, Jack J. J. M. Donners, René de Gelder, Jan M. M. Smits, and Anton W. Gal*

Department of Inorganic Chemistry, University of Nijmegen,
Toernooiveld 1, 6525 ED Nijmegen, The Netherlands.
E-mail: gal@sci.kun.nl

Received November 3, 1997

Keywords: Rhodium / N ligands / Carbonyl complexes / Methoxycarbonyl / Dinuclear complexes

The reaction of 1,4,7-trimethyl-1,4,7-triazacyclononane (Cn*) with [{(CO)$_2$Rh(μ-Cl)}$_2$] in methanol at 0°C, followed by the addition of NH_4PF_6, results in the formation of the mononuclear carbonyl complex [Cn*Rh(μ-CO)$_2$]PF_6 ([**1**]PF_6), the dinuclear carbonyl complex [Cn*Rh(μ-CO)$_3$RhCn*](PF$_6$)$_2$ {[**2**](PF$_6$)$_2$} and the dinuclear methoxycarbonyl complex [Cn*Rh(C(O)OMe)(μ-CO)$_2$RhCn*]PF_6 ([**3**]PF_6). The reaction of [**2**](PF$_6$)$_2$ with NaOMe results in formation of [**3**]PF_6 by the attack of the methoxide at a bridging carbonyl. Treatment of [**3**]PF_6 with NH_4PF_6 regenerates [**2**](PF$_6$)$_2$, thus showing that the methoxylation of [**2**](PF$_6$)$_2$ is reversible. The structures of [**1**]PF_6, [**2**](PF$_6$)$_2$ and [**3**]PF_6 have been determined by single-crystal X-ray diffraction. For [**3**]PF_6 an unprecendented facile, reversible, migration of the C(O)OMe ligand between the two rhodium centres of the Rh(μ-CO)$_2$Rh core is observed.

Tridentate N-donor ligands ('N_3' ligands) have so far found a limited application in the area of the organometallic chemistry of rhodium. Interesting reactivities have however been reported for rhodium complexes with *fac*-coordinating 1,4,7-trimethyl-1,4,7-triazacyclononane (Cn*) and [hydrotris(3,5-pyrazolyl)borate] (Tp^{Me2}) [1][2], and *mer*-coordinating pyridine-2,6-diimine (2,6-(C(R)=N-R')$_2$-C_5H_3N).[3] For ['N_3' Rh^I(cod)]$^+$, ['N_3' is Cn* or *N*-butyl-*N,N*-di-(2-pyridylmethyl)amine], we have recently reported on the oxidation of the cod ligand by H_2O_2 to a bicyclooxanonadiyl fragment.[4] In an extension of our explorative studies on the structure and reactivities of 'N_3' Rh sites, we now report on the carbonyl chemistry of Cn*Rh^I sites.

Results and Discussion

The reaction of the rigid *fac*-ligand Cn* with {[(CO)$_2$Rh(μ-Cl)]$_2$} in methanol at 0°C, followed by addition of NH_4PF_6, leads to the precipitation of a mixture of yellow [**2**](PF$_6$)$_2$ and orange [**3**]PF_6. Upon cooling of the filtrate, further precipitation of [**2**](PF$_6$)$_2$ and [**3**]PF_6 occurred, and a few bright-orange crystals of [**1**]PF_6 deposited (Scheme 1).

From the solid mixture that was obtained by filtration, the crystals of [**1**]PF_6 were removed by hand. We were able to interconvert [**2**](PF$_6$)$_2$ and [**3**]PF_6 in the resulting mixture; reaction with approx. 5.5 mol NaOMe per mol of [**2**](PF$_6$)$_2$ in MeOH resulted in the quantitative formation of [**3**]PF_6. Treatment of the same mixture with approx. 7 mol NH_4PF_6 per mol of [**3**]PF_6 in MeOH under reflux resulted in quantitative conversion to [**2**](PF$_6$)$_2$ (Scheme 1). [**2**](PF$_6$)$_2$ and [**3**]PF_6 were isolated as pure compounds via these procedures. Attempts to prepare [**2**](PF$_6$)$_2$ by refluxing an acetone solution of [**1**]PF_6 resulted in the almost quantitative recovery of [**1**]PF_6. Attempts to prepare [**1**]PF_6 by exposure of an acetone solution of [**2**](PF$_6$)$_2$ to 40 bar CO were also unsuccessful.

Scheme 1. Synthesis of [**1**]PF_6, [**2**](PF$_6$)$_2$ and [**3**]PF_6

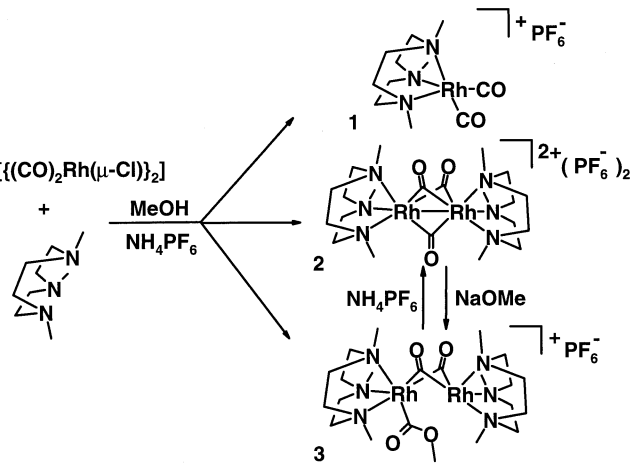

Structure of [**1**]PF_6

The structure of [**1**]PF_6 was determined by single-crystal X-ray diffraction (Figure 1). Selected bond lengths and angles are given in Tables 1 and 2.

The cation [**1**]$^+$ contains two terminal carbonyl groups. The coordination geometry can best be described as a pseudo trigonal bipyramid. The equatorial positions are occupied by one carbonyl and two nitrogens of the Cn* ligand; the axial-positions by the second carbonyl and the

 © WILEY-VCH Verlag GmbH, D-69451 Weinheim, 1998 1434–1948/98/0303–0401 $ 17.50+.50/0

Figure 1. Crystal structure of cation $[\mathbf{1}]^+$

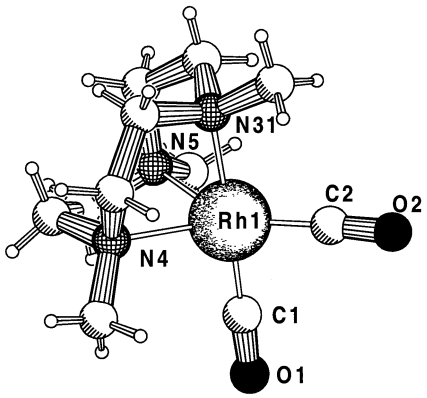

Table 1. Selected bond lengths [Å] for compounds $[\mathbf{1}]PF_6$, $[\mathbf{2}](PF_6)_2$ and $[\mathbf{3}]PF_6$[a]

	$[\mathbf{1}]^+$	$[\mathbf{2A}]^{+}$[b]	$[\mathbf{2B}]^{+}$[b]	$[\mathbf{3}]^+$
N31−Rh1	2.139(3)	2.220(8)	2.213(9)	2.265(5)
N32−Rh2		2.197(10)	2.200(11)	2.257(6)
N4−Rh1	2.261(3)	2.189(7)	2.190(8)	2.278(6)
N5−Rh1	2.320(3)	2.189(7)	2.190(8)	2.256(5)
N6−Rh2		2.200(7)	2.194(7)	2.275(5)
N7−Rh2		2.200(7)	2.194(7)	2.262(5)
C1−Rh1	1.842(4)	2.049(9)	1.999(10)	2.114(8)
C1−Rh2		2.050(10)	1.993(11)	2.709(10)
C2−Rh1	1.827(4)	1.995(8)	2.010(8)	1.998(6)
C2−Rh2		2.014(8)	1.999(9)	1.910(6)
C3−Rh1		1.995(8)	2.010(8)	1.986(7)
C3−Rh2		2.014(8)	1.999(9)	1.907(7)
C1−O1	1.136(5)	1.121(12)	1.170(13)	1.216(9)
C2−O2	1.141(5)	1.166(10)	1.167(11)	1.189(8)
C3−O3		1.166(10)	1.167(11)	1.202(8)
C1−O4				1.355(9)
C4−O4				1.436(9)
Rh1−Rh2		2.5888(14)	2.5930(12)	2.6512(6)

[a] For atom labelling see Figures 1, 2, and 3. − [b] In accord with the labelling for $[\mathbf{3}]^+$, the symmetry related atoms of N4, N6, C2 and O2 (obtained by applying m) in $[\mathbf{2A}]^{2+}$ and $[\mathbf{2B}]^{2+}$, are presented as N5, N7, C3 and O3, respectively, for reasons of comparison.

Table 2. Selected bond angles [°] for compounds $[\mathbf{1}]PF_6$, $[\mathbf{2}](PF_6)_2$, and $[\mathbf{3}]PF_6$[a]

	$[\mathbf{1}]^+$	$[\mathbf{2A}]^{+}$[b]	$[\mathbf{2B}]^{+}$[b]	$[\mathbf{3}]^+$
N31−Rh1−N4	81.87(10)	81.8(3)	81.1(3)	79.5(2)
N31−Rh1−N5	79.41(10)	81.8(3)	81.1(3)	79.2(2)
N4−Rh1−N5	76.41(11)	81.0(4)	80.8(4)	79.5(2)
N32−Rh2−N6		81.1(3)	81.3(3)	78.6(2)
N32−Rh2−N7		81.1(3)	81.3(3)	78.4(2)
N6−Rh2−N7		81.0(4)	81.2(4)	79.4(2)
N31−Rh1−C1	177.65(14)	179.6(4)	178.4(5)	172.5(3)
N32−Rh2−C1		179.2(4)	179.1(5)	
N31−Rh1−C2	95.91(14)	97.2(3)	97.6(4)	97.0(2)
N32−Rh2−C2		98.6(3)	97.7(3)	107.5(2)
N31−Rh1−C3		97.2(3)	97.6(4)	93.6(2)
N32−Rh2−C3		98.6(3)	97.7(3)	104.2(3)
N4−Rh1−C1	95.79(13)	98.5(3)	100.1(3)	96.6(3)
N4−Rh1−C2	144.29(18)	96.6(3)	97.3(4)	98.0(2)
N4−Rh1−C3		177.5(3)	177.8(3)	173.1(2)
N5−Rh1−C1	100.14(14)	98.5(3)	100.1(3)	93.8(3)
N5−Rh1−C2	138.52(17)	177.5(3)	177.8(3)	175.7(2)
N5−Rh1−C3		96.6(3)	97.3(4)	99.3(2)
N6−Rh2−C1		98.3(3)	99.4(3)	
N6−Rh2−C2		97.1(3)	96.8(3)	96.9(3)
N6−Rh2−C3		178.1(3)	177.9(3)	174.1(3)
N7−Rh2−C1		98.3(3)	99.4(3)	
N7−Rh2−C2		178.1(3)	177.9(3)	172.4(2)
N7−Rh2−C3		97.1(3)	96.8(3)	96.0(2)
O1−C1−Rh1	177.6(4)	140.8(8)	138.7(9)	126.6(6)
O1−C1−Rh2		140.9(8)	140.3(9)	
O2−C2−Rh1	176.8(4)	141.5(7)	139.1(8)	134.7(5)
O2−C2−Rh2		137.9(7)	140.2(8)	139.9(5)
O3−C3−Rh1		141.5(7)	139.1(8)	134.8(5)
O3−C3−Rh2		137.9(7)	140.2(8)	139.4(5)
Rh1−C1−Rh2		78.3(3)	81.0(4)	
Rh1−C2−Rh2		80.4(3)	80.6(3)	85.4(3)
Rh1−C3−Rh3		80.4(3)	80.6(3)	85.8(3)
C1−Rh1−C2	85.95(16)	82.5(3)	81.2(3)	89.9(3)
C1−Rh2−C2		82.0(3)	81.6(3)	
C1−Rh1−C3		82.5(3)	81.2(3)	90.3(3)
C1−Rh2−C3		82.0(3)	81.6(3)	
C2−Rh1−C3		85.8(5)	84.6(6)	82.7(3)
C2−Rh2−C3		84.8(5)	85.2(5)	87.2(3)
C1−Rh1−Rh2		50.8(3)	49.4(3)	68.2(3)
C2−Rh1−Rh2		50.1(2)	49.5(3)	45.9(2)
C3−Rh1−Rh2		50.1(2)	49.5(3)	45.8(2)
C1−Rh2−Rh1		50.8(2)	49.6(3)	
C2−Rh2−Rh1		49.5(2)	49.9(2)	48.7(2)
C3−Rh2−Rh1		49.5(2)	49.9(2)	48.4(2)
O1−C1−O4				120.3(7)
O4−C1−Rh1				112.6(5)
C1−O4−C4				115.2(6)

[a] For atom labelling see Figures 1, 2, and 3. − [b] In accord with the labelling for $[\mathbf{3}]^+$, the symmetry related atoms of N4, N6, C2, and O2 (obtained by applying m) in $[\mathbf{2A}]^{2+}$ and $[\mathbf{2B}]^{2+}$, are presented as N5, N7, C3, and O3, respectively, for reasons of comparison.

third nitrogen of Cn*. Remarkably, the N donors in the trigonal plane (N4 and N5) span the smallest N−Rh−N angle [76.41(11)°]. In order to be closer to the ideal 120° angle for a trigonal bipyramid, these N donors would be expected to span the largest N−Rh−N angle.

The axial Rh−N distance [Rh1−N31: 2.139(3) Å] is shorter than the equatorial Rh−N distances. [Rh1−N4: 2.261(3) Å, Rh1−N6: 2.320(3) Å]. The Rh−C and C−O distances of the equatorial and the axial carbonyl groups of cation $[\mathbf{1}]^+$ are equal within the experimental error (averaged distances: Rh−C: 1.83 Å, C−O: 1.14 Å) and are comparable to those in known five-coordinate $(L)_3Rh^I(CO)_2$ complexes.[5][6] In contrast to $[\mathbf{1}]^+$, these are all neutral complexes containing a monoanionic ligand, mostly a Cp-derivative. (Observed range in Rh−C distances: 1.824−1.867 Å, C−O distances: 1.109−1.154 Å.) Thus far, the hydrotrispyrazolylborate ($Tp^{R,R'}$) complex $[(Tp^{CF3,Me})Rh^I(CO)_2]$ was the only "five-coordinate" $'N_3'Rh^I(CO)_2$ complex with a reported X-ray structure.[6] In this complex, one of the three pyrazolyl groups is only weakly bound to the apical position in a square pyramidal geometry [Rh−N: 2.636(5)]. The basal Rh−N distances are 2.116(4) and 2.114(5) Å. Other reported bond lengths are: Rh−C: 1.824(7), 1.832(9) Å, C−O: 1.145(12), 1.146(9) Å. In solution $[(Tp^{CF3,Me})Rh^I(CO)_2]$ behaves like other $[Tp^{R,R'}Rh^I(CO)_2]$ derivatives in that it gives rise to equilibria between four and five coordination.[7]

The positions of the terminal ν_{CO} bands in the IR spectra of $[\mathbf{1}]PF_6$ in the solid state (KBr: 2054 and 1962 cm^{-1}) differ significantly from those in solution (CH_3CN: 2063 and 1980 cm^{-1}). A square pyramidal or even a square planar

geometry for [**1**]PF_6 in solution can therefore not be excluded. The latter geometry however seems unlikely, as it would require the rather rigid Cn* ligand to be κ^2-coordinated in solution. The ^{1}H-NMR spectrum of [**1**]PF_6 in [D$_6$]acetone or CD_3CN shows one singlet for the three N−CH_3 groups of the Cn* ligand, and one AA′BB′-multiplet pattern for its diastereotopic N−CH_aH_b− protons. The ^{13}C-spectrum of [**1**]PF_6 shows only one doublet at δ = 189 ($^1J_{C-Rh}$ = 73 Hz) for both carbonyl groups. The equivalence of its N−CH_2− and its N−CH_3 groups in the ^{1}H-NMR spectrum and the two carbonyls in the ^{13}C-spectrum must result from the rapid exchange of positions by Cn* nitrogens and carbonyl carbons at room temp.

Structure of [**2**]$(PF_6)_2$

Bright yellow crystals of compound [**2**]$(PF_6)_2$ were obtained from a saturated MeOH solution. From one of these crystals the structure of the cation [**2**]$^{2+}$ was determined by X-ray diffraction (Figure 2). Selected bond lengths and angles are given in Tables 1 and 2.

Figure 2. Crystal structure of cation [**2A**]$^{2+}$

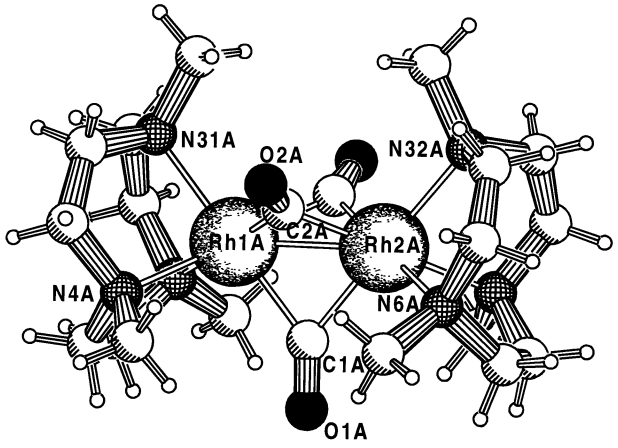

In the crystal structure two independent cations, [**2A**]$^{2+}$ and [**2B**]$^{2+}$, are found per unit cell. Each cation only slightly deviates from C_{2v} symmetry. A crystallographic mirror-plane passes through Rh1, Rh2, and C1. The two rhodium centers are bridged via three carbonyl groups. The coordination geometry of the two (μ-CO)$_3$ bridged rhodium atoms can best be described as distorted octahedral. In contrast to [**1**]$^+$, all N−Rh−N angles in [**2A**]$^{2+}$ and [**2B**]$^{2+}$ are found at approx. 81°.

The rather short Rh−Rh distances of the two independent cations, Rh1A−Rh2A 2.5888(14) and Rh1B−Rh2B 2.5930(12) Å, are in accordance with a Rh−Rh single bond, resulting from application of the 18 VE rule. Theoretical calculations however indicated that actual M−M binding in M(d8)(μ-CO)$_3$M(d8) systems is much weaker.[8] The various Rh−N, Rh−C, and C−O distances are equal within experimental error (averaged distances: Rh−N: 2.20 Å, Rh−C: 2.01 Å, C−O: 1.16 Å). There are a few literature reports of complexes containing the [Rh(μ-CO)$_3$Rh]$^{2+}$ core.[9] The distances and angles of the [Rh(μ-CO)$_3$Rh]$^{2+}$ core of [**2**]$(PF_6)_2$ compare well with those of [Rh(μ-CO)$_3$Rh]$^{2+}$ cores that have previously been characterized by single crystal X-ray diffraction; They involve ′N_3′ ligands, viz. methyl(trispyrazolyl)gallate[10] and two macrocyclic hexaamine-type ligands,[11] and a tripod ′O_3′ ligand.[12] On the basis of spectral and analytical data, complexes containing the [Rh(μ-CO)$_3$Rh]$^{2+}$ core have been proposed with the ′N_3′ ligands tris(pyrazolyl-1-yl)methane,[13] a macrocyclic hexaamine[14] and hydrotris(pyrazolyl)borate.[15] For the ′S_3′ ligand 2,5,8-trithia[9]-*o*-cyclophane it was reported that two [′S_3′Rh(CO)$_2$]$^+$ species exist in equilibrium with [′S_3′Rh(μ$_2$-CO)$_3$Rh′S_3′]$^{2+}$ [16], in marked contrast with our own observations for [′N_3′Rh(CO)$_2$]$^+$ and [′N_3′Rh(μ$_2$-CO)$_3$Rh′N_3′]$^{2+}$ (vide supra).

The IR band at 1810 cm^{-1} (CH_3CN) and the triplet ^{13}C-NMR signal at δ = 222 ($^1J_{C-Rh}$ = 28.7 Hz) indicate that the tri(μ-carbonyl) bridge is maintained in solution. The ^{1}H-NMR and ^{13}C-NMR signals for the two Cn* ligands show that [**2**]$^{2+}$ has an effective D_{3h} symmetry in solution. The N−CH_2− groups are observed as one singlet in the ^{1}H-NMR spectrum in [D$_6$]acetone, but the chemically inequivalent *endo*- and *exo*-protons are observed as the expected AA′BB′ multiplet in CD_3CN.

[**2**]$(PF_6)_2$ must be stored in the dark, since exposure to normal (glass-filtered) daylight results in a colour change from yellow, via intermediate green,[17] to dark blue, both in the solid state and in CH_3CN solution. The nature of the resulting blue compound is currently under investigation.[18]

Structure of [**3**]PF_6

Pale orange crystals of [**3**]PF_6 were obtained from a saturated MeOH solution, and the structure of cation [**3**]$^+$ was determined by X-ray diffraction (see Figure 3). Selected bond lengths and angles are given in Tables 1 and 2.

Figure 3. Crystal structure of cation [**3**]$^+$

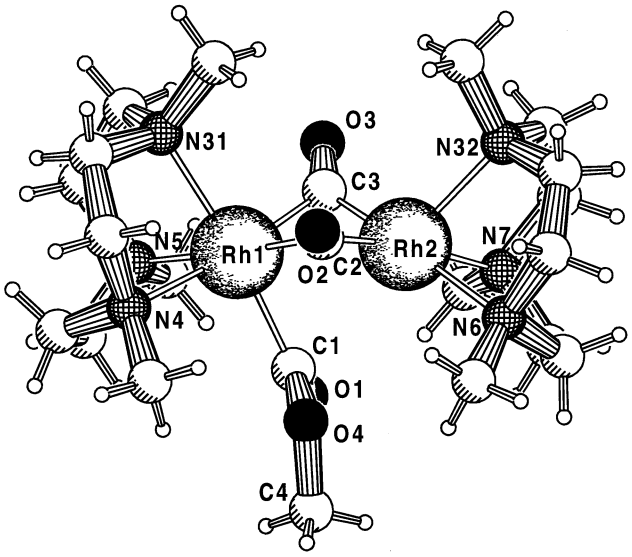

Comparison of Figures 2 and 3 shows that one of the three μ-carbonyl groups in [**2**]$^{2+}$ has been converted to a methoxycarbonyl group in [**3**]$^+$. This group is bound to

only one of the two rhodium centres, at a Rh1−C1 distance of 2.114(8) Å, thus leaving the other rhodium centre apparently coordinatively unsaturated at a Rh2−C1 distance of 2.709(10) Å. The Rh1−C1 distance in $[\mathbf{3}]^+$ is relatively long compared to those in previously reported Rh−C(O)OR complexes, viz. 1.918(9),[19] 2.041(5)[20] and 2.088(11)[21]Å. These complexes are all Rh^{III}-complexes. Ir−C distances in Ir−C(O)OR complexes have been found in the range 2.005 to 2.084 Å,[22] with the exception of a value of 2.20(4) Å reported for Ir−C(O)OMe in $[Ir_4(CO)_{11}\{C(O)OMe\}]^-$.[23] The Rh−Rh distance in $[\mathbf{3}]^+$, 2.6512(6) Å, is somewhat elongated compared to that in $[\mathbf{2}]^{2+}$, perhaps indicating the absence of a Rh−Rh bond in $[\mathbf{3}]^+$. This would make Rh1 a 18 VE, six-coordinate Rh^I site and Rh2 a 16 VE, five-coordinate Rh^I site. Strikingly, the Cn* ligands in $[\mathbf{3}]^+$ are found to be bound equally strongly to Rh1 and Rh2. Also there appear to be no significant differences between the Rh−N distances for N trans to μ-CO and N trans to the methoxycarbonyl-group or the vacant site. The average Rh−N distance in $[\mathbf{3}]^+$, 2.26 Å, is approx. 0.06 Å longer than that in $[\mathbf{2}]^+$. The largest difference between $[\mathbf{2}]^+$ and $[\mathbf{3}]^+$ is seen in the bonding of the bridging carbonyls. The addition of a methoxy anion to one of the three carbonyls in $[\mathbf{2}]^+$ has resulted in an asymmetric coordination of the remaining two bridging carbonyls. They are bound approx. 0.1 Å more tightly, and their O−C−Rh angles are approx. 5° less acute for the "coordinatively unsaturated" Rh2. The Rh1−C2 and Rh1−C3 distances in $[\mathbf{3}]^+$ are comparable to those found for $[\mathbf{2}]^+$. In the IR spectrum of $[\mathbf{3}]PF_6$ (KBr), three C−O stretching modes at 1771(w), 1708(s), and 1607(m) are observed. The first two are considered to be μ-CO vibrations, the latter is assigned to the carbonyl group of the C(O)OMe fragment. The appearance of a peak at *m/z* = 777 ($[M - OMe]^+$), besides peaks at *m/z* = 808 ($[M]^+$) and *m/z* = 663 ($[M-PF_6]^+$), in the FAB-MS spectrum shows loss of MeO^- under FAB conditions.

Fluxional Behaviour of in $[\mathbf{3}]^+$ *in Solution: C(O)OMe Migration*

The IR spectrum of $[\mathbf{3}]PF_6$ in CH_3CN [ν_{CO} 1774 (w), 1715 (s), 1618 (m)] is quite similar to that recorded in KBr, indicating that the structure of $[\mathbf{3}]^+$ is maintained in solution. In the ^{1}H-NMR spectrum of $[\mathbf{3}]^+$ the methoxy protons are observed as a singlet at δ = 3.5. In [D$_6$]acetone at room temperature only two singlets are observed for both Cn* groups, one singlet for all the N−CH_3 groups and one for all the N−CH_2− groups. In the ^{1}H-NOESY spectrum of $[\mathbf{3}]PF_6$ NOE contacts are observed between the methoxy group and the methyl and methylene protons of the Cn* ligands. As observed for $[\mathbf{2}]^{2+}$, in CD_3CN the N−CH_2− signal splits into an AA′BB′ pattern. Apparently $[\mathbf{3}]^+$ has effective D_{3h} symmetry in which the two Cn* ligands, and the N−CH_2− and N−CH_3 groups within the Cn* ligands are equivalent on the NMR timescale. In the room temperature ^{13}C-spectrum in CD_3CN, the 18 different carbons in the two distinct Cn* ligands found in the X-ray structure give only two averaged ^{13}C signals, one at δ = 58.0 for the twelve N−CH_2− groups and one at δ = 51.5 for the six N−CH_3 groups. This must result from a fast equilibrium in solution. Two triplet signals are observed for the carbonyl groups, one at δ = 248.1 ($^1J_{Rh-C}$ = 37.5 Hz) for the μ-CO groups and one at δ = 179.9 ($^1J_{Rh-C}$ = 17.3 Hz) for the carbonyl of the C(O)OMe ligand, with relative intensity of 2:1. The apparently equal coupling of the C(O)OMe carbonyl signal with both rhodium centres must be the result of a rapid migration of the methoxycarbonyl ligand between Rh1 and Rh2. (Figure 4) As a result, each Rh-atom becomes alternately five and six coordinate. The observed apparent $^1J_{Rh-C}$ of 17.3 Hz is quite small compared to that in other Rh−C(O)OR compounds (31−55 Hz)[19][20][21]. It converts to an actual value of 34.6 Hz, comparable to the literature values, under the assumption that $^3J_{Rh-C}$ in the static structure of $[\mathbf{3}]^+$ is close to zero.

Figure 4. Proposed mechanism of methoxycarbonyl migration in $[\mathbf{3}]PF_6$

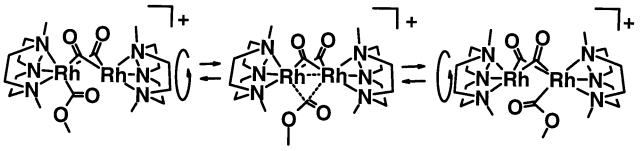

We propose that the observed averaging of NMR signals for the N−CH_2− and the N−CH_3 groups of the two Cn* ligands in $[\mathbf{3}]^+$ results from a combination of two fast processes: reversible migration of the C(O)OMe ligand between both Rh centres, and exchange of nitrogen donor atom positions at the five-coordinate rhodium centre. The latter is also observed in five-coordinate $[\mathbf{1}]^+$ (vide supra).

We thank *Unilever Research laboratory Vlaardingen* for a generous supply of 1,4,7-trimethyl-1,4,7-triazacyclononane.

Experimental Section

General Procedures: All reactions were performed under a nitrogen atmosphere using standard Schlenk techniques. Solvents (p.a.) were deoxygenated by bubbling through a stream of N_2, or by the freeze-pump-thaw method. $[\{(CO)_2Rh(\mu\text{-}Cl)\}_2]$ was prepared according to a literature procedure.[24] 1,4,7-trimethyl-1,4,7-triazacyclononane (Cn*) was generously supplied by Unilever Research. All other chemicals are commercially available and were used without further purification. − FT-IR: Perkin Elmer 1720X. − NMR: Bruker DPX200 (200 MHz and 50 MHz for ^{1}H and ^{13}C, respectively), Bruker AC300 (300 MHz and 75 MHz for ^{1}H and ^{13}C, respectively). Solvent shift reference for ^{1}H NMR: [D$_6$]acetone δ_H = 2.05, CD_3CN δ_H = 1.98. For ^{13}C NMR: [D$_6$]acetone δ_C = 29.50, CD_3CN δ_C = 1.28. − FAB-MS: VG7070E.

Preparation of a Mixture of $[\mathbf{1}]PF_6$, $[\mathbf{2}](PF_6)_2$ *and* $[\mathbf{3}]PF_6$: In a typical experiment 200 mg of (1.16 mmol) Cn* was dissolved in 15 ml of MeOH and the resulting solution was cooled to 0°C. 234 mg (0.6 mmol) of $[\{(CO)_2Rh(\mu\text{-}Cl)\}_2]$ was subsequently added and the orange solution was stirred for approximately 1 h. Evolution of a slight amount of gas was noticed. The addition of 800 mg (4.91 mmol) of NH_4PF_6, dissolved in 5 ml of MeOH, to the reaction mixture caused the precipitation of a mixture of $[\mathbf{2}](PF_6)_2$ and $[\mathbf{3}]PF_6$, which was collected by filtration. Combined yield 650 mg, ca. 60% based on $[\{(CO)_2Rh(\mu\text{-}Cl)\}_2]$. The filtrate was used to isolate a minor fraction of compound $[\mathbf{1}]PF_6$.

[**1**]PF_6: [**1**]PF_6 was obtained as bright orange crystals, suitable for X-ray diffraction, by cooling the filtrate of the reaction mixture described above to −30°C. Besides further precipitation of [**2**]$(PF_6)_2$ and [**3**]PF_6 a small amount of bright orange crystals of [**1**]PF_6 slowly deposited after some days. A few large crystals of [**1**]PF_6 could be isolated (hand-picking) from the resulting solid mixture.− ^{1}H NMR (200 MHz, CD_3CN): δ = 3.3−2.8 (m, 12 H, N−CH_2−), 3.19 (d, 9 H, $^3J_{Rh-H}$ = 1 Hz, N−CH_3). − ^{13}C NMR (50 MHz, CD_3CN): δ = 189 (d, $^1J_{Rh-C}$ = 73 Hz, Rh−*C*O), 59.6 (N−CH_2−), 55.3 (N−CH_3). − FT-IR (KBr): $\tilde{\nu}$ = 2054 cm^{-1}, 1962 (CO). − FT-IR (CH_3CN): $\tilde{\nu}$ = 2063 cm^{-1}, 1980 (CO). − FAB-MS; *m/z*: 273 [M−$(CO)_2$−PF_6−H]$^+$. − CHN analysis was not performed due to the small amount of pure [**1**]PF_6 obtained.

[**2**]$(PF_6)_2$: 800 mg (4.91 mmol) of NH_4PF_6 was added to 600 mg of the solid mixture of [**2**]$(PF_6)_2$ and [**3**]PF_6, prepared as decribed above. 15 ml of MeOH was subsequently added, and the mixture was refluxed (all solid material redissolved) for approximatly 10 min. After cooling to room temp., the MeOH solvent was partially evaporated. Compound [**2**]$(PF_6)_2$ crystallized as bright yellow cubes from the solution at −30°C, and was collected by filtration. Yield 550 mg (ca. 80%). − ^{1}H NMR (200 MHz, CD_3CN): δ = 3.30−2.90 (m, 24 H , N−CH_2−), 2.84 (s, 18 H, N−CH_3). − ^{1}H NMR (200 MHz, [D_6]-acetone): δ = 3.44 (s, 24 H , N−CH_2−), 3.14 (s, 18 H, N−CH_3). − ^{13}C NMR (50 MHz, [D_6]-acetone): δ = 221.9 (t, $^1J_{Rh-C}$ = 28.7 Hz, μ_2-CO), 58.5 (N−CH_2−), 52.0 (N−CH_3). − FT-IR (KBr): $\tilde{\nu}$ = 1803 cm^{-1} (μ-CO). − FT-IR (CH_3CN): $\tilde{\nu}$ = 1810 cm^{-1} (μ-CO). − FAB-MS; *m/z*: 777 [M−PF_6]$^+$, 748 [M−CO−PF_6]$^+$, 604 [M−CO−2PF_6]$^+$, 316 [M−2PF_6]$^{2+}$. − Calculated for $C_{21}H_{42}F_{12}N_6O_3P_2Rh_2$: C 27.35, H 4.59, N 9.11 Found: C 27.33, H 4.57, N 8.98.

[**3**]PF_6: 100 mg (1.9 mmol) of NaOMe was added to 300 mg of the solid mixture of [**2**]$(PF_6)_2$ and [**3**]PF_6, prepared as decribed above. 15 ml of MeOH was subsequently added, and the mixture was refluxed (all solid material redissolved) for approximatly 10 min. After cooling to room temp., the MeOH solvent was partially evaporated. Compound [**3**]PF_6 crystallized as pale orange needles from the solution at −30°C, and was collected by filtration. Yield 200 mg (ca. 70%). − ^{1}H NMR (200 MHz, [D_6]acetone): δ = 3.54 (s, 3 H, OCH_3), 2.90 (s, 24 H, N−CH_2−), 2.81 (d, $^3J_{C-Rh}$ = 0.8 Hz, 18 H, N−CH_3). − ^{13}C NMR (50 MHz, [D_6]acetone): δ = 57.7 (N−CH_2−), 51.1 (N−CH_3), 50.9 (OCH_3) (^{13}C-carbonyl signals undetected, due to low solubility). − ^{1}H NMR (300 MHz, CD_3CN): δ = 3.52 (s, 3 H, OCH_3), 2.90−2.55 (m, 24 H, N−CH_2−), 2.76 (d, $^3J_{H-Rh}$ = 0.80 Hz, 18 H, N−CH_3). − ^{13}C NMR (75 MHz, CD_3CN): δ = 248.1 (t, $^1J_{C-Rh}$ = 37.5 Hz, μ-CO), 179.9 (t, $^1J_{C-Rh}$ = 17.3 Hz, *C*(O)OMe), 58.0 (N−CH_2−), 51.5 (N−CH_3), 51.4 (OCH_3). − FT-IR (KBr): $\tilde{\nu}$ = 1771 cm^{-1} (w), 1708 (s) (μ-CO), 1607 (m) (C=O), 1048 (C−O). − FT-IR (CH_3CN): $\tilde{\nu}$ = 1774 cm^{-1} (w), 1715 (s) (μ-CO), 1618 (m) (C=O), (C−O) obscured by solvent vibrations. − FAB-MS; *m/z*: 808 [M]$^+$, 777 [M−OMe]$^+$, 663 [M−PF_6]$^+$, 604 [M−PF_6−OMe−CO]$^+$, 576 [M−PF_6−OMe−2CO]$^+$. − Calculated for $C_{22}H_{45}F_6N_6O_4PRh_2$: C 32.69, H 5.61, N 10.40 Found: C 32.33, H 5.37, N 10.06.

X-ray Structure Determination of [**1**]PF_6, [**2**]$(PF_6)_2$ *and* [**3**]PF_6: Crystals of [**1**]PF_6, [**2**]$(PF_6)_2$ and [**3**]PF_6 suitable for X-ray diffraction studies were obtained by cooling a saturated solution of the corresponding compound in MeOH to −30°C. Single crystals were mounted in air on glass fibres. Intensity data were collected at room temp. For all three compounds an Enraf-Nonius CAD4 single-crystal diffractometer was used, graphite monochromatized Cu-*Kα* radiation, θ-2θ-scan mode. Unit cell dimensions were determined from the angular setting of 25 reflections. Intensity data were corrected for Lorentz and polarization effects. Semi-empirical absorption correction (*Ψ*-scan) was applied for all three compounds.[25]

Table 3. Crystallographic data for compounds [**1**]PF_6, [**2**]$(PF_6)_2$, and [**3**]PF_6

	[**1**]PF_6	[**2**]$(PF_6)_2$	[**3**]PF_6
Emperical formula	$C_{11}H_{21}F_6N_3O_2PRh$	$C_{21}H_{42}F_{12}N_6O_3P_2Rh_2$	$C_{22}H_{45}F_6N_6O_4PRh_2$
Crystal size [mm]	0.60 × 0.35 × 0.28	0.42 × 0.18 × 0.11	0.32 × 0.16 × 0.10
Formula weight	475.19	922.37	808.43
Temperature [K]	293(2)	293(2)	293(2)
Crystal system	Monoclinic	Monoclinic	Monoclinic
Space group	*P* $2_1/n$	*C* 2/*m*	*P* $2_1/n$
a [Å]	8.87948(17)	20.790(3)	8.5949(4)
b [Å]	15.2246(3)	15.814(3)	13.1036(5)
c [Å]	12.9031(3)	22.051(5)	27.7555(13)
α [°]	90	90	90
β [°]	91.960(4)	116.61(2)	91.124(4)
γ [°]	90	90	90
V [Å^3]	1743.30(6)	6482(2)	3125.3(2)
$\rho_{calcd.}$ [gcm^{-3}]	1.811	1.890	1.718
Z	2	8	4
Wavelength [Å]	1.54184	1.54184	1.54184
F(000)	952	3696	1640
θ range [°]	4.49−69.88	40.158−46.695	40.113−46.904
Index ranges	$-10 \le h \le 10$	$-26 \le h \le 23$	$0 \le h \le 10$
	$-18 \le k \le 18$	$0 \le k \le 19$	$-15 \le k \le 0$
	$-15 \le l \le 15$	$0 \le l \le 27$	$-33 \le l \le 33$
Measured reflections	12510	7215	6340
Unique reflections	3303	7032	5926
Observed reflections [$I_o > 2\sigma(I_o)$]	3254	5747	5172
Refined parameters	302	439	377
Goodness-of-fit on F^2	1.104	1.086	1.032
R [$I_o > 2\sigma(I_o)$]	0.0332	0.0686	0.0599
*wR*2[all data]	0.0786	0.1922	0.1553
ρ_{fin} (max/min) [e Å^{-3}]	0.915/−0.623	1.845/−2.748	1.430/−2.186

Structures were solved by the program system DIRDIF[26] using the program PATTY[27] to locate the heavy atoms and were refined with standard methods (refinement against F^2 of all reflections with SHELXL97[28]) with anisotropic parameters for the nonhydrogen atoms. For **[1]**PF_6 the hydrogens were initially placed at calculated positions and were subsequently refined freely. For **[2]**$(PF_6)_2$ and **[3]**PF_6 all hydrogens were refined riding on the parent atoms. Details of the crystal parameters, data collections and structure refinements are given in Table 3. Crystallographic data (tables of structure determinations summaries, lists of anisotropic displacement parameters, lists of atom coordinates and full lists of bond lengths and angles, excluding structure factors) have been deposited with the Cambridge Crystallographic Data Centre as supplementary publication no. CCDC-179-100725. Copies of the data can be obtained free of charge on application to The Director, CCDC, 12 Union Road, Cambridge CB2 1EZ, UK [Fax: (internat.) +44(1223) 336-033; E-mail: deposit@ccdc.cam.ac.uk].

[1] $[(Cn^*)Rh^{III}(Me)]^+$ is active in the polymerisation of ethene: [1a] L. Wang, T. C. Flood, *J. Am. Chem. Soc*. **1992**, *114*, 3169. – [1b] L. Wang, R. S. Lu, R. Bau, T. C. Flood, *J. Am. Chem. Soc*. **1993**, *115*, 6999.

[2] $[(Cn^*)Rh^{I}(PMe_3)]^+$ and $[(Tp^{Me2})Rh^{I}(CO)]$ oxidatively add to C−H bonds: [2a] C. Wang, J. W. Ziller, T. C. Flood, *J. Am. Chem. Soc*. **1995**, *117*, 1647. – [2b] C. K. Ghosh, W. A. G. Graham, *J. Am. Chem. Soc*. **1987**, *109*, 4726. – [2c] C. K. Ghosh, W. A. G. Graham, *J. Am. Chem. Soc*. **1989**, *111*, 375. – [2d] P. E. Bloyce, J. Mascetti, A. J. Rest, *J. Organomet. Chem.* **1993**, *444*, 223. – [2e] A. A. Purwoko, A. J. Lees, *Inorg. Chem.* **1996**, *35*, 675.

[3] The α-chlorotolyl complex $[(2,6\text{-}(C(Me)=N\text{-}iPr)_2C_5H_3N)Rh^{III}Cl_2(CHClPh)]$ reacts with H_2O and O_2 to give benzaldehyde and H_2O_2: H. F. Haarman, F. R. Bregman, P. W. N. M. van Leeuwen, K. Vrieze, *Organometallics* **1997**, *16*, 979.

[4] B. de Bruin, M. J. Boerakker, J. J. J. M. Donners, B. E. C. Christiaans, P. P. J. Schlebos, R. de Gelder, J. M. M. Smits, A. L. Spek, A. W. Gal, *Angew. Chem*. **1997**, *109*, 2153 ; *Angew. Chem. Int. Ed. Eng*. **1997**, *36*, 2064.

[5] [5a] D. L. Lichtenberger, C. H. Blevins II, R. B. Ortega, *Organometallics* **1984**, *3*, 1614. – [5b] P. Braunstein, H. Lehner, D. Matt, A. Tiripicchio, M. Tiripicchio Camellini, *New J. Chem. (Nouv. J. Chim.)* **1985**, *9*, 597. – [5c] U. Behrens, F. Edelmann, *Z. Naturforsch., Teil B* **1986**, *41*, 1426. – [5d] A. K. Kakkar, N. J. Taylor, T. B. Marder, J. K. Shen, N. Hallinan, F. Basolo, *Inorg. Chim. Acta* **1992**, *198*, 219. – [5e] M. D. Rausch, W. P. Hart, J. L. Atwood, M. J. Zaworotko, *J. Organomet. Chem.* **1980**, *197*, 225. – [5f] A. K. Kakkar, N. J. Taylor, J. C. Calabrese, W. A. Nugent, D. C. Roe, E. A. Connaway, T. B. Marder, *J. Chem. Soc., Chem. Comm.* **1989**, 990. – [5g] P. Harter, J. Behm, V. Burkert, *J. Organomet. Chem.* **1992**, *438*, 297.

[6] E. Del Ministro, O. Renn, H. Rüegger, L. M. Venanzi, U. Burckhardt, V. Gramlich, *Inorg. Chim. Acta* **1995**, *240*, 631.

[7] [7a] N. Kitajima, W. B. Tolman, *Prog. Inorg. Chem*. **1995**, *43*, 419 (468). – [7b] A. L. Rheingold, R. Ostrander, B. S. Haggerty, S. Trofimenko, *Inorg. Chem.* **1994**, *33*, 3666.

[8] R. H. Summerville, R. J. Hoffmann, *J. Am. Chem. Soc*. **1979**, *101*, 3821.

[9] With Cp-ligand types, the $[Rh(CO)_3Rh]^{2+}$-core contains only one μ-CO, each Rh-atoms contains a terminal CO: O. S. Mills, J. P. Nice, *J. Organomet. Chem.* **1967**, *10*, 337.

[10] B. M. Louie, S. T. Rettig, A. Storr, J. Trotter, *Can J. Chem.* **1984**, *62*, 633.

[11] [11a] J.-P. Lecomte, J.-M. Lehn, D. Parker, J. Guilhem, C. Pascard, *J. Chem. Soc., Chem. Commun*. **1983**, 296. – [11b] J. M. Johnson, J. E. Bulkowski, A. L. Rheingold, B. C. Gates, *Inorg. Chem*. **1987**, *26* (16), 2645.

[12] W. Kläui, M. Scotti, M. Valderrama, S. Rojas, G. M. Sheldrick, P. G. Jones, T. Schroeder, *Angew. Chem*. **1985**, *97*, 697; *Angew. Chem. Int. Ed*. **1985**, *24*, 683.

[13] M. A. Esteruelas, L. A. Oro, R. M. Claramunt, C. López, J. L. Lavandera, J. Elguero, *J. Organomet. Chem*. **1989**, *366*, 245.

[14] D. Parker, *J. Chem. Soc, Chem. Commun.* **1985**, 1129.

[15] [15a] D. J. O′Sulivan, F. J. Lalor, *J. Organomet. Chem*. **1974**, *65*, C47. – [15b] M. Cocivera, T. J. Desmond, G. Ferguson, B. Kaitner, F. J. Lalor, D. J. O′Sulivan, *Organometallics* **1982**, *1*, 1125.

[16] H. A. Jenkins, S. J. Loeb, *Organometallics* **1994**, *13*, 1840.

[17] The colour of $[H(BPz)_3]Rh(\mu_2\text{-}CO)_3Rh[H(BPz)_3]$ is reported to be a pale green/yellow colour (ref.[15]).

[18] Exposure of a CH_3CN solution of **[2]**$(PF_6)_2$ to bright sunlight for 2 h results in a dark blue coloured solution: ^1H NMR (200 MHz, CD_3CN): δ = 3.1−2.8 (m, 24 H, $N-CH_2-$), 2.84 (d, $^3J_{H-Rh}$ = 0.9 Hz, 18 H, $N-CH_3$). – ^{13}C NMR (50 MHz, CD_3CN): δ = 241.1 (t, $^1J_{C-Rh}$ = 35.7 Hz, μ-CO), 59.0 (s, $N-CH_2-$), 52.9 ($N-CH_3$). – FT-IR (CH_3CN): $\tilde{\nu}_{CO}$ = 1794 (w), 1738 (s), 1633 (m) cm^{-1}.

[19] R. G. Miller, J. A. Kyle, G. W. Coates, D. J. Anderson, P. E. Fanwick, *Organometallics* **1993**, *12*, 1161.

[20] P. L. Burk, D. van Engen, K. S. Campo, *Organometallics* **1984**, *3*, 493.

[21] D. Carmona, F. J. Lahoz, L. A. Oro, J. Reyes, M. P. Lamata, *J. Chem. Soc., Dalton Trans.* **1990**, 3551.

[22] [22a] V. G. Albano, P. L. Bellon, M. Sansoni, *Inorg. Chem.***1969**, *8*, 298. – [22b] R. L. Harlow, J. B. Kinney, T. Herskovitz, *J. Chem. Soc., Chem. Comm.* **1980**, 813. – [22c] L. Garlaschelli, M. C. Malatesta, S. Martinengo, F. Demartin, M. Manassero, M. Sansoni, *J. Chem. Soc., Dalton Trans.* **1986**, 777. – [22d] M. R. Churchill, J. C. Fettinger, W. M. Rees, J. D. Atwood, *J. Organomet. Chem.* **1986**, *304*, 227. – [22e] A. Del Zotto, A. Mezzetti, G. Dolcetti, P. Rigo, N. B. Pahor, *J. Chem. Soc., Dalton Trans.* **1989**, 607.

[23] L. Garlaschelli, S. Martinengo, P. Chini, F. Canziani, R. Bau, *J. Organomet. Chem.* **1981**, *213*, 379.

[24] J. A. McCleverty, G. Wilkinson, L. G. Lipson, M. L. Maddox, H. D. Kaesz, *Inorganic Synthesis* **1990**, *28*, 84.

[25] A.C.T. North, D.C. Phillips, F.C. Mathews, *Acta Cryst*. **1968**, *A24*, 351.

[26] P. T. Beurskens, G. Beurskens, W. P. Bosman, R. de Gelder, S. Garcia-Granda, R. O. Gould, R. Israel, J. M. M. Smits. *DIRDIF-96*. A computer program system for crystal structure determination by Patterson methods and direct methods applied to difference structure factors; Laboratory of Crystallography, Department of Inorganic Chemistry, University of Nijmegen: The Netherlands, **1996**.

[27] P. T. Beurskens, G. Beurskens, M. Strumpel, C. E. Nordman. In *Patterson and Pattersons*; J. P. Glusker; Eds.: B. K. Patterson, M. Rossi; Clarendon Press: Oxford, **1987**; p. 356.

[28] G. M. Sheldrick, *SHELXL-97*; University of Göttingen: Germany, **1997**.

[97251]

Fluxionality and Phosphane Arm-off Reactions of Octahedral Ruthenium(II) Complexes with the Tripodal Polyphosphane $MeC(CH_2PPh_2)_3$

Claudia Landgrafe, William S. Sheldrick*, and Marc Südfeld

Lehrstuhl für Analytische Chemie der Ruhr-Universität Bochum,
D-44780 Bochum, Germany

Received November 14, 1997

Keywords: Ruthenium / Phosphorus / Triphos complexes / Fluxionality / Arm-off dissociation

Structural fluxionality is apparent in the ^{1}H- and ^{31}P-NMR spectra of compounds of the type [Ru(L)(MeCN)(triphos)](CF_3SO_3), **2**−**5**, at 25°C, where L represents a diorganyldithiocarbamate or a heterocyclic κ^2N,S coordinating thioamide. In contrast, complexes [Ru(Et_2NCS_2)(Y)(triphos)]$^{n+}$ (**6**, n = 1, Y = CO; **7**, n = 0, Y = CN^-; **8**, n = 0, Y = H^-) are stereochemically rigid in solution at this temperature, indicating that MeCN dissociation must occur for the crowded octahedral coordination spheres of **2**−**5**. Reaction of [Ru$(MeCN)_3$(triphos)]$(CF_3SO_3)_2$, **1**, with Na(Et_2NCS_2) at a 1:2 molar ratio yields [Ru$(Et_2NCS_2$-$\kappa^2S)(Et_2NCS_2$-$\kappa S)$(triphos)], **9**, which slowly converts to [Ru$(Et_2NCS_2$-$\kappa^2S)_2$(triphosO-κ^2P)], **10**, on recrystallization from ethanol/acetone under air [triphosO is O=P$(Ph)_2CH_2C(CH_3)(CH_2PPh_2)_2$]. A similar $\kappa^3P\rightarrow\kappa^2P$ arm-off dissociation leads to the formation of [Ru(mpy-$\kappa^2N,S)_2$(triphosO-κ^2P)] (**13**) and [Ru(mmim-$\kappa^2N,S)_2$(triphosO-κ^2P)] (**14**) (Hmpy = 2-mercaptopyridine, Hmmim = 2-mercapto-1-methylimidazole). Crystal structures are reported for [Ru(mbt-κ^2N,S)(MeCN)(triphos-κ^3P)](CF_3SO_3) (**4**) (Hmbt = 2-mercaptobenzothiazole), [Ru(mpym-κ^2N,S)(mpym-κS)(triphos-κ^3P)] (**11**) (Hmpym = 2-mercaptopyrimidine) and **14**, the latter of which is present as the OC-6-13 isomer.

The employment of transition metal complexes of tripodal polyphosphanes such as $CH_3C(CH_2PPh_2)_3$ (triphos) in homogeneous catalysis has attracted considerable interest[1][2][3][4].Although triphos is often regarded as a typical innocent ligand, whose neopentyl skeleton $CH_3C(CH_2)_3$ allows a relatively unstrained occupation of three facial sites in a square-pyramidal, trigonal-bipyramidal or octahedral coordination sphere[5], dissociation of a phosphane arm to provide the more flexible κ^2P binding mode has been implicated for a number of five-coordinate Rh^I and Ir^I complexes[6][7][8][9][10][11][12][13]. The kinetic lability of M^I-P bonds (M = Rh, Ir) can also lead to structural fluxionality at higher temperatures. For instance dissociation of a triphosphane arm in [IrCl(CO)(triphos)] at room temperature enables exchange between the two phosphorus environments and the ^{31}P-NMR spectrum consists solely of a singlet at $\delta = -16.1$[14]. An explanation for this behavior has been sought in the marked reduction in ring strain that may be achieved on going from the facial κ^3P geometry in an $18e^-$ trigonal-bipyramidal complex to the open κ^2P geometry of a square planar $16e^-$ species[11][15].

The idealized P−M−P angles in octahedral Rh^{III} or Ir^{III} complexes provide a relatively unstrained κ^3P geometry for a tripodal polyphosphane, so that the energetic advantage of an open κ^2P coordination mode should be less pronounced than for five-coordinated M^I complexes. However an arm-off dissociation has been implicated for the reaction of the octahedral Rh^{III} complexes [RhL_3(triphos)] (L = Me, H) with CO and H_2[7][15] and ^{1}H- and ^{31}P-NMR evidence have been presented for a $\kappa^3P\rightleftharpoons\kappa^2P$ equilibrium of the triphosphane ligand in solutions of [$RhMe_2$(MeCN)(triphos)]$^+$ at room temperature[11]. We ourselves have recently reported[16][17] the stereochemical non-rigidity of the complex cations [RhL(MeCN)(triphos)]$^{2+}$ in which L represents the bidentate diorganyldithiocarbamates $R_2NCS_2^-$ (R = Et, Bz) or the heterocyclic thioamide $mpym^-$ (Hmpym = 2-mercaptopyrimidine). Both CH_3CN and phosphane arm-off dissociation processes can be proposed to explain the fluxional behavior of such species. κ^2P coordinated complexes of the type [RhL_2(triphos-κ^2P)]$^+$ (L = $Et_2NCS_2^-$, $Me_2NCS_2^-$ $mpym^-$) may be obtained on treating the starting compound [Rh$(MeCN)_3$(triphos)]$^{3+}$ with two equivalents of the potentially chelating ligands L.

These results prompted the present comparative study of fluxionality and phosphane arm-off reactions for analogous isoelectronic octahedral Ru^{II} complexes. Our continuing choice of diorganyldithiocarbamates and heterocyclic thioamides as ligands L was motivated by their ability to coordinate in both a mono- or bidentate fashion[18][19], by the pronounced *trans* effect of their sulfur donor atoms and by their relatively restricted steric demands owing to a small chelating angle of bite. The ambidentate thioamides $mpym^-$, mpy^- (Hmpy = 2-mercaptopyridine), and $mmim^-$(Hmmim = 2-mercapto-1-methylimidazole) were employed for a mechanistic study of isomer formation for complex cations of the type [RuL_2(triphos-κ^2P)]$^+$ and [RuL_2(triphosO-κ^2P)]$^+$ [triphosO is O=P$(Ph)_2CH_2$-$C(CH_3)(CH_2PPh_2)_2$].

Results

Treatment of [Ru$(MeCN)_3$(triphos)]$(CF_3SO_3)_2$ (**1**) with selected anionic ligands L affords the octahedral complexes [Ru(Et_2NCS_2)(MeCN)(triphos)](CF_3SO_3) (**2**), [Ru(pyrdtc)(MeCN)(triphos)](CF_3SO_3) (**3**) (pyrdtc$^-$ = pyrrolidindithi-

 © WILEY-VCH Verlag GmbH, D-69451 Weinheim, 1998 1434−1948/98/0303−0407 $ 17.50+.50/0

ocarbamate), [Ru(mbt)(MeCN)(triphos)](CF_3SO_3) (**4**) (Hmbt = 2-mercaptobenzothiazole), and [Ru(mpym)(MeCN)(triphos)](CF_3SO_3) (**5**) (schemes 1 and 2). Mononuclear structures for the complex cations of **2**−**5** are confirmed by their highest FAB mass peaks, which each correspond to [M − MeCN − CF_3SO_3]$^+$. In contrast, the reduced steric demands of the facially coordinated cyclic thioether 1,4,7-trithiacyclononane ([9]aneS_3) allow the adoption of tridentate μ-1κ*S*:2κ^2*S*,*S*′ and μ-1κ*S*:2κ^2*N*,*S* bridging modes by respectively $Me_2NCS_2^-$ and mbt$^-$ in the dinuclear complexes [{Ru(μ-Me_2NCS_2)([9]aneS_3)}$_2$](CF_3SO_3)$_2$[20] and [{Ru(μ-mbt)([9]aneS_3)}$_2$](CF_3SO_3)$_2$[21]. The latter coordination pattern has also been reported for the organometallic half-sandwich complex [{Ru(μ-mtz)(C_6H_6)}$_2$Cl]Cl[18] (Hmtz = 2-mercapto-2-thiazoline).

Scheme 1. [Ru(Et_2NCS_2)(MeCN)(triphos)]$^+$ cation of **2** and [Ru(pyrdtc)(MeCN)(triphos)]$^+$ cation of **3**

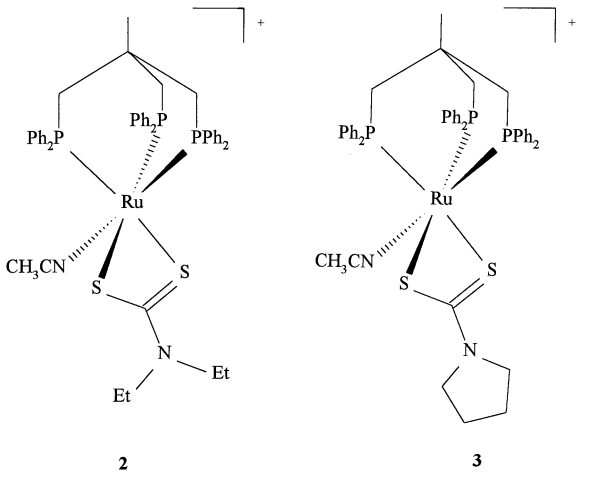

2 **3**

Scheme 2. [Ru(mbt)(MeCN)(triphos)]$^+$ cation of **4** and [Ru(mpym)(MeCN)(triphos)]$^+$ cation of **5**

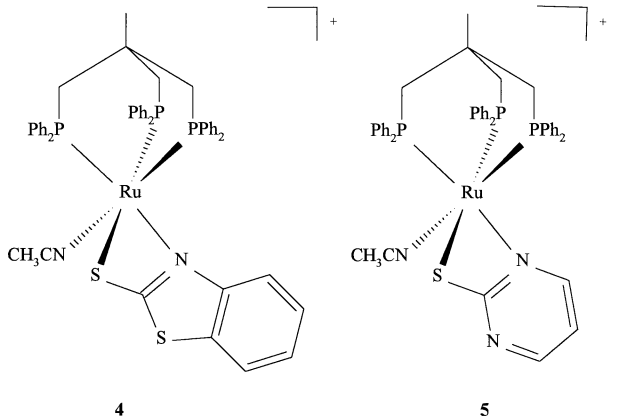

4 **5**

Figure 1 depicts the molecular structure of the monocation of **4**. As a result of the very small angle of bite [S(1)−Ru−N(1) = 66.1(2)°] of the coordinating heterocyclic thioamide mbt$^-$, an acetonitrile ligand can occupy the vacant sixth position of a coordination octahedron. However, the narrow S(1)−Ru−N(1) angle causes pronounced distortions in the geometry of the chelating polyphosphane cage. Whereas P(1)−Ru−P(2) [90.6(1)°] remains close to the idealised octahedral angle, both P(1)−Ru−P(3) and P(2)−Ru−P(3) narrow markedly [84.7(1), 86.4(1)°]. A marked *trans* influence of the thioamide sulfur atom is not apparent, indeed Ru−P(2) [2.302(2) Å] is slightly shorter than Ru−P(1) or Ru−P(3) [2.314(2), 2.307(2) Å]. It is instructive to contrast the formation of octahedral monocations in **2**−**5** with the recently reported five-coordinated product [Rh(bdt)(triphos)]$^+$ of the reaction of [$RhCl_3$(triphos)] with Na_2(bdt) [bdt = *o*-benzenedithiolate(2−)][22]. The angle of bite of the κ^2*S* coordinated *o*-benzenedithiolate ligand is no less than 20.3° wider than that of the κ^2*N*,*S* chelating 2-mercaptobenzothiazolate ligand in **4**. This finding suggests that the large Tolman cone angle of at least 220° for the tripodal polyphosphane ligand[23] will prevent the occupation of the potential sixth coordination site in [Rh(bdt)(triphos)]$^+$.

Figure 1. Molecular structure of the cation of **4**. Phenyl rings are omitted for clarity[a]

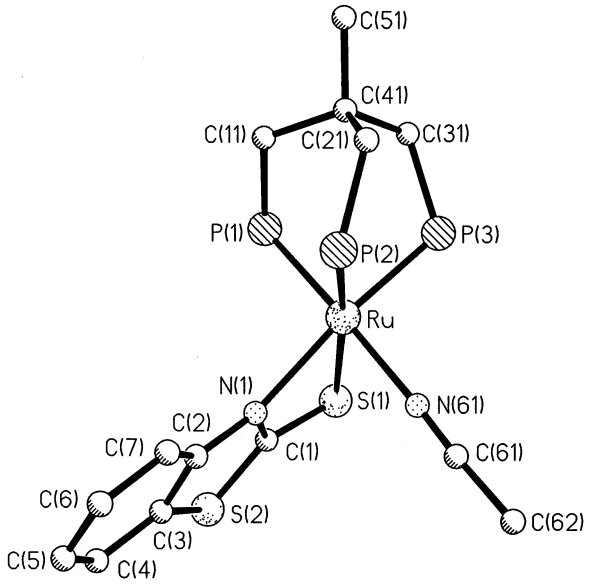

[a] Selected bond lengths [Å] and angles [°]: Ru−P(1) 2.314(2), Ru−P(2) 2.302(2), Ru−P(3) 2.307(2), Ru−S(1) 2.503(2), Ru−N(1) 2.242(6), Ru−N (61) 2.095(5), S(1)−C(1) 2.242(6), Ru−N(61) 2.095(5), S(1)−C(1) 1.714(8), S(2)−C(1) 1.723(8), S(2)−C(3) 1.735(9), S(1)−Ru−P(2) 168.9(1), N(1)−Ru−P(3) 169.9(2), N(61)−Ru−P(1) 178.2(2), P(1)−Ru−P(2) 90.6(1), P(1)−Ru−P(3) 84.7(1), P(2)−Ru−P(3) 86.4(1), S(1)−Ru−N(1) 66.1(2).

Stereochemical non-rigidity is observed for each of the monocations of **2**−**5** at room temperature. Whereas a doublet and triplet at an integral ratio of 2:1 would be expected for the magnetically inequivalent phosphorus atoms of the diorganyldithiocarbamate complexes **2** and **3**, their ^{31}P-NMR spectra in various solvents ($CDCl_3$, MeOD, [D_6]acetone) consist of a single broad uncontoured resonance (in $CDCl_3$ **2** δ = 22−36, **3** δ = 22−32) at ambient temperature [see Figure 2(a)]. As illustrated for **2** in Figure 2(b), cooling to −30°C provides the predicted spin pattern with resolved doublets (**2** δ = 26.10, **3** δ = 25.70) for the P atoms *trans* to the diorganyldithiocarbamate S atoms and a triplet (**2** δ = 27.44, **3** δ = 28.56) for the single P atom *trans* to acetonitrile. Each of the phosphorus atoms in the thioamide-con-

taining cations of **4** and **5** should generate its own separate ^{31}P-NMR resonance. In fact, the fluxional behavior of **4** in $CDCl_3$ solution leads to the observation of only two broad resonances at room temperature [Figure 3(a)]. Although three signals can be identified for **5** at this temperature, they are likewise broad and without fine structure. As may be seen for **4** in Figure 3(b), cooling to −30°C once again provides stereochemical rigidity and three individual triplets (**4** δ = 20.92, 31.52, 36.53; **5** δ = 19.89, 28.05, 37.59) appear in the ^{31}P-NMR spectrum at this temperature. The ^1H-NMR spectra of **2**−**5** are also in accordance with cation fluxionality at room temperature. For instance, whereas only a single broad resonance at δ = 2.43 can be observed for the triphos CH_2 protons of **2** at 25°C, three multiplets can be identified in $CDCl_3$ solution at −30°C: δ = 2.19, 2.30, 2.68). Restricted rotation about the diorganyldithiocarbamate C−N bond also leads to the observation of two signals for the ethyl CH_2 protons of this cation at −30°C (δ = 3.64, 3.84), which then coalesce to a single resonance (δ = 3.82) at ambient temperature.

Figure 2. ^{31}P-NMR spectrum of **2** in $CDCl_3$: (a) at room temperature, (b) at −30°C.

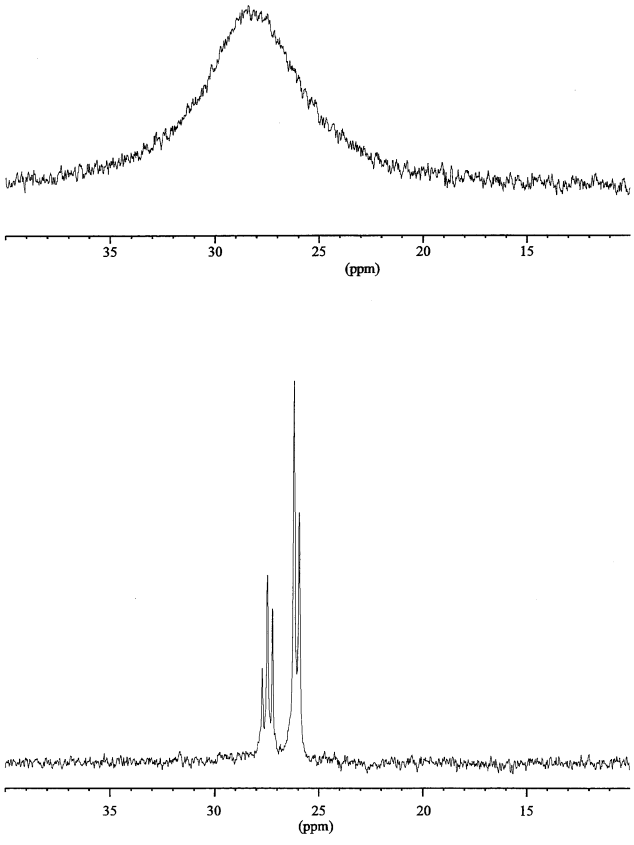

Both CH_3CN and phosphane arm-off dissociation can be discussed as possible mechanisms to explain the stereochemical non-rigidity of the cations $[Ru(L)(MeCN)(triphos)]^+$ of **2**−**5** in solution at 25°C. The position and width of the sharp MeCN singlets in the ^1H-NMR spectra of these complexes in $CDCl_3$ (−30°C: **2** δ = 1.80, **3** δ = 1.87, **4** δ = 1.87, **5** δ = 1.61) remain effectively unchanged on raising the solution temperature from −30°C to 25°C and, therefore, provide no evidence for a rapid acetonitrile exchange process. This finding prompted us to investigate whether fluxionality is also a general phenomenon for other sterically crowded Ru^{II} complexes of the type $[Ru(Et_2NCS_2)(Y)(triphos)]^{n+}$ (**6**, n = 1, Y = CO; **7**, n = 0, Y = CN^- **8**, n = 0, Y = H^-) depicted in Scheme 3. However, ^1H and ^{31}P NMR spectra for **6**−**8** in $[D_6]DMSO$ or $CDCl_3$ at both 25°C or 60°C indicate that these non-acetonitrile complexes are, in fact, all stereochemically rigid in solution. Pronounced highfield shifts are apparent for the P atom in *trans* position to the monodentate ligand Y in both **6** (**6**, L = CO, δ = 3.54) and the hydride complex **8** (δ = 5.29).

Figure 3. ^{31}P-NMR spectrum of **4** in $CDCl_3$: (a) at room temperature, (b) at −30°C.

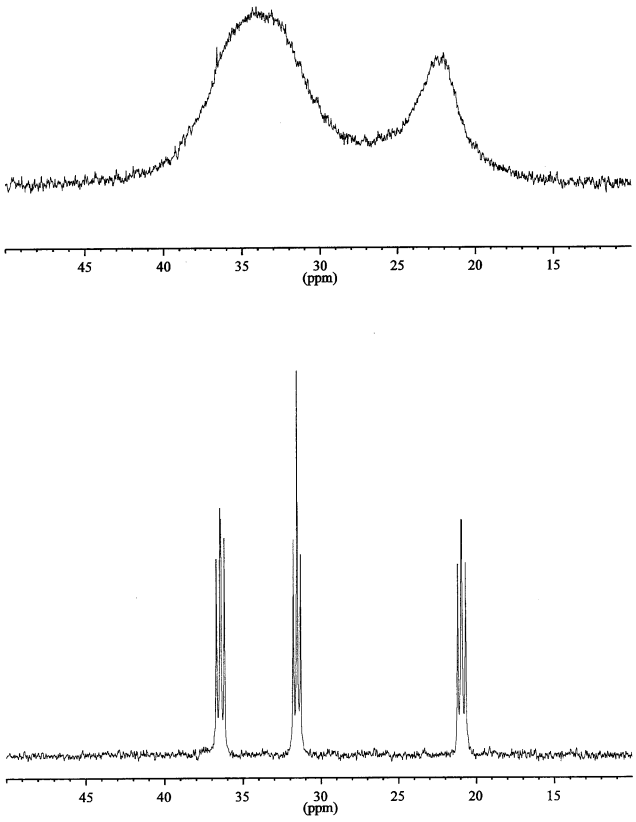

The implicated lack of triphos arm-off dissociation for Ru^{II} complexes of the type $[Ru(L)(Y)(triphos)]^{n+}$ in solution led us to investigate whether κ^2P coordinated triphos complexes with a dangling phosphone arm can be stabilized by the presence of an excess of a small bite chelating ligand such as $Et_2NCS_2^-$, $mpym^-$, mpy^-, or $mmim^-$. A facial replacement of one binding P atom is observed when $[Rh(MeCN)_3(triphos)]^{3+}$ is treated with two equivalents of bidentate ligands L, thereby yielding[16][17] κ^2P coordinated complexes such as $[Rh(R_2NCS_2\text{-}\kappa^2S)_2(triphos\text{-}\kappa^2P)][CF_3SO_3]$ (R = Et, Me) or $[Rh(mpym\text{-}\kappa^2N,S)_2(triphos\text{-}\kappa^2P)][CF_3SO_3]$. In contrast, retention of a κ^3S facial coordination mode has been reported for the cyclic thioether [9]$aneS_3$ in [Rh(mpym-κ^2N,S)(mpym-

Scheme 3. $[Ru(Et_2dtc)(CO)(triphos)]^+$ cation of **6** and molecules $[Ru(Et_2dtc)(L)(triphos)]^+$ [(L = CN (**7**), H (**8**)]

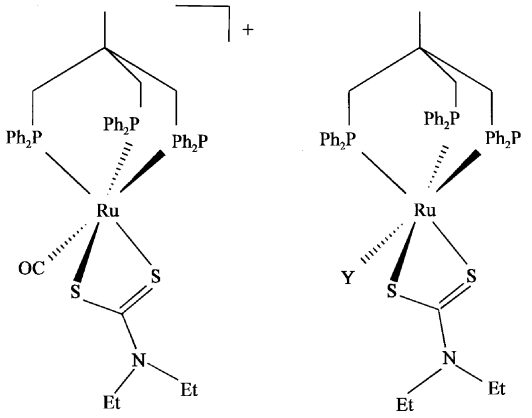

6 **7** (Y = CN^-), **8** (Y = H^-)

κS)([9]aneS$_3$-$\kappa^3 S$)][CF_3SO_3][19] and [Ru(mbt-$\kappa^2 N,S$)(mbt-κS)([9]aneS$_3$-$\kappa^3 S$)][21]. The presence of both mono- and bidentate dimethyldithiocarbamate ligands has been confirmed for the organometallic half-sandwich complex [Rh(η^5-C_5Me_5)(Me_2NCS_2-$\kappa^2 S$)(Me_2NCS_2-κS)][24].

Treatment of **1** with Na(Et_2NCS_2) at a 1:2 or 1:3 ratio affords the $\kappa^3 P$-triphos coordinated complex [Ru(Et_2NCS_2-$\kappa^2 S$)(Et_2NCS_2-κS)(triphos-$\kappa^3 P$)] (**9**), whose structure (Scheme 4) was established by elemental analysis, FAB mass spectrometry, and NMR spectroscopy. **9** exhibits a doublet at δ = 19.06 for the P atoms *trans* to the $\kappa^2 S$ coordinated chelating ligand and a triplet at δ = 32.37 for the remaining P atom *trans* to the monodentate $Et_2NCS_2^-$ ligand. The presence of a singlet at δ = ca. −25 to −30 would be characteristic for the P atom of a free dangling phosphane arm in a $\kappa^2 P$ coordinated complex[16][17]. Both the ^{1}H- and ^{31}P-NMR spectra are in accordance with stereochemical rigidity of **9** in $CDCl_3$ solution at 25°C. However attempts to recrystallize **9** from an ethanol/acetone solution under air led to formation of the $\kappa^2 P$ coordinated complex [Ru($EtNCS_2$-$\kappa^2 S$)$_2$(triphosO-$\kappa^2 P$)] (**10**) over a period of 14 d in relatively good yield (50%). The oxidation of the uncoordinated P atom is confirmed by the observation of a FAB MS basis peak *m*/*z* for $[M]^+$ at 1038, by a characteristic IR absorption band for $\tilde{\nu}$(PO) at 547 cm^{-1}, and by the presence of a typical ^{31}P-NMR resonance at δ = 26.86, a value very similar to that of 27.18 found for the analogous Rh^{III} complex [Rh(Et_2NCS_2-$\kappa^2 S$)$_2$(triphosO-$\kappa^2 P$)]Cl[16]. It is possible to follow the required $\kappa^3 P \rightarrow \kappa^2 P$ arm-off reaction of the initially $\kappa^3 P$ coordinated triphos in **9** by ^{31}P NMR spectroscopy. After 2d, respective singlets at δ = −26.00 and 26.86 for the dangling phosphorus atom in $\kappa^2 P$ coordinated triphos and its oxidation product triphosO in the final product **10** can be identified. These resonances also appear in the ^{31}P-NMR spectrum of the mixture of [Ru(Et_2NCS_2)$_2$(triphos-$\kappa^2 P$)] and [Ru(Et_2NCS_2)$_2$(triphos-O-$\kappa^2 P$)] present after 7 d in a $CDCl_3$ solution of **9** exposed to air. Whereas overlapping signals for the coordinated P atoms of these complexes may be located in the range δ = 38−40, the phosphorus resonances of **9** (δ = 19.06, 32.37) are now completely absent. It may be assumed that the driving force for the $\kappa^3 P \rightarrow \kappa^2 P$ arm-off reaction will be provided by the thermodynamic advantage of $\kappa^2 S$ chelation of both $Et_2NCS_2^-$ ligands. However, this process proceeds much more slowly than for the analogous Rh^{III} complexes, for which intermediate products of the type [Rh(R_2NCS_2-$\kappa^2 S$)(R_2NCS_2-κS)(triphos-$\kappa^3 P$)]$^+$ cannot be isolated[16].

Scheme 4. [Ru(Et_2dtc)$_2$(triphos)] (**9**) and [Ru(Et_2dtc)$_2$(triphosO)] (**10**)

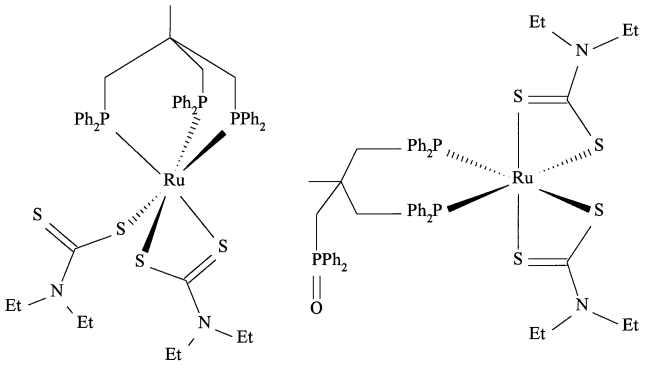

9 **10**

The reaction of **1** with 2 equivalents of the ambidentate heterocyclic thioamides $mpym^-$, mpy^-, and $mmim^-$ was studied to provide information on possible preferred isomer formation for products of the type [Ru(L)$_2$(triphosO-$\kappa^2 P$)]. As for diethyldithiocarbamate $Et_2NCS_2^-$, $\kappa^3 P$-triphos coordinated complexes [Ru(mpym-$\kappa^2 N,S$)(mpym-κS)-(triphos)] (**11**) and [Ru(mpy-$\kappa^2 N,S$(mpy-κS)(triphos)] (**12**) can be isolated in high yield at room temperature. Both are once again stereochemically rigid in solution at 25°C and may be characterized by their FAB MS basis peaks $[M]^+$ and the presence of three ^{31}P NMR triplets in the range δ = 21.5−29.2. In contrast to **10** or **12**, the 2-mercaptopyrimidinate complex **11** is stable in solution under air and may be recrystallized from $CHCl_3$/MeOH to afford crystals suitable for X-ray analysis (Figure 4). The small angle of bite [S(1)−Ru−N(1) 65.9(2)°] of the coordinating thioamide causes a marked narrowing of the opposite P(2)−Ru−P(3) angle to 85.0(1)°. As a result of the weaker *trans* influence of N, the Ru−P(2) distance of 2.291(2) Å is somewhat shorter than for the remaining triphos P atoms [2.301(2), 2.322(2) Å]. On leaving **12** to stand in $CHCl_3$ solution under air a color change from yellow to orange may be followed over a period of 3 d and the triphosO-$\kappa^2 P$ complex [Ru(mpy-$\kappa^2 N,S$)$_2$(triphosO-$\kappa^2 P$)] (**13**) may be isolated in effectively quantitative yield after 14 d. Rapid oxidation of the dangling phosphane arm is typical for analogous $\kappa^2 P$ coordinated Rh^{III} complexes[16][17] and has also been reported for square-planar Rh^I and Ni^{II} complexes[6][25]. Whereas **12** exhibits three triplets for its magnetically inequivalent P (δ 21.55, 26.60, 29.17 ppm) atoms, a singlet at δ = 25.89 and an AB pattern at δ = 42.45 for two nuclei with closely similar chemical shifts were recorded for **13**. The position of the former resonance is typical for the oxid-

ized phosphorus of triphosO and the latter spin system would be expected for either the OC-6-22 (N *trans* to N) or OC-6-13 (S *trans* to S) isomer but not the third possible OC-6-32 (S *trans* to N) isomer of Scheme 6. Although attempts to obtain crystals suitable for X-ray analysis remained unsuccessful, the molecular structure of the analogous κ^2P-triphosO complex [Ru(mmim-$\kappa^2N,S)_2$(triphosO-κ^2P)] (**14**) was determined. As previously also established for two Rh^{III} complexes [Rh(mpy-$\kappa^2N,S)_2$(triphosO-κ^2P)]Cl[16] and [Rh(mmim-$\kappa^2N,S)_2$(triphosO-κ^2P)]-[CF_3SO_3][17], **14** is present as the OC-6-13 isomer. The observation of individual resonances for the coordinated triphosO P atoms (δ = 47.8, 49.9) and the duplication of the $mmim^-$ methyl singlet (δ = 2.94, 2.98) and aromatic proton doublets (δ = 5.93, 6.09, 6.52, 6.61) indicates that the molecular geometry of **14** must deviate significantly from an idealized C_2 symmetry. This is confirmed by the observed distortions in the Ru^{II} coordination sphere of the X-ray structure (Figure 5). In view of the similarity of the ^{31}P NMR data for **13** and **14** it seems reasonable to assume that the former complex is also present as the OC-6-13 isomer with S atoms in *trans* position to one another.

Figure 4. Molecular structure of **11**. Phenyl rings are omitted for clarity[a]

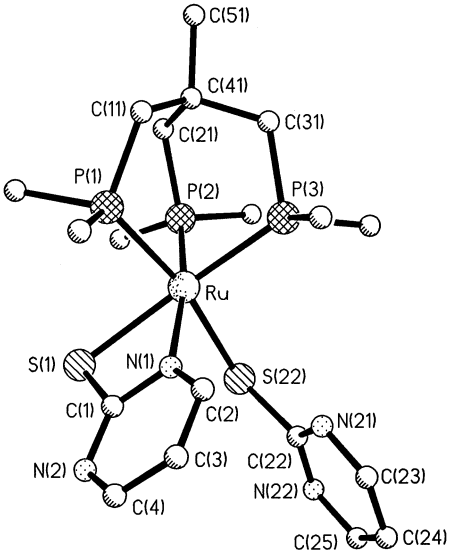

[a] Selected bond lengths [Å] and angles [°]: Ru−P(1) 2.301(2), Ru−P(2) 2.291(2), Ru−P(3) 2.322(2), Ru−S(1) 2.488(2), Ru−S(22) 2.451(2), Ru−N(1) 2.142(7), S(22)−Ru−P(1) 168.3(1), N(1)−Ru−P(2) 170.3(1), S(1)−Ru−P(3) 170.3(1), P(1)−Ru−P(2) 89.3(1), P(1)−Ru−P(3) 91.0(1), P(2)−Ru−P(3) 85.0(1), S(1)−Ru−N(1) 65.9(2).

Our present results indicate that the fluxionality of octahedral Ru^{II} complexes [Ru(L)(MeCN)(triphos-κ^3P)]$^+$ of bidentate ligands L^- results from a facile acetonitrile dissociation to a five-coordinate species [Ru(L)(triphos-κ^3P)]$^+$. In contrast to the analogous acetonitrile complexes, κ^3P-triphos compounds of the type [Ru(L)(Y)(triphos-κ^3P)]$^{n+}$ (n = 1, Y = CO; n = 0, Y = CN^-, H^-) are stereochemically rigid in solution at both 25°C and 60°C. Arm-off $\kappa^3P \rightarrow \kappa^2P$ reactions are apparently less favorable for Ru^{II} than for Rh^{III}, thereby allowing the isolation of com-

Figure 5. Molecular structure of **14**. Phenyl rings are omitted for clarity[a]

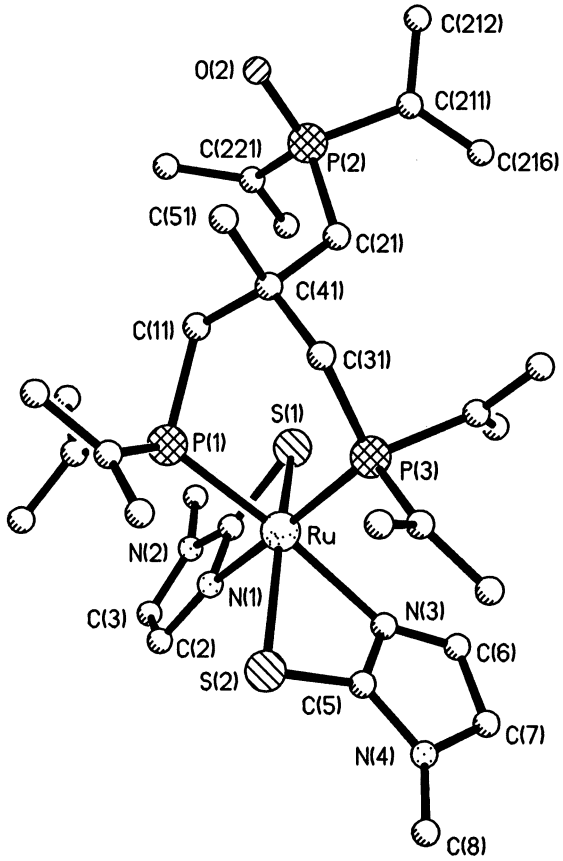

[a] Selected bond lengths [Å] and angles [°]: Ru−P(1) 2.239(5), Ru−P(3) 2.242(5), Ru−S(1) 2.480(6), Ru−S(2) 2.457(6), Ru−N(1) 2.155(4), Ru−N(3) 2.21(2), N(3)−Ru−P(1) 172.8(5), N(1)−Ru−P(3) 169.6(5), S(1)−Ru−S(2) 156.1(2), P(1)−Ru−P(3) 89.2(5), N(1)−Ru−S(1) 66.9(5), N(3)−Ru−S(2) 68.1(5).

Scheme 5. [Ru(mpym)$_2$(triphos)] (**11**) and [Ru(mpy)$_2$(triphos)] (**12**)

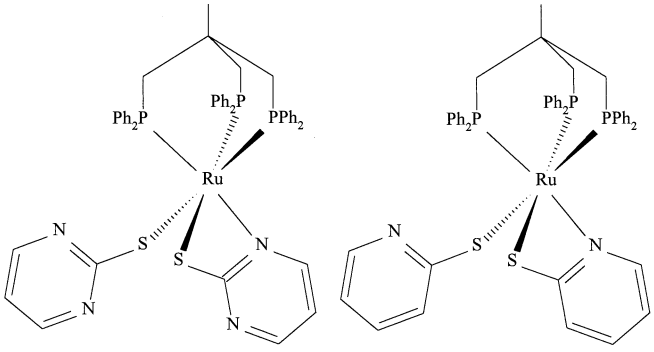

plexes such as [Ru(Et_2NCS_2-κ^2S)(Et_2NCS_2-κS)(triphos-κ^3P)] (**9**) or the analogous $mpym^-$ and mpy^- complexes **11** and **12**. However **9** and **12** do exhibit a slow arm-off phosphane dissociation and subsequent oxidation to afford the thermodynamically favorable bis-chelates [Ru(Et_2NCS_2-$\kappa^2S)_2$(triphosO-κ^2P)] (**10**) and [Ru(mpy-$\kappa^2N,S)_2$(triphosO-κ^2P)] **13**. As **13** and **14** are both formed from κ^3P-triphos

Scheme 6. Possible isomers of [Ru(mpy)$_2$(triphosO)] **13**

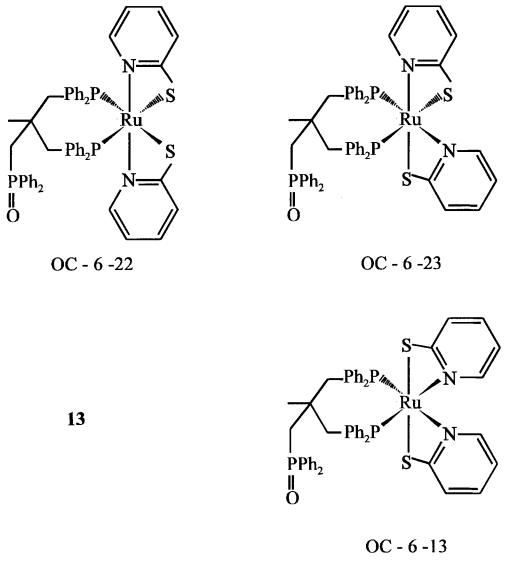

complexes it may be assumed that the first reaction stage will involve a slow $\kappa^3P \rightleftharpoons \kappa^2P$ dissociation. This must be followed by rapid isomerisation of the five-coordinated intermediate to allow nucleophilic attack of the N atom of the previously κS coordinated thioamide at a site *trans* to a κ^2P-triphos phosphorus. The resulting octahedral complex will then exhibit the observed OC-6-13 geometry. Relief of steric crowding and the energetic advantage of the associated formation of a second κ^2S or κ^2S,N chelate may be presumed to provide the driving force behind such a triphos arm-off dissociation.

Experimental Section

Where not otherwise stated reactions were performed under Ar in carefully dried solvents. − FAB MS: Fisons VG Autospec with 3-nitrobenzyl alcohol as the matrix. − FT-IR: KBr, Perkin-Elmer 1760. − ^{1}H and ^{31}P{^{1}H} NMR: Bruker AM 400; chemical shifts are reported as δ values relative to the signal of the deuterated solvent (for ^{1}H) or relative to 85% H_3PO_4 as external standard (for ^{31}P). − Elemental analyses: Carlo Erba 1106. − The starting compound [Ru(MeCN)$_3$(triphos)][CF_3SO_3] (**1**) was prepared according to the literature procedure[26] from $RuCl_3 \cdot x\ H_2O$, which was a gift from Degussa AG.

[Ru(Et$_2$NCS$_2$)(MeCN)(triphos)](CF$_3$SO$_3$) (**2**): Na(Et$_2$NCS$_2$)·3 H_2O (33.8 mg, 0,15 mmol) was added to a solution of **1** (172.0 mg, 0.15 mmol) in 10 ml of MeOH and the reaction mixture heated at reflux for 3 h. After filtration the red solution was reduced in volume to 3 ml and left to stand at room temperature to afford a yellow precipitate of **2** within 24 h. Recrystallisation from ethanol provided **2**·0.5 C_2H_5OH. Yield 111.0 mg (68%). − FAB MS, *m/z* (%): 874 (100) [M − MeCN − CF_3SO_3]$^+$. − ^{1}H NMR ($CDCl_3$, −30°C): δ = 1.24 (t, 6 H, CH_3 Et$_2$NCS$_2$), 1.58 (s, 3 H, CH_3 triphos), 1.80 (s, 3 H, MeCN), 2.19 (m, 2 H, CH_2 triphos), 2.30 (m, 2 H, CH_2 triphos), 2.68 (m, 2 H, CH_2 triphos), 3.64 (m, 2 H, CH_2 Et$_2$NCS$_2$), 3.84 (m, 2 H, CH_2 Et$_2$NCS$_2$), 6.87−7.38 (m, 30 H, Ph triphos). − ^{31}P NMR ($CDCl_3$, −30°C): δ = 26.10 (d, 2 P, *trans* to Et$_2$NCS$_2$), 27.44 (t, 1 P, *trans* to MeCN). − $C_{49}H_{52}F_3N_2O_3P_3RuS_3 \cdot 0.5\ C_2H_5OH$ (1088.2): calcd. C 55.2, H 5.1, N 2.6; found C 55.0, H 5.4, N 2.3.

[Ru(pyrdtc)(MeCN)(triphos)](CF$_3$SO$_3$) (**3**): The preparation of **3** was performed using **1** and NH_4(pyrdtc) (pyrdtc$^-$ = pyrrolidinedithiocarbamate) under conditions analogous to those for **2**. Yield 119.5 mg (75%). − FAB MS, *m/z* (%): 872 (100) [M − MeCN − CF_3SO_3]$^+$. − ^{1}H NMR ($CDCl_3$, −30°C): δ = 58 (s, 3 H, CH_3 triphos), 1.87 (s, 3 H, MeCN), 1.97, 2.08, 2.14 (3×2 H, 3 m, CH_2 pyrdtc$^-$ and triphos), 2.32 (m, 2 H, CH_2 triphos), 2.64 (m, 2 H, CH_2 triphos), 3.64 (m, 4 H, CH_2 pyrdtc$^-$), 6.87−7.39 (m, 30 H, Ph triphos). − ^{31}P NMR ($CDCl_3$, −30°C): δ = 5.70 (d, 2 P, *trans* to pyrdtc$^-$), 28.56 (t, 1 P, *trans* to MeCN). − $C_{49}H_{50}F_3N_2O_3P_3RuS_3$ (1062.1): calcd. C 55.4, H 4.7, N 2.6; found C 54.5, H 5.1, N 2.3.

[Ru(mbt)(MeCN)(triphos)](CF$_3$SO$_3$) (**4**): 2-Mercaptobenzothiazole Hmbt (25.2 mg, 0.15 mmol) was dissolved in 10 ml MeOH in the presence of 0.15 mmol 1 M NaOH. After addition of **1** (172.0 mg, 0.15 mmol) the reaction mixture was heated for 2 h at reflux and subsequently filtered; the volume of the red-brown solution was then reduced to 1 ml. Standing at −18°C led to crystallization of yellow-brown prisms of **4**·1/2 MeOH suitable for X-ray analysis. Yield 120.2 mg (73%). − FAB MS, *m/z* (%): 892 (100) [M − MeCN − CF_3SO_3]$^+$. − ^{1}H NMR ($CDCl_3$, −30°C): δ = 1.59 (s, 3 H, CH_3 triphos), 1.87 (s, 3 H, MeCN), 2.27 (m, 2 H, CH_2 triphos), 2.46 (m, 3 H, CH_2 triphos), 2.60 (m, 1 H, CH_2 triphos), 6.30 (d, 1 H, mbt), 6.80−7.39 (m, 32 H, Ph triphos and mbt), 7.68 (d, 1 H, mbt). − ^{31}P NMR ($CDCl_3$, −30°C): δ = 20.92 (t, 1 P), 31.52 (t, 1 P), 36.43 (t, 1 P). − $C_{51}H_{46}F_3N_2O_3P_3RuS_3 \cdot 0.5$ MeOH (1098.1): calcd. C 56.3, H 4.4, N 2.6; found C 55.9, H 4.4, N 2.4.

[Ru(mpym)(MeCN)(triphos)](CF$_3$SO$_3$) (**5**): The preparation of **5** was carried out with **1** and 2-mercaptopyrimidine (Hmpym) in a manner analogous to that employed for **4**. Yield 126.3 mg (82%). − FAB MS, *m/z* (%): 986 (2) [M$^+$], 837 (100) [M − MeCN − CF_3SO_3]$^+$. − ^{1}H NMR ($CDCl_3$, −30°C): δ = 1.61 (s, 3 H, MeCN), 1.63 (s, 3 H, CH_3 triphos), 2.05 (m, 1 H, CH_2 triphos), 2.26 (m, 2 H, CH_2 triphos), 2.78 (m, 3 H, CH_2 triphos), 6.60−7.56 (m, 31 H, Ph triphos and mpym), 7.78 (d, 1 H, mpym), 8.45 (d, 1 H, mpym). − ^{31}P NMR ($CDCl_3$, −30°C): δ = 19.89 (t, 1 P), 28.05 (t, 1 P), 37.59 (t, 1 P). − $C_{48}H_{45}F_3N_3O_3P_3RuS_2$ (1027.0): calcd. C 56.1, H 4.4, N 4.1; found C 55.4, H 5.1, N 3.6.

[Ru(Et$_2$NCS$_2$)(CO)(triphos)](CF$_3$SO$_3$) (**6**): CO was bubbled through a solution of **2** (119.7 mg, 0.11 mmol) in 20 ml CH_2Cl_2 leading to loss of the initial deep red color. After filtration and reduction in volume to 2 ml addition of 10 ml of diethyl ether led to precipitation of **6** which was centrifuged off and dried in vacuum. Yield 87.9 mg (76%). − FAB MS, *m/z* (%): 902 (26) [M − CF_3SO_3]$^+$, 874 (87) [M − CO − CF_3SO_3]$^+$. − ^{1}H NMR ([D$_6$]DMSO): δ = 1.14 (t, 6 H, CH_3 Et$_2$NCS$_2$), 1.70 (s, 3 H, CH_3 triphos), 2.53−2.85 (m, 6 H, CH_2 triphos), 3.54 (m, 2 H, CH_2 Et$_2$NCS$_2$), 3.71 (m, 2 H, CH_2 Et$_2$NCS$_2$), 6.94−7.49 (m, 30 H, Ph triphos). − ^{31}P NMR ([D$_6$]DMSO): δ = 3.54 (t, 1 P, *trans* to CO), 21.20 (d, 2 P, *trans* to Et$_2$NCS$_2$). − IR: $\tilde{\nu}$ = 2002 s cm^{-1} (CO). − $C_{48}H_{49}F_3NO_4P_3RuS_3$ (1051.1): calcd. C 54.9, H 4.7, N 1.3; found C 53.4, H 4.6, N 1.7.

[Ru(CN)(Et$_2$NCS$_2$)(triphos)] (**7**): NaCN (4.4 mg, 0.09 mmol) was added to **1** (95.2 mg, 0.09 mmol) in 10 ml of ethanol and the reaction mixture stirred for 18 h at room temperature. The resulting solid was filtered off and redissolved in 2 ml of CH_2Cl_2. Addition of 10 ml of diethyl ether led to precipitation of **7** which was dried in vacuum. Yield 54.3 mg (67%). − FAB MS, *m/z* (%): 900 (26) [M]$^+$, 874 (14) [M − CN]$^+$, 752 (3) [M − Et$_2$dtc]$^+$. − ^{1}H NMR ([D$_6$]DMSO): δ = 1.08 (t, 6 H, CH_3 Et$_2$NCS$_2$), 1.42 (s, 3 H, CH_3 triphos), 2.20−2.45 (m, 6 H, CH_2 triphos), 3.43 (m, 2 H, CH_2 Et$_2$NCS$_2$), 3.67 (m, 2 H, CH_2 Et$_2$NCS$_2$), 6.77−7.79 (m, 30 H, Ph triphos). − ^{31}P NMR ([D$_6$]DMSO): δ = 19.26 (t, 1 P, *trans* to CN),

27.40 (d, 2 P, *trans* to Et_2NCS_2). − IR: $\tilde{\nu}$ = 2094 s cm^{-1} (CN). − $C_{47}H_{49}N_2P_3RuS$ (900.0): calcd. C 62.7, H 5.5, N 3.1; found C 61.8, H 5.9, N 3.1.

[Ru(Et$_2$NCS$_2$)(H)(triphos)] (**8**): $NaBH_4$ (11.3 mg, 0.3 mmol) was added to **1** (108.8 mg, 0.1 mmol) in 20 ml at room temperature leading to gas formation and lightening of the solution color. After stirring at room temperature for 18 h the resulting solid was filtered off, washed with ethanol and ethyl ether and dried in vacuum. Yield 66.5 mg (76%). − FAB MS, *m/z* (%): 874 (100) $[M - H]^+$. − ^{1}H NMR ($CDCl_3$): δ = −5.47 (d, 1 H, $^2J_{PH}$ (*trans* to H) = 109.4 Hz, $^2J_{PH}$ (*trans* to S) = 16.6 Hz), 1.24 (t, 6 H, CH_3 Et_2NCS_2), 1.38 (s, 3 H, CH_3 triphos), 2.10−2.23 (m, 6 H, CH_2 triphos), 3.61 (m, 2 H, CH_2 Et_2NCS_2), 3.91 (m, 2 H, CH_2 Et_2NCS_2), 6.87−7.39 (m, 26 H, Ph triphos), 7.74 (s, 4 H, Ph triphos). − ^{31}P NMR ($CDCl_3$): δ = 5.29 (m, 1 P, *trans* to H), 47.10 (d, 2 P, *trans* to Et_2NCS_2). − IR: $\tilde{\nu}$ = 1846 s cm^{-1} (RuH). − $C_{46}H_{50}NP_3RuS_2$ (875.0): calcd. C 63.1, H 5.8, N 1.6; found C 61.9, H 5.8, N 1.4.

[Ru(Et$_2$NCS$_2$-κ^{2}S)(Et$_2$NCS$_2$-κS)(triphos)] (**8**): $Na(Et_2NCS_2)\cdot 3\ H_2O$ (67.0 mg, 0.3 mmol) was added to a solution of **1** (172.0 mg, 0.15 mmol) in 10 ml of MeOH and the reaction mixture heated at reflux for 3 h. After filtration and reduction in volume to 3 ml the resulting solution was left to stand at 4°C to afford a yellow precipitate of **9** within 24 h. Yield 127.3 mg (83%). − FAB MS, *m/z* (%): 874 (100) $[M - Et_2NCS_2]^+$. − ^{1}H NMR ($CDCl_3$): δ = 0.86, 1.01 (2 t, 2×6 H, CH_3 Et_2NCS_2), 1.52 (s, 3 H, CH_3 triphos), 2.23, 2.42 (m, 6 H, CH_2 triphos), 3.31, 3.54 (m, 8 H, CH_2 Et_2NCS_2), 6.60−7.70 (m, 30 H, Ph triphos). − ^{31}P NMR ($CDCl_3$): δ = 19.06 (d, 2 P, *trans* to Et_2NCS_2-κ^2*S*), 32.37 (t, 1 P, *trans* to Et_2NCS_2-κ*S*). − $C_{51}H_{59}N_2P_3RuS_4$ (1022.3): calcd. C 59.9, H 5.8, N 2.7; found C 59.8, H 5.0, N 2.6.

[Ru(Et$_2$NCS$_2$-κ^{2}S)$_2$(triphosO-κ^{2}P) (**10**): Slow crystallization of **9** from an ethanol/acetone solution at room temperature under air affords **10** in 50% yield over a period of 14 d. − FAB MS, *m/z* (%): 1038 (100) $[M]^+$, 890 (41) $[M - Et_2NCS_2]^+$. − ^{1}H NMR ($CDCl_3$): δ = 0.80−1.01 (m, 15 H, CH_3 of Et_2NCS_2 and triphosO), 2.13−3.60 (m, 14 H, CH_2 of Et_2NCS_2 and triphosO), 6.80−7.80 (m, 30 H, Ph triphosO). − ^{31}P NMR ($CDCl_3$): δ = 26.86 (s, 1 P, P=O) 38.96, 40.38 (2d, 2 P, *trans* to Et_2NCS_2). − IR: $\tilde{\nu}$ = 574 m cm^{-1} (δPO). − $C_{51}H_{59}N_2OP_3RuS_4$ (1038.3): calcd. C 59.0, H 5.7, N 2.7; found C 58.5, H 5.3, N 2.6.

[Ru(mpym-κ^{2}N,S)(mpym-κS)(triphos) (**11**): Hmpym (33.6 mg, 0.3 mmol) was dissolved in 10 ml of MeOH in the presence of 0.3 ml of 1 M NaOH. After addition of **1** (172.0 mg, 0.15 mmol) and refluxing for 3 h the solvent was removed and the resulting solid dissolved in a $CHCl_3$/MeOH mixture (2:3). Slow evaporation afforded yellow crystals of **11**. Yield 122.0 mg (74%). − FAB MS, *m/z* (%): 948 (1) $[M]^+$, 837 (100) $[M - mpym]^+$. − ^{1}H NMR ($CDCl_3$): δ = 1.53 (s, 3 H, CH_3 triphos), 2.05 (m, 1 H, CH_2 triphos), 2.45 (m, 2 H, CH_2 triphos), 2.68 (m, 3 H, CH_2 triphos), 5.62 (s, 1 H, mpym), 6.25 (s, 1 H, mpym) 6.60−8.00 (m, 34 H, mpym and Ph triphos). − ^{31}P NMR ($CDCl_3$): δ = 25.17 (t, 1 P), 26.39 (t, 1 P), 29.05 (t, 1 P). − $C_{49}H_{45}N_4P_3RuS_2\cdot MeOH\cdot CHCl_3$ (1099.4): calcd. C 55.7, H 4.6, N 5.1; found C 56.8, H 4.8, N 5.1.

[Ru(mpy-κ^{2}N,S)(mpy-κS)(triphos) (**12**): The preparation of **12** was performed with Hmpy and **1** under conditions analogous to those for **11**. It was recrystallized within 1 d from a $CHCl_3$ solution covered with hexane. Yield 100.7 mg (63%). − FAB MS, *m/z* (%): 947 (1) $[M]^+$, 836 (100) $[M - myp]^+$. − ^{1}H NMR ($CDCl_3$): δ = 1.43 (s, 3 H, CH_3 triphos), 2.39 (m, 6 H, CH_2 triphos), 5.94 (6, 1 H, mpy), 6.15 (d, 1 H, mpy), 6.53 (t, 1 H, mpy), 6.70−8.00 (m, 35 H, mpy and Ph triphos). − ^{31}P NMR ($CDCl_3$): δ = 21.55 (t, 1 P), 26.60 (t, 1 P), 29.17 (t, 1 P). − $C_{51}H_{47}N_2P_3RuS_2\cdot CHCl_3$ (1065.4): calcd: C 58.6, H 4.5, N 2.6; found C 58.0, H 4.9, N 2.6.

[Ru(mpy-κ^{2}N,S)$_2$(triphosO-κ^{2}P) (**13**): On leaving a reaction solution of **12** in $CHCl_3$ to stand under air the color changed over 3 d from yellow to orange. After 14 d the solution was reduced in volume to afford **13** as a yellow solid. $C_{51}H_{47}N_2OP_3RuS_2$ (962.1): calcd. C 63.7, H 4.9, N 2.9; found C 62.8, H 5.2, N 2.8. − FAB MS, *m/z* (%): 962 (84) $[M]^+$, 852 (30) $[M - mpy]^+$. − ^{1}H NMR ($CDCl_3$) 0.63 (s, 3 H, CH_3 triphosO), 2.19 (m, 2 H, CH_2 triphosO), 2.58, 2.79, 2.86, 3.19 (m, 4 H, CH_2 triphosO), 6.06 (m, 2 H, mpy), 6.22, 6.37 (d, 2 H, mpy), 6.76, 6.82 (m, 2 H, mpy) 6.90−7.70 (m, 32 H, Ph triphosO and mpy). − ^{31}P NMR ($CDCl_3$) 25.89 (s, 1 P, P=O), 42.45 (AB system, 2 P). − IR: $\tilde{\nu}$ = 1200 m (νPO), 568 m cm^{-1} (δPO).

[Ru(mmim-κ^{2}N,S)$_2$(triphosO-κ^{2}P) (**14**): Hmmim (34.2 mg, 0.3 mmol) was dissolved in 10 ml of MeOH in the presence of 0.3 ml of 1 M NaOH. After addition of **1** (172.0 mg, 0.15 mmol) the solution was refluxed for 4 h and then left to stand under air for 2 d. This was followed by filtration and reduction in volume to 1 ml to afford yellow-brown crystals of **14** at 4°C. Yield 100.2 mg (69%). − FAB MS, *m/z* (%): 968 (25) $[M]^+$, 855 (100) $[M - mmim]^+$. − ^{1}H NMR ($CDCl_3$): δ = 0.92 (s, 3 H, CH_2 triphosO), 2.94, 2.98 (s, 6 H, CH_3 mmim), 5.93, 6.09, 6.52, 6.61 (d, 4 H, CH mmim), 6.52 − 7.79 (m, 30 H, Ph triphosO). − ^{31}P NMR ($CDCl_3$): δ = 26.74 (s, 1 P, P=O), 47.8, 49.9 (AB system, 2 P). − IR: $\tilde{\nu}$ = 571 m cm $^{-1}$ (δPO). − $C_{49}H_{49}N_4OP_3RuS_2$ (968.1): calcd. C 60.8, H 5.1, N 5.8; found C 61.6, H 4.7, N 6.2.

X-Ray Structural Analyses Siemens P4 diffractometer, graphite-monochromated Mo-*Kα* radiation (λ = 0.71073 Å). Semi-empirical absorption corrections were applied to the intensity data by use of ψ scans. The structures were solved by a combination of Patterson and Fourier difference syntheses and refined by full-matrix least squares against *F* for **4**, **11**, and **14** (SHELXTL PLUS programs[27]). Hydrogen atoms were included where possible at calculated positions with isotropic temperature factors[28].

4·1/2 CH_3OH: $C_{51}H_{46}F_3N_2O_3P_3RuS_3\cdot 1/2\ CH_3OH$, M = 1098.1, orthorhombic, space group $Pca2_1$ (No. 29), a = 17.3490(3), b = 11.315(4), c = 25.440(6) Å, V = 4994(2) Å^3, Z = 4, D_{calc} = 1.460 g·cm^{-3}, μ = 0.59 mm^{-1}. Crystal size 0.42 × 0.48 × 0.49 mm; ω scan , scan range: 4 ≤ 2θ ≤ 50°(−20 ≤ h ≤ 0, −13 ≤ k ≤ 0, 0 ≤ l ≤ 30), 4963 reflections collected, 4530 symmetry-independent reflections (R_{int} = 0.049); max./min. transmission: 0.516/0.470; 613 parameters refined; $w^{-1} = \sigma^2(F_o) + 0.003\ F_o^2$, R = 0.040, R_w = 0.044 for 3896 reflections with $F_o^2 > 2\sigma(F_o^2)$; largest difference peak: 0.55 eÅ^{-3}. The $CF_3SO_3^-$ anion exhibits rotational disorder about the C−S axis and site occupation factors (s.o.fs) of 0.50 were employed for the F and O atoms of the two observed orientations. Anisotropic temperature factors were introduced for all nonhydrogen atoms of the cation, the anion S atoms and the C and O atoms of a disordered methanol molecule (s.o.fs = 0.5).

11·$CHCl_3\cdot CH_3OH$: $C_{49}H_{45}N_4P_3RuS_2\cdot CHCl_3\cdot CH_3OH$, M = 1099.4, monoclinic, space group $P2_1/c$ (No. 14), a = 12.611(3), b = 21.605(4), c = 18.757(4) Å, β = 91.01(3)°, V = 5110(2) Å^3, Z = 4, D_{calc} = 1.429 g·cm^{-3}, μ = 0.68 mm^{-1}. Crystal size 0.32 × 0.39 × 0.42 mm; ω scan , scan range: 4 ≤ 2θ ≤ 50° (0 ≤ h ≤14, −25 ≤ k ≤ 0, −22 ≤ l ≤ 22), 9602 reflections collected, 8898 symmetry-independent reflections (R_{int} = 0.032); max./min. transmission: 0.497/0.445; 512 parameters refined; $w^{-1} = \sigma^2(F_o) + 0.001\ F_o^2$, R = 0.061, R_w = 0.058 for 5639 refelctions with $F_o^2 > 2\sigma(F_o^2)$; largest difference peak: 1.13 eÅ^{-3}. Anisotropic temperature factors were introduced for all nonhydrogen atoms.

14·CH_3OH·1/2 H_2O: $C_{49}H_{49}N_4OP_3RuS_2$·CH_3OH·1/2 H_2O, M = 1009.1, triclinic, space group $P\bar{1}$(No. 2), a = 10.9610(4), b = 13.944(6), c = 17.590(3) Å, α = 76.90(3), β = 88.68(3), γ = 88.94(3)°, V = 2618(2) Å^3, Z = 2, D_{calc} = 1.280 g·cm^{-3}, μ = 0.50 mm^{-1}. Crystal size 0.28 × 0.34 × 0.40 mm; ω scan , scan range: 3 ≤ 2θ ≤ 45° (0 ≤ h ≤ 11, −15 ≤ k ≤ 15, −18 ≤ l ≤ 18), 7081 reflections collected, 6659 symmetry-independent reflections (R_{int} = 0.050); max./min. transmission: 0.804/0.627; 305 parameters refined; $w^{-1} = \sigma^2(F_o) + 0.005\ F_o^2$, R = 0.088, R_w = 0.081 for 2803 reflections with $F_o^2 > 2\sigma(F_o^2)$; largest difference peak: 1.13 eÅ^{-3}. The asymmetric unit contains a disordered water molecule and two disordered solvent methanols. S.o.fs of 0.5 were employed for the relevant O and C atoms. Anisotropic temperature factors were introduced for the Ru, S, P, and O atoms of **15**.

[1] C. Bianchini, C. Mealli, A. Meli, M. Peruzzini, F. Zanobini, *J. Am. Chem. Soc.* **1988**, 8725.
[2] C. Bianchini, A. Meli, M. Peruzzini, F. Vizza, Y. Fujiwara, T. Tintoku, H. Taniguchi, *J. Chem. Soc., Chem. Commun.* **1988**, 210.
[3] C. Bianchini, A. Meli, F. Laschi, J. A. Ramirez, P. Zanello, *Inorg. Chem.* **1988**, *27*, 4429.
[4] C. Bianchini, A. Meli, M. Peruzzini, F. Vizza, P. Frediani, J. A. Ramirez, *Organometallics* **1990**, *9*, 226.
[5] H. A. Mayer, W. C. Kaska, *Chem. Rev.* **1994**, *94*, 1239.
[6] W. O. Siegl, S. J. Lapporte, J. P. Collmann, *Inorg. Chem.* **1971**, *10*, 2158.
[7] J. Ott, L. M. Venanzi, C. A. Ghilardi, S. Midollini, A. Orlandini, *J. Organomet. Chem.* **1985**, *291*, 89.
[8] G. G. Johnston, M. C. Baird, *Organometallics* **1989**, *8*, 1894.
[9] G. G. Johnston, M. C. Baird, *J. Chem. Soc., Chem. Commun.* **1989**, 1008.
[10] E. G. Thaler, K. G. Caulton, *Organometallics* **1990**, *9*, 1871.
[11] D. J. Rauscher, E. G. Thaler, J. C. Huffmann, K. G. Caulton, *Organometallics* **1991**, *10*, 2209.
[12] C. Bianchini, A. Meli, M. Peruzzini, F. Vizza, A. Albinati, *Organometallics* **1990**, *9*, 2283.
[13] G. Kiss, I. T. Horváth, *Organometallics* **1991**, *10*, 3798.
[14] P. Janser, L. M. Venanzi, F. Bachechi, *J. Organomet. Chem.* **1985**, *296*, 229.
[15] E. G. Thaler, K. Folting, K. G. Caulton, *J. Am. Chem. Soc.* **1990**, *112*, 2664.
[16] K. Brandt, W. S. Sheldrick, *Chem. Ber.* **1996**, *129*, 1199.
[17] K. Brandt, W. S. Sheldrick, *Inorg. Chim. Acta* **1997**, in press.
[18] W. S. Sheldrick, C. Landgrafe, *Inorg. Chim. Acta* **1993**, *208*, 145.
[19] K. Brandt, W. S. Sheldrick, *J. Chem. Soc., Dalton Trans* **1996**, 1237.
[20] C. Landgrafe, W. S. Sheldrick, *J. Chem. Soc., Dalton Trans* **1994**, 1885.
[21] C. Landgrafe, W. S. Sheldrick, *J. Chem. Soc., Dalton Trans* **1996**, 989.
[22] C. A. Ghilardi, F. Laschi, S. Midollini, A. Orlandini, G. Scapacci, P. Zanello, *J. Chem. Soc., Dalton Trans* **1995**, 531.
[23] J. Ott, Dissertation, ETH Zürich, **1986**.
[24] D. R. Robertson, T. A. Stephenson, *J. Organomet. Chem.* **1976**, *107*, C46; D. R. Robertson, T. A. Stephenson, *J. Chem. Soc., Dalton Trans* **1994**, 1885.
[25] C. Bianchini, C. Mealli, A. Meli, M. Sabat, *Inorg. Chem.* **1984**, *23*, 2731; C. Bianchini, C. A. Ghilardi, A. Meli, A. Orlandini, *J. Organomet. Chem.* **1985**, *286*, 259.
[26] L. F. Rhodes, C. Sorato, L. M. Venanzi, F. Bachechi, *Inorg. Chem.* **1988**, *27*, 604.
[27] G. M. Sheldrick, *SHELXTL PLUS programs for use with Siemens X-ray systems, Göttingen, **1990***.
[28] Further details of the crystal structure investigations reported in this paper have been deposited with the Cambridge Crystallographic Data Centre as supplementary publication no. CCDC-100819. Copies of the data may be obtained free of charge on application to the Director, CCDC, 12 Union Road, Cambridge CB2 1EZ, UK (fax: int. code +44(0)1223/336−033, email: deposit@chemcrys.cam.ac.uk)

[97267]

A Zwitterionic Pentacoordinate Silicon Compound with an SiO_2N_2C Framework

Brigitte Pfrommer and Reinhold Tacke*

Institut für Anorganische Chemie, Universität Würzburg
Am Hubland, D-97074 Würzburg, Germany
Fax: (internat.) + 49 (0)931/8884609

Received September 29, 1997

Keywords: Pentacoordinate silicon / Zwitterionic λ^5*Si*-silicate / SiO_2N_2C framework / Hypervalent compounds / Main-group elements

The reaction of $(Me_2N)_3SiCH_2CH_2NMe_2$ with 2-amino-4-nitrophenol (molar ratio 1:2) in acetonitrile yields the zwitterionic spirocyclic λ^5*Si*-silicate [2-(dimethylammonio)ethyl]-bis[4-nitrobenzene-2-aminato-1-olato(2−)]silicate (**7**). Compound **7** was characterized by ^1H, ^{13}C, and ^{29}Si solution-state and ^{29}Si solid-state NMR spectroscopy, in addition to single-crystal X-ray diffraction. The SiO_2N_2C framework of **7** is characterized by five "normal" covalent bonds.

In the past few years, we have reported on the synthesis and structural characterization of a series of zwitterionic λ^5*Si*-silicates, such as **1**,[1a] **2** · H_2O,[1b] **3** · DMF,[1c] **4**,[1d] **5**,[1d] and **6**.[1e] These molecular pentacoordinate silicon compounds contain an SiO_4C (**1**, **2**), SiO_5 (**3**), SiF_4C (**4**), SiF_3C_2 (**5**), or SiO_2FC_2 (**6**) framework. With the synthesis of [2-(dimethylammonio)ethyl]bis[4-nitrobenzene-2-aminato-1-olato(2−)]-silicate (**7**), we have now succeeded in obtaining a zwitterionic λ^5*Si*-silicate with an SiO_2N_2C unit. To the best of our knowledge, this is the first pentacoordinate silicon compound which is characterized by two "normal" covalent Si−O and Si−N bonds (two of each) and one "normal" covalent Si−C bond, rather than a bonding system involving four "normal" covalent bonds and one significantly longer dative bond (4+1 coordination).[2][3]

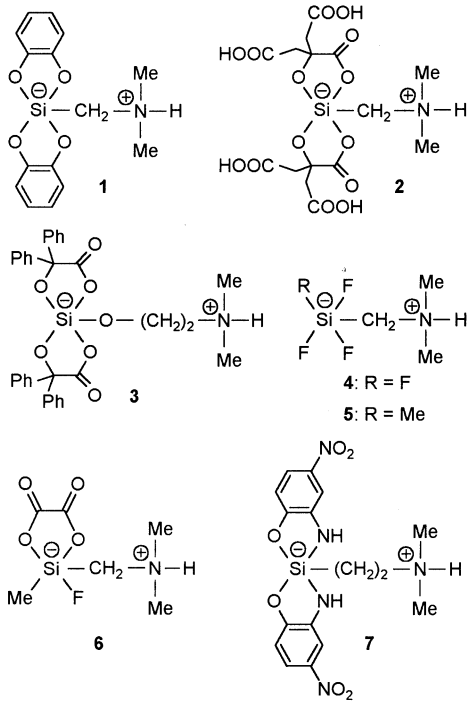

Results and Discussion

Compound **7** was synthesized according to Scheme 1, starting from trichloro(vinyl)silane. The reaction of trichloro(vinyl)silane with a mixture of $LiNMe_2$ and $HNMe_2$ in tetrahydrofuran gave tris(dimethylamino)[2-(dimethylamino)ethyl]silane (**8**), in a yield of 86%, which was then treated with two mol equivalents of 2-amino-4-nitrophenol in acetonitrile to give **7**, in a yield of 73%, as an orange-colored crystalline solid. The identity of **7** was established by elemental analysis (C, H, N), and both solution-state ([D_6]DMSO; ^1H, ^{13}C, ^{29}Si) and solid-state (^{29}Si CP/MAS) NMR studies. In addition, **7** was characterized by a single-crystal X-ray diffraction study.

Compound **7** crystallizes in the space group *Pc* with two crystallographically independent zwitterions in the asymmetric unit. The structures of these two molecules (see Figure 1) are very similar. The geometries of the coordination polyhedra surrounding the central silicon atoms Si and Si′ can be described as strongly distorted trigonal bipyramidal structures (transition trigonal bipyramid → square pyramid: 24.6%, Si; 35.7%, Si′; pivotal atoms C1 and C1′),[4] with each of the axial positions occupied by the oxygen atoms. The Si−O distances in the two molecules of **7** [1.806(6)−1.829(6) Å] are marginally longer than those observed for the axial Si−O distances of **1** and related spirocyclic zwitterionic λ^5*Si*-silicates containing ligands of the benzene-1,2-diolato(2−) type (typical values: 1.75−1.79 Å).[5] In contrast, the Si−C distances [1.875(9) Å, 1.867(8) Å] correspond to those observed for **1** and its derivatives (typical values: 1.87−1.89 Å).[5] The Si−N distances [1.741(7)−1.764(6) Å] are similar to those reported for the equatorial Si−N bonds of azasilatranes (typical values:

 © WILEY-VCH Verlag GmbH, D-69451 Weinheim, 1998 1434−1948/98/0303−0415 $ 17.50+.50/0

Scheme 1. Synthesis of the zwitterionic λ^5*Si*-silicate **7**

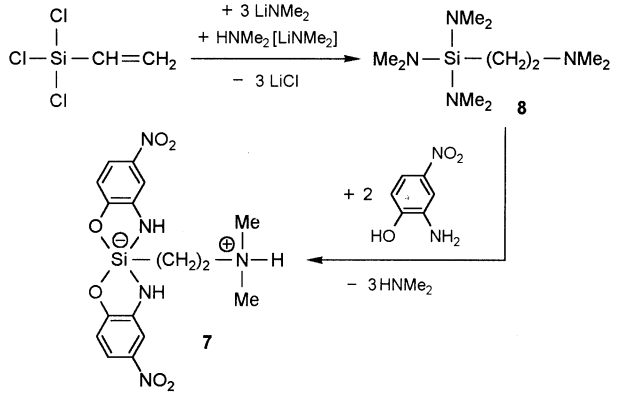

Figure 1. Structures of the two crystallographically independent zwitterions in the crystal of **7**[a]

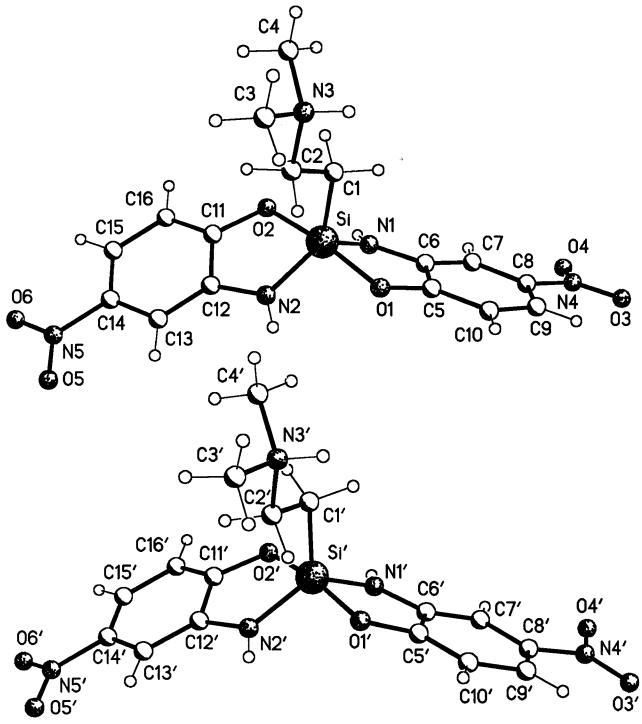

[a] Selected distances [Å] and angles [°] (standard deviations in parentheses): Si−O1 1.829(6), Si−O2 1.806(6), Si−N1 1.741(7), Si−N2 1.751(7), Si−C1 1.875(9); O1−Si−O2 171.8(3), O1−Si−N1 86.6(3), O1−Si−N2 89.3(3), O1−Si−C1 92.9(4), O2−Si−N1 90.0(3), O2−Si−N2 87.0(3), O2−Si−C1 95.3(4), N1−Si−N2 128.3(4), N1−Si−C1 114.4(4), N2−Si−C1 117.3(4). − Si′−O1′ 1.821(6), Si′−O2′ 1.809(6), Si′−N1′ 1.753(7), Si′−N2′ 1.764(6), Si′−C1′ 1.867(8); O1′−Si′−O2′ 167.3(3), O1′−Si′−N1′ 85.3(3), O1′−Si′−N2′ 89.2(3), O1′−Si′−C1′ 94.6(3), O2′−Si′−N1′ 89.0(3), O2′−Si′−N2′ 85.9(3), O2′−Si′−C1′ 98.1(3), N1′−Si′−N2′ 130.9(3), N1′−Si′−C1′ 116.5(3), N2′−Si′−C1′ 112.5(4).

1.73−1.77 Å).[3] All these data clearly demonstrate that the SiO_2N_2C framework of **7** is built up by five "normal" covalent bonds, and does not involve a bonding system in the sense of the 4+1 coordination usually observed for pentacoordinate silicon species with Si−N bonds.

As would be expected from the presence of the potential NH donor functions and acceptor atoms of **7**, several intermolecular N−H···O interactions are observed in the crystal, leading to the formation of a complex hydrogen bonding network.[6]

In the ^{29}Si CP/MAS NMR experiment, only one resonance signal was obtained for the two crystallographically independent silicon atoms (isotropic ^{29}Si chemical shift: δ = −77.2). As this chemical shift is very similar to that observed for **7** in [D_6]DMSO (δ = −78.6), it is concluded that the SiO_2N_2C framework is also present in solution. In addition, the ^{1}H chemical shifts observed for the NCH_3 (s, δ = 2.63), CCH_2N (m, δ = 3.18−3.23), and CNH groups (br. s, δ = 9.0) indicate the presence of an ammonium group. These and all other NMR data (see Experimental Section) are in accordance with the structure of **7** and thus clearly demonstrate that this zwitterionic compound is also present in solution.

This work was supported by the *Deutsche Forschungsgemeinschaft* and the *Fonds der Chemischen Industrie*. We would like to thank Professor *D. Stalke*, University of Würzburg, for helpful discussions in context with the crystal structure analysis.

Experimental Section

General: The syntheses were carried out under dry nitrogen. The solvents used were dried and purified according to standard procedures and stored under nitrogen. − Melting points: DuPont Instruments differential scanning calorimeter, type Thermal-Analyzer 910. − ^{1}H, ^{13}C, and ^{29}Si solution-state NMR spectra: recorded at room temp. on a Bruker DRX-300 NMR spectrometer (^{1}H, 300.1 MHz; ^{13}C, 75.5 MHz; ^{29}Si, 59.6 MHz); $CDCl_3$ and [D_6]DMSO were used as solvents; chemical shifts (ppm) were determined relative to internal $CHCl_3$ (^{1}H, δ = 7.24; $CDCl_3$), $CDCl_3$ (^{13}C, δ = 77.0; $CDCl_3$), [D_5]DMSO (^{1}H, δ = 2.49; [D_6]DMSO), [D_6]DMSO (^{13}C, δ = 39.5; [D_6]DMSO), and TMS (^{29}Si, δ = 0; $CDCl_3$, [D_6]DMSO); assignment of the ^{13}C-NMR data was supported by DEPT 135 experiments. − ^{29}Si CP/MAS NMR: recorded at room temp. on a Bruker DSX-500 NMR spectrometer at 11.74 T with double air bearing rotors of ZrO_2 (diameter 7 mm) containing 200 mg of sample [99.35 MHz; TMS as external standard (δ = 0)]. − Mass spectra: Finnigan MAT-711 mass spectrometer (EI MS, 70 eV); the selected *m/z* values given refer to the isotopes ^{1}H, ^{12}C, ^{14}N, and ^{28}Si.

[2-(Dimethylammonio)ethyl]bis[4-nitrobenzene-2-aminato-1-olato(2−)]silicate (**7**): The triaminosilane $(Me_2N)_3Si(CH_2)_2NMe_2$ (**8**) (3.05 g, 13.1 mmol) was added dropwise at room temp. within 2 min to a stirred solution of 2-amino-4-nitrophenol (4.04 g, 26.2 mmol) in acetonitrile (50 ml). After the mixture was stirred for 2 h at room temp., part of the solvent (ca. 25 ml) was removed at 40°C under reduced pressure (formation of a precipitate). The precipitate was filtered off and recrystallized from acetonitrile (slow cooling of a satd. boiling solution to room temp.) and dried in vacuo (0.01 Torr, 20°C, 6 h) to yield 3.88 g (73%) of orange-colored crystals, mp. 230°C (decomp.). − ^{1}H NMR ([D_6]DMSO): δ = 0.96−1.03 (m, 2 H, $SiCH_2C$), 2.63 (s, 6 H, NCH_3), 3.18−3.23 (m, 2 H, CCH_2N), 5.68 (s, 2 H, SiNH), 6.40 [d, $^3J_{HH}$ = 8.6 Hz, 2 H, 6-*H*, 4-nitrobenzene-2-aminato-1-olato(2−) (NBAO)], 7.21 (d, $^4J_{HH}$ = 2.8 Hz, 2 H, 3-*H*, NBAO), 7.39 (dd, $^3J_{HH}$ = 8.6 Hz, $^4J_{HH}$ = 2.8 Hz, 2 H, 5-*H*, NBAO), 9.0 (br. s, 1 H, CNH). − ^{13}C{^{1}H} NMR ([D_6]DMSO): δ = 15.0 ($SiCH_2C$), 38.9 (NCH_3), 53.7 (CCH_2N),

99.6 (*C*-3, NBAO), 105.3 (*C*-6, NBAO), 112.7 (*C*-5, NBAO), 135.4, 138.9, and 157.3 (odd NBAO C atoms). – $^{29}Si\{^1H\}$ NMR ([D$_6$]DMSO): δ = −78.6. – ^{29}Si CP/MAS NMR (spinning rate 4383 Hz, 308 transients, contact time 7 ms, 90° ^{1}H transmitter pulse length 6.8 μs, repetition time 25 s): δ = −77.2 ($\upsilon_{1/2}$ = 267 Hz). – $C_{16}H_{19}N_5O_6Si$ (405.4): calcd. C 47.40, H 4.72, N 17.27; found C 47.7, H 4.7, N 17.3.

Tris(dimethylamino)[2-(dimethylamino)ethyl]silane (**8**): A 1.6 M solution of *n*-butyllithium in hexane (312 ml, 499 mmol of *n*BuLi) was added dropwise at −25°C within 40 min to a stirred solution of dimethylamine (29.3 g, 650 mmol) in THF (150 ml). After the mixture was warmed to −15°C within 30 min and stirred for 1 h at this temp., a solution of trichloro(vinyl)silane (24.2 g, 150 mmol) in THF (150 ml) was added dropwise at −15°C within 30 min. The resulting mixture was stirred for 14 h at −5°C, and a solution of chlorotrimethylsilane (6.52 g, 60.0 mmol) in THF (20 ml) was added dropwise. The mixture was stirred for 2 h at −15°C and then allowed to warm to room temp. After the precipitate was filtered off and the solvent removed under reduced pressure, *n*-pentane (100 ml) was added to the residue. The resulting precipitate was filtered off, the solvent removed under reduced pressure, and the residue distilled in vacuo to give 30.1 g (86%) of a colorless liquid; bp. 54°C/0.02 Torr. – ^{1}H NMR ($CDCl_3$): δ = 1.05−1.12 (m, 2 H, $SiCH_2C$), 2.19 (s, 6 H, $CNCH_3$), 2.42−2.49 (m, 2 H, CCH_2N), 2.46 (s, 18 H, $SiNCH_3$). – $^{13}C\{^1H\}$ NMR ($CDCl_3$): δ = 12.8 ($SiCH_2C$), 38.6 ($SiNCH_3$), 45.8 ($CNCH_3$), 56.2 (CCH_2N). – $^{29}Si\{^1H\}$ NMR ($CDCl_3$): δ = −17.2. – EI MS: *m*/*z* = 232 (3) [M^+], 188 (80) [$M^+ - N(CH_3)_2$], 160 (100) [$M^+ - CH_2CH_2N(CH_3)_2$]. – $C_{10}H_{28}N_4Si$ (232.4): calcd. C 51.67, H 12.14, N 24.10; found C 51.5, H 12.1, N 24.0.

Crystal Structure Determination: A suitable single crystal of **7** was obtained by crystallization from acetonitrile (slow cooling of a satd. boiling solution to room temp.). The crystal was mounted in inert oil (RS 3000, Riedel-de Haën) on a glass fiber and then transferred to the cold gas stream of the diffractometer (Enraf-Nonius four-circle diffractometer; graphite-monochromated Mo-K_α radiation (λ = 0.71073 Å); for the low-temp. attachment, see ref.[7]). Cell parameters were obtained from least-squares fits to the settings of 25 reflections in the range of 20° ≤ 2θ ≤ 25°. No significant deviations in intensity were registered for two monitor reflections recorded at regular intervals. The structure was solved by direct methods (program SHELXS-96)[8a] and refined on F^2 (program SHELXL-96).[8b] The non-hydrogen atoms were refined anisotropically; for the refinement of the hydrogen atom positions a riding model was employed. Further information about the crystal data, data collection, and structure refinement is summarized in Table 1. Crystallographic data (excluding structure factors) for the structure reported in this paper have been deposited at the Cambridge Crystallographic Data Centre as supplementary publication no. CCDC-100592. Copies of the data can be obtained free of charge on application to CCDC, 12 Union Road, Cambridge CB2 1EZ, UK [Fax: (internat.) +44 (1223) 336-033; E-mail: deposit@ccdc.cam.ac.uk].

Table 1. Crystal data and experimental parameters for the crystal structure analysis of **7**

empirical formula	$C_{16}H_{19}N_5O_6Si$
formula mass [g mol^{-1}]	405.4
collection T_c[K]	173(2)
λ(Mo-K_α) [Å]	0.71073
crystal system	monoclinic
space group (no.)	*Pc* (7)
crystal dimensions [mm]	0.2 × 0.2 × 0.2
a [Å]	19.187(5)
b [Å]	8.652(2)
c [Å]	11.246(6)
β [°]	101.19(3)
V[Å^3]	1831.3(12)
Z	4
D(calcd.) [g cm^{-3}]	1.471
μ [mm^{-1}]	0.174
F(000)	848
2θ range [°]	4.32−46.04
index range	$-21 \le h \le 21$, $0 \le k \le 9$, $-12 \le l \le 12$
no. of collected/independent refl.	5089
no. of refl. used	5089
no. of parameters	510
no. of restraints	2
S[a]	1.016
weight parameters *a*/*b*[b]	0.045/0
*R*1[c] [$I > 2\sigma(I)$]	0.0681
*wR*2[d] (all data)	0.1399
max./min. resid. electron dens. [e Å^{-3}]	+0.242/−0.333

[a] $S = \{\Sigma[w(F_o^2 - F_c^2)^2] / (n - p)\}^{0.5}$; *n* = no. of reflections; *p* = no. of parameters. – [b] $w^{-1} = \sigma^2(F_o^2) + (aP)^2 + bP$, with $P = (F_o^2 + 2F_c^2)/3$. – [c] $R1 = \Sigma||F_o| - |F_c|| / \Sigma|F_o|$. – [d] $wR2 = \{\Sigma[w(F_o^2 - F_c^2)^2] / \Sigma[w(F_o^2)^2]\}^{0.5}$.

[1] [1a] R. Tacke, A. Lopez-Mras, J. Sperlich, C. Strohmann, W. F. Kuhs, G. Mattern, A. Sebald, *Chem. Ber.* **1993**, *126*, 851−861. – [1b] M. Mühleisen, R. Tacke, *Chem. Ber.* **1994**, *127*, 1615−1617. – [1c] R. Tacke, M. Mühleisen, *Inorg. Chem.* **1994**, *33*, 4191−4193. – [1d] R. Tacke, J. Becht, O. Dannappel, R. Ahlrichs, U. Schneider, W. S. Sheldrick, J. Hahn, F. Kiesgen, *Organometallics* **1996**, *15*, 2060−2077. – [1e] R. Tacke, O. Dannappel, M. Mühleisen in *Organosilicon Chemistry II − From Molecules to Materials* (Eds.: N. Auner, J. Weis), VCH, Weinheim, **1996**, pp. 427−446.

[2] Reviews and proceedings dealing with pentacoordinate silicon compounds: [2a] S. N. Tandura, M. G. Voronkov, N. V. Alekseev, *Top. Curr. Chem.* **1986**, *131*, 99−189. – [2b] W. S. Sheldrick in *The Chemistry of Organic Silicon Compounds, Part 1* (Eds.: S. Patai, Z. Rappoport), Wiley, Chichester, **1989**, pp. 227−303. – [2c] R. R. Holmes, *Chem. Rev.* **1990**, *90*, 17−31. – [2d] C. Chuit, R. J. P. Corriu, C. Reye, J. C. Young, *Chem. Rev.* **1993**, *93*, 1371−1448. – [2e] R. Tacke, J. Becht, A. Lopez Mras, J. Sperlich, *J. Organomet. Chem.* **1993**, *446*, 1−8. – [2f] Reference[1e]. – [2g] R. Tacke, O. Dannappel in *Tailor-made Silicon Oxygen Compounds − From Molecules to Materials* (Eds.: R. Corriu, P. Jutzi), Vieweg, Braunschweig/Wiesbaden, **1996**, pp. 75−86. – [2h] E. Lukevics, O. A. Pudova, *Chem. Heterocycl. Compd.* **1996**, *353*, 1605−1646. – [2i] R. R. Holmes, *Chem. Rev.* **1996**, *96*, 927−950.

[3] Azasilatranes are also pentacoordinate silicon species comprising covalent Si−N bonds. However, these compounds contain four "normal" covalent bonds (including the equatorial Si−N bonds; typical Si−N distances 1.73−1.77 Å) and one significantly longer axial dative Si←N bond (typical Si←N distances 2.03−2.25 Å) (4+1 coordination): [3a] A. A. Macharashvili, V. E. Shklover, Yu. T. Struchov, A. Lapsiņa, G. Zelcāns, E. Lukevics, *J. Organomet. Chem.* **1988**, *349*, 23−27. – [3b] D. Gudat, J. G. Verkade, *Organometallics* **1989**, *8*, 2772−2779. – [3c] Y. Wan, J. G. Verkade, *J. Am. Chem. Soc.* **1995**, *117*, 141−156. – In this context, see also: [3d] G. Klebe, J. W. Bats, K. Hensen, *Z. Naturforsch., B* **1983**, *38*, 825−829. – [3e] G. Klebe, J. W. Bats, K. Hensen, *J. Chem. Soc. Dalton Trans.* **1985**, 1−4.

[4] The quantification of the distortion in this form relates to the transition from the ideal trigonal bipyramid toward the ideal square pyramid along the reaction coordinate of the Berry pseudorotation. The degree of distortion was calculated according to the dihedral angle method described in the literature,[9] using the values given there for the reference geometry of the ideal square pyramid.

[5] R. Tacke, M. Mühleisen, A. Lopez-Mras, W. S. Sheldrick, *Z. Anorg. Allg. Chem.* **1995**, *621*, 779−788; and literature cited therein.

[6] Based on the N···O distances (in parentheses) determined, the existence of the following intermolecular hydrogen bonds can be discussed: N3−H···O3′/N3−H···O4′ [3.186(9)/2.875(9) Å,

bifurcated]。 and N3′−H′···O3/N3′−H′···O4 [3.018(10)/3.073(10) Å, bifurcated] (providing arrangement of the molecules to layers); N1−H···O1 [3.328(9) Å] (providing interaction between the layers in the crystal packing).

[7] T. Kottke, R. J. Lagow, D. Stalke, *J. Appl. Crystallogr.* **1996**, *29*, 465−468.

[8] [8a] *SHELXS-96*, University of Göttingen, Germany, **1996**; G. M. Sheldrick, *Acta Crystallogr., Sect. A* **1990**, *46*, 467−473. − [8b] *SHELXL-96*, University of Göttingen, Germany, **1996**.

[9] R. R. Holmes, J. A. Deiters, *J. Am. Chem. Soc.* **1977**, *99*, 3318−3326.

[97221]

Stability of Bridged and Unbridged η^2-Alkyne−titanocene and −zirconocene Complexes − Influence of Metals, Alkyne Substituents, Cp Substitution and Additional Ligands

Normen Peulecke[a], Wolfgang Baumann[a], Rhett Kempe[a], Vladimir V. Burlakov[b], and Uwe Rosenthal*[a]

Abteilung „Komplexkatalyse", Institut für Organische Katalyseforschung an der Universität Rostock e.V.[a],
Buchbinderstraße 5−6, D-18055 Rostock, Germany

Institute of Organo-Element Compounds, Russian Academy of Sciences[b],
Vavilov Str. 28, Moscow 117813, Russian Federation

Received September 1, 1997

Keywords: Alkyne complexes / Titanium / Zirconium / Coordination mode / Metallacycles / Cyclopentadienes

The influence of metals, alkyne substituents, Cp substitution and additional ligands on the stability of bridged and unbridged η^2-alkyne−titanocene and −zirconocene complexes has been investigated. The reduction of the complex [(η^5-C_5H_4)−$SiMe_2$−(η^5-C_5H_4)]$TiCl_2$ with magnesium in the presence of tolan (PhC_2Ph) does not give the expected alkyne−titanocene complex [(η^5-C_5H_4)−$SiMe_2$−(η^5-C_5H_4)]Ti(η^2-PhC_2Ph) but by coupling of two tolan molecules the corresponding titanacyclopentadiene [(η^5-C_5H_4)−$SiMe_2$−(η^5-C_5H_4)]TiC_4Ph_4 (**1**) was obtained. In the analogous reaction with $Me_3SiC_2SiMe_3$ the stable η^2-alkyne complex without additional ligands [(η^5-C_5H_4)−$SiMe_2$−(η^5-C_5H_4)]Ti(η^2-$Me_3SiC_2SiMe_3$) (**2**) was formed, due to the sterical influence of the alkyne substituents. The compounds without additional ligands $(thi)_2Ti(\eta^2\text{-}PhC_2Ph)$ (**3**) and $(thi)_2Ti(\eta^2\text{-}Me_3SiC_2SiMe_3)$ (**5**) were isolated from the unbridged titanocene complex $(thi)_2TiCl_2$ (thi = tetrahydroindenyl). Two equivalents of complex **3** reacted with one equivalent of water to yield the dimeric alkylidene-μ-oxo complex $[(thi)_2Ti(CPh{=}CHPh)]_2(\mu\text{-}O)$ (**6**). The reaction of the unbridged zirconocene compound $(thi)_2ZrCl_2$ gave the alkyne complex $(thi)_2Zr(THF)(\eta^2\text{-}Me_3SiC_2SiMe_3)$ (**7**) which is stabilized by THF. At higher temperature THF was eliminated from the orange complex **7** forming the green complex $(thi)_2Zr(\eta^2\text{-}Me_3SiC_2SiMe_3)$. This behaviour was investigated in detail using NMR spectroscopy and compared to similar complexes such as $Cp_2Zr(\eta^2\text{-}Me_3SiC_2SiMe_3)$ (not stable without THF), $(ebthi)_2Zr(\eta^2\text{-}Me_3SiC_2SiMe_3)$ (ebthi = ethylenebistetrahydroindenyl; stable without THF) and $Cp^*{}_2Zr(\eta^2\text{-}Me_3SiC_2SiMe_3)$ (Cp^* = pentamethyl-Cp, stable without THF). All complexes were characterized by spectroscopic methods. X-ray structural determinations were conducted for the complexes **1**, **3** and **7**. Compound **3** is the first example of a structurally characterized tolan−titanocene complex without additional ligands.

Introduction

Alkyne complexes of group-IV metallocenes can be used synthetically for many purposes.[1] We were the first to produce titanocene complexes of silylalkynes without additional ligands, e.g. $Cp_2Ti(\eta^2\text{-}Me_3SiC_2SiMe_3)$[2a] and also zirconocene complexes with additional ligands such as $Cp_2Zr(L)(\eta^2\text{-}Me_3SiC_2SiMe_3)$[2b][2c] as well as the first example of a zirconocene without additional ligands *rac*-$(ebthi)_2Zr(\eta^2\text{-}Me_3SiC_2SiMe_3)$.[3]

More recently, we reported the synthesis, spectral characteristics and X-ray structural determination of other examples such as Cp-bridged alkyne complexes of the type [(η^5-C_5H_4)-*ansa*-(η^5-C_5H_4)]Ti(η^2-$Me_3SiC_2SiMe_3$) (*ansa* = $Me_2Si{-}O{-}SiMe_2$) and [(η^5-C_5H_4)-*ansa*-(η^5-C_5H_4)]Zr(L)-(η^2-$Me_3SiC_2SiMe_3$) (*ansa* = $Me_2Si{-}O{-}SiMe_2$, L = py; *ansa* = $SiMe_2$, L = py).[4] The special feature of these reagents when used in conjunction with bis(trimethylsilyl)acetylene is their ability to generate the metallocene [Cp_2M] or *ansa* systems such as [(η^5-C_5H_4)$SiMe_2OSiMe_2$(η^5-C_5H_4)M], [(η^5-C_5H_4)$SiMe_2$(η^5-C_5H_4)M] and *rac*-[(ebthi)M], (M = Ti, Zr) under mild conditions. This tendency depends not only on the alkyne substituents but also on the nature of the additional ligands. The factors which determine whether alkyne complexes with or without additional ligands are formed remained unclear, because the stability and reactivity depend strongly on the character of this additional interaction. The use of different additional ligands allows a tuning of the stoichiometric[5a] and catalytic[5b][5c] reactions.

In this paper we report on the influence of metals, alkyne substituents, Cp substitution and additional ligands on the stability of bridged and unbridged η^2-alkyne−titanocene and −zirconocene complexes with and without additional ligands.

Complex Synthesis

The reduction of the complex [(η^5-C_5H_4)−$SiMe_2$−(η^5-C_5H_4)]$TiCl_2$[6] with magnesium in the presence of tolan (PhC_2Ph) in THF at room temperature does not give the expected alkyne−titanocene complex [(η^5-C_5H_4)−$SiMe_2$−(η^5-C_5H_4)]Ti(η^2-PhC_2Ph). Instead, the corresponding titanacyclopentadiene [(η^5-C_5H_4)−$SiMe_2$−(η^5-C_5H_4)]TiC_4Ph_4 (**1**) is obtained in 35% yield by coupling of two tolan molecules (Scheme 1).

This coupling with a second tolan molecule is typical behaviour for coordinatively and electronically unsaturated

 © WILEY-VCH Verlag GmbH, D-69451 Weinheim, 1998 1434−1948/98/0303−0419 $ 17.50+.50/0

Scheme 1

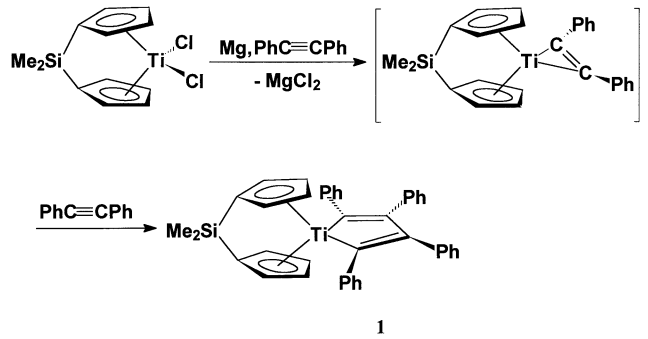

1

tolan complexes such as $Cp_2Ti(\eta^2\text{-}PhC_2Ph)$[7]; the titanacyclopentadiene with unbridged Cp ligands that is obtained is well-known. By using another alkyne, $Me_3SiC_2SiMe_3$, instead of tolan, the complex $[(\eta^5\text{-}C_5H_4)\text{-}SiMe_2\text{-}(\eta^5\text{-}C_5H_4)]Ti(\eta^2\text{-}Me_3SiC_2SiMe_3)$ (**2**) can be isolated (Scheme 2). This is explained by the special character of the silylalkyne which prevents a coupling reaction by sterical hindrance of the large substituents.

Scheme 2

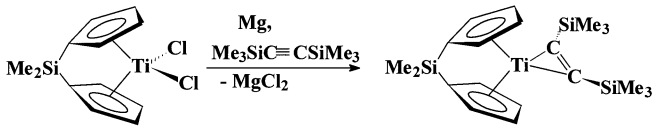

2

In the reaction of the unbridged complex $(thi)_2TiCl_2$[8] the compound without additional ligands $(thi)_2Ti(\eta^2\text{-}PhC_2Ph)$ (**3**) was isolated. The analogous complexes **4** and **5** were also obtained using other alkynes such as PhC_2SiMe_3 and $Me_3SiC_2SiMe_3$ (Scheme 3).

Scheme 3

3 $R^1=R^2=Ph$;
4 $R^1=Ph$, $R^2=SiMe_3$
5 $R^1=R^2=SiMe_3$

Two equivalents of complex **3** react with one equivalent of water to yield the dimeric alkenyl-μ-oxo complex $[(thi)_2Ti(CPh{=}CHPh)]_2(\mu\text{-}O)$ (**6**) (Scheme 4).

Scheme 4

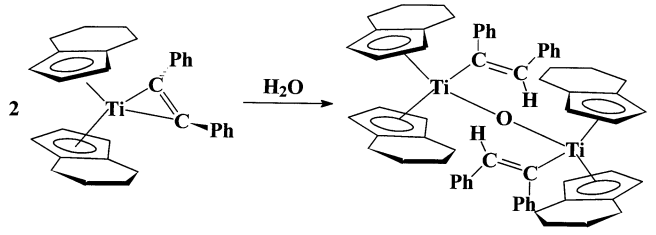

6

This reaction is a typical example of a tolan–titanocene complex, also found in the case of $Cp_2Ti(\eta^2\text{-}PhC_2Ph)$[7], but differs from those of the silylalkyne complex $Cp_2Ti(\eta^2\text{-}Me_3SiC_2SiMe_3)$, which gave only the elimination of the alkyne[9].

In the reaction of the unbridged zirconocene complex $(thi)_2ZrCl_2$[8] in THF at room temperature, the alkyne complex $(thi)_2Zr(THF)(\eta^2\text{-}Me_3SiC_2SiMe_3)$ (**7**), stabilized by THF, was formed (Scheme 5).

Scheme 5

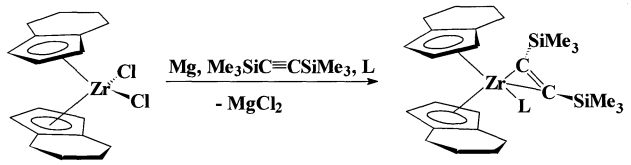

L = thf 7, L = py 8

Complex **7** is an analogue of the compound $Cp_2Zr(THF)(\eta^2\text{-}Me_3SiC_2SiMe_3)$[2b]. Just as for this Cp complex,[2c] coordination by py is also possible for the thi complex **7** which gives $(thi)_2Zr(py)(\eta^2\text{-}Me_3SiC_2SiMe_3)$ (**8**).

Spectral Characteristics

Complex **1** did not show any IR absorption of a complexed triple bond in the expected region of 1600–1800 cm^{-1}. IR absorptions for other complexes (**2**: 1683 cm^{-1}; **3**: 1671; **4**: 1652; **5**: 1629) and the ^{13}C-NMR-spectroscopic signals of the acetylenic C atoms (**2**: δ = 248.9; **3**: 198.8; **4**: 213.6, 220.0; **5**: 242.3) are typical of values for such alkyne complexes[10] and prove that complexes **2**, **3**, **4** and **5** have a titanacyclopropene structure. These data again show larger spectroscopic shifts (IR, NMR) for the potential π-acceptor groups $SiMe_3$ as alkyne substituents.

Complex **3** is the second example of a tolan–titanocene complex without additional ligands. The other complex $Cp_2Ti(\eta^2\text{-}PhC_2Ph)$[7] is characterized by an IR absorption at 1713 cm^{-1} and ^{13}C-NMR signals at δ = 196.5. Previously, only the complex with a stabilizing ligand, e.g. $Cp_2Ti(CO)(\eta^2\text{-}PhC_2Ph)$, had been reported.[11] In the latter, the alkyne formally acts as a two-electron donor, while it is regarded as contributing four electrons in **3**. This also follows from the frequencies of the C–C stretching vibrations (**3**: 1671 cm^{-1}; CO complex: 1780) in the IR spectra.

The IR and ^{13}C-NMR spectra of complex **7** are typical of those also found for the compound $Cp_2Zr(THF)(\eta^2\text{-}Me_3SiC_2SiMe_3)$.[2b] The higher shifts of complex **7**, e.g. the absorption in the IR spectra (Cp compound: 1581 cm^{-1}; **7**: 1559) and the ^{13}C-NMR signals of the acetylenic C atoms (Cp compound: 212.9; **7**: δ = 222.0) are typical of values[12] for substituted Cp ligands (Cp* and thi) which are stronger donors than Cp itself. At higher temperatures the orange complex **7** eliminates THF reversibly to give the green complex $(thi)_2Zr(\eta^2\text{-}Me_3SiC_2SiMe_3)$ (Scheme 6), a reaction

which is unknown for the Cp complex $Cp_2Zr(THF)(\eta^2\text{-}Me_3SiC_2SiMe_3)$.

Scheme 6

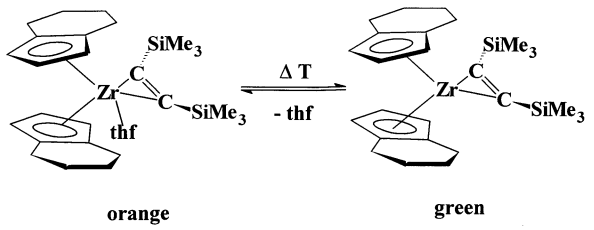

This reaction was identified using NMR spectroscopy after warming up to 343 K by a low-field shift from δ = 222.0 to 244.0. The same effect has been found for complexes similar to $Cp_2Zr(THF)(\eta^2\text{-}Me_3SiC_2SiMe_3)$ which are not stable without THF, *rac*-$(ebthi)_2Zr(\eta^2\text{-}Me_3SiC_2SiMe_3)$ being stable without THF at room temperature and $Cp^*_2Zr(\eta^2\text{-}Me_3SiC_2SiMe_3)$, which did not coordinate with THF at any of the temperatures investigated.[13]

Structural Investigations

The structure of **1** in the crystal is shown in Figure 1. The analogous complex with unsubstituted Cp has already been investigated by X-ray structure analysis.[14] Table 1 lists the relevant data of this complex in comparison with those of complex **1**.

Figure 1. Molecular structure of **1**; shown by an ORTEP plot (50% probability)[a]

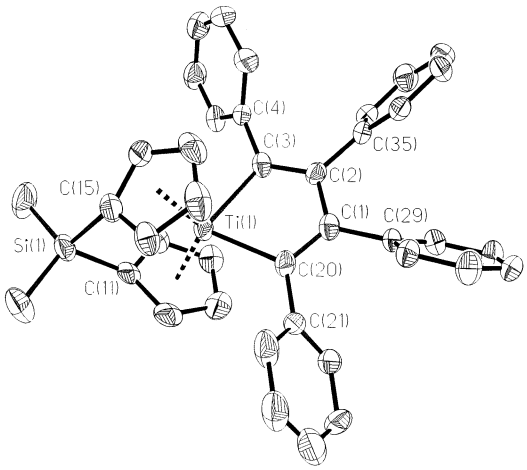

[a] Selected distances [Å] and angles [°]: C1−C20 1.364(5), C2−C3 1.362(5), Ti1−C3 2.172(4), Ti−C20 2.160(3); C4−C3−C2 124.5(3), C3−C2−C35 123.1(3), C1−C20−C21 123.0(3), C20−C1−C29 121.0(3), C15−Si−C11 92.7(2).

The bond lenghts and angles of the central five-membered titanacycle are nearly identical and are not influenced by the substitution at the Cp ligands. The structure of **3** in the crystal is shown in Figure 2.

Complex **3** is the first example of a structurally well-characterized tolan−titanocene complex that is stable without additional ligands. Previously, only the structures of complexes with stabilizing ligands, e.g. $Cp_2Ti(CO)(\eta^2\text{-}PhC_2Ph)$, have been described.[11] The comparison is between a complex with one alkyne group acting as a two-electron donor (CO complex) and in the other case as a four-electron donor (**3**). In Table 2 the relevant data of both complexes are listed and compared.

Table 1. Comparision of structural data of $Cp_2TiC_4Ph_4$ and **1**

	$Cp_2TiC_4Ph_4$	**1**
Distances [Å]		
Ti−C3	2.172(5)	2.172(4)
Ti−C20	2.141(5)	2.160(3)
C2−C3	1.369(6)	1.362(5)
C1−C2	1.495(6)	1.493(5)
C1−C20	1.370(6)	1.364(5)
Angles [°]		
C20−Ti−C3	80.3(2)	79.8(1)
Ti−C3−C2	112.5(3)	112.1(3)
Ti−C20−C1	111.0(3)	111.4(2)
C3−C2−C1	117.4(4)	117.2(3)
C20−C1−C2	118.5(4)	119.1(3)
Cp′−Ti−Cp′	134.8(3)	130.7(5)

Figure 2. Molecular structure of **3**, shown by an ORTEP plot (50% probability)[a]

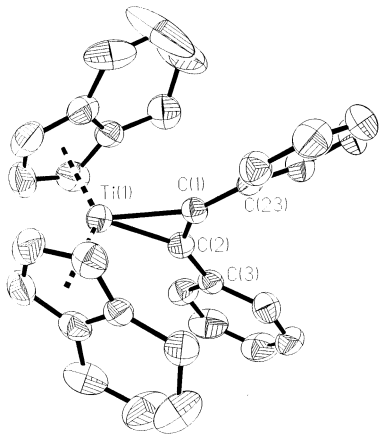

[a] Selected distances [Å] and angles [°]: C1−C2 1.287(6), Ti−C1 2.086(4), Ti−C2 2.044(5); C1−Ti−C2 36.3(2), C23−C1−C2 140.7(4), C3−C2−C1 138.7(5), Cp′−Ti−Cp′ 137.5(4).

Table 2. Comparison of structural data of $Cp_2Ti(CO)(\eta^2\text{-}PhC_2Ph)$ and **3**

Compound	$Cp_2Ti(CO)(\eta^2\text{-}PhC_2Ph)$	**3**
Distances [Å]		
C1−C2	1.29(1)	1.287(6)
Ti−C1	2.107(7)	2.086(4)
Ti−C2	2.230(7)	2.044(5)
Ti−C(O)	2.050(8)	−
Angles [°]		
C(O)−Ti−C2	71.9(3)	−
C1−Ti−C2	34.3(3)	36.3(2)
C23−C1−C2	138.8(7)	140.7(4)
C3−C2−C1	145.8(7)	138.7(5)
Cp′−Ti−Cp′	133.5(5)	137.5(4)

Both titanocene complexes contain different ligands (Cp and thi) and a detailed comparison and investigation of the influence of the additional CO ligand on the complexation

of tolan is therefore not possible. The Ti−C bond lengths are shorter in complex **3**, indicating a stronger complexation of the alkyne as expected. On the other hand, the additional ligand CO alone makes less space available in the coordination sphere at the central atom, reducing the interaction of the alkyne with the titanium atom. The structure of **7** in the crystal is shown in Figure 3.

Figure 3. Molecular structure of **7**, shown by an ORTEP plot (50% probability)[a]

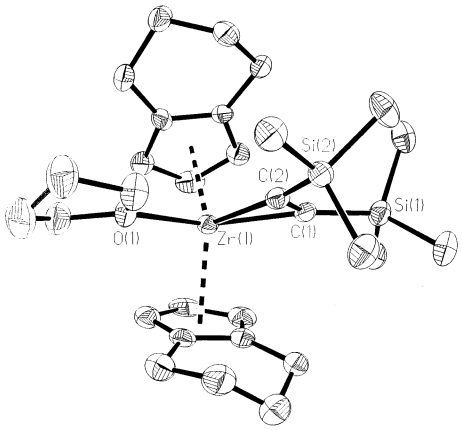

[a] Selected distances [Å] and angles [°]: C1−C2 1.340(7), Zr1−C1 2.218(5), Zr1−C2 2.271(5), Zr1−O1 2.404(4); C1−Zr1−C2 34.7(2), Si1−C1−C2 141.1(4), Si2−C2−C1 124.5(4), C2−Zr1−O1 86.7(1); the structural data of the Cp and the corresponding thi complex **7** are listed and compared in Table 3.

Table 3. Comparison of structural data of $Cp_2Zr(THF)(\eta^2\text{-}Me_3SiC_2SiMe_3)$ and **7**

Compound	$Cp_2Zr(THF)(\eta^2\text{-}Me_3SiC_2SiMe_3)$	**7**
Distances [Å]		
C1−C2	1.302(9)	1.340(7)
Zr−C1	2.204(7)	2.218(5)
Zr−C2	2.260(7)	2.271(5)
Zr−O1	2.390(5)	2.404(4)
Angles [°]		
C1−Zr−C2	33.9(2)	34.7(2)
C1−C2−Si2	134.4(6)	124.5(4)
C2−C1−Si1	143.5(6)	141.1(4)
C2−Zr−O1	86.8(2)	86.7(1)
Cp′−Zr−Cp′	130.5(3)	131.0(3)

The relatively small differences in the structures of both complexes again demonstrate that the above-mentioned spectroscopical shifts (IR, NMR) are better suited for the characterization of the interaction of the alkyne with the metal atom than the results of an X-ray crystal structural analysis.

Discussion

The influence of metals, alkyne substituents, Cp substitution and additional ligands on the stability of bridged and unbridged η^2-alkyne−titanocene and −zirconocene complexes with and without additional ligands are summarized in Tables 4 and 5 {Cp- and $[(\eta^5\text{-}C_5H_4)-SiMe_2-(\eta^5\text{-}C_5H_4)]$-ligated complexes are shown as Cp complexes because both show a similar behaviour}. For titanocene the existence of the complex **3** demonstrates clearly the stabilizing effects of the thi ligands compared to Cp {and also $[(\eta^5\text{-}C_5H_4)-SiMe_2-(\eta^5\text{-}C_5H_4)]$}. The effect of the thi ligands is not found for the zirconocene complexes because zirconium is larger.

Table 4. Existence of complexes $L_2M(\eta^2\text{-}RC_2R)$; influence of metals, alkyne substituents and Cp substitution

	R=SiMe$_3$		R=Ph	
L/L_2	Ti	Zr	Ti	Zr
Cp	+	−	+	−
thi	+	−	+	−
rac-ebthi	+	+	unknown	−
Cp*	+	+	+	+

Table 5. Existence of complexes $L_2Zr(L')(\eta^2\text{-}Me_3SiC_2SiMe_3)$; influence of Cp substitution in ligands L and additional ligands L′

L/L_2	without L′	L′ = THF	L′ = py
Cp	−	**+**	**+**
thi	> 320 K	< 320 K	+
rac-ebthi	**+**	< 194 K	**+**
Cp*	**+**	− until 77 K[13]	−

The complexes of the type $L_2Zr(\eta^2\text{-}Me_3SiC_2SiMe_3)$ can coordinate with additional ligands L′ to give the complexes $L_2Zr(L')(\eta^2\text{-}Me_3SiC_2SiMe_3)$. The restriction for this comes mostly from the nature of L/L_2. With ligands such as *rac*-ebthi and Cp*, complexes without additional ligands L′ are stable at room temperature. Due to the enhanced flexibility of these ligands at lower temperature in some cases, such as *rac*-ebthi, the coordination of L′ (< 194 K) was observed. With thi as the ligand L the coordination of L′ occurs at room temperature and the complex with an additional THF ligand is stable, but eliminates L′ at higher temperature (< 320 K). With Cp no complex without L′ is stable and with Cp* no complex with L′.

The reason for the stability of the THF complexes toward dissociation of THF seems to come mostly from sterical interactions of alkyne substituents and the ligands L/L_2 and L′ and not from electronic effects. Complexes with the flat pyridine ligand are more stable compared to the corresponding THF complexes.

Conclusion

Complexes of the type $L_2M(\eta^2\text{-}RC_2R)$ without stabilizing ligands are sterically and electronically unsaturated. The size of zirconium is larger than that of titanium and as a result, it has a greater tendency to coordinate additional ligands; complexes without additional ligands are very rare and exist only with large alkyne substituents ($SiMe_3$) *and* sterical demanding Cp substitution (*rac*-ebthi[15], Cp*[13]). For the smaller titanium atom, sterically demanding alkyne *or* Cp substituents alone make alkyne complexes without additional ligands possible.

On the basis of these results it seems that it is now possible to understand the stability as well as the reactivity of bridged and unbridged alkyne−titanocene and −zir-

conocene complexes better. Control of stability is possible only by empirical tailoring of the complexes using different metals, alkyne substituents, Cp substitution and additional ligands.

This research was supported by the *Max-Planck-Gesellschaft* and the *Fonds der Chemischen Industrie*.

Experimental Section

All operations were carried out in argon with standard Schlenk techniques. Solvents were freshly distilled from sodium tetraethylaluminate under argon prior to use. Deuterated solvents were treated with sodium or sodium tetraethylaluminate, distilled and stored under argon. − The following spectrometers were used: NMR, Bruker ARX 400; IR, Nicolet Magna 550 (Nujol mulls using KBr plates); MS, AMD 402. − Melting points were measured in sealed capillaries with a Büchi 535 apparatus. − X-ray crystallographic study: Data were collected with a STOE-IPDS diffractometer using graphite-monochromated Mo-K_α radiation. The structures were solved by direct methods (SHELXS-86)[16] and refined by full-matrix least-squares techniques against F^2 (SHELXL-93).[17] The hydrogen atoms were included at calculated positions. All other nonhydrogen atoms were refined anisotropically. Cell constants and other experimental details are compiled in Table 6. XP (SIEMENS Analytical X-ray Instruments, Inc.) was used for structure representations.

Preparation of [(η⁵-C₅H₄)−SiMe₂−(η⁵-C₅H₄)]TiC₄Ph₄ (**1**): 1.10 g of [(η⁵-C_5H_4)−$SiMe_2$−(η⁵-C_5H_4)]$TiCl_2$ (3.62 mmol) was dissolved in 20 ml of THF and 0.09 g (3.62 mmol) of magnesium turnings and 0.64 g (3.62 mmol) of tolan were added. The solution was heated to 50°C and the colour changed from red to yellow-brown. The reaction mixture was stirred for 3 h at room temp. and the solvent was removed and replaced by *n*-hexane. After filtration at −30°C, red-brown crystals were formed. The crystals were washed in *n*-hexane and dried in vacuo to give 0.75 g (35%) of **1**, m.p. 203−204°C. − $C_{40}H_{34}SiTi$ (590.68): calcd. C 81.34, H 5.80; found C 81.22, H 5.85. − ^{1}H NMR (C_6D_6): δ = −0.04 $SiMe_2$ (s, 6 H); 4.99, 8.17 CH (d, 4 H each); 6.75−7.10 Ph (m, 20 H). − ^{13}C NMR (C_6D_6): δ = −6.2 $SiMe_2$; 105.0 $C_{q.}$; 117.4, 123.6 CH; 124.8, 125.9, 127.0, 128.1, 128.3, 131.4 Ph; 141.3, 148.7 Ph(q.); 135.3, 201.3 C(alkyne). − MS (70 eV); *m/z*: 590 [M^+], 234 [(η⁵-C_5H_4)−$SiMe_2$−(η⁵-C_5H_4)Ti^+], 178 [PhC_2Ph^+].

Preparation of [(η⁵-C₅H₄)−SiMe₂−(η⁵-C₅H₄)]Ti(η²-Me₃SiC₂SiMe₃) (**2**): Using the same procedure as described for **1**, the title compound was prepared using 0.37 g (1.20 mmol) of [(η⁵-C_5H_4)−$SiMe_2$−(η⁵-C_5H_4)]$TiCl_2$ in 15 ml of THF using 0.029 g of magnesium turnings and 0.27 ml (1.20 mmol) of bis(trimethylsilyl)-acetylene. Yield 0.20 g (41.2%) of a yellow-brown oily solid. − ^{1}H NMR (C_6D_6): δ = −0.3 $SiMe_3$ (s, 18 H); 0.27 $SiMe_3$ (s, 6 H); 5.05, 9.33 CH (4 H each). − ^{13}C NMR (C_6D_6): δ = −6.0 $SiMe_2$; 0.6 $SiMe_3$; 114.6 C(C_5H_4); 121.8, 126.9 C_5H_4; 248.9 C(alkyne). − IR (Nujol): $\tilde{\nu}$ = 1683 cm^{-1}, $\nu(C{=}C)_{coord.}$ = 1251 cm^{-1} [δ_s (CH_3−Si)]. − MS (70 eV); *m/z*: 234 [M − alkyne$^+$], 234 [(η⁵-C_5H_4)−$SiMe_2$−(η⁵-C_5H_4)Ti^+], 170 [alkyne$^+$].

Preparation of (thi)₂Ti(η²-PhC₂Ph) (**3**): To 0.30 g (0.84 mmol) of $(thi)_2TiCl_2$, dissolved in 15ml of THF, were added 0.02 g (0.84 mmol) of Mg turnings and 0.15 g (0.84 mmol) of diphenylacetylene. The colour turned from red to green-brown and the solution was stirred for 3 h at room temp. After removing the solvent and replacing it by *n*-hexane, the brown solution was filtered and allowed to stand at −30°C, to induce precipitation of dark brown crystals (yield 0.25 g, 64%), m.p. 111°C. − $C_{32}H_{32}Ti$ (464.49): calcd. C 82.75, H 6.94; found C 82.32, H 6.99. − ^{1}H NMR (C_6D_6): δ = 1.11−1.22, 1.43−1.58, 1.90−2.02, 2.50−2.62 CH_2 (4 H each); 5.45 CH (2 H); 6.14 CH (4 H); 6.80−6.92 Ph (m, 4 H); 7.10−7.28 Ph (m, 6 H). − ^{13}C NMR (C_6D_6): δ = 22.8, 24.7 CH_2; 126.1 $C_{q.}$; 110.7, 111.4 CH; 142.1 (*ipso*), 125.5, 126.6, 128.6 Ph; 198.8 C(alkyne). − IR (Nujol): $\tilde{\nu}$ = 1671 cm^{-1} $\nu(C{\equiv}C)_{coord.}$ = 1585 cm^{-1} Ph.

Preparation of (thi)₂Ti(η²-PhC₂SiMe₃) (**4**): 0.30 g (0.84 mmol) of $(thi)_2TiCl_2$ was dissolved in 20 ml of THF and treated with 0.02 g (0.84 mmol) of magnesium turnings and 0.28 ml (1.23 mmol) of phenyl(trimethylsilyl)acetylene. The solution was heated to 50°C until the colour changed to violet. Preparation was the same as described for **2**; violet crystals, yield 0.290 g (75%). m.p. 158−160°C. − $C_{29}H_{36}SiTi$ (460.57): calcd. C 75.63, H 7.88; found C 75.57, H 7.92. − ^{1}H NMR (C_6D_6): δ = 0.03 $SiMe_3$; 2.23−2.70 (10 H), 1.90−1.99 (2 H), 2.51−2.62 (2 H), 2.75−2.83 (2 H) CH_2; 5.66 (2 H), 5.93 (2 H), 6.16 (2 H) CH; 6.45 *o*-Ph (2 H); 6.80 *p*-Ph (1 H); 7.03 *m*-Ph (2 H). − ^{13}C NMR (C_6D_6): δ = 1.4 $SiMe_3$; 23.3, 23.4, 25.4, 25.5 CH_2; 111.2, 111.8, 112.1 CH; 127.8, 127.9 $C_{q.}$; 126.1, 126.8, 129.6, 141.2(q) Ph; 213.6, 220.0 C(alkyne). − IR (Nujol): $\tilde{\nu}$ = 1652 cm^{-1}, $\nu(C{=}C)_{coord.}$ = 1589 cm^{-1} Ph, 1242 cm^{-1} [δ_s (CH_3−Si)]. − MS (70 eV) *m/z*: 286 [$(thi)_2Ti^+$], 174 [alkyne$^+$].

Preparation of (thi)₂Ti(η²-Me₃SiC₂SiMe₃) (**5**): To a solution of 0.30 g (0.84mmol) of $(thi)_2TiCl_2$ in 15 ml of THF 0.10 ml of bis(trimethylsilyl)acetylene and 0.20 g of magnesium turnings were added. Reaction and workup according to **4** resulted in the formation of a dark yellow solid. − ^{1}H NMR (C_6D_6): δ = −0.14 $SiMe_3$ (18 H); 1.22−1.39 (4 H), 1.58−1.83 (8 H), 2.68−2.73 (4 H) CH_2; 5.68 CH (2 H); 6.05 CH (4 H). − ^{13}C NMR (C_6D_6): δ = 2.1 $SiMe_3$; 23.6, 25.4 CH_2; 112.2, 113.0 CH; 131.0 $C_{q.}$; 242.3 C(alkyne). − IR (Nujol): $\tilde{\nu}$ = 1629 cm^{-1}, $\nu(C{=}C)_{coord.}$ = 1243 cm^{-1} [δ_s (CH_3−Si)]. − MS (70 eV); *m/z*: 286 [$(thi)_2Ti^+$], 170 [alkyne$^+$].

Preparation of [(thi)₂Ti(CPh=CHPh)]₂(μ-O) (**6**): 0.20 g of **3** were dissolved in 15 ml of wet *n*-hexane. After standing for 3 d, 0.15 g (74.3%) of yellow needles appeared, m.p. 127−128°C. − $C_{64}H_{58}OTi_2$ (938.92): calcd. C 81.87 H 6.23; found C 81.25 H 6.30. − ^{1}H NMR (C_6D_6): δ = 1.39−1.49 (8 H) 1.50−1.59, 1.62−1.73, 2.10−2.18, 2.21−2.30, 2.45−2.54, 2.68−2.78 (4 H) CH_2; 4.84, 5.19, 6.15 (4 H) CH; 6.95−7.20 (20 H) Ph; 7.76 (2 H) CH. − ^{13}C NMR (C_6D_6): δ = 21.4, 21.5, 23.2, 23.4, CH_2; 105.3, 106.7, 115.4 CH; 122.5, 124.8 $C_{q.}$; 123.6, 125.2, 125.9, 126.4, 130.5, 131.0, 139.1 (q), 152.6 (q) Ph; 130.5, 193.5 C(alkene).

Preparation of (thi)₂Zr(THF)(η²-Me₃SiC₂SiMe₃) (**7**): 1.30 g (3.24 mmol) of $(thi)_2ZrCl_2$ was dissolved in 20 ml of THF and treated with 0.08 g magnesium turnings and an equimolar amount of bis(trimethylsilyl)acetylene. The solution was stirred at room temp. until all magnesium had disappeared. The honey-yellow solution was concentrated to dryness, the residue was dissolved in hexane/THF (3:1), filtered, and cooled to −30°C to give 0.65 g (35%) **7** after 3 d, m.p. up to 50°C (elimination of THF). − $C_{30}H_{48}OSi_2Zr$ (572.10): calcd. C 62.98 H 8.46; found C 62.57 H 8.54. − ^{1}H NMR ([D_8]THF): δ = 0.21 $SiMe_3$ (18 H); 1.56 CH_2 (8 H); 2.05, 2.30 CH_2 (4 H each); 1.75, 3.70 THF (4 H each); 5.33 CH (4 H); 5.55 CH (2 H). − ^{13}C NMR ([D_8]THF): δ = 5.1 $SiMe_3$; 24.0, 25.1 CH_2; 100.4, 107.5 CH; 124.3 $C_{q.}$; 222.0 C(alkyne). − IR (Nujol): $\tilde{\nu}$ = 1559 cm^{-1}, $\nu(C{=}C)_{coord.}$ = 1241 cm^{-1} [δ_s (CH_3−Si)]. − MS (70 eV); *m/z*: 500 [M − THF^+], 329 [$(thi)_2Zr^+$], 170 [alkyne$^+$].

Preparation of (thi)₂Zr(py)(η²-Me₃SiC₂SiMe₃) (**8**): As described for complex **7**, the title compound was formed by adding 0.32 ml (0.40 mmol) of pyridine after all magnesium had disappeared. The red-brown solution was concentrated to dryness and the residue was dissolved in *n*-hexane and filtered. After standing for 2 d at −30°C, 0.98 g (55%) of complex **8** deposited as orange-

brown crystals, m.p. 141−142°C. − $C_{31}H_{45}NSi_2Zr$ (579.10): calcd. C 64.30 H 7.83; found C 63.70 H 7.75. − ^{1}H NMR (C_6D_6): δ = 0.45 $SiMe_3$ (18 H); 1.25−1.40 CH_2 (br., 12 H); 2.10−2.20 CH_2 (4 H); 5.15 CH (br., 4 H); 5.80 CH (2 H); 6.53 (2 H), 6.80 (1 H), 9.04 (2 H) pyridine. − ^{13}C NMR (C_6D_6): δ = 3.8 $SiMe_3$; 23.8, 25.0 CH_2; 97.3, 107.2 CH; 112.9 C_q.; 123.3, 136.5, 155.5 pyridine; C(alkyne) not observed at 297 K, broad signal at 216.7 (337 K). − IR (Nujol): $\tilde{\nu}$ = 1548, 1595 cm^{-1}, $\nu(C{=}N)_{py}$ and $\nu(C{=}C)_{coord.}$ = 1240 cm^{-1} [δ_s (CH_3−Si)]. − MS (70 eV); *m/z*: 500 [M − py$^+$], 329 [$(THI)_2Zr^+$], 170 [alkyne$^+$].

Table 6. Crystallographic data of **1**, **3**, and **7**[17]

Compound	**1**	**3**	**7**
Formula	$C_{40}H_{34}SiTi$	$C_{32}H_{32}Ti$	$C_{30}H_{48}OSi_2Zr$
Mol. mass	590.66	464.48	572.10
Cryst. colour	yellow-brown	green-brown	orange
Cryst. description	prism	prism	prism
Cryst. size [mm]	0.5 × 0.4 × 0.3	0.3 × 0.2 × 0.1	0.5 × 0.4 × 0.3
Cryst. system	triclinic	monoclinic	monoclinic
Space group	$P\bar{1}$	$P2_1/n$	$P2_1$
a [Å]	11.344(2)	8.699(1)	8.775(1)
b [Å]	12.6000(2)	19.493(3)	17.004(2)
c [Å]	13.620(2)	14.441(2)	10.318(2)
α [°]	113.60(1)	90.06	90.00
β [°]	90.20(1)	91.63(1)	107.04(1)
γ [°]	115.95(1)	90.00	90.00
Z	2	4	2
T [K]	200(2)	293(2)	200(2)
μ [mm^{-1}]	0.339	0.367	0.475
Abs. cor.	no	no	no
θ range (°)	1.96−24.33	1.76−21.52	2.06−24.30
Largest diff. [e $Å^{-3}$] peak/hole	0.2/−0.5	0.2/−0.2	0.5/−0.6
No. of reflect. (measd.)	4715	4916	4349
No. of reflect. (indep.)	4715	2519	4261
R (int)	−	0.069	0.023
No. of reflect. (obsvd.)	3086	1430	4038
No. of parameters	379	298	356
$[I > 2\sigma(I)]$ *R*1 $[I > 2\sigma(I)]$	0.050	0.047	0.033
wR_2 (all data)	0.134	0.102	0.099

[1] [1a] E. Negishi, *Chem. Scr.* **1989**, *29*, 457−468. − [1b] E. Negishi, T. Takahashi, *Acc. Chem. Res.* **1994**, *27*, 124−130. − [1c] S. L. Buchwald, R. B. Nielsen, *Chem. Rev.* **1988**, *88*, 1047−1058. − [1d] A. Ohff, S. Pulst, C. Lefeber, N. Peulecke, P. Arndt, V. V. Burlakov, U. Rosenthal, *Synlett* **1996**, 111−118.

[2] [2a] U. Rosenthal, H. Görls, V. V. Burlakov, V. B. Shur, M. E. Vol′pin, *J. Organomet. Chem.* **1992**, *426*, C53−C57, and references therein. − [2b] U. Rosenthal, A. Ohff, M. Michalik, H. Görls, V. V. Burlakov, V. B. Shur, *Angew. Chem.* **1993**, *105*, 1228−1230, *Angew. Chem. Int. Ed. Engl.* **1993**, *32*, 1193−1195. − [2c] U. Rosenthal, A. Ohff, W. Baumann, A. Tillack, H. Görls, V. V. Burlakov, V. B. Shur, *Z. Anorg. Allg. Chem.* **1995**, *621*, 77−83.

[3] C. Lefeber, W. Baumann, A. Tillack, R Kempe, H. Görls, U. Rosenthal, *Organometallics* **1996**, *15*, 3486−3490.

[4] N. Peulecke, C. Lefeber, A. Ohff, W. Baumann, A. Tillack, R. Kempe, V. V. Burlakov, U. Rosenthal, *Chem. Ber.* **1996**, *129*, 959−962.

[5] [5a] U. Rosenthal, A. Ohff, W. Baumann, R. Kempe, A. Tillack, V. V. Burlakov, *Angew. Chem.* **1994**, *106*, 1946−1948; *Angew. Chem. Int. Ed. Engl.* **1994**, *33*, 1850−1852. − [5b] P. Arndt, D. Thomas, U. Rosenthal, *Tetrahedron Lett*. **1997**, *38*, 5467−5468. − [5c] N. Peulecke, D. Thomas, W. Baumann, C. Fischer, U. Rosenthal, *Tetrahedron Lett*. **1997**, *38*, 6655−6686.

[6] C. S. Bajgur, W. R. Tikkanen, J. L. Petersen, *Inorg. Chem.* **1985**, *24*, 2539−2546.

[7] V. B. Shur, V. V. Burlakov, M. E. Volpin, *J. Organomet. Chem.* **1988**, *347*, 77−83.

[8] Q. Yang, M. D. Jensen, *Synlett* **1996**, *6* 563.

[9] C. Lefeber, A. Ohff, A. Tillack, W. Baumann, R. Kempe, V. V. Burlakov, U. Rosenthal, *J. Organomet. Chem.* **1995**, *501*, 179−188.

[10] V. V. Burlakov, A. V. Polyakov, A. I. Yanovsky, V. B. Shur, M. E. Vol′pin, U. Rosenthal, H. Görls, *J. Organomet. Chem.* **1994**, *476*, 197−206, and references therein.

[11] G. Fachinetti, C. Floriani, F. Marchetti, M. J. Mellini, *J. Chem. Soc., Dalton Trans.* **1978**, 1398−1403.

[12] U. Rosenthal, C. Nauck, P. Arndt, S. Pulst, W. Baumann. V. V. Burlakov, H. Görls, *J. Organomet. Chem.* **1994**, *484*, 81−87.

[13] J. Hiller, U. Thewalt, M. Polášek, L. Petrusová, V. Varga, P. Sedmera, K. Mach, *Organometallics* **1996**, *15*, 3752−3759.

[14] J. L. Atwood, W. E. Hunter, H. Alt, M. D. Rausch, *J. Am. Chem. Soc.* **1976**, *98*, 2454−2459.

[15] H. H. Brintzinger, D. Fischer, R. Mühlhaupt, B. Rieger, R. Waymouth, *Angew. Chem.* **1995**, *107*, 1255; *Angew. Chem. Int. Ed. Engl.* **1995**, *34*, 1143.

[16] G. M. Sheldrick, *SHELXS-86*, *Acta Crystallogr.* **1990**, *A46*, 467.

[17] G. M. Sheldrick, *SHELXL-93*, University of Göttingen, Göttingen, Germany, **1993**.

[18] Crystallographic data (excluding structure factors) for the structures reported in this paper have been deposited with the Cambridge Crystallographic Data Centre as supplementary publication no. CCDC-100666. Copies of the data can be obtained free of charge on application to CCDC, 12 Union Road, Cambridge CB2 1EZ, UK [Fax: internat. + 44(1223)336033, e-mail: deposit@ccdc.cam.ac.uk].

[97205]

Ethylene Polymerization with Hydridotris(pyrazolyl)boratoniobium Complexes as Precursors

Joëlle Jaffart, Céline Nayral, Robert Choukroun, René Mathieu, and Michel Etienne*

Laboratoire de Chimie de Coordination, UPR CNRS 8241,
205 Route de Narbonne, F-31077 Toulouse Cedex 4, France
E-mail: etienne@lcc-toulouse.fr

Received November 17, 1997

Keywords: Ethylene polymerization / Group 5 metal complexes / Hydridotris(pyrazolyl)borates / Alkyne ligands / Migratory insertion

Substituted hydridotris(pyrazolyl)borato (Tp′) niobium complexes of the type [Tp′$NbMe_2$(PhC≡CMe)] polymerize ethylene (under 1 atm, at room temp. and in toluene) when treated with an equimolar amount of $B(C_6F_5)_3$. A clear relationship is observed between the stereoelectronic nature of the complex and catalytic activity. This is discussed on the basis of electrochemical data for the dichloro complexes [Tp′$NbCl_2$(PhC≡CMe)], and the rates of alkyl migration in [Tp′Nb(Cl)(R)(PhC≡CMe)] (R = CH_2Me, CH_2SiMe_3). For a given electron density at the metal, the bulky $Tp^{Me2,4\text{-}Cl}$ yields a catalyst which is more than 6 times as active as the unsubstituted Tp based catalyst.

Several attempts have recently been made, with related group 5 metal complexes, to mimic the outstanding activity in the polymerization of olefins of group 4 metal molecular complexes[1]. It is also hoped that the group 5 catalysts would be more tolerant to functionalized monomers, a highly desirable property if co-polymers are targeted. Most of the approaches have relied on an isoelectronic comparison with the 14-electron metallocene alkyl cations $[Cp_2MR]^+$, known to be the active species in group 4 catalysis[1]. As far as we are aware, a true Nb- or Ta-based catalyst, akin to $[Cp_2MR]^+$, has not so far been isolated, so we will base this discussion on its precursor. The combination [Cp′M(diene)X_2]/MAO (MAO = methylaluminoxane) gives polyethylene (PE) with a maximum activity of 39 (kg of PE) (mol of catalyst)$^{-1}$ h^{-1}. Interestingly the PE has a very narrow polydispersity (1.05)[2]. Based on the isolobal analogy, developed by Gibson and co-workers, between the bent metallocene Cp_2Zr and the imido CpNb(=NR) moieties[3], several systems have been explored. However, their activity is highly dependant on the substituents bound either to the metal or to the imido nitrogen, as well as on the activation mode[4]. The highest reported activity is 61 kg mol^{-1} h^{-1} for the [Cp*Ta(=N−Si*t*Bu_3)(η^1-allyl)(η^3-allyl)]/MAO system[4a], whereas some other imido complexes are, at best, only marginally active[4c]. The borollide−Cp ligand set leads to a deceptively low activity (2 kg mol^{-1} h^{-1} for [Cp*(η^5-$C_4H_4BNR_2$)$TaCl_2$/MAO)][5]. Imidovanadium complexes [LV(=NR)Cl_2] [L = Cp, Tp′ (Tp′ = a substituted hydridotris(pyrazolyl)borate)] generate active systems[4c][6], particularly with respect to propene polymerization.

Given the similarity between imido and (4e)-alkyne ligands[7] and between Cp and Tp′ ligands[8], we describe here preliminary results: (i) showing that complexes of the type [Tp′$NbMe_2$(alkyne)] do polymerize ethylene when properly activated; (ii) providing a basis for a stereoelectronic/activity relationship in this series of complexes, which has not been previously made for the group 5 metal catalysts. Related studies have been reported for Tp′-supported yttrium catalysts[9].

In Table 1, we summarize the data for ethylene polymerization by the system [Tp′$NbMe_2$(PhC≡CMe)]/$B(C_6F_5)_3$ (Tp′ = Tp, Tp^{Me2}, $Tp^{Me2,4\text{-}Cl}$, see Scheme 1)[10], electrochemical behaviour for the first monoelectronic reduction of the parent dichloro complexes [Tp′$NbCl_2$(PhC≡CMe)], and first-order rate constants k for alkyl migration to the alkyne in [Tp′Nb(Cl)(CH_2SiMe_3)(PhC≡CMe)] and [Tp′Nb(Cl)(CH_2Me)(PhC≡CMe)] (a reaction which ultimately yields [Tp′Nb(Cl)(Me)(PhC≡CCH_2SiMe_3)] and [Tp′Nb(Cl)(Me)(PhC≡CCH_2Me)] respectively, as shown elsewhere[11]). Several of these compounds are new and their syntheses and full characterization may be found in the Experimental Section.

Table 1. Ethylene polymerization activity for [Tp′$NbMe_2$-(PhC≡CMe)]/$B(C_6F_5)_3$, electrochemical data for [Tp′$NbCl_2$-(PhC≡CMe)] and first-order rate constants k for alkyl migration to the alkyne in [Tp′Nb(Cl)(R)(PhC≡CMe)], as a function of Tp′

Tp′	Activity[a]	$E_{1/2}$ (ΔE_p, i_a/i_c)[b]	$k \times 10^5$ [c]	$k \times 10^5$ [d]
Tp^{Me2}	100	−1.18 (0.15, 0.9)[e]	2.3[f]	3.0[f]
$Tp^{Me2,\ 4\text{-}Cl}$	130	−0.97 (0.10, 0.9)	2.2	4.75
Tp	20	−0.93 (0.25, 0.5)[e]	3.5	−

[a] Average of at least 3 runs, kg of PE (mol of catalyst)$^{-1}$ h^{-1}. − [b] V vs SCE. − [c] s^{-1}, R = CH_2SiMe_3. − [d] s^{-1}, R = CH_2Me. − [e] From ref.[10]. − [f] From ref.[11].

The first observation is that the dimethyl complexes [Tp′$NbMe_2$(PhC≡CMe)] do polymerize ethylene when activated by the methyl abstracting agent $B(C_6F_5)_3$ in a tolu-

 © WILEY-VCH Verlag GmbH, D-69451 Weinheim, 1998 1434−1948/98/0404−0425 $ 17.50+.50/0

Scheme 1

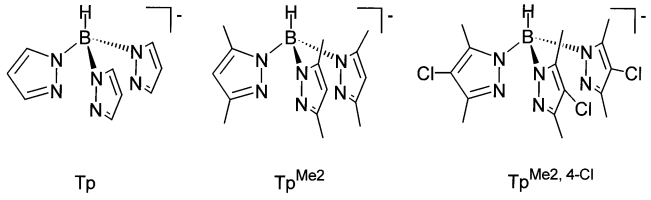

ene solution[12], with the activities being higher than those observed for previously described systems based on heavier group 5 metal complexes. When red-purple [$Tp^{Me2}NbCl_2$(PhC≡CMe)] is treated with 500 equiv. of MAO in toluene, a light yellow solution is obtained which fails to polymerize ethylene. The choice of the activator is critical in other group 5 systems[4a]. We have also verified (^{1}H NMR) that toluene solutions of yellow [$Tp^{Me2}NbMe_2$(PhC≡CMe)] do not react with ethylene (1 atm).

The second observation is that the activity is notably dependent on the nature of Tp′. Bulky Tp^{Me2} and $Tp^{Me2,4-Cl}$ lead to a much higher catalytic activity than the less sterically demanding, unsubstituted Tp. Increased electrophilicity, as probed by comparison of the reduction potential $E_{1/2}$ for the parent dichloro Tp^{Me2} and $Tp^{Me2,4-Cl}$ complexes, only slightly increases the catalytic activity. By way of contrast, steric protection is mandatory: Tp and $Tp^{Me2,4-Cl}$ offer virtually the same electron density at the metal (cf. $E_{1/2}$), but catalytic production is dramatically favored by the bulky ligand[13]. We propose that these effects result from a steric shielding of the metal center by Tp^{Me2} and $Tp^{Me2,4-Cl}$ which prevents decomposition of the catalytic species via some kind of association. Several decomposition processes of the group 4 catalysts involve the formation of dinuclear species[1].

Parallel experiments lend further support to this view. We have previously studied in detail the mechanism of alkyl exchange in [Tp^{Me2}Nb(Cl)(R)(PhC≡CMe)] that leads to [Tp^{Me2}Nb(Cl)(Me)(PhC≡CR)] via the rate determining step of migratory insertion of R on to the alkyne[11]. The disappearance of [Tp^{Me2}Nb(Cl)(R)(PhC≡CMe)] at 343 K occurs with first-order rate constants of $2.3\cdot10^{-5}$ s^{-1} and $3.0\cdot10^{-5}$ s^{-1} for R = CH_2SiMe_3 and CH_2Me, respectively[11]. The corresponding Tp and $Tp^{Me2,4-Cl}$ complexes have thus been synthesized and their thermolysis studied by ^{1}H NMR in [D_6]benzene at 343 K. The experimental first-order rate constants k provided in Table 1 indicate that, again, the steric bulk of the Tp′ ligand largely governs the stability of the complexes and the alkyl group migration on to the alkyne. On one hand, for similar electron density at the metal, the rate constant for alkyl migration is significantly higher when a less sterically demanding ligand is used (cf. rate and electrochemical data for Tp and $Tp^{Me2,4-Cl}$). On the other hand, ligands of similar size such as Tp^{Me2} and $Tp^{Me2,4-Cl}$ which significantly differ in their electron-donating ability provide a similar barrier to alkyl migration as soon as the migrating R becomes too bulky. When R = CH_2Me, the migration is slightly faster for $Tp^{Me2,4-Cl}$ as expected, whereas there is no difference for the bulkier R = CH_2SiMe_3. In addition, the rearrangement of [TpNb(Cl)(CH_2SiMe_3)(PhC≡CMe)], although faster, is accompanied by important decomposition while putative [TpNb(Cl)(CH_2Me)(PhC≡CMe)] decomposes during its attempted synthesis. In the same vein, the chemical and electrochemical reversibilities of the first one-electron reduction of the parent dichloro complexes are low for Tp only. These observations may be ascribed to steric protection of the metal by the bulkier Tp′.

Assuming that these alkyl to alkyne migrations mimic with sufficient reliability the migration of a growing alkyl chain to a coordinated ethylene at least with respect to steric interactions, we conclude that a more active catalyst is obtained when an efficient protection of the metal is realized at the expense of faster intramolecular migration of alkyl chains. Since ethylene coordination is expected to be easier for the less bulky Tp, the central role played by the size of Tp′ is to be emphasized.

Hydridotris(pyrazolyl)borato group 5 complexes can indeed be used as ethylene polymerization catalysts. Such ligands provide a high degree of steric control which prevents catalyst decomposition, a major feature of the polymerizations reported herein. Up to now, attempts at observing putative naked or base-stabilized alkyl cations such as [Tp′NbMe(PhC≡CMe)]$^+$ or [Tp′NbMe(PhC≡CMe)(L)]$^+$ have failed. Further studies aimed at improving the activity of ethylene polymerization and studying α-olefins are in progress.

We thank Dr. *D. de Montauzon* for the electrochemical experiments.

Experimental Section

General: All experiments were carried out under a dry dinitrogen atmosphere using either Schlenck tube or glove box techniques. THF was obtained after refluxing a purple solution of Na/benzophenone under dinitrogen. Toluene, *n*-hexane, and pentane were dried by refluxing over CaH_2 under dinitrogen. Toluene used for the polymerization reactions was treated with concentrated sulfuric acid, washed three times with water, stored over $CaCl_2$, then further dried by refluxing over CaH_2 under dinitrogen before use. [D_6]Benzene (used unless otherwise stated) and $CDCl_3$ were dried over molecular sieves and stored under dinitrogen. − ^{1}H and ^{13}C NMR (only pertinent $^1J_{CH}$ are quoted): Bruker AC 200 (200, 50 MHz resp) and AM 250 (250, 62.9 MHz resp). − Elemental analyses: Perkin Elmer 2400 Series II. DTA: Sétaram 92−16.18. − Cyclic voltammetry data (home-made potentiostat interfaced with a PC-computer, scan rate 100 mV s^{-1}): Pt disk (1 mm) working electrode, THF solution, 0.1 M Bu_4NBF_4 as supporting electrolyte, Pt wire as auxiliary electrode, SCE as reference electrode.

The new compounds [$Tp^{Me2,4-Cl}NbCl_2$(PhC≡CMe)], [$Tp^{Me2,4-Cl}NbMe_2$(PhC≡CMe)], [$Tp^{Me2,4-Cl}$Nb(Cl)(CH_2Me)(PhC≡CMe)], [$Tp^{Me2,4-Cl}$Nb(Cl)(CH_2SiMe_3)(PhC≡CMe)], [TpNb(Cl)(CH_2SiMe_3)(PhC≡CMe)] have been obtained following published procedures established for related Tp and Tp^{Me2} complexes[10][11]. Yields and full characterization of these new compounds are provided below. Tp^{Me2} and $Tp^{Me2,4-Cl}$ complexes exist as a mixture of discrete alkyne rotamers[10][11]. Some NMR resonances of the minor isomer may be obscured.

[TpNbMe$_2$(PhC≡CMe)] could not be obtained cleanly from [TpNbCl$_2$(PhC≡CMe)] and 2 equiv. of LiMe. Its synthesis from MeMgCl is described below. B(C_6F_5)$_3$ (ref.[14]) was sublimed in vacuo before use. Kinetic data on the rearrangement of [Tp′Nb(Cl)(R)(PhC≡CMe)] were obtained from [D_6]benzene solutions at 343 K as previously reported[11].

[Tp$^{Me2,4\text{-}Cl}$NbCl$_2$(PhC≡CMe)]: Yield 59%. − $C_{24}H_{27}BCl_5N_6Nb$ calcd: C 42.4, H 4.0, N 12.35; found: C 42.3, H 4.0, N 12.20. − ^{1}H NMR: Major isomer δ = 6.90−6.60 (m, 5 H, *Ph*C≡CMe), 3.84 (s, 3 H, PhC≡C*Me*), 2.94, 1.97 (s, 3 H each, Tp$^{Me2,4\text{-}Cl}$*Me*), 1.85, 1.79 (s, 6 H each, Tp$^{Me2,4\text{-}Cl}$*Me*). Minor isomer: δ = 8.3 (d, 2 H, *o-Ph*C≡CMe), 7.38 (t, 2 H, *m-Ph*C≡CMe), 2.97 (s, 3 H, PhC≡C*Me*), 2.21, 1.95 (s, 3 H each, Tp$^{Me2,4\text{-}Cl}$*Me*), 1.94, 1.81 (s, 6H each, Tp$^{Me2,4\text{-}Cl}$*Me*). − ^{13}C{^{1}H} NMR ($CDCl_3$): Major isomer: δ = 267.1, 221.4 (Ph*C*≡*C*Me), 150.3, 148.7, 141.4, 141.2 (Tp$^{Me2,4\text{-}Cl}$*C*Me), 136.9 (*ipsoPh*), 129.7, 128.9, 128.8 (*Ph*), 111.1 (Tp$^{Me2,4\text{-}Cl}$*C*Cl), 25.1 (PhC≡C*Me*), 13.4, 13.1, 11.2, 11.0 (Tp$^{Me2,4\text{-}Cl}$*Me*). Minor isomer: δ = 249.7, 234.5 (Ph*C*≡*C*Me), 136.2 *(ipsoPh*), 132.4, 131.1, 130.3 (*Ph*), 111.1 (Tp$^{Me2,4\text{-}Cl}$*C*Cl), 23.8 (PhC≡C*Me*), 13.6, 13.5, 10.8 (Tp$^{Me2,4\text{-}Cl}$*Me*).

[Tp$^{Me2,4\text{-}Cl}$NbMe$_2$(PhC≡CMe)]: Yield 50%. − $C_{26}H_{33}BCl_3N_6Nb$ calcd: C 48.8, H 5.2, N 13.1; found: C 49.1, H 5.2, N 12.9. − ^{1}H NMR: Major isomer δ = 7.10−6.90 (m, 5 H, *Ph*C≡CMe), 3.50 (s, 3 H, PhC≡C*Me*), 2.47, 2.12 (s, 3 H each, Tp$^{Me2,4\text{-}Cl}$*Me*), 1.97, 1.69 (s, 6 H each, Tp$^{Me2,4\text{-}Cl}$*Me*), 1.02 (s, 6 H, Nb*Me*). Minor isomer: δ = 7.93 (d, 2 H, *o-Ph*C≡CMe), 6.90 (t, 2 H, *m-Ph*C≡CMe), 2.52 (s, 3 H, PhC≡C*Me*), 2.09 (s, 3 H, Tp$^{Me2,4\text{-}Cl}$*Me*), 1.93, 1.89 (s, 6H each, Tp$^{Me2,4\text{-}Cl}$*Me*), 1.14 (s, 6 H, Nb*Me*). − ^{13}C NMR: Major isomer: δ = 250.1, 223.9 (Ph*C*≡*C*Me), 148.4, 148.2, 141.1, 141.0 (Tp$^{Me2,4\text{-}Cl}$*C*Me), 139.2 (*ipsoPh*), 130.0, 129.0, 128.9 (*Ph*), 110.9, 110.1 (Tp$^{Me2,4\text{-}Cl}$*C*Cl), 55.4 (q, J_{CH} = 120 Hz, Nb*Me*), 22.8 (PhC≡C*Me*), 14.3, 12.9, 12.8, 10.9 (Tp$^{Me2,4\text{-}Cl}$*Me*). Minor isomer: δ = 238.2, 235.8 (Ph*C*≡*C*Me), 56.4 (q, J_{CH} = 120 Hz, Nb*Me*), 23.2 (PhC≡C*Me*), 13.2, 13.1, 12.7, 10.7 (Tp$^{Me2,4\text{-}Cl}$*Me*).

[Tp$^{Me2,4\text{-}Cl}$Nb(Cl)(CH$_2$Me)(PhC≡CMe)]: Yield 45%. − $C_{26}H_{32}BCl_4N_6Nb$ calcd: C 46.3, H 4.8, N 12.5; found: C 46.8, H 5.2, N 12.2. − ^{1}H NMR: Major isomer δ = 7.30−6.80 (m, 5 H, *Ph*C≡CMe), 3.70 (dq, *J* = 12.8, 7.7 Hz, 1 H, NbC*H*$_2$Me), 3.54 (s, 3 H, PhC≡C*Me*), 2.75, 2.06, 1.96, 1.93, 1.87, 1.56 (s, 3 H each, Tp$^{Me2,4\text{-}Cl}$*Me*), 1.00 (dd, *J* = 7.7, 6.2 Hz, NbCH$_2$*Me*), 0.20 (dq, *J* = 12.8, 6.2 Hz, 1 H, NbC*H*$_2$Me). Minor isomer: δ = 8.10 (d, 2 H, *o-Ph*C≡CMe), 7.40 (t, 2 H, *m-Ph*C≡CMe), 3.90 (dq, *J* = 12.8, 7.7 Hz, 1 H, NbC*H*$_2$Me), 2.79 (s, 3 H, PhC≡C*Me*), 2.30, 2.08, 2.02, 1.90, 1.89, 1.74 (s, 3 H each, Tp$^{Me2,4\text{-}Cl}$*Me*), 0.97 (dd, *J* = 7.7, 6.2 Hz, NbCH$_2$*Me*), 0.30 (m, 1 H, NbC*H*$_2$Me). − ^{13}C NMR: Major isomer: δ = 249.6, 216.5 (Ph*C*≡*C*Me), 150.3, 149.6, 147.4, 141.6, 141.3, 141.0 (Tp$^{Me2,4\text{-}Cl}$*C*Me), 138.5 (*ipsoPh*), 131.9, 129.8, 129.0 (*Ph*), 111.0, 110.6, 110.4 (Tp$^{Me2,4\text{-}Cl}$*C*Cl), 88.4 (dd, J_{CH} = 105, 126 Hz, Nb*C*H$_2$Me), 23.1 (PhC≡C*Me*), 13.2, 13.1, 12.2, 11.1, 10.9, 10.8, 10.7 (Tp$^{Me2,4\text{-}Cl}$*Me* and CH$_2$*Me*). Minor isomer: δ = 235.8, 227.8 (Ph*C*≡*C*Me), 149.5, 149.2, 146.1, 141.4, 141.3, 140.9 (Tp$^{Me2,4\text{-}Cl}$*C*Me), 91.2 (dd, J_{CH} = 105, 126 Hz, Nb*C*H$_2$Me), 23.0 (PhC≡C*Me*), 13.4, 11.9, 10.5 (Tp$^{Me2,4\text{-}Cl}$*Me* and CH$_2$*Me*).

[Tp$^{Me2,4\text{-}Cl}$Nb(Cl)(CH$_2$SiMe$_3$)(PhC≡CMe)]: Yield 34%. − $C_{28}H_{38}BCl_4N_6NbSi$ calcd: C 45.9, H 5.2, N 11.5; found: C 46.5, H 5.5, N 10.8. − ^{1}H NMR: Major isomer δ = 7.00−6.80 (m, 5 H, *Ph*C≡CMe), 3.65 (s, 3 H, PhC≡C*Me*), 3.06 (d, *J* = 12.4 Hz, 1 H, NbC*H*$_2$SiMe$_3$), 2.82, 2.09, 2.06, 1.91, 1.73, 1.65 (s, 3 H each, Tp$^{Me2,4\text{-}Cl}$*Me*), 0.27 (d, *J* = 12.4 Hz, 1 H, NbC*H*$_2$SiMe$_3$), −0.17 (s, 9 H, Si*Me*$_3$). Minor isomer: δ = 8.14 (d, 2 H, *o-Ph*C≡CMe), 7.40 (t, 2 H, *m-Ph*C≡CMe), 3.45 (d, *J* = 11.8 Hz, 1 H, NbC*H*$_2$SiMe$_3$), 2.87 (s, 3 H, PhC≡C*Me*), 2.30, 2.09, 2.02, 1.98, 1.85 (s, 3 H each, Tp$^{Me2,4\text{-}Cl}$*Me*), 0.37 (d, *J* = 11.8 Hz, 1 H, NbC*H*$_2$SiMe$_3$), −0.44 (s, 9 H, Si*Me*$_3$). − ^{13}C NMR: Major isomer: δ = 251.5, 221.4 (Ph*C*≡*C*Me), 149.7, 149.6, 148.2, 141.2, 138.2 (Tp$^{Me2,4\text{-}Cl}$*C*Me), 138.3 (*ipsoPh*), 129.8, 129.6, 128.9 (*Ph*), 111.4, 110.9, 110.5 (Tp$^{Me2,4\text{-}Cl}$*C*Cl), 81.5 (dd, J_{CH} = 106, 124 Hz, Nb*C*H$_2$SiMe$_3$), 24.0 (PhC≡C*Me*), 14.5, 14.0, 12.9, 11.0, 10.7, 10.6 (Tp$^{Me2,4\text{-}Cl}$*Me*), 2.3 (Si*Me*).

[TpNbMe$_2$(PhC≡CMe)]: 0.7 ml of a 3.0 M THF solution of MeMgCl was added dropwise to a stirred cooled (0°C) toluene solution (50 ml) of [TpNbCl$_2$(PhC≡CMe)] (0.49 g, 1.0 mmol). Stirring was continued at 0°C for 4 h as the colour of the solution turned from red-purple to yellow greenish. The solution was then pumped to dryness. Extraction with pentane (30 ml), and filtration through a Celite pad, followed by several washings, afforded a yellow solution which was then evaporated to dryness. Crystallization from pure pentane afforded yellow crystals of the title compound (0.20 g, 0.44 mmol, 44%). The yield is limited by the high solubility of the compound. −$C_{20}H_{25}BN_6Nb$ calcd: C 53.1, H 5.5, N 18.6; found: C 53.1, H 4.9, N 18.3. − ^{1}H NMR: δ = 7.98, 7.45 (br s, 1 H each, Tp-3-C*H* and Tp-5-C*H*), 7.40−7.10 (m, 5 H, *Ph*C≡CMe), 7.45, 6.92 (br s, 2 H each, Tp-3-C*H* and Tp-5-C*H*), 6.06 (br s, 1 H, Tp-4-C*H*), 5.69 (br s, 2 H, Tp-4-C*H*), 3.28 (s, 3 H, PhC≡C*Me*), 1.14 (s, 6 H, Nb*Me*). − ^{13}C NMR: δ = 242.0, 227.7 (Ph*C*≡*C*Me), 143.3, 142.4, 135.0, 134.4 (br, Tp-3-*C*H and Tp-5-*C*H), 139.3 (*ipsoPh*), 130.7, 128.8, 128.4 (*Ph*), 105.7, 104.9 (br, Tp-4-*C*H), 55.0 (q, J_{CH} = 118 Hz, Nb*Me*), 22.0 (PhC≡C*Me*).

[TpNb(Cl)(CH$_2$SiMe$_3$)(PhC≡CMe)]: Yield 88%. − $C_{22}H_{29}BClN_6NbS$ calcd: C 48.5, H 5.4, N 15.4; found: C 48.9, H 5.0, N 15.1. − ^{1}H NMR: δ = 8.40, 7.42, 7.31, 7.00, 6.93 (d, *J* = 2.2 Hz, 1 H each, Tp-3-C*H* and Tp-5-C*H*), 7.30−7.00 (m, 5 H, *Ph*C≡CMe), 5.99, 5.71, 5.50 (t, *J* = 2.2 Hz, 1 H each, Tp-4-C*H*), 3.34 (s, 3 H, PhC≡C*Me*), 1.93 (s, 2 H, NbC*H*$_2$SiMe$_3$), −0.09 (s, 9 H, Si*Me*$_3$). − ^{13}C NMR: δ = 242.8, 225.9 (Ph*C*≡*C*Me), 144.7, 144.5, 144.0, 135.0, 134.9, 134.4 (Tp-3-*C*H and Tp-5-*C*H), 138.0 (*ipsoPh*), 131.1, 129.2, 128.7 (*Ph*), 105.8, 106.3 (Tp-4-*C*H), 83.1 (t, J_{CH} = 108 Hz, Nb*C*H$_2$SiMe$_3$), 23.3 (PhC≡C*Me*).

Typical Ethylene Polymerization Run: In the glove box [Tp$^{Me2,4\text{-}Cl}$NbMe$_2$(PhC≡CMe)] (12.8 mg, 0.02 mmol), a magnetic stir bar and purified toluene (5 ml) were introduced in a Fischer-Porter bottle equiped with a side arm. To this side arm was attached (Teflon joint, screw connection, Teflon stopcock) a glass vessel containing B(C_6F_5)$_3$ (10.4 mg, 0.02 mmol) dissolved in toluene (5 ml). The apparatus was removed from the glove box, and attached to a double manifold vacuum line connected to an ethylene tank through molecular sieves and CuO purifying devices. The main Fischer-Porter volume, containing the vigorously stirred (500 rpm) yellow solution of the niobium complex, was saturated with ethylene under 1 atm. No reaction occured at that stage. The Teflon stopcock of the side arm was opened to allow instantaneous mixing of the co-catalyst, then closed again. A chronometer was started. Virtually instantaneous precipitation of a whitish powder commenced together with temp. increase. Methanol (10 ml) containing a few drops of an aqueous HCl solution was introduced through the side arm after 5 min to quench the polymerization reaction. The precipitate was collected on a frit in air, washed several times with methanol and then diethyl ether, and dried to a constant weight in an oven (75°C). 0.212 mg of a white solid, corresponding to a catalytic activity of 125 kg mol^{-1} h^{-1}, were obtained. − $(C_2H_4)_n$ calcd: C 85.6, H 14.4, N 0.0; found: C 85.6, H 15.2, N 0.0. − DTA: m.p. 133.5°C.

[1] [1a] M. Bochman, *J. Chem. Soc., Dalton Trans.* **1996**, 255−270. − [1b] H. H. Brintzinger, D. Fischer, R. Mulhaupt, B. Rieger, R. M. Waymouth, *Angew. Chem., Int. Ed. Engl.* **1995**, *34*, 1143−1170. − [1c] R. F. Jordan, *Adv. Organomet. Chem.* **1991**, *32*, 325−387. − [1d] G. Fink, R. Mülhaupt, H. H. Brintzinger (Eds.), *Ziegler Catalysts*; Springer-Verlag, Berlin, **1995**.

[2] [2a] K. Mashima, S. Fujikawa, Y. Tanaka, H. Urata, T. Oshiki, E. Tanaka, A. Nakamura, *Organometallics* **1995**, *14*, 2633−2640. − [2b] K. Mashima, S. Fujikawa, H. Urata, E. Tanaka, A. Nakamura, *J. Chem. Soc., Chem. Commun.* **1994**, 1623−1624. − [2c] K. Mashima, S. Fujikawa, A. Nakamura, *J. Am. Chem. Soc.* **1993**, *115*, 10990−10991. − [2d] A. Nakamura, K. Mashima, *Jpn. Tokkyo Koho* JP5310828 (**1993**, to Mitsubishi).

[3] D. N. Williams, J. P. Mitchell, A. D. Poole, U. Siemeling, W. Clegg, D. C. R. Hockless, P. A. O′Neil, V. C. Gibson, *J. Chem. Soc., Dalton Trans.* **1992**, 739−751.

[4] [4a] D. M. Antonelli, A. Leins, J. F. Stryker, *Organometallics* **1997**, *16*, 2500−2502. − [4b] D. M. Antonelli, P. T. Gomes, M. L. H. Green, A. M. Martins, P. Mountford, *J. Chem. Soc., Dalton Trans.* **1997**, 2435−2444. − [4c] M. P. Coles, V. C. Gibson, *Polym. Bull.* **1994**, *33*, 529−533.

[5] G. C. Bazan, S. J. Donnelly, G. Rodriguez, *J. Am. Chem. Soc.* **1995**, *117*, 2671−2672.

[6] S. Scheuer, J. Fischer, J. Kress, *Organometallics* **1995**, *14*, 2627−2629.

[7] [7a] D. S. Williams, R. R. Schrock, *Organometallics* **1993**, *12*, 1148−1160. − [7b] V. C. Gibson, *J. Chem. Soc., Dalton Trans.* **1994**, 1607−1618. − [7c] J. L. Templeton, *Adv. Organomet. Chem.* **1989**, *29*, 1−100.

[8] S. Trofimenko, *Chem. Rev.* **1993**, *93*, 943−980.

[9] D. P. Long, P. A. Bianconi, *J. Am. Chem. Soc.* **1996**, *118*, 12453−12454.

[10] [10a] M. Etienne, F. Biasotto, R. Mathieu, J. L. Templeton, *Organometallics* **1996**, *15*, 1106−1112. − [10b] M. Etienne, B. Donnadieu, R. Mathieu, J. Fernandez−Baeza, F. Jalon, A. Otero, M. E. Rodrigo Blanco, *Organometallics* **1996**, *15*, 4597−4603.

[11] M. Etienne, R. Mathieu, B. Donnadieu, *J. Am. Chem. Soc.* **1997**, *119*, 3218−3228.

[12] X. Yang, C. L. Stern, T. J. Marks, *J. Am. Chem. Soc.* **1991**, *113*, 3623−3625; X. Yang, C. L. Stern, T. J. Marks, *J. Am. Chem. Soc.* **1994**, *116*, 10015−10031.

[13] Tp and Tp^{Me2} have cone angles of ca. 184° and 224°, respectively. We have found no mention of the cone angle of $Tp^{Me2,4\text{-}Cl}$ which can however be estimated to be close to that of Tp^{Me2}. S. Trofimenko, J. C. Calabrese, J. S. Thompson *Inorg. Chem.* **1987**, *26*, 1508−1514.

[14] A. G. Massey, A. J. Park *J. Organomet. Chem.* **1964**, *2*, 245−250.

[97263]

The Coordination and Structure of a Thiolate-Terminated "Molecular-Scale Wire" Linked to a Triosmium Cluster

Richard D. Adams*, Thomas Barnard, Adam Rawlett, and James M. Tour*

Department of Chemistry and Biochemistry, University of South Carolina,
Columbia, SC 29208, USA
Fax: (internat.) + 1-803/777-6781
E-mail: Adams@psc.sc.edu

Received November 24, 1997

Keywords: Osmium / Thiolate / Molecular wire / Molecular devices / Structure elucidation

The molecule (*p,p*)-$HSC_6H_4C{\equiv}CC_6H_4C{\equiv}CC_6H_5$ has been attached to a triosmium cluster and characterized crystallographically. The complex $Os_3(CO)_{10}(\mu\text{-}H)(\mu\text{-}SC_6H_4C{\equiv}CC_6H_4C{\equiv}CC_6H_5)$ (**1**) was obtained in 49% yield from the reaction of the thiol $HSC_6H_4C{\equiv}CC_6H_4C{\equiv}CC_6H_5$ with $Os_3(CO)_{10}(NCMe)_2$. The sulfur atom bridges two metal atoms on the edge of a triangular cluster of three osmium atoms. The three aryl rings are nearly coplanar. The ligand is 18.27(2) Å in length from the sulfur atom to the *para*-carbon atom of the third aryl ring. This compound may serve as a model for the coordination of thiol-terminated molecular wires to metallic probe surfaces.

Future computational systems will eventually consist of logic devices that are ultra dense, ultra fast, and ultra small[1][2][3]. The slow step in existing computational architectures is not usually the switching time, but the time it takes for an electron to travel through the circuit. By using molecular-scale electronic interconnects[4], electronic transmission times will be minimized and the resulting computational operations will occur at far greater speeds than those attainable from conventional patterned architectural arrays[1].

Although it is well documented that bulk conjugated organic materials can be semiconducting or even conducting when doped[5], recent studies have shown that oriented thiol-terminated conjugated rigid-rod molecules[6] can conduct electrons through a single undoped conjugated molecule, "molecular-scale wire", to and from a metallic surface[7]. However, initial studies have indicated the presence of a transmission barrier at the metal-organic interface[8]. A detailed knowledge of the bonding of thiols to metallic surfaces will be crucial to developing an understanding of electron-transport mechanisms and the constuction of devices involving the metal-organic interfaces. The metal-thiol linkage is usually regarded to be a single metal−sulfur bond with transfer of the hydrogen atom to the metal surface. Therefore, we have undertaken a study to determine the nature of the structures and modes of attachment of some thiol-terminated molecular wires to metal clusters serving as models for metal surfaces.

The complex $Os_3(CO)_{10}(\mu\text{-}H)(\mu\text{-}SC_6H_4C{\equiv}CC_6H_4C{\equiv}CC_6H_5)$ (**1**) was obtained in 49% yield from the reaction of (*p,p*)-$HSC_6H_4C{\equiv}CC_6H_4C{\equiv}CC_6H_5$ with $Os_3(CO)_{10}(NCMe)_2$. Crystals of **1**, suitable for X-ray crystallographic analysis, were obtained by slow evaporation of solvent from a solution in CH_2Cl_2 solvent at 25°C. An ORTEP diagram of the molecular structure of **1** is shown in Figure 1. The molecule consists of a linear $SC_6H_4C{\equiv}CC_6H_4C{\equiv}CC_6H_5$ ligand linked to the triosmium cluster by the sulfur atom bridging two of the three osmium atoms. The reaction has produced cleavage of the thiol sulfur−hydrogen bond and transfer of the hydrogen atom to the osmium cluster to become a hydride ligand. The position of the hydride ligand was located and refined crystallographically. It bridges the Os(1)−Os(2) bond of a triangular cluster of three osmium atoms, Os(1)−H(1) = 1.9(1) Å and Os(2)−H(1) = 1.81(8) Å, and exhibits the characteristic high-field resonance shift in the ^{1}H-NMR spectrum, $\delta = -17.04$. The sulfur atom bridges the same two metal atoms on the other side of the Os_3 plane, Os(1)−S = 2.423(3) Å and Os(2)−S = 2.421(4) Å. These values are similar to those found for other bridging thiolate−triosmium linkages that have been structurally characterized previously[9]. The alkyne C−C bonds are short, C(46)−C(47) = 1.16(2), C(54)−C(55) = 1.19(2) Å as expected for C−C triple bonds, and the alkyne groups are linear. The sulfur−carbon distance, S−C(40) = 1.82(1) Å, is typical of a carbon−sulfur single bond. The overall length of the ligand is an interesting feature. The distance from S to C(59) is 18.27(2) Å. Although the central aryl ring is twisted approximately 10° away from the planes of the two other rings, the three aryl rings are nearly coplanar. This is a feature that would facilitate electron transmission through the π-orbital network.

Figure 2 shows the packing of the molecules in the crystal. All aryl rings are nearly coplanar. The intermolecular spacings between the rings of the different molecules are determined largely by the size of the cluster.

Studies have shown that bis(phenylethynyl)arenes exhibit strong fluorescence and are effective receptors for chemiluminescence processes[10]. We have found that **1** exhibits a single strong UV absorption at 332 nm ($\varepsilon = 48500\ M^{-1}\ cm^{-1}$)

 © WILEY-VCH Verlag GmbH, D-69451 Weinheim, 1998 1434−1948/98/0404−0429 $ 17.50+.50/0

Figure 1. ORTEP diagram of the molecular structure of $Os_3(CO)_{10}(\mu\text{-}H)(\mu\text{-}SC_6H_4C{\equiv}CC_6H_4C{\equiv}CC_6H_5)$ (**1**)[a]

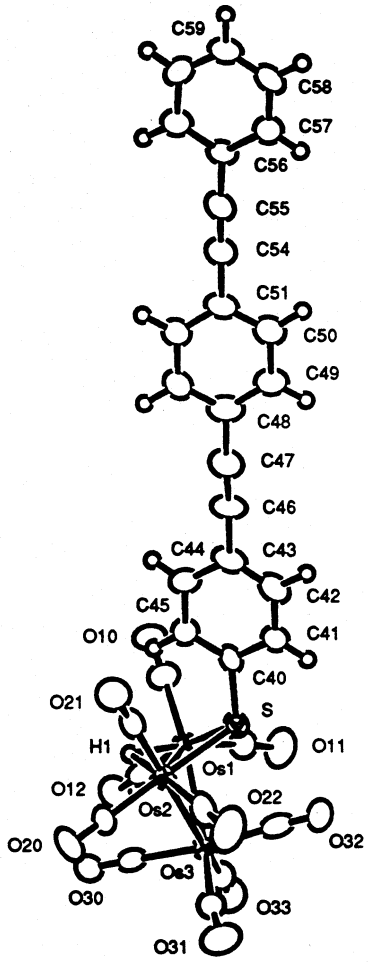

[a] Selected interatomic distances [Å] and angles [°] are: Os(1)−Os(2) = 2.8765(8), Os(1)−Os(3) = 2.8565(7), Os(2)−Os(3) = 2.8626(8), Os(1)−S = 2.423(3), Os(2)−S = 2.421(4), Os(1)−H(1) = 1.9(1), Os(2)−H(1) = 1.81(8), S−C(40) = 1.82(1), C(46)−C(47) = 1.16(2), C(54)−C(55) = 1.19(2), S···C(59) = 18.27(2); Os(1)−S−C(40) = 113.5(4), Os(2)−S−C(40) = 111.6(5).

Figure 2. Packing diagram of compound **1** showing the stacking of the $HSC_6H_4C{\equiv}CC_6H_4C{\equiv}CC_6H_5$ ligand in the solid state

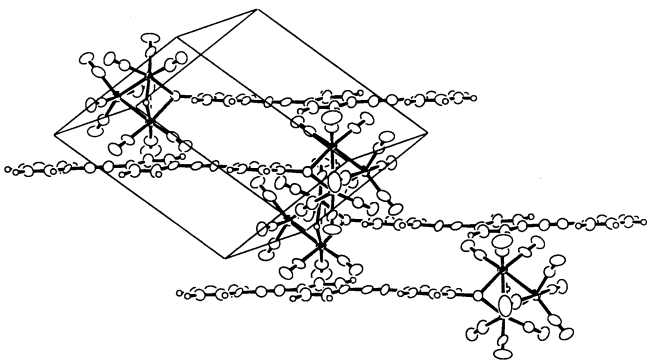

and a series of emissions at 348, 362, and 377 nm (λ_{ex} = 300 nm) which can be attributed to the $SC_6H_4C{\equiv}CC_6H_4C{\equiv}CC_6H_5$ ligand.

These studies were supported by the *Division of Chemical Sciences* of the *Office of Basic Energy Sciences of the U. S. Department of Energy*, Grant No. DE-FG05-95ER14548 to R. D. A. and the *Defense Advanced Research Projects Agency* to J. M. T. We thank Professor *Catherine J. Murphy* for assistance with the UV/Vis-spectral measurements.

Experimental Section

The reaction was performed under nitrogen. 24.0 mg of $HSC_6H_4C{\equiv}CC_6H_4C{\equiv}CC_6H_5$[6b] (0.0773 mmol), dissolved in 4 ml of CH_2Cl_2, was added to a solution of 75.0 mg of $Os_3(CO)_{10}(NCMe)_2$ (0.0804 mmol) in 50 ml of CH_2Cl_2. After stirring for 2 h at 25°C, the solvent was removed and the residue separated by TLC (in air) on silica gel by using a hexane/CH_2Cl_2 (3:1) solvent mixture. This yielded a yellow band containing 44.1 mg of $Os_3(CO)_{10}(\mu\text{-}H)(\mu\text{-}SC_6H_4C{\equiv}CC_6H_4C{\equiv}CC_6H_5)$ (**1**) (49%). − IR (νCO in hexane, cm^{-1}): 2110 (m), 2069 (vs), 2060 (m), 2026 (vs), 2020 (m), 2003 (m), 1992 (w), 1987 (w). − ^1H NMR (δ in $CDCl_3$): 7.52−7.25 (m, 13 H, Ph), −17.04 (s, 1 H, Os-H). − $C_{32}H_{14}O_{10}Os_3S$ (1161.12): calcd. C 33.10, H 1.22; found 32.98, 1.37.

Crystal Data: Space group = $P\bar{1}$, a = 15.019(3), b = 13.831(2), c = 9.299(1) Å, α = 90.21(1), β = 72.67(2), γ = 114.77°, Z = 2; 3221 reflections, R = 0.035. Diffraction measurements at 20°C were made on a Rigaku AFC6S four-circle diffractometer using Mo-K_α radiation. The structure solution and refinement were made by using the TEXSAN MOTIF structure-solving program library (v. 1.8) of the Molecular Structure Corp., The Woodlands, TX on a Silicon Graphics Indigo^2 computer. An absorption correction (DIFABS) was applied. − Crystallographic Data (excluding structure factors) for the structure reported in this paper have been deposited with the Cambridge Crystallographic Data Centre as supplementary publication no. CCDC-101062. Copies of the data can be obtained free of charge on application to CCDC, 12 Union Road, Cambridge CB2 1EZ [Fax: int code + 44(1223)336-033, E-mail: deposit@ccdc.cam.ac.uk).

[1] For some recent background work on molecular-scale electronics, see: [1a] A. Aviram (Ed.) in *Molecular Electronics: Science and Technology,* Confer. Proc. No. 262, American Institute of Physics: New York, **1992**. − [1b] J. S. Miller, *Adv. Mater.* **1990**, *2*, 378, 495, 601. − [1c] R. R. Birge (Ed.) in *Molecular and Biomolecular Electronics*, Advances in Chemistry Series 240, American Chemical Society, **1991**. − [1d] W. P. Kirk, M. A. Reed (Eds.) in *Nanostructures and Mesoscopic Systems*, Academic Press, New York, **1992**.

[2] For some theoretical considerations on molecular-scale wires, see: [2a] M. P. Samanta, W. Tian, S. Datta, J. I. Henderson, C. P. Kubiak, *Phys. Rev. B* **1996**, *53*, R7626. − [2b] V. Mujica, M. Kemp, A. Roitberg, M. Ratner, *J. Phys. Chem.* **1996**, *104*, 7296. − [2c] C. Joachim, J. F. Vinuesa, *Europhys. Lett.* **1996**, *33*, 635.

[3] For some recent background work on the formation of molecular-based transporters and devices, see: [3a] V. Grosshenny, A. Harriman, R. Ziessel, *Angew. Chem.* **1995**, *107*, 1211; *Angew. Chem. Int. Ed. Engl.* **1995**, *34*, 1100. − [3b] L. Langler, L. Stockman, J. P. Heremans, V. Bayor, C. H. Olk, C. Van Haesendonck, Y. Bruynseraede, J.-P. Issi, *Synth. Met.* **1995**, *70*, 1393. − [3c] J. I. Pascual, J. Méndez, J. Gómez-Herrero, A. M. Baró, N. Garcia, U. Landman, W. D. Luedtker, E. N. Bogachek, H.-P. Cheng, *Science* **1995**, *267*, 1793. − [3d] S. T. Purcell, N. Garcia, V. T. Binh, L. Jones II, J. M. Tour, *J. Am. Chem. Soc.* **1994**, *116*, 11985. − [3e] C. R. Martin, *Science* **1996**, *266*, 1961. − [3f] J. Seth, V. Palaniappan, T. Johnson, E. S. Prathapan, J. S. Lindsey, D. F. Bocian *J. Am. Chem. Soc.* **1994**, *116*, 10578. − [3g] D. Gust, *Nature* **1994**, *372*, 133. − [3h] C. Wu, T. Bein, *Science* **1994**, *266*, 1013. − [3i] R. W. Wagner, J. S. Lindsey, J. Seth, V. Palaniappan, D. F. Bocain, *J. Am. Chem. Soc.* **1996**,*118*, 3996. − [3j] M. J. Sailor, C. L. Curtis, *Adv. Mater.* **1994**, *6*, 688. − [3k] F. Brigelletti, L. Flamigni, V. Balzani, J. Collin, J. Sauvage, A.

Sour, E. C. Constable, A. M. W. C. Thompson, *J. Am. Chem. Soc*. **1994**, *116*, 7692. – [3l] C. Wu, T. Bein, *Science* **1994**, *264*, 1757. – [3m] W. E. Moerner, *Science* **1994**, *265*, 46. – [3n] J. L. Sessler, V. L. Capuano, A. Harriman, *J. Am. Chem. Soc*. **1993**, *115*, 4618. – [3o] A. Farazdel, M. Dupuis, E. Clementi, A. Aviram *J. Am. Chem. Soc*. **1990**, *112*, 4206. – [3p] J. M. Tour, R. Wu, J. S. Schumm, *J. Am. Chem. Soc.* **1991**, *113*, 7064. – [3q] H. Dai, E. Wong, C. M. Lieber, *Science* **1996**, *272*, 523. – [3r] R. Wu, J. S. Schumm, D. L. Pearson, J. M. Tour, *J. Org. Chem.* **1996**, *61*, 6906. – [3s] M. D. Ward, *Chem. Ind*. **1996**, 569.

[4] "Molecular electronics" is a poorly defined term since some authors refer to it as any molecular-based system such as a film or a liquid-crystalline array. Other authors, including us, have preferred to reserve the term "molecular electronics" for single-molecule tasks, such as single-molecule-based devices or single-molecular wires. Due to this confusion, we have chosen here to follow the Petty et al. [M. C. Petty, M. R. Bryce, D. Bloor (Eds.) in *Introduction to Molecular Electronics*, Oxford Univ. Press, New York, **1995**] terminology by using two subcategories, namely "molecular materials for electronics" for bulk applications and "molecular-scale electronics" for single-molecule applications.

[5] T. A. Skotheim (Ed.), *Handbook of Conducting Polymers*, Dekker, New York, **1986**.

[6] [6a] J. M. Tour, L. Jones II, D. L. Pearson, J. S. Lamba, T. Burgin, G. W. Whitesides, D. L. Allara, A. N. Parikh, S. Atre, *J. Am. Chem. Soc*. **1995**, *117*, 9529. – [6b] A. Dhirani, R. W. Zehner, R. P. Hsung, P. Guyot-Sionnest, L. R. Sita, *J. Am. Chem. Soc*. **1996**, *118*, 3319.

[7] L. A. Bumm, J. J. Arnold, M. T. Cygan, T. D. Dunbar, T. P. Burgin, L. Jones II, D. L. Allara, J. M. Tour, P. S. Weiss *Science* **1996**, *271*, 1705.

[8] [8a] C. Zhou, M. R. Deshpande, M. A. Reed, L. Jones II, J. M. Tour, *Appl. Phys. Lett.* **1997**,*71*, 611. – [8b] M. A. Reed, C. Zhou, C. J. Muller, T. P. Burgin, J. M. Tour, *Science* **1997**, *278*, 252.

[9] [9a] R. D. Adams, M. P. Pompeo, *Organometallics* **1992**, *11*, 103. – [9b] R. D. Adams, M. P. Pompeo, *Organometallics* **1992**, *11*, 1460. – [9c] R. D. Adams, N. M. Golembeski, J. P. Selegue, *J. Am. Chem. Soc.* **1981**, *103*, 546. – [9d] V. F. Allen, R. Mason, P. B. Hitchcock, *J. Organomet. Chem.* **1977**, *140*, 297. – [9e] R. D. Adams, Z. Dawoodi, D. F. Foust, B. E. Segmüller, *Organometallics* **1983**, *2*, 315. – [9f] E. W. Ainscough, A. M. Brodie, R. K. Coll, A. J. A. Mair, J. M. Waters, *Inorg. Chim. Acta* **1993**, *214* , 21. – [9g] A. M. Brodie, H. D. Holden, J. Lewis, M. J. Taylor, *J. Chem. Soc., Dalton Trans.* **1986**, 663. – [9h] H. D. Holden, B. F. G. Johnson, J. Lewis, P. Raithby, G. Uden, *Acta Crystallogr., Sect. C* **1983**, *39,* 1203. – [9i] H. D. Holden, B. F. G. Johnson, J. Lewis, P. Raithby, G. Uden, *Acta Crystallogr., Sect. C* **1983**, *39,* 1200.

[10] [10a] P. Nguyen, S. Todd, D. Van den Biggelaar, N. J. Taylor, T. J. Marder, Felix Wittmann, R. H. Friend, *Synlett* **1994**, 299. – [10b] P. J. Hanhela, D. P. Paul, *Aus. J. Chem.* **1981**, *34*, 1701. – [10c] P. J. Hanhela, D. P. Paul, *Aus. J. Chem.* **1981**, *34*, 1669.

[97278]

Bis(amidinate) Complexes of Silicon and Germanium

Hans H. Karsch*, Peter A. Schlüter, and Manfred Reisky

Technische Universität München, Institut für Anorganische Chemie,
Lichtenbergstr. 4, D-85747 Garching, Germany
Fax: (internat.) +49 (0)89/ 28914421
E-mail: Hans.H.Karsch@lrz.tu-muenchen.de

Received January 17, 1998

Keywords: Silicon amidinates / Germanium amidinates / Bidentate coordination

The synthesis of novel bis(amidinate) silicon and germanium complexes is described. The reaction of two equiv. of $[MeC(N\textit{i}Pr)_2]Li\cdot THF$ (**1**) with $SiCl_4$, $GeCl_4$ or $GeCl_2$·dioxane affords $[MeC(N\textit{i}Pr)_2]_2SiCl_2$ (**2**), $[MeC(N\textit{i}Pr)_2]_2GeCl_2$ (**3**) and $[MeC(N\textit{i}Pr)_2]_2Ge$ (**4**), respectively. The complexes **2** and **4** have been structurally characterized. The crystallographic results confirm a bidentate coordination of the amidinate ligands at the Si/Ge center, as indicated by spectroscopic studies.

Introduction

The coordination chemistry of amidinates is well established, not only for the transition metals[1][2] and the lanthanoides[3], but also for main group elements[4][5][6][7][8]. The main importance lies in the generation of element−nitrogen bonds as needed for CVD methods[9], and for the synthesis of new catalysts. However, the amidinate chemistry of Group 14 elements has hitherto only been investigated for tin and lead[10][11]. Amidinates of silicon and germanium are largely unknown, with only a few exceptions.

Thus, $PhC(NSiMe_3)[N(SiMe_3)_2]$[12] and $[PhC(NSiMe_3)_2]M\cdot(THF/Et_2O)_n$ (M = Li, Na, K, Rb)[11] are well known starting materials in amidinate chemistry. $PhC(NSiMe_3)[N(SiMe_3)_2]$ is the only compound of this type for which a crystal structure determination is available, and this confirms a monodentate amidinate coordination[11]. In contrast, a bidentate coordination was deduced from a $\delta^{29}Si$ value of −101.9 for the only other known amidinate silicon derivative, $PhC(NSiMe_3)_2SiCl_3$[14]. A report on structural investigations of two other silicon amidinate derivatives is currently in press[13]. With the aim of obtaining access to a new generation of molecular silicon−nitrogen compounds, which might easily be converted to polymeric materials of different but easily tunable structural units resembling silicate structures but with pseudochalcogenide bridges {i.e. $[N-C(R)-N(R')]^{2-}$ instead of O^{2-}}, and which further might be converted to Si/C/N/X materials, we have initiated a comprehensive study of silicon and germanium amidinate chemistry. We have found that modification of the organic substituents on the nitrogen as well as on the bridging carbon atom exerts a considerable effect on the coordination to the silicon or germanium center[15]. We report herein on preliminary results concerning the synthesis and characterization of novel bis(amidinate) complexes of Si^{IV}, Ge^{IV}, and Ge^{II}.

Results and Discussion

The anionic amidinate compound $[MeC(N\textit{i}Pr)_2]Li\cdot THF$ (**1**) was obtained by reaction of *i*Pr−N=C=N*i*Pr with MeLi (THF, room temp.) and was isolated as a white, crystalline solid in good yield according to the published procedure[16]. Reactions of 2 equiv. of **1** with 1 equiv. of $SiCl_4$, $GeCl_4$ or $GeCl_2\cdot$dioxane resulted in the formation of the new complexes $[MeC(N\textit{i}Pr)_2]_2SiCl_2$ (**2**), $[MeC(N\textit{i}Pr)_2]_2GeCl_2$ (**3**), and $[MeC(N\textit{i}Pr)_2]_2Ge$ (**4**) (Scheme 1), which were obtained as colorless, crystalline solids.

Scheme 1. Reactions of $SiCl_4$, $GeCl_4$, and $GeCl_2\cdot$dioxane with $[CH_3C(N\textit{i}Pr)_2]Li\cdot THF$ (**1**)

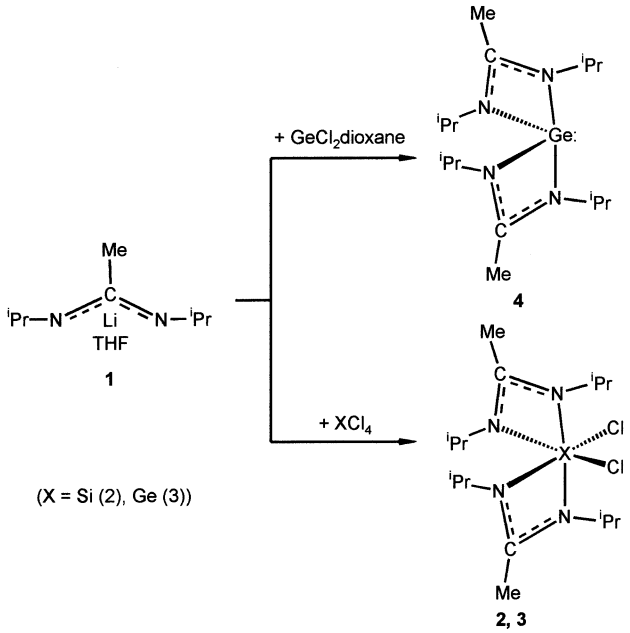

The constitutions of the complexes were established on the basis of their ^1H-, ^{13}C-NMR and mass spectra, as well as by elemental analyses.

The room-temperature ^1H-NMR spectrum of **2** shows four doublets of equal intensity in the aliphatic region due to the methyl protons of the isopropyl groups, and two septets due to the CH protons of the isopropyl groups of the amidinate ligands. The CH_3 group of the bridging unit is

 © WILEY-VCH Verlag GmbH, D-69451 Weinheim, 1998 1434−1948/98/0404−0433 $ 17.50+.50/0

observed as a singlet. Temperature-dependent NMR measurements establish a rigid molecular skeleton in the range −80 °C to +80 °C. In marked contrast, the analogous germanium compound **3** shows fluctional behavior. At room temp., four doublets are again observed for the isopropyl groups, but these broaden on heating and coalesce to one broad singlet at 80 °C.

However, the germanium(II) compound **4** exhibits a single set of amidinate resonances over the whole temperature range, indicating equivalence of the two donor nitrogen atoms and symmetrical coordination to the germanium center on the NMR timescale.

The ^{29}Si-NMR resonance of **2** ($\delta = -169.33$) indicates hexacoordination at silicon. All three complexes show remarkable thermal stability. For example, **2** can be heated in toluene at 100 °C for several days without noticeable decomposition. No reaction was observed upon treatment with potassium or sodium metal (THF, room temp.).

Confirmation of the bidentate coordination mode of the amidinate ligands was obtained from X-ray structure determinations of **2** and **4**.

X-ray Analysis of $[CH_3C(NiPr)_2]_2SiCl_2$ (**2**) *and* $[CH_3C(NiPr)_2]_2Ge$ (**4**): The X-ray analysis of the colorless crystals of compound **2** (from toluene) shows two identical molecules in the asymmetric unit (see Table 2). The molecular geometry and atom numbering scheme are shown in Figure 1; selected bond distances [Å] and angles [°] are listed in Table 1.

Figure 1. Molecular structure of **2**

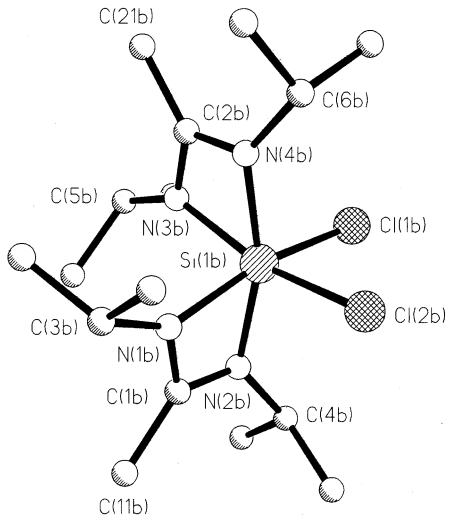

Both amidinate ligands are coordinated in a bidentate fashion, with one nitrogen in an axial and the other in an equatorial position of a distorted octahedron. Two chlorine atoms complete the *cis*-octahedral coordination sphere of the central silicon atom. As expected, the axial Si−N bond lengths [Si(1b)−N(2b): 1.837(2) Å, Si(1b)−N(4b): 1.841(2) Å] are slightly shorter than the equatorial distances [Si(1b)−N(1b): 1.915(2) Å, Si(1b)−N(3b): 1.914(2) Å]. This is accompanied by a slight shortening of the $C-N_{eq}$ bonds [N(1b)−C(1b): 1.312 Å, N(3b)−C(2b): 1.305(4) Å] compared to the $C-N_{ax}$ bonds [N(2b)−C(1b): 1.333(4) Å, N(4b)−C(2b): 1.341(4) Å] within the amidinate ligands, both being approximately intermediate between C−N double-bond and C−N(sp^2) single-bond distances. The four-membered Si−N−C−N rings are essentially planar, as are the arrangements about the nitrogen and carbon atoms. The overall structure of **2** resembles that of the structurally characterized tin compound $[MeC(NCy)_2]_2SnCl_2$[10a].

Table 1. Selected bond lengths [Å] and angles [°] of compounds **2** and **4**

	2		**4**
Cl(1b)−Si(1b)	2.185(1)	Ge(1)−N(1)	1.982(3)
Cl(2b)−Si(1b)	2.197(1)	Ge(1)−N(3)	2.300(2)
Si(1b)−N(4b)	1.841(2)	N(1)−C(1)	1.325(4)
Si(1b)−N(2b)	1.837(2)	N(3)−C(1a)	1.302(3)
Si(1b)−N(1b)	1.915(2)	N(1)−C(3)	1.459(4)
Si(1b)−N(3b)	1.914(2)	N(3)−C(5)	1.462(3)
N(1b)−C(1b)	1.312(4)		
N(2b)−C(1b)	1.333(4)		
N(3b)−C(2b)	1.305(4)		
N(4b)−C(2b)	1.341(4)		
N(2b)−Si(1b)−N(4b)	163.0(1)	N(1a)−Ge(1)−N(1)	100.7(1)
N(4b)−Si(1b)−N(1b)	98.0(1)	N(1)−Ge(1)−N(3)	96.20(9)
N(2b)−Si(1b)−N(1b)	69.0(1)	N(1)−Ge(1)−N(3a)	61.00(9)
N(4b)−Si(1b)−N(3b)	68.8(1)	C(1)−N(1)−C(3)	125.4(2)
N(2b)−Si(1b)−N(3b)	99.6(1)	C(3)−N(1)−Ge(1)	135.3(2)
N(3b)−Si(1b)−N(1b)	91.0(1)	C(1a)−N(3)−Ge(1)	85.5(2)
N(4b)−Si(1b)−Cl(1b)	96.8(8)	N(3a)−C(1)−N(1)	113.0(2)
N(2b)−Si(1b)−Cl(1b)	95.78(8)	N(3)−Ge(1)−N(3a)	145.7(1)
N(1b)−Si(1b)−Cl(1b)	164.75(8)	C(1)−N(1)−Ge(1)	99.2(2)
N(3b)−Si(1b)−Cl(1b)	90.81(8)	C(1a)−N(3)−C(5)	122.2(3)
N(3b)−Si(1b)−Cl(2b)	163.95(8)	C(5)−N(3)−Ge(1)	144.8(2)
N(1b)−C(1b)−N(2b)	107.0(2)		
N(3b)−C(2b)−N(4b)	106.7(2)		

Figure 2. Molecular structure of **4**

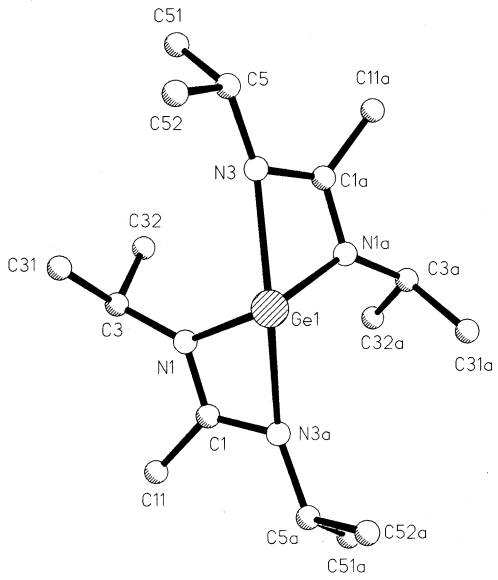

The X-ray structure determination of the colorless crystals of **4** (from pentane) reveals the presence of one-half of the molecule in the asymmetric unit (see Table 2). The whole molecule can be generated by symmetric transformations. The molecular geometry and atom numbering

scheme are shown in Figure 2; selected bond distances [Å] and angles [°] are listed in Table 1.

In the monomeric molecule, the germanium atom is surrounded by four nitrogen atoms originating from two amidinate ligands, each spanning an axial and an equatorial site of a heavily distorted Ψ-trigonal bipyramid, with the "lone pair" of germanium(II) occupying the third equatorial position. Although, as in the case of **2**, the four-membered rings are almost planar, only the equatorial nitrogen atoms N(1)/(1a) are planar [sum of angles at N(1)/(1a): 359.9°]. The respective Ge(1)−N(1)/(1a) bonds [1.982(3) Å] are significantly shorter than the axial Ge(1)−N(3)/(3a) bonds [2.300(1) Å], which coincides with a considerable deviation from planarity of the N(3)/(3a) atoms [sum of angles at N(3)/(3a): 352.5°]. The axial N(3)−Ge(1)−N(3a) bond angle [145.7(1)°] is very small compared the ideal tbp value of 180° and highlights the considerable ring strain in **4**. The angle N(1)−Ge(1)−N(1a) is also rather small (100.7°). Instead of a Ψ-tbp structure, the geometry might be classified as a distorted tetragonal pyramid − in fact, an intermediate state is the best compromise for an adequate description. In this regard, the structure resembles those of other Ge^{II} compounds bearing four-membered chelate rings[17]. As a consequence of this structural dilemma, fluctional behavior may be anticipated and is indeed observed (see above). Again, small element to nitrogen distances [Ge−N(1)/(1b): 1.982(3) Å] coincide with slightly longer C−N distances in the ligand [C(1)−N(1)/C(1a)−N(1a): 1.325(4) Å] and vice versa: the long Ge(1)−N(3)/(3a) bond [2.300(2) Å] corresponds to a short C(1)−N(3)/(3a) bond [1.302(3) Å]. The amidinate bite angle [N(1a)−Ge(1)−N(3)] is rather acute (61.0°), which is compensated by a concomitant widening of the N−C−N bond angle (125.4°).

Conclusions

Monoanionic, bidentate four-electron donor amidinates are highly suitable ligands for stabilizing low oxidation states and/or high coordination numbers at group 14 element centers (Si, Ge). The newly synthesized *cis*-dichlorosilicon bis(amidinate) complex **2** may be a potentially useful precursor for novel stable Si^{II} compounds. Work in this area is currently in progress.

We thank the *Deutschen Forschungsgesellschaft* for financial support.

Experimental Section

General: All reactions were carried out under dry nitrogen. The solvents used were distilled under nitrogen from Na/K alloy. MeLi (1.6 M in Et_2O) and *i*PrNCN*i*Pr were used as purchased. $SiCl_4$ and $GeCl_4$ were freshly distilled from K_2CO_3 prior to use. *$GeCl_2 \cdot dioxane$*[18] and *[MeC(NiPr)$_2$]Li·THF* (**1**)[16] were prepared according to literature procedures. Elemental analyses were obtained on a Vario EL CHN Automat Analyzer at the microanalytical laboratory of the TU München. − NMR: Jeol GX 270 and 400 FT-NMR spectrometers. All chemical shifts are reported in parts per million and coupling constants *J* in Hz. Spectra were recorded at 25 °C unless otherwise stated. − MS: Varian MAT 311A, CI.

Preparation of [MeC(NiPr)$_2$]$_2$SiCl$_2$ (**2**): To a suspension of 13.85 mmol (3.05 g) of **1** in 50 ml of Et_20, 6.58 mmol (0.83 ml) of $SiCl_4$ was added at −78 °C. The reaction mixture was allowed to warm to room temp. with stirring. After 18 h, the solvent was replaced by 40 ml of toluene and the resulting suspension was filtered. Evaporation of the solvent from the filtrate afforded 2.4 g (95%) of colorless crystals. − ^{1}H NMR (C_6D_6): δ = 0.96 (d, $^3J_{HH}$ = 8.0, 6 H, CH_3CH), 1.28 (d, $^3J_{HH}$ = 8.0, 6 H, CH_3CH), 1.37 (d, $^3J_{HH}$ = 8.0, 6 H, CH_3CH), 1.41 (s, 6 H, CH_3C), 1.48 (d, $^3J_{HH}$ = 8.0, 6 H, CH_3CH), 3.33 (sept, 2 H, $^3J_{HH}$ = 8.0, CH$_3$C*H*), 4.30 (sept, 2 H, $^3J_{HH}$ = 8.0, CH$_3$C*H*). − ^{13}C NMR (C_6D_6): δ = 12.37 (*C*H$_3$C), 21.76 (*C*H$_3$CH), 23.24 (*C*H$_3$CH), 23.32 (*C*H$_3$CH), 23.59 (*C*H$_3$CH), 45.19 (CH$_3$*C*H), 46.37 (CH$_3$*C*H), 166.77 (N*C*N). − ^{29}Si NMR (C_6D_6): δ = −169.33. − MS (CI, 150 eV): *m/z* (%) = 380 (2) [M$^+$], 345 (100) [M − Cl], 262 (11) [M − Cl − CN*i*Pr], 239 (50) [M − *i*PrNC(Me)N*i*Pr]. − $C_{16}H_{24}Cl_2N_4Si$ (381.46): calcd. C 50.38, H 8.98, N 14.69; found C 48.15, H 8.75, N 12.90.

Preparation of [MeC(NiPr)$_2$]$_2$GeCl$_2$ (**3**): To a suspension of 8.42 mmol (1.85 g) of **1** in 50 ml of THF, 4.00 mmol (0.46 ml) of $GeCl_4$ was added at −78 °C and the reaction mixture was allowed to warm to room temp. After stirring for 18 h at room temp., the solvent was replaced by 40 ml of pentane. The residue was extracted several times. The combined extracts were slowly concentrated in vacuo to afford 1.41 g (83%) of colorless crystals. − ^{1}H NMR (20 °C, [D$_8$]toluene): δ = 1.11 (d, $^3J_{HH}$ = 6.4, 6 H, CH_3CH), 1.46 (d, $^3J_{HH}$ = 6.4, 6 H, CH_3CH), 1.63 (d, $^3J_{HH}$ = 6.4, 6 H, CH_3CH), 1.65 (d, $^3J_{HH}$ = 6.4, 6 H, CH_3CH), 1.55 (s, 6 H, CH_3C), 3.49 (sept, $^3J_{HH}$ = 6.4, 2 H, CH$_3$C*H*), 4.22 (sept, $^3J_{HH}$ = 6.4, 2 H, CH$_3$C*H*). − ^{1}H NMR (80 °C, [D$_8$]toluene): δ = 1.51 (br, 24 H, CH_3CH), 1.62 (s, 6 H, CH_3C), 3.6−4.2 (br, 4 H, CH$_3$C*H*). − ^{13}C NMR (C_6D_6): δ = 11.06 (*C*H$_3$C), 21.68, 23.23, 23.46, 23.73 (*C*H$_3$CH), 46.34 (CH$_3$*C*H), 47.36 (CH$_3$*C*H), 162.46 (N=*C*N). − MS (CI, 150 eV): *m/z* (%) = 391 (58) [M − Cl], 285 (39) [M − MeC(N*i*Pr)$_2$], 141 (100) [MeC(N*i*Pr)$_2$]. − $C_{16}H_{34}Cl_2GeN_4$ (425.99): calcd. C 45.11, H 8.04, N 13.15; found C 45.28, H 8.00, N 12.61.

Preparation of [MeC(NiPr)$_2$]$_2$Ge (**4**): To a mixture of 8.12 mmol (1.79 g) of **1** and 3.45 mmol (0.8 g) of $GeCl_2 \cdot$dioxane, 40 ml of Et_2O was added at −78 °C. The reaction mixture was slowly allowed to warm to room temp. and stirred for a further 18 h. The solvent was then removed and the product was extracted with 50 ml of pentane. The pentane extract was concentrated and **4** was isolated as colorless crystals (1.02 g, 81%). − m.p. 41 °C. − ^{1}H NMR (C_6D_6): δ = 1.31 (d, $^3J_{HH}$ = 6.5, 24 H, CH_3CH), 1.53 (s, 6 H, CH_3C), 3.63 (sept, $^3J_{HH}$ = 6.5, 4 H, CH$_3$C*H*). − ^{13}C NMR (C_6D_6): δ = 11.91 (*C*H$_3$C), 24.89 (*C*H$_3$CH), 47.16 (CH$_3$*C*H), 162.53 (N*C*=N). − MS (CI, 150 eV): *m/z* (%) = 357 (15) [M], 183 (3) [M − 4 *i*Pr], 143 (100) [MeC(N*i*Pr)$_2$]. − $C_{16}H_{34}GeN_4$ (355.08): calcd. C 54.12, H 9.65, N 15.77; found C 51.93, H 9.50, N 14.77.

Crystal Structure Determination: Suitable crystals of **2** and **4** were sealed into glass capillaries. The structures were solved by direct methods and refined by full-matrix least-squares calculations against F^2 (SHELXL-93)[19]. Crystal data and numerical data of the structure determinations are given in Table 2. The thermal motion of all non-hydrogen atoms was treated anisotropically. All hydrogen atoms were calculated in ideal positions. Further information may be obtained from the Fachinformationszentrum Karlsruhe, D-76344 Eggenstein-Leopoldshafen (Germany), on quoting the depository numbers CSD-408153 (**2**) and CSD-408152 (**4**).

Table 2. Crystal data of the X-ray structural analyses of compounds **2** and **4**

	$[CH_3C(NiPr)_2]_2SiCl_2$ (**2**)	$[CH_3C(NiPr)_2]_2Ge$ (**4**)
Empirical formula	$C_{16}H_{34}N_4Cl_2Si$	$C_{16}H_{34}GeN_4$
Molecular mass [g/mol]	381.46	355.06
Temperature [K]	199(2)	185(2)
Crystal system	orthorhombic	tetragonal
Space group	*Pbca*	$P4_12_12_1$
a [Å]	15.089(2)	7.185(6)
b [Å]	17.224(2)	7.185(6)
c [Å]	32.622(3)	36.886(6)
α, β, γ [°]	90	90
Diffractometer	Enraf-Nonius CAD4-Turbo	Enraf-Nonius CAD4-Turbo
Radiation	Mo-K_α (λ = 0.71073 Å)	Mo-K_α (λ = 0.71073 Å)
Density (calculated) [Mg/m^3]	1.195	1.175
Absorption coefficient [mm^{-1}]	0.368	1.527
F (000)	3296	760
θ range for data collection [°]	3−26	3−27
Limiting indices	$0 \le h \le 18$, $0 \le k \le 21$, $0 \le l \le 40$	$-9 \le h \le -1$, $0 \le k \le 9$, $-49 \le l \le 48$
Reflections collected	8290	4237
Independent reflections	8238 (R_{int} = 0.000)	2168 (R_{int} = 0.0271)
Data/ restrained/ parameters	5910/ 0/ 415	1843/ 0/ 96
Goodness-of-fit on F^2	1.023	1.070
Final *R* indices [F_0>4σ(F_0)]	*R1* = 0.0400; *wR2* = 0.0976	*R1* = 0.0293; *wR2* = 0.0704
R indices (all data)	*R1* = 0.0785; *wR2* = 0.1392	*R1* = 0.0436; *wR2* = 0.0769
Largest diff. peak and hole	0.427; −0.330 e/Å^3	0.445; −0.376 e/Å^3
Scan modes	ω/θ	ω

[1] D. Walther, R. Fischer, M. Friedrich, P. Gebhardt, H. Görls, *Chem. Ber.* **1996**, *129*, 1389.
[2] W. Hiller, J. Stähle, A. Zinn, K. Dehnicke, *Z. Naturforsch.* **1989**, *44b*, 999.
[3] M. Wedler, M. Noltemeyer, U. Pieper, H. G. Schmidt, D. Stahlke, F. T. Edelmann, *Angew. Chem.* **1990**, *102*, 941; *Angew. Chem. Int. Ed. Engl.* **1990**, *29*, 894.
[4] Y. Zhou, D. S. Richeson, *Inorg. Chem.* **1996**, *35*, 1423.
[5] Y. Zhou, D. S. Richeson, *Inorg. Chem.* **1996**, *35*, 2448.
[6] M. P. Coles, D. C. Swenson, R. F. Jordan, *Organometallics* **1997**, *16*, 5183.
[7] U. Patt-Siebel, U. Müller, C. Ergezinger, B. Borgsen, K. Dehnicke, D. Fenske, G. Baum, *Z. Anorg. Allg. Chem.* **1990**, *582,* 30.
[8] J. Barker, N. C. Blacker, P. R. Phillips, N. W. Alcock, W. Errington, M. G. H. Wallbridge, *J. Chem. Soc., Dalton Trans.* **1996**, 431.
[9] R. Riedel, A. Greiner, G. Miehe, W. Dreßler, H. Fueß, J. Bill, F. Aldinger, *Angew. Chem.* **1997**, *109*, 657; *Angew. Chem. Int. Ed. Engl.* **1997**, *36*, 603.
[10] [10a] Y. Zhou, D. S. Richeson, *Inorg. Chem.* **1997**, *36*, 501. − [10b] S. Appel, F. Weller, K. Dehnicke, *Z. Anorg. Allg. Chem.* **1990**, *583*, 7. − [10c] J. D. Kildea, W. Hiller, B. Borgsen, K. Dehnicke, *Z. Naturforsch.* **1989**, *44b*, 889. − [10d] C. Ergezinger, F. Weller, K. Dehnicke, *Z. Naturforsch.* **1988**, *43b*, 1621.
[11] K. Dehnicke, *Chemiker Zeitung* **1990**, *114*, 295.
[12] A. R. Sanger, *Inorg. Nucl. Chem. Lett.* **1973**, *9*, 351.
[13] H. H. Karsch, P. A. Schlüter, F. Bienlein, M. Heckel, M. Herker, A. Sladek, E. Witt, *Z. Anorg. Allg. Chem.* **1998**, in press.
[14] H. Roesky, B. Miller, M. Noltemeyer, H. G. Schmidt, U. Scholz, G. M. Sheldrick, *Chem. Ber.* **1988**, *121,* 1403.
[15] H. H. Karsch, P. A. Schlüter, M. Reisky, **1998**, to be published.
[16] S. Hao, S. Gambarotta, C. Bensimon, J. J. H. Edema, *Inorg. Chim. Act*. **1993**, *213*, 65.
[17] [17a] H. H. Karsch, B. Deubelly, G. Hanika, J. Riede, G. Müller, *J. Organomet. Chem.* **1988**, *344*, 153. − [17b] H. H. Karsch, M. Hollstein, G. Müller, *Z. Naturforsch.* **1990**, *45b*, 775.
[18] W. A. Herrmann, M. Denk, *Deutsches Patent* DE 4214281.
[19] [19a] G. M. Sheldrick, C. Krüger, R. Goddard, *Oxford Univ. Press*, **1985**, 175. − [19b] G. M. Sheldrick, *Program for the refinement of structures*, **1993**, University of Göttingen. − [19c] J. Kopf, H. C. Rübcke, *Progr. CADHKL4*, **1993**, Universität Hamburg.

[98009]

Chemistry of Polyfunctional Molecules, 129[◇]

Synthesis and X-Ray Structures of Novel Lead(1+) and Indium(3+) Phosphazenide Complexes; Detailed ^{207}Pb-NMR Spectra of the ^{207}Pb-Labelled Dimeric Lead(1+) Species

Astrid Winkler[a], Walter Bauer*[b], Frank W. Heinemann[a], Veronica Garcia-Montalvo[a][+], Matthias Moll[a], and Jochen Ellermann*[a]

Institut für Anorganische Chemie der Universität Erlangen-Nürnberg[a],
Egerlandstrasse 1, D-91058 Erlangen, Germany
Fax: (internat.) +49(0)9131/85-7367

Institut für Organische Chemie der Universität Erlangen-Nürnberg[b],
Henkestrasse 42, D-91054 Erlangen, Germany
Fax: (internat.) +49(0)9131/85-9132
e-mail: bauer@organik.uni-erlangen.de

Received November 10, 1997

Keywords: Lead(1+) / Indium(3+) / Organylphosphanylamide complexes / Phosphazene / ^{207}Pb-NMR spectra

The reaction of $PbCl_2$ with $LiN(PPh_2)_2$ (**1**) at −78°C affords the P−P coupled phosphazene $Ph_2P-N{=}PPh_2-PPh_2{=}N-PPh_2$ (**2**) as an oxidation product and, as a reduction equivalent, the novel lead(1+) complex $[(Pb^{1+})_2(\mu\text{-}Ph_2P{=}N{=}PPh_2^-)_2](Pb-Pb)$ (**3**). The crystal structure determination of the red compound **3** shows a Pb−Pb bond length of 304.1(1) pm. The ^{31}P- and ^{207}Pb-NMR spectra of **3** are complicated due to the presence of a higher order spin system (AA′A′′A′′′X for the mono-^{207}Pb isotopomer, AA′A′′A′′′XX′ for the bis-^{207}Pb isotopomer). Simulations of the ^{31}P and ^{207}Pb spectra both on material with natural isotope abundance and on the ^{207}Pb-labelled compound (**3***) reveal a large Pb,Pb coupling constant of 7708 Hz, indicative of a covalent Pb−Pb bond. − Though $InCl_3$ is diagonally related to $PbCl_2$, no significant redox process is observed in the reaction between $InCl_3$ and **1**. The yellow crystals of $[In^{3+}(Ph_2P{=}N{=}PPh_2^-)_3]$ (**4**) that are obtained were also investigated by X-ray analysis. These show a propeller-like configuration of the three four-membered chelate rings with indium(3+) as the centre.

Previously[2][3][4] we published data on the unusual *oxidative splitting* and scrambling of lithium bis(diphenylphosphanyl)amide, $LiN(PPh_2)_2$ (**1**)[5][6][7][8], by MCl_2 (M = Co, Fe, Ni, Pd, Pt) that resulted in spirocyclic[2][3] and bicyclic[4] complexes of the types A, B, and C (Scheme 1). In contrast, the *oxidative coupling* of **1** with iodine[9] leads to the P−P coupled diphosphazene $Ph_2P-N{=}PPh_2-PPh_2{=}N-PPh_2$ (**2**), that can also be obtained by the reaction of **1** with anhydrous iron(3+) fluoride, copper(2+) fluoride[10], bismuth tribromide or antimony triiodide[11]. On the other hand, a mixture of arsenic triiodide and **1** in the molar ratio of 1:2 reacts at 20°C to yield **2** and the As(1+) complex D[11].

As a part of our studies on the chemical behaviour of **1** towards metal halides, we now report on the reaction of **1** with $PbCl_2$ and $InCl_3$, the latter having a diagonal relationship with $PbCl_2$.

Scheme 1

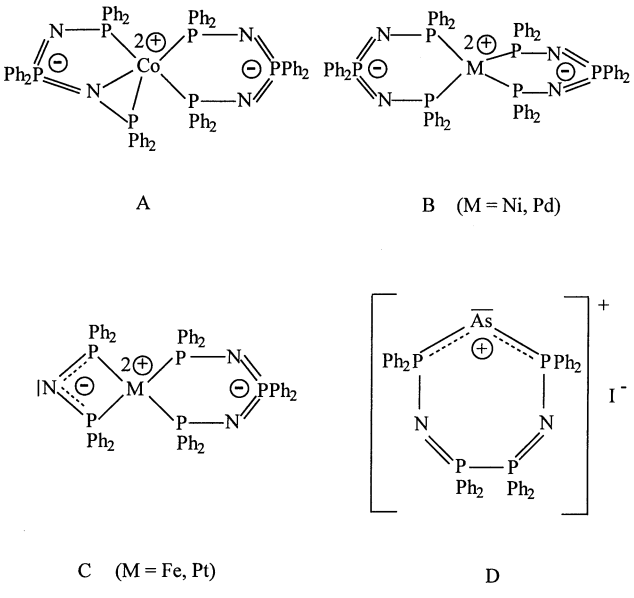

The Binuclear Lead(1+) Complex

The reaction of lead dichloride with two equivalents of **1** at −78°C, allowed to warm up to 20°C, in THF affords the diphosphazene **2** and a new complex, **3,** with lead in the rare oxidation state of 1+ (Scheme 2).

[◇] Part 128: Ref.[1].
[+] Present address: Instituto de Quimica, Universidad Nacional Autonoma de Mexico, Circuito Exterior, Ciudad Universitaria, 04510, Mexico D. F. (Mexico).

 © WILEY-VCH Verlag GmbH, D-69451 Weinheim, 1998 1434−1948/98/437−444 $ 17.50+.50/0

Scheme 2

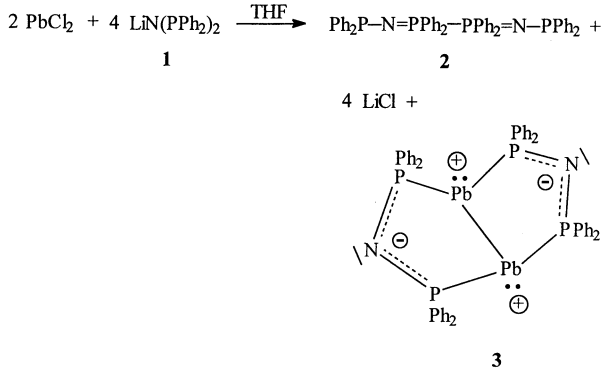

Compounds **2** and **3** can be isolated as pale yellow and deep red crystals, respectively, from THF by precipitation with *n*-pentane. In order to separate **2** and **3,** the crystal conglomerate was treated with cold toluene, in which **3** dissolves. Compound **2** was filtered off and identified by infrared spectroscopy[11].

Crystallization of **3** from toluene by slow solvent diffusion with *n*-pentane yielded large red rhombic crystals which were suitable for X-ray structural analysis.

The result of the structure determination of **3** is shown in Figure 1. The molecule contains a $[Pb^{1+}-Pb^{1+}]$ unit with an interatomic distance of 304.1(1) pm, which is considerably shorter than the interatomic Pb···Pb distance (349 pm)[12] in metallic lead. This indicates the possibility of a covalent $Pb^{1+}-Pb^{1+}$ bond in **3**, and this is confirmed by the ^{207}Pb-NMR spectrum of the ^{207}Pb-labelled **3** (= **3***) which shows a large ^{207}Pb,^{207}Pb coupling constant of 7708 Hz (see later). In the polylead anions Pb_5^{2-}, Pb_7^{4-}, Pb_9^{4-}, and in organometallic diplumbanes of type $R_3Pb-PbR_3$ (R = Ph, *c*-C_6H_{11}) Pb−Pb distances in the range of 284−324 pm are found[13]. The Pb(1)−Pb(2) bond of **3** is bridged by two bis(diphenylphosphanyl)amide anions, $[N(PPh_2)_2]^-$, forming a butterfly-like structure with P(1)−Pb(1)−P(4) and P(2)−Pb(2)−P(3) angles of 93.7(2)° and 95.5(2)°, respectively. All other angles at the Pb(1) and Pb(2) atoms also approach the "p-only" value of 90°. Therefore, the two vicinal lone electron pairs at the lead atoms (Scheme 2) have mainly s-character.

The average P−N bond length of 160(2) pm, which is typical for complexes with the *bridging* $[N(PPh_2)_2]^-$ entity[14][15][16], indicates a considerable amount of double-bond character. The two five-membered rings connected by the Pb(1)−Pb(2) bond show significant deviations from planarity (Figure 2). Whereas in the Pb(1)−P(1)−N(1)−P(2)−Pb(2) ring the P(1) atom is displaced by 30 pm from the least-squares plane, the deviation for the P(3) atom in the homologous Pb(1)−P(4)−N(2)−P(3)−Pb(2) ring is 26 pm. The dihedral angle between the two least-squares planes calculated for the two five-membered rings amounts to 89.4°. The P−N−P angles of 123.4(9)° and 125.2(11)°, respectively, are the same as those found in $(THF)_3LiN(PPh_2)_2$ [124.7(3)°][8].

Figure 1. Molecular structure (ORTEP plot) of **3**[a]

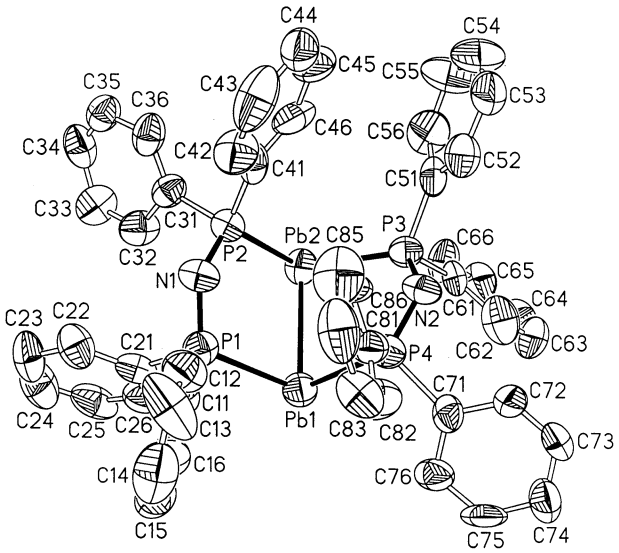

[a] Selected bond lengths [pm] and angles [°]: Pb(1)−P(1) 273.6(6), Pb(1)−P(4) 278.0(6), Pb(1)−Pb(2) 304.10(13), Pb(2)−P(3) 270.9(6), Pb(2)−P(2) 274.0(6), P(1)−N(1) 160(2), P(1)−C(11) 180(2), P(1)−C(21) 181(2), P(2)−N(1) 160(2), P(3)−N(2) 163(2), P(4)−N(2) 158(2); P(1)−Pb(1)−P(4) 93.7(2), P(1)−Pb(1)−Pb(2) 84.94(13), P(4)−Pb(1)−Pb(2) 88.93(12), P(3)−Pb(2)−P(2) 95.5(2), P(3)−Pb(2)−Pb(1) 84.32(12), P(2)−Pb(2)−Pb(1) 88.30(12), C(11)−P(1)−C(21) 99.7(10), N(1)−P(1)−Pb(1) 116.9(7), C(11)−P(1)−Pb(1) 113.6(8), C(21)−P(1)−Pb(1) 105.6(8), N(2)−P(3)−Pb(2) 120.1(7), N(2)−P(4)−Pb(1) 114.6(7), P(1)−N(1)−P(2) 123.4(9), P(4)−N(2)−P(3) 125.2(11).

Figure 2. Arrangement and distortion of the five-membered rings in **3**

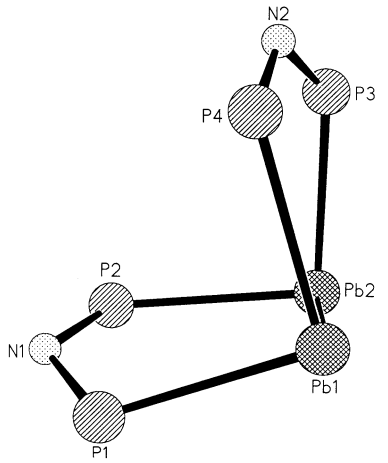

^{31}P- and ^{207}Pb-NMR Spectra

Whereas phosphorus is an element consisting of a pure isotope (100% ^{31}P, spin $I = 1/2$), lead consists of only 22.4% of the isotope ^{207}Pb (spin $I = 1/2$). Other stable lead isotopes are magnetically inactive (spin $I = 0$). Hence, according to the binomial coefficients, the natural isotope abundance distribution in **3** is 61%, 34%, and 5% for the presence of zero, one, and two ^{207}Pb isotopes, respectively.

The skeleton of magnetically active P and Pb nuclei in **3** is shown in Figure 3. For the sake of convenience we use the numbering shown in Figure 3 in the following discussion. In

the trivial case of the major isotopomer in which no ^{207}Pb isotope is present, the four ^{31}P nuclei are equivalent and give rise to a singlet at $\delta = 60.7$ in the ^{31}P-NMR spectrum (c.f. Figure 4). In the isotopomer shown in Figure 3a, with one ^{207}Pb isotope, an AA′A′′A′′′X spin system (A = A′ = A′′ = A′′′ = ^{31}P; X = ^{207}Pb) is present which results in rather complex ^{31}P and ^{207}Pb spectra (Figures 4a and 5a). Of crucial interest is the isotopomer with the lowest abundance, in which two ^{207}Pb nuclei are present (Figure 3b): here, an AA′A′′A′′′XX′ spin system exists with complex ^{31}P and ^{207}Pb spectra that are entirely different from those arising from the presence of only one ^{207}Pb isotope (Figures 4b and 5b).

Figure 3. Skeleton of magnetically active P and Pb nuclei in **3**. a) Isotopomer with one ^{207}Pb; b) isotopomer with two ^{207}Pb

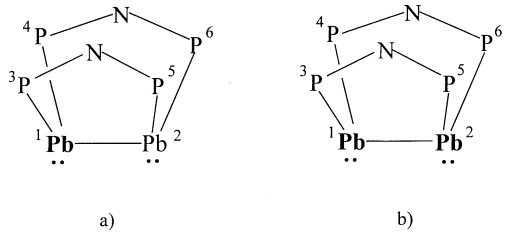

Figure 4. Simulated (a−c) and experimental (d) ^{31}P-NMR spectrum of **3**, natural isotope abundance, C_6D_6, satd. solution, +23°C. Spectrum (c) is a superposition of spectrum (a) (mono-^{207}Pb isotopomer) and spectrum (b) (bis-^{207}Pb isotopomer) with scaling to the appropriate isotopomer abundances. Signals in spectrum (d) which do not match the signals of the simulated spectrum are due to impurities from thermal decomposition

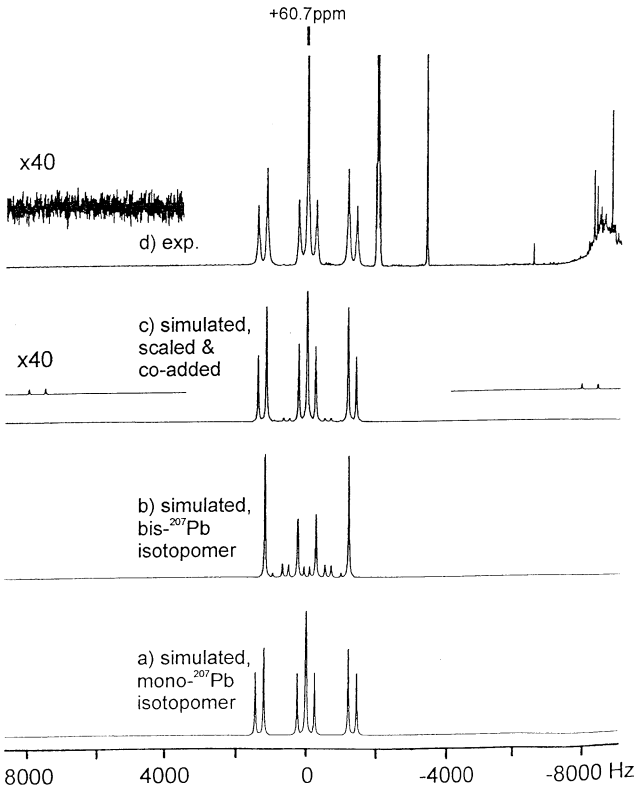

In order to elucidate the coupling constants involved, the ^{31}P- and ^{207}Pb-NMR spectra were simulated for the isotopomers with one and with two ^{207}Pb nuclei (Figures 4 and 5). The simulated spectra were scaled according to the abundances of the isotopomers and superimposed (Figures 4c and 5c). The corresponding experimental spectra are shown in Figures 4d and 5d. The ^{31}P- and ^{207}Pb-chemical shifts are $\delta = 60.7$ and $\delta = -608.0$, respectively. It should be noted that the simulation software employed cuts off signals below a certain intensity. Hence, simulations by using different software may reveal additional weak signals.

Figure 5. Simulated (a−c) and experimental (d) ^{207}Pb-NMR spectrum of **3**, natural isotope abundance, C_6D_6, satd. solution, +23°C. Spectrum (c) is a superposition of spectrum (a) (mono-^{207}Pb isotopomer) and spectrum (b) (bis-^{207}Pb isotopomer) with scaling to the appropriate isotopomer abundances

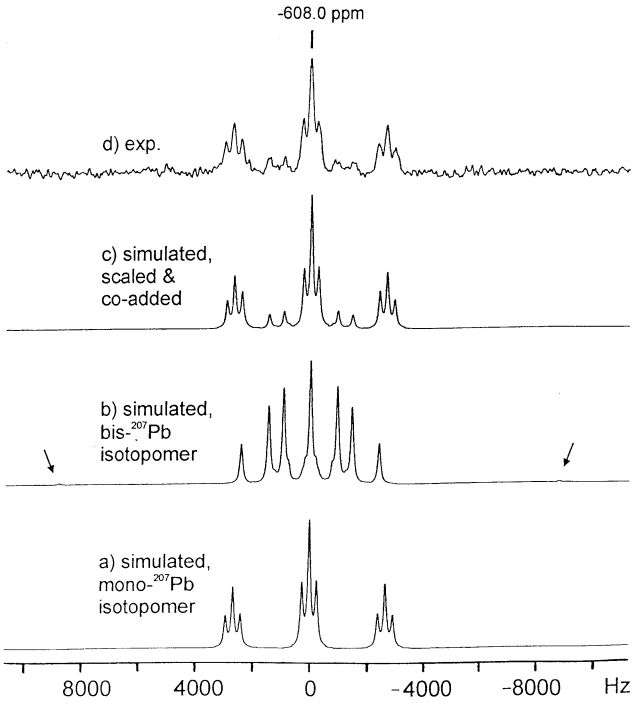

The coupling constants J_{13}, J_{15}, and J_{35} were relatively easily determined after some variation cycles. By contrast, the coupling constant "of interest", J_{12}, manifests only as very weak "satellites", which are visible in the simulation only after a large zoom of the vertical scale (Figures 4c and 5b). Variation of J_{12} over a wide range results in no significant changes in the center "multiplet". In the experimental ^{31}P and ^{207}Pb spectra of the natural abundance material these satellites are completely lost in the spectrum noise.

The simulated spectra are not sensitive to the sign of the homonuclear couplings J_{12} and J_{35} (J_{46}). Permutations of the signs of these coupling constants resulted in absolutely identical spectra. Hence, it is not possible to determine the signs of these coupling constants from the simulations. In contrast, the simulated spectra are sensitive to the relative signs of the heteronuclear coupling constants J_{13} and J_{15}. The simulations clearly indicate that the signs of J_{13} and J_{15} are unlike. Although many one bond (^1J)Pb,Pb couplings have been measured[17], the sign has been determined only recently[18] for a larger variety of compounds. Thus, J_{12} is

negative throughout for, e.g., tBu$_3$Pb-PbR$_3$ (R = Me, Et, iPr, n-C$_6$H$_{11}$, c-C$_6$H$_{11}$) and amounts up to −9200 Hz for R = n-C$_6$H$_{11}$. Only in Pb$_2$Me$_6$ J_{12} has been found to be positive[19]. It is save to assume that J_{12} is negative in **3**, especially when the influence of the 6s electron pairs is taken into account[20][21]. Tentatively, we hold the same to be true for J_{13} in **3**. Accordingly, the geminal coupling constant J_{15} must be positive.

In order to make visible the very weak "satellite" signals which are indicative of the Pb,Pb coupling constant in **3**, we carried out isotopic labelling. The synthesis of the labelled material is shown in Scheme 3. The ^{207}Pb-labelled compound is referred to as **3*** in the following text.

Scheme 3

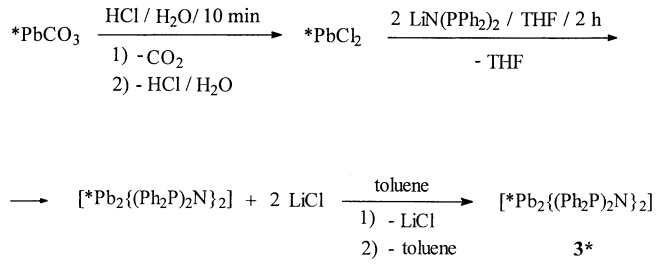

The ^{207}Pb enrichment of the initially employed ^{207}PbCO$_3$ is 92.8%. Hence, the distribution of the isotopomers of **3*** with zero, one, and two ^{207}Pb nuclei is 0.5%, 13.3%, and 86.2%, respectively. As for the ^{31}P- and ^{207}Pb-NMR measurements of the natural abundance material, crystals of **3*** were dissolved in [D$_6$]benzene. Due to the limited thermal stability of **3*** the ^{31}P spectrum (Figure 6d) is blurred due to the presence of signals from decomposition products. Unfortunately, these overlap heavily with the "satellite" signals of interest (Figure 6c) which would be indicative of the magnitude of the Pb,Pb coupling. Hence, even for the ^{207}Pb-labelled compound the relevant constant J_{12} could not be extracted from the ^{31}P spectrum.

Fortunately, however, the ^{207}Pb spectrum of **3*** (Figure 7d) finally yielded the desired information. The overall measuring time of this ^{207}Pb spectrum was 126 h. Spectra of several freshly prepared samples were superimposed. Although ^{207}Pb is generally a nucleus that is easy to detect, the broadness of the signals generally leads to a poor signal-to-noise ratio. This broadness is very likely due to chemical shift anisotropy (CSA) relaxation, a well known phenomenon with high field spectrometers[22]. When the simulation is carried out using the Pb,Pb coupling constant $|J_{12}|$ = 7708 Hz, the outer satellites in Figures 7b and 7c match the experimentally observed ones in Figure 7d.

Table 1 summarizes the results of the spin simulations. Diagonal numbers represent chemical shifts whereas off-diagonal numbers indicate coupling constants.

The large Pb,Pb coupling constant of 7.7 kHz clearly indicates that a covalent Pb−Pb bond must be present in **3**. Therefore, complex **3** bears a remote resemblance to [Ge$_2${C(SiMe$_3$)(PMe$_2$)$_2$}$_2$], which contains a covalent Ge−Ge bond[23].

Figure 6. Simulated (a−c) and experimental (d) ^{31}P-NMR spectrum of **3***, isotopically labelled by 92.8% ^{207}Pb, C$_6$D$_6$, satd. solution, +23°C. Spectrum (c) is a superposition of spectrum (a) (mono-^{207}Pb isotopomer) and spectrum (b) (bis-^{207}Pb isotopomer) with scaling to the appropriate isotopomer abundances. Signals in spectrum (d) which do not match the signals of the simulated spectrum are due to impurities from thermal decomposition

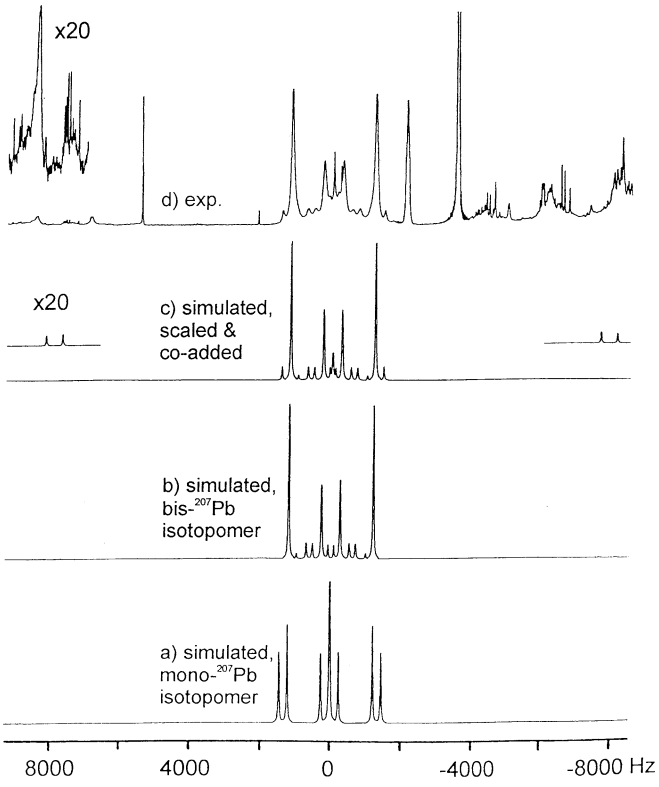

The ^{1}H-NMR spectrum of **3** is simple and does not have any unusual features. As a result of P,C coupling, the resonances for C-i and C-o of the phenyl groups in the ^{13}C{^{1}H}-NMR spectrum are split into multiplets. The IR spectroscopic data of **3** are listed in the Experimental Section. The assignments of the P−C$_6$H$_5$ modes[6] are based on the Whiffen nomenclature[24] in the more currently used description of Maslowsky[25]. The mass spectrum (EI) of **3** does not show the molecular ion peak of **3**$^+$, but instead shows the [M − PPh] fragment along with various peaks due to P−N and P−Ph fragments.

It is also worth pointing out that ligands which are similar to our system, i. e. [N(SiMe$_3$)$_2$]$^-$, [N(SiMe$_3$)(CMe$_3$)]$^-$, [N(SPPh$_2$)$_2$]$^-$, and [CH(PPh$_2$)$_2$]$^-$ generally yield different complexes with the lower main group-15 metal(2+) halides, e. g. [Pb{N(SiMe$_3$)$_2$}$_2$][26], [Pb{N(SiMe$_3$)(CMe$_3$)}$_2$][27], [Sn{N(SiMe$_3$)$_2$}$_2$][28], [Pb{(SPPh$_2$)$_2$N}$_2$][29], [Sn{CH(PPh$_2$)$_2$}$_2$][30], or [Pb{CH(PPh$_2$)$_2$}$_2$][30][31][32].

The Mononuclear Indium(3+) Complex

Reaction of InCl$_3$ with LiN(PPh$_2$)$_2$ (**1**) in the molar ratio of 1:3 in THF at 20°C affords LiCl and the yellow complex [In(Ph$_2$P=N=PPh$_2^-$)$_3$] (**4**), which was isolated after separation from LiCl with benzene/n-pentane as yellow moisture-sensitive crystals. These crystals were suitable for an X-

Figure 7. Simulated (a−c) and experimental (d) ^{207}Pb NMR spectrum of **3***, isotopically labelled by 92.8% ^{207}Pb, C_6D_6, satd. solution, +23°C. Spectrum (c) is a superposition of spectrum (a) (mono-^{207}Pb isotopomer) and spectrum (b) (bis-^{207}Pb isotopomer) with scaling to the appropriate isotopomer abundances

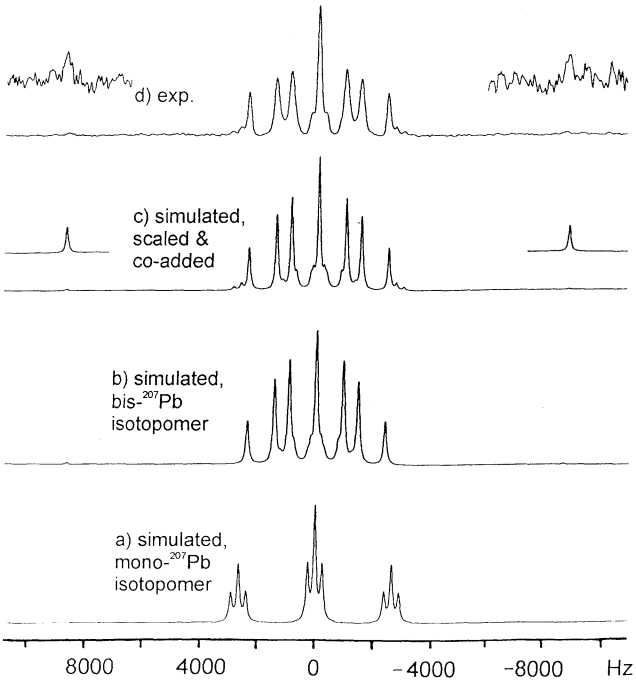

Table 1. ^{31}P- and ^{207}Pb-chemical shifts (δ, diagonal, ppm) and coupling constants (*J*, off-diagonal, Hz) in **3** and **3***, respectively, as derived from spectra simulations. The signs of the coupling constants are tentative (see text), however, it is certain that J_{13} (J_{14}, J_{25}, J_{26}) and J_{15} (J_{16}, J_{23}, J_{24}) have unlike signs

Nucleus #	1	2	3	4	5	6
1	−608.0	−7708	−2660	−2660	+240	+240
2		−608.8	+240	+240	−2660	−2660
3			+60.7	0	+240	0
4				+60.7	0	+240
5					+60.7	0
6						+60.7

ray crystal analysis. Surprisingly there is no reduction of $InCl_3$ to indium(1^+) derivatives by **1**.

The crystal structure determination shows that compound **4** consists of a tricyclic ring system with indium(3+) as the centre (Figure 8).

At the indium centre the four-membered P−N−P−In chelate rings are oriented in a propeller-like conformation. The main deviation from a regular octahedral arrangement is caused by the fact that the P−In−P angle for each bidentate $[N(PPh_2)_2]^-$ ligand is close to 58°. In the four-membered ring In(1)−P(3)−N(2)−P(4), the differences between the two P−N and In−P bond lengths as well as the two In−P−N angles are small. These differences in the related bond distances and angles increase in the In(1)−P(1)−N(2)−P(2) ring and are remarkable in the In(1)−P(5)−N(3)−P(6) ring [e.g. P(5)−N(3): 167.3(6), P(6)−N(3): 158.7; In(1)−P(5): 284.7(2), In(1)−P(6): 273.9(2) pm; In(1)−P(5)−N(3): 91.8, In(1)−P(6)−N(3): 97.9(2)°]. Accordingly, the tris(chelate) **4** does not contain a threefold symmetry axis and shows only C_1 symmetry. This clearly demonstrates that an octahedral or trigonal prismatic coordination polyhedron is not expected for **4**. The stereochemistry of complexes with coordination number 6 depends mainly on the normalized bite "*b*" of the bidentate ligand[33], which is defined in the case under discussion as *b* = P···P/In−P (distance between the donor atoms of the chelate/metal-donor atom distance). For the three four-membered rings mentioned above the *average* and normalized bites "*b*" are 1.02, 1.01, and 1.03, respectively. They are near the lowest limit known to date for tris(chelate) complexes with four-membered rings (*b* = 1.05 to 1.25)[33], e.g. $[Co(Ph-N=N-N-Ph^-)_3]$[34] *b* = 1.07[33]. The exceptional structure of **4** has no relationship with regular coordination polyhedras and is therefore best described as "propeller-like". The average value of the P−N bond lengths is 164.0(6) pm, and this is typical for complexes with the *chelating* $[N(PPh_2)_2]^-$ entity[4] and indicates π-electron delocalization.

Figure 8. Molecular structure (ORTEP plot) of **4**[a]

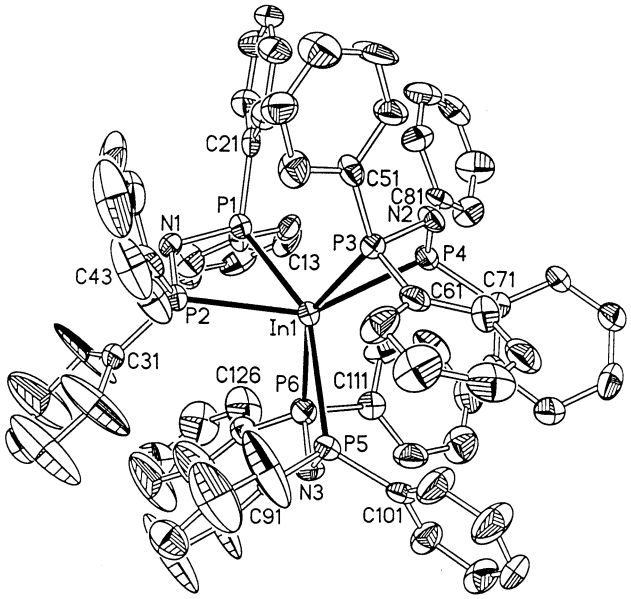

[a] Selected bond lengths [pm] and angles [°]: In(1)−P(1) 272.4(2), In(1)−P(6) 273.9(2), In(1)−P(4) 277.0(2), In(1)−P(2) 277.5(2), In(1)−P(3) 279.5(2), In(1)−P(5) 284.7(2), P(1)−N(1) 164.5(6), P(1)−C(21) 180.4(9), P(1)−C(11) 182.1(8), P(2)−N(1) 162.9(6), P(3)−N(2) 165.2(5), P(4)−N(2) 165.7(6), P(5)−N(3) 167.3(6), P(6)−N(3) 158.7(6), P(1)···P(2) 270.5(3), P(3)···P(4) 272.9(3), P(5)···P(6) 270.2(3); P(1)−In(1)−P(6) 101.14(7), P(1)−In(1)−P(4) 96.69(7), P(6)−In(1)−P(4) 106.61(6), P(1)−In(1)−P(2) 58.93(6), P(6)−In(1)−P(2) 99.34(6), P(4)−In(1)−P(2) 147.65(7), P(1)−In(1)−P(3) 105.26(7), P(6)−In(1)−P(3) 150.96(7), P(4)−In(1)−P(3) 58.71(6), P(2)−In(1)−P(3) 104.48(7), P(1)−In(1)−P(5) 149.72(7), P(6)−In(1)−P(5) 57.80(7), P(4)−In(1)−P(5) 109.65(6), P(2)−In(1)−P(5) 100.35(6), P(3)−In(1)−P(5) 101.17(7), N(1)−P(1)−C(21) 108.8(3), N(1)−P(1)−C(11) 109.3(3), C(21)−P(1)−C(11) 102.7(4), N(1)−P(1)−In(1) 95.3(2), C(21)−P(1)−In(1) 124.3(3), N(1)−P(2)−In(1) 93.8(2), N(2)−P(3)−In(1) 93.9(2), N(2)−P(4)−In(1) 94.7(2), N(3)−P(5)−In(1) 91.8(2), N(3)−P(6)−In(1) 97.9(2), P(2)−N(1)−P(1) 111.4(3), P(3)−N(2)−P(4) 111.1(3), P(6)−N(3)−P(5) 111.9(4).

Because it was impossible to record an IR spectrum in KBr under nitrogen, the air moisture caused sample decomposition during scanning, resulting in formation of $HN(PPh_2)_2$ (**5**) and decolorization. Compound **5** was identified by its IR spectrum[6]. It was not possible to anneal NMR tubes and so the NMR spectra of **4** contain signals of the impurity **5**.

This work was supported by the *Deutsche Forschungsgemeinschaft*, the *Fonds der Chemischen Industrie*, and the *Zerweck-Fonds* of the University of Erlangen-Nuernberg. We are also grateful to Prof. Dr. *D. Sellmann* for technical support concerning the X-ray analyses. We thank Prof. Dr. *B. Wrackmeyer* for valuable discussions. Dr. *V. Garcia-Montalvo* acknowledges *CONACYT* (Consejo Nacional de Ciencia y Tecnologia, México) for a post doctoral visiting fellowship.

Experimental Section

General: All operations were carried out under an atmosphere of pre-purified dry dinitrogen using standard Schlenk and vacuum line techniques. Solvents were dried and purified prior to use by conventional methods. Chemicals of the best available commercial grade were used: *n*-butyllithium (1.6 M solution in *n*-hexane, Merck-Schuchardt), $PbCl_2$ (Aldrich), $^{207}PbCO_3$ (Campro Scientific), $InCl_3$ (Aldrich). $HN(PPh_2)_2$ (**5**) was prepared according to literature procedures[6][35]. − IR: Perkin Elmer 983. − The NMR spectra of **3** and **3*** were recorded on a JEOL Alpha 500 spectrometer (11.7 Tesla) at 104.7 MHz (^{207}Pb) and 202.4 MHz (^{31}P), respectively. ^{207}Pb-NMR spectra are referenced to $Pb(NO_3)_2$ $\delta = -2961$ as a secondary reference ($PbMe_4$ $\delta = 0$). ^{31}P-NMR spectra are referenced to 85% H_3PO_4. No corrections for bulk susceptibilities have been applied. Samples of natural abundance and isotopically labelled compounds were prepared as saturated solutions of crystalline material in C_6D_6. Measurements were carried out at +23°C. A multinuclear 5 mm probehead was employed. ^1H-broadband decoupling was applied throughout. Samples were non-spinning. Spectral widths were 60 kHz (^{207}Pb) and 38 kHz (^{31}P), respectively. Recycle delays were 5 s (^{207}Pb) and 2.5 s (^{31}P). Pulse widths were 90° (13 μs, ^{207}Pb) and 60° (8 μs, ^{31}P). Measuring times were 43 h (Figure 4), 258 h (Figure 5), 20 h (Figure 6), and 126 h (Figure 7). Due to the thermal instability of **3** and **3***, the spectra of several freshly prepared samples were superimposed. Spectrum simulations were performed using the COMIC software package (JEOL). A Lorentzian line width of 30 Hz was used to match the experimental spectra. NMR of **4**: JEOL JNM-GX-270 (269.60 MHz for ^1H, 69.70 MHz for $^{13}C\{^1H\}$, 109.40 MHz for $^{31}P\{^1H\}$). Chemical shifts are relative to solvent signals, which in turn are referenced to TMS; for $^{31}P\{^1H\}$ NMR, 85% H_3PO_4 was employed as external standard. − MS: Varian MAT 212 (70 eV). − Microanalyses: Carlo Erba 1106 and 1108. − Melting points (uncorrected): Electrothermal IA 6304.

Preparation of Bis-μ-[bis(diphenylphosphanyl)amido-P,P']dilead(1+)(Pb−Pb) (**3**) *and Separation from 1.1.3.3.4.4.6.6-Octaphenyl-2.5-diaza-1.6-($\sigma^3\lambda^3$)diphospha-3.4-($\sigma^4\lambda^5$)diphosphahexane* (**2**): To a solution of 1.72 g (4.47 mmol) of $HN(PPh_2)_2$ (**5**) in 35 ml of THF was added 2.80 ml (4.48 mmol) of *n*-butyllithium (1.6 M solution in *n*-hexane) and the mixture was stirred for 30 min at −78°C. After addition of 0.62 g (2.23 mmol) of solid $PbCl_2$ and removal of the refrigerant, the colour of the suspension slowly changed from light yellow to deep red, while the mixture became a clear solution. Stirring was continued for 3 h at 20°C, then one third of the solvent was removed in vacuo. The residual clear deep red solution was layered with 85 ml of *n*-pentane and kept at 20°C for 5 d; deep red rhombic crystals of **3** and yellow cubes of **2** crystallized simultaneously. The two compounds were separated by decanting the solvent mixture of THF and *n*-pentane and treating the crystal conglomerate with cold toluene. While **3** dissolved, **2** was filtered off, washed with cold toluene and dried in vacuo to yield 0.45 g (52%). Mp. 155°C, mp.[10] 157°C.

Recrystallization of **3** from toluene by slow solvent diffusion (*n*-pentane) techniques afforded large red rhombic crystals after 3 d at 20°C; yield 0.84 g (63%), m.p. 140°C (dec.).

$Ph_2P-N=PPh_2-PPh_2=N-PPh_2$ (**2**): IR (KBr): $\tilde{\nu} = 3080\ cm^{-1}$ (w sh) + 3055 (w-m), 3030 (vw), 3025 (w) + 3010 (vw sh) [ν(CH)], 1586 (w-m) [ν(CC)k], 1568 (w) [ν(CC)l], 1475 (m) [ν(CC)m], 1431 (s) [ν(CC)n], 1389 (w) [2 × ϕ(CC)v], 1313 (w sh) + 1303 (w-m) [ν(CC)o], 1275 (w-m) [δ(CH)e], 1185 (vs), 1170 (vs) [ν(P=N)] + 1160 (s sh) [δ(CH)c], 1102 (m-s) [P^{IV}−Ph sens. q], 1090 (s) [P^{III}−Ph sens. q], 1068 (m) [δ(CH)d], 1027 (m) [δ(CH)b], 999 (w-m) [γ ring p, Ph], 975 (w) [γ(CH)j], 935 (vw) [γ(CH)h], 920 (w-m) [γ(CH)i], 848 (w) [γ(CH)g], 745 (s) [γ(CH)f], 720 (m-s), 714 (m-s) [P^{IV}−Ph sens. r], 699 (s) [P^{III}−Ph sens. r], 691 (m-s) [ϕ(CC)v], 661 (m-s) [ν(P−P) + γ(PNP)], 619 (w) + 605 (sh) [δ(CCC)s], 519 (m-s), 508 (s), 490 (m-s) [P−Ph sens. y], 458 (m-s), 441 (m) [P−Ph sens. t], 410 (w), 397 (w) [γ(CC)w], 382 (m), 371 (m) [δ(PNP)].

(**3**): IR (KBr): $\tilde{\nu} = 3070\ cm^{-1}$ (w-m sh) + 3055 (m), 3005 (w), 2990 (vw) [ν(CH)], 1585 (w-m) [ν(CC)k], 1570 (w-m) [ν(CC)l], 1478 (m) [ν(CC)m], 1432 (s) [ν(CC)n], 1385 (w) [2 × ϕ(CC)v], 1330 (w), 1305 (w) [ν(CC)o], 1275 (w) [δ(CH)e], 1180 (w-m) [δ(CH)a], 1159 (w-m) [δ(CH)c], 1128 (s) [ν(P⩬N)], 1105 (m-s), 1099 (m-s), 1088 (m-s) [P−Ph sens. q + ν(P⩬N)], 1070 (w-m) + 1048 (w) [δ(CH)d], 1026 (m) [δ(CH)b], 999 (w-m) [γ ring p, Ph], 970 (w) [γ(CH)j], 930 (vw) [γ(CH)h], 918 (vw) [γ(CH)i], 884 (w-m, br) [ν(P−N)], 850 (w) [γ(CH)g], 780 (m) [ν(P−N)], 748 (m), 738 (m-s) [γ(CH)f], 699 (vs) + 692 (s sh) [P−Ph sens. r + ϕ(CC)v], 620 (w), 603 (w) [δ(CCC)s], 555 (w), 548 (w-m) [γ(P⩬N⩬P)], 520 (vs), 490 (w-m), 480 (m) [P−Ph sens. y], 457 (w-m), 426 (m), 411 (w-m) [P−Ph sens. t], 376 (w), 358 (vw) [δ(NP_2)]. − ^1H NMR (C_6D_6, 21°C): δ = 6.45−6.90 (m, aromatic H). − $^{13}C\{^1H\}$ NMR (C_6D_6, 25°C): δ = 127.84 (s, C-*m*, Ph), 127.93 (s, C-*m*, Ph), 128.65 (s, C-*p*, Ph), 129.42 (s, C-*p*, Ph), 131.61 (m, C-*o*, Ph), 132.38 (m, C-*o*, Ph), 140.6 (m, C-*i*, Ph), 144.1 (m, C-*i*, Ph). − $^{31}P\{^1H\}$ NMR (C_6D_6, 22°C): δ = 58.9 (s). − EI-MS (70 eV, ref. to ^{208}Pb): *m/z* (%): 1076 (0.04) [M^+ − PPh], 768 (25) [**2**$^+$], 691 (6) [**2**$^+$ − Ph], 597 (65) [$(Ph_2PN)_3^+$], 583 (65) [$Ph_2P-N=PPh_2-N=PPh_2^+$], 520 (65) [$(Ph_2PN)_3^+$ − Ph], 460 (22) [$(Ph_2P)_2NPh^+$ − H], 384 (100) [$Ph_2P=N-PPh_2^+$], 306 (65) [$Ph_2P=N-Ph^+$], 262 (65) [PPh_3^+], 183 (92) [$(C_6H_4)_2P^+$], 122 (64) [$N\equiv P-Ph^+$]. − $C_{48}H_{40}N_2P_4Pb_2$ (1183.1): calcd. C 48.73, H 3.41, N 2.37; found C 49.14, H 3.45, N 2.38.

Preparation of [$^{207}Pb_2$(μ-$Ph_2P-N-PPh_2$−P,P')$_2$] (**3***): 0.155 g (0.580 mmol) of $^*PbCO_3$ was mixed with 12 ml of a concentrated aqueous solution of HCl. After the initially brisk foaming up had ceased the clear colourless solution was stirred for 10 min at 20°C. The solvent was removed under reduced pressure and the resulting $^*PbCl_2$ was dried at 100°C in vacuo for 4 h to exclude any traces of water. A conversion of 100% from $^*PbCO_3$ to $^*PbCl_2$ was assumed. 0.447 g of $HN(PPh_2)_2$ (**5**, 1.160 mmol) in 7 ml of THF was lithiated with 0.80 ml (1.280 mmol) of *n*-butyllithium (1.6 M solution in *n*-hexane), and the yellow solution was added to the solid $^*PbCl_2$ prepared as described above. After stirring for 2 h at 20°C the solvent from the red solution was evaporated in vacuo and the red residue was suspended in 7 ml of toluene for the separation of LiCl. Filtration with a D4 filter was followed by removal of the solvent from the filtrate to yield the red product [$^*Pb_2\{(Ph_2P)_2N\}_2$] that had traces of the by-product $Ph_2P-N=$

$PPh_2-PPh_2=N-PPh_2$ (**2**) as an impurity, but was nevertheless used for NMR experiments. Due to the low yield of the product [$*Pb_2\{(Ph_2P)_2N\}_2$] and its sensitivity to moisture, oxygen and various solvents we decided not to perform further purification. Yield 0.419 g (61%). The residue of the filtration consisted of traces of $Ph_2P-N=PPh_2-PPh_2=N-PPh_2$ (**2**) and LiCl that was detectable by $AgNO_3$ and flame spectrum.

Preparation of Tris[bis(diphenylphosphanyl)amido-P,P']-indium(3+) (**4**): To a solution of 1.49 g (3.87 mmol) of $HN(PPh_2)_2$ (**5**) in 50 ml of THF was added 2.60 ml (4.16 mmol) of *n*-butyllithium (1.6 M solution in *n*-hexane) and the mixture was stirred for 15 min at 20°C. Addition of 0.29 g of $InCl_3$ (1.29 mmol) resulted in a yellow suspension that turned into a clear yellow solution within 6 h. The solvent was removed in vacuo and the bright yellow residue was separated from LiCl by suspending it in 30 ml of benzene and filtering the mixture. The clear yellow filtrate was layered with 120 ml of *n*-pentane; after 48 h yellow crystals precipitated which were filtered off, washed with 5 ml of *n*-pentane and dried in vacuo, yielding 1.19 g (73%) of [$In\{(Ph_2P)_2N\}_3$], m.p. 182°C. – The crystals were suitable for an X-ray analysis. – ^1H NMR (C_6D_6, 21.5°C): δ = 7.65–6.60 (m, aromatic H), 3.55 (m, traces of THF), 3.02 (m, NH due to traces of moisture during sample preparation), 1.40 (m, traces of THF). – $^{13}C\{^1H\}$ NMR (C_4D_8O, 24.4°C): δ = 144.15 (m, C-*i*, Ph), 132.10 (pseudo-t, C-*o*, Ph), 129.05 (s, C-*p*, Ph), 128.75 (pseudo-t, C-*m*, Ph). – $^{31}P\{^1H\}$ NMR (C_6D_6, 22.0°C): δ = 80.06 (s); 40.74 [s, ≈ 5% of $(Ph_2P)_2NH$ due to traces of moisture during sample preparation]. – EI-MS (70 eV): *m/z* (%): 1270 (1.8) [$In\{HN(PPh_2)_2\}_3^+$], 385 (95) [$HN(PPh_2)_2^+$], 262 (95) [PPh_3^+]. – $C_{72}H_{60}InN_3P_6$ (1267.9): calcd. C 68.20, H 4.77, N 3.31; found C 67.54, H 5.15, N 2.89.

Table 2. Crystal data, data collection, and structure refinement for the complexes **3** and **4** (Siemens P4, Mo-K_α, 0.71073 A, graphite monochromator)

	3	**4**
Crystal data		
Formula	$C_{48}H_{40}N_2P_4Pb_2$	$C_{72}H_{60}InN_3P_6$
M_r	1183.08	1267.87
Crystal system	orthorhombic	orthorhombic
Space group	$P2_12_12_1$	$P2_12_12_1$
Crystal dimensions [mm]	0.80 × 0.60 × 0.60	0.50 × 0.30 × 0.20
a [pm]	1456.3(5)	1448.1(2)
b [pm]	3095 (1)	1452.6(5)
c [pm]	987.9(3)	2916.1(6)
α = β = γ [°]	90	90
V [nm^3]	4.453(3)	6.134(3)
Z	4	4
ρ_{calc} [gcm^{-3}]	1.765	1.373
F(000)	2264	2608
μ [mm^{-1}] Absorption coeff.	7.730	0.588
Data collection		
T [K]	293	200(2)
Scan mode	ω	ω
hkl range	$0 \le h \le 18$	$-1 \le h \le 18$
	$0 \le k \le 39$	$-1 \le k \le 18$
	$-12 \le l \le 7$	$-1 \le l \le 37$
Measured reflns.	6201	8835
Indep. reflns.	6030 (R_{int} = 0.0439)	8551 (R_{int} = 0.0462)
Observed reflns. [$F_o \ge 4.0\sigma(F)$]	3174	4073
Refinement	Full-matrix least-squares on F^2	
Data / Restraints / Parameter	6030 / 0 / 505	8551 / 0 / 739
Goodness-of-Fit on F^2	0.802[a]	0.704[a]
Final *R*-values	*R*1 = 0.0638[b]	*R*1 = 0.0459[b]
[$I < 2\sigma(I)$]	*wR*2 = 0.1539	*wR*2 = 0.0752
R-values (all data)	*R*1 = 0.0887	*R*1 = 0.1130
	*wR*2 = 0.1605[c]	*wR*2 = 0.0868[f]
Absolute structure parameter	0.03(2)[d]	−0.06(3)[d]
ρ_{fin}(*max*/*min*)(eÅ^{-3})	2.2233/−2.810[e]	0.756/−0.529

[a] GooF = $S = [\Sigma\{w(F_o^2 - F_c^2)^2\}/(n-p)]^{1/2}$ with n = 6030 (**3**), 8551 (**4**) and p = 505 (**3**), 739 (**4**). – [b] $R1 = [\Sigma(||F_o| - |F_c||/\Sigma|F_o|]$. – [c] $wR2 = [\Sigma\{w(F_o^2 - F_c^2)^2\}/\Sigma\{w(F_o^2)^2\}]^{1/2}$. – $w = 1/[\sigma^2(F_o^2)+(0.0950\cdot P)^2]$. – $P = (F_o^2)+2(F_c^2)/3$. – [d] H. D. Flack, *Acta Cryst.* **1983**, *A39*, 876–881. – [e] Residual electron densities (lower to 0.9 eÅ^{-3}) located close to the Pb atoms. – [f] $w = 1/[\sigma^2(F_o^2)]$.

Crystal Structure Determinations: Suitable single crystals of **3** and **4** were sealed into glass capillaries and used for measurement of precise cell constants and intensity data collection. Three standard reflections measured periodically during data collection showed no significant changes. Diffraction intensities were corrected for Lorentz and polarization effects. In the case of **3**, absorption effects were corrected empirically using Psi-scans of 40 reflections (min transmission = 0.002; max. transmission = 0.013). To minimize remaining absorption effects an additional correction using ΔF^2 methods[36] was applied (min. transmission = 0.089; max. transmission = 0.146). No absorption correction was applied in the case of **4**. The structures were solved by direct methods and refined by full-matrix least-squares calculations against F^2[37]. All non-hydrogen atoms were refined with anisotropic displacement parameters. The hydrogen atom positions of **3** and **4** were calculated and allowed to ride on their corresponding carbon atoms, their isotropic thermal parameters were tied to those of the adjacent carbon atoms by a factor of 1.5. Details of the crystal data, data collection, and structure refinement are summarized in Table 2. Crystallographic data (excluding structure factors) for the structures reported in this paper have been deposited with the Cambridge Crystallographic Data Centre as supplementary publication no. CCDC-100811. Copies of the data can be obtained free of charge on application to The Director, CCDC, 12 Union Road, Cambridge CB2 1EZ, UK [fax: int. code + 44(1223)336-033, e-mail: deposit@chemcrys.cam.ac.uk].

[1] J. Ellermann, M. Schütz, F. W. Heinemann, M. Moll, *Z. Anorg. Allg. Chem.* **1998**, *624*, 257–262.
[2] J. Ellermann, J. Sutter, F. A. Knoch, M. Moll, *Angew. Chem.* **1993**, *105*, 763–764; *Angew. Chem. Int. Ed. Engl.* **1993**, *32*, 700–701.
[3] J. Ellermann, J. Sutter, C. Schelle, F. A. Knoch, M. Moll, *Z. Anorg. Allg. Chem.* **1993**, *619*, 2006–2014.
[4] J. Ellermann, P. Gabold, C. Schelle, F. A. Knoch, M. Moll, W. Bauer, *Z. Anorg. Allg. Chem.* **1995**, *621*, 1832–1843.
[5] H. Schmidbaur, F. E. Wagner, A. Wohlleben-Hammer, *Chem. Ber.* **1979**, *112*, 496–500.
[6] J. Ellermann, M. Lietz, *Z. Naturforsch.* **1980**, *35b*, 64–67.
[7] A. Schmidpeter, F. Steinmüller, W. S. Sheldrick, *Z. Anorg. Allg. Chem.* **1989**, *579*, 158–172.
[8] Th. Kremer, F. Hampel, F. A. Knoch, W. Bauer, A. Schmidt, P. Gabold, M. Schütz, J. Ellermann, P. v. R. Schleyer, *Organometallics* **1996**, *15*, 4776–4782.
[9] P. Braunstein, R. Hasselbring, A. Tripicchio, F. Ugozzoli, *J. Chem. Soc., Chem. Commun.* **1995**, 37–38.
[10] J. Ellermann, P. Gabold, F. A. Knoch, M. Moll, A. Schmidt, M. Schütz, *Z. Naturforsch.* **1996**, *51b*, 201–208.
[11] M. Dotzler, A. Schmidt, J. Ellermann, F. A. Knoch, M. Moll, W. Bauer, *Polyhedron* **1996**, *15*, 4425–4433.
[12] A. F. Wells, *Structural Inorganic Chemistry*, 5th ed., Clarendon Press, Oxford, **1984**, p. 1279.
[13] M. Dräger, N. Kleiner in *Inorganic Reactions and Methods*, Vol.9: The Formation of Bonds to C, Si, Ge, Sn, Pb (Part 1), Founding Editor J. J. Zuckerman, Editor: A. P. Hagen, VCH, Weinheim, **1988**, p. 96–103.
[14] D. Pohl, J. Ellermann, F. A. Knoch, M. Moll, W. Bauer, *Chem. Ber.* **1994**, *127*, 2167–2171.
[15] D. Pohl, J. Ellermann, F. A. Knoch, M. Moll, W. Bauer, *J. Organomet. Chem.* **1994**, *481*, 259–274.

[16] J. Ellermann, P. Gabold, F. A. Knoch, M. Moll, D. Pohl, J. Sutter, W. Bauer, *J. Organomet. Chem.* **1996**, *525*, 89−107.
[17] B. Wrackmeyer in: G. A. Webb (Editor), *Annual Reports on NMR Spectroscopy*, Academic Press, London, **1990**, p. 249.
[18] M. Herberhold, V. Tröbs, B. Wrackmeyer, *J. Organomet. Chem.* **1997**, *541*, 391−400.
[19] J. D. Kennedy, W. McFarlane, B. Wrackmeyer, *Inorg. Chem.* **1976**, *15*, 1299−1302; J. D. Kennedy, W. McFarlane, G. S. Pyne, B. Wrackmeyer, *J. Organomet. Chem.* **1980**, *195*, 285−290.
[20] B. Wrackmeyer in: B. Krebs (Ed.), *Unkonventionelle Wechselwirkungen in der Chemie metallischer Elemente*, VCH, Weinheim, **1992**, 111−124.
[21] V. M. S. Gil, W. von Philipsborn, *Magn. Reson. Chem.* **1989**, *27*, 409−430.
[22] J. K. M. Sanders, B. K. Hunter, *Modern NMR Spectroscopy*, Oxford University Press, Oxford, **1993**, p. 214.
[23] H. H. Karsch, B. Deubelly, J. Riede, G. Müller, *Angew. Chem.* **1987**, *99*, 703−705; *Angew. Chem. Int. Ed. Engl.* **1987**, *26*, 673−675; H. H. Karsch, *Russ. Chem. Bull.* **1993**, *42*, 1937−1955.
[24] D. H. Whiffen, *J. Chem. Soc.* **1956**, 1350−1356.
[25] E. Maslowsky Jr., *Vibrational Spectra of Organometallic Compounds*, John Wiley and Sons, New York, London, Sydney, Toronto, **1977**, p. 399 and 402.
[26] M. J. S. Gynane, D. H. Harris, M. F. Lappert, P. P. Power, P. Riviere, M. Riviere-Baudet, *J. Chem. Soc., Dalton Trans.* **1977**, 2004−2009.
[27] D. H. Harris, M. F. Lappert, *J. Chem. Soc., Chem. Commun.* **1974**, 895−896.
[28] M. F. Lappert, P. P. Power, M. J. Slade, *J. Chem. Soc.,Chem. Commun.* **1979**, 369−370.
[29] J. S. Casa, A. Castineiras, J. Haiduc, A. Sanchez, J. Sordo, E. M. Velasquez-Lopez, *Polyhedron* **1994**, *13*, 2873−2879.
[30] A. L. Balch, D. E. Oram, *Organometallics* **1986**, *5*, 2159−2161.
[31] H. H. Karsch, A. Appelt, G. Hanika, *J. Organomet. Chem.* **1986**, *312*, C1−C5.
[32] A. L. Balch, D. E. Oram, *Inorg. Chem.* **1987**, *26*, 1906−1912.
[33] D. L. Kepert in *Progress in Inorganic Chemistry*, Vol. *23*, Aspects of the Stereochemistry of Six-coordination, Editor St. J. Lippart, John Wiley and Sons, New York, London, Sydney, Toronto, **1977**, p. 1−65.
[34] W. R. Krigbaum, B. Rubin, *Acta Cryst.* **1973**, *B29*, 749−756.
[35] H. Nöth, L. Meinel, *Z. Anorg. Allg. Chem.* **1967**, *349*, 225−240.
[36] S. Parkin, B. Moezzi, H. Hope, *J. Appl. Cryst.* **1995**, *28*, 53−56.
[37] SHELXTL 5.03 for Siemens Crystallographic Research Systems (**1995**), Siemens Analytical X-ray Instruments Inc., Madison, WI.

[97261]

Metal Complexes with Tetrapyrrole Ligands, LXXIII[◇]

Oxidation and Reduction of Cerium(IV) Sandwich Complexes with Porphyrin Ligands Linked by Aliphatic Diether Bridges of Variable Chain Length

Johann W. Buchler* and Torsten Dippell

Institut für Anorganische Chemie, Technische Universität Darmstadt,
Petersenstraße 18, D-64287 Darmstadt, Germany

Received September 22, 1997

Keywords: Cerium(IV) bisporphyrinates / Sandwich complexes / Diporphyrins / π Radical-cations and dications / Cerium(III) bisporphyrinate anions

Starting from 5-(4-hydroxyphenyl)-10,15,20-tris(4-methylphenyl)porphyrin (**2a**), the new bis(porphyrinyloxy)alkanes **4a** and **4d** were synthesized by ether formation with the α,ω-dibromoalkanes $Br(CH_2)_nBr$ (n = 8, 11; **3a**, **3d**). **4a** was obtained by a two-step reaction with the 5-[4-(8-bromooctyloxy)phenyl]-10,15,20-tris(4-methylphenyl)porphyrin (**2b**) as an intermediate. The diporphyrins **4a** and **4d** were metalated with cerium(III) acetylacetonate to yield the new (porphyrin)-cerium sandwich complexes **1a** and **1d** which were characterized by UV/Vis, IR, ^{1}H-NMR, ^{13}C-NMR spectroscopy and cyclic voltammetry. The mono- and dications and the cerium(III) bisporphyrinate anions of **1a-d** were produced by electrochemical oxidation and reduction, respectively, and were examined by UV/Vis/NIR spectroscopy. The length of the lateral chains does not have a specific effect on the first and second oxidation potentials of the porphyrin rings and the reduction potentials of the cerium ions in the bisporphyrinate systems, and on the energy of the NIR bands of the monocations.

Synthetic aggregates of porphyrins or metalloporphyrins and quinones are presently being studied in order to understand the elementary steps of light-induced charge separation in photosynthesis. Most of these contain covalent links between the individual functional groups or chromophores[1]. The (porphyrin-quinone)zinc systems prepared by Staab et al.[2] were especially stimulating for our work devoted to (porphyrin)cerium(IV) double-deckers in which the two porphyrin systems were linked by a quinone-containing bridge[3]. In the course of that work, cerium(IV) double-deckers of the type $Ce[ttpO(CH_2)_nOttp]$ (**1**)[4], namely **1b** and **1c**, were constructed in which the two porphyrin rings are bridged by aliphatic diether chains containing 9 or 10 methylene groups (n = 9 or 10), respectively. Since **1c** had shown unexpectedly high oxidation potentials at the porphyrin rings, the investigation was extended to the double-deckers **1a** and **1d** which have either a somewhat shorter (8 methylene groups, n = 8) or a longer "ansa" chain (11 methylene groups, n = 11). The electrochemical oxidations and reductions of all four species **1a**−**d** were coherently followed by cyclic voltammetry and digital coulometry[5]. The results are reported below.

Very recently, novel species have been added to those bisporphyrinate double-deckers of tetravalent metal ions mentioned[3] so far: Aida et al.[6] have obtained chiral zirconium(IV) and cerium(IV) bisporphyrinates and succeeded in the separation of their enantiomers.

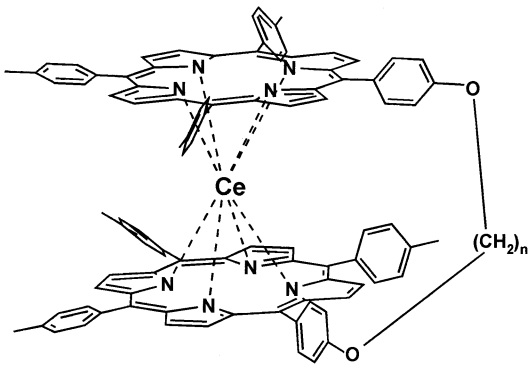

1

No.	1a	1b	1c	1d
n	8	9	10	11

Synthesis

The cerium double-deckers **1b** and **1c** had been prepared starting from the monofunctionalized tetraarylporphyrin H_2(HOttp) (**2a**) which is easily accessible from a mixed condensation-oxidation reaction of pyrrole, *p*-tolualdehyde, and *p*-hydroxybenzaldehyde[7] and can be transformed into a diporphyrin by ether formation with α,ω-dibromoalkanes, e. g. 1,9-dibromononane (**3b**) and 1,10-dibromodecane (**3c**),

[◇] Part LXXII: Ref.[3].

 © WILEY-VCH Verlag GmbH, D-69451 Weinheim, 1998 1434−1948/98/0404−0445 $ 17.50+.50/0

respectively[3][7]. Although sandwich formation leading to $Ce(HOttp)_2$ is possible with **2a**[8], the application of lateral bridges was unsuccessful because $Ce(HOttp)_2$ exists as a mixture of vicinal and transversal isomers. Thus, sandwich formation had been performed[3] starting from the respective diporphyrins **4b** or **4c** obtained from **2a** and **3b** or **3c**, respectively, and the new sandwiches **1a** and **1d** had to be prepared starting from **2a** by the diporphyrin route as well.

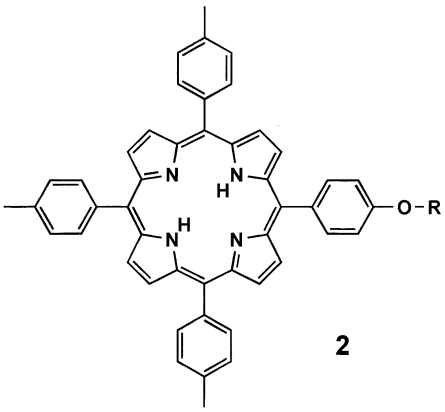

2

No.	R
2a	H
2b	$(CH_2)_8Br$
2c	$(CH_2)_9Br$
2d	$(CH_2)_{10}Br$
2e	$(CH_2)_{11}Br$

$Br—(CH_2)_n—Br$ **3** For n see **1**

Indeed, the diporphyrin **4d** could be made by directly coupling two equivalents of **2a** with **3d** in the presence of cesium carbonate in dimethylformamide at 100°C (see Experimental Section, protocol 1; 93%). The monofunctionalized porphyrin **2e** was also formed as a byproduct as already observed for **2c** and **2d**[3] and could be separated by column chromatography. However, because of the formation of many decomposition products, the former procedure failed for **4a** which then was prepared stepwise[5] by first, formation of the [(bromoalkoxy)phenyl]porphyrin **2b** (protocol 2; 89%) from **2a** and **3a**, and then coupling of the resulting **2b** with another equivalent of **2a** (protocol 3; 28%).

The formation of the double-deckers **1a** (11%) and **1d** (15%; protocol 4) was managed as described previously[3] for **1b** (24%) and **1c** (11%), by lithiation of the diporphyrins **4a** and **4d**, respectively, with *n*-butyllithium and subsequent addition of cerium(III) acetylacetonate in trichlorobenzene (TCB). The yields (given above in parentheses) were comparably small for all four double-deckers with a small preference for the chain length $n = 9$. Thus, all these lateral chains appear to fit the gap between the vicinal pair of phenolic oxygen atoms in the cerium double-decker system of **1a–d**.

Analytical Characterization

All the new compounds were identified by their UV/Vis, ^{1}H-NMR, IR, and mass spectra (for individual data, see protocols 1–4). The new diporphyrins **4a** and **4d** were prepared in the same manner as the known[3] species **4b** and **4c**. An additional identification came from the determination of their R_f values which increase in the series **4a** < **4b** < **4c** < **4d** (see Experimental Section, Table 4) indicating a decrease in polarity as the chain length of the diether bridge increases.

The new double-deckers **1a** and **1d**, as well as newly prepared[5] samples of **1b** and **1c**, which otherwise showed spectra identical with those of the original samples[3], were additionally characterized by ^{13}C-NMR data which are compiled in Table 1. The assignments were corroborated by DEPT experiments.

UV/Vis Spectra

The UV/Vis spectra of the new alkane-bridged double-deckers **1a** and **1d** resemble those of their unbridged analogs $Ce(ttp)_2$[9] and $Ce(HOttp)_2$[8] as much as the spectra of the double-deckers **1b** and **1c**, see Table 2a. All complexes show the typical Soret (B) band and four characteristic Q

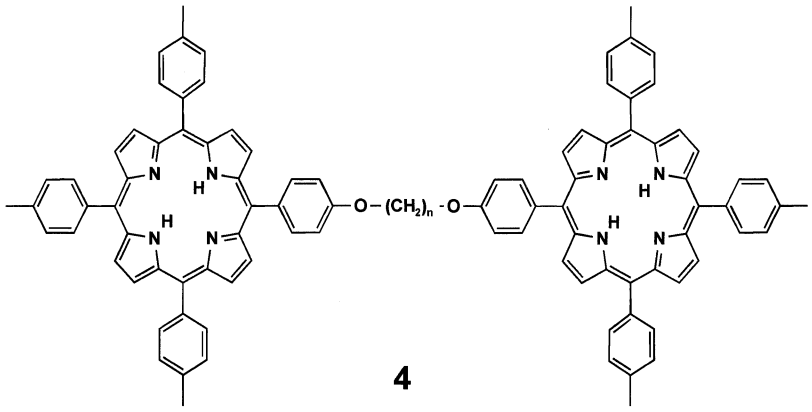

4

For n see **1**

Table 1. ^{13}C-NMR data of **1a–d** (δ values at 25°C in $CDCl_3$)

	CH_3[a]	CH_2[b]	CH_2[c]	CH_2–O[d]	C=C[e]	=C–O[f]
1a	21.59	25.44–28.06	28.86	68.41	123.88–153.34	158.18
1b	21.59	25.67–29.16	29.81	68.70	123.78–153.25	158.34
1c	21.59	25.89–29.34	29.81	68.41	123.72–153.43	158.55
1d	21.59	26.00–29.50	29.81	68.52	123.69–153.24	158.58

[a] CH_3, tolyl. – [b] $C_{aliphat.}$. – [c] $C_{aliphat.}$. – [d] $C_{aliphat.}$–O. – [e] $C_{arom.}$, $C_{heteoarom.}$. – [f] $C_{arom.}$–O.

bands which are labeled as discussed for cofacial porphyrin ligands in sandwich complexes[3][10]. The lateral aliphatic chain connecting the porphyrin ligands in the cerium sandwiches does not have any effect on the intensity and the location of the B and the Q bands (for data, see Experimental Section, protocol 4).

Table 2. UV/Vis/NIR data (λ_{max} [nm], lg ε in parentheses, at 25°C in CH_2Cl_2) of a) the double-deckers **1a–d**, b) the radical cations formed from **1a–d**, c) the dications formed from **1a–d** and d) the bisporphyrinate anions formed from **1a–d**

Table 2a

	B (Soret)	Q″	Q(1,0)	Q(0,0)	Q′
1a	398 (5.27)	483 (4.04)	544 (3.91)	586 (3.37)	647 (3.34)
1b	398 (5.27)	483 (4.04)	544 (3.91)	586 (3.37)	647 (3.34)
1c	398 (5.12)	480 (3.92)	544 (3.80)	582 (3.33)	648 (3.30)
1d	398 (5.29)	478 (4.09)	545 (3.94)	584 (3.42)	648 (3.40)

Table 2b

	E [V]	UV/Vis/NIR absorbance {λ_{max} [nm], (lg ε)}
1a	0.9	393 (5.28), 673 (3.90), 801 (3.57), 1386 (3.94)
1b	0.9	393 (5.13), 678 (3.69), 805 (3.45), 1385 (3.95)
1c	0.9	393 (5.04), 679 (3.80), 794 (3.66), 1383 (3.79)
1d	0.9	394 (5.21), 678 (3.67), 806 (3.40), 1383 (3.75)

Table 2c

	E [V]	UV/Vis/NIR absorbance {λ_{max} [nm], (lg ε)}
1a	1.3	389 (5.23), 668 (4.15), 802 (3.94), 1049 (3.97)
1b	1.3	389 (5.07), 675 (3.96), 805 (3.79), 1043 (3.85)
1c	1.3	388 (4.96), 678 (3.97), 802 (3.75), 1046 (3.75)
1d	1.3	389 (5.15), 674 (4.02), 801 (3.75), 1046 (3.77)

Table 2d

	E [V]	UV/Vis absorbance {λ_{max} [nm], (lg ε)}
1a	–0.6	415 (5.71), 515 (4.09), 555 (4.13), 646 (3.82)
1b	–0.6	415 (5.74), 518 (4.10), 558 (4.16), 643 (3.92)
1c	–0.6	415 (5.47), 515 (3.82), 556 (3.88), 643 (3.55)
1d	–0.6	415 (5.78), 519 (4.01), 554 (4.05), 643 (3.86)

Cyclic Voltammetry

In dichloromethane, cerium(IV) bisporphyrinates $Ce^{IV}(p)_2$ [e. g. $Ce(tpp)_2$, $Ce(ttp)_2$, or $Ce(oep)_2$] usually show two reversible oxidations (E_1, E_2) occuring at the porphyrin system and producing the π cation $[Ce(p)_2]^+$ and the π dication $[Ce(p)_2]^{2+}$, respectively[11]. The first quasireversible reduction (E_3) occurs at the metal center[11a] and generates a cerium(III) double-decker anion, $[Ce^{III}(p)_2]^-$. These essential processes are characterized in Eq. (1) by their respective reduction steps.

$$[Ce^{IV}(p^\bullet)(p^\bullet)]^{2+} + e^- \rightarrow [Ce^{IV}(p^\bullet)(p)]^+ + e^- \rightarrow Ce^{IV}(p)_2 + e^- \rightarrow [Ce^{III}(p)_2]^- \quad (1)$$

In order to clarify whether the previously found abnormally high oxidation potential of **1b** could be reproduced, and if it existed, were due to some steric abnormity of **1b**, the whole series **1a–d** was studied by cyclic voltammetry. New samples of **1b** and **1c** were prepared[5] as previously described[3] and measured anew. To our disappointment, all the double-deckers **1a–d** showed the three redox steps E_1, E_2, and E_3 at potentials very close to those of the reference compound $Ce(ttp)_2$ (see Table 3). A typical voltammogram is shown in Figure 1.

Figure 1. Cyclic voltammogram of the bridged double-decker **4a** (CH_2Cl_2, room temperature, NBu_4PF_6 as supporting electrolyte, calomel electrode)

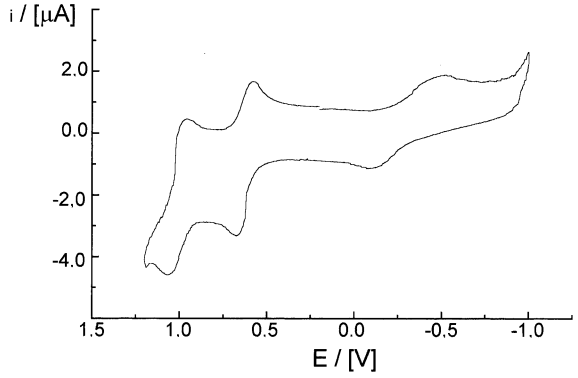

Table 3. Comparison of the redox potentials of the double-deckers $Ce(ttp)_2$ and **1a–d** (CH_2Cl_2, room temperature, NBu_4PF_6 as supporting electrolyte, saturated calomel electrode)

	E_1 [V]	E_2 [V]	E_3 [V]
$Ce(ttp)_2$	1.000	0.620	–0.290
1a	1.000	0.605	–0.300
1b	1.019	0.632	–0.303
1c	1.018	0.627	–0.310
1d	1.020	0.630	–

The similarity of all the redox potentials implies that the variation of the chain length ($8 < n < 11$) in the four double-deckers does not alter the mutual π-π interactions of the two porphyrin rings in these double-deckers. Thus, contrary to our previous speculation, the relative orientation of the two porphyrin ligands may not be altered by this variation of the length of the lateral chain.

Oxidation and Reduction

In order to record the UV/Vis/NIR spectra of the species connected by the redox processes defined by Eq. (1), the laterally bridged sandwich complexes **1a–d** were subjected

to electrolysis at controlled potentials (see protocol 5). The oxidations occurring at the porphyrin system produce the π radical-cation $[Ce(p^{\bullet}-p)]^{+}$ and the π dication $[Ce[p^{\bullet}-p^{\bullet})]^{2+}$, respectively, $(p-p)^{2-}$ symbolizing the diporphyrinate ligands derived from **3a**−**d**. The reduction takes place at the metal center and generates the double-decker anion $[Ce^{III}(p-p)]^{-}$.

On oxidation, the UV/Vis/NIR spectra show a hypsochromic shift of the B band from 398 via 393 (π radical-cation) to 389 nm (π dication; see Tables 2b and 2c). The typical feature of the π radical-cations $[Ce^{IV}(p^{\bullet})(p)]^{+}$ is a broad NIR band, found at 1350 nm for $[Ce^{IV}(tpp^{\bullet})(tpp)]^{+}$.[12] For $[Ce(p^{\bullet}-p)]^{+}$ it appears at 1383 nm. For the π dications $[Ce^{IV}(tpp^{\bullet})(tpp^{\bullet})]^{2+}$ and $[Ce^{IV}(p^{\bullet}-p^{\bullet})]^{2+}$, similar bands are observed at 1017[12] and 1044 nm, respectively. Reduction at the cerium ion yielding the double-decker anions $[Ce^{III}(p-p)]^{-}$ is indicated by a bathochromic shift of the B band to 415 nm (Table 2d), as found earlier for a series of lanthanoid(III) bisporphyrinate anions $[Ln(tpp)_2]^{-}$[13] An NIR band does not appear.

Financial support by the *Deutsche Forschungsgemeinschaft* and the *Fonds der Chemischen Industrie* is gratefully acknowledged. The authors thank Prof. Dr. *J. J. Veith* and Mr. *M. Fischer* for performing mass spectra, Dr. *S. Braun*, *K. Jungk*, and *K.-O. Runzheimer* for performing NMR spectra and the *Bayer AG* for a gift of trichlorobenzene.

Experimental Section

Spectrometers and chemicals used were specified in a previous paper of this series[8]. − Electrochemistry: Princeton Applied Research potentiostat M 173 contolled by an interface M 175 with the software M 270/250. − 1,8-Dibromooctane, 1,11-dibromoundecane, Cs_2CO_3, and DMF were obtained from Fluka Chemie AG, *n*-butyllithium (1.6 M in *n*-hexane) from Acros, and $Ce(acac)_3 \times H_2O$ from Aldrich. − *p*-(Hydroxyphenyl)tris(*p*-tolyl)porphyrin[7] (**2a**) was prepared by a literature method. − Elemental analyses were performed by Analytical Laboratories, P.O.B. 1106, D-51779 Lindlar. − Analytical thin layer chromatography was performed on commercial aluminium sheets coated with silica gel 60 F_{254} (Merck). A comparison of the R_f values found for the diporphyrins **4a**−**4d** is given in Table 4.

Table 4. Comparison of the R_f values of the diporphyrins **4a**−**d** determined by thin-layer chromatography (silica gel, toluene, room temperature)

4a	**4b**	**4c**	**4d**
0.50	0.55	0.59	0.64

Protocol 1: 1,11-Bis[4-{10,15,20-tris(4-methylphenyl)porphyrin-5-yl}phenoxy]undecane (**4d**): To a solution of 310 mg (0.46 mmol) of **2a** and 1.3 g (3.99 mmol) of anhydrous cesium carbonate in 15 ml of DMF a solution of 339 mg (1.08 mmol) of **3d** in 25 ml of DMF was added dropwise under nitrogen at 100°C. After cooling and filtration, the solvent was removed in vacuo. The residue was treated with 10 ml of toluene and chromatographed on an alumina column (II, neutral, 15 × 3.5 cm). Fractions were obtained as follows: with toluene a violet forerun of the monofunctionalized [(ω-bromoundecyloxy)phenyl]porphyrin **2e** and with CH_2Cl_2 the violet fraction of the diporphyrin **4d**. Evaporation of the solvent in vacuo and crystallization from CH_2Cl_2/MeOH (1:1) yielded the diporphyrin **4d** as a violet powder. 319 mg (93%). − MS; *m/z* (%): 748 (100) $[M^{2+}]$, 1496 (69) $[M^{+}]$. − UV/Vis (CH_2Cl_2): λ_{max} (lg ε) = 420 nm (5.78), 517 (4.36), 553 (4.15), 592 (3.93), 648 (3.93). − IR (KBr), 6 most intensive bands and NH band: $\tilde{\nu}$ [cm^{-1}] = 803, 970, 1247, 1470, 1512, 2925, 3314 (NH). − ^1H NMR (CD_2Cl_2): δ = −2.84 (s, 4 H, NH), 1.55−1.70 [m, 14 H, $OCH_2CH_2(CH_2)_7CH_2CH_2O$], 1.97−2.02 [m, 4 H, $OCH_2CH_2(CH_2)_7CH_2CH_2O$], 2.66−2.68 (m, 18 H, CH_3, tolyl), 4.24 [t, *J* = 8 Hz, 4 H, $OCH_2CH_2(CH_2)_7CH_2$-CH_2O], 7.26 (d, *J* = 8 Hz, 4 H, *m*-phenoxy-H), 7.51−7.56 (m, 12 H, *m*-tolyl-H), 8.04−8.09 (m, 16 H, *o*-tolyl- and *o*-phenoxy-H), 8.84−8.88 (m, 16 H, pyrrole-H).

Protocol 2: 5-[4-(8-Bromooctyloxy)phenyl]-10,15,20-tris(4-methylphenyl)porphyrin (**2b**): 1.68 g (6.2 mmol) of **3a** were added under nitrogen to a solution of 424 mg (0.63 mmol) of **2a** and 1.74 g (5.34 mmol) of anhydrous cesium carbonate in 50 ml of DMF. After stirring at 50°C for 5 h, the solution was filtered and the solvent removed in vacuo. 484 mg (89%) of the porphyrin **2b** were obtained as a violet powder after chromatography on an alumina column (II, neutral, 15 × 3.5 cm, isolation of the first violet fraction) with toluene and crystallization from CH_2Cl_2/MeOH (1:1). − MS; *m/z* (%): 863 (100) $[M^{+}]$. − UV/Vis (CH_2Cl_2): λ_{max} (lg ε) = 420 nm (5.64), 517 (4.23), 553 (3.98), 592 (3.70), 648 (3.70). − IR (KBr), 6 most intensive bands and NH band: $\tilde{\nu}$ [cm^{-1}] = 801, 967, 1177, 1246, 1472, 1506, 3319 (NH). − ^1H NMR (CD_2Cl_2): δ = −2.79 (s, 2 H, NH), 1.49−1.63 [m, 8 H, $OCH_2CH_2(CH_2)_4CH_2CH_2Br$], 1.70−2.00 [m, 4 H, $OCH_2CH_2(CH_2)_4CH_2CH_2Br$], 2.69 (s, 9 H, CH_3, tolyl), 3.40 [t, *J* = 8 Hz, 2 H, $OCH_2CH_2(CH_2)_4CH_2CH_2Br$], 4.23 [t, *J* = 8 Hz, 2 H, $OCH_2CH_2(CH_2)_4CH_2CH_2Br$], 7.27 (d, *J* = 8 Hz, *m*-phenoxy-H), 7.55 (m, 6 H, *m*-tolyl-H), 8.08 (m, 8 H, *o*-tolyl- and *o*-phenoxy-H), 8.85 (m, 8 H, pyrrole-H).

Protocol 3: 1,8-Bis{4-[10,15,20-tris(4-methylphenyl)porphyrin-5-yl]phenoxy}octane (**4a**): A suspension of 172 mg (0.20 mmol) of **2b**, 316 mg (0.47 mmol) of **2a** and 1.3 g (3.99 mmol) of Cs_2CO_3 in 25 ml of DMF was stirred for 5 h under nitrogen at 100°C. After cooling, 100 ml of water was added and the mixture was filtered. The violet residue was dried at 100°C and chromatographed on an alumina column (II, neutral, 15 × 3.5 cm). Fractions were obtained as follows: with toluene a violet forerun of the remaining monofunctionalized [(8-bromooctyloxy)phenyl]porphyrin **2b** and with CH_2Cl_2 the violet fraction of the diporphyrin **4a**. Evaporation of the solvent in vacuo and crystallization of the residue from CH_2Cl_2/MeOH (1:1) yielded 82 mg (28%) of **4a** as a violet powder. − MS; *m/z* (%): 1454 (100) $[M^{+}]$. − UV/Vis (CH_2Cl_2): λ_{max} (lg ε) = 420 nm (5.66), 517 (4.25), 553 (4.01), 592 (3.74), 648 (3.74). − IR (KBr), 6 most intensive bands and NH band: $\tilde{\nu}$ [cm^{-1}] = 801, 969, 1179, 1245, 1472, 1508, 3320 (NH). − ^1H NMR (CD_2Cl_2): δ = −2.78 (s, 4 H, NH), 1.59−1.76 [m, 8 H, $OCH_2CH_2(CH_2)_4CH_2$-CH_2O], 2.02−2.09 [m, 4 H, $OCH_2CH_2(CH_2)_4CH_2CH_2O$], 2.67−2.69 (m, 9 H, CH_3, tolyl), 4.29 [t, *J* = 8 Hz, 4 H, $OCH_2CH_2(CH_2)_4CH_2CH_2O$], 7.29 (d, *J* = 8 Hz, *m*-phenoxy-H), 7.51−7.56 (m, 12 H, *m*-tolyl-H), 8.06−8.13 (m, 16 H, *o*-tolyl- and *o*-phenoxy-H), 8.84−8.88 (m, 16 H, pyrrole-H).

Protocol 4: General procedure of the metalation of the diporphyrins **4a** and **4d** with $Ce(acac)_3 \times H_2O$: A solution of 1.6 mmol of BuLi in 0.25 ml of *n*-hexane was added to a solution of 100 mg of **4a** (0.069 mmol) or **4d** (0.067 mmol) in 50 ml of TCB under nitrogen. The resulting solution was stirred for 10 min at room temperature. After the addition of 313 mg (0.69 mmol) or 303 mg (0.67 mmol) of $Ce(acac)_3 \times H_2O$, the solution was heated at reflux for 6 h. After cooling and filtration, the solvent was evaporated in vacuo. The residue was purified on an alumina column (II, neutral,

15 × 3.5 cm) with toluene. The first brown fraction contained the double-decker followed by the second violet fraction of the corresponding diporphyrin. After evaporation of the solvent from the first fraction and recrystallization of the residue from CH_2Cl_2/MeOH (1:1) the following double-deckers were isolated as brown powders:

1,8-Bis{4-[10,15,20-tris(4-methylphenyl)porphyrin-5-yl]-phenoxy}octanatocerium(IV) (**1a**): 9 mg (11%). − MS; *m/z* (%): 1590 (100) [M^+]. − UV/Vis (CH_2Cl_2): λ_{max} (lg ε) = 399 nm (5.38), 478 (4.14), 545 (4.02), 584 (3.52), 646 (3.45). − IR (KBr), 9 most intensive bands: $\tilde{\nu}$ [cm^{-1}] = 802, 983, 1023, 1096, 1178, 1263, 1325, 1511, 2930. − ^{1}H NMR ($CDCl_3$): δ = 1.77−1.82 [m, 8 H, $OCH_2CH_2(CH_2)_4CH_2CH_2O$], 2.11−2.25 [m, 4 H, $OCH_2CH_2(CH_2)_4CH_2CH_2O$], 2.72−2.74 (m, 18 H, CH_3, tolyl), 4.46/4.58 [m, 4 H, $OCH_2CH_2(CH_2)_4CH_2CH_2O$], 6.29 (m, 8 H, *exo* *o*-tolyl- and *o*-phenoxy-H), 6.50 (m, 2 H, *exo* *m*-phenoxy-H), 7.07 (m, 6 H, *exo* *m*-tolyl-H), 7.50 (m, 2 H, *endo* *m*-phenoxy-H), 7.93 (m, 6 H, *endo* *m*-tolyl-H), 8.15−8.54 (m, 16 H, pyrrole-H), 9.48 (m, 8 H, *endo* *o*-tolyl- and *o*-phenoxy-H). − ^{13}C NMR ($CDCl_3$): δ = 21.59 (CH_3, tolyl), 25.44−28.06 [$OCH_2CH_2(CH_2)_4CH_2CH_2O$], 28.86 [$OCH_2CH_2(CH_2)_4CH_2CH_2O$], 68.42 [$OCH_2CH_2(CH_2)_4CH_2CH_2O$], 123.88−153.34 ($C_{arom.}$, $C_{heteroarom.}$), 158.18 ($C_{arom.}$−O). − CV (CH_2Cl_2/NBu_4PF_6): *E* = 1.000 V, 0.605, −0.300. − $C_{102}H_{82}CeN_8O_2 \times 4\ H_2O$ (1664.00): calcd. C 73.62, H 5.45, N 6.73; found C 73.95, H 5.82, N 6.26.

1,11-Bis{4-[10,15,20-tris(4-methylphenyl)porphyrin-5-yl]-phenoxy}undecanatocerium(IV) (**1d**): 16 mg (15%). − MS; *m/z* (%): 1632 (100) [M^+]. − UV/Vis (CH_2Cl_2): λ_{max} (lg ε) = 398 nm (5.29), 478 (4.09), 545 (3.94), 584 (3.42), 638 (3.40). − IR (KBr), 9 most intensive bands: $\tilde{\nu}$ [cm^{-1}] = 801, 981, 1026, 1100, 1178, 1261, 1326, 1512, 2970. − ^{1}H NMR ($CDCl_3$): δ = 1.64−1.80 [m, 14 H, $OCH_2CH_2(CH_2)_7CH_2CH_2O$], 2.03−2.15 [m, 4 H, $OCH_2CH_2(CH_2)_7CH_2CH_2O$], 2.71−2.72 (m, 18 H, CH_3, tolyl), 4.34/4.48 [m, 4 H, $OCH_2CH_2(CH_2)_7CH_2CH_2O$], 6.28 (m, 8 H, *exo* *o*-tolyl- and *o*-phenoxy-H), 6.50 (m, 2 H, *exo* *m*-phenoxy-H), 7.05 (m, 6 H, *exo* *m*-tolyl-H), 7.60 (m, 2 H, *endo* *m*-phenoxy-H) 7.93 (m, 6 H, *endo* *m*-tolyl-H), 8.17−8.41 (m, 16 H, pyrrole-H), 9.48 (m, 8 H, *endo* *o*-tolyl- and *o*-phenoxy-H). − ^{13}C NMR ($CDCl_3$): δ = 21.59 (CH_3, tolyl), 26.00−29.50 [$OCH_2CH_2(CH_2)_4CH_2CH_2O$], 29.81 [$OCH_2CH_2(CH_2)_4CH_2CH_2O$], 68.52 [$OCH_2CH_2(CH_2)_4CH_2CH_2O$], 123.69−153.24 ($C_{arom.}$, $C_{heteroarom.}$), 158.58 ($C_{arom.}$−O). − CV (CH_2Cl_2/NBu_4PF_6): *E* = 1.020 V, 0.630, −0.305. − $C_{105}H_{88}CeN_8O_2 \times 5\ H_2O$ (1724.10): calcd. C 73.15, H 5.73, N 6.50; found C 73.40, H 5.68, N 6.04.

Protocol 5: General procedure for the electrochemical oxidations and reductions of the cerium(IV) bisporphyrinates **1a**−**d**: A solution of 1.40 mg (8.8×10^{-4} mmol) of **1a**, 1.45 mg (9.04×10^{-4} mmol) of **1b**, 1.63 mg (1.01×10^{-3} mmol) of **1c**, or 1.64 mg (1.01×10^{-3} mmol) of **1d** in 60 ml of a 0.1 M solution of NBu_4PF_6 in CH_2Cl_2 was electrolyzed by a three-potential cycle. Along the first two oxidations at +0.9 V and +1.3 V, charges of about 81 to 95 mC and 87 to 95 mC, respectively, were transferred while the solutions changed their colors from orange/brown via yellow to yellow/green. Thereafter, the solutions were reduced by a constant potential at −0.6 V. During this three-step reduction of the dications to the double-decker anions the color changes reversed with the appearance of orange/brown and then yellow/green for the last reduction step with total charges between 200 and 254 mC being transferred. After the first two oxidations and the total reduction, samples were taken, appropriately diluted, and placed into cuvettes for UV/Vis/NIR spectroscopy producing the spectral data given in Tables 2b−d.

[1] H. Kurreck, M. Huber, *Angew. Chem.* **1995**, *107*, 929−947; *Angew. Chem. Int. Ed. Engl.* **1995**, *34*, 849−866 and references cited therein.

[2] T. Häberle, J. Hirsch, F. Pöllinger, H. Heitele, M. E. Michel-Beyerle, C. Anders, A. Döhling, C. Krieger, A. Rückemann, H. A. Staab, *J. Phys. Chem.* **1996**, *100*, 18269−18274 and references cited therein.

[3] J. W. Buchler, G. Heinz, *Chem. Ber.* **1996**, *129*, 1073−1081.

[4] Abbreviations used: M, metal; $(p)^{2-}$, $(ttp)^{2-}$, $(Hottp)^{2-}$, dianions of general porphyrin, 5,10,15,20-tetrakis(methylphenyl)-porphyrin, 5-hydroxyphenyl-10,15,20-tritolylporphyrin (**1a**); $[ttpO(CH_2)_nOttp]^{4-}$, tetraanion of a diporphyrin (see **4**); H(acac), acetylacetone; TCB, 1,2,4-trichlorobenzene.

[5] T. Dippell, Diplomarbeit, Technische Universität Darmstadt, **1996**.

[6] K. Tashiro, K. Konishi, T. Aida, *Angew. Chem.* **1997**, *109*, 882−884; *Angew. Chem. Int. Ed. Engl.* **1997**, *36*, 856−858.

[7] R. G. Little, *J. Heterocycl. Chem.* **1978**, *15*, 203−208.

[8] J. W. Buchler, V. Eiermann, H. Hanssum, G. Heinz, H. Rüterjans, *Chem. Ber.* **1994**, *127*, 589−595.

[9] J. W. Buchler, H. G. Kapellmann, M. Knoff, K. L. Lay, S. Pfeifer, *Z. Naturforsch., B* **1983**, *38B*, 1339−1345.

[10] [10a] O. Bilsel, J. W. Buchler, P. Hammerschmitt, J. Rodriguez, D. Holten, *Chem. Phys. Lett.* **1991**, *182*, 415−421. − [10b] O. Bilsel, J. Rodriguez, S.N. Milam, P.A. Gorlin, G. S. Girolami, K. S. Suslick, D. Holten, *J. Am. Chem. Soc.* **1992**, *114*, 6528−6538. − [10c] K. M. Kadish, G. Moninot, Y. Hu, D. Dubois, A. Ibnlfassi, J.-M. Barbe, R. Guilard, *J. Am. Chem. Soc.* **1993**, *115*, 8153−8166.

[11] [11a] J. W. Buchler, K. Elsässer, M. Kihn-Botulinski, B. Scharbert, *Angew. Chem.* **1986**, *98*, 257−258; *Angew. Chem. Int. Ed. Engl.* **1986**, *25*, 286−287. − [11b] J. W. Buchler, *Comments Inorg. Chem.* **1987**, *6*, 175−191. − [11c] J. W. Buchler, B. Scharbert, *J. Am. Chem. Soc.* **1988**, *110*, 4272−4276.

[12] J. W. Buchler, A. De Cian, J. Fischer, P. Hammerschmitt, R. Weiss, *Chem. Ber.* **1991**, *124*, 1051−1058.

[13] J. W. Buchler, P. Hammerschmitt, I. Kaufeld, J. Löffler, *Chem. Ber.* **1991**, *124*, 2151−2159.

[97216]

Complexation Studies with a Calix[4]arene-Derived Phosphinite − Divergent Arrays of Cavities Linked by MCl_2 Fragments (M = Pd, Pt)

Pascale Faidherbe[a], Catherine Wieser[a], Dominique Matt*[a], Anthony Harriman[b], André De Cian[c], and Jean Fischer[c]

Groupe de Chimie Inorganique Moléculaire, Université Louis Pasteur, UMR 7513[a],
1 rue Blaise Pascal, F-67008 Strasbourg Cedex, France

Ecole Européenne de Chimie, Polymères et Matériaux, Université Louis Pasteur[b],
1 rue Blaise Pascal, F-67008 Strasbourg Cedex, France

Laboratoire de Cristallochimie et Chimie Structurale, Université Louis Pasteur[c],
4 rue Blaise Pascal, F-67070 Strasbourg Cedex, France

Received November 24, 1997

Keywords: Calixarene / Phosphinite / Calixphosphane / Transition metals / X-ray diffraction

A cone-shaped calix[4]arene-derived monophosphinite, 25,27-di(ethoxycarbonylmethoxy)-26-hydroxy-28-(diphenylphosphinooxy)calix[4]arene (**L¹**), has been prepared in two steps from calix[4]arene. Treatment of **L¹** with [AuCl(tetrahydrothiophene)] in tetrahydrofuran gave the phosphinite complex [AuCl**L¹**] (**1**). Reaction of $[PdCl_2(PhCN)_2]$ with two equivalents of **L¹** gave selectively *trans*-$[PdCl_2\mathbf{L^1}_2]$ (**2**). Complex **2** · 2 CH_2Cl_2 crystallizes in the triclinic space group $P\bar{1}$. The molecule is centrosymmetric, leading to a divergent array of the two calixarene moieties. The palladium atom resides outside both cones. As a result of steric interactions, the *meta* and *para* carbon atoms of the PPh_2-bearing aryl ring are significantly pushed to the interior of the cavity. The related platinum complex *trans*-$[PtCl_2\mathbf{L^1}_2]$ (**3**), was obtained similarly from $[PtCl_2(PhCN)_2]$ and presents in the solid state a structure which is isomorphous to that of **2**. The diphosphinite 25,27-di(ethoxycarbonylmethoxy)-26,28-bis(diphenylphosphinoxy)calix[4]arene (cone) (**L²**) has also been prepared and reacts with $[PtCl_2(PhCN)_2]$ to yield oligomeric material.

The calix[4]arene structural framework has been extensively used as an important building block for the preparation of cavernous multifunctional podands[1][2][3][4][5][6][7]. Many of these ligands appear suitable for the selective recognition and complexation of metal cations[8][9][10][11][12][13][14][15][16][17] and/or for use as sensorial devices for anionic species[18][19]. An important feature which contributes to the valuable binding properties of functionalized calix[4]arenes in the *cone* conformation concerns the plasticity of the calixarene matrix. The flexibility of the cavity allows adoption of numerous geometries ranging from an almost C_4-symmetrical structure[20][21] to that of a so-called "pinched cone"[22][23]. In most structures where the latter shape has been encountered, two of the opposite aryl rings of the calixarene matrix lie almost coparallel, with the other two being essentially perpendicular.

As an extension of our earlier studies on calixarene-derived ligands suitable for transition metal complexation[24][25][26][27][28][29] we now report new examples of bulky calix[4]arene-derived phosphinites that form stable gold(I), palladium(II), and platinum(II) complexes. By reference to X-ray crystallography and NMR data, we describe the unusual structural attributes resulting from coordination of two such bulky ligands to a single metal center and, in particular, the resultant stereochemically-induced modification of the calixarene matrix. The present study complements previous results obtained with somewhat related compounds in which the calixarene ligands bear *tert*-butyl groups in the *para* positions, and for which inadequate X-ray crystallographic data were obtained[23]. In order to isolate the effects of metal complexation on the structural properties of the calixarenes of the macrocycle from steric effects relating to organic substituents, we have focussed our attention on the synthesis of calixarenes with freely accessible cavities. In fact omission of the *t*Bu groups allows intimate structural details to be elucidated. In addition such open cavities being equipped with a metal center at the bottom of the well may provide access to novel catalytic systems based on molecular recognition properties[30][31]. Here we describe the synthesis of open-ended calixarenes bearing two remote ester functions specifically designed to allow complexation of transition metals. Note, that investigations on the complexation properties of calixphosphinite ligands with three[9] and four[9][32][33] phosphorus atoms have recently been published.

Results and Discussion

Monophosphinite **L¹**, described here for the first time, was prepared in a two-step synthesis in which the first stage involved blocking of two distal hydroxy groups of calix[4]arene (Scheme 1). Intermediate **L⁰**, which is a key reactant for the formation of both **L¹** and **L²**, was obtained in 55% yield using conventional alkylation procedures[5]. It was deduced that of the four conformations possible for **L⁰**, the cone conformer was the only species detectable by ^{1}H- and ^{13}C-NMR spectroscopy. In particular, a unique ^{13}C-chemi-

 © WILEY-VCH Verlag GmbH, D-69451 Weinheim, 1998 1434−1948/98/0404−0451 $ 17.50+.50/0

cal shift of $\delta = 31.32$ was observed for the bridging methylene carbon atoms which, according to the diagnostic criteria outlined by Jaime et al. corresponds exactly to that expected for the cone conformation[34]. In fact similar studies made for the other non-metallated calixarene derivatives described here confirmed that these also persisted in the cone conformation.

Scheme 1. (*i*) K_2CO_3 (1 equiv.), RT, 15 h, acetone; then $BrCH_2CO_2Et$ (2 equiv.), 24 h , reflux; (*ii*) NEt_3 (2.5 equiv.), 0°C, in THF, 1 h; then addition of Ph_2PCl (2 equiv.); (*iii*) $LiNiPr_2$ (2 equiv.), 0.5 h, in THF (−78°C); then Ph_2PCl (2 equiv.)

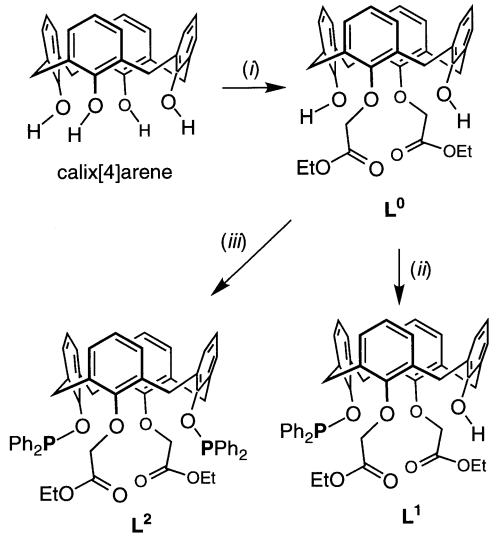

Monophosphination of $\mathbf{L^0}$ was achieved under mild conditions using NEt_3 as base. A signal typical of phosphinite residues is apparent at $\delta = 123.8$ in the ^{31}P-NMR spectrum. The IR (KBr) spectrum of $\mathbf{L^1}$ shows two strong absorption bands in the ester region (1760, 1737 cm^{-1}). The lower-energy band, located at 1737 cm^{-1}, is attributed to an ester having the carbonyl group hydrogen-bonded to a neighbouring hydroxy group. On this basis, the higher-energy band must arise from a non-hydrogen bonded carbonyl group. More surprisingly, precursor $\mathbf{L^0}$ also exhibits two well-resolved carbonyl bands in the IR spectrum (1761, 1742 cm^{-1}). This situation, which we have observed in other functionalized calixarenes bearing appended carbonyl moieties[23], is tentatively interpreted in terms of a mixture of free and hydrogen-bonded esters within the same molecule. X-ray investigations performed on complexes obtained from $\mathbf{L^1}$ corroborate this interpretation (vide infra).

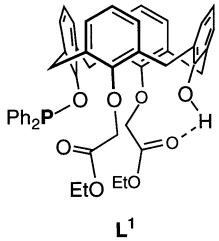

$\mathbf{L^1}$

Despite using forcing conditions, it was not possible to attach two phosphinites to the calixarene using mildly basic reagents (such as NEt_3). Synthesis of the bis-phosphinite $\mathbf{L^2}$ required more basic conditions, but was conveniently accomplished using two equivalents of $LiNiPr_2$ (Scheme 1). The ^{31}P-NMR spectrum of this compound displays a single peak at $\delta = 122.0$, indicating magnetic equivalence of the two phosphinites. The four bridging methylene groups of the macrocycle give a typical AB spectrum, as expected for a cone conformation. Interestingly, the aromatic region of the ^{1}H-NMR spectrum of $\mathbf{L^2}$ displays an AB_2 signal (6 H, $\delta = 6.21$, *p*-ArH_{calix}, 5.92, *m*-ArH_{calix}) significantly shifted upfield with respect to the other aromatic hydrogen atoms. Presumably, the two bulky phosphino groups cause steric crowding around the ester groups and thereby push the *meta* and *para* hydrogen atoms of two opposite aryl rings into the shielding zone of the other two aromatic rings of the calixarene matrix. These studies however do not allow distinction of which of the two aryl rings, namely those bearing the PPh_2 groups or those connected to the esters, are pinched together.

To show that phosphinite $\mathbf{L^1}$ is suitable for transition metal complexation, we investigated its coordinative properties towards a relatively small metal fragment, namely the "AuCl" unit. Thus, treatment of $\mathbf{L^1}$ with [AuCl(THT)] (THT = tetrahydrothiophene) in tetrahydrofuran gave the gold complex **1** as a white solid. The FAB mass spectrum of **1** shows an intense peak at 977.0 (with the expected isotopic profile) corresponding to the $[M^+ - Cl]$ ion. As for $\mathbf{L^1}$, the ^{1}H-NMR spectrum of **1** contains two AB patterns for the $ArCH_2Ar$ hydrogen atoms and an AB pattern for the two opposite $OCH_2C(O)$ groups. The ^{31}P-NMR spectrum displays a single peak at $\delta = 118.4$; this chemical shift is in agreement with those reported recently by Puddephatt et al. for other phosphinito-calixarene gold(I) complexes[9].

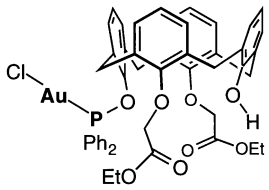

1

Reaction of $\mathbf{L^1}$ with $[PdCl_2(PhCN)_2]$ resulted in formation of complex **2** with high yield (Scheme 2). The *trans* stereochemistry around the metal center was inferred from the FAR IR spectrum which shows a single ν(Pd−Cl) band at 360 cm^{-1} and was confirmed by an X-ray diffraction study (vide infra). Despite the presence of the bridging P−Pd−P unit, the cone conformation of the two terminal calixarenes is retained. In marked contrast to the behaviour described above for $\mathbf{L^2}$, only a single aryl ring appears to be distorted out of its regular (i.e. non-metallated) position. Thus, NMR studies made with **2** indicate that there is an enhanced shielding effect for the *meta* and *para* hydrogens of only one aryl ring from each calixarene whereas with $\mathbf{L^2}$ two opposite rings are mutually distorted. Presumably,

deformation in **2** refers to the aryl rings lying closest to the metal center.

Scheme 2. (*i*) $[MCl_2(PhCN)_2]$ (M = Pd, Pt) in CH_2Cl_2

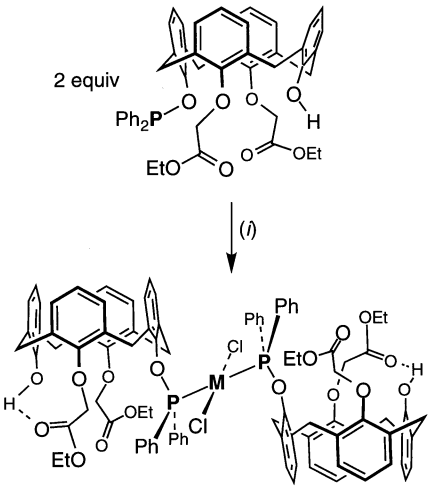

2, M = Pd ; **3**, M = Pt

The corresponding platinum analogue, **3**, also having *trans* sterochemistry [*J*(PPt) = 3006 Hz[35]] was obtained in a similar manner but starting from $[PtCl_2(PhCN)_2]$ (Scheme 2). Comparable upfield shifts on *meta* and *para* H atoms of a single aryl ring of each calixarene were observed. In fact, the ^{1}H-NMR properties of **2** and **3** were very similar, suggesting that a common structural feature persists in both metallated calixarenes. It is noteworthy that for complex **1** bearing the relatively small Au−Cl fragment all *m*-ArH hydrogen atoms lie above δ = 6.61 so that it appears reasonable to assign the upfield shifts observed for certain aromatic CH atoms in **2** and **3** to steric effects.

Both metal complexes, **2** and **3**, were fully characterized by X-ray structural analyses, but since these complexes are isomorphous, only one of them, namely the palladium complex **2**, will be described below. A summary of the crystal data is given in Table 1 (complex **2**) and Table 3 (complex **3**). Important distances and angles may be found in Table 2 (complex **2**) and Table 4 (complex **3**) . A view of **2** is represented in Figure 1. Examination of Figure 1 shows that half of the molecule is symmetry-generated since the palladium atom lies at the centre of symmetry. This leads to a solid-state structure with two divergent cavities, as defined by the calixarene units. The overall length of the molecule is ca. 18 Å. The complex exhibits square-planar coordination around the metal center with Pd−Cl and Pd−P bond lengths of 2.3014(6) and 2.3251(6) Å, respectively. The shape of the calixarene units strongly deviates from an ideal cone. In particular, two opposite aryl rings lie nearly perpendicular (dihedral angle Δ = 86°) with the other two making an angle of 12°. Each phosphorus atom is directed away from the cavity defined by the calixarene, the O−P−Pd plane being essentially orthogonal to the corresponding O-aryl ring (dihedral angle ca. 80°).

Several interesting facets emerge from the solid state structure (Fig. 1). Firstly, it is noticeable that the bulky diphenylphosphino groups adopt the position that causes minimal steric perturbation to the terminal calixarene units. Secondly, it is clearly demonstrated that the upper end of the phosphinated aryl ring is pushed towards the center of the cavity. The dihedral angle between the calixarene reference plane and the P-bearing phenoxy ring is 57.7(1)°. This "perturbation" of a single aryl unit was inferred from the NMR studies but is now shown unequivocally to exist in the solid state. Several complementary factors contribute to this effect. Although interactions between the d_{z^2} orbital on the palladium center and the adjacent aryl ring provide some minor repulsive force [Pd···C(1), 3.313 Å], the primary perturbing influence arises from steric interaction with the distant PPh_2 moiety {contacts: H(13)···C′(5) = 3.21 Å and H(13)···C′(6) = 3.33 Å [H(13) on C(18)]}. Thirdly, the above mentioned structural distorsion results in a rather narrow entrance to the cavity. This effect is illustrated by the comparatively short C(4)−C(33) separation of 4.64 Å and is reminiscent of the so-called *bis-roof* structure recently described by Shinkai et al.[36][37][38]. In the latter case, two distal aryl rings are made to approach each other by their involvment in π-complexes with $Cr(CO)_3$ fragments. This is a very different perturbing mode than that outlined for **2** and **3**, since the major structural feature of pinching of the calixarene unit results from mutual attraction of electron-deficient walls. In our case, a *single* wall is forced inwards by external steric influences. Finally, the short O(7)−O(5) distance (2.87 Å) indicates hydrogen bonding between the hydroxy function and the C(45)−O(7) carbonyl group. This finding corroborates our interpretation of the IR spectra.

Figure 1. MolView drawing of complex **2** with partial labeling scheme. The distance between C(4) and C(33) is 4.64 (1) A

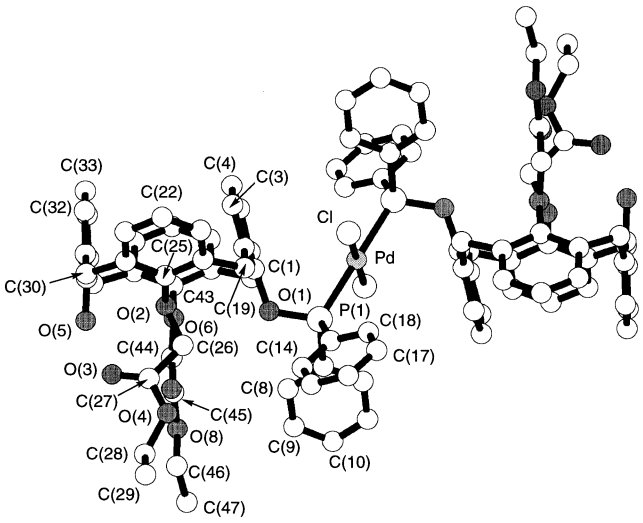

Considerable effort was expended to generate the corresponding cis isomers of **2** and **3**, but to no avail; examination of molecular models suggests that the bulky calixarene fragment provide undue steric barriers to formation of the cis complexes.

Reaction of $\mathbf{L^2}$ with $[PtCl_2(PhCN)_2]$ in CH_2Cl_2 gave a sparingly soluble white material in keeping with the overall formulation of $[PtCl_2(\mathbf{L^2})]_n$ to which we assign a polymeric

structure. The ^{31}P-NMR spectrum shows a broad peak at δ = 102.8, with a J(PPt) coupling constant of 3009 Hz, indicating that the stereochemistry about platinum is exclusively *trans*. The ^{1}H-NMR spectrum shows broad signals, suggesting the formation of a polymer and/or a mixture of oligomeric compounds. Because of its poor solubility, a molecular weight determination could not be performed. It is worth mentioning here that with previously reported diphosphinites having Bu^{t} groups occupying the *p*-positions of the calixarene moiety, cyclic tetrameric compounds were obtained[23]. The driving force for formation of oligomeric arrays arises from the fact that each of the phosphino groups in the bis derivative **L^{2}** is forced to lie outside of the cavity. Formation of bis(phosphinite) complexes with large metallo fragments such as "$PdCl_2$" or "$PtCl_2$" is then most easily accomplished by taking phosphorus from two separate calixarenes. With considerably smaller metallo-fragments such as CuCl, it is feasible that a mononuclear chelate could be generated[32]. Similar behaviour has also recently been observed with smaller phosphorus substituents[33].

In summary, we have described two novel phosphinites having open-ended cavities. Conditions are described which permit the selective attachment of one or two phosphino groups to the lower rim of a 1,3-difunctionalized calix[4]arene. The appended phosphino groups remain accessible for complexation with appropriate metallo-fragments and well-defined complexes have been observed with $PdCl_2$ and $PtCl_2$. In these cases and regardless of the presence of *t*Bu groups on the upper rim, it was only possible to isolate complexes demonstrating *trans* stereochemistry at the metal atom. The bulkyness of the two *trans* arranged phosphinites causes subtle modification to the structure of the calixarene unit, pushing one phenoxy ring into the cavity. In view of the fact that metallocalixarenes **2** or **3** contain two divergent cavities suitable for inclusion of neutral species, such nanostructures may provide further valuable complexation and/or catalytic opportunities.

We are grateful to *C. B. Dieleman* for his kind assistance. We are indebted to *Johnson Matthey* for a generous loan of precious metals.

Experimental Section

Reagents and Physical Measurements: All manipulations were performed in Schlenk-type flasks under argon. Solvents were dried by conventional methods and distilled immediately prior to use. $CDCl_3$ was eluted from a 5 cm thick alumina column and stored under argon over molecular sieves (0.4 nm). − IR spectra were recorded on a Perkin Elmer 1600 spectrometer (4000−400 cm^{-1}) and a Bruker FIR spectrometer (500−90 cm^{-1}). − ^{1}H-, ^{31}P{^{1}H}-, and ^{13}C{^{1}H}-NMR spectra were recorded with a FT Bruker WP-200 SY instrument. The ^{1}H-NMR data were referenced to residual protiated solvents (7.27 for $CDCl_3$), ^{13}C chemicals shifts are reported relative to deuterated solvents (δ = 77.0 for $CDCl_3$, δ = 67.40 for [D$_8$]THF) while the ^{31}P-NMR data are given relative to external H_3PO_4. − Mass spectra of complexes **2** and **3** were recorded on a ZAB HF VG Analytical instrument with *m*-nitrobenzyl alcohol as a matrix. The mass spectrum of **L^{2}** was recorded on a TSQ-70 spectrometer. Calix[4]arene[39], [AuCl(THT)] (THT = tetrahydrothiophene)[40], $[PdCl_2(PhCN)_2]$[41], and $[PtCl_2(PhCN)_2]$[41], were prepared using literature procedures.

Preparations

25,27-Di(ethoxycarbonylmethoxy)-26,28-(dihydroxy)calix[4]arene (**L^{0}**): A suspension of calix[4]arene (6.000 g, 14.13 mmol) was treated with K_2CO_3 (2.150 g, 15.55 mmol) in acetone (150 cm^3) for 15 h at room temperature. $BrCH_2CO_2Et$ (4.957 g, 29.68 mmol) was then added and the resultant mixture was heated under reflux for 24 h. After filtration, the solvent was removed in vacuo. The residue was recrystallized from CH_2Cl_2-MeOH, yielding **L^{0}** as a white analytically pure solid (6.600 g, 78%), R_f = 0.12 (SiO_2, CH_2Cl_2), m.p. 180°C. − IR (KBr): $\tilde{\nu}$ = 3387 br (OH), 1761 (C=O), 1742 (C=O···HO). − ^{1}H NMR ($CDCl_3$): δ = 7.66 (s, 2 H, OH), 7.07 (d, 4 H, *m*-ArH, ^{3}J = 7.5 Hz), 6.92 (d, 4 H, *m*-ArH, ^{3}J = 7.5 Hz), 6.75 (t, 2 H, *p*-ArH, ^{3}J = 7.5 Hz), 6.67 (t, 2 H, *p*-ArH, ^{3}J = 7.5 Hz), 4.75 (s, 4 H, OCH_2), 4.50 and 3.41 (AB spin system, 8 H, $ArCH_2Ar$, ^{2}J = 13 Hz), 4.34 (q, 4 H, OCH_2CH_3, ^{3}J = 7.1 Hz), 1.37 (t, 6 H, CH_3, ^{3}J = 7.1 Hz). − ^{13}C{^{1}H} NMR ($CDCl_3$): δ = 168.70 (CO), 152.82, 152.20, 132.95, 127.98 (4 C aromatic), 128.97, 128.34, 125.44, 118.95 (4 CH aromatic), 72.29 ($ArOCH_2$), 61.24 (OCH_2CH_3), 31.32 ($ArCH_2Ar$), 13.97 (CH_3). − $C_{36}H_{36}O_8 \cdot 0.5$ MeOH (596.68 + 16.02): calcd. C 71.55; H 6.25; found: C 71.03; H 5.70. The formation of a solvate was confirmed by ^{1}H-NMR spectroscopy.

25,27-Di(ethoxycarbonylmethoxy)-26-hydroxy-28-(diphenylphosphinooxy)calix[4] arene (**L^{1}**): To a solution of **L^{0}** (3.320 g, 5.60 mmol) in THF (100 cm^3) at 0°C was added triethylamine (1.420 g, 14.01 mmol). After stirring for 1 h, a solution of Ph_2PCl (1.360 g, 6.16 mmol) in THF (25 cm^3) was added slowly accompanied by formation of Et_3NHCl. The mixture was shaken for a further 24 h and the precipitate was removed by filtration before the solvent was evaporated in vacuo. Recrystallization of the residue from toluene-hexane gave **L^{1}** as a white solid (3.500 g, 80%), R_f = 0.43 (SiO_2, CH_2Cl_2), m.p. 148−150°C. − IR (KBr): $\tilde{\nu}$ = 3409 (OH), 1760 (C=O), 1737 (C=O···HO). − ^{1}H NMR ($CDCl_3$): δ = 7.80−7.78 and 7.49−7.47 (10 H, $OPPh_2$), 7.05−6.60 (12 H, ArH_{calix}), 4.62 and 3.31 (AB spin system, 4 H, $ArCH_2Ar$, ^{2}J = 13.5 Hz), 4.51 and 4.08 (AB spin system, 4 H, OCH_2CO_2, ^{2}J = 15.6 Hz), 4.29 and 3.01 (AB spin system, 4 H, $ArCH_2Ar$, ^{2}J = 13.2 Hz), 4.13 (q, 4 H,OCH_2CH_3, ^{3}J = 7.0 Hz), 3.67 (s, 1 H, OH), 1.24 (t, 6 H, OCH_2CH_3 , ^{3}J = 7.0 Hz). − ^{13}C {^{1}H} NMR ($CDCl_3$): δ = 169.44 (s, CO), 154.26−118.50 (s, C_{arom}), 71.75 (s, OCH_2CO), 60.78 (s, OCH_2CH_3), 31.17 and 30.95 (s, $ArCH_2Ar$), 13.97 (s, OCH_2CH_3). − ^{31}P{^{1}H} NMR ($CDCl_3$): δ = 123.8. − $C_{48}H_{45}O_8P$ (780.86): calcd. C 73.83; H 5.81; found: C 73.57; H 5.55.

25,27-Di(ethoxycarbonylmethoxy)-26,28-bis(diphenylphosphinooxy)calix[4]arene (**L^{2}**): To a cold (−78°C) solution of BuLi (1.5 M, 4.05 cm^3, 6.07 mmol) in THF (50 cm^3) was added slowly a solution of diisopropylamine (0.614 g, 6.07 mmol) in THF (20 cm^3), pre-cooled at −78°C. The mixture was kept at this temperature for 30 min before slow addition of a solution of the precursor **L^{0}** (1.800 g, 3.03 mmol) in THF (20 cm^3, −78°C). After 1 h, Ph_2PCl (1.339 g, 6.07 mmol) was added dropwise. The solution was stirred for 2 h, filtered through Celite, and evaporated to dryness. The residue was dissolved in toluene (50 cm^3) and the resulting suspension filtered through Celite in order to remove LiCl. Concentration of the filtrate and addition of hexane precipitated **L^{2}** as a white solid (2.490 g, 85%), R_f = 0.89 (SiO_2, CH_2Cl_2-MeOH, 95:5, v/v). − IR (KBr): $\tilde{\nu}$ = 1762 (C=O). − ^{1}H NMR ($CDCl_3$): δ = 7.76−6.70 (24H aromatics), 6.20 (t, 2 H, *p*-ArH, ^{3}J = 7.6 Hz), 5.91 (d, 4 H, *m*-ArH, ^{3}J = 7.6 Hz), 4.76 (s, 4 H, OCH_2), 4.41 and 2.84 (syst. AB, 8 H, $ArCH_2Ar$, ^{2}J = 14.5 Hz), 3.99 (q, 4 H, OCH_2CH_3,

^3J = 7.2 Hz), 1.37 (t, 6 H, CH_3, ^3J = 7.2 Hz). − $^{31}P\{^1H\}$ NMR ($CDCl_3$): δ = 122.0 (s, $OPPh_2$). This product is very sensitive to hydrolysis. We detected by NMR the formation of **L¹** and **L⁰** when traces of water were present. − MS (EI); *m/e* (%): 964.2 (10) [M^+]. − $C_{60}H_{54}O_8P_2$ (965.042): calcd. C 74.68; H 5.64; found: C 74.72; H 5.80.

Chlorobis[25,27-di(ethoxycarbonylmethoxy)-26-hydroxy-28-(diphenylphosphinooxy)calix[4]arene]gold(I) (**1**)**:** A solution of [AuCl(THT)] (0.160 g, 0.50 mmol) in THF (15 cm^3) was added to a solution of compound **L¹** (0.390 g, 0.50 mmol) in THF (15 cm^3). After 1 h the resultant solution was concentrated to ca. 5 cm^3; addition of pentane gave **1** as a white powder which was recrystallised from THF-pentane (0.380 g, 75%), m.p. 112−114°C (dec). − IR (KBr): $\tilde{\nu}$ = 3430 br (OH), 1752 (C=O), 1728 (C=O···HO). − ^1H NMR ([D_8]THF): δ = 8.27−8.17 and 7.74−7.73 (10 H, $OPPh_2$), 7.32−6.57 (12 H, ArH_{calix}), 4.68 and 3.13 (AB spin system, 4 H, $ArCH_2Ar$, ^2J = 13.3 Hz), 4.39 and 4.19 (AB spin system, 4 H, OCH_2CO_2, ^2J = 16.0 Hz), 4.31 and 3.32 (AB spin system, 4 H, $ArCH_2Ar$, ^2J = 13.5 Hz), 4.23 (q, 4 H,OCH_2CH_3, ^3J = 7.0 Hz), 3.76 (s, 1 H, OH), 1.30 (t, 6 H, OCH_2CH_3 , ^3J = 7.0 Hz). − $^{13}C\{^1H\}$ NMR ([D_8]THF): δ = 179.90 (s, CO), 154.80−119.18 (s, C_{arom}), 72.70 (s, OCH_2CO), 61.40 (s, OCH_2CH_3), 32.36 and 31.74 (s, $ArCH_2Ar$), 14.41 (s, OCH_2CH_3). − $^{31}P\{^1H\}$NMR ($CDCl_3$): δ = 118.4. − MS (FAB MS); *m/e* (%): 977 (100) [M^+ − Cl]. − $C_{48}H_{45}AuClO_8P$ (1013.28): calcd. C 56.90; H 4.48; found: C 57.22; H 4.77.

Table 1. Crystallographic data for *trans*-[$PdCl_2$(**L²**)$_2$] · 2 CH_2Cl_2 (**2** · 2 CH_2Cl_2)

formula	$C_{96}H_{90}Cl_2O_{16}P_2Pd$ · 2 CH_2Cl_2		
fw	1908.9	T [K]	293
a [Å]	11.393(3)	λ [Å]	0.71073
b [Å]	11.767(3)	space group	$P\bar{1}$
c [Å]	18.933(5)	Z	1
α [deg]	77.16(2)	D_{calcd} [g cm^{-3}]	1.382
β [deg]	87.04(2)	θ range [deg]	2−28
γ [deg]	68.05(2)		
μ [cm^{-1}]	4.720		
V [$Å^3$]	2294.0	R[a]	0.045
no of data collected	10309	R_w[b]	0.066
no of data with I>3σ(I)	7418		

[a] $R = \Sigma(||F_o|-|F_c||)/\Sigma|F_o|$. − [b] $R_w = [\Sigma w(|F_o|-|F_c|)^2/\Sigma w|F_o|^2]^{1/2}$; $w^{-1} = \sigma^2(F_o)$.

Table 2. Selected structural parameters for **2** (lengths in Å, angles in°)

Bond Lengths			
Pd−Cl	2.3014(6)	O2−C26	1.417(3)
Pd−P1	2.3251(6)	C26−C27	1.508(4)
P1−C7	1.811(2)	C27−O4	1.319(4)
P1−C13	1.812(2)	C27−O3	1.211(4)
O1−P1	1.621(2)	O6−C44	1.417(3)
C1−C2	1.396(3)	C44−C45	1.494(4)
C2−C3	1.402(4)	C45−O7	1.186(3)
C3−C4	1.369(4)	C45−O8	1.321(3)
C4−C5	1.388(4)	O8−C46	1.458(3)
C2−C19	1.515(3)	C46−C47	1.455(5)
C5−C6	1.395(3)	O5···O3	2.87(1)
C43−O6	1.397(3)	C4···C33	4.64(1)
C36−O5	1.372(3)	H13···C′5	3.21(1)
C25−O2	1.387(3)	H13···C′6	3.33(1)
Bond Angles			
Cl−Pd−P1	90.67(2)	C6−C48−C42	108.3(2)
O1−P1−C7	101.8(1)	C35−C37−C38	110.2(2)
O1−P1−C13	104.5(1)	C44−C45−O7	126.2(3)
C7−P1−C13	100.3(1)	C26−C27−O3	126.0(3)
C1−O1−P1	118.8(1)	C43−O6−C44	109.3(2)
C2−C19−C20	110.4(2)	C25−O2−C26	114.8(2)

trans-Dichlorobis[25,27-di(ethoxycarbonylmethoxy)-26-hydroxy-28-(diphenylphosphinooxy)calix[4]arene]palladium(II) (**2**): A solution of [$PdCl_2$(PhCN)$_2$] (0.384 g, 0.310 mmol) in THF (50 cm^3) was added slowly to a solution of **L¹** (0.484 g, 0.620 mmol) in THF (40 cm^3). After 2 h the solution was reduced to one-third and hexane was added, yielding **2** as a yellow solid (0.456 g, 84%), R_f = 0.84 (SiO_2, MeOH-CH_2Cl_2, 5/95, v/v), m.p. 238−240°C (dec). − IR spectrum (KBr): $\tilde{\nu}$ = 3414 (OH), 1750 (CO) , 1731 (C=O···HO). − Far FT-IR: $\tilde{\nu}$ = 360 (PdCl). − ^1H NMR ($CDCl_3$): δ = 7.84−6.32 (19 H, CH aromatic), 7.74 (1 H, OH, exchanges with D_2O), 6.21 (t, 1 H, *p*-ArH_{calix}, ^3J = 7.5 Hz), 5.92 (d, 2 H, *m*-ArH, 3J = 7.5 Hz), 5.11 and 4.59 (AB spin system, 4 H, OCH_2, ^2J = *1*6 Hz), 4.67 and 3.22 (AB spin system, 4 H, $ArCH_2$, ^2J = *1*3 Hz), 4.35 and 3.22 (AB spin system, 4 H, $ArCH_2Ar$, ^2J = 16.8 Hz), 4.24 (q, 8 H, OCH_2CH_3, ^3J = 7.1 Hz), 1.28 (t, 6 H, OCH_2CH_3, ^3J = 7.1 Hz). − $^{13}C\{^1H\}$ NMR ($CDCl_3$): δ = 171.35 (s, CO), 157.09−119.02 (C aromatic), 71.64 (OCH_2CO), 60.93 (OCH_2CH_3), 32.57 and 31.97 (2s, $ArCH_2Ar$), 13.97 (OCH_2CH_3). − $^{31}P\{^1H\}$ NMR ($CDCl_3$): δ = 111 (s). − MS (FAB MS); *m/e* (%): 1703 (0.5) [M^+ − Cl]. − $C_{96}H_{90}Cl_2O_{16}P_2Pd$ (1739.03): calcd. C, 66.31; H, 5.22; found: C, 66.34; H, 5.33.

trans-Dichlorobis[25,27-di(ethoxycarbonylmethoxy)-26-hydroxy-28-(diphenylphosphinooxy)calix[4]arene]platinum(II) (**3**)**:** To a solution of **L¹** (0.303 g, 0.390 mmol) in THF (40 cm^3) was added slowly a solution of [$PtCl_2$(PhCN)$_2$] (0.091 g, 0.195 mmol) in THF (50 cm^3). After 2h the solution was concentrated and hexane was added, yielding **3** as a white solid (0.293 g, 82%) which was dried in vacuo overnight, R_f = 0.8 (SiO_2, MeOH/CH_2Cl_2, 5/95, v/v), m.p. 271−275°C. − IR (KBr): $\tilde{\nu}$ = 3415br (OH), 1756 (C=O), 1731 (C=O···HO). − Far FT-IR: $\tilde{\nu}$ = 349 (PtCl). − ^1H NMR ($CDCl_3$): δ = 7.86−6.32 (19 H, CH aromatics), 7.72 (s, 1 H, OH, exchanges with D_2O), 6.22 (t, 1 H, *p*-ArH, ^3J = 7.6 Hz), 5.89 (d, 2 H, *m*-ArH, ^3J = 7.6 Hz), 5.14 and 4.65 (AB spin system, 4 H, OCH_2CO_2, ^2J = 16.4 Hz), 4.67 and 3.23 (AB spin system, 4 H, $ArCH_2Ar$, ^3J = 13.7 Hz), 4.42 and 3.20 (AB spin system, 4 H, $ArCH_2Ar$, ^2J = 14.8 Hz), 4.26 (q, 8 H, OCH_2CH_3, ^3J = 7.1 Hz), 1.29 (t, 6 H, OCH_2CH_3, ^3J = 7.1 Hz). − $^{13}C\{^1H\}$ NMR ($CDCl_3$): δ = 171.39 (CO), 157.20−119.07 (C aromatics), 71.63 (OCH_2CO_2), 60.97(OCH_2CH_3), 32.56 ($ArCH_2Ar$), 31.11 ($ArCH_2Ar$), 14.00 (OCH_2CH_3). − $^{31}P\{^1H\}$ NMR ($CDCl_3$): δ = 102.7 [s with Pt satellites, ^2J(PPt) = 3006.3 Hz]. − MS (FAB MS); *m/e* (%): 1827 (1) [M^+], 1790 (7) [M^+ − Cl]. − $C_{96}H_{90}Cl_2O_{16}P_2Pt$ (1827.72): calcd C, 63.09; H, 4.96; found: C, 62.79; H, 4.89.

Reaction of [PtCl₂(PhCN)₂] with **L²**: A solution of [$PtCl_2$(PhCN)$_2$] (0.168 g, 3.56 mmol) in CH_2Cl_2 (30 cm^3) was added to a solution of **L²** (0.344 g, 3.56 mmol) in CH_2Cl_2 (20 cm^3). After 1 h the solution was concentrated and hexane was added, yielding a white precipitate (0.329 g, 75%) which was poorly soluble in $CHCl_3$, CH_2Cl_2, and THF, m.p. 263−266°C. − ^1H NMR ($CDCl_3$): δ = 1.19 (t, OCH_2CH_3, ^3J = 7.0 Hz); all other signals are broad probably owing to a fluxional behaviour in solution or to the presence of several oligomeric compounds. $^{31}P\{^1H\}$ NMR ($CDCl_3$): δ 102.8 [s with Pt satellites, ^2J(P-Pt) = 3009 Hz]. − $C_{60}H_{54}Cl_2O_8P_2Pt$ (1231.04): calcd. C, 58.04; H, 4.42; found: C, 58.11; H, 4.32.

X-ray Crystallographic Studies: Complex **2**: Crystal data are given in Table 1. A suitable crystal of **2** · 2 CH_2Cl_2 was obtained by slow diffusion of hexane into a solution of complex **2** in CH_2Cl_2 at room temperature. Data were collected on an ENRAF-NONIUS MAC3 diffractometer at room temperature with graphite mono-

chromatic Mo-K_α radiation $\lambda = 0.7107$ Å. The cell parameters were obtained by fitting a set of 25 high-theta reflections. The data collection ($\omega/2\theta$ scan type, $2\theta_{max} = 56°$, $+h \pm k \pm l$), intensity controls without appreciable decay (0.2%) gives 10309 reflections from which 7418 were independant with $I>3\sigma(I)$. After Lorenz polarization and absorption (ψ scan) corrections, the structure was solved by direct methods. After refinement of the heavy atoms, a Fourier-difference map revealed maxima of residual electronic density close to the positions expected for hydrogen atoms; they were introduced into structure-factor calculations by their computed coordinates (C−H 0.95 Å) and isotropic thermal parameters such as B(H) = 1.3 B_{eq}(C) Å but not refined. Full least squares refinements against F with weights $\omega = 1/\sigma^2(F)$, $\sigma^2(F^2) = \sigma^2$ (counts) + $(pI)^2$. Anisotropic thermal parameters were assigned to all non-hydrogen atoms except for C(28), C(29), C′(28), and C′(29). Final positive and negative electron density residues: 0.81/−0.24 e·Å^{-3}. Atomic scattering factors were from International Tables for X-ray Crystallography (1983)[42]. All calculations were performed on a DEC AXP 3100 computer with the OpenMolEN[43] package (Enraf-Nonius, 1990). The ethyl group of one ester (C28) was found to be disordered over two positions in the ratio 1:1. The plot of **2** was drawn using MolView[44].

Complex **3**·*2 CH_2Cl_2:* Crystal data are given in Table 3. Crystals of **3** · 2 CH_2Cl_2 were obtained by slow diffusion of hexane into a solution of complex **3** in CH_2Cl_2. Data collection as described above. The data collection ($\omega/2\theta$ scan type, $2\theta_{max} = 52°$, $+h \pm k \pm l$), intensity controls without appreciable decay (0.2%) gives 9588 reflections from which 8843 were independant with $I>3\sigma(I)$. After Lorenz polarization and absorption (ψ scan) corrections, the structure was solved by direct methods. After refinement of the heavy atoms, a Fourier-difference map revealed maxima of residual electronic density close to the positions expected for hydrogen atoms; they were introduced into structure-factor calculations by their computed coordinates (C−H 0.95 Å) and isotropic thermal parameters such as B(H) = 1.3 B_{eq}(C) Å but not refined. Full least squares refinements against F with weights $\omega = 1/\sigma^2(F)$, $\sigma^2(F^2) = \sigma^2$ (counts) + $(pI)^2$. Anisotropic thermal parameters were assigned to all non-hydrogen atoms. Final positive and negative electron density residues: 0.771/−0.112 e·Å^{-3}. Complete atomic coordinates, thermal parameters and bond lengths and angles for both complexes have been deposited at the Crystallographic Data Centre (CCDC number 100858).

Table 3. Crystallographic data for *trans*-[$PtCl_2$(**L**^{2})$_2$] · 2 CH_2Cl_2 (**2** · 2 CH_2Cl_2)

formula	$C_{96}H_{90}Cl_2O_{16}P_2Pt$·2 CH_2Cl_2		
fw	1997.59	T [K]	294
a [Å]	11.3891(7)	λ [Å]	0.71073
b [Å]	11.7494(7)	space group	$P\bar{1}$
c [Å]	18.941(1)	Z	1
α [deg]	77.296(5)	D_{calcd} [g cm^{-3}]	1.45
β [deg]	87.064(5)	θ range [deg]	2.5−26
γ [deg]	68.052(5)		
μ [cm^{-1}]	1.819		
V [Å^3]	2291.9 (3)	R[a]	0.029
no of data collected	9588	R_w[b]	0.041
no of data with $I>3\sigma(I)$	8843		

[a] $R = \Sigma(\|F_o|-|F_c\|)/\Sigma|F_o|$. − [b] $R_w = [\Sigma w(|F_o|-|F_c|)^2/\Sigma w|F_o|^2]^{1/2}$; $w^{-1} = \sigma^2(F_o)$.

Table 4. Selected structural parameters for **3** (lengths in Å, angles in°)

Bond Lengths			
Pt−Cl	2.3066(7)	O2−C26	1.418(4)
Pt−P1	2.3024(7)	C26−C27	1.492(6)
P1−C7	1.815(3)	C27−O4	1.328(5)
P1−C13	1.820(3)	C27−O3	1.203(5)
O1−P1	1.625(2)	O6−C44	1.422(4)
C1−C2	1.386(4)	C44−C45	1.498(4)
C2−C3	1.399(5)	C45−O7	1.172(4)
C3−C4	1.374(5)	C45−O8	1.325(4)
C4−C5	1.381(5)	O8−C46	1.452(4)
C2−C19	1.515(4)	C46−C47	1.464(7)
C5−C6	1.384(4)	O5···O3	2.86(1)
C43−O6	1.398(3)	C4···C33	4.627(6)
C36−O5	1.372(4)	H13···C′5	3.21(1)
C25−O2	1.383(4)	H13···C′6	3.32(1)
Bond Angles			
Cl−Pt−P1	90.78(2)	C6−C48−C42	108.1(2)
O1−P1−C7	101.9(1)	C35−C37−C38	110.2(3)
O1−P1−C13	104.3(1)	C44−C45−O7	127.0(3)
C7−P1−C13	100.2(1)	C26−C27−O3	126.1(4)
C1−O1−P1	118.7(2)	C43−O6−C44	109.2(2)
C2−C19−C20	109.9(3)	C25−O2−C26	115.0(2)

[1] C. D. Gutsche in *Calixarenes, Monographs in Supramolecular Chemistry,* (Ed.: J. F. Stoddart), The Royal Society of Chemistry, Cambridge, England, **1989**.

[2] *Calixarenes, a versatile class of macrocyclic compounds* (Ed.: J. Vicens and V. Böhmer), Kluwer, Dordrecht, The Netherlands, **1990**.

[3] V. Böhmer, M. A. McKervey, *Chemie in unserer Zeit* **1991**, *25,* 195−207.

[4] J. L. Atwood, G. W. Orr, F. Hamada, R. L. Vincent, S. G. Bott, K. D. Robinson, *J. Am. Chem. Soc.* **1991**, *113,* 2760−2761.

[5] J.-D. van Loon, W. Verboom, D. N. Reinhoudt, *Organic Preparations and Procedures Int.* **1992**, *24,* 437−462.

[6] S. Shinkai, *Tetrahedron* **1993**, *49,* 8933−8968.

[7] C. Wieser, C. B. Dieleman, D. Matt, *Coord. Chem. Rev.* **1997**, *165,* 93−161.

[8] J.-C. G. Bünzli, J. M. Harrowfield in *Calixarenes, a versatile class of macrocyclic compounds* (Ed.: J. Vicens and V. Böhmer), Kluwer, Dordrecht, The Netherlands, **1990**, pp 211−231.

[9] W. Xu, R. J. Puddephatt, L. Manojlovic-Muir, K. W. Muir, C. S. Frampton, *J. Incl. Phenom.* **1994**, *19,* 277−290.

[10] P. D. Beer, Z. Chen, A. J. Goulden, A. Grieve, D. Hesek, F. Szemes, T. Wear, *J. Chem. Soc., Chem. Commun.* **1994**, 1269−1271.

[11] C. Hill, J.-F. Dozol, V. Lamare, H. Rouquette, S. Eymard, B. Tournois, J. Vicens, Z. Asfari, C. Bressot, R. Ungaro, A. Casnati, *J. Incl. Phenom.* **1994**, *19,* 399−408.

[12] R. Ungaro, A. Casnati, F. Ugozzoli, A. Pochini, J.-F. Dozol, C. Hill, H. Rouquette, *Angew. Chem., Int. Ed. Engl.* **1994**, *33,* 1506−1509.

[13] A. T. Yordanov, J. T. Mague, D. M. Roundhill, *Inorg. Chem.* **1995**, *34,* 5084−5087.

[14] D. M. Roundhill, *Progr. Inorg. Chem.* **1995**, *43,* 533−592.

[15] I. Neda, H.-J. Plinta, A. Fischer, P. G. Jones, R. Schmutzler, *Phosphorus, Sulfur, and Silicon* **1996**, *109−110,* 113−116.

[16] F. Arnaud-Neu, V. Böhmer, F. Dozol, C. Grüttner, R. A. Jakobi, D. Kraft, O. Mauprivez, H. Rouquette, M.-J. Schwing-Weill, N. Simon, W. Vogt, *J. Chem. Soc., Perkin Trans. 2* **1996**, 1175−1182.

[17] P. D. Beer, *J. Chem. Soc., Chem. Commun.* **1996**, 689−696.

[18] A. Arduini, E. Ghidini, A. Pochini, R. Ungaro, G. D. Andreetti, G. Calestani, F. Ugozzoli, *J. Incl. Phenom.* **1988**, *6,* 119−134.

[19] P. D. Beer, M. G. B. Drew, P. B. Leeson, M. I. Ogden, *J. Chem. Soc., Dalton Trans.* **1995**, 1273−1283.

[20] E. Dahan, S. E. Biali, *J. Org. Chem.* **1991**, *56,* 7269−7274.

[21] M. Conner, V. Janout, S. L. Regen, *J. Am. Chem. Soc.* **1991**, *113,* 9670−9671.

[22] C. Loeber, D. Matt, A. De Cian, J. Fischer, *J. Organomet. Chem.* **1994**, *475,* 297−305.

[23] C. Loeber, D. Matt, P. Briard, D. Grandjean, *J. Chem. Soc., Dalton Trans.* **1995**, 513−524.

[24] C. Loeber, C. Wieser, D. Matt, A. De Cian, J. Fischer, L. Toupet, *Bull. Soc. Chim. Fr.* **1995**, *132,* 166−177.

[25] C. Loeber, C. Wieser, D. Matt in *Stereoselective reactions of metal-activated molecules* (Ed.: H. Werner and J. Sundermeyer), Vieweg, Braunschweig, Germany, **1995**, pp191−194 ,
[26] C. Dieleman, C. Loeber, D. Matt, A. De Cian, J. Fischer, *J. Chem. Soc., Dalton Trans.* **1995**, 3097−3100.
[27] C. Wieser, D. Matt, L. Toupet, H. Bourgeois, J.-P. Kintzinger, *J. Chem. Soc., Dalton Trans.* **1996**, 4041−4043.
[28] C. Wieser, D. Matt, J. Fischer, A. Harriman, *J. Chem. Soc., Dalton Trans.* **1997**, 2391−2042.
[29] C. B. Dieleman, D. Matt, P. G. Jones, *J. Organomet. Chem.* **1997**, 461−473.
[30] H. K. A. C. Coolen, P. W. N. M. van Leuwen, R. J. M. Nolte, *Angew. Chem. Int. Ed. Engl.* **1992**, *31,* 905−907.
[31] M. T. Reetz, J. Rudolph, *Tetrahedron Assymetry* **1993**, *4,* 2405−2406.
[32] C. Floriani, D. Jacoby, A. Chiesi-Villa, C. Guastini, *Angew. Chem., Int. Ed. Engl.* **1989**, *28,* 1376−1377.
[33] M. Stolmàr, C. Floriani, A. Chiesi-Villa, C. Rizzoli, *Inorg. Chem.* **1997**, *36,* 1694−1701.
[34] C. Jaime, J. de Mendoza, P. Prados, P. M. Nieto, C. Sánchez, *J. Org. Chem.* **1991**, *56,* 3372−3376.
[35] P. S. Pregosin, R. W. Kunz in ^{31}P and ^{13}C NMR of Transition Metal Phosphine Complexes, n° 16 of Basic Principles and Progress (Ed.: P. Diehl, E. Fluck, R. Kosfeld), Springer, Berlin-Heidelberg, Germany, **1979**.
[36] H. Iki, T. Kikuchi, H. Tsuzuki, S. Shinkai, *Chem. Lett.* **1993**, 1735−1738.
[37] H. Iki, T. Kikuchi, S. Shinkai, *J. Chem. Soc., Perkin Trans. 1* **1993**, 205−210.
[38] H. Iki, T. Kikuchi, H. Tsuzuki, S. Shinkai, *J. Incl. Phenom.* **1994**, *19,* 227−236.
[39] C. D. Gutsche, L.-G. Lin, *Tetrahedron* **1986**, *42,* 1633−1640.
[40] R. Uson, A. Laguna, M. Laguna, *Inorg. Synthesis* **1989**, *26,* 85−87.
[41] F. R. Hartley, *The Chemistry of Platinum and Palladium,* Wiley, New York, USA, **1973**.
[42] *International Tables for X-Ray Crystallography*, Boston, MA, **1983**, p. A.183.
[43] C. K. Fair in *MolEN. An Interactive Intelligent System for Crystal Structure Analysis.* Enraf-Nonius, Delft, The Netherlands, **1990**.
[44] J.-M. Cense, *MolView*, Ecole Nationale Supérieure de Chimie de Paris, **1997**.

[97274]

Carbon Monoxide and Isonitrile Insertion into the B−B Bond of Five-Membered Cyclic Organo-1,2-diboranes☆

Jens Teichmann, Harald Stock, Hans Pritzkow, and Walter Siebert*

Anorganisch-Chemisches Institut der Universität Heidelberg,
Im Neuenheimer Feld 270, D-69120 Heidelberg, Germany

Received October 22, 1997

Keywords: 1,2-Diboraheterocycles / Carbon monoxide insertion / Isonitrile insertion / Dimerisation / Spiro insertion products

The insertion of CO into the B−B bond of 1,2-bis(diisopropylamino)-2,5-dihydro-1*H*-1,2-diborole (**1b**) and 1,2-bis(diisopropylamino)-3-methylidene-1,2-diborolane (**1c**) leads to the dimeric spiro products 1,7,9,14-tetrakis(diisopropylamino)-6,13-dioxa-1,7,9,14-tetraboradispiro[4.2.4.2]tetradeca-2,10-diene (**4b**) and 1,7,9,14-tetrakis(diisopropylamino)bismethylidene-6,13-dioxa-1,7,9,14-tetraboradispiro[4.2.4.2]tetradecane (**4c**). Insertions of CO into the B−B bonds of the cyclic organo-1,2-diborane compounds **5**, **6**, and **7** are not observed. The reaction of **1b** with *tert*-butyl isocyanide and 2,6-dimethylphenyl isocyanide in THF leads to the formation of the monomeric insertion products 1,3-bis(diisopropylamino)-2-*tert*-butylimino-1,3-diboracyclohex-4-ene (**10b**) and 1,3-bis(diisopropylamino)-2-(2′,6′-dimethylphenylimino)-1,3-diboracyclohex-4-ene (**11b**). The treatment of **1c** with the isonitriles yields 2-*tert*-butylimino-1,3-bis(diisopropylamino)-4-methylidene-1,3-diboracyclohexane (**10c**) and 1,3-bis(diisopropylamino)-2-(2′,6′-dimethylphenylimino)-4-methylidene-1,3-diboracyclohexane (**11c**). The steric requirements of the isonitrile insertion products **10b**, **c** and **11b**, **c** prevent their dimerisation and rearrangement. **11b** rearranges to 1-(diisopropylamino)-2-(diisopropylaminohydroxyboryl)-2-(2′,6′-dimethylphenylamino)-1-boracyclopent-3-ene (**12b**) upon reaction with water from sodium sulfate decahydrate. The compositions of the compounds are derived from the ^{1}H-, ^{11}B-, ^{13}C-NMR data as well as from mass-spectral and C, H, N analyses. In the cases of of **4b** and **12b** they have been proven by X-ray structure analyses.

The synthesis and structural characterization of the η^4-(4-boryl-1-borabutadiene)-η^5-cyclopentadienylcobalt complexes **2a**[1] from the 4-methylene-1,2-diborolane **1a**,[2] as well as **2b**[3] from the 1*H*-1,2-diborole **1b**[3] and bis(ethene)-cyclopentadienylcobalt, led to the expectation that related compounds should be formed with other 14 VE complex fragments. However, **1b** and either $Fe(CO)_5$ or $Fe_2(CO)_9$ did not yield the corresponding η^4-(4-boryl-1-borabutadiene)-tricarbonyliron complex **3b**. A few colorless crystals could be separated from the reaction mixture and mass-spectrometric data indicated the presence of a dimer of a reaction product of carbon monoxide and **1b**. Its constitution was elucidated by an X-ray structure analysis (see below) which showed the presence of the dimeric spiro compound **4b**.[4]

Reactions of CO with organoboranes are long since known and are well documented.[5] The insertion of CO into the B−B bond of three-membered heterocycles was first observed by Paetzold et al.[6] Tri-*tert*-butylazadiboriridine [$NB_2(CMe_3)_3$] and CO yield the tricyclic compound 1,3,4,5,7,8-hexa-*tert*-butyl-4,9-dioxa-1,7-diaza-2,5,8,10-tetraboradispiro[2.2.2.2]decane. The proposed mechanism describes, in the first step, the insertion of CO into the B−B bond to give a four-membered $NB_2C{=}O$ ring, which then undergoes a [3+3] cyclodimerisation of the BC=O chain to yield the corresponding six-membered ring. Sigmatropic migrations of the amino groups from the boron to the carbon atoms result in the final product.

Analogously, isonitriles (RNC) insert into the B−B bond of $NB_2(CMe_3)_3$ to form the corresponding four-membered rings $NB_2C{=}NR$. With R = Me, Et the primary products undergo a [3+3] cyclodimerisation of the BC=N chain to result in the tricyclic compounds.[7]

Scheme 1

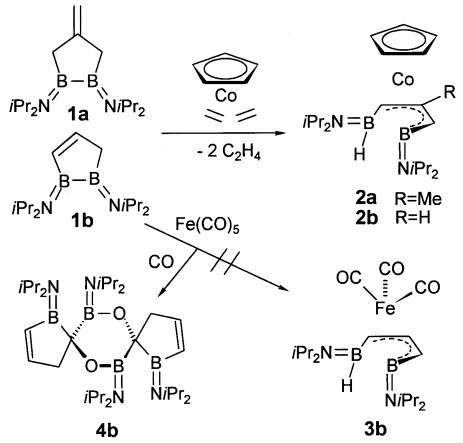

In the following we report on our findings concerning CO and C=NR insertion into the B−B bond of five-membered cyclic organodiboranes.

Results and Discussion

Reactions of Cyclic Organo-1,2-diboranes with Carbon Monoxide

The compound **4b**[4] is formed in a good yield when dried CO is bubbled into a THF solution of **1b**.[3] Due to its weak

 © WILEY-VCH Verlag GmbH, D-69451 Weinheim, 1998 1434−1948/98/0404−0459 $ 17.50+.50/0

solubility **4b** precipitates as a solid which is less sensitive to air and moisture. The reaction between the 3-methylidene-1,2-diborolane **1c**[1] and CO leads to the analogous dimeric spiro product 1,7,9,14-tetrakis(diisopropylamino)bismethylidene-6,13-dioxa-1,7,9,14-tetraboradispiro[4.2.4.2]tetradecane (**4c**).[4] We assume that, besides **4c**, two other isomers have been formed due to various positions of the exocyclic double bonds. Mass-spectral data and C, H, N analyses were obtained, but no NMR data could be obtained due to its very low solubility in organic solvents. The mass spectra of the reaction product of **1c** and $Fe(CO)_5$ indicate that the η^4-(1-boryl-2-methyl-1-borabutadiene)-tricarbonyliron complex (analogous to **3b**) was present[4], however, it could not be isolated. The reaction of **1a** with $Fe(CO)_5$ also led to traces of the analogous complex.

Scheme 2

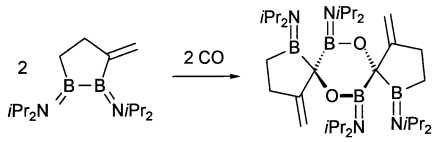

1c **4c**

In addition to **1a–c**, the cyclic organo-1,2-diborane compounds 1,2-bis(diisopropylamino)-1,2-diboret (**5**)[8], 1,2-bis(diisopropylamino)-1,2-benzodiboret (**6**)[9], and 1,2,4-tris(diisopropylamino)-3,5-dimethyl-1,2,4-triboracyclopentan (**7**)[10] were treated with dried CO. None of the expected insertion products were formed and the starting materials were recovered.

Scheme 3

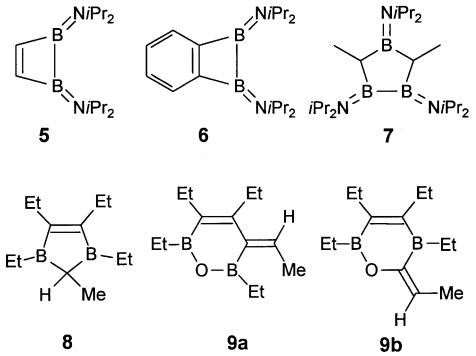

5 **6** **7**

8 **9a** **9b**

It is of interest to note that we did not observe any insertion into the B–C bonds of the compounds **1a–c**. This is in contrast to the reaction of CO with the 1,3,4,5-tetraethyl-2-methyl-2,3-dihydro-1,3-diborole (**8**), which leads to product **9a** and **9b**.[11] The formation of **9b** can be explained by insertion of CO into the B–CHMe bond of **8**, and exchange of the CHMe group for the oxygen of the inserted CO. The product **9a** is formed analogously by insertion of CO into the B–CEt bond and exchange of the CHMe group for the oxygen of the inserted CO, which yields the B–O–B bridge. When **8** is treated with $Ni(CO)_4$,[11] presumably **9a** is the precursor for the formation of a nickel complex with two cyclic allyl ligands.

Reactions of Organo-1,2-diboranes with Isonitriles

The failure of CO to insert into the B–B bond of the compounds **5–7** is also observed with the isonitriles. The reaction of the 1,2-diborole **1b** with *tert*-butyl isocyanide and with 2,6-dimethylphenyl isocyanide at −30°C in THF leads to colorless, slightly soluble monomeric products, 2-*tert*-butylimino-1,3-diboracyclohex-4-ene (**10b**) and 2-(2′,6′-dimethylphenylimino)-1,3-diboracyclohex-4-ene (**11b**). As a sideproduct in the reaction with **1b** its rearrangement to the known 1,3-bis(diisopropylamino)-2,3-dihydro-1,3-diborole[12][13] was observed. MS and ^{1}H-, ^{11}B-, and ^{13}C-NMR data confirmed the composition of the products formed.

Scheme 4

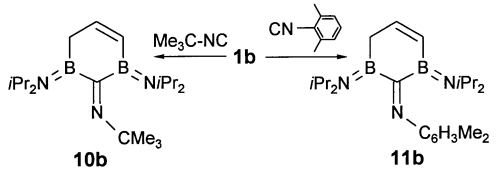

10b **11b**

In the ^{1}H-NMR spectra all four septuplets of the methine protons of the isopropyl groups of **10b** have different chemical shifts, whereas the compound **11b** shows only one multiplet and one septuplet for the four groups. This result indicates a rigid structure at room temperature.[10] There is a high double-bond character between the boron and nitrogen atoms.

Because of the quadrupole effect of the boron atoms the signals of the protons at the vicinal carbon atoms have very low intensities. The methylene protons can be detected near $\delta = 2.2$ as a doublet, and the methine protons of the double bond in the ring are not detected. The signal for the proton in 4-position is observed at $\delta = 6.30$, and that for the 5-position at $\delta = 6.85$. In **11b** the signal of the proton in the 5-position cannot be observed, because the signals of the aromatic substituent appear between $\delta = 6.8$ and 7.1.

The reaction between the 3-methylidene-1,2-diborolane **1c** and the two isonitriles leads to the 2-*tert*-butylimino-4-methylidene-1,3-diboracyclohexane **10c** and the 2-(2′,6′-dimethylphenylimino)-4-methylidene-1,3-diboracyclohexane **11c.**[10]

Scheme 5

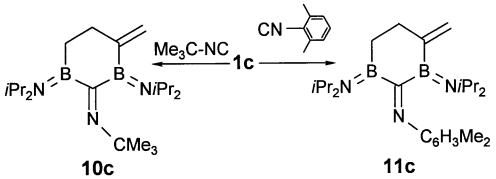

10c **11c**

The ^{11}B-NMR shifts of **10c** and **11c** are $\delta = 38$ and 39, which are within the expected region.[14] The ^{1}H-NMR data of **11c** are comparable to those of **11b**. The products are soluble only in THF.

The steric demand of the five-membered rings **1b** and **1c**, and that of the alkyl substituents of the isonitriles both prevent dimerization and rearrangement of the corresponding insertion products **10b**, **c** and **11b**, **c**. To induce a rearrange-

ment a small dipolar reagent such as water is needed. Therefore, **10b** and sodium sulfate decahydrate were heated in THF to yield the hydrolysis product **12**, which was characterized by an X-ray structure analysis. **12** can be described as one half of a spiro dimer, formed by ring contraction. The five-membered ring in **12** contains the terminal carbon atom of the isonitrile and only one boron atom.

Scheme 6

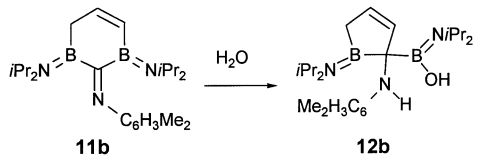

The formation of the dimeric insertion and rearrangement products **4a**, **b**, the insertion compounds **10b**, **c** and **11b**, **c** and the product of hydrolysis **12**, give evidence for the reaction path of insertion and rearrangement to the dimeric molecules. As proposed, the first step is an insertion of carbon monoxide or isonitrile into the B−B bond of the boron heterocycles.[6] The formed products are stable, if the steric requirements of the isonitriles or the heterocycles are suitable as in the isonitrile insertion products **10b**, **c** and **11b**, **c**. Rearrangement under ring contraction is the following step. This is supported by using water as a dipolar reagent to induce rearrangement with formation of **12**. In the case of CO insertion the dimeric spiro compounds **4b**, **c** are formed. The proposed reaction paths are in agreement with the mechanistic conclusions of Paetzold et al.[6][7]

Scheme 7

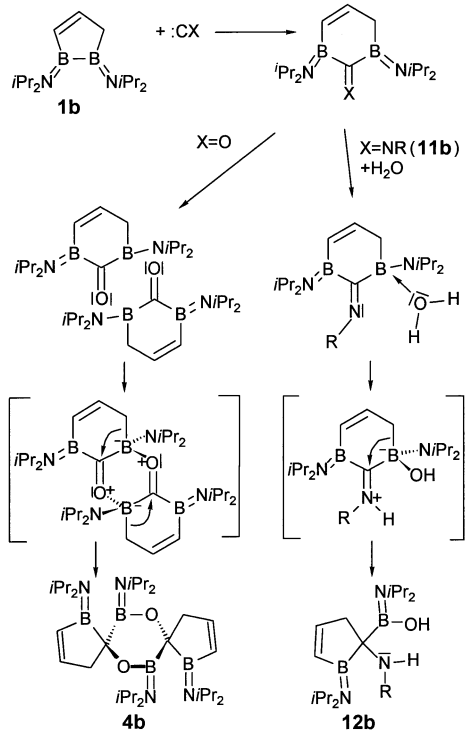

Crystal Structures of 4b and 12b

The centrosymmetric molecule in **4b** is built up by the central planar 6-membered ring (max. deviation ±0.01 Å) and, almost perpendicular (88.5°) to it, by the outer BC_4 rings, which are slightly puckered (±0.05 Å). The B−N units are planar indicating π interaction. The lengths of the B−C and B−N distances differ, which can be rationalized in terms of the other atoms connected to the boron atoms. The B−N distance at B2, bonded to C1 and C4, is slightly shorter than that at B1, which is bonded to O1 and C1′. The B−C distance involving an sp^2 carbon atom (B2−C4) is significantly shorter than those with sp^3 carbon atoms. In **12b** the same 5-membered ring is present, but instead of the 6-membered ring two independent groups are attached to C1, one of which [B(N*i*Pr$_2$)O] is similar to that part of

Figure 1. Molecular structure of **4b**[a]

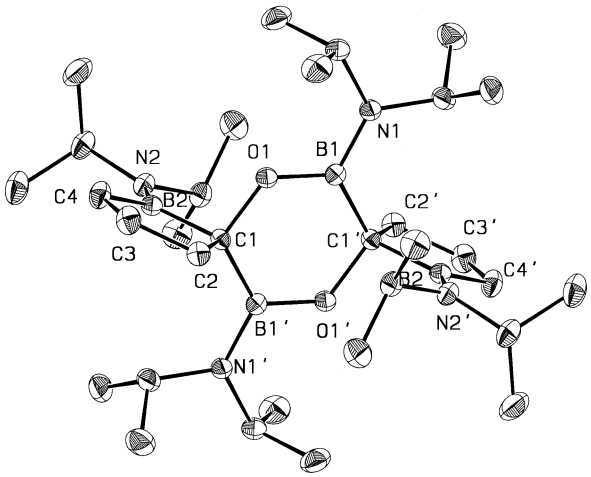

[a] Selected bond lengths [Å] and angles [°]: C1−B1′ 1.592(2), C1−O1 1.481(2), C1−C2 1.557(2), C1−B2 1.624(2),O1−B1 1.368(2), B1−N1 1.422(2), B2−N2 1.397(2), B2−C2 1.569(2); C2−C1−B2 103.1(1), B1′−C1−O1 112.5(1), C1−B2−C4 105.1(2), C1−B1′−O1′ 121.2(1), C1−O1−B1 126.3(1).

Figure 2. Molecular structure of **12b**[a]

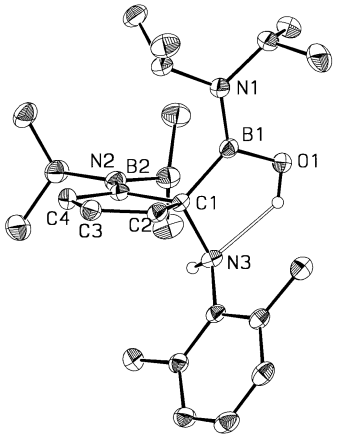

[a] Selected bond lengths [Å] and angles [°]: C1−B1 1.617(2) C1−N3 1.548(2), C1−C2 1.556(2), C1−B2 1.6 29(2), O1−B1 1.376(2), B1−N1 1.416(2), B2−N2 1.402(2), B2−C2 1.562(2); C2−B1−B2 102.4(1), B1−C1−N3 106.0(1), C1−B2−C4 105.7(1), C1−B1−O1 115.9(1).

the ring in **4b**, while the other [$HN(C_6H_3Me_2)$] substitutes for the oxygen in **4b**. The distances exhibit the same range of values as found in **4b** and the angles are almost identical, apart from those around C1. The 5-membered ring is planar, in contrast to **4b** where the steric repulsion of the diisopropylamino group at B1 pushes the 5-membered ring towards O1 and causes the distortion of the ring which adopts a slight envelope form. In **12b** this is not possible, as the dimethylphenyl group at N3 does not allow a tipping of the ring, which remains planar and lies symmetrically between the two groups. The angles at C1 in **4b** also show the effect of the distortion. A rotation around the bond C1−N3 would suspend the steric repulsion of the dimethylphenyl group, but the hydrogen atom at O1 forms an intramolecular hydrogen bond with N3, hindering the rotation around C1−N3.

Support of this work by the *Deutsche Forschungsgemeinschaft* (SFB 247), the *Fonds der Chemischen Industrie*, and the *BASF AG* is gratefully acknowledged.

Experimental Section

All reactions and manipulations were performed in dry glassware under nitrogen by using standard Schlenk techniques. Solvents were distilled from appropriate drying agents under nitrogen before use. The commercial carbon monoxide was bubbled through KOH for drying. − $Et_2O \cdot BF_3$ was used as the external standard for ^{11}B NMR. Internal standards for ^1H and ^{13}C were the signals of the deuterium-labeled solvents. NMR: $CDCl_3$ and C_6D_6 solutions, Jeol-FX-90 and Bruker AC 200. − MS: Varian MAT CH7 and Finnigan Mat 8230. − The following starting materials were prepared by previously described methods: 1,2-bis(diisopropylamino)-2,5-dihydro-1*H*-1,2-diborole (**1b**)[3], 1,2-bis(diisopropylamino)-3-methylidene-1,2-diborolane (**1c**)[3], 1,2-bis(diisopropylamino)-1,2-benzodiboret (**6**)[9], 1,2,4-tris(diisopropylamino)-3,5-dimethyl-1,2,4-triboracyclopentane (**7**).[10]

1,7,9,14-Tetrakis(diisopropylamino)-6,13-dioxa-1,7,9,14-tetraboradispiro[4.2.4.2]tetradeca-2,10-diene (**4b**): CO was bubbled through a solution of 950 mg (3.6 mmol) of **1b** in 40 ml of THF at room temp. for 1 h. After 15 min, a colorless solid was formed. Filtration of the mixture and washing of the residue with THF and hexane yielded 520 mg (0.9 mmol, 50%) of **4b**, m.p. 282°C. The remaining **1b** in the filtrate can be used for further reactions. − ^1H NMR ($CDCl_3$, 200 MHz): δ = 0.86, 0.88, 0.89, 1.12, 1.15, 1.27 (m, 48 H), 2.75, 2.94, 3.25, 3.75 (sept, 8 H), 7.05 (d, 2 H, $^3J_{H,H}$ = 7.95 Hz), 6.19 (d, 2 H, $^3J_{H,H}$ = 7.95 Hz), 2.33 (d, 2 H, $^3J_{H,H}$ = 19.0 Hz), 2.70 (d, 2 H, $^3J_{H,H}$ = 19.5 Hz). − ^{11}B NMR ($CDCl_3$, 29 MHz): δ = 44 (C_2BN), 32 (CB(N)O). − ^{13}C NMR ($CDCl_3$, 50 MHz): δ = 23.0, 23.3, 23.6, 24.9, 25.5, 26.0, 26.4 ($CHCH_3$), 44.6, 45.3, 47.6, 49.3 (NCH), 32.5 (CCH_2C), 159.3 ($CCHC$), (CB not detected). − MS (EI), *m/z* (%): 580 (100) [M^+], 453 (85) [M^+ − $BON(CH(CH_3)_2)_2$], 289 (45) [$M^+/2$ − H], 43 (74) [$CH(CH_3)_2$]. − $C_{32}H_{64}O_2B_4N_4$ (580.1) calcd. C 66.25, H 11.12, N 9.66; found C 65.70, H 11.12, N 9.65.

1,7,9,14-Tetrakis(diisopropylamino)bismethylidene-6,13-dioxa-1,7,9,14-tetraboradispiro [4.2.4.2]tetradecane (**4c**): 700 mg (2.54 mmol) of **1c** were treated with CO as in the previous experiment. The workup furnished 440 mg (0.72 mmol, 44%) of the colorless solid **4c**, m.p. 289°C (decomp.). The product was almost insoluble in all organic solvents. − MS (EI), *m/z* (%): 608 (45) [M^+], 303 (27) [$M^+/2$ − H], 481 (36) [M+ − $BON(CH(CH_3)_2)_2$], 43 (73) [$CH(CH_3)_2$], 28 (100) [CO; C_2H_4]. − $C_{34}H_{68}O_2B_4N_4$ (608.2) calcd. C 67.15, H 11.27, N 9.21; found C 66.80, H 11.23, N 9.18.

2-tert-Butylimino-1,3-bis(diisopropylamino)-1,3-diboracyclohex-4-ene (**10b**): 415 mg (5 mmol) of *tert*-butyl isocyanide, dissolved in 20 ml of THF, was added to a solution of 1.30 g (5 mmol) of **1b** in 30 ml of THF at −30°C. After 15 h at room temp., the solvent was removed under vacuum. Distillation yielded 600 mg (2.3 mmol, 46%) of colorless **10b**, b.p. 63°C/5·10^{-2} Torr. − ^1H NMR (C_6D_6, 200 MHz): δ = 0.9−1.4 [br., 24 H, $CH(CH_3)_2$], 1.43 [s, 9 H, $C(CH_3)_3$], 2.21 (d, 2 H, BCH_2), 2.95 (m, 1 H, NCH), 3.18 (m, 1 H, NCH), 3.53 (m, 1 H, NCH), 4.81 (m, 1 H, NCH), 6.25 (d, br., 1 H, BCH), 6.85 (m, br., 1 H, CH_2CHCH). − ^{11}B NMR (C_6D_6, 64 MHz): δ = 40 (sh), 45.

1,3-Bis(diisopropylamino)-2-(2',6'-dimethylphenylimino)-1,3-diboracyclohex-4-ene (**11b**): A preparation analogous to **10b,** using 660 mg (5 mmol) of 2,6-dimethylphenyl isocyanide and 1.3 g (5 mmol) of **1b,** resulted in 900 mg (3.5 mmol, 69%) of colorless **11b**, b.p. 80°C/5·10^{-2} Torr. − ^1H NMR (C_6D_6, 200 MHz): δ = 0.8−1.4 [m, 24 H, $CH(CH_3)_2$], 2.11 (s, 6 H, H_3CAr), 2.21 (d, 2 H, $CHCHCH_2$), 3.15 [m, 3 H, $CH(CH_3)_2$], 4.5 [sept, 1 H, $CH(CH_3)_2$], 6.25 (d, 1 H, $BCHCH$), 6.9 (m, 1 H, $CHCHCH_2$), 6.95 (m, 3 H, C_6H_3). − ^{11}B NMR (C_6D_6, 64 MHz): δ = 40. − MS (EI), *m/z* (%): 394 (36) [M^+ + 1], 378 [M^+ − CH_3], 43 (100) [$CH(CH_3)_2$].

2-tert-Butylimino-1,3-bis(diisopropylamino)-4-methylidene-1,3-diboracyclohexane (**10c**): 1.4 g (5 mmol) of **1c** was treated with 415 mg (5 mmol) of *tert*-butyl isocyanide under the same reaction conditions as in the previous experiments to yield 300 mg (0.8 mmol, 16%) of **10c**, b.p. 75°C/5·10^{-2} Torr. − ^{11}B NMR (C_6D_6, 64 MHz)): δ = 39. − MS (EI), *m/z* (%): 360 (87) [M^+ + 1], 57 (100) [C_4H_9], 43 (89) [C_3H_7].

1,3-Bis(diisopropylamino)-2-(2',6'-dimethylphenylimino)-4-methylidene-1,3-diboracyclohexane (**11c**): The preparation analogous to **10b** using 1.4 g (5 mmol) of **1c** and 660 mg (5 mmol) of 2,6-dimethylphenyl isocyanide yielded 800 mg (1.8 mmol, 36%) of **11c**, b.p. 105°C/5·10^{-2} Torr. − ^1H NMR (C_6D_6, 200 MHz): δ = 0.93 [m, 6 H, $CH(CH_3)_2$], 1.2 (m, 2 H, CH_2CH_2C), 1.45 [m, 18 H, $CH(CH_3)_2$], 2.16 (s, 6 H, H_3CAr), 2.75(m, 2 H, BCH_2CH_2), 3.3 [m, 3 H, $CH(CH_3)_2$], 3.95 [m, 1 H, $CH(CH_3)_2$], 5.2 (m, 1 H, $C=CH_2$), 7.00 (m, 1 H, $C=CH_2$), 7.06 (m, 3 H, C_6H_3). − ^{11}B NMR (C_6D_6, 64 MHz): δ = 38.

1-(Diisopropylamino)-2-(diisopropylaminohydroxyboryl)-2-(2',6'-dimethylphenylamino)-1-boracyclopent-3-ene (**12**): 390 mg (1 mmol) of **11c** and 33 mg (0.1 mmol) of $Na_2SO_4 \cdot\cdot 10\ H_2O$, dissolved in 50 ml of THF, were refluxed for 2 h. The hot solution was filtered through a G3 sintered-glass funnel. Crystallisation from a THF solution at 5°C gave 220 mg (0.5 mmol, 50%) of **12**, m.p. 60°C. − ^{11}B NMR (C_6D_6, 64 MHz): δ = 38.

Crystal-Structure Determinations of **4b** *and* **12b**: Crystal data and details of the structure determinations are listed in Table 1. Unique sets of intensity data were collected at −70°C with a four-circle diffractometer (Mo-K_α radiation λ = 0.7107 Å, graphite monochromator, ω scan). An empirical absorption correction (ψ scans) was applied. The structures were solved by direct methods [SHELXS86][15] and refined by least-squares methods based on F^2 with all measured reflections [SHELXL97].[16] All non-hydrogen atoms were refined anisotropically. Hydrogen atoms were included in calculated positions (CH in **4b**), or as part of the rigid group (CH_3 in **4b** and **12b**). All other hydrogen atoms were located in difference Fourier maps and refined.

Crystallographic data (excluding structure factors) for the structures reported in this paper have been deposited with the Cam-

Table 1. Crystal data and structure refinement for **4b** and **12b**

	4b	**12b**
Empirical formula	$C_{32}H_{64}B_4NO_2$	$C_{24}H_{43}B_2N_3O$
Formula weight	580.11	411.23
Crystal system	monoclinic	monoclinic
Space group	$P2_1/c$	$P2_1/c$
Unit-cell dimensions		
a [Å]	11.027(6)	8.147(5)
b [Å]	10.288(5)	18.337(13)
c [Å]	16.804(8)	17.479(11)
β [°]	108.27(2)	100.80(5)
Volume [Å^3]	1810.2(16)	2565(3)
Z	2	4
Calcd. density [g/cm^3]	1.064	1.065
Absorp. coeff. [mm^{-1}]	0.064	0.064
F(000)	640	904
Crystal size [mm]	0.5 × 0.5 × 0.3	0.7 × 0.6 × 0.6
θ range	1.9−25.0	1.6 - 27.0
Index ranges	−13/12, 0/12, 0/19	−10/10, 0/23, 0/22
No. of reflections		
unique	3180	5600
observed [$I > 2\sigma(I)$]	2355	4232
Transmission	0.94−0.99	0.95−0.99
Parameters	217	337
Goodness-of-fit on F^2	1.006	1.006
Final R indices		
$R1$ [$I > 2\sigma(I)$]	0.041	0.042
$wR2$ (all data)	0.103	0.108
Largest diff. peak/hole [e Å^{-3}]	0.23/−0.14	0.27/−0.14

bridge Crystallographic Data Centre as supplementary publication no. CCDC-100715. Copies of the data can be obtained free of charge on application to CCDC, 12 Union Road, Cambridge CB2 1EZ, UK [fax: (internat.) + 44(1223)336-003; e-mail: deposit@ccdc.cam.ac.uk].

[☆] Dedicated to Professor *Hartmut Bärnighausen* on the occasion of his 65th birthday.

[1] G. Gabbert, W. Weinmann, H. Pritzkow, W. Siebert, *Angew. Chem.* **1992**, *104*, 1670; *Angew. Chem. Int. Ed. Engl.* **1992**, *31*, 1603.

[2] G. E. Herberich, C.Ganter, L. Wesemann, R. Boese, *Angew. Chem.* **1990**, *102*, 914; *Angew. Chem. Int. Ed. Engl.* **1990**, *29*, 912.

[3] G. Gabbert, H. Pritzkow, M. Kaschke, W. Siebert, *Chem. Ber.* **1994**, *127*, 1363.

[4] J. Teichmann, Diploma Thesis, Universität Heidelberg, **1995**.

[5] A. Pelter, K. Smith, H. C. Brown, *Borane Reagents*, Academic Press, London, **1988**, 239.

[6] P. Paetzold, B. Redenz-Stormanns, R. Boese, *Angew. Chem.* **1990**, *102*, 910; *Angew. Chem. Int. Ed. Engl.* **1990**, *29*, 900.

[7] S. Luckert, E. Eversheim, M. Müller, B. Redenz-Stormanns, K. Englert, P. Paetzold, *Chem. Ber.* **1995**, *128*, 1029−1035.

[8] M. Hildenbrand, H. Pritzkow, W. Siebert, *Angew. Chem.* **1985**, *97*, 769*; Angew. Chem. Int. Ed. Engl.* **1985**, *24*, 759; M. Hildenbrand, H. Pritzkow, U. Zenneck, W. Siebert, *Angew. Chem.* **1984**, *96*, 371; *Angew. Chem. Int. Ed. Engl.* **1984**, *23*, 371.

[9] D. E. Kaufmann, R. Boese, A. Scheer, *Chem. Ber.* **1994**, *127*, 2349.

[10] H. Stock, Ph. D. Dissertation, Universität Heidelberg, **1997**.

[11] J. Edwin, W. Siebert, C. Krüger, *J. Organomet. Chem.* **1981**, *215*, 255−262.

[12] W. Weinmann, Ph. D. Dissertation, Universität Heidelberg, **1994**.

[13] G. Gabbert, Ph. D. Dissertation, Universität Heidelberg, **1993**.

[14] H. Nöth, B. Wrackmeyer, *Nuclear Magnetic Resonance Spectroscopy of Boron Compounds*, Springer-Verlag, Berlin, Heidelberg, New York, **1978**.

[15] G. M. Sheldrick, SHELXS86, Univ. Göttingen, **1986**.

[16] G. M. Sheldrick, SHELXL97, Univ. Göttingen, **1997**.

[97242]

Boryl- and Bridging Boryleneiron Complexes from Aminodichloroboranes

Holger Braunschweig*, Carsten Kollann, and Ulli Englert

Institut für Anorganische Chemie der Technischen Hochschule,
Templergraben 55, D-52056 Aachen, Germany
E-mail: holger.braunschweig@ac.rwth-aachen.de

Recieved October 30, 1997

Keywords: Boron / Iron / Boryl complexes / Borylene complexes / Iron−boron bond

Depending on the nature of the amino group bound to the boron atom, the reactions of various aminodichloroboranes R_2NBCl_2 with $Na[(\eta^5\text{-}C_5R'_5)Fe(CO)_2]$ yield either boryl or bridging borylene complexes of iron. The compounds $[(C_5R'_5)(CO)_2Fe\{BCl(NR_2)\}]$ (**1a**, $C_5R'_5 = C_5H_5$, R = Me; **1b**, $C_5R'_5 = C_5H_4Me$, R = Me; **1c**, $C_5R'_5 = C_5Me_5$, R = Me) and $[(\eta\text{-}BNR_2)(\mu\text{-}CO)\{(C_5R'_5)Fe(CO)\}_2]$ (**2a**, $C_5R'_5 = C_5H_5$, R = $SiMe_3$; **2b**, $C_5R'_5 = C_5H_4Me$, R = $SiMe_3$) were isolated as orange (**1a−c**) or red (**2a**, **b**) crystalline solids, and characterized by multinuclear NMR methods and IR spectroscopy. The structures of **1c** and **2b** in the crystalline state were determined by single-crystal X-ray studies.

Since 1990, when the first transition-metal complex with a two-center, two-electron bond between the metal and a threefold coordinated boron atom was structurally characterized[1], such boryl complexes have become of increasing interest, as they are known to be important intermediates in transition-metal-catalyzed hydroboration[2][3][4], and, very recently, the selective functionalization of alkanes in terminal position was achieved by photolysis of a boryl-tungsten complex[5]. During the last seven years a large number of structurally authentic boryl complexes have been described and the 1,2-dioxobenzo or "catechol" group, as ligand to boron, has had a pivotal role in obtaining these compounds, since most of them were either obtained by the reaction of an anionic transition-metal complex with CatBCl (Cat = 1,2-$O_2C_6H_4$)[6a][6b][6c][6d], or by oxidative addition of CatBH or CatBBCat to a suitable transition-metal center[7a][7b][7c][7d][7e][7f].

In contrast to the well-developed chemistry of boryl transition metal complexes, knowledge about the corresponding borylene complexes is restricted to only one example (and derivatives of this). Originally, this compound, a bridging dinuclear manganese complex, was obtained by an unprecedented and unexpected reaction of different diboranes(4) with $Na[(C_5H_4Me)Mn(SiMePh_2)(CO)_2]$[8]; more recently, the syntheses of these highly unusual compounds has been significantly improved by employing the corresponding manganese hydride complex $Na[(C_5H_4Me)MnH(CO)_2]$[9]. Interestingly, the borylene complexes of the type $[\eta\text{-}BX\{(C_5H_5)Mn(CO)_2\}_2]$ (X = NMe_2, Cl), undergo substitution reactions at the boron atom with preservation of the central Mn_2B core[10]. Due to their kinetic lability[11], however, boryl complexes generally react with cleavage of the boryl moiety[6a][6d][7e][11], regardless of the strength of the metal−boron bond, which in certain cases was calculated to be stronger than corresponding metal−carbon bonds[12a][12b].

In the course of our investigations on transition-metal complexes of boron with alternative boron-bound ligands[13a][13b], we report on the reactions of different aminodichloroboranes R_2NBCl_2 with $Na[(\eta^5\text{-}C_5R'_5)Fe(CO)_2]$ to yield amino-substituted boryl or bridging borylene complexes of iron.

Results and Discussion

The reaction of $Na[(\eta^5\text{-}C_5R'_5)Fe(CO)_2]$ with Me_2NBCl_2 in benzene at room temperature according to Scheme 1 affords the aminoboryl complexes $[(C_5R'_5)(CO)_2Fe\{BCl(NR_2)\}]$ (**1a**, $C_5R'_5 = C_5H_5$, R = Me; **1b**, $C_5R'_5 = C_5H_4Me$, R = Me; **1c**, $C_5R'_5 = C_5Me_5$, R = Me).

Scheme 1

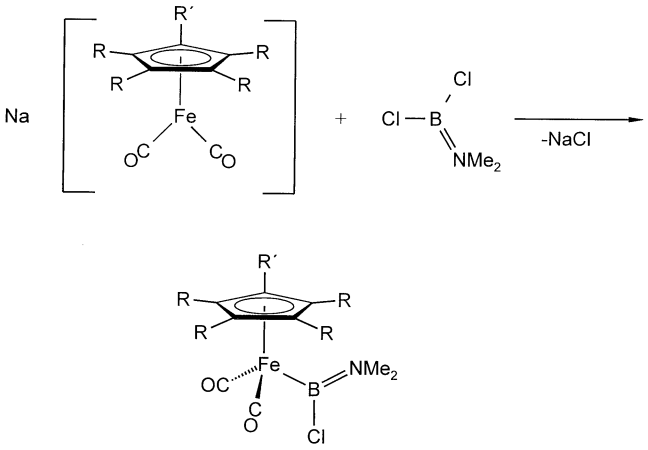

1a, R = R′ = H
1b, R = H; R′ = Me
1c, R = R′ = Me

The products were obtained from hexane at −30°C as air- and moisture-sensitive dark-orange materials in yields

 © WILEY-VCH Verlag GmbH, D-69451 Weinheim, 1998 1434−1948/98/0404−0465 $ 17.50+.50/0

of up to 65%. While **1a**, **c** show melting points of 35°C and 120°C, respectively, **1b** proved to be an oil at room temperature. As might be expected, the spectroscopic data of **1a**−**c** in solution are to some extent related to those of the corresponding diborane(4)yl complex $[(C_5H_5)Fe(CO)_2\{B_2(NMe_2)_2Cl\}]$[13a]. The ^{1}H- and ^{13}C-NMR spectra show double sets of signals for the dimethylamino group, due to the restricted rotation with respect to the B−N double bond. In the case of **1b** the variable-temperature ^{1}H-NMR studies show a coalescence of the two corresponding resonances at 83°C, from which a value for the rotation barrier of $\Delta G^{\neq} = 72.3$ kJ/mol can be calculated. This is in the range expected for aminosubstituted boranes[14a][14b]. The formation of the boron−iron bond results in characteristically deshielded ^{11}B-NMR signals at $\delta = 56.4$ (**1a**), 56.9 (**1b**), and 59.1 (**1c**), which are shifted to low field with respect to the signal of Me_2NBCl_2 at $\delta = 30.5$[15]. For a similar boryliron complex, $[CpFe(CO)_2BCat]$ (Cat = 1,2-$O_2C_6H_4$), a modest Fe−B π bonding in solution was deduced from the high CO stretching frequencies at 2024 cm^{-1} and 1971 cm^{-1}[6c]. In the case of **1a**−**c** the IR spectra gave no evidence for a metal−boron backbonding, since the CO stretching frequencies (**1a**, 2005 cm^{-1}, 1946 cm^{-1}; **1b**, 2002 cm^{-1}, 1944 cm^{-1}; **1c**, 1988 cm^{-1}, 1928 cm^{-1}) are equal to, or even lower than, those for the corresponding alkyliron complexes at 1999−2005 cm^{-1} and 1938−1944 cm^{-1}[16]. So far this finding is true for all fully characterized nitrogen-substituted boryliron complexes, e.g. $\{(C_5H_5)Fe(CO)_2[B_2(NMe_2)_2Cl]\}$[13a] and $\{[(C_5H_4Me)Fe(CO)_2]_2ClB_3N_3H_3\}$[13b].

As a representative of the new complexes, an X-ray structure analysis was carried out for $[(C_5Me_5)(CO)_2Fe\{BCl(NMe_2)\}]$ (**1c**) (Figure 1). Suitable crystals of **1c** were obtained, after some days, from solutions in hexane at −30°C. The complex crystallizes in the noncentrosymmetric space group $P2_12_12_1$, and the molecule adopts C_1 symmetry in the crystal. The almost perpendicular orientation (87.4°) of the N−B−Cl plane with respect to the Cp(centroid)−Fe−B plane provides no evidence for an iron−boron π interaction in the crystalline state[6c][17]. This is supported by an Fe−B distance of 202.7(5) pm, which is significantly longer than that in $[CpFe(CO)_2BCat]$ [195.6(6) pm]. For the latter compound a π interaction in the solid state is facilitated by the different orientation of the boryl ligand[6c]. A boron−nitrogen double bond, already established for the aminoboryl complexes **1a**−**c** in solution, is also found for **1c** in the crystal, as indicated by a B−N distance of 137.7(6) pm.

The corresponding bridging borylene complexes $[(\eta\text{-}BNR_2)(\mu\text{-}CO)\{(C_5R'_5)Fe(CO)\}_2]$ (**2a**, $C_5R'_5 = C_5H_5$, R = $SiMe_3$; **2b**, $C_5R'_5 = C_5H_4Me$, R = $SiMe_3$) were obtained by a similar reaction of $[(Me_3Si)_2N]BCl_2$ at room temperature with two equivalents of $Na[(C_5R'_5)Fe(CO)_2]$ in benzene (Scheme 2).

The products, which are formed with loss of one CO group from the initial iron complex, were isolated from hexane at low temperatures as dark-red solids in yields of about 25%, and proved to be extremely sensitive to air and moisture. This is in contrast to the known characteristics of the related borylenemanganese complex $[(\eta\text{-}BNMe_2)\{(C_5H_5)Mn(CO)_2\}_2]$[10]. Interestingly the formation of the borylene complexes **2a**, **b**, as the only boron-containing products, was observed under all conditions, even with an excess of $[(Me_3Si)_2N]BCl_2$, while the reaction of Me_2NBCl_2 with $Na[(C_5R'_5)Fe(CO)_2]$ always led to the formation of the boryl complexes $[(C_5R'_5)(CO)_2Fe\{BCl(NR_2)\}]$ (**1a**, $C_5R'_5 = C_5H_5$, R = Me; **1b**, $C_5R'_5 = C_5H_4Me$, R = Me; **1c**, $C_5R'_5 = C_5Me_5$, R = Me). In the latter cases a further exchange of a boron-bound chloride ligand could not be achieved. We attribute this result to the electronic influence of the silyl groups, which despite their size make the $[(Me_3-$

Figure 1. Structure of **1c** in the crystal (ellipsoids at 30% probability[25])[a]

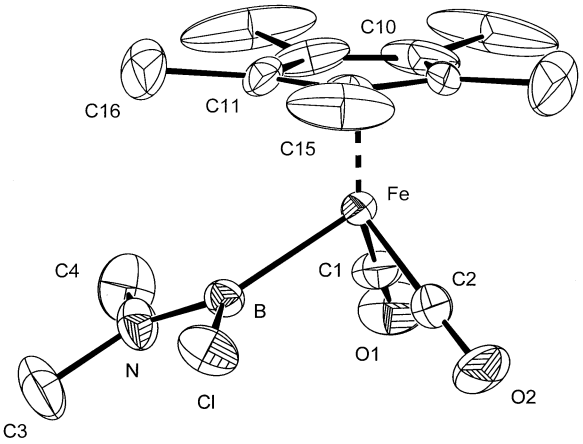

[a] Selected distances [pm] and angles [°]: Fe−B 202.7(5), B−N 137.7(6), B−Cl 183.4(5), Fe−centroid 173.5(1); Fe−B−Cl 116.0(2), Fe−B−N 131.9(4), Cl−B−N 112.0(3).

Scheme 2

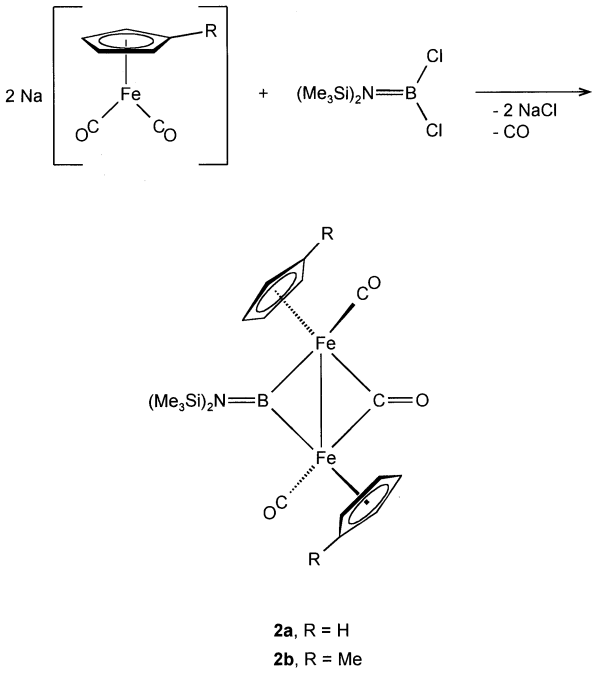

2a, R = H
2b, R = Me

$Si)_2N]BCl_2$ more reactive by weakening the boron−nitrogen double bond.

The structure of **2a**, **b** in solution is derived from the NMR and IR spectra. Due to the formation of two iron−boron linkages the borylene complexes show ^{11}B-NMR signals at $\delta \approx 119$. These are significantly shifted to low field with respect to the signals found for the boryl complexes **1a**−**c**. The IR and ^{13}C-NMR data resemble those of the isoelectronic vinylidenediiron complexes, where the presence of one bridging and two terminal CO groups has already been established[18].

Suitable single crystals of **2b** were obtained in a similar manner to those of **1c**, and the results of the X-ray structure analysis (Figure 2) showed that the compound crystallizes in the monoclinic space group $P2_1/c$.

Figure 2. Structure of **2b** in the crystal (ellipsoids at 30% probability[25])[a]

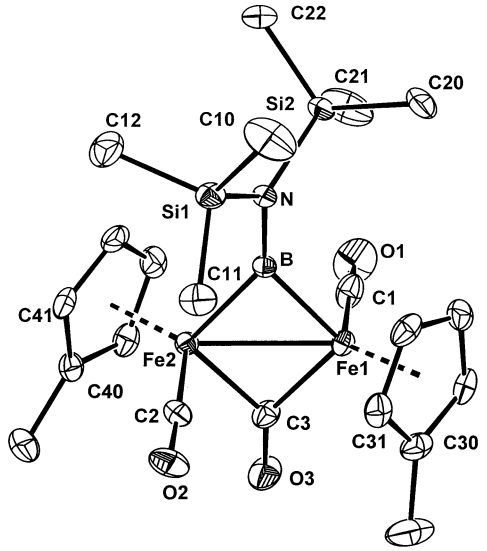

[a] Selected distances [pm] and angles [°]: Fe1−Fe2 254.8(1), Fe1−B 200.7(3), Fe2−B 200.2(3), B−N 141.2(4), Fe1−centroid1 175.5, Fe2−centroid2 174.6; Fe1−B−Fe2 78.9(1), Fe1−C3−Fe2 83.6(1).

In the crystal the borylene complex **2c** shows a *trans* orientation of the MeC_5H_4 and CO groups with respect to the Fe_2B unit. These three atoms form an isosceles triangle with Fe−B distances of 200.7(3) and 200.2(3) pm, and an Fe−Fe distance of 254.8(1) pm. Obviously, the Si1−B−Si2 plane is twisted by 53.7(1)° with respect to the Fe1−B−Fe2 plane due to the bulky Me_3Si groups. Hence, in connection with the extended B−N distance of 141.2(4) pm, a less effective backbonding from the nitrogen to the boron atom can be assumed. The overall molecular structure of **2c** resembles that of the structurally characterized vinylidenediiron complexes[18].

Conclusion

This study presents the synthesis and characterization in solution and in the crystal of various amino-substituted boryl and bridging borylene complexes of the type $[(C_5R'_5)(CO)_2Fe\{BCl(NR_2)\}]$ (**1a**, $C_5R'_5 = C_5H_5$, R = Me; **1b**, $C_5R'_5 = C_5H_4Me$, R = Me; **1c**, $C_5R'_5 = C_5Me_5$, R = Me) and $[(\eta\text{-}BNR_2)(\mu\text{-}CO)\{(C_5R'_5)Fe(CO)\}_2]$ (**2a**, $C_5R'_5 = C_5H_5$, R = $SiMe_3$; **2b**, $C_5R'_5 = C_5H_4Me$, R = $SiMe_3$). The formation of the products is obviously dominated by electronic rather than steric criteria, since the more bulky, but also more electrophilic, $[(Me_3Si)_2N]BCl_2$ yields the borylene complexes **2a**, **b** by substitution of both boron-bound chloride ligands by $[(\eta^5\text{-}C_5R'_5)Fe(CO)_2)]$ moieties, whereas the boryl complexes **1a**−**c** are formed from Me_2NBCl_2 by substitution of only one chloride ligand. These results show that aminodichloroboranes may serve as the starting materials for different types of transition-metal complexes of boron, and that the access to bridging borylene complexes is no longer restricted to the use of diborane(4) derivatives.

This work was supported by the *Deutsche Forschungsgemeinschaft* and the *Fonds der Chemischen Industrie*.

Experimental Section

All manipulations were carried out under dry nitrogen in Schlenk glassware. Solvents and reagents were dried by standard procedures, distilled and stored under nitrogen and molecular sieves. $Na[(\eta^5\text{-}C_5R_5)Fe(CO)_2]$[19], Me_2NBCl_2[20], and $[(Me_3Si)_2N]BCl_2$[21] were synthesized according to the literature. − NMR: Varian Unity 500 at 499.843 (^{1}H, standard TMS internal), 150.364 (^{11}B, standard $BF_3\cdot OEt_2$ in C_6D_6 external), 125.639 MHz ($^{13}C\{^1H\}$, APT, standard TMS internal); all NMR spectra were recorded in C_6D_6 as solvent. − Elemental analyses (C, H, N): Carlo-Erba elemental analyzer, model 1106. − IR: Perkin-Elmer FT-IR 1720x.

[Dicarbonyl{chloro(dimethylamino)boryl}(η^5-cyclopentadienyl)iron] (**1a**): 1.92 g (9.60 mmol) of $Na[(C_5H_5)Fe(CO)_2]$ was suspended in 50 ml of benzene and 1.21 g (9.60 mmol) of Me_2NBCl_2 was added dropwise by a syringe at ambient temp. After stirring for 20 min, all volatiles were removed in vacuo and the solid residue was treated with 40 ml of hexane, filtered, and the remaining solid washed with 20 ml of hexane, 1.65 g (65%) of **1a** was recovered from the filtrate at −30°C as orange crystals, m.p. 35°C. − ^{1}H NMR: δ = 2.70 (s, 3 H, NMe), 2.91 (s, 3 H, NMe), 4.11 (s, 5 H, C_5H_5). − ^{11}B NMR: δ = 56.4. − ^{13}C NMR: δ = 41.14 (NMe), 43.60 (NMe), 83.80 (C_5H_5), 215.76 (CO). − IR (toluene): $\tilde{\nu}$ = 2006 cm^{-1}, 1946 (CO). − $C_9H_{11}BClFeNO_2$ (267.29): calcd. C 40.44, H 4.15, N 5.24; found C 39.88, H 4.32, N 5.30.

[Dicarbonyl{chloro(dimethylamino)boryl}(η^5-methylcyclopentadienyl)iron] (**1b**): As described for **1a**, 0.93 g (4.35 mmol) of $Na[(C_5H_4Me)Fe(CO)_2]$ was treated with 0.55 g (4.35 mmol) of Me_2NBCl_2, and 0.78 g (64%) of **1b** was obtained as a dark orange oil by evaporating the filtrate in vacuo. − ^{1}H NMR: δ = 1.57 (s, 3 H, C_5H_4Me), 2.77 (s, 3 H, NMe), 2.93 (s, 3 H, NMe), 4.09 (m, 4 H, C_5H_4Me). − ^{11}B NMR: δ = 56.9. − ^{13}C NMR: δ = 12.90 (C_5H_4Me), 41.17 (NMe), 43.66 (NMe), 82.55, 84.62, 101.28 (C_5H_4Me), 216.19 (CO). − IR (toluene): $\tilde{\nu}$ = 2002 cm^{-1}, 1944 (CO). − $C_{10}H_{13}BClFeNO_2$ (281.33): calcd. C 42.69, H 4.66, N 4.98; found C 42.06, H 4.85, N 4.72.

[Dicarbonyl{chloro(dimethylamino)boryl}(η^5-pentamethylcyclopentadienyl)iron] (**1c**): As described for **1a**, 0.24 g (0.90 mmol) of $Na[(C_5Me_5)Fe(CO)_2]$ was treated with 0.11 g (0.90 mmol) of Me_2NBCl_2, and 0.17 g (55%) of **1c** was obtained as orange crystals, m.p. 120°C. − ^{1}H NMR: δ = 1.53 (s, 15 H, C_5Me_5), 2.87 (s, 3 H, NMe), 2.96 (s, 3 H, NMe). − ^{11}B NMR: δ = 59.1. − ^{13}C NMR: δ = 9.76 (C_5Me_5), 41.37 (NMe), 43.82 (NMe), 95.23 (C_5Me_5), 217.60 (CO). − IR (toluene): $\tilde{\nu}$ = 1988 cm^{-1}, 1928 (CO). −

$C_{14}H_{21}BClFeNO_2$ (337.42): calcd. C 49.83, H 6.27, N 4.15; found C 49.68, H 6.52, N 4.13.

[μ-{Bis(trimethylsilyl)aminoboranediyl}-bis{(η⁵-cyclopentadienyl)dicarbonyliron}Fe-Fe] (**2a**): As described for **1a**, 2.69 g (13.45 mmol) of $Na[(C_5H_5)Fe(CO)_2]$ were reacted with 1.30 g (5.38 mmol) of $[(Me_3Si)_2N]BCl_2$ and 0.70 g (26%) of **2a** isolated as dark red crystals. – ^{1}H NMR: δ = 0.32 (s, 18 H, $SiMe_3$), 4.41 (s, 10 H, C_5H_5). – ^{11}B NMR: δ = 118.4 . – ^{13}C NMR: δ = 4.75 ($SiMe_3$), 87.75 (C_5H_5), 215.52 (CO), 276.63 (μ-CO). – IR (hexane): $\tilde{\nu}$ = 1924 cm^{-1}, 1770 (CO). – $C_{19}H_{28}BFe_2NO_3Si_2$ (497.11): calcd. C 45.90, H 5.68, N 2.82; found C 45.84, H 5.80, N 2.67.

[μ-{Bis(trimethylsilyl)aminoboranediyl}bis{dicarbonyl(η⁵-methylcyclopentadienyl)iron}Fe–Fe] (**2b**): As described for **1a**, 1.76 g (8.23 mmol) of $Na[(C_5H_4Me)Fe(CO)_2]$ was treated with 0.99 g (4.11 mmol) of $[(Me_3Si)_2N]BCl_2$ and 0.86 g (25%) of **2b** isolated as dark-red crystals. – ^{1}H NMR: δ = 0.36 (s, 18 H, $SiMe_3$), 1.96 (s, 6 H, Me), 4.01–4.61 (br., 8 H, C_5H_4). – ^{11}B NMR: δ = 119.1. – ^{13}C NMR: δ = 4.82 ($SiMe_3$), 12.29 (C_5H_4Me), 84.39, 85.09, 88.30, 90.35, 103.73 (C_5H_4Me), 215.83 (CO), 279.26 (μ-CO). – IR (hexane): $\tilde{\nu}$ = 1925 cm^{-1}, 1770 (CO). – $C_{21}H_{32}BFe_2NO_3Si_2$ (525.14): calcd. C 48.03, H 6.14, N 2.67; found C 48.30, H 6.28, N 2.61.

X-ray Structure Determination for **1c**: $C_{14}H_{21}BClFeNO_2$, M = 337.44 g mol^{-1}, crystal data a = 8.2617(6), b = 9.915(1), c = 20.100(3) Å, V = 1646.5(3) Å^3, orthorhombic, $P2_12_12_1$ (No. 19), Z = 4, $\rho_{calcd.}$ = 1.361 g cm^{-3}, μ(Mo-K_α) = 10.77 cm^{-1}, F(000) = 704. Orange platelet, crystal size [mm] 0.6 × 0.6 × 0.4. ENRAF-Nonius CAD4; Mo-K_α radiation (λ = 0.7107 Å, graphite monochromator); intensity data from ω-2-Θ scans at 203 K. 7812 reflections in the range 3° < Θ < 27°, structure solution[23] with 3592 independent reflections, refinement[24] with 2819 observations with $I > \sigma(I)$ for 181 variables; H atoms were included as riding in idealized geometry [C–H = 98 pm, U_{iso}(H) = 1.3 · U_{eq}(C)]. Pronounced anisotropic displacement parameters were encountered for the carbon atoms in the pentamethylcyclopentadienyl ring and these indicate librational or static disorder of this moiety. Convergence at R = 0.051, R_w = 0.056, $w^{-1} = \sigma^2(F_o)$. Crystallographic data (excluding structure factors) for the structure reported in this paper have been deposited with the Cambridge Crystallographic Data Centre as supplementary publication no. CCDC-100790. Copies of the data can be obtained free of charge on application to CCDC, 12 Union Road, Cambridge CB2 1EZ, UK [Fax: (int. code) + 44(1223)336-033, E-mail: deposit@ccdc.cam.ac.uk, World Wide Web: http://www.ccdc.cam.ac.uk].

X-ray Structure Determination for **2b**: $C_{21}H_{32}BFe_2NO_3Si_2$, M = 525.17 g mol^{-1}, unit cell dimensions a = 10.684(2), b = 28.917(5), c = 8.337(5) Å, β = 108.26(3)°, V = 2446(2) Å^3, monoclinic, $P2_1/c$ (No. 14), Z = 4, $D_{calcd.}$ = 1.426 g cm^{-3}, μ(Mo-K_α) = 13.03 cm^{-1}, F(000) = 1096; dark-red transparent platelet, crystal size [mm] 0.65 × 0.54 × 0.15. ENRAF-Nonius CAD4; Mo-K_α radiation (λ = 0.7107 Å, graphite monochromator); intensity data from ω-2-Θ scans at 203 K., 6443 reflections in the range 3° < Θ < 26°, numerical absorption correction (transmission min. 0.528, max. 0.830) by Gaussian integration[22], 3680 independent observations with $I > \sigma(I)$ in structure solution[23] and refinement[24] for 271 variables; H atoms were included as riding in idealized geometry [C–H = 98 pm, U_{iso}(H) = 1.3 · U_{eq}(C)]. Convergence at R = 0.039, R_w = 0.047, $w^{-1} = \sigma^2(F_o)$. Crystallographic data (excluding structure factors) for the structure reported in this paper have been deposited with the Cambridge Crystallographic Data Centre as supplementary publication no. CCDC-100790. Copies of the data can be obtained free of charge on application to CCDC, 12 Union Road, Cambridge CB2 1EZ, UK [Fax: (int. code) + 44(1223)336-033, E-mail: deposit@ccdc.cam.ac.uk, World Wide Web: http://www.ccdc.cam.ac.uk].

[1] R. T. Baker, D. W. Ovenall, J. C. Calabrese, S. A. Westcott, N. J. Taylor, I. D. Williams, T. B. Marder, *J. Am. Chem. Soc.* **1990**, *112*, 9399–9400.
[2] D. Männig, H. Nöth, *Angew. Chem.* **1985**, *97*, 854–855; *Angew. Chem. Int. Ed. Engl.* **1985**, *24*, 878–879.
[3] K. Burgess, M. J. Ohlmeyer, *Chem. Rev.* **1991**, *91*, 1179–1191.
[4] A. E. Dorigo, P. von Ragué Schleyer, *Angew. Chem.* **1995**, *107*, 108–110; *Angew. Chem. Int. Ed. Engl.* **1995**, *34*, 115–117.
[5] J. F. Hartwig, K. M. Waltz, *Science* **1997**, *277*, 211–213.
[6] [6a] J. F. Hartwig, S. Huber, *J. Am. Chem. Soc.* **1993**, *115*, 4908–4909. – [6b] J. F. Hartwig, S. R. de Gala, *J. Am. Chem. Soc.* **1994**, *116*, 3661–3662. – [6c] D. R. Lantero, D. H. Motry, D. L. Ward, M. R. Smith, *J. Am. Chem. Soc.* **1994**, *116*, 10811–10812. – [6d] K. M. Waltz, X. He, C. Muhoro, J. F. Hartwig, *J. Am. Chem. Soc.* **1995**, *117*, 11357–11358.
[7] [7a] J. R. Knorr, J. S. Merola, *Organometallics* **1990**, *9*, 3008–3010. – [7b] S. A. Westcott, N. J. Taylor, T. B. Marder, R. T. Baker, N. J. Jones, J. C. Calabrese, *J. Chem. Soc., Chem. Commun.* **1991**, 304–305. – [7c] K. Burgess, W. A. van der Donk, S. A. Westcott, T. B. Marder, R. T. Baker, J. C. Calabrese, *J. Am. Chem. Soc.* **1992**, *114*, 9350–9359. – [7d] C. N. Iverson, M. R. Smith, *J. Am. Chem. Soc.* **1995**, *117*, 4403–4404. – [7e] J. F. Hartwig, Xiaoming He, *Angew. Chem.* **1996**, *108*, 352–354, *Angew. Chem. Int. Ed. Engl.* **1996**, *35,* 315–317. – [7f] C. Dai, G. Stringer, F. F. Corrigan, N. J. Taylor, T. B. Marder, N. C. Norman, *J. Organomet. Chem.* **1996**, *513*, 273–275.
[8] H. Braunschweig, T. Wagner, *Angew. Chem.* **1995**, *107*, 904–905; *Angew. Chem. Int. Ed. Engl.* **1995**, *34*, 825–826.
[9] H. Braunschweig, B. Ganter, *J. Organomet. Chem.* **1997**, *545*, 163–167.
[10] H. Braunschweig, M. Müller, *Chem. Ber.* **1997**, *130*, 1295–1298.
[11] X. He, J. F. Hartwig, *Organometallics* **1996**, *15*, 400–407.
[12] [12a] P. R. Rablen, J. F. Hartwig, S. P. Nolan, *J. Am. Chem. Soc.* **1994**, *116*, 4121–4122. – [12b] S. Sakaki, T. Kikuno, *Inorg. Chem.* **1997**, *36*, 226–229.
[13] [13a] H. Braunschweig, B. Ganter, M. Koster, T. Wagner, *Chem. Ber.* **1996**, *129*, 1099–1101. – [13b] H. Braunschweig, C. Kollann, M. Müller, *Chem. Ber.*, in press.
[14] [14a] C. Brown, R. H. Cragg, T. J. Miller, D. O. Smith, *J. Organomet. Chem.* **1983**, *244*, 209–215. – [14b] A. J. Ashe III, W. Klein, R. Rousseau, *J. Organomet. Chem.* **1994**, *468*, 21–23.
[15] H. Nöth, H. Vahrenkamp, *Chem. Ber.* **1967**, *100*, 3353–3356.
[16] N. DeLuca, A. Wojcicki, *J. Organomet. Chem.* **1980**, *193*, 359–364.
[17] B. E. R. Schilling, R. Hoffmann, J. W. Faller, *J. Am. Chem. Soc.* **1979**, *101*, 592–598.
[18] M. Akita, S. Kato, M. Terada, Y. Masaki, M. Tanaka, Y. Morooka, *Organometallics* **1997**, *16*, 2392–2412.
[19] D. L. Reger, V. Fauth, M. D. Dukes, *Syn. React. Inorg. Metal-Org. Chem.* **1977**, *7*, 151–154.
[20] A. J. Banister, N. N. Greenwood, *J. Chem. Soc.* **1964**, 995–1000.
[21] P. Geymeyer, E. G. Rochow, U. Wannagat, *Angew. Chem.* **1964**, *76*, 499–500; *Angew. Chem. Int. Ed. Engl.* **1964**, *3*, 633.
[22] P. Coppens, L. Leiserowitz, D. Rabinovich, *Acta Crystallogr.* **1965**, *18*, 1035–1038.
[23] G. M. Sheldrick, *SHELXS-86*, Göttingen, **1988**.
[24] B. A. Frenz and ENRAF-Nonius, *SDP*, version 5.0, **1989**.
[25] A. L. Spek, *PLATON 94*, Utrecht, **1994**.

[97249]

The Synthesis and Structure of Trimetaphosphimato Complexes of Hafnium and Zirconium

Norbert Stock*[a], Wolfgang Herrendorf[b], Johannes Beck[b], and Wolfgang Schnick*[a]

Laboratorium für Anorganische Chemie der Universität[a],
D-95440 Bayreuth, Germany
Fax: (internat.) + 49(0)921/55-2788
E-mail: wolfgang.schnick@uni-bayreuth.de

Institut für Anorganische und Analytische Chemie, Justus-Liebig-Universität[b],
D-35390 Giessen, Germany

Received November 4, 1997

Keywords: Cage compounds / Crystal structure / Hafnium / Trimetaphosphimates / Zirconium

The (trimetaphosphimato)hafnates and -zirconates $Na_4\{Hf_4(\mu_4\text{-}O)(\mu\text{-}OH)_6[(PO_2NH)_3]_4\}\cdot 18\ H_2O$ [**1**, $Pa\bar{3}$, a = 22.687(3) Å, Z = 8], $Na_4\{Hf_4(\mu_4\text{-}O)(\mu\text{-}OH)_6[(PO_2NH)_3]_4\}\cdot 21\ H_2O$ [**2**, $R\bar{3}$, a = 14.350(2), c = 50.348(10) Å, Z = 6], $Na_4\{Zr_4(\mu_4\text{-}O)(\mu\text{-}OH)_6[(PO_2NH)_3]_4\}\cdot 18\ H_2O$ [**3**, $Pa\bar{3}$, a = 22.693(3) Å, Z = 8], and $Na_4\{Zr_4(\mu_4\text{-}O)(\mu\text{-}OH)_6[(PO_2NH)_3]_4\}\cdot 21\ H_2O$ [**4**, $R\bar{3}$, a = 14.303(2), c = 50.284(10) Å, Z = 6] were obtained by the stoichiometric reaction of $HfOCl_2\cdot 8\ H_2O$ and $ZrOCl_2\cdot 8\ H_2O$ with an aqueous solution of $Na_3(PO_2NH)_3\cdot 4\ H_2O$, followed by the diffusion-controlled addition of methanol. During these reactions compounds **1** and **2**, or **3** and **4**, crystallized simultaneously and the hafnium and zirconium complexes **1** and **3**, as well as **2** and **4**, were found to be isostructural and isomorphous. The characteristic structural feature which is central to **1**, **2**, **3**, and **4** is the complex tetranuclear anion $\{M_4(\mu_4\text{-}O)(\mu\text{-}OH)_6[(PO_2NH)_3]_4\}^{4-}$ with M = Zr or Hf. The anion consists of five corner-sharing adamantanoid cages. The central cage, $\{M_4(\mu_4\text{-}O)(\mu\text{-}OH)_6\}^{8+}$, has a tetracoordinated oxygen atom in the middle, and the other cages are formed by the trimetaphosphimate ions acting as tridentate ligands which coordinate to Hf or Zr. The water content of the compounds **1**−**4** could not be determined unequivocally by chemical analyses since the compounds are always obtained as mixtures of the rhombohedral (**2/4**) and cubic (**1/3**) phases. Thermal decomposition of compounds **1**−**4** starts above 120 °C and leads to the formation of HfP_2O_7 and ZrP_2O_7/$NaZr_2(PO_4)_3$, with the evolution of H_2O and NH_3. DSC measurements gave no evidence that the compounds **1** and **2,** or **3** and **4**, might be transformed into each other by heating.

In contrast to the cyclotrimetaphosphates[1], whose structures have been well investigated, little is known concerning the X-ray-crystallographic results of the cyclotrimetaphosphimates (tri-μ-imidocyclotriphosphates), although the first synthesis of cyclotrimetaphosphimates was described in 1896.[2] Since there is the possibility of tautomeric forms, $[P(NH)O_2]_3^{3-}$ and $[PNO(OH)]_3^{3-}$, these compounds have been investigated intensively using IR spectroscopy,[3] but until now only a few crystal structures of the trimetaphosphimates have been known.[4] The two tautomeric forms of trimetaphosphimic acid are shown in Figure 1. IR spectroscopy, as well as single-crystal structure analyses, have confirmed the existence of the μ-imido form in both the solid state and solution. In principle coordination by both nitrogen and oxygen is possible, but up to the present exclusively coordination via oxygen has been found. Nevertheless, interactions between Ag and N are observed in $Ag_3(PO_2NH)_3$, leading to a strong distortion of the P_3N_3 ring.[4c] This interaction is also confirmed by the existence of $Ag_6(PO_2N)_3$, which was first described by Stokes;[2] however, the crystal structure has not yet been determined. The trimetaphosphimate ion can act as a monodentate ligand in combination with monovalent ions such as Na^+, K^+, Ag^+, NH_4^+, or $C(NH_2)_3^+$,[4] as bidentate and bridging ligand with the divalent ions Cu^{2+}, Co^{2+}, Zn^{2+} in $Na_4\{Cu[(PO_2NH)_3]_2\}\cdot 10\ H_2O$ and $Na\{M(PO_2NH)_3\}\cdot 7\ H_2O$ (M = Zn, Co),[5] as a tridentate ligand with Ga^{3+} in $Na_3\{Ga[(PO_2NH)_3]_2\}\cdot 12\ H_2O$,[6] and as tridentate and bridging ligand in $K_{1.3}(NH_4)_{1.7}\{Pr[(PO_2NH)_3]_2\}\cdot 8\ H_2O$.[7]

Figure 1. Tautomeric forms of trimetaphosphimic acid $H_3(PO_2NH)_3$

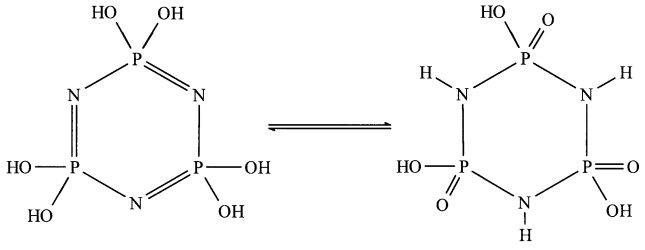

Because of the interesting properties of zirconium phosphates and zirconium phosphorus oxide nitrides, which means that they can be used as ion exchangers and catalysts,[8][9] we investigated the reaction of $Na_3(PO_2NH)_3\cdot 4H_2O$ with zirconium or hafnium salts, and the use of these trimetaphosphimates as nitrogen-containing precursors for the synthesis of oxonitridophosphates.

 © WILEY-VCH Verlag GmbH, D-69451 Weinheim, 1998 1434−1948/98/0404−0469 $ 17.50+.50/0

Figure 2. Adamantanoid metal-oxygen cage in the $[M_4(\mu_4\text{-}O)(\mu\text{-}OH)_6]^{8+}$ core (M = Zr, Hf)

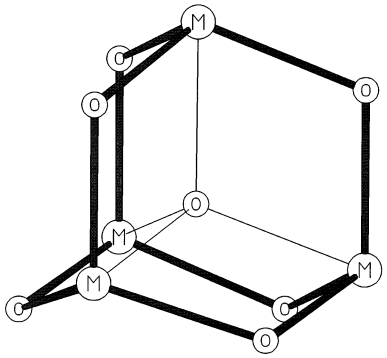

Results

The reaction of $Na_3(PO_2NH)_3 \cdot 4\ H_2O$ with $HfOCl_2 \cdot 8\ H_2O$ or $ZrOCl_2 \cdot 8\ H_2O$, leads to the formation of the four new compounds $Na_4\{Hf_4(\mu_4\text{-}O)(\mu\text{-}OH)_6[(PO_2NH)_3]_4\} \cdot 18\ H_2O$ (**1**), $Na_4\{Hf_4(\mu_4\text{-}O)(\mu\text{-}OH)_6[(PO_2NH)_3]_4\} \cdot 21\ H_2O$ (**2**), $Na_4\{Zr_4(\mu_4\text{-}O)(\mu\text{-}OH)_6[(PO_2NH)_3]_4\} \cdot 18\ H_2O$ (**3**) and $Na_4\{Zr_4(\mu_4\text{-}O)(\mu\text{-}OH)_6[(PO_2NH)_3]_4\} \cdot 21\ H_2O$ (**4**) which are always obtained as mixtures (**1/2** and **3/4**) of the rhombohedral (**2/4**) and cubic (**1/3**) phases. The respective Zr and Hf compounds (**1/3** and **2/4**) are isotypic and isomorphous, with distinct crystals of cubic and rhombohedral habit. The characteristic structural feature of all four compounds are the tetranuclear complex anions $\{M_4(\mu_4\text{-}O)(\mu\text{-}OH)_6[(PO_2NH)_3]_4\}^{4-}$ with M = Hf, Zr. Despite the topologically differing crystal structures of **1/3** (cubic phase) and **2/4** (rhombohedral phase) the anions $\{M_4(\mu_4\text{-}O)(\mu\text{-}OH)_6[(PO_2NH)_3]_4\}^{4-}$ have almost exactly the same topology in both cases. The cores of the $\{M_4(\mu_4\text{-}O)(\mu\text{-}OH)_6[(PO_2NH)_3]_4\}^{4-}$ ions consist of a slightly distorted tetrahedral arrangement of the transition metal, Hf or Zr (Table 1), with six edge-bridging OH groups (μ-OH) and one tetracoordinated O atom (μ_4-O) at the center of the M_4 tetrahedron, thus forming an adamantanoid cage $M_4(\mu_4\text{-}O)(\mu\text{-}OH)_6^{8+}$ as shown in Figure 2. The H atoms of the bridging μ-OH groups have not been localized, but on the basis of the analytical results which show the molar ratio to be Na/P/N/M = 1:3:3:1 for all four compounds, the μ-OH groups have to be assumed to be connecting the Zr and Hf atoms. In addition to this centered cage, four more adamantanoid cages are formed by tridentate coordination of the trimetaphosphimate ions, $(PO_2NH)_3^{3-}$, to the metal ions. The trimetaphosphimate ions exhibit the chair conformation and are bound to the metal centers through the three oxo groups. The entire complex ion $\{M_4(\mu_4\text{-}O)(\mu\text{-}OH)_6[(PO_2NH)_3]_4\}^{4-}$, consisting of five corner-linked adamantanoid cages, is shown in Figure 3. Similar to monoclinic ZrO_2 (baddeleyite), and one polymorphic form of HfO_2, the metal atoms exhibit the coordination number seven. The anions have the crystallographic symmetry C_3 with the tetracoordinated oxygen atom and one of the metal atoms (M2, M = Hf, Zr) situated on the threefold axes. The M−O bond lengths of the adamantanoid central cages in **1**−**4** (Table 1) compare well with the average bond lengths

Figure 3. View of the $\{M_4(\mu_4\text{-}O)(\mu\text{-}OH)_6[(PO_2NH)_3]_4\}^{4-}$ ions (M = Hf, Zr) in the cubic phase and rhombohedral phase [top: ball-stick model; bottom: polyhedron formed by metal (grey) and P atoms (white)]

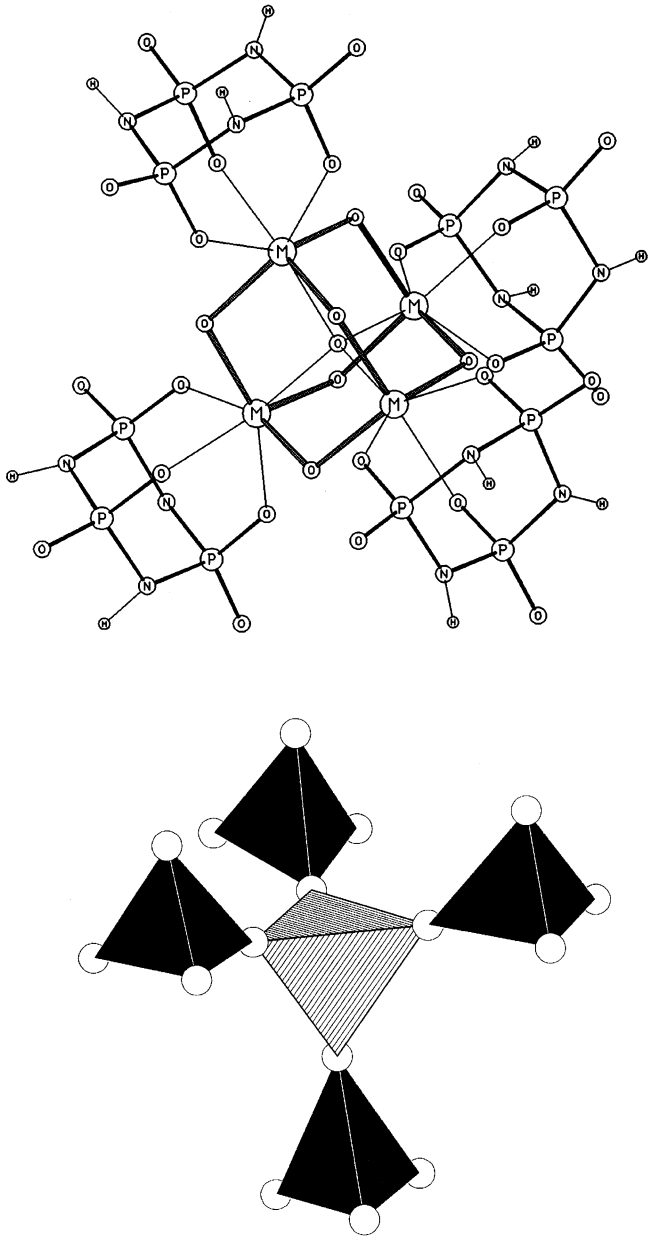

in corresponding compounds which have a coordination number of seven $\{[Zr_4(\mu_4\text{-}O)(\mu\text{-}O\mathit{n}Pr)_6]^{8+}$/Zr−O: 215−223 pm[10], monoclinic HfO_2: 203−225 pm[11], monoclinic ZrO_2: 205−227 pm[12]$\}$. The $M_4(\mu_4\text{-}O)(\mu\text{-}OH)_6^{8+}$ cage is only slightly distorted from the ideal tetrahedral symmetry. Unlike the situation for the trimetaphosphimato zirconates, where the distortion of the $Zr_4(\mu_4\text{-}O)(\mu\text{-}OH)_6^{8+}$ cage in the cubic phase (**3**) is slightly smaller than in the rhombohedral phase (**4**), the opposite is found for the distortion of the $Hf_4(\mu_4\text{-}O)(\mu\text{-}OH)_6^{8+}$ cages in the (trimetaphosphimato)hafnates **1** and **2** (Table 1). Therefore, within the accuracy of the measurements, the metal atoms of the central ada-

Table 1. Interatomic distances [pm] and angles [°] of **1** and **2**

$Na_4\{Hf_4(\mu_4\text{-}O)\text{-}(\mu\text{-}OH)_6[(PO_2NH)_3]_4\}\cdot 18\ H_2O$ (cubic, **1**)		$Na_4\{Hf_4(\mu_4\text{-}O)\text{-}(\mu\text{-}OH)_6[(PO_2NH)_3]_4\}\cdot 21\ H_2O$ (rhomb., **2**)	
Hf(1)−Hf(1)	348.7(1)	Hf(1)−Hf(1)	351.0(1)
−Hf(2)	349.4(1)	−Hf(2)	351.0(1)
$-\mu_4$O	214.3(2)	$-\mu_4$O	214.6(2)
−O(11)	211.7(4), 209.6(4)	−O(11)	211.9(3), 212.8(3)
−O(12)	211.4(4)	−O(12)	211.6(3)
−O(1A)	216.8(4)	−O(1A)	213.5(3)
−O(2A)	213.5(4)	−O(2A)	214.2(3)
−O(3A)	213.8(4)	−O(3A)	212.8(3)
Hf(2)−μ_4O	212.0(6)	Hf(2)−μ_4O	216.1(5)
−O(12)	210.7(4)	−O(12)	210.1(3)
−O(4A)	214.4(4)	−O(4A)	213.9(3)
P(1)−N(1)	167.4(5)	P(1)−N(1)	168.3(4)
P(1)−N(3)	167.8(5)	P(1)−N(3)	167.3(4)
P(1)−O(1A)	151.6(4)	P(1)−O(1A)	151.7(3)
P(1)−O(1B)	148.2(5)	P(1)−O(1B)	147.9(4)
P(2)−N(2)	167.3(5)	P(2)−N(2)	167.4(4)
P(2)−N(1)	168.9(5)	P(2)−N(1)	167.2(4)
P(2)−O(2A)	151.9(4)	P(2)−O(2A)	152.6(3)
P(2)−O(2B)	147.2(4)	P(2)−O(2B)	148.8(3)
P(3)−N(3)	167.2(5)	P(3)−N(3)	166.7(4)
P(3)−N(2)	166.6(5)	P(3)−N(2)	168.1(4)
P(3)−O(3A)	152.1(4)	P(3)−O(3A)	152.3(3)
P(3)−O(3B)	148.7(4)	P(3)−O(3B)	148.3(3)
P(4)−N(4)	168.6(5)	P(4)−N(4)	168.1(4)
P(4)−N(4)	167.8(5)	P(4)−N(4)	168.0(4)
P(4)−O(4A)	151.4(4)	P(4)−O(4A)	151.8(3)
P(4)−O(4B)	146.8(4)	P(4)−O(4B)	147.7(4)
Na(1)−O	234.6(8)−256.6(6)	Na(1)−O	239.4(4)−249.5(5)
Na(2)−O	236(2)−276(2)	Na(2)−O	217(7)−277(6)
Hf(2)−Hf(1)−Hf(1)	60.068(4)	Hf(2)−Hf(1)−Hf(1)	59.99(1)
Hf(1)−Hf(1)−Hf(1)	60	Hf(1)−Hf(1)−Hf(1)	60
Hf(1)−Hf(2)−Hf(1)	59.857(8)	Hf(1)−Hf(2)−Hf(1)	60.00(1)
N(3)−P(1)−N(1)	104.8(2)	N(3)−P(1)−N(1)	105.0(2)
N(1)−P(2)−N(2)	104.6(2)	N(1)−P(2)−N(2)	104.8(2)
N(2)−P(3)−N(3)	104.4(2)	N(2)−P(3)−N(3)	104.2(2)
N(4)−P(4)−N(4)	105.7(3)	N(4)−P(4)−N(4)	105.9(3)
P(1)−N(1)−P(2)	117.6(3)	P(1)−N(1)−P(2)	117.9(2)
P(2)−N(2)−P(3)	119.4(2)	P(2)−N(2)−P(3)	118.3(2)
P(3)−N(3)−P(1)	118.7(3)	P(3)−N(3)−P(1)	119.5(2)
P(4)−N(1)−P(4)	118.4(3)	P(4)−N(1)−P(4)	118.2(2)
O(1A)−P(1)−O(1B)	116.8(2)	O(1A)−P(1)−O(1B)	117.9(2)
O(2A)−P(2)−O(2B)	117.8(2)	O(2A)−P(2)−O(2B)	116.0(2)
O(3A)−P(3)−O(3B)	115.1(2)	O(3A)−P(3)−O(3B)	115.6(2)
O(4A)−P(4)−O(4B)	117.2(2)	O(4A)−P(4)−O(4B)	117.8(2)
O−P(1)−N	111.3(3), 105.1(2), 110.6(3), 107.5(2)	O−P(1)−N	110.7(2), 106.0(2), 110.7(2), 105.5(2)
O−P(2)−N	110.6(3), 105.7(2), 111.1(3), 106.0(2)	O−P(2)−N	111.7(2), 105.4(2), 110.4(2), 107.7(2)
O−P(3)−N	111.5(3), 105.2(2), 112.9(2), 107.0(2)	O−P(3)−N	111.3(2), 105.5(2), 112.9(2), 106.4(2)
O−P(4)−N	110.3(3), 106.1(2), 111.8(3), 104.9(2)	O−P(4)−N	111.1(2), 104.7(2), 110.4(2), 106.3(2)

mantanoid cage $M_4(\mu_4\text{-}O)(\mu\text{-}OH)_6^{8+}$ in **1** and **4** exhibit the ideal tetrahedral symmetry.

The trimetaphosphimate rings in $\{M_4(\mu_4\text{-}O)(\mu\text{-}OH)_6[(PO_2NH)_3]_4\}^{4-}$ M = Zr, Hf exhibit the chair conformation. The average P−O bond lengths of the oxygen atoms (O1A to O4A) coordinating to the metal (Zr: 152.1, 151.7 pm and Hf: 151.8, 152.1 pm for the cubic and the rhombohedral phase, respectively) are significantly longer than the average P−O bond lengths of oxygen atoms (O1B to O4B) coordinating to Na^+ or water molecules (Zr: 148.0, 147.7 pm and Hf: 147.7, 148.2 for the cubic and the rhombohedral phase, respectively). These values, as well as the corresponding P−N bond lengths and angles, differ only slightly among the compounds **1**, **2**, **3**, and **4**. Thus, the average P−N bond length is 167.6 pm and the average P−N−P angle is 118.4°. These findings are in accordance with the results obtained from trimetaphosphimates of monovalent cations, where there is a larger range of values but they are nevertheless similar to the results obtained in this work. The μ-imido H atoms have been unambiguously located in all four compounds by difference Fourier analyses. In comparison to other trimetaphosphimates these μ-imido groups are structurally directing, by forming hydrogen bonds between the trimetaphosphimate rings as can be

seen by comparing the structures of analogous trimetaphosphates with the corresponding trimetaphosphimates.[4] In the latter compounds the N−H groups of the $(PO_2NH)_3^{3-}$ are usually involved in extensive hydrogen-bonding interactions, forming a three-dimensional network in $(NH_4)_3(PO_2NH)_3 \cdot H_2O$[4a], bilayers in $Ag_3(PO_2NH)_3$,[4c] and pairs in $Na_3(PO_2NH)_3 \cdot H_2O$,[4b] and $K_3(PO_2NH)_3$.[4c]

Arrangement of the Complex Ions $\{M_4(\mu_4\text{-}O)(\mu\text{-}OH)_6[(PO_2NH)_3]_4\}^{4-}$ in the Cubic Phase

The two cubic compounds $Na_4\{M_4(\mu_4\text{-}O)(\mu\text{-}OH)_6[(PO_2NH)_3]_4\} \cdot 18\ H_2O$ (**1/3**) with M = Zr, Hf were found to be isostructural and isomorphous. The arrangement of the $\{M_4(\mu_4\text{-}O)(\mu\text{-}OH)_6[(PO_2NH)_3]_4\}^{4-}$ ions is shown in Figure 4. The anions are interconnected by coordination to the sodium ions and by hydrogen bonding, forming a three-dimensional network. Thus all H atoms of the μ-NH groups are bound to O atoms of the trimetaphosphimato ligands [N1−H1···O1B, N2−H2···O3B, N2−H2···O4B, N3−H3···O1B, N4−H4···O3B, N···O: 289−315 pm, N−H···O: 121−142° for **1** and N···O: 288−313 pm, N−H···O: 121−142° for **3**]. Na1 is octahedrally surrounded by three oxygen atoms of the water molecules [Na1−Ow1, −Ow2, −Ow3: 248.7(8), 234.6(8), 254.6(11) pm for **1** and 247.1(6), 234.1(6), 253.8(8) pm for **3**] and three oxygen atoms of the trimetaphosphimate rings [Na1−O2B, −O3B, −O4B: 237.9(5), 256.6(6), 236.0(5) pm for **1** and 236.7(4), 257.8(4), 235.2(4) pm for **3**]. The other sodium ion Na2 is located in a general position with an occupancy factor 1/3. Na2 is surrounded by five oxygen atoms of the water molecules [Na2−Ow1, −Ow2, −Ow3, −Ow4, −Ow6: 252(2), 276(2), 236(2), 262(2), 243(2) pm for **1** and 252(2), 281(2), 245(2), 252(2), 244(2) pm for **3**], as well as by two oxygen atoms of the trimetaphosphimate rings [Na2−O1B, −O2B: 276(2) and 242(2) for **1** and 274(2), 240(2) pm for **3**]. The residual electron density found for **1** (2.75 $e^-/Å^3$) and **3** (3.10 $e^-/Å^3$) is located on a special position $^1/_2{}^1/_2 0$. No other atoms are located within a radius of 3 Å around this site.

Figure 4. Crystal-packing diagram of the $\{M_4(\mu_4\text{-}O)(\mu\text{-}OH)_6[(PO_2NH)_3]_4\}^{4-}$ ions (M = Hf, Zr) in the cubic phase, view along [111]

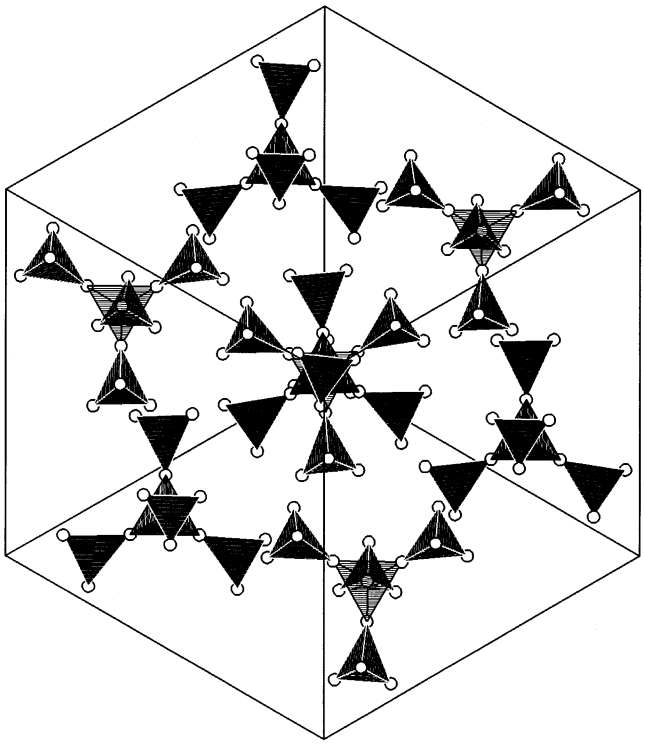

Arrangement of the Complex Ions $\{M_4(\mu_4\text{-}O)(\mu\text{-}OH)_6[(PO_2NH)_3]_4\}^{4-}$ in the Rhombohedral Phase

The two rhombohedral compounds $Na_4\{M_4(\mu_4\text{-}O)(\mu\text{-}OH)_6[(PO_2NH)_3]_4\} \cdot 21\ H_2O$ (**2/4**) with M = Zr, Hf, were found to be isostructural and isomorphous. The arrangement of the $\{M_4(\mu_4\text{-}O)(\mu\text{-}OH)_6[(PO_2NH)_3]_4\}^{4-}$ ions is shown in Figure 5. The structure consists of bilayers with a stacking sequence $A_\downarrow B_\uparrow C_\downarrow A_\uparrow B_\downarrow C_\uparrow$ of the anionic layers along [001]. The arrows describe the direction of the tip of the anion, i.e. the position of M2 (M = Hf, Zr), relative to the center of gravity of the cages with respect to [001]. Within the bilayers the anions are connected by hydrogen bonds N−H···O between the trimetaphosphimate rings [N3−H3···O3, N3−H3···O4, N4−H4···O3, N···O: 290−321 pm, N−H···O: 122−136° for **2** and N···O: 286−320 pm, N−H···O: 121−137° for **4**] and by coordination to Na1. The sodium ion Na1 is coordinated by six O atoms, three oxygen atoms of the water molecules Ow1, Ow2, Ow3 [Hf: $d_{av.}$ Ow−Na: 244.1 pm, Zr: $d_{av.}$ Ow−Na: 244.1 pm] and three O atoms of the trimetaphosphimate rings O1B, O3B, O4B [Hf: $d_{av.}$ O−Na: 241.8 pm, Zr: $d_{av.}$ O−Na: 241.8 pm], forming a distorted octahedron. The other sodium ion Na2 is located on a general position with an occupancy factor of 1/3. These Na2 ions are surrounded by six oxygen atoms, two oxygen atoms of the trimetaphosphimate rings [O1B, O2B: 278(6), 266(6) pm for **2**, 258(3), 278(3) pm for **4**] and four oxygen atoms of the water molecules [Ow2, Ow5, Ow7, Ow7′: 277(6), 217(7), 241(7) 246(7) pm for **2**, 260(3), 228(3), 241(6), 265(4) pm for **4**] thus connecting the bilayers. This connection is reinforced by extensive hydrogen bonding with O2B acting as a bridging atom [N1−H1···O2B···H2−N2; N1···O2···N2: 296, 299 for **2** and 295, 293 for **4**]. Thus a void centered at $00^1/_2$ is formed by connecting six $\{M_4[(PO_2NH)_3]_4(\mu_4\text{-}O)(\mu\text{-}OH)_6\}^{4-}$ units by hydrogen bonding between the $(PO_2NH)_3^{3-}$ rings. The hole has a radius of approximately 3 Å. The residual electron density which is found for **2** (2.27 $e^-/Å^3$) is located on the special position $^1/_3{}^2/_3{}^1/_6$ and no other atoms are located within a radius of 3 Å. In **4** no notable residual electron density was observed.

Discussion

In the (trimetaphosphimato)hafnates and -zirconates having the general composition $Na_4\{M_4(\mu_4\text{-}O)(\mu\text{-}OH)_6[(PO_2NH)_3]_4\} \cdot 18\ H_2O$ (**1**, **3**) and $Na_4\{M_4(\mu_4\text{-}O)(\mu\text{-}OH)_6[(PO_2NH)_3]_4\} \cdot 21\ H_2O$ (**2**, **4**) with M = Zr, Hf, for the

first time a metal oxide fragment incorporating four metal atoms was stabilized by trimetaphosphimate ions acting as tridentate ligands, thus stabilizing the tetranuclear anion. The synthesis of the compounds **1**−**4** succeeded when zirconyl chloride and hafnyl chloride were used, whereas the use of $ZrCl_4$ or $ZrSO_4 \cdot 4\ H_2O$ led to the formation of X-ray-amorphous products. The assumption that the preformed eight-membered rings $\{M(OH)_2\}_4^{8+}$ in the solutions of $HfOCl_2 \cdot 8\ H_2O$ and $ZrOCl_2 \cdot 8\ H_2O$ is preserved during the syntheses could not unambiguously be confirmed since the use of a mixture of $HfOCl_2 \cdot 8\ H_2O$ and $ZrOCl_2 \cdot 8\ H_2O$ in one reaction led to the formation of mixed crystals, containing Hf as well as Zr, in a 1:1 ratio. This was confirmed by EDX analysis.

Neither the cubic nor the rhombohedral phase of the (trimetaphosphimato)zirconates or -hafnates have been obtained as a single-phase product. Although the addition of NaCl during the synthesis of (trimetaphosphimato)zirconates resulted in the formation of some large single crystals of the cubic phase (**4**) analogous experiments using $HfOCl_2 \cdot 8\ H_2O$ did not lead to a pure single-phase cubic product **1**. In the same way neither varying the reaction temperature, nor varying the pH value by the addition of NaOH or HCl, resulted in single-phase products. Since the formulas of the cubic and rhombohedral phases obtained from the single-crystal structure determination differ only in their water content, and because the characteristic structural feature in the compounds **1**−**4** are the discrete tetranuclear complex anions $\{M_4(\mu_4\text{-}O)(\mu\text{-}OH)_6[(PO_2NH)_3]_4\}^{4-}$, a direct structural correlation between the respective cubic and rhombohedral phases was anticipated. However, a direct structural correlation (e.g. stacking variants, group-subgroup relations) can be ruled out since strongly differing arrangements of the anions occur.

Conclusion

Unlike the known trimetaphosphimato complexes where only monometallic complexes are formed in the title compounds, the trimetaphosphimato groups stabilize the metal oxide fragments $\{M_4(\mu_4\text{-}O)(\mu\text{-}OH)_6\}^{8+}$ (M = Zr, Hf) by acting as tridentate ligands. Thus the tetranuclear complex anion $\{M_4(\mu_4\text{-}O)(\mu\text{-}OH)_6[(PO_2NH)_3]_4\}^{4-}$ is obtained. The existence of a tetranuclear ring in $\{M_4[(OH)_2]_4(H_2O)_{16}\}^{8+}$ as the starting material seems to be important for the formation of the adamantanoid cage $\{M_4(\mu_4\text{-}O)(\mu\text{-}OH)_6\}^{8+}$, which is then stabilized by trimetaphosphimate ions. Despite the similarity of the characteristic anion $\{M_4(\mu_4\text{-}O)(\mu\text{-}OH)_6[(PO_2NH)_3]_4\}^{4-}$ in the four title compounds, cubic (**1**/**3**) and rhombohedral (**2**/**4**) products have been obtained exhibiting strongly differing topologies. As with many other Hf and Zr compounds isotypic products (**1**/**3** and **2**/**4**) are formed.

Figure 5. Crystal-packing diagram of the $\{M_4(\mu_4\text{-}O)(\mu\text{-}OH)_6[(PO_2NH)_3]_4\}^{4-}$ ions (M = Hf, Zr) in the rhombohedral phase, view along [010]

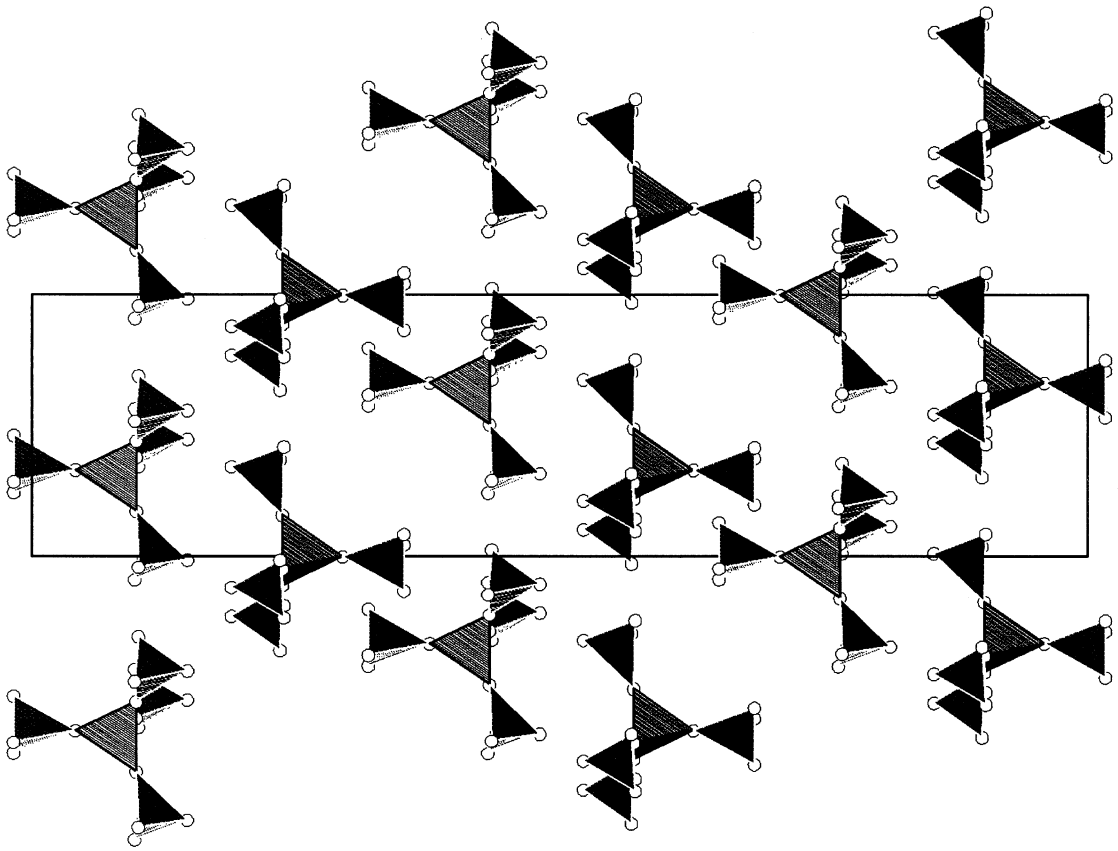

This work was supported by the *Fonds der Chemischen Industrie* and, in particular, by the *Deutsche Forschungsgemeinschaft* (Gottfried-Wilhelm-Leibniz-Programm).

Experimental Section

$Na_3(PO_2NH)_3 \cdot 4\ H_2O$ was obtained by a procedure described previously {Eq. (a)[13]}. $(PNCl_2)_3$ (Fluka, purum, 5 g, 14.38 mmol) was dissolved in 20 ml of dioxane (Merck, p.a.) in a round-bottom flask. A solution of $NaOOCCH_3 \cdot 3\ H_2O$ (Merck, p.a., 25 g, 0.184 mol) in 40 ml of H_2O was added while stirring (60°C, 24 h). The product precipitated as a white microcrystalline powder which was filtered and washed with ethanol and acetone. The product was recrystallized from water by the addition of ethanol (yield: 4.5 g, 83%).

$$(PNCl_2)_3 + 9\ Na(OOCCH_3) \cdot 3\ H_2O \rightarrow Na_3(PO_2NH)_3 \cdot 4\ H_2O + 6\ NaCl + 9\ HOOCCH_3 + 17\ H_2O \quad (a)$$

$HfOCl_2 \cdot 8\ H_2O$ (Alfa) was used as obtained, and $ZrOCl_2 \cdot 8\ H_2O$ (Fluka, puriss.) was recrystallized, from hydrochloric acid according to the literature.[14] For the synthesis of the (trimetaphosphimato)hafnates and -zirconates equimolar (3.35×10^{-5} M) aqueous solutions of $Na_3(PO_2NH)_3 \cdot 4\ H_2O$ (25 mg, 6.67×10^{-2} mmol in 2 ml of H_2O) and $HfOCl_2 \cdot 8\ H_2O$ (27.3 mg, 6.67×10^{-2} mmol in 2 ml of H_2O) or $ZrOCl_2 \cdot 8\ H_2O$ (21.5 mg, 6.67×10^{-2} mmol in 2 ml of H_2O) were mixed together at room temperature in a small glass vessel (V = 8 ml). The mixtures became turbid at once but cleared after 5 min without further stirring. They were cautiously covered with methanol and placed in a larger vessel (V = 40 ml) filled with 25 ml of methanol allowing very slow diffusion. The mixture was kept undisturbed at room temperature. After 3 d, crystals were observed growing on the inner glass wall of the smaller vessels. The crystallization was complete after approximately 8 d and led to the formation of two distinct types of crystals, exhibiting rhombohedral and quadratic habit. The reaction of $HfOCl_2 \cdot 8\ H_2O$ resulted in large crystals with rhombohedral as well as quadratic contours. In the case of $ZrOCl_2 \cdot 8\ H_2O$ the same procedure led to the formation of large crystals of only rhombohedral contour (however, small quadratic crystals of 10 μm edge length were observed under the scanning electron microscope). Large crystals of the (trimetaphosphimato)zirconate with a quadratic shape were obtained by adding sodium chloride (12 mg, 0.2 mmol) to the solution of $Na_3(PO_2NH)_3 \cdot 4\ H_2O$.

After the precipitation was complete, the mother liquor was removed and the crystals were washed with acetone (yield: 70%). Energy-dispersive X-ray microanalyses (Fa. Leo, Oberkochen) showed the atomic ratio Na/P/M (M = Hf, Zr) to be 1:3:1 for all four compounds. Chemical analysis of **4** was performed for Na, Zr, O, N, P, H and for **1** and **2** for Na and Hf, to confirm the occupancy factor of $^1/_3$ for Na2 in the general position. Phase separation was accomplished manually according to the shape of the crystals and due to their optical properties under the polarization microscope. $Na_4\{Hf_4(\mu_4\text{-}O)(\mu\text{-}OH)_6[(PO_2NH)_3]_4\} \cdot 18\ H_2O$ (**1**, 2184.11 g/mol): calcd. Hf 32.69, Na 4.21; found Hf 31.6, Na 4.06. $Na_4\{Hf_4(\mu_4\text{-}O)(\mu\text{-}OH)_6[(PO_2NH)_3]_4\} \cdot 21\ H_2O$ (**2**, 2238.16 g/mol): calcd. Hf 31.90, Na 4.11; found Hf 31.5, Na 4.06. $Na_4\{Zr_4(\mu_4\text{-}O)(\mu\text{-}OH)_6[(PO_2NH)_3]_4\} \cdot 21\ H_2O$ (**4**, 1889.08 g/mol): calcd. H 3.20, N 8.89, Na 4.87, O 44.04, P 19.68, Zr 19.32; found H 3.3, N 8.63, Na 4.96, O 42.0, P 19.3, Zr 18.6.

As the products **1/2** and **3/4** are always obtained as mixtures, the water content was not determined by chemical analysis but taken from the structural determination. Powder-diffraction investigations (Siemens D5000) revealed the existence of only two phases, **1/2** and **3/4**. All reflections have been indexed and their observed intensities correspond to a calculated diffraction pattern based on the single-crystal-structural data.

All four compounds are obtained as colorless solids and transparent crystals with well developed faces. They are stable in air and are water-soluble, however recrystallization from these solutions was not possible. Furthermore the existence of a ^{31}P-NMR signal [δ^{31}P (D_2O) = −0.544] in the solution NMR spectra (Bruker ARX 250) of **1/2** indicated decomposition of the complex anion $\{M_4(\mu_4\text{-}O)(\mu\text{-}OH)_6[(PO_2NH)_3]_4\}^{8-}$ (M = Hf, Zr) in water. This NMR shift is in accordance with the ^{31}P-NMR signal of the free $(PO_2NH)_3^{3-}$ ion as found in aqueous solutions of $K_3(PO_2NH)_3$ [δ^{31}P (D_2O) = −0.553].[4c]

Thermal decomposition of the products starts above 120°C with evolution of H_2O and NH_3. Reaction of mixtures of (**1/2**) or (**3/4**), respectively, for 2 d at 200−700°C were carried out in sealed quartz ampoules. The only X-ray crystalline products detectable were HfP_2O_7 and ZrP_2O_7 as well as $NaZr_2(PO_4)_3$. Therefore, nitrogen was not incorporated into the products, but NH_3 was formed as a condensation product.

IR spectra (Bruker IFS 66v; KBr pellets) of the cubic and rhombohedral (trimetaphosphimato)hafnates have been obtained after the separation of the crystals according to their shape and optical properties under the polarization microscope. The IR spectra of **1**−**4** are very similar, exhibiting the following IR absorptions $\tilde{\nu}$ [cm^{-1}] = 3600, 3270, 2704, 1642, 1316, 1256, 1110, 1052, 919, 825, 642, 553, 415.

Crystal Structure Analyses: X-ray diffraction data were collected on an image-plate diffractometer (STOE IPDS). Reflections shaded by the goniometer head were removed. The data sets were employed in the crystal shape optimization and the subsequent numerical absorption correction using HABITUS.[15] Afterwards identical reflections, which were measured multiply due to the measurement method, were averaged, and their mean values were used for the structure determination. Relevant crystallographic data and details of the data collection of the compounds **1**−**4** are listed in Table 2. According to the observed extinctions for the cubic phases the space group $Pa\bar{3}$ (no. 205) was unequivocally determined and the structures were solved by direct methods using SHELXTL-Plus.[16] For the rhombohedral phases the space groups $R3$ (no. 146) and $R\bar{3}$ (no. 148) have been considered. The crystal structures of these compounds were solved by direct methods using SHELXTL-Plus[16] in the centrosymmetric space group $R\bar{3}$. After the anisotropic refinement of the displacement parameters of all non-hydrogen atoms except Na2 for the cubic and the hexagonal phases, the μ-imido hydrogen atoms were located and refined using a riding model with a fixed N−H distance of 86 pm. The sodium ions Na2 in **1**−**4** were located on the basis of bonding lengths and coordination. They were located on general positions occupied to $^1/_3$. Therefore these partially occupied Na positions were only refined using isotropic displacement parameters. Since the compounds were always obtained as mixtures of the cubic and rhombohedral phase, the water content was determined exclusively from the diffraction data. Tables 3 and 4 show the positional parameters and the equivalent isotropic displacement parameters U_{equiv} for **1** and **2**. Corresponding parameters of the isotypic zirconium compounds (**3** and **4**) are omitted. Table 1 gives interatomic distances and angles in **1** and **2**.[17]

Table 2. Crystallographic data of the compounds **1**−**4**

Formula	$Na_4\{M_4(\mu_4\text{-}O)(\mu\text{-}OH)_6[(PO_2NH)_3]_4\cdot 18\ H_2O$		$Na_4\{M_4(\mu_4\text{-}O)(\mu\text{-}OH)_6[(PO_2NH)_3]_4\cdot 21\ H_2O$	
M	Hf (**1**)	Zr (**3**)	Hf (**2**)	Zr (**4**)
form. mass [g mol^{-1}]	2184.11	1835.03	2238.16	1889.08
crystal system	cubic		trigonal	
space group	$Pa\bar{3}$ (no. 205)		$R\bar{3}$ (no. 148)	
diffractometer	STOE-IPDS			
radiation (monochromator)	Mo-K_α (graphite)			
unit cell	a = 22.678(3)	a = 22.693(3)	a = 14.350(2), c = 50.348(10)	a = 14.303(2), c = 50.284(10)
V [10^6 pm^3]	11663.9(23)	11685.7(23)	8979.2(25)	8908.4(25)
Z	8	8	6	6
X-ray density [g cm^{-3}]	2.488	2.086	2.481	2.113
abs. coefficient [cm^{-1}]	75.75	11.72	73.87	11.6
temperature [K]	293(2)	293(2)	293(2)	293(2)
crystal size [mm]	0.326 × 0.282 × 0.174	0.320 × 0.164 × 0.144	0.153 × 0.113 × 0.104	0.208 × 0.176 × 0.126
F(000)	8336	7312	6420	5664
θ range [°]	4.02−24.08	2.54−28.12	5.42−28.01	4.62−26.03
h, k, l	−25/25, −25/25, −25/25	−30/27, −29/30, −27/27	−18/18, −18/17, −66/66	−17/17, −17/17, −60/61
total no. of reflections	57257	86460	22606	18379
independent reflections	3053	4750	4769	3828
observed reflections	2786 [I_o>2σ(I_o)]	3848 [I_o>2σ(I_o)]	3942 [I_o>2σ(I_o)]	3375 ([I_o>2σ(I_o)]
refined parameters	246	255	255	255
corrections	Lorentz, polarization, extinction			
absorption corrections	numerical using HABITUS[15]			
min./max. transm. ratio	0.1110/0.3026	0.8201/0.9050	0.3408/0.5139	0.7916/0.8926
min./max. resid. e$^-$ dens.	−0.551/2.746	−0.662/3.098	−0.916/2.270	−0.661/1.041
extinction coefficient	0.00005(2)	−	0.00008(2)	0.00002(2)
GOF	1.140	1.156	1.138	1.084
R indices: $R1$/$wR2$	0.0267/0.0795	0.041/0.1439	0.0292/0.0799	0.0422/0.1154

Table 3. Atomic coordinates and anisotropic displacement parameters [pm^2] for $Na_4\{Hf_4(\mu_4\text{-}O)(\mu\text{-}OH)_6[(PO_2NH)_3]_4\}\cdot 18\ H_2O$ (cubic phase)

Atom	Wyckoff symbol	x/a	y/b	z/c	U_{equiv}[a]
Hf1	24d	0.7649(1)	0.3716(1)	0.1245(1)	155(1)
Hf2	8c	0.7647(1)	0.2647(1)	0.2353(1)	155(1)
OT	8c	0.8186(2)	0.3186(2)	0.1814(2)	145(2)
O11	24d	0.8240(2)	0.3195(2)	0.0745(2)	243(2)
O12	24d	0.7127(2)	0.3203(2)	0.1822(2)	289(2)
P1	24d	0.6517(1)	0.4665(1)	0.1032(1)	199(3)
P2	24d	0.7430(1)	0.4698(1)	0.0152(1)	194(3)
P3	24d	0.6613(1)	0.3724(1)	0.0184(1)	185(3)
P4	24d	0.6549(1)	0.1657(1)	0.2501(1)	202(3)
O1A	24d	0.6949(2)	0.4341(2)	0.1426(2)	207(9)
O1B	24d	0.6070(2)	0.5038(2)	0.1329(2)	318(10)
O2A	24d	0.7820(2)	0.4359(2)	0.0578(2)	191(8)
O2B	24d	0.7718(2)	0.5097(2)	−0.0270(2)	318(10)
O3A	24d	0.7036(2)	0.3409(2)	0.0598(2)	200(8)
O3B	24d	0.6264(2)	0.3332(2)	−0.0210(2)	285(10)
O4A	24d	0.6951(2)	0.2044(2)	0.2135(2)	213(8)
O4B	24d	0.6103(2)	0.1310(2)	0.2184(2)	286(10)
N1	24d	0.6936(2)	0.5063(2)	0.0573(2)	220(11)
H1	24d	0.6901(2)	0.5440(2)	0.0552(2)	260
N2	24d	0.7032(2)	0.4188(2)	−0.0202(2)	220(10)
H2	24d	0.7043(2)	0.4165(2)	−0.0581(2)	260
N3	24d	0.6190(2)	0.4161(2)	0.0600(2)	226(11)
H3	24d	0.5812(2)	0.4129(2)	0.0593(2)	270
N4	24d	0.7007(2)	0.1224(2)	0.2895(2)	238(11)
H4	24d	0.6990(2)	0.0847(2)	0.2867(2)	290
Na1	24d	0.7789(2)	0.4937(2)	−0.1305(2)	504(80)
OW1	24d	0.7760(3)	0.4999(4)	−0.2399(3)	820(20)
OW2	24d	0.7930(6)	0.5961(4)	−0.1332(4)	1410(50)
OW3	24d	0.8898(4)	0.4807(6)	−0.1429(6)	1440(40)
OW4	24d	0.8776(5)	0.5952(6)	−0.2363(5)	1390(40)
OW5	24d	0.6596(4)	0.0401(3)	0.1525(4)	910(30)
OW6	24d	0.5921(3)	0.3031(4)	0.1701(5)	1170(40)
Na2	24d[b][c]	0.5195(9)	0.2467(9)	0.1148(9)	1280(60)

[a] U_{equiv} is defined as one third of the trace of the U_{ij} tensors. − [b] Only isotropically refined. − [c] SOF = 1/3.

Table 4. Atomic coordinates and anisotropic displacement parameters [pm^2] for $Na_4\{Hf_4(\mu_4\text{-}O)(\mu\text{-}OH)_6[(PO_2NH)_3]_4\}\cdot 21\ H_2O$ (rhombohedral phase)

Atom	Wyckoff symbol	x/a	y/b	z/c	U_{equiv}[a]
Hf1	18f	0.5559(1)	0.3816(1)	0.0981(1)	162(1)
Hf2	3c	0.6667	0.3333	0.0412(1)	164(1)
O11	18f	0.5122(3)	0.2261(3)	0.1125(1)	239(7)
O12	18f	0.5541(3)	0.3728(3)	0.0562(1)	230(7)
OT	3c	0.6667	0.3333	0.0841(1)	134(9)
P1	18f	0.3069(1)	0.3469(9)	0.1002(1)	205(2)
P2	18f	0.4382(1)	0.4509(1)	0.1459(1)	207(2)
P3	18f	0.4790(1)	0.5673(1)	0.0967(1)	195(2)
P4	18f	0.7531(1)	0.2879(1)	−0.0169(1)	225(2)
O1A	18f	0.3863(2)	0.3108(3)	0.0927(1)	211(6)
O1B	18f	0.1932(3)	0.2775(3)	0.0923(1)	307(8)
O2A	18f	0.5132(3)	0.4105(3)	0.1368(1)	217(6)
O2B	18f	0.4331(3)	0.4648(3)	0.1750(1)	308(8)
O3A	18f	0.5544(3)	0.5256(2)	0.0891(1)	199(6)
O3B	18f	0.5052(3)	0.6725(3)	0.0851(1)	307(8)
O4A	18f	0.7517(3)	0.2914(3)	0.0132(1)	223(6)
O4B	18f	0.8215(3)	0.2506(3)	−0.0296(1)	319(8)
N1	18f	0.3175(3)	0.3638(3)	0.1334(1)	233(8)
H1	18f	0.2626(3)	0.3288(3)	0.1435(1)	280
N2	18f	0.4746(3)	0.5667(3)	0.1301(1)	254(8)
H2	18f	0.4907(3)	0.6244(3)	0.1388(1)	310
N3	18f	0.3565(3)	0.4709(3)	0.0877(1)	226(8)
H3	18f	0.3190(3)	0.4847(3)	0.0768(1)	270
N4	18f	0.6243(3)	0.2107(3)	−0.0265(1)	265(8)
H4	18f	0.6048(3)	0.1541(3)	−0.0360(1)	320
Na1	18f	0.1058(2)	0.3247(2)	0.0596(1)	485(6)
OW1	18f	−0.0164(5)	0.3567(6)	0.0329(1)	750(2)
OW2	18f	−0.0601(7)	0.1882(10)	0.0816(2)	1450(40)
OW3	18f	0.0874(12)	0.1759(12)	0.0326(3)	1970(60)
OW4	18f	0.4077(6)	0.3734(7)	0.0236(1)	820(20)
OW5	18f	0.3202(7)	0.0929(8)	0.1381(2)	1250(40)
OW6	18f	−0.1496(10)	0.1189(11)	0.0240(4)	2060(70)
OW7	18f	−0.0185(17)	−0.1248(18)	0.1515(6)	2820(110)
Na2	18f[b][c]	0.1548(53)	−0.0301(50)	0.1300(12)	3470(250)

[a] U_{equiv} is defined as one third of the trace of the orthogonalized U_{ij} tensors. − [b] Only isotropically refined. − [c] Na2: SOF = 1/3.

[1] A. Durif, *Crystal Chemistry of Condensed Phosphates*, Plenum Press, New York, **1995**.
[2] H. N. Stokes, *Am. Chem. J.* **1896**, *18*, 629.
[3] [3a] K. Lunkwitz, E. Steger, *Spectrochim. Acta* **1967**, *23A*, 2593. – [3b] J. V. Pustinger, W. T. Cave, M. L. Nielsen, *Spectrochim. Acta* **1959**, *11*, 909.
[4] [4a] N. Stock, W. Schnick, *Acta Crystallogr.* **1996**, *C52*, 2645. – [4b] N. Stock, W. Schnick, *Acta Crystallogr.* **1997**, *C53*, 532. – [4c] N. Stock, W. Schnick, *Z. Naturforsch.* **1997**, *52b*, 251. – [4d] R. Olthof, T. Migchelsen, A. Vos, *Acta Crystallogr.* **1965**, *19*, 499. – [4e] R. Attig, D. Mootz, *Z. Anorg. Allg. Chem.* **1976**, *419*, 139.
[5] [5a] V. I. Sokol, L. Ya. Medvedeva, L. A. Butman, I. A. Rozanov, *Koord. Khim.* **1976**, *2*, 576. – [5b] V. I. Sokol, M. A. Porai-Kohits, V. R. Berdnikov, I. A. Rozanov, L. A. Butman, *Koord. Khim.* **1975**, *1*, 429.
[6] V. I. Sokol, M. A. Porai-Koshits, L. A Butman, I. A. Rozanov, V. A. Berdnikov, *Izv. Akad. Nauk SSR, Ser. Khim.* **1974**, *2*, 485.
[7] L. K. Shubochkin, O. V. Popov, E. F. Shubochkina, V. I. Sokol, I. A. Rozanov, L. A. Butman, *Koord. Khim.* **1977**, *3*, 902.
[8] A. Clearfield, G. D. Smith, *Inorg. Chem.* **1969**, *8*, 431.
[9] N. Fripiat, P. Grange, *J. Chem. Soc., Chem. Commun.* **1996**, 1409.
[10] P.Tolédano, M. In, C. Sanches, *C. R. Acad. Sci. Paris, Série II* **1990**, *311*, 1161.
[11] R. E. Hanu, P. R. Suitch, J. L. Pentecost, *J. Am. Ceram. Soc.* **1985**, *68*, 285.
[12] C. J. Howard, R. J. Hill, B. E. Reichert, *Acta Crystallogr.* **1988**, *B44*, 116.
[13] M. L. Nielsen, T. J. Morrow, *Inorg. Synth.* **1960**, *6*, 99.
[14] G. Brauer, *Handbuch der Präparativen Anorganischen Chemie*, Ferdinand Enke Verlag, Stuttgart, **1975**.
[15] W. Herrendorf, HABITUS: *A Program for Crystal Shape Optimization and Numerical Absorption Correction,* Universität Giessen, **1996**.
[16] G. M. Sheldrick, *SHELXTL-PLUS V4.2 Crystallographic System*, Siemens Analytical X-Ray Instruments Inc., Madison, WI, **1992**.
[17] Further details of the crystal-structure investigations may be obtained from the Fachinformationszentrum Karlsruhe, D-76344 Eggenstein-Leopoldshafen (Germany) by quoting the depository numbers CSD-407897 ($Na_4\{Hf_4(\mu_4\text{-}O)(\mu\text{-}OH)_6[(PO_2NH)_3]_4\}\cdot 18\ H_2O$), -407895 ($Na_4\{Hf_4(\mu_4\text{-}O)(\mu\text{-}OH)_6[(PO_2NH)_3]_4\}\cdot 21\ H_2O$), -407898 ($Na_4\{Zr_4(\mu_4\text{-}O)(\mu\text{-}OH)_6[(PO_2NH)_3]_4\}\cdot 18\ H_2O$) and -407896 ($Na_4\{Zr_4(\mu_4\text{-}O)(\mu\text{-}OH)_6[(PO_2NH)_3]_4\}\cdot 21\ H_2O$).
[97253]

Synthesis of a New Multidentate Phosphane Ligand $C_6H_2(CH_2PPh_2)_4$-1,2,4,5 − X-ray Structure of a Dinuclear Ruthenium(II)-Bridged Complex: [{$RuCl_2(PPh_3)$}$_2${$C_6H_2(CH_2PPh_2)_4$-1,2,4,5-*P,P′,P′′,P′′′*}]

Pablo Steenwinkel[a], Sebastiaan Kolmschot[a], Robert A. Gossage[a], Paulo Dani[a], Nora Veldman[b], Anthony L. Spek[b][+], and Gerard van Koten*[a]

Debye Institute, Department of Metal-Mediated Synthesis, Utrecht University[a],
Padualaan 8, NL-3584 CH Utrecht, The Netherlands
Fax: (internat.) + 31-30/252-3615
E-mail: g.vankoten@chem.ruu.nl

Bijvoet Center for Biomolecular Research, Department of Crystal and Structural Chemistry, Utrecht University[b],
Padualaan 8, NL-3584 CH Utrecht, The Netherlands

Received November 14, 1997

Keywords: Ruthenium / Bridging bis(bidentate) tetraphosphane ligand / Diruthenium(II) coordination complex / Cyclometallation versus *o-P,P′* chelation

The tetrakis(phosphane oxide) $C_6H_2\{CH_2P(O)Ph_2\}_4$-1,2,4,5 (**5**), has been prepared in high yield from the Arbuzov reaction of $C_6H_2(CH_2Br)_4$-1,2,4,5 (**4**), with excess (7 equiv.) of Ph_2POEt. Subsequent reduction of **5** with $HSiCl_3$ (12 equiv.) in $C_6H_4Cl_2$-1,2 afforded the new tetraphosphane $C_6H_2(CH_2PPh_2)_4$-1,2,4,5 (**6**), in high yield. The reaction of **6** with $[RuCl_2(PPh_3)_4]$ in CH_2Cl_2 afforded the green dinuclear ruthenium(II) coordination complex [{$RuCl_2(PPh_3)$}$_2${C_6H_2-$(CH_2PPh_2)_4$-1,2,4,5-*P,P′,P′′,P′′′*}]·0.5 CH_2Cl_2 (**8**), in 39% isolated yield. The solid-state molecular geometry of **8**, determined by X-ray analysis, shows that the tetraphosphane is *ortho-P,P′*-chelated to each of the two $[Ru^{II}Cl_2(PPh_3)]$ units.

Introduction

In recent years there has been an increasing interest in dinuclear organometallic complexes and such species have been used to model fundamental properties of multi- and polymeric organometallic materials[1] that have potential optical and/or electronic applications. Recently, we reported on the selective synthesis of 4,4′-biphenylene- and 1,4-phenylene-bridged bimetallic complexes of some platinum-group metals containing anionic *N,C,N′*-terdentate ligands (Figure 1)[2]. In addition to their interesting photochemical behavior[2a], these complexes have potential in the development of multimetallic materials, such as "molecular wires".

Figure 1. Some examples of 4,4′-biphenylene- and 1,4-phenylene-bridged organometallic complexes containing ligands with anionic *N,C,N′*-terdentate coordination moieties

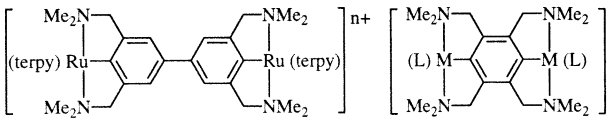

We have also investigated the synthesis of ruthenium(II) complexes of monoanionic (functionalized) *N,C,N′*-terdentate ligands $[C_6H_2(CH_2NMe_2)_2$-2,6-R-4$]^-$ (= NCN-R-4) and *P,C,P′*-terdentate ligands $[C_6H_2(CH_2PPh_2)_2$-2,6-R-4$]^-$ (= PCP-R-4) (Figure 2). The use of these ligands, which can be derived from the aryl compounds $C_6H_3(CH_2ER'_2)_2$-1,3-R-5 (**1**), either by transmetallation (of **1a**-Li) or direct cyclometallation (of **1b**), has resulted in a new series of stable organoruthenium complexes (see Scheme 1)[3].

Figure 2. Schematic representation of the monoanionic aryl ligands NCN-R-4 (R = H, Ph, $Me_3SiC{\equiv}C$, Me_3Si) and PCP-R-4 (R = H, Ph) and the dianionic C_2N_4 ligand

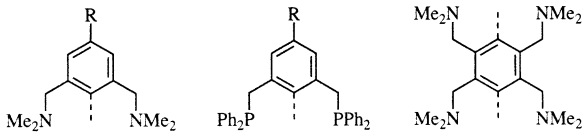

The PCP-R-4 ruthenium(II) complexes **2b** can be obtained directly by cyclometallation[4] of the corresponding diphosphanes **1b** with $[RuCl_2(PPh_3)_4]$. In contrast, the NCN-R-4 ruthenium(II) complexes **2a** were prepared by transmetallation of organolithium reagents $[LiC_6H_2$-$(CH_2NMe_2)_2$-2,6-R-4$]_2$ derived from the aryldiamines **1a**. Some NCN-R-4 and PCP-R-4 ruthenium(II) complexes have also been used as catalysts in various hydrogen-transfer reactions[5].

Recently, we have also developed a synthetic strategy for the preparation of homo- and heterodinuclear organometallic complexes of the bis(*N,C,N′*-terdentate) coordinating dianionic 1,4-phenylene-bridging ligand $[C_6(CH_2NMe_2)_4$-2,3,5,6$]^{2-}$ (= C_2N_4; Figure 2)[6] and extension of this re-

[+] Address correspondence pertaining to crystallographic studies to this author; E-mail: spea@xray.chem.ruu.nl

 © WILEY-VCH Verlag GmbH, D-69451 Weinheim, 1998 1434−1948/98/0404−0477 $ 17.50+.50/0

Scheme 1. Synthesis of ruthenium(II) complexes **2** and **3** derived from (functionalized) *N,C,N′*- and *P,C,P′*-terdentate-coordinating ligands **1**, by transmetallation (of **1a**-Li) or direct cyclometallation (of **1b**)

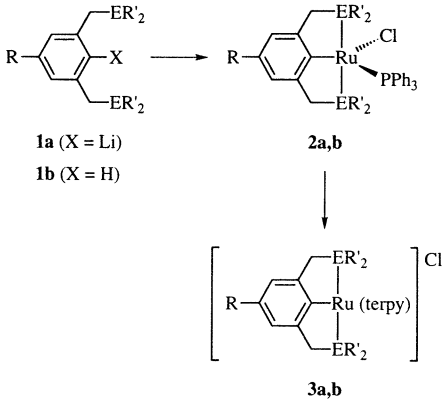

1,2,3 a: $ER'_2 = NMe_2$; R = H, Ph, $Me_3SiC{\equiv}C$, Me_3Si

1,2,3 b: $ER'_2 = PPh_2$; R = H, Ph

search has been aimed at the generation of the related dianionic 1,4-phenylene ligand with two potentially *P,C,P′*-terdentate coordination motifs, i.e., an analog to the tetraaminophenylene dianion C_2N_4 shown in Figure 2. As part of this research we have explored the synthesis of the tetraphosphane $C_6H_2(CH_2PPh_2)_4$-1,2,4,5 (**6**), which is a potential precursor to the ligand $[C_6(CH_2PPh_2)_4\text{-}1,2,4,5]^{2-}$. We now report the successful synthesis of **6** and its complexation reaction with $[RuCl_2(PPh_3)_4]$.

Results

The target compound of this study is tetraphosphane-substituted benzene $C_6H_2(CH_2PPh_2)_4$-1,2,4,5 (**6**). The synthetic protocol used involves an Arbuzov reaction[7] of a phosphanic ester (i.e., Ph_2POEt) with a benzylic bromide [i.e., $C_6H_2(CH_2Br)_4$-1,2,4,5 (**4**)] to afford a P^V oxide compound, **5**[8]. The latter is then reduced to the corresponding desired tetraphosphane **6** (see Scheme 2).

Synthesis of $C_6H_2(CH_2PPh_2)_4$-1,2,4,5 (5)

Compound **5** can be obtained in high yield, as a white solid, by treatment of the known $C_6H_2(CH_2Br)_4$-1,2,4,5 (**4**)[9] with excess of ethyldiphenylphosphanite (Ph_2POEt) in *m*-xylene at 140°C in a slight modification of a previously described procedure that gives an improved yield[8]. The ^{1}H-NMR data of the poorly soluble tetrakis(phosphane oxide) **5** (in warm CD_3OD solution) were identical to those reported previously[8].

Typical procedures described for the reduction of phosphane oxides to phosphanes failed to completely reduce compound **5** to phosphane **6**. For example, $HSiCl_3$ reduction of **5** in benzene, toluene or xylene at reflux temperature[10] did not result in the formation of the desired phosphane. Similarly, $LiAlH_4$ (or $LiAlH_4 \cdot CeCl_3$) reductions[11] in THF also failed to reduce **5** selectively. In the latter case, a new product formed in ca. 10% yield with over 85% of the starting material still present. This new product has not been isolated in a pure form but on the basis of ^{31}P-NMR data of the crude material, its air stability and its water solubility we believe that it is likely to be an ionic phosphonium species (vide infra). It was felt that the poor reactivity of **5** in the attempted reduction reactions was possibly due to its inherent low solubility. Therefore, alternative solvents were examined and it has been found that for the reduction of **5** with $HSiCl_3$, hot 1,2-dichlorobenzene was the solvent of choice. In practice, a suspension of **5** in 1,2-dichlorobenzene was heated to 180°C and kept at this temperature for 10 min to dissolve all solid material. The solution temperature was then reduced to 140°C and $HSiCl_3$ was added by syringe. The reaction mixture was kept for 1 h at this temperature and, after appropriate work-up, the desired tetraphosphane **6** was obtained as a white solid in very good yield (96%). Compound **6** is air-sensitive and reasonably soluble in aromatic and chlorinated solvents. Analytically pure crystals of **6** can be obtained by slow diffusion of MeOH into a solution of **6** in benzene.

Scheme 2. Synthesis of the tetraphosphane $C_6H_2(CH_2PPh_2)_4$-1,2,4,5 (**6**). – *i:* Ph_2POEt, *m*-xylene, 140°C, –EtBr. – *ii:* $HSiCl_3$, $C_6H_4Cl_2$–1,2, 140°C, 1 h.

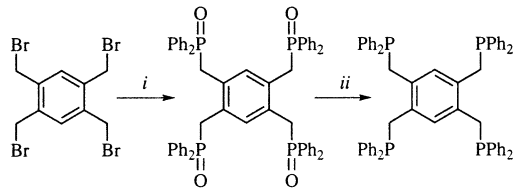

Reaction of Tetraphosphane 6 with $[RuCl_2(PPh_3)_4]$

It was anticipated that phosphane **6** would be susceptible to cyclometallation and that with $[RuCl_2(PPh_3)_4]$[12] the product of this reaction would be a bimetallic species related to the ruthenium(II) complex **3b** (Scheme 1) obtained when $C_6H_3(CH_2PPh_2)_2$-1,3-R-5 (**1b**), is used as the phosphane[3c][3d]. To test the reactivity of the new tetraphosphane **6** towards $[RuCl_2(PPh_3)_4]$, these two species were mixed in a 1:2 molar ratio in CH_2Cl_2 (Scheme 3) at room temperature and after 1 h a green precipitate had been formed. After appropriate work-up, this precipitate was isolated as a green solid, whose poor solubility in common organic solvents (benzene, toluene, THF, CH_2Cl_2, etc.) has prevented us from identifying this material, **8**, by solution-NMR spectroscopy and also prevented successful recrystallization. However, elemental microanalysis data suggested that this crude product has an overall formula $[\{RuCl_2(PPh_3)\}_2(\mathbf{6})] \cdot 0.5\ CH_2Cl_2$.

In a second experiment, aimed at directly obtaining a purer, more crystalline product **8**, we carried out the original reaction under slightly different conditions. To this end, a CH_2Cl_2 solution of two equivalents of $[RuCl_2(PPh_3)_4]$ was

carefully layered with a solution of tetraphosphane **6** in CH_2Cl_2 and the reaction mixture was left undisturbed for 24 h at room temperature. This produced analytically pure green crystals of **8** (isolated yield: 38%) which were suitable for an X-ray crystallographic study. This study afforded a solid-state structure (vide infra) which shows this product to be $[\{RuCl_2(PPh_3)\}_2\{C_6H_2(CH_2PPh_2)_4$-1,2,4,5-*P,P′,P″,P‴*$\}]\cdot 0.5\ CH_2Cl_2$ (**8**); the molecular geometry is depicted in Figure 3 and selected geometrical details are collected in Table 1. Complex **8** has a composition that corresponds to the original microanalytical data and it can be seen to be a dinuclear coordination complex of **6** in which this tetraphosphane functions as a bridging ligand that coordinates in a *P,P′*-bidentate manner to each of the identical metal centers. Thus, under the experimental conditions used or at reflux temperature in CH_2Cl_2, compound **6** does not undergo cyclometallation with the ruthenium(II) center to afford a product such as **7**. This behavior is different to that of aryldiphosphane $C_6H_4(CH_2PPh_2)_2$-1,3 which cyclometallates with $[RuCl_2(PPh_3)_4]$ under identical conditions to afford $[RuCl\{C_6H_3(CH_2PPh_2)_2$-2,6$\}(PPh_3)]$[3].

Scheme 3. Reactivity of **6** with $[RuCl_2(PPh_3)_4]$ in CH_2Cl_2 to afford coordination complex **8** rather than the cyclometallated species **7**. − *i:* 2 equiv. $[RuCl_2(PPh_3)_4]$, CH_2Cl_2, room temp., 1 h, −6 equiv. PPh_3.

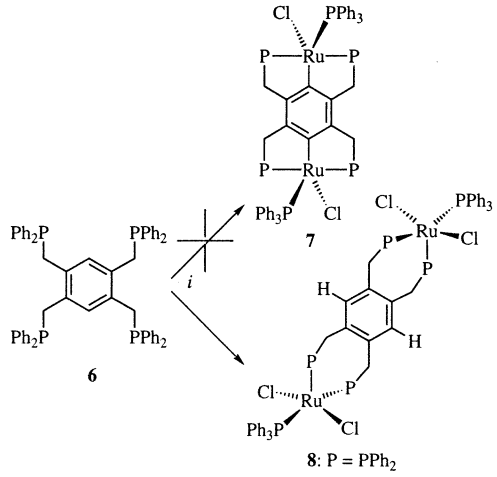

In the X-ray crystallographic structure of **8**, the tetraphosphane ligand bridges between the two identical 5-coordinate ruthenium(II) metal centers that have approximate square-pyramidal geometries; the molecule has a center of inversion positioned in the central aromatic ring of this tetraphosphane. The square pyramidal ligand array comprises in the basal plane plane two *trans*-Cl atoms [Cl(1) and Cl(2)] and two *trans*-P atoms [P(2) of the bridging ligand and P(3) of PPh_3] and at the apex there is a phosphorus atom P(1) of the bridging ligand. The bridging phosphane employs two mutually *ortho*-CH_2PPh_2 substituents for *ortho-P,P′* chelation to each metal center, thus forming a 7-membered chelate ring in which the bite angle P(1)−Ru(1)−P(2) is 97.46(9)°. The geometrical parameters found for **8**, including Ru−P bond lengths in the range of 2.208(3) to 2.391(2) Å and a Cl(1)−Ru(1)−Cl(2) bond angle of 160.96(9)°, are similar to those reported for related complexes with the general formula $[RuCl_2(Ph_2PR)_3]$[13a][13b] (see Discussion). The $P-C_{aryl}$ bond lengths fall in the range of 1.815(10) to 1.853(9) Å and the $Ru-P-C_{aryl}$ bond angles vary from 100.0(3) to 124.7(3)°. Interestingly, the proton H(31) situated on triphenylphosphane *ortho*-carbon atom C(31) is fairly close to the ruthenium(II) center with a Ru(1)···H(31) distance of 2.82 Å that is substantially shorter than the sum of the van der Waals radii (3.40 Å).

In further experimental studies aimed at promoting cyclometallation of the neutral phosphane **6** present in complex **8**, this latter complex was suspended in 1,2-dichlorobenzene and heated to 140°C together with PPh_3 and trioctylamine as a base. Although NMR-spectroscopic studies of the resulting solution indicated that a new orthometallated product had been formed, it was in fact the coordinated PPh_3 ligand, and not **6**, that had been cyclometallated. Unfortunately, a pure sample of this new cyclometallated product could not be separated for further identification.

Discussion

Synthesis of the Tetraphosphane

The choice of the Arbuzov-reaction/reduction sequence for the synthesis of tetraphosphane **6** is a consequence of the poor results that we achieved in preliminary experiments using the tetrabromide **4** as starting material in the well-known nucleophilic substitution of a benzylic bromide with $NaPPh_2$ in liquid ammonia[3c][14]. The main product of this latter reaction is not the desired phosphane **6**, but a mixture of phosphonium salts. These phosphonium salts are probably formed as a result of an intramolecular nucleophilic substitution reaction of a CH_2Br group with an *ortho*-positioned CH_2PPh_2 group that has been produced by an initially successful intermolecular nucleophilic substitution (see Scheme 4). The success of the route we employ to form **6** (Scheme 2) comes from the fact that the product of the Arbuzov reaction is a non-nucleophilic phosphane oxide and the initially formed $CH_2P(O)Ph_2$ unit is inert to intramolecular attack by an *ortho*-positioned benzylic bromide.

The solvent used in the $HSiCl_3$-mediated reduction reaction of the tetrakis(phosphane oxide) **5** to the tetraphosphane **6** was found to be crucial and the best experimental conditions that we found was the use of 1,2-dichlorobenzene at high temperature. It appears that for phosphane oxides like **5**, which have poor solubility characteristics, it is important to use a solvent that not only has a high boiling point but also one that has a good degree of polarity, and this combination of physical properties is found in 1,2-dichlorobenzene.

Solid-State Structure of 8

The complex formed by the undisturbed reaction of $[RuCl_2(PPh_3)_4]$ with **6** in CH_2Cl_2 was not one containing the expected cyclometallated tetraphosphane ligand **7**. In-

Figure 3. ORTEP drawing (50% probability atomic displacement ellipsoids) of [{$RuCl_2(PPh_3)$}$_2${$C_6H_2(CH_2PPh_2)_4$-1,2,4,5-*P,P′,P″,P‴*}] (**8**); hydrogen atoms and cocrystallized CH_2Cl_2 molecules have been omitted for clarity

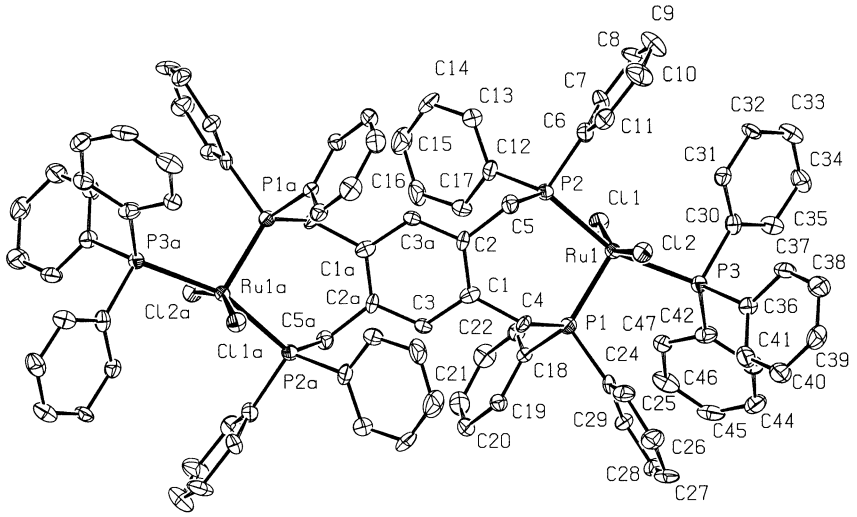

Table 1. Selected bond parameters of [{$RuCl_2(PPh_3)$}$_2${$C_6H_2(CH_2PPh_2)_4$-1,2,4,5-*P,P′,P″,P‴*}] (**8**)

Bond lengths [Å]		Bond angles [°]	
Ru(1)−Cl(1)	2.389(2)	Cl(1)−Ru(1)−Cl(2)	160.96(9)
Ru(1)−Cl(2)	2.383(2)	P(1)−Ru(1)−P(2)	97.46(9)
Ru(1)−P(1)	2.208(3)	P(1)−Ru(1)−P(3)	101.74(9)
Ru(1)−P(2)	2.318(2)	P(2)−Ru(1)−P(3)	160.49(9)
Ru(1)−P(3)	2.391(2)	Ru(1)−P(1)−C(4)	114.8(3)
P(1)−C(4)	1.846(8)	Ru(1)−P(1)−C(18)	120.1(3)
P(1)−C(18)	1.853(9)	Ru(1)−P(1)−C(24)	116.3(3)
P(1)−C(24)	1.834(9)	Ru(1)−P(2)−C(5)	118.3(3)
P(2)−C(5)	1.847(9)	Ru(1)−P(2)−C(6)	100.0(3)
P(2)−C(6)	1.815(10)	Ru(1)−P(2)−C(12)	124.7(3)
P(2)−C(12)	1.816(10)	Ru(1)−P(3)−C(30)	103.1(3)
P(3)−C(30)	1.844(10)	Ru(1)−P(3)−C(36)	120.2(3)
P(3)−C(36)	1.828(8)	Ru(1)−P(3)−C(42)	121.5(3)
P(3)−C(42)	1.821(9)	P(3)−C(30)−C(31)	116.9(7)
Ru(1)···H(31)	2.8118	P(3)−C(30)−C(35)	123.5(7)
		P(3)−C(36)−C(37)	120.8(7)
		P(3)−C(36)−C(41)	120.6(7)
		P(3)−C(42)−C(43)	122.9(7)
		P(3)−C(42)−C(47)	118.9(7)

Scheme 4. Schematic formation of phosphonium species from the reaction of $NaPPh_2$ with *ortho*-bis(bromomethyl)arenes

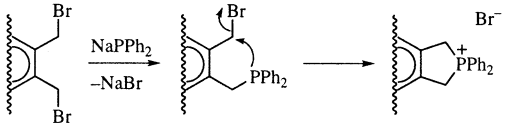

stead, the product is a bimetallic coordination complex of neutral tetraphosphane **6** in which two *ortho*-positioned phosphane donor substituents are coordinated to a ruthenium(II) metal center. The related tetraphosphane ligand 1,2,4,5-tetrakis(diphenylphosphano)benzene has been reported to form similar, non-metallated, bridged bimetallic (and polymeric) coordination complexes with several transition metals[15]. It appears that this type of initial *P,P′*-chelation forms a species that is relatively inert to Ru−P bond cleavage and as a consequence the C_{aryl}−H bond of the central aromatic ring cannot approach the metal center for intramolecular activation and subsequent C−Ru bond formation.

Bisruthenium(II) complex **8** is one of only a few structurally characterized 5-coordinate ruthenium(II) species in which the ligand array comprises two halide atoms and three phosphanes. Moreover, in complex **8** the presence of a close contact between the metal center and an *ortho* H atom of one of the PPh_3 C_{aryl}−H units is a noteworthy feature; interestingly, the structure of [$RuCl_2(PPh_3)_3$] has a similar interaction which was concluded to be substantially repulsive,[13a] and not to be an agostic interaction[13c][13d] of this C_{aryl}−H bond with the metal center. The authors described the overall structure of this complex as a distorted square pyramid with this *ortho*-H atom occupying the open coordination site of an octahedral ligand array. More recently, Cotton and Matusz[13b] have reported the solid-state structure of another square-pyramidal ruthenium complex, [$RuCl_2(Ph_2PCH_2SiMe_3)_3$], in which this type of M···H−C interaction was not found and the bulky benzylic substituent would appear to be shielding the vacant sixth coordination site in this 16-electron species. Comparison of some selected bond lengths and interbond angles collected in Table 2, shows that the overall solid-state structures of bimetallic **8** with *P,P′*-chelation and the mononuclear complexes [$RuCl_2(Ph_2PR)_3$] (R = Ph, CH_2SiMe_3) with monodentate-bonded phosphanes are surprisingly similar.

P,P′-Chelation versus Cyclometallation

Cyclometallation of aryldiphosphanes with ruthenium(II) species is a well-known reaction and has been successfully employed by us[3c] and others[3e] in earlier studies to form a series of complexes containing [$C_6H_2(CH_2PPh_2)_2$-2,6-R-4]$^-$, PCP-R-4 (Scheme 1). However, as reported here, the neutral tetraphosphane **6** has to date not been found to undergo such cyclometallation reactions and it is worthwhile considering the unique aspects of this compound that result in it having a different reactivity

Table 2. Selected bond parameters of **8** and the known ruthenium(II) complexes $[RuCl_2(Ph_2PR)_3]$ (R = Ph, CH_2SiMe_3)

	8	$[RuCl_2(PPh_3)_3]$[a]	$[RuCl_2(Ph_2PCH_2SiMe_3)_3]$[b]
Bond lengths [Å]			
Ru(1)−Cl(1)	2.389(2)	2.387(7)	2.395(2)
Ru(1)−Cl(2)	2.383(2)	2.388(7)	2.390(2)
Ru(1)−P_A[c]	2.208(3)	2.230(8)	2.210(2)
Ru(1)−P_B[c]	2.318(2)	2.374(6)	2.348(2)
	2.391(2)	2.412(6)	2.379(2)
Ru(1)···H	2.8118	2.59	not present
Bond angles [°]			
Cl(1)−Ru(1)−Cl(2)	160.96(9)	157.2(2)	163.93(7)
P_B−Ru(1)−P_B[c]	160.49(9)	156.4(2)	165.91(7)
P_A−Ru(1)−P_B[c]	97.46(9)	101.1(2)	96.83(7)
	101.74(9)	101.4(2)	99.24(7)

[a] Data obtained from ref.[12a]. – [b] Data obtained from ref.[12b]. – [c] P_A and P_B are the apical and basal phosphorus atoms, respectively.

pattern. For reaction of the neutral aryldiphosphanes $C_6H_3(CH_2PPh_2)_2$-1,3-R-5 (**1b**), with $[RuCl_2(PPh_3)_4]$ we proposed that prior to cyclometallation an 8-membered cyclic coordination complex is formed by replacement of PPh_3 ligands of $[RuCl_2(PPh_3)_3]$ (vide supra) by the more basic phosphorus donor substituents of **1b**[3c]. In this resulting intermediate complex the two *meta*-positioned CH_2PPh_2 substituents are coordinated to the ruthenium(II) metal center in a bidentate *P,P′*-chelate mode. As a consequence the metal center is brought into proximity to the C−H bond which can then be activated. Because this intermediate has not been detected by NMR-spectroscopic methods we assume that the formation of this intermediate is rate-determining and that the following step, i.e. C−H bond cleavage and generation of the new Ru−C σ bond, is a much faster process. In one rare and unique case, an example of an agostic interaction of a C_{aryl}−H bond of an aryldiphosphane, **1b** (R = H), at an Ru^{II} center afforded by *P,P′*-chelate bonding has been confirmed by an X-ray crystallographic study[3d]; the molecular geometry of the monocationic complex reported in this study is schematically presented in Figure 4.

Figure 4. Schematic representation of aryl C−H bond activation at a Ru^{II} center in an intermediate whose structure has been determined by an X-ray crystallographic study

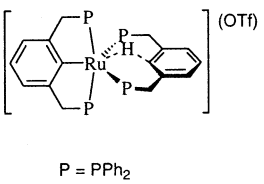

Tetraphosphane **6** should, like diphosphanes **1b**, displace PPh_3 from $[RuCl_2(PPh_3)_3]$ since the CH_2PPh_2 groups are more basic P donors than PPh_3. Several different coordination complexes could be formed, and two of these based on *P,P′*-chelation are the observed dinuclear coordination complex **8** as well as the alternative chelation complex **A** (See Figure 5). The difference between these complexes is that in **8** there is chelation of two *ortho*-positioned CH_2PPh_2 groups, whereas in **A** there is chelation two *meta*-positioned CH_2PPh_2 groups.

Figure 5. Schematic representation of two different coordination complexes **8** and **A** which could be formed from **6** and $[RuCl_2(PPh_3)]_4$

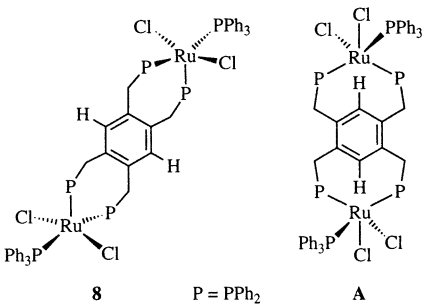

In complex **A**, there are two 8-membered chelate rings that allow the metal centers to be brought close to the aryl C−H bonds at positions 3 and 6 on the central aromatic ring; as a result of geometric (steric) restraints each ring has limited flexibility. In contrast, complex **8** contains two 7-membered chelate rings that have a good degree of conformational flexibility, and therefore this situation is energetically more favorable than that in **A**. However, unlike the situation in **A** the ruthenium(II) centers in **8** are unable to approach the central C−H bonds to undergo cyclometallation and form complex **7** (Scheme 3). The favorable situation found in complex **8** is emphasized by the fact that this complex does not undergo cycloruthenation during the synthetic procedure. In principle, the excess of free PPh_3 present in the reaction mixture (see Scheme 2) could induce the formation of an η^1-*P*-coordinated ligand **6** in complex **8**, and this would be sufficient to generate a situation where the an aryl C−H bond (as in **A**) is close enough to the metal center for cyclometallation to occur. However, the poor solubility characteristics of **8** in common organic solvents prevents the possibility of this situation.

Conclusion

In this report we have shown that the new neutral tetraphosphane ligand $C_6H_2(CH_2PPh_2)_4$-1,2,4,5 (**6**) can be easily prepared in high yield. The synthetic strategy, which involves an Arbuzov reaction, has great potential as an alternative (and less hazardous) route to many other aryl- and alkylphosphanes. In this strategy the choice of 1,2-dichlorobenzene as a high-temperature solvent for the reduction of the corresponding phosphane oxide was crucial. With ruthenium(II) centers the new tetraphosphane **6** affords *P,P′*-bidentate chelation from two *ortho*-positioned, rather than *meta*-positioned, CH_2PPh_2 substituents such that C−H bond activation and formation of a *P,C,P′*-terdentate-coordinated ruthenium(II) species does not occur.

This work was supported in part (P. S., N. V., A. L. S.) by the *Netherlands Foundation for Chemical Research (SON)* with financial aid from the *Netherlands Organization for Scientific Research (NWO)*.

Table 3. Crystal Data and Details of the Structure Determination for [{$RuCl_2(PPh_3)$}$_2${$C_6H_2(CH_2PPh_2)_4$-1,2,4,5-*P,P′,P″,P‴*}] (**8**)

	Crystal Data		
empirical formula	$C_{94}H_{80}Cl_4P_6Ru_2 \cdot 8\ CH_2Cl_2$		
formula weight	2418.92	crystal size [mm]	0.15 × 0.15 × 0.63
crystal system	triclinic	space group	*P*1 (no. 2)
a [Å]	10.2378(13)		
α [°]	106.139(10)		
b [Å]	14.227(2)		
β [°]	97.707(10)		
c [Å]	20.237(2)		
γ [°]	106.822(11)		
V [Å^3]	2635.4(6)	$D_{calcd.}$ [g cm^{-3}]	1.524
Z	1	*F*(000) [e]	1226
μ(Mo-K_α) [cm^{-1}]	9.3		
	Data Collection		
T [K]	150		
θ_{min}, θ_{max} [°]	1.1, 25.0		
wavelength (Mo-K_α) [Å]	0.71073	scan range [°]	1.10 + 0.00 tanθ
hor. aperture	3.00	vert. aperture	4.00
data set	−8/12, −17/17, −25/25		
total data	10839		
total unique data	9273		
observed data [$I > 2.0\ \sigma(I)$]	5094		
	Refinement		
N_{ref}, N_{par}	9273, 586	final *R*1[a]	0.0748
final *wR2*[b]	0.1660	goodness of fit	1.01
w^{-1}	$\sigma^2(F^2) + (0.0474P)^2 + 1.8922P$, where $P = (F_o^2+2F_c^2)/3$		
$(\Delta.\sigma)_{av}$, $(\Delta.\sigma)_{max}$	0.00, 0.00		
min. and max. resid. density [e Å^{-3}]	−0.74, 0.64		

[a] $R1 = \Sigma\|F_o|-|F_c\|/\Sigma|F_o|$. − [b] $wR2 = [(|F_o|^2-|F_c|^2)^2/\Sigma w(|F_o|^2)^2]^{1/2}$.

Experimental Section

General: All synthetic procedures were performed under dry dinitrogen. Hexane and benzene were freshly distilled from sodium benzophenone ketyl, CH_2Cl_2 from CaH_2, and xylenes and 1,2-dichlorobenzene from molecular sieves (5 Å). − Spectroscopic measurements ($^{1\ H,\ 13}C\{^1H\}$ and $^{31}P\{^1H\}$ NMR) were performed with a Bruker AC200 or AC300 spectrometer, with chemical shifts referenced to either Me_4Si or 85% H_3PO_4. − Elemental analyses were carried out by Dornis und Kolbe, Mikroanalytisches Laboratorium, Mülheim, Germany. − The compounds $C_6H_2(CH_2Br)_4$-1,2,4,5 (**4**)[9], Ph_2POEt[16], and $[RuCl_2(PPh_3)_4]$[17] were prepared according to previously described methods. $RuCl_3 \cdot 3\ H_2O$ was purchased from Degussa.

$C_6H_2(CH_2P(O)Ph_2)_4$-1,2,4,5 (**5**): A modification of a procedure described in the literature[8] was used. In a two-necked 100-ml round bottom flask, a stirred colorless solution of Ph_2POEt (20.52 g, 89 mmol) and $C_6H_2(CH_2Br)_4$-1,2,4,5 (5.35 g, 11.9 mmol) in xylenes (20 ml) was heated at 140°C for 0.5 h, while a gentle stream of nitrogen was bubbled through the reaction mixture. After this time, the reaction mixture was cooled to 50°C (ice bath) and the white solid which had precipitated was filtered off. This solid was washed once with hot benzene (100 ml), filtered off and dried in vacuo to afford the tetraphosphoryl compound **5** as a white solid which was sufficiently pure for further synthesis. Yield: 9.53 g (86%), mp > 220°C (ref.[8]: 315−317°C). − ^1H NMR (CD_3OD, 200 MHz, 335 K): δ = 7.62 (m, 40 H, ArH), 6.42 (s, 2 H, ArH), 3.52 (d, 8 H, $^2J_{P\text{-}H}$ = 12 Hz, CH_2P). − $^{31}P\{^1H\}$ NMR (CD_3OD, 81 MHz, 335 K): δ = 32.4 (s).

$C_6H_2(CH_2PPh_2)_4$-1,2,4,5 (**6**): In a two-necked 100-ml round bottom flask equipped with a reflux condensor and a septum, was heated a stirred suspension of the tetraphosphoryl compound **5** (1.89 g, 2.02 mmol) in 1,2-dichlorobenzene (50 ml) at reflux temperature until all solids had dissolved. The resulting clear solution was then allowed to cool to 140°C and $HSiCl_3$ (2.46 ml, 24.4 mmol) was carefully added through the septum over a period of 5 min by means of a syringe. The reaction mixture was then stirred at 140°C for 1 h, after which a clear solution was obtained. This solution was then cooled to 0°C with an ice bath. Degassed aqueous NaOH (50 ml, 4 M) was carefully added through the septum over a period of 5 min by means of a syringe while the mixture was stirred vigorously. This resulted in the formation of a two-layer system, from which the organic layer was collected. The aqueous layer was extracted with CH_2Cl_2 (2 × 25 ml) and the combined organic fractions were dried with $MgSO_4$ and filtered. The filtrate was concentrated in vacuo to ca. 10 ml. Hexane (50 ml) was slowly added, which induced the crystallization of a white solid. This solid was collected by filtration, washed with hexane (2 × 25 ml) and dried in vacuo to afford analytically pure tetraphosphane **6** as white crystals. Yield: 1.68 g (96%), mp 125°C. − ^1H NMR ($CDCl_3$, 300 MHz, 298 K): δ = 7.28 (m, 40 H, ArH), 6.22 (s, 2 H, ArH), 2.96 (s, 8 H, CH_2P). − $^{13}C\{^1H\}$ NMR ($CDCl_3$, 75 MHz, 298 K): δ = 138.4 (d, $^1J_{P\text{-}C}$ = 16 Hz, Ar), 133.0 (d, $^2J_{P\text{-}C}$ = 19 Hz, Ar), 131.2 (d, $^3J_{P\text{-}C}$ = 12 Hz, Ar), 128.4 (d, $^3J_{P\text{-}C}$ = 23 Hz, Ar), 32.6, 32.4 (d, $^1J_{P\text{-}C}$ = 15 Hz, CH_2P). − $^{31}P\{^1H\}$ NMR ($CDCl_3$, 81 MHz, 298 K): δ = −12.3 (s). − $C_{58}H_{50}P_4$: calcd. C 79.99, H 5.79; found C 79.84, H 5.72.

[{$RuCl_2(PPh_3)$}$_2${$C_6H_2(CH_2PPh_2)_4$-1,2,4,5-P,P′,P″,P‴}]·0.5 CH_2Cl_2 (**8**): A colorless solution of tetraphosphane **6** (0.38 g, 0.44 mmol) in CH_2Cl_2 (20 ml) was added to a brown solution of $[RuCl_2(PPh_3)_4]$ in CH_2Cl_2 (20 ml) at room temperature and the resulting reaction mixture was stirred for 2 h at this temperature. During this time a green precipitate formed. After 2 h, the green precipitate was filtered off, washed with CH_2Cl_2 (2 × 20 ml) and dried in vacuo to afford the pure bisruthenium(II) complex **8** in 38% yield as a green insoluble solid (mp > 200°C). − $C_{94}H_{78}Cl_4P_6Ru_2 \cdot 0.5\ CH_2Cl_2$: calcd. C 63.69, H 4.58; found C 63.83, H 4.65. − When a CH_2Cl_2 solution of $[RuCl_2(PPh_3)_4]$ was

layered with a CH_2Cl_2 solution of tetraphosphane **6** and the resulting reaction mixture was left undisturbed for 24 h, green-brown X-ray quality crystals (mp > 200°C) of bisruthenium complex **8** were obtained. These crystals were collected by filtration, washed with CH_2Cl_2 (2 × 20 ml), dried in vacuo and subsequently subjected to an X-ray structure determination.

X-ray Structure Determination of **8**: X-ray data were collected with an ENRAF-NONIUS CAD4 diffractometer on rotating anode for a needle-shaped green-brown crystal. Numerical data are collected in Table 3. The structure was solved by Direct Methods (SHELXL86)[18] and refined on F^2 using SHELXL96[19]. Data were corrected for absorption effects using the DIFABS algorithm as implemented in PLATON[20]. Hydrogen atoms were introduced at calculated positions and refined riding on their carrier atoms. Geometrical calculations and the ORTEP illustration were done with PLATON.

[1] [1a] N. Hagihara, K. Sonogashira, S. Takahashi, *Adv. Polym. Sci.* **1981**, *41*, 149. – [1b] J. E. Shears, C. E. Carraher, Jr., C. U. Pittmann, Jr., *Metal-Containing Polymer Systems*, Plenum, New York, **1985**. – [1c] S. J. Loeb, G. K. H. Shimizu, *J. Chem. Soc., Chem. Commun.* **1993**, 1395. – [1d] M. S. Khan, A. K. Kakkar, S. L. Ingham, P. R. Raithby, J. Lewis, B. Spencer, F. Wittmann, R. H. Friend, *J. Organomet. Chem* . **1994**, *472*, 247. – [1e] H. L. Anderson, S. J. Martin, D. D. C. Bradley, *Angew. Chem.* **1994**, *106*, 711; *Angew. Chem. Int. Ed. Engl.* **1994**, *33*, 655.

[2] [2a] J.-P. Sutter, M. Beley, J.-P. Collin, N. Veldman, A. L. Spek, J.-P. Sauvage, G. van Koten, *Mol. Cryst. Liq. Cryst.* **1994**, *253*, 215. – [2b] .-P. Sutter, D. M. Grove, M. Beley, J.-P. Collin, N. Veldman, A. L. Spek, J.-P. Sauvage, G. van Koten, *Angew. Chem.* **1994**, *106*, 1359; *Angew. Chem. Int. Ed. Engl.* **1994**, *33*, 1282. – [2c] P. Steenwinkel, N. Veldman, A. L. Spek, D. M. Grove, G. van Koten, *Organometallics*, submitted. – [2d] S. L. James, N. Veldman, A. L. Spek, G. van Koten, *Chem. Commun.* **1996**, 253. – [2e] P. Steenwinkel, S. L. James, N. Veldman, H. Kooijman, A. L. Spek, D. M. Grove, G. van Koten, *Organometallics* **1997**, *16*, 513. – [2f] P. J. Davies, D. M. Grove, G. van Koten, *Organometallics* **1997**, *16*, 800. – [2g] P. Steenwinkel, J. T. B. H. Jastrzebski, B.-J. Deelman, D. M. Grove, H. Kooijman, N. Veldman, W. J. J. Smeets, A. L. Spek, G. van Koten, *Organometallics*, in press. – [2h] M.-C. Lagunas, R. A. Gossage, A. L. Spek, G. van Koten, *Organometallics* **1997**, *16*, 5486 .

[3] [3a] J.-P. Sutter, S. L. James, P. Steenwinkel, T. Karlen, D. M. Grove, N. Veldman, W. J. J. Smeets, A. L. Spek, G. van Koten, *Organometallics* **1996**, *15*, 941. – [3b] P. Steenwinkel, S. L. James, N. Veldman, H. Kooijman, A. L. Spek, D. M. Grove, G. van Koten, *Chem. Eur. J.* **1996**, *2*, 1440. – [3c] T. Karlen, P. Dani, D. M. Grove, P. Steenwinkel, G. van Koten, *Organometallics* **1996**, *15*, 5687. – [3d] P. Dani, T. Karlen, R. A. Gossage, A. L. Spek, G. van Koten, *J. Am. Chem. Soc.* **1997**, *119*, 11317. – [3e] G. Jia, H. M. Lee, H. P. Xia, I. D. Williams, *Organometallics* **1996**, *15*, 5453.

[4] P. Steenwinkel, R. A. Gossage, G. van Koten, *Chem. Eur. J.* in press.

[5] [5a] M. H. P. Rietveld, D. M. Grove, G. van Koten, *New J. Chem.* **1997**, *21*, 751. – [5b] T. Karlen, P. Dani, P. Steenwinkel, D. M. Grove, G. van Koten, manuscript in preparation.

[6] [6a] P. Steenwinkel, S. L. James, D. M. Grove, H. Kooijman, A. L. Spek, G. van Koten, *Organometallics* **1997**, *16*, 513. – [6b] P. Steenwinkel, J. T. B. H. Jastrzebski, B.-J. Deelman, D. M. Grove, H. Kooijman, N. Veldman, W. J. J. Smeets, A. L. Spek, G. van Koten, *Organometallics* **1997**, accepted. – [6c] P. Steenwinkel, S. L. James, D. M. Grove, H. Kooijman, N. Veldman, W. J. J. Smeets, A. L. Spek, G. van Koten, *Organometallics*, submitted.

[7] J. March, *Advanced Organic Chemistry, Mechanisms and Structure*, 4th ed., Wiley, New York, **1992**, p. 171.

[8] G. V. Bodrin, M. I. Kabachnik, N. E. Kochetkova, T. Ya. Medved, B. F. Myasoedov, M. Yu. Polykarpov, M. K. Chmutova, *Izv. Akad. Nauk SSSR, Ser Khim.* **1979**, 2572 (*Engl. Transl.* **1980**, 2388; *Chem. Abstr.* **1980**, *92*, 146846b).

[9] W. Ried, H. Bodem, *Chem. Ber.* **1956**, *89*, 2328.

[10] [10a] H. Fritzsche, U. Hasserodt, F. Korte, *Chem. Ber.* **1964**, *97*, 1988. – [10b] H. Fritzsche, U. Hasserodt, F. Korte, *Chem. Ber.* **1965**, *98*, 171. – [10c] L. Horner, W. D. Balzer, *Tetrahedron Lett.* **1965**, 1157.

[11] T. Imamoto, T. Takeyama, T. Kusumoto, *Chem. Lett.* **1985**, 1491.

[12] It is known that in CH_2Cl_2 solution $[RuCl_2(PPh_3)_4]$ is predominantly present as a 1:1 mixture of $[RuCl_2(PPh_3)_3]$ and free PPh_3: P. R. Hoffman, K. G. Caulton, *J. Am. Chem. Soc.* **1975**, *97*, 4221.

[13] [13a] S. J. La Placa, J. A. Ibers, *Inorg. Chem.* **1965**, *4*, 778. – [13b] F. A. Cotton, M. Matusz, *Inorg. Chim. Acta* **1987**, *131*, 213. – [13c] Crabtree, R. H.; Hamilton, D. G. *Adv. Organomet. Chem.* **1988**, *28*, 299. – [13d] Brookhart, M.; Green, M. L. H. *J. Organomet. Chem.* **1983**, *250*, 395.

[14] See for example: H. Rimml, L. M. Venanzi, *J. Organomet. Chem.* **1983**, *259*, C6.

[15] [15a] G. Hogarth, *J. Organomet. Chem.* **1991**, *406*, 391. – [15b] M. A. Fox, D. A. Chandler, *Adv. Mater.* **1991**, *3*, 381. – [15c] P. W. Wang, M. A. Fox, *Inorg. Chem.* **1994**, *33*, 2938. – [15d] P. W. Wang, M. A. Fox, *Inorg. Chem.* **1995**, *34*, 36. – [15e] G. Hogarth, T. Norman, *Inorg. Chim. Acta* **1996**, *248*, 167.

[16] A. E. Arbuzov, A. I. Razumov, *Bull. Acad. Sci. U.R.S.S., Classe Sci. Chim.* **1945**, 167 (*Chem. Abstr.* **1945**, *40*, 3411[4]).

[17] P. S. Hallman, T. A. Stephenson, G. Wilkinson, *Inorg. Synth.* **1970**, *12*, 237.

[18] G. M. Sheldrick, *SHELXS86, Program for crystal structure determination*, University of Göttingen, Germany, **1986**.

[19] G. M. Sheldrick, *SHELXL96, Program for crystal structure refinement*, University of Göttingen, Germany, **1996**.

[20] A. L. Spek, *Acta Crystallogr.* **1990**, *A46*, C34.

[97268]

Metal Complexes of Biologically Important Ligands, CII[◇]

Organometallic Complexes of Iridium, Palladium, Chromium and Iron from 2-Phenyl-5(4*H*)-oxazolones − Organometallic Labelled Dipeptides

Werner Bauer[a], Markus Prem[a], Kurt Polborn[b][2], Karlheinz Sünkel[a][2], Wolfgang Steglich[b], and Wolfgang Beck*[a]

Institut für Anorganische Chemie der Ludwig-Maximilians-Universität[a],
Meiserstraße 1, D-80333 München, Germany

Institut für Organische Chemie der Ludwig-Maximilians-Universität[b],
Karlstr. 23, D-80333 München, Germany

Received November 14, 1997

Keywords: 2-Phenyl-4-R-5(4*H*)-oxazolones / Iridium / Palladium / Platinum / Iron / Chromium / *C-o,N*-Bridging 2-phenyloxazolone / Peptide labelling

Reactions of 2-phenyl-4-R-5(4*H*)-oxazolones (R = Me, CH_2Ph, CHMeEt) with $[(\eta^5\text{-}C_5Me_5)IrCl_2]_2$ afforded the cyclometallated complexes $(\eta^5\text{-}C_5Me_5)(Cl)Ir(L)$ (**1**−**3**) [L = 2-phenyl-4-R-5(4*H*)-oxazolone(*C-o,N*)]. 2-Phenyl-5(4*H*)-oxazolone reacts with $[(\eta^5\text{-}C_5Me_5)IrCl_2]_2$ and palladium(II) acetate to give complexes with a *C-o,N*-bridging oxazolone $[(\eta^5\text{-}C_5Me_5)(Cl)Ir]_2(\mu\text{-}Cl)(\mu\text{-L-H}^+)$ (**4**) and $Pd_3(\mu\text{-ac})_5(\mu\text{-L-H}^+)$ (**5**). 2-Phenyloxazolone anions were added to the π ligands of $[(\eta^5\text{-}C_6H_7)Fe(CO)_3]^+$ and $[(\eta^7\text{-}C_7H_7)Cr(CO)_3]^+$ to give the adducts **6**−**11**. Dipeptide derivatives **12**−**18** were obtained by reaction of **1**, **2** and by reaction of the adduct **6** from $[(\eta^5\text{-}C_6H_7)Fe(CO)_3]^+$ and the anion of 2-phenyloxazolone with α-amino acid esters. These reactions may be used for the labelling of peptides. Saponification of **15**−**18** yields the organometallic substituted peptide acids **19**−**22**. Their dianions (deprotonation of COOH and peptide amide) were used as ligands towards $(Ph_3P)_2PtCl_2$ to yield the bimetallic complexes **23**−**25**. The structures of **4**, **5**, **9** and **10** were determined by X-ray diffraction.

5(4*H*)-Oxazolones which can be considered as activated α-amino acid derivatives are important intermediates and starting materials in organic synthesis.[3] Recently, we reported on some metal complexes with neutral 2-phenyl-5(4*H*)-oxazolones.[4] In the following some cyclometallated complexes from these oxazolones and the use of the delocalized oxazolone anion[5] as nucleophile for the addition to π-coordinated ligands are described. Some of the compounds obtained may be of use for the labelling of peptides[6].

Results and Discussion

1. Cyclometallated Complexes

The reaction of the chloro-bridged iridium(III) complex $[Cp^*IrCl_2]_2$ with the substituted 2-phenyl-4-R-5(4*H*)-oxazolones gave the complexes **1**−**3**. Cyclometallation with phenyl-containing donors has been observed for several iridium complexes[7].

The complexes **1**−**3** contain an "asymmetric" metal center which causes doubling of the ^{1}H-NMR signals of the C_5Me_5 ligands (**1**: 5:1; **2**: 20:1; **3**: 1:1), due to diastereoisomer formation.

An unexpected complex **4** was obtained from the unsubstituted 2-phenyl-5(4*H*)-oxazolone and its structure was established by X-ray diffraction. In the complex **4** the two iridium atoms are bridged by a chlorine atom and a *C-o,N*-bound 2-phenyloxazolone ligand.

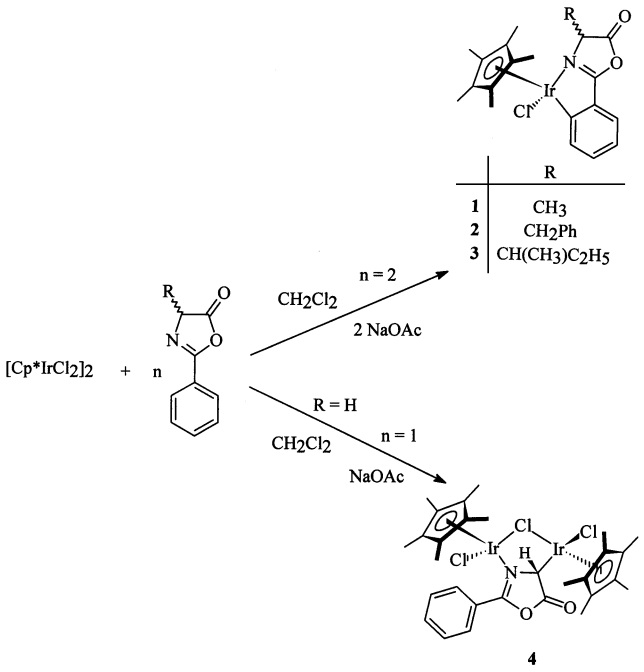

In the five-membered ring Cl−Ir−C−N−Ir the C atom is situated outside the almost planar arrangment of the other four atoms. The ^{1}H-NMR spectrum of **4** exhibits only

[◇] Part CI: Ref.[1].

 © WILEY-VCH Verlag GmbH, D-69451 Weinheim, 1998 1434−1948/98/0404−0485 $ 17.50+.50/0

Figure 1. Molecular structure of **4**[a] in the crystal

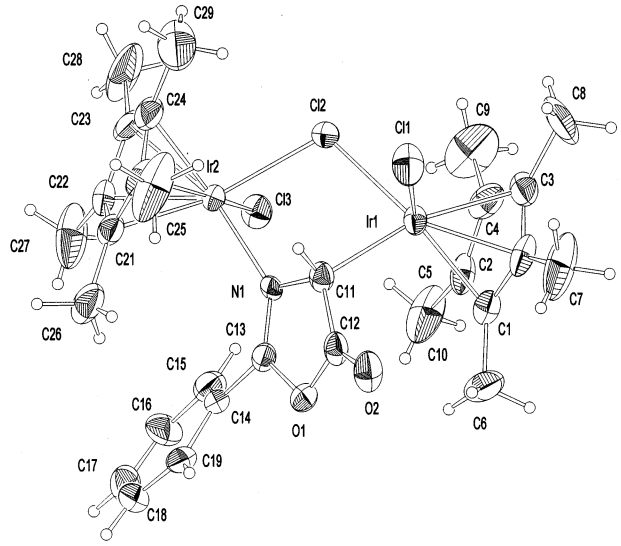

[a] Selected bond lengths [Å] and angles [°]: Ir2−N1 2.117(9), Ir1−C11 2.152(12), N1−C13 1.29(2), N1−C11 1.461(14), C11−C12 1.44(2), Ir2−Cl2 2.446(3), Ir1−Cl2 2.436(3); N1−Ir2−Cl2 82.7(2), C11−Ir1−Cl2 80.4(3), C13−N1−C11 106.4(10), N1−Ir2−Cl2−Ir1 3.53(0.27), Cl2−Ir2−N1−C11 37.00(0.72), C11−Ir1−Cl2−Ir2 110.45(0.17), N1−C13−C14−C15 46.68(2.04).

Figure 2. Molecular structure of **5**[a] in the crystal

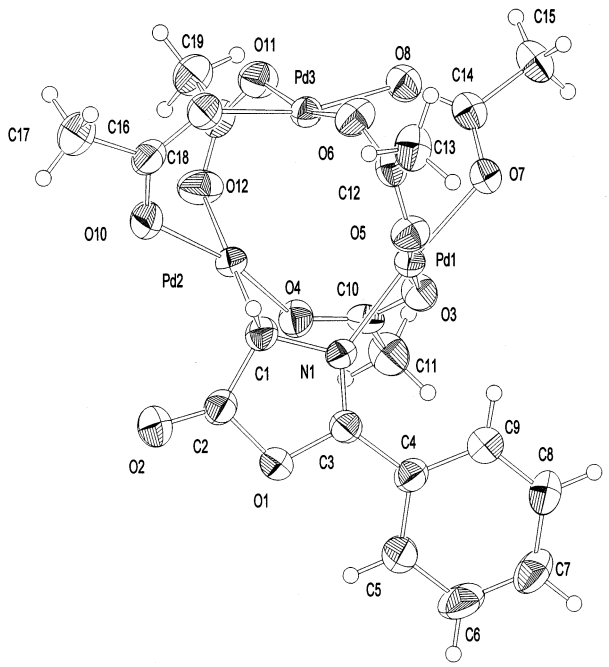

[a] Selected bond lengths [Å] and angles [°]: Pd3−O8 1.995(3), Pd3−O11 2.002(3), Pd2−O12 2.087(3), Pd2−O10 2.019(3), Pd2−C1 2.025(4), Pd1−N1 2.003(3), Pd1−O7 2.015(3), Pd1−O5 2.005(3); O11−Pd3−O6 166.40(13), O12−Pd2−C1 179.57(15), O7−Pd1−N1 175.47(13), O10−Pd2−O4 166.48(12).

two C_5Me_5 signals which implicates that only one diastereoisomer is formed. The same bridging occurs in the trinuclear palladium complex **5** which was obtained from Pd^{II} acetate and 2-phenyl-5(4*H*)-oxazolone. In **5** one acetate bridge of Pd_3ac_6[8] is substituted by a *C-o,N*-bridging 2-phenyloxazolone.

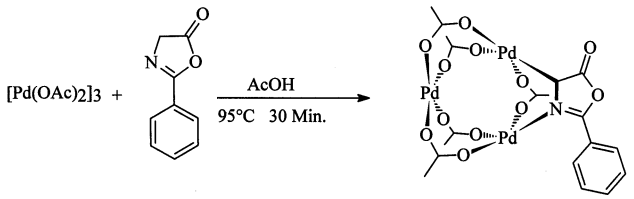

5

The molecular structure of **5** is very similar to that of Pd_3ac_6[8] with the exception that the Pd2−O12 distance [2.087(3) Å] is longer than the other Pd−O bonds (ca. 2.01 Å). This can be attributed to the *trans* influence of the strong C donor.

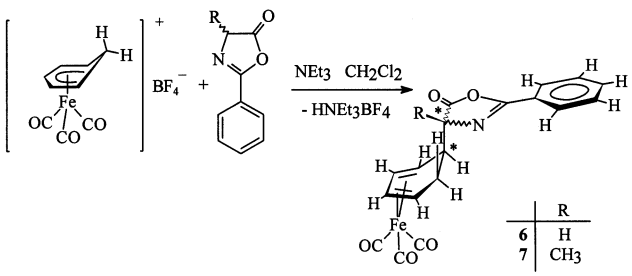

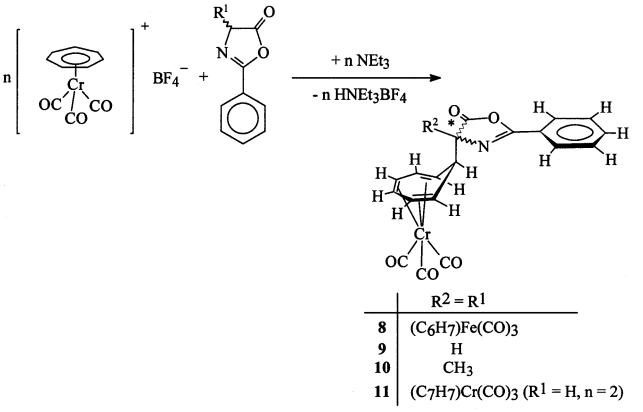

2. Addition of the 2-Phenyloxazolone Anion to Unsaturated Hydrocarbons of Cationic Complexes

The addition of organic and organometallic nucleophiles to π-coordinated hydrocarbons is a very well studied and important reaction[9]. The addition of the 2-phenyl-5(4*H*)-oxazolone anion to the cyclopentadienyl and the cycloheptatrienyl ligand afforded the complexes **6**−**11**.

In **6** and **7** two stereogenic centers are formed and the two diastereoisomers (**6**: 1:1.2; **7**: 1:1.8) can be detected in their ^{1}H- and ^{13}C-NMR spectra. For almost all atoms two sets of signals are observed. Interestingly, for **8** one diastereoisomer is formed in high excess. In the ^{1}H-NMR spectrum only some weak signals can be assigned to the second isomer; *exo* addition is proven for **6** and **7** by the signals of

the $CH-CH_2$ group and for **9** and **10** by X-ray structure determination.

Figure 3. Molecular structure of **9**[a] in the crystal

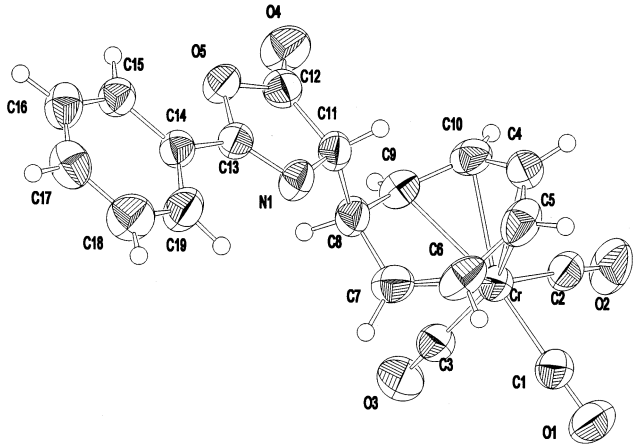

[a] Selected bond lengths [Å] and angles [°]: Cr−C1 1.853(4), Cr−C2 1.849(4), Cr−C3 1.858(4), C1−O1 1.151(4), Cr−C5 2.196(4), Cr−C6 2.201(4), Cr−C7 2.340(4), C8−C11 1.549(5), C13−N1 1.266(4), C13−C14 1.472(4); O5−C13−N1 117.5(3), C14−C13−N1 126.3(3), O4−C12−O5 122.0(3).

Figure 4. Molecular structure of **10**[a] in the crystal

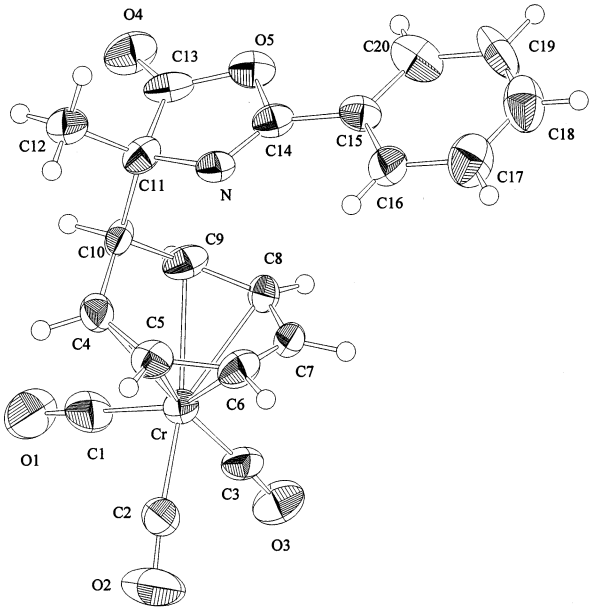

[a] Selected bond lengths [Å] and angles [°]:Cr−C1 1.840(9), Cr−C2 1.867(8), Cr−C3 1.840(8), C1−O1 1.164(8), Cr−C6 2.175(7), Cr−C5 2.228(7), Cr−C4 2.352(7), C10−C11 1.560(9), C14−N 1.255(8), C15−C14 1.459(10); O5−C14−N 116.3(7), C15−C14−N 129.8(7), O4−C13−O5 121.6(7).

3. Formation of Dipeptide Derivatives from 1, 2 and 6

The nucleophilic addition of α-amino acid esters[10] to **1**, **2** and **6** gave the dipeptide derivatives **12**−**18**.

The shift of the carbonyl IR absorption to lower wavenumbers (ca. 1590 cm^{-1}) in **12**−**14** is characteristic for coordination of the CO function[11]. The two stereogenic centers of **15** give rise to two diastereoisomers (1:1.2), whereas four diastereoisomers of **16**−**18** (1:1:1.2:1.2) (from three

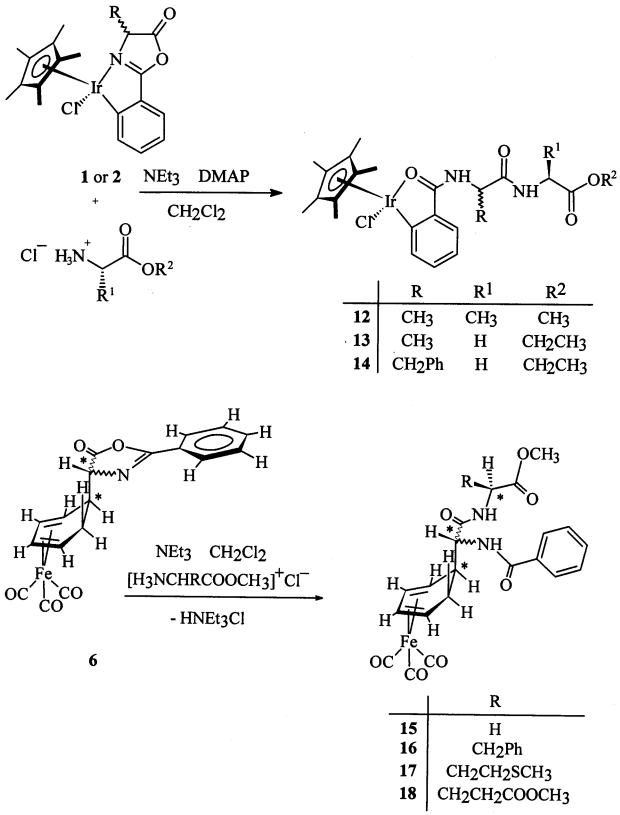

	R	R^1	R^2
12	CH_3	CH_3	CH_3
13	CH_3	H	CH_2CH_3
14	CH_2Ph	H	CH_2CH_3

	R
15	H
16	CH_2Ph
17	$CH_2CH_2SCH_3$
18	$CH_2CH_2COOCH_3$

stereogenic centers) were observed in their ^{1}H-NMR spectra (from the methoxy signals). Saponification of **15**−**18** could be accomplished to give the free acids **19**−**22**.

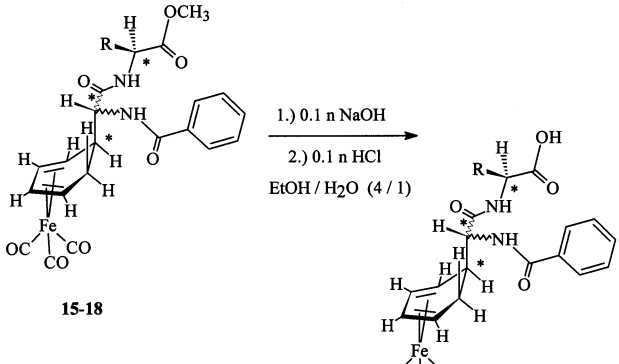

	R
19	H
20	CH_2Ph
21	$CH_2CH_2SCH_3$
22	CH_2CH_2COOH

Compounds **19**−**22** were used as dianionic chelate ligands (deprotonation of the amide and carboxylic group) towards $(Ph_3P)_2PtCl_2$ to afford the heterobimetallic complexes **23**−**25**. Recently, several examples for complexes with dianionic *N*-acyl-α-amino carboxylates have been reported[12] which can be considered as simple models for *O*,*N* coordination of peptides.

Two diastereoisomers of **23** (as for **15**) and four isomers of **24** and **25** (as for **16** and **17**) were observed in the ^{31}P-NMR spectra.

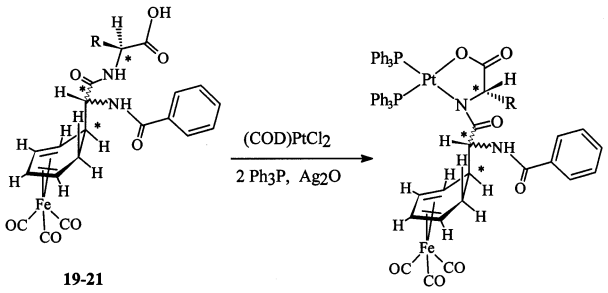

19-21

	R
23	H
24	CH_2Ph
25	$CH_2CH_2SCH_3$

Conclusions

The reaction of oxazolones with organometallic complexes leads to a versatile chemistry and the reaction of **1**, **2** and **6** with α-amino acid esters (or peptide esters) provides a method for the labelling of peptides at the amino terminus.

Support by the *Deutsche Forschungsgemeinschaft*, the *Fonds der Chemischen Industrie* and the *Wacker Chemie, München,* is gratefully acknowledged.

Experimental Section

All reactions were carried out in dry solvents under nitrogen. − NMR: Jeol GSX 270 or Jeol EX 400, using the solvent as internal standard. − IR: Nicolet 520 FT-IR. − The starting materials were prepared according to literature procedures ($[Cp^*IrCl_2]_2$[13], $[(C_6H_7)Fe(CO)_3]BF_4$[14], $[(C_7H_7)Cr(CO)_3]BF_4$[15], $(COD)PtCl_2$[16], 2-phenyl-5(4*H*)-oxazolones[17]). Pd^{II} acetate was purchased from Aldrich and purified by dissolving it in hot benzene, filtering and evaporating off the solvent. Glacial acetic acid was refluxed over $KMnO_4$ for several hours and distilled prior to use. The α-amino acid ester hydrochlorides were purchased from Merck or Fluka. − PE = polyethylene.

General Procedure for the Preparation of **1**−**3**: To a mixture of the oxazolone and 66 mg (0.81 mmol) of NaOAc in 5 ml of CH_2Cl_2 a deep red solution of 319 mg (0.4 mmol) of $[Cp^*IrCl_2]_2$ in 5 ml of the same solvent was added. After stirring overnight, the light-red mixture was filtered to remove NaCl, and the solvent was removed in vacuo. The yellow product was washed twice with 3 ml of Et_2O and dried in vacuo at 60°C for 5 h.

1: 142 mg (0.81 mmol) of 4-methyl-2-phenyl-5(4*H*)-oxazolone was used. Yellow powder. − IR (KBr): $\tilde{\nu}$ = 1844 cm^{-1} s (C=O), 1627 s (C=N); (PE): $\tilde{\nu}$ = 288 cm^{-1} s (M−Cl). − ^1H NMR (400 MHz, $CDCL_3$): δ = 1.66 (d, ^3J = 7.5 Hz, 3 H, CH_3), 1.76/*1.82* [each s, 15H 5:*1*, $C_5(CH_3)_5$], 4.43 (q, ^3J = 7.5 Hz, 1 H, C*H*CH_3), 7.04 (m, 1 H, C_6H_4), 7.27 (m, 1 H, C_6H_4), 7.53 (m, 1 H, C_6H_4), 7.82 (m, 1 H, C_6H_4). − ^{13}C NMR (100.5 MHz, $CDCl_3$): δ = 9.44/9.94 [$C_5(CH_3)_5$], 15.97 (CH_3), 58.86 (*C*HCH_3), 88.53/89.27 [$C_5(CH_3)_5$], 122.53, 127.63, 128.84, 134.05, 135.85 (C_6H_4), 166.37 (OC=N), 174.91 (Ir−C), 177.94 (C=O). − $C_{20}H_{23}ClIrNO_2$ (536.7): calcd. C 44.71, H 4.28, N 2.60; found C 44.46, H 4.75, N 2.41.

2: 204 mg (0.81 mmol) of 4-benzyl-2-phenyl-5(4*H*)-oxazolone was used. Yellow powder. − IR (KBr): $\tilde{\nu}$ = 1845 cm^{-1} s (C=O), 1623 s (C=N); (PE): $\tilde{\nu}$ = 292 cm^{-1} s (M−Cl). − ^1H NMR (270 MHz, $CDCl_3$): δ = 1.79/*1.83* [each s, 15H 20:*1*, $C_5(CH_3)_5$], 3.06 (dd, ^2J = 15.0 Hz, ^3J = 10.7 Hz, 1 H, C*H*H′), 3.64 (dd, ^2J = 15.0 Hz, ^3J = 4.6 Hz, 1 H, CH*H*′), 4.60 (dd, ^3J = 4.6 Hz, ^3J = 10.6 Hz, 1 H, C*H*CH_2Ph), 7.07 (m, 1 H, C_6H_4), 7.32 (m, 6 H, C_6H_4 and C_6H_5), 7.55 (m, 1 H, C_6H_4), 7.84 (m, 1 H, C_6H_4). − ^{13}C NMR (100.5 MHz, $CDCl_3$): δ = 9.30/9.40 [$C_5(CH_3)_5$], 36.80 (*C*H_2Ph), 62.20 (*C*HCH_2Ph), 88.40/86.20 [$C_5(CH_3)_5$], 122.30, 127.40, 127.50, 128.50, 128.70, 129.40, 133.90, 134.70, 135.60 (C_6H_4 and C_6H_5), 166.50 (OC=N), 172.40 (Ir−C), 177.90 (C=O). − $C_{26}H_{27}ClIrNO_2$ × 0.5 CH_2Cl_2 (655.6): calcd. C 48.53, H 4.27, N 2.13; found C 48.06, H 4.30, N 2.07.

3: 176 mg (0.81 mmol) of 4-(2′-butyl)-2-phenyl-5(4*H*)-oxazolone was used. Yellow powder. − IR (KBr): $\tilde{\nu}$ = 1844 cm^{-1} s (C=O), 1626 s (C=N); (PE): $\tilde{\nu}$ = 283 cm^{-1} s (M−Cl). − ^1H NMR (270 MHz, $CDCl_3$): δ = 1.28 (m, 2 H, CH_2), 0.83−1.09 (m, 6 H, 2 × CH_3), 1.74/*1.75* [each s, 15H 1.2:*1*, $C_5(CH_3)_5$], 4.29 [m, 1 H, C*H*(C_4H_9)], 7.07 (m, 1 H, C_6H_4), 7.28 (m, 1 H, C_6H_4), 7.52 (m, 1 H, C_6H_4), 7.81 (m, 1 H, C_6H_4). − ^{13}C NMR (100.5 MHz, $CDCl_3$): δ = 9.40/9.80 [$C_5(CH_3)_5$], 11.80 (CH_2CH_3), 14.80 ($CHCH_3$), 25.80 (CH_2CH_3), 36.60 (*C*HCH_3), 67.80 (*C*HC_4H_9), 88.40 [$C_5(CH_3)_5$], 122.40, 127.30, 131.50, 133.90, 135.90 (C_6H_4), 166.90 (OC=N), 173.20 (Ir−C), 178.30 (C=O). − $C_{23}H_{29}ClIrNO_2$ (655.6): calcd. C 47.70, H 5.05, N 2.42; found C 48.56, H 5.53, N 2.89.

4: To a mixture of 51 mg (0.32 mmol) of 2-phenyl-5(4*H*)-oxazolone and 26 mg (0.32 mmol) of NaOAc in 5 ml of CH_2Cl_2 a deep red solution of 247 mg (0.31 mmol) of $[Cp^*IrCl_2]_2$ in 5 ml of the same solvent was added. After stirring for 5 h the light red mixture was filtered to remove NaCl, and concentrated in vacuo to about 2 ml. The yellow product was precipitated with 15 ml of Et_2O, washed twice with 3 ml Et_2O and dried in vacuo at 60°C for 5 h. Crystals were obtained from a CH_2Cl_2/pentane mixture. − IR (KBr): $\tilde{\nu}$ = 1792 cm^{-1} s (C=O), 1608 w (C=N); (PE): $\tilde{\nu}$ = 262 cm^{-1} s, 288 s, 299 m (M−Cl). − ^1H NMR (270 MHz, $CDCl_3$): δ = 1.39 [s, 15 H, $C_5(CH_3)_5$], 1.58 [s, 15 H, $C_5(CH_3)_5$], 6.12 (s, 1 H, C*H*Ir), 7.27−7.56 (m, 3 H, 3,4,5-C_6H_5), 8.61 (d, ^3J = 7.9 Hz, 2 H, 2,6-C_6H_5). − ^{13}C NMR (100.5 MHz, CD_2Cl_2): δ = 8.57 [$C_5(CH_3)_5$], 8.63 [$C_5(CH_3)_5$], 67.79 (*C*HIr), 86.86 [$C_5(CH_3)_5$], 87.12 [$C_5(CH_3)_5$] 125.91, 128.56, 129.83, 132.49 (C_6H_5), 161.15 (OC=N), 179.00 (C=O). − $C_{29}H_{36}Cl_3Ir_2NO_2$ (921.4): calcd. C 37.76, H 3.90, N 1.51; found C 37.41, H 3.89, N 1.55.

5: A brown suspension of 123 mg (0.55 mmol) of palladium(II) acetate and 88 mg (0.55 mmol) of 2-phenyl-5(4*H*)-oxazolone in 2 ml of glacial acetic acid was heated to 95°C for 30 min whereby the product began to precipitate. After cooling, the mixture was centrifuged. The dark brown residue was washed with 1ml of glacial acetic acid and twice with 2 ml of water. After drying in vacuo at 50°C for 3 h, the dark brown product was dissolved in 5 ml of trichloromethane, filtered and added to 30 ml of *n*-hexane. The orange precipitate was centrifuged off, washed with pentane and *n*-hexane and dried in vacuo at 50°C for 8 h. Slow concentration of a solution in CH_2Cl_2/hexane (1:10) gave orange prisms, suitable for X-ray analysis. − IR (KBr): $\tilde{\nu}$ = 1807 cm^{-1} s (C=O), 1608 s, 1592 s, 1569 s (antisym. COO), 1421 s (sym. COO). − ^1H NMR (400 MHz, $CDCl_3$): δ = 1.48 (s, 3 H, CH_3COO), 1.94 (s, 3 H, CH_3COO), 1.97 (s, 3 H, CH_3COO), 2.00 (s, 3 H, CH_3COO), 2.05 (s, 3 H, CH_3COO), 5.41 (s, 1 H, CHPd), 7.70 (BB′, 2 H, 3,5-C_6H_5), 7.79 (A, 1 H, 4-C_6H_5), 9.15 (CC′, 2 H, 2,6-C_6H_5). − ^{13}C NMR (100.5 MHz, $CDCl_3$): δ = 22.19 (*C*H_3COO), 22.76 (*C*H_3COO), 23.00 (*C*H_3COO), 23.33 (*C*H_3COO), 23.39 (*C*H_3COO), 38.99

(CHPd), 123.78, 129.15, 129.96, 135.00 (C_6H_5), 165.50 (OC=N), 172.93 (C=O), 185.41 (CH_3COO), 185.47 (CH_3COO), 186.86 (CH_3COO), 188.13 (CH_3COO), 188.59 (CH_3COO). − $C_{19}H_{21}NO_{12}Pd_3$ (774.6): calcd. C 29.46, H 2.73, N 1.81; found C 29.38, H 3.18, N 1.75.

General Procedure for the Preparation of **6** *and* **7**: A stirred mixture of 150 mg (0.49 mmol) of $[(C_6H_7)Fe(CO)_3]BF_4$ and the appropriate oxazolone in 15 ml of CH_2Cl_2 was cooled (see below). A solution of 64.8 µl (0.47 mmol) of triethylamine in 5 ml of CH_2Cl_2 was slowly added. After 30 min of stirring at low temp., the yellow solution was allowed to warm up to room temp. and stirred for another 2 h. After concentrating to about 4 ml, triethylammonium chloride was precipitated with 40 ml of pentane and filtered off. The filtrate was concentrated and the residue was dissolved in 30 ml of pentane. This yellow solution was filtered through Celite and concentrated in vacuo to about 4 ml. Cooling to −78°C for 3 min gave a colourless precipitate which was filtered off. Removal of the solvent from the filtrate in vacuo gave the yellow, oily product which was dried in vacuo at room temp. for a few days.

6: 75 mg (0.47 mmol) of 2-phenyl-5(4*H*)-oxazolone was used. The addition of NEt_3 was carried out at −15°C. − IR (film NaCl): $\tilde{\nu}$ = 2045 cm^{-1} s (Fe−CO), 1964 s br. (Fe−CO), 1824 s (C=O), 1653 s (C=N). − ^{1}H NMR (400 MHz, $CDCl_3$): δ = *1.77* (dm, *1 H*, $^2J_{6endo}$ = 15.3 Hz, 6*exo*-C_6H_7)/1.61 (ddd, 1 H, $^2J_{6endo}$ = 15.0 Hz, $^3J_1$ = 3.7 Hz, $^3J_5$ = 2.6 Hz, 6*exo*-C_6H_7), *2.14*/2.06 (each ddd, *1 H*/1 H, $^2J_{6exo}$ = 15.1 Hz, $^3J_1$ = 11.1 Hz, $^3J_5$ = 4.0 Hz, 6*endo*-C_6H_7), 2.74 (m, *1 H* + 1 H, 1-C_6H_7), *2.92* (ddd, *1 H*, $^3J_3$ = 6.3 Hz, $^3J_1$ = 3.3 Hz, $^4J_4$ = 1.4 Hz, 2-C_6H_7)/3.06, 3.06 [m, *1 H* + 1 H (+ 1 H, 2-C_6H_7), 5-C_6H_7], *4.20*/4.24 [each d, *1 H*/1 H, $^3J_1$ = 6.0 Hz, NC*H*(C_6H_7)COO], *5.32* (ddd, *1 H*, $^3J_2$ = 6.1 Hz, $^3J_4$ = 4.4 Hz, $^4J_5$ = 1.6 Hz, 3-C_6H_7)/5.39, 5.39 [m, *1 H* + 1 H (+ 1 H, 3-C_6H_7), 4-C_6H_7], 7.43−7.60 (ABB′, *3 H* + 3 H, 3,4,5-C_6H_5), 7.96−8.00 (CC′, *2 H* + 2 H, 2,6-C_6H_5). − ^{13}C NMR (100.5 MHz, $CDCl_3$): δ = *27.77*/26.50 (6-C_6H_7), *40.25*/40.98 (1-C_6H_7), *59.38*/59.39, *59.26*/58.83 (2,5-C_6H_7), *70.03*/69.99 [CN*C*H(C_6H_7)COO], *86.06*/86.51, *85.83*/85.48 (3,4-C_6H_7), *125.95, 128.20, 129.14, 133.16,* 126.11, 128.22, 129.12, 133.14 (C_6H_5), *162.07*/161.95 [*C*NCH(C_6H_7)COO], *176.90*/177.29 [CNCH(C_6H_7)*C*OO], 211.69 (Fe−*C*O). Diastereomeric ratio *1.0*:1.15. − $C_{18}H_{13}FeNO_5$ (379.2): calcd. C 57.02, H 3.46, N 3.69; found C 57.38, H 4.14, N 3.48.

7: 86 mg (0.49 mmol) of 4-methyl-2-phenyl-5(4*H*)-oxazolone was used. The addition of NEt_3 was carried out at 0°C. − IR (film NaCl): $\tilde{\nu}$ = 2048 cm^{-1} s (Fe−CO), 1969 s br. (Fe−CO), 1816 s (C=O), 1658 s (C=N). − ^{1}H NMR (400 MHz, $CDCl_3$): δ = *1.41*/1.43 [each s, *3H*/3 H, NCC*H*$_3$(C_6H_7)COO], *1.78* (dm, *1 H*, $^2J_{6endo}$ = 15.3 Hz, 6*exo*-C_6H_7)/1.70 (dm, 1 H, $^2J_{6endo}$ = 15.1 Hz, 6*exo*-C_6H_7), *2.04*/1.99 (each ddd, *1 H*/1 H, $^2J_{6exo}$ = 15.2 Hz, $^3J_1$ = 11.0 Hz, $^3J_5$ = 4.3 Hz, 6*endo*-C_6H_7), 2.58 (m, *1 H*/1 H, 1-C_6H_7), *2.72*/2.99 (each ddd, *1 H*/1 H, $^3J_3$ = 6.2 Hz, $^3J_1$ = 3.2 Hz, $^4J_4$ = 1.3 Hz, 2-C_6H_7), 3.04 (m, *1 H*/1 H, 5-C_6H_7), *5.21*/5.31 (each ddd, *1 H*/1 H, $^3J_2$ = 5.6 Hz, $^3J_4$ = 4.3 Hz, $^4J_5$ = 1.4 Hz, 3-C_6H_7), *5.30* (m, *1 H*, 4-C_6H_7)/5.35 (dd, 1 H, $^3J_3$ = 5.0 Hz, $^3J_5$ = 6.0 Hz, 4-C_6H_7), 7.42−7.60 (ABB′, *3 H* + 3 H, 3,4,5-C_6H_5), 7.98−7.99 (CC′, *2 H* + 2 H, 2,6-C_6H_5). − ^{13}C NMR (100.5 MHz, $CDCl_3$): δ = *22.44*/22.56 (CH_3), *26.29*/25.43 (6-C_6H_7), *46.33*/45.45 (1-C_6H_7), *59.16*/59.25, *57.63*/58.13 (2,5-C_6H_7), *72.85*/72.80 [CN*C*CH$_3$(C_6H_7)COO], *86.01*/86.32, *85.59*/85.38 (3,4-C_6H_7), *126.21, 133.06,* 126.01, 128.21, 129.12, 133.02 (C_6H_5), *160.27*/159.94 [*C*NCCH$_3$(C_6H_7)COO], *180.48*/179.87 [CNCCH$_3$(C_6H_7)*C*OO], 211.72 (Fe−*C*O). Diastereomeric ratio *1.0*:1.8. − $C_{19}H_{15}FeNO_5$ (393.2): calcd. C 58.04, H 3.85, N 3.56; found C 57.50, H 3.79, N 2.84.

General Procedure for the Preparation of **8**−**11**: A stirred mixture of $[(C_7H_7)Cr(CO)_3]BF_4$ and the appropriate oxazolone in 15 ml of THF was cooled to 0°C. A solution of triethylamine in 5 ml of THF was slowly added. After stirring overnight, the red solution was concentrated to about 4 ml, triethylammonium chloride was precipitated with 40 ml of Et_2O and filtered off. The filtrate was taken to dryness and the residue was dissolved in 30 ml of Et_2O. This solution was filtered through Celite and the solvent was removed in vacuo. The residue was dissolved in 1 ml of CH_2Cl_2 and added to excess pentane to give the product as orange solid which was washed twice with pentane and dried in vacuo at 50°C for several hours.

8: 98 mg (0.31 mmol) of $[(C_7H_7)Cr(CO)_3]BF_4$, 117 mg (0.31 mmol) of **6** and 43.5 µl (0.31 mmol) of NEt_3 were used. The reaction was carried out in CH_2Cl_2 instead of THF. The CH_2Cl_2/pentane mixture had to be slowly concentrated to give the product. − IR (KBr): $\tilde{\nu}$ = 2045 cm^{-1} s (Fe−CO), 1979 s br. (Fe−CO, Cr−CO), 1924 s, 1884 s, 1878s, 1870 s (Cr−CO), 1807 s (C=O), 1653 s (C=N). − ^{1}H NMR (270 MHz, $CDCl_3$): δ = 1.42 (ddd, 1 H, $^2J_{6endo}$ = 14.9 Hz, $^3J_1$ = 3.6 Hz, $^3J_5$ = 2.5 Hz, 6*exo*-C_6H_7), 1.87 (*2.00*) (ddd, 1 H, $^2J_{6exo}$ = 14.9 Hz, $^3J_1$ = 10.8 Hz, $^3J_5$ = 4.2 Hz, 6*endo*-C_6H_7), 2.59 (ddd, 1 H, $^3J_{6endo}$ = 10.6 Hz, $^3J_{6exo}$ = 3.5 Hz, $^3J_2$ = 3.5 Hz, 1-C_6H_7), 2.68 (ddd, 1 H, $^3J_3$ = 5.1 Hz, $^3J_1$ = 3.5 Hz, $^4J_4$ = 2.2 Hz, 2-C_6H_7), 2.94 (*3.06*) (ddd, 1 H, $^3J_4$ = 7.9 Hz, $^3J_{6endo}$ = 3.7 Hz, $^3J_{6exo}$ = 2.2 Hz, 5-C_6H_7), 3.61 (m, 3 H, 1,2,7-C_7H_7), 4.82 (*5.00*) (m, 2 H, 3,6-C_7H_7), 5.23 (*5.36*) (m, 2 H, 3,4-C_6H_7), 5.85 (m, 1 H, 4-C_7H_7), 5.98 (m, 1 H, 5-C_7H_7), 7.50 (BB′, 2 H, 3,5-C_6H_5), 7.60 (A, 1 H, 4-C_6H_5), 7.86 (*7.78*) (CC′, 2 H, 2,6-C_6H_5). Diastereoisomeric ratio about 13:*1*. − ^{13}C NMR (100.4 MHz, $CDCl_3$): δ = 26.70 (6-C_6H_7), 41.12 (1-C_7H_7), 44.44 (1-C_6H_7), 56.51, 58.62 (2,5-C_6H_7), 62.39, 64.27 (2,7-C_7H_7), 83.34 (N*C*RR′COO), 85.56, 86.18 (3,4-C_6H_7), 97.50, 98.03, (4,5-C_7H_7), 102.04, 102.29 (3,6-C_7H_7), 125.60, 128.25, 129.21, 133.23 (C_6H_5), 160.30 [O*C*(Ph)N], 176.91 (CRR′*C*OO), 211.52 (Fe−CO). − $C_{28}H_{19}CrFeNO_8$ (605.3): calcd. C 55.56, H 3.16, N 2.31; found C 55.50, H 3.05, N 2.24.

9: 250 mg (0.80 mmol) of $[(C_7H_7)Cr(CO)_3]BF_4$, 125 mg (0.78 mmol) of 2-phenyl-5(4*H*)-oxazolone and 108.1 µl (0.78 mmol) of NEt_3 were used. The product could not be obtained analytically pure. For X-ray analysis suitable crystals were grown in an CH_2Cl_2 pentane mixture. − IR (KBr): $\tilde{\nu}$ = 1981 cm^{-1} s, 1915 s, 1883 s (Cr−CO), 1820 s (C=O), 1651 s (C=N). − ^{1}H NMR (400 MHz, $CDCl_3$): δ = 3.12 [d, 1 H, NC*H*(C_7H_7)CO], 3.55 (m, 1 H, 2-C_7H_7), 3.65 (m, 1 H, 7-C_7H_7), 3.75 (m, 1 H, 1-C_7H_7), 4.90 (m, 1 H, 3-C_7H_7), 5.05 (m, 1 H, 6-C_7H_7), 6.00 (m, 1 H, 4-C_7H_7), 6.05 (m, 1 H, 5-C_7H_7), 7.40−7.65 (ABB′, 3 H, 3,4,5-C_6H_5), 7.88 (CC′, 2 H, 2,6-C_6H_5). − ^{13}C-NMR (100.4 MHz, $CDCl_3$): δ = 40.14 (1-C_7H_7), 61.79, 62.15 (2,7-C_7H_7), 70.96 [N*C*H(C_7H_7)CO], 97.99, 98.25 (4,5-C_7H_7), 100.90, 101.17 (3,6-C_7H_7), 125.67, 128.17, 129.12, 133.29 (C_6H_5), 162.42 [O*C*(C_6H_5)N], 175.00 [NCH(C_7H_7)*C*OO].

10: 500 mg (1.59 mmol) of $[(C_7H_7)Cr(CO)_3]BF_4$, 279 mg (1.59 mmol) of 4-methyl-2-phenyl-5(4*H*)-oxazolone and 222 µl (1.59 mmol) of NEt_3 were used. − IR (KBr): $\tilde{\nu}$ = 1980 cm^{-1} s, 1915 s, 1887 s (Cr-CO), 1806 s (C=O), 1651 s (C=N). − ^{1}H NMR (400 MHz, $CDCl_3$): δ = 1.24 [s, 3 H, NCC*H*$_3$(C_7H_7)CO], 3.43 (2-C_7H_7), 3.67 (7-C_7H_7), 3.69 (1-C_7H_7), 4.73 (3-C_7H_7), 5.01 (6-C_7H_7), 5.84 (4-C_7H_7), 6.04 (5-C_7H_7) (each pseudo-t, $^3J \approx 8$ Hz), 7.47 (BB′, 2 H, 3,5-C_6H_5), 7.57 (A, 1 H, 4-C_6H_5), 7.88 (CC′, 2 H, 2,6-C_6H_5). − ^{13}C-NMR (100.4 MHz, $CDCl_3$): δ = 18.63 (CH_3), 45.93 (1-C_7H_7), 62.79, 63.62 (2,7-C_7H_7), 76.19 [N*C*(CH_3)(C_7H_7)CO], 97.34, 98.01 (4,5-C_7H_7), 102.33, 102.47 (3,6-C_7H_7), 125.68, 128.24, 129.15, 133.14 (C_6H_5), 160.00 [O*C*(C_6H_5)N], 178.69 [NC(CH_3)(C_7H_7)*C*OO]. − $C_{20}H_{15}CrNO_5$ (401.3): calcd. C 59.86, H 3.77, N 3.49; found C 59.42, H 3.96, N 3.29.

11: 200 mg (0.64 mmol) of $[(C_7H_7)Cr(CO)_3]BF_4$, 50 mg (0.31 mmol) of 2-phenyl-5(4*H*)-oxazolone and 86.5 µl (0.62 mmol) of NEt_3 were used. − IR (KBr): $\tilde{\nu}$ = 1980 cm^{-1} s, 1915 s, 1887 s (Cr−CO), 1807 s (C=O), 1651 s (C=N). − ^1H NMR (400 MHz, $CDCl_3$): δ = 3.32 (2-C_7H_7), 3.49 (7-C_7H_7), 3.69 (1-C_7H_7), 4.77 (3-C_7H_7), 4.85 (6-C_7H_7), 5.85 (4-C_7H_7), 5.96 (5-C_7H_7) (each pseudo-t, $^3J \approx 8$ Hz), 7.49 (BB′, 2 H, 3,5-C_6H_5), 7.58 (A, 1 H, 4-C_6H_5), 7.77 (CC′, 2 H, 2,6-C_6H_5). − ^{13}C NMR (100.4 MHz, $CDCl_3$): δ = 40.32 (1-C_7H_7), 61.46, 63.30 (2,7-C_7H_7), 85.49 [N*C*(C_7H_7)$_2$CO], 97.57, 98.05 (4,5-C_7H_7), 101.93, 102.42 (3,6-C_7H_7), 125.22, 128.19, 129.12, 133.34 (C_6H_5), 160.45 [O*C*(C_6H_5)N], 175.08 [NC(C_7H_7)$_2$*C*OO]. − $C_{29}H_{19}Cr_2NO_8$ (613.5): calcd. C 56.78, H 3.12, N 2.28; found C 56.03, H 3.45, N 2.19.

General Procedure for the Preparation of **12**−**14**: To a mixture of **1** or **2** respectivly, α-amino acid ester hydrochloride and about 2 mg of DMAP in 10 ml of CH_2Cl_2 69.6 µl (0.5 mmol) of NEt_3 was added. After stirring for about 20 h, the solvent was removed in vacuo. The residue was washed twice with 5 ml of water and dried in vacuo at 60°C for 5 h.

12: 268 mg (0.5 mmol) of **1** and 70 mg (0.5 mmol) of L-alanine methyl ester hydrochloride were used. Yellow powder. − IR (KBr): $\tilde{\nu}$ = 1745 cm^{-1} w ($COOCH_3$), 1628 m (free C=O), 1592 m (coord. C=O); (PE): $\tilde{\nu}$ = 286 cm^{-1} w (M−Cl). − ^1H NMR (270 MHz, $CDCl_3$): δ = 1.20−1.80 [m, 21 H, $C_5(CH_3)_5$ and 2 × CH_3], 3.75 (m, 3 H, $COOCH_3$), 4.49 [m, 1 H, NHC*H*(CH_3)$COOCH_3$], 4.68 [m, 1 H, NHC*H*(CH_3)CONH] 6.95 (m, 1 H, C_6H_4), 7.27 (m, 1 H, C_6H_4), 7.42 (m, 1 H, C_6H_4), 7.75 (m, 1 H, C_6H_4). − $C_{24}H_{32}ClIrN_2O_4$ (639.7): calcd. C 45.02, H 5.00, N 4.37; found C 44.95, H 5.08, N 4.63.

13: 268 mg (0.5 mmol) of **1** and 70 mg (0.5 mmol) of glycine ethyl ester hydrochloride were used. Yellow powder. − IR (KBr): $\tilde{\nu}$ = 1752 cm^{-1} s (COOEt), 1655 m (free C=O), 1593 m (coord. C=O); (PE): $\tilde{\nu}$ = 283 cm^{-1} w (M−Cl). − ^1H NMR (270 MHz, $CDCl_3$): δ = 1.24 (m, 3 H, $COOCH_2CH_3$), 1.48 [m, 3 H, NHCH(C*H*$_3$)CONH], 1.68 [m, 15 H, $C_5(CH_3)_5$], 3.80 (m, 1 H, NHC*H*H′COOEt), 3.95 (m, 1 H, NHCH*H*′COOEt), 4.14 (m, 2 H, $COOCH_2CH_3$), 4.64 [m, 1 H, NHC*H*(CH_3)CONH], 6.92 (m, 1 H, C_6H_4), 7.26 (m, 1 H, C_6H_4), 7.52 (m, 1 H, C_6H_4), 7.75 (m, 1 H, C_6H_4). − $C_{24}H_{32}ClIrN_2O_4$ (639.7): calcd. C 45.02, H 5.00, N 4.37; found C 44.14, H 5.02, N 4.67.

14: 328 mg (0.5 mmol) of **2** and 70 mg (0.5 mmol) of glycine ethyl ester hydrochloride were used. Yellow powder − IR (KBr): $\tilde{\nu}$ = 1743 cm^{-1} m (COOEt), 1670 m (free C=O), 1592 s (coord. C=O); (PE): $\tilde{\nu}$ = 282 cm^{-1} w (M−Cl). − ^1H NMR (270 MHz, $CDCl_3$): δ = 1.21 (m, 3 H, $COOCH_2CH_3$), 1.65 [m, 15 H, $C_5(CH_3)_5$], 3.27 (m, 2 H, NHCH_2COOEt), 4.14 (m, 2 H, CO-OCH_2CH_3), 4.77 [m, 1 H, NHC*H*(CH_2Ph)CONH], 6.94 (m, 1 H, C_6H_4), 7.31 (m, 1 H, C_6H_4), 7.59 (m, 1 H, C_6H_4), 7.75 (m, 1 H, C_6H_4). − $C_{30}H_{36}ClIrN_2O_4$ (716.3): calcd. C 50.30, H 5.07, N 3.91; found C 51.05, H 5.23, N 4.55.

General Procedure for the Preparation of **15**−**18**: Equimolar amounts of **6**, α-amino acid methyl ester hydrochloride and NEt_3 were stirred in about 20 ml of CH_2Cl_2 at room temp. for a few days (see below). The solvent was removed in vacuo, and the residue was taken up in Et_2O. Insoluble $HNEt_3BF_4$ was centrifuged off. The yellow solution was filtered through Celite, concentrated in vacuo to about 1 ml and added to excess pentane. The colourless precipitate was collected, washed once with pentane and dried in vacuo for a few days.

15: 59 mg (0.155 mmol) of **6**, 20 mg (0.159 mmol) of glycine methyl ester hydrochloride and 22.2 µl (0.159 mmol) of NEt_3 were used and stirred for 7 d. − IR (KBr): $\tilde{\nu}$ = 3283 cm^{-1} m br. (N−H), 2047 s (Fe−CO), 1975 s br. (Fe−CO), 1755 s ($COOCH_3$), 1637 s/1661 s (CONH-I), 1531 s/1550 s (CONH-II). − ^1H NMR (400 MHz, $CDCl_3$): δ = *1.52*/1.48 (each dm, *1 H*/1 H, $^2J_{6endo}$ = 14.5 Hz, 6*exo*-C_6H_7), *1.97*/2.04 (each ddd, *1 H*/1 H, $^2J_{6exo}$ = 15.0 Hz, $^3J_1$ = 11.0 Hz, $^3J_5$ = 5.0 Hz, 6*endo*-C_6H_7), *2.68*/2.73 (each dddd, *1 H*/1 H, $^3J_{6endo}$ = 10.6 Hz, $^3J_7$ = 6.9 Hz, $^3J_2$ = $^3J_{6exo}$ = 3.5 Hz, 1-C_6H_7), 3.04 (m, *2 H*/2 H, 2,5-C_6H_7), 3.72 (s, *1 H*/1 H, OCH_3), *3.92*/3.97 (each t, *1 H*/1 H, $^3J_{CHH'}$ = 5.2, CON*H*CH_2COOCH_3), 4.00, 4.05 (each dd, 1 H, 1 H, ^2J = 20.9 Hz, $^3J_{NH}$ = 5.4 Hz, NHC*H*′$COOCH_3$), *4.06*, *4.16* (each dd, *1 H*, *1 H*, ^2J = 27.0 Hz, $^3J_{NH}$ = 5.4 Hz, NHCH*H*′$COOCH_3$) *4.45*/4.51 [each dd, *1 H*/1 H, $^3J_{NH}$ = 8.4 Hz, $^3J_1$ = 6.9 Hz, C*H*(C_6H_7)CONH] *5.32* (m, *2 H*, 3,4-C_6H_7), 5.36 (dd, 1 H, $^3J_2$ = $^3J_4$ = 4.8 Hz, 3-C_6H_7), 5.41 (dd, 1 H, $^3J_3$ = $^3J_5$ = 4.7 Hz, 4-C_6H_7), *6.82*/6.90 (each d, *1 H*/1 H, $^3J_{CH}$ = 5.2 Hz, CHN*H*COPh), 7.40−7.53 (ABB′, *3 H*/3 H, 3,4,5-C_6H_5), 7.76−7.82 (CC′, *2 H*/2 H, 2,6-C_6H_5). − ^{13}C NMR (100.5 MHz, $CDCl_3$): δ = *26.93*/27.98 (6-C_6H_7), *40.47*/41.37 (1-C_6H_7), *57.86*/58.43, *59.27*/61.17 (2,5-C_6H_7), 59.79 (NH*C*H_2COOCH_3), *85.51*/85.19, *85.99*/86.27 (3,4-C_6H_7), *128.96, 132.27, 134.02,* 127.39, 129.02, 132.37, 133.81 (C_6H_5), *167.72, 171.36,* 167.74, 170.15, 171.31 (*C*$OOCH_3$, Ph*C*ONH, *C*ONH), 211.69 (Fe−*C*O). Diastereomeric ratio *1.0*:1.15. − $C_{21}H_{20}FeN_2O_7$ (468.2): calcd. C 53.87, H 4.31, N 5.98; found C 54.22, H 4.74, N 5.81.

16: 100 mg (0.264 mmol) of **6**, 58 mg (0.269 mmol) of phenylalanine methyl ester hydrochloride and 37.5 µl (0.269 mmol) of NEt_3 were used and stirred for 3 d. Four stereoisomers. − IR (KBr): $\tilde{\nu}$ = 3396 cm^{-1} m br., 3286 s br. (N−H), 2045 s (Fe−CO), 1967 s br. (Fe−CO), 1747 s ($COOCH_3$), 1636 s (CONH-I), 1534 s (CONH-II). − ^1H NMR (270 MHz, $CDCl_3$): δ = 1.39 (m, 1 H, 6*exo*-C_6H_7), 1.95 (m, 1 H, 6*endo*-C_6H_7), 2.59 (m, 1 H, 1-C_6H_7), 2.85−3.22 (m, 4 H, 2,5-C_6H_7, PhCH_2), 3.69, 3.71, 3.72, 3.73 (4 s, 3 H, OCH_3), 4.29−4.55 (m, 1 H, PhCONHC*H*), 4.85 [m, 1 H, CONHC*H*(CH_2Ph)], 5.32 (m, 2 H, 3,4-C_6H_7), 6.50 (m, 2 H, 2 NH), 7.02−7.19 (m, 5 H, $CH_2C_6H_5$), 7.42−7.55 (m, 3 H, 3,4,5-C_6H_5), 7.72−7.79 (m, 2 H, 2,6-C_6H_5). − $C_{28}H_{26}FeN_2O_7$ (558.4): calcd. C 60.23, H 4.69, N 5.02; found C 60.59, H 5.17, N 5.15.

17: 100 mg (0.264 mmol) of **6**, 54 mg (0.270 mmol) of methionine methyl ester hydrochloride and 37.6 µl (0.270 mmol) of NEt_3 were used and stirred for 7 d. Four stereoisomers. − IR (KBr): $\tilde{\nu}$ = 3440 cm^{-1} s br., 3290 s br. (N−H), 2044 s (Fe−CO), 1970 s br. (Fe−CO), 1745 s ($COOCH_3$), 1636 s (CONH-I), 1535 s (CONH-II). − ^1H NMR (270 MHz, $CDCl_3$): δ = 1.46 (m, 1 H, 6*exo*-C_6H_7), 1.88−2.20 (m, ca. 3 H, 6*endo*-C_6H_7, CH_2), 1.99, 2.01, 2.04, 2.05 (4 s, 3 H, SCH_3), 2.48 (m, 2 H, CH_2), 2.70 (m, 1 H, 1-C_6H_7), 3.03 (m, 2 H, 2,5-C_6H_7), 3.68, 3.69, 3.75, 3.76 (4 s, 3 H, OCH_3), 4.40−4.69 [m, 2 H, PhCONHC*H*, CONHC*H*(R)], 5.36 (m, 2 H, 3,4-C_6H_7), 6.67−7.08 (m, 2 H, 2 NH), 7.39−7.56 (m, 3 H, 3,4,5-C_6H_5), 7.75−7.83 (m, 2 H, 2,6-C_6H_5). − $C_{24}H_{26}FeN_2O_7S$ (542.4): calcd. C 53.15, H 4.83, N 5.16; found C 52.65, H 4.51, N 5.36.

18: 100 mg (0.264 mmol) of **6**, 57 mg (0.269 mmol) of glutamic acid dimethyl ester hydrochloride and 37.5 µl (0.269 mmol) of NEt_3 were used and stirred for 7 d. The product precipitated from the concentrated ether solution without adding pentane. Four stereoisomers. − IR (KBr): $\tilde{\nu}$ = 3440 cm^{-1} s br., 3287 s br. (N−H), 2045 s (Fe−CO), 1970 s br. (Fe−CO), 1741 s ($COOCH_3$), 1637 s (CONH-I), 1535 s (CONH-II). − ^1H NMR (270 MHz, $CDCl_3$): δ = 1.46 (m, 1 H, 6*exo*-C_6H_7), 1.99 (m, 2 H, CH_2), 2.18 (m, 1 H, 6*endo*-C_6H_7), 2.38 (m, 2 H, CH_2), 2.71 (m, 1 H, 1-C_6H_7), 3.00 (m, 2 H, 2,5-C_6H_7), 3.60, 3.61, 3.62, 3.63, 3.67, 3.68, 3.73, 3.74 (8 s, 6 H, 2 OCH_3), 4.50 [m, 2 H, PhCONHC*H*, CONHC*H*(R)], 5.36 (m, 2 H, 3,4-C_6H_7), 6.65−7.17 (m, 2 H, 2 NH), 7.42−7.56 (m, 3 H,

3,4,5-C_6H_5), 7.75−7.84 (m, 2 H, 2,6-C_6H_5). − $C_{25}H_{26}FeN_2O_9$ (554.3): calcd. C 54.17, H 4.73, N 5.05; found C 53.95, H 4.38, N 5.28.

General Procedure for the Preparation of **19**−**22**: To a solution of **15**−**18** in 10 ml of ethanol/water (4:1) a slight excess of NaOH (0.1 N) was slowly added. After stirring for a few hours, an equimolar amount of HCl (0.1 N) was added and after 30 min of further stirring the solvents were removed under reduced pressure. The residue was taken up in Et_2O/THF (1:1) (**19**), Et_2O/acetone (10:1) (**22**), or Et_2O (**20**, **21**) and filtered through Celite to remove NaCl. After concentrating in vacuo, the solution was added to excess pentane to precipitate the colourless product which was collected, washed once with pentane and dried in vacuo at 50°C for a few days.

19: 43 mg (0.092 mmol) of **15**, 0.93 ml of 0.1 N NaOH and 0.93 ml of 0.1 N HCl were used. − IR (KBr): $\tilde{\nu}$ = 3407 cm^{-1} m br., 3305 s br. (O−H, N−H), 2046 s (Fe−CO), 1973 s br. (Fe−CO), 1729 s (COOH), 1637 s (CONH-I), 1535 s (CONH-II). − ^{1}H NMR (400 MHz, [D$_6$]acetone): δ = 1.60 (m, 1 H, 6*exo*-C_6H_7), ca. 2.00 (m, 6*endo*-C_6H_7), 2.80 (m, 1 H, 1-C_6H_7), 3.27 (m, 2 H, 2,5-C_6H_7), 3.96 (m, 2 H, CH_2), 4.48 (m, 1 H, PhCONHC*H*), 5.61 (m, 2 H, 3,4-C_6H_7), 7.42−7.58 (m, 3 H, 3,4,5-C_6H_5), 7.88−8.00 (m, 2 H, 2,6-C_6H_5), 9.96 (s, 1 H, COOH). − $C_{20}H_{18}FeN_2O_7$ (454.2): calcd. C 52.89, H 3.99, N 6.17; found C 52.44, H 3.90, N 6.16.

20: 70 mg (0.125 mmol) of **16**, 1.3 ml of 0.1 N NaOH and 1.3 ml of 0.1 N HCl were used. Four stereoisomers. − IR (KBr): $\tilde{\nu}$ = 3428 cm^{-1} s br. (O−H, N−H), 2045 s (Fe−CO), 1970 s br. (Fe−CO), 1729 s (COOH), 1641 s (CONH-I), 1523 s (CONH-II). − ^{1}H NMR (270 MHz, $CDCl_3$): δ = 1.34 (m, 1 H, 6*exo*-C_6H_7), 1.91 (m, 1 H, 6*endo*-C_6H_7), 2.37−3.33 (m, 5 H, CH_2, 1-C_6H_7, 2,5-C_6H_7), 3.63, 4.38 (2 m, 1 H, PhCONHC*H*), 4.78 [m, 1 H, CONHC*H*(CH_2Ph)], 5.28 (m, 2 H, 3,4-C_6H_7), 6.72 (m, 1 H, NH), 6.96−7.60 (m, 9 H, NH, $CH_2C_6H_5$, 3,4,5-C_6H_5), 7.66−7.86 (m, 2 H, 2,6-C_6H_5). − $C_{27}H_{24}FeN_2O_7$ (544.3): calcd. C 59.58 H 4.44, N 5.15; found C 59.59, H 4.61, N 5.19.

21: 51 mg (0.094 mmol) of **17**, 0.98 ml of 0.1 N NaOH and 0.98 ml of 0.1 N HCl were used. Four stereoisomers. − IR (KBr): $\tilde{\nu}$ = 3403 cm^{-1} m br., 3300 s br. (O−H, N−H), 2047 s (Fe−CO), 1970 s br. (Fe−CO), 1723 s (COOH), 1636 s (CONH-I), 1532 s (CONH-II). − ^{1}H NMR (400 MHz, [D$_6$]acetone): δ = 1.60 (m, 1 H, 6*exo*-C_6H_7), ca. 2.00 (m, 6*endo*-C_6H_7, CH_2, SCH_3), 2.56 (m, 2 H, CH_2), 2.78 (m, 1 H, 1-C_6H_7), 3.24 (m, 2 H, 2,5-C_6H_7), 4.38−4.64 [m, 2 H, PhCONHC*H*, CONHC*H*(CH_2Ph)], 5.57 (m, 2 H, 3,4-C_6H_7), 7.43−7.57 (m, 3 H, 3,4,5-C_6H_5), 7.88−7.95 (m, 2 H, 2,6-C_6H_5). − $C_{23}H_{24}FeN_2O_7S$ (528.4): calcd. C 52.29, H 4.58, N 5.30; found C 52.73, H 4.70, N 5.27.

22: 95 mg (0.171 mmol) of **18**, 3.5 ml of 0.1 N NaOH and 3.5 ml of 0.1 N HCl were used. Four stereoisomers. − IR (KBr): $\tilde{\nu}$ = 3429 cm^{-1} s br. (O−H, N−H), 2047 s (Fe−CO), 1971 s br. (Fe−CO), 1723 s, 1720 s (2 COOH), 1644 s (CONH-I), 1527 s (CONH-II). − ^{1}H NMR (270 MHz, [D$_6$]acetone): δ = 1.59 (m, 1 H, 6*exo*-C_6H_7), ca. 2.00 (m, 6*endo*-C_6H_7, CH_2), 2.42 (m, 2 H, CH_2), 2.84 (m, 1 H, 1-C_6H_7), 3.20 (m, 2 H, 2,5-C_6H_7), 4.50 [m, 2 H, PhCONHC*H*, CONHC*H*(CH_2Ph)], 5.54 (m, 2 H, 3,4-C_6H_7), 7.41−7.62 (m, 3 H, 3,4,5-C_6H_5), 7.87−7.95 (m, 2 H, 2,6-C_6H_5). − $C_{23}H_{22}FeN_2O_9$ (526.3): calcd. C 52.49, H 4.21, N 5.32; found C 52.33, H 3.94, N 5.04.

General Procedure for the Preparation of **23**−**25**: To a solution of (COD)$PtCl_2$ in 10 ml of CH_2Cl_2 two equiv. of PPh_3, one equivalent of **19**−**21** and a slight excess of Ag_2O were added. This mixture was refluxed in the dark for 6 h and then, after cooling to room temp., filtered through Celite. The solvent was evaporated and the residue dried in vacuo for 2 h. After dissolving in 1 ml of CH_2Cl_2, petroleum ether was added to precipitate the colourless product which was washed with petroleum ether and dried in vacuo at room temp. for several days.

23: 9 mg (0.024 mmol) of (COD)$PtCl_2$, 11 mg (0.024 mmol) of **19**, 13 mg (0.05 mmol) of PPh_3 and 12 mg (0.052 mmol) of Ag_2O were used. − IR (KBr): $\tilde{\nu}$ = 3410 cm^{-1} s br. (N−H), 2042 s (Fe−CO), 1965 s br. (Fe−CO), 1653 s br. (coord. COO, CONH-I), 1512 s (CONH-II). − ^{1}H NMR (270 MHz, $CDCl_3$): δ = 1.55 (m, 1 H, 6*exo*-C_6H_7), 1.98 (m, 6*endo*-C_6H_7), 2.60 (m, 1 H, 1-C_6H_7), 3.05 (m, 4 H, 2,5-C_6H_7, NCH_2COO), 4.40 [m, 1 H, NHC*H*(C_6H_7)CON], 5.35 (m, 2 H, 3,4-C_6H_7), 6.99−7.82 (m, 35 H, 7 C_6H_5). − ^{31}P NMR: δ = 2.97 (d, $^2J_{P\text{-}P}$ = 18.6 Hz, $^1J_{P\text{-}Pt}$ = 3665 Hz, P *trans* to O), *4.08* (d, $^2J_{P\text{-}P}$ = 23.1 Hz, $^1J_{P\text{-}Pt}$ could not be determined, P *trans* to O), *10.36* (d, $^2J_{P\text{-}P}$ = 23.1 Hz, $^1J_{P\text{-}Pt}$ could not be determined, P *trans* to N), 18.61 (d, $^2J_{P\text{-}P}$ = 18.6 Hz, $^1J_{P\text{-}Pt}$ = 3921 Hz, P *trans* to N). Diastereomeric ratio 6:*1*. − $C_{56}H_{46}FeN_2O_7P_2Pt \times 0.5\ CH_2Cl_2$ (1214.3): calcd. C 55.89, H 3.90, N 2.31; found C 55.16, H 3.90, N 2.32.

24: 16 mg (0.043 mmol) of (COD)$PtCl_2$, 23 mg (0.042 mmol) of **20**, 22 mg (0.084 mmol) of PPh_3 and 20 mg (0.086 mmol) of Ag_2O were used. − IR (KBr): $\tilde{\nu}$ = 3430 cm^{-1} m br. (N−H), 2042 s (Fe−CO), 1967 s br. (Fe−CO), 1653 s br. (coord. COO, CONH-I), 1509 s (CONH-II). − ^{1}H NMR (270 MHz, $CDCl_3$): δ = 1.48 (m, 1 H, 6*exo*-C_6H_7), 1.85 (m, 6*endo*-C_6H_7), 2.24 (m, 1 H, 1-C_6H_7), 2.90 (m, 4 H, 2,5-C_6H_7, CH_2Ph), 3.72 [m, 1 H, NC*H*(CH_2Ph)COO], 4.30 [m, 1 H, NHC*H*(C_6H_7)CON], 5.25 (m, 2 H, 3,4-C_6H_7), 6.78−7.82 (m, 40 H, 8 C_6H_5). − ^{31}P NMR: δ = 2.85, 2.87, 2.92, 2.98 (each d, $^2J_{P\text{-}P}$ = 18.9 Hz, $^1J_{P\text{-}Pt}$ = 3669 Hz, P *trans* to O), 18.33, 18.36, 18.38, 18.41 (each d, $^2J_{P\text{-}P}$ = 18.3 Hz, $^1J_{P\text{-}Pt}$ = 3893 Hz, P *trans* to N). Diastereomeric ratio about 1:1:1.5:1.5. − $C_{63}H_{52}FeN_2O_7P_2Pt \times 0.5\ CH_2Cl_2$ (1304.5): calcd. C 58.01, H 4.02, N 2.15; found C 57.78, H 4.33, N 2.04.

25: 13.5 mg (0.036 mmol) of (COD)$PtCl_2$, 19 mg (0.036 mmol) of **21**, 18.9 mg (0.072 mmol) of PPh_3 and 18 mg (0.078 mmol) of Ag_2O were used. − IR (KBr): $\tilde{\nu}$ = 3415 cm^{-1} s br. (N−H), 2042 s (Fe−CO), 1967 s br. (Fe−CO), 1652 s br. (coord. COO, CONH-I), 1512 s (CONH-II). − ^{1}H NMR (270 MHz, $CDCl_3$): δ = 1.52 (m, 1 H, 6*exo*-C_6H_7), 1.85 (m, 6*endo*-C_6H_7, CH_2), 1.94, 2.01, 2.03 [each s, together 3 H, SCH_3 (1:1:2)], 2.50 (m, 3 H, 1-C_6H_7, CH_2), 2.98 (m, 2 H, 2,5-C_6H_7), 3.52, 3.74 [each m, together 1 H, NC*H*($CH_2CH_2SCH_3$)COO], 4.40 [m, 1 H, NHC*H*(C_6H_7)CON], 5.31 (m, 2 H, 3,4-C_6H_7), 7.08−7.89 (m, 35 H, 7 C_6H_5). − ^{31}P NMR: δ = 2.79, 2.80, 2.91, 2.97 (each d, $^2J_{P\text{-}P}$ = 19.2 Hz, $^1J_{P\text{-}Pt}$ = 3690 Hz, P *trans* to O), 18.24, 18.25, 18.34, 18.41 (each d, $^2J_{P\text{-}P}$ = 19.2 Hz, $^1J_{P\text{-}Pt}$ = 3881 Hz, P *trans* to N). Diastereomeric ratio about 1:1:1:2. − $C_{59}H_{52}FeN_2O_7P_2PtS \times CH_2Cl_2$ (1330.9): calcd. C 54.15, H 4.09, N 2.11; found C 53.53, H 4.23, N 2.31.

X-ray Diffraction Analyses[18]: Data collection: Enraf Nonius CAD4 Diffractometer (**4**, **5**), Siemens P4 Diffractometer (**9**, **10**), Mo-K_α radiation, λ = 0.71073 Å, graphite monochromator, cell constants from 25 centered reflections, ω-2Θ scan, intensity of three standard reflections checked every 2 h. Structure solution by SHELXS-86 and refinement by SHELXL-93 (G. M. Sheldrick, University of Göttingen, Germany), non-hydrogen atoms refined anisotropically, hydrogen atoms with U_i = 1.2 × U_{eq} of the adjacent carbon atom (**4**, **5**, **10**). For **9** hydrogen atoms found and refined freely. Full-matrix refinement against F^2. See Table 1 for crystal data and structure refinement.

Table 1. Crystal data and structure refinement for **4**, **5**, **9** and **10**

Compound number	**4** (M1403)[a]	**5** (M1550)	**9**	**10**
Empirical formula	$2 \times C_{29}H_{36}Cl_3Ir_2NO_2 \times 1.5\ CH_2Cl_2$	$C_{19}H_{21}NO_{12}Pd_3$	$C_{19}H_{13}CrNO_5$	$C_{20}H_{15}CrNO_5$
Formula weight	1970.06	774.57	387.30	401.33
T [K]	295(2)	294(2)	293(2)	293(2)
Crystal system	monoclinic	triclinic	monoclinic	monoclinic
Space group	$P2_1/c$ (No. 14)	$P\bar{1}$ (No. 2)	$C2/c$	$P2_1/n$
Unit-cell dimensions				
a [Å]	18.0641(19)	8.562(3)	31.384(2)	9.0240(10)
b [Å]	17.3233(24)	941.8(3)	6.6040(10)	10.373(3)
c [Å]	21.5724(38)	15.907(4)	16.7890(10)	19.333(5)
α [°]	90	101.72(2)	90	90
β [°]	91.048(11)	92.73(2)	106.92(11)	101.040(10)
γ [°]	90	108.61(2)	90	90
V [Å^3]	6749.5(1.7)	1181.5(6)	3329.1(6)	1776.2(7)
Z	4	2	8	4
Density (calcd.) [g/cm^3]	1.939	2.177	1.546	1.501
μ (Mo-K_a) [mm^{-1}]	8.261	2.323	0.718	0.676
F(000)	3756	752	1584	824
Crystal size [mm]	$0.43 \times 0.37 \times 0.10$	$0.47 \times 0.27 \times 0.07$	$0.55 \times 0.23 \times 0.08$	$0.05 \times 0.10 \times 0.38$
2θ range [°]	4.96−48.02	4.68−47.94	5−50	4.3−50
Index ranges	$\pm h\ +k\ +l$	$-h\ \pm k\ \pm l$	$+h\ +k\ \pm l$	$+h\ +k\ \pm l$ and $-h\ -k\ \pm l$
Reflections collected	10544	3978	3680	6657
Independent reflections	10253 [R(int) = 0.0447]	3693 [R(int) = 0.0171]	2921 [R(int) = 0.0372]	3133 [R(int) = 0.1596]
Absorption correction	ψ scan	ψ scan	ψ scan	N/A
Max. and min. transmission	0.991 and 0.240	0.998 and 0.683	0.238 and 0.209	
Data/parameters	7643/798	3239/321	2921/274	3133/244
Goodness-of-fit on F^2	1.076	1.079	1.038	0.990
Final R indices [$I > 2\sigma(I)$]	$R1$ = 0.0451, $wR2$ = 0.1077	$R1$ = 0.0247, $wR2$ = 0.0640	$R1$ = 0.0434, $wR2$ = 0.0783	$R1$ = 0.0753, $wR2$ = 0.1057
R indices (all data)	$R1$ = 0.0685, $wR2$ = 0.1260	$R1$ = 0.0309, $wR2$ = 0.0686	$R1$ = 0.0847, $wR2$ = 0.0933	$R1$ = 0.1961, $wR2$ = 0.1412
Largest diff. peak and hole [eÅ^{-3}]	1.639 and −1.381	0.557 and −0.539	0.212 and −0.273	0.374 and −0.401

[a] Two independent molecules, 1.5 CH_2Cl_2 disordered, split, Cp* disordered, not split.

[1] B. Kayser, C. Missling, J. Knicek, H. Nöth, W. Beck, *Eur. J. Inorg. Chem.* **1998**, 375−379.

[2] X-ray structure analyses.

[3] W. Steglich, *Fortschr. Chem. Forsch.* **1969**, *12*, 77−118; R. Lohmar, W. Steglich, *Chem. Ber.* **1980**, *113*, 3706−3715; G. Schulz, W. Steglich, *Chem. Ber.* **1980**, *113*, 770−786; B. Kübel, P. Gruber, R. Hurnaus, W. Steglich, *Chem. Ber.* **1979**, *112*, 128−137; G. Schulz, P. Gruber, W. Steglich, *Chem. Ber.* **1979**, *112*, 3221−3236; W. Steglich, P. Gruber, H.-U. Heininger, F. Kneidl, *Chem. Ber.* **1971**, *104*, 3816−3830; J. Leyendecker, U. Niewohner, W. Steglich, *Tetrahedron Lett.* **1983**, *24*, 2375−2378; E. Bunuel, C. Cativiela, M. D. Diaz-de-Villegas, *Tetrahedron: Asym.* **1996**, *7*, 1431−1436; R. M. Ortuno, J. Ibarzo, J. d′Angelo, F. Dumas, A. Alvarez-Larena, J. F. Piniella, *Tetrahedron: Asym.* **1996**, *7*, 127−138; D. Obrecht, C. Abrecht, M. Altorfer, U. Bohdal, A. Grieder, M. Kleber, P. Pfyffer, K. Müller, *Helv. Chim. Acta* **1996**, *79*, 1315−1337; M. L. Gelmi, F. Clerici, A. Melis, *Tetrahedron* **1997**, *53*, 1843−1854; M. Hugener, H. Heimgartner, *Helv. Chim. Acta* **1995**, *78*, 1863−1878; F. Cavelier, J. Verducci, *Tetrahedron Lett.* **1995**, *36*, 4425−4428.

[4] B. Schreiner, M. Prem, W. Bauer, K. Polborn, W. Beck, *Z. Naturforsch., Part B*, in press.

[5] W. Steglich, P. Gruber, G. Höfle, W. König, *Angew. Chem.* **1971**, *83*, 725−728; *Angew. Chem. Int. Ed. Engl.* **1971**, *10*, 653−656; H. Wegmann, W. Steglich, *Chem. Ber.* **1981**, *114*, 2580−2594.

[6] G. Jaouen, A. Vessieres, I. S. Butler, *Acc. Chem. Res.* **1993**, *26*, 361−369; D. P. Smith, M. T. Criffin, M. M. Olmstead, M. F. Maestre, R. H. Fish, *Inorg. Chem.* **1993**, *32*, 4677−4678; F. V. Sloop, G. M. Brown, R. A. Sachleben, M. L. Garrity, J. E. Elbert, K. D. Jacobson, *New. J. Chem.* **1994**, *18*, 317−326; J. M. Wolff, W. S. Sheldrick, *Chem.Ber.* **1997**, *130*, 981−988 and ref. therein; B. Kayser, K. Polborn, W. Steglich, W. Beck, *Chem. Ber.* **1997**, *130*, 171−177; J. M. Wolff, W. S. Sheldrick, *J. Organomet. Chem.* **1997**, *531*, 141−149 and ref. therein; R. Krämer, *Angew. Chem.* **1996**, *108*, 1287−1289; *Angew. Chem. Int. Ed. Engl.* **1996**, *35*, 1197−1199; D. Osella, M. Ravera, M. Vincenti, M. Salmain, G. Jaouen, *Organometallics* **1996**, *15*, 3037−3041; S. Blanalt, M. Salmain, B. Malézieux, G. Jaouen, *Tetrahedron Lett.* **1996**, *37*, 6561−6564; M. Schweiger, T. Ederer, K. Sünkel, W. Beck, *J. Organomet. Chem.*, in press.

[7] S. Sprouse, K. A. King, P. J. Spellane, R. J. Watts, *J. Am. Chem. Soc.* **1984**, *106*, 6647−6653; J. F. van Baar, K. Vrieze, P. J. Stufkens, *J. Organomet. Chem.* **1975**, *85*, 249−263; M. Nonoyama, *J. Organomet. Chem.* **1975**, *86*, 263−267; P. L. Bellon, F. de Martin, M. Manassero, M. Sansoni, *J. Organomet. Chem.* **1978**, *157*, 209−217; N. Farrell, D. Sutton, *J. Chem. Soc., Dalton Trans.* **1977**, 2124−2128; J. A. Carroll, R. E. Cobbledick, F. W. B. Einstein, N. Farrell, D. Sutton, P. L. Vogel, *Inorg. Chem.* **1977**, *16*, 2462−2469; L. Dahlenburg, F. Mirzaei, *J. Organomet. Chem.* **1983**, *251*, 123−132; J. A. Carroll, D. Sutton, Z. Xiaoheng, *J. Organomet. Chem.* **1982**, *244*, 73−86; K. A. King, P. J. Spellane, R. J. Watts, *J. Am. Chem. Soc.* **1985**, *107*, 1431−1432; A. C. Albéniz, G. Schulte, R. H. Crabtree, *Organometallics* **1992**, *11*, 242−249; P. Didier, I. Ortmans, A. Kirsch-De Mesmaeker, R. J. Watts, *Inorg. Chem.* **1993**, *32*, 5239−5245.

[8] A. C. Skapski, M. L. Smart, *J. Chem. Soc., Chem. Commun.* **1970**, 658−659.

[9] W. Beck, B. Niemer, M. Wieser, *Angew. Chem.* **1993**, *105*, 969−996; *Angew. Chem. Int. Ed. Engl.* **1993**, *32*, 923−950; L. A. P. Kane-Maguire, E. D. Honig, D. A. Sweigart, *Chem. Rev.* **1984**, *84*, 525−543 and ref. therein; A. J. Pearson, *Trans. Met. Chem.* **1981**, *6*, 67−78 and ref. therein; A. J. Birch, L. F. Kelly, A. S. Narula, *Tetrahedron* **1982**, *38*, 1813−1823; J. A. Carrer, B. Fates, L. A. P. Kane-Maguire, *J. Chem. Soc., Chem. Commun.* **1993**, 928−929; L. A. P. Kane-Maguire, R. Kanitz, P. Jones, P. A. Williams, *J. Organomet. Chem.* **1994**, *464*, 203−213; H.-J. Knölker, *Synlett* **1992**, 371−387; H.-J. Knölker, *J. Prakt. Chem./Chem.-Ztg.* **1996**, *338*, 190−193.

[10] See, e.g.: S. Jaroch, T. Schwarz, W. Steglich. P. Zistler, *Angew. Chem.* **1993**, *105*, 1803−1805; *Angew. Chem. Int. Ed. Engl.* **1993**, *32*, 1771−1773.

[11] D. A. Buckingham, L. G. Marzilli, A. M. Sargeson, *J. Am. Chem. Soc.* **1967**, *89*, 2772−2773 and 4539−4540.

[12] T. G. Appleton, J. R. Hall, P. D. Prenzler, *Inorg. Chem.* **1989**, *28*, 815−819; Y.-Q. Gong, Y.-F. Cheng, J.-M. Gu, X.-R. Ha,

Polyhedron **1997**, 3743, R. D. W. Kemmitt, S. Mason, J. Fawcett, D. R. Russell, *J. Chem. Soc., Dalton Trans.* **1992**, 1165−1176; H. Sigel, R. B. Martin, *Chem. Rev.* **1982**, *82*, 385−426; A. Bonamartini Corradi, E. Gozzoli, L. Menabue, M. Saladini, L. P. Battaglia, P. Sgarabotto, *J. Chem. Soc., Dalton Trans.* **1994**, 273−278 and ref. therein; G. Battistuzzi, M. Borsari, L. Menabue, M. Saladini, *Inorg. Chem.* **1996**, *35*, 4239−4247 and ref. therein; D. B. Grotjahn, T. L. Groy, *Organometallics* **1995**, *14*, 3669−3682.

[13] J. W. Kang, M. Mosley, P. M. Maitlis, *J. Am. Chem. Soc.* **1969**, *91*, 5970−5977; P. M. Maitlis, *Acc. Chem. Res.* **1978**, *11*, 301−307.

[14] D. Jones, L. Pratt, G. Wilkinson, *J. Chem. Soc.* **1962**, 4458−4463.

[15] J. D. Munro, P. L. Pauson, *J. Chem. Soc.* **1961**, 3475−3486.

[16] D. Drew, J. R. Doyle, *Inorg. Synth.* **1990**, *28*, 346−347.

[17] R. Lohmar, W. Steglich, *Chem. Ber.* **1980**, *113*, 3706−3715.

[18] Further details of the crystal structure determinations are available from the Fachinformationszentrum Karlsruhe, D-76344 Eggenstein-Leopoldshafen (Germany), on quoting the depository numbers CSD-407619 (**4**), -407618 (**5**), and from the Cambridge Crystallographic Data Centre, 12 Union Road, Cambridge CB2 1EZ (UK) on quoting the depository number CCDC-100699 (**9**, **10**).

[97269]

Synthesis, Reactivity, and Molecular Structures of Bis(diphenylphosphanyl)-amine- and Bis(diphenylphosphanyl)amide-Bridged Heterobimetallic μ-Isonitrile- and μ-Aminocarbyne Complexes (*Fe−Pt*)

Michael Knorr*[a][+] and Carsten Strohmann[b]

Institut für Anorganische Chemie der Universität des Saarlandes[a],
Postfach 151150, D-66041 Saarbrücken, Germany,
E-mail: m.knorr@rz.uni-sb.de

Institut für Anorganische Chemie der Universität Würzburg[b],
Am Hubland, D-97074 Würzburg, Germany

Received November 17, 1997

Keywords: Heterobimetallics / μ-Isonitrile complexes / μ-Aminocarbyne complexes / Bis(diphenylphosphanyl)amine / Iron / Platinum

Addition of isonitriles to $[(OC)_3Fe(\mu\text{-}CO)(\mu\text{-}Ph_2PNHPPh_2)Pt(PPh_3)]$ **1** produces the μ-isonitrile complexes $[(OC)_3Fe(\mu\text{-}C{=}NR)(\mu\text{-}Ph_2PNHPPh_2)Pt(PPh_3)]$ **2**, which are transformed to the μ-aminocarbyne complexes $[(OC)_3Fe\{\mu\text{-}CN(El)R\}(\mu\text{-}Ph_2PNHPPh_2)Pt(PPh_3)]^+$ **3** and **4** by electrophilic addition of $[El][BF_4]$ or $[El][OSO_2CF_3]$ (El = H, Me). The dppa backbone of **4** is readily deprotonated by $KOSiMe_3$ to yield the very stable zwitterionic aminocarbyne complex $[(OC)_3Fe\{\mu\text{-}CN(Me)2,6\text{-}xylyl\}(\mu\text{-}Ph_2PNPPh_2)Pt(PPh_3)]$ **5**.

Isonitriles (RNC) are often employed as ligands in coordination chemistry, since steric and electronic variation of the group R permits a fine tuning of the properties of a metal complex.[1][2] In addition to the innumerable examples of mononuclear isonitrile complexes, many heterobimetallic complexes and higher-nuclearity clusters bearing *terminal* isonitrile ligands have now been documented. However, polymetallic systems containing an isonitrile bridge between *two different* metal centers are still extremely scarce.[3a][3b][3c] We recently obtained the bis(diphenylphosphanyl)methane-bridged μ-isonitrile complex $[(OC)_3Fe(\mu\text{-}C{=}N\text{-}xylyl)(\mu\text{-}dppm)Pt(PPh_3)]$ by treatment of $[(OC)_3Fe\{Si(OMe)_3\}(\mu\text{-}dppm)Pt(H)(PPh_3)]$ with 2,6-dimethylphenylisonitrile under formal loss of $HSi(OMe)_3$.[3c] We report here on a different route for the synthesis of the bis(diphenylphosphanyl)amine-bridged μ-isonitrile complexes $[(OC)_3Fe(\mu\text{-}C{=}NR)(\mu\text{-}dppa)Pt(PPh_3)]$ and on their transformation to μ-aminocarbyne complexes, which have been characterized by multinuclear NMR techniques and single-crystal X-ray diffraction studies.

Results

In a manner similar as described by Shaw. et al. for the synthesis of the dppm-bridged complex $[(OC)_3Fe(\mu\text{-}CO)(\mu\text{-}dppm)Pt(PPh_3)]$[4], we obtained the dppa-bridged analogue $[(OC)_3Fe(\mu\text{-}CO)(\mu\text{-}dppa)Pt(PPh_3)]$ **1** containing a μ-carbonyl ligand by reaction of $[(OC)_4Fe(dppa\text{-}P)]$[5] with $[Pt(H_2C{=}CH_2)(PPh_3)_2]$ in 79% yield, as shown in Scheme 1. Addition of *o*-anisylisonitrile or 2,6-xylylisonitrile in a 1:1 ratio to the latter complex yields *selectively* within 10 min. at ambient temperature the heterobimetallic species $[(OC)_3Fe(\mu\text{-}C{=}NR)(\mu\text{-}dppa)Pt(PPh_3)]$ (**2a**: R = 2,6-xylyl; **2b**: R = *o*-anisyl) by substitution of the bridging carbonyl in **1**. There was no indication for a competing formation of an isomer bearing a terminal isonitrile ligand.

The most significant change in the IR spectra that accompanies the conversion of **1** to **2** is the replacement of the ν(CO) stretch of the bridging carbonyl of **1** (1761 cm^{-1}) by a broadened ν(C=N) stretch of medium intensity (**2a**: 1674; **2b**: 1670 cm^{-1}). The latter bands fall in the typical range for bridging isonitrile ligands with a strongly *bent* C=N−R group. The $^{31}P\{^1H\}$-NMR spectra of all the compounds reported herein characteristically show three mutually coupled resonances, as exemplified by that of **2a**. The spectrum of this μ-isonitrile complex features a doublet of doublets at δ = 114.3, attributable to the iron-bound dppa-phosphorus atom, which shows a strong coupling [^{2+3}J(P−P) = 174 Hz] to the platinum-bound dppa phosphorus at δ = 90.3. These signals are split further due to the presence of the PPh_3 ligand. The latter gives rise to a doublet of doublets at δ = 40.4, with couplings of 44 and 6 Hz. All signals are flanked by ^{195}Pt satellites, the Pt−P couplings of which are also evident in the ^{195}Pt-NMR spectrum (see Experimental Section).

Addition of excess of $HBF_4 \cdot Et_2O$ or $HOSO_2CF_3$ to a solution of **2** in dichloromethane led instantaneously to formation of the stable *N*-protonated cationic μ-aminocarbyne complexes $[(OC)_3Fe\{\mu\text{-}CN(H)R\}(\mu\text{-}dppa)Pt(PPh_3)][X]$ (**3a**: R = 2,6-xylyl, X = BF_4^-; **3b**: R = *o*-anisyl, X = $OSO_2CF_3^-$) in almost quantitative yields. It seems that in

[+] Present address: Laboratoire de Chimie de Coordination UMR 7513, Université Louis Pasteur, 4, rue Blaise Pascal, F-67070 Strasbourg, France.

 © WILEY-VCH Verlag GmbH, D-69451 Weinheim, 1998 1434−1948/98/0404−0495 $ 17.50+.50/0

Scheme 1

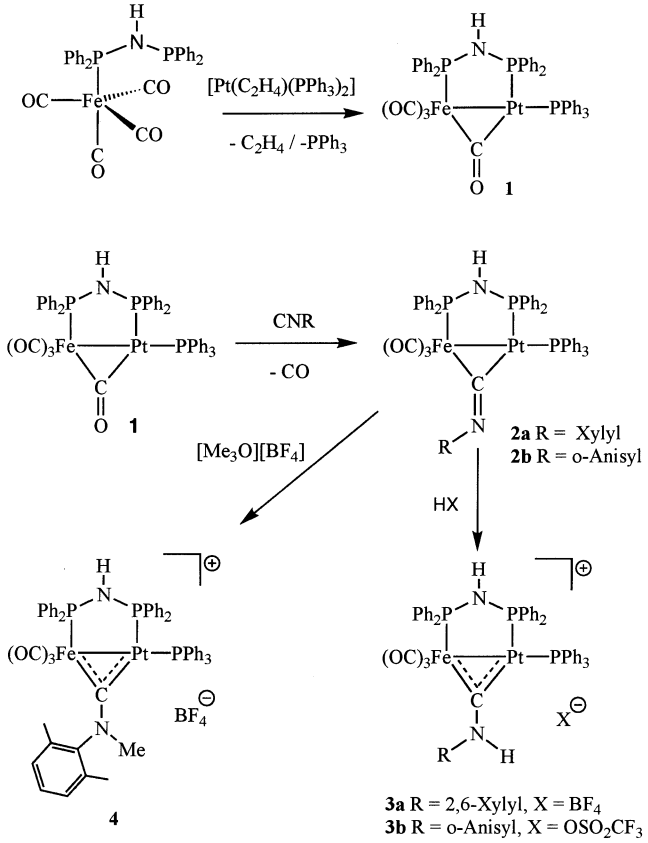

this case protonation of the nitrogen atom of the μ-CNR ligand is preferred to protonation of the metal-metal bond or a metal center yielding a heterometallic hydride complex, a reaction which would be a priori also conceivable. For example, protonation of $[(OC)_3Fe(\mu\text{-}CO)(\mu\text{-}dppm)Pt(PPh_3)]$ with HBF_4 is reported to give the cationic hydride-complex $[(OC)_4Fe(\mu\text{-}dppm)Pt(H)(PPh_3)][BF_4]$.[4]

The spectroscopic data obtained in solution were in agreement with the results of a single-crystal X-ray diffraction study performed on **3b**. The latter shows that the μ-aminocarbyne ligand symmetrically bridges [Fe−C(1) 1.975(6), Pt−C(1) 1.923(5) Å] the two metal centers, the separation of which, 2.5282(10) Å, is indicative of the presence of a metal-metal bond. Due to steric factors, only the isomer with the anisyl group oriented towards the iron center is formed. The short bond length between C(1) and N(1) of 1.263(7) Å reflects the partial C=N double-bond character of the μ-aminocarbyne unit, which, therefore, may alternatively be considered as a dimetallated iminium salt ligand. To date, to the best of our knowledge, only one other example of a *heterobimetallic* μ-aminocarbyne complex has been structurally described. A C−N distance of 1.29(2) Å was observed for this tungsten-gold complex bridged by a CN(Et)Me ligand.[6] The triflate counterion of **3b** is hydrogen-bonded to the N−H group {*d*[N(2)−H(2)...O(5)] 2.867 Å; H(2)···O(5) 2.10(7) Å} of the dppa ligand. The position of H(2) could be located and was isotropically refined. A comparable distance of 2.91 Å has been reported by Ellermann et al. for the hydrogen-bridged complex $[Cu(CN)(dppa)PPh_3]\cdot MeOH$.[7] Overall, the structure of **3b** shows strong similarities to that of the recently published μ-vinylidene complex $[(OC)_3Fe\{\mu\text{-}C{=}C(H)Ph\}(\mu\text{-}dppm)Pt(PPh_3)]$.[8]

Figure 1. View of the crystal structure of **3b** showing the atom-numbering scheme[a]

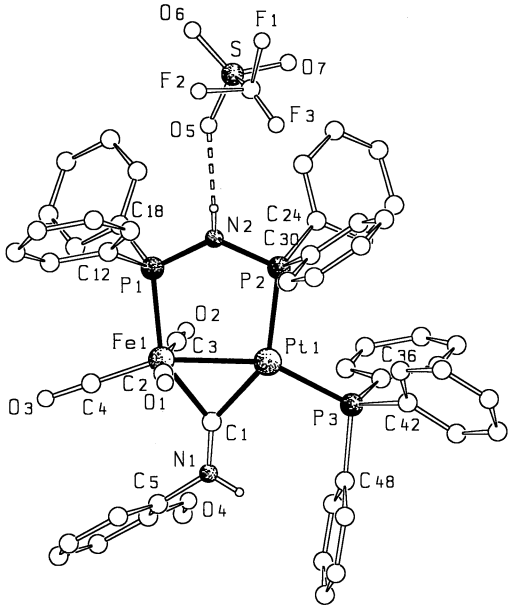

[a] Selected bond lengths [Å] and angles [°]: Fe−Pt 2.528(1), Fe−P(1) 2.226(3), Pt−P(2) 2.327(2), Pt−P(3) 2.291(1), Fe−C(1) 1.975(6), Pt−C(1) 1.923(5), C(1)−N(1) 1.263(7), P(1)−N(2) 1.668(9), P(2)−N(2) 1.697(9); C(1)−N(1)−C(5) 126.1(5), Pt−C(1)−Fe 80.9(2), Fe−Pt−C(1) 48.7(2), Pt−Fe−C(1) 50.5(2), C(1)−Fe−P(1) 146.9(2), C(1)−Pt−P(2) 144.2(2), C(1)−Pt−P(3) 103.5(2), P(1)−Fe−Pt 96.45(5), P(2)−Pt−P(3) 112.18(5), Fe−Pt−P(3) 151.32(4), P(1)−N(2)−P(2) 126.9(3).

In a similar manner, upon treatment of **2a** with a slight excess of $[Me_3O][BF_4]$, electrophilic addition affords the stable *N*-alkylated product $[(OC)_3Fe\{\mu\text{-}CN(Me)xylyl\}(\mu\text{-}dppa)Pt(PPh_3)][BF_4]$ **4**, which has been fully characterized by multinuclear NMR techniques and elemental analysis. Characteristic for this type of aminocarbyne complex is the ^{13}C resonance of the μ-C atom, which is observed in the lowfield region at $\delta = 311.7$ as a doublet of doublets of doublets with $^2J(P-C)$ coupling constants of 3, 11, and 82 Hz. Upon treatment of **3** with weak bases such as NEt_3 or $KOSiMe_3$, deprotonation of the μ-aminocarbyne ligand yields the precursor compounds **2**.

However, addition of $KOSiMe_3$ to a solution of **4** did not yield the anticipated μ-siloxycarbene complex.[9] Instead, deprotonation of the dppa backbone occurred, with formation of the stable zwitterionic μ-aminocarbyne complex $[(OC)_3Fe\{\mu\text{-}CN(Me)xylyl\}(\mu\text{-}Ph_2PNPPh_2)Pt(PPh_3)]$ **5**.

In addition to a detailed spectroscopic investigation in solution (see Experimental Section), the solid-state structure of **5** has been determined by a single-crystal X-ray diffraction study. Comparison with the structure of **3b** reveals that deprotonation of the dppa backbone has no significant influence on the metal-metal [Fe−Pt 2.517(1) Å] and metal-

Scheme 2

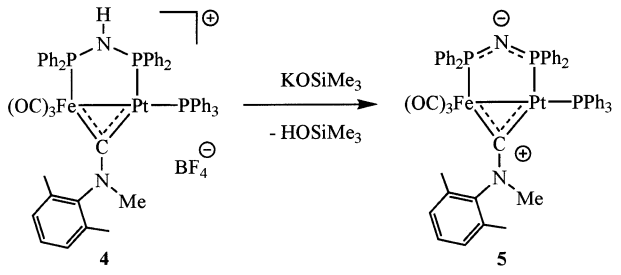

4 **5**

phosphorus distances. Only the shortened P(1)−N(2) and P(2)−N(2) distances of 1.608(4) and 1.633(4) Å may reflect a charge delocalization in the bis(diphenylphosphanyl)-amide bridge. These values are comparable to the P−N distances [1.626(7) and 1.598(7) Å] found in the bis(diphenylphosphanyl)amide-bridged dinuclear complex $[Co_2(\mu\text{-}CO)(CO)_4(\mu\text{-}Ph_2PNPPh_2)(\mu\text{-}PPh_2)]$ and the mononuclear chelate $[Pd(Cl)(Ph_2PNPPh_2)(PEt_3)]$, as reported recently by Ellermann[10] and Muller.[11] Compared to the P−N−P angle of **3b** [126.9(3)°], that of **5** is somewhat more acute and amounts to 123.4(2)°.

Figure 2. View of the crystal structure of **5** showing the atom-numbering scheme[a]

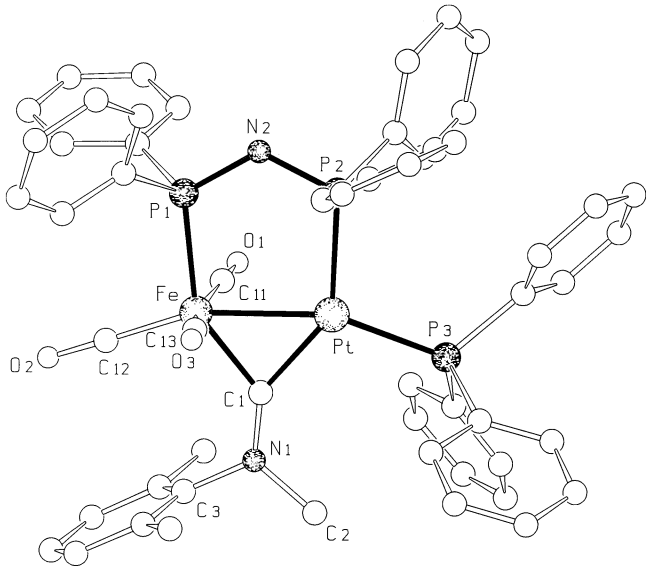

[a] Selected bond lengths [Å] and angles [°]: Fe−Pt 2.517(1), Fe−P(1) 2.276(2), Pt−P(2) 2.349(2), Pt−P(3) 2.277(1), Fe−C(1) 1.918(4), Pt−C(1) 1.996(5), C(1)−N(1) 1.296(6), P(1)−N(2) 1.608(4), P(2)−N(2) 1.633(4); C(1)−N(1)−C(2) 124.6(4), Pt−C(1)−Fe 80.0(2), Fe−Pt−C(1) 48.6(1), C(1)−Fe−Pt 51.3(2), C(1)−Fe−P(1) 146.9(2), C(1)−Pt−P(2) 141.40(13), C(1)−Pt−P(3) 109.5(1), P(1)−Fe−Pt 95.60(5), P(2)−Pt−P(3) 108.97(5), Fe−Pt−P(3) 157.14(4), P(1)−N(2)−P(2) 123.4(5).

To the best of our knowledge, the solid-state structures of **3b** and **5** represent the first examples of X-ray crystal-structure determinations performed on heterometallic bis(diphenylphosphanyl)amine- and bis(diphenylphosphanyl)amide-bridged systems. We are currently investigating the steric and electronic factors that govern the bonding mode of the coordinated isonitrile ligand (bridging vs. terminal)[12] and the reactivity of the amide bridge of $[(OC)_3Fe\{\mu\text{-}CN(R)(R')\}(\mu\text{-}Ph_2PNPPh_2)Pt(PPh_3)]$ towards electrophiles. Preliminary results using an $[AuPPh_3]^+$ fragment indicate that this route permits the synthesis of heterotrimetallic μ-aminocarbyne complexes of the type $[(OC)_3(L)Fe\{\mu\text{-}CN(R)(R')\}\{\mu\text{-}Ph_2PN(AuPPh_3)PPh_2\}Pt(PPh_3)]^+$ (L = CO, CNR).

The *Deutsche Forschungsgemeinschaft* and the *Fonds der Chemischen Industrie* is gratefully thanked for habilitation grants and financial support to M. K and C. S. and *Degussa AG* for a generous gift of Pt salts. We are also indebted to Prof. *M. Veith* for his support and for providing the institute facilities.

Experimental Section

All reactions were performed in Schlenk-tube flasks under purified nitrogen. Solvents were dried and distilled under nitrogen before use, toluene and hexane over sodium, dichloromethane from P_4O_{10}. Nitrogen was passed through BASF R3-11 catalyst and molecular-sieve columns to remove residual oxygen and water. Elemental C, H and N analyses were performed on a Leco Elemental Analyser CHN 900. − The ^1H-, $^{31}P\{^1H\}$-, and $^{13}C\{^1H\}$-NMR spectra were recorded at 200.13, 81.01 and 50.32 MHz, respectively, on a Bruker ACP 200 instrument. Phosphorus-chemical shifts were referenced to 85% H_3PO_4 in H_2O with downfield shifts reported as positive. ^{195}Pt-chemical shifts were measured on a Bruker ACP 200 instrument (42.95 MHz) and externally referenced to K_2PtCl_4 in water with downfield chemical shifts reported as positive. NMR spectra were recorded in pure $CDCl_3$, unless otherwise stated. The presence and amount of CH_2Cl_2 retained in **3a** and **4** was determined from the ^1H-NMR spectra. − The reactions were generally monitored by IR spectroscopy in the ν(CO) region. − $[Me_3O][BF_4]$ and 2,6-xylylisonitrile were obtained from Aldrich and Fluka and were used as received; dppa was prepared as described by Meinel and Nöth.[13]

Preparation of [(CO)$_3$Fe(μ-CO)(μ-dppa)Pt(PPh$_3$)] (**1**): To a solution of $[Pt(H_2C{=}CH_2)(PPh_3)_2]$ (751 mg, 1.0 mmol) in toluene (10 ml) one equivalent of $[(OC)_4Fe(dppa\text{-}P)]$ (553 mg, 1.0 mmol) was added. After stirring for 20 min. at ambient temperature, the orange-red solution was concentrated and **1** was precipitated by slow addition of hexane. The resulting crude yellow-orange product, which was sufficiently pure for further reactions, was then dried in vacuo. Yield: 798 mg (79%). Analytically pure **1** was obtained in form of red-orange crystals by recrystallization from toluene/Et_2O. − IR (KBr): $\tilde{\nu}$ = 2006 cm^{-1} (s), 1939 (vs), 1925 (sh), 1761 (m, br.) ν(CO). − ^1H NMR: δ = 4.97 [m, br., NH, $^3J(Pt-H)$ = 95.0 Hz], 7.00−7.69 (m, 35 H, phenyl). − $^{31}P\{^1H\}$ NMR: δ = 118.1 [dd, P^1(Fe), $^{2+3}J(P^1-P^2)$ = 213, $^{3+4}J(P^1-P^3)$ = 4, $^{2+3}J(Pt-P)$ = 30 Hz], 93.4 [dd, P^2(Pt), $^1J(Pt-P)$ = 2877 Hz], 42.0 [dd, P^3(Pt), $^2J(P^2-P^3)$ = 63, $^1J(Pt-P)$ = 4628 Hz]. − $^{195}Pt\{^1H\}$NMR: δ = −2543 [ddd, $^{2+3}J(Pt-P^1)$ = 30, $^1J(Pt-P^2)$ = 2877, $^1J(Pt-P^3)$ = 4628 Hz]. − $C_{46}H_{36}FeNO_4P_3Pt\cdot Et_2O$ (1010.65 + 74.12): calcd. C 55.36, H 4.27, N 1.29; found C 55.48, H 4.04, N 1.08.

Preparation of [(CO)$_3$Fe(μ-CN-xylyl)(μ-dppa)Pt(PPh$_3$)] (**2a**): To a solution of **1** (202 mg, 0.2 mmol) in CH_2Cl_2 (5 ml), one equivalent of 2,6-xylylisonitrile, dissolved in CH_2Cl_2 (5 ml), was added dropwise. After stirring for 15 min. at ambient temperature (evolution of CO), the orange-red solution was concentrated and **2a** was precipitated by the slow addition of hexane. The resulting microcrystalline yellow-orange product was dried in vacuo. Yield: 194

mg (87%). – IR (CH_2Cl_2): $\tilde{\nu}$ = 2004 cm^{-1} (s), 1934 (vs) ν(CO); 1671 (m, br.) ν(CN). – IR (KBr): $\tilde{\nu}$ = 3270 cm^{-1} (w) ν(NH); 2000 (m), 1934 (s), 1922 (s) ν(CO); 1674 (m, br.) ν(C=N). – ^1H NMR: δ = 2.07 (s, 3 H, xylyl-CH_3), 4.96 [m, br., NH, ^3J(Pt−H) = 89.0 Hz], 6.84−7.88 (m, 38 H, phenyl). – $^{31}P\{^1H\}$ NMR: δ = 114.3 [dd, P^1(Fe), $^{2+3}J(P^1-P^2)$ = 174, $^{3+4}J(P^1-P^3)$ = 6, ^{2+3}J(Pt−P) = 50 Hz], 90.3 [dd, P^2(Pt), ^1J(Pt−P) = 2866 Hz], 40.4 [dd, P^3(Pt), $^2J(P^2-P^3)$ = 44, ^1J(Pt−P) = 4326 Hz]. – $^{195}Pt\{^1H\}$NMR: δ = −2678 [ddd, $^{2+3}J(Pt-P^1)$ = 50, $^1J(Pt-P^2)$ = 2856, $^1J(Pt-P^3)$ = 4328 Hz]. – $C_{54}H_{45}FeN_2O_3P_3Pt$ (1113.82): calcd. C 58.23, H 4.07, N 2.51; found C 58.26, H 3.86, N 2.70.

Preparation of [(CO)$_3$Fe(μ-CN-o-anisyl)(μ-dppa)Pt(PPh$_3$)] (**2b**): This yellow derivative was prepared and isolated as described for **2a**. – IR (CH_2Cl_2): $\tilde{\nu}$ = 2008 cm^{-1} (m), 1940 (s) ν(CO); 1670 (m, br.) ν(C=N). – IR (KBr): $\tilde{\nu}$ = 3224 cm^{-1} (w) ν(NH); 2003 (m), 1933 (s) ν(CO); 1669 (m, br.) ν(C=N). – ^1H NMR: δ = 3.71 (s, 3 H, OCH_3), 5.04 [m, br., NH, ^3J(Pt−H) = 89.8 Hz], 6.75−7.75 (m, 39 H, phenyl). – $^{31}P\{^1H\}$ NMR: δ = 113.4 [dd, P^1(Fe), $^{2+3}J(P^1-P^2)$ = 173, $^{3+4}J(P^1-P^3)$ = 9, ^{2+3}J(Pt−P) = 40 Hz], 89.3 [dd, P^2(Pt), ^1J(Pt−P) = 2884 Hz], 40.0 [dd, P^3(Pt), $^2J(P^2-P^3)$ = 45, ^1J(Pt−P) = 4262 Hz]. – $^{195}Pt\{^1H\}$ NMR: δ = −2688 [ddd, $^{2+3}J(Pt-P^1)$ = 40, $^1J(Pt-P^2)$ = 2886, $^1J(Pt-P^3)$ = 4264 Hz]. – $C_{53}H_{43}FeN_2O_4P_3Pt$ (1115.79): calcd. C 57.05, H 3.88, N 2.51; found C 56.69, H 4.16, N 2.29.

Preparation of [(CO)$_3$Fe{μ-CN(H)xylyl}(μ-dppa)Pt(PPh$_3$)][BF$_4$] (**3a**): This complex was prepared by adding excess HBF_4ÆEt$_2$O to a solution of **2a** (0.111 g, 0.1 mmol) in CH_2Cl_2 (10 ml) at 253 K. After warming to ambient temperature, all volatiles were removed under reduced pressure. The orange-red residue was rinsed with Et_2O (3 ml) and dried in vacuo. – IR (CH_2Cl_2): $\tilde{\nu}$ = 2041 cm^{-1} (m), 1981 (vs) ν(CO); 1527 (w) ν(CN). – ^1H NMR: δ = 2.10 (s, 6 H, xylyl-CH_3), 6.53 [m, br., NH, ^3J(Pt−H) = 85 Hz], 6.85−7.85 (m, 38 H, phenyl), 9.08 (m, br., NH). – $^{31}P\{^1H\}$ NMR: δ = 103.6 [dd, P^1(Fe), $^{2+3}J(P^1-P^2)$ = 99, $^{3+4}J(P^1-P^3)$ = 13, $^{2+3}J(P^1-Pt)$ = 71 Hz], 80.5 [dd, P^2(Pt), $^2J(P^2-P^3)$ = 13, $^1J(P^2-Pt)$ = 2889 Hz], 37.2 [t, P^3(Pt), $^1J(P^3-Pt)$ = 3810 Hz]. – $C_{54}H_{46}BF_4FeN_2O_3P_3Pt\cdot 1.5\ CH_2Cl_2$ (1201.63 + 127.40): calcd. C 49.93, H 3.73, N 2.12; found C 49.99, H 3.88, N 2.20.

Preparation of [(CO)$_3$Fe{μ-CN(H)-o-anisyl}(μ-dppa)Pt(PPh$_3$)][BF$_4$] (**3b**): This complex was prepared by adding excess $HOSO_2CF_3$ to a solution of **2b** (0.112 g, 0.1 mmol) in CH_2Cl_2 (10 ml) at 253 K. After warming to ambient temperature, all volatiles were removed under reduced pressure. The orange-red residue was rinsed with Et_2O (3 ml) and dried in vacuo. – IR (CH_2Cl_2): $\tilde{\nu}$ = 2042 cm^{-1} (m), 1979 (vs) ν(CO); 1532 (w) ν(CN). – ^1H NMR: δ = 3.67 (s, 3 H, OCH_3), 6.94 [m, br., NH, ^3J(Pt−H) = 84 Hz], 6.87−7.42 (m, 39 H, phenyl), 7.91 (m, br., NH). – $^{31}P\{^1H\}$ NMR: δ = 102.2 [dd, P^1(Fe), $^{2+3}J(P^1-P^2)$ = 99, $^{3+4}J(P^1-P^3)$ = 14, $^{2+3}J(P^1-Pt)$ = 73 Hz], 79.0 [dd, P^2(Pt), $^2J(P^2-P^3)$ = 12, $^1J(P^2-Pt)$ = 2868 Hz], 37.3 [dd, P^3(Pt), $^1J(P^3-Pt)$ = 3791 Hz]. – $^{195}Pt\{^1H\}$ NMR: δ = −2510 [ddd, $^{2+3}J(P^1-Pt)$ = 73, $^1J(P^2-Pt)$ = 2868, $^1J(P^3-Pt)$ = 3791 Hz]. – $C_{54}H_{44}F_3FeN_2O_7P_3PtS$ (1265.83): calcd. C 50.18, H 3.70, N 2.17; found C 51.23, H 3.51, N 2.21.

Preparation of [(CO)$_3$Fe{μ-CN(Me)xylyl}(μ-dppa)Pt(PPh$_3$)][BF$_4$] (**4**): $[Me_3O][BF_4]$ (118 mg, 0.8 mmol) was added to a solution of **2a** (557 mg, 0.5 mmol) in CH_2Cl_2 (15 ml). After stirring for 16 h, the yellow solution was concentrated to a volume of ca. 10 ml and then layered with Et_2O. After 2 d, yellow air-stable crystals were formed, which were suitable for analysis by X-ray crystallography. Yield: 465 mg (74%). – IR (KBr): $\tilde{\nu}$ = 3217 cm^{-1} (w) ν(NH); 2028 (m), 1961 (vs) ν(CO); 1542 (w) ν(CN). – ^1H NMR: δ = 2.24 (s, 6 H, xylyl-CH_3), 2.83 (s, 3 H, NMe), 6.38 [m, br., NH, ^3J(Pt−H) = 91 Hz], 6.96−7.62 (m, 38 H, phenyl). – $^{13}C\{^1H\}$ NMR: δ = 311.7 [ddd, μ-C, ^2J(P−C) = 82, ^2J(P−C) = 11, ^2J(P−C) = 3 Hz], 209.3 [dd, 2 CO, ^2J(P−C) = 27, ^3J(P−C) = 5 Hz], 208.5 [d, 1 CO, ^2J(P−C) = 7 Hz], 117.9−138.4 (m, phenyl), 51.6 [dt, N−CH_3, ^4J(P−C) = 9, ^4J(P−C) = 3 Hz], 17.1 (s, xylyl-CH_3). – $^{31}P\{^1H\}$ NMR: δ = 102.6 [dd, P1(Fe), ^{2+3}J(P1−P2) = 110, ^{3+4}J(P1−P3) = 11, ^{2+3}J(P1−Pt) = 70 Hz], 81.1 [dd, P2(Pt), ^2J(P2−P3) = 8, ^1J(P2−Pt) = 2837 Hz], 37.2 [dd, P3(Pt), ^1J(P3−Pt) = 3810 Hz]. – $^{195}Pt\{^1H\}$ NMR: δ = −2717 [ddd, ^{2+3}J(P1−Pt) = 70, ^1J(P2−Pt) = 2837, ^1J(P3−Pt) = 3808 Hz]. – $C_{55}H_{48}BF_4FeN_2O_3P_3Pt\cdot 0.5\ CH_2Cl_2$ (1215.66 + 42.47): calcd. C 52.98, H 3.93, N 2.23; found C 52.55, H 4.05, N 2.20.

Preparation of [(CO)$_3$Fe{μ-CN(Me)xylyl}(μ-Ph$_2$PNPPh$_2$)Pt(PPh$_3$)] (**5**): $KOSiMe_3$ (3 mmol) was added to a suspension of **4** (0.5 mmol) in Et_2O (25 ml). The deprotonated product gradually dissolved within a period of 1 h. The yellow solution was then filtered and concentrated under reduced pressure. After addition of hexane, analytically pure **5** was precipitated. The product was filtered off and was dried in vacuo for 2 h. Yield: (447 mg, 84%). Suitable crystals for analysis by X-ray crystallography were obtained by layering a concentrated solution of **5** in CH_2Cl_2 with hexane. – IR (KBr): $\tilde{\nu}$ = ν(CO) 2002 cm^{-1} (m), 1934 (vs) ν(CO); ν(CN) 1538 (w) ν(CN). – ^1H NMR: δ = 2.22 (s, 6 H, xylyl-CH_3), 2.67 (s, 3 H, NMe), 7.01−7.85 (m, 38 H, phenyl). – $^{13}C\{^1H\}$ NMR: δ = 312.0 [dd, μ-C, ^2J(P−C) = 80, ^2J(P−C) = 19 Hz], 209.8 [dd, 2 CO, ^2J(P−C) = 27, ^3J(P−C) = 6 Hz], 208.6 [d, 1 CO, ^2J(P−C) = 8 Hz], 117.9−150.2 (m, phenyl), 51.4 [dt, N−CH_3, ^4J(P−C) = 9, ^4J(P−C) = 4 Hz], 17.4 (s, xylyl-CH_3). – $^{31}P\{^1H\}$ NMR: δ = 88.0 [br. d, P1(Fe), ^{2+3}J(P1−P2) = 130 Hz], 72.3 [br. d, P2(Pt), ^1J(P2−Pt) = 2554 Hz], 35.3 [d, P3(Pt), ^2J(P2−P3) = 12, ^1J(P3−Pt) = 3757 Hz]. – $^{195}Pt\{^1H\}$ NMR: δ = −2504 [br. dd, ^1J(P2−Pt) = 2554, ^1J(P3−Pt) = 3757 Hz]. – $C_{55}H_{47}FeN_2O_3P_3Pt$ (1127.85): calcd. C 58.57, H 4.20, N 2.48; found C 58.25, H 4.05, N, 2.10.

Crystal-Structure Determination of **3b**[14][15]: Collection of crystallographic data: Siemens Stoe AED 2 diffractometer; Mo-K_α radiation (λ = 0.71073 Å), graphite monochromator; intensity data were collected using the Ω/2Θ scan mode at 293 K. $C_{54}H_{44}F_3N_2FeO_7P_3PtS$: yellow crystals with approximate dimensions of 0.5 × 0.3 × 0.2 mm, triclinic, space group $P\bar{1}$; a = 13.105(3), b = 14.387(3), c = 14.997(7) Å, α = 81.29(3), β = 71.77(3), γ = 78.09(3)°, V = 2616.3(10) Å^3, Z = 2, ρ_{calcd} = 1.607 g cm^{-3}, F(000) = 1260; 9608 independent reflections in the scan range 2.38 < 2θ < 52.0°, of which 8455 with $I > 2\sigma(I)$ were used in the structure solution and refinement for 654 parameters; $R1 = \Sigma F_{o-Fc}/\Sigma F_o$ = 0.0411[$I > 2\sigma(I)$], $wR2 = [\Sigma w(F_o^2 - F_c^2)^2/\Sigma wF_o^4]^{1/2}$ = 0.1222 (all data), GoF = 1.114; anisotropic refinement for non-hydrogen atoms; hydrogen atoms in idealized geometries, except for H(2), which was refined isotropically. Highest residual electron density 0.793 eÅ^{-3}.

Crystal Structure Determination of **5**: Collection of crystallographic data: Siemens Stoe AED 2 diffractometer; Mo-K_α radiation (λ = 0.71073 Å), graphite monochromator; intensity data were collected using the Ω/2Θ scan mode at 293 K. $C_{55}H_{47}FeN_2O_3P_3Pt$: yellow crystals with approximate dimensions of 0.65 × 0.4 × 0.35 mm, monoclinic, space group $P2_1/c$; a = 11.026(6), b = 18.524(9), c = 23.708(12) Å, β = 90.49(4)°, V = 4842.4(4) Å^3, Z = 4, ρ_{calcd} = 1.547 g cm^{-3}, F(000) = 2256; 7614 independent reflections in the scan range 1.72 < 2θ < 48.0°, of which 6095 with $I > 2\sigma(I)$ were used in the structure solution and refinement for 589 parameters; $R1 = \Sigma|F_o - F_c|/\Sigma|F_o|$ = 0.0295 [$I > 2\sigma(I)$], $wR2 = [\Sigma w(F_o^2 - F_c^2)^2/\Sigma wF_o^4]^{1/2}$ = 0.0765 (all data), GoF = 1.036; anisotropic refine-

ment for non-hydrogen atoms; hydrogen atoms in idealized geometries. Highest residual electron density 0.793 eÅ^{-3}.

[1] Y. Yamamoto, H. Yamazaki, *Coord. Chem. Rev.* **1972**, *8*, 225−239.

[2] [2a] E. Singleton, H. E. Oosthuizen, *Adv. Organomet. Chem.* **1983**, *22*, 209−310. − [2b] D. Lentz, *Angew. Chem.* **1994**, *106*, 1377−1393; *Angew. Chem. Int. Ed. Engl.* **1994**, *33,* 1315−1331.

[3] [3a] K. S. Rattliff, P. E. Fanwick, C. P. Kubiak, *Polyhedron* **1990**, *9*, 2651−2653. − [3b] J. Fornies, F. Martinez, R. Navarro, A. Redondo, M. Tomas, A. J. Welch, *J. Organomet. Chem.* **1986**, *316*, 351−366. − [3c] M. Knorr, T. Faure, P. Braunstein, *J. Organomet. Chem.* **1993**, *447*, C4−C6.

[4] X. L. R. Fontaine, G. B. Jacobson, B. L. Shaw, M. Thornton-Pett, *J. Chem.Soc., Dalton Trans.* **1988**, 741−750.

[5] M. Knorr, P. Braunstein, A. Tiripicchio, F. Ugozzoli, *J. Organomet. Chem.* **1996**, *526*, 105−116.

[6] [6a] V. G. Albano, L. Busetto, M. C. Cassani, P. Sabatino, A. Schmitz, V. Zanotti, *J. Chem. Soc., Dalton Trans.* **1995**, 2087−2093. − [6b] For examples of X-ray structures of homobimetallic μ-aminocarbyne complexes see: S. Willis, A. R. Manning, *J. Chem. Soc., Dalton Trans.* **1979**, 23−27. − [6c] D. L. DeLaet, P. E. Fanwick, C. P. Kubiak, *Organometallics* **1986**, *5*, 1807−1811. − [6d] A. Schröder, W. Sperber, J. Fuchs, W. P. Fehlhammer, *Chem. Ber.* **1992**, *125*, 1001−1005.

[7] J. Ellermann, F. A. Koch, K. J. Meier, M. Moll, *J. Organomet. Chem.* **1992**, *428*, C44.

[8] M. Knorr, C. Strohmann, P. Braunstein, *Organometallics* **1996**, *15*, 5653−5663.

[9] M. Knorr, P. Braunstein, A. DeCian, J. Fischer, *Organometallics* **1995**, *14*, 1302−1309.

[10] D. Pohl, J. Ellermann, F. A. Knoch, M. Moll, W. Bauer, *J. Organomet. Chem.* **1994**, *481*, 259−274.

[11] [11a] M. Gomez, G. Muller, J. Sales, X. Solans, *J. Chem. Soc., Dalton Trans.* **1993**, 221−225. − [11b] See also: J. Geicke, I.-P. Lorenz, P. Mürschel, K. Polborn, *Z. Naturforsch* . **1997**, *52b*, 593−603.

[12] M. Knorr, C. Strohmann, poster abstract 98, 4th Anglo/German Inorganic Chemistry Meeting, University of Marburg **1997**.

[13] H. Nöth, E. Meinel, *Z. Anorg. Allg. Chem.* **1967**, *349,* 225−240.

[14] G. M. Sheldrick, *SHELXL-97, SHELXS-97*, Universität Göttingen, **1997**.

[15] Crystallographic data (excluding structure factors) for the structures reported in this paper have been deposited with the Cambridge Crystallographic Data Centre as supplementary publication no. CCDC-100733. Copies of the data can be obtained free of charge on application to The Director, CCDC, 12 Union Road, Cambridge CB2 1EZ, UK [Fax: (internat.) +44(0)1223/336033; e-mail: teched@chemcrys.cam.ac.uk].

[97270]

Mesomorphic Cyclometalated (Cyclopentadienyl)palladium and -platinum Complexes

Mauro Ghedini*, Francesco Neve, and Daniela Pucci

Dipartimento di Chimica, Università della Calabria,
I-87030 Arcavacata (CS), Italy
Fax: (internat.) + 39-984/492062
E-mail: ghedini@ccusc1.unical.it

Received December 25, 1997

Keywords: Metallomesogens / Azo compounds / Palladium / Platinum / Cyclopentadienyl complexes

The mesogenic 4,4′-bis[4-(*n*-octyloxy)benzoyloxy]azobenzene (HL) ligand reacts with $[(PhCN)_2PdCl_2]$ to give the dinuclear cyclometalated complex $[(\mu\text{-Cl})(L)Pd]_2$ (**1**), from which the mononuclear half-sandwich $[(\eta^5\text{-}C_5H_5)(L)Pd]$ (**2**) species has been obtained by reaction with $Tl(C_5H_5)$. The Pt^{II} analogue of **2**, $[(\eta^5\text{-}C_5H_5)(L)Pt]$ (**4**), has been prepared in a similar manner starting from $[(\mu\text{-Cl})(L)Pt]_2$ (**3**). Both dinuclear complexes **1** and **3** display a smectic C phase (S_C) stable over 80°C. Whereas **4** is the first example of an 18-electron Pt^{II} mesogen, both mononuclear **2** and **4** are mesomorphic materials that exhibit a nematic phase spanning a wide temperature range.

Introduction

Cyclometalation of group-10 metals[1] still attracts a steady interest since the pioneering work of early sixties.[2] The interest has been considerably revived upon the discovery of thermotropic mesomorphism (i.e. liquid-crystal behaviour under temperature variation) in some halo-bridged dinuclear *ortho*-palladated complexes.[3] Since then, the area of transition-metal-based mesogens (*metallomesogens*)[4] has enlarged considerably, becoming rapidly a hot topic in materials science.[5][6] Although the variety of species has increased in recent years,[7][8] most molecular organometallic mesogens are of the cyclometalated type (and cyclopalladated for the most part) and their chemistry is predominantly that of planar 16-electron complexes.

Recently, we became involved in the design of high-coordination-number mesogenic complexes, a challenging task currently pursued by many different groups.[9] In a previous communication we described the first examples of liquid-crystalline cyclopalladated azobenzene complexes containing the $\eta^5\text{-}C_5H_5$ ligand.[10] Our aim was to see whether the $(\eta^5\text{-}C_5H_5)Pd$ fragment could be incorporated into a thermotropic molecule without suppressing its mesomorphism. Following our communication, very recently, Lydon et al.[11] reported similar compounds derived from mesogenic Schiff bases. In particular, we proved that the use of symmetrically substituted nematogenic azobenzene ligands ($R = R' = C_6H_{13}$; $R = R' = OC_6H_{13}$) leads to the isolation of low-melting solids which do not exhibited liquid-crystal behaviour, whilst a more anisotropic ligand ($R = OC_6H_{13}$, $R' = OCOC_6H_4OC_8H_{17}$) gave a mesomorphic complex. However, although the latter ligand was able to compensate the reduction in structural anisotropy that originates from the lateral substitution of the organic molecule with a bulky $(\eta^5\text{-}C_5H_5)Pd$ group, a second problem arose. Metalation of the unsymmetrical azobenzene is not stereospecific, and a pair of isomers was obtained as a result of reaction at either one of the phenyl rings which form the azobenzene core.[10]

In order to gain more reliable mesogenic materials (in terms of a reproducible thermal behaviour), it is preferable to avoid isomeric mixtures with uncontrolled composition. Therefore, we decided to go back to symmetrically substituted azobenzene ligands. Thus, taking advantage of the observed beneficial role that the $OCOC_6H_4OC_8H_{17}$ group exerts on the mesomorphism, we considered the 4,4′-bis[4-(*n*-octyloxy)benzoyloxy]azobenzene (HL) ligand.

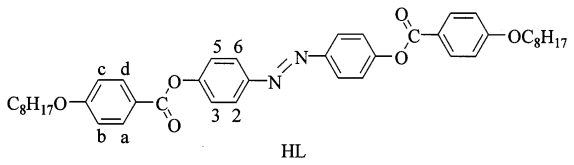

HL

We report here the synthesis of HL and its cyclometalated (cyclopentadienyl)palladium(II) and -platinum(II) derivatives. The mesomorphic properties of both the ligand and complexes are also reported and discussed.

Results and Discussion

Synthesis

The synthesis of HL was carried out by esterification of 4-(*n*-octyloxy)benzoic acid and 4,4′-dihydroxyazobenzene in the presence of 1,3-dicyclohexylcarbodiimide and catalytic amounts of 4-pyrrolidinopyridine. HL is a red solid which was characterized by ^{1}H-NMR spectroscopy (see Experimental Section).

The cyclopalladation of HL with $[(PhCN)_2PdCl_2]$ in benzene/methanol occurred with formation of the dinuclear species $[(\mu\text{-Cl})(L)Pd]_2$ (**1**) in good yield. Both the elemental

 © WILEY-VCH Verlag GmbH, D-69451 Weinheim, 1998 1434−1948/98/0404−0501 $ 17.50+.50/0

analysis and ^{1}H-NMR spectrum of **1** account for the expected formula (Experimental Section).

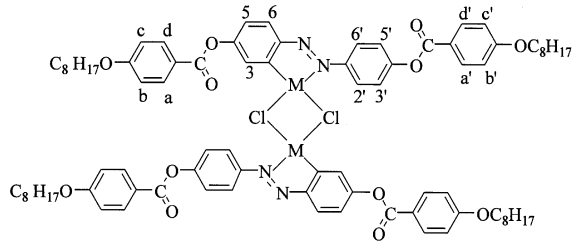

1 M = Pd
3 M = Pt

The subsequent bridge-splitting reaction with $Tl(C_5H_5)$[10][12] gives directly the monocyclopentadienyl complex [(η^5-C_5H_5)(L)Pd] (**2**). Compound **2** is a very soluble, purple-blue (λ_{max} = 574 nm), air-stable solid. Beside the signals of the *o*-deprotonated L ligand, the ^{1}H-NMR spectrum of **2** shows a singlet at δ = 5.88 which corresponds to a cyclopentadienyl ring bound in an η^5 fashion.[12b][13][14] The X-ray structure of the homologous [(η^5-C_5H_5)(pap)Pd] [pap = 2-(phenylazo)phenyl] has been previously reported. The C_5H_5 fragment was observed to assume an η^5 coordination with relevant asymmetry in the Pd−C bonds.[15]

Mesomorphic cycloplatinated complexes are still rare[16][17][18] compared to their palladium counterparts. Synthetic efforts were pushed forward when cycloplatination under mild conditions became affordable through the use of reagents such as [(μ-Cl)(η^3-C_4H_7)Pt]$_2$.[19] Thus, we set out to prepare complex **4**, the platinum analogue of **2**. The best procedure involves the formation of the dinuclear precursor [(μ-Cl)(L)Pt]$_2$ (**3**) through reaction of HL and [(μ-Cl)(η^3-C_4H_7)Pt]$_2$ under reflux conditions. Complex **3** is a dark-red solid wherein *o*-platination is apparent from its ^{1}H-NMR spectrum (see Experimental Section). On further treatment of the dinuclear species with $Tl(C_5H_5)$ no reaction occurred. As earlier noted by Cross et al.[20] this same reaction did not take place for [(μ-Cl)(pap)Pt]$_2$ whatever the excess of $Tl(C_5H_5)$. The reaction instead smoothly proceeds to the desired product if the addition of $Tl(C_5H_5)$ is preceded by bubbling CO through a solution of the chloro-bridged cycloplatinated dimer.[20] Starting from **3**, in situ formation of the orange complex [(CO)(Cl)(L)Pt] [$\tilde{\nu}_{CO}$ = 2102 cm^{-1} (KBr)] was followed by the chloride displacement reaction on addition of an excess of $Tl(C_5H_5)$. Complex [(η^5-C_5H_5)(L)Pt] (**4**) was recovered as a dark-red (λ_{max} = 520 nm), air-stable solid upon purification by cromatography on silica gel. The ^{1}H-NMR spectrum of **4** shows in the region of aromatic protons the pattern typical for an *o*-metalated phenyl ring with no $^nJ(^1H^{195}Pt)$ coupling. A singlet at δ = 5.87, showing satellites due to ^{195}Pt coupling ($^3J_{PtH}$ = 13 Hz), can be safely assigned to an η^5-C_5H_5 ligand.[12b]

Mesomorphic Properties

The mesomorphic properties of the parent ligand HL and complexes **1**−**4** are reported in Table 1. The mesophases were assigned on the basis of their optical textures observed by thermal polarizing microscopy. Thermal and thermodynamic data were obtained through differential scanning calorimetry (DSC).

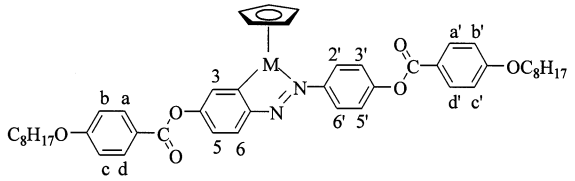

2 M = Pd
4 M = Pt

Table 1. Phase-transition data and assignments[a] for HL, [(μ-Cl)(L)M]$_2$ [M = Pd (**1**); Pt (**3**)], [(η^5-C_5H_5)(L)M] [M = Pd (**2**); Pt (**4**)]

Compound	Transition	*T* [°C]	ΔH [kJ mol^{-1}]
HL	C−S_C	140.0	26.5
	S_C−N	160.0	1.5
	N−I	314.1	3.2
1	C−C′	149.1	13.0
	C′−S_C	249.7	39.4
	S_C−I	330.7[b]	
2	C−N	142.8	37.5
	N−I	226.2	2.8
3	C−S_C	262.9	37.1
	S_C−I	342.0[b]	
4	C−N	160.4	40.8
	N−I	250.0[b]	

[a] C: crystal; S_C: smectic C; N: nematic; I: isotropic liquid. − [b] Decomposition.

HL exhibited enantiotropic smectic C (S_C) and nematic (N) phases, and both showed a marbled texture. Notwithstanding this, the S_C−N transition was clearly indicated by the appearance of characteristic transition bars.[21] The mesomorphism of HL is dominated by the nematic state which occurs over a wide range (some 150°C), whereas the fairly high clearing temperature is related to the high polarizability of the large rigid core of the molecule.

The dinuclear chloro-bridged complexes [(μ-Cl)(L)M]$_2$ (**1**, **3**) are mesogens which display only a smectic C phase (schlieren texture) between 249 and 330°C for **1** and between 262 and 342°C for **3** and decompose at the clearing point. The metal complexation in both cases narrows the mesomorphic range of the ligand with transition temperatures for the platinum complex **3** higher than those of the palladium homologue.

The mononuclear palladium complex **2** melted to a nematic phase which exhibited a marbled texture on heating and a schlieren one on cooling from the melt. Thus, the mesomorphism of the mononuclear palladium derivative becomes dominated by the nematic phase. This is not surprising if one considers the presence of a large substituent (i.e. the organometallic fragment) in the middle of the molecule (which opposes lateral interactions)[9c][22] and of the

two medium-sized alkyl chains (which are unable to stabilize smectic behaviour in this case). With respect to HL, the mononuclear compound **2** preserves a similar melting temperature although the stability of the nematic phase is much reduced. Both the presence of a single, nematic phase and the substantial lowering of the clearing point (some 90°C) are a likely consequence of the reduced anisotropy of molecular shape,[9d][9e][23][24] at least if no further effects (e.g. changes in the polarizability anisotropy and/or dipole moment variations following the lateral substitution) must be taken into account.

Changing palladium complex **2** for platinum complex **4** increases about 20°C both the melting and the clearing temperatures of the complex (Table 1), in line with the expected increase in polarizability by introduction of platinum. This trend has been seen at work in other Pd and Pt homologous series of calamitic mesogens.[15][18][25] However, more examples are needed to establish a general, less controversial behaviour since an opposite trend has occasionally been observed.[26] The increased stability of the nematic phase of **4** with respect to **2** is, however, thwarted by its lower thermal stability (toward decomposition) in the isotropic state.

Conclusions

Palladium(II) and platinum(II) mesogens are commonly available as planar, 16-electron species. In principle, the possibility to prepare metallomesogens with higher coordination numbers is restricted only by the loss of structural anisotropy as a consequence of extra coordination. However, from related studies on high-coordination-number calamitic mesogens we know that this disadvantage can be overcome by using ligands with high structural anisotropy.[22]

We have now demonstrated that the metalation of the highly anisotropic, mesogenic HL ligand through well-tested synthetic procedures allows the formation of 18-electron Pd^{II} and Pt^{II} species which are nematic liquid crystals. Interestingly, reporting the only other example of an 18-electron half-sandwich, isomerically pure palladium mesogen, the authors have pointed out the high tendency of this class of compounds to give preferentially nematic phases.[11][27] In conclusion, sterically demanding organometallic Pd^{II} and Pt^{II} mesogens can be conveniently prepared using the cyclopentadienyl group as a co-ligand. Whilst the only price to pay at this stage is a reduction in thermal stability of the mesogenic azobenzene precursor, this approach opens the way to further novel organometallic materials with interesting physical properties.

We thank the *Ministero dell' Università e della Ricerca Scientifica e Tecnologica* (MURST) and the *Consiglio Nazionale delle Ricerche* (CNR) for financial support.

Experimental Section

4-(*n*-Octyloxy)benzoic acid, 1,3-dicyclohexylcarbodiimide (DCC), 4-pyrrolidinopyridine (PPy), and thallium cyclopentadienide were available from Aldrich, and they were used as received. 4,4′-Dihydroxyazobenzene was prepared according to a published method.[28] − IR spectra were recorded as KBr pellets or nujol mulls with a Perkin Elmer System-2000 FT spectrophotometer. − ^{1}H-NMR spectra were obtained with a Bruker AC300 spectrometer with tetramethylsilane as an internal standard. − Elemental analyses were performed using a Perkin Elmer 2400 microanalyzer. − Absorption spectra were recorded with a Hitachi U-2000 spectrophotometer. − Phase transitions and optical textures were assigned by thermal optical microscopy by means of a Zeiss Axioskop polarizing microscope, equipped with a heating stage and a temperature-control unit. Transition temperatures and enthalpies were determined by differential scanning calorimetry (DSC) using a Perkin Elmer DSC-7 calorimeter operating at a scanning rate of 10°C min^{-1}.

4,4′-Bis[4-(n-octyloxy)benzoyloxy]azobenzene (HL): A mixture of 4,4′-dihydroxyazobenzene (0.40 g, 1.87 mmol), 4-(*n*-octyloxy)-benzoic acid (0.94 g, 3.74 mmol), DCC (0.85 g, 4.11 mmol), and PPy (0.055 g, 0.37 mmol) in dichloromethane (40 ml) was stirred at room temperature for 7 d. A grey solid was filtered off and the orange filtrate was washed with H_2O (2 × 30 ml), 5% CH_3COOH (2 × 25 ml), and H_2O (2 × 30 ml). The organic layer was dried with $NaSO_4$, then taken to dryness under reduced pressure. The yellow solid residue was recrystallized from dichloromethane/diethyl ether. Yield 0.69 g (54%). − ^{1}H NMR (300 MHz, $CDCl_3$): δ = 8.17 (d, *J* = 8.8 Hz, 2 H, $H^{a,d}$), 8.01 (d, *J* = 8.8 Hz, 2 H, $H^{2,6}$), 7.37 (d, *J* = 8.8 Hz, 2 H, $H^{3,5}$), 6.99 (d, *J* = 8.8 Hz, 2 H, $H^{b,c}$), 4.05 [t, *J* = 6.6 Hz, 2 H, $OCH_2(CH_2)_6CH_3$], 1.83 [m, 2 H, $OCH_2CH_2(CH_2)_5CH_3$], 1.50−1.29 [m, 10 H, $OCH_2CH_2(CH_2)_5CH_3$], 0.90 (t, *J* = 6.6 Hz, 3 H, CH_3). − IR (KBr): $\tilde{\nu}$ = 1740, 1730 cm^{-1} (COO). − $C_{42}H_{50}N_2O_6$ (678.9): calcd. C 74.31, H, 7.42, N, 4.13; found C 73.86, H, 7.45, N, 4.36.

Preparation of [(μ-Cl)(L)Pd]$_2$ (**1**): A suspension of the HL ligand (0.3 g, 0.44 mmol) in methanol (15 ml) was added to a stirred solution of an equimolar amount of $[(PhCN)_2PdCl_2]$ in benzene (15 ml) and the mixture was heated for 48 h at 100°C. The resulting orange solid was filtered off and recrystallized from hot methanol. Yield 0.29 g (80%). − ^{1}H NMR (300 MHz, $CDCl_3$): δ = 8.09 (d, 2 H, $H^{a,d}$), 8.07 (d, 2 H, $H^{a',d'}$), 7.92 (d, 2 H, $H^{2',6'}$), 7.89 (d, 1 H, H^6), 7.34 (d, 2 H, $H^{3',5'}$), 7.18 (d, 1 H, H^3), 7.13 (dd, 1 H, H^5), 6.92 (d, 2 H, $H^{b,c}$), 6.89 (d, 2 H, $H^{b',c'}$), 4.03 [t, 2 H, $OCH_2(CH_2)_6CH_3$], 3.97 [t, 2 H, $OCH_2(CH_2)_6CH_3$]. − $C_{84}H_{98}Cl_2N_4O_{12}Pd_2$ (1639.4): calcd. C 61.54, H 6.02, N 3.42; found C 61.35, H 6.11, N 3.07.

Preparation of [(η^5-C$_5$H$_5$)(L)Pd] (**2**): $Tl(C_5H_5)$ (0.03 g, 0.12 mmol) was added to a solution of $[Pd(\mu\text{-}Cl)(L)]_2$ (0.1 g, 0.06 mmol) in benzene (10 ml) and the mixture was stirred under nitrogen. After 4 h, the mixture was filtered and the dark filtrate was concentrated in a rotary evaporator. Recrystallization of the solid residue from chloroform/ethanol afforded the product as a dark blue microcrystalline solid. Yield 0.083 g (80%). − ^{1}H NMR (300 MHz, $CDCl_3$): δ = 8.28 (d, *J* = 8.6 Hz, 1 H, H^6), 8.17 (d, *J* = 8.8 Hz, 2 H, $H^{a,d}$), 8.16 (d, *J* = 8.8 Hz, 2 H, $H^{a',d'}$), 7.93 (d, *J* = 8.8 Hz, 2 H, $H^{2',6'}$), 7.72 (d, *J* = 2.3 Hz, 1 H, H^3), 7.27 (d, *J* = 9.0 Hz, 2 H, $H^{3',5'}$), 7.08 (dd, *J* = 8.6, 2.3 Hz, 1 H, H^5), 6.99 (d, *J* = 8.8 Hz, 4 H, $H^{b,c}$ + $H^{b',c'}$), 5.88 (s, 5 H, Cp), 4.06 [t, *J* = 6.6 Hz, 4 H, $OCH_2(CH_2)_6CH_3$], 1.84 [m, 4 H, $OCH_2CH_2(CH_2)_5CH_3$], 1.51−1.30 [m, 20 H, $OCH_2CH_2(CH_2)_5CH_3$], 0.90 (t, *J* = 6.6 Hz, 6 H, CH_3). − IR (nujol): $\tilde{\nu}$ = 1724 cm^{-1} (COO). − UV/Vis (3 × 10^{-5} M $CHCl_3$ solution): λ_{max} (ε) = 264 (56300), 331 (18100), 418 (11850), 574 nm (5780). − $C_{47}H_{54}N_2O_6Pd$ (849.3): calcd. C 66.46, H 6.41, N 3.30; found C 67.02, H 6.41, N 3.05.

Preparation of [(μ-Cl)(L)Pt]$_2$ (**3**): A solution of $[(\mu\text{-}Cl)(\eta^3\text{-}C_4H_7)Pt]_2$ (0.08 g, 0.15 mmol) and HL ligand (0.2 g, 0.30 mmol) in 15 ml of toluene was refluxed for 12 h and then cooled. The

precipitate was collected by filtration and purified by recrystallization from chloroform/diethyl ether to give a dark-red solid. Yield 0.174 g (65%). – ^{1}H NMR (300 MHz, $CDCl_3$): δ = 8.10 (d, *J* = 9.1 Hz, 2 H, $H^{a,d}$), 8.07 (d, *J* = 9.1 Hz, 2 H, $H^{a',d'}$), 7.96 (d, *J* = 8.4 Hz, 1 H, H^6), 7.86 (d, *J* = 8.8 Hz, 2 H, $H^{2',6'}$), 7.39 (d, *J* = 8.8 Hz, 2 H, $H^{3',5'}$), 7.13 (d, *J* = 2.0 Hz, 1 H, H^3), 7.09 (dd, *J* = 8.4, 2.0 Hz, 1 H, H^5), 6.94 (d, *J* = 9.1 Hz, 2 H, $H^{b,c}$), 6.89 (d, *J* = 9.1 Hz, 2 H, $H^{b',c'}$), 4.04 [t, *J* = 6.6 Hz, 4 H, $OCH_2(CH_2)_6CH_3$], 4.00 [t, *J* = 6.6 Hz, 4 H, $OCH_2(CH_2)_6CH_3$]. – $C_{84}H_{98}Cl_2N_4O_{12}Pt_2$ (1816.8): calcd. C 55.53, H 5.46, N 3.08; found C 56.23, H 5.64, N 3.31.

Preparation of [(η^5-C$_5$H$_5$)(L)Pt] (**4**): A brown suspension of $[(\mu\text{-Cl})(L)Pt]_2$ (0.14 g, 0.08 mmol) in benzene/diethyl ether (50 ml, 3:2, v/v) turned dark-orange after bubbling CO through the mixture and stirring was continued for 3 h. $Tl(C_5H_5)$ (0.21 g, 0.78 mmol) was added to the mixture which turned dark-red, then dark-violet within 1 h. After filtration of the greyish solid, the solution was concentrated in a rotary evaporator to give a sticky, dark solid. The crude product was chromatographed by using silica gel with *n*-hexane/diethyl ether (1:1) as eluent. The product was eluted first as a dark-red fraction. Removal of the solvent afforded **4** as a dark-red powder. Yield 0.083 g (55%). – ^{1}H NMR (300 MHz, $CDCl_3$): δ = 8.33 (d, *J* = 8.7 Hz, 1 H, H^6), 8.18 (d, *J* = 8.9 Hz, 2 H, $H^{a,d}$), 8.17 (d, *J* = 8.9 Hz, 2 H, $H^{a',d'}$), 7.84 (d, *J* = 8.9 Hz, 2 H, $H^{2',6'}$), 7.82 (d, *J* = 2.4 Hz, 1 H, H^3), 7.27 (d, *J* = 8.9 Hz, 2 H, $H^{3',5'}$), 7.01 (dd, *J* = 8.7, 2.4 Hz, 1 H, H^5), 6.98 (d, *J* = 8.8 Hz, 4 H, $H^{b,c}$ + $H^{b',c'}$), 5.87 [s, ^3J(PtH) = 13 Hz, 5 H, Cp], 4.06 [t, *J* = 6.6 Hz, 4 H, $OCH_2(CH_2)_6CH_3$], 1.84 [m, 4 H, $OCH_2CH_2(CH_2)_5CH_3$], 1.49–1.30 [m, 20 H, $OCH_2CH_2(CH_2)_5CH_3$], 0.90 (t, *J* = 6.6 Hz, 6 H, CH_3). – IR (nujol): $\tilde{\nu}$ = 1722 cm^{-1} (COO). – UV/Vis (3 × 10^{-5} M $CHCl_3$ solution): λ_{max} (ε) = 263 (30270), 342 (8400), 366 (8200), 520 nm (6450). – $C_{47}H_{54}N_2O_6Pt$ (938.0): calcd. C 60.18, H 5.80, N 2.99; found C 60.40, H 5.81, N 2.91.

[1] [1a] G. R. Newkome, W. E. Puckett, V. K. Gupta, G. E. Kiefer, *Chem. Rev.* **1986**, *86*, 451. – [1b] A. D. Ryabov, *Chem. Rev.* **1990**, *90*, 403. – [1c] E. W. Abel, F. G. A. Stone, G. Wilkinson, *Comprehensive Organometallic Chemistry II*, vol. 9, Pergamon, Oxford, **1995**.

[2] [2a] J. K. Kleiman, M. Dunbeck, *J. Am. Chem. Soc.* **1963**, *85*, 1544. – [2b] A. C. Cope, R. W Siekman, *J. Am. Chem. Soc.* **1965**, *87*, 3272.

[3] M. Ghedini, M. Longeri, R. Bartolino, *Mol. Cryst. Liq. Cryst.* **1982**, *84*, 207.

[4] [4a] P. Espinet, M. A. Esteruelas, L. A. Oro, J. L. Serrano, E. Sola, *Coord. Chem. Rev.* **1992**, *117*, 215. – [4b] S. Hudson, P. M. Maitlis ,*Chem. Rev.* **1993**, *93*, 861. – [4c] A. E. Polishchuk, T. V. Timofeeva, *Russ. Chem. Rev.* **1993**, *62*, 291. – [4d] L. Oriol, J. L. Serrano, *Adv. Mater.* **1995**, *7*, 348. – [4e] R. Deschenaux, J. W. Goobdy, in *Ferrocenes* (Eds.: A. Togni, T. Hayashi), VCH, Weinheim, **1995**. – [4f] F. Neve *Adv. Mater.* **1996**, *8*, 277.

[5] D. W. Bruce in *Inorganic Materials* (Eds.: D. W. Bruce, D. O′Hare), Wiley, Chichester, **1992**.

[6] J. L. Serrano, *Metallomesogens*, VCH, Weinheim, **1996**.

[7] [7a] T. Kaharu, R. Ishii, S. Takahashi, *J. Mater. Chem.* **1994**, *4*, 859. – [7b] T. Kaharu, R. Ishii, S. Takahashi, *J. Chem. Soc., Chem. Commun.* **1994**, 1349. – [7c] T. Kaharu, R. Ishii, T. Adachi, T. , T. Yoshida, S. Takahashi, *J. Mater. Chem.* **1995**, *5*, 687. – [7d] R. Ishii, T. Kaharu, N. Pirio, S. W. Zhang, S. Takahashi, *J. Chem. Soc., Chem. Commun.* **1995**, 1215. – [7e] S. W. Zhang, R. Ishii, S. Takahashi, *Organometallics* **1997**, *16*, 20.

[8] [8a] M. Benouazzane, S. Coco, P. Espinet, J. M. Martin-Alvarez, *J. Mater. Chem.* **1995**, *5*, 441. – [8b] P. Alejos, S. Coco, P. Espinet, J. M. Martin- Alvarez, *New J. Chem.* **1995**, *19*, 799. – [8c] S. Coco, P. Espinet, S. Falagan, J. M. Martin-Alvarez, *New J. Chem.* **1995**, *19*, 959. – [8d] S. Coco, P. Espinet, J. M. Martin-Alvarez, A. M. Levelut, *J. Mater. Chem.* **1997**, *7*, 19.

[9] [9a] H. Zheng, T. M. Swager, *J. Am. Chem. Soc.* **1994**, *116*, 761. – [9b] U. Stebani, G. Lattermann, M. Wittenberg, J. H. Wendorff, *Angew. Chem. Int. Ed. Engl.* **1996**, *35*, 1858. – [9c] E. Campillos, R. Deschenaux, A. M. Levelut, R. Ziessel, *J. Chem. Soc., Dalton Trans.* **1996**, 2533. – [9d] S. Morrone, D. Guillon, D. W. Bruce, *Inorg. Chem.* **1996**, *35*, 7041. – [9e] K. E. Rowe, D. W. Bruce, *J. Chem. Soc., Dalton Trans.* **1996**, 3913.

[10] M. Ghedini, D. Pucci, F. Neve, *Chem. Commun.* **1996,** 137.

[11] D. P. Lydon, G. W. V. Cave, J. P. Rourke *J. Mater. Chem.* **1997**, *7*, 403.

[12] [12a] G. K. Anderson, R. J. Cross, I. G. Phillips, *J. Chem. Soc., Chem. Commun.* **1978**, 709. – [12b] G. K. Anderson, R. J. Cross, S. Fallis, M. Rocamora, *Organometallics* **1987**, *6*, 1440.

[13] A. Albinati, S. Affolter, P. S. Pregosin, *Organometallics* **1990**, *9*, 379.

[14] S. Fallis, S. , L. Rodriguez, G. K. Anderson, N. P. Rath, *Organometallics* **1993**, *12*, 3851.

[15] G. K. Anderson, R. J. Cross, K. W. Muir, L. Manojlovic-Muir, *J. Organomet. Chem.* **1989**, *362*, 225.

[16] K. Praefcke, B. Bilgin, J. Pickardt, M. Borowsski, *Chem. Ber.* **1994**, *127*, 1543.

[17] K. Praefcke, B. Bilgin, N. Usol′tseva, B. Heinrich, D. Guillon, *J. Mater. Chem.* **1995**, *5*, 2257.

[18] J. Buey, L. Diez, L. , P. Espinet, H. S. Kitzerow, J. A. Miguel, *Chem. Mater.* **1996**, *8*, 2375.

[19] P. S. Pregosin, F. Wombacher, A. Albinati, F. Lianza, *J. Organomet. Chem.* **1991**, *418*, 249.

[20] R. J. Cross, N. H. Tennent, G. M. Warden, *J. Chem. Soc., Dalton Trans.* **1986**, 1059.

[21] D. Demus, L. Richter, *Textures of liquid crystals,* Verlag Chemie, Weinheim, **1978**.

[22] D. W. Bruce, *Adv. Mater.* **1994**, *6*, 699.

[23] M. J. Baena, P. Espinet, M. B. Ros, J. L. Serrano, *Angew. Chem. Int. Ed. Engl.* **1991**,*30*, 711.

[24] [24a] D. W. Bruce, X. –H. Lin, *J. Chem. Soc., Chem. Commun.* **1994**, 729. – [24b] D. W. Bruce, X. –H. Lin, *Liq. Cryst.* **1995**, *18*, 165.

[25] [25a] D. W. Bruce, E. Lalinde, P. Styring, D. A. Dunmur, P. M. Maitlis, *J. Chem. Soc., Chem. Commun.* **1986**, 581. – [25b] H. Adams, N. A. Bailey, D. W. Bruce, D. A. Dunmur, E. Lalinde, M. Marcos, C. Ridgeway, A. J. Smith, P. Styring, P. M. Maitlis, *Liq. Cryst.* **1987**, *2*, 381.

[26] T. Kaharu, S. Takahashi, *Chem. Lett.* **1992**, 1515.

[27] A referee raised the possibility for compounds **2** and **4** to observe the elusive phenomenon of nematic biaxiality. Although we have not investigated in this direction, we believe that the structural characteristics of such P-shaped compounds are not fully compatible with the steric requirements for thermotropic biaxial mesogens: [27a] S. Chandrasekar, B. R. Ratna, B. K. Sadashiva, V. N. Raja, *Mol. Cryst. Liq. Cryst.* **1988**, *165*, 123. – [27b] C. Versace, R. Bartolino, M. Ghedini, F. Neve, S. Armentano, M. Petrov, N. Kirov, *Liq. Cryst.* **1990**, *8*, 481. – [27c] J. Szydlowska, W. Pyzuk, A. Krowcynski, I. Bikchantaev, *J. Mater. Chem.* **1996**, *6*, 733.

[28] R. Willstätter, M. Benz, *Ber. Dtsch. Chem. Ges.* **1906**, *39*, 3495.

[97284]

Contributions to the Chemistry of Boron, 242[◇]

Rearrangement of Bis(dimethylamino)bis(1-indenyl)diborane(4) into Bis(dimethylamino)bis(3-indenyl)diborane(4)☆

Jörg Knizek, I. Krossing, Heinrich Nöth*, and Werner Ponikwar

Institute of Inorganic Chemistry, University of Munich
Meiserstraße 1, D-80333 München, Germany

Received October 15, 1997

Keywords: Chlorobis(dimethylamino)(3-indenyl)diborane(4) / Bis(dimethylamino)bis(1-indenyl)diborane(4) / Bis(dimethylamino)(1-indenyl)(3-indenyl)diborane(4) / Bis(dimethylamino)bis(3-indenyl)diborane(4) / Rearrangement / X-ray structures

Indenyllithium reacts with dichlorobis(dimethylamino)diborane(4) with formation of bis(dimethylamino)bis(1-indenyl)-diborane(4) which rearranges on heating to the isomer bis(dimethylamino)bis(3-indenyl)diborane(4). The "mixed" bis(dimethylamino)(1-indenyl)(3-indenyl)diborane(4) is obtained from indenyllithium and chlorobis(dimethylamino)(3-indenyl)diborane(4). The main structural differences between the two isomers **3** and **4** are a slightly shorter B−B bond in **4**, as well as a stronger twist about the B−B bond (89.9° vs. 67.4°) and, as expected, a shorter B−C bond. There is, however, no significant B−C π bonding.

Bis(dimethylamino)diorganyldiboranes(4) $(Me_2N)RB-BR(NMe_2)$ may either be reduced to their dianions $[B_2(NMe_2)_2R_2]^{2-}$ which feature a B=B double bond[2] or may be deprotonated to a diborabutadiene dianion $[R'_2=B(NMe_2)-B(NMe_2)=R']^{2-}$ (R′ = CHR'_2) provided that the organyl group carries a sufficiently acidic hydrogen atom[3]. The first route has been verified for R = phenyl,[2] the second for R′ = fluorenyl[3][4] and benzyl[5]. The alkali-metal salts of $B_2(NMe_2)_2(CR'_2)_2^{2-}$ not only show a noticeable variation of structures[3][5] but have also proved to be useful reagents for the preparation of new heterocycles such as 1-stanna-3,4-diborolanes or 1-plumba-3,4-diborolanes and 1,2-diboretanes[6]. Other diorganyldiboranes(4) that might readily be deprotonated are indenyl and cyclopentadienyl derivatives. These are expected to exhibit a different reactivity compared to the fluorenyldiborane(4) compounds because they are less acidic, are sterically less demanding, and their alkali-metal salts may therefore display different structural motifs. Here we report on the synthesis and structural characterisation of bis(dimethylamino)bis(indenyl)diboranes(4)[7].

Synthesis

There are at least four different synthetic pathways by which the synthesis of bis(dimethylamino)bis(indenyl)diboranes(4) can be achieved. These are summarized in Scheme 1.

The most straightforward pathway is described by eq. 1 while the route shown in eq. 2 may suffer from deprotonation of the indenyl group; this would lead to B−C bond formation in competition to B−B bond formation.

Scheme 1

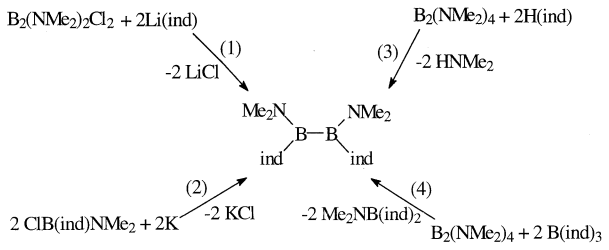

$$B_2(NMe_2)_2Cl_2 + Li(ind) \longrightarrow Me_2N(1\text{-ind})B\text{-}B(Cl)NMe_2 + LiCl \quad (5)$$

$$Me_2N(1\text{-ind})B\text{-}B(Cl)NMe_2 \xrightarrow{\Delta} Me_2N(3\text{-ind})B\text{-}B(Cl)NMe_2 \quad (6)$$

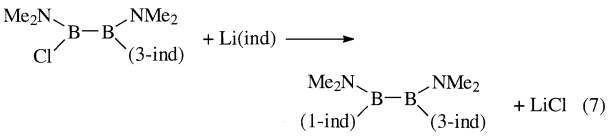

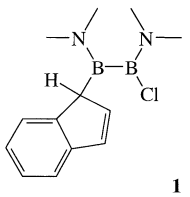

1

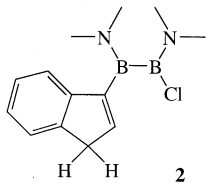

2

The results of eq. 3 depend on the acidity of indene and the Lewis acidity of the boron atoms in $B_2(NMe_2)_2(ind)_2$ which may prevent the liberation of Me_2NH and hence the synthesis of $B_2(NMe_2)_2(ind)_2$. The substituent exchange according to eq. 4 is prevented simply by the access to tri(in-

[◇] Part 241: Ref.[1].

 © WILEY-VCH Verlag GmbH, D-69451 Weinheim, 1998 1434−1948/98/0404−0505 $ 17.50+.50/0

denyl)borane, an as yet unknown triorganylborane. Consequently we studied the reaction described by eq. 1.

In toluene a surprising result was observed as even after 20 h at ambient temperature only monosubstitution with formation of chlorobis(dimethylamino)(indenyl)diborane(4) (**1**) occurred which was present in solution as the 1-indenyl isomer (eq. 5). On distillation **1** converted into the 3-indenyl isomer **2** (eq. 6).

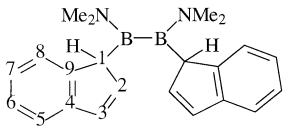

3

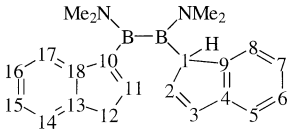

4

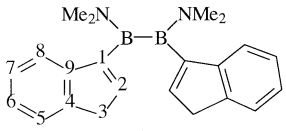

5

However, when a small amount of THF was added to the reaction mixture as described by eq. 1 then **1** was only an intermediate on route to bis(dimethylamino)bis(1-indenyl)diborane. Under these conditions **3** was formed and isolated in acceptable yields (55%).

Heating solutions of **3** in toluene under reflux converted this compound into its bis(3-indenyl)derivative **5**. Following this rearrangement using ^{1}H- and ^{13}C-NMR spectroscopy provided evidence that the "mixed" isomer **4** is an intermediate. Actually, **4** can be readily prepared from the chloro(3-indenyl)diborane(4) **2** by allowing it to react with Li(ind) at ambient temperature as shown in eq. 7.

Experiments designed to obtain bis(cyclopentadienyl)bis(dimethylamino)diborane(4) have so far failed. The reaction of TlCp with $(Me_2N)_2B_2Cl_2$ in toluene led to a solution that contained primarily the starting diborane(4) compound in addition to unidentified products (ratio 9:1 according to ^{11}B-NMR spectroscopy). Activation by ultrasound or replacement of TlCp by NaCp and the use of THF as a solvent lead to ether cleavage.

NMR Spectra

NMR-spectroscopic data on compounds **2**−**5** are summarized in the Experimental Section. Assignments were made from the analysis of ^{1}H-^{1}H-COSY and ^{1}H-^{13}C-HETCOR experiments.

The ^{11}B resonances of the indenyldiboranes(4) **3**−**5** all lie in a very narrow range, $\delta = 48 \pm 2$, irrespective of whether the indenyl group is present as the 1- or 3-isomer. However, the linewidth increases as the number of the 3-indenyl groups increases. The observed shielding corresponds to dialkylbis(dimethylamino)diboranes(4)[8]. 3-Indenyl groups should actually lead to a better shielding due to possible B−C π bonding as observed for amino(vinyl)boranes[9]. Therefore, we can assume that the 3-indenyl group is not coplanar with the B_2NC plane. Two ^{1}H- and ^{13}C-NMR signals for the dimethylamino group in **5** indicate hindered rotation about the B−N bonds. In the case of compound **4** there are even four ^{1}H-NMR signals of equal intensity as well as four ^{13}C resonances, which again demonstrate hindered rotation about the B−N bonds. Surprisingly, compound **3** displays eight signals for the Me_2N groups in the ^{1}H-NMR spectrum and shows six ^{13}C resonances. This fact can only be rationalized by assuming the presence of rotamers.

Compound **2** is exceptional in so far as one would expect two separated ^{11}B-NMR signals but only one is actually observed. This can be explained by an inductive effect of the B(Cl)NMe_2 group which brings about stronger B−N bonding on the neighbouring R(Me_2N)B group, as indicated by a deshielding of the protons of the dimethylamino groups. It is a well-known phenomenon that the ^{13}C resonances of carbon atoms bound to a boron atom are often difficult to detect due to the quadrupole-induced broadening of its resonance[8]. Thus only the ^{13}C resonances of the C atom of the 1-indenyl compounds could be determined but not those of the 3-indenyl groups.

The NMR data also suggest free rotation about the B−B bond. However, for the bis(1-indenyl)diborane(4) **3** hindered rotation about the B−C bonds may also be possible. Nevertheless, no firm conclusions as to the structure of the dominant conformation could be derived from NMR experiments. We therefore determined the molecular structures by X-ray crystallography although the results are, of course, restricted to the solid state.

Molecular Structures

Two of the indenyldiboranes(4) gave single crystals from hexane solutions suitable for an X-ray diffraction study. Figures 1 and 2 depict the results whilst Table 1 contains the bonding parameters.

The molecular structures of **3** and **4** confirm the conclusions drawn from the NMR data that **3** contains 1-indenyl groups only, while **4** carries both a 1-indenyl and 3-indenyl substituent.

A significant structural feature of both compounds is the B−B bond, which seems to be slightly longer in **3** than in **4**. However, both B−B bonds are longer than found for the comparable diborane(4) derivatives 1,2-difluorenyl-1,2-dipyrrolidinodiborane(4) [1.697(4) Å][10], 1,2-bis(dimethylamino)-1,2-bis(phenylethynyl)diborane(4) [1.696(8) Å][10], 1,2-bis(dimethylamino)-1,1-diphenyldiborane(4) [1.714(4) Å] and 1,2-bis(dimethylamino)-1,2-dimesityldiborane(4) [1.72(1) Å][11]. It appears from these data that the B−B bond length increases slightly when tetracoordinated C atoms are replaced by trigonal-planar C atoms.

B−N π bonding is indicated by the B−N bond lengths in compounds **3** and **4** which range from 1.386(4)−1.403(2) Å; this fits not only with the hindered rotation about the B−N bonds but also with many other B−N bond lengths of aminoboranes(4)[11]. However, one should note that in compound **4** the longer B−N bond is associated with the boron atom that carries the 1-indenyl substituent. The shorter B−N bond is found at the boron atom with the 3-

Table 1a. Selected bond lengths [Å] and bond angles [°] of compounds **3** and **4**; estimated standard deviations are given in parantheses

Bond lengths	**3**	**4**	Bond angles	**3**	**4**
B1−B2	1.726(4)	1.716(3)	N1−B1−C5	121.6(2)	119.3(2)
B1−N1	1.393(4)	1.403(2)	N1−B1−B2	122.1(3)	121.8(2)
B2−N2	1.386(4)	1.390(4)	C5−B1−B2	116.3(2)	118.8(1)
B1−C5	1.631(4)	1.621(3)	C14−B2−N2	118.0(3)	120.4(2)
B2−C14	1.640(5)	1.583(5)	N2−B2−B1	123.2(3)	125.7(2)
C5−C6	1.495(5)	1.512(2)	C14−B2−B1	118.6(3)	113.9(2)
C6−C7	1.341(4)	1.331(3)	B1−N1−C4	126.1(3)	126.7(2)
C7−C8	1.459(5)	1.470(3)	C4−N1−C3	111.4(3)	111.2(2)
C8−C9	1.401(4)	1.402(3)	B1−N1−C3	122.5(3)	122.1(2)
C9−C5	1.516(4)	1.509(3)	B2−N2−C2	122.9(3)	123.1(2)
C14−C15	1.537(5)	1.351(3)	B2−N2−C1	126.2(3)	124.9(2)
C15−C16	1.307(5)	1.505(3)	C1−N2−C2	110.9(3)	111.9(2)
C16−C17	1.498(5)	1.504(3)	B1−C5−C9	120.9(2)	107.0(1)
C17−C18	1.386(5)	1.403(3)	B1−C5−C6	113.1(2)	114.4(1)
C14−C18	1.484(5)	1.488(2)	B2−C14−C18	115.5(2)	127.3(2)
			B2−C14−C15	113.0(3)	125.8(2)

Table 1b. Selected torsion and interplanar angles [°] of compounds **3** and **4**

Torsion angles	**3**	**4**	Interplanar angles	**3**	**4**
N1−B1−B2−N2	67.4	89.9	C5−C9/C14−C18	104.2	3.4
C1−N2−B2−B1	177.6	−178.6	C8−C13/C17−C22	105.9	5.6
C4−N2−B1−B2	−174.4	168.8	C14−B2−N2/ C5−B−N1	65.3	92.3
C5−B1−B2−C14	63.6	85.9			

Figure 1. The molecular structure of the bis(1-indenyl)diborane(4) derivative **3** in the crystal; thermal ellipsoids are shown on a 25% probability level; hydrogen atoms (except those of the unique CH_2 groups) are omitted for clarity

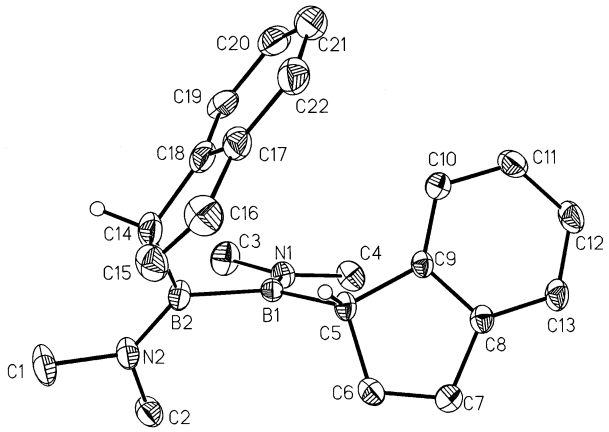

indenyl group; this atom is expected to participate in B−C π bonding with a consequent weakening of B−N π bonding.

As expected the lengths of the B−C bonds to the 1-indenyl groups are longer than the B−C bonds of the 3-indenyl substituent reflecting the different hybridization at the carbon atoms. Moreover, the C−C bond lengths clearly show that there is no electron delocalisation in the five-membered rings, and even the benzo rings show significantly different C−C bond lengths due to the disturbance by the *o*-disubstitution.

Figure 2. The molecular structure of the "mixed" bis(1-indenyl)diborane(4) derivative **4** in the crystal; thermal ellipsoids are drawn on a 25% probability level; hydrogen atoms (except for the unique CH and CH_2 group) are omitted for clarity

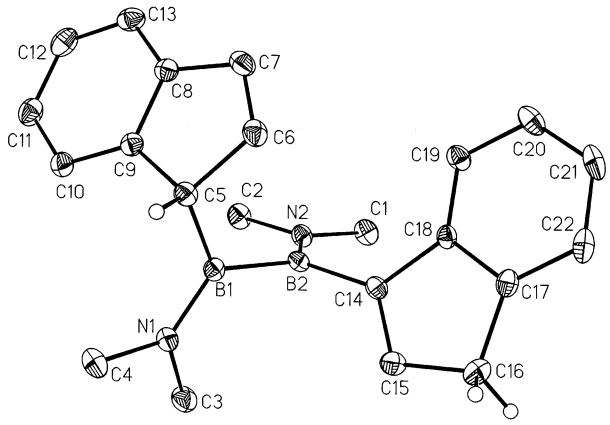

Strong B−N π bonding is indicated not only by short B−N bond lengths but also by planar geometry around the nitrogen and boron atoms. This is the case for these atoms in **3** and **4**. Moreover, the C_2N plane should be coplanar with the B_2C plane, e.g. the torsion angle C−N−B−B should be 0°. This is almost fulfilled for both compounds under consideration, the largest torsion angle being 11.0° (C11−N1−B1−B2 in **4**). While there is little difference between the two molecules there is a large conformational difference in the N−B−B−N torsion angle which is 67.4° for **3** but 89.9° for **4**. Another feature that determines the molecular shape of these molecules in the solid state is the orientation of the respective C^3 parts of the indenyl groups. For **3** the C5C6C9 plane is twisted against the N1B1B2 plane by 75.2°, and the C14C15C18 plane twisted against the N2B2B1 plane by 68.6°. In contrast, the C14C15C18 plane of the 3-indenyl group is rotated out of the N2B2B1 plane by 63.0° while the C5C6C9 plane is twisted against the N1B1B2 plane by 71.6°. As can be seen from Figure 1 the 1-indenyl groups are arranged in such a manner that the unique CH protons (on C5, C14) point in the same direction. This conformation is rather similar to that found in bis(dimethylamino)difluorenyldiborane(4)[10].

Discussion

The study of the indenyldiboranes(4) **2**−**5** show conclusively that the 1-indenyl derivatives represent the kinetic products while the 3-indenyl isomers are the stable thermodynamic products. The former are obtained from indenyllithium and $B_2Cl_2(NMe_2)_2$ at ambient temperature and rearrange to the latter on heating of their toluene solutions or on distillation. Although one might expect that the driving force for the rearrangement is due to B−C π bonding, the molecular structure of **4** provides no support for this assumption because the 3-indenyl group is oriented orthogonally to the NB_2 plane, thus ruling out any B−C π-bonding contribution. This, however, need not be the case in solution.

Similar behaviour has been observed for cyclopentadienylboranes. Grundke and Paetzold[12] have shown that cyclo-

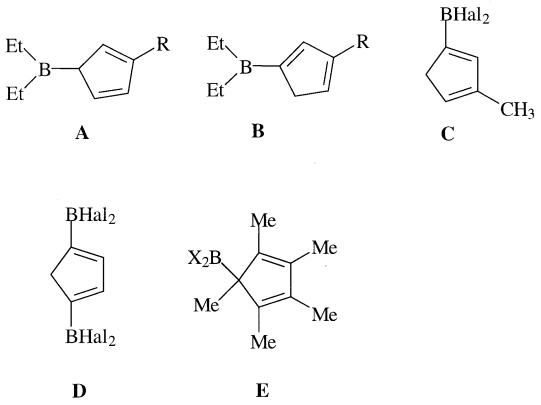

pentadienylboranes RCp−BEt_2 are present as the isomer **A**, and they found no NMR-spectroscopic evidence for isomer **B**.

Moreover, Jutzi and Seufert demonstrated that both the methyl and dihalogenoboryl group of the cyclopentadienyldihalogenoborane are only bonded to a vinylic carbon atom, e.g. like **C**, and the structure **D** follows for bis(dihalogenoborylcyclopentadiene) from NMR data[13]. When protic shifts are excluded, as is the case for (pentamethylcyclopentadienyl)boranes Cp*BX_2 (X = Cl, Br, I, NMe_2) rapid sigmatropic rearrangements are observed, except for X = NMe_2 which possesses a static structure **E** at ambient temperature showing both vinylic- and allylic-bound methyl groups[14]. The indenyldiboranes reported here therefore represent the first examples where both the allylic and the vinylic isomeric species could not only be detected by NMR methods but also isolated. This is due to the fact that the 1,3-sigmatropic rearrangement of the proton occurs slowly and, of course, raises the question of whether indenylboranes $(ind)_{3-x}BX_x$ behave similarly. We will report on these results in due course.

Experimental Section

General: All experiments were performed under anhydrous conditions using Schlenk techniques under N_2 or Ar. All reagents were purified before use either by distillation or crystallization. − Elemental analysis using a Haereus MX instrument were done at the Institute′s microanalytical laboratory. − IR: Perkin FT. − MS: Atlas CH7, 70 eV ionisation energy. − NMR: JEOL GSX 270 and JEOL EX 400, internal TMS (^1H, ^{13}C), external $BF_3 \cdot OEt_2$ (^{11}B). − X-ray: Siemens P4 with CCD area detector, SAINT software for data reduction; SHELX97 program package for structure solution and refinement. Numbering scheme of the NMR data refer to formulae **3**−**5**.

1-Chloro-1,2-bis(dimethylamino)-2-(3-indenyl)diborane(4) (**2**): By analogy to the preparation of **3**, $B_2Cl_2(NMe)_2$ (2.96 g, 16.4 mmol) in toluene (50 ml) was treated with a suspension of Li(ind) (2.0 g, 16.4 mmol) in toluene (30 ml) at −78°C. The insoluble material (found 0.67 g, calcd. for LiCl: 0.69 g) was removed after 2 d. **2** could not be crystallized from hexane, but was distilled at 95−98°C/10^{-3} Torr as a colourless viscous oil. Yield: 2.53 g of **2** (63%).− $C_{13}H_{19}B_2ClN_2$ (260.38): calcd. C 59.97, H 7.35, N 10.76; found C 59.48, H 7.37, N 10.59. − ^{11}B NMR (64 MHz, C_6D_6): δ = 43.6 [$h_{1/2}$ = 480 Hz, $B_2(NMe_2)_2(1\text{-ind})_2$] − ^1H NMR (400 MHz, C_6D_6): δ = 7.53 [d, 1 H, ^3J(H,H) = 7.7 Hz, indenyl: $H^{5/8}$], 7.37 [d, 1 H, ^3J(H,H) = 7.4 Hz, indenyl: $H^{5/8}$], 7.29 [t, 1 H, ^3J(H,H) = 7.7 Hz, indenyl: $H^{6/7}$], 7.15 [t, 1 H, ^3J(H,H) = 7.4 Hz, indenyl: $H^{6/7}$], 6.55 [t, 1 H, ^3J(H,H) = 2.1 Hz, indenyl: H^2], 3.21 [d, 2 H, ^3J(H,H) = 1.8 Hz, indenyl: H^3], 2.74 [s, 3 H, N(CH_3)], 2.61 [s, 3 H, N(CH_3)], 2.54 [s, 3 H, N(CH_3)], 2.52 [s, 3 H, N(CH_3)] − ^{13}C NMR (100 MHz, C_6D_6): δ = 148.5 (indenyl: C^4), 144.9 (indenyl: C^9), 137.1(indenyl: C^2), 126.5 (indenyl: C^8), 124.5 (indenyl: C^5), 124.1 (indenyl: C^7), 122.5 (indenyl: C^6), 44.2 [−N(CH_3)], 41.9 [−N(CH_3)], 41.1 [−N(CH_3)], 40.6 (indenyl: C^3), 37.5 [−N(CH_3)].

1,2-Bis(dimethylamino)-1,2-bis(1-indenyl)diborane(4) (**3**): $B_2(NMe_2)_2Cl_2$ [15] (5.06 g, 28.0 mmol) was dissolved in toluene (20 ml) and the solution cooled to −78°C. A suspension of lithiumindenide (6.84 g, 56.0 mmol), which had been freshly prepared from indene and butyllithium in toluene (90 ml), was added under vigorous stirring. The suspension was allowed to attain ambient temperature within 18 h, and was then heated for 3 h at 68°C, while stirring was continued. At this time the ^{11}B-NMR spectrum showed only a single-resonance signal of the monosubstituted product $Cl(Me_2N)B-B(NMe_2)$ind; 0.3 ml of THF was then added to the yellow suspension and the insoluble material was removed by centrifugation after 1h. After washing with toluene (20 ml) and drying in vacuum, 2.25 g (calcd. 2.38 g for LiCl) of the almost white insoluble material were obtained. Toluene was removed from the combined solutions in vacuum leaving behind a yellowish mass of honey-like appearance. It was then dissolved in hot hexane (75 ml). Some insoluble materials were removed by filtration, and crystals separated within 7 d at −20°C. Yield: 5.2 g of **3** (55%), m.p. 143−145°C. − $C_{22}H_{26}B_2N_2$ (340.08): calcd. C 77.70, H 7.71, N 8.24; found C 75.94, H 7.75, N 8.14. − ^{11}B NMR (64 MHz, C_6D_6): δ = 48.6 [$h_{1/2}$ = 520 Hz, $B_2(NMe_2)_2(1\text{-ind})_2$] − ^1H NMR (400 MHz, C_6D_6): δ = 7.44 (m, indenyl: H_{arom}), 7.38 (m, indenyl: H_{arom}), 7.23 (m, indenyl: H_{arom}), 6.88 [dd, 2 H, ^3J(H,H) = 5.4 Hz, ^4J(H,H) = 2.2 Hz, indenyl: H^3], 6.81 [dd, 4 H, ^3J(H,H) = 5.4 Hz, ^4J(H,H) = 2.2 Hz, indenyl: H^3], 6.78 [dd, 1 H, ^3J(H,H) = 5.4 Hz, ^4J(H,H) = 2.2 Hz, indenyl: H^3], 6.62 [dd, 2 H, ^3J(H,H) = 5.4 Hz, ^4J(H,H) = 2.0 Hz, indenyl: H^3], 6.29 (dd, 4 H, ^3J(H,H) = 5.4 Hz, ^3J(H,H) = 1.9 Hz, indenyl: H^2], 6.25 [dd, 2 H, ^3J(H,H) = 5.4 Hz, ^3J(H,H) = 1.8 Hz, indenyl: H^2], 6.24 [dd, 1 H, ^3J(H,H) = 5.4 Hz, ^3J(H,H) = 1.9 Hz, indenyl: H^2], 6.13 [dd, 2 H, ^3J(H,H) = 5.4 Hz, ^3J(H,H) = 1.8 Hz, indenyl: H^2], 3.42 (br. s, indenyl: H^1), 3.39 (br. s, indenyl: H^1), 3.37 (br. s, indenyl: H^1), 3.36 (br. s, indenyl: H^1), 2.58 [s, 6 H, N(CH_3)$_2$], 2.50 [s, 6 H, N(CH_3)$_2$], 2.48 [s, 3 H, N(CH_3)$_2$], 2.35 [s, 12 H, N(CH_3)$_2$], 2.34 [s, 12 H, N(CH_3)$_2$], 2.27 [s, 3 H, N(CH_3)$_2$], 2.23 [s, 36 H, N(CH_3)$_2$], 2.18 [s, 6 H, N(CH_3)$_2$]. − ^{13}C NMR (100 MHz, C_6D_6): δ = 148.9 ($C_{q(arom.)}$), 148.6 ($C_{q(arom.)}$), 148.3 ($C_{q(arom.)}$), 148.0 ($C_{q(arom.)}$), 145.9 ($C_{q(arom.)}$), 145.7 ($C_{q(arom.)}$), 139.8 (indenyl: C^2), 138.7 (indenyl: C^2), 138.3 (indenyl: C^2), 138.0 (indenyl: C^2), 129.6 (indenyl: C^3), 129.6 (indenyl: C^3), 129.4 (indenyl: C^3), 129.3 (indenyl: C^3), 125.3 ($C_{arom.}$), 125.3 ($C_{arom.}$), 124.2 ($C_{arom.}$), 124.1 ($C_{arom.}$), 124.0 ($C_{arom.}$), 123.9 ($C_{arom.}$), 123.9 ($C_{arom.}$), 123.8 ($C_{arom.}$), 123.8 ($C_{arom.}$), 123.7 ($C_{arom.}$), 121.3 (indenyl: $C^{5,8}$), 121.2 (indenyl: $C^{5,8}$), 121.2 (indenyl: $C^{5,8}$), 121.1 (indenyl: $C^{5,8}$), 49.4 (indenyl: C^1), 45.0 [N(CH_3)$_2$], 44.8 [N(CH_3)$_2$], 44.8 [N(CH_3)$_2$], 39.1 [N(CH_3)$_2$], 38.9 [N(CH_3)$_2$], 38.8 [N(CH_3)$_2$].

1,2-Bis(dimethylamino)-1-(1-indenyl)-2-(3-indenyl)diborane(4) (**4**): $Cl(Me_2N)B-B(NMe_2)$(3-ind) (750 mg, 2.88 mmol) was dissolved in toluene (10 ml) and the solution cooled to −78°C. The vigorously stirred solution was added to a suspension of Li(ind) (350 mg), 2.87 mmol) in toluene (20 ml). The suspension was allowed to attain ambient temperature within 2 h, and stirring was continued for additional 41 h. After that time, the ^{11}B-NMR spectrum revealed that no reaction had occurred. Addition of 0.2 ml

of THF caused the formation of an almost clear solution which became turbid within a few minutes. The insoluble product was removed using a centrifuge and provided 0.13 g of an off-white material soluble in water (calcd. 0.12 g for LiCl). Toluene was evaporated from the toluene solution. The slightly yellow, partly crystalline residue was redissolved in hexane (15 ml) and the crystals that grew from the solution at −20°C were recovered after 2 weeks. − Yield: 0.91 g of **4** (93%), m.p. 136−138°C. − $C_{22}H_{26}B_2N_2$ (340.08): calcd. C 77.70, H 7.71, N 8.24; found C 76.41, H 7.69, N 8.02. − ^{11}B NMR (64 MHz, C_6D_6): δ = 48.4 [$h_{1/2}$ = 600 Hz, $B_2(NMe_2)_2$(ind)$_2$] − ^{1}H NMR (270 MHz, C_6D_6): δ = 7.43 [d, 1 H, ^3J(H,H) = 7.2 Hz, indenyl: H$^{5/8}$], 7.38 (d, 1 H, bad resolution, indenyl: H$^{5/8}$), 7.28 (m, 2 H, H$_{arom.}$), 7.16 (m, 4 H, H$_{arom.}$), 6.78 [d, 1 H, ^3J(H,H) = 4.3 Hz, indenyl: H^3], 6.50 [d, 1 H, ^3J(H,H) = 4.5 Hz, indenyl: H^2], 6.34 [t, 1 H, ^3J(H,H) = 1.9 Hz, indenyl: H^{11}], 3.75 (s, 1 H, indenyl: H^1), 3.22 [d, 2 H, ^3J(H,H) = 2.1 Hz, indenyl: H^{12}], 2.77 [s, 3 H, N(CH_3)], 2.65 [s, 3 H, N(CH_3)], 2.38 [s, 3 H, N(CH_3)], 2.37 [s, 3 H, N(CH_3)] − ^{13}C NMR (68 MHz, C_6D_6): δ = 150.4 (indenyl: C$^{13/18}$), 148.5 (indenyl: C$^{13/18}$), 148.3 (indenyl: C$^{4/9}$), 144.7 (indenyl: C$^{4/9}$), 139.4 (indenyl: C^{11}), 136.0 (indenyl: C^{13}), 129.4 (indenyl: C^{11}), 126.0 (indenyl: C$^{8/17}$), 125.3 (indenyl: C$^{8/17}$), 124.1 (indenyl: C$^{5/14}$), 123.9 (indenyl: C$^{7/16}$), 123.7 (indenyl: C$^{7/16}$), 122.9 (indenyl: C$^{6/15}$), 121.2 (indenyl: C$^{6/15}$), 49.4 (indenyl: C^{10}), 45.0 [−N(CH_3)], 44.1 [−N(CH_3)], 41.1 (indenyl: C^{12}), 40.3 [−N(CH_3)], 39.1 [−N(CH_3)].

1,2-Bis(dimethylamino)-1,2-(3-indenyl)diborane(4) (**5**): A solution of **3** (200 mg, 0.59 mmol) in toluene (10 ml) was heated to reflux for 48 h. All volatiles were then removed in vacuum leaving behind **5** in colourless microcrystaline form. − Yield: 200 mg of **5** (100%), m.p. 148−151°C. − $C_{22}H_{26}B_2N_2$ (340.04): calcd. C 77.70, H 7.71, N 8.24, found: C 75.91 H 7.76, N 8.12. − ^{11}B NMR (64 MHz, C_6D_6): δ = 48.3 [$h_{1/2}$ = 650 Hz, $B_2(NMe_2)_2$(ind)$_2$] − ^{1}H NMR (270 MHz, C_6D_6): δ = 7.43 [d, 2 H, J^3(H,H) = 7.1 Hz, indenyl: H^{5,8}], 7.30 (m, 4 H, indenyl: H^{5,8}/H^{6,7}), 7.12 [pseudo t, 2 H, J^3(H,H) = 7.5 Hz, indenyl: H^{6,7}], 6.34 [t, 2 H, J^3(H,H) = 1.9 Hz, indenyl: H^2], 3.22 [d, 4 H, J^3(H,H) = 1.9 Hz, indenyl: H^3], 2.90 [s, 6 H, N(CH_3)$_2$], 2.59 [s, 6 H, N(CH_3)$_2$] − ^{13}C NMR (68 MHz, C_6D_6): δ = 148.6 (C^4), 148.1 (C^1), 144.7 (C^9), 138.7 (C^2), 126.6 (C^8), 124.3 (C^5), 124.0 (C^7), 122.6 (C^6), 44.9 [N(CH_3)$_2$], 41.2 (C^3), 40.5 [N(CH_3)$_2$].

X-ray Structure Determinations: Single crystals of compounds **3** and **4** were grown from hexane solutions at −20°C. The selected crystals were covered with perfluoroether oil, and mounted on a glass fibre, placed on the goniometer head and cooled with a gas flow of cold N_2. Preliminary dimensions of the unit cells were calculated from the reflection collected at four different settings of the crystal by recording 15 frames each with a CCD area detector. Data collection was performed with 10 s exposure time per frame by rotating the crystal by 0.3° in φ at two different χ settings. The data on 1350 frames were reduced by using the program SAINT[16] and the structures solved by direct methods using the XS and SHELX97 programs for structure solution and refinement. Non-hydrogen atoms were refined anisotropically, and the hydrogen atoms were included as a riding model in the final cycles of refinement. Relevant data are presented in Table 3.

Crystallographic data (excluding structure factors) have been deposited with the Cambridge Crystallographic Data Centre as supplementary publication no. 101104. Copies of the data can be obtained free of charge on application to CCCD, 12 Union Park, Cambridge, UK, CB2 1EZ [Fax: int. code + 44(0)1223/336033; E-mail: deposit@ccdc.cam.ac.uk].

Table 2. Selected crystallographic data for the structures of **3** and **4** and data refering to data collectiion and structure refinement

	3	**4**
Empirical formula	$C_{22}H_{26}B_2N_2$	$C_{22}H_{26}B_2N_2$
Formula mass	340.07	340.07
Crystal size [mm]	0.15 × 0.2 × 0.3	0.06 × 0.3 × 0.7
Crystal system	Monoclinic	Triclinic
Space group	*P*2(1)/*c*	*P*1bar
a [Å]	15.8977(3)	8.8466(1)
b [Å]	7.5756(1)	10.3594(2)
c [Å]	16.8297(3)	11.1737(3)
α [°]	90	77.403(1)
β [°]	93.323(1)	85.428(1)
γ [°]	90	83.222(1)
V [Å^3]	2023.47(6)	990.84(3)
Z	4	2
ρ(calcd.) [Mg/m^3]	1.116	1.140
μ [mm^{-1}]	0.064	0.065
F(000)	728	364
Index range	$-19 \le h \le 19$	$-11 \le h \le 11$
	$-9 \le k \le 9$	$-13 \le k \le 12$
	$-21 \le l \le 22$	$-14 \le l \le 14$
2 θ [°]	57.46	58.54
T [K]	193	193
Refl. collected	10800	5635
Refl. unique	3467	3048
Refl. observed (4σ)	2781	2640
R (int.)	0.0398	0.0249
No. of variables	339	263
Weighting scheme[a] x/y	0.0628/2.2247	0.0435/0.4055
GOOF	1.130	1.129
Final *R* (4σ)	0.0789	0.0474
Final *wR*2	0.1812	0.1141
Larg. res. peak [e/Å^3]	0.509	0.331

[a] $w^{-1} = \sigma^2 F_o^2 + (xP)^2 + yP$; $P = (F_o^2 + 2F_c^2)/3$.

[97232]

☆ Dedicated to Prof. Dr. *H.-P. Boehm* on the occasion of his 70th birthday.

[1] H. Nöth, H. Sachdev, *Z. Naturforsch. Part B* **1997**, *52*, 1345-1348.

[2] [2a] A. Moezzi, R. A. Bartlett, P. P. Power, *Angew. Chem.* **1992**, *104*, 1075−1076; *Angew. Chem. Int. Ed. Engl.* **1992**, *31*, 1082. − [2b] A. Moezzi, M. M. Olmstead, P. P. Power, *J. Am. Chem. Soc.* **1992**, *144*, 2715−2717.

[3] R. Littger, N. Metzler, H. Nöth, M. Wagner, M. Thomann, *Chem. Ber.* **1994**, *127*, 1901−1908.

[4] R. Littger, H. Nöth, in preparation.

[5] R. Littger, Dissertation, University of Munich, **1995**.

[6] R. Littger, H. Nöth, M. Wagner, *Angew. Chem.* **1993**, *32*, 295−297; *Angew. Chem. Int. Ed. Engl.* **1993**, *32*, 295−297.

[7] Part of the diploma thesis of W. Ponikwar, University of Munich, **1997**.

[8] H. Nöth, B. Wrackmeyer, *NMR Spectroscopy of Boron Compounds, NMR-Principles and Progress*, vol. 14 (Eds.: R. Diehl, E. Fluck, R. Kosfeld), Springer Publishers, Heidelberg, New York, **1973**.

[9] L. W. Hall, J. D. Odom, P. D. Ellis, *J. Am. Chem. Soc.* **1975**, *97*, 4527; B. Wrackmeyer, H. Nöth, *Chem. Ber.* **1976**, *109*, 1075−1088.

[10] H. Nöth, M. Wagner, *Chem. Ber.* **1991**, *124*, 1963−1972; H. Fußstetter, Dissertation, University of Munich, **1997**.

[11] A. Moezzi, M. M. Olmstead, P. P. Power, *J. Chem. Soc., Dalton Trans.* **1992**, 2429−2434.

[12] H. Grundke, P. Paetzold, *Chem. Ber.* **1971**, *104*, 1136−1146.

[13] P. Jutzi, A. Seufert, *Angew. Chem.* **1976**, *88*, 333−334; *Angew. Chem. Int. Ed. Engl.* **1976**, *15*, 295−296.

[14] P. Jutzi. A, Seufert, *Chem. Ber.* **1979**, *112*, 2481−1487.

[15] H. Nöth, W. Meister, *Z. Naturforsch., Part B* **1962**, *17*, 714−718; R. Littger, N. Metzler, H. Nöth, M. Wagner, M. Thomann, *Chem. Ber.* **1994**, *127*, 1901−1908.

[16] *SHELXTL,* Vers. 5, Siemens X-Ray Analytical Instruments, **1994**.

Multidonor Ligands, 1

Synthesis and Structural Characterization of Gold(I) and Silver(I) Complexes of the Multidonor Ligand 2-(Phenacylthio)pyridine − Crystal Structures of $[(AuPPh_3)\{py\{SCH_2C(O)Ph\}\text{-}2\}](ClO_4)$ and $[(AgPPh_3)(OClO_3)\text{-}\{py\{SCH_2C(O)Ph\}\text{-}2\}]$

José Vicente*[a], Maria-Teresa Chicote*[a], Sonia Huertas, M. Carmen Ramírez de Arellano[b], and Peter G. Jones*[b]

Grupo de Química Organometálica, Departamento de Química Inorgánica, Facultad de Química[a], Universidad de Murcia, Aptdo. 4021, E-30071 Murcia, Spain

Institut für Anorganische und Analytische Chemie, Technische Universität Braunschweig[b], Postfach 3329, D-38023 Braunschweig, Germany

Received October 20, 1997

Keywords: Gold(I) / Silver(I) / S-donor and N-donor ligand

The ligand properties of 2-(phenacylthio)pyridine towards gold(I) and silver(I) have been investigated. From the reactions of the ligand with acetone solutions of $[M(PPh_3)(acetone)]ClO_4$ (M = Ag, Au) under various experimental conditions, complexes $[(AuPPh_3)_n\{py\{SCH_2C(O)Ph\}\text{-}2\}](ClO_4)_n$ and $[(AgPPh_3)_n(OClO_3)_n\{py\{SCH_2C(O)Ph\}\text{-}2\}]$ ($n = 1-3$) have been obtained. The crystal structures of the complexes $[(AuPPh_3)\{py\{SCH_2C(O)Ph\}\text{-}2\}]ClO_4$ and $[(AgPPh_3)(OClO_3)\text{-}\{py\{SCH_2C(O)Ph\}\text{-}2\}]$ have been determined by X-ray diffraction. In the cationic gold complex the metal is linearly coordinated to nitrogen and phosphorus, whereas the corresponding silver complex displays a trigonal planar geometry with pyridine, phosphane and perchlorato ligands.

Introduction

The use of functionalized ligands, such as 2-(methylthio)pyridine, pyridine-2(1*H*)-thione, benzoxazole-2(3*H*)-thione,[1] or ylides derived from 2-pyridylmethylene(triaryl)-phosphonium salts,[2][3] has allowed us to synthesize a variety of mono- and polynuclear silver(I) and gold(I) derivatives including a new class of $[Au_3]^{3+}$, $[Au_2Ag]^{3+}$, and $[Au_2Cu]^{3+}$ clusters. Such polynuclear complexes offer the possibility of studying metal−metal interactions in d^{10} systems, which are the subject of considerable interest.[3][4][5][6][7][8][9][10][11][12]

The objective of the present work is to study the ligand properties of 2-(phenacylthio)pyridine [py{$SCH_2C(O)Ph$}-2], of which, as far as we are aware, there is no previously known complex. According to Scheme 1, this ligand could coordinate through the nitrogen, sulfur, or oxygen atoms while the anionic ligands resulting from deprotonation of the methylene group or the *ortho* position of the phenyl ring offer two additional coordination sites, together resulting in the possibility of coordinating up to eight metal centers. In this paper we explore the chemistry of gold(I) and silver(I) complexes with this ligand.

Gold(I) has a limited tendency to coordinate to neutral N or S donor ligands (L_N or L_S). In fact, only a few complexes of the type $[Au(L_N)(PR_3)]^+$ have been described with full experimental and spectroscopic details.[13][14][15][16][17][18][19][20][21] In this family, most complexes contain primary, secondary or tertiary amines while the only reported complexes with pyridinic ligands (L_{py}) are those with L_{py} = py,[22] or 2,2′-bipyridine,[23][24][25] and the dinuclear complex $[Au_2\{\mu_2\text{-}py(PPh_2)\text{-}2\}]^{2+}$.[19]

Scheme 1

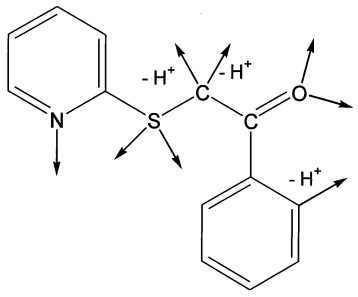

Gold(I) complexes with neutral sulfur donor ligands are less frequent and also less stable than those with thiolate and other anionic sulfur ligands.[22][25][24][26][27][28][29][30][31] Such low stability is attributable to the weakness of the Au^I-SR_2 bond. In fact, [AuCl(tht)] (tht = tetrahydrothiophene)[32] is the most widely used starting gold(I) complex because of the facile replacement of the sulfur ligand.[33] From [AuCl(tht)] other synthetic intermediates, such as $[Au(C_6F_5)_n(tht)]$ (n = 1, 3)[32][33][34] have been prepared and used as starting materials for many (pentafluorophenyl)gold(I) and -gold(III) complexes after replacement of tht.[35]

The similarly low tendency of gold(I) to coordinate to both N or S neutral donor ligands prompted us to study

 © WILEY-VCH Verlag GmbH, D-69451 Weinheim, 1998 1434−1948/98/0404−0511 $ 17.50+.50/0

the coordinative preferences of the mixed N-S ligand py{$SCH_2C(O)Ph$}-2 towards the $Au(PPh_3)^+$ moiety. In the absence of X-ray diffraction data, we have previously suggested that in complexes $[Au\{py(SMe)\text{-}2\}(L)]^+$ (L = tht, PPh_3) and $[Au\{py(SMe)\text{-}2\}_2]^+$ the mixed ligand would act as an S- rather than an N-donor ligand according to the preference of the soft gold(I) acid for the softer sulfur base. In fact, gold(I) complexes with pyridine-2-thiol or its conjugate base are always *S*-coordinated.[36][37] Similarly, in the complex $[Au\{py\{CS(=NC_6H_4OMe\text{-}2)\}\text{-}2\}(PPh_3)]$ the $AuPPh_3^+$ group is bonded to sulfur and interacts only weakly with the pyridine N atom.[38] Here we show for the first time the opposite preference of gold(I) for the N- rather than the S-donor atoms in the ligand py{$SCH_2C(O)Ph$}-2.

Synthesis of the Ligand

2-(Phenacylthio)pyridinium bromide was first obtained[39] by allowing 2-bromoacetophenone to react with 2-mercaptopyridine in refluxing ethanol for several hours. This and other sulfides resulting from the reaction of α-halo ketones or α-halo acetals with mercaptopyridine can be cyclized in good yield to form thiazolopyridinium salts.[39][40] We have found that equimolar amounts of 2-bromoacetophenone and 2-mercaptopyridine produce, after stirring in diethyl ether at room temperature for only 30 min, a quantitative yield of [Hpy{$SCH_2C(O)Ph$}-2]Br, which in turn reacts with aqueous NaOH to give 2-(phenacylthio)pyridine [py{$SCH_2C(O)Ph$}-2]. As far as we are aware the ligand properties of py{$SCH_2C(O)Ph$}-2 have not previously been explored.

Gold(I) and Silver(I) Complexes

When py{$SCH_2C(O)Ph$}-2 is treated with acetone solutions of $[M(PPh_3)(acetone)]ClO_4$ (M = Au, Ag) in 1:1, 1:2 or 1:3 molar ratios, complexes $[(AuPPh_3)_n\{py\text{-}\{SCH_2C(O)Ph\}\text{-}2\}](ClO_4)_n$ [*n* = 1 (**1**), 2 (**2**), 3 (**3**)] or $[(AgPPh_3)_n(OClO_3)_n\{py\{SCH_2C(O)Ph\}\text{-}2\}]$ [*n* = 1 (**4**), 2 (**5**), 3 (**6**)] are, respectively, obtained (Scheme 2). The reactions leading to polynuclear derivatives can be performed stepwise and thus **2** or **5** can be obtained from **1** or **4** and one equivalent of $[M(PPh_3)(acetone)]ClO_4$ while **3** or **6** can be prepared from **2** or **5** or from **1** or **4** upon addition of one or two equivalents, respectively, of the corresponding $[M(PPh_3)(acetone)]ClO_4$ complex. In the case of the gold complexes the purest products are obtained by the stepwise procedure.

We have shown that (acetylacetonato)gold(I) complexes react with a variety of organic substrates containing moderately acidic protons to give gold(I) complexes, including alkyl, alkynyl, ylide, diphenylphosphide, (diphenylphosphanyl)methanide, hydrosulfide and thiolato derivatives.[1][2][3][17][42][42a] However, the reaction of $[Au(acac)PPh_3]$ with 2-(phenacylthio)pyridine, meant to produce the organometallic complex **7** (Scheme 3), gave instead the known complex **A,** the structure of which we determined by X-ray diffraction methods; it had been previously reported.[36]

Scheme 2[a]

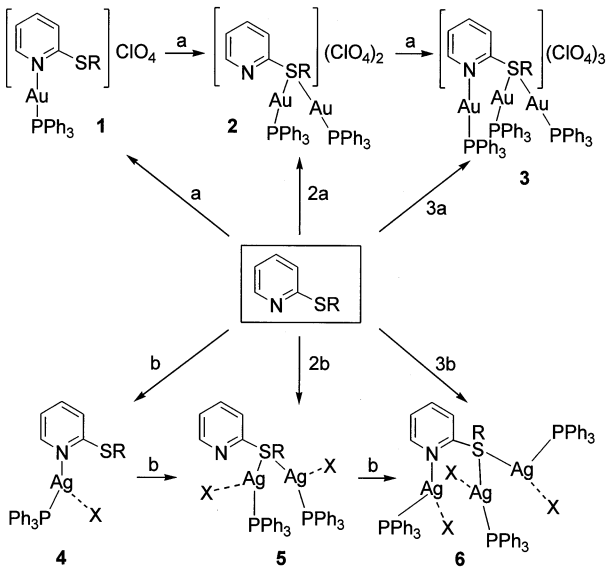

[a] R = $CH_2C(O)Ph$; X = $OClO_3$; a: + $[Au(PPh_3)(acetone)]ClO_4$; b: + $[Ag(PPh_3)(acetone)]ClO_4$.

Scheme 3[a]

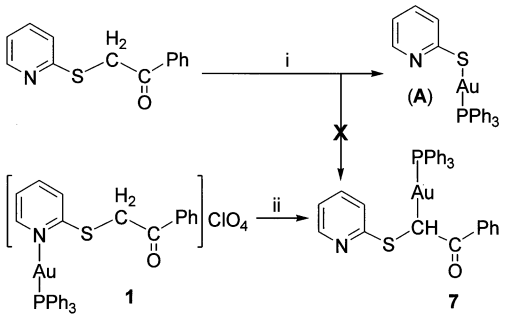

[a] i: + $[Au(acac)PPh_3]$ − Hacac; ii: + NaH − H_2 − $NaClO_4$.

The reaction of **1** with NaH (1:2.3, in dichloromethane, 2.5 h) gave the desired complex **7** resulting from deprotonation of the methylene group and the rearrangement of the $AuPPh_3^+$ group from N to C. The preference of gold for C rather than N donor ligands is well known. Although the elemental analyses of **7** were correct, it is difficult to separate it from traces of the starting material and some decomposition products (see below).

Crystal Structure of Complexes 1 and 4

Complex **1** crystallizes in the triclinic system with 3 molecules of acetone and two independent molecules in the asymetric unit. The crystal structure (Figure 1) shows cations in which the gold atoms are in almost linear environments, with N−Au−P angles of 175.46(12) and 173.91(12)° and tetrahedral ClO_4 anions. The Au−N distances [2.082(4) and 2.092(4) Å] are similar to the 2.086(16) Å found in $[Au_2\{\mu_2\text{-}py(PPh_2)\text{-}2\}]^{2+}$.[19] In $[Au(bipy)(PPh_3)]^+$ a distorted trigonal planar coordination leads as expected to Au−N bond lengths [2.166(2) and 2.406(2) Å] longer than those in **1**.[25]

The Au−P bond lengths [2.2359(13) and 2.2388(13) Å] in **1** are larger than those in $[Au_2\{\mu_2\text{-py}(PPh_2)\text{-}2\}]^{2+}$ [2.215(6) Å][19] or $[Au(bipy)(PPh_3)]^+$ [2.212(1) Å].

Figure 1. Structure of the cation of complex **1**[a]

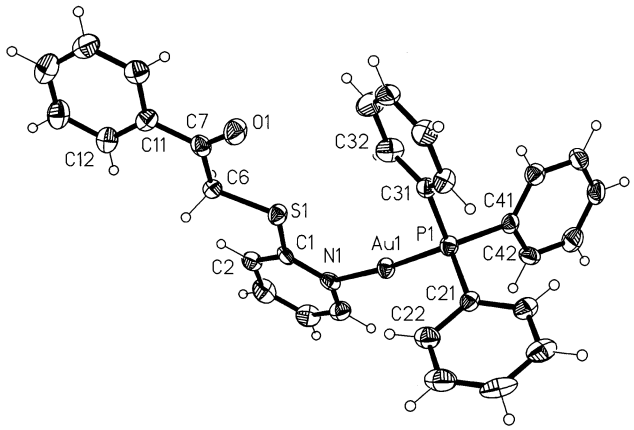

[a] 50% probability ellipsoids; selected bond lengths [Å] and angles [°]: Au(1)−N(1) 0.082(4), Au(2)−N(2) 2.092(4), Au(1)−P(1) 2.2359(13), Au(2)−P(2) 2.2388(13); N(1)−Au(1)−P(1) 175.46(12), N(2)−Au−P(2) 173.91(12).

The coordination of the $AuPPh_3^+$ group to N instead of S [Au···S, 3.071, 3.063(1) Å] is surprising because the soft gold(I) acid should prefer the softer sulfur base; when the ligand is pyridine-2-thiol or its conjugate base, gold(I) is always bonded to sulfur.[36][37] In addition, in the complex $[Au\{py\{C(S)(=NC_6H_4OMe\text{-}2)\}\text{-}2\}(PPh_3)]$ the $AuPPh_3^+$ group is bonded to sulfur (Au−S, 2.317 Å) and only weakly to the pyridine N atom (Au−N, 2.574 Å).[38] Probably the presence of the electron-withdrawing carbonyl group in **1** makes the sulfur atom less soft than usual.

Complex **4** crystallizes in the monoclinic system and its crystal structure (Figure 2) shows the silver atoms in a very distorted trigonal planar environment (the Ag atom lies 0.21 Å out of the plane of the donor atoms. The N−Ag−P [148.5(5)°], P−Ag−O [129.7(6)°], and N−Ag−O [79.0(5)°] bond angles show PPh_3 to be the most sterically demanding ligand. Two of the four Ag−N bond lengths [2.272, 2.268, 2.386, 2.407(4) Å] and the Ag−P [2.380, 2.377(1) Å] bond lengths at the two independent Ag atoms of $[Ag(8\text{-hydroxyquinoline})_2(PPh_3)]^+$ are similar to the Ag−N [2.263(2) Å] and Ag−P [2.3845(7) Å] bond lengths in **4**.[43] In the complex $[Ag(OClO_3)(O_2NO)\{py\{C(AuPPh_3)_2PPh_3\}\text{-}2\}]$[3] the Ag−N [2.178(8) Å] and Ag−$OClO_3$ [2.663(9) Å] bond lengths are shorter and similar, respectively, than the corresponding ones in complex **4** [Ag−O, 2.688(6) Å]. The long Ag−O bond length (compared with Ag−N [2.263(2) Å]) and the wide P−Ag−N [148.5(5)°] bond angle indicate the weak coordination of the anion to Ag^I, as does the wide Cl−O(1)−Ag angle [133.8(1)°]. The sulfur atom forms short intra- [3.097(1) Å] and intermolecular [2.998(1) Å] Ag−S contacts leading to weakly associated, centrosymmetric dimers.

Figure 2. Structure of complex **2**[a]

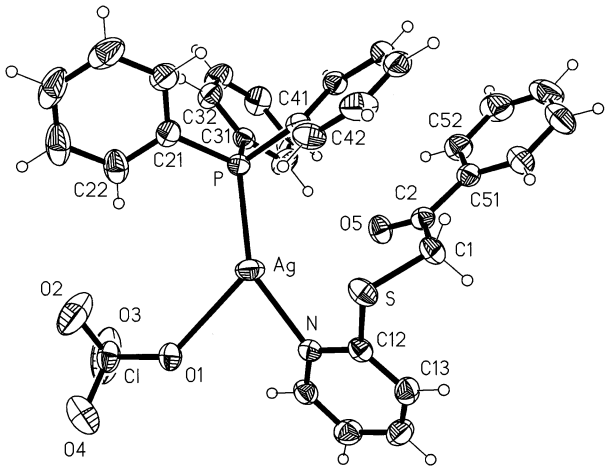

[a] 50% probability ellipsoids; selected bond lengths [Å] and angles [°]: Ag−N 2.263(2), Ag−P 2.3845(7), Ag−O(1) 2.688(6); N−Ag−P 148.47(6), P−Ag−O 129.7(6), N−Ag−O 79.0(5).

NMR Spectra

Because the resonance from the methylene protons in the ^{1}H-NMR spectrum of complex **1** at −60°C appears as a singlet, we propose that, in solution, the ligand acts as an N donor, as in its solid-state structure. Coordination through the sulfur atom would convert it into a chiral center and the methylene protons would be non-isochronous unless a rapid scrambling of the $AuPPh_3^+$ group between both sp^3 sulfur pairs occurred even at −60°C. In fact, at −60°C the *S*-bonded isomer of the silver complex **4** (**4**-S) is detected because the ^{1}H-NMR spectrum shows an AB system highfield of the CH_2 singlet, and in the ^{31}P-NMR spectrum four doublets corresponding to two different phosphorus nuclei (molar ratio 8:1) resonating at δ = 13.21 [$^1J(P^{109}Ag)$ = 742 Hz, $^1J(P^{107}Ag)$ = 643 Hz; **4**] and 11.69 [$^1J(P^{109}Ag)$ = 555 Hz, $^1J(P^{107}Ag)$ = 481 Hz; **4**-S] are observed. The $^1J(P^{109}Ag)$ and $^1J(P^{107}Ag)$ values are similar to those in complex **6** [$J(P^{109}Ag)$ = 770.6 Hz, $J(P^{107}Ag)$ = 667.6 Hz, *P*AgN; $J(P^{109}Ag)$ = 569 Hz, $J(P^{107}Ag)$ = 493 Hz, 2*P*AgS] where Ag^I is coordinated to both N and S.

The dinuclear complexes **2** and **5** show only one type of phosphorus nucleus at low temperature (−60°C), indicating that both $MPPh_3$ units coordinate to sulfur. This is also a surprising result because, according to the above explanation of the *N*-coordination, the sulfur atom has its donor ability reduced by the vicinity of the electron-withdrawing carbonyl group. However, a reasonable explanation for these facts is based on the marked tendency of gold(I) and silver(I) to establish short M···M contacts, a phenomenon termed aurophilicity,[7][8][9][10][11][12] or numismophilicity (from the Latin numisma = money, coin)[3] when it applies to gold or to the three coinage metals, respectively. Because the numismophilic interactions are weak (of similar energy to hydrogen bonds when the metal is gold)[44] the structure adopted is that in which there is a minimum of repulsion between the phosphane ligands, i.e., the double metalation of the sulfur atom is preferred to the alternative mixed *N*,*S*

metalation. At room temperature, the behavior of these complexes is different. Whereas the silver complex **5** shows a broad resonance, probably because of dissociative processes involving cleavage of S−AgPPh$_3$ and/or Ag−PPh$_3$ bonds, in the gold complex **2** such equilibria do not exist because its spectrum is not significantly different from that at −60°C.

The $^{31}P\{^1H\}$-NMR spectrum of **3** at −60°C consists of two singlets of 2:1 relative intensity, consistent with the structure proposed in Scheme 2, but at room temperature shows only a singlet, indicating that a fluxional process interchanging all three $AuPPh_3^+$ units occurs. Similarly, in the case of **6** the room-temperature $^{31}P\{^1H\}$-NMR spectrum shows a broad resonance, which at −60°C splits into two (2:1 relative intensities) pairs of doublets.

Resonances appearing at δ = 4.75 and 31.02 in the ^{1}H- and ^{31}P-NMR spectra, respectively, of **7** are due to the presence of traces of **1**, while a small amount of $[Au(PPh_3)_2]^+$ could account for the resonance at δ = 44.24. The slight conductivity of **7** (Λ_M = 11 Ω^{-1} cm^2 M^{-1}) is also consistent with the presence of both impurities.

IR Spectra

The bands assignable to the ν̃(CO) mode in the IR spectra of the ligand and the complexes appear in the narrow range of 1672−1680 cm^{-1}. The gold complexes **1**−**3** show the expected two bands for the tetrahedral ClO_4 anion in the ranges 1088−1094 and 621−622 cm^{-1}, respectively. This accords with the marked tendency of gold(I) to give dicoordinate complexes. In complexes **4**, **5** and **6**, a new band around 923 cm^{-1} and two bands in each of the two above-mentioned regions are observed. This is in agreement with the expected splitting when the symmetry of the ClO_4 decreases from T_d to C_{3v}. Therefore, it is reasonable to assume that, in the solid state, each ClO_4 anion is monocoordinated to one metal centre.

These differences among gold(I) and silver(I) complexes in the solid state disappear in acetone solutions, because all complexes show molar conductivities indicating the dissociation of all the perchlorate anions, i.e., complexes **1**−**6** behave as 1:1 electrolytes, **2** and **5** as 2:1 electrolytes, and **3** and **6** as 3:1 electrolytes.[45] Therefore, in acetone solutions of the silver complexes the solvent replaces the anion in the coordination sphere of the metal.

We thank the *DGES* and the *Fonds der Chemischen Industrie* for financial support. M. C. R. A. is grateful for an *Alexander von Humboldt Grant* and to the *Ministerio de Educación y Cultura* for a contract.

Experimental Section

General: The IR spectra, elemental analyses, conductance measurements in acetone and melting-point determinations were carried out as described earlier[42a]. − NMR: Varian Unity-300. Chemical shifts are referred to TMS [^{1}H, $^{13}C\{^1H\}$] or H_3PO_4 [$^{31}P\{^1H\}$]. − If not stated otherwise, the reactions were carried out at room temperature without special precautions against moisture. ***Warning:*** Perchlorate salts with organic cations may be explosive. − 2-Mercaptopyridine (HSpy) was purchased from Fluka and 2-bromoacetophenone [$BrCH_2C(O)Ph$] from Aldrich.

[Hpy{SCH$_2$C(O)Ph}-2]Br: A solution of equimolar amounts of pySH-2 (1.11 g, 10 mmol) and $BrCH_2C(O)Ph$ (1.99, 10 mmol) were stirred in diethyl ether (30 ml) for 0.5 h. The resulting yellow suspension was filtered off, the solid washed with diethyl ether (3 × 15 ml) and air-dried to give 3.07 g (99%) of colorless crystals, m.p. 200°C (ref.[39] 200°C). − IR (Nujol): ν̃ = 1693 cm^{-1} (CO). − $C_{13}H_{12}BrNOS$ (310.2): calcd. C 50.34, H 3.90, N 4.52, S 10.33; found: C 50.18, H 4.07, N 4.62, S 10.44.

py{SCH$_2$C(O)Ph}-2: To a solution of [Hpy{SCH$_2$C(O)Ph}-2]Br (2.48 g, 8 mmol) in water (50 ml) NaOH (0.5 M in water) was added dropwise until pH = 7. The resulting white suspension was extracted with dichloromethane (4 × 20 ml) and the organic layer was dried with anhydrous $MgSO_4$ and then filtered. Removing the volatiles in vacuo gave 514 mg of 2-(phenacylthio)pyridine (28%) as a pale yellow oil. − IR (Nujol): ν̃ = 1668 cm^{-1} (CO). − ^{1}H NMR ([D$_6$]acetone): δ = 4.79 (s, 2 H, C*H*$_2$), 6.93 [m, 1 H, *H4* (py)], 7.22 [m, 1 H, *H3* (py)], 7.3−7.8 [m, 4 H, *H5* (py) + *m-H* (Ph) + *p-H* (Ph)], 8.04 [d, ^3J(HH) = 7 Hz, 2 H, *o-H* (Ph)], 8.34 [m, 1 H, *H6* (py)]. − $C_{13}H_{11}NOS$ (229.3): calcd. C 68.10, H 4.84, N 6.11, S, 13.98; found: C 68.38, H 4.89, N 6.28, S 14.02.

[(AuPPh$_3$)$_n${py{SCH$_2$C(O)Ph}-2}](ClO$_4$)$_n$ [*n* = 1 (**1**), 2 (**2**), 3 (**3**)]. − *Preparation of Solutions of [Au(PPh$_3$)(acetone)]ClO$_4$:* An equimolecular mixture of [AuCl(PPh$_3$)] and $AgClO_4$ (1:1 molar ratio) in degassed acetone (25 ml mmol^{-1}) was stirred for 0.5 h under nitrogen and then the AgCl removed by filtration.

Complex **1**: A solution of [Au(PPh$_3$)(acetone)]ClO_4, from [AuCl(PPh$_3$)] (406 mg, 0.82 mmol) and $AgClO_4$ (107 mg, 0.82 mmol), was added dropwise under nitrogen to a solution containing py{SCH$_2$C(O)Ph}-2 (188 mg, 0.82 mmol) in degassed acetone (15 ml). The resulting suspension was stirred for 0.5 h and then filtered through Celite. The solvent was removed in vacuo and the oily residue was vigorously stirred with diethyl ether (20 ml) for 0.5 h to give 626 mg of **1** (97%), white solid, m.p. 137°C. − IR (Nujol): ν̃ = 1672 cm^{-1} (CO). − Λ_M = 144 Ω^{-1} cm^2 M^{-1}. − ^{1}H NMR (CD_2Cl_2, 20°C): δ = 4.90 (s, 2 H, C*H*$_2$), 7.48−7.67 [m, 20 H, C(O)*Ph* + P*Ph*$_3$], 7.83 [m, 1 H, *H3* (py)], 8.04 [m, 2 H, *H4* (py) + *H5* (py)], 8.50 [m, 1 H, *H6* (py)]. − ^{1}H NMR (CD_2Cl_2, −60°C): δ = 4.95 (s, 2 H, C*H*$_2$), 7.44 − 7.68 [m, 20 H, C(O)*Ph* + P*Ph*$_3$], 7.97 [m, 1 H, *H3* (py)], 8.08 [m, 2 H, *H4* (py) + *H5* (py)], 8.42 [m, 1 H, *H6* (py)]. − $^{31}P\{^1H\}$ NMR (CD_2Cl_2, 20°C and −60°C): δ = 29.44. − $C_{31}H_{26}AuClNO_5PS$ (788.0): calcd. C 47.25, H 3.33, N 1.78, S 4.07; found: C 47.42, H 3.79, N 1.73, S 3.71.

Complex **2**: A solution of [Au(PPh$_3$)(acetone)]ClO_4, from [AuCl(PPh$_3$)] (125 mg, 0.25 mmol) and $AgClO_4$ (53 mg, 0.25 mmol), was added dropwise to a solution containing **1** (200 mg, 0.25 mmol) in degassed acetone (15 ml). The resulting suspension was stirred for 1.5 h and then filtered through Celite. The solution was concentrated (2 ml) and diethyl ether added (20 ml) to give a suspension that was filtered, the solid washed with diethyl ether (5 ml), dried in the air and then in an oven at 60°C for 30 min to give 327 mg of **2** (97%), cream solid, m.p. 103°C. − IR (Nujol): ν̃ = 1672 cm^{-1} (CO). − Λ_M = 183 Ω^{-1} cm^2 M^{-1}. − ^{1}H NMR ([D$_6$]acetone, 20°C): δ = 5.28 (s, 2 H, C*H*$_2$), 7.40−8.36 [m, 38 H, *H3* (py) + *H4* (py) + *H5* (py)+ C(O)*Ph* + P*Ph*$_3$], 9.03 [m, 1 H, *H6* (py)]. − $^{31}P\{^1H\}$ NMR ([D$_6$]acetone, 20°C): δ = 29.66 (s). − $^{31}P\{^1H\}$ NMR ([D$_6$]acetone, −60°C): δ = 28.29 (s). − $C_{49}H_{41}Au_2Cl_2NO_9P_2S$ (1346.7): calcd. C 43.70, H 3.07, N 1.04, S 2.38; found: C 43.68, H 3.33, N 1.19, S 2.28.

Complex **3**: A solution of [Au(PPh$_3$)(acetone)]ClO_4, from [AuCl(PPh$_3$)] (92 mg, 0.19 mmol) and $AgClO_4$ (38 mg, 0.19 mmol), was added dropwise to a solution containing **2** (250 mg, 0.19 mmol) in degassed acetone (10 ml). The resulting suspension was stirred

for 2 h and then filtered through $MgSO_4$. The solvent was evaporated to dryness and the resulting solid stirred with diethyl ether (20 ml) to give a suspension that was filtered and dried under nitrogen to give 355 mg of **3** (98%), cream solid, m.p. 107°C. − IR (Nujol): $\tilde{\nu}$ = 1673 cm^{-1} (CO). − Λ_M = 285 Ω^{-1} cm^2 M^{-1}. − ^1H NMR ([D$_6$]acetone, 20°C): δ = 5.38 (s, 2 H, C*H*$_2$), 7.38−7.64 [m, 51 H, *H3* (py) + C(O)*Ph* + P*Ph*$_3$], 8.07 [m, 2 H, *H4* (py) + *H5* (py)], 8.78 [m, 1 H, *H6* (py)]. − $^{31}P\{^1H\}$ NMR([D$_6$]acetone, 20°C): δ = 29.12 (s). − $^{31}P\{^1H\}$ NMR([D$_6$]acetone, −60°C): δ = 28.21 (s, Ph$_3$*P*AuN), 29.68 (s, Ph$_3$*P*AuS). − $C_{67}H_{56}Au_3Cl_3NO_{13}P_3S$ (1905.4): calcd. C 42.23, H 2.96, N 0.74, S 1.68; found: C 42.14, H 3.27, N 0.62, S 1.70.

[(AgPPh$_3$)$_n$(OClO$_3$)$_n${py{SCH$_2$C(O)Ph}-2}] [*n* = 1 (**4**), (**5**), 3 (**6**)]. − *Preparation of Solutions of [Ag(PPh$_3$)*(acetone)]ClO_4: PPh_3 is added to an equimolecular amount of $AgClO_4$ in degassed acetone (15 ml $mmol^{-1}$).

Complex **4**: A solution of [Ag(PPh$_3$)(acetone)]ClO_4, from $AgClO_4$ (203 mg, 0.98 mmol) and PPh_3 (257 mg, 0.98 mmol), was added dropwise to a solution containing py{SCH$_2$C(O)Ph}-2 (225 mg, 0.98 mmol) in degassed acetone (5 ml) under nitrogen. The resulting suspension was stirred for 75 min and then concentrated to dryness. The residue was washed with diethyl ether (20 ml) and recrystallized from dichloromethane/diethyl ether to give 589 mg of **4** (86%), white solid, m.p. 137°C. − IR (Nujol): $\tilde{\nu}$ = 1677 cm^{-1} (CO). − Λ_M = 101 Ω^{-1} cm^2 M^{-1}. − ^1H NMR (CD_2Cl_2, 20°C): δ = 4.74 (s, 2 H, C*H*$_2$), 7.30−7.67 [m, 20 H, C(O)*Ph* + P*Ph*$_3$], 7.82 [m, 1 H, *H3* (py)], 7.97 [m, 2 H, *H4* (py) + *H5* (py)], 8.57 [m, 1 H, *H6* (py)]. − ^1H NMR (CD_2Cl_2, −60°C): δ = 3.93, 4.22 (AB system, $^2J_{HH}$ = 13 Hz, **4**-S, see Discussion), 4.55 (s, br., 2 H, C*H*$_2$), 7.03−7.77 [m, 21 H, *H3* (py) + C(O)*Ph* + P*Ph*$_3$], 8.05 [m, 2 H, *H4* (py) + *H5* (py)], 8.23 [m, 1 H, *H6* (py)]. − $^{31}P\{^1H\}$ NMR (CD_2Cl_2, 20°C): δ = 15.00 (s, br.). − $^{31}P\{^1H\}$ NMR (CD_2Cl_2, −60°C): δ = 13.21 [2 d, 88% P, $^1J(P^{109}Ag)$ = 742 Hz, $^1J(P^{107}Ag)$ = 643 Hz; **4**, see Discussion], 11.69 [2 d, 12% P, $^1J(P^{109}Ag)$ = 555 Hz, $^1J(P^{107}Ag)$ = 481 Hz; **4**-S, see Discussion]. − $C_{31}H_{26}AgClNO_5PS$ (698.9): calcd. C 53.28, H 3.75, N 2.00, S 4.59; found: C 53.31, H 3.76, N 1.96, S 4.48.

Complex **5**: A solution of [Ag(PPh$_3$)(acetone)]ClO_4, from $AgClO_4$ (612 mg, 2.96 mmol) and PPh_3 (775 mg, 2.96 mmol), was added dropwise to a solution containing py{SCH$_2$C(O)Ph}-2 (339 mg, 1.48 mmol) in degassed acetone (5 ml) under nitrogen. The resulting suspension was stirred for 2.5 min and then concentrated to dryness. The resulting solid was washed with *n*-hexane (20 ml) and the suspension filtered to give 1.61 g of **5** (99%), white solid, m.p. 150°C. − IR (Nujol): $\tilde{\nu}$ = 1680 cm^{-1} (CO). − Λ_M = 186 Ω^{-1} cm^2 M^{-1}. − ^1H NMR ([D$_6$]acetone, 20°C): δ = 5.01 (s, 2 H, C*H*$_2$), 7.40−7.80 [m, 35 H, C(O)*Ph* + P*Ph*$_3$], 7.93 [m, 1 H, *H3* (py)], 8.10 [m, 2 H, *H4* (py) + *H5* (py)], 8.61 [m, 1 H, *H6* (py)]. − $^{31}P\{^1H\}$ NMR ([D$_6$]acetone, 20°C): δ = 10−16 (br.). − $^{31}P\{^1H\}$ NMR ([D$_6$]acetone, −60°C): δ = 12.68 [2 d, $J(P^{109}Ag)$ = 759 Hz, $J(P^{107}Ag)$ = 658 Hz]. − $C_{49}H_{41}Ag_2Cl_2NO_9P_2S$ (1168.5): calcd. C 50.37, H 3.54, N 1.20, S 2.74; found: C 50.59, H 3.64, N 1.25, S 2.49.

Complex **6**: A solution of [Ag(PPh$_3$)(acetone)]ClO_4, from $AgClO_4$ (896 mg, 2.96 mmol) and PPh_3 (1.134 g, 2.96 mmol), was added dropwise to a solution containing of py{SCH$_2$C(O)Ph}-2 (330 mg, 1.48 mmol) in degassed acetone (5 ml) under nitrogen. The resulting suspension was stirred for 2.5 min and then concentrated to dryness. The resulting oil was washed with *n*-hexane (20 ml) and the resulting suspension filtered to give 2.33 g of **6** (99%), m.p. 138°C. − IR (Nujol): $\tilde{\nu}$ = 1681 cm^{-1} (CO). − Λ_M = 269 Ω^{-1} cm^2 M^{-1}. − ^1H NMR ([D$_6$]acetone, 20°C]: δ = 5.02 (s, 2 H, C*H*$_2$), 7.30−7.82 [m, 51 H, *H3* (py) + CO*Ph* + P*Ph*$_3$], 7.85−8.20 [m, 2 H, *H4* (py) + *H5* (py)], 8.61 [m, 1 H, *H6* (py)]. − $^{31}P\{^1H\}$ NMR ([D$_6$]acetone, 20°C): δ = 10−14 (br.). − $^{31}P\{^1H\}$ NMR ([D$_6$]acetone, −60°C): δ = 11.77 [2 d, $J(P^{109}Ag)$ = 569 Hz, $J(P^{107}Ag)$ = 493 Hz, 2 *P*AgS], 12.77 [2 d, $J(P^{109}Ag)$ = 770.6 Hz, $J(P^{107}Ag)$ = 667.6 Hz, *P*AgN]. − $C_{67}H_{56}Ag_3Cl_3NO_{13}P_3S$ (1638.1): calcd. C 49.13, H 3.45, N 0.86, S 1.96; found: C 50.21, H 3.62, N 0.90, S 2.05.

[Au{CH(Spy-2){C(O)Ph}}(PPh$_3$)] (**7**): To a solution of **1** (600.8 mg mg, 0.76 mmol) in dichloromethane (15 ml), NaH (Fluka, 50% in mineral oil, 86 mg, 1.79 mmol) was added. After 2.5 h of stirring, the resulting suspension was filtered through Celite. The solution was concentrated to dryness, the residue stirred with diethyl ether (2 × 15 ml) and the suspension filtered to give 290 mg of **7** (55%), pale cream solid, m.p. 106°C (dec.). − IR (Nujol): $\tilde{\nu}$ = 1638 (CO). − Λ_M = 11 Ω^{-1} cm^2 M^{-1}. − ^1H NMR ($CDCl_3$, 20°C): δ = 4.75 (s, traces, complex **1**, see Discussion), 5.42 [d, 1 H, C*H*, ^3J(PH) = 9.9 Hz], 6.42−7.56 (m, 19 H, PPh_3 + py). − $^{31}P\{^1H\}$ NMR: δ = 31.02 (s, traces, complex **1**, see Discussion), 39.24 (s), 44.24 (s, traces, $[Au(PPh_3)_2]^+$). − $C_{31}H_{25}AuNOPS$ (687.5): calcd. C 54.16, H 3.67, N 2.04, S 4.66; found: C 53.95, H 3.79, N 2.03S 4.55.

X-ray Crystallographic Studies: Crystal data are given in Table 1. Crystals of **1**·1.5 Me_2CO and **2** were mounted in inert oil on a glass fiber and transferred to the diffractometer (Siemens P4 with LT2 low-temperature attachment). Measurements were performed at −100°C using monochromated Mo-K_α radiation (λ = 0.71073 Å).

Table 1. Crystal Data for complexes **1**·1.5 Me_2CO and **2**

	1·1.5 Me_2CO	**2**
empirical formula	$C_{35.50}H_{35}AuClNO_{6.50}PS$	$C_{31}H_{26}AgClNO_5PS$
M	875.09	698.88
a [Å]	14.079(2)	13.5113(8)
b [Å]	14.663(2)	21.2262(14)
c [Å]	16.989(2)	11.1835(10)
α[°]	94.926(10)	90
β[°]	97.627(10)	113.332(6)
γ[°]	94.509(12)	90
Z	4	4
D_x [Mg/m^3]	1.685	1.576
crystal system	triclinic	monoclinic
space group	$P\bar{1}$	$P2_1/c$
crystal size [mm]	0.76 × 0.36 × 0.22	0.40 × 0.40 × 0.20
θrange [°]	3.01−25.00	3.18−27.50
reciprocal lattice segment	$-h, \pm k, \pm l$	$\pm h, +k, -l$
reflections measured	12737	8559
independent reflections	12092	6727
μ [mm^{-1}]	4.498	0.942
max/min transmission	0.767/0.915	0.925/0.821
parameters	853	370
F(000)	1736	1416
max Δρ [e Å^{-3}]	1.45	1.15
*R*1[a]	0.0313	0.0333
*wR*2[b]	0.0640	0.0819

[a] $R1 = \sigma||F_o| - |F_c||/\sigma|F_o|$ for reflections with $I > 2\sigma(I)$. − [b] $wR2 = \{\sigma[w(F_o^2 - F_c^2)^2]/\sigma[w(F_o^2)^2]\}^{0.5}$ for all reflections; $w^{-1} = \sigma^2(F^2) + (aP)^2 + bP$, where $P = (2F_c^2 + F_o^2)/3$ and *a* and *b* are constants set by the program.

Unit cell parameters were determined from a least-squares fit of ca. 80 accurately centered reflections (10° < 2θ < 27°). Intensities were registered using ω scans. Absorption corrections were based on ψ scans. The structures were solved by the heavy-atom method and refined anisotropically on F^2 (program SHELXL-93).[46] Hy-

drogen atoms were included using a riding model or as rigid methyl groups.

Crystallographic data (excluding structure factors) for the structures reported in this paper have been deposited with the Cambridge Crystallographic Data Centre under the number CCDC-100752. Copies of the data can be obtained free of charge on application to CCDC, 12 Union Road, Cambridge CB2 1EZ, UK (fax: int. code + (1223)336−033, e-mail: deposit@ccdc.cam.ac.uk).

[1] J. Vicente, M. T. Chicote, C. Rubio, *Chem. Ber.* **1996**, *129*, 327.
[2] J. Vicente, M. T. Chicote, M. C. Lagunas, P. G. Jones, *J. Chem. Soc., Chem. Commun.* **1991**, 1730.
[3] J. Vicente, M. T. Chicote, M. C. Lagunas, *Inorg. Chem.* **1993**, *32*, 3748.
[4] J. Vicente, M.-T. Chicote, M.-D. Abrisqueta, R. Guerrero, P. G. Jones, *Angew. Chem.* **1997**, *109*, 1252; *Angew. Chem. Int. Ed. Engl.* **1997**, *36*, 1203.
[5] I. G. Dance, M. L. Scudder, L. J. Fitspatrick, *Inorg. Chem.* **1985**, *24*, 2547.
[6] O. Steigelmann, P. Bissinger, H. Schmidbaur, *Angew. Chem.* **1990**, *102*, 1473; *Angew. Chem. Int. Ed. Engl.* **1990**, *29*, 1399.
[7] H. Schmidbaur, *Chem. Soc. Rev.* **1995**, 391.
[8] P. G. Jones, *Gold Bull.* **1981**, *14*, 102.
[9] P. G. Jones, *Gold Bull.* **1981**, *14*, 159.
[10] P. G. Jones, *Gold Bull.* **1983**, *16*, 114.
[11] P. G. Jones, *Gold Bull.* **1986**, *19*, 46.
[12] H. Schmidbaur, *Gold Bull.* **1990**, *23*, 11.
[13] A. Grohmann, J. Riede, H. Schmidbaur, *Z. Naturforsch., B* **1992**, *47*, 1255.
[14] E. G. Perevalova, K. I. Grandberg, V. P. Dyadchenko, T. V. Baukova, *J. Organomet. Chem.* **1981**, *217*, 403.
[15] J. F. Vollano, D. H. Picker, J. A. Statler, *Inorg. Chem. Acta*, **1989**, *155*, 31.
[16] E. M. Kinsch, D. W. Stephan, *Inorg. Chem. Acta*, **1984**, *91*, 263.
[17] J. Vicente, M. T. Chicote, R. Guerrero, P. G. Jones, *J. Chem. Soc., Dalton Trans.* **1995**, 1251.
[18] A. Burini, R. Galassi, B. R. Pietroni, G. Rafaiani, *J. Organomet. Chem.* **1996**, *519*, 161.
[19] Y. Inoguchi, B. Milewski-Mahrla, H. Schmidbaur, *Chem. Ber.* **1982**, *115*, 3085.
[20] J. M. Lopez de Luzuriaga, M. Soldner, A. Schier, H. Schmidbaur, *Z. Naturforsch., B* **1997**, *52*, 209.
[21] K. Angermaier, H. Schmidbaur, *J. Chem. Soc., Dalton Trans.* **1995**, 559.
[22] P. G. Jones, A. G. Maddock, M. J. Mays, M. M. Muir, A. F. Williams, *J. Chem. Soc., Dalton Trans.* **1977**, 1434.
[23] G. C. H. Jones, P. G. Jones, A. G. Maddock, M. J. Mays, P. A. Vergnano, A. F. Williams, *J. Chem. Soc., Dalton Trans.* **1977**, 1440.
[24] R. Usón, A. Laguna, A. Navarro, R. V. Parish, L. S. Moore, *Inorg. Chim. Acta* **1986**, *112*, 205.
[25] W. Clegg, *Acta Crystallogr.* **1976**, *B32*, 2712.
[26] M. G. B. Drew, M. J. Riedl, *J. Chem. Soc., Dalton Trans.* **1973**, 52.
[27] P. W. R. Corfield, H. M. M. Shearer, *Acta Crystallogr.* **1967**, *C23*, 156.
[28] S. Fuchs, J. M. Lopez de Luzuriaga, M. E. Olmos, A. Sladek, H. Schmidbaur, *Z. Naturforsch., B* **1997**, *52*, 217.
[29] A. J. Blake, R. O. Gould, J. A. Greig, A. J. Holder, T. I. Hyde, M. Schröder, *J. Chem. Soc., Chem. Commun.* **1989**, 876.
[30] A. Sladek, H. Schmidbaur, *Z. Naturforsch., B* **1996**, *51*, 1207.
[31] C. A. McAuliffe, R. V. Parish, P. D. Randall, *J. Chem. Soc., Dalton Trans.* **1979**, 1730.
[32] R. Usón, J. Laguna, J. Vicente, *J. Organomet. Chem.* **1977**, *131*, 471.
[33] For some selected and recent examples, see: V. G. Albano, L. Busetto, M. C. Cassani, P. Sabatino, A. Schmitz, V. Zanotti, *J. Chem. Soc., Dalton Trans.* **1995**, 2087. − Z. Assefa, B. G. McBurnett, R. J. Staples, J. P. Fackler, Jr., *Inorg. Chem.* **1995**, *34*, 4965. − P. J. Bonasia, D. E. Gindelberger, J. Arnold, *Inorg. Chem.* **1993**, *32*, 5126. − A. F. Chiffey, J. Evans, W. Levason, M. Webster, *Polyhedron* **1996**, *15*, 591. − S. Coco, P. Espinet, S. Falagan, J. M. Martín-Alvarez, *New J. Chem.* **1995**, *19*, 959. − J. Forniés, R. Navarro, E. P. Urriolabeitia, *J. Organomet. Chem.* **1993**, *452*, 241. − A. M. Gibson, G. Reid, *J. Chem. Soc., Dalton Trans.* **1996**, 1267. − M. C. Gimeno, E. Jambrina, A. Laguna, M. Laguna, H. H. Murray, R. Terroba, *Inorg. Chim. Acta* **1996**, *249*, 69. − S. Alvarez, O. Rossell, M. Seco, J. Valls, M. A. Pellinghelli, A. Tiripicchio, *Organometallics* **1991**, *10*, 2309. − C. G. Arena, D. Drommi, F. Faraone, M. Lanfranchi, F. Nicolo, A. Tiripicchio, *Organometallics* **1996**, *15*, 3170. − J. C. Jeffery, P. A. Jelliss, F. G. A. Stone, *Organometallics* **1994**, *13*, 2651. − L. K. Liu, L. S. Luh, Y. S. Wen, U. B. Eke, M. A. Mesubi, *Organometallics* **1995**, *14*, 4474. − I. Neda, A. Fischer, T. Kaukorat, P. G. Jones, R. Schmutzler, *Chem. Ber.* **1994**, *127*, 1579. − H. G. Raubenheimer, L. Lindeque, S. Cronje, *J. Organomet. Chem.* **1996**, *511*, 177. − V. Riera, M. A. Ruiz, A. Tiripicchio, M. Tiripicchio-Camellini, *Organometallics* **1993**, *12*, 2962. − I. D. Salter, V. Sik, S. A. Williams, T. Adatia, *J. Chem. Soc., Dalton Trans.* **1996**, 643. − M. Slany, M. Bardaji, M. J. Casanove, A. M. Caminade, J. P. Majoral, B. Chaudret, *J. Am. Chem. Soc.* **1995**, *117*, 9764. − A. M. Z. Slawin, M. B. Smith, J. D. Woollins, *J. Chem. Soc., Dalton Trans.* **1996**, 1283. − E. Zeller, A. Schier, H. Schmidbaur, *Z. Naturforsch., B* **1994**, *49*, 1243. − S. Ahrland, K. Dreisch, B. Noren, A. Oskarsson, *Mater. Chem. Phys.* **1993**, *35*, 281. − M. T. Bautista, P. S. White, C. K. Schauer, *J. Am. Chem. Soc.* **1994**, *116*, 2143. − M. Viotte, B. Gautheron, M. M. Kubicki, I. E. Nifant′ev, S. P. Fricker, *Met.-Based Drugs* **1995**, *2*, 311. − P. G. Jones, B. Ahrens, *Chem. Ber.* **1997**, *130*, 1813.
[34] R. Usón, A. Laguna, M. Laguna, E. J. Fernández, P. G. Jones, G. M. Sheldrick, *J. Chem. Soc., Dalton Trans.* **1982**, 1971.
[35] E. J. Fernandez, M. C. Gimeno, P. G. Jones, A. Laguna, M. Laguna, E. Olmos, *J. Chem. Soc., Dalton Trans.* **1996**, 3603.
[36] P. D. Cookson, E. R. T. Tiekink, *J. Chem. Soc., Dalton Trans.* **1993**, 259.
[37] R. Usón, A. Laguna, M. Laguna, J. Jimenez, M. P. Gómez, A. Sainz, P. G. Jones, *J. Chem. Soc., Dalton Trans.* **1990**, 3457.
[38] L. G. Kuzmina, K. I. Grandberg, L. G. Ilina, *Zh. Neorg. Khim.* **1995**, *40*, 1827 (*Chem. Abstr.* **1995**, *123*, 184068n).
[39] F. S. Babichev, V. N. Bubnowskaya, *Ukr. Khim. Zh.* **1964**, *30*, 848 (*Chem. Abstr.* **1965**, *62*, 1766c).
[40] C. K. Bradsher, D. F. J. Lohr, *J. Heterocycl. Chem.* **1966**, *3*, 27.
[41] A. A. Martynowskii, A. A. Brazhko, V. G. Bulakh, T. V. Panasenko, B. A. Samura, E. A. Krasnykh, *Khim.-Farm. Zh.* **1991**, *25*, 20 (*Chem. Abstr.* **1991**, *115*, 49360z).
[42] J. Vicente, M. T. Chicote, J. A. Cayuelas, J. Fernandez-Baeza, P. G. Jones, G. M. Sheldrick, P. Espinet, *J. Chem. Soc., Dalton Trans.* **1985**, 1163. − J. Vicente, M. T. Chicote, I. Saura-Llamas, J. Turpin, J. Fernandez-Baeza, *J. Organomet. Chem.* **1987**, *333*, 129. − J. Vicente, M. T. Chicote, I. Saura-Llamas, P. G. Jones, K. Meyer-Bäse, C. F. Erdbrügger, *Organometallics* **1988**, *7*, 997. − J. Vicente, M. T. Chicote, I. Saura-Llamas, *J. Chem. Soc., Dalton Trans.* **1990**, 1941. − J. Vicente, M. T. Chicote, I. Saura-Llamas, M. C. Lagunas, *J. Chem. Soc., Chem. Commun.* **1992**, 915. − J. Vicente, M. T. Chicote, P. G. Jones, *Inorg. Chem.* **1993**, *32*, 4960. − J. Vicente, M. T. Chicote, P. González-Herrero, P. G. Jones, B. Ahrens, *Angew. Chem.* **1994**, *106*, 1966; *Angew. Chem., Int. Ed. Engl.* **1994**, *33*, 1852. − J. Vicente, M. T. Chicote, P. González-Herrero, P. G. Jones, *J. Chem. Soc., Dalton Trans.* **1994**, 3183. − J. Vicente, M. T. Chicote, M. D. Abrisqueta, *J. Chem. Soc., Dalton Trans.* **1995**, 497. − J. Vicente, M. T. Chicote, P. González-Herrero, P. G. Jones, *J. Chem. Soc., Chem. Commun.* **1995**, 745. − J. Vicente, M. T. Chicote, R. Guerrero, P. G. Jones, *J. Am. Chem. Soc.* **1996**, *118*, 699. − J. Vicente, M. T. Chicote, R. Guerrero, P. G. Jones, M. C. Ramírez de Arellano, *Inorg. Chem.* **1997**, *36*, 4438. J. Vicente, M. T. Chicote, M. C. Lagunas, P. G. Jones, B. Ahrens, *Inorg. Chem.* **1997**, *36*, 4938. − [42a] J. Vicente, M. T. Chicote, M. C. Lagunas, P. G. Jones, *J. Chem. Soc., Dalton Trans.* **1991**, 2579.
[43] A. H. Othman, S.-C. Coh, H.-K. Fun, K. Sivakumar, *Acta Crystallogr.* **1996**, *C52*, 2760.
[44] H. Schmidbaur, W. Graf, G. Müller, *Angew. Chem.* **1988**, *100*, 439; *Angew. Chem., Int. Ed. Engl.* **1988**, *27*, 417.
[45] W. J. Geary, *Coord. Chem. Rev.* **1971**, *7*, 81.
[46] G. M. Sheldrick, University of Göttingen, **1993**.

[97239]

Oligomeric Solvent-Free Magnesium Bis(phosphanides) – Molecular Structure of Trimeric Magnesium Bis[bis(trimethylsilyl)phosphanide]☆

Matthias Westerhausen*, Matthias H. Digeser, Birgit Wieneke, Heinrich Nöth[+], and Jörg Knizek[+]

Institut für Anorganische Chemie der Ludwig-Maximilians-Universität,
Meiserstr. 1, D-80333 München, Germany
Fax: (internat.) + 49(0)89/5902-638
E-mail: maw@anorg.chemie.uni-muenchen.de

Received November 12, 1997

Keywords: Bis(silyl)phosphanes / Magnesium / NMR spectroscopy / Oligomers / Phosphorus

The metathesis reaction of (dme)$LiPH_2$ and chlorodiisopropylsilane yields $HP(SiHiPr_2)_2$ (**1**) and $P(SiHiPr_2)_3$ (**2**). The metalation of **1** by *n*/*sec*-dibutylmagnesium in heptane leads to the formation of dimeric magnesium bis[bis(diisopropylsilyl)-phosphanide] [(**3**)$_2$]. A toluene solution of magnesium bis[bis-(trimethylsilyl)phosphanide] (**4**) shows a dimer-trimer equilibrium in the $^{31}P\{^1H\}$-NMR spectrum at −40°C with an increasing amount of the dimer with increasing temperature. A molecular mass determination by freezing-point depression in benzene yields a value of 516 g·mol^{-1}, which lies between a monomeric and a dimeric molecule. Cooling of the toluene solution to −30°C leads to the precipitation of single crystals of monoclinic $\{(Me_3Si)_2P-Mg[\mu\text{-}P(SiMe_3)_2]_2\}_2Mg$ [(**4**)$_3$].

Several possibilities for the synthesis of the alkaline earth metal bis[bis(trialkylsilyl)amides] justified the vastly growing interest in the molecular chemistry of the heavier alkaline earth metals.[1][2] The alkaline earth metal bis(phosphanides) are easily accessible by the metalation of bis(trialkylsilyl)phosphane with the above-mentioned bis(trialkylsilyl)amides in toluene, where they precipitate, or in ethers such as tetrahydrofuran (thf) or 1,2-dimethoxyethane (dme), where ether adducts are formed.[3] Eq. (1) shows the preparation of the thf complexes of the alkaline earth metal bis[bis(trimethylsilyl)phosphanides].

$$M[N(SiMe_3)_2]_2 + 2\ HP(SiMe_3)_2 \xrightarrow{thf} (thf)_nM[P(SiMe_3)_2]_2 \quad (1)$$
$$M/n = Mg/2,\ Ca/4,\ Sr/4,\ Ba/4$$

The bis(trialkylsilyl)phosphanides of the heavier alkaline earth metals precipitate in the absence of neutral coligands such as ethers or amines. Therefore, the soluble ether adducts of the trialkylsilyl-substituted phosphanides[4] and a tmeda complex of $Mg[P(H)Ph]_2$[5] were investigated by solution NMR as well as X-ray crystallography. Further enhancement of the steric demand of the silyl groups reduces the reactivity of the phosphanes. For example, the metalation of bis(triisopropylsilyl)phosphane[6] by calcium bis-[bis(trimethylsilyl)amide] is neither possible in boiling toluene nor in refluxing thf nor a mixture of both.

Solvent-poor alkaline earth metal bis(phosphanides) are gaining interest especially due to the unexpected structures of the dimers in solution as well as the solid state. Ab-initio SCF calculations for $M_2(PH_2)_4$ show for magnesium the "conventional" monocyclic structure $H_2P-Mg(\mu\text{-}PH_2)_2Mg-PH_2$[6] whereas for calcium or strontium the bicyclic structure $H_2P-M(\mu\text{-}PH_2)_3M$ is the lowest in energy.[4d] In the case of dimeric barium bis(phosphanide) even the tricyclic isomer $Ba(\mu\text{-}PH_2)_4Ba$ has to be taken into consideration. Here, the synthesis of the first solvent-free dimeric and trimeric magnesium bis(phosphanides) is presented and the X-ray structure of trimeric magnesium bis-[bis(trimethylsilyl)phosphanide] is discussed in detail.

Preparation

To raise the reactivity of the P−H fragment compared to bis(triisopropylsilyl)phosphane[6][7] the diisopropylsilyl substituents are chosen. The second advantage of this substituent is the basicity of the Si−H moiety which allows an electrostatic attraction to the metal center as well as an agostic interaction between the metal atom and the Si−H bond. The metathesis reaction of (dme)$LiPH_2$ and chlordiisopropylsilane offers an easy approach to bis(diisopropylsilyl)-phosphane (**1**), which is obtained together with tris(diisopropylsilyl)phosphane (**2**) according to eq. (2). The metalation of **1** in toluene with dibutylmagnesium, dissolved in heptane, yields quantitatively dimeric magnesium bis[bis(diisopropylsilyl)phosphanide] [(**3**)$_2$]. However, the efforts of crystallization failed, and an oil remained after the work-up procedures.

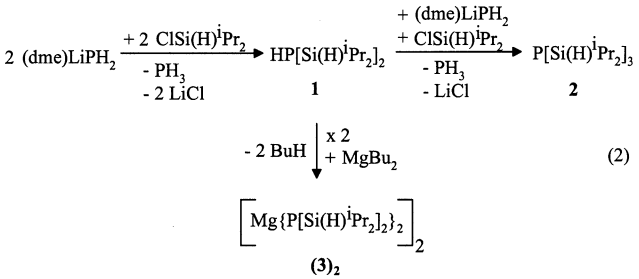

(2)

During the metalation of bis(trimethylsilyl)phosphane with commercially available *n*/*sec*-dibutylmagnesium a col-

[+] X-ray structure analysis.

 © WILEY-VCH Verlag GmbH, D-69451 Weinheim, 1998 1434−1948/98/0404−0517 $ 17.50+.50/0

orless solid precipitates, however, stirring for several hours at room temperature leads to a clear solution. Upon cooling to −30°C crystalline trimeric magnesium bis[bis(trimethylsilyl)phosphanide] [**(4)**$_3$], formed according to eq. (3), precipitates in the shape of colorless cuboids.

$$3\ MgBu_2 + 6\ HP(SiMe_3)_2 \longrightarrow \textbf{(4)}_3 \qquad (3)$$

The addition of tetrahydrofuran yields the already well-known bis(tetrahydrofuran)magnesium bis[bis(trimethylsilyl)phosphanide] (**4**·2 thf).[8] All these magnesium bis(phosphanides) are colorless and very moisture-sensitive.

Spectroscopic Characterization

The NMR data of the phosphanes **1** and **2** clearly show the existence of two chemically different methyl groups. This observation proves that the inversion of the phosphorus atom is very slow on the NMR time scale and the inversion barrier higher than at least 70 kJ·mol^{-1}. No line broadening is observable at room temperature.

The comparison between **1** and **2** shows the influence of the substitution of a hydrogen atom by a diisopropylsilyl group (Table 1). The effects are similar as described for $HP(SiMe_3)_2/P(SiMe_3)_3$.[9] The high-field shift of the ^{31}P signal is accompanied by a low-field shift of the ^{29}Si signal. The ^1J(P,Si) coupling constants of approximately 36 Hz are nearly not affected by this change in the ligand sphere of the phosphorus atom.

For compound **(3)**$_2$ the coupling pattern of two triplets between the bridging and the terminal phosphorus atoms clearly proves its dimeric appearance (Figure 1). Even at elevated temperatures up to 70°C the ligand-exchange processes are very slow on the NMR time scale. The $^2J(P_b,P_t)$ coupling constant of 22.2 Hz lies in the expected range. The ^1J(P,Si) coupling constant within the terminal ligand amounts nearly 39 Hz, whereas for the bridging ligand a value is not deducible, only a line broadening is observed.

For the ^1J(Si,H) coupling constants only a rough estimation can be given due to overlapping of the signals in the ^{29}Si-NMR spectrum and the expected pattern of higher order. For the bridging phosphanide ligand a line separation of approximately 140 Hz can be seen, whereas the ^1J(Si,H) coupling constant of the terminal ligand is clearly larger than 200 Hz. This difference could result from an agostic interaction between the magnesium atom and the Si−H bond[10] or from the different coordination numbers of the phosphorus atoms, in particular under consideration of the strongly differing ^1J(P,Si) coupling constants for the terminal and the bridging substituents. However, only one strong Si−H stretching vibration at 2101 cm^{-1} is observed in the characteristic region for Si−H moieties.

For magnesium bis[bis(trimethylsilyl)phosphanide] (**4**) the determination of the molecular mass by freezing-point depression in benzene yields a value of 516 g·mol^{-1} for a diluted solution, which lies between the mass of a monomer (379 g·mol^{-1}) and a dimer (758 g·mol^{-1}). The ^{1}H- and

Table 1. NMR parameters of the phosphanes **1** and **2** as well as magnesium bis[bis(diisopropylsilyl)phosphanide] [**(3)**$_2$] ([D$_6$]benzene, 30°C, t and b name the terminal and bridging position of the considered atom)

		1	**2**	**(3)**$_2$
^{1}H	δ(Me$_{Pr}$)	1.10	1.22	1.3[a]
	δ(Me$_{Pr}$)	1.10	1.19	
	δ(CH$_{Pr}$)	1.09	1.16	1.3[a]
	δ(PH)	0.41	–	–
	^1J(P,H)	187.3	–	–
	δ(Si$_t$H)	4.23	4.32	4.53
	^1J(Si$_t$,H)	188.2	188.1	
	^2J(P$_t$,H)	8.8	14.7	16.9
	^3J(H$_b$,H$_{Si}$)	3.1	–	–
	δ(Si$_b$H)	–	–	4.42
	^2J(P$_b$,H)	–	–	18.3
^{13}C{^{1}H}	δ(Me$_{Pr}$)	19.39	20.37	[b]
	^3J(P,C)	2.4	3.7	
	δ(Me$_{Pr}$)	19.22	19.62	
	^3J(P,C)	3.2	3.0	
	δ(CH$_{Pr}$)	13.28	14.56	15.78[c]
	^2J(P,C)	9.4	10.0	[c]
^{29}Si{^{1}H}	δ(Si$_t$)	10.29	7.46	9.19
	^1J(P$_t$,Si$_t$)	36.3	36.1	38.7
	δ(Si$_b$)	–	–	6.92
	^1J(P$_b$,Si$_b$)	–	–	< 4 Hz
^{31}P{^{1}H}	δ(P$_t$)	−307.49	−314.31	−347.00
	δ(P$_b$)	–	–	−301.41
	^2J(P$_t$,P$_b$)	–	–	22.2

[a] Broad signal. – [b] Four broad signals at δ = 19.7, 19.8, 20.7, and 21.4; assignment to terminal or bridging phosphanide ligands not possible – [c] Very broad signal due to overlapping of the dublets of the CH groups of the terminal and bridging phosphanide ligands; coupling constants not deducible.

Figure 1. ^{31}P{^{1}H}-NMR spectrum of a [D$_8$]toluene solution of magnesium bis[bis(diisopropylsilyl)phosphanide] [**(3)**$_2$] at 25°C; signals of the bridging (top) and terminal (bottom) (*i*Pr$_2$HSi)$_2$P ligands (109.365 MHz)

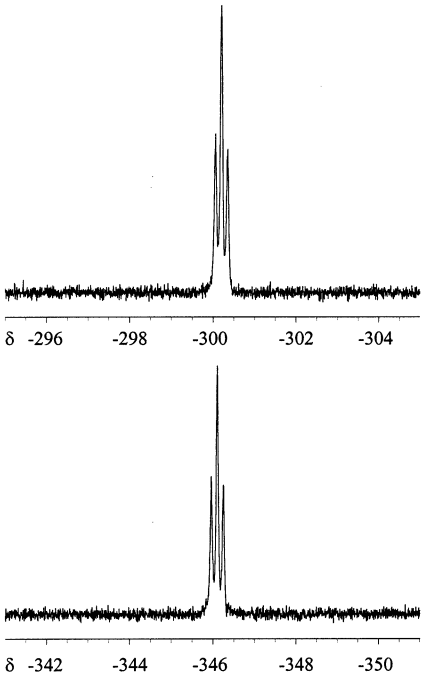

$^{13}C\{^1H\}$-NMR spectra show broad and overlapping signals, an assignment to certain oligomers is not possible. The $^{31}P\{^1H\}$-NMR spectrum recorded at −40°C shows two triplets at δ = −242.55 and −275.44 for the bridging and the terminal $(Me_3Si)_2P$ ligands with a $^2J(P,P)$ coupling constant of 17.9 Hz (Figure 2). In addition to this dimer another isomer with an intensity ratio for the bridging to terminal phosphanide ligands of 2:1 is observed and assigned to the trimer of the type $\{(Me_3Si)_2P-Mg[\mu\text{-}P(SiMe_3)_2]_2\}_2Mg$. This trimer can be crystallized from toluene at −30°C, and its structure is discussed below. Raising of the temperature (Figure 2) leads to an increasing concentration of the dimer at the expense of the trimer. At −40°C the amount of the trimer is 2.5 times higher than the one of the dimer, whereas at 0°C the dimer is 1.1 times more concentrated in solution. The equilibrium is shown in eq. (4), however, at room temperature and higher temperatures coalescence is observed, and the different oligomers are indistinguishable by $^{31}P\{^1H\}$-NMR spectroscopy.

Figure 2. Temperature-dependent $^{31}P\{^1H\}$-NMR spectra of a 0.5 M [D_8]toluene solution of magnesium bis[bis(trimethylsilyl)phosphanide] (**4**); all spectra are internally referenced to a small signal of $P(SiMe_3)_3$ at δ = −251.07 (161.835 MHz); at −40°C the dimeric and trimeric molecules coexist in toluene solution (see text)

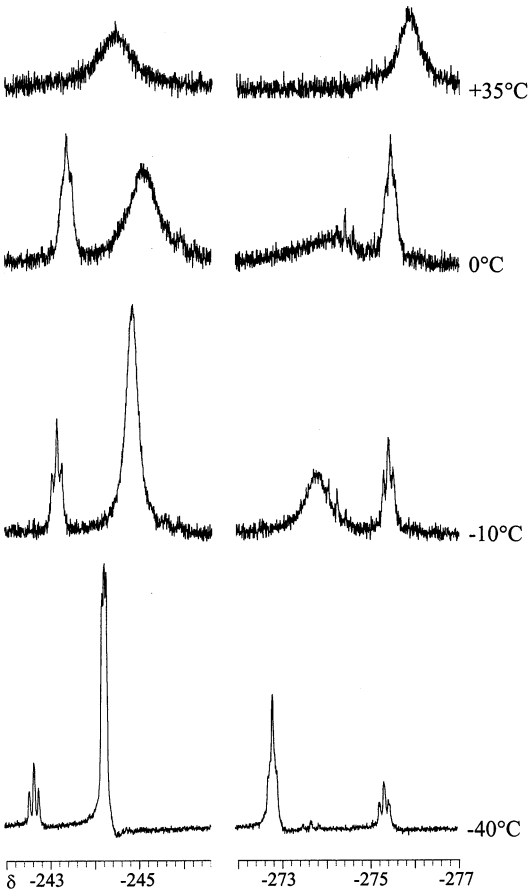

Magnesium bis[bis(trimethylsilyl)phosphanide] is monomeric in the gaseous phase as could be shown by mass spectrometry. The found isotopic pattern of the M^+ peak confirms the assignment.

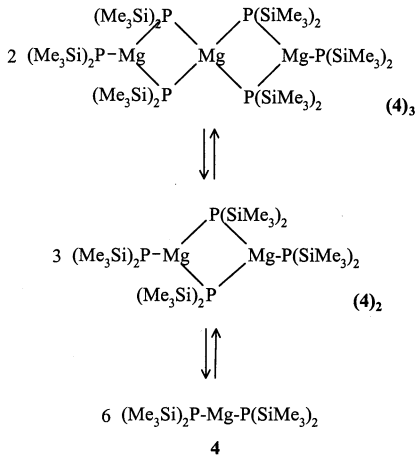

(4)

Molecular Structure of $(4)_3$

The molecular structure and numbering scheme of trimeric magnesium bis[bis(trimethylsilyl)phosphanide] [$(4)_3$] is shown in Figure 3. The coordination sphere around the magnesium atom Mg2 is a distorted tetrahedron, whereas Mg1 and Mg3 are surrounded by a trigonal planar coordination sphere. The four bridging phosphorus atoms are four-coordinate, and the angle sums of the terminal atoms P1 and P6 are 334.3° and 331.6°, respectively. Selected bond lengths and angles of $(4)_3$ are summarized in Table 2.

Figure 3. Molecular structure and the numbering scheme of trimeric magnesium bis[bis(trimethylsilyl)phosphanide] [$(4)_3$]; the ellipsoids represent a probability of 40%; the hydrogen atoms and the labelling of the carbon atoms are omitted for clarity

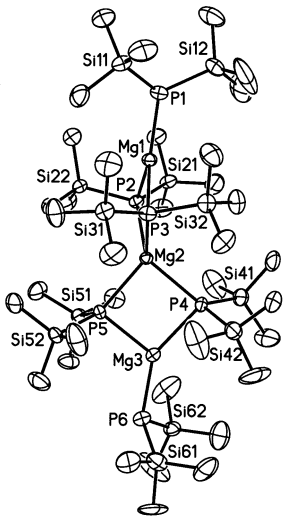

The influence of the coordination number is clearly seen. The terminal phosphanides show Mg−P bond lengths of approximately 245 pm, whereas the bridging phosphorus atoms show Mg−P distances to the triply coordinated magnesium atoms of 255 pm. A further increase of approximately 10 pm is observed for the bond lengths to the quadruply coordinated magnesium atom Mg2, however, the values lie in a wide range between 260 and 268 pm. The intramolecular strain due to the steric demand of the trimethylsilyl groups leads to a bending of the phosphanide

Table 2. Selected bond lengths [pm] and angles [°] of trimeric magnesium bis[bis(trimethylsilyl)phosphanide] [**(4)**$_3$]

n	1	2	3	4	5	6
Mg1−P(*n*)	245.1(2)	253.6(3)	255.3(2)			
Mg2−P(*n*)		261.7(2)	267.0(2)	267.8(2)	260.5(2)	
Mg3−P(*n*)				255.5(3)	254.1(3)	245.9(3)
P(*n*)−Si(*n*1)	221.6(3)	224.2(2)	224.8(2)	225.0(3)	224.9(2)	220.1(3)
P(*n*)−Si(*n*2)	221.2(3)	224.1(2)	223.6(3)	223.5(3)	223.7(2)	221.4(3)
Mg1−P(*n*)−Si(*n*1)	105.12(9)	107.68(9)	119.62(9)			
Mg1−P(*n*)−Si(*n*2)	121.3(1)	100.43(8)	96.75(9)			
Mg2−P(*n*)−Si(*n*1)		130.91(9)	128.04(9)	126.27(9)	114.75(9)	
Mg2−P(*n*)−Si(*n*2)		116.69(8)	114.90(9)	117.67(9)	129.17(9)	
Mg3−P(*n*)−Si(*n*1)				120.1(1)	95.55(8)	115.6(1)
Mg3−P(*n*)−Si(*n*2)				95.40(9)	113.79(9)	107.99(9)
Si(*n*1)−P(*n*)−Si(*n*2)	107.9(1)	106.04(9)	106.16(9)	105.6(1)	107.76(9)	108.0(1)
Mg1−P(*n*)−Mg2		87.89(7)	86.38(7)			
Mg2−P(*n*)−Mg3				87.10(7)	88.96(7)	

ligands towards the triply coordinated magnesium atoms Mg1 and Mg3. The bis(tetrahydrofuran)[8] as well as 1,2-dimethoxyethane complexes[11] show Mg−P bond lengths of approximately 250 pm between a triply coordinated phosphorus atom and a fourfold coordinated magnesium center.

The steric strain destabilizes the polymeric structures which presumingly lead to the precipitation of the magnesium bis[bis(trimethylsilyl)phosphanide] right after the metalation reaction. The polymeric structure breaks apart into trimers, which can then be crystallized. Due to longer M−P bonds for the heavier alkaline earth metals and consequently reduced intramolecular steric strain, solvent-free and soluble derivatives of oligomeric bis[bis(trimethylsilyl)phosphanides] are unknown thus far.

Conclusion

Solvent-free magnesium bis[bis(diisopropylsilyl)phosphanide] is soluble in common organic solvents such as toluene or benzene and dimeric in solution. In contrast to this derivative magnesium bis[bis(trimethylsilyl)phosphanide] shows monomeric molecules besides dimers by molecular-mass determination in benzene and a dimer-trimer equilibrium at −40°C in toluene in the $^{31}P\{^1H\}$-NMR spectrum at a 40 times more concentrated solution. Crystallization at −30°C from toluene solution yields single crystals of $\{(Me_3Si)_2P-Mg[\mu\text{-}P(SiMe_3)_2]_2\}_2Mg$. The Mg−P bond lengths vary between 245 and 268 pm depending on the coordination numbers of the metal and phosphorus atoms. In the gaseous phase monomeric magnesium bis[bis(trimethylsilyl)phosphanide] is observed.

This research was supported by the *Deutsche Forschungsgemeinschaft*, Bonn, and the *Fonds der Chemischen Industrie*, Frankfurt/Main. We also thank Prof. Dr. *J. Weidlein* of the University of Stuttgart for the recording of the Raman spectra.

Experimental Section

All experiments and manipulations were carried out under argon purified by passage through BTS catalyst and P_4O_{10}. Reactions were performed by using standard Schlenk techniques and dried, thoroughly deoxygenated solvents. The starting materials (1,2-dimethoxyethane-O,O′)lithium phosphanide[12] and bis(trimethylsilyl)phosphane[13] were prepared by literature procedures. − NMR spectra were recorded with Bruker spectrometers AM200, AC250, and AM400 or Jeol spectrometers GSX270 and EX400. − A Perkin-Elmer Paragon 1000 PC spectrophotometer was used to record the IR spectra; solid substances were measured in Nujol between CsBr windows (vs very strong, s strong, m medium, w weak, vw very weak, sh shoulder). The frequencies in the region of the Nujol vibrations are not listed.

Bis(diisopropylsilyl)phosphane (**1**) *and Tris(diisopropylsilyl)phosphane* (**2**): 5.0 g of $ClSi(H)iPr_2$ (33 mmol) were slowly added at −20°C to a solution of 4.3 g of $(dme)LiPH_2$ (33.2 mmol) in 80 ml of 1,2-dimethoxyethane. After complete addition, the reaction mixture was stirred for additional 2 h at room temperature. All volatile materials were removed in vacuum at room temperature and a subsequent vacuum distillation gave 2.5 g of $HP[Si(H)iPr_2]_2$ (**1**) (9.5 mmol, 57%) at 73°C/0.02 Torr. The residue was dissolved in 10 ml of *n*-pentane. Cooling to −60°C led to the crystallization of 1.3 g of $P[Si(H)iPr_2]_3$ (**2**) (3.5 mmol, 31%). At −60°C the mother liquor was decanted and the crystals which show a melting point of approximately −10°C were dried in vacuum. The NMR data of both compounds are summarized in Table 1.

Physical Data of **1**: IR (CsBr): $\tilde{\nu}$ = 2940 cm^{-1} vs, 2887 s, 2862 vs, 2722 vw, 2287 m (νPH), 2103 vs (νSiH), 1469 s, 1391 m, 1373 m, 1241 w, 1164 w, 1078 m, 1012 s, 922 m, 885 s, 783 vs, 764 vs, 706 w, 648 m, 612 m, 588 w, 563 vw, 482 m, 458 m, 409 w, 351 vw. − Raman: $\tilde{\nu}$ = 2941 cm^{-1} sh, 2919 s, 2889 s, 2863 vs, 2758 vw, 2716 vw, 2327 m, 2106 s, 1465 m, 1446 m, 1386 w, 1366 vw, 1290 w, 1234 s, 1160 w, 1076 m, 971 m, 920 vw, 882 s, 783 m, 761 w, 645 m, 618 s, 590 s, 565 m, 484 vs, 460 s, 408 m, 391 s, 361 w, 270 vs, 153 s. − MS (20 eV, source 490 K, sample 295 K); *m/z* (%): 262 (62.6) [M$^+$], 246 (19.8), 220 (60.0), 203 (100), 178 (16.5), 115 (12.7). − $C_{12}H_{31}PSi_2$ (262.52): calcd. C 54.90, H 11.90; found C 53.78, H 11.86.

Physical Data of **2**: IR (CsBr): $\tilde{\nu}$ = 2951 cm^{-1} vs, 2887 s, 2862 vs, 2098 vs (νSiH), 1469 s, 1390 m, 1373 m, 1241 w, 1163 vw, 1080 m, 1010 s, 972 vw, 922 m, 880 s, 795 sh, 760 vs, 649 m, 610 m, 592 w, 562 vw, 512 m, 361 vw. − MS (70 eV, source 470 K, sample 320 K); *m/z* (%): 376 (71.0) [M$^+$], 334 (48.3), 292 (55.9), 262 (7.6), 250 (36.3), 249 (37.9), 219 (13.2), 207 (18.8), 203 (17.6), 177 (19.8), 147 (9.6), 135 (21.2), 133 (23.8), 115 (10.2), 105 (15.3), 87 (20.0), 73 (44.3), 59 (100). − $C_{18}H_{45}PSi_3$ (376.78): calcd. C 57.38, H 12.04; found C 55.46, H 11.76.

Magnesium Bis[bis(diisopropylsilyl)phosphanide] (**3**): 1 ml of a 1.0 M solution of *n*/*sec*-dibutylmagnesium in heptane was added

dropwise slowly at 0°C to a solution of 530 mg of bis(diisopropylsilyl)phosphane (2.0 mmol) in 5 ml of toluene. After stirring for 5 additional hours at room temperature, all volatile materials were removed at reduced pressure at room temperature. Residues of toluene were removed at 60°C/10^{-2} mbar. A colorless pyrophoric oil remains, crystallization efforts from various solvents at −20°C and −60°C failed. The elemental analysis showed a low magnesium content and on the other hand high carbon and hydrogen values due to the grease still present in the sample. NMR data are listed in Table 1. − IR (CsBr): $\tilde{\nu}$ = 2940 cm^{-1} vs, 2886 sh, 2865 vs, 2755 vw, 2719 vw, 2101 vs (νSiH), 1462 vs, 1383 m, 1364 m, 1289 w, 1235 m, 1159 vw, 1069 s, 1006 vs, 969 w, 919 m, 879 s, 792 sh, 763 vs, 700 vw, 644 m, 611 s, 590 s, 566 w, 512 s, 483 sh, 410 w.

Magnesium Bis[bis(trimethylsilyl)phosphanide] (**4**): 1.75 ml of bis(trimethylsilyl)phosphane (8.03 mmol) was dissolved in 60 ml of toluene and 4.0 ml of a 1 M heptane solution of *n*/*sec*-dibutylmagnesium was added at room temperature. The precipitation of a colorless solid was observed immediately after complete addition, which dissolved within the next 12 h at room temperature. Reduction of the solution to 20 ml and storage at −30°C yielded 0.43 g of crystalline trimeric **(4)**$_3$ (0.38 mmol, 29%), m.p. 191°C. − NMR ([D_8]toluene, 0.5 mol/l, 25°C); ^{1}H: δ = 0.52 and 0.47 (broad, overlapping signals); ^{13}C{^{1}H}: δ = 5.65, 6.82, and 7.08 (broad overlapping signals); ^{29}Si{^{1}H}: δ = 3.74; ^{31}P{^{1}H}: see text above and Figure 2. − IR (Nujol, CsBr): $\tilde{\nu}$ = 1313 cm^{-1} vw, 1247 vs, 1073 vw, 1028 vw, 855 sh, 829 vs, 749 s, 683 s, 628 vs, 473 s, 460 s, 447 s, 419 s, 370 m, 314 m, 282 w. − MS (70 eV); *m*/*z* (%): 378 (17.0) [M^+], 305 (8.0) [$M^+ - SiMe_3$], 250 (35.1) [$PSi_3Me_9^+$], 178 (53.4) [$HPSi_2Me_6^+$], 163 (40.3) [$HPSi_2Me_5^+$], 147 (100) [$PSi_2Me_4^+$], 73 (89.5) [$SiMe_3^+$]. − $C_{12}H_{36}MgP_2Si_4$ (379.02): calcd. C 38.02, H 9.57; found C 36.93, H 9.22. − Molecular mass: calcd. for monomer: 379; found 516 (by freezing-point depression in benzene, 0.012 mol/l).

X-ray Crystallographic Study of **(4)**$_3$:[14] A suitable single crystal of **(4)**$_3$ was covered with nujol, sealed in a thin-walled capillary and mounted on a four-circle diffractometer Siemens P4 (graphite-monochromated Mo-K_α radiation and SMART area detector). Crystallographic parameters and details of data collection performed at −80°C are summarized in Table 3. No absorption or extinction corrections were applied. The structure was solved by direct methods with the software package SHELXTL Plus[17] and refined with the program SHELXL-93.[16] Neutral atom scattering factors were taken from Cromer and Mann[18] and for the hydrogen atoms from Stewart et al.[19] The non-hydrogen atoms were refined anisotropically whereas the hydrogen atoms were calculated in ideal positions. One of the trimethylsilyl groups shows a two-site disorder (C612, C613/C614, C615) with an occupation ratio of 0.59(3)/0.41(3).

Table 3. Crystallographic data of **(4)**$_3$ as well as details of the structure solution and refinement procedures

	(4)$_3$
Empirical formula	$C_{36}H_{108}Mg_3P_6Si_{12}$
Molecular mass (g·mol^{-1})	1137.05
T [K]	193
Crystal system	monoclinic
Space group[15]	$P2_1/n$
Unit cell dimensions:	
a [pm]	1290.65(1)
b [pm]	3529.33(5)
c [pm]	1633.51(1)
β [°]	99.46(1)
V [nm^3]	7.3397(1)
Z	4
$d_{calcd.}$ [g·cm^{-3}]	1.029
μ [mm^{-1}]	0.390
F(000)	2472
Scan range	1.2° ≤ θ ≤ 20.0°
Indices	$-13 \le h \le 13$; $-35 \le k \le 36$; $-17 \le l \le 17$
Measured data	22718
Unique data	6840 (R_{int} = 0.0809)
Number of parameters	533
R indices[a] with $I > -\sigma(I)$, data	6376
wR_2	0.0928
R_1	0.1067
R indices[a] with $I > 2\sigma(I)$, data	5099
wR_2	0.0899
R_1	0.0821
Goodness-of-fit σ[b] on F^2	1.946
Residual density [e·nm^{-3}]	354; −325

[a] Definition of the *R* values: $R_1 = (\Sigma\|F_o| - |F_c\|)/\Sigma|F_o|$. − $wR_2 = \{\Sigma[w(F_o^2 - F_c^2)^2]/\Sigma[w(F_o^2)^2]\}^{1/2}$ with $w^{-1} = \sigma^2(F_o^2) + (aP)^2$.[16] − [b] $\sigma = \{\Sigma[w(F_o^2 - F_c^2)^2]/(N_o - N_p)\}^{1/2}$.

☆ Dedicated to Professor Dr. *Hanns-Peter Boehm* on the occasion of his 70th birthday.

[1] M. Westerhausen, *Trends Organomet. Chem.* **1997**, *2*, 89.
[2] M. Westerhausen, *Coord. Chem. Rev.*, in press.
[3] M. Westerhausen, W. Schwarz, *J. Organomet. Chem.* **1993**, *463*, 51.
[4] [4a] M. Westerhausen, *J. Organomet. Chem.* **1994**, *479*, 141. − [4b] M. Westerhausen, M. Hartmann, W. Schwarz, *Inorg. Chem.* **1996**, *35*, 2421. − [4c] M. Westerhausen, W. Schwarz, *Z. Anorg. Allg. Chem.* **1996**, *622*, 903. − [4d] M. Westerhausen, G. Lang, W. Schwarz, *Chem. Ber.* **1996**, *129*, 1035.
[5] E. Hey, L. M. Engelhardt, C. L. Raston, A. H. White, *Angew. Chem.* **1987**, *99*, 61; *Angew. Chem. Int. Ed. Engl.* **1987**, *26*, 81.
[6] M. Westerhausen, R. Löw, W. Schwarz, *J. Organomet. Chem.* **1996**, *513*, 213.
[7] M. Driess, H. Pritzkow, *Z. Anorg. Allg. Chem.* **1996**, *622*, 1524.
[8] M. Westerhausen, A. Pfitzner, *J. Organomet. Chem.* **1995**, *487*, 187.
[9] E. Fluck, G. Heckmann in J. G. Verkade, L. D. Quin (Eds.): *Phosphorus-31 NMR Spectroscopy in Stereochemical Analysis*, VCH Publishers, Deerfield Beach, **1987**, p. 61.
[10] R. H. Crabtree, *Angew. Chem.* **1993**, *105*, 828; *Angew. Chem. Int. Ed. Engl.* **1993**, *32*, 789.
[11] M. Westerhausen, W. Schwarz, *Z. Anorg. Allg. Chem.* **1994**, *620*, 304.
[12] [12a] G. Fritz, H. Schäfer, W. Hölderich, *Z. Anorg. Allg. Chem.* **1974**, *407*, 266. − [12b] M. Baudler, K. Glinka, *Inorg. Synth.* **1990**, *27*, 228.
[13] H. H. Karsch, F. Bienlein, T. Rupprich, F. Uhlig, E. Herrmann, M. Scheer in W. A. Herrmann, H. H. Karsch (Eds.): *Synthetic Methods of Organometallic and Inorganic Chemistry (Herrmann/Brauer)*, vol. 3, Thieme, Stuttgart, New York, **1996**, p. 63.
[14] Further details of the crystal structure investigation are available on request from the Fachinformationszentrum Karlsruhe, D-76344 Eggenstein-Leopoldshafen, Germany, on quoting the depository number CSD-407914, the names of the authors, and the journal citation.
[15] T. Hahn (Ed.): *International Tables for Crystallography*, vol. A ("Space Group Symmetry"), 2nd ed., D. Reidel, Dordrecht, **1984**.
[16] G. M. Sheldrick, *SHELXL-93, Program for Crystal Structure Determination*, Universität Göttingen, **1993**.
[17] *SHELXTL PC 5.03*, Siemens Analytical X-Ray Instruments Inc., Madison, WI, **1990**; *SHELXTL Plus 4.0*, Siemens Analytical X-Ray Instruments Inc., Madison, WI, **1989**.
[18] D. T. Cromer, J. B. Mann, *Acta Crystallogr.* **1968**, *A24*, 321.
[19] R. F. Stewart, E. R. Davidson, W. T. Simpson, *J. Chem. Phys.* **1965**, *42*, 3175.

[97262]

The "Coloring Problem" in Solids: How It Affects Structure, Composition and Properties

Gordon J. Miller

Department of Chemistry, Iowa State University
Ames, IA 50011-3111, USA
E-mail: gmiller@iastate.edu

Received October 14, 1997

Keywords: Quantum chemistry / Intermetallic compounds / Transition metal cluster compounds / Crystallography / Electronic structure

The "coloring problem," as applied to the field of solid state chemistry, addresses the issues of structural preference as well as the distribution of different elements within a given structure. Both the connectivity and arrangement of elements in a solid affect physical and chemical properties, so a clear understanding of the forces controlling how elements will arrange themselves in a solid state structure creates the ability to predict structure-composition-property relationships. There are two fundamental energetic contributions that influence how elements in a structure order: the site energy and the bond energy. This review examines how these two parts of the total electronic energy work together to influence the observed structures, compositions, and properties of intermetallics and transition metal cluster compounds.

The study of chemical compounds fundamentally involves elucidation of the relationships among composition, structure, and properties. From a historical perspective, there are two types of compounds: Daltonides and Berthollides. All molecular and many solid state compounds follow the law of definite proportions, which demands integral ratios for their compositions. Berthollides, on the other hand, are nonstoichiometric compounds, and occur only in condensed matter (solids and liquids).[1] Although there are no general rules governing stoichiometry, simple electron counting rules like the octet rule, the 18-electron rule, and Wade's rules provide guidance for stable compositions.[2] Electronic structure theory gives theoretical justification for these simple rules, but application of these quantum mechanical models requires a knowledge of structure, both actual and hypothetical. An additional bonus from the results of electronic structure calculations is the possibility, in principle, of extracting information on physical and chemical properties. Of course, the quantitative accuracy of these predictions depends on the level of approximation used in the quantum mechanical calculations. Such theoretical studies combined with an experimental program involving synthesis, careful structural characterization, and measurements of physical properties allow a thorough examination of the fundamental relationships among composition, structure, and properties. Certain extended solids, in particular intermetallics and transition metal cluster compounds, provide superb examples for systematic investigations of these relationships.

Structure-property relationships can already be witnessed with the main-group elements,[3] and are strongly coupled to valence electron concentration (*vec*), which equals the number of valence *s* and *p* electrons per main-group atom (for the transition elements, valence *s*, *p*, and *d* electrons are

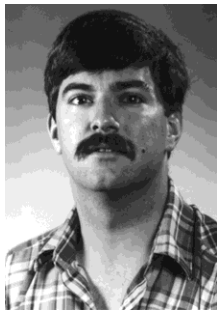

Gordon J. Miller was born in Utica, New York, USA. He received a B.S. degree in chemistry from the University of Rochester in 1982, and a Ph.D. in chemistry, under the supervision of Professor Jeremy K. Burdett, from the University of Chicago in 1986. He then began a postdoctoral research position in the group of Professor Arndt Simon at the Max-Planck-Institut für Festkörperforschung in 1987. In 1990, he joined the chemistry faculty at Iowa State University, where he is currently an Associate Professor. In 1995, he was awarded the Exxon Faculty Fellowship in Solid State Chemistry. His research group is studying structure-property relationships in extended solids, low temperature routes to new inorganic materials, and electronic structure theory of solids.

MICROREVIEWS: This feature introduces the readers to the authors' research through a concise overview of the selected topic. Reference to important work from others in the field is included.

 © WILEY-VCH Verlag GmbH, D-69451 Weinheim, 1998 1434–1948/98/0505–0523 $ 17.50+.50/0

needed; for lanthanides and certainly the actinides, valence *f* electrons must be included as well). For main-group elements with *vec* less than four, closed packed (ccp, hcp or bcc) metallic structures form.[4] If *vec* is greater than or equal to four, open network, nonmetallic structures occur.[4] The inert electron-pair effect in sixth-period elements, e.g., Tl, Pb, Bi, and Po, creates exceptions to these trends.[5] A theoretical technique called second moment scaling of the electronic energy density of states provides a rationale for the observed structural trends of the elements.[6] Complete electronic structure calculations are required, however, to assess observed properties. For example, the observed decrease in electrical conductivity as pressure increases for elemental Ca, Sr, and Ba has been explained by the results of detailed band structure calculations.[7]

As composition becomes a variable, potential structural complexity increases dramatically with respect to both the network of interatomic connections as well as the exact arrangement of the different atoms throughout the structure. The second aspect is also called the *site preference* problem, which is a specific application of the more general *coloring* problem.[*] How atoms are distributed within a network can influence not only to what extent different atoms occur in a compound, i.e., stoichiometry, but also the nature of the electronic structure, i.e., physical and chemical properties. Moreover, there is a synergism between composition and geometrical structure which are blended via the electronic structure that leads to further chemical diversity. Intermetallic and transition metal cluster compounds are well suited for examining these fundamental problems of extended solids: subtle changes can be made in their compound compositions which allow detailed investigation of site preference. The Hume-Rothery intermetallic phases[9] provide exceptional examples for studying both structural complexities mentioned at the beginning of this paragraph: not only does structure change with *vec*, but the distribution of atoms among the different crystallographic sites in a given Hume-Rothery phase is closely related to its structure. Therefore, for multicomponent systems adopting extended structures the following questions arise: (1) for a given composition, what controls the observed structure; (2) in a given structure, how do the different chemical elements arrange themselves; (3) how does this arrangement of atoms influence the observed physical and chemical properties of a given compound; and (4) what is the fundamental relationship among structure, property, and composition for a particular chemical system?

Background

The coloring problem, better known as the "four-color problem" in mathematics, was one of the best known, unsolved mathematical challenges until it was solved in 1976.[10] It defied solution for over one hundred years (since 1852), while attracting the attention of nearly every mathematician in the late nineteenth and throughout the twentieth century. The original basic problem is "to find the smallest number of colors necessary to color the countries of any map so that each two countries with a common border have different colors."[**] This problem belongs to the discipline of *graph theory.*[12] A *graph* is a collection of points, called *vertices*, with various pairs of points joined by a collection of arcs, called *edges.* A vertex has *valence m* if exactly *m* edges meet at that vertex. A *map* is a graph in which each vertex has valence at least three, and with edges that form simple closed curves, called *faces.* The application of this problem to chemistry is clear: the structures of chemical compounds are often represented by graphs in which atoms occupy *vertices*, and bonds often correspond to *edges* in the graph. The chemist wonders, which coloring has the lowest energy? In these chemical examples, however, "coloring" occurs at the vertices, and not at the faces.[***] the idea of reciprocity is important for justifying the equivalence of these two mathematical problems.[10]

The coloring problem occurs in some classic molecular examples: the simplest case being linear triatomic molecules. Both CO_2 and N_2O are linear molecules, but only CO_2 has inversion symmetry. The explanation for the arrangements OCO or NNO and not OOC or NON is simply that 16-electron triatomic molecules require the more electronegative component to occupy the terminal position, i.e., the site with lower coordination number.[14] This effect also occurs in the cage structures of S_4N_4 and As_4S_4,[15] (see Figure 1) which adopt identical molecular topologies: one site is two-bonded (N in S_4N_4; S in As_4S_4), the other is three-bonded (S in S_4N_4; As in As_4S_4). Since the Pauling electronegativities for these three elements increase from As to S to N, the arrangement of atoms in these molecules has the more electronegative element at the two-bonded position.

Figure 1. Molecular structures of As_4S_4 (left) and S_4N_4 (right); white circles are S atoms, black circles are As or N atoms

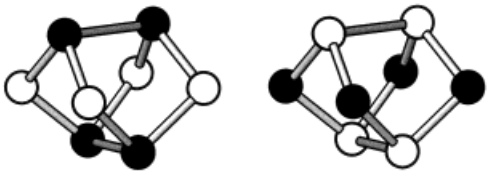

As_4S_4 S_4N_4

Molecular orbital theory can substantiate this conclusion through the principle of *topological charge stabilization.*[16] When a Mulliken population analysis[17] is applied to the

[*] A succinct statement of the coloring problem in chemical systems is, "Given a molecular or extended network and several different types of atoms or chemical groups, what is the best way to distribute them in the network for a fixed stoichiometry?"[8]

[**] The German mathematician Möbius is credited with its origination in the form of a puzzle to his students.[11]

[***] In terms of graph theory, another statement of the coloring problem is, "Consider a fixed molecule or solid state framework which is then populated with different sorts of atoms or atom groupings. Such a mapping of vertices to atoms is called a coloring, and the different atoms or units are associated with different colors."[13]

results of a molecular orbital calculation on a *homonuclear* molecular structure, differences in atomic populations, i.e., the number of valence electrons assigned to an atomic site in the molecule, usually occur. For an isostructural *heteronuclear* molecule, the most electronegative element will occupy the site with the largest Mulliken population. The simple Hückel theory can verify this conclusion. Consider a molecule composed of atoms, which are each described by a set of valence atomic orbitals $\{\chi_i\}$ with atomic orbital energies α_i ($\alpha_i < 0$). The strengths of the atomic orbital interactions in the molecule are prescribed by a set of resonance integrals β_{ij} ($\beta_{ij} < 0$). In the LCAO approximation, a molecular orbital is expressed as

$$\psi_n = \Sigma_i \, c_{ni} \, \chi_i \tag{1}$$

where c_{ni} is the numerical coefficient of the i^{th} atomic orbital in the n^{th} molecular orbital and the summation covers all valence atomic orbitals $\{\chi_i\}$ in the molecule. The energy of this molecular orbital can then be written as

$$E_n = \Sigma_i \, c_{ni}^2 \alpha_i + \Sigma_i \, \Sigma_{j \neq i} \, c_{ni} c_{ij} \beta_{ij} \tag{2}$$

The total valence electron energy, E_{mo}, is the sum of the molecular orbital energies E_n times their corresponding occupation numbers ($z_n = 0$, 1, or 2), which gives the result[18]

$$\begin{aligned} E_{\text{mo}} &= \Sigma_n \, z_n \, E_n = \Sigma_n \, z_n \, (\Sigma_i \, c_{ni}^2 \, \alpha_i + \Sigma_i \, \Sigma_{j \neq i} \, c_{ni} \, c_{nj} \, \beta_{ij}) \\ &= \Sigma_i \, (\Sigma_n \, z_n \, c_{ni}^2 \,) \, \alpha_i + \Sigma_i \, \Sigma_{j \neq i} \, (\Sigma_n \, z_n \, c_{ni} \, c_{nj}) \, \beta_{ij} \\ E_{\text{mo}} &= \Sigma_i \, q_i \, \alpha_i + \Sigma_i \, \Sigma_{j \neq i} \, p_{ij} \, \beta_{ij} \end{aligned} \tag{3}$$

where q_i is the atomic orbital population (Mulliken population in Hückel theory) and p_{ij} is the overlap population[17] (Coulson bond order index[19]) which are defined by the equations

$$q_i = \Sigma_n \, z_n \, c_{ni}^2 \tag{4}$$

$$p_{ij} = \Sigma_n \, z_n \, c_{ni} \, c_{nj} \tag{5}$$

The principle of topological charge stabilization uses just the first term of equation (3), i.e., the most stable coloring of a heteronuclear molecule is the one for which the most electronegative element, i.e., the one with the lowest α_i's, occupies the site with the greatest Mulliken population, q_i, in the *homonuclear* model of the molecule.

Figure 2. Simple representation of three-center four-electron bonding; in the trigonal bipyramidal molecule PF_4CH_3, the methyl group occupies the equatorial position; the linear F−P−F fragment along the axial direction involves three-center four-electron bonding, whose simple molecular orbital picture is shown; the nonbonding orbital has a node at the P atom, which results in the axial sites being generally preferred by the most electronegative ligands

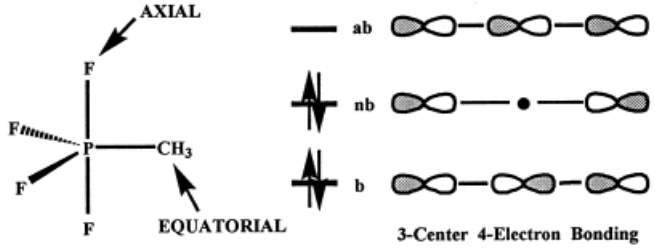

Additional examples of the application of this principle include five-coordinate main group molecules (see Figure 2), which adopt either trigonal bipyramidal or square pyramidal structures.[20] Both arrangements have two inequivalent sets of ligands, labeled axial and equatorial, which immediately lead to a site preference problem. In ten-electron trigonal bipyramidal molecules, e.g., PCl_3F_2 and $PF_4(CH_3)$,[2] the more electronegative F atoms prefer the axial sites, although these molecules undergo rapid pseudorotation. In each case, the more electronegative ligand is involved in three-center four-electron bonding along three collinear atoms.[21] The four electrons in this simple model occupy one bonding and one nonbonding molecular orbital (see Figure 2). The bonding orbital is delocalized throughout the three atomic orbitals, while the nonbonding molecular orbital has only ligand character, which provides the electronic driving force for the observed substitution pattern. Ligands in the equatorial sites of these molecules are involved in two-center two-electron bonding with the central atom. On the other hand, twelve-electron square pyramidal molecules like $XeOF_4$ have the more electronegative ligands (F atoms in $XeOF_4$) in the equatorial sites, which involve two three-center four-electron interactions.

When nonorthogonal atomic orbital basis sets are used in electronic structure calculations, as in the extended Hückel theory,[22] the expression for the total valence electron energy E_{mo} becomes slightly modified from equation (3). The overlap integrals S_{ij} are now explicitly included during calculation of the electronic energy levels, and expressions for the Mulliken population and overlap population become

$$q_i = \Sigma_n \, z_n \, (\, c_{ni}^2 + c_{ni} \, c_{nj} \, S_{ij}) \tag{6}$$

$$p_{ij} = \Sigma_n \, 2 \, z_n \, c_{ni} \, c_{nj} \, S_{ij} \tag{7}$$

Then, after some simple algebraic manipulations of the molecular orbital energy values, the total valence electron energy is

$$E_{\text{mo}} = \Sigma_i \, q_i \, \alpha_i + \Sigma_i \, \Sigma_{j \neq i} \, p_{ij} \, (\beta_{ij} - S_{ij} \, \alpha_i) \tag{8}$$

The first term in expressions (3) or (8) can be interpreted as the energy contribution from the valence electron configurations of the different atoms or ions in the structure, which is the *site energy*. The value of this term is sensitive to the degree of charge transfer between atoms as well as the coordination geometry at each site. The second term is a net two-center interaction term, the *bond energy*, and will be minimized when only bonding and nonbonding orbitals are occupied by providing maximum overlap populations p_{ij}.

This type of transformation of the total valence electron energy does not require a knowledge of the eigenstates of the system, i.e., $\{\psi_n\}$, provided another method can calculate the population terms, q_i and p_{ij}.[23] These chemical quantities are the matrix elements of the density matrix,[*]

[*] The density matrix elements are expansion coefficients of the total charge density in the atomic orbital basis set. Diagonal elements are the charge densities to associate with each orbital in the system; off-diagonal elements are bond orders between two different atomic orbitals on different atoms.

which can be determined without knowing the eigenstates by using, for example, the recursion method.[24] Furthermore, expressions (3) and (8) are general for all types of chemical systems: molecules, crystalline solids, amorphous solids, liquids, quasicrystalline solids, and defective crystalline materials. For solids, E_{band} replaces the symbol E_{mo} to describe the total valence electron energy from the occupation of energy bands rather than molecular orbitals. In subsequent discussions, we shall call this energy the total orbital energy, E_{orb}. This transformation of the total energy introduces a much more chemical approach to the analysis of electronic structure of solids. Furthermore, with respect to the "coloring" problem in chemical structures, the tight-binding expressions in equations (3) and (8) point to two contributions: atoms arrange themselves to provide the lowest site energy and to minimize the bond energy.

Figure 3. Structure of the quasi-infinite $^{1}_{\infty}[SnTe_5]^{2-}$ chain in K_2SnTe_5 and Tl_2SnTe_5;[25] white circles are Te atoms, black circles are Sn atoms

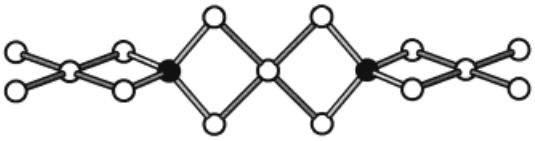

Consider one simple example of this problem: the quasi-infinite chain $^{\infty}_{1}[SbTe_5]^{2-}$ found in K_2SnTe_5 and Tl_2SnTe_5 (see Figure 3).[25] As the figure shows, this chain consists of tetrahedrally coordinated Sn atoms alternating with square planar coordinated, albeit slightly distorted, Te atoms, which we can formulate as $^{\infty}_{1}[(SnTe_{4/2})(TeTe_{4/2})]^{2-}$. X-ray diffraction studies are unable to differentiate between Sn ($Z = 50$) and Te ($Z = 52$) for these two sites, but their distribution has been inferred from the known crystal chemistry of these two elements. An extended Hückel calculation performed on a homonuclear chain (using only Te atomic orbital parameters) indicates that the more electropositive element [Sn; lower q_i's in equation (8)] would occupy the tetrahedrally coordinated site, and the more electronegative element [Te; higher q_i's in equation (8)] would occupy the site with square planar coordination. A direct comparison of the two different patterns shows the observed combination to be energetically preferred over the alternative by approximately 10.0 eV per formula unit if only nearest neighbor (four Sn−Te and four Te−Te) interactions are considered. Of this 10.0 eV energy difference, 1.2 eV is attributed to the difference in site energies and 8.8 eV is the difference in bond energies. The dominance of the bond energy difference reflects tetrahedral vs. square planar coordination at the two different sites. When second nearest neighbor interactions are included (Sn···Te along the chain in the tight-binding calculation), this total energy difference increases to 14.4 eV, of which 12.1 eV is due now to a difference in site energies, and 2.3 eV to a difference in bond energies. The dramatic change in how the two components contribute to the total energy arises from a significant difference in the coordination environment: Sn is surrounded by 4 + 2 Te atoms, whereas Te is coordinated by four Te atoms and two Sn atoms. Regardless, the Sn occupies the tetrahedral sites and Te, the square planar sites.

In extended solids the site preference problem has already been well documented for the spinels, $A^{2+}B_2{}^{3+}O_4$.[26] In these oxides, one-half the octahedral holes and one-eighth the tetrahedral holes are occupied by metal ions in the cubic closest packed oxide framework. A *normal* spinel would be $A_{(tet)}{}^{2+}B_{(oct)2}{}^{3+}O_4$, as in $Co_3O_4 \equiv Co_{(tet)}{}^{2+}Co_{(oct)}2^{3+}O_4$, whereas an *inverse* spinel would be $B_{(tet)}{}^{3+}$-$(A_{(oct)}{}^{2+}B_{(oct)}{}^{3+})O_4$, as in $CoFe_2O_4 \equiv Fe_{(tet)}{}^{3+}$-$(Co_{(oct)}{}^{2+}Fe_{(oct)}{}^{3+})O_4$. The crystal field theory achieved success by comparing the energies of octahedral and tetrahedral fields for different d^n electronic configurations. Strong preference for octahedral coordination occurs for d^1-d^4 and d^6-d^9 ions, which has been used to rationalize the different ionic arrangements in spinels. Of course, ligand field theory can also be applied to these examples with identical results.[2]

Perhaps a better example of the "coloring" problem is how to color the body-centered cubic (bcc) lattice with two different atoms at equal concentrations, i.e., AB. The cubic CsCl structure (Figure 4) is the alternant variant, with each A atom surrounded by eight nearest neighbor B atoms and six next nearest neighbor A atoms at a 15% larger distance. On the other hand, the CuTi structure (Figure 4) is a tetragonal modification of the bcc arrangement with alternating pairs of (001) planes of atoms. In CuTi, each A atom is coordinated by four A and four B nearest neighbors as well as four A and two B next nearest neighbors; each B atom is surrounded by four A and four B nearest neighbors and four B plus two A next nearest neighbors. In these two examples, the observed coloring depends on the *vec*, as also shown in Figure 4 for binary alloys of the transition metals.[27] Another possible coloring of this lattice is the NaTl structure (Figure 4),[28] which is limited to binary compounds of the pre- and post-transition elements. For the NaTl structure, there are four A and four B nearest neighbors plus six next nearest neighbor B atoms around each A atom. For this problem, semi-empirical calculations nicely reproduce the observed trend in structure.[27]

Therefore, with respect to these examples, the site preference problem is a specific corollary of the more general "coloring" problem. Extended solids offer the additional problem of disorder, which further complicates the problem. A general understanding (i.e., predictive algorithm) remains to be determined to elucidate solutions for the general case, but the following section examines a small number of examples from our research group to help build a body of data for the "coloring" problem in solids.

Applications

The remainder of this article focuses on specific examples of the "coloring problem" in extended solids from our group's research. The fundamental questions concern how structure, composition, and properties of extended solids are affected by the arrangement of different elements in a compound. Since intermetallic and transition metal cluster compounds are involved, these investigations reveal how

Figure 4. Structures of different AB colorings of the bcc lattice: (very top) CsCl structure; (center top) CuTi structure; (center bottom) NaTl structure; (very bottom) computed energy differences between the CsCl and CuTi arrangements vs. the average number of $s + d$ electrons; CsCl is the reference structure; the more stable structure has the lower value of ΔE for a given number of $s + d$ electrons; experimentally observed values are shown on the diagram

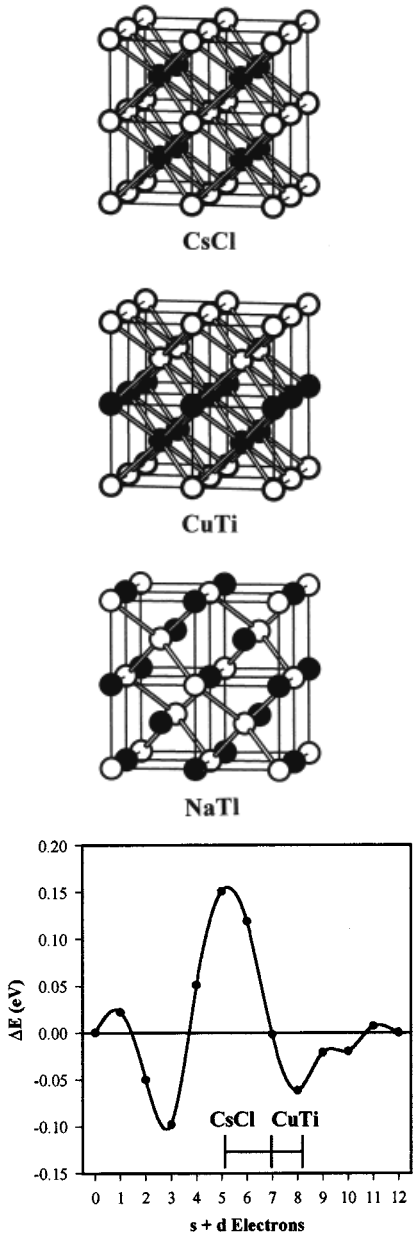

experiment and theory can work symbiotically to pursue some fundamental chemical questions. These applications are organized as follows: (1) kinetically vs. thermodynamically stable structures; (2) structural influences for a single composition but variable electron count; (3) site preferences and composition influenced by nearest neighbor interactions; (4) structure-composition relationships in intermetallics; and (5) composition-property effects.

Figure 5. Structures of the low and high temperature forms of Nb_3SI_7: (top) *o*-Nb_3SI_7; (bottom) *h*-Nb_3SI_7; black circles are Nb atoms, gray circles are S atoms, white circles are I atoms; figures on the left illustrate the two-dimensional layers of clusters, and those on the right show the local environments of the Nb_3 triangles; the point symmetry of the cluster in *o*-Nb_3SI_7 is C_s while in *h*-Nb_3SI_7 it is C_{3v}

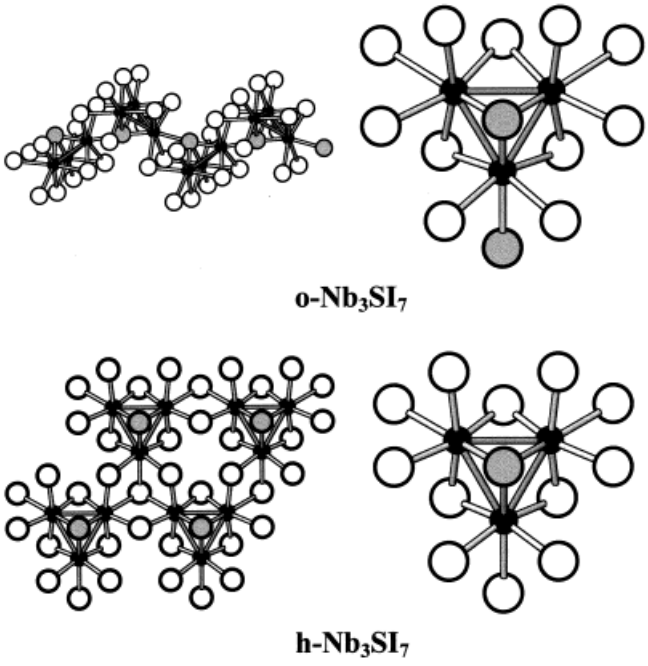

1. Kinetic versus Thermodynamic Products: Nb_3SI_7

The formation of solid state compounds is certainly controlled by both thermodynamic and kinetic factors. With temperature and pressure as fundamental variables, the complete study of a particular system involves numerous synthetic attempts under different conditions. Recent investigations with ternary transition metal/chalcogen/halogen systems containing metal clusters have uncovered a diverse collection of new layered compounds with various structures and properties.[29] One poignant example is Nb_3SI_7, which has been characterized in three topologically different layered structures (polymorphs, not polytypes!) depending upon the temperatures chosen for synthesis. All three structures, however, contain triangular Nb_3 clusters with capping sulfur atoms. Their differences arise in how these units are linked together. The coloring problem in this system addresses how sulfur and iodine form the anion matrix that contains the Nb_3 clusters.

At temperatures between ca. 300 °C and 650 °C, elemental niobium, sulfur, and iodine react in the molar ratio 3.0:1.0:3.5 to give a crystalline orthorhombic phase, *o*-Nb_3SI_7, whose structural formula is $Nb_3S_{1/2}{}^{i-a}I_3{}^{i}I_{6/2}{}^{a-a}$-$(I_{2/2}{}^{a-a}S_{1/2}{}^{a-i})$.[*] As seen in Figure 5, the Nb_3 triangle is capped by a single sulfur atom (S^i), and each edge is

[*] The notation for transition metal clusters differentiates between ligands bridging edges or faces of a cluster, i.e., X^i (i = *innen* = inner) and those connecting or terminating clusters, X^a (a = *aussen* = outer).[30]

bridged by an iodine atom (I^i). These $[Nb_3(\mu_3\text{-}S)(\mu_2\text{-}I)_3$ units are then connected together by six iodine atoms (I^{a-a}) linking two clusters and three ligands *trans* to the capping sulfur atom (two are I^{a-a} and one is S^{a-i}) linking three clusters. There is just one crystallographic type of sulfur atom in *o*-Nb_3SI_7: it caps an Nb_3 triangle, but it also bonds to an adjacent cluster (thus the S^{i-a} and S^{a-i} designations in the structural formula). In *o*-Nb_3SI_7 sulfur is 3+1 coordinated to Nb in a *cis*-divacant octahedral geometry. This local coordination structure at one of the anions gives rise to the undulating layered structure of *o*-Nb_3SI_7.

Figure 6. Schematic diagrams of the relationships in atomic orbital energies for three different elemental components of ternary compounds; the higher the electronegativity of an element, $\chi(X)$, the lower its valence orbital energies; for these schemes, $\chi(A) < \chi(B)$, so $E(A)'s > E(B)'s$; the interesting chemistry arises by considering how A and B relate to the third component C; (a) $\chi(A) < \chi(B) < \chi(C)$, (b) $\chi(A) < \chi(C) < \chi(B)$, (c) $\chi(C) < \chi(A) < \chi(B)$; electron transfer takes place until a constant electrochemical potential exists throughout the structure

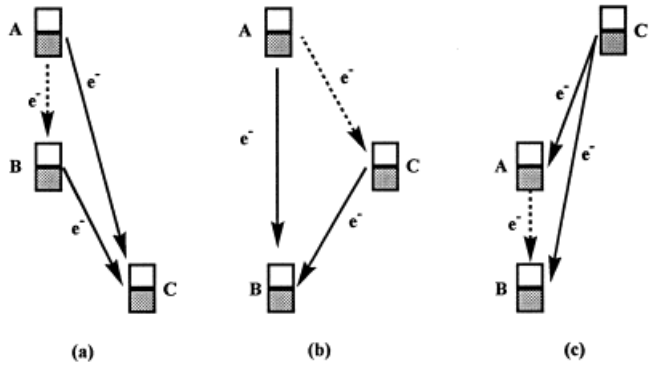

Above ca. 650°C, these elements form a layered hexagonal structure, *h*-Nb_3SI_7,[29] (see Figure 4) whose layers are related to those found in β-Nb_3I_8.[31] The corresponding structural formula for this compound is $Nb_3S_1{}^iI_3{}^iI_{6/2}{}^{a-a}I_{3/3}{}^{a-a}$. Each sulfur atom is just three-coordinated to Nb, and the layers are flat. The structures of *o*-Nb_3SI_7 and *h*-Nb_3SI_7 can be compared by examining the two different packing arrangements of anions: *o*-Nb_3SI_7 involves cubic closest packed anions $(\cdots c\cdots)$[32] with each (111) plane containing 1/8 sulfur and 7/8 iodine, while *h*-Nb_3SI_7 contains an alternating mixture of cubic closest packed and hexagonally closest packed layers $(\cdots hc\cdots)$[32] with sulfur occurring in alternate close packed layers to an extent 1/4 sulfur and 3/4 iodine. In *o*-Nb_3SI_7 the stacking arrangement of one anion "(111)" sheet (i.e., "SI_7") with respect to its two neighboring layers maximizes the S···S internuclear separation, or minimizes the electrostatic repulsion between neighboring sulfide ions. In both close packed anion arrays, Nb atoms occupy 3/8 of the total number of octahedral holes and are located close to the sulfur atoms. A combination of lattice energy[33] and extended Hückel[22] calculations on various models indicates that Nb−Nb bonding is optimized in *h*-Nb_3SI_7, but that the Madelung energy is lower for *o*-Nb_3SI_7. Quenching and annealing experiments conducted at different temperatures show that *o*-Nb_3SI_7 transforms to *h*-Nb_3SI_7 irreversibly at temperatures above ca. 650°C.

Thus, the coloring of the anion network in Nb_3SI_7 strongly influences the resultant total structure of the extended solid involving transition metal clusters. Ionic and covalent forces compete for the formation of a given atomic arrangement. At low temperatures, long range electrostatic interactions guide the formation of the kinetically stable *o*-Nb_3SI_7 by maximizing the separation between sulfide ions. At higher temperatures, however, the atoms rearrange to give a structure with lower internal energy, *h*-Nb_3SI_7, which retains certain structural features, e.g., the Nb_3 triangular cluster.[*]

The ternary niobium/sulfur/iodine system offers a further application of the coloring problem that is only possible in extended solids-nonstoichiometry. $Nb_3S_{1-x}I_{7+x}$ can be prepared from the elements for $x \leq 1$.[29][35] X-ray and neutron diffraction studies on polycrystalline powders and single crystals show that these layered compounds have structures related to β-Nb_3I_8 for $x > 0.6$ and *h*-Nb_3SI_7 for $x < 0.4$. A two-phase mixture of these structures exists for $0.4 < x < 0.6$. Throughout the series, moreover, sulfur and iodine atoms randomly occupy the anion site capping the Nb_3 cluster. Neutron powder diffraction on the compounds β-Nb_3I_8, $Nb_3S_{0.34}I_{7.66}$, and $Nb_3S_{0.64}I_{7.36}$ between 15 K and 300 K did not exhibit any ordering phenomena, i.e., no superstructure reflections nor any symmetry-lowering phase transitions. Magnetic susceptibility measurements give one unpaired electron per μ_3-I capped Nb_3 cluster, except in β-Nb_3I_8. We can understand the lack of superstructure from the electronic structures of μ_3-S capped Nb_3 groups and μ_3-I capped Nb_3 groups in the iodide matrix. Electronic and matrix effects work against each other to produce disorder: the six-electron Nb_3 cluster in Nb_3SI_7 has weaker Nb−Nb bonding but a smaller capping anion (sulfide) than the seven-electron cluster in β-Nb_3I_8. Thus, Nb−Nb distances remain nearly unchanged throughout the series $Nb_3S_{1-x}I_{7+x}$ and the Fermi levels do not vary with the composition variable *x*.

2. Coloring and Structure in Ternary MM′X Intermetallics

Intermetallic compounds adopt structures that are dependent, in part, on the number of valence electrons per formula unit. An understanding of this relationship between structure and electron count requires knowledge of the electronic structures and a good estimation of the structural energy differences for different arrangements of atoms. *Second moment scaling*[6] techniques and the *structural energy difference theorem*[4] have contributed greatly to the recent success of electronic structure calculations for sorting numerous binary intermetallic compounds. The second moment μ_2 for a quasi-continuous distribution of electronic states $\rho(E)$ (as one finds in an extended solid) is defined by the integral

$$\mu_2 = \int_{-\infty}^{\infty} E^2\rho(E)\mathrm{d}E \qquad (9)$$

[*] A new modification, *m*-Nb_3SI_7, has been recently characterized at temperatures exceeding 1000°C, but was first identified in the compound $Nb_7S_2I_{19} = [Nb_3SI_7]_2(NbI_5)$.[34]

Within the tight-binding (LCAO) approximation, this integral expression can be rewritten into a summation

$$\mu_2 = \Sigma_{i=1}^{N} \alpha_i^2 + \Sigma_{i<j} \beta_{ij}^2 \quad (10)$$

N is the number of atomic orbitals in the unit cell, α_i is the atomic orbital energy for the i^{th} atomic orbital, and β_{ij} is the resonance integral between different atomic orbitals i and j. For identical compositions, the first term in equation (10) is the same for all structural models. Second moment scaling, therefore, demands that for all structure types to be compared the unit cell and atomic positional parameters be selected to create equal second terms, $\Sigma_{i<j}\beta_{ij}^2$, and therefore equal μ_2 values. The structural energy difference theorem states that the energy difference between two structures is given to first order by the difference in the bonding contributions to the total energy, i.e., ΔE_{bond}. The total binding energy for a structure is generally the sum of a repulsive term, E_{rep}, and the bonding contribution, E_{bond}. E_{bond} can result from a Madelung (E_{mad}), molecular orbital or band structure (E_{orb}) calculation, while the repulsive term is a combination of short-range electrostatic and Pauli repulsion contributions, which are specifically proportional to coordination numbers. Heine has demonstrated that the second moment μ_2 is proportional to the average coordination number in a given structure.[36] Therefore, performing second moment scaling on various structural models creates equal E_{rep} terms in the total binding energy, and validates the structural energy theorem.[4]

Once the electronic structure calculations are completed, equation (3) or (8) can be used to provide a rationale, in chemical terms, for the predicted sorting diagram: an element will tend to adopt a single type of site that minimizes its site energy and bond energies. For a study of structural changes with valence electron concentration, the site energy changes rapidly with electron count due to the quadratic dependence of atomic orbital energies on charge. The relative electronegativities (χ) of the components in ternary A_x-B_yC systems give rise to three scenarios: (1) $\chi(C) > \chi(B) > \chi(A)$, (2) $\chi(B) > \chi(C) > \chi(A)$, and (3) $\chi(B) > \chi(A) > \chi(C)$. Figure 6 illustrates how electron transfer will take place as these elements form chemical bonds (the greater electronegativity implies lower atomic orbital energies). The sites ultimately selected by elements A and B in the C matrix will follow the ramifications of equation (8): lowest *site* and *bond* energies, which are governed by the extent of electron transfer and orbital overlap. In this first example, we highlight the subtle interplay between site potential and near neighbor interactions at controlling structure in metal-rich phosphides.

The recent synthesis and crystal structure determination of ZrNbP provide two unusual features:[37] (1) ZrNbP crystallizes in the Co_2Si structure type (oP12[*]), whereas Zr_2P (oC108) and Nb_2P (oP54) form other, quite complex structures; and (2) Zr and Nb are completely separated onto different crystallographic sites with no evidence for mixed site occupations nor of any variable composition, $Zr_{1\pm x}Nb_{1\mp x}P$. The miscibility of Zr and Nb is certainly manifested in their binary phase diagram, but does not seem to extend to this ternary compound. Furthermore, ZrNbP differs from ternary (Nb, Ta) sulfides,[38] in which there is only a partial segregation of Nb and Ta atoms onto inequivalent crystallographic sites. But ZrNbP is nonetheless similar to these ternary sulfides because they exist only for specific Ta:Nb ratios. Semi-empirical electronic structure calculations[39] were performed in our group in order to address the following questions: (1) what accounts for the complete segregation of Zr and Nb atoms in ZrNbP?, and (2) what controls the observed structure of ZrNbP with respect to viable alternative structures for the ternary MM′P phosphide system? As it turns out, both questions have the same answer, which relates to the nature of metal−metal bonding in this system. Moreover, the theoretical analysis predicted the structure for the new compound ZrMoP, which was subsequently confirmed by experiment. Therefore, the structure and existence of a new intermetallic compound could be predicted using crystal chemical principles and electronic structure calculations.

Figure 7. (Top) structure of ZrNbP and (bottom) structure of ZrMoP; black circles are Nb or Mo atoms, gray circles are Zr atoms, and white circles are P atoms; figures on the left illustrate metal−phosphorus contacts, figures on the right show metal−metal contacts

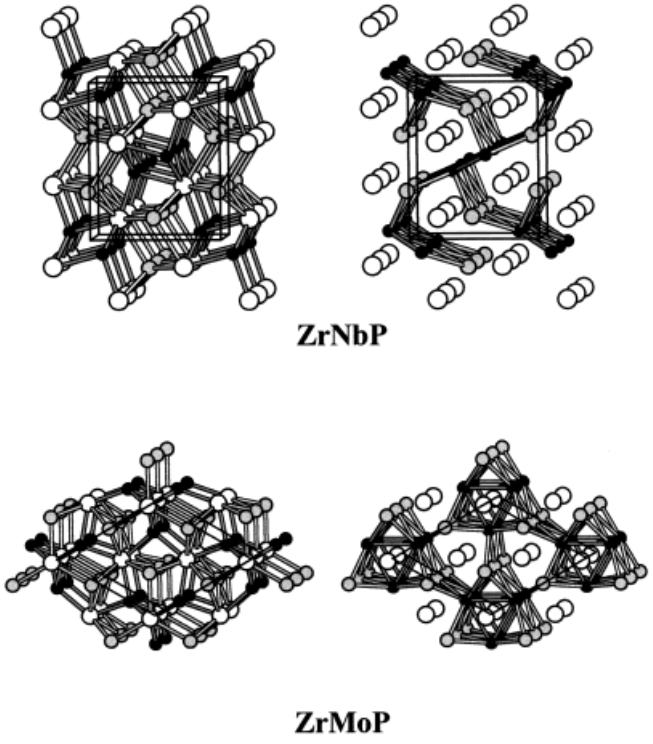

Figure 7 illustrates two projections of ZrNbP along the crystallographic b axis, one of which emphasizes the close metal−phosphorus contacts (d < 3.05 Å) while the other

[*] The Pearson symbol[32] describes for a given structure its Laue symmetry, lattice class, and number of atoms in the unit cell. oP12 means primitive orthorhombic with 12 atoms in the unit cell.

shows the metal−metal distances shorter than 3.30 Å. In ZrNbP, Nb is tetrahedrally coordinated and Zr is square pyramidally coordinated by P atoms. With respect to these coordination environments, there are two alternative structures common to many ABC intermetallics: (1) the Fe_2P-type and (2) the Cu_2Sb-type.[32][40] The Fe_2P structure type is also illustrated in Figure 7 to point out both the metal−phosphorus and metal−metal connectivities. In order to compare the total energies of the three structure types at valence electron counts around fourteen per formula unit, second moment scaling and the structural energy theorem were applied. Figure 8 illustrates these results as energy difference curves. Not only do these calculations reflect the stability of the observed structure for ZrNbP, but they also predict the structure of ZrMoP, if it exists, to be the Fe_2P-type. Direct synthesis and single crystal structural characterization of $Hf_{1.06}Mo_{0.94}P$ confirmed this prediction, and revealed the complete segregation of Hf and Mo, respectively, onto the square pyramidal and tetrahedral sites.[39] ZrMoP was also synthesized and characterized by X-ray powder diffraction.[39]

Figure 8. Energy difference curves vs. valence electron count for the Co_2Si-, Fe_2P-, and Cu_2Sb-structure types as possible models for the structure of ZrNbP; the energy of the Co_2Si-structure type is the reference energy ($\Delta E = 0$); the lowest ΔE curve for a given electron count represents the most stable structure among the three models; the electron counts for ZrNbP and ZrMoP are marked

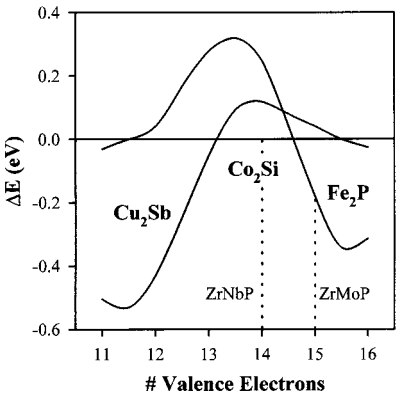

Why does the complete segregation of Zr and Nb in ZrNbP and of Hf and Mo in $Hf_{1.06}Mo_{0.94}P$ occur? The same electronic structure calculations[39] show that the observed, completely segregated sets of metal atoms give the lowest total valence electron energies over all other possible arrangements of metal atoms in ZrNbP and ZrMoP. From equation (8), this segregation provides the lowest site energies for these elements. In addition, analysis of the overlap populations[39][41] for the two shortest metal−metal contacts in each structure reveals that the *heteronuclear* Zr−Nb and Zr−Mo interactions are optimized, i.e., bonding and nonbonding orbitals are filled; antibonding orbitals are empty. At the corresponding Fermi levels, the homonuclear Nb−Nb interactions in ZrNbP are nonbonding whereas the Mo−Mo contacts in ZrMoP show significant antibonding overlap (see Figure 9). These theoretical results are well reflected in the observed bond lengths: the shortest heteronuclear metal−metal distances reflect the differences in atomic radii [d_{min} (Zr−Nb) = 3.014 Å in ZrNbP vs. d_{min} (Hf−Mo) = 2.915 Å in HfMoP], whereas the shortest homonuclear metal−metal distances demonstrate the nature of occupied electronic levels near the Fermi level [d_{min} (Nb−Nb) = 2.816 Å in ZrNbP vs. d_{min} (Mo−Mo) = 3.015 Å in HfMoP]. Thus, total segregation of Zr and Nb in ZrNbP or Hf and Mo in $Hf_{1.06}Mo_{0.94}P$ relies not only on the site energies in each structure, but also on the heteronuclear metal−metal interactions.

Figure 10 illustrates how the relationship between the site and bond energies arises. Phosphorus atoms create tetrahedral and square pyramidal ligand fields about the metals, which breaks the degeneracy of their valence *d* orbitals. According to electronegativities (see Figure 6) some of the metal valence electrons are transferred to phosphorus to form metal−phosphorus bonds. The electrons remaining in metal valence orbitals are utilized to form heteronuclear and homonuclear metal−metal bonds. Since the strength of orbital interactions is inversely proportional to the energy difference between the two isolated orbitals,[14] the strongest heteronuclear metal−metal interactions occur when the energy difference between occupied valence *d* orbitals of the

Figure 9. Overlap populations[17][41] for the shortest homonuclear and heteronuclear metal−metal bonds in ZrNbP (left) and ZrMoP (right); the dashed lines indicate calculated Fermi levels for 14 and 15 valence electrons per formula unit; positive values (bonding overlap) lie to the right and negative values (antibonding overlap) lie to the left; in ZrNbP, both Nb−Nb and Zr−Nb bonding is optimized; in ZrMoP, Zr−Mo bonding is optimized, but there is significant antibonding character for Mo−Mo bonding at the Fermi level

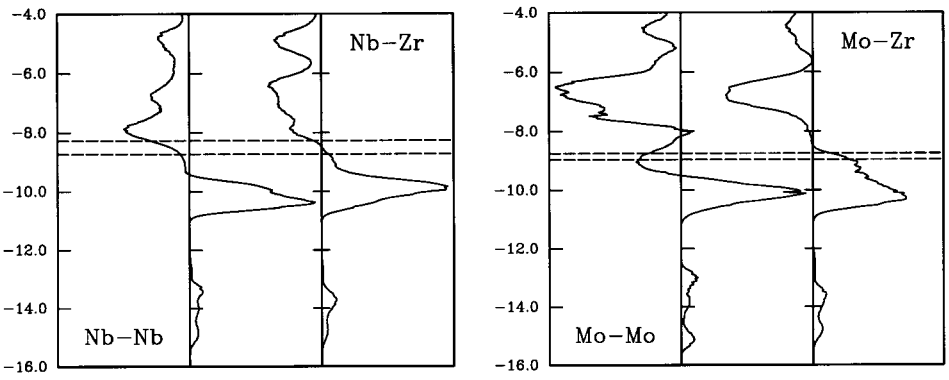

two different metals is smallest. In ZrNbP and ZrMoP this condition is met when Zr is in square pyramidal coordination and Nb or Mo are tetrahedrally coordinated by P: the difference in valence *d* orbital energies equals the free atomic orbital energy difference, Δ, plus the difference between the *d* orbital energy shifts from the π donor phosphorus ligands (expressed in units of e_π using the angular overlap model[2]). When the more electronegative Nb or Mo atoms are tetrahedrally coordinated, the resulting energy difference is less than when these elements are in the square pyramidal sites. In this manner, optimizing the site energy also minimizes the heteronuclear metal−metal bond energy.

Figure 10. Ligand field effects on the site preference problem in metal-rich ternary phosphides; in each section, the relative energies of the Zr and Nb 4*d* AOs are shown (Δ is energy difference between Nb and Zr 4*d* AOs); under the influence of either tetrahedral or square pyramidal ligand fields of phosphorus, these 4*d* orbitals are split and pushed up in energy by M−P σ* and π* interactions (e_π and e_π' are AOM parameters[2]); (left) $\Delta E = \Delta + 2e_\pi' - 2.7e_\pi$; (right) $\Delta E' = \Delta + 2.7e_\pi' - 2e_\pi$; $\Delta E < \Delta E'$

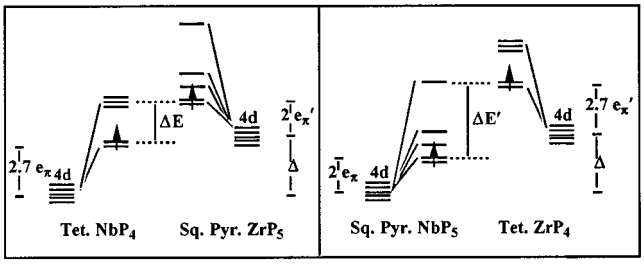

3. Coloring and Composition in Aluminides: Zintl Phases?

The question of chemical composition is closely linked to stable electronic configurations. For ionic and valence compounds (Zintl phases), the octet rule allows the chemist to "understand" chemical stability, since all bonding and nonbonding orbitals should be filled for "stable" chemical species.[42] When the electronegativity differences between elements in a compound are small, as in intermetallics, this rule becomes less well defined, and electronic structure calculations are necessary for a complete analysis. Nevertheless, the principle of bond order optimization by filling bonding and nonbonding orbitals is a compelling driving force for stable chemical compositions in a specific structure, i.e., equations (3) or (8).

Aluminides have been the focus of recent research towards an understanding of the transition from intermetallics to Zintl phases.[43] Post-transition elements form Hume-Rothery compounds[9] with *vec* < 2, while Zintl phases have networks of these elements with *vec* ≥ 4. Ternary aluminides involving an alkali or alkaline earth metal and an element from groups 11, 12, or 13 allow examination of compounds with *vec* values between two and four. A recent example of these efforts is $BaCu_5Al_8$,[44] which adopts the $NaZn_{13}$-type intermetallic structure. Further efforts have demonstrated that this structure occurs for compounds $ACu_{5\pm\varepsilon}Al_{8\mp\varepsilon}$, with A being Ba, Sr, La, or Eu and $\varepsilon \leq 1$.[45] The $NaZn_{13}$ structure type, shown in Figure 11, is a three-dimensional network of interconnected atom-centered (stuffed) icosahedra. Within the $[Cu_{5\pm\varepsilon}Al_{8\mp\varepsilon}]$ icosahedral substructure, there are two crystallographically inequivalent sites: (1) the center of each icosahedron, which is exclusively occupied by Cu; and (2) the surface of each icosahedron which is randomly decorated with $(4 \pm \varepsilon)$ Cu and $(8 \mp \varepsilon)$ Al atoms. Thorough synthetic and crystallographic investigations indicate that no ordering of Cu and Al on the icosahedra occurs even after months of annealing above 1000°C. Electronic structure calculations on various arrangements of Cu and Al in $BaCu_5Al_8$ demonstrate that bonding within the icosahedral framework is optimized (see Figure 11). Combinatorial methods indicate only ten unique ways of arranging four Cu and eight Al atoms in an icosahedron.[46][47] According to molecular orbital calculations, the lowest energy configurations of Cu and Al maximize the separations between Cu atoms. But, since there are six intericosahedral contacts per cluster, there is little energetic driving force for the ordering of Cu and Al. On the other hand, the overlap population curve in Figure 11 suggests that the stable compositions are influenced by the

Figure 11. (Top) structure of $BaCu_5Al_8$; shaded circles are Ba atoms, icosahedra correspond to the Cu-centered $[Cu_4Al_8]$ clusters which are tightly interconnected; (bottom) overlap populations for two types of bonds in the icosahedral network: (i) central Cu with surface atoms, and (ii) among difference surface atoms on the icosahedra; note that bonding orbitals are filled and antibonding orbitals are empty at the Fermi level for $BaCu_5Al_8$

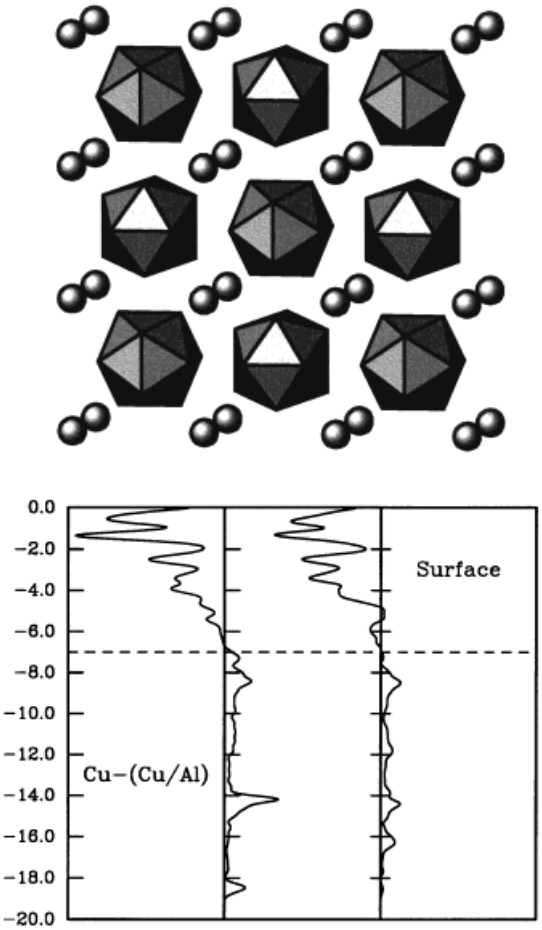

valence electron concentration and contribute to the narrow range of composition that has been observed.

Corresponding reactions with the more electronegative coinage metal, Au, rather than Cu produce a structure which is related to the $NaZn_{13}$-type, but the icosahedron is empty and there is an ordering of Au and Al atoms on the icosahedra (see Figure 12).[45] Both observations result from the repulsive Au−Au interactions that are present in this chemical environment: Au is the most electronegative component which attracts electrons from Al and increases the antibonding interaction between Au atoms. The arrangement of Au and Al corresponds to the lowest energy Au_4Al_8 icosahedron as calculated by molecular orbital methods.

Figure 12. Icosahedron found in $SrAu_{5+x}Al_{7-x}$; black circles are Au atoms, gray circles are a mixture of Au and Al atoms, white circles are Al atoms; the arrangement for the four black Au atoms corresponds to the lowest energy configuration of the icosahedron $[Au_4Al_8]$

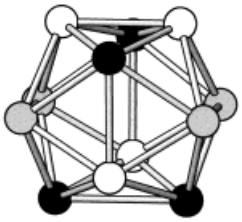

Further investigations with Au in this reducing environment produce new compounds[45][48][49] which allow an investigation of the chemistry and coloring problem involving the $BaAl_4$ structure, which is the most prolific intermetallic structure reported, known for more than 600 compounds.[50] This tetragonal structure contains two crystallographically distinct sets of aluminum atoms: one set forms planar square nets (Wyckoff site 4*e*) while the other set form dimers (Wyckoff site 4*f*) which link the square nets together to form a three-dimensional framework. There are numerous ternary variants of $BaAl_4$, in which the Al positions are occupied by two different elements in various ways (see Figure 13): (1) the $ThCr_2Si_2$-type, space group *I*4/*mmm*, with the different elements occupying the two inequivalent crystallographic sites; (2) the $CaBe_2Ge_2$-type, space group *P*4/*nmm*, in which the two elements alternate occupying the layers of square nets and the dimers so that only heteronuclear "Be−Ge" nearest neighbor contacts occur; and (3) the $BaNiSn_3$-type, space group *I*4*mm*, in which the Sn atoms form the square nets and the heteroatomic "Ni−Sn" pairs align in the same direction throughout the structure. The electronic structures of many compounds with these atomic arrangements have been extensively examined[51] and the results are summarized as follows: (1) for main group compounds, the structure is observed with 12−14 valence electrons per formula unit; (2) bonding within each dimer involves two-center two-electron σ bonds at 14 valence electrons, with an increasing π bonding character towards 12 valence electrons; and (3) optimum bonding between atoms on the 4*e* and 4*f* sites occurs at 12 valence electrons, and involves multi-center orbital interactions.

Figure 13. Three different colorings of $BaAl_4$ in ternary $LnAu_{1+x}Al_{3-x}$ intermetallics; black circles are Au atoms, dark gray circles (in center diagram only) are 50% Au/50% Al atoms, light gray circles are Al atoms, white circles are Ln atoms; (top) $LnAuAl_3$; (center) $LnAu_{1+x}Al_{3-x}$ ($0 < x \leq 0.5$); (bottom) $LnAu_2Al_2$

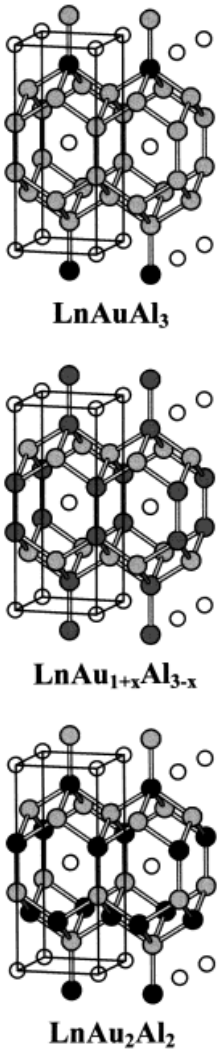

Recent investigations in ternary rare earth/gold/aluminum systems have shown interesting trends with respect to the "coloring" of Au and Al atoms in the covalent network of the $BaAl_4$ structure.[45][48] $LnAu_xAl_{4-x}$, $0.75 \leq x \leq 2$, have been reported for Ln ranging from La to Tb. When $x \geq 1.5$, the $CaBe_2Ge_2$ structure type occurs. For $x < 1.5$, i.e., higher Al concentrations, Au and Al partially disorder to give the $ThCr_2Si_2$-type until the composition $LnAuAl_3$, which shows both the ordered $BaNiSn_3$ and disordered $CeCuAl_3$ structure types. At $x = 0.75$, Au and Al are disordered on the 4*f* site, and show features of the $ThCr_2Si_2$ structure. Therefore, an interesting trend in coloring phenomenon occurs as the composition varies in $LnAu_xAl_{4-x}$ and for which the structural topology remains unchanged. Using equation (8) for these systems, the site energy is minimized when the most electronegative component occupies the 4*e* site, which is the place where Au replaces Al at low Au concentration ($x \leq 1$). As the Au

concentration increases, repulsive Au−Au interactions "force" Au atoms to occupy the square net positions 4*d*, until the maximum Au composition $LnAu_2Al_2$ is achieved. If the Au composition were to extend beyond this compound, Au−Au contacts would become necessary. Furthermore, the lowest possible Au concentration is $LnAu_{0.5}Al_{3.5}$ in order to maintain a maximum *vec* of fourteen electrons. When $x < 1$, entropic factors favor the body-centered tetragonal $BaAl_4$-type over the primitive tetragonal $BaNiSn_3$-type with no long range preference for the ordering of Au and Al in the dimers, which is observed for $EuAu_{0.75}Al_{3.25}$[45] Recent experiments have also shown that ordered vacancies enter the Au−Al framework as *vec* approaches fourteen electrons to give $Ln_3Au_2Al_9$ (Ln = Sm, Gd, Tb, Dy, and Yb).[45][49][52]

4. Coloring: Structure and Composition in Main Group Laves Phases

In the previous two sections, we have discussed how the coloring problem is tied to either structure or composition in intermetallic compounds. In general, however, these three aspects are closely interrelated, and are often difficult to separate and investigate systematically. An example of this problem occurs in the Ca−Li−Al ternary phase diagram along the line $CaLi_xAl_{2-x}$, which can be reformulated as $(CaLi_2)_y/(CaAl_2)_{1-y}$, $x = 2y$.[53] $CaLi_2$ and $CaAl_2$ form different Laves phase structures:[54] $CaLi_2$ adopts the hexagonal $MgZn_2$-type; and $CaAl_2$ forms the cubic $MgCu_2$-type. There exist many investigations concerning the influence of *vec* on the structures of Laves phases, but this study was the first which pointed out partial site preferences taking place in the framework of the majority component. Figure 14 illustrates how the volumes of the observed phases vary with Li content. When compared to a linear interpolation between the two binary compounds, there is a considerable volume reduction for the ternaries which strongly suggests covalent bonding within the aluminum framework, as found in Zintl phases. As x increases from zero in $CaLi_xAl_{2-x}$, the cubic $MgCu_2$-type structure changes to the hexagonal $MgNi_2$-type structure and then to the $MgZn_2$-type structure. Furthermore, stable compounds occur in $CaLi_xAl_{2-x}$ only for $x < 1$; when synthesis is attempted for phases with $x \geq 1$, disproportionation into $CaLi_2$ and $CaLi_yAl_{2-y}$, $y < 1$, occurs.

With respect to the coloring problem in Laves phases, the cubic $MgCu_2$-type structure has just one kind of majority site, whereas the hexagonal $MgNi_2$ and $MgZn_2$ types have three and two kinds of majority sites, respectively, which lead to potential site preferences. Li and Al show no site preferences in the hexagonal $MgNi_2$-type compounds, e.g., $CaLi_{0.33}Al_{1.67}$, and partial site preferences in the $MgZn_2$-type examples, e.g., $CaLi_{0.88}Al_{1.12}$. In this last compound, one of the majority sites (the kagomé nets; Wyckoff site 6*h*) is 50% Li and 50% Al, while the other crystallographic site (Wyckoff site 2*a*) attracts 75% Al and 25% Li. The reasons for these two coloring patterns stem from both the site energies as well as the driving force for Al in this reducing environment to establish an octet by forming Al−Al bonds.

Figure 14. $CaLi_xAl_{2-x}$ phases; (top) variation in volume per formula unit as the Li content varies from 0% to 100%; the dashed line connecting the two endpoints ($CaAl_2$ and $CaLi_2$) represents Zen's law for a linear variation with composition; the vertical dashed lines separate regions of the types of Laves phase structure observed for the experimental points; (bottom) trend in charges of the majority elements (Li_xAl_{2-x}) for the hexagonal $MgZn_2$-structure type as the number of valence electrons changes; the dashed line shows the maximum number of valence electrons allowed for this structure; the 2*a* site gains electrons, the 6*h* site loses electrons: thus, the more electronegative element would be attracted to the 2*a* site

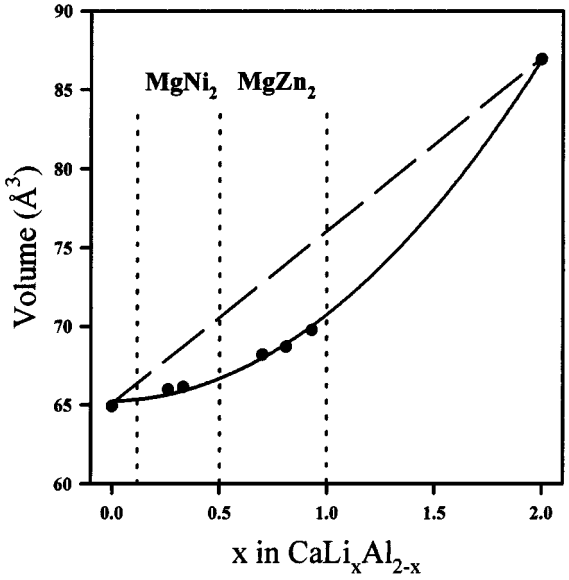

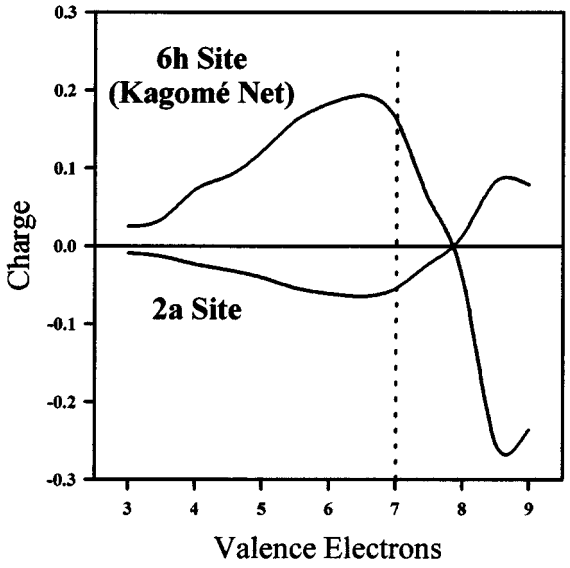

For the series of observed $CaLi_xAl_{2-x}$ compounds, both semiempirical and density functional theory show that Ca donates just one valence electron to the $[Li_xAl_{2-x}]$ framework. Figure 14 illustrates the deviations from the average Mulliken population for the two majority sites in the hexagonal $MgZn_2$-type structure as a function of valence electron count. Notice that the largest difference in atomic population occurs for six electrons per formula unit

("CaLiAl"), whereas the difference is nearly zero between seven and eight electrons. Thus, $CaAl_2$ (8 electrons) and $CaLi_{0.33}Al_{1.67}$ (7.33 electrons) adopt, respectively, the $MgCu_2$-type and the $MgNi_2$-type structures with no site preferences. On the other hand, $CaLi_{0.88}Al_{1.12}$ (6.25 electrons) do show segregation in agreement with the Mulliken population analysis. However, with respect to minimizing the bond energy component of the total orbital energy from equation (8), a completely random arrangement of Li and Al would be expected. If the Zintl-Klemm formalism is applied to Al in $CaLi_{0.88}Al_{1.12}$ with complete segregation of Li and Al into the two crystallographic sites as far as allowed by the composition, the Ca atoms would donate 1.2 electrons to the $[Li_{0.88}Al_{1.12}]$ framework, which opposes the conclusions from theoretical calculations. Table 1 summarizes three different scenarios for the arrangement of Li and Al atoms in $CaLi_{0.88}Al_{1.12}$: (1) minimum site energy, (2) minimum Al−Al bond energy, and (3) the observed configuration. These results demonstrate that the structure and the partial segregation of Li and Al arise from the synergistic interplay of both the site energy and bond energy terms in the total orbital energy. In addition, the observed structure optimizes the Ca−Ca orbital interactions, as has been shown by calculating pair potentials in $CaAl_2$.[55] In $CaLi_{0.33}Al_{1.67}$, both the site energy and bond energy terms allow for a completely random arrangement of Li and Al throughout the structure.

5. Coloring and Property Effects in Metal-Rich Tellurides

The cases discussed thus far demonstrate minor changes in physical or chemical properties as a function of atomic coloring. This is due primarily to the fact that either the electronic configurations are all closed shell (as in Nb_3SI_7), or the valence electron concentrations are sufficiently low (less than four per atom) as to preclude any significant change in electronic properties. In order to investigate effects of atomic coloring on conductivity properties, focus must be directed towards compounds involving the post-transition elements, whose structures lie close to the border between Zintl phases (valence compounds) and typical intermetallics (Hume−Rothery phases, for example). A particularly interesting set of examples involves the substitution of Sn atoms for Tl atoms in the low temperature superconductor Tl_5Te_3.

Tl_5Te_3 adopts a variation of the tetragonal Cr_5B_3-structure type with a smaller than typical *c*/*a* ratio for these compounds, which leads to a three-dimensional network of vertex-sharing octahedra, $^3_\infty[TlTe_{6/2}]$, stuffed with Tl atoms over each face of the octahedron, i.e., $[TlTe_{6/2}]Tl_{8/2} \triangleq Tl_5Te_3$ (see Figure 15).[56] Tl_5Te_3 has a superconducting transition at 2.2 K,[57] which according to a combination of band structure and lattice energy calculations,[58] can arise from an electronic instability in the electronic band structure that is frustrated by strong short-range repulsive forces which retard any structural distortion. Using simple electron counting, the octahedrally coordinated Tl atoms can be formulated as Tl^{2+}, which is unstable towards disproportionation into Tl^{+1} and Tl^{3+}.[20]

Figure 15. The structure of Tl_5Te_3 and its ternary derivatives; white circles are Te atoms, black circles are Tl atoms; Te octahedra are also illustrated; there is a Tl atom at the center of each octahedron

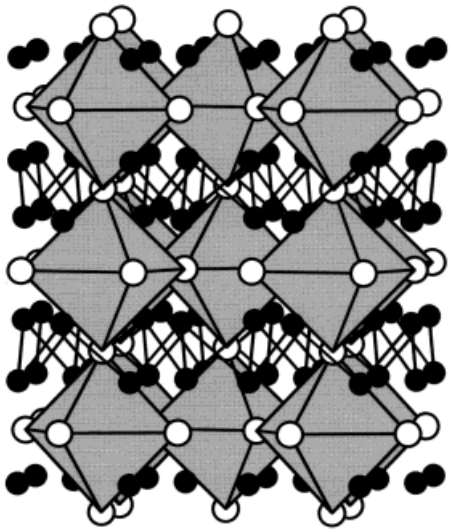

Böttcher and coworkers have recently synthesized ternary derivatives of Tl_5Te_3.[59] In particular, $SnTl_4Te_3$ was prepared and shown to be metallic. From crystallographic data, the Sn atoms occupy both Tl sites in the parent structure. Replacing a "Tl^{2+}" with a Sn^{2+} is a plausible chemical

Table 1. Analysis of various coloring models for the $MgZn_2$-type Laves phase $CaLi_{0.88}Al_{1.12}$ with respect to the Zintl-Klemm formalism; the $[Li_{0.88}Al_{1.12}]$ network is described by two crystallographic sites in the space group $P6_3/mmc$: the 2*a* and the 6*h* sites

Coloring Model		− 2*a* Site − Site Occ.	CN by Al[a]	Charge[b]	− 6*h* Site − Site Occ.	CN by Al[a]	Charge[b]	Role of Ca: Electrons, Bond Order
Minimum Site Energy	Al:	100.00%	2.500	−2.500	41.67%	3.667	−1.333	Ca donates 1.21 electrons;
	Li:	0.00%		+1.000	58.33%		+1.000	Ca−Ca Bond Order ca. 0.6
Minimum Bond Energy	Al:	56.25%	3.375	−1.625	56.25%	3.375	−1.625	Ca donates 0.95 electron;
	Li:	43.75%		+1.000	43.75%		+1.000	Ca−Ca Bond Order ca. 0.9
Observed Arrangement	Al:	75.00%	3.000	−2.000	50.00%	3.500	−1.500	Ca donates 1 electron;
	Li:	25.00%		+1.000	50.00%		+1.000	Ca−Ca Bond Order ca. 1.0

[a] CN = coordination number; it represents the average number of Al nearest neighbors. − [b] Charge for Al is based on the 8 − *N*rule; it equals 3 − (8 − CN) = CN − 5. The charge for Li is chosen to be +1 as the most electropositive element in this compound.

substitution, and with an increase the valence electron concentration to a closed subshell configuration, semiconducting behavior would be expected. Indeed, band calculations with Sn completely replacing the octahedrally coordinated Tl atoms produces an energy gap at the Fermi level (Model A: see Figure 16). A combination of electronic band structure and lattice energy calculations reveal that whereas covalent interactions prefer Sn atoms to substitute at the octahedral sites, ionic interactions would rather place Sn atoms at the other Tl sites.[58] When such a substitution mode takes place, $SnTl_4Te_3$ retains its metallic character, but yields a smaller density of states at the Fermi level (Model B: see Figure 16). Therefore, where the substitution for Tl takes place has a dramatic effect on the expected physical properties of the derivative compounds.

Figure 16. Densities of states for two models of Sn atom coloring in $SnTl_4Te_3$; (left) Model A: all Sn atoms occupy the octahedral sites shown as polyhedra in Figure 15; (right) Model B: all Sn atoms occupy the other Tl sites shown as black circles in Figure 15; note that the Fermi level occurs in an energy gap for Model A, but there is no gap in Model B

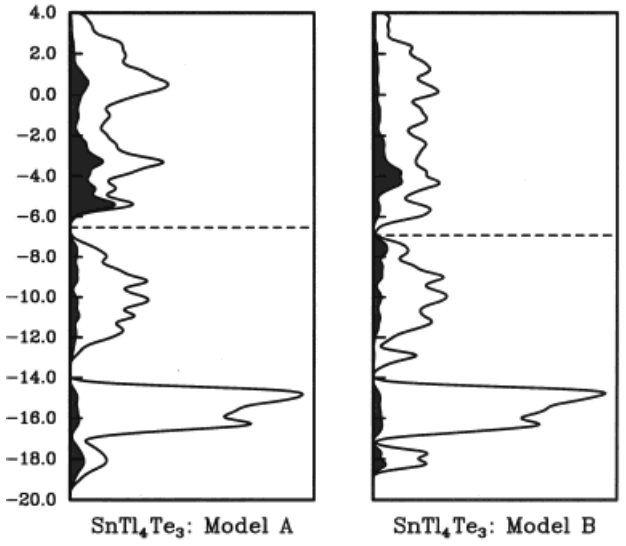

Summary, Implications, and Future Directions

The coloring problem has powerful ramifications in chemistry. Electronic structure theory provides a theoretical underpinning for its effects, and also allows a simple chemical understanding of the phenomenon. However, can theory really assist the synthetic chemist with this problem? One important goal of synthetic chemists is to prepare new materials, which is often motivated by trying to optimize certain chemical or physical properties, e.g., catalytic activity, thermoelectric behavior, or magnetism to name a few. For the solid state chemist, these efforts are largely Edisonian in nature. Of course, the discovery of some physical property in one example tends to attract attention to the particular structure type in question: for example, superconductivity in cuprates. A working knowledge of the coloring problem, which includes both an imagination for possible new structures as well as an analysis based upon existing structures, will greatly assist the synthetic solid state chemist as the search for new, exciting, and probably more complex materials continues. Complexity can be simply moving from binary to ternary to quaternary systems, where the number of possible new materials increases exponentially.

How atoms arrange themselves in extended solid state structures depends on the number of valence electrons and the differences in electrochemical potentials, which are related to electronegativity, size, and the types of valence electronic structure the atoms bring to the compound. This review attempted to demonstrate that not only is structure a concern, but also the decoration pattern once a network of atoms is in place. Structure-composition-property interrelationships can then be studied by a careful application of experiment and theory − in most cases involving intermetallic compounds, theory is essential in order to develop a description of the electronic structure that harks to the classical chemical ideas for valence compounds. A partitioning of the total electronic energy into a site energy and a bond energy creates two components to the coloring problem. Through the examples presented in this review, i.e., Nb_3SI_7, ZrNbP and ZrMoP, $BaCu_5Al_8$ and $SrAu_6Al_6$, $LnAu_xAl_{4-x}$, $CaLi_xAl_{2-x}$, and $Sn_xTl_{5-x}Te_3$, analysis of both components is necessary to understand the complete structural details of these compounds and to ultimately relate their structures to their physical properties.

Where does the coloring problem take us now? A couple of examples may provide an indication: (1) utilize the Klemm pseudoelement approach[60] to create possible mixed anion matrices for transition metals in order to study electronic transitions, e.g., metal-semiconductor or metal-superconductor transitions, and (2) rely on structural experience in crystalline solids to develop models for systems which lack translational symmetry and yet are beginning to show interesting properties and applications with little fundamental understanding, i.e., quasicrystals and amorphous metals.[61] Our group is beginning to address these questions using the elegant ideas surrounding the coloring problem.

My group's efforts in this field have benefited by the financial support of the *Department of Energy*, the Donors of the *Petroleum Research Fund*, administered by the *American Chemical Society*, and the *National Science Foundation* (DMR-96-27161). The author is indebted to *Jun Cheng*, *Chi-Shen Lee*, *Jianhua Lin*, *Karen Nordell*, and *Mark Smith* for significant contributions to some of the work presented in this microreview, and to *Carla Holbrook* for some of the figures.

☆ Dedicated to the memory of Professor *Jeremy K. Burdett*, who was a brilliant scientist and a superb mentor.

[1] H.-D. Hardt, *Die periodischen Eigenschaften der chemischen Elemente*, 2. Auflage, Georg Thieme Verlag, Stuttgart, **1987**, p. 126.
[2] J. K. Burdett, *Molecular Shapes*, Wiley Interscience, New York, **1980**.
[3] J. Donohue, *The Structure of the Elements*, Krieger, Malabar, Florida, **1982**.
[4] D. G. Pettifor, *Bonding and Structure of Molecules and Solids*, Oxford University Press, Oxford, **1995**.
[5] P. Pyykkö, *Adv. Quant. Chem.* **1978**, *11*, 353; P. Pyykkö, J. P. Desclaux, *Acc. Chem. Res.* **1979**, *12*, 276; P. Pyykkö, *Chem. Rev.* **1988**, *88*, 563.
[6] D. G. Pettifor, R. Podloucky, *Phys. Rev. Lett.* **1984**, *53*, 1080; J. K. Burdett, S. Lee, *J. Am. Chem. Soc.* **1985**, *107*, 3063; S. Lee,

Acc. Chem. Res. **1991**, *24*, 249; S. Lee, *J. Am. Chem. Soc.* **1991**, *113*, 101, 8611; L. Hoistad, S. Lee, *J. Am. Chem. Soc.* **1991**, *113*, 8216.
[7] T. L. Brennan, J. K. Burdett, *Inorg. Chem.* **1993**, *32*, 750.
[8] J. K. Burdett, S. Lee, T. J. McLarnan, *J. Am. Chem. Soc.* **1985**, *107*, 3083.
[9] W. Hume-Rothery, *J. Inst. Metals* **1926**, *35*, 295.
[10] D. Barnette, *Map Coloring, Polyhedra, and the Four-Color Problem*, The Mathematical Association of America, USA, **1983**.
[11] H. S. M. Coxeter, *Introduction to Geometry*, Wiley, New York, **1969**.
[12] F. Harary, *Graph Theory*, Addison-Wesley Publishing Co., Reading, MA, USA, **1972**.
[13] J. K. Burdett, E. Canadell, T. Hughbanks, *J. Am. Chem. Soc.* **1986**, *108*, 3971.
[14] T. A. Albright, J. K. Burdett,, M.-H. Whangbo, *Orbital Interactions in Chemistry*, Wiley-Interscience, New York, **1985**.
[15] S_4N_4: M. L. de Lucia, P. Coppens, *Inorg. Chem.* **1978**, *17*, 2336; As_4S_4: D. J. E. Mullen, W. Nowacki, *Z. Kristallogr. Kristallgeom. Kristallphys. Kristallochem.* **1972**, *136*, 48.
[16] B. M. Gimarc, *J. Am. Chem. Soc.* **1983**, *105*, 1979.
[17] R. Hoffmann, *Solids and Surfaces: A Chemist's View of Bonding in Extended Structures*, VCH Publishers, New York, **1988**; J. K. Burdett, *Prog. Solid State Chem.* **1984**, *15*, 173; R. S. Mulliken, *J. Chem. Phys.* **1955**, *23*, 1833, 2343.
[18] C. A. Coulson, *Proc. Roy. Soc. London, Ser. A* **1939**, *139*, 413.
[19] I. N. Levine, *Quantum Chemistry*, 2nd ed., Allyn, Bacon, Inc., Boston, **1974**, pp. 421-450.
[20] N. N. Greenwood, A. Earnshaw, *Chemistry of the Elements*, Pergamon Press, Oxford, **1984**.
[21] G. C. Pimentel, *J.Chem. Phys.* **1951**, *19*, 446; R. J. Hach, R. E. Rundle, *J. Am. Chem. Soc.* **1951**, *73*, 4321.
[22] R. Hoffmann, W. N. Lipscomb, *J. Chem. Phys.* **1962**, *36*, 2179, 3489; R. Hoffmann, *J. Chem. Phys.* **1963**, *39*, 1397; J. H. Ammeter, H.-B. Bürgi, J. C. Thibeault, R. Hoffmann, *J. Am. Chem. Soc.* **1978**, *100*, 3686.
[23] A. P. Sutton, *Electronic Structure of Materials*, Clarendon Press, Oxford, **1994**.
[24] R. Haydock, V. Heine, M. Kelly, *J. Phys. C* **1972**, *5*, 2845; V. Heine, R. Haydock, D. Bullett, M. Kelly, *Solid State Physics* **1980**, *35*, 1; D. G. Pettifor, D. L. Weaire (Eds.), *The Recursion Method and its Applications*, Springer-Verlag, Heidelberg, **1985**.
[25] K_2SnTe_5: B. Eisenmann, H. Schwerer, H. Schäfer, *Mater. Res. Bull.* **1983**, *18*, 383; Tl_2SnTe_5: V. Agafonov, P. Legendre, N. Rodier, J. M. Cense, E. Dichi, G. Kra, *Acta Crystallogr., Sect. C* **1991**, *47*, 850.
[26] J. B. Goodenough, A. L. Loeb, *Phys. Rev.* **1955**, *98*, 391.
[27] J. K. Burdett, T. J. McLarnan, *J. Solid State Chem.* **1984**, *53*, 382; J. K. Burdett, *Chemical Bonding in Solids*, Oxford University Press, Oxford, **1995**.
[28] E. Zintl, W. Dullenkopf, *Z. Phys. Chem.* **1932**, *B16*, 195.
[29] G. J. Miller, *J. Alloys Compd.* **1995**, *229*, 93; G. J. Miller, *J. Alloys Compd.* **1995**, *217*, 5.
[30] H. Schäfer, H. G. von Schnering, *Angew. Chem.* **1964**, *76*, 833.
[31] A. Simon, H. G. von Schnering, *J. Less-Common Met.* **1966**, *11*, 31.
[32] W. B. Pearson, *The Crystal Chemistry and Physics of Metals and Alloys*, Wiley, New York, **1972**.
[33] F. Seitz, *The Modern Theory of Solids*, Dover Publications, Inc., New York, **1987**, pp. 76−98.
[34] G. J. Miller, J. Lin, *Angew. Chem.* **1994**, *106*, 357; *Angew. Chem. Int. Ed. Engl.* **1994**, *33*, 334; P. Schmitz, University of Freiberg, private communication, **1997**.
[35] C.-S. Lee, M.Sc. Thesis, *The Site Preference Study of Trinuclear Niobium Compounds $Nb_3(S_xI_{1-x})I_7$ ($x = 0.0-1.0$)*, Iowa State University, **1997**; G. J. Miller, J. Lin, M. D. Smith, C. S. Lee, manuscript in preparation.
[36] V. Heine, I. J. Robertson, M. C. Payne in *Bonding and Structure of Solids*, The Royal Society, London, **1991**, p. 1.
[37] G. Marking, H. F. Franzen, *J. Alloys Compd.* **1994**, *204*, L16.
[38] B. Harbrecht, H. F. Franzen, *Z. Anorg. Allg. Chem.* **1987**, *551*, 74; B. Harbrecht, *Z. Kristallogr.* **1988**, *182*, 118; B. Harbrecht, H. F. Franzen, *Z. Kristallogr.* **1989**, *186*, 119; X. Yao, H. F. Franzen, *J. Less-Common Met.* **1990**, *161*, L37; X. Yao, H. F. Franzen, *J. Solid State Chem.* **1990**, *86*, 88; X. Yao, H. F. Franzen, *Z. Anorg. Allg. Chem.* **1991**, *598*, 353; X. Yao, H. F. Franzen, *J. Am. Chem. Soc.* **1991**, *113*, 1426; X. Yao, G. J. Miller, H. F. Franzen, *J. Alloys Compd.* **1992**, *183*, 7; H. F. Franzen, M. Köckerling, *Prog. Solid State Chem.* **1995**, *23*, 265.
[39] G. J. Miller, J. Cheng, *Inorg. Chem.* **1995**, *34*, 2962.
[40] B. G. Hyde, S. Andersson, *Inorganic Crystal Structures*, Wiley Interscience, New York, **1989**.
[41] T. Hughbanks, R. Hoffmann, *J. Am. Chem. Soc.* **1983**, *105*, 3528; S. Wijeyesekera, R. Hoffmann, *Organometallics* **1984**, *3*, 949.
[42] G. J. Miller in *Chemistry, Structure, and Bonding of Zintl Phases and Ions* (Ed.: S. M. Kauzlarich), VCH Publishers, Inc., New York, **1996**, p. 1.
[43] R. Nesper, *Angew. Chem.* **1991**, *103*, 805; *Angew. Chem. Int. Ed. Engl.* **1991**, *30*, 789; U. Häussermann, S. Wengert, P. Hofmann, A. Savin, O. Jepsen, R. Nesper, *Angew. Chem.* **1994**, *106*, 2147; *Angew. Chem. Int. Ed. Engl.* **1994**, *33*, 2069; U. Häussermann, S. Wengert, R. Nesper, *Angew. Chem.* **1994**, *106*, 2150; *Angew. Chem. Int. Ed. Engl.* **1994**, *33*, 2073; U. Häussermann, M. Wörle, R. Nesper, *J. Am. Chem. Soc.* **1996**, *118*, 11789.
[44] K. J. Nordell, G. J. Miller, *Croat. Chim. Acta* **1995**, *68*, 825.
[45] K. J. Nordell, Ph.D. Thesis, *Exploring Aluminum-Rich Intermetallics with Experiment and Theory*, Iowa State University, **1997**.
[46] T. J. McLarnan, P. B. Moore in *Structure and Bonding in Solids*, vol. II (Eds.: M. O′Keeffe, A. Navrotsky), Academic Press, New York, **1981**.
[47] B. K. Teo, H. Zhang, Y. Kean, H. Dang, X. Shi, *J. Chem. Phys.* **1993**, *99*, 2929.
[48] F. Hulliger, H.-U. Nissen, R. Wessicken, *J. Alloys Compd.* **1994**, *206*, 263; F. Hulliger, *J. Alloys Compd.* **1995**, *218*, 255.
[49] For related gallides, see also: Yu. Grin, M. Ellner, K.Hiebl, P. Rogl, O. M. Sichevich, O. M. Myakush, *J. Alloys Compd.* **1994**, *205*, 285.
[50] P. Villars, L. D. Calvert, *Pearson's Handbook of Crystallographic Data for Intermetallic Phases*, 2nd ed., ASM, Materials Park, OH, **1991**.
[51] C. Zheng, R. Hoffmann, *Z. Naturforsch.* **1986**, *41B*, 292; J. K. Burdett, G. J. Miller, *Chem. Mater.* **1989**, *2*, 12; C. Zheng, *J. Am. Chem. Soc.* **1993**, *115*, 1047.
[52] K. J. Nordell, G. J. Miller, *Angew. Chem.* **1997**, *109*, 2098; *Angew. Chem. Int. Ed. Engl.* **1997**, *36*, 2008.
[53] R. Nesper, G. J. Miller, *J. Alloys Compd.* **1993**, *197*, 109.
[54] C. Barrett, T. B. Massalski, *Structure of Metals*, 3rd ed., Pergamon Press, Oxford, **1980**.
[55] J. Hafner, *From Hamiltonians to Phase Diagrams*, Springer-Verlag, Berlin, **1987**, p. 58.
[56] I. Schewe, P. Böttcher, H. G. von Schnering, *Z. Kristallogr.* **1989**, *188*, 287.
[57] A. Judoakis, C. R. Kannewurf, *J. Appl. Phys.* **1968**, *39*, 3003.
[58] K. J. Nordell, G. J. Miller, *J. Alloys Compd.* **1996**, *241*, 51.
[59] S. Bradtmöller, P. Böttcher, *Z. Anorg. Allg. Chem.* **1993**, *619*, 1155; S. Bradtmöller, P. Böttcher, *Z. Kristallogr.* **1994**, *209*, 75; S. Bradtmöller, P. Böttcher, *Z. Kristallogr.* **1994**, *209*, 97; S. Bradtmöller, Ph.D. Thesis, *Ternäre Metallreiche Chalkogenide: Synthese, Strukturen und Eigenschaften*, University of Düsseldorf, **1995**; T. Doert, Ph.D. Thesis, *Chalkogenide mit In_5Bi_3-Typ-Struktur*, University of Düsseldorf, **1994**.
[60] W. Klemm, *Proc. Chem. Soc., London* **1959**, 329; W. Klemm, *Trab. Reun. Int. React. Solidos, 3rd* **1956**, *1*, 447.
[61] A. I. Goldman, K. F. Kelton, *Rev. Mod. Phys.* **1993**, *65*, 213.

[97231]

Carbonyl and Benzene Complexes of Lithium: Transition-Metal-Like Behaviour of Lithium in Organolithium Compounds☆

Matthias Tacke

Department of Chemistry, University College Dublin,
Belfield, Dublin 4, Ireland
E-mail: matthias.tacke@ucd.ie

Received November 29, 1997

Keywords: Lithium / (Benzene)lithium complex / (Carbonyl)lithium complex / Ab initio calculations

Complexes of CO and aromatic compounds were believed to be an exclusive domain of transition metals caused by their ability of backbonding to these ligands. But recently, (benzene)lithium and (carbonyl)lithium complexes were characterized by X-ray structure analysis and IR spectoscopy. In order to determine geometries of the complexes and the bonding energies of the benzene and CO molecule to the organolithium starting compound suitable models were chosen in combination with high-level ab initio calculations. For the carbonyl derivative a reaction enthalpy of −8 kcal/mol was found while the interaction with benzene reached unexpectedly −21 kcal/mol. This underlines the ability of lithium to act like a transition metal in subcoordinated organyl compounds without having d orbitals available for bonding.

Introduction

Aggregation is a nearly ubiquitous characteristic of organolithium compounds.[1] But if bulky substituents prevent aggregation monomeric organolithium compounds show in benzene solution lithium−benzene π interaction like a transition metal. So $(2,4,6\text{-}i\mathrm{Pr}_3\mathrm{C}_6\mathrm{H}_2)_2\mathrm{C}_6\mathrm{H}_3\mathrm{Li}$ crystallizes from benzene/hexane solution as a monomer with a coordination between the lithium center and the benzene molecule.[2]

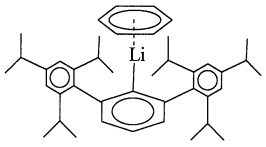

If the ligands have sterically less demanding *ortho*-substituted phenyl groups a small number of crystal structures show dimers exhibiting lithium−benzene interactions.[2][3] But X-ray crystallography is unable to measure the strength of this π interaction. This paper presents ab initio calculations on MP2 level for geometries and HF level for IR frequencies and zero-point energies which are able to fill the experimental gap. For these calculations there is no need for selecting highly substituted compounds of course. So three simple types of organolithium compounds are chosen (LiH, LiMe, LiPh)[4] which are allowed to interact with a benzene molecule to determine the reaction enthalpy of the process and to compare calculated and experimental structures.

In a recent spectroscopic study the very early steps of the reaction of organolithium compounds with CO or isonitrile were detected.[5] Liquid xenon (LXe) is used as the reaction medium because it suppresses electron-transfer reactions

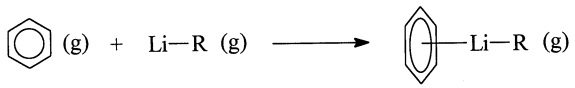

(R = H, Me, Ph)

which are known to complicate the reaction.[6] If this reaction is performed at sufficiently low temperature a coordination of CO is found firstly. This unexpected transition-metal-like behaviour of lithium is followed by insertion of carbon monoxide into the lithium−carbon bond which is again expected for transition metal complexes only.

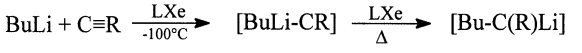

(R = O,NtBu)

Our investigations show that tetrameric methyllithium in combination with high-level MP2 calculations are a suitable model to determine reaction enthalpies and structures of the intermediates which allow comparison with the experimental data.

Results and Discussion

In a first attempt monomeric lithium hydride, which is the simplest model for an organolithium compound, is allowed to interact with benzene on MP2 level. Upon coordination we find a change in reaction enthalpy of −21 kcal/mol which is unexpectedly high. A weak interaction like a hydrogen bonding would give about −3 kcal/mol only. The Li−H stretching frequency decreases from 1420 cm^{-1} in free LiH to 1338 cm^{-1} in the coordinated LiH which means a total change of 6% indicating a major interaction as well. Correspondingly the Li−H bond length varies from 162.4

 © WILEY-VCH Verlag GmbH, D-69451 Weinheim, 1998 1434−1948/98/0505−0537 $ 17.50+.50/0

pm to 163.3 pm upon complexation. There is very little change in bond lengths in the benzene molecule. Even the hydrogen atoms stay nearly in the molecular plane. The resulting lithium−carbon bond length of the adduct in C_{6v} symmetry is 252.0 pm.

To verify this first result the reaction of Li^+ with benzene to form an adduct is calculated. Since this reaction enthalpy is measured to be -37 ± 2 kcal/mol applying ion cyclotron resonance technique[7] it is a unique chance to calibrate the ab initio calculations. The expected C_{6v} species exhibits an Li−C bond of 239.1 pm and a C−C bond of 140.6 pm which is slightly longer than in free benzene (139.6 pm). The enthalpy change is slightly overestimated by this calculation (−41 kcal/mol) showing that method (MP2) and basis set (6-31G**) are suitable to describe the system.

When using monomeric methyllithium as a model the calculation results in −19 kcal/mol for the reaction enthalpy with a new lithium−carbon distance of 251.7 pm. The most precise results are to be expected when monomeric phenyllithium is used since it is nearly the compound found to crystallize with benzene in an η^6-coordination mode. This time the enthalpy change is −21 kcal/mol and a lithium−carbon distance of 247.0 pm is found on average. Figure 1 illustrates the results on the MP2/6-31G** level of theory of the above-mentioned species.

These theoretical results give a consistent picture of the coordination of benzene to organolithium compounds. The calculated geometries of the complexes predict an atom distance of around 250 pm between lithium and carbon in the coordinated benzene. In the X-ray structure a significantly shorter value of 235 pm is determined. The calculations therefore give a reasonable but not excellent prediction of this important parameter. The interaction energy is with about −20 kcal/mol unexpectedly high and shows that the complexes formed are held together with more than weak Li−benzene π interactions as was suggested by the crystal-structure determination.[2] If bis(benzene)chromium is used as a reference compound for the bonding strength of the metal−benzene interaction an interesting comparison becomes available. From thermodynamical values it can be calculated that the reaction of $Cr(C_6H_6)_2$ to a chromium atom and two molecules of benzene needs around 80 kcal/mol.[8] Therefore, the bonding energy of each benzene unit to the chromium center is 40 kcal/mol which is only double the value of the lithium−benzene interaction. The high value is caused by the covalent nature of the lithium−carbon bond in the starting compound making it behave like a transition metal. Because lithium with its only three overall electrons is not able to build up highly ionic organo compounds as its heavier homologues it has to form a polar but covalent bond in a compound like phenyllithium. The subcoordination of lithium is normally moderated by formation of an oligomer with shared bonding electrons. But in the case of $(2,4,6\text{-}i\text{Pr}_3C_6H_2)_2C_6H_3Li$ the bulky substituents force the compound to remain a monomer with only two shared bonding electrons for the lithium center. In benzene solution this bonding type changes dramatically since the six-valence-electron donor benzene can form a stable

Figure 1. Molecular projections of adducts of benzene with LiH, LiMe, and LiPh; selected bond lengths in pm

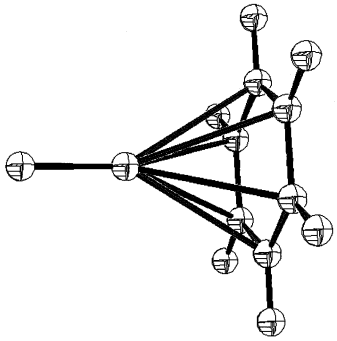

LiH: 163.3, LiC: 252.0, CC: 140.1

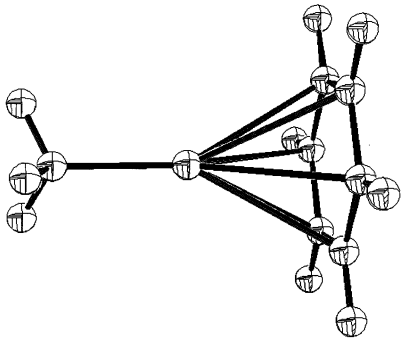

LiC(benzene): 251.7 (average)

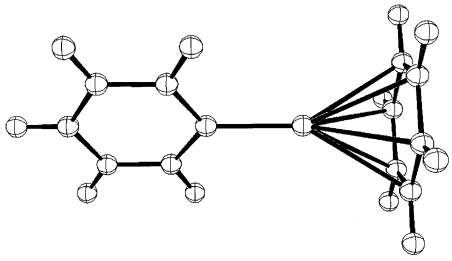

LiC(benzene): 247.0 (average)

complex and enables the lithium center to end up with an 8-valence-electron environment.

Recently, it was shown, that organolithium compounds are also able to interact with CO[5] in a newly developed LXe cell constructed from one piece of single-crystal silicon.[9] In a first step carbon monoxide is complexed with back bonding to *n*BuLi [ν(CO): 2047 cm^{-1}] and inserts in a second step at higher temperatures into the lithium−carbon bond [ν(CO): 1635 cm^{-1}]. Further warming-up to −20°C results in decomposition of the observed pentanoyllithium intermediate. Probably a lithiated oxycarbene is formed favoured by formation of a strong lithium−oxygen bond.

$$\text{nBuLi} + \text{CO} \xrightarrow[-100°C]{\text{LXe}} [\text{nBuLi-CO}] \xrightarrow[-30°C]{\text{LXe}} [\text{nBu-C(O)Li}]$$

$$\xrightarrow[-20°C]{\text{LXe}} \text{further reaction}$$

With tetrameric lithium hydride as a model substance for ab initio calculations of oligomeric organolithium species it was possible to obtain first structural information[5] about the complexation and insertion of the CO molecule. But the insertion turned out to be a sligthly exothermic partial reaction, which is hard to believe in the light of the successful experiment in liquid xenon. With tetrameric methyllithium as a much better substitute we can now show, that the wrong sign of the reaction enthalpy is caused by the inadequate model. The addition of CO to $(LiMe)_4$ releases −7.8 kcal/mol with the formation of a linear LiCO substructure with a relative long lithium−carbon distance of 234.0 pm. For comparison *d*(Li−C) in tetrameric methyllithium is calculated to 221.0 pm. In contrast to the experiment the calculated compound does not show backbonding to CO as indicated by a higher C−O stretching frequency in comparison to free carbon monoxide. The second possible isomer showing a likewise linear LiOC substructure is higher in energy. The insertion reaction of carbon monoxide into the lithium−carbon is now exothermic (−4.2 kcal/mol) and the resulting acetyl group coordinates with its carbon atom

Figure 2. Molecular projections of Li_4Me_4, Li_4Me_4CO, and $Li_4Me_3(COMe)$; selected bond lengths in pm

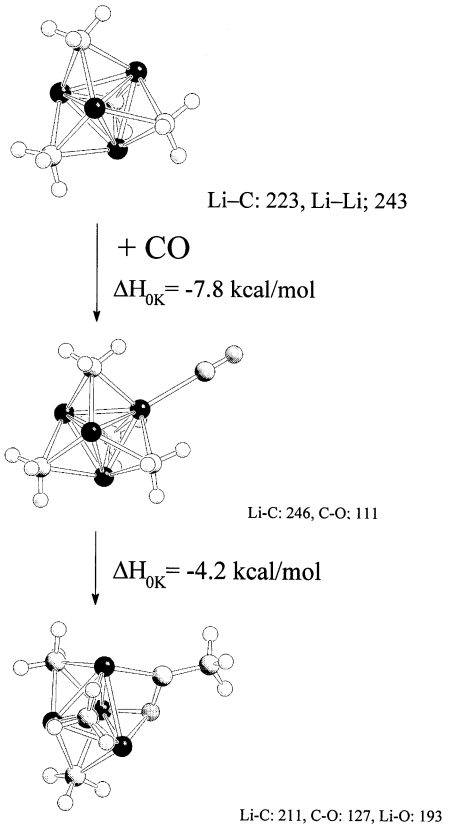

Table 1. Ab initio calculated energies and frequencies for the various intermediates

	electronic energy [Hartrees] (MP2)	zero-point energy [Hartrees] (HF)	ν(CO) [cm^{-1}]
CO	−113.021215	0.004825	2118
Li_4Me_4CO	−302.011968	0.156614	2475
$Li_4Me_3(COMe)$	−302.024139	0.162068	1626
Li^+·PhH	−238.808641	0.110077	
LiH·PhH	−239.538754	0.112874	
LiMe·PhH	−278.724527	0.143982	
LiPh·PhH	−469.881984	0.204110	

Table 2. Ab initio calculated geometries for the various intermediates

Li^+·PhH Standard orientation			
Center number	Coordinates [Å]		
	X	*Y*	*Z*
Li1	0.000000	0.000000	1.806913
C2	0.000000	1.405805	−0.126712
C3	1.217463	0.702903	−0.126712
C4	1.217463	−0.702903	−0.126712
C5	0.000000	−1.405805	−0.126712
C6	−1.217463	−0.702903	−0.126712
C7	−1.217463	0.702903	−0.126712
H8	0.000000	2.488179	−0.143186
H9	2.154826	1.244089	−0.143186
H10	2.154826	−1.244089	−0.143186
H11	0.000000	−2.488179	−0.143186
H12	−2.154826	−1.244089	−0.143186
H13	−2.154826	1.244089	−0.143186

LiH·PhH Standard orientation			
Center number	Coordinates [Å]		
	X	*Y*	*Z*
H1	0.000000	0.000000	3.508600
Li2	0.000000	0.000000	1.875200
C3	0.000000	1.401195	−0.219208
H4	0.000000	2.483028	−0.207116
C5	0.000000	−1.401195	−0.219208
H6	0.000000	−2.483028	−0.207116
C7	1.213471	0.700598	−0.219208
C8	1.213471	−0.700598	−0.219208
C9	−1.213471	0.700598	−0.219208
C10	−1.213471	−0.700598	−0.219208
H11	2.150365	1.241514	−0.207116
H12	2.150365	−1.241514	−0.207116
H13	−2.150365	1.241514	−0.207116
H14	−2.150365	−1.241514	−0.207116

LiMe·PhH Standard orientation			
Center number	Coordinates [Å]		
	X	*Y*	*Z*
Li1	0.000000	0.000000	1.268048
C2	0.000000	0.000000	3.268348
H3	0.000000	−1.010855	3.691113
C4	0.000000	1.400960	−0.822668
H5	−0.875426	0.505428	3.691113
H6	0.875426	0.505428	3.691113
C7	1.213267	−0.700480	−0.822668
C8	−1.213267	−0.700480	−0.822668
H9	0.000000	2.482902	−0.811488
H10	2.150256	−1.241451	−0.811488
H11	−2.150256	−1.241451	−0.811488
C12	0.000000	−1.400979	−0.822775
C13	−1.213283	0.700489	−0.822775
C14	1.213283	0.700489	−0.822775
H15	0.000000	−2.482922	−0.811711
H16	−2.150274	1.241461	−0.811711
H17	2.150274	1.241461	−0.811711

Table 2 *(continued)*

Center number	LiPh·PhH Standard orientation Coordinates [A] X	Y	Z
C1	0.000000	0.000000	1.308901
C2	0.000000	0.000000	4.191006
H3	0.000000	0.000000	5.275245
C4	0.000000	1.185759	2.083837
C5	0.000000	−1.185759	2.083837
H6	0.000000	2.152982	1.582074
H7	0.000000	−2.152982	1.582074
C8	0.000000	1.203397	3.484029
C9	0.000000	−1.203397	3.484029
H10	0.000000	2.146635	4.021178
H11	0.000000	−2.146635	4.021178
Li12	0.000000	0.000000	−0.687751
C13	−0.000007	1.401557	−2.721978
C14	0.000007	−1.401557	−2.721978
H15	−0.000011	2.483614	−2.711293
H16	0.000011	−2.483614	−2.711293
C17	1.213925	0.700759	−2.721400
C18	−1.213933	0.700747	−2.721404
C19	−1.213925	−0.700759	−2.721400
C20	1.213933	−0.700747	−2.721404
H21	2.150995	1.241532	−2.708094
H22	−2.151008	1.241512	−2.708094
H23	−2.150995	−1.241532	−2.708094
H24	2.151008	−1.241512	−2.708094

Center number	Li_4Me_4CO Standard orientation Coordinates [A] X	Y	Z
O1	0.000000	0.000000	4.016836
C2	0.000000	0.000000	2.869736
Li3	0.000000	0.000000	0.530136
Li4	−1.207885	0.697373	−1.501358
Li5	1.207885	0.697373	−1.501358
Li6	0.000000	−1.394746	−1.501358
C7	0.000000	2.100162	−0.307115
C8	1.818794	−1.050081	−0.307115
C9	−1.818794	−1.050081	−0.307115
C10	0.000000	0.000000	−3.221164
H11	−0.861692	0.497498	−3.695092
H12	0.861692	0.497498	−3.695092
H13	0.000000	−0.994996	−3.695092
H14	0.000000	2.249353	0.782519
H15	0.860769	2.703982	−0.639751
H16	−0.860769	2.703982	−0.639751
H17	1.947997	−1.124677	0.782519
H18	1.911332	−2.097438	−0.639751
H19	2.772101	−0.606543	−0.639751
H20	−1.947997	−1.124677	0.782519
H21	−2.772101	−0.606543	−0.639751
H22	−1.911332	−2.097438	−0.639751

to one [*d*(LiC) = 210.8 pm] and with the oxygen atom to two lithium atoms of a lithium tetrahedron plane [*d*(LiO) = 196.9 pm]. This coordination in a μ_3 fashion helps to find an exothermic reaction pathway for the insertion. Figure 2 illustrates the results on the MP2/6-31G** level of theory of the above-mentioned reaction steps. A summary of the theoretical results are given in Table 1 (energies and frequencies) while the coordinates of the optimized structures are found in Table 2.

In this second case the high-level calculations correspond with the experimental basis. In the early phase of the LXe experiment at low temperature a coordinated triple-bonded

Table 2 *(continued)*

Center number	Li_4Me_3COMe Standard orientation Coordinates [A] X	Y	Z
Li1	−1.034062	−1.931743	0.000000
Li2	1.231743	−0.850342	0.000000
C3	1.285637	1.256727	0.000000
O4	0.000000	1.396461	0.000000
C5	2.026287	2.568586	0.000000
Li6	−0.927215	0.156368	1.216750
Li7	−0.927215	0.156368	−1.216750
C8	0.174686	−1.660539	1.814355
C9	0.174686	−1.660539	−1.814355
C10	−2.674889	−0.457851	0.000000
H11	1.357455	3.431790	0.000000
H12	2.682286	2.594098	0.872794
H13	2.682286	2.594098	−0.872794
H14	−3.196468	−1.428345	0.000000
H15	−3.126195	0.062150	−0.860343
H16	−3.126195	0.062150	0.860343
H17	−0.086380	−1.163545	2.763242
H18	1.250917	−1.855296	1.940979
H19	−0.275216	−2.660100	1.936136
H20	−0.086380	−1.163545	−2.763242
H21	1.250917	−1.855296	−1.940979
H22	−0.275216	−2.660100	−1.936136

CO group is detected by IR spectroscopy and is assigned to the (carbonyl)lithium. Warming-up leads to the decomposition of this first species while a second one with a double-bonded CO group appears at the same time. It is plausible that the second intermediate is the organolithium-lithium species coordinating the RC=O group in a μ_3 fashion which shifts the carbonyl stretching frequency to 1635 cm^{-1} which, in turn, is only plausible in this extraordinary complexation mode. This second species finally reacts further resulting an IR spectrum with no C−O stretching frequencies above 1500 cm^{-1}.

Again a comparison of the bonding energy of carbon monoxide to lithium or chromium will help to classify the observed transition-metal-like behaviour of lithium. Chromium atoms react with carbon monoxide to $Cr(CO)_6$ and release nearly 180 kcal/mol which is interpreted as an (averaged) bonding energy between Cr and CO of 30 kcal/mol.[8] The result of the calculation for the lithium−CO bonding energy is less than 8 kcal/mol and indicates a relatively weak interaction. This is not unexpected in the second case since the subcoordination and therefore the transition-metal-like behaviour of lithium is markedly less because now a organolithium cluster is involved instead of a monomeric compound.

This work was supported by the *Deutsche Forschungsgemeinschaft*, the *Fonds der Chemischen Industrie* and the *Irish Research Organisation Forbairt*.

Experimental Section

With a view to determining the structures, IR frequencies and energies of formation the application of theoretical methods are proved advantageous. For this purpose the program package GAUSSIAN 92[10] implemented on an IBM-compatible Pentium computer with 64 MB RAM memory was used. Ab initio calculations were performed at the HF (Hartree-Fock) or MP2 (second

order Møller-Plesset) level of theory using 6-31G** basis set for the species of interest. Harmonic vibrational frequencies, calculated at the HF/6-31G** level only, characterized stationary points and gave the zero-point energy. Therefore, frequencies are scaled by using a factor of 0.89. Geometries were then optimized on MP2/6-31G** level to deliver the electronic energy and geometries for discussion. The sum of the electronic and the zero-point energy was used to calculate differences interpreted as reaction enthalpies at 0 K. For the visualisation of the calculated structures the program ORTEX 5[11] was used.

☆ Dedicated to Professor *Heinrich Nöth* on the occasion of his 70th birthday.

[1] J. L. Wardell, in *Comprehensive Organometallic Chemistry* (Eds.: G. Wilkinson, F. G. A. Stone, E. W. Abel), Pergamon, Oxford, England, **1982**; W. N. Setzer, P. von R. Schleyer, *Adv. Organomet. Chem.* **1985**, *24*, 353; *Lithium Chemistry* (Eds.: A.-M. Sapse, P. von R. Schleyer), Wiley, New York, USA, **1996**.

[2] B. Schiemenz, P. P. Power, *Angew. Chem. Int. Ed. Engl.* **1996**, *35*, 2150; *Angew. Chem.* **1996**, *108*, 2288.

[3] S. Kurz, E. Hey-Hawkins, *Organometallics* **1992**, *11*, 2729.

[4] K. N. Houk, N. G. Rondan, P. von R. Schleyer, E. Kaufmann, T. Clark, *J. Amer. Chem. Soc.* **1985**, *107*, 2821; E. Kaufmann, P. von R. Schleyer, K. N. Houk, Y.-D. Wu, *J. Amer. Chem. Soc.* **1985**, *107*, 5560; the interaction of LiH/LiMe with benzene is mentioned earlier using smaller basis sets: N. J. R. van Eikema Hommes, P. von R. Schleyer, *Angew. Chem. Int. Ed. Engl.* **1992**, *31*, 755; *Angew. Chem.* **1992**, *104*, 768; N. J. R. van Eikema Hommes, P. von R. Schleyer, *Tetrahedron* **1994**, *50*, 5903.

[5] M. Tacke, *Chem. Ber.* **1995**, *128*, 1051.

[6] D. Seyferth, R. C. Hui, R. M. Weinstein, W.-L. Wang, *Nova Acta Leopoldina* **1985**, *59*, 335.

[7] R. H. Staley, J. L. Beauchamp, *J. Amer. Chem. Soc.* **1975**, *97*, 5920.

[8] J. D. Cox, G. Pilcher, *Thermochemistry of Organic and Organometallic Compounds*, Acadamic Press, London, England, **1970**.

[9] M. Tacke, P. Sparrer, R. Teuber, H.-J. Stadter, F. Schuster, *J. Mol. Struct.* **1995**, *349*, 251.

[10] M. J. Frisch, G. W. Trucks, M. Head-Gordon, P. M. W. Gill, M. W. Wong, J. B. Foresman, B. G. Johnson, H. B. Schlegel, M. A. Robb, E. S. Replogle, R. Gomperts, J. L. Andres, K. Raghavachari, J. S. Binkley, C. Gonzalez, R. L. Martin, D. J. Fox, D. J. Defrees, J. Baker, J. J. P. Stewart, J. A. Pople, *Gaussian 92*, Revision E.1, Gaussian, Inc., Pittsburgh PA, **1992**.

[11] P. McArdle, *J. Appl. Cryst.* **1995**, *28*, 65.

[97287]

Synthesis of the First Lanthanoid(II) Pyrazolate Complex by Redox Transmetallation from Thallium and Mercury Reagents

Glen B. Deacon*[a], Ewan E. Delbridge[a], Brian W. Skelton[b], and Allan H. White[b]

Chemistry Department, Monash University[a],
Clayton, Victoria 3168, Australia
Fax: (internat.) +61 (0)399054597
E-mail: Glen.Deacon@sci.monash.edu.au

The Department of Chemistry, The University of Western Australia[b],
Nedlands, Western Australia, 6907, Australia
Fax: (internat.) +61(0)893801005

Received December 18, 1997

Keywords: Lanthanoid(II) complexes / Ytterbium / Thallium / η^2-Pyrazolate complexes / Diphenylmercury / Redox transmetallation / X-ray crystal structure

Ytterbium metal reacts with thallium(I) 3,5-diphenylpyrazolate, or with diphenylmercury and 3,5-diphenylpyrazole (Ph_2pzH) in tetrahydrofuran or 1,2-dimethoxyethane (DME) giving, after appropriate isolation, the first lanthanoid(II) pyrazolate complex, $[Yb(Ph_2pz)_2(DME)_2]$. The molecular structure reveals eight coordinate ytterbium(II) with two *cisoid* η^2-3,5-diphenylpyrazolate and two chelating 1,2-dimethoxyethane ligands.

Redox transmetallation between lanthanoid metals and metal complexes (eq. 1; $n = 2$ or 3; $m = an/b$) and redox transmetallation/ligand exchange involving mercurials (eq. 2; $n = 2$ or 3) provide simple halide free routes to lanthanoid complexes[1][2][3].

$$a\mathrm{Ln} + b\mathrm{M(L)}_m \rightarrow a\mathrm{Ln(L)}_b + b\mathrm{M} \downarrow \quad (1)$$

$$2\mathrm{Ln} + n\mathrm{HgR}_2 + 2n\mathrm{LH} \rightarrow 2\mathrm{Ln(L)}_n + n\mathrm{Hg} \downarrow + 2n\mathrm{RH} \quad (2)$$

Recent examples of eq. 1 involve mercury[4][5] and tin[6] compounds. Use of thallium(I) reagents is currently restricted to cyclopentadienyls[7][8][9][10] and phenolates[11]. We now report the synthesis of the first lanthanoid(II) pyrazolate, $Yb(Ph_2pz)_2$ (Ph_2pzH = 3,5-diphenylpyrazole), by redox transmetallation between thallium(I) 3,5-diphenylpyrazolate, and ytterbium metal and by redox transmetallation/ligand exchange between Yb, Ph_2pzH and $HgPh_2$, together with the X-ray crystal structure of $[Yb(Ph_2pz)_2(DME)_2]$ (DME = 1,2-dimethoxyethane). This opens the use of thallium-based redox transmetallation as a source of lanthanoid organoamides, and increases the versatility of reaction (2).

Thallium(I) 3,5-diphenylpyrazolate was obtained in high yield by reaction of thallium(I) ethoxide with 3,5-diphenylpyrazole in dichloromethane (eq. 3).

$$\mathrm{TlOEt} + \mathrm{Ph_2pzH} \longrightarrow \mathrm{Tl(Ph_2pz)} + \mathrm{EtOH} \quad (3)$$

Reaction of the thallium complex with ytterbium metal in the presence of mercury metal in tetrahydrofuran (THF) and evaporation and crystallisation from DME or reaction of Yb and $Tl(Ph_2pz)$ in DME gave $[Yb(Ph_2pz)_2(DME)_2]$ in good yield (eq. 4). Satisfactory crystallisation was not achieved from THF.

$$\mathrm{Yb} + 2\mathrm{Tl(Ph_2pz)} \xrightarrow{\mathrm{Hg}} \mathrm{Yb(Ph_2pz)_2} + 2\mathrm{Tl}\downarrow \quad (4)$$

The highly air-sensitive product was characterised by elemental analysis and infrared and ^{1}H-NMR spectra, whilst the visible/near infrared spectrum (no bands at 450−1200 nm) indicated the absence of Yb(III). The structure was established by X-ray crystallography below. Although a range of lanthanoid(III) pyrazolates are known[12], particularly $[Ln(R_2pz)_3(L)_n]$ complexes (R = Me, L = THF, n = 1[12c]; R = Ph or *t*Bu, L = THF, DME, or Ph_3PO, n = 1−3[12d-h]), no lanthanoid(II) pyrazolates have previously been reported. It is of particular interest that redox transmetallation/ligand exchange reactions of an excess of ytterbium metal with $Hg(C_6F_5)_2$ and 3,5-di-*tert*-butylpyrazole gave $[Yb((tBu)_2pz)_3(THF)_2]$ rather than a divalent complex[12d][12f], and analogous reactions with 3,5-diphenylpyrazole in this work gave an unidentifiable black insoluble material. However, with $HgPh_2$ as the reagent instead of the commonly used $Hg(C_6F_5)_2$, a smooth high yield synthesis of $[Yb(Ph_2pz)_2(DME)_2]$ was achieved (eq. 5).

$$\mathrm{Yb} + 2\mathrm{Ph_2pzH} + \mathrm{HgPh_2} \rightarrow \mathrm{Yb(Ph_2pz)_2} + 2\mathrm{PhH} + \mathrm{Hg} \downarrow \quad (5)$$

The successful outcome of eq. 5 compared with the failed preparation with $Hg(C_6F_5)_2$, shows that $HgPh_2$ has excellent prospects in redox transmetallation/ligand exchange (eq. 2), despite lower reactivity towards lanthanoid metals than $Hg(C_6F_5)_2$.

 © WILEY-VCH Verlag GmbH, D-69451 Weinheim, 1998 1434−1948/98/0505−0543 $ 17.50+.50/0

By contrast with eq. 4, treatment of thallium(I) 3,5-diphenylpyrazolate with a large excess of samarium metal gave impure (indicated by the Sm analysis) $[Sm(Ph_2pz)_3(DME)_2]$. The DME/Ph_2pz ratio was established by ^{1}H-NMR spectroscopy and corresponds to that in previously prepared $[Ln(Ph_2pz)_3(DME)_2]$ (Ln = La, Nd, or Er)[12h]. A significant high frequency shift of the Ph_2pz resonances from those for $[La(Ph_2pz)_3(DME)_2]$ is consistent with coordination to the paramagnetic ion. The oxidation state was established by the near infrared absorption, which was characteristic of Sm(III)[13], as well as by the typical pale yellow colour of the product solution, whilst the visible region lacked typical Sm(II) absorption near 600cm^{-1}[14]. Thus, even for lanthanoid metals giving accessible divalent compounds, reaction (1) $[M(L)_m = Tl(R_2pz)]$ does not necessarily give a lanthanoid(II) complex.

The molecular structure of $[Yb(Ph_2pz)_2(DME)_2]$ is displayed in Figure 1, together with selected bond distances and angles. Two η^2-Ph_2pz and two chelating DME ligands are bound to ytterbium, giving approximately dodecahedral YbN_4O_4 eight coordination. The common ligands are in a *cisoid* relationship to each other, as indicated by a N-N-centroid−Yb−N′-N′-centroid angle of 101.$_4$° and a O···O-centroid−Yb−O′···O′-centroid angle of 97.$_9$°. The dihedral angle between the two YbN_2 planes is 101.0(2)°. Observation of η^2-pyrazolate coordination for the first lanthanoid(II) pyrazolate is consistent with the predominance of this bonding mode in pyrazolatolanthanoid(III) complexes[12], but where μ-pyrazolate binding, the dominant mode for d-block metals[15], is also known[12a][12b][12c]. The first examples of η^2 coordination for d-block transition metals have recently been reported[15c][16]. With allowance for differences in oxidation state and coordination number[17], the Yb−N distances are comparable with those of lanthanoid(III) pyrazolates[12] and the Yb−O distances are consistent with those of the chelating DME of $[Er(Ph_2pz)_3(\eta^2\text{-DME})(\eta^1\text{-DME})]$[12h]. Thus, subtraction of the ionic radius for eight coordinate Yb^{2+} (1.14 Å)[17] from <Yb-N> gives 1.28 Å comparable (but at the low end) with values, 1.27−1.38 Å[12c-h], for a range of $[Ln(\eta^2\text{-}R_2pz)_3(L)_n]$ (R = Ph or *t*Bu) complexes, whilst a similar subtraction from <Yb-O> gives 1.39 Å, comparable with the 1.42 Å derived from the chelating DME of $[Er(Ph_2pz)_3(\eta^2\text{-DME})(\eta^1\text{-DME})]$[12h] and within the range derived from Ln−O of $[Ln(R_2pz)_3(THF)_n]$ (n = 2 or 3) (R = *t*Bu or Ph) complexes[12e][12f].

A wide ranging study of the syntheses and structures of pyrazolatolanthanoid(II) complexes, especially preparation by redox transmetallation reactions from free metals and thallium(I) pyrazolates, is in progress.

We are grateful to the *Australian Research Council* for financial support and for the award of an Australian Postgraduate Research Award to E. E. D

Figure 1. ORTEP plot of $[Yb(Ph_2pz)_2(DME)_2]$[a] showing 20% thermal ellipsoids for the non-hydrogen atoms

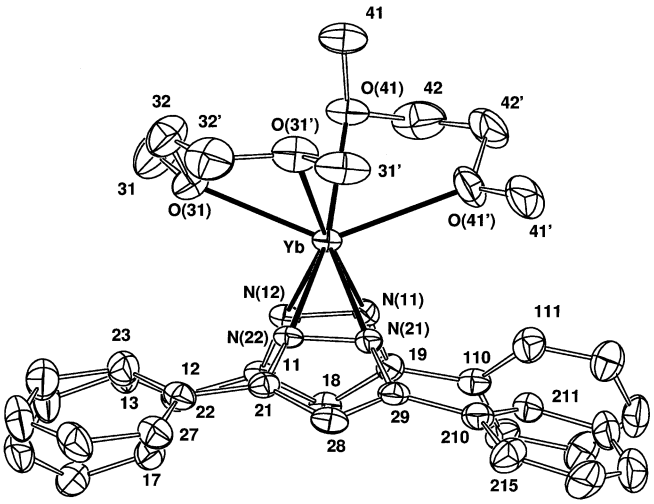

[a] Selected bond lengths [Å] and angles [°] data with estimated deviations in parentheses: Yb−N(11) 2.426(7), Yb−N(12) 2.414(7), Yb−N(21) 2.424(7), Yb−N(22) 2.430(7), Yb−O(31) 2.502(6), Yb−O(31′) 2.558(7), Yb−O(41) 2.484(6), Yb−O(41′) 2.576(7), N(11)−N(12) 1.362(9), N(21)−N(22) 1.357(9), N(11)−Yb−N(12) 32.7(2), N(11)−Yb−N(21) 95.5(2), N(11)−Yb−N(22) 107.3(2), N(11)−Yb−O(31) 116.7(2), N(11)−Yb−O(31′) 174.7(2), N(11)−Yb−O(41) 91.2(2), N(11)−Yb−O(41′) 87.7(2), N(12)−Yb−N(21) 102.8(2), N(12)−Yb−N(22) 96.4(2), N(12)−Yb−O(31) 86.8(2), N(12)−Yb−O(31′) 150.9(2), N(12)−Yb−O(41) 97.9(2), N(12)−Yb−O(41′) 119.7(2), N(21)−Yb−N(22) 32.5(2), N(21)−Yb−O(31) 122.8(2), N(21)−Yb−O(31′) 87.1(2), N(21)−Yb−O(41) 151.2(2), N(21)−Yb−O(41′) 86.7(2), N(22)−Yb−O(31) 91.0(2), N(22)−Yb−O(31′) 77.3(2), N(22)−Yb−O(41) 161.2(2), N(22)−Yb−O(41′) 116.8(2), O(31)−Yb−O(31′) 65.2(2), O(31)−Yb−O(41) 77.8(2), O(31)−Yb−O(41′) 136.6(2), O(31′)−Yb−O(41′) 84.4(2), O(31′)−Yb−O(41′) 87.9(2), O(41)−Yb−O(41′) 65.6(2).

Experimental Section

The compounds described here are extremely air- and moisture-sensitive and consequently all operations were carried out in an inert atmosphere (purified argon or nitrogen).

(3,5-Diphenylpyrazolato)thallium(I): Thallium(I) ethoxide (3.55 ml, 12.5g, 50.0 mmol) was added to a CH_2Cl_2 (200 ml) solution of 3,5-diphenylpyrazole (11.1g, 50.0 mmol). Addition of thallium(I) ethoxide caused undissolved 3,5-diphenylpyrazole to dissolve. Removal of the CH_2Cl_2 under vacuum yielded 19.4g (92%) of a white crystalline solid, m.p. 195°C (sealed capillary/argon). − IR: $\tilde{\nu}$ = 1600 cm^{-1} m, 1259 m, 1070 m, 1058 s, 1025 m, 972 m, 914 w, 799 m, 758 vs, 693 vs. − ^{1}H NMR (200 MHz, [D$_8$]THF): δ = 7.96 (s, 1 H, 4-H pz),7.12−7.21 (m, 2 H, *p*-H), 7.21−7.27 (m, 4 H, *m*-H), 7.68 (t, 4 H, *o*-H), − MS (70 eV, EI); *m*/*z* (%): 424 (50) [(^{205}Tl)M$^+$], 220 (80) [$C_{15}H_{11}N_2^+$], 205 (100) [^{205}Tl$^+$]. − $C_{15}H_{11}N_2Tl$ (423.6): calcd. C 42.53, H 2.62, N 6.61; found C 42.35, H 2.53, N 6.49.

Bis(1,2-dimethoxyethane)bis(η²-3,5-diphenylpyrazolato)-ytterbium(II) − Method A: A mixture of ytterbium powder (1.73g, 10.0 mmol), mercury metal (ca. 0.10 ml) and (3,5-diphenylpyrazolato)thallium(I) (2.12g, 5.0 mmol) in THF (30 ml) or DME (50 ml) was subjected to ultrasonication for 24 h. The resulting deep red solution with grey suspended solids was allowed to stand for several hours until the suspension settled out. The reaction mixture was then filtered using a filter cannula. In the case where THF was used, the filtrate was evaporated to dryness under vacuum yielding a red solid which was dissolved in DME (40 ml) and allowed to stand for several days at room temp. during which time 1.3 g (66%) of large red crystals formed. In the case where DME was used, evaporation of some DME (ca. 5 ml) and standing for several days

afforded large red crystals of similar appearance in similar yield, m.p. >350°C (sealed capillary/argon). – IR: $\tilde{\nu}$ = 1602 cm^{-1} m, 1156 w, 1121 w, 1099 m, 1071 s, 1025 m, 968 s, 914 w, 863 m, 859 m, 801 w, 757 vs, 722 m, 698 s, 685 s. – Visible/near IR (THF): λ_{max} (ε) = 410 nm (774). – ^{1}H NMR (300 MHz, [D_8]THF): δ = 3.24 (s, 12 H, CH_3O DME), 3.41 (s, 8 H, CH_2 DME), 7.07 (t, 4 H, *p*-H), 7.10 (s, 2 H, 4-H), 7.24 (t, 8 H, *m*-H), 7.92 (d, 8 H, *o*-H). – ^{171}Yb NMR (52.5 MHz, 0.04 M in DME): δ = 480 ($\Delta\nu_{1/2}$ 20 Hz) [relative to $Yb(C_5Me_5)_2(THF)_2$] – $C_{38}H_{42}N_4O_4Yb$ (791.8): calcd.: C 57.64, H 5.35, N 7.08, Yb 21.85; found C 56.88, H 5.24, N 7.59, Yb 22.43.

Method B: A mixture of ytterbium powder (1.73 g, 10.0 mmol), $HgPh_2$ (0.80 g, 2.3 mmol) and 3,5-diphenylpyrazole (1.00 g, 4.5 mmol) in THF (40 ml) was stirred and heated at 60°C for 2 d. The resulting red solution with grey suspended solids was filtered and the filtrate was evaporated to dryness. Recrystallisation of the resulting red solid from DME (20 ml) at −20°C gave 1.37 g (76%) of $[Yb(Ph_2pz)_2(DME)_2]$ as deep red crystals. – IR: Identical with that of the product from A. – $C_{38}H_{42}N_4O_4Yb$ (791.8): calcd. Yb 21.85; found Yb 21.48.

Reaction Between (3,5-Diphenylpyrazolato)thallium(I) and Samarium Metal: A mixture of samarium metal (1.50 g, 10.0 mmol), mercury metal (ca. 0.40 ml) and (3,5-diphenylpyrazolato)thallium(I) (0.85 g, 2.0 mmol) in THF (30 ml) was subjected to ultrasonication for 3 d. The resulting pale yellow solution with grey suspended solids was allowed to stand for several hours. Filtration and evaporation as above yielded a white solid which was recrystallised from a DME/light petroleum mixture giving $[Sm(Ph_2pz)_3(DME)_2]$ 0.42 g, (40%) as a white powder. – IR: $\tilde{\nu}$ = 1604 cm^{-1} m, 1513 w, 1422 w, 1282 w, 970 s, 906 w, 864 s, 800 w, 759 vs, 696 s, 684 s. – Visible/near IR (THF): λ_{max} (ε) = 369 nm (1.5), 402 (2.0), 977 (1.0), 1074 (2.0), 1328 (3.5), 1368 (1.0) . – ^{1}H NMR (300 MHz, [D_8]THF): δ = 3.27 (s, 12 H, CH_3O), 3.39 (s, 8 H, CH_2), 7.30 (t, 6 H, *p*-H), 7.54 (t, 12 H, *m*-H), 7.94 (s, 3 H, 4-H), 9.28 (d, 12 H, *o*-H). – $C_{53}H_{53}N_6O_4Sm$ (988.5): calcd. Sm 15.22; found Sm 16.64.

X-ray Crystallography of [Yb(Ph$_2$pz)$_2$(DME)$_2$]: Single crystals were grown from a saturated DME solution at room temperature over several days. $C_{38}H_{42}N_4O_4Yb$ (791.82), monoclinic, space group $P2_1/a$ (no. 14). a = 7.882(4), b = 18.959(3), c = 24.080(14) Å, β = 91.03(2)°, V = 3598(3) Å^3, Z = 4, D_c = 1.462 g cm^{-3}, μ_{Mo} = 26.4 cm^{-1}, $F(000)$ = 1600, $A^*_{min,max}$ 1.64, 2.17. For X-ray crystallography single crystals 0.20 × 0.38 × 0.33 mm were covered in a heavy oil and sealed into glass capillaries under purified argon. From 6331 diffractometer reflections ($2\theta_{max}$ 50°, $2\theta/\theta$ scan mode; monochromatic Mo K_α radiation; λ = 0.7107$_3$ Å; $T \approx$ 295 K; 18381 total reflections merged (R_{int} = 0.048), 50% crystal decomposition compensated by scaling), 3670 "observed" [$I > 3\sigma(I)$)] used after absorption correction in the final least squares refinement [anisotropic thermal parameters for non-hydrogen atoms, (x, y, z, U_{iso})$_H$ constrained]. R, Rw on $|F|$ were 0.044, 0.044 (statistical weights). Crystallographic data (excluding structure factors) for the structure reported in this paper have been deposited with the Cambridge Crystallographic Data Centre as supplementary publication no. CCDC-101118. Copies of the data can be obtained from The Director, CCDC, 12 Union Road, Cambridge CB2 1EZ, UK [Fax: (int. Code) +44(1223)336-033, E-mail: deposit@chemcrys.cam.ac.uk, World Wide Web: http://www.ccdc.cam.ac.uk].

[1] H Schumann, J. A. Meese-Marktscheffel, L. Esser, *Chem. Rev.* **1995**, *95*, 865–986.
[2] F. T. Edelmann, in *Comprehensive Organometallic Chemistry*, 2nd ed. (Eds.: G. Wilkinson, F. G. A. Stone, E. W. Abel), Pergamon, Oxford, **1995**, chapter 2.
[3] M. N. Bochkarev, L. N. Zakharov, G. S. Kalinina, *Organoderivatives of Rare Earth Elements* Kluwer Academic Press, Dordrecht, **1995**.
[4] L. N. Bochkarev, T. A. Stepantseva, L. N. Zakharov, G. K. Fukin, A. I. Yanovsky, Y. T. Struchkov, *Organometallics.* **1995**, *14*, 2127–2129.
[5] G. B. Deacon, G. D. Fallon, C. M. Forsyth, H. Schumann, R. Weimann, *Chem. Ber.* **1997**, *130*, 409–415.
[6] B. Cetinkaya, P. B. Hitchcock, M. F. Lappert, R. G. Smith, *J. Chem. Soc., Chem. Comm.* **1992**, 932–934.
[7] [7a] G. B. Deacon, A. J. Koplick, T. D. Tuong, *Aust. J. Chem.* **1984**, *37*, 517–525. – [7b] G. B Deacon, C. M. Forsyth, R. H. Newnham, T. D. Tuong, *Aust. J. Chem.* **1987**, *40*, 895–906.
[8] [8a] G. B. Deacon, G. N. Pain, T. D. Tuong, *Inorg. Synth.* **1990**, *28*, 291–297. – [8b] G. B. Deacon, A. J. Koplick, G. N. Pain, T. D. Tuong, in *Herrmann-Brauer, Synthetic Methods of Organometallic and Inorganic Chemistry*, 3rd edn (Eds.: W. A. Herrmann) *Vol. 6*, 52–55, 86–87.
[9] [9a] G. B. Deacon, A. Dietrich, C. M. Forsyth, H. Schumann, *Angew. Chem.* **1989**, *101*, 1374–1375; *Angew. Chem. Int. Ed. Engl.* **1989**, *28*, 1370–1371. – [9b] G. B. Deacon, C. M. Forsyth, W. C. Patalinghug, A. H. White, A. Dietrich, H. Schumann, *Aust. J. Chem.* **1992**, *45*, 671–683. – [9c] G. B. Deacon, C. M. Forsyth, B. M. Gatehouse, A. Philosof, B. W. Skelton, A. H. White, P. A. White, *Aust. J. Chem.* **1997**, *50*, 959–970.
[10] [10a] G. Y. Lin, T. W. Wong, *J. Organomet. Chem.* **1995**, *495*, 203–208. – [10b] G. Y. Lin, T. W. Wong, *J. Organomet. Chem.* **1996**, *523*, 93–98.
[11] [11a] G. B. Deacon, P. B. Hitchcock, S. A. Holmes, M. F. Lappert, P. MacKinnon, R. H. Newnham, *J. Chem. Soc. Chem. Comm.* **1989**, 935–937. – [11b] G. B. Deacon, T. Feng, S. Nickel, M. I. Ogden, A. H. White, *Aust. J. Chem.* **1992**, *45*, 671–683. – [11c] G. B. Deacon, T. Feng, P. MacKinnon, R. H. Newnham, S. Nickel, B. W. Skelton, A. H. White, *Aust. J. Chem.* **1993**, *46*, 387–399.
[12] [12a] H. Schumann, Pil Ryul Lee, J. Loebel, *Angew. Chem.* **1989**, *101*, 1073–1074; *Angew. Chem. Int. Ed. Engl.* **1989**, *28*, 1033–1035. – [12b] H. Schumann, J. Loebel, J. Pickardt, Changtao Qian, Zuowei Xie, *Organometallics* **1991**, *10*, 215–219. – [12c] G. B. Deacon, B. M. Gatehouse, S. Nickel, S. N. Platts, *Aust J. Chem.* **1991**, *44*, 613–621. – [12d] J. E. Cosgriff, G. B. Deacon, B. M. Gatehouse, H. Hemling, H. Schumann, *Angew. Chem.* **1993**, *105*, 906–907; *Angew. Chem. Int. Ed. Engl.* **1993**, *32*, 874–875. – [12e] J. E. Cosgriff, G. B. Deacon, B. M. Gatehouse, *Aust J. Chem.* **1993**, *46*, 1881–1896. – [12f] J. E. Cosgriff, G. B. Deacon, B. M. Gatehouse, H. Hemling, H. Schumann, *Aust J. Chem.* **1994**, *47*, 1223–1235. – [12g] J. E. Cosgriff, G. B. Deacon, B. M. Gatehouse, Pil Ryul Lee, H. Schumann, *Z. Anorg. allg. Chem.* **1996**, *622*, 1399–1403. – [12h] J. E. Cosgriff, G. B. Deacon, G. D. Fallon, B. M. Gatehouse, H. Schumann, R. Weimann, *Chem. Ber.* **1996**, *129*, 953–958. – [12i] G. Bielang, Doctoral Dissertation, Hamburg, **1979**.
[13] W. T. Carnall, in *The Absorption and Fluorescence Spectra of Rare Earth Ions in Solution* in *Handbook on the Physics and Chemistry of Rare Earths*, (Eds.: K. A. Gschneidner and L. Eyring) vol. 3, chapter 24, North-Holland, Amsterdam, **1979**.
[14] [14a] G. S. Ofelt, *J. Chem. Phys.* **1963**, *38*, 2171–2180. – [14b] A. N. Kamenskaya, N. B. Mikheev, N. A. Konovalova, *Russ. J. Inorg. Chem.* **1977**, *22*, 1152–1155.
[15] [15a] S. Trofimenko, *Prog. Inorg. Chem.* **1986**, *34*, 115–120. – [15b] S. Trofimenko. *Chem. Rev.* **1972**, *72*, 497–509. – [15c] J. E. Cosgriff, G. B. Deacon, *Angew Chem.* **1998**, *110*, 298–299; *Angew. Chem. Int. Ed. Engl.* **1998**, *37*, 286–287.
[16] [16a] I. A. Guzei, A. G. Baboul, G. P. A Yap, A. L. Rheingold, H. B. Schlegel, C. H. Winter, *J. Am. Chem. Soc.* **1997**, *119*, 3387–3388. – [16b] I. A. Guzei, G. P. A. Yap, C. H. Winter, *Inorg. Chem.* **1997**, *36*, 1738–1739. – [16c] D. Röttger, G. Erker, M. Grehl, R.Frölich, *Organometallics*, **1994**, *13*, 3897–3902.
[17] R. D. Shannon, *Acta Crystallogr., Sect. A* **1976**, *32*, 751–767.

[97312]

A Unique Copper-Controlled Template Synthesis of Tetradentate N4-Donor Ligands and Their Propeller-Type Linear Trinuclear Cu^{II} Complexes

Gerard A. van Albada[a], Ilpo Mutikainen[b], Urho Turpeinen[b], and Jan Reedijk*[a]

Leiden Institute of Chemistry, Gorlaeus Laboratories, Leiden University[a],
P. O. Box 9502, 2300 RA Leiden, Netherlands
E-mail: reedijk@chem.leidenuniv.nl

Laboratory of Inorganic Chemistry, Department of Chemistry[b],
P. O. Box 55 (A. I. Virtasen aukio 1), 00014 University of Helsinki, Finland

Received January 29, 1998

Keywords: Copper / Trinuclear / Formamidines / Magnetism / Crystal structure

In situ reaction of Cu^{II} triflate with aminopyridine or aminopyrimidine and triethylorthoformate in ethanol results in unique linear trinuclear Cu^{II} complexes with the general formula $[Cu_3(L^-)_4](CF_3SO_3)_2(EtOH)_x$ (L = dehydronated ligand *N,N′*-bis(pyridine-2-yl)formamidine or the new ligand *N,N′*-bis(pyrimidine-2-yl)formamidine). The structure [Cu−Cu−Cu angle 175.19(2)°] consists of four nearly flat molecules of the ligand which contribute to the propeller-type structure around the Cu−Cu−Cu axis. A strong antiferromagnetic interaction between the Cu^{II} ions is observed, resulting in an $S = 1/2$ ground state below 100 K.

Dinuclear and polynuclear exchange-coupled copper(II) complexes are well known, but the number of magnetically as well as structurally investigated trinuclear compounds is quite limited[1]. Also the theory for dinuclear and polynuclear systems is found adequate to describe the exchange parameter of magnetism[1][2], but linear trinuclear compounds are far less discussed. Dinuclear systems are also well documented because their relevance for bioinorganic model systems in copper enzymes[3].

Linear trinuclear Cu^{II} compounds are relatively rare and only few are studied magnetically[4]. A few are known with a CuN_{4-6} chromophore around each Cu^{II} ion[5]. We now wish to report a novel method for in situ synthesis of such trinuclear compounds, which have quite unusual propeller-type structure and a strong magnetic exchange coupling. Compounds $[Cu_3(pdf)_4](CF_3SO_3)_2(EtOH)_{1.5}$ (**1**), in which pdf is the dehydronated ligand *N,N′*-bis(pyridine-2-yl)formamidine, and $[Cu_3(pmf)_4](CF_3SO_3)_2(EtOH)_{0.5}$ (**2**), in which pmf is the dehydronated ligand *N,N′*-bis(pyrimidine-2-yl)-formamidine, were synthesized and characterised.

Structural analysis of **1** shows a linear arrangement of 3 Cu^{II} ions surrounded by 4 ligand molecules in a propeller mode, each of which being tetracoordinating to the 3 copper atoms (Figure 1). The central copper atom is distorted square-planar [angles of 163.46(11), 161.11(11)°] and normal Cu−N distances of ca. 2.0 Å. The outer copper ions are six coordinated with distorted square-based geometry, and a slightly different geometry for each copper. The angles of the basal plane of Cu1 (formed by N211−N311−N411−N125) are 176.84(11) and 158.53(11)° and of Cu3 (formed by N117−N217−N317−N423) are 178.50(11) and 156.83(11)°. The short Cu−N distances for Cu(1) and Cu(3) vary from 1.989(3) to 2.191(3) Å. The axial sites of the geometry are occupied by other nitrogens with Cu−N distances that vary from 2.267(4) to 2.543(3) Å. The axial angles slightly differ from linear [N325−Cu1−N111 = 160.81(11)° and N417−Cu3−N223 = 158.18(11)°], as a result of contraints caused by the ligandshape.

Figure 1. Plot of structure **1** with atom-labelling scheme. H- atoms and non-coordinating triflate anions and the ethanol molecules are omitted for clarity[a]

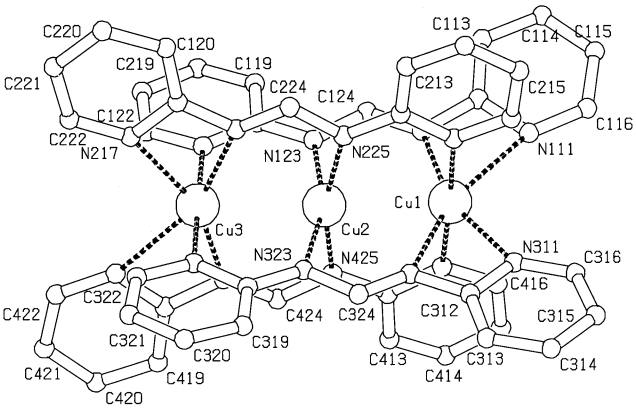

[a] Selected distances [Å] and angles [°]: Cu(1)−Cu(2) 2.6618(8), Cu(2)−Cu(3) 2.6676(8), Cu(1)−N(411) 1.989(3), Cu(1)−N(211) 1.992(3), Cu(1)−N(125) 2.033(3), Cu(1)−N(311) 2.168(3), Cu(1)−N(325) 2.272(3), Cu(1)−N(111) 2.543(3), Cu(2)−N(425) 1.997(3), Cu(2)−N(225) 2.026(3), Cu(2)−N(123) 2.036(3), Cu(2)−N(323) 2.050(3), Cu(3)−N(317) 2.001(3), Cu(3)−N(117) 2.011(3), Cu(3)−N(423) 2.032(3), Cu(3)−N(223) 2.191(3), Cu(3)−N(217) 2.267(4), Cu(3)−N(417) 2.500(3), N(411)−Cu(1)−N(211) 176.84(11), N(125)−Cu(1)−N(311) 158.53(11), N(111)−Cu(1)−N(325) 160.81(11), N(425)−Cu(2)−N(225) 163.46(11), N(123)−Cu(2)−N(323) 161.11(11), Cu(1)−Cu(2)−Cu(3) 175.19(2), N(317)−Cu(3)−N(117) 178.50(11), N(423)−Cu(3)−N(217) 156.83(11), N(223)−Cu(3)−N(417) 158.18(11).

The Cu−Cu distances of 2.6618(8) and 2.6676(8) Å, are only slightly longer than in the two other comparable

 © WILEY-VCH Verlag GmbH, D-69451 Weinheim, 1998 1434−1948/98/0505−0547 $ 17.50+.50/0

CuN_x-bridged linear copper(II) compounds[5a][5c], but shorter than in the azido-bridged trinuclear compounds[4][5b][5d].

The linear angle Cu1−Cu2−Cu3 is 175.19(2)°. Viewing along the Cu−Cu−Cu axis (Figure 2) a propeller type arrangement is visible in which the ligands are almost perpendicular to the axis with angles between the two rings of each ligand which vary from 27.73 to only 8.19°. Hydrogen bonds between the oxygens of the lattice ethanol and the triflate molecules (O···O 2.82 and 3.02 Å) stabilize the lattice.

Figure 2. View along the Cu−Cu−Cu axis of structure (**1**)

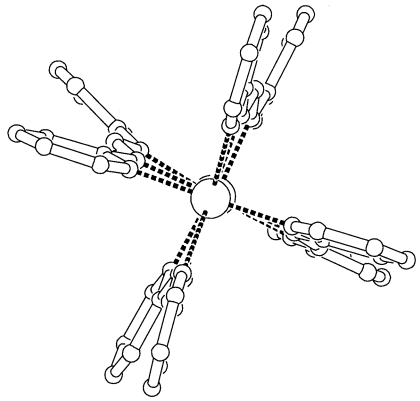

The ligand field spectrum of both compounds show a broad band with a double maximum at 16.3 and $20.8 \cdot 10^3$ cm^{-1} for **1** and at 16.9 and $20.9 \cdot 10^3$ cm^{-1} for **2**. These two absorptions are both d-d transitions[6a][6b], and it is tempting to assume that the highest energy is from the central Cu atom, although Cu2 is not perfectly square planar, and the lowest energy from the outer six-coordinated Cu atoms[5c][6c].

The EPR spectra at room temperature shows a broad absorption centered around g = 2.11 and a weaker broad absorption at ca. g = 3.6, which disappear upon cooling to 77 K. The EPR signal sharpens upon cooling and a very weak $g_{//}$ at ca. 2.3 is observed (no $A_{//}$ resolved). No structural conclusions can be drawn from these spectra. Preliminary temperature dependent magnetic susceptibility measurements down to 5 K, shows a magnetic moment of ca. 1.50 B.M. per copper(II) ion at 270 K, which decreases to ca. 1.0 B.M. at 20 K, which indicates an antiferromagnetic coupling between the copper(II) ions within the trinuclear units[6d][5c]. In the area 70−5 K $1/\chi$ vs. T is linear with $\Theta = 0$ and agrees with $\mu = 1.05$ (or 1.8 B.M./Cu_3) which agrees with a ground state only one unpaired electron per 3 Cu^{II}. A preliminary fit on the hamiltonian $H = -2J[(\mathbf{S}_A \cdot \mathbf{S}_B) + (\mathbf{S}_B \cdot \mathbf{S}_C)]$ shows that $J = -100$ cm^{-1} and assumes $J' = 0$.

Further work will deal with related ligands yielding this structure and with a full magnetic study. In summary, we have shown that copper ions can control the template synthesis of tetradentate formamidine ligands, simultanously resulting in linear trinuclear Cu^{II} complexes.

The work described in the present paper has been supported by the *Leiden University Study group WFMO* (Werkgroep Fundamenteel Materialen Onderzoek). Use of the services and facilities of the *Dutch National NWO/SURF Expertise Center CAOS/CAMM*, under grant numbers SON 326-052 and STW NCH99.1751, is gratefully acknowledged.

Experimental Section

General: Ligand field spectra were recorded on a Perkin-Elmer Lambda 900 spectrophotometer using the diffuse reflectance technique, with MgO as a reference. − X-band powder EPR spectra were obtained on a Jeol RE2x electron spin resonance spectrometer, using DPPH (g = 2.0036) as a standard. − Magnetic susceptibilities were measured in the temperature range 5−300 K with a Manics DSM-8 susceptometer. Data were corrected for magnetization of the sample holder and for diamagnetic contributions, which were estimated from the Pascal constants[8].

Synthesis: 2-Aminopyridine and 2-aminopyrimidine are obtained from Acros Organics; metal salts and solvents were commercially available and used without further purification. 1.2 mmol of $Cu(CF_3SO_3)_2$ and 1.2 mmol of 2-aminopyridine or 2-aminopyrimidine were each dissolved in ca. 10 ml of ethanol. To each solution ca. 5 ml of triethylorthoformate was added. The copper solution was added carefully to the amino compound solution and filtered to remove any un-dissolved material. After a few days black crystalline material was obtained, filtered, and air-dried.

Compound **1** $\{[Cu_3(pdf)_4](CF_3SO_3)_2(EtOH)_{1.5}\}$ can also be synthesized directly from the copper(II)triflate salt and the ligand Hpdf (which was synthesized in the literature[7]) in ethanol plus triethylorthoformate to remove the water from the ethanol. Satisfactory elemental analysis were obtained.

X-ray Crystal Structure Analysis: Crystal data for $[Cu_3(pdf)_4](CF_3SO_3)_2(EtOH)_{1.5}$: $C_{49}H_{45}Cu_3F_6N_{16}O_{7.5}S_2$, M = 1346.75, monoclinic, space group $P2_1/c$ (no. 14), a = 12.974(3), b = 17.769(4), c = 24.227(5) Å, β = 92.73(3)°, V = 5579(2) $Å^3$, Z = 4, D_c = 1.603 g cm^{-3}, T = 193 K, μ(Mo-K_α) = 1.295 mm^{-1}, $F(000)$ = 2736, 11365 reflections measured, 10881 independent, R_{int} = 0.0317, (2.52 < θ < 26.54°), a black crystal with dimensions of 0.30 × 0.30 × 0.25 mm was selected, mounted to the glass fiber using the oil drop method[9a]. Rigaku AFC-7S diffractometer, graphite-monochromated Mo-K_α radiation (λ = 0.71073 Å), ω-2θ scans. Data reduction using the TEXSAN[9b] package. The intensity data were corrected for Lorentz and polarization effects and for absorption and extinction. All non H atoms were refined anisotropically. H atoms were situated from difference Fourier map and refined isotropically. The structure was solved using direct methods SHELXS-86[9c]. The weighting scheme $w = 1/[\sigma^2(F_o^2) + (0.0970 P)^2 + 09.6067 P]$, where $P = (F_o^2 + 2 F_c^2)/3$ was adopted. Refinement method full-matrix least-squares on F^2 using SHELXL-93[9d] package converged to $R1$ [$I > 2\sigma(I)$] = 0.0475, $wR2$ = 0.1478 (all data) for 751 parameters, S = 0.892, largest difference peak and hole 1.080 and −0.437 e·$Å^{-3}$.

Crystallographic data (excluding structure factors) for the structure in this paper have been deposited with the Cambridge Crystallographic Data Centre as supplementary publication no. CCDC-101041. Copies of the data can be obtained free of charge on application to CCDC, 12 Union Road, Cambridge CB2 1EZ, UK [Fax: (internat.) +44(1223)336-033, E-mail: deposit@ccdc.cam.ac.uk].

[1] O. Kahn, *Molecular Magnetism*, VCH Publ., N. Y., **1993** and references cited therein.
[2] P. J. van Koningsbruggen, J. W. van Hal, R. A. G. de Graaff, J. G. Haasnoot, J. Reedijk, *J. Chem. Soc. Dalton Trans.* **1993**, 2163−2167.
[3] P. A. Vigato, S. Tamburini, *Coord. Chem. Rev.* **1990**, *106*, 25−170.
[4] [4a] F. Akagi, Y. Nakao, K. Matsumoto, S. Takamizawa, W. Mori, S. Suzuki, *Chem. Letters*, **1997**, 181−182. − [4b] R. Prins, M. Biagini-Cingi, M. Drillon, R. A. G. de Graaff, J. G. Haasnoot, A.-M. Manotti-Lanfredi, P. Rabu, J. Reedijk, F. Ugozzoli, *Inorg. Chim. Acta* **1996**, *248*, 35−44.
[5] [5a] G. J. Pyrka, M. El-Mekki, A. A. Pinkerton, *J. Chem. Soc. Chem. Commun.* **1991**, 84−85. − [5b] M. H. W. Lam, Y.-Y. Tang, K.-M. Fung, X.-Z. You, W.-T. Wong, *J. Chem. Soc. Chem. Commun.* **1997**, 957−958. − [5c] L.-P. Wu, P. Field, T. Morrissey, C. Murphy, P. Nagle, B. Hathaway, C. Simmons, P. Thornton, *J. Chem. Soc., Dalton Trans.* **1990**, 3835−3840. − [5d] M. A. S. Goher, F. A. Mautner, *Cryst. Res. and Technol.* **1992**, *27*, 817−823.
[6] [6a] B. J. Hathaway, in *Comprehensive Coordination Chemistry*, ed. G. Wilkinson, R. D. Gill, J. A. McCleverty, Pergamon Press, Oxford, **1987**, Vol. 5. − [6b] A. B. P. Lever, *Inorganic Electronic Spectroscopy*, 2nd. Ed, Elsevier, Amsterdam, **1984**. − [6c] A. M. Duda, A. Karaczyn, H. Kozłowski, I. O. Fritsky, T. Głowiak, E.V. Prisyazhnaya, T. Y. Sliva, J. Swiatek-Kozłowska, *J. Chem. Soc., Dalton Trans.* **1997**, 3853−3859. − [6d] G. Ferguson, C. R. Langrick, D. Parker, K. E. Matthes, *J. Chem. Soc., Chem. Commun.* **1985**, 1609−1610.
[7] [7a] P. Benkó, L. Pallos, *J. Prakt. Chemie* **1972**, *314*, 627−635. − [7b] P. Benkó, L. Pallos, F. Ordogh, B. Rosdy, Hungarian Patent no.155,429 (**1968**).
[8] I. M. Kolthoff, P. J. Elving, *Treatise on Analytical Chemistry*, Interscience Publ., New York, **1963**, Vol. 4, Part 1.
[9] [9a] T. Kottke, D. Stalke, *J. Appl. Crystallogr.* **1993**, *26*, 615−619. − [9b] TEXSAN. *Single Crystal Structure Analysis Software*, Version 1.6, Molecular Structure Corporation, The Woodlands, TX.77381, USA, **1993**. − [9c] G. M. Sheldrick, SHELXS86, *Program for crystal structure determination*. University of Göttingen, Germany, **1986**. − [9d] G. M. Sheldrick, SHELXL93, *Program for crystal structure refinement.* University of Göttingen, Germany, **1993**.

[98015]

Formation of Metallocene-Stabilized Planar-Tetracoordinate Carbon Compounds by a Protonation Route

Jörg Schottek, Gerhard Erker*, and Roland Fröhlich

Organisch-Chemisches Institut der Universität Münster
Corrensstraße 40, D-48149 Münster, Germany
Fax: (internat.) +49(0)251-83 39772
E-mail: erker@uni-muenster.de

Received December 17, 1997

Keywords: Planar-tetracoordinate carbon / Zirconocene / Acetylide complex / Selective protonation

Bis(alkynyl)zirconocene and -hafnocene complexes **4** react with (butadiene)zirconocene or -hafnocene, respectively, to yield the binuclear σ,π-acetylide bridged complexes $[(Cp_2M)_2(\mu\text{-}C{\equiv}C{-}R)_2]$ **7** (M = Zr, Hf; R = CH_3, C_2H_5, or CH_2Ph). The complexes **7** are selectively protonated upon treatment with *N,N*-dimethylanilinium tetraphenylborate or tetrakis(pentafluorophenyl)borate to yield the dinuclear metallocene cation complexes $[(Cp_2M^1)(\mu\text{-}RCC^1{-}H)(\mu\text{-}C{\equiv}C{-}R)M^2Cp_2^+]$ **13** ($M^1 = M^2$ = Zr, **a**–**c**; M^1 = Zr, M^2 = Hf, **h**; $M^1 = M^2$ = Hf, **i**) that contain a planar-tetracoordinate carbon atom (C^1-H) bearing a hydrogen substituent. Complex **13a** was characterized by X-ray diffraction. It reveals an agostic interaction of the C^1-H moiety with the M^2Cp_2 unit. The planar-tetracoordinate carbon unit C^1-H of **13a** exhibits $^{13}C/^1H$ NMR chemical shifts of δ = 161.0 and −0.11 and a coupling constant of $^1J_{CH}$ = 103 Hz. Selective protonation of (μ-alkynyl)bis(group 4 metallocene) complexes containing other additional bridging ligands provides a rather general synthetic entry to planar-tetracoordinate carbon containing complexes of this type: $[Cp_2M^1(\mu\text{-}C{\equiv}C{-}CH_3)(\mu\text{-}Cl)M^2Cp_2]$ (**10a**–**c**, M^1, M^2 = Zr, Hf) and $[Cp_2M^1(\mu\text{-}C{\equiv}C{-}CH_3)(\mu\text{-}CH_3)M^2Cp_2]$ (**11a**,**b**) selectively add a proton from $[(HNMe_2Ph)^+(BAr_4)^-]$ at carbon atom C^1 of the acetylide ligand to yield the corresponding "anti-van't Hoff/LeBel complexes" $[Cp_2M^1(\mu\text{-}CH_3CC^1\text{-}H)(\mu\text{-}X)M^2Cp_2^+]$ (**13d**–**g** and **k**, X = Cl, CH_3), respectively.

Introduction

Planar-tetracoordinate carbon has an electronic structure that is characterized by an electron-deficient σ-system (six electrons making four bonds) and a doubly occupied p-orbital perpendicular to the σ-plane.[1] Principally, σ-electron donor and π-acceptor substituents should stabilize this "unnatural" carbon coordination geometry.[1][2] We have previously prepared a large number of thermodynamically very stable "anti-van't Hoff/Le Bel" compounds of this general type, where the planar-tetracoordinate carbon atom is part of a C=C double bond and has two metal substituents that share a sp^2-orbital in the carbon σ-plane in a three-center-two-electron bond situation.[3] A very favourable situation arises when the two geminal metal substituents have slightly different σ-donor properties. Typical examples are a combination of Cp_2Zr and AlR_2[4] or Cp_2Zr and Cp_2Zr^+.[5] The complexes **1** and **2** are typical examples out of a large variety of such systems. The stabilization energy of planar-tetracoordinate vs. planar-tricoordinate carbon in these complexes is very high (ca. 35 kcal/mol calculated for **1**, ca. 12 kcal/mol experimentally determined for **2**).[6]

The synthetic routes developed and applied so far have allowed for the preparation of a great variety of examples of the complexes of the type **1** and **2** using various combinations of metal complex fragments, bridging ligands X and of the substituents attached at the carbon atoms C^1 (i.e. the planar-tetracoordinate carbon atom) and C^2, but systems bearing a hydrogen at C^1 were not available by these routes.[7] We have now found a rather simple method to solve this synthetic organometallic problem and have prepared a variety of cationic bis(metallocene) complexes of this general type by a regioselective protonation pathway.

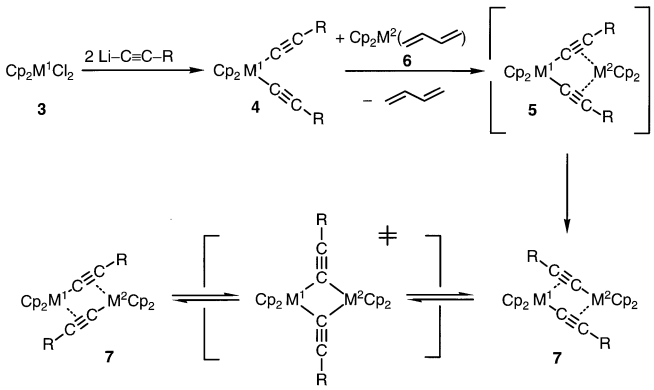

Results and Discussion

Synthesis of the Dinuclear Complexes

Dinuclear (μ-alkynyl)zirconocene and -hafnocene complexes were chosen as the starting materials for our new synthesis. We had previously shown that bis(alkynyl)group 4 metallocenes (**4**) react rapidly with in situ generated Cp_2M

 © WILEY-VCH Verlag GmbH, D-69451 Weinheim, 1998 1434–1948/98/0505–0551 $ 17.50+.50/0

Scheme 1

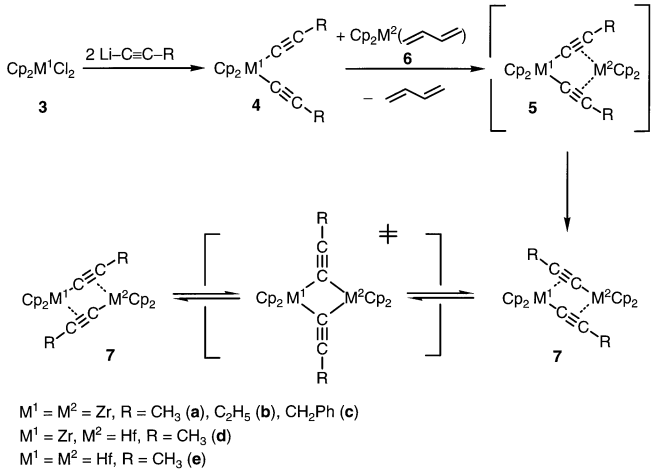

Scheme 2

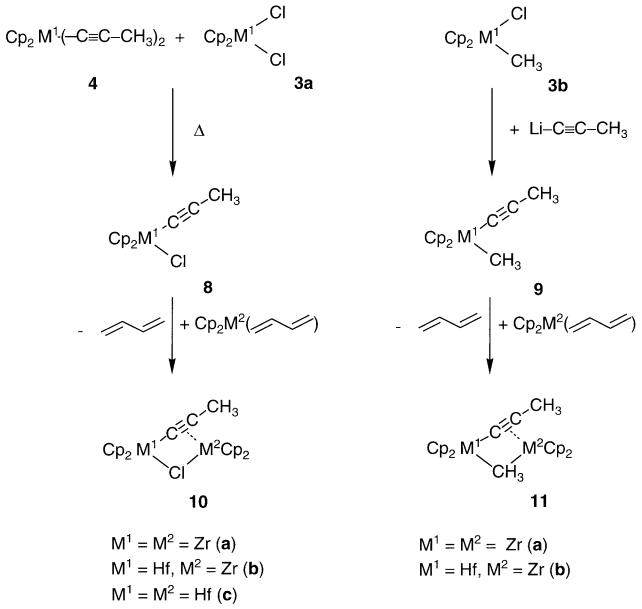

(M = Zr, Hf) reagents to cleanly form the [(μ-η^1:η^2-alkynyl)$_2$(MCp$_2$)$_2$] type complexes. There is evidence that the C_{2v}-symmetric species **5** are formed first, that subsequently rearrange to the C_{2h}-complexes **6** that are eventually isolated from the reaction.[8]

We have thus treated bis(propynyl)zirconocene **4a** (M^1 = Zr, R = CH$_3$) with (butadiene)zirconocene (**6a**, M^2 = Zr)[9] in benzene at ambient temperature (18 h) and obtained the dinuclear complex **7a** in 70% yield. Complex **7a**, like many examples of this type of complexes, is dynamic and undergoes an intramolecular exchange of the two μ-η^1:η^2-alkynyl ligands within the dinuclear metal complex framework that is rapid on the NMR time scale.[8][10]

Complexes **7b** and **7c** were prepared analogously by treatment of the respective bis(alkynyl)zirconocenes **4b** and **4c** with the (butadiene)zirconocene reagent. Treatment of bis(propynyl)hafnocene (**4a′**) with (butadiene)zirconocene cleanly gave the mixed-metal complex **7d**, and treatment of **4a′** with (butadiene)hafnocene furnished the bis(μ-η^1:η^2-propynyl)bis(hafnocene) complex **7e**. The latter reaction required more drastical reaction conditions (2 d at 60°C) to liberate Cp$_2$Hf in situ.

Thermally induced ligand exchange was used to prepare the (propynyl)metallocene chlorides **8**.[8] Subsequent treatment with the (butadiene)metallocenes then gave the (μ-η^1:η^2-propynyl)(μ-chloro)bis(metallocenes) **10a–c** (see Scheme 2). Treatment of **3b** with propynyllithium (to give **9**), followed by treatment with (butadiene)ZrCp$_2$, gave the (μ-η^1:η^2-propynyl)(μ-methyl)bis(metallocenes) **11a**, **b**.

In the synthesis of the μ-methyl bridged systems, only (butadiene)zirconocene was employed as the source for the in situ metallocene generation. Attempts to use the corresponding hafnocene reagent required higher temperatures that led to massive σ-ligand scrambling of the starting materials and precluded a clean product formation.

We then treated the dinuclear (μ-alkynyl)bis(metallocene) complexes **7**, **10**, and **11** with a suitable proton source. As reagents for the proton transfer reaction we choose the *N,N*-dimethylanilinium salts [HNMe$_2$Ph$^+$][B(C$_6$F$_5$)$_4^-$] (**12a**) or [HNMe$_2$Ph$^+$][BPh$_4^-$] (**12b**), respectively. Both reagents had previously been used for the synthesis of donor-ligand stabilized zirconocene derived cations, such as e.g. [Cp$_2$ZrCH$_3^+$] (from Cp$_2$Zr(CH$_3$)$_2$).[11] Thus, the here selected anions had shown to be of a sufficiently low nucleophilicity to not interfere with the formation of very electrophilic group 4 metallocene-based cation systems.

The protonation reactions in all cases led to the formation of the same cationic systems irrespective whether [BPh$_4^-$] or [B(C$_6$F$_5$)$_4^-$] was used as the counteranion. Thus, the bis(μ-η^1:η^2-propynyl)bis(zirconocene) complex **7a** was treated with one molar equivalent of the ammonium salt **12b** at −50°C in dichloromethane. After workup at room temperature a single cationic product was isolated in close to 60% yield that was identified as **13a** spectroscopically and by an X-ray crystal structure analysis (see below). The product exhibits a pair of ^{1}H/^{13}C-NMR Cp signals at δ = 6.03, 5.71 / 109.7, 108.4 (in [D$_2$]dichloromethane) and methyl group resonances at δ = 2.83, 2.44 / 25.1, 10.2. Noteworthy is the [Zr]-σ-alkenyl C^2 ^{13}C-NMR resonance at δ = 217.6 and the ^{1}H/^{13}C-NMR resonances of the planar-tetracoordinate carbon C^1-H group at δ = −0.11 (broad singlet) / 161.0 ($^1J_{CH}$ = 103 Hz). Thus, the planar-tetracoordinate carbon atom exhibits a chemical shift in the olefinic region, as it is expected for sp^2-hybridized carbon, but its $^1J_{CH}$ coupling constant is quite unusual at a very low value of close to 100 Hz. As we shall see, this is a very typical feature of the planar-tetracoordinate carbon compounds that bear a hydrogen substituent at C^1. It is probably the close vicinity of the C^1-H hydrogen to its adjacent zirconium center Zr^2 that results in such a marked decrease of the $^1J_{CH}$ value of this (sp^2)C-H moiety. According to the X-ray crystal structure analysis of **13a** (see below) an α-agostic interaction[12] between C^1-H and Zr^2 must be assumed.

Scheme 3

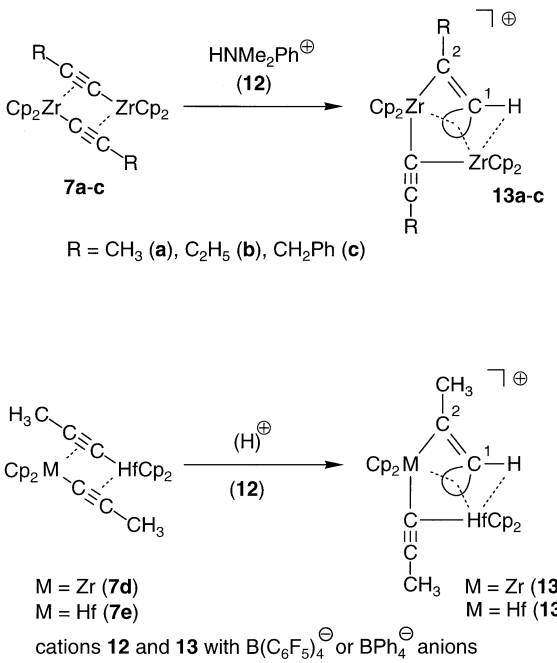

The protonation reactions of the related complexes **7b** and **7c** proceed analogously to yield the corresponding planar-tetracoordinate carbon complexes **13b** and **13c**, respectively. Some of their typical spectroscopic parameters are listed in Table 1. Protonation of the bis(μ-η^1:η^2-propynyl)bis(hafnocene) complex **7e** also proceeds cleanly to yield **13i**. Noteworthy is here that the C^1-*H* ^{1}H-NMR resonance is shifted markedly to a larger δ-value (+0.42) as compared to the zirconium-containing examples **10a**−**c** (see Table 1), whereas the $^1J_{C^1\text{-}H}$ coupling constant is still very low at 99 Hz. It thus may be that the ^{1}H-NMR C^1-*H* chemical shift is sensitive to the very nature of its closely adjacent metal center. This specific feature turned out to be of some diagnostic value in the protonation reactions of the heterodimetallic precursors.

Protonation of the bis(μ-η^1:η^2-propynyl)($HfCp_2$)($ZrCp_2$) complex **7d** could in principle lead to the formation of two regioisomeric products arising from H^+-addition to either the $CH_3-C\equiv C-HfCp_2$ or the $CH_3-C=C-ZrCp_2$ unit. The reaction of the heterodimetallic complex **7d** with **12b** resulted in the formation of a single organometallic product (**13h**) that was isolated in ca. 50% yield. The product exhibits ^{1}H/^{13}C-NMR pairs of Cp resonances at δ 5.94, 5.72 / 108.6, 108.1, and ^{13}C/^{1}H-NMR signals of the C^1-H unit at δ 162.5 ($^1J_{CH}$ = 100 Hz) and +0.38. The latter value is in the typical range expected of an α-agostic C^1-H moiety at $HfCp_2$. We therefore propose that protonation has occured regioselectively at the $CH_3-C\equiv C-HfCp_2$ part of the starting material **4e**, leading to the heterodinuclear planar-tetracoordinate carbon compound **13h**.

A very similar situation was found when the μ-chloro- and μ-methyl-bridged metallocene complexes were protonated. Treatment of (μ-η^1:η^2-propynyl)(μ-Cl)($ZrCp_2$)$_2$ **10a**

Scheme 4

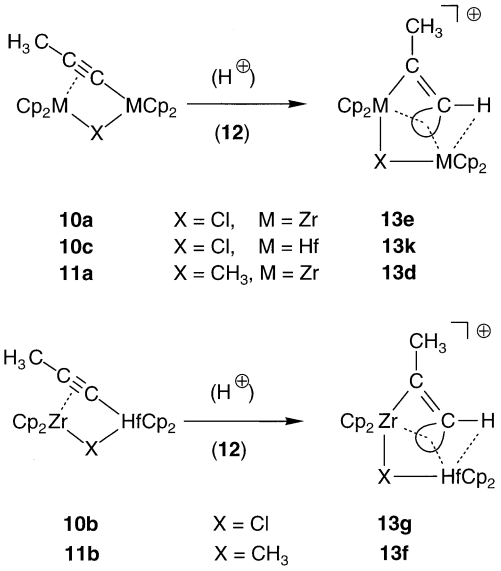

Table 1. Selected NMR data of the planar-tetracoordinate carbon complexes **13** and related reference compounds

Compd.	prepd. from	R	X	anion	M	δ C^2	δ C^1-H[d]		$^1J_{C^1\text{-}H}$ [Hz]
13a	**7a**	CH_3	[a]	[b]	Zr,Zr	217.6	161.0	−0.11	103
13b	**7b**	C_2H_5	[a]	[b][c]	Zr,Zr	227.6	160.4	−0.16	103
13c	**7c**	CH_2Ph	[a]	[b]	Zr,Zr	225.2	165.3	−0.47	[m]
13d	**11a**	CH_3	CH_3	[b][c]	Zr,Zr	229.8	159.3	0.83	108
13e	**10a**	CH_3	Cl	[b]	Zr,Zr	273.7	157.7	0.51	103
13f	**11b**	CH_3	CH_3	[c]	Zr,Hf	233.7	160.1	1.47	106
13g	**10b**	CH_3	Cl	[b]	Zr,Hf	227.1	156.4	1.12	99
13h	**7d**	CH_3	[a]	[b]	Zr,Hf	[e]	162.5	0.38	100
13i	**7e**	CH_3	[a]	[b]	Hf,Hf	225.1	167.4	0.42	99
13k	**10c**	CH_3	Cl	[b]	Hf,Hf	228.6	160.8	1.05	97
2a	–	CH_3	[a]	[c]	Zr,Zr	210.4	127.7[f]	[g][h]	–
2b	–	CH_3	[a]	[c]	Zr,Hf	217.1	129.5[f]	[g][h]	–
2c	–	*n*-C_3H_7	Cl	[c]	Zr,Zr	224.9	125.3	[g][h]	–
1a	–	CH_3	CCPh	–	Zr,Al	208.6	144.2[f]	[i][k]	–
1b	–	CH_3	CC−C_6H_{11}	–	Zr,Al	197.7	152.0[f]	[k][l]	–

[a] C≡C−R. – [b] $B(C_6F_5)_4^-$. – [c] BPh_4^-. – [d] NMR spectra in CD_2Cl_2. – [e] Not located. – [f] Tentative assignment. – [g] C^1-CH_3. – [h] From ref.[3][5][6]. – [i] C^1-Ph. – [k] From ref.[3][4]. – [l] C^1-cyclohexyl. – [m] Not determined.

with $[HNMe_2Ph^+][B(C_6F_5)_4^-]$ (**12b**) gave rise to the formation of the planar-tetracoordinate carbon compound **13e** ($^1H/^{13}C$ NMR of the C^1-H unit: δ = 0.51/157.7 ($^1J_{CH}$ = 103 Hz). Protonation of the corresponding mixed metal compound **10b** selectively led to a single product (**13g**) whose C^1-*H* ^{1}H-NMR resonance is found shifted to δ 1.12. A similar value was found in the planar-tetracoordinate carbon complex **13k** containing the $(\mu\text{-Cl})(Cp_2Hf)_2$ framework (see Table 1), and a similar trend was observed upon protonation of **11a** and **11b** giving rise to the selective formation of the planar-tetracoordinate carbon compounds **13d** and **13f**, respectively. In all these cases the $HfCp_2$ unit ended up in the "south-east position" of the planar-tetracoordinate carbon containing dimetallic framework, similarly as it was observed for a related series of mixed metal derivatives of the complex type **2** (see above).

X-ray Crystal Structure Analysis of 13a

Single crystals suited for the X-ray crystal structure analysis were obtained by allowing a solution of **13a** [· $B(C_6F_5)_4^-$] in dichloromethane to equilibrate with toluene by gas-phase diffusion in a closed system. The dimetallic cation **13a** and the $B(C_6F_5)_4^-$ anion are independent in the crystal. In the cation the two zirconocene units are well separated from each other (Zr1···Zr2 separation 3.477 Å). The zirconium centers are connected by means of two hydrocarbyl ligands, namely the $H_3C^3C^2C^1H$ unit and the $C^4C^5C^6H_3$ moiety. The special structural features of the former make complex **13a** so noteworthy. It contains the carbon atom C^1 that is planar-tetracoordinate. Carbon atom C^1 is bonded to C^2 [d C^1-C^2 1.255(9) Å], the metal atoms Zr^1 [d Zr^1-C^1 2.377(6) Å] and Zr^2 [d Zr^2-C^1 2.274(7) Å] and a hydrogen atom (crystallographically located, d C^1-H 0.91 Å). The atoms C^1, C^2, H^1, Zr^1, and Zr^2 are oriented coplanar (their neighboring atoms C^3, C^4, C^5, C^6 are located in the same plane, which is the typical σ-ligand plane of the two group 4 bent metallocene subunits).[13] The bonding angles around the planar-tetracoordinate carbon atom C^1 are 96.7(2)° ($Zr^1-C^1-Zr^2$), 74.1(5)° ($Zr^1-C^1-C^2$), 119° ($C^2-C^1-H^1$), and 70° ($Zr^2-C^1-H^1$) (sum of bonding angles at C^1: 359.8°).

Figure 1. A view of the molecular geometry of **13a**[a]

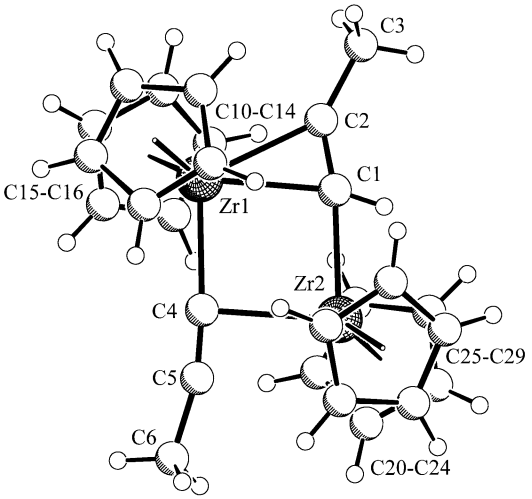

[a] Selected bond lengths [Å] and angles [°]: Zr1−C1 2.377(6), Zr1−C2 2.365(8), Zr1−C4 2.313(6), Zr2−C1 2.274(7), Zr2−C4 2.406(6), Zr2−C5 2.693(8), Zr2−H1 2.14(7), C1−C2 1.255(9), C1−H1 0.91(7), C2−C3 1.492(10), C4−C5 1.199(9), C5−C6 1.468(10), Zr1−C1−Zr2 96.7(2), Zr1−C4−Zr2 94.9(2), Zr1−C1−C2 74.1(5), Zr1−C1−H1 166(4), Zr1−C2−C1 75.2(5), Zr1−C2−C3 144.0(6), Zr2−C1−C2 170.1(6), Zr2−C1−H1 70(4), C1−C2−C3 140.8(8), Zr1−C4−C5 174.4(6), Zr2−C4−C5 90.3(5), C4−C5−C6 166.6(8).

In a comparison with typical planar-tetracoordinate carbon compounds and related complexes of this general structural type (see Table 2) it becomes apparent that the complexes **13** exhibit a few very special bonding parameters. The Zr^1-C^1 bond, the "extra bond" between the acceptor-metallocene Cp_2Zr^1 and the planar-tetracoordinate carbon center, is the shortest found in the overall series of complexes so far. This bond is by ca. 0.12 Å shorter than its equivalent in the related bis(zirconocene) complex **2a** ($M^1 = M^2 = Zr$, $R^1 = R^2 = CH_3$) (see Scheme 5 and Table 2). Only in the μ-N≡C−Ph complex **14** is this metal-to-bridgehead atom bond shorter. We also note that the C^1-C^2 bond in **13a** is rather short. Also the Zr^1-C^2 separation in **13a** [2.365(8) Å] is much larger than this was found in **2a** [2.182(5) Å]. We conclude that the $Cp_2Zr^1(\mu\text{-}\eta^1\text{:}\eta^2\text{-}H_3C^3-C^2C^1H)(Zr^2Cp_2)$ subunit in **13a** is in its structural details somewhat different from the bonding parameters of the related typical Zr/Zr^+ or Zr/Al containing planar-tetracoordinate carbon complexes (**2**, **1**). In some of its structural characteristics this unit in **13a** still resembles its Zr(μ-acetylide)Zr precursor unit. In some respect this unit behaves more as a "protonated alkynyl complex" than a (μ-alkyne)bis(zirconocene) cation [the $C^1\equiv C^2$ bond length in the $Cp_2Zr-C\equiv C-Ph$ dimer (**7f**) is 1.261(2) Å, the corresponding Zr^1-C^1 and Zr^1-C^2 distances are 2.431(2) and 2.407(2) Å, the Zr^2-C^1 bond length is 2.188(2) Å,[8] see Scheme 5].

The structural similarity between the cationic complex **13a** and its precursor, a neutral (acetylide)metallocene di-

Table 2. A comparison of selected structural parameters of dimetallic planar-tetracoordinate carbon complexes and related systems[a]

Compd.	M^1	M^2	C^1-R	Zr^1-C^1	Zr^1-C^2	C^1-C^2	M^2-C^1	ref.
13a	Cp_2Zr	Cp_2Zr^+	C−H	2.377(6)	2.365(8)	1.255(9)	2.274(7)	[b]
14	Cp_2Zr	Cp_2Zr^+	N	2.338(10)	2.266(14)	1.230(14)[c]	2.075(11)	[14]
1a	Cp_2Zr	$AlMe_2$	C−Ph	2.465(2)	2.163(3)	1.324(4)	2.103(3)	[4]
2a	Cp_2Zr	Cp_2Zr^+	$C-CH_3$	2.509(4)	2.182(5)	1.305(6)	2.324(5)	[5][6]

[a] For a schematic representation of the structures of these complexes see Scheme 5 and Figure 1. − [b] This work. − [c] C−N.

mer (**7**),[8][10] even is extending to the second bridging hydrocarbyl moiety, the μ-propynyl group.[15] In both planar-tetracoordinate carbon complexes **13** and **2** this bridge is rather unsymmetrically located between the two group 4 metallocene moieties. In **2a** it seems to be strongly σ-bonded to the metal atom Zr^2 [d Zr^2-C^4 2.263(4) Å] and leans over to Zr^1 [d Zr^1-C^4 2.472(4) Å, d Zr^1-C^5 2.814(5) Å][5][6] whereas in the complex **13a** we are encountered with the opposite geometric situation: Zr^1 is linked to C^4 by means of a strong σ-type interaction [d Zr^1-C^4 2.313(6) Å] and the C^4-C^5 triple bond [1.199(9) Å] is η^2-coordinated to Zr^2 [d Zr^2-C^4 2.406(6) Å, d Zr^2-C^5 2.693(7) Å]. The latter structural situation is similar as it is typically found in the related complexes **1** and **14** (see Scheme 5).

Scheme 5

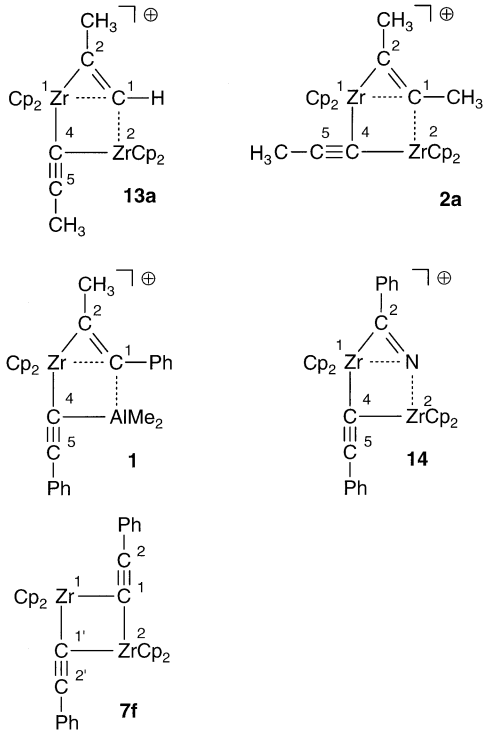

Conclusions

Protonation of dimetallic (μ-η^1:η^2-alkynyl)bis(group 4 metallocene) complexes apparently provides a simple and efficient route to stable and easily isolable cationic planar-tetracoordinate carbon compounds. The X-ray crystal structure analysis of a representative example (**13a**) has shown that four substituents (a carbon atom, two metal centers, and a hydrogen) are oriented coplanar with carbon atom C^1 and are all strongly bonded to it. In addition, there is evidence from the NMR spectra and the X-ray structural analysis that there is some electronic interaction of this hydrogen (C^1)-*H* with the adjacent metal center Zr^2. The $^1J_{C^1\text{-}H}$ coupling constant is rather small, and the C^1-H vector seems to be "leaning over" towards Zr^2 ($Zr^2\cdots H$ separation 2.136 Å). These features may indicate the presence of some α-agostic interaction between Zr^2 and the C^1-H bond, but we must also notice that the Zr^1-C^1 and Zr^1-C^2 separations are almost equal in lengths, and that the C^2-C^1 multiple bond is rather short as is the Zr^1-C^4 linkage. All these features seem to indicate some residual structural resemblance of **13a** with its (acetylide)metallocene dimer precursor. The participation of a hyperconjugative formula (**13′**) could possibly be used to illustrate this specific structural situation.

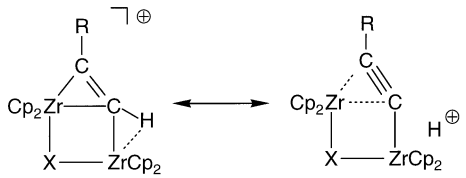

Despite these specific structural details the complexes **13** seem to represent additional examples of a large general class of stable easily prepared planar-tetracoordinate carbon compounds. It appears that the thermochemical stabilization of the planar-tetracoordinate carbon center in these dinuclear complexes is so pronounced that protonation routes typically found in other organometallic systems, such as e.g. protolytic cleavage of metal−carbon σ-bonds, become quite disfavored here. The presence of a (probably rather acidic) hydrogen atom at the "square planar" carbon may open up ways of detecting chemical reactions which are typical for this specific bonding situation of the element carbon and for synthesizing novel, potentially functionalized derivatives. We have begun to carry out such investigations in our laboratory.

Financial support from the *Fonds der Chemischen Industrie*, the *Ministerium für Wissenschaft und Forschung des Landes Nordrhein-Westfalen*, and the *Volkswagen-Stiftung* is gratefully acknowledged.

Experimental Section

Reactions with organometallic compounds were carried out in an inert atmosphere (argon) using Schlenk type glassware or in a glovebox. Solvents, including deuterated solvents used for NMR spectroscopy, were dried and distilled under argon prior to use. − The following instruments were used for physical characterization of the compounds: Bruker AC 200 P and Varian Unity plus (^{1}H: 600 MHz, ^{13}C: 150 MHz) NMR spectrometers; Nicolet 5 DXC FT-IR spectrometer; elemental analyses were carried out with a Foss-Heraeus CHN-Rapid elemental analyzer, melting points were determined by differential scanning calorimetry (2910 DSC, DuPont/STA Instruments). The spectral assignments were in most cases secured by 2D NMR methods (GHMBC, GHSQC, and GCOSY[16]). The $^1J_{C^1\text{-}H}$ coupling constants were usually determined by means of a selective 1D-GHMBC method. The (alkynyl)metallocene complexes **4** and **7**−**10**, and the (butadiene)metallocenes were prepared according to literature procedures.[8][9]

Preparation of [(μ-Methyl)(μ-propynyl)($ZrCp_2$)$_2$] **11a**: A solution containing 1.0 g (3.6 mmol) of methyl(propynyl)zirconocene and 1.0 g (3.6 mmol) of (butadiene)zirconocene in 25 ml of benzene was stirred for 24 h at room temperature. Pentane (10 ml) was added to precipitate the product, which was collected by filtration, washed three times with pentane and dried in vacuo to yield 790 mg (44%) of **11a**, m.p. 147°C (decomp.). − ^{1}H NMR (200.1 MHz,

300 K, [D$_6$]benzene): δ = 5.24, 5.17 (each s, each 10 H, Cp-H), 2.64 (s, 3 H, 3-H), −2.77 (s, 3 H, CH_3). − ^{13}C NMR (90.6 MHz, 300 K, [D$_6$]benzene): δ = 229.4 (C1), 179.7 (C2), 104.4, 102.5 (Cp), 21.5 (C≡C-CH_3), 6.08 (μ-CH_3). − $C_{24}H_{26}Zr_2$ (496.91): C 58.01, H 5.27; found C 58.13, H 5.72.

Preparation of [(μ-Methyl)(μ-propynyl)(ZrCp$_2$)(HfCp$_2$)] **11b**: Complex **11b** was prepared analogously as described above from 600 mg (1.66 mmol) of methyl(propynyl)hafnocene and 456 mg (1.66 mmol) of (butadiene)zirconocene in 25 ml of benzene (18 h, ambient temperature). Yield of **11b**: 630 mg (65%), m. p. 159°C (decomp.). ^{1}H NMR (200.1 MHz, 300 K, [D$_6$]benzene): δ = 5.22, 5.16 (each s, each 10 H, Cp-H), 2.65 (s, 3 H, 3-H), −3.09 (s, 3 H, CH_3). − ^{13}C NMR (90.6 MHz, 300 K, [D$_6$]benzene): δ = 224.6 (C1), 180.3 (C2), 104.3, 102.4 (Cp), 22.8 (C3), 5.87 (C4). − $C_{24}H_{26}HfZr$ (584.18): C 49.34, H 4.49; found C 47.72, H 4.46.

Protonation of the (μ-Propynyl)zirconocene Dimer **7a**: *Synthesis of* **13a**: A sample of complex **7a** (150 mg, 0.29 mmol) was mixed with solid *N,N*-dimethylanilinium tetrakis(pentafluorophenyl)borate **12a**. Dichloromethane (20 ml) was added at −20°C. The mixture was stirred for 1 h at this temperature and then allowed to warm to ambient temperature. Pentane (5 ml) was added. The precipitated product was collected by filtration, washed with pentane, and dried in vacuo to give 190 mg (59%) of **13a** [with $B(C_6F_5)_4^-$ anion], m.p. 229°C (decomp.). − ^{1}H NMR (599.9 MHz, 300 K, [D$_2$]dichloromethane): δ = 6.02, 5.73 (each s, each 10 H, Cp), 2.83 (d, 3 H, 3-H, $^4J_{HH}$ = 1.8 Hz), 2.44 (s, 3 H, 6-H), −0.11 (br, 1 H, 1-H). − ^{13}C NMR (150.9 MHz, 300 K, [D$_2$]dichloromethane): δ = 217.6 (C2), 161.0 (C1, $^1J_{CH}$ = 103 Hz), 109.7, 108.4 (Cp), 25.1 (C3, $^1J_{CH}$ = 129 Hz), 10.2 (C6, $^1J_{CH}$ = 133 Hz); $B(C_6F_5)_4^-$: 148.5 (*o*-C-F, $^1J_{CF}$ = 242 Hz), 138.5 (*p*-C-F, $^1J_{CF}$ = 245 Hz), 136.7 (*m*-C-F, $^1J_{CF}$ = 244 Hz), 124.2 (br, *i*-C). C4 and C5 not observed. − IR (KBr): ṽ = 3118, 2969, 2919, 2854, 2056 (C≡C), 1645, 1513, 1463, 1262, 1085, 1015, 979, 812 cm^{-1}. − $C_{50}H_{27}BF_{20}Zr_2$ (1200.97): C 50.00, H 2.27; found C 49.26, H 2.58.

X-ray Crystal Structure Analysis of **13a** [· $B(C_6F_5)_4^-$]: Single crystals were obtained by allowing a solution of **13a** in dichloromethane to equilibrate with toluene by diffusion through the gas phase over a period of several days. Formula $C_{50}H_{27}BF_{20}Zr_2$, M = 1200.97, 0.25 × 0.25 × 0.15 mm, a = 15.057(2), b = 16.618(4), c = 18.530(4) Å, β = 99.56(1), V = 4572(2) Å^3, ρ_{calc} = 1.745 g cm^{-3}, μ = 5.75 cm^{-1}, empirical absorption correction via ψ scan data (0.965 ≤ C ≤ 0.999), Z = 4, monoclinic, space group $P2_1/c$ (no. 14), λ = 0.71073 Å, T = 223 K, ω/2θ scans, 9449 reflections collected (±h, +k, −l), [(sinθ)/λ] = 0.62 Å^{-1}, 9156 independent and 5535 observed reflections [$I \geq 2\,\sigma(I)$], 663 refined parameters, R = 0.063, wR^2 = 0.137, max. residual electron density 0.71 (−0.75) e Å^{-3}, hydrogens calculated and riding, hydrogen at C1 found in Difference-Fourier map. Data set was collected with an Enraf Nonius CAD4 diffractometer equipped with a rotating anode FR 591. Programs used: data reduction MolEN, structure solution SHELXS-86, structure refinement SHELXL-93, graphics SCHAKAL-92. Crystallographic data (excluding structure factors) for the structure reported in this paper have been deposited with the Cambridge Crystallographic Data Centre as supplementary publication CCDC-100817. Copies of the data can be obtained free of charge on application to The Director, CCDC, 12 Union Road, Cambridge CB2 1EZ, UK [fax: int. code +44(1223)336-033, e-mail: deposit@ccdc.cam.ac.uk].

Preparation of **13b**. − a) *With $B(C_6F_5)_4^-$ Anion:* 150 mg (0.27 mmol) of bis(1-butynyl)zirconocene **7b** was treated with 220 mg (0.27 mmol) of the anilinium salt **12a** analogously as described above to give 220 mg (66%) of **13b**(· $B(C_6F_5)_4^-$), m.p. 216°C (decomp.). − ^{1}H NMR (200.1 MHz, 300 K, [D$_2$]dichloromethane): δ = 6.03, 5.71 (each s, each 10 H, Cp), 3.04 (dq, 2 H, 3-H, $^4J_{HH}$ = 1.7 Hz, $^3J_{HH}$ = 7.5 Hz), 2.69 (q, 2 H, 7-H, $^3J_{HH}$ = 7.5 Hz), 1.48 (t, 3 H, 8-H, $^3J_{HH}$ = 7.5 Hz), 1.37 (t, 3 H, 4-H, $^3J_{HH}$ = 7.5 Hz), −0.16 (br, 1 H, 1-H). − ^{13}C NMR (150.9 MHz, 300 K, [D$_2$]dichloromethane), cation only: δ = 227.6 (C2), 160.4 (C1, $^1J_{CH}$ = 103 Hz), 129.5 (C6), 108.5, 107.3 (Cp), 36.1 (C4, $^1J_{CH}$ = 129 Hz), 18.4 (C8, $^1J_{CH}$ = 133 Hz), 15.9 (C5, $^1J_{CH}$ = 125 Hz), 14.6 (C3, $^1J_{CH}$ = 124 Hz); C5 not observed. − IR (KBr): ṽ = 3119, 2962, 2918, 2851, 2054 (C≡C), 1642, 1513, 1463, 1262, 1089, 1020, 980, 812 cm^{-1}. − $C_{52}H_{31}BF_{20}Zr_2$ (1229.03): C 50.82, H 2.54; found C 50.09, H 2.68.

b) *With BPh_4^- Anion:* The preparation was carried out analogously as above. Treatment of 200 mg (0.36 mmol) of **7b** with [$HNMe_2Ph^+$][BPh_4^-] (**12b**) (150 mg, 0.37 mmol) gave 185 mg (59%) of **13b**(· BPh_4^-), m.p. 193°C (decomp.).

Preparation of **13c**: Treatment of 150 mg (0.22 mmol) of **7c** with 182 mg (0.22 mmol) of **12b** was carried out analogously as described above to yield 260 mg (87%) of **13c** (m. p. 165°C, decomp.), that was characterized spectroscopically. − ^{1}H NMR (599.9 MHz, 300 K, [D$_2$]dichloromethane): δ = 7.65−7.64 (m, 4 H, Ph-H), 7.38−7.37 (m, 4 H, Ph-H), 7.20−7.18 (m, 2 H, Ph-H), 5.86, 5.74 (s, each 10 H, Cp), 4.23 (d, 2 H, 3-H, $^4J_{HH}$ = 1.4 Hz), 4.04 (s, 2 H, 6-H), −0.47 (br, 1 H, 1-H). − ^{13}C NMR (150.9 MHz, 300 K, [D$_2$]dichloromethane), cation only: δ = 225.2 (C2), 165.3 (C1), 140.8, 126.4 (C4, C5), 132.0, 129.5, 126.6, 119.4 (Ph), 110.2, 107.8 (Cp), 46.6 (C3), 30.9 (C6). − IR (KBr): ṽ = 3123, 2960, 2924, 2853, 2050 (C≡C), 1643, 1514, 1462, 1274, 1085, 978, 813 cm^{-1}.

Preparation of **13d**. − a) *With $B(C_6F_5)_4^-$ Anion:* Analogously as described above, treatment of 150 mg (0.30 mmol) of **11a** with 240 mg (0.30 mmol) of **12a** at −50°C in 20 ml of dichloromethane followed by precipitation at room temperature (5 ml of pentane was added) gave **13d** as a yellow oil. Extensive stirring and washing with pentane eventually yielded **13d** as a sticky solid material, 120 mg (34%), m.p. 162°C (decomp.). − ^{1}H NMR (599.9 MHz, 300 K, [D$_2$]dichloromethane): δ = 6.11, 5.83 (s, each 10 H, Cp), 2.69 (d, 3 H, 3-H, $^4J_{HH}$ = 1.9 Hz), 0.84 (br, 1 H, 1-H), −0.79 (s, 3 H, 4-H). − ^{13}C NMR (150.9 MHz, 300 K, [D$_2$]dichloromethane), cation only: δ = 229.8 (C2), 159.3 (C1, $^1J_{CH}$ = 108 Hz), 110.8, 108.6 (Cp), 28.5 (C3), 13.5 (C4, $^1J_{CH}$ = 111 Hz). − IR (KBr): ṽ = 3123, 2961, 2918, 2850, 1644, 1511, 1470, 1275, 1263, 1095, 1018, 973, 810 cm^{-1}.

b) *With BPh_4^- Anion:* A sample of 150 mg (0.30 mmol) of **11a** was treated with 120 mg (0.30 mmol) of **12b** in 20 ml of dichloromethane at −50°C. The mixture was stirred for 30 min at −50°C, then for 1 h at room temperature. 10 ml of toluene was added dropwise with stirring to precipitate the product that was collected by filtration, washed several times with pentane and dried in vacuo to yield 154 mg (63%) of **13d**(· BPh_4^-), m.p. 210°C (decomp.). − $C_{48}H_{47}Zr_2$ (817.15): C 70.55, H 5.80; found C 69.14, H 5.85.

Preparation of **13e**: Treatment of 150 mg (0.30 mmol) of **10a** with 230 mg (0.30 mmol) of **12a** in 20 ml of dichloromethane analogously as described above gave, after precipitation with 5 ml of pentane, 173 mg (48%) of **13e**, m. p. 193°C (decomp.). − ^{1}H NMR (599.9 MHz, 300 K, [D$_2$]dichloromethane): δ = 6.15, 5.79 (s, each 10 H, Cp), 2.79 (d, 3 H, 3-H, $^4J_{HH}$ = 1.8 Hz), 0.50 (br, 1 H, 1-H). − ^{13}C NMR (150.9 MHz, 300 K, [D$_2$]dichloromethane), cation only: δ = 273.7 (C2), 157.7 (C1, $^1J_{CH}$ = 103 Hz), 112.5, 109.4 (Cp), 25.3 (C3, $^1J_{CH}$ = 129 Hz). − IR (KBr): ṽ = 3126, 2966, 2924, 2853, 1644, 1515, 1463, 1276, 1262, 1086, 979, 816 cm^{-1}. − $C_{47}H_{24}BClF_{20}Zr_2$ (1197.37): C 47.15, H 2.02; found C 47.18, H 2.18.

Preparation of **13f**: 150 mg (0.26 mmol) of **11b** was treated with 114 mg (0.28 mmol) of **12b** in 20 ml of dichloromethane at room temperature (45 min). Precipitation with 10 ml of toluene gave a solid that was washed with pentane and dried in vacuo. Yield of **13f**(· BPh_4^-) 180 mg (77%), m.p. 219°C (decomp.). − ^{1}H NMR (599.9 MHz, 300 K, [D$_2$]dichloromethane): δ = 5.92, 5.83 (s, each 10 H, Cp), 2.75 (d, 3 H, 3-H, $^4J_{HH}$ = 1.8 Hz), 1.48 (br, 1 H, 1-H), −0.72 (s, 3 H, 4-H); BPh_4: 7.41−7.33 (m, 8 H, Ph-H), 7.10−7.07 (m, 8 H, Ph-H), 6.96−6.89 (m, 4 H, Ph-H). − ^{13}C NMR (150.9 MHz, 300 K, [D$_2$]dichloromethane), cation only: δ = 233.7 (C2), 160.1 (C1, $^1J_{CH}$ = 106 Hz), 110.1, 109.2 (Cp), 27.0 (C3), 13.3 (C4, $^1J_{CH}$ = 111 Hz). − IR (KBr): $\tilde{\nu}$ = 3109, 3053, 3029, 2981, 2919, 2893, 1579, 1478, 1426, 1366, 1264, 1015, 816, 741, 705, 607 cm^{-1}. − $C_{48}H_{47}BHfZr$ (904.42): C 63.75, H 5.24; found C 61.28, H 5.20.

Preparation of **13g**: A sample of 150 mg (0.25 mmol) of **10b** was treated with 200 mg (0.25 mmol) of **12a** at −30°C in dichloromethane. After stirring for 30 min at −30°C and 30 min at room temperature the product was precipitated by slowly adding pentane (10 ml) at 0°C. The product was collected by filtration, washed with pentane and dried in vacuo to yield 210 mg (65%) of **13g** [· $B(C_6F_5)_4^-$], m.p. 147°C (decomp.). − ^{1}H NMR (599.9 MHz, 300 K, [D$_2$]dichloromethane): δ = 6.13, 5.85 (s, each 10 H, Cp-H), 2.83 (d, 3 H, 3-H, $^4J_{HH}$ = 1.8 Hz), 1.12 (q, 1 H, 1-H, $^4J_{HH}$ = 1.8 Hz). − ^{13}C NMR (150.9 MHz, 300 K, [D$_2$]dichloromethane), cation only: δ = 227.1 (C2), 156.4 (C1, $^1J_{CH}$ = 99 Hz), 111.3, 109.5 (Cp), 26.2 (C3, $^1J_{CH}$ = 129 Hz). − IR (KBr): $\tilde{\nu}$ = 3251, 3121, 2960, 2921, 2871, 1644, 1514, 1463, 1273, 1087, 979, 819, 661 cm^{-1}. − $C_{47}H_{24}BClF_{20}HfZr$ (1284.64): C 43.94, H 1.88; found C 43.14, H 2.38.

Preparation of **13h**: A sample of 160 mg (0.26 mmol) of **7d** was treated with 190 mg (0.26 mmol) of **12a** at −50°C in 30 ml of dichloromethane. The mixture was stirred at −50°C for 1 h and then warmed up to room temperature. Addition of 5 ml of pentane gave a red oil, that was solidified by means of a prolonged treatment with 20 ml of pentane to give 170 mg (51%) of **13h** [· $B(C_6F_5)_4^-$], m.p. 206°C (decomp.). − ^{1}H NMR (599.9 MHz, 300 K, [D$_2$]dichloromethane): δ = 5.94, 5.72 (s, each 10 H, Cp), 2.84 (d, 3 H, 3-H, $^4J_{HH}$ = 1.8 Hz), 2.53 (s, 3 H, 6-H), 0.37 (br, 1 H, 1-H). − ^{13}C NMR (150.9 MHz, 300 K, [D$_2$]dichloromethane), cation only: δ = 162.5 (C1, $^1J_{CH}$ = 100 Hz), 108.6, 108.1 (Cp), 25.6 (C3), 10.5 (C6). C2, C4, C5 not found. − IR (KBr): $\tilde{\nu}$ = 3126, 2961, 2923, 2853, 1644, 1514, 1467, 1272, 1087, 980, 813 cm^{-1}. − $C_{50}H_{27}BF_{20}HfZr$ (1288.25): C 46.62, H 2.11; found C 47.13, H 2.60.

Preparation of **13i**: Treatment of 150 mg (0.22 mmol) of **7e** with 173 mg (0.22 mmol) of **12a** at −50°C in 20 ml of dichloromethane analogously as described above, followed by addition of 10 ml of toluene gave a brown oil that was solidified by treatment with pentane. Yield of **13i** [· $B(C_6F_5)_4^-$]: 190 mg (63%), m.p. 224°C (decomp.). − ^{1}H NMR (599.9 MHz, 300 K, [D$_2$]dichloromethane): δ = 5.97, 5.65 (s, each 10 H, Cp), 2.90 (d, 3 H, 3-H, $^4J_{HH}$ = 1.8 Hz), 2.46 (s, 3 H, 6-H), 0.41 (br, 1 H, 1-H). − ^{13}C NMR (150.9 MHz, 300 K, [D$_2$]dichloromethane), cation only: δ = 225.1 (C2), 167.4 (C1, $^1J_{CH}$ = 99 Hz), 109.0, 107.4 (Cp), 27.5 (C3, $^1J_{CH}$ = 128 Hz), 12.0 (C6). − IR (KBr): $\tilde{\nu}$ = 3117, 2961, 2920, 2855, 1643, 1514, 1463, 1374, 1263, 1086, 1016, 979, 817 cm^{-1}. − $C_{50}H_{27}BF_{20}Hf_2$ (1375.52): C 43.66, H 1.98; found C 42.99, H 2.44.

Preparation of **13k**: A sample of 150 mg (0.22 mmol) of **10c** was treated with 173 mg (0.22 mmol) of **12a** at −30°C in 20 ml of dichloromethane. After stirring for 1 h at −30°C and 1 h at room temperature the product was precipitated by addition of 5 ml of pentane. The resulting oil was washed with toluene and then solidified by prolonged treatment with 20 ml of pentane to yield 110 mg (37%) of **13k** [· $B(C_6F_5)_4^-$], m.p. 136°C (decomp.). − ^{1}H NMR (599.9 MHz, 300 K, [D$_2$]dichloromethane): δ = 6.12, 5.80 (s, each 10 H, Cp), 3.43 (d, 3 H, 3-H, $^4J_{HH}$ = 4.8 Hz), 1.04 (q, 1 H, 1-H, $^4J_{HH}$ = 4.8 Hz). − ^{13}C NMR (150.9 MHz, 300 K, [D$_2$]dichloromethane), cation only: δ = 228.6 (C2), 160.8 (C1, $^1J_{CH}$ = 97 Hz), 111.1, 108.4 (Cp), 26.3 (C3, $^1J_{CH}$ = 129 Hz). − IR (KBr): $\tilde{\nu}$ = 3129, 2959, 2925, 2854, 1643, 1514, 1463, 1273, 1088, 979, 822 cm^{-1}.

[1] R. Hoffmann, R. W. Alder, C. F. Wilcox, *J. Am. Chem. Soc.* **1970**, *92*, 4992; R. Hoffmann, *Pure Appl. Chem.* **1971**, *28*, 181.

[2] J. B. Collins, J. D. Dill, E. D. Jemmis, Y. Apeloig, P. v. R. Schleyer, R. Seeger, J. A. Pople, *J. Am. Chem. Soc.* **1976**, *98*, 5419.

[3] Reviews: G. Erker, *Comments Inorg. Chem*. **1992**, *13*, 111; G. Erker, *Nachr. Chem. Techn. Lab.* **1992**, *40*, 1099; M. Albrecht, G. Erker, C. Krüger, *Synlett* **1993**, 441; D. Röttger, G. Erker, *Angew. Chem*. **1997**, *109*, 840; *Angew. Chem. Int. Ed. Engl*. **1997**, *36*, 812.

[4] G. Erker, R. Zwettler, C. Krüger, R. Noe, S. Werner, *J. Am. Chem. Soc.* **1990**, *112,* 9620; M. Albrecht, G. Erker, M. Nolte, C. Krüger, *J. Organomet. Chem*. **1992**, *427*, C21; G. Erker, M. Albrecht, S. Werner, M. Nolte, C. Krüger, *Chem. Ber*. **1992**, *125*, 1953; G. Erker, M. Albrecht, C. Krüger, S. Werner, P. Binger, F. Langhauser, *Organometallics* **1992**, *11*, 3517; G. Erker, M. Albrecht, C. Krüger, S. Werner, *J. Am. Chem. Soc*. **1992**, *114*, 8531; P. Binger, F. Sandmeyer, C. Krüger, *Organometallics* **1995**, *14*, 2969; P. Binger, F. Sandmeyer, C. Krüger, J. Kuhnigk, R. Goddard, G. Erker, *Angew. Chem*. **1994**, *106,* 213; *Angew. Chem. Int. Ed. Engl.* **1994**, *33*, 197; P. Binger, F. Sandmeyer, C. Krüger, G. Erker, *Tetrahedron* **1995**, *51*, 4277.

[5] D. Röttger, J. Pflug, G. Erker, S. Kotila, R. Fröhlich, *Organometallics* **1996**, *15*, 1265; D. Röttger, G. Erker, R. Fröhlich, S. Kotila, *Chem. Ber*. **1996**, *129*, 1; D. Röttger, G. Erker, R. Fröhlich, *J. Organomet. Chem*. **1996**, *518*, 221; W. Ahlers, B. Temme, G. Erker, R. Fröhlich, F. Zippel, *Organometallics* **1997**, *16*, 1440; W. Ahlers, G. Erker, R. Fröhlich, U. Peuchert, *Chem. Ber.* **1997**, *130*, 1069.

[6] [6a] R. Gleiter, I. Hyla-Kryspin, S. Niu, G. Erker, *Angew. Chem.* **1993**, *105*, 753, *Angew. Chem. Int. Ed. Engl*. **1993**, *32*, 754. − [6b] G. Erker, D. Röttger, *Angew. Chem*. **1993**, *105*, 1691, *Angew. Chem. Int. Ed. Engl*. **1993**, *32*, 1623; D. Röttger, G. Erker, R. Fröhlich, M. Grehl, S. J. Silverio, I. Hyla-Kryspin, R. Gleiter, *J. Am. Chem. Soc.* **1995**, *117*, 10503.

[7] The hydrozirconation reaction of dialkylaluminum or gallium alkynyl complexes (R_2M^{III}−C≡C−R)$_2$ leads to the formation of mixed metal complexes [Cp_2Zr(μ-R−CC−H)(μ-Cl)$M^{III}R_2$] that may also contain a planar-tetracoordinate carbon atom bearing a H-substituent, but this interpretation must still await confirmation by an X-ray crystal structure analysis: M. Albrecht, doctoral dissertation, Univ. Münster, **1992**. For related hydrozirconation reactions of metallated alkynes see e.g. C. E. Tucker, P. Knochel, *J. Am. Chem. Soc.* **1991**, *113*, 9888.

[8] G. Erker, W. Frömberg, R. Mynott, B. Gabor, C. Krüger, *Angew. Chem.* **1986**, *98*, 456, *Angew. Chem. Int. Ed. Engl*. **1986**, *25*, 463; G. Erker, W. Frömberg, R. Benn, R. Mynott, K. Angermund, C. Krüger, *Organometallics* **1989**, *8*, 911; W. Frömberg, doctoral dissertation, Univ. Bochum, **1986**.

[9] G. Erker, C. Krüger, G. Müller, *Adv. Organomet. Chem*. **1985**, *24*, 1 and references cited therein.

[10] J. H. Teuben, H. J. de Liefde Meijer, *J. Organomet. Chem*. **1969**, *17*, 87; G. D. Stucky, D. G. Sekutowsky, *J. Am. Chem. Soc.* **1976**, *98*, 1376; H. Lang, W. Imhof, *Chem. Ber*. **1992**, *124*, 1307. H. Lang, M. Herres, L. Zsolnai, *Organometallics* **1993**, *12*, 5008; N. Metzler, H. Nöth, *J. Organomet. Chem*. **1993**, *454*, C5; J. R. Berenguer, L. R. Falvello, J. Forniés, E. Lalinde, M. Tomás, *Organometallics* **1993**, *12*, 6; U. Rosenthal, A. Ohff, W. Baumann, R. Kempe, A. Tillack, V. V. Burlakov, *Angew. Chem.* **1994**, *106*, 1678; *Angew. Chem., Int. Ed. Engl*. **1994**, *33*, 1605, and references cited therein; U. Rosenthal, A. Ohff, W. Baumann, R. Kempe, A. Tillack, V. V. Burlakov, *Organometallics* **1994**, *13*, 2903; U. Rosenthal, S. Pulst, P. Arndt, A. Ohff, A. Tillack, W. Baumann, R. Kempe, V. V. Burlakov, *Organometallics* **1995**, *14*, 2961; R. Lang, M. Weinmann, *Synlett* **1996**, 1; S.

Pulst, P. Arndt, B. Heller, W. Baumann, R. Kempe, U. Rosenthal, *Angew. Chem.* **1996**, *108*, 1175; *Angew. Chem., Int. Ed. Engl*. **1996**, *35*, 1112.
[11] M. Bochmann, A. J. Jaggar, J. C. Nicholls, *Angew. Chem.* **1990**, *102*, 830; *Angew. Chem., Int. Ed. Engl*. **1990**, *29*, 780; M. Bochmann, *J. Chem. Soc., Dalton Trans.* **1996**, 255 and references cited therein. See also: R. F. Jordan, *Adv. Organomet. Chem.* **1991**, *32*, 325.
[12] M. Brookhart, M. L. H. Green, *J. Organomet. Chem*. **1983**, *250*, 395; M. Brookhart, M. L. H. Green, L.-L. Wong, *Progr. Inorg. Chem*. **1988**, *36*, 1.
[13] H. H. Brintzinger, L. S. Bartell, *J. Am. Chem. Soc.* **1970**, *92*, 1105; W. Lauher, R. Hoffmann, *J. Am. Chem. Soc.* **1976**, *98*, 1729.
[14] D. Röttger, G. Erker, R, Fröhlich, *Chem. Ber*. **1995**, *128*, 1045.
[15] R. Nast, *Coord. Chem. Rev.* **1982**, *47*, 89; M. Cowie, S. J. Loeb, *Organometallics* **1985**, *4*, 852; P. N. V. P. Kumar, E. D. Jemmis, *J. Am. Chem. Soc.* **1988**, *110*, 125; M. H. Chisholm, C. M. Cook, J. C. Huffman, J. D. Martin, *Organometallics* **1993**, *12*, 2354; G. Erker, M. Albrecht, C. Krüger, M. Nolte, S. Werner, *Organometallics* **1993**, *12*, 4979; D. Röttger, G. Erker, R. Fröhlich, S. Kotila, *Chem. Ber*. **1996**, *129*, 5; L. R. Falvello, S. Fernández, J. Forniés, E. Lalinde, F. Martínez, M. T. Moreno, *Organometallics* **1997**, *16*, 1326; E. D. Jemmis, K. T. Gijin, *Angew. Chem.* **1997**, *109*, 633; *Angew. Chem., Int. Ed. Engl*. **1997**, *36*, 606.
[16] S. Braun, H. Kalinowski, S. Berger, *100 and More Basic NMR-Experiments*, VCH, Weinheim, **1996**, and references cited therein.

[97310]

Octanuclear Bis(triple-helical) Metal(II) Complexes

Rolf W. Saalfrank*[a], Norbert Löw[a], Stefan Trummer[a], George M. Sheldrick[b], Markus Teichert[b], and Dietmar Stalke[c]

Institut für Organische Chemie der Universität Erlangen-Nürnberg[a],
Henkestraße 42, D-91054 Erlangen, Germany
Fax: (internat.) + 49(0)9131/85-1165
E-mail: saalfrnk@organik.uni-erlangen.de

Institut für Anorganische Chemie der Universität Göttingen[b],
Tammannstr. 4, D-37077 Göttingen, Germany

Institut für Anorganische Chemie der Universität Würzburg[c],
Am Hubland, D-97074 Würzburg, Germany

Received November 6, 1997

Keywords: Metal(II) complexes / Octanuclear complexes / Supramolecular chemistry / Zinc / Cadmium / Manganese

The reaction of H_2L^1 and H_2L^2 with divalent metal ions leads to octanuclear bis(triple-helical) metal(II) complexes of the general composition $[Zn_8O_2L^2{}_6]$ (**3**) and $[M_8O_2L^1{}_6]$ (**4**: M = Cd^{2+}; **5**: M = Mn^{2+}). NMR studies of the diamagnetic cadmium complex **4c** show six equivalent ligands. Unambiguous characterisation of **5b** was achieved by X-ray crystallographic analysis.

There is considerable interest in the design of metallosupramolecular oligomers containing a defined number of metal ions in a determined spatial arrangement. In principle, it is possible to selectively generate a large variety of structures by choosing the appropriate ligands and metal ions.[1][2] Our interest in polynuclear supramolecular complexes, with two or more Fe^{III} ions bridged by oxygen and nitrogen donor ligands, stems mainly from the importance of oxo-centered polyiron aggregates as model compounds for metalloproteins, oxidation catalysts and corrosion inhibitors.[3]

Complexation of trivalent Fe ions with the doubly negatively charged, pentadentate ligand L^1 leads to the {2}-metallacryptate $[K\subset(Fe_2L^1{}_3)]PF_6$ (**1**).[4] In contrast to L^1, nucleation of iron with the isodentate ligand L^2 yields the triple-helical, oxo-centered, trinuclear mixed-valence iron complex $[Fe_3OL^{2A}{}_3]$ (**2**)[5] but, unexpectedly, no {2}-metallacryptate $[K\subset(Fe_2L^{2B}{}_3)]PF_6$. This result can be explained by the fact that the pentadentate ligand L^2 exists as two different rotamers, L^{2A} and L^{2B} in solution. In the case of L^{2A} the coordination donors are five nitrogen atoms, whereas in the case of L^{2B} the donor atoms are three nitrogen and two oxygen atoms. Due to the topological equivalency of the ligand L^1 and the rotamer L^{2B}, one expects to obtain, using appropriate transition metals, isostructural complexes by nucleation of L^1 and L^2.

Herein we describe the reaction of the pentadentate tritopic ligands L^1 and L^{2B} with divalent metal ions such as zinc, cadmium and manganese. Treatment of 0.75 equiv. of the pyridylene-spacered tetraketone[6] H_2L^1 or the bis(tetrazole)[7] H_2L^2, with one equiv. of zinc acetate, cadmium or manganese dichloride furnishes the coordination compounds **3**−**5** which range from colourless to orange in appearance.

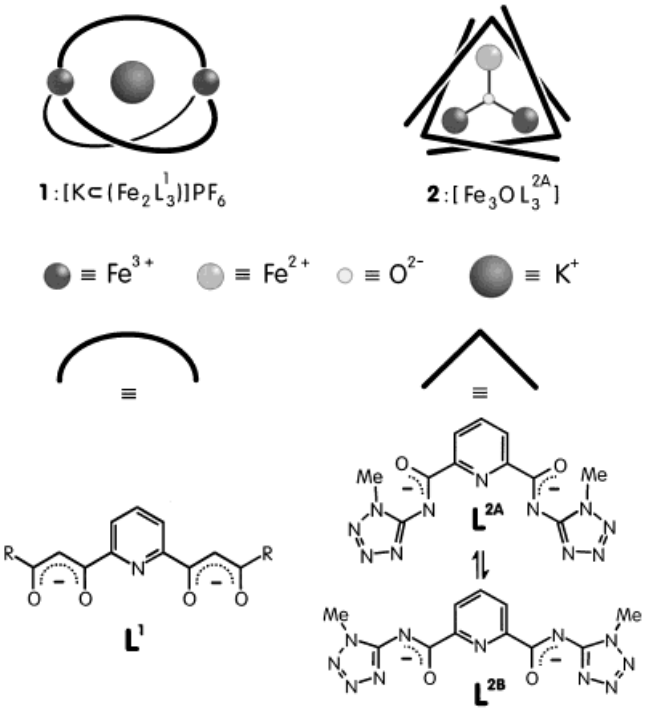

The compositions of these complexes were determined by FAB mass spectrometry (FAB = fast-atom bombardment). The FAB-MS spectrum of complex $[Zn_8O_2L^{2B}{}_6]$ (**3**) exhibits the correct molecular peak and isotopic pattern at *m*/*z* 2519 (Figure 1). According to their FAB-MS data, the corresponding cadmium (**4**) and manganese (**5**) complexes have the same composition.

 © WILEY-VCH Verlag GmbH, D-69451 Weinheim, 1998 1434−1948/98/0505−0559 $ 17.50+.50/0

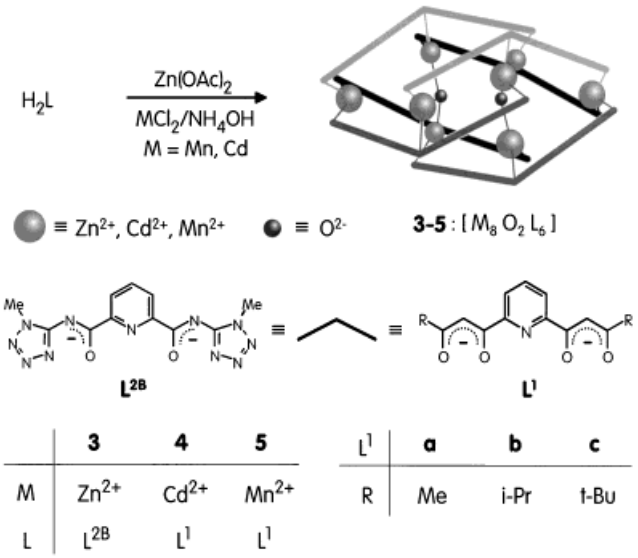

	3	4	5
M	Zn^{2+}	Cd^{2+}	Mn^{2+}
L	L^{2B}	L^{1}	L^{1}

L^1	a	b	c
R	Me	i-Pr	t-Bu

Figure 1. FAB-MS spectrum of zinc complex **3**

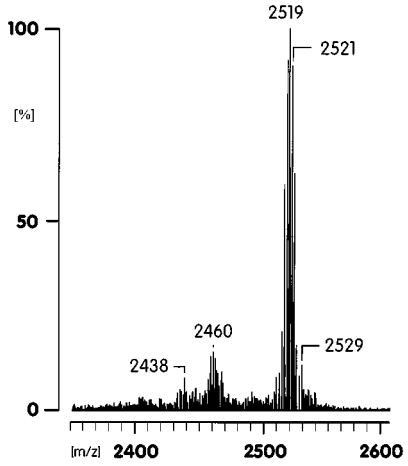

^{1}H- and ^{13}C-NMR studies of the diamagnetic cadmium complex [$Cd_8O_2L_6{}^{1c}$] (**4c**) reveals that, in solution, all six ligands are chemically identical, but that the two halves of each ligand are in different magnetic environments. Consequently, the ^{13}C-NMR spectrum of **4c** displays a double set of signals in contrast to the single set of the protonated free ligand H_2L^{1c}.

In order to unequivocally establish the structure of the polynuclear systems **3**−**5**, the manganese complex **5b** was taken as a representative example and we carried out an X-ray crystallographic analysis.[8] According to this analysis, **5b** is present in the crystal as a neutral, octanuclear bis(triple-helical) chelate complex. The core of **5b** consists of eight manganese(II) ions, forming a twofold capped, slightly twisted trigonal prism with a μ_3-O^{2-} ion centered in each of the two inner faces (Figure 2.). All the six doubly negatively charged pentadentate ligands L^{1b} link to three manganese atoms. The two antipodal manganese(II) ions are coordinated by three μ_1- and three μ_2-oxygen chelate atoms of three ligands. However, the six metal centers, constituting the trigonal prism, are coordinated by one pyridylene nitrogen and two μ_2-chelate oxygen atoms. Distorted octahedral coordination of these six manganese(II) ions is achieved by two extra μ_3-O^{2-} ions.

Figure 2. Left: Core of the octanuclear complex **5b** to highlight the bicapped distorted trigonal prism; right: Octanuclear core of **5b** showing two ligands and the μ_3-O^{2-} ions; H atoms omitted for clarity, O atoms hatched, C atoms shaded, N atoms empty, Mn atoms dotted

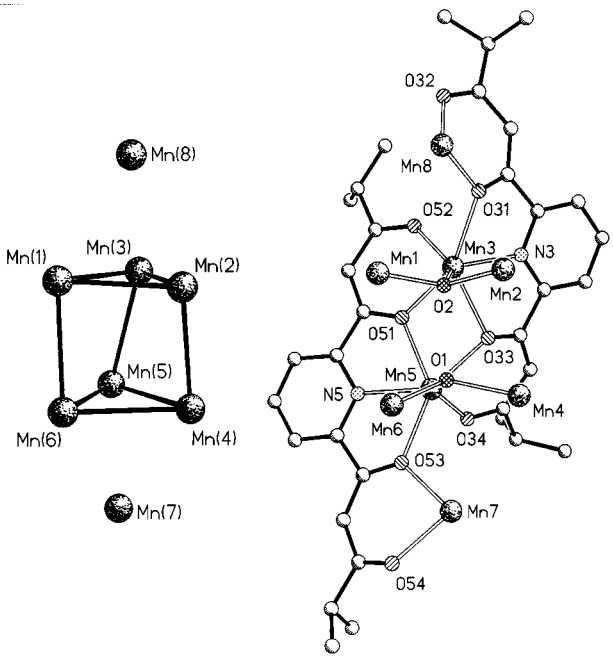

Consequently, in the neutral, octanuclear, bis(triple-helical) complex **5b** all the manganese(II) ions are octahedrally coordinated (Figure 3).

Figure 3. Molecular structure of the octanuclear complex **5b** in the crystal; H atoms omitted for clarity, O atoms hatched, C atoms shaded, N atoms empty, Mn atoms dotted

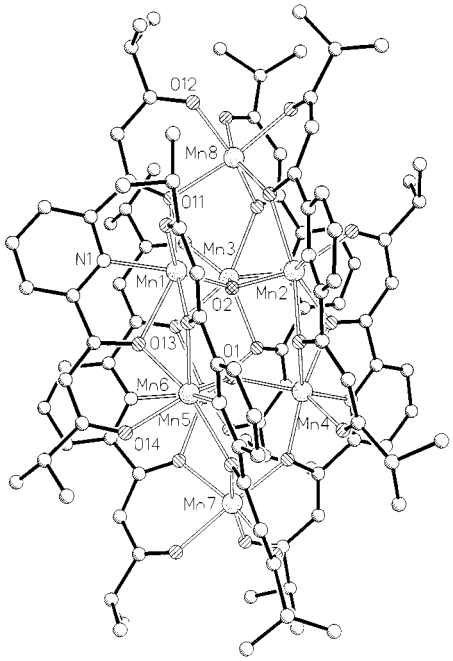

As shown by X-ray crystallographic analysis[12], the zinc complex **3** is isostructural with **5b**. The space-filling model

of **3** (Figure 4) illustrates the bis(triple-helical) arrangement of the ligands.

Figure 4. Space-filling model of bis(triple-helical) octanuclear $[Zn_8O_2L^{2B}{}_6]$ (**3**); top: view along the C_3 axis; bottom: view along the C_2 axis

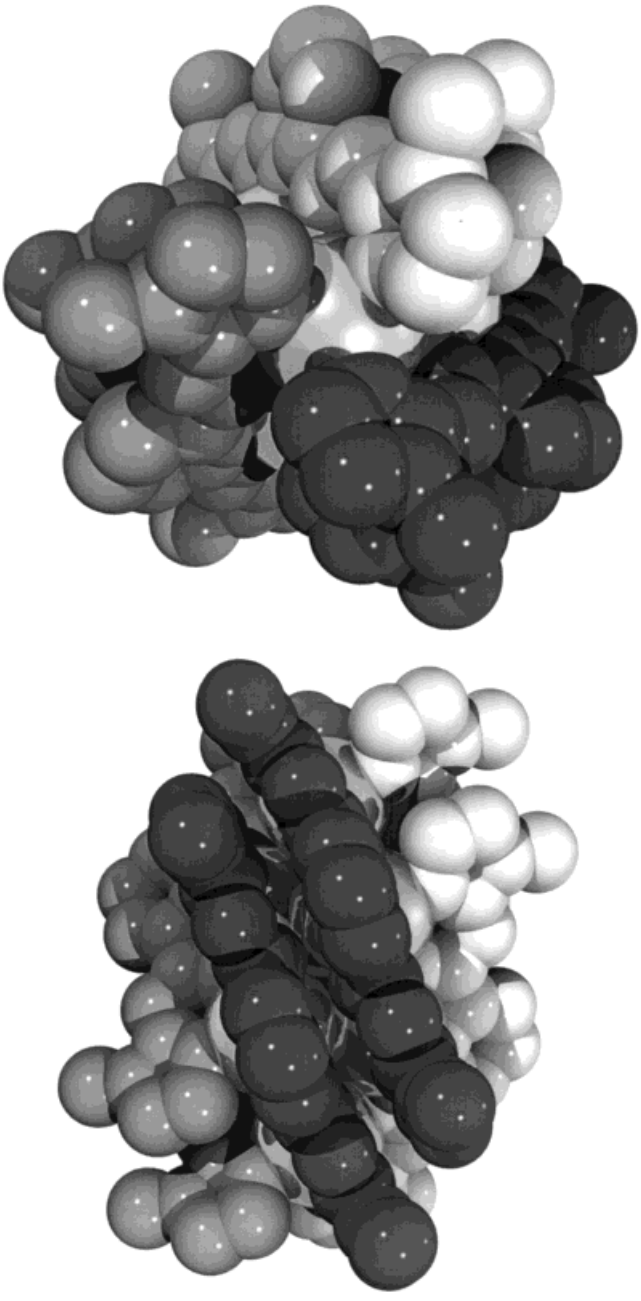

The similarity between the core of the octanuclear complex **3** and the metal framework of the iron-molybdenum co-factor of the nitrogenase MoFe protein[13] is noteworthy (Figure 5).

In conclusion these results demonstrate clearly that the formation of metalla-supramolecular structures is highly sensitive with respect to the metal ions, the ligands and their conformation. In contrast to the {2}-iron(III) cryptate **1** and the oxo-centered iron(III) complex **2,** both ligands $(L^1)^{2-}$ and $(L^{2A}/L^{2B})^{2-}$ lead to the isostructural bis(triple-helical) octanuclear complexes, i.e. $[Zn_8O_2L^{2B}{}_6]$ (**3**), $[Cd_8O_2L^1{}_6]$ (**4**) and $[Mn_8O_2L^1{}_6]$ (**5**).

Figure 5. Top: Core of the iron-molybdenum co-factor of nitrogenase[13]; bottom: torso of $[Zn_8O_2L^{2B}{}_6]$ (**3**)

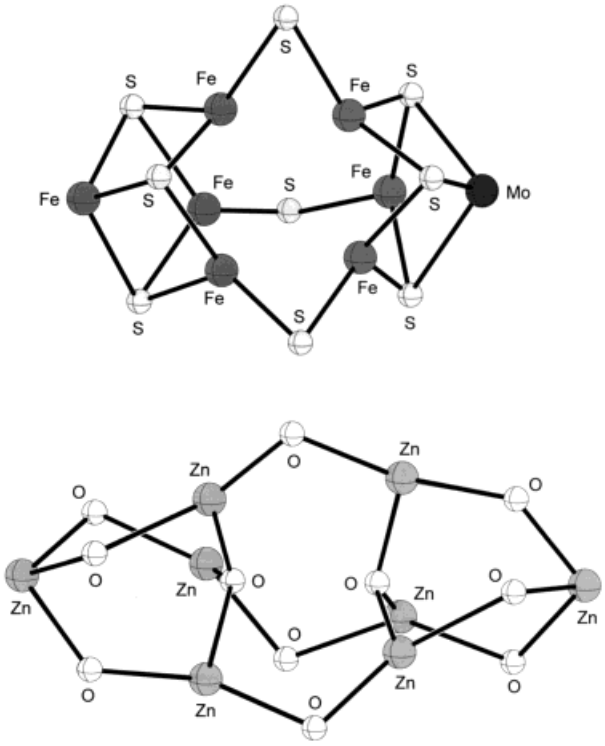

Financial support from the *Deutsche Forschungsgemeinschaft*, the *Volkswagen-Stiftung* and the *Fonds der Chemischen Industrie* is gratefully acknowledged. We would like to thank Prof. Dr. *K.-P. Zeller*, University of Tübingen, for the FAB-MS measurements.

Experimental Section

^{1}H- and ^{13}C-NMR spectra: Jeol JNM-GX-400 (400 MHz; 100 MHz) spectrometer with TMS as internal standard, chemical shifts are given in ppm. − Mass spectra: Varian MAT 3rA (EIMS) or a Finnigan MAT TSQ 70 instrument (ion desorption from *m*-NBA matrix: 10 keV xenon atoms, FAB MS). − Microanalyses: Heraeus CHN-Mikroautomat. − IR: Perkin−Elmer 1420 Ratio-Recording Infrared Spectrophotometer.

General Procedure for the Synthesis of the Bis(tetrazole) Ligand **H_2L^2**: A cooled suspension of 2.0 g (20 mmol) *N*-methylaminotetrazole and 2.0 g (47 mmol) of dry lithium chloride was placed in a three-necked, round-bottom flask, fitted with a condenser. The contents of the flask were stirred, while 2.03 g (10 mmol) of 2,6-pyridinedicarboxylic dichloride was slowly added. The solution was poured into ice-cold water (400 ml), stirred for 2 h and the white precipitate was filtered off, washed with water and dried in vacuo (oil pump).

N,N′-Bis(1-methyl-1H-tetrazol-5-yl)pyridyl-2,6-dicarboxamide (**H_2L^2**): Yield 2.77 g (84%), white powder, m.p. > 250°C (decomp.). − IR (KBr): $\tilde{\nu}$ = 3340 cm^{-1}, 3120 (NH), 3020 (=CH), 2920 (CH_3), 1690 (C=O), 1550 (C=C). − ^{1}H NMR (CD_3CN/CF_3COOD): δ = 4.25 (s, 6 H, 2 CH_3), 8.39 (t, $^3J_{H,H}$ = 7.7 Hz, 1 H, 4-pyridyl-CH), 8.63 (d, $^3J_{H,H}$ = 7.7 Hz, 2 H, 3,5-pyridyl-CH). − ^{13}C NMR

(CD_3CN/CF_3COOD): δ = 37.08 (2 CH_3), 129.84 (3,5-pyridyl-CH), 142.56 (4-pyridyl-CH), 148.13 (2,6-pyridyl-C=), 150.25 (2 CN_2), 164.19 (2 C=O). − MS (EI, 70 eV); *m/z*: 330 [M^+]. − $C_{11}H_{11}N_{11}O_2$ (329.32): calcd. C 40.12, H 3.37, N 46.80; found C 39.55, H 3.74, N 45.93.

General Procedure for the Synthesis of the Octameric Zinc Complex **3**: A solution of 293 mg (1.33 mmol) of $Zn(OAc)_2 \cdot 2\ H_2O$ in methanol (50 ml) was added to a solution of 329 mg (1.0 mmol) bis(tetrazole) H_2L^2 in acetonitrile (400 ml). The reaction mixture was stirred and heated under reflux for 24 h. The resulting precipitate was filtered off washed with diethyl ether and dried in vacuo. The resulting solid was recrystallized from hot acetonitrile.

[$Zn_8O_2L^{2b}{}_6$]$_2$ (**3**): Yield 365 mg (87%) of colourless crystals from acetonitrile, m.p. > 250°C (decomp.). − IR (KBr): $\tilde{\nu}$ = 1640 cm^{-1} (C=O), 1550 (C=C), 1450 (C=N). − MS (FAB, *m*-NBA); *m/z*: 2519 [M^+]. − $C_{66}H_{54}N_{66}O_{14}Zn_8$ (2518.70): calcd. C 31.48, H 2.16, N 36.70; found C 31.53, H 2.98, N 36.16.

General Procedure for the Synthesis of the Pyridyl-Spacered Tetraketones (**H_2L^1**): A suspension of 1.0 g (44 mmol) of freshly cut sodium and diethyl 2,6-pyridinedicarboxylate (4.90 g, 22 mmol) in dry benzene (50 ml) was placed in a three-necked, round-bottom flask, fitted with a condenser. The contents of the flask were stirred, while a solution of the corresponding methyl ketone (44 mmol) in benzene (25 ml) was added dropwise. Stirring at room temp. was continued for 30 min until the yellow sodium salt had precipitated out of the solution. The reaction mixture was heated gently for about 2−4 h. The sodium salt was collected by filtration and washed thoroughly with petroleum ether before drying. The dry solid was added to dilute hydrochloric acid (2 N, 50 ml) and the resulting solid was collected by filtration. The crude products were recrystallized from the mentioned solvents.

1,1′-(2,6-Bispyridyl)bis-1,3-butanedione (**H_2L^{1a}**): [The ^{1}H-NMR spectrum shows the presence of keto-enol tautomers. In the following we describe only the main tautomer (90%), the bis(keto-enol) system.] Yield 2.30 g (42%), yellow microcrystals from methanol, m.p. 60°C. − IR (KBr): $\tilde{\nu}$ = 3450 cm^{-1} (OH), 2920 (CH), 1720 (C=O), 1620 (C=C). − ^{1}H NMR ($CDCl_3$): δ = 2.30 (s, 6 H, 2 CH_3), 6.87 (s, 2 H, 2 =CH), 7.99 (t, $^3J_{H,H}$ = 7.7 Hz, 1 H, 4-pyridyl-CH), 8.24 (d, $^3J_{H,H}$ = 7.7 Hz, 2 H, 3,5-pyridyl-CH), 15.75 (br. s, 2 H, 2 =C−OH). − ^{13}C NMR ($CDCl_3$): δ = 26.13 (2 CH_3), 97.27 (2 =CH), 124.29 (3,5-pyridyl-CH), 138.16 (4-pyridyl-CH), 151.71 (2,6-pyridyl-C=), 180.43 (2 =C−OH), 194.92 (2 C=O). − MS (EI, 70 eV); *m/z*: 247 [M^+]. − $C_{13}H_{13}NO_4$ (247.25): calcd. C 63.15, H 5.31, N 5.67; found C 63.23, H 5.49, N 5.63.

1,1′-(2,6-Bispyridyl)bis-4-methyl-1,3-pentanedione (**H_2L^{1b}**): [The ^{1}H-NMR spectrum shows the presence of keto-enol tautomers. In the following we describe only the main tautomer (75%), the bis-(keto-enol) system.] Yield 2.40 g (36%), yellow microcrystals from methanol, m.p. 44°C. − IR (l, $CHBr_3$): $\tilde{\nu}$ = 3480 cm^{-1} (OH), 2950 (CH), 1600 (C=O), 1550 (C=C). − ^{1}H NMR ($CDCl_3$): δ = 1.27 (d, $^3J_{H,H}$ = 7.0 Hz, 12 H, 4 CH_3), 2.37 [sept, 2 H, 2 $CH(CH_3)_2$], 6.92 (s, 2 H, 2 =CH), 7.98 (t, $^3J_{H,H}$ = 7.7 Hz, 1 H, 4-pyridyl-CH), 8.19 (d, $^3J_{H,H}$ = 7.7 Hz, 2 H, 3,5-pyridyl-CH), 15.81 (br. s, 2 H, 2 =C−OH). − ^{13}C NMR ($CDCl_3$): δ = 19.23 (4 CH_3), 37.55 [2 $CH(CH_3)_2$], 94.67 (2 =CH), 124.63 (3,5-pyridyl-CH), 138.40 (4-pyridyl-CH), 151.80 (2,6-pyridyl-C=), 181.61 (2 =C−OH), 201.79 (2 C=O). − MS (EI, 70 eV); *m/z*: 303 [M^+]. − $C_{17}H_{21}NO_4$ (303.36): calcd. C 67.31, H 6.98, N 4.62; found C 67.02, H 6.88, N 4.69.

1,1′-(2,6-Bispyridyl)bis-4,4′-dimethyl-1,3-pentanedione (**H_2L^{1c}**): Yield 0.93 g (13%), colourless needles from methanol, m.p. 124°C: − IR (l, $CHBr_3$): $\tilde{\nu}$ = 3440 cm^{-1} (OH), 2970 (CH), 1610 (C=O), 1570 (C=C). − ^{1}H NMR ($CDCl_3$): δ = 1.30 (s, 18 H, 6 CH_3), 7.13 (s, 2 H, 2 =CH), 7.99 (t, $^3J_{H,H}$ = 7.8 Hz, 1 H, 4-pyridyl-CH), 8.19 (d, $^3J_{H,H}$ = 7.8 Hz, 2 H, 3,5-pyridyl-CH), 15.90 (br. s, 2 H, 2 = C−OH). − ^{13}C NMR ($CDCl_3$): δ = 27.24 (6 CH_3), 39.87 [2 $C(CH_3)_2$], 92.59 (2 =CH), 123.98 (3,5-pyridyl-CH), 138.21 (4-pyridyl-CH), 151.86 (2,6-pyridyl-C=), 182.39 (2 =C−OH), 202.78 (2 C=O). − MS (EI, 70 eV); *m/z*: 331 [M^+]. − $C_{19}H_{22}NO_4$ (331.41): calcd. C 68.86, H 7.58, N 4.23; found C 68.34, H 7.56, N 4.24.

General Procedure for the Synthesis of the Octameric Cadmium (**4a−c**) *and Manganese* (**5a−c**) *Complexes:* Aqueous ammonia (2 ml, 12%) was added dropwise to a solution of 184 mg (1.0 mmol) cadmium chloride or 126 mg (1.0 mmol) manganese(II) chloride and the appropriate pyridyl-spacered ligand H_2L^1 (0.75 mmol) in ethanol (100 ml), until no more turbidity was seen. To achieve complete precipitation of the products, water (100 ml) was added. The products were filtered off and dried in vacuo (oil pump) and recrystallized from the solvents described above.

[$Cd_8O_2L^{1a}{}_6$] (**4a**): Yield 180 mg (60%), yellow microcrystals from ethanol, m.p. 290°C (decomp.). Because of the total insolubility in all available solvents, detailed NMR investigations could not be carried out. − IR (KBr): $\tilde{\nu}$ = 2970 cm^{-1} (CH), 1610 (C=O), 1585 (C=C). − MS (FAB, *m*-NBA); *m/z*: 2402 [M^+]. − $C_{77}H_{66}Cd_8N_6O_{26}$ (2402.69): calcd. C 38.99, H 2.77, N 3.50; found C 41.60, H 3.99, N 3.61.

[$Cd_8O_2L^{1b}{}_6$] (**4b**): Yield 320 mg (94%), yellow microcrystals from ethanol, m.p. 275°C (decomp.). Because of the total insolubility in all available solvents, detailed NMR investigations could not be carried out. − IR (l, $CHBr_3$): $\tilde{\nu}$ = 2960 cm^{-1} (CH), 1610 (C=O), 1500 (C=C) − MS (FAB, *m*-NBA); *m/z*: 2740 [M^+]. − $C_{102}H_{114}Cd_8N_6O_{26}$ (2739.34): calcd. C 44.72, H 4.20, N 3.07; found C 43.55, H 4.48, N 3.07.

[$Cd_8O_2L^{1c}{}_6$] (**4c**): Yield 280 mg (77%), yellow microcrystals from ethanol, m.p. 285°C (decomp.). − IR (KBr): $\tilde{\nu}$ = 2950 cm^{-1} (CH), 1610 (C=O), 1450 (C=C). − ^{1}H NMR ($CDCl_3$): δ = 0.71, 1.24 (s, 54 H, 18 CH_3), 5.35, 6.22 (s, 6 H, 6 =CH), 7.57 (d, $^3J_{H,H}$ = 6.4 Hz, 6 H, 3-pyridyl-CH), 7.79 (d, $^3J_{H,H}$ = 7.3 Hz, 6 H, 5-pyridyl-CH), 7.89 (t, $^3J_{H,H}$ = 7.5 Hz, 6 H, 4-pyridyl-CH). − ^{13}C NMR ($CDCl_3$): δ = 27.92, 27.99 (18 CH_3), 42.50, 43.01 [6 $C(CH_3)_3$], 89.82, 94.20 (6 =CH), 121.11, 122.89 (3,5-pyridyl-CH), 138.98 (4-pyridyl-CH), 152.85, 155.99 (2,6-pyridyl-C), 172.05, 174.61, 207.62, 207.66 (24 C=O). − MS (FAB, *m*-NBA); *m/z*: 2908 [M^+]. − $C_{114}H_{138}Cd_8N_6O_{26}$ (2907.66): calcd. C 47.09, H 4.78, N 2.89; found C 40.07, H 4.50, N 2.51.

[$Mn_8O_2L^{1a}{}_6$] (**5a**): Yield 144 mg (59%), orange microcrystals from ethanol, m.p. 215°C (decomp.). − IR (KBr): $\tilde{\nu}$ = 2920 cm^{-1} (CH), 1620 (C=O), 1510 (C=C). − MS (FAB, *m*-NBA); *m/z*: 1942 [M^+]. − $C_{78}H_{66}Mn_8N_6O_{26}$ (1942.91): calcd. C 48.22, H 3.42, N 4.33; found C 48.93, H 4.63, N 5.22.

[$Mn_8O_2L^{1b}{}_6$] (**5b**): Yield 250 mg (88%), red crystals from toluene/pyridine, m.p. > 300°C. − IR (l, $CHBr_3$): $\tilde{\nu}$ = 2975 cm^{-1} (CH), 1625 (C=O), 1575 (C=C). − MS (FAB, *m*-NBA); *m/z*: 2280 [M^+]. − $C_{102}H_{114}Mn_8N_6O_{26}$ (2279.56): calcd. C 53.74, H 5.04, N 3.66; found C 55.53, H 4.64, N 3.44.

[$Mn_8O_2L^{1c}{}_6$] (**5c**): Yield 260 mg (85%), orange microcrystals from ethanol, m.p. > 300°C. − IR (KBr): $\tilde{\nu}$ = 2950 cm^{-1} (CH), 1610 (C=O), 1500 (C=C). − MS (FAB, *m*-NBA); *m/z*: 2448 [M^+]. − $C_{114}H_{138}Cd_8N_6O_{26}$ (2447.88): calcd. C 55.94, H 5.68, N 3.43; found C 57.03, H 6.30, N 3.68.

[1] D. Philp, J. F. Stoddart, *Angew. Chem.* **1996**, *108*, 1243−1286; *Angew. Chem. Int. Ed. Engl.* **1996**, *35*, 1154−1196; J.-M. Lehn, B. O. Kneisel, G. Baum, D. Fenske, *ibid.* **1996**, *108*, 1987−1990; *ibid.* **1996**, *35*, 1838−1840; J.-M. Lehn, *ibid.* **1990**, *102*, 1347−1362; *ibid.* **1990**, *29*, 1304−1319; I. Cragg-Hine, M. G. Davidson, O. Kocian, F. S. Mair, E. Pohl, P. R. Raithby, R. Snaith, N. Spencer, J. F. Stoddart, *ibid.* **1993**, *105*, 1254−1256; *ibid.* **1993**, *32*, 1182−1184; M. Simard, D. Su, J. D. Wuest, *J. Am. Chem. Soc.* **1991**, *113*, 4696−4698.

[2] R. W. Saalfrank, N. Löw, S. Kareth, V. Seitz, F. Hampel, D. Stalke, M. Teichert, *Angew. Chem.* **1998**, *110*, 182*; Angew. Chem. Int. Ed. Engl.* **1998**, *37*, 172; R. Saalfrank, I. Bernt, E. Uller, F. Hampel, *ibid.* **1997**, *109*, 2596−2599; *ibid.* **1997**, *36*, 2482−2485; R. W. Saalfrank, N. Löw, F. Hampel, H.-D. Stachel, *ibid.* **1996**, *108*, 2353−2354; *ibid.* **1996**, *35*, 2209−2210; R. W. Saalfrank, R. Burak, S. Reihs, N. Löw, F. Hampel, H.-D. Stachel, J. Lentmaier, K. Peters, E. M. Peters, H. G. von Schnering, *ibid.* **1995**, *107*, 1085−1087; *ibid.* **1995**, *34*, 993−995; R. W. Saalfrank, R. Burak, A. Breit, D. Stalke, R. Herbst-Irmer, J. Daub, M. Porsch, E. Bill, M. Müther, A. X. Trautwein, *ibid.* **1994**, *106*, 1697−1699; *ibid.* **1994**, *33*, 1621−1623.

[3] S.J. Lippard, J. M. Berg, *Bioanorganische Chemie*, Spektrum Akademischer Verlag, Heidelberg **1995**, chapter 5, p. 136f.; S. M. Gorun, G. C. Papaefthmiou, R. B. Frankel, S. J. Lippard, *J. Am. Chem. Soc.* **1987**, *109*, 4244−4255; S. J. Lippard, *Angew. Chem.* **1988**, *100*, 353−371; *Angew. Chem. Int. Ed. Engl.* **1988**, *27*, 344−361; K. Wieghardt, K. Pohl, I. Jibril, G. Huttner, *ibid.* **1984**, *96*, 66−67 and **1984**, *23*, 77−78.

[4] R. W. Saalfrank, S. Trummer, H. Krautscheid, V. Schünemann, A. X. Trautwein, S. Hien, J. Daub, *Angew. Chem.* **1996**, *108*, 2352−2350; *Angew. Chem. Int. Ed. Engl.* **1996**, *35*, 2206−2208.

[5] R. W. Saalfrank, A. Dresel, V. Seitz, S. Trummer, F. Hampel, M. Teichert, D. Stalke, C. Stadler, J. Daub, V. Schünemann, A. X. Trautwein, *Chem. Eur. J.* **1997**, *3*, 2058−2062.

[6] Syntheses of $\mathbf{H_2L^1}$ according to: D. E. Fenton, J. R. Tate, U. Castellato, S. Tamburini, P. A. Vigato, M. Vidali, *Inorg. Chim. Acta* **1984**, *83*, 23−31.

[7] Synthesis of $\mathbf{H_2L^2}$ according to: A. G. Oertli, W. R. Meyer, U. W. Suter, *Helv. Chim. Acta* **1992**, *75*, 184−189.

[8] Crystal structure determination of compound **5b**: $C_{102}H_{114}Mn_8N_6O_{26}$ + 6 C_5H_5N + LiCl (captured during crystallisation), M_r = 2279.56 + 6·79.10 + 42.39, monoclinic, space group $P2_1/c$, a = 1604.9(3), b = 4354.9(8), c = 1978.1(4) pm, β = 110.28(2)°, V = 12.968(4) nm^3, Z = 4, $\rho_{calcd.}$ = 1.432 Mg/m^3, $F(000)$ = 5792, λ = 71.073 pm, T = 153 K, μ(Mo-K_α) = 0.849 mm^{-1}, min/max transmission 0.630/0.883, crystal dimensions 0.60 × 0.35 × 0.15 mm, 6.54° ≤ 2Θ ≤ 46.52°; 103087 measured reflections of which 18490 were independent (R_{int} = 0.0671) and employed in the structure refinement (1779 parameters, 802 restraints). The R values are: $R1 = \Sigma|F_o - F_c|/\Sigma F_o$ = 0.0552 [I > 2σ(I)]; $wR_2 = [\Sigma w(F_o^2 - F_c^2)^2/\Sigma wF_o^4]^{1/2}$ = 0.1126 (all data); min/max residual electron density −407 e nm^{-3}/596 e nm^{-3}. Four isopropyl groups and one pyridine solvent molecule are disordered over two sites. The electron density at two pyridine nitrogen atoms was modelled as a lithium atom. A hydrogen atom attached to a bridging oxygen atom could not be located in the difference Fourier synthesis. In view of the possibility of disorder, X-ray analysis cannot provide a definite assignment in such a case. Crystallographic data for **5b** were collected with a Stoe-Siemens-Huber four-circle diffractometer with Siemens CCD area detector by using φ-scans on a shock-cooled crystal in an oil drop[9]. Data integration was performed with the program SAINT. A semiempirical absorption correction was applied. The structure was solved by direct methods (SHELXS-97)[10] and refined against F^2 by the least squares[11]. All non-hydrogen atoms were refined anisotropically. For the hydrogen atoms a riding model was employed. All disordered components were refined anisotropically with the assistance of distance and *ADP* restraints. Crystallographic data (excluding structure factors) for the structures reported in this paper have been deposited with the Cambridge Crystallographic Data Centre as supplementary publication no. CCDC-100830. Copies of the data can be obtained free of charge on application to CCDC, 12 Union Road, Cambridge CB2 1EZ, UK [Fax: (internat.) + (1223) 336-033; E-mail: deposit@ccds.cam.ac.uk].

[9] T. Kottke, D. Stalke, *J. Appl. Crystallogr.* **1993**, *26*, 615.

[10] G.M. Sheldrick, "SHELXS-97, Program for structure solution", *Acta Crystallogr.* **1990**, *A46*, 467.

[11] G.M. Sheldrick, *SHELXL-97*, *Program for structure refinement*, University of Göttingen, **1997**.

[12] The Zn complex **3** co-crystallises with ZnL^{2A}_2 (**6**). The asymmetric unit is composed of disordered **3** and **6**. The position of **6** is close to a C_2 axis which leads to two superimposed structures. The reason for that may be found in twinning. The reliability criteria for **3** are R_1 = 0.093 and wR_2 = 0.27. For red-green stereo presentations of **3** and **5b** see: http://www.organik.uni-erlangen.de/saalfrank/index/html

[13] J. B. Howard, D. C. Rees, *Chem. Rev.* **1996**, *96*, 2965−2982; B. K. Burgess, D. L. Lowe, *Chem. Rev.* **1996**, *96*, 2983−3011.

[97255]

A New Class of Oligonuclear Platinum-Thallium Compounds with a Direct Metal−Metal Bond
3. Unusual Equilibria in Aqueous Solution[◇]

Mikhail Maliarik[a][+], Julius Glaser*[a], Imre Tóth*[b], Mateus Webba da Silva[a], and László Zékány[b]

Department of Chemistry, Inorganic Chemistry, The Royal Institute of Technology (KTH),[a]
S-100 44 Stockholm, Sweden

Department of Analytical and Inorganic Chemistry, Lajos Kossuth University (KLTE),[b]
H-4010 Debrecen, Pf. 21, Hungary

Received December 5, 1997

Keywords: Equilibrium / Metal-metal bond / Stability constants / Platinum / Thallium / NMR

A new series of four binuclear platinum-thallium cyano compounds containing a direct and unsupported by ligands metal−metal bond has been prepared in aqueous solution. These compounds are represented by the formula $[(NC)_5Pt-Tl(CN)_{n-1}]^{(n-1)-}$ (n = 1−4 for compounds **I**, **II**, **III** **IV,** respectively) and $[(NC)_5Pt-Tl-Pt(CN)_5]^{3-}$ (for compound **V**). The oligonuclear complexes are synthesised according to the reaction $m Pt(CN)_4^{2-} + Tl^{3+} + nCN^- \rightleftharpoons [Pt_mTl(CN)_{4m+n}]^{3-2m-n}$. Thus, there occurs a change of the coordination number of the Pt center from four (square planar) to six (octahedral). Consequently, the formation of binuclear platinum-thallium cyano compounds involves at least two steps: (i) formation of metal−metal bond and (ii) formation of $(NC)_5Pt-$ unit by a cyanide transfer process. − The complexes exist in an equilibrium, which also includes the parent complexes $Pt(CN)_4^{2-}$ and $Tl(CN)_n^{3-n}$ (n = 0−4), and can be controlled by varying the cyanide concentration and/or pH of the solution. The stability constants of the compounds $\beta_N = [Pt_mTl(CN)_{4m+n}^{3-2m-n}] / \{[Pt(CN)_4^{2-}]^m \cdot [Tl^{3+}] \cdot [CN^-]^n\}$ have been determined by means of multinuclear NMR (^{195}Pt, ^{205}Tl): $\log\beta_N$ = 19.9±0.4, 30.7±0.3, 38.6±0.3, and 44.8±0.2 for **I**, **II**, **III**, and **IV** (m = 1, n = 1−4), and 32.1±0.3 for **V** (m = 2, n = 2), respectively, (in 1 M $NaClO_4$ as ionic medium, at 25 °C). To our knowledge, the present work constitutes the first detailed equilibrium study of metal−metal bonded compounds; it indicates that also other cluster formation reactions described in the literature may represent real equilibria.

Introduction

Starting from the report of Nagle et al. on the six-coordinated platinum in the structure of *trans*-$Tl_2Pt(CN)_4$,[3] a few oligometallic compounds containing platinum and thallium have been synthesised and their properties studied.[4][5][6][7][8][9] Recently, we have published a study of new binuclear platinum-thallium cyano compounds containing a direct metal−metal bond.[1] Their structure has been studied in solution[2] as well as in the solid state.[10] In the present study a new aspect of these small clusters′ chemistry is explored, namely their equilibrium behaviour in aqueous solution. The data on reversible equilibrium processes for metal−metal bonded compounds is practically non-existent.[11][12][13] Also for metal−carbon bonded compounds (excluding cyano complexes) the information is very scarce.[14][15] Equilibrium models, which are routinely used in coordination chemistry, would provide obvious advantages also for cluster chemistry, e.g. to increase the yield of a reaction by shifting the equilibrium in the direction of required species using the law of mass action in a quantitative way, or for catalytic studies providing speciation of the potentially active complexes, thus allowing the chemist to tune their redox potential, selectivity, etc.

Our interest on two-electron transfer reactions in solution prompted us to study the equilibria of the $Tl^{III}-Pt^{II}-CN^-$ system in water. The advantage of these components for a multinuclear NMR study is obvious, all atoms have suitable NMR active nuclei (see in refs.[1] and[2]). ^{205}Tl NMR is superior in sensitivity, and its huge chemical shift scale provides slow exchange regimes for the different species, thus allowing to follow the concentration distribution of the formed clusters. A further advantage of the direct spectroscopic detection of the different species was that the evaluation of the overall stability constant values of this relatively complicated system was possible without any sophisticated data treatment, using only molar ratios calculated from the NMR integrals and the mass balance equations. In this context, the structural change in the geometry of the platinum coordination sphere from four- to six-coordination in a two-step formation reaction of the platinum−thallium cluster is also discussed.

Results and Discussion

Preliminary experiments aimed at finding new complexes[2] indicated that the speciation of the Pt-Tl bimetallic complexes varies at different total concentrations of the

[◇] Part 1: Ref.[1]; Part 2: Ref.[2].
[+] Permanent address: Kurnakov Institute of General and Inorganic Chemistry, Russian Academy of Sciences, Leninsky Prospect 31, Moscow 117907, Russia.

 © WILEY-VCH Verlag GmbH, D-69451 Weinheim, 1998 1434−1948/98/0505−0565 $ 17.50+.50/0

components, Tl^{3+}, $Pt(CN)_4^{2-}$, CN^-, and H^+. Changing the concentration of any of the components shifted the distribution of the reactants and/or products, and demonstrated the existence of several types of chemical equilibria in the solutions.

In solutions with molar ratio Pt/Tl ≤ 1, bimetallic compounds are present only as binuclear species **I**−**IV**, at Pt/Tl > 1 a trimer **V** can be formed. The formation of the complexes in solution can be described by the following equilibrium:

$$m\ Pt(CN)_4^{2-} + Tl^{3+} + n\ CN^- \rightleftharpoons [Pt_mTl(CN)_{4+n}]^{(n-1)-} \quad (1)$$

giving the following overall stability constant:

$$\beta_N = [Pt_mTl(CN)_{4m+n}^{3-2m-n}] / \{[Pt(CN)_4^{2-}]^m \cdot [Tl^{3+}] \cdot [CN^-]^n\} \quad (1a)$$

where $m = 1$, $n = 1$, 2, 3, and 4 for **I**, **II**, **III**, and **IV**; and $m = 2$, $n = 2$ for **V**, respectively. The following simultaneous equilibria taking place in this system must also be considered:

$$Tl^{3+} + n\ CN^- \rightleftharpoons Tl(CN)_n^{3-n} \quad (2)$$

with $\beta_n = [Tl(CN)_n^{3-n}] / \{[Tl^{3+}] \cdot [CN^-]^n\}$,[20] and

$$CN^- + H^+ \rightleftharpoons HCN \quad (3)$$

with $K_H = K_a^{-1} = [HCN] / \{[CN^-][H^+]\}$.[21]

Although the stepwise formation/dissociation of platinum(II) cyano complexes could also be considered, the only species detected in ^{195}Pt-NMR spectra at the current experimental conditions were $Pt(CN)_4^{2-}$ and $[Pt_mTl(CN)_{4m+n}]^{3-2m-n}$ (and in some solutions also $Pt(CN)_6^{2-}$, which formed as a product of a slow photo-induced irreversible redox reaction). This finding is in accordance with the known properties of the complex, $Pt(CN)_4^{2-}$, namely its high stability (different values of $\log\beta_4$ can be found in the literature, ranging from 35 up to 65)[22] and kinetic inertness.[23] Based on these facts the species $Pt(CN)_4^{2-}$ was treated as a stable component.

The "addition reactions" between the complexes $Pt(CN)_4^{2-}$ and $Tl(CN)_n^{3-n}$ resulting in binuclear complexes:

$$Pt(CN)_4^{2-} + Tl(CN)_n^{3-n} \rightleftharpoons [PtTl(CN)_{4+n}]^{(n-1)-} \quad (4)$$

can be represented by the equilibrium constants,

$$K_N^{add} = [PtTl(CN)_{4+n}^{(n-1)-}] / \{[Pt(CN)_4^{2-}] \cdot [Tl(CN)_n^{3-n}]\} \quad (4a)$$

for $n = 1$, 2, 3, and 4, referring to complexes **I**, **II**, **III**, and **IV**, respectively. These constants can be calculated from the signal integrals of the Tl-containing species and the concentration of $Pt(CN)_4^{2-}$. The latter can be calculated from the following mass balance equation:

$$[Pt]_{tot} = [Pt(CN)_4^{2-}] + [\mathbf{I}] + [\mathbf{II}] + [\mathbf{III}] + [\mathbf{IV}] + [Pt(CN)_6^{2-}] \quad (5)$$

where the concentration of $Pt(CN)_6^{2-}$ can be assumed to be practically equal to that of Tl^+, due to the redox reaction: $Tl^{III} + Pt^{II} \rightleftharpoons Tl^+ + Pt^{IV}$. Equilibrium constants were determined and are: $\log K_{II}^{add} = 4.2$ (±0.3), (based on 10 experimental points); $\log K_{III}^{add} = 3.6$ (±0.3), (3 points); $\log K_{IV}^{add} = 2.3$ (±0.1), (21 points). The small number of points for measuring $\log K_{III}^{add}$ is due to the experimental finding that the complex $Tl(CN)_3$ is a minor species existing in an unbuffered region of the titration curve. $Tl(CN)^{2+}$ was not observed at any of the current experimental conditions; hence, a direct determination of K^{add} was not possible. The values of stability constants obtained for the complexes **II**−**IV** demonstrate high thermodynamic stability of the bimetallic Pt-Tl complexes as compared to the reagents.

The formation of the bimetallic species, **II**, **III**, and **IV** can also be described by a stepwise coordination of CN^- ions to **I**:

$$[PtTl(CN)_{4+(n-1)}]^{(n-2)-} + CN^- \rightleftharpoons [PtTl(CN)_{4+n}]^{(n-1)-} \quad (6)$$

giving equilibrium constants, $K_N = [PtTl(CN)_{4+n}^{(n-1)-}] / \{[PtTl(CN)_{4+(n-1)}^{(n-2)-}] \cdot [CN^-]\}$ for $n = 2$, 3 and 4, referring to the complexes $n =$ **II**, **III**, and **IV**, respectively. These constants, K_N, can be calculated from the signal integrals of the Pt-Tl-containing species, measured for suitable titration points and using $[CN^-]$ calculated from the mass balance equation:

$$[CN]_{tot} = [CN^-] + [HCN] + n\,[Tl(CN)_n^{3-n}] + 4\,[Pt(CN)_4^{2-}] + 5\,[\mathbf{I}] + 6\,[\mathbf{II}] + 7\,[\mathbf{III}] + 8\,[\mathbf{IV}] + 6\,[Pt(CN)_6^{2-}] \quad (7)$$

It should be noted, that the protonation equilibrium must also be considered when calculating values of K_N. Free cyanide concentrations were calculated by means of Eq. 3 from the equilibrium hydrogen ion concentration, $[H^+]$, obtained from the pH-potentiometric titrations (see Supplementary Material). The calculated values are: $\log K_{II} = 10.8$ (±0.2), (24 experimental points) and $\log K_{III} = 6.6$ (±0.4), (5 points). The latter one calculated for 5 points is less reliable; for $\log K_{IV}$ no trustworthy value could be calculated, due to the same reasons as discussed above for $\log K_{III}^{add}$. The trend of the constants follows the normal decrease of the stepwise stability constants, although the decrease is somewhat smaller compared to the corresponding values for the parent complexes, $Tl(CN)_2^+$ ($\log K_2 = 13.2$), $Tl(CN)_3$ ($\log K_3 = 8.5$).[20] The pronounced weakening of the bond between thallium and cyanide ligands in **II** and **III** compared to $Tl(CN)_2^+$ and $Tl(CN)_3$, respectively, can be attributed to the strong influence of the $(NC)_5Pt-$ unit coordinated to the thallium atom in these complexes.

In addition, a trinuclear complex **V** with the formula $[(NC)_5Pt-Tl-Pt(CN)_5]^{3-}$ is formed in solutions where the Pt/Tl ratio is larger than 1. This complex can be considered as an adduct of **II** and $Pt(CN)_4^{2-}$:

$$[PtTl(CN)_6]^- + Pt(CN)_4^{2-} \rightleftharpoons [Pt_2Tl(CN)_{10}]^{3-} \quad (8)$$

with an equilibrium constant,

$$K_V^{add} = [Pt_2Tl(CN)_{10}^{3-}] / \{[Pt(CN)_4^{2-}] \cdot [PtTl(CN)_6^-]\} \quad (8a)$$

K_v ^{add} can easily be calculated from the integral ratios of **II** and **V** (R = [**II**]/[**V**]) measured by ^{205}Tl NMR, and from the equilibrium concentration of $Pt(CN)_4^{2-}$ derived from ^{195}Pt NMR; K_v ^{add} = 1/(R·[$Pt(CN)_4^{2-}$]). It can be noted that no additional data are needed, and the experimental conditions for samples D1−D5 were selected in order to achieve comparable values of integrals for **II** and **V**, and to obtain measurable integrals for [$Pt(CN)_4^{2-}$] in order to minimize the uncertanties related to the integration (see Supplementary Material). Samples, D2−D5 are in fact a serial dilution of D1. The higher the total concentrations the larger the fraction of the trimer. From these data (5 experimental points), K_v ^{add} = 1.44 ±0.03 was calculated (see Scheme).

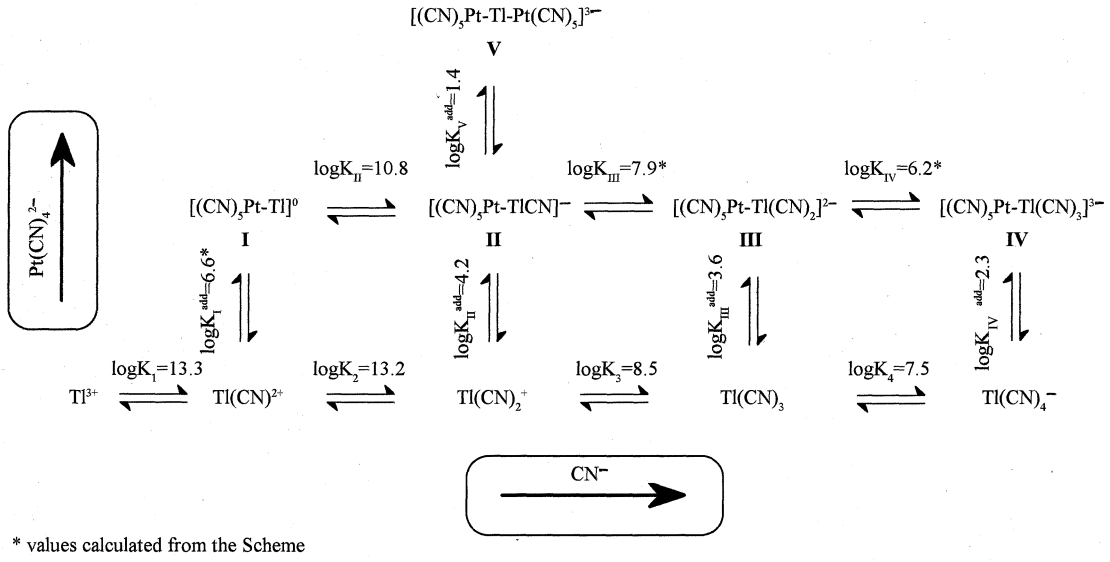

The equilibria describing the chemical system (components: $Pt(CN)_4^{2-}$, Tl^{3+} , CN^-, and H^+) are shown in the Scheme. It shows how the reactions 4, 6, and 8 result in formation of the different Pt-Tl complexes. These equilibria are related to each other and some of them can be calculated independently. From the known stepwise stability constants ($\log K_n$) for the parent complexes, $Tl(CN)_n^{3-n}$,[20] and the values of $\log K_{II}^{add}$, $\log K_{III}^{add}$, $\log K_{IV}^{add}$, and K_V^{add} determined in this work, we obtain

$\log K_{III} = \log K_3 + \log K_{III}^{add} - \log K_{II}^{add} = 7.9$ and
$\log K_{IV} = \log K_4 + \log K_{IV}^{add} - \log K_{III}^{add} = 6.2$.

In the following, when calculating the overall stability constants β_N, this value of $\log K_{III}$ is used instead of the directly determined and less reliable one (vide supra).

In addition the Scheme gives one more constant which is not directly measurable:

$\log K_I^{add} = \log K_2 + \log K_{II}^{add} - \log K_{II} = 6.6$.

These data can easily be converted to overall stability constants, $\log\beta_N = \log K_N^{add} + \log\beta_n$ (N = **I**−**IV**) and $\log\beta_V = \log\beta_{II} + \log K_V^{add}$ (cf. Eq. 1a); the values of $\log\beta$ are given in Table 1.

A typical distribution diagram of the studied chemical system, calculated using the data of Table 1 and ref.[20], is given in Figure 1. The increase of the free cyanide ion concentration with increasing pH causes further coordination of CN^- to the thallium atom of the binuclear Pt-Tl species and thus the equilibrium shifts towards the formation of Pt-Tl complexes with a higher number of cyanide ligands. In the presence of excess $Pt(CN)_4^{2-}$, compound **II** can also be transferred to **V**, but the formation of the trinuclear complex might be supressed by CN^- competition resulting in formation of compound **III**. At higher pH, the mononuclear complexes of platinum [$Pt(CN)_4^{2-}$] and thallium [$Tl(CN)_4^-$] are also present (i.e. equilibrium 4 is shifted to the left). Decrease of the pH shifts reaction 4 to the right, showing that the metal−metal bond formation in aqueous solution is reversible. Certainly, varying the pH shifts also

Table 1. Overall stability constants[a][b] of the Pt-Tl complexes I−V. $\beta_N = [Pt_mTl(CN)_{4m+n}^{3-2m-n}] / \{[Pt(CN)_4^{2-}]^m \cdot [Tl^{3+}]\cdot[CN^-]^n\}$, where m = 1, n = 1, 2, 3, and 4 for **I**, **II**, **III**, and **IV**; and m = 2, n = 2 for **V**, respectively. Temperature 25 °C, ionic medium ca. 1 M $NaClO_4$

Complex	$\log\beta_N$
I	19.9±0.4
II	30.7±0.3
III	38.6±0.3
IV	44.8±0.2
V	32.1±0.3

[a] Uncertainties are averaged deviations from the mean value calculated for the individual titration points; and attributed to uncertainties in the $\log K_N^{add}$ values (cf. Eqs. 4a and 8a), except for the error in **I**, which was estimated as the sum of uncertainties in $\log K_{II}^{add}$ and $\log K_{II}$. − [b] The value of $\log K_H$ = 9.3 (cf. eq 3) was estimated from pH-potentiometric titration (titration C) and was used for the calculation of the constants, K_N. Note that the ionic strength, $I \approx$ 1 M, was varying slightly during the titration and could reach up to 1.3 at high pH values.

Figure 1. Typical distribution of thallium-containing species in aqueous solution as a function of pH, as calculated from the determined stability constants (Table 1)[a]

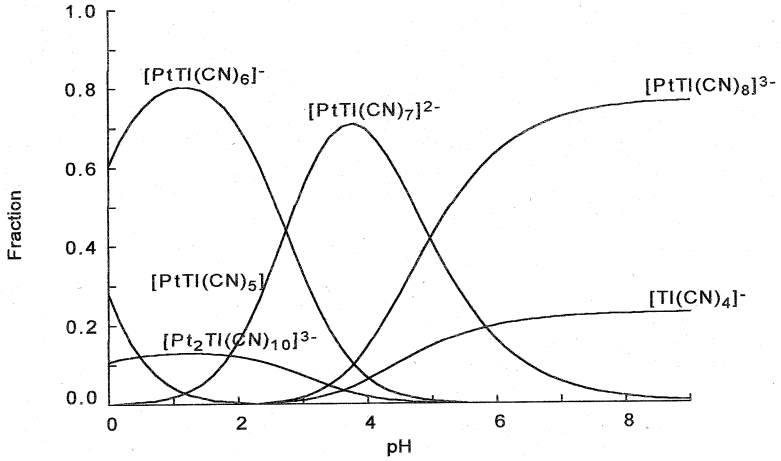

[a] $[Pt]_{tot}$ = 40 mM, $[Tl]_{tot}$ = 30 mM, $[CN]_{tot}$ = 280 mM.

the equilibrium of reaction 6, similarly as for the parent $Tl(CN)_n^{3-n}$ species.

These thermodynamic data (K_N^{add}) could be used as a quantitative measure of the stability or strength of the Pt−Tl bond only if the simple formation of an adduct between platinum and thallium cyanides took place by means of the reaction:

$$Pt(CN)_4^{2-} + Tl(CN)_n^{3-n} \rightleftharpoons (NC)_4Pt-Tl(CN)_n^{(n-1)-} \quad (9)$$

and if the entropy term is negligible. However, the structural data discussed in our recent paper[2] show that in all the bimetallic complexes five cyanides are coordinated directly to the Pt-center, and this $(NC)_5Pt-$ unit is, in turn, coordinated to the Tl atom. The species $[Pt^{II}CN)_5]^{3-}$ has not been reported previously and it is likely that it does not exist; accordingly, no formation constant has been measured.[24] When the free $[CN^-]$ is decreased, the equilibrium is shifted towards species with lower cyanide content, down to complex **I** with no cyanide ligands coordinated to the thallium atom, whereas the $(NC)_5Pt-$ unit remains unchanged. Thus, the stability constant for the coordination of the "fifth" cyanide to the Pt atom must be larger compared to all cyanides bound to thallium in the binuclear compounds.

It seems unreasonable that an extra cyanide ligand would be coordinated to the $Pt^{II}(CN)_4^{2-}$ complex without oxidation of platinum; hence, the formation of the $(NC)_5Pt-$ unit must be preceded or accompanied by an electron transfer from Pt to Tl leading to the formation of a Pt−Tl bond. Therefore, reaction 4 should involve at least two steps: (i) formation of metal−metal bond according to reaction 9 and (ii) formation of $(NC)_5Pt-$ unit by a cyanide transfer reaction. Whether these reactions are simultaneous or not should be subject of further study.

It can be noted that most information on complexes with metal−metal bonds in the literature has been obtained for the solid state; the reported solution studies were aimed mainly at structural characterisation of the species. In this context, the qualitatively studied $[Rh(CO)_2Cl]_2-[Co(CO)_4]^-$ system in toluene can be mentioned;[11] it exhibits some features similar to the bimetallic Pt-Tl cyanide compounds. Heteropolynuclear complexes formed in the Rh-Co solutions are in equilibrium which is governed by the Rh/Co ratio. The presumed bimetallic compound $(R_4N)[Rh(CO)_2ClCo(CO)_4]$ decomposes by addition of either Cl^- or OH^- ions to give mononuclear species. In another carbonyl mixed metal cluster, $[Re_7C(CO)_{21}Tl]^{2-}$, dissociation of μ_3-Tl^I was followed by infrared spectroscopy in acetone and a dissociation constant $K = 2.1 \cdot 10^{-3}$ M was calculated.[13] Also for the related cyano metal clusters equilibrium data are very scarce. A study of a stepwise coordination of cyanide to Mo−Mo and W−W bonded clusters has been published, but a formation of the metal−metal bond is not involved in the qualitative description of the equilibria.[12][25] In another study, an estimated stability constant (10^6) has been reported for the CN-bridged iron-platinum species.[26]

In the case of metal−carbon bonds there are a few papers containing equilibrium data. In our earlier work[14][15] we characterized the formation of monoketonato-thallium(III) ion in aqueous solution. In this equilibrium ketonato and the chloride ligands are in competition for Tl^{III}.

Conclusions

Reaction between $Pt(CN)_4^{2-}$ and $Tl(CN)_n^{3-n}$ (n = 1−4) complexes in aqueous solution results in the formation of a family of heteropolynuclear cyano complexes. Depending on the molar ratio Pt/Tl, cyanide concentration and pH, four binuclear complexes **I−IV** with the general composition $[(CN)_5Pt-Tl(CN)_{n-1}]^{(n-1)-}$ (n = 1− 4) and a trinuclear species **V** with the formula $[(NC)_5Pt-Tl-Pt(CN)_5]^{3-}$ can be obtained.

If kept in dark, the complexes are in chemical equilibrium. The distribution between the bimetallic compounds can be altered by varying the cyanide concentration (e.g. by changing the pH), and/or by changing the Pt/Tl ratio. An

excess of cyanide shifts equilibria 4 and 8 from the Pt-Tl complexes to mononuclear platinum and thallium cyano species. The high values of stability constants calculated for the bimetallic complexes **I−V** imply thermodynamically favourable formation of both the metal−metal bond and the $(CN)_5Pt-$ unit; the latter can be considered to be a ligand coordinated to thallium. Comparison of the stepwise stability constants for $[(CN)_5Pt-Tl(CN)_{n-1}]^{(n-1)-}$ complexes with those for the corresponding parent $Tl(CN)_n^{3-n}$ compounds (cf. Scheme) demonstrates the strong influence of the platinum cyano unit resulting in a substantial weakening of the Tl−C bonds.

It is very unusual that equilibria are reported for metal−metal bonded compounds and, according to our knowledge, the present work constitutes the first detailed equilibrium study of such a system. These results suggest that many of the reactions resulting in cluster formation are real equilibria (although many can be dominantly shifted to one direction) and that they can be studied using the tools of equilibrium coordination chemistry. Further work is certainly required to confirm if this observation applies to other cluster formation reactions which have been reported in the literature.

Supplementary Material

Data of the equilibrium study (tables of titration data from 6 independent potentiometric and NMR titrations and a serial dilution) can be obtained from the authors.

The continuous financial support of the *Swedish Natural Science Research Council (NFR)* is gratefully acknowledged. The authors thank *Carl Trygger Foundation for Scientific Research*, the *Hungarian National Scientific Research Foundation* (OTKA T017152 and T026115) and the *European Commission INTAS Programme* for financial support. M. M. acknowledges the *Swedish Institute* for postdoctoral fellowship.

Experimental Section

Materials: A concentrated (1.45 M) aqueous solution of $Tl(ClO_4)_3$ in 3.77 M $HClO_4$ was obtained by anodic oxidation of $TlClO_4$.[16] Solutions of thallium(III) cyanide complexes were synthesised by addition of a calculated volume of a sodium cyanide solution (and NaOH when needed) to the stock solution of thallium(III) perchlorate. Potassium tetracyanoplatinate(II) trihydrate (Aldrich, reagent grade) was used without further purification. The solution of sodium tetracyanoplatinate(II) was prepared by precipitation of potassium perchlorate from the aqueous solution of $K_2Pt(CN)_4$ with an excess of aqueous sodium perchlorate at 275 K and was used as a stock platinum solution.

Equilibrium Studies: All the solutions were kept dark to avoid photochemical decomposition. Samples were prepared by mixing the solutions of $Na_2Pt(CN)_4$ and $Tl(CN)_2^+$ both containing 1 M $NaClO_4$ as ionic medium, and the solutions were kept at room temperature overnight prior to titrations. The complex, $Tl(CN)_2^+$, was prepared from thallium(III) perchlorate (1.45 mol/l Tl^{3+} and 3.77 mol/l H^+) and sodium cyanide solutions (molar ratio CN/Tl = 3) which resulted in exclusive formation of $Tl(CN)_2^+$ species (at the actual pH value). 2.00-ml samples containing $[Tl]_{tot}$ = 54.0 mM, $[Pt]_{tot}$ = 49.8 mM, $[CN]_{tot}$ = 334 mM, were titrated with an aqueous solution of: (titration A) 3.32 M $HClO_4$ (starting pH 4.7) or (titration B) 3.5 M NaCN (starting pH 3.6). In a different experiment, 2.26 ml sample with $[Tl]_{tot}$ = 44.3 mM, $[Pt]_{tot}$ = 57.5 mM, $[CN]_{tot}$ = 341 mM, $[HClO_4]$ = 382 mM was titrated with 3.5 M NaCN (titration C) (see Supplementary Material).

The titrations were performed by using a syringe to add aliquotes of the titrant (5−100 μl) into the NMR tube through a rubber seal, and subsequently recording ^{205}Tl-NMR spectra to measure the signal integrals of the Tl^{III}-containing species and Tl^+. Tl^+ was present as a contaminant in the thallium(III) stock solution and as a product of the slow, but not negligible redox reaction due to the some unavoidable exposure to light. Nevertheless, the Tl^+ content never exceeded 15% of the total thallium concentration.[1][17]

In order to study the formation of the trinuclear complex samples (titration D) were prepared where the Pt/Tl ratio was 2. D1−D5: pH = 1.7±0.2, $[Tl]_{tot}$ = 40.0 mM, 30.0 mM, 20 mM, 15 mM, and 10 mM; $[Pt]_{tot}$ = 2 $[Tl]_{tot}$, $[CN]_{tot}$ = 11 $[Tl]_{tot}$, respectively. ^{205}Tl-NMR spectra were recorded as for the titrations mentioned above, and the $[Pt(CN)_4^{2-}]$ was also measured by integration of the ^{205}Pt-NMR signal. Since the individual species were in the slow exchange regime on the actual ^{205}Tl- and ^{205}Pt-NMR time scales, the signal integrals could be measured and the mole ratios calculated.

In order to measure $[H^+]$, the samples identical to A, B, and C were used to measure the pH by potentiometric titrations. pH values were measured by a combination electrode connected to a pH-meter (Radiometer PHM93). The readings of the electrode were calibrated to pH values using the method of Irving for pH > 1,[18] and by direct determination for pH < 1. These data resulted in *stoichiometric stability constants.*

NMR Measurements: NMR spectra were recorded with Bruker AM400 and Bruker DMX500 spectrometers at a probe temperature of 298 (±0.5) K. The following, typical NMR parameters were used:

^{205}Tl NMR: (AM400) spectrometer frequency (SF) = 230.8 MHz; spectral window (SW) = 50 kHz; pulse width (PW) = 7 μs (flip angle ca. 30°); pulse repetition time 2.16 s; digital resolution 12 Hz/point; and number of scans = 200−1000; (DMX500) SF = 288.49 MHz; SW = 7.2 kHz; pulse width (p1) = 9.6 μs (flip angle 90^0); pulse repetition time 5.33 s; digital resolution 18 Hz/point; number of scans 500. The chemical shifts are referred in ppm toward higher frequency from the ^{205}Tl-NMR signal of an aqueous solution of $TlClO_4$, extrapolated to infinite dilution. The transmitter frequency (O1) was positioned at the resonance of the ^{205}Tl nuclei uncoupled to ^{195}Pt and the intensity of this signal was measured directly from the spectra. In the equilibrium study, the sum of the integrals (in the absolute intensity mode) measured at different points of the NMR titration was not constant because the 90° pulse varied with the acidity of the sample resulting in a non-equal excitation of the signals. This was, however, not a problem since the total concentration of thallium in the titrated solution was known throughout the titration. Aqueous solutions of 25 and 50 mM $TlClO_4$ in 1 M $NaClO_4$ were used to calibrate the signal integrals. The accuracy of the integrals was estimated to 3−5%.

^{195}Pt NMR: (AM400) SF = 85.6 MHz; SW = 50 kHz; PW = 6 μs (flip angle ca. 30°); pulse repetition time 2.16 s; digital resolution 8 Hz/point; number of scans = 1000−10000; (DMX500) SF = 107.03 MHz; SW = 16 kHz ; P(90^0) = 13.0 μs (flip angle 90^0); pulse repetition time 1.3 s; digital resolution 17 Hz/point; number of scans 1500. The chemical shifts were measured relative to an external standard of aqueous 0.1 M Na_2PtCl_6 which is 4533 ppm

to higher frequency from $\Xi(^{195}Pt) = 21.4$ MHz at 25 ^{0}C.[19] A 15.0 mM aqueous solution of $K_2Pt(CN)_4$ was used for calibration of intensities of signals when measuring quantitative integrals. The accuracy of the integrals was estimated to 3−5%.

[1] K. E. Berg, J. Glaser, M. C. Read, I. Tóth, *J. Am. Chem. Soc.* **1995**, *117*, 7550−7551.
[2] M. Maliarik, K. E. Berg, J. Glaser, M. Sandström, I. Tóth, *Inorg. Chem*. Accepted for publication.
[3] J. K. Nagle, A. L. Balch, *J. Am. Chem. Soc.* **1988**, *110*, 319−321.
[4] A. L. Balch, P. Steven, *J. Am. Chem. Soc.* **1990**, *112*, 6139−6140.
[5] O. L. Renn, B. Lippert, *Inorg. Chim. Acta* **1993**, *208*, 219−223.
[6] R. Uson, J. Fornies, M. Tomas, R. Garde, P. Alonso, *J. Am. Chem. Soc.* **1995**, *117*, 1837−38.
[7] O. J. Ezomo, M. P. Mingos, I. D. Williams, *J. Chem. Soc., Chem. Commun.* **1987**, 924−925.
[8] L. Hao, J. J. Vittal, R. Puddephatt, *Inorg. Chem.* **1996**, *35*, 269−270.
[9] L. Hao, J. Xiao, J. J. Vittal, R. J. Puddephatt, L. Manojlovic-Muir, K. W. Muir, A. A. Torabi, *Inorg. Chem.* **1996**, *35*, 658−666.
[10] M. Maliarik, et al., to be published.
[11] F. Joó, H. Alper, *Canadian Journal of Chemistry* **1985**, *83*, 1157.
[12] T. A. Budzichowski, M. H. Chrisholm, *Polyhedron* **1994**, *13*, 2035−2042.
[13] U. Brand, R. Sharply, *Inorg. Chem.* **1997**, *36*, 253−255.
[14] B. Györi, A. Sánchez, J. Glaser, *J. Organomet. Chem.* **1989**, *361*, 1.
[15] J. Glaser, I. Tóth, *J. Chem. Soc. Chem. Commun.* **1986**, 1336.
[16] G. Biedermann, *Arkiv för Kemi* **1953**, *5*, 441.
[17] K. E. Berg, Licentiate Thesis, KTH (The Royal Institute of Technology), Stockholm, Sweden, **1995.**
[18] H. M. Irving, *Anal. Chim. Acta* **1967**, *38*, 475.
[19] P. S. Pregosin, *Transition Metal Nuclear Magnetic Resonance*, Elsevier, Amsterdam, **1991**, Vol. 13, p. 351.
[20] J. Blixt, B. Györi, J. Glaser, *J. Am. Chem. Soc.* **1989**, *111*, 7784.
[21] I. Bányai, J. Blixt, J. Glaser, I. Tóth, *Acta Chem. Scand.* **1992**, *46,* 138.
[22] L. G. Sillén, A. E. Martell, *Stability Constants of Metal-Ion Complexes, Special Publication Nos. 17 and 25,* Chemical Society, London, **1964** and **1971**.
[23] J. J. Pesek, W. R. Mason, *Inorg. Chem.* **1983**, *22*, 2958−2959.
[24] We mentioned the formation of platinum(IV) pentacyano complex in two recent communications,[1][17] as aproduct of the redox reaction between Pt^{II} and Tl^{III}.
[25] S. L. Bartley, S. N. Bernstein, K. R. Dunbar, *Inorg. Chim. Acta* **1993**, *213*, 213−231.
[26] M. Zhou, B. W. Pfennig, J. Steiger, D. Van Engen, A. B. Bocarsly, *Inorg. Chem.* **1990**, *29*, 2456−2460.

[97283]

Chemistry of 2*H*-Azaphosphirene Complexes, 9[◇]

Syntheses of 3-Phenyl-2*H*-Azaphosphirene Chromium and Molybdenum Complexes − First Evidence for Reaction Intermediates☆

Rainer Streubel*, Frank Ruthe, and Peter G. Jones

Institut für Anorganische und Analytische Chemie der Technischen Universität Braunschweig
Postfach 3329, D-38023, Braunschweig, Germany
Fax: (internat.) +49 (0)531/391-5387
E-mail: r.streubel@ tu-bs.de

Received November 3, 1997

Keywords: Phosphorus heterocycles / 2*H*-Azaphosphirene complexes / Carbene complexes / Chromium / Molybdenum

The synthesis of 3-phenyl-substituted 2*H*-azaphosphirene pentacarbonylchromium and pentacarbonylmolybdenum complexes is reported. New information on the rearrangement cascade, which finally leads to 2*H*-azaphosphirene ring formation, has been obtained through isolation of a reactive intermediate. A comparison of the ^{13}C-, ^{15}N-, ^{31}P-NMR, and UV/vis spectroscopic data and single crystal X-ray structural data of 3-phenyl-substituted 2*H*-azaphosphirene chromium, molybdenum, and tungsten complexes is presented.

Over the last three years we have focussed our attention on the synthesis and chemistry of 2*H*-azaphosphirene tungsten complexes (**II**) (Scheme 1).[2] These complexes show a fascinating reactivity upon ring opening to give, depending on the reaction conditions, nitrilium phosphane ylide tungsten complexes (**III**)[1][3] and/or an electrophilic terminal phosphanediyl tungsten complex.[4] Meanwhile, both reactive intermediates have found several applications in the synthesis of heterocycles.[5]

Scheme 1. 2-Aza-1-phospha-4-metallabutadienes **I**, 2*H*-azaphosphirene metal complexes **II** and their acyclic isomers, the nitrilium phosphane ylide metal complexes **III**; **I**, **II**, **III**: R, R′ = alkyl, aryl; [M] = metal complex fragment

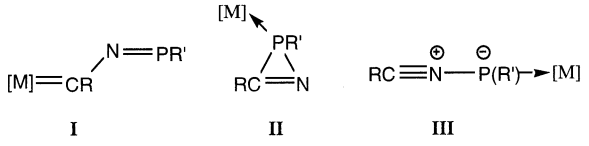

I **II** **III**

Our first synthetic route to 2*H*-azaphosphirene tungsten complexes used a rearrangement cascade in which transiently formed metallaheterobutadienes **I**, which are isomeric to **II** and **III**, were assumed to be key intermediates.[2a] The elucidation of the reaction course was an intriguing problem for us and, therefore, we decided to investigate the reaction of the aminobenzylidene chromium **1a**[6] and molybdenum complex **1b**[7] with [bis(trimethylsilyl)methylene]chlorophosphane (**2**).[8]

When we first carried out the reaction of complex **1a** with methylenechlorophosphane **2** in ether at ambient temperature and in the presence of triethylamine, we obtained a complicated product mixture. According to ^{31}P-NMR spectroscopic measurements the mixture contained approximately ten products, most of them appearing as singuletts in the spectra. Although these products could not be separated by column chromatography, the chromium complex **5** and the 2*H*-azaphosphirene chromium complex **6a**, the latter formed only in small amounts, were easily identified by their typical ^{31}P-nuclear magnetic resonances [**5**: δ = 95.4 (s) and **6a**: δ = −54.3 (s)]. Three other products showed chemical shift values at low field [δ = 518.6 (s)/425.4 (s), and δ = 476.3 (d)/445.1 (d), the latter with a $^{31}P,^{31}P$ coupling constant of 515 Hz]. Because of these typical chemical shift and coupling constant values, their identification was achieved by comparison with the data of compounds known in literature as bis[bis(trimethylsilyl)methyl]diphosphene [δ = 517 (s)][9] and the corresponding mono- and dinuclear diphosphene pentacarbonylchromium complexes, [{$(Me_3Si)_2HCP{=}PCH(SiMe_3)_2$}$Cr(CO)_5$]: δ = 475.8 and 444.3, $^1J(P,P)$ = 516 Hz and [{$(Me_3Si)_2HCP{=}PCH(SiMe_3)_2$}$[Cr(CO)_5]_2$]: δ = 425.9 (s).[10]

In contrast, the molybdenum complex **1b** gave the 2*H*-azaphosphirene molybdenum complex **6b** straight away, but only in low yields (28%). This reaction behavior underlines the close relationship between aminobenzylidene molybdenum and tungsten complexes. Significantly better yields of **6a** (30%) and **6b** (67%) were obtained if the reactions of **1a** and **1b** with **2** were carried out at low temperature (**1a**: −40°C; **1b**: −10°C). Apart from triethylammonium chloride, the 2*H*-azaphosphirene metal complexes **6a**, **b** and the phosphanediyl-bridged dinuclear chromium carbene complex **5a** were obtained in good yields after low-temperature column chromatography. The nature of complex **5a** as a long-lived intermediate was determined by reacting a pure sample of it with triethylamine under similar reaction conditions. Therefore we assume that the overall reaction pro-

[◇] Part 8: Ref.[1].

 © WILEY-VCH Verlag GmbH, D-69451 Weinheim, 1998 1434−1948/98/0505−0571 $ 17.50+.50/0

Scheme 2. Synthesis of 2*H*-azaphosphirene metal complexes **6a**, **b**

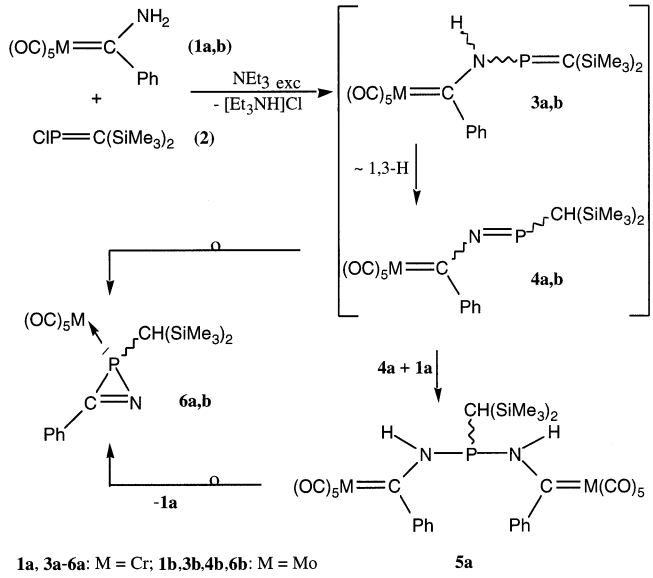

ceeds through the rearrangement cascade depicted in Scheme 2.

An additional experiment was carried out to shed more light on the formation of complex **5a**, which can a priori proceed through 1,2-addition reactions of aminobenzylidene chromium complex **1a** to the P−C and/or P−N double bond of the reactive intermediates **3a** and/or **4a**. In order to distinguish between these two pathways, we mimicked the hypothetical reaction of the first intermediate, **3a**, with the aminobenzylidene chromium complex **1a** by reacting **1a** with [bis(trimethylsilyl)methylene](*tert*-butylamino)phosphane **7**[11] under similar reaction conditions. After approximately one day at ambient temperature, only 18% of **7** was consumed, leading predominantly to one product, **8**, with a chemical shift at δ = 96.8 (Scheme 3). Unfortunately, we could not isolate this product because of subsequent chemical transformations and the lack of stability of **8** precluding chromatography. By comparison of the phosphorus chemical shift of **8** (δ = 96.8) with that of complex **5** (δ = 95.4), and because of the reaction selectivity, we tentatively assign the structure of complex **8** to this product. Nevertheless, the finding that complex **1a** reacted very slowly with compound **7** to give complex **8**, supports the interpretation that complex **5** resulted from a trapping of the 2-aza-1-phospha-4-chromabutadiene **4a**.

Interestingly, the NMR parameters of the carbon and nitrogen atoms of the three-membered ring of the 2*H*-azaphosphirene metal complexes **6a**, **b** and **9**[2b] vary very little with respect to metal exchange (Table 1). This is not the case with the phosphorus resonances, which differ significantly on going from chromium to the tungsten complex; this is a common feature of coordinated tervalent phosphorus compounds.[12] In order to obtain information about the electronic situation of the complexes **6a**, **b**, and **9**, UV/visible spectra were measured and λ_{max} values determined (Table 2). λ_{max} values of 200 and 240 nm should be

Scheme 3

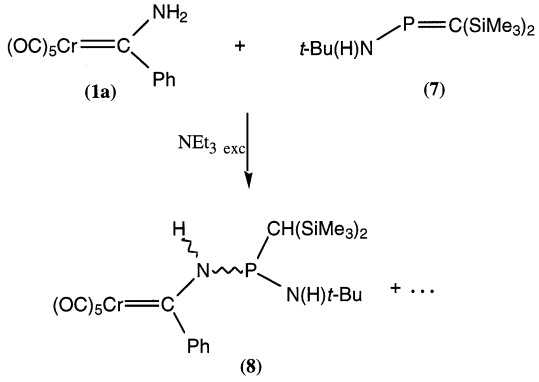

attributable to π-π* electron transitions related to the phenyl groups. Bands appearing as shoulders with λ_{max} values of 330 (**6b**) and 350 nm (**9**), with significantly lower lg ε values, are tentatively assigned to π-π*-electron transitions of the C−N double bonds. It should be noted that some metal carbonyl complexes also show charge-transfer transitions in the range of 300−350 nm.[13] A comparison of the values obtained for **6a**, **b**, and **9** with those of a mixture of related 3-phenyl-1*H*-thiazirene and benzonitrile sulfide (bands with λ_{max} values of 335, 324, 295, and 240 nm) is interesting.[14] This interpretation of these UV/visible spectra remains somewhat unsatisfactory because the bands of benzonitrile sulfide had been assigned unambigously, but those of 3-phenyl-1*H*-thiazirene had not.[14] EI-mass spectrometry experiments have shown that all of these 2*H*-azaphosphirene metal complexes predominantly undergo ring cleavage subsequent to the ionisation process.

Figure 1. Molecular structure of **6a** in the crystal (ellipsoids represent 50% probability levels, hydrogen atoms are omitted for clarity)

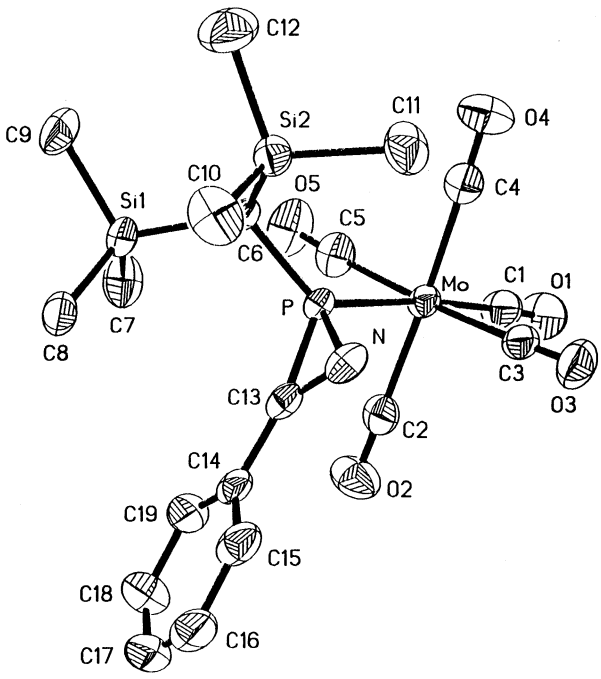

Table 1. Selected ^{13}C[a], ^{15}N[b], ^{31}P[a] NMR data (δ/[ppm], *J*/[Hz]) of 3-phenyl-2*H*-azaphosphirene metal complexes **6a**, **b**, and **9** (exclusively ring atoms of the 2*H*-azaphosphirene ring system)

complex	metal	$\delta^{13}C$	$\delta^{15}N$	$\delta^{31}P$	$^{(1+2)}J$(PC)	$^{(1+2)}J$(PN)
6a	Cr	193.3	−55.3	−54.3	1.7	38.3
6b	Mo	192.1	−56.3	−84.5	3.4	36.7
9	W	192.4	−53.2	−111.0	1.7	36.9

[a] C_6D_6, room temp. − [b] CD_2Cl_2, room temp.

Table 2. UV/vis spectroscopic data (hexane, r.t.; λ_{max}/[nm]) of 3-phenyl-2*H*-azaphosphirene metal complexes **6a**, **b**, and **9**

complex	metal	λ_{max} (lg ε)	λ_{max} (lg ε)	λ_{max} (lg ε)	λ_{max} (lg ε)
6a	Cr	−	208 (4.637)	240 (4.599)	−
6b	Mo	198 (4.625)	206 (4.610)	240 (4.697)	330 (3.394)
9	W	198 (4.655)	216 (4.657)	254 (4.590)	350 (3.544)

The molecular structures of the complexes **6a**, **b** were determined by X-ray crystallography (Figure 1 and Table 3).[15] The dimensions of the isostructural complexes **6a**, **b** (therefore, only **6a** is depicted in Figure 1) and the corresponding tungsten complex **9**[2b] differ mainly in their metal-phosphorus bond distances [**6a**: 2.3125(6), **6b**: 2.4772(12), and **9**: 2.470(2) Å] and, as a consequence of this, in the distance between the metal atom and the geometrical center of the C−N double bond (**6a**: 3.542, **6b**: 3.670, and **9**: 3.659 Å). These and previously reported findings[2b] seem to underline that the bonding situation of the heterocyclic ligand of 2*H*-azaphosphirene pentacarbonylmetal complexes should be described as a resonance hybrid of a three-membered ring system with a covalent bonding (**II**) and a π-electron donor-acceptor complex of benzonitrile and the phosphorus atom of the terminal phosphanediyl complex unit (**IV**) (Scheme 4).

Table 3. Selected bond lengths [pm] and angles [°] of complexes **6a**, **b**, and **9**

complex	P−C13	P−N	N−C13	C13−C14	M−P
6a	1.755(2)	1.811(2)	1.274(3)	1.458(3)	2.3125(6)
6b	1.762(4)	1.802(3)	1.273(5)	1.457(5)	2.4772(12)
9	1.759(5)	1.795(4)	1.272(7)	1.457(7)	2.470(2)
	C13−P−N	C13−N−P	N−C13−P	N−C13−C14	C6−P−M
6a	41.82(8)	66.75(11)	71.43(11)	133.3(2)	124.13(6)
6b	41.8(2)	67.4(2)	70.8(2)	134.4(3)	124.57(12)
9	41.9(2)	67.5(3)	70.6(3)	134.2(5)	124.3(2)

Scheme 4

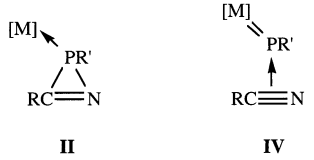

II **IV**

Support of the *Deutsche Forschungsgemeinschaft* and the *Fonds der Chemischen Industrie* and ^{15}N-NMR measurements of Priv.-Doz. Dr. *Dietrich Gudat* (Universität Bonn) are gratefully acknowledged.

Experimental Section

General: All operations were carried out under an inert atmosphere of deoxygenated dry nitrogen. Solvents were dried according to standard procedures. − NMR spectra were recorded on a Bruker AC-200 spectrometer (200 MHz for ^1H; 50.3 MHz for ^{13}C; 81 MHz for ^{31}P) using [D_6]chloroform and [D_6]benzene as solvents, the latter as internal standard, or a Bruker AMX-300 (30.4 MHz for ^{15}N) using dichloromethane as solvent and nitromethane as external standard; shifts are given relative to tetramethylsilane (^1H, ^{13}C), to nitromethane (^{15}N) and 85% H_3PO_4 (^{31}P). − MS: Finigan Mat 8430 (70 eV). − Elemental analyses: Carlo Erba analytical gas chromatograph. − IR: Biorad FT-IR-165; UV/vis: Hewlett Packard 8452A.

Procedure for the Preparation of 2H-Azaphosphirene Pentacarbonylmetal(0) Complexes: 0.34 g (1.5 mmol) of **2** and 5 ml of NEt_3 were added at −40°C or −10°C, respectively, to a solution of 1.5 mmol of aminobenzylidene chromium or molybdenum complex **1a**, **b** in 15 ml of diethyl ether. The reaction mixtures were stirred for approximately 40 and 48 hours, respectively, and allowed to warm up slowly to ambient temperature. The yellow/orange reaction mixtures were evaporated to dryness under reduced pressure (0.1 mbar). The residues were extracted with 30 ml of pentane and filtered. The filtration residues were washed twice with 5 ml of pentane, the organic phases combined and the solvent removed under reduced pressure. The residues were purified by column chromatography.

{[2-Bis(trimethylsilyl)methyl-3-phenyl-2H-azaphosphirene-κP]-pentacarbonylchromium(0)} (**6a**): separation by low-temperature chromatography (SiO_2, −40°C; hexane/ether, 9:1) afforded 0.22 g of **6a** (30%) as a yellow powder after removal of the solvent from the first yellow phase. M.p. 104°C (decomp.). − IR (KBr) $\tilde{\nu}$ = 2065 (s) cm^{-1}, 1988 (m), 1968 (vs), 1942 (vs), 1942 (vs) (CO), 1625 (s), 1618 (vw) (CN). − ^1H NMR (C_6D_6): δ = −0.01 (s, 9 H, $SiMe_3$), 0.27 (s, 9 H, $SiMe_3$), 0.57 [d, ^2J(P,H) = 3.97 Hz, 1 H, PC*H*], 7.01 (m_c, 3 H, *m,p*-Ph−*H*), 7.91 (m_c, 2 H, *o*-Ph−*H*). − $^{13}C\{^1H\}$ NMR (C_6D_6): δ = 1.2 [d, ^3J(P,C) = 3.1 Hz, $SiMe_3$], 2.1 [d, ^3J(P,C) = 2.9 Hz, $SiMe_3$], 28.3 [d, ^1J(P,C) = 29.8 Hz, P*C*H], 127.1 [d, ^2J(P,C) = 14.8 Hz, Ph−*C*1], 129.6 (s, Ph−*C*3/3′), 129.7 (s, Ph−*C*2/2′), 134.0 (s, Ph−C4), 193.3 [d, $^{(1+2)}J$(P,C) = 1.7 Hz, P*C*N], 215.9 [d, ^2J(P,C) = 16.8 Hz, *cis*-*C*O], 219.8 [d, ^2J(P,C) = 4.7 Hz, *trans*-*C*O]. − ^{15}N NMR (CH_2Cl_2): δ = −55.3 [d, $^{(1+2)}J$(P,N) = 38.3 Hz]. − $^{31}P\{^1H\}$ NMR (C_6D_6): δ = −54.3 (s). − UV/vis (hexane, c = $2.06 \cdot 10^{-5}$ M): λ_{max} (lg ε) = 208 (4.637), 240 (4.599). − MS (70 eV), [pos.-CI (NH_3)], (^{52}Cr); *m/z* (%): 486 (100) [(M + H)$^+$], 338 (40) [(M + H) − PhCN)$^+$]. − $C_{19}H_{24}CrNO_5PSi_2$ (485.5) calcd. C 47.00, H 4.98, N 2.88; found C 46.95, H 5.04, N 2.81.

N,N′-Bis{amino[(phenyl)carbene]pentacarbonylchromium(0)}bis(trimethylsilyl)methylphosphane (**5a**): Separation by low-temperature chromatography (SiO_2, −40°C; hexane/ether, 9:1) afforded 0.22 g of **5a** (20%) as a yellow orange powder after removal of the solvent from the second yellow phase. M.p. 106°C (decomp.). − IR (KBr) $\tilde{\nu}$ = 2061 (m) cm^{-1}, 1929 (vs, br), 1906 (vs, br) (CO). − ^1H NMR ($CDCl_3$): δ = 0.30 [d, ^4J(P,H) = 0.8 Hz, 18 H, $SiMe_3$], 0.39 [d, ^2J(P,H) = 1.8 Hz, 1 H, PC*H*], 6.52 (m_c, 8 H, *m*-Ph−*H*), 7.26 (m_c, 12 H, *o*-,*p*-Ph−*H*), 9.95 (br, 2 H, N*H*). − $^{13}C\{^1H\}$ NMR ($CDCl_3$): δ = 2.2 [d, ^3J(P,C) = 4.6 Hz, $SiMe_3$], 21.8 [d, ^1J(P,C) = 49.0 Hz, P*C*H], 119.5 [d, ^3J(P,C) = 5.7 Hz, Ph−*C*2/2′], 127.6 (s,

Ph−*C*4), 128.4 (s, Ph−*C*3/3′), 151.9 [d, ^3J(P,C) = 11.8 Hz, Ph−*C*1], 216.3 (s, *cis*-*C*O), 223.4 (s, *trans*-*C*O), 311.3 [d, ^2J(P,C) = 3.2 Hz, Cr=*C*R$_2$]. − ^{15}N NMR (CH_2Cl_2): δ = −161.1 [dd, ^1J(P,N) = 84, ^1J(N,H) = 84 Hz]. − ^{31}P{^{1}H} NMR ($CDCl_3$): δ = 95.4 (s). − ^{31}P{^{1}H} NMR (Et_2O/C_6D_6): δ = 92.8 (s). − MS (70 eV), [pos.-CI (NH_3)], (^{52}Cr); *m*/*z* (%): 727 (100) [(M + H)$^+$], 653 (6) [(M + H)$^+$ − Me_3SiH], 535 (14) {[M − $(Me_3Si)_2HCPH_2$)]$^+$}. − $C_{31}H_{31}Cr_2N_2O_{10}P$ (726.6): calcd. C 47.57, H 3.99, N 3.58; found C 47.00, H 3.79, N 3.46.

{[2-Bis(trimethylsilyl)methyl-3-phenyl-2H-azaphosphirene-κP]-pentacarbonylmolybdenum(0)} (**6a**): Separation by low-temperature chromatography (SiO_2, −15°C; hexane/ether, 9:1) afforded 0.53 g of **6a** (67%) as yellow powder after removal of the solvent from the first yellow phase. M.p. 105°C (decomp.). − IR (KBr) $\tilde{\nu}$ = 2074 (s) cm^{-1}, 1994 (s), 1973 (vs), 1945 (vs), 1928 (vs) (CO), 1619 (w) (CN). − ^{1}H NMR (C_6D_6): δ = 0.1 (s, 9 H, $SiMe_3$), 0.29 (s, 9 H, $SiMe_3$), 0.48 [d, ^2J(P,H) = 4.74 Hz, 1 H, PC*H*], 7.63 (m_c, 3 H, *m*-, *p*-Ph−*H*), 8.02 (m_c, 2 H, *o*-Ph−*H*). − ^{13}C{^{1}H} NMR (C_6D_6): δ = 1.4 [d, ^3J(P,C) = 3.7 Hz, $SiMe_3$], 2.2 [d, ^3J(P,C) = 3.1 Hz, $SiMe_3$], 27.9 [d, ^1J(P,C) = 30.6 Hz, P*C*H], 126.8 [d, ^2J(P,C) = 15.0 Hz, Ph−*C*1], 129.6 (s, Ph−*C*3/3′), 129.7 (s, Ph−*C*2/2′), 134.0 (s, Ph−*C*4), 192.1 [d, $^{(1+2)}J$(P,C) = 3.4 Hz, P*C*N], 204.5 [d, ^2J(P,C) = 11.5 Hz, *cis*-*C*O], 208.6 [d, ^2J(P,C) = 38.1 Hz, *trans*-*C*O]. − ^{15}N NMR (CH_2Cl_2): δ = −56.3 [d, $^{(1+2)}J$(P,N) = 36.7 Hz]. − ^{31}P{^{1}H} NMR (C_6D_6): δ = −84.5 [s, ^1J(Mo,P) = 166 Hz]. − UV/vis (hexane, *c* = 2.059·10^{-5} M): λ_{max} (lg ε) = 198 (4.625), 206 (4.610), 240 (4.697), 330 (3.394). − MS (70 eV), (^{98}Mo); *m*/*z* (%): 531 (2) [M$^+$], 400 (100) [(M − PhCN − CO)$^+$], 103 (82) [PhCN$^+$], 73 (78) [Me_3Si^+]. − $C_{19}H_{24}MoNO_5PSi_2$ (529.5): calcd. C 43.09, H 4.58, N 2.65; found C 43.36, H 4.77, N 2.72.

Reaction of [(Aminobenzylidene)pentacarbonylchromium(0)] (**1a**) *with [Bis(trimethylsilyl)methylene](tert-butylamino)phosphane* (**7**) *and Triethylamine*: To 150 mg (0.5 mmol) of **1a** in 6 ml of diethyl ether was added 130 mg (0.5 mmol) of **7** and 0.67 ml of triethylamine at −40°C with continuous stirring. The reaction mixture was allowed to warm up slowly and the reaction course was monitored after 24 h and 36 h by ^{31}P-NMR spectroscopy. The percentage of the compounds were estimated by signal integration, assuming that the relaxation times of the phosphorus nuclei are similar. The ratio of **7**/**8** (signal at δ = 96.8) was determined after 24 h as 82:18 and after 36 h as 64:29:7.

Crystal Structure Determination of **6a**[15]: $C_{19}H_{24}CrNO_5PSi_2$, *M* = 485.54, *P*$\bar{1}$, *a* = 9.1533(10), *b* = 10.7771(10), *c* = 13.5911(10) Å, α = 89.807(6)°, β = 85.161(8)°, γ = 64.298(8)°, *V* = 1202.9(2) Å^3, *Z* = 2, d_{calc} = 1.340 Mg/m^3, μ = 0.669 mm^{-1}, *T* = 173 K. A yellow needle (0.80 × 0.42 × 0.28 mm) was mounted in inert oil. 4502 intensities were measured (2Θ 6−50°, ω-scans, −10 < *h* < 0, −12 < *k* < 11, −16 < *l* < 16) using Mo-*K*α radiation (graphite monochromator) on a Siemens P4 diffractometer. After absorption correction (ψ-scans, min. and max. transmission: 0.847, 0.934), 4213 were unique (R_{int} = 0.0139) and 4208 used for all calculations (program SHELXL-93). The structure was solved by direct methods and refined anisotropically by full-matrix least squares on F^2. All hydrogen atoms (except rigid methyl groups) were refined with a riding model.The final *wR*(F^2) was 0.0724 with conventional *R*(F) 0.0275 for 268 parameters and 100 restraints. Highest peak 0.293, hole −0.235 e/Å.

Crystal Structure Determination of **6b**[15]: $C_{19}H_{24}MoNO_5PSi_2$, *M* = 529.48, *P*$\bar{1}$, *a* = 9.158(2), *b* = 10.782(2), *c* = 13.816(3) Å, α = 89.17(2)°, β = 85.83(2)°, γ = 65.03(2)°, *V* = 1233.2(4) Å^3, *Z* = 2, d_{calc} = 1.426 Mg/m^3, μ = 0.721 mm^{-1}, *T* = 143 K. A pale yellow tablet (0.70 × 0.70 × 0.30 mm) was mounted in inert oil. 4577 intensities were measured (2Θ 6−50°, ω/Θ-scans, −9 < *h* < 10, 0 < *k* < 12, −10 < *l* < 10) using Mo-*K*α radiation (graphite monochromator) on a Stoe STADI-4 diffractometer. After absorption correction (ψ-scans, min. and max. transmission: 0.767, 0.878), 4330 were unique (R_{int} = 0.0214) and used for all calculations (program SHELXL-93). The structure was solved by heavy atom method and refined anisotropically by full-matrix least squares on F^2. All hydrogen atoms (except rigid methyl groups) were refined with a riding model.The final *wR*(F^2) was 0.0926 with conventional *R*(*F*) 0.0382 for 268 parameters and 98 restraints. Highest peak 0.510, hole −0.452 e/Å.

☆ Dedicated to Professor *Wolfgang Beck* on the occasion of his 65th birthday.

[1] H. Wilkens, J. Jeske, P. G. Jones, R. Streubel, *J. Chem. Soc., Chem. Commun.* **1997**, 2317−2318.

[2] [2a] R. Streubel, J. Jeske, P. G. Jones, R. Herbst-Irmer, *Angew. Chem.* **1994**, *106*, 115−117; *Angew. Chem. Int. Ed. Engl.* **1994**, *33*, 80−82. − [2b] R. Streubel, A. Ostrowski, S. Priemer, U. Rohde, J. Jeske, P. G. Jones; *Eur. J. Inorg. Chem.* **1998**, 257−261.

[3] R. Streubel, H. Wilkens, A. Ostrowski, C. Neumann, F. Ruthe, P. G. Jones, *Angew. Chem.* **1997**, *109*, 1549−1550; *Angew. Chem. Int. Ed. Eng.* **1997**, *36*, 1492−1493.

[4] [4a] R. Streubel, A. Kusenberg, J. Jeske, P. G. Jones, *Angew. Chem.* **1994**, *106*, 2564−2566; *Angew. Chem. Int. Ed. Engl.* **1994**, *33*, 2427−2428. − [4b] A. Ostrowski, J. Jeske. P. G. Jones, R. Streubel, *J. Chem. Soc., Chem. Commun.* **1995**, 2507−2508.

[5] [5a] R. Streubel, L. Ernst, J. Jeske, P. G. Jones, *J. Chem. Soc., Chem. Commun.* **1995**, 2113−2114.− [5b] R. Streubel, A. Ostrowski, H. Wilkens, F. Ruthe, J. Jeske, P. G. Jones, *Angew. Chem.* **1997**, *109*, 409−413; *Angew. Chem. Int. Ed. Engl.* **1997**, *36*, 378−381.− [5c] A. Ostrowski, J. Jeske, F. Ruthe, P. G. Jones, R. Streubel, *Z. Anorg. Allg. Chem.* **1997**, *623*, 1897-1902.

[6] E. O. Fischer, H. J. Kollmeier, *Chem. Ber.* **1971**, *104*, 1339−1346.

[7] K. H. Dötz, *Chem. Ber.* **1980**, *113*, 3597−3604.

[8] R. Appel, A. Westerhaus, *Tetrahedron Lett.* **1981**, *22*, 2159−2160.

[9] J. Escudie, C. Couret, H. Ranaivonjatovo, J. Satgé, *J. Chem. Soc., Chem. Commun.* **1984**, 1621−1622.

[10] H. Lang, O. Orama, G. Huttner, *J. Organomet. Chem.* **1985**, *291*, 293−309.

[11] D. Gudat, Dissertation, Universität, Bielefeld, **1987**.

[12] J. Mason, *Multinuclear NMR*, Plenum Press, New York, **1987**.

[13] S. W. Kirtley in *Comprehensive Organometallic Chemistry*, Vol. 3, Ed.: G. Wilkinson, Pergamon Press, Oxford, **1982**.

[14] A. Holm, N. Harrit, I. Trabjerg, *J. Chem. Soc., Perkin Trans. 1*, **1978**, 746−750.

[15] Crystallographic data (excluding structure factors) for the structures reported in this paper have been deposited with the Cambridge Crystallographic Data Centre as supplementary publication no. CCDC-100668. Copies of the data can be obtained free of charge on application to The Director, CCDC, 12 Union Road, UK-Cambridge CB2 1EZ [fax: int. code +44(0)1223/336-033; E-mail: deposit@chemcrys.cam.ac.uk].

[97252]

Chemistry of 2*H*-Azaphosphirene Complexes, 10[◇]

Syntheses of 3-Heteroaryl-2*H*-Azaphosphirene Tungsten Complexes☆

Rainer Streubel*[a], Siegfried Priemer[a], Frank Ruthe[a], Peter G. Jones[a], and Dietrich Gudat[b]

Institut für Anorganische und Analytische Chemie der Technischen Universität Braunschweig[a],
Postfach 3329, D-38023, Braunschweig, Germany
Fax: (internat.) +49 (0)531/391-5387
E-mail: r.streubel@tu-bs.de

Institut für Anorganische Chemie der Universität Bonn[b],
Gerhard-Domagk-Straße 1, D-53121 Bonn, Germany
Fax: (internat.) +49 (0)228/73-5327
E-mail: dgudat@uni-bonn.de

Received December 1, 1997

Keywords: Phosphorus heterocycles / 2*H*-Azaphosphirene complexes / Carbene complexes / Tungsten / Cyclizations

The syntheses of 3-heteroaryl-substituted 2*H*-azaphosphirene pentacarbonyltungsten complexes are reported. The products were characterized by multinuclear NMR spectroscopy (^{1}H, ^{13}C, ^{15}N, ^{31}P, ^{183}W); the structure of the 3-*N*-methylpyrryl-substituted 2*H*-azaphosphirene complex was determined by single-crystal X-ray structure analysis.

2*H*-azaphosphirene tungsten complexes (**I**) are of current synthetic interest because of their widespread applicability in heterocycle synthesis. For example, we very recently demonstrated that 2*H*-azaphosphirene tungsten complexes provide a new access to five-membered heterocyclic complexes, through trapping reactions of transiently formed nitrilium phosphane ylide tungsten complexes (**II**) with an acetylene[2] and a nitrile derivative.[3] Therefore, we were interested in the synthesis of 3-heteroaryl-substituted 2*H*-azaphosphirene tungsten complexes. We also wished to test the limits of our initial synthetic approach[4] to 2*H*-azaphosphirene complexes.

Scheme 1. 2*H*-azaphosphirene tungsten complexes (**I**) and nitrilium phosphane ylide tungsten complexes (**II**) (**I**, **II**: R, R′ = alkyl, aryl; [M] = metal complex fragment)

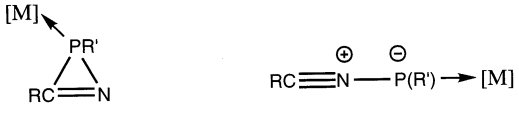

I **II**

Heteroaryl-substituted aminocarbene tungsten complexes **1a−c** were synthesized according to standard procedures[5] and reacted with [bis(trimethylsilyl)methylene]-chlorophosphane (**2**)[6] in the presence of triethylamine. In a similar way to our previously reported reactions of aryl-substituted aminocarbene complexes,[1][7] these reactions proceeded smoothly to give the 2*H*-azaphosphirene tungsten complexes **3a−c** (Scheme 2). These compounds were isolated in moderate to good yields after low-temperature column chromatography.

Scheme 2. Synthesis of 2*H*-azaphosphirene tungsten complexes **3a−c**

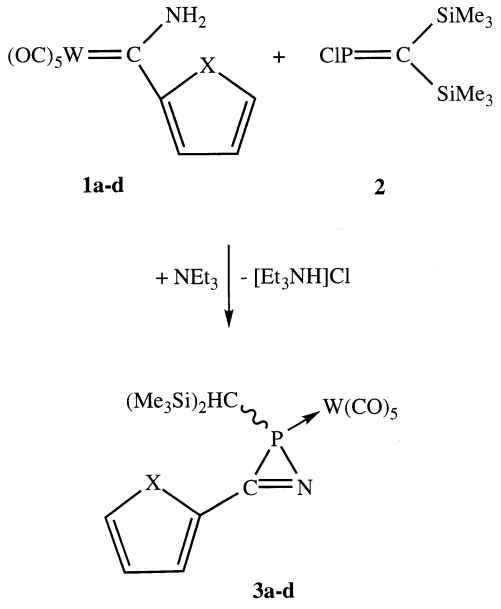

1a,3a: X = NMe; **1b,3b**: X = O; **1c,3c**: X = S; **1d,3d**: HC=CH

The proposed structures of the 2*H*-azaphosphirene tungsten complexes **3a−c** are unambiguously confirmed by their typical NMR data. The assignment of the ^{1}H- and ^{13}C-NMR resonances of the aromatic substituents in **3a−c** is based on a comparison with the corresponding data of 2-formyl-substituted heteroarenes.[8] The chemical shift of the

[◇] Part 9: See ref.[7].

 © WILEY-VCH Verlag GmbH, D-69451 Weinheim, 1998 1434−1948/98/0505−0575 $ 17.50+.50/0

pyrryl nitrogen atom in **3a** compares to reported values of *N*-alkyl pyrroles.[9] The chemical shifts of the atoms in the three membered rings of **3b,c** match those of the phenyl substituted derivative, **3d**, [1] while for the *N*-methylpyrryl-substituted compound, **3a**, both the ^{31}P and ^{15}N resonances display marked shifts to higher field (Table 1). The origin of this phenomenon arises presumably from π-interactions between the five- and three-membered rings and is in accord with the higher π-donor capability of a pyrryl as compared to a thienyl or phenyl substituent. The magnitudes of the carbon-phosphorus coupling constants in **3a−c** [$^{(1+2)}J_{PC}$ = 4.0−8.2 Hz] are larger than in **3d** and related *para*-substituted derivatives (1−3 Hz, ref.[7]) and increase in the same order (**3c** < **3b** < **3a**) as [$^{(1+2)}J_{PN}$]. The values of $\delta^{183}W$ and $^1J_{WP}$ for **3a−c** are essentially constant and lie in the known range for complexes of the type $[W(CO)_5(PR_3)]$.[10] CI EI mass spectrometric experiments revealed that, although only the [(M + H)$^+$] and not the [(M − H)$^-$] ions were detected, these 2*H*-azaphosphirene complexes preferentially show PCN-ring cleavage subsequent to the ionisation processes; this was observed in the positive and negative CI mode. Additionally, the resulting fragment ions indicate subsequent loss of carbon monoxide.

Table 1. Comparison of selected ^{13}C[a], ^{15}N[b], ^{31}P[b], ^{183}W[b] NMR data (δ values, *J*[Hz]) of 3-heteroaryl-2*H*-azaphosphirene tungsten complexes **3a−c**, **d**[7] (exclusively atoms of the three-membered ring and tungsten)

	δ ^{31}P	$^1J_{W,P}$	δ ^{13}C	$^{(1+2)}J_{C,P}$	δ ^{15}N	$^{(1+2)}J_{N,P}$	δ ^{183}W
3a	−127.9	294	179.2	8.2	−85.3	40.1	3249.8
3b	−108.3	298	181.7	7.0	−60.7	39.7	3252.5
3c	−103.0	296	185.0	4.0	−62.6	38.7	3255.3
3d	−108.8	294	192.3	1.3	−53.9	36.7	3255.9

[a] $CDCl_3$, room. temp. − [b] CH_2Cl_2, room. temp.

Figure 1. Molecular structure of **3a** in the crystal (ellipsoids represent 50% probability levels, hydrogen atoms are omitted for clarity). Selected bond lengths [A] and angles [°]: P−C(6) 1.760(4), P−N(1) 1.789(3), N(1)−C(6) 1.296(5), W−P 2.4741(13); C(6)−P−N(1) 42.8(2), C(6)−N(1)−P 67.4(2), N(1)−C(6)−P 69.8(2), N(1)−C(6)−C(14) 138.0(4).

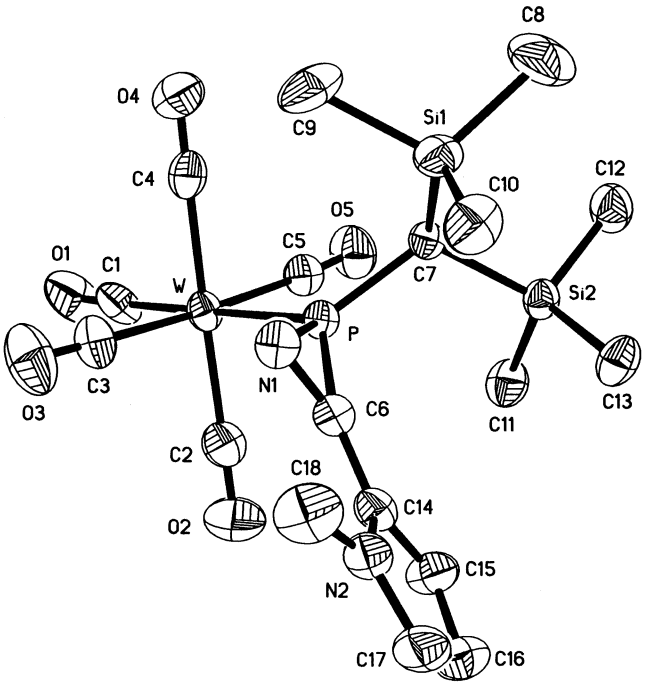

The molecular structure of complex **3a** was confirmed for the solid state by X-ray crystallography (Figure 1).[11] One of the most interesting structural features of **3a** is the almost coplanar arrangement of the two ring systems (interplanar angle 6.4°) which allows an effective π-electron interaction between the *N*-methylpyrryl group (π-donor) and the PCN-ring (π-acceptor). This is strongly supported by the observed bond length equalization of the carbon−carbon bonds in the pyrryl ring [C14−C15 1.389(5), C15−C16 1.385(6), C16−C17 1.396(6) Å] and the inter-ring bond [C6−C14 1.404(5) Å]. The latter is also significantly shorter than the corresponding distance in **3d** [1.457(7) Å][7], while at the same time the C−N double bond [N1−C6 1.296(5) Å] is longer than there [1.272(7) Å[7]].

Support by the *Deutsche Forschungsgemeinschaft* and the *Fonds der Chemischen Industrie* is gratefully acknowledged.

Experimental Section

General: All operations were carried out under deoxygenated dry nitrogen as inert gas, solvents were dried according to standard procedures. − NMR spectra were recorded on a Bruker AC-200 or a Bruker AMX-300 spectrometer (AC-200: 200 MHz for ^1H; 50.3 MHz for ^{13}C; 81 MHz for ^{31}P; AMX-300: 30.4 MHz for ^{15}N; 12.5 MHz for ^{183}W) using [D]chloroform and dichloromethane as solvent and internal standard; shifts are given relative to ext. tetramethylsilane (^1H, ^{13}C), H_3CNO_2 (^{15}N), 85% H_3PO_4 (^{31}P) and WO_4^{2-} (^{183}W). ^{15}N-NMR spectra were recorded using ^{31}P- and ^1H-based polarisation transfer techniques (INEPT); ^{183}W-NMR data were obtained from two dimensional ^{31}P-detected ^{31}P, $^{183}W\{^1H\}$ HMQC spectra. − MS: Finigan Mat 8430 (70 eV). − Elemental analyses: Carlo Erba analytical gas chromatograph. − IR: Biorad FT-IR-165.

General Procedure for the Preparation of Amino(heteroaryl)carbene Tungsten Complexes: The ethoxy(heteroaryl)-carbene tungsten complexes were prepared according to ref.[5] and reacted, without purification, with ammonia. A gentle flow of ammonia was bubbled through a solution of 5 mmol of the ethoxy-(heteroaryl)carbene tungsten complexes in 60 ml of ether until a yellow colour persisted and thin layer chromatography (SiO_2) indicated that all starting material had reacted. All volatile compounds were removed under reduced pressure (0.1 mbar) and the yellow residue was purified by column chromatography. The assignment of the ^1H and ^{13}C resonances of the aromatic heterocyclic substituents of **1a−c** accords with related chromium complexes.[12]

{[Amino(1-methyl-2-pyrryl)carbene]pentacarbonyltungsten(0)} (**1a**): 1.7 g of **1a** (79%) was obtained as a yellow powder after low temperature chromatography (SiO_2, −10°C; hexane/ether 1:1). M.p. 120°C (decomp.). − IR (KBr): $\tilde{\nu}$ = 3451 (m) cm^{-1}, 3351 (m), 3256 (m), (NH), 2061 (m), 1978 (m), 1903 (s), (CO). − ^1H NMR ($CDCl_3$): δ = 3.80 (s, 3 H, N−CH_3), 6.22 (dd, $^3J_{HH}$ = 4.0 Hz, $^3J_{HH}$ = 2.6 Hz, 1 H, pyrryl-C4-*H*), 6.85−6.91 (m, 2 H, pyrryl-C3/5-*H*), 8.07 (br, 2 H, NH_2). − $^{13}C\{^1H\}$ NMR ($CDCl_3$): δ = 37.1 (s, N−*C*H_3), 110.3 (s, pyrryl-*C4*), 123.7 (s, pyrryl-*C5*), 132.0 (s, pyrryl-*C3*), 143.6 (s, pyrryl-*C2*), 198.9 (s, $^1J_{CW}$ = 127.6 Hz, *cis*-*C*O), 202.9

(s, *trans*-*C*O), 240.6 (s, W=*C*R_2). − MS (70 eV), (^{184}W) *m*/*z* (%): 432 (8) [M^+], 404 (11) [M^+ − CO], 352 (53) [M^+ − C_5H_6N], 296 (40) [M^+ − 2 × CO − C_5H_6N], 268 (100) [M^+ − 3 × CO − C_5H_6N], 240 (41) [M^+ − 4 × CO − C_5H_6N], 212 (43) [M^+ − 5 × CO − C_5H_6N], 184 (33) [M^+ − 5 × CO − C_5H_6N − CNH_2]. − $C_{11}H_8N_2O_5W$ (432.0): calcd. C 30.58, H 1.87, N 6.48; found C 30.67, H 1.90, N 6.48.

{[Amino(2-furyl)carbene]pentacarbonyltungsten(0)} (**1b**): 1.5 g of **1b** (71%) was obtained as a yellow-orange powder after low temperature chromatography (SiO_2, −10°C; hexane/ether 1:1). M.p. 95°C (decomp.). − IR (KBr): $\tilde{\nu}$ = 3457 (m) cm^{-1}, 3341 (m), 3256 (m), (NH), 2064 (m), 1976 (m), 1928 (s), 1888 (s), (CO). − ^{1}H NMR ($CDCl_3$): δ = 6.56 (dd, $^3J_{HH}$ = 3.7 Hz, $^3J_{HH}$ = 1.8 Hz, 1 H, furyl-C4-*H*), 7.45−7.47 (m, 1 H, furyl-C3-*H*), 7.54−7.55 (m, 1 H, furyl-C5-*H*), 7.91 (br, 1 H, NH_2), 8.94 (br, 1 H, NH_2). − ^{13}C{^{1}H} NMR ($CDCl_3$): δ = 114.5 (s, furyl-*C4*), 129.4 (s, furyl-*C3*), 145.6 (s, furyl-*C5*), 159.0 (s, furyl-*C2*), 198.4 (s, $^1J_{CW}$ = 129.9 Hz, *cis*-*C*O), 202.6 (s, *trans*-*C*O), 229.8 (s, W=*C*R_2). − MS (70 eV), (^{184}W); *m*/*z* (%): 419 (56) [M^+], 391 (18) [M^+ − CO], 335 (55) [M^+ − 3 × CO], 307 (51) [M^+ − 4 × CO], 279 (100) [M^+ − 5 × CO], 252 (56) [M^+ − 3 × CO − NH_2 − C_4H_3O], 224 (35) [M^+ − 4 × CO − NH_2 − C_4H_3O]. − $C_{10}H_5NO_6W$ (419.0): calcd. C 28.67, H 1.20, N 3.34; found C 28.73, H 1.21, N 3.32.

{[Amino(2-thienyl)carbene]pentacarbonyltungsten(0)} (**1c**): 1.8 g of **1c** (84%) was obtained as a yellow powder after low temperature chromatography (SiO_2, −10°C; hexane/ether 1:1). M.p. 101°C (decomp.). − IR (KBr): $\tilde{\nu}$ = 3426 (m) cm^{-1}, 3343 (m), 3266 (m), (NH), 2064 (m), 1969 (m), 1922 (vs), 1911 (vs), 1888 (s), 1872 (vs), (CO). − ^{1}H NMR ($CDCl_3$): δ = 7.16 (dd, $^3J_{HH}$ = 5.0 Hz, $^3J_{HH}$ = 3.9 Hz, 1 H, thienyl-C4-*H*), 7.60 (dd, $^3J_{HH}$ = 3.9 Hz, $^4J_{HH}$ = 1.1 Hz, 1 H, thienyl-C3-*H*), 7.66 (dd, $^3J_{HH}$ = 5.0 Hz, $^4J_{HH}$ = 1.1 Hz, 1 H, thienyl-C5-*H*), 8.02 (br, 1 H, NH_2), 8.52 (br, 1 H, NH_2). − ^{13}C{^{1}H} NMR ($CDCl_3$): δ = 129.0 (s, thienyl-*C4*), 132.7 (s) and 133.2 (s) (thienyl-*C3*/*C5*), 153.5 (s, thienyl-*C2*), 198.4 (s, $^1J_{CW}$ = 127.2 Hz, *cis*-*C*O), 202.6 (s, *trans*-*C*O), 243.8 (s, W=*C*R_2). − MS (70 eV), (^{184}W); *m*/*z* (%): 435 (49) [M^+], 407 (30) [M^+ − CO], 351 (28) [M^+ − 3 × CO], 295 (100) [M^+ − 5 × CO], 268 (41) [M^+ − 3 × CO − C_4H_3S]. − $C_{10}H_5NO_5SW$ (435.1): calcd. C 27.61, H 1.16, N 3.22, S 7.37; found C 27.68, H 1.16, N 3.15, S 7.40.

General Procedure for the Preparation of 2H-Azaphosphirene-(pentacarbonyl)tungsten Complexes: To a solution of 1.5 mmol of amino(heteroaryl)carbene tungsten complexes **1a−c** in 15 ml of ether was added 0.34 g (1.5 mmol) of **2** and 5 ml of NEt_3 at 0°C. The reaction mixture was stirred at ambient temp. until **2** was consumed (^{31}P-NMR control). The yellow-orange reaction mixture was evaporated to dryness under reduced pressure (0.1 mbar). The residue was extracted with 30 ml of pentane and filtered. The filtration residue was washed twice with 5 ml of pentane, the organic phases combined and the solvent removed under reduced pressure. The residue was purified, if necessary, by low temperature column chromatography (SiO_2, −10°C; hexane/ether 10:1).

{[2-Bis(trimethylsilyl)methyl-3-(1-methyl-2-pyrryl)-2H-azaphosphirene-κP]pentacarbo-nyltungsten(0)} (**3a**): 0.35 g of **3a** (56%) was obtained, after stirring for 20 hours, as a yellow powder. M.p. 112°C (decomp.). − IR (KBr): $\tilde{\nu}$ = 2073 (m) cm^{-1}, 1990 (m), 1952 (s, sh), 1936 (s), 1919 (vs), (CO), 1618 (w) (CN). − ^{1}H NMR ($CDCl_3$): δ = 0.14 (s, 9 H, $SiMe_3$), 0.28 (s, 9 H, $SiMe_3$), 0.58 (d, $^2J_{HP}$ = 2.9 Hz, 1 H, PC*H*), 4.01 (d, $^4J_{HH}$ = 0.5 Hz , 3 H, N−CH_3), 6.37 (dd, $^3J_{HH}$ = 4.1 Hz, $^3J_{HH}$ = 2.5 Hz, 1 H, pyrryl-C4-*H*), 7.04−7.06 (m, 1 H, pyrryl-C3-*H*), 7.10 (m, 1 H, pyrryl-C5-*H*). − ^{13}C{^{1}H} NMR ($CDCl_3$): δ = 1.3 (d, $^3J_{CP}$ = 3.5 Hz, $SiMe_3$), 2.2 (d, $^3J_{CP}$ = 3.1 Hz, $SiMe_3$), 27.2 (d, $^1J_{CP}$ = 24.2 Hz, P*C*H), 36.2 (s, N−*C*H_3), 111.0 (s, pyrryl-*C4*), 120.2 (d, $^2J_{CP}$ = 19.2 Hz, pyrryl-*C2*), 122.3 (s, pyrryl-*C3*), 132.6 (s, pyrryl-*C5*), 179.2 (d, $^{(1+2)}J_{PC}$ = 8.2 Hz, P*C*N), 196.0 (d, $^2J_{CP}$ = 8.9 Hz, *cis*-*C*O), 198.1 (d, $^2J_{CP}$ = 35.6 Hz, *trans*-*C*O). − ^{15}N NMR (CH_2Cl_2): δ = −85.3 (d, $^{(1+2)}J_{NP}$ = 40.1 Hz, PC*N*), −224.3 (d, $^3J_{NP}$ = 1.4 Hz, pyrryl-*N*). − ^{31}P{^{1}H} NMR ($CDCl_3$): δ = −125.8 (s, $^1J_{PW}$ = 293.1 Hz). − ^{31}P{^{1}H} NMR (CH_2Cl_2): δ = −127.9 (s, $^1J_{PW}$ = 294.0 Hz). − ^{183}W NMR (CH_2Cl_2): δ = −3249.8 (d, $^1J_{PW}$ = 294.0 Hz). − MS (pos.-CI, NH_3), (^{184}W) *m*/*z* (%): 621 (100) [(M + H)$^+$], 515 (18) [(M + H)$^+$ − $C_6H_6N_2$], 106 (5) [$C_6H_6N_2^+$]. − MS (neg.-CI, NH_3), (^{184}W) *m*/*z* (%): 513 (100) [(M − H)$^-$ − $C_6H_6N_2$], 485 (18) [(M − H)$^-$ − $C_6H_6N_2$ − CO], 457 (2) [(M − H)$^-$ − $C_6H_6N_2$ − 2 × CO]. − $C_{18}H_{25}N_2O_5PSi_2W$ (620.4): calcd. C 34.85, H 4.06, N 4.52; found C 35.08, H 4.03, N 4.62.

{[2-Bis(trimethylsilyl)methyl-3-(2-furyl)-2H-azaphosphirene-κP]pentacarbonyltungsten(0)} (**3b**): 0.35 g of **3b** (58%) was obtained, after stirring for 25 hours, as a yellow powder. M.p. 106°C (decomp.). − IR (KBr): $\tilde{\nu}$ = 2074 (s) cm^{-1}, 1991 (m), 1965 (s), 1945 (vs), 1935 (s), 1923 (vs), 1907 (vs) (CO), 1636 (w) (CN). − ^{1}H NMR ($CDCl_3$): δ = 0.14 (s, 9 H, $SiMe_3$), 0.28 (s, 9 H, $SiMe_3$), 0.65 (d, $^2J_{HP}$ = 3.8 Hz, 1 H, PC*H*), 6.74 (dd, $^3J_{HH}$ = 3.5 Hz, $^3J_{HH}$ = 1.8 Hz, 1 H, furyl-C4-*H*), 7.42 (d, $^3J_{HH}$ = 3.5 Hz, 1 H, furyl-C3-*H*), 7.88 (d, $^3J_{HH}$ = 1.8 Hz,1 H, furyl-C5-*H*). − ^{13}C{^{1}H} NMR ($CDCl_3$): δ = 1.0 (d, $^3J_{CP}$ = 3.4 Hz, $SiMe_3$), 2.0 (d, $^3J_{CP}$ = 3.2 Hz, $SiMe_3$), 28.0 (d, $^1J_{CP}$ = 23.6 Hz, P*C*H), 113.6 (s, furyl-*C3*), 120.6 (s, furyl-*C4*), 143.3 (d, $^2J_{CP}$ = 17.1 Hz, furyl-*C2*), 149.2 (s, furyl-*C5*), 181.7 (d, $^{(1+2)}J_{CP}$ = 7.0 Hz, P*C*N), 195.6 (d, $^2J_{CP}$ = 8.9 Hz, *cis*-*C*O), 197.6 (d, $^2J_{CP}$ = 37.0 Hz, *trans*-*C*O). − ^{15}N NMR (CH_2Cl_2): δ = −60.7 (d, $^{(1+2)}J_{NP}$ = 39.7 Hz). − ^{31}P{^{1}H} NMR ($CDCl_3$): δ = −105.4 (s, $^1J_{PW}$ = 297.9 Hz). − ^{31}P{^{1}H} NMR (CH_2Cl_2): δ = −108.3 (s, $^1J_{PW}$ = 298.0 Hz). − ^{183}W NMR (CH_2Cl_2): δ = −3252.5 (d, $^1J_{PW}$ = 298.0 Hz). − MS (pos.-CI, NH_3), (^{184}W); *m*/*z* (%): 608 (100) [(M + H)$^+$], 515 (4) [(M + H)$^+$ − C_5H_3NO]. MS (neg.-CI, NH_3), (^{184}W); *m*/*z* (%): 513 (100)[(M − H)$^-$ − C_5H_3NO], 485 (8) [(M − H)$^-$ − C_5H_3NO − CO]. − $C_{17}H_{22}NO_6PSi_2W$ (607.4): calcd. C 33.56, H 3.64, N 2.30; found C 33.78, H 3.55, N 2.28.

{[2-Bis(trimethylsilyl)methyl-3-(2-thienyl)-2H-azaphosphirene-κP]-pentacarbonyltungsten(0)} (**3c**): 0.35 g of **3c** (56%) was obtained, after stirring for 22 hours, as a yellow powder. M.p. 110°C (decomp.). − IR (KBr): $\tilde{\nu}$ = 2072 (s) cm^{-1}, 1988 (m), 1963 (s), 1936 (vs, br), 1920 (vs), (CO), 1612 (w) (CN). − ^{1}H NMR ($CDCl_3$): δ = 0.15 (s, 9 H, $SiMe_3$), 0.29 (s, 9 H, $SiMe_3$), 0.70 (d, $^2J_{HP}$ = 3.3 Hz, 1 H, PC*H*), 7.34 (dd, $^3J_{HH}$ = 4.9 Hz, $^4J_{HH}$ = 3.8 Hz, 1 H, thienyl-C4-*H*), 7.87−7.94 (m, 2 H, thienyl-C3/5-*H*). − ^{13}C{^{1}H} NMR ($CDCl_3$): δ = 1.3 (d, $^3J_{CP}$ = 3.5 Hz, $SiMe_3$), 2.1 (d, $^3J_{CP}$ = 3.3 Hz, $SiMe_3$), 28.2 (d, $^1J_{CP}$ = 24.3 Hz, P*C*H), 129.2 (s, thienyl-*C5*), 130.0 (d, $^2J_{CP}$ = 17.9 Hz, thienyl-*C2*), 134.9 (s) and 135.7 (s), thienyl-*C3*/*C4*, 185.0 (d, $^{(1+2)}J_{PC}$ = 4.0 Hz, P*C*N), 195.7 (d, $^2J_{CP}$ = 8.9 Hz, *cis*-*C*O), 197.7 (d, $^2J_{CP}$ = 36.7 Hz, *trans*-*C*O). − ^{15}N NMR (CH_2Cl_2): δ = −62.6 (d, $^{(1+2)}J_{PN}$ = 38.7 Hz). − ^{31}P{^{1}H} NMR ($CDCl_3$): δ = −100.8 (s, $^1J_{PW}$ = 296.3 Hz). − ^{31}P{^{1}H} NMR (CH_2Cl_2): δ = −103.0 (s, $^1J_{PW}$ = 296.0 Hz). − ^{183}W NMR (CH_2Cl_2): δ = −3255.3 (d, $^1J_{PW}$ = 296.3 Hz). − MS (pos.-CI, NH_3), (^{184}W) *m*/*z* (%): 624 (50) [(M + H)$^+$], 515 (15) [(M + H)$^+$ − C_5H_3NS], 112 (100) [(C_5H_3NS + 3 H)$^+$], 74 (14) [($SiMe_3$ + H)$^+$]. − MS (neg.-CI, NH_3), (^{184}W) *m*/*z* (%): 513 (100) [(M − H)$^-$ − C_5H_3NS], 485 (44) [(M − H)$^-$ − C_5H_3NS − CO]. − $C_{17}H_{22}NO_5PSSi_2W$ (623.4): calcd. C 32.75, H 3.56, N 2.25, S 5.14; found C 32.82, H 3.61, N 2.11, S 5.17.

Crystal Structure Determination of **3a**[11]: $C_{18}H_{25}N_2O_5PSi_2W$, *M* = 620.40, $P\bar{1}$, *a* = 9.330(3), *b* = 9.522(3), *c* = 14.275(3) Å, α =

89.13(3), β = 83.66(3), γ = 79.80(3)°, V = 1240.5(5) Å^3, Z = 2, d_{calc} = 1.661 Mg/m^3, μ = 4.846 mm^{-1}, T = 143 K. A pale brown block (0.6 × 0.3 × 0.3 mm) was mounted in inert oil. 8349 intensities were measured (2Θ 6−50°) using Mo-*Kα* radiation on a Stoe STADI-4 diffractometer. After absorption correction (ψ-scans) 4383 were unique (R_{int} = 0.0256) and used for all calculations (program SHELXL-93). All hydrogen atoms (except rigid methyl groups) were refined with a riding model. The final $wR(F^2)$ was 0.052 with conventional $R(F)$ 0.023 for 269 parameters and 90 restraints. Highest peak 640, hole −969 e/nm^3.

☆ Dedicated to Professor *Hans Bock* on the occasion of his 70th birthday.

[1] R. Streubel, A. Ostrowski, S. Priemer, U. Rohde, J. Jeske, P. G. Jones, *Eur. J. Inorg. Chem.* **1998**, 257−261.

[2] R. Streubel, H. Wilkens, A. Ostrowski, C. Neumann, F. Ruthe, P. G. Jones, *Angew. Chem.* **1997**, *109*, 1549−1550; *Angew. Chem. Int. Ed. Eng.* **1997**, *36*, 1492−1493.

[3] H. Wilkens, J. Jeske, P. G. Jones, R. Streubel, *J. Chem. Soc., Chem. Commun.* **1997**, 2317−2318.

[4] R. Streubel, J. Jeske, P. G. Jones, R. Herbst-Irmer, *Angew. Chem.* **1994**, *106*, 115−117; *Angew. Chem. Int. Ed. Engl.* **1994**, *33*, 80−82.

[5] [5a] E. O. Fischer, H. J. Kollmeier, *Chem. Ber.* **1971**, *104*, 1339−1346. − [5b] J. A. Connor, E. M. Jones, *J. Chem. Soc.(A),* **1971**, 1974−1979.

[6] R. Appel, A. Westerhaus, *Tetrahedron Lett.* **1981**, *22*, 2159−2160.

[7] R. Streubel, F. Ruthe, P. G. Jones, *Eur. J. Inorg. Chem.* **1998**, 571−574.

[8] See: E. Breitmaier, W. Voelter, *Carbon-13 NMR Spectroscopy*, third ed., VCH, Weinheim, **1993**, p. 281.

[9] See: M. Witanowski, L. Stefaniak, G. A. Webb, *Ann. Rep. NMR Spectrosc.* (G.A. Webb, Ed.), Academic Press, London, **1981**, Vol. 11B, p 310.

[10] J. Mason, *Multinuclear NMR*, Plenum Press, New York, **1987**.

[11] Crystallographic data (excluding structure factors) for the structure reported in this paper have been deposited with the Cambridge Crystallographic Data Centre as supplementary publication no. CCDC-100855. Copies of the data can be obtained free of charge on application to The Director, CCDC, 12 Union Road, UK-Cambridge CB2 1EZ [fax: int. code +44(1223)336-033; E-mail: deposit@chemcrys.cam.ac.uk].

[12] J. A. Connor, E. M. Jones, E. W. Randall, E. Rosenberg, *J. Chem. Soc., Dalton Trans.* **1972**, 2419−2424.

[97288]

Transition Metal Substituted Acyl Phosphanes and Phosphaalkenes, 36[◇]

Synthesis and Structure of the First Carbyne Complex Functionalized Zwitterionic α-Carbenium Phosphinates [Tp′(CO)$_2$M≡C−P(O)$_2$−C(NR$_2$)$_2$] (M = Mo, W; R = Me, Et)

Lothar Weber*, Gottfried Dembeck, Hans-Georg Stammler, and Beate Neumann

Fakultät für Chemie der Universität Bielefeld,
Postfach 100131, D-33501 Bielefeld, Germany
Fax: (internat.) +49(0)5201-106-6146
E-mail: lothar.weber@uni-bielefeld.de

Received November 6, 1997

Keywords: Carbyne complexes / Molybdenum complexes / Oxidations / Tungsten

Oxidation of the phosphaalkenyl-substituted carbyne complexes [Tp′(CO)$_2$M≡C−P=C(NR$_2$)$_2$] (**1a**: M = Mo, R = Me; **1b**: M = W, R = Me; **2a**: M = Mo, R = Et; **2b**: M = W, R = Et) with molecular dioxygen cleanly affords the orange carbyne complexes [Tp′(CO)$_2$M≡C−P(O)$_2$C(NR$_2$)$_2$] [**3a**: M = Mo, R = Me; **3b**: M = W; R = Me; **4a**: M = Mo, R = Et; **4b**: M = W, R = Et; Tp′ = HB(3,5-Me$_2$HC$_3$N$_2$)$_3$], which are functionalized at the methylidyne carbon atom by an α-carbenium phosphinate moiety. The novel compounds have been characterized by IR, ^{1}H-, ^{13}C-, and ^{31}P-NMR spectroscopy. In addition, the molecular structure of **4a** has been determined by a single-crystal X-ray structure analysis.

Introduction

In search for transition-metal complexes with terminal isophosphaalkyne ligands R−P≡C[2][3][4][5][6] we recently obtained phosphaalkenyl-substituted carbyne complexes of the type Tp′(CO)$_2$M≡C−P=C(NR$_2$)$_2$ (**1**, **2**)[1]. These molecules possess electrophilic and nucleophilic centres in close proximity which renders them promissing as precursors for a number of chemical transformations.

Herein we report on the facile oxidation of the phosphaalkenyl carbyne complexes **1**, **2** (M = Mo, W; R = Me, Et) with molecular dioxygen.

Results and Discussion

When crystalline samples of the phosphaalkenyl carbyne complexes **2a** and **2b** were exposed to air for two weeks, a color change from deep-red to orange-red took place. The same oxidation process could be achieved within 2 h using pure oxygen at a pressure of 80 bar. Similarly, compounds **1a** and **1b** were rapidly oxidized under O_2 pressure, whereas in air complete oxidation took about three weeks (eq. 1).

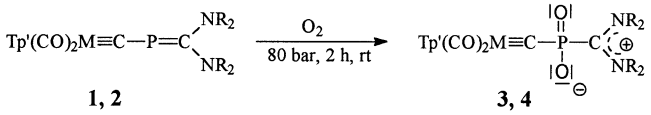

1, 2 **3, 4**

Tp′ = HB(3,5-Me$_2$HC$_3$N$_2$)$_3$
M = Mo **(a)**, W **(b)**
R = Me **(1, 3)**; R = Et **(2, 4)** (1)

Purification of the products was effected by column chromatography on silanized silica, using CH_2Cl_2 and ethanol as eluents, followed by crystallization of the orange-red powdery solids from a CH_2Cl_2/pentane mixture. Compared to the starting materials [**1a**: $\tilde{\nu}$(CO) = 1946, 1864 cm^{-1}; **1b**: 1935, 1848 cm^{-1}; **2a**: 1943, 1859 cm^{-1}; **2b**: 1933, 1845 cm^{-1}], the bands of the carbonyl stretching vibrations in the IR spectra of the products are significantly shifted to higher wavenumbers [**3a**: $\tilde{\nu}$(CO) = 2005, 1918 cm^{-1}; **3b**: 1987, 1893 cm^{-1}; **4a**: 2002, 1923 cm^{-1}; **4b**: 1989, 1894 cm^{-1}]. This observation is consistent with a decreased σ-donor/π-acceptor behavior of the novel organophosphorus carbyne ligands, compared with the phosphaalkenyl carbyne ligands in the precursors **1** and **2**. The PO_2 group of the carbenium phosphinate unit of the products gives rise to medium intensity bands at 1202−1205 and 1066−1068 cm^{-1}, which, by analogy with the IR data of numerous previously described phosphinates[7][8][9], are attributed to the asymmetric and symmetric PO_2 stretching vibrations.

The ^{13}C{^{1}H}-NMR spectra of **3a**, **b** and **4a**, **b** are especially interesting in the low field region, where doublets are observed at δ = 298.7−314.4 for the metal-bound carbon atoms of the carbyne ligands. In the ^{13}C{^{1}H}-NMR spectra of the starting materials, the corresponding resonances are observed at considerably lower field [**1a**: δ = 337 (d, $^1J_{PC}$ = 111.3 Hz); **1b**: 318.3 (d, $^1J_{PC}$ = 101.2 Hz); **2a**: 338.8 (d, $^1J_{PC}$ = 115.6 Hz); **2b**: 319.0 (d, $^1J_{PC}$ = 108.3 Hz)]. More remarkable is the dramatic decrease in the carbon-phosphorus coupling constants from the aforementioned values in **1**, **2a**, **b** to $^1J_{PC}$ = 28.2−54.0 Hz in the products. These observations can be explained in terms of a decreased

[◇] Part 35: Ref.[1].

 © WILEY-VCH Verlag GmbH, D-69451 Weinheim, 1998 1434−1948/98/0505−0579 $ 17.50+.50/0

electron transfer from the organophosphorus ligand to the metal and a decreased 3s orbital contribution in the C−P bond. Doublets at δ = 178.3−181.9 ($^1J_{PC}$ = 91.9−98.1 Hz) are assigned to the tricoordinate carbon atom of the [PC(NMe$_2$)$_2$] moiety of **3a**, **b** and **4a**, **b**. The oxidation of **1**, **2a**, **b** is accompanied by a considerable upfield shift of the resonance of this carbon atom [Δδ = 17.7−24.4], whereas the coupling constants $^1J_{PC}$ remain almost unaffected. The decreased donor capacity of the novel organophosphorus ligands in **3a**, **b** and **4a**, **b** is also reflected in the chemical shifts of the carbonyl carbon atoms, which are shifted from δ = 228.1−230.7 in **1**, **2a**, **b** to δ = 225.9−227.3 in the oxidation products.

The $^{31}P\{^1H\}$-NMR spectra of **3a**, **b** and **4a**, **b** display singlets (δ = −6.85 to +7.0) at higher fields compared to those of the precursors (δ = 49.0−65.9). Interestingly, in the tungsten derivatives **3b** and **4b**, the coupling constants $^2J_{PW}$ = 152.9 and 151.7 Hz clearly exceed the values measured from the spectra of **1b** ($^2J_{PW}$ = 51.4 Hz) and **2b** ($^2J_{PW}$ = 61.6 Hz). The ^{31}P-chemical shifts of our products may be compared to the ^{31}P-NMR data of $(Me_4Sb)^+(O_2PH_2)^-$ (δ = +1.70 in CH_2Cl_2) or $(Me_4Sb)^+(O_2PMe_2)^-$ (δ = −24.50 in CH_2Cl_2)[10].

The mass spectra (LSIMS) show the peaks of the molecular ions of **3a**, **b** and **4a**, **b** as parent ion peaks, underlining the fact that two oxygen atoms are added at the phosphorus centre of the starting materials.

X-ray Structural Analysis of 4a

Single crystals of **4a** were grown from CH_2Cl_2/hexane at 5°C. The results of the structural determination are shown in Figure 1. Selected bond lengths and angles for the complex are given in the caption. Crystalline **4a** consists of monomeric molecules with distorted octahedral geometry. The bond angles between the organophosphorus ligand and the two carbonyl ligands [C(16)−Mo(1)−C(18) = 82.91(14)°; C(17)−Mo(1)−C(18) = 83.53(13)°] are more acute than those in **2b** [85.5(3)°; 88.1(3)°][1]. The angles between the nitrogen donor atoms N(2), N(4) and N(5) of the Tp′ ligand are comparable in **4a** [79.96(9)−83.68(9)°] and **2b** [80.3(2)−82.9(2)°], and are markedly smaller than the ideal 90°. The metal atom lies in the plane defined by the carbon atoms C(5), C(9), and C(14) (deviation 0.083 Å). The most interesting structural feature of the molecule is the geometry of the organophosphorus ligand. The bond length Mo(1)−C(18) of 1.813(3) Å compares well with the corresponding bond length in Tp′(CO)$_2$Mo≡C−S−C$_6$H$_4$NO$_2$-*p* [1.801(4) Å][11], hence this bond has to be regarded as a metal−carbon triple bond.

The valence angle at the *sp*-hybridized methylidene carbon atom Mo(1)−C(18)−P(1) of 166.8(2)° shows only slight deviation from linearity, as was also found for the corresponding valence angle W−C−P in **2b** [167.9(4)°] and for that in the ion [Tp′(CO)$_2$W≡C−PMe$_2$Ph]$^+$ [168.1(5)°][12]. However, unlike in **2b**, the bonds between the phosphorus atom and carbon atoms C(18) [P(1)−C(18) = 1.788(3) Å] and C(19) [P(1)−C(19) = 1.909(3) Å] differ significantly. The standard value for a P−C single bond is 1.85 Å[13]. The tetracoordinate phosphorus atom can be considered as being part of a phosphinate unit $[R^1R^2PO_2]^-$. The phosphorus−oxygen atomic distances differ in length [1.496(3) and 1.467(3) Å] and are shorter than the P−O bond lengths in the hypophosphite ion (1.51 Å)[14].

The fourth substituent at the phosphorus atom is a trigonal-planar bis(diethylamino)carbenium unit [sum of bond angles at C(19) = 359.9(2)°]. Accordingly, the carbon−nitrogen bond lengths N(7)−C(19) [1.333(4) Å] and N(8)−C(19) [1.347(4) Å] are shortened compared to the calculated value of a $C_{sp^2}-N_{sp^2}$ single bond [1.450 Å][15].

Figure 1. Molecular structure of **4a**[a]

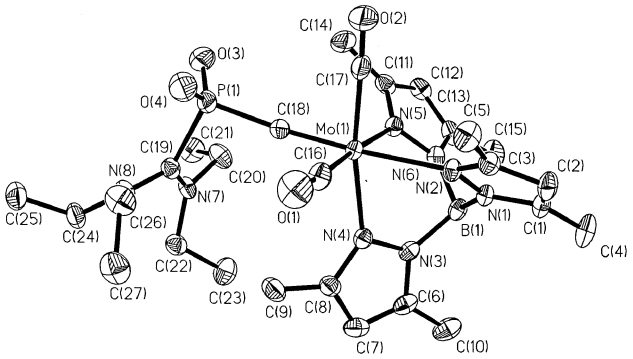

[a] Selected bond lengths [C] and bond angles [°]: Mo(1)−C(18) 1.813(3), Mo(1)−C(16) 2.004(3), Mo(1)−C(17) 2.000(3), Mo(1)−N(2) 2.326(2), Mo(1)−N(4) 2.227(2), Mo(1)−N(5) 2.219(2), P(1)−O(3) 1.496(3), P(1)−O(4) 1.467(3), P(1)−C(18) 1.788(3), P(1)−C(19) 1.909(3), O(1)−C(16) 1.147(4), O(2)−C(17) 1.139(4), N(7)−C(19) 1.333(4), N(8)−C(19) 1.347(4); C(16)−Mo(1)−C(18) 82.91(14), C(17)−Mo(1)−C(18) 83.53(13), C(16)−Mo(1)−C(17) 87.54(14), C(16)−Mo(1)−N(5) 175.87(11), C(16)−Mo(1)−N(4) 94.70(12), C(17)−Mo(1)−N(4) 170.26(11), N(4)−Mo(1)−N(5) 83.68(9), N(2)−Mo(1)−N(4) 79.96(9), N(2)−Mo(1)−N(5) 82.84(9), N(2)−Mo(1)−C(18) 172.93(12), Mo(1)−C(18)−P(1) 166.8(2), C(18)−P(1)−O(3) 110.81(15), C(18)−P(1)−O(4) 111.03(15), C(18)−P(1)−C(19) 98.57(14), C(19)−P(1)−O(3) 105.24(14), C(19)−P(1)−O(4) 109.94(15), O(3)−P(1)−O(4) 119.10(16), P(1)−C(19)−N(7) 120.4(2), P(1)−C(19)−N(8) 119.4(2), N(7)−C(19)−N(8) 120.1(3).

Figure 2. View along the vector P(1)−C(18)−Mo(1); only the ligating atoms N(2), N(4) and N(5) of the tripod are drawn for clarity

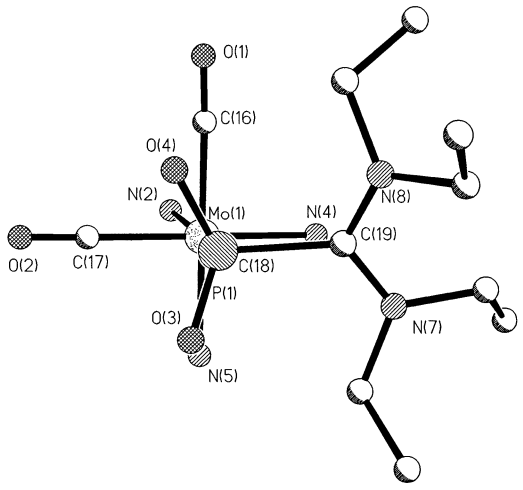

The valence angle C(18)−P(1)−C(19) of 98.57(14)° is significantly compressed, compared with the corresponding C−P−C angle in **2b** [105.7(3)°]. The remarkably long interatomic distance P(1)−C(19) [1.909(3) Å] between the phosphinato and carbenium centres is surprising. It is conceivable that the positively charged carbon atom and the positively polarized phosphorus centre repel each other. The diaminocarbenium unit is oriented towards the tripod ligand in such a way that the bonds P(1)−C(19) and Mo(1)−N(4) are eclipsed (Figure 2).

The *trans*-influence of the methylidyne ligand is reflected in the Mo(1)−N(2) bond length of 2.326(2) Å, which significantly exceeds the lengths of the other two Mo−N bonds [2.219(2) and 2.227(2) Å], which are *trans*-oriented with respect to the carbonyl ligands.

Experimental Section

Unless stated otherwise, standard inert-atmosphere techniques were used for the manipulation of all reagents and reaction products. − Infrared spectra were recorded on a Bruker FT-IR IFS66 spectrometer. − ^{1}H-, ^{13}C-, and ^{31}P-NMR spectra were recorded in CD_2Cl_2 solution on Bruker AC 100 and Bruker AM Avance DRX 500 instruments. Standards: $SiMe_4$ (^{1}H, ^{13}C), external 85% H_3PO_4 (^{31}P). − Elemental analyses were performed in the Microanalytical Laboratory of the University of Bielefeld and in the Microanalytical Laboratory, H. Kolbe, Mülheim, Germany. − Mass spectra (LSIMS) (matrix: *p*-nitrobenzyl alcohol) were obtained with a Varian MAT-CH5-DF spectrometer.

The precursors [Tp′(CO)$_2$M≡C−P=C(NR$_2$)$_2$] (**1a**: M = Mo, R = Me; **1b**: W, Me; **2a**: Mo, Et; **2b**: W, Et) were synthesized according to literature procedures[1]. Dioxygen was taken from a cylinder. Silanized silica gel (Merck) was purchased commercially.

[Tp′(CO)$_2$Mo≡C−P(O)$_2$C(NMe$_2$)$_2$] (**3a**): A solution of [Tp′(CO)$_2$Mo≡C−P=C(NMe$_2$)$_2$] (**1a**) (0.80 g, 1.35 mmol) in 15 ml of dichloromethane was treated with dioxygen in an autoclave at 20°C and 80 bar for 3 h. Thereafter, the ^{31}P{^{1}H}-NMR spectrum of the solution displayed a singlet at δ = −6.8. The solvent and volatile components were then removed in vacuo (ca. 0.1 Torr), and the yellow-brown residue was chromatographed on silanized silica 60 (column: *l* = 15 cm, *d* = 2 cm). Elution with *n*-hexane (300 ml) afforded a yellow fraction, which was discarded. The column was developed with 200 ml of CH_2Cl_2. An orange-red zone was then eluted with ethanol (100 ml) and this fraction was concentrated to dryness. The powdery, ochre residue was dissolved in 25 ml of a CH_2Cl_2/hexane mixture (1:2), and the solution was stored for 7 days at −5°C. Orange-red needles of **3a** separated (0.55 g, 65.3%). − IR (KBr): $\tilde{\nu}$ = 2551 cm^{-1} w [ν(BH)], 2005 vs, 1918 vs [ν(CO)], 1202 m [ν_{as}(PO$_2$)], 1067 m [ν_s(PO$_2$)]. − ^{1}H NMR: δ = 2.36 (s, 3 H, Tp′CH$_3$), 2.41 (s, 3 H, Tp′CH$_3$), 2.64 (s, 6 H, Tp′CH$_3$), 2.78 (s, 6 H, Tp′CH$_3$), 3.42 (s, 12 H, NCH$_3$), 5.80 (s, 1 H, Tp′-H), 5.95 (s, 2 H, Tp′-H). − ^{13}C{^{1}H} NMR: δ = 12.3 (s, Tp′*C*H$_3$), 13.9 (s, Tp′*C*H$_3$), 15.7 (s, Tp′*C*H$_3$), 38.1 (s, NCH$_3$), 106.0 (s, Tp′*C*H), 144.9 (s, Tp′*C*CH$_3$), 145.5 (s, Tp′*C*CH$_3$), 150.8 (s, Tp′*C*CH$_3$), 178.3 (d, $^{1}J_{PC}$ = 93.2 Hz, PCN$_2$), 226.5 (s, CO), 312.6 (d, $^{1}J_{PC}$ = 30.3 Hz, Mo≡C). − ^{31}P{^{1}H} NMR: δ = −6.85 (s). − MS: *m/z* = 626 [M$^+$] (^{98}Mo), 570 [M$^+$ − 2 CO] (^{98}Mo). − $C_{23}H_{34}BMoN_8O_4P$ (624.31): calcd. C 44.25, H 5.49, N 17.95; found C 42.20, H 5.52, N 17.19. Solid samples retained varying amounts of CH_2Cl_2 despite prolonged drying in vacuo.

[Tp′(CO)$_2$W≡C−P(O)$_2$C(NMe$_2$)$_2$] (**3b**): Analogously to the preparation of **3a**, a sample of 0.49 g (58.5%) of orange-red **3b** was obtained by the oxidation of 0.80 g (1.18 mmol) of **1b**. − IR (KBr): $\tilde{\nu}$ = 2551 cm^{-1} w [ν(BH)], 1987 vs [ν(CO)], 1893 vs [ν(CO)], 1202 m [ν_{as}(PO$_2$)], 1067 m [ν_s(PO$_2$)]. − ^{1}H NMR: δ = 2.35 (s, 3 H, Tp′CH$_3$), 2.38 (s, 3 H, Tp′CH$_3$), 2.41 (s, 6 H, Tp′CH$_3$), 2.66 (s, 6 H, Tp′CH$_3$), 3.41 (s, 12 H, NCH$_3$), 5.82 (s, 1 H, Tp′-H), 5.99 (s, 2 H, Tp′-H). − ^{13}C{^{1}H} NMR: δ = 12.6 (s, Tp′*C*H$_3$), 15.0 (s, Tp′*C*H$_3$), 16.9 (s, Tp′*C*H$_3$), 45.1 (s, NCH$_3$), 106.8 (s, Tp′*C*H), 145.4 (s, Tp′*C*CH$_3$), 146.2 (s, Tp′*C*CH$_3$), 152.2 (s, Tp′*C*CH$_3$), 152.4 (s, Tp′*C*CH$_3$), 179.4 (d, $^{1}J_{PC}$ = 91.9 Hz, PCN$_2$), 225.9 (s, CO), 298.7 (d, $^{1}J_{PC}$ = 46.2 Hz, W≡C). − ^{31}P{^{1}H} NMR: δ = 6.6 ($^{2}J_{PW}$ = 152.9 Hz). − MS: *m/z* = 713 [M$^+$], 656 [M$^+$ − 2 CO]. − $C_{23}H_{34}BN_8O_4PW$ (712.22): calcd. C 38.78, H 4.81, N 15.73; found C 38.39, H 4.78, N 15.66.

[Tp′(CO)$_2$Mo≡C−P(O)$_2$C(NEt$_2$)$_2$] (**4a**): As described above, a sample of **2a** (0.90 g, 1.39 mmol) was converted into orange-red **4a** by treatment with molecular dioxygen (yield: 0.67 g, 70.8%). − IR (KBr): $\tilde{\nu}$ = 2551 cm^{-1} w [ν(BH)], 2002 vs [ν(CO)], 1923 vs [ν(CO)], 1203 m [ν_{as}(PO$_2$)], 1066 m [ν_s(PO$_2$)]. − ^{1}H NMR: δ = 1.27 (t, $^{3}J_{HH}$ = 7.1 Hz, 12 H, CH$_2$C*H*$_3$), 2.31 (s, 6 H, Tp′CH$_3$), 2.37 (s, 6 H, Tp′CH$_3$), 2.62 (s, 6 H, Tp′CH$_3$), 3.89 (q, $^{3}J_{HH}$ = 7.1 Hz, 8 H, C*H*$_2$CH$_3$), 5.75 (s, 1 H, Tp′-H), 5.89 (s, 2 H, Tp′-H). − ^{13}C{^{1}H} NMR: δ = 12.9 (s, Tp′*C*H$_3$), 13.9 (s, NCH$_2$*C*H$_3$), 14.5 (s, Tp′*C*H$_3$), 16.4 (s, Tp′*C*H$_3$), 48.1 (s, N*C*H$_2$CH$_3$), 106.6 (s, Tp′*C*H), 145.3 (s, Tp′*C*CH$_3$), 145.9 (s, Tp′*C*CH$_3$), 151.4 (s, Tp′*C*CH$_3$), 181.0 (d, $^{1}J_{PC}$ = 95.3 Hz, PCN$_2$), 227.3 (s, CO), 314.4 (d, $^{1}J_{PC}$ = 28.2 Hz, Mo≡C). − ^{31}P{^{1}H} NMR: δ = −6.51 (s). − MS: *m/z* = 682 [M$^+$] (^{98}Mo), 626 [M$^+$ − 2 CO] (^{98}Mo). − $C_{27}H_{42}BMoN_8O_4P$ (680.42): calcd. C 47.66, H 6.22, N 16.47; found C 46.20, H 6.21, N 15.99. Solid samples retained varying amounts of CH_2Cl_2 despite prolonged drying in vacuo.

[Tp′(CO)$_2$W≡C−P(O)$_2$C(NEt$_2$)$_2$] (**4b**): As described above, 0.65 g (77.9%) of orange-red **4b** was prepared by oxidation of 0.80 g (1.09 mmol) of **2b** with dioxygen at 80 bar. − IR (KBr): $\tilde{\nu}$ = 2552 cm^{-1} w [ν(B−H)], 1989 vs [ν(CO)], 1894 vs [ν(CO)], 1205 m [ν_{as}(PO$_2$)], 1068 m [ν_s(PO$_2$)]. − ^{1}H NMR: δ = 1.30 (t, $^{3}J_{HH}$ = 6.8 Hz, 12 H, CH$_2$C*H*$_3$), 2.34 (s, 3 H, Tp′CH$_3$), 2.37 (s, 3 H, Tp′CH$_3$), 2.40 (s, 6 H, Tp′CH$_3$), 2.69 (s, 6 H, Tp′CH$_3$), 3.92 (q, $^{3}J_{HH}$ = 6.8 Hz, 8 H, C*H*$_2$CH$_3$), 5.81 (s, 1 H, Tp′-H), 5.97 (s, 2 H, Tp′-H). − ^{13}C{^{1}H} NMR: δ = 12.7 (s, Tp′*C*H$_3$), 13.9 (s, NCH$_2$*C*H$_3$), 15.0 (s, Tp′*C*H$_3$), 17.1 (s, Tp′*C*H$_3$), 47.9 (s, N*C*H$_2$CH$_3$), 106.8 (s, Tp′*C*H), 145.4 (s, Tp′*C*CH$_3$), 146.2 (s, Tp′*C*CH$_3$), 152.5 (s, Tp′*C*CH$_3$), 181.9 (d, $^{1}J_{PC}$ = 98.1 Hz, PCN$_2$), 226.5 (s, CO), 299.9 (d, $^{1}J_{PC}$ = 54.0 Hz, W≡C). − ^{31}P{^{1}H} NMR: δ = 7.0 (s, $^{2}J_{WP}$ = 151.7 Hz). − MS: *m/z* = 769 [MH$^+$], 712 [M$^+$ − 2 CO]. − $C_{27}H_{42}BN_8O_4PW$ (768.33): calcd. C 42.21, H 5.51, N 14.58; found C 41.91, H 5.51, N 14.35.

X-ray Crystal Structure Determination of **4a**: Single crystals of **4a** were grown from CH_2Cl_2/hexane at 5°C. A red crystal with the approximate dimensions 0.1 × 0.15 × 0.3 mm^3 was examined with a Siemens SMART CCD area detector system with three axis geometry using Mo-K_α radiation at 173 K. Crystal data and refinement details: Cell dimensions *a* = 16.8674(9), *b* = 15.8355(8), *c* = 13.6762(7) Å, β = 102.9790(10)°, *V* = 3559.6(3) Å^3, *Z* = 4, d_{calcd} = 1.428 g cm^{-3}, μ = 0.608 mm^{-1}, space group $P2_1/c$, data collection of 7737 unique intensities ($2\theta_{max}$ = 54°), semiempirical absorption correction from equivalents, structure solution by direct methods and anisotropic refinement with full-matrix least-squares methods on F^2 for all non-hydrogen atoms, programs used: Siemens SHELXTL-PLUS, SHELXL-97, R_F = 0.0478 for 6115 reflections with $I > 2\ \sigma(I)$, wR_F^2 = 0.0965 for all data, largest diff. peak 0.775 eÅ^{-3}.[16]

[1] L. Weber, G. Dembeck, R. Boese, D. Bläser, *Chem. Ber./Recueil* **1997**, *130*, 1305−1308.
[2] S. J. Goede, F. Bickelhaupt, *Chem. Ber.* **1991**, *124*, 2677−2684.
[3] M. Yoshifuji, T. Niitsu, N. Inamoto, *Chem. Lett.* **1988**, 1733−1734.
[4] L. N. Markovskii, G. N. Koidan, A. P. Marchenko, V. D. Romanenko, M. I. Povolotskii, A. M. Pinchuk, *Zh. Obshch. Khim.* **1989**, *59*, 2133 (*Chem. Abstr.* **1990**, *122*, 98672z).
[5] V. D. Romanenko, M. Sanchez, T. V. Sarina, M.-R. Mazières, *Tetrahedron Lett.*, **1992**, *33*, 2981−2982.
[6] S. Ho, K. Toyota, M. Yoshifuji, *Chem. Commun.* **1997**, 1637−1638.
[7] L. C. Thomas, R. A. Chittenden, *Spectrochim. Acta* **1970**, *26A*, 781−800.
[8] M. Abenoza, V. Tabcik, *J. Mol. Struct.* **1975**, *26*, 95−106.
[9] J. Weidlein, U. Müller, K. Dehnicke, *Schwingungsfrequenzen I*, Thieme, Stuttgart **1981**, p.106−107.
[10] B. Eberwein, J. Weidlein, *Z. Anorg. Allg. Chem.* **1976**, *420*, 229−239.
[11] T. Desmond, F. J. Lalor, G. Ferguson, M. Parvez, *J. Chem. Soc., Chem. Commun.* **1984,** 75−77.
[12] G. M. Jamison, P. S. White, J. L. Templeton, *Organometallics* **1991**, *10*, 1954−1959.
[13] D. E. C. Corbridge, *The Structural Chemistry of Phosphorus*, Elsevier Scient. Publ. Comp., Amsterdam, **1974**, p. 393.
[14] Holleman-Wiberg, *Lehrbuch der Anorganischen Chemie*, 101. Ed., de Gruyter, Berlin, **1995**, p. 768.
[15] A. N. Chernega, A. V. Ruban, V. D. Romanenko, L. N. Markovskii, A. A. Korkin, M. Y. Antipin, Y. T. Struchkov, *Heteroatom. Chem.* **1991**, *2*, 229−241.
[16] Crystallographic data (excluding structure factors) for the structure reported in this paper have been deposited with the Cambridge Crystallographic Data Centre as supplementary publication no. CCDC-100859. Copies of the data can be obtained free of charge on application to CCDC, 12 Union Road, Cambridge CB2 1EZ, UK [Fax: int. code +44(1223)336-033; E-mail: deposit@ccdc.cam.ac.uk].

[97258]

The Conformational Flexibility of Oxidized Cytochrome c Studied through Its Interaction with NH_3 and at High Temperatures

Lucia Banci, Ivano Bertini*, Georgios A. Spyroulias, and Paola Turano

Department of Chemistry, University of Florence,
Via Gino Capponi, 7, I-50121 Florence, Italy
Fax: (internat.) + 39(0)55/275-7555
E-mail: bertini@lrm.fi.cnr.it

Received November 21, 1997

Keywords: Cytochrome c / Hyperfine shift / Magnetic susceptibility anisotropy / NMR spectroscopy / Heme proteins

The binding of ammonia to oxidized horse heart cytochrome c has been studied by ^{1}H-NMR, EPR, and CD spectroscopy at pH = 8.0. The affinity constant of the ligand is in the range 1.5−4 M^{-1}. The ^{1}H-NMR spectra of the heme group have been found to be similar to those of the high-pH forms, high-temperature forms, and cyanide adduct of the Met80Ala mutant of *S. cerevisiae* iso-1-cytochrome c. The assignment of a number of signals has led to the determination of the values of the magnetic anisotropy and of the orientation of its axes. The latter are similar to those of the Met80Ala cyanide derivative. The assignment of the high-temperature species has been further pursued during this research. The analysis of the NMR data of the NH_3 adduct leads to the conclusion that substitution of Met80 at high pH or high temperature occurs through a ligand with cylindrical symmetry. This supports the suggestion that Met80 is substituted by a lysine at high pH.

The structure of the native cytochromes c has been extensively characterized by both X-ray crystallography[1][2][3][4][5][6][7] and NMR spectroscopy[8][9][10][11][12]. Several partially unfolded states of the oxidized species have also been detected spectroscopically as a function of temperature, pH, and denaturating agents[13−26] but the structural characterization for these protein forms is not available up to now. One important feature of cytochrome c folding/unfolding processes concerns the involvement of the covalently attached heme group and its axial ligands. The coordination of His and Met stabilizes the native state. Indeed, one of the first steps of ferricytochrome c unfolding upon increasing pH and/or temperature involves the detachment of Met80 from iron coordination[13−26]. In this respect NMR spectroscopy turns out to be a powerful technique for the detection of changes in the iron coordination in ferricytochrome c because the hyperfine shifted resonances are heavily affected by changes in the axial coordination of heme iron[27][28][29][30][31][32][33]. Indeed, through NMR spectroscopy, Hong and Dixon detected two forms of the alkaline isomerized species in slow exchange with the native form on the NMR time scale[34][35]. At neutral pH and temperature above 42°C, Ångstrom et al.[36] observed new species that closely resemble the alkaline isomerized forms. All these species contain low-spin iron(III). Recently, Taler et al. have further characterized the high-temperature species of horse cytochrome c and identified the ^{1}H-NMR resonances of the ε-CH_3 of Met80 in the high-temperature species at typical diamagnetic shift values[14].

It has been proposed that in oxidized cytochrome c at high pH values or at high temperatures the Nζ of a Lys residue substitutes Met80 in binding iron with a pK_a of 8.5−9.5[17][34][35][37][38][39][40][41][42][43][44][45][46][47][48][49]. It is known that pyridine and imidazole bind to iron by replacing Met80[50][51]. We report here an investigation on NH_3 binding to horse heart cytochrome. The results are compared with those related to the high-temperature species, whose characterization has been further extended during this research, with those on the cyanide adduct of the Met80Ala mutant of *S. cerevisiae* cytochrome *c*, and with those on the alkaline forms.

Results

NH_3 Adduct

The formation of the NH_3 adduct of horse heart cytochrome c (hh cyt c, hereafter) upon addition of increasing amounts of a solution of NH_4Br was monitored by ^{1}H-NMR spectroscopy at pH = 8.0 and at 293 K. At this pH this protein is largely in its physiologically relevant conformation, as shown by its ^{1}H-NMR spectrum (Figure 1, A).

Small traces of the alkaline forms are revealed by the peaks marked with asterisks. Upon addition of NH_4Br new resonances appear at δ = 25.2, 23.5, 15.7, 15.5, 11.6, 10.9 whereas the signals of native hh cyt c decrease in intensity (Figure 1, B−D). A broad feature is observed upfield at δ = −11.9. All the above-mentioned resonances are due to non-exchangeable protons because they remain when the spectra are recorded in D_2O.

Analogous titration was performed by circular dichroism spectroscopy (CD) in the Soret region. In the native form, the CD spectrum (Figure 2, A) is characterized by a negative absorption at 417 nm and a positive band at 400 nm, as already reported[40].

 © WILEY-VCH Verlag GmbH, D-69451 Weinheim, 1998 1434−1948/98/0505−0583 $ 17.50+.50/0

Figure 1. 600-MHz ^{1}H-NMR spectra of hh cyt c recorded in H_2O solution (100 mM phosphate buffer, pH = 8.0, T = 293 K) at increasing amounts of NH_4Br; (A) [NH_4Br] = 0 M; (B) [NH_4Br] = 0.5 M; (C) [NH_4Br] = 0.9 M; (D) [NH_4Br] = 2.7 M

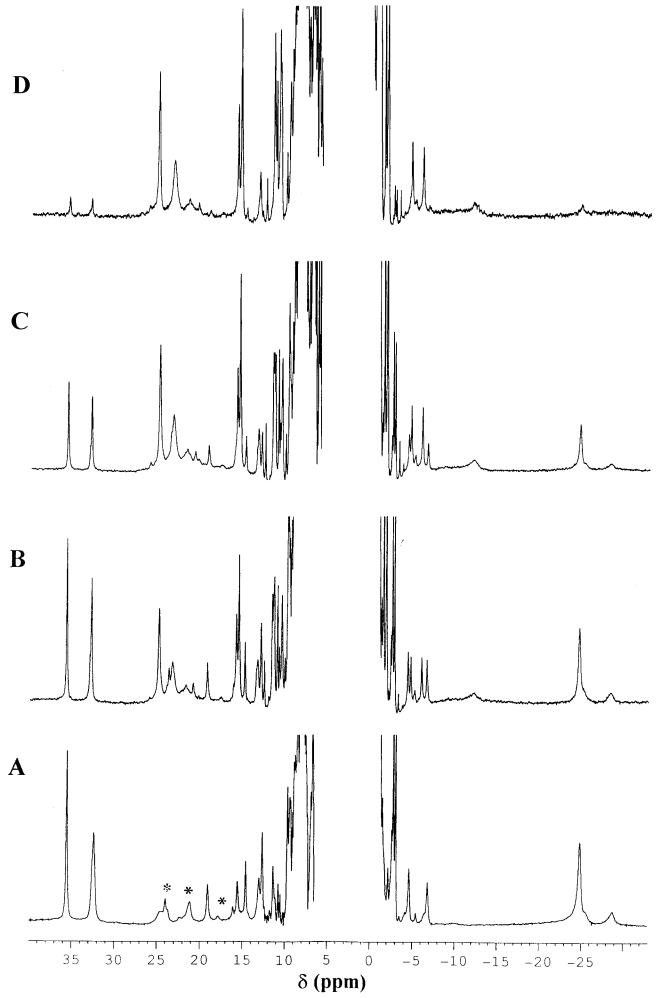

Figure 2. CD spectra on the native hh cyt c (A) and on the NH_3 adduct ([NH_4Br] = 2.7 M) recorded in 100 mM phosphate buffer (pH = 8.0, room temperature)

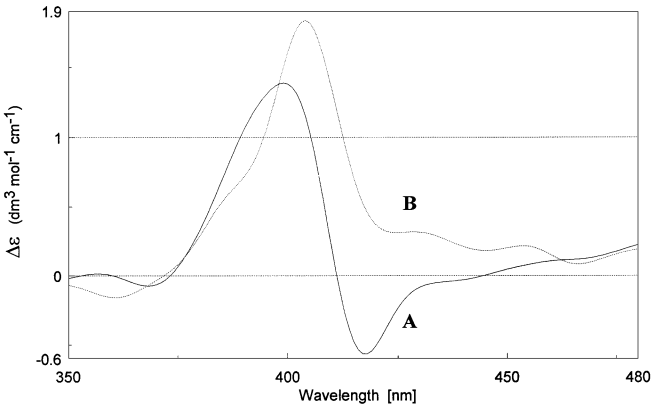

Figure 3. Downfield region of the 600-MHz ^{1}H-NMR EXSY spectrum recorded in H_2O solution (100 mM phosphate buffer, pH = 8.0, T = 293 K) on a sample with a ratio between native and NH_3-bound protein of about 1:1; broken lines indicate EXSY cross peaks between the heme methyl groups in the two protein forms

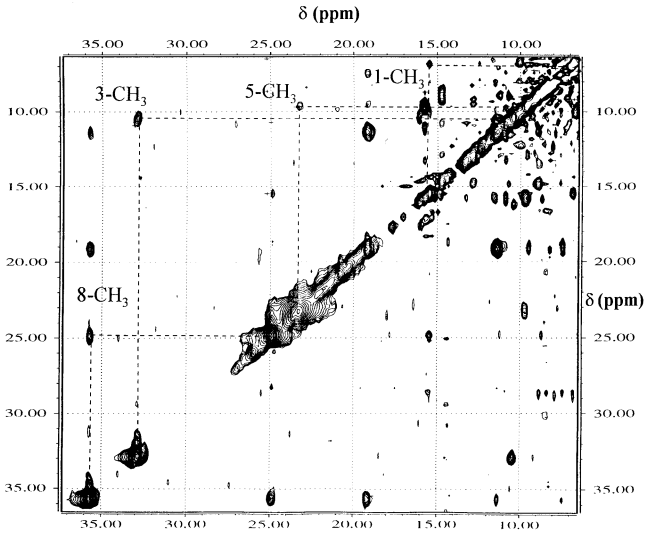

As the ligand concentration increases, the negative band becomes smaller and the positive absorption gains in intensity and moves towards higher wavelenghts. The final spectrum shows an intense positive band with maximum at 407 nm (Figure 2, B). A similar behavior has been reported as a function of an increase in pH and explained with the hypothesis that the negative 417-nm CD band is related to the ligation of the heme iron by Met80[40]. This idea is supported by chemical modification studies on cytochrome c[52].

From the circular dichroism and the ^{1}H-NMR titration, an apparent affinity constant in the range of 1.5−4 M^{-1} can be estimated.

The ^{1}H-NMR spectrum of the NH_3 derivative of hh cyt c was assigned by means of EXSY and NOESY spectroscopy. An EXSY cross peak is clearly detected between 8-CH_3 of the native form and the resonance at δ = 25.2 (Figure 3).

Other EXSY cross peaks have been observed at δ = 11.0 for 3-CH_3, δ = 15.5 for 1-CH_3, and δ = 23.5 for 5-CH_3. The δ-*meso* proton was assigned to the peak at δ = −6.0, thanks to its NOESY connectivities to both 8-CH_3 and 1-CH_3 of the NH_3-bound form. The 7-Hα proton was assigned at δ = 1.8 based on its EXSY connectivity with the 7-Hα of the native protein and on a strong NOESY connectivity with the 8-CH_3 resonance of the NH_3-bound form. The ε-CH_3 of Met80 gives an EXSY cross peak with a signal at δ = −3.3 (data not shown) which is then the corresponding signal in the NH_3 adduct, thus indicating that, in the presence of ammonia, Met80 is detached from iron and moves towards a position characterized by diamagnetic shift values. The β-CH_2 protons of His18 were assigned in the NH_3 adduct at δ = 15.7 and δ = 9.6. Indeed, an exchange cross peak is observed between one β-CH_2 signal at δ = 14.7 in the native form and that at δ = 15.7 in the NH_3 adduct. The resonances of the other β-CH_2 proton in the NH_3-bound and unbound forms are too close to each other to resolve the EXSY connectivity. The resonance was as-

signed by an NOESY experiment. All the above assignments are summarized in Table 1.

The shift pattern for the heme methyl groups is 8-CH_3 > 5-CH_3 > 1-CH_3 > 3-CH_3. The shift spreading is 14.2 ppm and the mean shift value is 18.5 ppm. At the same temperature the mean shift value for the four heme methyl groups of the native species is 21.3 ppm and the shift spreading is 28.9 ppm. At 2.7 M ligand concentrations, the native species is only about 10% of the NH_3-bound form. NOESY and TOCSY experiments were performed to further assign the spectrum of the adduct. The NOESY connectivities observed within the heme moiety are summarized in Scheme 1 (A).

The NOESY experiment allowed us to assign the Hα1 and Hα2 protons of Gly29 from their connectivities with 5-CH_3. The chemical shift of these two protons in the NH_3 adduct is very similar to that of the native form and therefore the EXSY cross peaks are too close to the diagonal to be clearly resolved. Other spin patterns were clearly identified in the TOCSY spectrum recorded in D_2O solution and are reported in Table 2.

Table 1. Shift values for the hyperfine shifted signals of NH_3 adduct of hh cyt c (pH = 8.0, T = 293 K), alkaline yeast Iso-1-cyt *c*, high-temperature forms of hh cyt *c*, (pH = 7.0, T = 335 K) and cyanide adduct of Met80Ala cyt c (T = 303 K)

Assignment	hh cyt c-NH_3 293 K (δ, ppm)	Alkaline yeast iso-1-cyt *c* 298 K (δ, ppm)[a]	hh cyt c 335 K (δ, ppm)	Various forms[b]	Met80Ala *c*-CN^- 303 K (δ, ppm)[d]
		Heme			
		24.8	22.3	A	
8-CH_3	25.2	24.0	22.0	B	22.5
			20.7	C	
		14.0	12.4	A	
3-CH_3	11.0	12.0	13.6	B	11.3
			11.3	C	
		21.5	20.6	A	
5-CH_3	23.5	19.0	18.9	B	19.5
			20.2	C	
			12.7	A	
1-CH_3	15.5		12.4	B	15.4
			13.4	C	
			4.0	A	
7-Hα	1.8		3.9	B	6.3
			3.7	C	
			0.8	A	
7-Hα′	−0.5		0.9	B	1.4
			0.4	C	
			−0.2	A	
7-Hβ	−1.5		0.1	B	0.6
			−0.4	C	
			1.1	A	
7-Hβ′	0.8		1.4	B	0.8
			1.7	C	
6-Hα	2.2		2.6		1.8
6-Hα′	−1.6		1.6		1.6
6-Hβ	−0.7		0.3		0.2
6-Hβ′	2.9		5.0		—[e]
2-Hα	0.8		−0.3	A	6.3
			−0.2	B	
2-CH_2	2.5		0.6	A	−0.2
			0.5	B	
4-CH_2	0.2		0.8		0.3
4-Hα	2.6		2.2		−0.1
α-*meso*	4.3		6.1		4.1
β-*meso*	1.4		−0.6		−0.8
γ-*meso*	—[c]		—[c]		—[e]
δ-*meso*	−6.0		−2.8	A	−4.3
			−1.9	B	
		His18			
Hα	10.9		—[c]		9.8
Hβ1	9.6		8.5	A	7.7
			9.0	B	
Hβ2	15.7		13.7	A	12.0
			14.1	B	
Hδ1	—[c]		—[c]		16.6
Hδ2	—[c]		18.3	A	16.1
			20.1	B	
Hε1			—[c]		−3.4
		Met80			
ε-CH_3	−3.3		2.6	A	
			2.3	B	

[a] Estimated chemical shifts taken from ref.[14]. — [b] The relative intensity of the EXSY peaks between the native and high-temperature species of hh cyt c follows the order : A > B > C. — [c] Not observed. — [d] Taken from ref.[60]. — [e] Not reported.

Table 2. Shift values for some residues in the NH_3 adduct of horse heart cyt c (100 mM phosphate buffer, pH = 8.0, T = 293 K)

Signal	hh cyt c-NH_3 (δ, ppm)
Gly1	
Hα1	3.5
Hα2	3.8
Gly6	
Hα1	3.2
Hα2	3.9
Phe10	
Hζ	9.3
Hε2	7.8
Hε1	8.9
Hδ2	6.9
Hδ1	7.3
Ala15	
Hα	6.1
β-CH_3	1.7
Cys17	
Hα	6.1
Hβ	6.9
Thr19	
Hα	6.7
Hβ	5.8
γ-CH_3	2.1
Gly23	
Hα1	3.7
Hα2	4.0
Gly29	
Hα1	−1.8
Hα2	−4.7
Asn31	
Hα	7.0
Hβ1	2.7
Hβ2	3.2
Phe36	
Hδ′s	7.4
Hε′s	6.5
Hζ	6.6
Gly45	
Hα1	3.7
Hα2	4.4
Asn54	
Hα	5.7
Hβ1	3.0
Hβ2	3.2
Gly56	
Hα1	3.8
Hα2	4.0
Trp59	
Hζ2	7.1
Hε3	6.8
Hζ3	6.5
Hη2	6.3
Leu64	
Hα	2.1
Hβ2	0.7
Hγ	0.4
δ1-CH_3	−0.3
δ2-CH_3	−0.6
Leu68	
Hα	2.8
Hβ2	−0.1
Hγ	0.6
δ1-CH_3	−0.9
δ2-CH_3	−1.8
Asn70	
Hα	6.0
Hβ1	3.3
Hβ2	3.4
Tyr74	
Hδ′s	8.1
Hε′s	7.1
Phe82	
Hδ′s	6.2
Hε′s	6.1
Hζ	5.9
Leu94	
Hα	2.1
Hβ1	1.4
Hβ2	0.6
Hγ	0.0
δ1-CH_3	−0.4
δ2-CH_3	−0.8
Tyr97	
Hδ2	7.4
Hε2	7.2
Hδ1	6.4
Hε1	5.6

Scheme 1. Schematic representation of a c-type heme; the dipolar connectivities observed between the heme resonances in hh cyt c NH_3 (A) and in the major high-temperature form (B) are also shown

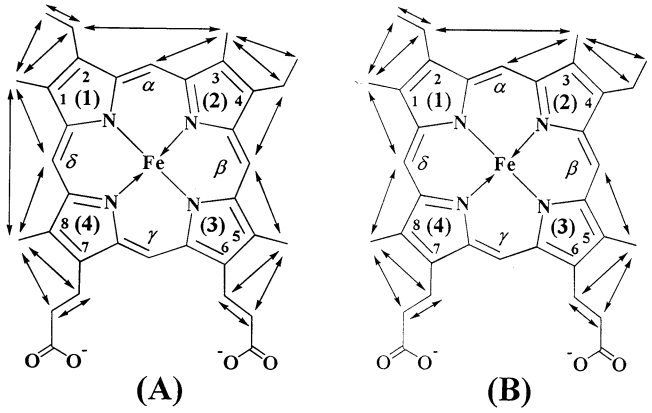

A broad resonance at δ ≈ 280 was also detected in the ^{1}H-NMR spectrum recorded in H_2O, which is probably due to the bound NH_3. No corresponding signal was detected in analogous spectra recorded in D_2O solutions. The broad signal observed at δ = −11.9, which does not exchange in D_2O, remains unassigned. However, its short T_1 value (< 2 ms) supports the idea that it is one of the two not-exchangeable protons of the proximal histidine ring. Non-selective T_1 values were also measured for the heme methyl groups, which are of the order of 70−80 ms.

From the EXSY cross-peak intensity observed between the heme methyl groups and from the above measured T_1 values, an exchange rate of 2−10 s^{-1} can be estimated.

The shift values of the assigned resonances reported in Table 2 allowed us to estimate the magnetic susceptibility tensor parameters for this protein form. The tensor has $\Delta\chi_{ax}$ and $\Delta\chi_{rh}$ values of 4.2 ± 0.2 × 10^{-32} and −2.2 ± 0.1 × 10^{-32} m^3, respectively. The χ_{xx} and χ_{yy} axes are close, although not exactly alligned, to the directions defined by the *meso* protons (the deviation is about 11°), while the χ_{zz} axis deviates by about 16° from the heme normal.

Figure 4. X-band EPR spectra of the NH_3 adduct ([NH_4Br] = 2.7 M, 100 mM phosphate buffer, pH = 8.0) recorded at 4.2 K using 30 dB microwave power and a gain of 800,000 (A), and 20 dB microwave power and a gain of 500,000 (B)

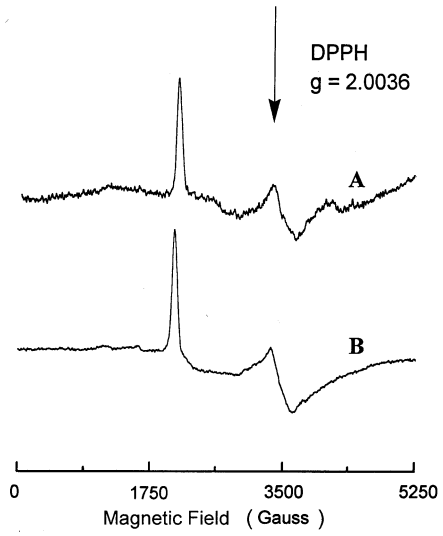

Figure 5. 600-MHz ^{1}H-NMR spectra of native hh cyt c recorded in H_2O solution (100 mM phosphate buffer, pH = 7.0) at various temperatures: (A) T = 293 K; (B) T = 300 K; (C) T = 310 K; (D) T = 320 K; (E) T = 330 K; (F) T = 335 K

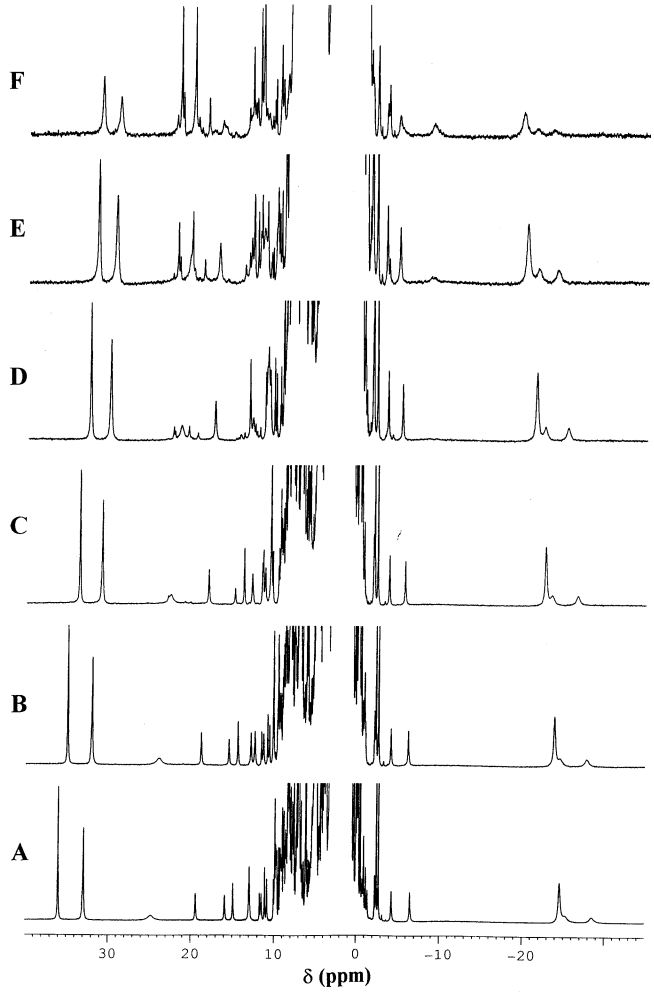

The EPR spectra of the final adduct (2.7 M of NH_4Br) at 4.2 K (Figure 4) show g values of 3.28, 2.01, and 1.66. The g values measured for the NH_3-bound cytochrome c are characteristic for a low-spin iron(III) and are within the range expected for a heme iron coordinated axially by a histidine and an amine group as exemplified by cytochrome f[53].

^{1}H-NMR Spectroscopy on the High-Temperature Species

In Figure 5 the ^{1}H-NMR spectra of oxidized hh cyt c in 100 mM phosphate buffer at pH = 7.0 are shown as a function of temperature in the 293−335 K range. At 293 K only the resonances of the native form are detected[10][54].

Upon increasing the temperature, new hyperfine shifted resonances appear in the 25−20 and 10−13 ppm ranges; a broad signal is also observed at δ = −10. At 335 K the intensity of the signals belonging to the new species is considerably enhanced, being twice as large as the intensity of the native-form resonances. At 335 K, the ^{1}H-NMR resonances due to three out of four heme methyl groups of the native form are well resolved at δ = 31.6, 29.5, and 12.4, while the fourth is at δ = 9.0. Three exchange cross peaks between the native and the high-temperature forms are observed for each methyl group, indicating that three new species are formed (Figure 6).

Figure 6. Downfield region of the 600-MHz ^{1}H-NMR EXSY spectrum of native hh cyt c recorded in H_2O solution (100 mM phosphate buffer, pH = 7.0) at 335 K with a mixing time of 40 ms; broken lines indicate EXSY cross peaks between the heme methyl groups in the native and high-temperature forms; cross peaks due to the three different high-temperature species are labelled accordingly to the concentration of the species: A > B > C

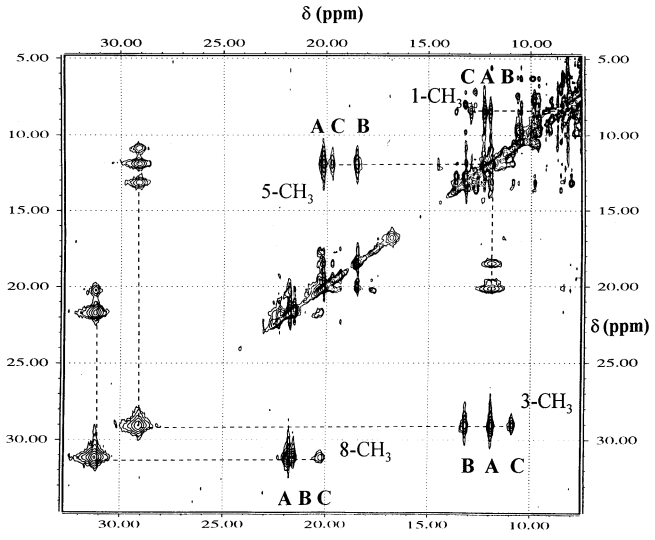

This implies that three different conformations involving the heme and the surrounding residues are present at this temperature. The shifts for these new species are compiled in Table 1. From the peak intensity, the A species is the major one, while the C species has the lowest concentration. The shift range for these resonances corresponds to that reported by Taler et al.[14]. From the EXSY cross-peak intensities, an exchange rate between the native and the

high-temperature forms of the order of 10 s^{-1} can be estimated. EXSY peaks are also observed between the corresponding resonances of the three forms A, B, and C.

EXSY experiments allowed us to identify the 7-propionate Hαs. The 7-propionate Hβs have been assigned on the basis of their NOE connectivities with the 7-Hαs of the same species. Dipolar connectivities were also observed between the 8-CH_3 resonances of the high-temperature forms and the corresponding 7-propionate protons. NOESY cross peaks have been also used to identify the other resonances reported in Table 1. Cross peaks between 5-CH_3 and the α-protons of 6-propionate are detected only for the major of the new species. All the dipolar connectivities between heme resonances observed at 335 K for form A are summarized in Scheme 1 (B).

As already observed by Taler et al.[14] through monodimensional saturation-transfer experiments, two exchange cross peaks were detected in the EXSY experiments between the ε-CH_3 of Met80 of the native form and two resonances at δ = 2.3 and 2.6 of the high-temperature species. Upon saturation of the Hγ proton of Met80 of the native species, located at δ = −22.7, saturation transfer is observed at δ = 3.2 and 2.7. From these assignments, it is clear that all the shift values observed for Met80 in the high-temperature species are typical of a "diamagnetic" methionine and therefore they constitute an additional demonstration that Met80 is detached from the heme iron under these experimental conditions.

By EXSY experiments also some of the His18 resonances were assigned, as reported in Table 1. Only two high-temperature species are detected for this residue.

For the native cytochrome c the heme methyl shift pattern is 8-CH_3 > 3-CH_3 > 5-CH_3 > 1-CH_3. At 335 K the mean shift value for the four heme methyl groups of the native species is 20.6 ppm while the spreading is 22.6 ppm. For the three high-temperature species the observed mean shift values are 17.0, 16.8, and 16.4 ppm for species A, B, and C, respectively. The spreading for the three species is 9.8, 9.6, and 9.4 ppm , in that order. The shift pattern is 8-CH_3 > 5-CH_3 > 1-CH_3 ≈ 3-CH_3.

Discussion

The present data show that NH_3 binds to iron(III) in oxidized hh cyt c by displacing Met80. The system has been characterized by EPR, CD and ^{1}H-NMR spectra. The ^{1}H-NMR spectra of the NH_3 adduct are different from that of the native hh cyt c because Met80 is not bound anymore, but they are, however, very similar to those of the high-temperature forms which experience the detachment of Met80 as well, the binding of another ligand to keep the low-spin nature of the iron. In fact, a heme with only a histidine bound in the fifth position gives rise to a high-spin species as observed in peroxidases[55][56][57][58][59]. Unfortunately, the previous[14] and the present data do not provide evidence for the nature of the sixth ligand. The comparison of the spectra of the NH_3 adduct and of the high-temperature species on one hand, and the spectra of the cyanide derivative of the Met80Ala yeast cytochrome c mutant[60] and of the high-pH species[34] on the other, may be instructive with respect to the conformational and unfolding properties[61][62] of cyt c. It is known[34] that cyt c undergoes a pH-dependent transition with a pK_a of 9.5 at 293 K. Interestingly, the pK_a decreases with increasing temperature, indicating that both pH and temperature cause similar effects. Indeed, Met80 is detached also at high pH[26]. As it results from Table 1, the NMR signals of the high-temperature species are close to those of the alkaline species. The ^{1}H-NMR spectra at high pH and high temperature have been reported also for the cyanide-free Met80Ala yeast cytochrome c[63], where no methionine is bound to the iron. They closely resemble those observed for the native protein under the same experimental conditions, although only one of the two alkaline forms in the mutant has been detected[63].

The ^{1}H-NMR heme shift pattern observed for the high-temperature forms, for the alkaline form, and for the NH_3 adduct closely resembles that of the cyanide adduct of Met80Ala mutant of yeast iso-1-cytochrome c (last column of Table 1)[60]. For the latter protein (at 303 K) the heme methyl resonances order is 8-CH_3 > 5-CH_3 > 1-CH_3 > 3-CH_3, the mean shift value is 17.2 ppm, and the heme methyl signal spreading is 11.2 ppm.

The cyanide adduct of Met80Ala mutant of yeast iso-1-cytochrome c has been extensively characterized by NMR both in terms of structure[60][64] and electronic properties[65][66]. The magnetic susceptibility tensor axes and anisotropies have been evaluated[65] and the contact contribution to the shift for the heme and the axial ligand has been separated from the pseudocontact one (Table 3). The pattern of the contact and pseudocontact contributions to the shift of the porphyrin methyl protons are determined by the orientation of the axial ligands[67−78]. In native cytochrome c both the His and the Met are contributing, whereas in the cyanide adduct of Met80Ala cytochrome c the orientation of the p_π nitrogen orbital of the His ring defines the shift pattern. In the latter system this orbital lies approximately parallel to the β/δ-*meso* direction and the smallest spin density is found for the 3-CH_3 (second column of Table 3)[65]. In native cytochrome c the contact shift pattern is completely different due to the contribution of Met80 which imparts a pairwise pattern to the heme methyl groups on opposite pyrrole rings, the 8-CH_3 and 3-CH_3 having significantly larger shifts than 1-CH_3 and 5-CH_3 (Table 3, third and fourth columns).

Table 3. Contact shift values (ppm) calculated for the NH_3 adduct of hh cyt *c*, the cyanide adduct of Met80Ala *S. cerevisiae* iso-1-cytochrome c (Met80Ala-CN^-)[65], native *S. cerevisiae* cytochrome c (yeast cyt c)[9], hh cyt c[10]

	hh cyt c-NH_3	Met80Ala-CN^-	yeast cyt c	hh cyt c
1-CH_3	24.0	16.9	4.5	3.4
3-CH_3	11.5	10.5	27.1	29.0
5-CH_3	32.0	20.8	7.4	6.1
8-CH_3	27.8	24.6	32.4	33.5

The orientation of the axial ligand determines the in-plane orientation of the magnetic susceptibility tensor axes[72][73][74][75][76][77][78] and then contributes to differentiate the shifts of the methyl signals. The directions of the tensor determined for the NH_3 adduct compare well with those of the cyanide adduct of Met80Ala for which the in-plane axes are essentially aligned with the *meso* proton directions and the *z* direction forms an angle of 6° with the direction of the perpendicular to the heme plane. The contact shift values for the heme methyl groups in the NH_3 adduct are also listed in Table 3 for comparison purposes. Analogously to the cyanide adduct of Met80Ala, the 3-CH_3 experiences the smallest shift.

Unfortunately, the NMR spectrum of the high-temperature species is complicated by the coexistence of four species at the same time. (At higher temperatures the protein denaturates). This prevented us from further extending the assignment of the A, B, and C forms and from calculating the magnetic susceptibility parameters. However, the comparison of the shift patterns of the high-temperature cytochrome c with the NH_3 adduct and with that of the cyanide adduct of the Met80Ala mutant, clearly supports the idea that the sixth axial ligand is axially symmetric. The same indication comes for the high-pH species.

Concluding Remarks

The assignment of the protons of the iron ligands reported in Table 1 for the NH_3 adduct and for the high-temperature species indicates a meaningful similarity between the two species. The similarity extends to the high-pH form of cytochrome c and the cyanide adduct of the Met80Ala mutant. The directions of the magnetic susceptibility anisotropy tensor for the NH_3 adduct are similar to those found in the cyanide adduct of the Met80Ala mutant. All of this has been rationalized in terms of the orientation of the axial histidine being the only factor determining the heme proton shift pattern. This suggests that the other axial ligand in the high-pH and the high-temperature forms has cylindrical symmetry. The results presented here are consistent with the hypothesis of a lysine substituting Met80 at high pH. They also shed further light on the conformational flexibility of the protein under various conditions.

This work was supported by the *E.U. BIOMED* program (BMH4-CT96/1492) and by *CNR-Comitato Nazionale Biotecnologia e Biologia Molecolare* (95.02860.CT14).

Experimental Section

Sample Preparation: Horse heart cytochrome c (Type VI) was purchased from Sigma Chemical Co. and used without further purification. The ^{1}H-NMR samples were prepared by dissolving the lyophilized protein in 100 mM phosphate buffer to give 2−4 mM solutions. The pH of the NMR samples was adjusted by addition of small volumes of concentrated solutions of NaOH or H_3PO_4. The pH was measured with an Orion Model 720 pH meter and a Microelectrodes, Inc., Model MI-410 microcombination pH probe. The NH_3 adduct was prepared by adding increasing amounts of a concentrated solution of NH_4Br at pH = 8.0. The same sample was used for EPR measurements. Circular dichroism spectra were obtained with a Jasco J500 dicrograph by titrating with NH_4Br a 8.0 μM ferricytochrome c solution (pH = 8.0, 100 mM phosphate buffer).

NMR Spectroscopy: The ^{1}H-NMR spectra were recorded with Bruker DRX 500 and AMX 600 spectrometers. T_1 measurements at 500 MHz were performed with the inversion-recovery method[79]. The 1D saturation-transfer experiments were performed with the superWEFT pulse sequence[80] and were collected using the standard methodology used for nuclear Overhauser effect (NOE) experiments of paramagnetic macromolecules[81]. All other spectra were acquired using presaturation during relaxation delay. EXSY experiments with the native cytochrome c were performed over the full spectral width with mixing times of 25, 40, and 60 ms at different temperatures (300, 310, 320, 330, 335 K). NOESY[82] and TOCSY[83] maps on a smaller spectral width (21 ppm) were collected in H_2O solutions at 335 K with a mixing time of 100 ms and a spin-lock time of 90 ms, respectively. EXSY experiments with a sample containing about 50% of the NH_3 adduct and 50% of the unbound form of cytochrome c were acquired with a mixing time of 40 ms at 293 K. NOESY and TOCSY maps of the completely NH_3-bound species were collected over a smaller spectral width (21 ppm) in H_2O and D_2O solutions at 293 K with a mixing time of 100 ms and a spin-lock time of 90 ms, respectively. − The 2D maps consisted of 4 K or 2 K data points in the F2 dimension. From 512 to 1024 experiments were recorded in the F1 dimension, using 64−512 scans per experiment. Raw data were multiplied in both dimensions by a pure cosine-squared and Fourier transformed to obtain 2048 × 2048 real data points. A polynomial base-line correction was applied in both directions. Data processing was performed using the standard Bruker software package. The 2D maps were analyzed by means of IBM RISC 6000 computers with the aid of the program XEASY (ETH, Zürich)[84].

EPR Spectroscopy: EPR experiments were performed at about 4.2 K with a Bruker ER200 spectrometer, operating at 9.6 GHz, equipped with an Oxford cryostat. The *g* values were calibrated by taking the 2,2-diphenyl-1-pycrylhydrazyl (DPPH) peak as reference (g = 2.0036). Spectra have been recorded using 30 dB microwave power and a gain of 800,000 or 20 dB microwave power and a gain of 500,000.

Magnetic Susceptibility Tensor Parameters: The hyperfine shift, i.e. the difference in shift of a proton in a paramagnetic system from that in an analogous diamagnetic system, includes contact and pseudocontact contributions[85][86][87][88]. The contact coupling is due to the presence of unpaired spin density on the resonating nucleus and vanishes a few chemical bonds away from the metal center. The pseudocontact contribution (δ_{pc}) arises from the magnetic susceptibility anisotropy and depends on the nuclear position with respect to the principal axes of the magnetic susceptibility tensor. Within the metal-centered point-dipole point-dipole approximation, the following equation holds[89]:

$$\delta_{pc} = \frac{1}{12\pi r_i^3}\left[\Delta\chi_{ax}(3n_i^2 - 1) + \frac{3}{2}\Delta\chi_{rh}\left(l_i^2 - m_i^2\right)\right] \quad (1)$$

where $\Delta\chi_{ax}$ and $\Delta\chi_{rh}$ are the axial and the rhombic anisotropies of the magnetic susceptibility induced by the paramagnetic ion, r_i is the distance of the nucleus *i* from the metal ion, and l_i, m_i, and n_i are the direction cosines of the position vector of atom *i* (r_i) with respect to the orthogonal reference system formed by the principal axes of the magnetic susceptibility tensor. − Pseudocontact shifts were determined by subtracting the chemical shifts measured in the reduced species of hh cyt c[90] from those of the NH_3-bound oxidized form of the same protein. The resonances of cysteines 14 and

17, of histidine 18, and of methionine 80 would experience non-negligible contact shifts and therefore were not included in the calculations. The 5 independent parameters (i.e. $\Delta\chi_{ax}$, $\Delta\chi_{rh}$, and three independent direction cosines which define the principal directions of the χ tensor with respect to a metal-centered axis system) were determined by finding the best fit of eq. 1 to a set of pseudocontact shifts[65][66], using the solution structure of horse heart cytochrome c[10].

[1] M. E. P. Murphy, B. T. Nall, G. D. Brayer, *J. Mol. Biol.* **1992**, *227*, 160−176.
[2] G. W. Bushnell, G. V. Louie, G. D. Brayer, *J. Mol. Biol.* **1990**, *214*, 585−595.
[3] H. Ochi, Y. Hata, N. Tanaka, M. Kakudo, T. Sakuri, S. Achara, Y. Morita, *J. Mol. Biol.* **1983**, *166*, 407−418.
[4] A. M. Berghuis, G. D. Brayer, *J. Mol. Biol.* **1992**, *223*, 959−976.
[5] G. V. Louie, G. D. Brayer, *J. Mol. Biol.* **1990**, *214*, 527−555.
[6] T. Takano, R. E. Dickerson, *J. Mol. Biol.* **1981**, *153*, 95−155.
[7] T. Takano, R. E. Dickerson, *J. Mol. Biol.* **1981**, *153*, 79−94.
[8] P. Baistrocchi, L. Banci, I. Bertini, P. Turano, K. L. Bren, H. B. Gray, *Biochemistry* **1996**, *35*, 13788−13796.
[9] L. Banci, I. Bertini, K. L. Bren, H. B. Gray, P. Sompornpisut, P. Turano, *Biochemistry* **1997**, *36*, 8992−9001.
[10] L. Banci, I. Bertini, H. B. Gray, C. Luchinat, T. Reddig, A. Rosato, P. Turano, *Biochemistry* **1997**, *36*, 9867−9877.
[11] P. X. Qi, D. L. Di Stefano, A. J. Wand, *Biochemistry* **1994**, *33*, 6408−6417.
[12] P. X. Qi, R. A. Beckman, A. J. Wand, *Biochemistry* **1996**, *35*, 12275−12286.
[13] A. Schejter, P. George, *Biochemistry* **1965**, *3*, 1045−1049.
[14] G. Taler, A. Schejter, G. Navon, I. Vig, E. Margoliash, *Biochemistry* **1995**, *34*, 14209−14212.
[15] G. R. Moore, G. W. Pettigrew, *Cytochromes c; Evolutionary, Structural and Physicochemical Aspects*, Springer-Verlag, Berlin, **1990**.
[16] H. Theorell, A. Akesson, *J. Am. Chem. Soc.* **1941**, *63*, 1804−1811.
[17] P. B. Barker, A. G. Mauk, *J. Am. Chem. Soc.* **1992**, *114*, 3619−3624.
[18] D. W. Dixon, X. Hong, S. E. Woehler, *Biophys. J.* **1989**, *56*, 339−351.
[19] T. Jordan, J. C. Eads, T. G. Spiro, *Protein Sci.* **1995**, *4*, 716−728.
[20] J. Babul, E. Stellwagen, *Biopolymers* **1971**, *10*, 2359−2361.
[21] J. Babul, E. Stellwagen, *Biochemistry* **1972**, *11*, 1195−1200.
[22] T. Y. Tsong, *Biochemistry* **1975**, *14*, 1542−1547.
[23] K. Muthukrishnan, B. T. Nall, *Biochemistry* **1991**, *30*, 4706−4710.
[24] W. Colon, L. P. Wakem, F. Sherman, H. Roder, *Biochemistry* **1997**, *36*, 12535−41.
[25] B. T. Nall in *Cytochrome c. A Multidisciplinary Approach* (Eds.: R. A. Scott, A. G. Mauk), University Science Books, Sausalito, CA, **1996**,chapter 4.
[26] M. T. Wilson, C. Greenwood, in *Cytochrome c. A Multidisciplinary Approach* (Eds.: R. A. Scott, A. G. Mauk), University Science Books, Sausalito, CA, **1996**, chapter 19.
[27] A. V. Xavier, D. L. Turner, H. Santos, *Methods Enzymol.* **1993**, *227*, 1−16.
[28] H. Santos, D. L. Turner, *Eur. J. Biochem.* **1992**, *206*, 721−728.
[29] H. Santos, D. L. Turner, *Biochim. Biophys. Acta* **1988**, *954*, 277−286.
[30] Y. Q. Feng, H. Roder, S. W. Englander, *Biophys. J.* **1990**, *57*, 15−22.
[31] G. Williams, N. J. Clayden, G. R. Moore, R. J. P. Williams, *J. Mol. Biol.* **1985**, *183*, 447−460.
[32] Y. Gao, J. Boyd, G. J. Pielak, R. J. P. Williams, *Biochemistry* **1991**, *30*, 1928−1934.
[33] D. L. Turner, R. J. P. Williams, *Eur. J. Biochem.* **1993**, *211*, 555−562.
[34] X. Hong, D. W. Dixon, *FEBS Lett.* **1989**, *246*, 105−108.
[35] L. L. Pearce, A. L. Gartner, M. Smith, A. G. Mauk, *Biochemistry* **1989**, *28*, 3152−3156.
[36] J. Angstrom, G. M. Moore, R. J. P. Williams, *Biochim. Biophys. Acta* **1982**, *703*, 87−94.
[37] D. L. Brautigan, B. A. Feinberg, B. M. Hoffman, E. Margoliash, J. Peisach, W. E. Blumberg, *J. Biol. Chem.* **1977**, *252*, 574−582.
[38] D. O. Lambeth, K. L. Campbell, R. Zand, G. Palmer, *J. Biol. Chem.* **1973**, *248*, 8130−8136.
[39] L. A. Davis, A. Schejter, G. P. Hess, *J. Biol. Chem.* **1974**, *249*, 2624−2632.
[40] Y. Looze, E. Polastro, M. Deconinck, J. Leonis, *Int. J. Peptide Protein Res.* **1978**, *12*, 233−236.
[41] C. Greenwood, M. T. Wilson, *Eur. J. Biochem.* **1971**, *22*, 5−10.
[42] N. Osheroff, D. Borden, W. H. Koppenol, E. Margoliash, *J. Biol. Chem.* **1980**, *255*, 1689−1697.
[43] H. T. Smith, F. Millet, *Biochemistry* **1980**, *19*, 1117−1120.
[44] G. Gupta, S. H. Koenig, *Biochem. Biophys. Res. Commun.* **1971**, *45*, 1134−1143.
[45] J. B. Wooten, J. S. Cohen, I. Vig, A. Schejter, *Biochemistry* **1981**, *20*, 5394−5402.
[46] K. E. Falk, P. A. Jovall, J. Angstrom, *Biochem. J.* **1981**, *193*, 1021−1024.
[47] P. M. A. Gadsby, J. Peterson, N. Foote, C. Greenwood, A. J. Thomson, *Biochem. J.* **1987**, *246*, 43−54.
[48] T. Kitagawa, Y. Ozaki, J. Teroaka, Y. Kyogoku, T. Yamanaka, *Biochim. Biophys. Acta* **1977**, *494*, 100−114.
[49] J. C. Ferrer, J. G. Guillemette, R. Bogumil, S. C. Inglis, M. Smith, A. G. Mauk, *J. Am. Chem. Soc.* **1993**, *115*, 7507−7508.
[50] W. Shao, Y. Yao, G. Liu, W. Tang, *Inorg. Chem.* **1993**, *32*, 6112−6114.
[51] W. Shao, J. Sun, Y. Yao, W. Tang, *Inorg. Chem.* **1995**, *34*, 680−687.
[52] Y. P. Myer, *Biochemistry* **1972**, *11*, 4203−4208.
[53] S. E. J. Rigby, G. R. Moore, J. C. Gray, P. M. A. Gadsby, S. J. George, A. J. Thomson, *Biochem. J.* **1988**, *256*, 571−577.
[54] Y. Q. Feng, H. Roder, S. W. Englander, A. J. Wand, D. L. Di Stefano, *Biochemistry* **1989**, *28*, 195−203.
[55] G. N. La Mar, J. S. de Ropp, K. M. Smith, K. C. Langry, *J. Biol. Chem.* **1980**, *255*, 6646−6652.
[56] J. D. Satterlee, J. E. Erman, G. N. La Mar, K. M. Smith, K. C. Langry, *Biochim. Biophys. Acta* **1983**, *743*, 246−255.
[57] L. Banci, I. Bertini, P. Turano, M. Tien, T. K. Kirk, *Proc. Natl. Acad. Sci. USA* **1991**, *88*, 6956−6960.
[58] J. S. de Ropp, G. N. La Mar, H. Wariishi, M. H. Gold, *J. Biol. Chem.* **1991**, *266*, 15001−15008.
[59] L. Banci, I. Bertini, E. A. Pease, M. Tien, P. Turano, *Biochemistry* **1992**, *31*, 10009−10017.
[60] K. L. Bren, H. B. Gray, L. Banci, I. Bertini, P. Turano, *J. Am. Chem. Soc.* **1995**, *117*, 8067−8073.
[61] T. Pascher, J. P. Chesick, J. R. Winkler, H. B. Gray, *Science* **1996**, *271*, 1558−1560.
[62] J. R. Winkler, P. Wittung, J. Leckner, B. G. Malmström, H. B. Gray, *Proc. Natl. Acad. Sci. USA* **1997**, *94*, 4246−4249.
[63] K. L. Bren, H. B. Gray, L. Banci, I. Bertini, P. Turano, *Chem. Biol.* **1995**, *2*, 355−363.
[64] L. Banci, I. Bertini, K. L. Bren, H. B. Gray, P. Sompornpisut, P. Turano, *Biochemistry* **1995**, *34*, 11385−11398.
[65] L. Banci, I. Bertini, K. L. Bren, M. A. Cremonini, H. B. Gray, C. Luchinat, P. Turano, *JBIC* **1996**, *1*, 117−126.
[66] L. Banci, I. Bertini, G. Gori Savellini, A. Romagnoli, P. Turano, M. A. Cremonini, C. Luchinat, H. B. Gray, *Proteins Struct. Funct. Genet.* **1997**, *29*, 68−76.
[67] F. A. Walker, J. Buehler, J. T. West, J. L. Hinds, *J. Am. Chem. Soc.* **1983**, *105*, 6923−6929.
[68] F. A. Walker, U. Simonis, in *NMR of Paramagnetic Molecules* (Eds.: L. J. Berliner, J. Reuben), Plenum Press, New York, **1993**.
[69] N. V. Shokhirev, F. A. Walker, *J. Phys. Chem.* **1995**, *99*, 17795−17804.
[70] F. A. Walker, M. Benson, *J. Phys. Chem.* **1982**, *86*, 3495−3499.
[71] F. A. Walker, D. Reis, V. L. Balke, *J. Am. Chem. Soc.* **1984**, *106*, 6888−6898.
[72] R. G. Shulman, S. H. Glarum, M. Karplus, *J. Mol. Biol.* **1971**, *57*, 93−115.
[73] D. L. Turner, C. A. Salgueiro, P. Schenkels, J. LeGall, A. V. Xavier, *Biochim. Biophys. Acta* **1995**, *1246*, 24−28.
[74] D. L. Turner, *Eur. J. Biochem.* **1995**, *227*, 829−837.
[75] L. Banci, A. Rosato, P. Turano, *JBIC* **1996**, *1*, 364−367.
[76] S. D. Emerson, G. N. La Mar, *Biochemistry* **1990**, *29*, 1556−1566.
[77] K. Rajarathnam, G. N. La Mar, M. L. Chiu, S. G. Sligar, *J. Am. Chem. Soc.* **1992**, *114*, 9048−9058.
[78] L. Banci, R. Pierattelli, D. L. Turner, *Eur. J. Biochem.* **1996**, *232*, 522−527.
[79] R. L. Vold, J. S. Waugh, M. P. Klein, D. E. Phelps, *J. Chem. Phys.* **1968**, *48*, 3831−3832.

[80] T. Inubushi, E. D. Becker, *J. Magn. Reson.* **1983**, *51*, 128−133.
[81] L. Banci, I. Bertini, C. Luchinat, M. Piccioli, A. Scozzafava, P. Turano, *Inorg. Chem.* **1989**, *28*, 4650−4656.
[82] S. Macura, K. Wüthrich, R. R. Ernst, *J. Magn. Reson.* **1982**, *47*, 351−357.
[83] A. Bax, D. G. Davis, *J. Magn. Reson.* **1985**, *65*, 355−360.
[84] C. Eccles, P. Güntert, M. Billeter, K. Wüthrich, *J. Biomol. NMR* **1991**, *1*, 111−130.
[85] R. H. Holm, C. J. Hawkins, in *NMR of Paramagnetic Molecules. Principles and Applications* (Eds.: G. N. La Mar, W. D. Horrocks, Jr., R. H. Holm), Academic Press, New York, **1973**, chapter 7.
[86] I. Bertini, C. Luchinat, *NMR of Paramagnetic Molecules in Biological Systems*, Benjamin/Cummings, Menlo Park, CA, **1986**,
[87] I. Bertini, C. Luchinat, "NMR of Paramagnetic Substances", *Coord. Chem. Rev. 150*, Elsevier, Amsterdam, **1996**, p. 1.
[88] I. Bertini, P. Turano, "NMR of Paramagnetic Macromolecules", *NATO ASI Series* (Ed.: G. N. La Mar), Kluwer Academic, Dordrecht, **1994**.
[89] H. M. McConnell, R. E. Robertson, *J. Chem. Phys.* **1958**, *29*, 1361−1365.
[90] A. J. Wand, D. L. Di Stefano, Y. Q. Feng, H. Roder, S. W. Englander, *Biochemistry* **1989**, *28*, 186−194.

[97273]

Cyclopentadienyl Complexes of Yttrium Aminotroponiminates: An Example for an Improved Alternative Ligand System

Peter W. Roesky

Institut für Anorganische Chemie, Universität Karlsruhe,
Engesserstraße, Geb. 30.45, D-76128 Karlsruhe, Germany
Fax: (internat.) +49 (0)721/661921

Received November 25, 1997

Keywords: Yttrium / Aminotroponiminate / Cyclopentadienyl / Dynamic NMR

Mixed aminotroponiminate ([ATI]$^-$) cyclopentadienyl complexes were prepared using two different synthetic routes. Reaction of $[[(i\text{Pr})_2\text{ATI}]\text{YCl}_2(\text{THF})_2]_2$ (**1**) with KCp* (Cp* = C_5Me_5) or $\text{Li}[C_5H_3(SiMe_3)_2]$ affords $[(i\text{Pr})_2\text{ATI}]\text{YCp}_2$* (**2a**) and $[(i\text{Pr})_2\text{ATI}]\text{Y}[C_5H_3(SiMe_3)_2]_2$ (**2b**), respectively. Moreover, $[(i\text{Pr})_2\text{ATI}]\text{YCp}_2$* has also been obtained from the reaction of Cp_2*$\text{Y}(\mu\text{-Cl})_2\text{Li}(\text{OEt}_2)_2$ (**3**) and $[(i\text{Pr})_2\text{ATI}]$K. The single crystal X-ray structure of $[(i\text{Pr})_2\text{ATI}]\text{YCp}_2$* shows that the steric demand of the $[(i\text{Pr})_2\text{ATI}]^-$ ligand is somewhat similar to that of the well-known cyclopentadienyl group and diazadiene ligand. $[(i\text{Pr})_2\text{ATI}]\text{Y}[C_5H_3(SiMe_3)_2]_2$ shows a dynamic behavior in solution (^{1}H NMR), which is essentially caused by rotation of the cyclopentadienyl group rather than by migration of the $[(i\text{Pr})_2\text{ATI}]^-$ ligand.

Introduction

Recently, there has been significant interest in early transition metal chemistry for the replacement cyclopentadienyl (or related systems) by other ligands in order to generate a similar steric and electronic environment.[1] For example, a number of metal complexes of the lanthanides and group 3 elements have been synthesized in which cyclopentadienyl is replaced by anionic bidentate nitrogen ligands such as amides,[2] benzamidinates,[3] and diazadienes.[4]

The aminotroponiminates ([ATI]$^-$) **A**, have been introduced as cyclopentadienyl alternatives for group 3,[5] group 4,[6] and the lanthanide elements.[5] [ATI]$^-$ is a bidentate mono-anionic ligand that features a 10 π electron backbone.[7] Upon coordination to a metal atom, [ATI]$^-$ forms a five-membered metallacycle adjacent to the seven-membered carbon ring. Recently, it was shown that the heteroleptic yttrium amides $[\text{ATI}]\text{Y}[\text{N}(\text{SiMe}_3)_2]_2$ and $[\text{ATI}]_2\text{Y}[\text{N}(\text{SiMe}_3)_2]$ are active catalysts for the hydroamination/cyclization reaction of aminoalkynes.[8] The new catalysts were obtained by transmetallation of the corresponding chloro precusors $[[\text{ATI}]\text{YCl}_2(\text{THF})_2]_2$ and $[\text{ATI}]_2\text{YCl}$ using $\text{K}[\text{N}(\text{SiMe}_3)_2]$.

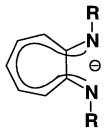

A

In order to compare the coordination behavior and the steric demands of both [ATI]$^-$ and cyclopentadienyl groups, our main interest is now focused on mixed cyclopentadienyl-[ATI]$^-$ complexes. In this paper, the synthesis of new cyclopentadienyl-[ATI]$^-$ yttrium complexes starting from the isopropyl derivative $[[(i\text{Pr})_2\text{ATI}]\text{YCl}_2(\text{THF})_2]_2$ (**1**)[5] is reported. These reactions lead to complexes of the general formula $[(i\text{Pr})_2\text{ATI}]\text{YCp}_2$ [Cp = C_5Me_5, $C_5H_3(SiMe_3)_2$]. **1** can be obtained from $[(i\text{Pr})_2\text{ATI}]$K and YCl_3 (Scheme 1).

Results and Discussion

Transmetallation of **1** with a slight excess of potassium pentamethylcyclopentadienyl (KCp*) in THF (Scheme 1), followed by workup in pentane, yields the corresponding dicyclopentadienyl complex $[(i\text{Pr})_2\text{ATI}]\text{YCp}_2$* (**2a**) as a pure yellow solid in fairly good yield. **2a** can also be obtained by the "classical" route using Cp_2*$\text{Y}(\mu\text{-Cl})_2\text{Li}(\text{OEt}_2)_2$ (**3**)[9] as the starting material. Reaction of **3** with 1 equivalent of $[(i\text{Pr})_2\text{ATI}]$K in toluene, followed by extraction with pentane, also affords **2a** (Scheme 1). **2a** is an air and moisture sensitive compound and has been characterized by MS, ^{1}H- and ^{13}C-NMR spectroscopy, and elemental analysis. The ^{1}H-NMR spectrum shows a sharp singlet for the protons of the Cp* unit, and this signal is shifted slightly downfield (δ = 1.94) compared with that of **3** (δ = 1.83).[9] The room temperature ^{1}H- and ^{13}C-NMR spectra point to a symmetrical coordination of the $[(i\text{Pr})_2\text{ATI}]^-$ ligand in solution, which is in agreement with the coordination observed in the solid state (see below). The signal of the isopropyl C*H* of **2a** is well resolved into a septet, but shows a marked upfield shift (δ = 3.82) compared to the starting material **1** (δ = 4.04).[5] In contrast to the anionic dicyclopentadienyl diazadiene complex of lanthanum, $[\text{Cp}_2\text{*La(DAD)}]^-$ {DAD = (Ph)N=C(Ph)C(Ph)=N(Ph)},[10] and the dicyclopentadienyl diazadiene complexes of group 4 metals, Cp_2*M(DAD) (M = Zr, Hf),[11] **2a** does not show a rapid dynamic exchange of the chelating ligand in solution at room temperature. Whereas DAD

 © WILEY-VCH Verlag GmbH, D-69451 Weinheim, 1998 1434−1948/98/0404−0593 $ 17.50+.50/0

Scheme 1

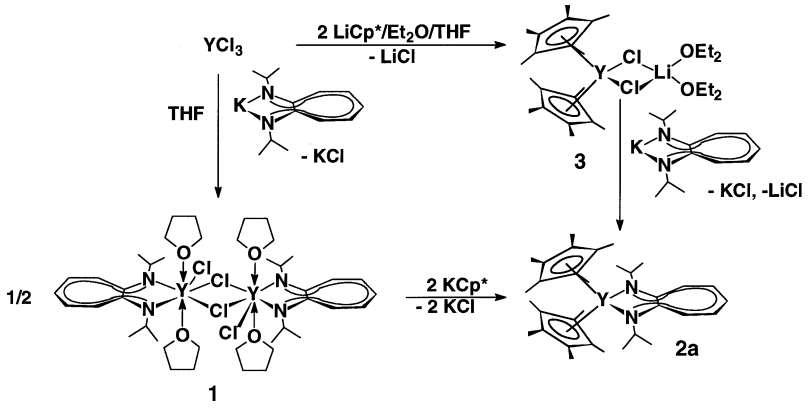

complexes show a rapid migration of the Cp*M unit from one side of the reduced DAD ligand to the other, the rigid geometry of the $[(i\mathrm{Pr})_2\mathrm{ATI}]^-$ ligand (also seen in the single crystal X-ray structure of **2a**) prevents such a strong movement of the Cp_2*Y moiety.

The solid-state structure of **2a** was investigated by single-crystal X-ray diffraction (Figure 1). Suitable crystals were obtained by slow evaporation of a saturated heptane solution of **2a**. The structure reveals a pseudo-tetrahedral arrangement of the ligands around the yttrium atom. The C_g−Y (C_g = Cp*-ring centroids) distances (C_g1−Y 244.6 pm and C_g2−Y 244.2 pm) are in the expected range of other Cp_2*Y^{III} compounds [e.g. 240.8(4) pm in Cp_2*Y(DAD)[10] and 266(2) pm in Cp_2*Y(μ-Cl)$_2$Li(THF)$_2$[12]]. The angle C_g1−Y−C_g2 (133.95°) is approximately five degrees smaller than that in Cp_2*Y(DAD) [138.6(2)°]. Similar bonding modes are observed for Cp_2*Sm[N(*t*Bu)=CHCH=N(*t*Bu)].[13] Both Cp* rings in **2a** are located in a staggered position with respect to each other. A C_2-symmetric coordination of the $[(i\mathrm{Pr})_2\mathrm{ATI}]^-$ ligand along the Y−C5 axis with symmetric N−Y distances [N1−Y 239.8(2) and N2−Y 239.0(3) pm] is observed. The whole $[(i\mathrm{Pr})_2\mathrm{ATI}]^-$ framework is twisted, i.e. the atom C1 (C2) is located about 40 pm above (below) the least-squares mean plane defined by the seven membered ring (C1−C7). This observation is in sharp contrast to the comparable group 4 complexes, $[(i\mathrm{Pr})_2\mathrm{ATI}]_2\mathrm{MCl}_2$ (M = Zr, Hf),[6] which show a planar coordination of the ligand. The N1−Y1−N2 angle [69.38(9)°] is in the range of comparable compounds such as **1** [67.4(2)°][5] and also of Cp_2*Y(DAD) [70.1(1)°], suggesting a similar steric demand for $[(i\mathrm{Pr})_2\mathrm{ATI}]^-$ and DAD.

$[(i\mathrm{Pr})_2\mathrm{ATI}]\mathrm{Y}[\mathrm{C}_5\mathrm{H}_3(\mathrm{SiMe}_3)_2]_2$ (**2b**) is prepared in a similar way to **2a**. Transmetallation of **1** with lithium bis[1,3-(trimethylsilyl)cyclopentadienyl], $\mathrm{Li}[\mathrm{C}_5\mathrm{H}_3(\mathrm{SiMe}_3)_2]$ in toluene in a 2:1 molar ratio (equation 1), followed by workup in pentane, leads to **2b** as a yellow solid in very high yields. **2b** has been characterized by MS, IR, ^{1}H-NMR spectroscopy, and elemental analysis. In contrast to **2a** the ^{1}H-NMR spectrum of **2b** shows a dynamic behavior in solution. At low temperature (213 K) two doublets for the methyl protons of the isopropyl groups of the $[(i\mathrm{Pr})_2\mathrm{ATI}]^-$ ligand are observed along with two singlets for the Me_3Si groups. These

Figure 1. Solid-state structure of **2a** showing the atom labeling scheme, omitting hydrogen atoms (SCHAKAL drawing)[a]

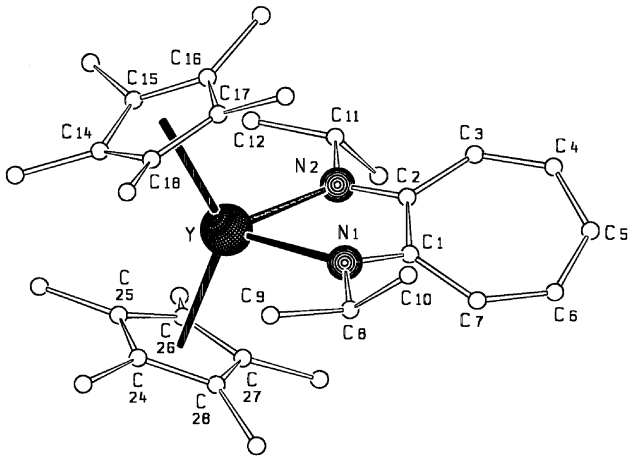

[a] Selected distances [pm] and angles [°]: C1−N1 132.7(4), C2−N2 132.9(4), C14−Y 277.5(3), C15−Y 275.4(3), C16−Y 270.8(3), C17−Y 271.8(3), C18−Y 276.4(3), C24−Y 269.0(4), C25−Y 271.1(3), C26−Y 275.5(3), C27−Y 273.3(3), C28−Y 271.1(4), N1−Y 239.8(2), N2−Y 239.0(3), C_g1−Y 244.6, C_g2−Y 244.2; N2−Y−N1 69.38(9), N1−Y−C14 127.52(10), N2−Y−C14 131.12(10), N1−Y−C15 132.13(10), N2−Y−C15 102.46(10), N1−Y−C16 103.40(9), N2−Y−C16 84.06(10), N1−Y−C17 84.22(9), N2−Y−C17 98.73(10), N1−Y−C18 97.93(10), N2−Y−C18 128.48(10), C_g1−Y−C_g2 133.95 (C_g = ring centroid).

signals start to coalesce with increasing temperature and have a coalescence temperature of about T_c = 273 K. At higher temperatures (313 K and above) the signals due to the methyl protons of the isopropyl groups appear as one doublet and the signal of the Me_3Si groups as a singlet. Since the $[(i\mathrm{Pr})_2\mathrm{ATI}]^-$ ligand does not show a fluctionality in **2a**, these results were interpreted as evidence that the two diastereotopic isopropyl groups exist in different chiral environments and, due to the reciprocal nature of this effect, so do the Me_3Si groups. It was shown earlier that $[\mathrm{C}_5\mathrm{H}_3(\mathrm{SiMe}_3)_2]_2\mathrm{ZrX}_2$ (X = F, Br, I) complexes crystallize in a staggered conformation.[14] These conformations are chiral in the absence of rotation of the cyclopentadienyl groups. In accordance with these results, two enantiomeric conformations are depicted in Figure 2 by considering a stronger repulsion of the Me_3Si groups in the back of the

bent metallocene than in the front. At high temperature both enantiomers interconvert rapidly, thus showing only one set of signals. A similar diastereotopic splitting of the isopropyl signals of the $[(i\mathrm{Pr})_2\mathrm{ATI}]^-$ ligand was observed earlier for the chiral homoleptic compounds $[(i\mathrm{Pr})_2\mathrm{ATI}]_3\mathrm{Ln}$ (Ln = Y, La, Sm).[5]

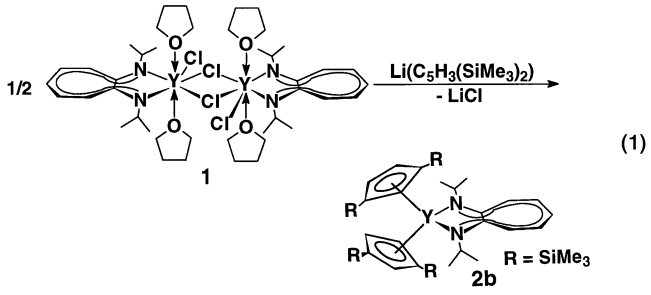

(1)

Figure 2. Schematic representation of both enantiomers of **2b** observed at low temperature in the ^{1}H NMR (considering the absence of a suitable scrambling mechanism at these temperatures)

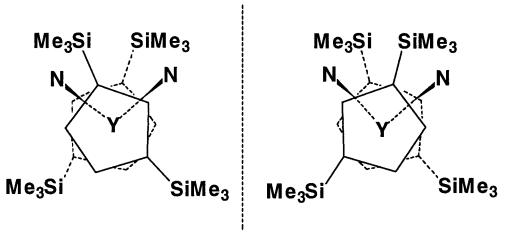

From the coalescence temperature (T_c = 273) and the separation ($\Delta\nu$ = 33.21 s^{-1}, 250 MHz NMR) of the two coalescing doublets of the isopropyl groups in the absence of any exchange, the free energy for the rotation about the Y−C_g axis was calculated to be $\Delta G_{Tc}^{\geq}$ = 56.95 kJ/mol, according to equation 2.[15]

$$\Delta G_{Tc}^{\ddagger} = -RT_c\ln(\pi\Delta\nu\, h/\sqrt{2}\, k_b T_c) \quad (2)$$

In summary, new mixed cyclopentadienyl−$[ATI]^-$ complexes of yttrium have been prepared. It has been demonstrated that the steric demand of the $[(i\mathrm{Pr})_2\mathrm{ATI}]^-$ ligand is comparable to that of the well-known cyclopentadienyl groups and diazadiene ligands. The fluctional behavior of $[(i\mathrm{Pr})_2\mathrm{ATI}]\mathrm{Y}[\mathrm{C_5H_3(SiMe_3)_2}]_2$ (**2b**) is essentially caused by rotation of the cyclopentadienyl groups and not by migration of the $[(i\mathrm{Pr})_2\mathrm{ATI}]^-$ ligand.

This work was supported by the *Deutsche Forschungsgemeinschaft* and the *Fonds der Chemischen Industrie* (Liebig fellowship). Additionally, generous support from Prof. Dr. *D. Fenske* is gratefully acknowledged.

Experimental Section

General: All manipulations of air-sensitive materials were performed with the rigorous exclusion of oxygen and moisture in flame-dried Schlenk-type glassware either on a dual manifold Schlenk line, or interfaced to a high vacuum (10^{-4} Torr) line, or in an argon-filled Braun Atmospheres glove box. Ether solvents (tetrahydrofuran and diethyl ether) were pre-dried over Na wire and distilled under nitrogen from Na/K alloy benzophenone ketyl. Hydrocarbon solvents (toluene and pentane) were distilled under nitrogen from Na wire. All solvents for vacuum line manipulations were stored in vacuo over Na/K alloy in resealable flasks. Deuterated solvents were obtained from Aldrich Inc. (all 99 atom% D) and were degassed, dried, and stored in vacuo over Na/K alloy in resealable flasks. NMR spectra were recorded on a Bruker AC 250 spectrometer. Chemical shifts are referenced to internal solvent resonances and are reported relative to tetramethylsilane. IR spectra were performed on a Bruker IFS 28, mass spectra were recorded at 70 eV on Varian MAT 711. Elemental analyses were performed in the micro analytical laboratory of the Institut für Anorganische Chemie der Universität Karlsruhe (S. Ariman). KCp*[16], $\mathrm{Li[C_5H_3(SiMe_3)_2]}$,[13] $\mathrm{Cp_2^*Y(\mu\text{-}Cl)_2Li(OEt_2)_2}$,[9] $[(i\mathrm{Pr})_2\mathrm{ATI}]\mathrm{K}$,[5] and $[[(i\mathrm{Pr})_2\mathrm{ATI}]\mathrm{YCl_2(THF)}]_2$,[5] were prepared by literature procedures.

Preparation of [(iPr)$_2$ATI]YCp$_2$* (**2a**) − *Route A:* THF was condensed at −196°C onto a mixture of 189 mg (0.21 mmol) of $\{[(i\mathrm{Pr})_2\mathrm{ATI}]\mathrm{YCl_2(THF)_2}\}_2$ and 174 mg (1.0 mmol) of KCp*, and the mixture was stirred for 18 h at room temperature. The solvent was evaporated in vacuum, and pentane was condensed onto the mixture. The solution was then filtered, and the solvent removed. This procedure was repeated twice. The remaining solid was recrystallized from pentane. − Yield 130 mg (56%).

Route B: THF was condensed at −196°C onto a mixture of 390 mg (0.21 mmol) of $\mathrm{Cp_2^*Y(\mu\text{-}Cl)_2Li(OEt_2)_2}$, and 161 mg (1.0 mmol) of $[(i\mathrm{Pr})_2\mathrm{ATI}]\mathrm{K}$ and the mixture was stirred for 18 h at room temperature. The solvent was evaporated in vacuum, and pentane was condensed onto the mixture. The solution was then filtered, and the solvent removed. The remaining solid was recrystallized from pentane. − Yield 180 mg (49%). − ^{1}H NMR (C_6D_6, 250 MHz, 25°C): δ = 1.17 [d, 12 H, $(CH_3)_2CH$, J(H,H) = 6.3 Hz], 1.94 (s, 30 H, CH_3Cp), 3.82 [sept, 2 H, $(CH_3)_2CH$, J(H,H) = 6.4 Hz], 6.09−6.24 (m, 3 H, $H^{3,5,7}$), 6.84 (dd, 2 H, $H^{4,6}$). − $^{13}C\{^1H\}$ NMR (C_6D_6, 62.9 MHz, 25°C): δ = 13.4 (CH_3Cp), 22.9 [$(CH_3)_2CH$], 49.4 [$(CH_3)_2CH$], 115.1 (C^5), 115.3 (Cp), 119.6 ($C^{3,7}$), 133.4 ($C^{4,6}$), 164.2 ($C^{1,2}$). − EI/MS (70 eV) *m/z* (%): 562 ($[M]^+$, rel. int. 11), 427 ($[M - Cp^*]^+$, 100), 223 ($[Cp^*Y - H]^+$, 64), 204 ($[C_{13}H_{20}N_2]^+$, 87). − $\mathrm{C_{33}H_{49}N_2Y}$ (562.67): calcd. C 70.44, H 8.78, N 4.98; found C 70.03, H 8.57, N 5.31.

Preparation of [(iPr)$_2$ATI]Y(C$_5$H$_3$(SiMe$_3$)$_2$)$_2$ (**2b**): THF was condensed at −196°C onto a mixture of 217 mg (0.25 mmol) of $\{[(i\mathrm{Pr})_2\mathrm{ATI}]\mathrm{YCl_2(THF)_2}\}_2$ and 216 mg (1.0 mmol) of $\mathrm{Li[C_5H_3(SiMe_3)_2]}$, and the mixture was stirred for 18 h at room temperature. The solvent was evaporated in vacuum, and pentane was condensed onto the mixture. The solution was then filtered, and the solvent removed. This procedure was repeated twice. −Yield 335 mg (94%). − IR (KBr) $\tilde{\nu}$ = 1592 cm^{-1} (st), 1506 (vs), 1470 (st), 1249 (st), 833 (vs). − ^{1}H NMR ([D$_8$]toluene, 250 MHz, 70°C): δ = 0.20 (s, 36 H, CH_3Si), 1.38 [d, 12 H, $(CH_3)_2CH$, J(H,H) = 6.6 Hz], 3.56 [sept, 2 H, $(CH_3)_2CH$], 6.09−6. 20 (m, 3 H, $H^{3,5,7}$), 6.16 (d, 2 H, Cp), 6.35 (d, 2 H, Cp), 6.64 (dd, 2 H, $H^{4,6}$), 6.71 (s, 1 H, Cp). − $^{13}C\{^1H\}$ NMR ([D$_8$]toluene, 62.9 MHz, 25°C): δ = 1.4 (CH_3Si), 20.7 [$(CH_3)_2CH$], 46.3 [$(CH_3)_2CH$], 110.6 (Cp), 115.3 (C^5), 117.9 (Cp), 119.5 ($C^{3,7}$), 133.4 ($C^{4,6}$), 164.2 ($C^{1,2}$). − ^{29}Si NMR ([D$_8$]toluene, 49.7 MHz, 25°C): δ = −9.5. − EI/MS (70 eV) *m/z* (%): 710 ($[M]^+$, rel. int. 11), 637 ($[M - C_3H_{15}Si]^+$, 8), 501 $[M - (C_9H_{11}N_2)]^+$, 100), 297 ($[C_{11}H_{21}YSi_2)]^+$ 37). − $\mathrm{C_{35}H_{61}N_2Si_4Y}$ (711.23): calcd. C 59.12, H 8.65, N 3.94; found C 58.75, H 8.71, N 4.50.

Crystal Structure Analysis of **2a**: Stoe-IPDS diffractometer (Mo-K_α radiation); T = 203(3) K; data collection and refinement: SHELXS-86[17], SHELXL-93[18]; monoclinic, space group P-1; lattice constants a = 9.694(2), b = 10.284(2), c = 15.730(3) Å, α = 88.39(2), β = 89.57(2), γ = 75.18(2)°, V = 1515.6(5) Å^3, Z = 2;

μ(Mo-K_α) = 2.666 mm^{-1}; $2\theta_{max.}$ = 26.00; 5511 independent reflections measured, of which 4539 were considered observed with $I > 2\sigma(I)$; max. residual electron density 0.526 and −0.367 e/A^{-3}; 339 parameters (all non hydrogen atoms were calculated anisotropically; the positions of the H atoms were calculated for idealized positions) R_1 = 0.0427. − Further details of the crystal structure investigation are available from the Fachinformationszentrum Karlsruhe, D-76344 Eggenstein-Leopoldshafen (Germany) on quoting the depository number CSD-407970, the name of the author, and the journal citation.

[1] Review: F. T. Edelmann, *Angew. Chem.* **1995**, *107*, 2647−2669; *Angew. Chem. Int. Ed. Engl.* **1995**, *34*, 2466−2488.

[2] [2a] R. Duchateau, T. Tuinstra, E. A. C. Brussee, A. Meetsma, P. T. van Duijnen, J. H. Teuben, *Organometallics*, **1997**, *16*, 3511−3522. − [2b] D. Dress, J. Magull, *Z. Anorg. Allg. Chem.* **1994**, *620*, 814−818.

[3] Review: F. T. Edelmann, *Top. Curr. Chem.* **1996**, *179*, 113−148. − Catalysis: R. Duchateau, C. T. van Wee, J. H. Teuben, *Organometallics* **1996**, *15*, 2291−2302.

[4] [4a] F. G. N. Cloke, H. C. de Lemos, A. A. Sameh, *J. Chem. Soc., Chem. Commun.* **1986**, 1344−1345. − [4b] F. G. N. Cloke, *Chem. Soc. Rev.* **1993**, 17−24. − [4c] H. Görls, B. Neumüller, A. Scholz, J. Scholz, *Angew. Chem.* **1995**, *107*, 732−735; *Angew. Chem. Int. Ed. Engl.* **1995**, *34*, 673−676.

[5] P. W. Roesky, *Chem. Ber.* **1997**, *130*, 859−862.

[6] H. V. R. Dias, W. Jin, Z. Wang, *Inorg. Chem.* **1996**, *35*, 6074−6079.

[7] H. V. R. Dias, W. Jin, R. E. Ratcliff, *Inorg. Chem.* **1995**, *34*, 6100−6105.

[8] M. R. Bürgstein, H. Berberich, P. W. Roesky, *Organometallics* **1998**, *17*, in press.

[9] K. H. den Haan, J. H. Teuben, *J. Organomet. Chem.* **1987**, *322*, 321−329.

[10] A. Scholz, K.-H. Thiele, J. Scholz, R. Weimann, *J. Organomet. Chem.* **1995**, *501*, 195−200.

[11] J. Scholz, A. Dlikan, D. Ströhl, A. Dietrich, H. Schumann, K.-H. Thiele, *Chem. Ber.* **1990**, *123*, 2279−2285.

[12] W. J. Evans, T. J. Boyle, J. W. Ziller, *Inorg. Chem.* **1992**, *31*, 1120−1122.

[13] A. Recknagel, M. Noltemeyer, F. T. Edelmann, *J. Organomet. Chem.* **1991**, *410*, 53−61.

[14] A. Antiñolo, M. F. Lappert, A. Singh, D. J. W. Winterborn, L. M. Engelhardt, C. L. Raston, A. H. White, A. J. Carty, N. J. Taylor, *J. Chem. Soc., Dalton. Trans.* **1987**, 1463−1472.

[15] H. Kessler, *Angew. Chem.* **1970**, *82*, 237−253; *Angew. Chem. Int. Engl.* **1970**, *9*, 219−235.

[16] H. Schumann, I. Albrecht, J. Loebel, E. Hahn, M. B. Hossain, D. van der Helm, *Organometallics*, **1986**, *5*, 1296−1304.

[17] G. M. Sheldrick, University of Göttingen, Germany, **1986**.

[18] G. M. Sheldrick, University of Göttingen, Germany, **1993**.

[97279]

Chiral Bisphosphanes, III[◇]

P-Alkylated (1*S*,2*S*)-Cyclopentane-1,2-diylbisphosphanes with Four Stereogenic Centers and Some Group 10 Metal(II) Complexes Containing the (1*S*,2*S*)-$C_5H_8[P(CH_3)C_8H_{15}$-*cyclo*$]_2$ Ligand

Lutz Dahlenburg* and Volker Kurth

Institut für Anorganische Chemie der Universität Erlangen-Nürnberg,
Egerlandstrasse 1, D-91058 Erlangen, Germany
Fax: (internat.) +49 (0)9131/85-7353
E-mail: dahlbg@anorganik.chemie.uni-erlangen.de

Received December 2, 1997

Keywords: Chirality / P ligands / Nickel / Palladium / Platinum

Radical-initiated P−H addition of (1*S*,2*S*)-$C_5H_8(PH_2)_2$ to cycloalkenes gave bis(secondary phosphanes), (1*S*,2*S*)-$C_5H_8[P(H)C_nH_{2n-1}$-*cyclo*$]_2$ (n = 5−8), as mixtures of $R_P,R_{P'}$, $S_P,S_{P'}$, and $R_P,S_{P'}$ diastereomers. The three diastereomers of the peralkylated chiral P_2 ligand (1*S*,2*S*)-$C_5H_8[P(CH_3)C_8H_{15}$-*cyclo*$]_2$ and its complexes with $NiCl_2$, PdI_2, and PtI_2 were prepared. The structures of [(1*S*,2*S*)-$C_5H_8\{P(CH_3)C_8H_{15}$-*cyclo*-(*R*)$\}_2NiCl_2$]·[(1*S*,2*S*)-$C_5H_8\{P(CH_3)C_8H_{15}$-*cyclo*-(*S*)$\}_2NiCl_2$], (1*S*,2*S*)-$C_5H_8\{P(CH_3)C_8H_{15}$-*cyclo*-(*R*)$\}_2PdI_2$, and (1*S*,2*S*)-$C_5H_8\{P(CH_3)C_8H_{15}$-*cyclo*-(*R*)$\}_2PtI_2$ were determined by X-ray diffraction.

The development of novel chiral ligands for applications in catalysis continues to be an important field of synthetic organic and organometallic chemistry[3]. Optically stable bidentate phosphanes exhibiting C_2 chirality in their carbon frameworks are among the most successful ligands employed in a variety of transition metal-catalyzed enantioselective hydrogenations[4]. In many of these widely used chelating bisphosphanes the phosphorus atoms bear two aryl substituents. The correct orientation of these aryl substituents in the coordination sphere has been identified as a stereochemically important feature contributing to the "recognition ability" of the metal complex[5]. The traditional route to this class of compounds involves the nucleophilic substitution with alkali metal diarylphosphides of enantiopure ditosylates derived from optically active natural precursors. This approach suffers the disadvantage that it cannot be applied to the preparation of *P*-alkylated analogs. Attempted replacement reactions using alkali metal dialkylphosphides thus resulted in products originating from P−P coupling and elimination rather than substitution[6]. Our objective has been the development of more variable methods for the synthesis of chiral bidentate phosphorus ligands, starting from the *resolved enantiomers* of chiral bis(primary phosphanes)[1], $H_2P{\cap}PH_2$, and bis(phosphonous dichlorides)[7], $Cl_2P{\cap}PCl_2$, respectively. In this report we describe how the radical-chain addition of the P−H bonds of (1*S*,2*S*)-cyclopentane-1,2-diylbis(phosphane), (1*S*,2*S*)-$C_5H_8(PH_2)_2$ (**1**)[1], across the >C=C< double bonds of several cycloalkenes can conveniently be exploited for the high-yield synthesis of bis(secondary) and bis(tertiary) P_2 ligands (1*S*,2*S*)-$C_5H_8[P(R')R]_2$ (R = cycloalkyl, R′ = H, Me) having chiral phosphorus centers supported on an asymmetric carbon backbone.

Results and Discussion

The AIBN-initiated addition of the $-PH_2$ functions of optically pure **1** across the carbon−carbon double bonds of cycloalkenes C_nH_{2n-2} [AIBN = α,α′-azobis(isobutyronitrile); n = 5−8] in the absence of a diluting solvent (Scheme 1) was employed as a method for the synthesis of (1*S*,2*S*)-cyclopentane-1,2-diyl-linked bis(secondary phosphanes) (1*S*,2*S*)-$C_5H_8[P(H)R]_2$, where R = *cyclo*-C_5H_9 (**2**), *cyclo*-C_6H_{11} (**3**), *cyclo*-C_7H_{13} (**4**), or *cyclo*-C_8H_{15} (**5**). Formation of higher alkylated by-products resulting from consecutive P−H/>C=C< addition steps did not occur in any of the preparations leading to **3**−**5**. We note, however, the observation of threefold and/or completely alkylated derivatives in reactions between **1** and cyclopentene if the latter was employed in a higher than 30-fold excess.

As anticipated for a free-radical-initiated reaction, no diastereoselectivity was observed in any of the examples studied; i. e., a more or less statistical mixture of $R_P,R_{P'}$, $R_P,S_{P'}$ (= $S_P,R_{P'}$), and $S_P,S_{P'}$ diastereomers was obtained in each case. Those compounds with like chirality at phosphorus ($R_P,R_{P'}$ and $S_P,S_{P'}$) are C_2-symmetric and, hence, show ^{31}P-NMR singlet signals; the presence of unlike configurations at the phosphorus atoms of the $R_P,S_{P'}$ isomers renders the two ^{31}P nuclei inequivalent, thus giving rise to AB doublets. For example, the stereoisomeric mixture of bisphosphanes **5** displayed ^{31}P-NMR singlets at δ = −29.30

[◇] Parts I and II: Refs.[1][2]

 © WILEY-VCH Verlag GmbH, D-69451 Weinheim, 1998 1434−1948/98/0505−0597 $ 17.50+.50/0

Scheme 1

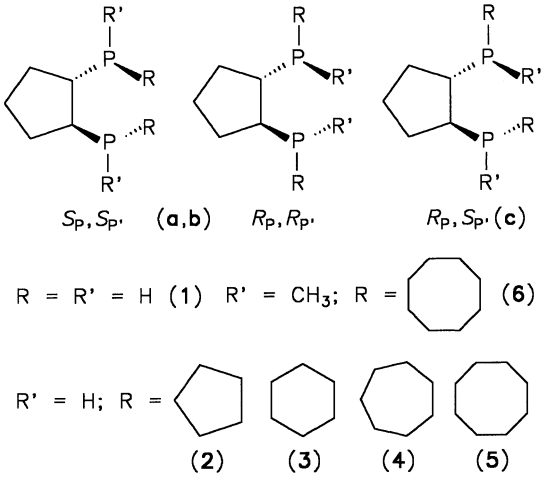

(C_2-symmetric diastereomer **5a**; 31%) and δ = −22.79 (C_2-symmetric diastereomer **5b**, 19%), together with an AB spectrum characterized by $\delta(P_A)$ = −22.45, $\delta(P_B)$ = −29.52, and $^3J(P_A,P_B)$ = 6.8 Hz ($R_P,S_{P'}$ diastereomer **5c**; 50%).

While the >PH signals of compound **2** suffered from spectral overlap, the >PH groups of one of the two C_2-symmetric diastereomers of bisphosphanes **3**−**5** emerged as (deceptively simple) AA′ subspectra of AMNXX′N′M′A′ spin systems, as expected for $H_AP_X(CH_M<)$-$CH_NCH_{N'}P_{X'}(CH_{M'}<)H_{A'}$ building blocks of symmetry C_2 [$\delta(^1H) \approx 3.3$; $^1J(P,H) \approx 195$, $^3J(H,H) \approx 5$ Hz]. Two-dimensional $\delta(^{31}P\{^1H\})-\delta(^1H\{^{31}P\})$-correlated NMR spectroscopy showed the resonating protons H_A and $H_{A'}$ to be associated with those ^{31}P nuclei that gave rise to the "lower frequency"-singlets, assigned to stereoisomers "**3a**"−"**5a**" [−36 < $\delta(^{31}P)$ < −29]. Furthermore, chemical shift correlation was evident for the "diastereomer **b**"-^{31}P singlet resonances located at higher frequencies [−28 < $\delta(^{31}P)$ < −22] and >P*H* multiplets centered at $\delta(^1H) \approx 3.0$. The contour map demonstrated that the latter proton resonances are also associated with ^{31}P doublets resulting from those phosphorus nuclei P_A of $R_P,S_{P'}$-configurated diastereomers **3c**−**5c**, which were found to resonate at high frequencies, close to the mutually equivalent nuclei of diastereomers **3b**−**5b**. Finally, the correlation spectra enabled the chemical shifts $\delta(P_B)$ of diastereomers **3c**−**5c**, having values similar to those of diastereomers **3a**−**5a**, to be associated with >P*H* multiplets centered around δ = 3.5.

Deprotonation of **5** using 2 equiv. of methyllithium in diethyl ether, followed by hydrolysis of the dilithio derivative so generated, caused the diastereomeric distribution to change in favor of the one diastereomer, **5b**, having its ^{31}P chemical shift at δ = −22.79; diastereomeric distribution after de- and re-protonation: **5a** (16%), **5b** (40%), **5c** (44%). An even more pronounced diastereoselectivity was encountered if the diastereomeric mixture of the dilithiated phosphanes (1*S*,2*S*)-$C_5H_8[P(Li)C_8H_{15}$-*cyclo*$]_2$ was allowed to interact with methyl iodide as an electrophile. The bis(tertiary phosphane) (1*S*,2*S*)-$C_5H_8[P(CH_3)C_8H_{15}$-*cyclo*$]_2$ (**6**) obtained in this way gave ^{31}P-NMR singlets at δ = −11.82 (C_2-symmetric diastereomer **6a**; 72%) and δ = −10.02 (C_2-symmetric diastereomer **6b**; 4%), along with two AB doublets at $\delta(P_A)$ = −6.01 and $\delta(P_B)$ = −14.04 [$^3J(P_A,P_B)$ = 6.2 Hz] originating from the $R_P,S_{P'}$-configurated donor atoms of diastereomer **6c** (24%).

While unequivocal assignment of $R_P,R_{P'}$ or $S_P,S_{P'}$ configuration was not feasible for the C_2-symmetric isomers **a** and **b** in the family of bisphosphanes **2**−**5**, differentiation between the $R_P,R_{P'}$ and $S_P,S_{P'}$ diastereomers was achieved for the bis(tertiary) ligand **6** by structural characterization of three of its nickel, palladium, and platinum complexes [**6**·MX_2] (X = Cl, I). Stirring the diastereomeric mixture **6a**−**c** with $NiCl_2 \cdot 6\,H_2O$ in ethanol or with (1,5-C_8H_{12})PdI_2 or (1,5-C_8H_{12})PtI_2 in dichloromethane cleanly produced the MX_2 adducts (1*S*,2*S*)-$C_5H_8\{P(CH_3)C_8H_{15}$-*cyclo*$\}_2NiCl_2$ (**7**), (1*S*,2*S*)-$C_5H_8\{P(CH_3)C_8H_{15}$-*cyclo*$\}_2PdI_2$ (**8**), and (1*S*,2*S*)-$C_5H_8P(CH_3)C_8H_{15}$-*cyclo*$\}_2PtI_2$ (**9**). The diastereomeric distributions of metal complexes **7**−**9** were found to be largely identical with those of the free ligand **6**. For example, the isomeric mixture of palladium complex **8** contained the C_2-symmetric stereoisomers **8a** [$\delta(^{31}P)$ = 42.83] and **8b** [$\delta(^{31}P)$ = 43.93] accompanied by the $R_P,S_{P'}$-configurated diastereomer **8c** [$\delta(P_A)$ = 47.66, $\delta(P_B)$ = 40.97; $J(P_A,P_B)$ = 20.7 Hz] in proportions of 70%, 3%, and 27%, respectively, suggesting that non-selective coordination rather than preferential binding of one particular stereoisomer **6a**, **6b**, or **6c** had occurred during complex formation.

For the platinum complex, selective precipitation of the prevalent isomer **9a** [$\delta(^{31}P)$ = 24.94] from solution was observed upon crystallzing the mixture of diastereomers **9a**−**c** from chloroform. Column chromatography on silica gel was used to separate the predominant stereoisomers of the nickel and palladium homologues **7a** [$\delta(^{31}P)$ = 42.28] and **8a** [$\delta(^{31}P)$ = 42.83] from their isomeric mixtures. Elution with ethyl acetate/acetone and dichloromethane provided palladium complex **8a** as diastereomerically pure crystals. For the nickel compound, on the other hand, the overall separation remained somewhat unsatisfactory as ^{31}P-NMR spectroscopy showed the predominant diastereomer **7a** to persistently contain ca. 5% of its minor C_2-symmetric diastereomer **7b** [$\delta(^{31}P)$ = 41.17], even after repeated attempts at chromatographic purification.

The configuration at phosphorus in **8a** (= [**6a**·PdI_2]) was established by X-ray diffraction as $R_P,R_{P'}$ (Figure 1), indicating that the uncoordinated bisphosphane diastereomer **6a** has to be assigned $S_P,S_{P'}$ stereochemistry. According to the results of an X-ray structure determination, platinum complex **9a** also has the $R_P,R_{P'}$ configuration (Figure 2). Moreover, crystals of **8a** and **9a** showed isotypism, both belonging to the same tetragonal space group $P4_1$ with virtually identical lattice constants and atomic positions. Samples of (1*S*,2*S*)-C_5H_8 $\{P(CH_3)C_8H_{15}$-*cyclo*$\}_2NiCl_2$ (**7**), largely enriched in diastereomer **7a** (vide supra) by chromatographic work-up, were found to crystallize with difficulty. Eventually, an X-ray diffraction study of a suitable speci-

men grown from acetone revealed that **7a** and its minor C_2-symmetric stereoisomer **7b** tend to co-crystallize, forming $[(1S,2S)\text{-}C_5H_8\{P(CH_3)C_8H_{15}\text{-}cyclo\text{-}(R)\}_2NiCl_2]\cdot[(1S,2S)\text{-}C_5H_8\{P(CH_3)C_8H_{15}\text{-}cyclo\text{-}(S)\}_2NiCl_2]$, **7a·7b** (see Figures 3 and 4), irrespective of their divergent concentrations present in solution.

Figure 1. Molecular Structure of $(1S,2S)\text{-}C_5H_8\{P(CH_3)C_8H_{15}\text{-}cyclo\text{-}(R)\}_2PdI_2$ (**8a**)[a]

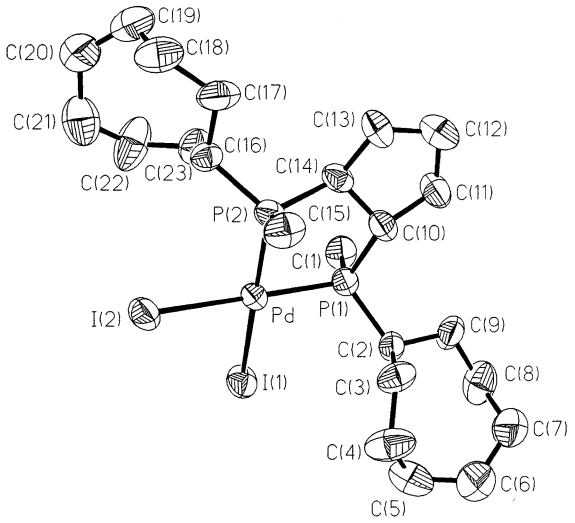

[a] Selected bond lengths [Å] and angles [°]: Pd−P(1), 2.257(2); Pd−P(2), 2.256(2); Pd−I(1), 2.6483(9); Pd−I(2), 2.6442(9). P(1)−Pd−P(2), 87.22(7); P(1)−Pd−I(1), 89.81(5); P(1)−Pd−I(2), 175.71(6); P(2)−Pd−I(1), 175.54(6); P(2)−Pd−I(2), 89.75(5); I(1)−Pd−I(2), 93.38(2).

Figure 2. Molecular Structure of $(1S,2S)\text{-}C_5H_8\{P(CH_3)C_8H_{15}\text{-}cyclo\text{-}(R)\}_2PtI_2$ (**9a**)[a]

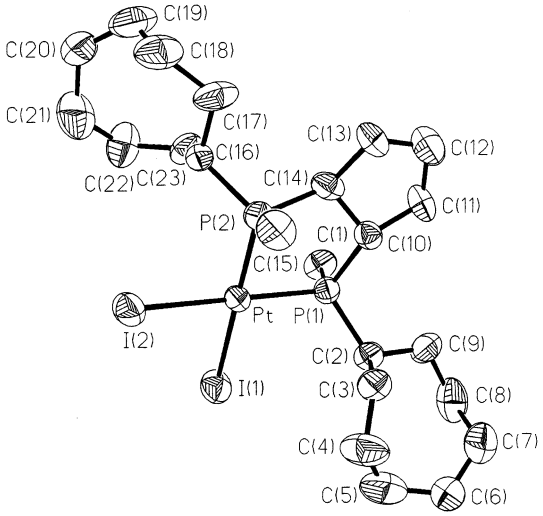

[a] Selected bond lengths [Å] and angles [°]: Pt−P(1), 2.236(3); Pt−P(2), 2.237(3); Pt−I(1), 2.6480(9); Pt−I(2), 2.6481(9). P(1)−Pt−P(2), 87.7(1); P(1)−Pt−I(1), 90.39(7); P(1)−Pt−I(2), 176.63(8); P(2)−Pt−I(1), 176.74(8); P(2)−Pt−I(2), 90.38(8); I(1)−Pt−I(2), 91.62(3).

The three X-ray structure analyses revealed the expected presence of square planar molecules, as evidenced (i) from the sum of the four interligand *cis* angles, 360.1°, and (ii) from the angles between the normals to the two planes de-

Figure 3. Molecular Structure of $(1S,2S)\text{-}C_5H_8\{P(CH_3)C_8H_{15}\text{-}cyclo\text{-}(R)\}_2NiCl_2$ (**7a**)[a]

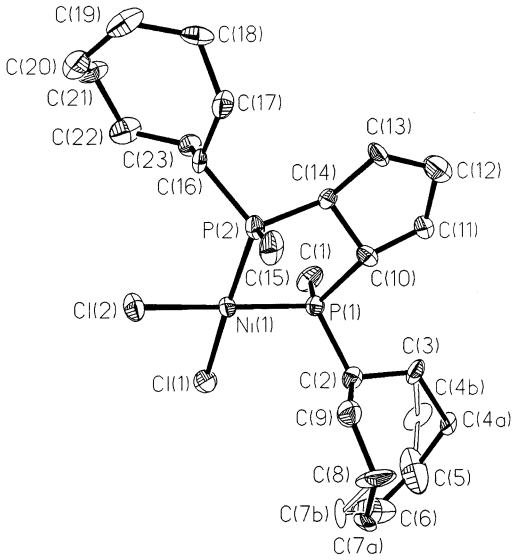

[a] Selected bond lengths [Å] and angles [°]: Ni(1)−P(1), 2.161(3); Ni(1)−P(2), 2.158(3); Ni(1)−Cl(1), 2.214(3); Ni(1)−Cl(2), 2.215(3). P(1)−Ni(1)−P(2), 88.4(1); P(1)−Ni(1)−Cl(1), 87.9(1); P(1)−Ni(1)−Cl(2), 175.8(1); P(2)−Ni(1)−Cl(1), 175.7(1); P(2)−Ni(1)−Cl(2), 88.5(1); Cl(1)−Ni(1)−Cl(2), 95.3(1).

Figure 4. Molecular Structure of $(1S,2S)\text{-}C_5H_8\{P(CH_3)C_8H_{15}\text{-}cyclo\text{-}(S)\}_2NiCl_2$ (**7b**)[a]

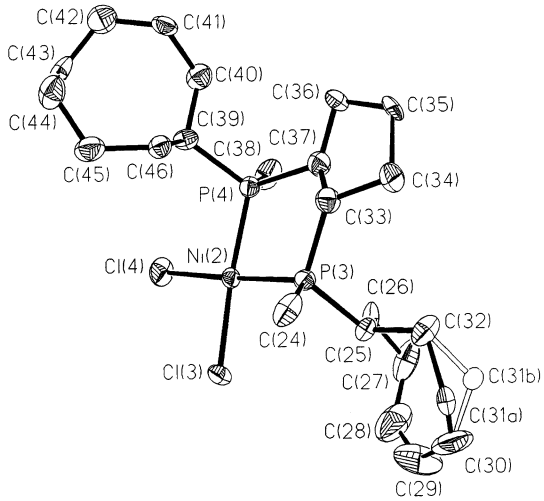

[a] Selected bond lengths [Å] and angles [°]: Ni(2)−P(1), 2.157(3); Ni(2)−P(2), 2.166(3); Ni(2)−Cl(3), 2.216(3); Ni(2)−Cl(4), 2.208(3). P(3)−Ni(2)−P(4), 89.0(1), P(3)−Ni(2)−Cl(3), 87.7(1); P(3)−Ni(2)−Cl(4), 177.3(1); P(4)−Ni(2)−Cl(3), 175.4(1); P(4)−Ni(2)−Cl(4), 88.6(1); Cl(3)−Ni(2)−Cl(4), 94.7(1).

fined by the MX_2 and MP_2 fragments. These dihedral angles amount to only 3.5° in molecules **7a** and **7b** of the nickel compound, the values for the palladium and platinum complexes **8a** and **9a** being 4.4° and 3.8°, respectively. The P−M−P bite-angle of the chelate ligand is almost the same in **8a** [87.22(7)°] and **9a** [87.7(1)°] and increases only slightly to 88.4(1)° and 89.0(1)° on going to structures **7a** and **7b**. The M−P distances range from 2.157(3) to 2.166(3) Å for *d*(Ni−P) in **7a·7b**, but are 2.256(3) and 2.257(3) Å

for *d*(Pd−P) in molecule **8a**. The M−P bonds of platinum complex **9a**, with lengths of 2.236(3) and 2.237(3) Å, are somewhat shorter than those of its lower homologue **8a**, whereas the lengths of the M−I bonds in the two molecules, 2.649(1) Å (M = Pd) and 2.648(1) Å (M = Pt), are equal within their standard deviations. While the torsion angle between the two planes through P(1), C(10), C(14) and C(10), C(14), P(2) within the chelate back-bones of the three $R_P,R_{P'}$-configurated diastereomers decreases marginally from 50.8° to 50.5° and 48.8° on going from **7a** to **8a** and **9a**, the corresponding value for the P(3)−C(33)−C(37)−P(4) framework of $S_P,S_{P'}$ diastereomer **7b** amounts to only 39.0°. Front views of the complexes, shown schematically for **7b** and **8a** in Figures 5 and 6, identify the puckering of the chelate rings in the λ,δ notation as δ. In the $R_P,R_{P'}$-configurated diastereomers the methyl substituents occupy axial positions with respect to the coordination plane, the torsion angles P−M−P−CH_3 being close to −105° in all three molecules **7a**, **8a**, and **9a**. The orientation of the equatorial pairs of cyclooctyl groups (torsion angles P−M−P−CH<, 130.1−132.5°) can be described as approximately "face-on" (Figure 6), similar to the alignment of the equatorial aryl groups in a variety of structurally characterized transition metal complexes containing perphenylated chelating bisphosphane ligands[5]. The $S_P,S_{P'}$ form of nickel complex **7b**, on the other hand, displays little differentiation between axially and equatorially oriented substituents, the torsion angles being −115.0° and −119.0° for the P−M−P−CH_3 fragments P(4)−Ni(2)−P(3)−C(25) and P(3)−Ni(2)−P(4)−C(39) and 125.8° and 120.7° for the two P−M−P−CH< chains of atoms P(4)−Ni(2)−P(3)−C(24) and P(3)−Ni(2)−P(4)−C(38). The conformation of the cyclooctyl rings can be approximated as "boat-chair"-like in the palladium and platinum complexes, and thus corresponds to the lowest-energy conformation of cycloctane[8][9]. In the two nickel complexes, on the other hand, the C_8H_{15} conformation comes close to "boat-only" if conformational disorder is neglected.

Figure 5. Schematic front view of (1*S*,2*S*)-C_5H_8{P(CH_3)C_8H_{15}-*cyclo*-(*S*)}$_2$$NiCl_2$ (**7b**)

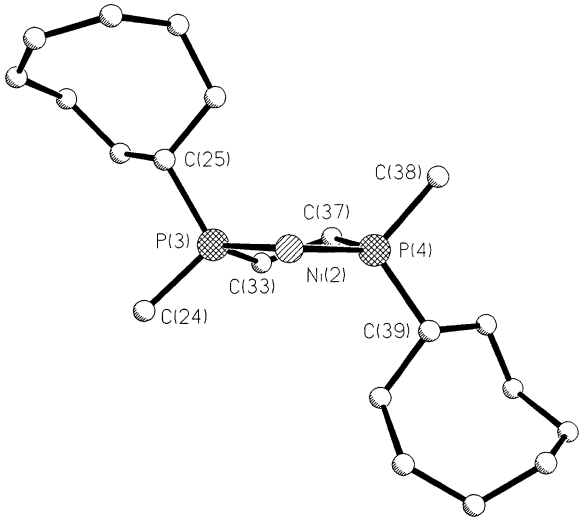

Figure 6. Schematic front view of (1*S*,2*S*)-C_5H_8{P(CH_3)C_8H_{15}-*cyclo*-(*R*)}$_2$$PdI_2$ (**8a**)

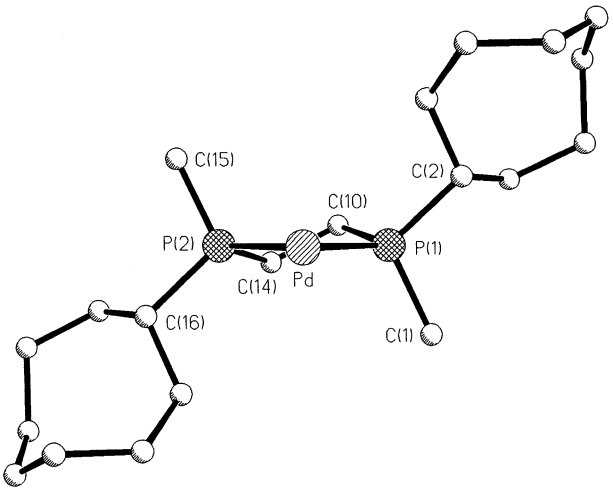

Conclusions

This work has shown that the free-radical-initiated P−H addition of enantiomerically pure bis(primary phosphanes), e.g. (1*S*,2*S*)-$C_5H_8(PH)_2$[1], across the carbon−carbon double bonds of cycloalkenes containing five to eight ring atoms provides an attractive method for the synthesis of the preparation of asymmetric bis(secondary phosphanes). The latter can be derivatized further by metalation and alkylation to give bis(tertiary) P_2 ligands, such as (1*S*,2*S*)-C_5H_8[P(CH_3)C_8H_{15}-*cyclo*]$_2$ (**6**), combining phosphorus-based asymmetry with backbone chirality. Only a few bisphosphanes with asymmetric phosphorus atoms connected to a chiral carbon framework have been reported before[10][11][12][13][14][15]. None of these contains peralkylated phosphanyl substituents −P(R′)R. It was therefore a challenge to isolate the $S_P,S_{P'}$-configurated diastereomer **6a**, observed to predominate in the isomeric mixture of bisphosphanes **6a**−**c**, in optically pure form. Attempts to liberate **6a** from its palladium or platinum complexes **8a** and **9a** were hampered, however, by extensive epimerization at phosphorus, which occurred upon reacting **8a** with excess sodium cyanide in the two-phase system toluene/water. Configurational inversion at phosphorus appears to be facile due to the fact that cyanolysis of **8a** under the conditions outlined before resulted in the liberation of **6** as an isomeric mixture containing 52% of the desired **6a** accompanied by 27% of **6b** and, 21% of **6c**.

Financial support from the *Deutsche Forschungsgemeinschaft* (Bonn) and the *Fonds der Chemischen Industrie* (Frankfurt/Main) is gratefully acknowledged. We are also indebted to *Degussa AG* (Hanau) for generous gifts of palladium and platinum salts.

Experimental Section

All manipulations were performed under nitrogen using standard Schlenk techniques. Solvents were distilled from the appropriate drying agents prior to use. − IR: Mattson Polaris. − NMR: Bruker

DPX 300 (300.1 MHz for ^{1}H, 75.5 MHz for ^{13}C, 121.5 MHz for ^{31}P) and Jeol FT-JNM-EX 270 (109.4 MHz for ^{31}P; for compounds **2**−**4** only) at 20 ± 2°C with TMS as internal or with H_3PO_4 as external standard (downfield positive). − Mass spectra: Jeol MS 700.

(1S,2S)-C_5H_8[P(H)C_5H_9-cyclo]$_2$ (**2**): A suspension of 0.2 g of AIBN in 1.63 g (23.9 mmol) of cyclopentene was added in two portions within 2 h to a gently refluxing solution of 0.64 g (4.77 mmol) of **1**[1] in 1.63 g (23.9 mmol) of cyclopentene. The mixture was stirred at reflux temperature for 4 d. Excess cyclopentene was then removed at room temperature under reduced pressure, and any remaining volatile material was removed from the product by heating at 60°C under a dynamic vacuum. The yield was 1.10 g (85%) of a colorless liquid, which was characterized as the desired bis(secondary phosphane) **2** on the basis of its spectroscopic properties. − MS (FD; toluene, 35 mA, 10 kV): *m*/*z* = 270 [M$^+$]. − IR (film): $\tilde{\nu}$ = 2295 (PH) cm^{-1}. − ^{1}H NMR (C_6D_6): δ = 1.1−2.3 (m, 26 H, C_5H_8 and C_5H_9), 2.86 [dm, ^1J(P,H) = 191 Hz; PH of C_2-symmetric diastereomer **2b** superimposed by P_AH of $R_P,S_{P'}$ diastereomer **2c**], 3.21 [dm, ^1J(P,H) = 193 Hz; PH of C_2-symmetric diastereomer **2a**], 3.45 [dm, ^1J(P,H) = 192 Hz; P_BH of $R_P,S_{P'}$ diastereomer **2c**]. − ^{31}P NMR (C_6D_6): δ = −41.2 (br; C_2-symmetric diastereomer **2a** overlapped by P_B of $R_P,S_{P'}$ diastereomer **2c**), −34.0 (br; C_2-symmetric diastereomer **2b** overlapped by P_A of $R_P,S_{P'}$ diastereomer **2c**); ^3J(P,P) not resolved.

(1S,2S)-C_5H_8[P(H)C_6H_{11}-cyclo]$_2$ (**3**): The preparation of this compound was carried out as described for **2** by reacting 0.68 g (5.07 mmol) of **1** with a total of 3.50 g (42.6 mmol) of cyclohexene, in the presence of a catalytic amount of AIBN (0.2 g), at 60°C for 3 d; yield 1.35 g (89%) of a colorless, viscous liquid. − IR (film): $\tilde{\nu}$ = 2263 (PH) cm^{-1}. − ^{1}H NMR (C_6D_6): δ = 1.1−2.2 (m, 30 H, C_5H_8 and C_6H_{11}), 3.0 [dm (br), ^1J(P,H) = 194 Hz; PH of C_2-symmetric diastereomer **3b** superimposed by P_AH of $R_P,S_{P'}$ diastereomer **3c**], 3.32 ["ddd", ^1J(P,H) = 194, ^3J(H,H) = 3.4, 5.9 Hz; PH of C_2-symmetric diastereomer **3a**], 3.4 [dm (br), ^1J(P,H) = 196 Hz; P_BH of $R_P,S_{P'}$ diastereomer **3c**]. − ^{31}P NMR (C_6D_6): −35.9 [AB-d, ^3J(P,P) = 5 Hz; P_B of $R_P,S_{P'}$ diastereomer **3c**], −35.5 (s; C_2-symmetric diastereomer **3a**), −28.4 (s; C_2-symmetric diastereomer **3b**), −28.2 [AB-d, ^3J(P,P) = 5 Hz; P_A of $R_P,S_{P'}$ diastereomer]; diastereomeric distribution: **3a**, 38%; **3b**, 20%; **3c**, 42%.

(1S,2S)-C_5H_8[P(H)C_7H_{13}-cyclo]$_2$ (**4**): The preparation of this compound was carried out as described for **2** and **3**, by reacting 0.30 g (2.24 mmol) of **1** with 3.00 g (31.2 mmol) of cycloheptene, in the presence of 0.2 g of AIBN, at 60°C for 3 d; yield 0.65 g (89%) of a colorless oil. − MS (FD; toluene, 35 mA, 10 kV): *m*/*z* = 326 [M$^+$]. − IR (film): $\tilde{\nu}$ = 2263 (PH) cm^{-1}. − ^{1}H NMR (C_6D_6): δ = 1.3−2.1 (m, 34 H, C_5H_8 and C_7H_{13}), 3.0 [dm (br), ^1J(P,H) = 194 Hz; PH of C_2-symmetric diastereomer **4b** superimposed by P_AH of $R_P,S_{P'}$ diastereomer **4c**], 3.35 ["ddd", ^1J(P,H) = 194, ^3J(H,H) = 3.4, 6.1 Hz; PH of C_2-symmetric diastereomer **4a**], 3.5 [dt (br), ^1J(P,H) = 196, ^3J(H,H) = 6 Hz; P_BH of $R_P,S_{P'}$ diastereomer **4c**]. − ^{31}P NMR (C_6D_6): −32.7 [AB-d, ^3J(P,P) = 7 Hz; P_B of $R_P,S_{P'}$ diastereomer **4c**], −32.4 (s; C_2-symmetric diastereomer **4a**), −26.4 (s; C_2-symmetric diastereomer **4b**), −26.0 [AB-d, ^3J(P,P) = 7 Hz; P_A of $R_P,S_{P'}$ diastereomer **4c**]; diastereomeric distribution: **4a**, 30%; **4b**, 27%; **4c**, 43%.

(1S,2S)-C_5H_8[P(H)C_8H_{15}-cyclo]$_2$ (**5**): This material was prepared as described above by stirring 0.50 g (3.73 mmol) of **1** in 4.00 g (36. 3 mmol) of cyclooctene, containing AIBN (0.2 g), at 60°C for 3 d; yield 1.12 g (85%) of colorless liquid **5**. MS (FD; toluene, 35 mA, 10 kV): *m*/*z* = 354 [M$^+$]. − IR (film): $\tilde{\nu}$ = 2265 (PH) cm^{-1}. − ^{1}H NMR (C_6D_6): δ = 1.3−2.2 (m, 38 H, C_5H_8 and C_8H_{15}), 3.0 [dm (br), ^1J(P,H) = 192 Hz; PH of C_2-symmetric diastereomer **5b** superimposed by P_AH of $R_P,S_{P'}$ diastereomer **5c**], 3.32 ["ddd", ^1J(P,H) = 194, ^3J(H,H) = 3.4, 5.3 Hz; PH of C_2-symmetric diastereomer **5a**], 3.46 [dt (br), ^1J(P,H) = 196, ^3J(H,H) = 5 Hz; P_BH of $R_P,S_{P'}$ diastereomer **5c**]. − ^{31}P NMR (C_6D_6): −29.52 [AB-d, ^3J(P,P) = 6.8 Hz; P_B of $R_P,S_{P'}$ diastereomer **5c**], −29.30 (s; C_2-symmetric diastereomer **5a**), −22.79 (s; C_2-symmetric diastereomer **5b**), −22.45 (AB-d; P_A of $R_P,S_{P'}$ diastereomer **5c**); diastereomeric distribution: **5a**, 31%; **5b**, 19%; **5c**, 50%.

(1S,2S)-C_5H_8[P(CH_3)C_8H_{15}-cyclo]$_2$ (**6**): A solution of **5** (0.72 g, 2.03 mmol) in 25 ml of THF was treated with 2.60 ml of a 1.6 M hexane solution of *n*-butyllithium (4.16 mmol) at room temperature. The resulting orange solution was stirred for 10 min and then cooled to −25°C. Methyl iodide (7.6 ml of a 0.54 M solution in THF, 4.10 mmol) was then added and the decolorized mixture was evaporated to dryness in vacuo at −25°C. The oily residue was allowed to warm to room temperature, dissolved in toluene, and washed with degassed water. After separation of the organic layer and removal of solvent, the product was extracted from the residue into boiling hexane. Removal of all volatile material from the extracts left ligand **6** as a clear viscous oil; yield 0.73 g (94%). − ^{1}H NMR (C_6D_6): δ = 0.84 ("t", ^2J(P,H) + ^5J(P′,H) = 3.5 Hz; PCH_3 of predominating $S_P,S_{P'}$ diastereomer **6a**), 0.94 ("d", ^2J(P,H) + ^5J(P′,H) = 3.7 Hz; PCH_3 of minor $R_P,R_{P'}$ diastereomer **6b**), 0.81, 1.19 (both "d", ^2J(P,H) + ^5J(P,H) = 3.5 Hz; both PCH_3 of $R_P,S_{P'}$ diastereomer **6c** present in intermediate concentration), 1.3−2.0 (m; 38 H, C_5H_8 and C_8H_{15}). − ^{31}P NMR (C_6D_6): δ = −14.04 [AB-d, ^3J(P_A,P_B) = 6.2 Hz; P_B of $R_P,S_{P'}$ diastereomer **6c**], −11.82 (s; $S_P,S_{P'}$ diastereomer **6a**), −10.02 ($R_P,R_{P'}$ diastereomer **6b**), −6.01 (AB-d; P_A of $R_P,S_{P'}$ diastereomer **6c**); diastereomeric distribution: **6a**, 72%; **6b**, 4%; **6c**, 24%.

(1S,2S)-C_5H_8[P(CH_3)C_8H_{15}-cyclo]$_2$NiCl$_2$ (**7**): To a stirred solution of **6** (0.58 g, 1.52 mmol) in 20 ml of CH_2Cl_2 was added a solution of $NiCl_2 \cdot 6\,H_2O$ (0.37 g, 1.56 mmol) in 30 ml of ethanol. The resulting red-brown mixture was stirred for 8 h and then the solvent was evaporated to give a quantitative yield (0.78 g) of **7** as a brown powder. − $C_{23}H_{44}Cl_2NiP_2$ (512.13): calcd. C 53.9, H 8.7; found C 54.00, H 8.87. − MS (EI, 70 eV, 180°C): *m*/*z* (%) = 512 (21%) [M$^+$], 475 (58) [M$^+$ − Cl], 438 (9%) [M$^+$ − 2Cl], 364 (61%) [M$^+$ − Cl − C_8H_{15}]. − ^{31}P NMR ($CDCl_3$): 38.51 [AB-d, J(P_A,P_B) = 84.6 Hz; P_B of $R_P,S_{P'}$ diastereomer **7c**], 41.17 (s; $S_P,S_{P'}$ diastereomer **7b**), 42.28 (s; $R_P,R_{P'}$ diastereomer **7a**), 45.23 (AB-d; P_A of $R_P,S_{P'}$ diastereomer **7c**); diastereomeric distribution: **7a**, 75%; **7b**, 4%; **7c**, 21%.

The $R_P,S_{P'}$ diastereomer **7c** was removed by chromatography on a column containing silica gel/acetone, which was charged with 0.78 g (1.52 mol) of **7** as a suspension in acetone. Elution with 5% ethyl acetate in acetone, followed by elution with dichloromethane, gave a yellow fraction, which on evaporation of solvent yielded 0.12 g (22%) of microcrystalline **7a**, contaminated by ca. 5% of **7b** (diastereomeric purity estimated by ^{31}P NMR). − ^{13}C{^{31}P,^{1}H} NMR ($CDCl_3$): 3.41 (CH_3), 23.39, 25.44, 25.55, 26.18, 26.89, 27.13, 27.97, 30.53, 31.52 (all CH_2), 34.02 (C_8H_{15}-CH), 44.03 (C_5H_8-CH); the CH_3 and CH resonances showed deceptively simple AA′*X* triplet splitting in the ^{31}P-coupled spectrum: J(P,C) + J(P′,C) = 23.4 Hz (CH_3), 30.2 Hz (C_8H_{15}-CH), and 45.3 Hz (C_5H_8-CH), respectively.

(1S,2S)-C_5H_8[P(CH_3)C_8H_{15}-cyclo]$_2$PdI$_2$ (**8**): To a solution of **6** (1.77 g, 4.65 mmol) in 100 ml of CH_2Cl_2 was added 1.52 g (5.34 mmol) of solid (1,5-C_8H_{12})$PdCl_2$[16]. The orange solution was stirred at room temperature for 10 min and then treated with sodium iodide (2.07 g, 13.81 mmol) to give a brown mixture, which

was stirred for additional 10 h. After filtration and evaporation of the filtrate to dryness, excess (1,5-C_8H_{15})$PdCl_2$ was removed by flash chromatography on a silica gel column with dichloromethane/ethyl acetate (19:1) as the eluent. Evaporation of solvent from the eluate left complex **8** as yellowish red powder; yield 2.95 g (85%). − $C_{23}H_{44}I_2P_2Pd$ (742.72): calcd. C 37.20, H 5.97; found C 37.53, H 6.14. − MS (EI, 70 eV, 180°C): *m/z* (%) = 742 (19%) [M^+], 615 (100%) [M^+ − I]. − ^{31}P NMR ($CDCl_3$): 40.97 [AB-d, $J(P_A,P_B)$ = 20.7 Hz; P_B of $R_P,S_{P'}$ diastereomer **8c**], 42.83 (s; $R_P,R_{P'}$ diastereomer **8a**), 43.93 (s; $S_P,S_{P'}$ diastereomer **8b**), 47.66 (AB-d; P_A of $R_P,S_{P'}$ diastereomer **8c**); diastereomeric distribution: **8a**, 70%; **8b**, 3%; **8c**, 27%.

For isolation of diastereomerically pure **8a**, the isomeric mixture **8a−c** (2.95 g) was chromatographed on a silica gel column, eluting first with with 5% ethyl acetate in acetone and then with dichloromethane as described above for nickel complex **7**. The residue remaining after removal of solvent from the CH_2Cl_2 eluate was thoroughly washed with acetone to give 0.32 g (15%) of **8a** as yellow-red microcrystals. − ^{1}H NMR ($CDCl_3$): 1.3−1.9 (m, 30 H, CH_2), 1.71 ["d", J(P,H) + J(P′,H) = 10.2 Hz; 6 H, CH_3], 2.25−2.55 (m, 6 H, CH and CH_2), 3.15−3.35 (m, 2 H, CH). − ^{13}C{^{31}P,^{1}H} NMR ($CDCl_3$): 6.05 (CH_3), 23.06, 25.31, 25.55, 26.83, 27.48, 28.30, 30.58, 31.86 (all CH_2), 37.32 (C_8H_{15}-CH), 45.47 (C_5H_8-CH); apparently simple AAX' patterns were observed for the CH_3 and CH resonances in the ^{31}P-coupled spectrum: J(P,C) + J(P′,C) = 24.3 Hz (CH_3), 30.6 Hz (C_8H_{15}-CH), and 45.8 Hz (C_5H_8-CH), respectively.

(1S,2S)-C_5H_8[P(CH_3)C_8H_{15}-cyclo]$_2PtI_2$ (**9**): Solid (COD)PtI_2[17] (0.49 g, 0.88 mmol) was added to a stirred solution of 0.33 g (0.86 mmol) of **6** in 40 ml of dichloromethane. After stirring for 10 h the solvent was removed in vacuo to leave a virtually quantitative yield of 0.72 g of the product as a dark yellow solid. − $C_{23}H_{44}I_2P_2Pt$ (831.41): calcd. C 33.23, H 5.33; found C 32.78, H 5.37. − MS (EI, 70 eV, 180°C): *m/z* (%) = 831 (17%) [M^+], 704 (100%) [M^+ − I]. − ^{31}P NMR ($CDCl_3$): 21.90 [AB-d with ^{195}Pt satellites, $J(P_A,P_B)$ = 2.3, ^1J(Pt,P) = 3320 Hz; P_B of $R_P,S_{P'}$ diastereomer **9c**], 24.94 [s with ^{195}Pt satellites, ^1J(Pt,P) = 3333 Hz; $R_P,R_{P'}$ diastereomer **9a**], 26.39 [s with ^{195}Pt-satellites, ^1J(Pt,P) = 3362 Hz; $S_P,S_{P'}$ diastereomer **9b**], 29.04 [AB-d with ^{195}Pt satellites, ^1J(Pt,P) = 3336 Hz; P_A of $R_P,S_{P'}$ diastereomer **9c**]; diastereomeric distribution: **9a**, 76%; **9b**, 6%; **9c**, 18%. − Crystallization of the diastereomeric mixture from chloroform resulted in preferential precipitation of **9a**.

Cyanolysis of Palladium Complex **8a**: A vigorously stirred suspension of 370 mg (0.5 mmol) of **8a** in 10 ml of water and 15 ml of toluene was treated with a ten-fold excess of solid potassium cyanide at room temperature. Stirring was continued for 8 h to produce a colorless two-phase system. The organic layer was separated and the organic phase was extracted twice with 10 ml of water to remove any residual KCN. Evaporation of the combined organic phases left the free ligand **6** as a 52:27:21 mixture of diastereomers **6a**, **6b**, and **6c**.

X-ray Structure Determinations: Single-crystals of (1*S*,2*S*)-C_5H_8{P(CH_3)C_8H_{15}-*cyclo*-(*R*)}$_2NiCl_2$·(1*S*,2*S*)-C_5H_8{P(CH_3)-C_8H_{15}-*cyclo*-(*S*)}$_2NiCl_2$ (**7a·7b**) (size 0.03 × 0.3 × 0.55 mm), (1*S*,2*S*)-C_5H_8{P(CH_3)C_8H_{15}-*cyclo*-(*R*)}$_2PdI_2$ (**8a**) (size = 0.20 × 0.25 × 0.50 mm), and (1*S*,2*S*)-C_5H_8{P(CH_3)C_8H_{15}-*cyclo*-(*R*)}$_2PtI_2$ (**9a**) (size 0.26 × 0.26 × 0.28 mm) were grown from acetone (**7a·7b**), CH_2Cl_2/hexane (**8a**), and $CHCl_3$ (**9a**), respectively. The measurements were made at −95 ± 2°C (**7a·7b**) and at 20 ± 2°C (**8a**, **9a**) on an Enraf-Nonius CAD 4 diffractometer using graphite-monochromated Mo-K_α radiation (λ = 0.7107 Å): orientation matrices and unit cell parameters from the setting anlges of 25 centered medium-angle reflections (**7a·7b**: 12 < 2θ < 16°; **8a**: 15 < 2θ < 34°; **9a**: 17 < 2θ < 26°); collection of the diffraction intensities of Ni complex **7a·7b** by ω scans (data uncorrected for absorption); intensity measurements of Pd and Pt compounds **8a** and **9a** by the ω/2θ scan technique (data corrected for absorption by ψ-scans; **8a**: T_{min} = 0.41, T_{max} = 0.99; **9a**: T_{min} = 0.86, T_{max} = 0.99). The structures were solved by direct methods employing the SIR-92[18] program system and subsequently refined by full-matrix least-squares procedures on F^2 (SHELXL-93[19]) with allowance for anisotropic thermal motion of all non-hydrogen atoms. According to the U_{ij} values of three of the cyclooctyl carbon atoms of **7a·7b**, twofold conformational disorder was suggested for these atoms, which was accounted for by assigning the particular carbon positions split occupancies of 0.45 [C(4a), C(7a)] and 0.55 [C(4b), C(7b)] and of 0.40 [C(31a)] and 0.60 [C(31b)], respectively. H atoms were included in the final structural models assuming ideal geometry and using appropriate riding models. − **7a·7b**: $C_{23}H_{44}Cl_2NiP_2$ (512.13); monoclinic, $P2_1$, a = 12.016(3), b = 16.538(4), c = 12.986(7) Å, β = 103.44(3)°, V = 2510(2) Å^3, Z = 4, $d_{calcd.}$ = 1.355 g cm^{-3}, μ(Mo-K_α) = 1.122 mm^{-1}; 5 ≤ 2θ ≤ 45°, 6843 reflections collected (−12 ≤ h ≤ 12, 0 ≤ k ≤ 17, 0 ≤ l ≤ 13, together with Friedel pairs), 6514 reflections independent ($R_{int.}$ = 0.0359); R_{w2} = 0.1115 for all data and 535 parameters, $w = \{\sigma^2(F_o^2) + [0.0433(F_o^2 + 2F_c^2)/3]^2 + 3.2250(F_o^2 + 2F_c^2)/3\}^{-1}$, R = 0.0463 for 4823 data with $I > 2\sigma(I)$, absolute structure parameter[20]: 0.03(3). − **8a**: $C_{23}H_{44}I_2P_2Pd$ (742.72); tetragonal, $P4_1$, a = 11.205(2), c = 21.650(9) Å, V = 2718(1) Å^3, Z = 4, $d_{calcd.}$ = 1.815 g cm^{-3}, μ(Mo-K_α) = 3.080 mm^{-1}; 5 ≤ 2θ ≤ 54°, 12730 reflections collected (−14 ≤ h ≤ 14, 0 ≤ k ≤ 14, 0 ≤ l ≤ 27, together with Friedel pairs), 5917 reflections independent ($R_{int.}$ = 0.0460); R_{w2} = 0.0906 for all data and 257 parameters, $w = \{\sigma^2(F_o^2) + [0.0386(F_o^2 + 2F_c^2)/3]^2 + 0.5985(F_o^2 + 2F_c^2)/3\}^{-1}$, R = 0.0379 for 4732 data with $I > 2\sigma(I)$, absolute structure parameter[20]: −0.01(3). − **9a**: $C_{23}H_{44}I_2P_2Pt$ (831.41); tetragonal, $P4_1$, a = 11.198(1), c = 21.685(5) Å, V = 2719.2(7) Å^3, Z = 4, $d_{calcd.}$ = 2.031 g cm^{-3}, μ(Mo-K_α) = 7.557 mm^{-1}; 5 ≤ 2θ ≤ 52°, 11460 reflections collected (−13 ≤ h ≤ 13, 0 ≤ k ≤ 13, 0 ≤ l ≤ 26), 5313 reflections independent ($R_{int.}$ = 0.0483); R_w2 = 0.0756 for all data and 254 parameters, $w = \{\sigma^2(F_o^2) + [0.0287(F_o^2 + 2F_c^2)/3]^2 + 0.6041(F_o^2 + 2F_c^2)/3\}^{-1}$, R = 0.0381 for 4102 data with $I > 2\sigma(I)$, absolute structure parameter[20]: −0.005(9). − Further details of the crystal structure determinations may be obtained from the Fachinformationszentrum Karlsruhe, D-76344 Eggenstein-Leopoldshafen (Germany), on quoting the depository numbers CSD-408020 (**7a·7b**), CSD-408024 (**8a**), or CSD-408023 (**9a**).

[1] C. Eckert, L. Dahlenburg, A. Wolski, *Z. Naturforsch.* **1995**, *50b*, 1004−1008.
[2] A. Saare, L. Dahlenburg, *Z. Naturforsch.* **1995**, *50b*, 1009−1017.
[3] W. A. Herrmann, B. Cornils in *Applied Homogeneous Catalysis with Organometallic Compounds* (Eds.: B. Cornils, W. A. Herrmann), VCH, Weinheim, **1996**, Vol. 2, chapter 4.1.
[4] H. Brunner in *Applied Homogeneous Catalysis with Organometallic Compounds* (Eds.: B. Cornils, W. A. Herrmann), VCH, Weinheim, **1996**, Vol. 1, chapter 2.2.
[5] J. M. Brown, P. A. Chaloner in *Homogeneous Catalysis with Metal Phosphine Complexes* (Ed.: L. H. Pignolet), Plenum, New York, **1983**, chapter 4.
[6] K. Tani, K. Suwa, E. Tanigawa, T. Ise, T. Yamagata, Y. Tatsuno, S. Otsuka, *J. Organomet. Chem.* **1989**, *370*, 203−221.
[7] L. Dahlenburg, Ger. Pat. Appl. 197 32 805.9, **1997**.
[8] E. L. Eliel, *Stereochemie der Kohlenstoffverbindungen*, Verlag Chemie, Weinheim, **1966**, chapter 9.2.
[9] J. P. Glusker, M. Lewis, M. Rossi, *Crystal Structure Analysis for Chemists and Biologists*, VCH, New York, **1994**, chapter 12.1.5.

[10] U. Nagel, B. Rieger, *Chem. Ber.* **1988**, *121*, 1123−1131.
[11] U. Nagel, B. Rieger, A. Bublewitz, *J. Organomet. Chem.* **1989**, *370*, 223−229.
[12] U. Nagel, B. Rieger, *Organometallics* **1989**, *8*, 1534−1538.
[13] U. Nagel, Bublewitz, *Chem. Ber.* **1992**, *125*, 1061−1072.
[14] U. Nagel, Th. Krink, *Chem. Ber.* **1993**, *126*, 1091−1100.
[15] K. Burgess, M. J. Ohlmeyer, K. H. Whitmire, *Organometallics* **1992**, *11*, 3588−3600.
[16] D. Drew, R. Doyle, A. G. Shavev, *Inorg. Synth*. **1972**, *13*, 52−53.
[17] D. Drew, R. Doyle, A. G. Shavev, *Inorg. Synth.* **1972**, *13*, 50−52.
[18] A. Altomare, M. C. Burla, M. Camalli, G. Cascarano, C. Giacovazzo, A. Guagliardi, G. Polidori, *SIR-92 − Program Package for Solving Crystal Structures by Direct Methods*, Bari, Perugia, and Rome, Italy, **1992**; *J. Appl. Crystallogr.* **1994**, *27*, 435−436.
[19] G. M. Sheldrick, *SHELX-93 − Program for the Refinement of Crystal Structures from Diffraction Data*, Göttingen, Germany, **1993**.
[20] H. D. Flack, *Acta Crystallogr., Sect. A*, **1983**, *39*, 876−881.
[97289]

Sulfur(IV) Compounds as Ligands, 23[◇]

C−C Coupling Reactions of (Sulfene)ruthenium Complexes with Enolates

Wolfdieter A. Schenk* and Jürgen Bezler

Institut für Anorganische Chemie der Universität Würzburg,
Am Hubland, D-97074 Würzburg, Germany
Fax: (internat.) + 49(0)931/888-4605
E-mail: wolfdieter.schenk@mail.uni-wuerzburg.de

Received December 2, 1997

Keywords: Enolates / Nucleophilic additions / Ruthenium / S ligands / Sulfenes

Sulfene complexes $[CpRu(PR'_3)_2(RHC{=}SO_2)]PF_6$ (**2a**−**d**) are obtained from the corresponding sulfur dioxide complexes **1a**−**c** and diazomethane or -ethane. Reaction of $[CpRu(dppm)(SO_2)]Cl$ (**1d**) and phenyldiazomethane gives the chlorobenzylsulfinato complex $[CpRu(dppm)(SO_2CHPhCl)]$ (**3**). Alternatively, **2a** may be synthesized by sulfur dioxide addition to the carbene complex $[CpRu(dppm)(CH_2)]PF_6$ (**5**) which, in turn, is obtained from the corresponding methyl complex $[CpRu(dppm)(CH_3)]$ and $[Ph_3C]PF_6$. Treatment of **2a**−**d** or **3** with the enolates of cyclic 2-methyl-1,3-diketones, methyl malonates, open-chain cyano or β-oxo esters, and cyclic β-oxo esters gives the C−C coupling products **6a**, **b**, **7a**−**e**, **8a**−**c**, **9a**−**c** in high yields and, in one case, with high diastereoselectivity as well. The functionalized sulfinate ligands thus formed may be alkylated and subsequently removed from the metal center by ligand substitution with acetonitrile. After $MeCN/SO_2$ exchange, the ruthenium complex can be recycled.

Highly reactive and unstable molecules can often be stabilized by coordination to a transition metal − this principle is certainly one of the most fascinating aspects of organic transition-metal chemistry.[1] In an ideal case, the species under consideration is not only "tamed", but is sufficiently modified such that it undergoes novel types of reactions. Sulfenes $R^1R^2C{=}SO_2$ are short-lived intermediates that may be generated for example by 1,2-elimination or [2 + 4]-cycloreversion reactions.[2] Their typical transformations include 1,2-additions across the C=S double bond, nucleophilic addition at sulfur, and cycloadditions.[2][3][4][5][6][7] Recently, we have synthesized $\eta^2(C,S)$-sulfene complexes of the type $[CpRu(PR_3)_2(CH_2{=}SO_2)]^+$ by methylene addition to the corresponding sulfur dioxide complexes.[8][9] In these species, the formal polarity of the sulfene is reversed. Nucleophiles such as halide or pseudohalide ions, amines and phosphanes are added at the carbon atom. With enamines, C−C coupling occurs with high yield and chemoselectivity.[9] We now report on the addition of enolates to sulfene complexes.

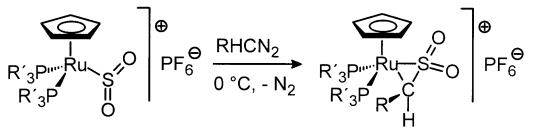

1a - c **2a - d** (1)

R′3P	dppm	dppe	(Me3P)2	dppm
R	H	H	H	Me
	1a	**1b**	**1c**	
	2a	**2b**	**2c**	**2d**

Results

Synthesis of Sulfene Complexes

The reaction of the sulfur dioxide complex **1a** with diazomethane or -ethane to give the sulfene complexes **2a**,**d** has been described previously.[9] Similarly, **1b**, **c** give the sulfene complexes **2b**, **c** (eq. 1).

Attempts to perform analogous reactions of **1a** with phenyldiazomethane, diphenyldiazomethane, or diazoacetic acid esters were unsuccessful. However, when we treated the chloride salt **1d** with phenyldiazomethane, we obtained the chlorobenzylsulfinate complex **3** in high yield (eq. 2). Complex **3** represents a synthetic equivalent for the corresponding phenylsulfene complex (see below).

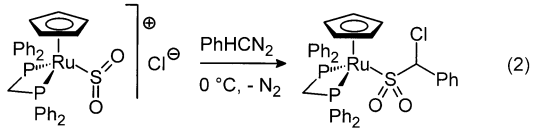

1d **3** (2)

An alternative synthetic access to sulfene complexes is provided by the addition of SO_2 to carbene complexes.[10][11] Thus, when the methyl complex **4** is treated at low temperature with triphenylmethyl hexafluorophosphate, a red solution of the carbene complex **5** is obtained,[12] which, upon addition of SO_2, undergoes immediate discoloration to yield **2a** (eq. 3). However, in spite of

[◇] Part 22: Ref.[15].

 © WILEY-VCH Verlag GmbH, D-69451 Weinheim, 1998 1434−1948/98/0505−0605 $ 17.50+.50/0

numerous attempts, we have not been able to extend this reaction to complexes of substituted sulfenes.

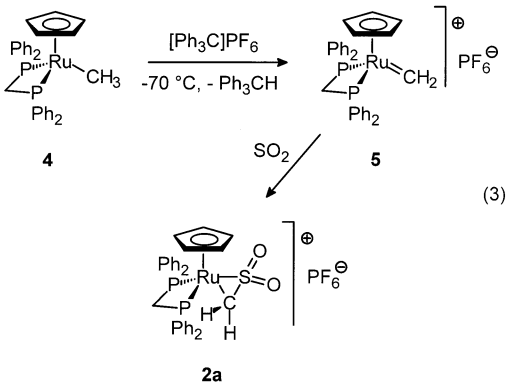

(3)

2b, **c** are slightly yellow crystalline compounds which, even at −20°C, decompose within a few days. **2c** has spectroscopic properties very similar to those of **2a** and the crystallographically characterized complex $[Cp^*Ru(PMe_3)_2(\eta^2\text{-}CH_2{=}SO_2)]PF_6$.[9] **2b**, on the other hand, is unusual in that it is fluxional on the NMR timescale due to a rapid rotation of the sulfene ligand. Standard treatment[13] of the temperature-dependent ^{31}P-NMR spectra using a two-site exchange model[14] yields an activation barrier of $\Delta G^{\neq} = 60$ kJ mol^{-1}. A similar ligand rotation has been found for the analogous sulfur trioxide complex $[Cp^*Ru(PMe_3)_2(\eta^2\text{-}O{=}SO_2)]PF_6$.[15] In the ^{1}H-NMR spectra, the two non-equivalent protons of the methylene groups give rise to two widely separated signals with the typical geminal coupling of ca. 4 Hz. The high-field signals show additional splitting due to strong coupling with one of the two phosphorus atoms. The ^{13}C resonance of the sulfene carbon atom appears as a doublet at $\delta = -20$. Finally, two fairly strong absorptions in the infrared spectrum at $\tilde{\nu} \approx 1230$ and 1100 cm^{-1} are typical for the $\eta^2(C,S)$-coordinated sulfene ligand.[9]

The chlorobenzylsulfinato complex **3** is a yellow, crystalline, air-stable compound. The two diastereotopic phosphorus atoms give rise to a narrow AB system in the ^{31}P-NMR spectrum, while the resonance of the α-carbon nucleus at the sulfur atom is split into a narrow doublet of doublets due to coupling with the two non-equivalent phosphorus nuclei. Here, the ν(SO) absorptions fall in the typical range of *S*-sulfinato complexes.[16]

Reactions with Enolates

Reactions of **2a** in THF with the sodium enolates of 2-methylcyclopentane-1,3-dione and 2,5,5-trimethylcyclohexane-1,3-dione gave the expected addition compounds **6a**, **b** in good yields (eq. 4).

Similarly, treatment of **2a**, **b** and **d** with the lithium enolates of the diethyl or isopropylidene esters of methylmalonic acid yielded the C−C coupling products **7a**−**d**, while

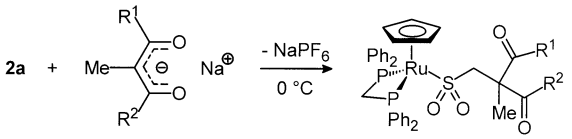

R^1, R^2	$-CH_2CH_2-$	$-CH_2CMe_2CH_2-$
	6a	**6b**

(4)

the analogous phenyl derivative **7e** was obtained from the chlorobenzylsulfinate complex **3** (eq. 5).

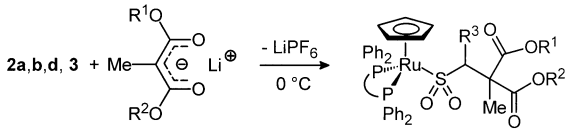

R^1, R^2	Et, Et	$-CMe_2-$	Et, Et	Et, Et	Et, Et
R^3	H	H	H	Me	Ph
$Ph_2P\frown PPh_2$	dppm	dppm	dppe	dppm	dppm
	7a	**7b**	**7c**	**7d**	**7e**

(5)

Products **6** and **7** were obtained as light-yellow crystalline solids. Due to their symmetrical structure they have fairly simple NMR spectra, which are in full accord with the constitutions shown in eqs. 4 and 5. Of note is the significant downfield shift (> 90 ppm) of the resonance of the former sulfene carbon atom that accompanies its release from the ruthenium atom. In similar experiments, the sulfene complexes **2a**, **b** were treated with the ester enolates of 2-methyl-3-oxobutyric acid and 2-cyanopropionic acid (eq. 6), while **2a**, **d** were allowed to react with the deprotonated esters of 2-oxocyclopentane- and 2-oxocyclohexane-1-carboxylic acids (eq. 7).

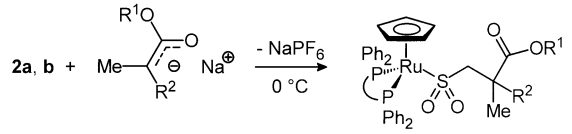

R^1	Et	Et	*t*-Bu
R^2	C(O)Me	CN	C(O)Me
$Ph_2P\frown PPh_2$	dppm	dppm	dppe
	8a	**8b**	**8c**

(6)

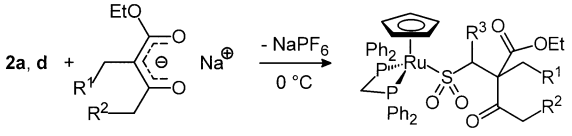

R^1, R^2	$-CH_2-$	$-CH_2CH_2-$	$-CH_2-$
R^3	H	H	Me
	9a	**9b**	**9c**

(7)

Again, the expected coupling products were obtained in good yields as light-yellow, air-stable, crystalline materials.

Since a stereocenter adjacent to the sulfene carbon atom is formed in this reaction, the methylene protons as well as the phosphorus nuclei become diastereotopic. **9c** was isolated in 71% yield as a single diastereoisomer. NMR-spectroscopic analysis of the crude reaction mixture revealed an almost quantitative formation of **9c** and none of the opposite diastereomer. Unfortunately, this compound crystallized only as stacks of very thin platelets, which were unsuitable for X-ray structure determination.

Release of the Sulfinate Ligands

The reactions of **7a** and **8c** with oxonium salts in dichloromethane (eq. 8) gave the expected *O*-alkylation[17] products **10a−c**, which were isolated in almost quantitative yield as yellow, crystalline, highly moisture-sensitive materials. Alkylation of one of the S=O functions introduces a new stereocenter at the sulfur atom and renders the methylene protons as well as the phosphorus nuclei diastereotopic. Only negligible diastereoselectivity (2%) is observed in the formation of **10c**.

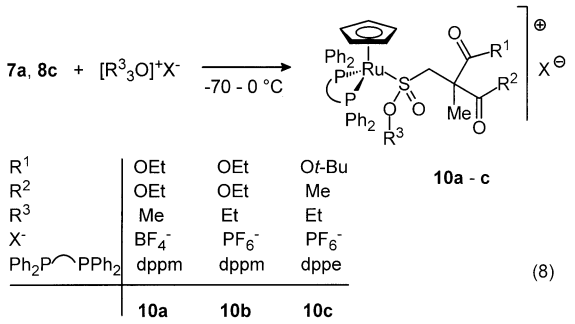

(8)

The role of sulfinic acid esters as ligands in coordination compounds has received very little attention.[17][18] Compared to sulfoxides, they are expected to be quite weak donors. Indeed, when **10a**, **b** are heated in acetonitrile a slow ligand substitution takes place yielding the known acetonitrile complex **11**[19] along with the free esters **12a**, **b** (eq. 9).

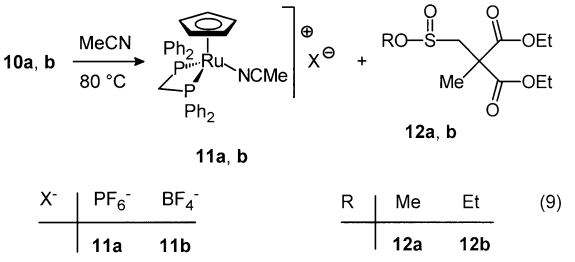

(9)

Despite the long reaction time, we observed no rearrangement[20] to the corresponding sulfones. The mixtures could be readily separated by extraction with diethyl ether, leaving **12a**, **b** in quantitative yields as colorless oils. **11** may be converted back into the starting SO_2 complex **1a** or its BF_4^- salt **1e** simply by dissolving it in liquid sulfur dioxide and allowing it to react for a few days at 20°C (eq. 10).

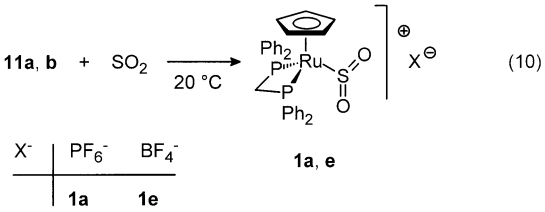

(10)

Discussion

The methylene transfer outlined in eq. 1 is initiated by nucleophilic attack of the diazo compound on the coordinated sulfur dioxide.[9] This explains why less nucleophilic diazo compounds do not react − phenyldiazomethane seems to represent the limiting case. The expected phenylsulfene complex was too unstable to be isolated but, due to its high electrophilicity,[9] could be trapped by the addition of chloride ions. The "inverse synthesis" of the sulfene complex **2a** as outlined in eq. 3 indicates that low-valent cationic carbene complexes such as **5**, which are normally seen as role models of electrophilic carbenes,[21] may also exhibit some nucleophilic character. A further extension of this synthesis to complexes of substituted sulfenes, however, was thwarted by the inaccessibility of the corresponding carbene complexes.

The rapid rotation of the sulfene ligand in **2b** deserves some comment. On the basis of steric considerations alone, it might be tempting to assume that the sulfene ligand can rotate more freely in the less congested dppm complex **2a**. The rotational barrier of a single-faced π-acceptor ligand, however, depends to a large extent on the spatial extension and energy difference of the occupied a′ and a″ frontier orbitals of the [$CpML_2$] fragment.[22] The antisymmetric a″ is the HOMO which is also M−L antibonding. With increasing pyramidalization of the [$CpML_2$] fragment, that is with decreasing L−M−L angle, the energy of this orbital is increased,[23] leading to a stronger fixation of the π-acceptor ligand perpendicular to the symmetry plane of the [$CpML_2$] complex.

Even in the early stages of this project, it soon became apparent that cationic sulfene complexes are highly reactive electrophiles.[8] Compared to uncoordinated sulfene, which adds nucleophiles at the sulfur atom,[2][3] the sulfene complexes studied here exhibit a reversed polarity;[9] only hard nucleophiles such as alkoxides are added at the sulfur atom.[8] Initial attempts to treat **2a** with Na[acac] gave intractable product mixtures, the spectral analyses of which indeed indicated competing C−C and C−O coupling, as well as further reactions initiated by deprotonation of the products. All these problems could readily be overcome by employing salts of tertiary C−H acidic compounds. In these cases, the reactions are clean and give the desired addition products in high yields. Particularly noteworthy is the high diastereoselectivity of the formation of **9c** (eq. 7). This is certainly a result of the rigid fixation of the methylsulfene

ligand in a sterically congested environment, which allows the prochiral enolate to approach in one orientation only.

The alkylation of the sulfinate function to give complexes of sulfinic acid esters provides a means of removing the metal complex from the organic moiety under mild conditions. Furthermore, the ionic acetonitrile complex thus obtained is easily separated from the organic component and can be converted back to the sulfur dioxide complex. A closed cycle is thus created, which allows the assembly of chain-extended sulfinic acid esters from sulfur dioxide, diazomethane or -ethane, and enolates (Scheme 1). Pertinent literature reports sulfinic acid esters to be prone to rearrangement to the corresponding sulfones.[20] Under our conditions, no such rearrangement could be detected, but we have at present no clear explanation as to the unexpected stability of **12a**, **b**.

Scheme 1

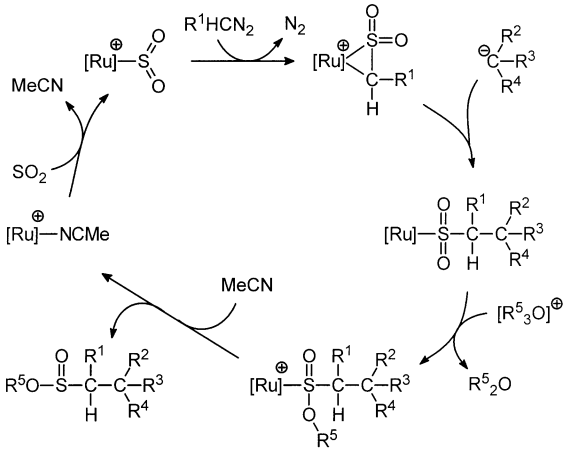

Esters of sulfinic acids have a number of important applications in organic synthesis.[24] Most pertinent work has been carried out on arenesulfinic acid esters, which seem to be much more readily accessible than their alkane counterparts. It is thus particularly gratifying that the reaction sequence outlined here not only provides esters of aliphatic sulfinic acids, but also tolerates a number of different functional groups.

This work has been supported by the *Deutsche Forschungsgemeinschaft* (SFB 347 "Selektive Reaktionen Metall-aktivierter Moleküle").

Experimental Section

All experiments were carried out in Schlenk tubes under nitrogen using suitably purified solvents. The crystallization of oily products was often conveniently induced by immersing the Schlenk tube in a small ultrasonic cleaning bath. − IR: Perkin-Elmer 283, Bruker IFS 25. − ^{1}H NMR: Bruker AMX 400, δ values relative to TMS; diastereotopic methylene protons of ethoxy groups invariably gave well-resolved ABX_3 spectra with ^2J(H,H) = 10.5 Hz and ^3J(H,H) = 7.1 Hz; for the sake of simplicity they are denoted in the following as "res. m" (resolved multiplet). − ^{13}C NMR: Bruker AMX 400, δ values relative to TMS; assignments were routinely checked by DEPT; in some cases the ^{13}C-NMR signals of quaternary carbon atoms were too weak to be detected. − ^{31}P NMR: Bruker AMX 400, δ values relative to 85% H_3PO_4. The ^{1}H- and ^{13}C-NMR signals of the phosphane ligands and the ^{31}P-NMR signals of the PF_6^- ion are very similar for all compounds and have therefore been omitted from the lists of spectral data. − Elemental analyses: Analytical Laboratory of the Institut für Anorganische Chemie. − The following starting materials were obtained as described in the literature: $[CpRu(PR_3)_2(SO_2)]X$ (**1a−d**),[25] [CpRu(dppm)Cl],[19] $[CpRu(dppm)(RHC{=}SO_2)]PF_6$ (**2a**, **d**),[9] diazomethane, diazoethane,[26] phenyldiazomethane.[27] Enolates were obtained from the corresponding 1,3-dicarbonyl compounds by deprotonation using lithium diisopropylamide or sodium bis(trimethylsilyl)amide. All other reagents were used as purchased.

[CpRu(dppe)(H$_2$C=SO$_2$)]PF$_6$ (**2b**): To a solution of **1b** (177 mg, 0.23 mmol) in dichloromethane (20 ml) a solution of diazomethane in diethyl ether (1 ml, 0.30 mmol) was added at −70°C. Gas evolution and a rapid color change to light-yellow were observed. The mixture was allowed to warm to 0°C, and all volatiles were removed in vacuo. After recrystallization from dichloromethane/pentane, a tan-colored microcrystalline powder was obtained. Yield 160 mg (89%), m.p. 156°C (dec.). − ^{1}H NMR (400 MHz, CD_2Cl_2, −70°C): δ = 0.02 [dd, ^2J(H,H) = 4.4 Hz, ^3J(P,H) = 16.8 Hz, 1 H, HC=SO_2], 3.30 (br. m, 1 H, HC=SO_2), 5.68 (s, 5 H, C_5H_5). − ^{13}C NMR (100 MHz, CD_2Cl_2, −70°C): δ = −20.2 [d, ^2J(P,C) = 6 Hz, $H_2C{=}SO_2$], 85.6 (s, C_5H_5). − ^{31}P NMR (162 MHz, CD_2Cl_2, −70°C): δ = 73.8 [d, ^2J(P,P) = 20 Hz], 78.7 [d, ^2J(P,P) = 20 Hz]. − IR (Nujol): $\tilde{\nu}$ = 1236, 1093 cm^{-1} (S=O). − $C_{32}H_{31}F_6O_2P_3RuS$ (787.6): calcd. C 48.80, H 3.97, S 4.07; found C 48.88, H 4.14, S 4.01.

[CpRu(PMe$_3$)$_2$(H$_2$C=SO$_2$)]PF$_6$ (**2c**): This compound was prepared analogously from **1c** (120 mg, 0.23 mmol) and diazomethane (0.45 mmol). Yield 109 mg (89%), m.p. 91°C (dec.). − ^{1}H NMR (400 MHz, [D_6]acetone, 20°C): δ = 0.71 [dd, ^2J(H,H) = 3.9 Hz, ^3J(P,H) = 17.6 Hz, 1 H, HC=SO_2], 2.57 (br. m, 1 H, HC=SO_2), 5.92 (s, 5 H, C_5H_5). − ^{13}C NMR (100 MHz, [D_6]acetone, 20°C): δ = −22.3 [d, ^2J(P,C) = 5 Hz, $H_2C{=}SO_2$], 96.0 (s, C_5H_5). − ^{31}P NMR (162 MHz, [D_6]acetone, 20°C): δ = 7.7 [d, ^2J(P,P) = 43 Hz], 9.7 [d, ^2J(P,P) = 43 Hz]. − IR (Nujol): $\tilde{\nu}$ = 1220, 1104 cm^{-1} (S=O). − $C_{12}H_{25}F_6O_2P_3RuS$ (541.4): calcd. C 26.62, H 4.65; found C 26.95, H 4.72.

[CpRu(dppm)(SO$_2$CHClPh)] (**3**): This compound was prepared analogously from **1d** (85 mg, 0.13 mmol) and phenyldiazomethane (0.25 mmol). The crude product was purified by chromatography on a short silica gel column using acetone/dichloromethane (2:1) as eluent. Yield 68 mg (71%), m.p. 171°C (dec.). − ^{1}H NMR (400 MHz, C_6D_6, 20°C): δ = 4.50 (s, 1 H, CHClPh), 4.89 (s, 5 H, C_5H_5). − ^{13}C NMR (100 MHz, C_6D_6, 20°C): δ = 83.2 [t, ^2J(P,C) = 2 Hz, C_5H_5], 83.3 [dd, ^2J(P,C) = 2 Hz, ^2J(P,C) = 1 Hz, CHClPh]. − ^{31}P NMR (162 MHz, C_6D_6, 20°C): δ = 11.0 [d, ^2J(P,P) = 90 Hz], 12.2 [d, ^2J(P,P) = 90 Hz]. − IR (Nujol): $\tilde{\nu}$ = 1184, 1032 cm^{-1} (S=O). − $C_{37}H_{33}ClO_2P_2RuS$ (740.2): calcd. C 60.04, H 4.49; found C 60.65, H 4.57.

[CpRu(dppm)(CH$_3$)] (**4**): A solution of [CpRu(dppm)Cl] (300 mg, 0.51 mmol) in toluene (10 ml) was treated at 20°C with methylmagnesium chloride in THF (1.54 mmol). After 20 h, the excess Grignard reagent was quenched by adding methanol (5 ml). All volatile material was then removed in vacuo and the solid residue was redissolved in toluene (20 ml). The resulting solution was filtered through Celite, and the filtrate was concentrated to a volume of 2 ml. Addition of pentane resulted in the deposition of the product as yellow crystals. Yield 185 mg (64%), m.p. 176°C (dec.). − ^{1}H NMR (400 MHz, C_6D_6, 20°C): δ = 0.20 [t, ^3J(P,H) = 7.1 Hz, 3 H, $RuCH_3$], 4.87 (s, 5 H, C_5H_5). − ^{13}C NMR (100 MHz, C_6D_6,

20°C): δ = −23.1 [t, ^2J(P,C) = 13 Hz, $RuCH_3$], 80.3 [t, ^2J(P,C) = 2 Hz, C_5H_5]. − ^{31}P NMR (162 MHz, C_6D_6, 20°C): δ = 22.8 (s). − $C_{31}H_{30}P_2Ru$ (565.6): calcd. C 65.83, H 5.35; found C 65.52, H 5.42.

[CpRu(dppm)(H$_2$C=SO$_2$)]PF$_6$ (**2a**). − *From* **4**: To a solution of **4** (185 mg, 0.33 mmol) in dichloromethane (20 ml), a solution of $[Ph_3C]PF_6$ (130 mg, 0.34 mmol) in the same solvent (2 ml) was added at −70°C. Sulfur dioxide was then introduced into the deep-red solution, and the mixture allowed to warm to 0°C. After concentration to a volume of 2 ml, the product was precipitated by adding pentane. Yield 218 mg (86%), colorless crystalline powder, identical (NMR, IR) with the known **2a**.[9]

Addition of Enolates: To a solution of Li[N(*i*Pr)$_2$] (25 mg, 0.22 mmol) or Na[N(SiMe$_3$)$_2$] (40 mg, 0.22 mmol) in THF (5 ml), an equimolar amount of the respective C−H acidic compound was added at −70°C. The resulting slurry was then added to a solution of 0.20 mmol of the sulfene complex in THF (10 ml). The mixture was allowed to warm to 20°C and stirred for 2 h. The solvent was then removed in vacuo, the oily residue was taken up in dichloromethane and chromatographed (neutral alumina, activity grade I, acetone/dichloromethane, 2:1). A broad, light-yellow band containing the product was collected. The solvent was evaporated and the product was recrystallized from benzene/pentane.

6a: Yield 76 mg (51%), m.p. 232°C (dec.). − ^{1}H NMR (400 MHz, CD_2Cl_2, 20°C): δ = 0.58 (s, 3 H, CH_3), 2.34−2.48, 2.87−2.92 (m, 4 H, CH_2CH_2), 2.89 (s, 2 H, SO_2CH_2), 4.95 (s, 5 H, C_5H_5). − ^{13}C NMR (100 MHz, CD_2Cl_2, 20°C): δ = 20.2 (s, CH_3), 35.2 (s, CH_2CH_2), 52.9 (s, C_{quat}), 82.3 (s, CH_2SO_2), 84.0 [t, ^2J(P,C) = 2 Hz, C_5H_5], 216.2 (s, CO). − ^{31}P NMR (162 MHz, CD_2Cl_2, 20°C): δ = 12.9 (s). − IR (Nujol): $\tilde{\nu}$ = 1715 (C=O), 1144, 1024 cm^{-1} (S=O). − $C_{37}H_{36}O_4P_2RuS$ (739.8): calcd. C 60.07, H 4.91; found C 60.54, H 5.30.

6b: Yield 124 mg (79%), m.p. 221°C (dec.). − ^{1}H NMR (400 MHz, CD_2Cl_2, 20°C): δ = 0.64 (s, 3 H, CH_3), 0.91 (s, 3 H, CH_3), 1.00 (s, 3 H, CH_3), 2.07 [d, ^2J(H,H) = 14.3 Hz, 2 H, CH_2], 2.82 [d, ^2J(H,H) = 14.3 Hz, 2 H, CH_2], 2.78 (s, 2 H, SO_2CH_2), 4.97 (s, 5 H, C_5H_5). − ^{13}C NMR (100 MHz, CD_2Cl_2, 20°C): δ = 19.1 (s, CH_3), 27.1 (s, CH_3), 30.6 (s, CH_3), 30.9 (s, CMe_2), 52.4(s, CH_2), 62.4 (s, C_{quat}), 78.2 (s, CH_2SO_2), 83.8 (s, C_5H_5), 209.0 (s, CO). − ^{31}P NMR (162 MHz, CD_2Cl_2, 20°C): δ = 13.5 (s). − IR (Nujol): $\tilde{\nu}$ = 1716, 1688 (C=O), 1144, 1032 cm^{-1} (S=O). − $C_{40}H_{42}O_4P_2RuS$ (781.9): calcd. C 61.44, H 5.41; found C 60.96, H 5.26.

7a: Yield 125 mg (78%), m.p. 183°C (dec.). − ^{1}H NMR (400 MHz, $CDCl_3$, 20°C): δ = 1.19 [t, ^3J(H,H) = 7.1 Hz, 6 H, CH_3], 1.36 (s, 3 H, CH_3), 2.86 (s, 2 H, SO_2CH_2), 4.10 (res. m, 4 H, OCH_2), 4.93 (s, 5 H, C_5H_5). − ^{13}C NMR (100 MHz, $CDCl_3$, 20°C): δ = 14.0 (s, CH_3), 19.4 (s, CH_3), 53.2 (s, C_{quat}), 61.0 (s, OCH_2), 73.3 (s, CH_2SO_2), 83.6 (s, C_5H_5), 171.5 (s, CO). − ^{31}P NMR (162 MHz, $CDCl_3$, 20°C): δ = 12.6 (s). − IR (Nujol): $\tilde{\nu}$ = 1740, 1712 (C=O), 1152, 1028 cm^{-1} (S=O). − $C_{39}H_{42}O_6P_2RuS$ (801.8): calcd. C 58.42, H 5.28; found C 57.96, H 5.59.

7b: Yield 129 mg (82%), m.p. 207°C (dec.). − ^{1}H NMR (400 MHz, CD_2Cl_2, 20°C): δ = 1.48 (s, 3 H, CH_3), 1.56 (s, 3 H, CH_3), 1.74 (s, 3 H, CH_3), 2.94 (s, 2 H, SO_2CH_2), 4.95 (s, 5 H, C_5H_5). − ^{13}C NMR (100 MHz, $CDCl_3$, 20°C): δ = 27.0 (s, CH_3), 27.6 (s, CH_3), 30.2 (s, CH_3), 43.4 (s, C_{quat}), 75.3 (s, CH_2SO_2), 83.6 (s, C_5H_5), 106.5 (s, O_2CMe_2), 168.5 (s, CO). − ^{31}P NMR (162 MHz, $CDCl_3$, 20°C): δ = 13.1 (s). − IR (Nujol): $\tilde{\nu}$ = 1744, 1732 (C=O), 1160, 1028 cm^{-1} (S=O). − $C_{38}H_{38}O_6P_2RuS$ (785.8): calcd. C 58.08, H 4.87; found C 58.17, H 4.87.

7c: Yield 124 mg (76%), m.p. 209°C (dec.). − ^{1}H NMR (400 MHz, $CDCl_3$, 20°C): δ = 1.18 [t, ^3J(H,H) = 7.1 Hz, 6 H, CH_3], 1.36 (s, 3 H, CH_3), 2.57 (s, 2 H, SO_2CH_2), 4.07 (res. m, 4 H, OCH_2), 4.85 (s, 5 H, C_5H_5). − ^{13}C NMR (100 MHz, $CDCl_3$, 20°C): δ = 14.0 (s, CH_3), 19.2 (s, CH_3), 53.2 (s, C_{quat}), 61.0 (s, OCH_2), 72.3 (s, CH_2SO_2), 85.6 (s, C_5H_5), 171.4 (s, CO). − ^{31}P NMR (162 MHz, $CDCl_3$, 20°C): δ = 83.0 (s). − IR (Nujol): $\tilde{\nu}$ = 1741, 1725 (C=O), 1142, 1024 cm^{-1} (S=O). − $C_{40}H_{44}O_6P_2RuS$ (815.9): calcd. C 58.89, H 5.44; found C 58.18, H 5.22.

7d: Yield 117 mg (72%), m.p. 207°C (dec.). − ^{1}H NMR (400 MHz, $CDCl_3$, 20°C): δ = 0.41 [t, ^3J(H,H) = 7.3 Hz, 3 H, CH_3], 1.15 [t, ^3J(H,H) = 7.1 Hz, 3 H, CH_3], 1.21 [t, ^3J(H,H) = 7.1 Hz, 3 H, CH_3], 1.43 (s, 3 H, CH_3), 3.66 [q, ^3J(H,H) = 7.3 Hz, 1 H, SO_2CHMe], 4.02 (res. m, 2 H, OCH_2), 4.17 (res. m, 2 H, OCH_2), 5.02 (s, 5 H, C_5H_5). − ^{13}C NMR (100 MHz, $CDCl_3$, 20°C): δ = 11.2 (s, CH_3), 14.2 (s, CH_3), 15.6 (s, CH_3), 57,5 (s, C_{quat}), 61.0 (s, OCH_2), 61.1 (s, OCH_2), 74.5 (s, SO_2CHMe), 82.7 (s, C_5H_5), 171.3 (s, CO), 171.4 (s, CO). − ^{31}P NMR (162 MHz, $CDCl_3$, 20°C): δ = 8.8 [d, ^2J(P,P) = 86 Hz], 11.1 [d, ^2J(P,P) = 86 Hz]. − IR (Nujol): $\tilde{\nu}$ = 1744, 1704 (C=O), 1156, 1024 cm^{-1} (S=O). − $C_{40}H_{44}O_6P_2RuS$ (815.9): calcd. C 58.89, H 5.44; found C 57.99, H 5.07.

7e: This compound was obtained from **3**. To ensure complete reaction the mixture was refluxed for 2 h. Yield 142 mg (81%), m.p. 156°C (dec.). − ^{1}H NMR (400 MHz, C_6D_6, 20°C): δ = 0.75 [t, ^3J(H,H) = 7.1 Hz, 3 H, CH_3], 0.94 [t, ^3J(H,H) = 7.1 Hz, 3 H, CH_3], 2.33 (s, 3 H, CH_3), 3.64 (res. m, 2 H, OCH_2), 3.95 (res. m, 1 H, OCH_2), 4.13 (res. m, 1 H, OCH_2), 4.35 (s, 5 H, C_5H_5), 4.55 (s, 1 H, SO_2CHPh). − ^{13}C NMR (100 MHz, C_6D_6, 20°C): δ = 13.8 (s, CH_3), 14.0 (s, CH_3), 18.2 (s, CH_3), 58,4 (s, C_{quat}), 60.5 (s, OCH_2), 60.8 (s, OCH_2), 78.4 (s, $CHPhSO_2$), 82.6 (s, C_5H_5), 170.3 (s, CO), 170.5 (s, CO). − ^{31}P NMR (162 MHz, C_6D_6, 20°C): δ = 9.9 [d, ^2J(P,P) = 90 Hz], 14.0 [d, ^2J(P,P) = 90 Hz]. − IR (Nujol): $\tilde{\nu}$ = 1725, 1713 (C=O), 1141, 1022 cm^{-1} (S=O). − $C_{45}H_{46}O_6P_2RuS$ (877.9): calcd. C 61.56, H 5.28; found C 61.72, H 5.19.

8a: Yield 114 mg (74%), m.p. 221°C (dec.). − ^{1}H NMR (400 MHz, $CDCl_3$, 20°C): δ = 1.19 [t, ^3J(H,H) = 7.1 Hz, 3 H, CH_3], 1.37 (s, 3 H, CH_3), 1.98 [s, 3 H, $C(O)CH_3$], 2.85 [d, ^2J(H,H) = 13.7 Hz, 1 H, SO_2CH_2], 2.94 [d, ^2J(H,H) = 13.7 Hz, 1 H, SO_2CH_2], 4.10 [q, ^3J(H,H) = 7.1 Hz, 2 H, OCH_2], 4.94 (s, 5 H, C_5H_5). − ^{13}C NMR (100 MHz, $CDCl_3$, 20°C): δ = 14.0 (s, CH_3), 19.3 (s, CH_3), 26.3 (s, CH_3), 58.8 (s, C_{quat}), 61.0 (s, OCH_2), 74.2 (s, CH_2SO_2), 83.7 (s, C_5H_5), 172.2 (s, CO), 205.8 (s, CO). − ^{31}P NMR (162 MHz, $CDCl_3$, 20°C): δ = 12.6 [d, ^2J(P,P) = 90 Hz], 12.9 [d, ^2J(P,P) = 90 Hz]. − IR (Nujol): $\tilde{\nu}$ = 1728, 1708 (C=O), 1148, 1036 cm^{-1} (S=O). − $C_{38}H_{40}O_5P_2RuS$ (771.8): calcd. C 59.14, H 5.22; found C 58.90, H 5.08.

8b: Yield 47 mg (31%), m.p. 211°C (dec.). − ^{1}H NMR (400 MHz, $CDCl_3$, 20°C): δ = 1.28 [t, ^3J(H,H) = 7.1 Hz, 3 H, CH_3], 1.37 (s, 3 H, CH_3), 2.51 [d, ^2J(H,H) = 13.2 Hz, 1 H, SO_2CH_2], 2.75 [d, ^2J(H,H) = 13.2 Hz, 1 H, SO_2CH_2], 4.22 (res. m, 1 H, OCH_2), 4.23 (res. m, 1 H, OCH_2), 4.95 (s, 5 H, C_5H_5). − ^{13}C NMR (100 MHz, $CDCl_3$, 20°C): δ = 13.9 (s, CH_3), 22.2 (s, CH_3), 40.6 (s, C_{quat}), 62.5 (s, OCH_2), 73.0 (s, CH_2SO_2), 83.6 (s, C_5H_5), 119.7 (s, CN), 168.6 (s, CO). − ^{31}P NMR (162 MHz, $CDCl_3$, 20°C): δ = 12.5 [d, ^2J(P,P) = 90 Hz], 13.0 [d, ^2J(P,P) = 90 Hz]. − IR (Nujol): $\tilde{\nu}$ = 1744 (C=O), 1168, 1032 cm^{-1} (S=O). − $C_{37}H_{37}NO_4P_2RuS$ (754.8): calcd. C 58.88, H 4.94, N 1.86; found C 59.09, H 4.45, N 1.23.

8c: Yield 127 mg (78%), m.p. 216°C (dec.). − ^{1}H NMR (400 MHz, $CDCl_3$, 20°C): δ = 1.35 (s, 12 H, *t*Bu and CH_3), 2.04 [s, 3 H, $C(O)CH_3$], 2.32 [d, ^2J(H,H) = 14.0 Hz, 1 H, SO_2CH_2], 2.87 [d, ^2J(H,H) = 14.0 Hz, 1 H, SO_2CH_2], 4.84 (s, 5 H, C_5H_5). − ^{13}C NMR (100 MHz, $CDCl_3$, 20°C): δ = 19.5 (s, CH_3), 26.9 (s, CH_3),

27,7 (s, *t*Bu), 59.1 (s, C_{quat}), 73.5 (s, CH_2SO_2), 80.7 (s, CMe_3), 85.6 (s, C_5H_5), 170.7 (s, CO), 206.1 (s, CO). − ^{31}P NMR (162 MHz, $CDCl_3$, 20°C): δ = 82.1 [d, ^2J(P,P) = 19 Hz], 84.2 [d, ^2J(P,P) = 19 Hz]. − IR (Nujol): $\tilde{\nu}$ = 1725, 1702 (C=O), 1140, 1022 cm^{-1} (S=O). − $C_{41}H_{46}O_5P_2RuS$ (813.9): calcd. C 60.51, H 5.70; found C 60.39, H 5.92.

9a: Yield 111 mg (71%), m.p. 190°C (dec.). − ^{1}H NMR (400 MHz, $CDCl_3$, 20°C): δ = 1.12 [t, ^3J(H,H) = 7.1 Hz, 3 H, CH_3], 1.56 (m, 2 H, CH_2), 1.99 (m, 2 H, CH_2), 2.22 [d, ^2J(H,H) = 13.6 Hz, 1 H, SO_2CH_2], 2.50 (m, 2 H, CH_2), 2.95 [d, ^2J(H,H) = 13.6 Hz, 1 H, SO_2CH_2], 4.02 (res. m, 1 H, OCH_2), 4.03 (res. m, 1 H, OCH_2), 4.87 (s, 5 H, C_5H_5). − ^{13}C NMR (100 MHz, $CDCl_3$, 20°C): δ = 14.1 (s, CH_3), 19.4 (s, CH_2), 30.4 (s, CH_2), 37.4 (s, CH_2), 59.6 (s, C_{quat}), 61.1 (s, OCH_2), 71.1 (s, CH_2SO_2), 83.8 (s, C_5H_5), 170.1 (s, CO), 214.6 (s, CO). − ^{31}P NMR (162 MHz, $CDCl_3$, 20°C): δ = 12.4 [d, ^2J(P,P) = 90 Hz], 13.1 [d, ^2J(P,P) = 90 Hz]. − IR (Nujol): $\tilde{\nu}$ = 1745, 1716 (C=O), 1149, 1022 cm^{-1} (S=O). − $C_{39}H_{40}O_5P_2RuS$ (783.8): calcd. C 59.76, H 5.14; found C 58.47, H 5.02.

9b: Yield 123 mg (77%), m.p. 172°C (dec.). − ^{1}H NMR (400 MHz, $CDCl_3$, 20°C): δ = 1.14 [t, ^3J(H,H) = 7.0 Hz, 3 H, CH_3], 1.28−1.54 (m, 4 H, CH_2), 2.05 (m, 4 H, CH_2), 2.79 [d, ^2J(H,H) = 13.0 Hz, 1 H, SO_2CH_2], 2.90 [d, ^2J(H,H) = 13.0 Hz, 1 H, SO_2CH_2], 4.06 [q, ^3J(H,H) = 7.0 Hz, 2 H, OCH_2], 4.88 (s, 5 H, C_5H_5). − ^{13}C NMR (100 MHz, $CDCl_3$, 20°C): δ = 14.1 (s, CH_3), 21.2 (s, CH_2), 26.4 (s, CH_2), 32.4 (s, CH_2), 39.6 (s, CH_2), 60.9 (s, C_{quat}), 60.9 (s, OCH_2), 72.0 (s, CH_2SO_2), 83.7 (s, C_5H_5), 171.1 (s, CO), 207.7 (s, CO). − ^{31}P NMR (162 MHz, $CDCl_3$, 20°C): δ = 12.6 [d, ^2J(P,P) = 90 Hz], 12.8 [d, ^2J(P,P) = 90 Hz]. − IR (Nujol): $\tilde{\nu}$ = 1731, 1701 (C=O), 1153, 1028 cm^{-1} (S=O). − $C_{40}H_{42}O_5P_2RuS$ (797.9): calcd. C 60.22, H 5.31; found C 59.92, H 5.37.

9c: Yield 113 mg (71%), m.p. 191°C (dec.). − ^{1}H NMR (400 MHz, $CDCl_3$, 20°C): δ = 0.79 [t, ^3J(H,H) = 6.3 Hz, 3 H, CH_3], 1.26 [t, ^3J(H,H) = 7.1 Hz, 3 H, CH_3], 1.66−1.91 (m, 2 H, CH_2), 2.08 (m, 1 H, CH_2), 2.43 (m, 1 H, CH_2), 2.52 (m, 2 H, CH_2), 3.72 [q, ^3J(H,H) = 6.3 Hz, 1 H, SO_2CH], 4.15 (res. m, 1 H, OCH_2), 4.16 (res. m, 1 H, OCH_2), 5.07 (s, 5 H, C_5H_5). − ^{13}C NMR (100 MHz, $CDCl_3$, 20°C): δ = 13.7 (s, CH_3), 14.6 (s, CH_3), 19.1 (s, CH_2), 29.3 (s, CH_2), 32.1 (s, CH_2), 59.3 (s, OCH_2), 82.4 (s, C_5H_5), 98.6 (s, $CHSO_2$), 165.3 (s, CO), signals of C_{quat} and CO (ketone) not detected due to low intensity. − ^{31}P NMR (162 MHz, $CDCl_3$, 20°C): δ = 11.9 [d, ^2J(P,P) = 88 Hz], 10.0 [d, ^2J(P,P) = 88 Hz]. − IR (Nujol): $\tilde{\nu}$ = 1672, 1613 (C=O), 1153, 1028 cm^{-1} (S=O). − $C_{40}H_{42}O_5P_2RuS$ (797.9): calcd. C 60.22, H 5.31; found C 59.99, H 5.12.

O-Alkylation of the Sulfinato Complexes: To a solution of the sulfinato complex (0.1 mmol) in dichloromethane (10 ml), a solution of the oxonium salt in the same solvent was added at −70°C. After being allowed to warm to 20°C, the mixture was concentrated to a volume of 1 ml and the product was precipitated by the addition of pentane. In some instances, **10a** separated as an oil. In this event, it was found that crystallization could be induced by ultrasound treatment under pentane.

10a: Yield 85 mg (94%), m.p. 88°C (dec.). − ^{1}H NMR (400 MHz, CD_2Cl_2, 20°C): δ = 1.10 (s, 3 H, CH_3), 1.20 [t, ^3J(H,H) = 7.2 Hz, 6 H, CH_3], 2.82 (s, 3 H, $SOCH_3$), 3.07 [d, ^2J(H,H) = 15.0 Hz, 1 H, SO_2CH_2], 3.63 [d, ^2J(H,H) = 15.0 Hz, 1 H, SO_2CH_2], 4.15 (res. m, 4 H, OCH_2), 5.31 (s, 5 H, C_5H_5). − ^{13}C NMR (100 MHz, CD_2Cl_2, 20°C): δ = 14.1 (s, CH_3), 14.2 (s, CH_3), 19.3 (s, CH_3), 52.0 (s, $SOCH_3$), 55.7 (s, C_{quat}), 62.2 (s, OCH_2), 62.6 (s, OCH_2), 74.4 (s, CH_2SO_2), 84.6 (s, C_5H_5), 169.7 (s, CO), 169.9 (s, CO). − ^{31}P NMR (162 MHz, CD_2Cl_2, 20°C): δ = 2.6 [d, ^2J(P,P) = 86 Hz], 5.8 [d, ^2J(P,P) = 86 Hz]. − IR (Nujol): $\tilde{\nu}$ = 1726 (C=O) cm^{-1}. − $C_{40}H_{45}BF_4O_6P_2RuS$ (903.7): calcd. C 53.16, H 5.02; found C 52.69, H 5.35.

10b: Yield 91 mg (93%), m.p. 135°C (dec.). − ^{1}H NMR (400 MHz, [D_6]acetone, 20°C): δ = 1.10 [t, ^3J(H,H) = 7.1 Hz, 3 H, CH_3], 1.16 [t, ^3J(H,H) = 7.1 Hz, 3 H, CH_3], 1.21 [t, ^3J(H,H) = 7.1 Hz, 3 H, $SOCH_3$], 1.22 (s, 3 H, CH_3), 2.95 [dq, ^3J(H,H) = 7.1 Hz, ^2J(H,H) = 9.6 Hz, 1 H, OCH_2], 3.07 [d, ^2J(H,H) = 15.1 Hz, 1 H, SO_2CH_2], 3.62 [dq, ^3J(H,H) = 7.1 Hz, ^2J(H,H) = 9.6 Hz, 1 H, OCH_2], 3.88 [d, ^2J(H,H) = 15.1 Hz, 1 H, SO_2CH_2], 4.10 (res. m, 4 H, OCH_2), 5.55 (s, 5 H, C_5H_5). − ^{13}C NMR (100 MHz, [D_6]acetone, 20°C): δ = 13.9 (s, CH_3), 14.0 (s, CH_3), 14.1 (s, CH_3), 19.2 (s, CH_3), 54.1 (s, C_{quat}), 61.9 (s, OCH_2), 62.4 (s, OCH_2), 63.1 (s, OCH_2), 73.6 (s, CH_2SO_2), 85.6 (s, C_5H_5), 169.7 (s, CO), 170.0 (s, CO). − ^{31}P NMR (162 MHz, [D_6]acetone, 20°C): δ = 2.6 [d, ^2J(P,P) = 85 Hz], 5.5 [d, ^2J(P,P) = 85 Hz]. − IR (Nujol): $\tilde{\nu}$ = 1733 (C=O), 1150 (S=O) cm^{-1}. − $C_{41}H_{47}F_6O_6P_3RuS$ (975.9): calcd. C 50.46, H 4.85; found C 50.82, H 4.99.

10c: Yield 90 mg (91%), m.p. 118°C (dec.). − ^{1}H NMR (400 MHz, [D_6]acetone, 20°C) (assignment to the two different diastereomers was not possible): δ = 0.75 [t, ^3J(H,H) = 7.0 Hz, 3 H, CH_3], 1.20 (s, 3 H, CH_3), 1.40 (s, 9 H, *t*Bu), 1.93, 2.04 [s, 3 H, C(O)CH_3], 2.71, 2.86, 3.30, 3.32 [d, ^2J(H,H) = 15.2 Hz, 2 H, SO_2CH_2], 2.95 (m, 2 H, $SOCH_2$), 5.41, 5.42 (s, 5 H, C_5H_5). − ^{13}C NMR (100 MHz, [D_6]acetone, 20°C): δ = 13.8, 14.6 (s, CH_3), 18.9, 19.4 (s, CH_3), 25.6, 26.2 (s, CH_3), 27.6, 27.7 (s, *t*Bu), 60.6, 60.7 (s, C_{quat}), 62.4, 62.6 (s, $SOCH_2$), 73.9, 74.2 (s, CH_2SO_2), 83.0, 83.1 (s, CMe_3), 87.4, 87.5 (s, C_5H_5), 169.6, 169.7 (s, CO), 202.3, 202.7 (s, CO). − ^{31}P NMR (162 MHz, [D_6]acetone, 20°C), major (51%) diastereomer: δ = 69.2 [d, ^2J(P,P) = 21 Hz], 73.3 [d, ^2J(P,P) = 21 Hz], minor (49%) diastereomer: δ = 66.2 [d, ^2J(P,P) = 21 Hz], 72.8 [d, ^2J(P,P) = 21 Hz]. − IR (Nujol): $\tilde{\nu}$ = 1716 (C=O), 1150 cm^{-1} (S=O). − $C_{43}H_{51}F_6O_5P_3RuS$ (987.9): calcd. C 52.28, H 5.20, S 3.25; found C 51.99, H 5.33, S 3.15.

Liberation of the Sulfinic Acid Esters: The respective ester complexes **10a**, **b** (0.2 mmol) were dissolved in acetonitrile (10 ml) and heated under reflux (15 h). Thereafter, the mixtures were concentrated to dryness and the resulting residues were suspended in diethyl ether. The acetonitrile complexes **11a**, **b** separated as yellow powders upon ultrasound treatment. In each case, the supernatant was concentrated to dryness, leaving the esters **12a**, **b** as colorless, spectroscopically pure oils in almost quantitative yields.

12a: ^{1}H NMR (400 MHz, $CDCl_3$, 20°C): δ = 1.24 [t, ^3J(H,H) = 7.1 Hz, 6 H, CH_3], 1.58 (s, 3 H, CH_3), 3.16 [d, ^2J(H,H) = 13.6 Hz, 1 H, SO_2CH_2], 3.34 [d, ^2J(H,H) = 13.6 Hz, 1 H, SO_2CH_2], 3.72 (s, 3 H, $SOCH_3$), 4.19 [q, ^3J(H,H) = 7.1 Hz, 4 H, OCH_2]. − ^{13}C NMR (100 MHz, $CDCl_3$, 20°C): δ = 13.9 (s, CH_3), 20.5 (s, CH_3), 51.4 (s, C_{quat}), 62.0 (s, OCH_2), 62.1 (s, OCH_2), 63.0 (s, CH_2SO_2), 170.1 (s, CO).

12b: ^{1}H NMR (400 MHz, $CDCl_3$, 20°C): δ = 1.25 [t, ^3J(H,H) = 7.1 Hz, 6 H, CH_3], 1.32 [t, ^3J(H,H) = 7.1 Hz, 3 H, CH_3], 1.58 (s, 3 H, CH_3), 3.19 [d, ^2J(H,H) = 13.6 Hz, 1 H, SO_2CH_2], 3.36 [d, ^2J(H,H) = 13.6 Hz, 1 H, SO_2CH_2], 4.06 (res. m, 2 H, $SOCH_2$), 4.19 (res. m, 2 H, OCH_2), 4.20 (res. m, 2 H, OCH_2). − ^{13}C NMR (100 MHz, $CDCl_3$, 20°C): δ = 13.9 (s, CH_3), 15.8 (s, CH_3), 20.4 (s, CH_3), 51.5 (s, C_{quat}), 62.0 (s, OCH_2), 62.1 (s, OCH_2), 63.2 (s, $SOCH_2$), 65.0 (s, CH_2SO_2), 170.1 (s, CO), 170.2 (s, CO).

Acetonitrile/SO_2 Exchange: In a small pressure tube, equipped with a Teflon needle valve, liquid sulfur dioxide (5 ml) was condensed onto the acetonitrile complex **11a**, **b** (0.1 mmol). After 7 d at 20°C, the tube was vented and the yellow residue was recrystallized from dichloromethane/pentane.

1a: Yield 72 mg (95%), spectroscopically identical to authentic material.[19]

1e: Yield 67 mg (96%) m.p. 158°C. – ^{31}P NMR (162 MHz, [D$_6$]acetone, 20°C): δ = −3.2 (s). – IR (Nujol): $\tilde{\nu}$ = 1279, 1115 (S=O) cm^{-1}. – $C_{30}H_{27}BF_4O_2P_2RuS$ (701.4): calcd. C 51.37, H 3.88, S 4.57; found C 50.94, H 3.88, S 4.50.

[1] J. P. Collman, L. S. Hegedus, J. R. Norton, R. G. Finke, *Principles and Applications of Organotransition Metal Chemistry*, University Science Books, Mill Valley, **1987**, pp. 1−18.
[2] J. F. King, R. Rathore in *The Chemistry of Sulfonic Acids, Esters, and Their Derivatives* (Eds.: S. Patai, Z. Rappoport), Wiley, New York, **1991**, pp. 583−669.
[3] B. G. Lenz, B. Zwanenburg in *Methoden der Organischen Chemie (Houben-Weyl)*, vol. E11, part 2, Thieme, Stuttgart, **1985**, pp. 1326−1344.
[4] W. Sundermeyer, J. Waldi, *Chem. Ber.* **1990**, *123*, 1687−1690.
[5] G. Opitz, W. Wiehn, M. L. Ziegler, B. Nuber, *Chem. Ber.* **1992**, *125*, 1621−1626.
[6] M. J. Pregel, E. Buncel, *J. Am. Chem. Soc.* **1993**, *115*, 10−14.
[7] E. Block, A. Wall, *J. Org. Chem.* **1987**, *52*, 809−818.
[8] W. A. Schenk, P. Urban, *J. Organomet. Chem.* **1991**, *411*, C27−C31.
[9] W. A. Schenk, P. Urban, E. Dombrowski, *Chem. Ber.* **1993**, *126*, 697−684.
[10] W. A. Herrmann, C. Bauer, J. Weichmann, *Chem. Ber.* **1984**, *117*, 1271−1286.
[11] A. K. Burrell, G. H. Clark, C. E. F. Rickard, W. R. Roper, A. H. Wright, *J. Chem. Soc., Dalton Trans.* **1991**, 609−614.
[12] W. B. Studabaker, M. Brookhart, *J. Organomet. Chem.* **1986**, *310*, C39−C41.
[13] G. Binsch, H. Kessler, *Angew. Chem.* **1980**, *92*, 445−463; *Angew. Chem. Int. Ed. Engl.* **1980**, *19*, 411.
[14] M. L. H. Green, L. L. Wong, A. Sella, *Organometallics* **1992**, *11*, 2660−2668.
[15] E. Dombrowski, W. A. Schenk, *Angew. Chem.* **1995**, *107*, 1098−1099; *Angew. Chem. Int. Ed. Engl.* **1995**, *34*, 1008−1009.
[16] G. Vitzthum, E. Lindner, *Angew. Chem.* **1971**, *83*, 315−327; *Angew. Chem. Int. Ed. Engl.* **1971**, *10*, 315.
[17] C. A. Poffenberger, A. Wojcicki, *Inorg. Chem.* **1980**, *19*, 3795−3803.
[18] S. E. Livingstone in *Comprehensive Coordination Chemistry*, vol. 2 (Eds.: R. D. Gillard, J. A. McCleverty), Pergamon, Oxford, **1987**, pp. 633−659.
[19] G. S. Ashby, M. I. Bruce, I. B. Tomkins, R. C. Wallis, *Aust. J. Chem.* **1979**, *32*, 1003−1016.
[20] S. Bravermann in *The Chemistry of Sulfinic Acids, Esters, and Their Derivatives* (Ed.: S. Patai), Wiley, New York, **1990**, pp. 297−349.
[21] M. Brookhart, Y. Liu in *Advances in Metal Carbene Chemistry* (Ed.: U. Schubert), Kluwer, Dordrecht, **1989**, pp. 251−270.
[22] B. E. R. Schilling, R. Hoffmann, D. L. Lichtenberger, *J. Am. Chem. Soc.* **1979**, *101*, 585−591.
[23] P. Hofmann, *Angew. Chem.* **1977**, *89*, 551−553; *Angew. Chem. Int. Ed. Engl.* **1977**, *16*, 536.
[24] J. Drabowicz, P. Kielbasinsky, M. Mikolajczyk in *The Chemistry of Sulfinic Acids, Esters, and Their Derivatives* (Ed.: S. Patai), Wiley, New York, **1990**, pp. 351−429.
[25] W. A. Schenk, U. Karl, M. R. Horn, *Z. Naturforsch., B* **1989**, *44*, 1513−1518.
[26] T. H. Black, *Aldrichim. Acta* **1983**, *16*, 3−10.
[27] X. Creary, W. W. Tam, K. F. Albizati, R. V. Stevens, *Org. Synth.* **1986**, *64*, 207−216.

[97290]

Towards New Iron(III) Chelators: Synthesis and Complexing Ability of a Water-Soluble Tripodal Ligand Based on 2,2′-Dihydroxybiphenyl Subunits

Paul Baret*, Virginie Beaujolais, Claude Béguin, Didier Gaude, Jean-Louis Pierre, and Guy Serratrice*

Laboratoire de Chimie Biomimétique, LEDSS, UMR CNRS 5616, Université J. Fourier,
BP 53, F-38041 Grenoble Cedex 9, France
Fax: (internat.) + 33(0)4/76 51 48 36
E-mail: Paul.Baret@ujf-grenoble.fr; Guy.Serratrice@ujf-grenoble.fr

Received December 4, 1997

Keywords: Dihydroxybiphenyl / Iron chelation / Formation constants / Protonation constants

A new water-soluble iron(III) sequestering agent has been designed. The tris-bidentate tripodal ligand consists of three 2,2′-dihydroxybiphenyl subunits connected via amide linkages at their *meta* (4-) positions to a framework of the "tren" type. The key step of the synthesis involves the coupling of suitably substituted monophenyl moieties in order to obtain the biphenyl precursor. The deprotonation constants of the ligand, and the formation and deprotonation constants of the Fe^{III} complex have been determined from potentiometric and spectrophotometric measurements. The results are compared with those of a previously described homologous ligand in which the chelating subunits are attached to the tren framework via the *ortho* (3-) position of the biphenyl rather than the 4-position.

Introduction

Iron overloading is a significant health problem, for which iron chelation therapy is required[1]. A number of limitations to the use of desferrioxamine, the only approved drug for treatment of iron overload (parenteral administration, prohibitive price, short plasma half-life), underline the need for the development of a truly orally effective drug. The search for effective ferric ion chelating agents was originally centered on mimics of natural siderophores [tris(catecholate) or tris(hydroxamate) ligands][2]. Catechol-based ligands are the most powerful in the thermodynamic sense [enterobactin, a tris(catecholate) siderophore produced by *E. Coli* has been shown[3] to have a stability constant for Fe^{III} complexation of 10^{49}], but these ligands are extremely air-sensitive and they have been shown to promote bacterial infections. Hydroxamate-based ligands seem to suffer limitations inherent to all the hydroxamate chelating agents. Recently, potential drugs for iron chelation therapy incorporating "non-natural" chelating subunits have been studied, such as hydroxypyridinone[4], pyridoxal isonicotinoyl hydrazone[5], and 8-hydroxyquinoline[6].

In a previous publication[7], we described tripodal ligands based on three 2,2′-dihydroxybiphenyl subunits connected to a tris(2-aminoethyl)amine (tren) framework via the *ortho* (3-) positions of their phenolic groups (an example, L_o, is depicted in Figure 1). The results obtained with these water-soluble and air-stable ligands were promising[8]. Nevertheless, the complexing ability of these ligands was found to be lower than that of tris(catecholates) or tris(hydroxamates) on the basis of the respective pFe values. The interpretation of molecular modelling studies suggested that connection of the 2,2′-dihydroxybiphenyl chelating pendant arms to the tren framework via the 4-position, i.e. *meta* to the hydroxy group, rather than via the 3-position (*ortho* to the hydroxy group), should be more conducive to an octahedral arrangement of the ligation sites around the metal center. However, this new mode of connection renders impossible the so-called salicylate-like binding of the metal[9] (which generally occurs at low pH). On the other hand, the presence of an amide group at the position *ortho* to the hydroxy group has been shown by Shanzer et al.[10] to result in hydrogen bonding in the complex between the amide and the oxygen coordinated to Fe^{III}. These interactions suggest a preorganization of the ligand around the metal center that improves its binding properties. In order to examine the effect of the position of the amide linkage (*ortho* or *meta* to the phenolic group) on the complexing ability of the ligand, we report herein on the synthesis and iron(III) complexing properties of L_m, a tripodal ligand in which the biphenyl subunits are attached via their 4-positions (Figure 1).

Figure 1. Structural formulae of tris-2,2′-dihydroxybiphenyl ligands

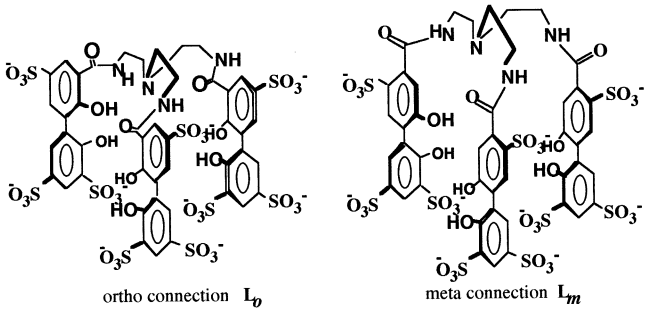

 © WILEY-VCH Verlag GmbH, D-69451 Weinheim, 1998 1434−1948/98/0404−0613 $ 17.50+.50/0

Results and Discussion

Synthesis of Ligands

The synthesis of tripodal ligands based on 2,2′-hydroxy-1,1′-biphenyl subunits, attached either via the 3-position[7a] or the 4-position (this work, Figure 2), is centered on the formation of amide links from carboxylate moieties, which are activated and then conjugated with the tetraamine, tris(2-aminoethyl)amine (tren). Coupling of the protected 2,2′-dimethoxy-1,1′-diphenyl-4-carboxylic acid **9** with tren was most conveniently accomplished using *N*,*N*′-carbonyldiimidazole (CDI).[18] For comparative complexation studies, simple bidentate ligands **14** and **15** were also prepared (Figure 2).

Figure 2. Synthesis of the ligands

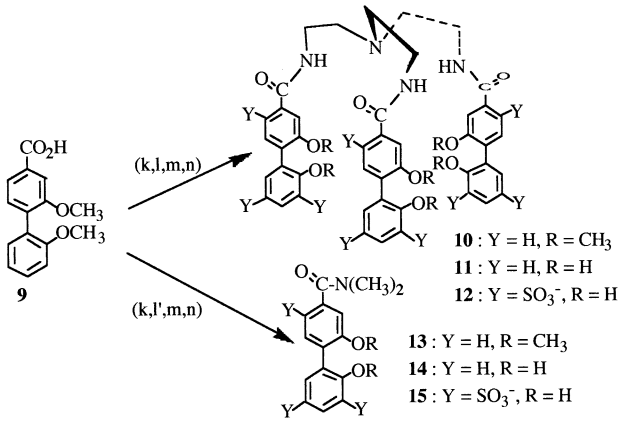

(k) CDI, THF, nitrogen ; then (l) TREN ,(l') $HN(CH_3)_2$
(m) BBr_3, CH_2Cl_2, 0 °C ; (n) H_2SO_4, ,SO_3

Sulfonation, using H_2SO_4/oleum, of tripod **11** and of bidentate ligand **14** afforded the water-soluble products **12** and **15**, respectively.

In the previously studied[7a] series of ligands, in which the connection with the spacer tren was at the 3-position of the biphenyl group, the starting material for the synthesis was commercially available 2,2′-hydroxy-1,1′-biphenyl. Functionalization at the position *ortho* to the phenolic hydroxy group was readily and regiospecifically effected by various methods. The synthesis of 2,2′-dimethoxy-1,1′-diphenyl-4-carboxylic acid (**9**) involves heterocoupling[13][19][20] (Figure 3) of the iodo derivative **5** of methyl 2-methoxybenzoate (**4**) and 2-methoxyphenylboronic acid (**7**) (Figure 3B). The iodo derivative was obtained[12] from 5-methyl-2-nitroanisole (**1**) (Figure 3A).

Ligand Deprotonation Constants

The ligand L_m possesses six hydroxy groups and one tertiary amine function and is denoted LH_7^{8-} taking into account the negative charges of the nine sulfonate groups. The deprotonation constants were determined by potentiometric titration of the fully protonated ligand with NaOH in 0.1 M $NaClO_4$ at 25°C (Figure 4a). Analysis of the titration curve yielded only the following five pK_a values: 10.62 ± 0.07; 7.48 ± 0.11; 6.23 ± 0.12; 5.85 ± 0.13, and 4.88 ± 0.13.

Figure 3. Synthesis of 2,2′-dimethoxy-1,1′-diphenyl-4-carboxylic acid **9**

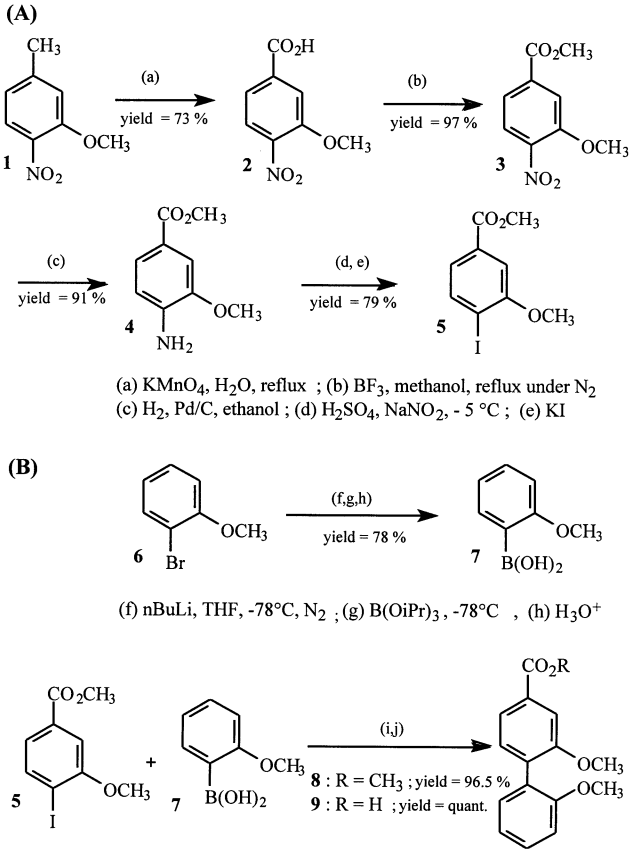

Figure 4. Potentiometric titration curves for (a) 0.5 mmol dm^{-3} ligand L_m; (b) ligand L_m + Fe^{3+} 1:1 0.5 mmol dm^{-3}; m = moles of base added per mol of ligand; all solutions were at 25°C and I = 0.1 mol dm^{-3} ($NaClO_4$); the deprotonation constants of the ligand and the complexation constants were calculated using the SUPERQUAD program[15]

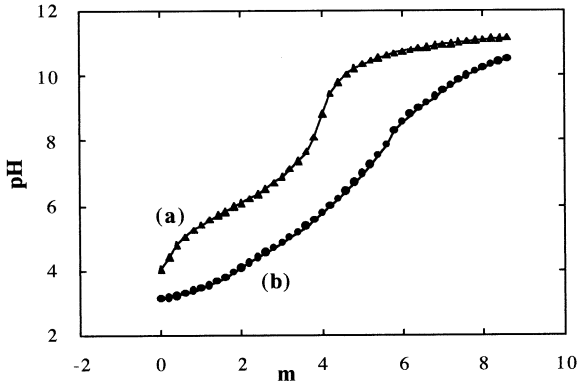

The deprotonation constants of LH_2^{13-} and LH^{14-} species are too high to be accurately determined by direct potentiometry. Spectrophotometric titration was carried out at pH = 10.2−12.7 and revealed one buffer region. The corresponding UV spectra exhibit isosbestic behavior, indicating the presence of only two absorbing species (Figure 5). The data were analyzed using the LETAGROP-

SPEFO[16][17] program (absorbance values at 4 wavelengths). The model delineated involves a single-proton step for the deprotonation equilibrium, yielding a pK_a value of 11.70 ± 0.03. The pK_a values of the monomeric analogue **15** (5,3′,5′-trisulfonate derivative of compound **14**) were also determined: 5.50 ± 0.01 by potentiometry in the acidic range, and 11.68 ± 0.03 by UV/Vis spectrophotometry in the basic range. The value of 5.50 befits a hydroxy group *meta* to the electron-withdrawing amide group.

Figure 5. UV/Vis absorption spectra of the L_m ligand as a function of pH; 1: pH = 10.2; 2: pH = 12.4; $[L_m]$ = 0.05 mmol dm^{-3}; I = 0.1 mol dm^{-3} ($NaClO_4$)

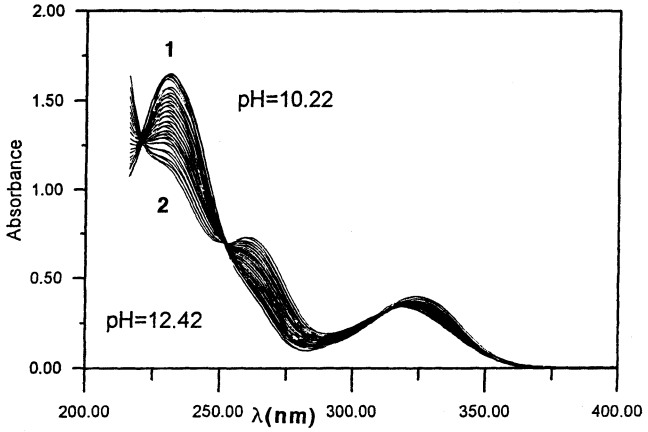

The three lower pK_a values (4.88, 5.85, and 6.23) and the two higher pK_a values (10.62 and 11.70) were assigned to hydroxy groups. The former reflect a roughly statistical separation (log 3 or 0.48), which is consistent with non-interacting arms if one allows for a difference up to one pK unit, as is encountered in several tripodal structures containing 2,2′-dihydroxybiphenyl[7b], catechol[21] or hydroxamate[22] binding units. It should be noted that the average value of these three pK_a′s, 5.65, is very close to the value of 5.50 determined for the monomeric analogue. A similar behavior is expected for the pK_a′s of the three remaining hydroxy groups, the value of 11.70 being very close to that of 11.68, measured for the monomeric analogue. Furthermore, it is assumed that the deprotonation of at least two OH groups, each borne by two different pendant arms of the tripod, induces a change in the UV spectrum. We can thus estimate the third pK_a in this range as having a value of 12.7 on the basis of a statistical separation (see above). The pK_a of 7.48 was attributed to the tertiary amine group by comparison with the value of 7.1 determined for tripodal ligands containing 2,2′-dihydroxybiphenyl subunits[7b].

Stability Constants of Ferric Complexes

Stability constants for the Fe^{III} complexes were determined by means of spectrophotometric and potentiometric titrations. The spectrophotometric behavior of the ferric complexes at a 1:1 metal-to-ligand molar ratio was investigated as a function of pH. The spectrum changed significantly over the pH range 0.7−5.3. The ligand reacts with Fe^{III} in acidic media, as indicated by the absorption spectra (Figure 6a). As the pH was increased from 1 to 2.5, the charge transfer band was found to shift from 520 nm ($\varepsilon \approx$ 600 mol^{-1} dm^3 cm^{-1}) to 470 nm ($\varepsilon \approx$ 1400 mol^{-1} dm^3 cm^{-1}). The absorbance data were processed with the LETAGROP-SPEFO program. The best fit was obtained by considering the formation of the $[FeLH_6]^{6-}$ and $[FeLH_5]^{7-}$ species, generating the values log β_{116}[23] = 61.9 ± 0.1 and log β_{115} = 60.0 ± 0.1, with ε_{max} = 580 mol^{-1} dm^3 cm^{-1} (λ = 520 nm) for $[FeLH_6]^{6-}$ and 1510 mol^{-1} dm^3 cm^{-1} (λ = 480 nm) for $[FeLH_5]^{7-}$. Increasing the pH to 5.3 led to an increase in the band intensity, which was accompanied by a shift to lower wavelength (Figure 6b). The best fitting model for the interpretation of spectrophotometric data was obtained by considering the equilibrium between $[FeLH_5]^{7-}$ and $[FeLH_3]^{9-}$. The calculated value of log β_{113} is 51.8 ± 0.1, with ε = 2600 mol^{-1} dm^3 cm^{-1} at 420 nm (shoulder). Only a marginal spectral change was observed over the pH range 5.3−7.5. At pH > 7.5, absorbances in the range 400−550 nm were found to decrease.

Figure 6. UV/Vis absorption spectra of Fe^{3+}−L_m ligand as a function of pH; (a) 1: pH = 0.7; 2: pH = 2.45; (b) 1: pH = 2.5; 2: pH = 5.3; $[Fe^{3+}]$ = $[L_m]$ = 0.25 mmol dm^{-3}; I = 0.1 mol dm^{-3} ($NaClO_4$)

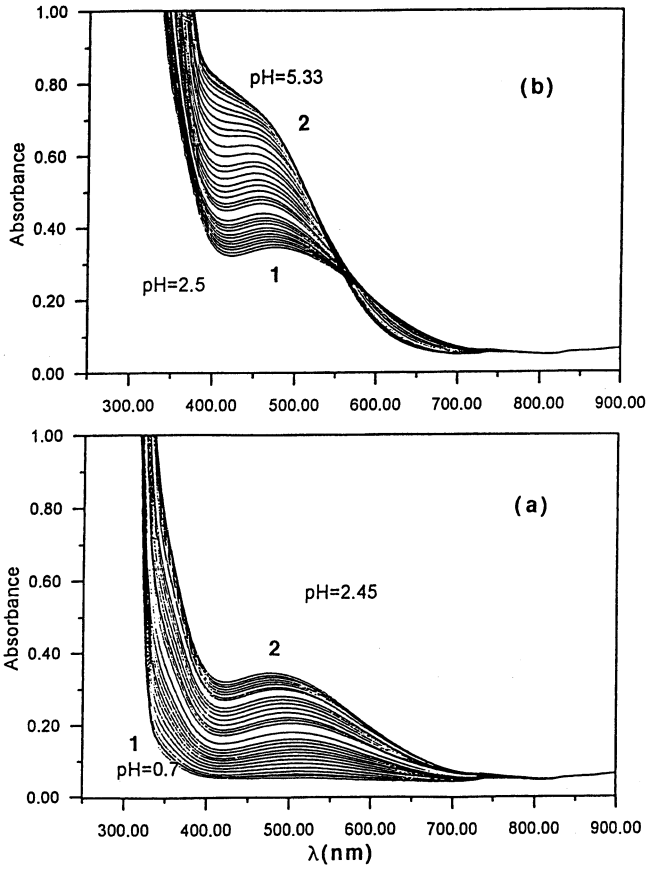

Potentiometric titration on 1:1 solutions in ferric ion and ligand was also carried out over the pH range 3−10 (Figure 4b). Data were analyzed using the SUPERQUAD program by considering the $[FeLH_5]^{7-}$ species at the beginning of the titration and using the value of β_{115} calculated from the spectrophotometric titration. The model was best fitted (σ_{fit} = 2.9) with six Fe^{III} complex species $[FeLH_4]^{8-}$,

$[FeLH_3]^{9-}$, $[FeLH_2]^{10-}$, $[FeLH]^{11-}$, $[FeL]^{12-}$, and $[FeLOH]^{13-}$ giving the following values of log β_{11h}: log $\beta_{114} = 56.49 \pm 0.02$; log $\beta_{113} = 51.86 \pm 0.03$; log $\beta_{112} = 46.26 \pm 0.04$; log $\beta_{111} = 39.11 \pm 0.06$; log $\beta_{110} = 30.03 \pm 0.08$; log $\beta_{11-1} = 20.26 \pm 0.08$.

From these values, the following deprotonation constants can be deduced for the complexes: $pK_{FeLH5} = 3.51$; $pK_{FeLH4} = 4.63$; $pK_{FeLH3} = 5.60$; $pK_{FeLH2} = 7.15$; $pK_{FeLH} = 9.08$; $pK_{FeL} = 9.77$.

It should be noted that the value of log $\beta_{113} = 51.86$ is in good agreement with that of 51.8 determined from the spectrophotometric study, thus validating the proposed model.

Structural attributes of these complexes can be proposed on the basis of their spectral characteristics. For $[FeLH_5]^{7-}$, the band at 470 nm ($\varepsilon = 1400$ mol^{-1} dm^3 cm^{-1}) is indicative of a dihydroxylate mode of coordination involving one arm of the ligand, as is apparent from comparison with the system Fe^{III} sodium 2,2′-dihydroxybiphenyl-3,5,3′,5′-tetrasulfonate[9]. Over the pH range 2.5−5.3, the observed increase in absorbance and shift to shorter wavelength (shoulder at $\lambda = 430$ nm with $\varepsilon = 2600$ mol^{-1} dm^3 cm^{-1}) suggest a bis(dihydroxylate) coordination involving two arms of the ligand in the $[FeLH_3]^{9-}$ species. A region of constant specific absorbance at pH = 5.3−7.5 indicates no increased degree of coordination to the dihydroxylate groups. At pH > 7.5, a decrease in the absorption in the range 400−550 nm may correspond to the formation of hydroxo complexes. The successive deprotonation constants of the complex $[FeLH_3]^{9-}$ may thus be attributed to deprotonation of the tertiary amine group, of one hydroxy group of the uncoordinated arm, and of the two water molecules that complete the coordination sphere around Fe^{III}. The fact that only two arms of the ligand L_m are involved in coordination of Fe^{III} might be explained in terms of repulsive effects between the negative charges on the sulfonate groups in the 3′-positions. It is assumed that such interactions prevent the formation of a hexadentate coordination cavity involving all three arms.

The pFe ($-\log [Fe^{3+}]$) values have been calculated to provide a comparison of the relative ability of the ligands to complex Fe^{III} (under biologically reasonable conditions, i.e. pH = 7.4, $[L]_{tot} = 10^{-5}$ mol dm^{-3}, $[Fe]_{tot} = 10^{-6}$ mol dm^{-3}). The calculated value for ligand L_m is 19.7. This value shows that the ligand L_m is less effective than the analogous tripodal L_o (pFe = 22.8),[7b] in which the subunits are connected via their 3-positions, i.e. *ortho* to the hydroxy groups. This lower affinity of L_m for Fe^{III} can be partly related to the available coordination modes. The structure of the ligand L_o favours an initial coordination of the salicylate type (with oxygen atoms of the carbonyl and hydroxy groups). A preorganization of the ligand is thus expected for a complexation of the metal ion by the other arms. This cannot occur for L_m.

Conclusion

A multistep synthesis of the tris-bidentate tripodal ligand L_m has been described. This ligand incorporates three 2,2′-dihydroxybiphenyl subunits, which are attached to a central "tren" framework via amide linkages at their 4-positions, i.e. *meta* to the phenolic hydroxy groups. The aim of this work was to compare the complexing ability of L_m with that of L_o, a previously described iron chelator in which the chelating pendant arms are attached via their 3-positions, i.e. *ortho* to the phenolic groups.

The ligand deprotonation constants (six hydroxy groups and one tertiary amine function) and the stability constants β_{11h} of the ferric complexes (in a pH range of 1−10) have been determined. The pFe value of 19.7 calculated for L_m as compared to the value of 22.8 for L_o[7b] reveals an interesting structural effect. Since molecular models suggested that the *meta* connection (L_m) should be more conducive to the formation of an octahedral coordination cavity than the *ortho* connection (L_o), the observed result was unexpected. The structure of the ligand L_o favours an initial coordination of the salicylate type (with oxygen atoms of the carbonyl and hydroxy groups), which is assumed to "preorganize" the ligand for a complexation of the metal ion by the other arms. This is not possible for L_m, thus diminishing its complexing ability towards Fe^{III}. Furthermore, as the coordination changes from a salicylate to a dihydroxylate mode of bonding upon deprotonation of the complex, an amide conformational change is assumed to occur for the complexation of the metal center by L_o. Thus, hydrogen bonding between the amide group and the coordinated oxygen atom (six-membered ring) can occur, which is not possible in the complex of Fe^{III} with L_m. The importance of the preorganization of the ligand was emphasized by Shanzer et al.[10], and seems to play a major role in determining the complexing ability of a given ligand. Thus, for the design of novel ligands, geometry of the octahedral coordination sphere around the metal center is not the sole criterion for the prediction of complexation stability.

We are grateful to Dr. *Hakim Boukhalfa* (L.E.D.S.S., Grenoble) for performing the UV/Vis spectrophotometric measurements.

Experimental Section

Materials and Equipment: Solvents were purified by standard techniques; 5-methyl-2-nitroanisole and 2-bromoanisole are commercially available (Aldrich). The amine "tren" was distilled from sodium. All other compounds were of reagent grade and were used without further purification. Iron(III) stock solutions were prepared by dissolving appropriate amounts of ferric perchlorate hydrate (Aldrich) in standardized $HClO_4/NaClO_4$ solutions. The solutions were standardized for ferric ion spectrophotometrically by using a molar extinction coefficient of 4160 mol^{-1} dm^3 cm^{-1} at 240 nm[11]. − IR spectra were recorded with Perkin-Elmer 397 or Nicolet Impact 400 spectrometers. UV/Vis absorption spectra were recorded using 1.000-cm path length quartz cells with a Perkin-Elmer Lambda 2 spectrometer connected to a COMPAQ Deskpro 386s microcomputer. − Mass spectra were recorded with a NERMAG R 10 1 C mass spectrometer. − ^{1}H- and ^{13}C-NMR spectra were obtained using 5-mm tubes at 25°C with a Bruker AC 200 or a Bruker AM 400 spectrometer. − Microanalyses were performed by the Central Service of CNRS, Solaise (France). − Melting points were determined with a Büchi apparatus and are not corrected.

3-Methoxy-4-nitrobenzoic Acid (**2**): A mixture of 5-methyl-2-nitroanisole (**1**) (25.0 g, 0.15 mol), potassium permanganate (97.5 g, 0.62 mol), and sodium hydrogen carbonate (12.3 g, 0.12 mol) in 1.5 l of water was refluxed for 4 h. Thereafter, the MnO_2 formed was filtered off. The filtrate was cooled to 0°C and acidified with 20% sulfuric acid to pH = 1. The yellow solid thus produced was washed with water, dried, and purified by recrystallization from ethanol (white crystals, 21 g, 73%). – M.p. 226°C (ref.[12] 230–233°C). – ^{1}H NMR (200 MHz, [D$_6$]DMSO): δ = 4.01 (s, 3 H, OCH_3), 7.71 (dd, J_1 = 8.3, J_2 = 1.4 Hz, 1 H), 7.79 (d, J = 1.4 Hz, 1 H), 7.83 (d, J = 8.3 Hz, 1 H). – ^{13}C NMR (50 MHz, [D$_6$]DMSO): δ = 56.8 (OCH_3), 114.6 (CH), 121.3 (CH), 125.0 (CH), 135.8, 141.9, 151.5 (C–O), 165.8 (C=O). – IR (KBr): $\tilde{\nu}$ = 3250–2200 cm^{-1} [ν(OH)], 1680 [ν(C=O)].

Methyl 3-Methoxy-4-nitrobenzoate (**3**): 3-Methoxy-4-nitrobenzoic acid (**2**) (21.0 g, 0.11 mol) was dissolved in methanol (350 ml) under nitrogen. BF_3 (40 ml, 50% w/w in methanol) was added and the mixture was stirred under reflux for 12 h. The solvent was then removed, the residue was treated with water (300 ml), and the resulting suspension was filtered. The collected yellow solid was washed with water (500 ml) and then dried in vacuo (21.9 g, 0.10 mol, 91%). – M.p. 91°C (ref.[12] 90–91°C). – ^{1}H NMR (200 MHz, $CDCl_3$): δ = 3.97 (s, 3 H, CO_2CH_3), 4.02 (s, 3 H, OCH_3), 7.67 (dd, J_1 = 8.3, J_2 = 1.5 Hz, 1 H), 7.71 (d, J = 1.5 Hz, 1 H), 7.84 (d, J = 8.3 Hz, 1 H). – ^{13}C NMR (50 MHz, $CDCl_3$): δ = 52.8 (CO_2CH_3), 56.7 (OCH_3), 114.6 (CH), 121.4 (CH), 125.3 (CH), 134.8, 142.0, 152.4 (C–O), 165.2 (C=O). – IR (KBr): $\tilde{\nu}$ = 1740 cm^{-1} [ν(C=O)].

Methyl 4-Amino-3-methoxybenzoate (**4**): Compound **3** (10.0 g, 47.4 mmol) was dissolved in a mixture of dichloromethane (50 ml) and ethanol (300 ml). The resulting solution was stirred for 12 h under hydrogen in the presence of Pd/charcoal (10% Pd, 923 mg). The catalyst was subsequently removed by filtration and the solvent was evaporated. The yellow solid thus obtained was purified by recrystallization from ethanol (7.84 g, 43.3 mmol, 91%). – M.p. 128°C (ref.[12] 127–128°C). – ^{1}H NMR (200 MHz, $CDCl_3$): δ = 3.86 (s, 3 H, OCH_3), 3.89 (s, 3 H, OCH_3), 4.22 (m, 2 H, NH_2), 6.66 (d, J = 8.0 Hz, 1 H), 7.45 (d, J = 1.7 Hz, 1 H), 7.54 (dd, J_1 = 8.0, J_2 = 1.7 Hz, 1 H). – ^{13}C NMR (50 MHz, $CDCl_3$): δ = 51.6 (CO_2CH_3), 55.5 (OCH_3), 111.1 (CH), 113.1 (CH), 119.5, 124.0 (CH), 141.0, 146.1 (C–O), 167.3 (C=O). – IR (KBr): $\tilde{\nu}$ = 3450–3330 cm^{-1} [ν(NH_2)], 1670 [ν(C=O)].

Methyl 4-Iodo-3-methoxybenzoate (**5**): To a mixture of **4** (8.1 g, 44.7 mmol), water (110 ml) and 20% H_2SO_4 (24 ml), a solution of sodium nitrite (3.47 g, 49.6 mmol) in water (20 ml) was slowly added at 0°C. At the end of the reaction, the excess nitrous acid was destroyed by the addition of urea (800 mg). Then, 20 ml of aqueous KI (7.74 g, 46.6 mmol) was added dropwise and the mixture was stirred for 2 h at 50°C. To the resulting brown mixture was added an aqueous solution of $Na_2S_2O_5$. The product was isolated by extraction with diethyl ether, neutralization with 1 N NaOH (to pH = 5), washing with brine, and drying with Na_2SO_4. The solvent was evaporated and the iodo compound was purified by column chromatography (alumina, pentane containing 3% ethyl acetate), giving a white solid (10.4 g, 33.6 mmol, 72%). – M.p. 50–52°C (ref.[12] 52–53°C). – ^{1}H NMR (200 MHz, $CDCl_3$): δ = 3.92 (s, 3 H, OCH_3), 3.94 (s, 3 H, OCH_3), 7.36 (dd, J_1 = 8.1, J_2 = 1.8 Hz, 1 H), 7.44 (d, J = 1.8 Hz, 1 H), 7.84 (d, J = 8.1 Hz, 1 H). – ^{13}C NMR (50 MHz, $CDCl_3$): δ = 52.3 (CO_2CH_3), 56.5 (OCH_3), 92.6 (CI), 111.2 (CH), 123.3 (CH), 131.6, 139.5 (CH), 158.2 (C–O), 166.5 (C=O). – IR (KBr): $\tilde{\nu}$ = 1720 cm^{-1} [ν(C=O)].

2-Methoxyphenylboronic Acid (**7**): At –78°C, *n*BuLi (80 ml, 1.6 M in hexane, 0.128 mol) was added to a solution of 2-bromoanisole (**6**) (13.3 ml, 0.107 mol) in diethyl ether (100 ml) and the mixture was stirred at this temperature for 30 min. With a protective nitrogen atmosphere, the lithio derivative was then cannulated into a solution of triisopropyl borate (32 ml, 0.214 mol) in diethyl ether. After stirring at –78°C for 30 min, then at room temperature, the mixture was poured into aqueous HCl (10%, 300 ml). The product was extracted with diethyl ether, the combined extracts were washed with water (100 ml), and dried with Na_2SO_4. The oily, crude product was stored in a refrigerator for 24 h, giving white crystals. These somewhat unstable crystals were rapidly washed with cold pentane and then dried in vacuo (11 g, 0.072 mol, 68%). – M.p. 104–105°C (ref.[13] 105–106°C). – ^{1}H NMR (200 MHz, $CDCl_3$): δ = 3.85 (s, 3 H, OCH_3), 6.85 (d, J = 8.3 Hz, 1 H, ArH), 6.93–7.01 (m, 1 H, ArH), 7.34–7.43 (m, 1 H, ArH), 7.77 (dd, J_1 = 7.3, J_2 = 1.8 Hz, 1 H, ArH). – ^{13}C NMR (50 MHz, $CDCl_3$): δ = 55.3 (OCH_3), 109.9 (CH), 121.1 (CH), 132.7 (CH), 136.8 (CH), 164.4 (C–O).

Methyl 2,2′-Dimethoxy-1,1′-diphenyl-4-carboxylate (**8**): To a solution of **5** (1.0 g, 3.42 mmol) in freshly distilled DMF (15 ml) under nitrogen were added **7** (78 mg, 5.13 mmol), Et_3N (1.4 ml, 10.3 mmol), $Pd(OAc)_2$ (23 mg, 0.103 mmol), and P(*o*-Tol)$_3$ (65 mg, 0.212 mmol). The orange solution was heated at 100°C for 3 h, whereupon it became black. The solvent was evaporated and the residue was treated with dichloromethane and 10% ammonia. The organic phase was washed with water and then dried with Na_2SO_4. The orange oil was purified by column chromatography (silica gel; pentane/diethyl ether, 9:1). **8** was obtained as a white solid (0.9 g, 3.3 mmol, 97%). – M.p. 112°C. – R_f = 0.55 (pentane/diethyl ether, 2:1). – ^{1}H NMR (200 MHz, $CDCl_3$): δ = 3.33 (s, 3 H, CO_2CH_3), 3.39 (s, 3 H, OCH_3), 3.50 (s, 3 H, OCH_3), 6.53–6.62 (m, 2 H, ArH), 6.62–6.90 (m, 2 H, ArH), 6.87 (d, J = 7.7 Hz, 1 H), 7.20 (d, J = 1.4 Hz, 1 H), 7.25 (dd, J_1 = 7.7, J_2 = 1.4 Hz, 1 H). – ^{13}C NMR (50 MHz, [D$_6$]DMSO): δ = 52.2 (CO_2CH_3), 55.4 and 55.6 (OCH_3), 111.3 (CH), 111.4 (CH), 120.2 (CH), 121.2 (CH), 126.3, 129.2 (CH), 130.7 (CH), 131.1, 131.4 (CH), 132.2, 156.6 (C–O), 156.7 (C–O), 167.2 (C=O). – IR (KBr): $\tilde{\nu}$ = 1710 cm^{-1} [ν(C=O)]. – MS (EI); *m/z*: 272 [M$^+$], 241, 225, 213, 198. – $C_{16}H_{16}O_4$: calcd. C 70.58, H 5.29; found C 70.40, H 5.47.

2,2′-Dimethoxy-1,1′-diphenyl-4-carboxylic Acid (**9**): Ester **8** (2.0 g, 7.34 mmol) was refluxed with ethanolic KOH (excess) for 3 h. The mixture was then concentrated and 10% HCl was added. The resulting precipitate was filtered off, washed with water, and dried in vacuo to give **9** as a white solid (1.9 g, quant.). – M.p. 170°C. – ^{1}H NMR (200 MHz, $CDCl_3$): δ = 3.78 (s, 3 H, OCH_3), 3.85 (s, 3 H, OCH_3), 6.98–7.07 (m, 2 H, ArH), 7.23–7.28 (m, 1 H, ArH), 7.33–7.41 (m, 1 H, ArH), 7.36 (d, J = 7.8 Hz, 1 H), 7.77 (d, J = 1.5 Hz, 1 H), 7.8 (dd, J = 7.8, 1.5 Hz, 1 H). – ^{13}C NMR (50 MHz, [D$_6$]DMSO): δ = 55.4 and 55.5 (OCH_3), 111.4 (CH), 111.5 (CH), 120.2 (CH), 121.4 (CH), 126.5, 129.1 (CH), 130.8 (CH), 131.1, 131.3 (CH), 132.2, 156.6 (C–O), 156.7 (C–O), 167.2 (C=O). – IR (KBr): $\tilde{\nu}$ = 3600–2300 cm^{-1} [ν(OH)], 1680 [ν(C=O)]. – MS (EI); *m/z*: 258 [M$^+$], 184.

N,N′,N″-(Nitrilotri-2,1-ethanediyl)tris(2,2′-dimethoxy-4-biphenylcarboxamide) (**10**): Under nitrogen, acid **9** (1.0 g, 3.87 mmol) was treated with CDI (690 mg, 4.26 mmol) in freshly distilled THF (50 ml) and the mixture was stirred for 12 h; tren (160 µl, 1.06 mmol) was added and the mixture was stirred overnight at room temperature. The solvent was then evaporated and the brown oil was purified by column chromatography (silica gel, dichloromethane containing 2% isopropylamine) giving **10** as a white solid (1.0 g, 3.50

mmol, 90%). − M.p. 116°C. − R_f = 0.6 (CH_2Cl_2/MeOH, 9:1). − ^{1}H NMR (200 MHz, $CDCl_3$): δ = 2.77 (br. s, 6 H, NCH_2), 3.61 (m, 24 H, NCH_2, OCH_3), 6.84−7.04 (m, 12 H, ArH), 7.24−7.44 (m, 9 H, ArH), 7.50 (br. s, 3 H, NH). − ^{13}C NMR (50 MHz, $CDCl_3$): δ = 38.4 (CH_2), 54.7 (CH_2), 55.3 and 55.4 (OCH_3), 110.2 (CH), 110.9 (CH), 118.6 (CH), 120.1 (CH), 126.7, 128.7 (CH), 131.0 (CH), 131.2 (CH), 134.0, 156.6 (C−O), 156.9 (C−O), 167.8 (C=O). − IR (KBr): $\tilde{\nu}$ = 1635 cm^{-1} [ν(C=O)]. − MSM [FAB(+), NBA matrix]; *m/z*: 867 [M + H^+], 596, 284, 257, 241, 213. − $C_{51}H_{54}N_4O_9 \cdot 3H_2O$: calcd. C 66.64, H 6.36, N 6.10; found C 66.65, H 6.04, N 6.15.

N,N′,N′′-(Nitrilotri-2,1-ethanediyl)tris(2,2′-dihydroxy-4-biphenylcarboxamide) (**11**): A solution of BBr_3 in dichloromethane (1 M, 20 ml) was cooled to 0°C under nitrogen. Podand **10** (860 mg, 0.99 mmol) was added and the mixture was stirred for 12 h at room temperature, resulting in the deposition of a white precipitate. The mixture was treated with methanol and the solvents were evaporated. The residue was dissolved in 30 ml of 10% aq. NaOH. Subsequent addition of 10% HCl at 0°C gave **11** as a white precipitate, which was dried in vacuo (700 mg, 0.89 mmol, 90%). − M.p. 170°C. − ^{1}H NMR (200 MHz, [D_6]DMSO): δ = 3.48 (br. s, 6 H, CH_2), 3.73 (br. s, 6 H, CH_2), 6.76−6.92 (m, 6 H, ArH), 7.10−7.21 (m, 9 H, ArH), 7.34−7.41 (m, 6 H, ArH), 8.81 (br. s, 3 H, NH), 9.37 (br. s, 3 H, OH), 9.50 (br. s, 3 H, OH). − ^{13}C NMR (50 MHz, [D_6]DMSO): δ = 34.3 (CH_2), 52.1 (CH_2), 115.1, 115.8, 117.4, 118.8, 128.5, 129.3, 131.4, 133.8, 154.6 (C−O), 166.9 (C=O). − IR (KBr): $\tilde{\nu}$ = 3650−2300 cm^{-1} [ν(OH)], 1640 [ν(C=O)]. − MS [FAB(+), NBA matrix]; *m/z*: 783 [M + H^+], 613, 540, 528. − $C_{45}H_{42}N_4O_9 \cdot HBr \cdot H_2O$: calcd. C 61.35, H 5.15, N 6.36; found C 61.61, H 5.12, N 6.27.

N,N′,N″-(Nitrilotri-2,1-ethanediyl)tris(2,2′-dihydroxy-5,3′,5′-trisulfo-4-biphenylcarboxamide) (**12**): The hydroxylated tripod **11** (830 mg, 1.06 mmol) was dissolved in 60 ml of oleum (H_2SO_4 + 15% SO_3) at 0°C. The mixture was then stirred at 90°C for 3 h. After cooling to room temperature, the brown solution was cautiously poured onto crushed ice with stirring. With cooling, the solution was brought to pH = 4 by the slow addition of 10% aq. NaOH. Sodium sulfate was eliminated by repeated precipitations by adding methanol. − M.p. > 286°C. − ^{1}H NMR (200 MHz, D_2O): δ = 3.80 (m, 2 H, CH_2), 4.00 (m, 2 H, CH_2), 7.17 (s, 1 H), 7.91 (s, 1 H), 7.94 (d, *J* = 2.3 Hz, 1 H), 8.22 (d, *J* = 2.3 Hz, 1 H). − ^{13}C NMR (50 MHz, CD_3OD): δ = 37.4 (CH_2), 55.3 (CH_2), 118.6 (CH), 128.4 (CH), 129.4, 131.4, 134.1 (CH), 134.5, 134.9 (CH), 137.1, 138.0, 156.4 (C−O), 159.2 (C−O), 174.2 (C=O).

2,2′-Dimethoxy-4-(N,N-dimethylcarbamoyl)-1,1′-biphenyl (**13**): Under nitrogen at room temperature, acid **9** (0.9 g, 3.48 mmol) was treated with CDI (623 mg, 3.84 mmol) in THF (100 ml) for 12 h. The mixture was then cooled to 0°C, dimethylamine (5 ml) was added, and stirring was continued overnight at room temperature. The solvent was then evaporated and the residual brown oil was purified by column chromatography (silica gel, dichloromethane containing 2% isopropylamine) to afford **13** as a white solid (800 mg, 2.80 mmol, 80%). − M.p. 123°C. − ^{1}H NMR (200 MHz, $CDCl_3$): δ = 3.04 (s, 6 H, NCH_3), 3.69 (s, 3 H, OCH_3), 3.71 (s, 3 H, OCH_3), 6.89−6.98 (m, 4 H, ArH), 7.13−7.31 (m, 3 H, ArH). − ^{13}C NMR (50 MHz, $CDCl_3$): δ = 36.0 (NCH_3), 40.0 (NCH_3), 55.6 (OCH_3), 55.7 (OCH_3), 110.0 (CH), 111.1 (CH), 118.7 (CH), 120.3 (CH), 127.0, 128.8 (CH), 129.2, 131.1 (CH), 131.2 (CH), 136.3, 156.9 (C−OMe), 157.0 (C−OMe), 171.5 (C=O). − MS (EI): *m/z*: 285 [M], 257, 213.

2,2′-Dihydroxy-4-(N,N-dimethylcarbamoyl)-1,1′-biphenyl (**14**): To a solution of BBr_3 in dichloromethane (1 M, 20 ml) at 0°C under nitrogen, **13** (900 mg, 3.15 mmol) was added and the mixture was stirred for 12 h at room temperature. The mixture was then treated with methanol and the solvents were evaporated. The residue was redissolved in 20 ml of 10% aq. NaOH and subsequent addition of 10% HCl at 0°C gave **14** as a white precipitate, which was dried in vacuo (800 mg, 3.10 mmol, 98%). − M.p. 186°C. − ^{1}H NMR (200 MHz, [D_6]DMSO): δ = 2.96 (s, 6 H, NCH_3), 6.77−6.90 (m, 4 H, ArH), 7.10−7.88 (m, 3 H, ArH), 9.23 (s, 1 H, OH), 9.43 (s, 1 H, OH). − ^{13}C NMR (50 MHz, [D_6]DMSO): δ = 34.8 (NCH_3), 114.4 (CH), 115.7 (CH), 117.3 (CH), 118.8 (CH), 125.2, 127.0, 128.3 (CH), 131.3 (CH), 131.4 (CH), 136.2, 154.4 (C−OH), 154.6 (C−OH), 154.6 (C=O). − IR (KBr): $\tilde{\nu}$ = 3500−2300 cm^{-1} [ν(OH)], 1600 [ν(C=O)]. − MS (EI); *m/z*: 275 [M], 213.

2,2′-Dihydroxy-4-(N,N-dimethylcarbamoyl)-3,3′,5′-trisulfo-1,1′-biphenyl (**15**): Sulfonation of **14** was performed as for **12**. − M.p. > 286°C. − ^{1}H NMR (200 MHz, CD_3OD): δ = 2.87 (s, 3 H, CH_3), 3.03 (s, 3 H, CH_3), 6.64 (s, 1 H), 7.7 (d, *J* = 2.3 Hz, 1 H), 7.75 (s, 1 H), 8.16 (d, *J* = 2.3 Hz, 1 H). − ^{13}C NMR (50 MHz, CD_3OD): δ = 35.3 (CH_3), 39.8 (CH_3), 114.5 (CH), 126.3, 126.5 (CH), 127.2, 129.9, 132.6 (CH), 132.7 (CH), 133.5, 136.3, 137.0, 154.3 (C−N), 158.0 (C−N), 172.9 (C=O).

Potentiometric Experiments: All measurements were made at 25°C. Solutions were prepared with deionized, doubly distilled water. The ionic strength was fixed at 0.1 M with sodium perchlorate (PROLABO puriss). The pH measurements were performed using a TACUSSEL Ionoprocesseur-II millivoltmeter equipped with glass and calomel electrodes (TACUSSEL). The electrodes were calibrated to read p[H] according to the classical method[14]. Potentiometric titrations employed a TACUSSEL Electroburex burette and a pH meter (Ionoprocesseur-II) connected to a Hewlett Packard microcomputer. The titrations were automated using software developed in our laboratory. The ligands and their iron(III) complexes at concentrations of ca. 0.001 M were titrated with standardized 0.05 M sodium hydroxide. The titration data were refined by the nonlinear least-squares refinement program SUPERQUAD[15] in order to determine the equilibrium constants (protonation and complexation).

Spectrophotometric Experiments: The deprotonation constant of one hydroxy group was determined in the UV region (the ligand concentration in aqueous solution was ca. $5 \cdot 10^{-5}$ M). The ferric complexes were investigated by spectrophotometry: The UV/Vis spectrum of a solution containing equal amounts of ligand and Fe^{III} (10^{-4} M) was monitored as a function of pH over the range 1−10 (adjusted with $HClO_4$ or NaOH); an aliquot was taken from the solution after each adjustment of the pH (which was measured using a pH meter) and its spectrum was recorded. The ionic strength was fixed at 0.1 M with $NaClO_4$/$HClO_4$ for this second set of experiments. The spectrophotometric data were fitted with the LETAGROP-SPEFO program[16][17]. The program uses a nonlinear least-squares method and calculates the thermodynamic constants of the absorbing species and their corresponding electronic spectra. The calculations were performed on the basis of absorbance data at about 6−8 wavelengths (between 400 and 600 nm).

[1] [1a] P. S. Dobbin, R. C. Hider, *Chem. Ber.* **1990**, 565. − [1b] C. Herschko, D. J. Weatherall, *Crit. Rev. Clin. Lab. Sc.* **1988**, *26*, 303.
[2] R. J. Bergeron, G. M. Brittenham, *The Development of Iron Chelators for Clinical Use*, CRC Press, Boca Raton, **1992**.
[3] L. D. Loomis, K. N. Raymond, *Inorg. Chem.* **1991**, *30*, 906.
[4] E. R. Huehns, J. B. Porter, R. C. Hider, *Hemoglobin* **1988**, *12*, 593.
[5] G. M. Brittenham, *Semin. Hematol.* **1990**, *27*, 112.

[6] P. Baret, C. G. Béguin, H. Boukhalfa, C. Caris, J.-P. Laulhère, J.-L. Pierre, G. Serratrice, *J. Am. Chem. Soc.* **1995**, *117*, 9760.
[7] [7a] P. Baret, C. G. Béguin, D. Gaude, G. Gellon, C. Mourral, J.-L. Pierre, G. Serratrice, A. Favier, *Tetrahedron* **1994**, *50*, 2077. – [7b] G. Serratrice, C. Mourral, A. Zeghli, C. G. Béguin, P. Baret, J.-L. Pierre, *New J. Chem.* **1994**, *18*, 749.
[8] S. Rachidi, C. Coudray, P. Baret, G. Gellon, J.-L. Pierre, A. Favier, *Biol. Trace Elem. Res.* **1994**, *41*, 77.
[9] G. Serratrice, A. Zeghli, C. G. Béguin, P. Baret, J.-L. Pierre, *New J. Chem.* **1993**, *17*, 297.
[10] A. Shanzer, J. Libman, S. Lifson, *Pure Appl. Chem.* **1992**, *64*, 1421.
[11] R. Bastian, R. Weberling, F. Palilla, *Anal. Chem.* **1956**, *28*, 459.
[12] M. A. Rizzacasa, M. V. Sargent, *J. Organometal. Chem.* **1976**, *10*, 529.
[13] W. J. Thomson, J. Gaudino, *J. Org. Chem.* **1984**, *49*, 5237.
[14] A. E. Martell, R. J. Motekaitis, *Determination and Use of Stability Constants*, 2nd ed., VCH Publishers, New York, **1992**.
[15] P. Gans, A. Sabatini, A. Vacca, *J. Chem. Soc., Dalton Trans.* **1985**, 1195.
[16] L. G. Sillen, B. Warsquist, *Ark. Kemi* **1969**, *31,* 377 (*Chem. Abstr.* **1969**, *71*, 85125h).
[17] M. Meloun, J. Havel, E. Hogfeldt, *Computation of Solution Equilibria*, Ellis Horwood, Chichester, **1988**.
[18] H. A. Staab, H. Rohr, *Newer Methods Prep. Org. Chem.* **1988**, *5*, 61.
[19] M. Miyaura, T. Yanagi, A. Suzuki, *Synth. Commun.* **1981**, *11*, 513.
[20] G. Bringman, R. Walter, R. Weirich, *Angew. Chem.* **1990**, *102*, 1006; *Angew. Chem. Int. Ed. Engl.* **1990**, *29*, 977.
[21] S. J. Rodgers, C. W. Lee, C. Y. Ng, K. N. Raymond, *Inorg. Chem.* **1987**, *26*, 1622.
[22] C. Y. Ng, S. J. Rodgers, K. N. Raymond, *Inorg. Chem.* **1989**, *28,* 2062.
[23] $\beta_{11n} = [FeLH_n]/[Fe^{3+}]\,[L]\,[H^+]^n$ is the equilibrium constant for $Fe^{3+} + L + nH^+ \rightleftharpoons FeLH_n$.

[97293]

Syntheses and Structures of Molecular Diphenolatonickel Compounds Containing Trimethylphosphane Ligands

Hans-Friedrich Klein*[a], Attila Dal[a], Thomas Jung[a], Siegmar Braun[b], Caroline Röhr[c], Ulrich Flörke[d], and Hans-Jürgen Haupt[d]

Institut für Anorganische Chemie der Technischen Universität Darmstadt[a],
Petersenstraße 18, D-64285 Darmstadt, Germany

Institut für Organische Chemie der Technischen Universität Darmstadt[b],
Petersenstraße 22, D-64285 Darmstadt, Germany

Institut für Anorganische Chemie der Universität Freiburg[c],
Albertstraße 21, D-79104 Freiburg, Germany

Anorganische und Analytische Chemie der Universität/GH Paderborn[d],
Warburger Strasse 100, D-33095 Paderborn, Germany

Received December 4, 1997

Keywords: Nickel / Oxidation / Phenols / Structure, dynamic NMR spectroscopy

The reaction of substituted phenols and dioxygen with $Ni(PMe_3)_4$ yields the low-spin tetracoordinate diphenolatonickel compounds $Ni(OAr)_2(PMe_3)_2$ [ArOH = 2-*tert*-butylphenol (**1**), 2-*tert*-butyl-4-methylphenol (**2**), 2-*tert*-butyl-6-methylphenol (**3**), 2,4-di(*tert*-butyl)phenol (**4**), 2-*tert*-butyl-4-methoxophenol (**5**), 2-chloro-4-*tert*-butylphenol (**6**), 2-isopropylphenol (**7**), 3-*tert*-butylphenol (**8**)]. As is revealed by variable temperature ^1H- and ^{13}C-NMR spectroscopy the complexes constitute a mixture of two isomers, each of which can be observed separately at lower temperatures when interconversion is slower. An additional 6-carbaldehyde function transforms the phenolate into a chelating ligand, giving rise to a high-spin hexacoordinate compound $Ni(OAr)_2(PMe_3)_2$ (**9**). X-ray crystal-structure determinations of **2** and **3** show a *trans* square-planar structure, and that of **9** shows a *trans* octahedral arrangement of donor atoms P_2O_4. Bulky substituents in the 3- or 4-position, or non-demanding substituents in the 2-position, are less effective in stabilizing molecular diphenolatonickel complexes.

Many low-valent metal compounds, if combined with a proton source and dioxygen, form an oxidizing system. Examples are Fentons reagent, Bartons Gif systems and the Wacker process. Peroxometal complexes are believed to be key intermediates in these reactions.[1] Strongly reducing phosphane complexes of zerovalent nickel are known to form peroxo species according to Eq. 1. In exceptional cases these may be isolated, e.g. with space-filling tricyclohexylphosphane ligands.[2]

$$Ni(PR_3)_4 + O_2 \rightarrow (R_3P)_2NiO_2 \rightarrow Ni + 2\ R_3P{=}O \qquad (1)$$

With the small trimethylphosphane the peroxo intermediate is explosive, and for this reason even small crystals of $Ni(PMe_3)_4$ crackle upon contact with air. Using mol-equivalent amounts of oxygen in solution the system becomes a mild oxidant. On this basis we have developed a new synthesis of molecular diphenolatonickel complexes containing trimethylphosphane ligands.

Conventionally, but not conveniently, unsolvated diphenolatonickel compounds may be prepared in an anhydrous medium as insoluble coordination polymers. Methods using $NiCl_2$ and sodium or lithium phenolates usually afford products which pertinaciously occlude halide impurities.

Some *ortho*-substituted phenols form diphenolatonickel dihydrates that can be converted into anhydrous compounds. These materials cannot be dissolved without reaction.[3] However, with nitrogen donor atoms in a suitable configuration numerous soluble chelate complexes, e. g. with 8-hydroxoquinolines or salicylaldimines, have been shown to exist as molecular compounds with square-planar coordination at the nickel atom. These complexes usually do not accommodate additional phosphane ligands.

In this contribution a novel method of synthesis is described which smoothly affords crystalline diphenolatobis(trimethylphosphane)nickel compounds starting from substituted phenols, $Ni(PMe_3)_4$, and dioxygen.

Results and Discussion

Pale-yellow solutions of $Ni(PMe_3)_4$ and two mol-equivalents of a phenol in hydrocarbon or ether solvents turn dark-red when treated with one mol-equivalent of dioxygen[4] according to Eq. 2. One of the trimethylphosphanes serves as a co-reductant, in this respect resembling the natural methane monooxygenase system.[5]

Using sterically shielding 2-*tert*-butylphenols, mononuclear diphenolatonickel complexes containing trimethylphosphane are obtained in good to excellent yields. Separation from moist trimethylphosphane oxide[6] is conveniently achieved by filtration, and trace impurities can be sublimed from the product in vacuo at 20°C.

 © WILEY-VCH Verlag GmbH, D-69451 Weinheim, 1998 1434–1948/98/0505–0621 $ 17.50+.50/0

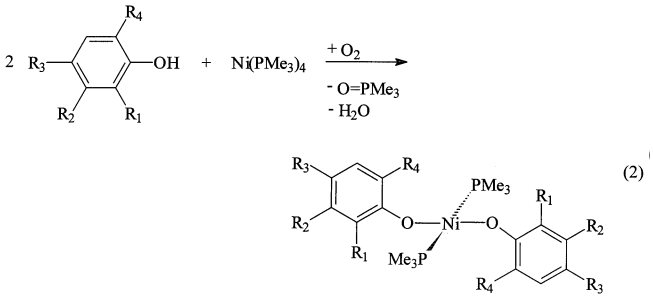

	1	2	3	4	5	6	7	8	9
R_1	*t*Bu	*t*Bu	*t*Bu	*t*Bu	*t*Bu	*t*Bu	*i*Pr	H	*t*Bu
R_2	H	H	H	H	H	H	H	*t*Bu	H
R_3	H	Me	H	*t*Bu	OMe	Cl	H	H	Me
R_4	H	H	Me	H	H	H	H	H	CHO
Yield [%]	52	78	86[a]	70	54	48	11	8	83

[a] Yield of crude product.

Recrystallization from pentane or ether affords red crystals that can be dried in vacuo without loss of phosphane ligands. While coordination of substoichiometric amounts of triorganophosphanes by diphenolatonickel polymers has been noticed,[7] to the best of our knowledge the molecular trimethylphosphane complexes **1**−**8** constitute a novel type of compound. The 2-*tert*-butyl groups not only prevent formation of coordination polymers by steric shielding but also enhance the reactivity of the phenolic function, when compared with the unsubstituted phenol. In a sluggish reaction with $Ni(PMe_3)_4$ and oxygen this parent phenol gives low yields of insoluble material which, according to the infrared data, appears to be a mixture of nickel oxide and diphenolatonickel containing residual trimethylphosphane ligands.

To investigate the limits of steric demand, the size and positions of phenolic substituents were varied.

Steric Protection of the Phenolate Function

Reducing the size of the substituent in 2-position induces loss of trimethylphosphane while forming insoluble coordination polymers at the expense of molecular diphenolatonickel compounds. This tendency increases from R = CMe_3 to R = H. Moving the protecting *tert*-butyl group to the 3- or 4-position dramatically reduces the yields of molecular complexes.

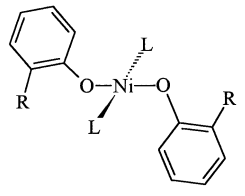

L = $P(CH_3)_3$

R	CMe_3	$CHMe_2$	2,4,6-Me_3	H
Yield [%]	52	11	0	0
R	2-CMe_3	3-CMe_3	4-CMe_3	
Yield [%]	52	8	0	

Neither steric nor electronic changes in the 4-position can affect the reasonably constant yields of bis(2-*tert*-butylphenolato)bis(trimethylphosphane)nickel compounds.

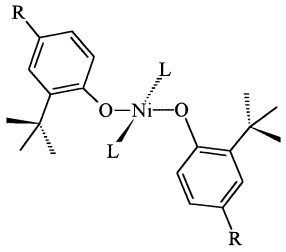

L = $P(CH_3)_3$

R	CMe_3	Me	H	OMe	Cl
Yield [%]	70	78	52	54	48

Thus, the stability of molecular diphenolatonickel complexes containing trimethylphosphane appears to be controlled by the size of the phenolic substituent in 2-position.

NMR Spectroscopy

For steric reasons an optimum configuration of the bis(2-*tert*-butylphenolato)nickel complexes **2** and **3** in solution is likely to be the same as that in the solids, and is characterized by CMe_3 groups pointing away from the plane of coordination (Figures 1 and 2). In the crystal a *transoid* arrangement of CMe_3 substituents (A) is favored, while in solution a second minimum of energy is populated through rotation of phenolato ligands (B), as shown by dynamic ^{1}H-NMR spectroscopy.

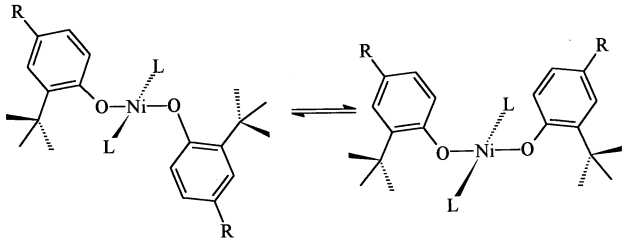

L = $P(CH_3)_3$

The room-temperature ^{1}H-NMR spectra (300 MHz) of the complexes **1**, **2**, **4**, **5**, and **7** (Table 1) show a broad one-proton signal at $\delta_H \approx 9 \pm 0.5$, whereas the other protons of the benzene ring show clearly resolved multiplets, e.g. for **2** a doublet of 1.9 Hz for the signal at $\delta_H = 6.65$ and a double doublet of 7.7 and 1.9 Hz for that at $\delta_H = 6.90$. From an analysis and comparison of the NMR data the broad high-frequency signal has to be assigned to 6-H, which is deshielded by the nearby nickel atom. On cooling the solution (e.g. **2** was cooled to 233 K) two clearly resolved doublets are observed for 6-H at $\delta_H = 9.21$ and 8.63 in an intensity ratio of about 2:1 with $J_{6\text{-H},5\text{-H}} = 7.8$ Hz for both signals. Line separations, albeit amounting to only a few Hz (ca. 0.01 ppm), can be seen also for the other protons, an exception being the 4-CH_3 protons. An H,H-COSY spectrum proves that the signals of 5-H of both species overlap at $\delta_H = 6.90$ and those of the 3-H atoms at $\delta_H = 6.65$. On the other hand, when heating a solution of **2** in

Figure 2. Molecular structure of **3** (ORTEP plot without hydrogen atoms)[a]

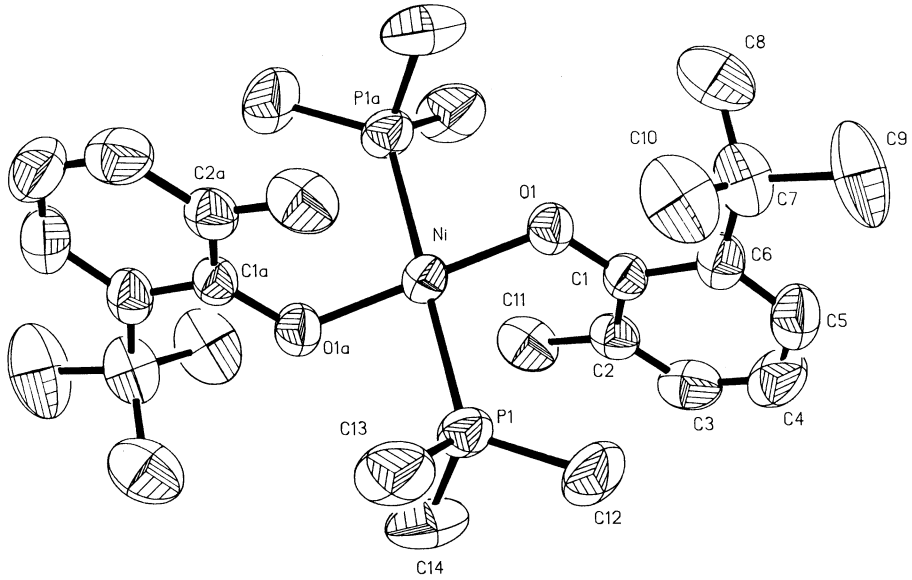

[a] Selected bond lengths [Å] and angles [°]: Ni−O1 1.861(3), Ni−P1 2.268(2), O1−C1 1.331(6), C2−C11 1.495(7), C6−C7 1.535(8); O1−Ni−P1 98.6(1), O1−Ni−P1a 81.5(1), C1−O1−Ni 127.3(3).

$[D_8]$toluene to 373 K, one doublet at $\delta_H = 9.07$ with $J = 7.8$ Hz appears.

Analogous results are obtained from the ^{13}C-NMR spectra (Table 2), e.g. that of **2**. At 305 K one set of signals is obtained, the one at $\delta_C = 123.0$ exhibiting some line broadening; according to 2D-H,C correlation it has to be attributed to C-6. At 233 K two sets of signals in a ratio of about 2:1 are observed for most C atoms, exceptions being those of C-3 and of both types of CMe_3 under the routine measurement conditions applied.

From these results it has to be concluded that there is a mixture of two rotamers, A and B, which can be observed separately when interconversion is slow on the NMR time scale.

Coordination Number 6

In a suitable conformation an aldehyde or ketone function can serve as additional O-donor ligand. This chelating property has been previously observed in equilibria of ligand dissociation involving pentacoordinate species which are formed in a ligand dismutation reaction from iodo(phenolato)nickel precursors.[8]

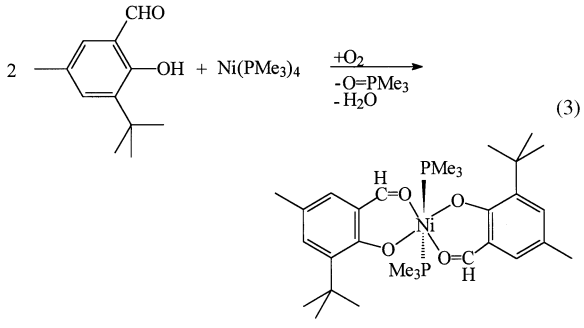

Trimethylphosphane is smoothly added to produce hexacoordinate **9** according to Eq. 3. Involvement of both aldehyde groups is evident from a bathochromic coordination shift of the ν(C=O) bands. Both types of diphenolatonickel complexes have been characterized by single-crystal X-ray diffraction.

Figure 1. Molecular structure of **2** (ORTEP plot without hydrogen atoms)[a]

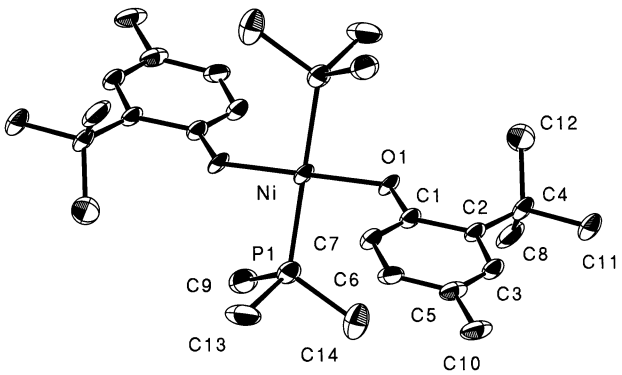

[a] Selected bond lengths [Å] and angles [°]: Ni−O1 1.868(3), Ni−P1 2.233(1), O1−C1 1.355(6), C1−C7 1.382(8), C6−C7 1.402(8); O1−Ni−P1 94.1(1), O1−Ni−P1′ 85.9(1), C1−O1−Ni 120.6(3).

Molecular Structures of 2, 3, and 9

Single crystals were obtained from pentane solutions at −20°C. Figures 1−3 give the atom numberings and the principal bond lengths and angles.

In all three molecular structures the nickel atom lies on a crystallographic inversion center. Bond lengths show significant deviations only between the hexacoordinate species **9** and the two square-planar complexes. Thus, in **9** the

Table 1. Dynamic ^{1}H-NMR spectra ([D$_8$]THF) of compounds **1**, **2**, **4**, **5**, and **8**[a]

Comp. T [K]	PCH_3	CCH_3	R	2-H	3-H	4-H	5-H	6-H
1	0.95	1.22			6.78	6.32	7.09	9.15
293	18 H	18 H	–	–	2 H	2 H	2 H	1 H
	s (br.)	s			d, J = 7.4	t, J = 7.4	t, J = 7.4	s (br.)
1a								8.75
233	–	–						0.7 H
	0.92	1.20			6.78	6.33	7.11	d, J = 6.7
	18 H	18 H			2 H	2 H	2 H	
	s (br.)	s			s (br.)	s (br.)	s (br.)	9.34
1b								1.3 H
233								d, J = 7.4
2	0.95	1.22	2.17		6.65		6.90	8.99
305	18 H	18 H	6 H	–	2 H	–	2 H	2 H
	s (br.)	s	s		d, J = 1.3		dd, J = 6.5/1.3	s (br.)
2a	0.92	1.20	2.17		6.63		6.90	8.63
233	18 H	18 H	6 H	–	2 H	–	2 H	0.7 H
	t′, N = 8.0	s	s		s (br.)		m	d, J = 8.0
2b	0.94	1.21	2.18					9.21
233	t′, N = 8.0	s	s					1.3 H
								d, J = 8.0
4	0.93	1.23	1.25		6.89		6.90	9.00
305	18 H	18 H	18 H	–	2 H	–	2 H	2 H
	t″, N = 6.3	s	s		d, J = 2.5		dd, J = 8.1/2.5	s (br.)
4a								8.82
233								1 H
	0.92	1.23	1.25		6.87		7.14	d, J = 8.1
	18 H	18 H	18 H	–	2 H	–	2 H	
4b	t′, N = 8.2	s	s		t, J = 3.0		m	9.18
233								1 H
								d, J = 8.0
5	0.94	1.21	3.57		6.48		6.69	9.01
305	18 H	18 H	6 H	–	2 H	–	2 H	1 H
	t′, N = 6.4	s	s		d, J = 3.1		dd, J = 8.4/3.1	s (br.)
8	0.96	1.27		7.75		6.45	7.06	7.21
305	18 H	18 H	–	2 H	–	2 H	2 H	2 H
	s (br.)	s		s		d, J = 7.0	m	d, J = 6.7

[a] t′ = virtual triplet with N as distance of outer lines.

Table 2. Dynamic ^{13}C-NMR spectra ([D$_8$]THF) of compounds **1**, **2**, **4**, **5**, and **8**

Comp. T [K]	PCH_3	CCH_3	CCH_3	R	C-1	C-2	C-3	C-4	C-5	C-6
1	10.8	28.4	33.6	–	164.2	138.1	125.4	112.4	123.8	121.5
305	t′, N = 22									
2	10.9	28.5	33.5	19.1 (Me)	162.1	137.6	124.9	120.3	125.5	121.1
305	t′, N = 23									
2a	10.3				161.2	137.0		119.8	125.4	120.4
233	t′, N = 23									
		28.1	33.3	19.1 (Me)			124.7			
2b	10.6				161.6	137.1		119.9	125.5	121.1
233	t′, N = 23									
4	10. 8	28.5	32.6	30.5 (Me)	161.7	134.1	120.8	136.9	121,5	120.8
305	t′ (br.)			33.8 (CMe_3)						
5	10.8	28.2	33.7	53.8 (OMe)	158.0	138.2	108.9	148.3	112.0	120.3
305	t′, N = 23									
8	9.7	29.9	33.2	–	165.0	111.4	150.2	109.9	116.4	126.8
305	t′, N = 24									

Ni−O distances of 1.995(2) and 2.060(2) Å, which are as expected for octahedral complexes of nickel,[9] exceed those of **2** and **3** by more than 10 pm. Also the large Ni−P distances of 2.482(1) Å are due to octahedral coordination in

Figure 3. Molecular structure of **9** (ORTEP plot without hydrogen atoms)[a]

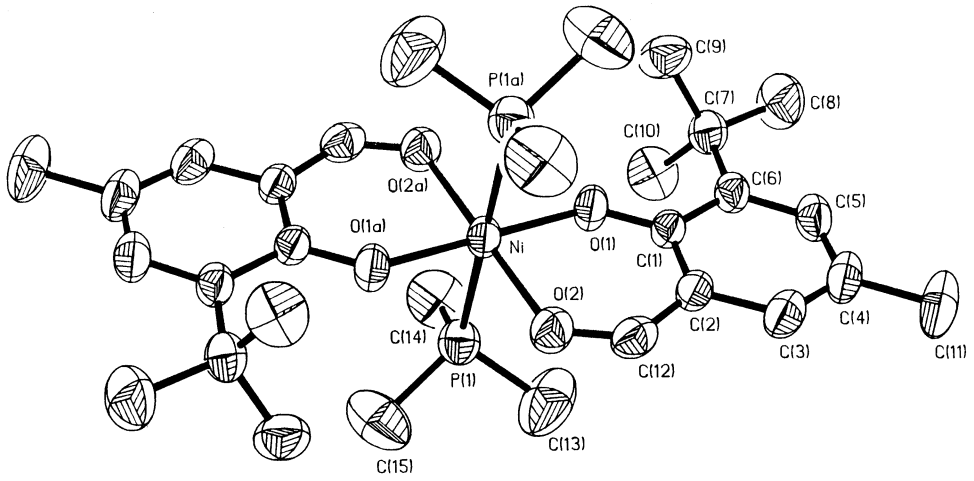

[a] Selected bond lengths [Å] and angles [°]: Ni−O1 1995(2), Ni−O2 2.060(2), Ni−P1 2.482(1), O1−C1 1.289(2), O2−C12 1.245(3), C4−C11 1.522(3), C6−C7 1.531(4); O1−Ni−P1 87.2(1), O1a−Ni−P1 92.8(1), O2−Ni−P1 89.9(1), O2a−Ni−P1 90.1(1), C1−O1−Ni 130.1(2), C12−O2−Ni 123.9(2).

the 20-electron complex **9** and are similar to those of octahedral nickel(IV) complexes[10] (18 electrons). The diamagnetic square-planar complexes **2** and **3** exhibit shorter Ni−O and Ni−P bond lengths. While Ni−P distances are as expected for 16-electron (trimethylphosphane)nickel complexes[11][12] the Ni−O distances of *trans*-bis(trimethylphosphane)nickel diphenolates are unprecedented as far as we are aware. When compared with a pentacoordinate tripyridinebis(2,4,6-trichlorophenolato)nickel(II)[13] [Ni−O = 2.014(4) Å] Ni−O distances such as 1.868(3) Å for **2** and 1.861(3) Å for **3** are considerably shorter. There is no structural indication for magnetic shielding of the aromatic 6-H nucleus by a close approach to the metal atom (see NMR Spectroscopy) because the calculated distance Ni−H(7) = 2.627 Å seems too large for such interaction. Similarly, in the 6-methyl-substituted compound **3** the distance between the 6-alkyl group and the nickel atom is beyond the radius of interaction.

Table 3. Distortions of square-planar geometries at nickel centres; L = $P(CH_3)_3$

formula	angles
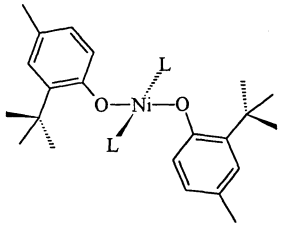	α=Ni-O-C(1)=120.6(3)° β=P(1)-Ni-O(1)=85.92(12)° γ=P(1a)-Ni-O(1)=94.08(12)°
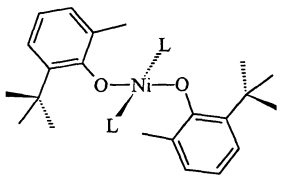	α=Ni-O-C(1)=127.3(3)° β=P(1)-Ni-O(1)=81.45(12)° γ=P(1a)-Ni-O(1)=98.55(12)°
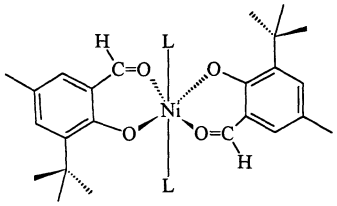	α=Ni-O-C(1)=130.1(2)° β=P(1)-Ni-O(1a)=92.8(1)° γ=P(1)-Ni-O(1)=97.2(1)°

Indeed, the substituent in 6-position points away from the nickel atom. While the angle α = 120.6(3)° in **2** (see Table 3) this angle in **3** is augmented by 6.7°. The sterically demanding 2-*tert*-butyl-6-methylphenolato ligand causes contraction of angles β from 85.92(12)°in **2** to 81.45(12)° in **3**. An even larger angle α in **9** is due to incorporation in the 6-membered chelate ring which also affects angles β and γ.

Conclusion

Molecular diphenolatobis(trimethylphosphane)nickel complexes can be prepared by convenient methods in high yields, if bulky substituents in the 2-position of the phenolato ligand prevent condensation reactions between metal centers. By dynamic NMR spectroscopy 2-*tert*-butyl groups are shown to hinder rotation of phenolato ligands around Ni−O bonds. X-ray crystallography reveals the nickel atoms to be surrounded by a meridian of two phenolato and two trimethylphosphane donors in mutual *trans* positions. These structures have been filed as the first reported for diamagnetic diphenolatonickel compounds. The five-membered chelate rings are all planar and show similar dimensions and the expected increase in bond lengths at the nickel atom as going from square-planar to octahedral coordination. Although in **9** the Ni−P distance represents an extremely long bond [2.482(1) Å], crystals of this compound

do not release trimethylphosphane at 20°C in vacuo. Further investigation of properties of (trimethylphosphane)nickel diphenolates are in progress in order to better understand the role of chelating phenols as active catalysts in olefin oligomerization reactions.[14]

Financial support of this work by the *Fonds der Chemischen Industrie* and the *Deutsche Forschungsgemeinschaft* is gratefully acknowledged.

Experimental Section

General Procedures and Materials: All air-sensitive and volatile materials were handled by standard vacuum techniques and kept under argon. Details have been given elsewhere.[8] $Ni(PMe_3)_4$ was prepared by literature methods,[15] phenols (Merck-Schuchardt) were used as purchased. Measured volumes of oxygen were admitted to the reaction mixture at −70°C and in vacuo.

Bis(2-tert-butylphenolato)bis(trimethylphosphane)nickel (**1**): 510 mg of $Ni(PMe_3)_4$ (1.37 mmol) and 414 mg of 2-*tert*-butylphenol (2.74 mmol) in 60 ml of THF were combined with 25 ml of dioxygen (1.04 mmol). Upon warming the light yellow solution turned dark-red. After 16 h at 20°C, the volatiles were removed in vacuo and the residue extracted with 50 ml of pentane through a glass-sinter disc (G3). Crystallization at −20°C afforded dark-red rhombs. Yield 362 mg (52% based on nickel), m.p. 184−186°C. − IR (Nujol): $\tilde{\nu}$ = 1574 cm^{-1} (C=C), 1044 (C−O), 944 [$\rho(PCH_3)$]. − $C_{26}H_{44}NiO_2P_2$ (509.3): calcd. C 61.32, H 8.71, P 12.16; found C 61.15, H 9.04, P 12.21.

Bis(2-tert-butyl-4-methylphenolato)bis(trimethylphosphane)nickel (**2**): 500 mg of $Ni(PMe_3)_4$ (1.37 mmol) and 452 mg of 2-*tert*-butyl-4-methylphenol (2.74 mmol) in 50 ml of THF at −70°C were combined with 33 ml of dioxygen (1.37 mmol). After warming the mixture to 20°C, the volatile components were removed in vacuo and the residue extracted with 60 ml of pentane. Keeping the dark-red solution at −20°C for 30 h afforded red-brown cubes. Yield 572 mg (78% based on nickel), m.p. 133−135°C. − IR (Nujol): $\tilde{\nu}$ = 1596 cm^{-1} (C=C), 1019 (C−O), 943 [$\rho(PCH_3)$]. − $C_{28}H_{48}NiO_2P_2$ (537.3): calcd. C 62.59, H 9.00, P 11.53: found C 62.96, H 9.48. P 11.78.

Bis(2-tert-butyl-6-methylphenolato)bis(trimethylphosphane)nickel (**3**): 870 mg of $Ni(PMe_3)_4$ (2.40 mmol) and 787 mg of 2-*tert*-butyl-6-methylphenol (4.80 mmol) in 50 ml of THF at −70°C were combined with 50 ml of dioxygen (2.08 mmol). After warming to 20°C, the light-yellow solution turned red-brown and was stirred for a further16 h. The volatiles were removed in vacuo, and the residue extracted with 50 ml of pentane. The crude product was collected as a brown oil (1110 mg, 86%) and used for spectroscopic measurements. Crystallization from 5 ml of pentane at −27°C starting with 900 mg of crude material afforded 260 mg of red-brown crystals (20%), m.p. 169−171°C. − IR (Nujol): $\tilde{\nu}$ = 1581 cm^{-1} (C=C), 950 [$\rho(PCH_3)$]. − ^{1}H NMR ([D$_8$]THF): δ = 0.61 [s (br.), 18 H, $P(CH_3)_3$], 1.30 (s, 6 H, CH_3), 1.50 [s, 18 H, $C(CH_3)_3$], 6.54 (t, J = 7.3 Hz, 1 H, 4-H), 7.00 (m, 2 H, 3-H, 5-H). − ^{13}C NMR ([D$_8$]toluene): δ = 11.88 [s (br.), $P(CH_3)_3$], 20.92 (s, CH_3), 29.94 [$C(CH_3)_3$], 35.21 [s, $C(CH_3)_3$], 114.89 (s, C-3), 124.80 (s, C-5), 128.90 (s, C-4); 141.45 (s, C-2), 143.96 (C-6), 163.07 (s, C-1).

Bis(2,4-di-tert-butylphenolato)bis(trimethylphosphane)nickel (**4**): 1350 mg of $Ni(PMe_3)_4$ (3.72 mmol) and 1530 mg of 2,4-di-*tert*-butylphenol (7.44 mmol) in 70 ml of THF at −70°C were combined with 90 ml of dioxygen (3.74 mmol). Upon warming to 20°C the yellow solution turned dark-red. After 16 h at 20°C, the volatiles were removed in vacuo and trimethylphosphane oxide sublimed from the residue at 30°C/0.1 mbar. Extraction with 60 ml of pentane and crystallization at −20°C afforded dark-red crystals. Yield 1620 mg (70% based on nickel), m.p. 169−171°C. − IR (Nujol): $\tilde{\nu}$ = 1591 cm^{-1} (C=C), 1016 (C−O), 942 [$\rho(PCH_3)$]. − $C_{34}H_{60}NiO_2P_2$ (621.5): calcd. C 65.71, H 9.73, P 9.97; found C 65.78, H 9.65, P 10.03.

Bis(2-tert-butyl-4-methoxyphenolato)bis(trimethylphosphane)nickel (**5**): 420 mg of $Ni(PMe_3)_4$ (1.16 mmol) and 417 mg of 2-*tert*-butyl-4-methoxyphenol (2.74 mmol) in 50 ml of THF at −70°C were combined with 30 ml of dioxygen (1.25 mmol). After warming the solution to 20°C and stirring for 16 h, the volatiles were removed in vacuo. Crystallization from 70 ml of pentane afforded 572 mg of dark-brown crystals (78% based on Ni), m.p. 133−135°C. − IR (Nujol): $\tilde{\nu}$ = 1603 cm^{-1} (C=C), 1018 (C−O), 948 [$\rho(PCH_3)$]. − $C_{28}H_{48}NiO_4P_2$ (569.3): calcd. C 59.07, H 8.50, P 10.88; found C 59.75, H 8.64, P 11.18.

Bis(2-tert-butyl-4-chlorophenolato)bis(trimethylphosphane)nickel (**6**): 770 mg of $Ni(PMe_3)_4$ (2.12 mmol) and 787 mg of 2-*tert*-butyl-4-chlorophenol (4.24 mmol) in 50 ml of THF at −70°C were combined with 50 ml of dioxygen (2.08 mmol). After warming up to 20°C, the volatiles were removed in vacuo and the resulting red-brown solid washed with ether (2 × 10 ml) and recrystallized from THF to afford 590 mg of brown-red crystals, m.p. 154−156°C. − IR (Nujol): $\tilde{\nu}$ = 1603 cm^{-1} (C=C), 1018 (C−O), 948 [$\rho(PCH_3)$]. − ^{1}H NMR ([D$_8$]THF): δ = 0.97 [s (br.), 18 H, $P(CH_3)_3$], 1.19 [s, 18 H, $C(CH_3)_3$], 6.79 [s (br.), 2 H, 3-H], 7.09 (s, 2 H, 5-H). − $C_{26}H_{42}Cl_2NiO_2P_2$ (580.2): calcd. C 53.83, H 7.30, P 10.68; found C 52.97, H 7.40, P 10.88.

Bis(2-isopropylphenolato)bis(trimethylphosphane)nickel(**7**): 620 mg of $Ni(PMe_3)_4$ (1.71 mmol) and 465 mg of 2-isopropylphenol (3.42 mmol) in 50 ml of THF at −70°C were combined with 50 ml of dioxygen (2.08 mmol). Stirring at −30°C for 1 h gave a dark red solution. Upon careful removal of volatiles in vacuo at −20°C (within 16 h) and extraction of the residue with 50 ml of pentane a large amount of red oil was obtained from which, after three months, dark-red crystals were deposited. These were isolated by washing with acetone in the cold, yielding 120 mg of red platelets (11% based on Ni), m.p. 109−112°C. − IR (Nujol): $\tilde{\nu}$ = 1591 cm^{-1} (C=C), 1036 (C−O), 948 [$\rho(PCH_3)$]. − ^{1}H NMR ([D$_8$]THF): δ = 0.97 [s, 18 H, $P(CH_3)_3$], 1.01 [d, J = 7 Hz, 12 H, $CH(CH_3)_2$], 3.08 [quint, J = 7 Hz, 2 H, $CH(CH_3)_2$], 6.34 (t, J = 7 Hz, 2 H, 3-H), 7.05 (m, 4 H, 2-H, 4-H), 8.71 [s (br.), 2 H, 6-H]. − ^{13}C NMR ([D$_8$]THF): δ = 9.79 [t′, N = 2 Hz, $P(CH_3)_3$], 21.49 [s, $CH(CH_3)_2$], 25.93 [$CH(CH_3)_2$], 113.57 (s, C-4), 122.99 (s, C-6), 124.82, 125.09 (s, C-3, C-5); 141.45 (s, C-2), 137.68 (s, C-2), 162.38 (s, C-1). − $C_{33}H_{52}NiO_2P_2$ (617.5): calcd. C 64.19, H 8.49; found C 64.70, H 8.60.

Bis(3-tert-butylphenolato)bis(trimethylphosphane)nickel (**8**): 880 mg of $Ni(PMe_3)_4$ (2.42 mmol) and 728 mg of 3-*tert*-butylphenol (4.85 mmol) in 70 ml of THF at −70°C were combined with 50 ml of dioxygen (2.08 mmol). Stirring at −30°C for 1 h gave a dark-red solution. Upon removal of volatiles in vacuo, and extraction of the residue with 50 ml of pentane at −30°C, 520 mg of $Ni(PMe_3)_4$ was recovered. A second extraction with 50 ml of pentane at 25°C gave 158 mg of red platelets (15% based on Ni), m.p. 112−117°C. − IR (Nujol): $\tilde{\nu}$ = 3430 cm^{-1} (OH), 1643 [δ(OH)], 1591 (C=C), 1036 (C−O), 948 [$\rho(PCH_3)$]. − $C_{46}H_{72}NiO_4P_2$ (809.7): calcd. C 68.23, H 8.89, P 7.65; found C 67.50, H 9.08, P 7.73.

Bis(2-tert-butyl-4-methyl-6-formylphenolato)bis(trimethylphosphane)nickel (**9**): 560 mg of $Ni(PMe_3)_4$ (1.54 mmol) and 580 mg of 3-*tert*-butyl-5-methylsalicylaldehyde (3.02 mmol) in 50 ml of THF

Table 4. Crystallographic data of compounds **2**, **3**, and **9**

	2	**3**	**9**
Formula	$C_{28}H_{48}NiO_2P_2$	$C_{28}H_{48}NiO_2P_2$	$C_{30}H_{48}NiO_4P_2$
Molecular mass	537.3	537.3	593.4
Crystal size [mm]	0.24 × 0.29 × 0.35	0.31 × 0.29 × 0.26	0.21 × 0.24 × 0.55
Crystal system	triclinic	monoclinic	triclinic
Space group	$P\bar{1}$	$P2_1/c$	$P\bar{1}$
a [Å]	8.314(2)	9.857(3)	9.762(2)
b [Å]	9.654(2)	12.867(3)	9.850(2)
c [Å]	11.344(2)	13.136(3)	9.363(2)
α [°]	93.81(2)	90	108.68(1)
β [°]	108.16(2)	110.25(2)	98.10(1)
γ [°]	114.51(2)	90	73.10(1)
V [Å^3]	766.8(3)	1563.1(7)	814.9
Z	1	2	1
$D_{calcd.}$ [g/cm^3]	1.164	1.142	1.209
μ(Mo-K_α) [mm^{-1}]	0.757	0.743	0.720
T [K]	293(2)	293(2)	293(2)
Data coll. range [°]	$5.5 \leq 2\Theta \leq 45$	$5.4 \leq 2\Theta \leq 55$	$3 \leq 2\Theta \leq 55$
h	$-11 \leq h \leq 11$	$-12 \leq h \leq 12$	$-12 \leq h \leq 12$
k	$-13 \leq k \leq 13$	$0 \leq k \leq 16$	$-12 \leq k \leq 12$
l	$0 \leq l \leq 11$	$0 \leq l \leq 17$	$0 \leq l \leq 12$
No. reflect. measured	2099	3751	7527
No. unique reflect.	1985	3598	3765
No. parameters refined	152	159	170
R_1 [$F \geq 4\sigma(F)$]	0.090	0.075	0.040
wR_2 [$F \geq 4\sigma(F)$][a]	0.251[b]	0.123[b]	0.041[c]

[a] $w = 1/\sigma^2(F) + 0.0001 \cdot F^2$. – [b] Refinement on F. – [c] Refinement on F.

at −70°C were combined with 38 ml of dioxygen (1.58 mmol). Upon warming the solution slowly turned brown. After 24 h at 20°C, the volatiles were removed in vacuo and the residue extracted with 50 ml of pentane. Keeping the solution at 8°C for 70 h afforded yellow-brown crystals. Yield 656 mg (83% based on nickel), m.p. 153−156°C. IR (Nujol): $\tilde{\nu}$ = 1596 cm^{-1} (C=O), 1024 (C−O), 943 [ρ(PCH_3)]. – ^{1}H NMR ([D_8]toluene): extremely broad signals at δ = 1.1−84.7. – $C_{30}H_{48}NiO_4P_2$ (593.4): calcd. C 60.73, H 8.15, P 10.44; found C 60.76, H 7.97, P 10.41.

Crystal-Structure Analyses: Crystal data are presented in Table 4.

Data Collection. – *Complex* **2**: A dark-red specimen was sealed under argon in a glass capillary and mounted on a Philips PW 1100 diffractometer. Using graphite-monochromated Mo-K_α radiation lattice parameters were obtained from 25 centered reflections. Intensities were collected (ω scan) and Lp corrections were applied. The structure was solved (SHELX 86) using a full-matrix least-squares refinement (SHELX 93). All non-hydrogen atoms were treated anisotropically, hydrogen atoms were held in idealized fixed positions. – *Complex* **3**: A dark-red specimen was sealed under argon in a glass capillary and mounted on a Siemens R3m/V diffractometer. Using graphite-monochromated Mo-K_α-radiation lattice parameters were obtained from 25 centered reflections. Intensities were collected (ω scan) and Lp and empirical absorption corrections were applied (4 scans). The structure was solved (SHELXS 86) and refined (SHELXL 93). Non-hydrogen atoms were refined anisotropically, hydrogen atoms were fixed in idealized positions. – *Complex* **9**: An orange-brown crystal was sealed and mounted as given for **3**. Lattice parameters were obtained from 25 centered reflections. Intensities were collected and four standard reflections were recorded every 400 measured reflections showing only random intensity fluctuations. Lp corrections and empirical absorption correction were applied (ψ scans, min./max. transmission 0.824/0.868). The structure was solved by Patterson and Fourier methods. Full-matrix least-squares refinement was based on F. All non-hydrogen atoms were refined anisotropically, hydrogen atoms were held in calculated positions. Scattering factors and structure refinement: SHELXTL-Plus (G. M. Sheldrick, **1990**).

Crystallographic data (excluding structure factors) for the structures reported in this paper have been deposited with the Cambridge Crystallographic Data Centre. Copies of the data [CCDC-100867 (**2**), -100866(**3**), -100880 (**9**)] can be obtained free of charge on application to CCDC, 12 Union Road, Cambridge CB2 1EZ, UK [Fax: (internat.) + 44(1223)336-033, E-mail: deposit@chemcrys.cam.ac.uk).

[1] G. W. Parshall, S. D. Ittel, *Homogeneous Catalysis*, 2nd ed., Wiley, New York, **1992**, chapter 6.
[2] P. W. Jolly, G. Wilke, *The Organic Chemistry of Nickel*, vol. 1, Academic Press, New York, **1972**, p. 317.
[3] J. I. Bullock, S. L. Jones, *J. Chem. Soc. (A)* **1970**, 2472.
[4] ***Caution:*** Solid Ni(PMe_3)$_4$ and dioxygen form an explosive mixture!
[5] R. H. Crabtree, *Chem. Rev.* **1995, 95**, 987.
[6] No stable hydrate of Me_3PO is formed at 20°C, and both components are easily removed in vacuo.
[7] H.-F. Klein, H. H. Karsch, *Chem. Ber.* **1976**, *109*, 2515.
[8] H.-F. Klein, A. Bickelhaupt, T. Jung, G. Cordier, *Organometallics* **1994**, *13*, 2557.
[9] H. Horrocks Jr., D.H. Tempelton, A. Zalkin, *Inorg. Chem.* **1968**, *7*, 1552.
[10] H.-F. Klein, A. Bickelhaupt, M. Lemke, T. Jung, C. Röhr, *Chem. Lett.* **1995**, 467−468.
[11] H.-F. Klein, *Angew. Chem.* **1973**, *85*, 403−404; *Angew. Chem. Int. Ed. Engl.* **1973**, *12*, 402−403.
[12] A. Mari, A. Gleizes, M. Dartiguenave, Y. Dartiguenave, *Inorg. Chim. Acta* **1981**, *52*, 83−92.
[13] M. F. Richardson, G. Wulfsberg, R. Marlow, S. Zaghonni, D. McCorkel, K. Shadid, J. Gagliardi, B. Farris, *Inorg. Chem.* **1993**, *32*, 1913−1919.
[14] W. Keim, *Angew. Chem.* **1990**, *102*, 251−260, *Angew. Chem. Int. Ed. Engl.* **1990**, *29*, 235−244..
[15] G. Stark, W. N. White, *J. Amer. Chem. Soc.* **1956**, *78*, 4606−4614.

[97295]

Replacement of One CO Unit in Dicarbonyl(η^5-cyclopentadienyl)cobalt Derivatives by Bis(*tert*-butylsulfonyl)acetylene

Christoph Benisch[a], Jorge Chávez[a], Rolf Gleiter*[a], Bernhard Nuber[b], Hermann Irngartinger[a], Thomas Oeser[a], Hans Pritzkow[b], and Frank Rominger[a]

Organisch-Chemisches Institut der Universität Heidelberg[a], Im Neuenheimer Feld 270, D-69120 Heidelberg, Germany

Anorganisch-Chemisches Institut der Universität Heidelberg[b], Im Neuenheimer Feld 270, D-69120 Heidelberg, Germany

Received December 8, 1997

Keywords: Alkyne complexes / Carbonyl complexes / Cobalt / CO-Replacement

The reaction of dicarbonyl(η^5-cyclopentadienyl)cobalt (**1**) and some of the Cp-ring substituted congeners with bis(*tert*-butylsulfonyl)acetylene (BTSA) results in the replacement of one CO group by the BTSA moiety. The variation of the yields and reaction times indicates a dependence of the reactivity of **1**−**6** with BTSA as a function of substituents. X-ray investigations of the products show that the alkyne unit is strongly bound to the metal.

So far, substitution reactions at dicarbonyl(η^5-cyclopentadienyl)cobalt [$CpCo(CO)_2$] (**1**)[1][2][3] with alkynes could not be stopped at the monosubstitution stages, although such complexes have been postulated as intermediates.[4] In the reported cases follow-up reactions led to cyclobutadiene complexes, cyclopentadienone complexes or benzene derivatives.[5][6][7][8][9][10][11] In order to contribute to the clarification of the mechanism of dimerization or trimerization of alkynes we investigated the reaction of $CpCo(CO)_2$ with alkynes having electron-acceptor groups. Acceptor groups were chosen because we thought that replacement of only one CO group could best be accomplished by a triple bond with stronger acceptor properties than diphenyl acetylene. Therefore bis(*tert*-butylsulfonyl)acetylene (BTSA) was our first choice because this compound has been found to be a powerful dienophile.[12][13] This led us to investigate the ligand properties of BTSA. In this paper we report experiments with **1**[3] and the substituted congeners dicarbonyl(η^5-methylcyclopentadienyl)- (**2**)[14], dicarbonyl(η^5-trimethylsilylcyclopentadienyl)- (**3**)[15][16], dicarbonyl(η^5-methoxycarbonylcyclopentadienyl)- (**4**)[17], dicarbonyl-(η^5−1-ethyl-2,3,4,5-tetramethylcyclopentadienyl)- (**5**)[18][19], and dicarbonyl(η^5-pentaallylcyclopentadienyl)cobalt (**6**)[20].

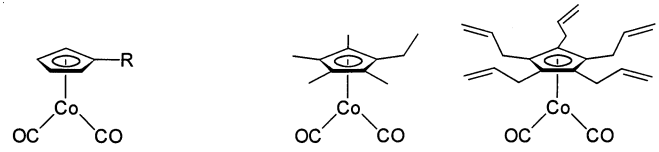

R = H, CH_3, $Si(CH_3)_3$, CO_2CH_3

1 **2** **3** **4** **5** **6**

Results and Discussion

The reaction of BTSA with **1**−**6** was accomplished by stirring solutions of **1**−**6** and BTSA in methylene chloride at room temperature. After 2−11 days the reaction was complete and the corresponding products could be isolated (Scheme 1). The monoalkyne complexes **7**−**12**, respectively, were obtained in yields between 36% and 85%. In addition to yields we list in Table 1 the reaction time which was required for complete conversion of starting materials. The data show that **4** having an electron withdrawing substituent on the Cp ring results in reduced yield (**10**, 39%) and increased reaction time (11 d) as compared to **1**. The lower yield encountered in the case of **12** we ascribe to steric effects. However, we can not exclude that the mechanism of the substitution might be different as compared to the other examples, because the five vinyl groups might act as ligands with formation of intermediate chelate complexes, which finally react to the observed, less strained product **12**.

Scheme 1

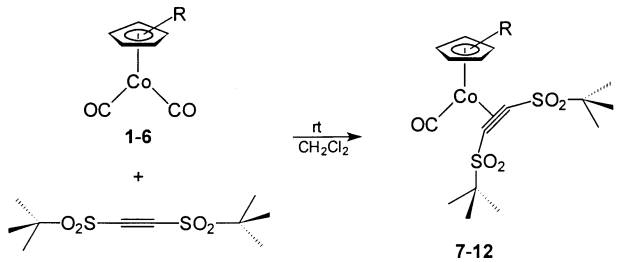

Table 1. reaction times, yields, and selected spectroscopical features of **7**−**12**

Compound	**7**	**8**	**9**	**10**	**11**	**12**
Reaction time [d]	3	2	6	11	2	3
Yield [%]	73	85	78	39	63	36
$\tilde{\nu}_{C\equiv C}$[cm^{-1}]	1772	1778	1779	1777	1752	1734
$\tilde{\nu}_{CO}$[cm^{-1}]	2017	2023	2022	2031	2010	2002
^{13}C δ (C≡C)	93.72	104.55	91.60	91.33	103.43	103.21

 © WILEY-VCH Verlag GmbH, D-69451 Weinheim, 1998 1434−1948/98/0505−0629 $ 17.50+.50/0

All resulting compounds (**7**−**12**) were characterized by their spectroscopic and analytical data. With the exception of **10** we were also able to grow single crystals allowing a more detailed study of the molecular parameters by using the X-ray technique. The molecular structures of **7** and **12** are shown in Figure 1.

Figure 1. Top: Molecular structure of one of both independent molecules of **7** in the unit cell. Bottom: Molecular structure of **12**. Ellipsoids are at the 50% probability level.

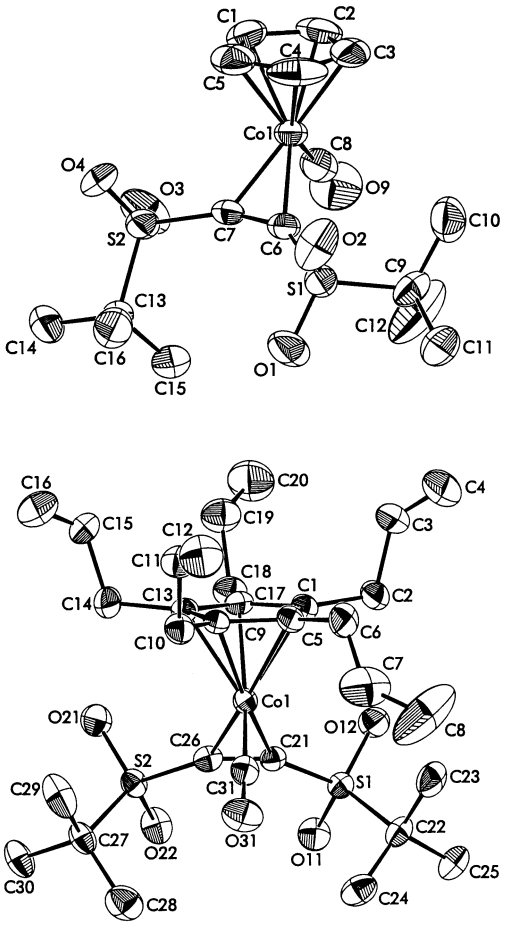

Table 2. Selected structural parameters of **7**−**9**, **11**, and **12**. The distances (*d*) are given in pm, the angles in degrees

Compound	**7**		**8**	**9**	**11**	**12**
d(C≡C)	126.4(5)	126.8(5)	127.0(3)	126.7(3)	126.9(3)	126.1(5)
d(≡C−Co)	194.2(3)	196.9(3)	194.7(3)	194.5(2)	195.2(2)	196.3(4)
	194.6(4)	196.8(3)	194.9(3)	195.9(2)	196.8(2)	196.4(4)
angle at C≡C−S	142.8(3)	142.2(3)	146.4(2)	145.0(2)	143.3(2)	140.9(3)
	158.5(3)	158.1(3)	158.9(2)	159.1(2)	155.9(2)	140.7(3)
torsion angle at S−C≡C−S	16(1)	13(1)	18(1)	15.6(1)	12.3(6)	3.0(1)
d(Co−CO)	176.1(4)	175.8(4)	177.0(3)	176.2(3)	175.3(2)	177.8(5)
d(C≡O)	113.5(5)	113.7(5)	113.1(4)	112.9(4)	113.9(2)	113.0(5)
d(Co−center of Cp)	170.2(2)	170.0(2)	169.6(2)	169.8(2)	170.2(1)	170.8(2)

The most relevant distances and angles of **7**−**9**, **11**, and **12** are listed in Table 2. A pronounced lengthening of the C−C bond of the alkyne unit was observed, from 119.1 pm in the uncomplexed state to 126.1−127.0 pm in the complexes. The deviation from linearity of up to 40° is considerable. These results are supported by vibrational spectra which show that the wave number for the uncomplexed BTSA unit (2160 cm^{-1} from Raman spectrum) is shifted to lower values (1734−1779 cm^{-1}).

Analogous results were reported by Yamazaki et al. for a related complex obtained by treating the diiodide of bis(triphenylphosphane)(η^5-cyclopentadienyl)cobalt (**13**) with tolane and isopropylmagnesium bromide.[21] The monosubstituted product **15** shows a C-C triple-bond stretching frequency of 1818 cm^{-1} which is considerably higher than that found in our examples.

Scheme 2

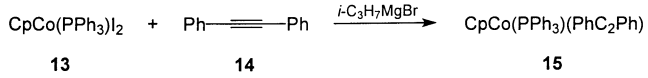

The complexes **7**−**12** are interesting intermediates on our endeavors to isolate a CpCo complex with two alkyne units and CpCo-capped push-pull cyclobutadiene complexes.

We are grateful to the *Deutsche Forschungsgemeinschaft*, the *Fonds der Chemischen Industrie* and the *BASF Aktiengesellschaft*, Ludwigshafen, for financial support. C. B. thanks the *Studienstiftung des deutschen Volkes* for a scholarship.

Experimental Section

General Methods. Moisture- and oxygen-sensitive reactions were conducted in oven-dried glassware under argon. Solvents were dried and distilled under argon before use; THF, diethylether, *n*-pentane, and *n*-hexane from sodium, dichloromethane from CaH_2. − Melting points are uncorrected. − Materials used for column chromatography: Silica gel 60 (Macherey-Nagel), alumina (Merck). − ^{1}H-NMR and ^{13}C-NMR: Bruker AS 200 (^{1}H at 200 MHz and ^{13}C at 50.33 MHz), Bruker WH 300 (^{1}H at 300 MHz, ^{13}C at 75.47 MHz) using the solvent as internal standard. − IR: Bruker Vector 22 FT-IR. − UV: Hewlett Packard HP8452A. − MS: Low resolution: ZAB-2F; high resolution: JEOL JMS-700. − Elemental analyses were carried out by the Mikroanalytisches Laboratorium der Universität Heidelberg. − The dicarbonyl(η^5-cyclopentadienyl)cobalt complexes **1**[3], **2**[14], **3**[15][16], **4**[17], and **5**[18][19] were prepared according to literature methods.

Dicarbonyl(η^5-pentaallylcyclopentadienyl)cobalt (**6**). Iodine (2.60 g, 10.2 mmol) was added at r.t. in portions to a stirred solution of 3.50 g (10.2 mmol) of dicobaltoctacarbonyl in 250 ml of anhydrous THF. The solution turned to a dark green color with vigorous foaming. After stirring for 1 h at room temperature, the solution was cooled to −40 °C and 6.17 g (20.3 mmol) of potassium pentaallylcyclopentadienide[20] was added. The reaction mixture was allowed to warm to room temperature overnight. After additional stirring for 1 d at room temperature the solvent was removed in vacuo, the residue dissolved in dichloromethane and chromatographed (alumina, 6% water, 30 × 3 cm). Elution with *n*-hexane yielded 2.51 g (33%) of **6** as a dark red, air-sensitive oil. − ^{1}H NMR (200 MHz, $CDCl_3$): δ = 2.92−2.96 (m, 10 H, CH_2), 4.81−5.00 (m, 10 H, =CH_2), 5.61−5.81 (m, 5 H, =CH). − ^{13}C NMR (50.32 MHz, $CDCl_3$): δ = 29.10 (CH_2), 99.62 (Cp-C), 115.40 (=CH), 137.21 (=CH_2), 183.85 (C≡O). − IR (film): $\tilde{\nu}$ = 3078 cm^{-1}, 3007, 2978, 2915, 2843, 2010, 1944, 1637, 1440, 1414, 1286, 993, 911,

617, 556. − UV/Vis (CH_2Cl_2): λ_{max} (lg ε) = 222 nm (5.00). − MS (EI, 70 eV): *m/z* = 352 [M^+ − CO], 324 [M^+ − 2CO].

General Procedure for the Preparation of the Carbonyl(η⁵-cyclopentadienyl)(η²-bis[tert-butylsulfonyl]acetylene)cobalt(I) Complexes. The dicarbonyl(η⁵-cyclopentadienyl)cobalt complex was added at ambient temperature to a solution of bis(*tert*-butylsulfonyl)acetylene (BTSA) in 50 ml of dichloromethane. After stirring for 2−11 d at r.t. the solvent was removed in vacuo and the product was isolated by silica gel chromatography (silica gel, *n*-pentane/diethyl ether).

Carbonyl(η⁵-cyclopentadienyl)(η²-bis[tert-butylsulfonyl]acetylene)cobalt(I) (**7**); Starting material: 300 mg (1.67 mmol) of dicarbonyl(η⁵-cyclopentadienyl)cobalt (**1**), 890 mg (3.34 mmol) of BTSA. Reaction time: 3 d. Silica gel chromatography (*n*-pentane/diethyl ether, 1:2). Yield: 508 mg (73%) of **7** as an orange solid, m.p. 110°C (decomposition). − ^{1}H NMR (300 MHz, $CDCl_3$): δ = 1.52 (s, 18 H, CH_3), 5.29 (s, 5 H, Cp-H). − ^{13}C NMR (75.47 MHz, $CDCl_3$): δ = 23.38 [C(*C*H_3)$_3$], 61.52 [*C*(CH_3)$_3$], 86.93 (Cp-C), 93.72 (≡C). − IR (KBr): $\tilde{\nu}$ = 3119 cm^{-1}, 2979, 2936, 2866, 2017, 1772, 1476, 1395, 1295, 1116. − UV/Vis (CH_2Cl_2): λ_{max} (lg ε) = 256 nm (4.14). − MS (EI, 70 eV): *m/z* = 390 [M^+ − CO], 270, 245, 214, 141, 124. − HRMS (FAB+): [M + H^+] $C_{16}H_{24}CoO_5S_2$: calcd. 419.0319; found 419.0332. − $C_{16}H_{23}CoO_5S_2$ (418.425): calcd. C 45.93, H 5.54; found C 45.79, H 5.61.

Carbonyl(η⁵-methylcyclopentadienyl)(η²-bis[tert-butylsulfonyl]acetylene)cobalt(I) (**8**); Starting material: 330 mg (1.70 mmol) of dicarbonyl(η⁵-methylcyclopentadienyl)cobalt (**2**), 906 mg (3.40 mmol) of BTSA. Reaction time: 2 d. Silica gel chromatography (*n*-pentane/diethyl ether, 3:1). Yield: 624 mg (85%) of **8** as an orange solid, m.p. 91°C (decomposition). − ^{1}H NMR (300 MHz, $CDCl_3$): δ = 1.44 (s, 3 H, Cp-CH_3), 1.53 (s, 18 H, C(CH_3)$_3$), 5.13/5.52 (pt, 4 H, Cp-H). − ^{13}C NMR (75.47 MHz, $CDCl_3$): δ = 11.55 (Cp-CH_3), 23.55 [C(*C*H_3)$_3$], 61.54 [*C*(CH_3)$_3$], 83.24/90.22 (Cp-C), 97.70 [Cp(*C*)-CH_3], 104.55 (≡C). − IR (KBr): $\tilde{\nu}$ = 3119 cm^{-1}, 2978, 2932, 2867, 2023, 1778, 1475, 1365, 1297, 1117. − UV/Vis (CH_2Cl_2): λ_{max} (lg ε) = 258 nm (4.32). − MS (FAB+): *m/z* = 433 [M + H^+], 405. − HRMS (FAB+): [M + H^+] $C_{17}H_{26}CoO_5S_2$: calcd. 433.0554; found 433.0554. − $C_{17}H_{25}CoO_5S_2$ (432.452): calcd. C 47.22, H 5.83; found C 47.03, H 5.86.

Carbonyl(η⁵-trimethylsilylcyclopentadienyl)(η²-bis[tert-butylsulfonyl]acetylene)cobalt(I) (**9**): Starting material: 420 mg (1.67 mmol) of dicarbonyl(η⁵-trimethylsilylcyclopentadienyl)cobalt (**3**), 890 mg (3.34 mmol) of BTSA. Reaction time: 6 d. Silica gel chromatography (*n*-pentane/diethyl ether, 1:1). Yield: 639 mg (78%) of **9** as a yellow solid, m.p. 116°C (decomposition). − ^{1}H NMR (300 MHz, $CDCl_3$): δ = 0.34 [s, 9 H, Si(CH_3)$_3$], 1.49 [s, 18 H, C(CH_3)$_3$], 5.20/5.35 (b, 4 H, Cp-H). − ^{13}C NMR (75.47 MHz, $CDCl_3$): δ = −0.62 [Si(CH_3)$_3$], 23.43 [C(*C*H_3)$_3$], 61.58 [*C*(CH_3)$_3$], 91.60 (≡C), 91.94/92.05 (Cp-C), 94.35 [Cp(*C*)-Si]. − IR (KBr): $\tilde{\nu}$ = 3092 cm^{-1}, 2980, 2956, 2867, 2022, 1779, 1459, 1393, 1295, 1115. − UV/Vis (CH_2Cl_2): λ_{max} (lg ε) = 258 nm (4.14). − MS (FAB+): *m/z* = 491 [M + H^+], 463, 389. − HRMS (FAB+): [M^+] $C_{19}H_{31}CoO_5S_2Si$: calcd. 490.0714; found 490.0779. − $C_{19}H_{31}CoO_5S_2Si$ (490.608): calcd. C 46.52, H 6.37; found C 46.55, H 6.46.

Carbonyl(η⁵-methoxycarbonylcyclopentadienyl)(η²-bis[tert-butylsulfonyl]acetylene)cobalt(I) (**10**): Starting material: 357 mg (1.50 mmol) of dicarbonyl(η⁵-methoxycarbonylcyclopentadienyl)-cobalt (**4**), 800 mg (3.00 mmol) of BTSA. Reaction time: 11 d. Silica gel chromatography (*n*-pentane/diethyl ether, 1:1). Yield: 280 mg (39%) of **10** as an orange solid, m.p. 114°C (decomposition).

Table 3. Crystallographic data of **7**, **8**, **9**, **11**, and **12**

Compound	**7**	**8**	**9**	**11**	**12**
Empirical formula	$C_{16}H_{23}CoO_5S_2$	$C_{17}H_{25}CoO_5S_2$	$C_{19}H_{31}CoO_5S_2Si$	$C_{22}H_{35}CoO_5S_2$	$C_{31}H_{43}CoO_5S_2$
Molecular mass [g/mol]	418.425	432.452	490.608	502.586	618.748
Solvent	*n*-pentane/diethyl ether	*n*-pentane/diethyl ether	*n*-pentane/diethyl ether	*n*-pentane/diethyl ether	*n*-pentane/diethyl ether
Crystal size [mm]	0.20×0.60×0.60	0.55×0.65×0.75	0.70×0.55×0.45	0.40×0.40×0.20	0.30×0.23×0.18
Crystal color	red	red	orange	red	orange
Crystal shape	irregular	prism	prism	irregular	needle
Crystal system	triclinic	triclinic	triclinic	monoclinic	monoclinic
Space Group	$P\bar{1}$	$P\bar{1}$	$P\bar{1}$	$P2_1/c$	$P2_1/c$
a [Å]	10.510(3)	9.601(3)	9.807(2)	15.270(4)	19.582(3)
b [Å]	12.431(3)	9.822(4)	9.920(1)	13.751(1)	9.518(1)
c [Å]	14.628(3)	12.710(4)	13.051(2)	11.961(2)	17.493(2)
α [°]	97.14(2)	70.04(3)	97.56(1)	90	90
β [°]	94.50(2)	78.31(3)	100.54(1)	100.28(2)	105.0920(10)
γ [°]	89.91(2)	63.07(3)	92.55(1)	90	90
V [Å^3]	1890.5(7)	1002.8(6)	1234.3(3)	2471.2(7)	3147.91(7)
$D_{calcd.}$ [Mg/m^3]	1.47	1.43	1.32	1.35	1.31
Z	4	2	2	4	4
F(000)	872	452	516	1064	1312
Temperature [K]	293	293	293	263	200
h_{min} / h_{max}	−12 / 12	0 / 12	−2 / 11	0 / 20	−23 / 23
k_{min} / k_{max}	−15 / 14	−10 / 12	−11 / 11	0 / 18	−11 / 11
l_{min} / l_{max}	0 / 17	−15 / 16	−15 / 15	−15 / 15	−12 / 20
μ [mm^{-1}]	1.15	1.09	0.94	0.89	0.71
Refl. collected	7161	4374	5504	6152	14195
Refl. unique	7062	4374	4343	5940	5328
Refl. observed	5603	3837	3844	4569	4309
Variables	434	227	281	282	358
R(*F*)	0.049	0.048	0.034	0.032	0.053
$R_w(F^2)$	0.116	0.121	0.089	0.079	0.127
S (Gof) on F^2	1.07	1.10	1.15	1.06	1.10
$(\Delta\rho)_{max}$ [e Å^{-3}]	0.44	0.34	0.40	0.49	0.80
$(\Delta\rho)_{min}$ [e Å^{-3}]	−0.55	−1.09	−0.26	−0.42	−0.59

– ^{1}H NMR (200 MHz, $CDCl_3$): δ = 1.51 [s, 18 H, $C(CH_3)_3$], 3.87 (s, 3 H, OCH_3), 5.37/5.79 (b, 4 H, Cp-H). – ^{13}C NMR (50.32 MHz, $CDCl_3$): δ = 23.55 [$C(CH_3)_3$], 52.40 (OCH_3), 61.90 [$C(CH_3)_3$], 88.87/89.57 (Cp-C), 90.31 [Cp(*C*)-CO_2Me], 91.33 (≡C), 164.44 (C=O). – IR (KBr): $\tilde{\nu}$ = 3094 cm^{-1}, 2977, 2868, 2031, 1777, 1726, 1477, 1374, 1300, 1196, 1149, 1119. – UV/Vis (CH_2Cl_2): λ_{max} (lg ε) = 260 nm (4.27). – MS (FAB+): *m*/*z* = 477 [M + H^+], 449. – HRMS (FAB+): [M + H^+] $C_{18}H_{26}CoO_7S_2$: calcd. 477.0452; found 477.0436.

Carbonyl(η^5–1-ethyl-2,3,4,5-tetramethylcyclopentadienyl)(η^2-bis[tert-butylsulfonyl]acetylene)cobalt(I) (**11**): Starting material: 396 mg (1.50 mmol) of dicarbonyl(η^5-1-ethyl-2,3,4,5-tetramethylcyclopentadienyl)cobalt (**5**), 800 mg (3.00 mmol) of BTSA. Reaction time: 2 d. Silica gel chromatography (*n*-pentane/diethyl ether, 3:1). Yield: 476 mg (63%) of **11** as an orange solid, m.p. 92°C (decomposition). – ^{1}H NMR (200 MHz, $CDCl_3$): δ = 1.01 (t, 3 H, CH_2CH_3, ^3J = 7.5 Hz), 1.47 [s, 18 H, $C(CH_3)_3$], 1.83 (s, 6 H, Cp-CH_3), 1.85 (s, 6 H, Cp-CH_3), 2.41 (q, 2 H, CH_2, ^3J = 7.5 Hz). – ^{13}C NMR (50.32 MHz, $CDCl_3$): δ = 9.28/9.43 (Cp-CH_3), 13.84 (CH_2CH_3), 17.81 (CH_2), 23.43 [$C(CH_3)_3$], 61.41 [$C(CH_3)_3$], 98.29/99.67 [Cp(*C*)-CH_3], 103.43 (≡C), 105.22 [Cp(*C*)-CH_2CH_3]. – IR (KBr): $\tilde{\nu}$ = 2974 cm^{-1}, 2914, 2871, 2010, 1752, 1458, 1380, 1291, 1115. – UV/Vis (CH_2Cl_2): λ_{max} (lg ε) = 272 nm (4.80). – MS (FAB+): *m*/*z* = 503 [M + H^+], 475. – HR-MS (FAB+): [M + H^+] $C_{22}H_{36}CoO_5S_2$: calcd. 503.1336; found 503.1452. – $C_{22}H_{35}CoO_5S_2$ (502.586): calcd. C 52.58, H 7.02; found C 52.38, H 7.11.

Carbonyl(η^5-pentaallylcyclopentadienyl)(η^2-bis[tert-butylsulfonyl]acetylene)cobalt(I) (**12**): Starting material: 304 mg (0.80 mmol) of dicarbonyl(η^5-pentaallylcyclopentadienyl)cobalt (**6**), 426 mg (1.60 mmol) of BTSA. Reaction time: 3 d. Silica gel chromatography (*n*-pentane/diethyl ether, 5:1). Yield: 180 mg (36%) of **12** as a yellow solid, m.p. 106°C (decomposition). – ^{1}H-NMR (300 MHz, $CDCl_3$): δ = 1.50 (s, 18 H, CH_3), 3.11–3.16 (td, 10 H, CH_2, ^3J = 6.2 Hz, ^4J = 1.6 Hz), 4.92–5.02 (dd, 5 H, CH=CH_{cis}H, $^3J_{trans}$ = 17.0 Hz, $^2J_{gem}$ = 1.4 Hz), 4.98–5.04 (dd, 5 H, CH=CH_{trans}H, $^3J_{cis}$ = 10.2 Hz, $^2J_{gem}$ = 1.4 Hz), 5.71–5.86 (tdd, 5 H, C*H*=CH_2, $^3J_{trans}$ = 17.0 Hz, $^3J_{cis}$ = 10.2 Hz, ^3J = 6.2 Hz). – ^{13}C NMR (75.47 MHz, $CDCl_3$): δ = 23.52 [$C(CH_3)_3$], 28.94 (CH_2), 61.91 [$C(CH_3)_3$], 101.50 (Cp-C), 103.21 (≡C), 116.81 (=CH_2), 135.14 (-CH=). – IR (KBr): $\tilde{\nu}$ = 3079 cm^{-1}, 2979, 2937, 2870, 2002, 1734, 1637, 1453, 1415, 1365, 1301, 1118, 993, 914, 636. – UV/Vis (CH_2Cl_2): λ_{max} (lg ε) = 294 nm (4.47). – MS (FAB+): *m*/*z* = 619 [M + H^+], 591. – HRMS (FAB+): [M + H^+] $C_{31}H_{44}CoO_5S_2$: calcd. 619.1962; found 619.2037. – $C_{31}H_{43}CoO_5S_2$ (618.748): calcd. C 60.18, H 7.00; found C 60.22, H 7.07.

X-ray Diffraction Analyses: The reflections were collected with a Nonius-CAD4 diffractometer (**11**), a Siemens Nicolet-Syntex-R3 diffractometer (**7**, **8**, **9**) and a Siemens CCD diffractometer (**12**). Intensities were corrected for Lorentz and polarisation effects. The structures were solved by direct methods (**7**, **8**, **9**, **12**: SHELXS-86[22]; **11**: SIR-92[23]). The structural parameters of the nonhydrogen atoms were refined anisotropically according to a full-matrix-least-squares technique (F^2). The hydrogen atoms were refined with fixed thermal parameters or calculated parameters. Refinement was carried out with SHELXL-93[24]. Table 3 contains the crystallographic data and details of the refinement procedure. Crystallographic data (excluding structure factors) have been deposited with the Cambridge Crystallograhic Data center as supplementary publication no CCDC–100891. Copies of data can be obtained free of charge on application to CCDC, 12, Union Road, Cambridge CB12 IEZ, UK [fax: int. code +44 (0)1223/336/033, email: deposit@ccdc.ac.uk].

[1] T. S. Piper, F. A. Cotton, G. Wilkinson, *J. Inorg. Nucl. Chem.* **1955**, *1*, 165.
[2] E. O. Fischer, R. Jira, *Z. Naturforsch. B.* **1955**, *10*, 355.
[3] M. D. Rausch, R. A. Genetti, *J. Org. Chem.* **1970**, *35*, 3888.
[4] W.-S. Lee, H. H. Brintzinger, *J. Organomet. Chem.* **1977**, *127*, 93.
[5] R. D. W. Kemmitt, D. R. Russell in G. Wilkinson, F. G. A. Stone, E. W. Abel (Ed.) *Comprehensive Organometallic Chemistry*, Pergamon Press, New York, **1982**, *Vol. 5*, 248.
[6] a) D. Seyferth, C. N. Ridue, J. S. Merola, *J. Organomet. Chem.* **1978**, *144*, C26. b) D. C. Müller, R. C. Gearhart, F. D. Brill, *J. Organomet. Chem.* **1979**, *169*, 395. c) M. C. Weiss, G. C. Gordon, V. L. Goedken, *J. Am. Chem. Soc.* **1979**, *101*, 857. d) H. J. Callot, E. Schaeffer, *J. Organomet. Chem.* **1978**, *145*, 91.
[7] A. Nakamura, N. Hagihara, *Bull. Chem. Soc. Jpn.* **1961**, *34*, 452.
[8] H. Sakurai, J. Hayashi, *J. Organomet. Chem.* **1974**, *70*, 85.
[9] R. Markby, H. W. Sternberg, I. Wender, *Chem. Ind.* **1959**, 1381.
[10] R. S. Dickson, G. Wilkinson, *J. Chem. Soc.* **1964**, 2699.
[11] K. P. C. Vollhardt, J. E. Bercaw, R. G. Bergman, *J. Am. Chem. Soc.* **1974**, *96*, 4996.
[12] [12] A. Riera, F. Cabré, A. Moyano, M. A. Péricas, J. Santamaria, *Tetrahedron Lett.* **1990**, *31*, 2169.– [12b] A. Riera, M. Marti, A. Moyano, M. A. Péricas, J. Santamaria, *Tetrahedron Lett.* **1990**, *31*, 2173.
[13] F. Ohlbach, R. Gleiter, T. Oeser, H. Irngartinger, *Liebigs Ann.* **1996**, 791.
[14] W. P. Weiner, R. G. Bergman, *J. Am. Chem. Soc.* **1983**, *105*, 3922.
[15] E. W. Abel, S. Moorhouse, *J. Organomet. Chem.* **1971**, *28*, 211.
[16] C. S. Kraihanzel, M.L. Losee, *J. Am. Chem. Soc.* **1968**, *90*, 4701.
[17] W. P. Hart, D. Shihua, M. D. Rausch, *J. Organomet. Chem.* **1985**, *282*, 111.
[18] T. Dooley, G. Fairhurst, C. D. Chalk, K. Tabatabaian, C. White, *Transition Met. Chem.* **1978**, *3*, 299.
[19] C. M. Fendrick, L. D. Schertz, V. W. Day, T. J. Marks, *Organometallics* **1988**, *7*, 1828.
[20] C. Batz, P. Jutzi, *Synthesis* **1996**, 1296.
[21] a) H. Yamazaki, N. Hagihara, *J. Organomet. Chem.* **1970**, *21*, 431. b) K. Yasafuku, H. Yamazaki, *J. Organomet. Chem.* **1976**, *121*, 405. c) H. Yamazaki, Y. Wakatsuki, *J. Organomet. Chem.* **1977**, *139*, 157.
[22] G. M. Sheldrick, *SHELXS-86*, Universität Göttingen, Germany, **1986**.
[23] A. Altomare, G. Cascarano, C. Giacovazzo, A. Guagliardi, M. C. Burla, G. Polidori, M. Camalli, *SIR-92*, Ist. di Ric. per lo Sviluppo di Metodologie Cristallografiche, CNR, Univ. of Bari, Italy, **1992**.
[24] G. M. Sheldrick, *SHELXL-93*, Universität Göttingen, Germany, **1993**.

[97300]

2,3,4-Tricarba-*nido*-hexaboranes(7) with a Bridging B−Ethyl−B Moiety

Bernd Wrackmeyer*[a], Hans-Jörg Schanz[a], Matthias Hofmann[b], and Paul von R. Schleyer[b]

Laboratorium für Anorganische Chemie, Universität Bayreuth[a]
D-95440 Bayreuth (Germany)
Fax: Int. code +49(0)921/552157
E-mail: b.wrack@uni-bayreuth.de

Institut für Organische Chemie, Universität Erlangen-Nürnberg[b]
Henkestr. 42, D-91054 Erlangen (Germany)
Fax: Int. code +49(0)9131/859132
E-mail: pvrs@organik.uni-erlangen.de

Received December 8, 1997

Keywords: Ab initio calculations / Boron / Carboranes / NMR spectroscopy

Hydroboration of diethyl(1-propynyl)borane **1** with tetraethyldiborane(6) in the presence of a catalytic amount of trimethyl- or tributyltin chloride gave two new organo-substituted carboranes **6** and **7** with 2,3,5-tricarba-*nido*-hexaborane(7) and 2,3,4-tricarba-*nido*-hexaborane(7) skeletons, respectively, along with polymeric material and the known organo-substituted 1-carba-*arachno*-pentaborane(10) (**3**) and pentaethyl-1,5-dicarba-*closo*-pentaborane(5) (**4**). Selective $^{11}B(5,6)$ decoupled ^{13}C-NMR spectra indicate an unprecedented B(5)−ethyl−B(6) bridge in **7**. This structure is supported by the agreement between experimental and calculated ^{11}B- and ^{13}C-chemical shifts on a model compound **7d** with methyl groups in the 1,2,3,5,6-positions and an ethyl group bridging B(5) and B(6).

Introduction

Treatment of tetraborane(10) with alkynes gave the first 2,3,4-tricarba-*nido*-hexaboranes(7) with a B(5)−H−B(6) bridge;[1] these early observations have, at least in part, been confirmed recently,[2] and the formation of the parent compound has been reported for the first time.[2b] Köster et al. have tentatively assigned (on the basis of mass spectra) the structure of 1,5,6-triethyl-2,3,4-trimethyl-2,3,4-tricarba-*nido*-hexaborane(7) to one of the minor products in the complex mixture which is obtained by dehalogenation of diethylboron chloride with lithium in THF.[3] An alternative route to small carboranes involves hydroboration of 1-alkynyl(diethyl)boranes in the presence of a large excess of Et_2BH,[5] which gives rise to hydroboration followed by Et_2BH-catalyzed condensations.[5][6][7] This method has afforded [Eq. (1)] the *arachno*-carborane **3**,[7] which is a precursor of the *closo*-carborane **4**. The formation of **3** in high yield requires that the hydroboration of **1** takes place stereoselectively to give **2** as a reactive intermediate prior to the condensation reactions. If this is not the case, products other than **3** will be formed, as reported in this work.

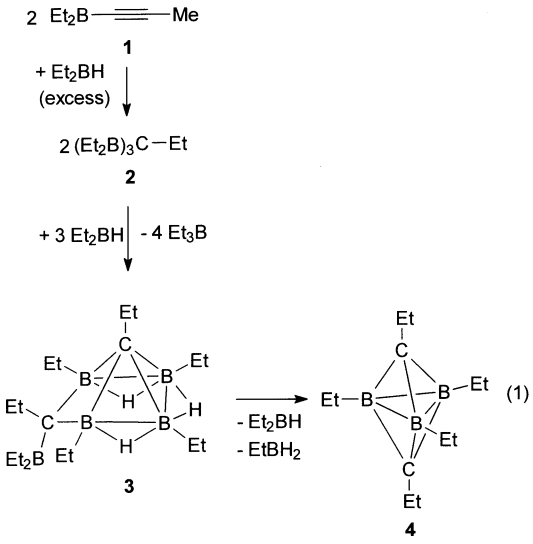

Results and Discussion

Synthesis. Conditions that reduce the stereoselectivity of the hydroboration of **1** will lead to mixtures containing compounds **2** and **5** [Eq. (2)]; hence, condensation reactions may give carboranes other than **3**. Therefore, we have studied the reaction of **1** with Et_2BH under various conditions. As long as a large excess of Et_2BH is used, **3** is the major product, although more side-products are formed if **1** is added to Et_2BH at room temperature or above, rather than at −78°C. The use of only a slight excess of Et_2BH (2.1 equivalents) results in mainly polymeric material containing just traces (< 1%, according to ^{11}B-NMR spectra) of carboranes, but the presence of a small amount of trimethyl- or tributyltin chloride leads to the formation of interesting products. Examination of the ^{11}B-NMR spectra of such reaction mixtures, after removing readily volatile material, shows not only the presence of polymers (ca. 60%), but also new types of carboranes **6** (ca. 15%) and **7** (ca. 10%) along with the known carboranes **3** (ca. 10%) and **4** (ca. 5%). Unlike **7**, pure carborane **6** could not be isolated. However, **6** was readily identified by its characteristic[8] ^{11}B-NMR data

 © WILEY-VCH Verlag GmbH, D-69451 Weinheim, 1998 1434−1948/98/0505−0633 $ 17.50+.50/0

[$\delta^{11}B(1) = -36.4$ and $\delta^{11}B(4,6) = 21.9$] as a 2,3,5-tricarba-*nido*-hexaborane(7) derivative. **6** is not stable to oxidation or hydrolysis but **7** is, meaning the latter can be separated and isolated. The compounds **7** do not react with Na[Et_3BH] after prolonged heating at 60°C in hexane, with Et_3Al in hexane at room temperature, or with bases such as pyridine.

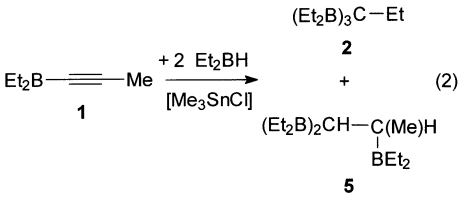

Potential intermediates prior to the formation of the carboranes **6** and **7** are shown in Scheme 1. It is suggested that the C_2-bridged compound **8** is formed in a similar way to **3**.[7] The C_2-bridged *arachno*-carborane **9** is comparable with a benzo derivative that has already been characterized.[9] The intermediacy of **9** (prior to elimination of $EtBH_2$[10][11] and rearrangement) has been proposed in order to explain the formation of 2,3,5-tricarba-*nido*-hexaborane(7) derivatives analogous to **6**.[8b] Although other rearrangements of **9** have not been observed before,[8b] it is conceivable that insertion of the formerly apical CEt group takes place not only into B−H−B bonds but also into B−C or C−C bonds, accompanied or followed by elimination of $EtBH_2$. This explains the formation of **10** and **10′** which, under the reaction conditions, can undergo irreversible H/Et exchange to give the isomers **7** and **7′** (in repeated experiments the ratio of **7**/**7′** varied from 3:1 to 2:3). The B(5)−Et−B(6) bridge in **7** is an unprecedented structural feature in borane and carborane chemistry. Bridging triorganosilyl, -germyl, and -stannyl groups have been observed previously, e.g. in the case of *nido*-pentaborane(9) derivatives.[12]

NMR Spectroscopic Results: The ^1H-, ^{11}B- and ^{13}C-NMR data of **7** (Table 1 and Experimental Section) are fully consistent with a 2,3,4-tricarba-*nido*-hexaborane(7) cage bearing terminal ethyl groups at all boron atoms, a hydrogen at C(4) and a methyl or a ethyl group at C(2) or C(3). There was no indication of the initially expected B−H−B group, either in the ^1H-NMR spectra (with or without ^{11}B decoupling) or in the ^{11}B-NMR spectra (with and without ^1H decoupling); this evidence definitely precludes the structures **10** and **10′**. However, there were additional signals due to an ethyl group for each isomer in the ^1H- and ^{13}C-NMR spectra. ^{13}C-NMR spectra of a mixture of **7** and **7′**, recorded under various conditions, are shown in Figure 1. The aliphatic region displays fourteen sharp ^{13}C resonances (two CH_2 and twelve CH_3 groups with carbon atoms not linked to boron), and in the region for the cage carbon atoms two sharp signals [$^{13}C(3,3')$] and four

Figure 1. 125.8-MHz ^{13}C-NMR spectra of a mixture of **7** and **7′** (ca. 10 mg in 0.5 ml of $CDCl_3$). **A**: Normal $^{13}C\{^1H\}$-NMR spectrum; the region of the boron bonded cage carbon atoms has been taken from a spectrum recorded at −30°C in order to show the broadened ^{13}C-NMR signals which are exceedingly broad in the spectrum at 25°C. **B**: The selective heteronuclear $^{13}C\{^{1\,H,\ 11}B(5,6)\}$ triple-resonance experiment shows sharpening of the B(5)−$^{13}CH_2$−B(6), $^{13}CH_2$−B(5,6), and $^{13}C(2, 2', 4, 4')$ signals. **C**: The selective heteronuclear $^{13}C\{^1H,^{11}B(1)\}$ triple-resonance experiment only gives rise to sharpening of the $^{13}CH_2$−B(1) signal.

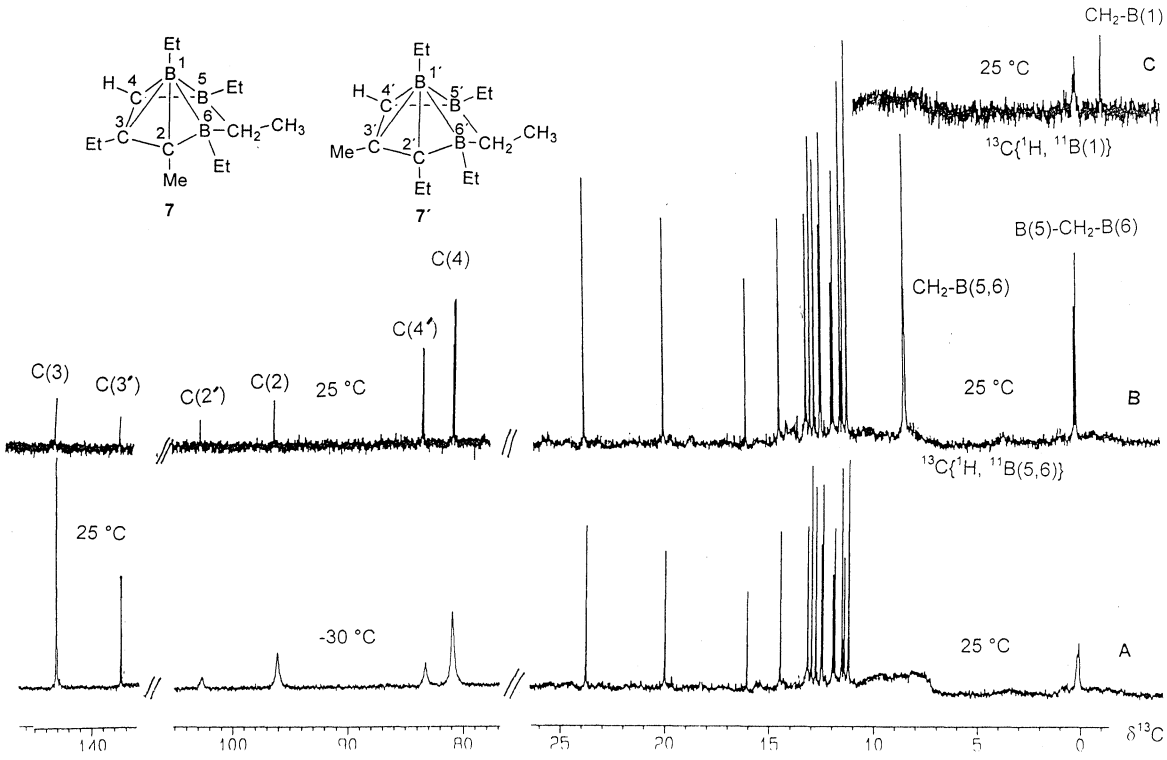

Scheme 1

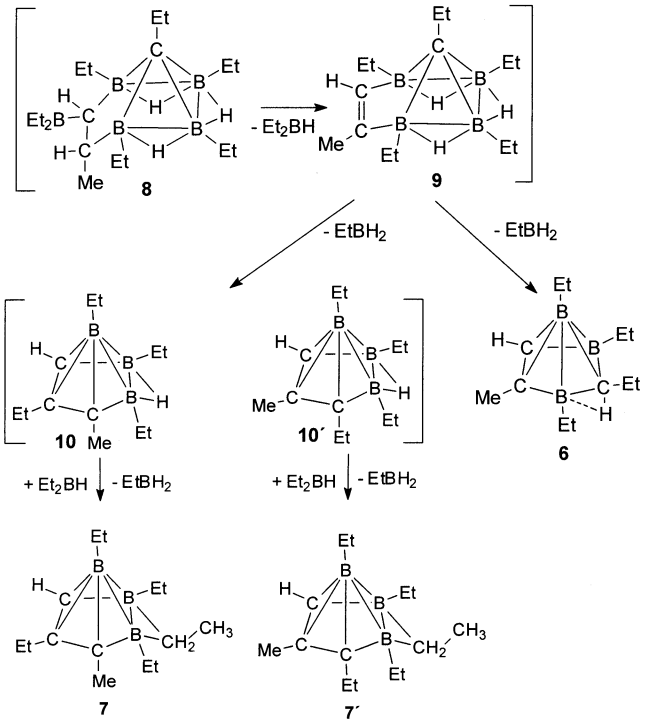

broad signals [^{13}C(2,2′) and 13C(4,4′)] are observed, as required for the two isomers **7** and **7′**. The unique μ-^{13}C(CH_2) signals (Figure 1, A and C) are significantly broadened [although less than the ^{13}C(CH_2) resonance of terminal BEt groups] as a result of scalar relaxation of the second kind[13][14] (partially relaxed scalar ^{13}C-^{11}B spin-spin coupling). This was proved by selective ^{11}B(5,6) decoupling (Figure 1, B) which, as expected, causes sharpening of the ^{13}C(2, 2′, 4, 4′) and ^{13}C(CH_2) signals of the terminal B(5,6)Et groups, and also the μ-^{13}C(CH_2) signal of the ethyl group in the B(5)−Et−B(6) bridge. Decoupling of B(1) (Figure 1, C) has no appreciable effect on the appearance of the ^{13}C-NMR spectrum except for sharpening of the ^{13}C(CH_2) resonance of the apical BEt group. The greater broadening of the terminal ^{13}C(CH_2) signal of the BEt groups with respect to that of the bridging B−Et−B [i.e. $^1J(^{13}C_{terminal},^{11}B) > {}^1J(^{13}C_{bridging},^{11}B)$] is reminiscent of the $^1J(^{11}B,^1H)$ in diborane(6) where the magnitude of the coupling constant of the terminal ^{1}H nucleus is approximately three times greater than that of the bridging ^{1}H nucleus.

MO Calculations: We applied the ab initio/GIAO/NMR method,[15][16] a powerful computational tool for the determination of polyhedral borane and carborane structures, to establish, in the absence of X-ray determinations the structural assignment for **7**.[17] The chemical shifts, computed for various optimized models, are compared with experimental NMR data. The methyl-bridged μ-Me-2,3,4-$C_3B_3H_6$ model compound **7b** not only allows the investigation of the chemical shifts of a bridging alkyl group (the new feature in **7** and **7′**, which is represented in **7b**) but also a thermodynamic stability assessment in comparison with the hydrogen bridge isomer (5-Me-2,3,4-$C_3B_3H_6$, **7a**, Figure 2). The 18.3 kcal mol^{-1} lower energy of **7a** than **7b** quantifies the extend to which methyl bridging is normally unfavourable. However, the methyl bridge has no large effect on the chemical shifts (compare **7b** to **7a**): The differences are ca. −10 ppm for C(2,4), +8 ppm for C(3), and ca. −5 ppm for B(6) (Table 1).[18] In particular, the apical B(1) has almost the same d^{11}B value of δ = −52 in **7a** and **7b**.

Figure 2 Geometries (bond lengths in pm) of model compounds **7a**−**d**, optimized at MP2(fc)/6-31G*[a]

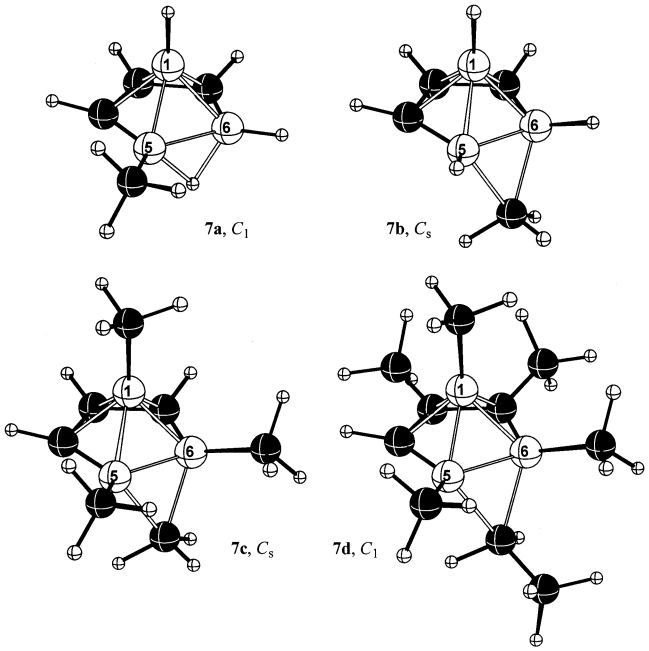

[a] **7a**: B1−C2 172.0, B1−C3 173.0, B1−C4 172.1, B1−B5 176.8, B1−B6 175.4, C2−C3 142.7, C3−C4 142.9, C2−B6 153.6, C4−B5 153.8, B5−B6 177.6, B5−μH 133.3, B6−μH 130.9. − **7b**: B1−C2 170.6, B1−C3 173.1, B1−B5 176.4, C2−C3 142.9, C2−B6 154.5, B5−B6 176.3, B5−μCH_3 179.5. − **7c**: B1−C2 171.2, B1−C3 173.7, B1−B5 176.9, C2−C3 142.9, C2−B6 154.9, B5−B6 177.4, B5−μCH_3 1.802. − **7d**: B1−C2 170.5, B1−C3 174.9, B1−C4 169.7, B1−B5 177.0, B1−B6 176.1, C2−C3 143.2, C3−C4 143.7, C2−B6 156.2, C4−B5 154.6, B5−B6 176.2, B5−μCH_2 185.1, B6−μCH_2 180.4.

Because of the large size of **7** and **7′** and the many possible orientations of the ethyl groups, model compounds were computed instead. The addition of methyl substituents to **7b** at B(1) and B(5,6) to give **7c** results in the expected d^{11}B increase of ca. 10 ppm but has no significant influece on the geometry (compare **7b** and **7c**, Figure 2). While the chemical shifts computed for **7c** correspond reasonably well with the measured values for **7** and **7′**, our best model, a 1,2,3,5,6-pentamethyl tricarbahexaborane(7) with a bridging ethyl group, gives better agreement with almost all the data in Table 1. The differences between **7c** and **7d** can be ascribed to electronic effects of the additional alkyl substituents to the cage in **7d**.[19] The constitution of **7** and **7′** with their unique B−alkyl−B bridge is supported by the above computations.

The B−μ-C and B(5)−B(6) distances computed for **7b**−**d** (Figure 2) show that the bridging alkyls are involved in deltahedral (three-centre) bonding. Corner protonated

cyclopropane (a CH_3^+ π complex of ethylene) provides an anology in carbon chemistry.[20]

Support of this work by the *Deutsche Forschungsgemeinschaft* and the *Fonds der Chemischen Industrie* is gratefully acknowledged.

Experimental Section

All synthetic work (except for the purification of **7** and **7′**) and handling of samples was carried out in an atmosphere of N_2 or Ar, observing all necessary precautions to exclude traces of oxygen or moisture. The starting materials were commercial samples (Me_3SnCl or nBu_3SnCl) or were prepared as described [Et_2BH[4], $Et_2B-C{\equiv}CMe$[6b]]. – NMR spectra: Bruker ARX 250 and DRX 500 spectrometers; the latter was equipped with a triple resonance probe head for the $^{13}C\{^{1\,H,\,11}B\}$ experiments; chemical shifts are reported with respect to Me_4Si [δ^1H ($CHCl_3/CDCl_3$) = 7.24; δ^1H ($C_6C_5CD_2H$) = 2.03; $\delta^{13}C$ ($CDCl_3$) = 77.0; $\delta^{13}C$ ($C_6D_5CD_3$) = 20.4] and Et_2O-BF_3 [$\delta^{11}B$ = 0 for $\Xi(^{11}B)$ = 32.083971 MHz]. – Electron impact (EI) mass spectra (70 eV): VARIAN MAT CH 7 with direct inlet.

5,6-μ-Ethyl-1,3,5,6-tetraethyl-2-methyl-2,3,4-tricarba-nido-hexaborane(7) (**7**) *and 5,6-μ-Ethyl-1,2,5,6-tetraethyl-3-methyl-2,3,4-tricarba-nido-hexaborane(7)* (**7′**): Et_2BH (1.326 g, 16.7 mmol hydride) was added at −78°C to diethyl(1-propynyl)borane **1** (1.799 g, 16.7 mmol) containing trimethyltin chloride (0.2 g) within 10 min. The reaction mixture was allowed to warm to room temperature and heated to 50°C. A further quantity of Et_2BH (1.344 g, 16.8 mmol hydride) diluted with BEt_3 (20 ml) was added over a period of 90 min, and the mixture was stirred at 50°C for a further 4 h. All volatile material was removed in vacuo, and fractional distillation of the residue gave a mixture (0.326 g; b.p. 70−80°C/10^{-3} Torr) of the carboranes **6** (55%), **7** and **7′** (35%) together with small amounts of unidentified products. The distillate was diluted with hexane (10 ml) and stirred in the presence of air for 10 h. The resulting solution was filtered, the solvent was removed in vacuo, and the residue was redistilled. The distillate [0.134 g (7%) of a colorless liquid; b.p. 74−77°C / 10^{-3} Torr] contained the carboranes **7** and **7′** in a ratio varying from 3:1 to 2:3 in repeated experiments, always in approximately the same yield.

7: ^1H NMR (500.1 MHz, 25°C, $CDCl_3$): δ = 4.03 [s, 1 H, C(4)H], 2.21 (m, 1 H), 2.01 (m, 1 H), 1.02 [t, 3 H, C(3)Et], 1.66 [s, 3 H, C(2)Me], 1.48 (m, 2 H), 0.18 (t, 3 H, μ-Et), 0.23 (m, 2 H), 0.68 [t, 3 H, B(1)Et], 0.88 (m, 2 H), 0.85 (m, 2 H), 1.18 (t, 3 H), 1.13 [t, 3 H, B(5,6)Et]. – ^{11}B NMR (160.6 MHz, 25°C, $CDCl_3$): δ = −34.4 [B(1)], 3.0, 5.4 [B(5,6)]. – ^{13}C NMR (125.8 MHz, 25°C, [D_8]toluene): δ = 143.3 [C(3)], 96.0 [broad, C(2)], 80.9 [broad, $^1J(^{13}C^1H)$ = 163.0 Hz, C(4)], 11.4 [C(3)*Me*], 24.0, 12.2 [C(2)*Et*], −0.3 (broad), 13.0 (μ-Et), −1.0 (broad), 11.8 [B(1)Et], 8.8 (broad), 8.7 (broad), 13.4, 11.7 [B(5,6)Et]. – EI-MS (70 eV): *m/z* (%) = 230 (5) [M^+], 201 (50) [M^+ − Et].

7′: ^1H NMR (500.1 MHz, 25°C, $CDCl_3$): δ = 4.12 [s, 1 H, C(4)H], 2.04 (m, 2 H), 1.09 [t, 3 H, C(2)Et], 1.81 [s, 3 H, C(3)Me], 1.60 (m, 2 H), 0.21 (t, 3 H, μ-Et), 0.15 (m, 2 H), 0.70 [t, 3 H, B(1)Et], 0.98 (m, 2 H), 0.86 (m, 2 H), 1.16 (t, 3 H), 1.12 [t, 3 H, B(5,6)Et]. – ^{11}B NMR (160.6 MHz, 25°C, $CDCl_3$): δ = −34.5 [B(1)], 2.9, 5.7 [B(5,6)]. – ^{13}C NMR (125.8 MHz, 25°C, [D_8]toluene): δ = 137.7 [C(3)], 102.7 [broad, C(2)], 83.2 [broad, $^1J(^{13}C^1H)$ = 161.1 Hz, C(4)], 15.7 [C(3)*Me*], 20.1, 15.0 [C(2)*Et*], −0.2 (broad), 13.4 (μ-Et), −1.1 (broad), 11.3 [B(1)Et], 8.9 (broad), 8.8 (broad), 11.7, 12.5 [B(5,6)Et].

Table 1. Experimental chemical shifts [ppm] of the cage nuclei of **7** and **7′** compared with computed values for model compounds **7a** to **7d** (compare Figure 1) at GIAO-SCF/6-31G*//MP2(fc)/6-31G* [a]

	7	**7′**	**7a**	**7b**	**7c**	**7d**
δ[^{11}B(1)]	−34.5	−34.4	−52.1	−52.3	−43.9	−39.4
δ[^{11}B(5,6)]	5.7, 2.9	5.4, 3.0	7.8, −0.4	−5.1	1.5	4.7, −2.2
δ[^{13}C(2)]	102.7	96.0	86.4	76.1	80.1	88.5
δ[^{13}C(3)]	137.7	143.3	119.5	127.5	132.3	140.0
δ[^{13}C(4)]	83.2	80.9	86.8	76.1	80.1	75.3
δ[^{13}C(μ-CH_2)]	−0.2	−0.3	–	−19.7	−8.5	−6.3

[a] Absolute energies [hartree]: **7a**: HF = −230.74721, MP2 = −231.53436; **7b**: HF = −230.71055, MP2 = −231.50560; **7c**: HF = −347.84152, MP2 = −349.04143; **7d**: HF = −464.94023, MP2 = −466.54612

[1] [1a] R. N. Grimes, *Carboranes*, Academic Press, London, **1970**. – [1b] C. L. Bramlett, R. N. Grimes, *J. Am. Chem. Soc.* **1966**, *88*, 4269−4270.

[2] [2a] M. A. Fox, R. Greatrex, *J. Chem. Soc., Chem. Commun.* **1995**, 667−668. – [2b] M. A. Fox, R. Greatrex, *J. Chem. Soc., Chem. Commun.* **1996**, 175−176.

[3] R. Köster, G. Benedikt, M. A. Grassberger, *Justus Liebigs. Ann. Chem.* **1968**, *719*, 187−209.

[4] The formula Et_2BH is used for simplicity. Tetraethyldiborane(6) is usually obtained and used as a mixture with triethylborane and small amounts of other ethyldiboranes(6): R. Köster, G. Bruno, P. Binger, *Justus Liebigs Ann Chem.* **1961**, *644*, 1−22.

[5] [5a] R. Köster, G. W. Rotermund, *Tetrahedron Lett*. **1964**, 1667. – [5b] P. Binger, *Tetrahedron Lett.*, **1966**, 2675. – [5c] R. Köster, H.-J. Horstschäfer, P. Binger, P. K. Matschei, *Liebigs Ann. Chem.* **1975**, 1339−1356.

[6] [6a] R. Köster, G. Seidel, B. Wrackmeyer, *Angew. Chem.* **1994**, *106,* 2380−2382; *Angew. Chem. Int. Ed. Engl.* **1994**, *33*, 2294−2296. – [6b] B. Wrackmeyer, H.-J. Schanz, *Collect. Czech. Chem. Commun.* **1997**, *62*, 1254−1262.

[7] R. Köster, R. Boese, H.-J. Schanz, B. Wrackmeyer, *J. Chem. Soc., Chem. Commun.* **1995**, 1691−1692.

[8] [8a] A. Feßenbecker, A. Hergel, R. Hettrich, V. Schäfer, W. Siebert, *Chem. Ber.* **1993**, *126*, 2205. – [8b] B. Wrackmeyer, H.-J. Schanz, *Main Group Met. Chem.* **1998**, *21*, 29−32.

[9] B. Gangnus, H. Stock, W. Siebert, M. Hofmann, P. v. R. Schleyer, *Angew, Chem.* **1994**, *106*, 2384; *Angew, Chem. Int. Ed. Engl.* **1994**, *33*, 2296.

[10] B. Wrackmeyer, H.-J. Schanz, W. Milius, *Angew. Chem.* **1997**, *109*, 98−99; *Angew. Chem. Int. Ed. Engl.* **1997**, *36*, 75−77.

[11] M. Hofmann, M. A. Fox, R. Greatrex, R. E. Williams, P. v. R. Schleyer, *J. Organomet. Chem.* in press.

[12] D.F. Gaines, *Acc. Chem. Res.* **1973**, *6*, 416−421.

[13] A. Abragam, *The Principles of Nuclear Magnetism,* Oxford University Press, Oxford **1961**, chapter 8.

[14] B. Wrackmeyer, *Annu. Rep. NMR Spectrosc.* **1988**, 20, 61−203.

[15] [15a] M. Bühl, P. v. R. Schleyer *J. Am. Chem. Soc.* **1992**, *114*, 477−491. – [15b] M. Bühl, J. Gauss, M. Hofmann, P. v. R. Schleyer *J. Am. Chem. Soc.* **1993**, *115*, 12385−12390. – [15c] See M. Diaz, J. Jaballas, J. Arias, H. Lee, T. Onak, *J. Am. Chem. Soc.* **1996**, *118*, 4405−4410 for an extensive bibliography.

[16] [16a] M. A. Fox, R. Greatrex, M. Hofmann, P. v. R. Schleyer, R. E. Williams *Angew. Chem.* **1997**, *109*, 1542−1544; *Angew. Chem. Int. Ed. Engl.* **1997**, *36*, 1498−1501. – [16b] M. Diaz, J. Jaballas, D. Tran, H. Lee, J. Arias, T. Onak, *Inorg. Chem.* **1996**, *35*, 4536−4540 and references cited therein.

[17] GIAO chemical shifts – [17a] K. Wolinski, J. F. Hinton, P. Pulay, *J. Am. Chem. Soc.* **1990**, *112*, 8251) and MP2(fc)6-31G* geometries – [17b] M. Häser, R. Ahlrichs, H. P. Baron, P. Weis, H. Horn, *Theor. Chim. Acta* **1992**, *83*, 455) were computed with the Gaussian 94 program – [17c] Gaussian 94, Revision D.3, M. J. Frisch, G. W. Trucks, H. B. Schlegel, P. M. W. Gill, B. G. Johnson, M. A. Robb, J. R. Cheeseman, T. Keith, G. A. Petersson, J. A. Montgomery, K. Raghavachari, M. A. Al-Laham, V. G. Zakrzewski, J. V. Ortiz, J. B. Foresman, J. Cioslowski, B. B. Stefanov, A. Nanayakkara, M. Challacombe, C. Y. Peng, P. Y.

Ayala, W. Chen, M. W. Wong, J. L. Andres, E. S. Replogle, R. Gomperts, R. L. Martin, D. J. Fox, J. S. Binkley, D. J. Defrees, J. Baker, J. P. Stewart, M. Head-Gordon, C. Gonzalez, and J. A. Pople, Gaussian, Inc., Pittsburgh PA, **1995**).

[18] For the parent 2,3,4-$C_3B_3H_7$ we get IGLO/DZ/MP2(fu)/6-31G* chemical shifts of −52.9 (B1), 0.7 (B5,6), 87.6 (C2,4) and 120.0 (C3); experimental δ^{11}B data :[2b] −57.9 [B(1)), −0.3 (B(5,6)].

[19] Geometric effects can be shown to be less important: A structure based on **7d** but with the methyl groups at C(2), C(3) and the bridging methylene group replaced by H (i.e. **7c** in the geometry of **7d**) gave computed chemical shifts [B(1): −42.3, B(5): 4.0, B(6): −3.1, C(2): 88.4, C(3): 138.0, C(4): −75.1, C(μ-CH_2): −9.7] close to those for the optimized **7c** geometry.

[20] W. Koch, P. v. R. Schleyer, P. Buzek, B. Liu, *Croat. Chim. Acta* **1992**, *65*, 655−672 and literature cited.

[97301]

A TXRF and Micro-Raman Spectrometric Reconstruction of Palettes for Distinguishing Between Scriptoria of Related Medieval Manuscripts

Guido Van Hooydonk*[a], Martine De Reu[a], Luc Moens[b], Joke Van Aelst[b][+], and Ludo Milis[c]

University of Ghent, Department of Library Sciences[a],
Rozier 9, B-9000 Ghent, Belgium
Fax (internat.): +32 9 264 38 52; Tel: +32 9 264 38 51
E-mail: guido.vanhooydonk@rug.ac.be

University of Ghent, Department of Analytical Chemistry[b],
Proeftuinstraat 86, B-9000 Ghent, Belgium

University of Ghent, Department of Medieval History[c],
Blandijnberg 2, B-9000 Ghent, Belgium

Received December 8, 1997

Keywords: Manuscripts / Scriptoria / TXRF / Micro-Ramanspectroscopy / Pigments / Middle Ages / Azurite / Gold initials / Workshops / Renaissance / Mercatellis / Codicology

Assigning related medieval manuscripts to different workshops on the basis of codicological characteristics, is not straightforward. We present the first attempt to distinguish between scriptoria by means of a large-scale total reflection X-ray fluorescence (TXRF) analysis of pigment elements and an identification of pigment molecules with micro-Raman spectroscopy. We analyzed 324 colored items in 10 medieval manuscripts, of which 7 are folio-sized illuminated manuscripts, all ordered by Raphael de Mercatellis in the late 15th and early 16th century. Palettes in miniatures were not yet examined. Blue palettes are exclusively azurite-based and are easily differentiated by means of the respective amounts of Ti, Ba, and As. Differences for green palettes are also pronounced. The green Cu-based pigment was not yet identified, but it certainly is not malachite or verdigris. Red pigments used are HgS, vermilion, and Pb_3O_4, red lead. The Flemish gold-leaf technique is used. The 7 Mercatellis manuscripts show two different palettes, both different from the non-Mercatellis manuscripts. The grouping of the Mercatellis manuscripts according to date and to palettes is, in general, consistent with a grouping on the basis of a classical codicological analysis, although some conflicting results are obtained. A quantitative and qualitative reconstruction of palettes by means of TXRF- and Raman-spectra, provides with a complimentary and objective tool for distinguishing between scriptoria.

Introduction

Confronting conclusions of (art-)historians about important artifacts from the past with those obtained by scientific experimental techniques, remains an intellectual challenge[1]. Well-known examples are the proton milliprobe analysis of Gutenberg's bible[2] and the debate that arose about the Shroud of Turin[3][4][5].

The late Middle Ages and the early Renaissance are crucial periods for the transfer of knowledge, since exactly then a large manuscript-production was confronted with the in-(ter)vention of printing. Many medieval manuscripts are illuminated and decorated. The quality of their miniatures not seldom compares well with that of paintings by illustrious contemporary artists[6]. But, whereas today almost everything is known about the contents of these manuscripts, in some intriguing cases little is known, until today, about the workshops (scriptoria) involved. Using a codicological approach, *distinguishing* between workshops producing *similar* manuscripts is very difficult, when no alternative historical sources are available, e.g. archives in abbeys or monasteries regarding their scriptoria or other identification means, sometimes left in the manuscript by scribes or illuminators[6].

Only recently, progress has been made in *identifying* pigment *elements* used in paintings and in medieval manuscripts[7][8] by TXRF (total reflection X-ray fluorescence) spectrometry, a technique conceived already in 1971[9][10]. The use of micro-Raman spectroscopy in manuscripts for identifying *molecules* started in 1984[11]. This technique was also recently applied by Clark et al.[12][13][14].

Sampling in manuscripts for these analyses is non-destructive and a large number of samples can be taken without damaging the manuscript. One sample provides enough material for both TXRF and Raman analyses. Despite all these possibilities, no large scale study has yet been reported on a *quantitative* reconstruction of palettes in a series of *related* medieval manuscripts. The 80 manuscripts, ordered by *Raphael de Mercatellis*[15], an illegitimate son of Philip the Good, Duke of Burgundy, represent such a series. A codicological analysis of the 60 remaining Mercatellis manuscripts, now held by libraries all over the world, has been carried out[16][17][18] and led to a classification of all

[+] Present address: Limburgs Universitair Centrum, Diepenbeek, Belgium.

 © WILEY-VCH Verlag GmbH, D-69451 Weinheim, 1998 1434–1948/98/0505–0639 $ 17.50+.50/0

Table 1. Manuscripts and samples

Ms	Short description (Date[a])	Codicological group[b]	Parts or hands[c]	TXRF-samples	Blue	Green	Gold	Red	UL[d]
M1	Georgius Reisch, Margarita Philosophica (1505 ?)	**3(3)**	2	56	19	7	8	22	Ms 7
M2	Richardus de Bury et al., several works (1492/4)	**3(2)**	3	27	9	1	3	14	Ms 67
M3	Plutarchus, De Viris Clarissimis (1492)	**2(1)**	≥1	25	6	5	4	10	Ms 109
M4	Decretum Gratiani (1505?)	**3(6)**	3	70	21	4	9	36	Ms 3
M5	Auctoritates Aristotelis (?)	**3(8)**	3	30	11	3	4	12	Ms 13
M6	Plato, Opera (?)	**3(8)**	3	37	10	4	5	18	Ms 1
M7	Petrus de Abano, Expositio problematum Aristotelis (1479)	**2(1)**	3	47	17	4	5	21	Ms 72
nM1	Hagiologicum Slavicum (?)	(Bulgaria)	1?	5	–	1	–	4	Ms 408
nM2	Thomas Aquinas (1280–1400 ?)	(Paris)	1?	19	9	–	–	10	Ms 117
nM3	Exercitiones (?)	(Cologne)	1?	8	–	–	–	8	Ms 211
		Total	≥18[e]	**324**	*102*	*29*	*38*	*155*	

[a] Probable date of production or acquisition from indications in the Ms. – [b] Classical codicological group(sub-group)[16]. – [c] If the number of hands >1, different hands or workshops *might* have been involved in the manufacturing of the manuscript[16]. – [d] Ghent University Library holding. – [e] M1–M7.

Mercatellis manuscripts in function of their codicological characteristics.

Given the technical and artistic skills required and the financial implications for producing manuscripts[6], the actual number of Mercatellis workshops must have been rather small, since these manuscripts were all made in the region Ghent-Bruges, where there was a tradition of manuscript-manufacturing in the late Middle Ages and early Renaissance. Scriptoria, working in this very typical and famous *Ghent-Bruges style*, however, did not make Mercatellis manuscripts[17]. Who exactly produced these 80 Mercatellis manuscripts remains an open and still intriguing question, although several suggestions have been made[16][17][18].

Therefore, we decided to use two analytical techniques to reconstruct both qualitatively (with Raman) and quantitatively (with TXRF) some Mercatellis palettes. The initials, the paragraph marks, the rubrication, and especially the very typical colored decorations *in margine* provide with an excellent basis for pigment analysis and palette reconstruction. This study is a first step in a larger project, aiming at an inventory of palettes of scriptoria, to be used for the identification of other historically important manuscripts of unknown or uncertain origin.

Manuscripts

Table 1 gives a short description (with date), the codicological group, determined by a number of visible characteristics, and the number of parts of the 7 Mercatellis manuscripts (M1–M7) studied. Three non-Mercatellis manuscripts (nM1–nM3) were also analyzed.

Results and Discussion

Elements Detected by TXRF: Table 1 also shows the distribution of the 324 samples, taken by rubbing a dry and clean cotton-wool swab (Q-tip) over the not-varnished colored surfaces (initial, paragraph-mark, rubrication, ...). With a Mo-tube, 12 elements were detected: Ca, Fe, Zn, Cu, Hg, Au, Pb, Ti, As, Mn, Ni, and Sr. With a W-tube Ba, Ag, Sn, and Sb could be retraced. Since nanogram samples can not be weighted, concentrations must be estimated by normalizing the sum of the elements detected to 100. This is by no means exact, since elements with atom number < 11 can not be detected.

Element Classification and Pigment Identification by Micro-Raman Spectra: Ca, Fe, and Zn are considered as *non-pigment elements*. Their presence in the majority of samples is due to the preparation of the parchment and to the presence of (traces of) ink. Although ink is not considered here as a pigment, samples taken from the inks predominantly contain Ca, Fe, and Zn and the latter two elements are highly correlated. Raman spectra of white grains show that Ca is mainly present as $CaSO_4$ (gypsum) and $CaCO_3$ (chalk).

The only *pigment key-element for blue and green* is Cu. The blue pigment used is azurite, easily identified by Raman. The green pigment, usually believed to be malachite or verdigris, must be another still unidentified but certainly Cu-based pigment (malachite and verdigris were not yet detected by Raman).

Two *pigment key-elements were found for red*: Hg in the pigment vermilion (HgS) and Pb in the pigment red lead (Pb_3O_4), both identified by Raman.

Two *precious elements* were detected Ag and Au (mainly in 38 gold initials).

Finally, 8 (to 11) *minor elements* were found: Ti, Ba, As, Sn, Ni, Mn, Sr, and Sb (to be combined with Cu, Hg, and Pb when *not* present as a main pigment element). The white pigment $BaSO_4$ was identified by Raman. All Raman spectra will be presented elsewhere[19].

Blue, Green, and Red Palettes: Figure 1 shows the experimental TXRF-results (percentages of elements found) for each of the 9 blue samples in nM2, without the main pigment element Cu and the non-pigment elements Ca, Fe, and Zn. For 7 samples, the overall constitution is very similar and amounts to an average of about 6% of the sample total. In the samples on pages 1 and 2, Ba is *not* detected.

This is not surprising, since Ba in this manuscript is the key-element in the whitener $BaSO_4$.

Figure 1. All 9 blue samples for nM2, without Cu and non-pigment elements (8% level)

The consistent reproduction of nearly the same percentages for each of the minor elements in the samples must result from the fact that a large number of basic manuscript elements (parchment, parchment preparation, pigment, pigment composition, granular structure, adhesion, resistance to rubbing, ...) remains invariant throughout the complete manuscript.

These observations lead to the conclusion that this 800-page *pecia* manuscript, made in Paris in the 14th century, was made in a single workshop, whereby the same technique and material (azurite) was used for blue initials and paragraph-marks. A specific whitener, $BaSO_4$, was used in the larger part of the manuscript (except in the first pages).

Conversely, these results demonstrate the consistency of the sampling and of the TXRF-analysis.

In Figure 2 on the other hand, the *average* composition for blue and green samples is given for all manuscripts.

Two very different *blue palettes* appear: one for the group M1-M4-M5 and another one for M2-M3-M6-M7, although the same pigment azurite is used in both cases. But, although within each group the palettes are very similar, the *averaged totals* of the element percentages differ significantly, in contrast with the results in Figure 1. For blue, the palette of nM2 resembles that found for M1, but the "absolute" amounts of material vary from 2.5% for M1 to over 5% for nM2 (a difference of a factor of 2).

In the hypothesis that the same, yet unidentified, Cu-based green pigment is used in all Mercatellis manuscripts M1−7, the *green palettes* confirm the group M1-M4-M5 but the pair M6-M7 emerges. Green for M2-M3 is intermediate. For green, the nM1 palette compares with those found for M2 and M3.

This grouping is further confirmed by the *red palettes* (not shown)[19]: two red pigments are identified by Raman (HgS, vermilion and Pb_3O_4, red lead).

The 7 Mercatellis manuscripts can therefore be divided in 2 distinct palette-groups:

Palette-group I: **M1**, *1505?*; **M4**, *1505?*, and **M5**, *date?.*

Palette-group II: (**M2**, *1492/94*))*?*; **M3**, *1492*; **M6**, *date?*, and **M7**, *1479*.

The detailed confrontation of this result with a codicological analysis is given below. A first conclusion is that the yet undated manuscript M5 can be situated around *1505* and the other one M6 in the period 1479−94 (with a preference for *1479*).

Group II is the oldest, as it goes back to pigments used from 1479 onwards, and remained active at least for some 15 years, using the same style and the same coloring technique.

Ba/Ti-Ratio in Blue Samples: Another detail on palettes revealed by TXRF spectrometry is shown in Figure 3, where %Ba is plotted against %Ti for 34 *blue* samples, in which Ba is detected. The average Ba/Ti ratio equals 2.8, with a correlation R^2 better than 0.86. The observed fluctuations in this ratio (not shown) remain between ± 40%, a result to be expected in the case of element ratio's on account of the accuracy of TXRF analyses. The origin of this ratio is not yet clear.

Figure 2. Average palettes for blue and green (without Cu and Ca) for all manuscripts

Figure 3. %Ba versus %Ti for 34 blue data points

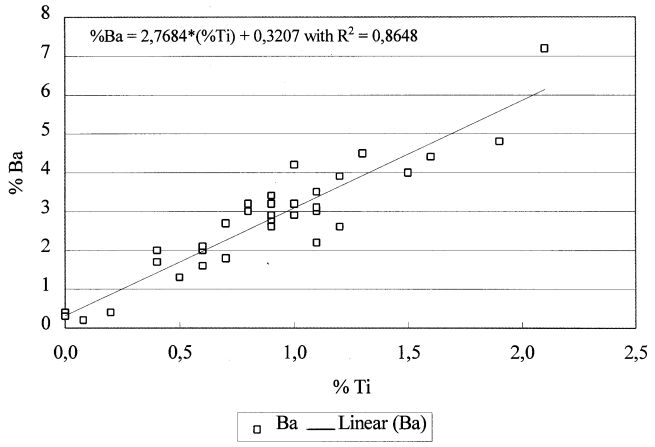

Raman spectra show that Ba is present as $BaSO_4$, a whitener (see also Figure 1). The molecule containing Ti remains a problem. Normally it would be $FeTiO_3$, but an Fe-Ti correlation was not (yet) found. TiO_2, a modern whitener, must be excluded, since it is generally accepted that this pigment was not known in the Middle Ages (although the mineral rutile, found in the Alps, is known as a gem from Antiquity). Raman did not reveal any traces of TiO_2. No correlation was found for Ti or Ba with any of the 14 other elements. Their presence as a pair is mainly restricted to blue samples in *group I* manuscripts *and in nM2*.

Almost no As is found in the blue samples of *Group I* manuscripts, where large amounts of Ti and Ba are found. The opposite situation applies for *Group II* (see Figure 2).

Gold: The two classical types of illuminations are present in Mercatellis manuscripts: *shell* (or liquid) *gold* is used mainly in *decorations in margine*, whereas *gold leaf* is reserved for *initials*. Shell gold was detected in 25 leaves and ranks out of 60 rubbed, although just rubbing of a colored surface was intended.

Gold initials continue to be real eye-catchers of medieval manuscripts, as intended 500 years ago. Gold is not always used for the initial itself but also for its *background*. Gold-leaf techniques can vary locally[6]: in Flanders and Germany, the parchment is first covered with a *brownish gesso* where an illumination is wanted, on which the gold leaf is fixed when the gesso was dry. In many Mercatellis manuscripts, this brownish gesso shows through the parchment at the back of the initial.

In most of the 38 gold initials, silver is detected and the Ag/Au ratio varies from 0.01 to 0.15. In one M2-initial 37% Ag was found, exactly as much as Au. Another initial (first page in M2) contains 4,4% Sn, which *could* indicate that mosaic or synthetic gold (SnS_2) was used, but this is highly improbable*. In *group II*, three initials are found with Pb/Au ratios between 6 and 1, whereas usually only a few percent Pb is found. In all three, gold leaf is used in the background. Here, lead is probably originating from white decorations in the initial (internal contamination, see also below).

In Figure 4, a logarithmic scale is used to plot the Cu/Au ratios for 37 gold initials (for one initial Cu/Au = 0). The majority of initials shows a low Cu "palette" (Ag, Cu, Hg, Pb, and Ni contribute 10 to 15% to the sample-total). However, for 10 initials in the two *palette-groups* (i.e. the 10 data points in Figure 4 with black background), the slope of the line connecting the data points almost vanishes and a plateau emerges at an average Cu/Au ratio of about 1:75. This *might* indicate that, irrespective of the palette-group, orders for gold (or gold leaves) were invariantly placed with the same merchant or that the same kind of coin was used for making gold leaves[6]. However, further work remains to be done on this point.

The first 12 gold initials in Figure 4 have a relatively high Cu/Au ratio (>0.1). High Cu/Au- and Pb/Au-ratios for gold initials must be explained by internal and/or external contamination. Sampling small decorated gold initials can easily lead to contamination by pigment elements in the initial's decorations (internal contamination). But, samples were also taken from large initials, where internal contamination can be avoided. Even then, as much as 30% Ca can be found, indicating that "external" contamination is substantial. This contamination is due to the intense contact between *facing pages* in a manuscript, kept closed almost constantly for about 500 years by means of straps. This kind of contamination is even clearly visible in M1: the white lower margin on f. 263r almost shows a "color-copy" of a decoration *in margine* on folio 262v.

TXRF and Raman Results versus Classical Codicological Results

Only the identification of pigments used in manuscripts by means of Raman spectroscopy allows one to reconstruct palettes on the basis of TXRF results. In this work, Raman spectra provided with conclusive evidence concerning the presence of some important (pigment-)molecules, such as $BaSO_4$, HgS, Pb_3O_4, $CaSO_4$, $CaCO_3$, $2CuCO_3 \cdot Cu(OH)_2$. Attempts to identify Ti molecules and lapis lazuli were not yet successful (miniatures were not yet analyzed in this work). Given the importance attached to blue pigments in the making of medieval manuscripts[1][6](see also below), it is a pity that *lapis lazuli* can not be detected by TXRF. So far, we did not yet find Raman evidence for lapis lazuli in any of the 93 blue samples but the Raman analysis shows that the blue pigment used in all manuscripts, studied here, is azurite. This observation allows us to confront the results of the palette reconstruction for blue illustrations, obtained in this work, with the results of codicological analyses on the same Mercatellis manuscripts. This confrontation is done on two levels: the complete manuscript and the sub-manuscripts (see Table 1).

The Complete Manuscripts

A classical codicological analysis is based upon a comparison of the visible characteristics of 60 Mercatellis

* Sn is found in only 7 of 324 samples (1 gold initial and *6 blue ranks*), and is highly correlated with Pb (%Pb = 5.456 × %Sn − 5.88 with R^2 = 0.9647). Here Pb, with Sn, is probably used as white lead (to be confirmed by Raman spectra).

Figure 4. Ratios Cu/Au for gold initials, descending order

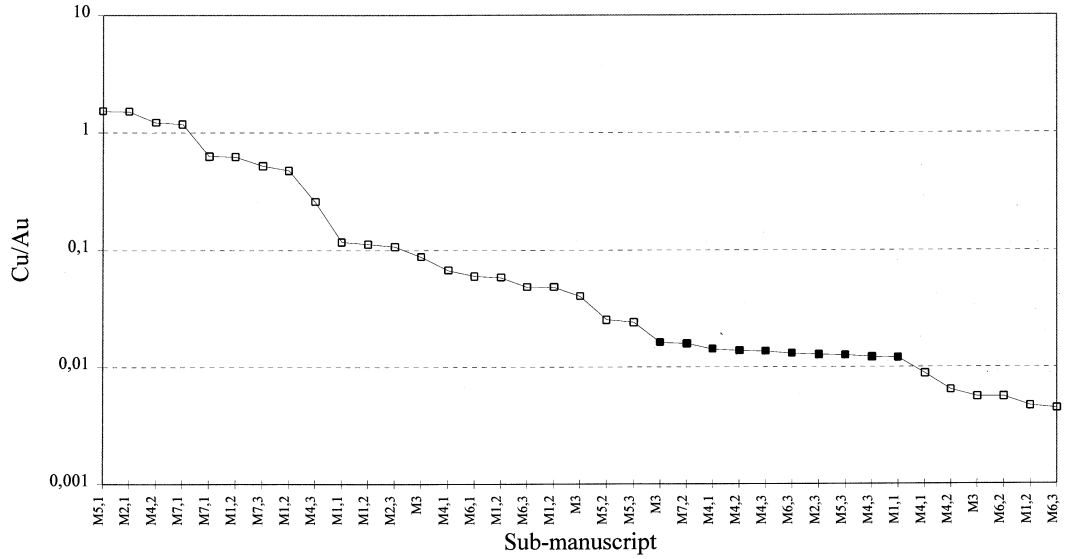

manuscripts still in existence[16][17][18]. Applying TXRF and Raman makes some invisible characteristics also visible.

The different codicological groups for the 7 Mercatellis manuscripts are given in Table 1. The result of the confrontation of the codicological with the analytical studies is given in Table 2.

Table 2. Confrontation of a codicological classification (CC) with palette-groups for 7 Mercatellis manuscripts

CC[a]/*Palette-group*[b]	**2(1)**	**3(2)**	**3(3)**	**3(6)**	**3(8)**
Palette-group I			M1	M4	M5
Palette-group II	M3, M7	M2			***M6***

[a] Taken from Table 1. – [b] This work.

For 6 out of 7 Mercatellis manuscripts, an acceptable result is obtained. However, the palette reconstruction suggests that the dividing line for the codicological classification should not be drawn between the major codicological groups **2** and **3** but between the codicological subgroups **3(2)** and **3(3)**, if the palette classification for M2 is valid (see above). In addition, M6 and M7 have similar palettes, whereas the codicological analysis reveals differences. This result for M6 is intriguing, so we further quantified and refined the palette reconstruction for blue decorations, which have always been important in manuscripts and since azurite is the only blue pigment found.

Correlation Between Sub-Manuscripts on the Basis of Blue Palettes

In Table 1, the 4th column gives the number of *parts* distinguished codicologically in the 7 Mercatellis manuscripts, giving a total of 18 sub-manuscripts (see bottom line in Table 1). Correspondingly, sub-manuscripts are distinguished as follows: the 2 different parts in M1 will be designated as $M_{1,1}$ and $M_{1,2}$ and so on for all 7 Mercatellis manuscripts.

Table 3 gives a correlation matrix for these 18 Mercatellis sub-manuscripts, calculated on the basis of the average percentages found for 10 *minor* elements in blue samples: Hg, Au, Ti, Ba, Ag, As, Sn, Ni, S and Sb. The correlation matrix consists of the Pearson product-moment correlation coefficients for the variables. A positive correlation between 0.6 and 1, rounded off, is given in bold; the identity in the diagonal is given by *1*.

The first 8 sub-manuscripts of *palette-group I* are similar (except in part for $M_{5,3}$) and the 10 sub-manuscripts of *palette-group II* form an even more homogenous set (in each case a *positive* correlation is found). There is no or a slightly negative correlation between sub-manuscripts of the two different *groups I and II* (except in part for $M_{6,3}$).

Parts $M_{5,3}$ and $M_{6,3}$ are slightly different from the other parts in M5 and M6. But, Table 3 also shows that most parts distinguished codicologically are not only consistent with the complete manuscript but also with the Mercatellis palette-groups *I and II*, the manuscript belongs to. Removing one (sub-)manuscript from one palette-group to the other, as suggested codicologically (see Table 2), would distort the symmetry of Table 3.

The blue palette of nM2 is correlated with *group I* and less with *group II* (see also Figure 1 and Figure 2). This is remarkable, since the *pecia* nM2 originates from Paris. The fact that a similar technique was used by geographically separated scriptoria in the 14th century for a completely different kind of manuscript, is an extra argument for distinguishing between two local Mercatellis workshops, which used different blues.

The refined analysis in Table 3 confirms that both M2 and M6 are members of *palette-group II*, which is in support of their position in Table 2. An extra codicological argument for the position of M6 is that the size and the ruling of this manuscript are the same as for Mercatellis manuscripts in group **2(3)**[16].

Table 3. Correlation matrix for blue data-points by palette-group and by sub-manuscripts on the basis of 10 minor elements

Sub-ms	$M_{1,1}$	$M_{1,2}$	$M_{4,1}$	$M_{4,2}$	$M_{4,3}$	$M_{5,1}$	$M_{5,2}$	$M_{5,3}$	$M_{2,1}$	$M_{2,2}$	$M_{2,3}$	M_3	$M_{6,1}$	$M_{6,2}$	$M_{6,3}$	$M_{7,1}$	$M_{7,2}$	$M_{7,3}$	nM_2
Palette Group I																			
$M_{1,1}$	*1*																		
$M_{1,2}$	**0.9**	*1*																	
$M_{4,1}$	**0.9**	**0.9**	*1*																
$M_{4,2}$	0.4	**0.7**	**0.6**	*1*															
$M_{4,3}$	0.5	**0.8**	**0.8**	**1**	*1*														
$M_{5,1}$	**1**	**0.9**	**0.8**	0.5	**0.6**	*1*													
$M_{5,2}$	**0.6**	**0.8**	**0.7**	**0.9**	**0.9**	**0.7**	*1*												
$M_{5,3}$	0.0	0.4	0.4	**0.8**	**0.8**	0.0	**0.6**	*1*											
Palette Group II																			
$M_{2,1}$	0.1	0.2	0.0	−0.1	−0.1	0.1	0.0	0.1	*1*										
$M_{2,2}$	−0.1	0.2	0.0	0.1	0.1	−0.1	0.1	0.5	**0.9**	*1*									
$M_{2,3}$	−0.2	0.1	−0.1	0.0	−0.1	−0.2	−0.1	0.4	**0.9**	**1**	*1*								
M_3	0.0	0.1	0.2	−0.2	0.0	−0.1	−0.2	0.3	**0.6**	**0.6**	**0.6**	*1*							
$M_{6,1}$	−0.1	0.0	−0.1	−0.2	−0.2	−0.2	−0.2	0.2	**1**	**0.9**	**1**	**0.7**	*1*						
$M_{6,2}$	−0.1	0.0	−0.1	−0.2	−0.2	−0.2	−0.2	0.2	**1**	**0.9**	**1**	**0.7**	**1**	*1*					
$M_{6,3}$	0.4	**0.6**	**0.6**	0.4	0.5	0.4	0.4	**0.6**	**0.7**	**0.7**	**0.7**	**0.7**	**0.6**	**0.6**	*1*				
$M_{7,1}$	−0.1	0.0	−0.1	−0.2	−0.2	−0.2	−0.2	0.2	**0.9**	**0.9**	**1**	**0.7**	**1**	**1**	**0.7**	*1*			
$M_{7,2}$	−0.2	0.0	−0.2	−0.2	−0.2	−0.2	−0.2	0.2	**0.9**	**0.9**	**1**	**0.7**	**1**	**1**	**0.6**	**1**	*1*		
$M_{7,3}$	−0.2	−0.1	−0.2	−0.2	−0.2	−0.2	−0.2	0.2	**0.9**	**0.9**	**1**	**0.7**	**1**	**1**	**0.6**	**1**	**1**	*1*	
non-Mercatellis group																			
nM_2	**0.9**	**0.8**	**0.7**	0.3	0.3	**0.9**	0.5	0.0	**0.6**	0.4	0.3	0.2	0.3	0.4	**0.7**	0.4	0.3	0.3	*1*

Conclusion

The 7 Mercatellis manuscripts analyzed were certainly made in Flanders using two different coloring techniques but also in two different periods, suggesting that also two different workshops were involved in their production. A large scale TXRF- and Raman-analysis can indeed lead to a quantitative reconstruction of palettes in medieval manuscripts and, even for related manuscripts, palette-differences can be detected. These differences must be attributed either to different hands or techniques, simultaneously available in the *same scriptorium*, to an evolution in manufacturing techniques in the *same scriptorium* or to *different scriptoria*.

The authors are greatly in debt to Prof. Dr. *R. Klockenkämper* and Dr. *A. von Bohlen* of the Institute for Spectroscopy and Applied Spectroscopy (ISAS), Dortmund. We also thank Dr. *W. De Vos*, Dr. *A. Arnould*, o.p., and Prof. Dr. *K. G. Van Acker* for their critical advise. A generous grant of the *Fund for Scientific Research-Flanders* (FWO-Vlaanderen) in support of this work is gratefully acknowledged.

Experimental Section

A description of the instrumentation used for TXRF and Raman is given elsewhere[7][8][19].

[1] M. V. Orna, *J. Chem. Educ*. **1997**, *74*, 373−382; M. V. Orna, T. F. Mathews, *Anal. Chem*., **1988**, *60(1)*, 47A−56A.
[2] B. H. Kusko, T. A. Cahill, R. A. Eldred, R. N. Schwab, *Nucl. Instr. Meth. B*, **1984**, *231*, N1−3, 699−694.
[3] W. McCrone, *Accounts Chem. Res.*, **1990**, *23*, 77−83.
[4] P. Damon et al., *Nature* **1989**, *337*, 611−615.
[5] A. D. Adler, ACS Symposium Series 625, **1996**, 223−228; D. A. Kouznetsov, A. A. Ivanov, R. Veletsky, ACS Symposium Series 625, **1996**, 229−247.
[6] C. De Hamel, *Medieval craftsman: scribes and illuminators*, Toronto University Press, **1992**.
[7] L. Moens, W. De Vos, R. Klockenkämper, A. Von Bohlen, *J. Trace Microprob. Tech*. **1995**, *13(2)*, 119−139.
[8] W. De Vos, Ph. D. Thesis, University of Ghent, **1996**.
[9] Y. Yoneda, T. Horiuchi, *Rev. Sci. Instr*. **1971**, *42*, 1069−1070; H. Aiginger, P. Wobrauschek, *Nucl. Instr. Methods* **1974**, *114*, 157−158; H. Aiginger, *Spectrochim. Acta*, **1991**, *46B*, 1313−1321.
[10] G. Tölg, R. Klockenkämper, *Spectrochim. Acta* **1993**, *48B*, 111−127.
[11] M. Delhaye, B. Guineau, J. Vezin, Courrier CNRS, **1984** (December), 20−31; *J. Forensic Sci*. **1984**, *29(2)*, 471−485.
[12] R. Clark, L. Cridland, B. Kariuki, K. Harris, R. Withnall, *J. Chem. Soc. Dalton Trans.* **1995**, 2577−2582.
[13] R. J. H. Clark, P. J. Gibbs, *J. Raman Spectr*. **1997**, *28 (2−3)*, 99; *Chem. Comm*. **1997**, 1003−1004 (June 7).
[14] L. Burgio, D. A. Ciomartan, R. J. H. Clark, *J. Molec. Struct*. **1997**, *405(1)*, 1−11.
[15] K. G. Van Acker, *Arch. Bibl. Belg*. **1977,** *48*, 143−198.
[16] A. Derolez, *The Library of Raphael de Mercatellis*, Story-Scientia, Gent, **1979**.
[17] A. Derolez, *Miscellania Neerlandica* **1987**, 479−503.
[18] A. Arnould, *J. Warburg Courtauld Inst*. **1988**, *55*, 197−209; Ph.D. Thesis, University of Ghent, **1992**.
[19] B. Wehling, P. Vandenabeele, L. Moens, R. Klockenkämper, A. von Bohlen, G. Van Hooydonk, M. De Reu, *Mikrochim. Acta*, submitted for publication.

[97302]

Aziridines as Complex Ligands: Coordination and Ring Opening

Ingo-Peter Lorenz*, Stephan von Beckerath, and Heinrich Nöth

Institut für Anorganische Chemie der Ludwig-Maximilians-Universität München,
Meiserstraße 1, D-80333 München, Germany
Fax (internat.): +0049 (0)89/5902-258
E-mail: ipl@anorg.chemie.uni-muenchen.de

Received November 14, 1997

Keywords: Aziridines / Coordination / Ring opening / Metallacyle / N-Chirality

The photolytically induced CO substitution reactions of $CpMn(CO)_3$ with *N*-phenylaziridine and of $W(CO)_6$ with 2,2-dimethylaziridine lead to the *N*-coordinated aziridine complexes $Cp(CO)_2Mn\{N(Ph)CH_2CH_2\}$ and $(CO)_5W\{N(H)CH_2CMe_2\}$. Both are stable with respect to thermal alkene elimination. The thermal reaction of $Cp(CO)_3MoCl$ with *N*-hydroxyethylaziridine leads to the metallaheterocyclic compound $Cp(CO)_2MoNH(CH_2CH_2OH)CH_2CH_2C(O)$. It might be formed by several reaction steps including a Cl migration with nucleophilic ring opening, a CO insertion reaction forming the β-aminoacyl ligand and finally a hydrolytic process. The X-ray structure analysis of $Cp(CO)_2Mn\{N(Ph)CH_2CH_2\}$ and $(CO)_5W\{N(H)CH_2CMe_2\}$ shows three-membered-ring ligands *N*-bonded to the metal atoms with a trigonal pyramidal configuration at the nitrogen atoms. The X-ray structure analysis of $Cp(CO)_2MoNH(CH_2CH_2OH)CH_2CH_2C(O)$ reveals a five-membered heterocyclic ring system, including the molybdenum atom, a carbonyl function and an ammonium center.

Introduction

The photolytic reactions of $CpMn(CO)_3$ with thiirane, C_2H_4S, or thiirane *S*-oxide, C_2H_4SO, lead to CO substitution and elimination of ethene with formation of the intensively colored S and SO complexes, $\{CpMn(CO)_2\}_2S$ (green) and $\{CpMn(CO)_2\}_2SO$ (violet)[1][2]. Both dinuclear compounds show a central, symmetrically-bridging 3c4e-π-system. With their planar Mn_2SO_n skeleton (n = 0, 1), they demonstrate isolobal bis-metalorganic analogues of SO_2 and SO_3. The coordination of C_2H_4S- and C_2H_4SO ligands to transition metals via sulfur was first reported to exist in $(Ph_3P)_2Pt\{S(O)_nC_2H_4\}$ (n = 0, 1)[3] and $[CpRu(PPh_3)_2(S\text{-}C_2H_4)]O_3SCF_3$[4]. Ring-opening and oxidative-addition reactions of C_2H_4S and C_2H_4SO onto transition metal complexes have not yet been observed.

The isoelectronic aziridine-derivatives $N(R)CH_2CR'R''$ are expected to react in a similar fashion. Firstly, the coordination of aziridines onto transition metal centers via its nitrogen atom should also be possible. Subsequent ethene elimination might result in the formation of mono- and dinuclear nitrene complexes. This would be a new synthetic approach to nitrene complexes. A third type of reaction could be ring-opening leading to four-membered ring systems by an oxidative-addition process. However, five-membered ring systems could also form, especially with hydrido complexes of transition metals e. g., by a nucleophilic attack of the alkylidene part on the electrophilic carbon atom of a carbonyl ligand.

Beck et al. have described the reactivity of aziridines with metalcarbonyl and metalcarbonylhydrido complexes[5]. They observed two types of reactions of aziridines: simple coordination as *N*-coordinate ligands, as well as ring-opening to give metallacycles. Both types of complexes were characterized mainly by their IR spectra[5][6][7][8]. Two examples of the five-membered metallacycles have been characterized by X-ray structure analysis[9][10][11][12]. Angelici et al. reported the reaction of aziridine with platinum(II)-nitrile complexes to give aziridino-amidines, 2-imidazolines and to *trans*-$[PtCl_2\{N(H)=C(Ph)NC_2H_4\}_2]$ complexes[13]. Coordination of the aziridine to the Pt-atom was not observed. In a recent paper, Beck et al.[14] described the reaction of a *N*-functionalized L-aziridine-2-carboxylate (ac) with some chloro-bridged transition-metal complexes to give e.g. $(OC)_2Rh(ac)$, $(\eta^5\text{-}C_5Me_5)(Cl)Ir(ac)$, $(\eta^3\text{-}C_3H_5)$-$Pd(ac)$, $Me_2NCH_2C_6H_4Pd(ac)$, $(R_3P)(Cl)Pd(ac)$ (R = Et, Bu, Ph), $(Ph_3P)(Cl)Pt(ac)$ and $[(Ph_3P)_2Pt(ac)]BF_4$. All these complexes are formed by HCl-elimination and by ring formation. They are the first structurally characterized N-aziridine complexes which possess an additional carboxylato-*O* bond to the transition metal (bidentate-*N*,*O*). Recently, the monodentate and *N*-coordinate benzylaziridine complex $Cp(CO)_2Mn\{N(Bz)CH_2CH_2\}$ was sucessfully synthesized and characterized[15].

In this paper the photolytic reactions of $CpMn(CO)_3$ and $W(CO)_6$ with different N- and C-substituted aziridines are reported. These lead to new *N*-coordinate mono-aziridine complexes. In addition, the thermal reaction of $Cp(CO)_3MoCl$ with *N*-hydroxyethylaziridine, which results in the formation of an interesting five-membered transition-metallacycle, is described.

Results and Discussion

$CpMn(CO)_3$ and *N*-phenylaziridine $N(C_6H_5)C_2H_4$ (**1a**) are photolysed for 3.5 h in *n*-pentane at −35°C. The clear

 © WILEY-VCH Verlag GmbH, D-69451 Weinheim, 1998 1434−1948/98/0505−0645 $ 17.50+.50/0

yellow solution turns orange after warming to r. t. Crystallisation provided monoclinic orange colored crystals of **2** (Scheme 1). **2** is neither light- nor air-sensitive. The formation of **2** results from a simple substitution reaction of one CO ligand for the nucleophilic nitrogen atom of the aziridine ligand (2e donor). **2** is also obtained by photolysing first $CpMn(CO)_3$ in thf to give the labile complex $CpMn(CO)_2$thf, which then is allowed to react with the aziridine ligand within 4 h to give **2**. The yield of **2** is higher for the "direct" synthesis in *n*-pentane (76%) than for the "indirect" in thf (56%).

Scheme 1

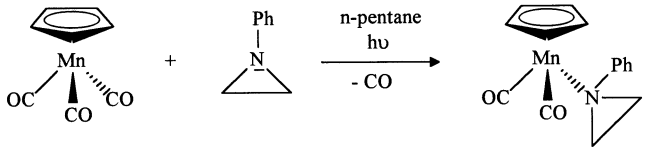

1a **2**

In accordance with the utilisation of *N*-substituted aziridines described later, the analagous reaction products of *C*-substituted N(H)-aziridines and further metal complexes are also of interest. By using such *C*-substituted aziridines the question as to whether the alkene elimination takes place by activation, therefore obtaining nitrene complexes by a new method, can be answered. In the case where alkene elimination is not observed, the N−H bond cleavage should be attempted by the nucleophilic attack of strong bases to obtain a new nucleophilic center at the N of the aziridine ligand. This would then be attempted to react with other electrophilic compounds. With 16e-fragments like $[CpMn(CO)_2]$, or 17e-fragments like $CpFe(CO)_2$ anionic or neutral μ_2-N bridged dimetallo complexes should be built up.

Thus, $W(CO)_6$ is first photolysed in thf for 2 h at r. t., followed by addition of one equivalent of 2,2-dimethylaziridine $N(H)CH_2CMe_2$ (**1b**). After evaporating the solution to dryness and removal of some $W(CO)_6$ by sublimation, the residue is dissolved in thf. Careful layering of n-pentane at −22°C yields yellow crystals of **3** (Scheme 2.). These are neither air, nor light sensitive and they are soluble in acetone, CH_2Cl_2 and thf. No $H_2C{=}CMe_2$ elimination was observed on heating.

Scheme 2

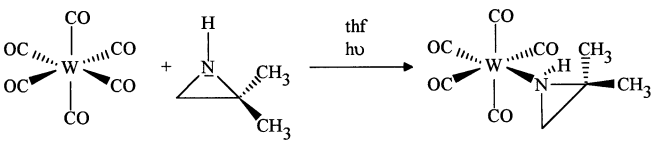

1b **3**

In contrast to both 16e complex fragments, where neutral addition products were obtained with aziridines, aziridines were reacted with 17e complex fragments in the hope of obtaining cationic addition products. Therefore, $CpMo(CO)_3Cl$ was reacted with *N*-hydroxyethylaziridine, $N(CH_2CH_2OH)C_2H_4$ (**1c**), in acetone at 60°C. After cooling to r. t., a dark red solution was obtained from which yellow-orange crystals of **4** separated on evaporation.

However, instead of the expected cationic complex $[Cp(CO)_2MoN(CH_2CH_2OH)CH_2CH_2)]Cl$, the new neutral metallacycle $Cp(CO)_2MoNH(CH_2CH_2OH)CH_2CH_2C(O)$ (**4**) was surprisingly obtained. Its formation requires several steps and the presence of traces of water. Firstly, a migration of the Cl onto the N atom giving the corresponding metallate and aziridinium ion. They undergo a nucleophilic ring opening process to give the β-aminoethyl ligand which as nucleophile attacks the electrophilic C atom of one of the CO ligands to give the β-aminoacyl ligand. The reaction is finished by the coordination of the amine to the metal to form the five-membered metallacycle. We believe that the replacement of the Cl substituent for H takes place during the long crystallization process. The presence of water could be derived from the hydroxyethyl substituent by condensation. Beck et al. have described a similar complex[5][10][11][14], the hydrido complex $CpMo(CO)_3H$ was used as a starting material. Therefore there was no hydrolytic process necessary.

The composition and structure of **2**, **3** and **4** were confirmed by elemental analyses, MS, ^{1}H-, $^{13}C\{^1H\}$-NMR and IR spectra, as well as by X-ray structure analyses.

The IR spectrum of **2** shows two ν(CO) vibrations at 1917.7 and 1839.1 cm^{-1} (in CH_2Cl_2), or 1915.8 and 1844.8 cm^{-1} (in KBr), respectively. The IR spectrum in KBr also shows the ν(CH) at 3106.4 and 3011.2 cm^{-1}, as well as the $\nu(C-N_{tert.})$ vibration at 1358.6 cm^{-1}. The IR spectrum of **3** exhibits three bands at 1974.7, 1924.8 and 1888.6 cm^{-1} for terminal CO groups ($2A_1 + E$, C_{4V} local symmetry). In the IR spectrum of **4**, ν(CO) bands at 2020.7 and 1936.3 cm^{-1} are observed for the two terminal ligands. A third ν(CO)-band at 1844.9 cm^{-1} is due to the carbonyl group within the ring.

In the EI-MS spectrum of **2**, the $[M^+]$ signal appears at 295.0 u, together with signals at 239.0 u and 120.0 u for $[M^+ - 2\ CO]$ and $[M^+ - 2\ CO - N(Ph)CH_2CH_2]$. In the EI-MS spectrum of **3**, the parent ion $[M^+]$ appears at 395.0 u, together with peaks at 367.0 for $[M^+ - CO]$, 339.0 for $[M^+ - 2\ CO]$, 309.0 for $[M^+ - 3\ CO - 2\ H]$, 281.0 for $[M^+ - 4\ CO]$, 253.0 for $[M^+ - 5\ CO]$ and 71.0 for $[HNCH_2CMe_2]$. **4** does not give the $[M^+]$ signal, the mass spectrum shows only fragments.

In the ^{1}H-NMR spectrum of **2**, the phenyl protons are found as singlets at 7.27 (*ortho*), 7.20 (*meta*) and 7.06 (*para*) ppm. In comparison with the free *N*-phenylaziridine ligand, these are deshielded by 0.11 to 0.40 ppm. The Cp protons give rise to a singlet at δ 4.25, which in comparison with $CpMn(CO)_3$ lies 0.51 ppm upfield. The aziridine ring protons are observed at 2.38 ppm as a broad singlet in **2**, whereas in **1a** two triplets are found at δ 3.58 and 3.38. The ^{1}H-NMR spectrum of **3** is characterized by 2 triplets at 2.50 and 2.35 ppm for the CH_2 ring protons, a triplett at δ 4.35 for the NH proton (ABX system), and two singlets at δ 1.40 and 1.35 for the methyl groups. In the ^{1}H-NMR spectrum of **4**, the Cp protons are observed at δ 5.32 as a singlet, shifted 0.56 ppm upfield from the $CpMo(CO)_3Cl$ starting

Scheme 3

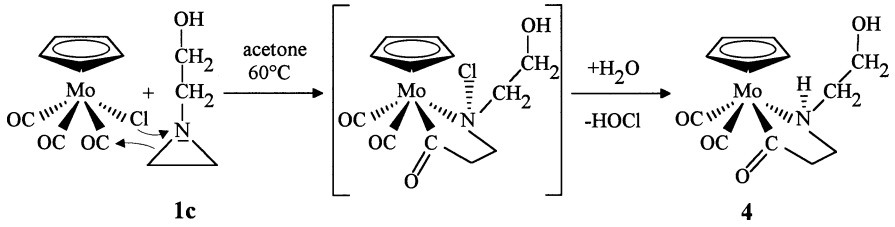

material. At 5.29 ppm, the OH proton of **4** is better shielded by 0.19 ppm relative to the free *N*-hydroxyethyl aziridine ligand. The signals for the *N*-2-hydroxyethyl and for the ethene group within the ring in **4** appear as 4 triplets at 3.80 (CH_2O), 3.63 (CH_2CO), 2.99 (CH_2N) and at δ 2.82 (CH_2N).

In the $^{13}C\{^1H\}$-NMR spectrum of **2**, the signals for the CO groups and the Cp ligand lie at δ 288.36 and 83.70, respectively. The different carbon atoms of the phenyl ring are detected between δ 129.28 and 122.70 (4 signals). Coordination of **1a** to the manganese atom in **2** leads to two signals which are very close together and shifted upfield for

Table 1. Crystal data and data collection of **2**, **3**, and **4**

	2	**3**	**4**
Empirical formula	$C_{15}H_{14}MnNO_2$	$C_9H_9NO_5W$	$C_{12}H_{15}MoNO_4$
Formula weight [g/mol]	295.21	395.02	333.19
Crystal size [mm^3]	0.40 x 0.40 x 0.12	0.25 x 0.10 x 0.05	0.35 x 0.30 x 0.26
Crystal color and habit	orange plate	yellow needle	orange-red plates
Crystal system	monoclinic	monoclinic	monoclinic
Space group	$P2_1/c$	$P2_1/n$	$P2_1/n$
Unit cell dimensions [Å],	a = 10.828(3)	a = 6.584(3)	a = 16.912(3)
	b = 9.326(3)	b = 10.608(4)	b = 8.707(2)
	c = 13.864(3)	c = 17.276(6)	c = 18.668(4)
[°]	β = 106.34(2)	β = 94.669(1)	β = 107.99(3)
Volume [Å^3]	1343.5(6)	1202.6(8)	2614.5(9)
Z	4	4	8
Density (calc.) [g/cm^3]	1.460	2.182	1.693
Absorption coefficient [mm^{-1}]	0.978	9.609	1.009
F(000)	608	736	1344
Scan type	ω-Scan	Hemisphere	ω-Scan
Temperature [K]	213(2)	183(2)	293(2)
2Θ range for data collection [°]	5.34−46.00	4.52−57.64	3.90−57.90
Index ranges	$-1 \le h \le 11$	$-8 \le h \le 8$	$-21 \le h \le 22$
	$0 \le k \le 10$	$-13 \le k \le 13$	$-10 \le k \le 11$
	$-15 \le l \le 14$	$-16 \le l \le 23$	$-20 \le l \le 23$
Reflections collected	2129	6600	12645
Independent reflections	1847 (R_{int} = 0.1357)	2104 (R_{int} = 0.0474)	5342 [R_{int} = 0.0492]
Observed reflections	1438 [$F > 4\sigma(F)$]	1827 [$F>4\sigma(F)$]	4235 [$F > 4\sigma(F)$]
Absorption correction	not necessary	semi empirical	semi empirical
Max. and min. transmission	0.465 and 0.694	0.159 and 0.394	0.6422 and 0.8542
Experimental details:			
Scan-speed in ω	variable; 3 to 60°/min		variable; 3 to 60°/min
Scan range (ω)	1.6°		1.2°
Solution and refinement			
Structure solution program	XS (Siemens)	XS (SHELXTL-Ver.5)	XS (Siemens)
Weighting scheme	$w^{-1} = \sigma^2Fo^2+(0.0862P)^2$ $+2.0719P$ where $P = (Fo^2+2Fc^2)/3$	$w^{-1} = \sigma^2Fo^2+(0.0330P)^2$ $+11.5843P$ where $P = (Fo^2+2Fc^2)/3$	$w^{-1} = \sigma^2Fo^2+(0.0690P)^2$ $+6.4669P$ where $P = (Fo^2+2Fc^2)/3$
Data/restraints/parameter	1841 / 0 / 214	1951 / 0 / 151	5337 / 0 / 325
Final R indices [$F>4\sigma(F)$]	R_1 = 0.0612, wR_2 = 0.1572	R_1 = 0.0396, wR_2 = 0.0929	R_1 = 0.0475, wR_2 = 0.1326
R indices (all data)	R_1 = 0.0831, wR_2 = 0.2026	R_1 = 0.0433, wR_2 = 0.0967	R_1 = 0.0678, wR_2 = 0.1522
Goodness-of-Fit on F^2	1.151	1.249	1.158
Largest and mean Δ/σ	0.002 0.000	0.001 0.000	−0.001 0.000
Largest difference peak / hole [eA^{-3}]	0.78 /−0.964	1.422 /−1.744	0.613 / −1.557

the two ring carbon atoms. They lie at 41.92 and 41.85 ppm, compared with δ 45.43 and 43.18 for free **1a**. In the $^{13}C\{^1H\}$-NMR spectrum of **3**, a signal at δ 191.21 for the tertiary carbon atom, at 68.05 ppm for the CH_2N ring group and only a singlet at 25.67 ppm for the two CH_3 substituents is observed. In the $^{13}C\{^1H\}$-NMR spectrum of **4**, signals are observed at 213.43 and 205.86 ppm (CO ligand and carbonyl function), 94.45 (Cp), 64.05 (s, C(12)H_2O) and at 52.09 ppm (s, C(11)H_2N). The C atoms of the five-membered ring are found at 50.66 ppm (s, C(10)H_2N) and 44.14 ppm (s, C(9)H_2CO).

Single crystals suitable for X-ray diffraction analysis of **2**, **3** and **4** were obtained. The crystal structure analysis data are summarized in Table 1 and the molecular structures and the most important bond lengths and angles are given in Figures 1, 2 and 3.

Figure 1. Molecular structure of **2**[a] in the crystal. Thermal ellipsoids are represented at a 25% probability scale

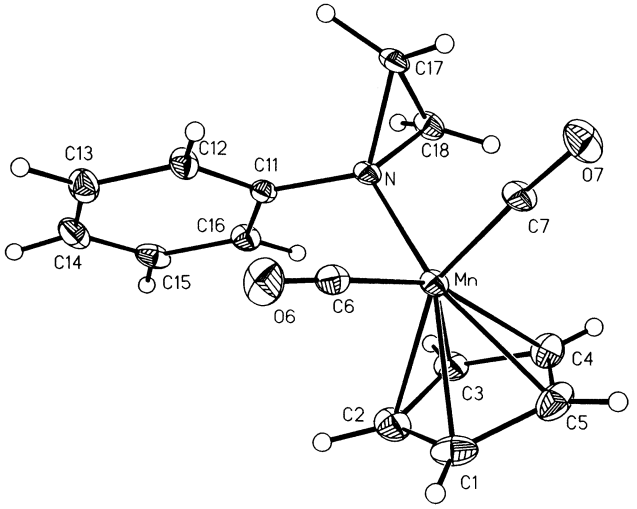

[a] Selected bond lenghts [Å] and bond angles [°]: Mn−N 2.096(5), Cp−$Mn_{average}$ 2.141(7), N−C11 1.446(7), N−C17 1.506(7), N−C18 1.491(8), C17−C18 1.480(9), C11−N−Mn 115.2(3), C17−N−Mn 121.7(4), C18−N−Mn 119.5(4), C7−Mn−C6 88.1(3), Mn−C6−O6 175.3(6), Mn−C7−O7 174.0(6), C18−N−C17 59.2(4), C17−C18−N 60.9(4), C18−C17−N 59.9(4), C11−N−C18 116.3(5), C11−N−C17 113.6(5).

The configuration at the Mn- and the N-atom of **2** is distorted tetrahedral. The Mn−N bond length of 2.096(5) Å indicates a single bond; the two bonds N−C17 (1.506(7) Å) and N−C18 (1.491(8) Å) are practically of equal length, while N−C11 (1.446(7) Å) is somewhat shorter. The bond length C17−C18 with 1.480(9) Å is a little bit shorter in comparison with typical C−C-single bonds and as found in aziridines[9]. While the C18−N−C17 angle within the ring is 59.2(4)°, the two angles C11−N−C17 and C11−N−C18 outside the ring lie between 116.3(5)° and 113.6(5)°. The angles C17−N−Mn (121.7(4)°) and C18−N−Mn (119.5(4)°), containing a manganese atom, are close to 120°. The angle C11−N−Mn (115.2(3)°), C11 being the *ipso*-carbon of the phenyl ligand, is also very large. The plane of the aziridine ligand nearly approaches orthogonality to the plane of the cyclopentadienyl ligand (71.3°).

Figure 2. Molecular structure of **3**[a] in the crystal. Thermal ellipsoids are represented at a 25% probability scale

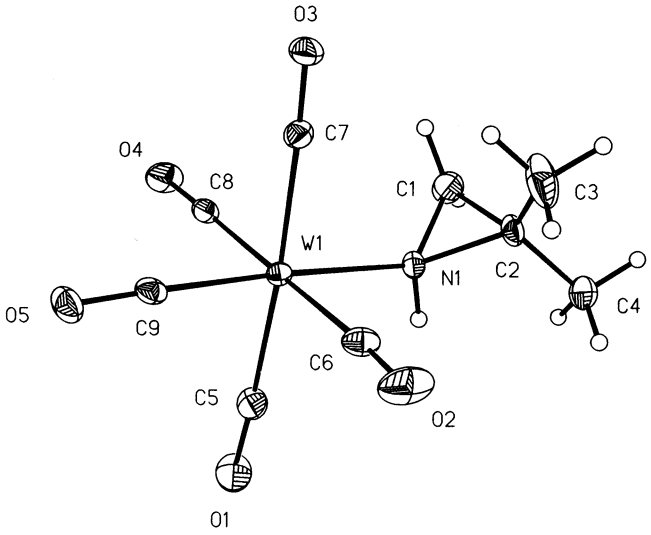

[a] Selected bond lenghts [Å] and bond angles [°]: W1−N1 2.307(8), N1−C1 1.488(14), N1−C2 1.500(13), C1−C2 1.48(2), C2−C3 1.49(2), C2−C4 1.504(14), C9−W1−C6 89.3(4), C6−W1−C8 177.9(3), C6−W1−C7 90.4(4), C7−W1−C5 176.2(4), C2−C1−N1 60.7(7), C1−C2−N1 59.9(7), C1−N1−C2 59.4(7), C1−N1−W1 128.8(6), C2−N1−W1 132.9(6), C8−W1−N1 91.0(4), C5−W1−N1 88.6(4), C3−C2−N1 116.8(9), C1−C2−C3 120.6(11), C3−C2−C4 115.0(10), N1−C2−C4 114.5(8).

The coordination sphere around the tungsten atom in **3** can be described as a distorted octahedron with maximum deviations of 4.8° for C7−W1−N1 and 3.5° for C9−W1−N1 from 90° and 180°, respectively. The W1−N1 bond length of 2.307(8) Å lies in the expected region for a single bond. The distance C1−C2 of 1.48(2) Å is again slightly shorter than that found for C−C single bonds and comparable to C17−C18 of **2**[9]. However, both bonds C2−C3 and C2−C4 are found to be somewhat longer (1.49(2) Å and 1.504(14) Å). The bond lengths N1−C1 and N1−C2 are to be considered to be of equal length (1.49(1) Å and 1.50(1) Å). Because of the C2 substituents both angles C1−N1−W1 and C2−N1−W1 are different (128.8(6)° and 132.9(6)°). The ring-angle C1−N1−C2 is again the smallest (59.4(7)°).

In **4**, the molybdenum atom possesses a distorted tetragonal pyramidal configuration with the Cp ligand in apical position. It is also part of the five-membered heterocyclic ring system, which is formed by the β-aminoacyl ligand[6][8][10][11]. Whereas the Mo1−N10 bond of 2.267(4) Å is very long, that of Mo1−C8 is remarkably shorter at 2.180(5) Å. The bonds N10−C10 and N10−C11 are almost equal (1.473(6) Å and 1.484(6) Å) and their length is typical for N−C single bonds. Of both C−C bonds within the ring, that of C8−C9 (1.536(7) Å) is significantly larger than that of C9−C10 (1.497(7) Å). While the atom distance O9−C8 of the carbonyl group is 1.233(6) Å, the bond length O12−C12, where O12 belongs to an OH group, corresponds with a single bond (1.432(6) Å). Within the five-membered ring with envelope conformation, the angle C8−Mo1−N10 of 73.4(2)° is the most acute and the angle

Figure 3. Molecular structure of **4**[a] in the crystal. Thermal ellipsoids are represented at a 25% probability scale

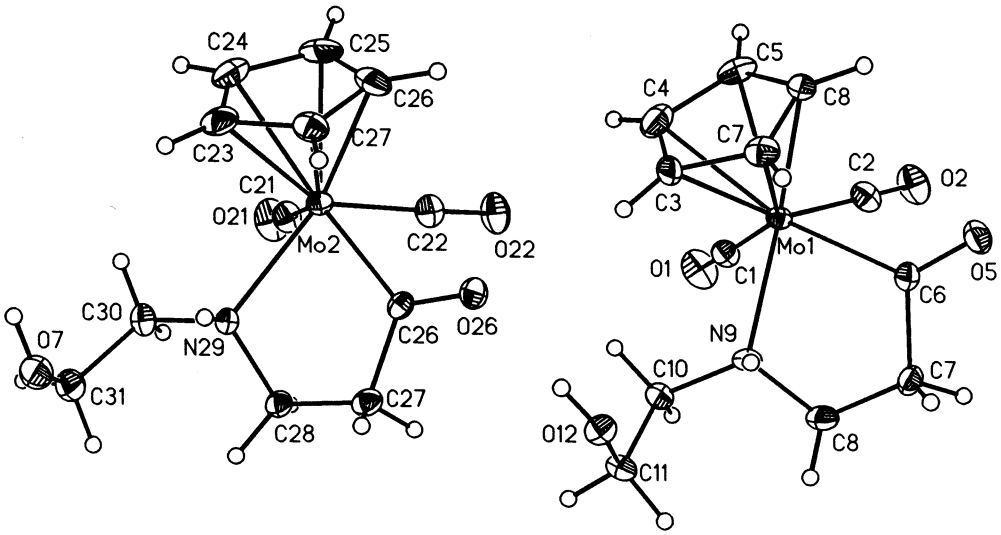

[a] Selected bond lenghts [Å] and bond angles[°]: Cp−$Mo1_{average}$ 2.348(5), Mo1−N10 2.267(4), Mo2−N31 2.280(4), Mo1−C8 2.180(5), Mo2−C28 2.162(4), Mo1−C6 1.929(6), O9−C8 1.233(6), O28−C28 1.239(5), C8−C9 1.536(7); C9−C10 1.497(7), N10−C10 1.473(6), N10−C11 1.484(6), C11−C12 1.523(6), C12−O12 1.432(6), C6−Mo1−C7 75.4(2), C7−Mo1−C8 121.3(2), C7−Mo1−N10 82.6(2), C8−Mo1−N10 73.4(2), Mo1−C6−O6 178.5(5), Mo1−C7−O7 175.5(4), N10−Mo1−C8 73.4(2), Mo1−C8−C9 127.5(4), C8−C9−C10 111.8(4), C9−C10−N10 108.7(4), C10−N10−Mo1 109.8(3).

C9−C8−Mo1 of 115.7(3)° the most open, because of the sp^2-hybridized C8 atom. The other three angles C8−C9−C10 (111.8(4)°), C9−C10−N10 (108.7(4)°) and C10−N10−Mo1 (109.8(3)°) are approximately equal. The ring shows envelope conformation, where N10 is placed −0.75 Å out of the plane Mo1−C8−C9−C10, with an interplanar angle to the Mo1−N10−C10 plane of 47.2° (respective data for N31 is −0.75 Å and for Mo2−C28−C29−C30 the interplanar angle to the Mo2−N31−C30 plane is 46.3°). The isolated crystals contain only one of the possible isomers with the relative configuration *RS*/*SR*.

Conclusion and Scopes

The results demonstrate that aziridine ligands coordinate much more effectively to transition metals than thiiranes. The latter prefer an ethene elimination and formation of sulfur complexes. The first aziridine complex has only recently been published[15]. **2** and **3** are two further examples. **3** is the first aziridine complex with a chiral N atom. We are continuing investigations in this field with more electrophilic, metalorganic-complex fragments to induce ethene elimination as a new synthetic approach to nitrene complexes. Moreover, aziridines can react, after coordination, with carbonyl ligands via ring-opening and by a redox reaction to produce the new metallaheterocycle **4**. We hope to elucidate the mechanism of its formation.

These complexes may find use in the therapeutic use of aziridines, which has been known since the fifties. Currently, there are detailed investigations on the cytostatic, cytotoxic and mutagenic activity of aziridine components[16][17][18][19][20][21][22]. In recent years organometallic transition complexes have gained a wide interest in cancer diagnostics[23]. It is planned to test such aziridine and aziridine-based complexes for such applications.

Experimental Section

To remove oxygen, all operations were carried out under an argon atmosphere in dry and argon-saturated solvents[24] . $CpMn(CO)_3$[25], $W(CO)_6$[25], $CpMo(CO)_3Cl$[25], *N*-phenylaziridine[26] and 2,2-dimethylaziridine[27] were prepared in accordance with literature procedures. *N*-hydroxyethylaziridine was used as purchased from Aldrich. The photolytic reactions were carried out by using a mercury-high-pressure lamp TQ 150 Hanau (as an inside dipping lamp) in a modified glass apparatus with an overflow tube, which allows a sufficient vertical mixing of the reaction solution. − IR: Perkin-Elmer 598 and Nicolet FT-IR. − NMR: Jeol EX-400 (^{1}H: 399.784 MHz and ^{13}C: 100.540 MHz) and Jeol GSX-270 (^{1}H: 240.0 MHz and ^{13}C: 61.0 MHz), both with [D_6]acetone and $CDCl_3$ as solvents and TMS as internal standard. − MS: Finnigan MAT 900 (20 kV), Varian MAT CH7 (70 eV).

N-Phenylaziridine-dicarbonyl-η^5-cyclopentadienyl-manganese(I) (**2**): 0.81 g (6.8 mmol) $CpMn(CO)_3$ and 2.73 g (13.4 mmol) of **1a** were photolysed at −35°C in 400 ml *n*-pentane for 3.5 h with strong stirring. The elimination of 1 mol of CO was controlled by IR spectroscopy. Thereafter, the clear orange solution was allowed to attain r. t. during 4 h and then the solvent was partially evaporated. After 24 h, orange crystals of **2** had formed; yield 1.54 g (76.6%); m.p. 149°C. − IR (CH_2Cl_2): $\tilde{\nu}$ [cm^{-1}] = 1917.7vs, 1839.1 vs (CO); IR (KBr): $\tilde{\nu}$ [cm^{-1}] = 3106.4 s, 3011.2 s (CH); 1915.8 vs, 1844.8 vs (CO); 1358.6 s (C-$N_{tert.}$). − ^{1}H-NMR ([D_6]acetone): δ = 7.27 (s, o-Ph, 2 H), 7.20 (s, m-Ph, 2 H), 7.06 (s, *p*-Ph, 1 H), 4.25 (s, Cp, 5 H), 2.38 (s, $(CH_2)_2$, 4 H). − ^{13}C{^{1}H}-NMR ([D_6]acetone): δ = 288.36 (s, CO), 129.28 (s, Ph, C_{ipso}), 129.25 (s, Ph, C_{ortho}), 123.06 (s, Ph, C_{meta}), 122.70 (s, Ph, C_{para}), 83.70 (s, Cp), 41.92 (s, CH_2), 41.85 (s, CH_2). − MS-EI (70 eV): 296.0 [M^+ + H], 295.0 [M^+], 239.0 [M^+ − 2 CO], 211.0 [M^+ − 2 CO − C_2H_4], 176.0 [M^+

− $N(Ph)C_2H_4$], 148.0 [M^+ − CO − $N(Ph)C_2H_4$], 120.0 [M^+ − 2 CO − $N(Ph)C_2H_4$]. − $C_{15}H_{14}MnNO_2$ (295.22): calcd. C 61.05, H 4.74, N 4.74; found. C 60.55, H 5.02, N 4.84.

2,2-Dimethylaziridine-pentacarbonyl-tungsten(0) (**3**): A solution of 1.0 g (2.8 mmol) of $W(CO)_6$ was photolysed while stirring in 400 ml thf at r. t. for 2 h. The elimination of 1 mole CO was observed by IR-spectroscopy. Then 0.20 g (2.8 mmol) of **1b** were added. The yellow solution turned orange within 1 h. After evaporating the solvent and sublimation of unreacted $W(CO)_6$ from the residue in vacuum at 60°C, the remaining material was dissolved in 50 ml of thf and covered with a layer of *n*-pentane (10 ml). After 48 h at −22°C yellow crystals of **3** had formed; yield 0.53 g (47%); m.p. 98°C. − IR (CH_2Cl_2): $\tilde{\nu}$ [cm^{-1}] = 1974.7 m, 1924.8 vs, 1888.6 m (CO). − ^{1}H-NMR ($CDCl_3$): δ = 1.85 (m, CH_2, 2 H), 1.40 (s, CH_3, 3 H), 1.35 (s, CH_3, 3 H). − $^{13}C\{^1H\}$-NMR ($CDCl_3$): δ = 191.21 (CMe_2), 68.05 (CH_2N), 25.67 (CH_3). − EI-MS (70 eV); *m/z* (%): 395.0 [M^+], 367.0 [M^+ − CO], 339.0 [M^+ − 2 CO], 309.0 [M^+ − 3 CO − 2 H], 281.0 [M^+ − 4 CO], 253.0 [M^+ − 5 CO], 71.0 [$HNCH_2CMe_2$]. − $C_9H_9NO_5W$ (395.02): calcd. C 27.36, H 2.30, N 3.54; found. C 27.00, H 2.03, N 2.68.

1,1-Dicarbonyl(η^5-cyclopentadienyl)-2-hydroxyethylmolybda(1)-aza(2)-cyclopentan(5)-one (**4**): To the red solution of 0.38 g (1.4 mmol) of $CpMo(CO)_3Cl$ in 125 ml acetone, were added two mol-equivalents of **1c** (0.22 ml, 2.7 mmol) while stirring. The solution was then heated to 60°C for 1 h, during which the color of the solution became darker. After cooling to r. t. and partially evaporating the solvent in a vacuum, yellow-orange crystals of **4** formed; yield 0.23 g (60%); m.p. 113°C. − IR (CH_2Cl_2): $\tilde{\nu}$ [cm^{-1}] = 2020.7 m, 1936.3 vs $(CO)_{terminal}$, 1844.9 s $(CO)_{carbonyl}$. − ^{1}H-NMR ([D_6]acetone): δ = 5.32 (s, Cp, 5 H), 5.29 (s, OH, 1 H), 3.80 (t, CH_2O, 2 H), 3.63 (t, C(11)H_2, 2 H), 2.99 (t, C(10)H_2, 2 H), 2.82 (t, C(9)H_2, 2 H). − $^{13}C\{^1H\}$-NMR ([D_6]acetone): δ = 213.43 $(CO)_{terminal}$, 205.86 $(CO)_{carbonyl}$, 94.45 (Cp), 64.05 (CH_2OH), 52.09 (C(11)H_2), 50.66 (C(10)H_2), 44.14 (C(9)H_2). − $C_{12}H_{15}MoNO_4$ (333.20): calcd. C 43.26, H 4.54, N 4.20; found. C 43.12, H 4.67, N 4.77.

X-Ray Structure Determinations of **2**, 3 and **4**[28]: The crystal structure, experimental specifications and refinement data are given in Table 1. Selected single crystals were mounted on in a glass fiber or a capillary with perfluoroether oil, and aligned on a Siemens P4 diffractometer in a N_2 cold stream equipped with a scintillation counter (**2**) or a CCD area detector (**3**, **4**). Data collection for the determination of the unit cell as well as for the structure determination was performed at −80°C (**2**), using MoK_α radiation (λ = 0.71073 Å) and a graphite monochromator. Data reduction was performed with programs XSCANX Ver. 2.2 or SAINT Ver. 4 (Siemens Analytical Instruments), and structure solution with direct (**2**, **4**) or heavy atom methods (**3**). The SHELXL and SHELX93 programs were used for structure refinement (on F^2) and documentation. Non hydrogen atoms are presented in anisotropic description. Hydrogen atoms were placed in calculated positions and refined with fixed isotropic U using the riding model (**3**) or freely unfined (**2**, **4**). In case of compound **3** the atom H1 was found in the difference Fourier synthesis and was freely refined isotropically.

[1] I.-P. Lorenz, J. Messelhäuser, W. Hiller, K. Haug, *Angew. Chem.* **1985**, *97*, 234−235; *Angew. Chem. Int. Ed. Engl.* **1985**, *24*, 228−229. − I.-P. Lorenz, J. Messelhäuser, W. Hiller, M. Conrad, *J. Organomet. Chem.* **1986**, *316*, 121−138. − I.-P. Lorenz, S. Drobnik, G. Beuter, A. Lubik, *Chem. Ber.* **1992**, *125*, 2363−2366. − S. Drobnik, Dissertation, Eberhardt-Karls-Universität Tübingen, **1995**.

[2] M. Höfler, A. Baitz, *Chem. Ber.* **1976**, *109*, 3147−3150. − M. Herberhold, D. Reiner, B. Zimmer-Gasser, U. Schubert, *Z. Naturforsch.* **1980**, *35b*, 1281−1285. − M. Herberhold, B. Schmidkonz, *J. Organomet. Chem.* **1988**, *358*, 301−320.

[3] I.-P. Lorenz, J. Kull, *Angew. Chem.* **1986**, *98*, 276−278, *Angew. Chem. Int. Ed. Engl.* **1986**, *25*, 261−262.

[4] J. Amaresekera, T. B. Rauchfuss, S. R. Wilson, *J. Am. Chem. Soc.* **1988**, *110*, 2332−2334.

[5] R. Höfer, A. Engelmann, W. Beck, *Chem. Ber.* **1973**, *106*, 2590−2600.

[6] W. Beck, W. Danzer, R. Höfer, *Angew. Chem.* **1973**, *85*, 87−88; *Angew. Chem. Int. Ed. Engl.* **1973**, *12*, 77−78.

[7] W. H. Knoth, *Inorg. Chem.* **1975**, *14*, 1566−1572.

[8] W. Danzer, R. Höfer, H. Menzel, B. Olgemöller, W. Beck, *Z. Naturforsch.* **1984**, *39b*, 167−179.

[9] G. A. Jones, L. J. Guggenberger, *Acta Crystallogr.* **1975**, *B 31*, 900−902.

[10] A. T. Liu, W. Beck, G. Huttner, H. Lorenz, *J. Organomet. Chem.* **1977**, *129*, 91−96.

[11] W. Beck, W. Danzer, A. T. Liu, G. Huttner, H. Lorenz, *Angew. Chem.* **1976**, *88*, 511−512; *Angew. Chem. Int. Ed. Engl.* **1976**, *15*, 495−496.

[12] J. Protas, Ph. Coutrot, A. El Gadi, *Acta Crystallogr.* **1989**, *C 45*, 1189−1192.

[13] R. Angelici, G. Bombieri, F. Benetollo, R. A. Michelin, M. Mozzon, R. Bertani, *Inorg. Chim. Acta* **1994**, *222*, 327−336.

[14] T. Hauck, K. Sünkel, W. Beck, *Inorg. Chim. Acta* **1995**, *235*, 391−396.

[15] S. von Beckerath, I.-P. Lorenz, R. Fawzi, M. Steimann, *Z. Naturforsch.* **1996**, *51b*, 959−962.

[16] O. C. Dermer, G. E. Ham, *Ethylenimines and other Aziridines*, Academic Press, New York, **1969**.

[17] J. A. Hendry, R. F. Homer, F. L. Rose, A. L. Walpole; *Brit. J. Pharm. Chemotherapy* **1951**, *6*, 357−410.

[18] S. G. Domagk, S. Peterson, W. Gauss, *Z. Krebsforschung* **1954**, *59*, 617−622.

[19] G. P. Wheeler, *Cancer Res.* **1962**, *22*, 651−688.

[20] W. J. Hayes, *Bull. World Health Organ.* **1964**, *31*, 721−736.

[21] B. S. Iyengar, S. M. Sami, S. E. Tarnow, W. A. Remers, W. T. Bradner, J. E. Schurig, *J. Med. Chem.* **1983**, *26*, 1453−1457.

[22] D. V. Lewis, *Xenobiotica* **1989**, *Vol. 19*, *Nr. 3*, 341−356.

[23] B. K. Keppler, *Metal Complexes in Cancer Chemotherapy*, VCH-Verlag, Weinheim-New York-Basel-Cambridge-Tokyo, **1993**.

[24] Organikum, VEB Deutscher Verlag der Wissenschaften, Berlin **1988**

[25] G. Brauer, *Handbuch der Präparativen Anorganischen Chemie*, 3. Auflage, 3. Bd., Ferdinand Enke Verlag Stuttgart, **1981**, 1866−1868, 1822−1823, 1947−1948

[26] R. Appel, R. Kleinstück, *Chem. Ber.* **1974**, *107*, 5−12

[27] T. L. Cairns, *J. Amer. Chem. Soc.* **1941**, *63*, 871−872.

[28] Crystallographic data (excluding structure factors) for the structures **2**, **3** and **4** reported in this paper have been deposited with the Cambridge Crystallographic Data Centre as supplementary publication no. CCDC 100778. Copies of the data can be obtained free of charge on application to CCDC, 12 Union Road, Cambridge CB2 1 EZ, UK (fax: int. code + 44(1223) 336−033, E-mail: deposit@ccdc.cam.ac.uk).

[97266]

Reactions and Coordination Properties of the First Secondary Carbaboranyldiphosphane: 1,2-Bis(phenylphosphanyl)-1,2-dicarba-*closo*-dodecaborane(12)☆

Viktor P. Balema, Fernando Somoza, Jr., and Evamarie Hey-Hawkins*

Institut für Anorganische Chemie der Universität
Talstraße 35, D-04103 Leipzig, Germany
Fax: (internat.) + 49(0)341/960-4600
E-mail: hey@server1.rz.uni-leipzig.de

Received November 20, 1997

Keywords: Secondary carbaboranyldiphosphane / Transition-metal complexes / Crystal structure

When a mixture of stereoisomers of *rac*- and *meso*-1,2-bis(phenylphosphanyl)-1,2-dicarba-*closo*-dodecaborane(12) (**1a**, **b**; **1a/1b** = 3:1) is treated with $[Cp_2ZrMe_2]$ in boiling toluene for 2 h, the formation of three phosphorus-containing products, namely *meso*-$[Cp_2Zr(PPh)_3]$ (**3**), $(PPh)_4$ (**4**) and $(PPh)_5$ (**5**), ratio 2.8:1.1:1.0, was observed by ^{31}P-NMR spectroscopy. In the ^{11}B-NMR spectrum of the reaction mixture, only signals for 1,2-dicarba-*closo*-dodecaborane(12) were observed. When zirconocene, prepared in situ from $[Cp_2ZrCl_2]$ and BuLi, was treated with **1a**, **b** at low temperature and then heated to reflux in toluene for 2 h, only formation of **3** and 1,2-dicarba-*closo*-dodecaborane(12) was observed. The mixture of stereoisomers of **1a**, **b** reacts with CuCl in THF to give *rac*- and *meso*-[CuCl(THF){1,2-$(PHPh)_2C_2B_{10}H_{10}$}] (**7a**, **b**), which is only stable in THF solution and loses THF in vacuo over several hours to yield the insoluble colorless complex $[CuCl\{1,2\text{-}(PHPh)_2C_2B_{10}H_{10}\}]_n$ (**8**). In THF solution, **7** reacts with PPh_3 to give the stable isolable complex $[CuCl(PPh_3)\{1,2\text{-}(PHPh)_2C_2B_{10}H_{10}\}]$ (**9**). No reaction of **1a**, **b** is observed with $[Cp'Mo(CO)_3]_2$ ($Cp' = C_5H_4Me$) in boiling THF, while only decomposition occurs in boiling toluene. However, [(NBD)Mo(CO)$_4$] (NBD = norbornadiene) reacts smoothly with **1a** in toluene at room temperature to give *cis*-*rac*-$[Mo(CO)_4\{1,2\text{-}(PHPh)_2C_2B_{10}H_{10}\}]$ (**10**). Compounds **7**, **9**, and **10** were characterized spectroscopically (^{1}H, ^{31}P, ^{11}B, ^{13}C NMR, IR), and an X-ray structure determination was carried out on **10**.

Organo-element and organic derivatives of dicarba-*closo*-dodecaboranes(12) have received increasing attention during the last decade due to their interesting chemical and physical properties. Thus, these compounds have been employed as catalysts[1][2], as doping reagents in semiconductor materials[3], as precursors for ceramic materials[4], and in medical areas[5][6][7]. Hence applications in medicine can be envisioned for related carbaboranylphosphanes and their transition-metal complexes[8].

While tertiary phosphanyl derivatives of dicarba-*closo*-dodecaboranes(12), which were first reported in 1963[9], have been employed as ligands in transition-metal chemistry and as starting materials for the preparation of other *closo*-carbaborane(12)-containing organophosphorus compounds[10], their secondary analogues have remained largely unexplored[11]. We have recently reported the synthesis and spectroscopic properties of the first secondary bis(phosphanyl)carbaboranes, *rac*- and *meso*-1,2-bis(phenylphosphanyl)-1,2-dicarba-*closo*-dodecaborane(12) (**1a**, **1b**), as well as the molecular structure of the *rac* isomer **1a**[12].

We now report reactions and coordination properties of **1a**, **b** towards transition-metal complexes.

Results and Discussion

Reactions of 1,2-Bis(phenylphosphanyl)-1,2-dicarba-*closo*-dodecaborane(12) (1)

We have studied the reaction of a mixture of stereoisomers of *rac*- and *meso*-1,2-bis(phenylphosphanyl)-1,2-dicarba-*closo*-dodecaborane(12) [**1** (mixture of stereoisomers), **1a** (*rac*), **1b** (*meso*)][12] with various transition-metal complexes, i.e., $[Cp_2ZrMe_2]$ ($Cp = C_5H_5$), $[Cp_2ZrCl_2]$/BuLi, CuCl, $[Cp'Mo(CO)_3]_2$ ($Cp' = C_5H_4Me$) and [(NBD)Mo(CO)$_4$] (NBD = norbornadiene) (Scheme 1). As already observed in the reaction of **1** with sulfur[12], the chemical reactivity of **1** differs markedly from that of comparable carbaboranyldiphosphanes with tertiary phosphanyl groups or alkyl- or aryl-substituted secondary diphosphanes. In the case of dimethylzirconocene, the course of reaction is similar to that observed with the primary phosphane $PhPH_2$[13].

Reaction of 1a, b with Dimethylzirconocene or Zirconocene

When a mixture of stereoisomers of **1** (**1a/1b** = 3:1) was treated with dimethylzirconocene in boiling toluene for 2 h (Scheme 1), the formation of three phosphorus-containing products − *meso*-$[Cp_2Zr(PPh)_3]$ (**3**)[13][14], $(PPh)_4$ (**4**)[15], and $(PPh)_5$ (**5**)[16] (ratio 2.8:1.1:1.0) − was observed by ^{31}P-NMR spectroscopy. The ^{1}H-NMR spectrum of the reaction mixture showed the presence of unreacted dimethylzirconocene (ca. 75%). **3** was isolated in 23% yield (based on reacted dimethylzirconocene) and characterized by comparison of its NMR data with those reported in the literature[13][14]. In the ^{11}B-NMR spectrum of the reaction mixture, only signals for 1,2-dicarba-*closo*-dodecaborane(12) were observed. As **1** exhibits remarkable thermal stability (up to 195°C in undecane solution), the formation of the

 © WILEY-VCH Verlag GmbH, D-69451 Weinheim, 1998 1434−1948/98/0505−0651 $ 17.50+.50/0

Scheme 1

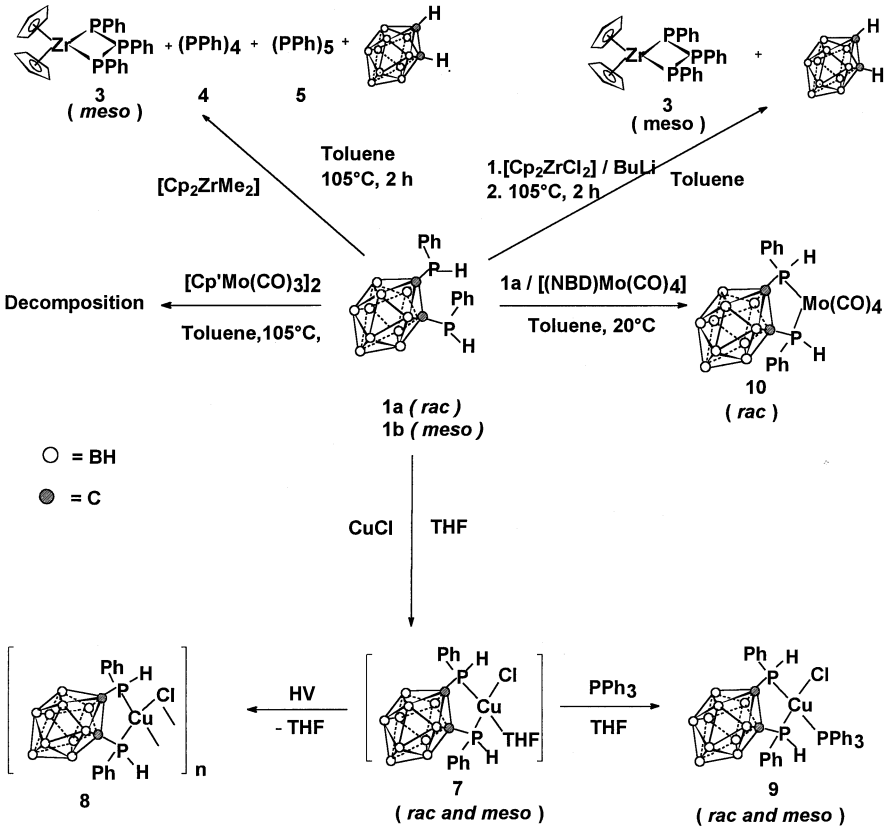

observed products **3**−**5** and 1,2-dicarba-*closo*-dodecaborane(12) must be due to reaction with dimethylzirconocene rather than decomposition of **1**.

When a mixture of stereoisomers of **1** (**1a/1b** = 3:1) is treated with "zirconocene", prepared in situ from $[Cp_2ZrCl_2]$ and BuLi by the Negishi method[17], followed by 2 h reflux in toluene, formation of **3** and 1,2-dicarba-*closo*-dodecaborane(12) is observed (Scheme 1); the cyclo-oligophosphanes **4** and **5** are not formed. The course of the reaction was monitored by ^{31}P-NMR spectroscopy. At room temperature, the spectrum of the burgundy red solution exhibits two major resonances at $\delta = -2.0$ ($^1J_{PH}$ = 233 Hz) and $\delta = -2.6$ ($^1J_{PH}$ = 230 Hz), which may be due to the *rac* and *meso* isomers of the intermediate $[Cp_2Zr\{1,2\text{-}(PHPh)_2C_2B_{10}H_{10}\}]$ (**6**). On heating the solution to reflux for 2 h, the signals corresponding to **6** are replaced by those of **3** and two low-intensity signals at $\delta = -24$ and $\delta = -31$ from an as yet unknown compound. Apparently, **6** decomposes with elimination of 1,2-dicarba-*closo*-dodecaborane(12) and formation of **3** as the final product.

The fact that **4** and **5** are not formed suggests the involvement of a different intermediate in the reaction between dimethylzirconocene and **1** in refluxing toluene. A phosphanylidenezirconocene complex, which is the most likely intermediate, was not observed.

Reaction of 1a, b with Copper(I) Chloride

A mixture of stereoisomers of **1** (**1a/1b** = 3:1) reacts with copper(I) chloride in THF over 1 h to give a yellow solution, which we believe contains the THF adduct *rac*- and *meso*-$[CuCl(THF)\{1,2\text{-}(PHPh)_2C_2B_{10}H_{10}\}]$ (**7**) (Scheme 1, Table 1), based on NMR studies. **7** is only stable in THF solution and as a solid loses THF in vacuo over several hours to yield the insoluble colorless complex $[CuCl\{1,2\text{-}(PHPh)_2C_2B_{10}H_{10}\}]_n$ (**8**). The latter is comparable to $[CuCl\{1,2\text{-}(PPh_2)_2C_2B_{10}H_{10}\}]$[18], which was obtained from $CuCl_2$ and 1,2-bis(diphenylphosphanyl)-1,2-dicarba-*closo*-dodecaborane(12). In THF solution, **7** reacts with PPh_3 to give the stable isolable complex $[CuCl(PPh_3)\{1,2\text{-}(PHPh)_2C_2B_{10}H_{10}\}]$ (**9**) in 92% yield (Scheme 1). **9** is soluble in THF and toluene. In the ^{31}P-NMR spectrum, only two broad signals are observed for coordinated PPh_3 and **1**, and this is due to the quadrupole moment of Cu. In the ^{1}H-NMR spectrum, signals for the P−H protons and the phenyl (PH*Ph* and P*Ph*$_3$) ligands are observed in the ratio 2:10:15. In contrast to complex **7** and the free ligand **1**, signals corresponding to *rac*- and *meso*-**9** were not observed. In the ^{13}C-NMR spectrum, the C atoms of the carbaborane cluster appear as a multiplet at $\delta = 81.3$. Signals corresponding to coordinated PPh_3 are observed in the us-

Table 1. NMR (^{31}P, ^{1}H, ^{13}C, ^{11}B) and IR data of compounds **1a**, **b**[12] (NMR in C_6D_6), **7** (NMR in [D_8]THF), **9** (NMR in C_6D_6) and **10** (NMR in C_6D_6)

	δ $^{31}P/J$ [Hz]	δ $^{1}H/J$ [Hz]	δ $^{13}C/J$ [Hz]	δ $^{11}B/^{1}J_{BH}$ [Hz]	$\tilde{\nu}$ [cm^{-1}] in KBr
1a	−15.15/246 ($^{1}J_{PH}$), 84 ($^{3}J_{PP}$)	7.30 m, 7.00 m (Ph), 4.78/244 ($^{1}J_{PH}$), 82 ($^{3}J_{PP}$) (PH), 3.5−1.6 br. m (B−H)	136.8 m, 131.0, 130.9, 129.0 (Ph), 76.3 m ($C_2B_{10}H_{10}$)	−0.9/142, −7.2/144, −9.4/225, −11.3	2626, 2606, 2583, 2561 (BH); 2323 (PH)
1b	−14.98/239 ($^{1}J_{PH}$), 87 ($^{3}J_{PP}$)	7.30 m, 7.00 m (Ph), 4.78/239 ($^{1}J_{PH}$), 87 ($^{3}J_{PP}$) (PH), 3.5−1.6 br. m (B−H)	136.8 m, 131.0, 130.9, 129.0 (Ph), 77.6 m ($C_2B_{10}H_{10}$)	−0.9/142, −7.2/144, −9.4/225, −11.3	2626, 2606, 2583, 2561 (BH); 2323(PH)
7	−14.5 v br.	7.76 m (**7a**), 7.53 m (**7b**), 7.41 m (Ph); 5.50/341 ($^{1}J_{PH}$), 172 ($^{3}J_{PP}$) (PH) (**7a**), 5.45/339 ($^{1}J_{PH}$), 179 ($^{3}J_{PP}$) (PH) (**7b**); 3.5−1.6 br. m (B−H)		−2.1, −5.4, −9.8	
9	1.08, −7.95/316 ($^{1}J_{PH}$)	8.23 br. m, 7.72 br. m, 7.05 m, 6.95 m (Ph), 5.12/320 ($^{1}J_{PH}$), 107 ($^{3}J_{PP}$) (PH), 3.5−1.6 br. m (B−H)	137.6 br. m, 134.75[a]/14.6 ($^{1}J_{CP}$), 133.0, 130.9[a], 130.1, 129.7[a], 129.6[a] (Ph), 81.3 m ($C_2B_{10}H_{10}$)	−1.6, −4.1, −9.1	2581 (BH); 2338 (PH)
10	67.70/358 ($^{1}J_{PH}$)	7.40 m, 6.97 m (Ph), 6.08/358 ($^{1}J_{PH}$), 19 ($^{2}J_{PP}$) (PH), 3.5−1.6 br. m (B−H)	212.3/9.9[b], 209.2/9.2[b] (CO), 134.7 m, 133.2, 130.1 m (Ph), 82.8 m ($C_2B_{10}H_{10}$)	−2.6/165, −3.9/151, −8.9, −11.4, −13.1	2593 (BH); 2034, 1955, 1936, 1905 (CO); 2342 (PH)

[a] PPh_3. − [b] Observed splitting in virtual triplet.

ual range for PPh_3−CuCl complexes[18][19] (Table 1). Molecular-mass determination with a vapor-pressure osmometer showed **9** to be monomeric in solution (calcd. 722, found 724). In conclusion, the data given are in agreement with a tetrahedral structure for **9**, in which the bis(phosphanyl)carbaborane is coordinated in a chelating fashion (Scheme 1). According to the NMR data (Table 1), the THF adduct **7** has a similar structure. Due to the low solubility of **8**, attempts to determine the molecular structure in solution were unsuccessful. A comparison with the CuCl complexes [CuCl{1,2-$(PPh_2)_2C_2B_{10}H_{10}$}][18] and [CuCl{1-$(PPh_2)C_2B_{10}H_{11}$}$_2$]$_n$[20] suggests an oligomeric structure.

Reaction of 1a, b with Carbonylmolybdenum Complexes

The reaction of **1a**, **b** with carbonylmolybdenum complexes depends on the nature of the Mo complex employed (Scheme 1). Thus, in contrast to primary and secondary alkyl- and arylphosphanes[21], no reaction is observed with [Cp′Mo(CO)$_3$]$_2$ (Cp′ = C_5H_4Me) in boiling THF. In boiling toluene reaction did occur, but a complex mixture of products was formed that could not be separated, isolated, or characterized.

However, [(NBD)Mo(CO)$_4$] reacts smoothly with **1a** in toluene at room temperature to give *cis-rac*-[Mo(CO)$_4${1,2-$(PHPh)_2C_2B_{10}H_{10}$}] (**10**; Scheme 1) in 73% yield. In the solid state, **10** is air- and moisture-stable. In solution, however, **10** slowly decomposes on exposure to air.

Molecular Structure of *cis-rac*-[Mo(CO)$_4${1,2-$(PHPh)_2C_2B_{10}H_{10}$}] (10)

Single crystals of **10** were obtained from toluene/hexane solution at −5°C. **10** crystallizes in the centrosymmetric space group $P2_1/c$. The X-ray structure determination (Figure 1) shows that both enantiomers of the racemic isomer are present in the unit cell. The bis(phosphanyl)carbaborane is coordinated in a chelating fashion. The structural parameters of **1a**[12] remain almost unchanged on coordination to the Mo atom [$C_{cluster}$−$C_{cluster}$ 1.683(2) (**1a**), 1.681(3) Å (**10**); P−$C_{cluster}$ 1.8727(13) (**1a**), 1.873(2), 1.872(2) Å (**10**); P−C_{Ph} 1.8244(14) (**1a**), 1.815(2), 1.813(2) Å (**10**)]. A comparison of **10** with *cis*-tetracarbonyl{1,4-η^2-[1,2-dimethyl-1,2-bis(phenylphosphanyl)disilane]}molybdenum(0) (*cis-rac*-**11**)[22], the only other structurally characterized complex of an $Mo(CO)_4$ fragment with a coordinated secondary diphosphane ligand (Figure 2), shows that the Mo−P bond lengths [2.4445(6), 2.4559(6) Å (**10**); 2.550(1) Å (**11**)] and P−Mo−P bond angle [84.31(2) (**10**); 89.4(1)° (**11**)] of **10** are smaller.

For the Mo−CO groups *trans* to the coordinated P atoms, the Mo−C distances are larger [2.015(3), 2.017(3)Å (**10**); 1.994(4) Å (**11**)] and the C−O bond lengths shorter [1.139(3), 1.140(3)Å (**10**); 1.152(5) Å (**11**)] in **10**. Similar trends, that is, lengthening of the Mo−P and C−O bonds and shortening of the Mo−C bonds, are observed for the complexes [$Mo(CO)_4(PMePhR)_2$] (R = Me, Ph)[23], [$Mo(CO)_4${1,2-$(PPh_2)_2C_2H_4$}][24] and [$Mo(CO)_4${1,2-$(PPh_2)_2C_2H_2$}][25] (Table 2), which are similar to **11**. This suggests increased π-acceptor properties of the P atoms in **1a**, in comparison with other phenyl-substituted phosphanes or diphosphanes[29], due to the presence of the electron-deficient carbaboranyl ligand in **1a**[30]. Accordingly, in the IR spectrum the CO vibrations of **10** are shifted to higher wavenumbers by 10−20 cm^{-1} compared with other tetracarbonyl(diphosphane)- or -bis(phosphane)molybdenum complexes[26][27][28] (Table 2).

Discussion of ^{31}P- and ^{1}H-NMR Data of 1, 7, 9, and 10

The mixture of stereoisomers of **1a**, **b** exhibits ^{31}P- and ^{1}H-NMR spectra in which the signals of the *HP*−CC−*PH* group appear as multiplets corresponding to an AA′XX′ spin system[12]. Simulation of the ^{1}H-NMR spectra allowed the corresponding coupling constants to be calculated [**1a**: $^{1}J_{PH}$ = 244 Hz, $^{3}J_{PP}$ = 84 Hz; **1b**: $^{1}J_{PH}$ = 239 Hz, $^{3}J_{PP}$ = 87 Hz][31]. Similar coupling patterns were observed in the ^{1}H-NMR spectra of **7**, **9** and **10**. The P-P coupling of the P−C−C−P fragment was observed only in the ^{1}H-NMR

Figure 1. Molecular structure of *cis-rac*-[Mo(CO)$_4${1,2-(PHPh)$_2$C$_2$B$_{10}$H$_{10}$}] (**10**); only one of the present enantiomers (*R*,*R*) with its atom-numbering scheme is shown (SHELXTL PLUS; XP)[37][a]

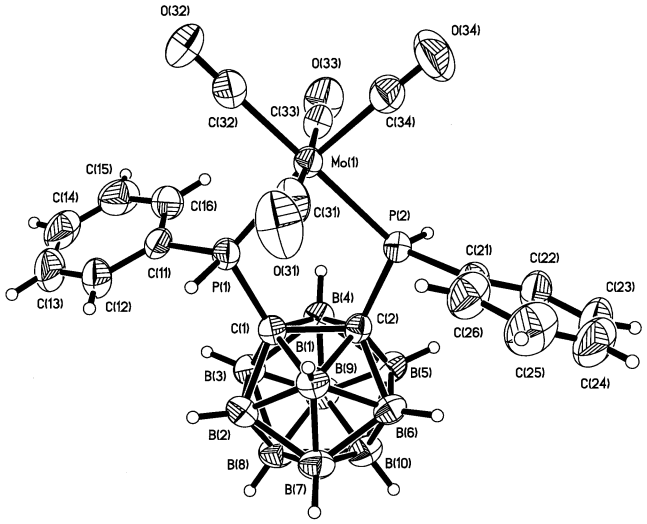

[a]Selected bond lengths [Å] and bond angles [°]: Mo(1)−P(1) 2.4559(6), Mo(1)−P(2) 2.4445(6), Mo(1)−C(31) 2.036(3), Mo(1)−C(32) 2.017(3), Mo(1)−C(33) 2.046(3), Mo(1)−C(34) 2.015(3), P(1)−C(11) 1.815(2), P(1)−C(1) 1.873(2), P(2)−C(21) 1.813(2), P(2)−C(2) 1.872(2), O(31)−C(31) 1.139(3), O(32)−C(32) 1.140(3), O(33)−C(33) 1.138(3), O(34)−C(34) 1.139(3), C(1)−C(2) 1.681(3); C(32)−Mo(1)−C(34) 92.85(11), C(31)−Mo(1)−C(34) 90.08(11), C(32)−Mo(1)−C(31) 88.67(12), C(33)−Mo(1)−C(34) 89.77(11), C(32)−Mo(1)−C(33) 87.80(11), C(31)−Mo(1)−C(33) 176.46(10), C(32)−Mo(1)−P(2) 175.00(9), C(34)−Mo(1)−P(1) 171.95(8), P(1)−Mo(1)−P(2) 84.31(2), Mo(1)−P(1)−C(1) 112.20(7), Mo(1)−P(2)−C(2) 112.56(7), C(11)−P(1)−C(1) 102.70(10), C(11)−P(1)−Mo(1) 127.10(8), C(1)−P(1)−Mo(1) 112.20(7), C(21)−P(2)−C(2) 102.06(10), C(21)−P(2)−Mo(1) 125.63(9), C(2)−P(2)−Mo(1) 112.56(7).

Figure 2. *cis*-Tetracarbonyl{1,4-η^2-[1,2-dimethyl-1,2-bis(phenylphosphanyl)disilane]}molybdenum(0)

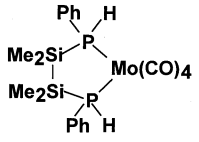

***rac*-11**

spectra of **7** and **9**. For **10**, the coupling constant of the P−Mo−P fragment ($^2J_{PP}$ = 19 Hz) was observed in the ^{1}H-NMR spectrum[27]. However, due to line broadening in the proton-coupled ^{31}P-NMR spectra, only P-H coupling was observed for **9** and **10**, and for **7** only one broad signal ($\nu_{1/2} \approx 600$ Hz) was present. As expected, for all complexes the coupling constant $^1J_{PH}$ increases on coordination (Table 1).

Conclusions

The reaction of the recently reported 1,2-bis(phenylphosphanyl)-1,2-dicarba-*closo*-dodecaborane(12) (**1a, b**)[12] with several transition-metal complexes is dependent on the metal and the complex employed (Scheme 1). With electron-poor zirconocene derivatives, reactions similar to those of primary phosphanes are observed[13]. In contrast, the electron-rich compounds CuCl and [(NBD)Mo(CO)$_4$] react with formation of the chelate complexes **7** and **10**, respectively. In vacuum **7** loses THF in the solid state and oligomerizes. With PPh_3, the stable monomeric complex **9** is obtained. In **10**, the carbaboranylbis(phosphane) ligand exhibits a higher π-acceptor ability compared to other diphosphanes in complexes of Mo(CO)$_4$, due to the presence of the electron-deficient carbaboranyl fragment.

We gratefully acknowledge support from the *Fonds der Chemischen Industrie. Chemetall GmbH* has provided a generous donation of alkyllithium compounds. F. S. thanks the *Alexander-von-Humboldt-Stiftung* for a fellowship.

Experimental Section

All experiments were carried out under purified dry argon. Solvents were dried and freshly distilled under argon. − The NMR spectra were recorded with an AVANCE DRX 400 spectrometer (Bruker); ^{1}H NMR: internal standard solvent (benzene), external standard TMS; ^{13}C NMR: external standard TMS, internal standard solvent; ^{31}P NMR: external standard 85% H_3PO_4; ^{11}B NMR: external standard $BF_3 \cdot Et_2O$. − The IR spectra were recorded with an FT-IR spectrometer Perkin-Elmer System 2000 in the range of 350−4000 cm^{-1}. − Molecular-mass determination: Vapour Pressure Osmometer (Knauer), in $CHCl_3$ at 35°C. − X-ray structural analysis: Siemens SMART CCD diffractometer. − The melting points were determined in sealed capillaries under argon and are uncorrected. − [Cp_2ZrMe_2][32], [Cp_2ZrCl_2][33], [Cp′Mo(CO)$_3$]$_2$[34]

Table 2. Comparison of selected bond lengths and CO vibrations of compound **10** with those of other Mo(CO)$_4$L$_2$ complexes with phenyl-substituted diphosphane and bis(phosphane) ligands

L$_2$	Mo−P [Å]	Mo−C *trans* to P [Å]	C−O *trans* to P [Å]	Ref.	ν(CO) [cm^{-1}]	Ref.
1,2-(PHPh)$_2$C$_2$B$_{10}$H$_{10}$	2.4445(6), 2.4559(6)	2.017(3), 2.015(3)	1.139(3), 1.140(3)	this work	2036, 1940, 1934, 1897 (hexane) 2034, 1955, 1936, 1905 (KBr)	this work
H(Ph)PSiMe$_2$SiMe$_2$P(Ph)H	2.550(1)	1.994(4)	1.152(5)	[22]		
Ph$_2$PCH$_2$CH$_2$PPh$_2$	2.500(2), 2.495(2)	1.999(8), 1.974(8)	1.140(8), 1.164(9)	[24]	2021, 1929, 1919, 1903 (C_6H_{12}) 2020, 1919, 1907, 1881 ($C_2H_4Cl_2$)	[26]
Ph$_2$PCH=CHPPh$_2$	2.501(1), 2.494(1)	1.993(5), 1.976(5)	1.152(6), 1.138(7)	[25]		
H(Ph)PCH$_2$CH$_2$P(Ph)H					2023, 1928, 1908, 1892 (CH_2Cl_2)[a] 2023, 1927, 1908, 1893 (CH_2Cl_2)[b]	[27]
(PPh$_3$)$_2$	2.576(2), 2.577(2)	1.972(8), 1.973(9)	1.158(8), 1.149(8)	[23]	2023, 1927, 1908, 1897 ($C_2H_4Cl_2$)	[28]
(PMePh$_2$)$_2$	2.545(1), 2.565(1)	1.981(6), 1.975(6)	1.153(7), 1.152(7)	[23]	2020, 1925, 1902, 1891 ($C_2H_4Cl_2$)	[28]
(PMe$_2$Ph)$_2$	2.525(2), 2.533(2)	1.981(6), 1.983(6)	1.150(7), 1.163(7)	[23]	2018, 1920, 1900, 1891 ($C_2H_4Cl_2$)	[28]

[a] *rac* isomer. − [b] *meso* isomer.

and [(NBD)Mo(CO)$_4$][35] were prepared by literature procedures. 1,2-Bis(phenylphosphanyl)-1,2-dicarba-*closo*-dodecaborane(12) (**1**) was prepared as described earlier[12]. CuCl and PPh_3 are commercially available.

Reaction of **1** *with Dimethylzirconocene:* A mixture of stereoisomers of **1** (1.2 g, 3.33 mmol, **1a/1b** = 3:1) and dimethylzirconocene (0.84 g, 3.35 mmol) were heated in toluene (20 ml) at 105°C for 2 h. After allowing the mixture to cool to room temperature, the solvent was distilled off. The resulting residue was characterized by ^{1}H-,^{11}B- and ^{31}P-NMR spectroscopy. *meso*-[$Cp_2Zr(PPh)_3$] (**3**) was isolated by washing the residue with hexane and ether, and then dissolving it in toluene. Filtration and cooling the solution to −30°C gave 0.4 g of **3** (23% based on [Cp_2ZrMe_2]). The spectroscopic data of **3** are in agreement with those reported previously[13][14].

Reaction of **1** *with Zirconocene Dichloride/BuLi:* At −80°C, BuLi in hexane (2 equiv.) was added slowly to a suspension of [Cp_2ZrCl_2] (0.29 g, 1.15 mmol) in toluene (10 ml) to generate "zirconocene" in situ. The mixture was stirred at −80°C for 1 h, then at −50°C for 15 min. The mixture was quickly brought to 20°C and a solution of **1** (0.35 g, 0.97 mmol, **1a/1b** = 3:1) in toluene (15 ml) was added. Samples for ^{11}B- and ^{31}P-NMR studies were taken after stirring the reaction mixture for 4 h at room temperature and for 2 h at 105°C.

Reaction of **1** *with CuCl. − [1,2-Bis(phenylphosphanyl)-1,2-dicarba-closo-dodecaborane(12)](tetrahydrofuran)copper(I) Chloride* (**7**) *and [1,2-Bis(phenylphosphanyl)-1,2-dicarba-closo-dodecaborane(12)]copper(I) Chloride* (**8**): A mixture of **1** (0.93 g, 2.58 mmol, **1a/1b** = 3:1) and CuCl (0.2 g, 2.22 mmol) in THF (25 ml) was stirred at room temperature for 1 h. The solvent was then removed from the clear yellow solution in vacuo to give a yellow solid (presumably the THF adduct **7**) which turned colorless after 2 h in vacuo, giving the final product **8**. The solid was washed with THF, toluene, and ether to give 0.78 g (76%) of **8**; dec. 267°C. − IR (KBr): $\tilde{\nu}$ = 3055 cm^{-1} (ν C−H), 2579 (ν B−H), 2350 (ν P−H). − $C_{14}H_{22}B_{10}ClCuP_2$ (459.39): calcd. C 36.60, H 4.83, Cl 7.72; found C 37.25, H 4.71, Cl 7.59. − **7** was characterized in [D_8]THF solution by ^{31}P-, ^{1}H- and ^{11}B-NMR spectroscopy (Table 1).

Reaction of **1** *with CuCl and PPh$_3$. − [1,2-Bis(phenylphosphanyl)-1,2-dicarba-closo-dodecaborane(12)](triphenylphosphane)copper(I) Chloride* (**9**): A mixture of **1** (0.7 g, 1.94 mmol, **1a/1b** = 3:1) and CuCl (0.19 g, 1.92 mmol) in THF (25 ml) was stirred at room temperature for 1 h. PPh_3 (0.5 g, 1.91 mmol) was added and the mixture stirred for 16 h. After filtration, the solvent was removed by distillation to give 1.28 g (92%) of **9** which can be recrystallized from THF/toluene; m.p. 218−219°C. − $C_{32}H_{37}B_{10}ClCuP_3$ (721.68): calcd. C 53.26, H 5.17, Cl 4.91; found C 53.55, H 5.17, Cl 5.59.

[1,2-Bis(phenylphosphanyl)-1,2-dicarba-closo-dodecaborane(12)]tetracarbonylmolybdenum(0) (**10**): A mixture of **1a** (0.7 g, 1.94 mmol) and [(NBD)Mo(CO)$_4$] (0.6 g, 1.93 mmol) in toluene (30 ml) was stirred at room temperature for 20 h. The solvent was removed in vacuo and the resulting solid was recrystallized from toluene/hexane (20 ml/10 ml). At −5°C crystals of **10** were obtained. Yield 0.8 g (73%); dec. 252−254°C. − $C_{18}H_{22}B_{10}MoO_4P_2$ (568.34): calcd. C 38.04, H 3.90; found 38.70, H 4.18.

Data Collection and Structural Refinement of **10**[36]: Data (Mo-K_α, λ = 0.71073 Å) were collected with a Siemens CCD (SMART). All observed reflections (2Θ range: 2−52°) were used for determination of the unit-cell parameters. The structures were solved by direct methods (SHELXTL PLUS[37]) and subsequent difference Fourier syntheses, and refined by full-matrix least squares on F^2 (SHELXTL PLUS[37]). Mo, O, P, B, and C atoms refined anisotropically, H atoms located and refined isotropically. Empirical absorption correction with SADABS[38]. − Crystal data: $C_{18}H_{22}B_{10}MoO_4P_2$, M = 568.34, white crystals, 0.4 × 0.3 × 0.2 mm, monoclinic, space group $P2_1/c$ (no. 14), T = 293(2) K, a = 22.012(1), b = 6.8393(4), c = 18.657(1) Å, β = 111.978(1)°, V = 2604.7(3) Å^3, Z = 4, $D_{calcd.}$ = 1.449 Mg m^{-3}, F(000) = 1136, μ(Mo-K_α) = 0.651 mm^{-1}, 11162 reflections collected with 1° < Θ < 26°; 4622 of these were independent; 404 parameters, *GOOF* = 1.100, residual electron density 0.321/−0.474 Å^{-3}, refinements converge to $R1$ = 0.0284, $wR2$ = 0.0734 [for reflections with $I > 2\sigma(I)$], $R1$ = 0.0335, $wR2$ = 0.0766 (all data).

☆ Dedicated to Professor Dr. *Hartmut Bärnighausen* on the occasion of his 65th birthday.

[1] F. A. Hart, D. W. Owen, *Inorg. Chim. Acta* **1985**, *103*, L1.
[2] B. Longato, S. Bresadola, *Inorg. Chem.* **1982**, *21*, 168.
[3] A. V. Bakun, Yu. P. Dokuchaev, I. I. Lapidis, Yu. V. Moskovskii, I. M. Skvortsov, B. G. Antokin, USSR Pat. 402241, **1986** (*Chem. Abstr.* **1986**, *105*, 16602).
[4] M. T. S. Hsu, T. S. Chen, S. R. Riccitiello, *J. Appl. Polym. Sci.* **1991**, *42*, 851.
[5] M. F. Hawthorne, *Angew. Chem.* **1993**, *105*, 997; *Angew. Chem. Int. Ed. Engl.* **1993**, *32*, 950.
[6] M. Gielen, A. Bouhdid, R. Willem, V. I. Bregadze, L. V. Ermanson, E. R. T. Tiekink, *J. Organomet. Chem.* **1995**, *501*, 277.
[7] N. N. Godovikov, V. P. Balema, E. G. Rys, Yu. G. Zhukovskiy, E. E. Sotchilina, S. N. Moralev, *Bioorganicheskja khimija (Bioorganic Chemistry Russ.)* **1993**, *19*, 1077.
[8] *Metal Complexes in Cancer Chemotherapy* (Ed.: B. K. Keppler), VCH Weinheim, New York, **1993**.
[9] R. P. Alexander, H. Schroeder, *Inorg. Chem*. **1963**, *2*, 1107.
[10] V. J. Bregadze, *Chem. Rev.* **1992**, *92*, 209.
[11] A. V. Kasantsev, M. N. Zhubekova, L. I. Zakharkin, *Zh. Obshch. Khim.* **1971**, *41*, 2027 (*Chem. Abstr.* **1972**, *76*, 59711).
[12] V. P. Balema, M. Pink, J. Sieler, E. Hey-Hawkins, L. Hennig, *Polyhedron*, in press.
[13] E. Hey, S. G. Bott, J. L. Atwood, *Chem. Ber*. **1988**, *121*, 561.
[14] H. Köpf, R. Voigtländer, *Chem. Ber.* **1981**, *114*, 2731.
[15] M. Baudler, B. Carlsohn, W. Böhm, G. Reuschenbach, *Z. Naturforsch.* **1976**, *31B,* 558.
[16] E. E. Nifant′ev, *Spektroskopija ^{31}P*, MGPI, Moskau, **1986**.
[17] E.-I. Negishi, F. E. Cederbaum, T. Takahashi, *Tetrehedron Lett.* **1986**, *27,* 2829.
[18] F. Teixidor, C. Viñas, M. M. Abad, R. Kivekäs, R. Sillanpää, *J. Organomet. Chem.* **1996**, *509*, 139.
[19] T. Kräuter, B. Neumüller, *Polyhedron* **1996**, *15*, 2851.
[20] J. G. Contreras, L. M. Silva-Trivino, M. E. Solis, *Inorg. Chim. Acta* **1988**, *142*, 51.
[21] J. R. Goerlich, R. Schmutzler, *Z. Anorg. Allg. Chem*. **1994**, *620*, 898; R. A. Jones, S. T. Schwab, A. L. Stuart, B. R. Whittlesey, T. C. Wright, *Polyhedron* **1985**, *4*, 1689.
[22] W. S. Sheldrick, A. Borkenstein, *Acta Crystallogr.* **1977**, *33B*, 2916.
[23] F. A. Cotton, D. J. Darensbourg, S. Klein, B. W. S. Kolthammer, *Inorg. Chem.* **1982**, *21*, 294.
[24] I. Bernal, G. M. Reisner, G. R. Dobson, C. B. Dobson, *Inorg. Chim. Acta* **1986**, *121*, 199.
[25] C.-H. Ueng, L.-C. Leu, *Acta Crystallogr.* **1991**, *47C,* 725.
[26] S. O. Grim, W. L. Briggs, R. C. Barth, C. A. Tolman, J. P. Jesson, *Inorg. Chem.* **1974**, *13*, 1095.
[27] B. R. Kimpton, W. McFarlane, A. S. Muir, P. G. Patel, J. L. Bookham, *Polyhedron* **1993**, *12*, 2525.
[28] D. J. Darensbourg, R. L. Kump, *Inorg. Chem.* **1978**, *17*, 2680.
[29] F. A. Cotton, G. Wilkinson, *Advanced Inorganic Chemistry*, 5th ed., John Wiley and Sons, New York, **1988**.
[30] R. N. Grimes, *Carboranes*, Academic Press, New York, **1970**.
[31] *VARIAN VNMR SOFTWARE*, version 4.1, revision C, SunOS™ 4.1.2, VARIAN Associates Inc., Palo Alto, **1992**.
[32] P. C. Wailes, H. Weigold, A. P. Bell, *J. Organomet. Chem.* **1972**, *34*, 155.
[33] E. Samuel, *Bull. Soc. Chim. Fr.* **1966**, 3548.

[34] S. W. Kirtley in *Comprehensive Organometallic Chemistry* (Ed.: G. Wilkinson), vol. 3, Pergamon Press, Oxford, **1982**, p. 1176ff.
[35] W. P. Fehlhammer, W. A. Herrmann, K. Öfele in *Handbuch der präparativen anorganischen Chemie* (Ed.: G. Brauer), vol. 3, E. Enke Verlag, Stuttgart, **1981**, p. 1884.
[36] Crystallographic data (excluding structure factors) for the structure reported in this paper have been deposited with the Cambridge Crystallographic Data Centre as supplementary publication no. CCDC-100919. Copies of the data can be obtained free of charge on application to CCDC, 12 Union Road, Cambridge, CB2 1EZ, UK (fax: int. code + (1223)336-033, e-mail: deposit@ccdc.cam.ac.uk).
[37] *SHELXTL PLUS*, Siemens Analyt. X-ray Inst. Inc., **1990** (XS: Program for Crystal Structure Solution, XL: Program for Crystal Structure Determination, XP: Interactiv Molecular Graphics).
[38] R. H. Blessing, *Acta Crystallogr.* **1995**, *51A*, 33.

[97276]

Controlled Degradation of a Ligand-Deficient Complex: From $[\{Cd(C_6F_5)(STrt)\}_4]$ to $[\{Cd(C_6F_5)(STrt)\}_3(OH)]^-$ and $[Cd(C_6F_5)(STrt)_2]^-$ (Trt = Triphenylmethyl)☆

Anne-Kathrin Duhme and Henry Strasdeit*

Fachbereich Chemie, Universität Oldenburg,
P. O. Box 2503, D-26111 Oldenburg, Germany
Fax: (internat.) +49(0)441/798-3329
E-mail: strasdeit@chemie.uni-oldenburg.de

Received December 2, 1997

Keywords: Cadmium / Crown compounds / Pentafluorophenyl / Potassium / S ligands

Bis(pentafluorophenyl)cadmium, $[Cd(C_6F_5)_2]$, reacts with equimolar amounts of triphenylmethanethiol, TrtSH, in toluene to give $[\{Cd(C_6F_5)(STrt)\}_4] \cdot 1.5$ tol (**1**). The cuboidal complex of **1** has been transformed into the heterometallic cuboidal complex $[\{Cd(C_6F_5)(STrt)\}_3(OH)K(THF)_3]$ (**2**) by reaction with KOH in tetrahydrofuran. In the presence of 18-crown-6, the compound $[K(18\text{-crown-6})(THF)_2][\{Cd(C_6F_5)(STrt)\}_3(OH)] \cdot THF$ (**3**) has been obtained instead of **2**. X-ray structure analysis shows the anion of **3** to be an incomplete cuboidal complex, which alternatively can be described as a cyclic trimer of the $\{Cd(C_6F_5)(STrt)\}$ unit stabilized by a μ_3-hydroxo ligand. The compound $[K(18\text{-crown-6})(THF)_2][Cd(C_6F_5)(STrt)_2]$ (**4**) has been isolated from reaction mixtures containing **1**, KSTrt and 18-crown-6. The cadmium atom in **4** is three-coordinated, in contrast to the cadmium atoms in **1**−**3**, which are situated in strongly distorted coordination tetrahedra. Intramolecular $C_6H_5\cdots C_6F_5\cdots C_6H_5$ stacks in **4** are interpreted as resulting from attractive ligand−ligand interactions. Spectroscopic data, particularly from ^{13}C-NMR and IR spectra, are consistent with the order of ligand deficiency: **1** > **2** > **3** > **4**. The macrocyclic, eight-coordinate complex $[K(18\text{-crown-6})(THF)_2]^+$ in **3** and **4** contains *trans* arranged THF ligands.

Metal complexes having an overall donor-to-metal ratio which is smaller than the typical coordination number adopted with the respective donors can be termed "ligand-deficient"[1]. Ligand deficiency is accompanied by low coordination numbers and/or the formation of oligomeric species with bridging ligands, and − most important − by the tendency to bind additional ligands[2]. Of course, the simple arithmetic of this concept is only useful, if the reactivity is not determined by other factors such as metal−metal bonding or the character of the metal−ligand bonds.

We found that bis(pentafluorophenyl)cadmium, $[Cd(C_6F_5)_2]$, is a suitable starting material for the synthesis of ligand-deficient chalcogenolato complexes of the general formula $[Cd_n(C_6F_5)_{2n-p}(ER)_p]$ (E = O or S; R = alkyl, aryl)[1][3]. A convenient method for the preparation of $[Cd(C_6F_5)_2]$ by thermal decarboxylation of $Cd(O_2CC_6F_5)_2$ has been described by Schmeißer and Weidenbruch[4]. Crystals of $[Cd(C_6F_5)_2]$ consist of two-coordinate monomers, as shown by X-ray structure determination[5]. Protolysis reactions with alcohols and thiols according to Eq. 1 allowed the syntheses of several new multinuclear complexes, most of which were also characterized by X-ray crystal structure analysis[1][3][6].

$$n\,[Cd(C_6F_5)_2] + p\,REH \rightarrow [Cd_n(C_6F_5)_{2n-p}(ER)_p] + p\,C_6F_5H \quad (1)$$

One of these complexes is $[\{Cd(C_6F_5)(STrt)\}_4]$ [Trt = triphenylmethyl ("trityl")], whose preparation and typical ligand-deficient behaviour towards the nucleophiles HO^- and $TrtS^-$ are described in this paper. The crystal structures of the resulting degradation products, a tri- and a mononuclear complex, respectively, are presented.

Syntheses

Starting from $[Cd(C_6F_5)_2]$, we have studied various reactions, which are shown in Schemes 1 and 2. The partial protolysis of $[Cd(C_6F_5)_2]$ with triphenylmethanethiol (TrtSH) in toluene (Eq. 2) yields $[\{Cd(C_6F_5)(STrt)\}_4] \cdot 1.5$ tol (**1**). X-ray structure analysis has revealed that **1** contains a cuboidal $\{Cd_4(\mu_3\text{-}SR)_4\}^{4+}$ core, which is structurally very similar to that of the already described *t*BuS$^-$ analogue[1]. The X-ray structure of **1** is therefore not included here, but will be detailed in a forthcoming paper together with the structure of the *di*nuclear alkoxo complex $[\{Cd(C_6F_5)(OTrt)\}_2]$[6].

1 exhibits the characteristic reactivity of a ligand-deficient complex towards potential ligands. It is degraded to the trinuclear complex $[\{Cd(C_6F_5)(STrt)\}_3(OH)]^-$ by reaction with the appropriate amount of hydroxide (Eqs. 3 and 4). The potassium hydroxide used in this reaction must be prepared in situ from potassium metal and water to be sufficiently reactive. Depending on whether or not 18-crown-6 has been added, $[K(18\text{-crown-6})(THF)_2][\{Cd(C_6F_5)(STrt)\}_3(OH)] \cdot THF$ (**3**) or $[\{Cd(C_6F_5)(STrt)\}_3(OH)K(THF)_3]$ (**2**), respectively, can be isolated. The anion of **3** is an incomplete cuboidal complex (see Scheme 2), whose structure will be discussed below. The structure of **2** has been unambiguously established from single-crystal X-ray diffraction data.

 © WILEY-VCH Verlag GmbH, D-69451 Weinheim, 1998 1434−1948/98/0505−0657 $ 17.50+.50/0

Scheme 1

$$4\,[Cd(C_6F_5)_2] + 4\,TrtSH \xrightarrow[-4\,C_6HF_5]{\text{toluene}} [\{Cd(C_6F_5)(STrt)\}_4]\cdot 1.5\,tol \quad (2)$$

1

$$3\,[\{Cd(C_6F_5)(STrt)\}_4] + 4\,KOH \xrightarrow{THF} 4\,[\{Cd(C_6F_5)(STrt)\}_3(OH)K(THF)_3] \quad (3)$$

2

$$3\,[\{Cd(C_6F_5)(STrt)\}_4] + 4\,KOH + 4\,18\text{-crown-6} \xrightarrow{THF} 4\,[K(18\text{-crown-6})(THF)_2][\{Cd(C_6F_5)(STrt)\}_3(OH)]\cdot THF \quad (4)$$

3

$$[\{Cd(C_6F_5)(STrt)\}_3(OH)K(THF)_3] + 18\text{-crown-6} \xrightarrow{THF} [K(18\text{-crown-6})(THF)_2][\{Cd(C_6F_5)(STrt)\}_3(OH)]\cdot THF \quad (5)$$

3

$$0.5\,[\{Cd(C_6F_5)(STrt)\}_4] + KSH + 18\text{-crown-6} \xrightarrow[-C_6HF_5]{THF} [K(18\text{-crown-6})(THF)_2][Cd(C_6F_5)(STrt)_2] + CdS\downarrow \quad (6)$$

4

$$[\{Cd(C_6F_5)(STrt)\}_4] + 4\,KSTrt + 4\,18\text{-crown-6} \xrightarrow[\text{toluene}]{THF/} 4\,[K(18\text{-crown-6})(THF)_2][Cd(C_6F_5)(STrt)_2] \quad (7)$$

4

Scheme 2

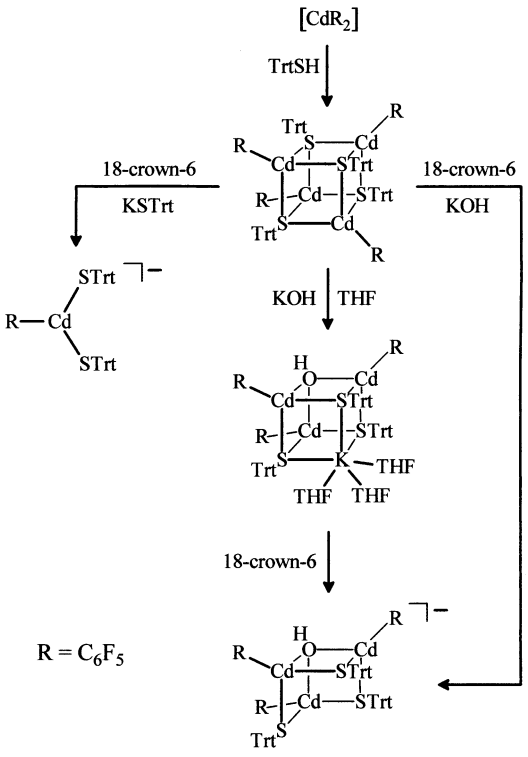

Unfortunately, the crystal quality was low, and thus the structure determination does not meet the usual standards. Therefore, only some basic crystal data are given here (see Experimental Section). **2** can be transformed into **3**: the $\{K(THF)_3\}^+$ group is removed by addition of 18-crown-6 (Eq. 5).

Interestingly, the reaction of **1** with monohydrogensulphide differs strongly from that with hydroxide. The SH^- ends up completely as cadmium sulphide (Eq. 6). We have already noticed the same type of different behaviour between H_2S and H_2O when reacted with $[Cd(C_6F_5)_2]$. With H_2S the only isolable product is CdS[1], while the partial hydrolysis of $[Cd(C_6F_5)_2]$ yields $[\{Cd(C_6F_5)(OH)\}_4]$, which could be isolated and structurally characterized by Weidenbruch et al.[7]. The second product in Eq. 6, namely the new compound $[K(18\text{-crown-6})(THF)_2][Cd(C_6F_5)(STrt)_2]$ (**4**), is more conveniently prepared from **1**, KSTrt and 18-crown-6 according to Eq. 7. The compounds **1**−**4** decompose on exposure to air, **4** apparently being most sensitive.

It is worth noting, that triphenylmethanethiolate has rarely been used as a sterically hindered ligand[8], especially when the wealth of data on bulky *aromatic* thiolate ligands is considered[9]. The main reason for this seems to be the fear, that C−S bond cleavage may occur. The C−S bonds of aliphatic thiols are in fact weaker than those of aromatic thiols. In some cases, C−S scission reactions have even led to isolable sulfido complexes[10]. However, in the syntheses of the compounds **1**−**4** the use of triphenylmethanethiol-(ate) has been found unproblematic[11].

Spectroscopic Properties

The ^{13}C-NMR spectra reflect the decrease of ligand deficiency, i. e. the decreasing electronic stress of the thiolate ligands, in the sequence **1**→**2**→**3**→**4**. The signal of the α-C atoms of the $TrtS^-$ groups is found at δ = 74.20 (**1**), 65.78 (**2**), 63.81 (**3**), and 63.30 (**4**), respectively. The chemical-shift difference between **2** and **3** may indicate, that for **2** the coordination of $\{K(THF)_3\}^+$ by the $[\{Cd(C_6F_5)(STrt)\}_3(OH)]^-$ anion, as found in the solid state, is retained in solution. However, the influence of the different solvents is difficult to estimate (**2**: C_6D_6, **3**: $CDCl_3$). A clear, but reverse trend is also observed for the *ipso*-C atoms of the $TrtS^-$ ligands: δ = 147.0 (**1**), 149.8 (**2**), 150.1 (**3**), and 153.6 (**4**), respectively. The remaining ^{13}C-NMR signals of the phenyl groups were found to be relatively insensitive to the coordi-

nation mode of the $TrtS^-$ ligand (μ_3, μ_2 or terminal). They span ranges of less than 2.0 ppm each.

The C_6F_5 ligands are terminally coordinated in all four compounds. Here, some less pronounced trends of the spectroscopic properties are observed: (i) for the ^{19}F-NMR signal of the *para*-F atom: $\delta = -156.7$ (**1**), -158.0 (**2**), and -160.4 (**3** and **4**), respectively, and (ii) for the C−F stretching frequency in the IR spectra: 954 (**1**), 949 (**2**), 948 (**3**), and 945 cm^{-1} (**4**), respectively. For the educt $[Cd(C_6F_5)_2]$ the C−F stretching vibration has been observed at 956 cm^{-1} [4]. A dependence of ν(C−F) on the metal oxidation state has been reported for pentafluorophenyl complexes of palladium and platinum: M^{IV} 968 ± 3, M^{II} 955 ± 6, and M^{I} 946 ± 6 cm^{-1} [12]. Thus, an increase in ligand deficiency shifts ν(C−F) into the same direction as an increasing oxidation state of the coordination centre does − in accordance with chemical intuition.

In the $TrtS^-$ ligands of **4** two types of *ortho*-H atoms can be distinguished by ^1H-NMR spectroscopy. Their intensity ratio of 2:1 is consistent with a structure that possesses an intramolecular $C_6H_5\cdots C_6F_5\cdots C_6H_5$ stack as observed in the solid state and discussed below.

X-ray Crystal Structures of 3 and 4

Crystals of **3** consist of $[\{Cd(C_6F_5)(STrt)\}_3(OH)]^-$ complexes, $[K(18\text{-crown-}6)(THF)_2]^+$ counterions and non-coordinating THF molecules. The trinuclear cadmium complex is shown in Figure 1. It can be regarded as a cyclic trimer of the $\{Cd(C_6F_5)(STrt)\}$ unit stabilized by a μ_3-hydroxo ligand. An alternative description is that of an incomplete cuboidal complex. As shown in Scheme 2, this complex can actually be prepared by removal of the $\{K(THF)_3\}^+$ corner from the heterometallic cuboidal complex $[\{Cd(C_6F_5)(STrt)\}_3(OH)K(THF)_3]$ (**2**). A structurally related, but homoleptic trinuclear complex has been described, namely $[Cd_3\{SC_6H_2(iPr)_3\text{-}2,4,6\}_7]^-$ [13].

The $[\{Cd(C_6F_5)(STrt)\}_3(OH)]^-$ complex in **3** closely approaches C_3 symmetry. Its central, chair-like Cd_3S_3 ring is strongly puckered, the metal part being contracted by the small μ_3-OH^- ligand. This contraction becomes obvious by comparison with the situation in $[\{Cd(C_6F_5)(STrt)\}_4]$ [6]: for **3** a shortening of the mean Cd···Cd distance (**3**: 3.57 Å) by 0.36 Å, an increase of the mean S−Cd−S angle by 9°, and a decrease of the mean Cd−S−Cd angle by 7° are observed. The coordination tetrahedra around the cadmium atoms are severely distorted with bond angles ranging from 87.6° for S−Cd−O to 130.4° for S−Cd−C (mean values). As may be expected from the different coordination modes of the thiolate, in **3** the mean Cd−S bond length (2.56 Å) is smaller than in **1** (2.65 Å), but larger than in **4** (2.467(1) Å) and in $[Cd(STrt)_2(tmeda)]$ (2.44 Å) [8b], where the ligands are terminally bonded.

Crystals of **4** are composed of $[Cd(C_6F_5)(STrt)_2]^-$ anions and $[K(18\text{-crown-}6)(THF)_2]^+$ cations. The cadmium complex (see Figure 2) is situated on a crystallographic twofold axis of rotation, which passes through the atoms Cd, C(1), C(4), and F(3). To our knowledge, $[Cd(C_6F_5)(STrt)_2]^-$ is the first cadmium complex reported to have an S_2C donor

Figure 1. View of the complex $[\{Cd(C_6F_5)(STrt)\}_3(OH)]^-$ in crystals of **3**; the hydrogen atoms of the thiolate ligands have been omitted for clarity; thermal ellipsoids are drawn with 30% probability[a]

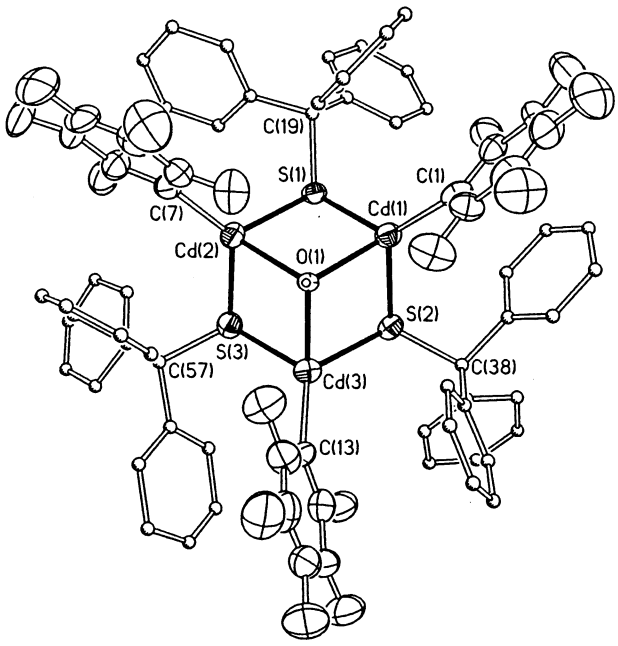

[a] Selected bond lengths [Å] and angles [°], mean values in brackets: Cd(1)−S(1) 2.542(3), Cd(1)−S(2) 2.586(3), Cd(2)−S(1) 2.568(3), Cd(2)−S(3) 2.545(3), Cd(3)−S(2) 2.563(3), Cd(3)−S(3) 2.583(3), Cd(1)−O(1) 2.395(6), Cd(2)−O(1) 2.408(7), Cd(3)−O(1) 2.368(7), Cd(1)−C(1) 2.16(1), Cd(2)−C(7) 2.18(1), Cd(3)−C(13) 2.20(1), S(1)−C(19) 1.87(1), S(2)−C(38) 1.89(1), S(3)−C(57) 1.87(1), S−Cd−S 90.91(9)−95.16(9) [93.0], S−Cd−O 86.0(2)−88.5(2) [87.6], S−Cd−C 126.1(3)−135.4(3) [130.4], O−Cd−C 111.4(4)−114.3(4) [113.1], Cd−S−Cd 87.4(1)−88.76(9) [88.2], Cd−O−Cd 95.7(3)−98.2(3) [96.6].

set [14][15]. The observed bond lengths and angles at the Cd atom are unexceptional. There is, however, a striking structural features of this complex, namely the mutual orientation of the trityl groups and the pentafluorophenyl ligand. The C_6H_5 ring containing the C atoms C(6) to C(11) and the symmetry related one in the same complex are arranged above and below the C_6F_5 group. A $C_6H_5\cdots C_6F_5\cdots C_6H_5$ intramolecular stack results, in which the plane of the C_6F_5 group forms an angle of 4.6° with each of the C_6H_5 planes. The atom C(1) lies nearly perpendicular over the centroid of the C_6 ring of the phenyl group (deviation: ca. 1.0°). The C(1)···centroid distance is 3.37 Å.

The alternating stacking in complexes between polyfluorinated and non-fluorinated aromatic molecules is a well-known structural phenomenon in organic chemistry. Dahl has studied a number of such molecular complexes containing hexafluorobenzene as the fluorinated component [16]. He has reported mean interplanar distances in the stacks ranging from 3.39 to 3.56 Å. These values correspond approximately to the van der Waals thickness of typical aromatic molecules of 3.4 Å [17]. When viewed perpendicular to the ring planes, a slipped orientation of adjacent rings is usually observed. This is also true for the $C_6H_5\cdots C_6F_5$ pairs in **4**. The close structural similarity to the molecular complex *p*-xylene−hexafluorobenzene [18] is shown in Figure 3. Recent

Figure 2. View of the complex $[Cd(C_6F_5)(STrt)_2]^-$ in crystals of **4**; hydrogen atoms have been omitted for clarity; thermal ellipsoids are drawn with 30% probability[a]

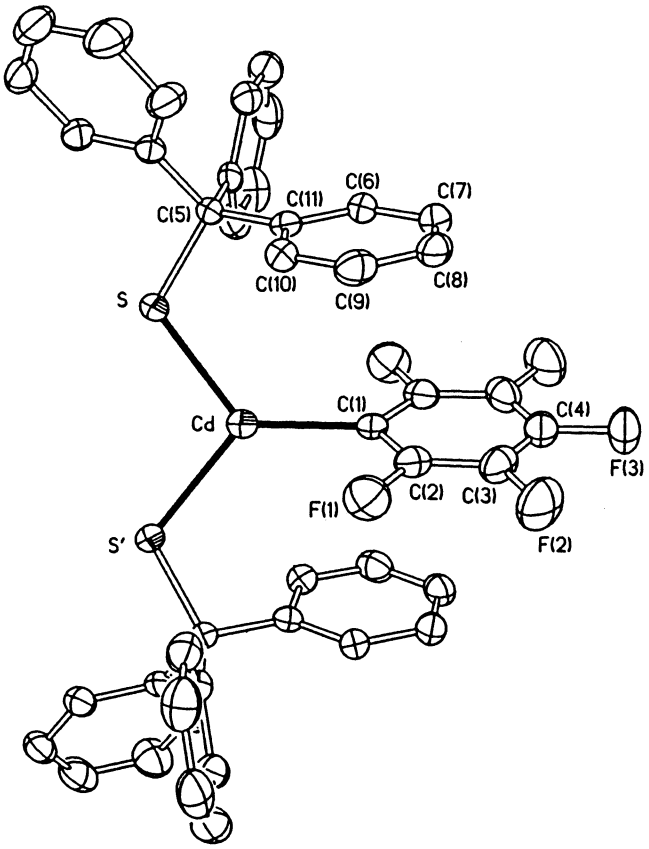

[a] Selected bond lengths [Å] and angles [°]: Cd−S 2.467(1), Cd−C(1) 2.180(6), S−C(5) 1.876(4), S−Cd−S′ 103.39(5), S−Cd−C(1) 128.31(3), Cd−S−C(5) 111.7(1).

results indicate, that the attractive forces between polyfluorinated and non-fluorinated aromatic molecules are largely electrostatic in nature[19].

Figure 3. The slipped parallel arrangement of aromatic rings in $[Cd(C_6F_5)(STrt)_2]^-$ (A) and in the *p*-xylene−hexafluorobenzene molecular complex[18] (B); the mean C_6 planes of the fluorine-containing groups are exactly parallel to the projection plane; small circles represent hydrogen atoms.

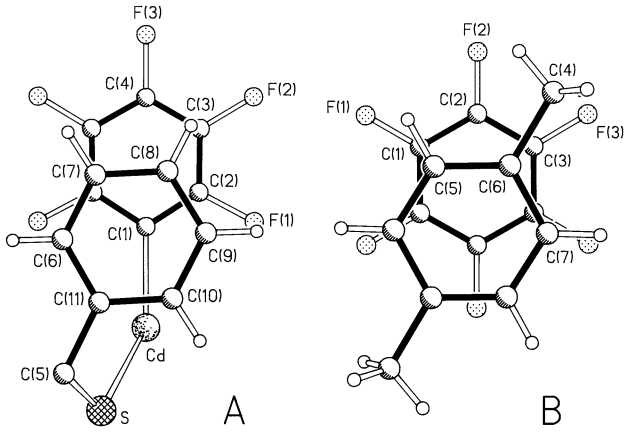

We believe, that attractive interligand interactions are the most probable cause of the $C_6H_5\cdots C_6F_5\cdots C_6H_5$ stacking in **4**. No other *intra*molecular causes can be recognized. In fact, the sterical demand of the thiolate ligands should favour other arrangements, especially those with one trityl group above and the other below the $CdS_2C(1)$ plane. The possibility cannot be ruled out, however, that packing forces contribute to determine the observed structure. Regarding the expected weakness of $C_6H_5\cdots C_6F_5$ interactions[19b][20], the ^{1}H-NMR results on **4** (see above) should not be interpreted as a proof, but merely as a possible indication of aromatic-ring stacking in solution. Intramolecular stacks of phenyl and pentafluorophenyl groups are also observed in crystals of the compounds **1**−**3** (cf. Figure 1). In these cases, it cannot be decided whether or not these arrangements are enforced by sterical crowding. The face-to-face orientation of C_6H_5 and C_6F_5 groups in metal complexes is not particularly rare, though it has mostly been neglected in structure discussions. The Cambridge Structural Database (CSD)[14] contains ca. 30 examples where in metal coordination spheres attractive interactions of the type described above seem possible. A detailed analysis is, however, beyond the scope of this paper.

In both **3** and **4**, the cationic part is formed by the macrocyclic complex $[K(18\text{-crown-}6)(THF)_2]^+$. The CSD[14] lists four other structures containing this complex[21]. The metal ion in $[K(18\text{-crown-}6)(THF)_2]^+$ is in an O_8 environment, the THF ligands being in *trans* position. The mean K−O(macrocycle) bond lengths are 2.79 (**3**) and 2.80 Å (**4**), respectively. Due to disorder of the THF ligands in both compounds, the K−O(THF) bond lengths are less accurate. Their mean values are 2.78 (**3**) and 2.76 Å (**4**), respectively.

This work was supported by the *Deutsche Forschungsgemeinschaft* and the *Fonds der Chemischen Industrie*. We are indebted to Prof. *H. Vahrenkamp* for the ^{19}F-NMR spectra and to Mr. *W. Saak* for collecting the diffraction data

Experimental Section

General: Bis(pentafluorophenyl)cadmium was prepared from $Cd(O_2CC_6F_5)_2$ according to a literature method[4]. Triphenylmethanethiol (Merck) was treated with activated charcoal in boiling ethanol and recrystallized twice from diethyl ether prior to use. Tetrahydrofuran was pretreated with KOH and subsequently destilled from $LiAlH_4$ under nitrogen. Toluene and *n*-hexane were refluxed over Na/K alloy and destilled under nitrogen. All other commercially available chemicals were used as received. The cadmium complexes described below were prepared and handled under an atmosphere of dry nitrogen in a glove box; storage was also under dry nitrogen. − IR: Bio-Rad FTS 7PC and Beckman IR-4220. − ^{1}H and $^{13}C\{^1H\}$ NMR: Bruker AM-300, chemical shifts relative to TMS, solvent signal as internal reference in the ^{13}C-NMR spectra ($CDCl_3$: δ_c = 77.00, C_6D_6: δ_c = 128.00). ^{19}F NMR: chemical shifts relative to $CFCl_3$. Prior to use, all NMR solvents were treated with molecular sieves to remove water. − Elemental analyses: Mikroanalytisches Laboratorium Beller, D-37004 Göttingen, Germany. − *Caution!* Cadmium compounds are highly toxic and probably carcinogenic. Therefore they should be handled with care to avoid exposure.

[{Cd(C$_6$F$_5$)(STrt)}$_4$]·1.5 tol (**1**): 2.76 g (10.0 mmol) of triphenylmethanethiol, dissolved in 10 ml of toluene, was added to a solution of 4.47 g (10.0 mmol) of $[Cd(C_6F_5)_2]$ in 25 ml of toluene.

After some minutes, a white, microcrystalline precipitate of **1** started separating from the yellow solution. The product was isolated within the next hour (on prolonged standing, a brown colouring occurred), thoroughly washed with toluene and dried in vacuo. Yield: 5.42 g (92%), m.p. 145°C (dec.). – IR (KBr): $\tilde{\nu}$ = 954 cm^{-1} (s, CF). – ^{13}C NMR (75.5 MHz, $CDCl_3$): δ = 21.44 (tol), 74.20 (Ph_3C), 125.3 (tol), 127.2 (Ph-*para* in Ph_3C), 127.9 (Ph-*meta* in Ph_3C), 128.2 (tol), 129.0 (tol), 129.7 (Ph-*ortho* in Ph_3C), 137.9 (tol), 147.0 (Ph-*ipso* in Ph_3C)[22]. – ^{19}F NMR (188.3 MHz, $CDCl_3$): δ = −109.3 (m, 8 F, C_6F_5-*ortho*), −156.7 (m, 4 F, C_6F_5-*para*), −162.0 (m, 8 F, C_6F_5-*meta*). – $C_{110.5}H_{72}Cd_4F_{20}S_4$ (2357.7): calcd. C 56.29, H 3.08, Cd 19.07, F 16.12, S 5.44; found C 55.81, H 3.02, Cd 19.14, F 16.2, S 5.63.

[{Cd(C_6F_5)(STrt)}$_3$(OH)K(THF)$_3$] (**2**): 39 mg (1.0 mmol) of freshly cut potassium metal was added to a solution of 18 µl (1.0 mmol) of water in 8 ml of tetrahydrofuran. After stirring overnight, a suspension of potassium hydroxide had formed. Traces of unreacted potassium were removed. 1.77 g (0.75 mmol) of **1**, dissolved in 12 ml of tetrahydrofuran, was added. The reaction mixture was stirred until the potassium hydroxide had completely reacted. Then the clear, colourless solution was carefully layered with *n*-hexane in the reaction flask. After 2 d, colourless crystals of **2** had separated, which were isolated on a large-pored glass filter, washed with *n*-hexane and dried in vacuo. Yield 1.20 g (62%), m.p. 146−147°C. – IR (KBr): $\tilde{\nu}$ = 949 cm^{-1} (s, CF). – ^1H NMR (300 MHz, CD_3CN): δ = 1.80 (m, 12 H, CCH_2C), 2.11 (br., 1 H, OH), 3.65 (m, 12 H, CH_2O), 6.91−7.03 (m, 27 H, Ph-*meta* and -*para*), 7.14 ("d", 18 H, Ph-*ortho*). – ^{13}C NMR (75.5 MHz, C_6D_6): δ = 25.68 (CCH_2C), 65.78 (Ph_3C), 67.77 (CH_2O), 126.8 (Ph-*para*), 127.7 (Ph-*meta*), 129.9 (Ph-*ortho*), 149.8 (Ph-*ipso*)[22]. – ^{19}F NMR (188.3 MHz, C_6D_6): δ = −110.8 (m, 6 F, C_6F_5-*ortho*), −158.0 (m, 3 F, C_6F_5-*para*), −161.9 (m, 6 F, C_6F_5-*meta*). – Crystallographic data (23°C): monoclinic, space group $P2_1/n$, a = 15.07(1), b = 21.75(1), c = 25.49(1) Å, β = 90.89(5)°, V = 8354 Å^3, Z = 4, $\rho_{calcd.}$ = 1.540 gcm^{-3}. – $C_{87}H_{70}Cd_3F_{15}KO_4S_3$ (1937.0): calcd. C 53.95, H 3.64, Cd 17.41, F 14.71, K 2.02, S 4.97; found C 53.07, H 3.70, Cd 17.57, F 14.1, K 2.10, S 4.62.

[K(18-crown-6)(THF)$_2$][{Cd(C_6F_5)(STrt)}$_3$(OH)]·THF (**3**): *Method A*: In tetrahydrofuran, potassium hydroxide was prepared as described above for **2**, but with the addition of 264 mg (1.00 mmol) of 18-crown-6. To the suspension 1.77 g (0.75 mmol) of **1**, dissolved in 12 ml of tetrahydrofuran, was added. After the reaction mixture had become clear, it was diluted with 15 ml of toluene and then layered with *n*-hexane. **3** separated as a colourless, crystalline solid, which was isolated, washed with *n*-hexane and dried in vacuo. Yield 1.49 g (68%), m.p. 165−166°C. – IR (KBr): $\tilde{\nu}$ = 948 cm^{-1} (s, CF). – ^1H NMR (300 MHz, CD_3CN): δ = 1.80 (m, 12 H, CCH_2C), 2.12 (br., 1 H, OH), 3.56 (s, 24 H, 18-crown-6), 3.64 (m, 12 H, CH_2O in THF), 7.02−7.13 (m, 27 H, Ph-*meta* and -*para*), 7.32 ("d", 18 H, Ph-*ortho*). – ^{13}C NMR (75.5 MHz, $CDCl_3$): δ = 25.58 (CCH_2C), 63.81 (Ph_3C), 67.93 (CH_2O in THF), 70.18 (18-crown-6), 125.6 (Ph-*para*), 126.8 (Ph-*meta*), 129.7 (Ph-*ortho*), 150.1 (Ph-*ipso*)[22]. – ^{19}F NMR (188.3 MHz, $CDCl_3$): δ = −110.9 (m, 6 F, C_6F_5-*ortho*), −160.4 (m, 3 F, C_6F_5-*para*), −163.7 (m, 6 F, C_6F_5-*meta*). – $C_{99}H_{94}Cd_3F_{15}KO_{10}S_3$ (2201.3): calcd. C 54.02, H 4.30, Cd 15.32, F 12.95, K 1.78, S 4.37; found C 53.98, H 4.35, Cd 15.14, F 13.0, K 1.92, S 4.50.

Method B: 0.97 g (0.50 mmol) of **2** was dissolved in 20 ml of tetrahydrofuran. To the stirred solution 132 mg (0.50 mmol) of 18-crown-6 was added. After the crown ether had dissolved, first toluene and then *n*-hexane were carefully layered over the reaction mixture. Nearly colourless crystals of **3** separated during the next 4 d. The product was isolated, washed with *n*-hexane and dried in vacuo. Yield 0.94 g (85%).

[K(18-crown-6)(THF)$_2$][Cd(C_6F_5)(STrt)$_2$] (**4**): 39 mg (1.0 mmol) of freshly cut potassium metal was added to a stirred solution of 276 mg (1.00 mmol) of triphenylmethanethiol in 2 ml of tetrahydrofuran. After ca. 4 h, the metal had completely reacted, and a clear, light yellow solution had formed. This solution was slowly dropped into a solution of 589 mg (0.250 mmol) of **1** in 2 ml of toluene. 264 mg (1.00 mmol) of 18-crown-6 was added. Then *n*-hexane was carefully layered over the light brown solution in the reaction flask. After 2 d, nearly colourless crystals of **4** had formed, which were isolated on a large-pored glass filter, washed with *n*-hexane, dried in vacuo, and finally stored in a refrigerator. Yield 1.01 g (79%). – IR (KBr): $\tilde{\nu}$ = 945 cm^{-1} (s, CF). – ^1H NMR (300 MHz, CD_3CN): δ = 1.80 (m, 8 H, CCH_2C), 3.56 (s, 24 H, 18-crown-6), 3.64 (m, 8 H, CH_2O in THF), 7.00−7.14 (m, 18 H, Ph-*meta* and -*para*), 7.33 ("d", 8 H, Ph-*ortho*), 7.47 ("d", 4 H, Ph-*ortho*). – ^{13}C NMR (75.5 MHz, C_6D_6): δ = 25.78 (CCH_2C), 63.30 (Ph_3C), 67.77 (CH_2O in THF), 70.16 (18-crown-6), 125.3 (Ph-*para*), 127.3 (Ph-*meta*), 130.7 (Ph-*ortho*), 153.6 (Ph-*ipso*)[22]. – ^{19}F NMR (188.3 MHz, C_6D_6): δ = −110.2 (m, 2 F, C_6F_5-*ortho*), −160.4 (m, 1 F, C_6F_5-*para*), −163.2 (m, 2 F, C_6F_5-*meta*). – $C_{64}H_{70}CdF_5KO_8S_2$ (1277.9): calcd. C 60.15, H 5.52, Cd 8.80, F 7.43, K 3.06, S 5.02; found C 59.87, H 5.65, Cd 8.37, F 7.3, K 4.03, S 5.10.

X-ray Crystal Structure Analysis of **3** *and* **4**: Intensity data were measured at 23°C on a Siemens/STOE AED2 diffractometer. Graphite-monochromated MoK_α radiation, ω scans, structure solutions by direct methods[23], refinements on F^2 values (full-matrix least-squares)[24].

A suitable single crystal of **3** was obtained by layering first a small amount of toluene and then *n*-hexane over a solution of the compound in tetrahydrofuran. $C_{99}H_{94}Cd_3F_{15}KO_{10}S_3$, M = 2201.3, pale brown crystal, crystal size 0.65 × 0.53 × 0.27 mm, monoclinic, space group $P2_1/c$, a = 25.464(3), b = 14.248(2), c = 28.421(4) Å, β = 104.40(3)°, V = 9988(2) Å^3, Z = 4, $\rho_{calcd.}$ = 1.464 gcm^{-3}, $F(000)$ = 4456, $\mu(MoK_\alpha)$ = 0.82 mm^{-1}. 11954 reflections collected, intensity variation during data collection: −24%, 3° ≤ 2Θ ≤ 43°, 0 ≤ h ≤ 26, 0 ≤ k ≤ 14, −29 ≤ l ≤ 28, empirical absorption correction, T_{min} = 0.3081, T_{max} = 0.4240. 11472 independent reflections (R_{int} = 0.0407) of which 11470 were used in the final refinement, 802 parameters, S (on F^2) = 1.022, $R1$ (all data) = 0.1415, $wR2$ (all data) = 0.1699, $R1$ [$I > 2\sigma(I)$] = 0.0678, max. and min. electron density in final difference map: +0.52 and −0.42 eÅ^{-3}. Each of the THF molecules was assumed to be disordered on two positions, occupied in the ratio of 3:2. A common isotropic U value was refined for the non-hydrogen atoms of each individual position. Anisotropic displacement parameters were refined for all other non-hydrogen atoms, except the C atoms of the trityl groups. All H atoms were included on idealized positions.

A single crystal of **4**, suitable for X-ray structure determination, was grown by layering *n*-hexane over a dilute solution of the compound in tetrahydrofuran. $C_{64}H_{70}CdF_5KO_8S_2$, M = 1277.9, pale yellow crystal, crystal size 0.76 × 0.53 × 0.46 mm, monoclinic, space group $C2/c$, a = 20.230(2), b = 13.897(1), c = 22.512(2) Å, β = 101.65(1)°, V = 6198.6(9) Å^3, Z = 4, $\rho_{calcd.}$ = 1.369 gcm^{-3}, $F(000)$ = 2648, $\mu(MoK_\alpha)$ = 0.55 mm^{-1}. 5721 reflections collected, intensity variation during data collection: −15%, 3.6° ≤ 2Θ ≤ 48°, 0 ≤ h ≤ 23, 0 ≤ k ≤ 15, −25 ≤ l ≤ 25, no absorption correction. 4868 independent reflections (R_{int} = 0.0312) of which all were used in the final refinement, 372 parameters, S (on F^2) = 1.107, $R1$ (all data) = 0.0977, $wR2$ (all data) = 0.1098, $R1$ [$I > 2\sigma(I)$] = 0.0510, max. and min. electron density in final difference map: +0.50 and

-0.32 eÅ^{-3}. Anisotropic displacement parameters were refined for the non-hydrogen atoms, except in the THF ligand, which was assumed to be disordered on three equally occupied positions. A common isotropic U value was refined for the non-hydrogen atoms of each individual position. A total of 30 restraints (DFIX instructions) were used to generate idealized geometries for the THF molecules. For practical reasons, an envelope conformation was chosen with metrical data (C−O 1.43, C−C 1.54 Å; C−O−C 106, O−C−C and C−C−C 104°) close to the values found for free THF[25]. All H atoms were included on idealized positions.

Crystallographic data (excluding structure factors) for the structures reported in this paper have been deposited with the Cambridge Crystallographic Data Centre as supplementary publication no. CCDC-100805. Copies of the data can be obtained free of charge on application to CCDC, 12 Union Road, Cambridge CB2 1EZ, UK [Fax: int. code +44(1223)336-033; E-mail: deposit@ccdc.cam.ac.uk].

☆ Dedicated to Professor *Manfred Weidenbruch* on the occasion of his 60th birthday.

[1] A.-K. Duhme, H. Strasdeit, *Z. Naturforsch.* **1994**, *49b*, 119−127.

[2] A textbook example is $[Pt_6Cl_{12}]$ (β-$PtCl_2$), which has a low donor-to-metal ratio (= 2) and on addition of chloride forms $[PtCl_4]^{2-}$ without change of the coordination number of platinum.

[3] I. Büsching, H. Strasdeit, *J. Chem. Soc., Chem. Commun.* **1994**, 2789−2790.

[4] M. Schmeißer, M. Weidenbruch, *Chem. Ber.* **1967**, *100*, 2306−2311; see also: P. Sartori, M. Weidenbruch, *Chem. Ber.* **1967**, *100*, 3016−3023.

[5] H. Strasdeit, I. Büsching, A.-K. Duhme, S. Pohl, *Acta Crystallogr. Sect. C* **1993**, *49*, 576−578.

[6] H. Strasdeit, I. Büsching, A.-K. Duhme, to be published.

[7] M. Weidenbruch, M. Herrndorf, A. Schäfer, S. Pohl, W. Saak, *J. Organomet. Chem.* **1989**, *361*, 139−145.

[8] For $TrtS^-$ metal complexes see e. g.: [8a] U. Brand, H. Vahrenkamp, *Chem. Ber.* **1996**, *129*, 435−440. − [8b] A. J. Edwards, A. Fallaize, P. R. Raithby, M.-A. Rennie, A. Steiner, K. L. Verhorevoort, D. S. Wright, *J. Chem. Soc., Dalton Trans.* **1996**, 133−137. − [8c] N. Kitajima, K. Fujisawa, M. Tanaka, Y. Moro-oka, *J. Am. Chem. Soc.* **1992**, *114*, 9232−9233. − [8d] M. M. Olmstead, P. P. Power, S. C. Shoner, *J. Am. Chem. Soc.* **1991**, *113*, 3379−3385. − [8e] R. D. Bach, A. T. Weibel, W. Schmonsees, M. D. Glick, *J. Chem. Soc., Chem. Commun.* **1974**, 961−962.

[9] J. R. Dilworth, J. Hu, *Adv. Inorg. Chem.* **1993**, *40*, 411−459.

[10] I. Dance, K. Fisher, *Prog. Inorg. Chem.* **1994**, *41*, 637−803.

[11] A $Cu^{II}-TrtS^-$ complex has been described that undergoes C−S bond cleavage already at room temp.: K. Fujisawa, Y. Moro-oka, N. Kitajima, *J. Chem. Soc., Chem. Commun.* **1994**, 623−624.

[12] R. Usón, J. Forniés, *Adv. Organomet. Chem.* **1988**, *28*, 219−297.

[13] K. Tang, X. Jin, A. Li, S. Li, Z. Li, Y. Tang, *J. Coord. Chem.* **1994**, *31*, 305−320.

[14] Cambridge Structural Database (CSD), Version 5.13 (April 1997, 167797 entries). − F. H. Allen, O. Kennard, *Chem. Des. Autom. News* **1993**, *8*, 1 and 31−37.

[15] For an overview on crystallographic and structural data of cadmium coordination compounds see: C. E. Holloway, M. Melník, *Main Group Met. Chem.* **1995**, *18*, 451−585.

[16] T. Dahl, *Acta Crystallogr. Sect. B* **1990**, *46*, 283−288, and literature cited therein.

[17] L. Pauling, *The Nature of the Chemical Bond*, 3rd ed., Cornell University Press, Ithaca, **1960**, p. 262.

[18] T. Dahl, *Acta Chem. Scand. A* **1975**, *29*, 170−174.

[19] [19a] M. Luhmer, K. Bartik, A. Dejaegere, P. Bovy, J. Reisse, *Bull. Soc. Chim. Fr.* **1994**, *131*, 603−606. − [19b] M. J. Duer, *J. Chem. Soc., Faraday Trans.* **1993**, *89*, 823−826. − [19c] J. H. Williams, *Acc. Chem. Res.* **1993**, *26*, 593−598. − [19d] J. H. Williams, *Chem. Phys.* **1993**, *172*, 171−186.

[20] R. Laatikainen, J. Ratilainen, R. Sebastian, H. Santa, *J. Am. Chem. Soc.* **1995**, *117*, 11006−11010.

[21] [21a] F. Paul, D. Carmichael, L. Ricard, F. Mathey, *Angew. Chem.* **1996**, *108*, 1204−1206; *Angew. Chem. Int. Ed. Engl.* **1996**, *35*, 1125−1127. − [21b] P. Müller, S. Huck, H. Köppel, H. Pritzkow, W. Siebert, *Z. Naturforsch.* **1995**, *50b*, 1476−1484. − [21c] T. A. Budzichowski, M. H. Chisholm, J. C. Huffman, O. Eisenstein, *Angew. Chem.* **1994**, *106*, 203−206; *Angew. Chem. Int. Ed. Engl.* **1994**, *33*, 191−193. − [21d] F. G. N. Cloke, P. B. Hitchcock, A. McCamley, *J. Chem. Soc., Chem. Commun.* **1993**, 248−250.

[22] The ^{13}C-NMR signals of the C_6F_5 group(s) could not be observed, because the solubility of the compound was too low. For typical ^{13}C-NMR data of C_6F_5 groups bonded to cadmium see refs.[1][5].

[23] G. M. Sheldrick, *SHELXTL PLUS*, Siemens Analytical X-ray Instruments Inc., Madison, WI, USA, **1990**.

[24] G. M. Sheldrick, *SHELXL-93, Program for Crystal Structure Refinement*, University of Göttingen, Germany, **1993**.

[25] [25a] W. I. F. David, R. M. Ibberson, *Acta Crystallogr. Sect. C* **1992**, *48*, 301−303. − [25b] C. W. Bird, G. W. H. Cheeseman in *Comprehensive Heterocyclic Chemistry* (Eds.: A. R. Katritzky, C. W. Rees), Vol. 4, Pergamon, Oxford, **1984**, pp. 1−38.

[97291]

Aminoethyl-Functionalized Cyclopentadienyl Complexes of d-Block Elements☆

Peter Jutzi* and Thomas Redeker

Fakultät für Chemie der Universität Bielefeld,
Universitätsstraße 25, D-33615 Bielefeld, Germany
Fax: (internat) + 49(0)521/106-6026
E-mail: P.Jutzi@uni-bielefeld.de

Received December 18, 1997

Keywords: Aminoethyl-functionalized cyclopentadienyl complexes / d-Block elements / Hemilabile N-ligands / Intramolecular coordination / Tethered aminoethyl groups / Water-soluble organometallics

The introduction of an aminoethyl side chain into cyclopentadienyl compounds of many d-block elements leads to interesting changes in structure and reactivity compared to the parent species: (i) A hemilabile bonding situation is observed in complexes with low-valent transition-metal centers; (ii) amino-group coordination to an adjacent metal or nonmetal center creates novel types of bimetallic compounds; (iii) complexes with a tethered ammoniumethyl group often show good solubility in protic solvents, relevant with regard to organometallic chemistry in water. These features together with others are described in this review, which informs about the synthesis and properties of this new type of transition-metal complexes.

Introduction

Undoubtedly, the cyclopentadienyl group, C_5H_5 (Cp), is one of the most important ligands in organometallic chemistry.[1] In the last decade, an increasing number of new ring-substituted cyclopentadienyl fragments has appeared in the literature. Variations in the Cp-ligand periphery often result in dramatic changes in physical and chemical properties of the corresponding compounds. These changes can be attributed to electronic and steric effects caused by the partial or full replacement of the hydrogen atoms by other groups.[2]

The chemistry of Cp complexes containing a donor-functionalized side chain is a rapidly growing area that is currently being explored by several research groups.[3][4][5][6][7][8][9] This review concentrates on complexes of d-block elements containing aminoethyl-substituted Cp ligands. The first complexes of this type were introduced by Green et al. in 1983; the dimethylamino func-

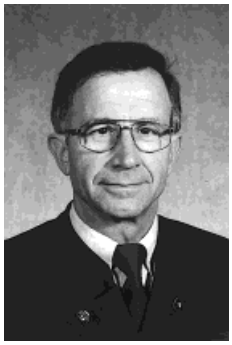

Prof. Dr. P. Jutzi studied chemistry at the Technical University of Munich and received his Ph.D. degree under the supervision of Prof. Dr. M. Schmidt at the University of Marburg .After his habilitation at the University of Würzburg in 1971 he was appointed associate professor in 1974. In 1978 he moved as full professor of Inorganic Chemistry to the University of Bielefeld. His scientific interest is in the field of experimental organometallic chemistry. Topics of research are: I) Cyclopentadienyl chemistry of p- and d-block elements, II) nanometer-sized materials.

Dr. Thomas Redeker studied chemistry at the University of Bielefeld and received his Ph.D degree in early 1997. The thesis entitled "Metallocenes of the elements titanium and zirconium with the diisopropylaminoethylcyclopentadienyl ligand" was performed in Prof. Jutzi's laboratories, supported by a fellowship of the "Fonds der Chemischen Industrie" and awarded with the "Abschlußzertifikat" of the "Fonds der Chemischen Industrie". Currently, he is working in the group of Prof. Dr. H. D. Kaesz (UCLA, USA) as a postdoctoral fellow. His project, the MOCVD of titanium films, is supported by a grant from the "Deutsche Forschungsgemeinschaft".

MICROREVIEWS: This feature introduces the readers to the authors' research through a concise overview of the selected topic. Reference to important work from others in the field is included.

 © WILEY-VCH Verlag GmbH, D-69451 Weinheim, 1998 1434–1948/98/0606–0663 $ 17.50+.50/0

tion was attached to a functionalized Cp ring only in the last step of the synthesis.[7a] The first synthesis of an aminoethyl-functionalized cyclopentadiene was described by Wang and co-workers in 1991. They prepared complexes with the (dimethylaminoethyl)cyclopentadienyl ligands Cp^{I} and Cp^{II} (Figure 1).[7f] Our laboratory contributed to this new field with compounds bearing the ligands Cp^{III} and Cp^{IV} (Figure 1).[9] Cyclopentadienyl ligands Cp^{V} and Cp^{VI} with pyrrolidyl and piperidyl functions as pendant groups were introduced by Herrmann and co-workers (Figure 1).[8c] The chiral dimethylaminoethyl-functionalized cyclopentadienyl ligand Cp^{VII} was described by van der Zeijden only recently (Figure 1).[8b][8l] The cyclopentadienyl ligand Cp^{VIII} with only one methyl substituent at the nitrogen atom was also introduced by Wang and co-workers.[8u] Tyler and Avey synthesized complexes with the Cp^{IX} ligand which contains the parent amino function.[7h]

Figure 1

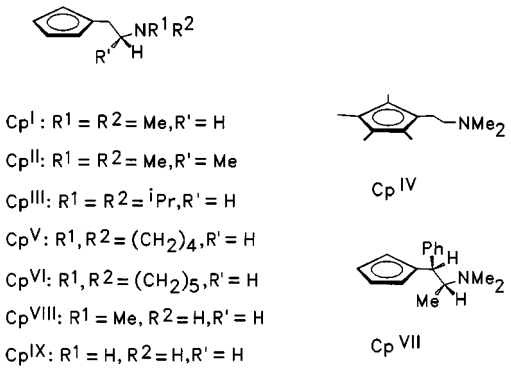

Apart from the general interest in novel ligand systems, we are investigating aminoethyl-functionalized Cp ligands for the following reasons (see Figure 2):

– The nitrogen atom of the aminoethyl group can coordinate to a metal center and block a vacant coordination site (see Figure 2a, d). Otherwise highly reactive intermediates or reaction products will be stabilized by this interaction, thus allowing unprecedented structures and chemical properties. Interesting bonding situations are expected as a function of the formal oxidation state of the respective metal. As documented by many examples, a cyclopentadienyl ligand stabilizes transition metals in high as well as in low oxidation states. On the other hand, the amino group favours coordination to metals in a high oxidation state (hard–hard interactions according to Pearson's concept). To metals in a low oxidation state, only weak interactions are anticipated, which might be strenghtened by the chelate effect; in this case, the aminoethyl-functionalized Cp ligand should behave as a hemilabile ligand. To metals in a high oxidation state, rather strong interactions are expected, which might allow the isolation of compounds even with cationic (aminoethyl)cyclopentadienyl units. In general, a ligated amino group will render the central atom much more electron-rich.

– The hemilabile bonding situation will allow an easy ligand exchange, as described in Figure 2g. The reversible

Figure 2

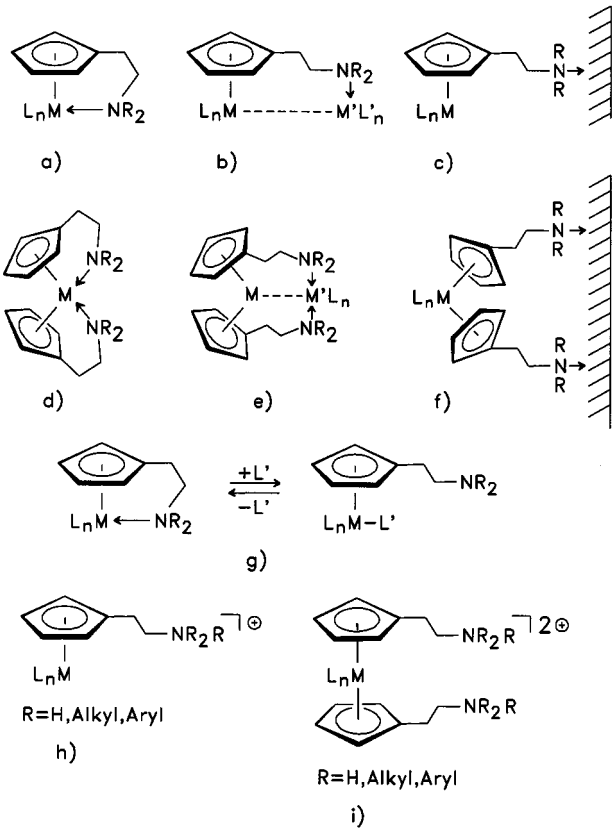

coordination to a reactive metal center is of special interest in connection with catalytic processes; it seems possible to stabilize a highly reactive, electronically and sterically unsaturated intermediate by weakly occupying the vacant coordination site, until the actual substrate coordinates and replaces the amino group. Such processes might increase the lifetime and also the selectivity of the catalyst. A versatile catalyst design is conceivable by modifying the aminoethyl group.

– The amino function can coordinate to an adjacent electron-deficient metal (or nonmetal) center (Figure 2b, e). The resulting homo- or hetero-bimetallic complexes might be stabilized by different kinds of additional interaction; synergetic effects are expected.

– The amino group allows an interaction with Lewis or Broensted acidic surfaces (see Figure 2c, f); this effect is of special interest with regard to the heterogenisation of homogenous catalysts.

– Pendant amino or ammonium groups might have drastical consequences concerning the solubility of respective complexes. The development of an organometallic chemistry in water[10] can be promoted by the application of protonated or alkylated (arylated) aminoethyl-functionalized Cp compounds (see Figure 2h, i).

– Amino or ammonium groups in the side chain might exert electronic and steric effects and thus might induce changes in the chemistry compared to that of the parent compounds. Electronic and steric effects can be altered by

variation of the substitution pattern at the cyclopentadienyl as well as at the amino fragment.

– The presence of N–H bonds in the side chain (Figure 1, compounds Cp^{VIII}, Cp^{IX}) allows further functionalization of the amino group by substitution reactions.

– The presence of protonated amino groups (Figure 2h, i; R′ = H) in principal permits proton-transfer reactions and thus opens new synthetic pathways.

This listing of effects unequivocally explains the current interest in aminoethyl-functionalized Cp complexes. In the following, we present a complete survey of d-block element complexes containing aminoethyl-functionalized cyclopentadienyl systems. Synthetic and structural aspects as well as important properties of these compounds are described with special emphasis to the effects of the tethered aminoethyl function.

Titanium and Zirconium Complexes

We started our efforts in this field synthesizing titanium compounds with the Cp^{I} and the Cp^{III} ligand. The titanium(III) complexes Cp^{I}_2TiCl (**1**) (Figure 3) and Cp^{III}_2TiCl (**2**) were prepared by the reaction of $Cp^{I}Li$ and $Cp^{III}Li$, respectively, with $TiCl_3$.[9m] A single-crystal X-ray structure analysis of **1** revealed a pseudo-tetrahedral coordination sphere and thus the interaction of only one of the two amino groups with the titanium center.[9m] The structure of **2** containing the bulkier diisopropylaminoethyl-functionalized cyclopentadienyl ligand Cp^{III} is still unknown.[9w] The extreme air sensitivity of **2** compared to **1** indicates the non-coordinating nature of the amino function. The organo derivatives Cp^{I}_2TiR (**3**: R = Me; **4**: R = Bz) could be synthesized by simple substitution reactions.[9m] Only very recently, the titanium(III) compound $[(Me_2NCH_2CH_2)Me_4C_5][C_5H_5]TiCl$ with an intramolecular amino-group coordination was synthesized and structurally characterized.[8aa]

In metallocene dichlorides of the type $Cp^{I}_2MCl_2$ (**5**: M = Ti; **6**: M = Zr) (Figure 3), the intramolecular interaction of the amino group turns out to be rather weak. Intermolecular interaction finally dominates due to the formation of insoluble coordination polymers; the structures of these species are still unknown.[8z][9m] The corresponding dimethyl-substituted compounds $Cp^{I}_2MMe_2$ (**7**: M = Ti; **8**: M = Zr) are highly reactive and were therefore only characterized by ^{1}H-NMR spectroscopy.

The metallocene dichlorides $Cp^{III}_2MCl_2$ (**9**: M = Ti; **10**: M = Zr) (Figure 3) could be characterized completely.[9q] A single-crystal X-ray structure analysis of the titanium species **9** reveals a monomeric structure with no intramolecular coordination of the diisopropylamino functions to the metal center. The non-coordinating nature in **9** and **10** can be attributed to steric effects of the isopropyl substituents.

The dialkylaminoethyl functions in this type of metallocene complexes dramatically change the physical as well as the chemical properties. In contrast to the parent complexes Cp_2MCl_2, both types $Cp^{I}_2MCl_2$ and $Cp^{III}_2MCl_2$ are extremely air- and moisture-sensitive. This is due to the effect

Figure 3

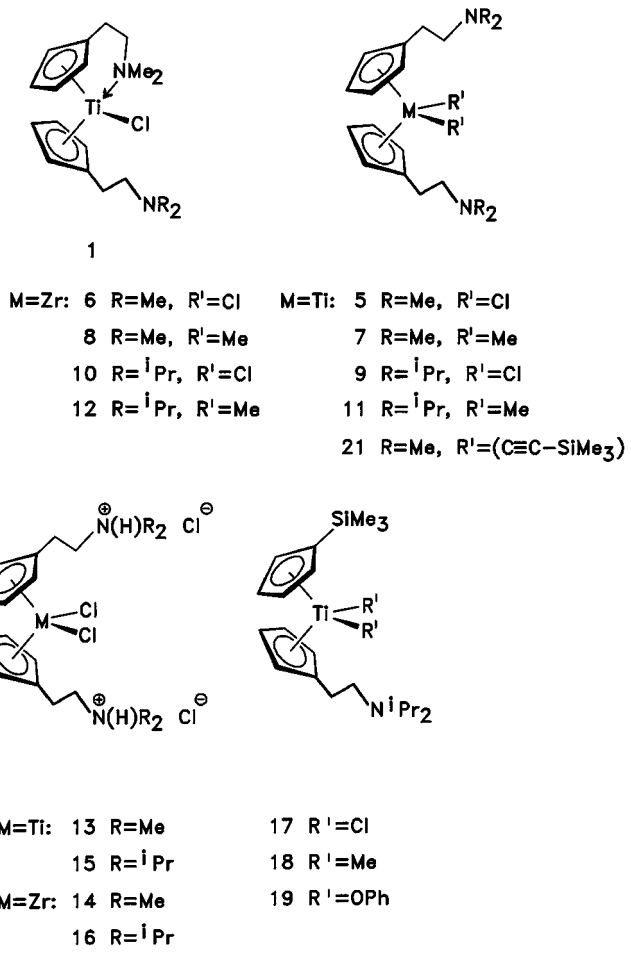

of the amino groups which facilitate the hydrolysis by enhancing the concentration of the attacking OH^- nucleophiles and by trapping the arising hydrogen chloride.

The methyl-substituted metallocenes $Cp^{III}_2MMe_2$ (**11**: M = Ti; **12**: M = Zr) (Figure 3) could be formed straightforwardly by the reaction of the corresponding metallocene dichlorides with methyllithium.[9q] The titanium derivative **11** exhibits a remarkable thermal stability. In contrast to the temperature- and light-sensitive complex Cp_2TiMe_2, for which an autocatalytic, "catastrophic" decomposition is reported[11], **11** is stable for several days under inert gas at room temperature. To explain this phenomenon, we propose a protecting effect of the N*i*Pr_2 group, which prohibits an α-elimination decomposition. Until now, an intramolecular coordination could not be proved unequivocally.

The metallocene dichlorides **5**, **6**, **9** and **10** could be converted quantitatively into the corresponding hydrochlorides $Cp^{I}_2MCl_2 \times 2$ HCl (**13**, **14**) and $Cp^{III}_2MCl_2 \times 2$ HCl (**15**, **16**) (Figure 3).[9q] In these compounds the protonated amino groups lead to drastic changes in the physical and chemical properties as compared to those of the non-protonated species. The hydrochlorides show an excellent solubility and stability in polar solvents such as chloroform or acetonitrile. Furthermore, solvolysis of the M–Cl bonds in protic solvents such as methanol or even water is prevented.

This is due to the effect of the ammonium groups which function as Broensted acids and reduce the concentration of the attacking OH^- nucleophiles, which are responsible for the hydrolytic process. Because of their exceptional stability, the hydrochlorides possess a long shelf life. Furthermore, they are useful starting materials for the synthesis of catalytically relevant species. For example, the metallocene dichloride dihydrochlorides **15** and **16** could be transformed with four equivalents of methyllithium into the dimethyl compounds **11** and **12** (Scheme 1).[9q] It is remarkable that a quantitative retransformation of the dimethyl compounds **11** and **12** back to the hydrochlorides **15** and **16** could be achieved by reaction with four equivalents of HCl in methanolic solution. No decomposition products were observed.

Scheme 1

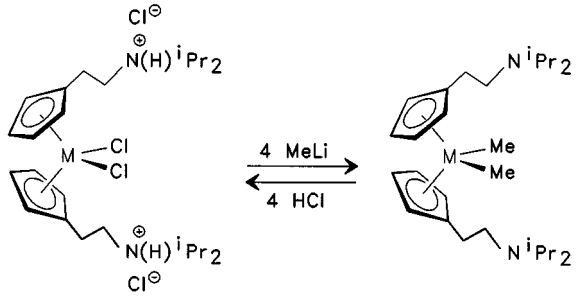

The mixed bent-sandwich complex $Cp^{III}Cp^{S}TiCl_2$ (**17**) (Cp^S = $CpSiMe_3$) containing only one (diisopropylaminoethyl)cyclopentadienyl ligand could be obtained by treating a solution of the halfsandwich complex $Cp^{S}TiCl_3$ with one equivalent of $Cp^{III}Li$ (Figure 3).[9r] The corresponding substituted derivatives $Cp^{III}Cp^{S}TiR_2$ [R = Me (**18**); PhO (**19**)] (Figure 3) as well as the hydrochloride $Cp^{III}Cp^{S}TiCl_2 \times HCl$ (**20**) can be synthesized in analogy to the symmetric titanocene complexes as described above.[9q] Only very recently, other titanocene derivatives with the Cp^{IV} ligand were synthesized and structurally characterized. They all show a non-coordinating amino group, but intermediate ligation was postulated to explain the observed reaction products.[8aa]

The metallocene dichlorides as well as the hydrochlorides containing the Cp^{III} ligand are catalyst precursors for the polymerization of ethylene; the productivities of the catalyst systems are comparable to those of the parent metallocene derivatives.[9q][9r] Furthermore, high catalytic activity in the dehydrocoupling of phenylsilane is observed for the methyl- and phenoxy-substituted derivatives.[9q][9r] The poly(phenylsilanes) obtained exhibit analytical data similar to those prepared with the parent catalyst system.

After the reaction, the catalytic species or its decomposition products generally remain in the polymer (leave-in catalysts) or are destroyed during the separation process and thus cannot be employed again. In our case, the influence of the diisopropylaminoethyl side chain provides sufficient stability to allow for efficient recycling of the pre-catalysts by a simple extraction procedure with methanol and aqueous HCl, as shown in Scheme 2 for complex **20**.[9v]

Scheme 2

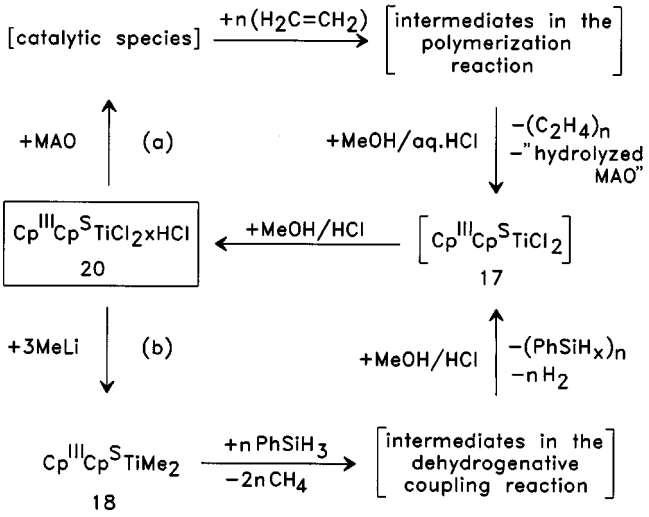

Enders et al. described the reaction of the polymeric titanocene $Cp^{I}_2TiCl_2$ (**5**) with two equivalents of $LiC{\equiv}CSiMe_3$ to afford the temperature-sensitive, monomeric bis(alkynyl)titanocene derivative $Cp^{I}_2Ti(C{\equiv}CSiMe_3)_2$ (**21**) (Figure 3).[8z] The reaction of **21** with AgCl and $Cu(SC_6H_4CH_2NMe_2)_2$, respectively, yielded the heterobimetallic titanium-silver and titanium-copper complexes $[Cp^{I}_2Ti(C{\equiv}CSiMe_3)_2][AgCl]$ (**22**) and $[Cp^{I}_2Ti(C{\equiv}CSiMe_3)_2][Cu(SC_6H_4CH_2NMe_2)_2]$ (**23**); a coordination of the N functions to the metal centers could not be observed.[8z]

Further mixed aminoethyl-functionalized zirconocene complexes have been prepared by Tanaka et al.[8t] $Cp(IndCH_2CH_2NMe_2)ZrCl_2$ (**24**) and $Cp^*(IndCH_2CH_2NMe_2)ZrCl_2$ (**25**) (Ind = C_9H_6, Cp* = C_5Me_5) (Figure 4) could be obtained by the reaction of the appropriately substituted indenyllithium with Cp^*ZrCl_3 and $CpZrCl_3$.[8t] NMR spectroscopy did not reveal any indication of an amino-group coordination. These complexes, activated with 2 equiv. of *n*BuLi, catalyze the dehydrocoupling polymerization of phenylsilane to afford high-molecular-weight poly(phenylsilanes). ^{29}Si-NMR spectroscopy indicates that the microstructure of the resulting polymers is predominantly syndiotactic.[8t]

Figure 4

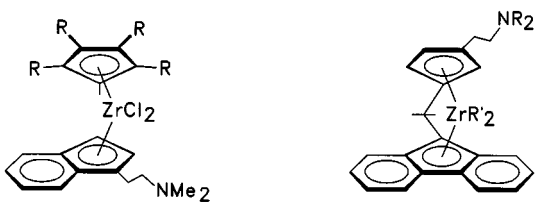

24 R=H
25 R=Me

26 R=Me,R'=Cl
27 R=iPr,R'=Cl
28 R=Me,R'=Me
29 R=iPr,R'=Me

In the context of our studies of metallocene complexes with early transition metals we focussed our efforts also on the synthesis of ansa-zirconocenes. There is considerable interest in the preparation of ansa-zirconocenes as precursors for olefin polymerization catalysts;[12] the bridging unit as well as the substituents of both Cp rings greatly influence the activity and the stereoselectivity of the polymerization reaction.

Very recently, we synthesized the compounds $[(C_{13}H_8)CMe_2(C_5H_3CH_2CH_2NMe_2)]ZrCl_2$ (**26**) and $[(C_{13}H_8)CMe_2(C_5H_3CH_2CH_2N\mathit{i}Pr_2)]ZrCl_2$ (**27**), which are the first examples of dialkylaminoethyl-functionalized ansa-zirconocenes (Figure 4).[9x] Single-crystal X-ray analyses reveal the monomeric structure of these complexes. The amino groups are not coordinating to the zirconium center. The dialkyaminoethyl-functionalized side chains in β-position to the C_1 bridge might be essential for affecting the stereoselectivity in the polymerization of propylene. The dimethyl derivatives **28** and **29** (Figure 4) were obtained in high yields by the reaction of **26** and **27**, respectively, with two equivalents of methyllithium.[9x] Complexes **28** and **29** are highly moisture-sensitive, orange-yellow oils with a good solubility in nonpolar aprotic solvents such as toluene. Examinations of these complexes with respect to their potential use in catalytic reactions are in progress.

Although group-4 metallocenes dominate the homogeneous Ziegler-Natta polymerizations of ethylene and propylene, also halfsandwich complexes are employed as precursors in many catalytic reactions. In this context, several titanium and zirconium halfsandwich complexes containing dialkylaminoethyl functionalized cyclopentadienyl ligands were synthesized.

The compound Cp^ITiCl_3 (**30**) is the first titanium halfsandwich complex with an intramolecularly coordinating amino function, as reported by Rausch and co-workers (Figure 5).[7n] The amino group affects significantly the catalytic reactivity of **30** as compared to that of the parent complex $CpTiCl_3$. The system **30**/MAO (MAO: methylaluminoxane) shows a considerably lower activity towards styrene and an impressively increased activity towards ethylene and propylene. This is most likely due to the coordination behaviour of the amino group which influence the coordination of the incoming monomer.[7n] Cyclopentadienyl complexes of titanium with tethered pyrrolidinyl and piperidinyl functions were introduced by Herrmann and co-workers.[8c] The titanium halfsandwich complexes Cp^VTiCl_3 (**31**) and $Cp^{VI}TiCl_3$ (**32**) were prepared by the reaction of the silylated cyclopentadiene precursor with $TiCl_4$. X-ray crystal-structure results confirm the intramolecular nitrogen coordination to the titanium(IV) center (Figure 5). Van der Zeijden designed the chiral dimethylaminoethyl-functionalized cyclopentadienyl titanium halfsandwich complex $Cp^{VI}TiCl_3$ (**33**) by the reaction of the trimethylsilyl derivative $Cp^{VII}SiMe_3$ with $TiCl_4$ (Figure 5).[8l] In the titanium compound **33** the nitrogen side chain is only weakly coordinated, NMR spectroscopy indicates a fluxional coordination of the amino side arm. This is in contrast to Cp^ITiCl_3 (**30**), where a rigid intramolecular coordination is observed.

Figure 5

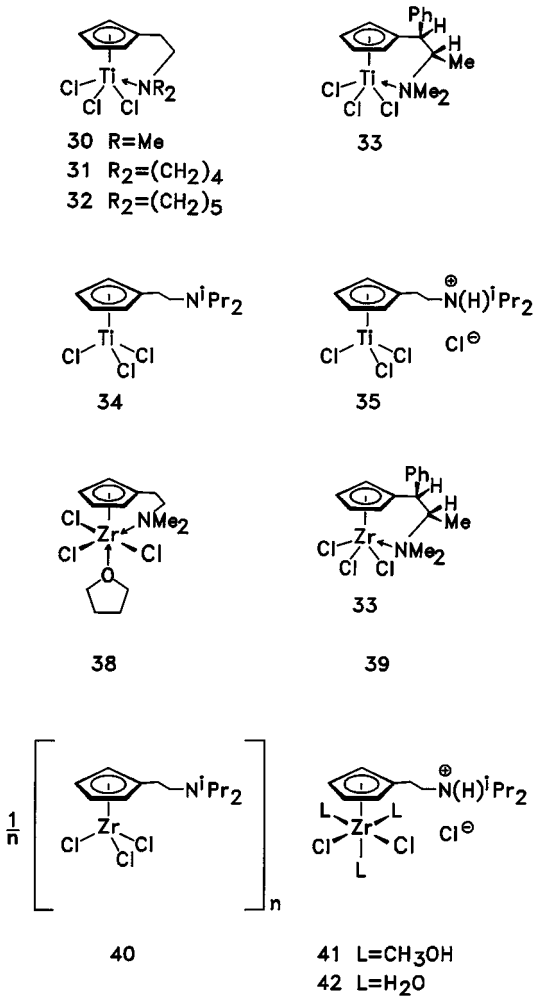

In the halfsandwich complex $Cp^{III}TiCl_3$ (**34**), synthesized by our group,[9u] the amino group is obviously not strongly coordinating intramolecularly to the titanium center (Figure 5); however, a weak intermolecular coordination was observed. The different coordination behaviour of **34** as compared to **30**−**33** can be attributed to steric effects of the bulkier isopropyl substituents at the amino function. Complex **34** reacted with one equivalent of HCl under protonation of the amino group to give the monomeric hydrochloride $Cp^{III}TiCl_3 \times HCl$ (**35**), which shows excellent solubility in polar solvents (Figure 5).[9u] Similar O-brigded dimers $[Cp^ITiCl]_2O \times 2HCl$ (**36**)[7n] and $[Cp^{VII}TiCl]_2O \times 2HCl$ (**37**)[8l] were obtained by the reaction of the halfsandwich complexes **30** and **33,** respectively, with traces of water.

In the trichlorozirconium complex $Cp^IZrCl_3 \times THF$ (**38**) an intramolecular coordination of the amino group takes place. (Figure 5). The monomeric structure of the THF adduct was proved by a single-crystal X-ray structure investigation.[9m] Van der Zeijden also synthesized the chiral zirconium species $Cp^{VII}ZrCl_3$ (**39**) (Figure 5).[8l] In contrast

to the corresponding titanium species $Cp^{VII}TiCl_3$ (**33**), the amino group is firmly coordinated to the metal center. Moreover, **39** still behaves as a moderate Lewis acid and catalyzes the Diels-Alder reaction of methacroleine with cyclopentadiene, but without measurable enantiomeric excess.[8l]

The zirconium compound $[Cp^{III}ZrCl_3]_x$ (**40**) (Figure 5) containing the bulkier diisopropylaminoethyl group forms a coordination polymer, comparable to the situation found for the analogous titanium species **34**.[9u] Compound **40** reacted with one equivalent of HCl under protonation of the amino group to give the monomeric air- and moisture-stable hydrochloride **41**, which crystallized with two additional methanol molecules in the coordination sphere of the zirconium atom (Figure 5).[9u] The reaction of **41** with water, which involves exchange of the donor ligands, led to the formation of the air- and water-stable hydrochloride **42** (Figure 5).[9u]

The extremely high air and moisture sensitivity of all described neutral halfsandwich complexes is worth mentioning. In contrast, the halfsandwich complexes with a protonated amino function are stable against air and moisture and soluble in protic solvents such as methanol. These properties of the protonated sandwich and halfsandwich compounds may be of special interest with regard to organometallic chemistry in water.

Vanadium, Chromium and Molybdenum Complexes

Only recently Enders and co-workers[8z] described the synthesis of the first dimethylaminoethyl-functionalized vanadocene and chromocene derivatives. The reaction of two equivalents of the metallated Cp^I ligand with in-situ prepared VCl_2 and $CrCl_2$, repectively, afforded the paramagnetic vanadocene and chromocene compounds $Cp^I{}_2M$ [M = V (**43**); M = Cr (**44**)]. The paramagnetic behaviour (spin-only value) is comparable to that of the parent complexes Cp_2Cr and Cp_2V. NMR data did not reveal any coordination of the N functions.

The first dimethylaminoethyl-functionalized bis(cyclopentadienyl)molybdenum complex was already synthesized by Green et al. in 1983.[7a] The functionalized molybdenum complex $[Mo(C_5H_4CH_2CH_2I)_2I_2]$ (**45**) (Scheme 3) reacted with dimethylamine and subsequently with ammonium hexafluorophosphate to give the ionic compound $[Mo(Cp^I)(C_5H_4CH_2CH_2NMe_2H)H]^{2+}[PF_6]^-{}_2$ (**46**) with the dimethylamino group intramolecularly coordinating to the molybdenum center. The structure of **46** as proposed on the basis of ^{1}H-NMR data is shown in Scheme 3.

Only very recently, the synthesis of halfsandwich complexes of chromium (type **46a**–**d**, Figure 5a) with an intramoleculary coordinating amino group was reported. These compounds were obtained as deep blue species by the reaction of $Cr(THF)_3Cl_3$ with the corresponding cyclopentadienyl alkali metal salts. In the mixture with MAO (MAO: methylaluminoxane), highly effective catalysts for olefin polymerisation are formed. Surprisingly, full catalytic activity is already reached in a molar Al/Cr ratio of 45–300:1.[*]

Figure 5a

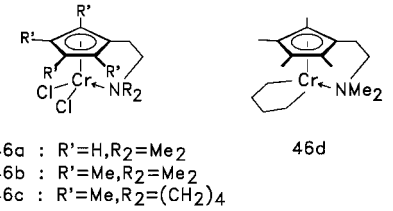

46a : R'=H, R_2=Me_2
46b : R'=Me, R_2=Me_2
46c : R'=Me, R_2=$(CH_2)_4$

46d

Wang and co-workers[7f] synthesized various molybdenum halfsandwich complexes in which the pendant dimethylaminoethyl group is coordinating intramolecularly to the metal center. Reaction of $Mo(CO)_6$ with Cp^ILi and subsequently with iodine led to the tricarbonyl complex $Cp^IMo(CO)_3I$ (**47**), which was transformed into the dicarbonyl compound $Cp^IMo(CO)_2I$ (**48**) (Scheme 4) by irradiation. Treatment of **48** with silver tetrafluoroborate led to the ionic molybdenum complex **49** (Scheme 4).[7f] An intramolecular coordination of the amino group takes place in **48** as well as in **49**.[7f]

Scheme 3

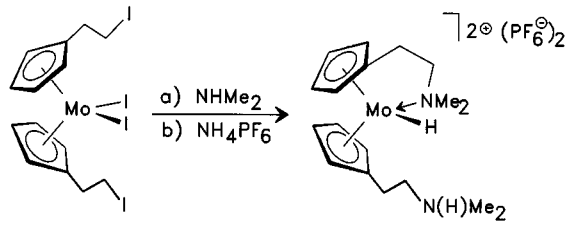

45 46

Scheme 4

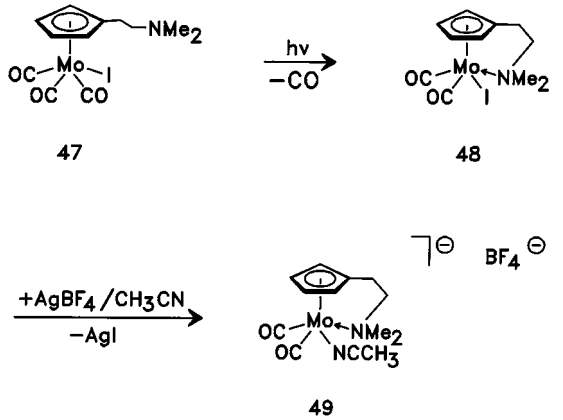

47 48

49

The dimethylaminoethyl-functionalized cyclopentadienylmolybdenum complex $(C_6H_9)Cp^IMo(CO)_2$ (**50**) (Scheme 5) was prepared by adding Cp^ILi to $(C_6H_8)Mo(CO)_2(CH_3CN)_2Br$.[7g] Reaction of **50** with trityl hexafluorophosphate provided the ionic compound $[(C_6H_8)Cp^IMo(CO)_2]^+[PF_6]^-$ (**51**) by hydride abstraction (Scheme 5). Treatment of **51** with trimethylamine *N*-oxide

[*] Note added in proof: P. Jolly, K. Ionas, G. P. I. Verkovnic, German Patent 19630580 A1, **1998**.

Scheme 5

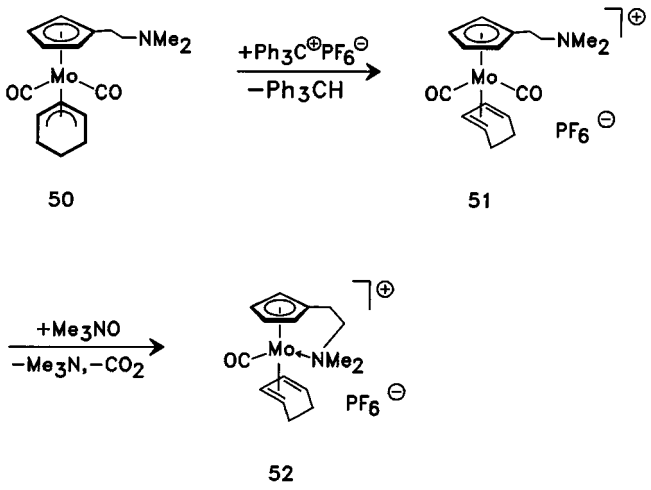

Scheme 6

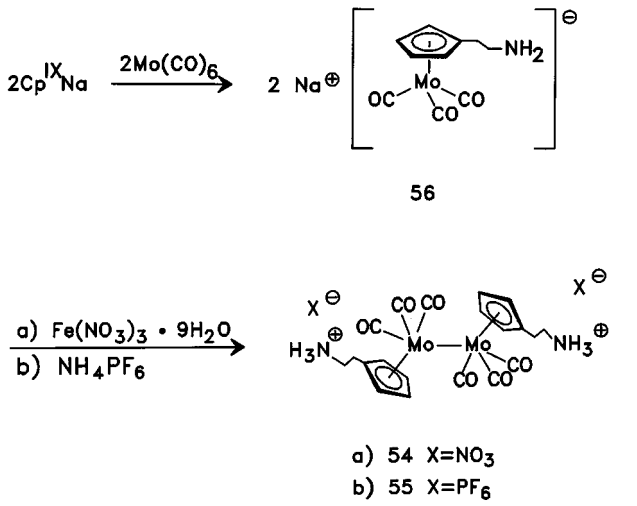

removed carbon monoxide to give $[(C_6H_8)(C_5H_4CH_2CH_2NMe_2)Mo(CO)]^+[PF_6]^-$ (**52**). (Scheme 5). A single-crystal X-ray structure analysis of **52** confirmes the intramolecularly coordinating dimethylamino group and the *exo* conformation of the cyclohexadiene ligand.[7g] Cationic dienylmolybdenum complexes are pertinent substrates for organic syntheses. Complexes of type **52** are particularly interesting because the electrophilicity is weakened as a result of amine coordination. Furthermore, the metal center is now chiral.

The dinuclear molydenum complex $[Cp^{IV}Mo(CO)_2]_2$ (**53**) was synthesized by our group.[9k] The structure analysis revealed that the side chains do not coordinate to the central metal atoms and lie on opposite sides of the Mo−Mo axis.[9k]

Avey and Tyler described the synthesis of the ammonioethyl-functionalized dimeric molybdenum complexes $Cp^{IX}{}_2Mo_2(CO)_6 \times 2$ HX (**54**: X = NO_3; **55**: X = PF_6) by reaction of $Cp^{IX}Na$ with $Mo(CO)_6$ and by subsequent oxidation of the anion $[Cp^{IX}Mo(CO)_3]^-$ (**56**) with $Fe(NO_3)_3 \cdot 9\ H_2O$ in water. The exchange of the anion in **54** with NH_4PF_6 afforded **55** (Scheme 6).[7h] It is noteworthy that in contrast to **55,** which is soluble in common organic solvents like THF, complex **54** is soluble and stable in aqueous solution.

Interestingly, the photochemistry of **55** differs from that of the parent complex $Cp^x{}_2Mo_2(CO)_6$ (**57**) (Cp^x = C_5H_4Me). Mechanistic work established that the different reactivities can be ascribed to a supramolecular effect of the tentacle ligand.[7l] Irradition of either dimer complex led to photolytic cleavage of the metal−metal bond. The photogenerated 17-electron radical complexes then reacted with THF (the solvent) to form 19-electron adducts; disproportionation then followed. The initial products were $[Cp^xMo(CO)_3(THF)]^+$, $[Cp^xMo(CO)_3]^-$ and

Scheme 7

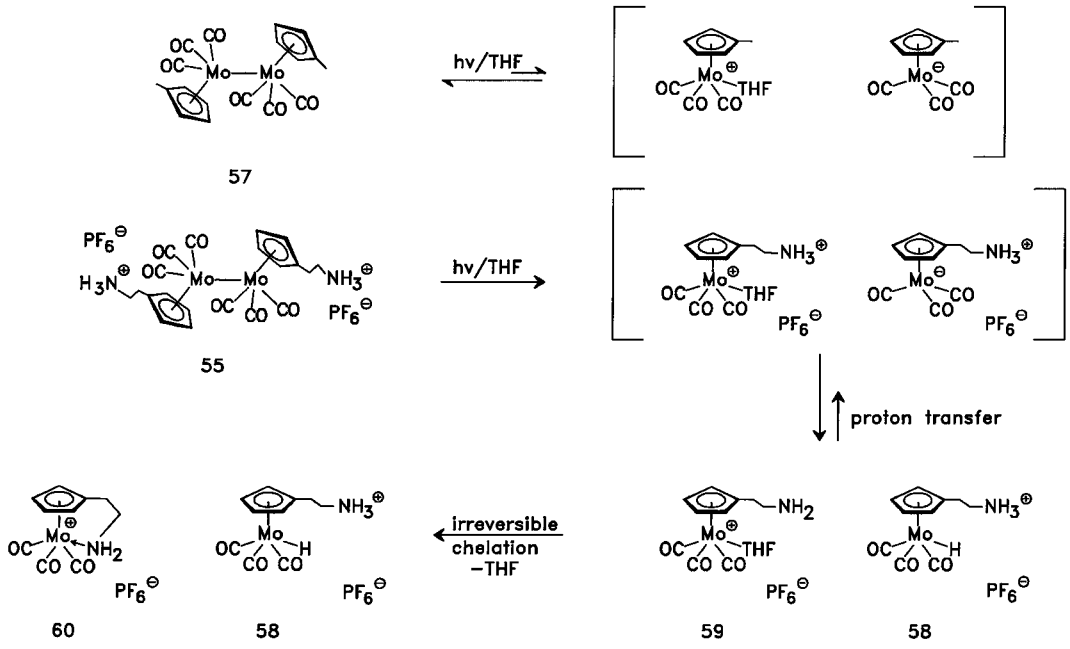

Scheme 8

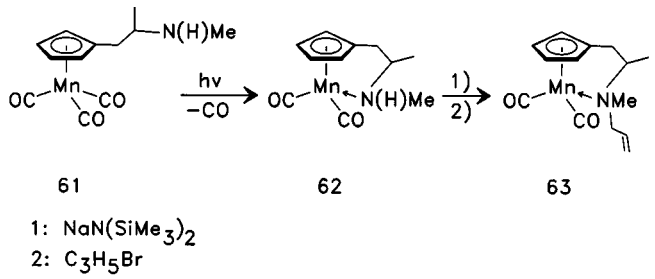

$[Cp^{IX}Mo(CO)_3(THF)]^+$, $[Cp^{IX}Mo(CO)_3]^-$, respectively (Scheme 7). In the case of the dimer **57**, a facile back reaction of these products ensued, and the net result was no reaction, even in the presence of an excess of $[C_6H_5CH_2CH_2NH_3]^+[PF_6]^-$.[7l] In the case of the tentacle dimer $Cp^{IX}{}_2Mo(CO)_6 \times 2\ HPF_6$ (**55**), proton transfer from the ammonium group to the anion yielded $Cp^{IX}Mo(CO)_3H \times HPF_6$ (**58**) and $[Cp^{IX}Mo(CO)_3THF]^+[PF_6]^-$ (**59**), and then facile coordination of the free amine by displacing the THF ligand effectively blocked the back reaction by forming $[Cp^{IX}Mo(CO)_3]^+[PF_6]^-$ (**60**) irreversibly.

The described cooperative interaction between the tentacle ligands and the unstable initial products of disproportionation to yield stable products is regarded as an example of supramolecular reactivity.[7l]

Manganese and Rhenium Complexes

Wang et al.[7e] synthesized the manganese complex $Cp^{VIII}Mn(CO)_3$ (**61**) by treating $Mn(CO)_5Br$ with $Cp^{VIII}Li$ (Scheme 8). Irradiation of **61** removed carbon monoxide and gave rise to an intramolecular amine-group ligation to provide complex **62** (Scheme 8).[7e] Deprotonation of **62** with $NaN(SiMe_3)_2$ and subsequent addition of allyl bromide led to the alkylation product **63** (Scheme 8). The X-ray analysis clearly shows that allylation occurred at the nitrogen atom and not at the manganese center.[7e] The sequence **62** → **63** is an example of further amino-group functionalization in complexes with aminoethyl-substituted Cp ligands still containing N−H functions.

The first rhenium complexes containing an *N*-functionalized cyclopentadienyl ligand and further interesting reaction sequences were reported by Wang et al.[8d] The lithium salts $Cp^{I}Li$ and $Cp^{VIII}Li$ were shown to react with $Re(CO)_5Br$ to provide the halfsandwich complexes $Cp^{I}Re(CO)_3$ (**64**) and $Cp^{VIII}Re(CO)_3$ (**65**) (Scheme 9). Irradiation of **64** and **65** afforded the complexes $Cp^{I}Re(CO)_2$ (**66**) and $Cp^{VIII}Re(CO)_2$ (**67**), respectively, in which the

Scheme 9

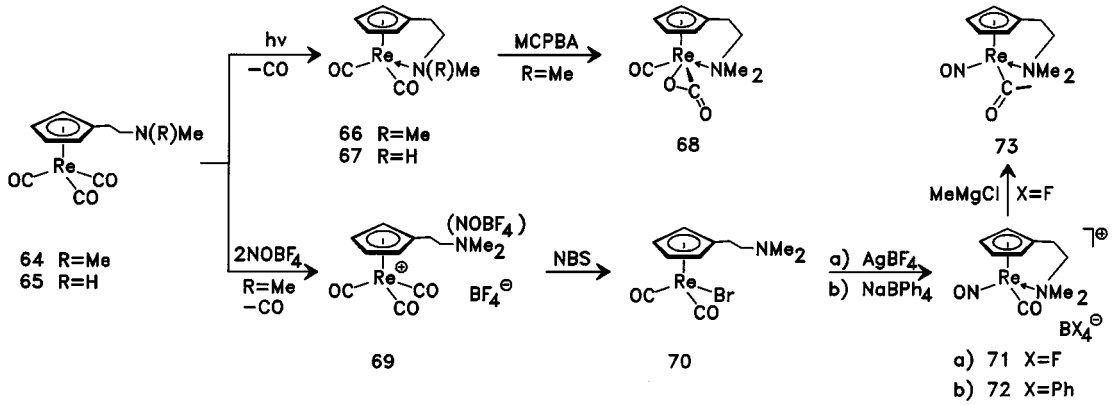

Scheme 10

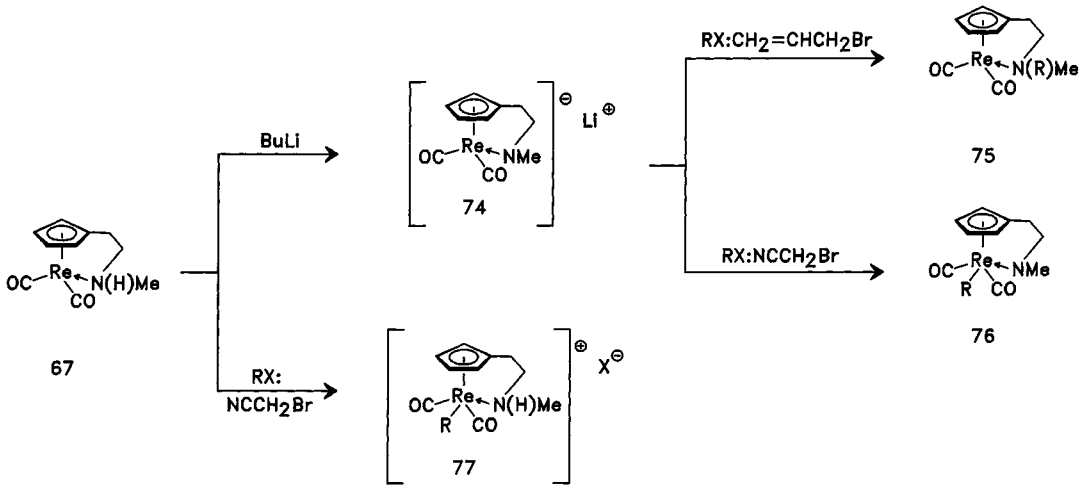

amino group is bound intramolecularly to the rhenium center (Scheme 9).[8d][8u] Oxidation of **66** with 3-chloroperoxybenzoic acid (MCPBA) provided the complex $Cp^IRe(CO)(CO_2)$ (**68**) (Scheme 9), the first example of a mononuclear CO_2 complex in rhenium chemistry. The structure of **68** is confirmed by X-ray crystallography.[8u] Reaction of **65** with two equivalents of $NOBF_4$ gave the nitrosylrhenium complex $[Cp^IRe(NO)(CO)_2]^+[BF_4]^- \times NOBF_4$ (**69**),[8k] which was treated with NBS to afford the bromo complex $Cp^IReBr(NO)(CO)$ (**70**) (Scheme 9). Removal of the bromide ion with $AgBF_4$ resulted in amino-group coordination to give the ionic complex $[Cp^IRe(CO)(NO)]^+[BF_4]^-$ (**71**) (Scheme 9). The X-ray diffraction study of the corresponding tetraphenylborate $[Cp^IRe(CO)(NO)]^+[BPh_4]^-$ (**72**) confirms the amino-group coordination.[8k] Reaction of the rhenium complex **71** with alkylating reagents occurred at the carbonyl carbon atom to provide acyl complexes. For instance, the reaction with methylmagnesium chloride led to the acyl derivative $Cp^IRe(NO)(COMe)$ (**73**) in which the amino group is still coordinating (Scheme 9).[8k] It is worth mentioning that the corresponding triphenylphoshane complex did not react with alkylmetal reagents to provide acyl complexes. Obviously, the influence of the amino function is necessary for this synthetic pathway.

Deprotonation of the N−H function in **67** with *n*BuLi led to the ionic compound **74** (Scheme 10), which reacted with electrophiles such as $CH_2{=}CHCH_2Br$ at the nitrogen center to provide the complex $[C_5H_4CH_2CH_2N(Me)(CH_2{=}CHCH_2)]Re(CO)_2$ (**75**) with to different substituents at the nitrogen atom (Scheme 10).[8u] This is another example of a further functionalization of an aminoethyl-substituted Cp ligand. However, **74** reacted with electrophiles such as $BrCH_2CN$ to give the alkylrhenium compound $Cp^IRe(CO)_2CH_2CN$ (**76**) (Scheme 10). Thus, the regioselectivity is dependent on the nature of the electrophile and can be explained on the basis of the hard-soft acid-base principle.[8u] Reaction of the neutral complex **66** with $BrCH_2CN$ gave exclusively the alkylrhenium compound $[Cp^IRe(CO)_2CH_2CN]^+[Br]^-$ (**77**).[8u] It is remarkable that the parent rhenium complex $CpRe(CO)_3$ does not react with $BrCH_2CN$. Thus, the electron donation of the amino ligand is important to promote the reactivity towards carbon electrophiles.

Iron Complexes

Treatment of $FeCl_2$ in THF with two equivalents of the lithiated ligand $Cp^{IV}Li$ yielded the dimethylaminoethyl-functionalized ferrocene $Cp^{IV}{}_2Fe$ (**78**).[9a] The analogous ferrocene $Cp^I{}_2Fe$ (**79**) could be synthesized in a similar manner.[7s] Not unexpectedly, no amino-group coordination is observed; the 18-electron rule is obeyed in both complexes by η^5-Cp bonding. Reaction of $Cp^{IV}H$ with $Fe(CO)_5$ led to the formation of the dimeric dicarbonyl(cyclopentadienyl)iron complex $[Cp^{IV}Fe(CO)_2]_2$ (**80**). In this compound, no intramolecular displacement of a CO ligand by the amino groups could be initiated.[9c] However, the cationic cyclopentadienyl iron halfsandwich complex $[Cp^{IV}Fe(CO)_2]^+[BF_4]^-$ (**81**), which was obtained by the reaction of **80** with $AgBF_4$, is stabilized by an intramolecular coordination of the amino group (Scheme 11).[9c]

Scheme 11

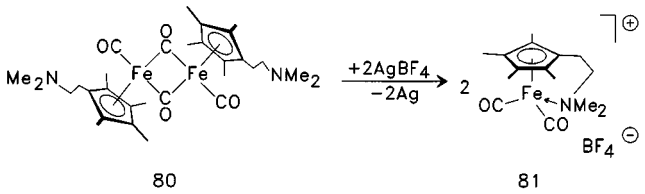

80 81

Cobalt, Rhodium and Iridium Complexes

Several halfsandwich complexes with the Cp^{IV} ligand and with the central atoms cobalt, rhodium and iridium were obtained by classical synthetic routes.[9b][9h] In compounds of the type $Cp^{IV}ML_2$ (M = Co, Rh, Ir; L = CO, C_2H_4) with the metals in the oxidation state +1, amino-group coordination is generally not observed. In compounds with the metals in the oxidation state +3, coordination depends on the further ligands present. The interplay between the donor ligands and the metal center can be tuned to a certain extent. An irreversible displacement was observed in the reaction of complexes of the type $Cp^{IV}MX_2$ (**82**) (M = Co, Rh, Ir; X = I; $X_2 = C_2O_4$) with stoichiometric amounts of trimethylphosphane or *tert*-butyl isonitrile to afford $Cp^{IV}M(L)X_2$ (**83**). With carbon monoxide, the displacement reaction leading to $Cp^{IV}M(CO)I_2$ (**84**) is reversible (Scheme 12).[9b][9h]

Scheme 12

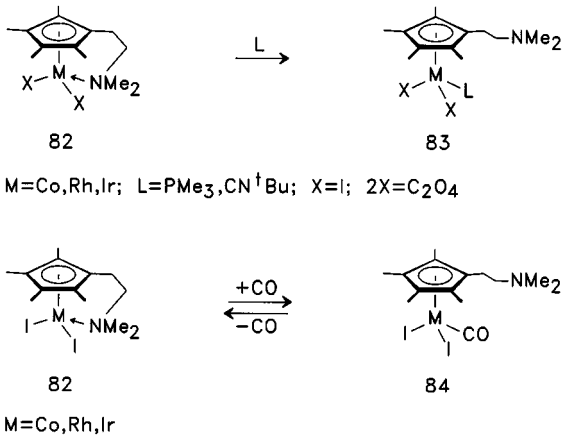

Poilblanc et al. described the synthesis of the rhodium(I) complex $Cp^IRh(cod)$ (**85**) (Scheme 13) by reaction of Cp^INa with $[Rh(cod)Cl]_2$.[8w] Oxidation with iodine resulted in the formation of the rhodium(III) complex Cp^IRhI_2 (**86**) (Scheme 13) with a coordinating amino group.

Scheme 13

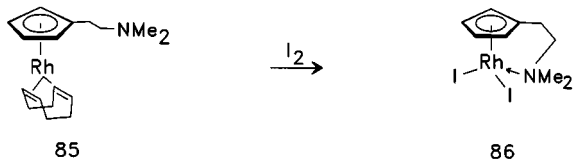

85 86

The reaction of **85** with HCl afforded the corresponding water-soluble hydrochloride $Cp^{I}Rh(cod) \times HCl$ (**87**). It is noteworthy that a reversible transformation to **85** could be achieved by treating **87** with a slight excess of *n*-butyllithium. The water-soluble rhodicinium complex $Cp^{I}_2RhCl \times 2\ HCl$ (**88**) was obtained by the reaction of the cyclopentadiene $Cp^{I}H$ with $Na_3RhCl_6 \times 12\ H_2O$.[8w]. Generally, the synthesis of this kind of compounds requires previous deprotonation of the cyclopentadiene by an auxiliary base. In case of the preparation of **88**, the role of the auxiliary basic reagent is probably adopted by the free amino group attached to the cyclopentadiene. The solubility of **87** and **88** in water is interesting in the context of a screening for antitumor activity.[8w]

Nickel, Palladium and Platinum Complexes

We were successful in the preparation of the dimeric carbonylnickel(I) complex $[Cp^{IV}Ni(CO)]_2$ (**89**) (Scheme 14) by the reaction of $Ni(CO)_4$ with $Cp^{IV}Li$ and subsequent oxidation with CuCl.[9n] The analogous complex $[Cp^{I}Ni(CO)]_2$ (**90**) (Scheme 14) containing the Cp^{I} ligand could be synthesized by Fischer and co-workers by a synproportionation of the nickelocene Cp^{I}_2Ni (**91**) with $Ni(CO)_4$.[8n][8o][8p] As expected, in both complexes no coordination of the pendant dimethylamino groups is observed.

Scheme 14

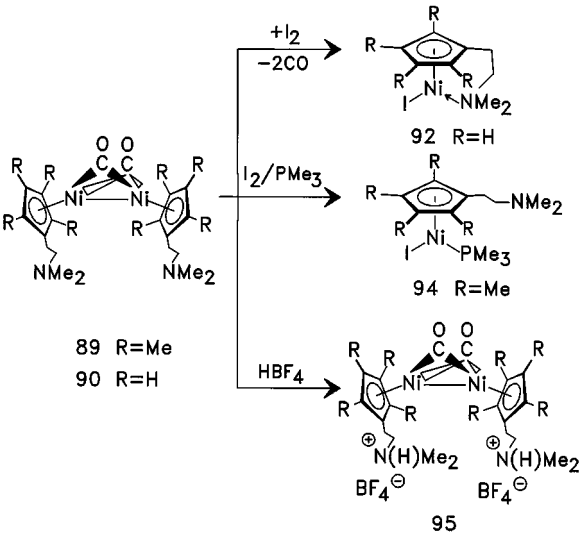

Cleavage of **90** with iodine gave the monomeric nickel complex $Cp^{I}NiI$ (**92**) with a coordinating amino group (Scheme 14).[8n][8o][8p] The CO-free complex **92** might be an interesting starting material for MOCVD studies. Attemps to prepare the corresponding permethylated complex $Cp^{IV}NiI$ (**93**) failed.[9g] Cleavage of **89** with iodine in the presence of PMe_3 afforded the monomeric nickel(II) halfsandwich complex $Cp^{IV}Ni(PMe_3)I$ (**94**) (Scheme 14).[9n] Complex **89** reacted with two equivalents HBF_4 under protonation of the amino groups to give the ionic, air stable compound $[Cp^{IV}Ni(CO)]_2 \times 2HBF_4$ (**95**) (Scheme 14), which shows excellent solubility and stability in polar solvents such as nitromethane and acetonitrile.[9n]

The reaction of **92** with $[(thf)_3Li\{Si[Si(CH_3)_3]_3\}]$ finally afforded the nickel halfsandwich complex **96** (Scheme 15). This is the first example in which the amino function coordinates to an element (silicon) directly attached to the central metal. The structure of **96** is proven by a single-crystal X-ray structure analysis. When **92** was treated with $[(thf)_3Li\{Si[Si(CH_3)_3]_3\}]$ in the presence of PPh_3, the "normal" substitution product $Cp^{IV}Ni(PPh_3)I$ (**97**) was obtained (Scheme 15).[8n][8o][8p]

Scheme 15

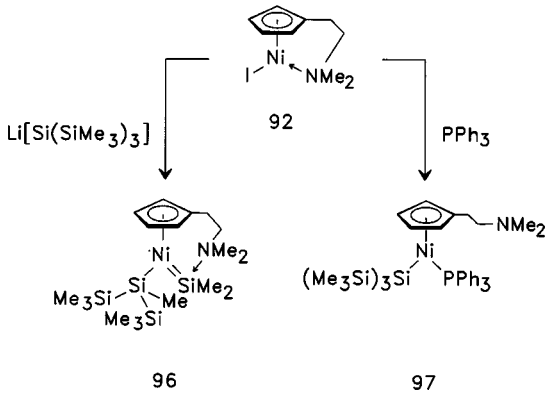

The reaction of **92** with PPh_3 and with low-valent indium bromide in the presence of NaI afforded the complex μ-$Cp^{I}Ni(PPh_3)InI_2$ (**98**) (Figure 16) with intramolecular coordination of the dimethylamino group.[8n][8o][8p] Another complex in which the amino group is coordinating to the adjacent electron-deficient metal center is the heterobimetallic compound μ-$Cp^{I}Ni(CO)GaCl_2$ (**99**) (Figure 6) which was obtained by the reaction of $[Cp^{I}Ni(CO)]_2$ (**90**) with Ga_2Cl_4.[8n][8o][8p] Both complexes **98** and **99** might be interesting as MOCVD precursors for nickel-indium and nickel-gallium alloy thin films.

Figure 6

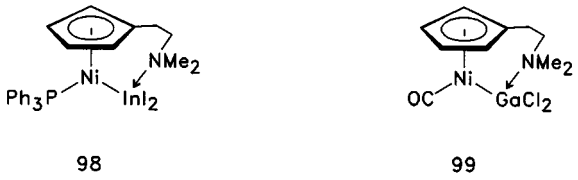

In the chemistry of palladium only dimethylaminoethyl-functionalized cyclopentadienyl complexes with the permethylated Cp^{IV} ligand are known. Reaction of $[Pd(CO)Cl]_n$ with $[Cp^{IV}MgCl]_2$ gave the thermally labile dimeric palladium complex $(Cp^{IV}PdCO)_2$ (**100**) in a mixture with $Cp^{IV}H$.[9n] The synthesis of the palladium halfsandwich complex $Cp^{IV}PdC_3H_5$ (**101**) demonstrated that even in complexes with the palladium metal in the +2 oxidation state, the amino group could not compete with a π-allyl ligand.[9n] The preparation of the dimeric platinum(I) complex $[Cp^{IV}Pt(CO)]_2$ (**102**) failed.[9g] However, the halfsandwich complex $Cp^{IV}PtMe_3$ (**103**) with a Pt^{IV} metal center was obtained in the reaction of $[IPtMe_3]_4$ with $Cp^{III}Li$ (Scheme 16).[9n] In this complex the 18-electron rule is obeyed, and thus no coordination of the amino group is ex-

pected. The reaction of **103** with one equivalent of HBF_4 did not result in an elimination of methane and subsequent amino coordination, but led to the formation of $Cp^{IV}PtMe_3 \times HBF_4$ (**104**) with a protonated amino group, which shows an excellent solubility in polar solvents (Scheme 16).[9n] With two equivalents of HBF_4, however, elimination of methane did occur, and **103** was transformed into the fluoro-substituted compound $Cp^{IV}Pt(F)Me_2 \times HBF_4$ (**105**) (Scheme 16).[9n]

Scheme 16

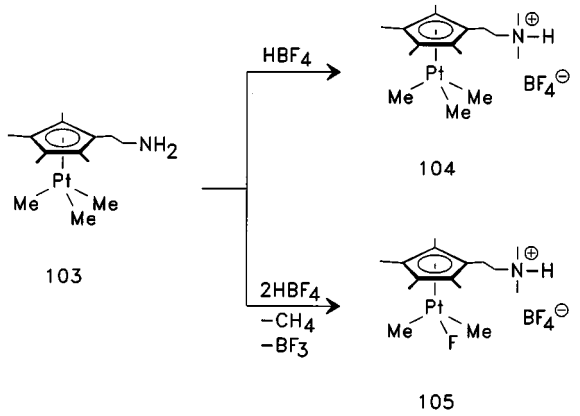

Conclusion

Similarly to the parent cyclopentadienyl ligand, aminoethyl-functionalized systems can be used as complexing agents for almost any transition metal. There are several good reasons to tether an amino group, as already pointed out in more detail in the introduction; many of the potential effects discussed have already been realized in very recent investigations. The possibility to modify at the cyclopentadienyl core as well as at the amino side group offers an enormous synthetic flexibility. In complexes containing (aminoethyl)cyclopentadienyl ligands, the following effects are of special interest:

− A hemilabile bonding situation is typical of compounds of low-valent transition metals. Amino-group coordination stabilizes otherwise highly reactive intermediates by a weak interaction (soft metal−hard ligand). The reversibility of this process should allow to control the reactivity and also the catalytic properties of the relevant metal complex in more detail.

− The amino group can bind to another metal (non-metal) center and thus create or stabilize novel types of bimetallic complexes.

− Compounds with a tethered ammonium group often show an exceptional stability against air and moisture and a high solubility in protic solvents; this phenomenon is important with regard to organometallic chemistry in water.

These features, together with the others described in this article, augur well for the development of a rich and interesting future chemistry of aminoethyl-functionalized cyclopentadienyl complexes of the transition metals.

The experimental work reported from our group was accomplished by *Jürgen Dahlhaus*, *Jürgen Kleimeier*, *Marc Oliver Kristen*, *Christian Müller*, and *Thomas Redeker*; X-ray crystal-structure analyses were performed by *Beate Neumann* and *Hans-Georg Stammler*. The dedication and expertise of these co-workers is very gratefully acknowledged. We thank *Marion Welschof* for preparing the drawings. Funding was kindly provided by the *Deutsche Forschungsgemeinschaft*, by the *Fonds der Chemischen Industrie*, and by the University of Bielefeld. We are grateful to the *BASF AG*, to the *Degussa AG*, and to the *Wittko AG* for gifts of chemicals.

☆ Dedicated to Professor *Heinrich Nöth* on the occasion of his 70th birthday.

[1] P. Jutzi, *J. Organomet. Chem.* **1990**, *400*, 1−17.

[2] For recent reviews see: [2a] P. Jutzi, *Adv. Organomet. Chem.* **1986**, *26*, 217−295. − [2b] C. Janiak, H. Schumann, *Adv. Organomet. Chem.* **1991**, *33*, 291−393. − [2c] J. Okuda, *Top. Curr. Chem.* **1991**, *160*, 97−145. − [2d] N. J. Coville, K. E. du Plooy, W. Pickl, *Coord. Chem Rev.* **1992**, *116*, 1−271. − [2e] J. Okuda, *Nachr. Chem. Tech. Lab.* **1993**, *41*, 8−14.

[3] Publications concerning alkenyl- and alkinyl-functionalized cyclopentadienyl ligands: [3a] J. F. Buzinkai, R. Schrock, *Organometallics* **1987**, *6*, 1447−1452. − [3b] J. Okuda, K. H. Zimmermann, *J. Organomet. Chem.* **1988**, *344,* C1-C4. − [3c] F. X. Kohl, R. Dickbreder, P. Jutzi, G. Müller, B. Huber, *Chem. Ber.* **1989**, *122*, 871−878. − [3d] J. A. Miguel-Garcia, P. M. Maitlis, *J. Chem. Soc., Chem. Commun.* **1990**, 1472−1473. − [3e] J. Okuda, K. H. Zimmermann, *Chem. Ber.* **1990**, *123*, 1641−1648. − [3f] M. Ogasa, D. T. Mallin, D. W. Macomber, M. D. Rausch, R. D. Rogers, A. N. Rollins, *J. Organomet. Chem.* **1991**, *405*, 41−52. − [3g] H. Lehmkuhl, J. Näser, G. Mehler, T. Keil, F. Danowski, R. Benn, R. Mynott, G. Schroth, B. Gabor, C. Krüger, P. Betz, *Chem. Ber.* **1991**, *124*, 441−452. − [3h] G. Erker, R. Aul, *Chem. Ber.* **1991**, *124*, 1301−1310. − [3i] J. Okuda, K. H. Zimmermann, *Chem. Ber.* **1992**, *125*, 637−641. − [3j] H. G. Alt, J. Han, U. Thewalt, *Organomet. Chem.* **1993**, *456*, 89−95. − [3k] J. Okuda, K. E. du Plooy, P. J. Foscano, *J. Organomet. Chem.* **1995**, *495,* 195−202. − [3l] R. E. v. H. Spence, W. E. Piers, *Organometallics* **1995**, *14*, 4617−4624. − [3m] K. A. Butakoff, D. A. Lemenovskii, P. Mountford, L. G. Kuz′mina, A. V. Churakov, *Polyhedron* **1996**, *15*, 489−499.

[4] Publications concerning *P*-functionalized cyclopentadienyl ligands: [4a] C. Charrier, F. Mathey, *J. Organomet. Chem.* **1979**, *170*, C41−C43. − [4b] J. C. Leblanc, C. Moise, A. Maisonnat, R. Poilblanc, C. Charrier, F. Mathey, *J. Organomet. Chem.* **1982**, *231*, C43−C48. − [4c] D. M. Bensley, Jr., E. A. Mintz, *J.Organomet. Chem.* **1988**, *353*, 93−102. − [4d] J. Szymoniak, J. Besançon, A. Dormond, C. Moise, *J. Org. Chem.* **1990**, *55*, 1429−1432. − [4e] M. Lin, K. A. Fallis, G. A Anderson, N. P. Rath, M. Y. Chiang, *J. Am .Chem. Soc.* **1992**, *114*, 4687−4693. − [4f] T. Cuenca, J. C. Flores, P. Royo, *J. Organomet. Chem.* **1993**, *462*,191−201. − [4g] R. T. Kettenbach, W. Bonrath, H. Butenschön, *Chem. Ber.* **1993**, *126*, 1657−1669. − [4h] I. Lee, F. Dahan, A. Maissonat, R. Poilblanc, *Organometallics* **1994**, *13*, 2743−2750. − [4i] D. Fryzuk, S. S. H. Mao, P. B. Duval,S. J. Rettig, *Polyhedron* **1995**, *14*, 11−23. − [4j] A. H. Cowley, C. S. King, A. Decken, *Organometallics* **1995**, *14*, 20−23. − [4k] J. Foerstner, R. Kettenbach, R. Goddard, H. Butenschön, *Chem. Ber.* **1996, 129**, 319−325. − [4l] O. J. Curnow, G. Huttner, S. J. Smail, M. M. Turnbull, *J. Organomet. Chem.* **1996**, *524*, 267−270. − [4m] I. Lee, F. Dahan, A. Maisonnat, R. Poilblanc, *J. Organomet. Chem.* **1997**, *532*, 59−170.

[5] Publications concerning *O*-functionalized cyclopentadienyl ligands: [5a] Q.Huang, Y. Qian, *Synthesis* **1987**, 910−912. − [5b] C. Qian, Z. Xie, Y. Huang, *J. Organomet. Chem.* **1987**, *323*, 285−294. − [5c] Y. Qian, G. Li, W. Chen, B. Li, X. Jin, *J. Organomet. Chem.* **1989**, *373*, 185−191. − [5d] D. Deng, C. Qian, G. Wu, P. Zheng, *J. Chem. Soc., Chem. Commun.* **1990**, 880−881. − [5e] D. Deng, B. Li, C. Qian, *Polyhedron* **1990**, *9*, 1453−1455. − [5f] H. Qichen, Q. Yanlong, L. Guisheng, T. Yongi, *Transition Met. Chem.* **1990**, *15*, 483−485. − [5g] R. Fandos, A. Meetsma, J. H. Teuben, *Organometallics* **1991**, *10*, 59−60. − [5h] Z. Xie, C. Qian, Y. Huang, *J. Organomet. Chem.* **1991**, *412*, 61−69. − [5i] C. Qian, B. Wang, D. Deng, G. Wu, P. Zheng, *J. Organomet. Chem.* **1992**, *427*, C29-C32. − [5j] U. Siemeling, *J. Organomet. Chem.* **1992**, *429*, C14-C18. − [5k] U. Siemeling, *J. Chem. Soc., Chem. Commun.* **1992**, 1335−1336. − [5l] Qian, G. Li, *Polyhedron* **1993**, *12*, 967−970. − [5m] D. Deng, C. Qian, F. Song, Z. Wang, G. Wu, P. Zheng, S. Jin, Y. Lin, *J.*

Organomet. Chem. **1993**, *458*, 83−88. − [5n] D. Laske, R. Duchateau, J. H. Teuben, A. L. Spek, *J. Organomet. Chem.* **1993**, *462*, 149−153. − [5o] U. Siemeling, B. Neumann, H.-G. Stammler, *Chem. Ber.* **1993**, 126, 1311−1316. − [5p] D. Deng, X. Zheng, C. Qian, J. Sun, L. Zheng, *J. Organomet. Chem.* **1994**, *466*, 95−100. − [5q] C.Qian, X. Zheng, Wang, D. Deng, J. Sun, *J. Organomet. Chem.* **1994**, *466*, 101−105. − [5r] D. Deng, Y. Jijang, C. Qian, G. Wu, P. Zheng, *J. Organomet. Chem.* **1994**, 470, 99−107. − [5s] P. Van de Weghe, C. Bied, J. Collin, J. Marçalo, I. Santos, *J. Organomet. Chem.* **1994**, *475*, 121−126. − [5t] U. Siemeling, G. Hüffmann, J.Organomet. Chem. **1994**, *475*, 229−232. − [5u] C. Qian, B. Wang, D. Deng, J. Hu, J. Chen, G. Wu, P. Zheng, *Inorg. Chem.* **1994**, *33*, 3382−3388.

[6] Recent publications concerning *O*-functionalized cyclopentadienyl ligands: [6a] Y. Mu, W. E. Piers, L. R. MacGillivary, M. J. Zawarotko, *Polyhedron* **1995**, *14*, 1−10. − [6b] U. Siemeling, *Chem. Ber.* **1995**, *128*, 1135−1136. − [6c] J. Christoffers, R. G. Bergman, *Angew. Chem.* **1995**, *107*, 2423−2425; *Angew. Chem. Int. Ed. Engl.* **1995**, *34*, 2226−2227. − [6d] A. A. H. van der Zeijden, C. Mattheis, R. Fröhlich, *Organometallics* **1997**, *16*, 2651−2658. − [6e] P. Foster, M. D. Rausch, J. C. W. Chien, *J. Organomet. Chem.* **1997**, *527*, 71−74. − [6f] O. V. Gusev, L. N. Morozova, T. A. Peganova, M. Yu. Antipin, K. A. Lyssenko, A. F. Noels, S. R. O'Leary, P. M. Maitlis, *J. Organomet. Chem.* **1997**, *536−537*, 191−196.

[7] Publications concerning *N*-functionalized cyclopentadienyl ligands: [7a] A. Baretta, K. S. Chong, F. G. N. Cloke, A. Feigenbaum, M. L. H. Green, *J. Chem. Soc., Dalton Trans.* **1983**, 861−864. − [7b] T. J. Clark, T. A. Nile, D. McPhail, A. McPhail, *Polyhedron* **1989**, *8*, 1804−1806. − [7c] P. J. Shapiro, E. Bunel, W. P. Schäfer, J. E. Bercaw, *Organometallics* **1990**, *9*, 867−869. − [7d] J. Okuda, *Chem. Ber.* **1990**, *123*, 1649−1651. − [7e] F. Wang, T.-Y. Lee, Y.-S. Wen, L.-K. Liu, *J. Organomet. Chem.* **1991**, *403*, 353−358. − [7f] T.-F. Wang, T.-Y. Lee, *J. Organomet. Chem.* **1992**, *423*, 31−38. − [7g] T.-F. Wang, Y.-S. Wen, *J. Organomet. Chem.* **1992**, *439*, 155−162. − [7h] A. Avey, D. R. Tyler, *Organometallics* **1992**, *11*, 3856−3863. − [7i] C. Qian, J. Guo, C. Ye, J. Sun, P. Zheng, *J. Chem. Soc., Dalton Trans.* **1993**, 3441−3445. − [7j] W. A. Herrmann, R. Anwander, F. C. Munck, W. Scherer, *Chem. Ber.* **1993**, *126*, 331−337. − [7k] R. Anwander, W. A. Herrmann, W. Scherer, F. C. Munck, *J. Organomet. Chem.* **1993**, *462*, 163−174. − [7l] A. Avey, T. J. R. Weakley, D. R. Tyler, *J. Am. Chem. Soc.* **1993**, *115*, 7706−7715. − [7m] A. K. Hughes, A. Meetsma, J. H. Teuben, *Organometallics* **1993**, *12*, 1936−1945. − [7n] J. C. Flores, J. C. W. Chien, M. D. Rausch, *Organometallics* **1994**, *13*, 4140−4142. − [7o] G. Paolucci, R. D'Ippolito, C. Ye, C. Qian, J. Gräper, D. R. Fischer, *J. Organomet. Chem.* **1994**, *471*, 97−104. − [7p] U. Böhme, K.-H. Thiele, *J. Organomet. Chem.* **1994**, *472,* 39−41. − [7q] H. Adams, N. A. Bailey, M. Colley, P. A. Schofield, C. White, *J. Chem. Soc., Dalton Trans.* **1994**, 1445−1451. − [7r] J. Okuda, *Comments Inorg. Chem*. **1994**, *16*, 185−205. − [7s] S. Rees, Jr., W. Lay, K. A. Dippel, *J. Organomet. Chem.* **1994**, *483*, 27−31.

[8] Recent publications concerning *N*-functionalized cyclopentadienyl ligands: [8a] S. Barry, A. Kucht, H. Kucht, M. D. Rausch, *J. Organomet. Chem.* **1995**, *489*, 195−199. − [8b] A. A. H. van der Zeijden, *Tetrahedron Asymm*. **1995**, 913−918. − [8c] W. A. Herrmann, M. J. A. Morawietz, T. Priermeier, K. Mashima, *J. Organomet. Chem.* **1995**, *486*, 291−295. − [8d] T.-F. Wang, J. P. Juang, K. J. Lin, *Bull. Inst. Chem., Acad. Sin*. **1995**, *42*, 41−48. − [8e] K.-H. Thiele, Ch. Schließburg, B. Neumüller, *Z. Anorg. Allg. Chem*. **1995**, *621*, 1106−1110. − [8f] U. Siemeling, U. Vorfeld, B. Neumann, H.-G. Stammler, *Chem. Ber.* **1995**, *128*, 481−485. − [8g] H. J. G. Luttikhedde, R. P. Leino, C.-E. Wileu, J. H. Näsman, M. J. Ahlgreu, T. A. Pakkanen, *Organometallics* **1996**, *15*, 3092−3094. − [8h] K. E. du Plooy, K. Moll, S. Wocadlo, W. Massa, J. Okuda, *Organometallics* **1995**, *14*, 3129−3131. − [8i] H. Pleino, D. Burth, *J. Organomet. Chem.* **1996**, *519*, 269−272. − [8j] J. Okuda, K. E. du Plooy, W. Massa, H.-C. Kang, U. Rose, *Chem. Ber.* **1996**, *129*, 275−277. − [8k] T.-F. Wang, C.-Y. Lai, Y.-S. Wen, *J. Organomet. Chem*. **1996**, *523*, 187−195. − [8l] A. A. H. van der Zeijden, *J. Organomet. Chem.* **1996**, *518*, 147−153. − [8m] M. Enders, R. Rudolph, H. Pritzkow, *Chem. Ber.* **1996**, *129*, 459−463. − [8n] R. A. Fischer, S. Nlate, H. Hoffmann, E. Herdtweck, J, Blümel, *Organometallics* **1996**, *15*, 5746−5752. − [8o] S. Nlate, E. Herdtweck, R. A. Fischer, *Angew. Chem*. **1996**, *108*, 1957−1959; *Angew. Chem. Int. Ed. Engl.* **1996**, 35, 1861−1863. − [8p] J. Weiß, E. Herdtweck, S. Nlate, M. Mattner, R. A. Fischer, *Chem. Ber.* **1996**, *129*, 297−303. − [8q] H. Schumann, F. Erbstein, R. Weimann, J. Demtschuk, *J. Organomet. Chem.* **1997**, *536−537*, 541−547. − [8r] T.-F. Wang, C.-C. Hwu, C.-W. Tsai, K.-J. Lin, *Organometallics* **1997**, *16*, 3089−3090. − [8s] A. Bertuleit, C. Fritze, G. Erker, R. Fröhlich, *Organometallics* **1997**, *16*, 2891−2899. − [8t] N. Choi, S. Onozawa, T. Sakakura, M. Tanaka, *Organometallics* **1997**, 16, 2765−2767. − [8u] T.-F. Wang, C.-Y. Lai, C.-C. Hwu, Y.-S. Wen, *Organometallics* **1997**, *16*, 1218−1223. − [8v] J. Okuda, T. Eberle, T. P. Spaniol, *Chem. Ber*. **1997**, *130*, 209−215. − [8w] A. I. Philippopoulos, N. Hadjiliadis, C. E. Hart, B. Donnadieu, P. C. Mc Gowan, R. Poilblanc, *Inorg. Chem*. **1997**, 36, 1842−1849. − [8x] P. C. McGowan, C. E. Hart, B. Donnadieu, R. Poilblanc, *J. Organomet. Chem.* **1997**, *528*, 191−194. − [8y] S. Sakanishi, D. A. Bardwell, S. Couchman, J. C. Jeffrey, J. A. McCleverty, M. D. Ward, *J. Organomet. Chem.* **1997**, *528*, 35−45. − [8z] M. Enders, K. Köhler, W. Frosch, H. Pritzkow, H. Lang, *J. Organomet. Chem.* **1997**, *538*, 163−170. − [8aa]R.Beckhaus, J. Oster, B. Ganter, U. Englert, *Organometallics* **1997**, *16*, 3902−3909.

[9] [9a] J. Dahlhaus, doctoral thesis, Universität Bielefeld, **1993**. − [9b] P. Jutzi, M. O. Kristen, J. Dahlhaus, B. Neumann, H.-G. Stammler, *Organometallics* **1993**, *12*, 2980−2985. − [9c] P. Jutzi, J. Dahlhaus, M. O. Kristen, *J. Organomet. Chem.* **1993**, *450*, C1−C3. − [9d] P. Jutzi, J. Dahlhaus,. M. Bangel, *J. Organomet. Chem.* **1993**, *460*, C13−C15. − [9e] J. Dahlhaus, P. Jutzi, M. Bangel, *J. Organomet. Chem.* **1993**, *474*, 55−58. − [9f] P. Jutzi. J. Dahlhaus, *Synthesis* **1993**, 684−686. − [9g] T. Redeker, diploma thesis, Universität Bielefeld, **1994**.− [9h] P. Jutzi, M. O. Kristen, B. Neumann, H.-G. Stammler, *Organometallics* **1994**, *13*, 3854−3861. − [9i] P. Jutzi, M. Bangel, *J. Organomet. Chem.* **1994**, *480*, C18-C19. − [9j] P. Jutzi, J. Dahlhaus, *Coord. Chem. Rev.* **1994**, *137*, 179−199. − [9k] H.-G. Stammler, P. Jutzi, B. Neumann, M. O. Kristen, *Acta Crystallogr*. **1995**, *C51*, 2496−2498. − [9l] H.-G. Stammler, P. Jutzi, B. Neumann, M. O. Kristen, H. Hölscher, *Acta Crystallogr*. **1995**, *C51*, 2494−2496. − [9m] P. Jutzi, J. Kleimeier, *J. Organomet. Chem.* **1995**, *486*, 287−289. − [9n] P. Jutzi, T. Redeker, H.-G. Stammler, B. Neumann, *J. Organomet.Chem*. **1995**, *498*, 127−137. − [9o] P. Jutzi, U. Siemeling, *J. Organomet. Chem.* **1995**, *500*, 175−185. − [9p] P. Jutzi, H. Schmidt, B. Neumann, H.-G. Stammler, *J. Organomet. Chem.* **1995**, *499*, 7−10. − [9q] P. Jutzi, T. Redeker, B. Neumann, H.-G. Stammler, *Organometallics* **1996**, *15*, 4153−4161. − [9r] P. Jutzi, T. Redeker, B. Neumann, H.-G. Stammler, *Chem. Ber.* **1996**, *129*, 1509−1515. − [9s] P. Jutzi, M. Bangel, B. Neumann, H.-G. Stammler, *Organometallics* **1996**, *15,* 747−752. − [9t] P. Jutzi, M. Bangel, B. Neumann, H.-G. Stammler, *Organometallics* **1996**, *15,* 4559−4564. − [9u] P. Jutzi, T. Redeker, B. Neumann, H.-G. Stammler, *J. Organomet. Chem.* **1997**, *533*, 237−245. − [9v] P. Jutzi, T. Redeker, *Organometallics* **1997**, *16*, 1343−1344. − [9w] Th. Redeker, doctoral thesis, Universität Bielefeld, **1997**. − [9x] P. Jutzi, C. Müller, B. Neumann, H.-G. Stammler, publication in preparation.

[10] [10a] M. Barton, J. M. Atwood, *J. Coord. Chem.* **1991**, *24*, 43−67. − [10b] P. Kalck, F. Monteil, *Adv. Organomet. Chem*. **1992**, *34*, 219−284. − [10c] W. A. Herrmann, C. Kohlpaintner, *Angew.Chem*. **1993**, *105*, 1588−1609; *Angew. Chem. Int. Ed. Engl.* **1993**, *32*, 1524−1544.

[11] [11a] K. Clauss, H. Bestian, *Justus Liebigs Ann. Chem*. **1962**, 654, 8−19. − [11b] F. N. Tebbe, G. W. Parshall, G. S. Reddy, *J. Am .Chem. Soc.* **1978**, *100*, 3611−3613. − [11c] U. Thewalt, T. Wöhrle, *J. Organomet. Chem.* **1994**, *464*, C17−C19.

[12] For recent reviews, see: [12a] R. F. Jordan, *Adv. Organomet. Chem*. **1991**, *32*, 325−387. − [12b] T. J. Marks, *Acc. Chem. Res.* **1992**, *25*, 57−77 − [12c] M. Bochmann, *Nachr. Chem. Tech. Lab.* **1993**, *41*, 1220−1228. − [12d] R. Mühlhaupt, *Nachr. Chem. Tech. Lab.* **1993**, *41*, 1341−1351. − [12e] M. Aulbach, F. Küber, *Chem. Unserer Zeit* **1994**, *28*, 197−208. − [12f] P. C. Möhring, N. J. Coville, *J. Organomet. Chem.* **1994**, 479, 1−29. − [12g] G. Fink, R. Mühlhaupt, H.-H. Brintzinger, *Ziegler Catalysts*, Springer-Verlag, Berlin, **1995**. − [12h] H.-H. Brintzinger, D. Fischer, R. Mühlhaupt, B. Rieger, R. Waymouth, *Angew. Chem.* **1995**, 107, 1255−1283; *Angew. Chem. Int. Ed. Engl.* **1995**, *34*, 1143−1170. − [12i] M. Bochmann, *J. Chem. Soc., Dalton Trans* **1996**, 255−270.

[97311]

Pyrazole as a Donor Function in Neopentane-Based Tripod Ligands $RCH_2C(CH_2pyrazol\text{-}1\text{-}yl)_{3-n}(CH_2PR_2)_n$ – Synthesis and Coordination Chemistry

Albrecht Jacobi, Gottfried Huttner*, Ute Winterhalter, and Sven Cunskis

Anorganisch-Chemisches Institut der Universität Heidelberg,
Im Neuenheimer Feld 270, D-69120 Heidelberg, Germany

Received October 6, 1997

Keywords: Tripodal ligands / Pyrazolyl donors / Molybdenum / Hydrogen bonds / 2D-NMR

The chlorine functions of $CH_3C(CH_2Cl)_3$, **1**, may be replaced by pyrazolyl (pz) as well as imidazolyl (im) residues under the conditions of nucleophilic substitution leading to tripodal ligands $CH_3C(CH_2X)_3$, X = pz, **2**; X = im, **3**. As a means of introducing two nitrogen donors and one phosphorus donor into a tripod ligand, substitution of the Br and OMs functions in $O(CH_2)_2C(CH_2Br)(CH_2OMs)$, **8**, by nitrogen nucleophiles and subsequent cleavage of the oxetane ring by a phosphide nucleophile to give $HOCH_2C(CH_2PPh_2)(CH_2X)_2$ has been developed, furnishing **10a** (X = pz) and **10d** (X = NEt_2), respectively. For the synthesis of **10a**, K-pz was used as the nucleophile, while **10d** was prepared using azide in the initial step, which then had to be transformed into NEt_2 in two subsequent steps. The nucleophugic functions of the oxetane **8** undergo selective substitution by K-pz and $KPPh_2$ in THF to produce $O(CH_2)_2C(CH_2PPh_2)(CH_2pz)$, **9b**. Phosphide cleavage of the oxetane function leads to $HOCH_2C(CH_2PPh_2)(CH_2PR_2)(CH_2pz)$, R = Ph, **10b**; R = 3,5-$Me_2(C_6H_3)$, **10c**. – The tris(pyrazolyl) tripod ligand **2** reacts with $(MeCN)_3Mo(CO)_3$ to give **2** · $Mo(CO)_3(MeCN)$, **12a**, in which only two of the three donor functions are coordinated. Upon reaction with **10a**, the same reagent gives **10a** · $Mo(CO)_4$, **12b**, with one pyrazolyl coordinated and the other involved in intramolecular hydrogen bonding to the CH_2OH function (N···H–O distance 280 pm). Blocking of the OH function of **10a** by etherification, i.e. to form $EtOCH_2C(CH_2PPh_2)(CH_2pz)_2$, **11**, does not dramatically affect the coordination capabilities with **11** · $Mo(CO)_3(MeCN)$, **12d**, being formed upon treatment with $(MeCN)_3Mo(CO)_3$. Again only one pz function is coordinated to the metal. Bidentate coordination by two phosphorus donors of **10c** is observed in **10c** · $Mo(CO)_3(MeCN)$, **12d**. The dangling arm pz donor function and the CH_2OH group are intermolecularly hydrogen-bonded in this case. When the bulky $P[3,5\text{-}Me_2(C_6H_3)]_2$ substituent of **10c** is replaced by the less sterically demanding PPh_2 donor in **10b**, η^3-coordination is finally observed with the formation of **10b** · $Mo(CO)_3$, **13**. The coordination capabilities of the new ligands are rationalized in terms of the size (six-, seven-, and eight-membered rings) and interference of the chelate cycles. All compounds have been characterized by the usual analytical and spectroscopic methods, with a complete assignment of the NMR data achieved by a combination of 2D-NMR techniques in some cases. The structures of the coordination compounds have additionally been deduced by X-ray methods.

Introduction

The coordination chemistry of tripod ligands has considerable potential in many fields of chemistry: Tripod ligands are essential constituents of many bioinorganic model compounds[1], the stabilization of unconventional ligands by tripod metal templates has found widespread application[2] and catalytic applications of tripod metal templates are a rapidly developing field[3]. As a special type of tripod ligands, molecules containing three different donor groups bonded to a neopentane backbone $CH_3C(CH_2X)(CH_2Y)(CH_2Z)$ have been shown to be productive in coordination chemistry, as well as in catalysis. Sacconi and his group, as well as the group of Bianchini, have made extensive contributions to the application of $CH_3C(CH_2PPh_2)_3$ in preparative and in catalytic chemistry[3][4]. Nevertheless, the potential offered by neopentane-based tripod ligands is still far from being fully exploited. Tripod ligands of this type with up to three different donor groups have only recently become available. While the synthetic strategies for introducing phosphorus donors are well developed[5a][5b][5c][5d][5e], including the EPC synthesis of chiral tripod ligands with three different phosphorus donor groups[5f][5g][5h], general strategies for the synthesis of tripod ligands containing, amongst others, nitrogen donor functions are still lacking. A special route into the chemistry of such ligands based upon the aminolytic cleavage of neopentane-based oxetanes has recently been reported[6] and some particular cases based on the nucleophilic substitution of functionalized neopentane derivatives by azide are known[7].

We report herein on our efforts to devise new methods by which tripod ligands **A** $RCH_2C(CH_2X)(CH_2Y)(CH_2Z)$ with the donor set X, Y, Z containing at least one nitrogen donor can be synthesized.

Special emphasis is put on the introduction of the pyrazolyl donor function, the reason being that this type of functionality has been shown to be highly efficient in tris(pyrazolyl)borate tripod ligands[8]. On the other hand, each

 © WILEY-VCH Verlag GmbH, D-69451 Weinheim, 1998 1434–1948/98/0606–0675 $ 17.50+.50/0

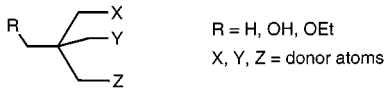

A

pyrazolyl donor function linked to the neopentane backbone in $RCH_2C(CH_2X)(CH_2Y)(CH_2Z)$ increases the ring size in the chelate cage $RCH_2C(CH_2X)(CH_2Y)(CH_2Z)M$ by one over the sterically ideal arrangement of three six-membered rings forming a bicyclooctane-type chelate cage that results when all three donor atoms of X, Y, Z are directly linked to the neopentane carbon skeleton. This increase in ring size (seven-membered chelate rings with one pyrazolyl entity and even eight-membered chelate rings with more than one of these entities) to some extent disfavours the tripodal coordination of such ligands. Given the excellent ligand properties of pyrazolyl ligands on one side and the expected destabilization of η^3-coordination by the introduction of pyrazolyl donor functions into neopentane-based tripod ligands, facile equilibration between η^3- and η^2-coordination modes in such ligand-metal templates may be envisaged. This means that introducing pyrazolyl donor functions into neopentane-based tripod ligands has the potential of allowing the synthesis of coordination compounds in which the pyrazolyl-containing arm of a tripod ligand is easily coordinated and decoordinated, thus reversibly protecting a coordination site at the metal center in the sense of an auxiliary ligand.

This paper deals with the synthesis of tripod ligands $RCH_2C(CH_2X)(CH_2Y)(CH_2Z)$ containing one to three nitrogen donor functions with the other donors being PR_2 groups. The coordination behaviour of these tripod ligands containing up to three pyrazolyl nitrogen donors is probed by characterization of their tricarbonylmolybdenum derivatives.

Synthesis of Tripod Ligands Starting from Tris(chloromethyl)ethane

Tris(chloromethyl)ethane **1**[9] reacts with an excess of potassium pyrazolate (K-pz) in DMSO with substitution of all three chlorine functions by pyrazolyl groups.

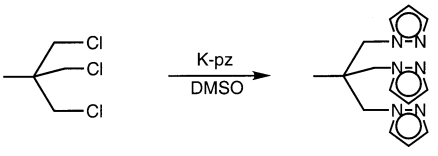

1 2

The tripod ligand **2** was obtained by bulb-to-bulb distillation in a kugelrohr apparatus in around 46% yield as a colourless oil, which solidified to give colourless needles after few days. Spectroscopic data and elemental analyses unequivocally confirmed its constitution (Tables 1 and 2, Exp. Section).

Since the reaction yielding **2** proceeded unexpectedly well – bearing in mind the sluggish reactivity of neopentane derivatives in nucleophilic substitution[7a][10] – it appeared worthwhile to attempt to introduce imidazolyl donors by the same type of straightforward approach. Imidazolyl residues at the neopentane backbone are appealing in so far as it has been shown that multidentate imidazolyl-functionalized ligands may be transformed into multidentate carbene ligands, with the additional merit of making use of the known stability of transition metal-imidazolinylidene carbene bonds[11]. Reaction of the trichloride **1** with potassium imidazolate in DMSO indeed resulted in the tripodal system **3**, albeit in modest yield only.

1 3

Compound **3** was isolated by bulb-to-bulb distillation from the ethereal extract after hydrolysis of the reaction mixture. As a consequence of the high boiling point of free imidazole and of the tripod ligand **3**, appreciable thermal decomposition occurred under the conditions of the distillation. Moreover, increasing the temperature and the reaction time in the synthesis of **3** did not increase the yield because of decomposition of the reaction system into a brown, viscous oil of unknown composition. Compound **3**, as obtained after distillation, consists of colourless needles. Spectroscopic data and elemental analyses confirm the given constitution (Tables 1 and 2, Exp. Section).

Synthesis of Tripod Ligands Starting from Monofunctionalized Oxetanes

Functionalized oxetanes $O(CH_2)_2C(CH_3)(CH_2X)$ have been shown to undergo aminolytic cleavage of the oxetane ring[6][12]. This method works when CH_2OR and CH_2SR substituents are present in the oxetane ring[6]. While this strategy failed in the presence of CH_2PR_2 substituents, we have now found that amino substituents are well tolerated. The pyrazolyl-substituted oxetane **5a** was obtained in good yields from the functionalized oxetane **4** by nucleophilic substitution with potassium 3,5-dimethylpyrazolate (K-3,5-Me_2pz).

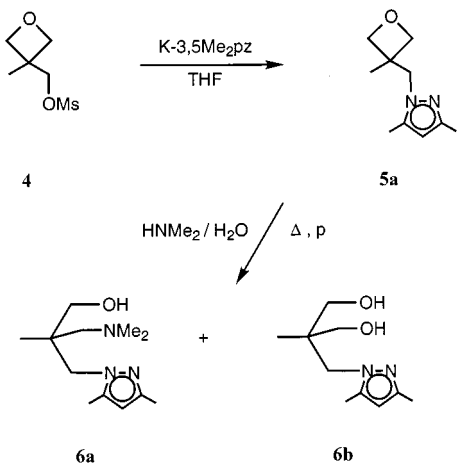

4 5a

6a 6b

Compound **5a** underwent aminolytic cleavage of the oxetane moiety upon treatment with $HNMe_2/H_2O$ at 40 bar/170°C. The product **6a** was accompanied by the bis(hydroxy) compound **6b**. Of course, under the drastic reaction conditions necessary to observe any reaction at all, hydrolytic cleavage effectively competes with aminolytic cleavage. Products **6a/6b** were not completely separable by Vigreux distillation; fractions containing **6a/6b** in ratios up to 4:1 were obtained at best. Compounds **6a/6b** could nevertheless be unequivocally characterized by derivatization (**7a/7b**).

Alternative and potentially more general methods for the exchange of the OMs group by an amine function have been examined. The standard procedure[13] of using potassium phthalimide (K-Phth) as the nitrogen nucleophile works well. While K-Phth is known to react with oxiranes with ring opening[13], the oxetane moiety in **4** stays intact and so this compound can be transformed to the phthalimide derivative **B** in high yields. **B** was fully characterized by its analytical and spectroscopic data (Exp. Section).

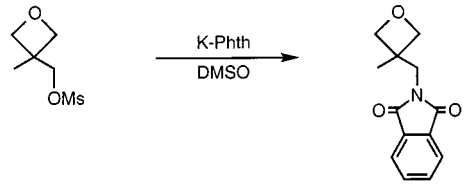

4 **B**

However, any attempt to transform the phthalimide group into an amine function proved problematic. While the cleavage of neopentane-bound phthalimide groups in $CH_3C(CH_2Phth)_3$ has been shown to proceed in the presence of 25% KOH over a period of a few days at room temperature[14], **B** showed no reaction under the same conditions. Hydrazinolysis of **B** was not very effective either; NMR control of the reaction mixture showed that the oxetane functionality was also affected under the drastic conditions necessary (boiling for 10 h). From the reaction mixture obtained after this time, the amine (**5c**) could not be separated.

An alternative strategy starting from **B** might have been possible through its reaction with $LiPPh_2$. If this nucleophile would selectively attack the oxetane ring[5d][5e] of **B**, a subsequent hydrazinolytic cleavage of the phthalimide moiety would no longer be impeded by the reactivity of the oxetane functionality (see above). However, when red $LiPPh_2$ was treated with a solution of colourless **B**, an immediate colour change to deep-green ensued, indicating a reaction at the phthalimide moiety[15]. Reaction control by ^{31}P-NMR spectroscopy showed that a multitude of PPh_2 derivatives of different kinds (^{31}P NMR: δ from −40 to +40) was formed under these conditions. In summary, potassium phthalimide does not appear to be the correct choice of nitrogen nucleophile for the problem at hand.

The use of azides as nitrogen nucleophiles is a well-established method, even for polyfunctional and sensitive compounds[16]. This method has previously proved successful in the synthesis of tripod ligands of type **A**[7], and it works as well with **4** as the starting compound. The transformation of **4** into the azide derivative **5b** has been reported in the patent literature, where no details of the procedure were given[17a]. We found that solutions of **4** in DMSO react with a threefold excess of NaN_3 to produce **5b**.

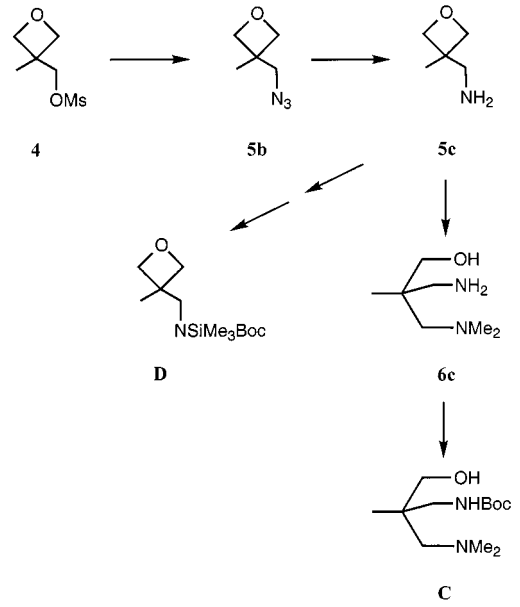

Optimum yields of around 90% were obtained after 30 h at 130°C. Shorter reaction times gave reduced yields (10 h: 50%), while prolonged heating or higher temperatures also reduced the yield (48 h: 55%) (caution: **5b** "AMMO" and several of its polymers are used as explosives[17b] and appropriate care has to be taken in its preparation and work-up). After dilution of the reaction mixture with two equiv. of water, **5b** was extracted into diethyl ether. The presence of **5b** in the ethereal solution was evidenced by an azide band at 2103 cm^{-1} in the IR spectrum. A small amount of the ethereal solution was concentrated to an extent that allowed the characterization of **5b** by ^1H NMR (Exp. Section). The reactivity of **5b** towards PPh_3 gave further proof of its identity: the corresponding iminophosphorane was formed immediately (^{31}P NMR: $\delta = +10.6$), which upon hydrolysis yielded **5c**. Compound **5c** was purified by distillation under reduced pressure, with appropriate care being taken in view of its volatility. The identity of **5c** was obvious from its analytical data (Exp. Section) as well as from its reaction with $HNMe_2/H_2O$ at 30 bar/130°C, which furnished **6c** (Exp. Section). This potential tripod ligand, containing two different nitrogen donors and one oxygen donor, was also fully characterized. Several attempts have been made to further derivatize **6c** with the aim of replacing its OH group by a PPh_2 group. This intended type of transformation requires protection of the NH_2 group. Boc-protection has been found to be adequate, allowing the formation of **C** as a colourless, microcrystalline solid (for analytical and spectroscopic data, see Exp. Section). However, deprotonation of **C** by a minimum of two equivalents of *n*BuLi, subsequent treatment of the product with an excess of MsCl, followed by addition of $LiPPh_2$, resulted in unseparable

product mixtures. These mixtures are not a result of cleavage of the Boc group by *n*BuLi, since **C** can be recovered after treatment with two equivalents of *n*BuLi under the same conditions after hydrolytic work-up. Selective deprotonation of the OH group in the presence of an NHBoc functionality has been reported to occur for HBocNCH(Me)CH_2OH[17c]. In this case, mesylation of the alcohol function was achieved using $MsCl/NEt_3$, whereas in the present case the use of NEt_3 as a base is not feasible since the product obtained after mesylation cannot be purified, presumably due to decomposition by internal cyclization[7a]. If the product mixture is treated with $LiPPh_2$ without any intermediate purification step, a complex mixture of compounds results, with the desired PR_2 substitution occurring only to a minor extent (< 10% according to ^{31}P-NMR data).

A solution to these problems might possibly have been found in replacing the NH function by an $NSiR_3$ function. When **C** was treated with one equivalent of *n*BuLi, and then the reaction mixture was quenched with TMSCl, the *N*-silylated product was obtained. However, mesylation and subsequent reaction with $LiPPh_2$ was again unselective and an unseparable mixture of products was obtained once more. Benzyl-protection of the NHBoc group might appear to be an alternative. However, we found that $CH_3C(CH_2PPh_2)_2(CH_2NBnBoc)$[6], which has been used as a model compound, does not allow for a straightforward debenzylation with the Li/NH_3/THF reagent[18a].

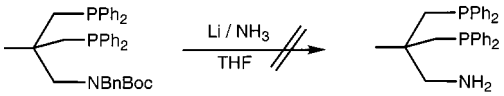

In the present case, only a small yield of $CH_3C(CH_2PPh_2)_2(CH_2NH_2)$ was obtained, which after chromatography was sufficiently pure for identification by NMR spectroscopy with reference to an authentic sample[7b]. Even though the transformation of carbamate-type NBn groups into NH_2 groups by alkali metal in liquid ammonia solutions under carefully controlled conditions is known to work in other cases[18b], the reluctance of the system to undergo a debenzylation reaction does not appear to be due to the presence of the PPh_2 group alone. While hydrogenolytic cleavage of the NBn function is not possible with the model compound due to phosphorus poisoning of the catalyst, it should work well with $CH_3C(CH_2OH)_2(CH_2NBnH)$[6]. With this compound, however, no reaction was observed under conditions using 10% Pd/C catalyst at 1 bar H_2 and 25°C. Only at 60°C under 60 bar H_2 and with reaction times of 12 h was the amine-functionalized product $CH_3C(CH_2OH)_2(CH_2NH_2)$ **E** obtained (Exp. Section).

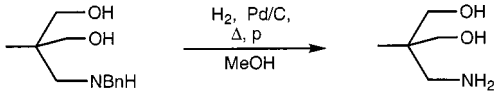

E

This result suggests that the difficulties observed in the debenzylation reactions are mainly due to the notoriously low reactivity of neopentane derivatives[10]. Even though $CH_3C(CH_2OH)_2(CH_2NH_2)$ is accessible by a debenzylation procedure, its further functionalization is impeded by the same sort of problems as already described for **6c**. The problem of functionalizing **6c** might also potentially be overcome by tracing back the synthesis of **6c** a few steps: Starting from **5c**, Boc-protection and subsequent silylation results in a product **D**, in which the CH_2NH_2 substituent is transformed into a $CH_2NBocSiMe_3$ functionality (see above). When this protected intermediate **D** is treated with $LiPPh_2$, an unseparable reaction mixture nevertheless results (^{31}P NMR: δ from −40 to +40). Tracing one step further back, **5b** produces the iminophosphorano-substituted oxetane $O(CH_2)_2C(CH_3)(CH_2N{=}PPh_3)$ in a clean reaction. If the oxetane moiety of this intermediate would undergo nucleophilic cleavage with $LiPPh_2$, a phosphorus donor might be introduced at such an early stage. However, in practice, this reaction also results in an unseparable mixture (^{31}P NMR) of different phosphorus-containing products.

In contrast to the reluctance of **6c** to undergo further functionalization, **6a** as well as **6b** can be transformed into the phosphorus-containing tripod ligands **7a** and **7b** by the standard procedure[6].

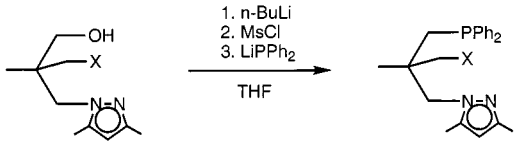

6a : X = NMe_2
6b : X = OH

7a : X = NMe_2
7b : X = PPh_2

While **6a** and **6b** are invariably obtained as mixtures (see above), their derivatives **7a** and **7b** can be easily separated by column chromatography owing to the fact that **7a** bearing an NMe_2 group migrates much more slowly than **7b**. Compounds **7** are obtained as colourless, analytically and spectroscopically pure oils (Tables 1 and 2, Exp. Section).

Synthesis of Tripod Ligands Starting from Difunctionalized Oxetanes

In the synthesis of neopentane-based tripod ligands, the use of difunctionalized oxetanes such as **8**[19] has the additional merit of producing a CH_2OH group at the backbone of the tripod ligand $HOCH_2C(CH_2X)(CH_2Y)(CH_2Z)$, which lends itself to further functionalization of the ligand. Compound **8** has successfully been used as a starting material in the synthesis of phosphorus-containing CH_2OH-functionalized tripod ligands[5d]. Its reaction with nitrogen nucleophiles allows access to mixed donor set tripod ligands containing a CH_2OH group at the quaternary carbon. Thus, **8** reacted with 2 equivalents of K-pz in THF to form the bis(pyrazolyl) derivative **9a**, which was purified by distil-

lation and obtained as a pale-yellow, viscous oil (Exp. Section).

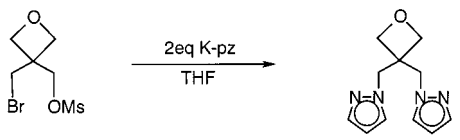

8 **9a**

When **8** was treated first with 1.2 equiv. of K-pz and then with 2 equiv. of $KPPh_2$, the substitution product **9b** was obtained in moderate yields. **9b** could be separated from some less polar co-products (including excess $HPPh_2$) by flash chromatography and was obtained as a colourless, microcrystalline solid.

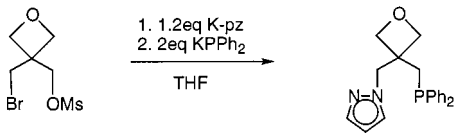

8 **9b**

The identity of the products **9** was established beyond doubt by elemental analyses and mass spectrometry, as well as by NMR spectroscopy (Exp. Section). As usual with 3,3-bis-substituted oxetanes, the symmetric (**9a**) and unsymmetric (**9b**) substitution patterns, respectively, are immediately evident from the multiplicity of the ^{1}H-NMR signals of the oxetane CH_2 groups (Exp. Section)[5d].

The use of azide as a nucleophile for the substitution of difunctional oxetanes has been reported previously[20a]. Use of **8** as the electrophilically-substituted oxetane instead of $O(CH_2)_2C(CH_2Cl)_2$[20a] was found to increase the yield of **9c** from 25% to around 90%, as inferred from the transformation of **9c** to the corresponding amine **9d** by PPh_3/H_2O.

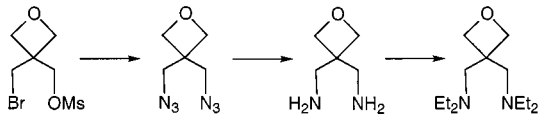

8 **9c** **9d** **9e**

The NH_2 functions of **9d** could be transformed into NEt_2 functions by treatment with ethyl iodide/K_2CO_3 in ethanol, resulting in a high yield of **9e**[20c]. The oxetane derivatives **9d** and **9e** were fully characterized by their analytical and spectroscopic data (Exp. Section). The potentially explosive **9c** was characterized by its ^{1}H-NMR spectrum, an azide band at 2105 cm^{-1} in the IR spectrum, and its derivatization to **9d**.

The difunctionalized oxetanes **9a**, **9b**, and **9e** underwent nucleophilic cleavage of the oxetane ring upon treatment with $LiPPh_2$ in boiling THF, resulting in the CH_2OH-functionalized tripod ligands **10**.

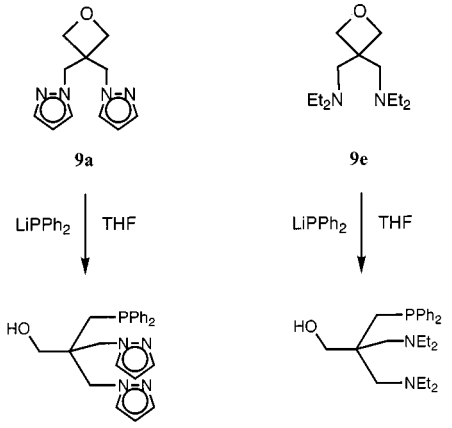

9a **9e**

10a **10d**

Compounds **10** were obtained as colourless oils upon chromatographic work-up. Elemental analyses, mass spectra, and NMR data were consistent with the given constitution in each case (Tables 1 and 2, Exp. Section).

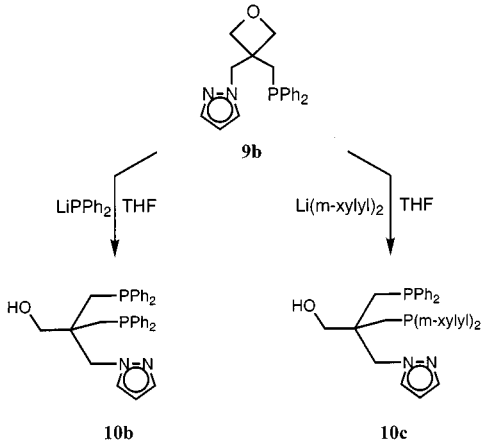

9b

10b **10c**

The diastereotopicity of the protons of some of the CH_2 groups in the neopentane framework is of considerable help in assigning the relevant signals to the individual CH_2 entities. For instance, the protons at the pyrazolyl-substituted CH_2 groups of **10a** are diastereotopic, while those of the CH_2PPh_2 and CH_2OH moieties, respectively, are not.

The appearance of the corresponding ^{1}H-NMR signals clearly reflects this difference (Table 1). Analogous arguments help in assigning the ^{1}H-NMR data of the other compounds **10**; the resolution obtainable at 200 MHz does, however, preclude a complete assignment of the ^{1}H-NMR spectra of **10c** and **10d** (Table 1).

Functionalization of the CH_2OH group at the backbone of tripod ligands is generally hampered by difficulties[21]. Problems arise because of the reduced reactivity of neopentane derivatives as well as due to the fact that tripod ligands, by definition, contain other nucleophilic groups (the ligand entities!) besides the CH_2OH entity. Thus, treatment of **10d** for example with KO*t*Bu/EtI in THF not unexpectedly results in a mixture of products, probably because of partial quaternization of the amine donor functions.

Table 1. Chemical shifts (δ values), integrals [*x*H] and coupling constants *J*[a] in the ^{1}H-NMR spectra of **2**, **3**, **7a**, **7b**, **10a**–**12d**, and **11** (solvent: $CDCl_3$)

	CH_2R	CH_2X	CH_2Y	CH_2Z	*pz-H* [b] *H4*	*H3*	*H5*	*aryl-H*	*other*
2	0.73s [3H] R=H	——4.23s [6H] X=Y=Z=pz——			6.30t [3H]	7.57d [3H]	7.74d [3H]	-	-
3	1.07s [3H] R=H	—3.96s [6H] X=Y=Z=imidazole——			-	-	-	-	6.89s, 7.17s, 7.47s [9H] *imidazole-H*
7a	0.86s [3H] R=H	——2.55m [4H]——— X=PPh_2, Y=NMe_2		3.99s [2H] Z=3,5Me_2-pz	5.76s [1H]	-	-	7.29-7.75m [10H]	2.22-2.48m [12H] pzCH_3, NCH_3
7b	0.93s [3H] R=H	——2.53bs [4H]——— X=Y=PPh_2		4.08s [2H] Z=3,5Me_2-pz	5.79s [1H]	-	-	7.30-7.44m [20H]	2.22s, 2.24s [6H] pzCH_3
10a	3.29s [2H] R=OH	2.15d [2H] *J*=3.6 X=PPh_2	—4.22d, 4.47d [4H]—— *J*=14.3 Y=Z=pz		6.27t [2H]	7.31d [2H]	7.60d [2H]	7.35-7.48m [10H]	-
10b	3.26s [2H] R=OH	——2.47bs [4H]——— X=Y=PPh_2		4.23s [2H] Z=pz	6.18t [1H]	7.09d [1H]	7.49d [1H]	7.30-7.45m [20H]	-
10c	3.25s [2H] R=OH	——2.42m [4H]——— X=PPh_2, Y=P(3,5-Me_2Ph)$_2$		4.25bs [2H] Z=pz	6.20t [1H]	———6.94-7.51[18H]———			2.27bs [12H] xylyl-CH_3
10d	3.25s [2H] R=OH	2.33m [4H] *J*=4.0 X=PPh_2	—2.44-2.78m [12H]—— Y=Z=NEt_2		-	-	-	7.32-7.57m [10H]	1.00t [12H] $^3J_{HH}$=7.2 NCH_2CH_3 6.66bs [1H] O*H*
11	3.11s [2H] R=OEt	2.31bs [2H] X=PPh_2	—4.38d, 4.50d [4H]—— *J*=14.2 Y=Z=pz		6.30t [2H]	———7.35-7.77[14H]———			1.08t [3H] $^3J_{HH}$=6.8, OCH_2CH_3, 3.06q [2H] $^3J_{HH}$=6.8, OCH_2CH_3

[a] $J = {}^2J_{HH}$ unless otherwise stated, coupling constants in Hz. – [b] All pyrazolyl-H′s (except for **7a** and **7b**) give broad signals due to $^3J_{HH}$ coupling (unresolved at 200 Mhz) and integrate as 1 H.

The pyrazolyl residues, being more resistant to electrophilic attack compared to the NEt_2 nucleophiles, should not be prone to problems resulting from quaternization and, indeed, **10a** is transformed to its ethyl ether derivative without complications. The complete set of analytical and spectroscopic data obtained for **11** is in accord with its proposed constitution (Tables 1 and 2, Exp. Section).

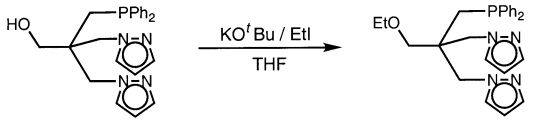

10a **11**

Coordination Chemistry

The coordination behaviour of the novel ligands was tested with $(MeCN)_3Mo(CO)_3$ as the substitution-labile precursor[22]. With the tris(pyrazolyl)-substituted ligand **2**, displacement of only two MeCN groups was observed, resulting in the $Mo(MeCN)(CO)_3$ derivative **12a**, in which **2** acts as a bidentate ligand.

On the basis of its mass spectrum and its ν(CO) IR data, **12a** might appear to be a compound of the composition **2**·$Mo(CO)_3$, containing η^3-coordinated **2** (Table 5, Exp. Section). The ^{1}H-NMR data obtained for **12a**, however, clearly demonstrate that only two pyrazolyl functions are coordinated, while the third one plays the role of a dangling arm (Table 3). The signals attributable to the CH_2pz groups show a clear 2:1 intensity pattern, with the signals of the coordinated residues significantly shifted compared to those of the dangling arm CH_2pz entity (Table 3). This 2:1 pattern is also evident in the ^{13}C-NMR data of **12a** on inspection of the signals of the CH_2pz and pyrazolyl carbons

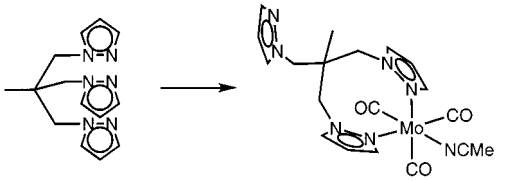

2 **12a**

(Table 4). The presence of a coordinated acetonitrile can also be deduced by NMR (Tables 3 and 4). Even if the shift imposed on the MeCN ligand by coordination is not always large enough to allow unequivocal differentiation between a coordinated and a non-coordinated acetonitrile, the relative intensity of the MeCN signal in the ^{1}H-NMR spectrum of **12a** shows that just one MeCN is present in each molecule (Table 3), which, in accord with the 18-electron rule and the findings described below (for **12c**, **12d**), leads to the given constitution for **12a**.

Table 2. Chemical shifts (δ values) and coupling constants J[a] in the $^{13}C\{^1H\}$-NMR spectra of **2**, **3**, **7a**, **7b**, **10a−10d**, and **11** (solvent: $CDCl_3$)

	CH_2R	CH_2X	CH_2Y	CH_2Z	*Cq*	pz-*C* [d]			*aryl-C*	*other*
						C4	*C3*	*C5*		
2	19.8 R=H	——56.2, X=Y=Z=pz——			42.8	105.7	140.0	132.2	-	-
3	19.3 R=H	——52.4, X=Y=Z=imidazole——			40.2	-	-	-	-	122.2,128.2 139.5, imidazole
7a	23.1d $^3J_{CP}$= 11.0 R=H	36.9d $^1J_{CP}$=14.7 X=PPh_2	55.6d $^3J_{CP}$=9.2 Y=pz	68.0d $^3J_{CP}$=7.4 Z= NMe_2	42.8d $^2J_{CP}$=12.9	104.9	147.3	140.0	128.7-133.6m	12.3, 14.0 pzCH_3, 49.3 NCH_3
7b	26.0m R=H	—40.6m X=Y=PPh_2——		57.4m Z=pz	41.2	105.1	148.0	140.3	129.2-133.8m	12.4, 13.9 pzCH_3
10a	65.2m R=OH	32.1m X=PPh_2	——54.9m Y=Z=pz——		46.7	105.6	140.0	132.3	128.9-139.8m	-
10b	68.8m R=OH	—35.0m X=Y=PPh_2——		58.4m Z=pz	46.7	105.5	139.8	131.7	128.9-139.3m	-
10c	68.9m R=OH	—34.9m X=Y=PPh_2——		58.4m Z=pz	45.5m	105.6	139.8	131.9	128.8-138.3m	21.8 xylyl-CH_3
10d	69.7 $^3J_{CP}$= 11.0 R=OH	34.3d $^1J_{CP}$=16.4 X=PPh_2	——61.6d $^3J_{CP}$=7.4—— Y=Z=NEt_2		44.7d $^2J_{CP}$=11.0	-	-	-	128.7-140.9m	12.1 NCH_2CH_3, 49.1 NCH_2CH_3
11	71.9 $^3J_{CP}$= 8.1 R=OEt	31.9d $^1J_{CP}$=17.6, X=PPh_2	—54.8m $^3J_{CP}$=9.1—— Y=Z=pz		45.5d $^2J_{CP}$=12.6	105.5	139.7	132.2	128.8-139.5m	15.5 OCH_2CH_3 65.5 OCH_2CH_3

[a] Coupling constants in Hz; all signals are singlets unless otherwise stated.

Table 3. Chemical shifts (δ values), integrals [xH] and coupling constants J[a] in the ^{1}H-NMR spectra of **12a−12d** and **13**

	CH_2R	CH_2X	CH_2Y	CH_2Z	pz-*H* [d]			*aryl-H*	*other*
					H4	*H3*	*H5*		
12a [b]	0.14s [3H] R=H	3.57d, 3.90d [2H] J=14.4 X=pz (c.)	3.90d, 4.31d [2H] J=14.4 Y=pz (c.)	4.13m, 4.40m [2H] Z=pz (n.c.)	6.36 (n.c.) 6.43, 6.51 (c.)	——7.45, 7.63 (n.c)—— ——7.47-8.43m (c.)——		-	0.49s [3H] *Me*CN
12b [c]	——1.39-1.57m, 2.43-2.95m, 3.28-3.43m, 3.64-3.76m, 4.12-4.28m [8H] CH_2P, CH_2N, CH_2O				6.20-6.48m [2H]	——7.36-8.60m [14H]——			-
12c [b]	2.31d, 2.62d [2H] $^3J_{HH}$ = 9.8, R=OEt	1.39d, 2.89d [2H] J=12.8 X=PPh_2	4.28d, 5.37d [2H] J=14.0 Y=pz (c.)	4.10d, 4.28d [2H] J=14.0 Z=pz (n.c.)	6.33 (n.c.) 6.47 (c.)	7.56 (n.c.) 7.84 (c.)	7.42 (n.c.) 8.85 (c.)	8.14m [4H] H_o, 7.32-7.35m [4H] H_m,7.36bs [2H] H_p	1.57s [3H] *Me*CN, 1.05t [3H] $^3J_{HH}$= 6.8 OCH_2CH_3, 2.17q, 2.76q [2H] $^3J_{HH}$ = 6.8 OCH_2CH_3
12d [c]	3.25bs [2H] R=OH	——2.42m [4H]—— X=PPh_2, Y=P(3,5-Me_2Ph)$_2$		4.21bs [2H] Z=pz (n.c.)	6.18 (n.c.)	——6.89-8.28m [18H]——			1.51s [3H] *Me*CN, 2.17-2.65bs [12H] xylyl-CH_3
13 [c]	3.54bs [2H] R=OH	—2.18dd, 2.64dd [4H]— J=14.0 $^2J_{HP}$ = 4.8/ 5.8 X=Y=PPh_2		4.00bs [2H] Z=pz	6.40 (c.)	——7.26-8.26m [22H]——			-

[a] $J = {}^2J_{HH}$ unless otherwise stated, coupling constants in Hz. − [b] Solvent: CD_2Cl_2; the CD_2Cl_2 was condensed into the NMR tubes prior to flame sealing. − [c] Solvent: $CDCl_3$. − [d] c. = coordinated, n. c. = non-coordinated; all pyrazolyl-H′s give broad signals and integrate as 1 H unless otherwise stated.

Table 4. Chemical shifts (δ values) and coupling constants J[a] in the $^{13}C\{^1H\}$-NMR spectra of **12a−12d** and **13**

	CH_2R	CH_2X	CH_2Y	CH_2Z	Cq	pz-C [d]			*aryl-C*	*other*
						C4	*C3*	*C5*		
12a [b]	19.2	54.7	54.8	55.7	43.9	105.9 (n.c.)	140.6 (n.c.)	132.1 (n.c.)	-	3.1
	R=H	X=pz (c.)	Y=pz (c.)	Z=pz (n.c.)		106.9 (c.)	147.1 (c.)	135.2 (c.)		*Me*CN
						107.1 (c.)	147.5 (c.)	135.7 (c.)		
12b[c]	68.4	28.4bs	52.3m	55.7m	45.5bs	105.9 (n.c.)	———	128.5-144.3 (m)	———	-
	R=OH	X=PPh_2	Y=pz (c.)	Z=pz (n.c.)		107.0 (c.)				
12c [b]	68.2	28.4d	51.4d	54.8d	45.1d	105.9 (n.c.)	139.6 (n.c.)	130.6 (n.c.)	128.4m C_m/C_i,	2.6, 121.3
	R=OEt	$^1J_{CP}$=7.4	$^3J_{CP}$=5.5	$^3J_{CP}$=12.9	$^2J_{CP}$=	107.0 (c.)	144.2 (c.)	135.2 (c.)	131.4d $^4J_{CP}$=	*Me*CN,
		X=PPh_2	Y=pz (c.)	Z=pz (n.c.)	3.7				10.1 C_p, 135.7d	15.2, 65.8
									$^2J_{CP}$= 14.7 C_o	OCH_2CH_3

[a] Coupling constants in Hz; all signals are singlets unless otherwise stated. − [b] Solvent: CD_2Cl_2; the CD_2Cl_2 was condensed into the NMR tubes prior to flame sealing. − [c] Solvent: $CDCl_3$. − [d] c. = coordinated, n. c. = non-coordinated.

Table 5. Chemical shifts (δ values) and coupling constants J in the $^{31}P\{^1H\}$-NMR spectra and ν_{CO} IR bands (CH_2Cl_2) of **12a−12d** and **13**

	^{31}P NMR [δ values]	IR {ν_{CO} [cm-1]}
12a[a]	-	1913 (vs), 1783 (s, br).
12b[b]	+ 18.4 (s).	2019 (s), 1903 (vs, br).
12c[a]	+ 18.4 (s).	1923 (vs), 1801 (s, br).
12d[b]	+16.6 (d, 1P, $^2J_{PP}$ = 23.7 Hz), +17.7 (d, 1P, $^2J_{PP}$ = 23.7 Hz).	1925 (vs), 1814 (s, br).
13[b]	+ 21.1 (s).	1936 (vs), 1825 (s, br).

[a] Solvent: CD_2Cl_2; the CD_2Cl_2 was condensed into the NMR tubes prior to flame sealing. − [b] Solvent: $CDCl_3$.

While η^3-coordination did not occur with **2**, having three pyrazolyl donor functions, it appeared probable that the exchange of one pz donor by a PPh_2 group might favour the facial coordination of ligands such as **10a**. While **2** would form a chelate cage with three condensed eight-membered chelate cycles, only one eight-membered cycle and two seven-membered cycles would result from the η^3-coordination of **10a**. However, reaction of **10a** with

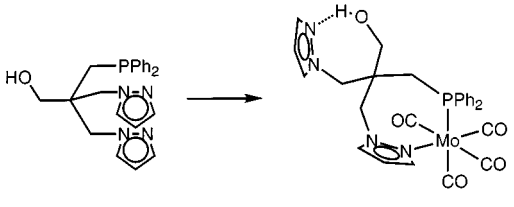

10a **12b**

$(MeCN)_3Mo(CO)_3$ affords **12b** as the only isolable product.

The presence of an $Mo(CO)_4$ group in **12b** is evident from the ν(CO) bands, as well as from its mass spectrum (Table 5, Exp. Section). The formation of $Mo(CO)_4$ derivatives from $(MeCN)_3Mo(CO)_3$ is well-documented in tripod coordination chemistry[6][21b]. The ^1H-NMR spectrum of **12b** cannot be completely resolved at 200 MHz; nevertheless, the groups of signals show the expected integral ratios (Table 3). For the bridging hydrogen evident in the solid-state structure (see below), no signal could be assigned, nor could an appropriate band be found in the IR spectrum of **12b**.

Crystals of **12b** suitable for X-ray analysis were obtained from dichloromethane by vapour-phase diffusion with petroleum ether (40/60). The structure of **12b**, as determined by single-crystal X-ray analysis (Table 8)[23a], is shown in Figure 1: η^2-coordination of the ligand by one pyrazolyl and one phosphorus donor results in the formation of a seven-membered chelate cycle. The tendency of the pyrazolyl ligand to enforce coplanarity between the bonds radiating from the two nitrogen centers in the ring (torsion angle Mo−N−N−C 1.9°, Table 6) results in a characteristic puckering at the other positions of the seven-membered ring, which is also observed for the corresponding entity in **12c** (Figure 1, Table 6).

A peculiar feature of the structure of **12b** is the formation of a strong OH−N hydrogen bond between the dangling arm pyrazolyl entity and the CH_2OH group. The corresponding N−O distance amounts to only 280 pm; the position of the bridging hydrogen has been successfully refined (Table 6).

A seven-membered ring is formed, with the OH group and the pyrazolyl entity linked by the hydrogen bond (Figure 1). With the coplanarity of the H−N−N−C fragment of this ring, its conformation is similar to that observed for the chelate ring (for torsion angles, see Table 6). Since it appears that in **12b** (see also **12d**) the OH proton competes successfully with the metal in coordinating the second pyrazolyl function of **10a**, η^3-coordination of a ligand of the type **10a** might possibly have resulted when the OH function of **10a** was transformed into the OEt function of **11**. However, it was found that **11** produces **12c** when reacted with $(MeCN)_3Mo(CO)_3$, in which again only two donor functions coordinate to the metal center (Figure 1). One pyrazolyl donor and the ethoxy group remain uncoordinated.

The conformation of the seven-membered chelate cycle closely resembles that observed for **12b** (for torsion angles, see Table 6). On the other hand, the rotational orientation

Figure 1. Conformations as observed for **12b**, **12c**, and **12d** in the solid state[a]

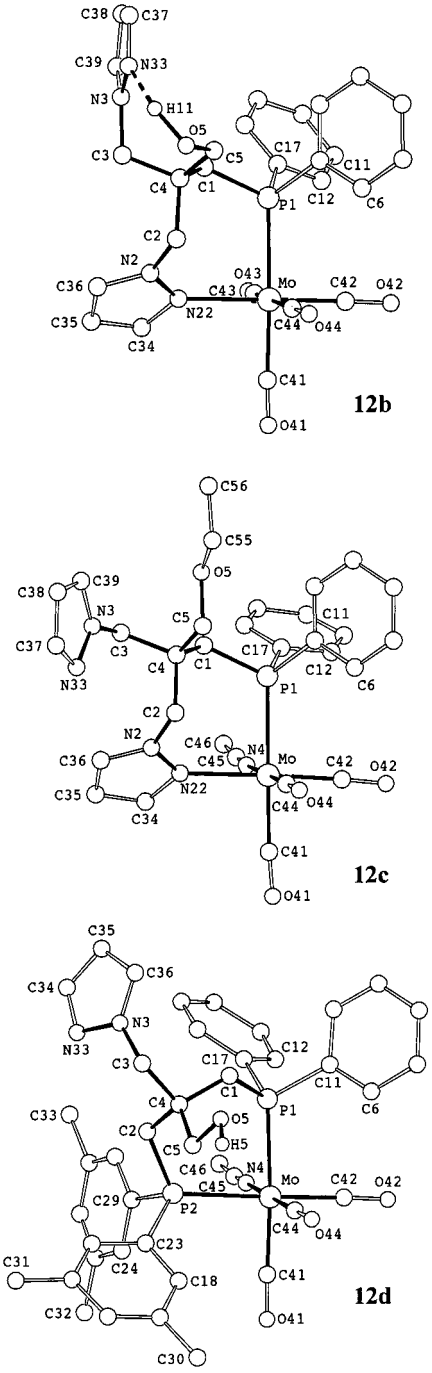

[a] The numbering scheme selected for compounds **12** allows direct comparison with the data given in ref.[6].

of the dangling arm functions is distinctly different from the situation in **12b**, where these donor functions are connected by a strong hydrogen bond (Table 6, Figure 1). Since the conformations of the chelate rings in **12b** and **12c** are nevertheless almost identical, this means that there is little interference between the conformation of the chelate ring at the metal center and the orientation of the substituents at C4 (Figure 1, Table 6). The spectroscopic data obtained

Table 6. Selected bond lengths [pm], bond angles [°], and torsion angles [°] for **12b**, **12c**, and **12d**[a]

	12b	**12c**	**12d**
Mo−P1	251.4 (1)	254.4 (2)	251.7 (1)
Mo−N22 (P2)	230.2 (2)	228.3 (4)	252.7 (1)
Mo−C41	200.6 (3)	197.2 (6)	198.1 (7)
Mo−C42	194.6 (3)	194.0 (5)	195.9 (5)
Mo−C43	204.1 (3)	–	–
Mo−C44	202.5 (3)	193.4 (5)	194.6 (5)
Mo−N4	–	222.0 (4)	220.6 (4)
P1−Mo−N22 (P2)	88.4 (1)	88.0 (1)	84.1 (1)
N33−H11	172 (6)	–	–
N33−H11−O1	143.3 (3)	–	–
Mo−P1−C11−C6	3.9 (2)	6.3 (3)	−22.5 (5)
Mo−P1−C17−C12	−52.3 (2)	−70.8 (5)	64.4 (6)
Mo−P2−C23−C18	–	–	2.3 (4)
Mo−P2−C29−C24	–	–	82.1 (4)
C44−Mo−P1−C1	−89.0 (1)	−92.6 (2)	−53.7 (2)
Mo−P1−C1−C4	61.7 (2)	62.7 (4)	−33.0 (4)
P1−C1−C4−C2	−50.0 (2)	−46.9 (5)	−30.3 (5)
C1−C4−C2−N2 (P2)	−52.3 (3)	−56.6 (5)	73.9 (5)
C4−C2−N2 (P2)−N22 (Mo)	91.6 (2)	93.4 (5)	−44.6 (4)
C2−N2−N22−Mo	1.9 (2)	5.5 (4)	–
(C2−P2−Mo−P1)	–	–	−9.9 (3)
N2−N22−Mo−P1	−51.5 (2)	−52.5 (3)	–
(P2−Mo−P1−C1)	–	–	42.4 (2)
N22−Mo−P1−C1	7.0 (1)	5.5 (2)	–
C4−C3−N3−N33	−82.5	68.4	80.5
C3−N3−N33−H11	15.0	–	–
N3−N33−H11−O1	40.3	–	–
N33−H11−O1−C5	7.9	–	–
H11 (C55)−O1−C5−C4	−75.5	−164.9	−172.4
O1−C5−C4−C3	43.7	−55.1	−62.2
C5−C4−C3−N3	55.3	−45.4	−174.9
C1−C4−C5−O5	162.6	61.0	54.7
C2−C4−C3−N3	170.9	71.3	−58.1

[a] The numbering scheme is such that chemically equivalent atoms have the same numbers in molecules **12b**, **12c** and **12d**.

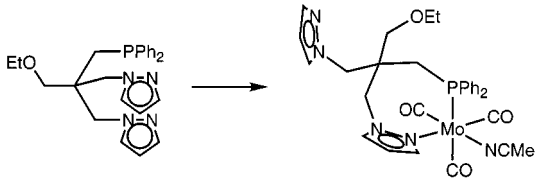

11 **12c**

for **12c** are roughly similar to those obtained for **12a** (Tables 3, 4, and 5). With the structure of **12c** known, this is an indirect proof of the validity of the constitution assigned to **12a**. The ^{1}H-NMR data of **12c** have been analysed in some detail (Table 3). Since at 200 MHz the signals of the five different types of CH_2 groups of **12c** are largely overlapped, a series of 2D-NMR experiments (see Exp. Section) was essential to allow complete assignment of all the individual signals (Tables 3 and 4). A rather astonishing result of these experiments was that the diastereotopic protons of the CH_2P group were found to have their resonances separated by about 1.5 ppm (Table 3). An equally large shift difference was observed for the two diastereotopic protons at the coordinated CH_2pz group (δ = 4.28, 5.37, Table 3). The dangling arm CH_2pz entity has a more normal shift difference (δ = 4.10, 4.28, Table 3) between its diastereotopic protons[6]. The observed strong differentiation between the two

hydrogens at the CH_2 groups in the chelate ring calls for an explanation, since correspondingly large shift differences have, to our knowledge, not hitherto been observed in compounds of neopentane-based ligands, nor in coordination compounds containing the CH_2pz group as part of a ligand[6][24]. It is assumed that the magnetic anisotropy of the dangling arm pyrazolyl entity is responsible for the observed difference in the magnetic shielding of the CH_2 groups within the chelate ring.

The two different types of pyrazolyl entities in **12c** give rise to several ^{1}H resonances in the aromatic region [Table 3; for the numbering scheme, see Figure 4 (Exp. Section)]. The resonance of the central CH group at C4 is well-separated on the highfield side of this range. The resonance of this group is significantly shifted downfield upon coordination (Table 3). An unequivocal assignment of the resonances of the CH groups at C3 and C5 was possible with the combined application of 2D-NMR experiments (Tables 3 and 4, Exp. Section). The ^{1}H signals of the phenyl substituents at the phosphorus could also be fully assigned (Table 3). The ^{13}C-NMR spectrum of **12c** shows an upfield shift for the methylene carbons bound to the coordinated PPh_2 and pyrazolyl entities and a downfield shift for the carbons of the coordinated pyrazolyl entity, while the ^{13}C signals of the non-coordinated CH_2pz group exhibit no shift at all (compared to the free ligand, see Tables 2 and 4). The information gleaned from these NMR experiments is important in so far as no data have hitherto been reported pertaining to the complete and absolute assignment of non-coordinated and coordinated pyrazolyl functions in the same coordination compound[24].

The fact that **11**, containing two pyrazolyl donor functions, acts only as a bidentate ligand, even though the OH group, which competes with the metal coordination of one pyrazolyl donor in the reactions of **10a**, is blocked as an OEt function, indicates that η^3-coordination of neopentane-based tripod ligands will tolerate at most one pyrazolyl donor. An attempt was therefore made to coordinate **10c**, which contains one pyrazolyl and two phosphorus donors, in an η^3-fashion to an $Mo(CO)_3$ fragment. Again, under standard conditions, only bidentate coordination of **10c** was observed, with the $Mo(MeCN)(CO)_3$ fragment coordinated to the two phosphorus donors of the ligand.

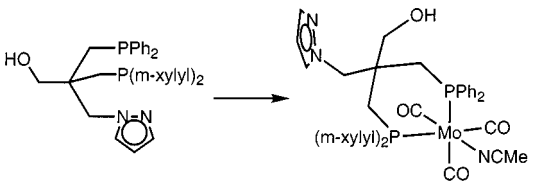

10c **12d**

The presence of a dangling arm pyrazolyl function is indicated by the ^{1}H-NMR data, where the CH_2pz group as well as the CH group at C4 of the pyrazolyl ring show their resonances in the ranges expected for non-coordinated CH_2pz groups (cf. **12c**, Table 5). The coordination of the two phosphorus donors is evident from the ^{31}P-NMR data (Table 3). From the mass spectrum of **12d**, the η^2-coordination of the ligand is not apparent since, as with **12a** and **12c**, the MeCN group is no longer present in the ions detected; [**10c**·$Mo(CO)_3^+$] is the ion with the highest *m*/*z* ratio observed.

The given constitution of **12d** was unequivocally proven by X-ray analysis. Small single crystals of **12d** were obtained by vapour-phase diffusion of petroleum ether (40/60) into the reaction mixture after it had been reduced to half of its original volume. The crystals were found to be very sensitive to air and moisture, but could be subjected to X-ray analysis when immersed in perfluorinated polyether oil and immediately cooled to −70°C (Exp. Section). The coordination of the two phosphorus donors leads to the formation of a six-membered chelate cycle (Figure 1). The conformation of the chelate ring does not correspond to a distinct chair-type arrangement (almost C_s symmetric), which has been observed in quite a number of related structures derived from neopentane-based tripod ligands in an η^2-coordination mode[6][25]. It does not conform to a twistboat arrangement either, which is again found in the structures of some closely related molecules[6][25]. In this context, the structure of $CH_3C(CH_2PPh_2)_2(CH_2Cl)Mo(CO)_4$[23b] is of interest, in which the chelate cycle adopts a distorted chair conformation (P1−C1−C2−P2 = 62.5°, see below). This compound was prepared in order to study the reactivity of the CH_2Cl group with the phosphorus donors protected by an $Mo(CO)_4$ entity − a strategy which has proved useful in certain ligand syntheses[26]. Its structure was analysed in order to get some appraisal of the accessibility of the CH_2Cl group to nucleophiles. The chlorine function has been found to point outwards, away from the molybdenum center[23b]. In contrast, the presence of two sterically demanding functionalities (CH_2pz, CH_2OH) at the central carbon atom in compound **12d** leads to some irregular distortion, which is best described as a chair conformation with some twist, as indicated by the torsion angle P1−C1−C2−P2 of 35.8°. This angle is close to 0° for a chair or boat conformation and around 70° for a pure twist-boat (see above)[6]. This type of distortion of the chelate ring in **12d** has not previously been observed in the coordination chemistry of neopentane-based tripod ligands acting in an η^2-coordination mode. One reason for the distortion observed in **12d** may be the fact that the pyrazolyl substituent and the OH group are both involved in intermolecular hydrogen bonding. The individual molecules are linked by this hydrogen bonding to form chains spiralling around the 2_1 axis, characterizing the symmetry of the crystal in the space group $P2_1/c$. Figure 2 shows a projection illustrating the arrangement in this infinite spiral.

In spite of the unconventional folding of the chelate ring of **12d**, the rotational position of the PPh_2 moieties relative to the idealized octahedral axis of the coordination polyhedron and the rotational position of the phenyl groups relative to the Mo−P axis are not dissimilar from those observed in quite a number of other essentially similar compounds (Table 6)[6].

Figure 2. Hydrogen bonding pattern as observed for **12d** in the crystal[a]

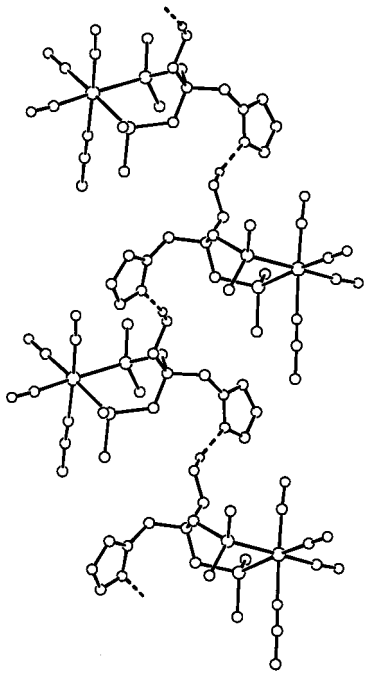

[a] For the sake of clarity, the aryl groups are represented by their *ipso*-carbon atom only; for structural features of **12d** see also Figure 1 and Table 6.

The idea that a tripod ligand of type **A** with only one pyrazolyl donor group and two phosphorus donors should be capable of η^3-coordination appears to be ruled out at first glance by the η^2-coordination observed for **12d**. However, it may be argued that the steric bulk introduced by the 3,5-dimethylphenyl substituents at P2 may be a factor in favouring η^2-coordination, which, as shown for the solid-state structure of **12d**, is then additionally stabilized by intermolecular hydrogen bonding. To verify this argument, the reactivity of **10b** towards $(MeCN)_3Mo(CO)_3$ was tested. While with this ligand intermolecular hydrogen bonding might also favour η^2-coordination, the reduced steric demand of **10b** − two PPh_2 groups instead of one PPh_2 and one $P(3,5\text{-}Me_2Ph)_2$ group − might successfully compete, such that η^3-coordination could result. Such a facial coordination of **10b** is in fact observed, with the $Mo(CO)_3$ derivative **13** being formed.

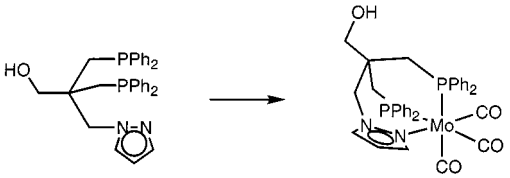

10b **13**

The fact that the ligand **10b** is coordinated in an η^3-binding mode cannot, of course, convincingly be deduced from the appearance of the molecular ion in the mass spectrum (see above), nor is it proved by the observation of the ν_{CO} IR pattern, even though this corresponds to the $A_1 + E$ envelope [Table 5, expected idealized local C_3 symmetry for this type of coordination of the $Mo(CO)_3$ chromophore]. The coordination of the two phosphorus donors on the other hand is clearly evident from the ^{31}P-NMR data (Table 5). The fact that the pyrazolyl donor is coordinated as well is at least not contradicted by the corresponding ^{1}H-NMR data (Table 3). The NMR data give convincing evidence for the fact that the OH group is not coordinated to the metal (Table 3).

Again, the constitution was unambiguously proved by an X-ray analysis performed on well-formed needles obtained from dichloromethane solutions of **13** by vapour-phase diffusion with petroleum ether (40/60). Two crystallographically independent molecules **13** are observed in the crystal (Figure 3). The overall conformations of the two molecules are rather similar, as shown by the torsion angles given in Table 7 (even the torsional positions of the aryl substituents are almost equivalent in the two symmetrically independent species within the crystal).

Figure 3. Conformation as observed for **13/1** in the solid state[a]

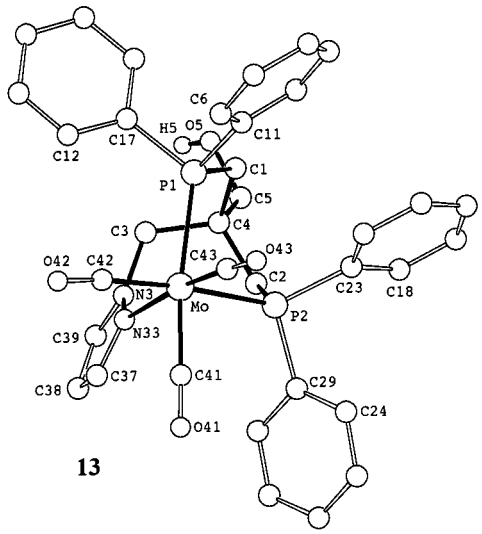

13

[a] **13/1** and **13/2** designate the two crystallographically independent molecules in the crystal of **13**. The structure of **13/2** corresponds in its overall arrangement to the structure shown for **13/1**. The numbering scheme chosen for **13** allows for the direct comparison with the data given in ref.[6].

The relative arrangement of the aryl substituents is in accord with a pattern previously described for η^3-coordinated tripod ligands containing two PPh_2 groups and one nitrogen donor[6], even though the chelate cage of **13** contains two seven-membered and only one six-membered cycle, while the cages of comparable molecules[6] contain the standard set of three condensed six-membered cycles. The main difference between the two individual molecules **12** within the crystal is a different orientation of the CH_2OH group relative to the chelate cage (Table 7). This difference in orientation results from the fact that, of the two independent molecules, one is engaged as a proton donor in a hydrogen bond, with one carbonyl group of the other molecule acting as the proton acceptor. The interaction is very weak (d_{O-O} = 299 pm, d_{O-H} = 229 pm, O−H−O =

Table 7. Selected bond lengths [pm], bond angles [°] and torsion angles [°] for **13/1** and **13/2**[a]

	13/1	13/2
Mo1−P1	254.7 (2)	253.9 (2)
Mo1−P2	250.7 (2)	250.9 (2)
Mo1−N3	232.4 (5)	230.3 (5)
Mo1−C41	194.4 (6)	194.1 (6)
Mo1−C42	196.9 (7)	196.6 (6)
Mo1−C43	192.5 (6)	191.7 (7)
P1−Mo1−P2	82.9 (1)	82.8 (1)
P1−Mo1−N3	94.8 (1)	95.1 (1)
P2−Mo1−N3	83.4 (1)	82.4 (1)
Mo1−P1−C1−C4	36.8 (5)	32.9 (5)
Mo1−P2−C2−C4	42.9 (5)	37.5 (5)
Mo1−N3−C3−C4	49.0 (5)	46.4 (5)
P1−C1−C2−P2	−39.7	−33.7
C1−C4−C5−O1	−60.7	55.6
Mo1−P1−C11−C6	−60.1 (5)	−77.1 (5)
Mo1−P1−C17−C12	11.2 (6)	2.3 (6)
Mo1−P2−C23−C18	−169.1 (4)	−159.4 (5)
Mo1−P2−C29−C24	−100.9 (5)	−100.7 (5)
H_z1−P1−C11−C6	−28.9	−45.1
H_z1−P1−C17−C12	−44.6	−52.6
H_z2−P2−C23−C18	142.0	154.6
H_z2−P2−C29−C24	−58.5	−56.7

[a] The numbering scheme adopted for **13/2** relates chemically equivalent atoms by adding 100 to the numbers used in **13/1** (not including molybdenum). The torsion angles given refer to a selection of enantiomers such that the skew of the chelate scaffolding has the same sense for both individual molecules.

144.2°), but is clearly present, as found in the solid-state structure. The OH group of the second molecule shows no close contacts to other hydrogen-accepting positions within the crystal.

The interatomic distances within the five individual molecules (**12b−d** and two molecules **13/1** and **13/2** in the crystal of **13**) are in rather close agreement. The Mo−P bond lengths span a range approximately between 250 and 255 pm (Tables 6 and 7). The Mo−N distances to the pyrazolyl donors are similarly found in a narrow range (228−233 pm), while the coordinated acetonitriles in **12c** and **12d** show significantly shorter Mo−N distances (220−222 pm). The Mo−C(CO) distances are in the usual range. A significant shortening of the Mo−C(CO) bond *trans* to to the pyrazolyl donor is observed in all molecules (Mo−C42 for **12b−d**, Mo−C43 for **13/1**, **13/2**). The Mo−C(CO) bonds *trans* to the acetonitrile ligands are also significantly shorter (Mo−C44 in **12c/d**) than the Mo−C(CO) bonds that are *trans* to an Mo−P bond. This observation reflects the higher donor/acceptor ratio of the nitrogen donors relative to a phosphane ligand. The bite angles P−Mo−N and P−Mo−P, respectively, span a range between 82° and 95° (Tables 6 and 7); angles smaller than 90° are generally observed. An angle of over 90° occurs only in **13**, where in both of the two independent molecules one of the P−Mo−N angles has a value around 95°. This large angle appears to be the result of the steric strain within the seven-membered chelate cycles. This strain leads to a folding of these cycles (Figure 3), which increases the steric burden on one of the phosphorus donors (P1), while relieving the burden on the other (P2). The angle P1−Mo−N33 responds to this strain by increasing accordingly. The presence of strain in the chelate cage of **13** is also indicated by the conformation of the six-membered chelate cycle, which, although in a situation where the chelate cage consists of three condensed six-membered rings, i.e. the normal tripod metal templates $RCH_2C(CH_2X)(CH_2Y)(CH_2Z)M$, is invariably found in an approximate boat arrangement[27]. In **13**, there is an appreciable twist in the boat conformation of this ring (P1−C1−C2−P2 = −39.7°, P101−C101−C102−P102 = −33.7°), which is similar to the twist observed in **12d**, where steric strain was also invoked as an explanation (see above).

Conclusions

1. It is found that pyrazolyl as well as imidazolyl donors may be incorporated into neopentane-based tripod ligands by means of nucleophilic substitution reactions with potassium pyrazolate and potassium imidazolate, respectively.

2. It is shown that the oxetane ring of substituted oxetanes $O(CH_2)_2C(CH_3)(CH_2X)$ undergoes aminolytic cleavage to furnish $CH_3C(CH_2X)(CH_2Y)(CH_2OH)$ systems, with X being an amine or a pyrazolyl substituent and Y being an amine function.

3. It is demonstrated that starting from $O(CH_2)_2$-$C(CH_2Br)(CH_2OMs)$, by selective substitution of the nucleophugic groups and subsequent nucleophilic cleavage of the oxetane moiety, chiral tripod ligands $HOCH_2C(CH_2PR_2)(CH_2Y)(CH_2Z)$ with mixed nitrogen/phosphorus donor sets may be obtained.

4. It is observed that potential tripod ligands $HOCH_2$-$C(CH_2pz)_{3-n}(CH_2PR_2)_n$ tend to act as bidentate chelate ligands when less than two phosphorus donors are present. The size of the chelate ring is invoked as an explanation, with this argument being corroborated by X-ray analysis.

We are grateful to the *German Science Foundation (DFG)*, *SFB 247*, the *VW Foundation (Stiftung Volkswagenwerk)*, and the *Fonds der Chemischen Industrie* for financial support. The author would especially like to thank *F. Rominger* for help with the data collection for the X-ray structure analysis of **12b** and **12c**. The technical support by *Th. Jannack* (mass spectrometry) and the *Microanalytical Laboratory of the Institute of Organic Chemistry* is gratefully acknowledged.

Experimental Section

All manipulations involving phosphanes were carried out under an argon atmosphere by means of standard Schlenk techniques and were monitored by TLC (Macherey-Nagel & Co., Polygram SIL G/UV_{254}). − The aminolytic cleavage of oxetanes was carried out in an HR 100 stainless steel high-pressure laboratory reactor (Berghof/Maasen GmbH) equipped with inlet and outlet valves and a manometer. − The bulb-to-bulb distillations were performed in a kugelrohr apparatus (Büchi). − All solvents were dried by standard methods[28] and distilled under argon. The solvents $CDCl_3$ and CD_2Cl_2 used for the NMR spectroscopic measurements were degassed by three successive "freeze-pump-thaw" cycles and dried over 4 A molecular sieves. − NMR: Bruker Avance DPX 200 at 200.13 MHz (^1H), 50.323 MHz ($^{13}C\{^1H\}$), 81.015 MHz ($^{31}P\{^1H\}$), T = 298 K, chemical shifts (δ) in ppm with respect to $CHCl_3$ (^1H: δ = 7.27, ^{13}C: δ = 77.0) and CH_2Cl_2 (^1H: δ = 5.32, ^{13}C: δ = 53.5)

as internal standards. ^{31}P chemical shifts (δ) in ppm with respect to 85% H_3PO_4 (^{31}P: δ = 0) as external standard. − 2D-NMR experiments: DQF-COSY[29a], TOCSY[29b], NOESY[29c], HMQC[29d], and HMBC[29e] experiments were performed in order to allow the complete assignment of protons and carbons in **12c**. − IR: Bruker FT-IR IFS-66, CaF_2 cells. − MS (EI): Finnigan MAT 8320; fast-atom bombardment (FAB) xenon, matrix: 4-nitrobenzyl alcohol. − Melting points: Gallenkamp MFB-595 010; uncorrected values. − Elemental analyses: Microanalytical Laboratory of the Organisch-Chemisches Institut, Universität Heidelberg. The procedures used for determining the carbon content often give falsely low values when Mo is present in a compound owing to the formation of incombustible Mo carbide; nitrogen values generally tend to be to low as well. − The silica gel (Kieselgel z.A. 0.06−0.2 mm, J. T. Baker Chemicals B.V.) used for chromatography was degassed at 1 mbar for 24 h and saturated with argon. A solution of 2.5 M *n*BuLi in hexanes was used for deprotonations. $Mo(CO)_6$ was sublimed before use. **1**[9], $(MeCN)_3Mo(CO)_3$[22], **4**[19] and **8**[5d] were prepared according to literature procedures. All other chemicals were obtained from commercial suppliers and used without further purification.

Figure 4. NMR numbering scheme for the pyrazolyl ring[24]

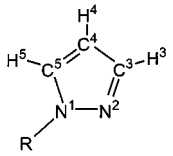

X-ray Structure Determinations: Suitable crystals were taken directly out of the mother liquor, immersed in perfluorinated polyether oil and fixed to a glass capillary at 200 K. The measurements for **12d** and **13** were carried out on a Siemens P4 four-circle diffractometer (equipped with a low temperature device) with graphite-monochromated Mo-K_α radiation. The measurements for **12b** and **12c** were carried out on a Siemens CCD/SMART System (equipped with a low temperature device) also with graphite-monochromated Mo-K_α radiation. All calculations were performed using the SHELXT-PLUS[30] software package. Structures were solved by direct methods with the SHELXS-86 program[30a] and refined with the SHELX-93 program[30b]. Graphical handling of the structural data during solution and refinement was performed with XPMA[31]. An absorption correction (ψ-scan, Δψ = 10°) was applied to the data for **12d** and **13**. An empirical absorption correction was applied in the cases of **12b** and **12c**. Atomic coordinates and anisotropic parameters of the non-hydrogen atoms were refined by full-matrix least-squares calculations. Data for the structure determination are compiled in Table 8.

Ligand Synthesis

1,1,1-Tris(pyrazol-1-yl-methyl)ethane (**2**): 3.40 g (50 mmol) of pyrazole was dissolved in 100 ml of DMSO and deprotonated at 0°C with 5.61 g (50 mmol) of KO*t*Bu. After warming to room temperature, 1.58 g (9 mmol) of tris(chloromethyl)ethane **1** in 10 ml of DMSO was added. The resulting mixture was stirred for 12 h at 120°C. The solution was then cooled and the DMSO was evaporated in vacuo (10^{-1} mbar). 60 ml of water was added to the oily brown residue and after stirring for 20 min., the brown solution was extracted with 50 ml portions of diethyl ether (5×). The combined organic phases were concentrated in vacuo (10^{-1} mbar). The brown residue was divided into three portions, which were separately purified by bulb-to-bulb distillation. After removing the pyrazole at 120°C (0.5 mbar), the temperature was raised further and 1.11 g (4.1 mmol, 46%) of **2** was obtained as colourless needles (200−250°C/0.5 mbar). − MS (EI); *m/z* (%): 270 (10) [M^+], 189 (100) [$M^+ - CH_2pz$], 121 (59) [$M^+ - CH_2pz - pz$], 81 (45) [CH_2pz^+]. − $C_{14}H_{18}N_6$ (270.34): calcd. C 62.19, H 6.71, N 31.10; found C 61.86, H 6.88, N 29.90.

1,1,1-Tris(imidazol-1-yl-methyl)ethane (**3**): 4.08 g (60 mmol) of imidazole was dissolved in 120 ml of DMSO and deprotonated at 0°C with 6.73 g (60 mmol) of KO*t*Bu. After warming to room temperature, 1.76 g (10 mmol) of tris(chloromethyl)ethane **1** in 10 ml of DMSO was added. The resulting mixture was stirred for 14 h at 120°C. The solution was then cooled and the DMSO was evaporated in vacuo (10^{-1} mbar). 70 ml of water was added to the reddish-brown residue. After stirring for 20 min, the brown solution was extracted with 30 ml portions of THF (5×) and subsequently with 20 ml portions of dichloromethane (3×). The combined organic phases were dried over $MgSO_4$, filtered, and concentrated in vacuo (10^{-1} mbar). The resulting orange-coloured oil was divided into three portions, which were separately purified by bulb-to-bulb distillation. 0.35 g (1.3 mmol, 13%) of **3** as colourless crystals (230°C/0.02 mbar) was obtained. − MS (EI); *m/z* (%): 271 (67) [M^+], 189 (28) [$M^+ - CH_2$imidazole], 121 (100) [$M^+ - CH_2$imidazole − imidazole], 81 (81) [CH_2imidazole$^+$]. − $C_{14}H_{18}N_6$ (270.34): calcd. C 62.19, H 6.71, N 31.10; found C 61.75, H 6.57, N 30.67.

3-Methyl-3-(3,5-dimethylpyrazol-1-yl-methyl)oxetane (**5a**); 4.80 g (60 mmol) of 3,5-dimethylpyrazole was dissolved in 150 ml of THF and deprotonated at 0°C with 6.74 g (60 mmol) of KO*t*Bu. The solution was then allowed to warm to room temperature. In a second flask, 9.00 g (50 mmol) of 3-methyl-3-(methylsulfonyloxymethyl)oxetane **4** in 100 ml of THF was cooled to 0°C. The potassium pyrazolate solution was then added and the reaction mixture was refluxed for 4 h. The jelly-like mixture was then quenched by the addition of 50 ml of water and the aqueous phase was extracted with 30 ml portions of diethyl ether (2×). The combined organic phases were washed with brine, dried over $MgSO_4$, filtered, and distilled through a 20 cm Vigreux column at 1 mbar. 6.85 g (38 mmol, 76%) of **9a** was obtained as a colourless oil (b.p. 128−133°C, 1 mbar). − ^1H NMR ($CDCl_3$): δ = 1.18 (s, 3 H, CqCH_3), 2.13, 2.15 (2s, 6 H, pzCH_3), 4.05 (s, 2 H, CH_2pz), 4.29, 4.70 (2d, 4 H, oxetane-CH_2, $^2J_{HH}$ = 5.8 Hz), 5.72 [s, 1 H, C*H(4)*pz]. − ^{13}C NMR ($CDCl_3$): δ = 11.8, 13.9 (2s, pzCH_3), 22.3 (s, CqCH_3), 41.5 (s, Cq), 54.5 (s, CH_2pz), 81.0 (s, oxetane-CH_2), 105.2 [s, *C(4)*pz], 139.5 [s, *C(5)*pz], 148.0 [s, *C(3)*pz]. − MS (EI); *m/z* (%): 180 (30) [M^+], 149 (55) [M^+ − CHO], 109 (100) [CH_2pz^+], 96 (22) [pz^+]. − $C_{10}H_{16}N_2O \cdot 1/3\ H_2O$* (180.25): calcd. C 64.49, H 9.02, N 15.04; found C 64.47, H 9.05, N 15.05. *The water content was inferred from the analytical results, which were well reproducible.

3-Azidomethyl-3-methyloxetane (**5b**): 18.0 g (0.1 mol) of 3-methyl-3-(methylsulfonyloxymethyl)oxetane **4** and 19.0 g (0.3 mol) of NaN_3 were dissolved in 300 ml of DMSO. This mixture was stirred vigorously for 30 h at 120°C. After cooling to room temperature, 600 ml water was added and the solution was carefully extracted with 100 ml portions of diethyl ether (4×). The combined organic phases were concentrated in vacuo (10^{-1} mbar) to half of the initial volume (CAUTION: explosive). A sample of 1 ml was concentrated to dryness at 10^{-2} mbar (0°C) in order to obtain spectroscopic data of **5b**. − IR (Et_2O): ν = 2103 (s, $-N_3$). − ^1H NMR ($CDCl_3$): δ = 1.28 (s, 3 H, CH_3), 3.48 (s, 2 H, CH_2N), 4.31, 4.39 (2d, 4 H, $^2J_{HH}$ = 6.0 Hz, oxetane-CH_2). − ^{13}C NMR ($CDCl_3$): δ = 23.1 (s, *C*H_3), 40.5 (s, *Cq*), 58.1 (s, *C*H_2N), 79.6 (s, oxetane-*C*H_2).

3-Aminomethyl-3-methyloxetane (**5c**): 23.7 g (90 mmol) of PPh_3 was added slowly to a well-stirred ethereal solution of **5b**. Evolution

Table 8. Crystal data for **12b**, **12c**, **12d**, and **13**

Compound	**12b**	**12c**	**12d**	**13**
Formula	$C_{27}H_{25}N_4O_5PMo$	$C_{30}H_{32}N_5O_4PMo$	$C_{41}H_{43}N_3O_4P_2Mo \cdot 0.5\ CH_2Cl_2 \cdot 1.5$ MeOH	$C_{35}H_{32}N_2O_4P_2Mo \cdot 2\ CH_2Cl_2$
molecular mass [g]	612.43	653.53	799.71	702.54
crystal size [mm]	0.3 × 0.3 × 0.3	0.3 × 0.3 × 0.2	0.05 × 0.05 × 0.2	0.3 × 0.3 × 0.2
crystal system	triclinic	monoclinic	monoclinic	triclinic
space group (No.)[30c]	*P*1 (2)	$P2_1/n$ (14)	$P2_1/c$ (14)	*P*1 (2)
a [pm]	936.62(2)	908.9(5)	1612.76(2)	1021.2(2)
b [pm]	1065.85(1)	2005.2(3)	1183.87(1)	1649.3(4)
c [pm]	1479.42(2)	1634.8(4)	2470.21(1)	2078.4(7)
α [°]	72.90(1)	90	90	93.02(2)
β [°]	72.12(1)	92.38(4)	93.71(1)	92.63(2)
γ [°]	72.94(1)	90	90	90.70(2)
V [10^6 pm^3]	1309.6(1)	2976.9(2)	4706.5(1)	3491.7(2)
Z	2	4	4	4
d_x [g cm^{-3}]	1.553	1.447	1.242	1.494
μ [mm^{-1}]	0.61	0.54	0.45	0.66
transition (min)	0.80	0.81	0.90	0.78
transition (max)	0.92	0.87	0.99	0.90
T [K]	200	200	200	200
no. rflns. for cell param. refinm.	all	25	all	26
scan range	6.4° ≤ 2Θ ≤ 54.6°	4.8° ≤ 2Θ ≤ 51.0°	3.3° ≤ 2Θ ≤ 51.8°	3.9° ≤ 2Θ ≤ 48.1°
scan speed [° min^{-1}]	–	ω = 6	–	ω = 12
no. rflns. measured	6881	5964	20889	11468
no. unique rflns.	5039	5531	7791	10683
no. rflns. observed	4730	4005	6519	7306
observation criterion	$I \geq 2\sigma$	$I \geq 2\sigma$	$I \geq 2\sigma$	$I \geq 2\sigma$
no. param. refined	443	462	514	868
resid. el. density [10^{-6} e pm^{-3}]	0.57	0.59	1.39[a]	0.71
R_1/R_w [%] (refinement on F^2)	3.1/10.4	5.5/11.3	6.1/23.6[a]	5.3/11.8

[a] Due to badly resolved, disordered solvent molecules.

of nitrogen was observed over a period of two hours. The reaction mixture was then stirred at room temperature for 10 h [reaction control: ^{31}P NMR: PPh_3, δ = −7.2, imidophosphorane (R−N=PPh_3), δ = +10.6; IR: ν = 2103 (s, R−N_3)]. Subsequently, addition of 1.8 ml of water and refluxing for two hours led to cleavage of the imidophosphorane (reaction control: ^{31}P NMR: O=PPh_3, δ = +28.2). The solvent was removed under reduced pressure (100 mbar) using a trap (−70°C). The residue was distilled through a 10 cm Vigreux column at 20 mbar while the head was cooled to −10°C (using a cryostat) and the collecting flask was ice-cooled. 9.1 g (82 mmol, 82%) **5c** was obtained as a colourless oil; b.p. of 40°C (20 mbar). − ^{1}H NMR ($CDCl_3$): δ = 1.21 (s, 3 H, CH_3), 2.86 (s, 2 H, CH_2N), 4.35, 4.41 (2d, 4 H, $^2J_{HH}$ = 5.8 Hz, oxetane-CH_2). − ^{13}C NMR ($CDCl_3$): δ = 21.1 (s, *C*H_3), 40.4 (s, *Cq*), 49.1 (s, *C*H_2S), 80.2 (s, oxetane-*C*H_2). − MS (EI), *m/z* (%): 129 (9) [$M^+ \cdot H_2O$], 101 (10) [M^+]. − $C_5H_{11}NO \cdot 1/10$ DMSO/H_2O* (110.76): calcd. C 56.39, H 10.74, N 12.65; found C 56.29, H 10.97, N 12.91. *The DMSO content was estimated by NMR; the water content was inferred from elemental analysis.

3-(tert-Butyloxycarbonyl)aminomethyl-3-methyloxetane (*Boc-***5c**): Boc-protection of **5c** was carried out on a 25 mmol sample according to a previously published procedure[6]. After work-up, Boc-**5c** was obtained as a colourless oil, which could be crystallized by overlayering a dichloromethane solution with petroleum ether (40/60). After two days, 4.07 g (20 mmol, 81%) of Boc-**5c** was isolated in the form of colourless needles. − ^{1}H NMR ($CDCl_3$): δ = 1.26 (s, 3 H, CqCH_3), 1.42 (s, 9 H, *Boc*), 3.26 (d, 2 H, $^3J_{HH}$ = 6.4 Hz, CH_2N), 4.31, 4.43 (2d, 4 H, $^2J_{HH}$ = 5.8 Hz, oxetane-CH_2), 5.25 (bs, 1 H, N*H*). − ^{13}C NMR ($CDCl_3$): δ = 22.3 (s, CqCH_3), 28.7, 79.7, 158.1 (3s, *Boc*), 40.5 (s, *Cq*), 47.4 (s, *C*H_2N), 80.5 (s, oxetane-*C*H_2). − MS (EI), *m/z* (%): 201 (2) [M^+], 145 (69) [$M^+ - C_4H_9$], 115 (100) [N*Boc*$^+$]. − $C_{10}H_{19}NO_3$ (201.27): calcd. C 59.68, H 9.52, N 6.96; found C 59.63, H 9.57, N 6.89.

3-(tert-Butyloxycarbonyl)(trimethylsilyl)aminomethyl-3-methyloxetane (**D**): Deprotonation of Boc-**5c** with 1 equiv. of *n*BuLi in THF at −70°C followed by addition of 1.2 equiv. TMSCl yielded **D** after removal of the solvent in vacuo (10^{-1} mbar). − ^{1}H NMR ($CDCl_3$): δ = 0.28 (s, 9 H, Si*Me*$_3$), 1.37 (s, 3 H, CqCH_3), 1.51 (s, 9 H, *Boc*), 3.18 (s, 2 H, CH_2N), 4.18, 4.68 (2d, 4 H, $^2J_{HH}$ = 5.8 Hz, oxetane-CH_2).

3-Phthalimidomethyl-3-methyloxetane (**B**): 9.0 g (50 mmol) of 3-methyl-3-(methylsulfonyloxymethyl)oxetane **4** and 10.2 g (55 mmol) of potassium phthalimide were dissolved in 400 ml of DMSO. This mixture was stirred vigorously for 4 h at 120°C. After cooling to 50°C, the DMSO was removed in vacuo (10^{-1} mbar) and 50 ml of water was added to the residue. The product was extracted with 40 ml portions of dichloromethane (4×). The combined organic phases were washed with brine, dried over $MgSO_4$, filtered, and concentrated at 10^{-1} mbar. The resulting light-yellow oil crystallized after 2 h at 0°C. 10.3 g (44.6 mmol, 89%) of **B** was obtained as colourless needles after washing the crystalline material with portions of petroleum ether (40/60) (3 × 20 ml). − ^{1}H NMR ($CDCl_3$): δ = 1.29 (s, 3 H, CqCH_3), 3.80 (s, 2 H, CH_2N), 4.27, 4.64 (2d, 4 H, $^2J_{HH}$ = 6.2 Hz, oxetane-CH_2), 7.66−7.81 (m, 4 H, *aromat. H*). − ^{13}C NMR ($CDCl_3$): δ = 22.6 (s, Cq*C*H$_3$), 41.1 (s, *Cq*), 44.7 (s, *C*H$_2$N), 80.9 (s, oxetane-*C*H$_2$), 123.6−134.5 (*aromat. C*). − MS (EI), *m/z* (%): 231 (67) [M^+], 201 (100) [$M^+ - CH_2O$]. − $C_{13}H_{13}NO_3$ (231.25): calcd. C 67.52, H 5.67, N 6.06; found C 67.25, H 5.66, N 6.05.

The aminolytic cleavage of the oxetanes **5a** and **5c** was performed in an autoclave (see above) according to a previously published procedure[6].

(±)-2-Dimethylaminomethyl-2-(3,5-dimethylpyrazol-1-yl-methyl)-2-methylpropan-1-ol (**6a**) *and 2-Methyl-2-(3,5-dimethylpyrazol-1-yl-methyl)propane-1,3-diol* (**6b**): 9.0 g (50 mmol) of **5a** was heated in an aqueous dimethylamine solution. After one week at 40 bar and 170°C, a product mixture of **6a/6b** in an overall yield of around 40% was obtained. The products **6a/6b** could not be completely separated by distillation through a 20 cm Vigreux column (10^{-1} mbar). Two fractions were collected above 100°C (**I**: 3.05 g, 130−150°C, **6a/6b** ratio = 4:1 and **II**: 1.81 g, 150−165°C, **6a**7**6b** ratio = 1:5; ratios estimated from ^{1}H-NMR data).

(±)-2-Aminomethyl-2-dimethylaminomethyl-2-methylpropan-1-ol (**6c**): 2.22 g (20 mmol) of **5c** was heated in an aqueous dimethylamine solution. The reaction was complete after 48 h at 30 bar and 140°C. After work-up, distillation through a micro Vigreux column in vacuo yielded 1.31 g (9 mmol, 45%) of **6c** as a colourless oil, b.p. 56°C (1.4 mbar). − ^{1}H NMR ($CDCl_3$): δ = 0.77 (s, 3 H, CqCH_3), 2.27 (s, 6 H, NMe_2), 2.37 (m, 2 H, CH_2N), 2.57, 2.80 (2bd, 2 H, $^2J_{HH}$ = 12.6 Hz, CH_2N), 2.95 (bs, 2 H, NH_2), 3.53 (bs, 2 H, CH_2O). − ^{13}C NMR ($CDCl_3$): δ = 20.0 (s, CqCH_3), 40.0 (s, *Cq*), 48.3, 67.2 (s, *C*H$_2$N), 48.8 (s, NMe_2), 71.1 (s, *C*H$_2$O). − $C_7H_{18}N_2O\cdot 1/4\ H_2O$ (146.23): calcd. C 55.78, H 12.37, N 18.58; found C 55.67, H 11.68, N 18.25.

(±)-2-(tert-Butyloxycarbonyl)aminomethyl-2-dimethylaminomethyl-2-methylpropan-1-ol (*Boc*-**6c**): Boc-protection of **6c** was carried out on a 6.4 mmol sample according to a previously published procedure[6]. After work-up, Boc-**6c** was obtained as a colourless oil, which solidified after a few days at 0°C yielding 1.56 g (6.3 mmol, 99%) of Boc-**6c** as colourless crystals. − ^{1}H NMR ($CDCl_3$): δ = 0.83 (s, 3 H, CqCH_3), 1.48 (s, 9 H, *Boc*), 2.29 (m, 2 H, CH_2N), 2.34 (s, 6 H, NMe_2), 2.93 (bs, 1 H, N*H*), 3.16, 3.45 (2m, 4 H, CH_2N, CH_2OH), 5.01 (bs, 1 H, O*H*). − ^{13}C NMR ($CDCl_3$): δ = 20.0 (s, Cq*C*H$_3$), 28.8, 79.8, 158.5 (3s, *Boc*), 40.7 (s, *Cq*), 45.6, 67.6, 68.9 (3s, *C*H$_2$N, *C*H$_2$O), 49.0 (s, NMe_2). − MS (EI), *m/z* (%): 246 [M$^+$], 173 [M$^+$ − C_4H_9O]. − $C_{12}H_{26}N_2O_3$ (246.35): calcd. C 58.51, H 10.64, N 11.37; found C 58.25, H 10.51, N 11.07.

2-Aminomethyl-2-methylpropane-1,3-diol (**E**): 3.95 g (19 mmol) of 2-benzylaminomethyl-2-methylpropane-1,3-diol[6] was dissolved in 50 ml of methanol. 0.6 g of 10% Pd/C was added and the mixture was stirred under 60 bar H_2 pressure at 60°C for 12 h (the reaction was monitored by ^{1}H NMR). The catalyst was then removed by filtration and the residue was distilled through a micro Vigreux column. 1.65 g (13.9 mmol, 73%) of **E** was obtained as a colourless oil (b.p. 63−65°C, 23 mbar). − ^{1}H NMR ($CDCl_3$): δ = 0.76 (s, 3 H, CqCH_3), 2.80 (s, 2 H, CH_2N), 3.58 (bs, 4 H, CH_2OH). − ^{13}C NMR ($CDCl_3$): δ = 18.3 (s, Cq*C*H$_3$), 40.1 (s, *Cq*), 48.2 (s, *C*H$_2$N), 68.8 (s, *C*H$_2$OH). − MS (EI), *m/z* (%): 120 [M$^+$]. − $C_5H_{13}NO_2$ (119.16): calcd. C 50.40, H 11.60, N 11.75; found C 49.59, H 10.41, N 10.75.

2-(tert-Butyloxycarbonyl)aminomethyl-2-methylpropane-1,3-diol (*Boc*-**E**): Boc-protection of **E** was carried out on a 10 mmol sample according to a previously published procedure[6]. After work-up, 2.1 g (9.6 mmol, 96%) of Boc-**E** was obtained as a colourless, microcrystalline solid. − ^{1}H NMR ($CDCl_3$): δ = 0.76 (s, 3 H, CqCH_3), 1.48 (s, 9 H, *Boc*), 3.24 (d, 2 H, $^3J_{HH}$ = 7.0 Hz, CH_2N), 3.42, 3.55 (2d, 4 H, $^2J_{HH}$ = 11.4 Hz, CH_2OH), 3.83 (bs, 1 H, N*H*). − ^{13}C NMR ($CDCl_3$): δ = 17.9 (s, Cq*C*H$_3$), 28.7, 80.7, 158.5 (3s, *Boc*), 41.4 (s, *Cq*), 43.8 (s, *C*H$_2$N), 68.5 (s, *C*H$_2$OH). − MS (EI), *m/z* (%): 220 (13) [M$^+$], 56 (100) [$C_4H_8^+$]. − $C_{10}H_{21}NO_4$ (219.28): calcd. C 54.77, H 9.65, N 6.39; found C 54.73, H 9.69, N 6.22.

Preparation of **7a** and **7b**: The transformation of alcohol functions into PPh_2 groups was performed according to a previously published procedure[6].

2-(Dimethylaminomethyl)-2-(diphenylphosphanylmethyl)-2-(3,5-dimethylpyrazol-1-ylmethyl)ethane (**7a**): Activation of **6a**[6] (fraction **I**, see above) and subsequent substitution with $LiPPh_2$ gave, after flash chromatography, 1.58 g (4 mmol, 33%) of a very viscous oil. − R_f = 0.2 (PE/Et_2O, 2:1). − ^{31}P NMR ($CDCl_3$): δ = −27.0 (s). − MS (EI); *m/z* (%): 393 (14) [M$^+$], 335 (34) [M$^+$ − CH_2NMe_2], 239 (14) [M$^+$ − CH_2NMe_2 − 3,5-Me_2pz], 183 (30) [PPh_2^+], 98 (39) [3,5-Me_2pz$^+$], 58 (100) [$CH_2NMe_2^+$]. − $C_{24}H_{32}N_3P$ (393.51): calcd. C 73.25, H 8.20, N 10.68, P 7.87; found C 72.05, H 8.30, N 10.14, P 7.55.

2,2-Bis(diphenylphosphanylmethyl)-2-(3,5-dimethylpyrazol-1-ylmethyl)ethane (**7b**): Activation of **6b**[6] (fraction **II**, see above) and subsequent substitution with $LiPPh_2$ gave, after flash chromatography, 1.71g (3.2 mmol, 40%) of **7b** as a viscous oil. − R_f = 0.6 (PE/Et_2O, 2:1). − ^{31}P NMR ($CDCl_3$): δ = −27.3 (s). − MS (EI); *m/z* (%): 534 (20) [M$^+$], 457 (100) [M$^+$ − Ph], 349 (5) [M$^+$ − CH_2PPh_2], 199 (8) [$CH_2PPh_2^+$], 185 (13) [PPh_2^+], 78 (4) [Ph$^+$]. − $C_{34}H_{36}N_2P_2$ (534.62): calcd. C 76.39, H 6.79, N 5.24, P 11.59; found C 75.79, H 7.00, N 5.01, P 11.42.

3,3-Bis(pyrazol-1-ylmethyl)oxetane (**9a**): 7.49 g (110 mmol) of pyrazole was dissolved in 300 ml of THF and deprotonated at 0°C with 12.35 g (110 mmol) of KO*t*Bu. After warming to room temperature and stirring for 20 min., a white precipitate of potassium pyrazolate was formed. This suspension was added at 0°C to a solution of 12.96 g (50 mmol) of **8** in 200 ml of THF and the reaction was completed by refluxing for 4 h. The jelly-like mixture was then quenched by the addition of 100 ml of water and the aqueous phase was extracted with 50 ml portions of diethyl ether (2×). The combined organic phases were washed with brine, dried over $MgSO_4$, filtered, and distilled through a 20 cm Vigreux column. 8.90 g (41 mmol, 82%) of **9a** was obtained as a pale-yellow oil (b.p. 138−145°C, 10^{-1} mbar). − ^{1}H NMR ($CDCl_3$): δ = 4.31 (s, 4 H, oxetane-CH_2), 4.68 (s, 4 H, CH_2pz), 6.23 [t, 2 H, $^3J_{HH}$ = 2 Hz, CH(4)pz], 7.37 [d, 2 H, $^3J_{HH}$ = 2 Hz, CH(3)pz], 7.52 [d, 2 H, $^3J_{HH}$ = 2 Hz, CH(5)pz]. − ^{13}C NMR ($CDCl_3$): δ = 45.4 (s, Cq), 54.3 (s, CH_2pz), 78.0 (s, oxetane-CH_2), 105.6 [s, C(4)pz], 131.4 [s, C(5)pz], 140.5 [s, C(3)pz]. − MS (EI); *m/z* (%): 218 (18) [M$^+$], 188 (99) [M$^+$ − OCH_2], 137 (57) [M$^+$ − CH_2pz], 120 (100) [M$^+$ − OCH_2 − pz], 81 (96) [CH_2pz^+], 69 (42) [pzH$^+$]. − $C_{11}H_{14}N_4O$ (218.26): calcd. C 60.53, H 6.47, N 25.67; found C 58.98, H 6.46, N 24.98.

3-(Diphenylphosphanylmethyl)-3-(pyrazol-1-ylmethyl)oxetane (**9b**): 1.63 g (24 mmol) of pyrazole was dissolved in 100 ml of THF and deprotonated at 0°C with 2.69 g (24 mmol) of KO*t*Bu. After warming to room temperature, a white precipitate of potassium pyrazolate was formed. This suspension was added at 0°C to a solution of 12.96 g (50 mmol) of **8** in 200 ml of THF and the reaction was completed by refluxing for 5 h. In another flask, 7.44 g (40 mmol) of $HPPh_2$ was dissolved in 50 ml of THF and deprotonated with 4.49 g (40 mmol) of KO*t*Bu at 0°C. After warming to room temperature and stirring for 20 min., the red potassium phosphide solution was added dropwise to the first reaction mixture, which was maintained at 0°C. After warming to room temperature and stirring for 10 h (the phosphide substitution was monitored by TLC), the then yellow solution was quenched by the addition of 100 ml of deoxygenated water. The aqueous phase was extracted with 50-ml portions of diethyl ether (2×). The combined organic phases were washed with deoxygenated brine, dried over $MgSO_4$, filtered, and concentrated in vacuo. The resulting viscous

oil was purified by column chromatography on silica gel using petroleum ether (40/60)/diethyl ether (1:1) as eluent to obtain 3.32 g (10 mmol, 49%) of **9b** as a colourless, microcrystalline powder. – R_f = 0.1 – ^{1}H NMR ($CDCl_3$): δ = 2.43 (bs, 2 H, CH_2P), 4.50 (2d, 4 H, CH_2O, $^2J_{HH}$ = 6.4 Hz), 4.65 (s, 2 H, CH_2N), 6.23 [t, 1 H, $^3J_{HH}$ = 2 Hz, C*H(4)*pz], 7.31 [d, 1 H, $^3J_{HH}$ = 2 Hz, C*H(3)*pz], 7.35–7.49 (10 H, *aromat. H*), 7.55 [d, 1 H, $^3J_{HH}$ = 2 Hz, C*H(5)*pz]. – ^{13}C NMR ($CDCl_3$): δ = 34.7 (d, *C*H_2P), 44.1 (d, *Cq*), 56.9 (s, CH_2N), 80.3 (d, CH_2O), 105.6 [s, *C(4)*pz], 129.0–140.3 (*aromat. C*), 131.1 [s, *C(5)*pz], 140.3 [s, *C(3)*pz]. – ^{31}P NMR ($CDCl_3$): δ = –26.8 (s). – MS (EI); *m/z* (%): 336 (29) [M^+], 305 (48) [M^+ – OCH_2], 199 (40) [$CH_2PPh_2^+$], 183 (100) [M^+ – PPh_2], 121 (73) [M^+ –OCH_2 –CH_2PPh_2], 81 (26) [CH_2pz^+]. – $C_{20}H_{21}N_2OP$ (336.37): calcd. C 71.41, H 6.29, N 8.33, P 9.21; found C 71.34, H 6.48, N 8.32, P 9.16.

3,3-Bis(azidomethyl)oxetane (**9c**)[20a]: Compound **9c** was prepared as described for compound **5b** (see above). Starting with 12.9 g (50 mmol) of **8**, two equiv. of NaN_3 were employed. After careful work-up (CAUTION: explosive), a sample of 1 ml was concentrated to dryness at 10^{-2} mbar (0°C) in order to obtain spectroscopic data of **9c**. – IR (Et_2O): ν = 2105 (s, –N_3). – ^{1}H NMR ($CDCl_3$): δ = 3.48 (s, 4 H, CH_2N), 4.35 (s, 4 H, oxetane-CH_2).

3,3-Bis(aminomethyl)oxetane (**9d**)[20b]: Compound **9d** was prepared as described for compound **5c** (see above). Two equiv. of PPh_3 and of water were employed. 3.9 g (31 mmol, 62%) of **9d** was obtained upon distillation as a colourless oil (b.p. 86°C, 3 mbar), which was found to contain 1/2 equivalent of water (as inferred from the elemental analysis, see also[20b]). – ^{1}H NMR ($CDCl_3$): δ = 1.10 (bs, 4 H, NH_2), 2.97 (s, 4 H, CH_2N), 4.37 (s, 4 H, oxetane-CH_2). – ^{13}C NMR ($CDCl_3$): δ = 43.9 (s, *C*H_2N), 44.6 (s, *Cq*), 78.3 (s, oxetane-*C*). – MS (EI); *m/z* (%): 117 (100) [M^+]. – $C_5H_{12}N_2O \cdot 1/2\ H_2O$ (125.17): calcd. C 47.98, H 10.47, N 22.38; found C 47.49, H 9.92, N 21.39.

3,3-Bis(diethylaminomethyl)oxetane (**9e**)[20c]: 2.32 g (20 mmol) of **9d** and 6.09 g (44 mmol) of K_2CO_3 were dissolved in 40 ml of EtOH. 11.5 ml (144 mmol) of EtI was slowly added, the reaction mixture was refluxed for 12 h, and then concentrated in vacuo to half of its initial volume. To the concentrate, 10 ml of aqueous NaOH (10%) was added and the mixture was extracted with 20 ml portions of dichloromethane (3×). The combined organic phases were washed with deoxygenated brine (2×), dried over $MgSO_4$, filtered, and concentrated in vacuo. Distillation through a 20 cm Vigreux column at 3 mbar furnished 3.01 g (13.2 mmol, 73%) of **9e** as a colourless oil (b.p. 91°C, 3 mbar). – ^{1}H NMR ($CDCl_3$): δ = 1.02 (t, 12 H, $^3J_{HH}$ = 7.2 Hz, NCH_2CH_3), 2.53 (q, 8 H, $^3J_{HH}$ = 7.2 Hz, NCH_2CH_3), 2.74 (s, 4 H, CH_2N), 4.45 (s, 4 H, oxetane-CH_2). – ^{13}C NMR ($CDCl_3$): δ = 11.8 (s, NCH_2CH_3), 44.8 (s, *Cq*), 47.8 (s, NCH_2CH_3), 57.7 (s, *C*H_2N), 80.0 (s, oxetane-*C*). – MS (EI); *m/z* (%): 228 (4) [M^+], 155 (39) [M^+ – NEt_2], 126 (63) [M^+ – NEt_2 – Et], 86 (100) [$CH_2NEt_2^+$]. – $C_{13}H_{28}N_2O$ (228.38): C 68.37, H 12.36, N 12.27; found C 67.70, H 11.71, N 12.14.

Preparation of **10a**–**10d**: 1 equiv. of the appropriately substituted oxetane was dissolved in THF (3 ml per mmol oxetane). In a second flask, 1.2 equiv. of $HPPh_2$ was dissolved in THF (2 ml per mmol $HPPh_2$) and deprotonated at 0°C with 1.2 equiv. of *n*BuLi. After warming to room temperature and stirring for 20 min., the red lithium phosphide solution was added dropwise to the oxetane solution at 0°C. The mixture was allowed to warm to room temperature, while the reaction progress was monitored by TLC. Upon completion (4–10 h), the reaction was quenched by the addition of deoxygenated water. The aqueous phase was extracted with small portions of diethyl ether (3×). The combined organic phases were washed with deoxygenated brine, dried over $MgSO_4$, filtered, and concentrated in vacuo yielding the crude products as colourless oils.

3-(Diphenylphosphanyl)-2,2-bis(pyrazol-1-ylmethyl)propan-1-ol (**10a**): The crude product was purified by column chromatography on silica gel using petroleum ether (40/60)/diethyl ether (1:1) and pure diethyl ether (after elution of $HPPh_2$) to obtain 5.57 g (13.8 mmol, 81%) of **10a** as a colourless, microcrystalline powder. – R_f = 0.15 (Et_2O) – ^{31}P NMR ($CDCl_3$): δ = –29.0 (s). – MS (EI); *m/z* (%): 403 (96) [M^+], 323 (68) [M^+ – CH_2pz], 255 (91) [M^+ – CH_2pz – pz], 199 (82) [$CH_2PPh_2^+$], 121 (100) [$CHPPh^+$], 81 (38) [CH_2pz^+]. – $C_{23}H_{25}N_4OP$ (404.45): calcd. C 68.30, H 6.23, N 13.85, P 7.66; found C 68.31, H 6.40, N 13.17, P 7.53.

2,2-Bis(diphenylphosphanylmethyl)-3-(pyrazol-1-yl)propan-1-ol (**10b**): The crude product was purified by column chromatography on silica gel using petroleum ether (40/60)/diethyl ether (3:2) and pure diethyl ether (after elution of $HPPh_2$) to obtain 2.78 g (5.3 mmol, 78%) of **10b** as a colourless, microcrystalline powder. – R_f = 0.3 (Et_2O) – ^{31}P NMR ($CDCl_3$): δ = –29.5 (s). – MS (EI); *m/z* (%): 522 (12) [M^+], 445 (100) [M^+ – Ph], 367 (55) [M^+ – 2 Ph], 183 (39) [PPh_2^+]. – $C_{32}H_{34}N_2OP_2$ (524.58): C 73.25, H 6.54, N 5.34, P 11.82; found C 73.37, H 6.24, N 5.31, P 11.78.

2-(Diphenylphosphanylmethyl)-2-(3,5-dimethylphenyl)-phosphanylmethyl]-3-(pyrazol-1-yl)propan-1-ol (**10c**): The crude product was purified by column chromatography on silica gel using petroleum ether (40/60)/diethyl ether (3:2) and pure diethyl ether (after elution of the diarylphosphanes) to obtain 1.75 g (3.0 mmol, 82%) of **10c** as a colourless, microcrystalline powder. – R_f = 0.25 (Et_2O) – m.p. 54.9°C. – ^{31}P NMR ($CDCl_3$): δ = –29.5 (d, $^4J_{PP}$ = 8.7 Hz), –29.8 (bs). – MS (EI); *m/z* (%): 577 (20) [M^+], 500 (55) [M^+ – Ph], 472 (35) [M^+ – (3,5-Me_2Ph)], 423 (43) [M^+ – 2 Ph], 241 (19) [P(3,5-Me_2Ph)$_2^+$], 101 (100) [(3,5-Me_2Ph)$^+$]. – $C_{36}H_{40}N_2OP_2$ (578.67): calcd. C 74.71, H 6.97, N 4.84, P 10.71; found C 74.57, H 7.19, N 4.67, P 10.47.

2,2-Bis(diethylaminomethyl)-3-(diphenylphosphanyl)propan-1-ol (**10d**): The crude product was purified by column chromatography on silica gel using petroleum ether (40/60)/diethyl ether (1:1) to obtain 2.23 g (5.4 mmol, 82%) of **10d** as a colourless, viscous oil. – R_f = 0.25. – ^{31}P NMR ($CDCl_3$): δ = –28.4 (s). – MS (EI); *m/z* (%): 413 (3) [M^+], 328 (10) [M^+ – CH_2NEt_2], 183 (12) [$CH_2PPh_2^+$], 86 (100) [$CH_2NEt_2^+$]. – $C_{25}H_{39}N_2OP$ (414.57): calcd. C 72.43, H 9.48, N 6.76, P 7.47; found C 72.34, H 9.56, N 6.65, P 7.48.

3-(Diphenylphosphanyl)-2,2-bis(pyrazol-1-yl-methyl)propyl Ethyl Ether (**11**): 855 mg (2.1 mmol) of **10a** was dissolved in 40 ml of THF and the solution was cooled to 0°C. Addition of 1.18 g (10.6 mmol) of KO*t*Bu yielded a clear, yellow solution. After 20 min., 0.84 ml (10.6 mmol) of EtI in 10 ml of THF was added dropwise. The reaction mixture was stirred overnight at room temperature [TLC control (PE/Et_2O, 3:2): **10a**: R_f = 0.1; **11**: R_f = 0.3]. The reaction was then quenched by the addition of 10 ml of deoxygenated water and the aqueous phase was extracted with 10 ml portions of diethyl ether (2×). The combined organic phases were washed with deoxygenated brine, dried over $MgSO_4$, filtered, and concentrated in vacuo. The resulting viscous oil was purified by column chromatography on silica gel using petroleum ether (40/60)/diethyl ether (3:2) to obtain 832 mg (1.9 mmol, 91%) of **11** as a colourless, viscous oil, which solidified after two days. – R_f = 0.3. – ^{31}P NMR ($CDCl_3$): δ = –29.0 (s). – MS (EI); *m/z* (%): 403 (96) [M^+], 323 (68) [M^+ – CH_2pz], 255 (91) [M^+ – CH_2pz – pz], 199 (82) [$CH_2PPh_2^+$], 121 (100) [$CHPPh^+$], 81 (38) [CH_2pz^+]. –

$C_{25}H_{29}N_4OP$ (432.51): calcd. C 69.43, H 6.76, N 12.95, P 7.16; found C 69.39, H 6.81, N 12.99, P 7.16.

Coordination Chemistry

Preparation of **12a**−**12d**, **13**: A stirred solution of 1 mmol ligand in 100 ml of dichloromethane was cooled to −70°C and 0.95 mmol (288 mg) of freshly prepared $(MeCN)_3Mo(CO)_3$ was added. After 2−4 h, all of the $(MeCN)_3Mo(CO)_3$ had dissolved, resulting in a clear, yellow solution. The solvent was then removed at 10^{-1} mbar without heating of the solution. The complexes were recrystallized at 0°C by vapour diffusion of petroleum ether (40−60) into a solution of the crude product in dichloromethane.

η^2-[1,1,1-Tris(pyrazol-1-yl-methyl)ethane]monoacetonitriletricarbonylmolybdenum(0) (**12a**): Yield 398 mg (0.81 mmol, 81%) of **12a** as a brown solid, m.p. 135−138°C (dec). − MS (FAB), *m/z* (%) [Frag.] : 452 (92) [$M^+ - CH_3CN$], 428 (43) [$M^+ - CH_3CN -$ CO], 396 (41) [$M^+ - CH_3CN - 2$ CO], 368 (100) [$M^+ - CH_3CN - 3$ CO]. − $C_{19}H_{21}MoN_7O_3$ (491.36): calcd. C 46.41, H 4.31, N 19.95; found C 44.20, H 4.18, N 18.30.

η^2-P,N-[3-(Diphenylphosphanyl)-2,2-bis(pyrazol-1-ylmethyl)propan-1-ol]tetracarbonylmolybdenum(0) (**12b**): Yield 514 mg (0.8 mmol, 84%) of **12b** as a light-brown solid. Recrystallization afforded 220 mg (0.36 mmol, 36%) of **12b** in the form of yellow crystals suitable for X-ray structural analysis, m.p. 200−205°C (dec). − MS (FAB), *m/z* (%): 614 (4) [M^+], 586 (13) [$M^+ -$ CO], 558 (7) [$M^+ - 2$ CO], 530 (16) [$M^+ - 3$ CO], 502 (21) [$M^+ - 4$ CO], 421 (100) [(**10a**-O)$^+$], 403 (41) [(**10a**)$^+$]. − $C_{27}H_{25}MoN_4O_5P$ (612.43): calcd. C 52.95, H 4.11, N 9.15, P 5.06; found C 51.55, H 3.88, N 8.91, P 5.00.

η^2-P,N-[3-(Diphenylphosphanyl)-2,2-bis-(pyrazol-1-yl-methyl)propyl Ethyl Ether]-monoacetonitriletricarbonylmolybdenum(0) (**12c**): Yield 516 mg (0.79 mmol, 79%) of **12c** as a light-yellow solid. Recrystallization afforded 131 mg (0.20 mmol, 20%) of **12c** in the form of colourless crystals suitable for X-ray structural analysis, m.p. 85°C (dec). − MS (FAB), *m/z* (%): 614 (41) [$M^+ - CH_3CN$], 586 (24) [$M^+ - CH_3CN -$ CO], 558 (39) [$M^+ - CH_3CN - 2$ CO], 530 (77) [$M^+ - CH_3CN - 3$ CO], 449 (100) [(**11**-O)$^+$], 433 (84) [(**11**)$^+$]. − $C_{30}H_{32}MoN_5O_4P$ (653.53): calcd. C 55.14, H 4.94, N 10.72, P 4.74; found C 54.84, H 4.67, N 10.40, P 4.60.

η^2-P,P-{2-(Diphenylphosphanylmethyl)-2-(3,5-dimethylphenyl)phosphanylmethyl]-3-(pyrazol-1-yl)propan-1-ol}monoacetonitriletricarbonylmolybdenum(0) (**12d**): The preparation of **12d** was carried out similarly to that of **12c** above. After 4 h, all of the $(MeCN)_3Mo(CO)_3$ had dissolved, resulting in a clear brown solution, which was concentrated to half of the initial volume and layered with petroleum ether (40−60). After one day at 0°C, small colourless needles suitable for X-ray structural analysis were obtained. The crystals were found to be very sensitive and turned black within seconds on exposure to air. − Yield 152 mg (0.19 mmol, 19%) of **12d**. − MS (FAB), *m/z* (%): 760 (16) [$M^+ - CH_3CN$], 732 (21) [$M^+ - CH_3CN -$ CO], 704 (16) [$M^+ - CH_3CN - 2$ CO], 676 (100) [$M^+ - CH_3CN - 3$ CO], 578 (26) [(**10c**)$^+$]. − $C_{41}H_{43}MoN_3O_4P_2$ (799.71): calcd. C 61.58, H 5.42, N 5.25, P 7.75; found C 61.79, H 6.15, N 4.63, P 7.83.

η^3-[2,2-Bis(diphenylphosphanylmethyl)-2-(pyrazol-1-ylmethyl)propan-1-ol]tricarbonylmolybdenum(0) (**13**): Yield 632 mg (0.9 mmol, 90%) of **13** as a light-yellow solid. Recrystallization afforded 197 mg (0.35 mmol, 35%) of **13** in the form of pale-yellow crystals suitable for X-ray structural analysis, m.p. 190−195°C (dec). − MS (FAB), *m/z* (%): 703 (48) [M^+], 674 (100) [$M^+ -$ CO], 648 (8) [$M^+ - 2$ CO], 619 (32) [$M^+ - 3$ CO]. − $C_{35}H_{32}MoN_2O_4P_2$ (702.54): calcd. C 59.84, H 4.59, N 3.99, P 8.82; found C 59.63, H 5.13, N 3.81, P 8.75.

[1] See for example: [1a] U. Bossek, H. Hummel, T. Weyhermüller, E. Bill, K. Wieghardt, *Angew. Chem.* **1995**, *107*, 2885−2888; *Angew. Chem. Int. Ed. Engl.* **1995**, *34*, 2885. − [1b] C. Titze, J. Hermann, H. Vahrenkamp, *Chem. Ber.* **1995**, *128*, 1095−1103. − [1c] A. Looney, G. Parkin, R. Alsfasser, M. Ruf, H. Vahrenkamp, *Angew. Chem.* **1992**, *104*, 57−58; *Angew. Chem. Int. Ed. Engl.* **1992**, *31*, 92. − [1d] P. Stavropoulos, M. C. Muetterties, M. Carrie, R. H. Holm, *J. Am. Chem. Soc.* **1991**, *113*, 8485−8492.

[2] [2a] L. Sacconi, F. Mani, *Transition Met. Chem.* **1982**, *8*, 179−252 and references cited therein. − [2b] S. Friedrich, H. Memmler, L. H. Gade, W.-S. Li, M. McPartlin, *Angew. Chem.* **1994**, *106*, 705−708; *Angew. Chem. Int. Ed. Engl.* **1994**, *33*, 676. − [2c] A. Barth, G. Huttner, M. Fritz, L. Zsolnai, *Angew. Chem.* **1990**, *102*, 956−958; *Angew. Chem. Int. Ed. Engl.* **1990**, *29*, 929. − [2d] P. Barbaro, C. Bianchini, P. Frediani, A. Meli, F. Vizza, *Inorg. Chem.* **1992**, *31*, 1523−1529.

[3] [3a] H. A. Mayer, W. C. Kaska, *Chem. Rev.* **1994**, *94*, 1239−1272. − [3b] C. Bianchini, A. Meli, M. Peruzzini, F. Vizza, F. Zanobini, *Coord. Chem. Rev.* **1992**, *120*, 193−208.

[4] [4a] C. Bianchini, A. Meli, A. Orlandini, L. Sacconi, *J. Organomet. Chem.* **1981**, *209*, 219−231. − [4b] C. Bianchini, D. Masi, A. Meli, M. Peruzzini, F. Zanobini, *J. Am Chem. Soc.* **1988**, *110*, 6411−6423. − [4c] C. Bianchini, A. Meli, M. Peruzzini, F. Vizza, *Organometallics* **1990**, *9*, 226−240.

[5] [5a] S.-T. Liu, K.-J. Liu, *Inorg. Chem.* **1990**, *29*, 4576−4579. − [5b] S.-C. Tsai, H.-E. Wang, S.-T. Wang, L.-M. Yiin, S.-T. Liu, *Chem. Ber.* **1995**, *128*, 151−155. − [5c] J. Scherer, G. Huttner, M. Büchner, *Chem. Ber.* **1996**, *129*, 697−713. − [5d] T. Seitz, A. Muth, G. Huttner, *Z. Naturforsch.* **1995**, *50b*, 1045−1049. − [5e] T. Seitz, A. Muth, G. Huttner, *Chem. Ber.* **1994**, *127*, 1837−1842. − [5f] H. Heidel, G. Huttner, G. Helmchen, *Z. Naturforsch.* **1993**, *48b*, 1681−1692. − [5g] H. Heidel, G. Huttner, R. Vogel, G. Helmchen, *Chem. Ber.* **1994**, *127*, 271−274. − [5h] H. Heidel, G. Huttner, L. Zsolnai, *Z. Naturforsch.* **1995**, *50b*, 729−734.

[6] A. Jacobi, G. Huttner, U. Winterhalter *Chem. Ber./Recueil* **1997**, *130*, 1279−1294.

[7] [7a] H.-E. Wang, C.-Y. Liu, M.-C. Cheng, S.-M. Peng, S.-T. Liu, *Phosphorus, Sulfur and Silicon* **1992**, *69*, 201−211. − [7b] S.-T. Liu, C.-Y. Liu, *J. Org. Chem.* **1992**, *57*, 6079−6080. − [7c] S.-T. Liu, C.-H. Yieh, H.-P. Dai, *Proc. Natl. Sci. Counc.(A)* **1995**, *19*, 1−4. − [7d] E. B. Fleischer, A. E. Gebala, A. Levey, P. A. Tasker, *J. Org. Chem.* **1971**, *36*, 3042−3044.

[8] S. Trofimenko, *Chem. Rev.* **1993**, *93*, 943−980.

[9] A. Mooradian, J. B. Cloke, *J. Am. Chem. Soc.* **1945**, *56*, 942−944.

[10] [10a] I. Dostrovsky, E. D. Hughes, C. K. Ingold, *J. Chem. Soc.* **1946**, 173−194. − [10b] D. Cook, A. J. Parker, *J. Chem. Soc. (B)* **1968**, 142−148. − [10c] M. H. Abraham, P. L. Grellier, M. J. Hogarth, *J. Chem. Soc., Perkin Trans. II,* **1975**, 1365−1371.

[11] [11a] F. E. Hahn, *Angew. Chem.*, **1993**, *105*, 681−696; *Angew. Chem. Int. Ed. Engl.* **1993**, *32*, 650−665. − [11b] K. Oefele, *J. Organomet. Chem.* **1968**, *12*, P42−P43. − [11c] K. Oefele, W. A. Herrmann, D. Mihalios, M. Elison, E. Herdtweck, T. Priermeier, P. Kiprof, *J. Organomet. Chem.* **1995**, *498*, 1−14. − [11d] W. A. Herrmann, M. Elison, J. Fischer, C. Köcher, G. R. J. Artus, *Chem. Eur. J.* **1996**, *2*, 772−780.

[12] [12a] H. Reiff, D. Dieterich, R. Braden, H. Ziemann, *Liebigs Ann. Chem.* **1973**, 365−374. − [12b] S. Searles, V. P. Gregory, *J. Am. Chem. Soc.* **1954**, *76*, 2789−2790.

[13] M. S. Gibson, R. W. Bradshaw, *Angew. Chem.*, **1968**, *80*, 986−996; *Angew. Chem. Int. Ed. Engl.* **1968**, *7*, 919.

[14] H. Stetter, W. Böckmann, *Chem. Ber.* **1951**, *84*, 834−839.

[15] D. Fenske, H. J. Becher, *Chem. Ber.* **1975**, *108*, 2115−2123.

[16] M. E. C. Biffin, J. Miller, D. B. Paul in *The Chemistry of the Azido Group*, (Ed.: S. Patai), *Interscience*, New York, **1971**, 57−119.

[17] [17a] A. A. Malik, G. E. Manser, R. P. Carson, T. G. Archibald, *Aerojet-General Corp., USA,* Pt.-No. *US 5523424 A,* 960604. − [17b] Y. Oyumi, T. B. Brill, *Combust. Flame* **1986**, *65(2)*, 127−135. − [17c] K. Higashiura, H. Morino, H. Matsuura, Y. Toyomaki, K. Ienaga, *J. Chem. Soc., Perkin Trans. I,* **1989**, 1479−1481.

[18] [18a] R. Soltek, G. Huttner, L. Zsolnai, A. Driess, *Inorg. Chim.*

Acta **1997**, *in press*. – [18b] R. Julina, T. Herzig, B. Bernet, A. Vasella, *Helv. Chim. Acta* **1986**, *69*, 368–374.

[19] J. Cheymol, P. Chabrier, J. Seyden-Penne, A. Habert-Somny, T. Strzalko, *Bull. Soc. Chim. Fr.* **1965**, 694–700.

[20] [20a] W. R. Carpenter, *J. Org. Chem*. **1962**, *27*, 2085–2088. – [20b] T. W. Campbell, *J. Org. Chem*. **1957**, *22*, 1029–1035. – [20c] As an alternative synthesis of **9e**, the substitution of functionalized oxetanes $O(CH_2)_2C(CH_2X)_2$ by $HNEt_2$ in a sealed tube has been reported by Cazier and Steyaert, *Bull. Soc. Chim. Belg.* **1948**, *57*, 224–229.

[21] [21a] T. Seitz, Doctorate Thesis, Universität Heidelberg, **1994**. – [21b] O. Walter, Doctorate Thesis, Universität Heidelberg, **1994**.

[22] D. P. Tate, W. R. Knipple, J. M. Augl, *Inorg. Chem.* **1962**, *1*, 433–434.

[23] [23a] Tables of the fractional atomic coordinates are available from the author on request. Further details of the crystal structure investigations may be obtained from the Fachinformationszentrum Karlsruhe, D-76344 Eggenstein-Leopoldshafen (Germany), on quoting the depository numbers CSD-407693 (**12b**), CSD-407692 (**12c**), CSD-407691 (**12d**), CSD-407690 (**13**). – [23b] A. Jacobi, Doctorate Thesis, Universität Heidelberg, **1997**. Deposited under A. Jacobi and G. Huttner, CSD-407694 $[CH_3C(CH_2PPh_2)_2(CH_2Cl)Mo(CO)_4]$.

[24] [24a] M. A. Esteruelas, L. A. Oro, M. C. Apreda, C. Foces-Foces, F. H. Cano, R. M. Claramunt, C. Lopez, J. Elguero, M. Begtrup, *J. Organomet. Chem.* **1988**, *344*, 93–108. – [24b] F. A. Jalon, B. R. Manzano, A. Otero, M. C. Rodriguez-Perez, *J. Organomet. Chem.* **1995**, *494*, 179–185.

[25] [25a] S.-T. Liu, H.-E. Wang, M.-C. Cheng, S.-M. Peng, *J. Organomet. Chem.* **1989**, *376*, 333–342. – [25b] S.-T. Liu, G.-J. Liu, C.-H. Yieh, M.-C. Cheng, S.-M. Peng, *J. Organomet. Chem.* **1990**, *387*, 83–94.

[26] P. Stössel, H. A. Mayer, C. Maichle-Mössmer, R. Fawzi, M. Steimann, *Inorg. Chem.* **1996**, *35*, 5860–5867.

[27] S. Beyreuther, J. Hunger, G. Huttner, S. Mann, L. Zsolnai, *Chem. Ber.* **1996**, *129*, 745–757.

[28] *Organikum*, Deutscher Verlag der Wissenschaften, Berlin **1990**, 638.

[29] [29a] U. Piantini, O. W. Sorensen, R. R. Ernst, *J. Am. Chem. Soc.* **1982**, *104*, 6800–6801. – [29b] L. Braunweiler, R. R. Ernst, *J. Magn. Reson.* **1983**, *53*, 521–528. – [29c] R. R. Ernst, *Angew. Chem.*, **1992**, *104*, 817–836; *Angew. Chem. Int. Ed. Engl*. **1992**, *31*, 805. – [29d] L. Müller, *J. Am. Chem. Soc.* **1979**, *101*, 4481–4484. – [29e] M. F. Summers, L. G. Marzilli, A. Bax, *J. Am. Chem. Soc.* **1986**, *108*, 4285–4294.

[30] [30a] G. M. Sheldrick, *SHELXS-86*, University of Göttingen, **1986**. – 30b] G. M. Sheldrick, *SHELX-93*, University of Göttingen, **1993**. – 30c] *International Tables for X-ray Crystallography, Vol. 4,* Kynoch Press, Birmingham, U.K. **1974**.

[31] L. Zsolnai, G. Huttner, *XPMA*, University of Heidelberg, **1994**.

[97228]

How to Derive Force Field Parameters by Genetic Algorithms: Modelling *tripod*-$Mo(CO)_3$ Compounds as an Example

Johannes Hunger, Stefan Beyreuther, Gottfried Huttner*, Kurt Allinger, Uwe Radelof, and Laszlo Zsolnai

Anorganisch-Chemisches Institut der Universität Heidelberg,
Im Neuenheimer Feld 270, D-69120 Heidelberg, Germany
Tel. (internat.): +49 (0)6221/549446
Fax (internat.): +49 (0)6221/545707
E-mail: GA@indi.aci.uni-heidelberg.de

Received October 28, 1997

Keywords: Genetic Algorithms / Force field calculations / Refinement of force field parameters / Tripod metal compounds / Conformational analysis

Force field parameters used to describe the conformation of coordination compounds involving transition metals are generally derived by a trial-and-error procedure, until a somehow satisfying agreement between the calculated and observed conformations of a few members of a class of related compounds is reached. It is shown in this paper that a more general and less biased alternative is available, applicable to many structures at a time. Genetic Algorithms will effectively optimize force field parameters in an automatic way, on the basis of a potentially exhaustive set of all the structural data available for a given class of compounds. The feasibility of this procedure has been demonstrated by the derivation of force field parameters describing the conformational behaviour of *tripod*-$Mo(CO)_3$ compounds [*tripod* = $RCH_2C(CH_2X)(CH_2Y)(CH_2Z)$, X,Y,Z = PR′R′′)] by simultaneous optimization based on the structure of ten individual molecules. With the force field parameters relevant to the organic part of these compounds taken from MM2*, the parameters involving contributions from the Mo center were refined. The agreement between observed and calculated structures is characterized by an rms deviation of around 0.3 Å for the ten structures contained in the data base. To assess the validity of this approach, the conformational space of $CH_3C(CH_2PPh_2)_3Mo(CO)_3$ was explored exhaustively. A contour diagram representing the relative energy of the molecule with respect to the rotational positions of its phenyl groups was found to effectively reproduce the scatter of these conformational parameters as earlier derived from an analysis of 82 relevant compounds. − As a further assessment, the conformational space of $CH_3C[CH_2P(o\text{-Tol})_2]_3Mo(CO)_3$, which was not included in the data base, has been analyzed. It is found that the structure corresponding to the global energy minimum corresponds to that observed in the crystal with an rms deviation of only 0.3 Å. The novel approach to problems of this type − Genetic Algorithms had not previously been applied in this context − thus appears promising.

Introduction

The reactivity of ligand-metal templates is largely determined by their conformations. Homogeneous catalysis by such templates has been shown to be strongly dependent on even minor changes in the conformation as well as in the conformational flexibility of the templates themselves.[1] Methods of predicting these conformational properties would hence be of considerable practical importance. "Understanding" conformations in the sense of being able to model them would be a crucial step in any attempt to understand homogeneous catalysis. In spite of the success quantum chemical methods nowadays have to rationalize and predict the properties of even relatively large ligand−metal templates[2][3], these methods are not yet in a state to allow for an extensive conformational search in a practicable amount of time. As an alternative, force field methods have become popular since N. L. Allinger and his group demonstrated how successful these methods can be.[4][5] Attractive as these methods are, they are hampered by difficulties when applied to inorganic compounds, especially those containing transition metals. Not only is it the broad span of coordination numbers and coordination geometries accessible to one and the same type of metal which is at the basis of these problems, but it is as well the lack of reliable spectroscopic and thermodynamic data which would allow for an appropriate assessment of force field parameters. Nevertheless, inorganic chemists have successfully addressed conformational problems by force field methods[6][7][8] and have devised different strategies to overcome the intrinsic difficulties. These methods rely by and large on an educated guess of the relevant parameters and the subsequent improvement of these initially chosen parameters by trial and error. The quality of the parameters is generally judged by the accuracy with which the chosen set of parameters will reproduce the structures of a few selected examples of the class of compounds to be modelled. There are two basic problems associated with this type of methodology:

(a) The structures which are used to assess the validity of a specific force field approach are taken from solid-state structure determinations. The approach of fitting force field

 © WILEY-VCH Verlag GmbH, D-69451 Weinheim, 1998 1434−1948/98/0606−0693 $ 17.50+.50/0

parameters to these structures is acceptable as a tool of parameter evaluation only if it is shown that these structures and the conformations represented by them reflect the "inner" molecular potential of the compounds and are not significantly influenced by the outer potential acting on the molecular entities within a crystal.

(b) The method of just selecting a few structures and then fitting the force field parameters on this reduced set of information by trial and error procedures does not appear to be the state of the art with respect to the computing capabilities now available.

In an attempt to understand the conformational flexibility of *tripod*−metal templates, an alternative strategy has been developed, which tries to make the maximum use of the information contained in molecular structures as determined by solid-state crystallography.

With regard to the problem outlined under (a) above, a statistical analysis of 82 structures containing the *tripod*−metal template $CH_3C(CH_2PPh_2)_3Co$ in compounds of the type *tripod*−CoL_2 and *tripod*−CoL_3 was performed in order to find out whether these structures might be taken as an unbiased sample representing the inner molecular forces, not largely disturbed by the crystal environment.[9][10] Irrespective of the statistical tools used (factor analysis, cluster analysis, partial least-squares, scattergraphs, neural networks), the analysis showed that the observed conformations are determined by the inner forces, and thus that they correspond to local minima on the molecular energy hypersurface. This result means that the conformations of *tripod*−metal compounds as determined by X-ray crystallography contain the information necessary for developing an appropriate force field: it is a necessary condition for a set of force field parameters to reproduce these conformations as at least local minima on the energy hypersurface described by it.

With regard to point (b) above, the task of deriving parameter sets from the observed conformations that give the optimal reproduction of the observed structures is a problem of global optimization. This class of mathematical problem has not yet found a unique solution in applied mathematics, nor is there a solution guaranteeing that the global minimum will be found in a finite number of steps in general. Nevertheless, several types of approaches exist, the practicability of which has been demonstrated in quite a number of optimization problems.[11][12] In the present work, Genetic Algorithms (GA) have been used as the optimizing tool. In this paper, we report how, by use of this approach, sets of force field parameters may be automatically derived from a structural database. Compounds of the type *tripod*−$Mo(CO)_3$ [*tripod* = $RCH_2C(CH_2X)(CH_2Y)(CH_2Z)$, X,Y,Z = PR′R″] serve as the specific example. The quality of the parameter sets thus derived is assessed by their ability to reproduce conformations as well as general conformational patterns. It is further validated by the correct prediction of the conformation of a specific *tripod*−$Mo(CO)_3$ compound that had not been part of the data basis.

Data Basis

Compounds of the type *tripod*−$Mo(CO)_3$ containing *tripod* ligands $RCH_2C(CH_2X)(CH_2Y)(CH_2Z)$ with up to three different donor groups X,Y,Z = PR′R″ are generally accessible by reacting $(CH_3CN)_3Mo(CO)_3$ with the appropriate *tripod* ligand.[13][14][15][16] The structures of a number of such compounds have been determined by X-ray crystallography.[13][14][15][16] When this work was commenced, nine relevant structure determinations had been reported[17] referring to ten crystallographically independent molecules of this type. To illustrate the overall structural characteristics of this type of compound, Figure 1 shows two mutually orthogonal projections of the structure of $CH_3C(CH_2PPh_2)_3Mo(CO)_3$.

Figure 1. Two orthogonal projections of the solid-state structure of $CH_3C(CH_2PPh_2)_3Mo(CO)_3$; the numbering scheme given is used throughout the text

The constitutions of all the structural examples included in the data base are given in Table 1.

In order to elaborate a force field description for this class of molecules, the parameters involving bonds to the molybdenum atom had to be evaluated from first principles.The force constants describing the organic part of the compounds on the other hand were taken from the well-established MM2* force field.[4][18] The force field parameters describing the force field interactions involving the metal were incorporated as defined by the expressions given in Figure 2. These parameters were in part refined by the methods described below.

Refinement of the Force Field: Any refinement of the force field will correspond to a search for the set (or sets) of parameter values that best reproduce the conformations present in the data base as local or even global minima on the corresponding energy hypersurface (surfaces). To perform this search in an automatic way, the strategy of Genetic Algorithms has been used throughout in this work. In the realm of molecular modelling, Genetic Algorithms have already been used to scan an energy hypersurface for minimum energy conformations. In the analysis and prediction of the conformation of biological macromolecules, the introduction of these algorithmic methods has in some cases dramatically improved the validity of the predictions.[19][20] To the problem of conformational search on an energy hypersurface, an inverse problem exists: given the confor-

Table 1. Compounds **1**−**10** and rms deviations between the conformations observed and calculated for the two different parameter sets *mm2f* and *mm2t*, and rms deviation between the conformations as calculated on the basis of the two different parameter sets. Compounds **6** and **7**, labelled with an asterisk, are two crystallographically independent conformations of $CH_3C(CH_2PEt)_3Mo(CO)_3$ as found in one and the same unit cell[a]

number	formula	RMS_{mm2f} [Å]	RMS_{mm2t} [Å]	$RMS_{mm2f/mm2t}$ [Å]
1	$CH_3C(CH_2PPh_2)_3Mo(CO)_3$	0.286	0.248	0.060
2	$CH_3C(CH_2PBzlPh)_3Mo(CO)_3$	0.417	0.357	0.190
3	$CH_3C(CH_2PMe_2)_3Mo(CO)_3$	0.197	0.190	0.071
4	$PhCOOCH_2C(CH_2PMe_2)_3Mo(CO)_3$	0.585	0.581	0.061
5	$CH_3C(CH_2PNap_2)_3Mo(CO)_3$	0.353	0.328	0.090
6*	$CH_3C(CH_2PEtPh)_3Mo(CO)_3$	0.252	0.240	0.075
7*	$CH_3C(CH_2PEtPh)_3Mo(CO)_3$	0.243	0.193	0.144
8	$ClCH_2C(CH_2PPh_2)_3Mo(CO)_3$	0.235	0.224	0.059
9	$CH_3C[CH_2P(DBP)_2]_3Mo(CO)_3$	0.312	0.284	0.062
10	$CH_3C(CH_2PEt_2)_3Mo(CO)_3$	0.248	0.235	0.074
mean		0.313	0.288	0.089

[a] Abbreviations: Et: ethyl, Me: methyl, Bzl: benzyl, Nap: naphthyl, DBP: dibenzophospholyl.

Figure 2. Definition of parameters involving the metal center

[a] Colour codes of atom types shown for a fragment of **2** (see Table 1). − [b] Parameter types and corresponding potential terms applied in the force field. − Abbreviations: E: energy; k_b: bonding constant; r: bond length; r_0: equilibrium bond length; k_a: force constant for angle bending; α/α_0: angle/equilibrium angle; $k_{t(1-3)}$: force constant 1−3 for torsion; ω: dihedral angle.

mations which correspond to − at least local − minima on the energy hypersurface, a search on the hypersurface defined by the force field parameters themselves should lead to an optimized parameter set.[21] With the efficiency of Genetic Algorithms in mind, and with the given formal logical analogy of these two problems, it appears natural to apply Genetic Algorithms to adapt a force field to a set of conformations. The formal logical complementarity of the two problems, (a) to find an optimized conformation on the basis of a given force field, and (b) to find an optimized force field on the basis of given conformations, is illustrated in Figure 3.

Figure 3. Complementary problems − analogous solutions

[a] Adaptation of a conformation to a given force field. − [b] Adaptation of force field parameters to a given conformation

In case (a), the conformation − symbolized by a circle, a square and a triangle, connected in a gear-like arrangement − has to be changed such that it optimally fits into a given pre-designed matrix, the structure of which is strictly defined by the force field used. In case (b), on the other hand, the conformation of the object is fixed and it is the matrix which has to adapt its shape to the conformation presented by the object, i.e. the force field parameters defining the shape of the matrix have to be changed to this end. To solve

these problems in both cases, even if they are logically complementary an optimization procedure must be invoked.

To devise such a procedure, whatever form it takes, the relative quality of a given approximation has to be defined by some numerical qualifiyer that numerically represents the overall performance of this particular approximation. In terms of the language of Genetic Algorithms, this qualifier is called the "fitness value" of a given approximation. In the case considered, the root-mean-square deviation between observed and calculated atom positions is a simple and efficient qualifier and is therefore used throughout in this work. An optimization procedure, whatever its form, has then to find approximations which minimize the discrepancy between observation and model, i.e., in the language of Genetic Algorithms, to find approximations with the optimal fitness values. Because of the a priori unpredictable shape of the hypersurface on which the minimization procedure is performed, analytical methods based on different types of gradients will not generally lead to the desired solution. Purely stochastic methods, on the other hand, will in principle solve the problem, albeit possibly only in an infinite amount of time. With these Monte Carlo type procedures, the hypersurface is probed at random and finding a solution basically relies on Cicero's old statement: "Quis est enim, qui totum diem iaculans, non aliquando conlineet ?"[22] Imagine how long it might take to find the highest elevation in the Alps by this purely stochastic procedure.[23] While completely deterministic analytical methods cannot generally solve the problem and while, as described, stochastic methods may be practically inapplicable, a combination of deterministic and stochastic strategies may well be successful.

Genetic Algorithms may be seen as an algorithmic implementation of both these principles.[24][25][26] The terminology associated with Genetic Algorithms is by and large the same as that used in biology to describe the evolutionary process. As far as we know, the Darwinian principle of "survival of the fittest" is based on two underlying basic molecular processes: crossing over and mutation. The higher the fitness of an individual within a given population, the higher its chance of reproducing; the offspring resulting from sexual reproduction will then have DNA blueprints from the mother as well as from the father, which will generally have fitness values well above the average. In this way and by occasional mutations, sufficient diversity is retained in each generation of a population such as to guarantee dynamic evolution. On the other hand transmithose DNA blueprints which have already led to a high fitness of the parent individuals is at the basis of the evolutionary optimization process and represents the deterministic part of it. Pieces of information which have already been evaluated as being efficient are at least in part inherited and used in the next evolutionary optimization step. To apply this evolutionary strategy to numerical problems, a set of parameters for which the optimized values are to be found is encoded as a binary string (Figure 4).

Figure 4. Force field parameter refinement with Genetic Algorithms

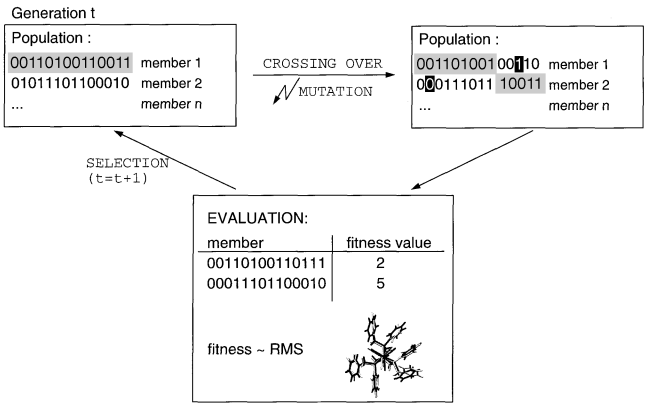

A "population" of such strings, each one representing a set of parameters, is generated at random. The fitness of all these parameter sets is then evaluated. For the problem at hand, this means that the set of parameters is applied to optimize the structures starting with the conformations as represented in the database. The rms deviations (see Experimental Section) between the structures as derived from the force field approach and those in the database are calculated, and taken to assess the fitness value for this specific set of parameters. This procedure is performed for all the members of a population (Figure 4). To produce the next generation with an intentionally increased fitness, those members of the parent population that are already ranked highly on the fitness scale are preferentially selected to reproduce. Mating is simulated by switching the information encoded in the binary strings, with the switching point being selected at random (Figure 4). By this crossover procedure, the population of the next generation is built up. To increase diversity, point mutations − changing a 0 to a 1 and vice versa − are occasionally performed at random. The procedure is then repeated to produce generation after generation and it is generally observed that the fitness increases from population to population. A typical result of the application of this procedure to the problem at hand is shown in Figure 5.

The dotted line represents the mean of the fitness values of all precedent populations at a given generation. It is seen that the discrepancy decreases exponentially. The lower curve represents the overall fitness of each individual population. It is seen that even after 160 generations, the fitness is still able to change. The population is not stuck in a niche, but is still capable of adapting. There is no guarantee that the optimal set of parameters has already been found, nor is there of course, by the very nature of the problem, any guarantee that a unique solution exists at all. The increase of the quality with which the best parameter set in a generation reproduces the conformation in the database is shown in Figure 5 as an overlay of the computed (grey) and the observed (red) conformations of **2** as an example.

A great advantage of applying Genetic Algorithms as minimizers stems from the fact that their algorithmic struc-

Figure 5. Genetic Algorithms at work[a]

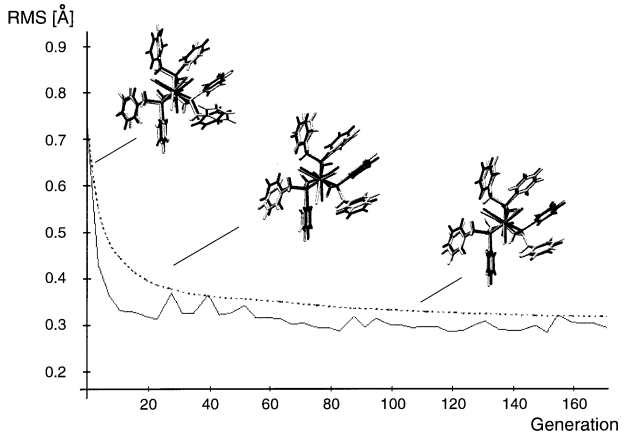

[a] The force field model is optimized such that the calculated conformations (i.e. grey) will reproduce the observed ones (i.e. red) increasingly well. The dotted line represents the cumulated fitness, which steadily increases as indicated. The average fitness of each individual population is represented by the continous line.

ture is inherently parallel, and hence the time-consuming steps (in the present case force field minimization of 10 structures) may naturally be distributed over the equivalent number of processors in a parallel computing environment (see Experimental Section). Yet another advantage may be seen in the fact that Genetic Algorithms have no problems in evaluating a whole subspace of solutions that will reproduce the observations equally well. Why should there exist a subspace of solutions and not just one optimal solution to a given problem? In the problem at hand, it is in fact to be expected that there will be several combinations of force field parameters, which − although individually numerically quite different − will reproduce the observations in conformational space equally well. This is to be expected owing to the fact that there are strong and sometimes even linear dependencies between the parameters. Consider a triangle with sides *a*, *b*, *c*. Given the length of the sides *a* and *b*, the length of *c* is as well determined by the angle subtended between *a* and *b* as it is by the value for the distance itself. In a force field approximation as applied the angle as well as the distance would be determined by individual potential functions for the angle and its deformation on the one hand and the distance and its change on the other. Trying to extract force constants for these two functions from a set of observations of triangles would inevitably lead to a multitude of solutions − in principal an infinite number of solutions − corresponding to the linear dependence between the angle and the distance. All these solutions will, of course, reproduce the observations equally well. While in spectroscopy this problem has been well delineated and is appropriately handled[27], molecular modelling as generally applied does not bother about it. As far as the refinement of force field parameters on the basis of a given set of conformations is concerned, the dependencies in parameter space would be cumbersome to handle by analytical refinement methods, while Genetic Algorithms would just produce a collection of solutions that would all reproduce the observations equally well.

With regard to the physical meaning of the parameters derived by such a refinement, it is evident from the above that individual parameters as such do not necessarily have to have a definite physical meaning. It is only the whole ensemble of parameters, which altogether have the physical meaning that, fed into the appropriate force field program, they will reproduce and hopefully predict conformations in agreement with empirical observations. Nevertheless, it is pleasing to apply, wherever possible, force constants that have been assessed by independent physical methods, and which then have a definite meaning even as individuals. With this in mind, the $Mo-C_{CO}$ stretching constant was set throughout at a value taken from the literature (Table 2), as was the Mo−C−O bending force constant.[28][29] Two parameter sets were finally refined (Table 2), with different degrees of freedom. The set designated as *mm2f* has the two aforementioned force constants at fixed values. The equilibrium distances and angles were set at the mean values observed for the sample in all cases, except for the $Mo-C_{CO}$ distance and the Mo−C−O angle, which were allowed to refine while the corresponding force constants were held at the fixed values (Table 2). Refinement thus mainly applied to the different types of force constants (Table 2). In the set of parameters designated as *mm2t*, the above set was augmented by allowing the torsion potentials involving contributions from molybdenum to refine (Table 2). This set was created for several reasons. Firstly, it seemed of interest to ascertain whether an augmented set of parameters would lead to a better refinement, as would in principle be expected, and whether the refinement procedure as applied would be able to converge on a set of values, even though these parameters are not so well-defined by the variance apparent in the data set. (The variance of values referring to these parameters in the data set would not lead one to expect that a stringent refinement would be possible at all). The second reason for deriving an augmented set of parameters was the curiosity to see how the introduction of these additional potentials would influence the values of the force field parameters common to both parameter sets. It is seen that the individual values for bond stretching and angle bending parameters are indeed quite different in both sets.

If these two sets of parameters are now applied to the ten compounds in the data base, to find the local minimum that best corresponds to the observed conformation, the results obtained (Table 1) are very similar for both parameter sets, even though individual parameters are grossly different in the two cases (Table 2). The rms deviation between observed and calculated structures as defined above is consistently somewhat smaller with the augmented force field *mm2t* than that derived using the *mm2f* approach (Table 1). This applies to the individual structures as well as to the sample as a whole (Table 1). With only a small difference between the quality of fit obtained from force field calculations based on the *mm2f* parameter set and that based on the *mm2t* set, the latter having 15 additional parameters, it

appears that on statistical reasoning the set *mm2f* is built on firmer grounds and should thus be preferred. Anyhow, the rms deviation between the two conformations for each compound obtained by applying one or the other set in the force field geometry optimization is considerably smaller than the rms of the difference between the observed and calculated structures in each case (Table 1). To illustrate the quality of fit obtained from the parameter set *mm2f*, Figure 6 shows an overlay of experimental and calculated conformations of four examples taken from the data set.

Figure 6. Overlay of calculated (grey) and observed (red) structures of compounds **1**, **3**, **5** and **6** (see Table 1)

The agreement is clearly quite satisfying. It may well be that the predominance of (mainly repulsive) interactions between the organic moieties of the ligands, which is characteristic of *tripod*-metal templates, is largely responsible for this degree of agreement. The conformations are thus dominated by forces that have been thoroughly modelled for organic compounds.[4][5]

If the parameters as evaluated here have the physical meaning of reproducing the conformational behaviour of *tripod*-metal compounds as a whole, the general trends and regularities observed for these compounds must be reliably reproduced by the force field approach. By analysis of 82 *tripod*-metal compounds[9], it has been found that the torsional positions occupied by the phenyl groups of the PPh_2 donors of *tripod* ligands form a regular pattern when plotted against each other in a type of scattergraph.[9] This analysis is shown in Figure 7 (black dots).[30]

Figure 7. Contour plot representing lines of equal energy as calculated for compound **1** based on the *mm2f* parameter set, with relative energies colour-coded as shown. The coordinates (φ) refer to the rotational positions of the two phenyl groups of a PPh_2 group in **1**. The black dots represent experimental points based on the analysis of 82 structures.[9] Pictograms of torsion angles φ refer to a projection of the molecule as presented in Figure 1 (left). For each PPh_2 group, φ_{2n+1} and φ_{2n} follow each other when counting in a clockwise sense referring to this projection. Grey lines represent energetically feasible pathways for rotational reorientation

This scattergraph is projected onto a contour-line diagram representing lines of equal energy as computed on the basis of the *mm2f* parameter set. It is evident from Figure 7 that regions of low energy (1, 2) correspond to regions which are densely occupied by experimental points. Regions of high energy (6) are not occupied at all. Region 3 corresponding to a two-ring flip transition[9] is in contrast quite densely populated. The contour plot shows that the energy differences between the regions 1 and 2 on the one hand and 3 are only small. Regions 4 and 5 correspond to one-ring flip transitions.[9] It has already been argued[9] that the extension of experimental points towards these regions indicates the feasibility of one-ring flip transitions. The potential pathways for a rotational rearrangement of the phenyl

rings at a PPh_2 grouphad already been delineated by lines as shown in Figure 7[9]. It is satisfying to see that the energy separation between the regions 3 and 2 and the transition point 4 is modest (roughly 10 kJ/mol), so that the free rotation of such phenyl groups as observed by NMR even at a temperature of −80°C finds is counterpart in the diagram.

Satisfying as the result shown by Figure 7 is, a more specific validation of the force field approach as developed would be the prediction of the conformation of a specific compound that had not already been included in the data set used to derive the force field. For this purpose, the conformational space available to $CH_3C[CH_2P(o\text{-Tol})_2]_3$-$Mo(CO)_3$ (**11**) was systematically analyzed by the above force field approach. It was not clear at that time that the compound could be prepared and even structurally characterized by X-ray analysis, and so it was especially satisfying to find that the subsequently determined crystal structure[31] agreed exceedingly well with the structure obtained as the global minimum from the force field calculations.

Figure 8. Overlay of the conformation of $CH_3C[CH_2P(o\text{-Tol})_2]_3$-$Mo(CO)_3$ as observed by X-ray analysis and calculated on the basis of the *mm2f* set (global minimum)

Figure 8 shows an overlay of the conformation as obtained from the conformational search (grey) and that observed in the crystal (red). Irrespective of the parameter set used (*mm2f*, *mm2t*), the global minimum was found at the same place in conformational space. The rms deviation between the two model conformations amounted to only 0.11 Å. The rms difference between the model conformations and the conformation observed in the crystal is very small as well (*mm2f*: 0.37 Å, *mm2t*: 0.42 Å)

The results obtained to date using this novel type of approach are sufficiently promising to warrant further investigations along such lines. While, from the results presented, it appears probable that the conformations of related molecules will be reliably predicted, it will be interesting to see whether the calculated energy hypersurfaces are approximately on scale with experimental data. The application of this method to problems pertaining to the conformational flexibility of *tripod*−$Mo(CO)_3$ compounds in solution (forthcoming paper) should give an answer to this question.

In summary, a novel approach to the derivation of force field parameters for metal-containing compounds is presented. It is shown that refinement of force field parameters on the basis of solid-state structures can be efficiently performed by the application of Genetic Algorithms. These algorithms are robust and allow for the simultaneous refinement of many force field parameters on an extended data basis containing many structures. When applied to *tripod*−$Mo(CO)_3$ compounds, the approach leads to models with a high predictive power with respect to specific conformations of these molecules, as well as to their overall conformational behaviour.

Financial support by the *German Science Foundation* (DFG HU 151/24-1), the *Fonds der Chemischen Industrie* and the Graduiertenkolleg "*Selektivität in der organischen und metallorganischen Synthese und Katalyse*" is gratefully acknowledged. The computations were made possible by grants of computing time at *Parsytec (IWR Heidelberg*) and CRAY (*KFA Jülich*) parallel computing environments. One of us (J. H.) wishes to thank the Graduiertenkolleg "*Modellierung und wissenschaftliches Rechnen in Mathematik und Wissenschaft*" (*IWR Heidelberg*).

Experimental Section

(a) *Force Field Calculations:* In order to apply the methodology of Genetic Algorithms to the problem of refining sets of force constants, it is necessary to have the force field program available as a source text. Since almost all modern force field programs are nowadays only commercially available and are delivered to the customer as executable files that will run only on a specific type of machine, these commercial programs are of no help. Instead of writing a whole new package for force field calculations, YAMMP[32], a program set written by R. K. Z. Tan et al. in ″C″, which is available as a public domain source code, was used as the core. The force field expressions implemented in this program were changed to correspond to the potentials applied in MacroModels MM2*.[18] Test runs on a vast sample of different compounds were performed with both programs to ensure that the results produced by MacroModel and those produced by the modified YAMMP program were numerically identical. Two converters which transform the MacroModel data format into the YAMMP data format were implemented and YAMMP was embedded in a number of shells so as to allow its use on different types of single processor machines (e.g. Pentium, SGI) as well as on different types of parallel computing systems (Parsytec GC, CRAY T3E).

To evaluate the rms deviation between two structural models, the mutual translational and rotational positions of the two models were optimized by a least-squares procedure using in part the *quatfit* program of D. Heisterberg[33] and in part a program based on the same algorithmic approach written by K. Allinger. The root-mean-square deviation was defined as the square root of the sum of the squares of the deviations between all n corresponding pairs of atoms divided by the square root of n (hydrogen atoms were included in these calculations throughout).

(b) *Optimization by Genetic Algorithms:* The force field parameter refinement was performed with the program *GAPAO*, written in ″C″, which uses functions from the *PGA-Genetic Algorithm Package.*[34] These functions are fully parallelized and are based on the *Message Passing Interface Library.*[35] This standard parallelization platform is available for all types of Unix systems, even for a net-

work of Linux PC's, and thus *GAPAO* has been installed on a Parsytec GC/Power Plus as well as on a CRAY T3E. Parallelization in this case means that all the evaluations of the parameter sets − implying the time-consuming energy minimizations of all the basis conformations − are performed on different processors. This leads to a tremendous economization of time and is thus another important advantage of the optimization procedure as applied.

Different crossing-over types and different selection routines are available.[34] In the cases reported, the approach of uniform crossing-over has been used.[36] To this end a mask of 0s and 1s with the length of the corresponding bitstring is generated at random. Applied according to the crossing over probability this mask then indicates which bits from the parents have to be taken to produce offspring. This type of crossing-over turned out to be especially useful in the treatment of large-scale parameterization problems.

The traditional "fortune wheel" selection type has been used as the selection routine.[25] This type of selection means that the probability of a given bitstring to be chosen to produce an offspring is proportional to its fitness value. Furthermore, an elitistic optimization strategy[25] has been adopted throughout, i.e. the best parameter set found in a given population is always left unchanged and taken into the next generation.

Evaluation was performed by energy minimization of all the structures contained in the data basis. To this end, the function *KA MMOPTfct*, written in C by K. Allinger, was used. The Polak-Ribière conjugate gradient minimization method[11][12] was employed and minimization was always driven to convergence (convergence criterion: 0.01 Å/iteration).

Parameters referring to force constants for bond stretching were encoded in the range 0.0−2.0 mdyn/Å. Parameters referring to force constants for angle bending were encoded in the range 0.0−1.5 mdyn/(rad^2). Torsional force constants k_{t1}, k_{t2}, and k_{t3} (see Figure 2) were encoded in a range between −1.5 and +1.5 kcal/mol. The refined Mo−C−O angle (see Table 2) was optimized in an interval between 170° and 180°; the Mo−C bond length was allowed to refine in an interval from 1.7 Å to 2.2 Å. Different subsequent runs were performed, each taking as its starting point the best results of the foregoing process, gradually augmenting the number of bits encoding the corresponding parameters in a stepwise manner from 5 to 8, and thus improving the resolution of the refined parameters.

Another way of overcoming the problem of discreteness in the optimization process was to apply a "hill climbing heuristic" to the best parameter set found and thus to locally optimize the corresponding parameters. This feature is implemented in the *GAPAO* program (*GAPAO-h)* by the strategy of altering or diminishing in a stepwise manner one parameter after another in the best parameter set, such that the resulting rms deviations become smaller. This is done until no further amelioration is achieved by such adjustments.

The method as described lends itself to a principally unlimited number of variations and it is a matter of experience to select appropriate values for the size of a population, and for the rates of crossing-over and mutation. This is exemplified in Figures 9a and b, which refer to different refinement runs for the parameters characterized by *mm2f*.

The rates of crossing-over and mutation were left unchanged for the three runs shown in Figure 9, with values that were found to be especially appropriate for the parameterization problem at hand (values given in Figure 9). The size of the population was different for the three runs. Not unexpectedly, the cumulated overall fitness,

Figure 9. How to find the appropriate GA protocol. Parameters used in the GA runs presented in a and b: crossing-over rate = 0.8, mutation rate = 0.02

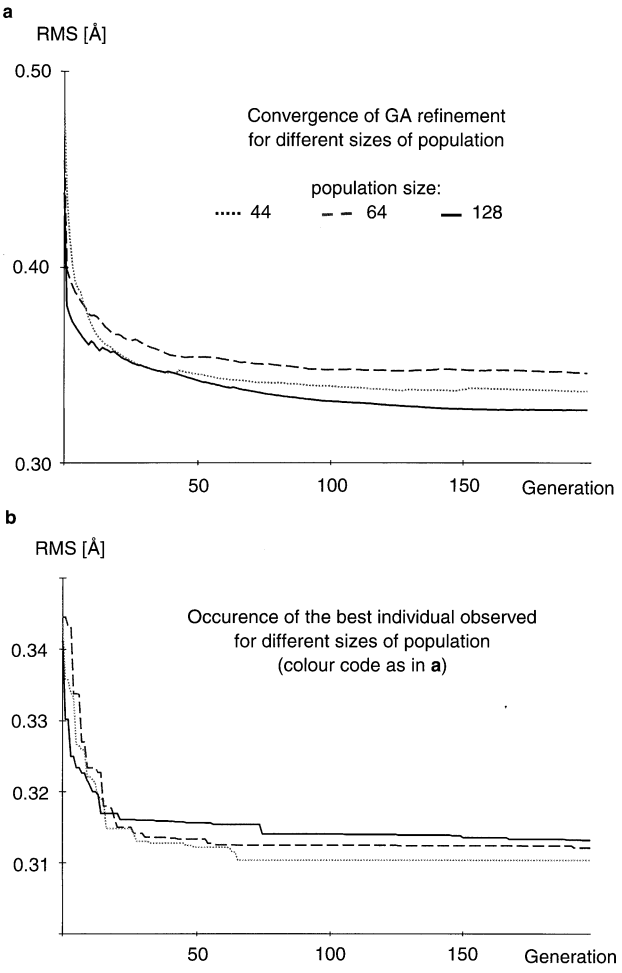

which is the mean of all the previously assessed fitness values, improves with the size of the population (see Figure 9a). However, the real aim of the optimization is not to find the population with the maximum overall fitness, but rather to find one member of a population − from which ever generation − which is the fittest individual of all, i.e. the search is aimed at the best set of force field parameters. Figure 9b illustrates that of the three runs described, the one based on a population of 60 randomly selected parameter sets produces the optimal solution after about 60 generations, with no better solution being found after more than 100 subsequent generations. The run based on a population size of 128 obviously takes far longer to converge. The run based on 44 individuals shows rapid convergence, but appears to be stuck at a lower quality solution.

In summary, it may be said that quite some experience and in some respects "green fingers" are needed to successfully apply Genetic Algorithms. However, this statement applies to other methods of global optimization as well and is not specific to the physical model analyzed here.

Calculations were performed on a CRAY T3E-512 with 512 compute nodes (600 MFLOPS/processor, 128 MB/processor, 333 MHz) and a Parsytec GC/Power Plus-192 (192 Power PC 601, 80 MHz, 32 MB/processor).

(c) *Conformational Analyses:* The φ_1/φ_2 contour plot of the PPh_2 conformations in **1**, as shown in Figure 7, is based on a grid search with a resolution of 5° for each P−Ph rotation φ (a φ value of 0° corresponds to an orientation of the phenyl ring perpendicular to the plane defined by the three P atoms, see Figure 7). Due to the C_2 symmetry of the phenyl groups, their rotation is periodic with a period of 180°, thus leading to 36 × 36 = 1296 grid points to describe one PPh_2 group. To account for the molecule as a whole, the multitude of orientations accessible to the remaining PPh_2 groups and to the chelate scaffolding have to be appropriately represented in the corresponding calculations. To this end, the torsion of the scaffolding τ[9] was uniformly set to starting values of 11° or 34°, respectively, leading to 2 × 1296 = 2592 starting geometries. In these conformations, the rotational arrangement at the remaining PPh_2 groups was set such that it corresponded to the regularites derived from an extensive analysis of such compounds ($\tau_{1/2/3}$ = 11°: $\varphi_{3/5}$ = 36°; $\varphi_{4/6}$ = 49°; $\tau_{1/2/3}$ = 34°: $\varphi_{3/5}$ = −50°, $\varphi_{4/6}$ = −29°; for the meaning of the numbers, see Figures 1 and 7).[9] (The conformations of a molecule such as **1** are chiral in general; only one of the enantiomers needs to be considered in the grid search due to this mirror symmetry in conformational space.)

A total of 2592 starting geometries were generated by the program *confgenrub* (written in "C" for that purpose) and then minimized by the program *bmin* as included in Version 5.0 of the molecular modelling software package MacroModel[18], using the force field MM2* and the parameter set *mm2f* described above. In order to evaluate the energy at each of the 1296 grid points, the rotational positions at the selected PPh_2 group at P1 (the orientation of the phenyl group as defined by the coordinate values of the grid point) had to be fixed during minimization. This was achieved by the technique of using a dummy atom, Du: A dummy atom was placed at a distance of 1 Å from the atom P_1, perpendicular to the plane defined by the 3 phosphorous positions, in the direction pointing towards the metal atom. Technically, this was achieved by imposing 3 restraints on its position: the distance P_1−Du as well as the angles P_2−P_1−Du and P_3−P_1−Du were fixed by giving them suitably steep potentials. The torsion angles φ_1 and φ2 were kept at the preordained values by imposing a corresponding restraint on the relevant torsion angles Du−P_1−C_{ipso}−C_{ortho}. Force constants as applied for this purpose were: distances: 500 kJ/Å^2, angles: 9999 kJ/rad^2, torsion angles: 9999 kJ/mol for k_{t1} (see Figure 2).

The refinement was performed using the Polak-Ribière minimizer with a gradient of 0.01Å/iteration and a maximum of 500 iteration steps as the limiting criteria. No cut-off was set for nonbonded interactions.

After minimization of each pair of conformations (two different τ values, see above) calculated for every grid point, the one with the lower energy was chosen to represent the energy (diagram in Figure 7).

The final contour plot as shown in Figure 7 was obtained by taking into account the isoenergetic enantiomeric conformation in each case. The mirror symmetry of the problem is apparent by a diagonal mirror plane characterizing the symmetry of the plot. The *plot2D* option of MacroModel was used to prepare the contour plot shown in Figure 7. The result of this procedure as depicted was obtained using the *mm2f* parameter set. Repeating the same procedure with the *mm2t* set produced a contour plot with the same overall characteristics.

A complete conformational search was performed for **11**. To generate the starting conformations for the search, the rotations of the tolyl groups about their P−C_{ipso} bonds were set at the initial values of φ = −135°, −45°, 135°. These torsional positions were defined with respect to a dummy atom, the position of which was generated as described above. The φ values refer to the torsion angle Du−P−C_{ipso}−$C_{ortho(Me\text{-}substituted)}$. The torsional arrangement of the cage was set by assigning a value of 20° to each of the 3 torsion angles τ.

Combining the four predefined orientations of each tolyl group in all possible combinations for the six tolyl groups present in the molecule gives a total of 4^6 = 4096 starting conformations. In this set, there are 16 (2^4) conformations that occur only once because of the C_3-symmetry of the molecule. The remaining 4096 − 16 = 4080 conformations occur in isoenergetic triplets. While physically indeterminable, they differ in assigning the same values of the six tolyl rotations φ to the P(*o*-Tol)$_2$ groups at P1P2P3, P2P3P1 or P3P1P2 in this sequence of cyclic permutations. Thus only (4096 − 16)/3 + 16 = 1376 starting geometries had finally to be taken into account. Minimization was performed as described above, with the criteria of a limiting gradient of 0.001Å/iteration and the maximum number of 2000 iterations allowed.

The calculations were carried out on two Silicon Graphics Indigo^2 MIPS R4400 workstations, 200 MHz, 128 MB RAM, operating under IRIX 5.3.

Table 2. Parameter sets *mm2t* and *mm2f*. Refined parameters are labelled with an asterisk

(a) Bond stretching

	parameter set *mm2f*		parameter set *mm2t*	
	r_0 [Å]	k_b [mdyn/ Å]	r_0 [Å]	k_b [mdyn/ Å]
Mo−C1	1.99*	2.00	1.94*	2.00
Mo−P	2.53	1.98*	2.53	0.75*

(b) Angle bending

	parameter set *mm2f*		parameter set *mm2t*	
	α_0 [°]	k_a [mdyn/rad^2]	α_0 [°]	k_a [mdyn/rad^2]
P−Mo−P	83.70	1.18*	83.70	0.53*
C1−Mo−C1	87.10	0.33*	87.10	0.39*
C1−Mo−P	94.90/175.90	0.1*	94.90/175.90	0.25*
Mo−C1−O	173.0*	0.47	170.00*	0.47
Mo−P−C2	119.0	0.29*	119.00	0.43*
Mo−P−C3	114.50	0.02*	114.50	0.29*

(c) Torsion

	parameter set *mm2f*			parameter set *mm2t*		
	k_{t1}[a]	k_{t2}[a]	k_{t3}[a]	k_{t1}[a]	k_{t2}[a]	k_{t3}[a]
P−Mo−P−C3	0.00	0.00	0.00	−0.90*	−0.58*	0.71*
P−Mo−P−C2	0.00	0.00	0.00	1.05*	0.26*	−0.24
Mo−P−C3−C3	0.00	0.00	0.00	−0.37*	−0.55*	0.11*
Mo−P−C2−C2	0.00	0.00	0.00	−1.06*	−0.19*	1.14*
Mo−P−C3−H	0.00	0.00	0.00	0.72*	−0.92*	1.20*

[a] In kcal/mol.

[1] See for example: [1a] H. Brintzinger, D. Fischer, R. Muhlhaupt, B. Rieger, R. M. Waymouth, *Angew. Chem. Int. Ed. Engl.* **1995**, *34(11)*, 1143−1170. − [1b] C. R. Landis, C. R. Halpern, *J. Am. Chem. Soc.* **1987**, *109*, 1746−1754. − [1c] G. Helmchen, S. Kudis, P. Sennhenn, H. Steinhagen, *Pure Appl. Chem.* **1997**, *69*, 513−518.

[2] G. Frenking, I. Antes, M. Boehme, S. Dapprich, A. W. Ehlers, V. Jonas, A. Neuhaus, M. Otto, R. Stegmann, A. Veldkamp, S. F. Vyboishchikov, in *Reviews in Computational Chemistry*, *Vol. 8* (Eds.: K. B. Lipkowitz, D. B. Boyd), VCH Publishers, Inc., New York, **1996**, p. 63−130

[3] L. J. Bartolotti, K. Flurchick, in *Reviews in Computational Chemistry*, *Vol. 7* (Eds.: K. B. Lipkowitz, D. B. Boyd), VCH Publishers, Inc., New York, **1996**, p. 187−259.
[4] N. L. Allinger, *J. Am. Chem. Soc.* **1977**, *99*, 8127−8134.
[5] U. Burkert, N. L. Allinger, *Molecular Mechanics*, ACS monograph, Washington, **1992**.
[6] P. Comba, T. W. Hambley, *Molecular Modelling of Inorganic Compunds*, VCH, Weinheim, **1995**.
[7] B. J. Hay, *Coord. Chem. Rev.* **1993**, *126*, 177−236.
[8] C. R. Landis, D. M. Root, T. Cleveland, in *Reviews in Computational Chemistry*, *Vol. 6* (Eds.: K. B. Lipkowitz, D. B. Boyd), VCH Publishers, Inc., New York, **1995**, 73−148.
[9] S. Beyreuther, J. Hunger, G. Huttner, S. Mann, L. Zsolnai, *Chem. Ber.* **1996**, *129*, 745−757.
[10] G. Huttner, S. Beyreuther, J. Hunger, in *Software-Entwicklung in der Chemie 10* (Ed.: J. Gasteiger), GDCH, Frankfurt am Main, **1996**, 201−207.
[11] W. H. Press, *Numerical Recipes: The Art of Scientific Computation*, Cambridge University Press, Cambridge, **1986**.
[12] P. E. Gill, W. Murray, M. H. Wright, *Practical Optimization*, Wiley, New York, **1988**.
[13] O. Walter, Th. Klein, G. Huttner, L. Zsolnai, *J. Organomet. Chem.* **1993**, *458*, 636−640.
[14] A. Muth, O. Walter, G. Huttner, A. Asam, L. Zsolnai, *J. Organomet. Chem.* **1994**, *468*, 149−163.
[15] Th. Seitz, A. Muth, G. Huttner, Th. Klein, O. Walter, M. Fritz, L. Zsolnai, *J. Organomet. Chem.* **1994**, *469*, 155−162.
[16] Th. Seitz, A. Asam, G. Huttner, O. Walter, L. Zsolnai, *Z. Naturforsch.* **1995**, *50b*, 1287−1306.
[17] The structures **3**, **8** and **10** (see Table1) have not yet been published, but have now been submitted. Details of the crystal structure investigations may be obtained from the Fachinformationszentrum Karlsruhe, D-76344 Eggenstein-Leopoldshafen (Germany), on quoting the depository numbers CSD-406278 (**3**), CSD-406277 (**8**) and CSD-406275 (**10**).
[18] The mm2 force field as implemented in Macromodel 5.0 (mm2*) has been used throughout (see F. Mohamadi, N. G. J. Richards, W. C. Guida, R. Liskamp, M. Lipton, C. Caufield, G. Chang, T. Hendrickson, W. C. Still, *J. Comp. Chem.* **1990**, *11*, 440−467).
[19] J. Devillers (Ed.), *Genetic Algorithms in Molecular Modelling*, Academic Press, San Diego, **1996**.
[20] R. Judson, in *Reviews in Computational Chemistry*, *Vol. 10* (Eds.: K. B. Lipkowitz, D. B. Boyd), VCH Publishers, Inc., New York, **1997**, 1−73.
[21] The idea of applying global minimizers to the inverse problem of finding optimized force field parameters has also been mentioned by van Gunsteren: − [21a] P. Ulrich, W. R. P. Scott, W. F. van Gunsteren, A. E. Torda, *Protein Structure Prediction Force Fields: Parameterization With Quasi-Newtonian Dynamics*; *Proteins* **1997**, *27*, 367−384. In contrast, local minimizers have routinely been used to locally improve parameters − [21b] S. Lifson, A. Warshel, *J. Chem. Phys.* **1968**, *49*, 5116−5128.
[22] Cicero, *De divinatione*, II, 59, "If somebody shoots the whole day, shouldn't he occasionally hit?"
[23] The problem is not drastically reduced when instead of the Alps, the Scottish Highlands or the Rocky Mountains are considered.
[24] J. Holland, *Adaption in Natural and Artificial Systems*, MIT Press, Michigan, **1975**.
[25] D. E. Goldberg, *Genetic Algorithms in Search, Research and Machine Learning*, Addison-Wesley, New York, **1989**.
[26] The strategy of simulated annealing is yet another way of combining deterministically analytic and stochastic strategies. See for example: [26a] S. Kirkpatrick, C. D. Gelatt, M. P. Vecchi, *Science* **1983**, *220*, 671−680. This methodology has been successfully applied to problems of conformational search, see for example: [26b] S. R. Wilson, W. Cui, J. W. Moskowitz, K. E. Schmidt, *Tetrahedron Lett.* **1988**, *29*, 4373−4376.
[27] E. B. Wilson, J. C. Decious, P. C. Cross, *Molecular Vibrations - The Theory of Infrared and Raman Vibrational Spectroscopy*, Maple Press Company, New York, **1955**.
[28] L. H. Jones, R. S. MacDowell, M. Goldblatt, *Inorg. Chem.* **1960**, *8*, 11, 2349−2363.
[29] Since bending force constants derived from spectroscopy may not be too accurate (see for instance ref.[5]), refinement was also performed including the Mo−C−O force constant in the subset of variable parameters. The force field parameters derived for this augmented set did not show an improvement over those with the bending force constants at the value given. It was observed, however, that the refined values of this force constant tended to be smaller than the value taken from the literature.
[30] In the scattergraph published previously for the same data (ref.[9]), a distortion by a partially incorrect treatment of symmetry had been introduced; this is now corrected in the diagram presented in Figure 7. We thank H. B. Bürgi for helpful discussions.
[31] P. Schober, Ph.D thesis, Heidelberg 1997.
[32] R. K. Z. Tan, S. C. Harvey, *J. Comp. Chem.* **1993**, *14*, 455−470.
[33] D. Heisterberg, **1990**, unpublished results; the program is available from the software archive of the Computational Chemistry List (CCL) at http://ccl.osc.edu/chemistry.html.
[34] D. Levine, Argonne National Laboratory, **1995**; the package is available at http://www.mcs.anl.gov/pgapack.html.
[35] W. Gropp, E. Lusk, Argonne National Laboratory, **1996** (available from http://www.mcs.anl.gov/mpi).
[36] G. Syswerda, *Proc. 3rd Int. Conference on Genetic Algorithms*, Morgan Kaufman Publishing, **1989**.

[97246]

Four-Coordinate Group-14 Elements in the Formal Oxidation State of Zero – Syntheses, Structures, and Dynamics of $[\{(CO)_5Cr\}_2Sn(L_2)]$ and Related Species☆

Peter Kircher, Gottfried Huttner*, Katja Heinze, Berthold Schiemenz, Laszlo Zsolnai, Michael Büchner, and Alexander Driess

Anorganisch-Chemisches Institut der Universität Heidelberg
Im Neuenheimer Feld 270, D-69120 Heidelberg, Germany
Fax: (internat.) + 49(0)6221/545707

Received February 2, 1998

Keywords: Germanium / Tin / Lead / ^{119}Sn NMR / Dynamic NMR / Salt metathesis

The sodium salts $Na_2[\{(CO)_5M\}_2EX_2]$ (M = Cr, Mo, W; E = Ge, Sn, Pb; X = Cl, I, $OOCCH_3$) react with 2,2′-bipyridine (bipy) to form neutral compounds $[\{(CO)_5M\}_2E(bipy)]$ (E = Sn: **1a–1c**; E = Ge: **3a**; E = Pb: **4**). 1,10-Phenanthroline (phen) analogues of compounds **1a–1c** and **3a** $[\{(CO)_5M\}_2E(phen)]$ (E = Sn: **1d–1f**, E = Ge: **3b**) are as well accessible. The 2,2′-bipyridine ligand in **1** may be formally replaced by two pyridine (py) ligands resulting in $[\{(CO)_5M\}_2Sn(py)_2]$ (**1g**: M = Cr, **1h**: M = W). The bis-bidentate ligand 2,2′-bipyrimidine (bpmd) is found to coordinate just one $[\{(CO)_5M\}_2Sn]$ entity in $[\{(CO)_5M\}_2Sn(bpmd)]$ (**2b**: M = Cr, **2c**: M = W). The biimidazolato (biim) ligand binds two $[\{(CO)_5Cr\}_2Sn]$ moieties in $[\{(CO)_5Cr\}_2Sn(biim)Sn\{Cr(CO)_5\}_2]^{2-}$, **2a**. It is shown by ^{1}H-NMR that the pyrimidine entities in these compounds (**2b**, **2c**) are able to rotate by a full 180° turnaround with respect to one another. This process must involve complete de-coordination of at least one of the two nitrogen donors in again at least one of the chelate cycles, the activation energy for this process being around 60 kJ/mol. By ^{119}Sn-NMR spectroscopy of almost all of the tin compounds described it is shown that equilibria between $[\{(CO)_5M\}_2Sn(L_2)]$ and $[\{(CO)_5M\}_2Sn(L)]$ + L exist in all cases. From the temperature dependence of the δ values it is concluded that the activation barriers for this association/dissociation process is below 10 kJ/mol. The structures of all new compounds are documented by X-ray analyses and all compounds are characterized by the usual analytical and spectroscopical techniques.

Introduction

The chemistry of low-valent main-group compounds may considerably be expanded by using organometallic protective groups to electronically and sterically inhibit the decomposition of such species. Thus while neither Bi_2 nor Sn_6^{2-} are known as such at ambient temperature their organometallic derivatives $[\{(CO)_5W\}_3Bi_2]$[1] and $[\{(CO)_5Cr\}_6Sn_6]^{2-}$[2] are well characterized species. In order to exploit the unconventional chemistry of compounds containing low-valent tin aggregates embedded in an organometallic matrix, starting materials which contain reactive tin−halide bonds and have the tin centers already coordinated to organometallic building blocks should be useful. With this idea in mind syntheses of various salts containing anions of type **A** (Figure 1) had been developed[3][4].

Figure 1. Anions of type **A**

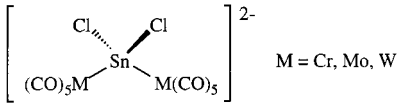

A

It had been found that the salts formed with $[Ph_4P]^+$ counter ions are quite unreactive and correspondingly indefinitely stable at room temperature under an inert atmosphere[4]. When, however, these salts are metathesized with $Na[BPh_4]$ the highly reactive sodium salts $[Na(solv)_x]_2[\{(CO)_5M\}_2SnCl_2]$ are formed[4]. The difference in reactivity of these two types of salts is illustrated by the observation that the phosphonium salts do not react with sodium 8-oxoquinolate, $Na[C_9H_6NO]$, while the sodium salt $[Na(solv)_x]_2[\{CO)_5Cr\}_2SnCl_2]$ instantaneously does[4]. The resulting anion $[\{(CO)_5Cr\}_2Sn(oxinato)]^-$ contains a tetrahedrally coordinated tin center (formal oxidation state: Sn^0) with two coordination positions occupied by the anionic chelate ligand[4].

We report here that an analogous procedure allows for the replacement of the two halide substituents in **A** by neutral nitrogen-based chelate ligands leading to neutral adducts of types **1** and **2** which as well contain tin in the formal oxidation state of zero. Analogous reactivity is observed for the homologues of type **A** anions containing germanium or lead instead of tin. 2,2′-Bipyridine or 1,10-phenanthroline adducts of Ge^0, **3**, and Pb^0, **4**, stabilized by coordination to two $[(CO)_5Cr]$ groups are thus obtained.

Results and Discussion

a) Compounds 1 Containing 2,2′-Bipyridine or 1,10-Phenanthroline as Chelating Ligands

THF solutions of the sodium salts of the anions of type **A**, $[\{(CO)_5M\}_2SnCl_2]^{2-}$, are prepared from $[Ph_4P]_2[\{(CO)_5M\}_2SnCl_2]$ by salt metathesis with $Na[BPh_4]$

 © WILEY-VCH Verlag GmbH, D-69451 Weinheim, 1998 1434−1948/98/0606−0703 $ 17.50+.50/0

as described[4]. Upon addition of 2,2′-bipyridine (bipy) or 1,10-phenanthroline (phen) the initially yellow solutions turn deep red immediately and take on a turbid appearance caused by the precipitation of NaCl.

Table 1. Complexes of type **1**

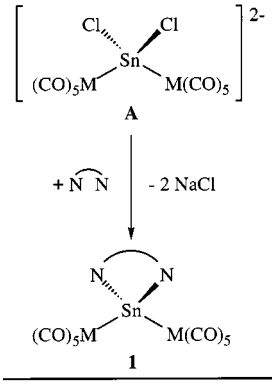

no.	M	N N
1a	Cr	bipy
1b	Mo	bipy
1c	W	bipy
1d	Cr	phen
1e	Mo	phen
1f	W	phen
1g	Cr	2 · py
1h	W	2 · py

Chromatographic workup, separating compounds **1** from the decomposition products $[M(CO)_6]$, $[M(CO)_4(bipy)]$, and $[M(CO)_4(phen)]$, respectively, leads to **1a**−**1f** in yields of around 50%. The compounds are obtained as microcrystalline deep red materials of analytical purity. Crystals suitable for X-ray analyses are obtained by vapour diffusion from THF/diethyl ether/petroleum ether (boiling range 40−60°C). **1a**−**1f** are analogues of the known species $[\{Cp'(CO)_2Mn\}_2Sn(bipy)]$[5] and $[\{Cp'(CO)_2Mn\}_2Sn(phen)]$[6].

The IR-ν_{CO} spectra of **1a**−**1f** show the three-band pattern (Table 4, Figure 2) characteristic of $[LM(CO)_5]$ species[7]; in a few cases an additional shoulder around 1960 cm^{-1} is observed (Table 4) indicating either a local symmetry lower than C_{4v} or coupling between the two $[(CO)_5M]$ chromophores. The IR-ν_{CO} absorptions of the neutral compounds **1** are shifted to somewhat higher energies relative to the absorptions of the dianionic starting materials (e.g. $[Na(THF)_x]_2[\{(CO)_5Cr\}_2SnCl_2]$: ν_{CO} (THF) = 2040 w, 2007 s, 1920 vs, 1895 sh cm^{-1}, Figure 2) as would be expected when reducing the charge in an $[LM(CO)_5]$ compound[8].

The ^{1}H-NMR spectra show the expected shifts of the proton resonances of the ligands (Table 2). The observed low-field shifts are somewhat higher than those found for the $[Cp'(CO)_2Mn]$ analogues of compounds **1**[5][6]. This indicates that the coordination of the chelate ligands is somewhat stronger for **1a**−**1f** as compared to their $[Cp'(CO)_2Mn]$ analogues[5][6].

This is in fact what would be expected taking into account the relative π-donor capabilities of $[Cp'(CO)_2Mn]$ and $[(CO)_5M]$ (M = Cr, Mo, W): with $[Cp'(CO)_2Mn]$ being the stronger π-donor[9] the cumulene-type compounds $[Cp^R(CO)_2Mn{=}Sn{=}Mn(CO)_2Cp^R]$ (Cp^R = Cp, Cp′, Cp*)[10] are available as such. Their 2,2′-bipyridine and 1,10-phenanthroline derivatives corresponding to **1a**−**1f** are directly obtained from the cumulenes by adding the chelate bases[5][6] and the compounds may thus be considered as Lewis base stabilized organometallic cumulenes. The interaction with the Lewis base chelate ligands remains weak in

Figure 2. Carbonyl region of the IR-absorption spectra of $[Na(THF)_x]_2[\{(CO)_5Cr\}_2SnCl_2]$ (A) and **1a** (B) in THF

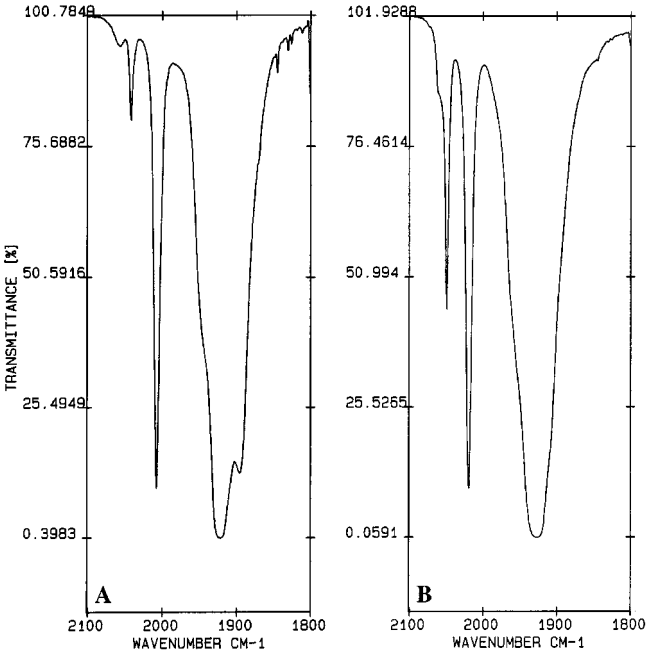

Table 2. ^{1}H-NMR-spectroscopic data ([D$_6$]acetone, 25°C) for the uncoordinated ligands and compounds **1**−**4**

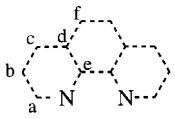

	H_a	H_b	H_c	H_d	H_f
bipyridine	8.67[a]	7.38[b]	7.89[c]	8.51[d]	–
1a	9.18[a]	8.17[b]	8.60[c]	9.12[d]	–
1b	9.25[a]	8.11[b]	8.55[c]	9.10[d]	–
1c	9.23[a]	8.14[b]	8.57[c]	9.08[d]	–
3a	9.13[a]	8.28[b]	8.67[c]	9.23[d]	–
4	9.13[a]	7.90[b]	8.37[c]	8.76[d]	–
phenanthroline	9.13[e]	7.72	8.42[f]	–	7.91[g]
1d	9.61[e]	8.48	9.19[f]	–	8.53[g]
1e	9.68[e]	8.42	9.13[f]	–	8.51[g]
1f	9.64[e]	8.44	9.13[f]	–	8.50[g]
3b	9.57[e]	8.59	9.26[f]	–	8.62[g]
pyridine	8.62[h]	7.32[j]	7.72[k]	–	–
1g	8.89[i]	8.00[j]	8.36[i]	–	–
1h	8.94[h]	7.96[j]	8.34[k]	–	–
bipyrimidine	9.00[l]	7.60[m]	–	–	–
2b[n]	9.71[l]	8.44[m]	9.68[l]	–	–
2c[n]	9.74[l]	8.39[m]	9.64[l]	–	

[a] $^3J(^1H,^1H)$ = 4.8−5.5 Hz. − [b] $^3J(^1H,^1H)$ = 8.0−8.4 Hz. − [c] $^3J(^1H,^1H)$ = 7.7−8.0 Hz. − [d] $^3J(^1H,^1H)$ = 4.7−5.8 Hz. − [e] $^3J(^1H,^1H)$ = 4.0−5.1 Hz. − [f] $^3J(^1H,^1H)$ = 8.0 Hz. − [g] $^3J(^1H,^1H)$ = 4.0−5.5/8.0 Hz. − [h] $^3J(^1H,^1H)$ = 6.4 Hz. − [i] broad signal, no coupling observable. − [j] $^3J(^1H,^1H)$ = 6.4/7.6 Hz. − [k] $^3J(^1H,^1H)$ = 7.6 Hz. − [l] $^3J(^1H,^1H)$ = 4.8−5.0 Hz. − [m] $^3J(^1H,^1H)$ = 4.8−5.0 Hz. − [n] Measured at −50°C.

this case reflecting the extensive Mn-d_π−Sn-p_π back-donation which effectively stabilizes even the base-free cumulenes. The weaker back-donation from the $[(CO)_5M]$ fragments makes the cumulene compounds $[(CO)_5M{=}Sn{=}M(CO)_5]$ so unstable that they have not yet been isolated as such[11]. Compounds **1a**−**1f** may be considered as base-stabilized forms of such species. Due to the inherent lack of sufficient back-donation from the metals the tin center in the hypothetical cumulenes $[(CO)_5M{=}Sn{=}M(CO)_5]$ is highly electron-deficient and will act as an effective Lewis acidic center towards the chelate bases. The shifts of the ^{1}H-NMR resonances of the ligands upon coordination are indicative of this interaction.

Table 3. ^{13}C-NMR-spectroscopic data ([D$_6$]acetone, 25°C) for the uncoordinated ligands and compounds **1**−**4**

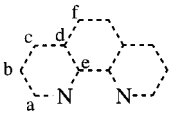

	CO_{ax}	CO_{eq}	C_a[a]	C_b[b]	C_c[c]	C_d[d]	C_e	C_f
bipyridine	−	−	149.9	124.6	137.5	121.3	156.7	−
1a	227.4	221.1	148.2	127.9	143.0	125.8	152.6	−
1b	−	210.6	148.0	127.4	142.3	125.8	−	−
1c	204.5	201.3	147.8	127.8	142.6	125.7	153.6	−
3a	227.1	220.4	145.8	127.6	142.8	125.6	146.0	−
4	221.3	219.3	148.8	126.6	141.0	125.1	152.3	−
phenanthroline	−	−	150.6	123.9	136.7	129.5	147.1	127.4
1d	227.0	220.9	149.4	126.3	141.8	132.2	140.4	129.1
1e	216.3	210.6	149.2	125.8	141.0	132.3	140.5	129.1
1f	206.0	201.4	148.9	126.2	141.3	132.2	140.4	129.1
3b	226.9	220.2	146.8	126.2	141.1	131.9	137.6	129.1
pyridine	−	−	150.6	124.4	136.5	−	−	−
1g	226.7	220.9	149.0	127.2	142.2	−	−	−
1h	204.7	201.5	149.7	127.6	142.0	−	−	−
bipyrimidine	−	−	158.2	122.0	−	−	164.4	−
2b[e]	226.5	220.8	156.4	125.0	163.9	−	−	−
2c[f]	203.6	200.9	155.5	124.3	162.8	−	155.7	

[a] C_a: $^1J(^1H,^{13}C;$ bipy) = 178 Hz; $^1J(^1H,^{13}C;$ **1a**) = 184 Hz; $^1J(^1H,^{13}C;$ **3a**) = 161 Hz. − [b] C_b: $^1J(^1H,^{13}C;$ bipy) = 165 Hz; $^1J(^1H,^{13}C;$ **1a**) = 171 Hz; $^1J(^1H,^{13}C;$ **3a**) = 165 Hz. − [c] C_c: $^1J(^1H,^{13}C;$ bipy) = 162 Hz; $^1J(^1H,^{13}C;$ **1a**) = 171 Hz; $^1J(^1H,^{13}C;$ **3a**) = 166 Hz. − [d] C_d: $^1J(^1H,^{13}C;$ bipy) = 163 Hz; $^1J(^1H,^{13}C;$ **1a**) = 165 Hz; $^1J(^1H,^{13}C;$ **3a**) = 170 Hz. − [e] Measured at 0°C. − [f] Measured at − 60°C.

This interaction is mirrored by the ^{13}C-NMR resonances (Table 3). With reference to the ^{13}C-NMR data of the free ligands the ^{13}C signals of the coordinated ligands consistently show the high-field (C_a, C_e) and low-field (C_b, C_c, C_d, and C_f) shifts which are known to be characteristic of the coordination of these chelate bases[12]. A theoretical explanation of this characteristic pattern of high- and low-field shifts has been put forward[13]. The individual resonances for the carbonyl carbon atoms C_{ax} and C_{eq} of the $[(CO)_5M]$ entities are generally well resolved (Table 3); only in the case of **1b** the quality of the spectroscopic data did not reveal the resonance of the axial carbonyl group.

Table 4. IR-$\tilde{\nu}_{CO}$ and ^{119}Sn{^{1}H}-NMR-spectroscopic data for compounds **1**−**4**

	IR ($\tilde{\nu}_{CO}$/cm^{-1})[a]					^{119}Sn{^{1}H} (δ/ppm)[b]
1a	2045 (m)	2016 (s)		1922 (vs)		1336
1b	2056 (m)	2034 (s)		1932 (vs)		1354
1c	2057 (m)	2035 (s)	1960 (sh)	1927 (vs)		1021[c]
1d	2045 (m)	2016 (s)		1922 (vs)		1327
1e	2056 (m)	2034 (s)		1932 (vs)		1349
1f	2057 (m)	2035 (s)	1959 (sh)	1926 (vs)		996[d]
1g	2046 (m)	2016 (s)		1924 (vs)		1515
1h	2058 (m)	2036 (s)		1928 (vs)		1200[e]
2a	2052 (w)	2011 (m)	1938 (sh)	1919 (vs)	1897 (sh)	1149
2b	2048 (m)	2018 (s)		1928 (vs)		1372
2c	2059 (m)	2038 (s)	1963 (sh)	1929 (vs)		1026[f]
3a	2047 (m)	2021 (s)	1956 (sh)	1923 (vs)		−
3b	2047 (m)	2021 (s)	1956 (sh)	1923 (vs)	1906 (sh)	−
4	2050 (m)	2017 (s)		1931 (vs)		

[a] In THF. − [b] In [D$_6$]acetone, 25°C. − [c] $^1J(^{183}W,^{119}Sn)$ = 578 Hz; intensity ratio of peaks 15:100:15. − [d] $^1J(^{183}W,^{119}Sn)$ = 520 Hz; intensity ratio of peaks 14:100:15. − [e] $^1J(^{183}W,^{119}Sn)$ = 575 Hz; intensity ratio of peaks 16:100:14. − [f] $^1J(^{183}W,^{119}Sn)$ = 540 Hz; intensity ratio of peaks 19:100:20. − [c]−[f] The intensity of the satellites is close to the value of 29% as expected from coupling of a tin nucleus with two equivalent tungsten nuclei.

The NMR data which are most characteristic for the particular bonding situation in compounds **1** are the ^{119}Sn-NMR resonances (Table 4). The absorptions occur at relatively low field in the broad range of shifts[14] hitherto observed for tin compounds of δ = − 2171 (Cp_2Sn[15]) to δ = + 3301 ([{Cp*(CO)$_2$Mn}$_3$Sn][16]).

The resonances observed for the tungsten compounds **1c** and **1f** consistently occur at higher fields similar to those of their chromium and molybdenum analogues[4].

The ^{119}Sn-NMR shifts of all compounds **1** are strongly temperature-dependent throughout. In the observable range of temperatures the shifts increase with a slope of around 1.5 ppm/K with increasing temperature. This increase is monotonic though not strictly linear (cf. Figure 3).

This behavior may be rationalized by the assumption of two different species which are close in energy to each other, but which have widely different ^{119}Sn-NMR shifts. One of these species should contain four-coordinate tin (type **B**, Figure 4) in accord with the solid-state structure (vide infra). The other one is assumed to be a species where one of the two nitrogen atoms of the chelate ligand is de-coordinated (type **C**, Figure 4). This type of arrangement would lead to a bonding situation close to the one characteristic of inidene-type compounds $L_n{=}X(R){=}ML_n$[17].

The 3-center-4-π system characterizing the bonding situation in inidene compounds has a dramatic effect on the NMR shift of the central atom X. It has been found that with phosphorus in this position ^{31}P-NMR shifts range from δ = 900 to δ = 1400, well out of the range of shifts documented for all other phosphorus compounds[18]. This strong low-field shift is in addition well correlated with the inverse of the energy ΔE ($^1/_{\Delta E}$) of the π-π* transition in these compounds[18]. Taken together these observations lend strong weight to an interpretation which relates the

Figure 3. Temperature-dependent ^{119}Sn-NMR spectrum of **1a** (left) and **1e** (right) and graphs obtained from Equation 1

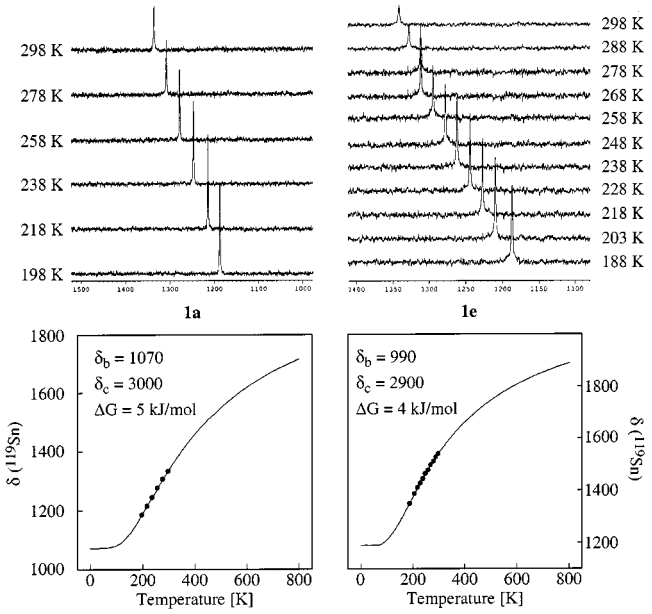

Figure 4. Equilibrium between four- and three-coordinated tin species **1d**−**1f**

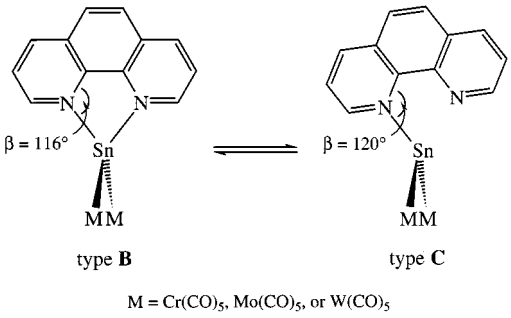

observed low-field shifts to the low HOMO-LUMO gap characterizing the 3-center-M⋯X⋯M-4π systems. The same type of arguments has been used to rationalize the extreme ^{119}Sn-NMR low-field shift of around δ = 3300 for a compound containing a M⋯X⋯M-π system as well[16]. A species of the type **C** as shown in Figure 4 would thus be expected to have its resonance around δ = 3000.

A guess for the shift which should be expected for a compound with four-coordinate tin (type **B**) may be based on the observation that $[Ph_4P]_2[\{(CO)_5Cr\}_2SnCl_2]$ shows one single temperature-independent signal at δ = 924 with its tungsten analogue $[Ph_4P]_2[\{(CO)_5W\}_2SnCl_2]$ resonating at δ = 605 again independent of temperature. The resonances of the chelate compounds of type **B** (Figure 4) would hence be expected somewhere around δ = 500 to δ = 1000.

An equilibrium as depicted in Figure 4 does not appear to be ruled out by MO considerations: EHT calculations[19] give an energy difference of only around 10 kJ/mol between the two isomeres (type **B** and **C**, Figure 4) with the chelate compound (type **B**) being the more stable.

The experimental observations are well in accord with the above assumptions. If a dynamic equilibrium as given in Figure 4 is assumed the ^{119}Sn-NMR shift of the equilibrium mixture of the two isomeres is given by $\delta_{obs.} = x_B\delta_B + x_C\delta_C$ with the molar fractions x_B and x_C and the shifts of the pure isomeres δ_B and δ_C, respectively. The observed temperature dependence of $\delta_{obs.}$ is then a consequence of the temperature dependence of the equilibrium constant pertaining to this isomerisation process and is given by Equation 1.

$$\delta_{obs.} = \frac{\delta_B + \delta_C \cdot e^{-\frac{\Delta G}{RT}}}{1 + e^{-\frac{\Delta G}{RT}}} \quad (1)$$

Fitting the parameters of δ_B, δ_C, and ΔG of the corresponding Equation 1 to the observed values results in a favorable agreement with the assumptions made above: the values for δ_B are estimated by this procedure in a range of δ = 990 to δ = 1070 for all four-coordinate compounds of type **B** (Figure 4). The values estimated for δ_C are in a range of δ = 2900 to δ = 3000. The values of ΔG range between 4 and 5 kJ/mol. All these values and ranges of values are completely independent of any guess made for the quantitative items δ_B, δ_C, and ΔG above. They are extracted from the observed material alone by the single assumption of a dynamic equilibrium as given in Figure 4 with no quantitative restrictions put on this equilibrium other than the experimental data. Graphs typical for the quality of fit obtained are shown for **1a** and **1e** in Figure 3. It is evident that quite some extrapolation is involved when the values δ_B and especially δ_C are to be determined by the fitting procedure. Nevertheless the ranges of δ_B and δ_C compare favorably with the expectations and the observed temperature dependence of $\delta_{obs.}$ is neatly reproduced.

The interpretation of the temperature dependence of the ^{119}Sn-NMR shifts in terms of an intramolecular equilibrium is further corroborated by the observation that addition of the free ligands (bipy, phen) to the solutions does not change the appearence of the ^{119}Sn-NMR spectra.

The equilibrium between species with η^2-coordinated ligands (type **B**) and η^1-coordinated ones (type **C**) as delineated should mirror itself into an appropriate behavior of the proton resonances of the ligands.

Figure 5. Temperature-dependent ^{1}H-NMR spectrum of **1e**

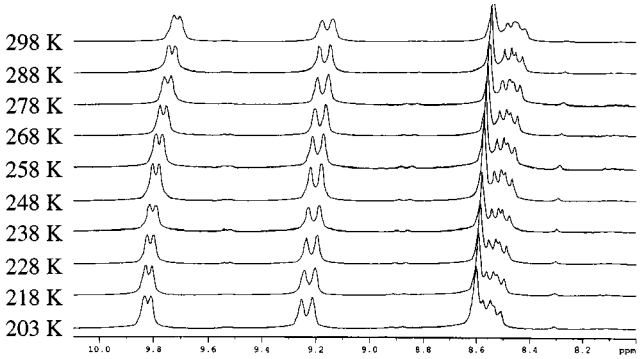

Figure 5 showing the temperature dependence of the ^{1}H-NMR spectrum of **1e** as an example demonstrates that with raising temperature all of the signals are continuously shifted to higher fields. Qualitatively this is well in accord with what would be expected on the basis of the partial de-coordination of the ligand characterizing the equilibrium depicted in Figure 4: with the ligands being less tightly bound in the mean with increasing temperature their signals should move towards the ones of the free ligands (Table 2).

Applying Equation 1 to the ^{1}H-NMR data of **1e** (Figure 5) with one set of limiting resonances fixed on the values of the free ligand [δ_C = 9.13 (H_a), 8.42 (H_c), 7.91 (H_f), 7.72 (H_b)] the other set of limiting resonances is derived as [δ_B = 9.96 (H_a), 9.57 (H_c), 8.87 (H_f), 8.70 (H_b)]. The value of ΔG characterizing the equilibrium is obtained as 2 kJ/mol and is − with respect to experimental accuracy (Figure 5) and the narrow range of temperatures studied − in satisfying agreement with the value of ΔG = 4 kJ/mol as extracted from ^{119}Sn-NMR measurements (vide supra). It is worth noting that the worst quality of fit is obtained for the data pertaining to the protons H_a of the α-CH groups. The sensitiveness of the resonances of these protons to minor changes in the coordination environment is amply been demonstrated in the literature[20]. Overall the successful modeling of the temperature dependence of the NMR spectra of compounds **1** and the qualitative agreement of the estimates made by these models for the reaction enthalpy, independent of whether ^{119}Sn- or ^{1}H-NMR data are analyzed, are in favor of the belief that the underlying basic assumption of an equilibrium (Figure 4) is correct.

The equilibrium (Figure 4) suggests that species with just one donor ligand should be stable as such without the necessity of a second donor ligand. Under these premises it appeared worthwhile to probe whether, excluding the chelate effect, one pyridine (py) molecule as a Lewis base would suffice to stabilize the underlying cumulene-type compounds to such an extent that inidene like adducts [$(CO)_5M{=}Sn(py){=}M(CO)_5$] could be isolated or whether a second pyridine molecule whould coordinate, leading to [$(CO)_5M{=}Sn(py)_2{=}M(CO)_5$], compounds, formally isoelectronic to the dianions [$\{(CO)_5M\}_2SnHal_2]^{2-}$[3][4].

b) Compounds 1 Containing Two Pyridine Donors

When THF solutions of the sodium salts [$Na(THF)_x$][$\{(CO)_5M\}_2SnCl_2$] (type **A**) are treated with a fourfold equimolar excess of pyridine, adduct formation is indicated by a change in the IR-ν_{CO} pattern. Isolation of the pyridine adducts **1g** and **1h**, albeit in yields below 20%, is possible by column chromatography. Compounds **1g** and **1h** are obtained as yellow microcrystalline solids. **1g** and **1h** are definitely less stable than the chelate adducts **1a**−**1f**: under conditions where **1a**−**1f** are indefinitely stable in THF solutions **1g** and **1h** gradually disintegrate to produce unsoluble greenish materials.

The IR-ν_{CO} absorptions (Table 4) of **1g** and **1h** are within a few wavenumbers found at the same positions as those of the corresponding 2,2′-bipyridine adducts **1a** and **1c**.

The ^{1}H-NMR spectra of **1g** and **1h** in [D_6]acetone (Table 2) with the corresponding low-field shifts relative to free pyridine clearly reveal the coordination of the pyridine ligands. The proton signals shift to lower fields as the temperature is lowered with the same type of observation having already been described for **1a**−**1f**.

The ^{13}C-NMR data (Table 3) equally well demonstrate the coordination of the heterocycles in **1g** and **1h**. Again the individual resonances of the carbonyl carbon atoms are observable and distinguishable (Table 3).

The ^{119}Sn-NMR data are indicative of dynamic equilibria in these cases as well. When CD_2Cl_2 is used as the solvent for **1h** sharp tungsten-modulated signals are observed over the whole range of temperatures (298−168 K). With decreasing temperature a monotonically increasing high-field shift of the signal is observed: at 298 K the resonance occurs at δ = 1271 at 168 K is is found at δ = 1164. If it is assumed that the underlying chemical process is again a coordination/de-coordination equilibrium similar to the one shown in Figure 4 and if it is further assumed that the pyridine, when de-coordinated remains close to the tin in the solvent cage an analysis as performed for the chelate compounds (vide supra) results in δ_B = 1100, δ_C = 2200, and ΔG = 5 kJ/mol, respectively, with the species of type **B** being the more stable. The quality of fit is similar to the one shown in Figure 3 for the chelate compounds **1a** and **1e**. This refers to the data from solutions of **1h** in CD_2Cl_2.

Solutions of **1h** in [D_6]acetone show the same type of temperature dependence of the ^{119}Sn-NMR signal with the additional complication that the signal starts to broaden at 240 K and is completely vanishing in the background at 230 K reappearing as a sharp signal at 210 K. It is assumed that some exchange with the [D_6]acetone solvent is responsible for this phenomenon. With the chelate compounds **1a** and **1e** this type of observation is not made; steric reasons are a rationale for this difference in behavior. Anyhow, the dynamic situation with **1h** is more complicated than the one described for **1a** and **1e** since addition of the free ligand pyridine is found to cause a high-field shift in the ^{119}Sn-NMR spectrum while starting with pure **1h** increasing dilution will shift the signal to the low-field side. These experiments indicate that coordination/de-coordination equilibria of the same type as depicted in Figure 4 must be at the basis of the observed phenomena.

c) Molecular Structures of Compounds 1a−1h

The molecular structures of all the compounds of **1a**−**1h** have been determined by X-ray analyses (Tables 5, 10, and 11). The similar allover geometry of the individual molecules within each class (**1a**−**1c**, **1d**−**1f**, **1g** and **1h**) warrants the discussion of the structures with reference to Figure 6, showing only the [$(CO)_5Cr$] derivatives[21].

This similarity is also illustrated by the fact that the crystal structures of **1a**−**1c** are isotypic (Table 10) as are those of **1d**−**1f** which include one THF solvate per molecule **1** (Tables 10 and 11) and those of **1g** and **1h** (Table 11). The environment of the tin centers in **1a**−**1h** is distorted tetrahedral (Table 5).

Figure 6. Molecular structures of compounds **1a**, **1c**, and **1g**

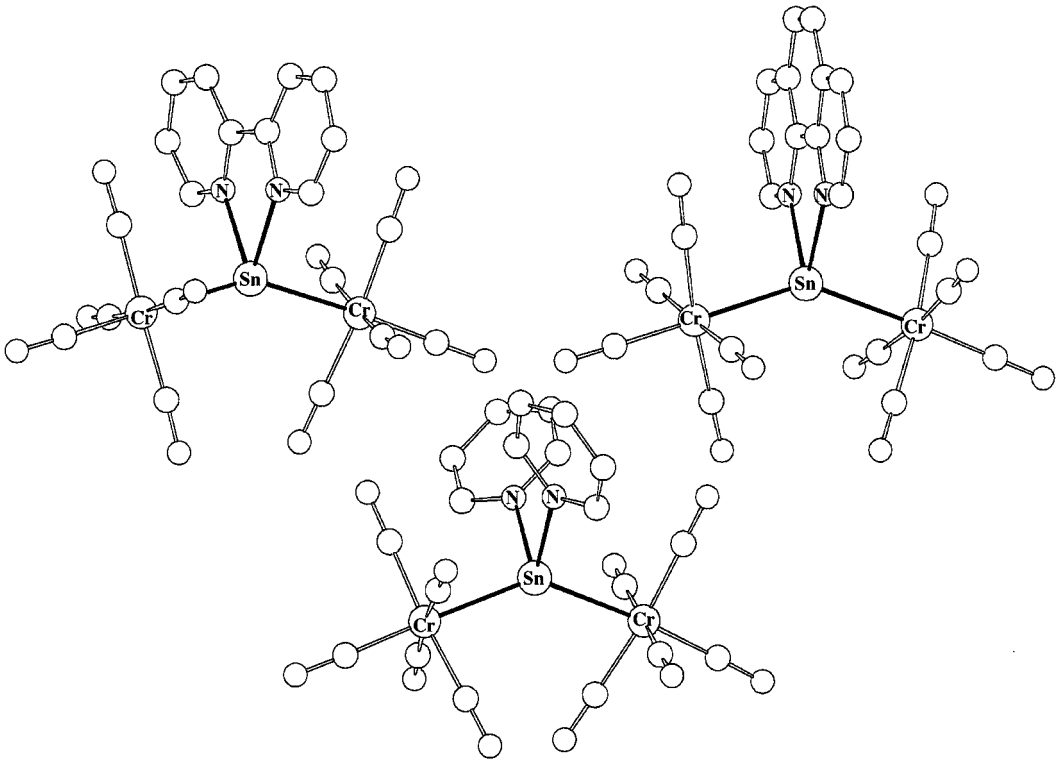

Table 5. Selected bond lengths [pm], angles [°] and torsion angles [°] of compounds **1a**−**1h**[a]

$[\{(CO)_5M\}_2Sn(N^{\frown}N)]$	**1a** M = Cr	**1b** M = Mo	**1c** M = W	**1d** M = Cr	**1e** M = Mo	**1f** M = W	**1g** M = Cr	**1h** M = W
M-Sn	262.2 (1)	276.1 (1)	276.0 (1)	262.3 (1)	274.4 (1)	275.3 (1)	260.3 (1)	277.9 (2)
	261.9 (1)	275.6 (1)	275.8 (1)	263.0 (1)	274.5 (1)	275.8 (1)	261.8 (1)	278.9 (2)
M-$C_{CO(ax)}$ [b]	186.5 (5)	200.1 (7)	201 (1)	188.3 (6)	200.5 (5)	200 (1)	186.4 (3)	203 (2)
M-$C_{CO(eq)}$ [b]	189.6 (5)	203.3 (7)	203 (1)	190.2 (6)	203.4 (5)	204 (1)	188.9 (4)	206 (2)
Sn-N	229.6 (3)	228.2 (5)	228 (1)	230.3 (4)	227.9 (3)	227.1 (9)	231.2 (3)	231 (1)
	227.5 (3)	227.2 (5)	227 (1)	230.5 (4)	228.0 (3)	229.1 (9)	232.9 (3)	236 (1)
M-Sn-M	148.66(3)	149.37(2)	149.07(4)	143.92(3)	146.09(2)	145.71(4)	139.24(2)	139.87(4)
N-Sn-N	71.5 (1)	71.2 (1)	71.3 (3)	72.3 (1)	72.4 (1)	72.4 (3)	86.9 (1)	86.1 (3)
M-Sn-N	103.98(8)	104.0 (1)	103.8 (3)	103.6 (1)	103.27(9)	104.7 (2)	102.96(7)	103.2 (3)
	100.62(8)	100.2 (1)	99.9 (2)	104.6 (1)	104.41(9)	103.4 (2)	108.01(7)	107.8 (3)
	101.60(8)	101.3 (1)	101.5 (3)	105.8 (1)	104.49(9)	102.6 (2)	106.00(7)	105.6 (2)
	104.48(8)	104.2 (1)	104.4 (2)	103.9 (1)	102.27(9)	104.3 (2)	101.56(7)	101.4 (2)
Sn-N-C_{ipso} [b]	117.9 (3)	118.7 (5)	118.7 (8)	116.3 (3)	116.3 (3)	116.4 (7)	-	-
Sn-M-$C_{CO(ax)}$ [b]	177.7 (1)	177.6 (2)	177.5 (4)	177.8 (2)	178.2 (2)	177.9 (4)	175.6 (1)	175.1 (4)
Sn-M-$C_{CO(eq)}$ [b]	88.0 (1)	87.7 (2)	87.7 (4)	87.7 (2)	87.3 (2)	87.3 (4)	87.9 (1)	88.2 (4)
$C_{CO(eq)}$-M-$C_{CO(ax)}$ [b]	92.0 (1)	92.3 (2)	92.3 (6)	92.3 (2)	91.4 (2)	92.7 (6)	92.0 (2)	91.9 (5)
$C_{CO(eq)}$-M-$C_{CO(eq)}$ [b]	89.9 (1)	89.9 (2)	89.9 (6)	89.9 (2)	89.9 (2)	89.7 (5)	89.9 (1)	89.9 (5)
	174.5 (1)	173.9 (2)	173.6 (6)	175.2 (2)	174.5 (2)	174.4 (5)	175.2 (1)	175.3 (5)
N-C-C-N	12 (1)	10.5 (8)	11 (1)	2.1 (8)	0.4 (5)	1.5 (9)	-	-
torsion angle α [c]	25	24	24	40	40	40	44	44

[a] Estimated standard deviations in units of the least significant figures given in each case are quoted in parentheses. − [b] Average values; the standard deviations refer to the largest individual esd in each set. − [c] α refers to the torsion angle $C_{CO(eq)}-M-M-C_{CO(eq)}$ as defined in Figure 7.

The tin−metal distances in compounds **1a**−**1h** are very similar (Table 5) within each class (Sn−Cr, Sn−Mo, Sn−W) for the three types of compounds (**1a**−**1c**, **1d**−**1f**, **1g**, and **1h**). Within each individual compound the two tin−

metal distances are close of being even numerically equal. The geometric data characterizing the Sn−{M(CO)$_5$} entities in each compound are again very similar (Table 5). While the distances are appropriately modulated by the kind of metal (Cr, Mo, or W) the same general trends are found in all compounds. The axial metal−carbonyl bonds are without exception some 2−4 pm shorter than the equatorial ones (Table 5). The equatorial M−CO entities tend to bend towards the tin center with the Sn−M−C_{eq} angles somewhat smaller than 90° throughout, and consequently the C_{ax}−M−C_{eq} angles somewhat larger than 90° (Table 5). The torsion angles α [$C_{CO(eq)}$−M−M−$C_{CO(eq)}$, Figure 7] are as well similar within each class of compounds (**1a**−**1c**, **1d**−**1f**, **1g**, and **1h**). While for **1a**−**1c** a more eclipsed orientation with α ≈ 24° is found to be preferred, a more staggered conformation is observed for **1d**−**1f** (α ca. 40°) and for **1g** and **1h** (α ≈ 44°) (Table 5).

Figure 7. Newman projection of a compound of type **1**; view along the M−M axis

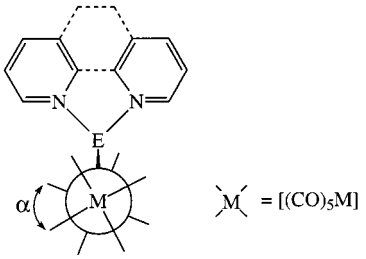

The Sn−N distances observed for **1a**−**1f** are close to their mean value of 229 pm within a few pm in all these compounds (Table 5). The quality of the data obtained for the tungsten compound **1c** is too low (Tables 10 and 11) to warrant a detailed discussion of individual differences; the same applies to the tungsten compound **1h**. A comparison of the 2,2′-bipyridine adduct **1a** and the bis-pyridine adduct **1g** suggests a somewhat weaker Sn−N interaction in **1g** (Sn−N: 232.0 pm) than in **1a** (Sn−N: 228.5 pm) (Table 5). The most apparent difference between the three classes of compounds (**1a**−**1c**, **1d**−**1f**, **1g**, and **1h**) is found in the angular distribution around the tin center: the M−Sn−M angles are close to 149° for the 2,2′-bipyridine adducts (Table 5) while they average at around 145° for the 1,10-phenanthroline adducts (Table 5). For the bis-pyridine adducts they are definitely smaller with values around 139° (Table 5).

The trend observed for the M−Sn−M angles is counterbalanced by an opposite trend in the N−Sn−N angles (Table 5, Figure 8): with 2,2′-bipyridine as the ligand this angle is constant at 71.3° (Table 5) within the limits of error for all three compounds **1a** −**1c**; with 1,10-phenanthroline (**1d**−**1f**) the angle stays at 72.4° (Table 5). For the bis-pyridine derivatives **1g** and **1h** angles of 86.5° (Table 5) are observed being again practically identical for the two compounds in this class. The rather small N−Sn−N angles observed for **1a**−**1c** and **1d**−**1f** are thus obviously a consequence of the chelate binding mode. While in the compounds **1g** and **1h** the two separate pyridine donors are

Figure 8. Correlation between the angles around the tin center

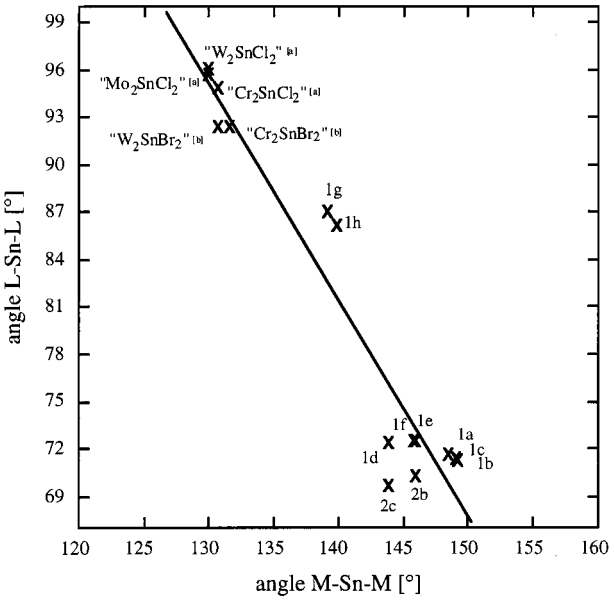

[a] Values for the chloride compounds [{(CO)$_5$M}$_2$SnCl$_2$]$^{2-}$ (M = Cr, Mo, W) are taken from ref.[3] − [b] Values for the bromide compounds [{(CO)$_5$M}$_2$SnBr$_2$]$^{2-}$ (M = Cr, W) are taken from ref.[4].

free to occupy the individually optimal positions, for the chemically related dianions [{(CO)$_5$M}$_2$SnHal$_2$]$^{2-}$ (M = Cr, Mo, W: Hal = Cl[3]; M = Cr, W: Hal = Br[4]), were two halide donors bind to the tin center, the angles Hal−Sn−Hal are around 94° so that it is propable to assume that an angle of around 90° is characteristic for an unstrained L−Sn−L arrangement in this type of compound. The trend apparent from the structures of **1a**−**1h** that a small N−Sn−N angle is accompanied by a large M−Sn−M angle is also apparent from the fact that the M−Sn−M angles observed for [{(CO)$_5$M}$_2$SnHal$_2$]$^{2-}$ are close to 131°[3][4]. The corresponding data for quite a number of compounds of the general formula [{(CO)$_5$M}$_2$SnL$_2$]^n (n = 0, L$_2$ = 2,2′-bipyridine, 1,10-phenanthroline, 2 pyridine, 2,2′-bipyrimidine; n = −2, L = Cl, Br) are collected in the diagram of Figure 8 which illustrates the correlation between M−Sn−M and L−Sn−L angles in this type of compounds.

d) Compounds 2 Containing Biimidazolato or 2,2′-Bipyrimidine Chelating Ligands

Since the bidentate chelate ligands 2,2′-bipyridine and 1,10-phenanthroline form the stable mononuclear adducts **1** bis-bidentate chelate bases should give dinuclear compounds. When disodium biimidazolate, $C_6H_4N_4Na_2$, is treated with [Na(THF)$_x$]$_2$[{(CO)$_5$Cr}$_2$SnCl$_2$][3][4] the dinuclear tin(0) compound **2a** is obtained (Scheme 1).

2a is separated from the reaction mixture by chromatographic workup. Crystals suitable for X-ray analysis are obtained by addition of 12-Crown-4 to a THF solution of **2a** followed by vapor diffusion from THF/diethyl ether/petroleum ether (boiling range 40−60°C).

Scheme 1. Reaction of $Na_2[\{(CO)_5Cr\}_2SnCl_2]$ with disodium biimidazolate

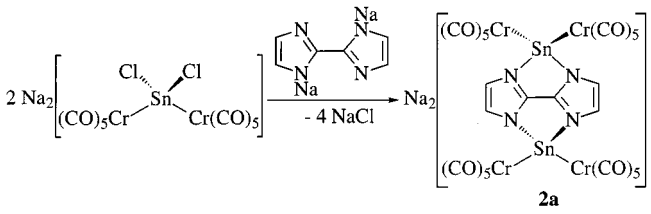

The IR-$\tilde{\nu}_{CO}$ spectrum in THF is consistent with the presence of $[(CO)_5Cr]$ groups (Table 4)[7]; in comparison with the IR-ν_{CO} spectra of **1a** and **1d** the absorption pattern observed for **2a** shows two additional resonances apparent as shoulders. The somewhat reduced local symmetry or some coupling between the individual $[(CO)_5Cr]$ chromophores may be the reason for this[7]. Relative to the absorptions observed for the neutral species **1a** and **1d** the center of gravity of the ν_{CO}-band pattern is shifted to slightly lower energies as expected.

The ^{1}H- and ^{13}C-NMR data of **2a** (see Experimental Section) are consistent with the ligand acting as a bis-bidentate chelate bridge.

A value of $\delta = 1149$ is observed for the ^{119}Sn-NMR resonance (Table 4) of **2a**. The ^{119}Sn-NMR shift is thus about 200 ppm upfield from the shifts observed for **1a** and **1d** and is close to the value observed for $[Ph_4P]_2[\{(CO)_5Cr\}_2SnCl_2]$ ($\delta = 924$)[4]. Even though no temperature-dependent ^{119}Sn-NMR data of **2a** could be obtained, the relatively strong high-field shift of the ^{119}Sn-NMR signal of **2a** suggests that there is no dynamic coordination/de-coordination equilibrium active for this compound.

Figure 9. Molecular structure of the dianion of **2a**

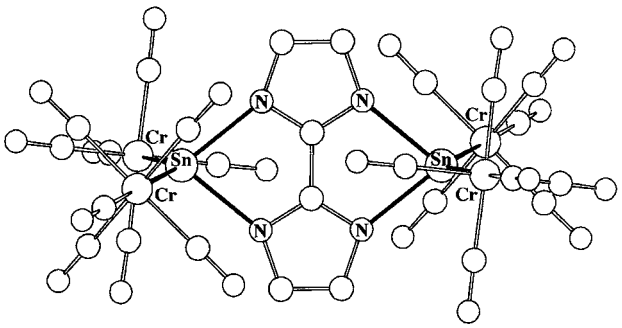

The X-ray analysis of **2a** (Tables 6 and 12, Figure 9) which is a centrosymmetric molecule in the solid state reveals the general type of bonding as inferred from the spectral data. The individual trends already discussed for compounds **1** are equally well seen in the structure of **2a** (Table 6). With respect to the diagram (Figure 8) correlating the bond angles M−Sn−M and N−Sn−N **2a** is an outlyer with values of 135° and 77°, respectively (Table 6) being found for **2a**. It is not clear whether it is the steric encumbrance in the dinuclear tin species **2a** or some peculiarity connected with the biimidazolato bridging ligand which causes this deviation.

Table 6. Selected bond lengths [pm], bond angles [°], and torsion angles [°] of compounds **2a**−**2c**[a]

$[(\{(CO)_5M\}_2Sn)_x(N\frown N)]^n$	**2a**·(12-Crown-4) M = Cr; $x = 2$; $n = -2$	**2b** M = Cr; $x = 1$; $n = 0$	**2c** M = W; $x = 1$; $n = 0$
M−Sn	260.1(1)	265.2(2)	275.2(1)
	262.1(2)	265.7(3)	275.4(1)
$M-C_{CO(ax)}$	183.2(9)	187(1)	196(2)
$M-C_{CO(eq)}$[b]	188.3(9)	191(3)	205(2)
Sn−N	229.2(5)	236.0(6)	231(1)
	226.9(5)	236.9(7)	234(1)
M−Sn−M	135.26(4)	146.05(5)	143.90(4)
N−Sn−N	77.2(2)	70.2(2)	69.6(4)
M−Sn−N	112.8(1)	101.2(2)	99.8(3)
	106.2(1)	104.7(2)	101.6(3)
	107.1(1)	101.3(2)	106.4(3)
	102.1(1)	107.9(2)	108.1(3)
$Sn-N-C_{ipso}$[b]	109.6(4)	118.4(5)	119.1(9)
$Sn-M-C_{CO(ax)}$	177.1(3)	179.1(5)	175.0(4)
$Sn-M-C_{CO(eq)}$[b]	86.7(2)	88.8(8)	87.4(5)
$C_{CO(eq)}-M-C_{CO(ax)}$[b]	93.3(4)	91.2(8)	92.6(7)
$C_{CO(eq)}-M-C_{CO(eq)}$[b]	89.8(3)	89(1)	89.9(7)
	173.3(3)	172(1)	174.2(7)
N−C−C−N torsion angle α[c]	0 33	6(1) 6	2(2) 10

[a] Estimated standard deviations in units of the least significant figures given in each case are quoted in parentheses. − [b] Average values; the standard deviations refer to the largest individual esd in each set. − [c] α refers to the torsion angle $C_{CO(eq)}-M-M-C_{CO(eq)}$ as defined in Figure 7.

Procedures analogous to the one which leads to the dinuclear compound **2a** with biimidazolate as the ligand gave, under the workup procedures applied to obtain compounds **1**, only the mononuclear species **2b** and **2c** with 2,2′-bipyrimidine (bpmd) as the potential bis-bidentate chelate ligand (Scheme 2).

Scheme 2. Reaction of $Na_2[\{(CO)_5M\}_2SnCl_2]$ (M = Cr, W) with 2,2′-bipyrimidine

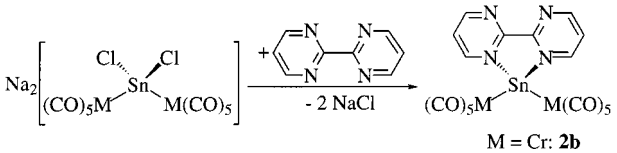

M = Cr: **2b**
M = W: **2c**

The IR-$\tilde{\nu}_{CO}$ data of **2b** and **2c** are in excellent qualitative accord with the corresponding data of compounds **1** (Table 4).

The mononuclearity of **2b** and **2c** is unequivocally proofed by X-ray analyses for both compounds (Tables 6 and 12, Figure 10). While the quality of the diffraction data obtained for the tungsten compound **2c** does not warrant a detailed discussion of individual geometric parameters the structure analysis of **2b** is of standard accuracy.

Since 2,2′-bipyridine is a direct analogue of 2,2′-bipyrimidine a comparison of structures **1a** and **2b** should be informative. Many of the general trends discussed for com-

Figure 10. Molecular structure of **2b**

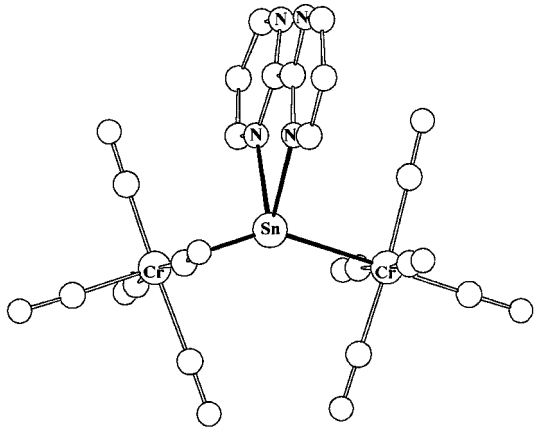

pounds **1** are as well observed for compounds **2** (Tables 5 and 6). The fact that the Cr−Sn bond is more than 3 pm longer than the one observed in **1a** (Table 5) has no explanation at the moment because at the same time the Sn−N distances in **2b** [236.5 (7) pm, Table 6] are definitely longer than the Sn−N bonds in the 2,2′-bipyridine derivative **1a** [228.5 (3) pm, Table 5]. Nevertheless, the angles characterizing the coordination at the tin center are very similar for both compounds as are the angles relevant to describe the coordination of the chromium centers in both compounds (Tables 5 and 6, Figure 9).

In contrast to the mononuclear structure of **2b** and **2c** the proton-NMR signals observed for these compounds at ambient temperature show a pattern (Figure 11) which indicates at least C_{2v} symmetry for the ligand surroundings while only C_s symmetry is possible with the static structure found in the solid state (Figure 10).

Figure 11. Temperature-dependent ^{1}H-NMR spectrum of **2c**

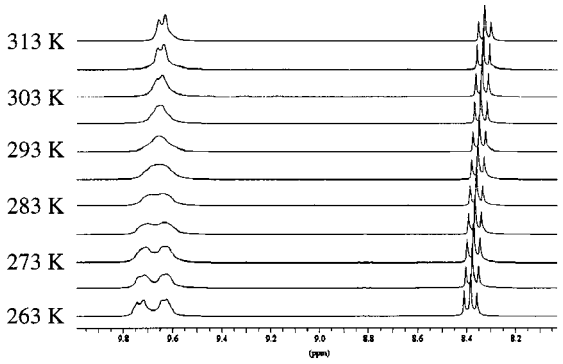

In the static structure the protons H_a and H_c (see insert, Table 2) have definitely different environments, while they give rise to only one broad signal at 298 K (Figure 11, $\delta \approx 9.6$). By variable-temperature NMR measurements (Figure 11) it is shown that upon cooling two doublets evolve from this envelope which are clearly resolved at 263 K (Figure 11). The appearance of the spectra at low temperatures thus corresponds to the static C_s-symmetric structure as is observed in the solid state (Figure 10). At higher temperatures the broad envelope observed at 298 K sharpens and a clear doublet is apparent at 313 K (Figure 11) indicating C_{2v} symmetry in the time average. The process which gives rise to this temperature dependence is then one which equilibrates all the four donor positions of the 2,2′-bipyrimidine ligand in **2c**.

According to the discussions made in the previous parts of this paper the most propable equilibration pathway is the one where one Sn−N bond is opened thus allowing the now uncoordinated pyrimidyl residue to rotate. Recoordination of this pyrimidyl entity necessarily leads to the equilibration of its donor functions. With the same type of process operating for the other pyrimidyl part of the chelate ligand all four donor positions are equilibrated on the time average. The coalescence temperature for this process as observed for **2c** (Figure 11) is around 288 K corresponding to an activation barrier of around 61±1 kJ/mol[22]. The same type of ^{1}H-NMR observation is made for **2b** with a coalescence temperature of 293 K. The activation energy (64±1 kJ/mol) is the same within the limits of error as the one found for **2c**. These energies refer to a process different from the one discussed in connection with the dynamic behavior of **1**: the process discussed there for 2,2′-bipyridine or 1,10-phenanthroline derivatives, respectively, involved nothing but a wagging motion of the chelate ligands with one of the nitrogen donors remaining tightly bound and the other one just shifting away from the tin by some 50 pm (Sn···N ca. 284 pm) without completely loosing the contact to its tin neighbor (type **C**, Figure 4). In the case of **2b** and **2c** this contact is completely lost by a full 180° rotation of the ring. Such a rotation is not possible for 1,10-phenanthroline and the observation that the 1,10-phenanthroline derivative **1e** behaves quite like the 2,2′-bipyridine derivative **1a** (vide supra) lends quite some credit to the interpretation of the dynamic processes in these cases. For **2b** and **2c** one Sn−N bond is completely broken and EHT calculations performed on [{(CO)$_5$Cr}$_2$Sn(bipy)] (**1a**) as a model compound suggest that quite some additional energy is needed for this process of completely breaking the bond.

The ^{13}C-NMR data of **2b** and **2c** are formally in accord with the static structure as observed in the solid state (Figure 10) and individual signals are observed for every type of chemically different carbon atoms (Table 3). This is due to the different time window of ^{1}H- and ^{13}C-NMR spectroscopy and especially to the large difference in resonance frequency of C_a and C_c (Table 3)[23]. At 313 K the resonances of C_a and C_c have just started to fade away yet without a time averaged signal being apparent. Further heating is precluded by the low boiling point of the [D$_6$]acetone solvent used.

The type of dynamic process as discussed for the 2,2′-bipyridine and 1,10-phenanthroline adducts **1** should likewise be apparent for **2b** and **2c** (Figure 12). In these cases the weakening of one of the two Sn−N bonds at each tin center should be a low lying pre-equilibrium step with reference to the complete bond breaking and rotation process which is evident by the coalscence experiments discussed above. If no further deep energy minima are met along the reaction coordinate of bond breaking and ring rotation −

Figure 12. Temperature-dependent ^{119}Sn-NMR spectrum of **2c**

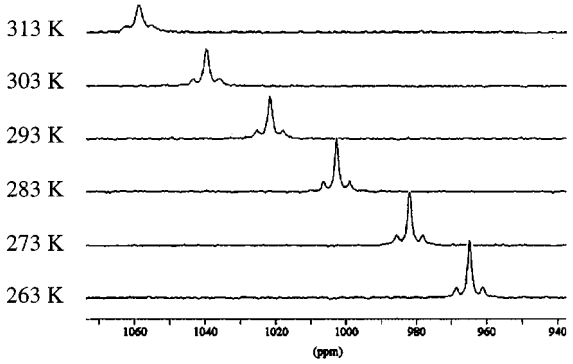

as is evident by the ^{1}H-NMR data – this additional dynamic process will not mirror itself into the temperature dependence of the ^{119}Sn-NMR spectrum and this is what is indeed observed. Fitting equation 1 as discussed for **1a** and **1e** to the shift values observed at different temperatures (Figure 12) for **2c** leeds to the values $\delta_B = 800$, $\delta_C = 3600$ and $\Delta G = 6$ kJ/mol with B and C refering to the use of the symbols in Figure 4. These values are in good agreement to the ones obtained for **1a** and **1e**.

Observations made for $[\{(CO)_5M\}_2SnCl_2]^{2-}$ (M = Cr, Mo, W) lend some additional credit to the above reasoning: the ^{119}Sn-NMR resonances of the salt $[Ph_4P]_2[\{(CO)_5Cr\}_2SnCl_2]$[4] occurs at $\delta = 924$ with a only slight temperature dependence as generally induced by solvation processes (Figure 13, B).

Figure 13. Comparison of the temperature dependence of the ^{119}Sn-NMR resonances of $[Na(solv)_x]_2[\{(CO)_5Cr\}_2SnCl_2]$ (A) and $[Ph_4P]_2[\{(CO)_5Cr\}_2SnCl_2]$ (B)

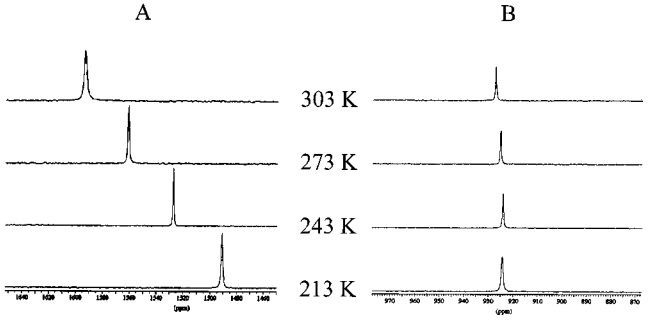

The disodium salt of the same dianion on the other hand shows a ^{119}Sn-NMR resonance which is strongly temperature dependent (Figure 13, A). The shift values observed between 213 K and 303 K span a range between $\delta = 1593$ and $\delta = 1490$. The IR-ν_{CO} absorptions of these two salts are different as well[4] with the absorption pattern observed for the disodium salt occuring at higher energies as compared to the one of the $[Ph_4P]$ salt[4]. A clue as to what the reason for these differences might be comes from the following observation: when THF solutions of the $[Ph_4P]_2[\{(CO)_5M\}_2SnCl_2]$ are treated with an equimolar amount of $CdCl_2$ the infrared band pattern changes to the one characteristic for the disodium salts $([Na(THF)_x]_2[\{(CO)_5M\}_2SnCl_2]$: $\tilde{\nu}_{CO}$ (THF): M = Cr: 2040 w, 2007 s, 2000 sh, 1920 vs, 1895 sh cm^{-1}, Figure 2; M = Mo: 2051 vw, 2025 s, 1949 sh, 1929 vs, 1901 s; M = W: 2052 w, 2027 m 1926 vs, 1894 s). The ^{119}Sn-NMR spectrum of solution of $[Ph_4P]_2[\{(CO)_5W\}_2SnCl_2 \cdot CdCl_2]$ for example taken at 300 K shows a signal at $\delta = 1250$, very similar to the one observed for the disodium salt ($\delta = 1268$). It is plausible to assume that $CdCl_2$ will interact with the $SnCl_2$ part of the dianion by association with the chlorine functions to produce an adduct of type **D** (Figure 14)

Figure 14. Possible form of an association between $[Ph_4P]_2[\{(CO)_5M\}_2SnCl_2]$ (M = Cr, Mo, W) and $CdCl_2$

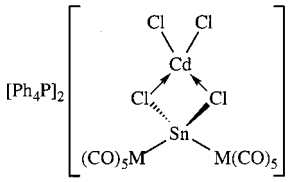

D

Several forms of association are of course conceivable with the extreme of a complete separation of the adduct into the two anions "$[CdCl_3]^-$" and $[\{(CO)_5Cr\}_2SnCl]^-$. The observed shift in the IR-ν_{CO} absorptions (vide supra) fits into this idea as does the observation that the ^{119}Sn-NMR spectra of $[Ph_4P]_2[\{(CO)_5M\}_2SnCl_2 \cdot CdCl_2]$ are strongly temperature-dependent while the ones of $[Ph_4P]_2[\{(CO)_5M\}_2SnCl_2]$ are not. Fitting the NMR data of $[Ph_4P]_2[\{(CO)_5W\}_2SnCl_2 \cdot CdCl_2]$ to an equilibrium of this type leads to a ΔG value of 5 kJ/mol for the relevant process and values of $\delta_B = 1000$ and $\delta_C = 3200$ with respect to Equation 1. These values are not to different from the ones estimated for a comparable equilibrium in the case of compounds **1** and **2**.

If THF solutions of $[Ph_4P]_2[\{(CO)_5M\}_2SnCl_2]$ are treated with equimolar amounts of $CoCl_2$, $FeCl_2$, or $MnCl_2$ the IR-ν_{CO} absorption pattern shifts accordingly with the resulting spectrum being equal to the one observed when $CdCl_2$ is used as the halide abstractor and altogether equal to the one observed for THF-solutions of $[Na(THF)_x]_2[\{(CO)_5M\}_2SnCl_2]$. When, on the other hand, solutions of $Na_2[\{(CO)_5M\}_2SnCl_2]$ in THF are treated with a large excess of [2.2.2]-Cryptand the IR-ν_{CO} absorption pattern as well as the ^{119}Sn-NMR resonances shift to the value characteristic for $[Ph_4P]_2[\{(CO)_5M\}_2SnCl_2]$[4]: the encrypted sodium ion can no longer act as a halide abstractor. Any attempts to isolate the product $[\{(CO)_5M\}_2SnCl]^-$ formed by halide abstraction from $[\{(CO)_5M\}_2SnCl_2]^{2-}$ have failed so far. The isolation of $[Ph_4P]_2[Zn_2Cl_6]$[24] from the reaction of $[Ph_4P]_2[\{(CO)_5Cr\}_2SnCl_2]$ and $ZnCl_2$ does however show that chloride abstraction is in fact occuring with the $ZnCl_2$ reagent.

e) Analogous Compounds with Germanium and Lead

The germanium analogue **3a** of **1a** is prepared from the reaction of $Na_2[Cr_2(CO)_{10}]$ with GeI_2 in the presence of

2,2′-bipyridine. The same procedure when performed with 1,10-phenanthroline instead of 2,2′-bipyridine as the chelating ligand leads to **3b** the germanium analogue of **1d** (Scheme 3).

Scheme 3. Reaction of $Na_2[Cr_2(CO)_{10}]$ with GeI_2 in the presence of a chelate ligand

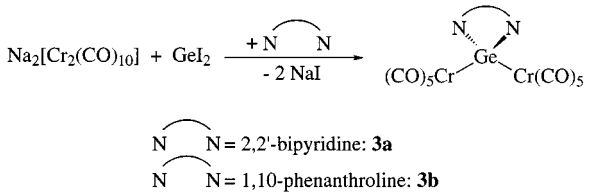

The lead analogue **4** of **1a** is accessible by the reaction of $[\{(CO)_5Cr\}_2Pb(OOCCH_3)_2]^{2-}$ [4] with 2,2′-bipyridine (Scheme 4).

Scheme 4. Reaction of the disodium salt $[\{(CO)_5Cr\}_2Pb(OOCCH_3)_2]^{2-}$ with 2,2′-bipyridine

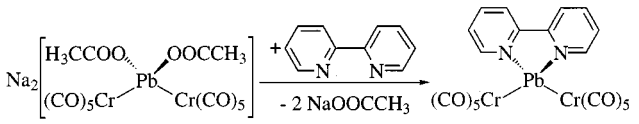

All three compounds are characterized by IR-$\tilde{\nu}_{CO}$, ^{1}H-NMR, and ^{13}C-NMR spectroscopy (Tables 2−4). The NMR shifts observed relative to the resonances of the free ligands clearly indicate a chelate type coordination in each case (Tables 2 and 3). The ^{1}H-NMR pattern observed for the resonances of the 2,2′-bipyridine ligands in the series of the germanium, tin, and lead compounds (**3a**, **1a**, and **4**) are compared to the ^{1}H-NMR pattern observed for the free ligand in Figure 15.

Figure 15. Comparison of the ^{1}H-NMR spectra of $[\{(CO)_5Cr\}_2E(bipy)]$ (E = Ge: **3a**; E = Sn: **1a**; E = Pb: **4**) with the ^{1}H-NMR spectrum of free 2,2′-bipyridine

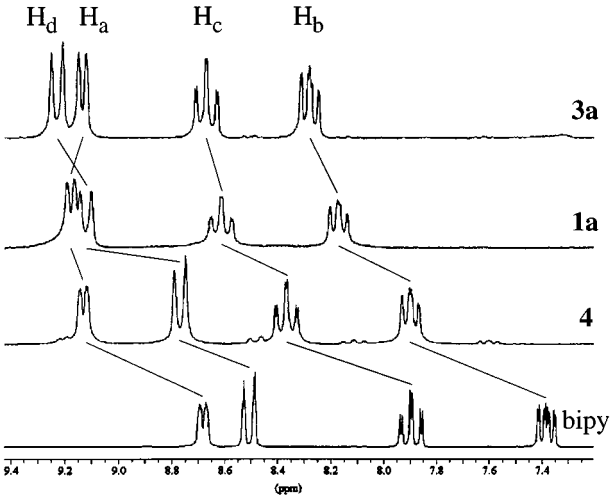

It is seen that the low-field shift upon coordination is smallest for the lead compound **4** and largest for the germanium compound **3a** (Table 2, Figure 15). This may be taken as an indication of the continuously stronger interaction between the main group center and the 2,2′-bipyridine ligand going from lead to germanium. An interesting special feature apparent from Figure 15 is that the signals originating from H_a and H_d change their relative position with respect to one another when going from the tin (**1a**) to the germanium compound **3a**. This type of observation had already been made with other coordination compounds of 2,2′-bipyridine and 1,10-phenanthroline and has prompted to some tentative explanations[20].

Table 7. Selected bond lengths [pm], bond angles [°], and torsion angles [°] of compounds **3a**−**4**[a]

$[\{(CO)_5Cr\}_2EL_2]$	**3a**/1 E = Ge L_2 = bipy	**3a**/2 E = Ge L_2 = bipy	**3b** E = Ge L_2 = phen	**4** E = Pb L_2 = bipy
Cr−E	247.1(3)	247.9(3)	247.5(1)	265.8(2)
	247.2(3)	249.6(3)	−	265.8(2)
$Cr-C_{CO(ax)}$[b]	186(1)	186(1)	184.5(7)	187.0(2)
$Cr-C_{CO(eq)}$[b]	187(1)	187(1)	187.8(8)	189.7(2)
E−N	206.1(9)	204.6(9)	206.9(4)	244(1)
	204.3(9)	205(1)	−	241(1)
Cr−E−Cr	133.26(9)	136.64(1)	137.94(5)	155.47(8)
N−E−N	76.7(3)	76.8(4)	78.1(2)	67.4(4)
Cr−E−N	103.7(3)	105.5(3)	104.4(1)	100.7(3)
	108.8(3)	108.8(3)	108.0(1)	99.4(3)
	112.1(3)	103.7(3)	−	99.4(3)
	107.8(3)	108.5(3)	−	101.2(3)
$E-N-C_{ipso}$[b]	118.1(8)	117.8(8)	115.0(4)	120.2(9)
$E-Cr-C_{CO(ax)}$[b]	174.7(5)	174.7(5)	177.9(2)	175.8(5)
$E-Cr-C_{CO(eq)}$[b]	88.9(5)	88.9(5)	88.0(2)	88.3(5)
$C_{CO(eq)}-Cr-C_{CO(ax)}$[b]	91.2(6)	91.2(6)	92.0(3)	91.8(7)
$C_{CO(eq)}-Cr-C_{CO(eq)}$[b]	90.0(6)	90.0(6)	89.9(3)	90.0(7)
	176.3 (7)	176.3(7)	175.7(7)	175.0(7)
N−C−C−N	7(1)	4(1)	0	16(1)
torsion angle α[c]	19	40	42	25

[a] Estimated standard deviations in units of the least significant figures given in each case are quoted in parentheses. − [b] Average values; the standard deviations refer to the largest individual esd in each set. − [c] α refers to the torsion angle $C_{CO(eq)}-M-M-C_{CO(eq)}$ as defined in Figure 7.

The structures of **3** and **4** have been determined by X-ray crystallography (Tables 7 and 13). The overall geometry closely corresponds to the one observed for the other 2,2′-bipyridine and 1,10-phenanthroline compounds described in this paper. The structures will therefore be discussed with implicit reference to Figure 2 which shows the general structural pattern with respect to the $[\{(CO)_5Cr\}_2Sn(L_2)]$ analogues **1a** and **1d**. The crystal of **3a** contains two crystallographically independent molecules designated as **3a**/1 and **3a**/2 in Table 7. The only very minor deviations in the scalar properties of the two crystallographically independent species **3a** (Table 7) demonstrate that the structures are to a very large extent determined by the inner molecular potential and not strongly influenced by the outer forces caused by the potential imposed onto the molecules by the crystal lattice. On the other hand the torsion angles characterizing the skew of the arrangement of the equatorial carbonyl groups of the $[(CO)_5Cr]$ entities relative to each other is different in the two individual molecules of **3a** (Table 7). This means that the corresponding torsional mode is a very soft one as expected. The Ge−N distances observed in **3a** (205 pm) are significantly shorter than the ones found in its

analogue [{Cp′(CO)$_2$Mn}$_2$Ge(bipy)] (Ge−N: 211.5 pm)[5]. The same trend is observed for the 1,10-phenanthroline compound **3b** (**3b** has crystallographic C_2 symmetry) with an Ge−N distance of 206.9 pm versus the equivalent distance in [{Cp′(CO)$_2$Mn}$_2$Ge(phen)] of 216.8 pm[6]. The Pb−N distances in the lead compound **4** fit to this trend as well. Due to absorption effects the structure analysis is not very accurate but it is still beyond doubt that the Pb−N distances in **4** (243 pm, Table 7) are significantly shorter than the ones found in [{Cp′(CO)$_2$Mn}$_2$Pb(bipy)] (Pb−N: 255.7 pm)[5]. An explanation for this trend based on the different π-donor capabilities of [Cp′(CO)$_2$Mn] versus [(CO)$_5$Cr] has already been given above. Yet another trend is seen when comparing the data collected in Tables 5 and 7: the M−E−M angle systematically increases along the series of germanium, tin, and lead compounds. This trend is as well apparent from the data known for the [Cp′(CO)$_2$Mn] analogues of **1a**, **3a**, and **4**[5][6] and their isoelectronic cationic analogues [{Cp′(CO)$_2$Mn}$_2$E(bipy)]$^+$ (E = As[25], Sb[25], Bi[26]).

f) Cyclovoltammetry of Compounds 1a−3b

Cyclovoltammetric data have been obtained (see Experimental Section) for all compounds but **4** and are listed in Table 8.

Table 8. Cyclovoltammetric data[a]

	Reduction		Oxidation	
1a	−1.16 rev.	−1.70 qrev.	+0.84 qrev.	+1.17 irrev.
1b	−1.22 rev.	−1.80 rev.	+0.70 irrev.	+1.08 irrev.
1c	−1.20 rev.	−1.76 rev.	+0.86 irrev.	+1.10 irrev.
1d	−1.16 irrev.	−	+0.84 qrev.	−
1e	−1.21 irrev.	−2.00 irrev.	+0.68 irrev.	−
1f	−1.20 irrev.	−	+0.83 irrev.	+1.09 irrev.
1g	−1.40 irrev.	−2.16 irrev.	+0.56 irrev.	+0.85 rev.
1h	−1.43 irrev.	−	+0.57 irrev.	+0.97 irrev.
2a	−	−	+0.54 irrev. +0.67 irrev.	+0.89 irrev.
2b	−0.86 rev.	−1.87 qrev.	+0.85 qrev.	−
2c	−0.92 rev.	−1.81 qrev.	+0.89 irrev.	+1.08 irrev.
3a	−1.09 rev.	−1.70 rev.	+0.78 irrev.	+0.85 qrev.
3b	−1.09 irrev.	−	+0.79 irrev.	+0.89 qrev.
4	−	−	−	

[a] Pt/SCE electrode/nBu$_4$NPF$_6$/CH$_3$CN; see Experimental Section.

A first reductive electron transfer occurs in the region between −0.8 and −1.4 V. Although the redox processes are only in part fully reversible a comparison of the observed potentials is revealing. For a given set of ligands reductions are found at closely similar values independent of the [(CO)$_5$M] groups to which the main-group center is bonded (compare: **1a**−**1c**, L$_2$ = bipy, −1.2 V; **1d**−**1f**, L$_2$ = phen, −1.2 V; **1g**−**1h**, L$_2$ = 2 py, −1.4 V; **1a**−**1c**, L$_2$ = bpmd, −0.9 V). Furthermore, the potential at which reduction occurs does appear to be independent of the kind of main-group center (compare: **1a**, Sn, L$_2$ = bipy, −1.2 V; **3a**, Ge, L$_2$ = bipy, −1.1 V). These observations indicate that the LUMO in all the compounds is ligand centered. Even the second reduction waves (Table 8) conform to this statement. Although some of the comparisons made are not completely sound on a thermodynamic basis due to partially irreversible electron transfer processes (Table 8) the trends are altogether clear. A reliable comparison can be made for **1a** (L$_2$ = bipy) and **2b** (L$_2$ = bpmd) because in each case the first reduction is fully reversible with the second one being quasireversible. It is observed that the first reduction of **1a** is by 30 kJ/mol more difficult than the first reduction of **2b**. The difference in electron affinity of the 2,2′-bipyridine versus the 2,2′-bipyrimidine ligand is mirrored by these data which again is in favour of the conclusion that the LUMO is ligand centered in each case.

While the reduction is thus ligand-centered the oxidation of the compounds **1a**−**3b** appears to be metal-centered: independent of the ligand but slightly dependent on the metal the oxidation waves are observed in the range of 0.7−1.0 V. In most cases the first oxidation wave occurs in this range (Table 8). In the case of **1g** and **1h**, where two pyridine molecules act as the L$_2$ donor set, the first irreversible oxidation is found at a lower potential of around 0.6 V already while the second one is again in the range discussed above. It is assumed that the first irreversible oxidation wave refers to the species which result from **1g** and **1h** by loss of one pyridine ligand. The corresponding dissociation equilibrium is evident from NMR and has been explained above. With the biimidazolato bridging ligand, species **2a**, which undergoes no reduction in the potential range studied, three oxidation waves are observed, all of them irreversible. But the last one with 0.9 V (Table 8) again being in the range characteristic of all the other compounds where this complication by several oxidation steps does not occur. Comparison of the oxidation potentials observed for **1a** (Sn) and **3a** (Ge) shows that the observed potentials are also practically independent of the main-group center. Taken together these findings indicate that the HOMO of the compounds is metal-centered with the exception of the dianionic compound **2a**.

Concluding Remarks

It is shown that even though the cumulene-type compounds [(CO)$_5$M=E=M(CO)$_5$] (E = Ge, Sn, Pb; M = Cr, Mo, W) are not yet known in the free state, their base adducts [{(CO)$_5$M}$_2$E(L$_2$)] are stable and well-characterized compounds. Their structures as determined by X-ray crystallography reveal a common bonding pattern for all the compounds of this type. By comparison of a series of compounds of the type [{(CO)$_5$M}$_2$Sn(L$_2$)] it is demonstrated that in an unstrained compound the angle sustained at the tin center by the donors of L$_2$ should be close to 90°. The M−E−M angles (E = Ge, Sn, Pb) are in the range between 133° and 155° systematically increasing from E = Ge over E = Sn to E = Pb. From NMR-spectroscopic data of the corresponding 2,2′-bipyridine adducts [{(CO)$_5$Cr}$_2$E(bipy)] it is inferred that the bonding interaction between the chelate ligand and the main-group element decreases in the series E = Ge to E = Pb. The temperature dependence of the ^{119}Sn-NMR shifts observed for compounds **1** and **2** is consistently interpreted in terms of an equilibrium [{(CO)$_5$M}$_2$E(L$_2$)] ⇌ [{(CO)$_5$M}$_2$E(L)] + L. With 2,2′-bi-

pyrimidine as a spectroscopic probe in $[\{(CO)_5M\}_2Sn(bpmd)]$ (M = Cr, W) this process of partial de-coordination is more directly evident from dynamic ^{1}H-NMR spectroscopy.

The financial support by the *Deutsche Forschungsgemeinschaft* (SFB 247) and the *Fonds der Chemischen Industrie* is gratefully acknowledged.

Experimental Section

General: All manipulations were carried out under argon by means of standard Schlenk techniques at 20°C unless mentioned otherwise. All solvents were dried by standard methods and destilled under argon. [D$_6$]acetone used for the NMR spectroscopic measurements was degassed by three successive "freeze-pump-thaw" cycles and dried over 4-A molecular sieves. Silica gel (Kieselgel z. A. 0.06−0.2 mm, J. T. Baker Chemicals B.V.) used for chromatography and Kieselgur (Kieselgur, gereinigt, geglüht, Erg. B.6, Riedel de Haen AG) used for filtration were degassed at 1 mbar at 180°C for 12 h and saturated with argon. − NMR: Bruker Avance DPX 200 at 200.13 MHz (^{1}H), 50.323 MHz (^{13}C{^{1}H}), 74.631 MHz (^{119}Sn{^{1}H}); chemical shifts (δ) in ppm with respect to [D$_6$]-acetone (^{1}H: δ = 2.04; ^{13}C: δ = 29.8) as internal standards and to $SnMe_4$ (^{119}Sn: δ = 0 at 25°C), respectively, as external standard. − IR: Bruker FT-IR IFS-66; CaF_2 cells. − UV/Vis/NIR: Perkin Elmer Lambda 19; cells (0.2 cm; Hellma 110 suprasil). − MS (FAB or EI): Finnigan MAT 8400; Nibeol (4-nitrobenzyl alcohol) or TEA (triethanol amine) matrices, respectively. − Elemental analyses: microanalytical laboratory of the Organisch-Chemisches Institut, Universität Heidelberg. − Melting points: Gallenkamp MFB-595 010; the values are not corrected. − Cyclic voltammetry: Methrohm "Universal Meß- und Titriergefäß", Methrohm GC electrode RDE 628, platinum electrode, SCE electrode, Princeton Applied Research potentiostat Model 273, 10^{-3} M in 0.1 M nBu$_4$NPF$_6$/CH_3CN. − The dinuclear sodium salts of the composition $Na_2[\{(CO)_5M\}_2EX_2]$ (E = Sn: M = Cr, Mo, W; X = Cl; E = Pb: M = Cr; X = $OOCCH_3$) were prepared by salt metathesis reaction from the corresponding stable phosphonium salts $[Ph_4P]_2[\{(CO)_5M\}_2EX_2]$ as described[4]. The biimidazole[27] and the metallates $Na_2[M_2(CO)_{10}]$ (M = Cr, Mo, W) were prepared as reported[28]. All other chemicals were commercially obtained and used without further purification.

Bis(pentacarbonylchromium)(2,2′-bipyridine)tin, [{(CO)$_5$Cr}$_2$-Sn(bipy)] (**1a**), *and Bis(pentacarbonylchromium)(1,10-phenanthroline)tin, [{(CO)$_5$Cr}$_2$Sn(phen)]* (**1d**): $Na_2[\{(CO)_5Cr\}_2SnCl_2]$ (310 mg; 0.5 mmol) was dissolved in THF (30 ml) and solid 2,2′-bipyridine (78 mg; 0.5 mmol) or solid 1,10-phenanthroline (90 mg; 0.5 mmol), respectively, was added in one portion. The clear orange solution turned deep red immediately. After stirring for 30 min, the solvent was removed in vacuo. The resulting red oil was dissolved in THF (3 ml) and chromatographed on silica gel (20 cm; Ø = 3 cm; diethyl ether). Elution with diethyl ether gave two bands. The first yellow band was identified by IR spectroscopy to be $[Cr(CO)_6]$[29]. The second pink band was also characterized by spectroscopic comparison (IR[30], ^{1}H-, and ^{13}C-NMR spectra) and found to be $[(CO)_4Cr(bipy)]$ or $[(CO)_4Cr(phen)]$, respectively. A third red-brown band which contained the compound **1a** or **1d** was eluted with THF. The resulting solution was taken to dryness leaving **1a** (230 mg; 71%) or **1d** (230 mg; 68%), respectively, as red solids. Single crystals of **1a** and **1d** were obtained within 3 d by applying the method described below.

Bis(pentacarbonylmolybdenum)(2,2′-bipyridine)tin, [{(CO)$_5$Mo}$_2$-Sn(bipy)] (**1b**), *and Bis(pentacarbonylmolybdenum)(1,10-phenanthroline)tin, [{(CO)$_5$Mo}$_2$Sn(phen)]* (**1e**): A yellow solution of $Na_2[\{(CO)_5Mo\}_2SnCl_2]$, obtained by salt metathesis reaction of $[Ph_4P]_2[\{(CO)_5Mo\}_2SnCl_2]$ (1340 mg; 1 mmol) with $Na[BPh_4]$ (684 mg; 2 mmol)[4], was filtered through Kieselgur (3 cm) into a Schlenk tube which already contained solid 2,2′-bipyridine (156 mg; 1 mmol) or solid 1,10-phenanthroline (180 mg; 1 mmol), respectively. The resulting deep red solution was filtered through Kieselgur (3 cm) and taken to dryness. The resulting red oil was redissolved in THF (3 ml) and slowly chromatographed (max. 50 drops/min) on silica gel (20 cm; Ø = 3 cm; diethyl ether). Two bands were obtained by elution with diethyl ether. The first yellow band was identified by IR spectroscopy to be $[Mo(CO)_6]$[29]. The second pink band was also characterized by spectroscopic comparison (IR[30], ^{1}H-, and ^{13}C-NMR spectra) and found to be $[(CO)_4Mo(bipy)]$ or $[(CO)_4Mo(phen)]$, respectively. A third red-brown band, containing the compound **1b** or **1d**, was eluted with THF. From the red-brown solution 310 mg (41%) of **1b** or 290 mg (38%) of **1d**, respectively, were obtained by removing the solvent in vacuo. Applying the method described below gave single crystals of **1b** and **1d** within 3 d.

Bis(pentacarbonyltungsten)(2,2′-bipyridine)tin, [{(CO)$_5$W}$_2$-Sn(bipy)] (**1c**), *and Bis(pentacarbonyltungsten)(1,10-phenanthroline)tin, [{(CO)$_5$W}$_2$Sn(phen)]* (**1f**). − *Method A:* The disodium salt $Na_2[\{(CO)_5W\}_2SnCl_2]$ (442 mg; 0.5 mmol) was dissolved in THF (30 ml). Solid 2,2′-bipyridine (78 mg; 0.5 mmol) or solid 1,10-phenanthroline (90 mg; 0.5 mmol), respectively, was added in one portion. The orange solution turned deep red immediately. After stirring for 30 min, the solvent was evaporated in vacuo. The oily red residue was redissolved in THF (3 ml) and chromatographed on silica gel (20 cm; Ø = 3 cm; diethyl ether). Elution with diethyl ether gave two bands. The first yellow band was found to contain $[W(CO)_6]$, the second pink band contained $[(CO)_4W(bipy)]$ or $[(CO)_4W(phen)]$, respectively. These compounds were characterized by comparison of spectroscopic data[29][30] (IR, ^{1}H-, and ^{13}C-NMR spectra). **1c** or **1f** were eluted with THF as a third red-brown band. The resulting solution was taken to dryness leaving 310 mg (67%) of **1c** or 350 mg (71%) of **1f**, respectively, as red microcrystalline powders.

Method B: To a stirred orange solution of the disodium metallate $Na_2[W_2(CO)_{10}]$ (347 mg; 0.5 mmol) in ethanol (30 ml) was added solid $SnCl_2$ (95 mg; 0.5 mmol) in one portion. The solution turned deep red immediately. After stirring for 30 min, the solution was filtered through Kieselgur (3 cm). By addition of solid 2,2′-bipyridine (78 mg; 0.5 mmol) or solid 1,10-phenanthroline (90 mg; 0.5 mmol), respectively, the corresponding chelate complex precipitated. After additional stirring for 30 min, the red solid was separated from the mother liquor by filtration, washed with ethanol (2 × 5 ml) and diethyl ether (2 × 5 ml), and taken to dryness. Yields: **1c**: 260 mg (57%); **1f**: 270 mg (56%).

Single crystals of **1c** or **1f** were obtained within 3 d by applying the method described below.

Bis(pentacarbonylchromium)bis(pyridine)tin, [{(CO)$_5$Cr}$_2$-Sn(py)$_2$] (**1g**), *and Bis(pentacarbonyltungsten)bis(pyridine)tin, [{(CO)$_5$W}$_2$Sn(py)$_2$]* (**1h**): To a stirred orange solution of $Na_2[\{(CO)_5Cr\}_2SnCl_2]$ (620 mg; 1 mmol) or $Na_2[\{(CO)_5W\}_2SnCl_2]$ (884 mg; 1 mmol), respectively, was added pyridine (316 mg; 4 mmol) in one portion. No colour change of the solution was observed upon the addition. After 30 min of stirring, the solution was

Table 9. Selected analytical data

	m.p. / °C	MS; *m/z* (%) [fragment]	UV / nm (THF) λ_{max} (ε)	mol. formula (mol. mass)	elemental analysis
1a	236 (dec.)	-	288 (32000); 448 (900)	$C_{20}H_8Cr_2N_2O_{10}Sn$ (659.0)	calcd. C 36.45 H 1.22 N 4.25 found C 36.64 H 1.40 N 4.22
1b	211 (dec.)	747 (100) [M^+]	306 (48600); 353 (13000, sh); 408 (4000); 485 (3500)	$C_{20}H_8Mo_2N_2O_{10}Sn$ (746.9)	calcd. C 32.17 H 1.08 N 3.75 found C 32.10 H 1.42 N 3.75
1c	145 (dec.)	-	287 (28700); 417 (3200); 464 (1100, sh)	$C_{20}H_8N_2O_{10}SnW_2$ (922.7)	calcd. C 25.92 H 1.09 N 3.02 found C 27.30 H 1.09 N 2.81
1d	228	683(18) [M^-]	280 (40000); 449 (1800, br)	$C_{22}H_8Cr_2N_2O_{10}Sn$ (683.9)	calcd. C 38.69 H 1.18 N 4.10 found C 37.37 H 2.06 N 3.99
1e	195 (dec.)	-	294 (26800); 307 (24400); 352 (7200, sh); 404 (3600); 478 (2900)	$C_{22}H_8Mo_2N_2O_{10}Sn$ (770.9)	calcd. C 34.28 H 1.05 N 3.63 found C 34.35 H 1.20 N 3.71
1f	212 (dec.)	946 (85) [M^-]	423 (3200); 485 (3000)	$C_{22}H_8N_2O_{10}SnW_2$ (946.7)	calcd. C 27.91 H 0.85 N 2.96 found C 28.03 H 0.90 N 2.96
1g	141 (dec.)	-	298 (17000); 378 (2600, sh)	$C_{20}H_{10}Cr_2N_2O_{10}Sn$ (661.0)	calcd. C 36.34 H 1.52 N 4.24 found C 35.97 H 2.47 N 3.51
1h	100 (dec.)	-	305 (16000); 405 (2300, sh)	$C_{20}H_{10}N_2O_{10}SnW_2$ (924.7)	calcd. C 25.98 H 1.09 N 3.03 found C 26.00 H 1.17 N 3.03
2a	178 (dec.)	-	293 (21000); 362 (1900, sh)	$C_{58}H_{68}Cr_4N_4Na_2O_{36}Sn_2$ (1888.5)	calcd. C 36.89 H 3.63 N 2.97 found C 34.45 H 3.57 N 2.47
2b	249 (dec.)	606 (28) [(M - 2 CO) $^-$]	285 (26000, sh) 331 (6800); 442 (2000)	$C_{18}H_6Cr_2N_4O_{10}Sn$ (660.9)	calcd. C 32.71 H 0.92 N 8.48 found C 32.76 H 1.06 N 8.44
2c	175 (dec.)	-	286 (24800); 345 (8300, sh); 419 (2600, sh); 469 (1500, sh)	$C_{18}H_6N_4O_{10}SnW_2$ (924.7)	calcd. C 23.38 H 0.65 N 6.06 found C 24.22 H 1.10 N 5.97
3a	255	613 (25) [M^-]	295 (60000); 426 (4400); 520 (1700, sh)	$C_{20}H_8Cr_2GeN_2O_{10}$ (612.9)	calcd. C 39.20 H 1.32 N 4.57 found C 39.34 H 1.83 N 4.48
3b	205 (dec.)	637 (25) [M^-]	291 (61400); 424 (5000)	$C_{22}H_8Cr_2GeN_2O_{10}$ (636.9)	calcd. C 41.49 H 1.27 N 4.40 found C 41.58 H 1.60 N 4.43
4	245 (dec.)	746 (5) [(M - 2 H) $^-$]	298 (13900); 310 (12000); 432 (2100)	$C_{20}H_8Cr_2N_2O_{10}Pb$ (747.5)	calcd. C 32.14 H 1.08 N 3.75 found C 32.17 H 1.27 N 3.71

Table 10. Crystal-structure data for **1a**–**1d**

compound	**1a**	**1b**	**1c**	**1d · THF**
formula	$C_{20}H_8Cr_2N_2O_{10}Sn$	$C_{20}H_8Mo_2N_2O_{10}Sn$	$C_{20}H_8N_2O_{10}SnW_2$	$C_{22}H_8Cr_2N_2O_{10}Sn$
molecular mass [g]	658.970	746.850	922.670	682.990
crystal dimensions [mm]	0.30 × 0.30 × 0.30	0.40 × 0.20 × 0.10	0.30 × 0.30 × 0.30	0.20 × 0.30 × 0.35
crystal system	orthorhombic	orthorhombic	orthorhombic	triclinic
space group (No.)	Pbca (61)	Pbca (61)	Pbca (61)	$P\bar{1}$ (2)
a [pm]	1260.5 (3)	1281.4 (3)	1278.4 (3)	1132.1 (6)
b [pm]	1650.3 (5)	1655.7 (5)	1652.7 (5)	1141.6 (6)
c [pm]	2158.5 (5)	2198.6 (5)	2192.8 (5)	1194.7 (6)
α [°]	90.00 (0)	90.00 (0)	90.00 (0)	81.03 (2)
β [°]	90.00 (0)	90.00 (0)	90.00 (0)	82.85 (2)
γ [°]	90.00 (0)	90.00 (0)	90.00 (0)	77.21 (2)
cell volume [10^6 pm^3]	4490 (2)	4665 (2)	4633 (2)	1481 (1)
molecular units / cell	8	8	8	2
density (calculated) [g cm^{-3}]	1.950	2.127	2.646	1.693
absorption coefficient [cm^{-1}]	21.15	21.27	110.36	16.17
temperature [K]	200	200	200	200
no. rflns. for cell parameter refinement	25	37	30	25
scan range	4.5° ≤ 2Θ ≤ 45.0°	4.4° ≤ 2Θ ≤ 49.0°	4.4° ≤ 2Θ ≤ 49.0°	4.7° ≤ 2Θ ≤ 44.0°
scan speed [° min^{-1}]	8.0 < $\dot{\omega}$ < 60.0	$\dot{\omega}$ = 10	$\dot{\omega}$ = 10	8.0 ≤ $\dot{\omega}$ ≤ 60.0
no. rflns. measured	2932	3861	3853	3844
no. unique rflns.	2932	3861	3853	3620
no. rflns. observed	2520	3105	2775	3452
observation criterion	2 σ (*I*)	2 σ (*I*)	2 σ (*I*)	2 σ (*I*)
no. parameters refined	317	317	312	381
residual electron density [· 10^{-6} e pm^{-3}]	0.43 / -0.70	0.65 / - 0.73	1.15 / - 1.54	1.31 / - 1.74
R_1 / R_W [%] (refinement on F^2)	3.1 / 8.4	3.6 / 10.4	4.3 / 10.0	4.0 / 13.0

filtered through Kieselgur (3 cm) and the solvent was evaporated in vacuo. The yellow oily residue was redissolved in THF (3 ml) and chromatographed slowly on silica gel (20 cm; Ø = 3 cm; diethyl ether). A yellow band was eluted with diethyl ether containing

Table 11. Crystal-structure data for **1e**−**1h**

compound	**1e** · **THF**	**1f** · **THF**	**1g**	**1h** · **THF**
formula	$C_{22}H_8Mo_2N_2O_{10}Sn$	$C_{22}H_8N_2O_{10}SnW_2$	$C_{20}H_{10}Cr_2N_2O_{10}Sn$	$C_{20}H_{10}N_2O_{10}SnW_2$
molecular mass [g]	770.880	946.700	660.990	924.690
crystal dimensions [mm]	0.40 × 0.50 × 0.50	0.20 × 0.30 × 0.30	0.50 × 0.40 × 0.40	0.50 × 0.40 × 0.40
crystal system	triclinic	triclinic	triclinic	triclinic
space group (No.)	$P\bar{1}$ (2)	$P\bar{1}$ (2)	$P\bar{1}$ (2)	$P\bar{1}$ (2)
a [pm]	1129.6 (2)	1133.4 (5)	895.5 (1)	931.4 (6)
b [pm]	1136.3 (1)	1141.7 (3)	1003.8 (2)	1028.2 (6)
c [pm]	1206.4 (1)	1212.1 (2)	1433.6 (2)	1464.9 (9)
α [°]	82.69 (1)	82.79 (2)	86.16 (1)	86.36 (2)
β [°]	81.27 (1)	81.18 (3)	76.46 (1)	77.54 (2)
γ [°]	77.61 (1)	77.36 (2)	68.55 (1)	67.46 (2)
cell volume [10^6 pm^3]	1487.7 (3)	1505.5 (9)	1165.8 (3)	1265 (3)
molecular units / cell	2	2	2	2
density (calculated) [g cm^{-3}]	1.864	2.230	1.883	2.428
absorption coefficient [cm^{-1}]	17.22	85.04	20.36	101.10
temperature [K]	200	200	200	200
no. rflns. for cell parameter refinement	28	18	34	25
scan range	4.8° ≤ 2Θ ≤ 48.0°	3.4° ≤ 2Θ ≤ 42.0°	4.4° ≤ 2Θ ≤ 52.0°	4.3° ≤ 2Θ ≤ 44.0°
scan speed [° min^{-1}]	$\dot{\omega}$ = 11	7.0 ≤ $\dot{\omega}$ ≤ 60.0	$\dot{\omega}$ = 11	8.0 ≤ $\dot{\omega}$ ≤ 60.0
no. rflns. measured	4926	3449	4894	3570
no. unique rflns.	4660	3235	4584	3104
no. rflns. observed	4467	2793	4385	2875
observation criterion	2 σ (*I*)	2 σ (*I*)	2 σ (*I*)	2 σ (*I*)
no. parameters refined	413	371	356	317
residual electron density [· 10^{-6} e pm^{-3}]	1.13 / - 1.15	1.34 / - 1.20	0.68 / - 1.31	2.02 / - 2.84
R_1 / R_W [%] (refinement on F^2)	3.2 / 9.1	3.6 / 12.9	2.6 / 8.5	4.6 / 13.2

$[Cr(CO)_6]$ or $[W(CO)_6]$, respectively (identified by comparison of IR spectroscopic data[29]). A second yellow band, eluted with diethyl ether, consisted of a mixture of $[Cr(CO)_6]$ and $[(CO)_5Cr(py)]$ or $[W(CO)_6]$ and $[(CO)_5W(py)]$, respectively, as identified by IR spectroscopy[29][30]. With THF a third yellow band was obtained consisting of pure **1g** or **1h**, respectively. Evaporation of the solvent left **1g** and **1h** as yellow oils. Yield: **1g**: 100 mg (15%); **1h**: 140 mg (15%). Single crystals of **1g** and **1h** were obtained within 8 d by applying the method given below.

Bis[bis(12-crown-4)sodium] Tetrakis(pentacarbonylchromium)-(biimidazolato)distannate(0), [Na-(12-crown-4)$_2$]$_2$[{(CO)$_5$Cr}$_2$-Sn(biim)Sn{Cr(CO)$_5$}$_2$] (**2a**): $Na_2[\{(CO)_5Cr\}_2SnCl_2]$ (310 mg; 0.5 mmol) was dissolved in THF (30 ml). Upon addition of solid disodium biimidazolate [45 mg; 0.25 mmol; obtained by heterogenous reaction of biimidazole (34 mg; 0.25 mmol) and NaH (14 mg; 0.6 mmol) in THF without further purification] no colour change was observed. After 30 min, the yellow solution was filtered through Kieselgur (3 cm). 12-Crown-4 (90 mg; 0.5 mmol) was added to the reaction mixture. Evaporation of the solvent in vacuo left 760 mg (80%) of **2a** as a yellow-brown solid. Applying the method described below gave single crystals of **2a** within 14 d.

2a·(12-crown-4)$_2$: ^{1}H NMR ([D$_6$]acetone, 25°C): δ = 7.22 (s, 4 H, imidazolato-H), 3.65 [s, 64 H, CH_2-(12-crown-4)]. − ^{13}C NMR ([D$_6$]acetone, 25°C): δ = 230.0 (CO_{ax}), 222.5 (CO_{eq}), 144.0 (*C*-2, biimidazolate), 127.1 (*C*-4 and *C*-5, biimidazolate), 62.5 (CH_2, 12-crown-4).

Bis(pentacarbonylchromium)(2,2′-bipyrimidine)tin, [{(CO)$_5$-Cr}$_2$Sn(bpmd)] (**2b**), *and Bis(pentacarbonyltungsten)(2,2′-bipyrimidine)tin, [{(CO)$_5$W}$_2$Sn(bpmd)]* (**2c**): $Na_2[\{(CO)_5Cr\}_2SnCl_2]$ (620 mg; 1 mmol) or $Na_2[\{(CO)_5W\}_2SnCl_2]$ (884 mg; 1 mmol), respectively, was dissolved in THF (50 ml). Upon the addition of solid 2,2′-bipyrimidine (79 mg; 0.5 mmol) the orange solution turned deep red immediately. The solvent was evaporated in vacuo after stirring the solution for 30 min. The red oily residue was dissolved in THF (3 ml) and chromatographed on silica gel (20 cm; Ø = 3 cm; diethyl ether). Two bands were obtained by elution with diethyl ether. The first yellow band was identified by comparison of IR spectra[29] and found to be $[Cr(CO)_6]$ or $[W(CO)_6]$, respectively. The second pink band was identified to be $[(CO)_4Cr(bpmd)]$ or $[(CO)_4W(bpmd)]$, respectively, by comparison of their IR spectra with the IR spectra of the corresponding 2,2′-bipyridine complexes (vide supra)[30]. With THF a third red-brown band was eluted which contained **2b** or **2c**, respectively. Evaporation of the solvent left **2b** and **2c** as red solids. Yield: **2b**: 150 mg (45%); **2c**: 170 mg (36%). Single crystals of **2b** and **2c** were obtained within 12 d by applying the method described below.

Bis(pentacarbonylchromium)(2,2′-bipyridine)germanium, [{(CO)$_5$-Cr}$_2$Ge(bipy)] (**3a**), *and Bis(pentacarbonylchromium)(1,10-phenanthroline)germanium, [{(CO)$_5$Cr}$_2$Ge(phen)]* (**3b**): To a stirred, orange solution of $Na_2[Cr_2(CO)_{10}]$ (430 mg; 1 mmol) in THF (50 ml) was added solid GeI_2 (326 mg; 1 mmol) in one portion. After 5 min of stirring, solid 2,2′-bipyridine (156 mg; 1 mmol) or solid 1,10-phenanthroline (180 mg; 1 mmol), respectively, was added and the deep red solution was filtered through Kieselgur (3 cm). After 30 min of stirring, the solvent was evaporated. The solid residue was redissolved in THF (3 ml) and chromatographed on silica gel (20 cm; Ø = 3 cm; diethyl ether). Elution with diethyl ether gave two bands. The first yellow band was identified by IR spectroscopy to be $[Cr(CO)_6]$[29]. The second pink band was found to consist of $[(CO)_4Cr(bipy)]$ or $[(CO)_4Cr(phen)]$, respectively, by comparison of IR[30], ^{1}H-, and ^{13}C-NMR spectra. The compounds **3a** and **3b** were eluted with THF as the third red-brown band. Evaporation of the solvent left the compounds as red microcrystalline powders. Yields:

Table 12. Crystal-structure data for **2a**−**2c**

compound	**2a** · **12-Crown-4**	**2b**	**2c**
formula	$C_{58}H_{68}Cr_4N_4Na_2O_{36}Sn_2$	$C_{18}H_6Cr_2N_4O_{10}Sn$	$C_{18}H_6N_4O_{10}SnW_2$
molecular mass [g]	188.520	660.960	924.660
crystal dimensions [mm]	0.30 × 0.20 × 0.10	0.30 × 0.20 × 0.20	0.30 × 0.30 × 0.20
crystal system	triclinic	monoclinic	monoclinic
space group (No.)	$P\bar{1}$ (2)	C2/c (15)	C2/c (15)
a [pm]	996.1 (2)	2977 (4)	3358.5 (6)
b [pm]	1415.2 (5)	950 (1)	1228.9 (2)
c [pm]	1581.7 (7)	1792 (2)	1253.9 (2)
α [°]	114.95 (2)	90.00 (0)	90.00 (0)
β [°]	95.86 (3)	92.22 (2)	93.20 (1)
γ [°]	103.08 (2)	90.00 (0)	90.00 (0)
cell volume [10^6 pm^3]	1919 (1)	5064 (11)	5167 (2)
molecular units / cell	1	8	8
density (calculated) [g cm^{-3}]	1.634	1.734	2.443
absorption coefficient [cm^{-1}]	12.89	18.77	99.02
temperature [K]	188	295	200
no. rflns. for cell parameter refinement	31	30	34
scan range	2.9° ≤ 2Θ ≤ 52.0°	2.7° ≤ 2Θ ≤ 50.0°	4.8° ≤ 2Θ ≤ 53.0°
scan speed [° min^{-1}]	$\dot{\omega}$ = 15	$\dot{\omega}$ = 10	$\dot{\omega}$ = 14
no. rflns. measured	7659	4542	5449
no. unique rflns.	7213	4451	5359
no. rflns. observed	4617	2731	3777
observation criterion	2 σ (*I*)	2 σ (*I*)	2 σ (*I*)
no. parameters refined	546	389	337
residual electron density [· 10^{-6} e pm^{-3}]	0.57 / - 0.61	0.66 / - 0.64	1.64 / - 1.36
R_1 / R_W [%] (refinement on F^2)	5.6 / 15.0	5.2 / 14.8	5.1 / 13.7

3a: 150 mg (25%); **3b**: 160 mg (25%). Single crystals of **3a** and **3b** suitable for X-ray structural analyses were obtained within 7 d by the method described below.

Bis(pentacarbonylchromium)(2,2′-bipyridine)lead, [{(CO)$_5$Cr}$_2$Pb(bipy)] (**4**): The disodium salt $Na_2[\{(CO)_5Cr\}_2Pb(OOCCH_3)_2]$ (694 mg; 0.5 mmol) was dissolved in dichloromethane (30 ml) and solid 2,2′-bipyridine (78 mg; 0.5 mmol) was added in one portion. The orange solution turned deep red immediately. After 30 min of stirring, the solution was taken to dryness. The oily red residue was dissolved in THF (3 ml) and chromatographed slowly (max. 50 drops/min) on silica gel (20 cm; Ø = 3 cm) with diethyl ether. The first yellow band was identified by spectroscopic comparison (IR spectra) to be $[Cr(CO)_6]$[29]. A second red band consisted of a mixture of **4** and $[(CO)_4Cr(bipy)]$ (identified by comparison of spectroscopic data[30]). A third red band contained pure **4**. The ethereal solution was taken to dryness leaving **4** as a red microcrystalline powder. Yield: **4**: 170 mg (45%). To grow single crystals of **4** the method described below was applied.

Procedure of Growing Single Crystals of **1**−**4**: A concentrated THF solution (5 ml) of the chelate complex **1**−**4** was shared out between three test tubes (Ø = 1 cm) which were brought into a Schlenk tube (250 ml). Diethyl ether (30 ml), which was in the tube, was allowed to diffuse through the gas-phase into the THF solutions (3 h). After this period of time, the diethyl ether was replaced by petroleum ether (boiling range 40−60°C; 50 ml). Vapor diffusion of the petroleum ether (boiling range 40−60°C) gave single crystals of **1**−**4** suitable for X-ray structure analyses.

X-ray Structure Determinations: The measurements for **1**−**4** were carried out with a Siemens P4 four-circle diffractometer with graphite-monochromated Mo-K_α radiation. The intensities of three check reflections (measured every 100 reflections) remained constant throughout the data collection, thus indicating crystal and electronic stability. All calculations were performed using the SHELXT PLUS software package. The structures were solved by direct methods with the SHELXS-86 program and refined with the SHELX93 program[31]. The program XPMA[32] was used for the graphical handling of the data. Absorption corrections (ψ scan, Δψ = 10°) were applied to the data. The structures were refined in fully or partially anisotropic models by full-matrix least-squares calculations. Hydrogen atoms were introduced at calculated positions. Tables 10−13 compile the data for the structure determinations. Peculiarities about the structures are as follows: **1c**: In this tungsten-containing compound one carbon atom of an equatorial carbonyl group could only be refined isotropically. **1d**: The crystal analyzed contained one THF per molecule **1d** with one of the THF carbon atoms refined isotropically in a disordered position (occupation: 0.6:0.4). **1e**: The crystal used contained one THF per molecule as well; again one of the THF carbon atoms was found in a split position (occupation: 0.7:0.3; anisotropic refinement). **1f**: All atoms of the solvent molecule THF included in the unit cell of **1f** showed some disorder (occupation: 0.6:0.4) and thus were refined only isotropically. **2a**: One of the crown ether molecules showed disorder. **2b**: The equatorial carbonyl groups at one chromium atom had to be refined in split positions (Δα ≈ 25°, with α defined as shown in Figure 7; occupation: 0.52:0.48). **2c**: The crystal analyzed contained 0.4 THF per unit cell with the oxygen atom showing some disorder (occupation: 0.5:0.5). Further details of the crystal-structure investigations may be obtained from the Fachinformationszentrum Karlsruhe, D-76344 Eggenstein-Leopoldshafen (Germany), on quoting the depository numbers CSD-408203 (**1a**), -408201 (**1b**), -408206 (**1c**), -408197 (**1d**), -408204 (**1e**), -408196 (**1f**), -408205 (**1g**), -408207 (**1h**), -408198 (**2a**), -408209 (**2b**), -408199 (**2c**), -408231 (**3a**), -408202 (**3b**), -408200 (**4**).

 © WILEY-VCH Verlag GmbH, D-69451 Weinheim, 1998 1434−1948/98/0606−0703 $ 17.50+.50/0

Table 13. Crystal-structure data for **3a**–**4**

compound	**3a**	**3b · THF**	**4**
formula	$C_{40}H_{16}Cr_4Ge_2N_4O_{20}$	$C_{22}H_8Cr_2GeN_2O_{10}$	$C_{20}H_8Cr_2N_2O_{10}Pb$
molecular mass [g]	1225.750	636.890	747.470
crystal dimensions [mm]	0.30 × 0.30 × 0.20	0.30 × 0.30 × 0.30	0.20 × 0.30 × 0.30
crystal system	monoclinic	orthorhombic	orthorhombic
space group (No.)	$P2_1/c$ (14)	Pnna (52)	Pbca (61)
a [pm]	869.6 (1)	1445.2 (1)	1272.2 (3)
b [pm]	4226.2 (5)	1727.8 (5)	1638.9 (5)
c [pm]	1295.1 (4)	1178.6 (1)	2178.4 (5)
α [°]	90.00 (0)	90.00 (0)	90.00 (0)
β [°]	107.52 (1)	90.00 (0)	90.00 (0)
γ [°]	90.00 (0)	90.00 (0)	90.00 (0)
cell volume [10^6 pm^3]	4539 (2)	2943.0 (9)	4542 (2)
molecular units / cell	4	4	8
density (calculated) [g cm^{-3}]	1.794	1.577	2.186
absorption coefficient [cm^{-1}]	23.16	17.99	83.94
temperature [K]	293	295	200
no. rflns. for cell parameter refinement	30	45	25
scan range	3.4° ≤ 2Θ ≤ 45.0°	4.2° ≤ 2Θ ≤ 50.0°	4.5° ≤ 2Θ ≤ 50.0°
scan speed [° min^{-1}]	$\dot{\omega}$ = 10	$\dot{\omega}$ = 13	$\dot{\omega}$ = 10
no. rflns. measured	6390	5057	4455
no. unique rflns.	5937	2600	4455
no. rflns. observed	3198	1471	2692
observation criterion	2 σ (*I*)	2 σ (*I*)	2 σ (*I*)
no. parameters refined	631	201	318
residual electron density [· 10^{-6} e pm^{-3}]	0.49 / - 0.69	0.52 / - 0.33	2.05 / - 2.13
R_1 / R_w [%] (refinement on F^2)	5.8 / 15.6	4.7 / 12.4	6.2 / 17.4

☆ Dedicated to Professor *Heinrich Nöth* on the occasion of his 70th birthday.

[1] G. Huttner, U. Weber, L. Zsolnai, *Z. Naturforsch.* **1982**, *37b*, 707–710.

[2] B. Schiemenz, G. Huttner, *Angew. Chem.* **1993**, *105*, 295–296; *Angew. Chem. Int. Ed. Engl.* **1993**, *32*, 159–166.

[3] B. Schiemenz, B. Antelmann, G. Huttner, L. Zsolnai, *Z. Anorg. Allg. Chem.* **1994**, *620*, 1760–1767.

[4] P. Kircher, G. Huttner, B. Schiemenz, K. Heinze, L. Zsolnai, O. Walter, A. Jacobi, A. Driess, *Chem. Ber.* **1997**, *130*, 687–699.

[5] F. Ettel, G. Huttner, W. Imhof, *J. Organomet. Chem.* **1990**, *397*, 299–307.

[6] F. Ettel, M. Schollenberger, B. Schiemenz, G. Huttner, L. Zsolnai, *J. Organomet. Chem.* **1994**, *476*, 153–162.

[7] [7a] J. K. Ruff, *Inorg. Chem.* **1967**, *6*, 1502–1504. – [7b] D. Uhlig, H. Behrens, E. Lindner, *Z. Anorg. Allg. Chem.* **1973**, *401*, 233–242. – [7c] T. Kruck, H. Breuer, *Chem. Ber.* **1974**, *107*, 263–269. – [7d] T. Kruck, F.-J. Becker, H. Breuer, K. Ehlert, W. Rother, *Z. Anorg. Allg. Chem.* **1974**, *107*, 95–100. – [7e] E. E. Isaacs, W. A. G. Graham, *Can. J. Chem.* **1975**, *53*, 467–473. – [7f] T. Kruck, W. Molls, *Z. Anorg. Allg. Chem.* **1976**, *420*, 159–176.

[8] C. Elschenbroich, A. Salzer, *Organometallchemie*, 3rd ed., Teubner, Stuttgart, **1990**, p. 277.

[9] [9a] W. Strohmeier, *Angew. Chem.* **1964**, *76*, 873–881; *Angew. Chem. Int. Ed. Engl.* **1964**, *3*, 730–738. – [9b] U. Honrath, H. Vahrenkamp, *Z. Naturforsch. B* **1979**, *34*, 1190–1194. – [9c] T. Madach, H. Vahrenkamp, *Z. Naturforsch. B* **1979**, *34*, 1195–1198.

[10] [10a] W. A. Herrmann, H.-J. Kneuper, E. Herdtweck, *Chem. Ber.* **1989**, *122*, 437–444. – [10b] F. Ettel, Ph. D. Thesis, University of Heidelberg, **1991**.

[11] The properties described for materials which were tentatively assigned the formulas $[(CO)_5M{=}Sn{=}M(CO)_5]$ (M = Cr, W) cast some doubt on this assignment. – G. K.-I. Magomedov, L. V. Morozova, Y. I. Markova, *Zh. Obshch. Khim.* **1983**, *53*, 1684–1685; *J. Gen. Chem. USSR (Engl. Trans.)* **1983**, *53*, 1515–1516.

[12] [12a] T. A. Annan, B. R. McGarvey, A. Ozarowski, D. G. Tuck, R. K. Chadha, *J. Chem. Soc., Dalton Trans.* **1989**, 439–446. – [12b] P. Jutzi, P. Galow, S. Abu-Orabi, A. M. Arif, A. H. Cowley, N. C. Norman, *Organometallics* **1987**, *6*, 1024–1031. – [12c] N. S. Hosmane, P. de Meester, N. N. Maldar, S. B. Potts, S. S. C. Chu, R. H. Herber, *Organometallics* **1986**, *5*, 772–778.

[13] R. J. Pugmire, D. M. Grant, *J. Am. Chem. Soc.* **1968**, *90*, 697–706.

[14] B. Wrackmeyer, *Annu. Rep. NMR Spec.* **1985**, *16*, 73–186.

[15] J. D. Kennedy, W. Mc Farlane in *NMR and the Periodic Table* (Eds.: R. K. Harris, B. Z. Mann), Academic Perss, London, **1978**, p. 342.

[16] B. Schiemenz, G. Huttner, L. Zsolnai, P. Kircher, T. Diercks, *Chem. Ber.* **1995**, *128*, 187–191.

[17] In this paper the term "inidene" is used instead of the IUPAC term "anediyl" (e.g.: F. Ettel, G. Huttner, L. Zsolnai, C. Emmerich, *J. Organomet. Chem.* **1991**, *414*, 71–87).

[18] G. Huttner, *J. Organomet. Chem.* **1986**, *308*, C11–C13.

[19] *CAChe*, Ext Hückel, Release 3.6 with given parameters for Cr and Sn, basis STO-6G, **1989**.

[20] J. D. Miller, R. H. Prince, *J. Chem. Soc.* **1965**, 3185–3194.

[21] Despite of the close similarity of the structures of compounds **1** within each series (**1a**–**1c**, **1d**–**1f**, **1g**, and **1h**) the molydenum derivatives **1b** and **1e** differ from their chromium and tungsten analogues in their solubility. In contrast to the latter the molybdenum compounds are soluble in toluene and their solubility in diethyl ether is definitely higher than the one observed for the corresponding chromium and tungsten species which are only sparingly soluble in this solvent. In accord to the known relative substitution lability of $[(CO)_5Mo]$ derivatives relative to their $[(CO)_5Cr]$ and $[(CO)_5W]$ analogues which is assumed to be due to an additional associative pathway operative in the molybdenum case, it may be inferred that the above solvents solubilize the molybdenum compounds **1b** and **1e** by some kind of association (J. P. Collman, L. S. Hegedus, J. R. Norton, R. G. Finke, *Principles and Applications of Organotransition Metal Chemistry*, University Science Books, Mill Valley, California, **1987**, pp. 235–278.).

[22] J. Sandström, *Dynamic NMR Spectroskoy*, Academic Perss, London, **1982**.

[23] H. Friebolin, *Ein- und zweidimensionale NMR-Spektroskopie*, VCH, Weinheim, **1988**.

[24] P. Kircher, Ph. D. Thesis, University of Heidelberg, **1998**, in preparation.

[25] A. Strube, G. Huttner, L. Zsolnai, *J. Organomet. Chem.* **1990**, *399*, 255−266.
[26] S. J. Davies, N. A. Compton, G. Huttner, L. Zsolnai, S. E. Garner, *Chem. Ber.* **1991**, *124*, 2731−2738.
[27] F. Holmes, K. M. Jones, E. G. Torrible, *J. Chem. Soc.* **1961**, 4790−4794.
[28] E. Lindner, H. Behrens, S. Birkle, *J. Organomet. Chem.* **1968**, *15*, 165−175.
[29] F. A. Cotton, C. S. Kraihanzel, *J. Am. Chem. Soc.* **1962**, *84*, 4432−4438.
[30] [30a] M. H. B. Stiddard, *J. Chem. Soc.* **1962**, 4712−4715. − [30b] R. J. Angelici, J. R. Graham, *Inorg. Chem.* **1967**, *6*, 988−992. − [30c] C. S. Kraihanzel, F. A. Cotton, *Inorg. Chem.* **1963**, *2*, 533−540. − [30d] R. J. Angelici, M. D. Malone, *Inorg. Chem.* **1967**, *6*, 1731−1736.
[31] G. M. Sheldrick, *SHELX86*, University of Göttingen, **1986**; G. M. Sheldrick, *SHELX93*, University of Göttingen, **1993**.
[32] L. Zsolnai, G. Huttner, *XPMA*, Universität Heidelberg, **1998**; http://www.rzuser.uni-heidelberg.de/v54/xpm.html

[98018]

 © WILEY-VCH Verlag GmbH, D-69451 Weinheim, 1998 1434−1948/98/0606−0703 $ 17.50+.50/0

Synthesis, Structure, Electronic, Redox, and Magnetic Properties of a New Mixed-Valent Mn-Oxo Cluster: $[Mn_2^{III,IV}O_2(N,N\text{bispicen})_2]^{3+}$ (*N*,*N*bispicen = *N*,*N*-bis(2-pyridylmethyl)-1,2-diaminoethane)

Olivier Horner[a,b], Marie-France Charlot[a], Alain Boussac[b], Elodie Anxolabéhère-Mallart[a], Lyuba Tchertanov[c], Jean Guilhem[c], and Jean-Jacques Girerd*[a]

Laboratoire de Chimie Inorganique, URA CNRS 420, Université Paris-Sud[a],
F-91405 Orsay, France

Section de Bioenergétique, URA CNRS 2096, CEA Saclay[b],
F-91191 Gif-sur-Yvette, France

Laboratoire de Cristallochimie, Institut de Chimie des Substances Naturelles UPR CNRS 2301[c],
F-91198 Gif-sur-Yvette, France

Received December 8, 1997

Keywords: Manganese / EPR spectroscopy / Spectroelectrochemistry / Mixed-valent compounds / Tripodal ligands

The synthesis and structural characterization of the novel $[Mn^{III,IV}{}_2O_2(N,N\text{bispicen})_2](ClO_4)_3{\cdot}CH_3CN$ complex employing the tetradentate ligand *N*,*N*bispicen = *N*,*N*-bis(2-pyridylmethyl)-1,2-diaminoethane are reported. Magnetic properties were determined and show that the ground state is a spin doublet. This can be quantitatively interpreted by antiferromagnetic coupling between a Mn(III) high spin and a Mn(IV) ($J = -316\ cm^{-1}$). The 16 line solution EPR spectrum exhibits an unusual splitting in the low field resonances.The following rhombic tensors were needed to simulate the EPR spectrum: $|A_{1x}| = 160\ 10^{-4}\ cm^{-1}$, $|A_{1y}| = 144\ 10^{-4}\ cm^{-1}$, $|A_{1z}| = 109\ 10^{-4}\ cm^{-1}$, $|A_{2x}| = 69\ 10^{-4}\ cm^{-1}$, $|A_{2y}| = 72\ 10^{-4}\ cm^{-1}$, $|A_{2z}| = 75\ 10^{-4}\ cm^{-1}$, $g_x = 2.001$, $g_y = 1.996$, $g_z = 1.984$. The classical ligand field theory of local $[g^{III}]$ and $[g^{IV}]$ tensors implemented with the first order perturbation theory to describe the properties of the pair does not result in a satisfying description of the $[g^{1/2}]$ tensor unless a large reduction in the spin-orbit constant is invoked. A simplified version of second-order perturbation theory leads to effects in qualitative agreement with experiment but weak as expected from the large $|J|$ value. The magnitude of these effects depends, however, on the anisotropy effects on each Mn ion. It is suggested that determination of the anisotropy of the magnetic properties of the monomeric Mn(III) and Mn(IV) moieties would be a valuable goal for a future study of these mixed valent di-manganese-di-μ-oxo complexes. The complex exhibits two quasi-reversible waves in the cyclic voltammogram, one at $E_{1/2} = 0.18$ V vs SCE for the III/IV ↔ III/III couple and the other at $E_{1/2} = 0.98$ V vs SCE for the III/IV ↔ IV/IV couple. The UV-Vis spectra of the three redox states have been recorded spectroelectrochemically.

During the last twenty years, several di-μ-oxo dimanganese complexes have been structurally characterized. There is still a continuing interest in these compounds due to their relevance to the water-oxidizing enzyme in photosystem II[1][2] and their redox catalytic properties, as shown with the mixed-valent complex $[Mn_2O_2(bpy)_4]^{3+}$[3][4][5] and its 1,10-phenantroline analogue.[4] Similar complexes using linear tetradentate ligands like *N*,*N*′-bis(2-pyridylmethyl)-1,2-diaminoethane (bispicen)[6] have been prepared in order to study their redox properties in relation to their structures.[7] We report herein the synthesis and characterization of a new dinuclear mixed-valence di-μ-oxo manganese complex with the tetradentate ligand *N*,*N*-bis(2-pyridylmethyl)-1,2-diaminoethane (*N*,*N*bispicen), an isomer of bispicen which presents a tertiary amino group as well as a primary amino group instead of the two secondary amino groups in bispicen. *N*,*N*bispicen is thus a tripodal ligand similar to tris(2-pyridylmethyl)amine (TPA)[8] and tris(2-aminoethyl)-amine (tren)[9] as shown in Scheme 1.

Scheme 1

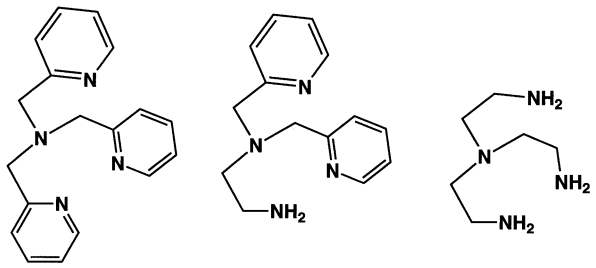

The *N*,*N*bispicen ligand has recently been used in the preparation of Fe(II) spin transition systems.[10] Unexpectedly the two primary amino groups of the two *N*,*N*bispicen ligands in the $[Mn_2O_2(N,N\text{bispicen})_2]^{3+}$ cation studied here

 © WILEY-VCH Verlag GmbH, D-69451 Weinheim, 1998 1434−1948/98/0721−0727 $ 17.50+.50/0

were found in a "*cis*" configuration relatively to the Mn_2O_2 diamond core. This unusual feature gives the potential to assemble two such dimanganese complexes in a dimer of dimers.

Results and Discussion

Structure: The structure of the $[Mn_2O_2(N,N\text{bispicen})_2]^{3+}$ cation is represented in Figure 1. This cation contains a dimanganese-di-μ-oxo unit which presents no axis of symmetry. The geometry about each manganese center is approximately octahedral, with ligating atoms from the two oxo bridges and the four nitrogen atoms from the *N,N*bispicen ligand. The Mn−Mn distance is 2.646(2) Å, which is comparable to the value found in dimanganese(III,IV)-di-μ-oxo complexes previously reported.[6][8][9][11][12] The two primary amino groups from the two *N,N*bispicen ligands are situated in the same half-space delimited by the Mn_2O_2 plane. This arrangement is probably due to a combination of two different effects. Firstly, a network of hydrogen bonds can be identified involving both NH_2 groups and the two ClO_4^- anions as represented in Scheme 2.

Figure 1. ORTEP diagram of the $[Mn_2O_2(N,N\text{bispicen})_2]^{3+}$ cation with thermal ellipsoids at 50% probability; the atom labels are shown for only one chemically symmetrical part of molecule; the labeling of the Part A and Part B of molecule are similar

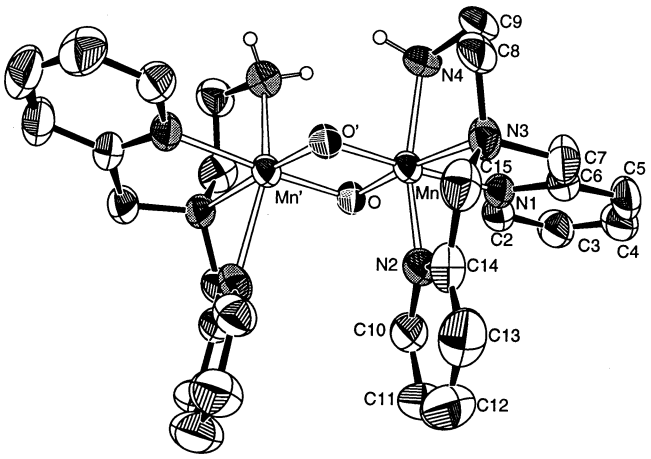

Scheme 2

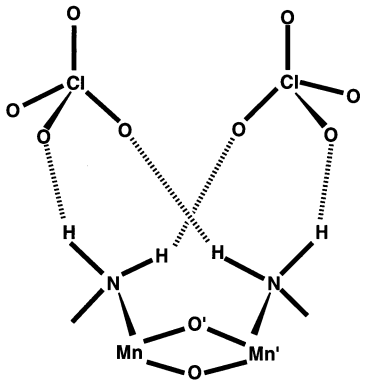

This network can be described as a cycle made of 2 Cl, 2 N, 4 O and 4 H atoms. The four distances O−N are 3.153 Å, 2.964 Å, 2.951 Å and 3.193 Å, all consistent with the presence of H bonds. Secondly a π-π interaction between the two pyridine groups appears to participate in the stabilisation of this structure. The shortest distance is that between the carbon atoms C10 and C10′ which is equal to 3.291 Å. The N2−N2′ distance is 3.412 Å.

The inequivalence between the Mn(IV) (Mn) and Mn(III) (Mn′) ions is easily recognizable from the bond distances (Table 1). The Mn equatorial pyridine distances Mn−N1 and Mn′−N′1 are, respectively 2.036(5) Å and 2.057(5) Å and the Mn-equatorial tertiary amine distances Mn−N3 and Mn′−N′3 are respectively 2.069(5) Å and 2.121(5) Å. These distances are less sensitive to the oxidation state of manganese than the axial ones. The Mn axial pyridine distances Mn−N2 and Mn′−N′2 are respectively equal to 2.015(6) Å and 2.238(6) Å and the axial Mn primary amine distances Mn−N4 and Mn′−N4′ are respectively 2.047(5) and 2.283(6) Å. This is in agreement with a $d_p^3d_{z^2}$ configuration for the Mn(III) ion (with the *z* axis perpendicular to the Mn_2O_2 plane).[12] An antibonding molecular orbital which is half occupied for the Mn(III) ion and empty for the Mn(IV) ion results fom the interaction of the d_{z^2} orbital with the σ orbitals of the axial pyridine N2 atom and the axial primary amino-group N4 atom. In previous studies it has been found that the average axial Mn(III) primary amine distance is 2.276 Å[9] in $[Mn_2O_2(tren)_2]^{3+}$ and the average axial Mn(III) pyridine distance in $[Mn_2O_2(TPA)_2]^{3+}$ is 2.233 Å.[8] These distances are similar to those found here.

Table 1. Selected bond lengths (Å) and angles (deg) for $[Mn^{III,IV}{}_2O_2(N,N\text{bispicen})_2](ClO_4)_3{\cdot}CH_3CN$

Bond lengths			
Mn−O	1.783(4)	Mn′−O	1.836(4)
Mn−O′	1.788(4)	Mn′−O′	1.838(4)
Mn−N(1)	2.036(5)	Mn′−N(1′)	2.057(5)
Mn−N(2)	2.015(6)	Mn′−N(2′)	2.238(6)
Mn−N(3)	2.069(5)	Mn′−N(3′)	2.121(5)
Mn−N(4)	2.047(5)	Mn′−N(4′)	2.283(6)
Mn···Mn′	2.646(2)		
Bond angles			
O−Mn−O′	87.6(2)	O−Mn′−N(1′)	174.7(2)
O−Mn−N(2)	96.6(2)	O′−Mn′−N(1′)	97.6(2)
O′−Mn−N(2)	95.0(2)	O−Mn′−N(3′)	96.8(2)
O−Mn−N(1)	94.7(2)	O′−Mn′−N(3′)	174.1(2)
O′−Mn−N(1)	177.2(2)	N(1′)−Mn′−N(3′)	81.6(2)
N(2)−Mn−N(1)	86.2(2)	O−Mn′−N(2′)	95.3(2)
O−Mn−N(4)	100.9(2)	O′−Mn′−N(2′)	98.9(2)
O′−Mn−N(4)	89.5(2)	N(1′)−Mn′−N(2′)	89.2(2)
N(2)−Mn−N(4)	162.0(2)	N(3′)−Mn′−N(2′)	75.3(2)
N(1)−Mn−N(4)	88.5(2)	O−Mn′−N(4′)	88.6(2)
O−Mn−N(3)	174.3(2)	O′−Mn′−N(4′)	106.7(2)
O′−Mn−N(3)	96.3(2)	N(1′)−Mn′−N(4′)	86.1(2)
N(2)−Mn−N(3)	79.0(2)	N(3′)−Mn′−N(4′)	79.1(2)
N(1)−Mn−N(3)	81.5(2)	N(2′)−Mn′−N(4′)	154.4(2)
N(4)−Mn−N(3)	83.2(2)	Mn−O−Mn′	94.0(2)
O−Mn′−O′	84.6(2)	Mn−O′−Mn′	93.7(2)

This structure can be compared in more general terms to the numerous examples already reported containing the $[Mn_2O_2]^{3+}$ core.[6][7][8][9][12][13][14] The difference between the average Mn−N(axial ligand) distances around both Mn ions reflects the asymmetry in electron distribution between the two Mn ions.[6] Here the value is 0.230 Å, which is comparable to that found for $[Mn_2O_2(bisimMe_2en)_2]^{3+}$ (0.204

Å).[12] In summary the $[Mn_2O_2(N,N\text{bispicen})_2]^{3+}$ cation is a new example of a complex of this family where the valences are profoundly differentiated.

Magnetic Susceptibility: The molar magnetic susceptibility χ_M of ground crystals of $[Mn_2O_2(N,N\text{bispicen})_2](ClO_4)_3.CH_3CN$ was measured as a function of the temperature *T*. The results are shown in Figure 2 in the form of the $\chi_M T$ versus *T* plot.

Figure 2. Product of the magnetic susceptibility per mole by temperature for $[Mn_2O_2(N,N\text{bispicen})_2](ClO_4)_3.CH_3CN$; the solid line was generated by the best fit parameters given in the text

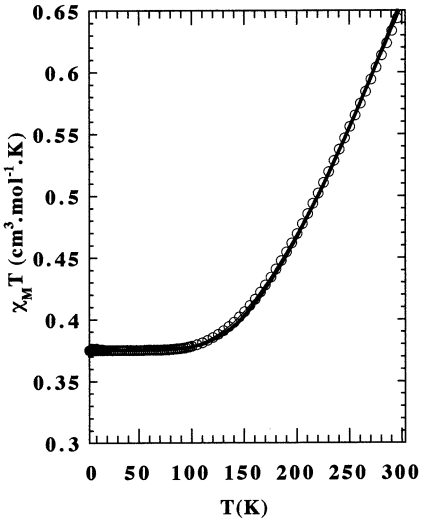

$\chi_M T$ decreases from 0.64 $cm^3mol^{-1}K$ at 292 K to a plateau at 0.38 $cm^3mol^{-1}K$ around 60 K. This is characteristic of an antiferromagnetic coupling between the electronic spins of the Mn(III) and Mn(IV) ions which produces a spin S = 1/2 ground state. This coupling is expressed by the Heisenberg hamiltonian $= -J\,\mathbf{S}_1\cdot\mathbf{S}_2$.The susceptibility was calculated according to:

$$\chi_M T = (N\beta^2 g^2/3k)(\Sigma S(S+1)(2S+1) \exp[J(S(S+1)/2kT)])/\Sigma(2S+1)\exp[J(S(S+1)/2kT)]$$

The best fit was obtained with $g = 2$ (kept constant) and $J = -316$ cm^{-1}. This value is close to that found for $[Mn_2O_2(\text{bispicMe}_2\text{en})_2](ClO_4)_3.H_2O$ ($J = -320$ cm^{-1})[11] and $[Mn_2O_2(bpy)_4](ClO_4)_3.2H_2O$ ($J = -300 \pm 14$ cm^{-1})[15] but clearly smaller than that of the strongest antiferromagnetic couplings, *J* down to -544 cm^{-1}, found in some $[Mn_2O_2L_2]^{3+}$ complexes (L representing a tetradentate ligand of the bispicen family) of ref[7], for which unfortunately no structural data is available.

EPR Spectrum: The EPR spectrum of $[Mn_2O_2(N,N\text{bispicen})_2]^{3+}$ was recorded at 10 K in acetonitrile (Figure 3a). As a first approximation this spectrum can be described as containing 16 lines, as previously observed for related complexes. Actually one may observe on closer inspection that the two lowest field lines are split. To our knowledge this feature is not generally observed in dimanganese (III,IV)-di-μ-oxo units. Another example can be found in the published spectrum of $[Mn_2O_2(TPA)_2]^{3+}$ although this was not commented upon by the authors.[16] It should be noted that the topologies of both complexes are similar. A simulation (not shown) with an axial constraint was first achieved with the following parameters: $|A_{1xy}| = 148\cdot10^{-4}$ cm^{-1}, $|A_{1z}| = 106\cdot10^{-4}$ cm^{-1}, $|A_{2xy}| = 72\cdot10^{-4}$ cm^{-1}, $|A_{2z}| = 72\cdot10^{-4}$ cm^{-1}, $g_{xy} = 1.999$, $g_z = 1.984$. The tensors were taken parallel to each other. The agreement factor *R* was found equal to 0.06. An improved simulation with $R = 0.02$, (Figure 3b) was obtained by letting the tensors become rhombic (but parallel): $|A_{1x}| = 160\cdot10^{-4}$ cm^{-1}, $|A_{1y}| = 144\cdot10^{-4}$ cm^{-1}, $|A_{1z}| = 109\cdot10^{-4}$ cm^{-1}, $|A_{2x}| = 69\cdot10^{-4}$ cm^{-1}, $|A_{2y}| = 72\cdot10^{-4}$ cm^{-1}, $|A_{2z}| = 75\cdot10^{-4}$ cm^{-1}, $g_x = 2.001$, $g_y = 1.996$, $g_z = 1.984$, $g_{iso} = 1.994$ with a line width equal to 11 G. This new set of values reproduced the splitting in the two lowest field lines mentioned above. It can be observed that the $[Mn_2O_2(tren)_2]^{3+}$ does not present this low-field feature although the ligand is also of the tripodal type. However the structure of this dimer is quite different, with the ligand bridging the two metal ions.[9]

Figure 3. X-band cw-EPR spectrum of $[Mn_2O_2(N,N\text{bispicen})_2]^{3+}$ in an 0.1 M NBu_4ClO_4 acetonitrile solution. Spectrometer setting: modulation amplitude, 1.91 G; $T = 10$ K; $\nu = 9.4384$ GHz; (a) experimental spectrum; (b) simulated spectrum

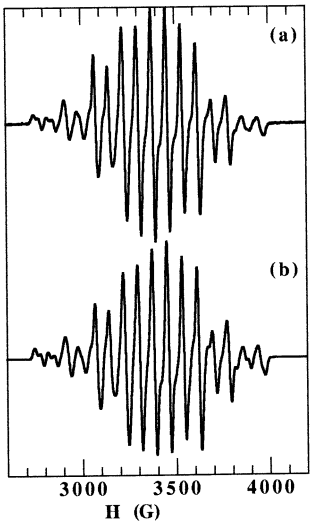

In general the spectra of the Mn(III)Mn(IV) pairs have been simulated using axial *g* and *A* tensors.[9][12][17] A rhombic simulation has been proposed for $[Mn_2O_2(bpy)_4]^{3+}$[18] (1.998, 1.992, 1.982, iso: 1.991). A ^{55}Mn ENDOR study of the same compound has used axial hyperfine tensors.[17] An X and Q band EPR and ^{55}Mn ENDOR study of $[(TACN)MnO_2(CH_3CO_2)Mn(TACN)]^{2+}$[19] has lead to rhombic tensors, in particular $g = 2.000$, 1.998, 1.984, iso: 1.994. The expression for a rhombic *g* tensor for Mn(III) has been given in ref[20]

$$\begin{aligned} g_x &= 2 - 2(\lambda/\Delta)(\cos\delta - \sqrt{3}\sin\delta)^2 \\ g_y &= 2 - 2(\lambda/\Delta)(\cos\delta + \sqrt{3}\sin\delta)^2 \\ g_z &= 2 - 8(\lambda/\Delta)(\cos\delta)^2 \end{aligned} \quad (1)$$

where λ is the spin orbit constant, Δ the energy gap between the "t_{2g}" and the "e_g"-like orbitals and δ a parameter reflecting the composition of the ground state as $|\phi> =$

$\cos\delta\ |d_{xz}d_{yz}d_{xy}d_{z^2}> + \sin\delta\ |d_{xz}d_{yz}d_{xy}d_{x^2-y^2}>$. It is also known that for the ground state of an antiferromagnetically coupled Mn(III)Mn(IV) pair one has

$$[g^{1/2}] = 2[g^{III}] - [g^{IV}] \quad (2)$$

The anisotropy of $[g^{III}]$ ($g_{perpendicular}{}^{III} = 1.990$, $g_{//}{}^{III} = 1.960$ for an elongated Mn(III) complex)[21] is larger than that of $[g^{IV}]$ ($g_{perpendicular}{}^{IV} = 1.991$, $g_{//}{}^{IV} = 1.995$ for Mn(IV) in TiO_2).[22] Initially assuming $[g^{IV}] = g^{IV}$ is isotropic, the three parameters δ, λ/Δ and g^{IV} can then be adjusted to reproduce the g values obtained. One finds $\delta = 8.14°$ ($\cos\delta = 0.9899$, $\sin\delta = 0.1416$), $\lambda/\Delta = 0.0012875$, and $g^{IV} = 1.996$. Consequently the system would be largely described by the $|d_{xz}d_{yz}d_{xy}d_{z^2}>$ wave function on Mn(III). From the type of distorsion observed in the structure it is tempting to consider the EPR z axis parallel to the axis of elongation observed in the structure. Although the g^{IV} and δ values seem reasonable, the λ/Δ ratio is smaller than expected. Indeed using $\lambda = 88\ cm^{-1}$ for the free Mn(III) ion,[20] one gets $\Delta = 68000\ cm^{-1}$ which is too large a value. This straightforward approach is thus not satisfying.

If isotropy for $[g^{IV}]$ is not assumed, the following general expression, deduced from equations 1 and 2, can be used to estimate λ/Δ.

$$g_{iso}{}^{1/2} = 4 - 8(\lambda/\Delta) - g^{IV}{}_{iso} \quad (3)$$

For instance with the value $g^{IV}{}_{iso} = 1.992$ for Mn(IV) in TiO_2[22] and $\lambda = 88\ cm^{-1}$, one finds $\Delta = 50300\ cm^{-1}$ which is still unlikely. The Δ value can be decreased by taking into account a reduction of λ reflecting covalency effects and decreasing $g^{IV}{}_{iso}$.

One may wonder if eq 2 is fully appropriate and if the extra terms due to anisotropy effects discussed by Zheng et al.[18] play a role. These terms are due to the perturbation of the spin doublet ground state by the excited spin levels. These effects have been studied for Fe(II)Fe(III) dimers in ref[23] and[24]. For the spin doublet ground state of an Mn(III)Mn(IV) pair one obtains the following modification of eq 2.

$$[g^{1/2}] = 2[g^{III}] - [g^{IV}] + (2/5)([g^{III}] - [g^{IV}])(7[D^{III}] + 2[D^{IV}])(2/-J) \quad (4)$$

Due to the large value of J, the correction introduced is expected to be small. Preliminary calculations for an elongated Mn(III) system ($\Delta g^{III} = g_{perpendicular}{}^{III} - g_{//}{}^{III} = 6\lambda/\Delta > 0$, $D^{III} < 0$) and assuming an isotropic Mn(IV) ion ($D^{IV} = 0$), show that

$$g_{iso}{}^{1/2} = 4 - 8(\lambda/\Delta) - g^{IV}{}_{iso} + (2/5)(14D^{III}/3(-J))(-2/3)(6\lambda/\Delta) \quad (5)$$

For $D^{III} < 0$, this indeed decreases the computed value for Δ by an amount proportional to D^{III} (1.6% for $D^{III} = -5\ cm^{-1}$, 3.1% for $D^{III} = -10\ cm^{-1}$). Due to the large J value as said above, this effect is weak unless the anisotropy energies be large. Nevertheless we feel that this problem has to be studied in more details for the following reasons. Little is known about the zero-field splitting energy value for Mn(III) and Mn(IV) ions in these dimers. It could well be that the zero-field splitting energy value for Mn(III) is substantial in these dimers due to a mixing of the $^3T_1$ state into the ^5E ground state of the Mn(III) ion, an effect shown recently by Caneschi et al. in a Mn(III) monomer.[21] Examination of the Tanabe-Sugano diagram for a d^4 ion shows that for a strong ligand field the $^3T_1$ state comes close to the ^5E ground state as one could sensibly predict in the case of dimers with nitrogeneous ligands. The properties of the Mn(IV) moiety also certainly deserve to be studied. In summary we propose that in order to understand in depth the electronic structure of these dimers, a better knowledge of the monomeric moieties has first to be achieved.

As for the A values, the $[A^{III}]$ presents the usual anisotropy with the lowest absolute value along the axis corresponding to the lowest g value (z) and the highest absolute principal value of the $[A^{IV}]$ tensor along the same axis.[19]

Redox Properties: The cyclic voltamogram of $[Mn_2O_2(N,N\text{bispicen})_2]^{3+}$ obtained in acetonitrile is shown in Figure 4. It shows two quasi-reversible waves, one at 0.18 V and the other at 0.98 V vs SCE. The $E_{1/2}$ value of 0.18 V corresponds to the one-electron couple III/IV $\leftrightarrow$ III/III, while that at 0.98 V represents the couple III/IV $\leftrightarrow$ IV/IV. Those two potentials are very similar to those previously reported for similar complexes with tetradentate ligands.[25]

Figure 4. Cyclic voltammetry of $[Mn_2O_2(N,N\text{bispicen})_2](ClO_4)_3.CH_3CN$ in acetonitrile, with 0.1 M $(TBA)ClO_4$ as supporting electrolyte; potentials are referenced vs SCE

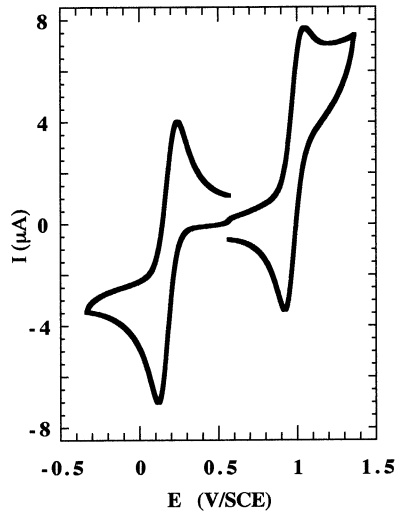

UV-Vis Spectroelectrochemistry: The spectrum of the $[Mn_2O_2(N,N\text{bispicen})_2]^{3+}$ complex as recorded in acetonitrile, is shown in Figure 5. It is comparable to those previously described for analogous dimanganese (III,IV)-di-μ-oxo units, the characteristic parameters of which have been summarized in ref[25]. It consists of a shoulder in the UV region and two bands of medium intensity in the visible region, which can be attributed as follows[26]: the 433 nm ($1080\ M^{-1}cm^{-1}$) band corresponds to a mixed contribution of Mn(IV) oxo LMCT and Mn(IV) d-d transitions, that at

Figure 5. Visible spectroelectrochemistry of the mixed-valent complex $[Mn_2O_2(N,N\text{bispicen})_2](ClO_4)_3\cdot CH_3CN$ in acetonitrile: (___) no potential applied; (–···–) oxidation at +1.14 V/SCE; (···) reduction at −0.13 V/SCE

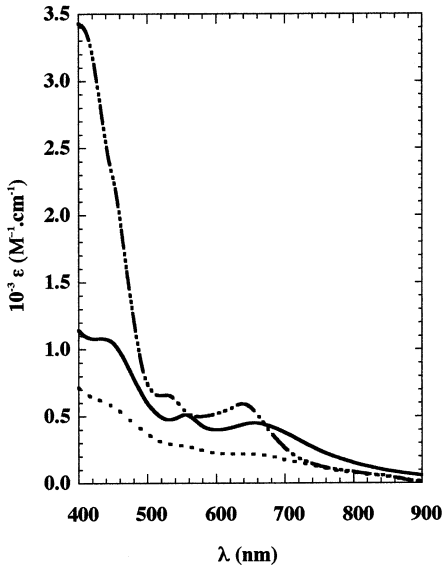

555 nm (511 $M^{-1}cm^{-1}$) to a Mn(IV) d-d transition and that at 654 nm (450 $M^{-1}cm^{-1}$) to Mn(IV) oxo LMCT.

After oxidation at +1.14 V/SCE, the spectrum of the Mn(IV)Mn(IV) form was obtained. The intensity of the absorption at 433 nm increases dramatically. This can be understood on the basis of the oxidation of the Mn(III) ion to Mn(IV). Apparently the Mn(IV) d-d band has shifted from 555 to 528 nm and its intensity has increased to 657 $M^{-1}cm^{-1}$. The band at 654 nm shifts to higher energy (637 nm) and also increases in intensity (592 $M^{-1}cm^{-1}$). This is in agreement with the attribution of such a band to an oxo Mn(IV) LMCT. After electrolysis at −0.13 V/SCE, a large decrease in the intensity of the spectrum is observed. Features at 661 (213 $M^{-1}cm^{-1}$), 556 (274 $M^{-1}cm^{-1}$) and 443 nm (595 $M^{-1}cm^{-1}$) are detected. At this potential, the Mn(III)Mn(III) form is obtained. The modifications described above are reversible by varying the potential applied appropriately. The observations reported above are very similar to those made by Brewer et al.[27] on $[Mn_2O_2(14\text{-}aneN_4)_2]^{3+}$ where 14-aneN$_4$ stands for 1,4,8,11-tetraazacyclotetradecane.

Conclusion

We have characterized a new di-μ-oxo bridged mixed valence manganese complex employing the tetradentate ligand *N,N*bispicen. The structure of the Mn(III)Mn(IV) complex has been resolved. Unexpectedly, the two primary amino groups from the two *N,N*bispicen ligands of the complex are situated on the same side of the space delimited by the Mn_2O_2 plane. Electronic, magnetic and redox properties have been reported. The EPR spectrum presents splitting of the resonances at low field which are most probably due to the rhombicity in the $[A^{III}]$ tensor. We remarked that the usual theory of the [*g*] tensor is not satisfactory unless λ is much reduced. We propose that second-order perturbation by excited spin levels on the spin doublet ground state, of the type described by Sage et al. for Fe(II)Fe(III) complexes and by Zheng et al. for Mn(III)Mn(IV), could lead to a better description if the zero-field splitting energy in those systems is important. Measurement of this energy by magnetization study and high-field EPR will be undertaken in a near future on the monomeric moieties corresponding to these dimers. The opportunity to use the two amino groups from the two *N,N*bispicen ligands in order to link two dinuclear complexes to form a tetranuclear complex will be explored.

This work has been supported in part by the *European Training and Mobility of Researchers* "Ru-Mn Artificial Photosynthesis" program (contract EU HMC network ERBXCT 94 0524).

Experimental Section

Compound Preparation: All chemical reagents were supplied by Aldrich and used without further purification. The ligand *N,N*-bis(2-pyridylmethyl)-1,2-diaminoethane (abbreviation: *N,N*bispicen) was prepared by following the procedure in ref[28]. This ligand has also recently been described in ref[10].

Caution: *Perchlorate salts of compounds containing organic ligands are potentially explosive. Only small quantities of those compounds should be prepared and handled behind suitable protective shields.*

$[Mn^{III,IV}{}_2O_2(N,N\text{bispicen})_2](ClO_4)_3\cdot CH_3CN$: 190 mg of *N,N*bispicen (0.785 mmol) were dissolved in 4 ml of absolute ethanol. To this solution 210.5 mg of $Mn(O_2CCH_3)_3.2H_2O$ (0.785 mmol) were added. After stirring for 1/2 hour, the resulting brown solution was filtered, and to the filtrate was added an absolute ethanol solution (4 ml) of $NaClO_4\cdot H_2O$ (220.5 mg, 1.57 mmol). A brown microcrystalline solid started to precipitate immediately. The solid was collected by filtration, washed thoroughly with absolute ethanol and dried under vacuum. The elemental analysis corresponds to a Mn(III)Mn(III) dimer $[Mn_2O_2(N,N\text{bispicen})_2](ClO_4)_2\cdot 1.3H_2O\cdot 1.3C_2H_5OH$. This powder was EPR silent. − $C_{30.6}H_{46.4}Cl_2Mn_2N_8O_{12.6}$: calcd C 40.43, H 5.11, Cl 7.82, Mn 12.11, N 12.33; found C 40.48, H 5.00, Cl 7.84, Mn 12.11, N 12.01. Dark single crystals characterized as $[Mn^{III,IV}{}_2O_2(N,N\text{bispicen})_2](ClO_4)_3\cdot CH_3CN$ were grown by slow diffusion of a mixture of CH_2Cl_2-$CHCl_3$ (1:1) into a concentrated solution of the powder in CH_3CN under air. − $C_{30}H_{39}Cl_3Mn_2N_9O_{14}$: calcd C 37.30, H 4.07, Cl 11.01, Mn 11.39, N 13.05; found C 37.47, H 3.94, Cl 10.95, Mn 11.38, N 13.0. − IR: $\tilde{\nu}$ = 3429 (br) cm^{-1}, 1607 (s), 1571 (w), 1480 (m), 1466(m), 1444(m), 1292 (m), 1144 (w), 1091 (vs), 766 (m), 697 (m), 660 (m), 625 (s). Symbols: br broad; vs very strong; s strong; m medium; w weak; sh shoulder. The single crystals of $[Mn^{III,IV}{}_2O_2(N,N\text{bispicen})_2](ClO_4)_3\cdot CH_3CN$ were used for all subsequent physical measurements.

Electrochemical Measurements: Cyclic voltammetry was measured using a EGG PAR potentiostat (M 273 model). The working electrode was a Pt disk of 3 mm diameter, carefully polished with diamond pastes and ultrasonically rinsed in ethanol before use. A Pt wire was used as counter electrode and as reference, a Ag/$AgClO_4$ electrode, prepared in acetonitrile and separated by a fritted disk from the main solution (270 mV above the potential of the saturated calomel electrode). The experiment was carried out on a carefully degassed solution by argon flushing.

Magnetic Susceptibility Measurements: Magnetic susceptibility measurements in the 4.2−300 K temperature range were carried

out with a MPMS5 SQUID magnetometer (Qantum Design Inc.). The calibration was made at 298K using palladium reference sample furnished by Quantum Design Inc. Ground crystals of $[Mn^{III,IV}_2O_2(N,N\text{bispicen})_2](ClO_4)_3.CH_3CN$ were used.

Crystallographic Data Collection and Refinement of the Structure of $[Mn^{III,IV}_2O_2(N,N\text{bispicen})_2](ClO_4)_3\cdot CH_3CN$: The crystal data of $[Mn^{III,IV}_2O_2(N,N\text{bispicen})_2](ClO_4)_3\cdot CH_3CN$ and the parameters of data collection are summarized in Table 2. A prismatic black crystal with the dimensions 0.9 × 0.25 × 0.15 mm was mounted in a glass capillary with 0.5 mm diameter. The unit-cell and intensity data were measured with an Enraf-Nonius CAD-4 diffractometer with graphite monochromated Mo-K_α radiation (λ = 0.71073 Å). The cell constants were obtained by least-squares procedures based upon the 2Θ values of 25 reflections measured in the ranges $20.8° < 2\Theta < 21.6°$ at ambient temperature. All reflection intensities were collected in the range $4° < 2\Theta < 50°$ within [$-19 \le h \le 19$, $-13 \le k \le 13$, $0 \le l \le 29$]. The total number of the collected and independent reflections are 16114 and 7870. Due to the peculiar form of the single crystal an empirical absorption correction was carried out. The structure was solved by direct methods with the program SHELXS86[29] and refined by using the SHELXL93[30] programs. The figure was prepared with ORTEP II.[31] The molecular cation was located in a general crystallographic position as well as three perchlorate anions and the molecule of acetonitrile. Observed disorder in the stucture involved the anions; all were disordered over two sites with non-identical occupations (0.60 and 0.40). The stucture was refined by full-matrix least-squares approximation based on F^2. Refinement was anisotropic for non-H atoms. Hydrogen positions were calculated by assuming geometrical positions and were included in the structural model (In addition, a cluster of electron density with seven different peak positions was found and these were not identified). Final refinement of this model was continued until convergence when $R1$ = 0.066 for $F^2 > 2\sigma(F^2)$ and R_w = 0.242. The final difference map showed two largest residual peaks of 0.68 and −0.66 eÅ^{-3}. Crystallographic data (excluding structure factors) for the structure reported in this paper have been deposited with the Cambridge Crystallographic Data Centre as supplementary publication no. CCDC-100897. Copies of the data can be obtained free of charge on application to The Director, CCDC, 12 Union Road, Cambridge CB2 1EZ, UK [Fax: (int. Code) +44(1223)336-033, E-mail: deposit@chemcrys.cam.ac.uk, World Wide Web: http://www.ccdc.cam.ac.uk].

Table 2. Crystallographic data for $[Mn^{III,IV}_2O_2(N,N\text{bispicen})_2](ClO_4)_3 \cdot CH_3CN$

Formula	$Mn_2C_{28}H_{36}N_8Cl_3O_{14}\cdot CH_3CN$
fw	965.93
Radiation	Mo-K_α (0.71073 Å)
Temp (K)	293
Space group	*P*21/*c*
a (Å)	16.511(9)
b (Å)	11.113(5)
c (Å)	24.55(2)
α (deg)	90
β (deg)	91.33(8)
γ (deg)	90
V (Å^3)	4503(5)
Z	4
μ (mm^{-1})	0.818
N_{meas}	16114
N_{obs}	7870
R	0.066
R_w	0.242

EPR Spectroscopy: EPR spectrum was recorded on Bruker ER 200 D spectrometer at X-band. For low temperature studies, an Oxford Instruments continuous flow liquid helium cryostat and a temperature control system were used. In order to get a good quality glass a 0.1 M solution of NBu_4ClO_4 in acetonitrile was used as solvent.

EPR Simulation: Simulation of the EPR spectrum was performed using a FORTRAN program originally developed by Drs L. K. White and R. L. Belford at University of Illinois. The program simulates powder spectra for S = 1/2 systems and can include four different hyperfine interactions using perturbation theory. It was modified to allow for calculation of the hyperfine contributions to the spectra to the second order.[32] Briefly, for each transition, the resonant field was calculated using perturbation theory up to the second order for the hyperfine coupling terms and the resulting stick spectrum was then convolved with Gaussian functions. This simulation program is coupled to a minimization program in order to find the set of parameters giving the lowest possible value of the agreement factor defined as $R = \Sigma_i(Y_i^{calc} - Y_i^{exp})^2/\Sigma_i Y_i^{exp\ 2}$.

[1] V. K. Yachandra, K. Sauer, M. P. Klein, *Chem. Rev.* **1996**, *96*, 2927−2950.
[2] W. Rüttinger, G. C. Dismukes, *Chem. Rev* . **1997**, *97*, 1−24.
[3] Abbreviations used: bispicMe$_2$en = *N*,*N*′-dimethyl-*N*,*N*′-bis(2-pyridylmethyl)ethane-1,2-diamine; bpy = 2,2′-bipyridine; bisimMe$_2$en = *N*,*N*′-Dimethyl-*N*,*N*′-bis(imidazol-4-ylmethyl)ethane-1,2-diamine); *N*,*N*bispicen = *N*,*N*-bis(2-pyridylmethyl)-1,2-diaminoethane; TPA = tris(2-pyridylmethyl)amine; tren = tris(2-aminoethyl)amine.
[4] S. R. Cooper, M. Calvin, *J. Am. Chem. Soc.* **1977**, *99*, 6623−6630.
[5] A. Gref, G. Balavoine, H. Riviere, C. P. Andrieux, *Nou. J. Chim.* **1984**, *8*, 615−618.
[6] M. A. Collins, D. J. Hodgson, K. Michelsen, D. K. Towle, *J. Chem. Soc., Chem. Commun.* **1987**, 1659−1660.
[7] P. A. Goodson, J. Glerup, D. J. Hodgson, K. Michelsen, H. Weihe, *Inorg. Chem* . **1991**, *30*, 4909−4914.
[8] D. K. Towle, C. A. Botsford, D. J. Hodgson, *Inorg. Chim. Acta* **1988**, *141*, 167−168.
[9] K. S. Hagen, W. H. Armstrong, H. Hope, *Inorg. Chem.* **1988**, *27*, 967−969.
[10] G. S. Matouzenko, A. Bousseksou, S. Lecocq, P. J. van Koningsbruggen, M. Perrin, O. Kahn, A. Collet, *Inorg. Chem.* **1997**, *36*, 2975−2981.
[11] J. Glerup, P. A. Goodson, A. Hazell, R. Hazell, D. J. Hodgson, C. J. Mc Kenzie, K. Michelsen, U. Rychlewska, H. Toflund, *Inorg. Chem* . **1994**, *33*, 4105−4111.
[12] Y.-M Frapart, A. Boussac, R. Albach, E. Anxolabéhère-Mallart, M. Delroisse, J.-B. Verlhac, G. Blondin, J.-J. Girerd, J. Guilhem, M. Cesario; A. W. Rutherford, D. Lexa, *J. Am. Chem. Soc.* **1996**, *118*, 2669−2678.
[13] P. M. Plaskin, R. C. Stoufer, M. Mathew, G. J. Palenik, *J. Am. Chem. Soc* . **1972**, *94*, 2121−2122.
[14] M. Stebler, A. Ludi, H.-B. Bürgi, *Inorg. Chem.* **1986**, *25*, 4743−4750.
[15] S. R. Cooper, G. C. Dismukes, M. P. Klein, M. Calvin, *J. Am. Chem. Soc.* **1978**, *100*, 7248−7252.
[16] X.-L Tan, Y. Gultneh, J. Sarneski, C. P. Scholes, *J. Am. Chem. Soc.* **1991**, *113*, 7853−7858.
[17] D. W. Randall, B. E. Sturgeon, J. A. Ball, G. A. Lorigan, M. K. Chan, M. P. Klein, W. H. Armstrong, R. D. Britt, *J. Am. Chem. Soc.* **1995**, *110*, 11780−11789.
[18] M. Zheng, S. V. Khangulov, G. C. Dismukes, V. V. Barynin, *Inorg. Chem.* **1994**, *33*, 382−387.
[19] W. Zweygart, R. Bittl, K. Wieghardt, W. Lubbitz, W. *Chem. Phys. Letters*, **1996**, *261*, 272−276.
[20] A. Abragam, B. Bleaney, *Electron Paramagnetic Resonance of Transition Ions,* Oxford University Press **1970**.
[21] A. Caneschi, D. Gatteschi, R. Sessoli, *J. Chem. Soc. Dalton Trans.* **1997**, 3963−3970. A.-L. Barra, D. Gatteschi, R. Sessoli, G. L. Abbati, A. Cornia, A. C. Fabretti, M. G. Uytterhoeven, *Angew. Chem. Int. Ed. Engl.* **1997**, *36*, 2329−2331.
[22] H. G. Andresen, *Phys. Rev.* **1961**, *35*, 1090−1096.

[23] J. T. Sage, Y. M. Xia, P. G. Debrunner, D. T. Keough, J. de Jersey, B. Zerner, *J. Am. Chem. Soc.* **1989**, *111*, 7239−7247.
[24] B. Guigliarelli, P. Bertrand, J.-P. Gayda, *J. Chem. Phys.* **1986**, *85*, 1689−1692.
[25] P. A. Goodson, J. Glerup, D. J. Hodgson, K. Michelsen, E. Pedersen, *Inorg. Chem* . **1990**, *29*, 503−508.
[26] D. R. Gamelin, M. L. Kirk, T. L. Stemmler, S. Pal, W. H. Armstrong, J. E. Penner-Hahn, E. I. Solomon, *J. Am. Chem. Soc.* **1994**, *116,* 2392−2399.
[27] K. J. Brewer, M. Calvin, R. S. Lumpkin, J. W. Otvos, L. O. Spreer, *Inorg. Chem.* **1989**, *28*, 4446−4451.
[28] O. Horner, E. Anxolabéhère-Mallart, M. F. Charlot, L. Tchertanov, J. Guilhem, A. Boussac, J.-J. Girerd, submitted for publication.
[29] G. M. Sheldrick, *SHELXS86, Program for Crystal Structure Solution;* University of Göttingen, Germany, **1986**.
[30] G. M. Sheldrick, *SHELXL93, Program for Crystal Structure Solution*; University of Göttigen, Germany, **1993**.
[31] C. K. Johnson, *ORTEPII.* Report ORNL-5138. Oak Ridge National Laboratory, Tennessee, USA., **1976**
[32] J. Bonvoisin, G. Blondin, J.-J. Girerd and J.-L. Zimmermann, *Biophys. J.* **1992**, *61*, 1076−1086.

[97299]

Metal Complexes of Biologically Important Ligands, 105[◇]

Catalytic Formation of Oligopeptides from α-Amino Acid Esters with (*p*-Cymene)ruthenium(II) Complexes☆

Winfried Hoffmüller, Michael Maurus, Kay Severin, and Wolfgang Beck*

Institut für Anorganische Chemie der Ludwig-Maximilians-Universität,
Meiserstraße 1, D-80333 München, Germany
Fax: (internat.) + 49(0)89/5902-214

Received December 23, 1997

Keywords: Catalysis / Oligomerization / Organometallics / Oligopeptides / Ruthenium complexes

Consecutive addition of one-equivalent portions of glycine ethyl ester to [(*p*-cymene)Ru(GGGOMe−H^+)Cl] leads to considerable amounts of (tetra- to nonapeptide)ruthenium complexes in a one-pot reaction, in which the (*p*-cymene)RuCl fragment acts as a catalyst. The analogous reaction with alanine methyl ester affords AGGG and AAGGG complexes as the main products. The course of these metal-catalyzed peptide oligomerizations has been followed by mass spectrometry. The synthesis and characterization of the pentapeptide complex [(C_6Me_6)Ru(GGGGGOMe−H^+)] is reported.

Introduction

There have been several reports on the formation of peptides from α-amino acid esters[2] or α-amino acids[3] in the presence of metal ions or metal complexes. Recently, our group reported a metal-promoted peptide synthesis in which non-activated α-amino acid esters are assembled in the coordination spheres of half-sandwich complexes of ruthenium, rhodium, and iridium.[4] This method permits the elongation of a coordinated peptide ester at its *N*-terminus with a defined amino acid sequence. In previous studies[4] we focused on stoichiometric reactions between peptide complexes and amino acid esters. However, according to the proposed mechanism, it should be possible to produce polypeptides using only catalytic amounts of these organometallic complexes (Scheme 1).

Scheme 1

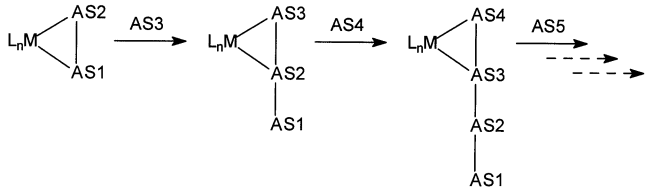

Therefore, we became interested in ascertaining whether longer peptide chains could be obtained by repetitive additions of α-amino acid esters to half-sandwich (peptide)metal complexes. In this paper, we report on the formation of tetra- to nonapeptides by means of a one-pot reaction of [(*p*-cymene)Ru(GGGOMe−H^+)Cl] (**1**) with glycine or alanine esters according to Scheme 1.

[◇] Part 104: Ref.[1].

Results and Discussion

Repetitive additions (every 24 h) of one equivalent of glycine ethyl ester (GlyOEt) to [(*p*-cymene)Ru(GGGOMe−H^+)Cl] (**1**) in the presence of triethylamine gave ruthenium complexes with increased chain length of the peptide (Scheme 2). The reaction resembles living polymerization processes.[5] A large excess of α-amino acid ester was avoided in order to reduce autocondensation reactions.

Scheme 2

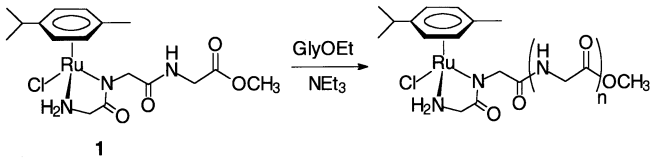

1

The course of the metal-catalyzed peptide oligomerization was followed by FAB mass spectrometry. This analytical tool allows the simultaneous determination of the various intact (peptide)Ru^{II} complexes that are present in the reaction mixture.[6] The relative amount of each peptide complex was estimated by comparing the appropriate peak heights. Table 1 and Figure 1A show how the distribution of the higher peptides changes as the complex is "fed" with successive one-equivalent portions of glycine ester. Significant amounts of hepta- to nonapeptides are obtained after the addition of 8 equivalents of GlyOEt. The time course of product formation reflects the statistical growth of the peptide chain. The limiting factor of this reaction was the increased viscosity of the solution after the addition of several portions of the amino acid. It should be emphasized, however, that the presence of the lipophilic (*p*-cymene)Ru^{II} fragment strongly increases the solubility of the otherwise

 © WILEY-VCH Verlag GmbH, D-69451 Weinheim, 1998 1434−1948/98/0729−0731 $ 17.50+.50/0

notoriously insoluble polyglycine peptides in organic solvents.

Figure 1. Catalytic formation of polypeptide complexes by consecutive addition (every 24 h) of glycine ethyl ester (A) or alanine methyl ester (B)

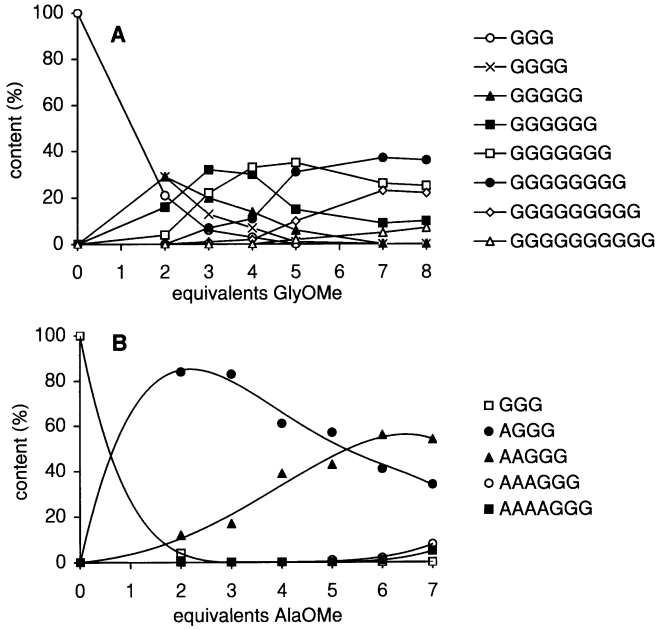

Table 1. Formation of (oligoglycine)ruthenium complexes following successive additions of one-equivalent portions of glycine ethyl ester

Peptide	Start	Portion no. 2	3	4	5	7	8
triglycine	100	21	6	3	0	0	0
tetraglycine	0	29	13	7	1	0	0
pentaglycine	0	29	20	14	6	0	0
hexaglycine	0	17	32	30	15	9	10
heptaglycine	0	4	22	33	35	26	25
octaglycine	0	0	7	11	31	37	26
nonaglycine	0	0	1	2	10	23	22
decaglycine	0	0	0	0	2	5	7

For comparison, a (pentaglycine methyl ester)ruthenium complex **2** was prepared directly from $[(C_6Me_6)RuCl_2]_2$ and GGGGGOMe. *N*,*N*-coordination in **2** is proven by the IR absorptions at 1660 and 1579 cm^{-1}.[4]

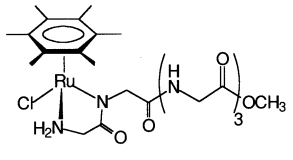

2

While with glycine ethyl ester and **1** the relative amount of any single product does not exceed 40% because of similar reactivities of all the products, with alanine methyl ester (AlaOMe) and **1** a different situation is encountered. Scheme 3 illustrates the reaction of **1** with one equivalent of AlaOMe. The larger steric bulk of this amino acid seems to prevent it from undergoing successive condensation reactions. Therefore, a substantial build-up of the AGGG complex (up to 84%) and the AAGGG complex (up to 56%) is observed (Figure 1B). Only minor amounts of peptide complexes with more than two alanine residues are produced, even after the addition of 7 equivalents of AlaOMe.

Scheme 3

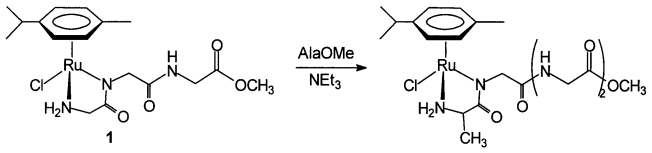

The experiments described herein demonstrate that (*p*-cymene)Ru^{II} complexes are able to catalyze the formation of oligopeptides from simple amino acid esters. We are currently investigating whether this strategy can be applied to generate oligopeptides with a different amino acid content and/or a longer chain length. In certain cases, this new synthetic approach might be an interesting alternative to conventional methods of peptide synthesis.

We are deeply indebted to Prof. Dr. *W. Steglich* for providing a series of mass spectra. Generous support by the *Deutsche Forschungsgemeinschaft* and the *Fonds der Chemischen Industrie* is gratefully acknowledged.

Experimental Section

Reactions were carried out in Schlenk tubes under N_2 or Ar. Methanol (puriss., < 0.05% H_2O) was saturated with N_2 and stored over molecular sieves (3 Å). $[(p\text{-cymene})RuCl_2]_2$ and $[(C_6Me_6)RuCl_2]_2$ were prepared according to literature procedures.[7] The free amino acid esters were prepared from the hydrochlorides by treatment with NEt_3 in dichloromethane. NEt_3·HCl precipitated upon addition of pentane. − IR: Perkin-Elmer 841, Nicolet 520; PE = polyethylene. − NMR: JEOL EX 400. − MS: Finnigan MAT 90 mass spectrometer.

[(p-Cymene)Ru(GGGOMe−H⁺)Cl] (**1**): A solution of 288 mg (1.2 mmol) of GGGOMe·HCl and 1.2 mmol of NaOMe in 10 ml of methanol was added to a suspension of 367 mg (0.6 mmol) of $[(p\text{-cymene})RuCl_2]_2$ in 20 ml of methanol. After stirring for 2 h, the mixture was concentrated in vacuo to a volume of 2 ml. NaCl precipitated upon the addition of 10 ml of dichloromethane and 3 ml of pentane and was separated by centrifugation. The solvent was then removed in vacuo. After the addition of pentane, an oily red compound was obtained. The product was purified by recrystallization from methanol/diethyl ether. Yellow powder. Yield 543 mg (94%). − M.p. 203−206°C (decomposition). − IR (KBr): $\tilde{\nu}$ = 3333 cm^{-1} (m), 3275 (m, sh), 3128 (m, NH), 1748 (s, C=O, ester), 1665 (s, amide I, uncoord.), 1583 (vs, amide I, coord.), 1535 (m, amide II). − IR (PE): $\tilde{\nu}$ = 286 cm^{-1} (w), 253 (m, RuCl). − ^{1}H NMR (400 MHz, $CDCl_3/CD_3OD$): δ = 1.27 [d, ^3J = 7 Hz, 6 H, $CH(CH_3)_2$], 2.21 (s, 3 H, $ArCH_3$), 2.83 [sept, ^3J = 7 Hz, 1 H, $CH(CH_3)_2$], 3.15 (m, 2 H, NH_2CH_2), 3.76 (s, 3 H, OCH_3), 3.94 (m, 2 H, CH_2CO_2), 4.11 (d, ^2J = 17 Hz, 1 H, NCH_2CO), 4.78 (d, ^2J = 16 Hz, 1 H, NCH_2CO), 5.36−5.58 (m, 4 H, C_6H_4). − ^{13}C NMR (68 MHz, $CDCl_3/CD_3OD$): δ = 18.63 ($ArCH_3$), 22.00, 23.10 [$CH(CH_3)_2$], 31.13 [$CH(CH_3)_2$], 40.94 (CH_2CO_2), 46.76 (NH_2CH_2), 52.54 (OCH_3), 54.74 (NCH_2CONH), 80.83, 81.95, 82.10, 82.47, 96.46, 101.76 (C_6H_4), 170.71 (CO_2Me), 174.45, 180.36 (CON). − $C_{17}H_{26}ClN_3O_4Ru \cdot 1/2\ H_2O$ (481.9): calcd. C 42.37, H 5.65, N 8.72; found C 42.56, H 5.87, N 8.55.

[(C$_6$Me$_6$)Ru(GGGGGOMe−H$^+$)Cl] (**2**): 311 µl (0.19 mmol) of NaOMe/MeOH (1.19 M) was added dropwise to a suspension of 65 mg (0.19 mmol) of GGGGGOMe·HCl and 62 mg (0.09 mmol) of $[(C_6Me_6)RuCl_2]_2$ in 15 ml of methanol. After 1 h, a small amount of a precipitate was separated by centrifugation and the solvent was removed in vacuo. The residue was treated with 5 ml of dichloromethane, 1 ml of methanol, and 2.5 ml of pentane and NaCl was removed by centrifugation. The product precipitated upon addition of 30 ml of pentane and was purified by recrystallization from methanol/dichloromethane (2:1)/diethyl ether. Orange crystals. Yield 40 mg (35%). − M.p. 198°C (decomposition). − IR (KBr): $\tilde{\nu}$ = 3289 cm^{-1} (s, NH), 3243 (sh, NH), 1758 (m, C=O, ester), 1743 (m, C=O, ester), 1691 (sh, amide I, uncoord.), 1660 (vs, amide I, uncoord.), 1579 (vs, amide I, coord.). − ^{1}H NMR (400 MHz, CD_3OD): δ = 2.13 (s, 18 H, $ArCH_3$), 3.14 (s, 2 H, NH_2CH_2), 3.31 (CH_2 together with CD_2HOD), 3.37 (s, 2 H, CH_2), 3.73 (s, 3 H, OCH_3), 3.89 (br. s, 2 H, CH_2), 3.95 (s, 2 H, CH_2). − $C_{23}H_{36}ClN_5O_6Ru\cdot H_2O$ (633.1): calcd. C 43.63, H 6.05, N 11.06; found C 44.01, H 6.24, N 11.02.

Peptide Synthesis: 213 mg (0.45 mmol) of $[(p\text{-cymene})RuCl_2]_2$ was dissolved in 20 ml of methanol and 347 µl (2.5 mmol) of NEt_3 was added as co-catalyst. Once per day one portion of 57 µl (0.55 mmol) of GlyOEt was added to the solution. Just before adding the third portion, a sample of 1.9 ml (first data point) was removed from the reaction vessel. Peptide complexes were isolated after precipitation with 30 ml of diethyl ether and were analyzed by mass spectrometry. The reaction volume was kept constant by adding 2 ml of methanol. Subsequent data points were obtained similarly. As the amount of complex in the solution decreased, the amount of GlyOEt added was decreased accordingly. After addition of the seventh portion, the viscosity increased and magnetic stirring became problematic. The solution showed thixotropic properties. − Peptide synthesis with AlaOMe was performed analogously using 152 mg (0.32 mmol) of $[(p\text{-cymene})RuCl_2]_2$ and 250 µl of NEt_3 dissolved in 20 ml of methanol.

MS Analysis: FAB-MS measurements were performed using *m*-NBA as the matrix. For each peptide complex present, three to four well-separated peak groups can be identified, corresponding to [M − Cl$^-$], [M − Cl$^-$ + H$^+$ + Na$^+$], [M + H$^+$], and [M + Na$^+$]. Ionization occurs without decomposition of the complex. Semi-quantitative analyses were performed by comparing the sums of the relevant peak heights.

☆ Dedicated to Professor *Heinrich Nöth* on the occasion of his 70th birthday as a mark of friendship and respect.

[1] A. Böhm, K. Polborn, K. Sünkel, W. Beck, *Z. Naturforsch. B.*, in press.

[2] [2a] D. A. Buckingham, L. G. Marzilli, A. M. Sargeson, *J. Am. Chem. Soc.* **1967**, *89*, 2772−2773. − [2b] D. R. Knighton, D. R. K. Harding, M. J. Friar, W. S. Hancock, G. D. Reynolds, C. R. Clark, R. F. Tasker, D. A. Buckingham, *J. Am. Chem. Soc.* **1981**, *103*, 7025−7026. − [2c] P. A. Suton, D. A. Buckingham, *Acc. Chem. Res.* **1987**, *20*, 357−364. − [2d] J. P. Collman, E. Kimura, *J. Am. Chem. Soc.* **1967**, *89*, 6096−6103. − [2e] Y. Wu, D. H. Bush, *J. Am. Chem. Soc.* **1972**, *94*, 4115−4122. − [2f] S. Yamada, M. Wagatsuma, Y. Takeuchi, S. Terashima, *Chem. Pharm. Bull. Tokyo* **1971**, *19*, 2380. − [2g] S. Terashima, M. Wagatsuma, S. Yamada, *Tetrahedron* **1973**, *29*, 1487−1496, 1497−1502.

[3] [3a] M. G. Schwendinger, B. M. Rhode, *Anal. Sci.* **1989**, *5*, 411. − [3b] B. M. Rhode, *Spektrum Wiss.* **1991**, *March*, 26−32. − [3c] H. Eder, S. Saetia, B. M. Rhode, *Inorg. Chim. Acta* **1993**, *207*, 3−10.

[4] [4a] W. Beck, R. Krämer, *Angew. Chem.* **1991**, *103*, 1492−1493; *Angew. Chem. Int. Ed. Engl.* **1991**, *30*, 1467−1468. − [4b] R. Krämer, M. Maurus, K. Polborn, K. Sünkel, C. Robl, W. Beck, *Chem. Eur. J.* **1996**, *2*, 1518−1526.

[5] Recently, a nickel(0)-catalyzed in vivo polycondensation of α-amino acid *N*-carboxyanhydrides was reported: T. J. Denning, *Nature* **1997**, *390*, 386−389.

[6] It has been demonstrated that selective interactions of peptides with one or more metal ions can be observed by mass spectrometry: [6a] T. W. Hutchens, R. W. Nelson, T.-T. Yip, *FEBS* **1992**, *296*, 99. − [6b] C. L. Gatlin, F. Turecek, T. Vaisar, *Anal. Chem.* **1994**, *66*, 3950−3958. − [6c] C. L. Gatlin, F. Turecek, T. Vaisar, *J. Mass Spectrom.* **1995**, *30*, 1617. − [6d] P. Hu, J. A. Loo, *J. Am. Chem. Soc.* **1995**, *117*, 11314−11319. − [6e] C. L. Gatlin, R. D. Rao, F. Turecek, T. Vaisar, *Anal. Chem.* **1996**, *68*, 263−270.

[7] M. A. Bennett, T.-N. Huang, T. W. Matheson, A. K. Smith, *Inorg. Synth.* **1982**, *21*, 74−76.

[97317]

The π-Electron-Accepting Ability of the Boron Atom in Ethynylboranes and Related Compounds – An Approximate Weight Computation for Resonance Structures☆

Vinzenz Bachler*, and Nils Metzler-Nolte*

Max-Planck-Institut für Strahlenchemie,
Stiftstrasse 34–36, D-45470 Mülheim a.d. Ruhr, Germany
Fax: (internat.) +49(0)208/306-3951
E-mail: nils@mpi-muelheim.mpg.de; bachler@mpi-muelheim.mpg.de

Received December 23, 1997

Keywords: Aminoboranes / Ab initio calculations / Valence-bond theory / Resonance structures / Alkynes

A theoretical analysis was performed to quantify the π-electron-accepting ability of the boron atom in ethynylboranes. An expansion technique was employed which permits to obtain a set of localized bonding schemes and their weights from a delocalized molecular orbital determinantal wavefunction. The derived manifold of bonding schemes is close to the classical resonance hybrid used in organic chemistry (valence-bond description). We quantified the π-electron transfer into the empty π-orbital of the boron atom by investigating nine model compounds where substituents with π-electron-donating ability are adjacent to a boron atom. This led to an ordering of the substituents according to their electron-donating ability towards boron. The boron atom hesitates to accept π-electrons from the ethynyl group in ethynylboranes in particular when good π-donors like amino groups are present. The π-electron donation from the vinyl group to the adjacent boron centre is slightly stronger than from the ethynyl group. Nitrogen lone-pair electrons are easily transferred to a neighbouring boron centre. Bonding schemes and their weights are in line with computed bond lengths and rotational barriers. Moreover, our theoretical results rationalize previous NMR and X-ray experiments and are in line with the reactivity of related compounds. It is demonstrated that bond lengths alone do not necessarily correlate with the degree of π-bonding and should be discussed with caution. The analysis is substantiated by showing that weights for covalent bonding schemes, as obtained from the simple restricted closed-shell MO determinant, correlate with bond strengths. Furthermore, a correlation of bonding-scheme weights with quantities based on the fragment orbital approach is presented. This novel correlation elucidates molecular properties which determine the extent of the π-electron transfer to the boron atom and permits a quantitative interpretation and prediction of intramolecular π-bonding.

Introduction

Ethynylboranes are characterized by a carbon−carbon triple bond directly attached to a Lewis acid boron atom[1]. Its electron-accepting ability may lead to an electron transfer from the adjacent alkynyl π-electron system into the empty π-orbital of the boron atom. This is illustrated in Scheme 1 for the parent compound ethynylborane **1a**.

Scheme 1. Two resonance structures symbolizing the electron-accepting ability of the boron atom

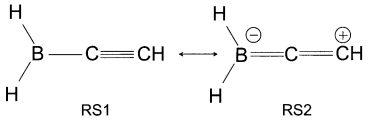

The π-electron structure of ethynylborane is described by the two resonance structures RS1 and RS2 which symbolize an alkynylborane and a heteroallene, respectively. In the heteroallene resonance structure RS2 one of the two π-electrons delocalized above and below the molecular plane is transferred to the boron atom. This transfer leads to a partial double bond between the boron atom and the alkynyl group accompanied by a formal negative and a positive charge at the boron and the terminal carbon atom, respectively (see Scheme 1). The relative weights of RS1 and RS2 in the resonance hybrid for those compounds have been debated for some time. X-ray crystallographic results[2] do not show a significant lengthening of the carbon−carbon triple bond or a shortening of the boron−carbon bond. In analogy to phenyl- and vinylboranes, NMR data for ethynylboranes have been interpreted in the light of a substantial B=C double bond character[3]. Calculated bond lengths and rotational barriers[2h][2i] of several alkynylboranes support a rather weak B=C double bond. Thus, the various findings appear partially contradictory. Moreover, they permit only indirect conclusions about the electronic structure of ethynylboranes and have not been quantified in a concise manner up to now.

Ab initio quantum chemistry provides a more direct access to the electronic structure of ethynylboranes. The predominantly applied computational methods are based on the molecular orbital method[4]. There, spin-coupled electron pairs are located in molecular orbitals delocalized over the whole molecule. Scheme 1, however, represents a set of valence-bond resonance structures which describe spin-coupled electron pairs strictly localized in bonds. Thus, a valence-bond calculation for ethynylboranes would be the ap-

 © WILEY-VCH Verlag GmbH, D-69451 Weinheim, 1998 1434−1948/98/0606−0733 $ 17.50+.50/0

propriate method for computing the weights of RS1 and RS2 contained in the valence-bond wave function. They would indicate the importance of RS1 and RS2 for the electronic structure of ethynylboranes. An alternative way is to compute a molecular orbital wave function and to analyze this wave function a posteriori in terms of resonance structures and their weights[5]. Recently, a concise method was proposed for expanding a determinantal wave function composed of delocalized molecular orbitals into a set of determinantal wave functions consisting of localized atomic orbitals[6]. The procedure permits to obtain from a delocalized molecular orbital wave function weights for localized bonding schemes which are close to the resonance structures of organic chemistry. Thus, the method is suited to discuss the frequent problem about the weight of a particular resonance structure in a resonance hybrid. In the following sections we use this technique to investigate the π-electron-accepting ability of the boron atom in ethynylboranes. We do this by obtaining weights for localized bonding schemes for a characteristic set of molecules. Our set of model compounds is represented in Scheme 2.

Scheme 2. The set of model compounds selected for quantifying the π-electron donation into the empty π-AO of boron

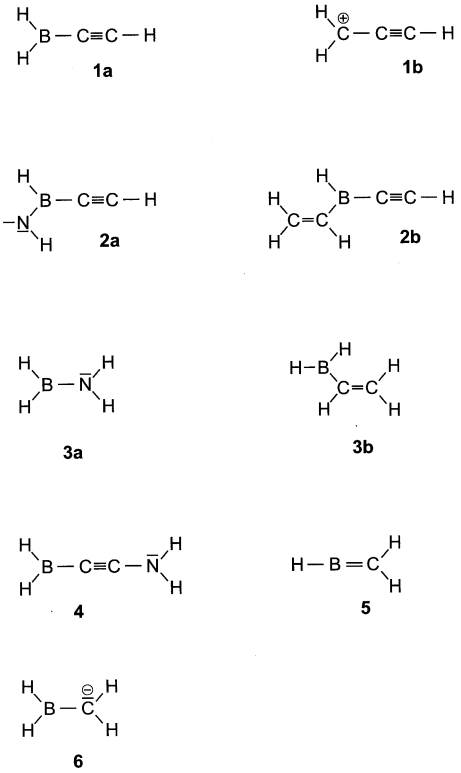

Ethynylborane (**1a**) is the parent compound of alkynylboranes and the main objective of our investigation. The BH_2 group is isoelectronic with the methylene cation CH_2^+. The differences in their π-electron-accepting properties are illustrated by compairing **1a** and the ethynylmethylene cation (**1b**). In **1a** and **1b**, only the ethynyl groups donate π-electrons to the BH_2 and the CH_2^+ group, respectively. However, the π-electron-donating properties of amino and vinyl groups are also well established[3b][7]. In **2a** and **2b** competitive π-electron donation may occur and we investigate the competitive electron-donating abilities of the amino, vinyl and ethynyl groups, for which aminoborane (**3a**) and vinylborane (**3b**) serve as reference compounds. Our set of model compounds comprised also 2-aminoethynylborane (**4**) where the electron attraction of the BH_2 group and the electron donation of the NH_2 group are mediated by the ethynyl group. This should lead to a push-pull π-electron transfer in **4**. In methyleneborane (**5**) the sp-hybridized boron atom itself provides a π-electron and a full carbon−boron double bond exists. In the methylborane carbanion (**6**) only a partial B=C double bond is formed which stabilizes the carbanion by delocalizing the negative charge. Compounds **5** and **6** were included in this study to put the amount of B=C double bonding (as expected from resonance structure RS2) in perspective.

Computational Methods

Applied Programs and the Expansion Technique

Quantum chemical calculations were performed by using the Gaussian 92/DFT suite of ab initio programs operating under OpenVMS[8]. The restricted Hartree-Fock (RHF) method[9] and the 6−311G** basis sets[10] were applied to optimize the geometries of the molecules.

We used the recently proposed technique[6] to expand a molecular orbital (MO) determinantal wave funtion Ψ^{mo} into N_D determinantal wave functions Ψ_i^{ao} composed of atomic orbitals (AOs).

$$\Psi^{mo} = \sum_{i=1}^{N_D} c_i \Psi_i^{ao} \qquad (1)$$

The expansion coefficients c_i in (1) are determinants of matrices which contain definite selections of the canonical MO coefficients. The weight w_i of a definite Ψ_i^{ao} in the expansion (1) was computed by means of

$$w_i = \frac{c_i^2}{\sum_{j=1}^{N_D} c_j^2} \qquad (2)$$

Equation 1 leads to an expansion of the delocalized wave function Ψ^{mo} into wave functions Ψ_i^{ao} which are strictly localized. Any Ψ_i^{ao} represents a definite occupation pattern of the localized atomic spin orbitals. Hence, we analyze the delocalized MO wave function in terms of local spin occupations and their weights[6]. Furthermore, local bonding schemes are obtained by drawing lines between electrons of opposite spin-localized at adjacent atoms of the molecule. These bonding schemes are close to the resonance structures drawn by organic chemists[6]. We are mainly interested in the π-electron distribution. Therefore, MO determinants Ψ^{mo} composed of π-MOs were expanded.

The Expansion Technique and Extended AO Basis Sets

We employed the extended basis set 6−311G[11] to expand Ψ^{mo} into the Ψ_i^{ao}s. We note, that eq. 1 holds also when extended basis sets are employed[6]. Thus, the Ψ_i^{ao}s contain the various groups of contracted gaussian functions which represent the π-AOs. Use of the 6−311G basis set requires a recipe for computing the total weights of the various local spin occupations.

Consider a planar molecule with four π-electrons distributed over four adjacent π-AOs. Each of them is represented by three groups of primitive gaussians. Consequently, various types of spin occupations can occur in the Ψ_i^{ao}s[12] (Scheme 3).

Scheme 3. Several types of local spin occupations occuring when the 6−311G basis is applied in the expansion technique; the occupation schemes are used to obtain local atomic spin occupations

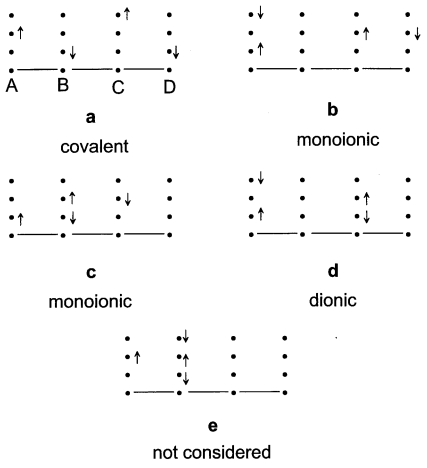

The covalent spin occupation of type (a) describes a complete spin alternation. We obtain the total weight of the local covalent spin occupation by adding up all weights of those 81 Ψ_i^{ao}s which describe the general spin-occupation pattern given by (a). The total weight for a local monoionic spin occupation is obtained by sampling the weights for Ψ_i^{ao}s with occupation patterns of type (b). A similar sampling is performed to compute the total weight for further monoionic and diionic spin occupations resulting from cases (c) and (d), respectively. However, eq. 1 produces also Ψ_i^{ao}s for energetically unfavourable spin occupations of type (e) which allocate three electrons at one atom. Those spin occupations have very small weights and are neglected in our weight sampling.

Relating Weights and Bond Strengths

We also relate weights for bonding schemes to the strengths of the bonds designated by the bonding schemes. For this purpose the second derivatives of the molecular energy with respect to definite internal coordinates are needed. These coordinates are the bond lengths in the *z*-matrix[13] defining the molecular geometries. We computed the second derivatives by repeating the last step in the geometry optimization but we used an analytic hessian (FOPT=CALCALL)[8]. The second derivatives of the energy with respect to the internal coordinates of the *z*-matrix were printed out by means of the option IOP(1/33 = 1)[8].

Results

π-Electron Donation from the Alkynyl Group to the Isoelectronic BH_2 and CH_2^+Groups

In ethynylborane (**1a**) the Lewis acidic BH_2 group is directly attached to the ethynyl group (see Scheme 1). Two π-electrons of this group can be transferred to the BH_2 group by partially occupying the empty π-orbital of the boron atom. Thus, two π-electrons of the ethynyl group can delocalize over three π-AOs and a partial boron−carbon π-bond can be formed (see Scheme 1). In order to investigate the extent of this π-bonding we expanded a restricted closed-shell MO determinant for the two π-electrons into the set of all 81 AO determinants. We derived local spin occupations by sampling the corresponding AO determinants as outlined above. Local spin occupations and their weights are given in the first column of Table 1.

Table 1. Bonding schemes and their weights for ethynylborane (**1a**); the covalent weights show that the boron atom hesitates to accept π-electrons from the ethynyl group

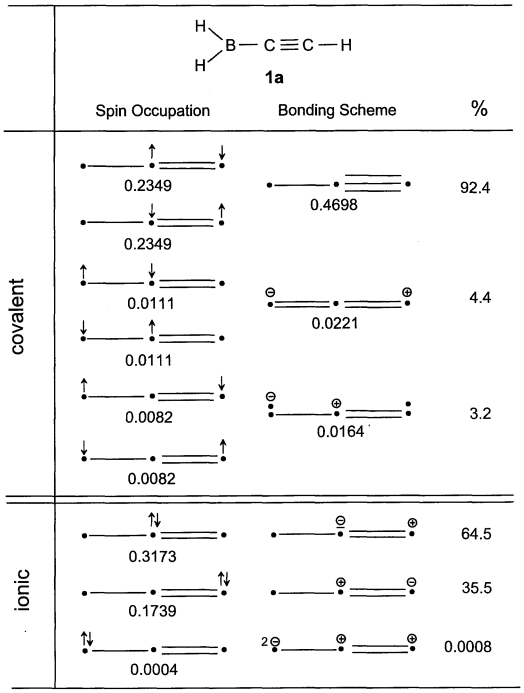

Generally, a line in a bonding scheme represents a spin-coupled electron pair localized in bonds or at an atom by forming a lone pair[14]. In the second column of Table 1 spin occupations of the first column are converted into bonding schemes. Equal weights of spin-inverted spin occupations are added up to derive weights for bonding schemes. All covalent AO determinants give rise to three covalent bonding schemes. All ionic AO determinants make up three ionic bonding schemes (see Table 1). It is well known that expanding an uncorrelated restricted MO determinant produces weights for the covalent and ionic bonding schemes which are too small and too large, respectively[15].

This problem could be alleviated by using a correlated wavefunction to obtain localized bonding schemes, the procedure for which is, however, computationally more involved. Former work has demonstrated that geometries for boron compounds are reproduced reasonably well by RHF calculations. Moreover, it was shown previously that *within the subspaces* of the covalent and ionic bonding schemes the weights can be expected to appear in correct relative order[16]. Therefore, the weights of covalent bonding schemes in Table 1 should indicate their relative importance. Because this work concentrates solely on the relative importance of covalent bonding schemes, all ionic bonding schemes have been omitted for clarity for the other compounds in this study. In the following we estimate the importance of a covalent bonding scheme by its weight precentage value, where 100% is the weight sum of all covalent bonding schemes. Table 1 shows that the two π-electrons reside mainly on the alkynyl group (92.4%). A heteroallene structure with a B=C double bond is only of minor importance (4.4%). The weight for the singlet diradicaloid bonding scheme is small (3.2%) but of comparable magnitude. These results suggest that the boron atom hesitates to accept a single π-electron from the alkynyl group. It also avoids to accept a spin-coupled electron pair as indicated by the very small weight of the respective charge-separated bonding scheme. These conclusions seem to be supported by the optimized geometries. The carbon−carbon triple bond length of the alkynyl group is 1.1927 Å, a value close to the carbon−carbon triple bond length of acetylene (1.204 Å)[17]. Thus, the C≡C bond in **1a** is in essence an acetylene triple bond. A value of 1.5250 Å is computed for the B−C bond length in **1a**. This value is close to the computed B−C bond length in BH_2-CH_3 (1.578 Å)[18]. The small bond shortening is in line with the different carbon hybridizations present in **1a** and BH_2-CH_3 (sp vs. sp^3). All results support the notion that the double-bond character of the B−C bond in **1a** is small.

In **1b** the ethynyl group is adjacent to the positively charged CH_2^+ group which is isoelectronic to the BH_2 group of **1a**, but expected to be a much stronger π-acceptor due to its positive charge. As for **1a**, the covalent AO determinants for **1b** lead to three local covalent spin occupations and bonding schemes as recorded in Table 2.

Table 2. Bonding schemes and their weights for model compound **1b**; the covalent weights indicate the two π-electrons are delocalized

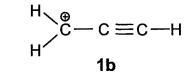

1b

Spin Occupation	Bonding Scheme	%
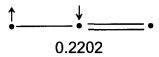 0.2202	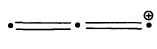	42.2
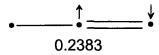 0.2383	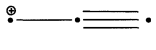	45.7
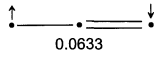 0.0633	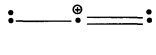	12.1

They show that the two π-electrons are almost equally localized in the CH_2-CCH bond region (42.2%) and in the $CH_2C{\equiv}CH$ bond region (45.7%). Hence, the carbon−carbon triple bond experiences a removal of π-electrons but also positive charge is accumulated in this bond region as indicated by the first bonding scheme of Table 2. These two effects have an opposite influence on the carbon−carbon triple bond length which therefore remains unaffected. In contrast, the carbon−carbon single bond CH_2-CCH should have a significant double-bond character. Both conclusions are supported by the optimized bond lengths: The CH_2-CCH bond length of 1.3414 Å is close to the carbon−carbon bond length in ethylene (1.337 Å)[19], but the $CH_2C{\equiv}CH$ bond length is 1.2096 Å, a value near 1.204 Å which is the carbon−carbon bond length in acetylene[17]. Thus, in spite of the *massive* π-electron withdrawal from the triple bond its bond length remains virtually unchanged. This fact emphasizes that geometrical parameters are at best an indirect measure of electronic properties. The leading covalent bonding schemes of Table 2 describe the well-known delocalization of the positive charge[20] among the two terminal carbon atoms. A feature of cation **1b** seems to be its notable singlet biradical character. This is indicated by the appreciable weight of the third covalent bonding scheme (12.1%). This conclusion illustrates an advantage of the applied procedure: The singlet biradical character of a closed-shell molecule is contained in a restricted closed-shell MO determinant. However, it remains hidden but is revealed by the expansion technique[6].

The effective charge delocalization in alkynyl-substituted carbocations has been demonstrated by Olah et al.[21] using NMR spectroscopy.

Scheme 4. A set of alkynyl-substituted compounds where π-electron delocalization operates; compound **C** serves as a comparison

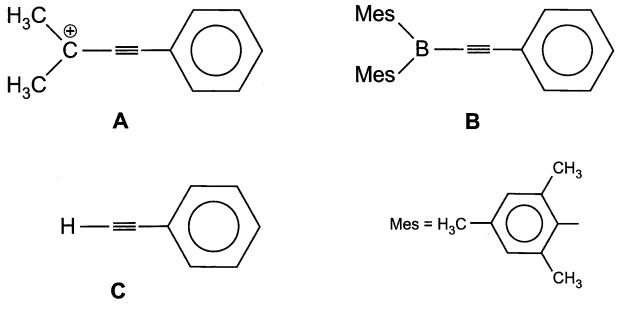

In **A** (see Scheme 4), the ^{13}C chemical shift of the *para*-carbon atom of the phenyl ring is $\delta_p = 145.5$ or $\Delta\delta_p = 16.8$ downfield from that of the respective carbon atom in **C**[21]. In **B**, $\Delta\delta_p$ is only 1 ppm[3d] supporting our notion that despite of their isoelectronic nature, the X−C≡C π-interaction is much weaker in ethynylboranes (X = R_2B) than in the carbocation (X = R_2C^+). By comparing the results for model compounds **1b** and **1a** we have presented two extreme cases of a strong and weak electron delocalization, respectively, which are most likely inaccessible preparatively. In those ethynylboranes known, competitive π-electron donation from other substituents to boron might diminish the

B−C≡C π-interaction even further. A quantitative estimate of these substituent effects is presented in the next section.

Competitive π-Electron Donations from the Amino, Vinyl, and Ethynyl Groups to the BH_2 Group

There is ample experimental evidence for the formation of a partial boron−nitrogen double bond in aminoboranes. For example, NMR spectroscopy shows a hindered rotation about the B−N bond and a rotational barrier of ca. 20 kcal/mol is measured[7f][7i] and confirmed by computational methods[22]. In aminoboranes with three-coordinate boron atoms the B−N bond length is ca. 1.40 Å and the nitrogen atom is planar[7a][7f][7i]. In related compounds with tetra-coordinated boron atoms, however, the B−N bond is ca. 0.05 Å longer and the nitrogen atom is pyramidal[7a][7f][7i]. π-Electron donation from a vinyl group to a neighbouring boron centre is considered to be much weaker, but firmly established[1d]. We have calculated the relative weights for all covalent bonding schemes in amino(ethynyl)borane (**2a**) and ethynyl(vinyl)borane (**2b**) in order to determine the relative π-donating abilites of the three substituents.

The four π-electrons in **2a** occupy two π-MOs delocalized over four π-AOs. By expanding a restricted closed-shell MO determinant we obtained a set of 4356 AO determinants for the four π-electrons. The results for the local covalent spin occupations and their weights as obtained by sampling the corresponding AO determinants are displayed in Table 3.

Table 3. Covalent bonding schemes and their weights for the amino(ethynyl)borane (**2a**)

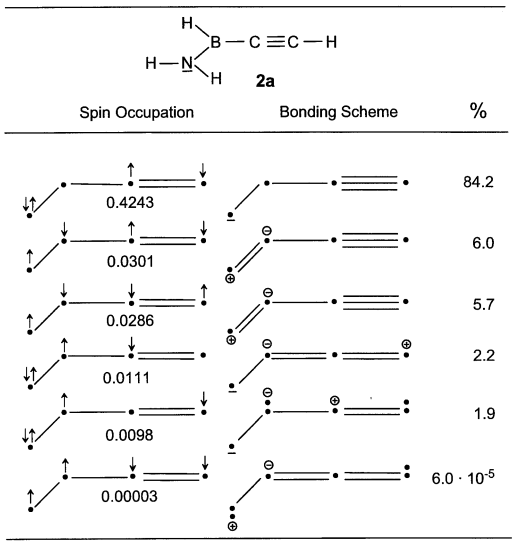

As before, any line in a bonding scheme symbolizes a spin-coupled electron pair present in the corresponding local spin occupation. A single local spin occupation, however, may be compatible with various ways of drawing lines and its weight contributes to the weights of several bonding schemes[6]. Such a case is the second spin occupation in Table 3 contributing at least to a biradical scheme with a central double bond and to a scheme with a triple bond in the alkynyl group and an N=B double bond. The alkynyl carbon−carbon bond is much shorter (1.1904 Å) than the boron−carbon bond (1.5495 Å) and the bonding scheme comprising an alkynyl triple bond should be energetically much more favourable. Therefore, we attributed the weight of the second spin occupation solely to the bonding scheme with the alkyne triple and the N=B double bond (see Table 3). Similar arguments have been applied previously to derive bonding schemes from local spin occupations where the conversion is non-unique[6].

Weights in Table 3 indicate that the four π-electrons in **2a** prefer the ethynyl group and the nitrogen lone pair (84.2%). However, the boron atom accepts an electron from the nitrogen lone pair by forming a partial nitrogen−boron double bond $H_2N{=}BHCCH$ (11.7%). The formation of a π-bond between the boron atom and the ethynyl group is rather unfavourable (2.2%). The singlet biradical character of **2a** is also negligible (1.9%). In aminoborane (**3a**) (36 AO determinants for two π-electrons delocalized over two centres) the weight for the resonance hybrid with a B=N double bond is 11.2%. These results imply that the boron atom readily accepts an electron from the nitrogen lone pair, but much less from the ethynyl group. In addition, the ethynyl group is a fairly electronegative substituent at the boron centre. Its electron withdrawal through the σ bond is balanced by a slightly stronger π-electron donation from the nitrogen atom (11.7% vs. 11.2%). This idea had been advanced previously but remained unsubstantiated until now. Former computations[23] have shown that a barrier of 32.4 kcal/mol exists for a rotation about the nitrogen−boron bond. This barrier height points to a partial double-bond character and is in line with the exceptional stability of aminoboranes. Lone-pair electron donation has been exploited frequently for stabilizing otherwise inaccessible boron compounds e.g. diborane compounds[2g][24], boranes with B=C[25], B=N[26] and B=P[27] bonds. ^{13}C chemical shifts for compounds similar to **2a** have been analyzed in some detail. They are in line with an ethynyl group without electron deficit[2d][2e][2f][2h][28]. These experimental findings corroborate our theoretical result that the boron atom avoids to accept π-electrons from the C≡C triple bond provided a good π-donor like the amino group in **2a** is present. A direct comparison between two weak π-donors is possible in compound **2b** (Table 4). In **2b**, four π-electrons are distributed over five π-AOs and we obtained 11025 AO determinants.

The results in Table 4 highlight the preference of the four π-electrons for the vinyl and the ethynyl groups (83.5%). The boron atom accepts only weakly a π-electron from the vinyl group by forming the boron−carbon double bond $H_2CCH{=}BHCCH$ [5.6%, compared to 5.2% in vinylborane (**3b**)]. Electron donation from the ethynyl group by forming an $H_2CCHBH{=}CCH$ boron−carbon double bond is even less favourable (3.5%). The various singlet biradical bonding schemes appear only with small weights. However, *the vinyl group is a slightly better π-electron donator than the alkynyl group.* Our conclusions are substantiated by the optimized carbon−carbon bond lengths for the vinyl and the ethynyl group which are 1.3300 Å and 1.1921 Å, respectively. They are close to the bond lengths of ethylene (1.337

Table 4. Covalent bonding schemes and their weights for the ethynyl(vinyl)borane (**2b**); the boron atom accepts only weakly π-electrons; the π-donation is slightly stronger from the vinyl than from the ethynyl group

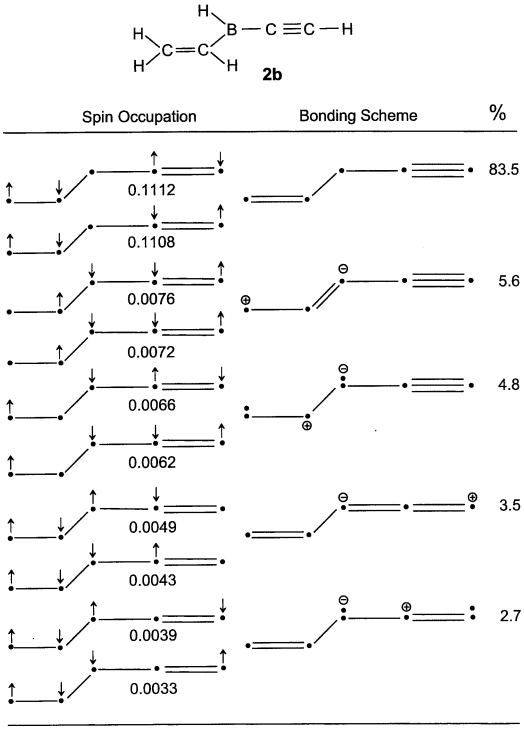

Å)[19] and of acetylene (1.204 Å)[17], respectively. The boron−carbon bonds $H_2CCH-BHCCH$ and $H_2CCHBH-CCH$ in **2b** have lengths of 1.5491 Å and 1.5358 Å, respectively. Again, these values reflect the trend imposed by the different hybridization states of the carbon atoms.

Conclusions from the Expansion Results

The following picture emerges consistantly from the above expansion results. The lone-pair electrons of an amino group are donated efficiently into the empty π-orbital of boron. Adjacent carbon−carbon double or triple bonds are an order of magnitude weaker π-electron donors. In the absence of a good π-electron donor, however, the boron centre excerts its full Lewis acidity and the extent of B=C bonding is doubled but still remains small (2.2% in **2a**, Table 3, vs. 4.4% in **1a**, Table 1). In the presence of a comparably potent π-donor, e.g. the vinyl group, an ethynyl group will only excert half of its maximal electron-donating ability (3.5%, Table 4). Moreover, the weights show that the vinyl group is more electron-donating than the ethynyl group (5.6% vs. 3.5%, Table 4). This is corroborated by ^{13}C-NMR data on dimesitylboranes[29].

Electron Donation from an NH_2 to the BH_2 Group Mediated by an Alkynyl Group

2-Aminoethynylborane (**4**) is of push-pull type and the electron transfer is mediated by the π-electrons of the alkynyl group perpendicular to the molecular plane. Due to this intramolecular electron transfer a partial $H_2B=CCNH_2$ double bond is expected. In order to verify this assumption we expanded a restricted MO determinant[6] for the four π-electrons and we obtained 4356 AO determinants. Subsequently, we derived covalent local spin occupations and their weights by sampling weights of the corresonding AO determinants. The results are compiled in Table 5.

Table 5. Covalent bonding schemes and their weights for the "push-pull" 2-aminoethynylborane (**4**)

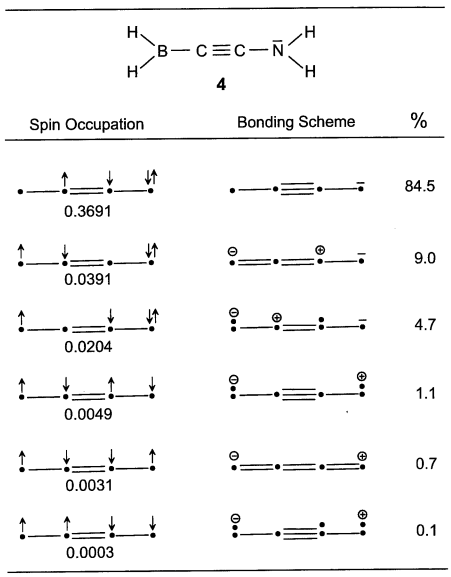

Spin occupation four is characterized by complete spin alternation and its weight can contribute to the weights of several bonding schemes. Again, we attributed the total weight solely to the bonding scheme conceived to have the lowest energy. Table 5 shows that the four π-electrons prefer the alkynyl group and the nitrogen atom by forming a lone pair (84.5%). The weight for the second bonding scheme illustrates that the boron atom accepts also a π-electron from the ethynyl group by forming a partial boron−carbon double bond (9.0%) but two π-electrons remain at nitrogen as a lone pair. This result accords with the notion that the coulomb repulsion between the nitrogen lone pair and the π-electrons of the alkynyl group is important. It is reduced when two alkynyl π-electrons leave the alkynyl group by forming the partial $H_2B=CCNH_2$ double bond. A push-pull character of a molecule is frequently described by resonance structures with a maximal number of covalent bonds[30] similar to the fifth bonding scheme of Table 5. Its small weight, however, shows that the formation of a completely delocalized push-pull system is highly unfavourable. The boron−carbon double-bond character in **4** (9.0%) is larger than in **1a** (4.4%). This accords with the computed boron−carbon bond lengths which are 1.4932 Å in **4** and 1.5250 Å in **1a**. Nöth et al. synthesized compound **D**[31] (see Scheme 5) which contains the "push-pull" part of model compound **4**. B=C π-bonding in **D**, however, is diminished by the two amino groups at the boron atom.

None of the spectroscopic data [δ ^{13}C, $\delta^{11}B$, ν_{CC} (IR)] of **D** are significantly different from other ethynylboranes.

Scheme 5: An alkynylborane which contains a push-pull entity; the push-pull character is dwarfed by two amino substituents at the boron centre

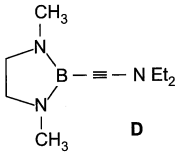

D

These findings are in line with the analysis for the model compounds **2a** and **3a**. The boron atom in **D** accepts lone-pair electrons from the adjacent nitrogen atoms but not from the ethynyl group. Accordingly, **D** could not be photodimerized to form a push-pull-stabilized cyclobutadiene[30].

Strong Carbon−Boron Double Bonds

So far we have concentrated on the formation of a partial B=C double bond through π-donation from an adjacent ethynyl or vinyl group. We will now use our expansion technique to investigate two compounds with strong B=C double bonds. In methyleneborane (**5**), the sp-hybridized boron atom provides itself one π-electron and a full boron−carbon double bond is present[32]. In contrast, the methylborane carbanion (**6**) will develop a partial (but probably strong) B=C double bond because a π-electron of the negatively charged carbon centre may be transferred to the empty π-orbital of the sp^2-hybridized boron atom. We expanded the restricted MO determinants for the two π-electrons and sets of 36 AO determinants were obtained. Weights for covalent and ionic local spin occupations were obtained by sampling the weights of the corresponding AO determinants (Tables 6 and 7).

Table 6. Bonding schemes and their weights for methyleneborane (**5**)

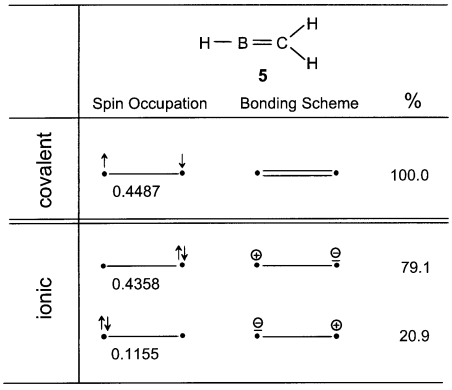

The only covalent bonding scheme for **5** evolves with a weight of 44.9% when referred to the weights of all bonding schemes. This value is close to 50% which is the weight for the covalent bonding scheme of ethylene when a restricted MO determinant is expanded[33]. The proximity of both values shows that a pronounced boron−carbon π-bond is present in methyleneborane (**5**). The π-bond in $H_2C{=}BH$ is further substantiated by its computed short bond length of 1.3741 Å. The weights for the two ionic bonding schemes show that the π-bond is polar and the electrons prefer the carbon atom. As mentioned before, when an uncorrelated wavefunction is expanded the absolute weights for all ionic bonding schemes will be overestimated at the expense of the covalent bonding schemes. Table 6 exemplifies for compound **5** that the covalent weight is only 10% smaller than the covalent weight in ethylene.

Table 7. Bonding schemes and their weights for the methylborane carbanion (**6**)

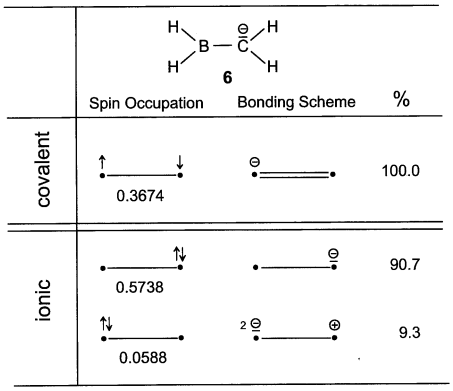

Evidently, the boron−carbon bond in **6** possesses significant double-bond character (36.7%). This supports the notion that the sp^2-hybridized boron atom efficiently stabilizes the carbanion centre by forming a partial double bond accompanied by a delocalization of the negative charge. A decrease of the negative charge at the sp^2-hybridized carbon atom is supported by ^{13}C-NMR data: For the methylene carbon atom in a dialkylmethyleneborane anion, a ^{13}C chemical shift of $\delta = 54.5$ was observed[34]. This value suggests a significant deshielding of the methylene carbon atom as a consequence of π-electron delocalization. The B=C double-bond character in **6** is also corroborated by the calculated B−C bond length of 1.4446 Å. This value is much smaller than 1.5250 Å which is the boron−carbon bond length in the alkynylborane **1a**. Moreover, a rotation about the B−C bond leads to a local minimum located 26.7 kcal/mol higher in energy than the planar ground state[35].

Computed Weights and Bond Strength

We have applied weights for localized bonding schemes to evaluate the electron-accepting ability of a boron atom bonded to a π-electron-donating group. A large electron attraction is indicated by a large weight for those covalent bonding schemes which describe a π-bond between the boron atom and the electron-donating group. Thus, we assume that the weights for covalent bonding schemes are obtained in the correct relative order. The weights were obtained by expanding a restricted closed-shell MO determinant for the π-electrons into the set of AO determinants. It is well known that expanding such an uncorrelated MO determinant leads to covalent and ionic weights which are too small and too large, respectively[15]. Expansions of correlated MO wave functions, however, produce correct weights[36]. In this section we show that even the uncorrelated restricted MO determinant leads to meaningful covalent weights whose relative magnitudes correlate with bond strengths.

Consider the leading bonding scheme RS1 for **1a**. It locates two π-electrons into the C=C bond region and an alkynyl group is indicated. A large or a small weight for this bonding scheme designates the triple bond as strong or weak, respectively. A measure for the C≡C triple-bond strength at the equilibrium geometry is the energy increase ΔE which occurs when the bond is elongated by an amount ΔR (see Appendix for details). Figure 1 correlates this energy increase ΔE with the computed weights for all covalent bonding schemes of Tables 1−7 with at least one C≡C triple bond.

Figure 1. A correlation between weights for bonding schemes and computed ΔE values; bonding schemes are considered where at least one C≡C triple bond occurs

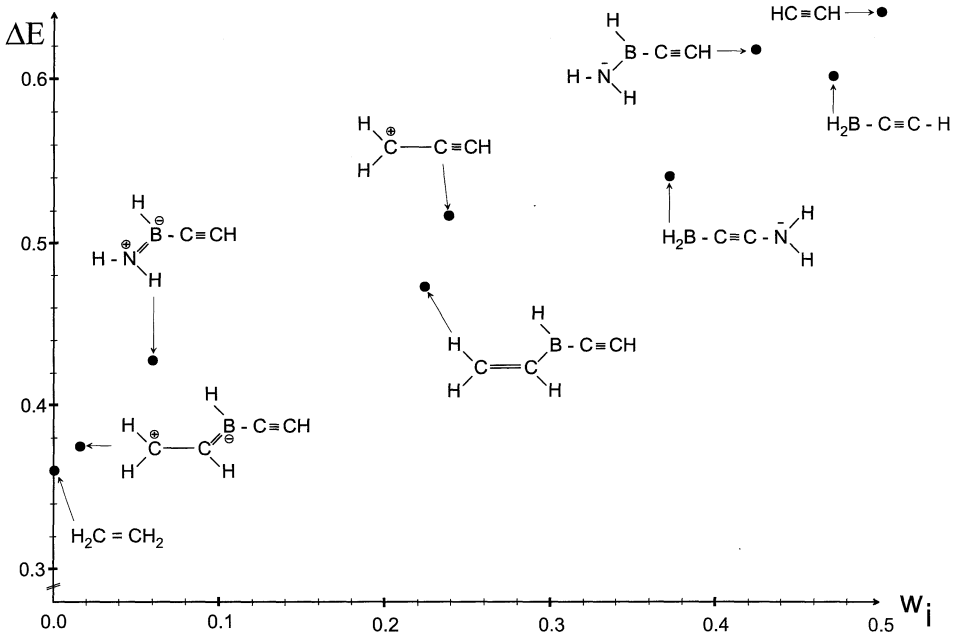

On the abscissa their weights are given and on the ordinate the corresponding energy increases ΔE are recorded (computed by means of eq. 5 or eq. 9). The needed second derivatives were obtained at the RHF/6−311G** level of theory as described in "Computational Methods". Figure 1 shows that a correlation exists between ΔE values and the weights for covalent bonding schemes. The entry for acetylene (0.5) confines the rightmost upper end of the correlation line. In our context, ethylene can be considered as an acetylene molecule devoid of one π-bond and we attribute weight zero to ethylene. Its entry marks the leftmost lower end of the correlation line. The fact that acetylene and ethylene are members of the correlation line supports a qualitative weight rationalization. All leading covalent bonding schemes for **1a**, **2a**, and **4** locate two π-electrons into the alkynyl groups. Their entries appear near acetylene, which shows that the π-systems in **1a**, **2a** and **4** are acetylene-like. The leading covalent bonding scheme for **2b** locates two π-electrons into the alkynyl but also two π-electrons into the vinyl group (see Figure 1). Its intermediate weight shows that both groups are relevant. At the leftmost lower part of the correlation line, different covalent bonding schemes of **2a** and **2b** appear. They attribute two π-electrons to the ethynyl group and two π-electrons to the N=B and C=B double bonds, respectively. Their small weights, however, indicate that an occurrence of N=B, and C=B double bonds in combination with an ethynyl C≡C triple bond is unfavourable in **2a** and **2b**. The small weights suggest the notion that the ΔE values for these bonding schemes are determined by the bonds which remain when the π-bonds of the bonding schemes are not drawn. Thus, the small ΔE values should be determined by the strongest remaining bond which is the double bond of the alkynyl groups and hence appear near the value for ethylene (see Figure 1).

A similar treatment was carried out for bonding schemes with double bonds. On the abscissa of Figure 2, weights are recorded for covalent bonding schemes of Tables 1−7 which comprise at least one double bond.

The corresponding ΔE values are given on the ordinate. Figure 2 shows that a fair correlation between weights and ΔE values exists. The ethylene entry confines the righmost upper part of the correlation line with a weight of 0.5 and ethane (attributed weight zero) delimits the leftmost lower part of the correlation line. The dominating covalent bonding schemes for **3b** and **5** appear near the ethylene entry (see Figure 2). This proximity shows that the π-bonds in **3b** and **5** are similar to the strong π-bond in ethylene. The bonding schemes for the $H_2C{=}CCH$ double bond in **1b** and the $H_2N{=}BH_2$ double bond in **3a** appear at the middle of the correlation line. This intermediate location, between ethylene and ethane, shows that these π-bonds have a significant single-bond character. The covalent bonding schemes for C=B double bonds in **1a**, **3b** and **4** are located at the lower left part of the correlation line. Their small weights show that drawing of double bonds is unjustified. These boron−carbon bonds are in essence single bonds and the entries appear near ethane. The location of two π-electrons

Figure 2. A correlation between weights for bonding schemes and computed ΔE values; the bonding schemes comprise at least one C=C double bond

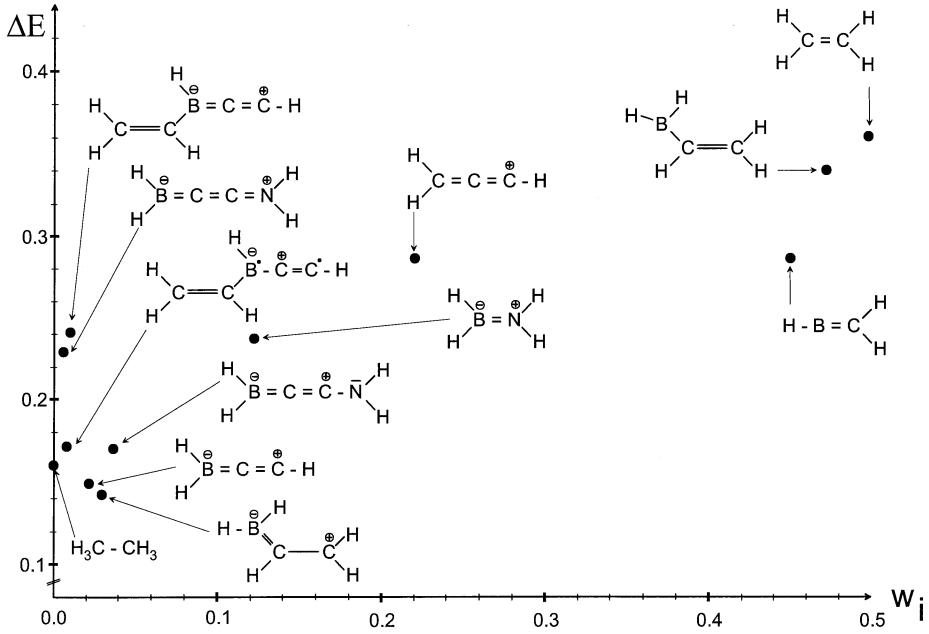

into the vinyl group combined with a singlet biradical arrangement of the remaining two π-electrons is unfavourable for **2b**. The corresponding bonding scheme appears with a small weight (see Figure 2). At the lower leftmost part of the correlation line, deviations are found for two covalent bonding schemes of **2b** and **4**. They both locate four π-electrons into two π-bonds. However, their small weights show that they should be regarded as *two* single bonds. This may explain the deviation from the correlation line where small Δ*E* values are determined by only *one* single bond.

Discussion and Conclusion

In the previous sections we have evaluated the π-electron-accepting ability of an sp^2-hybridized boron atom bonded to a π-electron-donating entity. The π-electron-attraction can be viewed as an intramolecular π-electron transfer. It leads to a partial B=X double bond where X is an atom of the electron-donating substituent. This double-bond character increases in the sequence of model compounds **1a** < **3b** < **3a** < **6**. Our analysis is rooted in the framework of valence-bond theory. An alternative way, however, is to analyse the π-bond character of the B=X bonds by means of the qualitative perturbational approach in terms of fragment molecular orbitals[38]. In the following we show that a correlation between computed weights and quantities based on the fragment-orbital approach exists. This correlation leads to an elucidation of factors which are responsible for the extent of the B=X double-bond character.

Consider the parent ethynylborane (**1a**) where an intramolecular π-electron transfer may occur from the alkynyl group to the BH_2 group. The acceptor (A) fragment orbital is the lowest unoccupied molecular orbital (LUMO) of the borane BH_3. The donor (D) orbital is one of the degenerate π-orbitals of acetylene. Electron transfer occurs within the model compound **1a** which can be viewed as donor acceptor complex (DA). The π-electron transfer transforms the π-orbital of D into the π-orbital of (DA). This occurs by mixing the LUMO of A into the π-orbital of D[38]. An efficient π-electron transfer is manifested by an π-orbital energy in (DA) which is significantly lower than in D[38]. For model compounds **1a**, **3b**, **3a**, **1b** and **6** the operation of this concept is illustrated in Table 8.

In the first column the computed orbital energies of the acceptor fragment orbitals are recorded. These are the LUMOs of BH_3 and of CH_3^+. In the third column the energies of the donor fragment orbitals of the reference donor molecules D are given. Electron transfer in the model compounds (DA) leads to new π-orbitals and their computed MO energies are given in column two. The energy differences Δ*E* between the π-orbital energies in (DA) and (D) are recorded in column four. The Δ*E* values show the intramolecular electron transfer increases in the sequence **1a** < **3b** < **3a** < **6**. This ordering accords with the weights for the corresponding covalent bonding schemes. However, the Δ*E* value for compound **1b** is far too large and incompatible with the intermediate weight for the covalent bonding scheme. The donor orbitals for the substituted boranes are energy lowered only by mixing in the acceptor orbitals of BH_3 and the overall net charges of (D) and (DA) are identical. In **1b**, however, a positive charge is present which is absent in the donor fragment (D). This leads to an additional energy lowering of the donor π-orbital and the Δ*E* value is exaggerated. A better interpretation is given in the following by interrelating computed weights to quantities derived from the fragment molecular orbital approach. Any bonding scheme for the B=X double bonds is charcterized by a definite expansion coefficient c_i (see eq. 1). For the

Table 8. The fragment orbital approach as applied to a selection of model compounds; they are considered as donor acceptor molecules (DA) where a π-electron donation occurs from the donor fragments D to the acceptors fragments A; the relevant MO energies ε and the energie decreases ΔE are given

A	(AD)	D	ΔE	$\frac{1}{\varepsilon_D^\circ - \varepsilon_A^\circ}$	$\lg \frac{\Delta E}{\varepsilon_D^\circ - \varepsilon_A^\circ}$
	$H_2B-C\equiv CH$ $\varepsilon_g = -0.42235$	$HC\equiv CH$ $\varepsilon_7 = -0.41440$	-0.00795	-2.0772	-1.782
BH_3 $\varepsilon_5 = 0.06701$ (LUMO)	$H_2B-CH=CH_2$ $\varepsilon_{11} = -0.39237$	$H_2C=CH_2$ $\varepsilon_8 = -0.37678$	-0.01559	-2.2533	-1.454
	$H_2B-\bar{N}H_2$ $\varepsilon_8 = -0.43956$	 $\varepsilon_5 = -0.38496$	-0.0546	-2.2125	-0.918
	$H_2B-\overset{\ominus}{C}H_2$ $\varepsilon_8 = -0.06231$	 $\varepsilon_5 = 0.03434$	-0.09665	-30.6091	0.471
$CH_3^{\oplus}$ $\varepsilon_5 = -0.28526$ (LUMO)	$H_2C=C=\overset{\oplus}{C}H$ -0.70486	$HC\equiv CH$ $\varepsilon_7 = -0.41440$	-0.29046	-7.7435	0.352

molecules in Table 8, c_i is simply the product between the π-MO coefficients $c_{\mu\pi}$ and $c_{\nu\pi}$.

$$c_i = c_{\mu\pi}c_{\nu\pi} \qquad (3)$$

Here, μ and ν refer to an AO of boron and of the adjacent atom X, respectively. The boron coefficients $c_{\mu\pi}$ are much smaller than the coefficients $c_{\nu\pi}$ for atom X. Moreover, $c_{\nu\pi}$ can be reasonably approximated by the unperturbed MO coefficient of the donor orbital. The small boron coefficients $c_{\mu\pi}$, however, are determined in the perturbational fragment approach by a first-order improvement of the donor MO[38]. This improvement is proportional to a first-order coupling integral divided by the energy difference between the donor and the acceptor orbital, namely $(\varepsilon_D - \varepsilon_A)$[39]. Weights w_i are proportional to the squares of the expansion coefficients c_i (see eq. 2). Therefore, the w_i should correlate linearly with a quantity which is the square of the first-order coupling integral divided by the square of $(\varepsilon_D - \varepsilon_A)$. The computed ΔE values of Table 8 can be considered as second-order perturbation energies[40]. The analytic form of the second-order perturbation energies[40] and the above reasoning leads us to conclude that the w_i values should correlate linearly with ΔE divided by $(\varepsilon_D - \varepsilon_A)$. The logarithm of the $\Delta E/(\varepsilon_D - \varepsilon_A)$ values are recorded in the last column of Table 8. Figure 3 shows that they correlate reasonably with the logarithms of the w_i values.

This correlation leads immediately to an explanation of the relative ordering of weights in terms of properties of the fragment orbitals. A small weight for the B=X double bond is expected provided the ΔE values are small and the energy difference $(\varepsilon_D - \varepsilon_A)$ is large. This situation holds for ethynylborane (**1a**) and vinylborane (**3b**). Large ΔE values supplemented by a small energy difference $(\varepsilon_D - \varepsilon_A)$ determine large B=X weights. This is valid for the ethynyl carbocation

Figure 3. A correlation between bonding-scheme weights and a quantity based on the fragment molecular orbital approach

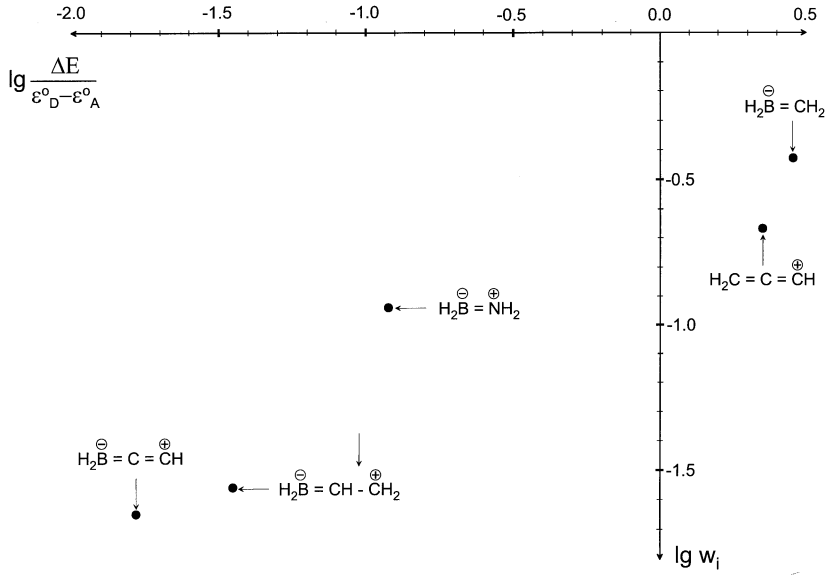

1b and the borane carbanion **6**. Aminoborane (**3a**) represents an intermediate case. Thus, a large B=X double-bond character is expected provided the donating fragment has a low π-electron ionization potential. This is certainly true for the carbanion fragment in **6**. The π-electron ionization potential of acetylene (11.4 eV)[41] and ethylene (10.5 eV)[41] are larger and the B=C double-bond character in **1a** and **3b** is rather small. Due to the ionization potentials, however, the B=C double-bond character in **3b** should be slightly larger than in **1a**. This accords with the corresponding weights which are 4.4% in **1a** and 5.2% in **3b**. Moreover, the extent of the double-bond character is also determined by the energy of the acceptor orbital. The high energy of the BH_3 acceptor orbital implies a small weight for the B=C double bond in ethynylborane (**1a**). On the contrary, the low energy of the acceptor orbital of CH_3^+ leads to a rather large weight for the C=C double bond in **1b**. The derived qualitative explanation holds also for the π-bond present in a planar borylphosphane H_2B-PH_2. The optimized geometry of H_2B-PH_2 is characterized by a pyramidal phosphanyl group and the lone pair at the PH_2 group is oriented away from the BH_2 group. Therefore, only a weak B=P π-bond is present in H_2B-PH_2 at the equilibrium geometry[42]. However, computational results at a *planar* C_{2v} geometry of H_2B-PH_2 indicate a B=P bond slightly *stronger* than the B=N bond in **3a**[43]. This finding is in line with the concepts determining the correlation line of Figure 3. The 3p electrons at the planar PH_2 fragment have a lower ionization potential than the 2p electrons at the NH_2 fragment. Consequently, the weight for the B=P bond should be larger than the weight for the B=N bond.

The authors are greatful to Prof. *K. Wieghardt* for his support of this work and to Prof. *R. Köster*, Dr. *G. Olbrich* and Dr. *F. Mark* for helpful discussions. The technical assistance of *K. Sand* is also gratefully acknowledged.

Appendix

Consider a bonding scheme with one bond of length R (exemplified for **1a** in Scheme 6).

Scheme 6. A bonding scheme where only one π-bond is indicated; the only bond parameter is the bond length R

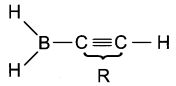

The energy E at a bond length R, elongated by ΔR, is given up to second order in ΔR by

$$E(0+\Delta R)=E(0)+\left(\frac{dE}{dR}\right)^{0}\Delta R+\frac{1}{2}\left(\frac{d^2E}{dR^2}\right)\Delta R^2+.. \qquad (4)$$

If we assume an optimized geometry for **1a**, the first derivative in eq. 4 vanishes. Furthermore, we apply a reference elongation with a squared norm of unity. Thus, ΔR^2 is unity and the energy increase ΔE is given by

$$\Delta E = E(0+1)-E(0)=\frac{1}{2}\left(\frac{d^2E}{dR^2}\right)^{0} \qquad (5)$$

We see, ΔE is given by half of the curvature when the reference elongation is applied. A representative covalent bonding scheme for two π-bonds is the leading scheme for the ethynyl(vinyl)borane (**2b**) represented in Scheme 7.

Scheme 7. A bonding scheme where two π-bonds are indicated; the two bonds have the bond lengths R_a and R_b

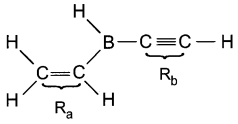

It locates four π-electrons into two π-bonds such that a C≡C triple and a C=C double bond is formed. A measure for their combined bond strength is the energy increase resulting when the two bonds are stretched by ΔR_a and ΔR_b (see Scheme 7). The energy up to second order in ΔR_a and ΔR_b at the distorted geometry is given by eq. 6.

$$E(0+\Delta R_a,0+\Delta R_b)=E(0,0)+\frac{1}{2}\left(\frac{\delta^2E}{\delta R_a^2}\right)^{00}\Delta R_a^2+\frac{1}{2}\left(\frac{\delta^2E}{\delta R_b^2}\right)^{00}\Delta R_b^2+... \qquad (6)$$

Here, we have applied the Taylor expansion for a function depending on two parameters[37]. The expansion is simplified by the vanishing of the first derivatives implied by the use of optimized geometries. Moreover, we neglected the mixed second derivatives. This is suggested by the fact that the double and the triple bonds are well separated. A coupling between the two bonds should be negligible. Again, a reference elongation is chosen such that the squared norm of the elongation vector is unity. Thus, we have

$$\Delta R_a^2+\Delta R_b^2=1 \qquad (7)$$

Moreover, we partition the elongations such that eq. 8 holds.

$$\Delta R_a^2=\Delta R_b^2=\frac{1}{2} \qquad (8)$$

Based on these assumptions, we obtain an energy increase ΔE given by eq. 9.

$$\Delta E = E\left(0+\sqrt{\frac{1}{2}},0+\sqrt{\frac{1}{2}}\right)-E(0,0)=\frac{1}{4}\left[\left(\frac{\delta^2E}{\delta R_a^2}\right)^{00}+\left(\frac{\delta^2E}{\delta R_b^2}\right)^{00}\right] \qquad (9)$$

The ΔE given by eq. 5 and eq. 9 are based on a different number of bond elongations, namely one and two, respectively. The squared norm of both elongations, however, is equal and unity. This property permits us to compare bonding schemes with a different number of bonds by computing ΔE values. Our notion is that covalent bonding schemes with large (small) weights indicate strong (weak) bonds and they should be characterized by large (small) ΔE values. In Figure 1, weights for bonding schemes and ΔE values are correlated.

☆ Dedicated to Professor *Heinrich Nöth* on the occasion of his 70th birthday.

[1] [1a] U. Krüerke, *Z. Naturforsch.* **1956**, *11b*, 364–365 (first synthesis of an alkynylborate). – [1b] E. C. Ashby, W. E. Foster, *J. Org. Chem.* **1964**, *29*, 3225–3229 (unsuccessful synthesis of a triethynylborane; see ref.[2j]). – [1c] R. Köster, H.-J. Horstschäfer, P. Binger, *Justus Liebigs Ann. Chem.* **1968**, *717*, 1–20 (first general synthesis and characterization of ethynylboranes). – For a review of the early literature see: [1d] R. Köster, *Methoden der Organischen Chemie (Houben/Weyl), Organoborverbindungen*, vol. 13, Georg Thieme Verlag, Stuttgart, **1984**.

[2] [2a] A. Meller, W. Maringgele, G. Elter, D. Bromm, M. Noltemeyer, G. M. Sheldrick, *Chem. Ber.* **1987**, *120*, 1437−1439. − [2b] H. Nöth, U. Wietelmann, *Chem. Ber.* **1987**, *120*, 863−865. − [2c] J. J. Eisch, B. Shafii, J. D. Odom, A. L. J. Rheingold, *J. Am. Chem. Soc.* **1990**, *112*, 1847−1853. − [2d] N. Metzler, Diplomarbeit, Ludwig-Maximilians-Universität München, **1991**. − [2e] B. Ederer, N. Metzler, H. Nöth, *Chem. Ber.* **1993**, *126*, 2003−2010. − [2f] H. Schulz, G. Gabbert, H. Pritzkow, W. Siebert, *Chem. Ber.* **1993**, *126*, 1593−1595. − [2g] H. Nöth, M. Wagner, *Chem. Ber.* **1991**, *124*, 1963−1972. − [2h] N. Metzler, Dissertation, Ludwig-Maximilians-Universität München, **1994**. − [2i] N. Metzler, H. Nöth, *Chem. Ber.* **1995**, *128*, 711−717. − [2j] J. E. Davies, P. R. Raithby, R. Snaith, A. E. H. Wheatley, *J. Chem. Soc., Chem.Commun.* **1997**, 1797−1798.

[3] [3a] B. Wrackmeyer, H. Nöth, *Chem. Ber.* **1977**, *110*, 1086−1094. − [3b] B. Wrackmeyer, *Progr. Nucl. Magn. Res. Spectrosc.* **1979**, *12*, 227−259, in particular p. 243. − [3c] B. Wrackmeyer, K. Horchler, *Progr. Nucl. Magn. Res. Spectrosc.* **1990**, *22*, 209−253, in particular p. 226. − [3d] N. M. D. Brown, F. Davidson, J. W. Wilson, *J. Organomet. Chem.* **1981**, *209*, 1−11. − [3e] B. Wrackmeyer, *Z. Naturforsch.* **1982**, *37 b*, 788−789. − [3f] B. V. Cheesman, L. Deloux, M. Srebnik, *Magn. Res. Chem.* **1995**, *33*, 724−728.

[4] For a comprehensive compilation of results obtained with the ab initio MO method see: W. J. Hehre, P. v. R. Schleyer, J. A. Pople, *Ab initio Molecular Orbital Theory*, Wiley, New York, **1986**.

[5] [5a] P. C. Hiberty, C. Leforestier, *J. Am. Chem. Soc.* **1978**, *100*, 2012−2017. − [5b] For a review of chemical applications see: P. C. Hiberty in *Valence Bond Theory and Chemical Structure* (Eds.: D. J. Klein, N. Trinjastic), Elsevier, Amsterdam, **1990**.

[6] V. Bachler, *Theor. Chem. Acc.* **1997**, *92*, 223−242.

[7] [7a] M. F. Lappert, P. P. Power, A. R. Sanger, R. C. Srivastava, *Metal and Metalloid Amides*, Ellis Horwood Limited, Chichester, **1980**. − [7b] H. Nöth, *Progress in Boron Chemistry*, vol. 3 (Eds.: H. J. Brotherton, H. Steinberg,) Pergamon Press, Oxford, **1968**. − [7c] H. Nöth, W. Storch, *Chem. Ber.* **1976**, *109*, 884−895. − [7d] B. Wrackmeyer, R. Köster in *Methoden der Organischen Chemie (Houben/Weyl)*, vol. 13/3c ("Organobor-verbindungen"), Georg Thieme Verlag, Stuttgart **1984**. − [7e] M. Bühl, P. v. R. Schleyer, M. A. Ibrahim, T. Clark, *J. Am. Chem. Soc.* **1991**, *113*, 2466−2471. − [7f] P. H. M. Budzelaar, A. J. Kos, T. Clark, P. v. R. Schleyer, *Organometallics* **1985**, *4*, 429−437. − [7g] H. Nöth, B. Wrackmeyer, *NMR Spectroscopy of Boron Compounds*, Springer Verlag, Heidelberg, **1978**.

[8] M.J. Frisch, G.W. Trucks, H.B. Schlegel, P.M.W. Gill, B.G. Johnson, M.W. Wong, J.B. Foresman, M.A. Robb, M. Head-Gordon, E.S Repogle, R. Gomperts, J.L Andres, K. Raghavachari, J.S. Binkley, C. Gonzales, R.L. Martin, D.J. Fox, J. Baker, J.J.P. Stewart, J.A. Pople, *Gaussian92/DFT*, Revision g.4, Gaussian Inc., Pittsburg, **1993**.

[9] C. C. J. Roothaan, *Rev. Mod. Phys.* **1951**, *23*, 69−89.

[10] R. Krishan, J. S. Binkley, R. Seeger, J. A. Pople, *J. Chem. Phys.* **1980**, *72*, 650−654.

[11] This basis set is also described in ref.[10].

[12] These types of local spin occupations were already discussed in previous expansion work where the extended 4−31G basis was applied, see: P. C. Hiberty, G. Ohanessian, *J. Am. Chem. Soc.* **1982**, *104*, 66−70.

[13] See for example: T. Clark, *Handbook of Computational Chemistry*, Wiley, New York, **1985**, sect. 3.3, p. 102.

[14] This is a basic notion in valence-bond theory. See for example: G.W. Wheland, *Resonance in Organic Chemistry*, Wiley, New York, **1961**, sect. 9.12, p. 587.

[15] See for example: P. C. Hiberty, G. Ohanessian, *Int. J. Quant. Chem.* **1985**, *27*, 245−257 in particular sect. 4 and 5, see also ref.[5b].

[16] P. C. Hiberty, G. Ohanessian, *Int. J. Quant. Chem.* **1985**, *27*, 259−272, in particular sect. 4, p. 270.

[17] *Tables of Interatomic Distances and Configuration of Molecules and Ions*, The Chemical Society, London, **1965**, M74s.

[18] N. Metzler, Dissertation, Ludwig-Maximilians-Universität München, **1994**, p. 44.

[19] See ref.[17],p. 78s.

[20] See for example: J. D. Roberts, R. Stewart, M. C. Caserio, *Organic Chemistry*, Benjamin, Menlo Park, **1971**, chapt. 6.4, p. 138.

[21] G. A. Olah, R. J. Spear, P. W. Westerman, J. M. Denis, *J. Am. Chem. Soc.* **1974**, *96*, 5855−5860.

[22] N. Metzler, H. Nöth, *Chem. Ber.* **1995**, *128*, 711−717.

[23] T. L. Allen, W. H. Fink, *Inorg. Chem.* **1993**, *32*, 4230−4234.

[24] [24a] H. Nöth, W. Meister, *Chem. Ber.* **1961**, *94*, 509−514. − [24b] H. Nöth, H. Pommerening, *Angew. Chem.* **1980**, *92*, 481−482; *Angew. Chem. Int. Ed. Engl.* **1980**, *19*, 482−483. − [24c] M. Wagner, Dissertation, Ludwig-Maximilians-Universität München, **1992**.

[25] B. Glaser, H. Nöth, *Chem. Ber.* **1986**, *119*, 3253−3267.

[26] J. Kroner, H. Nöth, K. Polborn, H. Stolpmann, M. Tacke, M. Thomann, *Chem. Ber.* **1993**, *126*, 1995−2002.

[27] G. Linti, H. Nöth, R. T. Paine, K. Polborn, *Angew. Chem.* **1990**, *102*, 715−717; *Angew. Chem. Int. Ed. Engl.* **1990**, *29*, 682−684.

[28] H. Feulner, N. Metzler, H. Nöth, *J. Organomet. Chem.* **1995**, *489*, 51−62.

[29] Y. Yamamoto, I. Moritani, *J. Org. Chem.* **1975**, *40*, 3434−3437.

[30] See for example: R. Gompper, G. Seybold, *Angew.Chem.* **1968**, *80*, 804−806; *Angew. Chem. Int. Ed. Engl.* **1968**, *7*, 824−826. − See also: J. March, *Advanced Organic Chemistry*, Wiley, New York, **1985**, p. 52 and references therein.

[31] H. O. Berger, H. Nöth, B. Wrackmeyer, *J. Organomet. Chem.* **1978**, *145*, 17−20.

[32] For a review see: A. Berndt, *Angew.Chem.* **1993**, 105, 1034−1058; *Angew. Chem. Int. Ed. Engl.* **1993**, *32*, 985−1009.

[33] This holds for all two electron homopolar bonds. For an outline see for example: R. McWeeny, *Coulson's Valence*, Oxford University Press, Oxford, **1979**, in particular chapt. 5.4, p. 127.

[34] [34a] B. Ederer, Dissertation, Ludwig-Maximilians-Universität München, **1991**, in particular p. 35. − [34b] H. Ederle, B. Ederer, R. Littger, H. Nöth, M. Wagner, *Adv. Boron Chem.* **1997**, *201*, 49−60.

[35] We computed the value at the RHF/6−311G** level of theory. The boron and the carbon atom are both pyramidalized in this local minimum.

[36] [36a] P. Karafiloglou, J. P. Malrieu, *Chem. Phys.* **1986**, 104, 383−398. − [36b] P. C. Hiberty, G. Ohanessian, *Int. J. Quant. Chem.* **1985**, 27, 259−272.

[37] See for example: M. R. Spiegel, *Mathematical Handbook*, Schaum's Outline Series, McGraw-Hill, New York, **1968**, p. 113, eq. 20.60.

[38] T. A. Albright, J. K. Burdett, M. H. Whangbo, *Orbital Interactions in Chemistry*, Wiley, New York, **1985**.

[39] See for example: H. Eyring, J. Walter, G. E. Kimball, *Quantum Chemistry*, Wiley, New York, **1944**, p. 96, eq. 7.31.

[40] See ref.[39], p. 95, eq. 7.30.

[41] *CRC Handbook of Chemistry and Physics* (Ed.: R. C. Weast), CRC Press Inc., Boca Rosta, **1986**, Table E-83.

[42] [42a] T. L Allen, A. C. Scheiner, H. F. Schaefer III, *Inorg. Chem.* **1990**, *29*, 1930−1936. − [42b] D. A. Hoic, M. DiMare, G. C. Fu, *J. Am. Chem. Soc.* **1997**, *119*, 7155−7156. − [42c] R. T. Paine, H. Nöth, *Chem. Rev.* **1995**, *95*, 343−379.

[43] See ref.[23] and references therein, in particular p. 4233−4234.

[97318]

On the Chemistry of Gallium, 14[◇]

Synthesis and Structure of Gallium/Silicon Heterocycles with a Ga_2Si_2 and a Ga_3Si Framework☆

Gerald Linti*, Wolfgang Köstler, and Alexander Rodig

Institut für Anorganische Chemie der Universität,
Engesserstr. Geb. 30.45, D-76128 Karlsruhe, Germany
Fax: (internat.) + 49(0)721/608-4854
E.mail: linti@achpc9.chemie.uni-karlsruhe.de

Received December 29, 1997

Keywords: Gallium / Silicon / Heterocycles / Main group elements

The reaction of $Ga_2X_4 \cdot 2$ dioxane with four equivalents of $(Me_3Si)_3SiLi(thf)_3$ (= hypersilyllithium) affords for X = Br a 1,3,2,4-disiladigalletane together with tetrahedral hypersilylgallium(I). For X = Cl an anionic 1,2,3,4-silatrigalletanate, a four-membered heterocycle with a Ga_3 unit, is isolated. These primary examples of gallium/group-14 heterocycles have been investigated by NMR spectroscopy as well as by X-ray single-crystal structure analysis. In addition, the synthesis and structure of bis(hypersilyl)gallium chloride is described. This monomeric molecule has a nearly T-shaped Si_2GaCl framework.

The tris(trimethylsilyl)silyl (= hypersilyl) group has proved to be a very useful substituent in gallium chemistry. Not only trivalent gallanes like $tmp_2GaSi(SiMe_3)_3$,[1] $Y_2GaSi(SiMe_3)_3 \cdot thf$ (Y = Me, Cl),[2] $Cl_2Ga[Si(SiMe_3)_3]_2 \cdot Li(thf)_2$[3], and $[(EtO)_2GaSi(SiMe_3)_3]_2$[2] are accessible but the hypersilyl group is also excellently capable of stabilizing a number of low-valent gallium compounds with gallium−gallium bonds. This includes hypersilyl-substituted digallanes $[(Me_3Si)_3Si]_2Ga-Ga[Si(SiMe_3)_3]_2$ and $[(Me_3Si)_3SiGa(Cl)-Ga(Cl)Si(SiMe_3)_3]_2$[4] as well as an anionic tetragallane $[(Me_3Si)_3SiGa\{Ga(I)Si(SiMe_3)_3\}_3]^-$ and the polyhedral nonagallane $[\{(Me_3Si)_3Si\}_6Ga_9]^-$.[5] The hypersilyl-substituted tetrahedral gallium(I) cluster $[(Me_3Si)_3SiGa]_4$ proved to be very stable towards dissociation into monomeric units.[6] In all these cases the hypersilyl group remained unaffected. Consequently, the central silicon atom is bonded to only one gallium atom and no cyclic compounds are known with gallium and silicon atoms as ring-building elements. In the following we describe results, where the inherent capability of the hypersilyl ligand for Si−Si bond cleavage is used for the synthesis of gallium−silicon heterocycles, which feature a tetracoordinate silicon atom bonded to two gallium atoms.

Reactions

By treating $[(Me_3Si)_3SiGa(Cl)-Ga(Cl)Si(SiMe_3)_3]_2$ (**1**) with two equivalents of $Li(thf)_3Si(SiMe_3)_3$ (Eq. 1) disproportionation of the gallium(II) species is achieved. Accompanying $[(Me_3Si)_3SiGa]_4$ (**2**), bis(hypersilyl)gallium chloride (**3**) is isolated in this reaction. Recently, we have described the synthesis of **2**[6] together with $Cl_2Ga[Si(SiMe_3)_3]_2 \cdot Li(thf)_2$ (**4**) and several not further characterized byproducts by reaction of $Ga_2Cl_4 \cdot 2$ dioxane with three equivalents $Li(thf)_3Si(SiMe_3)_3$ (Eq. 2). Another reaction course is observed, if $Ga_2Cl_4 \cdot 2$ dioxane, dissolved in tetrahydrofuran, is treated with four equivalents of $Li(thf)_3Si(SiMe_3)_3$ (Eq. 3). In this reaction the disproportionation of the gallium(II) species leads again to several hypersilylgallium compounds in oxidation state III, but no **2** is observed. Instead, black crystals of the unprecedented gallium/silicon heterocycle **5** are isolated. On the other hand, the analogous reaction of $Ga_2Br_4 \cdot 2$ dioxane with four equivalents of $Li(thf)_3Si(SiMe_3)_3$ affords **6** together with **2** (Eq. 4). The latter cocrystallizes with $Si(SiMe_3)_4$, which is formed during the reaction course. It is plausible, that **2** and bis(hypersilyl) gallium bromide are formed by disproportionation at first. **6** forms formally by elimination of bromotrimethylsilane from the sterically crowded $[(Me_3Si)_3Si]_2GaBr$. This takes place in the presence of excess $Li(thf)_3Si(SiMe_3)_3$, consequently the halosilane reacts further to produce $Si(SiMe_3)_4$ (Scheme 1). The pathway leading to **5** obviously also includes a step of disproportionation, but now an oligomeric hypersilylgallium(I) reacts with $Li(thf)_3Si(SiMe_3)_3$. Thus, a possible intermediate might be the three-membered gallacycle $[Ga_3\{Si(SiMe_3)_3\}_4]^-$. Migration of a trimethylsilyl group from an $Si(SiMe_3)_3$ group at the four-coordinate gallium center to a three-coordinate one and insertion of the remaining $Si(SiMe_3)_2$ unit into a Ga−Ga bond affords **5**.

Spectroscopic Characterization

[◇] Part 13: G. Linti, M. Bühler, H. Urban, *Z. Anorg. Allg. Chem.* **1998**, *624*, 517−520.

 © WILEY-VCH Verlag GmbH, D-69451 Weinheim, 1998 1434−1948/98/0606−0745 $ 17.50+.50/0

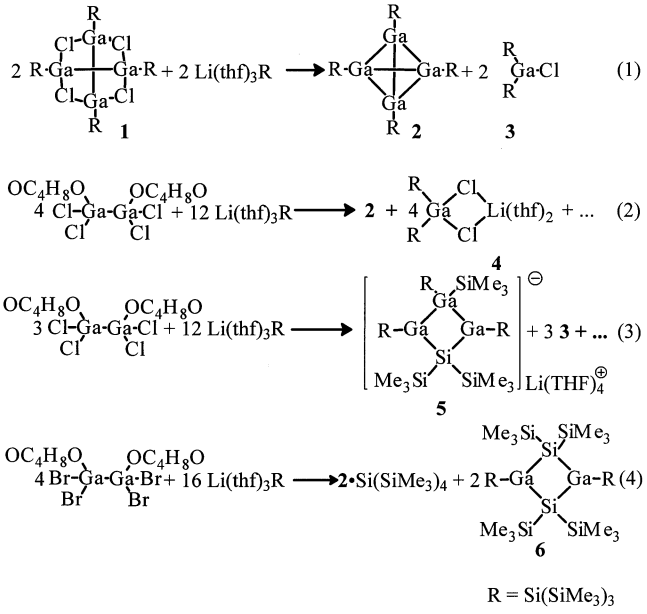

Scheme 1. Proposed reaction pathways to **6** (a) and **5** (b)

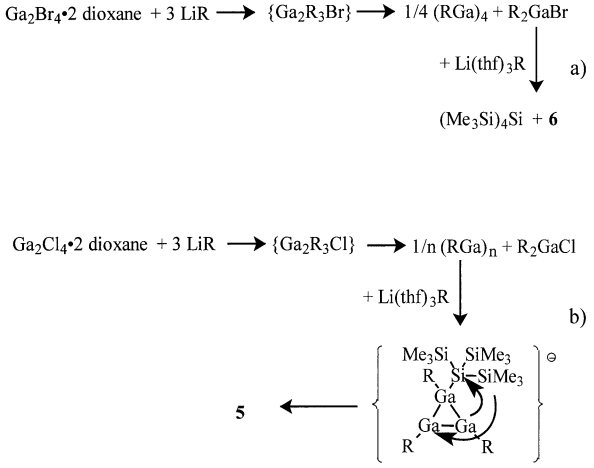

The ^{1}H- and ^{13}C-NMR spectra for **5** show two signals for the hypersilyl groups, one for the Ga−$SiMe_3$ group and two for the $Si(SiMe_3)_2$ unit, as is expected. In the ^{29}Si-NMR spectrum for the eight chemical different silicon atoms eight signals are observed. All trimethylsilyl groups, including the gallium-bonded one, resonate in the typical range between δ = −8.8 and −14.2. The central silicon atoms of the hypersilyl groups give rise to two signals at δ = −120.2 and −131.4. The signal for the ring silicon atom is identified at δ = −4.3. In **6** the signal for the ring silicon atoms is observed at δ = −3.3, that for the central atom of the hypersilyl group at δ = −103.8. Whereas there are no comparable data available for silicon atoms bonded to two gallium atoms, the chemical shifts for the hypersilyl silicon atoms are in the typical range known for other hypersilylgallium derivatives.[2] For example, the central silicon atom in $tmp_2GaSi(SiMe_3)_3$[1] resonates at δ = −115.3, in $Cl_2GaSi(SiMe_3)_3 \cdot thf$[2] at δ = −127.8, and in $[(PhO)_3GaSi(SiMe_3)_3]^-$[2] at δ = −141.7. Electron-precise compounds with Ga−Ga bonds like $[(Me_3Si)_3SiGa(Cl)-Ga(Cl)Si(SiMe_3)_3]_2$[4] have signals in this range (δ = −112.2), too. This is only a small variation compared to other hypersilyl derivatives; here chemical shifts from δ = −33.4 for $(Me_3Si)_3SiF$[7] to −189.4 for $Li(thf)_3Si(SiMe_3)_3$[15c] are known. The chemical shifts of the gallium compounds seem to be affected by the electron-withdrawing properties of the ligands at and the coordination number of the gallium center. But the bonding situation at the gallium center obviously has the largest impact. In the electron-deficient tetrahedral cluster **1**, the signal for the hypersilyl silicon atom is observed at δ = −68.7. This shift to higher frequencies compared to other gallium compounds must be due to the multicenter-bonding situation the gallium atoms are involved in.

In the mass spectrum (70 eV) of **6** not only the molecular peak at *m/z* = 980 and the typical fragmentation pathway, i.e. loss of CH_3, $SiMe_3$, and $Si(SiMe_3)_3$ are observed, but in addition at *m/z* = 490 the radical cation $[(Me_3Si)_3SiGaSi(SiMe_3)_2]^{+\cdot}$ and consequent fragmentation occurs.

X-ray Structure Analysis

3 crystallizes in the hexagonal space group $P6_122$ with $Z = 6$. The crystal consists of well-separated monomeric molecules of **3** with a severely distorted trigonal-planar coordinated gallium center (Figure 1). The Ga−Si distance is 240.3(2) pm, which is comparable to the one in $Me_2Ga(thf)-Si(SiMe_3)_3$ [d_{GaSi} = 241.1(3) pm],[2] but shorter than in $tmp_2Ga-Si(SiMe_3)_3$ [d_{GaSi} = 246.8(1) pm].[1] Here, due to the three versus only two space-filling substituents the hypersilyl groups must minimize their steric interactions by bond elongation. In **3** this is achieved by a wide SiGaSi bond angle [150.3(1)°]. This is very wide, compared to other monomeric R_2GaCl compounds like $[(Me_3Si)_2N]_2GaCl$[8] [N−Ga−N = 128.5(2)°], $(2,4,6\text{-}iPr_3C_6H_2)_2GaCl$[9] [C−Ga−C = 133.8(7)°], and $(2,4,6\text{-}tBu_3C_6H_2)_2GaCl$[10] [C−Ga−C = 135.6(2)°]. Only $(Mes_2C_6H_3)_2GaCl$ [C−Ga−C = 153.5(5)°] is even more T-shaped.[11]

Figure 1. View of a molecule of **3**[a]

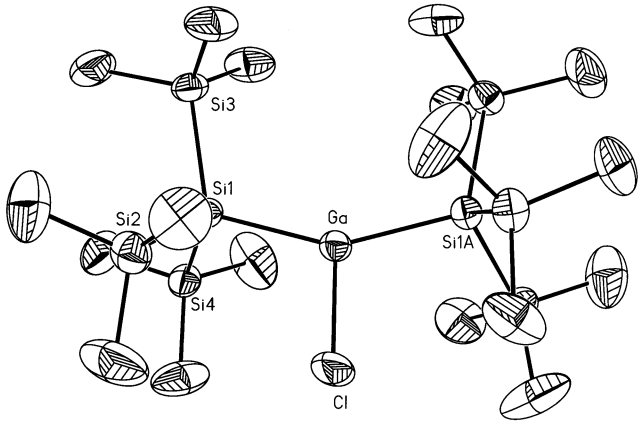

[a] Selected bond lengths [pm] and angles [°]: Ga−Cl 222.4(3), Ga−Si1 240.3(2), Si1−Si4 235.8(3), Si1−Si3 235.(3), Si1−Si2 236.1(3); Cl−Ga−Si1 104.83(5), Si1−Ga−Si1 150.33(10), Si4−Si1−Si3 110.1(1), Si4−Si1−Si2 113.96(10), Si3−Si1−Si2 110.9(1), Si4−Si1−Ga 102.42(8), Si3−Si1−Ga 113.79(9), Si2−Si1−Ga 105.36(9).

5 crystallizes monoclinic, space group $P2_1/n$, and consists of anionic Ga_3Si heterocycles (Figure 2) and isolated $Li(thf)_4$ cations. The heterocycle **5** is diamond-shaped with acute angles of 84.52(5)° at the ring silicon atom and of 81.39(3)° at the tetracoordinated gallium center. The wide angles [97.78(4), 95.96(4)°] are as expected at the three-coordinate gallium atoms. As is indicated by the sum of angles the ring adopts a flat butterfly structure; the Si1Ga1Ga2 and Si1Ga3Ga2 plane orthogonals intersect at 20.6°. Consequently, the two hypersilyl groups at Ga1 and Ga3 are on the same side of the ring, the hypersilyl group at Ga2 is in *trans* position to them. Nevertheless, the attachment of so many bulky substituents to that four-membered ring results in a considerable distortion of the bond angles and the coordination spheres around Ga2 and Ga3 (Figure 3a). Inspecting the ring silicon atom, at first, the Si2−Si1−Si3 angle, namely the angle between the trimethylsilyl groups is near the tetrahedral angle, but the trimethylsilyl group (Si2) on the inner side of the butterfly has very wide Si2−Si1−Ga2,3 angles. This means the Si1−Si2 bond has only an angle of 26.5° with the Si1Ga2Ga3 plane. In contrast, the Si1−Si3 bond is nearly perpendicular to this plane (Si3Si1//Si1Ga2Ga3: 100.5°). At the tetracoordinated gallium atom Ga2 the situation is similar. The Si8−Ga2−Si12 angle [110.37(6)°] is near the tetrahedral angle, too. The bond Ga2−Si8, involving the central atom of the attached hypersilyl group, has wide angles with the Ga2−Ga1,3 bonds [Si8−Ga2−Ga1 126.64(4)°; Si8−Ga2−Ga3 128.57(4)°], but, in contrast, the corresponding angles involving the trimethylsilyl silicon atom Si12 have values of only 105.67(5)° and 98.09(5)°. This means angles between the Ga2Ga1Ga3 plane and the Si8−Ga2 and Si12−Ga2 bonds of 36.4° and 106.8°, respectively. Furthermore, the steric crowding in **5** causes a no longer exactly planar arrangement around Ga1 and Ga3. Both atoms are 16 pm above the plane through their neighboring atoms. The Ga−Ga bond lengths in the trigallane unit of **5** [255.27(9), 252.88(9) pm] are in the typical range for other hypersilyl-substituted oligogallanes like $[(Me_3Si)_3SiGa(Cl)-Ga(Cl)Si(SiMe_3)_3]_2$ (d_{GaGa} = 250.5 pm),[4] $[(Me_3Si)_3SiGa\{Ga(I)Si(SiMe_3)_3\}_3]^-$ (d_{GaGa} = 253.3 pm)[5] and $[(Me_3Si)_3Si]_2Ga-Ga[Si(SiMe_3)_3]_2$ (d_{GaGa} = 259.9 pm).[4] Only one structurally investigated compound with a trigallane unit is known so far, $Ga_3I_5 \cdot 3\ PEt_3$.[12] In this gallium subhalide shorter Ga−Ga bond lengths [d_{GaGa} = 245.1(1), 246.0(1) pm] are observed. The Ga−Si($SiMe_3$) distances in **5** [d_{GaSi} = 248.4 pm] are very long compared to other hypersilylgallium compounds, as is discussed above. There is no difference between the Ga−Si bond lengths involving three- or four-coordinate gallium atoms in **5**. In contrast, the Ga−$SiMe_3$ bond length is 5 pm shorter. As we have noted earlier,[2] the Ga−Si bond lengths are very sensitive to steric requirements. In this sense, the shorter bond length to the trimethylsilyl group is expected, but further structural data on molecules with Ga−$SiMe_3$ bonds are not available, yet. The ring silicon atom is also in a novel environment. For this atom bonded to two gallium atoms Ga−Si bond lengths of 247.5(2) and 245.2(2) pm are observed, thus in the range of long Ga−Si bonds. The Si−Si and Si−C bond lengths are in the normal range for these bond types.

Figure 2. View of the heterocyclic anion in **5**; the methyl groups have been omitted for clarity[a]

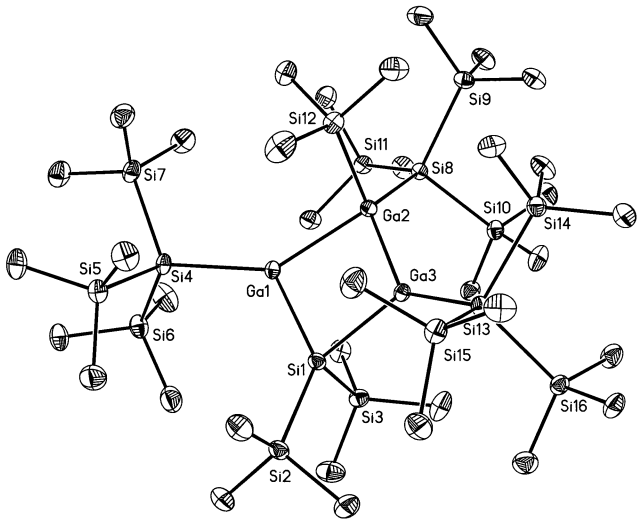

[a] Selected bond lengths [pm] and angles [°]: Ga1−Ga2 255.27(9), Ga2−Ga3 252.88(9), Ga1−Si1 247.5(2), Ga3−Si1 245.2(2), Ga1−Si4 248.4(2), Ga2−Si8 248.4(2), Ga2−Si12 243.6(2), Ga3−Si13 248.3(2), Si1−Si2 235.4(2), Si1−Si3 236.5(2), Si−$SiMe_3$ 235.5; Si1−Ga1−Ga2 94.78(4), Ga3−Ga2−Ga1 81.39(3), Si1−Ga3−Ga2 95.96(4), Ga3−Si1−Ga1 84.52(5), Si1−Ga1−Si4 119.60(6), Si4−Ga1−Ga2 144.07(5), Si12−Ga2−Si8 110.37(6), Si12−Ga2−Ga3 105.67(5), Si8−Ga2−Ga3 128.57(4), Si12−Ga2−Ga1 98.09(5), Si8−Ga2−Ga1 126.64(4), Si1−Ga3−Si13 125.63(5), Si13−Ga3−Ga2 136.59(5), Si2−Si1−Si3 106.12(8), Si2−Si1−Ga3 127.03(7), Si3−Si1−Ga3 98.00(7), Si2−Si1−Ga1 135.74(7), Si3−Si1−Ga1 97.47(7).

Figure 3. Side-on view of a) anionic **5**, b) one of the two independent molecules of **6**; the methyl groups have been omitted for clarity

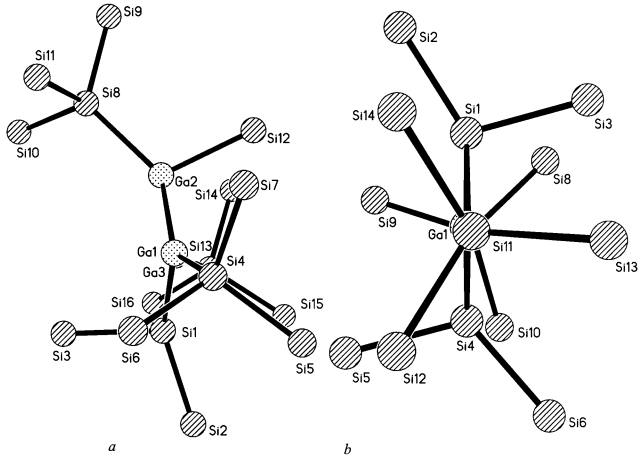

Compound **6** (Figure 4) crystallizes triclinic, space group $P\bar{1}$, with two independent molecules in the asymmetric unit. The nearly planar four-membered gallium/silicon heterocycles have an approximately quadratic alternating Ga_2Si_2 framework of distorted trigonal-planar coordinated gallium and tetrahedrally coordinated silicon centers. Thus, the inner ring angles at the gallium atoms are 91.6°, those at the silicon atoms 88.4°, on an average. The Ga−Si bond lengths in the ring (d_{GaSi} = 242.1 pm on an average) vary only by

2 pm. The exocyclic gallium−silicon bond lengths are similar to the innercyclic, too. But, if **5** and **6** are compared, it has to be noted, that all Ga−Si bonds are shortened by more than 5 pm. This is, at least in part, a consequence of the replacement of a $[Ga(SiMe_3)Si(SiMe_3)_3]^-$ unit by the less bulky $Si(SiMe_3)_2$ group. In spite of the reduction of steric crowding, the *anti*-standing trimethylsilyl groups are bonded either in a flat or nearly perpendicular manner to the heterocycle (Figure 3b). The corresponding angle pairs between Si−Si bonds and the Ga_2Si planes are 31 and 104.3° or 42.3 and 115.9°, respectively. It has to be noted, that the two independent molecules differ only a little in the orientation of the approximately staggered hypersilyl groups to one another.

Figure 4. View of a molecule of **6**[a]

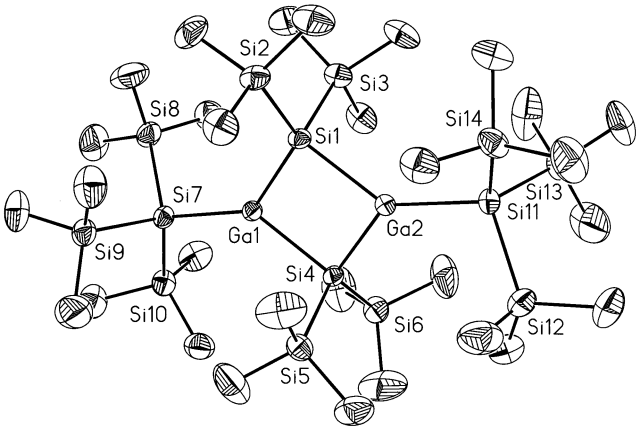

[a] Selected bond lengths [pm] and angles [°]: Ga1−Si1 242.89(9), Ga1−Si4 241.2(1), Ga1−Si7 241.5(1), Ga2−Si1 242.5(1), Ga2−Si4 241.68(9), Ga2−Si11 242.5(1), Si1−Si2 232.8(1), Si1−Si3 233.9(1), Si4−Si5 233.7(2), Si4−Si6 232.4(1), Si−$SiMe_3$ 234.0; Si4−Ga1−Si1 91.59(4), Si4−Ga2−Si1 91.57(4), Ga2−Si1−Ga1 88.11(3), Ga1−Si4−Ga2 88.68(3), Si4−Ga1−Si7 132.66(3), Si7−Ga1−Si1 135.74(3), Si4−Ga2−Si11 132.77(4), Si11−Ga2−Si1 135.64(3), Si2−Si1−Si3 107.27(5), Si2−Si1−Ga2 128.62(5), Si3−Si1−Ga2 96.78(5), Si2−Si1−Ga1 127.47(5), Si3−Si1−Ga1 102.77(5), Si6−Si4−Si5 116.52(5), Si6−Si4−Ga1 123.73(5), Si5−Si4−Ga1 100.53(5), Si6−Si4−Ga2 120.08(5), Si5−Si4−Ga2 101.97(5).

Conclusions

With **5** and **6** we have described two novel gallium- and silicon-containing heterocycles, which have both been prepared starting from gallium(II) halides, showing that the hypersilyl ligand is not only useful as a bulky substituent, but is also a valuable source for $Si(SiMe_3)_2$ units. **6** is formally a dimer of a hypothetical silagallene $RGa{=}SiR'_2$, **5** is a novel substituted trigallane derivative. Obviously, in all reactions described in this work disproportionation takes place. The different product distributions reflect the sensitivity of low-valent gallium halide reaction chemistry. Only small variations in the reaction conditions may either proceed in retention or cleavage of the initial Ga−Ga bond. In the latter case gallium(III) compounds and new oligogallanes are formed; in the worst case elemental gallium precipitates.

We thank Prof. Dr. *H. Schnöckel* for his support of this work. We are also indepted to Mr. *H. Piotrowski* and Prof. Dr. *P. Klüfers* for collecting the crystallographic data set for **5**. Financial support by the *Deutsche Forschungsgemeinschaft*, the *Fonds der Chemischen Industrie*, and *Chemetall GmbH* is gratefully acknowledged.

Experimental Section

General: All handling was performed under purified nitrogen or in vacuo using Schlenk techniques. − NMR: Bruker ACP 200 and 250. − MS: Varian MAT 711 with direct inlet. − Gallium halides were prepared from the elements,[14] $(Me_3Si)_3SiLi(thf)_3$[15] as described in the literature. Other chemicals were used as purchased. − X-ray Crystallographic Study:[13] Suitable crystals were mounted with a perfluorated polyether oil on the tip of a glass fiber and cooled immediately on the goniometer head. Data collections were performed in ω-scan with Mo-K_α radiation (graphite monochromator) on a Stoe STADI4 (**3**, **5**) or Stoe IPDS (**6**) diffractometer using the commercial software. Structures were solved using the program XS from Siemens SHELXTL (PC) and refined against F^2 (full matrix) with SHELXL93. All non-hydrogen atoms were refined anisotropically. All hydrogen atoms bonded to carbon atoms were included as riding model with fixed isotropic U's in the final refinement. For further details see Table 1.

Bis[tris(trimethylsilyl)silyl]gallium Chloride (**3**): Into a solution of $[(Me_3Si)_3Si]_4Ga_4Cl_4$ (**1**) (0.51 g, 0.36 mmol) in 20 ml of tetrahydrofuran a solution of $LiSi(SiMe_3)_3 \cdot 3$ thf (0.34 g, 0.73 mmol) in 15 ml of tetrahydrofuran was added dropwise at 60°C (at room temperature no reaction was observed). After stirring the resulting red solution for additional 12 h at room temperature all volatiles were removed in vacuo. The residue was suspended in 10 ml of pentane. Upon filtration the solution was reduced to a volume of 2 ml and cooled to −25°C. Yellow prisms of **3** crystallized followed by black violet plates of **2**.

Lithium 2,4,4-Tris(trimethylsilyl)-1,2,3-tris[tris(trimethylsilyl)silyl]-1,3-digalla-2-gallata-4-silacyclobutane · 4 THF (**5**): A solution of $Ga_2Cl_4 \cdot 2$ dioxane (0.49 g, 1.07 mmol) in 15 ml of tetrahydrofuran was added dropwise at −78°C to a solution of $LiSi(SiMe_3)_3 \cdot 3$ thf (2.00 g, 4.25 mmol) in 20 ml of tetrahydrofuran. After slowly warming to ambient temperature, the mixture was stirred for another 12 h, then all volatiles were removed in vacuo and the residue was extracted three times with 20 ml of pentane, each. The insoluble residue was treated with 15 ml of toluene and sonicated for 5 min. The red solution was filtered. Upon standing a dark red oil separated, which was redissolved in methylcyclohexane/tetrahydrofuran (25:1). At 0°C 0.15 g of **5** (14%) crystallized as black-red prisms. From the pentane fraction bis(hypersilyl)gallium chloride could be identified as one of the gallium(III) products. − ^{1}H NMR ([D$_8$]THF): δ = 0.30 [54 H, 1,3-Si($SiMe_3$)$_3$], 0.25 (9 H, 2-$SiMe_3$), 0.20 [27 H, 2-Si($SiMe_3$)$_3$], 0.17, 0.13 (9 H each, 4-$SiMe_3$). − ^{13}C NMR ([D$_8$]THF): δ = 11.8, 8.2 (4-$SiMe_3$), 5.8 [1,3-Si($SiMe_3$)$_3$], 5.6 [2-Si($SiMe_3$)$_3$], 3.6 (2-$SiMe_3$). − ^{29}Si NMR ([D$_8$]THF): δ = −4.3 (Si-4), −8.8 [2-Si(*Si*Me_3)$_3$], −9.4 [1,3-Si(*Si*Me_3)$_3$], −11.8 (4-$SiMe_3$), −12.7 ($GaSiMe_3$), −14.2 (4-$SiMe_3$), −120.2 [1,3-*Si*($SiMe_3$)$_3$], −131.4 [2-*Si*($SiMe_3$)$_3$]. − MS (70 eV, EI, ^{69}Ga): *m/z* (%) = 536 (5) $[Ga\{Si(SiMe_3)_3\}_2]^+$, 389 (16) $[Me_3SiGaSi(SiMe_3)_3]^+$, 316 (10) $[GaSi(SiMe_3)_3]^+$, 248 (94) $[HSi(SiMe_3)_3]^+$, 174 (83) $[Si(SiMe_3)_2]^+$, 160 (100) $[HSi(SiMe_3)(SiMe_2)]^+$, 73 (76) $[SiMe_3]^+$. − $C_{52}H_{140}Ga_3LiO_4Si_{16}$ (1495.2): calcd. C 41.77, H 9.44; found C 42.15, H 10.16.

1,1,3,3-Tetrakis(trimethylsilyl)-2,4-bis[tris(trimethylsilyl)silyl]-1,3,2,4-disiladigalletane (**6**): A solution of $LiSi(SiMe_3)_3 \cdot 3$ thf (4.66 g, 9.89 mmol) in 30 ml of tetrahydrofuran was treated at room temperature dropwise with a solution of $Ga_2Cl_4 \cdot 2$ dioxane (1.59 g, 2.50 mmol) in 40 ml of tetrahydrofuran. After stirring for an-

Table 1. Crystal data and data-collection parameters

Compound	**3**	**5**	**6**
Chem. formula	$C_{18}H_{54}ClGaSi_8$	$C_{52}H_{140}Ga_3LiO_4Si_{16}$	$C_{30}H_{90}Ga_2Si_{14}$
Form. weight	600.50	1495.18	983.72
Cryst. size [mm]	0.30×0.40×0.50	0.25×0.28×0.30	0.20×0.20×0.25
Cryst. system	hexagonal	monoclinic	triclinic
Space group	$P6_122$	$P2_1/n$	$P\bar{1}$
a [Å]	9.604(4)	14.054(2)	24.113(3)
b [Å]	9.604(4)	24.232(6)	25.480(4)
c [Å]	68.530(40)	26.036(4)	9.6617(10)
α [°]	90	90	100.191(15
β [°]	90	97.56(3)	80.874(13)
γ [°]	120	90	98.330(15)
V [Å^3]	5474.1(45)	8790(3)	5726.7(12)
Z	6	4	4
ρ(calcd.) [Mg/m^3]	1.093	1.130	1.141
μ [mm^{-1}]	1.096	1.164	1.253
F(000)	1932	3216	2112
Index range	$\pm h \pm k \pm l$	$\pm hkl$	$\pm h \pm k \pm l$
$2\theta_{max}$ [°]	46.04	49.98	48.24
Temp. [K]	210	200	193(2)
Refl. collected	8624	15607	31672
Refl. unique	2554	14661	17028
Refl. observed (4σ)	1964	9521	10226
R_{int}	0.1393	0.0485	0.0322
Absorption corr.	n. a.	semi-empirical	semi-empirical
Min/max. transm.	–	0.7493/0.6647	0.6369/0.8580
No. variables	137	721	889
Weighting scheme[a] x/y	0.0448/5.5264	0.0232/2.7117	0.0303/0.0000
GOOF	1.139	1.130	0.794
Final R (4σ)	0.0476	0.0527	0.0308
Final $wR2$	0.1074	0.0884	0.0679
Largest resid. peak [e/Å^3]	0.716	0.439	0.345

[a] $w^{-1} = \sigma^2 F_o^2 + (xP)^2 + yP$; $P = (F_o^2 + 2F_c^2)/3$.

other 12 h, the volatiles were removed in vacuo and the oily residue was suspended in 30 ml of pentane. After filtration, a dark red solution was obtained from which after separation of minor portions of **6** 0.43 g of **2** · $Si(SiMe_3)_4$ (43%) as blue-violet plates crystallized upon cooling to −30°C. The in pentane not soluble residue of filtration was extracted with 30 ml of toluene. From the solution obtained, 0.54 g of **6** (44%) crystallized as orange needles at −30°C. – **6**: ^{1}H NMR (C_6D_6): δ = 0.47. – ^{13}C NMR (C_6D_6): δ = 6.8 ($SiMe_3$), 5.5 [$Si(SiMe_3)_3$]. – ^{29}Si NMR (C_6D_6): δ = −3.3 ($Ga_2\mathit{Si}_2$), −7.1 ($SiMe_3$), −8.0 [$Si(\mathit{Si}Me_3)_3$], −103.8 [$\mathit{Si}(SiMe_3)_3$]. – MS (70 eV, EI, ^{69}Ga): m/z (%) = 980 (23) $[M]^{+\cdot}$, 965 (11) $[M - CH_3]^+$, 907 (2) $[M - SiMe_3]^+$, 733 (100) $[M - Si(SiMe_3)_3]^+$, 660 (1) $[M - Si(SiMe_3)_4]^{+\cdot}$, 645 (40) $[(660) - CH_3]^+$, 587 (28) $[(660) - SiMe_3]^+$, 490 (55) $[M/2]^{+\cdot}$, 475 (18) $[M/2 - CH_3]^+$, 417 (42) $[M/2 - SiMe_3]^+$, 316 (68) $[GaSi(SiMe_3)_3]^+$, 243 (40) $[M/2 - Si(SiMe_3)_3]^+$.– $C_{30}H_{90}Ga_2Si_{14}$ (983.7): calcd. C 36.63, H 9.22; found C 35.35, H 9.28. – **2** · $Si(SiMe_3)_4$: ^{1}H NMR (C_6D_6): δ = 0.47 [s, 27 H, $GaSi(SiMe_3)_3$], 0.27 [s, 9 H, $Si(SiMe_3)_4$]. – ^{13}C NMR (C_6D_6): δ = 4.4 [$GaSi(SiMe_3)_3$], 2.8 [$Si(SiMe_3)_4$]. – ^{29}Si NMR (C_6D_6): [= −8.3 ($GaSi(\mathit{Si}Me_3)_3$], −9.8 [$Si(\mathit{Si}Me_3)_4$], −68.7 [$Ga\mathit{Si}(SiMe_3)_3$], −135.5 [$\mathit{Si}(SiMe_3)_4$].

[☆] Dedicated to Professor *Heinrich Nöth* on the occasion of his 70th birthday.

[1] R. Frey, G. Linti, K. Polborn, *Chem. Ber.* **1994**, *127*, 101 – 103.
[2] G. Linti, R. Frey, W. Köstler, Horst Urban, *Chem. Ber.* **1996**, *129*, 561 – 569.
[3] A. M. Arif, A. H. Cowley, T. M. Elkins, R. A. Jones, *J. Chem. Soc., Chem. Commun.* **1986**, 1776−1777.
[4] G. Linti, W. Köstler, *Angew. Chem.* **1996**, *108*, 593−595; *Angew. Chem. Int. Ed. Engl.* **1996**, *35*, 550−552.
[5] G. Linti, W. Köstler, *Angew. Chem.* **1997**, *109*, 2758−2760; *Angew. Chem. Int. Ed. Engl.* **1997**, *36*, 2644−2645.
[6] G. Linti, *J. Organomet. Chem.* **1996**, *520*, 107 − 113.
[7] H. C. Marsmann, W. Raml, E. Hengge, *Z. Naturforsch., B: Anorg. Chem., Org. Chem.* **1980**, 35, 1541−1547.
[8] P. J. Brothers, R. J. Wehmschulte, M. M. Olmstead, K. Ruhlandt-Senge, S. R. Parkin, P. P. Power, *Organometallics* **1994**, *13*, 2792−2799.
[9] M. A. Petrie, P. P. Power, H. V. R. Dias, K. Ruhlandt-Senge, K. M. Waggoner, R. J. Wehmschulte, *Organometallics* **1993**, *12*, 1086−1093.
[10] A. Meller, S. Pusch, E. Pohl, L. Häming, R. Herbst-Irmer, *Chem. Ber.* **1993**, *126,* 2255−2257
[11] X.-W. Li, W. T. Pennington, G. H. Robinson, *Organometallics* **1995**, *14*, 2109−2111.
[12] A. Schnepf, C. Doriat, E. Möllhausen, H. Schnöckel, *Chem. Commun.* **1997**, 2111−2112.
[13] Crystallographic data (excluding structure factors) for the structures reported in this paper have been deposited with the Cambridge Crystallographic Data Centre as supplementary publication no. CCDC-100895. Copies of the data can be obtained free of charge on application to CCDC, 12 Union Road, Cambridge CB21EZ, UK (Fax: int code +44(0)1223/336-033; e-mail: deposit@ccdc.cam.ac.uk).
[14] Brauer, *Handbuch der präparativen Anorganischen Chemie*, F. Enke Verlag, Stuttgart, **1975**.
[15] [15a] H. Gilman, C. L. Smith, *J. Organomet. Chem.* **1968**, *14*, 91. – [15b] G. Gutekunst, A. G. Brook, *J. Organomet. Chem.* **1982**, *225*, 1. – [15c] A. Heine, R. Herbst-Irmer, G. M. Sheldrick, D. Stalke, *Inorg. Chem.* **1993**, *32*, 2694.

[97322]

The Role of 1-Azaallyllithium Compounds in Phosphorus Chemistry, 2[◇]

Aspects of the Chemistry of the Cyclic Phosphonium Salt $[Ph_2P^aP(Cl)N(SiMe_3)C(tBu)=C^bH(P^a–C^b)]Cl$ and the Related Diazadiphosphetidine $[ClP^aN(R)P(Cl)N^bR(P^a–N^b)]$ [R = C(*t*Bu)=C(H)SiMe$_3$]

Peter B. Hitchcock, Michael F. Lappert*, and Marcus Layh

The Chemistry Laboratory, University of Sussex,
Brighton, BN1 9QJ, UK

Received March 9, 1998

Keywords: Phosphorus chemistry / Phosphonium salts / Diazadiphosphetidines / Phosphazoles / 1-Azaallyl compounds

We report the preparation of the novel phosphonium salts $[Ph_2P^aP(NR'_2)N(R)C(tBu)=C^bH]A(P^a–C^b)$ (**2a**; R′ = Et, R = SiMe$_3$, A = Cl; **2b**: R′ = Me, R = SiMe$_3$, A = Cl; **2c**: R = Et, R′ = SiMe$_3$, A = [OSO_2CF_3]; **2d**: R′ = Et, R = SiMe$_3$, A = [BPh_4]; **4**: R′ = Et, R = H, A = Cl) and *trans*-1,3,2,4-diazadiphosphetidines $R'_2NP^aN(R)P(NR'_2)N^c(R)(P^a–N^c)$ [**3a**: R′ = Et, R = C(*t*Bu)=C(H)PPh_2; **3b**: R′ = Me, R = C(*t*Bu)=C(H)PPh_2; **7**: R′ = Me, R = C(*t*Bu)=C(H)SiMe$_3$]. Reaction of **3a** with Cu_2I_2 led to the *P*- and *P,P′*-centred complexes [Cu(I)(**3a**)] (**5a**) and [{Cu(I)}$_2$(**3b**)] (**5b**) [R = C(*t*Bu)=C(H)PPh_2]. The phosphazole $N^aC(tBu)C(H)C^cP^aN(Me)(CH_2)_2N^cMe(N^a–P^a)(C^c–N^c)$ (**8**) was obtained by a remarkable heterocycloaddition reaction from the diazadiphosphetidine $ClP^aN(R)P(Cl)N^bR(P^a–N^b)$ [**6**: R = C(*t*Bu)=C(H)SiMe$_3$] and the electron-rich olefin $[=C^aN(Me)(CH_2)_2N^aMe(C^a–N^a)]_2$ and was oxidised with S_8 yielding $N^aC(tBu)C(H)C^cP^a(S)N(Me)(CH_2)_2N^cMe(N^a–P^a)(C^c–N^c)$ (**9**). Compounds **2–9** were characterised by multinuclear NMR spectroscopy, mass spectrometry for **5–9**, while single-crystal X-ray diffraction data are provided for **3a** and **5a**.

Introduction

Recently we reported that treatment of the ketimine $Me_3SiN=C(Bu^t)CH(R')SiMe_3$ (**A**: R′ = PPh_2; **B**: R′ = SiMe$_3$) with PCl_3 gave the novel phosphonium salt $[Ph_2P^aP(Cl)N(SiMe_3)C(tBu)=C^bH]Cl(P^a–C^b)$ (**1a**) or the *trans*-1,3,2,4-diazadiphosphetidine **6** (Scheme 1)[1].

Scheme 1

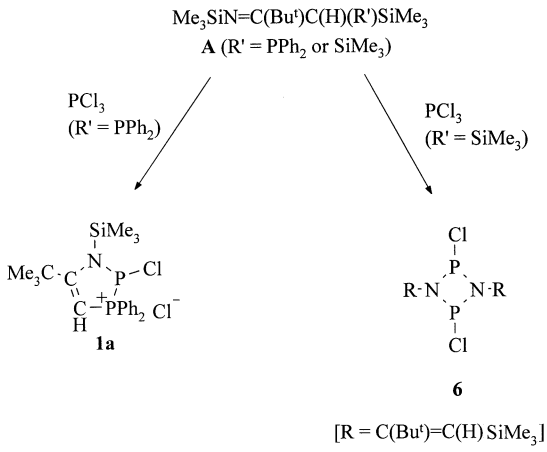

The chloride **1a** was thermolabile and decomposed during attempted recrystallisation, whereas the corresponding triflate or tetraphenylborate was stable. We now present further reactions of the two phosphorus-containing heterocycles **1a** and **6**.

[◇] Part 1: Ref.[1].

Results and Discussion

The reaction of **1a** with $Me_3SiNR'_2$ led (step i in Scheme 2), by Me_3SiCl elimination, to the P^{III}-dialkylamino derivatives **2a** and **2b**. Both compounds were thermally labile and were isolated as crude materials from the reaction mixture by removing the solvent and washing the residue with pentane. They were characterised solely by multinuclear NMR spectroscopy.

After resolvation in hot toluene, **2a** or **2b** eliminated a second equivalent of Me_3SiCl and cooling gave (step ii in Scheme 2) colourless crystals of the *trans*-diazadiphosphetidine **3a** or **3b** in nearly quantitative yield. Each gave satisfactory (parent ion) mass spectra and microanalyses. NMR-spectroscopic studies showed that the *P,P′*-bis(diethylamino) compound **3a** existed in solution as mixture of two *trans* isomers, which only differed in the orientation of their substituents at the endocyclic nitrogen atom. In the minor isomer (henceforth identified as *syn*), both diphenylphosphane end groups were close to the same endocyclic phosphorus atom (this conformation is also adopted in the CuI complex **5a**, see Figure 3), while in the major (*anti*) isomer they were close to endocyclic phosphorus atoms of adjacent molecules (as in the crystal, Figure 2). The bis(dimethylamino) analogue **3b**, by contrast, was found to exist solely as the *anti* isomer.

Replacing Cl^- of **2a** by a bulkier anion by treatment with $Ag[OSO_2CF_3]$ or $Na[BPh_4]$ gave (step iii in Scheme 2) the thermally stable five-membered heterocycle **2c** or **2d**. Each was recrystallised from a mixture of CH_2Cl_2 and pentane

 © WILEY-VCH Verlag GmbH, D-69451 Weinheim, 1998 1434–1948/98/0606–0751 $ 17.50+.50/0

Scheme 2. Some reactions of the phosphonium salt **1a**

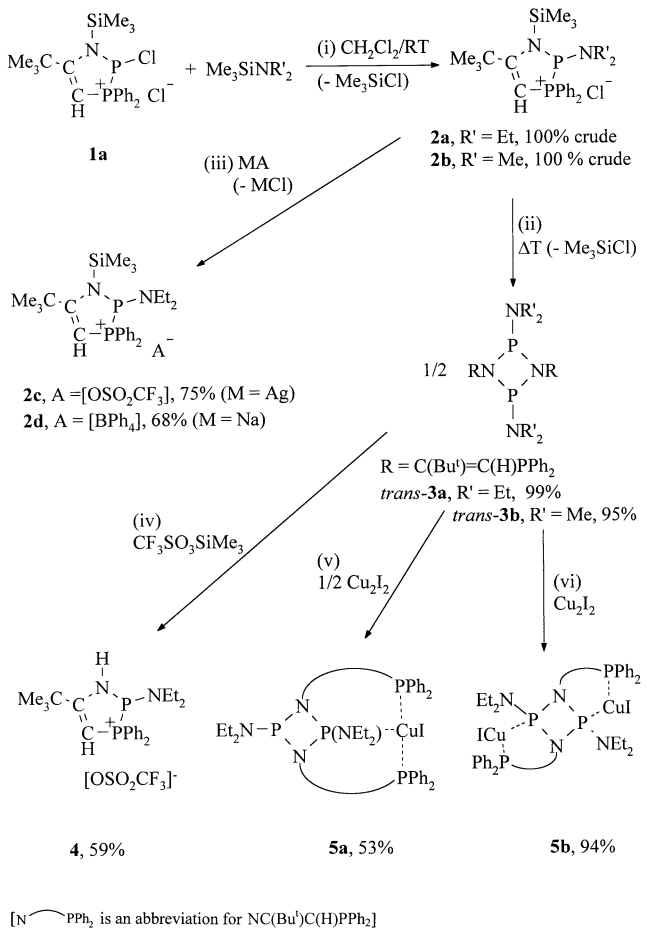

and was fully characterised. Remarkably, the conversion of the phosphonium chloride **2a** into the diazadiphosphetidine **3a** proved to be quasi-reversible as was shown by treatment of **3a** with $CF_3SO_3SiMe_3$ in hot toluene (80°C, 96 h) which yielded (step iv in Scheme 2) the phosphonium triflate **4**; the cation is the desilylated analogue of that in **2a**. The fate of the Me_3Si group at N was not established. A similar observation had, however, been made for the reaction of $Me_3SiN{=}C(t\text{Bu})CH(PPh_2)SiMe_3$ (**A**: R′ = PPh_2) with $PhPCl_2$ or $EtPCl_2$ (cf. Scheme 1) giving $Ph_2P^aP(R'')N(H)C(t\text{Bu}){=}C^bH(P^a{-}C^b)Cl$ (R'' = Ph or Et), with no trace of the $SiMe_3$-substituted product being detected[1].

The ability of a diazaphosphetidine to act as ligand is well documented[2] and is now demonstrated for **3a** by the synthesis (steps v or vi of Scheme 2) of the iodocopper(I) complexes **5a** or **5b** from a mixture of **3a** and Cu_2I_2 in hot toluene. Thus, compound **3a** behaved as a novel terminal tridentate (**5a**) or bridging bis(bidentate) (**5b**) ligand. The related reaction of **3b** with AgI led, under similar reaction conditions, to the disappearance of AgI, and the formation of a white precipitate, presumably an Ag analogue of **5b**, but its extreme insolubility in standard solvents including hot $CHCl_3$ or CH_3CN prevented its characterisation. This was not surprising, as even **5b** was only very sparingly soluble in hot toluene or $CHCl_3$, which may be due to its being a polymer of infinite chain length, with **5b** moieties bridging CuI units (*anti* isomer). The *syn* isomer of **5a** was, by contrast, a monomer both in the gas phase (parent ion in the mass spectrum) and in the crystal (see Figure 3). As a consequence, **5a** was much more soluble than **5b** in, for example, hot toluene.

Further reactions of the diazadiphosphetidine **6** are illustrated in Scheme 3. Treatment of **6** with Me_3SnNMe_2 led (i in Scheme 3) in a clean reaction to the *trans*-diazadiphosphetidine **7**, which with $LiNEt_2$ gave an inseparable mixture of products, whereas Me_3SiNEt_2 proved to be unreactive. The treatment of **6** with the electron-rich olefin [$=C^aN(Me)(CH_2)_2N^aMe(C^a{-}N^a)]_2$[3] led not, as we had anticipated, by chlorine abstraction to a stable phosphorus-centred radical, as had been reported for formation of PR'_2 from $ClPR'_2$ [R′ = $CH(SiMe_3)_2$][4], but (step ii in Scheme 3) to the fused bicyclic compound $N^aC(t\text{Bu})C(H)C^cP^aN(Me)(CH_2)_2N^cMe(N^a{-}P^a)(C^c{-}N^c)$ (**8**). The latter was distillable in a vacuum at 130°C and crystallised at room temperature after several days. Compound **8** was converted (step iii in Scheme 3) into its P^V derivative **9** by treatment with S_8 and crystallisation from Et_2O.

Scheme 3. Some reactions of the *trans*-diazadiphosphetidine **6** [R = C(*t*Bu)C(H)$SiMe_3$]

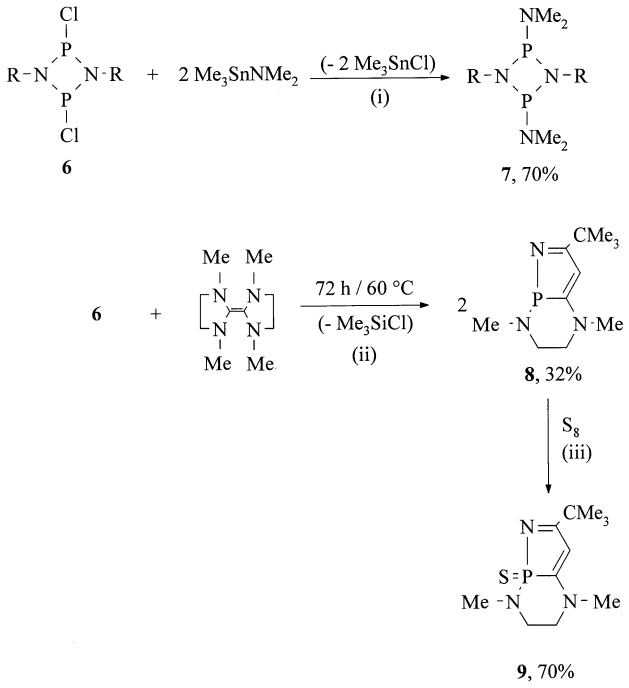

A plausible reaction pathway for the formation of **8** is outlined in Scheme 4. The first step (i in Scheme 4) is the dissociation of **6** into the transient monomer, the iminophosphane, which is subjected to nucleophilic attack (step ii in Scheme 4) by the electron-rich olefin known[5] to be a powerful C-centred nucleophile. A reversible dimerisation of an iminophosphane has been reported for *t*BuP=N*t*Bu[6]. In step (iii) (which may be synchronous with ii), a *spiro* bycyclic compound **B** is formed with electron-rich

carbene elimination (this can dimerise to reform the electron-rich olefin). Loss of Me_3SiCl from **B** thus leads (step iv in Scheme 4) to **C**, which isomerises (step v in Scheme 4) into the more stable bicyclic compound **8**.

Scheme 4. Proposed reaction pathway from **6** + [=$C^aN(Me)(CH_2)_2$-$N^aMe(C^a-N^a)]_2$ to **8**

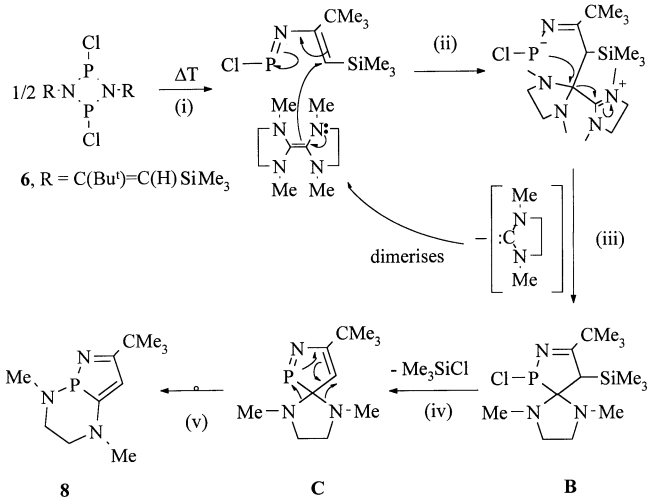

NMR-Spectra and Solution Behaviour

In the following discussion of the NMR spectra of the new cyclic phosphonium salts **2** and **4** we also include data on five related compounds $[Ph_2P^aP(R'')N(R')C(t\text{Bu})=C^bH(P^a-C^b)]$A {R′ = $SiMe_3$, R″ = Cl and A = Cl (**1a**), $[OSO_2CF_3]$ (**1b**), $[BPh_4]$ (**1c**); A = Cl, R′ = H, R″ = Ph (**10a**), Et (**10b**)} which had been reported earlier[1]. The data are summarised in Table 1. Each was insoluble in hydrocarbons or Et_2O, but readily soluble in CH_2Cl_2. As a general rule, the NH compounds (i.e., R′ = H) **4**, **10a** and **10b** were thermally stable and were easily crystallised from aromatic solvents, while solutions of the $NSiMe_3$ derivatives **1a**−**2d** were much less so and, in particular for A = Cl, decomposed at room temperature. Compounds with the bulkier anions (A = $[OSO_2CF_3]$ or $[BPh_4]$) were sufficiently stable to be purified by recrystallisation from mixtures of CH_2Cl_2 and Et_2O or pentane.

The ^{31}P-NMR spectral shift values for the λ^4P^+ (Table 1) were in the region reported for typical phosphonium salts[7]. The assignments of individual ^{31}P-NMR spectroscopic shift values and $J_{H\text{-}P}$ coupling constants were made on the basis of 2D-^{31}P-^{1}H correlation experiments for **2d**, **4**, **10a**, and **10b** (as an example, see Figure 1). These showed cross-peaks for NH, CH, and for each set of *o*-hydrogen atoms at the benzene rings of the λ^4P^+ and hence established the identity of the λ^4P^+. The remaining doublet is consequently attributed to λ^3P, an assignment further supported by its broadening attributable to the quadrupolar moment of the adjacent nitrogen atom.

The $^1J_{PP}$ coupling constants were on the low side of previously reported values (240−424 Hz)[8][9][10] in related systems, but showed the general trend[8] of increasing with increasing electron-donating strength of the substituent at the λ^3P (**2c** being an exception).

The comparatively small effect of changing the anion A^- (compounds **1a**−**1c**, **2a**, **2c**, **2d**) on the ^{31}P-NMR shift value for λ^3P, and in particular on the size of the $^1J_{PP}$ coupling constants makes it plausible to assume that in solution the phosphonium salts exist as separated ion pairs even for the comparatively small chloride anion. Larger differences in ^{31}P-NMR spectroscopic shifts {$\Delta\delta[^{31}P(\lambda^3P)]$ = 6−18 ppm} and coupling constants (Δ^1J_{PP} = 35−58 Hz) in the related urea-bridged derivatives [*t*Bu(Ph)P^aP(R)N(Me)-C(O)N^b(Me)(P^a-N^b)]A (R = Me, Et, *i*Pr, *t*Bu, Ph, Xyl, 9-Anth, $CHCl_2$, or CH_2SiMe_3) have been attributed to a change in structure from a zwitterionic form for the chloride to a separated ion pair for the tetraphenylborate[8].

Other interesting features were: (i) the ^{1}H-NMR spectroscopic shift of the ring C*H* adjacent to λ^4P^+ seemed to depend mainly on the nature of the counterion. Independent of other substituents they varied from $\delta \approx 10$ for A = Cl, through $\delta \approx 8$ for A = $[OSO_2CF_3]$ to $\delta \approx 6$ for A = $[BPh_4]$; (ii) the large $^4J_{H\text{-}\lambda^4P}$ coupling constants of 10−16 Hz for the NH compounds **4** and **10**; and (iii) $\delta[^{13}C\{^1H\}]$ = 78 for the ring *C*H and δ = 190 for the ring *C*N, a value usually associated with a carbon atom doubly bonded to an oxygen or nitrogen atom. Items (ii) and (iii) indicate a considerable delocalisation of π-electron density in the heterocycle between N and λ^4P^+.

The ^{31}P-NMR spectroscopic shift of $\delta \approx 186$ for the endocyclic phosphorus atom of the diazadiphosphetidine **3a**, **3b**, or **7** in $CDCl_3$ solution is appropriate for each having *trans*-orientated substituents at the phosphorus atom[11][12][13][14][15][16][17][18][19][20][21]. While **7** showed only a singlet for the magnetically equivalent phosphorus atoms of the PN heterocycle, the spectrum of **3a** indicated the presence of two isomers in a ratio of approximately 3:1. The set of signals of the major isomer assigned to be of the *anti* isomer (as in the crystal) showed an AA′XX′ spectral pattern with two pseudo triplets, one for the PPh_2 (X) groups at δ = −29.4 and the other for the ring phosphorus (A) at δ = 186.6. The spectrum was readily simulated on the basis of J_{AX} = 202.6 and $J_{AA'}$ = 20.4 Hz. The CP-MAS ^{31}P-NMR spectrum of **3a** showed the signals only of the major (δ = −29.4 and δ = 186.6, J_{PP} = 190 Hz), but not of the minor, isomer. It is, however, not inevitable that the minor isomer exists only in solution and not in the solid, because the larger line width and the less favourable signal-to-noise ratio of the solid-state NMR spectrum compared to that in solution may have obscured the CP-MAS signals of the minor isomer. The solution ^{31}P-NMR spectrum of the latter showed features consistent with its being the *syn* isomer, having a conformation similar to **5a**. Only a doublet was observed for the PPh_2 groups, while the ring phosphorus atom close to the PPh_2 groups gave rise to a triplet of doublets due to a coupling with *P*Ph_2 and the other endocyclic phosphorus atom, respectively. Variable-temperature solution ^{31}P-NMR spectroscopic studies on the isomeric mixture of **3a** showed no temperature dependence for the ratio

Table 1. Selected NMR-spectroscopic data of cyclic phosphonium salts

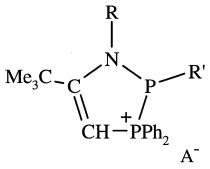

No.	R	R′	A	δ ^{31}P (λ^3P)	δ ^{31}P (λ^4P)	$^1J_{P\text{-}P}$	δ ^{1}H (CH)	δ ^{13}C (CH)	δ ^{13}C (CN)
1a	$SiMe_3$	Cl	Cl	69.2	54.9	227.9	10.26	[a]	191.0
1b	$SiMe_3$	Cl	OSO_2CF_3	73.0	61.7	233.5	8.77	78.2	191.5
1c	$SiMe_3$	Cl	BPh_4	69.5	63.1	241.0	6.15	–	–
2a	$SiMe_3$	NEt_2	Cl	74.4	29.4	269.1	10.08	–	–
2b	$SiMe_3$	NMe_2	Cl	74.9	30.1	263.5	9.90	69.0	190.6
2c	$SiMe_3$	NEt_2	OSO_2CF_3	84.5	31.2	190.4	8.23	[a]	188.8
2d	$SiMe_3$	NEt_2	BPh_4	86.5	33.2	279.5	6.11	72.5	188.5
4	H	NEt_2	OSO_2CF_3	82.3	10.6	304.9	8.19	65.0	184.0
10a	H	Ph	Cl	15.0	43.8	238.5	10.09	64.8	186.4
10b	H	Et	Cl	28.6	39.6	245.4	9.44	63.7	185.8

[a] Not identified.

Figure 1. 2D-^{31}P{^{1}H} ^{1}H-NMR correlation spectrum of $Ph_2P^aP(Ph)N(H)C(t\text{Bu})=C^bH(P^a-C^b)Cl$ (**10a**)

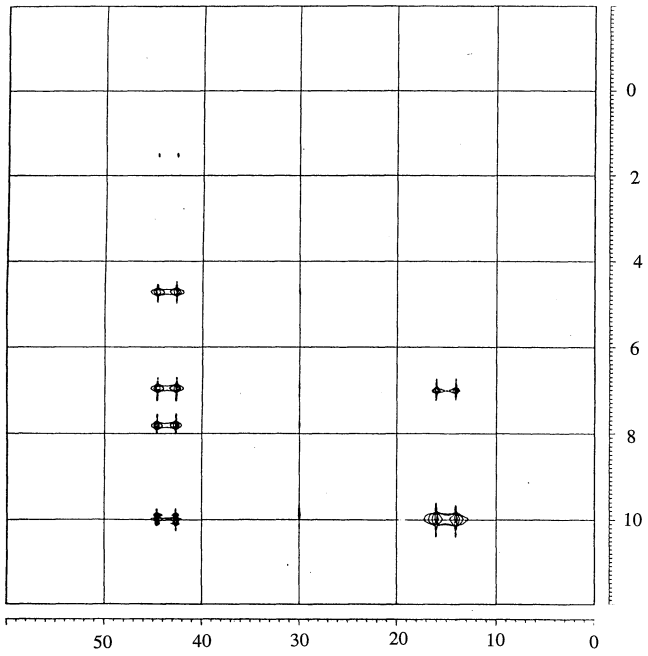

of the two isomers between −45 and +60°C, while prolonged heating (12 h at 60°C) led to complete decomposition of the sample. No signals attributable to the formation of a *cis* isomer were observed.

In solutions of the metal complexes **5a** or **5b**, the ^{31}P-NMR spectral signal for the metal-coordinated ring phosphorus atoms was shifted by ca. 50 ppm to lower frequency, whereas the influence on the chemical shifts of the PPh_2 groups was only small. Probably due to the quadrupolar moment of the coordinated copper centre, the lines were, particularly for **5a**, so broad that any coupling information was obscured. Slightly sharper lines were observed for **5b**, so that $J_{P(A)P(X)}$ = 297 Hz was determined, being ca. 100 Hz larger than in the free ligand **3a**. The unusual magnitude of these coupling constants in **3** and **5**, being in the lower range of reported directly bonded P-P coupling constants[11], is attributed to a through-space coupling rather than a $^4J(^{31}P\text{-}^{31}P)$. This is supported by the close P···P contacts between phosphane and ring phosphorus atoms in the crystal structures of **3a** [3.262(1) Å] and **5a** [3.252(3) and 3.319(3) Å]. A similar effect had been observed for **6**, where the closeness of the ring phosphorus atom and the trimethylsilyl group gave rise to a coupling ($J_{P\text{-}H}$ = 1.3 Hz[1]) between these two groups.

There has been much interest in the *cis*/*trans* isomerism in 1,3,2,4-diazadiphosphetidines, with the *cis* generally the thermodynamically and the *trans* the kinetically favoured isomer (refs.[14][15][16][17][18][19][20][21][22][23], and literature cited therein). For bulky ligands at N and P, the *trans* isomer is usually thermodynamically favoured. Studies into the relationship between isomer and the chemical shift δ(^{31}P) showed the signals of the *cis* isomer to be ca. 50−90 ppm at higher frequency than in the *trans* isomer[14][18][19][20][21][22][23]. Each of the diazadiphosphetidines having the bulky C(*t*Bu)=C(H)R′ (R′ = $SiMe_3$ and PPh_2) substituent at N, which we have so far characterised, has invariably adopted the *trans* conformation.

The ^{31}P-NMR spectroscopic shifts previously reported for *trans*-diazadiphosphetidines coordinated to metals were for most part in the same region (δ ≈ 130−170[2]) as observed for **5a** and **5b**. Only for Pd or Pt complexes, values of 40 or 80 ppm to lower frequency have been observed. The direction of the shift change, as between the free ligand and the complex upon coordination, seems largely to depend on the metal[2]. Since **5a** and **5b** are, to our knowledge, the first compexes of diazadiphosphetidines with copper, no comparative data are available.

The structures of **8** and **9** were determined with the help of multinuclear NMR spectra and MS. The assignments of the ^{13}C-NMR spectroscopic shifts were made on the basis of (i) their chemical shift values and (ii) the information derived from $J_{P\text{-}C}$ coupling constants (when compared with literature data[24]). The interpretation of the ^{1}H-NMR spectroscopic shift data required NOE-difference NMR-spectroscopic studies. Irradiation of an individual *t*Bu group gave a 6.4% enhancement for the olefinic CH signal, while irradiation of the CNMe group gave enhancements of 3.9 and 2.0% for the CH and the *exo*-H at the neighbouring CH_2 group, respectively. The hydrogen atoms of the remaining CH_2 groups were not unambiguously identified, as any NOE enhancement was obscured due to the closeness of these signals to the centre of irradiation.

The spectra of **9** were very similar to those of **8**, the major difference being a higher frequency shift of the CH proton in the ^{1}H-NMR spectrum and a similar effect in the ^{13}C-NMR spectrum for the carbon atom directly bonded to the phosphorus atom (**8**: C*H*: δ = 5.83; *C*P: δ = 183.2; **9**: C*H*: δ = 5.26; *C*P: δ = 166). A further difference was the magnitude of the coupling constants of the nuclei close to the phosphorus atom, being much larger for **9** [$^{3}J(^{1}H\text{-}^{31}P)$ = 30.0; $^{1}J(^{13}C\text{-}^{31}P)$ = 94.4; $^{2}J(^{13}C\text{-}^{31}P)$ = 46.4 Hz] than for **8** [$^{3}J(^{1}H\text{-}^{31}P)$ = 17.1; $^{1}J(^{13}C\text{-}^{31}P)$ = 4.1; $^{2}J(^{13}C\text{-}^{31}P)$ = 36.0 Hz].

X-ray Structural Analysis of 3a and 5a

The X-ray molecular structures of **3a** and **5a** are illustrated in Figures 2 and 3, with the atom-numbering scheme and selected bond lengths and angles being shown in Tables 2 and 3.

The crystalline compound **3a** is centrosymmetric and adopts a *trans* configuration with the substituents at N(1) being *anti* to one another. The $P^{a}NPN^{a}(P^{a}-N^{b})$ ring is planar, with the *N*-ligating sp^2-carbon atoms also coplanar, the sum of angles at nitrogen (Σ N) being 360°. The endocyclic ring angle at nitrogen, 100.8(1)°, is much larger than that at phosphorus, 79.2(1)°. The N(2)−P(2)−N(1) and N(2)−P(2)−N(1′) bond angles are significantly narrower than tetrahedral, indicating the presence of a stereochemically active lone pair at P(2). The alkenyl groups have the (*E*) configuration, so as to minimise steric effects, the *tert*-butyl group being *trans* to PPh_2. As a consequence, there are close contacts between the phosphorus atom of one diphenylphosphane group [P(1)] and one ring phosphorus atom [P(1)−P(2): 3.262(1) Å] which may account for the large coupling constant between P(1) and P(2) (J_{PP} = 190 Hz) observed in the solid-state ^{31}P-NMR spectrum. The *exo* P−N distances [P(2)−N(2): 1.671(3) Å] are much shorter than the *endo* ones [P(2)−N(1): 1.751(1); P(2)−N(1′): 1.730(2) Å].

In general, the skeletal geometry of **3b** closely resembles that of other known *trans*-1,3,2,4-diazadiphosphetidines, such as $[(MeO)PN(Ph)]_2$[25], $\{[F_3C(F_2C)_2H_2C]PN(tBu)\}_2$[21], $[(F_3CH_2CO)PN(Ph)]_2$[14], $[(Ph_2N)PN(Ph)]_2$[17], $[(C_6H_4Me\text{-}4)OPN(Ph)]_2$[20], $[Me_2C^{a}(CH_2)_3(Me)_2C^{b}NPN(SiMe_3)(C^{a}-C^{b})]_2$[26] and $\{[Me_3Si)_2N]PN(SiMe_3)\}_2$[27].

In the CuI complex **5a**, the copper centre is surrounded in a distorted tetrahedral fashion by the iodine, the ring phosphorus P(1) and the two phosphorus atoms P(3) and P(4) of the *exo*-diphenylphosphane groups, Figure 4. The coordination to the metal atom leads to a *syn* conformation in the diazadiphosphetidine and a slight puckering

Figure 2. Molecular structure of **3a**

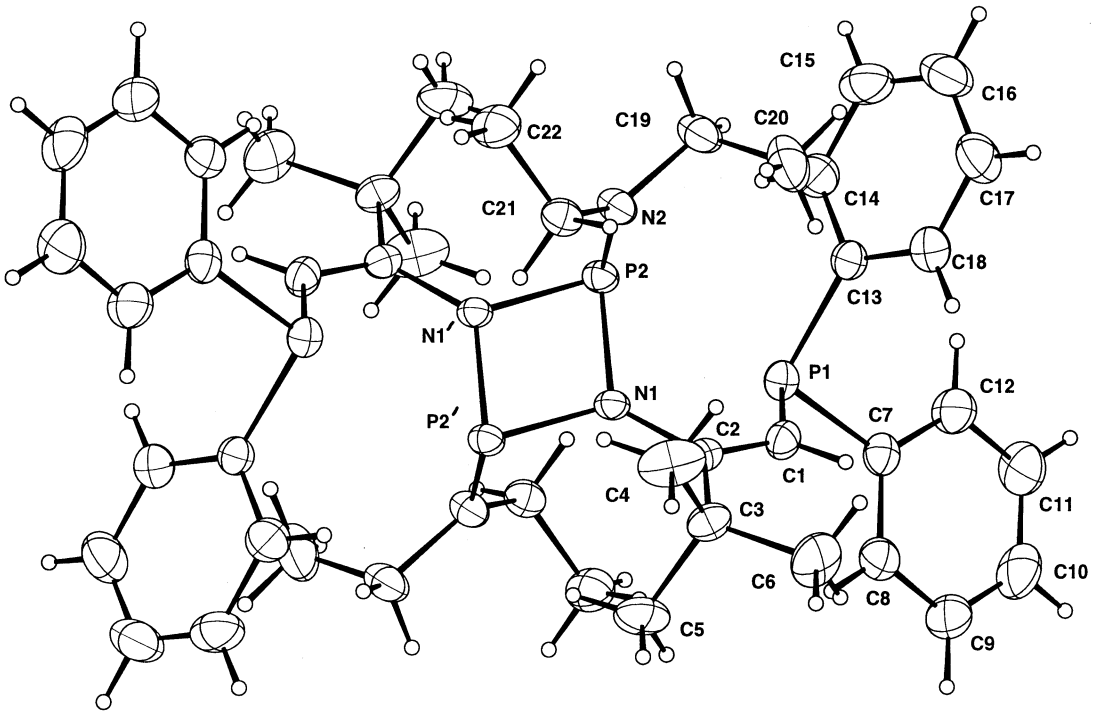

Figure 3. Molecular structure of **5a**

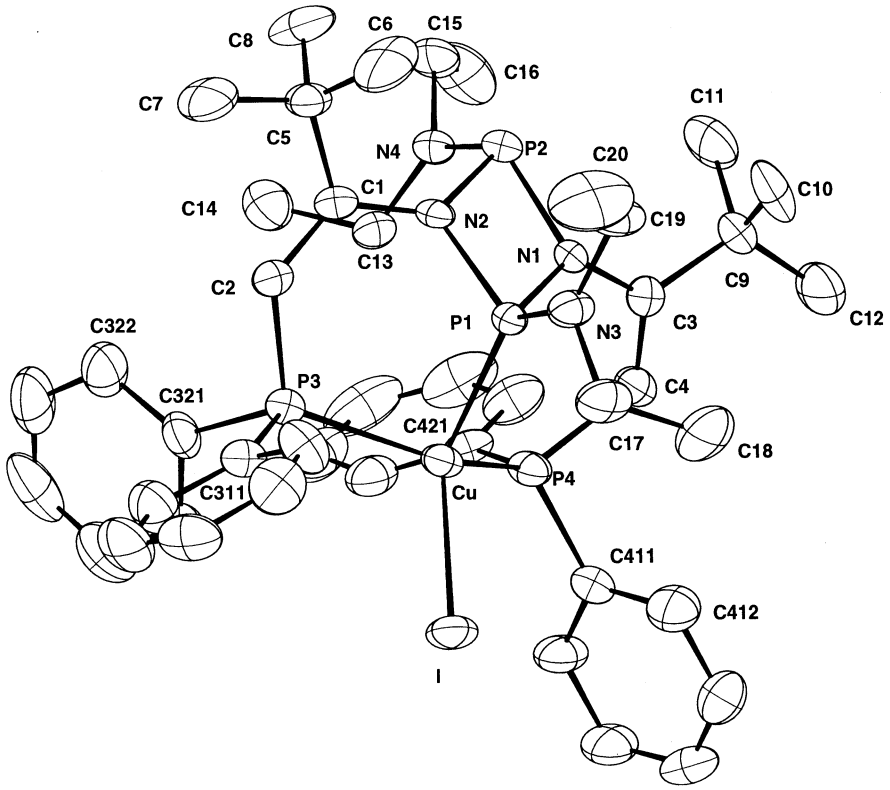

Table 2. Selected bond lengths [Å] and angles [°] for **3a**

P(1)−C(1)	1.805(3)	P(1)−C(13)	1.831(3)
P(1)−C(7)	1.846(3)	P(2)−N(2)	1.671(3)
P(2)−N(1)′	1.730(2)	P(2)−N(1)	1.751(2)
N(1)−C(2)	1.405(3)	N(2)−C(19)	1.458(4)
N(2)−C(21)	1.462(4)	C(1)−C(2)	1.340(4)
C(2)−C(3)	1.535(4)	C(3)−C(6)	1.527(5)
C(3)−C(4)	1.532(5)	C(3)−C(5)	1.536(4)
C(7)−C(12)	1.380(4)	C(7)−C(8)	1.384(4)
C(8)−C(9)	1.390(5)	C(9)−C(10)	1.355(5)
C(10)−C(11)	1.362(5)	C(11)−C(12)	1.382(5)
C(13)−C(18)	1.378(4)	C(13)−C(14)	1.381(4)
C(14)−C(15)	1.387(5)	C(15)−C(16)	1.360(6)
C(16)−C(17)	1.372(6)	C(17)−C(18)	1.373(5)
C(19)−C(20)	1.503(5)	C(21)−C(22)	1.518(4)
C(1)−P(1)−C(13)	104.60(14)	C(1)−P(1)−C(7)	98.9(2)
C(13)−P(1)−C(7)	99.80(14)	N(2)−P(2)−N(1)′	104.12(12)
N(2)−P(2)−N(1)	108.06(12)	N(1)−P(2)−N(1)′	79.18(12)
C(2)−N(1)−P(2)	125.3(2)	C(2)−N(1)−P(2)′	133.9(2)
P(2)−N(1)−P(2)′	100.82(12)	C(19)−N(2)−C(21)	116.6(2)
C(19)−N(2)−P(2)	117.1(2)	C(21)−N(2)−P(2)	126.1(2)
C(2)−C(1)−P(1)	126.7(2)	C(1)−C(2)−N(1)	120.3(3)
C(1)−C(2)−C(3)	122.8(3)	N(1)−C(2)−C(3)	116.8(2)
C(6)−C(3)−C(4)	108.9(3)	C(6)−C(3)−C(2)	112.1(3)
C(4)−C(3)−C(2)	109.7(3)	C(6)−C(3)−C(5)	107.4(3)
C(4)−C(3)−C(5)	109.1(3)	C(2)−C(3)−C(5)	109.6(3)
C(12)−C(7)−C(8)	117.7(3)	C(12)−C(7)−P(1)	122.3(3)
C(8)−C(7)−P(1)	119.7(2)	C(7)−C(8)−C(9)	120.5(3)
C(10)−C(9)−C(8)	120.5(4)	C(9)−C(10)−C(11)	120.1(4)
C(10)−C(11)−C(12)	119.9(4)	C(7)−C(12)−C(11)	121.4(4)
C(18)−C(13)−C(14)	117.9(3)	C(18)−C(13)−P(1)	123.6(3)
C(14)−C(13)−P(1)	118.5(3)	C(13)−C(14)−C(15)	120.5(4)
C(16)−C(15)−C(14)	120.5(4)	C(15)−C(16)−C(17)	119.6(4)
C(18)−C(17)−C(16)	120.0(4)	C(17)−C(18)−C(13)	121.5(4)
N(2)−C(19)−C(20)	114.0(3)	N(2)−C(21)−C(22)	112.6(3)

Table 3. Selected bond lengths [Å] and angles [°] for **5a**

I−Cu	2.574(1)	Cu−P(1)	2.223(2)
Cu−P(4)	2.292(3)	Cu−P(3)	2.306(3)
P(1)−N(3)	1.643(7)	P(1)−N(1)	1.723(7)
P(1)−N(2)	1.736(6)	P(2)−N(4)	1.649(8)
P(2)−N(1)	1.754(6)	P(2)−N(2)	1.755(7)
P(3)−C(2)	1.788(8)	P(3)−C(321)	1.813(10)
P(3)−C(311)	1.837(10)	P(4)−C(4)	1.812(9)
P(4)−C(411)	1.819(9)	P(4)−C(421)	1.839(10)
P(1)−Cu−P(4)	94.61(9)	P(1)−Cu−P(3)	91.77(9)
P(4)−Cu−P(3)	133.87(10)	P(1)−Cu−I	129.32(8)
P(4)−Cu−I	107.15(7)	P(3)−Cu−I	103.49(7)
N(3)−P(1)−N(1)	110.1(4)	N(3)−P(1)−N(2)	106.2(3)
N(1)−P(1)−N(2)	80.9(3)	N(3)−P(1)−Cu	121.9(3)
N(1)−P(1)−Cu	113.8(2)	N(2)−P(1)−Cu	116.5(2)
N(4)−P(2)−N(1)	108.3(3)	N(4)−P(2)−N(2)	105.9(3)
N(1)−P(2)−N(2)	79.5(3)	C(2)−P(3)−C(321)	106.5(5)
C(2)−P(3)−C(311)	96.9(4)	C(321)−P(3)−C(311)	102.0(5)
C(2)−P(3)−Cu	117.2(3)	C(321)−P(3)−Cu	119.5(3)
C(311)−P(3)−Cu	111.6(3)	C(4)−P(4)−C(411)	99.3(4)
C(4)−P(4)−C(421)	103.8(5)	C(411)−P(4)−C(421)	102.8(4)
C(4)−P(4)−Cu	113.2(3)	C(411)−P(4)−Cu	114.2(3)
C(421)−P(4)−Cu	120.8(3)	C(3)−N(1)−P(1)	125.9(5)
C(3)−N(1)−P(2)	133.4(6)	P(1)−N(1)−P(2)	100.0(3)
C(1)−N(2)−P(1)	127.5(5)	C(1)−N(2)−P(2)	130.6(5)
P(1)−N(2)−P(2)	99.4(4)	C(17)−N(3)−C(19)	114.6(7)
C(17)−N(3)−P(1)	117.9(6)	C(19)−N(3)−P(1)	126.0(6)
C(13)−N(4)−C(15)	116.4(7)	C(13)−N(4)−P(2)	126.0(6)
C(15)−N(4)−P(2)	117.6(6)		

of the PN heterocycle [angle between the planes P(1)N(2)P(2) and P(1)N(1)P(1): 5.7(7)°]. The *exo* P−N bond lengths [P(1)−N(3): 1.643(7); P(2)−N(4): 1.649(8) Å] are considerably shorter than the *endo* ones [P(1)−N(2):

1.736(6); P(2)−N(1): 1.754(6); P(1)−N(1): 1.723(7); P(2)−N(2): 1.755(7) Å], but the influence of metal coordination on the endocyclic P−N bonds is only small (Table 2). The Cu−I [2.574(1) Å] and Cu−P distances [Cu−P(1): 2.223(2); Cu−P(3): 2.306(3); Cu−P(4): 2.292(3) Å] are within the range of values reported for four- and three-coordinated phosphanecopper(I) complexes: $[CuI(PPh_3)_3]$ triclinic: $Cu-P_{av.}$ 2.34(1), Cu−I 2.686(1) Å[28]; $[CuI(PPh_3)_3]$ trigonal: $Cu-P_{av.}$ 2.355(8), Cu−I 2.67(1) Å[28]; $[(Cu\{\mu\text{-}I\}\{P(c\text{-}C_6H_{11})_3\})_2]$: Cu−P 2.23(1), $Cu-I_{av.}$ 2.58(1) Å[29]; $[(Cu\{\mu\text{-}I\}\{P(Ph)(CH_2CH_2PPh_2)_2\})_2]$: Cu−P 2.263(4)−2.325(5), Cu−I 2.614(2) Å[30]; $[Cu(PMe_3)(\mu\text{-}I)_2Cu(PMe_3)_2]$[31], $[\{Cu(\mu\text{-}I)(PPh_2Me)\}_2] \cdot SO_2$: $Cu-P_{av}$ 2.250(2), $Cu-I_{av}$ 2.719(1) Å[32]; $[(Cu\{\mu\text{-}I\}\{P(C_6H_4Me\text{-}4)_3\})_2](C_6H_5Me)_2$: Cu−P 2.238(4), $Cu-I_{av}$ 2.583(2) Å[33]. For two-coordinate phosphanecopper complexes, the observed Cu−P distances are usually slightly smaller: $[CuBr\{P(C_6H_2Me_3\text{-}2,4,6)_3\}]$ 2.193(2) Å[34]; $[CuX\{P(C_6H_2(OMe)_3\text{-}2,4,6\}_3]$ with X = Cl 2.177(1), X = Br 2.197(3), X = I, Cu−P 2.188(4) Å[35]; $[Cu\{N(SiMe_3)C(tBu)=C(H)SiMe_3\}(PPh_3)]$ 2.145(3) Å[36]. Apart from the already mentioned puckering of the ring, the nature of the backbone of the heterocycle in **5a** is similar to that of the free ligand **3a**.

Figure 4. Molecular structure of **5a** (core atoms only)

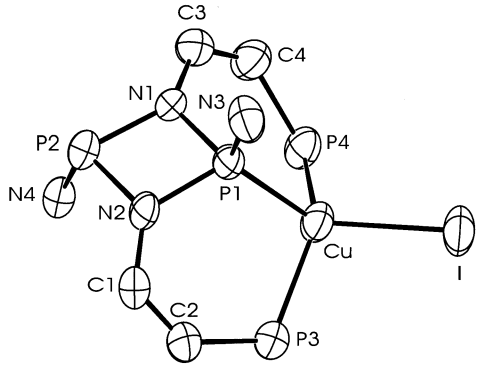

We are grateful to the *E.U.* for the award of a fellowship to M. L., within the framework of the HCM Programme (Contract No. ERBCHBGCT930264) and *ESPRC* for a follow-up grant for M. L. We also thank Dr. *A. C. Avent*, Mr. *C. Dadswell*, Dr. *G. Lawless*, and Professor *P. J. Parsons* for helpful discussions.

Experimental Section

All manipulations were carried out under argon, using standard Schlenk techniques. Solvents were distilled from drying agents and degassed. − The NMR spectra were recorded in C_6D_6 or $CDCl_3$ at 298 K using the following Bruker instruments: AC-P 250 (^{1}H 250.1 MHz; ^{11}B 80.3 MHz; ^{13}C 62.9 MHz; ^{31}P 101.2 MHz), DPX 300 (^{1}H 300.1 MHz; ^{13}C 75.5 MHz; ^{31}P 121.5 MHz), and AMX 500 (^{1}H 500.1MHz; ^{13}C 125.7 MHz) and referenced internally to residual solvent resonances in the case of ^{1}H and ^{13}C spectra. The ^{31}P and ^{11}B spectra were referenced externally to H_3PO_4 and $BF_3(OEt_2)$, respectively. Unless otherwise stated, all NMR spectra, other then ^{1}H, were proton-decoupled. − Electron-impact mass spectra were taken from solid samples using a Kratos MS 80 RF instrument. − Melting points were taken in sealed capillaries and are uncorrected. Elemental analyses were determined by Medac Ltd., Brunel University. Due to incorporation of solvent, some of the phoshonium salts and the copper complexes **5** gave unsatisfactory elemental analyses.

Preparation of the Phosphonium Chlorides $[Ph_2P^aP(NR'_2)N(SiMe_3)C(tBu)=C^bH(P^a-C^b)]A$ (**2a**: R′ = Et, A = Cl; **2b**: R′ = Me, A = Cl; **2c**: R′ = Et, A = OSO_2CF_3; **2d**: R′ = Et, A = BPh_4): Me_3SiNEt_2[2] (0.34 ml, 1.82 mmol) was added to a solution of $[Ph_2P^aP(Cl)N(SiMe_3)C(tBu)=C^bH(P^a-C^b)]Cl$ (**1**)[1] (0.83 g, 1.82 mmol) in CH_2Cl_2 (15 ml) at −50°C. The yellow solution was slowly warmed to room temperature and stirred for 1 h. Removal of volatiles in vacuo gave crude **2a** (0.90 g, 100%). − ^{1}H NMR ($CDCl_3$): δ = 0.15 [s, $SiMe_3$], 0.84 [s, broad, Me], 1.61 [s, *t*Bu], 2.2−3.1 [m, very broad, CH_2], 7.52−7.69 [Ph, 10 H], 10.08 [dd, CH, $J(^1H\text{-}^{31}P)$ 27.5 and 27.6 Hz]. − ^{31}P NMR ($CDCl_3$): δ = 74.4 [d, λ^3P, $^1J(^{31}P\text{-}^{31}P)$ = 269.1 Hz], 29.0 [d, λ^4P, $^1J(^{31}P\text{-}^{31}P)$ = 269.1 Hz].

Crude compound **2b** (1.45 g, 100%) was prepared in an identical fashion, from **1** (1.40 g, 3.07 mmol) and Me_3SiNMe_2 (0.49 ml, 3.07 mmol). − ^{1}H NMR ($CDCl_3$): δ = 0.13 [s, $SiMe_3$], 1.59 [s, *t*Bu], 2.60 [s, very broad, CH_3], 5.26 [s, CH_2Cl_2], 7.46−7.73 [Ph, 10 H], 9.90 [s, broad, CH]. − ^{31}P NMR ($CDCl_3$): δ = 74.9 [d, λ^3P, $^1J(^{31}P\text{-}^{31}P)$ = 263.5 Hz], 30.1 [s, broad, λ^4P^+]. − ^{13}C NMR ($CDCl_3$): δ = 5.2 [s, $SiMe_3$], 30.9 [s, $C(CH_3)_3$], 41.3 [d, $C(CH_3)_3$, $^3J(^{13}C\text{-}^{31}P)$ = 13.8 Hz], NMe_2 signal not observed, 53.4 [s, CH_2Cl_2], 69.0 [d, CH, $^1J(^{13}C\text{-}^{31}P)$ = 20.2 Hz], 120.1 [d, *ipso* C, $^1J(^{13}C\text{-}^{31}P)$ = 66.3 Hz], 127.3−133.7 [Ph], 190.6 [s, broad, CN].

Compound **2c** or **2d** was obtained by adding $Ag(OSO_2CF_3)$ (0.21 g, 0.81 mmol) or $Na[BPh_4]$ (0.46 g , 1.36 mmol) at −40°C to a solution of **2a** (0.4 g, 0.81 mmol; or 0.67 g, 1.36 mmol, respectively) in CH_2Cl_2 (15 ml). The mixture was allowed to warm to room temperature and was stirred for another 4 h or 2.5 h, then filtered and all volatiles were removed from the filtrate in vacuo. The crude product was recrystallised from a mixture of CH_2Cl_2 and pentane to give colourless crystals of **2c** (0.36 g, 75%) or **2d** (0.59 g, 68%).

2c: ^{1}H NMR ($CDCl_3$): δ = 0.13 [s, $SiMe_3$], 0.74 [m, broad, Me], 1.56 [s, *t*Bu], 2.50 [m, very broad, CH_2], 3.09 [m, very broad CH_2], 7.60−7.84 [Ph, 10 H], 7.97−8.04 [d, 2 H], 8.23 [dd, CH, $^3J(^1H\text{-}^{31}P)$ 27.7 Hz, $^2J(^1H\text{-}^{31}P)$ 19.7 Hz]. − ^{31}P NMR ($CDCl_3$): δ = 84.5 [d, λ^3P, $^1J(^{31}P\text{-}^{31}P)$ = 190.4 Hz], 31.2 [s, very broad, λ^4P^+]. − ^{13}C NMR ($CDCl_3$): δ = 5.0 [s, $SiMe_3$], 13.1 [s, Me], 30.3 [s, $C(CH_3)_3$], 41.4 [d, $C(CH_3)_3$, $^3J(^{13}C\text{-}^{31}P)$ = 13.0 Hz], 45 [s, very broad CH_2], CH and OSO_2CF_3 signals not identified, 116.9 [d, *ipso* C, $^1J(^{13}C\text{-}^{31}P)$ = 71.2 Hz], 118.7 [d, *ipso* C, $^1J(^{13}C\text{-}^{31}P)$ = 50.6 Hz], 130.1 [d, Ph, $J(^{13}C\text{-}^{31}P)$ = 12.4 Hz], 130.5 [d, Ph, $J(^{13}C\text{-}^{31}P)$ = 13.1 Hz], 132.7 [d, Ph, $J(^{13}C\text{-}^{31}P)$ = 9.9 Hz], 133.8 [s, Ph], 134.3 [s, Ph], 135.1 [d, Ph, $J(^{13}C\text{-}^{31}P)$ = 9.4 Hz], 188.8 [d, CN, $^2J(^{13}C\text{-}^{31}P)$ = 11.8 Hz].

2d · $(CH_2Cl_2)_{0.5}$: Mp 105°C (dec.). − $C_{49.5}H_{60}BClN_2P_2Si_2$ (819.41): calcd. C 72.6, H 7.38, N 3.42; found C 70.7, H 7.30, N 3.39. − ^{1}H NMR ($CDCl_3$): δ = 0.22 [s, $SiMe_3$], 0.69 and 0.80 [s, broad, Me], 1.40 [s, *t*Bu], 2.24−2.93 [m, very broad, CH_2], 5.28 [s, CH_2Cl_2], 6.11 overlapping dd, CH, $J(^1H\text{-}^{31}P)$ = 29.5 Hz], 6.94 [t, 4 H, $J(^1H\text{-}^{31}P)$ = 7.1 Hz], 7.07 [t, 8 H, $J(^1H\text{-}^{31}P)$ = 7.3 Hz], 7.48−7.69 [m, 16 H]. − ^{31}P NMR ($CDCl_3$): δ = 86.5 [d, λ^3P, $^1J(^{31}P\text{-}^{31}P)$ = 279.5 Hz], 33.2 [d, λ^4P^+, $^1J(^{31}P\text{-}^{31}P)$ = 279.5 Hz]. − ^{11}B NMR ($CDCl_3$): δ = −9.1. − ^{13}C NMR ($CDCl_3$): δ = 5.0 [s, $SiMe_3$], 14.8 [s, Me], 30.3 [s, $C(CH_3)_3$], 40.6 [d, $C(CH_3)_3$, $^3J(^{13}C\text{-}^{31}P)$ = 14.1 Hz], 41.5 [s, CH_2], δ 43.7 [d, CH_2 $^1J(^{13}C\text{-}^{31}P)$ = 37.0 Hz], δ 53.4 [s, CH_2Cl_2], δ 72.5 [d, CH, $^1J(^{13}C\text{-}^{31}P)$ = 16.9 Hz], 118.3 [d, *ipso* C, $^1J(^{13}C\text{-}^{31}P)$ = 68.0 Hz], 121.5 [s, BPh], 122.5 [d, *ipso*-C, $^1J(^{13}C\text{-}^{31}P)$ = 24.7 Hz], 125.4 [s, BPh], 130.1 [t, Ph], 132.0 [d, Ph, $J(^{13}C\text{-}^{31}P)$ = 6.4 Hz], 133.5 [d, Ph, $J(^{13}C\text{-}^{31}P)$ = 9.7 Hz],

134.1 [d, Ph, $J(^{13}C\text{-}^{31}P)$ = 19.9 Hz], 136.3 [s, BPh], 164.2 [q, *ipso* C, $^{1}J(^{13}C\text{-}^{11}B)$ = 49.4 Hz], 188.5 [d, CN, $^{2}J(^{13}C\text{-}^{31}P)$ = 9.4 Hz].

Preparation of cis/trans-[$Et_2NP^{a}N(R)P(NEt_2)N^{d}R(P^{a}-N^{d})$] [**3a**: R = C(*t*Bu)=C(H)PPh_2]: Crude **2a** (0.90 g, 1.82 mmol) was heated in toluene (15 ml) under reflux until a clear yellow solution had formed and was then allowed to cool to room temperature. After 1 d, colourless crystals of **3a** (0.6 g, 85%) had formed. A second crop of crystals (0.1 g, 14%) was obtained after removing part of the solvent from the mother liquor; mp 192°C (dec.). − $C_{44}H_{60}N_4P_4$ (768.89): calcd. C 68.7, H 7.86, N 7.29; found C 68.4, H 7.88, N 7.53. − MS; *m/z* (%): 768 (2) $[M_2]^+$, 696 (2) $[M_2 - NEt_2]^+$, 384 (43) $[M]^+$. − ^{1}H NMR ($CDCl_3$): δ = 0.68 [s, very broad, CH_3, *cis/trans*], 1.29 [s, *t*Bu, *cis/trans*], 2.72 [s, broad, CH_2, *trans*], 4.05 [s, broad, CH_2, *cis*], 5.38 [s, broad, CH, *cis*], 5.50 [t, CH, $^{2}J(^{1}H\text{-}^{31}P)$ = 4.2 Hz, *trans*], 7.15−7.30 [Ph, 8 H], 7.50−7.60 [*o*-Ph, 2 H]. − ^{31}P NMR ($CDCl_3$): *trans* isomer (AA′XX′ system): δ = −29.4 [t, PPh_2 $_J(^{31}P\text{-}^{31}P)_{AX}$ = 202.6 Hz], 186.6 [t, PN, $^{2}J(^{31}P\text{-}^{31}P)_{AA'}$ = 20.4 Hz]; *cis* isomer: δ = −30.1 [d, PPh_2, $J(^{31}P\text{-}^{31}P)$ = 198.0 Hz], 176.8 [s, PN uncoord., $^{2}J(^{31}P\text{-}^{31}P)$ = 20.7 Hz], 193.9 [dt, PN coord., $J(^{31}P\text{-}^{31}P)$ = 198.0 Hz, $^{2}J(^{31}P\text{-}^{31}P)$ = 20.7 Hz]. − ^{13}C NMR ($CDCl_3$): isomeric mixture: δ = 13.8 [s, broad, CH_3], 30.4 [s, $C(CH_3)_3$,], $C(CH_3)_3$ signal not identified, 39.8 [s, broad, CH_2], 103.8 [s, CH,], 126.5 and 127.8 [s, Ph], 131.2 and 134.3 [d, Ph, $J(^{13}C\text{-}^{31}P)$ = 15.9 and 19.0 Hz], 141.0 and 141.1 [s, Ph], 145.3 and 145.4 [s, Ph], 162.3 and 162.6 [s, CN]. − CP-MAS ^{31}P NMR: δ = −27.7 [d, PPh_2 $_J(^{31}P\text{-}^{31}P)$ = 191.6 Hz], 186.6 [s, broad, PN].

Preparation of trans-[$Me_2NP^{a}N(R)P(NMe_2)N^{c}R(P^{a}-N^{c})$] [**3b**: R = C(*t*Bu)=C(H)PPh_2]: Colourless crystals of **3b** (1.04 g, 95%) were obtained similarly to **3a**, from **2b** (1.45 g, 3.07 mmol) in hot toluene (20 ml); mp 185°C (dec.). − $C_{40}H_{52}N_4P_4$ (712.78): calcd. C 67.4, H 7.35, N 7.86; found C 67.0, H 7.43, N 7.70. − MS; *m/z* (%): 712 (3) $[M_2]^+$, 668 (22) $[M_2 - NMe_2]^+$, 357 (100) $[M + H]^+$, 356 (54) $[M]^+$, 342 (50) $[M - Me]^+$, 312 (97) $[M - NMe_2]^+$. − ^{1}H NMR ($CDCl_3$): δ = 1.23 [s, *t*Bu], 2.52 [s, broad, NCH_3], 5.24 [d, CH, $^{2}J(^{1}H\text{-}^{31}P)$ = 2.5 Hz], 7.19−7.29 [Ph, 8 H], 7.41−7.47 [*o*-Ph, 2 H]. − ^{31}P NMR ($CDCl_3$): δ = −28.7 [t, PPh_2 $_J(^{31}P\text{-}^{31}P)$ = 101.8 Hz], 184.9 [t, PN, $^{1}J(^{31}P\text{-}^{31}P)$ = 101.8 Hz]. − ^{13}C NMR ($CDCl_3$): δ = 30.2 [s, $C(CH_3)_3$,], 36.8 [s, broad, NCH_3], 38.7 [s, CH_2], 39.5 [s, $C(CH_3)_3$,], 102.8 [d, CH, $^{3}J(^{13}C\text{-}^{31}P)$ = 8.1 Hz], 127.3 [d, Ph, $J(^{13}C\text{-}^{31}P)$ = 26.4 Hz], 127.9 [s, Ph], 132.0 [d, Ph, $J(^{13}C\text{-}^{31}P)$ = 18.6 Hz], 132.6 [d, Ph, $J(^{13}C\text{-}^{31}P)$ = 18.5 Hz], 141.1 [d, Ph, $J(^{13}C\text{-}^{31}P)$ = 9.7 Hz], 161.7 [d, CN, $^{2}J(^{13}C\text{-}^{31}P)$ = 20.3 Hz].

*Preparation of the Phosphonium Salt [$Ph_2P^{a}P(NEt_2)$]*N(H)-C(tBu)=C^{b}*H*$(P^{a}-C^{b})$*][*OSO_2CF_3*]·*$^{1}/_{2}$ C_6H_6 (**4**): Compound **3a** (0.35 g, 0.46 mmol) and $CF_3SO_3SiMe_3$ (0.36 ml, 9.1 mmol) were stirred in toluene (20 ml) for 96 h at 80°C. After removing the volatiles, a colourless solid remained. Attempts to recrystallise it from toluene or a mixture of CH_2Cl_2/Et_2O or THF/pentane failed, but dissolving in hot benzene gave, on cooling to room temperature, colourless crystals of **4** (0.31 g, 59%); mp > 105°C (dec.). − $C_{26}H_{34}F_3N_2O_3P_2S$ (573.58): calcd. C 54.4, H 5.97, N 4.88; found C 56.5, H 6.03, N 4.53. − ^{1}H NMR ($CDCl_3$): δ = 0.82 [t, Me, $^{4}J(^{1}H\text{-}^{31}P)$ ′ = 7.1 Hz], 1.39 [s, *t*Bu], 2.92 [s, very broad, CH_2], 5.04 [d, NH, $^{4}J(^{1}H\text{-}^{31}P)$ = 10.5 Hz], 7.35 [s, C_6H_6], 7.54−7.66 [Ph, 10 H], 8.19 overlapping dd, CH, $J(^{1}H\text{-}^{31}P)$ = 29.0 Hz]. − ^{31}P NMR ($CDCl_3$): δ = 82.3 [d, λ^3P, $^{1}J(^{31}P\text{-}^{31}P)$ = 304.9 Hz], 10.6 [d, λ^4P, $^{1}J(^{31}P\text{-}^{31}P)$ = 304.9 Hz. − ^{13}C NMR ($CDCl_3$): δ = 14.5 [s, Me], 28.6 [s, $C(CH_3)_3$], 37.8 [d, $C(CH_3)_3$, $^{3}J(^{13}C\text{-}^{31}P)$ = 10.7 Hz], 43 [s, broad CH_2], 65.0 [d, CH $^{2}J(^{13}C\text{-}^{31}P)$ = 68.0 Hz], CF_3SO_3 signal not identified, 120.1 [d, *ipso* C, $^{2}J(^{13}C\text{-}^{31}P)$ = 70.8 Hz], 124.3 [d, *ipso* C, $^{2}J(^{13}C\text{-}^{31}P)$ = 76.6 Hz], 128.3 [s, C_6H_6], 130.0 [dd, *o*-C, $J(^{13}C\text{-}^{31}P)$ = 12.0 and 4.6 Hz], 132.2 [dd, *o*-C, $J(^{13}C\text{-}^{31}P)$ = 8.0 and 4.5 Hz], 133.1 [s, Ph], 133.2 [s, Ph], 133.5 [s, Ph], 133.9 [s, Ph], 184.0 [t, CN, $J(^{13}C\text{-}^{31}P)$ = 15.0 Hz].

*Preparation of trans-***5a**: The diazadiphosphetidine **3a** (0.47 g, 0.61 mmol) was suspended in toluene (20 ml) and Cu_2I_2 (0.12 g, 0.31 mmol) was added. The reaction mixture was heated until **3a** had completely dissolved, then stirred for 12 h at room temperature, whereafter a very fine precipitate had formed. Further toluene (15 ml) was added. The mixture was heated under reflux until most of the precipitate had dissolved. Hot filtration and cooling the filtrate to room temperature gave colourless crystals of **5b** (0.1 g, 14%). Removing ca. 2/3 of the solvent from the mother liquor and cooling at −20°C gave colourless crystals of **5a** (0.31 g, 53%); mp 175°C (dec.). − $C_{51}H_{68}CuIN_4P_4$ (1051.48): calcd. (**5a** + 1 molecule of toluene) C 58.3, H 6.52, N 5.33; found C 57.2, H 6.09, N 5.17. − MS; *m/z* (%): 958 (0.1) $[M]^+$, 831 (0.3) $[M - I]^+$, 574 (0.6) $[M - Et_2NPNC(tBu)=CHPPh_2]^+$, 511 (2.5) $[M - Et_2NPNC(tBu)=CHPPh_2 - Cu]^+$, 384 (35) $[Et_2NPNC(tBu)=CHPPh_2]^+$. − ^{1}H NMR ($CDCl_3$): δ = 0.04 [s, CH_3 coord., 3 H], 0.82 [s, CH_3 coord., 3 H], 1.20 [t, CH_3 coord., 6 H, $^{4}J(^{1}H\text{-}^{31}P)$ = 7.0 Hz], 1.25 [s, *t*Bu, 18 H], 2.45 [s, broad, CH_2 coord. 3 H], 2.95 [s, broad, CH_2 coord., 3 H], 3.69 [m, CH_2 uncoord., 3 H], 5.73 [s, broad, CH], 7.17−7.43 [mult. multiplets, Ph, 8 H, PhMe], 7.69 [t, *o*-Ph, 2 H, $^{2}J(^{1}H\text{-}^{31}P)$ = 8.3 Hz]. − ^{31}P NMR ($CDCl_3$): δ = − 24.9 [s, very broad, PPh_2], 142.6 [s, very broad, ring P coord.], 172.2 [s, ring P uncoord.]. − ^{13}C NMR ($CDCl_3$): δ = 11.3 and 12.5 [s, CH_3 coord.], 14.8 [s, CH_3 uncoord.], 30.6 [d, $C(CH_3)_3$, $^{4}J(^{13}C\text{-}^{31}P)$ = 8.4 Hz], 35.6 [s, CH_2], 38.7 [s, CH_2], 40.6 [s, $C(CH_3)_3$,], 105.9 [d, CH, $^{3}J(^{13}C\text{-}^{31}P)$ = 33.0 Hz], 128.0 [d, Ph, $J(^{13}C\text{-}^{31}P)$ = 36.2 Hz], 128.2 [s, Ph], 129.3 [d, Ph, $J(^{13}C\text{-}^{31}P)$ = 41.3 Hz], 131.8 [s, Ph], 133.3 [d, Ph, $J(^{13}C\text{-}^{31}P)$ = 17.0 Hz], 135.5 [dd, Ph, overlayed], 139.7 [d, Ph, $J(^{13}C\text{-}^{31}P)$ = 39.2 Hz], 163.1 [s, CN].

Preparation of **5b**: Cu_2I_2 (0.25 g, 0.65 mmol) was added to a solution of **3a** (0.5 g, 0.325 mmol) in hot (105°C) toluene (100 ml). The mixture was stirred for 15 h, whereafter the greyish Cu_2I_2 had disappeared and a white precipitate had formed. After 12 h at room temperature, the supernatant liquor was filtered off and the residue dried in vacuo to give **5b** (0.7 g, 94%), as a colourless, extremely insoluble, white powder; mp 260°C (dec.). − $C_{47.5}H_{64}Cu_2I_2N_4P_4$ (1195.85): calcd. C 56.8, H 6.42, N 5.57; found C 42.4, H 5.32, N 4.46. − MS (300°C); *m/z* (%): 831 (5) $[M - 2\,I - Cu]^+$, 574 (13) $[M - Et_2NPNC(tBu)=CHPPh_2]^+$; (250°C); *m/z* (%): 559 (22) $[M_{1/2} - Me]^+$, 480 (3) $[M_{1/2} - Et - Cu]^+$. − ^{1}H NMR ($CDCl_3$): δ = 0.46 [s, broad, CH_3], 0.69 [s, broad, CH_3], 1.53 [s, *t*Bu], 2.45 and 3.72 [m, very broad, NCH_2], 5.91 [t, CH, $^{2}J(^{1}H\text{-}^{31}P)$ = 3.82 Hz], 7.34−7.37 [m, Ph, 3 H], 7.40−7.42 [m, Ph, 3 H], 7.57−7.7.64 [m, Ph, 2 H], 7.75−7.82 [m, Ph, 2 H]. − ^{31}P NMR ($CDCl_3$): δ = −38.0 [d, PPh_2, $J(^{31}P\text{-}^{31}P)$ = 292.8 Hz], 131.3 [d, PN, $J(^{31}P\text{-}^{31}P)$ = 292.8 Hz]. − ^{13}C NMR ($CDCl_3$): δ = 11.2 [s, CH_3], 31.0 [d, $C(CH_3)_3$, $^{4}J(^{13}C\text{-}^{31}P)$ = 8.7 Hz], 39.3 [s, CH_2], $C(CH_3)_3$ signal not identified, 106.6 [d, CH, $^{3}J(^{13}C\text{-}^{31}P)$ = 33.2 Hz], 126.3−133.9 [phenyl C], 163.0 [s, CN].

Preparation of [$Me_2NP^{a}N(R)P(NMe_2)N^{c}R$]$(P^{a}-N^{c})$ [**7**: R = C(*t*Bu)=C(H)$SiMe_3$]: Me_3SnNMe_2 (0.13 g, 0.64 mmol) was added to a solution of [ClP^{a}N(R)P(Cl)N^{b}R$(P^{a}-N^{b})$][1] (0.15 g, 0.32 mmol) in CH_2Cl_2 (5 ml). The reaction mixture was stirred for 12 h at room temperature, whereafter a white solid had crystallised. All volatiles were removed and the resulting residue was extracted with hot toluene (10 ml). The hot mixture was filtered. Cooling the filtrate to −15°C gave colourless crystals of **7** (0.11 g, 70%); mp 170°C (dec.). − MS; *m/z* (%): 488 (5) $[M_2]^+$, 473 (1) $[M_2 - Me]^+$, 444 (9) $[M_2 - NMe_2]^+$, 415 (2.5) $[M_2 - SiMe_3]^+$, 244 (75) $[M]^+$, 229 (11) $[M - Me]^+$, 187 (72) $[M - tBu]^+$. − ^{1}H NMR (C_6D_6): δ = 0.16 [s,

Table 4. Crystallographic data for compounds **3a** and **5a**

Compounds	**3a**	**5a**
Empirical formula	$C_{44}H_{60}N_4P_4$	$C_{51}H_{68}CuIN_4P_4$
Formula weight	768.84	1051.41
Temperature [K]	293(2)	293(2)
Radiation, λ [Å]	Mo-K_α, 0.71073	0.71073
Crystal system	triclinic	triclinic
Space group	$P\bar{1}$ (No. 2)	$P\bar{1}$ (No. 2)
a [Å]	8.568(2)	11.021(2)
b [Å]	10.504(3)	12.114(2).
c [Å]	13.324(5)	21.816(3).
α [°]	110.59(3)	74.28(1)
β [°]	92.54(2)	76.15(1)
γ [°]	98.30(2)	72.86(1)
V [Å^3]	1104.9(6)	2638.6(7)
Z	1	2
$D_{calcd.}$ [g cm^{-3}]	1.16	1.323
μ [mm^{-1}]	0.21	1.16
F[000]	412	1088
Crystal size [mm]	0.4 × 0.2 × 0.1	0.3 × 0.2 × 0.2
θ min and max [°]	2 to 25	2 to 25
Dataset	0/10; −12/12; −15/15	0/13; −13/14; −24/25
Tot., uniq. data	3880, 3880	9249, 9249
Reflections with $I > 2\sigma(I)$	2609	4685
Structure solution	Direct methods	Direct methods
Refinement method	Full-matrix least squares on all F^2	Full-matrix least squares on all F^2
Parameters	235	520
Final R indices $I > 2\sigma(I)$	$R1$ = 0.051, $wR2$ = 0.099	$R1$ = 0.073, $wR2$ = 0.150
R indices (all data)	$R1$ = 0.091, $wR2$ = 0.115	$R1$ = 0.160, $wR2$ = 0.192
Largest diff. peak and hole [e/Å^3]	0.23 and −0.20	1.05 and −0.53
Abs.correction from ψ scans	not applied	T_{max} = 1.00, T_{min} = 0.91
Max. shift/error	0.005	0.002

$SiMe_3$], 1.19 [s, *t*Bu], 2.75 [d/t, NMe_2], 4.36 [s, CH]. − ^{31}P NMR (C_6D_6): δ = 187. − ^{13}C NMR (C_6D_6): δ = 2.0 [s, $SiMe_3$], 30.6 [s, $C(CH_3)_3$], 37.7 [t, NMe_2, $^2J(^{13}C\text{-}^1H)$ = 9.1 Hz], 39.8 [s, $C(CH_3)_3$], 100.4 [s, CH], 160.8 [s, CN].

Preparation of $N^aC(tBu)C(H)C^eP^aN(Me)(CH_2)_2N^cMe(N^a{-}P^a)(C^c{-}N^c)$ (**8**): A mixture of [$ClP^aN(R)P(Cl)N^bR(P^a{-}N^b)$] (**6**)[1] (0.71 g, 1.5 mmol) and [$=C^aN(Me)(CH_2)_2N^aMe(C^a{-}N^a)]_2$[3] (0.30 g, 1.5 mmol) in toluene (15 ml) was stirred for 60 h at 50°C. Removal of the solvent and distillation (130°C, 10^{-2} Torr) of the residue in vacuo gave the yellow oil **8** (0.22 g, 32%), which slowly crystallised; mp 58−60°C. − MS; *m*/*z* (%): 225 (80) $[M]^+$, 210 (67) $[M - Me]^+$, 197 (10) $[M - CH_2CH_2]^+$, 182 (90) $[M - MeNCH_2]^+$. −^{1}H NMR ($CDCl_3$): δ = 1.36 [s, *t*Bu], 2.08 [m, CH_2], δ 2.30 [m, CH_2], 2.37 [m, CH_2], 2.41 [d, NMe $^4J(^1H\text{-}^{31}P)$ = 2.7 Hz], 2.58 [d, NCH_3 $^3J(^1H\text{-}^{31}P)$ = 12.9 Hz], 3.06 [ddd, CH_2], 5.83 [d, CH, $^3J(^1H\text{-}^{31}P)$ = 17.1 Hz]. − ^{31}P NMR ($CDCl_3$): δ = 98.9 [s]. − ^{13}C NMR ($CDCl_3$): δ = 29.2 [d, $C(CH_3)_3$, $^4J(^{13}C\text{-}^{31}P)$ = 2.3 Hz], 38.4 [d, $C(CH_3)_3$, $^3J(^{13}C\text{-}^{31}P)$ = 7.5 Hz], 40.6 [s, NCH_3], 42.9 [d, NCH_3 $^2J(^{13}C\text{-}^{31}P)$ = 38.5 Hz], 51.5 [d, NCH_2, $^2J(^{13}C\text{-}^{31}P)$ = 3.1 Hz], 53.7 [s, NCH_2], 98.5 [d, CH, $^2J(^{13}C\text{-}^{31}P)$ = 36.0 Hz], 183.2 [d, CP, $^1J(^{13}C\text{-}^{31}P)$ = 4.1 Hz], 185.8 [s, CN].

Preparation of $N^aC(tBu)C(H)C^eP^a(S)N(Me)(CH_2)_2N^cMe(N^a{-}P^a)(C^c{-}N^c)$ (**9**): Sulfur (0.02 g, 0.63 mmol) was added to a solution of **8** (0.1 g, 0.44 mmol) in toluene (5 ml) and the mixture was stirred for 15 h, then filtered and the solvent removed from the filtrate in vacuo. Recrystallisation of the residue from Et_2O gave yellow crystals of **9** (0.07 g, 70%); mp 126°C (dec.). − HR-MS: calcd. for $C_{11}H_{20}N_3PS$ 257.1116; found 257.1118. − MS; *m*/*z* (%): 257 (100) $[M]^+$, 242 (15) $[M - Me]^+$, 224 (27) $[M - HS]^+$, 214 (65) $[M - MeNCH_2]^+$, 201 (15) $[M - Me_2C{=}CH_2]^+$. − ^{1}H NMR ($CDCl_3$): δ = 1.21 [s, *t*Bu], 2.05 [m, CH_2], 2.15 [s, NMe], 2.27 and 2.35 [m, CH_2], 2.56 [d, NMe, $^3J(^1H\text{-}^{31}P)$ = 12.0 Hz], 4.33 [ddd, CH_2], 5.26 [d, CH, $^3J(^1H\text{-}^{31}P)$ = 30.0 Hz]. − ^{31}P NMR ($CDCl_3$): δ = 83.6 [s]. − ^{13}C NMR ($CDCl_3$): δ = 28.2 [d, $C(CH_3)_3$], 35.3 [s, NCH_3], 35.3 [d, $C(CH_3)_3$, $^4J(^{13}C\text{-}^{31}P)$ = 25.0 Hz], 39.1 [d, NCH_3, $^2J(^{13}C\text{-}^{31}P)$ = 5.7 Hz], 46.8 [s, NCH_2], 50.9 [d, NCH_2, $^2J(^{13}C\text{-}^{31}P)$ = 12.4 Hz], 94.1 [d, CH, $^2J(^{13}C\text{-}^{31}P)$ = 46.4 Hz], 166.9 [d, CP, $^1J(^{13}C\text{-}^{31}P)$ = 94.4 Hz], 193.8 [d, CN, $^2J(^{13}C\text{-}^{31}P)$ = 7.5 Hz].

X-ray Structure Determination of the Diazadiphosphetidines **3a** *and* **5a**[37]: Data were collected with an Enraf-Nonius CAD4 diffractometer using monochromatic Mo-K_α radiation and single crystals sealed under argon in Lindemann capillaries. Cell dimensions were calculated from the setting angles for 25 reflections with 9° < θ < 13°. Intensities were measured by an ω-2θ scan. Corrections were made for Lorentz and polarisation effects and in the case of **5a** for absorption. There was no crystal decay as measured by two standard reflections. Positions of non-hydrogen atoms were derived by direct methods using SHELXS-86[38] and refined on F^2 with anisotropic thermal parameters by full-matrix least squares using SHELXL-93[39]. Further details are in Table 4.

☆ Dedicated to Prof. Dr. Dr. h. c. mult. *Heinrich Nöth* on the occasion of his 70th birthday as a mark of respect and (by M. F. L.) of friendship.

[1] P. B. Hitchcock, M. F. Lappert, M. Layh, *J. Organomet. Chem.* **1997**, *529*, 243.
[2] M. S. Balakrishna, V. S. Reddy, S. S. Krishnamurthy, J. F. Nixon, J. C. T. R. Burckett St. Laurent, *Coord. Chem. Rev.* **1994**, *129*, 1. For further examples of metal complexes see: [2a] J. C. T. R. Burckett St. Laurent, P. B. Hitchcock, J. F. Nixon, *J. Organomet. Chem.* **1983**, *249*, 243. − [2b] V. S. Reddy, S. S. Krishnamurthy, M. Nethaji, *J. Organomet. Chem.* **1992**, *438*, 99. − [2c] T. K. Prakasha, S. S. Krishnamurthy, S. E. Davies, M. F. Meidine, J. F. Nixon, *J. Organomet. Chem.* **1992**, *438*, 241. − [2d] D. A. Dubois, E. N. Duesler, R. T. Paine, *Organometallics* **1983**, *2*, 1903. − [2e] D. A. Dubois, E. N. Duesler, R. T. Paine, *Organometallics* **1983**, *3*, 1913.
[3] H. E. Winberg, J. E. Carnahan, D. D. Coffman, M. Brown *J. Am. Chem. Soc.* **1965**, *87*, 2055.
[4] M. J. S. Gynane, A. Hudson, M. F. Lappert, P. P. Power, H. Goldwhite, *J. Chem. Soc., Chem. Commun.* **1976**, 623.
[5] M. F. Lappert, *J. Organomet. Chem.* **1988**, *358*, 185.
[6] O. J. Scherer, W. Gläßel, *Chem. Ber.* **1977**, *110*, 3874.
[7] D. G. Gorenstein, *Progr. Nucl. Magn. Reson. Spectrosc.* **1983**, *16*, 1.
[8] R. Vogt, P. G. Jones, R. Schmutzler, *Chem. Ber.* **1993**, *126*, 1271.
[9] L. Ernst, P. G. Jones, P. Look-Herber, R. Schmutzler, *Chem. Ber.* **1990**, *123*, 35.
[10] H. Grützmacher, H. Pritzkow, *Chem. Ber.* **1989**, *122*, 1411.
[11] H. R. G. Bender, E. Niecke, M. Nieger, H. Westermann, *Z. Anorg. Allg. Chem.* **1994**, *620*, 1194.
[12] M. Baudler, C. Gruner, H. Tschäbunin, J. Hahn, *Chem. Ber.* **1982**, *115*, 1737.
[13] E. G. Finer, R. K. Harris, *Progr. Nucl. Magn. Reson. Spectrosc.* **1970**, *6*, 61.
[14] S. S. Kumaravel, S. S. Krishnamurthy, B. R. Vincent, T. S. Cameron, *Z. Naturforsch.* **1986**, *41b*, 1067.
[15] M. L. Thomson, A. Tarassoli, R. C. Haltiwanger, A. D. Norman, *Inorg. Chem.* **1987**, *26*, 684.
[16] R. Keat, A. N. Keith, A. Macphee, K. W. Muir, D. G. Thomson, *J. Chem. Soc., Chem. Commun.* **1978**, 372.
[17] H.-J. Chen, R. C. Haltiwanger, T. G. Hill, M. L. Thompson, D. E. Coons, A. D. Norman, *Inorg. Chem.* **1985**, *24*, 4725.
[18] D. A. Harvey, R. Keat, A. N. Keith, K. W. Muir, D. S. Rycroft, *Inorg. Chim. Acta* **1979**, *34*, L201.
[19] R. Keat, *Top. Curr. Chem.* **1982**, *102*, 89.
[20] V. S. Reddy, S. S. Krishnamurthy, M. Nethaji, *J. Chem. Soc., Dalton Trans.* **1994**, 2661.
[21] W. A. Kamil, M. R. Bond, R. D. Willett, J. M. Shreeve, *Inorg. Chem.* **1987**, *26*, 2829.
[22] S. S. Kumaravel, S. S. Krishnamurthy T. S. Cameron, A. Linden, *Inorg. Chem.* **1988**, *27*, 4546.

[23] R. Keat, L. Murray, D. S. Rycroft, *J. Chem. Soc., Dalton Trans.* **1982**, 1503.
[24] H.-O. Kalinowski, S. Berger, S. Braun *^{13}*C-NMR-Spektroskopie, Georg Thieme Verlag, Stuttgart, New York, **1984**.
[25] W. Schwarz, H. Hess, W. Zeiss, *Z. Naturforsch.* **1978**, *33b*, 723.
[26] V. Y. Antosyak, V. N. Biyushkin, *Zh. Strukt. Khim.* **1990**, *31*, 122 (*Chem. Abstr.* **1991**, *114*, 23804u).
[27] E. Niecke, W. Flick, S. Pohl, *Angew. Chem. Int. Ed. Engl.* **1976**, *15*, 309; *Angew. Chem.* **1976**, *88*, 305.
[28] P. F. Barron, J. C. Dyason, P. C. Healy, L. M. Engelhardt, C. Pakawatchai, V. A. Patrick, A. H. White, *J. Chem. Soc., Dalton Trans.* **1987**, 1099.
[29] G. L. Soloveichik, O. Eisenstein, J. T. Poulton, W. E. Streib, J. C. Huffman, K. G. Caulton, *Inorg. Chem.* **1992**, *31*, 3306.
[30] R. D. Hart, B. W. Skelton, A. H. White, *Aust. J. Chem.* **1991**, *44*, 919.
[31] G. A. Bowmaker, R. D. Hart, B. E. Jones, B. W. Skelton, A. H. White, *J. Chem. Soc., Dalton Trans.* **1995**, 3063.
[32] P. G. Eller, G. J. Kubas, R. R. Ryan, *Inorg. Chem.* **1977**, *16*, 2454.
[33] G. A. Bowmaker, J. V. Hanna, R. D. Hart, P. C. Healy, A. H. White, *Aust. J. Chem.* **1994**, *47*, 25.
[34] E. C. Alyea, G. Ferguson, J. Malito, B. L. Ruhl, *Inorg. Chem.* **1985**, *24*, 3720.
[35] L.-J. Baker, G. A. Bowmaker, R. D. Hart, P. J. Harvey, P. C. Healy, A. H. White, *Inorg. Chem.* **1994**, *33*, 3925.
[36] P. B. Hitchcock, M. F. Lappert, M. Layh, unpublished results.
[37] Crystallographic data (excluding structure factors) for the structures reported in this paper have been deposited with the Cambridge Crystallographic Data Centre as supplementary publication no. CCDC-101392. Copies of the data can be obtained free of charge on application to CCDC, 12 Union Road, Cambridge CB2 1EZ, UK [fax (internat.): +44(0)1223/336033; e-mail: deposit@ccdc.cam.ac.uk].
[38] G. M. Sheldrick, *SHELXS-86 − Program for the Solution of Crystal Structures*, University of Göttingen, **1985**.
[39] G. M. Sheldrick, *SHELXL-93 − Program for Crystal Structure Refinement*, University of Göttingen, **1993**.

[98054]

Organometallic Compounds of Group 13, 54[◇]

Novel Organoborane Lewis Acids via Selective Boron-Tin Exchange Processes − Steric Constraints to Electrophilic Initiation by the Boron Halide☆

John J. Eisch*, and Boguslaw W. Kotowicz

Department of Chemistry, The State University of New York at Binghamton,
Binghamton, New York 13902-6000, USA

Received March 12, 1998

Keywords: Organometallics / Boron / Lithium / Tin / Metal-metal exchange / Electrophilic reagents

With the purpose of preparing novel mono- and bidentate organoboron Lewis acids, the scope and limitations of synthesizing the requisite organoboranes by the boron-tin exchange between a boron halide and the appropriate organostannane have been examined in detail. The following organotin derivatives have been obtained either from the corresponding RMgBr or RLi reagent and Me_nSnCl_{4-n} or from a Barbier procedure using the organic halide, Me_3SnCl and magnesium metal: 1,2-bis(trimethylstannyl)ethyne, *o*-, *m*-, and *p*-bis(trimethylstannyl)benzenes, α,*o*-bis(trimethylstannyl)toluene, α,α-bis(trimethylstannyl)-*o*-xylene, and 2,2-dimethyl-2-stannaindane. The individual interaction of the 1,2-bis(trimethylstannyl)ethyne and the isomeric bis(trimethylstannyl)benzenes with Et_2BBr produced the corresponding bis(diethylboryl)-derivatives. By contrast, with Et_2BCl the α,*o*-bis(trimethylstannyl)toluene gave only *o*-diethylboryl-α-trimethylstannyltoluene and with BCl_3 the α,α′-bis(trimethylstannyl)-*o*-xylene formed only α,α′-bis(chlorodimethylstannyl)-*o*-xylene. Furthermore, in the attempted double boron-tin exchange between *o*-bis(trimethylstannyl)benzene and BCl_3, an unprecedented rearrangement of the 1-(dichloroboryl)-2-(trimethylstannyl)benzene intermediate into its 1-[chloro(methyl)boryl]-2-(chlorodimethylstannyl) isomer was observed. Likewise, *o*-bis(trimethylstannyl)benzene with $PhBCl_2$ produced by a similar rearrangement 1-[methyl(phenyl)boryl]-2-(chlorodimethylstannyl)benzene. The thermolysis of such boranes led variously to definite dimers or ill-defined oligomers. Preliminary studies of the properties of these organoboranes have identified the heightened Lewis acidity of 1,2-bis(diethylboryl)ethyne and the π-electron delocalization involving the $2p_z$-boron orbitals in the 9,10-dihydro-9,10-diboraanthracene system. Finally, an electronic mechanism for the boron-tin exchange has been developed to account for the selectivity of the boron halide's attack at unsaturated carbon–tin bonds.

As part of an ongoing investigation of Ziegler-Natta olefin-polymerization catalysis the present study has explored the synthesis of novel Group-13 Lewis acids for their potential suitability as cocatalysts with cyclopentadienyl transition metal derivatives in such homogeneous polymerizations.[1][2][3][4] In this contribution the preparation of organoborane Lewis acids bearing substituents of enhanced electron-withdrawing power (**1**) and diminished steric demand (**2**) and possibility multidentate boron centers (**3**) has been the principal focus of research. The electron-withdrawing group E in **1** could favorably be a halide (F > Cl > Br > I) and an organyl group other than alkyl (sp^3) having greater *p*-character, such as aryl (sp^2) or 1-alkynyl (sp). As to steric demands (**2**), smaller groups E (Me versus *t*Bu; 1-alkenyl versus alkyl; and 1-alkynyl versus 1-alkenyl) should engender less B-strain upon the boron center accepting the donor group D and rehybridizing to sp^3. Finally, the coordination of suitably sized donor D (**3**) should be stabilized by chelation, as has been abundantly established by the pioneering researches of Köster and coworkers with *cis*-1,2-diborylalkenes.[5]

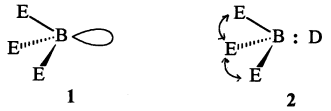

In order to synthesize the required organoborane Lewis acids, most of which are mixed or unsymmetrical boranes, such as $PhBCl_2$ or $Et_2B-C\equiv C-BEt_2$, a preparative route occurring under mild conditions is required, so as to minimize any tendency of the desired product E_2BE' to redistribute rapidly into E_3B and E'_3B.[6] For this desideratum it was found that the transmetallation reaction between the appropriate organostannane and a boron halide was generally a feasible route (Eq. 1).[7]

$$R{-}SnMe_3 + \underset{E = R, X}{Et_2B{-}X} \longrightarrow \underset{\mathbf{1}}{R{-}BE_2} + Me_3Sn{-}X \qquad (1)$$

In some situations where such a tin-boron exchange failed to produce the desired borane, it was instead found

[◇] Part 53: J. J. Eisch, X. Ma, M. Singh, G. Wilke, *J. Organomet. Chem.* **1997**, *527*, 301.

 © WILEY-VCH Verlag GmbH, D-69451 Weinheim, 1998 1434−1948/98/0606−0761 $ 17.50+.50/0

that the analogous tin-lithium exchange is more suitable and that the desired transformation is then attainable by treating the lithium derivative RLi with E_2B-X (Eqs. 2, 3).

$$R-SnMe_3 \xrightarrow[\text{eq. 2}]{Bu^nLi} R-Li \xrightarrow[\text{eq. 3}]{E_2B-X} R-BE_2 \quad \mathbf{1}$$
$$\text{- } Bu^nSnMe_3 \qquad \text{- LiX}$$

Finally, each of the successes or failures of the tin-boron exchanges in achieving its intended transformation has provided us with valuable insight into the reaction mechanisms of such processes.

Results

Preparation of Organotin Precursors

Where successfully applicable, the organotin precursors, such as 1,2-bis(trimethylstannyl)ethyne (**3**), phenyl(trimethyl)tin (**4**), benzyl(trimethyl)tin (**5**), and 2,2-dimethyl-2-stannaindane (**6**) were prepared from the appropriate lithium or magnesium reagent and either Me_3SnCl or Me_2SnCl_2, as required, and were generally attainable according to published procedures[8] or procedures given in this article (cf. infra). The other precursors, containing two trimethylstannyl groups, were individually prepared from the corresponding organyl dibromide or dichloride by preparing the organomagnesium intermediate from magnesium metal in THF in the presence of the organotin chloride reactant (Barbier procedure[9]). Small to moderate amounts of the trimethylstannyl derivative (**9**) were formed as a side product (Eq. 4).

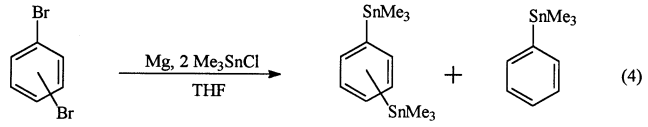

(4)

7a = o **8a** = 44% **9a** = 41%
7b = m **8b** = 49% **9b** = 23%
7c = p **8c** = 66% **9c** = 20%

In a similar manner, α,*o*-bis(trimethylstannyl)toluene (**10**) and α,α′-bis(trimethylstannyl)-*o*-xylene (**11**) were prepared from *o*-bromobenzyl bromide in 45% yield and from α,α′-dichloro-*o*-xylene in 85% yield, respectively.

Preparation of Organolithium Precursors

Unusual lithium reagents employed in this study were prepared by the following procedures: a) dilithioethyne (**12**) by either the action of 3 equivalents of *n*-butyllithium on trichloroethylene[10] or the action of 2 equivalents of the lithium reagent on acetylene; b) α,α′-dilithio-*o*-xylene (**13**) from stirring 2.2 equivalents of *n*-butyllithium and 1 equivalent of **11** vigorously for 96 h, whereupon a yellow precipitate of **13** formed; quenching such a reaction mixture with excess Me_3SiCl, hydrolytic work-up and distillation yielded 87% of α,α′-bis(trimethylsilyl)-*o*-xylene (**14**) and 90% of *n*-butyl(trimethyl)tin, indicating that **13** had been formed in at least 90% yield (Eqs. 5–6).

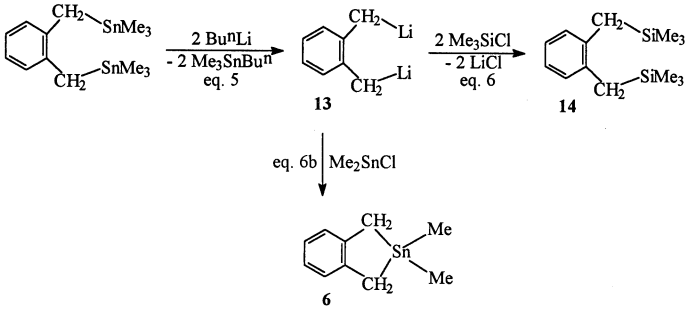

Similarly, the dissolution of **13** in anhydrous diethyl ether and the slow introduction of 1 equivalent of Me_2SnCl_2 led to the isolation of 75% of 2,2-dimethyl-2-stannaindane[11] (**6**) (Eq. 6b).

Preparation of Organoboranes by Boron-Tin Exchange Reactions

1,2-Bis(diethylboryl)ethyne (**15**): This organoborane could be prepared by the interaction of bromo(diethyl)borane (**16**) with dilithioethyne (**12**), but since the most convenient source of **12** involved the action of *n*-butyllithium on trichloroethylene in THF, **12** was generated as a solid complex with LiCl and 0.5 equiv. of THF. The complexed THF in 12 was then easily cleaved in the reaction of **12** with Et_2BBr, producing also **17** and lowering the yield of **15** (Eq. 7).

$$\underset{\mathbf{12}}{LiC\equiv CLi \cdot 0.5\ THF} \xrightarrow[(2.5\ \text{equiv.})]{Et_2BBr_2} \underset{\mathbf{15}\ 39\%}{Et_2B-C\equiv C-BEt_2} + \underset{\mathbf{17}\ 93\%}{Et_2B-O-(CH_2)_4Br} \quad (7)$$

The boron-tin exchange between **16** and 1,2-bis(trimethylstannyl)ethyne (**3**) in pentane precludes this side reaction and permits **15** to be isolated cleanly and in good yield (65%) by distillation. As with all such unsymmetrical boranes, their distillation had to be conducted at as low a temperature (and hence pressure) as possible to minimize redistribution and the formation of triethylborane (cf. infra) (Eq. 8).

$$\underset{\mathbf{3}}{Me_3Sn-C\equiv C-SnMe_3} \xrightarrow[\text{- } Me_3SnBr]{\mathbf{16}} \underset{\mathbf{15}}{Et_2B-C\equiv C-BEt_2} \xrightarrow{\Delta} Et_3B\uparrow \quad (8)$$

Attempts were made to reduce **15** selectively to (*Z*)-1,2-bis(diethylboryl)ethene (**18**) with dihydrogen and a Lindlar catalyst, but the hydrogenation could not be halted but proceeded to form 1,2-bis(diethylboryl)ethane (**19**) (Eq. 9). In recording the NMR spectra of **15** and **19** in various solvents, it was discovered that **15**, but not **19**, forms a complex with two equivalents of THF. For example, the ^{11}B signal of **15** in C_6D_6 occurs at $\delta = 72.0$ but in THF is found at $\delta = 36.9$.

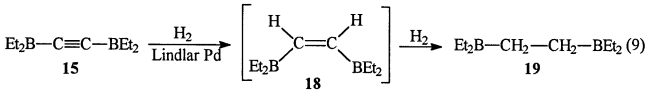

(9)

1,2-Bis(dichloroboryl)benzene (**20**): Despite the reported preparation of **20** in 88% yield from the interaction of **8a** with BCl_3 in a 1:3 ratio in CH_2Cl_2 at −78 °C,[12] attempts to

reproduce this result in our laboratory under the specified conditions or under a variety of modified procedures did not lead to high yields of isolable **20** but rather to the monomethylated derivative **24** when a large excess of BCl_3 was employed. Other reactions conducted with different ratios of reactants and in different solvents (alkanes, arenes, CH_2Cl_2) gave mixtures of **20**−**24**. An unmistakable sign that the reaction between **20** and BCl_3 (1:2 ratio) was taking an unexpected course was the isolation of a precipitate composed of 44% of the expected 2 equivalents of Me_3SnCl and 40% of 1 equivalent of the unexpected Me_2SnCl_2. The source of the Me_2SnCl_2 can best be explained by a relatively fast boron-tin exchange leading from **8a** to **21**, which rearranges relatively rapidly to **23** and this undergoes a second boron-tin exchange to produce **24** more rapidly than the diminished concentration of **21** can generate **20**. The small proportion of **22** produced could have arisen from either **20** or **24**.

Scheme 1

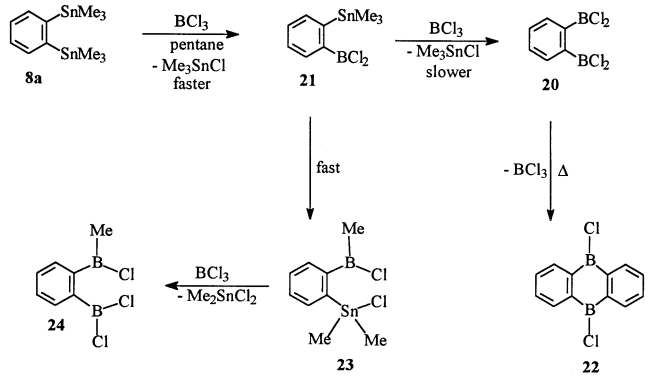

1-[Methyl(phenyl)bory]l-2-(chlorodimethylstannyl)benzene (**25**): Confirmation of the foregoing unusual rearrangement (**21**−**23**) came from the reaction of **8a** with phenylboron dichloride at −78°C. The by-product Me_3SnCl was isolated in 78% yield and **25** was isolated by distillation (Eq. 10), a clear indication that **26** is an intermediate in this novel transformation.

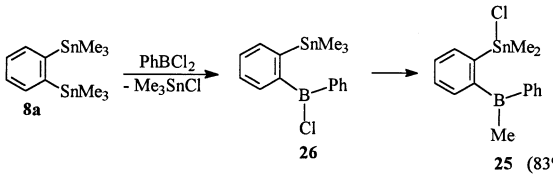

(10)

1,2-, 1,3-, and 1,4-Bis(diethylboryl)benzenes (**27**−**29**): These isomeric diborylbenzenes were readily prepared in high yield (> 80%) by treating the individual bis(trimethylstannyl)benzenes (**8a**−**8c**) with 2 equivs. of Et_2BBr or Et_2BCl and removing the Me_3SnX under reduced pressure at 50°C (Eq. 11).

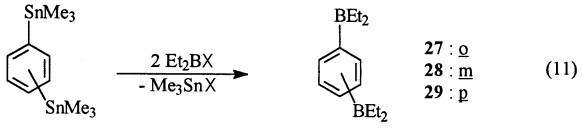

(11)

Diethyl(phenyl)borane could also be prepared similarly from trimethyl(phenyl)tin in 89% yield.

o-(Diethylboryl)-α-(trimethylstannyl)toluene (**30**): The interaction of α,*o*-bis(trimethylstannyl)toluene (**10**) with Et_2BCl (1:2 ratio) at 25°C led cleanly to 90% of **30** after all volatiles were removed (Eq. 12). When the reaction was conducted with Et_2BBr and with a 4-h heating period, boron-tin exchange had also occurred at tin−methyl bond of **30** as well, forming **31** also in 90% yield (Eq. 13).

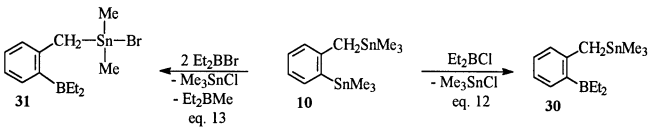

α,α′-Bis(dichloroboryl)-o-xylene (**32**) *(attempted):* The interaction of α,α′-bis(trimethylstannyl)-*o*-xylene (**11**) with BCl_3 (1:2 ratio) from −50 to 25°C led to the formation instead of 85% of α,α′-bis(chlorodimethylstannyl)-*o*-xylene (**32**), the product of the boron-tin exchange at the tin−methyl bond (eq. 14).

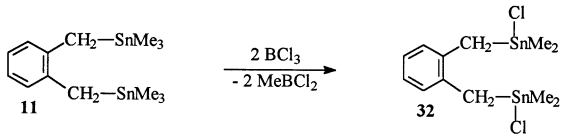

(14)

Thermolysis of Organoboranes

1,2-Bis(diethylboryl)ethyne (**15**): A neat sample of **15** was heated to 120°C and the evolved liquid permitted to reflux for 2 h. Evaporation of the evolved liquid under reduced pressure allowed the condensation of 1.0 equivalent of Et_3B and a red-brown viscous oil remained (**33**). Subsequent heating up to 700°C in a TGA apparatus left a shiny black residue of empirical formula (by elemental analyses) of $C_3B_2H_{0.14}$ (**34**) (Eq. 15).

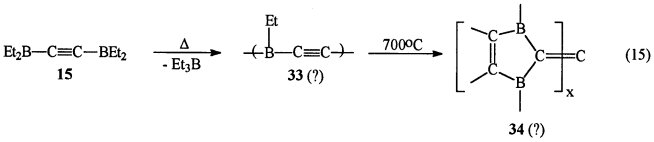

(15)

1,2-Bis(diethylboryl)ethane (**19**): Heating **19** to 180°C for 2 h and subsequent cooling similarly led to the evolution of 1.5 equiv. of Et_3B and a yellow residue (**35**) that lost no further weight up to 350°C in a TGA apparatus (Eq. 16).

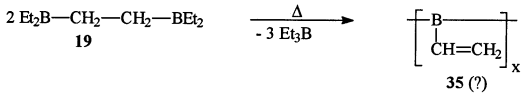

(16)

1,2-Bis(diethylboryl)benzene (**27**): Heating **27** in refluxing heptane for 18 h formed 9,10-diethyl-9,10-dihydro-9,10-diboraanthracene (**36**) almost quantitatively. The triethylborane eliminated was removed with the heptane by evaporation under reduced pressure. Yellow **36** was crystallized from pentane at −78°C (Eq. 17).

1,2-Bis(dichloroboryl)benzene (**20**) *or 1-(Dichloroboryl)-2-loro(methyl)boryl]benzene* (**24**): Individual samples or

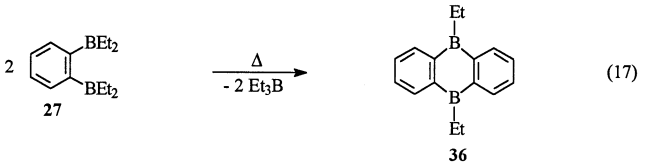

(17)

mixtures of **20** and **24** gradually formed 9,10-dichloro-9,10-dihydro-9,10-diboraanthracene (**22**) when heated at reflux in heptane (Eq. 18). Samples of **22** were purified by sublimation as yellow needles.

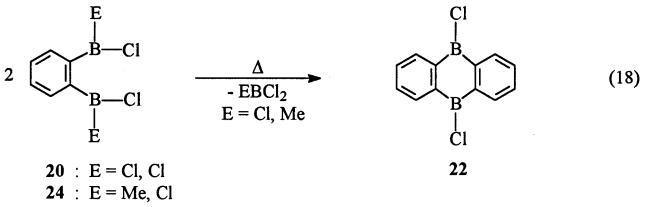

(18)

Discussion

Selectivity of Boron-Tin Exchange

The attack by a boron halide R_2B-X (**37**) on an organotin substrate (**38**) can be viewed as passing through a transition state (**39**) involving electrophilic attack of R_2B-X on the C−Sn bond or one involving concerted electrophilic attack by boron and nucleophilic attack by halide (**40**) (Scheme 2).

Scheme 2

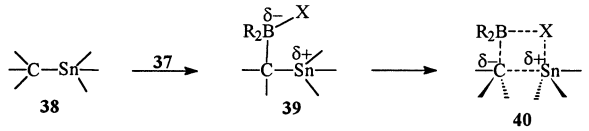

If the carbon in **38** is involved in π-bonding (sp- or sp^2-hybridized carbon), this situation would explain why transition state **39**, involving principally electrophilic attack by R_2B-X, should be relatively lower in energy and hence rate-determining for the boron-tin exchange. Furthermore, transition state **39** would account readily for the following: 1) the selective borylation of **3** at the acetylenic carbon−tin bonds rather than the methyl carbon−tin bonds; 2) the exclusive borylation of mono- and bis(trimethylstannyl)benzenes, such as **8a**, at the aryl carbon−tin bonds; and 3) the sole monoborylation of **10** at the aryl carbon−tin bond, even when 2 equiv. of the boron halide, Et_2BCl, were employed. Thus, generally when an sp- or sp^2-hybridized carbon−tin bond is pitted against an sp^3-hybridized carbon−tin bond in boron-tin exchange processes, the former carbon centers always react faster (cf. infra for an intramolecular exception to this conclusion.)

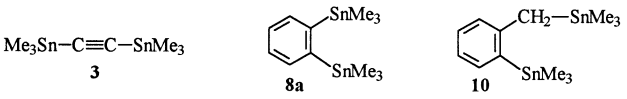

A further interesting structural example of such boron-tin exchanges are the benzylic trimethyltin derivatives, such as benzyltrimethyltin (**5**) and α,α-bis(trimethylstannyl)-*o*-xylene (**11**), which present competing carbon−tin bonds, namely benzylic C−Sn and methyl C−Sn bonds, both formally involving identical sp^3-hybridized carbon centers. When **5** and **11** were individually treated with an excess of BCl_3, they were converted into **41** and **42**, respectively. Thus, exchange took place selectively at the methyl carbon-tin bond. With the absence of any π-electron density at the carbon center, a transition state like **39** would no longer be a low-energy configuration and a bridging transition state resembling **40** may be more accessible. The carbon group bridging between tin and carbon would be more appropriate the smaller its steric requirements would be. Therefore, the greater reactivity of the methyl carbon−tin bond would stem from the methyl group's smaller steric size and better bridging property, compared with the bulkier benzyl group. It should be noted that trimethylaluminum exists as a stable dimer with bridging methyl groups, while tribenzylaluminum is monomeric.

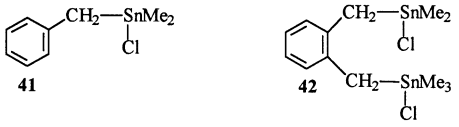

The exceptional instance where an sp^3-hybridized carbon−tin bond enters into a boron-tin exchange more readily than an available sp^2-hybridized carbon−tin bond is the facile intramolecular boron-tin exchange first observed in this study (Scheme 1 and Eq. 10) and depicted generally in Scheme 3. Undoubtedly, the failure of **21** or **26** to undergo the boron-tin exchange with the elimination of Me_3SnCl and the formation of benzoborirene **43** stems from the extremely strained transition state of type **39** that would have been required. A four-center transition state involving the methyl groups (**44**), on the other hand, is easily attainable.

Scheme 3

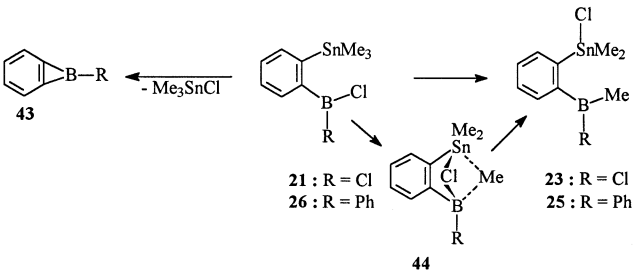

Thermal Redistribution of Unsymmetrical Organoboranes

The unsymmetrical organoboranes synthesized in this study uniformly underwent a redistribution of groups upon heating over 100°C. With diethylboryl derivatives the amount of evolved triethylborane corresponded rather well with the selective formation of defined oligomers or polymers. The formation of the dihydro-9,10-diboraanthracene (**36**, Eq. 17) from the 1,2-diborylbenzene **27** and the production of some polymeric structure of the Et−B−C≡C− unit (**33**, Eq. 15) are illustrative. If such thermolyses are continued up to 700°C, there are indications that boron carbides of unusual stoichiometry may result. Such thermoly-

sis of diborylacetylene **15** yields a glistening black solid of approximate composition C_3B_2. Further work is required to learn whether this solid **34** (Eq. 15) is a novel boron carbide or a mixture of B_4C and carbon.[13]

Unusual Properties of Unsymmetrical Organoboranes

An exploration of the boron-tin exchange route to organoboranes has been undertaken, in order to prepare such boranes that might exhibit novel properties, such as enhanced Lewis acidity and unusual spectral properties.[14] Both kinds of properties would involve the ability of the $2p_z$-orbital on tricoordinate boron to accept electron density, either intermolecularily from a Lewis base (Eq. 19) or from an adjacent π-electron cloud (resonance structure **45** and **46**, Scheme 4).

Scheme 4

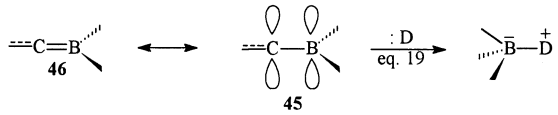

Although the study of the properties of such boranes has just begun, two observations are already noteworthy: 1) 1,2-bis(diethylboryl)ethyne (**15**) readily forms a stable bis-complex with THF (**47**), whereas the structurally similar 1,2-bis(diethylboryl)ethane (**19**) does not complex with THF at all nor do Et_3B, $PhBEt_2$, or the dihydro-9,10-diboraanthracene **36**; and 2) both the known 9,10-dichloro- (**22**) and the novel 9,10-diethyl- (**36**) -9,10-dihydro-9,10-diboraanthracenes absorb in the visible spectrum (yellow) and exhibit their ^{11}B-NMR signals shifted considerably upfield ($\delta <$ 70), that is, attributable to a more shielded boron nucleus, than those of $PhBEt_2$ or *o*-$(Et_2B)_2C_6H_4$ (**27**), whose ^{11}B signals occurs at $\delta = 78-80$. Both the electronic and the ^{11}B-NMR spectral data are consistent with the interaction of the $2p_z$-orbitals of boron in **22** and **36** with the adjacent π clouds (**48**).

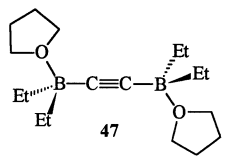

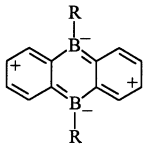

As to the enhanced Lewis acidity of **15** over **19**, it is to be expected that the steric F-strain generated in complex **47** by the neighboring C≡C group would be somewhat smaller than that of an adjacent CH_2-CH_2 group in such a complex formed by **19** and two THF units. But such steric factors alone seem inadequate in explaining the enhanced acidity of **15**. Therefore, we propose that the enhanced electronegativity of the sp-hybridized carbon centers in **15** withdraws electron density more effectively along the σ C−B bond, thereby enhancing the Lewis acidity of boron.

Our continuing studies will investigate the significance and consequences of π-electron interactions between boron and unsaturated carbon.[15]

This research was initiated as part of a materials science project sponsored by *Akzo Corporate Research America Inc.* and was completed under support of the *National Science Foundation* and a Senior Scientist Award to the principal investigator by the *Alexander von Humboldt Foundation*

Experimental Section

General Techniques: All preparations and purification procedures involving manipulations with oxygen- and moisture-sensitive reagents were carried out under an anhydrous, oxygen-free argon or nitrogen atmosphere employing Schlenk techniques.[16] Those procedures which did not require a protective atmosphere but involved working with toxic chemicals (such as boron and tin compounds) were carried out in an exhaust hood evacuating air at 100 ft/min. For the operations under reduced pressure the required vacuum was provided either by a rotary vacuum oil pump (down to 0.1 Torr) or by a water pump (down to 10 Torr) and toxic volatiles were condensed in cold baths.

In instances when acetylene and hydrogen were used, tanks were connected through purification columns directly to the one of the manifold′s outlets. Acetylene was purified by passing through a bubbler with concentrated sulfuric acid and a 25-cm column filled with activated charcoal and 4-Å molecular sieves. Hydrogen was delivered to the system after passing through a similar column filled only with 4-Å molecular sieves. When a volume of hydrogen needed to be measured, a calibrated gas buret was used.

Commercially available solvents of reagent grade were purified according to the recommended methods.[16] Solvents used in reactions were always freshly distilled under argon or nitrogen from the appropriate drying agents: aliphatic hydrocarbons from $LiAlH_4$; toluene from sodium; dichloromethane from CaH_2; and ethers from sodium/benzophenone combination. Deuteriated solvents (Cambridge Scientific) for NMR measurements of oxygen- and moisture-sensitive substance were vacuum-transferred to the Schlenk glass vessels and stored over 4-Å molecular sieves under argon. − Nuclear magnetic resonance (NMR) spectra were recorded with Bruker AM 360 (^{1}H: 360.0 MHz, ^{11}B: 115.5 MHz, ^{13}C: 90.5 MHz, ^{27}Al: 93.8 MHz, ^{119}Sn: 134.2 MHz) or Bruker-IBM AM 300 (^{1}H: 299.9 MHz, ^{11}B: 96.2 MHz, ^{13}C NMR: 75.4 MHz, ^{27}Al: 78.2 MHz, ^{119}Sn: 111.8 MHz) instruments. [D_6]Benzene, [D]chloroform, or 95% tetrachloromethane and 5% [D_6]benzene mixture were used as solvents. The chemical shifts are reported on a δ scale in parts per million (ppm) from the reference signals set as $\delta = 0$. The following substances served as references: ^{1}H and ^{13}C NMR: tetramethylsilane (TMS), internal; ^{11}B NMR: boron trifluoride−diethyl ether ($BF_3 \cdot Et_2O$), external; ^{119}Sn NMR: tetramethyltin (Me_4Sn), external. − Gas chromatographic analysis (GC) was performed with a Hewlett-Packard Chromatograph, model 5880A, with helium as the carrier gas.

Lithium Compounds

Dilithioethyne (**12**). − *Method 1:*[10] A flask was charged with a solution of *n*-butyllithium (231 ml of 2.0 M pentane solution, 0.462 mol) and then the pentane was removed under vacuum. With cooling a mixture of freshly distilled THF (50 ml) and Et_2O (50 ml) was slowly added to the residue. The resulted solution was cooled to −78°C and stirred for 0.5 h. Then a solution of trichloroethylene (20.2 g, 0.154 mol) in 50 ml of Et_2O was added dropwise. After completion of the addition the resulting clear yellow solution was stirred for 2 h at −78°C and then allowed to warm up to ambient temperature. A white precipitate gradually began to fill the flask and at approximately 0°C the flask was full of solid. The solvents

were removed partly by filtration and partly in vacuum. The yellow solid was washed with pentane (2 × 100 ml), filtered, and dried under vacuum (0.5 Torr, 40°C). Analysis of the resulting powder (20.4 g) allowed an estimation of its composition as $Li_2C_2 \cdot LiCl \cdot 0.5$ THF with 29.8% content of dilithioethyne (6.07 g, 96%).[17]

Method 2: A solution of *n*-butyllithium (70 ml of 2.5 M in hexane, 0.175 mol) was diluted with freshly distilled hexane (100 ml) and cooled to −15°C. With vigorous stirring acetylene was then passed through the solution at a rate maintaining the reaction temperature below −10°C. After approximately 15 min, a white precipitate started to form. When gas evolution was evident (bubbling through the check valve) a slow delivery of acetylene was continued for 0.5 h and then stopped. The reaction mixture was allowed to warm up to room temperature and then was heated at reflux for 2 h to expel all dissolved gas. The solvent was removed partly by filtration and partly by evaporation in vacuum. The remaining white solid residue was washed with hexane (2 × 100 ml), filtered and dried in vacuum (0.5 Torr, 60°C). The resulting fine, white powder (3.40 g) was analyzed and found to have 92% of dilithioethyne (**12**) (3.13 g, 82%).

1,4-Dilithiobenzene: The reaction of 1,4-bis(trimethylstannyl)-benzene (0.86 g, 2.1 mmol) with *n*-butyllithium (2.8 ml of 1.6 M hexanes solution, 4.3 mmol) in pentane/diethyl ether (1:1 v/v, 10 ml) after stirring for 2 d gave 0.75 g of colorless precipitate. The precipitate was derivatized with methyl iodide to give 92% of *p*-xylene. *n*-Butyl(trimethyl)tin was formed in 95% yield.[11]

1,4-Bis(trimethylsilyl)benzene: To a similarly prepared suspension of 1,4-dilithiobenzene was added 2.1 equiv. of chlorotrimethylsilane. Usual work-up provided crude solid 1,4-bis(trimethylsilyl)-benzene, which was washed with cold pentane (90%; recrystallized from hexane, mp 92−93°C).

α,α′-Dilithio-o-xylene (**13**): The reaction of α,α′-bis(trimethylstannyl)-*o*-xylene (0.80 g, 1.85 mmol with *n*-butyllithium (2.4 ml of 1.6 M hexanes solution, 3.8 mmol) in pentane/diethyl ether (1:1 v/v, 10 ml) after stirring for 2 d gave 0.62 g of a bright yellow precipitate. The precipitate was derivatized with methyl iodide to give 90% of 1,2-diethylbenzene. *n*-Butyl(trimethyl)tin was formed in 89% yield.

Tin Compounds

1,2-Bis(trimethylstannyl)ethyne (**3**): To a stirred suspension of dilithioethyne (1.22 g, 32.2 mmol) in 100 ml of dry pentane at −25°C was added dropwise over 40 min a solution of trimethyltin chloride (12.94 g, 65.0 mmol) in 100 ml of pentane. The reaction was then warmed to room temperature and heated at reflux for 1 h. The lithium chloride was filtered off and the filtrate upon concentration deposited pale yellow crystals. The crude product was recrystalized from pentane at −78°C and dried under vacuum (40°C, 5 Torr) to give off-white crystals of 1,2-bis(trimethylstannylethyne) (8.56 g, 76%); mp 57−59°C (mp 58−60°C). − ^{1}H NMR (C_6D_6): δ = 0.15 (s, 18 H, J_{Sn-H} = 58 Hz). − ^{13}C NMR (C_6D_6): δ = 8.0 (Sn-*C*H$_3$, J_{Sn-C} = 400 Hz), 115.8 (Sn−*C*≡*C*−Sn). − ^{119}Sn NMR (C_6D_6) δ = 80.9. − A corresponding reaction with trimethyltin bromide yielded 64% of the product.

1,2-Bis(trimethylstannyl)benzene (**8a**): Magnesium turnings (3.16 g, 130 mmol) in 20 ml of THF were activated with 0.3 ml of ethylene bromide. A fresh 50-ml portion of THF was then added and 0.2 ml more of ethylene bromide was injected. The mixture was heated at reflux until gas evolution stopped. At reflux a solution of 1,2-dibromobenzene (5.89 g, 25 mmol) in 30 ml of THF and trimethyltin chloride (50 ml of 1.0 M THF solution, 50 mmol) was added dropwise. As the reaction progressed, a green-brown solution developed. After the addition the reaction mixture was heated at reflux for 6 h, poured into 150 ml of a cold, saturated aqueous solution of ammonium chloride and then extracted with two 75-ml portions of ethyl ether. The extracts were washed with water, dried with anhydrous Na_2SO_4, and then concentrated under reduced pressure. Vacuum distillation of the remaining residue gave 1,2-bis(trimethylstannyl)benzene (**8a**) as a colorless, viscous liquid (4.46 g, 44%); bp 90−94°C/0.1 Torr (bp 92−94°C/0.145 Torr). − ^{1}H NMR (C_6D_6): δ = 0.28 (s, 18 H, J_{Sn-H} = 52 Hz), 7.15 (dd, *J* = 5.3, 3.5 Hz, 2 H), 7.52 (dd, *J* = 5.3, 3.5 Hz, 2 H). − ^{13}C NMR (C_6D_6) δ = −7.2 (Sn-*C*H$_3$), 127.4, 137.3, 151.6 (C_{ar}-Sn). − ^{119}Sn NMR (C_6D_6): δ = 34.1. − *Trimethyl(phenyl)tin* (**9**) (2.46 g, 41%) was isolated as a major by-product; bp 65−68°C/0.1 Torr). − ^{1}H NMR (C_6D_6): δ = 0.20 (s, 9 H, J_{Sn-H} = 54 Hz), 7.20 (m, 3 H), 7.43 (dd, 2 H). − ^{13}C NMR (C_6D_6) δ = −9.9 (Sn-*C*H$_3$), 128.5, 136.1, 142.0 (C_{ar}-Sn). − ^{119}Sn NMR (C_6D_6): δ = 29.9. − The following bis(trimethylstannyl) derivatives were also prepared analogously.

1,3-Bis(trimethylstannyl)benzene (**8b**): This compound was prepared from 1,3-dibromobenzene (5.89 g, 25 mmol) and trimethyltin chloride (50 ml of 1.0 M THF solution, 50 mmol). Vacuum distillation yielded trimethyl(phenyl)tin (**9**) (1.37 g, 23%) and the desired compound as a colorless liquid (4.93 g, 49%); bp 92−95°C/0.1 Torr. − ^{1}H NMR (C_6D_6): δ = 0.24 (s, 18 H, J_{Sn-H} = 54 Hz), 7.27 (t, *J* = 7 Hz, 1 H, J_{Sn-H} = 10 Hz), 7.44 (d, *J* = 7 Hz, 2 H, J_{Sn-H} = 46 Hz), 7.79 (s, 1 H, J_{Sn-H} = 42 Hz). − ^{13}C NMR (C_6D_6): δ = −9.7 (Sn-*C*H$_3$), 128.5, 136.2, 142.0, 143.3. − ^{119}Sn NMR (C_6D_6): δ = 30.4.

1,4-Bis(trimethylstannyl)benzene (**8c**): This compound was prepared from 1,4-dibromobenzene (6.63 g, 28 mmol) and trimethyltin chloride (56 ml of 1.0 M THF solution, 56 mmol). The crude product was recrystallized from pentane at −78°C to give 1,4-bis(trimethylstannyl)benzene as short, white needles (7.44 g, 66%); mp 125−127°C (mp 124°C).[18] − ^{1}H NMR (C_6D_6): δ = 0.24 (s, 18 H, J_{Sn-H} = 54 Hz), 7.49 (s, 4 H). − ^{13}C NMR (C_6D_6) δ = −9.9 (Sn-*C*H$_3$), 136.0, 142.1 (C_{ar}-Sn). − ^{119}Sn NMR (C_6D_6): δ = 30.8.

α,o-Bis(trimethylstannyl)toluene (**10**): This compound was prepared from 2-bromobenzyl bromide (5.61 g, 22.5 mmol) and trimethyltin chloride (50 ml of 1.0 M THF solution, 50 mmol). Vacuum distillation of the crude product yielded the compound as a colorless, viscous liquid (4.21 g, 45%); bp 89−92°C/0.1 Torr. − ^{1}H NMR (C_6D_6): δ = 0.03 (s, 9 H, J_{Sn-H} = 52 Hz), 0.28 (s, 9 H, J_{Sn-H} = 52 Hz), 2.38 (s, 2 H, J_{Sn-H} = 62 Hz), 6.97−7.00 (m, 2 H), 7.12 (d, *J* = 7 Hz, 1 H), 7.38 (d, *J* = 7 Hz, 1 H). − ^{13}C NMR (C_6D_6): δ = −9.6 (CH_2-Sn-*C*H$_3$), −8.2 (C_{ar}-Sn-*C*H$_3$), 24.2 (Sn-*C*H$_2$), 123.6, 126.8, 129.1, 136.7, 138.7, 149.9. − ^{119}Sn NMR (C_6D_6): δ = 36.6 [Ph-*Sn*-(CH$_3$)$_3$], −0.8 [Ph-CH$_2$-*Sn*-(Me)$_3$].

α,α′-Bis(trimethylstannyl)-o-xylene (**11**): This compound was prepared from α,α′-dichloro-*o*-xylene (4.34 g, 24.6 mmol) and trimethyltin chloride (50 ml of 1.0 M THF solution, 50 mmol). The crude product was distilled under vacuum to yield the pure derivative as a colorless, viscous liquid (9.14 g, 85%); bp 92−95°C/0.05 Torr. − ^{1}H NMR (C_6D_6): δ = 0.04 (s, 18 H, J_{Sn-H} = 54 Hz), 2.16 (s, 4 H, J_{Sn-H} = 62 Hz), 6.93 (s, 4 H). − ^{13}C NMR (C_6D_6): δ = −9.5 (Sn-*C*H$_2$), 124.3, 128.3, 138.4 (C_{ar}-Sn). − ^{119}Sn NMR (C_6D_6): δ = 2.7.

α-(Trimethylstannyl)-o-xylene was formed as a reaction by-product (0.51 g, 7%). − ^{1}H NMR (C_6D_6) δ = −0.02 (s, J_{Sn-H} = 50 Hz, 9 H), 2.05 (s, 2 H), 6.90 (m, 2 H), 6.92 (m, 2 H), 7.04 (d, 1 H). − ^{13}C NMR (C_6D_6): δ = −9.7 (Sn-*C*H$_3$), 18.2 (Sn-*C*H$_2$), 124.0, 126.4, 127.6, 130.3, 133.3, 141.5 (C_{ar}-Sn). − ^{119}Sn NMR (C_6D_6): δ = 2.4.

α,α′−Bis(chlorodimethylstannyl)-o-xylene (**32**): To a stirred solution of α,α′-bis(trimethylstannyl)-*o*-xylene (4.78 g, 11 mmol) in dry pentane (50 ml) at −50°C was added 22 ml of a 1.0 M hexane solution of boron trichloride in portions of 0.5 ml over 1.5 h. During the addition a white precipitate formed. After the addition the reaction was stirred at −50°C for 2 h and then allowed to reach ambient temperature. Upon warming the initially formed precipitate redissolved. When the reaction mixture reached room temperature, a new precipitate formed. The reaction mixture was stirred for 12 h at room temperature and the precipitate was then filtered off, washed twice with two 20-ml portions of dry pentane and dried under vacuum (1 Torr, room temp.) to give the desired derivative as a white, moisture-sensitive powder (4.04 g, 85%). − ^{1}H NMR (C_6D_6): δ = 0.27 (s, 12 H, J_{Sn-H} = 56 Hz), 2.48 (s, 4 H, J_{Sn-H} = 70 Hz), 6.90 (m, 4 H). − ^{13}C NMR (C_6D_6): δ = −2.0 (Sn-*C*H$_3$), 25.3 (Sn-*C*H$_2$), 125.7, 129.1, 135.8. − ^{119}Sn NMR (C_6D_6): δ = 2.44.

2,2-Dimethyl-2-stannaindane (**6**): A suspension of 10 mmol of α,α′-dilithio-*o*-xylene was prepared from 11 mmol of α,α′-bis(trimethylstannyl)-*o*-xylene and 22 mmol of *n*-butyllithium according to the aforementioned procedure. After dilution with dry diethyl ether, the lithium reagent was treated at 0°C with an ether solution of 10 mmol of dimethyltin dichloride. The reaction was stirred at reflux for 2 h and then poured into a solution of aqueous NH_4Cl. Usual work-up gave an orange-yellow oil with the desired stannaindane as the major component by NMR criteria. Distillation under reduced pressure gave an 85% yield of colorless product. − ^{1}H NMR (C_6D_6): δ = 0.09 (s, J_{Sn-H} = 55 Hz, 6 H), 2.20 (s, J_{Sn-H} = 41 Hz, 4 H), 7.03 (dd, *J* = 5.3, 3.5 Hz, 2 H), 7.03 (dd, *J* = 4.5, 3.5 Hz, 2 H). − ^{13}C NMR (C_6D_6): δ = −10.1 (Sn-*C*H$_3$), 17.95 (Sn-*C*H$_2$), 125.4, 131.2, 143.6 (C_{ar}-Sn).

Boron Compounds

1,2-Bis(diethylboryl)ethyne (**15**). − *Method A:* In this method the active dilithioethyne was prepared from trichloroethylene and *n*-butyllithium (cf. supra). The composition of solids from this reaction varied and the actual proportions of Li_2C_2, LiCl, and THF had to be analyzed after each preparation. The quantity of the dilithioethane used in the preparation described here refers to 14.7 g of a solid of the composition 33% Li_2C_2, 37% LiCl, and 30% THF by weight. An excess of Et_2BBr was used to allow for the formation of diethyl[(4-bromo)butoxy]borane ($Et_2B-O-[CH_2]_4Br$), a side-product formed from a THF ring cleavage reaction by Et_2BBr even at low temperatures.

A solution of diethylboron bromide (47.2 g, 0.317 mol) in 100 ml of dry pentane was added to a stirred suspension of the dilithioethyne (4.85 g, 0.128 mol) in 100 ml of pentane at such a rate as to maintain the temperature below 40°C. After the addition, the reaction mixture had turned red-brown. Lithium bromide was filtered off and the pentane was removed from the filtrate under reduced pressure. The residue was then distilled at 0.3 Torr to yield 1,2-bis(diethylboryl)ethyne as a colorless liquid (8.1 g, 39%); bp 40−50°C/0.3 Torr. − ^{1}H NMR (C_6D_6): δ = 1.08 (t, *J* = 7 Hz, 12 H), 1.19 (q, *J* = 7 Hz, 8 H). − ^{13}C NMR (C_6D_6): δ = 9.4 (CH$_2$-*C*H$_3$), 20.6 (br., CH$_2$-*C*H$_3$), 137.2 (br., B-*C*≡*C*-B). − ^{11}B NMR (C_6D_6): δ = 72.

Diethyl(4-bromobutoxy)borane was formed as a reaction by-product (12.52 g, 93%); recovered as a distillation residue. − ^{1}H NMR (C_6D_6): δ = 0.76 (q, *J* = 7 Hz, 4 H), 0.93 (t, *J* = 7 Hz, 6 H), 1.04 (m, 2 H), 1.62 (m, 2 H), 3.01 (t, *J* = 7 Hz, 2 H), 3.50 (t, *J* = 6 Hz, 2 H). − ^{13}C NMR ($CDCl_3$): δ = 8.0 (CH$_2$-*C*H$_3$), 12.1 (br., B-*C*H$_2$), 29.7, 30.3, 33.4, 64.2 (O-*C*H$_2$). − ^{11}B NMR (C_6D_6) δ = 53.2.

Method B: To a stirred solution of diethylboron bromide (0.68 g, 4.6 mmol) in 10 ml of dry pentane at −30°C was added a solution of bis(trimethylstannyl)ethyne (0.80 g, 2.3 mmol) in 20 ml of dry pentane. After the addition, the reaction mixture was stirred for 1 h at 25°C and then cooled to −78°C, upon which white trimethyltin bromide precipitated. After this solid was filtered off at −78°C, pentane was partly removed from the cold filtrate under reduced pressure and the residue was allowed to warm up to ambient temperature. A fresh 10-ml portion of dry pentane was added to the residue and the solution again cooled to −78°C whereupon further precipitate was filtered off. The pentane was partly removed from the filtrate in vacuo and the remaining residue distilled under vacuum to give 1,2-bis(diethylboryl)ethyne (0.24 g, 65%) containing less than 2 mol-% of trimethyltin bromide.

1,2-Bis(diethylboryl)ethane (**19**): The modified Lindlar catalyst used here refers to the commercial product $Pd/CaCO_3$. In the original Lindlar procedure the catalyst, $Pd/CaCO_3$, was partly deactivated by addition of quinoline. Since quinoline forms a pale yellow complex with bis(diethylboryl)ethyne and the hydrogenation then does not proceed at all, the palladium catalyst used in these experiments was not poisoned with quinoline. A suspension of the modified Lindlar catalyst (0.16 g) in 5 ml of cyclohexane was stirred at room temperature under a slow flow of hydrogen gas for 1 h. Thereafter a solution of bis(diethylboryl)ethyne (1.31 g, 8.1 mmol) in 10 ml of cyclohexane was introduced and the hydrogen flow was stopped. From there the reaction was carried out by admission of hydrogen gas from a calibrated gas burette. The reaction was stopped when the hydrogen consumption had ceased. Hydrogen was purged by a stream of argon passing through the flask. The cyclohexane was removed under reduced pressure and the residue distilled under vacuum to yield pure 1,2-bis(diethylboryl)ethane (1.2 g, 85%). bp 30−34°C/2 Torr. − ^{1}H NMR (C_6D_6): δ = 1.0−1.3 (m), no signals at δ = 2.0−10.0. − ^{13}C NMR (C_6D_6): signals at δ = 10−30, no signals at δ = 40−150. − ^{11}B NMR (C_6D_6): δ = 75.

Pyrolysis of 1,2-Bis(diethylboryl)ethyne (**15**): This compound (1.45 g, 9 mmol) was slowly heated under argon at about 100°C, whereupon a colorless liquid began to distill. The heating was continued until the internal temperature reached 120°C. Further gentle reflux was maintained for 2 more hours after which the reaction mixture was cooled to room temperature and the volatiles removed under vacuum. The distillate consisted of triethylborane (0.99 g, 10 mmol). The red-brown residue (0.45 g) was then heated to 350°C under vacuum to give a viscous dark oil and then up to 700°C in a TGA apparatus to yield a glistening black solid which contained 55.13% C, 38.12% B, and 2.68% H, approximating an empirical formula of $C_3H_2H_{0.14}$.

Pyrolysis of 1,2-bis(diethylboryl)ethane (**19**): 1,2-Bis(diethylboryl)ethane (**19**) (0.64 g, 3.9 mmol) was slowly heated under argon to 120°C where triethylborane started to distill. Further heating in a TGA apparatus was continued until the internal temperature reached approximately 350°C and the evolution of volatiles had stopped. The reaction was cooled to room temperature and volatile substances removed under vacuum, which proved to be triethylborane (0.59 g, 6.0 mmol). The composition of the yellow residue (0.03 g) was not determined.

1,2-Bis(dichloroboryl)benzene (**20**) *and 1-Dichloro-2-[chloro(methyl)boryl]benzene* (**24**): To a stirred solution of 1,2-bis(trimethylstannyl)benzene (**8a**) (2.31 g, 5.7 mmol) in 20 ml of dry pentane was added a solution of boron trichloride (11.4 ml of 1.0 M hexanes solution, 11.4 mmol) at −40°C. During the addition a white precipitate formed gradually. The precipitate was separated from the solution at −40°C and dried under vacuum to give 1.51 g of white

solid identified as a mixture of trimethyltin chloride (5.0 mmol, 44%) and dimethyltin dichloride (2.3 mmol, 40%). From the solution the solvents were removed in vacuo to give 1.23 g of a yellow oil. Since the separation of the substances present in the residue was unsuccessful, the components were identified spectroscopically.

1-Dichloroboryl-2-[chloro(methyl)boryl]benzene (40 mol-%) (**24**): ^{1}H NMR (C_6D_6): δ = 1.21 (s, 3 H), 7.19 (dd, *J* = 5.5, 3.3 Hz, 2 H), 8.18 (dd, *J* = 5.5, 3.3 Hz, 2 H). − ^{13}C NMR (C_6D_6): δ = 9.5, 133.9, 136.4. − ^{11}B (C_6H_6): δ = 33. − *1-[Chloro(methyl)boryl]-2-(chlorodimethylstannyl)benzene* (65 mol-%) (**23**): ^{1}H NMR (C_6D_6): δ = 0.24 (s, 6 H), 1.21 (s, 3 H), 7.42 (d, 1 H) 7.86 (td, 1 H), 7.92 (d, 1 H) 8.36 (td, 1 H). − ^{13}C NMR (C_6D_6): δ = −0.3 (Sn-*C*H$_3$), 10.0 (B-CH$_3$), 132.8, 133.8, 135.8, 136.4. − ^{11}B (C_6H_6): δ = 38.7. − ^{119}Sn (C_6H_6): δ = 172.1. − *9,10-Dichloro-9,10-Dihydro-9,10-diboraanthracene* (**22**)[19] (ca. 10 mol-%). − ^{1}H NMR (C_6D_6): δ = 7.27 (dd, *J* = 5.55, 3.5 Hz, 4 H), 7.68 (dd, J = 5.5, 3.5 Hz, 4 H). − ^{13}C NMR (C_6D_6): δ = 132.9, 137.1.

When the reaction was repeated by employing 6.0 mmol of 1,2-bis(trimethylstannyl)benzene and 24.0 mmol of boron trichloride, Me_3SnCl and Me_2SnCl_2 were filtered off from the chilled reaction solution (−40°C), the filtrate freed of volatiles and the residue distilled under vacuum to yield 80% of **24**.

Diethyl(phenyl)borane: A solution of trimethyl(phenyl)tin (2.65 g, 11 mmol) in 10 ml of dry pentane was added dropwise to a stirred solution of diethylboron bromide (1.80 g, 12 mmol) in 10 ml of pentane at room temperature. The reaction mixture was heated under atmospheric pressure until pentane started to distill. When distillation stopped, the reaction was heated and stirred at 70°C for 3 h. The volatiles were removed under vacuum to give a clear, brownish liquid which was identified as nearly pure diethyl(phenyl)borane (1.43 g, 89%). − ^{1}H NMR (C_6D_6): δ = 1.01 (t, *J* = 7.8 Hz, 6 H), 1.54 (q, *J* = 7.8 Hz, 4 H), 7.25 (m, 3 H), 7.75 (d, *J* = 6.5 Hz, 2 H). − ^{13}C NMR (C_6D_6): δ = 8.8 (-*C*H$_3$), 16.0 (br., B-*C*H$_2$), 128.2, 132.1, 134.5, 139.3 (C_{ar}-B). − ^{11}B NMR (C_6D_6): δ = 78.1.

1,2-Bis(diethylboryl)benzene (**27**): A solution of 1,2-bis(trimethylstannyl)benzene (1.81 g, 4.5 mmol) in 5 ml of dry pentane was added dropwise to a refluxing solution of diethylboron bromide (1.78 g, 12 mmol) in 10 ml of pentane. After the addition, the reaction mixture was heated at reflux for 1 h. The pentane and unreacted Et_2BBr were removed under reduced pressure and a fresh 10-ml portion of dry pentane was added to the yellow residue and the solution was cooled to −78°C. Upon cooling a precipitate was formed and was filtered off at −78°C. The pentane was removed from the filtrate under vacuum to give a crude product as a lemon-colored oil (1.16 g). Distillation of the crude product yielded **27** as a yellowish, viscous liquid (0.81 g, 84%). During distillation partial decomposition with the evolution of some triethylborane was observed. − ^{1}H NMR (C_6D_6): δ = 1.00 (t, *J* = 8 Hz, 12 H), 1.35 (q, *J* = 8 Hz, 8 H), 7.24 (dd, *J* = 5.0, 3.0 Hz, 2 H), 7.35 (dd, *J* = 5.0, 3.0 Hz, 2 H). − ^{13}C NMR (C_6D_6): δ = 8.2 (CH$_2$-*C*H$_3$), 21.6 (br., B-*C*H$_2$-CH$_3$), 128.6, 130.3, 139.7 (C_{ar}-B). − ^{11}B NMR (C_6D_6): δ = 80.8.

9,10-Diethyl-9,10-dihydro-9,10-diboraanthracene (**36**): A solution of 1,2-bis(diethylboryl)benzene (**27**) (0.98 g, 4.6 mmol) in dry heptane (10 ml) was heated under reflux for 12 h. The solvent was then gradually distilled off as the reaction temperature rose to 140°C. The residue was stirred at 140−150°C for 6 h and the volatiles then were removed under vacuum. The oily, yellow residue (0.63 g) contained (**36**) and unreacted (**27**) in an approximate molar ratio of 1.0:0.3. Freshly distilled pentane (10 ml) was added to the residue and the resulting solution was cooled to −78°C, whereupon a fine, pale yellow precipitate settled out. The colorless supernatant solution was decanted and the precipitate dried under vacuum. The precipitate was identified by spectral data as pure **36** (0.12 g, 23%). − ^{1}H NMR (C_6H_6): δ = 1.09 (t, *J* = 8.2 Hz, 6 H), 1.89 (q, *J* = 8.2 Hz, 4 H), 7.33 (dd, *J* = 5.4, 3.2 Hz, 4 H), 8.01 (dd, *J* = 5.3, 3.4 Hz, 4 H). − ^{13}C NMR (C_6H_6): δ = 10.3 (*C*H$_3$), 12.4 (br., B-*C*H$_2$), 132.7, 136.0, 145.6 (br., C_{ar}-B). − ^{11}B NMR (C_6H_6): δ = 67.5.

1,3-Bis(diethylboryl)benzene (**28**): A solution of 1,3-bis(trimethylstannyl)benzene (1.46 g, 3.6 mmol) in 3 ml of dry pentane and diethylboron chloride (0.85 g, 8.1 mmol) were stirred at room temperature for 1 h. Thereupon the reaction mixture was heated under atmospheric pressure until the pentane started to distill. Then, the reaction mixture was stirred and heated to 70°C for 3 h. Volatiles were removed under vacuum to leave a yellowish, oily residue that was identified as essentially pure 1,3-bis(diethylboryl)benzene (0.67 g, 87%). − ^{1}H NMR (C_6D_6): δ = 1.07 (t, *J* = 7.9 Hz, 12 H), 1.62 (q, *J* = 7.8 Hz, 8 H), 7.35 (t, *J* = 7.5 Hz, 1 H), 7.87 (d, *J* = 7.3 Hz, 2 H), 8.45 (s, 1 H). − ^{13}C NMR (C_6D_6): δ = 8.8 (*C*H$_3$), 17.3 (br., B-*C*H$_2$), 127.7, 137.8, 139.4, 140.3. − ^{11}B NMR (C_6D_6): δ = 78.5. − Attempts to further purify the crude product by distillation failed and resulted in its significant decomposition with the liberation of triethylborane.

A parallel procedure was conducted with 1,4-bis(trimethylstannyl)benzene (**8**) and diethylboron chloride to provide a 90% yield of 1,4-bis(diethylboryl)benzene (**29**) at the stage where volatiles had been removed from the reaction mixture. Attempted distillation again led to the evolution of triethylborane.

2-(Diethylboryl)-α-(trimethylstannyl)toluene (**30**): At room temperature a solution of α,2-bis(trimethylstannyl)toluene (1.71 g, 4 mmol) in 3 ml of dry pentane was added dropwise to a neat sample of diethylboron chloride (0.85 g, 8 mmol). The reaction mixture was stirred at room temperature for 1 h and then heated gradually until pentane started to distill. The reaction mixture then was stirred and heated at 70°C for 3 h. After that, volatiles were removed under reduced pressure to leave a pale yellow, oily mixture of **30** and unreacted tin derivative in approximately a 1:1 molar ratio. The residue was then allowed to react further with an excess of Et_2BCl (1.0 g, 10 mmol). After stirring the mixture at 60°C for 12 h, the volatiles were removed in vacuo. The clear yellow oil was identified by spectral data as 2-(diethylboryl)-α-(trimethylstannyl)-toluene. Further purification of the crude product by distillation resulted in its partial decomposition. − ^{1}H NMR (C_6D_6): δ = 0.03 (s, J_{Sn-H} = 52 Hz, 9 H), 1.03 (t, *J* = 7.6 Hz, 6 H), 1.49 (q, *J* = 7.6 Hz, 4 H), 2.20 (s, 2 H, J_{Sn-H} = 72 Hz), 6.93 (t, *J* = 7.5 Hz, 1 H), 6.94 (d, *J* = 6.2 Hz, 1 H), 7.00 (t, *J* = 7.4 Hz, 1 H), 7.12 (td, *J* = 7.4, 1.2 Hz, 1 H). − ^{13}C NMR (C_6D_6): δ = −9.5 (Sn-*C*H$_3$, *J* = 324, 308 Hz), 8.95 (B-CH$_2$-*C*H$_3$), 21.6 (Sn-*C*H$_2$, *J* = 300, 244 Hz), 22.0 (br., *C*H$_2$), 123.1, 127.6, 128.36, 128.42, 143.1 (*C*H$_{ar}$-B). − ^{11}B NMR (C_6D_6): δ = 85.3. − ^{119}Sn NMR (C_6D_6): δ = 3.7.

2-(Diethylboryl)-α-(bromodimethylstannyl)toluene (**31**): A solution of α,2-bis(trimethylstannyl)toluene (2.11 g, 5 mmol) in 5 ml of dry pentane was added to a solution of diethylboron bromide (1.78 g, 12 mmol) in 5 ml of pentane at room temperature. The reaction mixture was heated at reflux for 3 h and then the pentane was partly distilled off under atmospheric pressure. The residue was further heated at 70°C for 4 h. The volatiles were removed under vacuum to leave a colorless oil of almost pure **31** (1.75 g, 90%). − ^{1}H NMR (C_6D_6): δ = 0.31 (s, J_{Sn-H} = 55 Hz, 6 H), 0.97 (t, *J* = 7.5 Hz, 6 H), 1.44 (q, *J* = 7.5 Hz, 4 H), 2.58 (s, 2 H, J_{Sn-H} = 68 Hz); 6.85−7.05 (m, 4 H). − ^{13}C NMR (C_6D_6): δ = −2.6 (Sn-*C*H$_3$), 8.9 (B-CH$_2$-*C*H$_3$), 22.1 (br., B-*C*H$_2$), 27.9 (Sn-*C*H$_2$), 124.3, 127.9,

128.6, 128.7, 139.1 (C_{ar}-Sn). – ^{11}B NMR (C_6D_6): δ = 84.9. – ^{119}Sn NMR (C_6D_6): δ = 3.6.

1-[Methyl(phenyl)boryl]-2-(chlorodimethylstannyl)benzene (**25**): A solution of 1,2-bis(trimethylstannyl)benzene (1.85 g, 4.6 mmol) in 10 ml of pentane was added dropwise to a refluxing solution of dichloro(phenyl)borane (0.73 g, 4.6 mmol) in 10 ml of pentane. The reaction mixture was then heated at reflux for 1 h and thereafter cooled to −78°C. The precipitate of trimethyltin chloride (0.71 g, 78%) was filtered off at −78°C and the volatiles were removed from the filtrate under reduced pressure. The light yellow oil (1.69 g) was further distilled under vacuum (0.1 Torr, 60°C) to give partly decomposed **25** (1.03 g, 61%). – ^{1}H NMR (C_6D_6): δ = 0.16 (s, 6 H, J_{Sn-H} = 56 Hz), 1.26 (s, 3 H), 7.01 (t, J = 7.2 Hz, 2 H), 7.09 (d, J = 7.2 Hz, 1 H), 7.20−7.29 (m, 2 H), 7.42 (m, 2 H), 8.07 (d, 1 H). – ^{13}C NMR (C_6D_6): δ = 0.5 (Sn-CH_3), 12.5 (br., B-CH_3), 128.5, 128.7, 129.6, 132.4 (B-C_{ar}), 132.8, 133.1, 136.2, 137.2 (B-C_{ar}), 137.7, 147.0 (Sn-C_{ar}).

☆ Dedicated to Professor *Heinrich Nöth* on the occasion of his 70th birthday.

[1] J. J. Eisch, A. M. Piotrowski, S. K. Brownstein, E. J. Gabe, F. L. Lee, *J. Am. Chem. Soc.* **1985**, *107*, 7219.

[2] J. J. Eisch, K. R. Caldwell, S. Werner, C. Krüger, *Organometallics* **1991**, *10*, 3417.

[3] J. J. Eisch, K. R. Caldwell, *Advances in Chemistry*, vol. 230, American Chemical Society, Washington, D.C., **1992**, pp. 575−590.

[4] J. J. Eisch, S. I. Pombrik, G.-X. Zheng, *Organometallics* **1993**, *12*, 3856.

[5] R. Köster, G. Seidel, K. Wagner, B. Wrackmeyer, *Chem. Ber.* **1993**, *126*, 305.

[6] T. Onak, *Organoborane Chemistry*, Academic Press, New York, **1975**, pp. 24−26.

[7] H. Nöth, H. Vahrenkamp, *J. Organomet. Chem.* **1968**, *11*, 399.

[8] J. J. Eisch, *Organometallic Syntheses*, vol. 2, Academic Press, New York, **1981**, pp. 167−177.

[9] M. A. Tinga, G. Schat, O. S. Akkerman, F. Bickelhaupt, E. Horn, H. Kooijman, W. J. J. Smets, A. L. Spek, *J. Am. Chem. Soc.* **1993**, *115*, 2808.

[10] S. Ijadi-Maghsoodi, Y. Pang, T. J. Barton, *J. Poly. Sci. A: Polym. Chem.* **1990**, *28*, 955.

[11] A future publication will present the extensive scope and preparative applications of such lithium-tin exchange processes.

[12] D. Kaufmann, *Chem. Ber.* **1987**, *120*, 901.

[13] The feasibility of synthesizing novel boron carbides by the controlled thermolysis of poly(diethylboryl)-substituted precursors is under current study in this laboratory.

[14] Previous studies of the properties of cyclic borapolyenes are reported in the following: [14a] J. J. Eisch, J. E. Galle, S. Kozima, *J. Am. Chem. Soc.* **1986**, *108*, 379. – [14b] J. J. Eisch, B. Shafii, J. D. Odom, A. L. Rheingold, *J. Am. Chem. Soc.* **1990**, *112*, 1847. – [14c] J. J. Eisch, J.E. Galle, B. Shafii, A.L. Rheingold, *Organometallics* **1990**, *9*, 2342.

[15] A critical review of the nature and extent of π bonding between boron and carbon centers has recently appeared: J. J. Eisch, *Advances in Organometallic Chemistry*, vol. 39, Academic Press, Orlando, **1995**, pp. 355−391.

[16] J. J. Eisch, *Organometallic Syntheses*, vol. 2, Academic Press, New York, **1981**, pp. 1−84.

[17] The dilithioethyne available commercially proved to be totally unsuitable for the preparations of **3** and of **15**.

[18] C. D. Schaeffer, Jr., J. J. Zuckerman, *J. Organomet. Chem.* **1973**, *55*, 97.

[19] R. Clement, *C. R. Acad. Sci. Paris* **1965**, *261*, 4436.

[98057]

Asymmetric Catalysis, 117[◇]

Novel Chiral Oxazoline Ligands for Potential Charge-Transfer Effects in the Rh(I)-Catalysed Enantioselective Hydrosilylation☆

Henri Brunner*[a], Reinhard Störiko[a], and Frank Rominger[b]

Institut für Anorganische Chemie der Universität Regensburg[a],
D-93040 Regensburg, Germany
Fax: (internat.) +49 (0)941 9434439

Organisch-Chemisches Institut der Universität Heidelberg[b],
D-69120 Heidelberg, Germany
E-mail: henri.brunner@chemie.uni-regensburg.de

Received September 30, 1997

Keywords: Oxazolines / Charge-transfer / 4,4'-Bipyridine / Enantioselective hydrosilylation / Rh(I)-complexes

Novel 2-(4,4′-bipyridin-2-yl)oxazolines, bearing a chiral oxazoline moiety, were synthesised starting from 4,4′-bipyridine and selectively monomethylated in the *N′*-position. After coordination to rhodium these electron-poor ligands are supposed to exhibit charge-transfer effects with electron-donating substrates in the Rh(I)-catalysed enantioselective hydrosilylation (see next publication). Similar effects were expected from 4,4′-bipyridine- and pyrazine-bisoxazolines after complexation with rhodium. For comparison 2-(4-phenylpyridin-2-yl)oxazoline ligands were synthesised. Rh(I)-complexes of selected ligands were prepared and characterised, including an X-ray structure analysis.

Introduction

A well-known example in asymmetric catalysis is the Rh(I)-catalysed enantioselective hydrosilylation of prochiral ketones, which after hydrolysis gives chiral secondary alcohols[2][3][4]. Asymmetric induction is brought about by *in situ* Rh(I)-catalysts consisting of $[Rh(cod)Cl]_2$ and preferably nitrogen ligands[5][6][7]. In particular, ligands containing chiral oxazolines proved to be effective[8][9][10][11].

Our point of interest was a possible pre-orientation of the substrate to be hydrosilylated with respect to the catalytic centre. Such a pre-orientation of the metal bound prochiral ketone might result in a higher enantiodiscrimination. We propose charge-transfer interactions for this pre-orientation. Charge-transfer interactions usually appear in systems consisting of electron-donating and electron-accepting compounds[12][13][14][15]. In addition to the isolation of stable charge-transfer complexes, e.g. the paraquat-hydroquinone adduct[16][17] (Scheme 1), charge-transfer interactions were used as a template effect for ring closure reactions[18].

We tried to introduce charge-transfer interactions in the Rh(I)-catalysed hydrosilylation using the electron-rich 2,5-dimethoxyacetophenone as the substrate. The acceptor had to be a chiral ligand whose electron-accepting properties should be amplified by coordination to Rh(I). *N′*-Methylated 2-(4,4′-bipyridin-2-yl)oxazolines **1**, which resemble paraquat after coordination to Rh, promised to be a suitable

Scheme 1

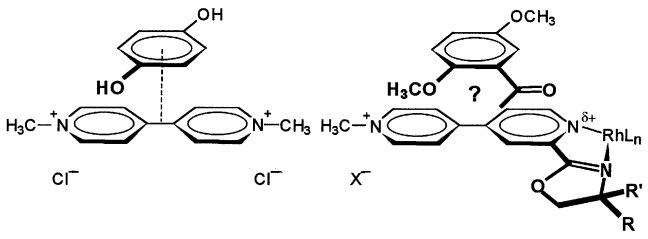

system (Scheme 1). The ligands of type **1** contain the same chelating unit as the ligands of type **2**, which were among the first successful chiral nitrogen ligands in enantioselective catalysis[11][19]. Since the formation of oxazoline rings is straightforward and the necessary enantiopure amino alcohols are accessible by reduction of amino acids, chirality should be easily introduced into 4,4′-bipyridine-oxazolines, provided a synthesis of the 2-cyano precursor is found. Another task is the selective methylation of the *N′*-position, which is necessary to increase the electron accepting properties of the 4,4′-bipyridine system.

Scheme 2

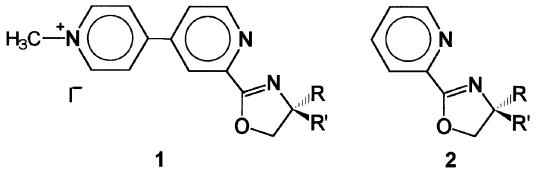

1 **2**

[◇] Part 116: See ref.[1].

 © WILEY-VCH Verlag GmbH, D-69451 Weinheim, 1998 1434–1948/98/0606–0771 $ 17.50+.50/0

In this paper we describe the synthesis and characterisation of 2-(4,4′-bipyridin-2-yl)oxazolines and their *N*′-methylated derivatives, 2-(4-phenylpyridin-2-yl)oxazolines, 4,4′-bipyridine- and pyrazine-bisoxazolines as well as some Rh(I)-complexes[20]. The next paper reports on the catalytic results.

The 2-(4,4′-Bipyridin-2-yl)oxazolines 3a-f

Six novel 2-(4,4′-bipyridin-2-yl)oxazolines **3a-f** were prepared from 4,4′-bipyridine via the four-step synthesis shown in Scheme 3.

Scheme 3

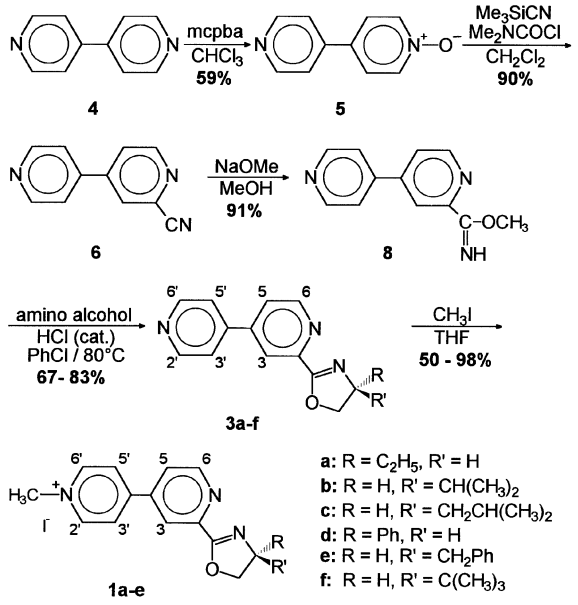

In a variation of known procedures[21][22][23], 4,4′-bipyridine (**4**) was oxidised to the *N*-oxide **5** with *m*-chloroperbenzoic acid (mcpba) in $CHCl_3$. Chromatography on SiO_2 using an acetone/methanol gradient was necessary to separate the desired **5** from unreacted 4,4′-bipyridine and 4,4′-bipyridine *N*,*N*′-dioxide. α-Cyanation of the *N*-oxide **5** with trimethylsilyl cyanide and dimethylcarbamoyl chloride in CH_2Cl_2[24] yielded the nitrile **6** in 90% (Scheme 3) which had been only prepared as *N*,*N*′-bisquarternised salts[25]. A small amount of a side-product was obtained, characterised as the previously unknown 4,4′-bipyridine-2-carboxamide **7** (Scheme 4), probably resulting from partially hydrolysed **6**. Conversion of **6** into the carboximidate **8** (91% yield) was accomplished by stirring **6** for 2 d in dry methanol containing catalytic amounts of methanolate[26], according to Scheme 3. The resulting iminoether **8** was air-stable and could be stored for months if kept dry. The acid-catalysed condensation of **8** and enantiopure amino alcohols gave the corresponding oxazolines **3a-f** (Scheme 3). After flash chromatography and recrystallisation all six new ligands were obtained analytically pure in good yields (67−83%). By $^{13}C/^{1}H$ correlation experiments for **3c** all its protons and carbon atoms could be assigned. Comparison of their chemical shifts with those of the other ligands allowed almost complete assignment of their signals, too.

The oxazolines were unstable towards acids. Crude **3a** in chlorobenzene was almost completely transferred into the aqueous layer while shaking with 2 N HCl, thereby hydrolysing to the hydroxyalkylamide **9** (Scheme 4). After treatment of **9** with *p*-tosyl chloride and triethylamine in $CHCl_3$ according to ref.[27] the original oxazoline **3a** was restored.

Scheme 4

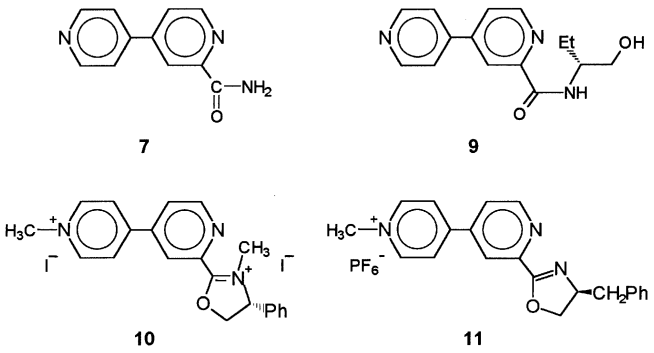

The *N*′-Methylated 2-(4,4′-Bipyridin-2-yl)oxazolines 1a−e and 11

The 2-(4,4′-bipyridin-2-yl)oxazolines **3a-e** were treated with excess methyl iodide in absolute THF at room temperature according to Scheme 3. A comparable selective *N*′′-methylation of 2,2′;4,4′′-terpyridine was reported by Persaud and Barbiero[28]. For **3e** nearly quantitative quarternisation of the *N*′-position occurred selectively and the product **1e** was isolated as an orange solid. The location of the methyl group was determined unequivocally by NMR spectroscopy. The AA′BB′ system of the Py′ ring in the ^{1}H NMR spectrum was shifted downfield compared to the non-methylated ligand **3e** and the CH_3 group showed a cross-peak with H-2′ and H-6′ in the NOESY spectrum. In the ^{13}C NMR spectrum the signals of C-2′ and C-6′ are broader than the other peaks due to the quadrupol momentum of the quarternised nitrogen.

For **3a-d** the analogous reactions gave the corresponding *N*′-methylated ligands **1a-d** (Scheme 3) in satisfying yields (50−63%). Here, the formation of a red side-product was observed. It could be removed by fractional crystallisation from methanol/ether solutions at −20°C. For **3d** the side-product was recrystallised from aqueous acetone/methanol yielding dark red tetrahedra, which were characterised as the dimethylated compound **10** (Scheme 4). 2D NMR experiments (NOESY and $^{13}C/^{1}H$ correlations) showed that the second methyl group is attached to the oxazoline-nitrogen. The methylated ligands **1a-e** are orange solids, which are hygroscopic and have to be stored under dry nitrogen. Spectroscopic characterisation including a $^{13}C/^{1}H$ NMR correlation spectrum for **1c** allowed almost complete assignment of all carbon and hydrogen atoms.

By treating **1e** (dissolved in water) with saturated aqueous NH_4PF_6 the iodide was substituted by hexafluorophosphate to yield **11** in 88% (Scheme 4), which was sparingly

soluble in methanol and could be recrystallised from boiling water.

The 2,2′-Bis(oxazolin-2-yl)-4,4′-bipyridine 15, the 2,5-Bis(oxazolin-2-yl)-3,6-dimethylpyrazine 19 and the 2-(4-Phenylpyridin-2-yl)oxazolines 23a,b

Since the *N*-oxidation of 4,4′-bipyridine **4** always yielded ca. 30% *N*,*N*′-dioxide **12**, the novel bisoxazoline **15** could be prepared via the dinitrile **13**[29] and the biscarboximidate **14**[30] (Scheme 5).

Scheme 5

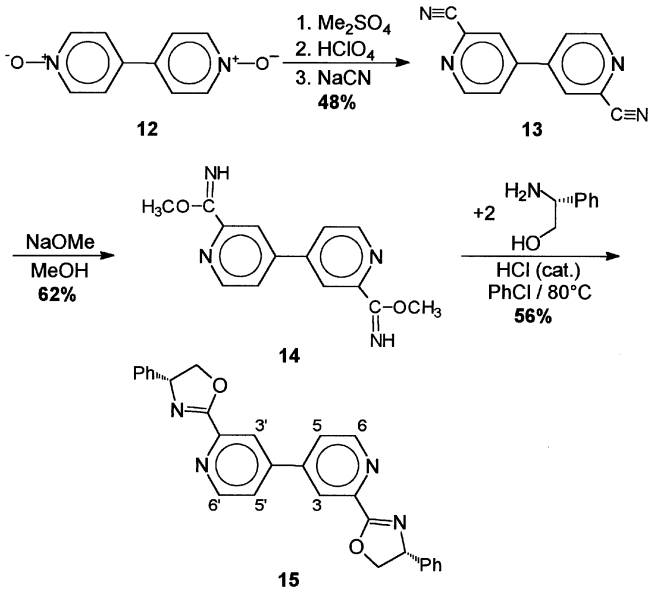

4,4′-Bipyridine *N*,*N*′-dioxide **12** as a single product was obtained in excellent yield (95%) by oxidation of 4,4′-bipyridine **4** with excess H_2O_2/urea adduct and phthalic anhydride in CH_2Cl_2 (80% yield were reported by using smaller amounts of oxidising agent[31]). Condensation of **14** with 2 equivalents of *(R)*-α-phenylglycinol yielded **15** as the first example of a chiral C_2-symmetrical 4,4′-bipyridine derivative, which is able to coordinate to two metal centres. The corresponding 2,2′-bipyridine-bisoxazoline was synthesised by Nishiyama et al.[32]. In the ^{1}H NMR spectra **15** and its mono-oxazoline counterpart **3d** display nearly identical chemical shifts for the oxazoline protons and the ABX system of the pyridine ring.

Since pyrazine is a ″shortened″ 4,4′-bipyridine, a Rh(I)-coordinated pyrazoline-bisoxazoline could also exhibit charge-transfer properties. Such a bisoxazoline was synthesised starting from dimethyl 3,6-dimethylpyrazine-2,5-dicarboxylate **16**[33]. After hydrolysis of **16** to **17**, the diacid chloride **18** was prepared using $SOCl_2$. Without isolation of intermediates the two oxazoline rings were condensed via a three-step reaction (Scheme 6). The pyrazine-bisoxazoline **19** was obtained in 46% yield.

For comparison two 2-(4-phenylpyridin-2-yl)oxazolines **23a,b** were synthesised from commercially available 4-phenylpyridine *N*-oxide **20** using the same reactions as for **3a-f** via the intermediates **21** and **22** (Scheme 7). **23a,b** differ from **3c** and **3e**, respectively, only in the nature of the 4-

Scheme 6

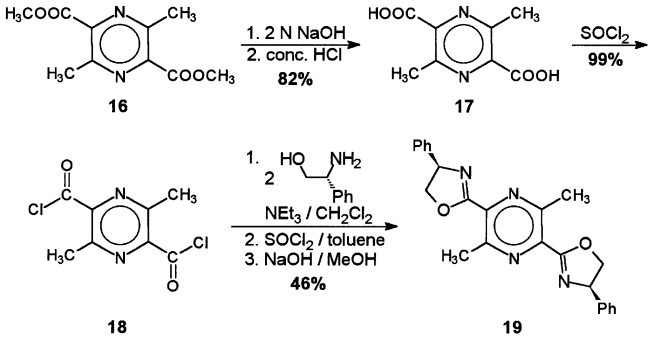

substituent (phenyl vs. 4′-pyridine). Thus, the spectroscopic data of **23a,b** are very similar to their 4,4′-bipyridine counterparts.

The Rh(I) Complexes 24−28

To ascertain that the 4,4′-bipyridine-oxazolines **3** prefer chelate coordination via pyridine- and oxazoline-*N* with regard to a monodentate coordination via *N*′, a series of Rh(I)-complexes was synthesised. All complexes were prepared by adding a solution of $[Rh(cod)Cl]_2$ in CH_2Cl_2 to the dissolved ligand. Exchange of chloride by PF_6^- (**24**, **25**) or BF_4^- (**26**) gave the corresponding red complexes in 82−92% yields (Scheme 8).

The ^{1}H NMR data (including COSY) proved the chelate coordination, because for **24** H-6 exhibited a strong downfield shift (0.87 ppm) compared to the free ligand **3d** due to the proximity of the rhodium. On the other hand H-2′/H-6′ did not shift at all. The $[Rh(cod)\mathbf{3e}]^+$-complexes were synthesised with two different anions (**25** = PF_6^-, **26** = BF_4^-). Interestingly, both the ^{1}H and ^{13}C NMR spectra showed significant differences especially for the pyridine signals. All three pyridine protons H-3, H-5 and H-6 and the carbon atoms C-5 and C-6 of **26** were shifted downfield compared to **25**. The olefinic ^{13}C atoms of 1,5-cyclooctadiene coupled with ^{103}Rh giving rise to doublets ($^1J_{C,Rh}$ = 12.6−12.9 Hz) in both ^{13}C NMR spectra.

The Rh(I)-complex **27** (Scheme 8) derived from the oxazoline **23a** (75% yield) showed broad signals for all 1,5-cyclooctadiene carbons in the ^{13}C NMR spectrum, but long-range couplings between ^{103}Rh and ^{13}C atoms of the ligand were identified. The carboxylic and the methine carbons of the oxazoline ring gave rise to doublets ($^2J_{C,Rh}$ =

Scheme 7

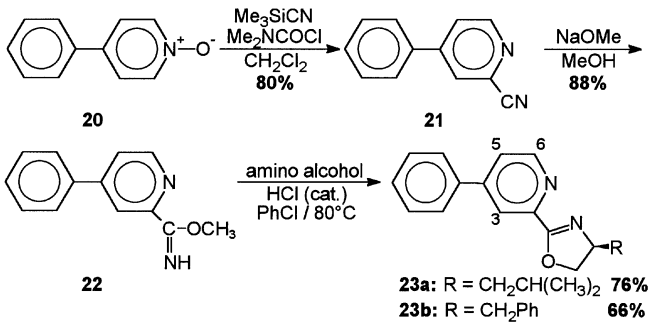

Scheme 8

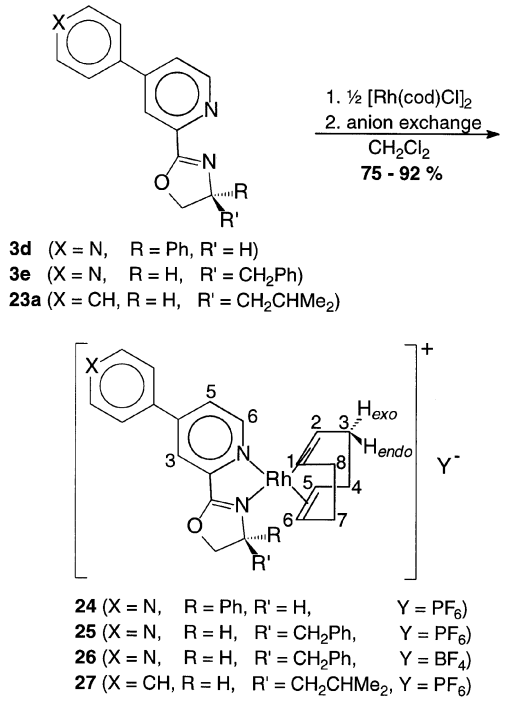

1.4 Hz and 2.1 Hz, respectively). Similarly, the pyridine carbons C-6, C-5 and C-3 appeared as doublets ($^2J_{C,Rh}$ = 0.6 Hz and $^3J_{C,Rh}$ = 0.9 Hz). Analogous couplings were not found for **25** and **26**.

By slow diffusion of ether into a $CHCl_3$ solution of **27** red needles suitable for an X-ray structure analysis were obtained. There are two independent species in the unit cell (Figure 1).

Figure 1. Molecular structure of the two different species in the unit cell of **27**

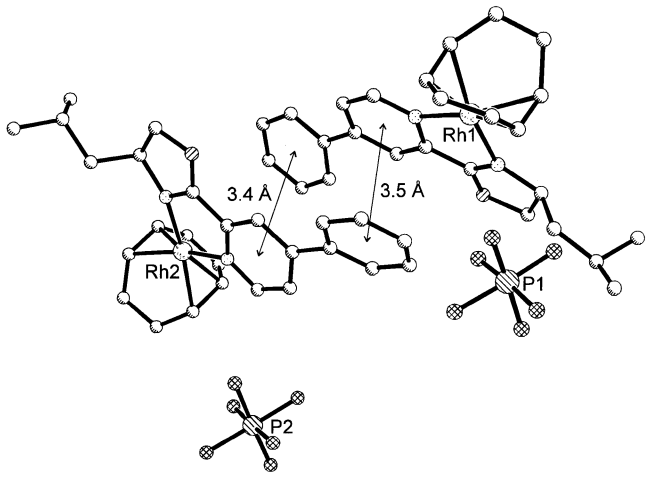

Both cations differ to some extent in the arrangement of the cod-ligands. The most interesting feature is the orientation of the two aromatic rings of both complexes. Each phenyl ring is oriented in a plane above the pyridine ring of the other cation and vice versa (arrows in Figure 1). The angles phenyl plane versus pyridine plane of the other cation are very small (2.7° and 6.7°, respectively). With 3.4−3.5 Å the distances of the aromatic rings are similar to that between graphite layers (3.35 Å). This π-stacking is probably amplified by charge-transfer interactions between the electron-rich phenyl and the electron-accepting pyridine ring.

Figure 2 shows the molecular structure of one of the cations of **27**, establishing the expected square planar coordination of rhodium by the two nitrogen atoms of ligand **23a** and the two double bonds of 1,5-cyclooctadiene. The (*S*)-configuration of the chiral carbon atom in the oxazoline ring was unequivocally proven. Selected bond lengths and angles are summarised in Table 1. For further details and the CSD number see Experimental Section.

Figure 2. Molecular structure of one of the cations of **27**[a]

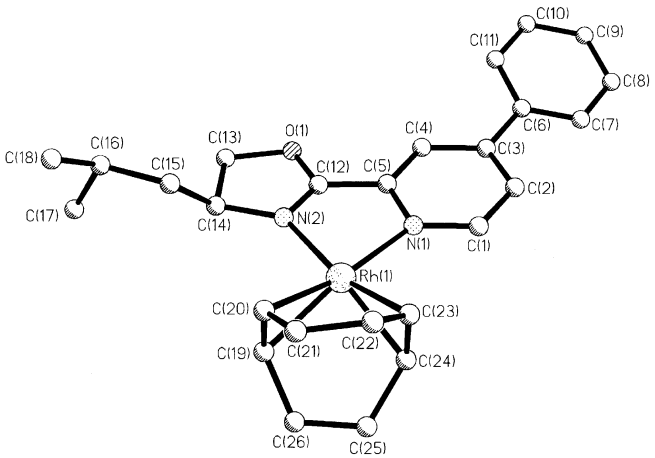

[a] Selected bond lengths [Å] and angles [°]: Rh1−N1 2.119, Rh1−N2 2.102, Rh1−(C23=C24)[b] 1.995, Rh1−(C19=C20)[b] 2.025, C23−C24 1.366, C19−C20 1.353, N2−C14 1.498, C14−C13 1.526, C13−O1 1.458, O1−C12 1.328 C12−C5 1.461, C12−N2 1.269; (C23=C24)-Rh1−(C19=C20)[b] 87.3, N1−Rh1−N2 79.4, Rh1−N1−C5 112.5, N1−C5−C12 113.8, C5−C12−N2 122.3, Rh1−N2−C12 111.8, N2−C12−O1 120.0, C12−O1−C13 104.7, O1−C13−C14 106.0, C13−C14−N2 102.2, C14−N2−C12 106.8, phenyl/pyridine (same cation) 20.7 and 27.1. − [b] C19=C20/C23=C24: statistical middle of the olefinic double bond.

Reaction of bisoxazoline **15** with $[Rh(cod)Cl]_2$ (2 equivalents of Rh) yielded the dinuclear complex **28** in 56% yield

Scheme 9

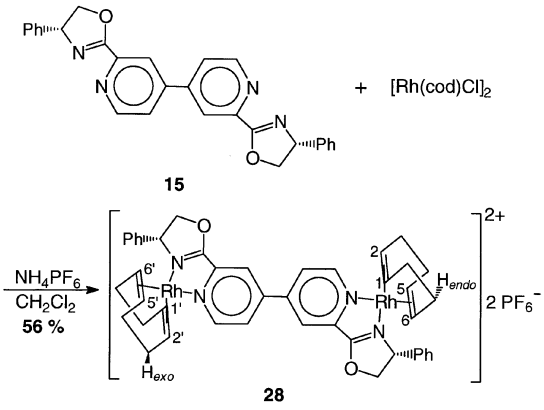

(Scheme 9). The symmetry introduced by the bridging of **15** between two Rh(cod) units showed up in the ^{1}H NMR spectrum of **28**, the signals of which were somewhat broadened (no sharpening even at −80°C, 250 MHz, CD_2Cl_2).

We thank the *Fonds der Chemischen Industrie* for providing a *Kekulé* scholarship for R.S. and for financial support.

Experimental Section

General: Chromatography: Merck silica gel 60 (63−200 mesh). − Melting points (not corrected): Büchi SMP 20 (open capillaries). − Elemental analyses: Microanalytical Laboratory, University of Regensburg. − ^{1}H/^{13}C NMR: Bruker AW-80 (80 MHz, T = 31°C), AC-250 (250/62.9 MHz, T = 24°C) and ARX-400 (400/100.6 MHz, T = 21°C), TMS or the solvent itself as internal standard. For optimal resolution some spectra were altered after acquisition using Bruker WIN NMR 5.0/5.1 software. The protons H-2′/H-6′ and H-3′/H-5′ in all 4,4′-bipyridine derivatives form AA′BB′ spin systems and were assigned as centred multiplets (AA′BB′). The two diastereotopic protons of the oxazoline CH_2 group are differentiated as H_Z and H_E (*cis* and *trans*, respectively, with regard to the methine proton). The abbreviations *qC* in the ^{13}C NMR data represent quarternary carbon atoms. − MS: Finnigan MAT 95 (FAB and FD), Finnigan MAT 311 A (EI, 70 eV). High-resolution mass spectra were recorded at the Max-Planck-Institut für medizinische Forschung in Heidelberg: VG Analytic ZAB 2E/70SE (FAB) and Joel JMS-SX102A (EI, 70 eV); the abbreviation K^+ represents the cationic species of salt like compounds. − IR: Beckman IR 4240 (solids as KBr pellets, liquids as films between NaCl plates); only characteristic bands are listed. − Optical rotation: Perkin-Elmer Polarimeter 241 (0.1 or 0.2 dm cuvettes).

Materials: Commercially available reagents were used without further purification. All anhydrous solvents were stored under nitrogen.

Abbreviations: cod = η^4-1,5-cyclooctadiene, *m*-NBA = *m*-nitrobenzyl alcohol, Ox = oxazoline, PE = petroleum ether (b.p. 40−60°C), TFA = trifluoroacetic acid.

4,4′-Bipyridine N-Oxide Hemihydrate (**5**): To a stirred solution of 10.0 g (64.0 mmol) of 4,4′-bipyridine (**4**) in $CHCl_3$ (200 ml) was added during 6 h a solution of 57−86% mcpba (12.9 g, max. 64.0 mmol) in $CHCl_3$ (500 ml). After 3 d four portions of mcpba (2.0 g each) in $CHCl_3$ (150 ml each) were added every 24 h. Stirring at r. t. was continued for a total of 17 d. The solution was reduced to ca. 30 ml and the mixture was separated by column chromatography (SiO_2, 20 × 5 cm). Elution with acetone yielded unreacted **4** (R_f = 0.5 [methanol]) and *m*-chlorobenzoic acid. After removing the acid by extracting a $CHCl_3$ solution with 2 N NaOH, 1.05 g (6.7 mmol, 10.5%) of 4,4′-bipyridine were reisolated. With an acetone/methanol gradient (4:1 → 3:1) the desired product **5** (R_f = 0.31 [methanol]) was obtained. Recrystallisation from acetone afforded 6.07 g (33.5 mmol, 55%) of **5**. Cream-coloured crystals, mp. 170°C (ref.[21]: 180°C, ref.[22]: 174−176°C). − ^{1}H NMR (250 MHz, D_2O): δ = 7.50 (AA′BB′, 2 H, H-3′, H-5′), 7.70 (AA′BB′, 2 H, H-3, H-5), 8.20 (AA′BB′, 2 H, H-2, H-6), 8.42 (AA′BB′, 2 H, H-2′, H-6′). − MS (EI): *m/z* (%) = 172 (100) [M^+], 156 (38) [M^+ − O], 155 (18), 116 (16), 90 (14), 89 (15), 63 (14), 51(14). − IR (KBr): $\tilde{\nu}$ (cm^{-1}) = 1250/1225 s (NO). − $C_{10}H_8N_2O$ Γ 1/2 H_2O (181.20): calcd. C 66.29, H 5.01, N 15.46; found C 66.11, H 5.22, N 15.15. With pure methanol as liquid phase 4.41 g (19.7 mmol, 31%) of 4,4′-bipyridine *N,N′*-dioxide **12** as the dihydrate were eluted (R_f = 0.1 [methanol]).

4,4′-Bipyridine-2-carbonitrile (**6**): 6.0 g (33.1 mmol) of **5** were dissolved under nitrogen in dry CH_2Cl_2 (70 ml). After adding 4.8 ml (38.4 mmol) of trimethylsilyl cyanide the solution was stirred for 5 min and then treated with 3.1 ml (33.7 mmol) of dimethylcarbamoyl chloride. Stirring at r. t. was continued for 2 d. The solvent was evaporated and the yellow residue treated with 10% aqueous K_2CO_3 (70 ml). The solid was sucked off and dried. Recrystallisation from acetone yielded 5.4 g (29.8 mmol, 90%) of **6**. White solid, m.p. 238−240°C. − ^{1}H NMR (250 MHz, [D_6]DMSO): δ = 7.93 (AA′BB′, 2 H, H-3′, H-5′), 8.21 (dd, ^3J = 5.2 Hz, ^4J = 1.9 Hz, 1 H, H-5), 8.57 (dd, ^4J = 1.9 Hz, ^5J = 0.9 Hz, 1 H, H-3), 8.78 (AA′BB′, 2 H, H-2′, H-6′), 8.90 (dd, ^3J = 5.2 Hz, ^5J = 0.9 Hz, 1 H, H-6). − ^{13}C NMR (100.6 MHz, [D_6]DMSO): δ = 117.6 (*C*N), 121.6 (C-3′, C-5′), 125.4/126.8 (C-3 and C-5), 133.8 (C-2), 142.6 (C-4), 146.2 (C-4′), 150.9 (C-2′, C-6′), 152.3 (C-6). − MS (EI): *m/z* (%) = 181 (100) [M^+], 180 (21), 57 (21). − IR (KBr): $\tilde{\nu}$ (cm^{-1}) = 2240 w (C≡N). − $C_{11}H_7N_3$ (181.20): calcd. C 72.92, H 3.89, N 23.19; found C 72.84, H 4.15, N 22.87.

If the crude product was purified by flash chromatography (SiO_2, 15 × 4.5 cm) with PE/acetone (1:1) 300 mg (1.5 mmol, 4.5%) of a side-product (R_f = 0.31 [acetone]) were obtained. It crystallised from ether and was characterised as *4,4′-bipyridine-2-carboxamide* (**7**). Colourless needles, m.p. 176−178°C. − ^{1}H NMR (250 MHz, $CDCl_3$): δ = 6.00 (br s, 1 H, N*H*H′), 7.61 (AA′BB′, 2 H, H-3′, H-5′), 7.71 (dd, ^3J = 5.1 Hz, ^4J = 1.9 Hz, 1 H, H-5), 7.92 (br s, 1 H, NH*H′*), 8.50 (dd, ^4J = 1.9 Hz, ^5J = 0.8 Hz, 1 H, H-3), 8.71 (dd, ^3J = 5.1 Hz, ^5J = 0.8 Hz, 1 H, H-6), 8.78 (AA′BB′, 2 H, H-2′, H-6′). − ^{13}C NMR (62.9 MHz, $CDCl_3$): δ = 120.3 (C-3 or C-5), 121.4 (C-3′, C-5′), 123.9 (C-5 or C-3), 144.7/147.2 (qC), 149.2 (C-6), 150.7 (qC), 150.8 (C-2′, C-6′), 166.3 (*C*=O). − MS (EI): *m/z* (%) = 199 (53) [M^+], calcd. for $C_{11}H_9N_3O$ 199.07456, found 199.07442, diff. −0.14 mmu/0.7 ppm, 157 (12), 156 (100) [M^+ − HNCO], 155 (41) [M^+ − $CONH_2$], 129 (16), 128 (14), 102 (11), 101 (11). − IR (KBr): $\tilde{\nu}$ (cm^{-1}) = 3415/3380/3290/3200 m (NH), 1795/1775/1690 s (C=O).

Methyl 4,4′-Bipyridine-2-carboximidate (**8**): 50 mg (2.2 mmol) of sodium were dissolved in dry methanol (35 ml) under nitrogen. Then 1.63 g (9.0 mmol) of **6** were added and allowed to react for 2 d at r. t. The suspension became finally a clear solution. After adding 0.1 ml (1.6 mmol) of acetic acid the solvent was evaporated. The residue was treated with warm ether (ca. 400 ml). Insoluble inorganic salts were removed by hot filtration. Cooling of the filtrate to −20°C afforded 1.74 g (8.2 mmol, 91%) of white crystals, m.p. 134−136°C. **8** is easily hydrolysed but can be stored for months if kept dry. − ^{1}H NMR (250 MHz, C_6D_6): δ = 3.94 (s, 3 H, C*H*$_3$), 6.76 (dd, ^3J = 5.1 Hz, ^4J = 1.9 Hz, 1 H, H-5), 6.78 (AA′BB′, 2 H, H-3′, H-5′), 7.86 (dd, ^4J = 1.9 Hz, ^5J = 0.9 Hz, 1 H, H-3), 8.33 (dd, ^3J = 5.1 Hz, ^5J = 0.9 Hz, 1 H, H-6), 8.53 (AA′BB′, 2 H, H-2′, H-6′), 9.98 (br s, 1 H, N*H*). − ^{13}C NMR (62.9 MHz, C_6D_6): δ = 53.7 (*C*H$_3$), 118.8 (C-3), 121.2 (C-3′, C-5′), 122.6 (C-5), 144.6/147.1/149.1 (qC), 150.1 (C-6), 151.1 (C-2′, C-6′), 166.2 (*C*=N). − MS (EI): *m/z* (%) = 213 (87) [M^+], 183 (15), 182 (83) [M^+ − OCH_3], 170 (17) [M^+ − CH_3 − CO], 157 (10), 156 (100) [M^+ − OCH_3 − CN], 155 (39) [M^+ − OCH_3 − HCN], 101 (13), 51 (11). − IR (KBr): $\tilde{\nu}$ (cm^{-1}) = 3310 w (NH), 1655 s (C=N), 1370 vs (CO). − $C_{12}H_{11}N_3O$ (213.24): calcd. C 67.59, H 5.67, N 19.71; found C 67.44, H 5.48, N 19.32.

General Procedure I (Preparation of Oxazolines): To a solution of **8** (2.3 g, 10.8 mmol) and 10.8 mmol of the amino alcohol in dry chlorobenzene (20 ml) one drop of conc. HCl was added and the solution was stirred at 80°C with a gentle stream of nitrogen bubbling through. After 47−68 h the cooled solution was directly purified by flash chromatography.

(+)-2-[4-(R)-Ethyloxazolin-2-yl]-4,4′-bipyridine (**3a**): Amino alcohol: 2-*(R)*-aminobutan-1-ol. 14 × 3.5 cm SiO_2 with PE/acetone (1:1) as eluent (R_f = 0.32 [acetone]). Recrystallisation from ether/PE yielded 1.83 g (7.2 mmol, 67%) of colourless crystals, m.p. 73−76°C. − ^{1}H NMR (250 MHz, $CDCl_3$): δ = 1.05 (t, ^3J = 7.4 Hz, 3 H, CH_3), 1.69 (″oct″, $^3J \approx$ 7.0 Hz, 1 H, CH_AH$_B$CH$_3$), 1.84 (m, 1 H, CH$_A$$H_BCH_3$), 4.18 (″t″, ^2J = ^3J = 8.1 Hz, 1 H, Ox-CH_ZH$_E$), 4.35 (m, 1 H, Ox-C*H*), 4.62 (dd, ^2J = 8.1 Hz, ^3J = 9.3 Hz, 1 H, Ox-CH$_Z$$H_E$), 7.60 (AA′BB′, 2 H, *H-3′, H-5′*), 7.64 (dd, ^3J = 5.1 Hz, ^4J = 1.8 Hz, 1 H, H-5), 8.32 (d, ^4J = 1.8 Hz, 1 H, H-3), 8.76 (AA′BB′, 2 H, H-2′, H-6′), 8.82 (d, ^3J = 5.1 Hz, 1 H, *H-6*). − ^{13}C NMR (62.9 MHz, $CDCl_3$): δ = 10.0 (*C*H$_3$), 28.5 (*C*H$_2$CH$_3$), 68.4 (Ox-*C*H), 72.9 (Ox-*C*H$_2$), 121.4 (C-3′, C-5′), 121.6 (C-3), 122.9 (C-5), 144.8/146.4/148.0 (qC), 150.5 (*C*-6), 150.8 (C-2′, C-6′), 162.4 (*C*=N). − MS (EI): *m/z* (%) = 253 (11) [M$^+$], 225 (28), 224 (100) [M$^+$ − C$_2$H$_5$], 208 (13), 196 (20), 182 (13), 169 (25), 155 (26). − IR (KBr): $\tilde{\nu}$ (cm^{-1}) = 3030 w, 2965/2930 m, 2870/2860 w (CH), 1640 s (C=N). − $C_{15}H_{15}N_3O$ (253.30): calcd. C 71.13, H 5.97, N 16.59; found C 70.76, H 6.06, N 16.40. − Optical rotation (*c* = 1.27, $CHCl_3$): [α]$^{21}_D$ = +36, [α]$^{21}_{578}$ = +38, [α]$^{21}_{546}$ = +45, [α]$^{21}_{436}$ = +94, [α]$^{21}_{365}$ = +197.

(−)-2-[4-(S)-Isopropyloxazolin-2-yl]-4,4′-bipyridine (**3b**): Amino alcohol: *(S)*-valinol. 12 × 3.5 cm SiO_2 with acetone as eluent (R_f = 0.32). Recrystallisation from ether/PE yielded a light yellow solid (70%), m.p. 76−78°C. − ^{1}H NMR (250 MHz, $CDCl_3$): δ = 0.98 (d, ^3J = 6.7 Hz, 3 H, CH_3), 1.08 (d, ^3J = 6.7 Hz, 3 H, CH_3′), 1.93 (″sept″, $^3J \approx$ 6.7 Hz, 1 H, C*H*Me$_2$), 4.16−4.30 (m, 2 H, Ox-CH_ZH$_E$ and Ox-C*H*?), 4.56 (m, 1 H, Ox-CH$_Z$$H_E$?), 7.60 (AA′BB′, 2 H, H-3′, H-5′), 7.64 (dd, ^3J = 5.1 Hz, ^4J = 1.7 Hz, 1 H, H-5), 8.33 (d, ^4J = 1.7 Hz, 1 H, *H-3*), 8.76 (AA′BB′, 2 H, H-2′, H-6′), 8.82 (d, ^3J = 5.1 Hz, 1 H, H-6). − ^{13}C NMR (62.9 MHz, $CDCl_3$): δ = 18.2 (*C*H$_3$), 19.0 (*C*H$_3$′), 32.8 (*C*HMe$_2$), 70.9 (Ox-*C*H$_2$), 73.2 (Ox-*C*H), 121.4 (C-3′, C-5′), 121.7 (C-3), 123.0 (C-5), 144.9/146.4/148.1 (qC), 150.6 (C-6), 150.8 (C-2′, C-6′), 162.4 (*C*=N). − MS (EI): *m/z* (%) = 267 (7) [M$^+$], 225 (21), 224 (100) [M$^+$-C$_3$H$_7$], 223 (23), 196 (17), 169 (21), 156 (11), 155 (22), 43 (10) [C$_3$H$_7^+$]. − IR (KBr): $\tilde{\nu}$ (cm^{-1}) = 3040 w, 2980 m, 2960 s, 2930/2910/2870 m (CH), 1645 s (C=N). − $C_{16}H_{17}N_3O$ (267.33): calcd. C 71.89, H 6.41, N 15.72; found C 71.78, H 6.63, N 15.55. − Optical rotation (*c* = 1.24, $CHCl_3$): [α]$^{20}_D$ = −29, [α]$^{20}_{578}$ = −30, [α]$^{20}_{546}$ = −34, [α]$^{20}_{436}$ = −73, [α]$^{20}_{365}$ = −155.

(−)-2-[4-(S)-(2-Methylpropyl)oxazolin-2-yl]-4,4′-bipyridine (**3c**): Amino alcohol: *(S)*-leucinol. Flash chromatography on SiO_2 (15 × 3.5 cm) with PE/acetone (1:1) as eluent (R_f = 0.32 [acetone]) yielded a yellow oil (73%), which neither crystallised nor could be distilled without decomposition. − ^{1}H NMR (250 MHz, $CDCl_3$): δ = 0.99 (d, $^3J \approx$ 6.0 Hz, 3 H, CH_3), 1.01 (d, ^3J = 6.5 Hz, 3 H, CH_3′), 1.44 (″dt″, ^2J = 13.3 Hz, $^3J \approx$ 7.1 Hz, 1 H, CH_AH$_B$CHMe$_2$), 1.78 (″dt″, ^2J = 13.3 Hz, $^3J \approx$ 6.6 Hz, 1 H, CH$_A$$H_B$CHMe$_2$), 1.90 (″sept″, $^3J \approx$ 6.6 Hz, 1 H, C*H*Me$_2$), 4.12 (″t″, ^2J = ^3J = 8.1 Hz, 1 H, Ox-CH_ZH$_E$), 4.44 (m, 1 H, Ox-C*H*), 4.65 (dd, ^2J = 8.1 Hz, ^3J = 9.4 Hz, 1 H, Ox-CH$_Z$$H_E$), 7.60 (AA′BB′, 2 H, H-3′, H-5′), 7.65 (dd, ^3J = 5.2 Hz, ^4J = 1.7 Hz, 1 H, H-5), 8.32 (d, ^4J = 1.7 Hz, 1 H, H-3), 8.76 (AA′BB′, 2 H, H-2′, H-6′), 8.82 (d, ^3J = 5.2 Hz, 1 H, H-6). − ^{13}C NMR (62.9 MHz, $CDCl_3$): δ = 22.69 (*C*H$_3$), 22.71 (*C*H$_3$′), 25.4 (*C*HMe$_2$), 45.5 (*C*H$_2$CHMe$_2$), 65.6 (Ox-*C*H), 73.8 (Ox-*C*H$_2$), 121.4 (C-3′, C-5′), 121.6 (C-3), 122.9 (C-5), 144.8/146.4/148.1 (qC), 150.5 (C-6), 150.7 (C-2′, C-6′), 162.2 (*C*=N). − MS (EI): *m/z* (%) = 281 (35) [M$^+$], 238 (24) [M$^+$ − C$_3$H$_7$], 225 (27), 224 (79) [M$^+$ − C$_4$H$_9$], 196 (26), 183 (21), 182 (33), 181 (46), 180 (60), 170 (36), 169 (25), 165 (45), 156 (54), 155 (62), 98 (26), 84 (68), 71 (28), 57 (100) [C$_4$H$_9^+$], 56 (22), 55 (26), 43 (45), 42 (30), 41 (57). − IR (film): $\tilde{\nu}$ (cm^{-1}) = 3030 w, 2975/2930 m, 2870 w (CH), 1645 m (C=N). − $C_{17}H_{19}N_3O$ (281.36): calcd. C 72.57, H 6.81, N 14.93; found C 71.89, H 7.06, N 14.86. − Optical rotation (*c* = 1.6, $CHCl_3$): [α]$^{20}_D$ = −39, [α]$^{20}_{578}$ = −40, [α]$^{20}_{546}$ = −48, [α]$^{20}_{436}$ = −100, [α]$^{20}_{365}$ = −208.

(−)-2-[4-(R)-Phenyloxazolin-2-yl]-4,4′-bipyridine (**3d**): Amino alcohol: *(R)*-α-phenylglycinol. 15 × 3.5 cm SiO_2 with PE/acetone (1:1) as eluent (R_f = 0.35 [acetone]). Recrystallisation from ether yielded a white foam (80%), m.p. 52−55°C. − ^{1}H NMR (250 MHz, $CDCl_3$): δ = 4.44 (″t″, ^2J = $^3J \approx$ 8.6 Hz, 1 H, Ox-CH_ZH$_E$), 4.94 (dd, ^2J = 8.7 Hz, ^3J = 10.2 Hz, 1 H, Ox-CH$_Z$$H_E$), 5.50 (dd, ^3J = 8.5 Hz, ^3J = 10.2 Hz, 1 H, Ox-C*H*), 7.27−7.41 (m, 5 H, Ph-*H*), 7.59 (AA′BB′, 2 H, H-3′, H-5′), 7.67 (dd, ^3J = 5.1 Hz, ^4J = 1.8 Hz, 1 H, H-5), 8.45 (dd, ^4J = 1.8 Hz, ^5J = 0.7 Hz, 1 H, H-3), 8.75 (AA′BB′, 2 H, H-2′, H-6′), 8.85 (dd, ^3J = 5.1 Hz, ^5J = 0.7 Hz, 1 H, H-6). − ^{13}C NMR (62.9 MHz, $CDCl_3$): δ = 70.5 (Ox-*C*H), 75.4 (Ox-*C*H$_2$), 121.4 (*C-3′*, *C-5′*), 122.0 (*C-3*), 123.2 (*C-5*), 126.8 (*o*- or *m*-Ph-*C*), 127.8 (*p*-Ph-*C*), 128.8 (*m*- or *o*-Ph-*C*), 141.6 (qC of Ph), 144.7/146.5/147.8 (qC), 150.6 (C-6), 150.8 (C-2′, C-6′), 163.7 (*C*=N). − MS (EI): *m/z* (%) = 301 (100) [M$^+$], 272 (25), 271 (96) [M$^+$ − CH$_2$O], 156 (44), 155 (36), 118 (36), 91 (22), 90 (31), 89 (32). − IR (KBr): $\tilde{\nu}$ (cm^{-1}) = 3055/3025/2980/2890 w (CH), 1650 s (C=N). − $C_{19}H_{15}N_3O$ (301.35): calcd. C 75.73, H 5.02, N 13.94; found C 75.28, H 5.24, N 13.81. − Optical rotation (*c* = 1.27, $CHCl_3$): [α]$^{22}_D$ = −52, [α]$^{22}_{578}$ = −54, [α]$^{22}_{546}$ = −63, [α]$^{22}_{436}$ = −107, [α]$^{22}_{365}$ = −156.

(+)-2-[4-(S)-Benzyloxazolin-2-yl]-4,4′-bipyridine (**3e**): Amino alcohol: *(S)*-phenylalaninol. 8 × 3.5 cm SiO_2 with ethyl acetate/acetone (1:1) as eluent (R_f = 0.39 [acetone]). Recrystallisation from ether yielded a white solid (83%), m.p. 95−98°C. − ^{1}H NMR (250 MHz, $CDCl_3$): δ = 2.79 (dd, ^2J = 13.8 Hz, ^3J = 9.0 Hz, 1 H, CH_AH$_B$Ph), 3.32 (dd, ^2J = 13.8 Hz, ^3J = 4.9 Hz, 1 H, CH$_A$$H_B$Ph), 4.27 (dd, ^2J = 8.6 Hz, ^3J = 7.8 Hz, 1 H, Ox-CH_ZH$_E$), 4.49 (dd, ^2J = 8.6, ^3J = 9.4 Hz, 1 H, Ox-CH$_Z$$H_E$), 4.71 (dddd, ^3J = 9.4 Hz, ^3J = 9.0 Hz, ^3J = 7.8 Hz, ^3J = 4.9 Hz, 1 H, Ox-C*H*), 7.21−7.35 (m, 5 H, Ph-*H*), 7.59 (AA′BB′, 2 H, H-3′, H-5′), 7.64 (dd, ^3J = 5.1 Hz, ^4J = 1.8 Hz, 1 H, H-5), 8.33 (d, ^4J = 1.8 Hz, 1 H, H-3), 8.76 (AA′BB′, 2 H, H-2′, H-6′), 8.83 (d, ^3J = 5.1 Hz, 1 H, H-6). − ^{13}C NMR (62.9 MHz, $CDCl_3$): δ = 41.7 (*C*H$_2$Ph), 68.2 (Ox-*C*H), 72.7 (Ox-*C*H$_2$), 121.4 (C-3′, C-5′), 121.7 (C-3), 123.1 (C-5), 126.6 (*p*-Ph-*C*), 128.6/129.2 (*o*- and *m*-Ph-*C*), 137.7 (qC of Ph), 144.8/146.5/147.9 (qC), 150.6 (C-6), 150.8 (C-2′, C-6′), 162.9 (*C*=N). − MS (EI): *m/z* (%) = 315 (10) [M$^+$], 225 (16), 224 (100) [M$^+$ − CH$_2$Ph], 196 (16), 169 (19), 155 (18), 91 (12) [PhCH$_2^+$]. − IR (KBr): $\tilde{\nu}$ (cm^{-1}) = 3030 m, 2985/2920/2880 w (CH), 1635 s (C=N). − $C_{20}H_{17}N_3O$ (315.37): calcd. C 76.17, H 5.43, N 13.32; found C 76.13, H 5.75, N 13.24. − Optical rotation (*c* = 1.26, $CHCl_3$): [α]$^{20}_D$ = +30, [α]$^{20}_{578}$ = +33, [α]$^{20}_{546}$ = +36, [α]$^{20}_{436}$ = +69, [α]$^{20}_{365}$ = +132.

(−)-2-[4-(S)-tert-Butyloxazolin-2-yl]-4,4′-bipyridine (**3f**): Amino alcohol: *(S)*-*tert*-leucinol. 11.5 × 2.5 cm SiO_2 with PE/acetone (3:2) as eluent (R_f = 0.09). Stirring in PE/ether and filtration gave a white solid (76%), m.p. 98−99°C. − ^{1}H NMR (250 MHz, C_6D_6): δ = 0.90 (s, 9 H, CH_3), 3.90 (dd, ^2J = 7.8 Hz, ^3J = 10.8 Hz, 1 H, Ox-CH_EH$_Z$?), 4.041 (d, ^2J = 7.8 Hz, 1 H, Ox-CH$_E$$H_Z$?), 4.044 (d, ^3J = 10.8 Hz, 1 H, Ox-C*H*?), 6.73 (AA′BB′, 2 H, H-3′, H-5′), 6.77 (dd, ^3J = 5.2 Hz, ^4J = 2.0 Hz, 1 H, H-5), 8.42 (dd, ^4J = 2.0 Hz, ^5J = 0.8 Hz, 1 H, H-3), 8.48 (AA′BB′, 2 H, H-2′, H-6′), 8.50 (dd, ^3J = 5.2 Hz, ^5J = 0.8 Hz, 1 H, H-6). − ^{13}C NMR (62.9 MHz, $CDCl_3$): δ = 26.0 (*C*H$_3$), 34.0 (*C*Me$_3$), 69.4 (Ox-*C*H$_2$), 76.7 (Ox-*C*H), 121.4 (C-3′, C-5′), 121.7 (C-3), 122.9 (C-5), 144.9/146.4/148.1 (qC), 150.5 (C-6), 150.7 (C-2′, C-6′), 162.2 (*C*=N). − MS (EI): *m/z* (%) = 281 (3) [M$^+$], 225 (100) [M$^+$ − C$_4$H$_8$], 224 (78) [M$^+$ −

C_4H_9], 223 (35), 196 (33), 170 (10), 169 (25), 156 (44), 155 (61), 57 (20) [$C_4H_9^+$], 41 (17). − IR (KBr): $\tilde{\nu}$ (cm^{-1}) = 3060 w, 2960/2950 m, 2905/2865 w (CH), 1665/1645 m (C=N). − $C_{17}H_{19}N_3O$ (281.36): calcd. C 72.57, H 6.81, N 14.93; found C 72.22, H 6.42, N 14.44. − Optical rotation (c = 1.1, $CHCl_3$): $[\alpha]^{20}_D$ = −30, $[\alpha]^{20}_{578}$ = −32, $[\alpha]^{20}_{546}$ = −38, $[\alpha]^{20}_{436}$ = −79, $[\alpha]^{20}_{365}$ = −156.

(+)-N-[2-(R)-(1-Hydroxybutyl)]-4,4′-bipyridine-2-carboxamide (**9**): 2.03 g (9.5 mmol) of **8** and 0.9 ml (9.5 mmol) of 2-*(R)*-aminobutan-1-ol were heated to 80°C in dry chlorobenzene (15 ml) for 66 h. After cooling the solvent was removed. The residue was treated with ether (30 ml) and extracted with 2 N HCl (2× 5 ml). Almost all the substance was transferred into the aqueous layer, which then was alkalised with 2 N NaOH. After extraction with $CHCl_3$ (3× 20 ml) the organic layer was dried over $MgSO_4$ and the solvent evaporated. Recrystallisation from cyclohexane/acetone afforded 910 mg (3.4 mmol, 35%) of **9**. Colourless crystals, m.p. 117−119°C. − ^{1}H NMR (250 MHz, $CDCl_3$): δ = 1.04 (t, ^3J = 7.4 Hz, 3 H, CH_3), 1.55−1.86 (m, 2 H, CH_2CH$_3$), 3.69−3.86 (br s, 1 H, OH), 3.73 (dd, ^2J = 11.1 Hz, ^3J = 5.5 Hz, 1 H, CH_AH$_B$), 4.01−4.15 (m, 1 H, CH), 3.82 (dd, ^2J = 11.1 Hz, ^3J = 4.0 Hz, 1 H, CH$_A$$H_B$), 7.53 (AA′BB′, 2 H, H-3′, H-5′), 7.60 (dd, ^3J = 5.1 Hz, ^4J = 1.7 Hz, 1 H, H-5), 8.18 (d, ^3J = 8.2 Hz, 1 H, NH), 8.38 (d, ^4J = 1.7 Hz, 1 H, H-3), 8.60 (d, ^3J = 5.1 Hz, 1 H, H-6), 8.69 (AA′BB′, 2 H, *H-2′*, *H-6′*). − ^{13}C NMR (62.9 MHz, $CDCl_3$): δ = 10.6 (*C*H$_3$), 24.3 (*C*H$_2$CH$_3$), 53.7 (*C*H), 65.0 (*C*H$_2$OH), 120.0 (C-3), 121.3 (C-3′, C-5′), 123.5 (C-5), 144.8/147.0 (qC), 149.0 (C-6), 150.7 (C-2′, C-6′), 151.0 (qC), 164.4 (*C*=O). − MS (EI): *m/z* (%) = 271 (1) [M^+], 241 (32) [M^+ − CH_2O], 240 (100) [M^+ − CH_2OH], 183 (12), 156 (26), 155 (86). − IR (KBr): $\tilde{\nu}$ (cm^{-1}) = 3450/3390/3345/3270 m (OH, NH), 2960/2930 m, 2880 w (CH), 1670 s (C=O). − $C_{15}H_{17}N_3O_2$ (271.32): calcd. C 66.40, H 6.32, N 15.49; found C 65.87, H 6.36, N 15.19. − Optical rotation (c = 0.16, $CHCl_3$): $[\alpha]^{22}_D$ = +45, $[\alpha]^{26}_{578}$ = +53, $[\alpha]^{26}_{546}$ = +64, $[\alpha]^{26}_{436}$ = +103, $[\alpha]^{26}_{365}$ = +138.

General Procedure II (N′-Methylation): 2.6 mmol of 2-(4,4′-bipyridin-2-yl)oxazoline (**3**) were dissolved in dry THF (30 ml) under nitrogen. After adding 3.0 ml (48.0 mmol) of methyl iodide the light-protected solution was stirred for 63−90 h at r. t. The resulting reddish precipitate was collected and washed with dry ether (3 × 5 ml). The red side-product was removed by dissolving the precipitate in dry methanol and adding dry ether till an appearing cloudiness just faded. After cooling (−20°C) only the side-product crystallised and was filtered off. Dry ether (5−15 ml) was added to the resulting filtrate and after cooling to −20°C the pure, hygroscopic product **1** was obtained.

(+)-N′-Methyl-2-[4-(R)-ethyloxazolin-2-yl]-4,4′-bipyridinium Iodide (**1a**): From oxazoline **3a**. Orange solid (51%), m.p. > 68°C (dec.). − ^{1}H NMR (250 MHz, CD_3OD): δ = 1.04 (t, ^3J = 7.4 Hz, 3 H, CH$_2$CH_3), 1.61−1.88 (m, 2 H, CH_2CH$_3$), 4.27 (″t″, ^2J = ^3J = 7.9 Hz, 1 H, Ox-CH_ZH$_E$), 4.29−4.44 (m, 1 H, Ox-CH), 4.51 (s, 3 H, N-CH_3), 4.69 (dd, ^2J = 7.9 Hz, ^3J = 9.2 Hz, 1 H, Ox-CH$_Z$$H_E$), 8.13 (dd, ^3J = 5.2 Hz, ^4J = 1.9 Hz, 1 H, H-5), 8.53 (dd, ^4J = 1.9 Hz, ^5J = 0.9 Hz, 1 H, H-3), 8.55 (AA′BB′, 2 H, H-3′, H-5′), 8.91 (dd, ^3J = 5.2 Hz, ^5J = 0.9 Hz, 1 H, H-6), 9.10 (AA′BB′, 2 H, H-2′, H-6′). − ^{13}C NMR (62.9 MHz, CD_3OD): δ = 10.1 (CH$_2$*C*H$_3$), 29.4 (*C*H$_2$CH$_3$), 49.0 (N-*C*H$_3$), 69.3 (Ox-*C*H), 74.4 (Ox-*C*H$_2$), 123.3 (C-3), 125.5 (C-5), 127.1 (C-3′, C-5′), 144.4 (qC), 147.6 (C-2′, C-6′), 149.1 (qC), 152.2 (C-6), 154.2 (qC), 164.1 (*C*=N). − MS (FAB, MeOH/glycerol): *m/z* = 663 [2 K^+ + I^-], 268 [K^+]. − IR (KBr): $\tilde{\nu}$ (cm^{-1}) = 3030/2960/2930 m, 2875 w (CH), 1645 s (C=N). − $C_{16}H_{18}IN_3O$ • 1/2 H_2O (404.25): calcd. C 47.54, H 4.74, N 10.39; found C 47.79, H 5.12, N 9.97. Optical rotation (c = 2.2, MeOH): $[\alpha]^{22}_D$ = +25, $[\alpha]^{22}_{578}$ = +26, $[\alpha]^{22}_{546}$ = +31.

(−)-N′-Methyl-2-[4-(S)-isopropyloxazolin-2-yl]-4,4′-bipyridinium Iodide (**1b**): From oxazoline **3b**. Orange solid (53%), m.p. > 130°C (dec.). − ^{1}H NMR (250 MHz, CD_3OD): δ = 0.99 (d, ^3J = 6.7 Hz, 3 H, CH_3), 1.08 (d, ^3J = 6.7 Hz, 3 H, CH_3′), 1.92 (m, 1 H, C*H*Me$_2$), 4.22−4.33 (m, 1 H, Ox-C*H*), 4.37 (″t″, ^2J = ^3J = 8.3 Hz, 1 H, Ox-CH_ZH$_E$), 4.51 (s, 3 H, N-CH_3), 4.63 (dd, ^2J = 8.3 Hz, ^3J = 9.6 Hz, 1 H, Ox-CH$_Z$$H_E$), 8.14 (dd, ^3J = 5.2 Hz, ^4J = 2.0 Hz, 1 H, H-5), 8.53 (dd, ^4J = 2.0 Hz, ^5J = 0.8 Hz, 1 H, H-3), 8.55 (AA′BB′, 2 H, H-3′, H-5′), 8.91 (dd, ^3J = 5.2 Hz, ^5J = 0.8 Hz, 1 H, H-6), 9.11 (AA′BB′, 2 H, H-2′, H-6′). − ^{13}C NMR (62.9 MHz, CD_3OD): δ = 18.5 (*C*H$_3$), 19.0 (*C*H$_3$′), 33.9 (*C*HMe$_2$), 49.0 (N-*C*H$_3$), 72.4 (Ox-*C*H$_2$), 73.9 (Ox-*C*H), 123.3 (C-3), 125.5 (C-5), 127.1 (C-3′, C-5′), 144.4 (qC), 147.6 (C-2′, C-6′), 149.1 (qC), 152.2 (C-6), 154.2 (qC), 164.1 (*C*=N). − MS (FAB, MeOH/glycerol): *m/z* = 282 [K^+]. − IR (KBr): $\tilde{\nu}$ (cm^{-1}) = 3020/2960 m, 2870 w (CH), 1645 s (C=N). − $C_{17}H_{20}IN_3O$ • 2 H_2O (445.30): calcd. C 45.85, H 5.43, N 9.44; found C 45.98, H 5.12, N 8.91. − Optical rotation (c = 2.2, MeOH): $[\alpha]^{22}_D$ = −23, $[\alpha]^{22}_{578}$ = −24, $[\alpha]^{22}_{546}$ = −28.

(−)-N′-Methyl-2-[4-(S)-(2-methylpropyl)oxazolin-2-yl]-4,4′-bipyridinium Iodide (**1c**): From oxazoline **3c**. Orange solid (50%), m.p. > 85°C (dec.). − ^{1}H NMR (250 MHz, CD_3OD): δ = 1.00 (d, ^3J = 6.6 Hz, 3 H, CH_3), 1.02 (d, ^3J = 6.6 Hz, 3 H, CH_3′), 1.48 (″dt″, ^2J = 13.3 Hz, ^3J = 7.3 Hz, 1 H, CH_AH$_B$CHMe$_2$), 1.78 (″dt″, ^2J = 13.3 Hz, ^3J = 6.6 Hz, 1 H, CH$_A$$H_B$CHMe$_2$), 1.89 (″sept″, ^3J = 6.6 Hz, 1 H, C*H*Me$_2$), 4.19 (″t″, ^2J = ^3J = 8.1 Hz, 1 H, Ox-CH_ZH$_E$), 4.41−4.56 (m, 1 H, Ox-C*H*), 4.51 (s, 3 H, N-CH_3), 4.73 (dd, ^2J = 8.1 Hz, ^3J = 9.5 Hz, 1 H, Ox-CH$_Z$$H_E$), 8.13 (dd, ^3J = 5.2 Hz, ^4J = 2.0 Hz, 1 H, H-5), 8.53 (dd, ^4J = 2.0 Hz, ^5J = 0.8 Hz, 1 H, H-3), 8.55 (AA′BB′, 2 H, H-3′, H-5′), 8.90 (dd, ^3J = 5.2 Hz, ^5J = 0.8 Hz, 1 H, H-6), 9.10 (AA′BB′, 2 H, H-2′, H-6′). − ^{13}C NMR (62.9 MHz, CD_3OD): δ = 23.1 (*C*H$_3$), 23.2 (*C*H$_3$′), 26.5 (*C*HMe$_2$), 46.5 (*C*H$_2$CHMe$_2$), 49.0 (N-*C*H$_3$), 66.5 (Ox-*C*H), 75.4 (Ox-*C*H$_2$), 123.3 (C-3), 125.5 (C-5), 127.1 (C-3′, C-5′), 144.4 (qC), 147.6 (C-2′, C-6′), 149.1 (qC), 152.2 (C-6), 154.2 (qC), 163.9 (*C*=N). − MS (FAB, MeOH/glycerol): *m/z* = 719 [2K^+ + I^-], 424 [MH^+], 268 [K^+]. − IR (KBr): $\tilde{\nu}$ (cm^{-1}) = 3020 m, 2950 s, 2865 m (CH), 1645 s (C=N). − $C_{18}H_{22}IN_3O$ • H_2O (441.32): calcd. C 48.98, H 5.48, N 9.52; found C 49.24, H 5.46, N 9.61. − Optical rotation (c = 2.2, MeOH): $[\alpha]^{22}_D$ = −31, $[\alpha]^{22}_{578}$ = −32, $[\alpha]^{22}_{546}$ = −36.

(−)-N′-Methyl-2-[4-(R)-phenyloxazolin-2-yl]-4,4′-bipyridinium Iodide (**1d**): From oxazoline **3d**. Orange solid (63%), m.p. > 135°C (dec.). − ^{1}H NMR (250 MHz, CD_3OD): δ = 4.40 (″t″, ^2J = ^3J ≈ 8.5 Hz, 1 H, Ox-CH_ZH$_E$), 4.50 (s, 3 H, N-CH_3), 5.03 (dd, ^2J = 8.7 Hz, ^3J = 10.3 Hz, 1 H, Ox-CH$_Z$$H_E$), 5.54 (dd, ^3J = 8.3 Hz, ^3J = 10.3 Hz, 1 H, Ox-C*H*), 7.29−7.38 (m, 5 H, Ph-*H*), 8.15 (dd, ^3J = 5.2 Hz, ^4J = 2.0 Hz, 1 H, H-5), 8.54 (AA′BB′, 2 H, H-3′, H-5′), 8.58 (dd, ^4J = 2.0 Hz, ^5J = 0.8 Hz, 1 H, *H-3*), 8.93 (dd, ^3J = 5.2 Hz, ^5J = 0.8 Hz, 1 H, H-6), 9.09 (AA′BB′, 2 H, H-2′, H-6′). − ^{13}C NMR (62.9 MHz, CD_3OD): δ = 49.1 (N-*C*H$_3$), 71.3 (Ox-*C*H), 77.1 (Ox-*C*H$_2$), 123.6 (C-3), 125.8 (C-5), 127.1 (C-3′, C-5′), 128.0 (*o*- or *m*-Ph-*C*), 129.0 (*p*-Ph-*C*), 130.0 (*m*- or *o*-Ph-*C*), 143.0 (qC of Ph), 144.4 (qC), 147.6 (C-2′, C-6′), 148.9 (qC), 152.4 (C-6), 154.1 (qC), 165.2 (*C*=N). − MS (FAB, MeOH/glycerol): *m/z* = 316 [K^+]. − IR (KBr): $\tilde{\nu}$ (cm^{-1}) = 3020 m (CH), 1645 s (C=N). − $C_{20}H_{18}IN_3O$ • H_2O (461.31): calcd. C 52.07, H 4.37, N 9.11; found C 52.08, H 4.55, N 8.96. − Optical rotation (c = 2.2, MeOH): $[\alpha]^{22}_D$ = −15, $[\alpha]^{22}_{578}$ = −17, $[\alpha]^{22}_{546}$ = −19.

In this case the red side-product was recrystallised from aqueous acetone/methanol to give dark-red tetrahedra, m.p. > 215°C (dec.), which were characterised as *N′,N″-dimethyl-2-[4-(R)-phenylox-*

azolinium-2-yl]-4,4′-bipyridinium Diiodide (**10**). − ^{1}H NMR (400 MHz, D_2O): δ = 3.14 (s, 3 H, Ox-N-CH_3), 4.40 (s, 3 H, N′-CH_3), 5.16 (dd, ^2J = 14.4 Hz, ^3J = 3.9 Hz, 1 H, Ox-CH_ZH$_E$), 5.40 (dd, ^2J = 14.4 Hz, ^3J = 4.7 Hz, 1 H, Ox-CH$_Z$$H_E$), 5.48 (″t″, $^3J \approx$ 4.3 Hz, 1 H, Ox-C*H*), 7.19−7.22 (m, 2 H, *o*-Ph-*H*), 7.30−7.36 (m, 3 H, *m*- and *p*-Ph-*H*), 8.47 (AA′BB′, 2 H, H-3′, H-5′), 8.55 (dd, ^3J = 6.3 Hz, ^4J = 2.4 Hz, 1 H, H-5), 8.90 (d, ^3J = 5.2 Hz, 1 H, H-6), 8.97 (AA′BB′, 2 H, H-2′, H-6′), 9.09 (d, ^4J = 2.4 Hz, 1 H, H-3). − ^{13}C NMR (100.6 MHz, D_2O): δ = 34.5 (Ox-N-*C*H$_3$), 48.7 (N′-*C*H$_3$), 58.8 (Ox-*C*H), 59.1 (Ox-*C*H$_2$), 126.7 (*o*-Ph-*C*), 126.9 (C-3), 127.0 (C-3′, C-5′), 129.2 (C-5), 129.6 (*p*-Ph-*C*), 129.7 (*m*-Ph-*C*), 133.7/141.9 (qC), 146.3 (C-6), 146.6 (C-2′, C-6′), 149.2/152.3 (qC), 156.7 (*C*=N). − MS (FAB, H_2O/glycerol)[34]: *m/z* = 332 (weak) [KH$^+$], 331 [K$^+$], 165.5 = 331/2 (very weak) [K^{++}]. − IR (KBr): $\tilde{\nu}$ (cm^{-1}) = 3060/2990 w (CH), 1675 s (C=N). − $C_{21}H_{21}I_2N_3O$ • 2H_2O (621.26): calcd. C 40.60, H 4.06, N 6.76; found C 40.71, H 4.32, N 6.53.

(+)-N′-Methyl-2-[4-(S)-benzyloxazolin-2-yl]-4,4′-bipyridinium Iodide (**1e**): 1.3 g (4.1 mmol) of **3e** and 5.0 ml (80.0 mmol) of methyl iodide in dry THF (50 ml) were stirred at r. t. for 40 h under nitrogen. The precipitated orange solid was filtered off and washed with dry ether (2× 10 ml). After recrystallisation from methanol/ether at −20°C 1.84 g (4.0 mmol, 98%) of pure **1e** were obtained. Light orange solid, m.p. > 165°C (dec.). − ^{1}H NMR (250 MHz, CD_3OD): δ = 2.92 (dd, ^2J = 13.7 Hz, ^3J = 7.1 Hz, 1 H, CH_AH$_B$Ph), 3.11 (dd, ^2J = 13.7 Hz, ^3J = 5.9 Hz, 1 H, CH$_A$$H_B$Ph), 4.33 (dd, ^2J = 8.5 Hz, ^3J = 7.5 Hz, 1 H, Ox-CH_ZH$_E$), 4.48 (s, 3 H, N-CH_3), 4.58 (dd, ^2J = 8.5 Hz, ^3J = 9.5 Hz, 1 H, Ox-CH$_Z$$H_E$), 4.75 (m, 1 H, Ox-C*H*), 7.15−7.33 (m, 5 H, Ph-*H*), 8.11 (dd, ^3J = 5.2 Hz, ^4J = 2.0 Hz, 1 H, H-5), 8.48 (dd, ^4J = 2.0 Hz, ^5J = 0.8 Hz, 1 H, H-3), 8.51 (AA′BB′, 2 H, H-3′, H-5′), 8.89 (dd, ^3J = 5.2 Hz, ^5J = 0.8 Hz, 1 H, H-6), 9.08 (AA′BB′, 2 H, H-2′, H-6′). − ^{13}C NMR (62.9 MHz, CD_3OD): δ = 42.2 (*C*H$_2$Ph), 49.0 (N-*C*H$_3$), 69.0 (Ox-*C*H), 74.0 (Ox-*C*H$_2$), 123.3 (C-3), 125.6 (C-5), 127.1 (C-3′, C-5′), 127.7 (*p*-Ph-*C*), 129.6/130.6 (*o*- and *m*-Ph-*C*), 138.9 (qC of Ph), 144.3 (qC), 147.6 (C-2′, C-6′), 149.0 (qC), 152.2 (C-6), 154.2 (qC), 164.4 (*C*=N). − MS (FAB, H_2O/glycerol): *m/z* = 787 [2K$^+$ + I$^-$], 330 [K$^+$]. − IR (KBr): $\tilde{\nu}$ (cm^{-1}) = 3020 m (CH), 1645 s (C=N). − $C_{21}H_{20}IN_3O$ • 1/2 H_2O (466.32): calcd. C 54.09, H 4.54, N 9.01; found C 54.21, H 4.66, N 8.69. − Optical rotation (*c* = 2.2, MeOH): $[\alpha]^{22}_D$ = +11, $[\alpha]^{22}_{578}$ = +12, $[\alpha]^{22}_{546}$ = +15, $[\alpha]^{22}_{436}$ = +27.

(+)-N′-Methyl-2-[4-(S)-benzyloxazolin-2-yl]-4,4′-bipyridinium Hexafluorophosphate (**11**): 460 mg (1.0 mmol) of **1e** were dissolved in water (15 ml) and treated with 1 ml of saturated aqueous NH_4PF_6. The precipitated yellow solid was collected after 30 min and washed with little water. After recrystallisation from boiling water 420 mg (0.9 mmol, 88%) of **11** were isolated. Light yellow, hygroscopic solid, m.p. > 120°C (dec.). − ^{1}H NMR (250 MHz, [D$_6$]acetone): δ = 2.90 (dd, ^2J = 13.9 Hz, ^3J = 7.5 Hz, 1 H, CH_AH$_B$Ph), 3.11 (dd, ^2J = 13.9 Hz, ^3J = 6.3 Hz, 1 H, CH$_A$$H_B$Ph), 4.24 (dd, ^2J = 8.3 Hz, ^3J = 7.5 Hz, 1 H, Ox-CH_ZH$_E$), 4.55 (dd, ^2J = 8.3 Hz, ^3J = 9.5 Hz, 1 H, Ox-CH$_Z$$H_E$), 4.69 (s, 3 H, N-C$H_3$), 4.67−4.86 (m, 1 H, Ox-C*H*), 7.13−7.38 (m, 5 H, Ph-*H*), 8.12 (dd, ^3J = 5.2 Hz, ^4J = 2.0 Hz, 1 H, H-5), 8.53 (dd, ^4J = 2.0 Hz, ^5J = 0.8 Hz, 1 H, H-3), 8.71 (AA′BB′, 2 H, H-3′, H-5′), 8.92 (dd, ^3J = 5.2 Hz, ^5J = 0.8 Hz, 1 H, H-6), 9.25 (AA′BB′, 2 H, H-2′, H-6′). − MS (FAB, MeOH/glycerol): *m/z* = 476 (weak) [MH$^+$], 330 [K$^+$]. − IR (KBr): $\tilde{\nu}$ (cm^{-1}) = 3150/3060/3030/2970/2910 w (CH), 1650 s (C=N), 840 vs, 555 s (PF). $C_{21}H_{20}F_6N_3OP$ • H_2O (493.39): calcd. C 51.12, H 4.49, N 8.52; found C 51.12, H 4.44, N 8.36. − Optical rotation (*c* = 2.2, acetone): $[\alpha]^{22}_D$ = +7.7, $[\alpha]^{22}_{578}$ = +8.6, $[\alpha]^{22}_{546}$ = +10, $[\alpha]^{22}_{436}$ = +20.

4,4′-Bipyridine N,N′-Dioxide Dihydrate (**12**): 5.4 g (57.4 mmol) of commercially available H_2O_2/urea adduct and 8.5 g (57.4 mmol) of phthalic anhydride were suspended in CH_2Cl_2 (60 ml). After 15 min 2.0 g (12.8 mmol) of 4,4′-bipyridine (**4**) were added and stirred for 3 d. Then the resulting suspension was poured into a saturated solution of aqueous $NaHCO_3$ (200 ml) and continuously extracted with $CHCl_3$ for 3 d. Removing the solvent and recrystallisation from water afforded 2.72 g (12.1 mmol, 95% [ref.[31]: 80%]) of 4,4′-bipyridine *N,N′*-dioxide as the yellow dihydrate, m.p. > 250°C (ref.: 305°C[31], 305−306°C[36], 335°C[21]). − ^{1}H NMR (250 MHz, D_2O): δ = 7.84 (AA′BB′, 4 H, H-3,3′, H-5,5′), 8.30 (AA′BB′, 4 H, H-2,2′, H-6,6′). − MS (FD, MeOH): *m/z* = 188 [M$^+$]. − IR (KBr): $\tilde{\nu}$ (cm^{-1}) = 1255 s, 1245 vs (NO). $C_{10}H_8N_2O_2$ • 2 H_2O (224.22): calcd. C 53.57, H 5.39, N 12.49; found C 53.98, H 5.42, N 12.26.

4,4′-Bipyridine-2,2′-dicarbonitrile (**13**): **12** (1.7 g, 7.6 mmol) and dimethyl sulfate (15 ml, 157.7 mmol) were heated at 140°C for 30 min. The cooled solution was treated with ethanol (30 ml) and 70% $HClO_4$ (10 ml). The precipitated solid was collected, dried, dissolved in water (90 ml), weakly alkalised with Na_2CO_3 and cooled on ice. A solution of 2.6 g (59 mmol) of NaCN in water (25 ml) was added and the precipitation completed by stirring for 1 h. After washing the filtered precipitate with ice water it was dried in vacuo over P_4O_{10}. Recrystallisation from ethanol yielded 760 mg (3.7 mmol, 48%) of the white dinitrile **13**. − ^{1}H NMR (250 MHz, [D$_6$]DMSO): δ = 8.29 (dd, ^3J = 5.2 Hz, ^4J = 1.9 Hz, 2 H, H-5, H-5′), 8.66 (dd, ^4J = 1.9 Hz, ^5J = 0.9 Hz, 2 H, H-3, H-3′), 8.95 (dd, ^3J = 5.2 Hz, ^5J = 0.9 Hz, 2 H, H-6, H-6′). − MS (EI): *m/z* (%) = 206 (100) [M$^+$]. − IR (KBr): $\tilde{\nu}$ (cm^{-1}) = 2230 m (C≡N).

Dimethyl 4,4′-Bipyridine-2,2′-dicarboximidate (**14**): 50 mg (2.2 mmol) of sodium were dissolved in dry methanol (40 ml) under nitrogen. 750 mg (3.6 mmol) of **13** were added and stirring at r. t. was continued for 4 d. After addition of acetic acid (0.1 ml, 1.6 mmol) the solvent was evaporated and the residue treated with warm ether (300 ml). Inorganic salts were removed by hot filtration. Cooling the filtrate to −20°C lead to 600 mg (2.2 mmol, 62%) of **14**. Colourless crystals, m.p. 211−214°C. − ^{1}H NMR (250 MHz, $CDCl_3$): δ = 4.07 (s, 6 H, CH_3), 7.66 (dd, ^3J = 5.1 Hz, ^4J = 1.8 Hz, 2 H, H-5, H-5′), 7.86 (dd, ^4J = 1.8 Hz, ^5J = 0.8 Hz, 2 H, H-3, H-3′), 8.79 (dd, ^3J = 5.1 Hz, ^5J = 0.8 Hz, 2 H, H-6, H-6′), 9.31 (br s, 2 H, N*H*). − ^{13}C NMR (62.9 MHz, $CDCl_3$): δ = 54.0 (*C*H$_3$), 118.8 (C-3, C-3′), 123.0 (C-5, C-5′), 146.7/148.8 (qC), 150.1 (C-6, C-6′), 166.2 (*C*=N). − MS (EI): *m/z* (%) = 270 (100) [M$^+$], 240 (15), 239 (63) [M$^+$ − OCH$_3$], 227 (20), 214 (14), 213 (83) [M$^+$ − OCH$_3$ − CH$_3$OH], 182 (13), 181 (15), 180 (23), 156 (12), 155 (18), 153 (13), 58 (17). − IR (KBr): $\tilde{\nu}$ (cm^{-1}) = 3300/3265 m (NH), 1645 s (C=N), 1365 vs (CO). − $C_{14}H_{14}N_4O_2$ (270.29): calcd. C 62.21, H 5.22, N 20.73; found C 62.21, H 5.18, N 20.32.

(−)-2,2′-Bis[4-(R)-phenyloxazolin-2-yl]-4,4′-bipyridine (**15**): Following general procedure I 580 mg (2.1 mmol) of **14** and 590 mg (4.3 mmol) of *(R)*-α-phenylglycinol were heated at 80°C in dry chlorobenzene (20 ml) for 6 d. Flash chromatography (SiO_2, 9.5 × 2.5 cm) with PE/acetone (1:1) as eluent (R_f = 0.37 [acetone]) followed by recrystallisation from PE/ether afforded 520 mg (1.2 mmol, 56%) of **15**. Light yellow foam, m.p. 102−105°C. − ^{1}H NMR (250 MHz, $CDCl_3$): δ = 4.44 (″t″, ^2J = ^3J = 8.6 Hz, 2 H, Ox-CH_ZH$_E$), 4.94 (dd, ^2J = 8.6 Hz, ^3J = 10.2 Hz, 2 H, Ox-CH$_Z$$H_E$), 5.50 (dd, ^3J = 8.6 Hz, ^3J = 10.2 Hz, 2 H, Ox-C*H*), 7.30−7.41 (m, 10 H, Ph-*H*), 7.74 (dd, ^3J = 5.0 Hz, ^4J = 1.9 Hz, 2 H, H-5, H5′), 8.50 (dd, ^4J = 1.9 Hz, ^5J = 0.9 Hz, 2 H, H-3, H-3′), 8.86 (dd, ^3J = 5.0 Hz, ^5J = 0.9 Hz, 2 H, H-6, H-6′). − ^{13}C NMR (62.9 MHz, $CDCl_3$): δ = 70.5 (Ox-*C*H), 75.5 (Ox-*C*H$_2$),

122.1/123.4 (C-3, C-3′ and C-5, C-5′), 126.9 (*o*- or *m*-Ph-*C*), 127.9 (*p*-Ph-*C*), 128.9 (*m*- or *o*-Ph-*C*), 141.6 (qC of Ph), 145.8/148.0 (qC), 150.7 (C-6, C-6′), 163.6 (*C*=N). − MS (EI): *m/z* (%) = 446 (100) [M^+], calcd. for $C_{28}H_{22}N_4O_2$ 446.1743, found 446.1737, diff. −0.5 mmu/1.2 ppm, 416 (28) [$M^+ - CH_2O$], 315 (20), 301 (20), 296 (21), 269 (31), 91 (44), 90 (42), 89 (24). − IR (KBr): $\tilde{\nu}$ (cm^{-1}) = 3055/3025/2890 w (CH), 1640 s (C=N). − Optical rotation (*c* = 1.27, $CHCl_3$): $[\alpha]^{22}_D = -78$, $[\alpha]^{22}_{578} = -82$, $[\alpha]^{22}_{546} = -95$, $[\alpha]^{22}_{436} = -168$, $[\alpha]^{22}_{365} = -271$.

3,6-Dimethylpyrazine-2,5-dicarboxylic Acid (**17**): 1.4 g (6.2 mmol) of dimethyl 3,6-dimethylpyrazine-2,5-dicarboxylate (**16**)[133] were refluxed in 2 N NaOH (50 ml) for 30 min. The cooled solution was acidified with conc. HCl and the precipitate filtered off. After recrystallisation from ethyl acetate 1.0 g (5.1 mmol, 82%) of **17** were obtained. Colourless crystals, m.p 195°C (ref. 194−195°C[37], 200−201°C[38]). − ^{1}H NMR (80 MHz, [D_6]acetone): δ = 2.78 (s, CH_3). − IR (KBr): $\tilde{\nu}$ (cm^{-1}) = 3465 s (OH), 1705 s (C=O).

3,6-Dimethylpyrazine-2,5-dicarboxylic Acid Chloride (**18**): 970 mg (5.1 mmol) of **17** and 1.1 ml of $SOCl_2$ were refluxed for 2 h. Excess $SOCl_2$ was removed in vacuo and the residue (1.18 g, 5.1 mmol, 99%), m.p. 98°C, was directly used in the next reaction. − ^{1}H NMR (80 MHz, $CDCl_3$): δ = 2.85 (s, CH_3). − MS (EI): *m/z* (%) = 234 (14)/232 (21) [M^+], 199 (33)/197 (100) [M^+ − Cl], 171 (24)/169 (74) [M^+ − Cl − CO], 143 (13)/141 (41) [M^+ − Cl − 2 CO], 106 (17) [M^+ − 2 Cl − 2 CO]. − IR (KBr): $\tilde{\nu}$ (cm^{-1}) = 1755 vs (C=O), 880/865 s (CCl).

(+)-2,5-Bis[4-(R)-phenyloxazolin-2-yl]-3,6-dimethylpyrazine (**19**): To a solution of (*R*)-α-phenylglycinol (1.36 g, 9.9 mmol) and dry triethylamine (1.4 ml) in CH_2Cl_2 (15 ml) was added during 15 min a solution of **18** (1.15 g, 4.9 mmol) in CH_2Cl_2 (12 ml) at 0°C under nitrogen. The mixture was stirred for 16 h at r. t. The solvent was removed and the residue treated with toluene (30 ml) and $SOCl_2$ (2.2 ml). After refluxing for 1 h the cooled solution was evaporated. A solution of NaOH (800 mg, 20.0 mmol) in methanol (40 ml) was added and refluxing continued for 3.5 h. To the cooled solution ether (100 ml) and brine (30 ml) were added. The organic layer was collected and the aqueous layer extracted with acetone (3× 30 ml). After washing with brine (20 ml) the combined organic layers were dried over $MgSO_4$ and evaporated. The oily residue was purified by flash chromatography (SiO_2, 10 × 3 cm) with PE/ethyl acetate (1:1) as eluent (R_f = 0.65 [ethyl acetate]). Recrystallisation from ether/acetone yielded 900 mg (2.3 mmol, 46%) of **19**. Light yellow solid, m.p. 143°C. − ^{1}H NMR (250 MHz, $CDCl_3$): δ = 2.99 (s, 6 H, CH_3), 4.35 (″t″, $^2J = {}^3J \approx 8.6$ Hz, 2 H, Ox-CH_ZH$_E$), 4.90 (dd, ^2J = 8.7 Hz, ^3J = 10.2 Hz, 2 H, Ox-CH$_Z$$H_E$), 5.56 (dd, ^3J = 8.5 Hz, ^3J = 10.2 Hz, 2 H, Ox-C*H*), 7.31 (m, 2 H, *p*-Ph-*H*), 7.34 (m, 4 H, *o*- or *m*-Ph-*H*), 7.38 (m, 4 H, *m*- or *o*-Ph-*H*). − ^{13}C NMR (62.9 MHz, $CDCl_3$): δ = 23.4 (*C*H_3), 71.1 (Ox-*C*H), 74.6 (Ox-*C*H_2), 126.7 (*o*- or *m*-Ph-*C*), 127.8 (*p*-Ph-*C*), 128.9 (*m*- or *o*-Ph-*C*), 141.0/141.7/151.6 (qC), 162.4 (*C*=N). − MS (EI): *m/z* (%) = 398 (100) [M^+], 307 (32), 121 (24), 118 (39), 104 (73), 103 (27), 91 (57), 89 (24). − IR (KBr): $\tilde{\nu}$ (cm^{-1}) = 3050/3020/2950/2920/2890 w (CH), 1645 s (C=N). − $C_{24}H_{22}N_4O_2$ (398.46): calcd. C 72.34, H 5.56, N 14.06; found C 72.21, H 5.57, N 13.90. − Optical rotation (*c* = 1.29, $CHCl_3$): $[\alpha]^{22}_D = +53$, $[\alpha]^{22}_{578} = +57$, $[\alpha]^{22}_{546} = +68$, $[\alpha]^{22}_{436} = +171$.

4-Phenylpyridine-2-carbonitrile (**21**): 5.0 g (29.2 mmol) of commercially available 4-phenylpyridine *N*-oxide (**20**) and 4.0 ml (32.0 mmol) of trimethylsilyl cyanide were dissolved in CH_2Cl_2 (50 ml) and stirred for 5 min under nitrogen. After adding 2.7 ml (29.3 mmol) of dimethylcarbamoyl chloride the resulting solution was stirred at r. t. for 2 d. A solution of 10% aqueous K_2CO_3 (50 ml) was added and stirring continued for 10 min. The organic layer was separated and the aqueous layer extracted with CH_2Cl_2 (2× 25 ml). The combined organic layers were washed with 25 ml of brine and dried over $MgSO_4$. Recrystallisation from PE (750 ml) yielded 4.2 g (23.3 mmol, 80%) of **21**. Colourless needles, m.p. 99°C (ref.: 99−100°C[39], 99°C[40][41], 98−99°C[42]). − ^{1}H NMR (250 MHz, $CDCl_3$): δ = 7.49−7.66 (m, 5 H, Ph-*H*), 7.72 (dd, ^3J = 5.2 Hz, ^4J = 1.6 Hz, 1 H, H-5), 7.90 (dd, ^4J = 1.6 Hz, ^5J = 0.8 Hz, 1 H, H-3), 8.75 (dd, ^3J = 5.2 Hz, ^5J = 0.8 Hz, 1 H, H-6). − ^{13}C NMR (62.9 MHz, $CDCl_3$): δ = 117.4 (*C*N), 124.6/126.4 (C-3 and C-5), 127.0/129.5 (*o*- and *m*-Ph-*C*), 130.2 (*p*-Ph-*C*), 134.6/136.0/149.9 (qC), 151.5 (C-6). − MS (EI): *m/z* (%) = 180 (100) [M^+], 179 (18), 153 (11). − IR (KBr): $\tilde{\nu}$ (cm^{-1}) = 2220 w (C≡N). − $C_{12}H_8N_2$ (180.21): calcd. C 79.98, H 4.47, N 15.54; found C 79.77, H 4.65, N 15.40.

Methyl 4-Phenylpyridine-2-carboximidate (**22**): 20 mg (0.9 mmol) of sodium were dissolved in dry methanol (8 ml) under nitrogen. 1.26 g (7.0 mmol) of **21** were added and stirring at r. t. was continued for 90 h. After addition of a few drops of acetic acid the solvent was evaporated and the residue treated with warm ether (70 ml). Inorganic salts were removed by hot filtration. After evaporation of the solvent and recrystallisation from PE 1.31 g (6.2 mmol, 88%) of the imino ether **22** were obtained as a light yellow solid, m.p. 81−83°C. − ^{1}H NMR (250 MHz, C_6D_6): δ = 3.93 (s, 3 H, CH_3), 6.95 (dd, ^3J = 5.1 Hz, ^4J = 1.8 Hz, 1 H, H-5), 6.99−7.28 (m, 5 H, Ph-*H*), 8.05 (dd, ^4J = 1.8 Hz, ^5J = 0.8 Hz, 1 H, H-3), 8.36 (dd, ^3J = 5.0 Hz, ^5J = 0.8 Hz, 1 H, H-6), 10.02 (br s, 1 H, N*H*). − ^{13}C NMR (62.9 MHz, C_6D_6): δ = 53.7 (*C*H_3), 119.0/122.9 (C-3 and C-5), 127.3/129.26 (*o*- and *m*-Ph-*C*), 129.27 (*p*-Ph-*C*), 138.2 (qC of Ph), 148.8/149.8 (qC), 149.9 (C-6), 166.7 (*C*=N). − MS (EI): *m/z* (%) = 212 (79) [M^+], 182 (17), 181 (83) [$M^+ - OCH_3$], 156 (13), 155 (100) [$M^+ - CH_3 - CN$], 154 (29) [$M^+ - CH_3 - HCN$], 153 (11), 128 (17), 127 (27), 77 (17), 43 (17). − IR (KBr): $\tilde{\nu}$ (cm^{-1}) = 3290 m (NH), 1655 s (C=N), 1365 vs (CO). − $C_{13}H_{12}N_2O$ (212.25): calcd. C 73.57, H 5.70, N 13.20; found C 73.57, H 5.90, N 12.61.

(−)-4-(S)-(2-Methylpropyl)-2-(4-phenylpyridin-2-yl)oxazoline (**23a**): Following general procedure I 1.35 g (6.3 mmol) of **22** and 750 mg (6.4 mmol) of *(S)*-leucinol were heated at 80°C in dry chlorobenzene (25 ml) for 64 h. Flash-chromatography (SiO_2, 9 × 3 cm) with PE/acetone (2:1) as eluent (R_f = 0.26) followed by recrystallisation from PE/ether afforded 1.35 g (4.8 mmol, 76%) of **23a**. Colourless needles, m.p. 43−44°C. − ^{1}H NMR (250 MHz, $CDCl_3$): δ = 0.98 (d, ^3J = 6.7 Hz, 3 H, CH_3), 1.00 (d, ^3J = 6.3 Hz, 3 H, CH_3′), 1.43 (″dt″, ^2J = 13.5 Hz, ^3J = 7.1 Hz, 1 H, C$H_A$$H_B$CHMe$_2$), 1.78 (″dt″, ^2J = 13.5 Hz, $^3J \approx 6.7$ Hz, 1 H, CH$_A$$H_B$CHMe$_2$), 1.89 (″sept″, $^3J \approx 6.3$ and 6.7 Hz, 1 H, C*H*Me$_2$), 4.10 (″t″, $^2J = {}^3J$ = 8.0 Hz, 1 H, Ox-CH_ZH$_E$), 4.43 (m, 1 H, Ox-C*H*), 4.65 (dd, ^2J = 8.0 Hz, ^3J = 9.5 Hz, 1 H, Ox-CH$_Z$$H_E$), 7.41−7.55 (m, 3 H, Ph-*H*), 7.59 (dd, ^3J = 5.2 Hz, ^4J = 1.6 Hz, 1 H, H-5), 7.66−7.72 (m, 2 H, Ph-*H*), 8.29 (dd, ^4J = 1.6 Hz, ^5J = 0.8 Hz, 1 H, H-3), 8.74 (dd, ^3J = 5.2 Hz, ^5J = 1.2 Hz, 1 H, H-6). − ^{13}C NMR (62.9 MHz, $CDCl_3$): δ = 22.7 (*C*H_3 and *C*H_3′), 25.5 (*C*HMe$_2$), 45.5 (*C*H_2CHMe$_2$), 65.5 (Ox-*C*H), 73.7 (Ox-*C*H_2), 121.8 (C-3), 123.1 (C-5), 127.1/129.1 (*o*- and *m*-Ph-*C*), 129.3 (*p*-Ph-*C*), 137.5 (qC of Ph), 147.6/149.1 (qC), 150.1 (C-6), 162.6 (*C*=N). − MS (EI): *m/z* (%) = 280 (21) [M^+], 224 (40), 223 (80) [$M^+ - C_4H_9$], 196 (21), 195 (35), 181 (42), 169 (100), 168 (30), 155 (47), 154 (63), 127 (34), 84 (30). − IR (KBr): $\tilde{\nu}$ (cm^{-1}) = 3055/3025 w, 2955 s, 2925/2875 m (CH), 1645 s (C=N). − $C_{18}H_{20}N_2O$ (280.37): calcd. C 77.11, H 7.19, N 9.99; found C 76.94, H 7.18, N 9.95. Optical rotation (*c* = 1.27, $CHCl_3$): $[\alpha]^{22}_D = -30$, $[\alpha]^{22}_{578} = -33$, $[\alpha]^{22}_{546} = -39$, $[\alpha]^{22}_{436} = -78$, $[\alpha]^{22}_{365} = -160$.

(+)-4-(S)-Benzyl-2-(4-phenylpyridin-2-yl)oxazoline (**23b**): Following general procedure I 580 mg (2.7 mmol) of **22** and 415 mg (2.7 mmol) of *(S)*-phenylalaninol were heated at 80°C in dry chlorobenzene (20 ml) for 64 h. Flash-chromatography (SiO_2, 10 × 3 cm) with PE/acetone (2:1) as eluent (R_f = 0.17) followed by recrystallisation from PE/ether afforded 560 mg (1.8 mmol, 66%) of **23b**. Ivory coloured needles, m.p. 156−157°C. − ^{1}H NMR (250 MHz, $CDCl_3$): δ = 2.78 (dd, ^2J = 13.8 Hz, ^3J = 9.1 Hz, 1 H, CH_AH$_B$Ph), 3.33 (dd, ^2J = 13.8 Hz, ^3J = 5.0 Hz, 1 H, CH$_A$$H_B$Ph), 4.25 (dd, ^2J = 8.6 Hz, ^3J = 7.7 Hz, 1 H, Ox-CH_ZH$_E$), 4.47 (dd, ^2J = 8.6 Hz, ^3J = 9.4 Hz, 1 H, Ox-CH$_Z$$H_E$), 4.69 (dddd, ^3J = 9.4 Hz, ^3J = 9.1 Hz, ^3J = 7.7 Hz, ^3J = 5.0 Hz, 1 H, Ox-C*H*), 7.19−7.35 (m, 5 H, Ox-Ph-*H*), 7.41−7.53 (m, 3 H, Py-Ph-*H*), 7.60 (dd, ^3J = 5.2 Hz, ^4J = 2.0 Hz, 1 H, H-5), 7.67−7.72 (m, 2 H, Py-Ph-*H*), 8.31 (dd, ^4J = 2.0 Hz, ^5J = 0.8 Hz, 1 H, H-3), 8.74 (dd, ^3J = 5.2 Hz, ^5J = 0.8 Hz, 1 H, H-6). − ^{13}C NMR (62.9 MHz, $CDCl_3$): δ = 41.7 (*C*H$_2$Ph), 68.2 (Ox-*C*H), 72.6 (Ox-*C*H$_2$), 121.9 (C-3), 123.4 (C-5), 126.6 (Ox-*p*-Ph-*C*), 127.1 (Ox-*o*- or *m*-Ph-*C*), 128.6 (Py-*o*- or *m*-Ph-*C*), 129.17/129.23 (Ox- and Py-*m*- or *o*-Ph-*C*), 129.4 (Py-*p*-Ph-*C*), 137.4 (qC of Py-Ph), 137.9 (qC of Ox-Ph), 147.4/149.2 (qC), 150.2 (*C*-6), 163.3 (*C*=N). − MS (EI): *m*/*z* (%) = 314 (5) [M$^+$], 224 (17), 223 (100) [M$^+$ − CH$_2$Ph], 195 (21), 168 (24), 167 (12), 154 (14), 127 (12). − IR (KBr): $\tilde{\nu}$ (cm^{-1}) = 3050/3030/2970/2955/2920/2890 w (CH), 1650 s (C=N). − $C_{21}H_{18}N_2O$ (314.39): calcd. C 80.23, H 5.77, N 8.91; found C 80.30, H 5.82, N 8.91. − Optical rotation (*c* = 1.26, $CHCl_3$): [α]$^{20}_D$ = +33, [α]$^{20}_{578}$ = +35, [α]$^{20}_{546}$ = +40, [α]$^{20}_{436}$ = +79, [α]$^{20}_{365}$ = +148.

General Procedure III [(η^4-1,5-Cyclooctadiene)oxazoline-rhodium(I) Complexes]: To a stirred solution of 1.0 mmol of oxazoline in dry CH_2Cl_2 (6 ml) were added 247 mg (0.5 mmol) of [Rh(cod)Cl]$_2$ in dry CH_2Cl_2 (6 ml) under nitrogen. The resulting dark red solution was stirred for 2 h, then excess (ca. 1.4 mmol) of solid NH_4PF_6 or $NaBF_4$ (for **26**) was added. After stirring for another 1−2 h, the inorganic salts were filtered off and rinsed with 2 ml of dry CH_2Cl_2. The filtrate containing the complex was treated as described for the individual compounds.

(−)-(η^4-1,5-Cyclooctadiene){2-[4-(R)-phenyloxazolin-2-yl]-4,4′-bipyridine-N,N′′}rhodium(I) Hexafluorophosphate (**24**): From oxazoline **3d**. By adding 6 ml of dry PE to the filtrate and cooling to −20°C 607 mg (0.9 mmol, 92%) of **24** were obtained. Red microcrystalline solid, m.p. > 245°C (dec.). − ^{1}H NMR (400 MHz, $CDCl_3$): δ = 1.72−1.80 (m, 2 H, cod-H$_{endo}$-3, H$_{endo}$-8), 1.89−1.94 (m, 2 H, cod-H$_{endo}$-4, H$_{endo}$-7), 2.19−2.28 (m, 2 H, cod-H$_{exo}$-3, H$_{exo}$-8), 2.43−2.52 (m, 2 H, cod-H$_{exo}$-4, H$_{exo}$-7), 3.93−4.00 (m, 2 H, cod-H-1, H-2), 4.41−4.48 (m, 2 H, cod-H-5, H-6), 4.67 (m, 1 H, Ox-C*H*?), 5.33 (m, 2 H, Ox-CH_2?), 7.31−7.33 (m, 2 H, *m*-Ph-*H*), 7.41−7.47 (m, 3 H, *o*- and *p*-Ph-*H*), 7.65 (AA′BB′, 2 H, H-3′, H-5′), 7.98 (″d″, ^3J = 5.6 Hz, 1 H, H-6), 8.06 (dd, ^3J = 5.6 Hz, ^4J = 2.0 Hz, 1 H, H-5), 8.17 (dd, ^4J = 2.0 Hz, ^5J = 0.5 Hz, 1 H, H-3), 8.75 (AA′BB′, 2 H, H-2′, H-6′). − MS (FD, CH_2Cl_2): *m*/*z* = 512 [K$^+$]. HR-MS (FAB, *m*-NBA + 1% TFA): *m*/*z* (%) = 512 (100%) [K$^+$], calcd. for $C_{27}H_{27}N_3ORh$ 512.1209, found 512.1215, diff. +0.6 mmu/1.2 ppm. − IR (KBr): $\tilde{\nu}$ (cm^{-1}) = 2985/2950/2885/2840 w (CH), 1645 w (C=N), 840 vs, 555 s (PF). − Optical rotation (*c* = 0.38, MeOH): [α]$^{22}_D$ = −6.6, [α]$^{22}_{578}$ = −6.6, [α]$^{22}_{546}$ = −15.

(+)-(η^4-1,5-Cyclooctadiene){2-[4-(S)-benzyloxazolin-2-yl]-4,4′-bipyridine-N,N′′}rhodium(I) Hexafluorophosphate (**25**): From oxazoline **3e**. The filtrate was evaporated, the residue was dissolved in dry acetone (5 ml) and dry ether (10 ml) was added. Crystallisation at −20°C yielded 550 mg (0.8 mmol, 82%) of **25**. Red needles, m.p. > 205°C (dec.). − ^{1}H NMR (250 MHz, $CDCl_3$): δ = 1.82−2.02 (m, 2 H, cod-H$_{endo}$-3, H$_{endo}$-8), 2.09−2.16 (m, 2 H, cod-H$_{endo}$-4, H$_{endo}$-7), 2.35−2.44 (m, 2 H, cod-H$_{exo}$-3, H$_{exo}$-8), 2.58−2.74 (m, 2 H, cod-H$_{exo}$-4, H$_{exo}$-7), 2.84 (dd, ^2J = 13.9 Hz, ^3J = 8.1 Hz, 1 H, CH_AH$_B$Ph), 3.03 (dd, ^2J = 13.9 Hz, ^3J = 4.4 Hz, 1 H, CH$_A$$H_B$Ph), 4.36−4.46 (m, 3 H, Ox-C*H*? and cod-H-1, H-2), 4.64−4.81 (m, 4 H, Ox-CH_2? and cod-H-5, H-6), 7.22−7.35 (m, 5 H, Ph-*H*), 7.60 (AA′BB′, 2 H, H-3′, H-5′), 7.98 (″s″, 1 H, H-3), 8.02 (″d″, $^3J \approx$ 5.4 Hz, 1 H, H-6), 8.08 (″d″, $^3J \approx$ 5.4 Hz, 1 H, H-5), 8.76 (AA′BB′, 2 H, H-2′, H-6′). − ^{13}C NMR (62.9 MHz, $CDCl_3$): δ = 29.7 (cod-C-3, C-8), 31.3 (cod-C-4, C-7), 40.5 (*C*H$_2$Ph), 63.9 (Ox-*C*H), 76.4 (Ox-*C*H$_2$), 82.6 (d, $^1J_{Rh,C}$ = 12.9 Hz, cod-C-1, C-2), 85.0 (d, $^1J_{Rh,C}$ = 12.6 Hz, cod-C-5, C-6), 121.5 (C-3′, C-5′), 123.3 (C-3), 127.5 (*p*-Ph-*C*), 127.9 (C-5), 129.0/129.6 (*o*- and *m*-Ph-*C*), 134.8 (qC of Ph), 142.2/145.6/150.1 (qC), 150.2 (C-6), 151.2 (C-2′, C-6′), 171.1 (*C*=N). − MS (FAB, CH_2Cl_2/*m*-NBA): *m*/*z* = 526 [K$^+$], 418 [K$^+$ − cod]. − IR (KBr): $\tilde{\nu}$ (cm^{-1}) = 2950/2925/2890/2840 w (CH), 1650 w (C=N), 845 vs, 565 s (PF). − $C_{28}H_{29}F_6N_3OPRh$ (671.43): calcd. C 50.09, H 4.35, N 6.26; found C 49.84, H 4.47, N 6.03. − Optical rotation (*c* = 0.29, MeOH): [α]$^{26}_D$ = +63, [α]$^{26}_{578}$ = +52, [α]$^{26}_{546}$ = +66.

(+)-(η^4-1,5-Cyclooctadiene){2-[4-(S)-benzyloxazolin-2-yl]-4,4′-bipyridine-N,N′′}rhodium(I) Tetrafluoroborate (**26**): From oxazoline **3e**. The filtrate was evaporated, the residue was dissolved in dry acetone (5 ml) and dry ether (5 ml) was added. Crystallisation at −20°C yielded 540 mg (0.9 mmol, 88%) of **26**. Red microcrystalline solid, m.p. > 150°C (dec.). − ^{1}H NMR (250 MHz, $CDCl_3$): δ = 1.79−1.93 (m, 2 H, cod-H$_{endo}$-3, H$_{endo}$-8), 2.04−2.17 (m, 2 H, cod-H$_{endo}$-4, H$_{endo}$-7), 2.30−2.44 (m, 2 H, cod-H$_{exo}$-3, H$_{exo}$-8), 2.59−2.74 (m, 2 H, cod-H$_{exo}$-4, H$_{exo}$-7), 2.87 (dd, ^2J = 13.9 Hz, ^3J = 7.6 Hz, 1 H, CH_AH$_B$Ph), 3.03 (dd, ^2J = 13.9 Hz, ^3J = 4.5 Hz, 1 H, CH$_A$$H_B$Ph), 4.40−4.51 (m, 3 H, Ox-C*H*? and cod-H-1, H-2), 4.59−4.86 (m, 4 H, Ox-CH_2? and cod-H-5, H-6), 7.21−7.35 (m, 5 H, Ph-*H*), 7.65 (AA′BB′, 2 H, H-3′, H-5′), 7.99 (″s″, 1 H, *H*-3), 8.14 (″d″, $^3J \approx$ 5.5 Hz, 1 H, H-6), 8.23 (″d″, $^3J \approx$ 4.0 Hz, 1 H, H-5), 8.77 (AA′BB′, 2 H, H-2′, H-6′). − ^{13}C NMR (62.9 MHz, $CDCl_3$): δ = 29.7 (cod-C-3, C-8), 31.3 (cod-C-4, C-7), 40.5 (*C*H$_2$Ph), 63.9 (Ox-*C*H), 76.5 (Ox-*C*H$_2$), 82.6 (d, $^1J_{Rh,C}$ = 12.7 Hz, cod-C-1, C-2), 85.1 (d, $^1J_{Rh,C}$ = 12.6 Hz, cod-C-5, C-6), 121.5 (C-3′, C-5′), 123.1 (C-3), 127.5 (*p*-Ph-*C*), 128.2 (C-5), 129.0/129.6 (*o*- and *m*-Ph-*C*), 134.8 (*qC* of Ph), 142.1/145.4/150.0 (qC), 150.7 (C-6), 151.2 (C-2′, C-6′), 171.2 (*C*=N). − MS (FD, CH_2Cl_2): *m*/*z* = 526 [K$^+$]. − IR (KBr): $\tilde{\nu}$ (cm^{-1}) = 2945/2915/2880/2835 w (CH), 1645 w (C=N), 1085/1060 vs (BF). − $C_{28}H_{29}BF_4N_3ORh \bullet H_2O$ (631.29): calcd. C 53.27, H 4.95, N 6.65; found C 53.36, H 4.79, N 6.43. Optical rotation (*c* = 0.58, MeOH): [α]$^{23}_D$ = +73°, [α]$^{23}_{578}$ = +70°, [α]$^{23}_{546}$ = +83°.

(+)-(η^4-1,5-Cyclooctadiene){4-(S)-(2-methylpropyl)-2-(4-phenylpyridin-2-yl)oxazoline-N,N′}rhodium(I) Hexafluorophosphate (**27**): From oxazoline **23a**. By adding 12 ml of dry ether to the filtrate and cooling to −20°C a bright orange solid (475 mg, 0.7 mmol, 75%) was obtained. Slow diffusion of ether into a $CHCl_3$ solution yielded **27** as red needles, m.p. > 185°C (dec.). − ^{1}H NMR (250 MHz, $CDCl_3$): δ = 0.93 (d, ^3J = 6.5 Hz, 3 H, CH_3), 0.98 (d, ^3J = 6.5 Hz, 3 H, CH_3′), 1.40−1.70 (m, 3 H, CH_2C*H*Me$_2$), 1.89 (m, 2 H, cod-H$_{endo}$-3, H$_{endo}$-8), 2.05−2.20 (m, 2 H, cod-H$_{endo}$-4, H$_{endo}$-7), 2.43 (m, 2 H, cod-H$_{exo}$-3, H$_{exo}$-8), 2.58−2.82 (m, 2 H, cod-H$_{exo}$-4, H$_{exo}$-7), 4.16−4.27 (m, 1 H, Ox-C*H*?), 4.30−4.80 (m, 4 H, cod-olefinic-*H*), 4.58 (dd, $^2J \approx$ 9.0 Hz, ^3J = 5.9 Hz, 1 H, Ox-CH_EH$_Z$?), 4.96 (″t″, ^2J = ^3J = 9.0 Hz, 1 H, Ox-CH$_E$$H_Z$?), 7.48−7.56 (m, 3 H, Ph-*H*), 7.66−7.73 (m, 2 H, Ph-*H*), 7.89−7.94 (m, 1 H, Py-*H*), 7.99−8.02 (m, 2 H, Py-*H*). − ^{13}C NMR (62.9 MHz, $CDCl_3$): δ = 21.5 (*C*H$_3$), 23.7 (*C*H$_3$′), 25.3 (*C*HMe$_2$), 29.3/30.4/31.2 (br, cod-*C*H$_2$), 44.1 (*C*H$_2$CHMe$_2$), 62.1 (d, $^2J_{Rh,C}$ = 2.1 Hz, Ox-*C*H), 77.3 (Ox-*C*H$_2$), 82.5/83.1/85.9 (br, cod-*C*H), 123.0 (d,

$^3J_{Rh,C}$ = 0.9 Hz, C-3), 127.2 (d, $^3J_{Rh,C}$ = 0.9 Hz, C-5), 127.4/129.7 (*o*- and *m*-Ph-*C*), 131.3 (*p*-Ph-*C*), 134.6 (qC of Ph), 145.2 (qC), 149.6 (d, $^2J_{Rh,C}$ = 0.6 Hz, *C-6*), 153.0 (qC), 170.9 (d, $^2J_{Rh,C}$ = 1.4 Hz, *C*=N). − MS (FAB, CH_2Cl_2/*m*-NBA): *m/z* = 491 [K^+]. − IR (KBr): $\tilde{\nu}$ (cm^{-1}) = 2965/2885 w (CH), 1645 w (C=N), 840 vs, 555 s (PF). − $C_{26}H_{32}F_6N_2OPRh$ (636.42): calcd. C 49.07, H 5.07, N 4.40; found C 49.07, H 5.25, N 4.43. − Optical rotation (*c* = 0.46, MeOH): $[\alpha]^{22}_D$ = +83, $[\alpha]^{22}_{578}$ = +88, $[\alpha]^{22}_{546}$ = +87.

X-ray Structure Analysis of **27**: $C_{26}H_{32}F_6N_2OPRh$ (636.42); crystal dimensions 0.32 × 0.13 × 0.13 mm^3; crystal system tetragonal; space group $I4_1$ (80); unit cell dimensions: *a* = *b* = 38.1211(1), *c* = 7.5213(1) Å, α = β = γ = 90°, *V* = 10930.1(2) $Å^3$, *Z* = 16; density $d_{calcd.}$ = 1.55 g/cm^3, μ(Mo-K_α) = 0.75 mm^{-1}, *T* = 293(2) K; θ range for data collection 1.5−25.6°; total no. of reflections 41381, independent reflections 9353 (R_{int} = 0.0523), observed reflections with $I > 2\sigma(I)$ 7346; data/restraints/parameters: 9349/29/691; goodness-of-fit on F^2 = 1.11; final *R* indices [$I > 2\sigma(I)$]: *R*1 = 0.044, *wR*2 = 0.092; absolute structure parameter: −0.05(3). Further details of the crystal structure investigation may be obtained from the Fachinformationszentrum Karlsruhe, D-76344 Eggenstein-Leopoldshafen (Germany), on quoting the depository number CSD-407778.

(+)-Di(η⁴-1,5-cyclooctadiene){2,2′-bis[4-(R)-phenyloxazolin-2-yl]-4,4′-bipyridine-N,N′′,N′,N′′′}dirhodium(I) Bis(hexafluorophosphate) (**26**): To a stirred solution of 150 mg (0.33 mmol) of **15** in dry CH_2Cl_2 (4 ml) were added 163 mg (0.33 mmol) of $[Rh(cod)Cl]_2$ in CH_2Cl_2 (5 ml) under nitrogen. The resulting dark red solution was stirred for 1.5 h, then solid NH_4PF_6 (165 mg, 1.0 mmol) was added. After stirring for another 1.5 h, the inorganic salts were filtered off and rinsed with 2 ml of CH_2Cl_2. The filtrate was evaporated and the residue was dissolved in dry acetone (5 ml). Adding dry ether (5 ml) and subsequent cooling to −20°C yielded 215 mg (0.2 mmol, 56%) of **26**. Dark red solid, m.p. > 110°C (dec.). − ^{1}H NMR (250 MHz, $CDCl_3$): δ = 1.60−2.00 (m, 8 H, cod-H_{endo}), 2.10−2.60 (m, 8 H, cod-H_{exo}), 3.96 (m, 4 H, cod-H-1, H-2, H-1′, H-2′), 4.42 (m, 4 H, cod-H-5, H-6, H-5′, H-6′), 4.62 (m, 2 H, Ox-C*H*?), 5.10−5.50 (m, 4 H, Ox-CH_2?), 7.10−7.50 (m, 10 H, Ph-*H*), 8.26 and 8.51 (m, 6 H, Py-*H*). − MS (FD, CH_2Cl_2): *m/z* = 1013 [$M^+ - PF_6$], 657 [Rh(cod)**15**$^+$], 434 = 868/2 [K^{++}]. − HR-MS (FAB, *m*-NBA + 1% TFA): *m/z* (%) = 657 (100%) [Rh(cod)**15**$^+$], calcd. for $C_{36}H_{34}N_4O_2Rh$ 657.1737, found 657.1713, diff. −2.4 mmu/3.7 ppm. − IR (KBr): $\tilde{\nu}$ (cm^{-1}) = 3060/3030/2940/2915/2875/2830 w (CH), 1645 w (C=N), 840 vs, 555 s (PF). − Optical rotation (*c* = 0.45, acetone): $[\alpha]^{23}_D$ = +16, $[\alpha]^{23}_{578}$ = +12, $[\alpha]^{23}_{546}$ = −3.3.

☆ Dedicated to Professor *H. Nöth* on the occasion of his 70th birthday.

[1] H. Brunner, A. Winter, B. Nuber, *Z. Naturforsch.*, submitted.
[2] H. Brunner, H. Nishiyama, K. Itoh, *Asymmetric Hydrosilylation* in *Catalytic Asymmetric Synthesis* (Ed.: I. Ojima), VCH Publishers, New York **1993**, 303−322.
[3] H. Brunner, *Transition Metal Catalyzed Reactions* in *Houben-Weyl, Vol. E 21d, Stereoselective Synthesis* (Eds.: G. Helmchen, R. W. Hoffmann, J. Mulzer, E. Schaumann), Thieme, Stuttgart, New York **1995**, 4074−4081.
[4] H. Brunner, W. Zettlmeier, *Handbook of Enantioselective Catalysis, Vol. I & II*, VCH, Weinheim **1993**.
[5] H. Brunner, G. Riepl, *Angew. Chem.* **1982**; *94*, 369−370; *Angew. Chem. Int. Ed. Engl.* **1982**, *21*, 377; *Angew. Chem. Suppl.* **1982**, 769−776.
[6] H. Brunner, G. Riepl, H. Weitzer, *Angew. Chem.* **1983**, *95*, 326; *Angew. Chem. Int. Ed. Engl.* **1983**, *22*, 331; *Angew. Chem. Suppl.* **1983**, 445−450.
[7] H. Brunner, R. Becker, G. Riepl, *Organometallics* **1984**, *3*, 1354−1359.
[8] H. Brunner, U. Obermann, *Chem. Ber.* **1989**, *122*, 499−507.
[9] G. Balavoine, J. C. Client, I. Lellouche, *Tetrahedron Lett.* **1989**, *30*, 5141−5144.
[10] H. Nishiyama, H. Sakaguchi, T. Nakamura, M. Horihata, M. Kondo, K. Itoh, *Organometallics* **1989**, *8*, 846−848.
[11] H. Nishiyama, M. Kondo, T. Nakamura, K. Itoh, *Organometallics* **1991**, *10*, 500−508.
[12] V. Gutmann, *The Donor-Acceptor Approach to Molecular Interactions*, Plenum Press, New York, London **1978**.
[13] G. Briegleb, *Elektronen-Donator-Akzeptor-Komplexe*, Springer, Berlin, Göttingen, Heidelberg **1961**.
[14] R. Foster, *Organic Charge-Transfer Complexes*, Academic Press, London, New York **1969**.
[15] For charge-transfer effects in catalysis see: K. Tamaru, M. Ichikawa, *Catalysis by Electron Donor-Acceptor Complexes*, Kodansha Ltd., Tokyo **1975**.
[16] A. Ledwith, H. J. Woods, *J. Chem. Soc. C* **1970**, 1422−1425.
[17] M. M. Mahmoud, S. C. Wallwork, *Acta Crystallogr., Sect. B* **1981**, *37*, 398−401.
[18] Review: J. F. Stoddart, D. B. Amabilino, *Chem. Rev.* **1995**, *95*, 2725−2728.
[19] H. Brunner, U. Obermann, P. Wimmer, *J. Organomet. Chem.* **1986**, *316*, C1-C3.
[20] R. Störiko, *Dissertation*, Universität Regensburg **1997**.
[21] R. Fielden, L. A. Summers, *J. Heterocycl. Chem.* **1974**, *11*, 299−301.
[22] D. B. Moran, G. O. Morton, J. D. Albright, *J. Heterocycl. Chem.* **1986**, *23*, 1071−1077.
[23] J.-C. Plaquevent, I. Chichaoui, *Tetrahedron Lett.* **1993**, *33*, 5287−5288.
[24] W. K. Fife, *J. Org. Chem.* **1983**, *48*, 1375−1377.
[25] T. Saika, T. Iyoda, T. Shimidzu, *Chem. Lett.* **1990**, 1955−1958.
[26] General procedure: F. C. Schaefer, G. A. Peters, *J. Org. Chem.* **1961**, *26*, 412−418.
[27] M. Peer, J. C. de Jong, M. Kiefer, T. Langer, H. Rieck, H. Schell, P. Sennhenn, J. Sprinz, H. Steinhagen, B. Wiese, G. Helmchen, *Tetrahedron* **1996**, *52*, 7547−7583.
[28] L. Persaud, G. Barbiero, *Can. J. Chem.* **1991**, *69*, 315−321.
[29] R. Fielden, L. A. Summers, *Experientia* **1974**, *30*, 843−844.
[30] Described as a non characterised intermediate in: J. Stanek, G. Caravatti, H.-G. Caparo, P. Furet, H. Mett, P. Schneider, U. Regenass, *J. Med. Chem.* **1993**, *36*, 46−54.
[31] L. Kaczmarek, R. Balicki, P. Nantka-Mamirski, *Chem. Ber.* **1992**, *125*, 1965−1966.
[32] H. Nishiyama, S. Yamaguchi, S.-B. Park, K. Itoh, *Tetrahedron: Asymmetry* **1993**, *4*, 143−150.
[33] F. Korte, K. Störiko, *Chem. Ber.* **1960**, *93*, 1033−1042.
[34] This compound has to accept an electron in the mass spectrometer, because otherwise no peak at *m/z* = 331 should occur. The expected peak for the dication at 165.5 (= 331/2) is extremely weak. The signal at *m/z* = 332 is not only due to the ^{13}C isotope pattern but must additionally represent a protonated species.
[35] I. Wölfle, J. Lodaya, B. Sauerwein, G. B. Schuster, *J. Am. Chem. Soc.* **1992**, *114*, 9304−9309.
[36] G. A. Tostikov, U. M. Jemilev, V. P. Jurjev, F. B. Gershanov, S. R. Rafikov, *Tetrahedron Lett.* **1971**, 2807−2808.
[37] C. Gastaldi, E. Princivalle, *Gazz. Chim. Ital.* **1928**, *58*, 412−416.
[38] S. Wleügel, *Ber. Dtsch. Chem. Ges.* **1882**, *15*, 1050−1056.
[39] F. H. Case, T. J. Kasper, *J. Am. Chem. Soc.* **1956**, *78*, 5842−5844.
[40] K. Kanematsu, R. T. Parfitt, A. E. Jacobsen, J. H. Ager, E. L. May, *J. Am. Chem. Soc.* **1968**, *90*, 1064−1065.
[41] K. Kanematsu, M. Takeda, A. E. Jacobsen, E. L. May, *J. Med. Chem.* **1969**, *3*, 405−408.
[42] J. Court, S. Vidal, J.-M. Bonnier, *Bull. Soc. Chim. Fr.* **1972**, 3107−3111.

[97224]

Asymmetric Catalysis, 118[◇]

Rh(I)-Catalysed Asymmetric Hydrosilylation using New Oxazoline Ligands with Potential Charge-transfer Properties☆

Henri Brunner* and Reinhard Störiko

Institut für Anorganische Chemie der Universität Regensburg,
D-93040 Regensburg, Germany
Fax: (internat.) +49(0)941/9434439
E-mail: henri.brunner@chemie.uni-regensburg.de

Received September 30, 1997

Keywords: Enantioselective hydrosilylation / Oxazoline ligands / Charge-transfer / 4,4-Bipyridine derivatives / 2,5-Dimethoxyacetophenone

Novel *N*′-methylated 2-(oxazolin-2-yl)-4,4′-bipyridinium salts, bearing a chiral oxazoline moiety, were tested in the Rh(I)-catalysed enantioselective hydrosilylation. After coordination to rhodium these electron-attracting ligands are supposed to exhibit charge-transfer effects with electron-donating substrates. Therefore, a new catalytic hydrosilylation reaction with 2,5-dimethoxyacetophenone as an electron-rich substrate was developed. The results were compared with those of the non-methylated 2-(oxazolin-2-yl)-4,4′-bipyridine and related ligands. In addition, the new ligands and Rh(I)-complexes were tested in the hydrosilylation of acetophenone.

Introduction

In the Rh(I)-catalysed enantioselective hydrosilylation of prochiral ketones, the substrate (e.g. acetophenone **1a**) reacts with diphenylsilane to yield the chiral silylalkyl ether **2a** (Scheme 1)[1][2][3]. After hydrolysis the chiral 1-phenylethanol **4a** is obtained. Asymmetric induction is brought about by in situ Rh(I)-catalysts consisting of $[Rh(cod)Cl]_2$ and preferably nitrogen ligands, e.g. chiral oxazolines[4][5][6][7].

Scheme 1

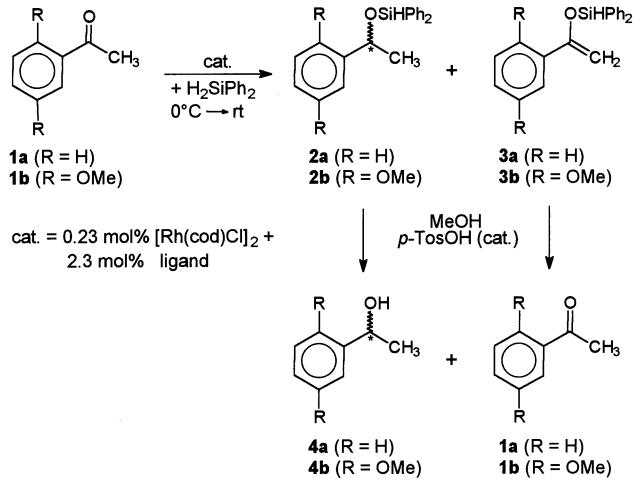

In the preceding paper, we proposed charge-transfer interactions for a possible pre-orientation of the substrate to be hydrosilylated with respect to the catalytic centre. We tried to find evidence for charge-transfer effects in the Rh(I)-catalysed hydrosilylation using the electron-rich 2,5-dimethoxyacetophenone as the substrate. As acceptor with electron-accepting properties we resorted to the Rh(I)-coordinated 2-(oxazolin-2-yl)-4,4′-bipyridinium salts **5**, described in the preceding publication. The adduct catalyst/substrate should resemble the charge-transfer complex paraquat/hydroquinone (both formulas are shown in the preceding paper, see Introduction). In the ligands of type **5** chirality is easily introduced into the oxazoline ring. Ligands **5** contain the same 2-(pyridin-2-yl)oxazoline chelating unit as the ligands of type **6** (Scheme 2), which were

Scheme 2

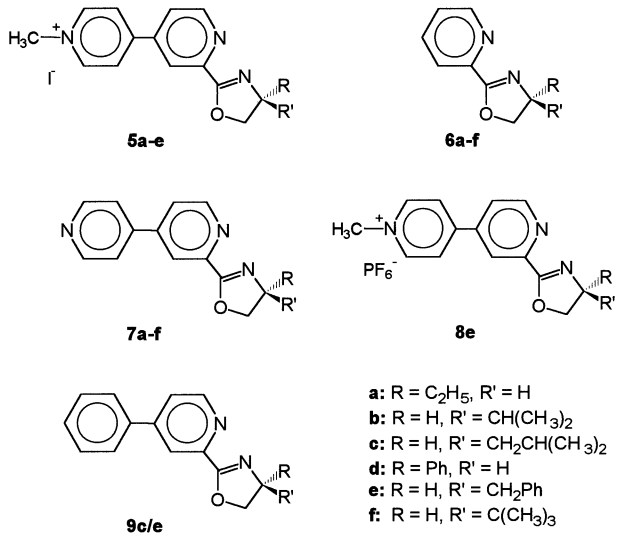

[◇] Part 117: H. Brunner, R. Störiko, F. Rominger, *Eur. J. Inorg. Chem.* **1998**, 771−781, preceding paper.

 © WILEY-VCH Verlag GmbH, D-69451 Weinheim, 1998 1434−1948/98/0606−0783 $ 17.50+.50/0

among the first successful chiral nitrogen ligands in enantioselective catalysis[4][8].

To establish charge-transfer effects in the Rh(I)-catalysed enantioselective hydrosilylation, the catalytic results of the ligands of type **5** were compared with those of similar but less electron-accepting ligands. Obvious differences in the optical yield might originate from a charge-transfer mediated pre-orientation.

Hydrosilylation of 2,5-Dimethoxyacetophenone

2,5-Dimethoxyacetophenone (**1b**) has already been tested in the asymmetric hydrosilylation[9] and in two recent papers it has been reduced with chiral auxiliaries[10][11]. A standard procedure for the hydrosilylation of 2,5-dimethoxyacetophenone with diphenylsilane was set up[12], similar to the acetophenone/diphenylsilane system. Since the racemic alcohol **4b** was not well characterised in the literature[13], it was synthesised by reduction of **1b** with KBH_4 in methanol and spectroscopically characterised. The catalytic intermediates **2b** and **3b** were analysed in situ by ^1H NMR spectroscopy. The silylenol ether **3b** originates from the enol tautomer of **1b** and on hydrolysis reverts to the ketone **1b** (Scheme 1). Hence, it reduces the chemical yield of the chiral alcohol **4b**.

For quantification of the catalytic results three parameters were calculated from the ^1H NMR spectra (80 MHz, $CDCl_3$), which were recorded for each catalysis (reproducibility about ±5%): (i) the amount of silylenol ether **3** in the hydrosilylation product: **3**/(**2**+**3**); (ii) the total degree of hydrosilylation (conversion): (**2**+**3**)/(**1**+**2**+**3**) and (iii) the chemical yield of the silylalkyl ether **2**, which on hydrolysis is converted to the chiral product **4**: (**2**)/(**1**+**2**+**3**). The enantiomeric excess of the alcohol **4** was determined by GC with a Chirasil-DEX CB column (reproducibility ±0.5%). The values in the tables were averaged over usually two independent runs, differing in most cases less than 5% (conversion and chemical yield) and 1% (ee), respectively.

To compare the *N*′-methylated ligands **5a−e** with the non-methylated ligands **7a−e** (Scheme 2) each pair was doubly tested in parallel runs. No CCl_4 (see later) was added due to the limited solubility of the ionic compounds **5a−e** in chlorinated solvents. For reaction conditions and results see Table 1.

All the *N*′-methylated ligands **5a-e** induced much higher optical inductions than their non-methylated counterparts **7a−e** (Figure 1). The pair **5c/7c** exhibited the largest difference with an average Δee of about 40%. The degree of hydrosilylation was generally high (>79%), in some cases even quantitative. The amount of silylenol ether scattered around 14−58%.

The non-methylated bipyridines **7a** and **7e** performed much better if CCl_4 was added. No silylenol ether was formed and the optical yield increased remarkably (Table 1). This significant increase in asymmetric induction on conducting the hydrosilylation in CCl_4 is known as the CCl_4 effect[4][14][15] and will be referred to later.

Table 1. Hydrosilylation of 2,5-dimethoxyacetophenone with **5a−e**, **7a−e**, **8e**, **9c** and **9e**; reaction time: 90 h (no solvent) or 18 h (in CCl_4); catalyst: 0.23 mol% $[Rh(cod)Cl]_2$ (0.46 mol% Rh) and 2.3 mol% ligand; substrate/Rh: 214:1

ligand	no of runs	silylenol ether [%]	conversion [%]	chemical yield [%]	ee (*config.*) [%]	
7a	2	26	95[a]	71	5.8	(*S*)
	2 (+ CCl_4)	0	77	77	38.5	(*S*)
5a	2	22	86[a]	68	27.0	(*S*)
7b	2	23	99[a]	77	3.2	(*R*)
5b	2	34	90[a]	60	28.1	(*R*)
7c	2	26	100	75	7.1	(*R*)
5c	2	19	86	70	44.4	(*R*)
9c	2 (18 h)	11	97[a]	88	46.3	(*R*)
7d	2	25	100	76	1.0	(*S*)
5d	2	50	93[a]	47	10.5	(*S*)
7e	4	21	96[a]	76	6.7	(*R*)
	2 (+ CCl_4)	0	96[a]	96	52.1	(*R*)
5e	4	26	91[a]	68	29.0	(*R*)
8e	2	30	78	55	9.4	(*R*)
9e	2 (18 h)	12	99[a]	87	44.8	(*R*)

[a] No more diphenylsilane detectable by ^1H NMR spectroscopy (80 MHz, $CDCl_3$).

Figure 1. Comparison of the enantioselectivities of the hydrosilylation of 2,5-dimethoxyacetophenone with the ligands **7a−e** and **5a−e**

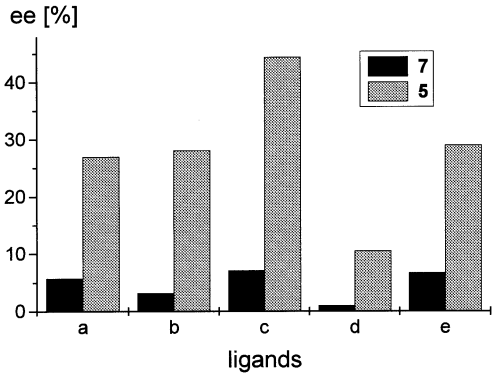

Unexpectedly, the anion exchanged **8e** (hexafluorophosphate instead of iodine in **5e**, Scheme 2) led to a much lower enantioselectivity than **5e** (Table 1), a result which does not fit into the picture of charge-transfer interactions between coordinated ligand and substrate.

The 2-(4-phenylpyridin-2-yl)oxazoline ligands **9c** and **9e** (Scheme 2) are sterically almost identical to **7c** and **7e**, respectively. As they are definitely less electron-attracting than **5c** and **5e**, no charge-transfer effects were expected in the hydrosilylation of 2,5-dimethoxyacetophenone. Surprisingly, both ligands yielded relatively high enantioselectivities (**9c**: 46.3% ee, **9e**: 44.8% ee, Table 1), which are slightly better than the *N*′-methylated ligands **5c** and **5e** and differ markedly from their sterically equivalent 4,4′-bipyridine counterparts **7c** and **7e**. An explanation of these findings might be the free *N*′-position in the ligands **7**. It is known that for the Rh(I)-catalysed hydrosilylation with nitrogen ligands, a ligand excess is beneficial. This points to equilibria involving catalytically active species containing at least two ligand molecules, one of which could be even monodentate[15]. Only the non-methylated ligands **7** can bind via

their free pyridine′ nitrogen and this might result in the low optical yields. Due to the methylation of this nitrogen in **5** and due to the phenyl substituent in **9** the formation of such species is impossible for these ligands.

Also, the bisoxazolines **10** and **11** (Scheme 3) were tested due to their potential charge-transfer properties if coordinated to two Rh-centres. A Rh/ligand ratio of 2:1 was used and CCl_4 was added (no precipitation as with ligands **5a−e** was observed). However, no asymmetric induction was observed with **10** and **11**[12].

Scheme 3

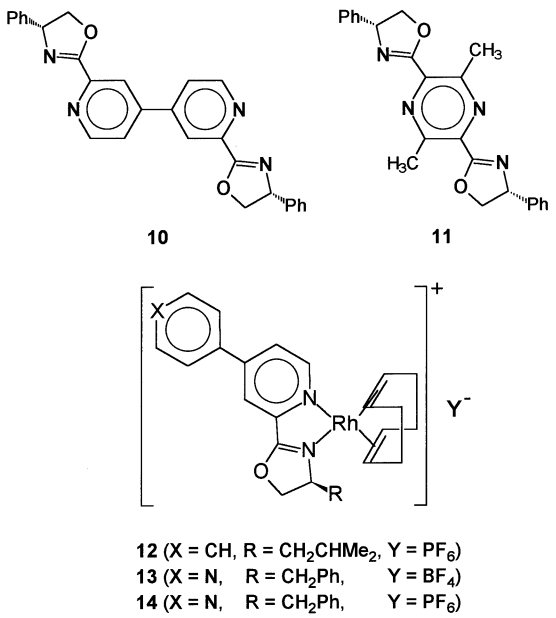

12 (X = CH, R = CH_2CHMe_2, Y = PF_6)
13 (X = N, R = CH_2Ph, Y = BF_4)
14 (X = N, R = CH_2Ph, Y = PF_6)

So far the hydrosilylation results did not provide definitive proof for charge-transfer interactions between coordinated ligand and substrate. Hence, we investigated the absorption behaviour of some presumed catalytic intermediates looking for charge-transfer transitions[16]. The UV spectra of equally concentrated methanol solutions of 2,5-dimethoxyacetophenone, [Rh(cod)**5e**]Cl (prepared in situ), and [Rh(cod)**5e**]Cl + 2,5-dimethoxyacetophenone (1:1) were recorded. 2,5-Dimethoxyacetophenone showed an absorption maximum at 330 nm in accord with the literature[17]. [Rh(cod)**5e**]Cl exhibited a maximum at 287 nm and a shoulder at ca. 380 nm. The spectrum of the 1:1 catalyst/substrate mixture was only a superposition of the compounds′ single spectra. No charge-transfer transitions were found up to 900 nm (Figure 2).

By substituting the electron-rich 2,5-dimethoxyacetophenone for the much less electron-donating acetophenone (to be described next), charge-transfer interactions should be strongly reduced. However, **5e** used as a cocatalyst in the hydrosilylation of acetophenone gave a higher optical induction than the non-methylated **7e** (17.8% compared to 9.6% ee, similar amounts of silylenol ether and chemical yields under identical conditions)[12].

All these experiments showed that the desired charge-transfer interactions, if existent at all, had only little influence on the catalytic results compared to other effects resulting from the nature of the ligands.

Figure 2. UV-Spectra in methanol (ca. 10^{-5} M)

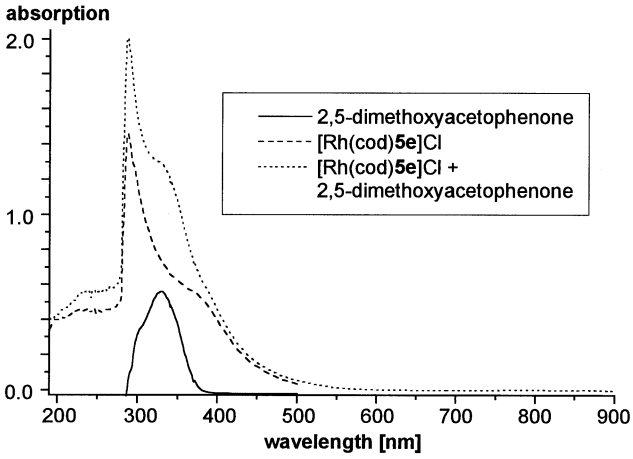

Hydrosilylation of Acetophenone

The new ligands were tested in the hydrosilylation of acetophenone with diphenylsilane in CCl_4. The results of the oxazolines **7a-f** and the bisoxazoline **10** are shown in Table 2. In general good chemical (up to 95%) and optical yields (up to 74% ee) were obtained. In most cases no silylenol ether was formed.

Table 2. Hydrosilylation of acetophenone with **7a-f** and **10**; reaction time: 18 h; catalyst: 0.24 mol% $[Rh(cod)Cl]_2$ (0.48 mol% Rh) and 2.35 mol% ligand; substrate/Rh: 210:1

ligand	no of runs (solvent)	silylenol ether [%]	conversion [%]	chemical yield [%]	ee (*config.*) [%]
7a	2 (CCl_4)	0	92[a]	92	59.8 (*S*)
7b	2 (CCl_4)	0	91[a]	91	66.5 (*R*)
7c	2 (CCl_4)	0	94[a]	94	73.9 (*R*)
7d	2 (CCl_4)	7	78[a]	70	62.9 (*S*)
10[b]	2 (CCl_4)	50	85[a]	42	29.8 (*S*)
7e	2 (CCl_4)	0	94[a]	94	67.9 (*R*)
7e[c]	2 (none)	34	98[a]	65	9.6 (*R*)
7e	1 (C_6F_6)	46	99[a]	53	4.3 (*R*)
7e	1 (C_6HF_5)	11	96[a]	85	37.1 (*R*)
7e	1 (Cl_2-C=CCl_2)	49	96[a]	49	*racemate*
7e	2 (CCl_3Br)	–	0	0	–
7f	2 (CCl_4)	14	81[a]	70	31.8 (*R*)

[a] No more diphenylsilane detectable by ^1H NMR spectroscopy (80 MHz, $CDCl_3$). – [b] 1.16 mol% ligand. – [c] Reaction time: 90 h.

Figure 3 compares the enantioselectivities obtained with the ligands **7a−f** and the reported values (comparable conditions) of the 2-(pyridin-2-yl)oxazolines **6a−f** (Scheme 1)[4].

The 2-(4,4′-bipyridin-2-yl)oxazolines **7a−c** and **7e** induced a slightly higher optical induction compared to the corresponding 2-(pyridin-2-yl)oxazolines **6**. Only **7d** and **7f** performed worse than their counterparts **6d** and **6f**. The results with the *tert*-butyl substituted **7f** were surprising, because the enantiomeric excess dropped appreciably with re-

Figure 3. Comparison of the enantioselectivities of the hydrosilylation of acetophenone with the ligands **7a−f** and **6a−f** (values of **6a−f** taken from the literature[4])

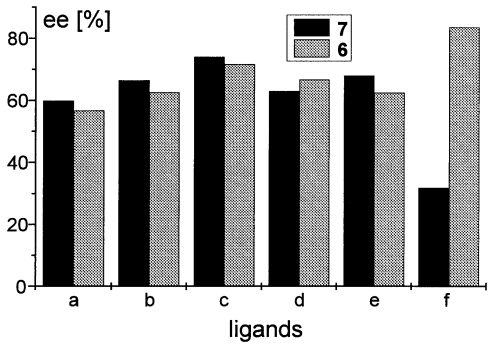

gard to **6f**, which still is the best 2-(pyridin-2-yl)oxazoline for asymmetric hydrosilylation[4].

With the bisoxazoline **10** less than half the optical yield of its mono-oxazoline equivalent **7d** was obtained (Table 2), while the amount of silylenol ether was more than sevenfold. The pyrazine ligand **11** did not yield any optically active product at all (three double experiments with different concentrations of **11**)[12].

It is well known, that Rh(I)-catalysed hydrosilylations with nitrogen ligands tend to give higher chemical and, in particular, optical yields in the presence of CCl_4 ("CCl_4 effect")[4][14][15]. So far the highest increase in the asymmetric induction by conducting the catalysis in CCl_4 has been 18.3% ee compared to toluene solution or the solvent-free procedure[15]. As already mentioned, the bipyridine ligands **7a** and **7e** improved the optical yields in the hydrosilylation of 2,5-dimethoxyacetophenone in CCl_4 by striking 32.7 and 45.4% ee, respectively (Table 1).

Using acetophenone as the prochiral substrate and **7e** as the cocatalyst the optical induction in CCl_4 increased by 58.3% compared to the solvent-free reaction (Table 2). Therefore, we studied the hydrosilylation of acetophenone using the ligand **7e** in other polyhalide solvents (Table 2). None of these solvents increased the enantioselectivity compared to CCl_4. Replacing hexafluorobenzene by pentafluorobenzene the content of silylenol ether decreased from 46 to 11%, while the optical yield increased from 4.3 to 37.1%. In perchloroethylene only racemic alcohol was produced, whereas CCl_3Br totally inhibited the hydrosilylation. This inhibition had been reported for similar reactions[14] and explained by an oxidative addition of CCl_3Br to Rh(I) yielding a catalytically inactive Rh(III)-species.

The activity of in situ catalysts consisting of $[Rh(cod)Cl]_2$ and the 2-(4-phenylpyridin-2-yl)oxazolines **9c** and **9e** depended on the stage, when the additive CCl_4 came into play (Table 3). If the in situ catalyst (always easily recognised by its red colour) was prepared in the presence of CCl_4, no hydrosilylation activity was observed. If the in situ catalyst was prepared in acetophenone and CCl_4 was added later together with the diphenylsilane, smooth reaction took place as usual.

Since the Rh-complex **12** (Scheme 3), containing **9c** as the ligand, had been synthesised (preceding paper), it was tested in three different catalytic runs (Table 3). **12** proved to be a poor catalyst with respect to the chemical and optical yield. However, by adding a fourfold amount of ligand establishing the Rh/ligand ratio of 1:5, a catalytic system resulted, which formed almost no silylenol ether and which gave 74.8% ee, exceeding the asymmetric induction of the in situ system (70.5% ee) to some extent.

Table 3. Hydrosilylation of acetophenone with the ligands **9c**, **9e** and the complexes **12−14**; reaction time: 18 h (if not otherwise stated); 0.48 mol% Rh; substrate/Rh: 210:1

catalytic system	no of runs (solvent)	silylenol ether [%]	conversion [%]	chemical yield [%]	ee (*config.*) [%]	
$[Rh(cod)Cl]_2$ + 2.35 mol% **9e**	1 (none)	13	99[a]	86	54.9	(*R*)
$[Rh(cod)Cl]_2$ + 2.35 mol% **9e**	3 (CCl_4 from the beginning)	−	0, 0[b]	0, 0[b]	−	
$[Rh(cod)Cl]_2$ + 2.35 mol% **9e**	1 (CCl_4 added with H_2SiPh_2)	0	93[a]	93	64.2	(*R*)
$[Rh(cod)Cl]_2$ + 2.35 mol% **9c**	2 (none)	22	100	78	45.0	(*R*)
$[Rh(cod)Cl]_2$ + 2.35 mol% **9c**	(CCl_4 from1 the beginning)	−	0	0	−	
$[Rh(cod)Cl]_2$ + 2.35 mol% **9c**	1 (CCl_4 added with H_2SiPh_2)	5	95[a]	90	70.5	(*R*)
12[c]	1 (CCl_4 from the beginning)	62	96[a]	36	2.9	(*R*)
12[c]	1 (CCl_4 added with H_2SiPh_2)	76	92[a]	22	2.6	(*R*)
12 + 1.9 mol% **9c**[d]	2 (CCl_4 added with H_2SiPh_2)	2	84	83	74.8	(*R*)
13	1 (CCl_4)[c]	17	81[a]	68	33.6	(*R*)
	1 (CCl_4)[d]	29	86[a]	61	34.6	(*R*)
14	2 (CCl_4)[d]	25	74[a]	57	14.4	(*R*)
14 + 1.9 mol% **7e**	2 (CCl_4)[c]	0	85	85	66.2	(*R*)

[a] No more diphenylsilane detectable by ^1H NMR spectroscopy (80 MHz, $CDCl_3$). − [b] After 90 h. − [c] Reaction time: 66 h. − [d] Reaction time: 42 h.

All these results show that the inhibition of the catalyst by CCl_4 is only possible during its formation. Once the catalyst is formed, CCl_4 cannot inhibit its activity. Instead, it leads to a lower amount of silylenol ether and a higher enantioselectivity compared to the hydrosilylation without CCl_4 (Table 3). The ″inertness″ of the prepared Rh(I)-complex **12** towards CCl_4 was also proven by recording ^1H NMR spectra of **12** in $CDCl_3$ before and after adding 25 vol% of CCl_4. Even 24 h after the addition no changes of the original spectrum were evident.

Two other Rh(I)-complexes **13** and **14** (Scheme 3) were tested in the hydrosilylation of acetophenone (Table 3). Although they only differ in the nature of their anion, the BF_4-complex **13** gave a much higher optical yield than the PF_6-complex **14**. The enantioselectivities of these complexes (Rh/ligand ratio: 1:1) are quite low compared to the in situ catalysts (Rh/ligand ratio: 1:5). In line with this, addition of a fourfold excess of **7e** to **14** resulted in similar chemical and optical yields as the in situ catalyst of $[Rh(cod)Cl]_2$ and **7e** (Tables 3 and 2).

We thank the *Fonds der Chemischen Industrie* for providing a *Kekulé* scholarship for R.S. and for financial support.

Experimental Section

Chromatography: Merck silica gel 60 (63−200 mesh). − Elemental analysis: Microanalytical Laboratory, University of Regensburg. − ^1H / ^{13}C NMR: Bruker AW-80 (80 MHz, T = 31°C) and AC-250 (250 / 62.9 MHz, T = 24°C), TMS as internal standard. − MS: Finnigan MAT 311 A (EI, 70 eV). − IR: Beckman IR 4240 (film between NaCl plates), only characteristic bands are listed. − UV/Vis: Kontron Instruments Spectrophotometer UVIKON 922. − All liquids were distilled and stored under argon. − η^4-1,5-Cyclooctadiene = cod.

Asymmetric Hydrosilylation of 2,5-Dimethoxyacetophenone: 8 mg (0.016 mmol) of $[Rh(cod)Cl]_2$ (0.032 mmol Rh) and ligand (0.16 mmol, if not otherwise stated) were dissolved in 2,5-dimethoxyacetophenone (1.1 ml, 7.0 mmol) under argon. Eventually, 1.7 ml of CCl_4 were added and the solution was stirred at r. t. for 30 min. After cooling to 0°C for at least 30 min diphenylsilane (1.3 ml, 7.0 mmol) was added and stirring in the ice bath, which was warming-up, continued for the period quoted.

To determine the amount of silylenol ether, the degree of hydrosilylation and the chemical yield, a sample was taken and a ^1H NMR spectrum ($CDCl_3$, 80 MHz) recorded. The following integrals were used: δ = 5.43 (s, Si*H*) and 5.36 (q, C*H*) together (silylalkyl ether I_A), δ = 5.10 and 4.77 (2 d, CH_2) together (silylenol ether I_E), and δ = 2.60 (s, CH_3, 2,5-dimethoxyacetophenone I_{DMAP}). Calculations: silylenol ether [%] = $[I_E/(I_A + I_E)]\cdot 100$, conversion [%] = $[(3\ I_E + 3\ I_A)/(3\ I_A + 3\ I_E + 2\ I_{DMAP})]\cdot 100$, and chemical yield [%] = $[3I_A/(3I_A + 3I_E + 2I_{DMAP})]\cdot 100$.

Hydrolysis was performed by adding methanol (8 ml) and a few crystals of *p*-TosOH. After stirring at r. t. for 30 min the solvents were evaporated. Ca. 0.1 ml of the residue were purified by chromatography (4−5 cm SiO_2 in a Pasteur pipette) with CH_2Cl_2 as eluent (R_f = 0.12). The first fraction (ca. 3 ml) was discarded, the following 10 ml were collected and evaporated. The enantiomeric excess was determined by injecting 0.4 µl of a solution of the resulting oil (1−2 drops) in 1 ml of CH_2Cl_2 (Merck Uvasol®) into a Fisons 8130 gas chromatograph. Column: Chrompack Chirasil-DEX CB (l = 25 m, ⊘ = 0.25 mm), integrator: Varian 4290, retention times (160°C): 8.6−8.8 min [*(R)*-1-(2,5-dimethoxyphenyl)ethanol] and 9.2−9.4 min [(*S*)-1-(2,5-dimethoxyphenyl)ethanol].

1-(2,5-Dimethoxyphenyl)ethyl Diphenylsilyl Ether (**2b**). − ^1H NMR (250 MHz, $CDCl_3$): δ = 1.45 (d, ^3J = 6.2 Hz, 3 H, CH_3), 3.65 (s, 3 H, OCH_3), 3.73 (s, 3 H, OCH_3'), 5.36 (q, ^3J = 6.2 Hz, 1 H, $CHCH_3$), 5.43 (s, 1 H, Si*H*), 6.71 / 6.72 / 7.19 (3 m, 3 H, H-3, H-4, H-6), 7.29−7.45 (m, 6 H, Ph-*H*), 7.56−7.65 (m, 4 H, Ph-*H*).

1-(2,5-Dimethoxyphenyl)ethenyl Diphenylsilyl Ether (**3b**)[18]. − ^1H NMR (250 MHz, $CDCl_3$): δ = 3.69 (s, 3 H, OCH_3), 3.72 (s, 3 H, OCH_3'), 4.77 (d, ^2J = 1.2 Hz, 1 H, C=C*H*H′), 5.10 (d, ^2J = 1.2 Hz, 1 H, C=CH*H*′), 5.64 (s, 1 H, Si*H*), 6.79−6.81 (m, 2 H, Ar-*H*), 7.15 (m, 1 H, Ar-H), 7.27−7.49 and 7.52−7.71 (m, 10 H, Ph-*H*).

rac-1-(2,5-Dimethoxyphenyl)ethanol (**4b**): 2,5-Dimethoxyacetophenone (1.5 ml, 9.5 mmol) and KBH_4 (800 mg, 14.8 mmol) in dry methanol (10 ml) were stirred for 15 h. After acidifying with 2 N HCl (10 ml) the solution was extracted with ether (3× 10 ml). The combined organic layers were washed with water (10 ml) and brine (10 ml), and dried over $MgSO_4$. Evaporation of the solvent yielded 1.73 g (100%) of the oily alcohol **4b**. − ^1H NMR (250 MHz, $CDCl_3$): δ = 1.48 (d, ^3J = 6.4 Hz, 3 H, CH_3), 2.76 (d, ^3J = 4.8 Hz, 1 H, O*H*), 3.76 (s, 3 H, OCH_3), 3.81 (s, 3 H, OCH_3'), 5.05 (dq, ^3J = 6.4 Hz, ^3J = 4.8 Hz, 1 H, CH_3CHOH), 6.74 (dd, ^3J = 8.7 Hz, ^4J = 2.8 Hz, 1 H, H-4), 6.79 (dd, ^3J = 8.7 Hz, ^5J = 0.8 Hz, 1 H, H-3), 6.94 (dd, ^4J = 2.8 Hz, ^5J = 0.8 Hz, 1 H, H-6). − ^{13}C NMR (62.9 MHz, $CDCl_3$): δ = 23.1 (CH_3), 55.8 and 55.9 (OCH_3), 66.4 (*C*HOH), 111.6 / 112.4 / 112.5 (C-3, C-4, C-6), 134.9 (C-1), 150.7 (C-2), 154.0 (C-5). − MS (EI): *m/z* (%) = 182 (100) [M^+], 167 (95) [$M^+ - CH_3$], 152 (24), 139 (88), 137 (32), 124 (33), 43 (29). − IR (film): $\tilde{\nu}$ (cm^{-1}) = 3400 s (O−H), 2960/2945 s (C−H), 2830 s (OC−H), 1275/1210/1070/1045/1020 s (C−O). − $C_{10}H_{14}O_3$ (182.22): calcd. C 65.91, H 7.74; found C 65.64, H 7.81.

Asymmetric Hydrosilylation of Acetophenone: 10 mg (0.02 mmol) of $[Rh(cod)Cl]_2$ (0.04 mmol Rh) and ligand (0.2 mmol, if not otherwise stated) were dissolved in acetophenone (1.0 ml, 8.5 mmol) under argon. Usually, 2.0 ml of CCl_4 were added and the solution was stirred at r. t. for 30 min. After cooling to 0°C for at least 30 min diphenylsilane (1.6 ml, 8.6 mmol) was added and stirring in the ice bath, which was warming-up, continued for the period quoted.

To determine the amount of silylenol ether, the degree of hydrosilylation and the chemical yield, a sample was taken and a ^1H NMR ($CDCl_3$, 80 MHz) recorded. The following integrals were used: δ = 5.70 ppm (s, Si*H*, silylenol ether I_E), δ = 5.40 (s, Si*H*, silylalkyl ether I_A), and δ = 2.50 (s, CH_3, acetophenone I_{AP}). Calculations: silylenol ether [%] = $[I_E/(I_A + I_E)]\cdot 100$, conversion [%] = $[(3\ I_E + 3\ I_A)/(3\ I_A + 3\ I_E + I_{AP})]\cdot 100$, and chemical yield [%] = $[3\ I_A/(3\ I_A + 3\ I_E + I_{AP})]\cdot 100$.

Hydrolysis was performed by adding methanol (10 ml) and a few crystals of *p*-TosOH. After stirring at r. t. for 30 min the solvents were evaporated and the residue was distilled in a kugelrohr apparatus at 100−120°C / ca. 1 Torr. The enantiomeric excess was determined by injecting 0.4 µl of a solution of the distillate (3−4 drops) in 1 ml of CH_2Cl_2 (Merck Uvasol®) into a Fisons 8130 gas chromatograph. Column: Chrompack Chirasil-DEX CB (l = 25 m, & osol; = 0.25 mm), integrator: Varian 4290, retention times (118°C): 7.3−7.7 min [(*R*)-1-phenylethanol] and 8.0−8.3 min [(*S*)-1-phenylethanol].

☆ Dedicated to Professor *H. Nöth* on the occasion of his 70th birthday.

[1] H. Brunner, H. Nishiyama, K. Itoh, *Asymmetric Hydrosilylation* in *Catalytic Asymmetric Synthesis* (Ed.: I. Ojima), VCH Publishers, New York **1993**, 303−322.
[2] H. Brunner, *Transition Metal Catalyzed Reactions* in *Houben-Weyl, Vol. E 21d, Stereoselective Synthesis* (Eds.: G. Helmchen, R. W. Hoffmann, J. Mulzer, E. Schaumann), Thieme, Stuttgart, New York **1995**, 4074−4081.
[3] H. Brunner, W. Zettlmeier, *Handbook of Enantioselective Catalysis, Vol. I & II*, VCH, Weinheim **1993**.
[4] H. Brunner, U. Obermann, *Chem. Ber.* **1989**, *122*, 499−507.
[5] G. Balavoine, J. C. Client, I. Lellouche, *Tetrahedron Lett.* **1989**, *30*, 5141−5144.
[6] H. Nishiyama, H. Sakaguchi, T. Nakamura, M. Horihata, M. Kondo, K. Itoh, *Organometallics* **1989**, *8*, 846−848.
[7] H. Nishiyama, M. Kondo, T. Nakamura, K. Itoh, *Organometallics* **1991**, *10*, 500−508.
[8] H. Brunner, U. Obermann, P. Wimmer, *J. Organomet. Chem.* **1986**, *316*, C1−C3.
[9] H. Brunner, A. Kürzinger, *J. Organomet. Chem.* **1988**, *346*, 413−424.
[10] P. Ramachandran, P. Veeraraghavan, B. Gong, H. C. Brown, *Tetrahedron Lett.* **1994**, *35*, 2141−2144.
[11] Y.-J. Cherng, J.-M. Fang, T.-J. Lu, *Tetrahedron: Asymmetry* **1995**, *6*, 89−92.
[12] R. Störiko, *Dissertation*, Universität Regensburg **1997**.
[13] M. Mayen, E. Marechal, *Bull. Soc. Chim. Fr.* **1972**, 4662−4681.
[14] H. Brunner, C. Huber, *Z. Naturforsch.* **1991**, *43b*, 1145−1148.
[15] H. Brunner, P. Brandl, *Tetrahedron: Asymmetry* **1991**, *2*, 919−930.
[16] See for example: L. J. Andrews, R. M. Keefer, *Molecular Complexes in Organic Chemistry*, Holden-Day, San Francisco, London, Amsterdam **1964**.
[17] R. Matsushima, Y. Hiramatsu, T. Kitanishi, *J. Chem. Soc., Perkin Trans. 2* **1988**, 847−850.
[18] Determined by analysis of a mixture consisting of ca. 25% **3b** and ca. 75% **2b**.

[97225]

Synthesis of Oxorhenium(V) Complexes Derived from 7α-Functionalized Testosterone: First Rhenium-Containing Testosterone Derivatives

Frank Wüst*[a], Dieter Scheller[b], Hartmut Spies[a], and Bernd Johannsen[a]

Forschungszentrum Rossendorf e.V., Institut für Bioanorganische und Radiopharmazeutische Chemie[a],
Postfach 510119, D-01314 Dresden, Germany

Institut für Organische Chemie der Technischen Universität Dresden[b],
Mommsenstraße 6, D-01062 Dresden, Germany

Received September 29, 1997

Keywords: Steroids / Rhenium / 7α-Substituted testosterone / Androgen receptor / Chelates

In an effort to assist in the preparation of metal-containing ligands for the androgen receptor, we have synthesized the first oxorhenium(V) complexes containing a pendant testosterone moiety. The key step in the synthesis involves the copper-catalysed, α-selective 1,6-Michael addition of a 4-pentenylmagnesium bromide to 6-dehydrotestosterone 17β-acetate. The α-stereoselectivity is governed by the presence of the C-19 methyl group. The absolute configurations of the epimers were investigated by ^{1}H-NMR studies. Further chemical transformations of the 7α-pentenyl spacer introduced the terminal thiol group, needed for complex formation. The complex formation was accomplished by the "3+1" mixed-ligand concept using two different rhenium precursors. The obtained complexes differ with respect to the central donor atom of the tridentate ligand part, namely, S and O.

Introduction

The development of radiolabeled ligands for the androgen receptor may make possible the imaging and detection of androgen-dependent tumors, such as prostate cancer, as well as greatly facilitate the study of androgen action in heterogeneous tissues[1]. Because of its wide availability, convenient half-life and appropriate γ energy, technetium-99m is frequently the radionuclide of choice for diagnostic imaging agents in nuclear medicine[2]. Therefore, the synthesis of technetium- and rhenium-containing steroids that are capable of binding to steroid-hormone receptors with high affinity has been a goal of many investigators[3]. A number of radiolabeled steroid ligands have been prepared as molecular probes for the estrogen and progesterone receptors[4]. A detailed study of the androgen receptor has lagged behind the other sex steroid receptors due in part to the low levels of androgen receptor present in most target tissues, and also to the relatively low stability of this receptor[5][6]. The recent developments of radiolabeled ligands for the androgen receptor involved only syntheses of radiohalogenated, C-11- and 3-H-labeled derivatives of testosterones, 19-nortestosterone and 5α-dihydrotestosterone[6][7][8]. To date, there are no reports using technetium or rhenium as androgen labels.

Recently, it has been shown that the androgen receptor can tolerate a bulky iodide at the 7α position[6]. Moreover, the access to 7α-alkyl and -(phenylalkyl) substituents is well known[9][10]. Therefore, we focused our attention on the introduction of a 7α-alkyl side-chain into the testosterone skeleton bearing a terminal oxorhenium(V) chelate according to the mixed-ligand concept[11][12]. In our preliminary investigations we used rhenium as a surrogate for the radioactive technetium.

Results and Discussion

In this paper we report the synthesis of 17β-hydroxy-7α-(5-mercaptopent-1-yl)-androst-4-en-3-one (**8**) and its conversion into the corresponding oxorhenium(V) "3+1" mixed-ligand complexes. The ω-mercaptoalkyl-functionalized testosterone derivative **8** binds as a monodentate ligand to the oxorhenium(V) core, with the remaining positions at the metal center occupied by a tridentate dithiolate ligand "SXS" . The latter ligand differs with respect to the central donor atom, which can be O or S. The key step of the synthesis of **8** (Scheme 1) involves the diastereoselective introduction of a 4-pentenyl group into the 7α position of the testosterone skeleton. This reaction succeeded by the copper-catalysed, 1,6-conjugate Michael addition of a 4-pentenyl chain to 6-dehydrotestosterone **1**[13]. We used a modification of the procedure by French et al.[10a], replacing pure THF as the solvent and 7 mol-% CuCN (related to 5-bromopentene) instead of a mixture of THF/Et_2O and 0.5 equiv. of CuI. The reaction proceeded with an α/β diastereoselectivity of 4.3:1 which is similar to that of French. The 19β-methyl group in **1** increases the steric bulk of the β face and therefore increases the α selectivity. The separation of both diastereomers of **2** was easily accomplished by flash chromatography to yield the desired diastereomers in 43% (**2a**) and 10% (**2b**). The 4-pentenyl group was used as nucleophilic component containing a masked primary alcohol. This strategy eliminates the need for protecting-group manipulations, contrary to other investigators who have used protected alcohols as nucleophilic compo-

 © WILEY-VCH Verlag GmbH, D-69451 Weinheim, 1998 1434−1948/98/0606−0789 $ 17.50+.50/0

nents[10b][10c]. The following transformation of **2a** into the required alcohol **5** was achieved by subsequent cleavage of the acetyl group of **2a** and introduction of a TBDMS protecting group followed by a hydroboration/oxidation step using 9-BBN, H_2O_2 and NaOH. The regeneration of the enone system in the A ring of **5** was accomplished by oxidation using *N*-bromoacetamide.

The introduction of a thiol group into the steroid molecule succeeded via a thiobenzoate by the Mitsunobu reaction[14] starting from alcohol **5**. This reaction is the method of choice for the introduction of a sulfur moiety under mild conditions in high yield. By treatment of alcohol **5** with the system PPh_3, DIAD and BzSH the thiobenzoate **6** was obtained in a satisfactory yield of 88%. The cleavage of the TBDMS ether in **6** by treatment with TBAF in THF as the otherwise usual TBDMS deprotecting agent failed. The removal of the silyl ether protecting group succeeded in the system 40% HF/acetonitrile in moderate yield of 68%. The last step of the synthesis involves the saponification of **7** by sodium methoxide in MeOH to give the desired thiol **8**. The overall yield for the end product **8** is 12% based on 6-dehydrotestosterone **1**.

The absolute configurations of the chromatographically separated compounds **2a** (7α isomer) and **2b** (7β isomer) were determined by ^{1}H-NMR measurements[10]. These measurements established the chemical shifts and the coupling pattern of the AB part of the 6α-H, 6β-H and 7-H ABX system of both diastereomers **2a** and **2b**. The assignment of 6α-H (**2a**: δ = 2.32, dd, $^2J_{6\alpha6\beta}$ = 14.3 Hz and $^3J_{6\alpha7\beta}$ = 2.5 Hz; **2b**: δ = 2.30, dd, $^2J_{6\alpha6\beta}$ = 14.5 Hz and $^3J_{6\alpha7\alpha}$ = 5.0 Hz) and 6β-H (**2a**: δ = 2.38, dd, $^2J_{6\alpha6\beta}$ = 14.3 Hz and $^3J_{6\beta7\beta}$ = 5.1 Hz; **2b**: δ = 2.18, dd, $^2J_{6\alpha6\beta}$ = 14.5 Hz and $^3J_{6\beta7\alpha}$ = 12.6 Hz) was confirmed by using the 2D-NOESY and COSY technique.

The large $^3J_{\text{axial-axial}}$ coupling constant of 12.6 Hz according to the Karplus curve between 6β-H and 7α-H indicates that the pentyl spacer at the 7-C of **2b** is β-substituted. This led us to the conclusion that compound **2a** therefore must be α-substituted.

The complex formation according to the "3+1" concept by the use of two different rhenium precursors **9**[12] and **10**[15] offers the access to oxorhenium(V) complexes which differ in the central donor atom of the tridentate ligand part, being S for **12** and O for **13**. The corresponding mixed-ligand complexes **12** and **13** could be obtained as reddish-brown and wine-red amorphous glasses in 71% (for **12**) and 14% (for **13**) yield, respectively (Scheme 2).

The common reaction of both the tridentate ligand "SOS" **11** and the thiol **8** with the oxorhenium(V) precursor **10** leads to the complex **13**. This reaction occurs immediately at 0°C due to the high reactivity of rhenium precursor **10**. For the preparation of rhenium complex **12** an alternative route is used, based on the chlorine-containing complex **9** as a precursor. The complex formation by exchange of the chlorine atom in **9** by the mercaptide sulfur of **8** requires heating for 2 hours. In the infrared spectra a strong absorption band at 961 cm^{-1} (for **12**) and 969 cm^{-1} (for **13**) is observed, which is indicative of the $Re{=}O^{3+}$ core. The ^{1}H-NMR spectrum of **12** shows at δ = 3.12, 3.91 and 4.30 complex coupling patterns of the tridendate "SSS" ligand protons. By using the "SOS" ligand resulting in complex **13** only broad signals could be observed.

The complexes **12** and **13** represent the first examples of rhenium-containing androgen receptor ligands. Further investigations concerning the biological evaluation of **12** and **13** and their technetium analogues under in vitro and in vivo conditions will be done in order to evaluate the useful-

Scheme 1. Synthesis of thiol **8**

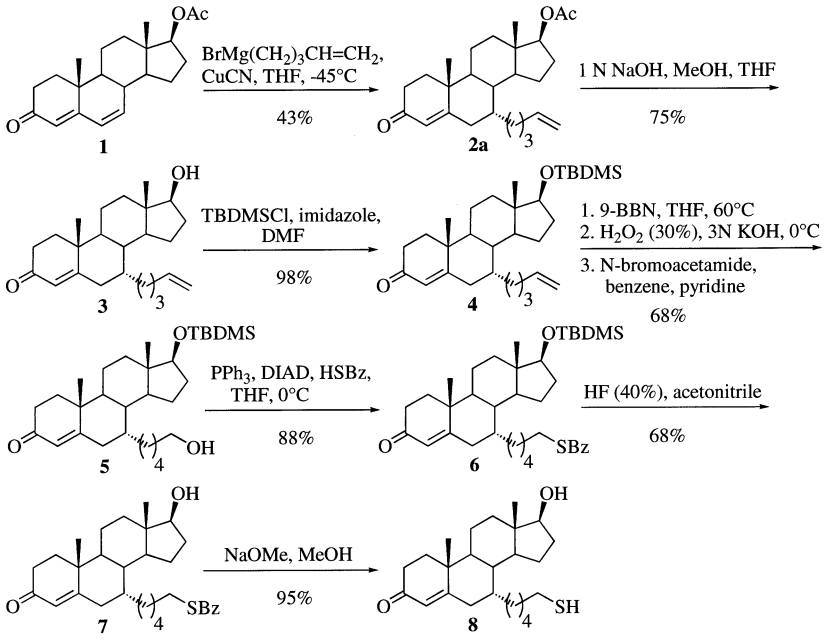

Scheme 2. Oxorhenium(V) complexes **12** (X = S) and **13** (X = O) according to the mixed-ligand concept

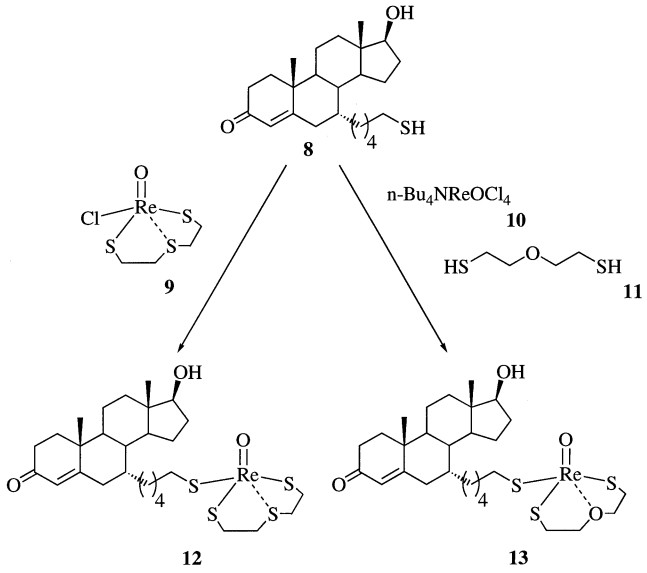

ness of complexes like **12** and **13** to act as radiotracers for the image of the androgen receptor.

Financial support of this work by the *Deutsche Forschungsgemeinschaft* is gratefully acknowledged.

Experimental Section

General: Solvents and reagents were purchased from the following commercial sources: Sigma, Fluka and Aldrich. THF was distilled from sodium/benzophenone ketyl prior to use. CuCN and magnesium turnings were dried prior to use. Other reagents were used as received. The synthesis involving air-sensitive compounds were carried out under argon using standard Schlenk technique. The standard workup procedure for product isolation involved quenching of the reaction mixture in an aqueous solution, followed by a thorough extraction with $CHCl_3$, washing of the extract, drying with $MgSO_4$, filtration and evaporation of the solvent under reduced pressure. Flash chromatography was performed according to Still[16], using Merck silica gel (0.040−0.063 mm). − IR: Specord M 80 Carl-Zeiss Jena. − NMR: Bruker DRX-500; Varian Inova-400. For ^1H NMR $CDCl_3$ as solvent $\delta_H = 7.26$; for ^{13}C NMR, $CDCl_3$ $\delta_C = 77.0$. − MS: Finnigan MAT 90.

17β-Acetoxy-7α-(4-penten-1-yl)androst-4-en-3-one (**2a**): 4.51 ml (38.16 mmol) of 5-bromopentene in 15 ml of dry THF was slowly added to 1.29 g (53 mmol) of magnesium turnings under argon. The resulting slurry was diluted with 5 ml of THF and heated for 1 h at 60°C while stirring. Afterwards, additional 60 ml of THF was added to adjust the Grignard solution to 0.75 M. The solution was cooled to −45°C and stirred for 30 min and 245 mg (2.73 mmol) of CuCN was added in one portion and stirring was continued for 30 min. Then 5 g (15.22 mmol) of dienone **1** in 60 ml of THF was added at −40°C over a period of 90 min. The solution was kept at −40 to −45°C for 30 min and then quenched with 5 ml of HOAc followed by filtration of the copper salts and standard workup. The resulting yellow oil contained the two diastereomers **2a** and **2b**. Separation of the diastereomers was accomplished by flash chromatography (EtOAc/*n*-hexane, 5:95). Yield: 2.6 g (43%) of the 7α product **2a** (pale yellow oil) and 0.6 g (10%) of the 7β-product **2b**. − IR ($CHCl_3$): $\tilde{\nu}$ = 1734 cm^{-1} (s, 17β-OAc), 1674 (s, 3-C=O), 1615 (m, C=C). − ^1H NMR ($CDCl_3$): δ = 0.82 (s, 3 H; 18-CH_3), 1.18 (s, 3 H; 19-CH_3), 2.02 (s, 3 H; 17β-$OCOCH_3$), 4.58 (t, ^3J = 8.4 Hz, 1 H; 17-H), 4.91−5.00 (m, 2 H; −CH=CH_2), 5.70 (s, 1 H; 4-H), 5.71−5.76 (m, 1 H; −CH=CH_2). − ^{13}C NMR ($CDCl_3$): δ = 199.0, 171.1, 169.7, 138.5, 125.8, 114.6, 82.4, 47.0, 45.8, 42.4, 38.7, 38.6, 36.6, 36.3, 36.3, 35.9, 33.9, 33.7, 27.3, 26.6, 24.5, 22.8, 21.1, 20.7, 18.0, 11.8. − HRMS (EI, 70 eV): calcd. for $C_{26}H_{28}O_3$ 398.2820, found 398.2812.

17β-Hydroxy-7α-(4-penten-1-yl)androst-4-en-3-one (**3**): 2.6 g (6.5 mmol) of the 17β-acetoxy steroid **2a** was dissolved in 60 ml of MeOH and 30 ml of THF and cooled to 0°C. 30 ml of 1 N NaOH was added drop by drop. The resulting mixture was stirred for 2 h at room temperature and 15 ml of 2 N HCl was added followed by standard workup and flash chromatography (EtOAc/*n*-hexane, 1:2). Yield 1.72 g (75%), m.p. 149−153°C. − IR (KBr): $\tilde{\nu}$ = 3455 cm^{-1} (s, OH), 3077 (w, =C−H), 1658 (s, 3-C=O), 1617 (m, C=C). − ^1H NMR ($CDCl_3$): δ = 0.79 (s, 3 H; 18-CH_3), 1.20 (s, 3 H; 19-CH_3), 3.66 (t, ^3J = 8.4 Hz, 1 H; 17-H), 4.92−5.01 (m, 2 H; CH=CH_2), 5.72 (s, 1 H; 4-H), 5.73−5.80 (m, 1 H; CH=CH_2). − ^{13}C NMR ($CDCl_3$): δ = 199.2, 170.0, 138.6, 125.8, 114.5, 81.6, 47.2, 46.0, 42.8, 39.0, 38.6, 36.6, 36.3, 36.2, 36.0, 34.0, 33.8, 30.3, 26.7, 24.6, 22.8, 20.9, 18.1, 10.9. − $C_{24}H_{36}O_2$ (356.54): calcd. C 80.85, H 10.18; found C 80.50, H 10.14.

17β-(tert-Butyldimethylsilyloxy)-7α-(4-penten-1-yl)androst-4-en-3-one (**4**): 1.24 g (18.2 mmol) of imidazole was dissolved in 12 ml of dry DMF. 1.37 g (9.1 mmol) of TBDMSCl in 6 ml of DMF was slowly added at 0°C. After 30 min, 1.3 g (3.64 mmol) of hydroxysteroid **3** in 5 ml of DMF was added in one portion and the mixture was stirred for 3 h at room temperature. After hydrolysis with a 0.1% K_2CO_3 solution, the mixture was extracted several times with $CHCl_3$, dried with $MgSO_4$ and the solvent was removed under reduced pressure. The residue was purified by flash chromatography (EtOAc/*n*-hexane, 1:3). Yield 1.7 g (98%), m.p. 117−119°C. − IR (KBr): $\tilde{\nu}$ = 3076 cm^{-1} (w, =C−H), 1676 (s, 3-C=O), 1616 (m, C=C). − ^1H NMR ($CDCl_3$): δ = 0.01 [s, 6 H; $Si(CH_3)_2$], 0.75 (s, 3 H; 18-CH_3), 0.88 [s, 9 H; $SiC(CH_3)_3$], 1.20 (s, 3 H; 19-CH_3), 3.57 (t, ^3J = 8.4 Hz, 1 H; 17-H), 4.93−5.01 (m, 2 H; CH=CH_2), 5.72 (s, 1 H; 4-H), 5.75−5.83 (m, 1 H; CH=CH_2). − ^{13}C NMR ($CDCl_3$): δ = 199.3, 170.3, 138.7, 125.8, 114.5, 81.6, 47.3, 45.6, 43.2, 39.1, 38.7, 36.7, 36.6, 36.4, 36.0, 34.1, 33.9, 30.7, 26.8, 25.8, 24.6, 22.9, 20.9, 18.1, 18.1; 11.2, −4.5, −4.8. − $C_{30}H_{50}O_2Si$ (470.81): calcd. C 76.53, H 10.70; found C: 76.35, H 10.46.

17β-(tert-Butyldimethylsilyloxy)-7α-(5-hydroxypent-1-yl)androst-4-en-3-one (**5**): 1.7 g (3.6 mmol) of the steroid **4** was dissolved in 15 ml of dry THF and cooled to 0°C. 44 ml of 9-BBN (0.5 M in THF; 22 mmol) was added dropwise to the stirred solution under argon. After the addition of 9-BBN was complete, the whole mixture was stirred at 60°C for 40 min. At 0°C 15 ml of water was added, followed by 15 ml of 3 N NaOH 5 min later. After another 5 min, 15 ml of 30% H_2O_2 was added very carefully and the mixture was stirred for 30 min. After standard workup using saturated $NaHCO_3$ solution a colorless oil containing the 3-hydroxy-7α-hydroxypentyl steroid was obtained. The residue was dissolved in a mixture of 13 ml of benzene and 26 ml of pyridine, and 0.75 g (5.43 mmol) of *N*-bromoacetamide was added. This was stirred overnight at room temperature. Standard workup involved treatment with 1 N HCl and flash chromatography (EtOAc/*n*-hexane, 1:1). Yield 1.2 g (68%), pale yellow oil. − IR ($CHCl_3$): $\tilde{\nu}$ = 3412 cm^{-1} (s, OH), 1673 (s, 3-C=O), 1614 (m, C=C). − ^1H NMR ($CDCl_3$): δ = −0.02 [s, 6 H; $Si(CH_3)_2$], 0.71 (s, 3 H; 18-CH_3), 0.84

[s, 9 H; $SiC(CH_3)_3$], 1.17 (s, 3 H; 19-CH_3), 3.53 (t, ^3J = 8.4 Hz, 1 H; 17-H), 3.59 (t, ^3J = 6.6 Hz, 2 H; CH_2OH), 5.68 (s, 1 H; 4-H). − ^{13}C NMR ($CDCl_3$): δ = 199.4, 170.5, 125.6, 81.5, 62.7, 47.3, 45.5, 43.1, 39.0, 38.6, 36.7, 36.6, 36.3, 35.9, 33.9, 32.6, 30.6, 27.1, 25.9, 25.8, 24.9, 22.8, 20.9, 20.5, 18.0, 18.0, 11.1, −4.6, −4.9. − LRMS (DCI positive, isobutane) for $C_{30}H_{52}O_3Si$: 489 [M+1].

7α-[(S)-5-Benzoylthiopent-1-yl]-17β-(tert-butyldimethylsilyloxy)androst-4-en-3-one (**6**): 880 µl (4.1 mmol) of 90% diisopropyl azodicarboxylate (DIAD) was added to an efficiently stirred solution of 1.08 g (4.1 mmol) of PPh_3 in 11 ml of dry THF at 0°C. The mixture was stirred at 0°C for 30 min and a white precipitate resulted. 1 g (2.05 mmol) of the hydroxy steroid **5** and 532 µl (4.1 mmol) of 95% thiobenzoic acid in 6 ml of dry THF were added dropwise over a period of 10 min and stirring of the mixture was continued for 1 h at 0°C and for 1 h at room temperature. To the resulting yellow solution 100 ml of $CHCl_3$ was added and the mixture was washed with saturated $NaHCO_3$ solution. After drying with $MgSO_4$ and evaporation of the solvent, a pale yellow residue was obtained which was purified by flash chromatography (EtOAc/*n*-hexane, 1:3). Yield 1.1 g (88%), pale yellow oil. − IR ($CHCl_3$): $\tilde{\nu}$ = 1666 cm^{-1} (s, 3-C=O), 1615 (m, C=C). − ^1H NMR ($CDCl_3$): δ = −0.02 [s, 6 H; $Si(CH_3)_2$], 0.73 (s, 3 H; 18-CH_3), 0.87 [s, 9 H; $SiC(CH_3)_3$], 1.18 (s, 3 H; 19-CH_3), 3.05 (t, ^3J = 7.3 Hz, 2 H; CH_2SBz), 3.56 (t, ^3J = 8.4 Hz, 1 H; 17-H), 5.71 (s, 1 H; 4-H), 7.41−7.97 (m, 5 H; $H_{aromat.}$). − ^{13}C NMR ($CDCl_3$): δ = 199.1, 191.9, 170.2, 137.1, 133.2, 128.5, 127.1, 125.7, 81.5, 47.3, 45.6, 43.1, 39.0, 38.6, 36.7, 36.6, 36.3, 35.9, 34.0, 30.6, 29.6, 29.3, 28.9, 26.9, 25.8, 24.9, 22.9, 20.9, 18.0, 18.0, 11.1, −4.6, −4.9. − LRMS (DCI positive, isobutane) for $C_{37}H_{56}O_3SSi$: 609 [M+1].

7α-[(S)-5-Benzoylthiopent-1-yl]-17β-hydroxyandrost-4-en-3-one (**7**): 3.5 ml of 40% aqueous HF was added to a solution of 0.9 g (1.48 mmol) of the steroid **6** in 20 ml of acetonitrile at room temperature. After stirring 1 h at room temperature, 20 ml of saturated $NaHCO_3$ solution was added and the product was extracted with $CHCl_3$. After drying with $MgSO_4$ and evaporation of the solvent, flash chromatography (EtOAc/*n*-hexane, 1:1) was used to isolate pure **7**. Yield 0.5 g (68%), m.p. 129−133°C. − IR (KBr): $\tilde{\nu}$ = 3060 cm^{-1} (w, =C−$H_{aromat.}$), 1662 (s, 3-C=O), 1615 (m, C=C). − ^1H NMR ($CDCl_3$): δ = 0.78 (s, 3 H; 18-CH_3), 1.19 (s, 3 H; 19-CH_3), 3.05 (t, ^3J = 7.3 Hz, 2 H; CH_2SBz), 3.64 (t, ^3J = 8.4 Hz, 1 H; 17-H), 5.71 (s, 1 H; 4-H), 7.41−7.97 (m, 5 H; $H_{aromat.}$). − ^{13}C NMR ($CDCl_3$): δ = 199.2, 192.0, 170.0, 137.1, 133.2, 128.5, 127.1, 125.8, 81.6, 47.1, 46.0, 42.8, 39.0, 38.6, 36.6, 36.3, 36.2, 35.9, 34.0, 30.3, 29.6, 29.0, 28.9, 26.9, 24.9, 22.8, 20.9, 18.0, 10.9. − $C_{31}H_{42}O_3S$ (494.74): calcd. C 75.26, H 8.56, S 6.48; found C 74.85, H 8.28, S 6.31.

17β-Hydroxy-7α-[5-mercaptopent-1-yl]androst-4-en-3-one (**8**): 70 mg (0.14 mmol) of the thiobenzoate **7** was dissolved in 4.5 ml of MeOH while stirring at room temperature under argon. To this solution 280 µl (0.28 mmol) of 1 N NaOMe was added. After 1.5 h, the pH was adjusted to 4−5 by 1 N HCl. Then, 5 ml of water was added and the solution was extracted with chloroform. Drying with $MgSO_4$ and evaporation of the solvent yielded a yellow residue which was purified by flash chromatography (EtOAc/*n*-hexane, 1:1). Yield 52 mg (95%), m.p. 150−153°C. − IR (KBr):$\tilde{\nu}$ = 3449 cm^{-1} (s, OH), 2551 (w, S−H), 1656 (s, 3-C=O), 1616 (m, C=C). − ^1H NMR ($CDCl_3$): δ = 0.79 (s, 3 H; 18-CH_3), 1.21 (s, 3 H; 19-CH_3), 1.59 (s-like, 1 H; SH), 3.76 (m, 1 H; 17-H), 5.72 (s, 1 H; 4-H). − ^{13}C NMR ($CDCl_3$): δ = 199.2, 170.0, 125.8, 81.7, 47.2, 46.0, 42.8, 39.0, 38.7, 36.7, 36.3, 36.2, 36.0, 34.0, 33.9, 30.3, 28.0, 26.9, 25.0, 24.6, 22.8, 20.9, 18.1, 10.9. − $C_{24}H_{38}O_2S$ (390.63): calcd. C 73.79, H 9.81, S 8.21; found C 73.54, H 10.06, S 7.86.

[5-(17β-Hydroxy-3-oxoandrost-4-en-7α-yl)pentan-1-thiolato]-oxo(3-thiapentane-1,5-dithiolato)rhenium(V)rhenium(V) (**12**): 78 mg (200 µmol) of chloro(3-thiapentane-1,5-dithiolato)oxorhenium(V) (**9**) was dissolved in 5 ml of hot acetonitrile while stirring. To this mixture a solution of the steroid **8** (117 mg, 300µmol) in 5 ml of acetonitrile was added . The mixture was refluxed for 2 h and then concentrated to dryness. The residue was purified by flash chromatography [*n*-hexane/ethylacetate, 1:1 and chloroform/methanol, 10:1]. After slow evaporation of the solvent, a brown glass was obtained. Yield 106 mg (71%). − IR (KBr): $\tilde{\nu}$ = 3437 cm^{-1} (s, OH), 1658 (s, C=O), 1613 (m, C=C), 961 (s, Re=O). − ^1H NMR ($CDCl_3$): δ = 0.79 (s, 3 H; 18-CH_3), 1.19 (s, 3 H; 19-CH_3), 3.12 (tt, 2 H, *J* = 14.3 Hz), 3.65−3.67 (m, 1 H; 17-H), 3.84 (t, 2 H, ^3J = 7.3 Hz; CH_2SReO"SSS"), 3.91 (br. d, 2 H, *J* = 10.2 Hz), 4.30 (br. d, 2 H, *J* = 13.2 Hz), 5.72 (s, 1 H; 4-H). − MS (FAB negative, tetraglyme); *m/z* (%): 741 (47.6), 742 (19.0), 743 (100) [M − 1], 744 (28.6), 745 (19.0), 746 (3.8). − $C_{28}H_{45}O_3S_4Re$ (744.13): calcd. C 45.20, H 6.10, S 17.24; found C 44.97, H 6.04, S 16.94.

[5-(17β-Hydroxy-3-oxoandrost-4-en-7α-yl)pentan-1-thiolato](3-oxapentane-1,5-dithiolato)oxorhenium(V) (**13**): 75 mg (128 µmol) of tetra-*n*-butylammonium tetrachlorooxorhenate(V) (**10**) was dissolved in 2 ml of EtOH and cooled to 0°C. At this temperature 50 mg (128 µmol) of the steroid **8** and 15 µl (128 µmol) of 3-oxapentane-1,5-dithiol (**11**) in 2 ml of chloroform was added while stirring. The color of the mixture immediately changed to red. The reaction mixture was stirred at 0°C for 2 h. The solution was then concentrated and the residue dissolved in chloroform yielding a red solution which was purified by flash chromatography [*n*-hexane/ethylacetate, 1:1 and chloroform/methanol, 10:1]. After slow evaporation of the solvent, a wine-red glass was obtained. Yield 13 mg (14%). − IR (KBr): $\tilde{\nu}$ = 3436 cm^{-1} (s, OH), 1659 (s, 3-C=O), 1613 (m, C=C), 969 (s, Re=O). − ^1H NMR ($CDCl_3$): δ = 0.79 (s, 3 H; 18-CH_3), 1.20 (s, 3 H; 19-CH_3), 2.87 (br. s, 1 H), 3.35 (br. s, 2 H), 3.52 (br. s, 2 H), 3.65−3.71 (m, 4 H), 3.94 (br. s, 1 H), 4.61 (br. s, 1 H), 4.70 (br. s, 1 H), 5.73 (s, 1 H, 4-H). − MS (FAB negative, tetraglyme); *m/z* (%): 725 (45.7), 726 (47.6), 727 (100) [M − 1], 728 (81.9), 729 (35.2), 730 (11.4). − $C_{28}H_{45}O_4S_3Re$ (728.05): calcd. C 46.19, H 6.23, S 13.21; found C 45.96, H 6.52, S 12.97.

[1] A. Liu, J. A. Katzenellenbogen, H. F. VanBrocklin, C. J. Mathias, M. J. Welch, *J. Nucl. Med.* **1991**, *32*, 81−88.
[2] J. A. Katzenellenbogen, *J. Nucl. Med.* **1995**, *36 Suppl.*, 8S−13S.
[3] [3a] J. P. O'Neil, K. E. Carlson, C. J. Anderson, M. J. Welch, J. A. Katzenellenbogen, *Bioconjugate Chem.* **1994**, *5*, 182−193. − [3b] J. P. DiZio, C. J. Anderson, A. Davison, G. J. Ehrhardt, K. E. Carlson, M. J. Welch, J. A. Katzenellenbogen, *J. Nucl. Med.* **1992**, *33*, 558−569. − [3c] J. P. DiZio, R. Fiaschi, A. Davison, A. G. Jones, J. A. Katzenellenbogen, *Bioconjugate Chem.* **1991**, *2*, 353−366. − [3d] S. Top, A. Vessières, G. Jaouen, *J. Chem. Soc., Chem. Commun.* **1994**, 453−454. − [3e] S. Top, H. El Hafa, A. Vessières, J. Quivy, J. Vaissermann, D. W. Hughes, M. J. McGlinchey, J.-P. Mornon, E. Thoreau, G. Jaouen, *J. Am. Chem. Soc.* **1995**, *117*, 8372−8380. − [3f] F. Wüst, H. Spies, B. Johannsen, *Bioorg. Med. Chem. Lett.* **1996**, *6*, 2729−2734. − [3g] B. Johannsen, H. Spies, *Transition Met. Chem.* **1997**, *22*, 318−320.
[4] M. J. Welch, J. B. Downer, J. A. Katzenellenbogen in *Current Directions in Radiopharmaceutical Research and Development*, chapter 9 (Ed.: S. J. Mather), Kluwer Academic Publishers, Dordrecht/Boston/London, **1996**, pp. 137−156.
[5] M. Salman, G. C. Chamness, *J. Med. Chem.*, **1991**, *34*, 1019−1024.
[6] R. M. Hoyte, K. Borderon, K. Bryson, R. Allen, R. B. Hochberg, T. J. Brown, *J. Med. Chem.* **1994**, *37*, 1224−1230.
[7] A. Liu, K. E. Carlson, J. A. Katzenellenbogen, *J. Med. Chem.* **1992**, *35*, 2113−2129.
[8] G. Berger, M. Maziere, C. Prenant, J. Sastre, D. Comar, *Int. J. Appl. Radiat. Isot.* **1981**, *32*, 811−815.

[9] C. J. Lovely, R. W. Brueggemeier, *Bioorg. Med. Chem. Lett.* **1995**, *5*, 2513−2516.
[10] [10a] A. N. French, S. R. Wilson, M. J. Welch, J. A. Katzenellenbogen, *Steroids* **1993**, *58*, 157−169. − [10b] J. Bowler, T. J. Lilley, J . D. Pittam, A. E. Wakeling, *Steroids* **1989**, *54*, 71−99. − [10c] P. Luppa, S. Hauck, I. Schwab, C. Birkmayer, H. Hauptmann, *Bioconjugate Chem*, **1996**, *7*, 332−337.
[11] H. Spies, T. Fietz, M. Glaser, H.-J. Pietzsch, B. Johannsen, in *Technetium and Rhenium in Chemistry and Nuclear Medicine 4* (Eds.: M. Nicolini, M. Mazzi, M. Bandoli), SGEditoriali, Padova, **1995**, pp. 243−246.
[12] T. Fietz, H. Spies, H.-J. Pietzsch P. Leibnitz, *Inorg. Chim. Acta* **1995**, *321*, 233−236.
[13] R. Bucourt, M. Wignau, V. Torelli, H. Richard-Foyh, C. Geynet, C. Secco-Millet, G. Redeulih, E. Baulieu, *J. Biol. Chem.* **1978**, *253*, 8221−8228.
[14] O. Mitsunobu, *Synthesis* **1981**, 1−28.
[15] R. Alberto, R. Schibli, A. Egli, P. A. Schubiger, W. A. Herrmann, G. M. Artus, U. Abram, T. A. Kaden, *J. Organomet. Chem.* **1995**, *493*, 119−127.
[16] W. C. Still, M. Kahn, A. Mitra, *J. Org. Chem.* **1978**, 43, 2923−2925.

[97285]

Crystal Structure and Formation of the Aluminium Hydroxide Chloride $[Al_{13}(OH)_{24}(H_2O)_{24}]Cl_{15} \cdot 13\ H_2O$

Wilhelm Seichter*, Hans-Jörg Mögel, Paul Brand, and Dhafer Salah

Faculty of Chemistry and Physics, TU Bergakademie Freiberg,
Leipziger Straße 29, D-09596 Freiberg, Germany
Fax: (internat.) + 49(0)3731/39-3170
E-mail: Seichter@orion.hrz.tu-freiberg.de

Received December 12, 1997

Keywords: Aluminium hydroxide chloride / Crystal structure / Tridecameric cation / Structure of cation / Formation

A basic aluminium chloride with high chlorine content (basicity 1.85) has been crystallized from a concentrated aqueous solution. Its crystal structure has been determined by X-ray structure analysis. The structure contains tridecameric cations of a novel type consisting only of interconnected AlO_6 octahedra. The formation of these polycations is discussed.

The structures of complex cations of basic aluminium chlorides, formed by hydrolysis and condensation, as well as the conditions of their formation, are of special interest because of their occurrence in natural water and their applications as antiperspirants and in water purification. Detailed information concerning the structures of similar complex cations has been provided by the crystal-structure analyses of basic aluminium sulfates and selenates carried out by Johansson and co-workers. They demonstrated the existence of a dimeric species[1] $[Al_2(OH)_2(H_2O)_8]^{4+}$, consisting of two octahedrally coordinated Al centres connected by a common edge (di-μ-OH^- bridge), and of a polycation $[Al_{13}O_4(OH)_{24}(H_2O)_{12}]^{7+}$ (Figure 1) with a Keggin-type structure.[2] The latter structure is characterized by a particular resonance shift in its ^{27}Al-NMR spectrum, even in solutions of basic aluminium chlorides,[3] caused by the tetrahedrally coordinated, central aluminium, which is surrounded by 12 other octahedrally coordinated Al atoms. Various crystalline basic aluminium chlorides have been prepared from solutions by Walter-Levy and Breuil.[4] The crystalline phases were characterized by means of X-ray powder analysis and their thermal decomposition was investigated. The powder diagrams of some of these crystalline phases were unambiguously indexed and the lattice constants were determined. This is also the case for a cubic phase prepared at Dow Chemical Co.[5] However, as far as we are aware, results of crystal structure analyses have hitherto not been reported.

In this paper, we report on a structure analysis of the most chlorine-rich of the basic aluminium chlorides described by Walter-Levy and Breuil.[4][6] These authors obtained the salt as a crystalline precipitate that formed after several days following dilution and storage of concentrated basic aluminium chloride solutions. Suitable monocrystals for our structure analysis were obtained serendipitously, in the course of studies on the colloid structures of basic aluminium chlorides. Colloid solutions with an Al:Cl ratio in the range 1−2 tend to form gels after evaporation of the solvent, and these were the subject of rheological and light-scattering investigations[7]. In basic aluminium chloride solutions, besides the aforementioned monomeric, dimeric and tridecameric species, further oligomeric and polymeric cations exist. To date, only vague statements have been made regarding their size and shape.[3] For comparison, we also studied solutions rich in chloride. It was known that crystalline phases could be precipitated from such media. After very slow evaporation of water from a concentrated solution of a basic aluminium chloride with an Al:Cl ratio of 0.7, besides very large crystals of $AlCl_3 \cdot 6H_2O$, crystals of another phase grew, which were the subject of our investigations.

Figure 1. Tridecameric cation after Johansson[2]

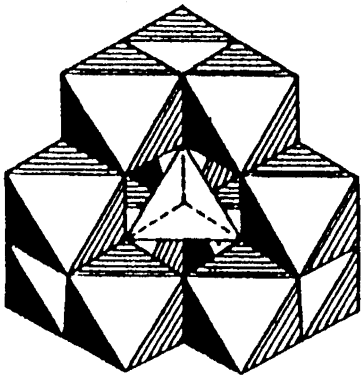

Results and Discussion

The lattice constants of the formed monocrystal were determined by means of single-crystal X-ray diffractometry. On the basis of the monoclinic unit cell obtained, the unindexed powder data reported by Breuil for the hydroxide chloride 5 $AlCl_3 \cdot 8\ Al(OH)_3 \cdot 37.5\ H_2O$[8] become indexable. Therefore, we conclude that a crystal of this phase was pre-

 © WILEY-VCH Verlag GmbH, D-69451 Weinheim, 1998 1434−1948/98/0606−0795 $ 17.50+.50/0

sent. The results of its X-ray structure analysis confirmed this assertion, although not all the positions of the hydrogen atoms could be determined. The water content in the formal unit was found to be slightly lower than reported, being consistent with the composition 5 $AlCl_3 \cdot 8\ Al(OH)_3 \cdot 37\ H_2O$. The cell contains 4 formal units. The atomic positions determined in the structure analysis show two analogous types of large units, built up from connected AlO_6 octahedra (Figure 2). Two of each kind are present in the unit cell. The chlorine atoms are situated outside of these complex units, along with the oxygen and hydrogen atoms obviously belonging to water molecules. Considering the charges (Al^{3+}, Cl^-), the large units must be viewed as polycations. Each polycation consists of 13 octahedra (Figure 3): a central one, 6 further octahedra surrounding the central unit and connected to it by common edges, and finally 6 peripherally arranged octahedra, with each one joined to the inner ring by two common corners. The Al^{3+} ion in the central octahedron lies at an inversion centre of the space group, and thus the polycations are centrosymmetric. The central Al^{3+} and the 6 Al^{3+} of the ring are coplanar and together form a centred, almost regular, hexagon. The oxygen positions correspond to octahedra with varying degrees of distortion. The Al−O distances in the central octahedron are virtually equal (188−189 pm), and the O−Al−O angles are approximately equal (97°), but differ from the octahedral ideal of 90°. The ring octahedra are distorted to a greater extent. The peripheral octahedra occupy alternate positions above and below the plane of the hexagon. Accordingly, they show a certain degree of deformation; the Al−O distances to the free corners are obviously longer than those to the corners that are shared with the adjacent octahedra. Since not all of the hydrogen atom positions could be determined, the question remains as to which oxygen atoms the hydrogen atoms should be assigned so as to form hydroxide ions or water molecules. Consideration of the charges may elucidate this matter. In the polycation, we find 13 Al^{3+} ions with 39 positive charges. On the other hand, there are 15 Cl^- ions, giving 15 negative charges per polycation. This leaves 39 − 15 = 24 negative charges in the polycation to account for. This number corresponds to the number of linkage oxygen atoms. We can thus assume that these oxygen atoms belong to hydroxide ions. Water molecules must then be present at the 24 free corners of the peripheral octahedra. An additional 13 water molecules are situated outside of the polycation. The basic aluminium chloride investigated can therefore be assigned the formula $[Al_{13}(OH)_{24}(H_2O)_{24}]Cl_{15} \cdot 13\ H_2O$.

Hence, a further tridecameric cation species has been detected in addition to Johansson′s tridecamer. The new species is characterized by a single resonance of octahedrally coordinated Al in its ^{27}Al-NMR spectrum and needs to be formally distinguished from the previously identified species. The notation Al_{13} is no longer unambiguous. It seems reasonable to distinguish the two tridecameric species by using an auxiliary index that denotes the different coordination of the central aluminium: $Al_{13}{}^t$ (t: tetrahedral) for the Johansson species and $Al_{13}{}^o$ (o: octahedral) for the new structure. The two tridecamers have OH^- ($Al_{13}{}^o$) or O^{2-} groups ($Al_{13}{}^t$) that form a common vertex of three octahedra. Therefore, Brown et al.[9] and Baes and Mesmer[10] discuss the formation of $Al_{13}{}^t$ in terms of the assembly of trimers $[Al_3(\text{tri-}\mu\text{-}OH)(OH)_3(H_2O)_9]^{5+}$ (Figure 4), which are in turn formed by the condensation of a dimer $[Al_2(OH)_2(H_2O)_8]^{4+}$ with a monomer $[Al(OH)(H_2O)_5]^{2+}$. It has been assumed that the Keggin tridecamer is formed by the reaction of the hydroxide ions of an $[Al(OH)_4]^-$ anion with the nucleophilic tri-μ-OH^- of trimeric units, building up a tetrahedral arrangement of linking oxygen ions with the liberation of water. In our tridecamer $Al_{13}{}^o$, there are OH^- groups that connect three octahedra. The central Al^{3+} is surrounded by six tri-μ-OH^-. The formation of this polycation structure can also be envisaged as starting from trimers, formed by condensation of dimeric and monomeric

Figure 2. Crystal structure of $[Al_{13}(OH)_{24}(H_2O)_{24}]Cl_{15} \cdot 13\ H_2O$; section of the unit cell: polycations with centres in $z = 1/2$

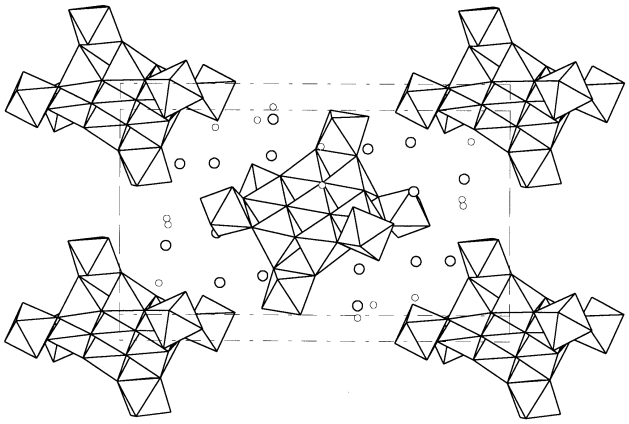

Figure 3. Structure of the polycation $[Al_{13}(OH)_{24}(H_2O)_{24}]^{15+}$; large circles: aluminium; small cirder: oxygen

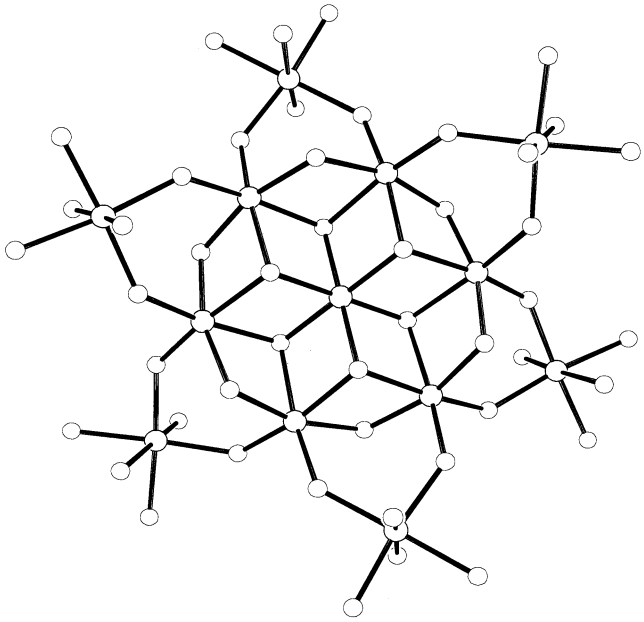

units. However, in this case, the process continues with the addition of other dimers, which condense together after further protolysis and form the ring surrounding the central atom. The peripheral octahedra could clearly be attached subsequently by the condensation of monomer units with the compact planar core.

We thank the *Fonds der Chemischen Industrie* and the *Deutsche Forschungsgemeinschaft* (Graduiertenkolleg "Crystal Engineering and Crystallization") for financial support.

Experimental Section

General: The Al_{13}° hydroxide chloride was crystallized from a basic aluminium chloride solution with an Al/Cl ratio of 0.7. The solution was prepared by dissolution of partially thermally decomposed $AlCl_3 \cdot 6\ H_2O$ in hot water (80°C) at a mass ratio of solid material/water of 1:1. The thermal decomposition of the starting material was carried out at about 180°C in a whirling air stream. The solution was placed in an open dish at ambient temperature. After 4 months, well-grown crystals of suitable dimensions for X-ray structure analysis were obtained. The quality of separated crystals was tested by polarization microscopy. Solid-state ^{27}Al-NMR analysis was performed with a Bruker MSL300 instrument at a frequency of 15 KHz.

X-ray Crystallographic Study: T = 295°C; crystal size 0.20 × 0.20 × 0.15 mm, formula weight 1957.27, monoclinic, space group $P2_1/c$, a = 13.901(1), b = 23.483(3), c = 22.345(2) Å, β = 90.36(1)°, V = 7294.1(12) Å^3, Z = 4, $D_{calcd.}$ = 1.782 g cm^{-3}. Enraf-Nonius CAD4 diffractometer, graphite-monochromated Cu-K_α radiation (λ = 1.5418 Å), F(000) = 4040, μ = 7.736 cm^{-1}, ω-2θ scan, scan range (θ) 2.73−74.73°, *hkl* range +17, +29, ±27, no. of unique reflections 14942, no. of observed reflections 11292 with $I > 2\sigma(I)$, refined parameters 903, $R1$ for observed reflections 0.00527, $R1$ for all reflections 0.0776, $wR2$ for observed reflections 0.1341, $wR2$ for all reflections 0.1497, GooF = 1.077 for the observed and GooF = 1.025 for all reflections, residual electron density 0.80/−0.62 e Å^{-3}. The structure was solved by direct methods (SHELXS-86) and refined by full-matrix least-squares methods with SHELXL-93. DIFABS was used for empirical absorption correction. Further details of the crystal structure investigations may be obtained from the Fachinformationszentrum Karlsruhe, D-76344 Eggenstein-Leopoldshafen (Germany) on quoting the depository number CSD-408095.

[1] G. Johannson, *Acta Chem. Scand.* **1962**, *16*, 403−420.
[2] G. Johannson, *Ark. Kemi* **1962**, *20*, 305−319, 321−342 (*Chem. Abstr.* **1963**, *58*, 12028e,f.
[3] J. J. Fitzgerald, in *Antiperspirants and Deodorants* (*Cosmetic Science and Technology Science*, vol. 7) (Eds.: K. Laden, C. B. Felger), Marcel Dekker, New York, **1988**, p. 119−292.
[4] H. Breuil, *Ann. Chim.* **1965**, *10*, 467−493.
[5] Joint Committee on Powder Diffraction Standards, International Center for Diffraction Data, Powder Diffraction File, Set 31, Number 6 (J. Belton, Henslee, Central Laboratoty, Dow Chemical Company, Freeport, Texas, USA, private communication, **1980**).
[6] L. Walter-Levy, H. Breuil, *C. R. Acad. Sci.* **1962**, *255*, 1744−1746.
[7] H.-J. Mögel, P. Brand, T. Angermann, *Progr. Colloid Polym. Sci.* **1994**, *97*, 93−96.
[8] Joint Committee on Powder Diffraction Standards, International Center for Diffraction Data, Powder Diffraction File, Set 20, Number 26[4].
[9] P. L. Brown, R. N. Sylva, G. E. Batley, J. Ellis, *J. Chem. Soc., Dalton Trans.* **1985**, 1967−70.
[10] C. E. Baes, R. E. Mesmer, *The Hydrolyses of Cations*, J. Wiley and Sons, New York, **1976**, p. 112−23.

[97303]

Oxovanadium(IV) and -(V) Complexes with Aminoalcohol Ligands: Synthesis, Structure, Electrochemical, and Magnetic Properties☆

Winfried Plass

Fakultät für Chemie, Universität Bielefeld,
Postfach 100131, D-33501 Bielefeld, Germany
Fax: (internat.) +49(0)521/106-6146
E-mail: winfried.plass@uni-bielefeld.de

Received December 22, 1997

Keywords: Aminoalcohol ligands / Hydrogen bonds / Magnetic properties / Oxo complexes / Vanadium

The aminoalcohol ligands diethanolamine (H_2dea) and triethanolamine (H_3tea) react with $[VO(acac)_2]$ to yield the tetranuclear oxovanadium(IV) complexes $[\{VO(dea)\}_2\{VO(acac)\}_2(\mu_2\text{-}OMe)_2]$ (**1**) and $[\{VO(Htea)\}_2\{VO(acac)\}_2(\mu_2\text{-}OMe)_2]$ (**2**). In the case of the potentially bridging aminoalcohol ligands *N,N,N′,N′*-tetrakis(2-hydroxyethyl)ethylenediamine (H_4edte) and *N,N,N′,N′*-tetrakis(2-hydroxypropyl)ethylenediamine (H_4edtp) the corresponding oxovanadium(IV) complexes could not be isolated. Instead after air oxidation the ligand supported binuclear oxovanadium(V) complexes $[\{VO(acac)\}]_2(edte)]$ (**3**) and $[\{VO(acac)\}_2(edtp)]$ (**4**) are obtained. The reaction of the ligand H_4edtp with ammonium *meta*-vanadate in methanol solution leads to the methoxy bridged binuclear oxovanadium(V) complex $[(VO)_2(edtp)(\mu_2\text{-}OMe)_2]$ (**5**). The tetranuclear oxovanadium(IV) complexes can be isolated as crystalline compounds **1**·2 MeOH and **2**·2 MeOH and have been characterized by IR, UV/Vis, and ESR spectroscopy as well as cyclic voltammetry and magnetic susceptibility measurements. Single-crystal diffraction studies reveal that the complexes **1** and **2** contain a tetranuclear $\{(VO)_4(\mu_3\text{-}OR)_2(\mu_2\text{-}OR)_4\}^{2+}$ core composed of three different types of edge-shared binuclear units, whereas the oxovanadium(V) complexes **3**, **4**, and **5** posses binuclear structures, that are either ligand supported as in the case of **3** and **4** or contain a μ_2-methoxy bridged $\{(VO)_2(\mu_2\text{-}OR)_2\}^{4+}$ core as in the case of **5**. ESR and magnetic data indicate a singlet ground state for **1**·2 MeOH and **2**·2 MeOH, although competing ferromagnetic exchange interactions are operative within the tetranuclear core structure. In the solid state compounds **1**·2 MeOH and **2**·2 MeOH hydrogen bridged supramolecular structures are found. The hydrogen bonding scheme of both compounds leads to the formation of a similar chain arrangement of the tetranuclear complexes **1** and **2**.

Introduction

The increasing interest in vanadium coordination chemistry is based on its well established biological function in the oxidations states +4 and +5, e.g. as essential element for enzymatic systems like vanadium-requiring haloperoxidases and nitrogenases and the insulin-mimetic action of vanadium compounds[1]. Related with this biological aspects the coordination chemistry of oxovanadium(IV) and -(V) complexes with aminoalcohols has found special attention[2][3][4][5]. In addition the coordination chemistry of oxovanadium(IV) complexes with aminoalcohols offers easy access to model systems for the magnetic behavior of corresponding polynuclear complexes and has already led to a magnetostructural relationship for such systems[6][7]. Similarly to the well established tris(hydroxymethyl)alkane family of ligands[8] aminoalcohols can be utilized as bridging units in the formation of higher nuclear oxovanadium(IV) complexes[9].

The present study describes a synthetic approach to oxovanadium(IV) and -(V) complexes with potentially bridging and/or chelating aminoalcohol ligands depicted in Scheme 1. Besides the structural and spectroscopic characterization of these complexes special emphasis is placed on their electrochemical and magnetic properties.

Scheme 1. Aminoalcohol ligands used in this study[a]

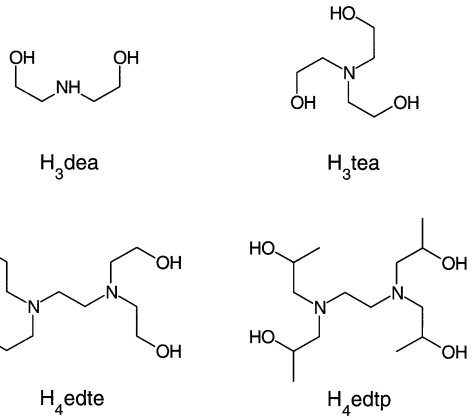

H_3dea H_3tea H_4edte H_4edtp

[a] Abbreviations: H_2dea = diethanolamine; H_3tea = triethanolamine; H_4edte = *N,N,N′,N′*-tetrakis(2-hydroxyethyl)ethylenediamine, H_4edtp = *N,N,N′,N′*-tetrakis(2-hydroxypropyl)ethylenediamine.

Results and Discussion

Syntheses

In methanol solution the aminoalcohol ligands diethanolamine (H_2dea) and triethanolamine (H_3tea) react with $[VO(acac)_2]$ (Hacac = 2,4-pentanedione) to form the neu-

 © WILEY-VCH Verlag GmbH, D-69451 Weinheim, 1998 1434–1948/98/0606–0799 $ 17.50+.50/0

tral tetranuclear oxovanadium(IV) complexes [{VO(dea)}$_2$-{VO(acac)}$_2$(μ_2-OMe)$_2$] (**1**) and [{VO(Htea)}$_2${VO(acac)}$_2$-(μ_2-OMe)$_2$] (**2**). The complexes **1** and **2** are obtained as green crystalline solid materials, which are insoluble in alcohols and water but readily soluble in DMF and DMSO. Under oxygen free reaction conditions the formation of the complexes **1** and **2** is virtually independent of the ligand to [VO(acac)$_2$] ratio. However, the vanadyl ion can easily be oxidized to the +5 oxidation state in the presence of either aminoalcohol ligand. With H_3tea the air oxidation leads to the well-known oxovanadium(V) triethanolaminate[4][10]. Similar reactions with the potentially bridging aminoalcohol ligands *N,N,N′,N′*-tetrakis(2-hydroxyethyl)ethylenediamine (H_4edte) and *N,N,N′,N′*-tetrakis(2-hydroxypropyl)-ethylenediamine (H_4edtp) did not yield any isolable vanadium(IV) complexes. Nevertheless after air oxidation the ligand supported binuclear oxovanadium(V) complexes [{VO(acac)}$_2$(edte)] **3**) and [{VO(acac)}$_2$(edtp)] (**4**) can be isolated, which are isoluble in common organic solvents. For both complexes **3** and **4** only one of the acetylacetonate ligands at the vanadyl ion is replaced by the aminoalcohol ligand. Utilizing ammonium *meta*-vanadate as starting material the reaction with the ligand H_4edtp in methanol solution afforded the methoxy bridged binuclear oxovanadium(V) complex [(VO)$_2$(edtp)(μ_2-OMe)$_2$] (**5**). **5** is readily soluble in DMF and DMSO but only sparingly soluble in alcohols.

Crystal Structure Descriptions

The molecular structures of the tetranuclear complexes **1** and **2** are shown in Figures 1 and 2. In both complexes the aminoalcohols, H_2dea and H_3tea, coordinate as tridentate ligands in their dianionic form and occupy three facial positions at the vanadium center V1 leading structurally similar {VO(dea)(OMe)}$^-$ and {VO(Htea)(OMe)}$^-$ fragments. Dimers of these fragments arranged in an *anti*-coplanar configuration constitute the central units of complexes **1** and **2** with the oxygen donors O3 and O3′ in the bridging positions. The formal condensation of two {VO(acac)}$^+$ fragments onto the trigonal faces of the central fragments established by the coordinated alkoxy ligands (O3, O4′, O5 and O3′, O4, O5′) leads to the tetranuclear complexes **1** and **2**. The resulting {(VO)$_4$(μ_3-OR)$_2$(μ_2-OR)$_4$}$^{2+}$ core structure of **1** and **2** generally resembles that of an earlier reported Schiff base substituted tetranuclear oxovanadium(IV) complex[9] and corresponds to the well-known {M_4O_{16}} condensation motif found for high valent transition-metal systems[8][11]. The actual orientation pattern of the oxo groups is directed by the *trans* effect generally observed for such strong terminal ligands, i.e. all are arranged *trans* to the μ_3-bridging oxygen donors O3 and O3′. Consequently, the {(VO)$_4$(μ_3-OR)$_2$(μ_2-OR)$_4$}$^{2+}$ core of **1** and **2** consists of five edge shared binuclear arrangements: one with *anti*-coplanar (V1···V1′: 329.0(2) pm for **1**, 326.6(2) pm for **2**), two with *syn*-coplanar (V1···V2 and V1′···V2′: 342.2(2) pm for **1**, 341.9(2) pm for **2**), and two with twist configuration (V1···V2′ and V1′···V2: 329.5(2) pm for **1**, 330.8(2) pm for **2**).

Figure 1. Molecular structure **1** in crystals of **1**·2 MeOH[a]

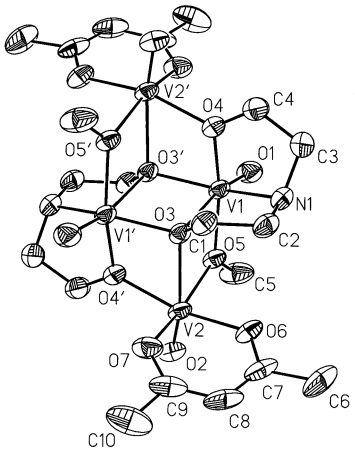

[a] The thermal ellipsoids are drawn at the 50% probability level; hydrogen atoms are omitted; atoms related by the crystallographic inversion center are denoted with a′ in the labelling scheme; selected bond lengths and metal−metal distances [pm]: C1−O1 160.5(2), V1−O3 222.1(2), V1−O3′ 201.5(2), V1−O4 195.1(2), V1−O5 201.1(2), V1−N1 215.2(3), V2−O2 159.8(2), V2−O3 235.6(2), V2−O4′ 201.0(2), V2−O5 199.1(2), V2−O6 199.9(2), V2−O7 200.2(2), V1···V2 342.2(2), V1···V2′ 329.5(2), V1···V1′ 329.0(2), V2···V2′ 585.8(3); selected bond angles [°]: O1−V1−O3 166.80(9), O2−V2−O3 164.75(9), V1−O3−V2 96.75(7), V1−O3−V1′ 101.80(8), V1′−O3−V2 97.51(8), V1−O4−V2′ 112.59(10), V1−O5−V2 117.58(9).

Figure 2. Molecular structure of **2** in crystals of **2**·2 MeOH[a]

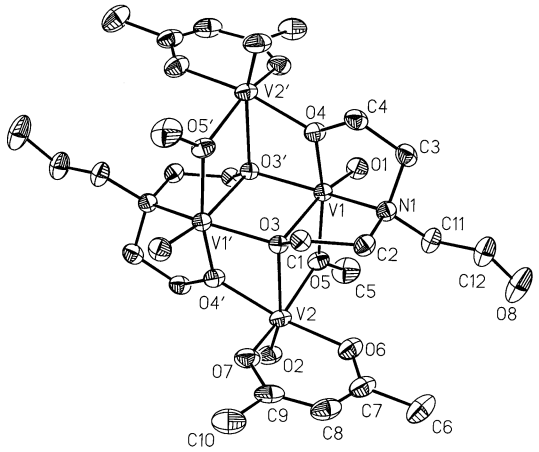

[a] The thermal ellipsoids are drawn at the 50% probability level; hydrogen atoms are omitted; atoms related by the crystallographic inversion center are denoted with a′ in the labelling scheme; selected bond lengths and metal−metal distances [pm]: V1−O1 160.8(2), V1−O3 219.8(2), V1−O3′ 201.4(2), V1−O4 193.9(2), V1−O5 203.5(2), V1−N1 217.7(3), V2−O2 159.6(2), V2−O3 237.3(2), V1−O4′ 200.4(2), V2−O5 197.5(2), V2−O6 200.8(3), V2−O7 200.1(3), V1···V2 341.9(2), V1···V2′ 330.8(2), V1···V1′ 326.6(2), V2···V2′ 588.2(2); selected bond angles [°]: O1−V1−O3 167.22(11), O2−V2−O3 163.32(11), V1−O3−V2 96.72(8), V1−O3−V1′ 101.57(9), V1′−O3−V2 97.54(9), V1−O4−V2′ 114.08(11), V1−O5−V2 116.97(11).

The crystal structures of the compounds **1**·2 MeOH and **2**·2 MeOH are characterized by the fact that both complexes contain hydrogen bond donors (**1**: NH, **2**: OH) as well as different possible acceptors. Moreover, also the additional molecules of methanol present in the crystal structures are involved in the hydrogen bonding networks. In the

hydrogen bonding scheme of **1** · 2 MeOH depicted in Figure 3 each tetranuclear oxovanadium(IV) complex takes part in the four equivalent hydrogen bonds with a N−H···O−H···O=V arrangement (N1, O1m, O1a). This leads to the formation of a hydrogen bridged chain along the [010] direction with a shortest V···V separation of 673 pm between neighboring complexes. Although the nitrogen atom of the H_3tea ligand present in **2** has lost its hydrogen donor ability due to the third substituted ethoxy group, the hydrogen bonding scheme observed for **2** · 2 MeOH depicted in Figure 4 is rather similar to that found for **1** · 2 MeOH. Nevertheless, in contrast to **1** · 2 MeOH the crystal structure of **2** · 2 MeOH exhibits two topologically different types of hydrogen bonds that can be characterized as bridging and terminal. The bridging of the oxovanadium(IV) complexes is facilitated by O−H···O=V hydrogen bonds between the dangling ethoxy groups and the oxo groups of the central binuclear unit (O8···O1a). As a result a hydrogen bridged chain along the [100] direction with a shortest V···V separation of 650 pm between neighboring complexes is formed. Whereas the methanol molecules present in **2** · 2 MeOH participate in terminal hydrogen bonds to one of the oxygen donors of the acetylacetonate ligands (O1m···O7).

Figure 3. Representation of the hydrogen bonding scheme of **1** · 2 MeOH[a]

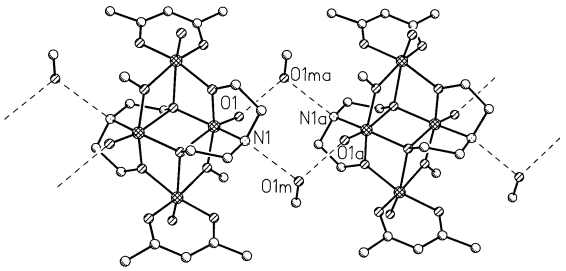

[a] Selected distances [pm]: O1−O1ma 274, N1−O1m 293.

Figure 4. Representation of the hydrogen bonding scheme of **2** · 2 MeOH[a]

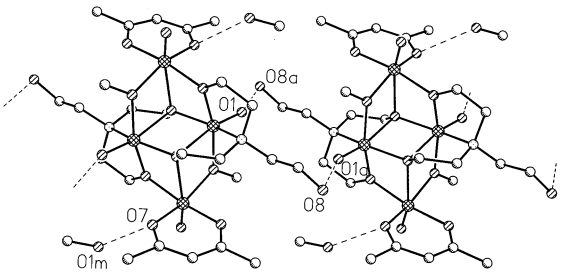

[a] The scheme is only shown for one of the enantiomeric chains; selected distances [pm]: O1−O8a 281, O1m−O7 289.

The centrosymmetric molecular structure of the ligand supported binuclear complex **3** is depicted in Figure 5. The oxovanadium(V) centers are coordinated by an acetylacetonate ligand and one of the diethanolamine fragments of the $edte^{4-}$ ligand affording an octahedral coordination environment. Basically the same molecular structure can be expected for the analogous binuclear oxovanadium(V) complex **4**, except that different stereochemical configurations are possible at the chiral carbon centers. Figure 6 shows the molecular structure derived for **4**. The observed disorder of the carbon atoms C14, C17, C20, and C23 is consistent with the occurrence of all possible stereochemical isomers in the solid state. As expected the observed bond lengths and angles for the oxovanadium(V) centers are the same for both complexes **3** and **4** within the estimated standard deviations.

Figure 5. Molecular structure of **3**[a]

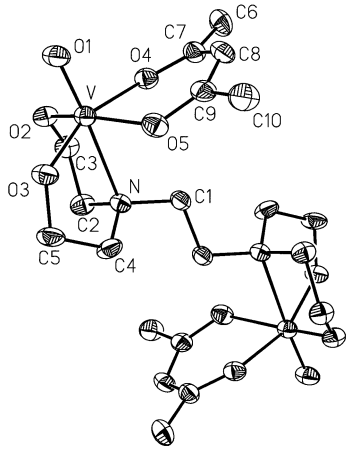

[a] The thermal ellipsoids are drawn at the 50% probability level; hydrogen atoms are omitted; selected bond lengths [pm]: V−O1 159.3(4), V−O2 181.6(4), V−O3 181.8(4), V−O4 200.5(4), V−O5 201.3(4), V−N 242.7(4); selected bond angles [°]: O1−V−O2 99.2(2), O1−V−O3 100.3(2), O1−V−O4 99.0(2), O1−V−O5 96.3(2), O1−V−N 176.6(2).

Figure 6. Molecular structure of **4**[a]

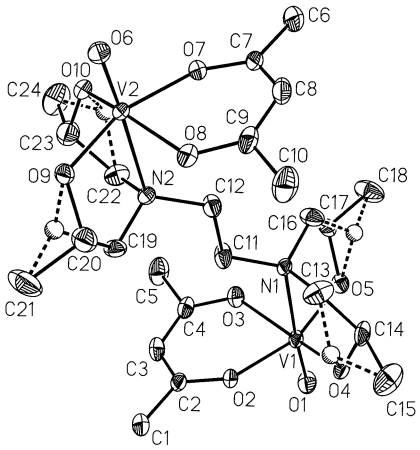

[a] The thermal ellipsoids are drawn at the 30% probability level; hydrogen atoms are omitted; C14, C17, C20, and C23 are disordered, the positions corresponding to the (*S*) configuration are represented by shaded circles and the corresponding bonds by broken lines; selected bond lengths [pm]: V1−O1 160.4(3), V1−O2 200.6(2), V1−O3 202.0(3), V1−O4 183.2(2), V1−O5 181.4(2), V1−N1 244.6(3), V2−O6 159.5(2), V2−O7 202.0(2), V2−O8 201.3(3), V2−O9 181.8(2), V2−O10 182.6(2), V2−N2 244.8(3); selected bond angles [°]: O1−V1−O2 98.76(12), O1−V1−O3 98.64(13), O1−V1−O4 99.78(13), O1−V1−O5 100.30(13), O1−V1−N1 176.43(12), O6−V2−O7 97.69(12), O6−V2−O8 98.93(13), O6−V2−O9 99.70(12), O6−V2−O10 101.31(13), O6−V2−N2 177.18(12).

The crystal structure analysis of **5** reveals the formation of a binuclear μ_2-methoxy bridged $\{(VO)_2(\mu_2\text{-}OR)_2\}^{4+}$ core

(see Figure 7). The coordination of the hexadentate aminoalcohol ligand edtp^{4-} leads to an octahedral coordination environment for both oxovanadium(V) centers. In contrast to **4** the crystal structure of **5** is consistent with the presence of just one diastereomer derived from the enantiomeric ligand pair (*R,R,R,R*)-H_4edtp and (*S,S,S,S*)-H_4edtp. In Figure 7 only the molecular structure of [$(VO)_2$\{(*S,S,S,S*)-edtp\}(μ_2-OMe)$_2$] is depicted, which is related to the enantiomeric structure of [$(VO)_2$\{(*R,R,R,R*)-edtp\}(μ_2-OMe)$_2$] by an crystallographic mirror plane (with V1, V2, O1, O2, and N1 lying on the mirror plane). Although not enforced by a crystallographic symmetry element the molecular structure of **5** is consistent with an approximate C_2 symmetry with the twofold axis perpendicular to the mean plane given by V1, O3, V2, and O3a ($\Sigma \measuredangle$ = 355°).

Figure 7. Molecular structure of **5**[a]

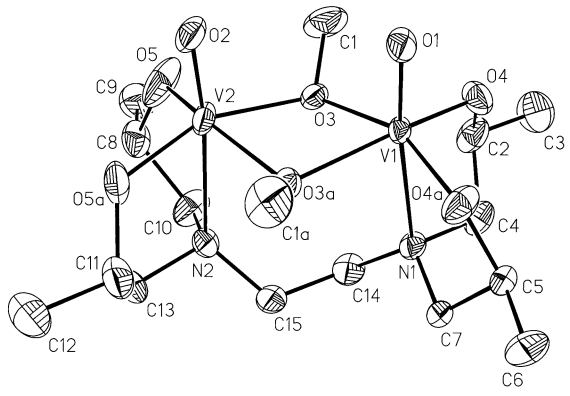

[a] The thermal ellipsoids are drawn at the 30% probability level; hydrogen atoms are omitted; atoms related by the crystallographic mirror plane are denoted with the suffix a in the labelling scheme; for the carbon and nitrogen atoms only the positions corresponding to the all (*S*) form of the edtp^{4-} ligand are shown; selected bond lengths [pm]: V1−O1 159.5(2), V1−O3 200.14(14), V1−O4 181.1(2), V1−N1 240.3(2), V2−O2 160.0(2), V2−O3 199.8(2), V2−O5 181.1(2), V2−N2 241.7(4); selected bond angles [°]: O1−V1−O3 99.60(8), O1−V1−O4 98.15(7), O1−V1−N1 173.75(1), O3−V1−O4 90.00(8), O3−V1−O3a 72.33(8), O3−V1−O4a 156.75(8), O2−V2−O3 99.70(8), O2−V2−O5 98.86(2), O2−V2−N2 170.93(12), O3−V2−O5 90.14(9), O3−V2−O3a 72.46(8), O3−V2−O5 90.14(9), V1−O3−V2 105.22(7).

Spectroscopic and Electrochemical Characterization

The IR spectra of the tetranuclear complexes **1** and **2** are consistent with their centrosymmetric core structure and the presence of vanadyl acetylacetonate fragments. The bands related with the V=O stretching vibrations are observed at 950 and 975 cm^{-1}, with the latter being characteristic for an octahedral coordinated vanadyl acetylacetonate fragment[6][9]. Although the complexes **3** and **4** contain an oxidized oxovanadium(V) group, their band related with the V=O stretching vibration is observed at a similar value of about 970 cm^{-1}. For **1** · 2 MeOH and **2** · 2 MeOH the observed IR bands due to their O−H and N−H stretching vibrations are in accord with their hydrogen bridged supramolecular structure found in the solid state (cf. Figures 3 and 4).

The NMR spectra recorded for **5** are consistent with the presence of only one diastereomer with C_2 symmetry in solution. According to the results of the crystallographic analysis this corresponds to the enantiomeric pair [$(VO)_2$\{(*S,S,S,S*)-edtp\}(μ_2-OMe)$_2$] and [$(VO)_2$\{(*R,R,R,R*)-edtp\}(μ_2-OMe)$_2$]. Consequently the protons of the methylene groups are diastereotopic. The observed coordination induced shifts of the ^{1}H and ^{13}C resonances (see Experimental Section) toward lower fields are consistent with the structure of the chelate rings and generally an intact molecular structure of **5** in solution[2][4][5][12].

To probe the electrochemical properties of the tetranuclear oxovanadium(IV) complexes **1** and **2** cyclic voltammetry measurements have been performed. Figure 8 shows representative cyclic voltammograms of a solution of **2** · MeOH in DMF measured at a gold working electrode. As expected the neutral oxovanadium(IV) complexes **1** and **2** can be oxidized. Figure 8 shows that four oxidation half waves can be observed in the cyclic voltammogram (A, B, C, and D). The first oxidative peak at E_a = 0.47 V (A) possesses a reductive counterpart at E_c = 0.37 V (G). Based on the scan rate dependence of the peak separation and the peak current ratio ($i_a/i_c \approx 1$) the wave given by A/G is found to be quasi-reversible. On the contrary, for the oxidative peaks B (E_a = 0.73 V) and C (E_a = 0.90 V) no related reduction half waves are observed as can be seen from the cyclic voltammogram measured with an anodic potential limit of about 1.0 V (see broken line in Figure 8). Upon scanning through the fourth oxidation half wave D (E_a = 1.17 V) two new reduction half waves E (E_c = 1.01 V) and F (E_c = 0.61 V) are observed. The reduction half waves E and F can be assigned to a new species derived by a chemical reaction of the positively charged complex after the last oxidation step D. This is further evidenced by the observed scan rate dependence of the two reduction half waves E and F.

Figure 8. Cyclic voltammograms of **2**[a]

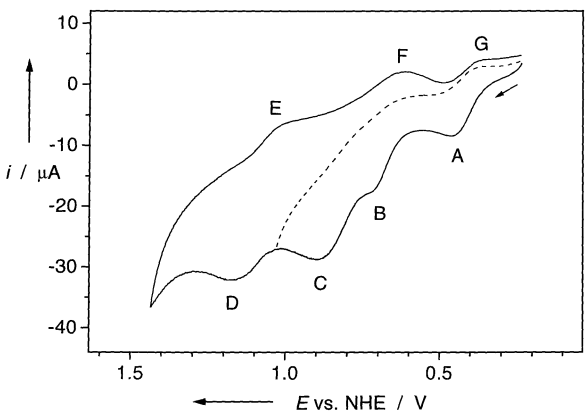

[a] Solvent DMF; tetra-*n*-buthylammonium perchlorate is used as supporting electrolyte at 0.1 M concentration and the concentration of the compound **2**·2 MeOH is about 1 mM; scan rate 50 mV/s; the broken line represents a scan with an anodic reversion potential of about 1.0 V; A, B, C, and D represent anodic peak potentials and E, F, and G stand for cathodic peak potentials (see text).

ESR Spectra and Magnetic Properties of 1 and 2

The X-band ESR powder spectra of **1** · 2 MeOH and **2** · 2 MeOH recorded at room temperature show a broad unstructured band at $g = 1.97$ and a second weak resonance at half-field, indicating the spectra are the result of exchange coupled spin systems[13]. The temperature dependence of the spectra indicates singlet ground states for **1** and **2**. At very low temperatures only the resonance signal of a residual monomeric oxovanadium(IV) impurity can be detected.

The magnetic susceptibility data of polycrystalline samples of **1** · 2 MeOH and **2** · 2 MeOH were measured in a temperature range from 4 to 280 K. The temperature dependence of the molar magnetic susceptibility χ_M in both cases goes through a maximum which is indicative for antiferromagnetic exchange interactions to be operative. At low temperatures χ_M is increasing again due to the presence of paramagnetic impurities. The $\chi_M T$ values at low temperatures are in accord with an $S = 0$ ground state of **1** and **2**, as suggested by the ESR spectra.

The observed ESR spectra and magnetic properties of **1** · 2 MeOH and **2** · 2 MeOH resemble those observed for an earlier reported oxovanadium(IV) complex with the same tetranuclear core structure[9]. On the basis of a general magneto-structural relationship for edge-shared binuclear oxovanadium(IV) units[6], both antiferro- and ferromagnetic interactions can be expected to be operative within the $\{(VO)_4(\mu_3\text{-}OR)_2(\mu_2\text{-}OR)_4\}^{2+}$ core of **1** and **2**. The spin topology and the notation of the magnetic exchange interaction parameters are depicted in Scheme 2. As a consequence of the given spin topology the expected antiferro- (J_{sc}) and ferromagnetic exchange interactions (J_{ac} and J_t) cannot be simultaneously satisfied.

Scheme 2. Spin topology of the $\{(VO)_4(\mu_3\text{-}OR)_2(\mu_2\text{-}OR)_4\}^{2+}$ core[a]

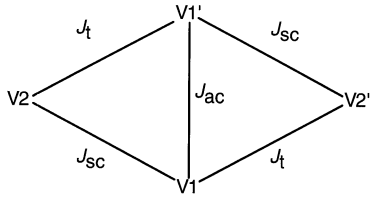

[a] The magnetic exchange coupling constants are denoted as follows: J_{ac} for *anti*-coplanar, J_{sc} for *syn*-coplanar, and J_t for twist configurations.

Based on data observed for other complexes with similar configurations of the binuclear oxovanadium(IV) units[6][9], the relative ratio of the exchange interaction parameters can be estimated as $-J_{sc} \gg J_{ac} \approx J_t$. Although competing magnetic interactions are operative within the tetranuclear core, a simplified binuclear model proved to be sufficient to describe the magnetic data of such a tetranuclear core structure with the given estimated parameter ratio[9]. This model refers to the picture that both pairs with *syn*-coplanar configuration (V1···V2 and V1′···V2′) should be predominantly coupled to form two virtually independent $S=0$ ground states. A quantitative analysis of the magnetic data has been performed using the Heisenberg−Dirac-van Vleck Hamiltonian given in Eq. 1.

$$\hat{\mathbf{H}} = -J(\hat{\mathbf{S}}_1 \cdot \hat{\mathbf{S}}_2 + \hat{\mathbf{S}}_{1'} \cdot \hat{\mathbf{S}}_{2'}) \quad (1)$$

Although only one exchange interaction constant is used in the analytical expression, reasonably good fits to the experimental data of **1** · 2 MeOH and **1** · 2 MeOH can be achieved. The magnetic parameters derived for the simplified isotropic spin Hamiltonian according to Eq. 1 are $g = 1.89$ and $J = -165$ cm^{-1} for **1** · 2 MeOH and $g = 1.94$ and $J = -171$ cm^{-1} for **2** · 2 MeOH. The rather strong antiferromagnetic coupling constants observed for both complexes are in good agreement with the data reported for other complexes containing binuclear units with *syn*-coplanar configuration (V···V 333 pm, $J = -334$ cm^{-1}[14] and V···V 341 pm, $J = -152$ cm^{-1}[9]) and can be explained on the basis of the possible superexchange mechanism through the bridging methoxy oxygen donors (O5 and O5′).

This work was supported by the *Deutsche Forschungsgemeinschaft*, the *Fonds der Chemischen Industrie*, and the *Herbert Quandt-Stiftung der VARTA AG.*

Experimental Section

NMR: ^{1}H, ^{13}C, ^{51}V, ^{1}H-^{1}H COSY, ^{1}H-^{13}C COSY, and ^{1}H-^{1}H NOESY NMR spectra were recorded on a Bruker DRX500 (^{1}H 500 MHz, ^{13}C 125.8 MHz, ^{51}V 131.5 MHz) spectrometer. Chemical shifts δ are reported with reference to external tetramethylsilan (^{1}H and ^{13}C) and $VOCl_3$ (^{51}V). − IR: Solid samples were measured either as KBr pellets or Nujol mulls between CsI plates using a Bruker IFS66 FT-IR spectrometer. − Raman: Solid samples were measured as powder on aluminium support using a Bruker IFS66/FRA106 (λ_e = 1064 nm) spectrometer. − UV/Vis: Spectra were recorded on Beckman Acta MIV (solid state reflection, cellulose as calibration standard) and Schimadzu UV-160A spectrometers (solution transmission). − Cyclic voltammetry: Princeton Applied Research VersaStat (Model 253). Cyclic voltammograms have been measured at room temperature with a three-electrode system composed of a gold working electrode, a platinum auxiliary electrode, and a platinum wire as reference electrode. The surface of the the gold working electrode was polished before each measurement. The reported potentials were referenced compared to the potential of the ferrocenium/ferrocene couple [$E^0(Fc^+/Fc) = 400$ mV vs. NHE] as internal standard[15]. The solvent DMF was dried and saturated with argon. Tetra-*n*-buthylammonium perchlorate was used as the supporting electrolyte at 0.1 M concentration and the solutions of the complexes were about 1 mM in concentration. − Powder diffraction: Powder diffraction diagrams were measured of solid samples on Al support with a Philips PW3710 powder diffractometer using Cu-$K\alpha$ radiation. − ESR: X-Band ESR spectra were recorded using a Bruker ECS106 spectrometer at a microwave frequencies of 9.48 GHz with 2,2-diphenyl-1-picrylhydrazyl as standard. − Magnetic susceptibility: Magnetic susceptibility measurements from 4 to 280 K were performed by using a Quantum Design MPMS2 SQUID magnetometer. All data were collected at an applied field of 10 kOe. The diamagnetic corrections were estimated from Pascal's constants. The susceptibility data were further corrected for temperature-independent paramagnetism (TIP) and the presence of paramagnetic impurity. For details see ref.[9]. − Melting points (uncorrected): Electrothermal melting point apparatus. − Elemental analyses: LECO CHNS-932 Analyzer.

Preparation of [{VO(dea)}$_2${VO(acac)}$_2$(μ_2-OMe)$_2$] · 2 MeOH (**1** · 2 MeOH) *and [{VO(Htea)}$_2${VO(acac)}$_2$(μ_2-OMe)$_2$] · 2 MeOH* (**2** · 2 MeOH): All manipulations were carried out under an argon atmosphere using Schlenk line techniques. The solvent methanol was purified and dried using standard methods. The ligand (9.5 mmol, i.e. 1.00 g of H_2dea or 1.42 g of H_3tea) dissolved in 5 ml methanol was added to a solution of 2.54 g (9.5 mmol) [VO(acac)$_2$] in 20 ml methanol. The resulting green solution was heated at reflux for 2 h and subsequently allowed to stand at room temperature. Within 3−4 days green crystals began to grow. After an additional week the crystalline compounds were isolated by filtration and washed with methanol. A second crop of material was obtained from the filtrate after removing solvent to about 1/3 of the original volume. The isolated solid materials can be handled in air. Within about 8 weeks the crystals start to decompose due to the loss of cocrystallized methanol.

1 · 2 MeOH: Yield 0.98 g (52%), dec. 165°C. − $C_{22}H_{46}N_2O_{16}V_4$ (798.4): calcd. C 33.10, H 5.81, N 3.51, found: C 33.31, H 5.69, N 3.68. − Selected IR data (Nujol mull between CsI plates, cm^{-1}): ν(OH) 3370 br. w, ν(NH) 3240 m, ν(C⩵C) + ν(C⩵O) 1583 vs and 1518 vs, ν(V=O) 978 vs (V2 cf. Figure 1), ν(V=O) 950 vs (V1 cf. Figure 1). − UV/Vis [DMF, $\tilde{\nu}_{max}$ in 10^3 cm^{-1} (ε in lmol^{-1} cm^{-1})]: 22.4 (23, sh), 16.0 (55), 11.5 (110). − UV/Vis (solid state, reflectance, $\tilde{\nu}_{max}$ in 10^3 cm^{-1}): 31.8, 26.7 (sh), 22.5 (sh), 16.2, 11.2.

2 · 2 MeOH: Yield 1.59 g (76%), dec. 159°C. − $C_{26}H_{54}N_2O_{18}V_4$ (886.5): calcd. C 35.23, H 6.14, N 3.16, found: C 35.01, H 5.82, N 3.11. − Selected IR data (Nujol mull between CsI plates, cm^{-1}): ν(OH) 3515 w, ν(OH) 3410 m, ν(C⩵C) + ν(C⩵O) 1582 vs and 1521 vs, ν(V=O) 973 vs (V2 cf. Figure 2), ν(V=O) 954 vs (V1 cf. Figure 2). − UV/Vis [DMF, $\tilde{\nu}_{max}$ in 10^3 cm^{-1} (ε in lmol^{-1} cm^{-1})]: 22.3 (20, sh), 16.1 (54), 11.7 (103). − UV/Vis (solid state, reflectance, $\tilde{\nu}_{max}$ in 10^3 cm^{-1}): 31.6, 26.3 (sh), 22.2 (sh), 16.4, 11.4.

Preparation of [{VO(acac)}$_2$(edte)] (**3**) *and [{VO(acac)}$_2$(edtp)]* (**4**): The ligand (7.5 mmol, i.e. 1.78 g of H_4edte or 2.19 g of H_4edtp, the latter being a mixture of all possible diastereomers) dissolved in 5 ml methanol was added to a solution of 4.00 g (15 mmol) [VO(acac)$_2$] in 40 ml methanol. At room temperature a slow stream of air was bubbled through the stirred green solution (for about 2 h). The resulting brown solution was kept at room temperature for crystallization. Orange needles began to grow after about 1 day and after additional 2 days the crystalline compound was isolated by filtration and washed with methanol. A second crop of material was obtained from the filtrate after reducing the solution volume to about 20 ml.

3: Yield 2.51 g (59%), dec. 148°C. − $C_{20}H_{34}N_2O_{10}V_2$ (564.4): calcd. C 42.56, H 6.07, N 4.96; found: C 42.37, H 6.28, N 4.68. − Selected IR data (Nujol mull between CsI plates, cm^{-1}): ν(C⩵C) + ν(C⩵O) 1574 s and 1527 s, ν(V=O) 970 vs. − Selected Raman data (powder on Al support, λ_e = 1064 nm, 35 mW, cm^{-1}): ν(V=O) 964 s.

4: Yield 2.32 g (50%), dec. 136°C. − $C_{24}H_{42}N_2O_{10}V_2$ (620.5): calcd. C 46.46, H 6.82, N 4.51; found: C 46.27, H 6.68, N 4.66. − Selected IR data (Nujol mull between CsI plates, cm^{-1}): ν(C⩵C) + ν(C⩵O) 1576 vs and 1531 vs, ν(V=O) 972 vs. − Selected Raman data (powder on Al support, λ_e = 1064 nm, 90 mW, cm^{-1}): ν(V=O) 969 s.

Preparation of [(VO)$_2$(edtp)(μ_2-OMe)$_2$] (**5**): NH_4VO_3 (2.8 g, 24 mmol) was added to a solution of H_4edtp (3.50 g, 12 mmol) in 50 ml methanol containing all possible diastereomers of the ligand. The resulting mixture was heated at reflux for 8 h. The hot reaction mixture was filtered to remove unreacted NH_4VO_3. Upon cooling the filtrate to room temperature orange crystals of **5** · *x* MeOH formed. The number of methanol molecules present in the crystalline material is estimated to x = 0.3 based on the elemental analysis and NMR data and is consistent with the crystal structure data.

5: Yield 0.38 g (6%), dec. 169°C. − $C_{16}H_{34}N_2O_8V_2$ · 0.3 MeOH (493.9): calcd. C 39.64, H 7.18, N 5.67; found: C 39.66, H 7.36, N 5.74. − Selected IR data (Nujol mull between CsI plates, cm^{-1}): ν(V=O) 963 vs. − Selected Raman data (powder on Al support, λ_e = 1064 nm, 150 mW, cm^{-1}): ν(V=O) 961 m. − ^{1}H NMR (500 MHz, [D$_6$]DMSO): δ = 1.00 (d, ^3J = 6.0 Hz, 6H, CH_3), 1.18 (d, ^3J = 6.0 Hz, 6H, CH_3), 2.23−2.31 [m; 6H, CH_2NCH_2CH(CH$_3$)OV], 2.62−2.67 (m, 2H, NCH_2CH(CH$_3$)OV), 2.80−2.85 [m, 2H, NCH_2CH(CH$_3$)OV], 3.23−3.31 (m, 2H, CH_2N), 4.21 (s, 6H, OCH_3), 4.70 (m, 2H, NCH$_2$CH(CH$_3$)OV], 4.81 (m, 2H, NCH$_2$CH(CH$_3$)OV). − ^{13}C NMR (125.8 MHz, [D$_6$]DMSO): δ = 19.7 (CH_3), 21.4 (CH_3), 51.6 (CH_2N), 59.7 [NCH_2CH(CH$_3$)OV], 63.7 [NCH_2CH(CH$_3$)OV], 67.5 (OCH_3), 76.3 [CH_2CH(CH$_3$)OV], 78.2 [CH_2CH(CH$_3$)OV]. − ^{51}V NMR (131.5 MHz, [D$_6$]DMSO): δ = −444.

Crystal Structure Determinations of **1** · 2 MeOH, **2** · 2 MeOH *and* **3**: The crystallographic data of **1** · 2 MeOH, **2** · 2 MeOH, and **3** were collected with ω-scan technique on a Siemens R3m/V diffractometer using graphite monochromated Mo-$K\alpha$ (λ = 71.073 pm) radiation. The unit cell parameters were obtained by least-squares refinement of the angular settings from well centered reflections in the 2Θ range of 18−30°. Lorentz and polarization corrections as well as an absorption correction based on azimuthal ψ scans were applied to the diffraction data. The structures were solved by direct methods (SHELXTL)[16] and subsequent full-matrix least-squares refinement of the function $\Sigma w(F_o^2 - F_c^2)^2$ $\{w = 1/[\sigma^2(F_o^2) + (A \cdot P)^2 + B \cdot P]$ with $P = (F_o^2 + 2F_c^2)/3\}$[17]. All non-hydrogen atoms were refined with anisotropic displacement parameters. The hydrogen atoms were treated using the riding model with their isotropic displacement parameters fixed at 1.2 times the value of the non-hydrogen atom attached. For the hydrogen atoms of the methyl as well as hydroxyl groups their conformation was additionally fitted to the difference Fourier map.

1 · 2 MeOH: $C_{22}H_{46}N_2O_{16}V_4$; formula weight 798.4; crystal size 0.5 × 0.5 × 0.4 mm; triclinic space group $P\bar{1}$ (No. 2); T = 188 K;; a = 773.5(3), b = 998.7(3), c = 1241.6(4) pm, α = 103.10(2), β = 107.69(2), γ = 106.13(2)°; V = 0.8255(5) nm^3; Z = 1; $\rho_{calcd.}$ = 1.606 g/cm^3; μ(Mo-K_α) = 1.168 mm^{-1}; 2Θ range 4−54°; 3553 independent reflections ($R_{int.}$ = 0.022); 204 parameters; A = 0.08, B = 0.5; $wR2$ = 0.137; $R1$ = 0.047 for 3064 reflections with $F > 4\sigma(F)$; max./min. residual electron density in the final difference Fourier map 0.9/−0.6 · 10^{-6} e/pm^3.

2 · 2 MeOH: $C_{26}H_{54}N_2O_{18}V_4$; formula weight 886.5; crystal size 0.3 × 0.2 × 0.2 mm; monoclinic space group $P2_1/c$ (No. 14); T = 188 K; a = 965.4(2), b = 1677.0(4), c = 1677.0(4) pm, β = 104.65(2)°; V = 1.8622(8) nm^3; Z = 2; $\rho_{calcd.}$ = 1.581 g/cm^3; μ(Mo-K_α) = 1.048 mm^{-1}; 2Θ range 4−54°; 4095 independent reflections ($R_{int.}$ = 0.020); 232 parameters; A = 0.05, B = 2.7; $wR2$ = 0.122; $R1$ = 0.046 for 3028 reflections with $F > 4\sigma(F)$; max./min. residual electron density in the final difference Fourier map 0.5/−0.5 · 10^{-6} e/pm^3.

3: $C_{20}H_{34}N_2O_{10}V_2$; formula weight 564.4; crystal size 0.25 × 0.15 × 0.05 mm; monoclinic space group $P2_1/n$ (No. 14); T = 188 K; a = 812.2(3), b = 1165.2(5), c = 1298.3(6) pm, β = 102.65(3)°; V = 1.1989(9) nm^3; Z = 2; $\rho_{calcd.}$ = 1.563 g/cm^3; μ(Mo-K_α) = 0.837 mm^{-1}; 2Θ range 4−54°; 2632 independent reflections ($R_{int.}$ = 0.030); 156 parameters; A = 0.07, B = 2.5; $wR2$ = 0.176; $R1$ = 0.067 for 1675 reflections with $F > 4\sigma(F)$; max./min. residual electron density in the final difference Fourier map 0.6/−0.4 · 10^{-6} e/pm^3.

Crystal Structure Determinations of **4** *and* **5**: The crystallographic data of **4** and **5** were collected on a Siemens SMART-CCD diffractometer (ω-scans with 0.3° per frame) using graphite monochromated Mo-$K\alpha$ (λ = 71.073 pm) radiation. The intensities of the reflections of a hemisphere have been measured (SMART). Lorentz and polarization corrections as well as an empirical absorption correction based on the intensities of equivalent reflections measured at different angular settings have been performed (SAINT and SADABS). The structure was solved by direct methods (SHELXTL)[16] and subsequent full-matrix least-squares refinement of the function $\Sigma w(F_o^2 - F_c^2)^2$ $\{w = 1/[\sigma^2(F_o^2) + (A \cdot P)^2 + B \cdot P]$ with $P = (F_o^2 + 2F_c^2)/3\}$[17]. All non-hydrogen atoms were refined with anisotropic displacement parameters. The hydrogen atoms were treated using the riding model with their isotropic displacement parameters fixed at 1.2 times the value of the non-hydrogen atom attached. For the hydrogen atoms of the methyl as well as hydroxyl groups their conformation was additionally fitted to the difference Fourier map.

For **4** the observed systematic absences suggest either of the orthorhombic space groups $Pca2_1$ and *Pbcm*. Attempts to solve the structure in the centrosymmetric space group *Pbcm* were unsuccessful. This led in agreement with intensity statistics to the noncentrosymmetric orthorhombic space group $Pca2_1$ as final choice. The refinement afforded a Flack parameter[18] of about 0.4, which could not be reduced upon inversion of the parameter set. Therefore the final structure refinement was performed assuming racemic twinning, which led to a refined Flack parameter of 0.42(2). Also the refinement in the chiral subgroup $P2_1$ was attempted but did not give any evidence for the presence of any particular chiral molecular structure. The presence of all possible diastereomers is consistent with the observed disorder of the chiral carbon atoms of the edtp^{4-} ligand (C14, C17, C20, and C23) on two positions corresponding to their respective (*R*) and (*S*) configurations (in Figure 6 only the positions for the (*R*) configurations are represented as ellipsoids).

The additional methanol molecule present in **5** is highly disordered and only the respective oxygen atom could be located from the difference Fourier map and refined with an isotropic displacement parameter.

4: $C_{24}H_{42}N_2O_{10}V_2$; formula weight 620.5; crystal size 0.4 × 0.4 × 0.4 mm; orthorhombic space group $Pca2_1$ (No. 29); T = 183 K; a = 2553.18(4), b = 823.11(1), c = 1396.16(1) pm; V = 2.93410(6) nm^3; Z = 4; $\rho_{calcd.}$ = 1.405 g/cm^3; μ(Mo-K_α) = 0.691 mm^{-1}; 2Θ range 4−54°; 5897 independent reflections ($R_{int.}$ = 0.027); 3298 reflections for Friedel opposites merged; 379 parameters; A = 0.06, B = 2.1; $wR2$ = 0.109; $R1$ = 0.039 for 5331 reflections with $F > 4\sigma(F)$; Flack parameter x = 0.42(2); max./min. residual electron density in the final difference Fourier map 0.5/−0.6 · 10^{-6} e/pm^3.

5: $C_{16}H_{34}N_2O_8V_2 \cdot 0.3$ MeOH; formula weight 493.9; crystal size 0.4 × 0.4 × 0.06 mm; orthorhombic space group *Pbcm* (No. 57); T = 183 K; a = 903.85(1), b = 1453.37(2), c = 1757.92(3) pm; V = 2.30925(6) nm^3; Z = 4; $\rho_{calcd.}$ = 1.421 g/cm^3; μ(Mo-M_α) = 0.852 mm^{-1}; 2Θ range 4−54°; 2593 independent reflections ($R_{int.}$ = 0.028); 208 parameters; A = 0.04, B = 1.8; $wR2$ = 0.097; $R1$ = 0.038 for 2204 reflections with $F > 4\sigma(F)$; max./min. residual electron density in the final difference Fourier map 0.5/−0.4 · 10^{-6} e/pm^3.

Further details of the crystal structure investigations may be obtained from the Fachinformationszentrum Karlsruhe; D-76344 Eggenstein-Leopoldshafen (Germany), on quoting the depository numbers CSD-408105 (**1** · 2 MeOH), CSD-408106 (**2** · 2 MeOH); CSD-408107 (**3**), CSD-408108 (**4**), and CSD-408109 (**5**).

☆ Dedicated to Professor *Achim Müller* on the occasion of his 60th birthday.

[1] [1a] H. Sigel, A. Sigel (Eds.), *Metal Ions in Biological Systems,* vol. 31: *Vanadium and Its Role in Life*, Marcel Dekker, New York, **1995**. – [1b] N. D. Chasteen (Ed.), *Vanadium in Biological Systems*, Kluwer Academic Publishers, Dordrecht, **1990**. – [1c] R. Wever, K. Kustin, *Adv. Inorg. Chem.* **1990**, *35*, 81−115.

[2] [2a] W. Plass, *Z. Anorg. Allg. Chem.* **1997**, *623*, 461−477. – [2b] W. Plass, *Inorg. Chim. Acta* **1996**, *244*, 221−227. – [2c] W. Plass, *Z. Anorg. Allg. Chem.* **1994**, *620*, 1635−1644.

[3] [3a] D. C. Crans, A. D. Keramidas, S. S. Amin, O. P. Anderson, S. M. Miller, *J. Chem. Soc. Dalton Trans.* **1997**, 2799−2812. – [3b] D. C. Crans, P. M. Ehde, P. K. Shin, L. Pettersson, *J. Am. Chem. Soc.* **1991**, *113*, 3728−3736. – [3c] D. C. Crans, R. L. Bunch, L. A. Theisen, *J. Am. Chem. Soc.* **1989**, *111*, 7597−7607. – [3d] D. C. Crans, P. K. Shin, *Inorg. Chem.* **1988**, *27*, 1797−1806. – [3e] G. J. Colpas, B. J. Hamstra, J. W. Kampf, V. L. Pecoraro, *Inorg. Chem.* **1994**, *33*, 4669−4675. – [3f] C. R. Cornman, G. J. Colpas, J. D. Hoeschele, J. Kampf, V. L. Pecoraro, *J. Am. Chem. Soc.* **1992**, *114*, 9925−9933.

[4] D. C. Crans, H. Chen, O. P. Anderson, M. M. Miller, *J. Am. Chem. Soc.* **1993**, *115*, 6769−6776.

[5] D. C. Crans, K. P. Shin, *J. Am. Chem. Soc.* **1994**, *116*, 1305−1315.

[6] W. Plass, *Angew. Chem.* **1996**, *108*, 699−703; *Angew. Chem. Int. Ed. Engl.* **1996**, *35*, 627−631.

[7] W. Plass, *Z. Anorg. Allg. Chem.* **1997**, *623*, 1290−1298.

[8] M. I. Khan, J. Zubieta in *Progress in Inorganic Chemistry* (Ed.: K. D. Karlin), Wiley-Interscience, New York, **1995**, vol. 43, pp. 1−149.

[9] W. Plass, *Inorg. Chem.* **1997**, *36*, 2200−2205.

[10] [10a] M. G. Voronkov, A. F. Lapsin, U.S.S.R. Patent 187,793 and 187,792 **1966** [*Chem. Abstr.* **1967**, *67*, 4452e, 4453f]. – [10b] R. K. Mittal, *Z. Anorg. Allg. Chem.* **1967**, *351*, 309−312.

[11] [11a] M. Mikuriya, T. Kotera, F. Adachi, S. Bandow, *Chem. Lett.* **1993**, 945−948. – [11b] I. Cavaco, J. C. Pessoa, M. T. Duarte, P. M. Matias, R. T. Henriques, *Polyhedron* **1993**, *12*, 1231−1237.

[12] M. M. Caldeira, M. L. Ramos, N. C. Oliveira, V. M. S. Gil, *Can. J. Chem.* **1987**, *65*, 2434−2440.

[13] A. Bencini, D. Gatteschi, *Electron Paramagnetic Resonance of Exchange Coupled Systems*, Springer, Berlin, **1990**.

[14] M. I. Khan, Y.-D. Chang, Q. Chen, J. Salta, Y.-S. Lee, C. J. O'Connor, J. Zubieta, *Inorg. Chem.* **1994**, *33*, 6340−6350.

[15] R. R. Gagné, C. A. Koval, G. C. Lisensky, *Inorg. Chem.* **1980**, *19*, 2854−2855.

[16] *SHELXTL,* Siemens Analytical X-Ray Instruments Inc., Madison, Wisconsin, USA, **1994**.

[17] G. M. Sheldrick, *SHELXL-93*, Universität Göttingen, **1993**.

[18] [18a] H. D. Flack, *Acta Crystallogr.* **1983**, *A39*, 876−881. – [18b] G. Bernardinelli, H. D. Flack, *Acta Crystallogr.* **1985**, *A41*, 500−511.

[97314]

Three-Dimensional Assemblies of Gold Colloids in Nanoporous Alumina Membranes☆

Taka-aki Hanaoka[a,b], Hans-Peter Kormann[a], Michael Kröll[a], Thomas Sawitowski[a], and Günter Schmid*[a]

Institut für Anorganische Chemie, Universität Essen,[a]
Universitätsstrasse 5–7, D-45177 Essen, Germany
Fax: (internat.) + 49 (0)201/183 2402
E-mail: guenter.schmid@uni-essen.de

National Institut of Materials and Chemical Research,[b]
Higashi 1-1, Tsukaba 305, Japan
Fax: (internat.) + 81 (0)298/544487
E-mail: hanaoka@nimc.go.jp

Received December 22, 1997

Keywords: Gold colloids / Self-assembly / Nanoporous alumina / Three-dimensional organization

Examples of a new class of three-dimensionally arranged gold colloids have been prepared in the nanoscale pores of alumina membranes. Immobilization of the colloid particles was achieved by a modification of the inner walls with alkoxysilanes $Y–(CH_2)_x–Si(OR)_3$ and $Y–(CH_2)_x–SiR(OR)_2$ bearing suitable functional groups (Y = NH_2, SH), followed by anchoring of the colloids by self-assembly onto the modified surface. This procedure gives tight and stable ensembles of colloids on the walls. TEM analyses revealed uniform and random colloidal dispersions on the walls in the form of sub-monolayers without any aggregation. UV/Vis spectra of the filled membranes showed an absorption maximum at ca. 525 nm arising from an excitation of the plasmon resonance of the gold colloids. The dimensions of the pores can be "tuned" and given the diverse range of different colloids available, routes to novel catalysts and sensors can be envisaged.

Introduction

Over the past decade, a wide variety of approaches have been proposed for the construction of nanostructured materials from nanoparticles. Organization of nanoscale particles is considered as a promising route for the development of new materials that can be classified as nanostructures. Since metal colloids represent one of the most extensively studied classes of nanoscale materials, and because they have the advantage of well-defined size and character, such systems are promising candidates for use as building blocks in the construction of nanostructured materials.[1] Nanostructures constructed from colloids are of interest for a wide range of applications[2] as a result of their chemical, catalytic, electrochemical, magnetic, and optical properties. For example, in catalysis they can be regarded as offering intermediate situations between homogeneous and heterogeneous catalysts[3], and unique catalytic features in reactions such as hydrogenation[4], hydrosilylation[5], and photocatalytic reactions[6] have been reported. Meanwhile, the adsorption of metal colloids onto organic and inorganic supports has been investigated as a means of preparing well-defined heterogeneous catalysts.[7]

Immobilization of metal colloid particles on a suitable structured matrix using a self-assembly technique is one of the most promising strategies for the construction of colloidal nanostructures.[8] Based on such a strategy, the preparation of two-dimensional metal colloid arrays on a flat surface has been reported by Natan et al.[9] and by Sato et al.[10] The use of colloids offers several advantages: (i) essentially monodispersed metal particles are easily obtained, (ii) the preparation and characterization of many kinds of colloidal metals has been well-researched, (iii) ordering of colloids is expected by self-assembly, (iv) anchoring on supports increases stability against agglomeration, and (v) new characteristics originate from an interaction between the colloidal particles and supports.

Since the construction of three-dimensional ensembles is necessary for the practical use of colloids, the development of three-dimensional structures from two-dimensional arrays is necessary.[11] Three-dimensional colloid arrangements have been reported to be produced from multi-layer films by sequential self-assembling[12] and by using sol-gel techniques[13], as well as from the use of reversed micelles[14], and by an external electric field induced layering of colloid crystals.[15] Assembling a homogeneous dispersion in a well-defined three-dimensional nanostructure offers an alternative route to these "stepwise"[12][13][14][15] constructions. Such a strategy requires careful selection of the appropriate matrix. Since a porous alumina membrane, which can be prepared by anodic oxidation of aluminum in diprotic acid solution, has a huge number of parallel pores of uniform diameter, we chose it as a promising matrix for supporting assemblies of colloids. The dimensions of the pores can be controlled by adjusting the anodization con-

 © WILEY-VCH Verlag GmbH, D-69451 Weinheim, 1998 1434–1948/98/0606–0807 $ 17.50+.50/0

ditions; by varying the applied voltage their diameter can be varied from 5 to 150 nm and their depth, i.e. the thickness of the membrane, from 1 to >100 μm.[16] Such a porous alumina membrane has also been used as a unique template in the assembly of nanostructures.[17] The anodization procedure is readily applicable for the preparation of a membrane of large area and of appropriate shape. Here, we describe the assembly of gold colloids in the well-ordered pores of alumina membranes using a self-assembly technique. These materials belong to a new class of three-dimensional nanostructures, the structures of which can be "tuned" by modification of the matrix. Therefore, this strategy should be a potentially useful technique in the development of diverse applications in optics, as sensors, and as catalysts.

Results and Discussion

Immobilized Colloids in Membranes: Scheme 1 illustrates our strategy for the preparation of the target material and the colloid coordination. The procedure consists of the anodization of aluminum, the derivatization of pores in the alumina membrane with a functionalized alkoxysilane such as $Y-(CH_2)_x-Si(OR)_3$ or $Y-(CH_2)_x-SiR(OR)_2$ (Y = SH, NH_2), and the immobilization of colloidal particles.

Scheme 1. Modification of alumina membranes with functionalized alkoxysilane molecules and chemisorption of gold colloids

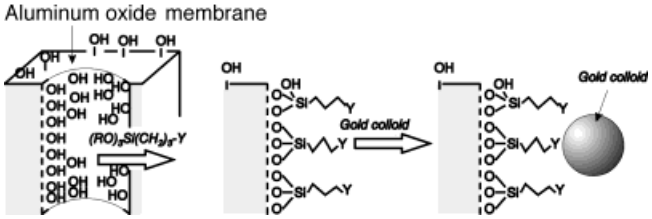

Aluminum plates form porous membranes on the surface upon anodization in 2% phosphoric acid solution. Pore size and pore density is largely governed by the applied voltage.[16] Membranes containing pores of 150 ± 10 nm in diameter are obtained by constant voltage anodization at 150 V. Detachment of the membrane by treatment with sulfuric acid gives a self-standing alumina membrane with a thickness of between 20 and 90 μm depending on the anodization period.

The hydroxyl groups present on the alumina surface are highly reactive and react readily with alkoxysilane molecules generating covalent Al−O−Si moieties. Functional groups Y are selected such that they show good affinity to the metal colloid. Reactions of the alkoxysilanes with the pore walls proceed smoothly in toluene solution under reflux conditions. The IR spectrum of a membrane reacted with 3-aminopropylmethyldiethoxosilane (APDMS) shows two signals at 2960 and 2930 cm^{-1}, which can be attributed to C−H stretching vibrations of the alkyl chains.[18] By monitoring the peak intensity during the course of the reaction, saturation is observed after ca. 14 h. The reactivity of the reagents is modified by the nature of the functional group Y and by the number of alkoxy groups. Compared to dialkoxysilanes, trialkoxysilanes show lower reactivity. On the other hand, aminoalkoxysilanes are highly reactive compared to mercapto derivatives.

The immobilization of gold colloids in the pores can be performed by one of two types of vacuum incorporation. In the first, the modified membrane is placed on a short plastic tube connected to a water pump, and the gold colloid solution is sucked through the membrane. Alternatively, the membrane is placed in a flask and the colloid solution is added. Evacuation of the flask causes the solution to penetrate into the pores. In both cases it is necessary to exhaustively wash out remaining silane before the filling process. Even small amounts of unreacted reagents cause immediate aggregation of the gold colloids. Well-washed membranes take on a dark-red color upon incorporation of gold colloids. Figure 1 shows a schematic depiction of a membrane containing immobilized gold.

Figure 1. Model structure of a colloid-charged porous alumina membrane

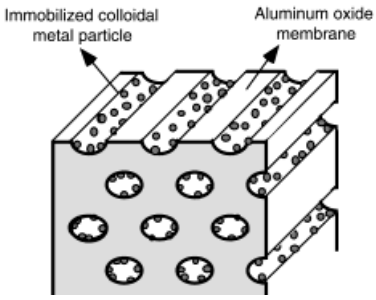

Optical Properties: UV/Vis spectra of gold colloid solutions, prepared as described[21], show an absorption maximum at ca. 520 nm originating from an excitation of plasmon resonance.

Figure 2. UV/Vis spectra of immobilized gold colloids in nanoporous membranes derivatized with different alkoxysilanes − A: derivatized with APDMS; B: derivatized with MPDMS

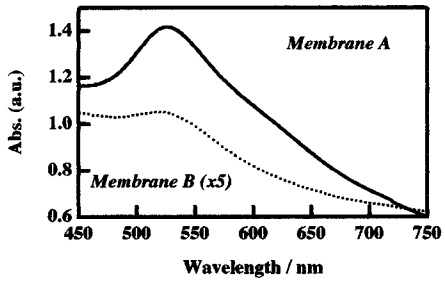

The spectra of colloids in membranes show resonances at approximately the same position. Figure 2 shows the spectra of two colloid-containing membranes. Membrane A was modified with APDMS, membrane B with 3-mercaptopropylmethyldimethoxysilane (MPDMS). Both spectra show a peak at λ_{max} = ca. 525 nm, but the relative ab-

sorbances differ markedly. The peak position is close to that of the original solution, albeit slightly shifted to longer wavelengths. This shift can be explained in terms of interparticle coupling between the colloids[19], i.e. a reduction of the distance between particles compared to that in solution.

The difference in the absorbances of membranes A and B can be attributed to the different amounts of colloid that are immobilized. The different degree of immobilization can be explained by preferred interactions between the amino functions of APDMS and the colloids bearing citric acid molecules on the surface. The SH functions in MPDMS could be expected to form strong bonds to gold particles, but this effect is less in evidence compared to the acid-base interaction. Since neither spectrum shows aggregation peaks between 600 and 800 nm, aggregation of the colloids by migration can be excluded. The lack of aggregation indicates that the colloids are tightly bound to the surface through their interaction with the functional groups of anchored molecules. Assuming that the pores have a diameter of 160 nm and that there is a pore density of $1.1 \cdot 10^9$ cm^{-2}, in accordance with the data of Rigby and co-workers[16c], the internal surface area of the pores can be roughly calculated as $4 \cdot 10^2$ cm^2 for 1 cm^2 of membrane. The outer surface area is thus less than 1% of this value. Since the density of surface hydroxy groups on the alumina was reported to be 10 per nm^2 after treatment at 100°C[20], the total number of OH groups in the pores can be estimated as $4 \cdot 10^{16}$ for 1 cm^2 of membrane. If all OH groups are derivatized by silane molecules, about 23 nmol of functional groups are fixed in the pores. Considering the size of the colloid (13 nm), more than ca. 450 of the functional groups can be expected to be present within the area corresponding to the dimensions of one colloid particle. Of course, not all functional groups are able to interact with the colloids, but strong interactions by multi-anchoring between the surface and the particle are very reasonable as an interpretation of the absence of aggregation.[22]

Transmission Electron Microscopy: To confirm the dispersion of the colloids on the derivatized surface of the pores, transmission electron microscopy (TEM) investigations were carried out on sectioned samples. Figure 3 shows a TEM image of a porous membrane following derivatization with APDMS and treatment with a gold colloid by vacuum incorporation.

The gold colloid particles can clearly be recognized on the pore walls. Apart from the region near the surface of the membrane, the particles are randomly and uniformly distributed and cover the wall surface as a sub-monolayer extending over a large area. No aggregated or chained particles can be observed in either direction, i.e. in the plane of, or perpendicular to the wall. In contrast, a TEM image of an underivatized porous membrane following treatment with the colloid revealed only the presence of partly aggregated colloids of low density. Therefore, the random arrangement indicated by the UV/Vis spectrum is clearly confirmed by the TEM observation.

The average diameter of the immobilized colloids on the wall is found to be ca. 15 nm (for 131 measured particles).

Figure 3. TEM image of immobilized gold colloids (ca. 13 nm) in opened pores of alumina

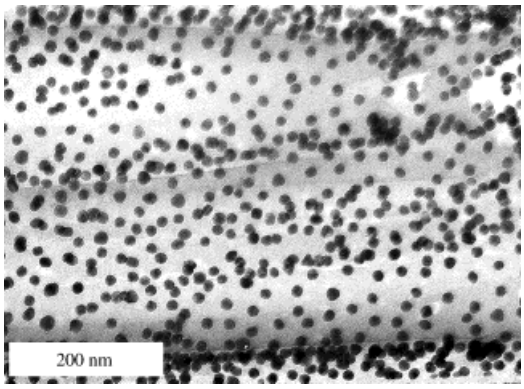

This value is slightly larger but close to the size of the original colloids in aqueous solution, i.e. the colloidal particles do not grow or aggregate during immobilization. The sub-monolayer coverage of the wall with the gold colloids was found to represent ca. 25% of a full monolayer. Incomplete coverage of the wall can be attributed to an electrostatic repulsion between particles. This is consistent with previous observations on a two-dimensional array of gold colloids on a derivatized SiO_2 surface.[9]

Since the pores are cylindrical in shape, the walls are concave. Therefore, the particle density projected on the film appears to vary with position in the pore. Differently sectioned TEM photographs clearly show the effect of pore shape. Figures 4a to 6a show images of apparently different dispersions according to the sectioning, along with schematic depictions.

In order to make TEM imaging easy, Anopore™ with 250 nm pore widths was used for this special purpose. The sample was derivatized with APDMS and sectioned into sheets of thickness 100 nm. A part of the sample gave images showing the particles located only near the pore walls (Figure 4a). In this micrograph, closely packed, vertically overlapped particles are observed along the walls. This arrangement is interpreted as illustrated in Figure 4b. In this image, thin sectioning is considered to remove both walls, i.e. the upper and lower faces, of the pore. Since particles near the wall are viewed from the perpendicular direction, particles aligned vertically give a projected image of overlapped particles. As the result, the density of particles near the wall appears to increase. Figure 5a shows an image of an area similar to that depicted in Figure 4a (bottom), but additionally shows a pore with an intact rear side (upper part). Figure 5b illustrates a tubular pore cut in half, with immobilized particles on the surface. In accordance with the curvature of the bottom side, the apparent density of particles appears to be higher near the vertical walls and gradually decreases towards the center.

Figure 6a depicts two distinct areas in one pore (parts A and B). The two areas are distinguishable by the following criteria: (i) the observed density of particles in part A is much higher than that in part B, (ii) overlapped images of particles are apparent only in part A, (iii) the darkness

Figure 4. (a) TEM image of gold colloids in the pores. Both the upper and lower walls have been removed by sectioning; (b) schematic representation illustrating the situation

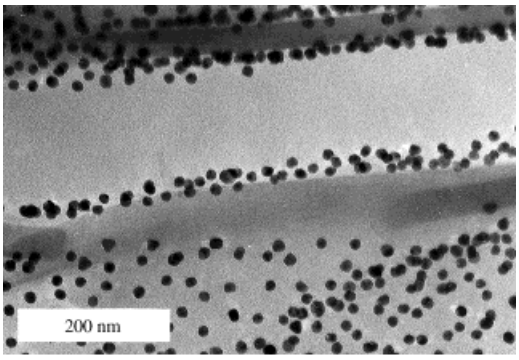

a

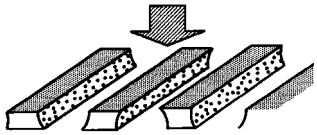

b

Figure 5. (a) TEM image of gold colloids in alumina pores opened on one side, (b) schematic representation to clarify the photograph

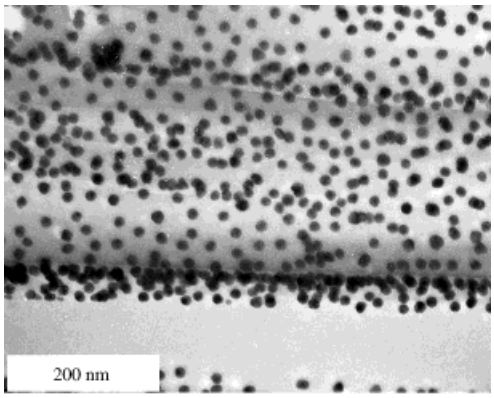

a

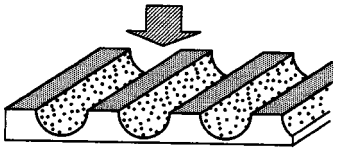

b

Figure 6. (a) Some distinct areas in a piece of membrane supporting gold colloids. Area B shows part of a pore opened on one side, while area A depicts a view through a thin, but colloid-bearing alumina wall; the density of colloids appears higher in A than in B due to the simultaneous imaging of particles on both the front and rear sides. The schematic representation in Figure 6b helps to clarify the relatively complicated situation in Figure 6a.

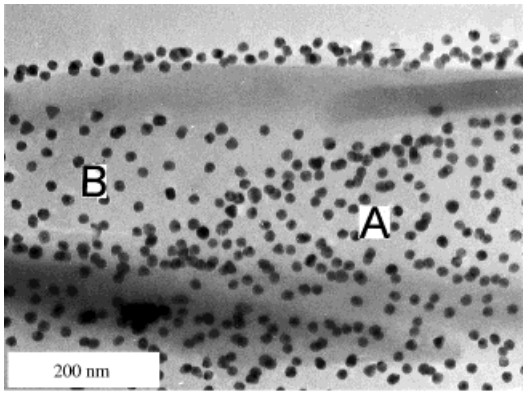

a

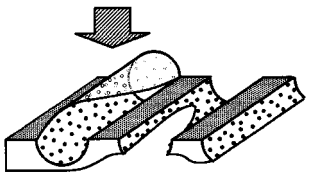

b

around the colloids in area A is more pronounced than that in area B. Part B is considered to be similar to the bottom part of a wall, as in Figure 4b. Figure 6b illustrates a cylindrical pore sliced slantwise. This scheme depicts two parts; one part is modelled in Figure 5b, while the other consists of a whole pore wall. The image of area A is assigned to a transmission view of the whole tube, i.e. the overlapped image of both upper and lower walls of one pore. This view can be considered to give an almost double particle density and an overlapped image of particles through projection of both walls within the same area. The model shown in Figure 6b interprets all characteristics of Figure 6a.

These three TEM photographs are consistent with the results of spectroscopic studies and clearly confirm the situation with gold colloids immobilized on the tubular walls of alumina membranes.

Conclusions

Gold colloids have been successfully immobilized in the parallel and uniform pores of alumina membranes. The ensemble of colloids forms a sub-monolayer on the pore walls (coverage = ca. 0.25), as shown by TEM and UV/Vis spectroscopy. The observations show that the colloids are tightly anchored on the surface, randomly and uniformly, without any aggregation. Thus, three-dimensionally arranged colloidal particles are distributed over a large area, as a result of their self-assembly on the derivatized surfaces of the structurally well-defined alumina. The thickness of the membranes in which the colloids are arranged ranges from 10 to 100 μm, and the pore size can be "tuned" by variation of the anodization conditions. Variation of the anchored colloids should be easily achieved by means of suitable combinations of derivatizing reagents and colloidal metals.

Experimental Section

General: Aluminum plates of 99.5% of purity were used. Of the alkoxysilanes used as derivatizing reagents, 3-mercaptopropylmethyldimethoxysilane (MPDMS) was purchased from ABCR GmbH & Co., Germany, while 3-aminopropylmethyldiethoxysilane (APDMS) was purchased from Fluka GmbH, Switzerland. Toluene was obtained as analytical grade and was dried by distillation from sodium benzophenone ketyl. Analytical grade methanol was used without further purification. Gold colloid solutions were prepared by an established method[21] through reduction of $HAuCl_4$ with sodium citrate. The average diameter of the colloids was measured as 13 ± 1 nm. Commercially available porous aluminum oxide membrane, Anopore™ (Merck, Germany; average pore diameter 250 nm), was also used as a porous alumina membrane.

Physical Measurements: IR spectra of derivatized membranes were recorded on a BIO-RAD FTS-175 infrared spectrometer. Electronic spectra of membranes containing gold colloids were measured on a Varian Cary-1 UV/Vis spectrometer equipped with a small aperture fitted to the sample. TEM images were obtained using a Philips CM 200 FEG microscope. Samples for TEM were embedded in a resin and sectioned. The thickness of the sample was varied from 100 to 50 nm. An Ultra Cut Microtom, Leica, Germany, was used for sectioning.

Preparation of Porous Alumina Membranes: Aluminum plates (99.5%, 70 × 55 × 2 mm) were electropolished before anodization in a mixture of sulfuric acid and phosphoric acid. Anodic oxidation was carried out in 2% (w/w) phosphoric acid under a constant voltage of 150 V at 6°C. The maximum current density was ca. 2.5 mA cm^{-2}. Anodization was allowed to proceed for 6 to 48 h depending on the required thickness of the membrane. Thereafter, the applied voltage was reduced in a stepwise manner from 150 V to 0.5 V and then stopped. The anodized plates were washed with water and dried in air, then immersed in 12.5% sulfuric acid at room temperature in order to detach the porous alumina membranes. The membranes were carefully washed with water and then immersed in 10% sulfuric acid for 10 min to remove the barrier layer on the rear side, so as make through pores. Subsequently, the membrane was rinsed with water and methanol, and dried.

Derivatization of Porous Alumina: A typical procedure for the derivatization with MPDMS and APDMA was as follows: the membrane was cut to a size of ca. 1 × 2 cm, then washed with methanol, and dried in air. Subsequent procedures were carried out under nitrogen. The specimen was placed in a 50 ml flask under anhydrous conditions. A dry toluene solution of the derivatization reagent (5%) was added to the flask, heated to reflux temperature, and maintained under these conditions for 18 h without stirring. After cooling, the solution was removed and the membrane was thoroughly rinsed with dry toluene. In order to ensure complete reaction of the surface hydroxy groups with the alkoxysilanes, each specimen was subsequently subjected to the reaction conditions for a further 1 h. Afterwards, the sample was repeatedly washed with hot toluene to ensure complete removal of the unreacted reagent.

Immobilization: The implantation of gold colloids into the modified pores was carried out by one of two vacuum filling methods. (a) The membrane was washed with water and then placed on a short plastic tube (⊘ = 5 mm) connected to a water pump via a 3-way control valve. A drop of gold colloid solution was applied to the other side of the membrane and drawn into the pores by applying a vacuum. (b) The washed membrane was placed in a 50-ml round-bottomed flask and 10 ml of the gold colloid solution was added. The flask was then carefully evacuated to water-pump pressure and maintained under these conditions overnight. In both methods, immobilization of the colloids was checked by observing the color of the membrane. After incorporation, the membrane was washed thoroughly with distilled water and dried in air at room temperature.

☆ Dedicated to Professor *Hartmut Bärnighausen* on the occasion of his 65th birthday.

[1] [1a] *Clusters and Colloids* (Ed.: G. Schmid), VCH, Weinheim, **1994**, chapter 1. – [1b] G. Schmid, *Chem. Rev.* **1992**, *92*, 1709–1727. – [1c] G. Schön, U. Simon, *Colloid Polym. Sci.* **1995**, *273*, 101–117. – [1d] J. H. Fendler, F. C. Meldrum, *Adv. Mater.* **1995**, *7*, 607–632; M. Giersig, P. Mulvaney, *J. Phys. Chem.* **1997**, *97*, 6334–6336. – [1e] R. G. Freeman, K. C. Grabar, K. J. Allison, R. M. Bright, J. A. Davis, A. P. Guthrie, M. B. Hommer, M. A. Jackson, P. C. Smith, D. G. Walter, M. J. Natan, *Science* **1995**, *267*, 1629–1632.

[2] *Nanomaterials: Synthesis, Properties, and Application* (Eds.: A. S. Edelstein, R. C. Cammarata), Institute of Physical Publishing, Bristol, **1996**, p. 111–140.

[3] D. R. Anton, R. H. Crabtree, *Organometallics* **1983**, *2*, 855–859.

[4] [4] H. Hirai, H. Chawanya, N. Toshima, *Macromol. Chem., Rapid Commun.* **1981**, *2*, 99–103. – [4b] N. Toshima, T. Takahashi, *Bull. Chem. Soc. Jpn.* **1992**, *65*, 400–409. – [4c] H. Bönnemann, W. Brijoux, R. Brinkmann, E. Dinjus, R. Fretzen, T. Joussen, B. Korall, *J. Mol. Cat.* **1992**, *74*, 323–333. – [4d] M. Brust, J. Fink, D. Bethell, D. J. Schiffrin, C. Kiely, *J. Chem. Soc., Chem. Commun.* **1995**, 1655–1656.

[5] [5a] L. N. Lewis, N. Lewis, *J. Am. Chem. Soc.* **1986**, *108*, 7228–7231. – [5b] L. N. Lewis, R. J. Uriarte, N. Lewis, *J. Mol. Catal.* **1991**, *66*, 105–113.

[6] [6a] A. Harriman, *J. Chem. Soc., Faraday Trans.* **1986**, *82*, 2267–2274. – [6b] C. K. Grätzel, M. Grätzel, *J. Am. Chem. Soc.* **1979**, *101*, 7741–7743. – [6c] G. S. Nahor, L. C. T. Shoute, P. Neta, A. Harriman, *J. Chem. Soc., Faraday Trans.* **1990**, *86*, 3927–3933. – [6d] T. Hanaoka, H. Arakawa, K. Takeuchi, T. Matsuzaki, Y. Sugi, *Chem. Express* **1989**, *4*, 137–140. – [6e] T. Hanaoka, Y. Kubota, K. Takeuchi, T. Matsuzaki, Y. Sugi, *J. Mol. Catal. A - Chemical* **1995**, *98*, 157–160.

[7] [7a] G. Schmid, M. Harms, J.-O. Malm, J.-O. Bovin, J. van Ruitenbeck, H. W. Zandbergen, W. T. Fu, *J. Am. Chem. Soc.* **1993**, *115*, 2046–2048. – [7b] K. J. Klabunde, Y.-X. Li, B.-J. Tan, *Chem. Matter.* **1991**, *3*, 30–39.

[8] [8a] A. Badia, S. Singh, L. Demers, L. Cuccia, G. R. Brown, R. B. Lennox, *Chem. Eur. J.* **1996**, *2*, 359–363. – [8b] A. Ulman, *Chem. Review* **1996**, *96*, 1533–1554.

[9] [9a] K. C. Grabar, K. J. Allison, B. E. Baker, R. M. Bright, K. R. Brown, R. G. Freeman, A. P. Fox, C. D. Keating, M. D. Musick, M. J. Natan, *Langmuir* **1996**, *12*, 2353−2361. − [9b] K. C. Grabar, R. G. Freeman, M. B. Hommer, M. J. Natan, *Anal. Chem*. **1995**, *67*, 735−743. − [9c] K. C. Grabar, P. C. Smith, M. D. Musick, J. A. Davis, D. G. Walter, M. A. Jackson, A. P. Guthrie, M. J. Natan, *J. Am. Chem. Soc*. **1996**, *118*, 1148−1153.
[10] [10a] T. Sato, D. Brown, B. F. G. Johnson, *J. Chem. Soc., Chem. Commun*. **1997**, 1007−1008. − [10b] T. Sato, D. G. Hasko, H. Ahmed, *J. Vac. Sci. Technol. B* **1997**, *15*, 45−48.
[11] D. L. Feldheim, K. C. Grabar, M. J. Natan, T. E. Mallouk, *J. Am. Chem. Soc*. **1996**, *118*, 7640−7641.
[12] J. Schmitt, G. Decher, W. J. Dressick, S. L. Brandow, R. E. Geer, R. Shashidhar, J. M. Calvert, *Adv. Mater*. **1997**, *9*, 61−65.
[13] H. Fan, Y. Zhou, G. P. Lopez, *Adv. Mater*. **1997**, *9*, 728−731.
[14] L. Motte, F. Billoudet, E. Lacaze, M.-P. Pilenti, *Adv. Mater*. **1996**, *8*, 1018−1020.
[15] M. Trau, D. A. Saville, A. Aksay, *Science*, **1996**, *272*, 706−709.
[16] [16a] J. P. O′Sullivan, G. C. Wood, *Proc. Roy. Soc. Lond. A* **1970**, *317*, 511−543. − [16b] J. W. Diggle, T. C. Downie, C. W. Goulding, *Chem. Rev*. **1969**, *69*, 365−405. − [16c] R. C. Furneaux, W. R. Rigby, A. P. Davidson, *Nature* **1989**, *337*, 147−149.
[17] [17a] H. Masuda, K. Fukuda, *Science* **1995**, *268*, 1466−1468. − [17b] H. Masuda, M. Satoh, *Jpn. J. Appl. Phys*. **1996**, *35*, 126−129. − [17c] P. Hoyer, N. Baba, H. Masuda, *Appl. Phys. Lett*. **1995**, *66*, 2700−2702. − [17d] C. A. Huber, T. E. Huber, M. Sadoqi, J. A. Lubin, S. Manalis, C. B. Prater, *Science* **1994**, *263*, 800−802. − [17e] J. C. Hulteen, C. R. Martin, *J. Mater. Chem*. **1997**, *7*, 1075−1087.
[18] D. E. Weisshaar, B. D. Lamp, M. D. Porter, *J. Am. Chem. Soc*. **1992**, *114*, 5860−5862.
[19] G. L. Hornyak, C. J. Patrissi, C. R. Martin, *J. Phys. Chem*. **1997**, *101*, 1548−1555.
[20] Y. Iwasawa, *Hyoumen*, **1981**, *19*, 161.
[21] [21a] J. Turkevich, P. C. Stevenson, J. Hillier, *Disc. Faraday Soc*. **1951**, *11*, 55−75. − [21b] G. Schmid, A. Lehnert, U. Kreibig, Z. Adamczyk, P. Belouscheck, *Z. Naturforsch*. **1990**, *45b*, 989−994.
[22] G. Schmid, St. Peschel, Th. Sawitowski, *Z. Anorg. Allg. Chem*. **1997**, *623*, 719−723.

[97315]

Silsesquioxanes as Ligands for Gold Clusters☆

Günter Schmid*[a], Raphael Pugin[a], Jan-Olle Malm[b], and Jan-Olov Bovin[b]

Institut für Anorganische Chemie, Universität Essen[a],
Universitätsstrasse 5−7, D-45117 Essen, Germany
Fax: (internat.) + 49(0)201/183-2402
E-mail: guenter.schmid@uni-essen.de

National Center for HREM, Inorganic Chemistry 2, Lund University[b],
P.O. Box 124, S-22100 Lund, Sweden
Fax: (internat.) + 46(0)46/2224012
E-mail: jan-olle.malm@oorg2.lth.se

Received February 6, 1998

Keywords: Silsesquioxanes / Gold clusters / Self assembly

A new type of gold cluster has been synthesized using the silsesquioxane derivative (cyclopentyl)$_7$Si$_8$O$_{12}$(CH$_2$)$_3$SH (T_8-OSS−SH) to exchange the PPh_3 ligands in $(PPh_3)_{12}Au_{55}Cl_6$ by T_8-OSS−SH quantitatively. This exchange causes several important changes in the physical and chemical behavior of the compound. Owing to the presence of cyclopentyl substituents, the cluster becomes soluble in non-polar solvents such as pentane. The stability of this compound compared with that of the PPh_3-protected cluster is considerably higher meaning that decomposition in solution, and even under the high-energetic irradiation in the microscope, is not observed over longer periods of time. The increase in the total diameter from 2.1 to ca. 4.4 nm is probably responsible for these advantageous properties, supported by strong S−Au bonds. The increase in size is also expressed as an increase in the activation energy for electron-tunneling processes through the ligand shells of neighboring clusters in a densely packed pellet. This increase is from 0.16 eV for $(PPh_3)_{12}Au_{55}Cl_6$ to 0.26 eV for the T_8-OSS−SH-protected cluster.

Introduction

In nanoscale structures, the effect of size on the electronic properties (Quantum Size Effect) is an active area of research.[1][2] The main motivation for this work is to understand the change in the electronic properties on the way from the bulk to the nanosized species. By reducing the size of a three-dimensional metal particle, initially having bulk properties, to a zero-dimensional arrangement containing dozens or a few hundreds of atoms, a dramatic change in the electronic properties is observed. The electrons, which are free in all three dimensions, now behave like electrons in a box and the continuous density of states is replaced by a more discrete energy level structure. This band-gap structure can be considered as an intermediate between the typical band structure in the bulk and the bonding and antibonding system in a molecular state. In this way, if a metal cluster has a diameter in the order of the de Broglie wavelength of the valence electrons, the metal core could be regarded as a zero-dimensional quantum dot.

For the two-shell cluster $(PPh_3)_{12}Au_{55}Cl_6$, physical investigations have clearly indicated the existence of Quantum Size Effects.[2][3] Electronic inter-cluster tunneling processes through the ligand shell have been observed and are caused by an electron jump from one metal island to the other.

This class of small metal particle needs a protective ligand shell to prevent uncontrolled growth and the formation of macroscopic metal particles. It therefore seemed interesting to modify the nature and the size of this ligand shell in order to evaluate the influence of the latter on the chemical, physical, and electronic properties. Our investigations are based principally on functionalized organosilsesquioxane ligands (OSS) for several reasons. Firstly, it is likely that they should represent a satisfactory class of spacers to obtain well-separated ligand-stabilized quantum dots. On the other hand, the incomplete T_7-OSS (**1**; T = number of $RSiO_{3/2}$ units), which is used as a precursor in the synthesis of different functionalized OSS, has been subject to great attention since this molecule has a close similarity with the β-cristobalite form of silica.[4]

Figure 1. Formalized structure of the incompletely condensed silsesquioxane (cyclopentyl)$_7$Si$_7$O$_9$(OH)$_3$ (**1**)

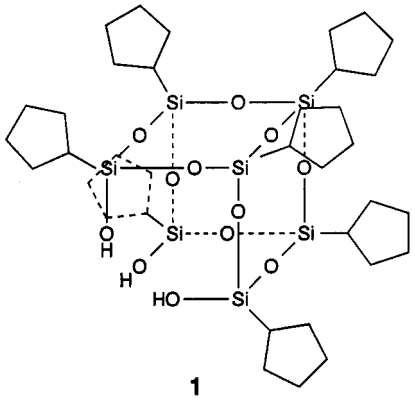

1

 © WILEY-VCH Verlag GmbH, D-69451 Weinheim, 1998 1434−1948/98/0606−0813 $ 17.50+.50/0

During the last few years, Feher et al. have focused a great deal of effort to describe a new approach for modeling the chemistry of silica-supported transition-metal complexes.[5][6] After corner-capping reactions with metal complexes, they obtained representative models for catalysts supported on hydroxylated silica. It appears fundamental to try to adapt this approach to cluster chemistry. Previous work with the functionalized T_8-OSS−ethyldiphenylphosphane ligand has already given good precursors to achieve gold clusters but has never led to the isolation of such materials.[7] We have therefore extended these studies with SH-functionalized OSS. We describe here the synthesis of a new thiol-substituted OSS that is obtained by treating 3-mercaptopropyltrimethoxysilane with the incompletely condensed $(cyclopentyl)_7Si_7O_9(OH)_3$. Subsequent use of this functionalized OSS as a protective ligand has allowed us to isolate a new Au_{55} cluster whose numerous advantages are reported.

Results and Discussion

Trichloro(cyclopentyl)silane, $(cyclopentyl)SiCl_3$, is obtained by hydrosilylation of cyclopentene and trichlorosilane in the presence of H_2PtCl_6 as catalyst.[8] The hydrolysis of $(cyclopentyl)SiCl_3$ in a mixture of water/acetone leads to the incompletely condensed $(cyclopentyl)_7Si_7O_9(OH)_3$ (**1**) after two weeks. The reaction between **1** and the (3-mercaptopropyl)trimethoxysilane allows the isolation of the thiol-substituted OSS **2**, whose elemental analysis, IR, ^{1}H-, $^{13}C\{^1H\}$-, and $^{29}Si\{^1H\}$-NMR data are given in the Experimental Section.

Marsmann et al. have already reported the synthesis of a similar thiol-functionalized OSS by co-hydrolysis of trichloro(*n*-propyl)silane with the (3-mercaptopropyl)trimethoxysilane in a 7:1 ratio.[9][10] In the case reported here, we have preferred to perform two successive hydrolyses in order to avoid the statistically possible formation of polythiol-functionalized OSS as products of a competitive reaction.

Although it is difficult to evaluate the exact size of **2** due to the flexibility of the propyl chain, the total diagonal length of this ligand should be in a range of 1.4−1.5 nm. As explained in the introduction, this size allows one to predict the possibility of obtaining well-separated quantum dots.

In previous works we described the exchange of the PPh_3 ligand shell in $(PPh_3)_{12}Au_{55}Cl_6$ by $Ph_2PC_6H_4SO_3Na$ in a phase-transfer reaction to give a water-soluble gold cluster.[11] Owing to the well-known affinity of thiol functions to gold atoms[12] and the labile nature of the phosphane ligands bound to the surface gold atoms,[13] we tried to use this method to synthesize thiol-functionalized OSS gold clusters (Equation 1).

$$(PPh_3)_{12}Au_{55}Cl_6 + 12\ T_8\text{-OSS}-SH \rightarrow (T_8\text{-OSS}-SH)_{12}Au_{55}Cl_6\ (\mathbf{3}) + 12\ PPh_3 \quad (1)$$

This approach has been successfully applied and allowed us to obtain the expected cluster in almost quantitative yield. However, to prevent coalescence special precautions should be taken (see Experimental Section). ^{1}H-, $^{31}P\{^1H\}$-NMR spectroscopy, and elemental analysis prove that all

Scheme 1. Synthesis of the silsequioxane ligand $(cyclopentyl)_7Si_8O_{12}[CH_2]_3SH$ (T_8-OSS−SH) (**2**)

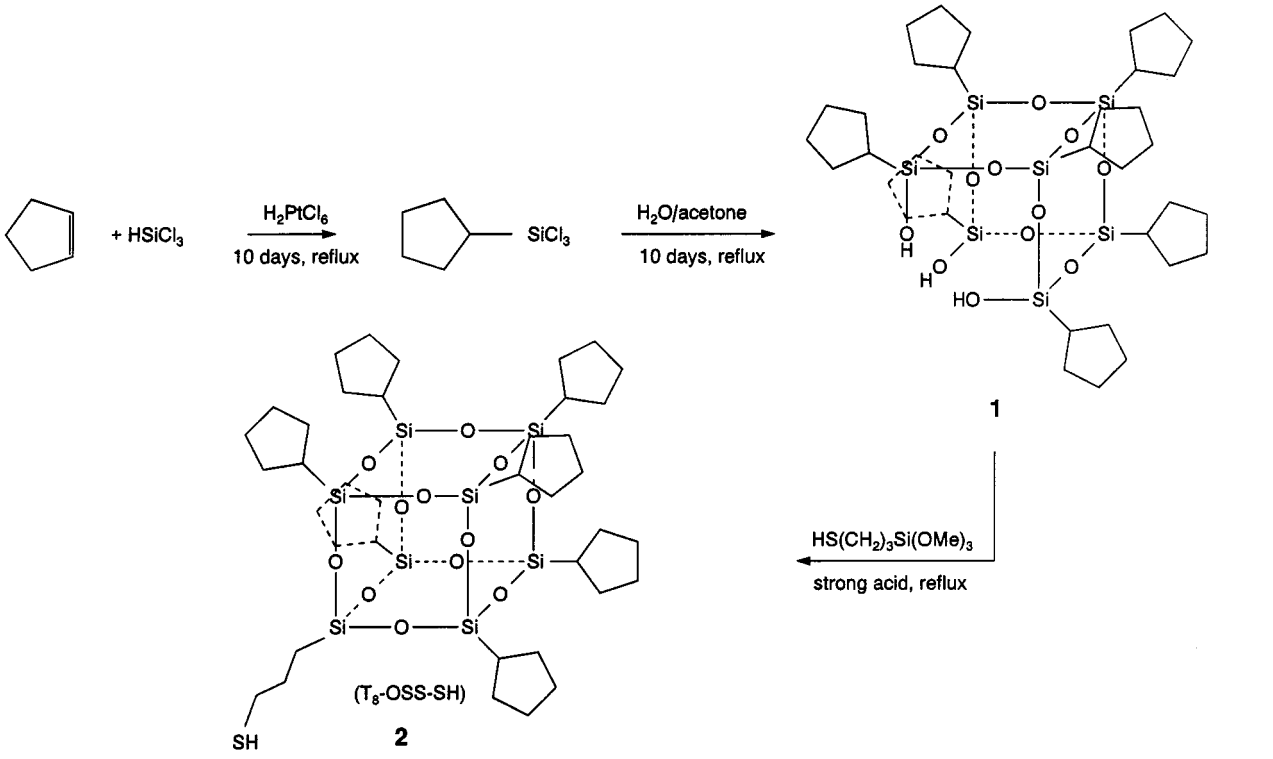

twelve phosphane ligands are replaced by thiol-functionalized oligosilsesquioxanes.

The most remarkable changes in behavior are found in the solubility and in the stability of this new cluster. It is soluble in pentane as well as in dichloromethane and the solutions are stable over several months. This behavior is in contrast to the very labile $(PPh_3)_{12}Au_{55}Cl_6$ cluster which degrades, if dissolved, in the course of hours. Transmission electron microscopy (TEM) investigations show monodisperse particles (Figure 2).

Figure 2. Transmission electron microscopy image of a ca. 145 × 200 nm area of randomly oriented $(T_8\text{-OSS}-SH)_{12}Au_{55}Cl_6$ clusters

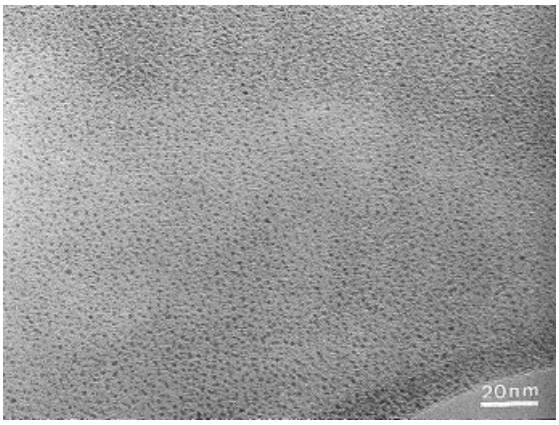

Figure 3 shows a high resolution electron microscopy (HRTEM) image of an area of a well-ordered two-dimensional arrangement of $(T_8\text{-OSS}-SH)_{12}Au_{55}Cl_6$ (**3**) clusters. The formation of ordered monolayers of nanosized metal particles has been observed previously.[14] Ordering seems to happen preferentially if clusters can arrange from solution on a support without chemical interactions between each other and the surface. In this way ideal arrangements may occur owing to the mobility of the clusters. If strong chemical interaction between cluster and surface is provoked organization is clearly hindered, as has been shown in numerous studies of cluster assemblies on chemically modified surfaces.[15] The quality of the ordered area in Figure 3 also becomes visible from a Fourier transform (insert in Figure 3). The angle between the visible peaks can be measured as ca. 75°. The size of the individual clusters can be determined as 1.4 ± 0.1 nm, a value that is in good agreement with the calculated value (1.4 nm). HRTEM results of this quality with other Au_{55} clusters, e.g. $(PPh_3)_{12}Au_{55}Cl_6$, have not been obtained in the past due to very fast coalescence and aggregation processes occurring under the influence of the electron beam[16] and so have led to misinterpretation of HRTEM work by other groups.[17]

The increase in the thickness of the ligand shell on changing from PPh_3 to T_8-OSS−SH, i.e. from 2.1 to ca. 4.4 nm for the total size of the cluster, leads to considerable changes in the interelectronic relation between neighboring clusters. Recently, we determined the activation energy for electron-tunneling processes in densely packed Au_{55} cluster pellets containing different ligand shells or spacer molecules,[18] and this resulted in a linear relation between cluster spacing and activation energy. $(T_8\text{-OSS}-SH)_{12}Au_{55}Cl_6$ fits well into this series and shows a Coulomb gap of 0.26 eV, corresponding to a distance of the cluster nuclei of ca. 3 nm, a value that is in agreement with the theoretical value of 4.4 nm − 1.4 nm = 3.0 nm.[19]

Figure 3. High resolution transmission electron microscopy image of a 52 × 52 nm area of oriented $Au_{55}(T_8\text{-OSS}-SH)_{12}Cl_6$ clusters; the insert shows the Fourier transform of that area

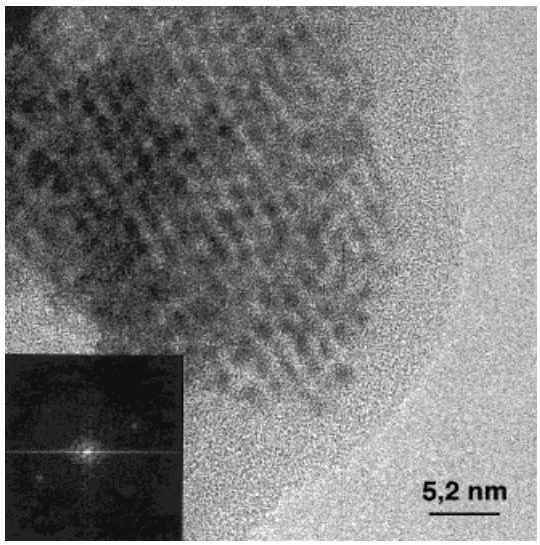

These results impressively show that a change in the nature of the ligand molecules causes drastic effects in the physical properties. The solubility in pentane is explained by the presence of many non-polar cyclopentyl groups on the ligand. To understand the unusual stability we should consider the total cluster diameter including the metal gold core and the ligand shell. The diameter is close to 4.4 nm [2.1 nm for $(PPh_3)_{12}Au_{55}Cl_6$] and this is probably the main reason that agglomeration among clusters is efficiently prevented. However, this phenomenon is also due to the good affinity of thiols for gold atoms, even if at present we cannot assert anything about the nature of the sulfur−gold bond. Indeed two approaches can be considered. The first involves an elimination or migration of hydrogen and the formation of a covalent bond between gold and the ligand. The second is to consider an interaction of intact thiol with gold atoms and the formation of a dative bond.

Theoretically, there is also one other way that should allow us to synthesize this new cluster by a phase-transfer reaction, according to Equation 2.

$$(PPh_2C_6H_4SO_3Na)_{12}Au_{55}Cl_6 + 12\ T_8\text{-OSS}-SH \rightarrow (T_8\text{-OSS}-SH)_{12}Au_{55}Cl_6 + 12\ PPh_2C_6H_4SO_3Na \quad (2)$$

However, we did not observe any exchange of $PPh_2C_6H_4SO_3Na$ by T_8-OSS−SH. Despite this failure we do not believe that $PPh_2C_6H_4SO_3Na$ ligands have better affinity to gold atoms than T_8-OSS−SH. One hypothesis could be to consider that non-polar thiol-functionalized OSS encounters difficulties in crossing the water phase and the water layer surrounding the water-soluble gold cluster. The fact that no phase-transfer reaction is observed be-

tween $(T_8\text{-OSS}-SH)_{12}Au_{55}Cl_6$, dissolved in dichloromethane, and $PPh_2C_6H_4SO_3Na$, dissolved in water, supports this assumption and indicates clearly that we cannot have any doubts about the affinity of thiol groups for gold atoms.

Following this synthetic work, a number of investigations were undertaken to assess physical properties and applications.

In nanoporous membranes science, the size and the high stability of this newly synthesized gold cluster turned out to be very advantageous. Recent works have shown that in alumina membrane pores near 7 nm in diameter can be filled with this new Au_{55} cluster, leading to a monodisperse helical arrangement.[20] These results are very promising in terms of the elaboration of 1D quantum wires and are all the more interesting since it is still difficult, in practice, to make smaller pores near 3 nm in order to fill them with usual $(PR_3)_{12}Au_{55}Cl_6$ clusters, the size of which does not exceed 2.1−2.2 nm.

Conclusions

The 3-propylthiol-substituted T_8-OSS (T_8-OSS−SH) has allowed us to synthesize, for the first time and in very high yield, a new Au_{55} cluster stabilized with thiol-functionalized OSS ligands.

This work clearly demonstrates the dramatic influence of this new ligand on the cluster properties. Among these properties, the size and the high stability are the greatest advantages for future physical investigations and applications.

This newly synthesized Au_{55} cluster can also be considered as a valuable model for transition-metal complexes or clusters supported on silica surface since OSS show great similarities with the cristobalite form of silica.

Following these first results many future possibilities can be suggested. It should first be possible to modify the length of the functionalized OSS carbon chain to investigate inter-tunnel conductivity and quantum-size effects. Moreover, the functional group could also be changed to synthesize other ligands to stabilize different metal centers in clusters or colloids. In this way the trisilanol part of the incompletely condensed $(cyclopentyl)_7T_7(OH)_3$ allowed us to complex nickel clusters.[21]

G. S. and R. P. thank the *Bundesministerium für Bildung, Wissenschaft, Forschung und Technologie*, Bonn for supporting this work under project FKZ 03N1012A7 and the *Fonds der Chemischen Industrie* for their continued financial support.

Experimental Section

All reactions using air-sensitive reagents and products were performed under nitrogen using standard Schlenk techniques. In the work described here only the (3-mercaptopropyl)trimethoxysilane is highly sensitive in the presence of water and humidity. All solvents were dried and purified using standard procedures. − NMR spectra were recorded with a Bruker DPX working at 300 MHz for ^1H, 75.5 MHz for $^{13}C\{^1H\}$, 121.5 MHz for $^{31}P\{^1H\}$ and 59.6 MHz for $^{29}Si\{^1H\}$. − Infrared spectra were recorded with a Perkin-Elmer FT-IR 1600 spectrometer. − TEM images were recorded using Philips FEG-CM 200 and JEM-4000 EX machines working with 200 and 400 kV accelerating voltages, respectively. − Elemental analyses were carried out by the Analytical Laboratory of the Chemistry Department of the University of Essen.

(Cyclopentyl)SiCl$_3$ and (Cyclopentyl)$_7$T$_7$(OH)$_3$ (**1**): (Cyclopentyl)$SiCl_3$ and **1** were synthesized by well-known literature procedures. **1** was obtained with yields as high as 80% and the purity of this product was assessed by comparison of the NMR and IR data and elemental analysis. − IR: ν = 3200 cm^{-1} m ν(OH), 2949 s, 2865 s, ν(alkyl), 1452 m, 1250 s, δ(C−H), 1120 vs ν_{asym}(Si−O−Si), 498 m ν_{sym}(Si−O−Si). − ^1H NMR ($CDCl_3$): δ = 0.95−1.2 (m, 7 H, CH pentyl), 1.45−1.95 (m, 56 H, CH_2 pentyl), 6.10 (br., 3 H, OH). − $^{13}C\{^1H\}$ NMR ($CDCl_3$): δ = 21.97, 22.10, 22.48 (s, CH, pentyl), 26.72, 26.75, 26.78 (s, CH_2), 26.99, 27.01, 27.02 (s, CH_2). $C_{35}H_{66}O_{12}Si_7$ (875.5): calcd. C 48.02, H 7.60; found C 47.98, H 7.68.

(Cyclopentyl)$_7$T$_8$(CH$_2$)$_3$SH (**2**): 272 mg (1.39 mmol) of $HS(CH_2)_3Si(OMe)_3$ was placed in a dry 100-ml three-necked round-bottomed flask filled with nitrogen. 30 ml of dried benzene and, with vigorous stirring, 1.2 g (1.39 mmol) of **1** and 10 mg of *p*-toluenesulfonic acid, diluted in few ml of dried acetone, were added. The solution was stirred for 20 h under reflux, then cooled with an ice bath, concentrated to 10 ml and carefully layered with 60 ml of acetonitrile whereupon **2** precipitated. In order to simplify the filtration, the resulting white solid was allowed to stand overnight in a cold place. After filtration and washing with acetonitrile, pure **2** was dried under vacuum. Yield 1.03 g (78%). − IR: ν = 2950 cm^{-1} s ν(alkyl), 2866 s, 2590 w ν(S−H), 1452 m δ(C−H), 1250 s, 1121 vs, ν_{asym}(Si−O−Si), 733 w ν(Si−CH_2), 693 w, 507 m ν_{sym}(Si−O−Si). − ^1H NMR (C_6D_6): δ = 0.75 (t, 2 H, CH_2−Si), 1.10 (t, 1 H, SH), 1.18−1.28 (m, 7 H, CH-pentyl), 1.45−1.90 (m, 56 H, CH_2-pentyl, m, 2 H, $CH_2-CH_2-CH_2SH$), 2.27 (m, 2 H, CH_2−SH). − $^{13}C\{^1H\}$ NMR (C_6D_6): δ = 11.38 (d, CH_2−Si), 22.70, 22.71, 22.73 (s, CH-pentyl, 3:3:1), 27.35 (s, CH_2−SH), 27.43, 27.45, 27.46, 27.83, 27.85, 27.86 (s, CH_2-pentyl, 3:3:1:3:1:3), 28.24 (s, CH_2-CH_2SH). − $^{29}Si\{^1H\}$ NMR (C_6D_6): δ = −66.56 (Si−cyclopentyl, 3), −66.59 (Si−cyclopentyl, 1), −66.62 (Si−cyclopentyl, 3), −66.96 ($SiCH_2$, 1). − $C_{38}H_{70}O_{12}SSi_8$ (975.7): calcd. C 46.77, H 7.23; found C 46.35, H 7.32.

(T$_8$-OSS-SH)$_{12}$Au$_{55}$Cl$_6$ (**3**): 20 mg (1.41 μmol) of $(PPh_3)_{12}Au_{55}Cl_6$ and 16.5 mg (16.9 μmol) of **2** were placed in a dry 100-ml three-necked round-bottomed flask filled with nitrogen. 50 ml of dried benzene and, a few minutes later, 5 × 10 ml of dried dichloromethane were added with vigorous stirring. After evaporation of the solvents, the brown product was extracted with 50 ml of pentane and filtered through an ANOTOP® filter (20 nm). The pentane was removed under vacuum and the new gold cluster was precipitated with 30 ml of acetonitrile and filtered. The filtration pad was washed with copious amounts of acetonitrile in order to remove triphenylphosphane and dried overnight under vacuum. At this stage, the black powder obtained still contained an excess of T_8-OSS−SH due to a slight amount of decomposition during the ligand-exchange reaction. Usual purification methods such as extraction, recrystallisation or chromatography did not allow the isolation of the pure gold cluster and mainly led to progressive decomposition. The best way to purify **3** was found to be ultra-fast centrifuging. This method was successfully applied with a concentrated pentane solution with 28000 rpm (34000 *g*) over 24 h. Yield: 20−30 mg (60−90%). − The spectroscopic data (IR, ^1H, $^{13}C\{^1H\}$ NMR) are the same as for the free ligand (see above). ^{31}P-NMR signals could no longer be observed. − $C_{456}H_{840}Au_{55}Cl_6O_{144}S_{12}Si_{96}$ (22754.5): calcd. C 24.07, H 3.72, S 1.69; found C 25.36, H 3.81, S 1.53. − The slight excess of carbon and hydrogen, as well as the

low value for sulphur, can be explained by the presence of solvent molecules on the cluster surface. Indeed, if this cluster is sterically well covered and protected by functionalized OSS there would still be enough space in between to trap a few solvent molecules.

☆ Dedicated to Professor *Heinrich Nöth* on the occasion of his 70th birthday.

[1] G. Nimtz, P. Marquard, H. Gleiter, *J. Cryst. Growth* **1988**, *86*, 66.

[2] U. Simon, G. Schön, G. Schmid, *Angew. Chem.* **1993**, *105*, 264; *Angew. Chem. Int. Ed. Engl.* **1993**, *32*, 250.

[3] B. A. Smith, J. Z. Zhang, U. Giebel, G. Schmid, *Chem. Phys. Lett.* **1997**, *270*, 139.

[4] F. J. Feher, D. A. Newman and J. F. Walzer, *J. Am. Chem. Soc.* **1989**, *111*, 1741.

[5] F. J. Feher, *J. Am. Chem. Soc.* **1986**, *108*, 3850.

[6] F. J. Feher and R. L Blanski, *Makromol. Chem., Macromol. Symp.* **1993**, *66*, 95.

[7] G. Schmid, V. Ruffieux, unpublished results.

[8] F. J. Feher, T. A. Budzichowski, R. L. Blanski, K. J. Weller, J. W. Ziller, *Organometallics* **1991**, *10*, 2526.

[9] B. J. Hendan, H. C. Marsmann, *J. Organomet. Chem.* **1994**, *483*, 33.

[10] U. Dittmar, B. J. Hendan, U. Floerke, H. C. Marsmann, *J. Organomet. Chem.* **1995**, *489*, 185.

[11] G. Schmid, N. Klein, L. Korste, U. Kreibig, D. Schönauer, *Polyhedron* **1988**, *7*, 605.

[12] [12a] G. Schmid, S. Peschel, T. Sawitowski, *Z. Anorg. Allg. Chem.* **1997**, *623*, 719. – [12b] P. Fenter, P. Eisenberger, K. S. Liang, *Phys. Rev. Lett.* **1993**, *70*, 2447.

[13] G. Schmid, *Struct. Bonding (Berlin)* **1985**, *62*, 51.

[14] [14a] R. P. Andres, J. D. Bielefeld, J. I. Hendersen, D. B. Janes, V. R. Kolagunat, C. P. Kubiak, W. J. Mahoney, R. G. Osifchin, *Science* **1996**, *273*, 169. – [14b] M. Brust, J. Bethell, D. J. Shiffrin, C. J. Kieley, *Adv. Mater.* **1995**, *7*, 795.

[15] G. Schmid, S. Peschel, *New. J. Chem.*, in press.

[16] G. L. Hornyak, S. Peschel, T. Sawitowski, G. Schmid, *Micron*, in press.

[17] D. H. Rapaport, W. Vogel, H. Cölfer, R. Schlögl, *J. Phys. Chem.* **1997**, *101*, 4175.

[18] U. Simon, R. Flesch, H. Wiggers, G. Schön, G. Schmid, *J. Mater. Chem.*, in press.

[19] U. Simon, H. Wiggers, R. Pugin, G. Schmid, unpublished results.

[20] G. Hornyak, M. Kröll, R. Pugin, T. Sawitowski, G. Schmid, J.-O. Bovin, G. Karsson, H. Hofmeister, S. Hopfe, *Chem. Eur. J.* **1997**, *3*, 1951.

[21] G. Schmid, R. Pugin, unpublished results.

[98025]

Transition Metal Complexes with Sulfur Ligands, 131[◇]

Synthesis, Structure, and Properties of Osmium Complexes Containing [Os('S_4')] and [Os('S_2')$_2$] Fragments ('S_4'$^{2-}$ = 1,2-Bis(2-mercaptophenylthio)-ethane(2−), 'S_2'$^{2-}$ = 1,2-Benzenedithiolate)☆

Dieter Sellmann*, Andreas C. Hennige, and Frank W. Heinemann

Institut für Anorganische Chemie der Universität Erlangen-Nürnberg,
Egerlandstr. 1, D-91058 Erlangen, Germany
Fax: (internat.) +49(0)9131/857367
E-mail: sellmann@anorganik.chemie.uni-erlangen.de

Received December 22, 1997

Keywords: S ligands / P ligands / Osmium / Solvent effects

In search for osmium complexes with sulfur-dominated coordination spheres that potentially bind and activate or stabilize nitrogenase relevant small molecules, several osmium−sulfur complexes containing 1,2-bis(2-mercaptophenylthio)ethane(2−) ('S_4'$^{2-}$) and benzenedithiolate ('S_2'$^{2-}$) ligands were synthesized. [Os^{II}(PR_3)$_2$('S_4')] [R = Ph (**1**), Et (**2**)], [Os^{IV}(PR_3)$_2$('S_2')$_2$] [R = Et (**3**), Pr(**4**), Me(**5**), Ph(**6**)], [Os^{IV}(PCy_3)('S_2')$_2$] (**7**), ($PHCy_3$)[Os^{III}('S_2')$_2$] (**8a**), (NMe_4)-[Os^{III}('S_2')$_2$] (**8b**), and (NBu_4)$_2$[Os^{IV}('S_2')$_3$] (**9b**) were obtained in reactions starting from commercially available osmium compounds and the sulfur and phosphane ligands. The presence or absence of reducing solvents strongly influenced these reactions. Octahedral (**3**), (**4**), and ($PHCy_3$)$_2$[Os^{IV}('S_2')$_3$] (**9a**) were characterized by X-ray structure analysis, leading to the conclusion that despite the high oxidation state of the osmium centers, innocent dithiolate ligands are present. The stabilization of the Os^{IV} centers is traced back to S→M π donation. Close inspection of **1** and **2** revealed a large influence of the phosphane ligands on the stability of Os^{II} thioether complexes. While **1** is reasonable stable, **2** readily gives **3** and ethylene via intramolecular 'S_4'$^{2-}$ ligand reduction and Os^{II} → Os^{IV} oxidation. UV-Vis spectra of **3**−**5** indicate phosphane dissociation in solution leading to pentacoordinate [Os(PR_3)('S_2')$_2$] complexes. This was confirmed by the synthesis of pentacoordinate [Os(PCy_3)('S_2')$_2$] (**7**).

Introduction

Transition metals in sulfur-dominated coordination spheres form the active centers of numerous oxidoreductases such as nitrogenases, hydrogenases and CO dehydrogenase[1]. In the search for low-molecular compounds that combine structural and reactivity features of these [MS] enzymes we have found that transition metal complexes containing [M('S_4')] (**A**) or [M('S_2')$_2$] fragments (**B** and **C**) ['S_4'$^{2-}$ = 1,2-bis(2-mercaptophenylthio)ethane(2−); 'S_2'$^{2-}$ = 1,2-benzenedithiolate(2−)] can bind and activate or stabilize a considerable number of small molecules that are key intermediates in enzymatic processes[2]. In a few cases, catalytic reaction cycles could be developed[3]. For example, [Rh(L)('S_4')]$^+$ complexes (L = CO, PCy_3) catalyze the heterolytic cleavage of dihydrogen and D_2/H^+ exchange that are features of hydrogenases[4].

Iron and ruthenium [M('S_4')] complexes bind key intermediates of N_2 fixation such as N_2H_2, N_2H_4 and NH_3[2]. However, attempts to coordinate also dinitrogen to such fragments have as yet remained unsuccessful. In this context it is to be noted that transition metal N_2 complexes with sulfur dominated coordination spheres are conspicuously rare. In fact, [Mo(N_2)$_2$(octamethyltetrathiacyclohexadecane)] is the only example for the coordination of N_2 to a metal center carrying exclusively sulfur coligands[5].

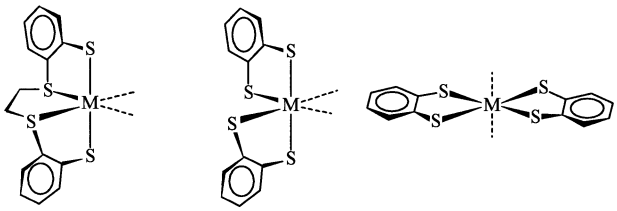

For this reason, we have started to explore the osmium chemistry of 'S_4'$^{2-}$ and 'S_2'$^{2-}$ ligands, anticipating that with [Os('S_4')] or [Os('S_2')$_n$] species complexes could become accessible that proved inaccessible with the iron and ruthenium homologues. [Os('S_4')] complexes have been unknown as yet, the chemistry of osmium benzene-1,2-dithiolate and related ligands is largely unexplored[6]. No benzenedithiolate complex was known, and only a very few complexes with toluenedithiolate, maleonitriledithiolate and similar ligands have been described[7].

[◇] Part 130: D. Sellmann, T. Gottschalk-Gaudig, F. W. Heinemann, *Inorg. Chem*, submitted.

 © WILEY-VCH Verlag GmbH, D-69451 Weinheim, 1998 1434−1948/98/0606−0819 $ 17.50+.50/0

Results

[Os($'S_4'$)] Complexes

Two target complexes containing [Os($'S_4'$)] cores could be obtained from commercially available $OsCl_3 \cdot x\,H_2O$ by the reaction according to eq. (1).

$$OsCl_3{\cdot}xH_2O + {'S_4'}\text{-}H_2 + PR_3\ \text{exc.} \xrightarrow[\text{reflux}]{\text{THF / MeOH}} [Os(PR_3)_2({'S_4'})] \quad (1)$$

R = Ph (**1**), Et (**2**)

Heating to reflux, an excess of the respective phosphane, and the use of the solvent mixture MeOH/THF proved necessary. The excess of phosphane and the methanol probably serve as reducing reagents for $OsCl_3 \cdot x\,H_2O$. The methanol additionally causes precipitation of the resultant yellow to yellow-green [Os(PR_3)$_2$($'S_4'$)] complexes **1** (PPh_3) and **2** (PEt_3) from the reaction solutions. When pure THF was used as solvent, neither **1** nor **2** could be isolated.

In these experiments, it was noted that **2** is rather thermolabile. The reaction leading to its formation according to eq. (1) had to be quenched after ca. one hour of refluxing in order to avoid a drastic decrease in yield. Already at room temperature, [Os(PEt_3)$_2$($'S_4'$)] (**2**) slowly decomposes according to eq. (2).

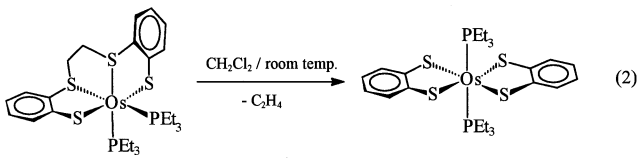

(2)

2 **3**

An intramolecular redox reaction leads to release of C_2H_4 and formation of the Os^{IV} complex [Os(PEt_3)$_2$($'S_2'$)$_2$] (**3**). The evolving ethylene could be detected by its ^{1}H-NMR signal at $\delta = 5.24$[8].

Complexes **1** and **2** were characterized by the common spectroscopic methods. For example, the ^{1}H-NMR spectra of **1** and **2** exhibit signal patterns that are typical of C_2 symmetrical [ML_2($'S_4'$)][9] complexes. Cyclic voltammetry of **2** further revealed two reversible redox waves at $E_{1/2} = -20$ mV and $E_{1/2} = 950$ mV that can be assigned to the formation of the $[\mathbf{2}]^+$ and $[\mathbf{2}]^{2+}$ cations.

Attempts to substitute one PPh_3 ligand of **1** by N_2H_4 or CO remained unsuccessful. Complex **1** proved substitution inert even at elevated temperatures and pressures. In this respect, **1** contrasts the homologous [Ru(PPh_3)$_2$($'S_4'$)] which readily exchanges one PPh_3 ligand for numerous two electron donors at room temperature[10].

The facile formation of the Os^{IV} complex [Os(PEt_3)$_2$($'S_2'$)$_2$] (**3**) from the Os^{II} complex [Os(PEt_3)$_2$($'S_4'$)] (**2**) and the rareness of osmium benzene dithiolate complexes in higher oxidation states prompted us to investigate these species more closely, which are also potentially suited to yield complexes with [Os($'S_4'$)] cores via template alkylations[9].

Synthesis and Characterization of the Hexa- and Pentacoordinate Os^{IV} Complexes [Os(PR_3)$_2$($'S_2'$)$_2$] (R = Me, Et, Pr, Ph), and [Os(PCy_3)($'S_2'$)$_2$]

[Os(PR_3)$_2$($'S_2'$)$_2$] complexes were obtained with various PR_3 ligands according to eq. (3).

$$(NH_4)_2[OsBr_6] + 2\ {'S_2'}\text{-}Li_2 + 2\ PR_3 \xrightarrow[\text{reflux / 19 h}]{\text{THF / MeOH}} [Os(PR_3)_2({'S_2'})_2] \quad (3)$$

R = Et (**3**), Pr (**4**), Me (**5**), Ph(**6**)

The resultant complexes **3**–**6** are gray-black to black-violet and diamagnetic. While the PMe_3 and PPh_3 complexes **5** and **6** are only very sparingly soluble, the PEt_3 and PPr_3 complexes **3** and **4** readily dissolve in common organic solvents. The complexes were characterized by elemental analyses and spectroscopic methods, and **3** and **4** also by X-ray structure analyses. The Os^{IV} complexes **3** and **4** each exhibit a characteristic low field shifted ^{31}P-NMR signal in the region of $\delta = -200$ and contrast in this respect the Os^{II} complexes **1** and **2** whose ^{31}P-NMR signals appear at δ ca. -20. No ^{31}P-NMR spectrum could be recorded of the sparingly soluble PMe_3 complex **5**. The ^{31}P-NMR spectrum of the PPh_3 complex **6** revealed one broad signal at $\delta = -46.5$. The shift of this signal indicates dissociation of **6** to give pentacoordinate [Os(PPh_3)($'S_2'$)$_2$] (vide infra).

When the reaction according to eq. (3) was carried out with the sterically very demanding phosphane PCy_3, no hexacoordinate complex but the pentacoordinate [Os(PCy_3)($'S_2'$)$_2$] (**7**) formed. This even occurred when a fourfold excess of PCy_3 was applied. Complex **7** was obtained as violet microcrystals that proved diamagnetic and well soluble in organic solvents. The number and splitting of the ^{1}H- and ^{13}C-NMR signals of **7** indicate that **7** possesses lateral symmetry. The ^{31}P-NMR spectrum exhibits one signal at $\delta = -29.2$ whose chemical shift contrasts the ^{31}P-NMR shifts (-200 ppm) of the bisphosphane complexes **3** and **4**. The FD mass spectrum of **7** revealed the molecular ion at $m/z = 752$ and no ions of higher masses. These results and, in addition, the UV-Vis-NIR spectroscopic properties of **7** versus those of **3**–**5** (vide infra) indicate that **7** is mononuclear possessing the structure indicated by formula **D**.

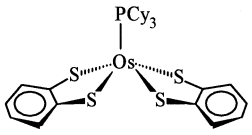

D

X-ray Structure Determination of [Os(PEt_3)$_2$($'S_2'$)$_2$] (3) and [Os(PPr_3)$_2$($'S_2'$)$_2$] (4)

The molecular structures of **3** and **4** are depicted in Figure 1.

Complexes **3** and **4** both possess crystallographically imposed inversion symmetry and exhibit pseudo-octrahedral coordination with the phosphane ligands in *trans* positions. The corresponding Os–P and Os–S distances in **3** and **4**

Figure 1. ORTEP plots of a) $[Os(PEt_3)_2(′S_2′)_2]$ (**3**) and b) $[Os(PPr_3)_2(′S_2′)_2]$ (**4**) drawn with 50% probability ellipsoids (H atoms omitted)[a]

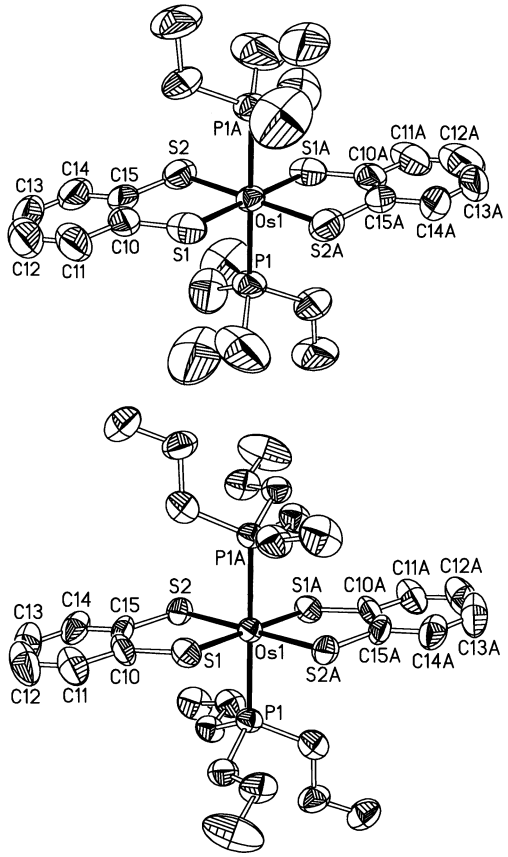

[a] Selected distances [pm] and angles [°]: **3**: Os(1)−S(1) 231.1(2), Os(1)−S(2) 232.8(2), Os(1)−P(1) 244.8(2), S(1)−C(10) 174.8(8), S(2)−C(15) 173.1(8), C(10)−C(11) 142.4(10), C(11)−C(12) 138(2), C(12)−C(13) 130(3), C(14)−C(15) 141.2(9), C(10)−C(15) 139.0(11). S(1)−Os(1)−P(1) 90.58(7), S(2)−Os(1)−P(1) 90.46(7), S(1)−Os(1)−S(2) 86.33(7). − **4**: Os(1)−S(1) 231.2(2), Os(1)−S(2) 231.7(2), Os(1)−P(1) 244.2(2), S(1)−C(10) 172.8(11), S(2)−C(15) 172.6(9), C(10)−C(11) 137.9(13), C(11)−C(12) 137(2), C(12)−C(13) 136(2), C(14)−C(15) 138.1(12), C(10)−C(15) 145.3(14), S(1)−Os(1)−P(1) 89.85(8), S(2)−Os(1)−P(1) 90.65(8), S(1)−Os(1)−S(2) 86.29(8).

are identical within the 3σ criterion. The averaged Os−S distances of **3** and **4** [231.7(2) pm] are identical to the Ru−S distances of the analogous $[Ru(PMe_3)_2(′S_2′)_2]$ [231.7(1) pm][11] and are in the usual range of osmium(IV) thiolate complexes. Os−S distances of osmium(IV) thiolate complexes cover a range from 220 to 241 pm and depend on the coordination number and geometry[12].

Detailed inspection of the C−C and C−S bond distances in the $C_6H_4S_2^{2-}$ ligands revealed no evidence for a partial oxidation of the benzenedithiolate ligands to give dithiocyclohexadiene units according to eq. (4).

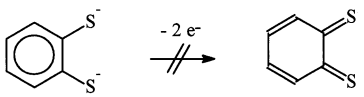

(4)

In this respect, the Os^{IV} complexes **3** and **4** behave identical to the homologous Fe^{IV} complex $[Fe(PMe_3)_2(′S_2′)_2]$ and related species, which have been extensively discussed previously[13]. They allow to conclude that benzenedithiolate behaves as "innocent" dithiolate ligand such that stabilization of higher metal oxidation states is rather due to increasing S→M π donation.

Reversible Dissociation of $[Os(PR_3)_2(′S_2′)_2]$ Complexes; UV-Vis-NIR Spectra

The UV-Vis-NIR spectra of the hexacoordinate complexes **3**−**5** exhibit very intense absorptions (ε > 40000 $l·mol^{-1}·cm^{-1}$) in the region of 950−1050 nm. These bands can be assigned to sulfur-metal LMCT transitions, and they slowly decrease in intensity when dilute solutions of **3**−**5** are kept at room temperature. Simultaneously, the solutions change color from deep red to violet blue. Addition of the respective phosphane reverses these effects (Figure 2).

Figure 2. UV-Vis-NIR spectra of a) **4** in CH_2Cl_2 (λ_{max} = 1043 nm, ε = 42740 $lmol^{-1}cm^{-1}$), b) after 12 h, c) after addition of excessive PPr_3

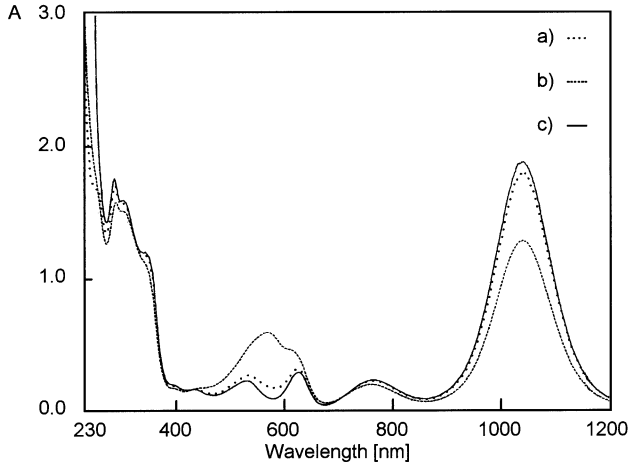

These observations indicate that the hexa-coordinate complexes reversibly dissociate in solution to yield pentacoordinate species according to eq. (5).

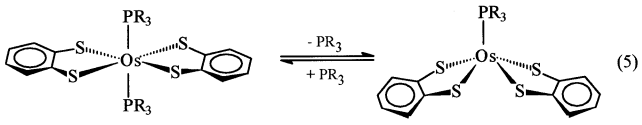

(5)

4

This assumption is supported by the electronic spectrum of the pentacoordinate complex $[Os(PCy_3)(′S_2′)_2]$ (**7**) which does not exhibit an absorption in the NIR region. It is further corroborated by the FD mass spectra of complexes **3**−**5**, which all show intensive signals of the fragment ions $[Os(PR_3)(′S_2′)_2]^+$ in addition to the molecular ions.

Synthesis and Properties of the Os^{III} Complex $(PHCy_3)[Os(′S_2′)_2]$ (8a)

The $[Os(PR_3)_2(′S_4′)]$ complexes **1** and **2** had shown that the solvent and reaction time could markedly influence the course of synthesis reactions. This was also observed when $(NH_4)_2[OsBr_6]$, $′S_2′$-Li_2 and an excess of PCy_3 were com-

bined not in THF as in the reaction according to eq. (3), but in a mixture of THF and MeOH, and refluxed for three days. In this case, not the Os^{IV} complex **7** but the Os^{III} complex $(PHCy_3)[Os('S_2')_2]$ (**8a**) formed as major product according to eq. (6).

$$(NH_4)_2[OsBr_6] + 2\ 'S_2'\text{-}Li_2 + \text{exc. } PCy_3 \xrightarrow[3\ d,\ reflux]{THF\ /\ MeOH} (PHCy_3)[Os('S_2')_2] \quad (6)$$

8a

Complex **8a** precipitated as orange micro-crystals from the boiling reaction mixture. The violet-blue $[Os(PCy_3)('S_2')_2]$ (**7**) formed only as minor by-product and could be isolated in negligible amounts when the mother liquors were cooled to −20 °C.

Apparently, in the reaction according to eq. (6) the solvent MeOH and possibly also the excess PCy_3 act as reducing reagents upon $(NH_4)_2[OsBr_6]$. Complex **8a**, whose elemental composition differs from that of the Os^{IV} complex $[Os(PCy_3)('S_2')]$ (**7**) only by one proton, was identified by its spectra, magnetism, and by the metathesis reaction with NMe_4OH yielding the NMe_4^+ salt $(NMe_4)[Os('S_2')_2]$ (**8b**) according to eq. (7).

$$(PHCy_3)[Os('S_2')_2] + \text{exc. } NMe_4OH \xrightarrow{THF} (NMe_4)[Os('S_2')_2] + (PHCy_3)OH \quad (7)$$

8a **8b**

The presence of the $PHCy_3^+$ cation in **8a** could further be concluded from the ^{1}H-NMR spectrum of **8a** which revealed the characteristic ^1J(PH) coupling constant (475 Hz) of the $PHCy_3^+$ cation.

8a is paramagnetic and exhibits a magnetic moment of μ_{eff} = 3.04 μ_B. The magnetic moment is compatible with three unpaired electrons at Os^{III} centers in square planar or tetragonal pyramidal coordination. In contrast octahedral Os^{III} thiolate phosphane complexes with one unpaired electron exhibit magnetic moments in the range μ_{eff} = 1.85−1.98 μ_B[14]. The structure of the anion in **8a** remains unknown, however, the dinuclear structure of the homologous iron complex that was revealed by X-ray structure analysis[15] suggests a similar structure for **8a** as indicated by formula **E.**

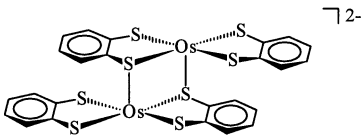

E

Complex **8a** is sparingly soluble in THF or MeOH, but readily dissolves in CH_2Cl_2. Also in the absence of air, the resultant orange CH_2Cl_2 solutions are unstable and turn to deep violet in the course of a few hours, because **8a** spontaneously forms **7** according to eq. (8).

$$(PHCy_3)[Os('S_2')_2] \xrightarrow[room\ temp.]{CH_2Cl_2} [Os(PCy_3)('S_2')_2] + H^+ + e^- \quad (8)$$

8a **7**

This reaction involves an $Os^{III} \rightarrow Os^{IV}$ oxidation, but the oxidizing reagent as well as the fate of the formally released proton and electron remain unknown. Evolution of H_2 could not be observed[16].

Synthesis and Properties of $(NBu_4)_2[Os('S_2')_3]$ and $(PHCy_3)_2[Os('S_2')_3]$

Single crystals that precipitated in minor amounts from the mother liquors of the $[Os(PCy_3)('S_2')_2]$ (**7**) synthesis could be characterized by X-ray structure analysis revealing that the crystals contained the salt $(PHCy_3)_2[Os('S_2')_3]$ (**9a**). The NBu_4^+ salt $(NBu_4)_2[Os('S_2')_3]$ (**9b**) was subsequently obtained in the straight forward synthesis according to eq. (9).

$$(NH_4)_2[OsBr_6] + 6\ NBu_4OH + 3\ 'S_2'\text{-}H_2 \xrightarrow[2\ h,\ reflux]{MeOH} (NBu_4)_2[Os('S_2')_3] \quad (9)$$

9b

9b was isolated in form of dark red crystals, which were characterized by elemental analysis and spectroscopic methods. **9b** is diamagnetic. Its cyclic voltammogramm shows one irreversible (−580 mV) and two reversible anodic redox waves (−80 mV and 180 mV). They can be assigned to the redox steps indicated by eq. (10).

$$[Os('S_2')_3]^{3-} \underset{-e^-}{\overset{+e^-}{\leftarrow}} [Os('S_2')_3]^{2-} \underset{+e^-}{\overset{-e^-}{\rightleftharpoons}} [Os('S_2')_3]^{-} \underset{+e^-}{\overset{-e^-}{\rightleftharpoons}} [Os('S_2')_3]^{0} \quad (10)$$

- 580 mV - 80 mV 180 mV

Figure 3 depicts the molecular structure of the anion of $(PHCy_3)_2[Os('S_2')_3]$ (**9a**).

Figure 3. ORTEP plot of the anion of $(PHCy_3)_2[Os('S_2')_3]$ (**9a**) drawn with 50% probability ellipsoids (H atoms omitted)[a]

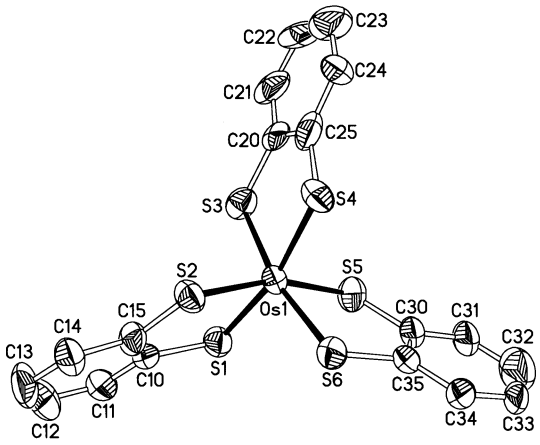

[a] Selected distances [pm]: Os(1)−S(1) 236.6(2), Os(1)−S(2) 235.7(2), Os(1)−S(3) 235.6(2), Os(1)−S(4) 234.5(3), Os(1)−S(5) 235.0(3), Os(1)−S(6) 236.0(3), S(1)−C(10) 175.8(9), S(2)−C(15) 173.6(9), S(3)−C(20) 177.4(10), S(4)−C(25) 172.7(11), S(5)−C(30) 176.7(11), S(6)−C(35) 177.2(10); average S−S(intra) 3.190, S−S(inter) 3.385. − Selected angles [°]: S(1)−Os(1)−S(4) 167.40(9), S(2)−Os(1)−S(5) 163.53(9), S(3)−Os(1)−S(6) 168.23(8), S(1)−Os(1)−S(2) 85.06(8), S(3)−Os(1)−S(4) 85.40(9), S(5)−Os(1)−S(6) 85.23(10).

The average Os−S distances in **9a** [235.6(3) pm] are longer than those in the neutral $[Os(PR_3)_2('S_2')_2]$ complexes **3** and **4** [231.7(2) pm]. This can be traced back to reduced

S→M π donation in **9a** which unlike **3** and **4** does not exhibit π acceptor phosphane ligands. As for **3** and **4**, scrutinizing the C−C and C−S distances yielded no evidence for cyclohexadienedithioketone-like structures of the $C_6H_4S_2$ ligands.

An important structural feature of numerous dithiolene type $[M(S_2C_2R_2)_3]$ complexes (R = H, Ph) is their trigonal prismatic coordination geometry. Potential factors, e.g., S···S interactions between vicinal S donors, metal-ligand π bonding and the overall charge of the complexes, stabilizing the trigonal pyramidal versus the octahedral coordination geometry have been elucidated[17]. The analysis of the S−Os−S angles in **9a** shows that **9a** is best described to possess pseudo-octahedral geometry. Due to the chelate bite of the $C_6H_4S_2$ units, the ideal S−M−S angle which can be reached for *'trans'* sulfur donors in octahedral complexes is 170° (instead of 180°)[18]. The corresponding angle in trigonal prismatic complexes is 136°. The respective S−Os−S angles in **9a** vary between 163.5(1)° and 168.2(1)° and are thus close to the ideal angle for octahedral coordination.

A literature search revealed that there are only two other dianionic $[M('S_2')_3]^{2-}$ complexes (M = Ti[19], Zr[18]) that exhibit octahedral geometry. The anion in $(AsPh_4)_2[W('S_2')_3]$ shows average S−W−S angles of 151.6°[20]. It thus represents an intermediate between octahedral and trigonal prismatic coordination comparable to the structure of the monoanion in $(AsPh_4)[Nb('S_2')_3]$[21].

Discussion and Summary

The Os^{II} complexes $[Os(PR_3)_2('S_4')]$ (**1**) (R = Ph) and **2** (R = Et) could be directly synthesized from $'S_4'^{2-}$, the respective phosphane and commercially available $OsCl_3 \cdot x\ H_2O$. Complexes **1** and **2** revealed a remarkable influence of the phosphane coligands upon the complex stability and reactivity. **1** proved temperature stable and substitution inert contrasting the homologous $[Ru(PPh_3)_2('S_4')]$, which readily exchanges one PPh_3 ligand. **2** is so labile that already at room temperature it readily releases C_2H_4 and forms the Os^{IV} complex $[Os(PEt_3)_2('S_2')_2]$ (**3**) via an intramolecular redox reaction. Evidently, the strongly electron donating PEt_3 and the a priori high electron density of the Os^{II} center destabilize the $'S_4'^{2-}$-ligand to such an extent that its C_2H_4 bridge is reductively eliminated. Such C_2H_4 eliminations from the $'S_4'^{2-}$-ligand have been observed previously with electron rich Fe and Mo species[22]. In this respect, **2** unexpectedly strongly differs from its iron and ruthenium alkylphosphane $[M(PR_3)_2('S_4')]$ counterparts which are perfectly stable at ambient conditions. Complex **3** and the PMe_3 **5**, PPr_3 **4**, and PPh_3 **6** analogues were directly obtained from $[OsBr_6]^{2-}$, $'S_2'^{2-}$ and the respective phosphanes. X-ray structure analyses of **3** and **4** revealed that these complexes possess planar $[Os('S_2')_2]$ cores and *trans* phosphanes. UV-Vis-NIR spectroscopy further showed that the hexacoordinate complexes **3** to **5** have very intense NIR bands and reversibly dissociate yielding pentacoordinate $[Os(PR_3)('S_2')_2]$ complexes. When PR_3 is the sterically very bulky PCy_3, only the pentacoordinate species $[Os(PCy_3)('S_2')_2]$ (**7**) could be isolated. The influence of solvents upon the course of reactions became particularly evident when the synthesis of (**7**) was tried in MeOH instead of THF. In this case, the Os^{III} complex $(PHCy_3)[Os('S_2')_2]$ (**8a**) formed. Complex **8a** probably possesses a dinuclear anion, is paramagnetic and spontaneously oxidizes in CH_2Cl_2 to give **7**. Cyclic voltammetry revealed redox activity also for **2**, **3**, and $(NBu_4)_2[Os('S_2')_3]$ (**9b**) which forms from stoichiometric amounts of $[OsBr_6]^{2-}$, NBu_4^+, and $'S_2'^{2-}$. X-ray structure analysis of the analogous $(PHCy_3)_2[Os('S_2')_3]$ (**9a**) revealed pseudo-octahedral coordination geometry of the $[Os('S_2')_3]^{2-}$ anion.

Scrutinizing the C−C and C−S distances in the $C_6H_4S_2$ units of **3**, **4**, and **9a** corroborates previous results. They indicate that benzenedithiolate behaves as "normal" dithiolate also when binding to metal centers in higher oxidation states. The stabilization of these oxidation states thus is better traced back to increasing S→M π donation than to a "non-innocence" of benzenedithiolate that involves a break-up of the aromatic benzene system.

In summary, first examples of complexes containing $[Os('S_4')]$ and $[Os('S_2')_2)]$ fragments have been synthesized and characterized. The complexes differ unexpectedly strongly from their iron and ruthenium homologues. While with $'S_4'^{2-}$ or $'S_2'^{2-}$ ligands the metal oxidation state +IV is found only in very few iron and only unsignificantly more ruthenium complexes, it is well accessible with Os complexes.

Financial Support of this work by the *Deutsche Forschungsgemeinschaft* and the *Fonds der Chemischen Industrie* is gratefully acknowledged.

Experimental Section

General Methods: Unless noted otherwise, all reactions were carried out under an atmosphere of dinitrogen at room temperature by using standard Schlenk techniques. Solvents were dried and distilled before use. − Physical measurements were carried out with the following instruments: IR spectra, Perkin Elmer 16PC FTIR spectrometer (IR spectra of solutions were recorded in CaF_2 cuvettes with compensation of the solvent bands, solids were measured as KBr pellets); mass spectra, Varian MAT 212; UV/Vis/NIR spectra, Shimadzu UV3101 PC spectrometer; NMR spectra, Jeol FT-JNM-GX 270, EX 270 and LA 400; Magnetic susceptibility: Johnson Matthey susceptibility balance; Cyclic voltammograms, EG&G potentiostat PAR model 264A with glassy carbon working electrode, Pt counter electrode and Ag/AgCl reference electrode. Conducting electrolyte: 0.1 M NBu_4PF_6. Potentials are referred to NHE via $Cp_2Fe^{0/+}$ as internal standard. $Cp_2Fe^{0/+}$ = 0.40 V vs. NHE[23]. − 1,2-benzenedithiol[24] and 1,2-bis(2-mercaptophenylthio)ethane $'S_4'$-H_2[25] were prepared as described in the literature.

[Os(PPh$_3$)$_2$('S$_4$')] (**1**): $OsCl_3 \cdot x\ H_2O$ (335 mg, 1.1 mmol), PPh_3 (1 g, 3.8 mmol), and $'S_4'$-H_2 (350 mg, 1.1 mmol) were suspended in MeOH (20 ml) and THF (40 ml) and refluxed for 24 h. The resultant suspension was cooled to room temperature, the precipitating yellow-green crystals were separated, recrystallized from CH_2Cl_2 (20 ml), and dried in vacuo. Yield: 500 mg of **1**·0.25 CH_2Cl_2 (44%). − $C_{50.25}H_{42.5}OsP_2S_4$ (1044.5): calcd. C 57.78, H 4.10, S 12.28; found C 57.55, H 4.15, S 12.22. − ^{1}H NMR (CD_2Cl_2): δ = 6.4−7.5 (m, 38 H, C_6H_4, C_6H_5), 2.15−2.4 (m, 2 H,

C_2H_4), 1.6−1.8 (m, 2 H, C_2H_4). − $^{13}C\{^1H\}$ NMR (CD_2Cl_2): δ = 159.6, 136.2 (m), 135.4 (t), 133.1, 130.8, 129.8, 129.2, 128.1, 126.7 (t), 121.6 (C_6H_4, C_6H_5), 43.3 (C_2H_4). − $^{31}P\{^1H\}$ NMR (CD_2Cl_2) δ = −14.4 (s, *P*Ph_3).

[Os(PEt$_3$)$_2$('S$_4$')] (**2**): $OsCl_3 \cdot x\ H_2O$ (360 mg, 1.2 mmol), PEt_3 (4 ml, 26 mmol), and 'S$_4$'-H_2 (380 mg, 1.2 mmol) were suspended in MeOH (35 ml) and THF (20 ml) and refluxed for 1 h. The resultant solution was filtered and cooled to −20°C. Yellow crystals precipitated that were separated after one week, washed with MeOH (50 ml) and *n*-hexane (20 ml), and dried in vacuo. Yield: 550 mg of **2** (62%). − $C_{26}H_{42}OsP_2S_4$ (735.0): calcd. C 42.49, H 5.76, S 17.45; found C 42.85, H 5.75, S 17.54. − FD MS (CH_2Cl_2); *m/z*: 736 [M^+]. − ^1H NMR (CD_2Cl_2), δ = 7.3−7.6 (m, 4 H, C_6H_4), 6.65−7.0 (m, 4 H, C_6H_4), 2.45−2.7 (m, 2 H, C_2H_4), 1.7−2.2 (m, 12 H, CH_2), 1.4−1.7 (m, 2 H, C_2H_4), 0.8−1.2 (m, 18 H, CH_3). − ^{31}P NMR (CD_2Cl_2), δ = −26.3 (s, *P*Et_3). − CV (CH_2Cl_2, room temp., [mV]); *E* = −20 (rev.), −950 (rev.).

[Os(PR$_3$)$_2$('S$_2$')$_2$] with R = Me, Et, Pr, Ph

General Procedure: At −78°C, 2.5 M *n*BuLi in *n*-hexane (0.8 ml, 2 mmol) was added to a solution of 'S$_2$'-H_2 (0.12 ml, 1 mmol) in THF (10 ml). The solution was warmed to room temperature and added to a suspension of $(NH_4)_2[OsBr_6]$ (350 mg, 0.5 mmol) and PR_3 (0.15 ml, 1 mmol) in MeOH or THF (10 ml). The resultant suspension was heated under reflux for 19 h, filtered, and cooled to room temperature or −20°C. The resultant complexes precipitated as black crystals or gray-black powders that were collected after one week, washed with MeOH (20 ml) and dried in vacuo. Complex **6** required recrystallization from THF (20°C → −20°C) in order to obtain correct elemental analyses.

[Os(PEt$_3$)$_2$('S$_2$')$_2$] (**3**): Yield: 225 mg of **3** (50%). − $C_{24}H_{38}OsP_2S_4$ (707.0): calcd. C 40.78, H 5.42, S 18.14; found C 40.66, H 5.72, S 18.10. − FD MS (CH_2Cl_2); *m/z*: 590 [M^+ − PEt_3]. − ^1H NMR (CD_2Cl_2), δ = 7.5−7.7 (m, 4 H, C_6H_4), 5.3−5.5 (m, 4 H, C_6H_4), 0.4−0.6 (quint, 18 H, CH_3), −0.7 (m, 12 H, CH_2). − $^{13}C\{^1H\}$ NMR (CD_2Cl_2), δ = 148.0, 125.0, 120.7 (C_6H_4), 10.7 (t, CH_2), 6.7 (s, CH_3). − $^{31}P\{^1H\}$ NMR (CD_2Cl_2), δ = −195.4 (s, *P*Et_3). − UV/VIS/NIR (CH_2Cl_2): λ_{max} (lg ε) = 1043 nm (4.61), 765 (3.64), 626 (3.78), 531 (3.67). − CV (CH_2Cl_2, room temp., [mV]); *E* = 340 (rev.), −760 (rev.), 1030 (irrev.).

[Os(PPr$_3$)$_2$('S$_2$')$_2$] (**4**): Yield: 290 mg of **4** (73%). − $C_{30}H_{50}OsP_2S_4$ (791.1): calcd. C 45.55, H 6.37, S 16.21; found C 45.50, H 6.40, S 15.75. − FD MS (CH_2Cl_2); *m/z*: 792 [M^+], 632 [M^+ − PPr_3]. − ^1H NMR (CD_2Cl_2), δ = 7.5−7.7 (m, 4 H, C_6H_4), 5.35−5.55 (m, 4 H, C_6H_4), 0.6−0.9 (m, 12 H, $^{\beta}CH_2$), 0.5 (t, 18 H, CH_3), −0.75−(−0.6) (m, 12 H, $^{\alpha}CH_2$). − $^{13}C\{^1H\}$ NMR (CD_2Cl_2), δ = 147.9, 124.9, 120.7 (C_6H_4), 21.1 (t, $^{\alpha}CH_2$), 16.3 (s, CH_3), 16.0 (t, $^{\beta}CH_2$). − $^{31}P\{^1H\}$ NMR (CD_2Cl_2), δ = −201.1 (s, *P*Pr_3). − UV/VIS/NIR (CH_2Cl_2, λ_{max} (lg ε) = 1043 nm (4.63), 761 (3.74), 625 (3.88).

[Os(PMe$_3$)$_2$('S$_2$')$_2$] (**5**): Yield: 155 mg of **5** (50%). − $C_{18}H_{26}OsP_2S_4$ (622.8): calcd. C 34.71, H 4.21; found C 34.96, H 4.17. − ^1H NMR (C_6D_6), δ = 7.9−8.1 (m, 4 H, C_6H_4), 5.4−5.6 (m, 4 H, C_6H_4), −1.2 (t, 18 H, CH_3). − UV/VIS/NIR (CH_2Cl_2): λ_{max} (lg ε) = 985 nm (4.53), 750(3.71), 622(3.56).

[Os(PPh$_3$)$_2$('S$_2$')$_2$] (**6**): Yield: 410 mg of **6** (82%). − $C_{48}H_{38}OsP_2S_4$ (995.2): calcd. C 57.93, H 3.85; found C 57.90, H 3.84. − ^1H NMR (CD_2Cl_2), δ = 7.5−7.6 (m, 4 H, C_6H_4), 6.9−7.25 (m, 30 H, C_6H_5), 5.9−6.05 (m, 4 H, C_6H_4). − $^{13}C\{^1H\}$ NMR (CD_2Cl_2), δ = 134.1 (d), 132.3 (d), 132.2, 129.4, 128.8 (d), 128.1, 122.8, 134.1 (d) (C_6H_4, C_6H_5). − $^{31}P\{^1H\}$ NMR (CD_2Cl_2), δ = −46.5 (s, *P*Ph_3).

*[Os(PEt$_3$)$_2$('S$_2$')$_2$] (**3**) from OsCl$_3$·x H$_2$O, 'S$_4$'-H$_2$ and PEt$_3$*: $OsCl_3 \cdot x\ H_2O$ (360 mg, 1.2 mmol), PEt_3 (4 ml, ca. 25 mmol), and 'S$_4$'-H_2 (380 mg, 1.2 mmol) were combined in MeOH (35 ml) and THF (20 ml) and heated under reflux for 3 d. The resultant solution was filtered while hot and cooled to room temperature. Black crystals precipitated that were collected after 7 d, washed with MeOH (40 ml) and *n*-hexane (20 ml) and dried in vacuo. They were identified by comparison with an authentic sample of **3**. Yield: 620 mg of **3** (73%). − $C_{24}H_{38}OsP_2S_4$ (707.0): calcd. C 40.78, H 5.42, S 18.14; found C 40.80, H 5.67, S 18.36.

[Os(PCy$_3$)('S$_2$')$_2$] (**7**): At −78°C, 2.5 M *n*BuLi in *n*-hexane (0.4 ml, 1 mmol) was added to a solution of 'S$_2$'-H_2 (0.16 ml, 0.5 mmol) in THF (10 ml). The solution was warmed to room temperature and added to a suspension of $(NH_4)_2[OsBr_6]$ (176 mg, 0.25 mmol) and PCy_3 (280 mg, 1 mmol) in THF (20 ml). The resultant violet suspension was heated under reflux for 19 h, filtered and cooled to −20°C. The precipitating violet crystals were collected after 8 d, washed with MeOH (20 ml) and dried in vacuo. When the THF/MeOH mother liquor was kept at −20°C, a few single crystals separated in the course of 14 d, which were identified as $(PHCy_3)_2[Os('S_2')_3]$ (**8a**) by X-ray structure determination. Yield: 125 mg of **7** (67%). − $C_{30}H_{41}OsPS_4$ (751.1): calcd. C 47.98, H 5.50, S 17.08; found C 47.88, H 5.51, S 17.27. − FD MS (CH_2Cl_2); *m/z*: 752 [$M]^+$. − ^1H NMR (CD_2Cl_2), δ = 8.25−8.45 (m, 4 H, C_6H_4), 6.55−6.75 (m, 4 H, C_6H_4), 0.7−2.0 (m, 33 H, C_6H_{11}). − $^{13}C\{^1H\}$ NMR (CD_2Cl_2), δ = 164.4, 129.0, 123.7 (C_6H_4), 28.8, 28.1, 28.0, 26.4 (C_6H_{11}). − $^{31}P\{^1H\}$ NMR (CD_2Cl_2), δ = −29.2 (s, *P*Cy_3). − UV/VIS/NIR (CH_2Cl_2, λ_{max} (lg ε) = 563 nm (3.66), 753 (3.22).

(PHCy$_3$)[Os('S$_2$')$_2$] (**8a**): At −78°C, 2.5 M *n*BuLi in *n*-hexane (0.8 ml, 2 mmol) was added to a solution of 'S$_2$'-H_2 (0.12 ml, 1 mmol) in THF (10 ml). The solution was warmed to room temperature and added to a suspension of $(NH_4)_2[OsBr_6]$ (355 mg, 0.5 mmol) and PCy_3 (560 mg, 2 mmol) in MeOH (10 ml) and THF (10 ml). The resultant violet suspension was heated under reflux for 3 d and cooled to room temperature. Orange crystals precipitated that were separated, washed with MeOH (20 ml) and Et_2O (40 ml) and dried in vacuo. Yield: 195 mg of (**8a**) (52%). − $C_{30}H_{42}OsPS_4$ (752.1): calcd. C 47.91, H 5.63, S 17.05; found C 47.83, H 5.68, S 16.96. − ^1H NMR (CD_2Cl_2), δ = 7.4−7.6 (m, 4 H, C_6H_4), 6.55−6.75 (m, 4 H, C_6H_4), 5.46 (d, $^1J_{PH}$ = 475 Hz, 1 H, P*H*Cy_3), 0.8−1.9 (m, 33 H, C_6H_{11}). − $^{13}C\{^1H\}$ NMR (CD_2Cl_2, −70°C), δ = 148.3, 127.7, 121.8 (C_6H_4), 26.1, 25.8, 25.5, 24.2 (C_6H_{11}). − $^{31}P\{^1H\}$ NMR (CD_2Cl_2), δ = 20.7 (s, *P*HCy_3).

(NMe$_4$)[Os('S$_2$')$_2$] (**8b**): An orange-brown suspension of (**8a**) (75 mg, 0.1 mmol) in THF (5 ml) was treated with a 2.2 M solution of NMe_4OH in MeOH (0.1 ml, 0.2 mmol). The resultant orange-brown powder was separated, washed with MeOH (5 ml) and dried in vacuo. Yield: 50 mg of (**8b**) (92%). − $C_{16}H_{20}NOsS_4$ (544.8): calcd. C 35.28, H 3.70, N 2.57; found C 35.52, H 3.46, N 2.47. − ^1H NMR ([D$_6$]DMSO), δ = 7.30−7.45 (m, 4 H, C_6H_4), 6.55−6.70 (m, 4 H, C_6H_4), 3.1 (s, 12 H, NMe_4^+).

(NBu$_4$)$_2$[Os('S$_2$')$_3$] (**9b**): NBu_4OH (3 ml of 1 M solution in MeOH, 3 mmol) 'S$_2$'-H_2 (0.18 ml, 1.5 mmol), and $(NH_4)_2[OsBr_6]$ (355 mg, 0.5 mmol) were combined in MeOH (50 ml) and heated under reflux for 2 h. The resultant brown-red solution was filtered while hot, and cooled to room temperature. Brown-red crystals precipitated that were separated after 4 h, washed with MeOH (30 ml) and Et_2O (30 ml), and dried in vacuo. Yield: 500 mg of (**9b**) (91%). − $C_{50}H_{84}N_2OsS_6$ (1095.8): calcd. C 54.80, H 7.73, N 2.56, S 17.56; found C 54.61, H 7.97, N 2.54, S 17.84. − ^1H NMR (CD_2Cl_2), δ = 6.55−7.90 (m, C_6H_4), 3.00 (m, 16 H, CH_2), 1.70 (m, 16 H, CH_2), 1.42 (m, 16 H, CH_2), 1.0 (t, 24 H, CH_3), 0.22 (s, C_6H_4), −0.90 (s,

Table 1. Selected crystallographic data for $[Os(PEt_3)_2('S_2')_2]$ (**3**), $[Os(PPr_3)_2('S_2')_2]$ (**4**), and $(PHCy_3)_2[Os('S_2')_3]$ (**9a**)

compound	$[Os(PEt_3)_2('S_2')_2]$ (**3**)	$[Os(PPr_3)_2('S_2')_2]$ (**4**)	$(PHCy_3)_2[Os('S_2')_3]$ (**9a**)
Formula	$C_{24}H_{38}P_2S_4Os$	$C_{30}H_{50}P_2S_4Os$	$C_{54}H_{78}P_2S_6Os$
MW [g/mol]	706.92	791.08	1171.66
Crystal size. [mm]	0.4 × 0.3 × 0.2	0.3 × 0.2 × 0.1	0.5 × 0.2 × 0.2
$F(000)$	704	800	2416
Crystal system	monoclinic	monoclinic	monoclinic
Space group	$P2_1/n$	$P2_1/c$	$P2_1/n$
a [pm]	968.9(7)	1001.5(5)	1801.7(4)
b [pm]	1163.7(6)	1320.8(6)	1705.4(5)
c [pm]	1285.6(7)	1354.7(4)	1942.4(5)
β [°]	93.38(5)	95.09(3)	112.72(2)
Cell volume [nm³]	1.447(2)	1.785(1)	5.505(3)
Z	2	2	4
$d_{calcd.}$ [g/cm³]	1.622	1.472	1.414
μ [mm^{-1}]	4.817	3.913	2.636
Temperature [K]	293(2)	293(2)	200(2)
θ-range	2.36−27.04	2.04−27.05	2.27−27.06
Measured reflections	5442	4852	14605
Independent reflections	3177	3354	11812
Observed reflections	2169	1943	4086
Refined parameters	145	169	605
R_1 [$F_0 \geq 4\sigma(F)$]	0.0330	0.0434	0.0488
wR_2 (all data)	0.0865	0.1074	0.1115

C_6H_4). − CV (CH_2Cl_2, room temp., [mV]); E_1 = −80 (rev.), 180 (rev.), −580 (irrev.).

X-ray Structure Analysis of $[Os(PEt_3)_2('S_2')_2]$ (**3**), $[Os(PPr_3)_2('S_2')_2]$ (**4**), *and* $(PHCy_3)_2[Os('S_2')_3]$ (**9a**): Black single crystals of $[Os(PEt_3)_2('S_2')_2]$ (**3**) and $[Os(PPr_3)_2('S_2')_2]$ (**4**) were grown from MeOH (**3**) or MeOH/THF (**4**) solutions at −20°C. A few black single crystals of $(PHCy_3)_2[Os('S_2')_3]$ (**9a**) were obtained as minor by-product from the THF/MeOH mother liquor resulting from the synthesis of $[Os(PCy_3)('S_2')_2]$ (**7**). Suitable single crystals were sealed under N_2 in glass capillaries. The data were collected using a Siemens P4 diffractometer. The structures were solved with direct methods and refined using full-matrix least-squares procedures on F^2 values (SHELXTL 5.03)[26]. Non-hydrogen atoms were refined anisotropically, hydrogen positions were taken from the difference Fourier synthesis and fixed on their positions with a common isotropic thermal parameter in case of **4**, while for **3** and **9a** all H-atoms are geometrically positioned. One cyclohexyl group (C70−C75) of the cation in **9a** is disordered. Two different orientations were refined, with a site occupancy of 50%. Table 1 lists selected crystallographic data of **3**, **4**, and **9a**[27].

☆ Dedicated to Professor *Heinrich Nöth* on the occasion of his 70th birthday.

[1] [1a] B. K. Burgess in *Molybdenum Enzymes, Cofactors, and Model Systems*, (Eds.: E. I. Stiefel, D. Coucouvanis, W. E. Newton), ACS Symposium Ser. **1993**, *535*, 144−170. − [1b] D. J. Lowe, R. N. F. Thorneley, B. E. Smith in *Metalloproteins Part 1, Metal Proteins with Redox Roles*; (Ed.: P. Harrison), Verlag Chemie, Weinheim, **1985**. − [1c] R. R. Eady in *Perspectives in Bioinorganic Chemistry*, (Eds.: R. W. Hay, J. R. Dilworth, K. B. Nolan), JAI Press, London, **1991**, p. 225.

[2] [2a] D. Sellmann, H. Friedrich, F. Knoch, M. Moll, *Z. Naturforsch.* **1994**, *48b*, 76−88. − [2b] D. Sellmann, M. Waeber, *Z. Naturforsch.* **1986**, *41b*, 877−884. − [2c] D. Sellmann, E. Böhlen, M. Waeber, G. Huttner, L. Zsolnai, *Angew. Chem.* **1985**, *97*, 984−985; *Angew. Chem. Int. Ed. Engl.* **1985**, *24*, 981−982. − [2d] D. Sellmann in *Molybdenum Enzymes, Cofactors, and Model Systems*, (Eds.: E. I. Stiefel, D. Coucouvanis, W. E. Newton), ACS Symposium Ser. **1993**, *535*, 332−345. − [2e] D. Sellmann in *Sulfur Coordinated Transition Metal Complexes: Biological and Industrial Significance*, (Eds.: E. I. Stiefel, K. Matsumoto), ACS Symposium Ser. **1996**, *653*, 101−116.

[3] [3a] D. Sellmann, B. Seubert, *Angew. Chem.* **1992**, *104*, 200−201; *Angew. Chem. Int. Ed. Engl.* **1992**, *31*, 205−207. − [3b] D. Sellmann, D. Häußinger, F. Knoch, M. Moll, *J. Am. Chem. Soc.* **1996**, *118*, 5368−5374.

[4] D. Sellmann, J. Käppler, M. Moll, *J. Am. Chem. Soc.* **1993**, *115*, 1830−1835.

[5] T. Yoshida, T. Adachi, M. Kaminaka, T. Ueda, T. Higuchi, *J. Am. Chem. Soc.* **1988**, *110*, 4872−4873.

[6] W. P. Griffith in *Comprehensive Coordination Chemistry Vol. 4* (Ed.: G. Wilkinson), Pergamon Press, Oxford, **1987**, p. 606.

[7] [7a] B. J. McCormick, D. S. Rinehart, *J. Inorg. Nucl. Chem.* **1980, 42**, 928−930. − [7b] R. E. De Simone, *J. Am. Chem. Soc.* **1973**, *95*, 6238−6244. − [7c] G. N. Schrauzer, H. W. Fink, V. P. Mayweg, *Angew. Chem.* **1964**, *76*, 715; *Angew. Chem. Int. Ed. Engl.* **1964**, *3*, 639. − [7d] A. M. Dix, J. M. Diesveld, J. G. M. van der Linden, *Inorg. Chim. Acta* **1977**, *24*, L51−52. − [7e] P. B. Critchlow, S. D. Robinson, *J. Chem. Soc. Dalton Trans.* **1975**, 1367−1372.

[8] M. Hesse, H. Meier, B. Zeeh, *Spektroskopische Methoden in der organischen Chemie*, 3rd ed., Georg Thieme Verlag, Stuttgart, **1987**, p. 171.

[9] D. Sellmann, H.-E. Jonk, H.-R. Pfeil, G. Huttner, J. v. Seyerl, *J. Organomet. Chem.* **1980**, *191*, 171−179.

[10] D. Sellmann, E. Böhlen, *Z. Naturforsch.* **1982**, *37b*, 1026−1033.

[11] D. Sellmann, M. Geck, F. Knoch, M. Moll, *Inorg. Chim. Acta* **1991**, *186*, 187−198.

[12] [12a] M. Arroyo, J. A. Chamizo, D. L. Hughes, R. L. Richards, P. Roman, P. Sosa, H. Torrens, *J. Chem. Soc. Dalton Trans.* **1994**, 1819−1824. − [12b] J. P. Collman, D. S. Bohle, A. K. Powell, *Inorg. Chem.* **1993**, *32*, 4004−4011. − [12c] C. M. Che, W. K. Cheng, T. C. W. Mak, *Inorg. Chem.* **1986**, *25*, 703−706.

[13] D. Sellmann, M. Geck, F. Knoch, G. Ritter, J. Dengler, *J. Am. Chem. Soc.* **1991**, *113*, 3819−3828.

[14] [14a] M.-L. Abasq, C. J. Pickett, R. L. Richards, M. Arroyo, J. A. Chamizo, A. Calderón, P. Sosa, H. Torrens, *Polyhedron* **1996**, *15*, 3623−3629. − [14b] R. L. Lintvedt, W. E. Lynch, X. Q. Shui, *Inorg. Chem.* **1991**, *30*, 1014−1019.− [14c] A. Earnshaw, *Introduction to magnetochemistry*, Academic Press, London, **1968**, p. 70−71.

[15] B. S. Kang, L. H. Weng, D. X. Wu, F. Wang, Z. Guo, L. R. Huang, Z. Y. Huang, H. Q. Liu, *Inorg. Chem.* **1988**, *27*, 1128−1130.

[16] D. Sellmann, M. Geck, M. Moll, *J. Am. Chem. Soc.* **1991**, *113*, 5259−5264.

[17] [17a] R. Eisenberg, E. I. Stiefel, R. C. Rosenberg, H. B. Gray, *J. Am. Chem. Soc.* **1966**, *88*, 2874−2876. − [17b] R. Eisenberg, E. I. Stiefel, R. C. Rosenberg, H. B. Gray, *J. Am. Chem. Soc.* **1966**, *88*, 2956−2966. − [17c] R. Eisenberg, J. A. Ibers, *J. Am. Chem.*

Soc. **1965**, *87*, 3776−3778. − [17d] G. N. Schrauzer, V. P. Mayweg, *J. Am. Chem. Soc.* **1966**, *88*, 3235−3242. − [17e] G. N. Schrauzer, A. E. Smith, V. P. Mayweg, W. Heinrich, *J. Am. Chem. Soc.* **1965**, *87*, 5798−5799. − [17f] J. Takats, J. L. Martin, *Inorg. Chem.* **1975**, *14*, 1358−1364.
[18] M. Cowie, M. J. Bennett, *Inorg. Chem.* **1976**, *15*, 1595−1603.
[19] M. Könemann, W. Stüer, K. Kirschbaum, D. M. Giolando, *Polyhedron* **1994**, *13*, 1415−1425.
[20] [20a] D. Sellmann, W. Kern, F. Knoch, *Z. Kristallogr.* **1993**, *205*, 300−302. − [20b] D. Sellmann, W. Kern, M. Moll, *J. Chem. Soc. Dalton Trans.* **1991**, 1733−1736.
[21] M. Cowie, M. J. Bennett, *Inorg. Chem.* **1976**, *15*, 1589−1595.
[22] [22a] D. Sellmann, W. Reißer, *J. Organomet. Chem.* **1985**, *297*, 319−329.− [22b] D. Sellmann, W. Reißer, *J. Organomet. Chem.* **1985**, *294*, 333−346.
[23] H. Koepp, H. Wendt, H. Strehlow, *Z. Elektrochem.* **1960,** *64*, 483−491.
[24] J. Degani, R. Fochi, *Synthesis* **1976**, *7*, 471−472.
[25] D. Sellmann, W. Reißer, *Z. Naturforsch.* **1984,** *39b*, 1268−1275.
[26] SHELXTL 5.03 for Siemens Crystallographic Research Systems, Release 4 21/V, Copyright **1995** by Siemens Analytical X-Ray Instruments Inc., Madison; WI.
[27] Further details of the crystal structure investigations are available on request from Cambridge Crystallographic Data Centre, The Director, 12 Union Road, Cambridge CB2 1EZ (Telefax: Int. + 1223/336-033; E-mail: deposit@chemcrys.cam.ac.uk), on quoting the "supplementary publication no. CCDC-100408", the names of the authors, and the journal citation.
[97316]

Zinc Complexes of Tripodal N_3O Ligands☆

Alexander Trösch and Heinrich Vahrenkamp*

Institut für Anorganische und Analytische Chemie der Universität Freiburg,
Albertstr. 21, D-79104 Freiburg, Germany

Received December 30, 1997

Keywords: Zinc complexes / Tripodal ligands / Ligand bridging / Halide, phenolate, thiophenolate, and phosphate coligands

The tripodal N,O ligands bis(2-pyridylmethyl)(*o*-hydroxybenzyl)amine ($\mathbf{L}^1$) and bis(2-pyridylmethyl)(2-carboxyethyl)amine ($\mathbf{L}^2$) were tested for their ligating properties towards zinc. Zinc halides yielded $\mathbf{L}^1{\cdot}Zn{-}Hal$ (**1a**−**c**, Hal = Cl, Br, I) and $\mathbf{L}^2{\cdot}Zn{-}Hal$ (**2a**−**c**, Hal = Cl, Br, I). Subsequent treatment of $\mathbf{L}^1$ with $ZnEt_2$ or $Zn[N(SiMe_3)_2]_2$ and phenol, thiophenols or diphenylphosphate led to $\mathbf{L}^1{\cdot}Zn{-}OPh$ (**3**), $\mathbf{L}^1{\cdot}Zn{-}SAr$ (**4**) and $\mathbf{L}^1{\cdot}Zn{-}OPO(OPh)_2$ (**5**). Zinc salts of noncoordinating anions yielded oligonuclear ligand-bridged complexes $[\mathbf{L}^1{\cdot}Zn]ClO_4$ (**6**), $[\mathbf{L}^2{\cdot}Zn]ClO_4$ (**7**) and $[\mathbf{L}^2{\cdot}Zn]NO_3$ (**8**), of which **6** was identified as a phenolate bridged dimer and **8** as a η^1-η^2-carboxylate bridged polymer.

The challenge of modern coordination chemistry is the design of complexes in which an inert ligand matrix provides the metal ion with appropriate electronic properties and the right number of labile coordination sites to effect specific metal-mediated reactions. In practice this means the use of polydentate ligands, and specifically in the field of functionalized macrocycles a high level of sophistication has been reached for this purpose.

We are trying to contribute to this area of research in the field of zinc chemistry. Zinc ion catalysis, in organic synthesis as well as in biological systems, involves zinc complexes of low coordination numbers, e.g. 4 or 5[1]. Hence most macrocyclic ligands which favour coordination numbers 5 and 6 are not ideally suited for mechanistic or bioinorganic model studies here. The ligands of choice are the tripods of which very many have been synthesized in recent years. If constructed right, those of type **A** should favour tetrahedral zinc and those of type **B** should favour trigonal-bipyramidal zinc, each with one labile coordination site.

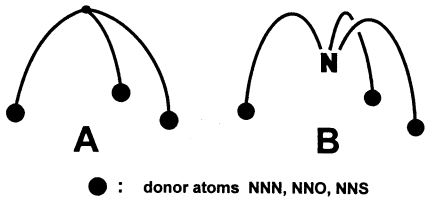

A typical representative of type **A** is the class of pyrazolylborate ligands[2] to which we have contributed synthetic, model complex, and complex reactivity studies[3]. One of the simplest representatives of type **B** is tris(picolyl)amine[4] which so far has been used sparsely in zinc chemistry[5]. In contrast to the pyrazolylborates, the type **B** tripods can easily be obtained with different donor "arms" in the same ligand. A recent example which has the additional advantage of bearing one negative charge is dipicolylglycinate[6] of which we have prepared the $[\mathbf{L}{\cdot}Zn{-}OH_2]^+$ complex and studied its reactivity[7].

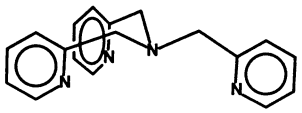
tris(picolyl)amine

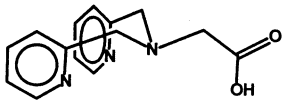

dipicolylglycine

Ligands like tris(picolyl)amine and dipicolylglycinate have an arrangement of donor atoms corresponding to that of ethylenediamine, i.e. they support valence angles near 90° and hence octahedral coordination at the metal ion, as we have experienced for zinc complexes of the latter[7]. In order to relax their bite, the length of their "arms" should be extended. Some reports on zinc complexes having type **B** ligands with "longer arms" seem to support this idea[8]. We therefore looked for such ligands to include them in our reactivity studies. Of the various possibilities we opted for the two dipicolylamine derivatives $H\mathbf{L}^1$ with a phenolate unit and $H\mathbf{L}^2$ with a carboxylate unit as the third "arm". Both could be expected to bind to zinc as the monoanions $\mathbf{L}^1$ and $\mathbf{L}^2$ and thereby ensure a reasonably good complex stability.

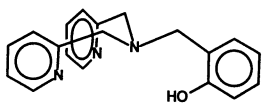

$H\mathbf{L}^1$

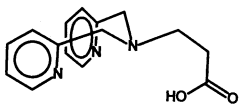

$H\mathbf{L}^2$

Both $H\mathbf{L}^1$[9] and $H\mathbf{L}^2$[10] have been described before and used for bioinorganic model studies[9][10][11][12][13]. The coordination chemistry of ligands like $\mathbf{L}^1$ with varying "arm lengths" was developed extensively by D. E. Fenton[13][14][15][16] including the modelling of the structure and reactivity of zinc enzymes[15][16] and the preparation of dinuclear copper and zinc complexes of $\mathbf{L}^1$[13][15]. One of the attractions in the zinc chemistry of $\mathbf{L}^1$ and $\mathbf{L}^2$ is that they

 © WILEY-VCH Verlag GmbH, D-69451 Weinheim, 1998 1434−1948/98/0606−0827 $ 17.50+.50/0

allow to mimick the fivefold N_xO_y coordination of zinc in enzymes like the peptidase astacin [histidine (3×), tyrosine, H_2O][17] or Escherichia coli alkaline phosphatase [histidine (2×), aspartate (2×), H_2O][18]. With this in mind we intended to explore the basic zinc coordination chemistry of $\mathbf{L}^1$ and $\mathbf{L}^2$ (coordination numbers, ligand bridging) and to find complexes like $[\mathbf{L}\cdot Zn]^+$, $[\mathbf{L}\cdot Zn-OH_2]^+$ or $[\mathbf{L}\cdot Zn-OH]$ for reactivity studies involving a labile coordination site or a hydrolytically active function at the zinc ion.

L·Zn−X Complexes

In order to test the ligating abilities of $\mathbf{L}^1$ and $\mathbf{L}^2$ their zinc halide complexes were prepared. This could be achieved with $ZnHal_2$ in methanol, using NaOH to deprotonate **L**H. All six complexes (**1** and **2**) were obtained. Complexes **1** are soluble in polar organic solvents like dichloromethane or ethanol, complexes **2** dissolve only in water or water/alcohol mixtures. The presence of the intact ligands **L** in the complexes is evident from their ^{1}H-NMR spectra (see experimental), their binding to zinc can be deduced from the low-field shifts of the signals for the pyridyl-H_α atoms.

$\mathbf{L}^1\cdot Zn-Hal$		$\mathbf{L}^2\cdot Zn-Hal$	
1a	Hal = Cl	**2a**	Hal = Cl
1b	Br	**2b**	Br
1c	I		

Proof for the molecular nature of complexes **L**·Zn−Hal was obtained by the structure determination of **1a**, see Figure 1. The geometry at zinc in **1a** is close to trigonal-bipyramidal, and it can be compared with that in related zinc complexes of tris(benzimidazolylmethyl)amine[19] or dipicolylglycinate[7]. This includes the bending along the trigonal axis (165°) and the lengthening of the axial Zn−N distance compared to the equatorial ones. The axial Zn−Cl distance (2.33 Å) seems long when compared to those in pyrazolylborate zinc complexes (2.14−2.18 Å)[20]. But it compares well with that in trigonal-bipyramidal (tren)Zn−Cl (2.31 Å)[21].

Figure 1. Molecular structure of $\mathbf{L}^1\cdot Zn-Cl$ (**1a**)[a]

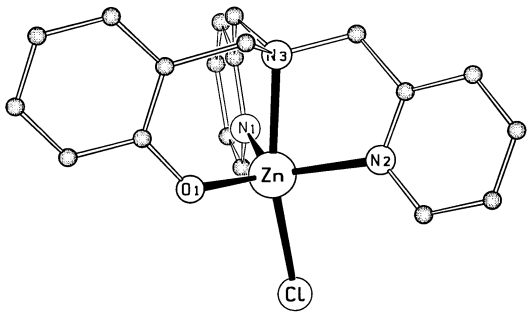

[a] Bond lengths and angles around zinc: Zn−N1 2.109(5), Zn−N2 2.116(4), Zn−N3 2.240(4), Zn−O1 1.928(3), Zn−Cl 2.326(2) Å. − N1−Zn−N3 77.6(2), N2−Zn−N3 76.7(2), O1−Zn−N3 91.9(2), Cl−Zn−N3 165.1(1), Cl−Zn−N1 96.5(2), Cl−Zn−N2 95.3(1), Cl−Zn−O1 102.9(1), N1−Zn−N2 121.2(2), N1−Zn−O1 117.0(2), N2−Zn−O1 115.8(2)°.

In the subsequent derivatizations it turned out to be advantageous to use an acid-sensitive zinc compound {$ZnEt_2$ or $Zn[N(SiMe_3)_2]_2$} for the deprotonation of ligands **L**H. The resulting labile complexes {$\mathbf{L}\cdot Zn-Et$ or $\mathbf{L}\cdot Zn-N(SiMe_3)_2$} were then treated with the corresponding acid HX of the coligand X. This way the $\mathbf{L}^1\cdot Zn$ unit was converted to the phenolate **3** by treatment with $ZnEt_2$ and phenol. Likewise thiophenol could be incorporated as the thiophenolate **4a** via the $Zn-N(SiMe_3)_2$ intermediate. **4a** could, however, not be obtained in a pure form. Therefore alternatively *p*-chlorothiophenol was used, leading to **4b** which was fully characterized. Finally, using $ZnEt_2$ and diphenylphosphate the phosphate complex **5** was prepared. Complexes **3**−**5** are again soluble in moderately polar organic solvents, thereby indicating their molecular nature. Their ^{1}H-NMR spectra (see Experimental Section) are proof for their constitutions.

$\mathbf{L}^1\cdot Zn-OPh$ **3**	$\mathbf{L}^1\cdot Zn-SPh$ **4a**
$\mathbf{L}^1\cdot Zn-SC_6H_4-p\text{-}Cl$ **4b**	$\mathbf{L}^1\cdot Zn-O-PO(OPh)_2$ **5**

Crystals for a structure determination were obtained of **5**. Figure 2 shows that the coordination environment of zinc is very similar to that in **1a**, including the moderate deformation of the trigonal-bipyramidal geometry, the lengthening of the axial vs. equatorial Zn−X bonds and the bending of the N3−Zn−O2 axis. The orientation and the bonding situation of the phosphate ligand can be compared to that in a considerable number of pyrazolylborate−zinc−organophosphate complexes.[22] Specifically, the close similarity of the P−O2 and P−O5 bond lengths and the wide Zn−O−P angle are as observed before. This holds also for organophosphate complexes of dipicolylglycinate[7] and tris(picolyl)amine[5].

[L·Zn]$^+$ Complexes

The main purpose of this study was the preparation of zinc complexes in which the tripodal ligands **L** encapsulate the zinc ion such that they stabilize $[\mathbf{L}\cdot Zn]^+$ cations or cationic $[\mathbf{L}\cdot Zn-OH_2]^+$ complexes which can give access to reactive substrates **S** for zinc-mediated or zinc-catalyzed interconversions via intermediate complexes $[\mathbf{L}\cdot Zn-\mathbf{S}]$. To obtain such cationic complexes ligands **L** were treated with zinc salts of noncoordinating anions. In case of $\mathbf{L}^1$ and $\mathbf{L}^2$ this worked with $Zn(ClO_4)_2 \cdot 6\ H_2O$. When using methanol as a solvent and NaOH as a base the products **6** and **7** were isolated. Of these **6** was impure and insoluble while **7** could be recrystallized from water yet not obtained in the form of good single crystals. A form of **6** suitable for X-ray analysis was obtained by runing the reaction in CH_2Cl_2/methanol with KOH as a base, removing $KClO_4$ by filtration and allowing the product to crystallize from chloroform. This product **6** was not soluble in chloroform after isolation but could be subjected to NMR spectroscopy in DMSO. The ^{1}H-NMR and IR data of **6** and **7** (see Experimental Section) confirm the presence of **L** and ClO_4^- but give no indication of the complexes' structures. The insoluble form of **6** seems to be polymeric. **7** is likely to be a carboxylate-

Figure 2. Molecular structure of $\mathbf{L}^1$·Zn−OPO(OPh)$_2$ (**5**)[a]

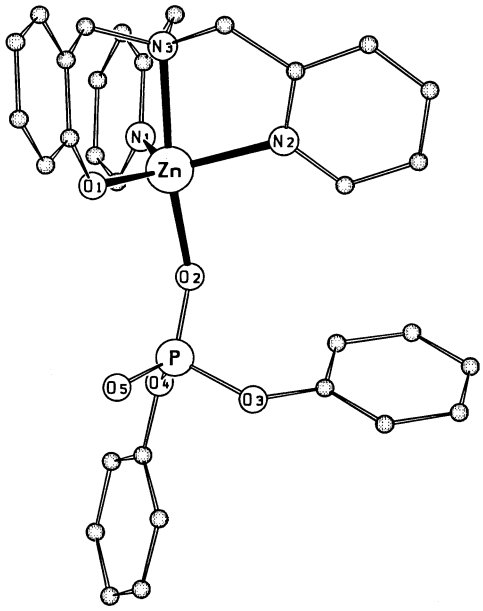

[a] Pertinent bond lengths and angles: Zn−N1 2.073(4), Zn−N2 2.096(3), Zn−N3 2.221(3), Zn−O1 1.926(3), Zn−O2 2.030(3), P−O2 1.486(3), P−O3 1.598(3), P−O4 1.601(3), P−O5 1.461(3) Å. − N3−Zn−N1 79.5(1), N3−Zn−N2 77.5(1), N3−Zn−O1 91.7(1), N3−Zn−O2 168.5(1), N1−Zn−N2 111.9(1), N1−Zn−O1 121.0(2), N1−Zn−O2 93.3(2), N2−Zn−O1 122.6(2), N2−Zn−O2 97.4(1), O1−Zn−O2 99.8(1), Zn−O2−P 151.9(2)°.

bridged oligomer, possibly a polymer like **8** (see below) or a trimer like the analogous dipicolylglycinate complex[7].

$[\mathbf{L}^1\cdot Zn]ClO_4$ **6** $\qquad$ $[\mathbf{L}^2\cdot Zn]ClO_4$ **7**

The structure determination of the soluble form of **6** showed it to be a chloroform-solvated dimer (see Figure 3). The unit cell contains two independent centrosymmetric dinuclear entities which differ slightly in their conformations but only marginally in the coordination environments of the zinc ions (bond lengths ±0.01 Å , angles ±2°). The coordination geometry of zinc is trigonal-bipyramidal, and all details associated therewith correspond to those for **1a** and **5**. The phenolate oxygen atoms provide the bridging function, as has been observed before, typically in zinc complexes of dinucleating ligands with central phenolate units[23]. The basic type of $[N_3Zn(\mu\text{-}O)_2]$ coordination is realized in $[\mathbf{L}\cdot Zn{-}OH]_2^{2+}$ with L = triazacyclononane[24] or tris(picolyl)amine[5] and zinc in a square-pyramidal environment. The Zn−N and Zn−O distances in **6** compare well with those in the reference compounds. The closest relation to **6** exists in the corresponding copper derivative of $\mathbf{L}^1$ which, however, contains square-pyramidal copper[13]. Fenton has also described two phenoxide-bridged dizinc complexes derived from $\mathbf{L}^1$-related tripod ligands with longer arms[15]:

When using zinc nitrate, a pure product, **8**, could only be obtained with $\mathbf{L}^2$. The structure determination showed this to be a polymeric methanol solvate with noncoordinating

Figure 3. Molecular structure of the cations of **6**[a]

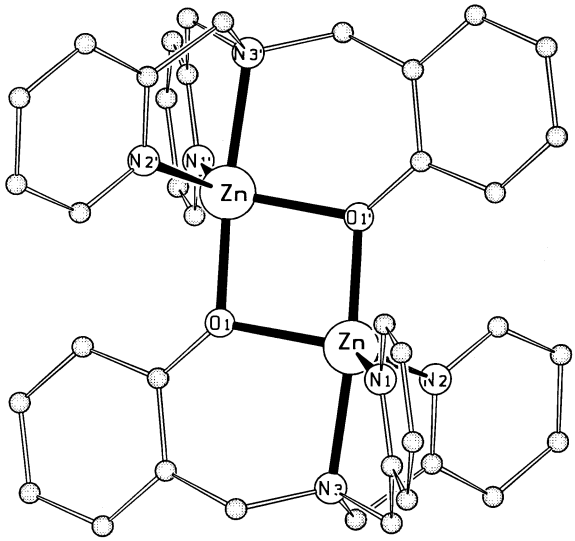

Average bond lengths and angles about zinc: Zn−O1 2.029(3), Zn−O1′ 2.002(4), Zn−N1 2.066(4), Zn−N2 2.066(4), Zn−N3 2.161(4), Zn···Zn 3.064(2) Å. N3−Zn−N1 80.4(2), N3−Zn−N2 79.9(2), N3−Zn−O1 93.0(2), N3−Zn−O1′ 172.5(2), N1−Zn−N2 126.6(2), N2−Zn−O1 122.8(2), N2−Zn−O1′ 99.6(2), O1−Zn−N1 112.6(2), O1′−Zn−N1 106.0(2), O1−Zn−O1′ 81.0(2), Zn−O1−Zn′ 99.0(2)°.

nitrate anions (see Figure 4). The linkage between the monomeric units is provided by the carboxylate groups in a manner which to our knowledge has not been observed for zinc before: one oxygen atom is bridging while the other is coordinated to the neighbouring zinc ion (η^1-η^2-carboxylate bridging)[25]. In contrast the trimeric complex $[\mathbf{L}\cdot Zn]ClO_4$ with L = dipicolylglycinate has one oxygen coordinating the ipso zinc ion and the other the neighbouring one[7]. The coordination geometry of the zinc ions in **8** is severley distorted octahedral with O1−Zn−O2 (58.7°) as the smallest and N3−Zn−O1′ (113.9°) as the largest *cis* angles and *trans* angles of 169.6 (N3−Zn−O2′), 150.0 (O1−Zn−O1′), and 154.8° (N1−Zn−N2). Carboxylate bridging between zinc ions is quite common[26], and all types of bridging[27] except for the η^1-η^2 type have been observed.

Figure 4. Solid-state arrangement of polymeric $[\mathbf{L}^2\cdot Zn]^+$ in **8**[a]

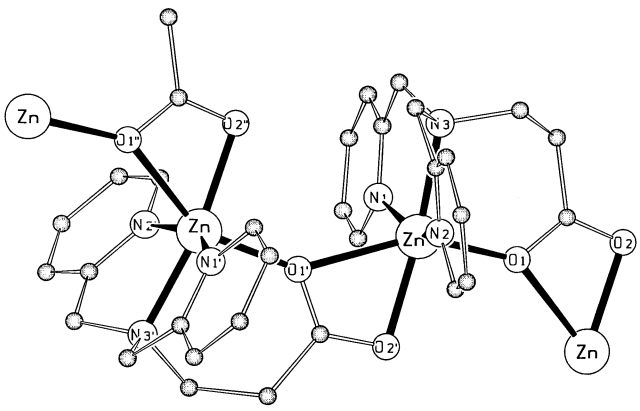

[a]Bond lengths: Zn−N1 2.084(3), Zn−N2 2.076(3), Zn−N3 2.179(3), Zn−O1 2.013(2), Zn−O1′ 2.302(2), Zn−O2′ 2.132(2) Å.

As can be seen from the Zn−N and Zn−O bond distances the coordination of $\mathbf{L}^2$ to zinc can be viewed as that in a trigonal-bipyramidal $\mathbf{L}^2$·Zn−X complex, i.e. the Zn−N3 bond is longer than the three other Zn−L bonds. Carboxylate atom O2′ then occupies the second axial ligand position, viz. Zn−O2′ is comparable in length to Zn−N3. The Zn−O1′ bond, i.e. the one that provides bridging to the neighbouring zinc ion, is the weakest, and O1 also occupies the most distorted octahedral ligand position. The distorted nature of the bridging assembly points to weak bridging, in accordance with the solubility of **8** in methanol.

Conclusions

The results of this paper indicate that ligands $\mathbf{L}^1$ and $\mathbf{L}^2$ are suitable for monofunctional zinc complexes L·Zn−X. Anionic coligands X providing Zn−Cl, −Br, −I, −OR, −SR, and −oxoanion linkages can be incorporated. The structures of the complexes are trigonal-bipyramidal with the pivotal N atom of the tripod and the coligand X on the axial positions. The complexes derived from $\mathbf{L}^1$ complement previous work on zinc complexes of similar tripodal ligands with one phenolate and two pyridyl donors[13][14][15][16].

In terms of functionality and possibly catalytic activity the complexes derived from $\mathbf{L}^2$ seem to be better suited. In case of $\mathbf{L}^1$ phenolate bridging and consequently oligomerization seem to be so preferred that we could not obtain a soluble $[\mathbf{L}^1{\cdot}Zn]^+$ complex or a species $[\mathbf{L}^1{\cdot}Zn{-}\mathbf{S}]^+$ with a labile solvent ligand **S** like H_2O. On the other hand the oligomeric $[\mathbf{L}^2{\cdot}Zn]^+$ complexes **7** and **8** are soluble in methanol and/or water indicating the presence of species $[\mathbf{L}^2{\cdot}Zn{-}\mathbf{S}]^+$. If such a species is [L·Zn−OH] it should be a catalyst for the cleavage of esters or peptides[15][28]. Our subsequent work in this field will therefore focus on the solution chemistry of the $\mathbf{L}^2$·Zn complexes, their acid-base behaviour and their reactivity towards hydrolysable substrates.

This work was supported by the *Fonds der Chemischen Industrie*. We thank Dr. *W. Deck*, Dr. *B. Müller*, and *M. Tesmer* for spectra and X-ray work.

Experimental Section

General experimental methods and measuring techniques: see ref.[29]. The ligands $\mathbf{L}^1$[9] and $\mathbf{L}^2$[10] were prepared according to the published procedures.

1a: 400 mg (1.31 mmol) of $\mathbf{L}^1$ and 52 mg (1.31 mmol) of NaOH were dissolved in 40 ml of methanol. 177 mg (1.31 mmol) of $ZnCl_2$ in 10 ml of methanol were added, and the mixture was stirred for 2 h. Upon addition of 200 ml of ether the raw product **1a** was precipitated and filtered off. Recrystallization from methanol/water (1:1) yielded 218 mg (41%) **1a** as colourless crystals, m.p. 263°C (dec.). − $C_{19}H_{18}ClN_3OZn$ (405.2), calcd.: C 56.32, H 4.48, N 10.37, found: C 55.76, H 4.40, N 10.15. − ^{1}H NMR ($CDCl_3$): δ = 3.76 [s, 2 H, NCH_2Ph], 3.85 [d, J = 15.6 Hz, 2 H, NCH_2Py], 4.10 [d, J = 15.6 Hz, 2 H, NCH_2Py], 6.42−7.10 [m, 4 H, Ph], 7.29 [d, J = 7.8 Hz, 2 H, H_δ(Py)], 7.47 [dd, J = 5.4 Hz, 6.5 Hz, 2 H, H_β(Py)], 7.87 [dd, J = 7.8 Hz, 5.4 Hz, 2 H, H_γ(Py)], 9.45 [d, J = 6.5 Hz, 2 H, H_α(Py)]. − IR (KBr): $\tilde{\nu}$ = 1604s, 1479vs, 1438s, 1309vs.

1b: Like **1a** from 200 mg (0.66 mmol) of $\mathbf{L}^1$, 26 mg (0.66 mmol) of NaOH, and 149 mg (0.66 mmol) of $ZnBr_2$. Yield 229 mg (77%) of **1b**, colourless crystals, m.p. 259°C. − $C_{19}H_{18}BrN_3OZn$ (449.7), calcd.: C 50.75, H 4.03, N 9.34, found: C 48.80, H 3.88, N 9.06. − ^{1}H NMR ($CDCl_3$): δ = 3.73 [s, 2 H, NCH_2Ph], 3.85 [d, J = 15.8 Hz, 2 H, NCH_2Py], 4.08 [d, J = 15.8 Hz, 2 H, NCH_2Py], 6.39−7.08 [m, 4 H, Ph], 7.30 [d, J = 9.2 Hz, 2 H, H_δ(Py)], 7.43 [dd, J = 6.6 Hz, 5.2 Hz, 2 H, H_β(Py)], 7.86 [dd, J = 9.2 Hz, 6.6 Hz, 2 H, H_γ(Py)], 9.47 [d, J = 5.2 Hz, 2 H, H_α(Py)]. − IR (KBr): $\tilde{\nu}$ = 1605s, 1480vs, 1451m, 1433m, 1307s.

1c: Like **1a** from 200 mg (0.66 mmol) of $\mathbf{L}^1$, 26 mg (0.66 mmol) of NaOH, and 211 mg (0.66 mmol) of ZnI_2. Yield 268 mg (82%) of **1c**, colourless crystals, m.p. 168°C. − $C_{19}H_{18}IN_3OZn$ (496.7), calcd.: C 45.95, H 3.65, N 8.46, found: C 44.37, H 3.55, N 8.12. − ^{1}H NMR (DMSO): δ = 3.84 [s, 2 H, NCH_2Ph], 4.15 [s, 4 H, NCH_2Py], 6.39−7.06 [m, 4 H, Ph], 7.65−7.69 [m, 4 H, H_β(Py), H_δ(Py)], 8.17 [dd, J = 7.5 Hz, 6.6 Hz, 2 H, H_γ(Py)], 8.79 [d, J = 4.2 Hz, 2 H, H_α(Py)]. − IR (KBr): $\tilde{\nu}$ = 1609s, 1482vs, 1441m, 1293m, 1273s.

2a: 200 mg (0.74 mmol) of $\mathbf{L}^2$ and 30 mg (0.74 mmol) of NaOH were dissolved in 10 ml of methanol. 101 mg (0.74 mmol) of $ZnCl_2$ in 10 ml of methanol were added. A flask containing diethyl ether was then connected to the reaction flask by a glass tube. After 2 d, the product had precipitated and was filtered off. Recrystallization from methanol/water (1:1) yielded 96 mg (35%) **2a** as colourless microcrystals, m.p. 258°C (dec.). − $C_{15}H_{16}ClN_3O_2Zn$ (371.2), calcd.: C 48.54, H 4.34, N 11.32, found: C 48.07, H 4.16, N 10.95. − ^{1}H NMR (D_2O): δ = 2.15 [t, J = 7.1 Hz, 2 H, $CH_2(C_2)$], 3.89 [t, J = 7.1 Hz, 2 H, $CH_2(C_1)$], 4.23 [s, 4 H, NCH_2Py], 7.45−7.56 [m, 4 H, H_β(Py), H_δ(Py)], 8.00 [dd, J = 7.8 Hz, 7.7 Hz, 2 H, H_γ(Py)], 8.57 [d, J = 5.2 Hz, 2 H, H_α(Py)]. − IR (KBr): $\tilde{\nu}$ = 1605vs, 1441m, 1395m.

2b: Like **2a** from 150 mg (0.55 mmol) of $\mathbf{L}^2$, 22 mg (0.55 mmol) of NaOH, and 124 mg (0.55 mmol) of $ZnBr_2$. Yield 98 mg (43%) of **2b**, colourless microcrystals, m.p. 259°C (dec.). − $C_{15}H_{16}BrN_3O_2Zn$ (415.6), calcd.: C 43.35, H 3.88, N 10.11, found: C 42.43, H 3.81, N 9.79. − ^{1}H NMR (D_2O): δ = 1.99 [t, J = 6.9 Hz, 2 H, $CH_2(C_2)$], 2.75 [t, J = 6.9 Hz, 2 H, $CH_2(C_1)$], 4.12 [s, 4 H, NCH_2Py], 7.36−7.43 [m, 4 H, H_β(Py), H_δ(Py)], 7.87 [dd, J = 7.8 Hz, 7.7 Hz, 2 H, H_γ(Py)], 8.43 [d, J = 4.1 Hz, 2 H, H_α(Py)]. − IR (KBr): $\tilde{\nu}$ = 1600vs, 1440m, 1365m.

2c: Like **2a** from 200 mg (0.74 mmol) of $\mathbf{L}^2$, 30 mg (0.74 mmol) of NaOH, and 236 mg (0.74 mmol) of ZnI_2. Yield 282 mg (82%) of **2c**, colourless needles, m.p. 223°C (dec.). − $C_{15}H_{16}IN_3O_2Zn$ (462.6), calcd.: C 38.95, H 3.49, N 9.08, found: C 38.39, H 3.93, N 8.57. − ^{1}H NMR (D_2O): δ = 2.18 [t, J = 5.8 Hz, 2 H, $CH_2(C_2)$], 2.93 [t, J = 5.8 Hz, 2 H, $CH_2(C_1)$], 4.28 [s, 4 H, NCH_2Py], 7.50−7.60 [m, 4 H, H_β(Py), H_δ(Py)], 8.03 [dd, J = 7.8 Hz, 7.7 Hz, 2 H, H_γ(Py)], 8.60 [d, J = 4.8 Hz, 2 H, H_α(Py)]. − IR (KBr): $\tilde{\nu}$ = 1607s,1539vs, 1441m.

3: 200 mg (0.66 mmol) of $\mathbf{L}^1$ were dissolved in 10 ml of toluene. Diethylzinc (0.66 ml, 0.66 mmol) was added as a 1 M solution in hexane. Then, 62 mg (0.66 mmol) of phenol dissolved in 5 ml of toluene were added while stirring. Upon addition of the phenol the raw product **3** was precipitated and filtered off. Recrystallization from ethanol/water (1:1) yielded 162 mg (53%) of **3** as colourless crystals, m.p. 224°C. − $C_{25}H_{23}N_3O_2Zn$ (462.9), calcd.: C 64.87, H 5.01, N 9.08, found: C 63.74, H 4.98, N 8.97. − ^{1}H NMR ($CDCl_3$): δ = 3.68 [s, 2 H, NCH_2Ph], 3.70 [d, J = 15.8 Hz, 2 H, NCH_2Py], 4.00 [d, J = 15.8 Hz, 2 H, NCH_2Py], 6.42−7.23 [m, 13 H, Ph, H_β(Py), H_δ(Py), O-Ph], 7.72 [dd, J = 7.1 Hz, 6.3 Hz, 2 H, H_γ(Py)],

8.90 [d, J = 5.7 Hz, 2 H, H_α(Py)]. − IR (KBr): $\tilde{\nu}$ = 1607s, 1591s, 1478vs, 1454m, 1437m, 1308vs.

4a: 200 mg (0.66 mmol) of $\mathbf{L}^1$ were dissolved in 10 ml of toluene. $Zn[N(SiMe_3)_2]_2$ (255 mg, 0.66 mmol) were added. Then, 67 µl (73 mg, 0.66 mmol) of thiophenol dissolved in 5 ml of toluene were added while stirring. Upon addition of the thiophenol the raw product **4a** was precipitated and filtered off. Recrystallization from ethanol yielded 130 mg (41%) of **4a** as a colourless solid, m.p. 104°C. − $C_{25}H_{23}N_3OSZn$ (479.0), calcd.: C 62.70, H 4.84, N 8.77, found: C 57.38, H 4.17, N 7.91. − ^{1}H NMR ($CDCl_3$): δ = 3.67 [s, 2 H, NCH_2Ph], 3.78 [d, J = 15.7 Hz, 2 H, NCH_2Py], 3.98 [d, J = 15.7 Hz, 2 H, NCH_2Py], 6.30−7.73 [m, 15 H, Ph, H_β(Py), H_δ(Py), H_γ(Py), S-Ph], 9.02 [d, J = 5.4 Hz, 2 H, H_α(Py)]. − IR (KBr): $\tilde{\nu}$ = 1603s, 1478vs, 1437m, 1312s.

4b: Like **4a** from 200 mg (0.66 mmol) of $\mathbf{L}^1$, 255 mg (0.66 mmol) of $Zn[N(SiMe_3)_2]_2$, and 95 mg (0.66 mmol) of 4-chloro-thiophenol. Yield 149 mg (44%) of **4b** as colourless crystals, m.p. 142°C. − $C_{25}H_{22}ClN_3OSZn$ (513.4), calcd.: C 58.49, H 4.32, N 8.19, found: C 58.47, H 4.39, N 7.91. − ^{1}H NMR ($CDCl_3$): δ = 3.67 [s, 2 H, NCH_2Ph], 3.80 [d, J = 15.8 Hz, 2 H, NCH_2Py], 3.91 [d, J = 15.8 Hz, 2 H, NCH_2Py], 6.35−7.28 [m, 12 H, Ph, H_β(Py), H_δ(Py), S-Ph], 7.70 [dd, J = 9.5 Hz, 8.7 Hz, 2 H, H_γ(Py)], 9.00 [d, J = 5.5 Hz, 2 H, H_α(Py)]. − IR (KBr): $\tilde{\nu}$ = 1604s, 1477vs, 1438m, 1309s, 1093s.

5: Like **3** from 200 mg (0.66 mmol) of $\mathbf{L}^1$, 0.66 ml (0.66 mmol) of diethylzinc as a 1 M solution in hexane, and 164 mg (0.66 mmol) of diphenylphosphate. Yield 303 mg (74%) of **5** as colourless crystals, m.p. 91°C. − $C_{31}H_{28}N_3O_5PZn \cdot 2\ H_2O \cdot CH_3OH$ (618.9 + 36.0 + 32.0), calcd.: C 55.95, H 5.28, N 6.12, found: C 56.09, H 4.51, N 6.31. − ^{1}H NMR ($CDCl_3$): δ = 3.77 [s, 2 H, NCH_2Ph], 3.81 [d, J = 15.8 Hz, 2 H, NCH_2Py], 4.03 [d, J = 15.8 Hz, 2 H, NCH_2Py], 6.42−7.46 [m, 18 H, Ph, H_β(Py), H_δ(Py), P-O-Ph], 7.78 [dd, J = 7.6 Hz, 6.4 Hz, 2 H, H_γ(Py)], 9.04 [d, J = 4.4 Hz, 2 H, H_α(Py)]. − ^{31}P NMR ($CDCl_3$): δ = −11.63. − IR (KBr): $\tilde{\nu}$ = 1608s, 1595s, 1485vs, 1453m, 1437m, 1296s, 1267s, 1205s, 1104vs.

6: 200 mg (0.66 mmol) of $\mathbf{L}^1$ were dissolved in 10 ml of methylene chloride. 37 mg (0.66 mmol) of KOH in 5 ml of methanol were added, and the mixture was stirred for 10 min. Then, 244 mg (0.66 mmol) of $Zn(ClO_4)_2 \cdot 6\ H_2O$ in 5 ml of methanol were added while stirring. The solution became cloudy and was then refluxed for 30 min. After this, another 37 mg (0.66 mmol) of KOH in 5 ml methanol were added and the solution stirred overnight. The precipitate formed was removed by filtration. The filtrate was evaporated to dryness . Recrystallization from chloroform yielded 90 mg (23%) of **6** as colourless crystals, m.p. 274°C (dec.). − $C_{19}H_{18}ClN_3O_5Zn \cdot CHCl_3$ (469.2 + 119.4), calcd.: C 40.81, H 3.25, N 7.14, found: C 40.23, H 3.16, N 6.93. − ^{1}H NMR (DMSO): δ = 3.76 [s, 2 H, NCH_2Ph], 4.08 [s, 4 H, NCH_2Py], 6.36−6.99 [m, 4 H, Ph], 7.58−7.62 [m, 4 H, H_β(Py), H_δ(Py)], 7.91 [dd, J = 7.9 Hz, 7.7 Hz, 2 H, H_γ(Py)], 8.70 [d, J = 4.3 Hz, 2 H, H_α(Py)]. − IR (KBr): $\tilde{\nu}$ = 1611s, 1485s, 1445m, 1274m, 1090vs.

7: 200 mg (0.74 mmol) of $\mathbf{L}^2$ and 30 mg (0.74 mmol) of NaOH were dissolved in 10 ml of methanol. 244 mg (0.74 mmol) of $Zn(ClO_4)_2 \cdot 6\ H_2O$ in 10 ml of methanol were added, and the mixture was stirred for 10 min. The solution became cloudy and after 5 min, **7** precipitated as a white solid. Recrystallization from water yielded 171 mg (53%) of **7** as colourless microcrystals, m.p. 296°C (dec.). − $C_{15}H_{16}ClN_3O_6Zn$ (435.2), calcd.: C 41.40, H 3.71, N 9.66, found: C 41.14, H 3.49, N 9.56. − ^{1}H NMR (D_2O): δ = 2.10 [t, J = 7.0 Hz, 2 H, $CH_2(C_2)$], 2.85 [t, J = 7.0 Hz, 2 H, $CH_2(C_1)$], 4.19 [s, 4 H, NCH_2Py], 7.40−7.50 [m, 4 H, H_β(Py), H_δ(Py)], 7.96 [dd, J = 7.9 Hz, 7.7 Hz, 2 H, H_γ(Py)], 8.51 [d, J = 5.0 Hz, 2 H, H_α(Py)]. − IR (KBr): $\tilde{\nu}$ = 1607s, 1548s 1484m, 1441m, 1088vs.

8: 200 mg (0.74 mmol) of $\mathbf{L}^2$ and 30 mg (0.74 mmol) of NaOH were dissolved in 10 ml of methanol.193 mg (0.74 mmol) of

Table 1. Crystallographic details

	1a	**5**	**6**	**8**
formula	$C_{19}H_{18}ClN_3OZn$	$C_{31}H_{29}N_3O_5PZn \cdot CH_3OH \cdot 2\ H_2O$	$C_{38}H_{36}Cl_2N_6O_{10}Zn_2 \cdot 2\ CHCl_3$	$C_{15}H_{16}N_4O_5Zn \cdot CH_3OH$
mol. mass	405.18	686.98	1177.10	429.73
cryst. from	CH_2Cl_2/hexane	CH_3OH/H_2O	$CHCl_3$	CH_3OH
crystal size [mm]	0.3 × 0.5 × 1.0	0.4 × 0.5 × 0.5	0.3 × 0.4 × 0.5	0.5 × 0.6 × 0.6
space group	$P-1$	$P-1$	$P-1$	$P2_1/n$
Z	2	2	2	4
a [Å]	6.835(1)	9.503(2)	12.641(5)	9.968(2)
b [Å]	12.586(2)	12.855(3)	14.085(8)	7.866(2)
c [Å]	13.168(2)	13.453(3)	15.555(11)	23.089(5)
α [°]	107.26(1)	90.87(3)	89.92(5)	90
β [°]	101.38(1)	93.49(3)	68.06(5)	94.79(3)
γ [°]	102.32(1)	106.90(3)	66.09(4)	90
V [Å^3]	1014.8(3)	1568.6(6)	2311(2)	1804.0(7)
d(calc.) [g·cm^{-3}]	1.33	1.45	1.69	1.58
temp. (K)	293	293	183	293
µ(Mo-$K\alpha$) [mm^{-1}]	1.35	0.89	1.56	1.40
Θ range [°]	3.7−26.0	2.4−26.1	2.7−26.0	2.7−26.0
hkl range	h: −8 to 8 k: −15 to 14 l: 0 to 16	h: −11 to 0 k: −15 to 15 l: −16 to 16	h: −15 to 14 k: −17 to 0 l: −19 to 19	h: 0 to 12 k: 0 to 9 l: −28 to 28
refl. measd.	4152	6556	9423	3735
indep. refl.	3972	6164	9035	3524
obs. refl. [$I>2\sigma(I)$]	3392	4621	6879	2881
parameters	226	406	595	244
refl. refined	3972	4621	9021	3524
R (obs. refl.)	0.065	0.053	0.051	0.040
R (all refl.)	0.211	0.163	0.175	0.119
min. / max. residual el. density [e·Å^{-3}]	+1.1 / −1.2	+0.8 / −0.8	+1.0 / −1.1	+1.0 / −0.7

$Zn(NO_3)_2 \cdot 4\ H_2O$ in 10 ml of methanol were added. A flask containing diethyl ether was then connected to the reaction flask by a glass tube. After 2 d, crystallization yielded 191 mg (65%) of **8** as colourless crystals, m.p. 238°C (dec.). − $C_{15}H_{16}N_4O_5Zn \cdot CH_3OH$ (397.7 + 32.0), calcd.: C 44.72, H 4.69, N 13.04, found: C 43.24, H 4.13, N 13.36. − ^1H NMR (D_2O): δ = 2.17 [t, J = 5.6 Hz, 2 H, $CH_2(C_2)$], 3.91 [t, J = 5.6 Hz, 2 H, $CH_2(C_1)$], 4.27 [s, 4 H, NCH_2Py], 7.52−7.59 [m, 4 H, H_β(Py), H_δ(Py)], 8.03 [dd, J = 7.7 Hz, 7.6 Hz, 2 H, H_γ(Py)], 8.59 [d, J = 4.8 Hz, 2 H, H_α(Py)]. − IR (KBr): $\tilde{\nu}$ = 1609s, 1541m, 1384vs, 1363vs.

Structure Determinations[30]: Crystals were obtained from the reaction solutions. Diffraction data were recorded with the ω/2θ technique on a Nonius CAD4 diffractometer fitted with a molybdenum tube (K_α, λ = 0.7107 Å) and a graphite monochromator. No absorption corrections were applied. The structures were solved with direct methods and refined anisotropically with the SHELX program suite[31]. Hydrogen atoms were included with fixed distances and isotropic temperature factors 1.2 times those of their attached atoms. Parameters were refined against F^2. The R values are defined as $R_1 = \Sigma|F_o - F_c|/\Sigma F_o$ and $wR_2 = [\Sigma[w(F_o^2 - F_c^2)^2/\Sigma[w(F_o^2)^2]]^{1/2}$. Drawings were produced with SCHAKAL[32]. Table 1 lists the crystallographic data.

☆ Dedicated to Prof. *H. Nöth* on the occasion of his 70th birthday.

[1] cf. *Comprehensive Coordination Chemistry* (Eds.: G. Wilkinson, R. D. Gillard, J. A. McCleverty), Pergamon Press, Oxfrod, **1987**, vol. 5. *Comprehensive Organometallic Chemistry* (Eds.: G. Wilkinson, F. G. A. Stone, E. W. Abel), Pergamon Press, Oxfrod, **1982**, vol. 2.

[2] S. Trofimenko, *Chem. Rev.* **1993**, *93*, 943−980.

[3] K. Weis, H. Vahrenkamp, *Inorg. Chem.* **1997**, *36*, 5592−5596, and references cited therein.

[4] G. Anderegg, F. Wenk, *Helv. Chim. Acta* **1967**, *50*, 2330−2332.

[5] G. Anderegg, E. Hubmann, N. G. Podder, F. Wenk, *Helv. Chim. Acta* **1977**, *60*, 123−140. N. N. Murthy, K. D. Karlin, *J. Chem. Soc. Chem., Commun.* **1993**, 1236−1238. H. Adams, N. A. Bailey, D. E. Fenton, Q.-Y. He, *J. Chem. Soc., Dalton Trans.* **1997**, 1533−1539. C. S. Allen, C.-L. Chuang, M. Cornebise, J. W. Canary, *Inorg. Chim. Acta* **1995**, *239*, 29−37. Z. W. Mao, Q. W. Hang, W. X. Tang, S. X. Liu, Z. M. Wang, J. L. Huang, *Polyhedron* **1996**, *15*, 321−325.

[6] D. D. Cox, S. J. Benkovic, L. M. Bloom, F. C. Bradley, M. J. Nelson, L. Que, D. E. Wallick, *J. Am. Chem. Soc.* **1988**, *110*, 2026−2032.

[7] A. Abufarag, H. Vahrenkamp, *Inorg. Chem.* **1995**, *34*, 2207−2216.

[8] P. M. Schaber, J. C. Fettinger, M. R. Churchill, D. Nalewajek, K. Fries, *Inorg. Chem.* **1988**, *27*, 1641−1646. G. Alzuet, L. Casella, A. Perotti, J. Borras, *J. Chem. Soc., Dalton Trans.* **1994**, 2347−2351. R. Luckay, T. E. Chantson, J. H. Reibenspies, R. D. Hancock, *J. Chem. Soc., Dalton Trans.* **1995**, 1363−1367. M. L. Turoneck, P. Moore, H. J. Clase, N. W. Alcock, *J. Chem. Soc., Dalton Trans.* **1995**, 3659−3666.

[9] S. Yan, L. Que, *J. Am. Chem. Soc.* **1988**, *110*, 5222−5224. S. Yan, X. Pan, L. F. Taylor, J. H. Zhang, C. J. O′Connor, D. Britton, O. P. Anderson, L. Que, *Inorg. Chim. Acta* **1996**, *243*, 1−8.

[10] A. Hazell, K. B. Jensen, C. J. McKenzie, H. Toftlund, *J. Chem. Soc., Dalton Trans.* **1993**, 3249−3257.

[11] D. Karlin, B. I. Cohen, J. C. Hayes, A. Farook, J. Zubieta, *Inorg. Chem.* **1987**, *26*, 147−153.

[12] S. Menage, L. Que, *New J. Chem.* **1991**, *15*, 431−438.

[13] H. Adams, N. A. Bailey, I. K. Campbell, D. E. Fenton, Q.-Y. He, *J. Chem. Soc., Dalton Trans.* **1996**, 2233−2237.

[14] H. Adams, N. A. Bailey, C. O. Rodriguez de Barbarin, D. E. Fenton, Q.-Y. He, *J. Chem. Soc., Dalton Trans.* **1995**, 2323−2331.

[15] H. Adams, N. A. Bailey, D. E. Fenton, Q.-Y. He, *J. Chem. Soc., Dalton Trans.* **1996**, 2857−2865.

[16] C. O. Rodriguez de Barbarin, N. A. Bailey, D. E. Fenton, Q.-Y. He, *J. Chem. Soc., Dalton Trans.* **1997**, 161−166.

[17] W. Bode, F. X. Gomis-Rüth, R. Huber, R. Zwilling, W. Stöcker, *Nature* **1992**, *358*, 164−167.

[18] E. E. Kim, H. W. Wyckoff, *J. Mol. Biol.* **1991**, *218*, 449−464.

[19] U. Hartmann, R. Gregorzik, H. Vahrenkamp, *Chem. Ber.* **1994**, *127*, 2123−2127. R. Gregorzik, U. Hartmann, H. Vahrenkamp, *Chem. Ber.* **1994**, *127*, 2117−2122.

[20] K. Yoon, G. Parkin, *J. Am. Chem. Soc.* **1991**, *113*, 8414−8418. F. Hartmann, W. Kläui, A. Kremer-Aach, D. Mootz, A. Strerath, H. Wunderlich, *Z. anorg. allg. Chem.* **1993**, *619*, 2071−2076.

[21] R. J. Sime, R. L. Dodge, A. Zalkin, D. H. Templeton, *Inorg. Chem.* **1971**, *10*, 537−541.

[22] K. Weis, M. Rombach, M. Ruf, H. Vahrenkamp, *Eur. J. Inorg. Chem.* **1998**, 263.

[23] K. Schepers, B. Bremer, B. Krebs, G. Henkel, E. Althaus, B. Mosel, W. Müller-Warmuth, *Angew. Chem.* **1990**, *102*, 582−584; *Angew. Chem. Int. Ed. Engl.* **1990**, *29*, 531−533. S. Ohtsuka, M. Kodera, K. Motoda, M. Ohba, H. Okawa, *J. Chem. Soc. Dalton Trans.* **1995**, 2599−2604.

[24] P. Chaudhuri, C. Stockheim, K. Wieghardt, W. Deck, R. Gregorzik, H. Vahrenkamp, B. Nuber, J. Weiss, *Inorg. Chem.* **1992**, *31*, 1451−1457.

[25] We found one reference for this type of bridging between zinc and magnesium or calcium, respectively: W. Clegg, I. R. Little, B. P. Straughan, *Inorg. Chem*. **1988**, *27*, 1916−1923.

[26] The Cambridge Crystallographic Data File yields 94 structures with carboxylate or carbonate bridges between two zinc ions.

[27] C. Oldham in *Comprehensive Coordination Chemistry* (Eds.: G. Wilkinson, R. D. Gillard, J. A. McCleverty), Pergamon Press, Oxford, **1987**, vol. 2, pp. 435−456.

[28] S. H. Gellmann, R. Petter, R. Breslow, *J. Am. Chem. Soc.* **1986**, *108*, 2388−2395.

[29] M. Förster, R. Burth, A. K. Powell, T. Eiche, H. Vahrenkamp, *Chem. Ber.* **1993**, *126*, 2643−2648.

[30] The crystallographic data of the structures described in this paper were deposited with the Cambridge Crystallographic Data Centre as "supplementary publication no. CCDC-100944". Copies of these data are available free of charge from the following address: The Director, CCDC, 12 Union Road, GB-Cambridge CB2 1EZ (Telefax: Int. +44-12 23/3 36 0 33; E-mail: deposit@chemcrys.cam.ac.uk).

[31] G. M. Sheldrick, *SHELX-86 and SHELXL-93*, Programs for Crystal Structure Determination, Universität Göttingen, **1986** and **1993**.

[32] E. Keller, Program *SCHAKAL*, Universität Freiburg, **1993**.

[97324]

Supersilyl Compounds of Phosphorus, IV[1]
Silicon Compounds, 118[2]

The Triphosphide $(t\mathrm{Bu_3Si})_2\mathrm{P_3Na}$: Formation, X-ray and Ab initio Structure Analyses, Protonation and Oxidation to Triphosphane $(t\mathrm{Bu_3Si})_2\mathrm{P_3H}$ and Hexaphosphanes $(t\mathrm{Bu_3Si})_4\mathrm{P_6}$☆

Nils Wiberg*[a], Angelika Wörner[a], Hans-Wolfram Lerner[a], Konstantin Karaghiosoff[a][+], Dieter Fenske[b][++], Gerhard Baum[b][++], Alk Dransfeld[c][+++], and Paul von Ragué Schleyer[c][+++]

Institut für Anorganische Chemie der Universität München[a], Meiserstraße 1, D-80333 München, Germany

Institut für Anorganische Chemie der Universität Karlsruhe[b], Engesserstraße, Geb. Nr. 30.45, D-76128 Karlsruhe, Germany

Institut für Organische Chemie der Universität Erlangen[c], Henkestraße 42, D-91054 Erlangen, Gemany

Received January 15, 1998

Keywords: Silicon / Phosphorus / Oligophosphides and -phosphanes / NMR spectra / X-ray structure analysis / Ab initio calculations

The violet THF adduct $(t\mathrm{Bu_3Si})_2\mathrm{P_3Na(THF)_4}$ (**1a**) of the triphosphide $(t\mathrm{Bu_3Si})_2\mathrm{P_3Na}$ (**1**) is prepared, (i) by protolysis of the tetraphosphide $(t\mathrm{Bu_3Si})_2\mathrm{P_4Na_2}$ (**2**) with an equimolar amount of $\mathrm{CF_3CO_2H}$ in THF (transformation of **2** into **1**), (ii) by the reaction of $t\mathrm{Bu_3SiNa}$ and the oligophosphane $(t\mathrm{Bu_3SiP_3})_n$ in THF (building-down of P_n), and (iii) by the action of $t\mathrm{Bu_3SiNa}$ on $\mathrm{PCl_3}$ in THF (building-up of P_n). According to X-ray structural analysis, the SiPPPSi skeleton of the anionic part $[t\mathrm{Bu_3SiPPPSi}t\mathrm{Bu_3}]^-$ of **1a** is W-shaped with two P–P $1^1/_2$ bonds; in addition, **1a** contains a planar deltoid $\mathrm{P_3Na}$ backbone with the 4 THF molecules coordinated to Na. The protolysis of **1a** leads to cyclotriphosphane $(t\mathrm{Bu_3Si})_2\mathrm{P_3H}$ (**11**), and the oxidation of **1a** leads to 1,1′-bicyclotriphosphane $(t\mathrm{Bu_3Si})_2\mathrm{P_3}$–$\mathrm{P_3}(\mathrm{Si}t\mathrm{Bu_3})_2$ (**12**) as the main product and bicyclo[3.1.0]hexaphosphane $(t\mathrm{Bu_3Si})_4\mathrm{P_6}$ (**13**) as an isomer of **12**. The structures of **11**, **12**, and **13** as well as the structure of **1a** have been unambiguously determined by ^{31}P-NMR studies. Ab initio structure and energy calculations show that the acyclic $\mathrm{P_3H_2^-}$ with allylic conjugation and P–P $1^1/_2$ bonds is thermodynamically more stable than the cyclic isomer whereas, in contrast, the neutral compound $\mathrm{P_3H_3}$ prefers the cyclic form. The exceptional downfield shift of the NMR signal of the central phosphorus in **1a** is in agreement with DFT NMR calculations for a model compound $[\mathrm{H_3SiPPPSiH_3}]\mathrm{Na}$ with P–P $1^1/_2$ bonds.

While nitrogen hydrides of the formula $\mathrm{N}_n\mathrm{H}_n$ and their derivatives have an acyclic structure with a double bond, phosphorus hydrides $\mathrm{P}_n\mathrm{H}_n$ and their derivatives show, in accordance with the double-bond rule, cyclic structures without a double bond[3]. This is demonstrated by a comparison of the structures of $\mathrm{N_3H_3}$ and $\mathrm{N_4H_4}$ with those of $\mathrm{P_3H_3}$ and $\mathrm{P_4H_4}$, (see Scheme 1).

Scheme 1

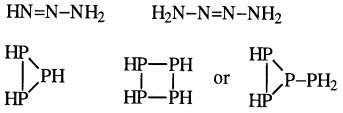

In contrast the tendency of phosphanes $\mathrm{P}_n\mathrm{H}_n$ to form unsaturated acyclic structures increases after deprotonation, because the negative charges of the phosphides obtained may be better stabilized by a π system containing a phosphorus chain. This is suggested by our studies in connection with the triphosphide $(t\mathrm{Bu_3Si})_2\mathrm{P_3Na}$ (see Scheme 2) and the tetraphosphide $(t\mathrm{Bu_3Si})_2\mathrm{P_4Na_2}$ (cf. refs.[4][5]) which have the structures **1** (disupersilyltriphosphenide) and **2** (disupersilyltetraphosphenediide), respectively.

Scheme 2

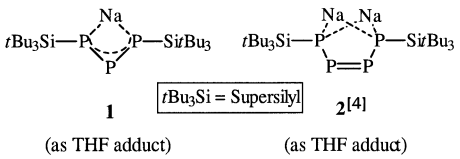

The unsaturated cluster anion $\mathrm{R_2P_3^-}$ with substituents R which are sterically constrained (such as supersilyl $t\mathrm{Bu_3Si}$[5]) is readily formed. Thus, **2** converts into **1** under suitable conditions (see below). The compounds $\mathrm{Mes^*{}_2P_2ELi}$ (Mes* = Supermesityl, E = P, As) and $(t\mathrm{Bu_3Si})_2\mathrm{E_3Na}$ (E = N, As) were both synthesized by Jutzi et al.[6] and this

[+] Simulation of NMR spectra.
[++] X-ray structure analysis.
[+++] Ab initio structure and NMR calculations.

 © WILEY-VCH Verlag GmbH, D-69451 Weinheim, 1998 1434–1948/98/0606–0833 $ 17.50+.50/0

group[7][8]. Finally the anions $[(Me_3Si)_2CPPPC(SiMe_3)_2]^-$[9a] and $[RPPPR]^-$ (RR = $-CH_2CH_2-$ and $-CHPhCHPh-$)[9b] containing a P_3 skeleton with a π system were prepared as alkali metal salts.

In this publication we deal with the syntheses and the structure of **1,** as well as with the protolysis and oxidation of the compound, which proceed by the formation of the triphosphane $(tBu_3Si)_2P_3H$ and two isomers of hexaphosphane $(tBu_3Si)_4P_6$, respectively. In addition, the question concerning the relative stabilities of cyclic and acyclic P_3H_3 and $P_3H_2^-$ is answered by ab initio calculations.

Formation of $(tBu_3Si)_2P_3Na$ (1)

As has already been mentioned, **1** is prepared by transformation of **2**. In addition, **1** may be formed from supersilylphosphanes $(tBu_3Si)_mP_n$ or supersilyldihalogenephosphanes tBu_3SiPX_2 by building-down or building-up the phosphorus framework. In the latter cases, supersilyl sodium tBu_3SiNa in tetrahydrofuran (THF) serves as the reaction partner. Details of the syntheses of **1** are discussed below. In this connection, not only **2**, but also the phosphides **3** and **4** as well as the phosphanes **5**−**8** play a role (see Scheme 3).

Scheme 3

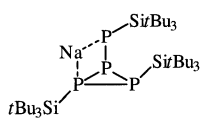

3[5]
(as THF adduct)

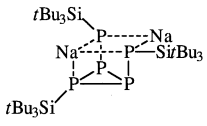

4 [5, 10]
(as THF adduct)

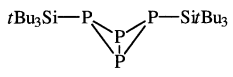

5 [4, 11]

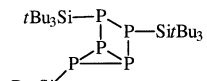

6 [10]

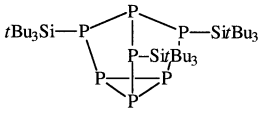

7 [11]

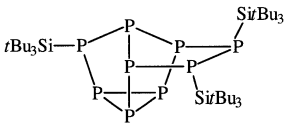

8 [5]

Transformation of 2

To convert the tetraphosphide **2**, which is easily prepared from P_4 and tBu_3SiNa in THF[4], into the triphosphide **1**, the former is protonated by equimolar amounts of a strong acid (CF_3CO_2H or CF_3SO_3H) in THF at −78°C. Then, by warming up the reaction mixture to room temp., **1** and tBu_3SiPH_2 are obtained according to Eq. 1.

$$3\ \mathbf{2} \xrightarrow[-4Na^+]{+4H^+} 2\ \mathbf{1} + 2\,tBu_3SiPH_2 \qquad (1)$$

In fact, **1** is produced simultaneously with the pentaphosphide **4** as well as oligophosphanes $(tBu_3SiP_3)_n$ (see below); in addition, the starting material **2** remains unreacted (**1**, **2**, and **4** exist in the molar ratio 2:1:1, increasing amounts of acid lead to a decrease in the amount of **2** and also of **1**[5][10]). As **1** cannot easily be separated from the other products, reaction (1) is less suitable for its preparation.

In the weak acid acetonitrile, **2** quickly transforms according to Eq. 1 ($NaCH_2CN$ may be another product), but the solutions obtained are unstable and after some weeks contain tBu_3SiPH_2 as the one and only soluble phosphorus compound.

Building-Down of Phosphorus Clusters

The reaction of oligophosphanes $(tBu_3SiP_3)_n$ (among others **8**[5]) with *n*-fold molar amounts of tBu_3SiNa is particularly suitable for the synthesis of **1**. In this way, the triphosphide **1** is obtained as the only product according to Eq. 2. The oligophosphanes, on the other hand, are prepared from **2** and a twofold molar amount of a strong acid (CF_3SO_3H) in pentane: $\mathbf{2} + 2H^+ \rightarrow 1/n\ (tBu_3SiP_3)_n + tBu_3SiPH_2$.

$$^1/_n\ (tBu_3SiP_3)_n \text{ (among others } \mathbf{8}) + tBu_3SiNa \rightarrow \mathbf{1} \qquad (2)$$

Reaction (2) demonstrates, as does reaction (1), the high tendency for the formation of **1**. The same holds for the reaction shown in (3): a twofold molar amount of tBu_3SiNa degrades the heptaphosphane **7** (which is easily prepared from P_4 and $tBu_3Si-SitBu_3$ in THF or toluene at 100°C together with the tetraphosphane **5**[11]) into the triphosphide **1** and the tetraphosphide **3**. The latter compound is also quantitatively obtained by reaction of the tetraphosphane **5** with equimolar amounts of tBu_3SiNa in THF[5].

$$\mathbf{7} + 2\ tBu_3SiNa \rightarrow \mathbf{1} + \mathbf{3} \qquad (3)$$

In addition, it is worth noting that the pentaphosphane **6** is transformed by tBu_3SiNa into the triphosphide **1** together with other phosphorus containing substances[10].

Building-Up of Phosphorus Clusters

To synthesize **1** by building-up the phosphorus chain, PCl_3 in pentane is slowly added dropwise to a solution of a threefold molar amount of tBu_3SiNa in THF, cooled to −78°C. While warming up the solution to room temp., the starting materials react according to (4a). In fact, **1** is produced simultaneously with the tetraphosphide **3**, the pentaphosphide **4** as well as some mono- and diphosphides (**1**, **3**, **4**, and the other phosphides are formed in the molar ratio 10:5:3:3).

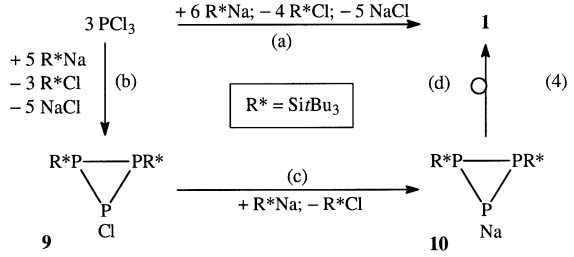

An insight into the formation pathway of **1** is given by the reaction of PCl_3 with an equimolar amount of tBu$_3$SiNa, the products of which are some chlorine-free and some chlorine-containing supersilylphosphanes[5]; this will be thoroughly discussed elsewhere[12]. Obviously, the chlorine containing compound **9** plays an important role in the building-up of **1**, as it may react with tBu$_3$SiNa with exchange of Cl for Na (Eq. 4c). An isomerization of the phosphide **10** obtained in this way leads to **1** (Eq. 4d).

The formation of **9**, summarized by Eq. 4b, may be interpreted as follows: As a first reaction product, tBu$_3$SiPCl$_2$ is formed from PCl_3 and tBu$_3$SiNa by exchange of Cl^- for tBu$_3$Si$^-$. For steric reasons supersilyldichlorophosphane does not undergo any further supersilanidation[5]. Instead, with the cooperation of PCl_3 and tBu$_3$SiNa, it enters a building-up of phosphorus clusters which proceeds according to the reactions formulated in Eq. 5[5].

$$>\!P\text{–}Cl + Cl\text{–}P< \xrightarrow[-\,t\mathrm{Bu_3SiCl}]{+\,t\mathrm{Bu_3SiNa}} >\!PNa + Cl\text{–}P< \qquad (5)$$

$$>\!PNa + Cl\text{–}P< \xrightarrow{-\mathrm{NaCl}} >\!P\text{–}P<$$

Hereafter, tBu$_3$SiPCl$_2$, PCl_3, and tBu$_3$SiNa first of all may react according to tBu$_3$SiPCl$_2$ + tBu$_3$SiNa → tBu$_3$Si-PClNa + tBu$_3$SiCl and 2 tBu$_3$SiPClNa + PCl_3 → tBu$_3$Si-PCl−PCl−PClSitBu$_3$ + 2 NaCl under formation of trichlorodisupersilyltriphosphane, which then converts according to Eq. 5 into **9**.

Characterization and Structure of (tBu$_3$Si)$_2$P$_3$Na(THF)$_4$ (1a)

If a solution of 2.8 mmol of **1**, prepared by reaction of (tBu$_3$SiP$_3$)$_n$ with tBu$_3$SiNa in 6 ml of THF (cf. Eq. 2), is concentrated to 2 ml and mixed with 2 ml of pentane, then over several days, deep violet crystals of the THF adduct (tBu$_3$Si)$_2$P$_3$Na(THF)$_4$ (**1a**) of the triphosphide **1** may be obtained. These are extremely sensitive to air and moisture but comparatively stable thermally. However, the tendency of **1** to crystallize from THF is quite low and exchanging THF for another solvent is not advisable, since **1** decomposes when the THF is removed.

A suitable crystal of the phosphide **1a** selected from many unsuitable crystals was investigated by X-ray structure analysis. The view of the molecule in the crystal (orthorhombic), all atomic positions of which seem to be splitted, is shown in Figure 1. As can be clearly seen, the three P atoms and the Na atom in **1a** occupy the edges of a planar deltoid (P−P−P = 104.2, P−P−Na = 95.2, P−Na−P = 64.3°; sum of the angles of the mean values of the split positions is 358.9°). For each of the outer P atoms a planar surrounding may be outlined, consisting of one P, one Si, and one Na atom, the central P atom has two P atoms as neighbours forming an obtuse angle and the Na atom is coordinated by two P and four O atoms forming a distorted octahedron with a sharp P−Na−P angle. The O atoms are each coordinated to one Na and two C atoms. The P−P distances have a mean value of 2.10 Å, in between those found for P−P single bonds (around 2.20 Å) and those for P−P double bonds (around 2.00 Å)[3]. As can be seen from Table 1, the two P−P distances and the two P−P−Na angles are indeed slightly different [P1−P2 = 2.12, P1−P3 = 2.07 Å; P1−P2−Na = 96.6, P1−P3−Na = 93.7° (mean values); an analogous situation is also observed for the two N−N bonds and the N−N−Na angle of (tBu$_3$Si)$_2$-N$_3$Na(THF)$_2$ in the crystal[13]]. The distance of the sodium atom to the outer phosphorus atom showing the longer P−P bond is shorter than the distance to the outer phosphorus atom showing the shorter −P bond [P2−Na = 3.05, P3−Na = 3.18 Å (mean values)].

As shown by the X-ray structure analysis, the anionic W-shaped part of **1a** with two P−P $1^1/_2$ bonds represents a triphosphaallylic anion, the bonding situation of which can be described by a resonance formula with two limiting structures, as is shown in Eq. 6 (the triphosphenide Mes$_2$*-P$_3$Li was not investigated by means of X-ray diffraction; however according to ^{31}P-NMR it also has an acyclic structure[6]).

The ^{31}P{^{1}H}-NMR spectrum of the anion in **1a** shows two signals with the splitting pattern of an AX$_2$ spin system in the range typical for the unsaturated twocoordinate phosphorus atom in diphosphenes[14], and in a range which is possible for an unsaturated anionic phosphorus atom[9b] (Figure 2). This is in accord with the *trans-trans* configuration of the anion, as found in the crystal. An isomeric anion with *trans-cis* configuration is, according to the NMR spectra, not present in the C_6D_6 solution, obviously as a consequence of the steric crowding of the supersilyl groups; an isomer with *cis-cis* configuration is not possible for steric reasons and can be definitely ruled out from the signal pattern in the ^{29}Si{^{1}H}-NMR spectrum, which suggests a large $^2J_{PP}$ coupling constant. (In the case of Mes*$_2$P$_3$Li with the less bulky supermesityl substituents, the compound exists as a mixture of the *cis-trans* and the *trans-trans* isomer[6].)

Protolysis and Oxidation of (tBu$_3$Si)$_2$P$_3$Na (1)

While the protolysis of the tetraphosphide **2** with trifluoroacetic acid in THF, as reported elsewhere[4][5], proceeds nonuniformly with the formation of a number of phosphanes and phosphides containing supersilyl groups, the triphosphide **1** is protolyzed with CF_3CO_2H in THF in a comparatively uniform reaction to form the ring compound **11**. The triphosphene tBu$_3$Si−P=P−PH−SitBu$_3$, which is expected to be the primary product of the protolysis of **1**, is presumably thermodynamically as well as kinetically unstable with respect to the cyclotriphosphane **11**. (In contrast, as product of the protolysis of Mes*$_2$P$_3$Li the unsaturated compound Mes*−P=P−PH−Mes* was obtained[6].)

The oxidation of **2** with tetracyanoethylene in THF proceeds, as reported[4][5], uniformly with the formation of the bicyclotetraphosphane **5**[4], i.e. with retention of the P$_4$ skeleton. On the other hand, the action of TCNE on the triphosphide **1** in THF leads to a doubling of the P$_3$ skeleton: the isomeric hexaphosphanes **12** and **13,** with connected and anellated rings of phosphorus atoms, respectively, are

Figure 1. Molecular structure of $(t\mathrm{Bu_3Si})_2\mathrm{P_3Na(THF)_4}$ (**1a**) in the crystal; top: atom numbering used; bottom: splitting of positions of atoms found (SCHAKAL plot; atoms drawn with arbitrarily chosen atom radii; without H atoms)[a]

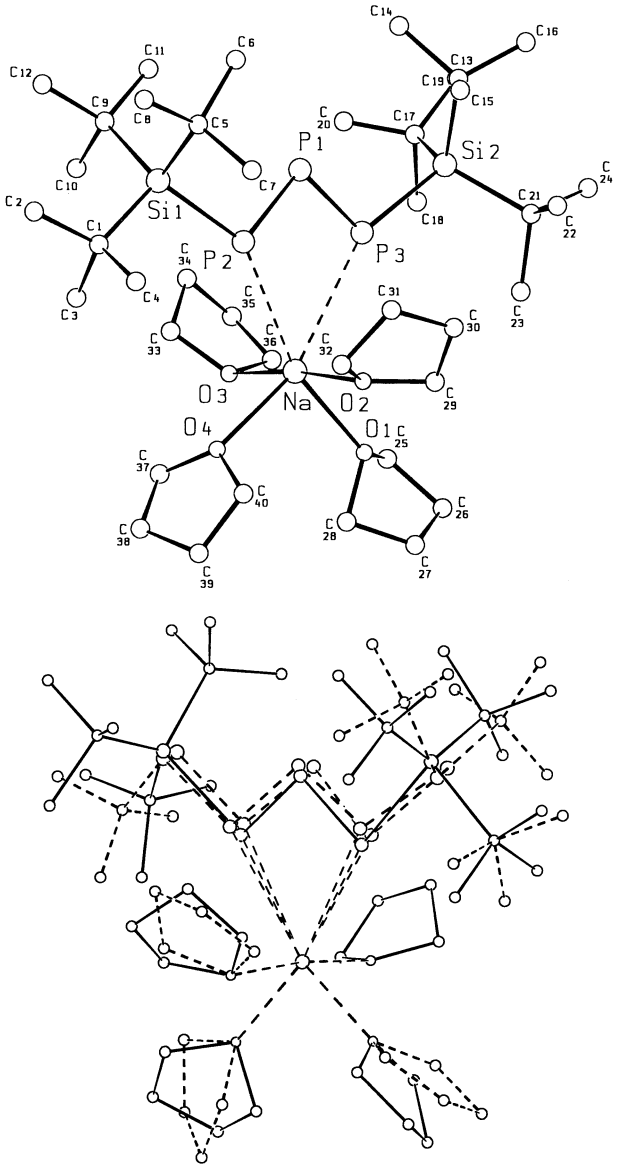

[a] Selected distances [Å] and angles [°] of the molecular structure of **1a** in the crystal with the standard deviations in units of the last significant position in parentheses (all positions of the P and Si atoms seem to be triply split): P(1A)−P(2A) 2.09(2), P(1B)−P(2B) 2.12(2), P(1C)−P(2C) 2.15(2), P(1A)−P(3A) 2.14(3), P(1B)−P(3B) 2.06(2), P(1C)−P(3C) 2.02(2), P(2A)−Si(1A) 2.47(2), P(2B)−Si(1B) 2.26(1), P(2C)−Si(1C) 2.23(2), P(3A)−Si(2A) 2.37(3), P(3B)−Si(2B) 2.26(1), P(3C)−Si(2C) 2.23(2), P(2A)−Na 2.92(2), P(2B)−Na 3.03(1), P(2C)−Na 3.19(2), P(3A)−Na 3.07(2), P(3B)−Na 3.20(1), P(3C)−Na 3.27(2), O(1)−Na 2.349(8), O(2)−Na 2.35(1), O(3)−Na 2.37(1), O(4)−Na 2.359(6); P(2A)−P(1A)−P(3A) 104.6(11), P(2B)−P(1B)−P(3B) 101.3(7), P(2C)−P(1C)−P(3C) 106.6(9), P(1A)−P(2A)−Na 96.2(8), P(1B)−P(2B)−Na 99.7(5), P(1C)−P(2C)−Na 93.9(6), P(1A)−P(3A)−Na 91.0(7), P(1B)−P(3B)−Na 96.1(5), P(1C)−P(3C)−Na 94.1(7), Si(1A)−P(2A)−Na 167.4(7), Si(1B)−P(2B)−Na 150.1(5), Si(1C)−P(2C)−Na 148.9(8), Si(2A)−P(3A)−Na 162.0(12), Si(2B)−P(3B)−Na 155.9(5), Si(2C)−P(3C)−Na 160.3(11), P(2A)−Na−P(3A) 68.0(4), P(2B)−Na−P(3B) 62.5(3), P(2C)−Na−P(3C) 62.4(5), Si(1A)−P(2A)−P(1A) 96.1(10), Si(1B)−P(2B)−P(1B) 104.3(6), Si(1C)−P(2C)−P(1C) 103.0(9), Si(2A)−P(3A)−P(1A) 97.3(11), Si(2B)−P(3B)−P(1B) 105.7(7), Si(2C)−P(3C)−P(1C) 105.5(12).

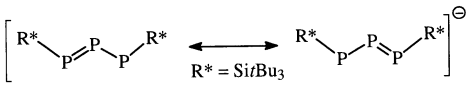

(6)

Figure 2. Observed $^{31}P\{^1H\}$-NMR spectrum of **1a** in C_6D_6 at 109.37 MHz (25°C; external 85% H_3PO_4); $^1J_{P1P2}$ = 552.6 Hz

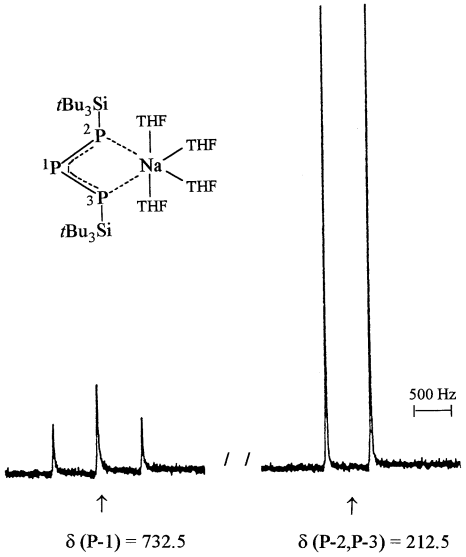

formed. Presumably, in the first step TCNE oxidizes the triphosphide **1** to form the resonance stabilized triphosphanyl radical $[t\mathrm{Bu_3Si{-}P{=}P{-}P{-}Si}t\mathrm{Bu_3} \rightleftharpoons t\mathrm{Bu_3Si{-}P{-}P{=}P{-}Si}t\mathrm{Bu_3}]^{\bullet}$, which therefore exists for a longer period of time and changes into the 1,1′-bicyclotriphosphane **12** and the bicyclohexaphosphane **13**.

Unfortunately, the compounds **11**−**13** (see Scheme 4) have not so far been isolated in their pure state; however, their structures, as shown by the formula, can be proved unambiguously from their ^{31}P-NMR spectra (see below). The ^{31}P-NMR data of phosphorus compounds of type **11** ($t\mathrm{Bu_2P_3H}$[15]), **12** ($\mathrm{P_6}t\mathrm{Bu_4}$[16]), and **13** ($\mathrm{P_6}t\mathrm{Bu_4}$[17], $\mathrm{P_6Cp^*_4}$[18]), which were already known, were also quite helpful for this purpose. Other isomers of the cyclophosphanes **11**−**13** could not be spectroscopically detected using NMR. The molecular structures shown for the compounds are obviously the most sterically favorable, and therefore energetically lowest lying.

Scheme 4

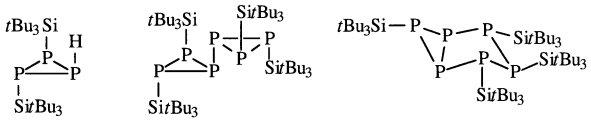

11 **12** **13**

The $^{31}P\{^1H\}$-NMR spectrum of the cyclotriphosphane **11** exhibits the signals of an ABC spin system [δ_A(P-1) = −246.9, δ_B(P-2) = −259.5, δ_C(P-3) = −260.1; $^1J_{P1P2}$ = −188.0 Hz, $^1J_{P1P3}$ = −141.3 Hz, $^1J_{P2P3}$ = −224.2 Hz]. In the proton coupled ^{31}P-NMR spectrum (Figure 3) it extends to an ABCX spin system ($^1J_{P3H}$ = 137.1 Hz, $^2J_{P1H}$ = 16.6 Hz, $^2J_{P2H}$ = 6.9 Hz; regarding the signs of $^1J_{PP}$ and

$^1J_{PH}$ see refs.[19][20][21]). Because of the small shift difference between the signals of P-2 and P-3 the spectra deviate strongly from first order. The difference in the PP couplings to P-3 allows an assignment of the signals to P-1 and P-2. The larger coupling constant between P-2 and P-3 indicates a *cis* orientation of the substituents H and Si*t*Bu$_3$ at these phosphorus atoms[22]. For **11** the ^{31}P-NMR chemical shifts, as well as the P−P coupling constants, fall in the range characteristic for cyclotriphosphanes[23][24].

Figure 3. Observed (a) and calculated[20] (b) ^{31}P-NMR spectrum of the cyclotriphosphane **11** at 161.84 MHz in C_6D_6 (0.01 M solution, 25°C, external 85% H_3PO_4); the shift difference between the NMR signals of P-2 and P-3 observed at this frequency is only 102.7 Hz; the relative signs of the coupling constants result from the iterative fitting of the spectrum assuming negative values for $^1J_{PP}$ and positive values for $^1J_{PH}$[19][20][21]: $^1J_{P1P2}$ = −188.0, $^1J_{P1P3}$ = −141.3, $^1J_{P2P3}$ = −224.2, $^1J_{P3H}$ = 137.1, $^2J_{P1H}$ = 16.6, $^2J_{P2H}$ = 6.9 Hz

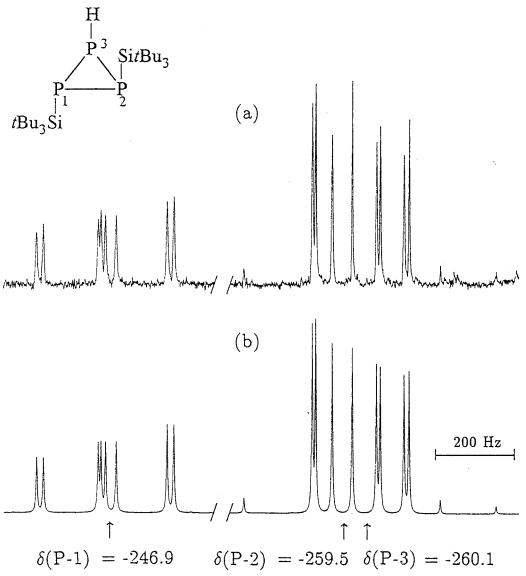

The ^{31}P{^{1}H}-NMR spectrum of the 1,1′-bicyclotriphosphane **12** shows three multiplets with the classical splitting pattern of an AA′BB′MM′ spectrum. Approximate values for δ_P and J_{PP} can be estimated by simple examination of the experimental spectrum[19]; starting from these values the spectrum can be solved by iterative fitting[20] (Figure 4). The ^{31}P-NMR data of **12** parallel, to a large degree, those of *t*Bu$_2$P$_3$−P$_3$*t*Bu$_2$[16]. The chemical shifts of the phosphorus nuclei appear at high field [δ(P-1) = −142.6, δ(P-2) = −194.8, δ(P-3) = −210.8], as is generally found for δ^{31}P in cyclotriphosphanes[23][24]. The direct connection of the two P_3 rings is indicated by the large and negative coupling constant between P-1 and P-1′. The spatial neighbourhood of the lone pairs at P-3 and P-1′ as well as P-1 and P-3′ causes a large and positive coupling constant (57.7 Hz) between these phosphorus atoms, while for $^2J_{P1'P2}$ and $^2J_{P1P2'}$ a much smaller value (1.7 Hz) is observed. This proves the *trans* orientation of the supersilyl substituents at the adjacent phosphorus atoms P-2 and P-3 as well as P-2′ and P-3′. In accord with this is also the sequence of magnitudes of $^1J_{P1P2}$ (−284.7 Hz) and $^1J_{P1P3}$ (−174.9 Hz)[22]. Obviously, like *t*Bu$_2$P$_3$−P$_3$*t*Bu$_2$[16], **12** also forms the sterically most favorable all *trans* isomer. In the case of **12**, however, coupling constants $^3J_{P2P2'}$ (7.6 Hz) and $^3J_{P3P3'}$ (0.4 Hz) are found to have the reverse order of magnitude. This difference, as well as the clearly more negative coupling constant $^3J_{P2P3'}$ (−14.1 Hz) observed for **12,** is presumably caused by a larger population of the rotamers with a wider torsion angle P-2,P-1,P-1′,P-2′.

Figure 4. Observed (a) and calculated[20] (b) ^{31}P{^{1}H}-NMR spectrum of **12** at 109.36 MHz in C_6D_6 (25°C; external 85% H_3PO_4): $^1J_{P1P1'}$ = −301.1, $^1J_{P1P2}$ = $^1J_{P1'P2'}$ = −284.7, $^1J_{P1P3}$ = $^1J_{P1'P3'}$ = −174.9, $^1J_{P2P3}$ = $^1J_{P2'P3'}$ = −171.8, $^2J_{P1P2'}$ = $^2J_{P1'P2}$ = 1.7, $^2J_{P1P3'}$ = $^2J_{P1'P3}$ = 57.7, $^3J_{P2P2'}$ = 7.6, $^3J_{P3P3'}$ = 0.4, $^3J_{P2P3'}$ = $^3J_{P2'P3}$ = −14.1 Hz; the relative signs of the coupling constants result from the iterative fitting of the spectra assuming negative values for $^1J_{PP}$[21]

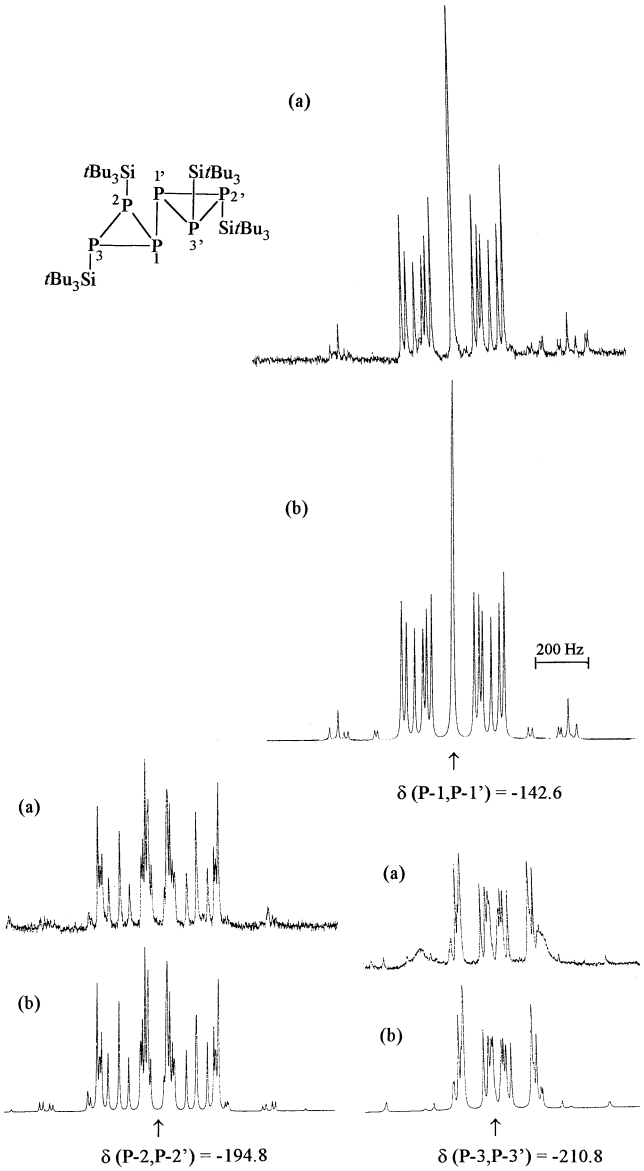

The structure of the bicyclo[3.1.0]hexaphosphane **13** can be derived from the NMR data after a complete analysis of its ^{31}P{^{1}H}-NMR spectrum. It shows, as in the case for the analogous hexaphosphanes P$_6$*t*Bu$_4$[17] and P$_6$Cp*$_4$[18] the four multiplets of an AA′BB′MX spin system (Figure 5). The signal of P-2 (X part) appears at high field (δ =

Figure 5. Observed (a) and calculated[20] (b) $^{31}P\{^1H\}$-NMR spectrum of **13** at 109.37 MHz in C_6D_6 (25°C; external 85% H_3PO_4): $^1J_{P1P2} = {}^1J_{P2P3} = -159.5$, $^1J_{P1P3} = -245.9$, $^1J_{P1P6} = {}^1J_{P3P4} = -397.1$, $^1J_{P4P5} = {}^1J_{P5P6} = -487.7$, $^2J_{P1P4} = {}^2J_{P3P6} = 23.2$, $^2J_{P1P5} = {}^2J_{P3P5} = 11.7$, $^2J_{P2P4} = {}^2J_{P2P6} = 105.4$, $^2J_{P4P6} = 34.7$, $^3J_{P2P5} < 1.0$ Hz; the relative signs of the coupling constants result from the iterative fitting of the spectrum assuming negative values for $^1J_{PP}$[21]

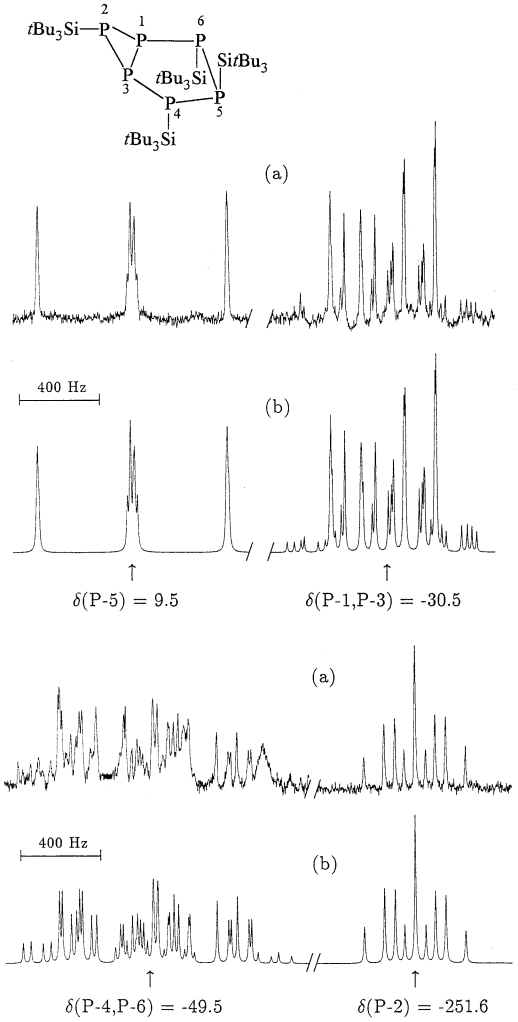

−251.6) as a triplet of triplets and can be understood, practically, according to a first order interpretation. On the other hand the signal of P-5 (M part, δ = 9.5) deviates considerably from the first order $(J_{P\text{-}4P\text{-}5})/\nu_0[\delta(P\text{-}4) - \delta(P\text{-}5)] = 0.08$ at 109.37 MHz). For the phosphorus atoms P-1 and P-3 at the bridgehead positions δ = −30.5, and for the adjacent phosphorus atoms P-4 and P-6 in the pentaphospholane ring δ = −49.5; the characteristic splitting pattern for the A and the B part of an AA′BB′M spin system[19] is observed, each doubled by coupling with P-2. The presence of a cyclotriphosphane ring in **13** is indicated by the chemical shift at high field for P-2 as well as by the large and negative coupling constant $^1J_{P1P3} = -245.9$ Hz (regarding the sign see ref.[21]). As in the case of P_6tBu_4[17] $^1J_{P1P6}$ and $^1J_{P5P6}$ are clearly larger than $^1J_{PP}$ in the cyclotriphosphane ring, and here have values of −397.1 Hz and −487.7 Hz, respectively, which are remarkably large values. The large and positive coupling constant between P-2, P-4 and P-6 (+105.4 Hz) indicates that the lone pairs at these phosphorus atoms are facing each other. The tBu_3Si substituents at P-2 as well as at P-4 and P-6 must therefore occupy in the first case the axial position and in the last two cases the equatorial positions, as shown by the X-ray structure analyses for P_6tBu_4[17] and $P_6Cp^*_4$[18] in the crystal.

Cyclic versus Acyclic $P_3H_2^-$, P_3H_3 and Derivatives: Ab initio Structure, Energy and NMR Calculations

Figure 6 comprises the results of ab initio calculations concerning structure and relative energies of cyclic P_3H_3 (**14**) and $P_3H_2^-$ (**18**) as well as of their acyclic isomers (**15**, **16**, **17**, **19**) and two derivatives of *cyclo*-P_3H_3 (**20**, **21**). Our RMP2/6-31+G* calculations of the parent $P_3H_2^-$ anion show that the acyclic planar *trans-trans* form **19** with allylic conjugation[25], $[HP\cdots P\cdots PH]^-$, and P−P $1^1/_2$ bonds[25] is thermodynamically 6.1 kcal/mol more stable than the cyclic isomer **18** (isomerization of **19** via **17** to a *trans-cis* isomer has a barrier of 23.1 kcal/mol, see Figure 6). With silyl substituents the allyl preference increases slightly [E_{rel} for cyclic $(H_3Si)_2P_3^-$ is 7.6 kcal/mol]. In contrast, neutral compounds with a P_3 framework like P_3H_3 (**14**)[26], $(H_3Si)_2P_3H$ (**20**), $(H_3Si)_2P_3Cl$ (**21**) prefer the cyclic form. Structural alternatives with a terminal PH_2 group are less stable than the global minimum for the neutral *cyclo*-P_3H_3 [E_{rel} (H_2PPPH, **15**) with respect to **14** is 11.7 kcal/mol, Figure 6] as well as for the anionic *acyclo*-$P_3H_2^-$ [E_{rel} (H_2PPP^-) with respect to **19** is 12.7 kcal/mol)]. Therefore, cyclization of the "protonated anion" **1** to **11** and ring opening of the "reduced halogenide" **9** to **1** is in agreement with our ab initio results for the simple models R_2P_3X and $R_2P_3^-$ with R = H or SiH_3 and X = H or Cl.

Both the acyclic anion $R_2P_3^-$ (in **1** with R = Si*t*Bu$_3$; calcd. for R = H, SiH_3) and the cyclic isomer could have two ^{31}P-NMR signals. The question is which R_2P_3Na model structure provides computed NMR data which are in agreement with the experiment? Unfortunately, ab initio NMR calculations which neglect electron correlation give $\delta^{31}P$ values for the model complexes, (RP⩬P⩬PR,Na) (R = H or SiH_3), with unusually large deviations of several hundred ppm. However, density functional NMR calculations (SOS-DFPT[27]), which include correlation are in good agreement with GIAO-MP2[28] (explicit consideration of correlation) and should only deviate by the order of 37 ppm from the experiment[29]. Our SOS-DFPT/Perdew-Wang functional '91/B3///RMP2/6-31G*, NMR values for an appropriate model of **1** (modeling the silyl substituent by SiH_3 and the solvated sodium by bare Na^+) are in reasonable agreement with the experiment for the W-shaped, C_S-symmetric acyclic form with a folded deltoid P_3Na moiety ($\delta DPB3^{31}P = 720$ and 176, corresponding to 733 and 213) and exclude any cyclic form[30]. The $\delta DPB3^{31}P$ values for the strictly planar Si_2P_3Na framework indicate that this transition structure of the molecule, in solution or in the crystalline framework, occurs only intermittently during the permanent internal motion of the molecule.

Figure 6. RMP2/6-31G* (and 6-31+G* for anions) geometries (bond length in [A], angles in [°] and relative energies (in [kcal/mol]) for P_3H_3, $P_3H_2^-$ and $(H_3Si)_2P_3X$ (X = H, Cl)

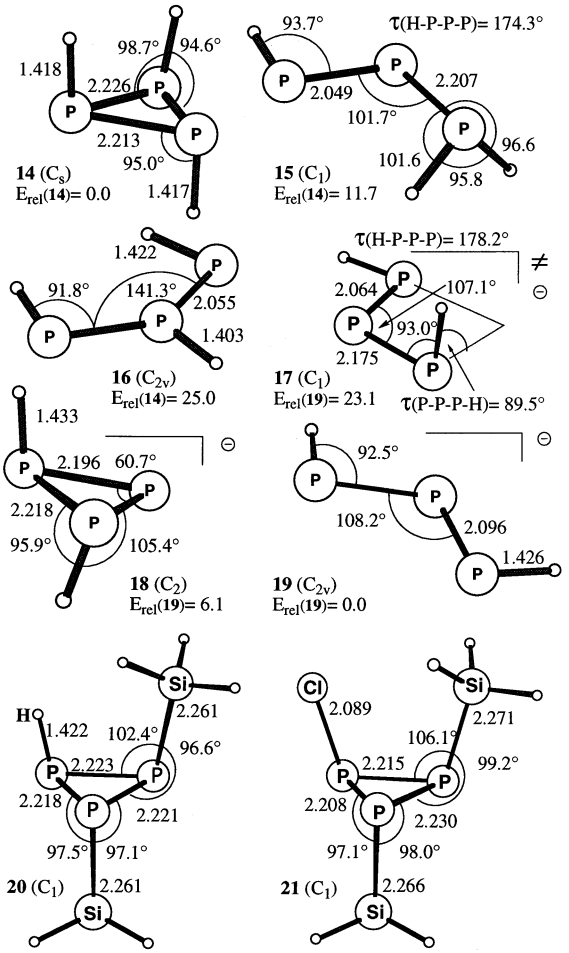

We would like to thank the *Deutsche Forschungsgemeinschaft* for supporting our research and the *Computer-Chemie-Centrum Erlangen* for computer time on an HP735 platform.

Experimental Section

All experiments were carried out under dry argon with strict exclusion of air and moisture. CF_3SO_3H, CF_3CO_2H, TCNE, CD_3CN, and PCl_3 were commercially available. $(t\mathrm{Bu_3Si})_2P_4Na_2$ (**2**) in THF[4], $t\mathrm{Bu_3SiNa}$ in THF[31], and $(t\mathrm{Bu_3Si})_3P_7$ (**7**)[11] were prepared according to literature procedures. The solvents (pentane, benzene, tetrahydrofuran) were distilled from sodium/benzophenone immediately before use.

The NMR spectra were recorded with a JEOL FX-90-Q (^{1}H/^{13}C/^{29}Si: 89.55/22.52/17.79 MHz), a JEOL GXS-270 (^{1}H/^{13}C/^{29}Si/^{31}P: 270.17/67.94/53.67/109.37 MHz), and a JEOL EX-400 (^{1}H/^{13}C/^{31}P: 399.78/100.53/161.84 MHz) spectrometer. The ^{29}Si-NMR spectra were recorded with the INEPT pulse sequence using empirically optimized parameters for polarization transfer from the *t*Bu substituents. The mass spectra (electron impact) were recorded with a Varian CH7 instrument.

Conversion of **2** *into* **1**: a) 5.22 mmol (0.4 ml) of CF_3CO_2H in 2 ml of pentane was added dropwise with stirring to a cooled (−78°C) solution of 5.22 mmol of **2** in 50 ml of THF and the resulting deep red reaction mixture was warmed up after 1 h to ambient temp. While warming, the solution changed colour to red-violet. According to the ^{31}P-NMR spectrum (C_6D_6) the reaction solution contained, in addition to $t\mathrm{Bu_3SiPH_2}$ and small amounts of $t\mathrm{Bu_3Si}$-PHNa (identified by comparison with authentical samples[32]), the phosphorus compounds **1** (see below), **2** (unreacted starting material) and **4** (identified by comparison with an authentic sample[10]) in a molar ratio of 2:1:1, as well as the oligophosphane $(t\mathrm{Bu_3SiP_3})_n$ (see below).

b) From a solution of 0.138 mmol of **2** in 2 ml of THF the solvent was removed in vacuo and 1 ml of CD_3CN added to the remaining deep red solid to yield a violet solution. According to the ^{31}P-NMR spectrum of this solution, **1** (identified by comparison with an authentic sample, see below) and $t\mathrm{Bu_3SiPD_2}$ (identified by comparison with an authentic sample[32]) were formed as the only phosphorus-containing products in a molar ratio of 1:1. After removing the CD_3CN in vacuo, $t\mathrm{Bu_3SiPD_2}$ was separated from the residue by sublimation (100°C/10^{-3} mbar) and isolated as colourless needles. − ^{1}H NMR (CD_3CN, internal TMS): δ = 1.14 (d; $^4J_{PH}$ = 0.46 Hz; 3 *t*Bu). − ^{13}C{^{1}H} NMR (CD_3CN, internal TMS): δ = 22.8:30.9 (d/d; $^2J_{CP}/^3J_{CP}$ = 6.1/3.0 Hz; 3 *t*Bu). − ^{29}Si NMR (CD_3CN, external TMS): δ = 24.0 (d; $^1J_{SiP}$ = 30.7 Hz; Si*t*Bu$_3$). − ^{31}P{^{1}H} NMR (CD_3CN, external 85% H_3PO_4): δ = −268.9 (quint; $^1J_{PD}$ = 29.4 Hz; PD_2).

Note: In the course of a few weeks the violet colour of the reaction solution vanished and it then contained, according to the ^{31}P-NMR spectrum, $t\mathrm{Bu_3SiPD_2}$ as the only phosphorus compound. According to the ^{29}Si-NMR spectrum $t\mathrm{Bu_3SiCN}$ also formed (identified by comparison with an authentic sample[33]).

c) **2**, dissolved in a pentamethyldiethyltriamine (PMDTA)/benzene mixture, converted in the course of several months at ambient temp. into **1** and $t\mathrm{Bu_3SiPHNa}$ (as PMDTA adducts); at the same time additional, and as yet unidentified, phosphorus-containing products were formed.

Formation of **1** *from Supersilylpolyphosphanes:* a) 3.45 mmol of **2** in 50 ml of THF was added dropwise to a solution of 6.94 mmol (0.61 ml) of CF_3SO_3H in 5 ml of pentane at ambient temp. The deep red colour of the solution of **2** changed to yellow on contact with the acid. According to the ^{31}P-NMR spectrum (C_6D_6) polyphosphanes together with $t\mathrm{Bu_3SiPH_2}$ were formed (molar ratio of the polyphosphane phosphorus to the monophosphane phosphorus in accord with Eq. 2 is 3:1). The solvent and all volatile materials were removed in vacuo, the residue dissolved in 10 ml of pentane and all insoluble material (CF_3SO_3Na) separated by filtration. After several days at −25°C, a yellow solid precipitated from the filtrate, which was separated, dissolved in heptane and precipitated again at −25°C. Repetition of this procedure several times afforded 0.820 g of a yellow and very air-sensitive solid polyphosphane product. According to the ^{31}P-NMR spectrum, this product was free of $t\mathrm{Bu_3SiPH_2}$, and according to elemental analysis had the composition $t\mathrm{Bu_3SiP_3}$[34]. After removal of the pentane and heptane in vacuo from the respective filtrates, solid $t\mathrm{Bu_3SiPH_2}$ was obtained from the remaining residue by sublimation at 100°C/10^{-3} mbar (identified by comparison with an authentic sample[32]).

A solution of 2.80 mmol of $t\mathrm{Bu_3SiNa}$ in 6 ml of THF was slowly added dropwise to a solution of 0.820 g (2.80 mmol with respect to the formula $t\mathrm{Bu_3SiP_3}$) of the solid yellow polyphosphane (see above) in 10 ml of THF. The colour of the reaction solution changed from yellow to deep violet. According to the ^{31}P-NMR spectrum, **1** was quantitatively formed, which proved the identity of the polyphosphane to be $(t\mathrm{Bu_3SiP_3})_n$. The reaction solution was concentrated to 5 ml and mixed with 2 ml of pentane. In the course of 10 d violet, and very air- and moisture-sensitive crystals of so-

dium 2,3-bis(tri-*tert*-butylsilyl)triphosphenide−tetrahydrofuran(1/4) (**1a**) separated. − ^{1}H NMR (C_6D_6/THF, internal TMS): δ = 1.38 (br.; 2 Si*t*Bu$_3$). − ^{13}C{^{1}H} NMR (C_6D_6/THF, internal TMS): δ = 25.3 (br.; 6 *C*Me$_3$), 32.3 (br.; 6 C*Me*$_3$). − ^{29}Si NMR (C_6D_6/THF, external TMS): δ = 18.3 (td; $^1J_{SiP}$ + $^3J_{SiP}$ = 47.1 Hz; $^2J_{SiP}$ = 7.1 Hz; 2 Si*t*Bu$_3$). − ^{31}P{^{1}H} NMR (C_6D_6/THF, external 85% H_3PO_4): cf. Figure 1. − X-ray structure investigation [cf. section on characterization and structure of (*t*Bu$_3$Si)$_2$P$_3$Na(THF)$_4$ (**1a**)].

b) A solution of 0.445 mmol *t*Bu$_3$SiNa in 1 ml of THF was added dropwise to 0.181 g (0.222 mmol) of **7** at ambient temp. The reaction mixture immediately adopted a red-violet colour. According to the ^{31}P-NMR spectrum **1** (identified by comparison with an authentic sample, see above) and **3** formed in a molar ratio of 1:1. After a longer period of time dark red crystals of highly air- and moisture-sensitive 1-[tri-*tert*-butylsilyl(sodio)phosphanidyl]-2,3-*trans*-bis(tri-*tert*-butylsilyl)cyclotriphosphane−tetrahydrofuran-(1/*n*) (**3**) were formed from the red-violet reaction solution (identified by comparison with an authentic sample[12]).

Note: The phosphide **3** was also formed quantitatively from the reaction of **5** with an equimolar amount of *t*Bu$_3$SiNa in THF.

Formation of **1** *from Phosphorus Trichloride:* A solution of 0.184 g (1.35 mmol) of PCl_3 in 0.5 ml of heptane was added dropwise to a cooled (−78°C) solution of 4.6 mmol *t*Bu$_3$SiNa in 10 ml of THF (procedure A); alternatively a solution of 11.5 mmol *t*Bu$_3$SiNa in 25 ml of THF was added dropwise to a cooled (−78°C) solution of 0.623 g (4.98 mmol) of PCl_3 in 20 ml of THF (procedure B). The resulting reaction mixtures were then warmed up to ambient temp. According to the ^{31}P-NMR spectrum the triphosphide **1** (see above), the tetraphosphide **3**[5], the pentaphosphide **4**[5][10], monophosphides (see below), and diphosphides (see below) were formed in a molar ratio of about 10:5:3:1:2 for procedure A, and of about 7:4:3:1:4 for procedure B [the compounds were identified by comparison of the ^{31}P-NMR data with those of authentical samples; cf. references given with the numbers of the compounds; the mono- and diphosphides were formed in only small amounts (giving one and two ^{31}P-NMR signals, respectively) and are not yet identified.

Note: After the insoluble materials from the reaction solution, obtained according to procedure B, were separated by filtration, and the solution was concentrated to 15 ml and cooled to −25°C, a microcrystalline precipitate of a mixture of the compounds mentioned above was obtained. The filtrate ("mother liquor"), which contains **1**, **3**, **4**, and other phosphides in a molar ratio of 8:5:3:3, was further treated with CF_3CO_2H and with TCNE (see below).

Reaction of **1** *with Trifluoracetic Acid:* A solution of 0.060 g (0.53 mmol) of CF_3CO_2H in 0.5 ml of heptane was added dropwise at ambient temp. to 2 ml of the "mother liquor" (described above and obtained from PCl_3 and *t*Bu$_3$SiNa in THF) which contained, as shown from titration, 0.56 mmol/ml of anionic phosphorus. The solvents and all volatile materials were removed in vacuo, the residue was dissolved in pentane, the insoluble material (CF_3CO_2Na) separated by filtration, and the pentane then removed in vacuo and the residue dissolved in 1 ml of C_6D_6. According to the ^{31}P-NMR spectrum, protonated **1** (≡ **11**), protonated **3**[5] and protonated **5**[5][10] were formed in a molar ratio of about 3:5:3, together with monophosphanes, diphosphanes, and other phosphanes. The structure of *trans*-bis(supersilyl)cyclotriphosphane (**11**), which could not be isolated from the reaction mixture, was unambiguously proved from the ^{31}P-NMR spectra [cf. section on the protolysis and oxidation of (*t*Bu$_3$Si)$_2$P$_3$Na (**1**)]. The ^{1}H-, ^{13}C-, and ^{29}Si-NMR spectra revealed no additional information for **11** because of superposition of its signals with the signals of other compounds present in the mixture.

Reaction of **1** *with Tetracyanethylene:* 2 ml of the "mother liquor" described above (obtained from PCl_3 and *t*Bu$_3$SiNa in THF, and which contained, as shown from a titration, 0.56 mmol/ml anionic phosphorus) was added dropwise to 0.059 g (0.46 mmol) of TCNE at ambient temp. The solvent and all volatile materials were removed in vacuo, the residue was dissolved in pentane, unsoluble materials were removed by filtration, and finally the pentane was evaporated in vacuo and the residue dissolved in 0.8 ml of C_6D_6. According to the ^{31}P-NMR spectrum, **5**[4][11], **6**[10], **12**, and **13** are formed in a molar ratio of 2:7:8:1 together with other phosphanes. Assuming, that **4** was oxidized uniformly to **6** and **1** was oxidized only to **12** and **13**, the compounds **1** and **4**, present in the "mother liquor" in a molar ratio of 8:3, must be found in the reaction solution, after the oxidation, in a molar ratio of 4:3 (experimentally observed 9:7 ≡ 4:3.1). The structures of 2,2′,3,3′-tetrasupersilyl-1,1′-bicyclotriphosphane (**12**) and 2,4,5,6-tetrasupersilylbicyclo[3.1.0]hexaphosphane (**13**), which could not be isolated from the reaction mixture, were unambiguously derived from the ^{31}P-NMR spectra [cf. section on the protolysis and oxidation of (*t*Bu$_3$Si)$_2$P$_3$Na (**1**)]. The ^{1}H-, ^{13}C-, and ^{29}Si-NMR spectra revealed no additional information for **12** and **13**, due to the superposition of their NMR signals with the signals of other compounds present in the mixture.

X-ray Structure Determination of (tBu$_3$Si)$_2$P$_3$Na(THF)$_4$ (**1a**): Diffractometer STOE IPDS, Mo-K_α radiation, λ = 0.71069 Å. A small violet crystal was fixed in perfluoroether and analyzed in a Mark-tube at T = 200(2) K. Crystallographic data: $C_{40}H_{86}NaO_4P_3Si_2$, M_f = 803.17, orthorhombic, space group $Pna2_1$ (No. 33), a = 24.433(6), b = 17.439(7), c = 12.005(6) Å, V = 5115(4) Å^3, Z = 4, $d_{calcd.}$ = 1.043 g cm^{-3}, μ = 0.204 mm^{-1}, F(000) = 1768. − Data collection: ω scans, 2Θ = 2.38−21.00° in $-32 \le h \le 32$, $-22 \le k \le 8$, $-15 \le l \le 15$. 10985 measured reflections, of which 4866 symmetry independent. − Solution of the structure: Restraints, 390 parameters optimized, $R1[I > 2\sigma(I)]$ = 0.0787, $wR2$ = 0.1802, GOF = 2.128; residual electron density = 0.389 and −0.388 e Å^{-3}. For further details of the crystal structure investigation (for example splitting of the positions of the atoms) see ref.[35].

☆ Dedicated to Professor Dr. *Heinrich Nöth* on the occasion of his 70th birthday.

[1] Part III: Ref.[4].

[2] Part 117: N. Wiberg, K. Amelunxen, H.-W. Lerner, H. Nöth, J. Knizek, I. Krossing, *Z. Naturforsch.* **1998**, *52b*, 333.

[3] Holleman-Wiberg, *Lehrbuch der Anorganischen Chemie*, 101 Aufl., Verlag DeGruyter, Berlin, **1995**. Cf. also for cyclic phosphanes: M. Baudler, K. Glinka, *Chem. Rev.* **1993**, *93*, 1623; for acyclic phosphanes: M. Baudler, K. Glinka, *Chem. Rev.* **1994**, *94*, 1273.

[4] N. Wiberg, A. Wörner, K. Karaghiosoff, D. Fenske, *Chem. Ber.* **1997 130**, 135.

[5] N. Wiberg, *Coord. Chem. Rev.* **1997 163**, 217. Preliminary communications about NMR and X-ray structure analyses of **4**: N. Wiberg, A. Wörner, H. Nöth, K. Karaghiosoff in *Organosilicon Chemistry II* (Eds.: N. Auner, J. Weis), VCH, Weinheim, **1996**, p. 197.

[6] P. Jutzi, U. Meyer, *Phopshorus Sulfur* **1988**, *40*, 275.

[7] N. Wiberg, P. Karampatses, E. Kühnel, M. Veith, V. Huch, *Z. Anorg. Allg. Chem*. **1988 562**, 91.

[8] N. Wiberg, H.-W. Lerner, unpublished results.

[9] [9a] V. Thelen, D. Schmidt, M. Nieger, E. Niecke, W. W. Schoeller, *Angew. Chem*. **1996, 108**, 354; *Angew. Chem. Int. Ed. Engl.* **1996 35**, 313. − [9b] M. Baudler, J. Hahn, *Z. Naturforsch.* **1990**, *45b*, 1139; N. Maigrot, M. Sierra, C. Charrier, F. Mathey, *Bull. Soc. Chim. Fr.* **1994**, *131*, 397.

[10] N. Wiberg, A. Wörner, H.-W. Lerner, K. Karaghiosoff, H. Nöth, in preparation.

[11] I. Kovács, G. Baum, G. Fritz, D. Fenske, N. Wiberg, H. Schuster, K. Karaghiosoff, *Z. Anorg. Allg. Chem.***1993**, *619,* 453.

[12] N. Wiberg, A. Wörner, H.-W. Lerner, K. Karaghiosoff, in preparation.
[13] N. Wiberg, H.-W. Lerner, M. Veith, V. Huch, in preparation.
[14] K. Karaghiosoff in *Multiple Bonds and Low Coordination in Phosphorus Chemistry* (Eds.: M. Regitz, O. J. Scherer), Thieme, Stuttgart, **1990**, p. 463.
[15] M. Baudler, B. Makowka, K. Langerbeins, *Z. Naturforsch.* **1985**, *40b*, 1274.
[16] M. Baudler, B. Makowka, *Angew. Chem.* **1984**, *96*, 976; *Angew. Chem. Int. Ed. Engl.* **1984**, *23*, 987.
[17] M. Baudler, Y. Aktalay, K.-F. Tebbe, T. Heinlein, *Angew. Chem.* **1981**, *93*, 1020; *Angew. Chem. Int. Ed. Engl*. **1981**, *20*, 967.
[18] P. Jutzi, R. Kroos, A. Müller, H. Bögge, M. Penk, *Chem Ber.* **1991**, *124*, 75.
[19] R. J. Abraham, *The Analysis High Resolution NMR Spectra*, Elsevier, New York, **1971**.
[20] L. Cassidei, O. Sciacovelli, *LAOCOON*, QCPE program no. 458; PC version: K. J. Tupper, Program QCMP program no. 049.
[21] K. Karaghiosoff in *Encyclopedia of Nuclear Magnetic Resonance* (Eds.: D. M. Grant, R. K. Harris) Wiley, Chichester, **1996**, p. 3612.
[22] J. Hahn in *Phosphorus-31 NMR Spectroscopy in Stereochemical Analysis* (Eds.: G. Verkade, L. D. Quin) VCH, Dearfield Beach, **1987**, ch. 10.
[23] Y. Leroux, R. Burgada, S. G. Kleemann, E. Fluck in *Handbook of Phosphorus-31 Nuclear Magnetic Resonance Data* (Ed.: J. C. Tebby) CRC Press, Boca Raton, **1991**.
[24] J. Hahn, M. Baudler, C. Krüger, Y.-H. Tsay, *Z. Naturforsch.* **1982**, *37b*, 797.
[25] P. v. R. Schleyer, *J. Am. Chem. Soc.* **1985**, *107*, 4793; M. N. Glukhovtsev, A. Dransfeld, P. v. R. Schleyer, *Phys. Chem.* **1996**, *100*, 13447.
[26] W. W. Schoeller, T. Busch, *Chem. Ber.* **1993**, *204*, 80.
[27] V. G. Malkin, O. L. Malkina, *Chem. Phys. Lett.* **1993**, *204*, 80.
[28] J. Gauss, *Chem. Phys. Lett.* **1992**, *191*, 614.
[29] D. B. Chesnut, E. F. C. Byrd, *Heteroatom Chem.* **1996**, *7*, 307.
[30] Computational details at http://www.ccc.uni.erlangen.de/sharc/
[31] N. Wiberg, K. Amelunxen, H.-W. Lerner, H. Schuster, H. Nöth, I. Krossing, M. Schmidt-Amelunxen, T. Seifert, *J. Organomet. Chem.* **1997**, *542*, 1.
[32] N. Wiberg, H. Schuster, *Chem. Ber.* **1991**, *124*, 93.
[33] M. Weidenbruch, H. Pesel, *Z. Naturforsch.* **1978**, *33b*, 1465.
[34] N. Wiberg, A. Wörner, H.-W. Lerner, K. Karaghiosoff, T. Klapötke, in preparation.
[35] Crystallographic data (excluding structure factors) for the structure reported in this paper has been deposited with the Cambridge Crystallographic Data Centre as supplementary publication No. CCDC-101056. Copies of the data can be obtained free of charge on application to CCDC, 12 Union Road, Cambridge CB2 1EZ, UK [Fax: (internat.) code + 44(0)1223/336-033; E-mail: deposit@ccdc.cam.ac.uk).

[98008]

Borane-Substituted Imidazol-2-ylidenes: Syntheses, Structures, and Reactivity☆

Andreas Wacker, Hans Pritzkow, and Walter Siebert*

Anorganisch-Chemisches Institut der Universität,
Im Neuenheimer Feld 270, D-69120 Heidelberg, Germany
Fax: +49-(0)6221/54-5609
ci5@ix.urz.uni-heidelberg.de

Received January 26, 1998

Keywords: Boranes / Carbenes / Carbene complexes / Heterocycles / Imidazoles

Reactions of the Lewis acids BH_3 and BEt_3 with trimethylimidazole (**1**) lead to the borane adducts **2a** and **2b**. Deprotonation of **2a** with *n*-butyllithium results in the formation of the novel *N*-borane-substituted imidazol-2-ylidene anion **3a**$^-$ whereas deprotonated **2b** rearranges unexpectedly to the anionic compound **3b**$^-$. This can be transformed into the carbene–borane adduct **4** by methylation. The reaction of **3a**$^-$ with $[Mn(CO)_5Br]$ yields the carbene complex **5**. Surprisingly, **3a**$^-$ attacks $Fe(CO)_5$ at a carbon atom which leads to the iron acyl complex anion **6**$^-$. The compositions of the products follow from spectroscopic and analytical data and from X-ray structure analyses for $Li(thp)^+$**3a**$^-$, $Li(thf)_2^+$**3b**$^-$ and $Li(thp)_3^+$**6**$^-$.

Introduction

The chemistry of nucleophilic carbenes has become an area of particular interest since the discovery of the first stable carbenes, synthesized by Arduengo et al. in 1991[1]. Several derivatives of the imidazol-2-ylidene **A** as well as the imidazolin-2-ylidene **B**[2] and the chain-like carbene compound **C** have been reported[3]. Based on the heterocycles triazole and thiazole, the carbenes **D**[4] and **E**[5] have also been synthesized. Recently, a review of the chemistry of N-heterocyclic carbenes was published by Herrmann et al.[6].

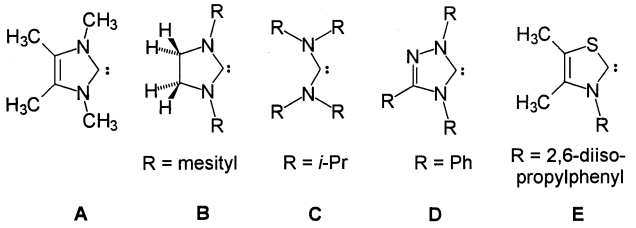

Compounds **A**–**E** have in common the presence of only organic substituents attached to the nitrogen atoms, whereas other main-group element substituted carbenes are not known. Fehlhammer et al.[7] synthesized a tris(carbene)iron complex in which the carbene units are connected via a BH group.

In 1994 Contreras, Wrackmeyer, et al.[8] published the synthesis of the imidazabole **F** (R = H) which may also be regarded as an intramolecular carbene–borane adduct **F′**. Its BH_2 groups function as Lewis acid centers for the carbene carbon atoms (see below).

Imidazol-2-ylidenes (e.g. **A**) have also proved to be excellent ligands in transition-metal complexes[9]. In particular, ligand exchange reactions with carbonylmetal compounds work easily yielding the expected carbene complexes. The

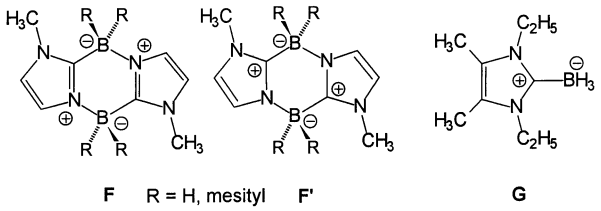

reactions occur at room temperature and, depending on the stoichiometry of the reactants, mono-substituted products of type **H** are formed as well as bis- and tris(carbene) complexes in the case of Mo, W, and Ni[10][11]. Beside complexes with the monodentate ligand **A**, compounds **J** with a bidentate ligand are known as well[10][11].

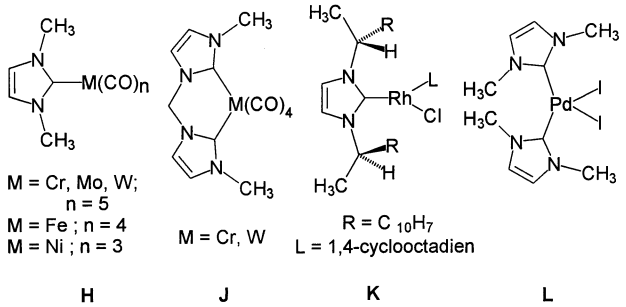

In complexes of imidazol-2-ylidenes the metal–carbene bond has weak π-backbonding character[6][10]. Therefore, these carbenes appear comparable to phosphanes, and could therefore also prove important in homogeneous catalytic processes[6][9e][10]. In fact, **K** and **L** are examples of useful carbene catalysts for asymmetric hydrosilylations (**K**)[12] and for the Heck reaction (**L**)[13].

In the following we report the deprotonation of the trimethylimidazol–borane adducts **2a** and **2b** with *n*-butyl-

 © WILEY-VCH Verlag GmbH, D-69451 Weinheim, 1998 1434–1948/98/0606–0843 $ 17.50+.50/0

lithium which results in the formation of the novel anions **3a**$^-$ and **3b**$^-$. **3a**$^-$ forms the metal complexes **5** and **6**$^-$.

Results and Discussion

Synthesis

Analogous to the reaction of imidazoles with boranes[14], 1,4,5-trimethylimidazole (**1**) reacts with $BH_3 \cdot$ thf at 0 °C to yield 3-borane-1,4,5-trimethylimidazole (**2a**), a colorless, crystalline, and air-stable solid. Its composition follows from NMR and MS data. Deprotonation of **2a** leads to the formation of the 3-borane−1,4,5-trimethylimidazol-2-ylidene anion **3a**$^-$. The salt Li(thp)$^+$**3a**$^-$, thp being tetrahydropyran, is obtained as a colorless crystalline solid, which is sensitive to air and moisture. This first example of a borane-substituted nucleophilic carbene is dimeric in the solid state (see below). It is derived from **A** by formal substitution of a methyl group by the isoelectronic BH_3^- unit.

Scheme 1

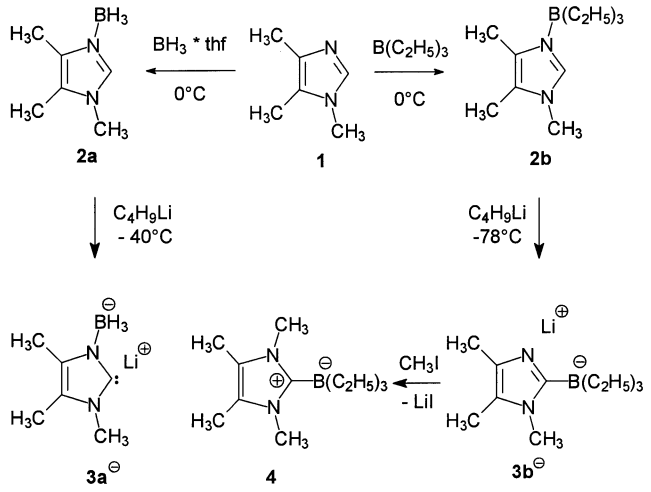

A characteristic feature of nucleophilic carbenes is the low-field ^{13}C-NMR shift of the carbene carbon atom signal (δ = 211−256 for **A**−**E**)[1][2][3][4][5]. **3a**$^-$ shows a resonance at δ = 191.3 which is shifted 22.4 ppm to high field compared to that of the corresponding carbene **A**[1]. Obviously, there is a transfer of electron density from the negatively charged boron atom to the carbene carbon atom. The remaining ^{13}C-NMR data are very similar to those of **A**. The signals for C4 and C5 appear at δ = 121.8 and 128.7 while those for the three methyl groups appear at δ = 8.3, 10.4, and 33.8. The ^{11}B-NMR spectrum shows one signal at δ = −21.1 which is broadened so that coupling with the hydrogen atoms is not observed, in contrast to **2a** ($^1J_{B\text{-}H}$ = 94 Hz).

Treatment of **1** with BEt_3 at 0 °C leads to 3-(triethylborane)−1,4,5-trimethylimidazole (**2b**) in quantitative yield. **2b** is a crystalline, colorless solid which is, in contrast to **2a**, sensitive to air. By analogy to the formation of **3a**$^-$, treatment of **2b** with *n*-butyllithium was expected to yield a carbene; however, surprisingly the rearranged anion **3b**$^-$ was obtained. After deprotonation, migration of the triethylborane from the nitrogen to the carbene carbon atom took place. This follows from the NMR data and from an X-ray structural analysis of Li(thf)$_2^+$**3b**$^-$. Obviously, the different Lewis acidities of BH_3/BEt_3 are responsible for this result.

The ^{13}C-NMR spectrum of **3b**$^-$ exhibits two signals at δ = 119.9 and 123.8 for the C4 and C5 atoms, the one for C2 not being observed. The resonances for the methyl groups are found at δ = 8.3, 9.4, and 32.0 while the ethyl substituents show two signals at δ = 10.7 and 14, the latter for the CH_2 carbon atom being broadened.

The different electronic behavior of BH_3 and BEt_3 as Lewis acids is reflected in the ^{11}B-NMR spectra. **2a** exhibits a resonance at δ = −20.9 whereas for **2b** a low-field shift to δ = −1.5 is observed. Comparing the shifts of **2a** and **2b** with those of **3a**$^-$ and **3b**$^-$ it is striking that for **3a**$^-$ (δ = −21.1) there is only a slight difference relative to **2a** whereas in the case of **3b**$^-$ (δ = −14.6) compared with **2b** a significant shift to higher field is observed. These data indicate that the migration of the triethylborane from the nitrogen to the carbon atom results in a larger electronic saturation of the boron atom. This is supported by comparing the ^{11}B-NMR shifts for tetraalkyl- and trialkyl(amino)-borates. $[BEt_4]^-$ shows a resonance at δ = −17.5[15] whereas for $[Et_3BNH_2]^-$ a low-field shift to δ = −9.8 is observed[16].

The reaction of **3b**$^-$ with iodomethane results in the formation of the 2-(triethylborane)−1,3,4,5-tetramethylimidazoline (**4**). Carbene adducts of this kind are known for a large variety of electrophiles and are usually obtained by addition of the Lewis acid to the free imidazol-2-ylidene[17]. Thus, carbene adducts with BH_3 and BF_3 have been described[18]. The method presented herein is a new route to generate triethylborane−carbene adducts. In the first step the trialkylborane is introduced, which on deprotonation and rearrangement gives **3b**$^-$. In the last step methylation of the anion **3b**$^-$ with CH_3I leads to the carbene adduct **4**.

4 is characterized by ^{1}H-, ^{13}C-, ^{11}B-NMR spectroscopy, and mass spectrometry. The ^{1}H-NMR spectrum shows the expected two signals at δ = 1.29 and 3.26 for the two sets of equivalent methyl substituents. In the ^{13}C-NMR spectrum only one signal for the imidazole carbon atoms C4 and C5 (δ = 123.6) is found, while that of C2 is, as for **3b**$^-$, not observed. The methyl substituents give rise to two signals at δ = 12.1 and 32.9. The ^{11}B-NMR shift of δ = −12.6 is comparable with that of **3b**$^-$.

Complex Formation

The reactivity of **3a**$^-$ in ligand-exchange reactions was studied. When $[Mn(CO)_5Br]$ is added to a solution of **3a**$^-$, the expected complex **5** is obtained. In contrast to this, the reaction of **3a**$^-$ with $Fe(CO)_5$ results in the formation of the acyl complex **6**$^-$. Treatment of **3a**$^-$ with chlorobis(dimethylamino)borane leads to the borane compound **7** (Scheme 2).

The orange-yellow complex **5** is extremely sensitive to air and moisture, and is obtained by reaction of the in situ generated carbene **3a**$^-$ with $[Mn(CO)_5Br]$ at −40 °C. The IR spectrum of the reaction mixture indicates the presence of several products, for which pure **5** can be isolated by column chromatography in 33% yield. **5** is characterized by

^{1}H-, ^{13}C-, ^{11}B-NMR, IR spectroscopy, and mass spectrometry. The ^{1}H-NMR spectrum shows two signals at δ = 2.22 and 2.24 for the C-CH_3 groups and one for the N-CH_3 group at δ = 3.81. In the ^{13}C-NMR spectrum the signals of the imidazole carbon atoms are found at δ = 129.0, 130.9 (C4, C5) and 146.9 (C2). This high-field shift of 44.4 ppm relative to that of **3a**$^-$ is in the same range as those for other carbenes and their complexes[10]. For the carbonyl ligands two signals at δ = 214.6 and 256.1 are observed. The assumption that **5** possesses a structure analogous to **6**$^-$ can be ruled out on the basis of the NMR data. The ^{11}B-NMR shift of δ = −22.3 is comparable with the data mentioned above. Again the signal is broadened so that no coupling to the hydrogen atoms can be observed. The IR spectrum of **5** shows four absorptions at $\tilde{\nu}$ = 2081, 2004, 1992 and 1974 cm^{-1}. In the mass spectrum (EI) of **5** the molecular ion of *m*/*z* = 318 with the expected isotopic distribution is observed as well as the fragmentation pattern for the sequential loss of up to five CO molecules, with the resulting base peak at *m*/*z* = 178 [M$^+$ − 5 CO].

Scheme 2

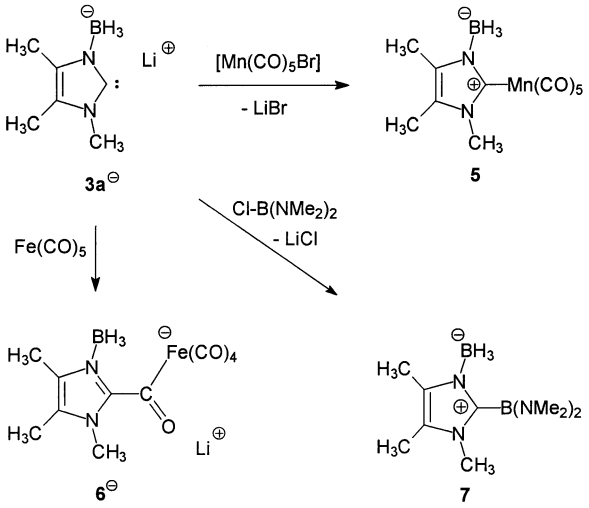

At room temperature **3a**$^-$ attacks one carbonyl ligand in $Fe(CO)_5$, analogously to the reaction of alkyllithium with carbonyl complexes[19], with formation of the complex anion **6**$^-$. The reaction occurs rapidly and quantitatively as monitored by IR spectroscopy. This behavior represents an important difference relative to the reactivity of the imidazol-2-ylidenes known today. Obviously, **3a**$^-$ is much more nucleophilic than the classic nucleophilic carbenes. In the presence of tetrahydropyran, $Li(thp)_3^+$**6**$^-$ is obtained as a crystalline yellow solid which is extremely sensitive to air and moisture. It decomposes slowly even at temperatures < −10°C.

For the anion **6**$^-$ two structures may be expected, the acyl complex **6**$^-$ with an Fe−C single bond or the carbene complex **6′**$^-$. The X-ray diffraction study of $Li(thp)_3^+$**6**$^-$ reveals that in the solid state the complex has the acyl structure **6**$^-$ (see below). In case of an equilibrium between the two structures in solution, it should be possible to transform the complex into a Fischer carbene complex by methylation as preliminary experiments indicate.

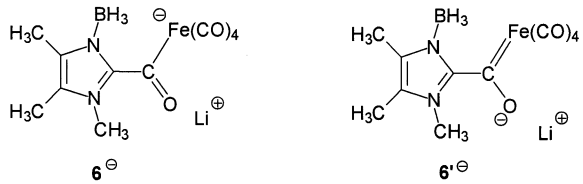

The NMR data for **6**$^-$ reveal the expected pattern: In the ^{13}C-NMR spectrum a low-field shift to δ = 154.3 for the C2 atom is observed, compared with δ = 135.7 in **2a**. This can be explained by the electron-withdrawing effect of the acyl group. Its carbon atom shows a resonance at δ = 280.8 while for the four other carbonyl groups only one signal is observed at δ = 219.4. The ^{11}B-NMR shift of δ = −22.9 differs little from those for **2a** and **3a**$^-$. Again, the signal is broadened so that no coupling with the hydrogen atoms can be observed. Its IR spectrum shows four CO absorptions at $\tilde{\nu}$ = 2031, 1949, 1928, and 1911 cm^{-1}.

The reaction of **3a**$^-$ with chlorobis(dimethylamino)borane at −30°C leads to **7** in 72% yield. It was characterized by ^{1}H-, ^{13}C-, ^{11}B-NMR spectroscopy, and mass spectrometry. The ^{1}H-NMR spectrum shows two signals for the aminoboryl and the N-CH_3 groups at δ = 2.56 and 3.39, in an intensity ratio of 4:1. This indicates a free rotation of the dimethylamino substituents. The two C-CH_3 groups show resonances at δ = 2.10 and 2.11. In the ^{13}C-NMR spectrum two signals can be found in the aromatic region at δ = 123.4 and 131.0 for the atoms C4 and C5, while that of C2 is not observed. The four CH_3 substituents resonate at δ = 8.5, 10.0, 31.4, and 40.0. The ^{11}B-NMR shift of the BH_3 group is nearly unchanged with δ = −21.8, and the second boron signal is observed at δ = 27.8, a typical shift for a diamino(organo)borane.

Crystal Structures

To elucidate the structure of **3a**$^-$, an X-ray diffraction study was carried out (crystal data and structure refinement for **3a**$^-$, **3b**$^-$, and **6**$^-$ are shown in Table 1). A single crystal of $Li(thp)^+$**3a**$^-$ was grown from a tetrahydropyran solution at 4°C. Its structure (Figure 1) is built up by dimeric units of two carbene anions which are connected by the two lithium cations.

It was found that for imidazoles and imidazol-2-ylidenes the distances and angles at C2 show characteristic differences[1]. In imidazol-2-ylidenes the angle N1−C2−N3 (101.4−102.2°) is significantly smaller than that in imidazoles and imidazolium ions (107−109°)[20]. The C2−N distances are a little elongated and approximately equal (1.363−1.373 Å)[1], while in imidazoles an alternation of bond lengths is observed (e.g. 1.32 and 1.37 Å[21]). The C2−N1 and C2−N3 bond lengths (1.373 and 1.368 Å) in **3a**$^-$ are in good agreement with those of **A**[1], while the N1−C2−N3 angle of 104.0° is enlarged by 2.5°. This slight increase can be explained by the interaction of the carbene center with the lithium cation. The imidazole ring is almost planar with deviations from the best plane through the ring

Table 1. Crystal data and structure refinement for Li(thp)$^+$**3a**$^-$, Li(thf)$_2^+$**3b**$^-$, and Li(thp)$_3^+$**6**$^-$

	Li(thp)$^+$**3a**$^-$	Li(thf)$_2^+$**3b**$^-$	Li(thp)$_3^+$**6**$^-$
Empirical formula	$C_{11}H_{22}BLiN_2O$	$C_{20}H_{40}BLiN_2O_2$	$C_{26}H_{42}BFeLiN_2O_8$
Formula weight	216.1	358.3	584.2
Crystal system	triclinic	monoclinic	monoclinic
Space group	$P\bar{1}$	$P2_1/n$	$P2_1/n$
Unit cell			
a [Å]	8.218(4)	9.723(11)	10.873(8)
b [Å]	8.669(4)	13.853(14)	14.426(11)
c [Å]	11.108(6)	17.274(19)	20.307(15)
α [°]	79.44(3)	90	90
β [°]	75.19(3)	93.03(9)	93.37(6)
γ [°]	61.89(3)	90	90
Volume [Å^3]	673.0(6)	2323(4)	3180(4)
Z	2	4	4
Calc. density [g/cm^3]	1.066	1.024	1.220
Adsorp.coeff. [mm^{-1}]	0.066	0.063	0.519
F(000)	236	792	1240
Crystal size [mm]	0.65×0.55×0.50	0.7×0.5×0.5	0.7×0.7×0.5
Θ-range [°]	1.9−25.0	1.9−26.0	1.7−27.0
Index-ranges	−9/+9, −9/+10, 0/+13	−11/+11, 0/+17, 0/+21	−13/+13, 0/+18, 0/+25
No. of reflections			
unique	2375	4558	6932
observed [I>2σ(I)]	1619	2604	4836
Transmission	0.933−1.00	0.94−1.00	0.87−1.00
Parameters	228	239	527
Final R indices			
$R1$ [I > 2σ(I)]	0.059	0.091	0.045
$wR2$	0.165	0.271	0.117
Largest diff.peak/hole[e/Å^3]	+0.17 / −0.40	+0.48 / −0.43	+0.31 / −0.22

atoms being less than 0.006 Å. The B6−N1 distance of 1.572 Å is characteristic for a B−N single bond. For each of the lithium cations a short (Li−C2′ 2.169 Å) and a longer contact (Li1−C2 2.339 Å) with the carbene carbon atoms are observed. The coordination around the Li cation is completed by the thp molecule and a weak interaction with the BH_3 group.

Figure 1. Structure of Li(thp)$^+$**3a**$^-$ in the crystal[a]

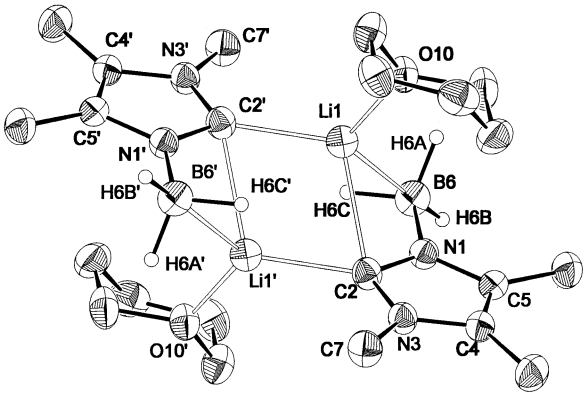

[a] Selected bond lengths [Å] and angles [°]: N1−C2 1.373(3), C2−N3 1.368(3), N3−C4 1.393(3), C4−C5 1.355(3), C5−N1 1.398(3), B6−N1 1.572(3), Li1−B6 2.417(5), Li1−N1 2.489(5), Li1−C2 2.339(5), Li1−C2′ 2.169(5), Li1−H1 2.315(5), Li1−H3 2.214(5), B6−H1 1.156(32), B6−H3 1.185(30), B6−H2 1.102(30), N1−C2−N3 104.0(2), C2−N3−C4 112.2(2), N3−C4−C5 105.7(2), C4−C5−N1 107.9(2), C5−N1−C2 110.3(2).

3a$^-$ is the first example of an isolable borane-substituted imidazol-2-ylidene, although carbene−borane adducts such as 2-borane−1,3-diethyl-4,5-dimethylimidazoline (**G**) are already known[18]. **F** has not attracted any attention as a carbene although the structural data[8] support the assumption that it may be regarded as a carbene−borane adduct (**F′**) as well.

In **F′** (R = mesityl)[8b] the C2−N bonds (1.356 and 1.357 Å) are nearly identical and match the distances found in **G**. The N−C−N angle of 106.4° has increased by 1.7° compared with that in **G**, but is still significantly smaller than in an imidazole or imidazolium ion. The C2−B distance in **F′** is 1.635 Å (**G**: 1.603 Å) which may be explained by the effect of the sterically demanding mesityl substituents. In contrast, **F** represents a description as an adduct in which the BH_2 group of a 2-boryl-substituted imidazole acts as Lewis acid and the imidazole nitrogen atom as Lewis base. This should lead to a characteristic imidazole structure with alternation of the C2−N bond lengths and a larger N−C−N angle. Another indication for the carbene character of **F′** (R = H) is its ^{13}C-NMR shift of δ = 161.0[8a] which is observed in the typical low-field area of carbene adducts and is comparable with the shift of δ = 166.6 for **G**[18].

A different structure is found for Li(thf)$_2^+$**3b**$^-$. A single crystal was grown from a hexane solution at 4°C and the structure is shown in Figure 2. The crystal-structure determination reveals the occurrence of a migration of the BEt_3 group from the nitrogen to the carbon atom, leading to a 1-methyl-2-borane-substituted imidazole anion.

The C2−N1 and C2−N3 bond lengths of 1.337 Å and 1.373 Å show the typical alternation of a 1-substituted imi-

Figure 2. Structure of $Li(thf)_2^+\mathbf{3b}^-$ in the crystal[a]

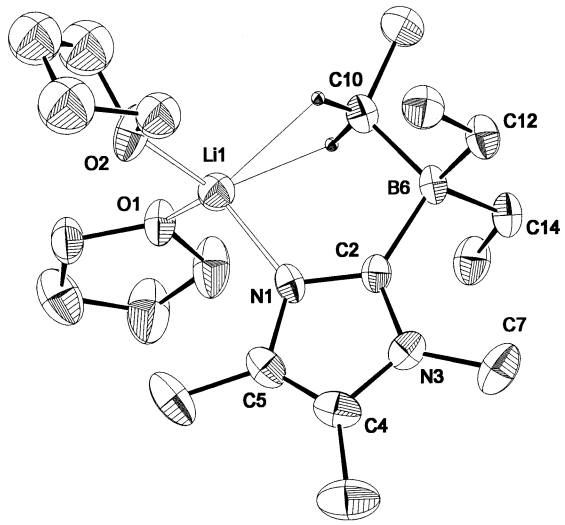

[a] Selected bond lenghts [Å] and angles [°]: N1−C2 1.337(4), C2−N3 1.373(4), N3−C4 1.389(5), C4−C5 1.346(5), C5−N1 1.388(5), N2−C7 1.464(5), B6−C2 1.645(5), B6−C10 1.655(5), B6−C12 1.646(5), B6−C14 1.639(5), Li1−N1 1.932(7), Li1−C10 2.511(7), N1−C2−N3 107.4(3), N1−C5−C4 109.4(3), C2−N1−N3 108.2(3), N3−C4−C5 105.7(3), C2−N3−C4 109.3(3).

dazole[21] and the N1−C2−N3 angle of 107.4° has increased considerably when compared to that of **A**[1] and $Li(thp)^+\mathbf{3a}^-$. The N1 atom interacts strongly with the lithium cation (Li1−N1 1.932 Å), whose coordination is completed by the two thf molecules and weak agostic interactions with the hydrogen atoms of the methylene group at C10.

Figure 3. Structure of $Li(thp)_3^+\mathbf{6}^-$ in the crystal[a]

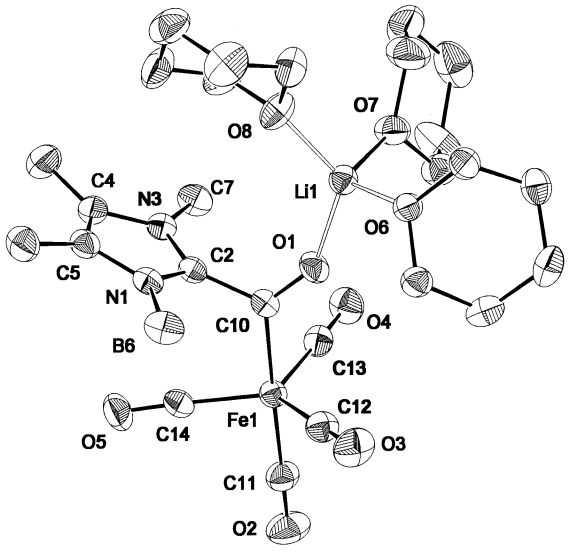

[a] Selected bond lengths [Å] and angles [°]: N1−C2 1.326(3), C2−N3 1.347(3), N3−C4 1.395(3), C4−C5 1.351(4), C5−N1 1.397(4), N1−B6 1.596(4), N3−C7 1.465(4), C2−C10 1.512(4), Fe1−C10 1.966(3), C10−O1 1.237(3), Li1−O1 1.905(5), Fe1−C11 1.800(3), Fe1−C12 1.792(3), Fe1−C13 1.781(3), Fe1−C14 1.787(3), N1−C2−N3 109.4(2), C2−N1−C5 107.7(2), C2−N3−C4 108.3(2), N3−C4−C5 106.4(2), N1−C5−C4 108.2(2), C2−C10−O1 114.6(2), C2−C10−Fe1 118.7(2), Fe1−C10−O1 126.6(2), C10−Fe1−C11 178.3(1).

The bonding in $Li(thp)_3^+\mathbf{6}^-$ is of significant interest in order to distinguish whether it is an acyl or a carbene compound. The answer was found by carrying out an X-ray diffraction study. Single crystals were grown from a thp solution at 4°C. The X-ray structure of $\mathbf{6}^-$ shows the complex anion with $Li(thp)_3^+$ as counter ion that is attached to the acyl oxygen atom (Figure 3). There is no doubt that $\mathbf{6}^-$ must be regarded as an acyl complex. It exhibits a trigonal-bipyramidal coordination of the iron atom by four CO ligands and the acyl group, derived from the addition of $\mathbf{3a}^-$ to one of the axial carbon monoxide in $Fe(CO)_5$. The C10−Fe1−C11 axis is nearly linear with an angle of 178.7°. The $Li(thp)_3^+$ ion is coordinated by the oxygen atom of the acyl group. The length of the Fe1−C10 bond (1.966 Å) is in agreement with the formulation as an acyl complex, for which Fe−C distances between 1.92 and 1.99 Å[22] are typically observed, compared with 1.84−1.87 Å for carbene complexes[23]. The C2−C10 (1.512 Å) and C10−O1 (1.237 Å) distances also fit with the data found for acyl complexes[22]. Obviously the acyl ligand has nearly no influence on the *trans*-CO group, with the Fe1−C11 bond length of 1.800 Å being comparable to those for the equatorial carbonyl groups (1.781−1.792 Å). The distances and angles of the imidazole ring indicate the loss of carbene character. The alternating bond lengths N1−C2 (1.326 Å) and C2−N3 (1.347 Å) as well as the large N1−C2−N3 angle of 109.4° are typical for an imidazole.

Experimental Section

General: Reactions were carried out under dry argon, using standard Schlenk techniques. Solvents were dried, distilled, and saturated with nitrogen. Glassware was dried with a heat-gun in high vacuum. − ^{1}H-, ^{13}C-, ^{11}B-NMR: Bruker AC 200 spectrometer, NMR references are $(CH_3)_4Si$ and $BF_3 \cdot Et_2O$. − IR spectra were recorded with a Bruker IFS 28 Fourier transformation spectrometer with CaF_2 cells. − Mass spectra were obtained with a Finnigan MAT 8200 plus spectrometer using the EI technique. − Melting points (uncorrected) were obtained with a Büchi apparatus, using a capillary which was filled under argon and sealed. − 1,4,5-trimethylimidazole (**1**)[24a] and $[Mn(CO)_5Br]$[24b] were prepared according to literature procedures.

3-Borane−1,4,5-trimethylimidazole (**2a**): To a solution of 790 mg (7.2 mmol) of **1** in 20 ml of thf, 7.2 ml of $BH_3 \cdot$ thf (1.0 M in thf) was added dropwise at 0°C, after which the mixture was allowed to warm to room temp. and stirred for 24 h. By that time a white solid had precipitated. The product was dissolved by heating and then allowed to crystallize at −30°C. Yield: 760 mg (85%) colorless, air-stable needles, m.p.: 160°C. − ^{1}H NMR (200.1 MHz, $CDCl_3$): δ = 2.10 (s, 3 H, C-CH_3), 2.14 (s, 3 H, C-CH_3), 3.53 (s, 3 H, N-CH_3), 7.62 (s, 1 H, N=CH-N). − ^{13}C NMR (50.3 MHz, $CDCl_3$): δ = 9.2 (C-*C*H_3), 10.6 (C-*C*H_3), 33.2 (N-CH_3), 125.3 (C=*C*-N), 132.2 (C=*C*-N), 135.7 (N=CH-N). − ^{11}B NMR (64.2 MHz, $CDCl_3$): δ = −20.9 (q, $^1J_{B\text{-}H}$ = 94 Hz). − $C_6H_{13}BN_2$ (124.0): calcd. C 58.12, H 10.56, N 22.59; found C 57.72, H 10.40, N 22.43.

3-(Triethylborane)−1,4,5-trimethylimidazole (**2b**): To a solution of 1.52 g (13.8 mmol) of **1** in 20 ml of toluene, 2.2 ml of BEt_3 was added dropwise at 0°C. The mixture was allowed to warm to room temp. and stirred for 24 h. The solvent was evaporated in vacuo and the colorless oil was allowed to crystallize at −30°C, and then washed with pentane and dried. Yield: 2.84 g (99%); colorless crys-

tals, m.p.: 65°C. – ^{1}HNMR (200.1 MHz, $CDCl_3$): δ = 0.37 (t, 9 H, CH_2-CH_3), 0.57 (q, 6 H, CH_2-CH_3), 2.11 (s, 3 H, C-CH_3), 2.20 (s, 3 H, C-CH_3), 3.54 (s, 3 H, N-CH_3), 7.45 (s, 1 H, N=CH-N). – ^{13}C-NMR (50.3 MHz, $CDCl_3$): δ = 8.0 (C-*C*H_3), 9.3 (CH_2-*C*H_3), 11.0 (C-*C*H_3), 14 (br., *C*H_2-CH_3), 32.2 (N-CH_3), 124.5 (C=C-N), 130.8 (C=C-N), 134.2 (N=CH-N). – ^{11}B-NMR (64.2 MHz, $CDCl_3$): δ = −1.5 ($\Delta\nu_{1/2}$ = 290 Hz).

Lithium 3-Borane−1,4,5-trimethylimidazol-2-ylidene [Li(thp)$^+$-**3a**$^-$]: To a suspension of 860 mg (6.9 mmol) of **2a** in 25 ml of thf 3.2 ml of *n*-butyllithium (2.5 N in hexane) was added dropwise at −40°C. The mixture was allowed to warm to room temp. and stirred for 24 h. The solvent was evaporated in vacuo and the resulting solid was recrystallized from thf/hexane at −30°C. Yield: 1.14 g (82%) colorless crystals, m.p.: 210−220°C (decomp.). – ^{1}H NMR (200.1 MHz, C_6D_6): δ = 1.38 (m, 12 H, thf), 1.74 (s, 3 H, C-CH_3), 2.34 (s, 3 H, C-CH_3), 3.43 (s, 3 H, N-CH_3), 3.57 (m, 12 H, thf). – ^{13}C NMR (50.3 MHz, C_6D_6): δ = 8.3 (C-*C*H_3), 10.4 (C-*C*H_3), 25.1 (thf), 33.8 (N-CH_3), 67.6 (thf), 121.8 (C=C-N), 128.7 (C=C-N), 191.3 (N=C-N). – ^{11}B NMR (64.2 MHz, C_6D_6): δ = −21.1 ($\Delta\nu_{1/2}$ = 290 Hz).

Lithium Triethyl(1,4,5-trimethylimidazolyl)borate [Li(thf)$_2^+$**3b**$^-$]: To a suspension of 950 mg (4.6 mmol) of **2b** in 20 ml of thf 2.0 ml of *n*-butyllithium (2.5 N in hexane) were added dropwise at −78°C. The mixture was allowed to warm to room temp. and stirred for 24 h. The solvent was evaporated in vacuo and the resulting white solid was recrystallized from thf/hexane. Yield: 1.07 g (77%) colorless crystals, m.p.: 150−160°C (decomp.). – ^{1}H NMR (200.1 MHz, $CDCl_3$): δ = 0.29 (q, 6 H, CH_2-CH_3), 0.59 (t, 9 H, CH_2-CH_3), 1.83 (m, 8 H, thf), 2.06 (s, 3 H, C-CH_3), 2.10 (s, 3 H, C-CH_3), 3.58 (s, 3 H, N-CH_3), 3.72 (m, 8 H, thf). – ^{13}C NMR (50.3 MHz, $CDCl_3$): δ = 8.3 (C-*C*H_3), 9.4 (C-*C*H_3), 10.7 (CH_2-*C*H_3), 14.0 (br., *C*H_2-CH_3), 25.6 (thf), 32.0 (N-CH_3), 67.9 (thf), 119.9 (C=C-N), 123.8 (C=C-N), C2 not observed. – ^{11}B NMR (64.2 MHz, C_6D_6): δ = −14.6.

2-(Triethylborane)−1,3,4,5-tetramethylimidazoline (**4**): 810 mg (3.9 mmol) of **2b** was dissolved in 15 ml of thf and 1.7 ml of *n*-butyllithium (2.5 N in hexane) was added dropwise at −78°C. The mixture was allowed to warm to room temp. and stirred for 1 h. Then 0.5 ml of iodomethane was added at −30°C, the solution was warmed to room temp. and stirred for another hour. The solvent was evaporated in vacuo, the resulting white solid was dissolved in hexane and filtered. After cooling to −30°C, a white precipitate had formed which was filtered and dried. Yield: 600 mg (69%) white powder. – ^{1}H NMR (200.1 MHz, C_6D_6): δ = 1.01 (q, 6 H, CH_2-CH_3), 1.18 (t, 9 H, CH_2-CH_3), 1.29 (s, 6 H, C-CH_3), 3.26 (s, 6 H, N-CH_3). – ^{13}C NMR (50.3 MHz, C_6D_6): δ = 8.3 (C-*C*H_3), 12.1 (CH_2-*C*H_3), 15.0 (br., CH_2-CH_3), 32.9 (N-CH_3), 123.6 (C=C-N), C2 signal not observed. – ^{11}B NMR (64.2 MHz, C_6D_6): δ = −12.6. – EI-MS; *m/z* (%): 193 (45) [$M^+ - C_2H_5$], 137 (100), 124 (44) [$M^+ - BEt_3$].

(3-Borane−1,4,5-trimethylimidazol-2-ylidene)pentacarbonylmanganese (**5**): To a suspension of 240 mg (1.9 mmol) of **2a** in 20 ml of thp was added 0.85 ml of *n*-butyllithium (2.5 N in hexane) dropwise at −40°C. The reaction mixture was allowed to warm to room temp. and stirred for 1 h. Then 535 mg (1.9 mmol) of [$Mn(CO)_5Br$] were added at −40°C and the solution was again warmed to room temp. and stirred for another hour. While warming, the solid dissolved, the solution became orange-colored and at room temp. deep red. The solvent was evaporated in vacuo, the residue dissolved in toluene and separated by column chromatography (SiO_2/toluene). Yield: 200 mg (33%) yellow powder. – ^{1}H NMR (200.1 MHz, [D_8]thf): δ = 2.22 (s, 3 H, C-CH_3), 2.24 (s, 3 H, C-CH_3), 3.81 (s, 3 H, N-CH_3). – ^{13}C NMR (50.3 MHz, [D_8]thf): δ = 8.3 (C-*C*H_3), 9.6 (C-*C*H_3), 32.3 (N-CH_3), 129.0 (C=C-N), 130.9 (C=C-N), 146.9 (N-C-N), 214.6 (CO), 256.1 (CO). – ^{11}B NMR (64.2 MHz, C_6D_6): δ = −22.3. – IR (hexane): $\tilde{\nu}$(CO) [cm^{-1}] = 2081 (w), 2004 (s), 1992 (vs), 1974 (s). – EI-MS; *m/z* (%): 318 (22) $[M]^+$, 290 (17) $[M - CO]^+$, 262 (20) $[M - 2\ CO]^+$, 234 (48) $[M - 3\ CO]^+$, 206 (29) $[M - 4\ CO]^+$, 178 (100) $[M - 5\ CO]^+$.

Lithium (3-Borane−1,4,5-trimethylimidazol-2-ylcarbonyl)tetracarbonyliron [Li(thp)$_3^+$**6**$^-$]: To a suspension of 500 mg (4.0 mmol) of **2a** in 20 ml of thp was added 1.8 ml of *n*-butyllithium (2.5 N in hexane) dropwise at −40°C. The mixture was allowed to warm to room temp. and stirred for 1 h. Then 0.55 ml of $Fe(CO)_5$ was added at −40°C. At −30°C a yellow solid was formed which dissolved at 5°C. The orange-colored solution was stirred for 1 h at room temp. and afterwards half of the solvent was removed in vacuo. Crystallization at −30°C yielded 1.29 g (78%) yellow needles, m.p.: 120−127°C (decomp.). – ^{1}H NMR (200.1 MHz, C_6D_6): δ = 1.29 (m, 24 H, thp), 1.44 (s, 3 H, C-CH_3), 2.01 (s, 3 H, C-CH_3), 3.42 (s, 3 H, N-CH_3), 3.52 (m, 16 H, thp). – ^{13}C NMR (50.3 MHz, [D_8]thf): δ = 8.2 (C-*C*H_3), 10.0 (C-*C*H_3), 24.7 (thp), 27.8 (thp), 31.1 (N-CH_3), 69.3 (thp), 121.1 (C=C-N), 128.1 (C=C-N), 154.3 (N-C-N), 219.4 (CO), 280.8 (CO). – ^{11}B NMR (64.2 MHz, C_6D_6): δ = −22.9 (br.). – IR (thp): $\tilde{\nu}$(CO) [cm^{-1}] = 2031 (s), 1949 (s), 1928 (vs), 1911 (vs).

3-Borane−2-[bis(dimethylamino)boryl]-1,4,5-trimethylimidazoline (**7**): To a suspension of 500 mg (4.0 mmol) of **2a** in 20 ml of thf was added 1.6 ml of *n*-butyllithium (2.5 N in hexane) dropwise at −40°C with dissolving of the solid. The mixture was allowed to warm to room temp. and stirred for 1 h. Then 540 mg (4.0 mmol) of chlorobis(dimethylamino)borane was added at −30°C, the solution warmed to room temp. and stirred for another hour. The solvent was removed in vacuo and the white precipitate dissolved in toluene. LiCl was separated by filtration and the product was allowed to crystallize from a toluene/hexane solution. Yield: 640 mg (72%) colorless needles, m.p.: 74°C. – ^{1}H NMR (200.1 MHz, $CDCl_3$): δ = 2.10 (s, 3 H, C-CH_3), 2.17 (s, 3 H, C-CH_3), 2.56 (s, 12 H, N-CH_3), 3.39 (s, 3 H, N-CH_3). – ^{13}C NMR (50.3 MHz, $CDCl_3$): δ = 8.5 (C-*C*H_3), 10.0 (C-*C*H_3), 31.4 (N-CH_3), 40.0 (N-CH_3), 123.4 (C=C-N), 131.0 (C=C-N), C2 signal not observed. – ^{11}B NMR (64.2 MHz, $CDCl_3$): δ = −21.9 (br., BH_3), 27.8 [br., $B(NMe_2)_2$]. – EI-MS; *m/z* (%): 221 (13) [$M^+ - H$], 207 (7) [$M^+ - CH_3$], 123 (100) [$M^+ - B(NMe_2)_2$].

Crystal-Structure Determinations of Li(thp)$^+$**3a**$^-$, Li(thf)$_2^+$**3b**$^-$, *and* Li(thp)$_3^+$**6**$^-$: Crystal data and details of the structure determinations are listed in Table 1. Unique sets of intensity data were collected at −70°C with a four-circle diffractometer (Mo-K_α radiation λ = 0.7107 Å, graphite monochromator, ω-scan). Empirical absorption corrections (ψ-scans) were applied. The structures were solved by direct methods [SHELXS86][25] and refined by least-squares methods based on F^2 with all measured reflections [SHELXL97][26]. All non-hydrogen atoms were refined anisotropically. Hydrogen atoms in **3b**$^-$ were included in calculated positions or as part of rigid groups (CH_3), in **3a**$^-$ and **6**$^-$ hydrogen atoms were located in difference Fourier maps and refined. The thf molecules in **3b**$^-$ and one of the thp molecules in **6**$^-$ are disordered.

Crystallographic data (excluding structure factors) for the structures reported in this paper have been deposited with the Cambridge Crystallograhpic Data Center as supplementary publication no. CCDC-101057. Copies of the data can be obtained free of charge on application to CCDC, 12 Union Road, Cambridge CB2 1EZ, UK; fax: int. code + 44(0)1223/336-001; e-mail: deposit@ccdc.cam.ac.uk

[☆] Dedicated to Prof. Dr. *Heinrich Nöth* on the occasion of his 70th birthday.

[1] [1a] A. J. Arduengo, R. L. Harlow, M. Kline, *J. Am. Chem. Soc.* **1991**, *113*, 361−363. − [1b] A. J. Arduengo, H. V. Rasika Dias, R. L. Harlow, M. Kline, *J. Am. Chem. Soc.* **1992**, *114*, 5530−5534.

[2] A. J. Arduengo, J. R. Görlich, W. J. Marshall, *J. Am. Chem. Soc.* **1995**, *117*, 11027−11028.

[3] R. W. Alder, P. R. Allen, M. Murray, A. G. Orpen, *Angew. Chem.* **1996**, *108*, 1211−1213; *Angew. Chem. Int. Ed. Engl.* **1996**, *35*, 1121−1123.

[4] D. Enders, K. Breuer, G. Raabe, J. Runsink, J. H. Teles, J.-P. Melder, K. Ebel, S. Brode, *Angew. Chem.* **1996**, *108*, 1119−1122; *Angew. Chem. Int. Ed. Engl.* **1996**, *35*, 1021−1024.

[5] A. J. Arduengo, J. R. Görlich, W. J. Marshall, *Liebigs Ann.* **1997**, 365−374.

[6] W. A. Herrmann, C. Köcher, *Angew. Chem.* **1997**, *109*, 2256−2282; *Angew. Chem. Int. Ed. Engl.* **1997**, *36*, 2162−2187.

[7] W. P. Fehlhammer, U. Kernbach, M. Ramm, R. Luger, *Angew. Chem.* **1996**, *108*, 333−335; *Angew. Chem. Int. Ed. Engl.* **1996**, *35*, 310−312.

[8] [8a] I. I. Padilla-Martinez, M. de Jesus Rosalez-Hoz, R. Contreras, S. Kerschl, B. Wrackmeyer, *Chem. Ber.* **1994**, *127*, 343−346. − [8b] K. Okada, R. Suzuki, M. Oda, *J. Chem. Soc., Chem. Commun.* **1995**, 2069−2070.

[9] [9a] A. J. Arduengo, M. Tamm, S. J. McLain, J. C. Calabrese, F. Davidson, W. J. Marshall, *J. Am. Chem. Soc.* **1994**, *116*, 7927−7928. − [9b] H. Schumann, M. Glanz, J. Winterfeld, H. Hemling, N. Kuhn, T. Kratz, *Angew. Chem.* **1994**, *106*, 1829−1830; *Angew. Chem. Int. Ed. Engl.* **1994**, *33*, 1804−1805. − [9c] W. P. Fehlhammer, T. Bliss, U. Kernbach, I. Brüdgam, *J. Organomet. Chem.* **1995**, *490*, 149−153. − [9d] W. A. Herrmann, O. Runte, G. Artus, *J. Organomet. Chem.* **1995**, *501*, C1−C4. − [9e] W. A. Herrmann, M. Elison, J. Fischer, C. Köcher, G. R. J. Artus, *Chem. Eur. J.* **1996**, *2*, 772−780. − [9f] W. A. Herrmann, C. Köcher, L. J. Gooßen, G. R. J. Artus, *Chem. Eur. J.* **1996**, *2*, 1627−1636. − [9g] D. Enders, H. Gielen, G. Raabe, J. Runsink, J. H. Teles, *Chem. Ber.* **1996**, *129*, 1483−1488.

[10] K. Öfele, W. A. Herrmann, D. Mihalios, M. Elison, E. Herdtweck, W. Scherer, J. Mink, *J. Organomet. Chem.* **1993**, *459*, 177−184.

[11] K. Öfele, W. A. Herrmann, D. Mihalios, M. Elison, E. Herdtweck, T. Priermeier, P. Kiprof, *J. Organomet. Chem.* **1994**, *498*, 1−14.

[12] W. A. Herrmann, L. J. Gooßen, C. Köcher, G. R. J. Artus, *Angew. Chem.* **1996**, *108*, 2980−2982; *Angew. Chem. Int. Ed. Engl.* **1996**, *35*, 2805−2807.

[13] W. A. Herrmann, M. Elison, J. Fischer, C. Köcher, G. R. J. Artus, *Angew. Chem.* **1995**, *107*, 2602−2604; *Angew. Chem. Int. Ed. Engl.* **1995**, *34, 2371−2373.*

[14] H. Nöth, B. Wrackmeyer, *Chem. Ber.* **1974**, *107*, 3070−3088.

[15] R. J. Thompson, J. C. Davis, Jr., *Inorg. Chem.* **1965**, *4*, 1464.

[16] H. Nöth, B. Wrackmeyer, *NMR Spectroscopy of Boron Compounds*, Springer Verlag, Heidelberg, **1978**.

[17] [17a] A. J. Arduengo, H. V. Rasika Dias, J. C. Calabrese, F. Davidson, *J. Am. Chem. Soc.* **1992**, *114*, 9724−9725. − [17b] A. J. Arduengo, H. V. Rasika Dias, F. Davidson, R. L. Harlow, *J. Organomet. Chem.* **1993**, *462*, 13−18. − [17c] N. Kuhn, H. Bohnen, G. Henkel, *Z. Naturforsch.* **1994**, *49b*, 1473−1480. − [17d] N. Kuhn, T. Kratz, D. Bläser, R. Boese, *Chem. Ber.* **1995**, *128*, 245−250. − [17e] A. J. Arduengo, S. F. Gamper, M. Tamm, J. C. Calabrese, F. Davidson, H. A. Craig, *J. Am. Chem. Soc.* **1995**, *117*, 572−573. − [17f] A. J. Arduengo, R. Krafczyk, W. J. Marshall, R. Schmutzler, *J. Am. Chem. Soc.* **1997**, *119*, 3381−3382. − [17g] L. Weber, E. Dobbert, H.-G. Stammler, B. Neumann, R. Boese, D. Bläser, *Chem. Ber.* **1997**, *130*, 705−710.

[18] N. Kuhn, G. Henkel, T. Kratz, J. Kreutzberg, R. Boese, A. H. Maulitz, *Chem. Ber.* **1993**, *126*, 2041−2045.

[19] E. O. Fischer, A. Maasböl, *Chem. Ber.* **1967**, *100*, 2445−2456.

[20] [20a] V. Langer, K. Huml, *Acta Crystallogr., Sect. B* **1982**, *38*, 298−300. − [20b] A. K. Abdul-Sada, A. M. Greenway, P. B. Hitchcock, T. J. Mohammed, K. R. Seddon, J. A. Zora, *J. Chem. Soc., Chem. Comm.* **1986**, 1753−1754.

[21] G. Bruno, F. Nicolo, *Acta Crystallogr.* **1994**, *C50*, 428−430.

[22] [20a] T. G. Attig, R. G. Teller, S.-M. Wu, R. Bau, A. Wojicicki, *J. Am. Chem. Soc.* **1979**, *101*, 619−627. − [20b] H. Y. Liu, L. L. Koh, K. Eriks, W. P. Giering, A. Prock, *Acta Crystallogr.* **1990**, *C46*, 51−54. − [20c] L.-K. Liu, L.-S. Luh, *Organometallics* **1994**, *13*, 2816−2824.

[23] [23a] H. Adams, N. A. Bailey, M. Grayson, C. Ridgway, A. J. Smith, P. Taylor, M. J. Winter, *Organometallics* **1990**, *9*, 2621−2628. − [23b] D. J. Crowther, Z. Zhang, G. J. Palenik, W. M. Jones, *Organometallics* **1992**, *11*, 622−628.

[24] [24a] E. Schaumann, *Methoden Org. Chem. (Houben-Weyl)*, vol. E8c, p. 6−7. − [24b] W. E. Silverthorn, *Adv. Organomet. Chem.* **1975**, *13*, 47−49.

[25] G.M. Sheldrick, *SHELXS86*, Univ. Göttingen, **1986**.

[26] G.M. Sheldrick, *SHELXS97*, Univ. Göttingen, **1997**.

[98014]

Neutron Diffraction Study of [K(18-crown-6)] $[(PPh_3)_2ReH_6Cr(CO)_3]$, a Bimetallic Donor-Acceptor Complex☆

Mary H. Drabnis[a], Robert Bau*[a], Sax A. Mason[b], Jeffrey W. Freeman[c], and Richard D. Ernst[c]

Department of Chemistry, University of Southern California,[a]
Los Angeles, CA, 90089, U.S.A

Institut Laue-Langevin,[b]
F-38042 Grenoble, France

Department of Chemistry, University of Utah,[c]
Salt Lake City, UT 84112, U.S.A.

Received February 2, 1998

Keywords: Neutron diffraction / Donor-acceptor complex / Bridging hydride ligand / Rhenium / Chromium

A neutron diffraction analysis was carried out at 120 K on a single crystal of $[K(18\text{-crown-6})][(PPh_3)_2ReH_6Cr(CO)_3]\cdot THF$ in order to locate the hydride ligands. Three of the hydrides are bound terminally to the Re atom while the other three bridge the Re–Cr bond; the bridging hydrides are closer to the Re atom. This compound can be thought of as a donor–acceptor complex, with $[(PPh_3)_2ReH_6]^-$ acting as the donor to the $Cr(CO)_3$ fragment. Average distances and angles: Re–Cr = 2.58(1), Re–H(br) = 1.75(1), Cr–H(br) = 1.92(2), Re–H(t) = 1.69(1) Å; Re–H–Cr = 89.1(7)°. Final agreement factors: $R(F)$ = 6.4% for 3443 reflections with $I > 2\sigma(I)$, and $R(F)$ = 8.3% for all data (4195 reflections).

The concept of a transition metal hydride complex functioning as a ligand has been attracting an increasing amount of attention.[1][2][3][4][5][6][7] In recent years, several cases have been documented in which a metal hydride acts as a donor to a second (otherwise electron-deficient) metal atom. The donor-acceptor interaction in the resulting compound takes place through the bridging hydride ligands, much as in a borohydride complex.[8] In this communication we report the neutron structure determination of one such compound, the $[(PPh_3)_2ReH_6Cr(CO)_3]^-$ anion, and provide the first accurate characterization of a Re−H−Cr bridging system.

$[K(18\text{-crown-6})][(PPh_3)_2ReH_6Cr(CO)_3]$ is made by reaction of $[K(18\text{-crown-6})]$ $[(PPh_3)_2ReH_6]$ with $(CH_3CN)_3Cr(CO)_3$ in THF.[1] Crystals were obtained by the addition of diethyl ether to a THF solution of the title compound. Neutron diffraction data were collected at the Institut Laue-Langevin at 120 K on a sample with volume 4 mm^3, and the structure was refined to a final agreement factor of $R(F)$ = 6.4% (Experimental Section).

The structure of the $[(PPh_3)_2ReH_6Cr(CO)_3]^-$ unit is shown in Figure 1, and selected distances and angles listed in Table 1. Three of the H ligands bridge the Re−Cr bond and three are terminal on Re, as predicted.[1] The bridging H atoms are closer to the Re atom [average Re−H = 1.75(1) Å, average Cr−H = 1.92(2) Å], despite the smaller size[9] of chromium. This suggests that the complex as a whole is best viewed as a donor-acceptor complex in which an 18-electron $[(PPh_3)_2ReH_6]^-$ moiety serves as a 6−electron donor, through the three bridging H atoms, to a 12-electron $Cr(CO)_3$ fragment. The average Re−H−Cr angle is 89.1(7)°, comparable to other compounds having M−(μ−H)$_3$−M bridges.[10] The Re−Cr bond length, 2.58(1) Å, is much shorter than the single-bonded Re−Cr distance of 3.05 Å,[11] suggesting some level of multiple bonding. Indeed, $[(PPh_3)_2ReH_6Cr(CO)_3]^-$ as a whole is isoelectronic with $[Re_2H_9(triphos)]^-$, a compound considered to have a formal triple bond.[3]

Figure 1. A plot of the core of the $[(PPh_3)_2ReH_6Cr(CO)_3]^-$ anion, with all but the *ipso* carbons of the phenyl groups removed for clarity

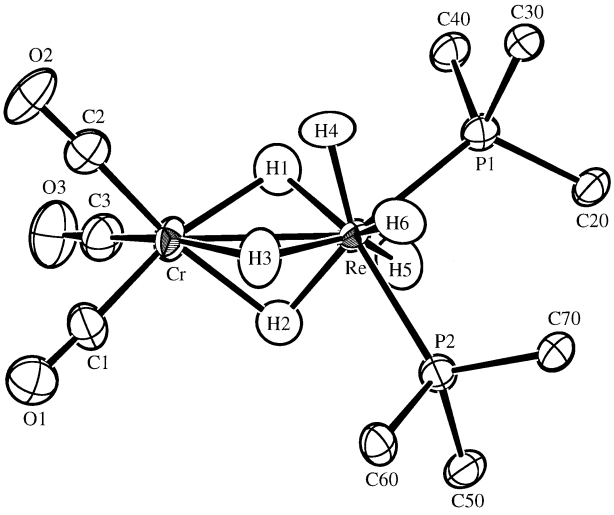

As anticipated earlier,[1] the eight ligands around the Re atom (not counting the Re−Cr bond) define the familiar dodecahedral arrangement[12] of two interpenetrating trapezoids. Figure 2 shows this clearly: atoms H1, H4, H6, and P2 are virtually co-planar (within ±0.01 Å), and define one trapezoid, which is essentially perpendicular to the other

 © WILEY-VCH Verlag GmbH, D-69451 Weinheim, 1998 1434−1948/98/0606−0851 $ 17.50+.50/0

Table 1. Selected distances [Å] and angles [°]

Re−Cr	2.58(1)		
Re−P(1)	2.39(1)	Re−P(2)	2.38(1)
Re−H(1)	1.75(1)	Re−H(4)	1.69(1)
Re−H(2)	1.76(1)	Re−H(5)	1.70(1)
Re−H(3)	1.74(1)	Re−H(6)	1.69(1)
Cr−H(1)	1.94(2)	Cr−C(1)	1.81(1)
Cr−H(2)	1.95(2)	Cr−C(2)	1.80(1)
Cr−H(3)	1.87(2)	Cr−C(3)	1.82(1)
P(1)−Re−H(1)	88.0(5)	P(2)−Re−H(1)	156.4(5)
P(1)−Re−H(2)	139.3(5)	P(2)−Re−H(2)	81.9(5)
P(1)−Re−H(3)	148.1(5)	P(2)−Re−H(3)	92.3(5)
P(1)−Re−H(4)	75.2(5)	P(2)−Re−H(4)	133.9(5)
P(1)−Re−H(5)	66.6(5)	P(2)−Re−H(5)	85.3(5)
P(1)−Re−H(6)	84.3(5)	P(2)−Re−H(6)	67.3(5)
H(1)−Re−H(2)	76.9(6)	H(1)−Re−H(3)	90.3(6)
H(1)−Re−H(4)	69.2(6)	H(1)−Re−H(5)	78.8(6)
H(1)−Re−H(6)	135.7(7)	H(2)−Re−H(3)	70.5(6)
H(2)−Re−H(4)	130.4(6)	H(2)−Re−H(5)	73.5(6)
H(2)−Re−H(6)	132.1(6)	H(3)−Re−H(4)	74.5(6)
H(3)−Re−H(5)	143.8(7)	H(3)−Re−H(6)	74.9(6)
H(4)−Re−H(5)	130.5(7)	H(4)−Re−H(6)	66.6(6)
H(5)−Re−H(6)	135.2(7)		
Cr−Re−H(4)	81.2(5)	Cr−Re−P(1)	136.1(3)
Cr−Re−H(5)	105.2(5)	Cr−Re−P(2)	121.1(4)
Cr−Re−H(6)	119.2(5)	P(1)−Re−P(2)	101.8(3)
H(1)−Cr−H(2)	68.2(6)	C(1)−Cr−H(1)	167.9(8)
H(2)−Cr−H(3)	63.6(6)	C(2)−Cr−H(2)	168.0(8)
H(1)−Cr−H(3)	80.9(7)	C(3)−Cr−H(3)	168.3(8)
C(1)−Cr−Re	127.4(6)	Re−H(1)−Cr	88.4(6)
C(2)−Cr−Re	125.9(6)	Re−H(2)−Cr	88.0(6)
C(3)−Cr−Re	128.9(6)	Re−H(3)−Cr	91.0(7)

trapezoid, defined by atoms H3, H2, H5, and P1 (co-planar within ±0.05 Å). The Re atom is slightly out of plane of both trapezoids. Because of the unsymmetrical positioning of the Re−Cr bond relative to these two interpenetrating trapezoids (one trapezoid contains two bridging H ligands while the other one has only one bridging hydride), the Cr−Re−P angles are unequal [Cr−Re−P1 = 136.1(4), Cr−Re−P2 = 121.1(4)°]. The closest H···H non-bonding contacts are those along the "sides" of the trapezoids (Figure 2): H4···H6 = 1.85, H1···H4 = 1.96, H2···H3 = 2.02, H2···H5 = 2.07 Å.

The average terminal Re−H distance in the title compound [1.69(1) Å] is, as expected,[3][13] shorter than the average bridging Re−H distance [1.75(1) Å]. The former is comparable to terminal Re−H distances found from other neutron structure determinations (range 1.66 to 1.69 Å),[10] but the latter is unusually short (standard Re−H bridging bond lengths range from 1.81 to 1.88 Å[10]). This suggests that the Re−H bridge in $[(PPh_3)_2ReH_6Cr(CO)_3]^-$ is stronger than a normal bridge (i.e., is somewhat more "terminal" in character).

The Cr atom has the expected distorted octahedral geometry, with C−Cr−H (*trans*) angles that have a mean value of 168.1(8)°. The average Cr−H bond length [1.92(2) Å] is much longer than normal bridging Cr−H distances

Figure 2. An alternative view of the $[(PPh_3)_2ReH_6Cr(CO)_3]^-$ core, plotted in such a way as to show the coordination around the Re atom, which consists of two intepenetrating trapezoids. The coplanar atoms H3, H2, H5, and P1 define one trapezoid, which is approximately perpendicular (87°) to the other trapezoid, defined by the coplanar atoms H1, H4, H6, and P2. Because of this arrangement, the three H−Re−H angles are decidedly unequal to each other, as are the three H−Cr−H angles

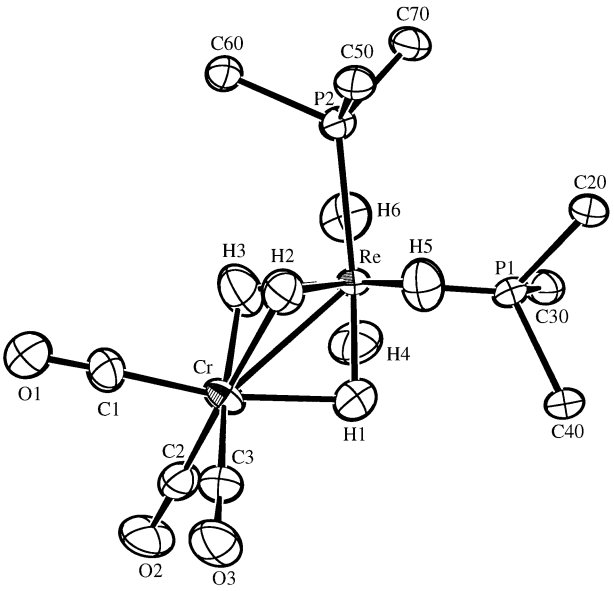

[range: 1.72−1.73 Å],[14] suggesting a weaker-than-usual chromium-hydrogen interaction.

Curiously, the H−Cr−H angles show an unequal distribution [63.6(6), 68.2(6), 80.9(7)°] as do the H−Re−H angles [70.5(6), 76.9(6), 90.3(7)°], presumably because of the steric requirement for maintaining a dodecahedral arrangement of ligands around rhenium.

The K^+ coordination sphere is quite interesting, being made up of the 18-crown-6 ligand and two CO oxygens from separate $Cr(CO)_3$ fragments. This approximately D_{6h}, 8-fold coordination is shown in Figure 3. The THF solvate molecule, which does not bind to the potassium ion and has no other strong interactions, is disordered and was refined as a rigid body in two orientations.

The present structure determination represents the first time that a Re−H−Cr bridging system has been analyzed by neutron diffraction. An earlier X-ray analysis[15] on the single-hydride-bridged complex $(OC)_5Re(H)Cr(CO)_5$ revealed a Re−Cr distance of 3.435(1) Å, but did not locate the bridging H atom. It was originally proposed that the Re−H−Cr bridge in that compound was linear,[15] but that suggestion was made before it became generally accepted that 3-center/2-electron M−H−M bridge bonds are inherently bent.[7][14][16]

Only a few metal hydride complexes of the donor-acceptor type have been accurately analyzed by neutron diffraction. Earlier examples include $[Re_2H_9(triphos)]^-$ {in which $[ReH_9]^{2-}$ is formally a ligand to a $[Re(triphos)]^+$ moiety},[3] $[Pt_2H_3(dppe)_2]^+$ {a complex between $PtH_2(dppe)$ and $[PtH(dppe)]^+$},[4] $[PtIrH_4(PEt_3)_4]^+$ {a complex between $PtH_2(PEt_3)_2$ and $[IrH_2(PEt_3)_2]^+$},[5] and

Figure 3. The coordination around the K^+ ion, which is surrounded by six oxygen atoms from the 18-crown-6 ligand and two carbonyl oxygen atoms in an approximately D_{6h} arrangement. The two axial ligands are the O2 and O3 atoms of the $H_3Cr(CO)_3$ portions of two neighboring anions

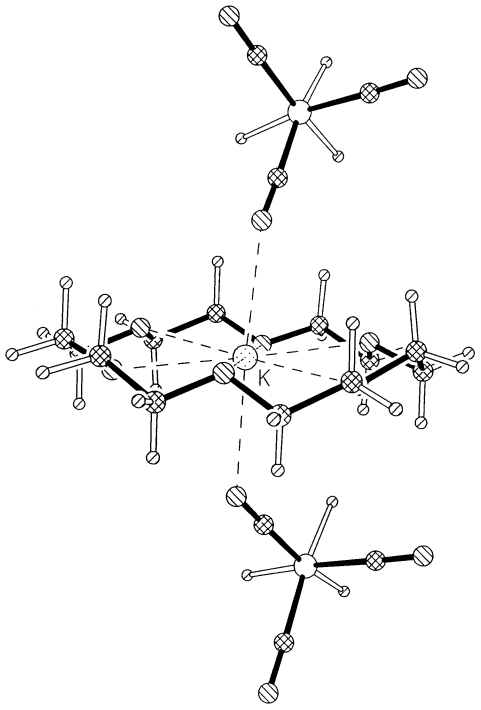

$[(PEt_3)_2(C_6Cl_5)PtHAg(H_2O)]^+$, in which a Pt−H bond is a donor to a Ag^+ ion.[6] Also worthy of mention are two complexes in which $[Na(18\text{-crown-}6)]^+$ and $[K(18\text{-crown-}6)]^+$ act as acceptors from a $[WH_5(PMe_3)_3]^-$ fragment.[17] In most cases {except $[Re_2H_9(triphos)]^-$},[3] the hydride ligands are unsymmetrically bridging in such a way as to indicate that they are held much more tightly to the donor atom than the acceptor atom. The structure of the title compound is consistent with this general trend: the short/long pattern of distances in the Re−H−Cr linkage is certainly suggestive of a higher bond order for the Re−H portion than the H−Cr portion of the bridge.

This research was supported by the *National Science Foundation* and the *American Chemical Society* (Petroleum Research Fund).

Experimental Section

The neutron diffraction data set was collected at the Institut Laue-Langevin, Grenoble, France, on the thermal-beam instrument D19, which is equipped with a 4° × 64° position-sensitive detector.[18] A platelike single crystal of dimensions 1.2 × 1.6 × 2.0 mm, volume 4 mm^3, was sealed in epoxy on an Al pin and placed in a Displex cryorefrigerator.[19] It was then indexed and cooled at 2 degrees per minute while the strong (0, 0, 4) reflection was being monitored. Below 117 K the mosaic spread increased and at 95 K the peak was much broader and weaker, so the temperature was raised to 120 K where the mosaic spread was acceptable and the peak intensity restored. Data were initially collected at a neutron wavelength of 1.3139 Å, but this was changed to 1.5394 Å to increase the intensity of the reflections. Bragg intensities were integrated in three dimensions using the ILL program RETREAT.[20] The two sets of intensities were then scaled and merged, and corrected for attenuation by the cylindrical heat shields, and for absorption effects (μ = 2.31 cm^{-1} at 1.3139 Å; 2.55 cm^{-1} at 1.5394 Å) using the program D19ABS, based on the ILL version of the CCSL system.[21] Refinement was begun using the positions of the non-hydrogen atoms obtained from the x-ray structure determination;[1] the positions of the organic hydrogen atoms were calculated and subjected to several cycles of least-squares refinement. The hydride ligands were readily found in a difference Fourier map. All atoms except those of the disordered THF molecule were refined anisotropically[22a] to yield final agreement factors of $R(F) = 6.4\%$ for 3443 reflections with $I > 2\sigma(I)$, and $R(F) = 8.3\%$ for all data (4195 reflections). The neutron scattering lengths used in the refinement were those tabulated by Sears.[22b]

Supplementary Material: A summary of the results of the neutron diffraction study, with final atomic positions and a complete listing of distances and angles in the title compound, have been deposited with the Cambridge Crystallographic Data Centre as Supplementary Publication No. CCDC−100889. Copies of the data can be obtained free of charge on application to CCDC, 12 Union Road, Cambridge CB2 1EZ, UK (e-mail: deposit@ccdc.cam.ac.uk; fax: +44(0)1223/336-033).

☆ Dedicated to the 70th birthday of Prof. *Heinrich Nöth.*

[1] J. W. Freeman, A. M. Arif, R. D. Ernst, *Inorg. Chim. Acta* **1995**, *240*, 33.

[2] [2a] L. S. van der Sluys, M. M. Miller, G. J. Kubas, K. G. Caulton, *J. Am. Chem. Soc.* **1991**, *113*, 2513. − [2b] D. Alvarez, Jr., E. G. Lundquist, J. W. Ziller, W. J. Evans, K. G. Caulton, *J. Am. Chem. Soc.* **1989**, *111*, 8392. − [2c] J. W. Bruno, J. C. Huffman, M. A. Green, K. G. Caulton, *J. Am. Chem. Soc.* **1984**, *106*, 8310. − [2d] J. T. Poulton, K. Folting, K. G. Caulton, *Organometallics* **1992**, *11,* 1364.

[3] S. C. Abrahams, A. P. Ginsberg, T. F. Koetzle, P. Marsh, C. R. Sprinkle, *Inorg. Chem.* **1986**, *25*, 2500.

[4] M. Y. Chiang, R. Bau, G. Minghetti, A. L. Bandini, G. Banditelli, T. F. Koetzle, *Inorg. Chem.* **1984**, *23*, 122.

[5] A. Albinati, T. J. Emge, T. F. Koetzle, S. V. Meille, A. Musco, L. M. Venanzi, *Inorg. Chem.* **1986**, *25*, 4821.

[6] A. Albinati, S. Chaloupka, F. Demartin, T. F. Koetzle, H. Regger, L. M. Venanzi, M. K. Wolfer, *J. Am. Chem. Soc.* **1993**, *115*, 169.

[7] R. M. Bullock, L. Brammer, A. J. Schultz, A. Albinati, T. F. Koetzle, *J. Am. Chem. Soc.* **1992**, *114*, 5125.

[8] T. J. Marks and J. R. Kolb, *Chem. Rev.* **1977**, *77*, 263.

[9] The Re and Cr covalent radii can be estimated as 1.371 and 1.249 A, respectively, using half of the Re−Re distance in rhenium metal and half of the Cr−Cr distance in chromium metal: see *Interatomic Distances Supplement*, Chemical Society, London, **1965**. From these values one can estimate that Cr is about 0.12 A smaller than Re. Essentially the same difference (0.11 A) can be obtained by comparing average Re−H (1.837 A) and Cr−H (1.728 A) bridging distances (see ref.[10]).

[10] R. Bau, M. H. Drabnis, *Inorg. Chim. Acta* **1997**, *259*, 27.

[11] J. A. Abad, E. Delgado, M. E. Garcia, M. J. Grosse-Ophoff, I. J. Hart, J. C. Jeffery, M. S. Simmons, F. G. A. Stone, *J. Chem. Soc., Dalton Trans.* **1987**, 41.

[12] For a review on eight-coordinate complexes, see S. J. Lippard, *Prog. Inorg. Chem.* **1967**, *8*, 109. The geometrical arrangement around Re in the title complex is similar to that found in $[K(THF)_2ReH_6(PPh_3)_2]_2$ (ref.[2b]) and in $OsH_6[P(iPr)_2Ph]_2$ [J. A. K. Howard, O. Johnson, T. F. Koetzle, J. L. Spencer, *Inorg. Chem.* **1987**, *26*, 2930].

[13] R. Bau, W. E. Carroll, R. G. Teller, T. F. Koetzle, *J. Am. Chem. Soc.* **1977**, *99*, 3872.

[14] [14a] J. Roziere, J. M. Williams, R. P. Stewart, Jr., J. L. Petersen, L. F. Dahl, *J. Am. Chem. Soc.* **1977**, *99*, 4497. − [14b] J. L. Petersen, R. K. Brown, J. M. Williams, R. K. McMullan, *Inorg. Chem.* **1979**, *18*, 3493. − [14c] J. L. Petersen, R. K. Brown, J. M. Williams, *Inorg. Chem.* **1981**, *20*, 158.

[15] A. S. Foust, W. A. G. Graham, R. P. Stewart, Jr., *J. Organometal. Chem.* **1973**, *54*, C22.

[16] R. Bau, R. G. Teller, S. W. Kirtley, T. F. Koetzle, *Accts. Chem. Res.* **1979**, *12*, 176.

[17] A. Berry, M. L. H. Green, J. A. Bandy, K. Prout, *J. Chem. Soc (Dalton)*, **1991**, 2185.
[18] M. Thomas, R. F. D. Stansfield, M. Berneron, A. Filhol, G. Greenwood, J. Jacobe, D.Feltin, S. A. Mason, in *Position-sensitive Detection of Thermal Neutrons*, edited by P. Convert and J. B. Forsyth, p. 344, London: Academic Press, **1983**.
[19] J. Archer and M. S. Lehmann, *J. Appl. Cryst.* **1986**, *19*, 456.
[20] C. Wilkinson, H. W. Khamis, R. F. D. Stansfield, G. J. McIntyre, *J. Appl. Cryst.* **1988**, *21*, 471.
[21] J. C. Matthewman, P. Thompson, P. J. Brown, *J. Appl. Cryst.* **1982**, *15*, 167.
[22] [22a] G. M. Sheldrick, *SHELXL-93*, University of Göttingen, Germany, **1993**. – [22b] V. F. Sears, *Neutron News* **1992**, *3*, 26.
[98020]

Synthesis of Silylborazines and Their Utilization as Precursors to Silicon-Containing Boron Nitride☆

Dileep Srivastava, Eileen N. Duesler, and Robert T. Paine*

Department of Chemistry, University of New Mexico
Albuquerque, New Mexico 87131, USA

Received February 12, 1998

Keywords: Borazines / Silyl borazines / Oligomers / Pyrolysis / Ceramics

The reactions of $LiSi(SiMe_3)_3$ with $Cl(Me)_2B_3N_3(Me)_3$, $Cl_2(Me)B_3N_3(Me)_3$, $(ClBNMe)_3$, and $(ClBNH)_3$ result in the formation of molecular species $(Me_3Si)_3Si(Me)_2B_3N_3(Me)_3$, $[(Me_3Si)_3Si]_2(Me)B_3N_3(Me)_3$, $[(Me_3Si)_3SiBNMe]_3$, and $[(Me_3Si)_3SiBNH]_3$. The new compounds have been characterized by spectroscopic techniques, and a single-crystal X-ray diffraction analysis for $[(Me_3Si)_3SiBNMe]_3$ has been completed. The monomer $(Me_3Si)_3Si(Cl)_2B_3N_3H_3$ was also prepared and combined with $(Me_3Si)_2NH$ in hexane to form an organic solvent soluble oligomer. Pyrolysis of this oligomer provides composites containing BN and an $Si_XN_YC_Z$ phase that suppresses the crystallization of BN.

After about a decade of intense study, it has been demonstrated that inorganic and organometallic polymers may be used to produce a number of ceramic powders including SiC, Si_3N_4, BN, B_4C, and AlN[1][2][3], albeit at greater expense than traditional metallurgical routes. Despite the economic drawback, many polymer precursors offer the advantage that they can be processed into useful physical forms (e.g., fibers, coatings, binders, and porous bodies) that cannot be achieved by classical powder-processing approaches. One additional area where polymer precursors are showing potentially useful benefits and applications is in the fabrication of composite materials[2][3][4][5]. Polymer-derived syntheses of ceramic-ceramic composites have most often been accomplished by three chemical approaches: blending and pyrolysis of a liquid or soluble polymeric precursor with an elemental filler, blending and pyrolysis of two or more processible polymeric precursors, and pyrolysis of a "single-source" preceramic polymer[4][5]. Successes have been demonstrated with each approach. However, until very recently the least attention and fewest successes have been realized with the "single-source" approach, primarily due to the lack of appropriate monomers and polymers. This situation has begun to change. In particular, several groups have noted that addition of boron to silicon-based ceramics can produce enhanced stability in the resulting composite, as well as improve property performances[6]. These observations, in turn, have resulted in new efforts to obtain processible single-source preceramic polymers that convert readily to so-called SiNCB ceramic composites[7][8][9][10][11][12][139][14][15][16][17][18][19][20][21]. In this report, the syntheses of model molecular silyl-substituted borazines and a silylborazine oligomer are described along with our initial efforts to define the pyrolysis chemistry of the polymer that results in formation of SiNCB composites.

Results and Discussion

Relatively few compounds with boron−silicon bonds have been prepared, and the interesting development of this chemistry has been briefly summarized by Berry and coworkers[22]. Pertinent to our work, two reports of the formation of *B*-silylborazines, $(Ph_3SiBNMe)_3$ and $(Ph_3SiBNPh)_3$, formed from salt-elimination reactions, have appeared[23][24]. Similarly, salt-elimination reactions involving the *B*-chloroborazines, $Cl(Me)_2B_3N_3(Me)_3$, $Cl_2(Me)B_3N_3(Me)_3$, $(ClBNMe)_3$, and $(ClBNH)_3$ with $LiSi(SiMe_3)_3$ produce *B*-silylborazines $[(Me_3Si)_3Si](Me)_2B_3N_3(Me)_3$ (**2**), $[(Me_3Si)_3Si](Me)B_3N_3(Me)_3$ (**3**), $[(Me_3Si)_3SiBNMe]_3$ (**4**), and $[(Me_3Si)_3SiBNH]_3$ (**5**) in high yields as summarized in Eq. 1. Compound **2** is obtained as a white solid, which when recrystallized from benzene gives blocky, colorless crystals. The remaining compounds are isolated as waxy or gummy solids. Each compound is soluble in Et_2O, THF, benzene, and pentane and is moisture-sensitive in both the solid state and in solutions.

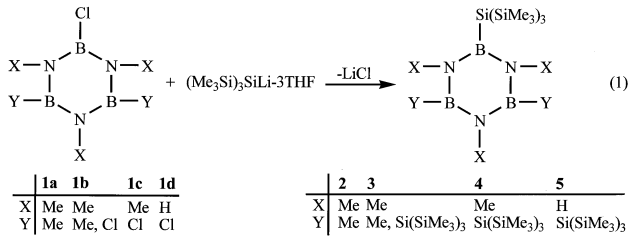

(1)

	1a	1b	1c	1d
X	Me	Me	Me	H
Y	Me	Me, Cl	Cl	Cl

	2	3	4	5
X	Me	Me	Me	H
Y	Me	Me, $Si(SiMe_3)_3$	$Si(SiMe_3)_3$	$Si(SiMe_3)_3$

Compounds **2**−**4** give satisfactory CHN analyses; however, **5** retains small amounts of reactants and adequate analyses are not obtained. All of the compounds display a moderately intense parent ion peak in the EI-mass spectrum that provides confirmation of the molecular composition. The $^{11}B\{^1H\}$-NMR spectra for **2** and **3** show two reso-

 © WILEY-VCH Verlag GmbH, D-69451 Weinheim, 1998 1434−1948/98/0606−0855 $ 17.50+.50/0

nances; one resonance, in the range $\delta = 36.3-37.1$, is assigned to the BMe group[25] and the second resonance, in the range $\delta = 42.2-42.8$, is assigned to the $BSi(SiMe_3)_3$ group. Compounds **4** and **5** produce a single resonance at $\delta = 42.2$ and 38, respectively which are assigned to the $BSi(SiMe_3)_3$ group. The ^1H- and $^{13}C\{^1H\}$-NMR spectra are also consistent with the proposed structures showing resonances assigned to BMe, $BSi(SiMe_3)$, and NMe groups.

The molecular structure of compound **2** was determined by single-crystal X-ray diffraction analysis. A view of the molecule is shown in Figure 1 and selected bond lengths and angles are given in Table 1. As expected, the B_3N_3 ring is planar and the $(Me_3Si)_3Si$ group occupies an *exo* position bonded to B(1). The average B−N distance, 1.434 Å [range 1.453(6)−1.407(8) Å] is identical to the average values in several borazine compounds: $(HNBH)_3$[26], 1.436 Å; $(Me_2NBNH)_3$[27], 1.433 Å; and $(Me_3N_3Me_2B_3)_2NH$[28], 1.438 Å. Four of the B−N distances are within one standard deviation of the average value, while the two distances associated with B(3) vary from the average by slightly more than 3σ. Such a variation is not typical for borazine rings although a similar behavior was found in $[Me_3N_3Me_2B_3]_2NMe$[28] [B−N distance range 1.463(6) Å−1.414(7) Å]. The average $B-CH_3$ and $N-CH_3$ distances, 1.593 and 1.475 Å, are comparable with the values in $(Me_3N_3Me_2B_3)_2NH$, 1.580 and 1.476 Å, and in $(Me_3N_3Me_2B_3)_2NMe$, 1.586 and 1.479 Å[28]. The terminal B−Si bond length, 2.097(4) Å, is somewhat unique. We are unaware of structural data for closely comparable compounds containing an *exo*, two-center, two-electron B−Si bond with the boron atom having formal sp^2 hybridization. The observed distance is longer than the sum of covalent radii: 0.88 Å (B) + 1.17 Å (Si) = 2.05 Å[29], and not surprisingly it is significantly longer than the distance in tBuN≡B−Si$(SiMe_3)_3$, 1.976(4) Å[30], which contains a formally sp-hybridized B atom (N≡B−Si, 176.6°). On the other hand, the B−Si distances in $Cy_3P \cdot B(H)_2SiMe_3$, 2.007(4) Å[31] and in $Cp_2Ta[\eta^2\text{-}BH_3\{Si(t\text{Bu})_2H\}]$, 2.02(1) Å[22], which contain sp^3-hybridized boron atoms, are also significantly shorter than the distance in **2**. The long distance in **2** may result from steric interactions between the bulky Me_3Si groups on the Si atom and the Me groups on the *ortho* N atoms in the borazine ring. The molecular structure of the *B,B′,B′′*-trisilyl derivative **4** was also determined[32], but disorder in several silylmethyl carbon atoms led to a large *R* value. Nonetheless, the composition and anticipated structure of **4** is confirmed. It is also noteworthy that the B−Si bond lengths are long: 2.11(2) Å (average).

In previous reports[28][33] we have described the syntheses of polyborazinylamine oligomers by reaction of chloroborazine with hexamethyldisilazane and heptamethyldisilazane. Extending this approach, the borazine monomer $H_3N_3B_3(Cl)_2Si(SiMe_3)_3$ was prepared from the 1:1 reaction of $(HNBCl)_3$ and $LiSi(SiMe_3)_3$ in hexane. The reaction mixture was filtered to remove LiCl and the monomer solution containing **6** was combined with $(Me_3Si)_2NH$ at 23°C. This produces a glassy, colorless solid (**7**), following solvent evaporation, that is soluble in pentane, hexane, benzene,

Figure 1. Molecular structure and atom-labeling scheme for $[(Me_3Si)_3Si](Me)_2B_3N_3(Me)_3$ (**2**)

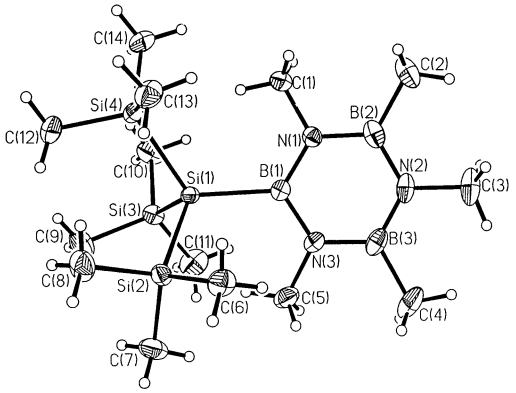

and Et_2O. The oligomer formation is summarized in Eq. 2. Elemental analysis (CHN) of the oligomer is in close agreement with the calculated values for **7** although a small amount of residue is typically found according to the combustion analysis. The ^1H-NMR spectrum displays a sharp resonance at $\delta = 0.25$ that is assigned to the $Si(SiMe_3)_3$ groups in the oligomer and a broad peak at $\delta = 0.35$ is assigned to N−H groups. The ^{11}B-NMR spectrum displays two broad resonances centered at $\delta = 18$ and 38. No further attempts were made to characterize the structure of the oligomer.

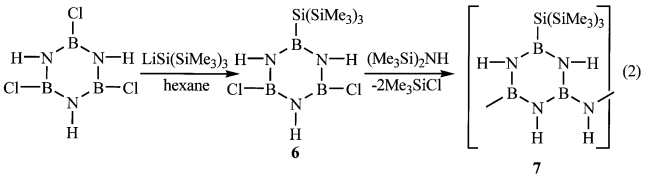

The pyrolysis behavior of **7** was initially surveyed by TGA from 50−1400°C under argon. There are two primary weight loss ranges. From 100−300°C about 35% of the mass is lost and from 350−500°C another 18% of the mass is lost. No significant further change occurs above 600°C. The overall ceramic yield is ca. 47%. Bulk samples of the polymer were initially pyrolyzed at 1200°C for 12 h under a slow stream of pure nitrogen. The product is a shiny black hard solid. The infrared spectrum of the material shows a strong, broad peak centered at ca. 1400 cm^{-1} and a medium-intensity band at ca. 800 cm^{-1}. These bands closely resemble those of a standard sample of turbostratic BN[33]. In addition, weaker bands appear at 1030, 840, and 470 that may be tentatively assigned to Si_3N_4. The XRD pattern (Figure 2) for this sample shows only a weak, broad peak centered at $2\theta = 42°$ ($d = 2.1$ Å). This is interesting since pyrolyzed samples of polyborazinylamine polymers typically show a strong reflection at $2\theta = 26°$ ($d = 3.3$ Å) and weaker, broad reflections centered at $2\theta = 34°$ and 42° following pyrolysis at temperatures as low as 900°C. This leads to the tentative conclusion that the crystallization of the boron nitride formed in this study is depressed by the pres-

ence of the silicon present as amorphous Si_3N_4, SiC, and/or a ternary SiNC material.

Figure 2. Powder XRD patterns from pyrolysis of polymer precursor **7**; lower trace: 1200°C, 12 h under N_2; upper trace: 1400°C, 12 h under N_2

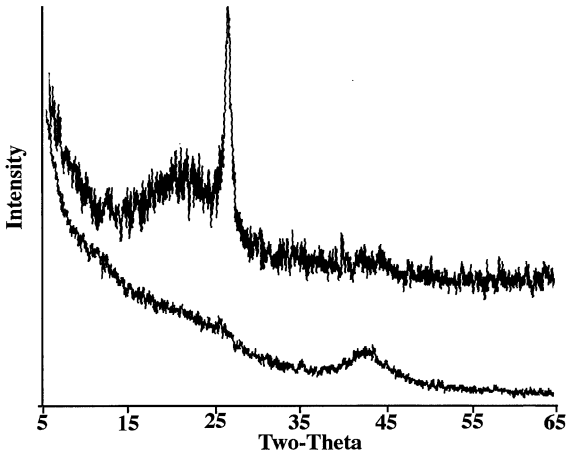

Further heating of the black, glassy solid to 1400°C under nitrogen gave a gray solid. The sample analyzed as $B_{1.0}N_{1.28}Si_{0.29}C_{0.12}$. An infrared spectrum shows a strong, broad band at ca. 1400 cm^{-1} and a sharper band at ca. 800 cm^{-1} that are assigned to BN and additional bands at 1080, 930, 470, and 420 cm^{-1}. The XRD pattern (Figure 2) shows a broad reflection at 2θ = 26° (*d* = 3.37 Å) and very weak peaks at 2θ = 21° (*d* = 4.0 Å, broad), 39° (*d* = 2.28 Å), 44° (*d* = 2.06 Å), 50° (*d* = 1.83 Å) and 57° (*d* = 1.60 Å). Further heating of this material at 1600°C under Ar leads to gray solid that analysed as $B_{1.0}N_{1.26}Si_{0.25}C_{0.10}$. The XRD pattern (Figure 3) for this material now shows a sharp reflection at 2θ = 22° (*d* = 4.06 Å) and very weak reflections at 2θ = 28° (*d* = 3.13 Å), 32° (*d* = 2.84 Å), 36° (*d* = 2.48 Å), 47° (*d* = 1.93 Å), 48° (*d* = 1.87 Å), 60° (*d* = 1.53 Å). The reflection at 2θ = 22° and weak reflections at 2θ = 32° and 48° may be tentatively ascribed to α-Si_3N_4 that has begun to form in this sample. Other weak reflections may correspond to Si and β-SiC.

Figure 3. Powder XRD pattern from pyrolysis of polymer **7** at 1600°C, 12 h under N_2

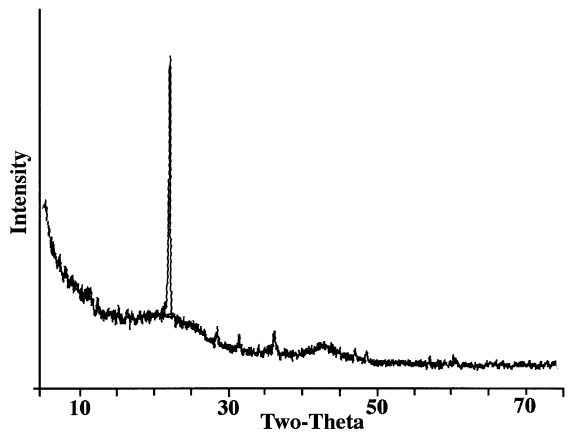

A sample of the glassy polymer **7** was also heated at 350°C for 12 h under a flowing stream of NH_3 and then for 6 h under N_2. The resulting residue was heated at 1200°C for 12 h under N_2. The remaining solid was cream-colored, displayed no crystallinity, and analyzed as $B_{1.0}N_{1.42}Si_{0.27}$.

The silyl-substituted monomer molecules **2**−**5** have been prepared and characterized by spectroscopic techniques, and the molecular structure determination for **2** confirms substitution of the very bulky $(Me_3Si)_3Si$ group on the borazine ring at a boron atom. The monomer **6** has also been produced but not isolated. It has been combined with hexamethyldisilazane to provide an organic solvent soluble $(Me_3Si)_3Si$-derivatized polyborazinylamine oligomer **7**. Pyrolysis of this oligomer in nitrogen produces a ceramic product rich in boron and nitrogen containing small amounts of silicon and carbon. The Si appears to suppress the crystallization of BN at 1200°C. At approximately 1400°C the Si present begins to form crystalline phases that at 1600°C show some evidence for formation of α-Si_3N_4. These results are similar to findings reported by Sneddon and coworkers on the pyrolysis of borazine/silazane backbone copolymers. The results suggest that related silyl-substituted borazine monomers should be explored as potential SiNCB precursors.

This work was supported by the *UNM/NSF Center for Microengineered Materials* and its industrial partners.

Experimental Section

Standard vacuum-line and inert-atmosphere techniques were used for the manipulation of reactants and products. − Infrared spectra were obtained with a Nicolet 6000 FT-IR spectrometer and NMR spectra were recorded with Bruker AC-250 and JEOL GSX-400 spectrometers. − NMR spectra were recorded from C_6D_6 solutions and referenced with Me_4Si (^1H, ^{13}C) and $BF_3 \cdot OEt_2$ (^{11}B). − Mass spectra were obtained with a Finnegan mass spectrometer through a solids probe. − Reagents $(Me_3Si)_3SiLi \cdot 3THF$[34], $(ClBNMe)_3$ (**1c**)[35], $(ClBNH)_3$ (**1d**)[36], $Cl_2(Me)B_3N_3(Me)_3$ (**1b**)[37], and $Cl(Me)_2B_3N_3(Me)_3$ (**1a**)[38] were prepared as described in the literature. Solvents were dried by standard procedures and vacuum-transferred from storage vessels into reaction flasks immediately before use.

Synthesis of Molecular Model Compounds [(Me$_3$Si)$_3$Si]-(Me)$_2$B$_3$N$_3$(Me)$_3$ (**2**): A sample of $LiSi(SiMe_3)_3 \cdot 3$ THF (1.0 g, 2.1 mmol) was added over 10 min to a stirred solution (−78°C) of 2-chloro-1,3,4,5,6-pentamethylborazine, $(Cl(Me)_2B_3N_3(Me)_3$; 0.4 g, 2.1 mmol) in 40 ml of hexane. The reaction mixture was warmed to 25°C and stirred overnight. Volatile materials were removed in vacuo. The white residue was combined with hexane (50 ml) and filtered. Solvent removal from the filtrate afforded a solid **2** that was recrystallized from a minimum of hexane. Yield: 0.75 g (90%); mp 85°C; soluble in Et_2O, pentane, THF, benzene. − IR (KBr): $\tilde{\nu}$ = 2953 cm^{-1} (m), 2899 (m), 1477 (s,sh), 1447 (s), 1400 (s), 1388 (s), 1244 (m), 1105 (m), 1075 (m), 997 (m), 863 (s,sh), 836 (s), 682 (m), 625 (m), 515 (w), 430 (w). − MS (50 eV); *m/z* (%): 397 (28) $[M^+]$, 382 (24) $[M - CH_3^+]$, 324 (32) $[M - SiMe_3^+]$, 250 (17) $[M - 2\ SiMe_3^+]$, 150 (11) $[M - (Me_3Si)_3Si^+]$, 73 (100) $[Me_3Si^+]$. − ^1H NMR: δ = 0.36 (CH_3−Si, 27 H), 0.43 (CH_3−B, 6 H), 2.68 (CH_3−N, 3 H), 3.09 (CH_3−N, 6 H). − $^{13}C\{^1H\}$ NMR: δ = 1.92 (CH_3−B), 4.22 (CH_3−Si), 34.2 (CH_3−N), 41.8 (CH_3−N). −

$^{11}B\{^1H\}$ NMR: δ = 36.3 (B−CH_3, 2 B), 42.2 [B−Si($SiMe_3$)$_3$, 1 B]. − $C_{14}H_{42}B_3N_3Si_4$ (397.28): calcd. C 42.32, H 10.60, N 10.60; found C 42.28, H 10.77, N 10.67.

[(Me$_3$Si)$_3$Si]$_2$(Me)B$_3$N$_3$(Me)$_3$ (**3**): A sample of LiSi($SiMe_3$)$_3$ · 3 THF (1.4 g, 3.0 mmol) was added over 15 min to a stirred solution (−78°C) of 2,4-dichloro-1,3,5,6-tetramethylborazine ($Me_3N_3B_3(Me)Cl_2$; 0.32 g, 1.5 mmol) in hexane (40 ml). The mixture was subsequently warmed to 25°C and stirred for 12 h. The volatile components were evaporated leaving a white residue that was extracted with hexane (50 ml). The solution was filtered, the filtrate concentrated and a white waxy solid **3** was recovered. Yield: 0.80 g (85%); mp 103−106°C; soluble in Et_2O, pentane, benzene, and THF. − IR (KBr): $\tilde{\nu}$ = 2520 cm^{-1} (m), 2509 (m), 1484 (m), 1433 (m), 1381 (s,sh), 1357 (s), 1239 (s), 1107 (w), 1064 (m), 984 (m), 947 (w), 832 (s), 696 (w), 684 (m), 608 (m). − MS (50 eV); *m/z* (%): 629 (35) [M^+], 614 (20) [M − CH_3^+], 556 (40) [M − $SiMe_3^+$], 382 (18) [M − Si($SiMe_3$)$_3^+$], 73 (100) [Me_3Si^+]. − ^1H NMR: δ = 0.36 (CH_3−Si, 54 H), 0.44 (CH_3−B, 3 H), 3.07 (CH_3−N, 6 H), 3.56 (CH_3−N, 3 H). − $^{13}C\{^1H\}$ NMR: δ = 4.27 (CH_3−Si), (CH_3−N), 47.8 (CH_3−N). − $^{11}B\{^1H\}$ NMR: δ = 37.1 (B−CH_3, 1 B), 42.8 [B−Si($SiMe_3$)$_3$, 2 B]. − $C_{22}H_{66}N_3B_3Si_8$ (629.90): calcd. C 41.97, H 10.50, N 6.67; found C 40.92, H 10.99, N 6.91.

[(Me$_3$Si)$_3$Si]B$_3$N$_3$(Me)$_3$ (**4**): A sample of LiSi($SiMe_3$)$_3$ · 3 THF (1.95 g, 4.2 mmol) was added over 15 min to a stirred solution (−78°C) of 1,3,5-trimethyl-2,4,6-trichloroborazine ($Me_3N_3B_3Cl_3$; 0.32 g, 1.4 mmol) in hexane (40 ml). The reaction mixture was warmed to 25°C and stirred overnight. Removal of the volatiles from the reaction mixture afforded a white residue that was extracted with hexane (50 ml) and filtered. The solvent was removed from the filtrate under vacuum leaving a white waxy solid. Yield: 1.06 g (88%); soluble in Et_2O, pentane, benzene, and THF. − IR (KBr): $\tilde{\nu}$ = 2952 cm^{-1}(s), 2893 (s), 1924 (w), 1864 (w), 1472 (m), 1434 (w), 1348 (br., s) 1261 (m, sh), 1244 (s), 1074 (s), 967 (m), 838 (s, br.), 748 (m), 681 (m), 622 (m), 438 (w). − MS (50 eV); *m/z* (%): 862 (15) [M^+], 847 (15) [M − $SiMe_3^+$], 789 (35) [M − $SiMe_3^+$], 614 (52) [M − Si($SiMe_3$)$_3^+$]. − ^1H NMR: δ = 0.38 (CH_3−Si), 3.58 (CH_3−N). − 13{^1H} NMR: δ = 4.37 (CH_3−Si), 47.7 (CH_3−N). − $^{11}B\{^1H\}$ NMR: δ = 42.2. − $C_{30}H_{90}B_3N_3Si_{12}$ (862.52): calcd. C 41.80, H 10.50, N 4.88; found C 42.10, H 10.54, N 5.29.

[(Me$_3$Si)$_3$Si]$_3$B$_3$N$_3$H$_3$ (**5**): A sample of (Me_3Si)$_3$SiLi · 3 THF (1.55 g, 3.38 mmol) was added to a cooled (−78°C), stirred solution of $Cl_3B_3N_3H_3$ (0.208 g, 1.13 mmol) in hexane (40 ml). The solution was warmed slowly to 23°C and stirred overnight. The solvent was removed by vacuum evaporation leaving a white residue that was redissolved in fresh hexane (50 ml) and filtered to remove entrained LiCl. The filtrate was concentrated leaving a gummy solid **5** that was vacuum-dried. Yield: 0.81 g (88%); mp 78−83°C. Further attempts to purify this compound by sublimation and recrystallization were unsuccessful. − MS (50 eV); *m/z* (%): 819 (4) [M^+], 804 (1) [M − Me^+], 746 (1) [M − Me_3Si^+], 731 (1) [M − (Me_3Si)(Me)$^+$], 658 (4) [M − (Me_3Si)$_2$(Me)$^+$, 247 (4) [Si($SiMe_3$)$_3^+$]. − ^1H NMR: δ = 0.36 (CH_3Si). − $^{13}C\{^1H\}$ NMR: δ = 1.94 (CH_3Si). − $^{11}B\{^1H\}$ NMR: δ = 38.

Synthesis of Polymer **7**: In a typical reaction, LiSi($SiMe_3$)$_3$ · 3 THF (1.3 g, 2.9 mmol) was added with stirring over 15 min to (ClBNH)$_3$ (0.53 g, 2.9 mmol) in hexane (60 ml) cooled to −78°C. The mixture was warmed to 23°C and stirred overnight. The resulting mixture was filtered to remove LiCl, and the filtrate containing **6** was combined with (Me_3Si)$_2$NH (0.6 ml, 2.9 mmol). This mixture was stirred (23°C) for 24 h and the volatiles removed by vacuum evaporation. This left a glassy, colorless solid **7**. Yield: 0.9 g (90%); soluble in hexane, pentane, benzene, and Et_2O. − IR (KBr): 3446 cm^{-1} (s), 2956 (s), 2922 (s, sh), 2900 (s), 1456 (s), 1413 (s), 1251 (m), 1186 (w), 1111 (w), 1064 (m), 836 (s), 754 (m), 712 (w), 687 (m), 623 (w), 609 (w). − ^1H NMR: δ = 0.35−0.25 (br., m). − $^{13}C\{^1H\}$ NMR: δ = 3.9−1.9 (br.). − $C_9H_{31}B_3N_4Si_4$ (340.14): calcd. C 31.76, H 9.11, N 16.47; found C 32.29, H 8.52, N 14.43.

Polymer Pyrolysis: The TGA of the polymer was recorded under Ar (50−1400°C, 10°C/min). There is a significant weight loss (ca. 35%) between 100 and 350°C and a more gradual weight loss (ca. 18%) up to 500°C. Beyond this temperature, there is minimal weight loss. − Bulk pyrolyses were performed under a variety of conditions, and some representative results are summarized. Typically, a sample (0.35 g) of glassy polymer was placed in a Pt boat in a quartz pyrolysis tube, and the tube was evacuated and backfilled with dry N_2. The sample was then heated at 1200°C under a slow stream of N_2 purge gas. After 12 h, a black solid was collected and characterized. − IR (KBr): $\tilde{\nu}$ = 1410 cm^{-1} (vs), 1030 (vs), 830 (m), 800 (m), 470 (m). − XRD: *d* = 2.1 Å (br.). − The sample was further heated to 1400°C under N_2 for 12 h, and the resulting gray solid was characterized. − IR (KBr): $\tilde{\nu}$ = 1400 cm^{-1} (vs), 1130 (m), 1080 (s), 930 (m), 800 (s), 470 (m), 420 (w). − XRD: *d* = 4.0 Å, 3.38, 2.28, 2.06, 1.83, 1.60. − Found C 3.76, B 28.21, N 46.78, Si 21.25. − Continued heating of this sample at 1600°C for 12 h under N_2 results in a dark gray solid. − IR (KBr): $\tilde{\nu}$ = 1382 cm^{-1}, 1088, 894, 784, 476. − XRD: *d* = 4.06 Å, 3.13, 2.84, 2.48, 1.93, 1.87, 1.53. − Found C 3.27, B 29.47, N 48.11, Si, 19.14. − A sample (0.35 g) of glassy polymer was also heated at 350°C under

Table 1. Crystallographic data for [(Me_3Si)$_3$Si](Me)$_2$B$_3$N$_3$(Me)$_3$ (**2**)

empirical formula	$C_{14}H_{42}B_3N_3Si_4$
formula weight	397.3
T [°C]	22
crystal system	monoclinic
space group	$P2_1/c$
a [Å]	9.346(2)
b [Å]	11.677(2)
c [Å]	24.027(5)
α [°]	90.0
β [°]	98.82
γ [°]	90.0
V [Å^3]	2591.2(9)
Z	4
$D_{calcd.}$ [g cm^{-3}]	1.018
μ [cm^{-1}]	0.227
F(000)	872
reflections collected	$-h\ -k\ \pm l$
measured	5109
independent	4542
observed [$F > 3\sigma(F)$]	3023 [$F > 3\sigma(F)$]
R_F [%]	6.42
R_{wF} [%]	5.93

Table 2. Selected bond lengths and bond angles for [(Me_3Si)$_3$Si]-(Me)$_2$B$_3$N$_3$(Me)$_3$ (**2**)

Bond lengths [Å]			
B(1)−Si(1)	2.097(4)	Si(1)−Si(2)	2.382(2)
B(1)−N(1)	1.432(6)	Si(1)−Si(3)	2.362(2)
B(1)−N(3)	1.440(6)	Si(1)−Si(4)	2.385(2)
B(2)−N(1)	1.439(6)	N(1)−C(1)	1.470(6)
B(2)−N(2)	1.428(8)	N(2)−C(3)	1.488(6)
B(3)−N(2)	1.407(8)	N(3)−C(5)	1.470(6)
B(3)−N(3)	1.453(6)	B(2)−C(2)	1.585(8)
		B(3)−C(4)	1.601(9)
Bond angles [°]			
N(1)−B(1)−N(3)	115.6(3)	B(1)−N(1)−B(2)	123.4(4)
N(1)−B(2)−N(2)	117.8(4)	B(2)−N(2)−B(3)	122.0(4)
N(2)−B(3)−N(3)	118.2(5)	B(1)−N(3)−B(3)	122.5(4)

NH_3 for 12 h, then under N_2 at 350°C for 6 h, and 1200°C for an additional 12 h. The resulting solid was cream-colored. − IR (KBr): 1388 cm^{-1} (s), 1033 (s), 788 (m), 696 (w), 448 (w). − Found B 28.24, N 51.95, Si 19.81.

Crystallographic Measurements and Structure Solution: A suitable crystal of **2** was mounted in a glass capillary and centered on a Syntex P3/F automated diffractometer. Determinations of the crystal class, orientation matrix, and unit-cell dimensions were performed in a standard fashion. Data were collected with use of Mo-K_α radiation (λ = 0.71069 Å), a highly oriented graphite crystal monochromator, a scintillation counter, and pulse-height analyzer. Selected data-collection parameters are summarized in Table 2. The space-group assignment was made by inspection of a small data set[39], and no absorption correction was required. Redundant and equivalent data were averaged and converted to unscaled $|F_o|$ values following corrections for Lorentz and polarization effects. Standard intensities decayed by about 10% during data collection and intensities were scaled accordingly. All calculations were performed with the SHELXTL PLUS structure solution package[40]. The structure was solved by direct methods and refined with full-matrix least-squares techniques[41]. The heavy atoms were refined anisotropically, and the H atoms were initially refined (riding model) in idealized positions with fixed U_{iso} = 1.2 U_{equiv} of the parent atom. The hydrogen positions were then allowed to vary to achieve the final *R* value. Further information on the X-ray crystallographic structure determination for $(Me_3Si)_3SiBB_2Me_2N_3Me_3$ may be obtained from the Cambridge Crystallographic Data Centre, 12 Union Road, Cambridge CB21EZ, England, and may be ordered by quoting the depository number CCDC-101122.

☆ Dedicated to Professor *Heinrich Nöth* on the occasion of his 70th birthday.

[1] C. K. Narula, *Ceramic Precursor Technology and Its Applications*; Marcel Dekker, New York, **1995** and references therein.
[2] M. Birot, J.-P. Pillot, J. Dunogués, *Chem. Rev.* **1995**, *95*, 1443 and references therein.
[3] R. M. Laine, F. Babonneau, *Chem. Mater.* **1993**, *5*, 260 and references therein.
[4] R. T. Paine, J. F. Janik, M. Fan, *Polyhedron* **1994**, *13*, 1225 and references therein.
[5] H.-P. Baldus, M. Jansen, *Angew. Chem.* **1997**, *109*, 338; *Angew. Chem. Int. Ed. Engl.* **1997**, *36*, 328 and references therein.
[6] T. Wideman, E. Cortez, E. E. Remsen, G. A. Zank, P. J. Carroll, L. G. Sneddon, *Chem. Mater.* **1997**, *9*, 2218 and references therein.
[7] T. Wideman, K. Su, E. E. Remsen, G. A. Zank, L. G. Sneddon, *Chem. Mater.* **1995**, *7*, 2203.
[8] K. Su, E. E. Remsen, G. A. Zank, L. G. Sneddon, *Chem. Mater.* **1993**, *5*, 547.
[9] T. Wideman, K. Su, E. E. Remsen, G. A. Zank, L. G. Sneddon, *Mater. Res. Soc. Symp. Proc.* **1996**, *410*, 185.
[10] R. Riedel, A. Kienzle, V. Szabó, J. Mayer, *J. Mater. Sci.* **1993**, *28*, 3931.
[11] J. Bill, A. Kienzle, M. Sasaki, R. Riedel, F. Aldinger, *Adv. Sci. Technol.* **1995**, *3B*, 1291.
[12] J. Bill, F. Aldinger, *Adv. Mater.* **1995**, *7*, 775.
[13] R. Riedel, A. Kienzle, W. Dressler, L. Ruwisch, J. Bill, F. Aldinger, *Nature* **1996**, *382*, 796.
[14] S. Schaible, R. Riedel, R. Boese, E. Werner, U. Klingebiel, M. Nieger, *Appl. Organomet. Chem.* **1994**, *8*, 491.
[15] R. Riedel, W. Dressler, *Ceram. Int.* **1996**, *22*, 233.
[16] H.-P. Baldus, O. Wagner, M. Jansen, *Mater. Res. Soc. Symp. Proc.* **1992**, *271*, 821.
[17] H.-P. Baldus, M. Jansen, O. Wagner, *Key. Eng. Mater.* **1994**, *89−91*, 75.
[18] H.-P. Baldus, G. Passing, *Mater. Res. Soc. Symp. Proc.* **1994**, *346*, 617.
[19] H.-P. Baldus, G. Passing, D. Sporn, A. Thierauf, *Ceram. Trans.* **1995**, *58*, 75.
[20] R. Riedel, J. Bill, A. Kienzle, *Appl. Organomet. Chem.* **1996**, *10*, 241
[21] J. Löffelholz, M. Jansen, *Adv. Mater.* **1995**, *7*, 289.
[22] Q. Jiang, P. J. Carroll, D. H. Berry, *Organometallics* **1993**, *12*, 177.
[23] D. Seyferth, H. P. Kögler, *J. Inorg. Nucl. Chem.* **1960**, *15*, 99.
[24] A. H. Cowley, H. H. Sisler, G. E. Ryschkewitsch, *J. Amer. Chem. Soc.* **1960**, *82*, 501.
[25] H. Nöth, B. Wrackmeyer, *Nuclear Magnetic Resonance Spectroscopy of Boron Compounds.* In the series *NMR Basic Principles and Progress*; Springer-Verlag, Berlin, **1978**, vol. 14.
[26] W. Harshbarger, G. H. Lee, R. F. Porter, S. H. Bauer, *Inorg. Chem.* **1969**, *8*, 1683.
[27] H. Hess, B. Reiser, *Z. Anorg. Allgem Chem.* **1971**, *381*, 91.
[28] C. K. Narula, D. A. Lindquist, M. Fan, T. T. Borek, E. N. Duesler, A. K. Datye, R. Schaeffer, R. T. Paine, *Chem. Mater.* **1990**, *2*, 377.
[29] L. Pauling, in *The Nature of the Chemical Bond*, 3rd ed., Cornell University, Ithaca, NY, **1960**, p. 246.
[30] M. Haase, V. Klingebiel, R. Boese, M. Polk, *Chem. Ber.* **1986**, *119*, 1117.
[31] A. Blumenthal, P. Bissinger, H. Schmidbaur, *J. Organometal. Chem.* **1993**, *462*, 107.
[32] Crystal data for **4** ($C_{30}H_{90}B_3N_3Si_{12}$): triclinic, space group $P\bar{1}$, a = 14.112(12), b = 14.204(14) Å, c = 17.794(11) Å, α = 74.34(6), β = 74.77(5), γ = 60.22(6)°, V = 2945.4 $Å^3$, Z = 2. Several methyl carbon atoms displayed large anisotropic thermal parameters and C(7) was equally disordered over two sites.
[33] R. T. Paine, C. K. Narula, *Chem. Rev.* **1990**, *90*, 73; R. T. Paine, L. G. Sneddon, *ACS Symp. Ser.* **1994**, *572*, 358 and references therein.
[34] G. Gutekunst, A. G. Brook, *J. Organomet. Chem.* **1982**, *225*, 13.
[35] C. H. Brown, A. W. Laubengayer, *J. Am. Chem. Soc.* **1955**, *77*, 3699.
[36] C. K. Narula, D. A. Lindquist, M. Fan, T. T. Borek, E. N. Duesler, A. K. Datye, R. Schaeffer, R. T. Paine, *Chem. Mater.* **1990**, *2*, 377 and references therein.
[37] R. H. Toeniskoetter, F. R. Hall, *Inorg. Chem.* **1963**, *2*, 29.
[38] A. Meller, H. Marecek, *Monatsch. Chem.* **1968**, *99*, 1666.
[39] Space-group notations as given in: *International Tables for X-ray Crystallography*; Reidel, Dordrecht, Holland, **1983**, vol. I, pp. 73−346.
[40] G. M. Sheldrick, Nicolet SHELXTL Operations Manual, Nicolet XRD Corp., Cupertino, CA, **1981**. SHELXTL uses absorption, anomalous dispersion, and scattering data compiled in: *International Tables for X-ray Crytstallography*, Kynoch, Birmingham, England, **1974**, vol. IV, pp. 55−60, 99−101, 149−150. Anomalous dispersion terms are included for all atoms with $Z > 2$.
[41] A general description of the least-squares algebra is found in: *Crystallographic Computing* (Eds.: F. R. Ahmed, S. R. Hall, C. P. Huber), Munksgaard, Copenhagen, **1970**, p. 187. The least-squares refinements minimize $\Sigma w(|F_o| - |F_c|)^2$, where $w = 1/[\sigma(F)^2 + gF^2]$, g = 0.0004; $R = \Sigma||F_o| - |F_c||/\Sigma|F_o|$, $R_{wF} = [\Sigma w(|F_o| - |F_c|)^2/\Sigma w|F_o|^2]^{1/2}$ and GOF = $[\Sigma w(|F_o| - |F_c|)^2/(NO - NV)]^{1/2}$, where NO = number of observations and NV = number of variables.

[98030]

A Trinuclear Palladium(II) Complex with Bridging 2-Hydroxyacetophenone N^4-Ethylthiosemicarbazone Ligands − An Unusual Dimethylformamide Promoted Deprotonation and Aggregation

Dimitra Kovala-Demertzi*[a], Nikolaos Kourkoumelis[a], Douglas X. West[b], Jesús Valdés-Martínez[c], and Simon Hernández-Ortega[c]

Department of Chemistry, University of Ioannina[a],
45110 Ioannina, Greece
E-mail: dkovala@cc.uoi.gr

Department of Chemistry, Illinois State University[b],
Normal, IL 61790-4160, USA

Instituto de Química, Universidad Nacional Autonoma de Mexico[c],
Circuito Exterior, Ciudad Universitaria, Coyoacán 04510, México DF

Received August 8, 1997

Keywords: Trinuclear *triangulo* palladium complex / 2-Hydroxyacetophenone N^4-ethylthiosemicarbazone / Dimethylformamide aggregation

The X-ray crystal structure of a palladium(II) complex of 2-hydroxyacetophenone N^4-ethylthiosemicarbazone (H_2Ap4E) shows it to be a *triangular,* trinuclear complex with bridging thiosemicarbazonato sulfur atoms. This species can be formed from a monomer on dissolution in DMF or directly from Li_2PdCl_4 and the thiosemicarbazone in methanol-ammonia solution.

Thiosemicarbazones of aromatic *ortho*-hydroxy aldehydes and ketones have recently attracted considerable attention because of their potential biological properties[1] and catalytic activity[2]. These aromatic thiosemicarbazones most often coordinate as the dianion on loss of the phenoxy hydrogen and thiosemicarbazone moiety′s to form mononuclear [M(ONS)X] (ONS represents the dianionic thioseicarbazone ligand coordinated via the phenoxy oxygen, azomethine nitrogen and thiolato sulfur and X represents a neutral molecule such as ammonia or pyridine)[3], or dinuclear $[M(ONS)]_2$ {M=Ni(II) or Cu(II) and M−O,O−M bridging pattern}[4][5][6][7] have been isolated on deprotonation of the ring hydroxy group and loss of the N(2) hydrogen of the thiosemicarbazone (tsc) moiety. Most recently, a trinuclear nickel(II) complex with both Ni−O,O−Ni and Ni−S,O−Ni bridging patterns has been reported[8]. Two monomers combine to form a butterfly-shaped dimer by Ni−O,O−Ni bonding and a third monomer binds to the dimer via Ni−S,O−Ni bridging. Palladium(II) complexes of tscs of 2-acetylpyridine have been studied with regard to their structural and biological properties, and some of them show remarkable antitumour activity[9][10][11]. Therefore, we expanded our studies of palladium(II) complexes to include other potentially tridentate tsc ligands and report here the structure of $[Pd(Ap4E)]_3 \cdot$DMF (Ap4E is the dianion of 2-hydroxyacetophenone N^4-ethylthiosemicarbazone) with Pd−S−Pd bridging.

Although numerous dinuclear palladium complexes are known, only a few trinuclear palladium complexes have been reported[12][13]. Triangular complexes[12][13], as well as linear complexes[14], have been structurally characterized. Linear tripalladium structures have been found for the complexes $Pd_3[\eta^3$-1,3-di(pyvaloyl)allyl$]_2(\mu,\eta^2$-acetate$)_4$[14b], $Pd_3[1\text{-}3\eta^3$-6-(α-chloroethyl)cyclooctenyl$]_2Cl_4$[14c] and $[Pd_3(\mu\text{-}SCy)_4Cl_2(PMe_3)2]$[14h] with four bridging ligands and palladium atoms at non-bonding distances. Bent trimetallic structures have been proposed for $[Pd_3(\mu\text{-}PPh_2)_2(\mu\text{-}Cl)_2(PPh_3)_2]$[14f], $[NEt_4]_2[Pd_3(\mu\text{-}Cl)_4Cl_2(C_6F_5)_4]$[14g], $[Pd_3(\eta^3$-1,2,3-tri(*p*-methoxyphenyl)allyl$)_2(acac)_2]$[14d] and $[Pd_3(\eta^3$-2-methylallyl$)_2(Cl)_4]$[14e]. In the case of allyl complexes, it is believed that the bent structures may result from crystal packing forces rather than steric interactions.

Palladium acetate has been found to be trinuclear with a triangular arrangement of non-bonded palladium[12f] and $[Pd_3(\mu\text{-}O_2CMe)_3(\mu\text{-}MeSCHR)_3]$[13a] is a mixed-sphere palladium complex in which the solid state nuclearity and structure of palladium acetate is retained. Complexes that are cationic and triangular trinuclear with two triply bridging ligands include $[Pd_3(\mu_3\text{-}SPPh_2)_2(PhN{=}NC_6H_4)(PPh_3)_2]ClO_4$[13c] and $[Pd_3(C_6H_4CH_2NMe_2)_3(pyS)_2]BF_4$[13d] and with three bridging ligands, capped by a lone sulfur atom as $[Pd_3(\mu_3\text{-}S)(SC)(\mu\text{-}Ph_2PCH_2PPH_2)_3][SCN]\cdot 3C_2H_4Cl_2$[13b] have been studied. Neutral tripalladium triangular complexes with two bridging ligands $[Pd_3(\mu\text{-}SO_2)_2(BuNC)_5]\cdot 2(C_6H_6)$[12b] and with three bridging ligands

 © WILEY-VCH Verlag GmbH, D-69451 Weinheim, 1998 1434−1948/98/0606−0861 $ 17.50+.50/0

Figure 1. The reaction path for the synthesis of $[Pd(Ap4E)]_3 \cdot DMF$

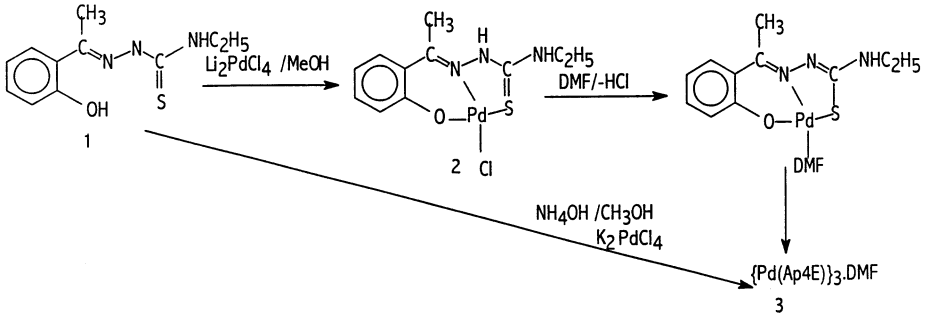

$[Pd_3(\mu\text{-}Pcy)_2(m\text{-}SPh)(PCyH)_2(SPh)]$[13e] have been studied. However, to our knowledge this is the first report of an approximately symmetric, *triangular* palladium(II) complex, $[Pd(Ap4E)]_3 \cdot DMF$, with three bridging ligands having the same formal charge and bonding pattern.

Results and Discussion

The reaction of Li_2PdCl_4 with HAp4E afforded the complex **2**. The microanalytical data are consistent with the empirical formula $C_{36}H_{46}N_{10}O_4Pd_3S_3$, which indicates the structure $[Pd(HAp4E)Cl]_n$, and suggests a mononuclear or binuclear structure. A mononuclear is suggested by the IR spectrum, which revealed the appearance of a strong band at 346 cm^{-1} consistent with a terminal $\nu(Pd-Cl)$ bond. Figure 1 shows the reactions used to form the trinuclear complex $[Pd(Ap4E)]_3 \cdot DMF$ with three doubly deprotonated phenolato-thiosemicarbazonato ligands and its molecular structure is shown in Figure 2. Each Ap4E ligand coordinates via its phenoxy oxygen and azomethine nitrogen atoms and bridges to another palladium(II) with its thiolato sulfur atom. The metal-ligand bond distances are as follows: Pd1−O1, 1.967(5) Å; Pd2−O1a, 1.993(5) Å and Pd3−O1b, 1.994(6) Å; Pd1−N1, 2.005(6) Å; Pd2−N1a, 2.002(6) Å and Pd3−N1b, 2.020(5) Å; Pd1−S1, 2.226(2) Å; Pd2−S1a, 2.250(2) Å and Pd−S1b, 2.231(2) Å. The bridging sulfur atoms are closer (ca. 0.1 Å) to one Pd atom, having distances of 2.332(2) Å, 2.315(2) Å and 2.337(2) Å to the second Pd atom. The distances between the palladium centres [Pd1−Pd2, 3.945(1); Pd2−Pd3, 4.146(1); Pd1−Pd3, 3.500(1)] indicate that there are no metal-metal bonds. The three bond angles involving bridging sulfur atoms are as follows: Pd1−S1−Pd2, 120.6(1)°; Pd2−S1a−Pd3, 129.3(1)° and Pd3−S1b−Pd1, 100.2(1)°.

Figure 2. Molecular structure of $[Pd(Ap4E)]_3 \cdot DMF$ and numbering scheme

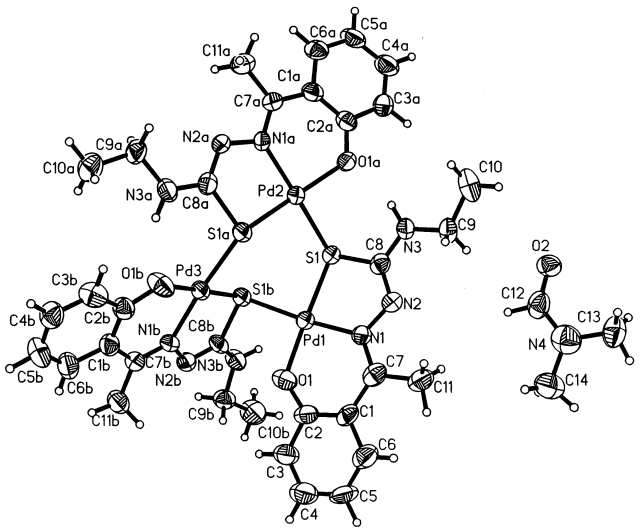

Figure 3. a) UV spectra of 5×10^{-5} M H_2Ap4E (——) [Pd(HAp4E)Cl] and (----) $[Pd(Ap4E)]_3 \cdot DMF$ (− −) in DMF and b) in $CHCl_3$

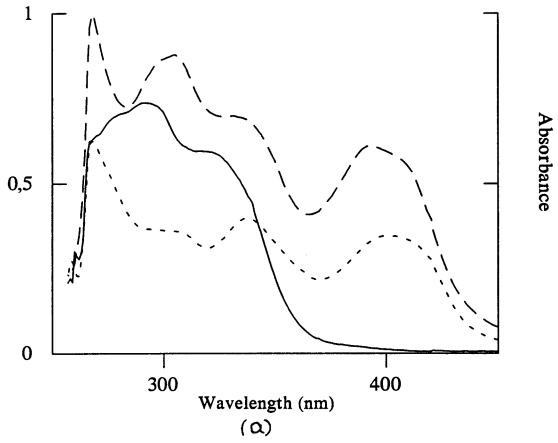

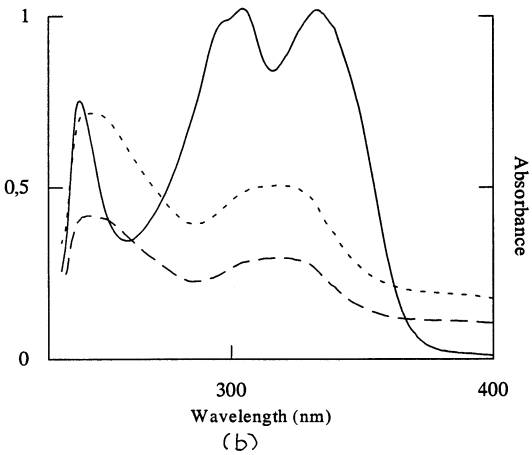

The coordination planes Pd1−O1−N1−S1−S1b, Pd2−O1a−N1a−S1a-S1 and Pd3−O1b−N1b−S1b−S1a have mean plane deviations of 0.066, 0.157 and 0.048 Å, respectively, and form dihedral angles of 42.24(6)°, 20.23(5)° and 43.98(6)° respectively, with Pd1−S1−Pd2−S1a−Pd3−S1b, which has a mean plane deviation of 0.436 Å.

A kinetically labile ligand and polar solvent like dimethylformamide affords the elimination of hydrogen chloride from **2** and the deprotonation of H_2Ap4E to form [Pd(Ap4E)]$_3$·DMF (Figure 1). The electronic spectra of the complexes **2** and **3** exhibit the same spectral pattern in $CHCl_3$, suggesting conversion of the trinuclear to the mononuclear complex (Figure 3). A different spectral pattern is shown in DMF solution, consistent with the slow transformation of the monomer to the trinuclear complex. Although transformation of **2** to **3** occurs in DMF solution (and the trinuclear complex can be prepared by this method), a non-coordinating, non-polar solvent such as $CHCl_3$ causes **3** to be reverted to **2** (Figure 3b). In contrast dinuclear complexes of copper(II)[5] and nickel(II)[6][7][8] when dissolved in solvents like DMSO and DMF are able to partly monomerize and crystals of a monomer were isolated from DMF solution[7].

Experimental Section

H_2Ap4E = 2-hydroxyacetophenone N^4-ethylthiosemicarbazone, **1**, was prepared by reacting equimolar amounts of 2-hydroxyacetophenone (2 mmol) and N^4-ethyl-3-thiosemicarbazide (2 mmol) in 30 ml ethanol. Two drops of concentrated sulfuric acid were added and the reaction mixture was refluxed for three hours. On partial evaporation of the solvent a white solid formed, which was filtered, washed with cold 2-propanol and dried. [Pd(HAp4E)Cl], **2**, was prepared by reacting lithium tetrachloropalladate (1.2 mmol) prepared in situ from palladium chloride and lithium chloride in methanol and H_2Ap4E (1 mmol) in methanol. The reaction mixture was stirred for 24 hours at room temperature and the resulting yellow powder was filtered, washed with methanol followed by ether and dried in vacuo over silica gel. Calcd for [Pd(HAp4E)Cl]·H_2O: C, 33.35; H, 4.04; N, 10.65; Cl, 8.95. Found: C, 33.05; H, 4.02; N,10.52; Cl, 9.10. Yield 43%. Slow evaporation of **2** from dimethylformamide gives dark red crystals of the complex **3** suitable for X-ray structural analysis. Also, the complex [Pd(Ap4E)]$_3$ was prepared directly from the reaction of K_2PdCl_4 (1.2 mmol) and H_2Ap4E (1 mmol) in 25 ml of H_2O, by adjusting the pH of the reaction to *ca.* 9 with drops of a 1.5 M NH_3 solution. Figure 1 shows the two routes to the trinuclear [Pd(Ap4E)]$_3$. Calcd for [Pd(Ap4E)]$_3$: C 38.66; H 3.80; N 12.30; found: C 39.13, H 4.10; N 12.40. Yield 50%.

Crystal Data: $C_{36}H_{46}N_{10}O_4Pd_3S_3$, molecular mass 1098.2, triclinic, space group *P*1bar, α = 8.874(2) Å, b = 15.680(2) Å, c = 16.273(2) Å, α = 97.80(2)°, β = 105.76(2)°, γ = 103.31(2)°, U = 2072.5(5) Å^3, Z = 2 , d = 1.760 Mg/m^3, F(000) = 1100, Mo$K\alpha$ (λ = 0.71073 Å). A red-wine prism with dimensions 0.36 × 0.10 × 0.08 mm was mounted in random orientation on a glass fiber and data were acquired with a Siemens P4 Four-Circle Diffractometer. The structure was solved with direct methods and missing atoms were found by difference-Fourier synthesis. All non-hydrogen atoms were refined with anisotropic temperature factors. The H atoms were allowed to ride on the C atoms and assigned fixed isotropic temperature factor, U = 0.06 Å^2. Hydrogen atoms on a heteroatom, H3D, H3E and H3 C, were refined in found positions. Refinement of the structure was made by full-matrix least-squares. The minimized function was $S_w(F_o - F_c)^2$ with, $w^{-1} = [\sigma^2(F) + 0.0009(F)^2]$, with final g = 0.0005 for [Pd(Ap4E)]$_3$·DMF. Scattering factors were taken from International Tables for X-ray Crystallography (**1974**, Vol. IV). All calculations were done with the SHELXTL PC™ program package.

[1] D. X. West, S. B. Padhye, P. B. Sonawane, R. C. Chikate, *Asian J. Chem. Rev.*, **1990**, *1*, 125.
[2] D. E. Barber, Z. Lu, T. Richardson, R. H. Crabtree, *Inorg. Chem.*, **1992**, *31*, 4709.
[3] M. Soriano-Garcia, R. A. Toscano, J. Valdes-Martinez, J. M. Fernandez, *Acta Cryst.*, **1985**, *C41*, 498.
[4] Z. Lu, C. White, A. L. Rheingold and R. H. Crabtree, *Inorg. Chem.*, **1993**, *32*, 3991
[5] D. X. West, Y.-H. Yang, T. L. Klein, K. I. Goldberg, A. E. Liberta, J. Valdés-Martínez, R. A. Toscano, *Polyhedron*, **1995**, *14*, 1681.
[6] D. X. West, Y.-H. Yang, T. L. Klein, K. I. Goldberg, A. E. Liberta, J. Valdés-Martínez, R. A. Toscano, *Polyhedron*, **1995**, *14*, 3051.
[7] D. X. West, M. M. Salberg, G. A. Bain, A. E. Liberta, J. Valdés-Martínez, S. Hernández-Ortega, *Transition Met. Chem.*, **1996**, *21*, 206.
[8] A. Berkessel, G. Hermann, O.-T. Racuch, M. Buchner, A. Jacobi , G. Huttner, *Chem. Ber.*, **1996**, *129*, 1421.
[9] D. Kovala-Demertzi, A. Domopoulou, M. A. Demetrzis, C. P. Raptopoulou, A. Terzis, *Polyhedron*, **1994**, *13*, 1917.
[10] D. Kovala-Demertzi, A. Domopoulou, M. A. Demetrzis, J. Valdés-Martínez, S. Hernández-Ortega, G. Espinosa-Perez. D. X. West, M. M. Salberg, G. A. Bain, P. D. Bloom, *Polyhedron*, **1996**, *15*, 2587.
[11] A. Papageorgiou, Z. Iakovidou, D. Mourelatos, E. Mioglou, L. Boutis, A. Kotsis, D. Kovala-Demertzi, A. Domopoulou, D. X. West, M.A. Demertzis, *Anticancer Res.*, **1997**, *17*, 247.
[12] [12a] E. M. McPartlin and N. C. Stephenson, *Acta Cryst.*, **1969**, B25, 165. – [12b] S. Otsuka, Y. Tatsuno, M. Miki, M. Aoki, M. Matsumoto, H. Yasioka, K. Nakatsu, *J. Chem. Soc., Chem. Commun.*, **1973**, 445. – [12c] J. P. Fackler, W. J. Zegarski, *J. Am. Chem. Soc.*, **1973**, *95*, 8566. – [12d] G. W. Bushnell, K. R. Dixon, P. M. Moroney, A. D. Rattray, C. Wan, *J. Chem. Soc., Chem. Commun.*, **1977**, 709. – [12e] C. G. Francis, S. I. Kahn, P. R. Morton, *Inorg. Chem.*, **1984**, *23*, 3680; (f) A. C. Skapski, M. Smart, *J. Chem. Soc. Chem. Commun.*, **1970**, 658.
[13] [13a] M. Basato, A. Grassi, G. Valle, *Organometallics*, **1995**, *14*, 4439. – [13b] G. Ferguson, B. R. Loyd, L. Manojlovic-Muir, K. W. Muir, R. Puddephatt, *Inorg. Chem.*, **1986**, *25*, 4190. – [13c] J. Fornies, F. Martinez, R. Navarro, E. P. Urriolabeitia, A. Welch, *J. Chem Soc., Dalton Trans.*, **1995**, 2805. – [13d] A. Deeming, M. N. Meah, P.A. Beates, M.B. Hourthouse, *J. Chem. Soc., Dalton Trans.*, **1988**, 2193. – [13e] M. Sommovigo, M. Pasquall, F. Marchetti, P. Leoni, T. Beringhell, *Inorg. Chem.*, **1994**, *33*, 2651.
[14] [14a] A. L. Balch, J. R. Boehm, H. Hope, M. M. Olmstead, *J. Am. Chem. Soc.*, **1976**, *98*, 1431. – [14b] L.Y. Ukhin, N. A. Dolgopolova, L. G. Kuzmina, Y. Struchkov, *J. Organomet. Chem.*, **1981**, *210*, 263. – [14c] M. Parra-Hake, M. F. Retting, R. M.Wing, *Organometallics* **1983**, *2*, 1013. – [14d] P. M. Bailey, A. Kelly, P. M. Maitlis, *J. Chem. Soc., Dalton Trans.*, **1978**, 1825. – [14e] P. M. Bailey, A. Kelly, P. M. Maitlis, *J. Organomet. Chem.*, **1978**, *144*, C52. – [14f] S. G. Cartwright, K. R. Dixon, A. D. Rattray, *Inorg. Chem.*, **1980**, *19*, 1120. – [14g] R. Uson, J. Fornies, M. Tomas, B. Menjon, J. Crnicer, A. J. Welch, *J. Chem. Soc., Dalton Trans.*, **1990**, 151. – [14h] E. M. Padillia, C. M. Jensen, *Polyhedron,* **1991**, *10*, 89.

[97188]

Synthesis of Stable *N′,N′,N′′,N′′*-Tetramethylguanidine-Substituted σ^4(P)- and σ^3(P)-Organophosphorus Compounds with *N*-Protonated P–N Bonds The First σ^3-Phosphorus-Substituted Ammonium Salts☆

Volker Plack, Jochen Münchenberg, Holger Thönnessen, Peter G. Jones, and Reinhard Schmutzler*

Institut für Anorganische und Analytische Chemie der Technischen Universität,
Postfach 3329, D-38023 Braunschweig, Germany

Received December 15, 1997

Keywords: *N′,N′,N′′,N′′*-Tetramethylguanidine / Triphenylmethyl / Phosphorus-substituted ammonium salts / Steric hindrance / Cleavage reactions

The dependence of the protolytic decomposition rate of phosphorus amides on the substituents at phosphorus is decribed. On treatment with HCl, the *N′,N′,N″,N″*-tetramethylguanidine(= TMG)-substituted σ^4(P) compounds **5** and **9** formed salts that were protonated at the imino nitrogen atoms and were completely stable in the solid state, and surprisingly stable in solution. Even with a large excess of HCl, only the imino nitrogen atom underwent protonation, with formation of HCl_2^- as a counter anion, without cleavage of the P–N bond. The basicity of the imino nitrogen atom also protected σ^3(P) species from electrophilic attack, and the ionic compounds **12**, **14**, and **20c** were formed, providing examples of the first stable σ^3(P) amides with one or two protonated P-N bonds. Such unusual stability is associated with steric protection by the Ph_3C (= trityl) group and charge delocalization over the TMG-moiety. In contrast, $MeP(TMG)_2$ was unstable towards HCl, whereas treatment with $HSbF_6$ led to the phosphonium salt **24**, where protonation had occurred at phosphorus. The same result was obtained when triphenylmethylphosphonous dichloride **1** was allowed to react with 3 equivalents of HTMG, forming the stable phosphonium salt **19**, soluble in water, which was converted to the bicationic species **20c** upon treatment with HCl. – The basicity of the tritylated phosphorus compounds was found to increase in the order **5** < **2** < **19** < **13** < HTMG < **21**; the basic centre is the phosphorus atom in **21** and the imino nitrogen atom in all other compounds. The fluorinating agent $Et_3N \cdot 3$ HF caused rapid conversion of compound **6** to **25**, the nucleophilic attack of fluoride ion at phosphorus could not be prevented by the stabilizing effects mentioned. – All compounds were investigated by ^{1}H- and ^{31}P-NMR spectroscopy. The crystal structures of compounds **5**, $Ph_3CP(=O)$-(H)TMG,and **6**, [**5** · 2 HCl], were determined; **6** is protonated at the imino nitrogen, leading to a longer P–N bond [**5**: 161.6(2), **6**: 168.7(2) pm], and the counterion is HCl_2^-. In the structure of **20c**, $[Ph_3CP(TMG)_2] \cdot 3$ HCl, the cation is protonated at both imino N atoms and the counterions are Cl^- and HCl_2^- (one of each).

Introduction

The bond between phosphorus and nitrogen is particularly susceptible to attack by acids; this is exploited in a general method of forming phosphorus halides from the corresponding phosphorus amides (Eq. 1). The hydrolytic cleavage of the P−N bond is complex and takes place under mild conditions to give an ammonium salt and the corresponding phosphorus halide[1][2].

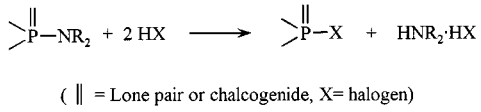

(1)

(‖ = Lone pair or chalcogenide, X= halogen)

Because alkyl groups are the most widely used substituents at nitrogen, and in connection with our own studies on *N′,N′,N′′,N′′*-tetramethylguanidine (TMG)-derivatives[3], we wished to apply the method to TMG-substituted phosphorus compounds. In particular, we wanted to prepare the monochloride of (triphenylmethyl)phosphonous acid **8**, which could, in principle, be formed by the process described in Eq. 1, via compound **5**.

In contrast to expectation, the reaction of **5** with HCl furnished the ionic compound **6**, an intermediate that was reasonably stable in solution and completely stable in the solid state.

Such cases of protonation of the nitrogen atom with preservation of the P−N bond are scarce in the literature. However, a few examples of compounds are known in which the P−N bond was not affected by protonic acids; e.g., Riess et al. were able to isolate stable ammonium salts with tetra- and penta-coordinated phosphorus[4]. Furthermore, Schmidpeter et al. have investigated 5-membered ring systems containing −P=N− moieties, from which stable ammonium salts could also be obtained[6]. However, σ^3(P) compounds with protonated phosphorus-nitrogen single bonds have only been postulated as reaction intermediates[7][8][9][10]. Most reactions of phosphorus amides with protonic acids proceed via protonation at phosphorus, which is due mainly to the nucleophilic character of the phosphorus atom; a few examples of such phosphonium salts with various counterions have been reported[11][12].

Thus, the intermediates formed by HCl attack on TMG-substituted phosphanes need to be identified and investi-

 © WILEY-VCH Verlag GmbH, D-69451 Weinheim, 1998 1434−1948/98/0606−0865 $ 17.50+.50/0

gated with regard to their stability (e.g., by varying the environment of the phosphorus atom). The protolytic stability of the P−N bond must be determined by electronic (a conjugative delocalization of the cationic charge on phosphorus or at TMG) and steric factors (shielding of the phosphorus atom by a bulky substituent). In our investigations we used trityl-TMG substituted phosphorus compounds, which proved suitable in forming intermediates of interest, especially in the acid-catalysed nucleophilic substitution at σ^3(P) amides[8][12][13].

Results and Discussion

The phosphonous dichloride **1**, which has been known since 1933[14], was used as starting material for the preparation of compounds containing the trityl-moiety bonded to phosphorus. It reacted vigorously with 2 equivalents of HTMG, forming compound **2** (Scheme 1).

Scheme 1

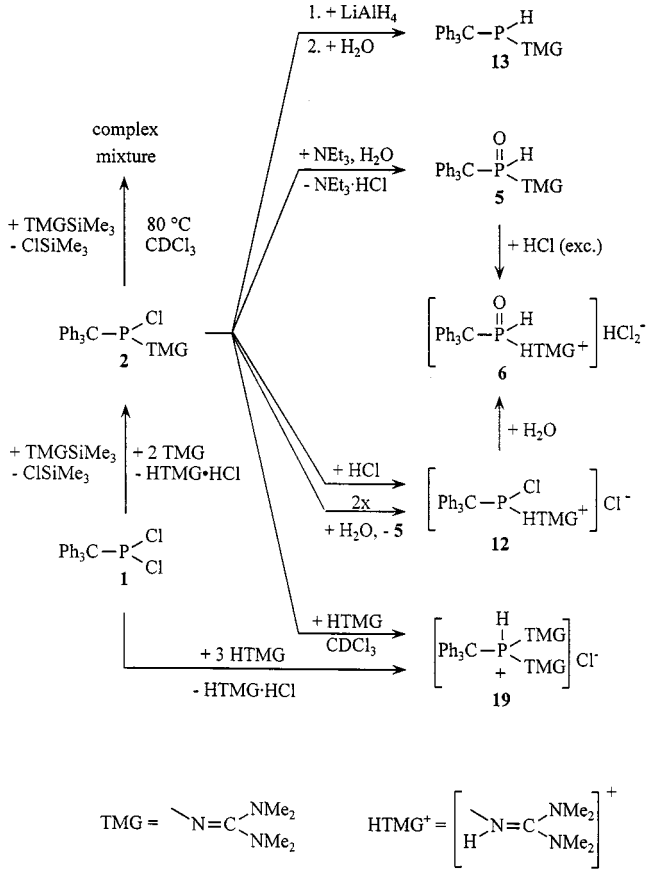

Using the less reactive agent Me_3SiTMG (Scheme 1) partial aminolysis of **1** was also effected. The reaction of triphenylmethylphosphonous difluoride **3** and HTMG, however, involved an unusual preferential cleavage of the phosphorus−carbon rather than the phosphorus−fluorine bond, with formation of the known phosphonous difluoride **4**[15] (Eq. 2); this interesting phenomenon had previously been observed by Nixon in connection with aminolysis reactions of Cl_3CPF_2[16].

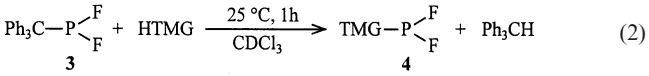

(2)

Treatment of **2** with H_2O and NEt_3 led spontaneously to triphenylmethylphosphonous *N′,N′,N′′,N′′*-tetramethylguanidinide **5** (Scheme 1). The attempted preparation of the monochloride of triphenylmethylphosphonous acid **8** using excess HCl led to the hydrogendichloride **6** (formally **5**·2 HCl), which was stable at room temperature and was converted to Ph_3CPCl_2 **1** and $Ph_3CPH(O)OH$ **7** upon heating in excess HCl at 80°C (Eq. 3).

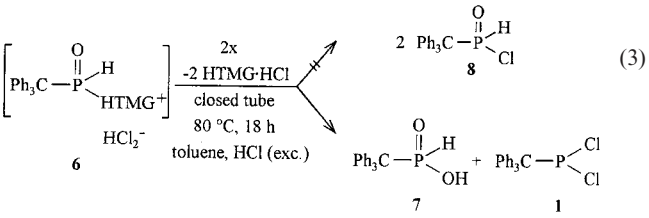

(3)

This result is at variance with the observation that organo(chloro)phosphonous acids are usually stable when they contain sterically demanding substituents[17].

Figure 1. Structure of **5** in the crystal. The solvent has been omitted for clarity[a]

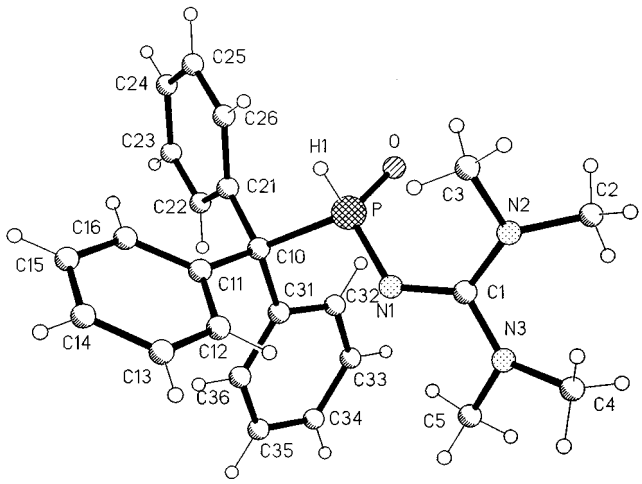

[a] Selected bond lengths [pm] and angles [°]: P−O 148.1(2), P−H(1) 136(2), P−N(1) 161.6(2), P−C(10) 187.5(2), N(1)−C(1) 131.5(3), N(2)−C(1) 137.3(3), N(2)−C(3) 145.5(3), N(2)−C(2) 145.5(3), N(3)−C(1) 134.5(3), N(3)−C(5) 145.0(4), N(3)−C(4) 146.6(4), O−P−N(1) 117.35(11), O−P−C(10) 114.13(11), N(1)−P−H(1) 107.6(9), C(10)−P−H(1) 101.7(9), O−P−H(1) 110.0(9), N(1)−P−C(10) 104.76(11), C(1)−N(1)−P 126.8(2), C(1)−N(2)−C(3) 120.4(2), C(1)−N(2)−C(2) 121.8(2), C(3)−N(2)−C(2) 114.8(2), C(1)−N(3)−C(5) 120.0(2), C(1)−N(3)−C(4) 122.9(2), C(5)−N(3)−C(4) 115.7(2), N(1)−C(1)−N(3) 119.4(2), N(1)−C(1)−N(2) 124.8(2), N(3)−C(1)−N(2) 115.7(2).

Discussion of the X-Ray Structures of 5 and 6

Compound **5** crystallises with half a molecule of dichloromethane (disordered over an inversion centre) in the asymmetric unit. The hydrogen atom H2 of the cation of **6**

Figure 2. Structure of **6** in the crystal[a]

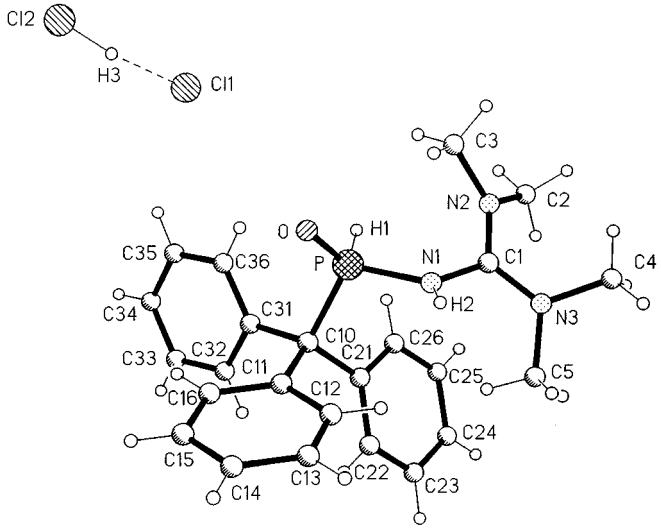

[a] Selected bond lengths [pm] and angles [°]: P−O 147.2(2), P−N(1) 168.7(2), P−C(10) 186.0(2), P−H(1) 132(2), N(1)−C(1) 137.8(3), N(1)−H(2) 90(3), N(2)−C(1) 133.0(3), N(2)−C(3) 145.8(3), N(2)−C(2) 146.7(3), N(3)−C(1) 132.2(3), N(3)−C(4) 145.8(3), N(3)−C(5) 146.6(3), Cl(1)−H(3) 187(3), Cl(2)−H(3) 135(3), O−P−N(1) 112.38(10), O−P−C(10) 113.61(10), N(1)−P−C(10) 108.25(11), O−P−H(1) 114.9(8), N(1)−P−H(1) 103.3(8), C(1)−N(1)−P 126.3(2), C(1)−N(1)−H(2) 114.5(1.7), P−N(1)−H(2) 118.6(1.7), C(1)−N(2)−C(3) 123.5(2), C(1)−N(2)−C(2) 121.2(2), C(3)−N(2)−C(2) 115.2(2), C(1)−N(3)−C(4) 121.6(2), C(1)−N(3)−C(5) 123.1(2), C(4)−N(3)−C(5) 114.9(2), N(3)−C(1)−N(2) 121.6(2), N(3)−C(1)−N(1) 118.8(2), N(2)−C(1)−N(1) 119.6(2), Cl(1)−H(3)−Cl(2) 173(2).

was located at the imino nitrogen N1; this hydrogen and all other non-C-bonded hydrogen atoms of **5** and **6** were refined freely.

The P−O, P−C, and P−H bonds are marginally shorter in **6** than in **5** [**5**: P−O 148.1(2), P−C10 187.5(2), P−H1 136(2) pm; **6**: P−O 147.2(2), P−C10 186.0(2), P−H1 132(2) pm]. The increase in coordination number at the imino nitrogen leads, as expected, to a marked increase in the P−N bond length [**5**: P−N 161.6(2), **6**: P−N 168.7(2) pm]. In compound **5** the imino N−C bond [N1−C1 131.5(3) pm] is naturally shorter than the amino N−C bonds [N2−C1 137.3(3), N3−C1 134.5(3) pm]. In compound **6** the N1−C1 bond [137.8(3) pm] is about 5 pm longer than N2−C1 [133.0(3) pm] and N3−C1 [132.2(3) pm]; this indicates that the positive charge is delocalized over the two dimethylamino groups. The average $N-C_{methyl}$ bond lengths differ insignificantly [**5**: 145.6, **6** 146.22 pm].

The phosphorus atom, as expected, displays somewhat distorted tetrahedral coordination geometry, with the largest angles involving the doubly bonded O atom. In the case of **5** O−P−N1 [117.35(11)°] is the largest, C10−P−H1 [101.7(9)°] the smallest angle; in **6** O−P−H1 [114.9(8)°] and C10−P−H1 [103.5(8)°].

The counteranion in compound **6** is the hydrogendichloride anion. The angle at H3 is 173(2)°. One Cl−H bond is significantly longer than the other [Cl1−H3 187(3), Cl2−H3 135(3) pm], so the negative charge is mainly located at Cl1. The Cl−Cl distance is 320.8(1) pm, which is normal for hydrogendichloride anions (cf. [(4-$CH_3OC_6H_4$)$(CH_3)PCl_2$] [ClHCl]: Cl···Cl 321.0(3) pm; [(4-$C_2H_5OC_6H_4$)PCl_3] [ClHCl]: Cl···Cl 318.9(1) pm)[18].

The H2 atom forms a hydrogen bond to Cl1 at [1.5 − x, 0.5 + y, −0.5 − z], with the following dimensions: H2···Cl1 237(3) pm, N1···Cl1 321.9(2) pm and N1−H2···Cl1 157(2)°. The H1 atom is linked to O [at 1.5 − x, 0.5 + y, 0.5 − z] via short contacts that may be interpreted as hydrogen bonds [H1···O 255(2), P···O 386.6(2) pm, P−H1···O 170.4(1.2)°].

The formation of compounds **1** and **7** from **6** would appear to be the result of the conversion of $Ph_3CPH(=O)Cl$ **8**, formed as an intermediate by nucleophilic attack of chloride anion on **6**. This process is complex and will be discussed in a subsequent publication.

The unusual stability of **6** is caused by the kinetically stabilizing effect of the trityl group[19], and the possibility of charge delocalisation in TMG-substituted phosphorus compounds[3]. The latter might be the reason for the possibility of the isolation of compound **10**, a doubly protonated species whose formation was concluded from analytical data (Eq. 4).

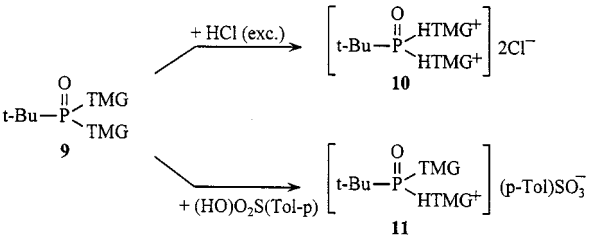

(4)

The possibility of rearrangement of the dichloride **10** to the hydrogendichloride in the solid state was considered, in the mass spectrum, from the observation of only the monoprotonated parent ion. The cation **11** was formed in good yield by treatment of **9** with *p*-tolylsulfonic acid. This counterion, of low nucleophilicity, gave rise to additional stabilization, compared to the chloride ion.

The displacement of halogen by water was of particular importance and led, as mentioned above, to compound **5** in the presence of NEt_3, or to a mixture of **5** and **12**, in which a second molecule of **2** acted as a scavenging agent for the HCl liberated (Scheme 1). In the presence of excess water the same treatment afforded compound **6**. Compound **12** was also formed by reaction of **2** with HCl (Scheme 1) and **5** with phosgene (Eq. 5), respectively.

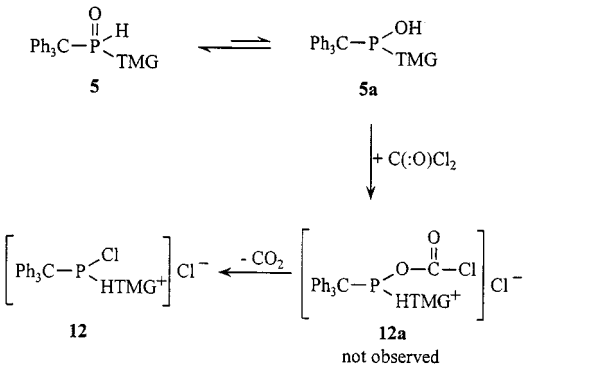

(5)

The latter reaction was preceded by the formation of the tautomeric parent acid **5a**, where the proton was more strongly acidic than in **5**, and the reaction with $C(=O)Cl_2$ took place rapidly. The assumed intermediate **12a** was unstable and was transformed to **12**. This salt was stable as a solid, but in solution slowly decomposed to **1**, **2**, and HTMG·HCl (Eq. 6).

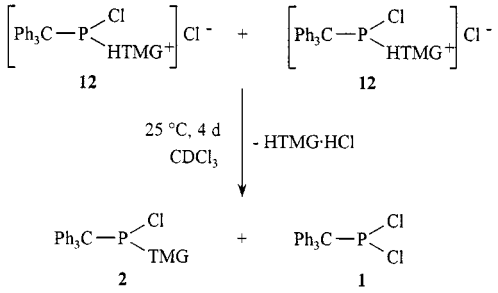

(6)

To define the effects causing the unusual stability of **12**, further investigations were conducted that involved variation of the nucleophilicity and steric congestion at the phosphorus atom. Thus, the nucleophilicity of the tritylated phosphorus compounds should increase if the chlorine atom in **2** were substituted by hydrogen. This was realized when **2** was allowed to react with $LiAlH_4$ (Scheme 1). The isolation of **13** was not possible because Ph_3CH was also formed and could not be separated from the reaction mixture. A toluene solution of the resulting crude product was, therefore, treated with excess HCl, and the colourless solid precipitated was identified as the hydrogendichloride **14**, where protonation had occurred at the imino nitrogen atom (Eq. 7).

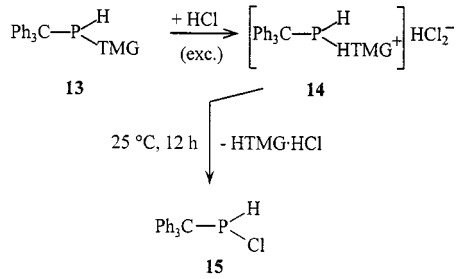

(7)

The identity of **14** was established by analytical and NMR spectral data, and by its decomposition to triphenylmethylphosphonous chloride **15**. Compounds like **15** are sufficiently stable only in the presence of bulky groups, and only a few examples, mainly referred to as intermediates, are mentioned in the literature[20][21][22]. Compound **15**, which is completely stable, will be described elsewhere in connection with alternative synthetic routes and further investigations.

To exclude the steric hindrance effect of the trityl group, the protonation reaction was repeated with compound **16** where, moreover, the nucleophilicity of phosphorus should be higher than in both **2** and **13** (Eq. 8).

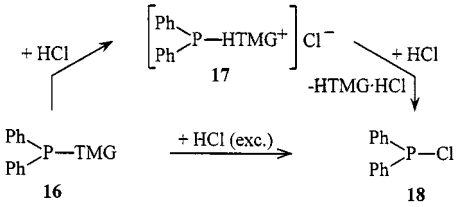

(8)

The reaction pathway is not clear. The solid that precipitated from toluene consisted of HTMG·HCl and a phosphorus compound separated that could not be isolated (in a 1:1 ratio). The product soluble in toluene was characterized by ^{31}P NMR as diphenylphosphinous chloride **18**, which was formed as shown (Eq. 8). The precise location of the proton in **17** could not be established, because the ^{1}H NMR resonance of the proton bonded to phosphorus or nitrogen was not observed.

Scheme 2

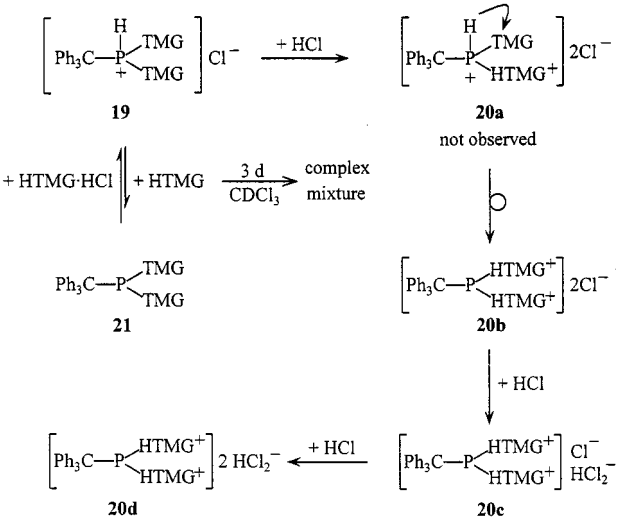

When the reaction of HTMG with **1** was carried out in a molar ratio 3:1, the final product was the phosphonium salt **19**, which was also obtained when **2** was allowed to react with HTMG (Scheme 1). In both cases, the strongly basic properties of the phosphorus atom of $Ph_3C-P(TMG)_2$ **21** were evident (based on ^{31}P NMR studies). The equilibrium between **19** and **21** was established spontaneously (molar ratio **19/21** = 6:4). After removing the volatile products, the phosphonium salt **19** was isolated.

The isolation of **21** from this equilibrium mixture was, however, not possible. After the components were left in solution in $CDCl_3$ for 3 d, a complex mixture was obtained (Scheme 2). The attempted preparation of **21** via reaction of **2** with Me_3SiTMG was also unsuccessful because under the reaction conditions (temperature ca. 80°C), decomposition with formation of an oily product took place (Scheme 1). The above-mentioned acid-base equilibrium could not be observed when **19** was treated with excess NEt_3. This provides additional evidence of the high basicity of **21**. The basic properties of the phosphorus atom in amino-substi-

tuted phosphorus compounds are well known[23][24]. However, it should be noted that in the preparation of $RP(TMG)_2$ (R = Me, *t*Bu, and Ph) by treatment of $RPCl_2$ with HTMG (molar ratio: 1:4) these compounds could be obtained readily and in good yield by distillation of the corresponding crude products[3]. The formation of **19** took place quantitatively, but the separation from HTMG·HCl by washing with H_2O resulted in low yields, because **19** also showed hydrophilic properties. The phosphorus atom in $Ph_3C-P(TMG)_2$ seemed to be more basic than the imino nitrogen atom in HTMG and, therefore, **19** showed (in contrast to the conversion of compounds **12** and **14**) no decomposition to the chlorinated compound **2** and the unprotonated species **21**, respectively (Eq. 9).

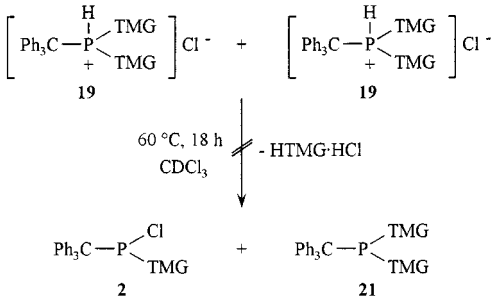

(9)

The TMG moieties in $[Ph_3C-PH(TMG)_2]^+$ also were found to display basic properties at the imino nitrogen atoms and additional HCl should lead to a doubly protonated species. Surprisingly, the product resulting from the reaction of **19** with HCl was, instead of the expected compound **20a**, the σ^3(P) compound **20b**, where both imino nitrogen atoms were protonated (Scheme 2).

The migration of the proton in **20a** is caused by the electron-withdrawing effect of the $HTMG^+$ moiety, which is comparable to that of a chlorine atom. The electron density at the phosphorus atom in **20b** is comparable to that in **12**, and a decreasing tendency of electrophilic attack was established by treatment of **20b** with excess hydrogen chloride, leading to HCl_2^- as counter anion. There was no protonation at the phosphorus atom. Treatment of **19** with HCl (ratio 1:1) led to the ionic species **20b** with chloride as counterion. Compound **20b** was insoluble in $CDCl_3$, whereas the corresponding hydrogendichloride **20d** was well soluble in chlorinated solvents and, as expected from its structure, insoluble in nonpolar solvents. The crystals, obtained from the reaction mixture (in CH_2Cl_2/Et_2O, ratio: 7:1) at room temperature by treatment of **19** with HCl (ratio: 1:3), contained both chloride and hydrogendichloride anions (see below). The solubility of this compound (**20c**) lies between that of **20b** and **20d**. Surprisingly, the attempted conversion of **20c** did not afford the expected compounds **12** and HTMG·HCl, and reflected the increasing influence of steric congestion by the second $HTMG^+$ moiety (Eq. 10). Thus, in contrast to **12** and **14**, nucleophilic attack at the phosphorus atom was not possible, even on raising the temperature (60 °C).

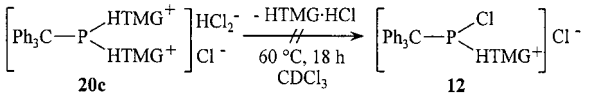

(10)

Figure 3. Structure of **20c** in the crystal. Methyl and phenyl hydrogen atoms and solvent have been omitted for clarity[a]

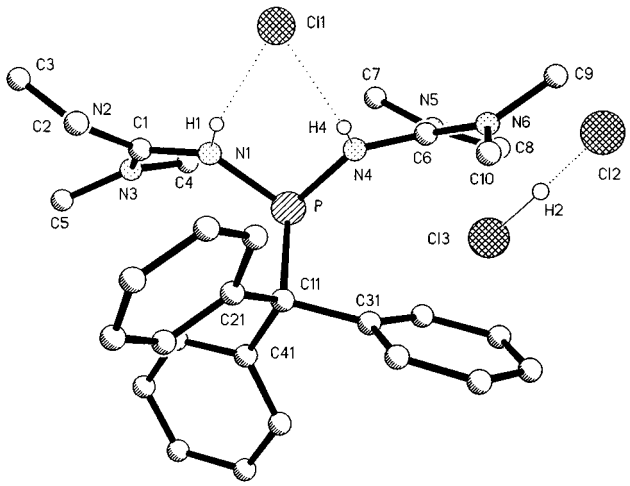

[a] Selected bond lengths [pm] and angles [°]: P−N(4) 171.7(3), P−N(1) 173.4(2), P−C(11) 195.8(3), N(1)−C(1) 135.4(4), N(1)−H(1) 81.9(40), N(2)−C(1) 133.9(4), N(2)−C(2) 146.1(4), N(2)−C(3) 146.8(4), N(3)−C(1) 133.4(4), N(3)−C(4) 146.1(4), N(3)−C(5) 146.5(4), N(4)−C(6) 135.9(4), N(4)−H(4) 74.4(36), N(5)−C(6) 133.7(4), N(5)−C(7) 146.1(4), N(5)−C(8) 146.8(4), N(6)−C(6) 133.0(4), N(6)−C(10) 145.8(4), N(6)−C(9) 146.3(4), Cl(2)−H(2) 170.1(54), Cl(3)−H(2) 145.5(54), N(4)−P−N(1) 93.07(12), N(4)−P−C(11) 104.53(12), N(1)−P−C(11) 105.30(12), C(1)−N(1)−P 130.2(2), P−N(1)−H(1) 114(3), C(1)−N(1)−H(1) 115(3), C(1)−N(2)−C(2) 121.7(3), C(1)−N(2)−C(3) 120.7(3), C(2)−N(2)−C(3) 115.4(3), C(1)−N(3)−C(4) 123.4(2), C(1)−N(3)−C(5) 121.8(3), C(4)−N(3)−C(5) 114.7(3), C(6)−N(4)−P 124.8(2), P−N(4)−H(4) 119(3), C(6)−N(4)−H(4) 115(3), C(6)−N(5)−C(7) 122.1(2), C(6)−N(5)−C(8) 122.8(3), C(7)−N(5)−C(8) 114.9(2), C(6)−N(6)−C(10) 121.5(2), C(6)−N(6)−C(9) 123.2(3), C(10)−N(6)−C(9) 114.9(2), N(3)−C(1)−N(2) 120.0(3), N(3)−C(1)−N(1) 122.2(3), N(2)−C(1)−N(1) 117.7(3), N(6)−C(6)−N(5) 121.8(3), N(6)−C(6)−N(4) 118.1(3), N(5)−C(6)−N(4) 120.1(3), Cl(2)−H(2)−Cl(3) 177(4).

Discussion of the X-ray Structure of 20c

Compound **20c** crystallises as a dichloromethane solvate. All three non-C-bonded hydrogen atoms were refined freely.

The P−N bonds in **20c** [P−N1 173.4(2), P−N4 171.7(3) pm] are longer than those of $Ph_2P(TMG)$ **A**[25] [P−N1 169.6(3) pm]. The N1−C1 [135.4(4) pm] and N4−C6 [135.9(4) pm] bonds are about 5 pm longer [**A**: P−N1 129.3(4) pm], but the amino N−C bonds [133.0(4) (N6−C6) to 133.9(4) (N2−C1) pm] are much shorter than those of **A** [N2−C1 138.2(4), N3−C1 136.4(4) pm]. In compound **20c** the formal imino N−C double bond is longer than the amino N−C bonds, which means that the positive charge is effectively delocalized via π bonding to N2, N3, N5, and N6. The N−methyl bond lengths vary from 145.8(4) pm (N6−C10) to 146.8(4) pm (N2−C2 and N5−C8).

The phosphorus atom displays a pyramidal configuration, lying 82 pm out of the plane of its α-substituents. The smallest angle at phosphorus is between the two TMG substituents [N1−P−N4 93.07(12)°], the angles involving C11 of the triphenylmethyl group are 105.30(12)° (N1−P−C11) and 104.53(12)° (N4−P−C11), respectively. The P−C11 bond [195.8(3) pm] is extremely long.

The hydrogendichloride anion displays dimensions of 145(5) pm (Cl3−H2), 170(5) pm (Cl2−H2), 177(4)° (Cl2−H2−Cl3). The distance between Cl2 and Cl3 is 315.5(1) pm. The other counterion is a chloride ion, which forms hydrogen bonds to both N−H groups; the Cl···H distances are 247(4) pm (Cl1···H1) and 237(4) pm (Cl1···H4).

In compound **22** the steric hindrance effect of the organic group was essentially absent, and treatment with excess HCl afforded the chlorinated product **23**, with no P- or N-protonated intermediates being observed (Eq. 11).

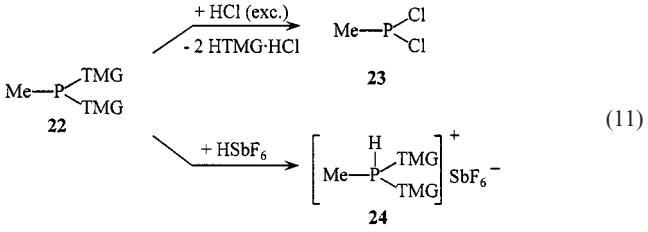

(11)

The ^{31}P-NMR spectrum of the adduct between **22** and $HSbF_6$ also suggested that electrophilic attack on the polar P−N bond led to the phosphonium cation, an intermediate that was stable in combination with weakly nucleophilic anions but not in the presence of chloride ions.

A measure of the relative basicity of compounds **2**, **5**, **13**, and **19** was obtained through the acid-base reactions outlined in Scheme 3.

The basicity of the tritylated compounds increased in the order shown in Figure. 4 (in comparison to HTMG and NEt_3) and, in agreement with this, the acidity of the corresponding acids (**6**, **12**, **20**, **14**, and **19**) increased in the reverse order, as was evident from ^{1}H NMR studies.

Figure 4. The relative basicities of tritylated *N′,N′,N″,N″*-tetramethylguanidino-substituted phosphorus compounds in comparison to NEt_3 and HTMG (**bold print**: main basic centres)

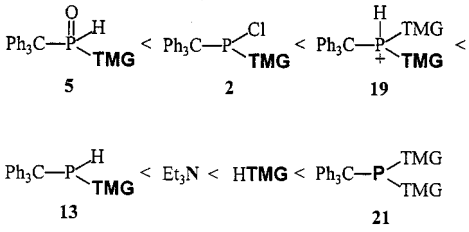

Increasing acidity effects an increasing tendency to proton exchange and influences the observed ^{1}H NMR spectra. Figure. 5 shows the ^{1}H-NMR spectra of **5** observed after interaction with HCl in various ratios (employing the corresponding mixtures of **5** and **6**).

The ^1J(PH) values may be considered as diagnostic of the extent of the protonation of compound **5**, and of the deprotonation of **6**. These values lay between 494 Hz (sharp doublet, compound **5**) and 550 Hz (broad doublet, compound **6**). If the ratio of HCl to **5** was increased to 1:1, HCl_2^- was formed and because of proton exchange processes δ(^{1}H)(P*H*) and ^1J(PH) could not observed. A dynamic phenomenon that can be explained by a fast bond exchange, relative to the NMR time scale, also led to the averaging of the NMR signals in the ^{31}P-NMR spectra and caused the absence of the N*H* proton resonance in the ^{1}H NMR. In contrast, in the ^{31}P-NMR spectra ^1J(PH)-coupling of the phosphorus nuclei of **5** was observed, even in the presence of HCl. The δ(^{31}P) values observed for mixtures of **5** and HCl showed a linear relationship, and ranged between δ = 24.8 (compound **5**) and δ = 27.4 (compound **6**) (Figure. 6).

Scheme 3

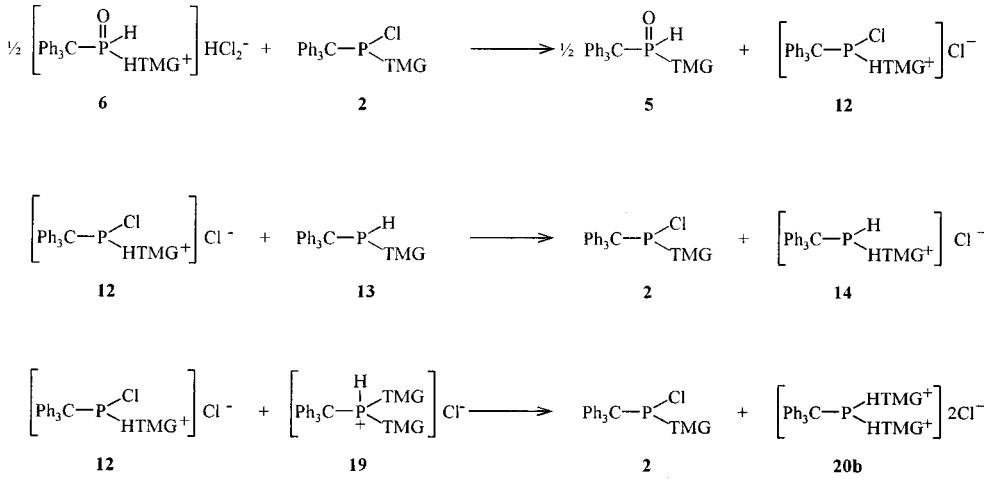

Figure 5. ^{1}H NMR spectra of mixtures of **5** with various ratios of HCl

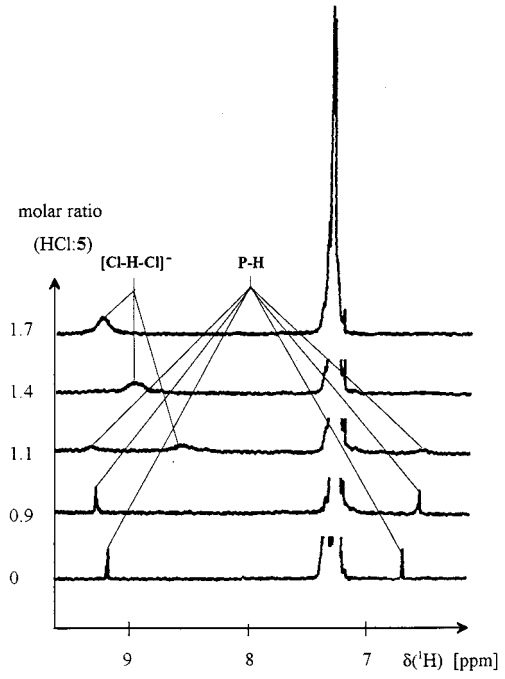

Figure 6. Dependence of $\delta(^{31}P)$ (upper curve) and $^1J(PH)$ (lower curve) of **5** on the degree of protonation at the imino nitrogen atom

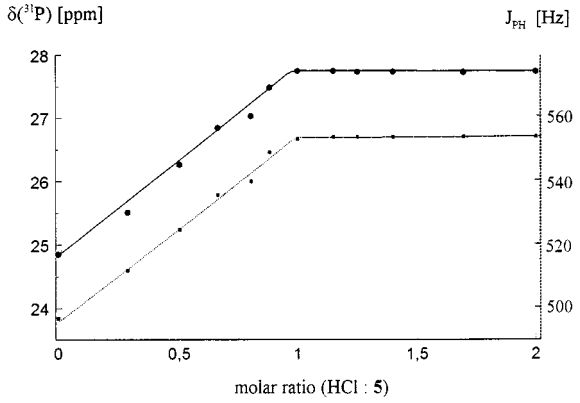

The ^{1}H NMR signal of the HCl_2^- proton moved significantly downfield when the proportion of HCl was increased (broad hump at room temperature).

The ^{1}H-NMR spectra of compounds **10**, **11**, and **17** were also influenced by such dynamic phenomena, whereas the NMR spectra of **12** and **14** were more informative, and clear evidence for the presence of hydrogen atoms in both compounds came from ^{1}H-NMR spectra. The increasing basicity in the series led to restricted proton interactions, and the NMR spectra of **12**, **14**, and **20c** exhibited broadened singlets, caused by the protons bonded to the imino nitrogen atoms. Furthermore, in **14** the resonance of the P*H* proton was observed as a broad doublet of doublets, making the accurate determination of $^1J(PH)$ and $^3J(HH)$ impossible. However, the observed value of $J(PH)$ (ca. 235 Hz) is typical of $\sigma^3(P)$ compounds[26], and suggested the structure proposed for **14**.

The restricted proton exchange (as concluded from the ^{1}H-NMR spectra) was also proved by ^{31}P-NMR spectroscopy. Mixtures of compounds **2** and **13** with the corresponding protonated species (**12** and **14**) did not give rise to single averaged peaks. Furthermore, both systems (**2/12**; **13/14**) showed, in contrast to the system **5/6**, separate resonances for the protonated and unprotonated species.

For TMG·HCl, the signals of the $N(CH_3)_2$ protons of all protonated compounds (**6**, **10**, **11**, **12**, **14**, **17**, and **20c**) were shifted downfield, compared to those of the related unprotonated species. All the spectra exhibited sharp singlets, and demonstrated the chemical equivalence of the $N(CH_3)_2$ groups, caused by a three step isomerisation via, a: deprotonation, b: inversion of configuration at the imino nitrogen atom, and c: reprotonation; a mechanism that was reported previously for other TMG-substituted compounds[27][28][29].

In addition to structural parameters (see X-ray studies), the ^{31}P-NMR data also could be used as a sensitive probe to evaluate the electronic structure of the C=N double bond. Surprisingly, the ^{31}P-NMR signals of the protonated $\sigma^3(P)$ species (**12**, **14**, **20c**) were markedly shifted to high field, relative to the corresponding unprotonated compounds (**2**, **13**, **21**). This phenomenon can be rationalized as a consequence of the delocalisation of the positive charge along the $P-N=C(NMe_2)_2$ grouping (Figure. 7).

Figure. 7. Possible charge delocalisation over the TMG moiety (illustrated for molecule **6**)

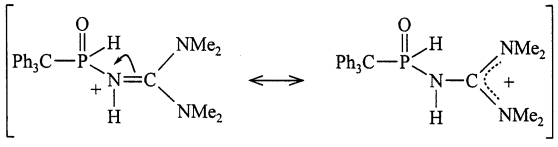

6

Thus, the ^{31}P-NMR data of the protonated species should generally be comparable to those of the corresponding amino-substituted phosphorus compounds. A compilation of such data is shown in Table 1, supporting this assumption through similar $\delta(^1H)$ values of corresponding N(H)−*t*Bu-substituted phosphorus compounds.

Table 1. $\delta(^{31}P)$ values of unprotonated and protonated tritylated *N′,N′,N″,N‴*-tetramethylguanidino-substituted phosphorus compounds, compared to those of the corresponding *tert*-butyl derivatives

R =	TMG	HTMG⁺	-N(H)t-Bu [30]
$Ph_3C-P(Cl)R$	154.7 ppm **2**	122.1 ppm **12**	129.1 ppm
$Ph_3C-P(=O)(H)R$	24.7 ppm **5**	27.7 ppm **6**	26.3 ppm
$Ph_3C-P(H)R$	33.1 ppm **13**	15.4 ppm **14**	18.7 ppm
Ph_3C-PR_2	114.3 ppm **21**	83.5 ppm **20**	-

The observation that the resonance of the phosphorus atom in **17** was shifted downfield, in the direction of the unprotonated precursor **16**, cannot be explained. Compounds **19** and **24** were characterized from their ^1J(PH) values, which were typical of σ^4(P) compounds[26].

Reactivity of Protonated Compounds

Because of the protonation at the imino nitrogen atom of aminosubstituted trityl-phosphane compounds, the phosphorus becomes more electrophilic and thus more susceptible to nucleophilic attack (e.g. by H_2O). In agreement with this it has been found that the chemical behaviour of protonated species is similar to that of the corresponding halogenated compounds. Thus **6** reacted slowly with H_2O, forming triphenylmethylphosphonous acid **7** (Eq. 12), whereas hydrolysis of the unprotonated compound **5** was not observed.

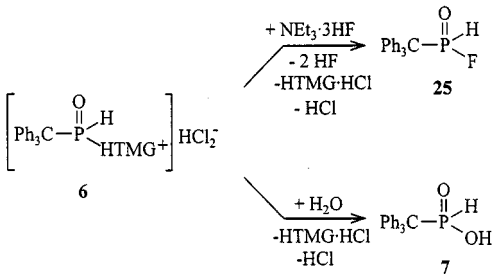

(12)

However, the sensitivity to nucleophilic attack at the protonated P−N bond of these species appeared to be lower than at the P−Cl bond, because hydrolysis of **12** initially led to the displacement of the chlorine atom (Scheme 1).

The bis(TMG)-substituted phosphorus compound **19** was attacked by H_2O to a lesser extent, forming **6** and additional phosphorus compounds that could not be characterized (decomposition of **19** after 7d at room temperature in dichloromethane and excess H_2O: ca. 10%). Unexpectedly, **20c** was soluble in water, and showed no conversion to the expected compounds (**6** or **7**, and HTMG · HCl). This must be due to steric congestion.

On changing the counterion to F^-, the displacement of $HTMG^+$ took place rapidly. For instance, the reaction of **6** with $NEt_3 \cdot 3$ HF in a 1:1 molar ratio spontaneously led to triphenylmethylphosphonous fluoride **25** (Eq. 12), providing an alternative convenient synthesis to that reported previously[19].

We are grateful to *BASF AG, Bayer AG* and *Hoechst AG* for generous supplies of chemicals used in this research, and to *Fonds der Chemischen Industrie* for financial assistance.

Experimental Section

All experiments were carried out with exclusion of air and moisture; solvents were purified and dried according to the usual methods[31][32]. – NMR spectra were recorded in $CDCl_3$ (unless otherwise noted) at 298 K, using a Bruker AC-200 instrument at 200.1 MHz (^{1}H), 81.3 MHz (^{31}P) and 50.3 MHz (^{13}C) and referenced internally to residual solvent resonances. – Electron impact mass spectra were recorded on solid samples, using a Finnigan MAT 8430 (70 eV) instrument. – Melting points were taken in sealed capillaries and are uncorrected (Instrument: Büchi 510). – IR spectra were recorded on a BIO-RAD IR-165 instrument. – The abbreviation "in vacuo" indicates a pressure of 0.1 mm Hg.

The following compounds were synthesized according to the literature: Ph_3CPCl_2[14], Ph_3CPF_2[19], (*t*Bu)P(=O)(TMG)$_2$[33], Ph_2P(TMG) and MeP(TMG)$_2$[3], Me_3SiTMG[34]. All other compounds were obtained commercially.

Reactions which were investigated solely by ^{31}P-NMR spectroscopy in $CDCl_3$ are not described in the Experimental Section, because the products were synthesized by alternative methods reported in the present work, and also in previous publications.

Chloro Triphenylmethylphosphonous N′,N′,N″,N″-Tetramethylguanidinide (**2**). – *Method A: Reaction of Triphenylmethylphosphonous Dichloride* **1** *with HTMG:* HTMG (1.80 g, 15.64 mmol) was added dropwise with stirring over 10 min at room temperature to a solution of **1** (2.70 g; 7.82 mmol) in 30 ml of dichloromethane. The solvent was evaporated and toluene (50 ml) was added to the residue. The precipitate was filtered off and the solvent from the filtrate was removed in vacuo. The residue was dissolved in 15 ml of dichloromethane and the product was obtained as an amorphous, colourless solid. Yield 2.1 g (63.3%); m.p. 145°C (dec.). – ^{1}H NMR: δ = 2.59 (s, 12 H, N(CH$_3$)$_2$), 7.16−7.37 (m, 15 H, Ph_3C). $C_{24}H_{27}ClN_3P$ (423.92): calcd. C 68.00, H 6.42, N 9.91; found C 67.70, H 6.64, N 9.91.

Method B: From **1** *and* Me_3SiTMG: To a solution of 1.0 g (2.9 mmol) **1** in 7 ml of toluene, 543 mg (2.9 mmol) of Me_3SiTMG was added at room temperature. After 3 h the precipitate was filtered off, washed with 5 ml of diethyl ether and dried in vacuo. Yield 1.03 g (83.9%); m.p. 143°C (dec.).

Triphenylmethylphosphonous N′,N′,N″,N″-Tetramethylguanidinide (**5**): *N′,N′,N″,N″*-Tetramethylguanidine (1.6 g; 13.9 mmol) was added dropwise with stirring over 10 min at room temperature to a solution of **1** (2.40 g, 6.95 mmol) in 40 ml of toluene. To this solution a solution of H_2O (0.5 g; 27.76 mmol) in HTMG (0.8 g; 6.95 mmol) was added with stirring at 0°C during 30 min. The reaction mixture was allowed to reach room temperature and the precipitate was filtered off. The solvent was removed from the filtrate in vacuo, and the product was left as a colourless solid. Yield 2.4 g (85.1%); m.p. 175°C (dec.). – ^{1}H NMR: δ = 2.61 [s, 12 H, N(CH$_3$)$_2$], 7.18−7.35 (m, 15 H, Ph_3C), 7.92 [d, ^1J(PH) = 493.7 Hz, 1 H, PH]. – ^{13}C NMR: δ = 39.73 (s, CH$_3$), 62.96 [d, ^1J(PC) = 90.7 Hz, Ph_3C], 143.25 [d, ^2J(PC) = 3.1 Hz, C_6H_5], 130.73 [d, ^3J(PC) = 6.5 Hz, C_6H_5], 127.88 (s, C_6H_5), 126.45 [d, ^5J(PC) = 2.0 Hz, C_6H_5], 162.58 (s, C=N). – ^{31}P NMR: δ = 24.8 (s). – IR (KBr): ν = 1339 (P=O), 2307 (P−H). – $C_{24}H_{28}N_3OP$ (405.48): calcd. C 71.09, H 6.96, N 10.36; found C 70.53, H 6.91, N 10.04.

[Triphenylmethylphosphonous N′,N′,N″,N″-Tetramethylguanidinide] · 2 HCl (**6**): To a solution of $Ph_3CPH(O)$TMG **5** (1.01 g; 2.5 mmol) in 10 ml of toluene were added at room temperature 3 equivalents of HCl (7.5 ml of a 1 M solution in diethyl ether; 7.5 mmol HCl). The precipitate was filtered off and the product was obtained as a colourless solid. Yield 1.12 g (95.6%); m.p. 220°C (dec.). – ^{1}H NMR: δ = 2.88 [s, 12 H, N(CH$_3$)$_2$], 7.13−7.32 (m, 15 H, Ph_3C), 9.58 (s, 1 H, HCl_2^-), no resonances for P*H* and N*H* were observed. – ^{13}C NMR: δ = 41.65 (s, CH$_3$), 63.32 [d, ^1J(PC) = 77.7 Hz, Ph_3C], 139.12 [d, ^2J(PC) = 2.4 Hz, C_6H_5], 130.38 [d, ^3J(PC) = 7.3 Hz, C_6H_5], 129.02 (s, C_6H_5), 128.04 [d, ^5J(PC) = 2.6 Hz, C_6H_5], 159.65 (s, C=N). – ^{31}P NMR: δ = 27.7 (s). – IR (KBr): ν = 1291 (P=O), 2340 (P−H). – $C_{24}H_{30}Cl_2N_3OP$ (478.40): calcd. C 60.25, H 6.32, N 8.78; found C 60.33, H 6.21, N 8.82.

6 (*Preparation of Crystals*): A solution of $Ph_3CPH(=O)$TMG **5** (1.01 g; 2.5 mmol) in 10 ml of toluene was combined with a solu-

tion of 2 equivalents of HCl (5.0 ml; 5 mmol HCl of a 1 M solution in diethyl ether) in toluene (20 ml). After 4 d the resulting colourless crystals were filtered off. Yield 1.15 g (98.1%).

Decomposition of **6**; *Formation of* **1** *and* **7**: A solution of **5** (1.0 g; 2.5 mmol) in toluene (20 ml) was treated with gaseous hydrogen chloride for (ca.) 2 min but the precipitate (**6**) formed instantaneously was found to be dissolved again after prolonged action of HCl. This solution was heated in a sealed tube for 18 h at 80°C. The solvent was removed in vacuo and the products were characterized by ^{31}P NMR spectroscopy. The data were identical to those of **1** and **7**[19].

[tert-Butylphosphonic Bis(N′,N′,N′′,N′′-tetramethylguanidinide)] · 2 HCl (**10**): Addition of 2 equivalents of HCl (4.52 ml of a 1 M solution in diethyl ether; 4.52 mmol) to a stirred solution of **9** (0.75 g; 2.26 mmol) in toluene (20 ml) at room temperature resulted in a yellow oil. After decanting the solvent the oil was washed with n-hexane (2× 10 ml), was dried in vacuo and **10** was obtained as a colourless solid. Yield 0.89 g (97.3%); m.p. 79°C (dec.). − ^{1}H NMR: δ = 1.42 [d, ^3J(PH) = 18.72, 9 H, PC(CH$_3$)$_3$], 3.21 [s, 24 H, N(CH$_3$)$_2$], no resonance for N(*H*)=C< was observed. − ^{31}P NMR: δ = 31.70 (s). − FAB-MS chemical ionization with nitrobenzyl alcohol (= NBA)]: positive *m/z* (%): 666 (2) [(*t*BuP(=O)(TMG)$_2$·H)$_2$]$^+$, 333 (78) [*t*BuP(=O)(TMG)$_2$·H]$^+$, 218 (100) [*t*BuP(=O)TMG]$^+$, 71 (12) [HNCNMe$_2$]$^+$; negative (*m/z*) (%): 188 (100) [Cl$^-$·NBA]$^-$. − IR (KBr): ν = 1253 (P=O). − $C_{14}H_{35}Cl_2N_6OP$ (405.35): calcd. C 41.48, H 8.70, N 20.73; found: C 41.60, H 8.73, N 20.46.

tert-Butylphosphonic Bis(N′,N′,N′′,N′′-tetramethylguanidinide)] · (p-Tol)SO$_3$H (**11**): A solution of a mixture of **9** (0.45 g; 1.35 mmol) and *p*-toluenesulphonic acid (0.25g; 1.31 mmol) in 10 ml of toluene was stirred at room temperature for 16 h. The oily precipitate formed was separated from the solvent and after washing with n-hexane (two 5 ml portions) **11** was obtained as a colourless solid. Yield 0.62 g (94.5%); m.p. 135°C (dec.). − ^{1}H NMR: δ = 1.23 [d, ^3J(PH) = 16.85, 9 H, PC(CH$_3$)$_3$], 2.31 (s, 12 H, *Me*C$_6$H$_4$SO$_3^-$), 2.98 [s, 12 H, N(CH$_3$)$_2$], 7.10/7.74 [m (AA′XX′), 4 H, MeC$_6$*H*$_4$SO$_3^-$]. − ^{31}P NMR: δ = 20.28 (s). − FAB-MS (NBA): positive *m/z* (%): 333 (86) [*t*BuP(=O)(TMG)$_2$·H]$^+$, 218 (100) *t*BuP(=O)TMG]$^+$, 71 (14) [HNCNMe$_2$]$^+$; negative (*m/z*) (%): 324 (16) [MeC$_6$H$_4$SO$_3$·NBA]$^-$, 171 (100) [MeC$_6$H$_4$SO$_3$]$^-$. − $C_{21}H_{37}N_6O_4PS$ (500.60): calcd. C 50.39, H 7.45, N 16.79, S 6.40; found: C 50.02, H 8.07, N 16.53, S 6.21.

[Chloro Triphenylmethylphosphonous N′,N′,N′′,N′′-Tetramethylguanidinide] · HCl (**12**): − *Method A : Treatment of* **5** *with Phosgene:* A solution of C(=O)Cl$_2$ (0.27 g; 2.7 mmol) in toluene (1.4 ml) was added to a solution of **5** (1.1 g; 2.7 mmol) in toluene (20 ml) at room temperature. After 10 min the evolution of CO_2 had ceased, and the solid product was separated and washed with diethyl ether (10 ml). The product was dried in vacuo and the product was obtained as an amorphous solid. Yield 1.0 g (80.0%); m.p. 168°C (dec.). − ^{1}H NMR: δ = 2.95 [s, 12 H, N(CH$_3$)$_2$], 7.13−7.41 (m, 15 H, Ph$_3$C), 7.85 (s, 1 H, NH$^-$). − $C_{24}H_{28}Cl_2N_3P$ (460.4): calcd. C 62.61, H 6.13, N 9.13; found: C 62.80, H 6.29, N 8.94.

Method B: Treatment of **2** *with HCl:* To a solution of **2** (1.0 g, 2.36 mmol) in 10 ml of toluene was added at room temperature 1 equivalent of HCl (2.36 ml of a 1 M solution in diethyl ether; 2.36 mmol HCl). After 5 min the colourless precipitate of **12** was collected by filtration, washed with diethyl ether (5 ml), and dried in vacuo. Yield 1.0 g (91.7%), m.p. 167°C (dec.).

Method C: Via Hydrolysis of **2**: To a solution of **2** (1.0 g; 2.36 mmol) in 10 ml of toluene were added at room temperature 0.5 equivalents of H_2O (21 mg; 1.18 mmol). After 15 min the colourless precipitate of **12** was collected by filtration, washed with diethyl ether (5 ml), and dried in vacuo. Yield 0.48 g (88.4%), m.p. 166°C (dec.).

Triphenylmethylphosphonous N′,N′,N′′,N′′-Tetramethylguanidinide (**13**): To a solution of 1.3 g (3.1 mmol) of **2** in 20 ml of diethyl ether 0.2 g (5.3 mmol) of LiAlH$_4$ were added at 0°C with stirring. The mixture was allowed to warm up to room temperature and stirring was continued for another hour. The reaction was quenched by addition of water (20 ml), using a water bath for cooling. The precipitate was filtered off and the solvent was removed from the filtrate in vacuo. To the residue 10 ml of diethyl ether was added and the product was obtained as a colourless amorphous substance, containing small amounts of Ph$_3$CH (4%), on cooling this solution to −20°C. Yield 0.81 g (67.8%); m.p. 118°C (dec.). − ^{1}H NMR: δ = 2.55 [s, 12 H, N(CH$_3$)$_2$], 7.25 (s, 15 H, Ph$_3$C), 5.67 (d, ^1J(PH) = 188.4 Hz, 1 H, PH).

[Triphenylmethylphosphonous N′,N′,N′′,N′′-Tetramethylguanidinide]·2 HCl (**14**): To a solution of Ph$_3$CPH(TMG) **13** (0.6 g; 1.5 mmol) in 10 ml of toluene were added at room temperature 3 equivalents of HCl (4.5 ml of a 1 M solution in diethyl ether; 4.5 mmol HCl). The precipitate was filtered off and the product was obtained as a colourless solid. Yield 0.51 g (71.6%); m.p. 145°C (dec.). − ^{1}H NMR: δ = 2.84 [s, 12 H, N(CH$_3$)$_2$], 7.09−7.43 (m, 15 H, Ph$_3$C), 5.81 [dd, 1 H, J(PH) = 235.6 Hz, J(HH) = 4.6 Hz, P-H], 7.99 (m, 1 H, NH), 10.60 (s, 1 H, HCl$_2^-$). − $C_{24}H_{30}Cl_2N_3P$ (462.4): calcd. C 62.34, H 6.54, N 9.08; found C 62.49, H 6.52, N 8.96.

Decomposition of **14**: A 60 mg (0.13 mmol) sample of **14** was dissolved in CDCl$_3$ (0.5 ml) and placed into a 5-mm NMR tube, capped with a rubber septum. The decomposition was monitored by ^{31}P NMR; it was complete after 18 h. Product **15** was characterized by comparison of its ^{1}H and ^{31}P NMR data to those of an authentic sample[30].

[Diphenylphosphinous N′,N′,N′′,N′′-Tetramethylguanidinide] · HCl (**17**): A solution of **16** (0.61 g; 2.01 mmol) in toluene (30 ml) was treated with gaseous hydrogen chloride until precipitation of a colourless solid commenced. The solid product was separated by filtration and investigated by ^{31}P- and ^{1}H-NMR spectroscopy. The spectra indicated a mixture of **17** and HTMG·HCl. In the ^{31}P-NMR spectrum of the filtrate a signal was observed which was due to Ph$_2$PCl [δ(^{31}P) in C$_6$D$_6$ = 82.2[35]]. − ^{1}H NMR: δ = 2.98 [s, 12 H, N(CH$_3$)$_2$], 7.12−7.79 (m, 5 H, C$_6$H$_5$); no resonance for N(*H*)=C< was observed. − ^{31}P NMR: δ = 41.2 (s).

Bis(N′,N′,N′′,N′′-tetramethylguanidino) Triphenylmethyl Phosphonium Chloride (**19**): *N′,N′,N′′,N′′*-Tetramethylguanidine (2.0 g; 17.4 mmol) was added dropwise with stirring over 10 min at room temperature to a solution of **1** (2.0 g, 5.80 mmol) in 20 ml of dichloromethane. After stirring for 0.5h at room temperature the reaction mixture was washed with water (10 ml) and was cooled to 0°C. The dichloromethane layer was separated from the mixture and dried over Na$_2$SO$_4$ (5.0 g). The solvent was removed in vacuo, and the residue was washed with 10 ml of diethyl ether, resulting in a colourless, amorphous substance. Yield 1.59 g (50.9%); m.p. 146°C (dec.). − ^{1}H NMR: δ = 2.70 [s, 24 H, N(CH$_3$)$_2$], 7.05−7.25 (m, 15 H, Ph$_3$C), 8.23 [d, ^1J(PH) = 471.5 Hz, 1 H, PH]. − ^{31}P NMR: δ = 5.1. − $C_{29}H_{40}ClN_6P$ (539.1): calcd. C 64.61, H 7.48, N 15.59; found C 62.19, H 7.63, N 14.24.

[Triphenylmethylphosphonous Bis(N′,N′,N′′,N′′-tetramethylguanidinide)] · 3 HCl (**20c**): To a solution of [Ph$_3$CPH-(TMG)$_2$]$^+$Cl$^-$ (**19**) (0.5 g; 0.93 mmol) in 10 ml of dichloromethane were added at room temperature 3 equivalents of HCl (2.8 ml of a

Table 2. Crystal data of **5**, **6**, and **20c**

	5·0.5 CH_2Cl_2	**6**	**20c**·CH_2Cl_2
Formula	$C_{24.5}H_{29}ClN_3OP$	$C_{24}H_{30}Cl_2N_3OP$	$C_{30}H_{44}Cl_5N_6P$
M_r	447.93	478.38	696.93
Crystal habit	colourless prism	colourless prism	colourless prism
Crystal size (mm)	0.60 x 0.40 x 0.30	0.60 x 0.45 x 0.20	0.80 x 0.65 x 0.20
Temperature (°C)	-130	-100	-130
Crystal system	triclinic	monoclinic	triclinic
Space group	$P\bar{1}$	$P2_1/n$	$P\bar{1}$
Cell constants			
a (pm)	883.9(2)	1271.2(2)	881.6(2)
b (pm)	937.5(2)	913.18(12)	1248.9(3)
c (pm)	1465.4(3)	2134.6(3)	1624.3(3)
α (°)	80.99(3)	90	72.51(2)
β (°)	85.76(3)	95.734(8)	87.95(2)
γ (°)	77.87(3)	90	85.81(2)
U (nm^{-3})	1.1716(4)	2.4656(6)	1.7010(6)
Z	2	4	2
D_X (Mg m^{-3})	1.270	1.289	1.361
μ (mm^{-1})	0.253	0.349	0.504
$F(000)$	474	1008	732
$2\theta_{max}$ (°)	50	50	50
absorption correction	none	none	psi-scans
min. and max. transmission			0.794 and 0.906
No. of refins.:			
measured	4415	4375	8507
independent	4130	4338	6013
R_{int}	0.018	0.034	0.019
$wR(F^2$, all refl.)	0.121	0.090	0.135
$R(F,>4\sigma(F))$	0.049	0.040	0.054
No. of parameters	297	296	399
S	1.04	0.89	1.02
max. Δ/σ	< 0.001	< 0.001	< 0.001
max. $\Delta\rho$ (e nm^{-3})	296	368	1843

1 M solution in diethyl ether; 2.79 mmol HCl). After leaving the resulting solution at room temperature for 18 h the product was obtained as colourless crystals. Yield 0.55 g (84.8%); m.p. 146°C (dec.). – ^{1}H NMR: δ = 2.92 [s, 24 H, $N(CH_3)_2$], 7.06–7.41 (m, 15 H, Ph_3C), 8.55 (s, 2 H, NH), 12.2 (s, 1 H, HCl_2^-). – ^{31}P NMR [a striking solvent effect on δ(^{31}P) was noted]: δ ($CDCl_3$) = 83.5, δ (D_2O) = 61.4, δ (CD_3OD) = 72.5. – $C_{29}H_{42}Cl_3N_6P \cdot CH_2Cl_2$ (696.96): calcd. C 51.70, H 6.36, N 12.06; found C 52.96, H 6.55, N 12.65.

Attempted Preparation of [Methylphosphonous Bis(N′,N′,N″,N″-tetramethylguanidinide)] · 4 HCl; Formation of Methylphosphonous Dichloride (**23**): The reaction was carried out in a manner similar to that for **17**, using $MeP(TMG)_2$ (0.5 g; 1.82 mmol) in toluene (30 ml). The ^{31}P-NMR spectrum of the filtrate exhibited one signal only, which was due to **23** [δ(^{31}P) in C_6D_6 = 191.2][36].

Methyl Bis(N′,N′,N″,N″-tetramethylguanidino)phosphonium Hexafluoroantimonate (**24**): Addition of $HSbF_6$ (0.50 g, 2.11 mmol) to a stirred solution of **22** (0.54 g; 1.97 mmol) in n-hexane (10 ml) at room temperature resulted in a colourless oil. After removal of the solvent, the oil was redissolved in dichloromethane (5 ml) and reprecipitated by addition of *n*-hexane (10 ml). This process was repeated twice, giving only a mixture of **24** and $HSbF_6$. – ^{1}H NMR: δ = 0.81 (s, br, 3 H, PCH_3), 2.61 [s, br, 24 H, $N(CH_3)_2$], 6.82 [d, 1 H, J(PH) = 483 Hz, PH]. – ^{31}P NMR: δ = 17.43 (s).

Attempted Preparation of [Triphenylmethylphosphonous N′,N′,N″,N″-Tetramethylguanidinide] · 2 HF; Formation of Triphenylmethylphosphonous Fluoride (**25**): $Et_3N \cdot 3$ HF (337 mg; 2.1 mmol) was added dropwise with stirring over 2 min at room temperature to a solution of **6** (1.0 g, 2.1 mmol) in 10 ml of dichloromethane. The solvent was evaporated in vacuo, and toluene (20 ml) was added to the residue. The precipitate was filtered off and the solvent from the filtrate was removed in vacuo. The product was obtained as an amorphous, colourless solid. Yield 0.6 g (92.5%); m.p. 159°C (dec.)[19].

Determination of Crystal Structures – Data Collection and Reduction: Crystals were mounted on glass fibres in inert oil and transferred to the cold gas stream of the diffractometer (Stoe STADI-4 for **5** and **20c**, Siemens P4 for **6**, both with LT-2 low temperature attachment). The cell constants for **5** and **20c** were refined from ±ω angles of 52 reflections in the 2θ range 20–23°. The orientation matrix for **6** was refined from setting angles of 62 reflections in the 2θ range 5–25° (monochromated Mo-K_α radiation).

Structure Solution and Refinement: The structures were solved by direct methods and refined anisotropically on F^2 (program system: SHELXL-93, G.M.Sheldrick, University of Göttingen). H atoms were included using a riding model or rigid methyl groups, except for P–H, N–H and Cl–H hydrogens, which were refined freely. Weighting schemes of the form $w^{-1} = [\sigma^2(F_o^2) + (aP)^2 + bP]$ were employed, with $P = (F_o^2+2F_c^2)/3$. Full details of the crystal structure determinations (except structure factors) have been deposited under the number 100815 at the Cambridge Crystallographic Data Centre. Copies may be obtained free of charge from: The Director, CCDC, 12 Union Road, GB-Cambridge CB2 1EZ [Telefax: Int. +44 (0)1223/336–033; E-mail: fileserv@chemcrys.cam.ac.uk.]

☆ Dedicated to Professor *Manfred Weidenbruch* on the occasion of his 60th birthday.

[1] A. B. Burg, P. J. Slota, *J. Am. Chem. Soc.* **1958**, *80*, 1107–1109.
[2] K. Issleib, W. Seidel, *Chem. Ber.* **1959**, *92*, 2681–2694.
[3] J. Münchenberg, O. Böge, A.K. Fischer, P.G. Jones, R. Schmutzler, *Phosphorus, Sulfur, and Silicon* **1994**, *86*, 103–121.
[4] J. Febvay, F. Casabianca, J. G. Riess, *J. Am. Chem. Soc*. **1984**, *106*, 7985–7986.
[5] F. Bouvier, J.-M. Dupart, J. G. Riess, *Inorg. Chem*. **1988**, *27*, 427–430.
[6] J. H. Weinmaier, J. Luber, A. Schmidpeter, S. Pohl, *Angew. Chem*. **1979**, *91*, 442–443; *Angew. Chem., Int. Ed. Engl*. **1979**, *18*, 412–413.
[7] T. A. van der Knaap, F. Bickelhaupt, *Phosphorus and Sulfur* **1984**, *21*, 227–236.
[8] E. E. Nifantyev, M. K. Gratchev, S. Yu. Burmistrov, L. K. Vasyanina, M. Yu. Antipin, Yu. T. Struchkov, *Tetrahedron* **1991**, *47*, 9839–9860.
[9] A. N. Pudovik, E. S. Batyeva, V.A. Al′fonsov, *Phosphorus, Sulfur, and Silicon* **1990, 49/50**, 221–214.
[10] O. Dahl, *Tetrahedron Lett*. **1982**, *23*, 1493–1496.
[11] E. E. Nifantyev, M. K. Gratchev, S. Yu. Burmistrov, *Phosphorus, Sulfur, and Silicon* **1992**, *70*, 159–174.
[12] E. E. Nifantyev, M. K. Gratchev, *Phosphorus, Sulfur, and Silicon* **1990**, *49/50*, 203–206.
[13] E. E. Nifantyev, M. K. Gratchev, *Uspekh. Khim*. **1994**, *63*, 602–637.
[14] H.H. Hatt, *J. Chem. Soc*. **1933**, 776–786.
[15] J. Münchenberg, unpublished results.
[16] J.F. Nixon, *J. Chem. Soc*. **1964**, 2469–2471.
[17] A.G. Cook, *J. Org. Chem*. **1965**, *30*, 1262–1263.
[18] D. Mootz, W. Poll, H. Wunderlich, H.-G. Wussow, *Chem. Ber*. **1981**, *114*, 3499–3504.
[19] V. Plack, J. R. Goerlich, A. Fischer, H. Thönnessen, P. G. Jones, R. Schmutzler, *Z. Anorg. Allg. Chem*. **1995**, *621*, 1080–1092.
[20] C. Couret, J. Escudie, H. Ranaivonjatovo, J. Satge, *Organometallics* **1986**, *5*, 113–117.

 © WILEY-VCH Verlag GmbH, D-69451 Weinheim, 1998 1434–1948/98/0606–0865 $ 17.50+.50/0

[21] J. Satge, J. Escudie, C. Couret, H. Ranaivonjatovo, M. Andrianarison, *Phosphorus and Sulfur* **1986**, *27*, 65−74.
[22] J. Escudie, C. Couret, H. Ranaivonjatovo, J. Satge, *J. Chem. Soc., Chem. Commun.* **1984**, *24*, 1621−1622.
[23] R. D. Kroshefsky, J. G. Verkade, *Inorg. Chem*. **1975**, *14*, 3090−3095.
[24] R. G. Pearson, H. Sobel, J. Songstad, *J. Am. Chem. Soc*. **1968**, *90*, 319−326.
[25] J. Münchenberg, Dissertation, Technische Universität, Braunschweig **1996**.
[26] S. Berger, S. Braun and H.-O. Kalinowski, *NMR-Spektroskopie von Nichtmetallen;* Georg Thieme Verlag, Stuttgart-New York **1994**, Vol. 3, p. 126.
[27] H. Kessler, D. Leibfritz, *Tetrahedron Lett*. **1969**, 427−430.
[28] V. J. Bauer, W. Fulmor, G. O. Morton, S. R. Safir, *J. Am. Chem. Soc*. **1968**, *90*, 6846−6847.
[29] K. Kanamori, J. D. Roberts, *J. Am. Chem. Soc*. **1983**, *105*, 4698−4701.
[30] V. Plack, unpublished results.
[31] Autorenkollektiv, *Organikum*, Reprint of the 15th ed.; VEB Deutscher Verlag der Wissenschaften, Berlin **1977**, p. 783.
[32] D. D. Perrin, W. L. F. Armarego, D. R. Perrin, *Purification of Laboratory Chemicals*, 3rd edn.; Pergamon Press, Oxford, London, Edinburgh, New York, Toronto, Paris, Braunschweig, **1988**.
[33] J. Münchenberg, J.R. Goerlich, A.K. Fischer, P.G. Jones and R. Schmutzler, *Z. Anorg. Allg. Chem*. **1996**, *622*, 348−354.
[34] S.C. Chaudhry, D. Kummer, *J. Organomet. Chem*. **1988**, *339*, 241−252.
[35] D. G. Gorenstein, *Progr. NMR Spectrosc***. 1983,** *16*, 1.
[36] D. Houalla, T. Mouheich, M. Sanchez, R. Wolf, *Phosphorus* **1975**, *5*, 229−240.

[97306]

Palladacycles as Reactive Intermediates

Gerald Dyker

Chem. Ber./Recueil **1997**, *130*, 1567−1578

Reference[5] *on page 1576 should read as follows:*

[5] A special case of a 9-membered palladacycle annelated by four cyclopentane units has been reported: P. Binger, H. M. Büch, R. Benn, R. Mynott, *Angew. Chem.* **1982**, *94*, 66; *Angew. Chem. Int. Ed. Engl.* **1982**, *21* 62−63.

G. Dyker
[C97132]

 © WILEY-VCH Verlag GmbH, D-69451 Weinheim, 1998 1434−1948/98/0606−0877 $ 17.50+.50/0

Reaction of *ortho*-Methylbenzonitrile with Lithium *N,N,N′*-Trimethylethylenediamide: Assembly and Crystal Structure of a Primary Isoquinolinoamidolithium–Secondary Amine Complex

Neil Feeder, Ronald Snaith, and Andrew E. H. Wheatley*

Department of Chemistry, University of Cambridge,
Lensfield Road, Cambridge, CB2 1EW, U.K.
Fax: (internat.) + 44-1223/336362
E-mail: rs10003@cam.ac.uk

Received February 6, 1998

Keywords: Isoquinoline / Lithium / Self-condensation / Solid-state structure / Solution structure

The product of reaction between *ortho*-methylbenzonitrile (*o*-MeC_6H_4CN) and lithium *N,N,N′*-trimethylethylenediamide [$LiN(Me)(CH_2)_2NMe_2$], the 1:1 complex 1-lithioamido-3-(2-methylphenyl)isoquinoline–*N,N,N′*-trimethylethylenediamine (**1**-Li·HTriMEDA), has a solid-state structure which shows a new type of $(NCNLi)_2$ core and a solution structure in which the coordination mode of the diamine by-product varies with temperature.

The reactions of organolithium reagents with benzonitrile have long been known to induce cyclotrimerisation[1] to yield, amongst other products, fully unsaturated 2,4,6-triphenyl-1,3,5-triazine[2] by 1,4-elimination of organolithium from a lithio-1,4-dihydrotriazine precursor. More recently, we reported a nitrile addition product, an imidolithium species of the type which probably acts as an initial intermediate in the cyclisation reaction[3]. Given this latter result, we sought to investigate the reactions of organolithium reagents with *ortho*-methylbenzonitrile, for which addition across the nitrile triple bond is known to be in competition with *ortho* lithiation[4]. It has also been reported[5] for this system that a nitrile self-condensation product, a substituted 1-aminoisoquinoline (**1**-H), can result in various yields (2−80%) depending on the organolithium reagent employed and on the reaction conditions.

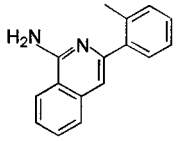

1-H

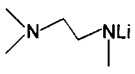

LiTriMEDA

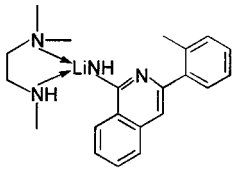

1-Li·HTriMEDA

The reaction of lithium *N,N,N′*-trimethylethylenediamide (LiTriMEDA) with *o*-methylbenzonitrile in toluene at −78°C affords a red solution which becomes yellow at room temperature. Addition of hexane and storage at ambient temperature overnight yields orange crystals identified as the 1:1 complex, 1-lithioamido-3-(2-methylphenyl)isoquinoline−*N,N,N′*-trimethylethylenediamine (**1**-Li·HTriMEDA). X-ray crystallography shows that in the solid state **1**-Li·HTriMEDA is a transoid dimer (Figure 1), in which the primary amidolithium centre[6] in the self-assembled 1-lithioamidoisoquinolino moiety is chelated by the concomitantly formed secondary amine. This dimer demonstrates several unusual structural features. At first sight it appears to incorporate a straightforward four-membered Li(1)−N(2)−Li(1A)−N(2A) ring at its core, with further stabilisation of the metal being afforded by isoquinoline N centre donation to lithium. However, closer inspection reveals that, within the supposed four-membered ring, two of the N−Li distances are short [Li(1A)−N(2) 2.055(6) A] while the other two are unusually long [Li(1)−N(2) 2.394(7) A]. It seems, therefore, to be the relatively short (isoquinoline)N−Li interactions [N(1)−Li(1) 2.081(6) A] which are mainly responsible for dimerisation. Consequently, the central unit of the structure is best viewed as being an eight-membered [(isoquinoline)N−C−(amido)N−Li]$_2$ ring resulting from inter-monomer (isoquinoline)N−Li interactions, with very weak (amido)N−Li cross-ring interactions. A search of the Cambridge Crystallographic Database locates only two examples of eight-membered $(NCNLi)_2$ rings[7], neither of which shows any cross-ring interactions whatsoever. Thus the structure of **1**-Li·HTriMEDA, containing as it does partial cross-ring contacts, is unique. The coordination sphere of each metal centre is completed by chelation of the HTriMEDA ligands which, unusually, have also been formed during the reaction. While at 2.130(7) A the Li(1)−N(4) bond is of a length normal for such an interaction, the Li(1)−N(3) bond is, at 2.358(7) A, surprisingly long. Alkali metal complexes containing protic amine bases are not common, and those which are known have generally been synthesised by allowing an organolithium compound to react with an excess of amine[8], by having the amine ligand present in a 1:1 reaction between a lithiating agent and a (more acidic) organic substrate, or by adding the amine after the lithiation reaction

 © WILEY-VCH Verlag GmbH, D-69451 Weinheim, 1998 1434−1948/98/0707−0879 $ 17.50+.50/0

is complete. Indeed, the last method has been used to give enolatolithium and amidolithium complexes containing HTriMEDA itself[9]. In both of these cases diamine chelation of the metal centre was accompanied by a hydrogen bonding interaction involving the acidic proton of HTriMEDA. While in $[H_2C{=}C(NMe_2)OLi{\cdot}HTriMEDA]_2$ the interaction was directed towards the enamine N-centre, in $[H_2C{=}C(t\text{Bu})OLi{\cdot}HTriMEDA]_2$ it was directed towards the enolato π system [N−H···C distances 2.62 and 2.73 A]. This last structural feature pinpoints a final interesting facet of the structure of **1**-Li·HTriMEDA in that here a somewhat analogous, but rather stronger, interaction is observed. The N(3)−H(3N) bond points approximately at the *centre* of the 3-(2-methylphenyl) ring [H(3N)···ring centroid 2.440 A, N(3)−H(3N)−ring centroid 172.3°]. This interaction appears to account for the massive N(1)C(9)C(10)C(11) torsional angle of 114.3°. However, it is also noticeable that in $[H_2C{=}C(t\text{Bu})OLi{\cdot}HTriMEDA]_2$, where the hydrogen bonding interaction is somewhat weaker than in **1**-Li·HTriMEDA, bonds between the lithium centre and the chelating diamine are essentially equivalent and, at 2.11(1) and 2.09(1) A[9], of lengths typical for such interactions. It seems, therefore, that the relative strength of the hydrogen bond in **1**-Li·HTriMEDA is the most likely reason for the surprising length of the Li(1)−N(3) interaction.

o-methylbenzonitrile in THF/HMPA [HMPA = $O{=}P(NMe_2)_3$] at −78°C afforded predominantly *o*-lithiomethylbenzonitrile, **1**-H was best synthesised by the 1:1 reaction of Me_2NLi with the nitrile in THF/HMPA at −78°C, subsequent addition of a second equivalent of nitrile and heating at 60°C for 1 hour resulting, after workup, in the high yield formation (80%) of **1**-H. In this current work, a 2:2 reaction of LiTriMEDA with *o*-methylbenzonitrile affords **1**-Li·HTriMEDA, the immediate precursor to **1**-H, essentially quantitatively (first batch yield of crystals 90%, with respect to nitrile) in non-donor media (toluene) at ambient or sub-ambient temperature. The yield of the complex, with respect to nitrile, is unaffected if the correct stoichiometry (2:1 nitrile/LiTriMEDA) is used. It is logical, therefore, that the initial 1:1 reaction, which yields either an imidolithium (**2a**, which rapidly isomerises to *o*-lithiated imine **2b**) or, more probably, a complexed *o*-lithiated nitrile (**2c**) (Scheme 1) is *slow* relative to subsequent insertion of the second equivalent of *o*-methylbenzonitrile (yielding **3b/c**). Presumably ring closure by **3b/c** yields **4b/c** which, in turn, gives the title complex via a simple rearrangement (accompanied by elimination of HTriMEDA in the case of **4b**). It is presently impossible to say whether the first stage of the reaction is addition/isomerisation or *o*-lithiation, although it has been observed that in the presence of benzonitrile, LiTriMEDA readily gives an extremely stable addition product[3].

Figure 1. Structure of dimeric **1**-Li·HTriMEDA; hydrogen atoms (except the primary amidolithium and secondary amine hydrogen atoms) have been omitted for clarity; the symmetry operation which relates original atoms to their "A" equivalents is $-x+1, -y+1, -z+1$

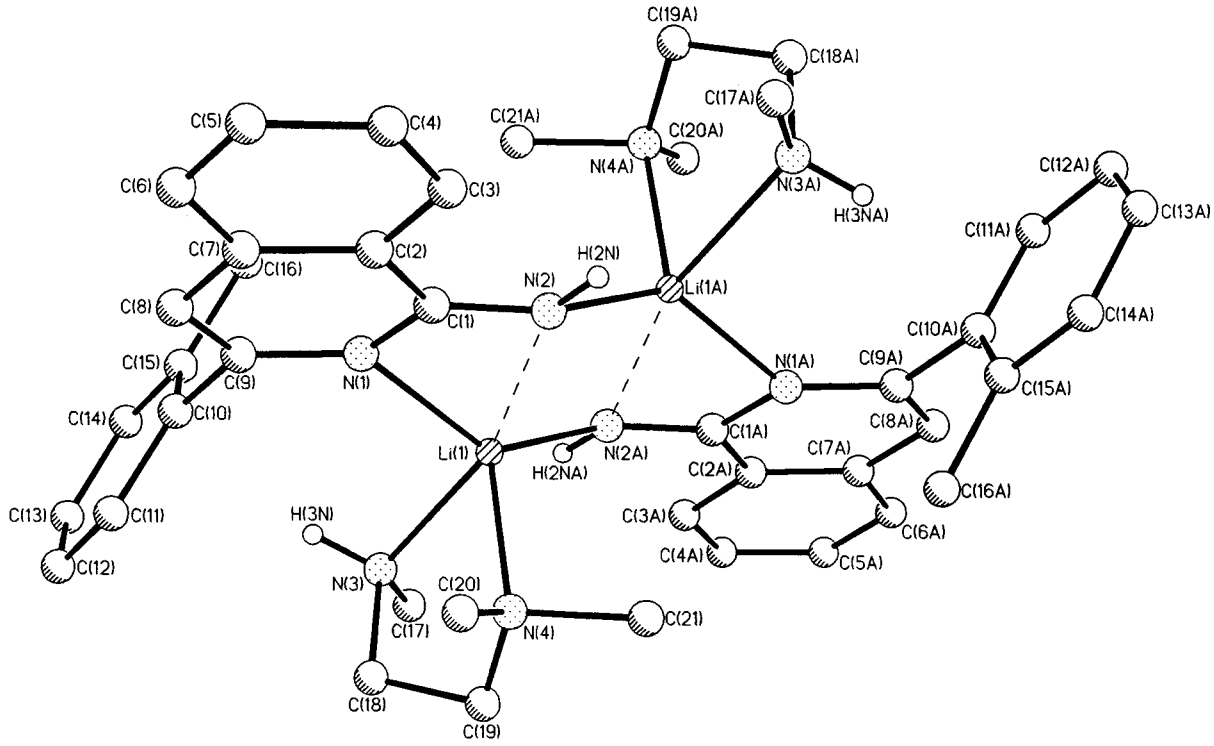

Although the self-condensation reaction of two equivalents of *o*-methylbenzonitrile in the presence of one equivalent of certain lithium reagents has been reported earlier[5], no lithiated intermediates have been isolated previously. Given the finding[4] that the reaction of Me_2NLi with

A solution of **1**-Li·HTriMEDA (12.0 mg ml^{-1} in $[D_6]$benzene) yields a ^{1}H-NMR spectrum in which, unusually, extensive coupling is observed through the secondary amine

Scheme 1

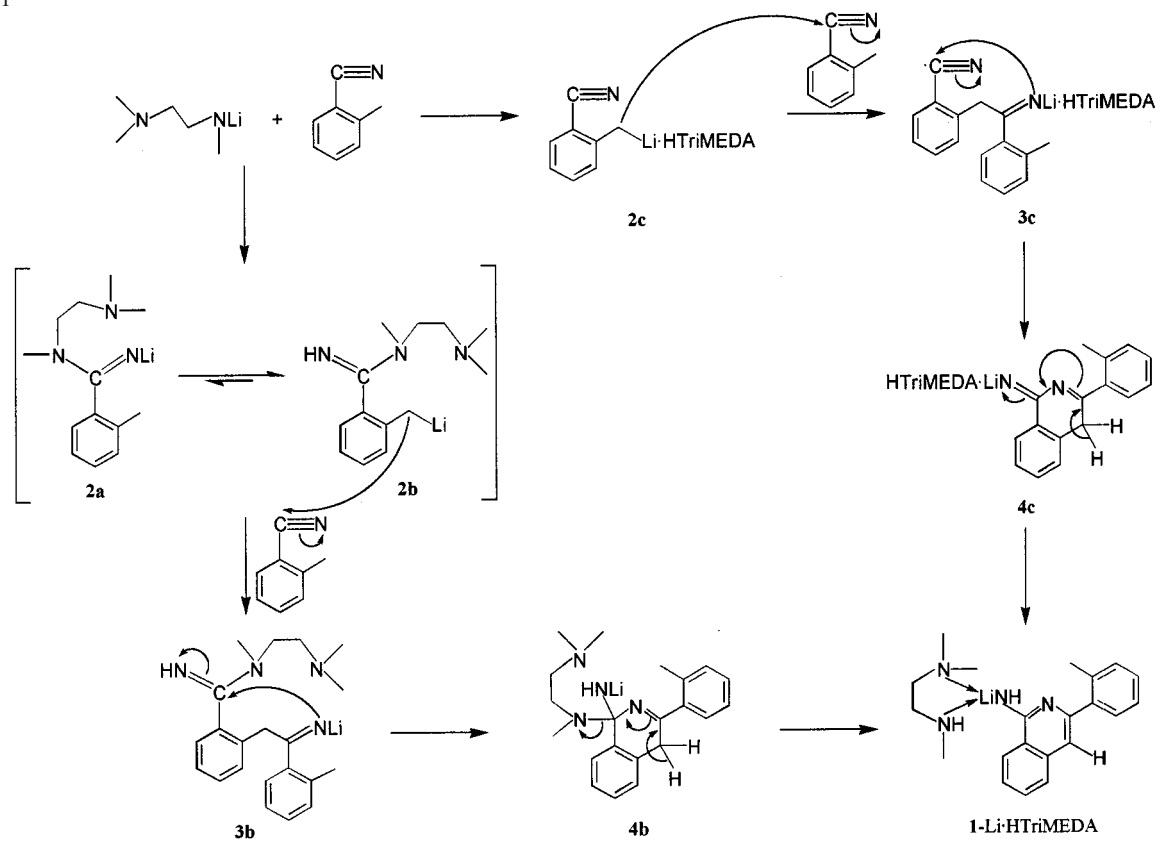

N centre. Consequently, therefore, the $H_3C(H)NCH_2$ triplet at δ = 2.46 ($^3J_{H\text{-}(C)H}$ = 5.46 Hz) is split into two ($^3J_{H\text{-}(N)H}$ = 6.64 Hz) and the $H_3C(H)N$ resonance at δ = 2.26 is a doublet ($^3J_{H\text{-}(N)H}$ = 6.43 Hz); irradiation of the $H_3C(H)N$ multiplet at δ = 0.93 causes these signals to appear as a triplet and singlet respectively. At the same concentration, ^{1}H-NMR spectroscopy in [D_8]toluene indicates that as a function of temperature there is a significant change in the behaviour of the HTriMEDA with respect to the metal centre. It appears either to change from (i) free base to mono- or bidentate coordinated ligand or (ii) monodentate ligand to bidentate chelate of the lithium centre. This is suggested by the observation that while at 60°C the HTriMEDA methylene protons bonded to either N centre (Table 1, H^c and H^d) demonstrate chemical shifts downfield of the (same species) *N*-methyl protons (H^b and H^e) bonded to *the same N-centre* [i. e. δ(H^c) > δ(H^b) and δ(H^d) > δ(H^e)], as the temperature is lowered so the former protons drift to positions *upfield* relative to their methyl counterparts [i. e. δ(H^b) > δ(H^c) and δ(H^e) > δ(H^d)]. This observation is consistent with the known behaviour of free and complexed TMEDA [$(H_3C)_2N(CH_2)_2N(CH_3)_2$][10], and indeed a comparison of the spectra of **1**-Li·HTriMEDA with those of pure HTriMEDA in toluene suggests that it is only in the range 25−60°C that the base is essentially free. Moreover, extensive coordination of the metal centres by HTriMEDA at low temperature is suggested by variable-temperature ^{7}Li-NMR spectroscopy. In toluene the dominant lithium

Table 1. ^{1}H-NMR data for the secondary amine ligand in **1**-Li·HTriMEDA in [D_8]toluene over the range 60°C to −80°C; (−) indicates that the signal was not observable at that temperature; the H^a signal was obscured by that of H^e at low temperature while those of H^b and H^c were obscured by the [D_8]toluene resonance

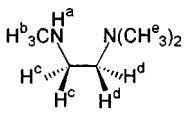

Temp. [°C]	δ [ppm]				
	H^a	H^b	H^c	H^d	H^e
60	0.84	2.26	2.46	2.20	2.03
40	0.91	2.25	2.42	2.18	2.01
25	1.10	2.17	2.29	2.03	1.93
0	1.41	−	−	1.87	1.84
−25	−	−	2.05	1.72	1.76
−50	−	−	1.95	1.61	1.71
−80	−	−	1.90	1.48	1.65

Table 2. Cryoscopic data for **1**-Li·HTriMEDA in benzene over the concentration range 2.0−15.4 mg ml^{-1}

Conc. [mg ml^{-1}]	Av. mol. mass (±5)	*n* (±0.1)
2.0	274	0.8
3.9	305	0.9
7.0	349	1.0
10.3	386	1.1
15.4	413	1.2

environment moves from δ = 1.79 (at 60°C) to δ = 1.43 (at 25°C) to δ = 0.90 (at 0°C) and finally to δ = 0.53 (at −80°C). Clarification comes from cryoscopy in benzene. Results suggest (Table 2) that whereas at low concentration (2.0 mg ml^{-1}) HTriMEDA is ostensibly free in solution, at higher concentrations (ca. 10−15 mg ml^{-1}) the secondary amine and metal centre interact. This clearly suggests, given the evidence from NMR spectroscopy, that at these higher concentrations **1**-Li·HTriMEDA dissolves in non-donor solvents to give a species in which, at or about cryoscopy temperature (5°C), the secondary amine acts as a *monodentate* ligand, probably [judging from the relative Li(1)−N(3) and Li(1)−N(4) distances observed in the solid-state structure] through its $(H_3C)_2N$ centre, and as a *bidentate* one only at much lower temperatures.

The reaction of LiTriMEDA with *o*-methylbenzonitrile clearly demonstrates the significant effect of ring substituents on the chemistry of benzonitriles. The observed condensation reaction is enabled by the contrasting behaviour of LiTriMEDA as either a nucleophile (with benzonitrile)[3] or a base (with *o*-methylbenzontrile)[4], the isolated complex, **1**-Li·HTriMEDA, demonstrating a variety of interesting features in both the solid state and in non-polar solution.

We thank the *U.K. EPSRC* (A.E.H.W) for financial support and Dr. *Basil J. Wakefield* and Dr. *Gregory P. Shields* for useful discussions.

Experimental Section

General: All operations were carried out using standard inert-atmosphere Schlenk techniques with a dual nitrogen/vacuum line. Schlenk tubes were pre-dried at 180°C prior to evacuation to less than 0.1 Torr three times, being filled with dry nitrogen from the house supply between each evacuation. *N,N,N′*-Trimethylethylenediamine and *o*-methylbenzonitrile were used as received from Aldrich Chemical Company and stored over 4 A molecular seive. Toluene (freshly distilled and maintained at reflux over sodium), hexane (freshly distilled and maintained at reflux over sodium-potassium amalgam) and *n*-butyllithium were added directly to the nitrogen-filled Schlenk tube using standard syringe techniques. − NMR spectroscopy: Bruker AM 400 and DRX 400 (400.137 MHz and 155.508 MHz, for ^1H and ^7Li, respectively). For ^1H-NMR spectroscopy, [D_6]benzene and [D_8]toluene as solvents, TMS at 25°C as external standard; for ^7Li-NMR spectroscopy, [D_6]benzene and [D_8]toluene as solvents, PhLi in [D_6]benzene and [D_8]toluene respectively at 25°C as external standards.

N,N,N′-Trimethylethylenediamine (HTriMEDA): ^1H NMR (60°C, 3.6 mg ml^{-1} in [D_8]toluene): δ = 2.52 [t, 2 H, $H_3C(H)NCH_2$, $^3J_{H\text{-}(C)H}$ = 6.01 Hz], 2.32 [s, 3 H, $H_3C(H)N$], 2.27 [t, 2 H, $CH_2N(CH_3)_2$, $^3J_{H\text{-}(C)H}$ = 6.01 Hz], 2.07 [s, 6 H, $N(CH_3)_2$], 0.88 [s, br., 1 H, $H_3C(H)N$]. Spectra at 60, 40, 25, 0, −25, −50, and −80°C showed no significant variation.

1-Lithioamido-3-(2-methylphenyl)isoquinoline−N,N,N′-trimethylethylenediamine (**1**-Li·HTriMEDA): *n*-Butyllithium (1.88 ml, 1.6 M in hexanes, 3.0 mmol) was added to *N,N,N′*-trimethylethylenediamine (0.38 ml, 3.0 mmol) in toluene (2 ml) at −78°C under nitrogen. After stirring for 15 min, *o*-methylbenzonitrile (0.36 ml, 3.0 mmol) was added and the resultant red solution was stirred for a further 15 min at −78°C. Warming to room temp. gave a yellow solution, to which hexane (1 ml) was added. Storage overnight at room temp. afforded orange crystals of **1**-Li·HTriMEDA, yield 90% (with respect to nitrile), m.p. > 300°C. − $C_{21}H_{27}LiN_4$ (342.41): calcd. C 73.68, H 7.89, Li 2.05, N 16.37; found C 73.06, H 7.97, Li 2.00, N 16.07. − ^1H NMR (60°C, 12.0 mg ml^{-1} in [D_6]benzene): δ = 7.50 (d, 1 H, Ar, $^3J_{HH}$ = 8.16 Hz), 7.38 (d, 1 H, Ar, $^3J_{HH}$ = 7.69 Hz), 7.32 (dd, 1 H, Ar, $^3J_{HH}$ = 6.92, 5.94 Hz), 7.14 (dd, 1 H, Ar), 7.07 (br., 1 H, Ar), 6.93 (br., dd, 1 H, Ar), 6.85 (d, 1 H, Ar, $^3J_{HH}$ = 6.66 Hz), 6.69 (br., 1 H, Ar), 6.43 (s, 1 H, Ar), 4.71 (s, br., 1 H, NHLi), 2.46 (dt, 2 H, $H_3C(H)NCH_2$, $^3J_{H\text{-}(C)H}$ = 5.46 Hz, $^3J_{H\text{-}(N)H}$ = 6.64 Hz), 2.26 [d, 3 H, $H_3C(H)N$, $^3J_{H\text{-}(N)H}$ = 6.43 Hz], 2.21 [t, 2 H, $CH_2N(CH_3)_2$, $^3J_{H\text{-}(C)H}$ = 5.97 Hz], 2.03 [s, 6 H, $N(CH_3)_2$], 1.99 (s, br., 3 H, $ArCH_3$), 0.93 [m, br., 1 H, $H_3C(H)N$]. − ^7Li NMR (25°C, 12 mg ml^{-1} in [D_6]benzene): δ = 1.69 (s, 1 Li), 1.38 (s, ca. 13 Li). − ^7Li NMR (25°C, 12 mg ml^{-1} in [D_8]toluene): δ = 1.86 (s, 1 Li), 1.43 (s, ca. 14 Li); (0°C): δ = 1.81 (s, 1 Li), 0.90 (s, ca. 18 Li); (−25°C): δ = 0.78 (s); (−50°C): δ = 0.55 (s); (−80°C): δ = 0.69 (s, 1 Li), 0.53 (s, ca. 11 Li).

X-ray Crystallographic Study of **1**-Li·HTriMEDA: $C_{21}H_{27}LiN_4$, triclinic, space group *P*1, *a* = 10.093(2), *b* = 11.523(4), *c* = 8.700(2) A, α = 93.28(2), β = 100.050(10), γ = 96.97(2)°, *V* = 985.7(5) A^3, M_r = 342.41, *Z* = 2, D_c = 1.154 Mg m^{-3}, μ(Mo-K_α) = 0.069 mm^{-1}, *F*(000) = 368. Data were collected by the ω/2θ scan method on a Rigaku AKC5R four-circle diffractometer at 150(2) K using graphite-monochromated Mo-K_α radiation (λ = 0.71069 A) in the range 5.10 < 2θ < 50.00°, +*h*, ±*k*, ±*l*; 3691 reflections of which 3474 were independent (R_{int} = 0.0391) and used in all calculations. The structure was solved using direct methods[11] and subsequent Fourier difference syntheses and refined[12] by full-matrix least-squares on F^2 with anisotropic thermal parameters for all non-hydrogen atoms. H(2N), H(2NA), H(3N) and H(3NA) were located from the Fourier difference map and their coordinates and isotropic temperature factors were allowed to refine. All other hydrogen atoms were placed in geometrically idealised positions and refined using a riding model or as rigid methyl groups. Methylene groups in the HTriMEDA chelates were disordered over two positions. In the final cycles of refinement a weighting scheme of the form $w^{-1} = [\sigma^2(F_o^2) + (0.0840P)^2 + 0.63P]$, where $P = (F_o^2 + 2F_c^2)/3$, was employed which produced a flat analysis of variance. Final $R(F)$ = 0.0623 for 3462 reflections with $[I > 2\sigma(I)]$, $wR(F^2)$ = 0.1865 for all data; 277 parameters; goodness of fit = 1.165. Maximum peak and hole in final Fourier difference map 0.297 and −0.210 eA^{-3} respectively. Crystallographic data (excluding structure factors) for the structure reported in this paper have been deposited with the Cambridge Crystallographic Data Centre as supplementary publication no. CCDC-101025. Copies of the data can be obtained free of charge on application to CCDC, 12 Union Road, Cambridge CB2 1EZ, UK [Fax: (int. code) + 44-1223/336-033, E-mail: deposit@ccdc.cam.ac.uk, www: http://www.ccdc.cam.ac.uk].

[1] [1a] R. M. Anker, A. H. Cook, *J. Chem. Soc.* **1941**, 323−331. − [1b] L. S. Cook, B. J. Wakefield, *J. Chem. Soc., Perkin Trans. 1* **1980**, 2392−2397.
[2] [2a] D. R. Armstrong, W. Clegg, M. MacGregor, R. E. Mulvey, P. A. O′Neil, *J. Chem. Soc., Chem. Commun.* **1993**, 608−610. − [2b] D. R. Armstrong, K. W. Henderson, M. MacGregor, R. E. Mulvey, M. J. Ross, W. Clegg, P. A. O′Neil, *J. Organomet. Chem.* **1995**, *486*, 79−93.
[3] R. P. Davies, P. R. Raithby, G. P. Shields, R. Snaith, A. E. H. Wheatley, *Organometallics* **1997**, *16*, 2223−2225.
[4] E. M. Kaiser, J. D. Petty, *J. Organomet. Chem.* **1976**, *107*, 219−228.
[5] E. M. Kaiser, J. D. Petty, L. E. Solter, W. R. Thomas, *Synthesis* **1974**, 805−806.
[6] For solid-state examples of primary amidolithium species see: [6a] B. Cetinkaya, P. B. Hitchcock, M. F. Lappert, M. C. Misra, A.

J. Thorne, *J. Chem. Soc., Chem. Commun*. **1984**, 148−149. − [6b] T. Fjeldberg, P. B. Hitchcock, M. F. Lappert, A. J. Thorne, *J. Chem. Soc., Chem. Commun*. **1984**, 822-824. − [6c] L. M. Engelhardt, G. E. Jacobsen, P. C. Junk, C. L. Raston, B. W. Skelton, A. H. White, *J. Chem. Soc., Dalton Trans.* **1988**, 1011−1020. − [6d] D. Barr, W. Clegg, L. Cowton, L. Horsburgh, F. M. Mackenzie, R. E. Mulvey, *J. Chem. Soc., Chem. Commun*. **1995**, 891−892. − [6e] W. Clegg, L. Horsburgh, F. M. Mackenzie, R. E. Mulvey, *J. Chem. Soc., Chem. Commun*. **1995**, 2011−2012. − [6f] W. Clegg, L. Horsburgh, P. R. Dennison, F. M. Mackenzie, R. E. Mulvey, *J. Chem. Soc., Chem. Commun*. **1996**, 1065−1066. − [6g] R. von Bülow, H. Gornitzka, T. Kottke, D. Stalke, *J. Chem. Soc., Chem. Commun*. **1996**, 1639−1640. − [6h] N. D. R. Barnett, W. Clegg, L. Horsburgh, D. M. Lindsay, Q.-Y. Liu, F. M. Mackenzie, R. E. Mulvey, P. G. Williard, *J. Chem. Soc., Chem. Commun*. **1996**, 2321−2322. − [6i] A. Avent, A. D. Frankland, P. B. Hitchcock, M. F. Lappert, *J. Chem. Soc., Chem. Commun*. **1996**, 2433−2434. − [6j] W. Clegg, L. Horsburgh, F. M. Mackenzie, R. E. Mulvey, *J. Am. Chem. Soc*. **1996**, *118*, 4721−1422.

[7] [7a] D. R. Armstrong, F. A. Banbury, I. Cragg-Hine, M. G. Davidson, F. S. Mair, E. Pohl, P. R. Raithby, R. Snaith, *Angew. Chem*. **1993**, *105*, 1801−1803; *Angew. Chem. Int. Ed. Engl*. **1993**, *32*, 1769−1771. − [7b] M. S. Eisen, M. Kapon, *J. Chem. Soc., Dalton Trans.* **1994**, 3507−3510.

[8] G. Boche, I. Langlotz, M. Marsch, K. Harms, N. E. S. Nudelman, *Angew. Chem*. **1992**, *104*, 1239-1240; *Angew. Chem. Int. Ed. Engl*. **1992**, *31*, 1205−1207.

[9] T. Laube, J. D. Dunitz, D. Seebach, *Helv. Chim. Acta* **1985**, *68*, 1373−1393.

[10] D. S. Wright, Ph.D. Thesis, Cambridge, **1989**.

[11] G. M. Sheldrick, *Acta Crystallogr., Sect. A* **1990**, *A46*, 467−473.

[12] G. M. Sheldrick, *SHELXL-93, Program for Crystal Structure Refinement*, University of Göttingen, **1993**.

[98024]

Chiral Bisphosphanes, VII[◇]

(1*S*,2*S*)-Cyclopentane-1,2-diyl-bis(phosphonous dichloride), (1*S*,2*S*)-$C_5H_8(PCl_2)_2$ − A Versatile Optically Active Reagent

Lutz Dahlenburg* and Anja Kaunert

Institut für Anorganische Chemie der Universität Erlangen-Nürnberg,
Egerlandstrasse 1, D-91058 Erlangen, Germany
Fax: (internat.) +49 (0)9131/85-7387
E-mail: dahlbg@anorganik.chemie.uni-erlangen.de

Received March 12, 1998

Keywords: Chirality / P ligands / Synthetic methods / Triphosgene

Treatment of (1*S*,2*S*)-$C_5H_8(PH_2)_2$ (**1**) with $OC(OCCl_3)_2$ gave (1*S*,2*S*)$C_5H_8(PCl_2)_2$ (**2**) as the first example of an optically active bis(phosphonous dichloride). **2** was converted to (1*S*,2*S*)-$C_5H_8(PX_2)_2$ [PX_2 = $P(OMe)_2$ (**3**), $P(OPh)_2$ (**4**), P[OCH(Me)Et-(*S*)]$_2$ (**5**), P[2-$OC_{10}H_6C_{10}H_6O$-2′-(*R*)] (**6**), $P(NC_4H_8O$-*cyclo*$)_2$ (**7**), $P(C_6H_{11}$-*cyclo*$)_2$ (**8**)] by reactions with oxygen, nitrogen, and carbon nucleophiles.

The design of new chiral phosphanes for use in transition metal-based asymmetric catalysis continues to play an important role in synthetic organic and organometallic chemistry[2]. Our current research in this field has been focused on the development of variable methods of synthesis for chiral bidentate phosphorus ligands with electron-rich and/or electron-poor donor atoms, starting from the resolved enantiomers of chiral bis(primary phosphanes)[3][4]. We herein report the details of a synthetic procedure that allows the facile transformation of (1*S*,2*S*)-cyclopentane-1,2-diyl-bisphosphane, (1*S*,2*S*)-$C_5H_8(PH_2)_2$[3] (**1**), into its PCl_2 homologue (1*S*,2*S*)-$C_5H_8(PCl_2)_2$ (**2**) and present selected examples of how the optically pure multi-purpose P−Cl reagent **2** is easily converted to the 1*S*,2*S* enantiomers of various $C_5H_8(PX_2)_2$ ligands containing sterically and electronically different P−C-, P−N-, or P−O-bonded substituents X on phosphorus.

Results

Formerly, primary phosphanes RPH_2 were reported to produce bis(phosphonous dichlorides) $RPCl_2$ on treatment with chlorine in inert halogenated solvents[5]. These results could not be reproduced, however, in later work where it was shown that both phosphonous and phosphinous chlorides are more readily prepared from a primary or secondary phosphane by oxidizing the P−H bond with $COCl_2$ ("phosgene") rather than with Cl_2[6][7]. Bis(trichloromethyl) carbonate, $OC(OCCl_3)_2$ ("triphosgene"), has served as a convenient crystalline alternative to the highly toxic phosgene in miscellaneous laboratory reactions and its use as an electrophile, dehydrating agent, or specific oxidant in the preparation of many classes of organic compounds has been studied thoroughly during the past decade[8]. We reasoned that triphosgene would also turn out useful as a synthetic auxiliary in the conversion of the easily accessible (1*S*,2*S*)-$C_5H_8(PH_2)_2$[3] (**1**) to the more reactive and, hence, more versatile (1*S*,2*S*)-$C_5H_8(PCl_2)_2$ (**2**). Actually, bis(phosphonous dichloride) **2** formed smoothly when bis(primary phosphane) **1** and $OC(OCCl_3)_2$ where combined in THF at 50°C in 3:4 stoichiometry, as required for the quantitative transformation of the two $-PH_2$ groups into $-PCl_2$ functions. This procedure provided solutions of **2** exhibiting no extraneous signals in their ^{31}P-NMR spectra, from which the pure product was isolated in 66% yield by vacuum distillation.

Compound **2** represents the hitherto only example of an optically active P_2 ligand possessing reactive P−Cl bonds, opening up variable synthetic routes to a wide range of enantiomerically pure electron-rich and electron-poor P−C-, P−N-, and P−O-bonded derivatives (1*S*,2*S*)-$C_5H_8(PX_2)_2$, potentially useful as supporting ligands in asymmetric catalysis. So far, we have prepared bidentates of the former type with PX_2 = $P(OMe)_2$ (**3**), $P(OPh)_2$ (**4**), P[OCH(Me)Et-(*S*)]$_2$ (**5**), P[2-$OC_{10}H_6C_{10}H_6O$-2′-(*R*)] (**6**), $P(NC_4H_8O$-*cyclo*$)_2$ (**7**), and $P(C_6H_{11}$-*cyclo*$)_2$ (**8**) by conventional reactions of **2** with mono- and difunctional alcohols, secondary amines, and Grignard reagents (Scheme 1). The ease of synthesis of ligands **3**−**8**, starting from enantiopure **2**, may be contrasted with, e. g., the previously described tedious preparation of **8**, which involved oxidation of *rac*-$C_5H_8[P(C_6H_{11}$-*cyclo*$)_2]_2$ to *rac*-$C_5H_8[P(O)(C_6H_{11}$-*cyclo*$)_2]_2$, followed by optical resolution of the *P*,*P*′-dioxide with (+)-di-*O*-benzoyl tartaric acid and reduction of the resolved P=O enantiomers in neat diphenylsilane at 150°C[9].

[◇] Part VI: Ref.[1]

 © WILEY-VCH Verlag GmbH, D-69451 Weinheim, 1998 1434−1948/98/0707−0885 $ 17.50+.50/0

Scheme 1

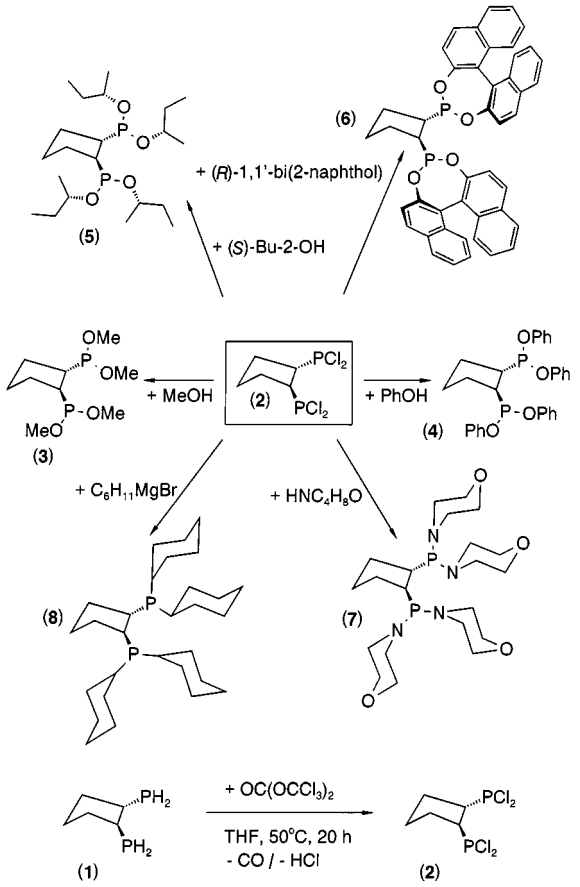

Discussion

The usefulness of the above procedures for the synthesis of optically active P_2 ligands rests on the following features[10]: First, the formation of bis(phosphonous dichlorides) or bis(phosphinous chlorides) by chlorination with triphosgene of bis(primary phosphanes) or bis(secondary phosphanes) can conceivably be performed with any other suitable chiral $H_2P{\cap}PH_2$ or H(R)P∩P(R)H precursor, as will be examplified elsewhere for the correspondent transformations of systems as different as $C_5H_8[P(H)R]_2$[11] and $Fe(C_5H_4PH_2)_2$[12]. Second, substitution reactions undergone by P−Cl functional phosphorus(III) compounds upon treatment with carbon, nitrogen or oxygen nucleophiles are among the most general and most easily accomplished coupling methods in organic chemistry. Finally, the fact that it is possible to incorporate virtually any other P−O-, P−N-, or P−C-bonded residue R into chiral $Cl_2P{\cap}PCl_2$ or Cl(R)P∩P(R)Cl frameworks makes it possible to utilize the method for the preparation of a wide range of optically active P_2 ligands having fine-tunable and, perhaps, rationally designed steric and electronic requirements.

Financial support from the *Deutsche Forschungsgemeinschaft* (Bonn) and the *Fonds der Chemischen Industrie* (Frankfurt/Main) is gratefully acknowledged. We are also indebted to *Hoechst AG* (plant Vlissingen/NL) for a generous gift of P_4.

Experimental Section

All manipulations were performed under nitrogen using standard Schlenk techniques. Solvents were distilled from the appropriate drying agents prior to use. − NMR: Bruker DPX 300 (300.1 MHz for ^1H, 75.5 MHz for ^{13}C, 121.5 MHz for ^{31}P) at ambient temperature with TMS as internal or H_3PO_4 as external standard (downfield positive). − Mass spectra: Jeol MS 700. − Optical rotation: Schmidt & Haensch POLARTRONIC E.

CAUTION: Although at the time of writing this article no conclusive data on the toxicity of triphosgene were available to the authors, the reagent should be handled using similar precautions as for the more dangerous phosgene, even if $OC(OCCl_3)_2$ is safer because of its lower vapor pressure and higher stability[8][13].

(1S,2S)-$C_5H_8(PCl_2)_2$ (**2**): A solution of 23.7 g (80 mmol) of $OC(OCCl_3)_2$ (Aldrich) in 250 ml of THF was added dropwise within 2 h to a stirred solution of 8.1 g (60 mmol) of (1*S*,2*S*)-$C_5H_8(PH_2)_2$[3] in 400 ml of THF, heated to 50°C. The mixture was stirred overnight at 50°C, solvent was then evaporated, and the residue was distilled in the vacuum of an oil pump at 80 to 110°C (pot temperature) to give 10.8 g (66%) of **2** as a colorless liquid. − ^1H NMR (C_6D_6): δ = 1.25 [qui, ^3J(H,H) = 7.1 Hz; 2 H, CH_2-4], 1.60 (m; 4 H, CH_2-3,5), 2.36 (m; 2 H, CH-1,2). − $^{13}C\{^1H\}$ NMR (C_6D_6): δ = 26.9 [t, ^3J(P,C) = 3.1 Hz; C-4], 29.6 [*A*XX′-d, ^2J(P,C) + ^3J(P′,C) = 14.5 Hz; C-3,5], 50.5 [dd, ^1J(P,C) = 51.8, ^2J(P,C) = 13.6 Hz; C-1,2]. − $^{31}P\{^{13}C\}$ NMR (C_6D_6): δ = 188.6 (s). − $[\alpha]_D^{25}$ = −19.8 (neat).

(1S,2S)-$C_5H_8\{P[OCH(Me)Et\text{-}(S)]_2\}_2$ (**5**): At dry-ice temperature, a quantity of 1.95 g (7.1 mmol) of **2**, dissolved in 20 ml of diethyl ether, was added dropwise, within 30 min, to a stirred solution containing 2.65 ml (28.7 mmol) of (*S*)-(+)-butan-2-ol (Aldrich) and 4.0 ml (28.7 mmol) of triethylamine in 200 ml of diethyl ether. Precipitation of $[Et_3NH]Cl$ occurred immediately to give a pasty suspension which was diluted by adding additional quantities of solvent in order to maintain stirring. After warming to room temperature overnight, the mixture was filtered and evaporated to leave bis(phosphinite) **5** as an opaque oil. Occasionally, this material contained impurities which in view of their $^{31}P\{^1H\}$ NMR signals (δ ca. 40−45) were strongly suspected to be onium salts, e. g., $[(1S,2S)\text{-}C_5H_8\{P[OCHC(Me)Et\text{-}(S)]_2\}_2H_n]Cl_n$ (*n* = 1, 2). These could be removed quantitatively by stirring the crudes with excess sodium amide in toluene. Subsequent filtration and evaporation of solvent afforded diastereomerically pure **5** as a colorless liquid (1.37 g; 45%), spectroscopically free from contaminating admixtures. − $^{13}C\{^1H\}$ NMR (C_6D_6): δ = 9.9, 10.1 (both s; both $CH_2\mathit{C}H_3$, pairwise diastereotopic), 22.0, 22.1 (both s; both $CH\mathit{C}H_3$, pairwise diastereotopic), 27.5 [m; $(CH_2)_3$], 31.6, 31.7 (both s; both $\mathit{C}H_2CH_3$, pairwise diastereotopic), 43.5 [dd, *J*(P,C) = 10.8 and 18.0 Hz; PCH], 75.5, 76.6 [both *A*XX′-t, Σ*J*(P,C) = 16.5 Hz; both POCH, pairwise diastereotopic]. − $^{31}P\{^1H\}$ NMR (C_6D_6): δ = 179.6 (s). − MS (FD; toluene, 35 mA, 10 kV): *m*/*z* = 423 [M^+].

(1S,2S)-$C_5H_8\{P[2\text{-}OC_{10}H_6C_{10}H_6O\text{-}2'\text{-}(R)]\}_2$ (**6**) was obtained analogously from 1.78 g (6.5 mmol) of **2** and 3.75 g (13.1 mmol) of (*R*)-(+)-1,1′-bi(2-naphthol) (Aldrich) in 200 ml of diethyl ether containing 3.68 ml (26.4 mmol) of added triethylamine; yield: 3.69 g (81%) of a yellow waxy solid. − $^{13}C\{^1H\}$ NMR (CD_2Cl_2): δ = 21.5 (s; $CH_2\mathit{C}H_2CH_2$), 27.0 [*A*XX′-t, ^2J(P,C) + ^3J(P′,C) = 20.3 Hz; $\mathit{C}H_2CH_2\mathit{C}H_2$], 41.9 [dd, ^1J(P,C) = 38.6, ^2J(P,C) = 17.9 Hz; PCH], 121.4, 122.2, 123.6, 124.7, 125.2, 125.6, 126.5, 126.9, 127.1, 128.5, 128.7, 129.3, 130.1, 130.8, 131.4, 131.7, 133.0, 133.2 (all s; 18 anisochronous aromatic C), 149.5, 150.7 th d, ^2J(P,C) = 6.9 Hz; both POC]. − $^{31}P\{^1H\}$ NMR (C_6D_6): δ = 203.5 (s). − MS (FD; toluene, 35 mA, 10 kV): *m*/*z* = 698 [M^+].

Compounds **3**, **4**, **7**, and **8** were prepared as described previously for the associated racemats[1][9]. As expected, the products exhibited NMR and MS data corresponding in all respects to those reported for the racemic mixtures.

[1] L. Dahlenburg, C. Becker, J. Höck, S. Mertel, *J. Organomet. Chem.*, in press.
[2] W. A. Herrmann, B. Cornils in *Apllied Homogeneous Catalysis with Organometallic Componds* (Eds.: B. Cornils, W. A. Herrmann), VCH, Weinheim, **1996**, Vol. 2, chapter 4.1.
[3] C. Eckert, L. Dahlenburg, A. Wolski, *Z. Naturforsch*. **1995**, *50b*, 1004−1008.
[4] L. Dahlenburg, V. Kurth, *Eur. J. Inorg. Chem*. **1998**, 597−603.
[5] C. Walling (E. I. Du Pont de Nemours & Co.), U. S. 2437798, **1948** [*Chem. Abstr.* **1948**, *42*, P4199c].
[6] W. A. Henderson, Jr., S. A. Buckler, N. E. Day, M. Grayson, *J. Org. Chem.* **1961**, *26*, 4470−4471.
[7] E. Steininger, *Chem. Ber.* **1963**, *96*, 3184−3194.
[8] L. Cotarca, P. Delogu, A. Nardelli, V. Sunjic, Synthesis **1995**, 553−576.
[9] A. Saare, L. Dahlenburg, *Z. Naturforsch*. **1995**, *50b*, 1009−1017.
[10] L. Dahlenburg, Ger. Pat. Appl. 197 32 805.9, **1997**.
[11] V. Kurth, Dissertation, Universität Erlangen-Nürnberg, in progress.
[12] S. Nückel, Diploma Thesis, Universität Erlangen-Nürnberg, **1998**.
[13] S. B. Damle, Chem. Eng. News **1993**, *71 (6)*, 4.

[98058]

Zirconocene−(μ-Organyl)borate Betaines Derived by Treatment of a (σ-Alkenyl)(σ-alkynyl)zirconocene Complex with Tris(pentafluorophenyl)borane☆

Wolfgang Ahlers, Gerhard Erker*, and Roland Fröhlich

Organisch-Chemisches Institut der Universität Münster,
Corrensstraße 40, D-48149 Münster, Germany
Fax: +49(0)251-83 36503
E-mail: erker@uni-muenster.de

Received January 7, 1998

Keywords: Zirconocene / Metallocene cation / Isonitrile insertion / Isonitrile complex

Hydrozirconation of propyne followed by treatment with propynyllithium yields the (σ-propenyl)(σ-propynyl)zirconocene complex **11**. Its treatment with the organometallic Lewis acid $B(C_6F_5)_3$ results in transfer of the σ-propynyl group from zirconium to boron followed by insertion of the alkynylborate triple bond into the zirconium carbon bond of the remaining metallaallyl cation to furnish the zirconocene–(μ-hydrocarbyl)borate betaine complex **14**. This reacts with three molar equivalents of *tert*-butyl isocyanide to give **16**. Complex **16** contains a five-membered carbocyclic ring, formed by carbon-carbon coupling of the former propenyl and propynyl groups with the C≡N–R reagent, to which a (η^2-iminoacyl)(κ-*tert*-butyl isocyanide)zirconocene moiety is attached. Complex **16** was characterized by an X-ray crystal structure analysis.

Introduction

Allyl- and propargyl-conjugation effects are of great importance in organic chemistry. They greatly influence the chemistry of allylic and propargylic substrates due to the thermodynamic stabilization of the respective cations, radicals or anions.[1] Organometallic group 4 metallocene cations [$^{R}Cp_2Zr-R^+$] play a very important role as the active species of the homogeneous metallocene Ziegler catalysts.[2] It is therefore of interest to know about the electronic effects that influence and alter the properties of such cationic organometallic systems, i.e. whether allylic[3] or propargylic conjugation effects may lead to chemical consequences in such cations. We have recently investigated two potential synthetic entries into "metallapropargyl"-cation systems of the type [$^{R}Cp_2Zr-C\equiv C-R^+$].[4][5] Such species can be generated in situ, but they are extremely reactive. Their interesting chemical behavior has led to the development of a variety of rather simple synthetic pathways to a number of novel organometallic frameworks. Here are two representative examples: treatment of bis(propynyl)zirconocene (**1**) with trityltetraphenylborate[6] generated the reactive intermediate [$Cp_2Zr-C\equiv C-CH_3^+$] that instantaneously attacked an equivalent of the starting material **1** to form the CC-coupled product **3** which contains a planar-tetracoordinate carbon atom (C^3) at a bridgehead-position of the dimetallabicyclic framework.[3]

When **1** is treated with the strong organometallic Lewis acid tris(pentafluorophenyl)borane (**4**)[7] a propynyl anion equivalent is transferred[8] from zirconium to boron with generation of a 1,1-bis(cyclopentadienyl)zircona-propargyl cation intermediate (**5**). This then inserts the alkynyl moiety of the resulting anion to give the observed product **6**. The

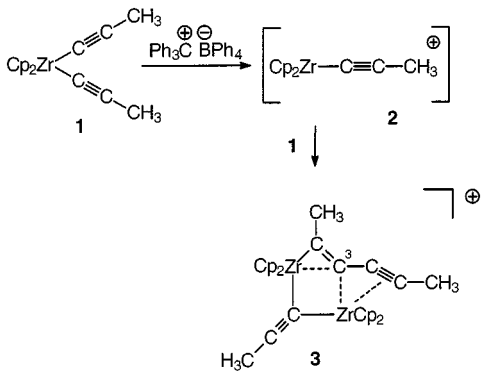

metallocene (μ-hydrocarbyl)borate betaine **6** exhibits a unique reactivity. It seems to be in an (endothermic) equilibrium with its isomer **7**, formally obtained by an intramolecular alkyne insertion reaction into the Zr−C(sp^2) σ-bond, from which the stable corresponding methylenecyclopropene derivatives are obtained in high yield by treatment with suitable insertion reagents, e.g. isonitriles (see Scheme 1). Subsequent hydrolysis of **8** led to interesting novel organic three-membered ring systems.[5][9]

It would be interesting to know whether this chemistry of conjugated metallocene cations could be extended from metallapropargyl to metallaallyl systems.[3] Which of the two cations is preferrentially formed in a competitive situation? Do ring closure reactions of the **6** ⟹ **7** type require the presence of two acetylide-derived building blocks (i.e. to make cyclopropenylium product stabilization possible as in **8**) or would building blocks of lower unsaturation being tolerable in the chemistry depicted in Scheme 1? To address these and related questions experimentally we have pre-

 © WILEY-VCH Verlag GmbH, D-69451 Weinheim, 1998 1434−1948/98/0707−0889 $ 17.50+.50/0

Scheme 1

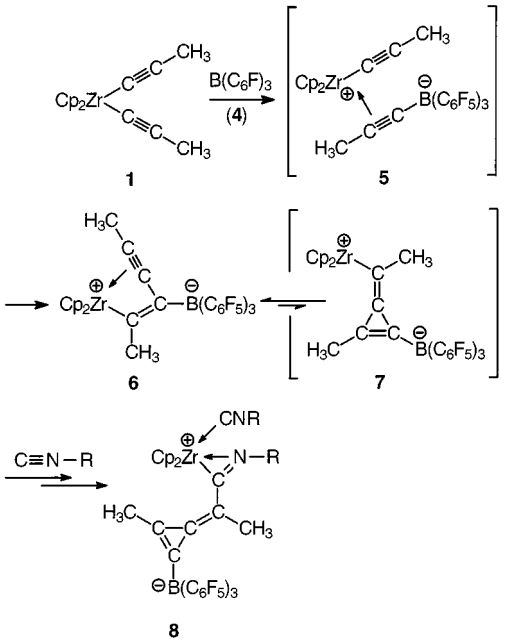

pared a "mixed" (σ-alkenyl)(σ-alkynyl)metallocene and investigated its metallocene cation chemistry initiated by treatment with $B(C_6F_5)_3$.

Results and Discussion

(σ-Propenyl)(σ-propynyl)zirconocene **11** was synthesized in the following way. Propyne was hydrozirconated by treatment with the oligomeric $[Cp_2Zr(H)Cl]_n$ reagent **9** in toluene at ambient temperature[10] to give the (*trans*-1-propenyl)zirconocene chloride complex **10** (74%). Subsequent treatment with propynyllithium in toluene furnished **11** in good yield (>90%). It shows the characteristic spectroscopic features of the *trans*-1-metallated alkene (^{1}H NMR: δ 6.98, 5.88, ^3J = 17.4 Hz; ^{13}C NMR: δ 182.2 (C1); IR: ν = 1635 cm^{-1}) and of the σ-alkynyl unit [IR: ν = 2086 cm^{-1}; ^{13}C NMR: δ 129.1, 118.1 ($C^4{\equiv}C^5$)].

Scheme 2

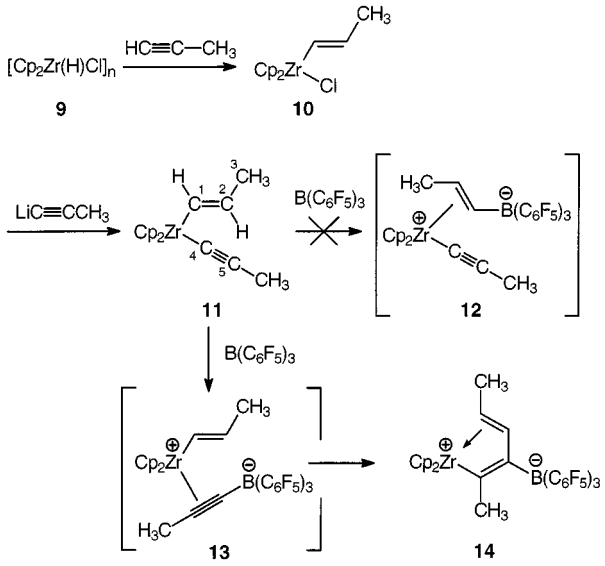

Complex **11** reacts instantaneously with $B(C_6F_5)_3$ at room temperature. A mixture of products is formed containing a major component (**14**) that amounts to ca. 80%, but this product has turned out not to be very stable. In the course of several hours it decomposes unspecifically. Therefore, the product **14** was not isolated but only characterized spectroscopically from freshly prepared solutions (in [D_6]benzene, [D_8]toluene, or [D_5]bromobenzene). The NMR spectra clearly showed that carbon-carbon coupling of the two unsaturated σ-ligands at zirconium had occurred under the influence of the borane Lewis acid. The product exhibits the signals of a terminal *trans*-$H_3C^6-C^5H=C^4H$ moiety [233 K, [D_8]toluene: ^{1}H NMR: δ 7.40, 5.78, ^3J = 16 Hz; ^{13}C NMR: δ 158.8 (C4), 115.5 (C5)].

The C4=C5 double bond is probably coordinated to the electrophilic zirconium center, according to the corresponding ^{13}C-NMR chemical shifts and a comparison with typical reference data from the literature.[12a] Compound **14** at 233K in [D_8]toluene at 564 MHz exhibits a set of 15 ^{19}F NMR signals, which indicates hindered rotation about the C(sp^2)−B bonds. In addition, complex **14** exhibits a pair of diastereotopic cyclopentadienyl ligands (^{1}H-/^{13}C-NMR signals in [D_8]toluene at 233 K: δ 5.16, 5.02/112.8, 111.0). Raising the temperature results in a coalescence of the Cp-signals [T_{coal} (^{1}H NMR, 600 MHz) = 304 K], and a Gibbs activation energy of $\Delta G^{\ddagger}_{isom}$ (304 K) = 15.5 ± 0.5 kcal mol^{-1} for the dynamic exchange process.[11] This NMR behavior has precedence for substituted (1-butadienyl) ligand systems bonded to a cationic Cp_2M^+ unit: we assume a weak π-interaction of the $C^4=C^5$ double bond with the very electrophilic group 4 metallocene unit in **14**.[12] Conformational equilibration of the helically arranged C_4 unit in **14** may then occur by reversible cleavage of this weak π-complexation similarly as it was previously observed in the structurally and chemically related betaine system **15** (see Scheme 3).[13][14]

Scheme 3

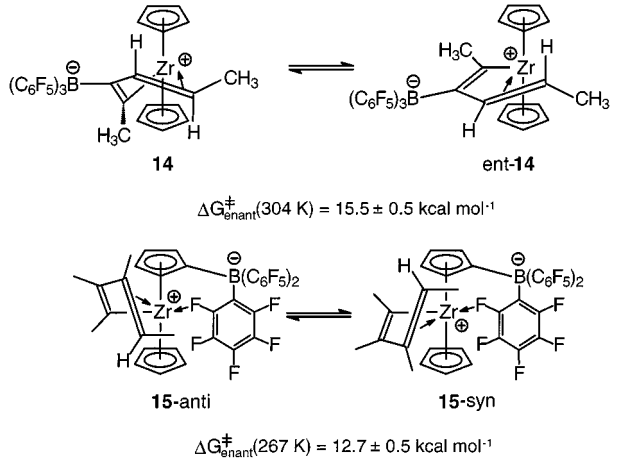

Complex **14** reacts readily with *tert*-butyl isocyanide (it consumes three equivalents of this reagent) to give an insertion/addition product **16**, that was isolated in >80% yield as a very pale yellow amorphous solid. Recrystallization from chloroform by slow evaporation of the solvent eventually

gave single crystals that were suited for an X-ray crystal structure analysis (see Figures 1 and 2). An overall view of the structure is given in Figure 1.

Figure 2 shows a projection of the central core of atoms of the newly formed product. This reveals that two equivalents of the isonitrile reagent were inserted. The first was used to couple the alkenyl- and alkynyl-derived moieties of the starting material together to form a five-membered carbocycle (C1−C5). The carbon framework $H_3C^6-C^2=C^1[B]-C^5H_2-C^4-C^7H_3$ of the product **16** corresponds exactly to the connectivity of the framework of its precursor **14**, only that the number of hydrogen atoms at carbon centers C5 and C4 does not correspond with the starting material.

Figure 1. A view of the molecular structure of **16**

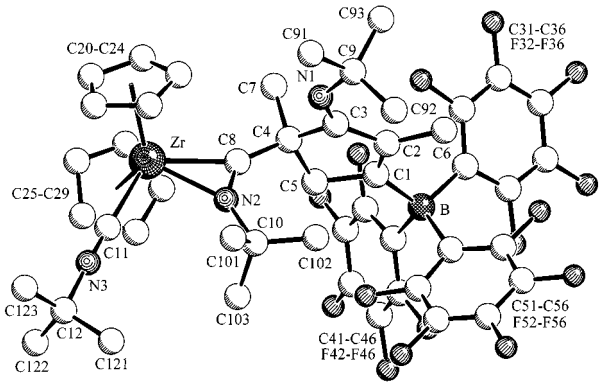

Unfortunately, we could not find any intermediate along the reaction pathway. Therefore, a detailed mechanistic picture of the **14**→**16** transformation must remain speculative at this time. A possible pathway is formulated in Scheme 4, starting with isonitrile insertion followed by electrophilic addition of the activated iminoacyl group at the C=C double bond to form the five-membered ring. We must assume a subsequent 1,2-hydride migration, potentially assisted by zirconium−carbon σ-bond formation to form the likely intermediate **19**. This is then trapped by insertion of an additional *tert*-butyl isocyanide insertion into the Zr−C σ-bond, followed by coordination of the third C≡NR molecule to give the observed stable reaction product.[15]

The X-ray crystal structure analysis of **16** shows the presence of the newly formed carbocyclic five-membered ring system (C1−C5) that contains the C1−C2 double bond [1.346(7) A] in conjugation to the ketimine functionality [C3−N1 1.266(7) A]. The bulky $-B(C_6F_5)_3$ substituent is attached to the sp^2-carbon atom C1 [C1−B 1.662(8) A]. Noteworthy is the presence of a η^2-iminoacyl group at the group 4 bent metallocene unit. The corresponding Zr−C8 bond length is 2.209(5) A, the Zr−N2 distance is 2.234(4) A. The angles inside the organometallic three-membered ring system are small [C8−Zr−N2 32.9(2)°, Zr−C8−N2 74.7(3)°, Zr−N2−C8 72.4(3)°]. The C8−N2 bond length is 1.258(6) A which is marginally shorter than the uncomplexed N1=C3 imino double bond at the adjacent five-membered ring (see above).

Figure 2. A view of the central atom framework of **16** with atom numbering scheme[a]

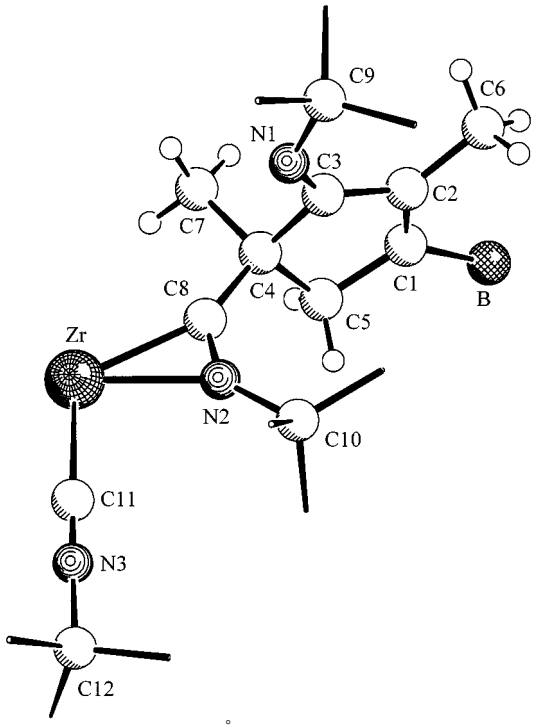

[a] Selected bond lengths [A] and angles [°]: Zr−C8 2.209(5), Zr−N2 2.234(4), Zr−C11 2.338(7), C11−N3 1.153(7), N3−C12 1.477(8), N2−C8 1.258(6), N2−C10 1.498(6), C8−C4 1.525(7), B−C1 1.662(8), C1−C2 1.346(7), C1−C5 1.517(7), C2−C3 1.500(7), C2−C6 1.503(7), C3−C4 1.545(7), C3−N1 1.266(7), N1−C9 1.471(7), C4−C5 1.548(7), C4−C7 1.537(7); Zr−C8−C4 148.8(4), Zr−C8−N2 74.7(3), Zr−N2−C8 72.4(3), Zr−N2−C10 148.5(3), Zr−C11−N3 175.5(5), C11−N3−C12 175.8(7), C11−Zr−N2 84.1(2), C11−Zr−C8 117.0(2), N2−Zr−C8 32.9(2), C8−N2−C10 139.0(5), N2−C8−C4 136.4(5), C8−C4−C5 111.8(4), C8−C4−C3 115.0(4), C8−C4−C7 108.4(4), B−C1−C2 126.3(5), B−C1−C5 122.4(5), C1−C2−C3 111.9(5), C1−C2−C6 123.1(5), C2−C3−C4 114.8(5), C2−C3−N1 140.1(5), C3−C4−C5 104.7(4), C3−C4−C7 106.6(4), C3−N1−C9 130.8(5), C5−C4−C7 110.2(4), C4−C5−C1 104.4(4); α(Zr,C8,N2)/(C1,C2,C3,C4,C5) 85.4.

The complex framework of **16** corresponds to a zirconium−borate-betaine structure, which means that the zirconium center bears a partial positive charge. Its high electrophilicity and coordinative unsaturation has led to the complexation of the *tert*-butyl isocyanide ligand. In view of the special stereoelectronic features of the group 4 bent metallocene framework[16] it is likely that the metal−isonitrile coordination is dominated by ligand to metal σ-donation of electrons, without a significant π-backbonding contribution. This is confirmed by the bonding parameters of the Zr←C≡NR unit of **16** and its spectroscopic properties.[17] The C≡N bond length in the free isonitrile is 1.145 A. The C11−N3 distance of the coordinated *tert*-butyl isonitrile ligand in **16** is only marginally elongated at 1.153(7) A. The RN≡C→Zr unit is close to linear [angle N3−C11−Zr 175.5(3)°], and the Zr−C11 distance is 2.338(7) A. Thus the $Cp_2Zr^+\leftarrow C\equiv N-CMe_3$ unit in **16** shows very similar bonding features as found in the pure donor/acceptor adduct $[Cp_3Zr\leftarrow C\equiv N-CMe_3^+]$ (**20**)

Scheme 4

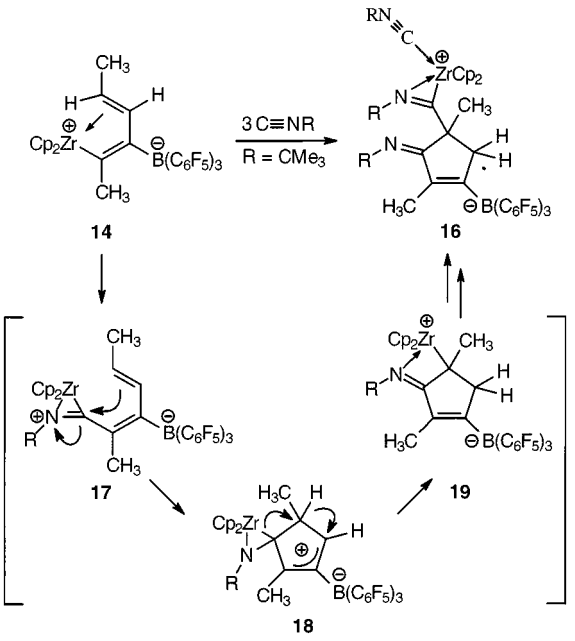

[Zr−C: 2.313(3) Å, C−N 1.145(4) (identical with the uncomplexed ligand); angle Zr−C−N 178.4(2)°].[18] The IR (C≡NR) band of **16** is at ν = 2197 cm^{-1} (**20**: 2209 cm^{-1}) which is above the free ligand value of ν = 2140 cm^{-1} as expected.[17]

The η^2-iminoacyl ligand and the isonitrile donor ligand are both oriented in the σ-ligand plane of the bent metallocene group, as expected. Therefore, two isomeric arrangements of these ligands are possible, which are characterized by central or lateral positioning of the iminoacyl nitrogen atom, respectively.[19] In the crystal we have only found the N-inside isomer (**16a**). But an investigation of the system in solution has revealed the presence of the other, the N-outside isomer (**16b**) and shown that the two stereoisomers **16a** and **16b** are interconverted on the NMR time scale.

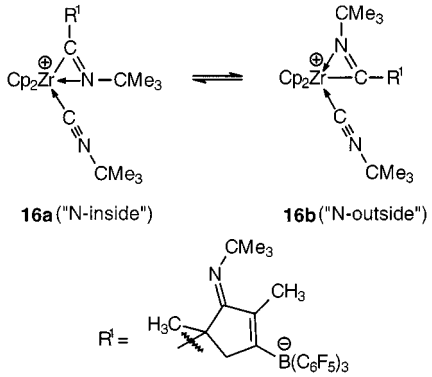

In [D$_8$]THF solution complex **16** exhibits two complete sets of ^{1}H- and ^{13}C-NMR signals at 213 K in a ratio of 70:30 which correspond to the two isomers **16a** and **16b**. The chemical shifts of the sets of signals are mostly very similar, some of them are overlapping. The presence of the two isomers can clearly be monitored e.g. by observing six ^{13}C NMR signals of the $-C(CH_3)_3$ substituents at the nitrogen atoms (major isomer **16a**: δ 30.57, 26.61, 26.30; minor isomer **16b**: 30.66, 26.56, 25.58) or the narrowly separated Cp signals at δ 105.23/103.87 (**16a**) and δ 105.28/103.91 (**16b**). Two of the ^{1}H-NMR Cp resonances of the isomers are isochronous (δ 6.00), but the others are split into a 70:30 intensity pair of signals at 5.80 (**16a**) and 5.82 (**16b**). Upon increasing the temperature, coalescence of the two sets of spectra takes place to give an averaged single set of signals corresponding to the equilibrated chiral isomers (leading e.g. to a single pair of ^{1}H-NMR signals of the diastereotopic Cp-ligands at δ 5.94 and 5.75). From the temperature dependent ^{1}H NMR spectra the activation barrier of the **16a** ⟹ **16b** isomerization reaction was determined at $\Delta G^{\neq}_{isom}$ (273 K) = 14 ± 1 kcal mol^{-1} using the DNMR5 dynamic NMR simulation program.[20]

It is very clear that the dynamic process monitored by the temperature dependent ^{1}H- and ^{13}C-NMR spectra as described above corresponds to the iminoacyl N-inside ⟹ N-outside isomerization reaction and not from an equilibration process that solely involves the advent or disappearance of a persistent propeller conformation at the $-B(C_6F_5)_3$ borate group attached at the sp^2-C carbon atom C1 of the five-membered ring system. We are quite sure about this interpretation since we were able to observe this "freezing" of the chiral propeller-geometry at the boron center[5] independently by temperature dependent ^{19}F-NMR spectroscopy (at 564 MHz). As expected for this overall scenario we have observed a total of 30 ^{19}F-NMR resonances of the $B(C_6F_5)_3$ residues at 233 K in [D$_8$]THF, 15 arising from the major isomer **16a** (70% intensity) [δ −128.4, −130.2, −130.7, −133.3, −134.8, −135.6 (*ortho*), −164.6, −165.3, −165.6 (*para*), and −167.4, −168.3, −168.5, −168.6, −169.2, −169.3 (*meta*)] and 15 of lower intensity (30%) due to the minor isomer **16b** [δ −128.9, −130.5, −131.2, −133.2, −133.9, −135.3 (*ortho*), −164.9, −165.2, −165.9 (*para*), and −167.6, −167.8, −168.7, −169.2, −169.7, −169.9 (*meta*)]. Increasing the temperature results in massive line broadening which is first due to giving the (sp^2-C)−B rotation free and thus leading to individual equilibration of the six −*o*-F, three −*p*-F, and six −*m*-F signals for each of the isomers − which gives rise to the observation of a set of two *ortho*-F, two *meta*-F and two *para*-F resonances, each in a ca. 70:30 ratio. Raising the temperature further eventually leads to rapid **16a** ⟹ **16b** equilibration also on the ^{19}F-NMR time scale and thus gives rise to a very simple limiting high temperature spectrum showing only three remaining lines corresponding to the *o*-, *m*-, and *p*-F substituents at the $B(C_6F_5)_3$ unit under rapidly equilibrating conditions.

Conclusions

In principle, the reaction of the (σ-propenyl)(σ-propynyl)zirconocene complex **11** with the strong organometallic Lewis acid $B(C_6F_5)_3$ proceeds very similar to the reaction of bis(σ-propynyl)ZrCp_2 with tris(pentafluorophenyl)borane.[5][9] The propynyl ligand is transferred, followed by an insertion reaction with carbon-carbon coupling to give the group 4 metallocene−(μ-hydrocarbyl)borate betaine com-

plex **14**. The reaction of **11** with $B(C_6F_5)_3$ proceeds rather selectively. Within the limits of detection it is the σ-propynyl group that is transferred. The σ-propenyl ligand remains bonded to zirconium in the first step, it is only used subsequently as a reactive reagent in the insertion reaction. This pronounced selectivity might indicate an increased thermochemical stabilization of the 1,1-bis(cyclopentadienyl) "zircona-allyl" cation over the corresponding "zircona-propargyl" cation system, but this experimental result could also merely reflect the higher mobility of the σ-propynyl group in the transfer step. In any case the resulting "zircona-allyl" cation complex is extremely unstable and rapidly reacts with the in situ generated alkynyl-functionalized borate anion by insertion to yield the metallocene−betaine complex **14**. We conclude that metalla-allyl type reagents can readily be generated by the synthetic route applied in this study, but we must note that such systems seem to be very reactive. If there should be any thermodynamic stabilization at all it is certainly overruled by a very high kinetic reactivity of this organometallic cationic system.

The reaction of **14** with *tert*-butyl isocyanide yields the product **16** which is very interesting in view of its specific bonding features that are derived from the dipolar (i.e. betaine) structure of this metal complex. The connection of the borate anion part $[R-B(C_6F_5)_3^-]$ with the $Cp_2Zr(\eta^2$-iminoacyl) group by means of the bridging carbocyclic framework in fact creates a situation where the zirconocene unit effectively behaves like a metallocene cation that is completely separated from its anion.[21] This shows up in its property to serve as an organometallic Lewis acid strongly coordinating an isonitrile donor ligand. The structural and spectroscopic features of the resulting local $[Cp_2Zr(R')\leftarrow C\equiv NR^+]$ moiety are as expected for an (isonitrile)-zirconocene cation donor-acceptor adduct. This provides additional evidence that a variety of group 4 metallocene−(μ-organyl)borate betaines are very suited organometallic molecules to detect, study, and eventually use a typical metallocene cation reactivity in an overall *neutral* molecule.

Financial support from the *Fonds der Chemischen Industrie*, the *Bundesminister für Bildung, Wissenschaft, Forschung und Technologie (BMBF)*, the *Deutsche Forschungsgemeinschaft*, and the *Ministerium für Wissenschaft und Forschung des Landes Nordrhein-Westfalen* is gratefully acknowledged.

Experimental Section

All reactions were carried out in an inert atmosphere (argon) using Schlenk-type glassware or in a glovebox. Solvents, including deuterated solvents, were dried and distilled under argon prior to use. For additional general information, including a list of spectrometers used, see ref.[5] and ref.[9]. The reagents (hydrido)zirconocene chloride[10] and tris(pentafluorophenyl)borane[7] were prepared according to literature procedures.

Preparation of (1-Propenyl)zirconocene Chloride (**10**): (Hydrido)-zirconocene chloride (1.10 g, 4.32 mmol) was suspended in 10 ml of toluene. The Schlenk flask was evacuated and filled with propyne. The mixture was stirred and additional propyne was entered into the gasphase in ca. 20 min intervals. A clear solution was obtained after ca. 4 h. Solvent was removed in vacuo and the residue stirred with pentane (3 ×) to give 950 mg (74%) of **10** as a pale yellow solid, m. p. 78°C (decomp.). − ^{1}H NMR ([D$_6$]benzene): δ 6.88 (dq, ^3J = 17.2 Hz, ^4J = 1.5 Hz, 1 H, Zr-C^1*H*=), 5.89 (dq, ^3J = 17.2 Hz, 6.0 Hz, 1 H, =C^2*H*-), 5.81 (s, 10 H, Cp), 1.79 (dd, ^3J = 6.0 Hz, ^4J = 1.5 Hz, 3 H, CH_3). − ^{13}C NMR ($CDCl_3$): δ 177.2 (C1), 138.6 (C2), 112.8 (Cp), 23.8 (CH_3).

Preparation of (1-Propenyl)(1-propynyl)zirconocene (**11**): (Propenyl)zirconocene chloride **10** (1.00 g, 3.47 mmol) and propynyllithium (165 mg, 3.59 mmol) were mixed as solids. At −78°C 10 ml of cold toluene was added with stirring. The cooling bath was removed after 1 h and the mixture allowed to warm to room temperature. After stirring overnight a lithium chloride precipitate was removed by filtration and the solvent evaporated in vacuo from the filtrate. The oily residue was solidified by treatment with pentane (12 h stirring) and the product dried in vacuo to yield 956 mg (91%) of **11**, m.p. 129°C (decomp.). − ^{1}H NMR ([D$_6$]benzene): δ 6.98 (dq, ^3J = 17.4 Hz, ^4J = 1.2 Hz, 1 H, Zr-CH=), 5.95 (s, 10 H, Cp), 5.88 (dq, ^3J = 17.4 Hz, 5.8 Hz, 1 H, =CH-), 1.78 (s, 3 H, C=C-CH_3), 1.77 (dd, ^3J = 5.8 Hz, ^4J = 1.2 Hz, 3 H, =CH-C*H*$_3$). − ^{13}C NMR ([D$_6$]benzene): δ 182.2 (Zr-*C*H=), 135.6 (=CH-), 110.6 (Cp), 129.1, 118.1 (-C=C-), 23.9 (=CH-*C*H$_3$), 5.90 (=C-*C*H$_3$). − IR (KBr): ν = 2086 (C=C), 1635 (C=C). − $C_{16}H_{18}Zr$ (301.5): C 63.67, H 5.97; found: C 62.68, H 5.49%.

Reaction of **11** *with B(C$_6$F$_5$)$_3$: Generation of* **14**: 5 mg (16.6 μmol) of **11** and 8.5 mg (16.6 μmol) of $B(C_6F_5)_3$ were mixed as solids. 0.5 ml of the respective deuterated solvent (see below) was added and the clear orange colored solution characterized spectroscopically. The solutions were not stable for prolonged periods of time. They turned brownish and a dark colored oil precipitated. Spectroscopic characterization of **14**: ^{1}H NMR ([D$_8$]toluene, 600 MHz, 233 K): δ 7.40 (d, ^3J = 16.2 Hz, 1 H, 4-H), 5.78 (br. s, 1 H, 5-H), 5.16 (s, 5 H, Cp), 5.02 (s, 5 H, Cp), 1.86 (s, 3-H, 2-CH_3), 0.80 (d, ^3J = 6.0 Hz, 3 H, 5-CH_3). − ^{13}C NMR ([D$_8$]toluene, 150 MHz, 233 K): δ 158.8 (C4), 149.3 [$^1J_{CF}$ = 253 Hz, o-$B(C_6F_5)_3$], 115.5 (C5), 112.8 (Cp), 111.0 (Cp), 26.9 (2-CH_3), 19.1 (5-CH_3) [C2, C3, *m*-, *p*-, and *ipso*-C of $B(C_6F_5)_3$ not observed]; the spectral assignment was secured by GCOSY, GHSQC, and GHMBC-NMR experiments[22]. − ^{11}B NMR ([D$_6$]benzene): δ −13.2. − ^{19}F NMR ([D$_8$]toluene, 233K, 564 MHz): δ −128.7, −129.2, −129.8, −133.3, −133.8, −138.2 (*o*-), −160 to −164 (*p*-), −164.5, −164.7, −165.7, −167.0, −167.3, −168.3 [*m*-$B(C_6F_5)_3$]. From the temperature-dependent dynamic NMR spectra (^{1}H-NMR coalescence of the Cp-signals) a Gibbs activation energy of the enantiomerization process of **14** was derived at $\Delta G^{\neq}_{enant}$ (T_c = 304 K) = 15.5 ± 0.5 kcal mol^{-1} (Δν = 20.6 Hz, in [D$_8$]toluene) using the Gutowsky-Holm approximation.[11]

Reaction of **14** *with tert-Butyl Isocyanide: Preparation of* **16**: The betaine **14** was generated in situ by treatment of 200 mg (0.66 mmol) of **11** with 340 mg (0.66 mmol) of $B(C_6F_5)_3$ in 8 ml of toluene at −78°C. The mixture was stirred for 30 min at −78°C and then allowed to warm to 0°C during 1 h. 1 ml of *tert*-butyl isocyanide was added to the orange colored turbid solution. The reaction mixture was stirred overnight at ambient temperature. Volatiles were removed in vacuo and the residue washed twice with 5 ml of pentane. The resulting solid was dissolved in 5 ml of dichloromethane and the product precipitated by the addition of 10 ml of pentane, collected by filtration and dried in vacuo; yield of **16** 527 mg (81%). Single crystals of **16** suited for the X-ray crystal structure analysis were obtained from $CDCl_3$ by a slow evaporation of the solvent. Characterization of **16**: m.p. 141°C (decomp.). In solution two isomers **16a** and **16b** were detected in a 70:30 ratio. − ^{1}H NMR ([D$_8$]THF, 600 MHz, 213 K) major isomer (**16a**): δ 6.00 (s, 5 H, Cp), 5.80 (s, 5 H, Cp), 2.75, 2.68 (AB, ^2J = 16 Hz, each 1 H, 5-H,

5-H′), 1.86 (s, 3 H, 4-CH_3), 1.65 (s, 3 H, 2-CH_3), 1.75, 1.35, 1.30 [s, each 9 H, C(CH_3)$_3$]; minor isomer (**16b**): δ 6.00 (s, 5 H, Cp), 5.82 (s, 5 H, Cp), 2.78, 2.36 (AB, ^2J = 16 Hz, each 1 H, 5-H, 5-H′), 1.92 (s, 3 H, 4-CH_3), 1.88 (s, 3 H, 2-CH_3), 1.72, 1.30, 1.02 [s, each 9 H, C(CH_3)$_3$]. – ^{13}C NMR ([D$_8$]THF, 150 MHz, 213 K) major isomer (**16a**): δ 230.0 (Zr-C=N), 179.4 (C3), 147.8 (Zr←C≡NR), 146.2 ($^1J_{CF}$ = 246 Hz), 136.6 ($^1J_{CF}$ = 240 Hz), and 135.0 [$^1J_{CF}$ = 254 Hz, *o*-, *p*-, *m*-B(C_6F_5)$_3$], 133.2 (C2), 122 [*ipso*-C of B(C_6F_5)$_3$], 105.23 and 103.87 (Cp), 58.8, 58.1, and 51.9 (*ipso*-C of *tert*-butyl), 55.1 (C4), 48.9 (C5), 28.1 (4-CH_3), 30.57, 26.61, and 26.30 [C(CH_3)$_3$], 16.6 (2-CH_3), C1 not observed; minor isomer (**16b**): δ 230.0 (Zr-C=N), 179.4 (C3), 147.3 (Zr←C≡NR), 146.2 ($^1J_{CF}$ = 246 Hz), 136.6 ($^1J_{CF}$ = 254 Hz), and 135.0 [$^1J_{CF}$ = 240 Hz, *o*-, *p*-, *m*-B(C_6F_5)$_3$], 132.6 (C2), 122 [*ipso*-C of B(C_6F_5)$_3$], 105.28 and 103.91 (Cp), 58.3, 52.00 (*ipso*-C of *tert*-butyl, 1 signal not observed), 54.2 (C4), 48.3 (C5), 30.66, 26.56, and 25.58 [C(CH_3)$_3$], 29.4 (4-CH_3), 16.2 (2-CH_3), C1 not observed. – These assignments were supported by the results of GCOSY, GHSQC and GHMBC NOE-difference, and ROESY NMR experiments[22]. – ^{11}B NMR ($CDCl_3$): δ −15.1. – ^{19}F NMR ([D$_8$]THF, 564 MHz, 233 K) major isomer (**16a**): δ −128.4, −130.2, −130.7, −133.3, −134.8, −135.6 (*ortho*-), −164.6, −165.3, −165.6 (*para*-), −167.4, 168.3, −168.5, −168.6, −169.2, −169.3 [*meta*-B(C_6F_5)$_3$]; minor isomer (**16b**): δ −128.9, −130.5, −131.2, −133.2, −133.9, −135.3 (*ortho*-), −164.9, −165.2, −165.9 (*para*-), −167.6, −167.8, −169.2, −169.7, −169.9 [*meta*-B(C_6F_5)$_3$]. IR (KBr): ν = 2197 (N≡CR), 1611 (C=C). – UV/Vis (dichloromethane): λ_{max} = 306 nm (ε = 34500), 254 (ε = 36000), 233 (ε = 21700). – $C_{49}H_{45}BF_{15}N_3Zr$ (1062.9): C 55.37, H 4.27, N 3.97; found: C 55.41, H 4.50, N 4.26%.

X-ray Crystal Structure Analysis of **16**: Formula $C_{49}H_{45}BF_{15}N_3Zr \cdot 1.5\ CHCl_3$, M = 1241.96, 0.30 × 0.20 × 0.10 mm, a = 12.105(1), b = 13.146(1), c = 17.167(1) A, α = 88.97(1), β = 82.62(1), γ = 82.29(1)°, V = 2684.7(4) A^3, ρ_{calc} = 1.536 g cm^{-3}, μ = 5.19 cm^{-1}, empirical absorption correction via φ scan data (0.891 ≤ C ≤ 0.999), Z = 2, triclinic, space group P1bar (No. 2), λ = 0.71073 A, T = 223 K, ω/2θ scans, 9916 reflections collected (±h, +k, ±l), [(sinθ)/λ] = 0.59 A^{-1}, 9463 independent and 4891 observed reflections [$I \geq 2\ \sigma(I)$], 705 refined parameters, R = 0.061, wR^2 = 0.141, max. residual electron density 1.06 (−0.75) e A^{-3}, hydrogens calculated and refined as riding atoms.

Data set was collected with an Enraf Nonius MACH3 diffractometer. Programs used: data reduction MolEN, structure solution SHELXS-86, structure refinement SHELXL-93, graphics SCHAKAL-92.

Crystallographic data (excluding structure factors) for the structure reported in this paper have been deposited with the Cambridge Crystallographic Data Centre as supplementary publication no. CCDC-100939. Copies of the data can be obtained free of charge on application to The Director, CCDC, 12 Union Road, Cambridge CB2 1EZ, UK [fax: int. code +44(1223)336-033, e-mail: deposit@ccdc.cam.ac.uk].

☆ Dedicated to Professor *Heinrich Nöth* on the occasion of his 70th birthday.

[1] W. R. Roth, H.-W. Lennartz, W. v. E. Doering, L. Birladeanu, C. A. Guyton, T. Kitegawe, *J. Am. Chem. Soc.* **1990**, *112*, 1722; W. v. E. Doering, T. Kitegawa, *J. Am. Chem. Soc.* **1991**, *113*, 4288; W. v. E. Doering, W. R. Roth, F. Bauer, M. Boenke, R. Breuckmann, J. Ruhkamp, O. Wortmann, *Chem. Ber.* **1991**, *124*, 1461; W. R. Roth, O. Adamczak, R. Breuckmann, H.-W. Lennartz, R. Boese, *Chem. Ber.* **1991**, *124*, 2499.

[2] H. Sinn, W. Kaminsky, *Adv. Organomet. Chem*. **1980**, *18*, 99; R. F. Jordan, *Adv. Organomet. Chem*. **1991**, *32*, 325; M. Aulbach, F. Küber, *Chemie Unserer Zeit* **1994**, *28*, 197; H.-H. Brintzinger, D. Fischer, R. Mülhaupt, B. Rieger, R. Waymouth, *Angew. Chem.* **1995**, *107*, 1255; *Angew. Chem., Int. Ed. Engl*. **1995**, *34*, 1143; M. Bochmann, *J. Chem. Soc., Dalton Trans.* **1996**, 255 and references cited in these articles.

[3] J. J. Eisch, A. M. Piotrowski, S. K. Brownstein, E. J. Gabe, F. L. Lee, *J. Am. Chem. Soc.* **1985**, *107*, 7219; C. McDade, J. E. Bercaw, *J. Organomet. Chem*. **1985**, *279*, 281. A. D. Horton, A. G. Orpen, *Organometallics* **1991**, *10*, 3910; *Organometallics* **1992**, *11*, 8; A. S. Guram, Z. Guo, R. F. Jordan, *J. Am. Chem. Soc.* **1993**, *115*, 4902; A. S. Guram, R. F. Jordan, D. F. Taylor, *J. Am. Chem. Soc.* **1991**, *113*, 1833; R. Beckhaus, J. Sang, T. Wagner, B. Ganter, *Organometallics* **1996**, *15*, 1176.

[4] W. Ahlers, B. Temme, G. Erker, R. Fröhlich, F. Zippel, *Organometallics* **1997**, *16*, 1440.

[5] B. Temme, G. Erker, R. Fröhlich, M. Grehl, *Angew. Chem*. **1994**, *106*, 1570, *Angew. Chem. Int. Ed. Engl*. **1994**, *33*, 1480; B. Temme, G. Erker, R. Fröhlich, M. Grehl, *J. Chem. Soc., Chem. Commun*. **1994**, 1713; W. Ahlers, B. Temme, G. Erker, R. Fröhlich, T. Fox, *J. Organomet. Chem*. **1997**, *527*, 191.

[6] J. C. W. Chien, W.-M. Tsai, M. D. Rausch, *J. Am. Chem. Soc.* **1991**, *113*, 8570.

[7] A. G. Massey, A. J. Park, F. G. A. Stone, *Proceedings Chem. Soc*. **1963**, 212; A. G. Massey, A. J. Park, *J. Organomet. Chem*. **1964**, *2*, 245; A. G. Massey, A. J. Park, *Organometallic Synthesis* (Eds.: R. B. King, J. J. Eisch), Elsevier, New York, **1986**, Vol. 3, p. 461.

[8] X. Yang, C. L. Stern, T. J. Marks, *J. Am. Chem. Soc.* **1994**, *116*, 10015.

[9] G. Erker, W. Ahlers, R. Fröhlich, *J. Am. Chem. Soc*. **1995**, *117*, 5853; W. Ahlers, G. Erker, R. Fröhlich, F. Zippel, *Chem. Ber.* **1997**, *130*, 1079.

[10] P. C. Wailes, H. Weigold, A. P. Bell, *J. Organomet. Chem*. **1971**, *27*, 373; J. Schwartz, *Pure Appl. Chem*. **1980**, *52*, 733; J. Jubb, J. Song, D. Richeson, S. Gambarotta, *Comprehensive Organometallic Chemistry*, (Eds.: E. W. Abel, F. G. A. Stone, G. Wilkinson), Pergamon, New York, **1995**, Vol. 4, p.556−572.

[11] H. S. Gutowsky, C. H. Holm, *Chem. Phys.* **1956**, *25*, 1228; M. L. H. Green, L.-L. Wong, A. Sella, *Organometallics* **1992**, *11*, 2660, and references cited therein.

[12] [12a] Z. Wu, R. F. Jordan, J. L. Petersen, *J. Am. Chem. Soc.* **1995**, *117*, 5867; C. P. Casey, S. L. Hallenbeck, D. W. Pollock, C. R. Landis, *J. Am. Chem. Soc.* **1995**, *117*, 9770; C. P. Casey, S. L. Hallenbeck, J. M. Wright, C. L. Landis, *J. Am. Chem. Soc.* **1997**, *119*, 9680. – [12b] B. Temme, J. Karl, G. Erker, *Chem. Eur. J.* **1996**, *2*, 919; J. Karl, G. Erker, *J. Mol. Catal*. in press; J. Karl, G. Erker, *Chem. Ber.* **1997**, *130*, 1261.

[13] J. Ruwwe, G. Erker, R. Fröhlich, *Angew. Chem*. **1996**, *108*, 108, *Angew. Chem. Int. Ed. Engl.* **1996**, *35*, 80.

[14] From the observed experimental data two slightly different stereochemical situations can be envisaged for the characterization of **14**. If the C(sp^2)-B(C_6F_5)$_3$ unit (under ″frozen″ static NMR conditions) contains a *chiral* borate propeller geometry, than two diastereomeric isomers of **14** would result. However, it could also be possible that the C(sp^2)-B(C_6F_5)$_3$ unit favours a *prochiral* conformation that only leads to 15 diastereotopic ^{19}F NMR signals due to the presence of the adjacent chiral metal complex framework (for a discussion of such an example see e.g. S. Döring, G. Erker, R. Fröhlich, O. Meyer, K. Bergander, *Organometallics*, in press.) In the case of **14** we cannot decide between these two alternative stereochemical interpretations at present because it was not possible to identify the minor components of the obtained product mixture.

[15] See for a comparison: C. Valero, M. Grehl, D. Wingbermühle, L. Kloppenburg, D. Carpenetti, G. Erker, J. L. Petersen, *Organometallics* **1994**, *13*, 415.

[16] H. H. Brintzinger, L. S. Bartell, *J. Am. Chem. Soc.* **1970**, *92*, 1105. J. W. Lauher, R. Hoffmann, *J. Am. Chem. Soc.* **1976**, *98*, 1729.

[17] A. S. Guram, D. C. Swenson, R. F. Jordan, *J. Am. Chem. Soc.* **1992**, *114*, 8991; Z. Guo, D. C. Swenson, A. S. Guram, R. F. Jordan, *Organometallics* **1994**, *13*, 766; P. K. Hurlburt, J. J. Rack, J. S. Luck, S. F. Dec, J. D. Webb, O. P. Anderson, S. H. Strauss, *J. Am. Chem. Soc.* **1994**, *116*, 10003; D. M. Antonelli, E. B. Tjaden, J. M. Stryker, *Organometallics* **1994**, *13*, 763.

[18] G. Erker, R. Fröhlich, *Organometallics* **1997**, *16*, 531; T. Brackemeyer, G. Erker, R. Fröhlich, J. Prigge, U. Peuchert, *Chem. Ber.* **1997**, *130*, 899.

[19] [19a] K. Tatsumi, A. Nakamura, P. Hofmann, P. Stauffert, R. Hoffmann, *J. Am. Chem. Soc.* **1985**, *107*, 4440. – [19b] R. D.

Adams, D. F. Chodosh, *Inorg. Chem.* **1978**, *17*, 41; G. Erker, *Acc. Chem. Res.* **1984**, *17*, 103; F. H. Elsner, T. D. Tilley, *J. Organomet. Chem.* **1988**, *358,* 169; review; L. D. Durfee, I. P. Rothwell, *Chem. Rev.* **1988**, *88,* 1059; G. Erker, R. Zwettler, C. Krüger, *Chem. Ber.* **1989**, *122,* 1377; R. F. Jordan, D. F. Taylor, *J. Am. Chem. Soc.* **1989**, *111,* 778; R. F. Jordan, D. F. Taylor, N. C. Baenziger, *Organometallics* **1990**, *9,* 1546; A. S. Guram, R. F. Jordan, *Organometallics* **1990**, *9,* 2116, 2190; S. M. Beshouri, D. E. Chebi, P. E. Fanwick, I. P. Rothwell, J. C. Huffman, *Organometallics* **1990**, *9,* 2375; F. R. Lemke, D. J. Szakla, R. M. Bullock, *Organometallics* **1992**, *11,* 876; A. S. Guram, R. F. Jordan, *J. Org. Chem.* **1993**, *58,* 5595; P. G. Cozzi, T. Carofiglio, C. Floriani, A. Chiesi-Villa, C. Rizzoli, *Organometallics* **1993**, *12,* 2845; A. S. Guram, Z. Guo, R. F. Jordan, *Organometallics* **1991**, *10,* 3470.

[20] D. S. Stephenson, G. Binsch, DNMR5: A Computer Program for Iterative Analysis of Exchange-Broadened NMR spectra, *QCPE* **1978**, *10*, 365; G. Binsch, *Dyn. Nucl. Magn. Reson. Spectrosc*. **1975**, 45; G. Binsch, H. Kessler, *Angew. Chem.* **1980**, *92*, 455; *Angew. Chem., Int. Ed. Engl*. **1980**, *11*, 2660, and references cited therein.

[21] B. Temme, G. Erker, J. Karl, H. Luftmann, R. Fröhlich, S. Kotila, *Angew. Chem*. **1995**, *107*, 1867; *Angew. Chem. Int. Ed. Engl*. **1995**, *34*, 1755; J. Karl, G. Erker, R. Fröhlich, *J. Organomet. Chem*. **1997**, *535*, 59; J. Karl, G. Erker, R. Fröhlich, *J. Am. Chem. Soc.* **1997**, *119*, 11165.

[22] S. Braun, H. Kalinowski, S. Berger, *100 and More Basic NMR Experiments*, VCH, Weinheim **1996**, and references cited therein.

[98003]

Transition Metal Stannyl Complexes, 12[◇]

Chelate-Assisted Oxidative Addition of Phenyl- and Alkyltin Groups to Nickel and Platinum

Hilmar Gilges and Ulrich Schubert*

Institut für Anorganische Chemie, Technische Universität Wien,
Getreidemarkt 9, A-1060 Wien, Austria
Fax: (internat.) + 43(0)1/5816668
E-mail: uschuber@fbch.tuwien.ac.at

Received January 19, 1998

Keywords: Platinum / Nickel / Stannyl complexes / Oxidative addition / Tin

Reaction of $Ni(COD)_2$ (COD = 1,5-cyclooctadiene) with two equivalents of $Ph_2PCH_2CH_2SnPh_3$ or of $(Ph_3P)_2Pt(C_2H_4)$ with two equivalents of $Ph_2PCH_2CH_2SnR_3$ (R = Ph, Me, Bu) results in the immediate formation of the complexes $(R_3SnCH_2CH_2Ph_2P)M[PPh_2CH_2CH_2SnPh_2(M–Sn)](R)$ (M = Ni, Pt) with a *cis* arrangement of the two phosphorus atoms. The structure of $(Me_3SnCH_2CH_2Ph_2P)Pt[PPh_2CH_2CH_2SnMe_2(Pt–Sn)](Me)$ was confirmed by an X-ray structure analysis. In the presence of PPh_3, this complex shows dynamic behavior in solution due to $Ph_2PCH_2CH_2SnMe_3$/PPh_3 exchange. When the phosphanylalkylstannanes $Ph_2PCH_2CH_2SnPh_{3-x}Me_x$ (x = 1, 2) are employed in the reaction with $Ni(COD)_2$ or $(Ph_3P)_2Pt(C_2H_4)$, the Sn–Ph groups are more prone to oxidative addition than the Sn–Me groups. When $Ni(COD)_2$ is treated with one equivalent of $Ph_2PCH_2CH_2SnPh_3$ and PR'_3 (PCy_3 or PMe_2Ph) each, the complexes $(R'_3P)M(PPh_2CH_2CH_2SnPh_2)(Ph)(M–Sn)$ are formed. Heating of $(Ph_3SnCH_2CH_2Ph_2P)Ni[PPh_2CH_2CH_2SnPh_2(Ni–Sn)](Ph)$ to 70 °C induces the oxidative addition of a Sn–Ph group of the dangling ligand, and *cis*-$Ni[PPh_2CH_2CH_2SnPh_2(Ni–Sn)]_2$ is obtained. The same complex is formed upon reaction of $Ni(COD)_2$ with $Ph_2PCH_2CH_2SnPh_2H$. Reaction of $Ni(COD)_2$ with $Ph_2PCH_2CH_2SnMe_3$ results in the immediate formation of *trans*-$Ni[(PPh_2CH_2CH_2SnMe_2(Ni–Sn)]_2$.

Contrary to Sn−H bonds that readily add to a variety of transition-metal complex fragments,[2] there are only few examples for the oxidative addition of non-activated Sn−C bonds. For example, $SnPh_4$ only adds to electron-rich fragments such as $(Ph_3P)_2Pt$ to give $(Ph_3P)_2Pt(SnR_3)(Ph)$.[3][4][5] Sn−Me bonds are even less reactive than Sn−Ph bonds.[6] The weaker Sn−C bonds in alkynylstannanes also add to less electron-rich metal centers.[7][8]

One of the possibilities to promote oxidative addition reactions is "chelate assistance", introduced by Stobart et al. for phosphanylalkylsilyl ligands with Si−H bonds.[9] We previously used this option to add Sn−C bonds to electron-rich Pd and Pt fragments[10] as well as to the less reactive $Fe(CO)_4$ fragment,[11] using ligands of the type $Ph_2P(CH_2)_nSnR_3$. Richmond et. al. observed reversible Sn−Ph addition in the reaction of a $SnPh_3$-substituted ethylenediamine derivative with $W(CO)_3(CH_3CN)_3$.[12] The concept was also extended to Si−Si and Si−Sn bonds.[13][14]

In the present paper, we first describe the reaction of $Ni(COD)_2$ with $Ph_2PCH_2CH_2SnR_3$. The results led us to re-examine some of our experiments with Pt compounds and to correct some of our previous results.[10]

[◇] Part 11: Ref.[1].

Results and Discussion

When $Ni(COD)_2$ (COD = 1,5-cyclooctadiene) was treated with two equivalents of $Ph_2PCH_2CH_2SnPh_3$ in THF, the color of the yellow solution changed to deep orange, and a broad signal in the ^{31}P-NMR spectrum at $\delta \approx 28$ indicated the immediate formation of phosphanenickel complexes. Additional stirring for 2.5 h resulted in the almost quantitative formation of the oxidative addition product **1** (Eq. 1) according to the ^{31}P-NMR spectrum.

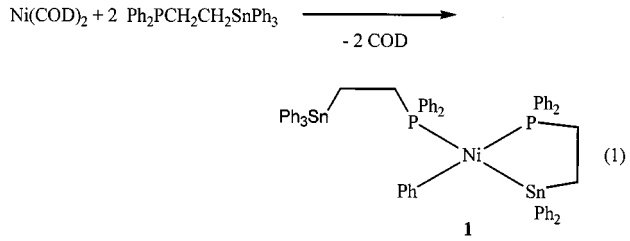

(1)

1

We were not able to separate traces of $Ph_2P(O)CH_2CH_2SnPh_3$ and unreacted $Ph_2PCH_2CH_2SnPh_3$. However, the structure of the complex was unequivocally confirmed by multinuclear NMR spectroscopy. The spectra are discussed in detail in the following paragraph because they are representative for most of the complexes reported in this paper.

 © WILEY-VCH Verlag GmbH, D-69451 Weinheim, 1998 1434−1948/98/0707−0897 $ 17.50+.50/0

The $^{31}P\{^1H\}$-NMR spectrum of **1** showed the expected two doublet signals of an AB system. The resonance at δ = 58.3 is attributed to the phosphorus atom in a five-membered ring because of the significant downfield shift of ca. 32 ppm relative to the resonance of the other phosphorus nucleus at δ = 26.1. This downfield shift is a well-known phenomenon upon chelation,[15] and was also observed in the related Pt complexes $Pt[Ph_2PCH_2CH_2SiR_2(Pt-Si)]_2$[9] and $(Ph_3P)Pt(Ph_2PCH_2CH_2SiR_2)(SiR_3)(Pt-Si)$.[13] The $^2J_{PNiP}$ coupling constant of 6.1 Hz proved the *cis* disposition of the phosphorus nuclei. The $J_{117/119SnP}$ coupling constant of 219.8 Hz between the Sn and P nucleus at δ = 58.3 of the chelate ring is typical for the *cis* position of both nuclei. On the other hand, the signal at δ = 26.1 showed the typical *trans*-$^2J_{SnNiP}$ (^{117}Sn: 1065.9 Hz; ^{119}Sn: 1109.3 Hz) and an additional set of Sn satellites attributed to the $^3J_{117/119SnCCP}$ coupling within the dangling ligand. The NMR data confirm the *trans* position of the non-chelated ligand and the metal-bonded tin atom. The ^{119}Sn-NMR spectrum corroborates the assignment of the phosphorus resonances by showing a doublet of doublets at δ = 23.6 for the tin atom bound to nickel, with *trans* $^2J_{119SnNiP}$ of 1116.9 Hz and J_{SnP} of 223 Hz. This resonance is distinctly shifted downfield by ca. 120 ppm relative to the resonance at δ = −97.6 for the non-coordinated $SnPh_3$ group. This resonance appears as a doublet with the appropriate $^3J_{119SnCCP}$ of 183.8 Hz.

The ^{1}H-NMR spectrum lacked essential structural information because the methylene proton signals appear as complex multiplets superimposing each other (see Experimental Section). The only interesting feature is the resonance of the protons of the *Ni*-bonded phenyl group. Their multiplet was significantly shifted to higher field (δ = 6.75−7.05), compared to the other phenyl resonances. This highfield shift seems to be a typical phenomenon for complexes of this kind because it is also reported for $(CO)_3Fe(Ph_2PCH_2CH_2SnPh_2)(Ph)(Fe-Sn)$[11] and $(Ph_3P)Pt(Ph_2PCH_2CH_2SnPh_2)(Ph)(Pt-Sn)$.[10] The ^{13}C-NMR spectrum confirms that there are two different phosphanylalkylstannane units in the molecule because of two separate resonances for the $SnCH_2$ and the PCH_2 group. While the resonances for the methylene carbon atoms of the dangling ligand appear as doublets due to the coupling with the phosphorus atom within the ligand, the resonances of the CH_2 groups of the chelating ligand appear as doublet of doublets because of the additional coupling with the other phosphorus nucleus. This observation seems reasonable if one takes into account that in this case the second phosphorus atom is in a kind of *transoid* position with respect to the carbon nuclei while in the first case the second phosphorus nucleus is *cisoid*. In the very complex range of the phenyl carbon signals no assignment for the *ipso*-carbon atom of the metal-bonded phenyl group was possible.

Since the second $Ph_2PCH_2CH_2SnPh_3$ in **1** just acts as a monodentate ligand, we also treated $Ni(COD)_2$ with a 1:1 mixture of $Ph_2PCH_2CH_2SnPh_3$ and $PPhMe_2$ or PCy_3 (Eq. 2). $(PhMe_2P)Ni(Ph_2PCH_2CH_2SnPh_2)(Ph)(Ni-Sn)$ (**2**) was

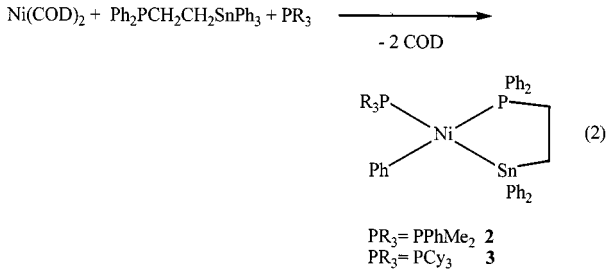

formed in 90% yield (^{31}P NMR) together with **1** and a small amount of $PhP(O)Me_2$ as by-products.

Unfortunately, **2** was even more difficult to purify than **1**. The reaction of PCy_3 resulted in almost quantitative formation of $(Cy_3P)Ni(Ph_2PCH_2CH_2SnPh_2)(Ph)(Ni-Sn)$ (**3**) (^{31}P-NMR). It was possible to isolate the complex analytically pure as a yellow-brown powder by column chromatography. Contrary to **1**, it was even possible to assign the resonance for the *ipso*-carbon atom of the metal-bonded phenyl group. It appears at δ = 155.6 (dd) with two $^2J_{PNiC}$ couplings of 59.2 and 7.9 Hz due to the *trans*- and *cis*-phosphorus nuclei. These values are in good agreement with those found for the *ipso*-carbon atom in $(Me_3P)_2Ni[CH_2C(CH_3)_2C_6H_4(Ni-C)]$ (δ = 171.1, *trans*-$^2J_{PNiC}$ = 79 Hz).[16]

In the reaction with $Ph_2PCH_2CH_2SnPh_3$, nickel resembles platinum and does not parallel the reactivity pattern of palladium that formed the product of a double oxidative SnPh addition and consecutive reductive biphenyl elimination, *trans*-$Pd[Ph_2PCH_2CH_2SnPh_2(Pd-Sn)]_2$.[10] Therefore, the possibility to induce a second SnPh oxidative addition was probed. Crude **1** was dissolved in toluene and heated to about 70°C for 9 h. Monitoring the reaction by ^{31}P-NMR spectroscopy showed a new singlet resonance at δ = 63.3 with a double set of tin satellites. The coupling constants of 930.1 Hz (^{119}Sn), 891.0 Hz (^{117}Sn), and 161.1 Hz ($^{119/117}$Sn) are in the typical range for a *trans*- and a *cis*-tin nucleus relative to the phosphorus atoms, thus excluding *trans*-$Ni[Ph_2PCH_2CH_2SnPh_2(Ni-Sn)]_2$.

The singlet resonance in the ^{31}P-NMR spectrum is due to two equivalent phosphorus nuclei in molecules where both tin atoms are ^{118}Sn isotopes. A doublet-of-doublet resonance at δ = 56.8 was observed (*trans*-J_{119SnP} = 933.3 and *cis*-J_{119SnP} = 164.0 Hz) in the ^{119}Sn-NMR spectrum. Even if one takes into account that the values given for the couplings are based on a first-order interpretation of the spectra because the resolution was too poor to observe all couplings needed for a interpretation as an ABXY spin system, the data clearly indicate the formation of the *cis* product **4** resulting from the oxidative addition of a second Sn−Ph bond (Eq. 3). Unfortunately, the course of the reaction was not completely straightforward because some decomposition occurred, and the resulting product still contained small amounts of **1** besides the impurities present in the starting complex.

We therefore prepared **4** independently from $Ni(COD)_2$ with two equivalents of $Ph_2PCH_2CH_2SnPh_2H$, utilizing the fact that Sn−H bonds are more prone to oxidative addition

than Sn−C bonds. On addition of the phosphanylalkylstannane at room temperature, the color of the solution changed immediately, and gas evolution was observed after a short period. The yellow oil resulting after work-up showed the same resonances in the ^{31}P- and ^{119}Sn-NMR spectra as were observed in the thermal reaction of **1**. This proves that for SnH the second oxidative addition is facilitated, as expected (Eq. 3).

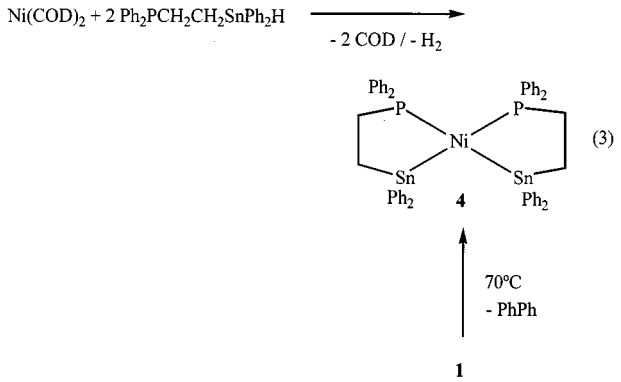

(3)

In the reaction of $Pd(PPh_3)_4$ with either $Ph_2PCH_2CH_2SnPh_3$ or $Ph_2PCH_2CH_2SnMe_3$, the *trans* complexes $Pd[PPh_2CH_2CH_2SnR(Pd-Sn)]_2$ were formed.[10] Because of the somewhat surprising formation of the *cis* product **4** from **1** at elevated temperatures the question arises which isomer is obtained when $Ph_2PCH_2CH_2SnMe_3$ is treated with $Ni(COD)_2$ (Eq. 4).

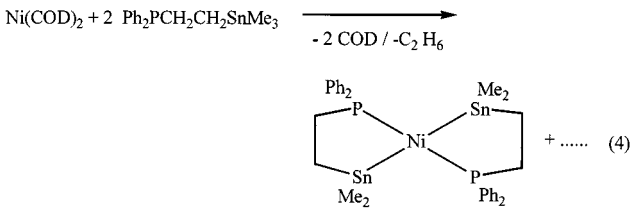

(4)

The ^{31}P-NMR spectrum of the residue obtained after removal of all volatiles showed two resonances. The one at $\delta = 30.6$ with an Sn coupling of 149 Hz was assigned to $Ph_2P(O)CH_2CH_2SnMe_3$ as shown by the ^{31}P-NMR spectrum of a sample of $Ph_2P(O)CH_2CH_2SnMe_3$, independently prepared by oxidation of the phosphane with H_2O_2. Despite of the fact that all solvents were thoroughly dried and degassed, and air was excluded as far as possible by standard Schlenk techniques, it was impossible to suppress the formation of phosphane oxides completely. The fact that Ni^0 complexes, that are intermediates in the reactions, are very good catalysts in the phosphane oxidation by oxygen may be the reason that even very small traces of air led to significant phosphane oxidation. The singlet resonance at $\delta = 41.5$ was assigned to *trans*-$Ni[Ph_2PCH_2CH_2SnMe_2(Ni-Sn)]_2$ because of the typical *cis* coupling to $^{117/119}$Sn of 137.9 Hz and the equivalence of the two phosphorus nuclei (if both are ^{118}Sn). The *trans* conformation was confirmed by the virtual triplet observed in the ^{119}Sn spectrum at $\delta = 5.9$ due to the inequivalence of the two phosphorus atoms in molecules with a ^{118}Sn and a ^{119}Sn nucleus. The triplet pattern is caused by the fact that $^2J_{SnNiP}$ and the "mixed" $^2J_{SnNiP}/^3J_{SnCCP}$ coupling constant have approximately the same value. Thus, in the case of $Ph_2PCH_2CH_2SnMe_3$, the outcome of the reaction of $Ni(COD)_2$ parallels that of Pd.

Comparing the higher reactivity of Sn−Ph bonds with that of Sn−Me it is somewhat surprising that elevated temperatures are needed to induce oxidative addition of a second Sn−Ph bond while the addition of a second Sn−Me bond takes place at room temperature. This may have steric reasons. Steric effects may also be responsible for the formation of different isomers in both reactions. In the reaction of the $SnPh_3$ derivative, the stereochemical outcome of the reaction is probably controlled by electronic reasons because all atoms bonded to the Ni center are equally substituted by phenyl groups. Contrary to that, steric factors may dominate in the reaction of the trimethylstannyl derivative, leading to the *trans* arrangement that minimizes the steric repulsion between the bulkier phosphane substituents.

The ligand $Ph_2PCH_2CH_2SnPh_2Me$ offers the possibility of either Sn−Ph or Sn−Me addition. Unfortunately, the reaction carried out as before was not straightforward. Nevertheless, the evolution of small amounts of gas was observed during the reaction. The ^{31}P-NMR spectrum of the residue after work-up showed two characteristic doublet resonances at $\delta = 57.9$ and 25.3 ($^2J_{PNiP} = 6.1$ Hz) for the main product. The reasonably close agreement of the NMR data with those of **1** ($\delta = 58.3$, 26.1; $^2J_{PNiP} = 6.1$ Hz) suggested that $(MePh_2SnCH_2CH_2Ph_2P)Ni[(PPh_2CH_2CH_2SnPhMe)(Ni-Sn)](Ph)$ with a dangling phosphanylalkylstannane ligand is the main product. The tin satellites at the downfield signal with $J_{SnP} = 213$ Hz supported this interpretation. However, due to the poor resolution of the spectrum no tin satellites at the highfield signal were observed. A compound with a singlet resonance at $\delta = 42.5$ was formed as a minor product. No tin satellites were resolved at this signal, but it can be supposed that due to the chemical shift and the gas evolution observed during reaction, *trans*-$Ni[Ph_2PCH_2CH_2SnPh_2(Ni-Sn)]_2$ may be the by-product.

The somewhat different results for the oxidative addition of Sn−C bonds to Ni^0 compared to Pd^0 and the fact that we had found complexes of the type $(R_3Si-SiR_2CH_2CH_2Ph_2P)Pt[PPh_2CH_2CH_2SiR_2(Pt-Si)](SiR_3)$ in our previous investigations on chelate-assisted Si−Si oxidative addition to $(Ph_3P)_2Pt(C_2H_4)$, we re-checked the experiments on the Sn−C addition of phosphanylalkylstannanes to Pt^0 published by us some years ago.[10] First, we treated $(Ph_3P)_2Pt(C_2H_4)$ with two molar equivalents of $Ph_2PCH_2CH_2SnPh_3$ according to the published procedure and observed almost quantitative formation of a complex with the ^{31}P-NMR data in good agreement with those previously assigned to $(Ph_3P)Pt[Ph_2PCH_2CH_2SnPh_2-(Pt-Sn)](Ph)$ as product of this reaction. However, on scrutinizing the better data obtained now, we have to correct the assignment. Instead of the PPh_3 derivative, the complex

$(Ph_3SnCH_2CH_2Ph_2P)Pt[PPh_2CH_2CH_2SnPh_2(Pt-Sn)](Ph)$ (**5**) was formed (Eq. 5).

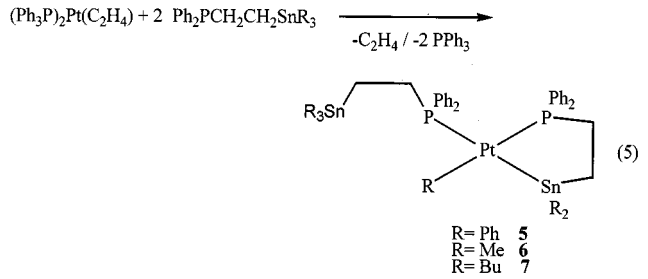

This is confirmed by the fact that a coupling to Sn (179.9 Hz) in the typical range for a $^3J_{SnCCP}$ was now observed at the resonance for the phosphorus of the non-chelated ligand. The ^{119}Sn-NMR spectrum also corroborates that there is a dangling phosphanylalkylstannane ligand because there is an additional doublet at $\delta = -97.5$ with the correct phosphorus coupling besides the doublet of doublets resonance for the chelated tin nucleus at $\delta = 97.2$. Complex **5** corresponds to the analogous Ni complex **1**. It therefore seemed reasonable to study whether a second oxidative Sn−Ph addition is also possible for Pt. However, a toluene solution of **5** heated to 70°C for 10 h and then analyzed by ^{31}P-NMR spectroscopy did not indicate any formation of the product of a second oxidative addition.

This led us to re-examine also the reaction of two equivalents $Ph_2PCH_2CH_2SnMe_3$ with $(Ph_3P)_2Pt(C_2H_4)$, for which we had previously postulated the formation of the Pt^{IV} complex $Pt[PPh_2CH_2CH_2SnMe_2(Pt-Sn)]_2(Me)_2$.[10] On inspection of the better spectroscopic data obtained now we realized that the formerly observed doublet resonance in the ^{119}Sn-NMR spectrum is contradicting the proposed structure. The product was instead the Pt^{II} complex $(Me_3SnCH_2CH_2Ph_2P)Pt[PPh_2CH_2CH_2SnMe_2(Pt-Sn)](Me)$ (**6**) (Eq. 5). The spectrum of the yellow oil left after removal of all volatiles from the reaction mixture mainly showed two broad resonances at $\delta \approx 55$ and 27, and a broad signal at $\delta = -3$ in the ^{31}P-NMR spectrum. The signals sharpened on lowering the temperature, and at 240 K the dynamic process was completely frozen. At this temperature, the expected spectrum for **6,** the typical AB pattern with the corresponding Sn satellites, was observed in addition to a sharp resonance for free PPh_3. The fact that the resonances of the dangling phosphorus ligand and the PPh_3 continually broaden on rising the temperature from 240 K to 360 K while the resonance of the ring-integrated phosphorus first broadens to a much smaller extend, and then re-sharpens (starting at about 310 K) indicates that the dynamic process is a $Ph_2PCH_2CH_2SnMe_3/PPh_3$ exchange at the Pt^{II} center. This suggestion is in agreement with results obtained for the complexes *cis*-$(Ph_3P)_2Pt(SiR_3)(H)$ where similar interchange processes with excess PPh_3 were observed[17]. The authors also observed the phenomenon that the resonance of the PPh_3 ligand *cis* to the silyl ligand that does not take part in the dynamic process is only slightly broadened.

To elucidate the role of the PPh_3 in the dynamic process, **6** was independently prepared from $Pt(COD)_2$. As expected, the product **6** formed in almost quantitative yield showed no dynamic features at room temperature because of the absence of PPh_3. On addition of PPh_3, a dynamic process was initiated similar to that observed for the product resulting from the reaction of $(Ph_3P)_2Pt(C_2H_4)$ at room temperature.

Colorless crystals of **6** suitable for an X-ray crystal structure analysis were obtained by diffusion of heptane into a concentrated benzene solution of the complex. The structure analysis proved the *cis* arrangement of the two phosphorus ligands with one dangling phosphanylalkylstannane (Figure 1). The Pt−C(1) distance [214 (1) pm] is in the normal range for $Pt-CH_3$ compounds (202−220 pm).[18]The Pt−Sn(1) bond length of 259.36(8) pm is significantly shorter than that in *trans*-$(Ph_3P)_2Pt(SnPh_3)(H)$ (265.4 pm).[19] This difference is reasonable if one takes into account the different influence of a hydride and a phosphane ligand. The P(1)−Pt−P(2) angle is widened [104.30(9)°] due to the steric repulsions between the bulky phenyl groups at the phosphorus atoms. This distortion from the regular square-planar arrangement is compensated by the angles C(1)−Pt−P(2), C(1)−Pt−Sn(1) and P(1)−Pt−Sn(1) being smaller than 90° [87.8(3), 85.3(3), and 82.55(7)°]. The latter is partially due to chelation. The methyl groups at the tin atom of the dangling ligand are disordered in the crystal.

Figure 1. ORTEP diagram of **6**; the hydrogen atoms are omitted for clarity[a]

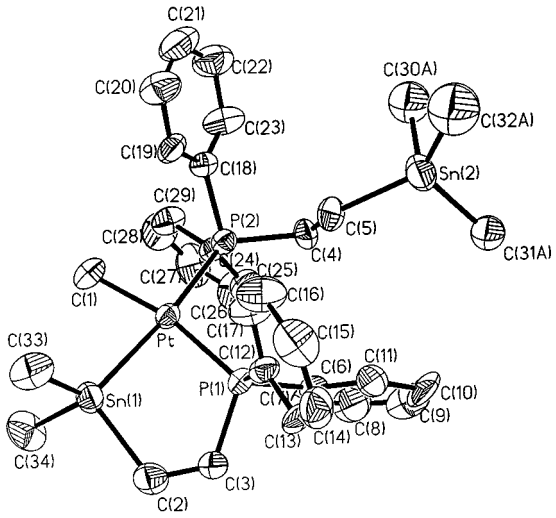

[a] Selected bond lengths [pm] and angles [°]: Pt−C(1) 213.7(11), Pt−P(1) 227.4(3), Pt−P(2) 232.7(3), Pt−Sn(1) 259.36(8), Sn(1)−C(2) 213.7(11), P(1)−C(3) 184.5(10), P(2)−C(4) 187.2(9), Sn(2)−C(5) 213.1(10), Sn(1)−C(33) 213.0(11), Sn(1)−C(34) 215.0(12); C(1)−Pt−P(1) 167.4(3), C(1)−Pt−P(2) 87.8(3), P(1)−Pt−P(2) 104.30(9), C(1)−Pt−Sn(1) 85.3(3), P(1)−Pt−Sn(1) 82.55(7), P(2)−Pt−Sn(1) 173.13(7), C(33)−Sn(1)−C(34) 104.4(5), C(33)−Sn(1)−C(2) 109.2(5), C(34)−Sn(1)−C(2) 106.4(5), C(33)−Sn(1)−Pt 118.2(3), C(34)−Sn(1)−Pt 115.6(4), C(2)−Sn(1)−Pt 102.5(3), C(24)−P(2)−Pt 110.8(3), C(18)−P(2)−Pt 115.3(4), C(4)−P(2)−Pt 121.3(4), C(12)−P(1)−C(3) 103.7(5), C(6)−P(1)−C(3) 100.2(4), C(12)−P(1)−Pt 114.6(3), C(6)−P(1)−Pt 120.0(4), C(5)−C(4)−P(2) 114.8(7), C(3)−C(2)−Sn(1) 107.9(8), C(2)−C(3)−P(1) 113.2(7), C(4)−C(5)−Sn(2) 113.9(7).

Attempts to induce the oxidative addition of one of the SnMe bonds of the dangling ligand by heating a toluene solution of **6** to about 90°C for 10 h failed. The ^{31}P-NMR spectrum did not indicate any reaction.

Contrary to the results obtained for Ni^0, an increase of the steric bulk at the Sn atom by changing the methyl groups in the phosphanylethylstannane against butyl groups did not influence the general outcome of the reaction. Besides the main product $(Bu_3SnCH_2CH_2Ph_2P)Pt[PPh_2CH_2CH_2SnBu_2(Pt-Sn)](Bu)$ (**7**) (formed in 90% yield according to the ^{31}P-NMR spectrum), a minor amount of $(Ph_3P)Pt[PPh_2CH_2CH_2SnBu_2(Pt-Sn)](Bu)$ was observed as a by-product [^{31}P NMR(C_6D_6): δ = 53.9 (d, $^2J_{PPtP}$ = 9.7 Hz, $J_{117/119SnP}$ = 105.0 Hz, $^1J_{PtP}$ = 1914.1 Hz), 32.1 (d, $^2J_{PPtP}$ = 9.7 Hz, $^2J_{119SnNiP}$ = 1666.3 Hz, $^2J_{117SnPtP}$ = 1597.9, $^1J_{PtP}$ = 2119.2].

The use of the previously unknown derivative $Ph_2PCH_2CH_2SnMe_2Ph$, synthesized similar to its congeners by radical addition of $PhMe_2SnH$ to $CH_2{=}CHPPh_2$, led to the formation of $(PhMe_2SnCH_2CH_2Ph_2P)Pt[PPh_2CH_2CH_2SnMe_2(Pt-Sn)](Ph)$ (**8**) and thus corroborates the fact that SnPh addition is favored over SnMe addition. The exclusive formation of the product of Sn−Ph activation was proven in the ^{1}H-NMR spectrum by a slightly broadened singlet resonance for the methyl groups at the metal-bonded Sn with a coupling to platinum of 7.3 Hz. This coupling constant was too small a value for $^2J_{PtCH}$, but in good agreement with a $^3J_{PtSnCH}$ coupling. The proton signals of the Pt−Ph moiety once again show the significant high-field shift and appear at δ = 6.87−6.98. The ^{13}C-NMR spectrum in the range for the sp^2-carbon atoms and their Pt satellites is very complex. Therefore, no assignments are possible. The complexes **7** and **8** are not dynamic at room temperature in the presence of PPh_3.

Conclusions

The present and our previous results on corresponding palladium complexes,[10] allow to draw a complete picture on the reactivity pattern of $Ph_2PCH_2CH_2SnR_3$ (R = Me, Ph) with complexes of the zero-valent metals of the nickel triad. For R = phenyl, the reactivity of $Ni(COD)_2$ parallels that of $(Ph_3P)_2Pt(C_2H_4)$. Complexes of the type $(Ph_3SnCH_2CH_2Ph_2P)M[PPh_2CH_2CH_2SnPh_2(M-Sn)](Ph)$ [M = Ni (**1**), Pt (**5**)], with a dangling $Ph_2PCH_2CH_2SnR_3$ ligand and a *cis* disposition of the two phosphorus atoms, were formed in both cases. For the nickel complex **1**, the oxidative addition of an Sn−Ph bond of the dangling $Ph_2PCH_2CH_2SnR_3$ ligand was observed at elevated temperatures during which the *cis* arrangement of the phosphorus atoms was retained. The resulting complex is *cis*-$Ni[PPh_2CH_2CH_2SnPh_2(Ni-Sn)]_2$ (**4**). The same reaction was not observed for the corresponding Pt complex **5**. The higher reactivity of Ni for the formation of the second chelate ring by oxidative addition of an Sn−Ph bond of the dangling phosphanylalkylstannyl ligand is somewhat surprising, because the heavier metals in a group are more prone to oxidative addition reactions. The driving force for the formation of **4** from **1** therefore may be the easier reductive elimination of biphenyl from the intermediate Ni^{IV} complex.

In the corresponding reactions of the tri*methyl*stannyl derivative $Ph_2PCH_2CH_2SnMe_3$ the reactivity pattern of $Ni(COD)_2$ parallels that of $Pd(PPh_3)_4$. In both cases the bischelated complexes *trans*-$M[PPh_2CH_2CH_2SnMe_2(M-Sn)]_2$ were formed, while the reaction with $(Ph_3P)_2Pt(C_2H_4)$ stopped at the stage of the mono-chelated complex *cis*-$(Me_3SnCH_2CH_2Ph_2P)Pt[(PPh_2CH_2CH_2SnMe_2)(Pt-Sn)](Me)$ (**6**). The change in geometry of $Ni[PPh_2CH_2CH_2SnMe_2-(Ni-Sn)]_2$ compared to the $SnPh_2$ derivative (**4**) is probably caused by steric effects overriding the electronic preference of the *cis* isomer.

When the phosphanylalkylstannanes $Ph_2PCH_2CH_2-SnPh_{3-x}Me_x$ (x = 1, 2) are employed, there is the possibility of either Sn−Ph or Sn−Me oxidative addition. For both Ni^0 and Pt^0, the Sn−Ph groups are more prone to oxidative addition than the Sn−Me groups, as was previously observed by us for Fe complexes.[11]

Complex **6**, whose structure was unambiguously confirmed by an X-ray structure analysis, showed dynamic behavior in the presence of PPh_3 that may be attributed to a $PPh_3/Ph_2PCH_2CH_2SnMe_3$ exchange process.

This work was supported by the *Fonds zur Förderung der wissenschaftlichen Forschung* (*FWF*). We thank Dr. *K. Mereiter* for valuable discussions.

Experimental Section

All operations were carried under dry and oxygen-free argon by standard Schlenk-tube techniques. All solvents were dried by standard procedures, saturated with argon and stored over molecular sieves. The THF used was freshly distilled from potassium. The phosphanylalkylstannanes were synthesized according to literature procedures[11][20] from $Ph_2P(C_2H_3)$ and $HSnR_3$. − The NMR spectra were recorded with a Bruker AC 250 spectrometer. ^{1}H- and ^{13}C-NMR data were referenced against the solvent resonances, while ^{31}P- and ^{119}Sn-NMR data were referenced against the external standards 85% H_3PO_4 and $SnMe_4$. Integrations of the ^{1}H-NMR signals are omitted if there are overlaps with residual proton resonances of the deuterated solvents (especially C_6D_6). − DSC analyses were performed with a Shimadzu Thermal Analyzer DSC 50. The expression J_{XY} is used for those cases where coupling is possible through different nuclei.

Preparation of (Ph$_3$SnCH$_2$CH$_2$PPh$_2$)Ni(Ph)[Ph$_2$PCH$_2$CH$_2$-SnPh$_2$(Ni−Sn)] (**1**): An amount of 922 mg (1.63 mmol) of $Ph_2PCH_2CH_2SnPh_3$ was added to a solution of 213 mg (0.77 mmol) of $Ni(COD)_2$ in 25 ml of THF. The color of the yellow solution immediately turned to deep orange. After additional 2.5 h of stirring at room temperature, the reaction mixture was yellowish brown. Then the solvent and most of the COD was removed in vacuo at 40°C, leaving a slightly oily golden brown residue that contained **1** as the main product, according to the ^{31}P-NMR spectrum. Neither recrystallisation nor column chromatography on silica with common organic solvents resulted in analytically pure samples of **1**. − ^{31}P NMR (101.25 MHz, C_6D_6): δ = 58.3 (d, $^2J_{PNiP}$ = 6.1 Hz, $J_{117/119SnP}$ = 219.8 Hz), 26.1 (d, $^2J_{PNiP}$ = 6.1 Hz, $^2J_{119SnNiP}$ = 1109.3 Hz, $^2J_{117SnNiP}$ = 1065.9 Hz, $^3J_{SnCCP}$ = 183.0 Hz). − ^{119}Sn NMR (93.276 MHz, C_6D_6) δ 23.6 (dd, $^2J_{SnNiP}$ = 1116.7 Hz, J_{SnP} = 223 Hz), −97.6 (d, $^3J_{SnCCP}$ = 183.8 Hz). − ^{13}C NMR (62.90 MHz, C_6D_6): δ = 3.9 (d, $SnCH_2$, $^2J_{PCC}$ = 5.1 Hz),

6.3 (dd, $SnCH_2$, $^2J_{PCC}$ = 31.7 Hz, J_{PC} = 13.4 Hz), 23.7 (d, PCH_2, $^1J_{PC}$ = 11.5 Hz), 32.6 (dd, PCH_2, $^1J_{PC}$ = 24.5 Hz, J_{PC} = 7.9 Hz), 127.8−146.5 (C_6H_5). − ^{1}H NMR (250.130 MHz, C_6D_6): δ = 1.01−1.38 (m, overlapping $SnCH_2$), 1.59−1.84 (m, PCH_2), 2.40−2.61 (m, PCH_2), 6.75−7.05 (m, NiC_6H_5), 7.00−7.62 (m, C_6H_5).

Preparation of (PhMe$_2$P)Ni(Ph)[Ph$_2$PCH$_2$CH$_2$SnPh$_2$(Ni−Sn)] (**2**): A solution of 51 mg (0.37 mmol) of $PhPMe_2$ and 207 mg (0.37 mmol) of $Ph_2PCH_2CH_2SnPh_3$ in 6 ml of THF was added to a solution of 101 mg (0.37 mmol) of $Ni(COD)_2$ in 10 ml of THF. The mixture turned orange and, during further stirring for 4 h, yellow-brown. After removal of all volatiles, a sticky yellowish brown residue was obtained. It contained 90% of **2** and some **1** and $PhP(O)Me_2$ according to the NMR spectra. − ^{31}P NMR (101.25 MHz, C_6D_6): δ = 60.0 (d, $^2J_{PNiP}$ = 4.2 Hz, $J_{117/119SnP}$ = 239.0 Hz), −6.8 (d, $^2J_{PNiP}$ = 4.2 Hz, $^2J_{119SnNiP}$ = 1199.5 Hz, $^2J_{117SnNiP}$ = 1150.3 Hz). − ^{119}Sn NMR (93.276 MHz, C_6D_6): δ = 35.0 (dd, $^2J_{SnNiP}$ = 1199.1 Hz, J_{SnP} = 239.1 Hz). − ^{13}C NMR (62.90 MHz, C_6D_6): δ = 6.2 (dd, $SnCH_2$, $^2J_{PCC}$ = 31.1 Hz, $^3J_{PNiSnC}$ = 11.0 Hz), 12.9 (d, PCH_3, $^1J_{PC}$ = 22.6 Hz), 32.9 (dd, PCH_2, $^1J_{PC}$ = 33.0 Hz, $^3J_{PNiPC}$ = 9.2 Hz, 126.7−146.8 (C_6H_5). − ^{1}H NMR (250.130 MHz, C_6D_6): δ = 0.73 (d, PCH_3, $^2J_{PCH}$ = 6.1 Hz), 1.17−1.33 (m, $SnCH_2$), 2.59−2.78 (m, PCH_2), 6.90−7.73 (m, C_6H_5).

Preparation of (Cy$_3$P)Ni(Ph)[Ph$_2$PCH$_2$CH$_2$SnPh$_2$(Ni−Sn)] (**3**): A solution of 258 mg (0.92 mmol) of PCy_3 and 518 mg (0.92 mmol) of $Ph_2PCH_2CH_2SnPh_3$ in 5 ml benzene was added to a suspension of 252 mg (0.92 mmol) of $Ni(COD)_2$ in 15 ml of heptane. A red-brown solution formed almost immediately. After additional stirring for 4 h, during which the color slightly lightened, the solution was filtered through glass wool. From the resulting deep red solution all volatiles were removed in vacuo. The remaining golden-red oil was chromatographed on silica gel with Et_2O/petroleum ether (1:50). The complex **3** was eluted as a deep yellow zone. After removal of the solvent, 620 mg (75%) of **3** was obtained as a brown-yellow powder. M.p. 69°C (dec.). − $C_{50}H_{62}P_2NiSn$ (902.3): calcd. C 66.6, H 6.93; found C 65.9, H 6.81. − ^{31}P NMR (101.250 MHz, C_6D_6): δ = 51.9 (d, $^2J_{PNiP}$ = 8.6 Hz, J_{119SnP} = 222.2 Hz, J_{117SnP} = 206 Hz), 22.5 (d, $^2J_{PNiP}$ = 8.6 Hz, $^2J_{119SnNiP}$ = 1036.3 Hz, $^2J_{117SnNiP}$ = 991.2 Hz). − ^{119}Sn NMR (93.276 Hz, C_6D_6): δ = 16.7 (dd, $^2J_{119SnNiP}$ = 1036.3 Hz, $^2J_{119SnNiP}$ = 218.7 Hz). − ^{13}C NMR (62.90 MHz, C_6D_6): δ = 5.2 (dd, $SnCH_2$, $^2J_{PCC}$ = 29.6 Hz, $^3J_{PNiSnC}$ = 12.2 Hz), 32.7 (dd, PCH_2 $^1J_{PC}$ = 31.4 Hz, $^2J_{PNiPC}$ = 6.9 Hz), 34.7 (d, $^1J_{PC}$ = 11.6 Hz), 30.7 (s), 27.8 (d, J_{PC} = 9.4 Hz), 26.8 (s), signals of PCy_3, 121.1−156.2 (C_6H_5), 155.6 (dd, NiC, $^2J_{PNiC}$ = 59.2 Hz, $^2J_{PNiC}$ = 7.9 Hz). − ^{1}H NMR (250.130 MHz, C_6D_6): δ = 0.93−0.98 (m, $SnCH_2$, 2 H), 1.15 (s, br.) 1.51−1.80 (m) (cyclohexyl, 33 H), 2.65−2.87 (m, PCH_2, 2 H), 6.95−7.10 (m, NiC_6H_5), 7.07−7.79 (m, C_6H_5).

Thermal Reaction of **1**: An amount of 350 mg of the crude complex **1** was dissolved in 20 ml of toluene and heated in a sealed Schlenk tube for 9 h to 70°C. Then the solvent was removed in vacuo. The oily yellowish brown residue was analyzed by ^{31}P- and ^{119}Sn-NMR spectroscopy, which showed partial formation of $Ni[Ph_2PCH_2CH_2SnPh_2(Ni-Sn)]_2$ (**4**) and some decomposition. The reaction products could not be separated. The NMR data are given in the next paragraph.

Preparation of Ni[(Ph$_2$PCH$_2$CH$_2$SnPh$_2$(Ni−Sn)]$_2$ (**4**) *from Ph$_2$PCH$_2$CH$_2$SnPh$_2$H*: A solution of 400 mg (0.82 mmol) of $Ph_2PCH_2CH_2SnPh_2H$ in 6 ml of THF was added to a yellow solution of 108 mg (0.41 mmol) of $Ni(COD)_2$ in 10 ml of THF. The reaction mixture immediately turned red, and a gas was evolved. During additional 3 h of stirring, the color of the solution lightened to yellowish brown with further weak gas evolution. Then all volatiles were removed in vacuo leaving a yellowish brown oily residue containing **4** in about 85% yield, as confirmed by ^{31}P- and ^{119}Sn-NMR spectroscopy. Washing the residue twice with 3 ml of pentane each left a slightly oily yellowish brown powder that still contained some impurities that could not be removed. − ^{31}P NMR (101.250 MHz, C_6D_6): δ = 63.3 (s, $^2J_{119SnNiP}$ = 930.5 Hz, $^2J_{117SnNiP}$ = 891.1 Hz, $J_{117/119SnP}$ = 161.1 Hz. − ^{119}Sn NMR (93.276 MHz, C_6D_6): δ = 56.8 (dd, $^2J_{PNiSn}$ = 933.3 Hz, J_{SnP} = 164.0 Hz).

Reaction of Ni(COD)$_2$ with Ph$_2$PCH$_2$CH$_2$SnMe$_3$: A solution of 1.47 g (3.86 mmol) of $Ph_2PCH_2CH_2SnMe_3$ in 8 ml of THF was added to a solution of 532 mg (1.93 mmol) of $Ni(COD)_2$ in 40 ml of THF. The resulting red solution was stirred for 3 h during which a gas evolved and the color of the solution deepened. The red-brown solution was concentrated in vacuo, and the resulting yellow-brown slightly sticky residue was analyzed by ^{31}P- and ^{119}Sn-NMR spectroscopy. − ^{31}P NMR (101.250 MHz, C_6D_6): δ = 41.5 (s, J_{SnP} = 137.9 Hz). − ^{119}Sn NMR (93.276 MHz, C_6D_6): δ = 5.9 (t).

Reaction of Ni(COD)$_2$ with Ph$_2$PCH$_2$CH$_2$SnPh$_2$Me: A solution of 1.08g (2.16 mmol) of $Ph_2PCH_2CH_2SnPh_2Me$ in 5 ml of THF was added to 297 mg (1.08 mmol) $Ni(COD)_2$, dissolved in 20 ml of THF. The deep red solution was stirred for 4 h while a small amount of gas was evolved. Removal of all volatiles in vacuo left a brown oil. − ^{31}P NMR (101.250 MHz, C_6D_6): δ = 57.9 (d, $^2J_{PNiP}$ = 6.1 Hz, $J_{117/119SnP}$ = 213 Hz), 25.3 (d, $^2J_{PNiP}$ = 6.1 Hz).

Preparation of (Ph$_3$SnCH$_2$CH$_2$Ph$_2$P)Pt[PPh$_2$CH$_2$CH$_2$SnPh$_2$-(Pt−Sn)](Ph) (**5**): A solution of 193 mg (0.35 mmol) of $Ph_2PCH_2CH_2SnPh_3$ in 3 ml of benzene was added to a solution of 117 mg (0.17 mmol) of $(Ph_3P)_2Pt(C_2H_4)$ in 12 ml of benzene. An immediate color change to bright yellow and gas evolution occurred. The solution was stirred for additional 10 h at room temperature, resulting in a pale yellow solution. A yellow oil remained after removal of all volatiles in vacuo. Complex **5** was obtained as a pale yellow powder on washing the oil three times with 5 ml of petroleum ether each at 0°C and drying in vacuo. Yield 128 mg (57%). M.p. 95°C (dec.). − $C_{64}H_{58}P_2PtSn_2$ (1321.6): calcd. C 58.2, H 4.42; found C 57.9, H 4.30. − ^{31}P NMR (101.250 MHz, C_6D_6): δ = 51.8 (d, $^2J_{PPtP}$ = 11.0 Hz, $^1J_{PtP}$ = 2020.2 Hz, J_{SnP} = 115.0 Hz), 24.1 (d, $^2J_{PPtP}$ = 11.0 Hz, $^1J_{PtP}$ = 2184.9 Hz, $^2J_{119SnPtP}$ = 1712.6 Hz, $^2J_{117SnPtP}$ = 1635.7 Hz, $^3J_{SnCCP}$ = 179.4 Hz). − ^{119}Sn NMR (93.276 MHz, C_6D_6): δ = 97.2 (dd, $^2J_{119SnPtP}$ = 1711.5 Hz, J_{119SnP} = 117.0 Hz), −97.5 (d, $^3J_{119SnCCP}$ = 180.6 Hz). − ^{13}C NMR (62.90 MHz, C_6D_6): δ = 4.1 (d, $^2J_{PCC}$ = 7.5 Hz, $SnCH_2$), 5.2 (dd, $^2J_{PCC}$ = 23.6 Hz, $^3J_{PPtSnC}$ = 12.0 Hz, $SnCH_2$), 24.4 (d, $^1J_{PC}$ = 20.8 Hz, PCH_2) 36.6 (dd, $^1J_{PC}$ = 37.5 Hz, J_{PC} = 8.8 Hz, PCH_2), 124.3−156.3 (C_6H_5, no assignment was possible due to different phenyl groups and Pt satellites). − ^{1}H NMR (250.130 MHz, C_6D_6): δ = 0.80−1.28 (m, overlapping, 4 H, $SnCH_2$), 2.15−2.32 (m, 2 H, PCH_2), 2.45−2.68 (m, 2 H, PCH_2), 6.78−7.73 (m, C_6H_5).

Preparation of (Me$_3$SnCH$_2$CH$_2$Ph$_2$P)Pt[PPh$_2$CH$_2$CH$_2$SnMe$_2$-(Pt−Sn)](Me) (**6**). − *Method a:* A solution of 128 mg (0.17 mmol) of $(Ph_3P)_2Pt(C_2H_4)$ in 10 ml of benzene was treated with 130 mg (0.35 mmol) of $Ph_2PCH_2CH_2SnMe_3$ in 4 ml of benzene at room temperature for 12 h. After removal of the solvent in vacuo, an orange oil remained. The product was crystallized from a concentrated benzene solution by heptane diffusion as pale yellow crystals in 55% yield (89 mg). M.p. 132°C. − $C_{34}H_{46}P_2PtSn_2$ (949.2): calcd. C 43.0, H 4.88, found C 43.4, H 4.65.

Method b: To a beige solution of 131 mg (0.32 mmol) of $Pt(COD)_2$ in 3 ml of benzene, 242 mg (0.64 mmol) of

$Ph_2PCH_2CH_2SnMe_3$ was added, resulting in a color change to yellow-brown. On stirring for 16 h, the color of the reaction mixture became lighter. All volatiles were removed in vacuo after filtration through glass wool, and the remaining slightly oily solid was washed twice at 0°C with 3 ml of pentane each. After drying, **6** was obtained as a beige powder (210 mg, 69%).

^{31}P NMR (101.250 MHz, C_6D_6): δ = 55.9 (d, $^2J_{PPtP}$ = 7.3 Hz, $^1J_{PtP}$ = 2152.2 Hz, J_{SnP} = 108.6 Hz), 27.9 (d, $^2J_{PPtP}$ = 7.3 Hz, $^1J_{PtP}$ = 2065.5 Hz, $^2J_{119SnPtP}$ = 1726.2 Hz, $^2J_{117SnPtP}$ = 1696.8 Hz, $^3J_{SnCCP}$ = 213.6 Hz). – ^{119}Sn NMR (93.276 MHz, C_6D_6): δ = 147.2 (dd, $^2J_{119SnPtP}$ = 1732.1 Hz, J_{119SnP} = 111.9 Hz), −29.5 (d, $^3J_{119SnCCP}$ = 218.7 Hz). – ^{13}C NMR (62.90 MHz, [D$_8$]toluene): δ = −11.7 (dd, *trans*-$^2J_{PPtC}$ = 82.9 Hz, *cis*-$^2J_{PPtC}$ = 7.6 Hz, $PtCH_3$), −9.6 (s, $SnCH_3$), −6.5 (d, $^3J_{PPtSnC}$ = 8.2 Hz, $^2J_{PtSnC}$ = 78.5 Hz, $SnCH_3$), 5.8 (s, br., $SnCH_2$), 6.1 (d, J_{PC} = 13.1 Hz, $SnCH_2$), 25.4 (d, br., $^1J_{PC}$ = 12.0 Hz, PCH_2), 39.4 (dd, $^1J_{PC}$ = 39.2 Hz, J_{PC} = 8.7 Hz, PCH_2). – ^{1}H NMR (250.130 MHz, [D$_8$]toluene): δ = −0.11 (s, $^2J_{SnCH}$ = 51.3 Hz, 9 H, $SnCH_3$), 0.55 (s, $^2J_{SnCH}$ = 41.5 Hz, $SnCH_3$, 6H), 0.65 (d, $^3J_{PPtCH}$ = 6.1 Hz, $PtCH_3$), 0.71− 0.95 (m, $SnCH_2$), 1.44−1.52 (m, $^2J_{117/119SnCH} \approx$ 59 Hz, 2 H, $SnCH_2$), 2.03−2.12 (m, PCH_2), 2.48−2.61 (m, PCH_2, 2 H), 6.98−7.75 (m, C_6H_5).

Preparation of (Bu$_3$SnCH$_2$CH$_2$Ph$_2$P)Pt[PPh$_2$CH$_2$CH$_2$SnBu$_2$-(Pt−Sn)](Bu) (**7**): The reaction was carried out in benzene as described for **6**, using 160 mg (0.22 mmol) of $(Ph_3P)_2Pt(C_2H_4)$ and 227 mg (0.45 mmol) of $Ph_2PCH_2CH_2SnBu_3$. Removal of all volatiles in vacuo resulted in a yellow oil (consisting of **7** in about 90% yield according to the ^{31}P-NMR spectrum). By washing the oil twice with 8 ml of pentane each and drying in vacuo, a yellow powder was obtained that contained **7** and only traces of impurities according to the ^{31}P-NMR spectrum. – ^{31}P NMR (101.25 MHz, C_6D_6): δ = 53.2 (d, $^2J_{PPtP}$ = 9.3 Hz, $^1J_{PtP}$ = 1899.5 Hz, $J_{117/119SnP}$ = 110.2 Hz), 27.9 (d, $^2J_{PPtP}$ = 9.3 Hz, $^1J_{PtP}$ = 2097.2 Hz, $^2J_{119SnPtP}$ = 1671.2 Hz, $^2J_{117SnPtP}$ = 1596.7 Hz, $^3J_{119SnCCP}$ = 185.6 Hz, $^3J_{117SnCCP}$ = 178.2 Hz). – ^{119}Sn NMR (93.276 MHz, C_6D_6): δ = 175.8 (dd, $^2J_{119SnPtP}$ = 1673.4 Hz, J_{119SnP} = 111.9 Hz), −4.8 (d, $^3J_{PCC119Sn}$ = 185.7 Hz). – ^{1}H NMR (250.130 MHz, C_6D_6): δ = 0.75−1.96 (complex overlapping multiplets of butyl groups and $SnCH_2$), 2.20−2.51 (m, PCH_2), 2.65−2.80 (m, PCH_2) 6.99−7.90 (m, C_6H_5).

Preparation of (PhMe$_2$SnCH$_2$CH$_2$Ph$_2$P)Pt[PPh$_2$CH$_2$-CH$_2$SnMe$_2$(Pt−Sn)](Ph) (**8**): An amount of 123 mg (0.16 mmol) of $(Ph_3P)_2Pt(C_2H_4)$ and 144 mg (0.16 mmol) of $Ph_2PCH_2CH_2SnMe_2Ph$ was treated as described above. After removal of all volatiles, the yellow oil was analyzed by multinuclear NMR which indicated the almost quantitative formation of **8** according to ^{31}P NMR. – ^{31}P NMR (101.250 MHz, C_6D_6): δ = 52.8 (d, $^2J_{PPtP}$ = 11.0 Hz, $^1J_{PtP}$ = 2116.0 Hz, $J_{117/119SnP}$ = 104.1 Hz), 24.4 (d, $^2J_{PPtP}$ = 11.0 Hz, $^1J_{PtP}$ = 2046.2 Hz, $^2J_{119SnPtP}$ = 1572,3 Hz, $^2J_{117SnPtP}$ = 1503.7 Hz, $^3J_{119/117SnCCP}$ = 200.0 Hz). – ^{119}Sn NMR (93.276 MHz, C_6D_6): δ = 161.2 (dd $^2J_{119SnPtP}$ = 1572.9 Hz, J_{119SnP} = 104.4 Hz) −25.5 (d, $^3J_{119SnCCP}$ = 208.0 Hz). – ^{13}C NMR (62.90 MHz, C_6D_6): δ = −11.1 [s, $Sn(CH_3)_2Ph$], −7.4 [d, $^3J_{PPtSnC}$ = 6.9 Hz, $^2J_{PtSnC}$ = 74.9 Hz, $Sn(CH_3)_2$], 3.7 (d, $^2J_{PCC}$ = 7.4 Hz, $SnCH_2$), 6.6 (d, $^2J_{PCC}$ = 16.2, $SnCH_2$), 25.4 (d, br., $^1J_{PC}$ = 18.5 Hz, PCH_2) 37.6 (dd, $^1J_{PC}$ = 38.4 Hz, J_{PC} = 8.8 Hz, PCH_2), 121.9−156.6 (C_6H_5, no assignment possible due to different phenyl groups and Pt satellites). – ^{1}H NMR (250.13 MHz, C_6D_6): δ = 0.04 (s, $^2J_{SnCH}$ = 53.0 Hz, 6 H, $SnCH_3$), 0.36 (s, br, $^3J_{PtSnCH}$ = 8.1 Hz, 6 H, $SnCH_3$), 0.58−0.73 (m, $SnCH_2$), 1.05−1.19 (m, $SnCH_2$), 2.09−2.21 (m, 2 H, PCH_2), 2.53−2.67 (m, 2 H, PCH_2), 6.87−6.98 (m, 5 H, PtC_6H_5), 7.10−7.86 (m, C_6H_5).

X-ray Structure Analysis of **6**: Triclinic, space group *P*1, *a* = 1241.42(1), *b* = 1280.91(2), *c* = 1578.98(3) pm, α = 66.396(1), β = 69.796(1), γ = 66.749(1)°, *V* = 2060.91·10^6(3) pm^3, $d_{calcd.}$ = 1.655 g cm^{-3} for *Z* = 2. *F*(000) = 1000, μ(Mo-K_α) = 4.690 mm^{-1}, λ = 71.073 pm, *T* = 302 K, crystal size = 0.5 × 0.4 × 0.25 mm. A crystal was sealed in a glass capillary and mounted on a Siemens SMART diffractometer with a CCD area detector. A hemisphere of data was collected by a combination of three sets of exposures (17343 reflections). Each set had a different φ angle for the crystal, and each exposure took 15 s and covered 0.3° in ω (2.9° ≤ 2Θ ≤ 60.1°). The crystal-to-detector distance was 3.85 cm. The data were corrected for polarization and Lorentz effects, and an empirical absorption correction (SADABS) was applied (11897 unique reflections). The structure was solved by the Patterson method (SHELS86). Refinement was carried out with the full-matrix least-squares method based on F^2 (SHELXL93) with anisotropic thermal parameters for all non-hydrogen atoms. Hydrogen atoms were inserted in calculated positions and refined riding with the corresponding atom. Refinement converged at R_1 = 0.0595 [for 1847 reflections with $I > 2\sigma(I)$], wR_2 = 0.1344 {$w = [\sigma^2(F_o)^2 + (0.0 \cdot x P)^2 + x \cdot P]^{-1}$, where $P = (F_o^2 + 2F_c^2)/3$}; final GOF = 0.511. The final difference map showed no peak larger than +2.008 e^{-3} and no hole larger than −1.243 e^{-3}.[21]

[1] Part 11: U. Schubert, S. Grubert, *Organometallics* **1996**, *15*, 4707.
[2] U. Schubert, *Angew. Chem.* **1994**, *106*, 435; *Angew. Chem. Int. Ed. Engl.* **1994**, *33*, 419.
[3] G. Butler , C. Eaborn, A. J. Pidcock, *Organomet. Chem.* **1979**, *181*, 47.
[4] T. A. K.Al-Allaf, C. Eaborn, K. Kundu, A. J. Pidcock, *J. Chem. Soc., Chem. Commun*. **1981**, 55.
[5] G. Butler, C. Eaborn, A. J. Pidcock, *Organomet. Chem.* **1985**, *185*, 367.
[6] C. Eaborn, K. Kundu, A. Pidcock, *J. Chem. Soc*. **1981**, 1223.
[7] B. Cetinkaya, M. F. Lappert, J. McMeeking, D. E. Palmers, *J. Chem. Soc., Dalton Trans.* **1973**, 1202.
[8] H. Werner, O. Gevert, P. Haquette, *Organometallics* **1997**, *16*, 803.
[9] M. J. Auburn, R. D. Holmes Smith, S. R. Stobart, *J. Am. Chem. Soc.* **1984**, *106*, 1314.
[10] C. Müller, U. Schubert, *Chem. Ber.* **1991**, *124*, 2181.
[11] U. Schubert, S. Grubert, U. Schulz, S. Mock, *Organometallics* **1992**, *11*, 3165.
[12] B. P. Buffin, M. J. Poss, A. M. Arif, T. G. Richmond, *Inorg. Chem*. **1993**, *32*, 3805.
[13] H. Gilges, U. Schubert, *J. Organomet. Chem.* **1997**, 548, 57; M. Murikami, T. Yoshida, Y. Ito, *Organometallics* **1994**, *13*, 2900; M. Murikami, T.Yoshida, Y. Ito, *Chem. Lett.* **1996**, 13.
[14] H. Weichmann, *J. Organomet. Chem*. **1982**, *238*, C49.
[15] P. E. Garrou, P. E. *Chem. Rev.* **1981**, *81*, 229.
[16] E. Carmona, E. Gutierrez-Puebla, J. M. Marin, A. Monge, M. Paneque, M. L. Poveda, C. Ruiz, *J. Am. Chem. Soc.* **1989**, *111*, 2883.
[17] H. Azizian, K. R. Dixon, C. Eaborn, A. Pidcock, N. M. Shuaib, J. Vinaixa, *J. Chem. Soc.* **1982**, 1020.
[18] *Comprehensive Organometallic Chemistry*, vol. 9 (Eds.: E. W. Abel, F. G. A. Stone, G. Wilkinson), Pergamon Press, Oxford, **1995**, p. 454.
[19] H. C. Clark, G. Ferguson, M. J. Hampden-Smith, H. Ruegger, B. L. Ruhl, *Can. J. Chem.* **1988**, *66*, 3120.
[20] H. Weichmann, G. Quell, A. Tzschach, *Z. Anorg. Allg. Chem.* **1983**, *503*, 7.
[21] Crystallographic data (excluding structure factors) for the structure reported in this paper have been deposited with the Cambridge Crystallographic Data Centre. Copies of the data can be obtained free of charge on application to CCDC, 12 Union Road, Cambridge C82 1EZ, UK [fax: int. code +(1223)336-033; e-mail: deposit@ccdc.cam.ac.uk] quoting the depository number CCDC-101015.

[98011]

Phosphane Complexes of Alkaline Earth Metals

Hans H. Karsch* and Manfred Reisky

Technische Universität München, Institut für Anorganische Chemie
Lichtenbergstraße 4, D-85747 Garching, Germany
Fax: (internat.) +49 (0)89/ 28914421
E-mail: Hans.H.Karsch@lrz.tu-muenchen.de

Received March 9, 1998

Keywords: Phosphane complexes / Alkaline earth metal compounds / Phosphanomethanides

The reaction of lithium[bis(dimethylphosphanyl)(trimethylsilyl)methanide] Li[$(PMe_2)_2C(SiMe_3)$] with $BeCl_2$ gave the homoleptic compound Be[$(PMe_2)_2C(SiMe_3)]_2$ (**5**) with four beryllium–phosphorus bonds constituting a distorted tetrahedron around the beryllium center. The reaction of $MgCl_2$ with Li[$(PMe_2)_2C(SiMe_3)$] resulted in the formation of the bis-chelate complex Mg[$(PMe_2)_2C(SiMe_3)]_2 \cdot 2$ THF (**7**), where the distorted *cis*-octahedral magnesium center is additionally coordinated by two THF ligands. In the reaction of **7** with an additional equivalent of Li[$C(PMe_2)_2(SiMe_3)$], THF is released and the magnesate anion {Mg[$(PMe_2)_2C(SiMe_3)]_3$}$^-$ (**8**) was obtained. This compound is not only the first reported hexacoordinated magnesate, but also the first magnesium compound with six magnesium–phosphorus bonds. With $CaCl_2$ and Li[$C(PMe_2)_2(SiMe_3)$], a heptacoordinated complex Ca[$(PMe_2)_2C(SiMe_3)]_2 \cdot 3$ THF (**10**) with three coordinating THF ligands was isolated. The complexes were characterized using ^{9}Be{^{1}H}-, ^{31}P{^{1}H}-, ^{1}H-, ^{13}C{^{1}H}-NMR spectroscopy, and elemental analysis and by X-ray diffraction. The neutral compounds are highly soluble in nonpolar solvents.

Introduction

The alkaline earth metals are very hard coordination centers. In general, they do not form stable complexes with soft donors such as phosphanes and it seems a challenging task to create stable alkaline earth metal−phosphane donor bonds. Only three complexes of diorganometal centers R_2M with "normal" (i.e. neutral) phosphane ligands R_3P, two examples for beryllium[1] and one for magnesium[2], have been reported in the literature, but none have been well characterized. Phosphane complexes of alkaline earth metals are promising precursors for chemical vapor deposition (CVD) processes and possible candidates for metal-mediated organic synthesis. Moreover, with phosphane donor ligands it might be possible to stabilize low-valency alkaline earth metal compounds and mixed alkaline earth/transition-metal bi- or multinuclear complexes. A promising strategy for creating alkaline earth metal to phosphorus bonds makes use of *anionic* phosphanide ligands containing phosphorus of formal valency number two, and in fact several alkaline earth metal compounds with phosphanide ligands **1** have been described[3]. Bridged heterobimetallic phosphanides **2** may also be formed in this way[4].

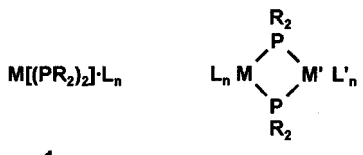

1 **2**

An alternative class of anionic phosphane donor ligands is established by diphosphanomethanides **3**[5].

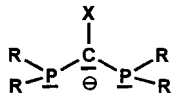

3

In this class of ligands, in contrast to phosphanides, the negative charge is not localized at the phosphorus atom and the phosphorus valency number is three, as is typical for phosphanes. Anionic diphosphanomethanides have been ligated to hard metal centers (e.g. aluminium[6] and rare earth metals[7]) and they often enable high phosphane coordination numbers even at these metal centers.

Thus, it emerged that phosphane coordination to alkaline earth metals might be achieved by using anionic diphosphanomethanide ligands. Meanwhile, using a related strategy, a hexacoordinated magnesium compound **4** with four magnesium−phosphorus bonds has been successfully synthesized[8].

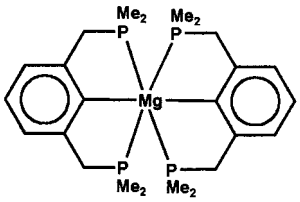

4

The use of diphosphanomethanides additionally might provide access to homoleptic species exhibiting exclusively metal−phosphorus bonds. Furthermore, the monoanionic nature of these ligands and their tendency to form four-

 © WILEY-VCH Verlag GmbH, D-69451 Weinheim, 1998 1434−1948/98/0707−0905 $ 17.50+.50/0

membered chelates allows comparisons to be made with other recently synthesized compounds of alkaline earth metals derived from amidinates and aminoiminophosphoranates[9]. Additionally, for the heavier alkaline earth metals the question of d-orbital participation may be considered.

This paper is concerned with the synthesis and full characterization of phosphane donor adducts to alkaline earth metal centers ranging from beryllium to calcium, including the first homoleptic examples of beryllium and magnesium with exclusive metal−phosphorus bonds.

Results and Discussion

$Be[(PMe_2)_2C(SiMe_3)]_2$ (5)

This first molecular compound with beryllium exclusively joined to phosphorus was obtained by treating anhydrous $BeCl_2$ with two equivalents of $Li[(PMe_2)_2C(SiMe_3)]$ according to Eq. (1) and isolated from pentane as colorless crystals **5**. The substance is extremely air and moisture sensitive.

$$BeCl_2 + 2\ Li[C(PMe_2)_2(SiMe_3)] \xrightarrow{THF} \mathbf{5} \qquad \text{(eq.1)}$$

The first $^9Be\{^1H\}$-NMR spectrum of a beryllium−phosphorus compound was obtained from **5** in C_6D_6 at room temperature. It exhibits a quintet at $\delta = 6.4$ with a $^1J_{Be-P}$ coupling constant of 33.5 Hz. The same coupling constant can be extracted from the $^{31}P\{^1H\}$-NMR quartet signal ($\delta = -30.8$). This is an indication of a highly symmetrical structure with four equivalent phosphorus atoms in solution. As expected, the coupling constant is smaller than that observed in the $^{31}P\{^1H\}$-NMR spectrum of the phosphanide compound Cp*BeP(*t*Bu)$_2$ (**6**) ($^1J_{Be-P} = 50$ Hz), the only other hitherto known, sufficiently characterized molecular beryllium−phosphorus compound[10].

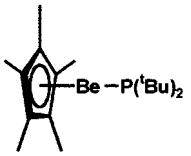

6

The spectra are essentially temperature independent (−80 to +40°C).

X-ray analysis reveals 1/2 (**A**) and 1/4 (**B**) molecule in the asymmetic unit. The whole molecules can be generated by symmetric transformations (#1: $x + 1 - 1, -y + 1/2, -z + 3/2$; #2: $-x, y, -z + 1/2$; #3: $-x + 1 - 1, -y + 1/2, z$; #4: $-x, y, -z + 3/2$). The bond lengths and angles are nearly identical for both molecules **A** and **B**, but the $SiMe_3$ group in **B** is disordered and could not be resolved computationally. Therefore, only molecule **A** will be discussed.

In the solid state, compound **5** is a monomer. The central beryllium dication is coordinated by two chelating $[(PMe_2)_2C(SiMe_3)]^-$ monoanions resulting in a distorted tetrahedral BeP_4 arrangement. The normals to the two BeP_2 planes intersect at an angle of 90°. Both BePCP four-membered rings are planar, as is the environment of the endocyclic C atoms C1 and C1a. The Be−P bond lengths are remarkably short; a comparison with the only two structurally characterized beryllium−phosphorus compounds shows that the bond lengths in **5** [2.134(2) and 2.137(3) Å] are just between the respective bond lengths in **6** (2.083 Å)[10] and in the binary solid-state phase Be_3P_2 (2.20 Å)[11], but in both cases anionic phosphanide- and phosphide-type ligating atoms, respectively, are involved. The endocyclic P−C bond lengths [1.740(4) and 1.744(4) Å] are quite short and of nearly equal length, as is the case in a variety of other diphosphanomethanide complexes[5]. This has been explained in terms of an ylidic bonding model with some charge delocalization within the PCP moiety. The nonbonding P1−P2 distance [2.685(1) Å] is significantly shorter than the van der Waals radii, as is the case with other chelating diphosphanomethanide derivatives and must be regarded as a consequence of the geometric restraints[12].

Figure 1. Crystal structure of **5** (only molecule A is shown)

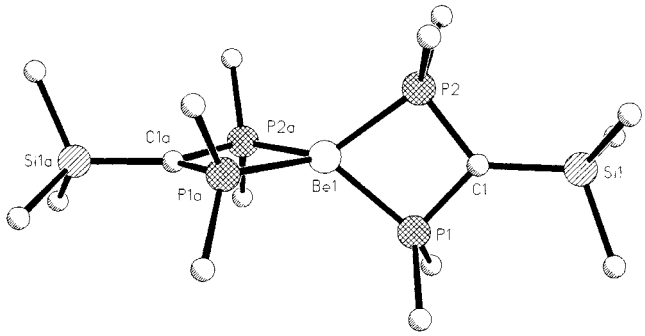

$Mg[(PMe_2)_2C(SiMe_3)]_2 \cdot 2$ THF (7)

Diphosphanomethanides can span tetrahedral coordination sites only with centers from the second period (lithium[13], beryllium: this paper, boron[14]). With increasing atomic radii, i.e. with the heavier elements, either higher coordination numbers at the coordination center M (which decreases the P−M−P angle; Si[15], P[12]) or a monodentate ligating mode is observed (Si[15], P[16]). Consequently, in the analogous reaction of anhydrous $MgCl_2$ with $Li[(PMe_2)_2C(SiMe_3)]$, the formation of the bis-chelate complex **7** is observed.

In contrast to the beryllium compound, where the central atom is tetrahedrally coordinated by four phosphorus atoms, the magnesium center in **7** is additionally coordinated by two THF molecules, completing a distorted octahedral environment at the metal center.

$^{31}P\{^1H\}$-NMR variable-temperature experiments at −80°C show a multi-line, symmetric pattern, tentatively assigned to a not completely resolved AA′BB′ spin system

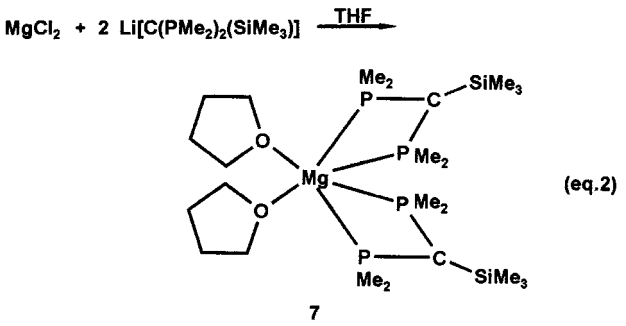

7

(centered at $\delta = -16.7$). At room temperature only one singlet ($\delta = -16.2$) was detected, due to a fast exchange of axial and equatorial sites. These experiments indicate a *cis*-octahedral coordination, in contrast to the only hitherto known magnesium−phosphorus compound **4** with four Mg−P bonds[8]. The *cis*-octahedral coordination was confirmed by X-ray analysis.

Figure 2. Crystal structure of **7**

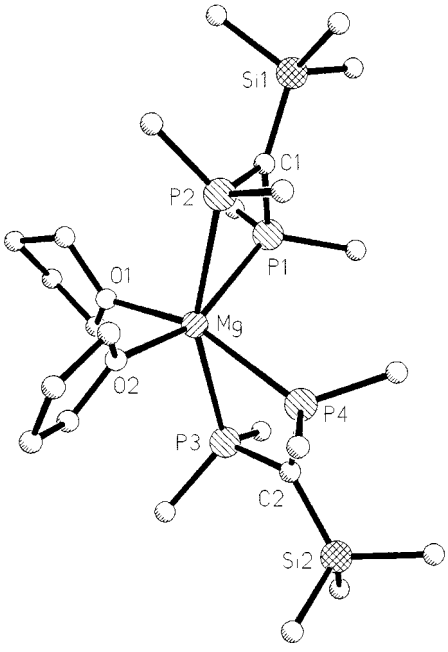

The Mg−P bond lengths [2.654(1)−2.684(1) Å] are equal within one standard deviation and are significantly shorter than in **4** [2.761(1) and 2.770(1)[8]], but more comparable with those in tetracoordinated magnesium−phosphanide compounds, e.g. in $[Mg(PHPh)_2(TMEDA)]$ [2.592(5) and 2.587(5) Å][17].

In contrast, the Mg−O bond lengths [2.137(2) and (2.122(2) Å] are significantly longer than in tetrahedral reference compounds [e.g. $Ph_2Mg(THF)_2$: 2.03 Å][18], and therefore it seems possible to remove the THF ligands. In fact, a substitution of the THF ligands by a third diphosphanomethanide ligand is possible (see below).

The average bond lengths of P1/2−C1 and P3/4−C2 (1.75 Å) range between the bond lengths of an ylidic P−C bond (typically around 1.68 Å) and a single P−C bond (ca. 1.83 Å), consistent with the carbanionic character of C1 and C2. The mean lengths of $P-C_{methyl}$ bonds (1.85 Å) are roughly within this latter range.

The sums of the angles in the four-membered rings MgPCP are 359.8° and 359.9° respectively, which indicates the planarity of chelate rings. The environment of the carbanionic carbon atoms is also planar, the silicon atom of the $SiMe_3$ groups adopting a position in the same plane as the four-membered chelate rings.

$[Li(12\text{-crown-}4)_2]^+\{Mg[(PMe_2)_2C(SiMe_3)]_3\}^-$ (8)

The homoleptic "magnesate" anion **8** is obtained as described in Eq. 3. Hitherto known "magnesate" anions exhibit coordination numbers of four[19] or five[20]. It is also the first molecular magnesium compound with six magnesium−phosphorus bonds.

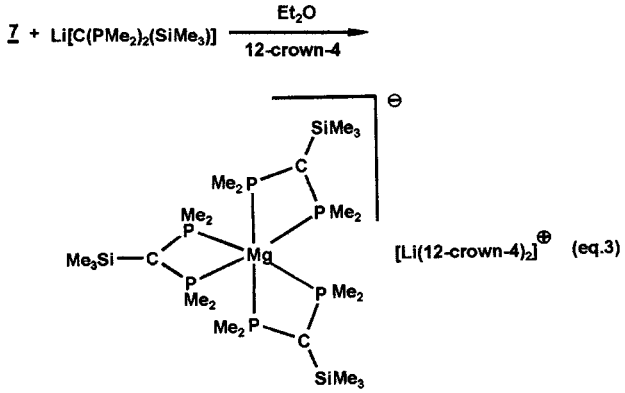

8

The $^{31}P\{^1H\}$-NMR spectrum (C_6D_6) shows a singlet ($\delta = -15.8$), which does not vary with temperature and thus indicates the equivalence of all six phosphorus atoms.

The ^1H-NMR spectrum (C_6D_6) reveals, besides the signals of the phosphanomethanide ligand, the presence of two 12-crown-4 molecules ($\delta = 2.9$) per anion. Colorless crystals of **8** have been grown from diethyl ether solution. The X-ray analysis shows the structure containing a $Li[12\text{-crown-}4]_2^+$ cation[21], two molecules of C_6H_6 and a hexacoordinated "magnesate" anion, which is isoelectronic with the neutral aluminium complex **9**[6]. The cation and anion units are well separated without any noticeable interionic contacts.

The $Li[12\text{-crown-}4]_2^+$ cation shows considerable disorder, which influences the *R* values, but has no influence on the structural findings concerning the anion. Again, as in **5** and **7**, the three four-membered chelate rings in **8** are planar, as are the environments of the carbanionic carbon atoms. The deviation from the ideal octahedral geometry at magnesium can be described by the torsion angle ϕ of the trigonal P_3 planes P1, P3, P5 and P2, P4, P6 ($\phi = 32.2°$). This angle indicates a slightly enhanced torsion towards a trigonal-prismatic coordination compared to **9** ($\phi = 35.9°$)[6].

A magnesium ion of coordination number six can also be assigned in the polymeric solid-state phase of MgP_4[22],

Figure 3. Crystal structure of **8** (only the anion is shown)

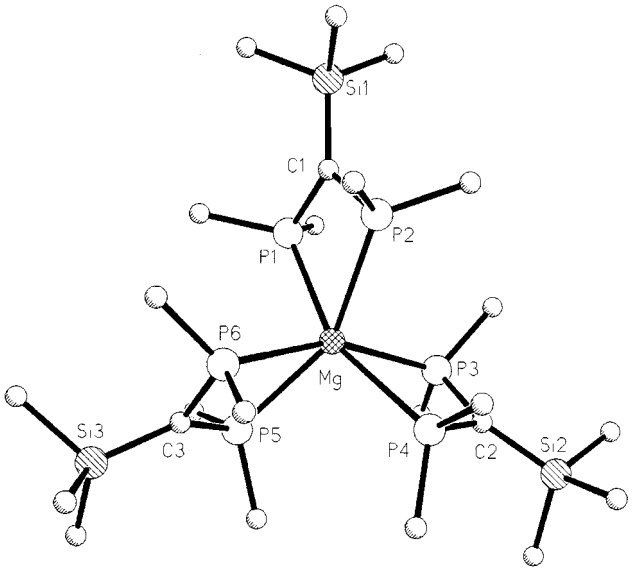

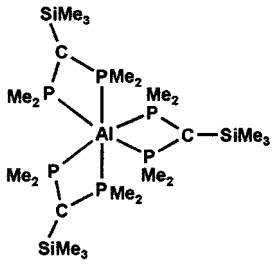

9

although a description in terms of 4 + 2 coordination may be more appropriate. There are two quite different Mg−P distances in MgP_4 (four short contacts: 2.608 A and two long contacts: 2.862 A), in marked contrast to the case of **8**. In **8**, the Mg−P bond lengths are more similar, ranging from 2.635(3) to 2.698(3) A, with a mean Mg−P bond length of 2.66 A. In **9**, the Al−P distance amounts to 2.490 A[6]. Altogether, as expected, a high ionic contribution to the metal to ligand bonding in both **8** and **9** may be extracted from these data.

$Ca[(PMe_2)_2C(SiMe_3)]_2 \cdot 3$ THF

The diphosphanomethanides are also suitable phosphane donor ligands for the heavier alkaline earth metals. An example is given by Eq. 4. Colorless crystals of **10** are obtained from the pentane extraction of the reaction mixture.

The $^{31}P\{^1H\}$-NMR spectrum displays a singlet (δ = −28.6) which essentially remains unchanged on cooling (−80°C).

The X-ray analysis of the colorless crystals of **10** shows two identical molecules in the asymmetric unit and reveals phosphane coordination to a calcium atom for the first time. Three THF molecules and two chelating diphosphanomethanide ligands generate a distorted pentagonal-bipyramidal coordination polyhedron. Two of the THF ligands are in a *trans*-axial position with a bond angle

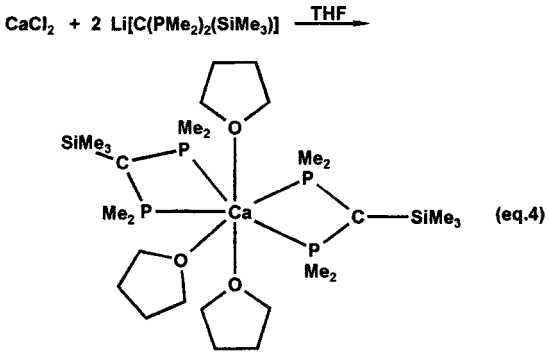

10

O1−Ca1−O3 of 177.0(1)°; the third THF ligand and the two planar four-membered chelate rings of the diphosphanomethanides complete the pentagon. The sum of internal angles is 361.3° indicating the near planarity of the pentagon. The higher coordination number of Ca^{2+} can easily be understood in terms of the increasing ion radius in going from Mg^{2+} to Ca^{2+}.

Figure 4. Crystal structure of **10** (only molecule A is shown)

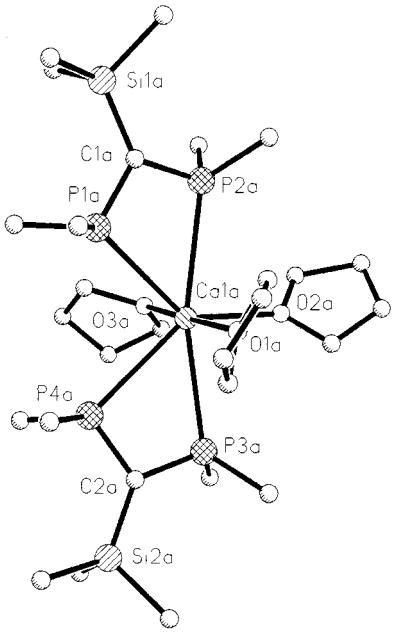

The angles P2−Ca1−O2 and P3−Ca1−O2 are close to rectangular (81.96° and 81.95°, respectively) indicating that the two chelating diphosphanomethanide ligands are located essentially in one hemisphere of the central atom, as is the case in the magnesium compound **7** (which in the case of **10** is more or less trivial, however). The partial ylidic character of the $P-C_{carbanion}$ bond again is evident from the average bond lengths of 1.75 A (see above). The mean Ca−P (3.043 A) and Ca−O bond lengths (2.391 A) are within the range found in known phosphanide and THF complexes of calcium[3][23]. An indication of d-orbital participation is not obvious, at least as extracted from the planarity of the chelate rings and of the endocyclic C atoms,

as it also was found in most other diphosphanomethanide complexes, including **5**, **7**, **8**, and **9**. In marked contrast to **10**, the chelate rings in the scandium complex $Sc[(PMe_2)_2C(SiMe_3)]_3$[7] show a considerable deviation from planarity.

Comparison of 5, 7, and 10

All three compounds are monomeric and contain chelating diphosphanomethanides. As a consequence of the monomeric nature, these alkaline earth metal−phosphane complexes are soluble in nonpolar organic solvents such as pentane. With increasing metal radii, the coordination number increases from 4 (beryllium) to 6 (magnesium) to 7 (calcium), resulting in more or less distorted tetrahedral, octahedral, and pentagonal-bipyramidal coordination geometry, respectively. The additional coordination sites are occupied by two (magnesium) or three (calcium) THF donor molecules. In all cases the four-membered chelate rings including the metal atom are planar. For the magnesium and the calcium compounds a cisoid coordination of the diphosphanomethanide ligands is observed. The P−C bond lengths within the four-membered rings in all cases are close to 1.75 A which is well between the bond lengths of a single and an ylidic P−C double bond. This is in accordance with other diphosphanomethanide chelate rings and reflects the partial ylidic character of this bond. Since all P−C and M−P endocyclic bond lengths within a given compound are almost identical, an "unisobidentate" coordination mode, as present in some diphosphanomethanide[14] and related complexes with potentially bidenate ligands[24], is not observed. One may speculate whether the restriction of the diphosphanomethanide coordination to one hemisphere of the metal (magnesium, calcium) may be attributed to effects which are also responsible for the bending in simple MX_2 molecules[25]. It is interesting to note that similar behavior has been observed in amidinate and aminoiminophosphoranate complexes of the heavier alkaline earth metals[9]. This observation can now be extended: it is no longer restricted to N-donor-type ligands, but includes also P-donor-type ligands and is probably a quite general phenomenon. Moreover, magnesium coordination centers can also be added to the series, which is particularly noteworthy since d orbitals are not available for this element.

The proposed generality of this observation is augmented by the fact that the chelate rings in **5**, **7**, and **10** not only span quite different coordination polyhedra but also vary considerably in the M−P bond lengths in going from beryllium to magnesium to calcium. Likewise, as a consequence of this bond lengthening, the endocyclic angles at phosphorus increase and at the metal decrease (see Table 1). Hence, although the geometric constraints are quite different, the cisoid arrangement of the anionic ligands is retained.

Comparison of 7 and 8

The replacement of the two THF ligands in **7** by a third diphosphanomethanide ligand leads to the first reported hexacoordinated "magnesate" anion **8** with six magnesium−phosphorus bonds.

The Mg−P bond lengths in both compounds are nearly equal, as are the bond lengths and angles in all four-membered chelate rings. This shows that the anionic nature of **8** has no influence on the radius of the Mg^{2+} dication; the bonding thus seems to be mainly ionic.

In accord with the long Mg−O bonds in **7**, the THF ligands can be removed thermally by heating **7** in vacuo. However, a simple THF-free derivative of **7** was not ob-

Table 1. Comparison of structural features of **5**, **7**, **8**, and **10**

$Be[(PMe_2)_2C(SiMe_3)]_2$, **5** (molec. A)	$Mg[(PMe_2)_2C(SiMe_3]_2\cdot 2$ THF, **7**	$\{Mg[(PMe_2)_2C(SiMe_3]_3\}^-$, **8**	$Ca[(PMe_2)_2C(SiMe_3]_2\cdot 3$ THF, **10** (molec. A)
Be−P1: 2.137(3)	Mg−P1: 2.667(1)	Mg−P1: 2.635(3)	Ca−P1: 3.041(1)
Be−P2: 2.134(3)	Mg−P2: 2.678(1)	Mg−P2: 2.689(3)	Ca−P2: 3.049(1)
	Mg−P3: 2.654(1)	Mg−P3: 2.674(3)	Ca−P3: 3.045(1)
	Mg−P4: 2.684(1)	Mg−P4: 2.668(3)	Ca−P4: 3.038(1)
	Mg−O1: 2.137(2)	Mg−P5: 2.644(3)	Ca−O1: 2.393(3)
	Mg−O2: 2.122(2)	Mg−P6: 2.682(3)	Ca−O2: 2.410(3)
			Ca−O3: 2.370(3)
P1−C1: 1.740(4)	P1−C1: 1.752(2)	P1−C1: 1.753(9)	P1−C1: 1.758(4)
P2−C1: 1.744(4)	P2−C1: 1.750(2)	P2−C1: 1.766(8)	P2−C1: 1.758(4)
	P3−C2: 1.753(2)	P3−C2: 1.754(7)	P3−C2: 1.765(4)
	P4−C2: 1.753(2)	P4−C2: 1.753(7)	P4−C2: 1.751(4)
		P5−C3: 1.761(7)	
		P6−C3: 1.745(8)	
P1−Be−P2: 77.92(4)	P1−Mg−P2: 63.48(2)	P1−Mg−P2: 63.55(8)	P1−Ca−P2: 55.62(3)
Be−P1−C1: 90.6(2)	Mg−P1−C1: 94.93(7)	Mg−P1−C1: 96.5(3)	Ca−P1−C1: 98.4(1)
Be−P2−C1: 90.5(2)	Mg−P2−C1: 94.61(7)	Mg−P2−C1: 94.3(3)	Ca−P2−C1: 98.1(1)
P1−C1−P2: 100.9(2)	P1−C1−P2: 106.8(1)	P1−C1−P2: 105.7(4)	P1−C1−P2: 107.8(2)
	P3−Mg−P4: 63.69(2)	P3−Mg−P4: 63.36(7)	P3−Ca−P4: 55.20(3)
	Mg−P3−C2: 95.16(8)	Mg−P3−C2: 95.0(2)	Ca−P3−C2: 98.2(1)
	Mg−P4−C2: 94.12(7)	Mg−P4−C2: 95.2(2)	Ca−P4−C2: 98.8(1)
	P3−C2−P4: 106.9(1)	P3−C2−P4: 106.3(3)	P3−C2−P4: 106.5(2)
P1−Be−P1#: 124.8(3)	P3−Mg−P2: 157.04(3)	P5−Mg−P6: 63.47(8)	P3−Ca−P2: 163.89(4)
P1−Be−P2#: 126.61(5)	P3−Mg−P1: 102.18(3)	Mg−P5−C3: 95.6(3)	P3−Ca−P1: 140.46(4)
P2−Be−P1#: 126.61(5)	P4−Mg−P2: 100.03(3)	Mg−P6−C3: 94.7(3)	P4−Ca−P2: 140.61(4)
P2−Be−P2#: 130.6(3)	P4−Mg−P1: 101.18(3)	P5−C3−P6: 106.1(4)	P4−Ca−P1: 86.12(4)

Table 2. Crystal data of **5**, **7**, **8,** and **10**

	5	**7**	**8**	**10**
formula	$C_{16}H_{42}BeP_4Si_2$	$C_{24}H_{48}MgO_2P_4Si_2$	$C_{40}H_{95}MgLiO_8P_6Si_3 \cdot 2\ C_6H_6$	$C_{28}H_{66}CaO_3P_4Si_2$
formula weight	423.571	583.071	1161.721	670.951
space group	*Ccca*	$P2_1/c$	$P2_1/c$	$P2_12_12_1$
crystal system	orthorhombic	monoclinic	monoclinic	orthorhombic
a [A]	18.230(1)	16.934(1)	12.567(1)	17.309(2)
b [A]	28.256(2)	12.556(1)	24.569(2)	20.907(2)
c [A]	15.963(1)	18.591(2)	24.987(2)	22.583(2)
α [°]	90	90	90	90
β [°]	90	116.0(1)	101.1(1)	90
γ [°]	90	90	90	90
Z	12	4	4	8
ρ ($mg \cdot m^{-3}$)	1.026	1.090	1.019	1.091
μ (mm^{-1})	0.361	0.315	0.237	0.393
F(000)	2760	1272	2520	2928
2θ range (deg)	6−50	6−50	6−48	6−50
reflections collected	7746	6920	12118	15054
reflections unique	4018	6198	11830	14266
refined params	163	312	661	713
GooF[a] s on F^2	1.034	1.026	1.056	1.020
$R1[F_0>4\sigma(F_0)]$[b]	0.056	0.036	0.095	0.046
$wR2[F_0>4\sigma(F_0)]$[b]	0.149	0.092	0.286	0.095
Largest diff. peak and hole [$e \cdot A^{-3}$]	0.576, −0.485	0.614, −0.274	1.563, −0.389	0.400, −0.204

[a] Definition of the *R* values: $R1 = (\Sigma||F_o| - |Fc||)/\Sigma|F_o|$, $wR2 = \{\Sigma[w(F_o^2 - F_c^2)^2]/\Sigma[w(F_o^2)^2]\}^{1/2}$ with $w^{-1} = \sigma^2(F_o^2) + (aP)^2 -$ [b] Definition of goodness-of-fit, *s*: $s = \{\Sigma[w(F_o^2 - F_c^2)^2]/(N_o - N_p)\}^{1/2}$.

tained, the nature of the resulting compound being currently under investigation.

Conclusion

For the first time it has been demonstrated that not only phosphanide donors (with two-coordinated phosphorus), but also "normal" phosphane donors (with three-coordinated phosphorus) are able to coordinate to alkaline earth metal centers. Even "classic" ligands for alkaline earth metals, such as halides, diethylether, or THF can be replaced successfully by diphosphanomethanides. These results emphasize the exceptional role of diphosphanomethanides in phosphane coordination chemistry. The preference for a cisoid arrangement of anionic ligands in alkaline earth metal compounds can be emphasized and further extended. This seems to be a quite general phenomenon that is not restricted to the heavier metal centers but has now also been established for magnesium compounds.

The neutral compounds described are soluble in nonpolar solvents and represent promising precursors for chemical vapor deposition (CVD) processes. In addition they are possible candidates for metal-mediated organic synthesis and for a wide range of reactions in nonpolar solvents.

H. H. K. thanks the *Deutsche Forschungsgemeinschaft* and the *Fonds der Chemischen Industrie* for Financial Support. We also thank Dr. *E. Witt* for assistance with structural refinements.

Experimental Section

General: All reactions were performed in a two-armed glass vessel as described elsewhere[26]. Exclusion of air and moisture was essential and glassware was treated accordingly. All solvents were dried over Na/K alloy and distilled prior to use. − For ^1H- and $^{13}C\{^1H\}$-NMR spectra TMS (δ = 0) was used as an internal standard. The $^{31}P\{^1H\}$-NMR spectra were obtained in C_6D_6 ([D_8]toluene for low temperature experiments) with H_3PO_4 (85%) as the external reference on a JEOL GX 270 spectrometer. The ^9Be-NMR spectrum was obtained in C_6D_6 with $BeSO_4 \cdot 7\ H_2O$ as the external standard on a JEOL Lambda 400 spectrometer.

The alkaline earth metal chlorides were used in the anhydrous form and prepared as described[27]. 12-crown-4 was purchased from commercial sources and dried over molecular sieve (4 A). Li[(P-$Me_2)_2C(SiMe_3)$] was prepared as described previously[28].

Elemental analyses were performed by the Mikroanalytisches Labor des Anorganisch-chemischen Instituts der Technischen Universität München.

Hazard: Beryllium compounds are extremely toxic and may cause cancer[29]. Handle with care! Avoid inhalation and any skin contact!

Preparation of the Diphosphanomethanide Complexes with Be, Mg, and Ca: 7.0 mmol of $Li[(PMe_2)_2C(SiMe_3)]$[28] and 3.5 mmol of MCl_2 (M = Be, Mg, Ca) were dissolved in 40 ml of THF at −78°C. After being stirred overnight at room temperature, the solvent was removed and replaced by pentane. After filtration, colorless crystals were isolated from pentane in all cases by slowly cooling the solutions.

Preparation of $[Li(12\text{-crown-}4)_2]^+\{Mg[(PMe_2)_2C(SiMe_3)]_3\}^-$: 2.20 mmol of $Li[(PMe_2)_2C(SiMe_3)]$[28] were dissolved in ether (40 ml) at −78°C. After adding 2.20 mmol of 12-crown-4 and 2.06 mmol of $Mg[(PMe_2)_2C(SiMe_3)]_2 \cdot 2$ THF (**7**), the mixture was warmed up to room temperature and stirred overnight. The ether was removed and the remaining solid was washed with 30 ml of pentane. After replacing pentane by ether, colorless crystals were grown from the solution by cooling.

All compounds were extremely air and moisture sensitive. Therefore, elemental analysis were not completely satisfactory in all cases.

Be[(PMe$_2$)$_2$C(SiMe$_3$)]$_2$ (**5**): *M* = 423.571 g/mol, yield: 87.2%. – ^{1}H (C_6D_6): δ = 0.20 (s, 18 H), 1.21 (s, 24 H). – ^{31}P{^{1}H} (C_6D_6): δ = −30.8 (1:1:1:1 quart., $^1J_{Be-P}$ = 33.5 Hz). – ^{13}C{^{1}H} (C_6D_6): δ = 4.70 [s, Si(CH_3)$_3$] 20.17 ["quint.", P(CH_3)$_2$], 22.31 (s, P$_2$*C*Si). – ^{9}Be (C_6D_6): δ = 6.4 (quint., $^1J_{Be-P}$ = 33.5 Hz). – $C_{16}H_{21}BeP_4Si_2$: calcd. (found): C, 45.40 (43.74); H, 10.01 (9.64).

Mg[(PMe$_2$)$_2$C(SiMe$_3$)]$_2$·2 THF (**7**): *M* = 583.071 g/mol, yield: 91.0%. – ^{1}H (C_6D_6): δ = 0.53 (s, 18 H), 1.28 (m, THF, 8 H), 1.36 (s, 24 H), 3.47 (m, THF, 8 H). – ^{31}P{^{1}H} (C_6D_6): δ = −16.2 (s); ^{31}P{^{1}H} ([D$_8$]toluene, −100°C): δ = −16.7 (AA′BB′ spin system, *N* = 34.2 Hz). – ^{13}C{^{1}H} (C_6D_6): δ = 6.37 [s, Si(*C*H$_3$)$_3$], 21.63 ["quint.", P(*C*H$_3$)$_2$], 22.67 (s, P$_2$*C*Si), 25.46 (s, THF), 68.57 (s, THF). – $C_{16}H_{21}MgP_4Si_2$: calcd. (found): C, 49.26 (49.11); H, 10.33 (10.07).

{Mg[(PMe$_2$)$_2$C(SiMe$_3$)]$_3$}$^-$Li(12-crown-4)$_2^+$ (**8**): *M* = 1005.494 g/mol, yield: 55.0%. – ^{1}H (C_6D_6): δ = 0.40 (s, 27 H), 1.49 (s, 36 H), 2.90 (s, 32 H). – ^{31}P{^{1}H} (C_6D_6): δ = −15.5 (s); ^{31}P{^{1}H} ([D$_8$]toluene, −80°C): δ = −14.8 (s, br). – ^{13}C{^{1}H} (C_6D_6): δ = 6.94 [s, Si(*C*H$_3$)$_3$], 22.05 ["quint.", P(*C*H$_3$)$_2$], 22.63 (s, P$_2$*C*Si), 65.46 (s, 12-crown-4).

Ca[(PMe$_2$)$_2$C(SiMe$_3$)]$_2$·3 THF (**10**): *M* = 670.951 g/mol, yield: 85.7%. – ^{1}H (C_6D_6): δ = 0.46 (s, 18 H), 1.27 (m, THF, 12 H), 1.31 (s, 24 H), 3.50 (m, THF, 12 H). – ^{31}P{^{1}H} (C_6D_6): δ = −28.6 (s). – ^{13}C{^{1}H} (C_6D_6): δ = 7.75 [s, Si(*C*H$_3$)$_3$], 21.89 ["quint.", P(*C*H$_3$)$_2$], 22.70 (s, P$_2$*C*Si), 25.58 (s, THF), 68.71 (s, THF). – $C_{28}H_{45}CaO_3P_4Si_2$: calc, (found): C, 50.12 (48.57); H, 9.91 (9.79).

X-ray Measurements: The single crystals were sealed in thin-walled capillaries and mounted on a four-circle diffractometer CAD4 (Fa. ENRAF-NONIUS) with graphite-monochromated Mo-Kα radiation (λ = 0.71073 A). All data were collected at low temperatures (−74°C). The structures were solved by direct methods with the software package SHELXTL PC[30] and refined with the program SHELXL-93[31]. All non-hydrogen atoms were refined anisotropically, and a riding model was employed in the refinement of the hydrogen atom positions. Further details can be obtained from the Fachinformationszentrum Karlsruhe, D-76344 Eggenstein-Leopoldshafen under following CSD-numbers: Be[(PMe$_2$)$_2$C(SiMe$_3$)] 407270, Mg[(PMe$_2$)$_2$C(SiMe$_3$)]$_2$·2 THF 407238, {Mg[(PMe$_2$)$_2$C(SiMe$_3$)]$_3$}$^-${Li(12-crown-4)$_2$}$^+$ 407252, Ca[(PMe$_2$)$_2$C(SiMe$_3$)]$_2$·3 THF 407239.

[1] BePh$_2$·2 PMe$_3$: G. E Coates, M. Tranah, *J. Chem. Soc (A)* **1967**, 236; Be*t*Bu$_2$·PMe$_3$: G. E. Coates, P. D. Roberts, *J. Chem. Soc. (A)* **1968**, 2651.

[2] MgCp$_2$·2 PMe$_3$: H. Lehmkuhl, K. Mehler, R. Benn, A. Rufinska, C. Krüger, *Chem. Ber.* **1986**, *119*, 1054.

[3] M. Westerhausen, W. Schwarz, *J. Organomet. Chem.* **1993**, *463*, 51.

[4] M. Westerhausen, H.-D. Hausen, W. Schwarz, *Z. Anorg. Allg. Chem.* **1995**, *621*, 877. For further reading, see: M. Westerhausen, *Trends in Organometallic Chemistry* **1997**, *2*, 89.

[5] H. H. Karsch, *Russ. Chem. Bull*. **1993**, *42*, 1937.

[6] H. H. Karsch, A. Appelt, J. Riede, G. Müller, *Organometallics*, **1987**, *6*, 316.

[7] H. H. Karsch, G. Ferazin, O. Steigelmann, H. Kooijmann, W. Hiller, *Angew. Chem.* **1993**, *105*, 1814; *Angew. Chem., Int. Ed. Engl.* **1993**, *32*, 1739.

[8] A. Pape, M. Lutz,. G. Müller, *Angew. Chem.* **1994**, *106*, 2375; *Angew. Chem., Int. Ed. Engl.* **1994**, *33*, 2281.

[9] R. Fleischer, D. Stalke, *Inorg. Chem.* **1997**, *36*, 2413.

[10] J. L. Atwood, S. G Bott,. R. A. Jones, S. U. Koschmieder, *J. Chem. Soc., Chem. Comm.* **1990**, 693.

[11] A. El Maslout, J.-P. Motte, A. Courtois, J. Protas, C. Gleitzer, *J. Solid State Chem.* **1975**, *15*, 223.

[12] H. H. Karsch, E. Witt, E. Hahn, *Angew. Chem.* **1996**, *108*, 80; *Angew. Chem., Int. Ed. Engl.* **1996**, *35*, 2242.

[13] H. H. Karsch, A. Appelt, B. Deubelly, K. Zellner, J. Riede, G. Müller, *Z. Naturforsch.* **1988**, *43b*, 1416.

[14] K. Zellner, Dissertation TU München, **1990**; H. H. Karsch, K. Zellner, A. Schier, unpublished.

[15] H. H. Karsch, R. Richter, A. Schier, *Z. Naturforsch.* **1993**, *48b*, 1533.

[16] H. H. Karsch, E. Witt, A. Schneider, E. Herdtweck, M. Heckel, *Angew. Chem.* **1995**, *107*, 628; *Angew. Chem., Int. Ed. Engl.* **1995**, *34*, 557.

[17] E. Hey, L. M. Engelhardt, C. L. Raston, A. H. White, *Angew. Chem.* **1987**, *99*, 61; *Angew. Chem., Int. Ed. Engl.* **1987**, *26*, 81.

[18] P. R. Markies, O. S. Akkermann, F. Bickelhaupt, W. J. J. Smeets, A. L. Spek, *Adv. Organomet. Chem.* **1991**, *32*, 147.

[19] T. Greiser, J. Kopf, D. Thoennes, E. Weiss, *Chem. Ber.* **1981**, *114*, 209.

[20] B. Schubert, E. Weiss, *Chem. Ber.* **1984**, *117*, 366.

[21] P. P. Power, *Acc. Chem. Res.* **1988**, *21*, 147.

[22] H. G. v. Schnering, G. Menge, *Z. Anorg. Allg. Chem.* **1976**, *422*, 219.

[23] M. Westerhausen, M. Digeser, *Inorg. Chem.* **1997**, *36*, 521.

[24] C. Silvestru, I. Haiduc, S. Klima, U. Thewalt, M. Gielen, J. J. Zuckermann, *J. Organomet. Chem.* **1987**, *327*, 181; J. E. Drake, A. B. Sarkar, M. L. Y. Wong, *Inorg. Chem.* **1990**, *29*, 785.

[25] I. Bytheway, R. J. Gillespie, T.-H. Tang, R. F. Bader, W. *Inorg. Chem.* **1995**, *34*, 2407.

[26] H. H. Karsch, H. Reisacher, A. Schneider, T. Rupprich, in W. A Herrmann (ed.): *Synthetic Methods of Organometallic and Inorganic Chemistry (Herrmann, Brauer), Vol. 3*, (Ed.: H. H. Karsch), *Phosphorus, Arsenic, Antimony, and Bismuth*, Thieme, Stuttgart, New York, **1996**, p. 143f..

[27] *Gmelins Handbuch der anorganischen Chemie*, 8th edt, Vols.26−31, Verlag Chemie, Weinheim, **1930−1961**, (Be: p. 211f, Mg: p. 97f, Ca: p. 70f).

[28] H. H. Karsch, *Z. Naturforsch*. **1988**, *43b*, 1416.

[29] H. Schmidbaur, O. Kumberger, *Chem. Unserer Zeit* **1993**, *27*, 310.

[30] *SHELXTL-PC*: Siemens Analytical X-ray Instruments (**1990**), Inc. Madison USA, Release 4.1.

[31] *SHELXL-93*: G. M. Sheldrick, Progr. for the Refinement of Structures, University of Göttingen, **1993**.

[98051]

Diastereoselective Synthesis of Chiral (Triazolinylidene)rhodium Complexes Containing an Axis of Chirality

Dieter Enders*[a], Heike Gielen[a], Jan Runsink[a], Klaus Breuer[b], Stefan Brode[b], and Karlheinz Boehn[b]

Institut für Organische Chemie, Rheinisch-Westfälische Technische Hochschule Aachen[a],
Professor-Pirlet-Str. 1, D-52074 Aachen, Germany
Fax: (internat.) + 49(0)241/8888-127
E-mail: Enders@RWTH-Aachen.de

BASF AG, Ammoniaklaboratorium[b],
D-670056 Ludwigshafen, Germany

Received Feburary 4, 1998

Keywords: Chiral carbenes / Carbene complexes / Rhodium complexes / Axial chirality / Asymmetric hydrosilylation

Deprotonation of chiral triazolium salts **1** and reaction of the resulting nucleophilic carbenes with $[(COD)RhCl]_2$ or $[(NBD)RhCl]_2$ afforded square-planar complexes **2–6** in yields of 65–95%. The complexes contain an axis of chirality and a diastereomeric excess of up to 97% was achieved. The relative and absolute configurations of these complexes were determined by NMR spectroscopic investigations and X-ray structure analysis. The application of the rhodium(COD) complexes as catalysts in an asymmetric hydrosilylation reaction has been examined, resulting in enantiomeric excesses of up to 44%. Similar results were achieved for aromatic and aliphatic ketones and a nonlinear temperature effect (principle of isoinversion) was observed.

Introduction

Metal complexes of nucleophilic carbenes have already been investigated[1][2]. Recent investigations have included chiral modifications and the application of these complexes as catalysts in asymmetric synthesis. The first chiral carbene complexes bearing imidazolidinylidene ligands were introduced by Lappert et al. in 1983[3], followed by chiral imidazolinylidene complexes by Herrmann et al.[4] and by complexes containing chiral imidazolinylidenes and triazolinylidenes by our group[5][6]. Using the C_1-symmetrical triazolinylidenes as ligands, different rotamers were obtained as a result of hindered rotation about the carbene carbon−metal bond[5]. To prevent the formation of these various rotamers, one possibility is to employ chelating carbene ligands. These ligands have previously been used to prepare ruthenium and rhodium complexes bearing a stereogenic center at the metal atom[6]. Another possibility is to use nonchelating carbene ligands with hindered rotation about the carbene carbon−metal bond, causing an axis of chirality when in a perpendicular orientation to the square-plane of the metal complex. We now report the diastereoselective synthesis of rhodium(I) complexes containing this kind of chirality and the application of these complexes in a hydrosilylation reaction.

Results and Discussion

Following our work on palladium(II) complexes containing two carbene ligands and therefore two axes of chirality in the *cis* form (resulting in two diastereomers and one *meso* form according to our nomenclature[5]), we prepared square-planar rhodium complexes containing one carbene ligand perpendicular to the square-plane of the complex[3][7].

Scheme 1. Preparation of rhodium(COD) and -NBD complexes

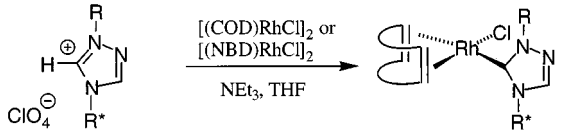

1 **2-6**

The axis of chirality is represented by the carbene carbon−rhodium bond. The two substituents of the first plane are the chlorine atom and the olefin *trans* to the chlorine, whereas the substituents of the second plane are the nitrogen atoms neighboring the carbene carbon atom (see Figure 1).

Figure 1. Axis of chirality

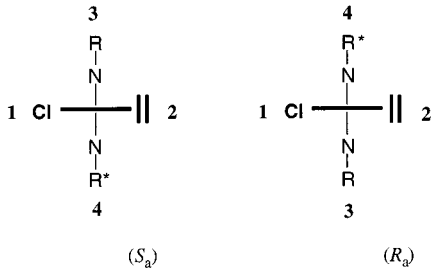

Rhodium(COD) Complexes: The rhodium(COD) complexes **2−4** were prepared by reaction of a triazolium salt **1** with$[(COD)RhCl]_2$ in THF with NEt_3 in yields of 65−95%, the yield depending on the substituent R at *N*1. With a

 © WILEY-VCH Verlag GmbH, D-69451 Weinheim, 1998 1434−1948/98/0707−0913 $ 17.50+.50/0

phenyl group as the substituent at *N*1, the yield was higher than with an alkyl group (see Table 1).

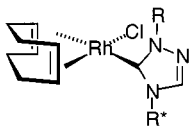

2 R = Ph R* =

3a R = Me
3b R = Ph R* =
3c R = *t*Bu

4a R = Me
4b R = Ph R* = 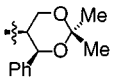
4c R = *t*Bu

Table 1. Yields and diastereomeric excesses (*de*) of rhodium(COD) complexes **2**–**4**

	Yield [%]	*de* [%][a]
2	90	–
3a	70	41
3b	95	40
3c	78	36
4a	79	93
4b	95	91
4c	65	97

[a] Determined by ^{1}H-NMR spectroscopy.

The benzyl group in complex **2** (two doublets of ^2J = 14 Hz for the two benzylic protons in the ^{1}H-NMR spectrum) indicates the existence of the axis of chirality within the complex, the two protons becoming diastereotopic because of the hindered rotation about the carbene carbon–rhodium bond. Calculation of the barrier for rotation of the carbene–carbon rhodium bond at the MP2/TZVP//RI-DFT/SV(P) level of theory yielded an energy of 93 kJ/mol, which is consistent with the experimentally found hindered rotation[8]. The diastereomeric excess of the complexes with chiral substituents R*, **3** and **4**, was determined by ^{1}H-NMR spectroscopy to be 36–41% for **3a–c** [R* = (*R*)-1-phenylethyl]. Using the 2,2-dimethyl-4-phenyl-1,3-dioxanyl residue as chiral substituent R* **4a–c**, diastereomeric excesses of up to 97% could be achieved, the best obtained being with the bulky *t*-butyl group (**4c**). Despite the mixture of diastereomers in solution, the major diastereomer of **4a** could be crystallized and its structure in the solid state was determined by X-ray structure analysis (Figure 2).[9][10]

The X-ray structure shows the rhodium atom with a square-planar arrangement of the ligands and a bond angle Cl–Rh–C(carbene) of 88.3(2)°. The interatomic distances within the triazolinylidene heterocycle are similar to those obtained for other (triazolinylidene)metal complexes[5][6]. The carbene carbon bond length amounts to 2.004(7) A, identical to the value obtained by Lappert et al. for an (imidazolidinylidene)rhodium(COD) complex [2.004(4) A][3]. The configuration of the axis of chirality was assigned as (S_a) for this complex **4a**.

Rhodium(NBD) Complexes: The rhodium(NBD) complexes **5–6** were prepared in the same way as the rhodium(COD) complexes.

Figure 2. Molecular structure of (S_a)-**4a**[a]

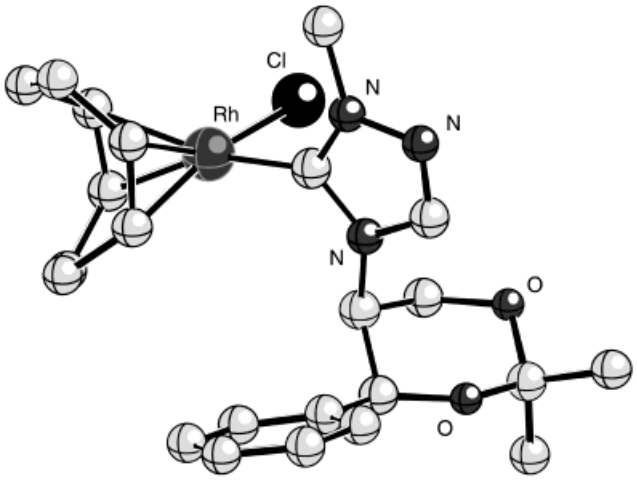

[a] Selected bond lengths (A) and angles (°): Rh–C(carbene) 2.004(7), Rh–Cl 2.366(2), Cl–Rh–C(carbene) 88.3(2).

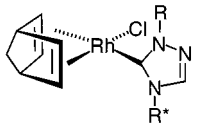

5 R = Ph R* =

6a R = Me
6b R = Ph R* = 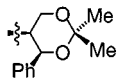
6c R = *t*Bu

Table 2. Yields and diastereomeric excesses (*de*) of rhodium(NBD) complexes **5** and **6**

	Yield [%]	*de* [%][a]
5	95	–[b]
6a	93	[b]
6b	95	[b]
6c	75	87

[a] Determined by ^{1}H-NMR spectroscopy. – [b] Due to broad signals (rotation of the ligand), a diastereomeric excess could not be determined.

They did not show the same hindrance of rotation about the carbene carbon–rhodium bond as the rhodium(COD) complexes. For the achiral benzyl group, at room temperature no splitting of the benzylic protons was observed in the ^{1}H-NMR spectrum. These findings were again supported by MP2/TZVP//RI-DFT/SV(P) calculations, which gave a rotational barrier of 58 kJ/mol for the rotation about the carbene carbon–rhodium bond in complex **5**, much lower than that of complex **2**[8]. This is probably due to the significantly smaller size of the NBD ligand compared to the COD ligand, which leads to a considerably decreased steric interaction in the course of the rotation. By analogy, no evidence for the existence of two diastereomers was observed in the NMR spectra of complexes **6a** and **6b** with a chiral ligand, and only very broad signals were observed for the triazolinylidene ligand. Nevertheless, complex **6c** with a bulky *t*-butyl substituent showed a hindered rotation. A diastereomeric excess of 87% was determined, lower than that for the rhodium(COD) complex **4c** (97%). NMR spectroscopic investigations (NOE′s and ring-current effects) re-

vealed the relative and therefore the absolute configuration of complex **6c**.

Figure 3. NMR spectroscopic investigations of complex **6c**

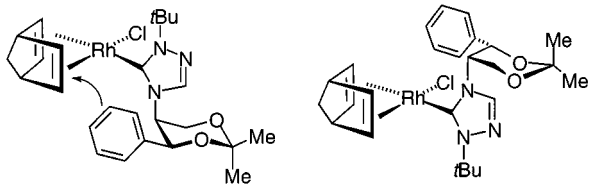

6c major diastereomer **6c** minor diastereomer

In both diastereomers, the dioxane ring in the chair conformation points away from the rhodium atom. For the major diastereomer (S_a), the phenyl substituent of the dioxanyl group points at the olefinic protons of the double bond *trans* to the chlorine atom, causing a ring-current effect and a NOE. The former leads to a significant highfield shift of these protons. For the minor diastereomer (R_a) with the phenyl group pointing at the chlorine atom, neither this ring-current effect nor the NOE was observed. This conformation and configuration of **6c** in solution is identical to the structure obtained for **4a** in the solid state. The lower diastereomeric excess of the rhodium(NBD) complex **6c** compared to rhodium(COD) complex **4c** and the rotation of the ligand in case of complexes **5, 6a−b** may be caused by a lower steric hindrance of the NBD ligand compared to the COD ligand. Upon cooling to −40°C, the broad signal of the benzylic protons of complex **5** in the ^{1}H-NMR spectrum sharpened due to a more hindered rotation, now appearing as two doublets. NMR spectroscopic investigations of Rh, Cr, Mo, and W complexes with hindered carbene ligand rotation at lower temperatures have already been reported[11].

Substitution Reactions: The chlorine atom of the complexes **2−6** was exchanged with iodine using NaI in MeOH and the resulting complexes were purified by column chromatography. Some examples for this substitution reaction are summarized in Table 3.

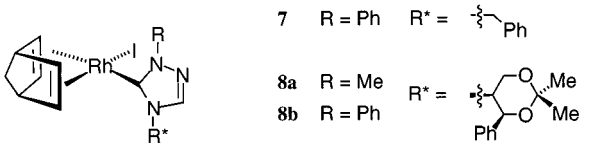

Table 3. Yields and diastereomeric excesses (*de*) of rhodium(NBD) complexes **7** and **8**

	Yield [%]	*de* [%][a]
7	90	–
8a	70	87
8b	83	87

[a] Determined by ^{1}H-NMR spectroscopy.

The (iodo)rhodium(NBD) complexes **7** and **8** showed a hindered rotation at room temperature, in contrast to the chloro complexes **5, 6a−b**. The diastereomeric excess of the complexes **8a−b** was determined to be 87%, identical to the result obtained for the chloro complex **6c**. For complex **7**, the barrier for the rotation about the carbene carbon−rhodium bond was again calculated at the MP2/TZVP//RI-DFT/SV(P) level of theory, yielding a barrier height of 73 kJ/mol[8]. The energy obtained is somewhat higher than for the corresponding chloro complex **5**, suggesting that the steric interaction of the iodine ligand is more significant. This is in agreement with experiment, since we did not observe rotation about the carbene carbon−rhodium bond in the NMR spectra.

Asymmetric Hydrosilylation: The hydrosilylation reaction with achiral (imidazolidinylidene)rhodium(COD) complexes, by Lappert et al.[12] was further developed by Herrmann et al. using chiral imidazolinylidene ligands, which gave enantiomeric excesses of up to 32%[4].

The potential of the (triazolinylidene)rhodium(COD) and -(NBD) complexes as catalysts was examined in a hydrosilylation reaction. The best enantioselectivities were achieved with complexes **4a−c**. In typical hydrosilylations, the methyl ketones **9−12** were reduced to the corresponding alcohols with diphenylsilane and 1 mol% of the catalyst in THF[13].

Scheme 2. Asymmetric hydrosilylation of methyl ketones **9−12**

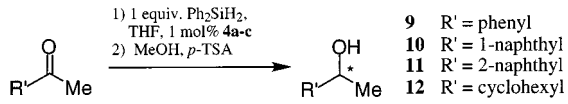

Enantiomeric excesses of up to 44% were achieved with similar results being observed for aromatic and aliphatic ketones. The configuration of the resulting alcohol depends upon the achiral group R at *N*1 of the triazolinylidene ligand. For example, the enantiomeric excess changes from 44% (*S*) (catalyst **4a**) to 43% (*R*) (catalyst **4c**) with acetylcyclohexane **12** as the starting material and no change of the chirality information within the catalyst.

Table 4. Reaction conditions, yields and enantiomeric excesses for the hydrosilylation reaction

Catalyst	Ketone	Temperature [°C]	Time	Yield [%]	*ee* [%]
4a	**9**	22	4h	90	20 (*S*)
4c	**9**	11	6d	60	40 (*R*)
4a	**10**	42	4h	80	37 (*R*)
4b	**10**	2	10d	40	32 (*R*)
4a	**11**	2	5d	90	19 (*S*)
4c	**11**	22	16h	40	24 (*R*)
4a	**12**	−10	6d	75	44 (*S*)
4b	**12**	2	4d	80	43 (*S*)
4c	**12**	22	3d	70	43 (*R*)

The optimum reaction temperature in order to achieve the highest enantioselectivities varies from +42°C to −10°C for the different systems. We found a decreasing enantioselectivity with increasing or decreasing temperature with respect to the optimum conditions (principle of isoinversion[14]). This nonlinear temperature effect has also been observed by Scharf et al.[15] for a hydrosilylation reaction with rhodium(NBD) complexes and chiral cyclic monophosphonite ligands.

Conclusion

Axially chiral (triazolinylidene)rhodium(COD) and -(NBD) complexes have been prepared with diastereomeric excesses of up to 97%. The NMR spectroscopic and theoretical investigations show the steric requirements needed for hindered rotation about the carbene carbon−rhodium bond. This new type of chiral complex was examined in asymmetric hydrosilylation reactions with enantiomeric excesses of up to 44% for aromatic and aliphatic ketones. This represents a good result for a nonchelating ligand, probably caused in part by the axis of chirality.

This work was supported by the *Fonds der Chemischen Industrie*, the *Deutsche Forschungsgemeinschaft* (*Leibniz* award) and the *Forschungsverbund Katalyse Nordrhein-Westfalen*. We are grateful to *BASF AG*, *Degussa AG*, *Boehringer Mannheim GmbH*, *Bayer AG* and *Hoechst AG* for the donation of chemicals.

Experimental Section

General: All solvents were dried and distilled before use. The triazolium perchlorates[16], $[(COD)RhCl]_2$ and $[(NBD)RhCl]_2$[17] were prepared according to literature procedures. − Column chromatography: Merck silica gel 60, 0.040−0.063 mm (230−400 mesh) (flash). − Optical rotation values: Perkin-Elmer P 241, solvent UVASOL-quality. − Melting points (uncorrected): Büchi 510. − IR: Perkin-Elmer FT 1750. − NMR: Varian VXR 300 and Gemini 300 (300 and 75 MHz for ^1H and ^{13}C, respectively), Varian Unity 500 (500 and 125 MHz for ^1H and ^{13}C, respectively), $CDCl_3$ as solvent, TMS as internal standard, room temperature if not otherwise noticed. − MS: Finnigan MAT (70 eV) and Finnigan SSQ 7000 (70 eV).

1. General Procedure for the Preparation of (Chloro)rhodium-(COD) Complexes **2−4**: $(COD)RhCl]_2$ (50 mg, 0.10 mmol), NEt_3 (0.2 ml, 1.4 mmol) and 1.1 equiv. of the corresponding triazolium perchlorate **1** (0.22 mmol) were dissolved in 40 ml of THF and the solution was stirred at room temperature for 14 h. The solution was evaporated to dryness in vacuo and the products were purified by column chromatography (silica gel, Et_2O/pentane, 2:1).

Chloro(η⁴-1,5-cyclooctadiene)(1-phenyl-4-benzyl-4,5-dihydro-1H-1,2,4-triazol-5-ylidene)rhodium(I) (**2**): Yield 86 mg (90%), m.p. 184°C. − IR (KBr): ν = 3110 cm^{-1} (m), 3047 (m), 3005 (m), 2931 (s), 2880 (s), 2833 (m), 1595 (s), 1545 (m), 1497 (s), 1476 (m), 1457 (m), 1435 (m), 1396 (s), 1355 (s), 1333 (s), 1222 (s), 766 (s), 723 (s), 706 (s), 650 (s). − ^1H NMR (300 MHz): δ = 1.66 (m, 1 H, CH_2CH_2), 1,84 (m, 4 H, CH_2CH_2), 2.12 (m, 1 H, CH_2CH_2), 2.30 (m, 2 H, CH_2CH_2), 2.74 (m, 1 H, CHCH), 3.08 (m, 1 H, CHCH), 5.12 (m, 1 H, CHCH), 5.22 (m, 1 H, CHCH), 5.86 (d, *J* = 14.83 Hz, 1 H, $PhCH_2$), 6.06 (d, *J* = 14.83 Hz, 1 H, $PhCH_2$), 7.50 (m, 8 H, C_6H_5), 7.90 (s, 1 H, N_2CH), 8.56 (m, 2 H, C_6H_5). − ^{13}C NMR (75 MHz): δ = 28.64, 28.87, 32.23, 32.60 (CH_2CH_2), 53.37 ($PhCH_2$), 69.07 (d, *J* = 14.3 Hz, CHCH), 70.35 (d, *J* = 14.3 Hz, CHCH), 98.83 (d, *J* = 7.4 Hz, CHCH), 99.53 (d, *J* = 7.4 Hz, CHCH), 123.75, 128.48, 128.73, 128.82, 128.90, 129.31 (C_5H_5CR), 134.70, 139.74 (C_5H_5CR), 142.42 (CHN), 186.94 (d, *J* = 51.0 Hz, NCRh). − MS (70 eV); *m/z* (%): 481.1 (38.2) [M^+], 445.0 (12.1) [M^+ − HCl], 372.9 (43.6) [M^+ − COD], 336.9 (100) [M^+ − COD − Cl]. − HR-MS; *m/z*: $C_{23}H_{25}ClN_3Rh$ [M^+]: calcd. 481.0785; found 481.0785.

(R)-Chloro(η⁴-1,5-cyclooctadiene)(1-methyl-4-(1-phenylethyl)-4,5-dihydro-1H-1,2,4-triazol-5-ylidene)rhodium(I) (**3a**): Yield 60 mg (70%), diasteromeric excess (*de*) 41%, m.p. 78−80°C − $[\alpha]_D^{25}$ = +63 (*c* = 0.1, $CHCl_3$). − IR (KBr): $\tilde{\nu}$ = 3029 cm^{-1} (m), 2978 (s), 2933 (s), 2875 (s), 2829 (s), 1531 (s), 1495 (s), 1474 (s), 1404 (s), 1383 (s), 1335 (s), 794 (s), 732 (s), 701 (s). − ^1H NMR (300 MHz): δ = 1.74 (m, 1 H, CH_2CH_2), 1.92 (d, *J* = 7.14 Hz, 3 H, $CHCH_3$), 2.00 (m, 3 H, CH_2CH_2), 2.40 (m, 4 H, CH_2CH_2), 2.93 (m, 1 H, CHCH), 3.36 (m, 2 H, CHCH), 4.27 (s, 3 H, NCH_3), 5.12 (m, 2 H, CHCH), 6.73 (q, J = 7.41 Hz, 1 H, $CHCH_3$), 7.33 (m, 2 H, C_6H_5), 7.40 (m, 2 H, C_6H_5), 7.60 (s, 1 H minor diastereomer, N_2CH), 7.64 (m, 1 H, C_6H_5), 7.92 (s, 1 H, N_2CH). − ^{13}C NMR (75 MHz): δ = 22.93 (CH_3), 28.35, 29.18, 32.20, 33.36 (CH_2CH_2), 39.98 (NCH_3), 58.48 ($CHCH_3$), 68.40 (d, *J* = 14.3 Hz, CHCH), 69.61 (d, *J* = 15.0 Hz, CHCH), 99.46 (d, *J* = 7.4 Hz, CHCH), 99.85 (d, *J* = 6.9 Hz, CHCH), 126.36, 128.36, 129.20 (C_5H_5CR), 138.80 (C_5H_5CR), 140.24 (N_2CH), 186.02 (d, *J* = 50.3 Hz, NCRh). − MS (70 eV); *m/z* (%): 433.0 (11.0) [M^+], 324.9 (100) [M^+ − COD], 288.8 (17.5) [M^+ − COD − Cl], 260.9 (45.5), 105.0 (42.8). − HR-MS; *m/z*: $C_{19}H_{25}ClN_3Rh$ [M^+]: calcd. 433.0785; found 433.0784.

(R)-Chloro(η⁴-1,5-cyclooctadiene)(1-phenyl-4-(1-phenylethyl)-4,5-dihydro-1H-1,2,4-triazol-5-ylidene)rhodium(I) (**3b**): Yield 94 mg (95%), *de* 40%, m.p. 207°C. − $[\alpha]_D^{25}$ = +142 (*c* = 0.1, $CHCl_3$). − IR (KBr): ν = 3031 cm^{-1} (m), 2995 (m), 2969 (m), 2935 (s), 2914 (s), 2874 (s), 2829 (s), 1597 (s), 1531 (s), 1500 (s), 1476 (m), 1452 (m), 1409 (s), 1387 (m), 1345 (s), 762 (s), 718 (s), 691 (s), 663 (s). − ^1H NMR (300 MHz): δ = 1.65 (m, 1 H, CH_2CH_2), 1.76 (m, 2 H, CH_2CH_2), 1.90 (m, 2 H, CH_2CH_2), 2.00 (d, *J* = 7.15 Hz, 3 H, $CHCH_3$), 2.15 (m, 1 H, CH_2CH_2), 2.35 (m, 2 H, CH_2CH_2), 2.68 (m, 1 H, CHCH), 2.81 (m, 2 H, CHCH), 5.15 (m, 2 H, CHCH), 7.02 (q, J = 7.14 Hz, 1 H, $CHCH_3$), 7.39 (m, 2 H, C_6H_5), 7.46 (m, 4 H, C_6H_5), 7.56 (m, 2 H, C_6H_5), 7.72 (s, 1 H minor diastereomer, N_2CH), 8.18 (s, 1 H, N_2CH), 8.55 (m, 2 H, C_6H_5). − ^{13}C NMR (75 MHz): δ = 22.79 (CH_3), 28.20, 29.17, 32.18, 32.76 (CH_2CH_2), 59.49 ($CHCH_3$), 68.76 (d, *J* = 14.3 Hz, CHCH), 71.02 (d, *J* = 13.8 Hz, CHCH), 98.50 (d, *J* = 7.5 Hz, CHCH), 99.42 (d, *J* = 7.4 Hz, CHCH), 123.95, 125.55, 128.41, 128.47, 128.84, 129.25 (C_5H_5CR), 138.28, 139.89 (C_5H_5CR), 140.67 (N_2CH), 186.85 (d, *J* = 51.0 Hz, NCRh). − MS (70 eV); *m/z* (%): 495.0 (36.3) [M^+], 386.9 (66.5) [M^+ −COD], 350.9 (64.3) [M^+ − COD − HCl], 246.9 (44.9), 105.0 (77.7). − HR-MS, *m/z*: $C_{24}H_{27}ClN_3Rh$ [M^+]: calcd. 495.0942; found 495.0942.

(R)-(1-tButyl-4-(1-phenylethyl)-4,5-dihydro-1H-1,2,4-triazol-5-ylidene)(chloro)(η⁴-1,5-cyclooctadiene)rhodium(I) (**3c**): Yield 74 mg (78%), *de* 36%, m.p. 81°C. − $[\alpha]_D^{25}$ = +38 (*c* = 0.1, $CHCl_3$). − IR (KBr): ν = 3047 cm^{-1} (m), 2976 (s), 2933 (s), 2876 (s), 2831 (s), 1545 (s), 1496 (m), 1475 (s), 1454 (s), 1406 (s), 1383 (s), 1365 (s), 762 (m), 703 (s), 673 (m). − ^1H NMR (300 MHz): δ = 1.87 (m, 4 H, CH_2CH_2), 1.97 (d, *J* = 7.69 Hz, 3 H, $CHCH_3$), 2.01 (s, 9 H, $C(CH_3)_3$), 2.36 (m, 1 H, CH_2CH_2), 3.20 (m, 1 H, CHCH), 3.35 (m, 1 H, CHCH), 5.04 (m, 2 H, CHCH), 7.36 (m, 5 H, C_6H_5, $CHCH_3$), 7.70 (m, 1 H, C_6H_5), 7.72 (s, 1 H minor diastereomer, N_2CH), 7.88 (s, 1 H, N_2CH). − ^{13}C NMR (75 MHz): δ = 23.37 (CH_3), 28.79, 28.86 (CH_2CH_2), 31.25 [$C(CH_3)_3$], 32.17, 32.70 (CH_2CH_2), 59.76 ($CHCH_3$), 61.95 [$C(CH_3)_3$], 68.51 (d, *J* = 14.3 Hz, CHCH), 69.74 (d, *J* = 14.9 Hz, CHCH), 95.63 (d, *J* = 7.5 Hz, CHCH), 97.63 (d, *J* = 7.4 Hz, CHCH), 126.08, 127.51, 129.19 (C_5H_5CR), 139.64 (C_5H_5CR), 140.67 (N_2CH), 184.10 (d, *J* = 56.7 Hz, NCRh). − MS (70 eV); *m/z* (%): 475.0 (37.1) [M^+], 440.1 (10.8) [M^+ − Cl], 402.8 (14.2), 366.9 (50.5) [M^+ − COD], 331.0 (24.3) [M^+ − COD − HCl], 310.9 (100.0) [M^+ − COD − C_4H_8], 105.1 (18.6). − HR-MS, *m/z*: $C_{22}H_{31}ClN_3Rh$ [M^+]: calcd. 475.1255; found 475.1255.

(S_a,4S,5S)-Chloro(η⁴-1,5-cyclooctadiene)(1-methyl-4-(2,2-dimethyl-4-phenyl-1,3-dioxan-5-yl)-4,5-dihydro-1H-1,2,4-triazol-5-

ylidene)rhodium(I) (**4a**): Yield 84 mg (79%), *de* 93%, m.p. >230°C − $[\alpha]_D^{25}$ = +80 (*c* = 0.1, $CHCl_3$). − IR (KBr): ν = 3174 cm^{-1} (w), 2990 (m), 2939 (s), 2914 (m), 2875 (s), 2833 (m), 1533 (m), 1499 (m), 1478 (m), 1448 (m), 1376 (s), 1204 (s), 1188 (s), 1165 (s), 1121 (s), 1078 (s), 1017 (m), 732 (s), 701 (s). − ^{1}H NMR (300 MHz): δ = 1.65 (s, 3 H, CCH_3), 1.69 (s, 3 H, CCH_3), 1.88 (m, 5 H, C$H_2$$CH_2$), 2.14 (m, 1 H, C$H_2$$CH_2$), 2.30 (m, 4 H, C$H_2$$CH_2$, C*H*CH), 2.96 (m, 1 H, C*H*CH), 4.19 (s, 3 H, NCH_3), 4.27 (br. d, *J* = 12.91 Hz, 1 H, OCH_2), 4.52 (d/d, *J* = 12.92/2.20 Hz, 1 H, OCH_2), 4.91 (m, 1 H, C*H*CH), 5.01 (m, 1 H, C*H*CH), 5.50 (d, *J* = 2.48 Hz, 1 H, OCH), 5.72 (d/d/d, *J* = 1.65/1.65/1.65 Hz, 1 H, OCHC*H*), 7.24 (m, 5 H, C_6H_5), 8.35 (s, 1 H minor diastereomer, N_2CH), 8.73 (s, 1 H, N_2CH). − ^{13}C NMR (75 MHz): δ = 18.44 (CCH_3), 28.48 (*C*$H_2$$CH_2$), 29.04 (*C*$H_2$$CH_2$), 29.73 (C$CH_3$), 32.28 (*C*$H_2$$CH_2$), 33.26 (*C*$H_2$$CH_2$), 39.76 ($NCH_3$), 57.25 (OCH*C*H), 64.89 (O*C*H_2), 68.26 (d, *J* = 13.8 Hz, *C*HCH), 69.13 (d, *J* = 14.3 Hz, *C*HCH), 73.09 (OCH), 99.31 (d, *J* = 6.8 Hz, *C*HCH), 99.64 (d, *J* = 7.4 Hz, *C*HCH), 100.47 [O*C*$(CH_3)_2$], 126.13, 128.52, 128.64 (*C*$_5H_5$CR), 137.35 (C_5H_5*C*R), 143.17 (N_2CH), 187.33 (d, *J* = 52.3 Hz, NCRh). − MS (70 eV); *m/z* (%): 519.0 (24.7) [M^+], 411.0 (100.0) [M^+ − COD], 376.9 (6.7) [M^+ −COD − Cl]. − HR-MS, *m/z*: $C_{23}H_{31}ClN_3O_2Rh$ [M^+]: calcd. 519.1153; found 519.1153.

(S$_a$,4S,5S)-Chloro(η^4-1,5-cyclooctadiene)(1-phenyl-4-(2,2-dimethyl-4-phenyl-1,3-dioxan-5-yl)-4,5-dihydro-1H-1,2,4-triazol-5-ylidene)rhodium(I) (**4b**): Yield 110 mg (95%), *de* 91%, m.p. >230°C − $[\alpha]_D^{25}$ = +8 (*c* = 0.1, $CHCl_3$). − IR (KBr): ν = 3161 cm^{-1} (m), 2991 (m), 2935 (s), 2910 (m), 2877 (s), 2831 (m), 1597 (m), 1538 (m), 1499 (s), 1464 (m), 1452 (m), 1430 (m), 1402 (s), 1382 (s), 1366 (s), 1187 (s), 1160 (s), 1112 (s), 1078 (s), 1010 (s), 763 (s), 736 (s), 719 (s), 699 (s). − ^{1}H NMR (300 MHz): δ = 1.43 (m, 1 H, C$H_2$$CH_2$), 1.61 (m, 2 H, C$H_2$$CH_2$), 1.68 (s, 3 H, CCH_3), 1.72 (s, 3 H, CCH_3), 1.75 (m, 3 H, C$H_2$$CH_2$), 2.06 (m, 1 H, C$H_2$$CH_2$), 2.19 (m, 1 H, C$H_2$$CH_2$), 2.27 (m, 2 H, C*H*CH), 4.42 (d/d, *J* = 12.91/1.37 Hz, 1 H, OCH_2), 4.60 (d/d, *J* = 12.91/2.20 Hz, 1 H, OCH_2), 4.90 (m, 1 H, C*H*CH), 5.11 (m, 1 H, C*H*CH), 5.58 (d, *J* = 2.47 Hz, 1 H, OCH), 6.00 (d/d/d, *J* = 1.64/1.64/1.64 Hz, 1 H, OCHC*H*), 7.23 (m, 1 H, C_6H_5), 7.30 (m, 4 H, C_6H_5), 7.42 (m, 1 H, C_6H_5), 7.51 (m, 2 H, C_6H_5), 8.43 (m, 2 H, C_6H_5), 8.45 (s, 1 H minor diastereomer, N_2CH), 8.95 (s, 1 H, N_2CH). − ^{13}C NMR (75 MHz): δ = 18.47 (CCH_3), 28.67 (*C*$H_2$$CH_2$), 28.78 (*C*$H_2$$CH_2$), 29.77 (C$CH_3$), 31.70 (*C*$H_2$$CH_2$), 33.09 (*C*$H_2$$CH_2$), 58.14 (OCH*C*H), 64.99 (O*C*H_2), 68.39 (d, *J* = 14.4 Hz, *C*HCH), 70.79 (d, *J* = 13.7 Hz, *C*HCH), 73.12 (OCH), 98.63 (d, *J* = 6.9 Hz, *C*HCH), 98.87 (d, *J* = 7.4 Hz, *C*HCH), 100.53 (O*C*$(CH_3)_2$), 124.13, 126.13, 128.41, 128.53, 128.66 (*C*$_5H_5$CR), 137.40, 139.73 (C_5H_5*C*R), 143.56 (N_2CH), 186.75 (d, *J* = 51.6 Hz, NCRh). − MS (70 eV); *m/z* (%): 581.2 (11.7) [M^+], 546.2 (16.8) [M^+ −Cl], 473.0 (14.9) [M^+ − COD], 437.0 (63.7) [M^+ − COD − Cl]. − HR-MS, *m/z*: $C_{28}H_{33}ClN_3O_2Rh$ [M^+]: calcd. 581.1309; found 581.1306.

(S$_a$,4S,5S)-(1-tButyl-4-(2,2-dimethyl-4-phenyl-1,3-dioxan-5-yl)-4,5-dihydro-1H-1,2,4-triazol-5-ylidene)(chloro)(η^4-1,5-cyclooctadiene)rhodium(I) (**4c**): Yield 72 mg (65%), *de* 97%, m.p. 228°C. − $[\alpha]_D^{25}$ = +39 (*c* = 0.1, $CHCl_3$). − IR (KBr): ν = 3031 cm^{-1} (w), 2990 (m), 2939 (m), 2914 (m), 2876 (s), 2833 (m), 1534 (m), 1478 (m), 1448 (m), 1376 (s), 1188 (s), 1121 (s), 1078 (s), 1016 (s), 732 (s), 701 (s). − ^{1}H NMR (300 MHz): δ = 1.65 (s, 3 H, CCH_3), 1.70 (s, 3 H, CCH_3), 1.77 (m, 2 H, C$H_2$$CH_2$), 1.88 (m, 2 H, C$H_2$$CH_2$), 1.92 [s, 9 H, C$(CH_3)_3$], 2.02 (m, 1 H, C*H*CH), 2.16 (m, 1 H, C$H_2$$CH_2$), 2.24 (m, 2 H, C$H_2$$CH_2$), 2.36 (m, 1 H, C$H_2$$CH_2$), 2.90 (m, 1 H, C*H*CH), 4.41 (d/d, *J* = 12.64/1.37 Hz, 1 H, OCH_2), 4.56 (d/d, *J* = 12.91/2.20 Hz, 1 H, OCH_2), 4.86 (m, 1 H, C*H*CH), 4.97 (m, 1 H, C*H*CH), 5.52 (d, *J* = 2.47 Hz, 1 H, OCH), 6.20 (d/d/d, *J* = 1.65/1.65/1.65 Hz, 1 H, OCHC*H*), 7.26 (m, 5 H, C_6H_5), 8.49 (s, 1 H minor diastereomer, N_2CH), 8.87 (s, 1 H, N_2CH). − ^{13}C NMR (75 MHz): δ = 18.50 (CCH_3), 28.19 (*C*$H_2$$CH_2$), 29.37 (*C*$H_2$$CH_2$), 29.68 (C$CH_3$), 30.88 (*C*$H_2$$CH_2$), 31.23 [C(*C*$H_3$)$_3$], 31.34 (*C*$H_2$$CH_2$), 58.53 (OCH*C*H), 61.70 [*C*$(CH_3)_3$], 65.09 (O*C*H_2), 68.01 (d, *J* = 14.3 Hz, *C*HCH), 68.99 (d, *J* = 14.99 Hz, *C*HCH), 73.69 (OCH), 95.90 (d, *J* = 7.5 Hz, *C*HCH), 97.70 (d, *J* = 8.0 Hz, *C*HCH), 100.51 [O*C*$(CH_3)_2$], 126.55, 128.53, 128.73 (*C*$_5H_5$CR), 137.25 (C_5H_5*C*R), 142.45 (N_2CH), 183.93 (d, *J* = 51.0 Hz, NCRh). − MS (70 eV); *m/z* (%): 561.2 (88.7) [M^+], 453.0 (100) [M^+ − COD], 417.0 (58.2) [M^+ − COD − Cl], 396.9 (81.4). − HR-MS, *m/z*: $C_{26}H_{37}ClN_3O_2Rh$ [M^+]: calcd. 561.1622; found 561.1620.

2. General Procedure for the Preparation of (Chloro)rhodium(NBD) Complexes **5** *and* **6***:* [(NBD)RhCl]$_2$ (46 mg, 0.1 mmol), NEt_3 (0.2 ml, 1.4 mmol) and 1.1 equiv. of the corresponding triazolium perchlorate **1** (0.22 mmol) were dissolved in 40 ml of THF and the solution was stirred at room temperature for 14 h. The solution was evaporated to dryness in vacuo and the products were purified by column chromatography (silica gel, Et_2O/pentane, 2:1).

Chloro(η^4-1,5-norbornadiene)(1-phenyl-4-benzyl-4,5-dihydro-1H-1,2,4-triazol-5-ylidene)rhodium(I) (**5**): Yield 88 mg (95%), m.p. 192°C. − IR (KBr): ν = 3118 cm^{-1} (m), 3047 (m), 3002 (m), 2958 (m), 2919 (m), 2841 (m), 1596 (s), 1541 (m), 1497 (s), 1456 (m), 1397 (s), 1338 (s), 1306 (s), 1222 (s), 763 (s), 726 (s), 705 (s). − ^{1}H NMR (500 MHz): δ = 1.10 (d/d/d, *J* = 8.51/1.38/1.38 Hz, 1 H, CHCH_2), 1.18 (d/d/d, *J* = 8.51/1.65/1.65 Hz, 1 H, CHCH_2), 2.69 (m, 2 H, CHC*H*CHCH_2), 3.47 (m, 2 H, CH_2C*H*), 4.87 (m, 2 H, CHC*H*CHCH_2), 5.80 (br. s, 2 H, PhCH_2), 7.48 (m, 4 H, C_6H_5), 7.61 (m, 4 H, C_6H_5), 8.01 (s, 1 H, N_2CH), 8.54 (m, 2 H, C_6H_5). − ^{1}H NMR (500 MHz, −40°C): δ = 1.09 (br. d, *J* = 8.55 Hz, 1 H, CHCH_2), 1.17 (br. d, *J* = 8.24 Hz, 1 H, CHCH_2), 2.59 (m, 2 H, CHC*H*CHCH_2), 3.46 (m, 2 H, CH_2C*H*), 4.85 (m, 1 H, CHC*H*CHCH_2), 4.91 (m, 1 H, CHC*H*CHCH_2), 5.50 (d, *J* = 14.65 Hz, 1 H, PhCH_2), 6.08 (d, *J* = 14.65 Hz, 1 H, PhCH_2), 7.48 (m, 2 H, C_6H_5), 7.54 (m, 2 H, C_6H_5), 7.62 (m, 2 H, C_6H_5), 7.69 (m, 2 H, C_6H_5), 8.31 (s, 1 H, N_2CH), 8.53 (m, 2 H, C_6H_5). − ^{13}C NMR (75 MHz): δ = 49.36 (m, CH_2CH*C*HCH), 50.67 (d, *J* = 2.9 Hz, CH_2*C*H), 52.97 (PhCH_2), 63.00 (d, *J* = 5.1 Hz, *C*H_2CHCH), 78.34 (d, *J* = 6.0 Hz, CH_2CH*C*HCH), 123.50, 128.56, 128.72, 128.78, 129.17 (*C*$_5H_5$CR), 135.32, 139.84 (C_5H_5*C*R), 142.63 (CHN), 189.00 (d, *J* = 57.5 Hz, NCRh). − MS (70 eV); *m/z* (%): 465.1 (3.6) [M^+], 429.0 (3.3) [M^+ −HCl], 372.9 (3.0) [M^+ − NBD], 336.9 (16.0) [M^+ − NBD − HCl], 91.0 (100.0). − HR-MS, *m/z*: $C_{22}H_{21}ClN_3Rh$ [M^+]: calcd. 465.0472; found 465.0477.

(4S,5S)-Chloro(1-methyl-4-(2,2-dimethyl-4-phenyl-1,3-dioxan-5-yl)-4,5-dihydro-1H-1,2,4-triazol-5-ylidene)(η^4-1,5-norbornadiene)rhodium(I) (**6a**): Yield 94 mg (93%), m.p. 199°C. − $[\alpha]_D^{25}$ = +128 (*c* = 0.1, $CHCl_3$). − IR (KBr): ν = 2994 cm^{-1} (s), 2953 (m), 2922 (m), 2882 (m), 2837 (m), 1533 (m), 1483 (m), 1451 (m), 1441 (m), 1407 (m), 1383 (s), 1305 (m), 1237 (s), 1204 (s), 1187 (s), 1162 (s), 1115 (s), 1079 (s), 762 (m), 734 (s), 705 (s). − ^{1}H NMR (300 MHz): δ = 1.29 (d/d, *J* = 1.37/1.37 Hz, 2 H, CHCH_2), 1.64 (s, 3 H, CCH_3), 1.68 (s, 3 H, CCH_3), 2.34 (m, 1 H, CH_2CHC*H*CH), 3.33 (m, 1 H, CH_2CHC*H*CH), 3.63 (m, 1 H, CH_2C*H*), 3.73 (m, 1 H, CH_2C*H*), 4.05 (s, 3 H, NCH_3), 4.14 (d/d, *J* = 12.91/1.37 Hz, 1 H, OCH_2), 4.54 (d/d, *J* = 12.91/2.20 Hz, 1 H, OCH_2), 4.78 (m, 1 H, CH_2CHC*H*CH), 4.85 (m, 1 H, CH_2CHC*H*CH), 5.55 (d, *J* = 2.47 Hz, OCH), 5.90 (d/d/d, *J* = 1.37/1.37/1.37 Hz, 1 H, OCH_2C*H*), 7.24 (m, 1 H, C_6H_5), 7.34 (m, 4 H, C_6H_5), 8.63 (s, 1 H, N_2CH). − ^{13}C NMR (75 MHz): δ = 19.04 (*C*CH_3), 30.27 (*C*CH_3), 40.05 (NCH_3), 49.60 (d, *J* = 11.9 Hz, CH_2CH*C*HCH), 50.03 (d, *J* = 12.5 Hz, CH_2CH*C*HCH), 51.52 (d, *J* = 5.7 Hz, CH_2*C*H), 57.21 (OCH_2), 64.29 (*C*H_2CHCHCH),

65.58 (OCH_2CH), 73.15 (OCH), 79.53 (d, J = 5.7 Hz, $CH_2CHCHCH$), 81.07 (d, J = 5.7 Hz, $CH_2CHCHCH$), 100.94 [$C(CH_3)_2$], 126.64, 128.86, 129.21 (C_5H_5CR), 137.89 (C_5H_5CR), 143.52 (N_2CH), 186.64 (d, J = 58.1 Hz, NCRh). − MS (70 eV); *m/z* (%): 503.1 (4.7) [M^+], 468.2 (54.6) [M^+ − Cl], 411.0 (71.3) [M^+ − NBD], 376.2 (17.7) [M^+ − NBD − HCl], 323.1 (41.1), 287.1 (36.6), 211.1 (60.8), 272.1 (9.0), 184.1 (80.6), 91.2 (100.0). − HR-MS, *m/z*: $C_{22}H_{27}N_3O_2Rh$ [M^+ − Cl]: calcd. 468.1151; found 468.1154.

(4S,5S)-Chloro(η⁴-1,5-norbornadiene)(1-phenyl-4-(2,2-dimethyl-4-phenyl-1,3-dioxan-5-yl)-4,5-dihydro-1H-1,2,4-triazol-5-ylidene)rhodium(I) (**6b**): Yield 108 mg (95%), m.p. 226°C. − $[\alpha]_D^{25}$ = +13 (c = 0.1, $CHCl_3$) − IR (KBr): ν = 3049 cm^{-1} (w), 2985 (s), 2922 (m), 2956 (s), 2937 (m), 2912 (m), 2837 (w), 1597 (m), 1533 (m), 1501 (s), 1453 (m), 1410 (m), 1383 (s), 1326 (m), 1234 (s), 1201 (s), 1161 (s), 1115 (s), 1074 (s), 1014 (s), 762 (s), 734 (s), 704 (s). − ^{1}H NMR (300 MHz): δ = 1.05 (d/d/d, J = 8.24/1.50/1.50 Hz, 1 H, $CHCH_2$), 1.16 (d/d/d, J = 8.52/1.38/1.38 Hz, 1 H, $CHCH_2$), 1.67 (s, 3 H, CCH_3), 1.71 (s, 3 H, CCH_3), 2.00 (m, 1 H, $CH_2CHCHCH$), 2.40 (m, 1 H, $CH_2CHCHCH$), 3.37 (m, 1 H, CH_2CH), 3.50 (m, 1 H, CH_2CH), 4.29 (br. d, J = 12.37 Hz, 1 H, OCH_2), 4.62 (d/d, J = 12.91/1.92 Hz, 1 H, OCH_2), 4.80 (m, 2 H, $CH_2CHCHCH$), 5.63 (d, J = 2.47 Hz, OCH), 6.11 (d/d/d, J = 1.65/1.65/1.65 Hz, OCH_2CH), 7.22 (m, 1 H, C_6H_5), 7.34 (m, 2 H, C_6H_5), 7.46 (m, 3 H, C_6H_5), 7.55 (m, 2 H, C_6H_5), 8.34 (m, 2 H, C_6H_5), 8.82 (s, 1 H, N_2CH). − ^{13}C NMR (75 MHz): δ = 18.51 (CCH_3), 29.74 (CCH_3), 48.71 (br. CH_2CH), 50.51 ($CH_2CHCHCH$), 50.80 (br. CH_2CH), 57.37 (OCH_2), 63.26 (d, J = 5.2 Hz, $CH_2CHCHCH$), 65.06 (OCH_2CH), 72.51 (OCH), 77.46 (d, J = 5.2 Hz, $CH_2CHCHCH$), 77.82 (d, J = 6.2 Hz, $CH_2CHCHCH$), 100.45 [$C(CH_3)_2$], 123.86, 126.05, 128.31, 128.53, 128.60, 128.62 (C_5H_5CR), 137.32, 139.55 (C_5H_5CR), 143.32 (N_2CH), 187.54 (d, J = 58.1 Hz, NCRh). − MS (70 eV); *m/z* (%): 565.2 (19.0) [M^+], 473.1 (19.9) [M^+ −NBD], 437.1 (100.0) [M^+ − NBD − HCl], 349.0 (12.8), 273.0 (16.6), 247.0 (15.1). − HR-MS, *m/z*: $C_{27}H_{29}ClN_3O_2Rh$ [M^+]: calcd. 565.0996; found 565.1001.

(Sₐ,4S,5S)-(1-tButyl-4-(2,2-dimethyl-4-phenyl-1,3-dioxan-5-yl)-4,5-dihydro-1H-1,2,4-triazol-5-ylidene)(chloro)(η⁴-1,5-norbornadiene)rhodium(I) (**6c**): Yield 82 mg (75%), *de* 87%, m.p. 113°C. − $[\alpha]_D^{25}$= +36 (c = 0.1, $CHCl_3$). − IR (KBr): ν = 3060 cm^{-1} (w), 2988 (s), 2939 (m), 2878 (m), 1543 (m), 1498 (m), 1475 (m), 1454 (m), 1400 (s), 1384 (s), 1306 (m), 1267 (s), 1234 (s), 1206 (s), 1192 (s), 1166 (s), 1112 (s), 1078 (s), 1010 (m), 754 (m), 704 (s). − ^{1}H NMR (500 MHz, major diastereomer): δ = 1.19 (d/d/d, J = 8.54/1.53/1.53 Hz, 1 H, $CHCH_2$), 1.22 (d/d/d, J = 8.54/1.53/1.53 Hz, 1 H, $CHCH_2$), 1.64 (s, 3 H, CCH_3), 1.71 (s, 3 H, CCH_3), 1.88 (s, 9 H, $C(CH_3)_3$), 2.26 (m, 1 H, $CH_2CHCHCH$), 3.13 (m, 1 H, $CH_2CHCHCH$), 3.63 (m, 2 H, CH_2CH), 4.26 (d/d, J = 12.82/1.53 Hz, 1 H, OCH_2), 4.55 (m, 1 H, $CH_2CHCHCH$), 4.59 (d/d, J = 12.82/1.53 Hz, 1 H, OCH_2), 4.70 (m, 1 H, $CH_2CHCHCH$), 5.59 (d, J = 2.44 Hz, OCH), 6.45 (d/d/d, J = 1.53/1.53/1.53 Hz, OCH_2CH), 7.25 (m, 1 H, C_6H_5), 7.28 (m, 2 H, C_6H_5), 7.30 (m, 2 H, C_6H_5), 8.78 (s, 1 H, N_2CH). − ^{1}H NMR (500 MHz, minor diastereomer): δ = 1.32 (d/d/d, J = 8.54/1.67/1.67 Hz, 1 H, $CHCH_2$), 1.35 (d/d/d, J = 8.54/1.60/1.60 Hz, 1 H, $CHCH_2$), 1.64 (s, 3 H, CCH_3), 1.73 (s, 3 H, CCH_3), 1.85 (s, 9 H, $C(CH_3)_3$), 2.23 (m, 1 H, $CH_2CHCHCH$), 3.39 (m, 1 H, $CH_2CHCHCH$), 3.76 (m, 2 H, CH_2CH), 4.29 (d/d, J = 11.52/1.83 Hz, 1 H, OCH_2), 4.75 (m, 2 H, $CH_2CHCHCH$), 4.82 (d/d, J = 12.51/2.90 Hz, 1 H, OCH_2), 5.61 (d, J = 2.83 Hz, OCH), 6.27 (d/d/d, J = 1.76/2.60/2.60 Hz, OCH_2CH), 7.12 (m, 1 H, C_6H_5), 7.22 (m, 2 H, C_6H_5), 7.44 (m, 2 H, C_6H_5), 8.40 (s, 1 H, N_2CH). − ^{13}C NMR (75 MHz): δ = 18.53 (CCH_3), 29.66 (CCH_3), 31.14 [$C(CH_3)_3$], 47.40 (d, J = 12.5 Hz, $CH_2CHCHCH$), 48.65 (d, J = 12.0 Hz, $CH_2CHCHCH$), 50.22 (d, J = 2.4 Hz, CH_2CH), 50.32 (d, J = 2.9 Hz, CH_2CH), 58.50 (OCH_2CH), 60.95 [$C(CH_3)_3$], 63.04 (d, J = 4.9 Hz, $CH_2CHCHCH$), 65.11 (OCH_2), 72.19 (d, J = 6.0 Hz, $CH_2CHCHCH$), 73.41 (OCH), 75.64 (d, J = 6.5 Hz, $CH_2CHCHCH$), 100.46 [$C(CH_3)_2$], 126.59, 128.51, 128.55 (C_5H_5CR), 137.35 (C_5H_5CR), 142.11 (N_2CH), 185.46 (d, J = 56.7 Hz, NCRh). − MS (70 eV); *m/z* (%): 545.2 (39.0) [M^+], 453.0 (100.0) [M^+ − NBD], 417.0 (98.7) [M^+ − NBD − HCl], 396.9 (95.7), 361.0 (49.0), 308.9 (47.7), 272.9 (55.4), 196.9 (41.1), 105.0 (63.1), 91.1 (69.9). − HR-MS, *m/z*: $C_{25}H_{33}ClN_3O_2Rh$ [M^+]: calcd. 545.1309; found 545.1308.

3. General Procedure for the Preparation of (Iodo)rhodium(NBD) Complexes **7** *and* **8**: Chloro)rhodium(NBD) complexes **5**, **6a−b** (0.1 mmol) and NaI (40 mg, 0.26 mmol) were dissolved in 10 ml of MeOH. The solution was stirred at room temperature for 6 h, evaporated to dryness in vacuo and the products were purified by column chromatography (silica gel, Et_2O/pentane, 1:1).

Iodo(η⁴-1,5-norbornadiene)(1-phenyl-4-benzyl-4,5-dihydro-1H-1,2,4-triazol-5-ylidene)rhodium(I) (**7**): Yield 50 mg (90%), m.p. 172°C. − IR (KBr): ν = 3120 cm^{-1} (m), 3052 (m), 3006 (m), 2949 (m), 2912 (m), 2863 (m), 2840 (m), 1595 (m), 1534 (m), 1498 (s), 1458 (m), 1384 (m), 1343 (m), 1303 (s), 761 (s), 732 (s), 697 (s). − ^{1}H NMR (500 MHz): δ = 1.09 (d/d/d, J = 8.51/1.65/1.65 Hz, 1 H, $CHCH_2$), 1.24 (d/d/d, J = 8.52/1.65/1.65 Hz, 1 H, $CHCH_2$), 2.91 (m, 2 H, $CH_2CHCHCH$), 3.47 (m, 2 H, CH_2CH), 5.06 (m, 1 H, $CH_2CHCHCH$), 5.10 (m, 1 H, $CH_2CHCHCH$), 5.56 (d, J = 14.55 Hz, 1 H, $PhCH_2$), 6.03 (d, J = 14.56 Hz, 1 H, $PhCH_2$), 7.48 (m, 4 H, C_6H_5), 7.58 (m, 4 H, C_6H_5), 7.98 (s, 1 H, N_2CH), 8.56 (m, 2 H, C_6H_5). − ^{13}C NMR (75 MHz): δ = 51.18 (d, J = 2.33 Hz, CH_2CH), 51.83 (d, J = 11.9 Hz, $CH_2CHCHCH$), 52.92 (d, J = 12.0 Hz, $CH_2CHCHCH$), 53.47 ($PhCH_2$), 64.39 (d, J = 5.1 Hz, CH_2CHCH), 75.48 (d, J = 8.0 Hz, $CH_2CHCHCH$), 75.58 (d, J = 5.7 Hz, $CH_2CHCHCH$), 123.02, 128.43, 128.66, 128.83, 129.14, 129.19 (C_5H_5CR), 135.01, 139.93 (C_5H_5CR), 142.70 (CHN), 190.80 (d, J = 55.2 Hz, NCRh). − MS (70 eV); *m/z* (%): 557.0 (0.3) [M^+], 430.0 (2.6) [M^+ − I], 337.2 (10.4) [M^+ − NBD − I], 126.0 (27.8), 72.1 (100.0). − HR-MS, *m/z*: $C_{22}H_{21}N_3Rh$ [M^+ − I]: calcd. 430.0783; found 430.0783.

(Sₐ,4S,5S)-Iodo(1-methyl-4-(2,2-dimethyl-4-phenyl-1,3-dioxan-5-yl)-4,5-dihydro-1H-1,2,4-triazol-5-ylidene)(η⁴-1,5-norbornadiene)rhodium(I) (**8a**): Yield 42 mg (70%), *de* 87%, m.p. 122−124°C. − $[\alpha]_D^{25}$ = +97 (c = 0.1, $CHCl_3$). − IR (KBr): ν = 2989 cm^{-1} (s), 2922 (m), 2873 (m), 1563 (m), 1532 (m), 1498 (m), 1451 (m), 1403 (m), 1383 (s), 1307 (m), 1203 (s), 1188 (s), 1163 (s), 1117 (s), 1078 (s), 761 (m), 732 (s), 701 (s). − ^{1}H NMR (300 MHz): δ = 1.24 (d, J = 8.12 Hz, 1 H, $CHCH_2$), 1.32 (d, J = 8.18 Hz, 1 H, $CHCH_2$), 1.64 (s, 3 H, CCH_3), 1.68 (s, 3 H, CCH_3), 2.23 (m, 1 H, $CH_2CHCHCH$), 3.47 (m, 1 H, $CH_2CHCHCH$), 3.57 (m, 1 H, CH_2CH), 3.71 (m, 1 H, CH_2CH), 4.04 (s, 3 H, NCH_3), 4.26 (br. d, J = 12.63 Hz, 1 H, OCH_2), 4.57 (d/d, J = 12.91/2.20 Hz, 1 H, OCH_2), 5.01 (m, 2 H, $CH_2CHCHCH$), 5.55 (d, J = 2.20 Hz, OCH), 5.73 (m, 1 H, OCH_2CH), 7.29 (m, 5 H, C_6H_5), 8.35 (s, 1 H minor diastereomer, N_2CH), 8.70 (s, 1 H, N_2CH). − ^{13}C NMR (75 MHz): δ = 18.44 (CCH_3), 29.70 (CCH_3), 39.32 (NCH_3), 51.43 (m, $CH_2CHCHCH$, CH_2CH), 53.14 (d, J = 12.0 Hz, $CH_2CHCHCH$), 56.48 (OCH_2), 64.55 (OCH_2CH), 65.08 (d, J = 5.2 Hz, $CH_2CHCHCH$), 73.00 (OCH), 77.34 (d, J = 6.0 Hz, $CH_2CHCHCH$), 100.51 [$C(CH_3)_2$], 126.41, 128.54, 128.72 (C_5H_5CR), 137.39 (C_5H_5CR), 143.16 (N_2CH), 188.20 (d, J = 55.9 Hz, NCRh). − MS (70 eV); *m/z* (%): 595.0 (1.6) [M^+], 502.9 (4.88) [M^+ − NBD], 468.0 (100.0) [M^+ − I], 376.0 (21.2) [M^+ − NBD

− I], 287.9 (16.2), 184.0 (23.1). − HR-MS, *m/z*: $C_{22}H_{27}N_3O_2Rh$ [M^+ − I]: calcd. 468.1151; found 468.1153.

(S_a,4S,5S)-Iodo(η^4-1,5-norbornadiene)(1-phenyl-4-(2,2-dimethyl-4-phenyl-1,3-dioxan-5-yl)-4,5-dihydro-1H-1,2,4-triazol-5-ylidene)rhodium(I) (**8b**): Yield 54 mg (83%), *de* 87%, m.p. > 230°C. $-[\alpha]_D^{25} = +79$ (c = 0.1, $CHCl_3$). − IR (KBr): ν = 2990 cm^{-1} (s), 2958 (m), 2922 (m), 2876 (m), 2838 (m), 1596 (m), 1536 (m), 1500 (s), 1460 (m), 1450 (m), 1427 (m), 1383 (s), 1368 (s), 1354 (s), 1199 (s), 1163 (s), 1117 (s), 1073 (s), 1017 (s), 831 (s), 708 (s), 698 (s). − ^{1}H NMR (300 MHz): δ = 0.98 (d/d/d, J = 8.52/1.50/1.50 Hz, 1 H, CHCH_2), 1.17 (d/d/d, J = 8.50/1.38/1.38 Hz, 1 H, CHCH_2), 1.68 (s, 3 H, CCH_3), 1.70 (s, 3 H, CCH_3), 1.85 (m, 1 H, CH_2CHC*H*CH), 2.51 (m, 1 H, CH_2CHC*H*CH), 3.29 (m, 1 H, CH_2C*H*), 3.44 (m, 1 H, CH_2C*H*), 4.35 (d/d, J = 13.18/1.10 Hz, 1 H, OCH_2), 4.53 (d/d, J = 12.91/2.47 Hz, 1 H, OCH_2), 4.95 (m, 2 H, CH_2CHC*H*CH), 5.58 (d, J = 2.19 Hz, OCH), 6.02 (d/d/d, J = 1.37/1.37/1.37 Hz, OCH_2C*H*), 7.23 (m, 1 H, C_6H_5), 7.36 (m, 4 H, C_6H_5), 7.45 (m, 1 H, C_6H_5), 7.54 (m, 2 H, C_6H_5), 8.36 (m, 2 H, C_6H_5), 8.54 (s, 1 H minor diastereomer, N_2CH), 8.92 (s, 1 H, N_2CH). − ^{13}C NMR (75 MHz): δ = 19.04 (CCH_3), 30.31 (CCH_3), 51.50 (m, CH_2*C*H, CH_2CH*C*HCH), 54.93 (d, J = 12.0 Hz, CH_2CH_2CH*C*HCH), 58.10 (OCH_2), 65.11 (d, J = 5.1 Hz, *C*H_2CHCHCH), 65.24 (OCH_2*C*H), 73.60 (OCH), 75.09 (d, J = 5.7 Hz, CH_2CH*C*HCH), 76.31 (d, J = 6.2 Hz, CH_2CH*C*HCH), 101.15 [*C*$(CH_3)_2$], 123.93, 127.00, 128.99, 129.14, 129.27 (C_5H_5CR), 138.06, 140.23 (C_5H_5*C*R), 144.07 (N_2CH), 189.87 (d, J = 56.3 Hz, NCRh). − MS (70 eV); *m/z* (%): 657.0 (1.8) [M^+], 530.1 (97.7) [M^+ − I], 437.9 (100.0) [M^+ − NBD − I], 349.9 (12.3), 246.9 (11.1). − HR-MS, *m/z*: $C_{27}H_{29}N_3O_2Rh$ [M^+ − I]: calcd. 530.1308; found 530.1309.

4. General Procedure for a Catalytic Hydrosilylation Reaction: Under a nitrogen atmosphere, the ketones **9−12** (1 mmol) and Ph_2SiH_2 (184 mg, 1 mmol) were added to a solution of the (triazolinylidene)rhodium(COD) complex **4a−c** (1 mol%) in 2 ml of THF stirred at reaction temperature. The reaction was quenched by addition of methanol (0.5 ml) containing 1% of *p*-toluenesulfonic acid (*p*-TSA). After evaporation of the solvent in vacuo and purification of the product by column chromatography (silica gel, pentane/Et_2O, 2:1), the enantiomeric excess of the product alcohol was determined by gas chromatography (LIPODEX E, CP-CHIRASIL-DEX CB, 7-CD PERME).

[1] W. A. Herrmann, C. Köcher, *Angew. Chem.* **1997**, *109*, 2257; *Angew. Chem., Int. Ed. Engl.* **1997**, *36*, 2162.

[2] M. Regitz, *Angew. Chem.* **1996**, *108*, 791; *Angew. Chem., Int. Ed. Engl.* **1996**, *35*, 725.

[3] [3a] A. W. Coleman, P. B. Hitchcock, M. F. Lappert, R. K. Maskell, J. H. Müller, *J. Organomet. Chem.* **1983**, *250*, C9. − [3b] A. W. Coleman, P. B. Hitchcock, M. F. Lappert, R. K. Maskell, J. H. Müller, *ibid.* **1985**, *296*, 173.

[4] [4a] W. A. Herrmann, L. J. Gooßen, C. Köcher, G. R. J. Artus, *Angew. Chem.* **1996**, *108*, 2980; *Angew. Chem., Int. Ed. Engl.* **1996**, *35*, 2805. − [4b] W. A. Herrmann, L. J. Gooßen, G. R. J. Artus, C. Köcher, *Organometallics* **1997**, **16**, 2472.

[5] D. Enders, H. Gielen, G. Raabe, J. Runsink, J. H. Teles, *Chem. Ber.* **1996**, *129*, 1483.

[6] D. Enders, H. Gielen, G. Raabe, J. Runsink, J. H. Teles, *Chem. Ber.* **1997**, *130*, 1253.

[7] [7a] C. Köcher, W. A. Herrmann, *J. Organomet. Chem.* **1997**, *532*, 261. − [7b] W. A. Herrmann, L. J. Gooßen, M. Spiegler, *ibid.* **1997**, *547*, 357.

[8] All ab initio calculations were performed using the TURBOMOLE program package. (For an overview of TURBOMOLE′s capabilities see: R. Ahlrichs, M. v. Arnim, in *Methods and Techniques in Computational Chemistry: METECC-95*, Eds.: E. Clementi, G. Corongiu)
Geometries have been calculated at the RI-DFT (K. Eichkorn, O. Treutler, H. Ihm, M. Häser, R. Ahlrichs, *Chem. Phys. Letters* **1995**, *242*, 652) level with the Becke−Perdew functional using TURBOMOLE′s SV(P) basis sets (K. Eichkorn, F. Weigend, O. Treutler, R. Ahlrichs, *Theor. Chem. Acc.* **1997**, *97*, 119). Energies were calculated at the MP2 level with TZVP basis sets by optimization for different rotation angles.

[9] Software used for the presentation: Ball & stick vers. 2.2, A. Falk, N. Müller, G. Schoppel, L.Webb, Linz (Austria), Stafford (Great Britain).

[10] Suitable crystals were obtained from CH_2Cl_2/pentane mixtures at room temp. The compound crystallizes in the orthorhombic space group $P2_12_12_1$; a = 10.601(5), $^\circ b$ = 11.441(3), c = 19.178(6) A. At a cell volume of 2326.1 A^3, Z = 4 and $M_{ber.}$ = 519.87, the calculated density and the absorption coefficient are ρ = 1.484 mg m^{-3} and μ = 7.180 mm^{-1}, respectively. The total number of electrons per unit cell amounts to F(000) = 1072. The data collection was performed at 203 K on a Siemens P4 diffractometer, Cu-K_α radiation (graphite monochromator, λ = 1.54178 A), 1735 reflections measured (+h, +k, +l), 1735 independent reflections, 4.50° < θ < 55.85°. Structure solved by direct methods [SHELXTL (G. M. Sheldrick, Univ. Göttingen, Germany), refinement on F^2]. The hydrogen atoms were located and refined isotropically. 1733 observed reflections [$I > 2\sigma$ (I)] were used in the final refinement of 295 parameters terminating at R = 0.0327 (R_W = 0.0738). Maximal residual electron density −0.314/+ 0.339 e A^{-3}. Crystallographic data (excluding structure factors) for the structure reported in this paper have been deposited with the Cambridge Crystallographic Data Centre as supplementary publication no. CCDC-101134. Copies of the data can be obtained free of charge on application to: The Director, CCDC, 12 Union Road, Cambridge CB2 1EZ, UK, [Fax: (internat.) +44 (0)1223 336033, e-mail: deposit@chemcrys.cam.ac.uk].

[11] [11a] M. J. Doyle, M. F. Lappert, *J. Chem. Soc., Chem. Commun.* **1974**, 679. − [11b] C. G. Kreiter, K. Öfele, G. W. Wieser, *Chem. Ber.* **1976**, *109*, 1749.

[12] M. F. Lappert, R. K. Maskell, *J. Organomet. Chem.* **1984**, *264*, 217.

[13] D. Enders, H. Gielen, K. Breuer, *Tetrahedron: Asymmetry* **1997**, *8*, 3571.

[14] [14a] H. Buschmann, H.-D. Scharf, N. Hoffmann, P. Esser, *Angew. Chem.* **1991**, *103*, 480; *Angew. Chem., Int. Ed. Engl.* **1991**, *30*, 452. − [14b] A. Gypser, P.-O. Norrby, *J. Chem. Soc., Perkin Trans. 2*, **1997**, 939.

[15] D. Haag, PhD thesis, RWTH Aachen, **1997**.

[16] For the preparation and further application of triazolium salts, see: [16a] D. Enders, K. Breuer, G. Raabe, J. Runsink, J. H. Teles, J.-P. Melder, K. Ebel, S. Brode, *Angew. Chem.* **1995**, *107*, 1119; *Angew. Chem., Int. Ed. Engl.* **1995**, *34*, 1021. − [16b] J. H. Teles, J.-P. Melder, K. Ebel, R. Schneider, E. Gehrer, W. Harder, S. Brode, D. Enders, K. Breuer, G. Raabe, *Helv. Chim. Acta* **1996**, *79*, 61. − [16c] D. Enders, K. Breuer, J. H. Teles, *Helv. Chim. Acta* **1996**, *79*, 1217. − [16d] D. Enders, K. Breuer, J. H. Teles, *Helv. Chim. Acta* **1996**, *79*, 1899. − [16e] D. Enders, K. Breuer, J. Runsink, J. H. Teles, *Liebigs Ann.* **1996**, 2019.

[17] G. Giordano, R. H. Crabtree, *Inorg. Synth.* **1979**, *19*, 218.

[98021]

A Methylene-Bridged Dialuminium Compound as a Chelating Lewis Acid: Complexation of Nitrite and Nitrate Anions by $R_2Al–CH_2–AlR_2$ [R = $CH(SiMe_3)_2$]☆

Werner Uhl*[a], Frank Hannemann[a], Wolfgang Saak[a], and Rudolf Wartchow[b]

Fachbereich Chemie der Universität[a],
Postfach 2503, D-26111 Oldenburg, Germany
Fax: (internat.) +49(0)441/798-3352

Institut für Anorganische Chemie der Universität[b]
Callinstraße 9, D-30167 Hannover, Germany
Fax: (internat.) +49(0)511/762-3006

Received March 16, 1998

Keywords: Aluminium / Chelates / Lewis acids

Sodium nitrite ($NaNO_2$) dissolves readily in THF, when the methylene-bridged dialuminium compound $R_2Al–CH_2–AlR_2$ [R = $CH(SiMe_3)_2$] **1** with two coordinatively unsaturated aluminium atoms is added. Compound **1** reacts as a chelating Lewis acid, and, as shown by a crystal structure determination of the $[Na([18]crown-6)(Et_2O)]^+$ derivative **5c**, a compound (**5**) is formed, in which one oxygen atom and the nitrogen atom of the nitrite ion are each coordinated by one aluminium atom to form a five-membered Al_2CNO heterocycle. The second oxygen atom of the nitrite anion is not affected. Similarly, lithium nitrate ($LiNO_3$) reacts with **1** to yield a THF soluble product (**6a**). Single crystals were obtained of the $[Li(N,N',N''\text{-trimethyltriazinane})_2]^+$ derivative **6c**, whose structure shows each aluminium atom to be coordinated by one oxygen atom of the nitrate ion to give a six-membered Al_2CNO_2 heterocycle.

Chelating Lewis bases for the effective coordination of cations are extraordinarily important in all areas of chemistry as can be seen from thousands of known compounds. In contrast, chelating Lewis acids as anion receptors for the complexation and recognition of anions are investigated to a much lower extent, and by far the most of these ligands were obtained by the protonation of amino groups of macrocyclic or polycyclic compounds[1]. Organoelement derivatives of the elements of the third main-group have a coordinatively unsaturated central atom and are therefore suitable as Lewis acids, but only few examples exist, which have more than one atom of those elements and could possibly be useful as a chelating ligand. Well documented and characterized[2] compounds of this type are for instance 1,8-naphthlenediylbis(dimethylborane)[3], $Cl_2Al-CH_2-AlCl_2$[4], $Cl_2Al-CH_2CH_2-AlCl_2$[5], $R_2Al-CH_2-AlR_2$ **1** [R = $CH(SiMe_3)_2$][6], $R(Cl)Al-CH_2-Al(Cl)R$ [R = $CH(SiMe_3)_2$][7], $Me_2(THF)AlOC_6H_4OAl(THF)Me_2$[8], $Cl_2In-CH_2-InCl_2 \cdot 2\,TMEDA$[9], and $Hg(C_6H_4-InCl_2 \cdot THF)_2$[10]. However, most of these compounds have up to now not been investigated concerning their ability to act as a chelating Lewis acid. Exceptions are the diborane compound with a single example of a hydrido bridge[3] and the methylene bridged tetraalkyl dialuminium derivative **1**, which was recently synthesized by our group[6]. Few chelate complexes of **1** have been isolated and characterized, in which heterocycles are formed by the coordination of both aluminium atoms to one hydride (**2**)[11], hydroxide[12], or thiomethanolate anion[13]. A remarkable five-membered ring (**3**) was obtained by the reaction of **1** with $LiCH(PMe_2)_2$, in which one Al atom is coordinated to the central carbanion and the other one to a phosphorus atom[14]. A terminal coordination of a neopentyl group is observed by the reaction of **1** with neopentyllithium (**4**)[15]. Much more interest deserve, however, the up to now unknown complexes with multidentate inorganic anions like nitrate, nitrite, azide, sulfate etc. in order to find specific anion receptors or in order to use a Lewis-acid like **1** as a phase transfer reagent to dissolve ionic compounds in organic solvents and to study their changed, possibly enhanced reactivity. We started now with systematic investigations into those reactions and wish to report here on the complexes of **1** with sodium nitrite and lithium nitrate. Carbon bridged dialuminium compounds have recently been used in organic syntheses to form for instance C=C double bonds, but they usually were only used as reactive intermediates, and they were not isolated or well characterized[16].

Reactions of the Methylene-Bridged Dialuminium Compound 1 with $NaNO_2$ and $LiNO_3$

Both, sodium nitrite and lithium nitrate are insoluble even in a large excess of THF. But upon addition of one equivalent of the chelating Lewis-acid μ-methylene tetraalkyldialuminium $R_2Al-CH_2-AlR_2$ **1** the complete dissolution of the crystalline salts occurred within several hours by stirring

 © WILEY-VCH Verlag GmbH, D-69451 Weinheim, 1998 1434–1948/98/0707–0921 $ 17.50+.50/0

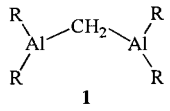

1

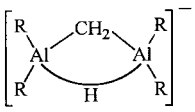

2

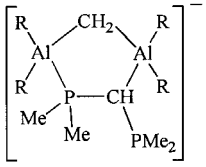

3

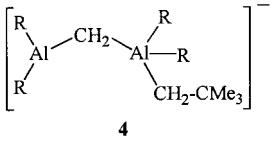

4

R = $CH(SiMe_3)_2$

at room temperature. Yellow solutions were formed, from which the yellow addition products **5a** and **6a** were isolated after concentration and cooling to −50°C in a high yield. The crystals rapidly became amorphous upon drying in vacuo and had low melting points of 92°C and 135°C (**5a** and **6a**, respectively). The ^{1}H- and ^{13}C-NMR spectroscopic characterization gave some important changes in comparison to the neutral starting compound **1**, and all signals of groups bound to aluminium showed a significant shift to high field. In **1** the protons of the Al−CH_2−Al group resonated at δ = −0.50, and we observed the methine protons at δ = −0.22 and the corresponding carbon atoms at δ = 13.2; in **5a** and **6a** these resonances were shifted to δ(Al-CH_2Al) = −1.24 and −1.27, δ(AlC*H*Si_2) = −1.06 and −1.05, δ(Al*C*HSi_2) = 4.1 and 4.3, respectively. Such shifts to a higher field are very indicative of the enhancement of the coordination number at the aluminium atoms from three to four[11][12][13][14][15][17].

Both compounds were stable in THF solutions, but slow decomposition by the precipitation of $NaNO_2$ or $LiNO_3$ and the formation of **1** was observed in more nonpolar solvents like diethyl and diisopropyl ether or in mixtures of ether with toluene or pentane. Single crystals of the nitrate derivative **6a** with the counterion $[Li(THF)_4]^+$ could not be obtained, while single crystals of **5a** showed a severe disorder of the $Na(THF)_3$ cation, and the structure could not be refined satisfactorily. Therefore, we synthesized several derivatives of **5** and **6** by using different chelating Lewis-bases like the crown ether [18]crown-6, tetramethylethylenediamine (TMEDA), tetramethylpropylenediamine (TMPDA), pentamethyldiethylenetriamine (PMDETA), and *N,N′,N′′*-trimethyltriazinane. Some of the isolated products are described in detail in the Experimental Section, the spectroscopic properties of their anions as well as their solubility in polar or nonpolar solvents differ only slightly from those of the THF adducts. But owing to the chelating coordination of the cations they show a significantly increased stability and can be stored in diethyl ether solution at room temperature without decomposition and precipitation of the corresponding salts. High quality single crystals were obtained of compounds **5c** {[Na([18]crown-6)(Et_2O)]$^+$} (Eq. 1) and **6c** {[Li(triazinane)$_2$]$^+$}; the last one crystallized from a dilute solution of the mixed triazinane/THF adduct **6b** (Eq. 2) in diethyl ether in the presence of triazinane.

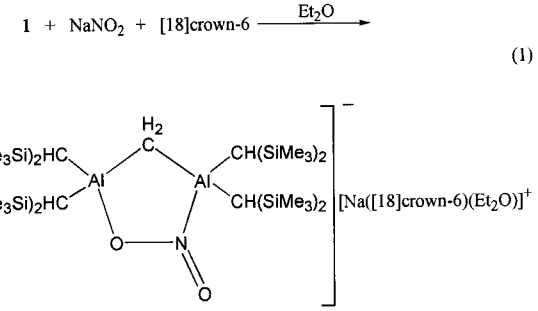

5c

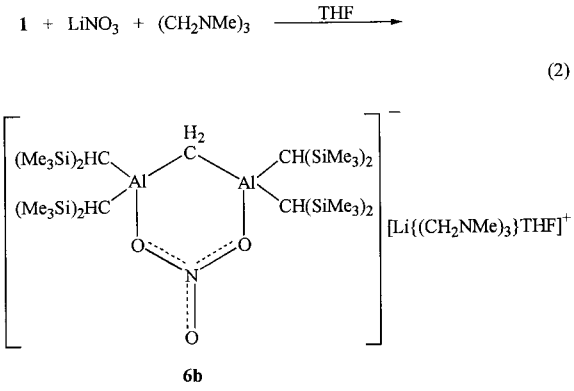

6b

As shown in Eq. (1), the structure of the complex **5c** comprises the nitrite anion coordinated by one oxygen atom and the lone pair at the central nitrogen atom. This structure should result in two chemical different AlR_2 moieties, but at room temperature only one singlet was detected in the ^{1}H-NMR spectrum for both the methine and the $SiMe_3$ protons. However, a splitting into two resonances was observed upon cooling a sample of **5**c dissolved in [D_{10}]diethyl ether to −70°C indicating a fast exchange process at elevated temperatures.

Crystal Structures of 5c and 6c

The molecular structures of the nitrito complex **5c** and the nitrato complex **6c** are depicted in Figures 1 and 2. To the best of our knowledge, it is the first time, that chelating Lewis-acids like compound **1** with coordinatively unsaturated atoms of the elements of group 13 are successfully used for the coordination of at least bidentate anions and that the coordination mode could be determined by crystal structure determinations. Both anions are coordinated in a chelating manner by both aluminium atoms of **1**. As expected, the nitrate anion in **6c** is bound by two oxygen atoms to form a six-membered Al_2CO_2N heterocycle, while a five-membered Al_2CNO heterocycle is observed in **5c** with the nitrite anion coordinated via one oxygen and the central

nitrogen atom. One oxygen atom of each anion is in a terminal position.

Figure 1. Molecular structure and numbering scheme of the anion of **5c**; the thermal ellipsoids are drawn at the 40% probability level; methyl groups are omitted for clarity[a]

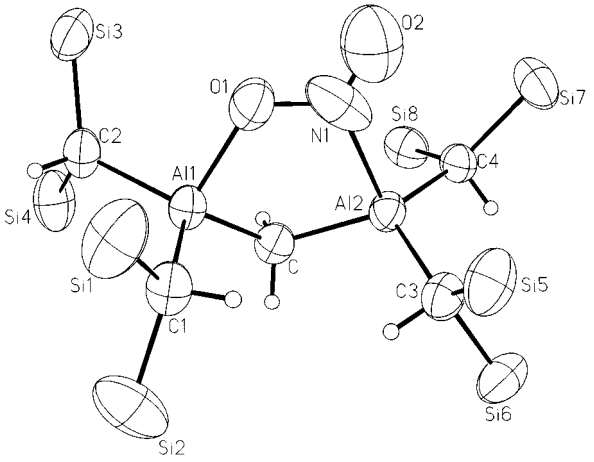

[a] Selected bond lengths [pm] and angles [°]: Al1−O1 196.0(3), Al2−N1 212.3(5), N1−O1 137.6(5), Al1−C 196.1(3), Al2−C 195.0(3), Al1−C1 202.7(3), Al1−C2 202.6(3), Al2−C3 199.9(3), Al2−C4 201.3(3), C−Al1−O1 96.8(1), Al1−O1−N1 114.4(2), O1−N1−Al2 119.2(2), N1−Al2−C 89.5(2), Al1−C−Al2 111.3(2).

Figure 2. Molecular structure and numbering scheme of the anion of **6c**; the thermal ellipsoids are drawn at the 40% probability level; methyl groups are omitted for clarity[a]

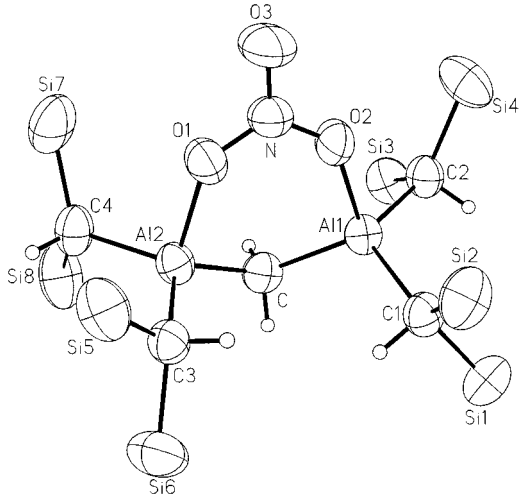

[a] Selected bond lengths [pm] and angles [°]: Al1−O2 193.9(3), Al2−O1 195.7(3), N−O1 126.1(4), N−O2 125.2(4), N−O3 121.4(4), Al1−C 194.5(4), Al2−C 195.0(4), Al1−C1 201.4(3), Al1−C2 202.7(4), Al2−C3 203.8(4), Al2−C4 200.8(4), C−Al2−O1 99.8(2), Al2−O1−N 136.0(3), O1−N−O2 121.3(4), N−O2−Al1 135.9(3), O2−Al1−C 100.4(2), Al1−C−Al2 116.2(2).

The methylene bridged tetraalkyldialuminium moieties of both compounds are quite similar. The Al−C distances of the $CH(SiMe_3)_2$ substituents are 201.6 (**5c**) and 202.2 pm (**6c**) on average, and the smallest distances are observed to the aluminium atom bound to nitrogen. The bond lengths to the carbon atom of the methylene bridge are 195.6 (**5c**) and 194.8 pm (**6c**). As expected from the enhancement of the coordination number at the aluminium atoms[11][12][13][14][15][17], all distances are lengthened compared with the starting compound **1**[6], which had the corresponding values at 195.7 and 193.8 pm. The structure of **1** showed a strongly enlarged Al−C−Al angle (129.6°) caused by steric and electrostatic repulsion between the bulky substituents and the positively charged Al atoms[6]. Owing to the formation of five and six membered heterocycles this angle is reduced in **5c** and **6c** to 111.3° and 116.2°, respectively.

The Al−O distance in the nitrito compound **5c** is slightly lengthened to 196.0 pm compared with complexes of trimethylaluminium with sulfate or nitrate anions (ca. 191 pm)[18][19]. The Al−N1 distance is long (212.3 pm) with respect to some [bis(trimethylsilyl)methyl]aluminium compounds recently obtained in our group[20], which may indicate only a weak coordinative interaction to the Al atom Al2. Unfortunately, the N−O distances N1−O1 137.6 pm and N1−O2 103.1 pm, which is in the range of the triple bond in NO^+, are incorrect due to a disorder of the atoms N1 and O2. Both atoms could not be refined in split positions to give acceptable positions. The same disorder was observed for the THF adduct, which could not be completely refined due to the severe disorder of the cation. The distances should therefore not further be discussed in detail, but it seems clear, that strong differing distances are present with one value approaching a double bond and one approaching a single bond similar to the situation in nitrous acid HONO (N−O = 142 and 118 pm)[21]. A similar coordination mode with bridging μ-NO_2-N,O groups has been observed before in several coordination compounds of the transition metals. As expected, the N−O distances of the bridging NO groups of these complexes are elongated compared to those of terminal N=O groups by up to 17 pm[22]. The atoms of the nitrito group (N1, O1, O2) and the aluminium atom coordinated by nitrogen (Al2) lie almost ideally within a plane (sum of the angles 359.8 pm). The most acute angles in the five-membered central heterocycle are at the Al atoms with 96.8° at Al1 and 89.5° at Al2, the last one is coordinated by the nitrogen atom. The heterocycle adopts an envelope conformation with the four atoms Al1, Al2, O1, and N1 almost ideally within a plane and the bridging carbon atom 58 pm above the plane. The angle between the normals of the planes (Al1O1N1Al2 and Al1-CAl2) is 31.7°.

In contrast to the strongly differing N−O distances of **5c**, a more delocalized electronic system is observed in the nitrato compound **6c** with three quite similar N−O distances. The N−O bond length to the terminal oxygen atom is 121.4 pm, which is only 4.5 pm shorter than the distance between nitrogen and the bridging oxygen atoms (125.7 pm on average). The longer distances are similar to the N−O bond lengths of the nitrate ions in many salt-like compounds, which are in the range of about 126 pm[23]. Two metal atoms bridged by two different oxygen atoms of a nitrato group as in **6c** are for instance observed in some aquo Zn-, Cu-, or Ni nitrato complexes[24]. The Al−O distances of **6c** are similar to **5c** (194.8 pm on average). The most acute angles of the six-membered heterocycle are

found at the aluminium atoms (100.1° on average), while the angles Al−O−N are much enlarged to 136°. As expected, the nitrogen atom is planar surrounded by three oxygen atoms (sum of the angles = 360.0°). The heterocycle has an envelope conformation similar to **5c** with the bridging carbon atom 59.2 pm above the plane spanned by the five atoms Al1, Al2, O1, O2, and N, which have a maximum deviation from this plane of only 2.5 pm (angle between the normals of the planes 34.9°).

No short bonding distances are observed between atoms of the complex anions and the corresponding cations in both compounds. The sodium atom in **5c** is coordinated by six oxygen atoms of the crown ether (Na−O = 248.7 to 271.8 pm) and one oxygen atom of an ether molecule (Na−O 247.0 pm) with a distorted coordination geometry. In **6c**, the Li atoms of the counterions $[Li(triazinane)_2]^+$ are located on a crystallographic inversion center; the Li atoms are coordinated by six nitrogen atoms with Li−N distances between 215.7 and 234.0 pm.

We are grateful to the *Deutsche Forschungsgemeinschaft* and the *Fonds der Chemischen Industrie* for generous financial support.

Experimental Section

General: All procedures were carried out under purified argon in dried solvents (THF and diethyl ether over Na/benzophenone). Compound **1** was synthesized as described in ref.[6], *N,N′,N″*-trimethyltriazinane and pentamethyldiethylenetriamine (PMDETA) were distilled over Na (PMDETA under reduced pressure) and stored over molecular sieve, commercially available crown ether 18-crown-6 (Merck-Schuchardt), $NaNO_2$ (Aldrich), and $LiNO_3$ (Riedl-deHaen) were thoroughly evacuated at room temperature and used without further purification.

Synthesis of $[(\mu\text{-}NO_2\text{-}N,O)R_2AlCH_2AlR_2]^-[Na(THF)_3]^+$ (**5a**): A solution of 0.362 g (0.514 mmol) of **1** in 25 ml of THF is added to an excess (0.057 g, 0.826 mmol) of solid $NaNO_2$. The mixture is vigorously stirred for 22 h, and the solution adopts a pale yellow color. After filtration the solution is concentrated in vacuo at room temp. and cooled to −50°C. The product is isolated as yellow crystals, which rapidly become amorphous at room temperature and normal pressure. Yield: 0.404 g (79%). − M. p. (argon, sealed capillary): 92°C. − ^{1}H NMR ($[D_{10}]Et_2O$, 300 MHz): δ = 3.66 (m, 12 H, OCH_2 of THF), 1.82 (m, 12 H, CH_2CH_2 of THF), 0.09 (s, 72 H, $SiMe_3$), −1.06 (s, 4 H, $AlCHSi_2$), −1.24 (s, 2 H, $AlCH_2Al$). − ^{13}C NMR ($[D_{10}]Et_2O$, 75.5 MHz): δ = 68.4 (OCH_2 of THF), 26.2 (CH_2CH_2 of THF), 5.9 ($SiMe_3$), 5.0 (br., $AlCH_2Al$), 4.1 ($AlCSi_2$). − IR (CsBr, paraffin): ν = 1497 m cm^{-1} νNO; 1462 vs, 1377 s paraffin; 1339 w, 1316 w, 1244 vs δCH_3; 1192 m, 1159 m, 1049 vs, 1028 s νCC, νCO; 1003 vs δCH; 934 vs, 918 vs, 899 vs, 843 vs, 777 vs, 750 vs, 725 s ρCH_3(Si); 698 s, 669 vs ν_{as}SiC; 629 m, 613 w ν_sSiC; 588 w, 561 s, 521 m, 503 w, 496 m, 448 w νAlC, νAlO; 386 vw, 366 vw δSiC. − UV/vis (diethyl ether) (ε): 240 (1750), 290 (sh, 700), 370 nm (sh, 90). − $C_{41}H_{102}Al_2NNaO_5Si_8$ (990.90): calcd. Al 5.4, Na 2.3; found Al 5.4, Na 2.2.

Synthesis of $[(\mu\text{-}NO_2\text{-}N,O)R_2AlCH_2AlR_2]^-[Na(PMDETA)_2]^+$ (**5b**): An excess of solid $NaNO_2$ (0.070 g, 1.01 mmol) is treated with a solution of 0.513 g (0.727 mmol) of **1** in 50 ml of diethyl ether. 2 ml of PMDETA is added to the suspension, and the mixture is vigorously stirred for 18 h. The solution adopts a pale yellow color. After filtration the solution is concentrated in vacuo at room temp. to about 4 ml and cooled to −50°C. The product is isolated as yellow crystals, which become amorphous at room temperature. Yield: 0.588 g (72%). − M. p. (argon, sealed capillary): 140°C. − ^{1}H NMR ($[D_{10}]Et_2O$, 300 MHz): δ = 2.48 and 2.38 (each: pseudo-t, 8 H, NCH_2 of PMDETA), 2.26 (s, 6 H, N-Me of PMDETA), 2.22 (s, 24 H, NMe_2 of PMDETA), 0.10 (s, 72 H, $SiMe_3$), −1.05 (s, 4 H, $AlCHSi_2$), −1.23 (s, 2 H, $AlCH_2Al$). − ^{13}C NMR ($[D_{10}]Et_2O$, 75.5 MHz): δ = 58.6 and 56.7 (NCH_2 of PMDETA), 46.4 (NMe_2 of PMDETA), 43.7 (NMe of PMDETA), 6.0 ($SiMe_3$), 4.9 (br., $AlCH_2Al$), 4.3 ($AlCSi_2$). − IR (CsBr, paraffin): ν = 1497 m cm^{-1} νNO; 1464 vs, 1377 s, 1366 s, 1355 m paraffin; 1341 vw, 1308 s, 1291 s, 1252 vs, 1242 vs, 1225 vs δCH_3; 1161 s, 1150 s, 1127 m, 1111 s, 1096 m, 1065 m, 1026 vs νCC, νCN; 1007 vs δCH; 930 vs, 901 vs, 843 vs, 777 vs, 750 vs, 727 s ρCH_3(Si); 667 vs ν_{as}SiC; 629 m, 615 w ν_sSiC; 590 w, 559 s, 517 m, 503 m, 496 m, 465 w, 449 w, 424 vw νAlC, νAlO; 380 w, 353 vw δSiC. − UV/vis (diethyl ether) (ε): 240 (2050), 270 nm (sh, br., 1230). $C_{47}H_{124}Al_2NaN_7O_2Si_8$ (1210.84): calcd. Al 4.8, Na 2.0; found Al 4.8, Na 2.0.

Synthesis of $[(\mu\text{-}NO_2\text{-}N,O)R_2AlCH_2AlR_2]^-[Na([18]crown\text{-}6)(Et_2O)]^+$ (**5c**): An excess of solid $NaNO_2$ (0.061 g, 0.884 mmol) is treated with a solution of 0.507 g (0.719 mmol) of **1** and 0.252 g (0.953 mmol) [18]crown-6 in 50 ml of diethyl ether. The mixture is vigorously stirred for 18 h, and the solution adopts a pale yellow color. After filtration the solution is concentrated in vacuo at room temp. and cooled to −50°C. The product is isolated as yellow crystals, which become amorphous upon thorough drying in vacuo and include about 0.4 molecules of diethyl ether in each formula unit. Yield: 0.455 g (59%). − M. p. (argon, sealed capillary): 163°C. − ^{1}H NMR ($[D_{10}]Et_2O$, 300 MHz, 300 K): δ = 3.69 (s, 24 H, [18]crown-6), 3.39 (q, 1.6 H, OCH_2 of Et_2O), 1.12 (t, 2.4 H, CH_3 of Et_2O), 0.11 (s, 72 H, $SiMe_3$), −1.04 (s, 4 H, $AlCHSi_2$), −1.23 (s, 2 H, $AlCH_2Al$). − ^{1}H NMR ($[D_{10}]Et_2O$, 500 MHz, 203 K): δ = 3.65 (s, 24 H, [18]crown-6), 3.38 (q, 1.6 H, OCH_2 of Et_2O), 1.15 (t, 2.4 H, CH_3 of Et_2O), 0.15 and 0.06 (each: s, 36 H, $SiMe_3$), −1.0 and −1.1 (each: br., 2 H, $AlCHSi_2$), $AlCH_2Al$ not detected. − ^{13}C NMR ($[D_{10}]Et_2O$, 75.5 MHz): δ = 69.8 ([18]crown-6), 6.0 ($SiMe_3$), 5.0 (br., $AlCH_2Al$), 4.2 ($AlCSi_2$). − IR (CsBr, paraffin): ν = 1501 m cm^{-1} νNO; 1462 vs, 1377 s, 1354 m paraffin; 1321 vw, 1296 m, 1244 vs δCH_3; 1157 m, 1111 s, 1100 s, 1026 m νCC, νCO; 1005 s δCH; 953 sh, 932 s, 899 s, 845 vs, 777 s, 750 s, 725 m ρCH_3(Si); 669 s ν_{as}SiC; 629 w, 610 w ν_sSiC; 588 w, 561 m, 517 w, 505 w, 498 w, 463 vw, 449 vw νAlC, νAlO; 388 vw, 359 vw δSiC. − UV/vis (diethyl ether) (ε): 230 (2530), 280 (sh, 870), 360 nm (90). $C_{41}H_{102}Al_2NaNO_8Si_8 \cdot 0.4\ C_4H_{10}O$ (1068.55): calcd. Al 5.1, Na 2.2; found Al 5.1, Na 2.0.

Synthesis of $[(\mu\text{-}NO_3\text{-}O,O')R_2AlCH_2AlR_2]^-[Li(THF)_4]^+$ (**6a**): Solid $LiNO_3$ (0.038 g, 0.554 mmol) is treated with a solution of an equimolar amount of 0.391 g (0.554 mmol) of **1** in 50 ml of THF. The mixture is vigorously stirred for 12 h. The yellow solution is concentrated to about 1 ml, and the product crystallizes as yellowish crystals upon cooling to −50°C. Yield: 0.490 g (83%). − M. p. (argon, sealed capillary): 135°C. − ^{1}H NMR ([D$_{10}$]diethyl ether, 300 MHz): δ = 3.64 (m, 16 H, OCH_2 of THF), 1.79 (m, 16 H, CH_2CH_2 of THF), 0.10 (s, 72 H, $SiMe_3$), −1.05 (s, 4 H, $AlCHSi_2$), −1.27 (s, 2 H, $AlCH_2Al$). − ^{13}C NMR ([D$_{10}$]diethyl ether, 75.5 MHz): δ = 68.2 (OCH_2 of THF), 26.3 (CH_2CH_2 of THF), 5.7 ($SiMe_3$), 5.0 (br., $AlCH_2Al$), 4.3 ($AlCSi_2$). − IR (CsBr, paraffin): ν = 1501 s cm^{-1} νNO; 1462 vs, 1377 vs paraffin; 1344 m, 1281 vs, 1248 vs δCH_3; 1179 w, 1067 s, 1044 vs νCC, νCO; 1007 s δCH; 930 vs, 912 s, 845 vs, 777 vs, 750 s, 725 s ρCH_3(Si); 667 s ν_{as}SiC; 629 m, 611 w ν_sSiC; 583 w, 556 s, 521 m, 505 m, 465 vw, 452 w, 421 w νAlC, νAlO, νLiO; 372 vw, 334 vw, 316 vw δSiC. − UV/vis (THF) (ε): 225 (2470), 260 nm (sh, br., 990). $C_{45}H_{110}Al_2LiNO_7Si_8$ (1062.96): calcd. Al 5.1, Li 0.6; found Al 5.1, Li 0.6.

Table 1. Crystal data, data collection parameters, and structure refinement for **5c** and **6c**[a] (crystal data of **5a** and **5d** [Na(TMPDA)$_2$] included)

	5a	**5c**	**5d**	**6c**
Formula	$C_{41}H_{102}NO_5NaAl_2Si_8$	$C_{45}H_{112}NO_9NaAl_2Si_8$	$C_{43}H_{114}N_5O_2NaAl_2Si_8$	$C_{41}H_{108}LiN_7O_3Al_2Si_8$
Crystal system	monoclinic	monoclinic	monoclinic	triclinic
Space group	*P*2(1)/*n*; No. 14[25]	*P*2(1)/*n*; No. 14[25]	*P*2(1)/*n*; No. 14[25]	*P*1; No. 2[25]
Z	4	4	4	2
Temperature [K]	297(1)	300(2)	297(1)	293(2)
$d_{calc.}$ [g/cm^3]	0.842	1.041	0.975	0.994
a [pm]	1816.2(2)	1496.0(1)	1989.6(3)	1404.5(2)
b [pm]	1837.1(2)	2766.5(3)	1507.0(3)	1437.6(2)
c [pm]	2385.9(3)	1716.0(1)	2393.1(5)	1935.3(2)
α [°]	90	90	90	78.97(2)
β [°]	100.98(2)	90.594(7)	100.78(3)	85.54(2)
γ [°]	90	90	90	64.09(1)
V [10^{-30} m^3]	7815(1)	7102(1)	7049(2)	3449.8(8)
μ [mm^{-1}]		0.223		0.215
Crystal size [mm]	0.65 × 0.65 × 0.04	0.67 × 0.70 × 0.33	1.06 × 0.72 × 0.61	0.65 × 0.53 × 0.53
Diffractometer	AED-2	Stoe-IPDS	AED-2	AED-2
Radiation	Mo-K_α; graphite monochromator			
2Θ range [°]		3.8 ≤ 2Θ ≤ 48.2		3.2 ≤ 2Θ ≤ 46
Index ranges		−15 ≤ *h* ≤ 17 −31 ≤ *k* ≤ 31 −19 ≤ *l* ≤ 17		−15 ≤ *h* ≤ 15 −15 ≤ *k* ≤ 15 0 ≤ *l* ≤ 21
Independent reflections		10572		9621
Reflections $F > 4\,\sigma(F)$		5380		5823
Parameters		621		630
$R = \Sigma\|\|F_o\| - \|F_c\|\|/\Sigma\|F_o\|$ [$F > 4\sigma(F)$]		0.0531		0.0873
$wR^2 = \{\Sigma w(\|F_o\|^2 - \|F_c\|^2)^2/\Sigma w(F_o^2)^2\}^{1/2}$ (all data)		0.0795		0.1068
Max./min. residual electron density [10^{30} e/m^3]		0.480/−0.280		0.295/−0.208

[a] Programmes SHELXL-93; SHELXTL[26]; solutions by direct methods, full matrix refinement with all independent structure factors.

Synthesis of [(μ-NO$_3$-O,O′)R$_2$AlCH$_2$AlR$_2$]$^-$[Li{(CH$_2$NMe)$_3$}-THF]$^+$ (**6b**): Solid $LiNO_3$ (0.048 g, 0.696 mmol) is treated with a solution of an equimolar amount of 0.490 g (0.694 mmol) of **1** and 2 ml of trimethyltriazinane in 45 ml THF. The mixture is vigorously stirred for 24 h. The yellow solution is evaporated, the residue is treated with 5 ml of diethyl ether, and THF is added dropwise until a clear solution is obtained. Product **6b** crystallizes as yellow crystals upon cooling to −50°C, which contain one molecule of THF and one molecule of trimethyltriazinane in each formula unit. The product (**6c**) with two trimethyltriazinane molecules coordinated to lithium, which was used for the crystal structure determination, was obtained on slow cooling of a dilute solution of **6b** in diethylether by the addition of a small amount of trimethyltriazinane. Yield of **6b**: 0.465 g (69%). − M. p. (argon, sealed capillary): 99°C. − ^{1}H NMR ([D$_8$]THF, 300 MHz): δ = 3.62 (m, 4 H, OCH$_2$ of THF), 3.10 (br., 6 H, NCH$_2$ of triazinane), 2.20 (s, 9 H, Me of triazinane), 1.78 (m, 4 H, CH$_2$CH$_2$ of THF), 0.10 (s, 72 H, SiMe$_3$), −1.06 (s, 4 H, AlCHSi$_2$), −1.28 (s, 2 H, AlCH$_2$Al). − ^{13}C NMR ([D$_8$]THF, 75.5 MHz): δ = 78.3 (NCN of triazinane), 40.5 (Me of triazinane), 5.8 (SiMe$_3$), 5.1 (br., AlCH$_2$Al), 4.4 (AlCSi$_2$). − IR (CsBr, paraffin): ν = 1503 m cm^{-1} νNO; 1466 vs, 1377 s paraffin; 1346 w, 1289 m, 1274 m, 1244 s δCH$_3$; 1159 m, 1119 s, 1051 vs νCC, νCO, νCN; 1015 s δCH; 916 s, 843 vs, 777 s, 737 m, 725 m ρCH$_3$(Si); 671 s ν$_{as}$SiC; 631 m, 611 w ν$_s$SiC; 579 m, 554 m, 519 s, 506 m, 465 m, 452 w, 419 w νAlC, νAlO; 395 w, 372 w, 339 w, 316 w δSiC. − UV/vis (THF) (ε): 240 (1710), 260 nm (sh, br., 1320). − $C_{39}H_{101}Al_2LiN_4O_4Si_8$ (975.84): calcd. Al 5.5, Li 0.7; found Al 5.6, Li 0.7.

Crystal Structure Determinations: Single crystals of compound **5c** were obtained by recrystallization from diethyl ether, the crystals of compound **6c** were grown by recrystallization of **6b** from a dilute solution in ether in the peresence of a small quantity of triazinane. Crystal data and structure refinement parameters are given in Table 1[27]. One of the [Li(triazinane)$_2$]$^+$ cations shows a disorder with a partial overlap of the atoms of the triazinane molecules. Crystal data of **5a** and of **5**[Na(TMPDA)$_2$] (**5d**) (TMPDA = tetramethylpropylenediamine) are also given in Table 1; both structures could not be satisfactorily refined due to the severe disorder of the cations. **5d** was obtained on the same route as compound **5b**, but was not isolated in a high yield.

☆ Dedicated to Prof. Dr. *Heinrich Nöth* on the occasion of his 70th birthday.

[1] B. Dietrich, *Pure Appl. Chem.* **1993**, *65*, 1457−1464. M. M. G. Antonisse, D. N. Reinhoudt, *Chem. Commun.* **1998**, 443−448. Polytin compounds as Lewis acids are published in: R. Altmann, K. Jurkschat, M. Schürmann, D. Dakternieks, A. Duthie, *Organometallics* **1997**, *16*, 5716−5723.

[2] Two compounds of the type R$_2$Al−CH$_2$−AlR$_2$ were described in literature, which are, however, probably mixtures of dismutation products: H. Lehmkuhl, R. Schäfer, *Tetrahedron Lett.* **1966**, 2315−2320. E. C. Ashby, R. S. Smith, *J. Organomet. Chem.* **1982**, *225*, 71−85.

[3] H. E. Katz, *J. Am. Chem. Soc.* **1985**, *107*, 1420−1421.

[4] M. R. Ort, E. H. Mottus, *J. Organomet. Chem.* **1973**, *50*, 47−52.

[5] H. Martin, H. Bretinger, *Z. Naturforsch., B: Chem. Sci.* **1991**, *46*, 615−620. Cited literature.

[6] M. Layh, W. Uhl, *Polyhedron* **1990**, *9*, 277−282. A methylene bridged dialuminium compound with coordinatively saturated aluminium atoms {Li$_2$[(Me$_3$SiCH$_2$)$_3$AlCH$_2$Al(CH$_2$SiMe$_3$)$_3$} is published in: W. Uhl, M. Layh, W. Massa, *Chem. Ber.* **1991**, *124*, 1511−1516.

[7] W. Uhl, M. Layh, *J. Organomet. Chem.* **1991**, *415*, 181−190.

[8] F. A. R. Kaul, M. Tschinkl, F. P. Gabbai, *ibid.* **1997**, *539*, 187−191. See also: T. Ooi, M. Takahashi, K. Maruoka, *J. Am. Chem. Soc.* **1996**, *118*, 11307−11308.

[9] M. A. Khan, C. Peppe, D. G. Tuck, *Organometallics* **1986**, *5*, 525−530.
[10] F. P. Gabbai, A. Schier, J. Riede, *Chem. Commun.* **1996**, 1121−1122. See also: F. P. Gabbai, A. Schier, J. Riede, D. Schichl, *Organometallics* **1996**, *15*, 4119−4121. M. Tschinkl. A. Schier, J. Riede, E. Schmidt, F. P. Gabbai, *ibid.* **1997**, *16*, 4759−4761. F. P. Gabbai, A. Schier, J. Riede, A. Sladek, H. W. Görlitzer, *Inorg. Chem.* **1997**, *36*, 5694−5698. M. Tschinkl, A. Schier, J. Riede, F. P. Gabbai, *ibid.* **1997**, *36*, 5706−5711.
[11] W. Uhl, M. Layh, *Z. Anorg. Allg. Chem.* **1994**, *620*, 856−862.
[12] W. Uhl, M. Layh, unpublished.
[13] W. Uhl, R. Gerding, F. Hannemann, *Z. Anorg. Allg. Chem.*, in press.
[14] W. Uhl, M. Koch, M. Heckel, W. Hiller, H. H. Karsch, *Z. Anorg. Allg. Chem.* **1994**, *620*, 1427−1433.
[15] W. Uhl, M. Koch, A. Vester, *ibid.* **1993**, *619*, 359−366.
[16] I. Marek, J. F. Normant, *Chem. Rev.* **1996**, *96*, 3241−3267.
[17] W. Uhl, A. Vester, *Chem. Ber.* **1993**, *126*, 941−945. W. Uhl, M. Koch, J. Wagner, *Z. Anorg. Allg. Chem.* **1995**, *621*, 249−257. W. Uhl, E. Schnepf, J. Wagner, *ibid.* **1992**, *613*, 67−75.
[18] R. D. Rogers, J. L. Atwood, *Organometallics* **1984**, *3*, 271−274. See also: H. Aeissen, K. Dehnicke, *Chem. Ber.* **1978**, *111*, 480−485.
[19] J. L. Atwood, K. D. Crissinger, R. D. Rogers, *J. Organomet. Chem.* **1978**, *155*, 1−14.
[20] W. Uhl, U. Schütz, W. Hiller, M. Heckel, *Chem. Ber.* **1994**, *127*, 1587−1592. W. Uhl, R. Gerding, S. Pohl, W. Saak, *ibid.* **1995**, *128*, 81−85.
[21] A. P. Cox, M. C. Ellis, C. J. Attfield, A. C. Ferris, *J. Mol. Struct.* **1994**, *320*, 91−106.
[22] V. McKee, M. Zvagulis, C. A. Reed, *Inorg. Chem.* **1985**, *24*, 2914−2919. D. A. House, V. McKee, P. J. Steel, *ibid.* **1986**, *25*, 4884−4889. U. Thewalt, R. E. Marsh, *ibid.* **1970**, *9*, 1604−1610. U. Thewalt, *Acta Crystallogr. B* **1970**, *26*, 81−88. B. F. G. Johnson, A. Sieker, A. J. Blake, R. E. P. Winpenny, *J. Chem. Soc., Chem. Commun.* **1993**, 1345−1346. A. Chiesa, R. Ugo, A. Sironi, A. Yatsimirski, *ibid.* **1990**, 350−351. A. J. Finney, M. A. Hitchman, C. L. Raston, G. L. Rowbottom, A. H. White, *Aust. J. Chem.* **1981**, *34*, 2125−2138 and 2139−2157. G. Bombieri, G. Bruno, M. Cusumano, G. Guglielmo, *Acta Crystallogr. C* **1984**, *40*, 409−412. F. Oberdorfer, B. Balbach, M. L. Ziegler, *Z. Naturforsch. B: Chem. Sci.* **1982**, *37*, 157−167. J. A. Halfen, S. Mahapatra, M. M. Olmstead, W. B. Tolman, *J. Am. Chem. Soc.* **1994**, *116*, 2173−2174.
[23] A. F. Wells, *Structural Inorganic Chemistry*, 5th ed., Clarendon Press, **1984**, p. 820ff.
[24] N. N. Greenwood, A. Earnshaw, *Chemistry of the Elements*, Pergamon Press, **1984**, p. 542.
[25] T. Hahn (Ed.), *International Tables for Crystallography, Space Group Symmetry*, Kluwer Academic Publishers, Dordrecht-Boston-London, **1989**, vol. A.
[26] SHELXTL-Plus REL. 4.1, Siemens Analytical X-RAY Instruments Inc., Madison, USA, **1990**; G. M. Sheldrick *SHELXL-93, Program for the Refinement of Structures*, Universität Göttingen, **1993**.
[27] The crystallographic data of **5c** and **6c** (excluding structure factors) were deposited with the Cambridge Crystallographic Data Centre as supplementary publication no. CCDC-101256. Copies of the data can be obtained free of charge on application to The Director, CCDC, 12 Union Road, GB-Cambridge CB2 1EZ, UK [fax: Int. Code+44(0)1223/ 336-033; e-mail: deposit-@chemcrys.cam.ac.uk].

[98061]

Bis(tetramethylpiperidino)aluminum Halide Adducts $tmp_2AlX \cdot Do$ and Tetrahaloaluminates of Tricoordinated Aluminum Cations $[tmp_2Al(Do)]AlX_4$

Ingo Krossing[1], Heinrich Nöth*, and Holger Schwenk-Kircher[2]

Institute of Inorganic Chemistry, University of Munich,
Meiserstraße 1, D-80333 Munich, Germany

Received December 3, 1997

Keywords: Bis(tetramethylpiperidino)aluminum halide complexes / Tricoordinated aluminum cations / ^{27}Al-NMR spectroscopy / X-ray crystal structure analysis / Ab initio calculations

Upon treatment with Lewis bases Do (Do = pyridine bases or THF), the Lewis acids tmp_2AlX (X = Cl, Br, I) are converted exclusively to the monoadducts $tmp_2AlX \cdot Do$ (**2–4**). The Al–X bonds of these addition compounds are considerably elongated, indicating a tendency towards the formation of ionic species $[tmp_2Al(Do)]X$. Due to the steric requirements of the bulky tmp ligands, addition of an excess of the Lewis base does not force these compounds to form tetracoordinated aluminum cations $[tmp_2Al(Do)_2]^+$ or pentacoordinated adducts $tmp_2AlX \cdot Do_2$. Attempts to prepare ionic representatives by reaction of $tmp_2AlX \cdot Do$ with "ate" complexes of comparatively low nucleophilicity [MY = $NaBPh_4$, $AgBPh_4$, $LiB(C_6F_5)_4$, $AgBF_4$, AgOtos] result in phenylation products [e.g. tmp_2AlPh (**5a**) and $BPh_3 \cdot py$ (**5b**)] or tetracoordinated addition compounds $tmp_2AlY \cdot Do$ (Y = anion). However, addition of one equivalent of AlX_3 (X = Br, I) initiates halide abstraction with formation of the ionic $[tmp_2Al(Do)]AlX_4$ species **6a–f**, as indicated by ^{27}Al-NMR data and conductivity measurements. Solid $[tmp_2Al(py)]AlI_4$ (**6b**) decomposes readily into $tmpAlI_2$ and $tmpAlI_2 \cdot py$ (**7c**). Addition of non-polar aliphatic solvents to solutions of $[tmp_2Al(Do)]AlX_4$ (**6**) leads to slow decomposition into tmp_2AlX and $AlX_3 \cdot Do$ (**7a–b**, **d**). This also occurs in polar donor solvents, where compounds $AlX_3 \cdot Do$ are favoured due to the formation of penta- or hexacoordinated species $AlX_3 \cdot Do \cdot Solv_n$ (n = 1, 2). Semiempirical AM1 calculations reveal the gas-phase stability of the tricoordinated bis(tmp)aluminum cation in the salt $[tmp_2AlPy]AlCl_4$ as the only representative in a series of calculated aluminum cations $[(R_2N)_2AlPy]AlCl_4$ (R_2N = Me_2N, Et_2N, iPr_2N, tmp). According to these calculations, the stability of a given cation increases when tetrachloroaluminate is replaced by tetraiodoaluminate. Ab initio calculations have been performed on two cations $[(H_2N)_2Al(Do)]^+$ (Do = NH_3, py) and indicate very short Al–N bond lengths owing to ionic bonding contributions.

As aluminum compounds exhibit the highest Lewis acidity amongst main group III species[3][4], tetra-, penta- and hexacoordinated Lewis acid−base complexes with many different neutral donor molecules have been described in the literature[5]. Due to their importance in industrial processes[6], complexes involving $AlCl_3$ and trimethylaluminum as Lewis acids [e.g. $AlCl_3 \cdot NMe_3$, $AlCl_3 \cdot (NMe_3)_2$, $AlBr_3 \cdot$diglyme (diglyme = diethylene glycol dimethyl ether), $AlMe_3 \cdot OMe_3$, etc.][4][7][8] have been particularly well studied. These addition compounds can exist as covalent molecules or as ion pairs, as shown by X-ray crystal structure determinations {e.g. $[AlCl_2(py)_4]AlCl_4$}[3], ^{27}Al-NMR and conductivity measurements, e.g. of solutions of $AlCl_3$ or $AlBr_3$ in THF, diglyme, DME etc.[8][9]. A fine example of this feature has recently been published by Atwood et al.[10]. They investigated reactions of Me_2AlX (X = Cl, Br, I) with tBuNH$_2$ as a donor molecule. Whereas the chloride gave the molecular adduct $Me_2AlCl \cdot NH_2t$Bu, the bromide and iodide were forced to dissociate upon addition of excess tBuNH$_2$, forming the salts $[Me_2Al(NH_2t$Bu$)_2]X$ (X = Br, I). The chemistry of tetracoordinated aluminum cations has so far been explored only fleetingly, and apart from the latter compounds, as far as we are aware, only two other species of this type have been reported, namely $[t$Bu$_2$Al(tmeda)$]^+$ by Uhl[11] and **A** by Raston[12].

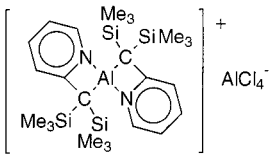

A

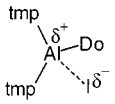

B

To the best of our knowledge, tricoordinated aluminum cations $[R_2Al(Do)]^+$ (Do = monofunctional ligand) have yet to be observed and characterized.

In contrast to the aminoboron halides, aminoaluminum halides can be expected to be sufficiently acidic to form addition compounds [see $(Me_3Si)_2NAl(H)(Cl) \cdot NMe_3$][13]. Even aminoorganylalanes form Lewis acid−base adducts, as exemplified by $Ph_2NAlMe_2 \cdot NMe_3$ and $Ph_2NAlMe_2 \cdot OEt_2$[14]. Thus, the question arose as to whether the recently synthesized series of monomeric bis(amino)aluminum halides, tmp_2AlX (tmp = 2,2,6,6-tetramethylpiperidino, X = Cl **1a**, Br **1b**, I **1c**)[15] and some products of nucleophilic substitution derived from these[16][17] would still show

 © WILEY-VCH Verlag GmbH, D-69451 Weinheim, 1998 1434−1948/98/0707−0927 $ 17.50+.50/0

Lewis acidity. This was indeed found to be the case for **1a–c**. Here, we report on the addition compounds $tmp_2AlX \cdot Do$ (X = Cl, Br, I) as well as the salts $[tmp_2Al(Do)]Y$ (Y = AlI_4).

Synthesis and Reactions

Addition of one equivalent of a donor molecule Do to *n*-hexane solutions of tmp_2AlX, **1a–c**, leads to immediate precipitation of the adducts $tmp_2AlX \cdot Do$ **2a**, **b**, **3a–c**, and **4a–c** in almost quantitative yield, according to Eq. 1.

$$tmp_2AlX + Do \xrightarrow{\text{hexane}} tmp_2AlX{*}Do \quad (1)$$

2-4

	2a	2b	3a	3b	3c	4a	4b	4c
X	Cl	Cl	Br	Br	Br	I	I	I
Do	iq	thf	thf	py	iq	py	iq	γ-pic

The adducts **2–4** are stable in vacuo and do not lose their donor molecules, even when subjected to high vacuum conditions at 50°C. On the other hand, Et_2O, tBuPH$_2$, NEt_3, and acridine do not give stable addition compounds (with respect to the application of vacuum). Moreover, tmp_2AlI (**1c**), the most Lewis acidic compound in the series of the halides **1a–c**, crystallizes from Et_2O as its tricoordinated monomer, as proven by NMR and by examination of its unit cell parameters[15]. Compounds **2–4** are readily soluble in aromatic hydrocarbons, CH_2Cl_2, CH_2Br_2, THF, and Et_2O. Addition of a large excess of donor (up to tenfold, or, in the case of THF, using the donor as solvent) does not force coordination of a further donor molecule (i.e. bring about pentacoordination at the aluminum atom), nor does it induce dissociation into ionic $[tmp_2Al(Do)_2]X$ species. The addition compounds **2–4** can be crystallized from THF and no replacement of Do by the solvent is observed.

Attempts to prepare low coordinated ionic species of the type $[tmp_2Al(py)]Y$ (Y = anion) by addition of $NaBPh_4$, $AgBPh_4$, or $LiB(C_6F_5)_4$ to solutions of $tmp_2AlI \cdot py$ in various solvents at ambient temperature, did not lead to substitution of the iodine atom by the weakly coordinating ions BR_4^-, even after a reaction time of several weeks. In the case of the reaction with $AgBPh_4$, the only species detectable after heating were tmp_2AlPh (**5a**) and $BPh_3 \cdot py$ (**5b**). This implies that $[tmp_2Al(py)]BPh_4$ is formed initially, which then decomposes to give **5a** and **5b**. The aluminum compound **5a** has been synthesized independently from PhLi and tmp_2AlCl[17].

Upon reaction with AgOtos (Otos = tosylate), **4a** gives only the tetracoordinated, covalent product of nucleophilic substitution, $tmp_2AlOtos \cdot py$ (**5c**). Likewise, a mixture of $AgBF_4$, 2,6-lutidine (= lut) and **1b** yields the adduct $tmp_2Al(BF_4) \cdot lut$ (**5d**). Replacing the sterically hindered, less powerful donor 2,6-lutidine by pyridine leads to $tmp_2Al(BF_4) \cdot py$ (**5e**). The latter compound, molecular in *n*-pentane solution, dissociates in CH_2Cl_2 to give an ion pair $[tmp_2Al(py)]BF_4$. This dissociation is accompanied by dramatic shifts of the ^{11}B- and ^{19}F-NMR resonances.

$$tmp_2AlI{*}py + \begin{matrix}+\ NaBPh_4\\ +\ AgBPh_4\\ +\ LiB(C_6F_5)_4\end{matrix} \xrightarrow[\text{weeks}]{\text{r.t., various solvents}} [tmp_2Al(py)^+]BPh_4^- \quad (2a)$$

4a

$$tmp_2AlI{*}py + \begin{matrix}NaBPh_4\\ +\ AgBPh_4\end{matrix} \xrightarrow[110\ °C,\ 3d]{\text{toluene}} \left[[tmp_2Al(py)^+]BPh_4^- \right] \quad (2b)$$

4a

$$\downarrow$$

$$tmp_2AlPh\ (\mathbf{5a}) + BPh_3{*}py\ (\mathbf{5b})$$

$$tmp_2AlI{*}py + AgOtos \xrightarrow[\text{r.t.; 12 h}]{\text{benzene}} tmp_2AlOtos{*}py \quad (2c)$$

4a **5c**

$$tmp_2AlBr + AgBF_4 + \text{N} \xrightarrow{\text{hexane}} tmp_2Al(FBF_3)(lut) \quad (2d)$$

lut = 2,6-lutidine **5d**

$$tmp_2AlX{*}py + AgBF_4 \xrightarrow{\text{hexane/ pentane}} \begin{matrix}tmp_2Al(py)BF_4\ \mathbf{5e}\\ [tmp_2Al(py)^+]BF_4^-\ (CH_2Cl_2/\ CDCl_3)\end{matrix} \quad (2e)$$

As all the tested tetraphenylborates and tetrafluoroborates turned out to be either unstable (due to dephenylation) or too basic (formation of adducts) to give ionic compounds of the type $[tmp_2Al(Do)]Y$, a different approach was evaluated, in which strong halide acceptors were employed in order to induce a reaction according to Eq. 3a.

$$tmp_2AlX{*}Do + AlX_3 \xrightarrow{\text{solv.}} tmp_2AlDo]^+[AlX_4]^- \quad \mathbf{6}$$

solv. = CH_2Cl_2, CH_2Br_2, Et_2O => -78°C
solv. = toluene, benzene => 0°C

	6a	6b	6c	6d	6e	6f
X	Br	I	I	I	I	I
Do	iq	py	γ-pic	4-tBu-Py	iq	acr

Addition of one equivalent of AlX_3 (X = Br, I) to solutions of $tmp_2AlX \cdot Do$ (X = Br, I) in CH_2Br_2 (for **6a**) or in aromatic solvents such as toluene leads smoothly to the ionic compounds $[tmp_2Al(iq)]AlBr_4$ (**6a**), $[tmp_2Al(py)]AlI_4$ (**6b**), $[tmp_2Al(4\text{-Me-py})]AlI_4$ (**6c**), $[tmp_2Al(4\text{-}t\text{Bu-py})]AlI_4$ (**6d**), $[tmp_2Al(iq)]AlI_4$ (**6e**), and $[tmp_2Al(acr)]AlI_4$ (**6f**), (iq = isoquinoline, acr = acridine). If a solution of $tmp_2AlCl \cdot thf$ (**2a**) in THF is treated with $AlCl_3$, only the adduct $AlCl_3 \cdot (thf)_2$ is formed, according to the ^{27}Al-NMR spectrum. In contrast to the iodide $[tmp_2Al(acr)]AlI_4$ (**6f**), ad-

dition of $AlBr_3$ to a 1:1 mixture of tmp_2AlBr (**1b**) and acridine leads to exclusive formation of $AlBr_3 \cdot acr$ (**7d**), leaving **1b** uncoordinated. The tetraiodoaluminates were found to be the most stable of all the tetrahaloaluminates. Nevertheless, NMR spectroscopic evidence was found even for the formation of ionic tetrachloroaluminates. Solutions of **6b−f** in aromatic hydrocarbons or CH_2Cl_2 are stable for weeks at ambient temperature, but addition of *n*-pentane (in an attempt to induce crystallization) results in slow decomposition to give tmp_2AlI (**1c**) and $AlI_3 \cdot Do$. This was proven by the isolation and full characterization of $AlI_3 \cdot iq$ (**7a**) and $AlI_3 \cdot$(4-*t*Bu-py) (**7b**), as well as by NMR spectroscopic characterization of tmp_2AlI (**1c**) (see Eq. 4a and 4b)[15]. The preparation of **6b** also proceeds smoothly in Et_2O, but storing the concentrated solution at −78°C in the hope of obtaining crystals leads to decomposition into soluble $AlI_3 \cdot py \cdot (OEt_2)_n$ and insoluble tmp_2AlI (**1c**), according to Eq. 4c[15]. Upon standing for one week at 35°C, solid **6b** disproportionates into $tmpAlI_2$ and $tmpAlI_2 \cdot py$ (**7c**).

$$[tmp_2AlDo]AlX_4 \xrightarrow[\text{weeks}]{Et_2O\ -78°C} tmp_2AlX\ (s) + AlX_3{*}Do{*}(OEt_2)_n\ (solv.) \quad (4a)$$

$$[tmp_2AlDo]AlX_4 \xrightarrow[\text{rapid}]{\text{n-pentane}} tmp_2AlX\ (solv.) + AlX_3{*}Do\ (s) \quad (4b)$$

$$\underset{\textbf{6b}}{[tmp_2Al(py)]AlI_4} \xrightarrow[T = 35°C]{\text{as a solid at}} \underset{\textbf{7c}}{tmpAlI_2{*}Py} + tmpAlI_2 \quad (4c)$$

Characterization

Compared to the shifts and half-widths of the ^{27}Al-NMR signals of the tricoordinated alanes tmp_2AlX **1a−c** ($\delta^{27}Al$ = 130−131, $\Delta_{1/2}$ = 9100−13700 Hz)[15], the signals of the adducts **2−4** are shifted by 30−60 ppm to higher field due to the higher electron-density at the aluminum center and are narrower. As compounds **2−4** have tetracoordinated aluminum atoms, and thus the local symmetry at the aluminum nuclei is increased (as compared to **1a−c**), the average half-widths of the ^{27}Al-NMR signals are reduced to approximately 6800 Hz (see Table 1)[18][19]. Single sets of lines are observed in the ^{1}H- and ^{13}C-NMR spectra of the tmp ligands, indicating free rotation about the Al−N bond as well as rapid inversion of the piperidinyl ring. Compared to the halides **1a−c**, the signals are shifted downfield [by about 0.3 ppm (^{1}H NMR) and 2.7 ppm (^{13}C NMR)]. Moreover, the chemical shifts show a strong solvent dependence. In $CDCl_3$, the signals are found at higher field than in C_6D_6. The decrease in Lewis acidity in the series Al−I > Al−Br > Al−Cl[3][4] and the bond enthalpy order Al−X (Al−I < Al−Br < Al−Cl)[6] are mirrored by the chemical shifts of the tmp methyl groups. For $tmp_2AlCl \cdot iq$ (**2b**), the methyl protons give rise to a signal at δ = 1.29; for $tmp_2AlBr \cdot iq$ (**3c**) at δ = 1.37, and for $tmp_2AlI \cdot iq$ (**4b**) at δ = 1.41. Similarily, the methyl protons resonate at δ = 1.58 in $tmp_2AlBr \cdot py$ (**3b**) and at δ = 1.62 in $tmp_2AlI \cdot py$ (**4a**). These changes point to a predissociation of the weakest Al−X bond (Al−I). The aluminum centre thus becomes more positively charged (see **B**), and the resonances appear at lower field.

Table 1. ^{27}Al chemical shifts and line-widths, and selected ^{1}H- and ^{13}C-NMR data of compounds **2b**, **3a−c**, and **4a−c**

Compound (solv.)	**2b** [$CDCl_3$]	**3b** [C_6D_6]	**3c** [$CDCl_3$]	**3a** [C_6D_6]	**4a** [C_6D_6]	**4b** [$CDCl_3$]	**4c** [C_6D_6]
$\delta^{27}Al$[a]	102	96	109	125	92	108	76
$\Delta_{1/2}$[b]	8.300	4.360	7.500	8.000	4.900	8.900	5.900
δ^1H[a]	10.07	s9.25 s	10.17	s3.76 t	9.06 s	10.21	s9.27 s
	9.11 d[e]		9.18 d[c]			9.21 d[d]	
$\delta^{13}C$[a]	155.1	150.4	155.7	68.3	148.0	155.3	150.2

[a] In ppm. − [b] In Hz. − [c] ^3J(H,H) = 7.4 Hz. − [d] ^3J(H,H) = 6.4 Hz. − [e] ^3J(H,H) = 6.6 Hz.

The chemical shifts of hydrogen and carbon atoms adjacent to the heteroatoms of the donor molecules proved to be valuable indicators in ascertaining whether or not a compound $tmp_2Al(Do)Y$ (Y = anion or ligand) is dissociated into an ion pair (see Table 2). In comparison with the free pyridine bases, the resonances for these bases in the adducts **2−4** are shifted downfield by 0.6 to 1 ppm (^{1}H-NMR) and by 0.6 to 3.5 ppm (^{13}C-NMR), respectively.

The decomposition products of the tetraphenylborate, as described by Eq. 2b, were identified by their ^{1}H-, ^{13}C-, and ^{27}Al-NMR shifts, as reported in the literature (tmp_2AlPh, **5a**)[17], or by the known ^{11}B-NMR shift of δ = 5.0[20]. Further evidence was provided by the ^{1}H-NMR spectrum, elemental analysis, and X-ray crystal structure determination of $BPh_3 \cdot py$ (**5b**)[21].

Since $tmp_2AlOtos \cdot py$ (**5c**) exhibits a ^{27}Al-NMR signal in the same range as the adducts **2−4** ($\delta^{27}Al$ = 97, $\Delta_{1/2}$ = 5500 Hz), as well as a similar shift of the *ortho*-protons on the pyridine ring (δ^1H = 9.29, cf. the data in Table 1), it appears that this species is not ionic. A very similar situation is found for $tmp_2Al(lut)BF_4$ (**5d**). In its ^{27}Al-NMR spectrum, a line at δ = 1 ($\Delta_{1/2}$ = 3400 Hz) is found, too narrow to be attributable to a tricoordinated aluminum centre. Moreover, the ^{11}B-NMR spectrum consists of a single, broadened line at $\delta^{11}B$ = 17.9. Due to the coordination at the aluminum centre, the resonance is deshielded by 18 ppm compared to the free, ionic tetrafluoroborate[20]. Similarly, a solution of $tmp_2Al(py)BF_4$ (**5e**) in pentane exhibits a signal at $\delta^{11}B$ = 19.3. If the spectrum is recorded in $CDCl_3$ or CH_2Cl_2, a line at $\delta^{11}B$ = 0.9 is observed, indicating the presence of uncoordinated, free BF_4^-[20]. This is accompanied by correspondingly dramatic differences in the ^{19}F-NMR signals. Whereas in pentane a broadened resonance at $\delta^{19}F$ = −111 (analogous to **5d**: $\delta^{19}F$ = −104.5 and −111.0) is found, in $CDCl_3$ a 1:1:1:1 quartet at $\delta^{19}F$ = −151 with ^1J(B,F) = 12 Hz supports the salt formation [*cf.* F_3BOH, ^1J(B,F) = 16.4 Hz; $F_3B \cdot N(H)_xMe_{3-x}$, x = 0−3,

^1J(B,F) = 15.1 to 16.4 Hz][20]. The ^{27}Al-NMR signal of **5e** in CH_2Cl_2 is additional evidence for the ionic behavior in polar solvents: a very broad signal is observed, covering the full spread of the spectrum. The ^{1}H-NMR signals of the *ortho*-protons on the pyridine ring also reflect this change: the shift for **5e** (δ = 8.71) is consistent with an ionic structure {cf. [tmp_2Al(py)]AlI_4, (**6b**), δ^1H = 8.59}, but not with the adduct $tmp_2AlI\cdot$py (**4a**), where the corresponding signal appears at δ = 9.06.

Compared to the adducts **2**–**4**, the formation of the ionic species **6a**–**f** is accompanied by dramatic changes in the line-widths of the ^{27}Al-NMR signals. Whereas **2**–**4** exhibit average line widths of 6800 Hz, a single sharp line attributable to the AlX_4^- fragment ($\Delta_{1/2}$ = 17 to 134 Hz) is found for compounds **6a**–**f**. The second aluminum nucleus, assumed to be tricoordinated, should contribute to the spectra with a very broad line. Due to the presence of highly symmetrical, NMR-sensitive and unsymmetrical, tricoordinated aluminum centres, this line is not usually detected {e.g. in the ambient temperature ^{27}Al-NMR spectrum of [Al(O*i*Pr)$_3$]$_4$ one sharp line, assigned to the central, hexacoordinated aluminum atom is readily detected (δ^{27}Al = −2.62, $\Delta_{1/2}$ = 102 Hz), while signals due to the tetracoordinated aluminum atoms are not seen[19]}. As the chemical shifts of the tetrahaloaluminates (**6a**: δ^{27}Al = 104; **6b**–**e**: δ^{27}Al = 50−55; **6f**: δ^{27}Al = −22) are, with the exception of **6f**, found at lower field than those reported in the literature [$AlBr_4^-$: δ^{27}Al = 80−83, AlI_4^-: δ^{27}Al = −27 (CH_2Cl_2)][19], a weak coordination of the anions to the cationic aluminum center is indicated. Considering the narrow line-width for **6a**–**f** ($\Delta_{1/2}$ = 17−134 Hz), this interaction cannot be very strong, since the aluminum nucleus is very sensitive to a disturbance of symmetry. Due to the positive charge of **6a**–**f**, the ^{1}H- and ^{13}C-NMR signals of the protons and the carbon atoms adjacent to the heteroatoms of the donor molecules are shifted by about 0.4 ppm (^{1}H NMR) and 1−3 ppm (^{13}C NMR), respectively, to higher field, compared to the corresponding signals in compounds **2**–**4**. This is a characteristic feature for these ionic compounds (see Table 2 and compare with the data in Table 1).

Table 2. Selected NMR data of compounds **6**

Compound	δ^{27}Al [ppm]	$\Delta_{1/2}$ [Hz]	δ^1H [ppm]	δ^{13}C [ppm]
6a [$CDCl_3$]	104	66	9.89 s[a], 8.94 d[b]	152.5
6b [C_6D_6]	50	134	8.59 s[a]	147.0
6c [C_6D_6]	51	35	8.47 s[a]	146.9
6d [C_6D_6]	51	75	8.54 s[a]	146.6
6e [$CDCl_3$]	55	17	9.70 s[a], 8.75 d[b]	152.4
6f [$CDCl_3$]	−22.0	70	8.80 s[a][c], 8.21 d[d]	148.7

[a] Broad. − [b] ^3J(H,H) = 6.4 Hz. − [c] At C7, *trans* to N1. − [d] ^3J(H,H) = 8.1 Hz.

Single sets of lines are observed for the tmp ligand in **6**, indicating free rotation about the Al−N bond and rapid inversion of the piperidinyl ring. Compared to the adducts **2**–**4**, the signals appear at higher field and resemble those found for the halides **1b**–**c**. This is in line with calculated AM1 data[29] for **1b**, **c** and [tmp_2Al(py)]AlX_4 (X = Br, I). As the calculated Al−N bond lengths and N−Al−N bond angles are very similar (to within ±0.01 A and ±1°), similar NMR spectroscopic data can be expected.

Addition of *n*-pentane to a solution of **6b** or **6d** in aromatic hydrocarbons leads to disproportionation according to Eq. 4c. In solution, the characteristic chemical shifts of tmp_2AlI (**1c**) could be detected (^{1}H-, ^{13}C-, ^{27}Al-NMR)[15]. Crystals of $AlI_3\cdot$4-*t*Bu-py (**7b**), which separated on cooling to 5°C, were characterized spectroscopically and analytically, as was a sample of $AlBr_3\cdot$acr (**7d**), obtained according to Eq. 3b. Due to the highly symmetrical coordination at the aluminum nuclei, these compounds give sharp lines at δ^{27}Al = 51 ($\Delta_{1/2}$ = 46 Hz) (**7b**) and δ = 83 ($\Delta_{1/2}$ = 34 Hz) (**7d**). Since only one distinct line was observed in each ^{27}Al-NMR spectrum, dissociation into ionic species as found for $AlCl_3\cdot py_2$ can be ruled out[5]. Moreover, $AlI_3\cdot$iq (**7a**) precipitated under these conditions as a molecular adduct. It was only characterized by its X-ray crystal structure.

In the solid state, **6b** decomposes into $tmpAlI_2$ and $tmpAlI_2\cdot$py (**7c**) (Eq. 4c). This is demonstrated by its ^{27}Al-NMR spectrum: one signal at δ^{27}Al = 69 ($\Delta_{1/2}$ = 2640 Hz) is observed for **7c**, the half-width of which resembles that of signals of other $tmpAlX_2\cdot$Do compounds[15][19]. The ^{1}H- and ^{13}C-NMR shifts of **7c** are very similar to those observed for $tmp_2AlI\cdot$py (**4a**), differing by only about 0.01 ppm (δ^1H) and 0.1 ppm (δ^{13}C). Thus, it is most likely that **7c** is present in solution as a tetracoordinated adduct.

Conductivity Measurements

To prove the formation of ions, conductivity measurements were carried out on well-defined CH_2Cl_2 solutions of **5d**, **6a**–**b**, **e** and the dissociation patterns were deduced from the calculated gradients of the resulting Fuoss-Kraus plots[22]. These salts are stable in CH_2Cl_2 solution and do not undergo halogen-exchange with the solvent, as is observed for AlX_3 solutions (X = Br, I). The gradient of these plots gives an indication of the ion pair formation from the undissociated parent species. An equilibrium as described by Eq. 5a corresponds to a gradient of −0.5, that according to Eq. 5b exhibits a gradient of 0, while a dissociation pattern described by Eq. 5c is represented by a value of 0.5.

$$AB \rightleftharpoons A^+ + B^- \quad (5a)$$

$$2\,AB \rightleftharpoons A^+ + A_2B \quad (5b)$$
$$2\,AB \rightleftharpoons A_2B^+ + B^-$$

$$3\,AB \rightleftharpoons A^+ + A_2B_3^- \quad (5c)$$
$$3\,AB \rightleftharpoons A_2B^+ + AB_2^-$$
$$3\,AB \rightleftharpoons A_3B_2^+ + B^-$$

A solution of **5d** in CH_2Cl_2 shows no electrical conductivity and thus this compound remains as a molecular adduct, as already shown by its NMR data. Solutions of **6a**, **b**, **e** exhibit electrical conductivity, indicating ion pair formation. The gradient of the plot for **6b** reaches a value of approximately −0.6, indicating a reaction according to Eq. 5a. However, the gradients for **6a**, **e** are −0.1 and −0.2,

respectively. This corresponds with ion formation according to Eq. 5a and Eq. 5b, with a greater percentage of the dissociation behavior conforming to Eq. 5b. **8a** and **8b** represent two possible structures of the ionic products formed according to Eq. 5b.

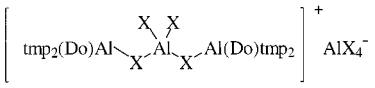

8a

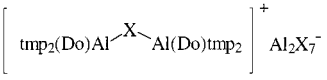

8b

Crystal Structures

The adducts of tmp_2AlCl (**2a**, **b**) and tmp_2AlBr (**3a**) crystallize in the monoclinic space group $P2_1/n$ with four molecules in the unit cell, while $tmp_2AlBr \cdot py$ (**3b**) and $tmp_2AlI \cdot py$ (**4a**) are isotypical having the monoclinic space group $C2/c$ ($Z = 8$). Structural parameters of these compounds are given in Table 3, crystallographic details in Table 6.

Table 3. Selected bonding parameters of compounds **2a**, **b**, **3a**, **b**, and **4a**

Compound	**2a**	**2b**	**3a**	**3b**	**4a**
Bond lengths [Å]					
d(Al−X)	2.227(3)	2.220(1)	2.408(2)	2.429(2)	2.704(1)
d(Al−N1)	1.836(5)	1.844(2)	1.836(4)	1.838(4)	1.849(3)
d(Al−N2)	1.843(6)	1.851(3)	1.844(4)	1.844(4)	1.854(4)
d(Al−N3/O1)	2.041(7)	1.913(2)	1.928(4)	2.030(4)	2.022(3)
Bond angles [°]					
N1−Al−N2	126.0(3)	126.6(1)	126.7(2)	125.7(2)	126.1(2)
N1−Al−X	106.3(2)	104.22(8)	104.9(2)	105.2(1)	104.4(1)
N2−Al−X	113.8(2)	115.40(8)	115.2(2)	115.5(1)	116.0(1)
N3/O1−Al−X	95.7(2)	95.13(7)	94.3(2)	93.6(1)	92.7(1)
N3/O1−Al−N1	111.6(3)	111.8(1)	111.9(2)	111.7(2)	111.9(2)
N3/O1−Al−N2	99.1(3)	99.2(1)	98.9(2)	100.4(2)	100.7(2)
Al−N1−C1	127.4(4)	127.4(2)	125.9(4)	127.5(3)	127.4(3)
Al−N1−C5	116.8(4)	117.0(2)	116.7(3)	114.9(4)	116.8(3)
Al−N2−C10	124.7(4)	123.9(2)	124.8(3)	125.8(3)	124.9(2)
Al−N2−C14	121.9(4)	121.5(2)	121.2(4)	120.8(3)	121.0(2)
Sum of bond angles [°]	Σ(N1)	358.9	358.8	358.8	359.4
Σ(N2)	359.5	359.8	359.7	359.6	359.6
Σ(N3/O1)	360.0	360.0	359.6	359.9	360.0
Torsion angles [°]					
C1−N1−Al−X	69.81	75.95	75.06	72.36	–
C5−N1−Al−X	57.20	60.41	60.49	59.88	–
C10−N2−Al−X	29.23	35.06	22.49	26.69	–
C14−N2−Al−X	19.68	19.39	16.27	18.36	–

Each of the aluminum centres in the five compounds is coordinated in a distorted tetrahedral fashion by one tmp ligand in the chair conformation, one tmp ligand in the twist conformation, the N or O atom of the donor molecule, and the halogen atom. The N and O atoms of the ligands are tricoordinated and exhibit bond angle sums close to 360° (358.8−360.0°). The most interesting feature of these adducts are the long Al−X bond lengths: 2.220(1) to 2.227(3) Å for X = Cl; 2.408(2) to 2.429(2) Å for X =

Figure 1. Molecular structure of **2a** in the solid state. Thermal ellipsoids are shown at a 25% probability level

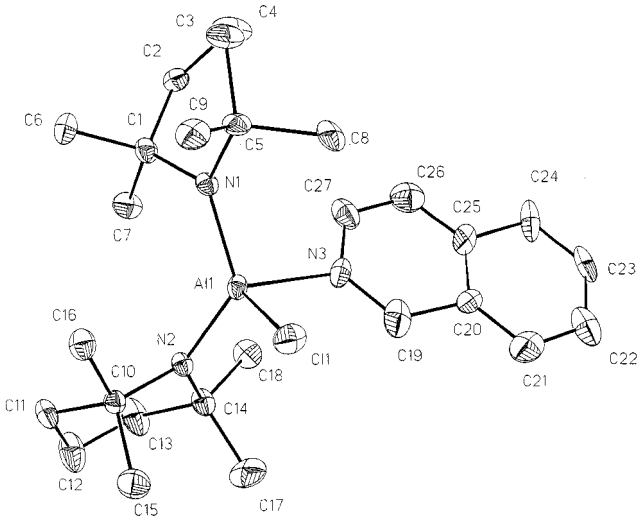

Figure 2. Molecular structure of **2b** in the solid state. Thermal ellipsoids are shown at a 25% probability level

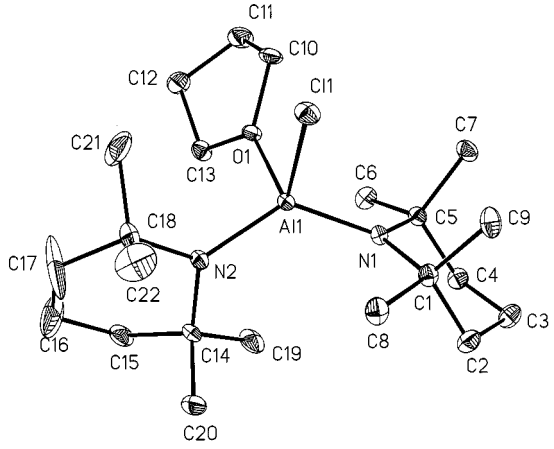

Figure 3. Molecular structure of **3a** in the solid state. Thermal ellipsoids are shown at a 25% probability level

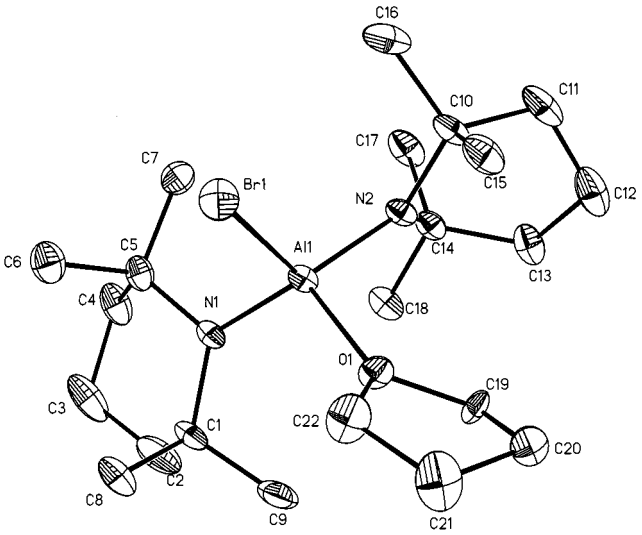

Figure 4. Molecular structure of **3b** in the solid state. Thermal ellipsoids are shown at a 25% probability level

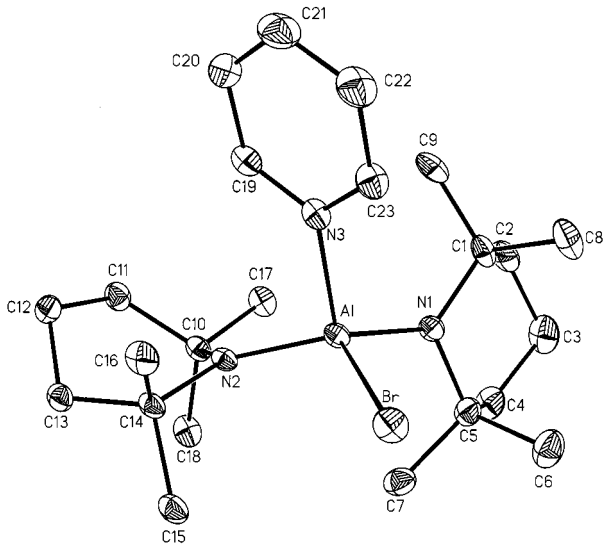

Figure 5. Molecular structure of **4a** in the solid state. Thermal ellipsoids are shown at a 25% probability level

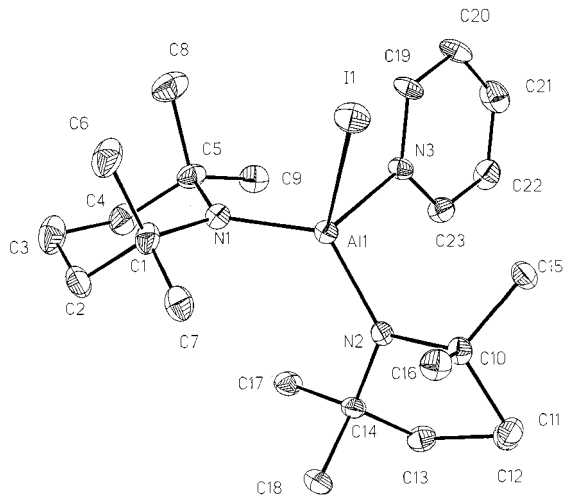

Br, and 2.704(1) A for X = I. The Al−N bond lengths fall in a narrow range, varying only from 1.836(5) to 1.854(4) A. There are no differences in the bond distances between the tmp ligand present in the chair conformation and that in the twist conformation. Al−Do distances range from 1.913(2) to 1.928(4) A (THF) and from 2.022(3) to 2.041(7) A (pyridine bases). As the tmp ligands are quite bulky, the N−Al−N bond angle [125.7(2) to 126.7(2)°] shows a considerable deviation from the tetrahedral bond angle of 109.5°.

Compared to the sums of their covalent radii (Al−Cl 2.10, Al−Br 2.28, Al−I 2.48 A, corrected for ionic contributions by the Schomaker-Stevenson method[23]), which normally correspond well with the experimental Al−X atom distances (X = Cl, Br, I), the bond lengths found for $tmp_2AlX\cdot Do$ (**2−4**) are unusually long. They exceed the sums of their covalent radii by 12 (Cl) to 23 pm (I). The bond lengths *d*(Al−Cl) in **2a**, **b** and the Al−Cl distance found in the molecular adduct $Me_2AlCl\cdot NH_2tBu$ [2.204(2) A][10] reveal that the adducts **2a**, **b** are in a state of predissociation {cf. the related salts $[Me_2Al(NH_2tBu)_2]X$, X = Br, I}[10]. Thus, Al−Cl bond lengths shorter than those in the adducts **2a**, **b** have been observed even for usually longer bridging Al−Cl−Al distances, e.g. in the centrosymmetric organoaluminum dichloride $Ar(Cl)Al(\mu\text{-}Cl)_2Al(Cl)Ar$ (Ar = 2,6-$Mes_2C_6H_3$), where the Al−Cl bond lengths amount to 2.195(2) A, terminal: 2.125(2) A][24]. This is also true for **3−4**, which exhibit long Al−X distances in the range typical of bridging Al−X−Al units, e.g. of the same order as those in $(tBu_2Al\mu\text{-}X)_2$ [X = Br 2.463(3) A, X = I 2.708 A][25] or in $(trip_2Al\mu\text{-}Br)_2$ [*d*(Al−Br) = 2.475(4) and 2.500(3) A; trip = 2,4,6-$iPr_3C_6H_2$][26]. This elongation can be viewed as the initial stage of dissociation. For the Al−I bond in particular, a strongly polar $Al^{\delta+}-I^{\delta-}$ bonding situation follows [cf. $Me_2AlI\cdot NMe_3$; *d*(Al−I) = 2.58 A][28], which also explains the poor solubility of these compounds in non-polar solvents.

Crystals of the adduct $AlI_3\cdot iq$ (**7a**) are monoclinic, space group *C*2/*c* (*Z* = 8, Figure 7). For compound $tmpAlI_2\cdot py$ (**7c**), the monoclinic space group $P2_1/n$ with four molecules in the unit cell has been determined (Figure 8). The aluminum atoms in these adducts are tetracoordinated by the pyridine base, the iodine atoms, and the tmp ligand. The latter substituent adopts the chair conformation and possesses a planarized nitrogen centre (sum of bond angles 356.2°). The Al−N distance to the donor molecule decreases from 1.978(5) A (**7c**) to 1.947(9) A (**7a**) (cf. the adducts **2−4** in Table 2) as the number of iodine atoms increases. This gives an indication that AlI_3 is a stronger Lewis acid than $tmpAlI_2$. For $AlCl_3\cdot NMe_3$, *d*(Al−N) amounts to 1.96 A[4], while for *cyclo*-$Me_2NCH_2CH_2(Et)\text{-}NAlCl_2$, this distance is 1.963(2) A[27]. However, in **7c**, the Al−N bond to the tmp ligand is short [1.809(5) A] and resembles that in $[tmp(Br)Al\mu\text{-}OEt]_2$, [*d*(Al−N) = 1.810(3) A][15]. Thus, the difference between the coordinative Al−N linkage and the covalent Al−N bond is about 0.17 A. Given these bonding parameters for **7a**, **c**, it is not surprising that the Al−I bond lengths in **7a** are − on average − 6.5 pm shorter than those in **7c** [**7a**: 2.500(4) to 2.510(4), **7c**: 2.572(2) and 2.573(2) A]. This is in accord with a decrease of the Lewis acidity of the aluminum centre in **7c** and compares well with the *d*(Al−I) of 2.58 A observed in $Me_2AlI\cdot NMe_3$[28].

Semiempirical and Ab Initio Calculations

Semiempirical AM1[29] calculations have been performed in order to investigate the extent of steric shielding and the bond strength factors that are necessary to favor ionization. Thus, the structures of the cations $[(R_2N)_2Al(py)]^+$ and the salts $[(R_2N)_2Al(py)^+]AlCl_4^-$, as well as of the halide-bridged adduct compounds $(R_2N)_2(py)Al-Cl-AlCl_3$ were computed (R = Me, Et, *i*Pr, and R_2N = tmp). The heats of formation of the respective minimum geometries and the shortest $Al-ClAlCl_3$ distances are presented in Table 4.

Figure 6. Molecular structure of **7b** in the solid state. Thermal ellipsoids are shown at a 25% probability level[a]

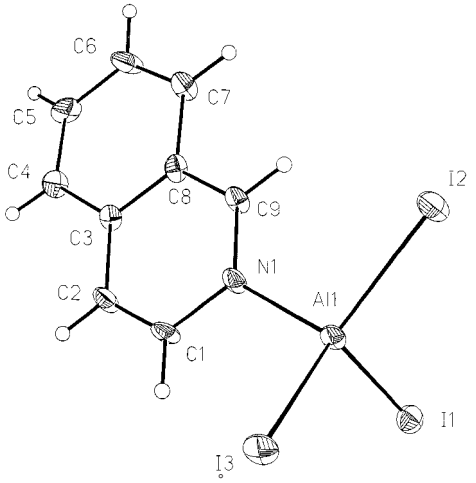

[a] Selected atom distances [A] and bond angles [°]: Al1−I1 2.500(4), Al1−I2 2.508(4), Al1−I3 2.510(4), Al1−N1 1.947(9); N1−Al1−I1 104.8(3), N1−Al1−I2 106.7(3), N1−Al1−I3 106.8(3), I1−Al−I2 112.2(1), I1−Al−I3 112.2(2), I2−Al1−I3 113.5(1).

Figure 7. Molecular structure of **7c** in the solid state. Thermal ellipsoids are shown at a 25% probability level[a]

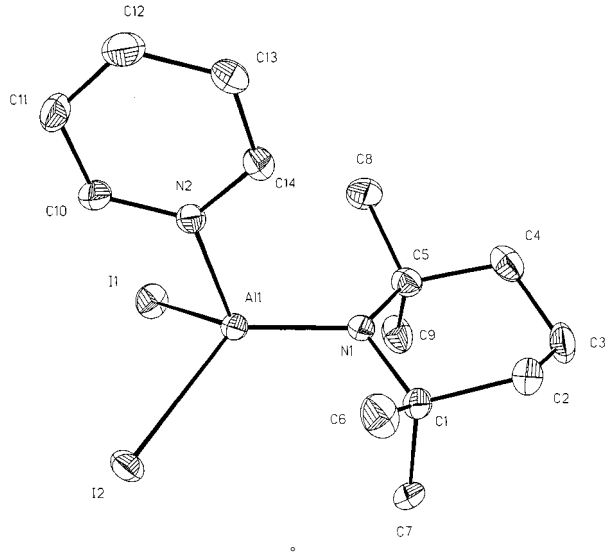

[a] Selected atom distances [A] and bond angles [°]: Al1−I1 2.573(2), Al1−I2 2.572(2), Al1−N1 1.809(5), Al1−N2 1.978(5); N1−Al1−I1 122.3(2), N1−Al1−I2 123.5(2), N1−Al1−N2 106.3(2), I1−Al−N2 103.4(2), I2−Al−N2 101.2(2), I1−Al1−I2 96.89(6), C1−N1−Al1 120.1(4), C5−N1−Al1 118.7(4), C1−N1−C5 117.4(5).

Table 4. AM1 calculated heats of formation of various model compounds

R_2N	Heat of formation $[(R_2N)_2Al(py)]^+$	Heat of formation $(R_2N)_2(py)Al\cdots Cl - AlCl_3$	$Al\cdots ClAlCl_3$ $d(Al-Cl)$ [A]
Me_2N	+113.1 kcal/mol	−231.1 kcal/mol	2.42
Et_2N	+93.3 kcal/mol	−251.7 kcal/mol	2.41
iPr_2N	+82.5 kcal/mol	−254.3 kcal/mol	2.42
tmp	+90.1 kcal/mol	−235.0 kcal/mol	4.45

The free cations exhibit positive heats of formation (in the range +82.5 to +113.1 kcal/mol), whereas the tetrachloroaluminum compounds are exergonic by −231.1 to −254.3 kcal/mol. Shielding of the aluminum center by the amido ligands R_2N (R = Me, Et, *i*Pr) is insufficient to prevent coordination of one chlorine atom [*d*(Al−Cl) of the tetrachloroaluminate to the aluminum center of the cation: 2.41−2.42 A]. It is only the sterically most demanding amido ligand, tmp, that allows the induction of ionization, as demonstrated by the shortest Al−Cl distance of 4.45 A. In another series of calculations, the enthalpies for the formation of $[tmp_2Al(py)]AlX_4$ (X = Cl, Br, I), as well as for the observed decomposition reactions of the salts into tmp_2AlX and $AlX_3 \cdot py$, were calculated from the computed heats of formation of every compound involved (see Scheme 1) using Hess′ rule.

Scheme 1. AM1 computed heats of formation and enthalpies of reaction for the formation and decomposition of $[tmp_2Al(py)]AlX_4$ (X = Cl, Br, I)

All enthalpies in kcal/mol

$$tmp_2AlCl + py + 0.5\ Al_2Cl_6 \xrightarrow[K = 3.56]{\Delta G_r = -0.7} [tmp_2Al(py)]AlCl_4$$

ΔG_f = -116.0 + 31.9 -150.2 -235.0

$$\xrightarrow[K = 4.4*10^5]{\Delta G_r = -7.7} tmp_2AlCl + AlCl_3{*}py \qquad (6a)$$

ΔG_f = -116.0 -126.7

$$tmp_2AlBr + py + 0.5\ Al_2Br_6 \xrightarrow[K = 133]{\Delta G_r = -2.9} [tmp_2Al(py)]AlBr_4$$

ΔG_f = -103.7 + 31.9 -124.5 -199.2

$$\xrightarrow[K = 113]{\Delta G_r = -2.8} tmp_2AlBr + AlBr_3{*}py \qquad (6b)$$

ΔG_f = -103.7 -98.3

$$tmp_2AlI + py + 0.5\ Al_2I_6 \xrightarrow[K = 5.28*10^{11}]{\Delta G_r = -16.0} [tmp_2Al(py)]AlI_4$$

ΔG_f = -76.8 + 31.9 -54.0 -116.9

$$\xrightarrow[K = 4.48*10\text{-}6]{\Delta G_r = 7.3} tmp_2AlI + AlI_3{*}py \qquad (6c)$$

ΔG_f = -76.8 -32.8

Two opposing trends are observed: whereas the heat of formation for the salt $[tmp_2Al(py)]AlX_4$ decreases on going from the chloride to the iodide (but still remains exergonic), the enthalpies for the formation of the salts increase in this direction. In fact, in the case of the iodide, the salt is stable with respect to decomposition into tmp_2AlI and $AlI_3 \cdot py$. This is partly due to the thermodynamically less favored Al−I bond [E(Al−Cl) = 494 kJ/mol; E(Al−I) = 364 kJ/mol][6], but is mainly attributable to the contribution of electrostatic stabilization of the tetraiodoaluminate, since the decomposition products, which also contain Al−X bonds, are less favored on going from the chloride to the iodide.

As no X-ray crystal structures of the ionic species could be determined, an ab initio study (MP2/6-31+G*)[30] of two model compounds $[(H_2N)_2Al(Do)]^+$ (Do = NH_3 **8a**, py **8b**) was performed, in order to assess the structural parameters of these cations. The minimum structures of the cations **8a**, **b** are depicted in Figure 9, and their structural parameters are given in Table 5.

Figure 8. Computed structures of $[(H_2N)_2Al(NH_3)]^+$ (**8a**) and $[(H_2N)_2Al(py)]^+$ (**8b**)

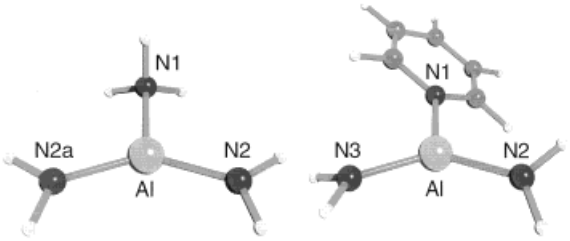

8a 8b

Table 5. Selected ab initio calculated bonding parameters for the two model cations, **8a**,**b**

Compound[a]	Sym.	*d*(Al−N) [A]	*d*(Al−L) [A]	N−Al−N [°]	*q*(Al) [e]	*q*(N) [e]	*q*(L) [e]	B.O. Al−N	LP*[b] (Al)
$[(H_2N)_2Al(NH_3)]^+$ **8a**	*C*s	1.758	1.996	139.34	2.12	−1.54	−1.26	0.62	0.19
$[(H_2N)_2Al(py)]^+$ **8b**	*C*1	1.764	1.947	136.86	2.14	−1.54	−0.78	0.60	0.13

[a] All calculations MP2/6-31+G*. − [b] Number of electrons in $3p_z$ orbital of Al.

The tricoordinated aluminum cations **8a**, **b** represent highly charged species [*q*(Al) = +2.12e and +2.14e, *q*(N) = −1.54e and −1.54e, *q*(Do-N) = −1.26e and −0.78e], with short Al−N bond lengths of 1.758 A (**8a**) and 1.764 A (**8b**) as well as wide N−Al−N bond angles of 139.3° and 136.8°, respectively. The Al−N distances to the nitrogen atoms of the donor molecules reflect their degree of hybridization. As expected, for the sp^3-hybridized donor NH_3, a longer Al−N bond length (1.996 A) was calculated, compared to that for the aromatic pyridine donor [*d*(Al−N) = 1.947 A]. According to NBO analysis, the $3p_z$(Al) orbital is populated with 0.19 (**8a**) and 0.13 (**8b**) electrons, indicating the presence of only weak pp(π) Al−N bonding. This compares well with the calculated minimum structures of $(H_2N)_2AlY$ [Y = Cl, OH, SH, NH_2, PH_2, CH_3, SiH_3, $Al(NH_2)_2$][17]. For these compounds, it was shown that the Al−N bond is highly polar and that the shorter the Al−N distance, the wider the N−Al−N bond angle[17]. Since the Al−N bond lengths in **8a**, **b** are 2 pm shorter than in $(H_2N)_2AlCl$ (**9**) [the compound with the shortest Al−N bond in the $(H_2N)_2AlY$ series, *d*(Al−N) = 1.782 A], the N−Al−N bond angles in **8a**, **b** of 139.3° and 136.8° are widened by about 16° compared to that in the chloride **9** (123.2°). The short Al−N bonds are mirrored by an increased positive charge of 0.16e and 0.18e residing on the aluminum centres of **8a**, **b**, compared to that calculated for the chloride **9**. Since the charge on the nitrogen atoms in **8a**, **b**, and **9** remains almost constant (−1.53 to −1.55e), a strongly polar Al−N bond is responsible for the short Al−N distances in **8a**, **b**.

Discussion

The aim of this study was the synthesis and characterization of low coordinated, cationic aluminum compounds. In contrast to the $R_2AlX/tBuNH_2$ system described by Atwood et al.[10], the compounds tmp_2AlX (X = Cl, Br, I) could not be forced to ionize by the addition of an excess of a donor molecule. The steric demand of the tmp and donor ligands prevents the formation of cations of the type $tmp_2Al(Do)_2^+$ and of adducts of the type $tmp_2AlX \cdot Do_2$. However, comparison of the Al−X bond lengths determined for **2**−**4**, having conventional terminal and bridging Al−X bonds, reveals that $tmp_2AlX \cdot Do$ shows the early stages of dissociation into $[tmp_2Al(Do)^+]X^-$. Dissociation of compounds of the type $tmp_2AlX \cdot Do$ should be facilitated by weakly coordinating anions X^-. However, such a strategy did not succeed with X = BPh_4^-, $B(C_6F_5)_4^-$, BF_4^-, or tosylate. Instead, decomposition reactions or coordination of the various anions occurred. Nevertheless, the tetrabromo- and tetraiodoaluminates turned out to be sufficiently non-basic (and suitably large) to stabilize the salts $[tmp_2Al(Do)]AlX_4$ (**6a**−**f**) in solution. The formation of the AlX_4^- units (X = Br, I) is favoured due to the decreasing strength of the Al−X bonds in $tmp_2AlX \cdot Do$ on proceeding from chlorine to iodine, so that the additional stabilization energy provided by ion pair formation governs the overall enthalpy for the decomposition of $[tmp_2Al(py)]AlI_4$ (as predicted by AM1 calculation). Since decomposition products of even tetraiodoaluminates have been found [e.g. $AlI_3 \cdot iq$ (**7a**), $AlI_3 \cdot 4$-*t*Bu-py (**7b**)], this seems to be contradictory. However, the calculations can only simulate gaseous species in vacuo. As the variations in the reaction enthalpies are small, solvent effects must play a role in the behavior of the tetrahaloaluminate salts. Nevertheless, both the experimental and theoretical approaches indicate that the iodo compounds represent the most stable species. Non-polar solvents disfavour the formation of ionic species of type $[tmp_2Al(Do)]AlX_4$ (**6a**−**f**), whereas polar donor solvents stabilize the ions, but may also abstract AlX_3 as $AlX_3 \cdot Do \cdot (Solv.)_n$ (*n* = 1, 2), providing an alternative decomposition pathway for the system.

Conclusion

The aluminum atoms in the tricoodinated bis(tetramethylpiperidino)aluminum halides **1a**−**c** are Lewis acidic and form monoadducts of the type $tmp_2AlX \cdot Do$ (**2**−**4**) with THF and pyridine bases. Since the Al−X (X = Cl, Br, I)

bonds in **2−4** are considerably longer than those in **1a−c**, a tendency towards dissociation into $tmp_2(Do)Al^+$ and X^- is indicated. Attempts to prepare salts of the type $[tmp_2Al(Do)]Y^-$ [Y = BPh_4, $B(C_6F_5)_4$, Otos] led either to decomposition or to the formation of molecular adducts. The solution behavior of $tmp_2Al(py)BF_4$ (**5e**) shows a solvent dependence: in pentane, a tetracoordinated molecular product is observed, while in CH_2Cl_2 or $CDCl_3$ solution, it dissociates into an ion pair. However, halide abstraction from $tmp_2AlX\cdot Do$ can be achieved by the addition of AlX_3 to generate salts of the type $[tmp_2Al(Do)]AlX_4$, as demonstrated by electrical conductivity in CH_2Cl_2 solution. These experimental results are supported by semiempirical AM1 calculations on the $[(R_2N)_2Al(py)]AlX_4$ species. The results show that the steric demand of the tmp ligand is essential for ion pair formation. The formation of tetraiodoaluminate compounds is favored over that of the corresponding tetrabromo- or tetrachloroaluminates. Further ab initio studies of some model systems explain the presence of short Al−N distances in terms of ionic contributions to the Al−N bond. Whether the Lewis acidic aluminum centre in these cations can act as catalyst, e.g. in olefin polymerization, needs to be evaluated experimentally. Since these salts are highly Lewis acidic, are soluble in aromatic hydrocarbons, and are sterically encumbered so as to possibly induce regioselectivity, these aspects will be investigated and communicated in forthcoming reports.

Once again, the tmp ligand is found to produce a remarkable stabilizing effect and allows the generation of unusual bonding situations, such as the tricoordinated aluminum cations. As yet, the most weakly coordinating anions $CB_{11}H_{11}X^-$ (X = H, Cl) have not been tested[31], but they are certainly good candidates for achieving the formation of $tmp_2Al(Do)^+$ cations, or the even more demanding goal of generating the dicoordinated cation tmp_2Al^+.

We are grateful to the *Fonds der Chemischen Industrie* and *Chemetall mbH* for supporting our studies. We also thank Mrs. *G. Käser* and Mrs. *C. Ullmann* for performing the elemental analyses, Mr. *P. Mayr*, Dr. *R. Waldhör* and Dr. *C. Miller* for recording many NMR spectra, Mrs. *D. Ewald* for mass spectra and Mrs. *E. Kiesewetter* for IR spectra. Access to the calculation facilities of *Leibniz Rechenzentrum* is also acknowledged.

Experimental Section

All manipulations were performed using Schlenk techniques under a dinitrogen or argon atmosphere. All solvents were rigorously dried prior to use and stored under N_2 or argon. Discrepancies in the elemental analyses of a number of compounds can be attributed to insufficient protection against oxidation and hydrolysis of the air- and moisture-sensitive compounds during the weighing procedures. − NMR: Bruker ACP 200, Jeol GSX400 and Jeol GSX270. − IR: Nicolet FT-IR spectrometer model 6000, CsI plates, Nujol. − MS: Varian Atlas CH7 spectrometer.

General Procedure for the Synthesis of the Adducts $tmp_2AlX\cdot Do$ **2−4**: The concentrations of stock solutions of tmp_2AlX (X = Cl, Br, I), **1a−c**, in *n*-hexane were determined by titration of aluminum and halide. At ambient temperature, the stoichiometric amount of the appropriate donor was added as a hexane solution. Most of the adducts precipitated immediately. After filtration and concentration of the filtrate to one-third of its original volume, storage at −20°C overnight led to the deposition of well-shaped crystals of **2−4**. Precipitates were washed twice with pentane and dried in vacuo. Yields varied between 80 and 95%. Where suitable crystals for X-ray diffraction studies were required, aromatic solvents or *n*-hexane/THF mixtures proved to be appropriate media for recrystallization.

$tmp_2AlCl\cdot iq$ (**2a**): tmp_2AlCl (43.2 ml, 0.11 M, 4.8 mmol); isoquinoline (0.99 g, 4.8 mmol), yield of **2a**: 1.95 g (86%), m.p. 148−151°C. − ^1H NMR ($CDCl_3$) (400 MHz): δ = 1.37 (t, 8 H, tmp-β-CH_2), 1.29 [s, 24 H, tmp-C(CH_3)$_2$], 1.62 (m, 4 H, tmp-γ-CH_2), 7.80 (t, 1 H, iq-C*H*), 7.93 (m, 3 H, iq-C*H*), 8.15 (d, 1 H, iq-C*H*), 9.14 [d, 1 H, ^3J(H,H) = 6.5 Hz, iq-C*H*], 10.10 (s, 1 H, iq-C*H*). − ^{13}C NMR ($CDCl_3$) (100 MHz): δ = 18.1 (tmp-*C*4), 34.0 (tmp-*C*7-10), 41.5 (tmp-*C*3/5), 52.7 (tmp-*C*2/6), 122.0 (iq-*C*), 126.8 (iq-*C*), 127.7 (iq-*C*), 129.2 (iq-*C*), 129.5 (iq-*C*), 134.3 (iq-*C*), 137.3 (iq-*C*), 141.1 (iq-*C*), 155.1 (iq-*C*). − ^{27}Al NMR ($CDCl_3$) (70 MHz): δ = 102 ($\Delta_{1/2}$ = 8300 Hz). − $C_{27}H_{43}AlClN_3$ (473.10): calcd. C 68.69, H 9.18, N 8.90; found C 67.67, H 8.62, N 8.68.

$tmp_2AlBr\cdot iq$ (**3c**): tmp_2AlBr (40.7 ml, 0.27 M, 11.0 mmol); isoquinoline (2.28 g, 11.0 mmol), yield of **3c**: 5.06 g (89%), m.p. 155−160°C. − ^1H NMR ($CDCl_3$) (400 MHz): δ = 1.41 (t, 8 H, tmp-β-CH_2), 1.37 [s, 24 H, tmp-C(CH_3)$_2$], 1.66 (m, 4 H, tmp-γ-CH_2), 7.78 (t, 1 H, iq-C*H*), 7.94 (m, 3 H, iq-C*H*), 8.13 (d, 1 H, iq-C*H*), 9.18 [d, 1 H, ^3J(H,H) = 7.4 Hz, iq-C*H*], 10.17 (s, 1 H, iq-C*H*). − ^{13}C NMR ($CDCl_3$) (100 MHz): δ = 17.9 (tmp-*C*4), 34.1 (tmp-*C*7-10), 41.5 (tmp-*C*3/5), 52.9 (tmp-*C*2/6), 121.8 (iq-*C*), 126.8 (iq-*C*), 127.7 (iq-*C*), 129.4 (iq-*C*), 129.5 (iq-*C*), 134.2 (iq-*C*), 137.5 (iq-*C*), 141.6 (iq-*C*), 155.7 (iq-*C*). − ^{27}Al NMR ($CDCl_3$) (70 MHz): δ = 109 ($\Delta_{1/2}$ = 7500 Hz). − IR (Nujol) [ν(Al−Br)]: ν = 332 cm^{-1} vs. − $C_{27}H_{43}AlBrN_3$ (516.54): calcd. C 62.78, H 8.39, N 8.13, Br 15.5; found C 58.75, H 8.13, N 7.42, Br 15.9.

$tmp_2AlI\cdot iq$ (**4b**): tmp_2AlI (84.9 ml, 0.10 M, 8.5 mmol); isoquinoline (1.76 g, 8.5 mmol), yield of **4b**: 3.93 g (82%), 152°C (decomp. to a black material), m.p. 168°C. − ^1H NMR ($CDCl_3$) (400 MHz): δ = 1.41 (t, 8 H, tmp-β-CH_2), 1.44 [s, 24 H, tmp-C(CH_3)$_2$], 1.65 (m, 4 H, tmp-γ-CH_2), 7.76 (t, 1 H, iq-C*H*), 7.93 (m, 3 H, iq-C*H*), 8.15 (d, 1 H, iq-C*H*), 9.21 [d, 1 H, ^3J(H,H) = 6.4 Hz, iq-C*H*], 10.21 (s, 1 H, iq-C*H*). − ^{13}C NMR ($CDCl_3$) (100 MHz): δ = 17.7 (tmp-*C*4), 34.1 (tmp-*C*7-10), 41.3 (tmp-*C*3/5), 53.1 (tmp-*C*2/6), 121.7 (iq-*C*), 126.8 (iq-*C*), 127.5 (iq-*C*), 129.4 (iq-*C*), 129.5 (iq-*C*), 134.0 (iq-*C*), 137.2 (iq-*C*), 141.8 (iq-*C*), 155.3 (iq-*C*). − ^{27}Al NMR ($CDCl_3$) (70 MHz): δ = 108 ($\Delta_{1/2}$ = 8900 Hz). − IR (Nujol) [ν(Al−I)]: ν = 341 cm^{-1} vs. − $C_{27}H_{43}AlIN_3$ (563.54): calcd. C 57.55, H 7.91, N 7.10, I 22.4; found C 56.55, H 7.69, N 7.46, I 22.5.

$tmp_2AlBr\cdot thf$ (**3a**): tmp_2AlBr (35.1 ml, 0.27 M, 9.5 mmol); THF (5 ml, excess), yield of **3a**: 3.97 g (91%), m.p. 50−53°C. − ^1H NMR (C_6D_6) (270 MHz): δ = 1.45 (s, 24 H, tmp-CH_3), 1.31 (t, 8 H, tmp-β-CH_2), 1.58 (m, 4 H, tmp-γ-CH_2), 3.76 (br s, 4 H, thf-α-CH_2), 1.84 (br s, 4 H, thf-β-CH_2). − ^{13}C NMR (C_6D_6) (100 MHz): δ = 18.2 (tmp-*C*4), 34.3 (tmp-*C*7-10), 40.0 (tmp-*C*3/5), 52.5 (tmp-*C*2/6), 25.6 (thf-β-*C*H$_2$), 68.3 (thf-α-*C*H$_2$). − ^{27}Al NMR (C_6D_6) (70 MHz): δ = 125 ($\Delta_{1/2}$ = 8080 Hz). − IR (Nujol) [ν(Al−Br)]: ν = 342 cm^{-1} vs. − $C_{22}H_{44}AlBrN_2O$ (459.49): calcd. C 57.51, H 9.65, N 6.10, Al 5.9, Br 17.4; found C 56.01, H 9.65, N 5.81, Al 5.4, Br 17.1.

$tmp_2AlBr\cdot py$ (**3b**): tmp_2AlBr (50.0 ml, 0.27 M, 13.5 mmol); pyridine (1.00 g, 13.5 mmol), yield of **3b**: 5.98 g (95%), m.p. 121−125°C. − ^1H NMR (C_6D_6) (400 MHz): δ = 1.51 (t, 8 H, tmp-β-CH_2), 1.58 [s, 24 H, tmp-C(CH_3)$_2$], 1.74 (m, 4 H, tmp-γ-CH_2), 6.43 (t, 2 H, py-C*H*), 6.75 (t, 1 H, py-C*H*), 9.25 (br. s, 2 H, py-C*H*). − ^{13}C NMR (C_6D_6) (100 MHz): δ = 18.6 (tmp-*C*4), 34.5

(tmp-*C*7-10), 42.2 (tmp-*C*3/5), 53.4 (tmp-*C*2/6), 124.1 (py-*C*), 140.4 (py-*C*), 150.4 (py-*C*). – ^{27}Al NMR (C_6D_6) (70 MHz): δ = 96 ($\Delta_{1/2}$ = 4360 Hz). – IR (Nujol) [ν(Al–Br)]: ν = 347 cm^{-1} vs. – $C_{23}H_{41}AlBrN_3$ (466.48): calcd. C 59.22, H 8.86, N 9.01, Al 5.7, Br 17.2; found C 57.59, H 8.74, N 8.49, Al 5.8, Br 16.5.

tmp$_2$AlI·py (**4a**): tmp$_2$AlI (64.5 ml, 0.10 M, 6.5 mmol); pyridine (0.48 g, 6.5 mmol), yield of **4a**: 3.17 g (95%), m.p. 134–137°C. – ^{1}H NMR (C_6D_6) (400 MHz): δ = 1.48 (t, 8 H, tmp-β-C*H*$_2$), 1.62 [s, 24 H, tmp-C(C*H*$_3$)$_2$], 1.76 (m, 4 H, tmp-γ-C*H*$_2$), 6.30 (t, 2 H, py-C*H*), 6.62 (t, 1 H, py-C*H*), 9.06 (br s, 2 H, py-C*H*). – ^{13}C NMR (C_6D_6) (100 MHz): δ = 17.8 (tmp-*C*4), 34.8 (tmp-*C*7-10), 42.7 (tmp-*C*3/5), 53.3 (tmp-*C*2/6), 125.0 (py-*C*), 141.9 (py-*C*), 148.0 (py-*C*). – ^{27}Al NMR (C_6D_6) (70 MHz): δ = 92 ($\Delta_{1/2}$ = 4900 Hz). – $C_{23}H_{41}AlIN_3$ (513.48): calcd. C 53.80, H 8.05, N 8.18, Al 5.3, I 24.7; found C 50.73, H 7.46, N 7.60, Al 5.7, I 25.0.

tmp$_2$AlI·pic (**4c**): tmp$_2$AlI (32.8 ml, 0.10 M, 3.3 mmol); γ-picoline (0.29 g, 3.3 mmol), yield of **2a**: 1.70 g (80%), m.p. 136–139°C. – ^{1}H NMR (C_6D_6) (400 MHz): δ = 1.52 (t, 8 H, tmp-β-C*H*$_2$), 1.66 [s, 24 H, tmp-C(C*H*$_3$)$_2$], 1.73 (m, 4 H, tmp-γ-C*H*$_2$), 1.54 (s, 3 H, γ-pic-C*H*$_3$), 6.32 (br s, 2 H, β-pic-C*H*), 9.27 (br s, 2 H, α-pic-C*H*). – ^{13}C NMR (C_6D_6) (100 MHz): δ = 18.3 (tmp-*C*4), 34.4 (tmp-*C*7-10), 42.2 (tmp-*C*3/5), 53.5 (tmp-*C*2/6), 125.0 (β-pic-*C*), 150.2 (α-pic-*C*). – ^{27}Al NMR (C_6D_6) (70 MHz): δ = 77 ($\Delta_{1/2}$ = 5900 Hz). – IR (Nujol) [ν(Al–I)]: ν = 318 cm^{-1} s. – $C_{24}H_{43}AlIN_3$ (527.51): calcd. C 54.65, H 8.22, N 7.39; found C 50.98, H 8.13, N 6.75.

Reaction of tmp$_2$AlI·py **4a** *with AgBPh$_4$ To Give BPh$_3$·py* (**5b**) *and tmp$_2$AlPh* (**5a**): $AgBPh_4$ (0.58 g, 1.36 mmol) was suspended in 10 ml of benzene. A solution of tmp$_2$AlI·py (18.1 ml, 0.075 M, 1.36 mmol) in benzene was added at ambient temperature. The mixture was heated to reflux for 3 days and the insoluble material was filtered off (0.46 g, calcd. AgI: 0.32 g). From the resulting filtrate, all volatiles were removed in vacuo. The residue was extracted with 20 ml of toluene and this solution was stored overnight at –78°C. A microcrystalline precipitate of BPh3·py (**5b**), (0.17 g, 39%) separated; tmp$_2$AlPh (**5a**) was characterized in solution by its NMR data[15].

5b: ^{1}H NMR (C_6D_6) (270 MHz): δ = 7.25 (t, 3 H, *p*-Ph-*H*), 7.32 (t, 6 H, *m*-Ph-*H*), 7.51 (d, 6 H, *o*-Ph-*H*), 6.15 (br s, 2 H, *m*-py-*H*), 6.57 (br. s, 1 H, *p*-py-*H*), 8.15 (br s, 2 H, *o*-py-*H*). – ^{11}B NMR (C_6D_6) (64 MHz): δ = 5.1 (br). – $C_{23}H_{20}BN$ (321.23): calcd. C 86.00, H 6.28, N 4.36; found C 84.20, H 6.61, N 4.28.

tmp$_2$AlOtos·py (**5c**): To a suspension of AgOtos (1.00 g, 3.6 mmol) and pyridine (0.29 ml, 3.6 mmol) in 30 ml of toluene, a solution of tmp$_2$AlBr (13.3 ml, 0.27 M, 3.6 mmol) in *n*-hexane was added at ambient temperature. Immediately, a yellow precipitate of tmp$_2$AlBr·py separated. The mixture was allowed to stir overnight, and then the insoluble material, which had become somewhat brown, was filtered off and weighed (2.41 g, calcd. AgBr 0.67 g). Extraction with 50 ml of benzene resulted in a yellow solution, which was concentrated in vacuo to a volume of 10 ml. Storage of this solution overnight at 8°C afforded tmp$_2$AlOtos·py as a colorless precipitate. Yield of **5c**: 0.54 g (28%), decomp. > 311°C. – ^{1}H NMR ($CDCl_3$) (270 MHz): δ = 1.27 (t, 8 H, tmp-β-C*H*$_2$), 1.09 [br s, 24 H, tmp-C(C*H*$_3$)$_2$], 1.54 (m, 4 H, tmp-γ-C*H*$_2$) 2.24 (s, 3 H, tos-C*H*$_3$), 7.55 (t, 2 H, *m*-py-*H*), 7.96 (t, 1 H, *p*-py-*H*), 9.29 (br s, 2 H, *o*-py-*H*). – ^{13}C NMR ($CDCl_3$) (100 MHz): δ = 18.1 (tmp-*C*4), 33.9 (tmp-*C*7-10), 40.9 (tmp-*C*3/5), 52.2 (tmp-*C*2/6), 21.4 (tos-*C*H$_3$), 125.0 (py-*C*), 141.8 (py-*C*), 149.8 (py-*C*), 127.0 (tos-*C*), 128.3 (tos-*C*), 128.8 (tos-*C*), 139.1 (tos-*C*). – ^{27}Al NMR (C_6D_6) (70 MHz): δ = 97 ($\Delta_{1/2}$ = 5500 Hz).

tmp$_2$Al(lut)(BF$_4$) (**5d**): $AgBF_4$ (1.65 g, 8.5 mmol) and 2,6-lutidine (0.86 g, 8.5 mmol) were suspended in 50 ml of *n*-hexane and the mixture was cooled to –78°C. A solution of tmp$_2$AlBr (22.9 ml, 0.35 M, 8.0 mmol) in *n*-hexane was then added slowly and the mixture was allowed to attain ambient temperature. After stirring overnight, the brownish insoluble material was filtered off (2.32 g, calcd. AgBr 1.61 g) and the resulting yellow filtrate was stored for several days at –78°C. Colorless crystals of tmp$_2$Al(lut)(BF_4) **5d** separated. Yield: 2.47 g (62%); m.p. > 328°C (decomp.). – ^{1}H NMR (C_6D_6) (400 MHz): δ = 1.23 (t, 8 H, tmp-β-C*H*$_2$), 1.06 [s, 24 H, tmp-C(C*H*$_3$)$_2$], 1.53 (m, 4 H, tmp-γ-C*H*$_2$), 2.41 (s, 6 H, lut-C*H*$_3$), 6.57 (d, 2 H, lut-*H*), 7.00 (t, 1 H, lut-*H*). – ^{13}C NMR (C_6D_6) (100 MHz): δ = 18.8 (tmp-*C*4), 32.0 (tmp-*C*7-10), 38.6 (tmp-*C*3/5), 49.6 (tmp-*C*2/6), 52.4 (lut-*C*H$_3$), 119.8 (lut-*C*), 136.9 (lut-*C*). – ^{27}Al NMR (C_6D_6) (70 MHz): δ = 1 ($\Delta_{1/2}$ = 3900 Hz). – ^{11}B NMR (C_6D_6) (64 MHz): δ = 17.9. – ^{19}F NMR (C_6D_6) (85 MHz): δ = –104.5 (s), –111.0 (s). – IR (Nujol): ν = 421 w, 452 m, 468 s, 507 vs, 527 vs, 551 vs, 568 s, 596 s, 745 w, 762 w, 851 w, 870 w, 900 m, 918 s, 936 vs, 957 vs, 982 vs, 997 vs, 1064 s, 1082 w, 1130 vs, 1180 s, 1202 m, 1236 vs, 1294 w, 1346 m, 1364 s, 1375 s, 1384 s, 1435 m, 1470 s, 1594 w, 1645 w, 1732 w, 2458 w, 2672 w, 2766 w, 2873–3007 vs. – $C_{25}H_{45}AlBF_4N_3$ (501.44): calcd. C 59.88, H 9.05, N 8.38, Al 5.4; found C 60.06, H 10.07, N 7.47, Al 6.0.

tmp$_2$Al(py)BF$_4$ (**5e**): To a solution of $AgBF_4$ (1.06 g, 4.96 mmol) in 35 ml of CH_2Cl_2, a solution of tmp$_2$AlI·py (37.0 ml, 0.134 M, 4.96 mmol) in toluene was added at ambient temperature. Immediately, a dark precipitate formed. After stirring the mixture overnight, the insoluble material was filtered off and the filtrate was concentrated in vacuo. The resulting yellow oil (1.89 g, 80%) was found to be soluble in aliphatic as well as in aromatic or chlorinated solvents. Crystallization could not be achieved. – ^{1}H NMR ($CDCl_3$) (270 MHz): δ = 0.83 (t, 8 H, tmp-β-C*H*$_2$), 1.23 [s, 24 H, tmp-C(C*H*$_3$)$_2$], 1.60 (m, 4 H, tmp-γ-C*H*$_2$), 7.75 (t, 2 H, py-*H*), 8.22 (t, 1 H, py-*H*), 8.71 (br s, 2 H, py-*H*). – ^{27}Al NMR ($CDCl_3$) (70 MHz): Only an extremely broad, poorly-defined signal was observed. – ^{11}B NMR ($CDCl_3$) (64 MHz): δ = 0.9; (pentane): δ = 19.3 (no BF coupling observed). – ^{19}F NMR ($CDCl_3$) (85 MHz): δ = –151.0 [q, ^1J(B,F) = 12 Hz]; (pentane): δ = –111.0 (br s).

[tmp$_2$Al(iq)]AlBr$_4$ (**6a**): To a solution of tmp$_2$AlBr·iq in CH_2Br_2 (33.1 ml, 0.178 M, 5.89 mmol), $AlBr_3$ (1.57 g, 5.89 mmol) in 10 ml of CH_2Br_2 was added dropwise at 0°C. After 30 min., the clear red solution was reduced to half of its original volume and stored overnight at –20°C. **6a** separated as an orange microcrystalline powder. Yield: 4.43 g (96%), m.p. > 302°C (decomp.). – ^{1}H NMR ($CDCl_3$) (270 MHz): δ = 1.34 (t, 8 H, tmp-β-C*H*$_2$), 1.47 [s, 24 H, tmp-C(C*H*$_3$)$_2$], 1.62 (m, 4 H, tmp-γ-C*H*$_2$), 7.94 (t, 1 H, iq-C*H*), 8.10 (m, 2 H, iq-C*H*), 8.28 (d, 1 H, iq-C*H*), 8.30 (d, 1 H, iq-C*H*), 8.94 [d, 1 H, ^3J(H,H) = 6.4 Hz, iq-C*H*], 9.89 (s, 1 H, iq-C*H*). – ^{13}C NMR ($CDCl_3$) (100 MHz): δ = 17.5 (tmp-*C*4), 34.2 (tmp-*C*7-10), 39.9 (tmp-*C*3/5), 52.5 (tmp-*C*2/6), 124.2 (iq-*C*), 127.0 (iq-*C*), 127.5 (iq-*C*), 130.1 (iq-*C*), 130.1 (iq-*C*), 136.4 (iq-*C*), 137.1 (iq-*C*), 137.7 (iq-*C*), 152.5 (iq-*C*). – ^{27}Al NMR ($CDCl_3$) (70 MHz): δ = 102 ($\Delta_{1/2}$ = 66 Hz); (CH_2Br_2): δ = 104 ($\Delta_{1/2}$ = 53 Hz). – IR (Nujol) [ν(Al–Br)]: ν = 429 cm^{-1} vs. – $C_{27}H_{43}Al_2Br_4N_3$ (783.24): calcd. C 41.40, H 5.53, N 5.36, Al 6.9, Br 40.8; found C 36.01, H 5.12, N 4.43, Al 7.2, Br 40.7 (C, H, N ratio: calcd. 9:14.33:1; found 9.48:16.06:1).

[tmp$_2$Al(py)]AlI$_4$ (**6b**): To AlI_3 (0.62 g, 1.5 mmol) dissolved in 5 ml of benzene, a solution of tmp$_2$AlI·py (20.0 ml, 0.075 M, 1.5 mmol) in benzene was added at ambient temperature. The mixture was stirred overnight. Subsequent addition of 5 ml of pentane led to the precipitation of yellowish **6b**. Yield: 1.10 g (79%), decomp. at *T* > 166 C (blackens). – ^{1}H NMR (C_6D_6) (270 MHz): δ = 1.31 (t, 8 H, tmp-β-C*H*$_2$), 1.48 [s, 24 H, tmp-C(C*H*$_3$)$_2$], 1.55 (m, 4 H,

tmp-γ-CH_2), 6.21 (t, 2 H, py-C*H*), 6.57 (t, 1 H, py-C*H*), 8.59 (br s, 2 H, py-C*H*). – ^{13}C NMR (C_6D_6) (100 MHz): δ = 18.1 (tmp-*C*4), 34.5 (tmp-*C*7-10), 40.2 (tmp-*C*3/5), 52.9 (tmp-*C*2/6), 125.5 (py-*C*), 142.2 (py-*C*), 147.0 (py-*C*). – ^{27}Al NMR (C_6D_6) (70 MHz): δ = 50 ($\Delta_{1/2}$ = 134 Hz). – IR (Nujol) [ν(Al–I)]: ν = 338 cm^{-1} vs. – $C_{23}H_{41}Al_2I_4N_3$ (921.18): calcd. C 29.99, H 4.49, N 4.56, Al 5.9, I 55.1; found C 29.55, H 4.62, N 3.67, Al 5.8, I 55.6.

[tmp$_2$Al(4-Me-py)]AlI$_4$ (**6c**): To a solution of tmp$_2$AlI (50 ml, 0.10 M, 5.0 mmol) in *n*-hexane, γ-picoline (0.50 ml, 5.0 mmol) was added at ambient temperature. From the resulting suspension, all volatiles were removed in vacuo. The residue was redissolved in 50 ml of diethyl ether and the solution was cooled to −78°C. After the addition of AlI_3 powder (2.04 g, 5.0 mmol), the mixture was allowed to warm to ambient temperature (1.5 h). The cloudy solution was filtered and the filtrate was concentrated to a volume of 25 ml. At this stage, the NMR spectra of **6c** were recorded by removal of all volatiles from a portion of the solution in vacuo and redissolving the residue in C_6D_6. Storage of the filtrate for several weeks at −78°C afforded colorless crystals of tmp$_2$AlI **1c** (2.07 g, 95%) (characterized by its NMR spectra and check of the unit cell parameters)[15].

6c: ^{1}H NMR (C_6D_6) (270 MHz): δ = 1.29 (t, 8 H, tmp-β-CH_2), 1.46 [s, 24 H, tmp-C(CH_3)$_2$], 1.56 (m, 4 H, tmp-γ-CH_2), 1.49 (s, 3 H, γ-pic-CH_3), 6.12 (d, 2 H, γ-pic-C*H*), 8.47 (br. s, 2 H, γ-pic-C*H*). – ^{13}C NMR (C_6D_6) (100 MHz): δ = 18.1 (tmp-*C*4), 34.5 (tmp-*C*7-10), 40.0 (tmp-*C*3/5), 52.8 (tmp-*C*2/6), 21.3 (γ-pic-*C*H$_3$) 126.5 (γ-pic-*C*), 145.9 (γ-pic-*C*), 156.9 (γ-pic-*C*). – ^{27}Al NMR (C_6D_6) (70 MHz): δ = 51 ($\Delta_{1/2}$ = 35 Hz).

[tmp$_2$Al(4-tBu-py)]AlI$_4$ (**6d**): To a solution of tmp$_2$AlI (25 ml, 0.10 M, 2.5 mmol) in *n*-hexane, 4-*t*Bu-py (0.36 ml, 2.5 mmol) was added at ambient temperature. From the resulting suspension of tmp$_2$AlI·4-*t*Bu-py, all volatiles were removed in vacuo and the yellow residue was redissolved in 35 ml of toluene. AlI_3 powder (1.01 g, 2.5 mmol) was then added in one portion. The mixture was stirred for 1 h, then the cloudy solution was filtered. After concentration of the filtrate to one-third of its original volume, the solution was cooled to −78°C. NMR spectra of **6d** were obtained from this solution. Even after weeks at various temperatures and at different concentrations, no crystals suitable for X-ray structure determination were formed. – ^{1}H NMR (C_6D_6) (270 MHz): δ = 1.28 (t, 8 H, tmp-β-CH_2), 1.45 [s, 24 H, tmp-C(CH_3)$_2$], 1.56 (m, 4 H, tmp-γ-CH_2), 0.69 (s, 9 H, *t*Bu-CH_3), 6.35 (d, 2 H, 4-*t*Bu-py-C*H*), 8.54 (br s, 2 H, 4-*t*Bu-py-C*H*). – ^{13}C NMR (C_6D_6) (100 MHz): δ = 18.1 (tmp-*C*4), 34.4 (tmp-*C*7-10), 40.0 (tmp-*C*3/5), 52.8 (tmp-*C*2/6), 29.5 (4-*t*Bu-*C*H$_3$) 127.8 (4-*t*Bu-py-*C*), 146.6 (4-*t*Bu-py-*C*), 156.9 (4-*t*Bu-py-*C*). – ^{27}Al NMR (C_6D_6) (70 MHz): δ = 51 ($\Delta_{1/2}$ = 74 Hz).

[tmp$_2$Al(iq)]AlI$_4$ (**6e**): To tmp$_2$AlI·iq (1.71 g, 3.03 mmol) dissolved in 15 ml of toluene, a solution of AlI_3 (1.24 g, 3.03 mmol) in 10 ml of toluene was added at a temperature of 5–10°C. After stirring for 1.5 h, the mixture was filtered and the clear filtrate was concentrated to dryness in vacuo. A reddish-brown residue of [tmp$_2$Al(iq)]AlI$_4$ was obtained. Yield: 2.91 g (99%); m.p. > 330°C (decomp.). – ^{1}H NMR ($CDCl_3$) (270 MHz): δ = 1.32 (t, 8 H, tmp-β-CH_2), 1.41 [s, 24 H, tmp-C(CH_3)$_2$], 1.61 (m, 4 H, tmp-γ-CH_2), 7.91 (t, 1 H, iq-C*H*), 8.08 (m, 2 H, iq-C*H*), 8.14 (d, 1 H, iq-C*H*), 8.26 (d, 1 H, iq-C*H*), 8.75 [d, 1 H, ^3J(H,H) = 8.4 Hz, iq-C*H*], 9.70 (s, 1 H, iq-C*H*). – ^{13}C NMR ($CDCl_3$) (100 MHz): δ = 17.6 (tmp-*C*4), 34.0 (tmp-*C*7-10), 39.5 (tmp-*C*3/5), 52.0 (tmp-*C*2/6), 124.4 (iq-*C*), 127.1 (iq-*C*), 127.7 (iq-*C*), 130.1 (iq-*C*), 130.8 (iq-*C*), 136.4 (iq-*C*), 137.0 (iq-*C*), 137.9 (iq-*C*), 152.4 (iq-*C*). – ^{27}Al NMR ($CDCl_3$) (70 MHz): δ = 55 ($\Delta_{1/2}$ = 17 Hz); (CH_2Cl_2): δ = 54 ($\Delta_{1/2}$ = 43 Hz). – IR (Nujol) [ν(Al–I)]: $\tilde{\nu}$ = 362 cm^{-1} vs. – $C_{27}H_{43}Al_2I_4N_3$ (783.24): calcd. C 33.39, H 4.46, N 4.33, Al 5.6, I 52.3; found C 35.54, H 4.97, N 3.98, Al 5.2, I 52.8 (C,H ratio: calcd. 1:1.59; found 1:1.65).

[tmp$_2$Al(acr)]AlI$_4$ (**6f**): To a solution of tmp$_2$AlI (0.81 g, 1.84 mmol) in 50 ml of CH_2Cl_2, a solution of acridine (8.80 ml, 0.209 M, 1.84 mmol) in CH_2Cl_2 was added at −78°C. The mixture was kept at this temperature for 1 h and then 0.75 g (1.84 mmol) of AlI_3 was added in one portion. The suspension was slowly allowed to warm to ambient temperature and then filtered. From the orange-red filtrate, all volatiles were removed in vacuo. The residue was characterized as **6f** (1.86 g, 99%). Attempts to crystallize the product from various solvents were not successful. – ^{1}H NMR ($CDCl_3$) (270 MHz): δ = 1.34 (t, 8 H, tmp-β-CH_2), 1.47 [s, 24 H, tmp-C(CH_3)$_2$], 1.65 (m, 4 H, tmp-γ-CH_2), 7.53 (t, 2 H, acr-C*H*), 7.78 (t, 2 H, acr-C*H*), 8.01 (d, 2 H, acr-C*H*), 8.21 (d, 2 H, acr-C*H*), 8.80 (s, 1 H, acr-C*H*). – ^{13}C NMR ($CDCl_3$) (100 MHz): δ = 17.7 (tmp-*C*4), 34.3 (tmp-*C*7-10), 39.8 (tmp-*C*3/5), 52.6 (tmp-*C*2/6), 125.8 (acr-*C*), 126.6 (acr-*C*), 128.3 (acr-*C*), 128.8 (acr-*C*), 136.6 (acr-*C*), 148.7 (acr-*C*). – ^{27}Al NMR ($CDCl_3$) (70 MHz): δ = −22 ($\Delta_{1/2}$ = 70 Hz); (CH_2Cl_2): δ = −27 ($\Delta_{1/2}$ = 65 Hz). – $C_{31}H_{45}Al_2I_4N_3$ (1021.28): calcd. Al 5.3, I 49.7; found Al 5.1, I 50.0.

AlBr$_3$·acr (**7a**): To a solution of tmp$_2$AlBr (50 ml, 0.12 M, 6.0 mmol) in *n*-hexane, a solution of acridine (4.88 ml, 1.23 M, 6.0 mmol) in toluene was added at ambient temperature. After the addition of $AlBr_3$ (1.60 g, 6.0 mmol), a greenish-yellow precipitate of $AlBr_3$·acr formed immediately. The insoluble material was filtered off and washed twice with pentane. Yield: 2.40 g (90%); decomp. at T > 186°C. – The ^{27}Al-NMR spectrum of the filtrate exhibited the chemical shift of tmp$_2$AlBr (**1b**) (d^{27}Al = 130; $\Delta_{1/2}$ = 10200 Hz)[15]. – ^{1}H NMR ($CDCl_3$) (270 MHz): δ = 7.68 (t, 2 H, acr-*H*), 7.96 (t, 2 H, acr-*H*), 8.16 (d, 2 H, acr-*H*), 8.45 (br d, 2 H, acr-*H*), 9.14 (s, 1 H, acr-*H*). – ^{27}Al NMR ($CDCl_3$) (70 MHz): δ = 83 ($\Delta_{1/2}$ = 38 Hz). – IR (Nujol) [ν(Al–Br)]: ν = 404 cm^{-1} vs, 460 vs. – $C_{13}H_9AlBr_3N$ (379.68): calcd. C 35.02, H 2.03, N 3.14; found C 35.59, H 3.18, N 3.28.

AlI$_3$·4-tBu-py (**7b**): A solution of tmp$_2$AlI (51.5 ml, 0.10 M, 5.15 mmol) in *n*-hexane was diluted with a further 150 ml of the solvent. Then, 4-*t*Bu-py (0.75 ml, 5.15 mmol) was added. To this clear solution, powdered AlI_3 (2.10 g, 5.15 mmol) was added at ambient temperature. On leaving the mixture to stand overnight, a copius amount of a colorless precipitate was deposited, which was removed by filtration. Washing the solid with pentane afforded (2.70 g, 96%) of **7b**, m.p. 154–158°C (becomes red). NMR analysis of the filtrate showed only the signals of **1c**. – ^{1}H NMR (C_6D_6) (400 MHz): δ = 0.65 [s, 9 H, *t*Bu-C(CH_3)$_3$], 6.42 (t, 2 H, py-C*H*), 8.63 (d, 2 H, py-C*H*). – ^{13}C NMR (C_6D_6) (100 MHz): δ = 29.3 [*t*Bu-C(*C*H$_3$)$_3$], 35.1 [*t*Bu-*C*(CH$_3$)$_3$], 122.9 (py-*C*), 146.6 (py-*C*). – ^{27}Al NMR (C_6D_6) (70 MHz): δ = 51 ($\Delta_{1/2}$ = 46 Hz). – IR (Nujol) [ν(Al–I)]: ν = 371 cm^{-1} vs, 385 vs. – $C_9H_{13}AlI_3N$ (542.89): calcd. C 19.91, H 2.41, N 2.58; found C 21.08, H 2.88, N 2.63.

tmpAlI$_2$·py (**7c**): To a solution of tmp$_2$AlI·py (28.7 ml, 0.134 M, 3.85 mmol) in toluene, AlI_3 (1.57 g, 3.85 mmol) was added at 0°C and the mixture was kept stirring overnight. The turbid solution was then filtered and the filtrate was concentrated to dryness in vacuo. The resulting brownish oil was stored for some days at temperatures up to 35°C. After one week, colorless crystals of **7c** formed. These were isolated from the oil (1.70 g, 88%) and washed twice with pentane; m.p. > 202°C (decomp.). – ^{1}H NMR (C_6D_6) (400 MHz): δ = 1.39 (t, 4 H, tmp-β-CH_2), 1.63 [s, 12 H, tmp-C(CH_3)$_2$], 1.60 (m, 2 H, tmp-γ-CH_2), 6.26 (t, 2 H, py-C*H*), 6.59 (t, 1 H, py-C*H*), 9.05 (br s, 2 H, py-C*H*). – ^{13}C NMR (C_6D_6) (100

Table 6. Crystallographic data and details relating to the data collection and structure solution of the compounds examined by X-ray diffraction analysis

Compound	$tmp_2AlCl \cdot iq$ **2a**	$tmp_2AlCl \cdot thf$ **2b**	$tmp_2AlBr \cdot thf$ **3a**	$tmp_2AlBr \cdot py$ **3b**	$tmp_2AlI \cdot py$ **4a**	$AlI_3 \cdot iq$ **7b**	$tmpAlI_2 \cdot py$ **7c**
Chem. formula	$C_{27}H_{43}AlClN_3$	$C_{22}H_{44}AlClN_2O$	$C_{22}H_{44}AlBrN_2O$	$C_{23}H_{41}AlBrN_3$	$C_{23}H_{40}AlIN_3$	$C_9H_7AlI_3N$	$C_{14}H_{23}AlI_2N_2$
Form wght.	472.07	415.02	459.48	466.48	512.46	536.84	500.12
Cryst. size [mm]	0.4 × 0.5 × 0.5	0.2 × 0.3 × 0.3	0.4 × 0.3 × 0.3	0.6 × 0.4 × 0.4	0.2 × 0.2 × 0.3	0.1 × 0.1 × 0.3	0.7 × 0.5 × 0.4
Cryst. system	monoclinic	monoclinic	monoclinic	monoclinic	monoclinic	monoclinic	monoclinic
Space group	$P2_1/n$	$P2_1/n$	$P2_1/n$	$C2/c$	$C2/c$	$C2/c$	$P2_1/n$
a [A]	10.685(3)	7.715(3)	8.104(3)	31.700(1)	32.21(1)	20.01(3)	9.861(3)
b [A]	16.945(1)	18.396(6)	16.986(6)	11.086(5)	11.063(6)	10.23(1)	18.133(1)
c [A]	14.745(5)	17.139(6)	17.576(9)	14.671(6)	14.886(8)	14.12(2)	10.113(4)
α [°]	90	90	90	90	90	90	90
β [°]	100.83(2)	94.444(5)	98.62(4)	108.64(3)	110.394(1)	107.27(5)	99.41(3)
γ [°]	90	90	90	90	90	90	90
V [A^3]	2622.0(2)	2425.0(2)	2392.1(2)	4885.3(3)	4971.2(4)	2759(7)	1784.0(1)
Z	4	4	4	8	8	8	4
ρ_{calcd} [Mg/m^3]	1.196	1.137	1.276	1.268	1.369	2.585	1.862
μ [mm^{-1}]	0.199	0.208	1.769	1.732	1.337	6.828	3.566
absol.	–	–	–	–	semiempirical	semiempirical	semiempirical
min./max. transm.	–	–	–	–	0.621 and 0.851	0.144 and 1.000	0.055, 0.107
F(000)	1024	912	984	1984	2120	1920	960
Index range	$0 \le h \le 12$	$-9 \le h \le 9$	$5 \le h \le 0$	$-35 \le h \le 0$	$-35 \le h \le 35$	$-24 \le h \le 24$	$-11 \le h \le 11$
	$0 \le k \le 19$	$-23 \le k \le 21$	$0 \le k \le 19$	$0 \le k \le 12$	$-13 \le k \le 13$	$-12 \le k \le 12$	$-3 \le k \le 21$
	$-16 \le l \le 16$	$-21 \le l \le 22$	$-19 \le l \le 19$	$-15 \le l \le 16$	$-18 \le l \le 18$	$-17 \le l \le 17$	$-4 \le l \le 12$
2 θ [°]	48.00	58.14	47.10	47.12	54.76	54.78	50.06
Temp. [K]	233	173	223	213(2)	213	213	223
Refl. collected	4267	13580	2899	3709	13202	7175	3081
Refl. unique	4030	4752	2618	3636	3735	2684	2948
Refl. observed (4σ)	2191	4159	2042	2581	3291	1561	2667
R_{int}	0.0826	0.0416	0.0383	0.0614	0.0725	0.0832	0.0868
No. variables	297	252	252	261	261	127	176
Weighting scheme x/y[a]	0.0841/12.9220	0.0225/3.8906	0.1000/0.0000	0.0539/9.6308	0.0622/13.5922	0.1334/18.0998	0.0783/ 5.0904
GooF	1.025	1.214	1.169	1.034	1.144	1.152	1.088
Final R (4σ)	0.0915	0.0669	0.0479	0.0495	0.0474	0.0669	0.0457
Final w$R2$	0.2043	0.1332	0.1467	0.1050	0.1116	0.1756	0.1241
Larg. res. peak [e/A^3]	0.894	0.577	0.658	0.768	0.885	2.760	1.785

[a] $w^{-1} = \sigma^2 F_o^2 + (xP)^2 + yP$; $P = (F_o^2 + 2F_c^2)/3$.

MHz): δ = 17.6 (tmp-*C*4), 34.8 (tmp-*C*7-10), 42.7 (tmp-*C*3/5), 53.3 (tmp-*C*2/6), 124.9 (py-*C*), 141.7 (py-*C*), 148.0 (py-*C*). – ^{27}Al NMR (C_6D_6) (70 MHz): δ = 69 ($\Delta_{1/2}$ = 2640 Hz). – IR (Nujol) [ν(Al–I)]: ν = 315 cm^{-1} vs, 335 vs, 355 vs. – $C_{14}H_{23}AlI_2N_2$ (500.14): calcd. C 33.62, H 4.64, N 4.80; found C 33.40, H 4.80, N 5.13.

X-ray Crystal Structure Determinations: Data collection for X-ray structure determinations was performed on a Syntex P4 or a Syntex R3 four-circle diffractometer using graphite-monochromated Mo-K_α (λ = 0.71073 A) radiation. Single crystals were mounted in Lindemann capillaries and sealed under argon atmosphere. Other data collection for X-ray structure determinations was performed on a Siemens P4 four-circle diffractometer equipped with a CCD area detector[32]. Single crystals were mounted in polyfluoroether oil and fixed on top of a glass fibre. Data was collected at −80 to −100°C. All calculations were performed on PC′s and workstations using the Siemens SHELXTL-Plus[33] or SHELX-93[34] software packages. The structures were solved by direct or heavy atom methods and successive interpretation of the difference Fourier maps, followed by least-squares refinement. All non-hydrogen atoms were refined anisotropically. The hydrogen atoms were included in the refinement in calculated positions by a riding model using fixed isotropic thermal parameters. Data relevant to the crystallography, data collection and refinement are compiled in Table 6. Further details of the crystal structure determinations are deposited at the Cambridge Crystallographic Data Centre and may be requested by quoting the depository number CSD-101038, the names of the authors, and the full journal citation.

[1] I. Krossing, Dissertation, University of Munich, **1997**.
[2] Responsible for some X-ray crystal structure determinations.
[3] J. D. Smith, I. J. Worrall, A. McKillop, *Dictionary of Organometallic Compounds*, Chapman and Hall, London **1984–1989**, *Aluminum* pp. 9–120, *Gallium* pp. 940–962, *Indium* pp. 1138–1151.
[4] A. Haaland, *Angew. Chem.* **1989**, *101*, 1017–1032; *Angew. Chem. Int. Ed. Engl.* **1989**, *28*, 992.
[5] [5a] P. Pullmann, K. Hensen, J. W. Bats, *Z. Naturforsch. Part B* **1982**, *37*, 1312–1316. – [5b] D. M. Brown, D. T. Stewart, D. E. H. Jones, *Spectrochim. Acta* **1973**, *29a*, 213–217. – [5c] M. Dalibart, J. Derouault, M. T. Forel, *J. Mol. Struct.* **1981**, *70*, 119–123. – [5d] I. R. Beattie, P. J. Jones, J. A. K. Howard, L. E. Smart, C. J. Gilmore, J. W. Akitt, *J. Chem. Soc., Dalton Trans.* **1979**, 528–541. – [5e] J. Meunier, M. T. Forel, *Can. J. Chem.* **1972**, *50*, 1157–1161.
[6] [6a] A. J. Downs (Ed.), *Chemistry of Aluminium, Gallium, Indium and Thallium*, Blackie Academic and Professional, London, **1993**. – [6b] N. N. Greenwood, K. Wade, *Friedel-Crafts and Related Reactions* (Ed.: G. Olah), Interscience, New York, **1963**.
[7] P. J. Olgren, J. P. Cannon, C. F. Smith Jr., *J. Phys. Chem.* **1971**, *75*, 282–289.
[8] L. Jakobsmeier, I. Krossing, H. Nöth, M. J. H. Schmidt, *Z. Naturforsch. Part B* **1996**, *51*, 1117–1126.
[9] H. Nöth, R. Rurländer, P. Wolfgardt, *Z. Naturforsch. Part B* **1982**, *37*, 29–35.
[10] D. A. Atwood, J. Jegler, *Inorg. Chem*. **1996**, *35*, 4277–4282.

[11] W. Uhl, J. Wagner, D. Fenske, G. Baum, *Z. anorg. allg. Chem.* **1992**, *612*, 25−33.
[12] U. Kynast, B. W. Skelton, A. H. White, M. J. Henderson, C. L. Raston, *J. Organomet. Chem.* **1990**, *384*, C1.
[13] K. Ruhlandt-Senge, P. P. Power, *Inorg. Chem.* **1991**, *30*, 2633−2639.
[14] M. G. Gardiner, M. G. Koutsantonis, S. M. Lawrence, F.-C. Lee, C. L. Raston, *Chem. Ber.* **1996**, *129*, 545−549.
[15] I. Krossing, H. Nöth, C. Tacke, M. Schmidt, H. Schwenk, *Chem. Ber.* **1997**, *130*, 1047−1052.
[16] I. Krossing, H. Nöth, B. N. Anand, *Inorg.Chem.* **1997**, *36*, 1979−1981.
[17] K. Knabel, I. Krossing, H. Nöth, H. Schwenk-Kircher, M. J. H. Schmidt-Amelunxen, T. Seifert, unpublished results.
[18] Low local symmetry leads to broad signals and vice versa. See refs.[19a] and[19b].
[19] [19a] J. Mason, *Multinuclear NMR*, Plenum Press, New York and London, **1987**, 259−278. − [19b] H. Lehmkuhl, *J. Organomet. Chem.* **1991**, *411*, 37−55.
[20] H. Nöth, B. Wrackmeyer, NMR Spectroscopy of Boron Compounds, Vol. 14 (Eds.: P. Diehl, E. Fluck, R. Korfeld), Springer Verlag, Berlin, Heidelberg, New York, **1978**. -
[21] $BPh_3 \cdot py$ (**5b**) precipitates in triclinic crystals of space group $P\bar{1}$ ($Z = 2$) from benzene/pentane solutions. As the B−N and C−C bonds are isoelectronic, the pyridine and phenyl ligands are site disordered, so that every phenyl position is occupied to 1/4 by the pyridine molecule. Therefore, bond lengths cannot be discussed, but the structure is an additional proof for the reaction described by Eq. 2b.
[22] R. M. Fuoss, C. A. Kraus, *J. Am. Chem. Soc.* **1933**, 55, 2387−2399.
[23] V. Shomaker, D. P. Stevenson, *J. Am. Chem. Soc.* **1941**, 63, 37−40.
[24] R. J. Wehmschulte, W. J. Grigsby, B. Schiemenz, R. A. Bartlett, P. P. Power, *Inorg. Chem.* **1996**, *35*, 6694−6702.
[25] I. Krossing, Dissertation, University of Munich, **1997**.
[26] M. A. Petrie, P. P. Power, H. V. Rasika Dias, K. Ruhlandt-Senge, K. M. Waggoner, R. J. Wehmschulte, *Organometallics* **1993**, *12*, 1086−1093.
[27] M. J. Zaworotko, J. L. Atwood, *Inorg. Chem.* **1980**, *19*, 268−271.
[28] J. L. Atwood, P. A. Milton, *J. Organomet. Chem.* **1973**, *52*, 275−279.
[29] Performed with the program *Hyperchem*, V3.0, Autodesk, **1993**.
[30] Performed with the program *Gaussian 94*, Revision B.2, M. J. Frisch, G. W. Trucks, H. B. Schlegel, P. M. W. Gill, B. G. Johnson, M. A. Robb, J. R. Cheeseman, T. Keith, G. A. Petersson, J. A. Montgomery, K. Raghavachari, M. A. Al-Laham, V. G. Zakrzewski, J. V. Ortiz, J. B. Foresman, C. Y. Peng, P. Y. Ayala, W. Chen, M. W. Wong, J. L. Andres, E. S. Replogle, R. Gomperts, R. L. Martin, D. J. Fox, J. S. Binkley, D. J. Defrees, J. Baker, J. P. Stewart, M. Head-Gordon, C. Gonzalez, and J. A. Pople, Gaussian, Inc., Pittsburgh PA, **1995**.
[31] S. H. Strauss, *Chem. Rev.* **1993**, *93*, 927−942.
[32] Siemens Industrial Automation, **1995**.
[33] *PC SHELXTL Rel. 5.03*, Siemens Analytical Instruments, Version 4.1, **1994**.
[34] G. M. Sheldrick, University of Göttingen, **1993**.

[97292]

Metal Tetrahydridoborates and Tetrahydridometallates, 22[◇]

Structural Chemistry of Lithium Tetrahydroborate Ether Solvates☆

Hans-Hermann Giese, Heinrich Nöth*, Holger Schwenk, and Steffen Thomas

Institute of Inorganic Chemistry, University of Munich,
Meiserstraße 1, D-80333 München, Germany

Received December 23, 1997

Keywords: Lithium tetrahydridoborate diethyl ether (1:1) / Lithium tetrahydridoborate diveron (1:1) / Lithium tetrahydridoborate dimethoxyethane (1:2) / Lithium tetrahydridoborate triglyme (1:1) / Lithium tetrahydridoborate tetrahydrofuran (1:3) / Lithiumtetrahydridoborate 1,3-dioxolane (1:1) / Hydride-bridge bonding

$LiBH_4 \cdot OEt_2$ (**1**) and $LiBH_4 \cdot O(Me)CMe_3$ (**2**) form double-stranded chains in the solid state. While 3 hydrides of the BH_4 group in **1** bind to three different Li atoms through Li···H–B interactions, the fourth H atom interacts with three adjacent Li centers. In contrast, in compound **2** there are two single Li···H–B bonds and two doubly bridging hydrogen atoms, the latter again interacting with three lithium centers. Moreover, the arrangements of the ether molecules in **1** and **2** are different. $LiBH_4 \cdot 2$ DME (**3**) (DME = dimethoxyethane) forms a molecular lattice, in which the BH_4^- anions are present in Li···H_2BH_2 bridges. The same structural feature is present in $LiBH_4 \cdot$ TG (**4**) (TG = triglyme = triethylene glycol dimethyl ether), but the TG molecule coordinates to two Li centers through two of its four oxygen atoms in such a manner that a chain structure results. The compound $LiBH_4 \cdot 3$ THF (**5**) exists as discrete molecules in the lattice. Its BH_4^- anion is triply bridging to the Li center. In contrast, $LiBH_4 \cdot C_3H_6O_2$ (**6**) (1,3-dioxolane) is polymeric. Due to the presence of two μ^2_2-BH_4 groups, a chain of the type ···Li(H_2BH_2)Li(H_2BH_2)··· is formed, and the 1,3-dioxolane molecules connect the chains through Li–O coordination to form a three-dimensional array. In spite of the variations in the bonding of the BH_4 group to Li centers, the Li atoms are hexacoordinated in **3** to **6** but are heptacoordinated in **1** and **2**.

Introduction

Lithium tetrahydridoborate is a commercially available reagent which surpasses $NaBH_4$ in terms of its reactivity[2]. It is widely used, and most reactions are performed in diethyl ether (OEt_2) or tetrahydrofuran (THF) as $LiBH_4$ is more rapidly hydrolyzed than $NaBH_4$[3]. Several ether solvates of $LiBH_4$ are known, but the only one to have been structurally characterized is 2 $LiBH_4 \cdot$18-crown-6[4] and more recently $LiBH_4 \cdot OEt_2$[17]. Most of the other ether solvates of $LiBH_4$ were first described in the period from 1950 to 1974[5], and only a few have subsequently been investigated in detail by vibrational and/or NMR spectroscopy[6]. To date, the following solvates have been characterized: $LiBH_4 \cdot n OEt_2$ (n = 0.5, 1, 2)[7][8], $LiBH_4 \cdot n$THF (n = 1, 2)[2c][8], $LiBH_4 \cdot O i Pr_2$[2c], and $LiBH_4 \cdot$1,4-dioxane[2c][9].

Meanwhile, several modes of bonding or interaction of the BH_4^- ion with metal centers have been established[5]. In mononuclear species $M(BH_4)_n$ or $L_mM(BH_4)_n$, μ_1-, μ_2-, or μ_3-BH_4 groups may be present, as shown in formulae **A**–**C**, which have local C_{3v}, C_{2v}, and C_{3v} point-group symmetry, respectively. BH_4 groups acting as bridges between two metal centers (type **D**) are found in solid $Be(BH_4)_2$[10], $Zr_3(BH_4)_6H_6 \cdot 4$ PMe_3[11], and $Cr_2(BH_4)_4 \cdot dipy_2 \cdot Cr(BH_4)_2 \cdot dipy \cdot$TMEDA[12]. Although the double μ_2-bridging mode **B** prevails, other bonding modes are possible as depicted in **E**–**I**. Type **G** has been observed in dimeric $LiBH_4 \cdot$TMEDA[13]. We use the notation shown in **A** to **I** to describe the hydride bridges. The subscripts indicate the number of hydrogen atoms of the BH_4 group that interact with *one* metal atom, while the superscripts denote the number of hydrogen atomss that interact with different metal centers. Thus, for example, μ_1^3 would indicate a hydrogen atom of the BH_4^- anion that forms bridges to three metal atoms. The examples given demonstrate that the BH_4^- anion is a very versatile ligand[14].

Synthesis

The synthesis of ether solvates of $LiBH_4$ can be achieved in various ways. One method is to dissolve $LiBH_4$ in the respective ether, and to crystallize the solvates either by cooling of the saturated solution or by removal of the solvent. A second method is to replace the solvate molecule with a more strongly coordinating ether. Thirdly, the ether can be added to a suspension of $LiBH_4$ in hexane or toluene. Using these methods, the following solvates have been obtained as single crystals (see Experimental Section for the method used): $LiBH_4 \cdot OEt_2$ (**1**), $LiBH_4 \cdot$DIV (**2**), $LiBH_4 \cdot 2$ DME (**3**), $LiBH_4 \cdot$TG (**4**), $LiBH_4 \cdot 3$ THF (**5**), $LiBH_4 \cdot$DIOXL (**6**) [DIV = $MeOCMe_3$, DME = $MeOCH_2CH_2OMe$, TG = $MeO(CH_2CH_2O)_3Me$, DIOXL = $C_3H_6O_2$, 1,3-dioxolane]. No single crystals could be obtained in the case of $LiBH_4 \cdot$1,4-dioxane[9] due to its very low solubility.

[◇] Part 21: Ref.[1].

 © WILEY-VCH Verlag GmbH, D-69451 Weinheim, 1998 1434–1948/98/0707–0941 $ 17.50+.50/0

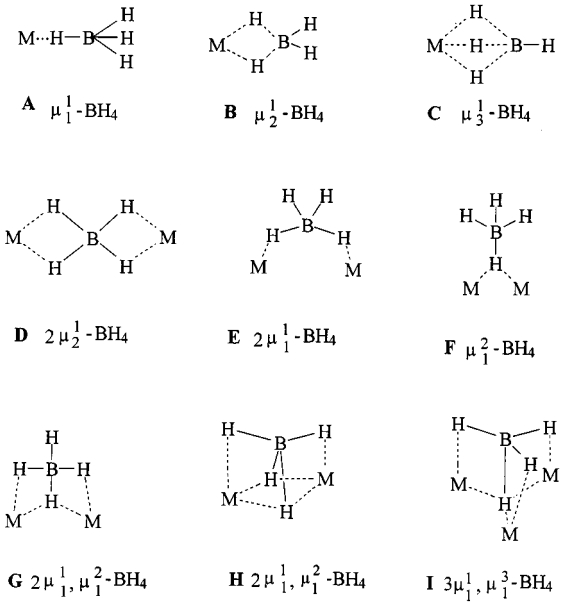

IR and NMR Spectra

In order to obtain some information on the interaction of the Li^+ center with the BH_4^- anion, IR spectra were recorded of the solid compounds as Nujol/Hostaflon mulls. The data attributable to BH stretching vibrations are summarized in Table 1. There are four strong bands in this region, irrespective of the type of ether solvate molecule present, and the pattern observed is not characteristic for a BH_4^- group of either T_d, C_{3v}, or C_{2v} symmetry. Bands due to $\nu^{10}BH_4$ are not resolved. The strong band at 2240 ± 65 cm^{-1} seems to be the overtone of the δBH_2 vibration at 1130 ± 10cm^{-1}. The IR spectra of solid $LiBH_4$ and $NaBH_4$ do not differ significantly[15]. It is only the triglyme solvate that shows a better resolution. Obviously, the bonding between the BH_4^- group and Li^+ is predominantly ionic, and the IR spectra do not allow any firm conclusions to be drawn regarding type of interaction of the BH_4 group with the Li center (μ_1, μ_2, or μ_3 bonding).

Table 1. IR bands in the stretching vibration region for the $LiBH_4$ ether solvates: crystalline material in Nujol/Hostaflon suspension

1[a]	**2**	**3**	**4**	**5**	**6**
2230 st	2180 m	2134	2198 m	2111 m	2180 st
2234 st	2277	2258	2264 st	2127 m	2256 st
2286 st	2306	2281	2295 st	2176 st	
2364 st	2320	2373	2560 st	2237 st	
	2410 sh		2330 m st	2272 st	2317 st
			2382 m st	2334 m st	
				2382 m st	

[a] In crystalline solid $LiBH_4$ the following bands were observed in the IR spectrum and assigned (in cm^{-1}): 2525 ($2\nu_2$), 2408 ($\nu_2 + \nu_4$), 2308 (ν_3), 2182 ($2\nu_4$)[15].

Likewise, the ^{11}B-NMR spectra of solutions of the $LiBH_4$ solvates in their respective ethereal solvents, or of the solid solvate in C_6D_6, did not yield any additional information (see Table 2). With the exception of $LiBH_4 \cdot TG$, each solvate gave rise to a 1:4:6:4:1 quintuplet with $^1J(^{11}B^1H)$ in the small range of 81−83 Hz, and $\delta^{11}B$ varying only within a range of ± 2.6 ppm. The shielding at the ^{11}B center decreases slightly when C_6D_6 is used as a solvent instead of the respective ether. This may be taken as evidence for a slightly stronger $Li(BH_4)$ interaction within an ion pair. No NMR data could be recorded for $LiBH_4 \cdot$1,4-dioxane, neither in dioxane nor in C_6D_6, due to its very low solubility in both solvents. This suggests that its structure in the solid state consists of an extended lattice. $LiBH_4 \cdot 3$ THF and $LiBH_4 \cdot$1,3-dioxolane are also practically insoluble in deuterated benzene. However, for a solution of $LiBH_4$ in triglyme, two additional signals are observed at $\delta = +3.7$ and $\delta = +7.5$. The signals in this case are broad, even that for the BH_4 anion at $\delta = -39.7$, and they show no resolved lines due to B-H coupling. The signal at $\delta = +3.7$ may be due to the presence of a BH_3 adduct to the ether (cf. $\delta^{11}B = 2.5$ for $H_3B \cdot OMe_2$)[16].

Table 2. ^{11}B- and ^{7}Li-NMR data of $LiBH_4$ solvates [δ is given in ppm, the coupling constant $^1J(^{11}B^1H)$ is given in Hz (in parentheses)

	$LiBH_4 \cdot OEt_2$ **1**	$LiBH_4 \cdot$ DIV **2**	$LiBH_4 \cdot 2$ DME **3**	$LiBH_4 \cdot$ TG **4**	$LiBH_4 \cdot 3$ THF **5**	$LiBH_4 \cdot$ DIOXL **6**
$\delta^{11}B$	−39.1 (81)[a]	−38.4 (81)[c]	−39.1 (83)[d]	−40.5, −14.6, −9.1 (br.)[e]	−41.0 (82)[e]	−40.4 (81)[g]
	−40.0 (87)[b]	−39.7 (br)[b]	−41.3 (82)[b]	−40.8 (71)[b]	–	–
δLi	1.78[a]	−1.83[c]	0.416[d]	1.300[e]	−2.331[f]	0.493[g]
	0.145[b]	0.119[b]	−0.154[b]	−0.679[b]	–	–

[a] In OEt_2. – [b] In C_6D_6. – [c] In diveron. – [d] In dimethoxyethane. – [e] In triglyme. – [f] In THF; in addition a weak doublet at $\delta^{11}B = 14$ (64 Hz) is observed. – [g] – In 1,3-dioxolane.

Table 3. Li···B atom distances in [A] of the $LiBH_4$-ether solvates

	$LiBH_4 \cdot OEt_2$	$LiBH_4 \cdot$ DIV	$LiBH_4 \cdot 2$ DME	$LiBH_4 \cdot$ TG	$LiBH_4 \cdot 3$ THF	$LiBH_4 \cdot$ DIOXL
Li···B	2.498(8)	2.560(4)	2.470(4)	2.478(6)	2.319(7)	2.445(3)
	2.53(1)	2.505(4)	–	–	–	2.447(3)
	2.54(1)	2.520(4)	–	–	–	2.431(3)

In benzene solution, the shielding of the ^{7}Li nucleus also varies considerably, but is more in line with the number of solvent molecules attached to the $LiBH_4$ molecule. This becomes evident by comparing the δ values for the DME and TG solvates with those of diethyl ether and diveron. The δ^7Li data for compounds **1**−**6** in their respective ether solutions are difficult to rationalize. The excellent shielding of the Li nucleus in **5** is most likely due to ion-pair formation $[Li(THF)_4]BH_4$, but then it is hard to understand why the Li center in **3** is less shielded than that in **2**, and why the Li resonance for **1** in diethyl ether solution is found at very low field. Since the degrees of association of $LiBH_4 \cdot OEt_2$ and $LiBH_4 \cdot$DIV in C_6D_6 solution are unknown, it is difficult to interpret the δ^7Li data, which suggest much stronger solvation in benzene (ratio Li/O only 1:1) than in ether. A

better shielding in benzene can only be expected when strong interactions between $LiBH_4$ molecules remain, while the indications seem contrary to this. Therefore, association through the BH_4 groups must remain in benzene solution. As both compounds have been found to be moderately soluble, it is evident that the chain structures present for these compounds in the solid state (vide infra) must be broken down into smaller $[LiBH_4 \cdot Do]_n$ units (Do = coordinated solvent).

Crystal and Molecular Structures

Coordination Compounds of $LiBH_4$ with Noncyclic Ethers: Neither the NMR data of solutions of $LiBH_4$ in the respective ethers nor the IR data of the solid ether solvates allowed an unambiguous assignment of the structure of the $LiBH_4$-ether solvates, particularly with respect to the type of Li···H−B interaction. Therefore, it was necessary to determine the molecular structures of the ether solvates of $LiBH_4$ by X-ray diffraction analysis.

$LiBH_4 \cdot OEt_2$ (**1**), whose crystal structure has recently been reported[17], crystallizes from a diethyl ether solution in colorless needles of the orthorhombic system and, therefore, only a few features will be discussed.

Figure 1 shows that three of the four H atoms of the BH_4^- anion each interact with one Li center and that the fourth hydrogen atom coordinates to three Li^+ ions. This hydrogen atom is tetracoordinated. Moreover, each Li center is coordinated by six hydrogen atoms and one ether oxygen atom. The sum of bond angles subtended at the ether oxygen atoms is 359.8°. Li−H atom distances range from 1.94(5) to 2.25(5) A, while bond angles at Li span the wide range from 48.0 to 161.4°, with many falling in the interval 90 ± 15°. This shows that the coordination polyhedron can be described as a very strongly distorted octahedron. As expected, the coordination polyhedron around the boron atom is close to a tetrahedron.

The units shown in Figure 1 are the building blocks for the formation of doubly stranded chains in the lattice of **1** as depicted in Figure 2. In the lattice, each BH_4 group has to be described as $3\mu_1{}^1$, $\mu_1{}^3$, i.e. all four hydrogen atoms of the BH_4^- ion are involved in coordination to Li^+ ions, which are heptacoordinated. The ether molecules are arranged in such a manner that an organophilic "skin" partially shields the $(LiBH_4)_n$ core. This most probably explains why $LiBH_4 \cdot OEt_2$ not only dissolves in ether but also to a small extent in toluene. The structure in solution will, of course, differ significantly from that in the solid state.

$LiBH_4 \cdot$ DIV (**2**) crystallizes from toluene solution in thin monoclinic plates. Figure 3 depicts a single molecule, showing a doubly bridging BH_4 anion. These molecules are associated as shown in Figure 4a. Here, it can be seen that each Li center shares hydrogen atoms with three BH_4 groups, and this leads to heptacoordination at Li (6 H atoms and 1 O atom). Of the four hydrogen atoms of each BH_4^- anion, two are involved in bridging two Li centers, while the other two are involved in single B−H···Li interactions ($2\ \mu_1{}^1$-, $2\ \mu_1{}^2$-BH_4). Figure 4a depicts the arrangement in a double-stranded chain. It also shows that the *tert*-butyl

Figure 1. ORTEP plot of four $LiBH_4 \cdot OEt_2$ (**1**) molecules; estimated standard deviations in parentheses[a]

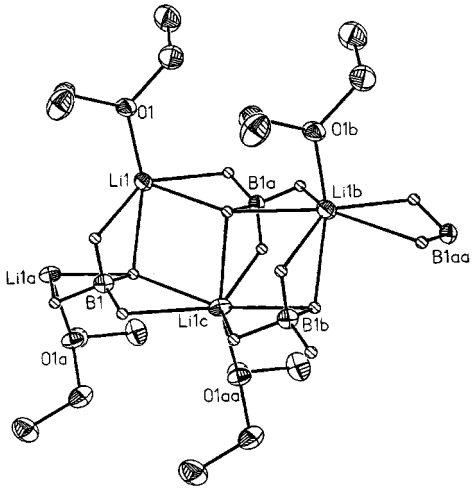

[a] Selected bond lengths and atom distances [A]: Li1−O1 1.927(6), Li1−H1 1.97(3), Li1−H2 2.11(3), Li1−H 42.08(3), B1−H1 1.12(3), B1−H2 1.14(3), B1−H3 1.01(5), B1−H4 1.19(4), Li1···B1 2.53(1), Li1···B1B 2.54(1). − Selected bond angles [°]: C1−O1−C3 115.0(3), C11−O1−Li1 122.3(4), C3−O1−Li 122.5(3), H1−B1−H3 109(3), H1−B1−H2 107(2), H1−B1−H4 110(3), H2−B1−H3 116(3), H2−B1−H4 107(3), H3−B1−H4 108(2), O1−Li1···B1 122.5(3), O1−Li1···B1A 106.2(4), Li1−H2−Li1A 161(2), Li1−H1−B1 105(2), Li1A−H3−B1 104(3), B1−H4−Li1B 105(3). − Atom Li1B is part of the adjacent chain (see Figure 2).

groups of the diveron molecules are ordered in such a manner that allows one methyl unit of each DIV molecule to be arranged in a zipper-like orientation. Thus, the organyl groups shield the $LiBH_4$ part of the $[(LiBH_4)_2]_\infty$ chain better than in **1** (Figure 4b). However, every second pair of *trans*-oriented ether molecules are turned by 69.7° to one another. Therefore, the arrangement of the molecules of **2** in the chain is different to that observed for **1**.

$LiBH_4 \cdot 2$ DME (**3**) forms colorless monoclinic crystals. There is half a molecule in the asymmetric unit. The Li and B atoms occupy special positions on a C_2 axis. Figure 5 depicts the molecular structure of compound **3**.

It is apparent that the hexacoordinated Li atoms are surrounded by four oxygen atoms of two DME molecules and two hydrogen atoms from a $\mu_2{}^1$-BH_4 group.

The B−H bonds to the bridging hydrogen atoms are slightly, although not significantly, longer than those to the terminal hydrogen atoms. In the case of the Li−O coordination, one Li−O distance is significantly shorter than the other [2.058(2) A for O2, 2.133(1) A for O1]. The rather acute O1−Li−O2 bond angle is due to the small bite angle of the DME molecule. Consequently, the deviation from octahedral symmetry around the Li ion is substantial; the smallest bond angle is 55.9(9)° (H2−Li1−H2a), the largest 150.8(5)° (H2−Li1−O2). Bond angles subtended at atoms O1 and O2 are rather different, the largest C−O−Li bond angles being those to the methyl groups of the DME molecule, which range from 122.0(1) to 126.30(9)°. More interesting in terms of the coordination geometry is the fact that the bond angle sums at atoms O1 and O2 are 321.1(3)° and 349.5(3)°, respectively. Considering the C−O−C bond

Figure 2. A space-filling model of a chain of $LiBH_4 \cdot OEt_2$

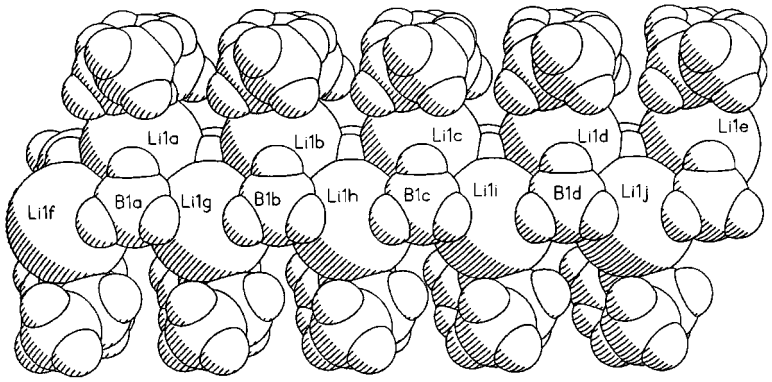

Figure 3. ORTEP plot of $LiBH_4 \cdot OMe(CMe_3)$ (**2**) in the asymmetric unit[a]

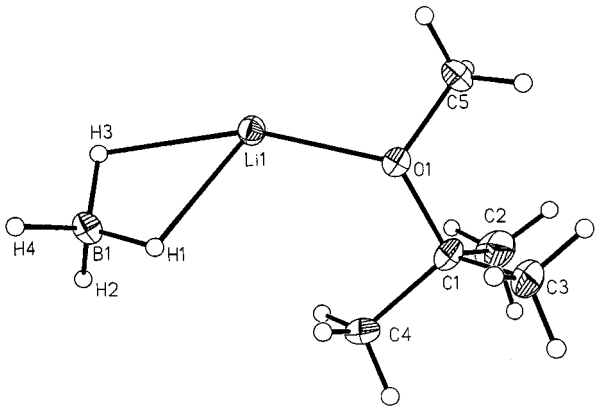

[a] Selected bond lengths and atom distances [A]: Li1−O1 2.000(4), Li1−H1 2.11(2), Li1−H3 2.16(2), Li1B−H1 2.16(2), H2−Li1A 2.00(2), H3−Li1A 2.08(2), Li1−H4B 2.08(2), Li1−HaB 2.16(2), B1−H1 1.11(2), B1−H2 1.12(3), B1−H3 1.14(2), B1−H4 1.11(3), Li1···B1 2.560(4), Li1−B1A 2.505(4), Li1−B1B 2.529(4). − Selected bond angles [°]: O1−Li1−H1 110.9(6), O1−Li1−H3 159.1(6), H1−B1−H2 110(2), H1−B1−H3 110(2), H1−B1−H4 108(2), H2−B2−H3 106(2), H2−B1−H4 114(2), H3−B1−H4 109(2), B1−H1−Li1 101(1), B1−H3−Li1 97(1), B1−H4−Li1B 100(1), B1−H2−Li1A 104(2) Σ∠ at O1: 356.0°.

angles of 112.6 and 111.3(3)°, respectively, it would appear that these oxygen atoms are best described as being sp^3-hybridized. The O1−Li−O2 bond angle of 79.49(6)° as well as the Li1−O1−C2 and Li1−O2−C3 bond angles [112.6(1)° and 111.87(8)°] indicate that the Li···O interaction is predominantly polar. However, it should be borne in mind that **3** is nevertheless a molecular compound.

The $LiBH_4 \cdot TG$ solvate **4** forms colorless, orthorhombic crystals. There are four molecules in the unit cell. However, the triglyme ligand does not coordinate to only one Li center. As shown in Figure 6, the triglyme ligand binds to *two* different Li centers through two of its four oxygen donor atoms. Therefore, a chain structure results, in which the Li centers are hexacoordinated. The Li ions are coordinated by four oxygen atoms of *two* different triglyme molecules, as well as by a $\mu_2{}^1$-bonding BH_4 group.

The C−O atom distances in **4** fall in the fairly narrow range from 1.425(2) (O1−C2) to 1.432(2) A (O2−C4). However, the sum of bond angles at atom O1 is only 335.4°, in contrast to atom O2, where the sum is 359.3°. This points to two different bonding situations for O1 and O2, as suggested also by the *shorter* Li1−O2 atom distance. On the other hand, the O2−Li1−O1 bond angle of 79.67(8)° does not deviate at all from the analogous bond angle in **3** [79.49(8) A], and we take this as evidence that the Li···O interactions in **4** are again primarily determined by polar factors, irrespective of the bond angle sums at the O atoms.

Coordination Compounds of $LiBH_4$ with Cyclic Ethers: Cyclic ethers such as THF, 1,4-dioxane, 1,3,5-trioxolane, and many others add to $LiBH_4$. However, to date we have been unsuccessful in obtaining good single crystals of these solvates, apart from the case of THF and 1,3-dioxolane solvates.

$LiBH_4 \cdot 3$ THF (**5**) crystallizes from a THF solution at −40°C in extensively intergrown platelets. Crystal selection at low temperature was difficult, as was the mounting using oxygen-free perfluoroether oil. Several crystals had to be examined and even the best one was comparatively weakly diffracting. Consequently, the quality of the structure determination is less than satisfactory. Nevertheless, a model structure was found that seems to be reliable, even though the hydrogen atoms at the boron center had to be fixed in their found positions in the final cycles of refinement. Figure 7 shows the result.

It is apparent that **5** is a molecular compound that may be regarded as a contact ion pair. The Li center is hexacoordinated by three oxygen atoms and three hydrogen atoms. Thus, the BH_4 group acts as a $\mu_3{}^1$-ligand. Li−O atom distances vary significantly, ranging from 1.952(6) to 2.017(6) A, while the O−Li−O bond angles span the small range from 100.6(3) to 102.5(3)°. On the other hand, the bite of the BH_4 group is very small, as exemplified by H−Li−H bond angles in the range 45.5−54.4°. The Li···B atom distance is 2.319(7) A, which is shorter than the Li···B distances found for $\mu_2{}^1$-BH_4 groups.

$LiBH_4 \cdot 1,3$-DIOXL (**6**) separates from saturated 1,3-dioxolane solutions. The crystals are monoclinic. The contents of the asymmetric unit is depicted in Figure 8. The structure features tricoordinated Li ions, which are, of course, coordinatively unsaturated. These units associate to

Figure 4. a) Four molecules of **2** in a chain; b) space-filling model

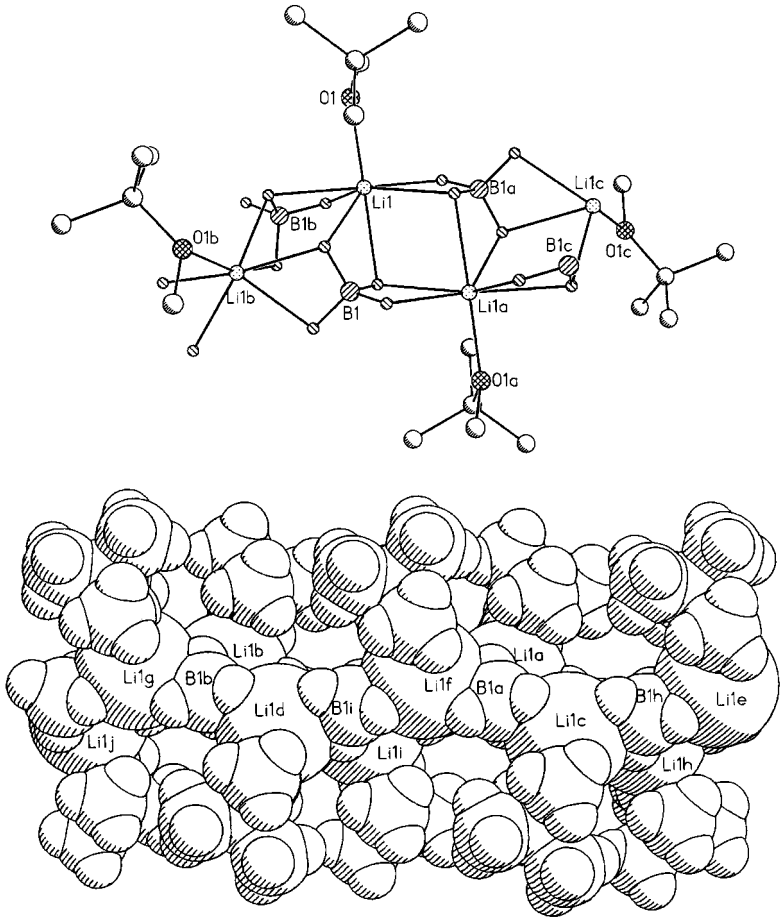

Figure 5. ORTEP plot of the molecular structure of $LiBH_4 \cdot 2$ DME (**3**)[a]

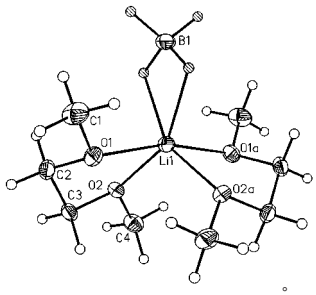

[a] Selected bond lengths and atom distances [A]: Li1−O1 2.133(1), Li1−O2 2.058(2), Li1−H2 1.17(2), B1−H1 1.15(2), B1−H2 1.17(2), Li1···B1 2.470(4). − Selected bond angles [°]: O1−Li1−O2 79.49(6), O1−Li1−O1a 165.9(2), O1−Li1−O2a 92.60(7), O2−Li1−O1a 92.60(7), O2−Li1−O2a 111.9(2), Li1−H2−B1 98.1(9), H1−B1−H1a 110(2), H1−B1−H2 111(1). Σ∠ O1 = 341.2°, O2 = 349.5°.

form an extended structure, as shown in Figure 9. The BH_4 groups join strands of Li(1,3-dioxolane) units.

The BH_4 groups are of the $4\mu_1{}^1$-type, i.e. there are four singly bridging hydrogen atoms to 4 Li centers. Moreover, both oxygen atoms of the 1,3-dioxolane are involved in coordination. This leads to hexacoordinated Li ions with an H_4O_2 environment. The two Li−O distances are 1.993(3) and 2.031(3) A, and the O−Li−O bond angles are 94.6(1)° for Li1 and 96.2(1)° for Li2. It is also interesting to note that the Li···B atom distances are 2.445(3) and 2.439(3) A, respectively. These are definitely longer than the Li···B distance in **4** as a result of the "unusual" Li−H−B interactions. The two OCO planes of the dioxolane molecules coordinated to a Li center are twisted by almost 90° with respect to one another. The symmetry at atom Li2 is higher than that at atom Li1. Moreover, the Li···B···Li angles differ considerably, amounting to 174.1(1)° at atom B1 and 162.8(1)° at atom B2.

Discussion

It is well known that $LiBH_4$ forms many well-defined solvates with various kinds of ethers[2]. Although the compositions of some of these solvates have been determined, their structures in the solid state and in solution have never been adequately described.

In the present study, it is demonstrated that an IR-spectroscopic investigation does not allow unambiguous conclusions to be drawn concerning the coordination mode of the anion BH_4^- to the Li centers. Such information can only be obtained from X-ray structure determinations, which are of course confined to the solid state. Thus, the structure of $(LiBH_4)_2 \cdot 18$-crown-6 has been determined, which reveals $\mu_1{}^1$-BH_4 interactions with the Li centers[4].

Figure 6. ORTEP plot of two molecules of $LiBH_4 \cdot TG$ (**4**)[a]

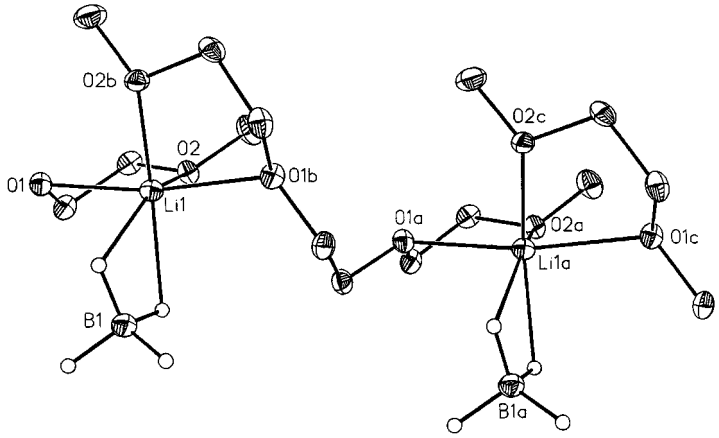

[a] Selected bond lengths and atom distances [A]: Li1−O1 2.192(2), Li1−O2 2.035(3), Li1−O1B 2.192(2), Li1−O2B 2.035(3), Li1···B1 2.487(6). − Selected bond angles [°]: O1−Li1−O2 79.67(8), O1−Li1−O2B 94.1(1), O1−Li1−O1B 169.6(2), O2−Li1−O1B 94.1(1), O2−Li1−O2B 107.3(2), O1B−Li1−O2B 79.68(8).

Figure 7. ORTEP plot of the molecular structure of $LiBH_4 \cdot 3$ THF (**5**); thermal ellipsoids are represented at the 25% probability level[a]

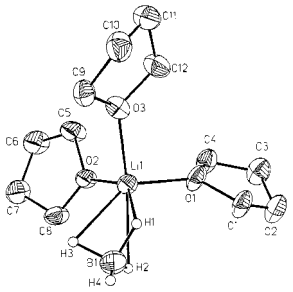

[a] Selected bond lengths and atom distances [A]: Li1−O1 1.952(6), Li1−O2 1.968(5), Li1−O3 2.017(6), Li1−H1 2.02(4), Li1−H2 2.10(5), Li1−H3 2.12(4), Li1···B1 2.319(7), B1−H1 1.15(3), B1−H2 1.15(3). − Selected bond angles [°]: O1−Li1−O2 102.5(3), O1−Li1−O3 100.6(3), O2−Li1−O3 101.4(2), O1−Li1···B1 114.2(3), O2−Li1···B1 117.8(3), O3−Li1···B1 117.8(3), H1−B1−H2 110.2(3), H1−B1−H3 102.7(3), H1−B1−H4 117.3(8), H2−B1−H3 90.3(3), H2−B1−H4 90.3(3), H3−B1−H4 115.7(3); Σ∠ at O atoms: O1: 358.1°, O2: 357.6°, O3: 354.9°

Figure 8. ORTEP plot of the molecular structure of $LiBH_4 \cdot 1,3$-dioxolane (**6**)[a]

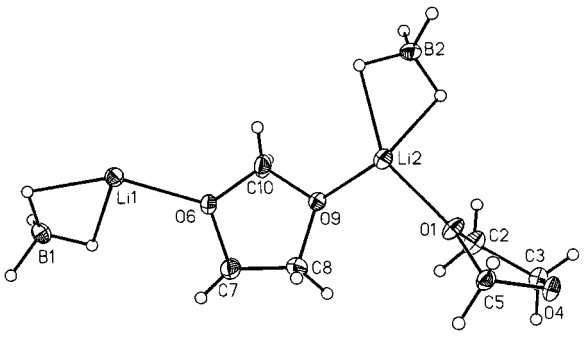

[a] Selected bond lengths and atom distances [A]: Li1−O6 2.004(3), Li1−O4A 1.993(3), Li1···B1 2.445(3), Li1−B2B 2.447(3) Li2···B2 2.431(3), Li2C−B1 2.428(3), Li2−O1 1.984(3), Li2−O9 2.031(3). Selected bond angles [°]: O6−Li1−B1 117.4(1), B1−Li1−O4A 100.6(1), O6−Li1−O4A 96.2(1), O4A−Li1···B2B 118.6(1), O6−Li1···B2B 98.7(1).

The compound can therefore be regarded as a "double" contact ion pair, in which each Li atom is coordinated by a hydrogen atom and four oxygen atoms. Although all the molecular solvates described herein, such as $LiBH_4 \cdot 2$ DME and $LiBH_4 \cdot 3$ THF, may also be regarded as contact ion pairs, this seems to be an inadequate description as the BH_4 group definitely favors μ_1, μ_2, or μ_3 interactions with the Li^+ center. The structure determinations presented in this study clearly show a preferential orientation of the BH_4 moiety. Using Edelstein's correlation of metal−boron distances as a measure of the denticity of the BH_4 group[18], it is shown that this holds not only for typical covalent metal tetrahydridoborates, but also for more polar metal tetrahydridoborates.

It is also evident that strongly coordinating ether ligands such as THF and DME lead to the formation of molecular $LiBH_4$ complexes, while more weakly bound ethers such as OEt_2 or diveron lead to polymers. This is apparent from ether/Li ratios of 1:1 with weak donors and ratios of up to 4:1 with strong donor molecules. As the O/Li ratio decreases, coordination unsaturation at the Li ion increases and this is counterbalanced by additional Li···H interactions. Therefore, we observe BH_4 groups of type **A** ($\mu_3{}^1$-BH_4) for $LiBH_4 \cdot 3$ THF, of type **B** ($\mu_2{}^1$-BH_4) for $LiBH_4 \cdot 2$ DME and $LiBH_4 \cdot TG$, and $4\mu_1{}^1$-BH_4 for $LiBH_4 \cdot 1,3$-DIOX. Type-**D** BH_4 groups ($2\mu_1{}^1$,$2\mu_1{}^1$-BH_4) are present in $LiBH_4 \cdot DIV$ and $3\mu_1{}^1$,$\mu_1{}^3$-bonding is found in $LiBH_4 \cdot OEt_2$. Thus, in these cases, each hydrogen atom of the BH_4 group is involved in interactions with the Li^+ ions. Amongst the $LiBH_4$−ether complexes described here, there are hydrogen atoms of the BH_4 group that coordinate to three Li centers, as for example, in **1**. Consequently, these are H^- ions in a tetracoordinated environment. However, in complexes of $LiBH_4$ with nitrogen ligands, the interaction of BH_4 hydride with three Li centers is more common than with ethers[19], and we have recently found an example where even four metal centers coordinate to one hydride, namely $LiAl_3H_5(OR)_5$[20].

Figure 9. View of the three-dimensional array of compound **6**

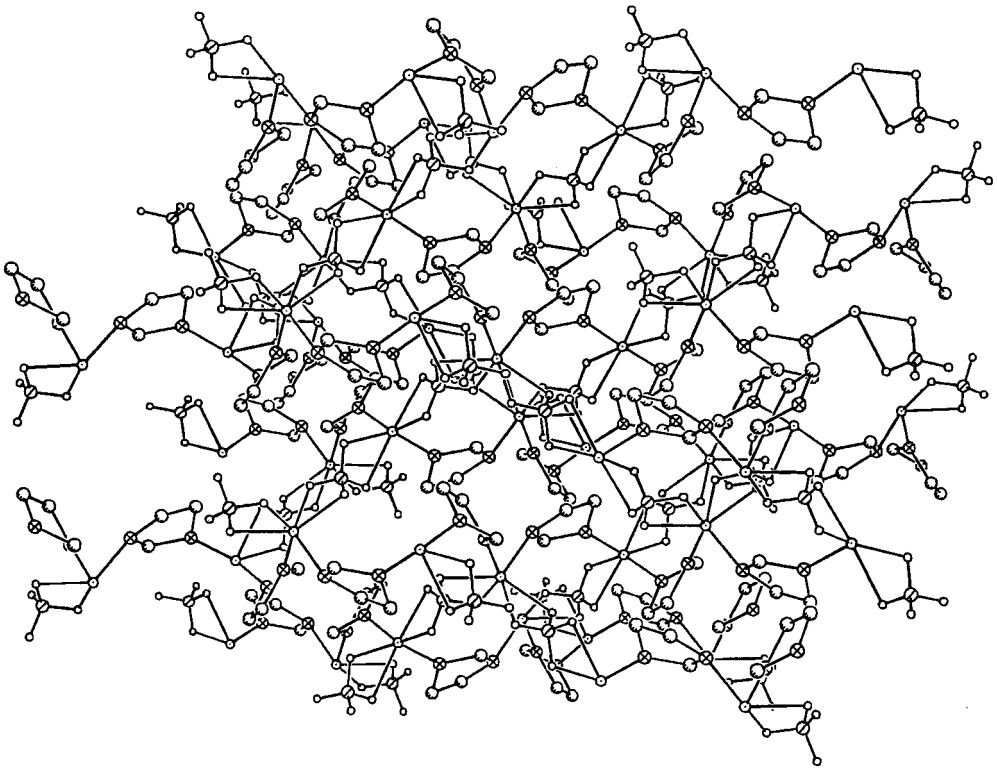

It is evident that the BH_4 group is a very versatile ligand, and it can be expected to show still further variations in coordination mode as a ligand in competition with ethers or other donor ligands. Studies in this area are currently in progress in our laboratory.

We thank *Chemetall GmbH* for support of this study. Moreover we are indebted to the *Fonds der Chemischen Industrie* for unbureaucratic help over many years, and we are also grateful to Mrs. *E. Kiesewetter* and Mrs. *G. Hanatschek* for recording the IR spectra.

Experimental Section

The hydrolytic sensitivity of $LiBH_4$ requires the exclusion of moisture in all experiments. Therefore, the Schlenk-tube technique was used with N_2 or Ar as the protecting gas. All solvents were carefully dried, and only flame-dried glassware was used. $LiBH_4$ (Chemetall GmbH) was crystallized from diethyl ether and dried in vacuum. NMR spectra were recorded with Jeol EX 270 and EX 400 instruments [standards: TMS (^1H, ^{13}C), 1 M LiCl (^7Li), $BF_3 \cdot OEt_2$ (^{11}B)]. – IR: Nicolet FT-IR.

Lithium Tetrahydridoborate–Diethyl Ether (**1**): Diethyl ether (35 ml) was added to $LiBH_4$ (0.94 g, 43 mmol) at 20°C with stirring. After heating to reflux for 4 h, a turbid solution formed, from which the insoluble material was removed by filtration (G3 glass frit). On cooling to 5°C, needles formed which were not suitable for X-ray crystallography. Yield: 3.36 g of **1** (81%), m.p. ca. 5°C. The ether adduct was dissolved in a minimum amount of an Et_2O/toluene (5:3) mixture. Single crystals of sufficient quality grew at −20°C. Isolation and the selection of suitable crystals was carried out at this temperature. **1** was found to be readily soluble in Et_2O and benzene, but insoluble in hexane. – $C_4H_{14}BLiO$ (95.91): calcd. B 11.27, Li 7.24; found B 11.09, Li 7.11 (by titration); B 10.33, Li 6.92 (by AAS).

Lithium Tetrahydridoborate–tert-Butyl Methyl Ether (**2**): Prepared analogously to **1** from $LiBH_4$ (0.76 g) and diveron (25 ml). **2** crystallized from the solution in very thin, interwoven needles. Yield: 3.07 g (79%), dec. 283°C. Single crystals were obtained from the saturated solution at 20°C by cooling to 5°C. The compound was found to be soluble in diveron and benzene, but insoluble in hexane. – $C_5H_{16}BLiO$ (128.08): calcd. B 9.83, Li 6.31; found B 9.69, Li 6.22 (by titration); B 8.93, Li 6.43 (by AAS).

Lithium Tetrahydridoborate–Bis(dimethoxyethane) (**3**): Prepared analogously to **1** from $LiBH_4$ (0.61 g, 28 mmol) and dimethoxyethane (60 ml). A clear solution resulted after heating. Since no crystals separated at 20°C, the solution was cooled to −20°C. Well-shaped needles separated. Yield: 2.4 g of **3** (42%). The compound was found to be soluble in DME, THF (reaction), and benzene, but insoluble in hexane. – $C_8H_{24}BLiO$ (154.03): calcd. B 5.35, Li 3.44; found B 5.41, Li 3.53 (by titration); B 5.45, Li 3.41 (by AAS).

Lithium Tetrahydridoborate–Triglyme (**4**): Obtained by dissolving $LiBH_4$ (250 mg, 11.5 mmol) in 10 ml of triglyme. After heating to reflux (20 min), the hot suspension was filtered and the clear solution was cooled to −20°C. Well-shaped needles formed, which were isolated by filtration. Yield: 600 mg of **4** (26%), m.p. 59°C. The compound was found to be soluble in triglyme and benzene, but insoluble in hexane. – $C_8H_{22}BLiO$ (152.01): calcd. B 5.41, Li 3.47; found B 5.40, Li 3.42 (by titration); B 5.28, Li 3.24 (by AAS).

Lithium Tetrahydridoborate–Tris(tetrahydrofuran) (**5**): To $LiBH_4$ (3.2 g, 146 mmol), tetrahydrofuran (50 ml, 615 mmol) was added with stirring. Most of the $LiBH_4$ dissolved exothermically. The turbid solution was heated to reflux for 10 min, and any insoluble material was then removed at ambient temperature by fil-

Table 4. Data relevant to crystallography, data collection and refinement of the structures of the $LiBH_4$-ether adducts

Compound	**1**	**2**	**6**	**4**	**9**	**3**
Chem. formula	$C_4H_{14}BLiO$	$C_5H_{16}BLiO$	$C_3H_{10}BLiO_2$	$C_8H_{22}BLiO_4$	$C_{12}H_{28}BLiO_3$	$C_8H_{24}BLiO_4$
Form. wght.	95.90	109.93	95.86	200.01	238.09	202.02
Cryst. size [mm]	0.15×0.2×0.4	0.3×0.4×0.55	0.33×0.4×0.6	0.1×0.15×0.3	0.1×0.3×0.9	0.2×0.3×0.3
Cryst. system	Orthorhombic	Monoclinic	Monoclinic	Orthorhombic	Tetragonal	Monoclinic
Space group	*Pna*2(1)	*I*2/*a*	*P*2(1)/*n*	*Pbcn*	*I*4(1)*cd*	*C*2/*c*
a [A]	11.806(12)	9.2598(7)	7.1656(5)	6.395(2)	18.2973(3)	14.376(5)
b [A]	13.617(9)	12.3190(9)	12.9452(9)	15.078(7)	18.2973(3)	7.895(3)
c [A]	4.531(5)	14.4108(14)	13.2702(8)	12.798(7)	18.4226(4)	12.258(5)
α [°]	90.00	90.00	90.00	90.00	90.00	90.00
β [°]	90.00	94.159(1)	101.523(1)	90.00	90.00	105.59(2)
γ [°]	90.00	90.00	90.00	90.00	90.00	90.00
V [A^3]	728.4(12)	1639.5(2)	1206.1(1)	1234.1(10)	6167.7(2)	1340.1(9)
Z	4	8	8	4	16	4
ρ(calcd.) [Mg/m^3]	0.875	0.891	1.056	1.076	1.026	1.001
μ [mm^{-1}]	0.053	0.053	0.076	0.079	0.068	0.073
F(000)	216	496	416	440	2112	448
Index range	$-13\le h\le 13$	$-11\le h\le 11$	$-7\le h\le 7$	$-5\le h\le 8$	$-20\le h\le 18$	$-15\le h\le 18$
	$-10\le k\le 10$	$-14\le k\le 14$	$-14\le k\le 14$	$-18\le k\le 18$	$-20\le k\le 20$	$-10\le k\le 10$
	$-5\le l\le 5$	$-17\le l\le 17$	$-13\le l\le 14$	$-15\le l\le 15$	$-20\le l\le 20$	$-15\le l\le 15$
2 θ [°]	46.50	56.26	46.50	58.12	46.48	57.52
Temp. [K]	193(4)	173(4)	203	173	153(5)	193
Refl. collected	2821	4174	4690	6273	12493	3729
Refl. unique	867	1518	1706	1184	2215	1295
Refl. observed (4σ)	714	1026	1548	627	1938	1140
R (int.)	0.0825	0.0555	0.0332	0.0650	0.1845	0.0216
No. variables	82	93	188	74	166	113
Weighting scheme[a] *x*/*y*	0.0000/0.5250	0.0728/2.2374	0.0409/0.5497	0.0281/0.4510	0.0835/3.1079	0.0341/0.6213
GOOF	1.219	1.089	1.076	1.164	1.122	1.235
Final *R* (4σ)	0.0627	0.0647	0.0386	0.0400	0.0658	0.0415
Final *wR*2	0.1109	0.1668	0.0943	0.0813	0.1697	0.0978
Larg. res. peak [e/A°^{3}]	0.150	0.660	0.183	0.124	0.196	0.098

[a] $w^{-1} = \sigma^2F_o^2 + (x\cdot P)^2 + y\cdot P$; $P = (F_o^2 + 2\cdot F_c^2)/3$.

tration. A 25-ml aliquot of the solution was cooled to −75°C. Extensively intergrown crystals were deposited. Single crystals were selected at −75°C and investigated crystallographically. The crystals, which proved to be $LiBH_4\cdot 3$ THF, melted at ca. −60°C. The remaining solution was subjected to NMR (^7Li, ^{11}B) and IR analysis. The compound loses THF readily at ambient temperature, and finally gives $LiBH_4\cdot$THF[8]. As yet, we have not been able to obtain the latter in the form of single crystals.

Lithium Tetrahydridoborate−1,3-Dioxolane (**6**): $LiBH_4$ (780 mg, 35.8 mmol) was added to 1,3-dioxolane (40 ml). The suspension was heated to reflux for 20 min, and insoluble material was removed by filtration at −30°C. On storing the clear solution at −30°C, colorless crystals formed within 3 d. Yield: 2.67 g of **6** (78%). Recrystallization from 20 ml of toluene at −30°C gave well-shaped single crystals of **6**. − $C_3H_{10}BLiO_2$ (95.86): calcd. C 37.62, H 10.44, B 11.27; found C 36.93, H 10.43, B 11.15.

Crystal-Structure Determinations: Single crystals were grown by slow evaporation of the solvent from the ethereal solutions ($LiBH_4\cdot OEt_2$, $LiBH_4\cdot$DIV, $LiBH_4\cdot 3$ THF) or by cooling solutions in toluene (all others) to low temperatures. The crystals of **1**, **2**, and **5** were removed from the cold solution and transferred directly into precooled perfluoroether oil at −60°C. The selected specimen was mounted on a glass fiber, which was rapidly transferred to the goniometer head. The crystal was cooled in an N_2 cold stream to −100°C. Most crystals of $LiBH_4\cdot$DIV and $LiBH_4\cdot 3$ THF were found to be weakly diffracting. Only the best data obtained are reported here. A Siemens P4 four-circle diffractometer equipped with a SMART-CCD detector was used for data collection with graphite-monochromated Mo-K_α radiation. Preliminary determinations of the cell constants used reflections of 4 different sets of 15 frames. The dimensions of the unit cell reported in Table 4 are those calculated from all data. Data reduction was performed using the program SAINT[21]. The structures were solved by the direct methods implemented in the SHELXTL and SHELX-93 program packages[22]. Hydrogen atoms bonded to the boron atom were refined freely, except for those in **3**. Non-hydrogen atoms were described anisotropically. Hydrogen atoms bonded to carbon atoms were placed in calculated positions and refined with a riding model. The positions of hydrogen atoms bonded to boron atoms were taken from difference Fourier maps. Crystallographic data have been deposited with the Cambridge Crystallographic Data Centre as supplementary publication CCDC-101311. Copies of the data can be obtained free of charge on application to CCCD, 12 Union Park, Cambridge CB2 1EZ, U.K. [Fax: (internat.) + 44(0)1223/336033; E-mail: deposit@ccdc.cam.ac.uk].

☆ Dedicated to my colleague Prof. Dr. *K.-H. Kompa* on the occasion of his 60th birthday.

[1] H. Nöth, S. Thomas, M. Schmidt, *Chem. Ber.* **1996**, *129*, 451−458.

[2] [2a] H. Hajos, *Komplexe Hydride*, VEB, Deutscher Verlag der Wissenschaften, Berlin, **1966**. − [2b] K. M. Mackay, *Hydrogen Compounds of the Metallic Elements*, E. & F. N. Spon Ltd., London, **1996**. − [2c] E. Wiberg, E. Amberger, *Hydrides of the Elements of Main Groups I−IV*, Elsevier Publ. Comp., Amsterdam, London, New York, **1971**. − [2d] Y. M. Choi, S. Narasimha, *Inorg. Chem*. **1981**, *20*, 4456−4457; **1982**, *21*, 3657−3661.

[3] R. E. Mesmer, W. L. Jolly, *Inorg. Chem*. **1962**, *1*, 608−612 and literature cited therein; J. A. Gardiner, J. W. Collat, *ibid*. **1965**, *4*, 1208−1212.

[4] A. S. Antsyshikina, G. G. Sadikov, M. A. Porai-Koshits, V. N. Konoplev, T. A. Silina, A. S. Sizareva, *Koord. Khim.* **1994**, *20*, 277−284.

[5] *Gmelin Handbuch der Anorganischen Chemie*, Supplement to 8th ed., vol. 33, Boron Compounds, part B, **1976**.
[6] T. L. Volski, H. B. Moore, L. E. Rott, K. J. Martin, G. W. Schaeffer, *J. Am. Chem. Soc*. **1958**, *80*, 522−549.
[7] G. W. Schaeffer, T. L. Kolski, D. L. Ekstedt, *J. Am. Chem. Soc*. **1957**, *79*, 5912−5915.
[8] E. Wiberg, H. Nöth, R. Uson, *Z. Naturforsch*., *Part B* **1956**, *11*, 490−491; T. L. Kolski, H. B. Moore, L. E. Roth, K. J. Martin, G. W. Schaeffer, *J. Am. Chem. Soc*. **1958**, *80*, 549−592.
[9] N. M. Joseph, R. E. Paul, French Patent, 1077048 (**1954**); *Chem. Abstr*. **1959**, *53*, 10681.
[10] D. S. Marynick, W. N. Lipscomb, *Inorg. Chem*. **1972**, *11*, 820.
[11] C. S. Mayo, M. Brown, V. K. Loyd, *Acta Crystallogr., Sect. C* **1994**, *50*, 367−369; J. E. Gozum, S. R. Wilson, G. S. Girolani, *J. Am. Chem. Soc*. **1992**, *114*, 4483−9492.
[12] M. Dionne, S. Hao, S. Gambarotta, *Can. J. Chem*. **1995**, *73*, 1126.
[13] D. R. Armstrong, W. Clegg, H. M. Colquhoun, J. A. Danils, R. E. Mulvey, I. R. Stephenson, K. Wade, *J. Chem. Soc., Chem. Comm*. **1987**, 630−631.
[14] H. Nöth, M. Thomann, M. Bremer, G. Wagner, *Current Topics in the Chemistry of Boron*, Royal Soc. Chem. Special Publ. No. 143, **1994**, p. 387−391.
[15] K. B. Harvey, N. R. M. Quaker, *Can. J. Chem*. **1971**, *49*, 3272−3281; V. V. Volkov, E. V. Sobolev, Z. A. Grankina, I. S. Kalina, *Zh. Neorg. Khim.* **1968**, *13*, 659−664.
[16] D. E. Young, G. E. McAchran, S. G. Shore, *J. Am. Chem. Soc*. **1966**, 88, 4390.
[17] A. Heine, D. Stalke, *J. Organomet. Chem*. **1997**, *542*, 25−28, have independently determined the structure of **1** in the solid state. Therefore, we restrict the discussion of the structure to some essentials necessary to compare **1** with the structure of **2**.
[18] H. Edelstein, *Inorg. Chem*. **1981**, *20*, 299−303.
[19] The preparation and structures of compounds $LiBH_4 \cdot n$ L [L = tBuNH$_2$, $(CH_3NCH_2)_3$], and others will be published soon.
[20] H. Nöth, A. Schlegel, J. Knizek, H. Schwenk, *Angew. Chem*. **1997**, *109*, 2754−2758; *Angew. Chem. Int. Ed. Engl*. **1997**, 36, 2640−2643.
[21] Siemens Analytical Instrum. Div., *SAINT*, Version 4.
[22] *SHELX-93* programs; G. W. Sheldrick, University of Göttingen, **1993**, and *SHELXTL*, Siemens Analytical Instruments, version 5, **1994**.

[97321]

1,2-Diphosphetes with Unusual Structures – A Quantum Chemical Investigation of Bonding Properties☆

Wolfgang W. Schoeller*[a], Ulrike Tubbesing[a], and Alexander B. Rozhenko[b]

Fakultät für Chemie, Universität Bielefeld,[a]
Postfach 100131, D-33501 Bielefeld, Germany

Institute of Organic Chemistry, National Academy of Sciences of Ukraine,[b]
5, Murmanskaya street, Kiev-94, 253 660 Ukraine

Received December 16, 1997

Keywords: Ab initio calculations / Phosphorus / Strained molecules / Substituent effects / Pericyclic reactions

According to quantum chemical calculations at an ab initio level parent 1,2-diphosphete is slightly more stable than its corresponding 1,4-diphosphabutadiene structural isomer. The quantum chemical calculations indicate that substituents at phosphorus and to a much less extent at carbon exert strong influences on the equilibrium geometries of 1,2-diphosphete structures: π donors at phosphorus strongly elongate the P–P bond while electronegative substituents at phosphorus increase the interflap angle of the four-membered ring systems, bringing an envelope conformation to the fore. The lengthening of the P–P bond gives rise to a Möbius-type delocalization within the ring moiety.

Introduction

Since the first described route for the syntheses of 1,2-diphosphetes **1** by condensation of cyclopolyphosphanes with alkynes[1] a variety of procedures have been reported, involving the [2+2] cycloaddition reaction of diphosphene complexes with alkynes[2], insertion of a phosphenium cation into a three-membered phosphirene ring[3], the reaction of sterically stabilized iminophosphanes with phosphirenes[4], the Zr-to-P metathetical exchange on 1-phospha-2-zirconacyclobutenes[5], and the reaction of butadiynes with terminal phosphanylidene complexes[6]. In addition a variety of other procedures exist[7]. The versatility of 1,2-diphosphetes has been summarized in recent reports[7].

Here we present quantum chemical calculations which reveal that substituents with strong donor capabilities have sizable effects on the P−P bond equilibrium geometries, ranging from usual (P−P = 2.2 A) to strongly stretched (P−P = 2.5 A) bonds. Furthermore, the substituents strongly affect the interflap angle of the four-membered ring system. On this basis we propose 1,2-diphosphetes with noticeable irregular geometries, which are best described by a cyclic delocalized ring system with 4 electrons (Möbius-type aromaticity).

We note that the recent experimental effort in the synthesis of 1,2-diphosphophosphetes has opened a new convenient general access to symmetrically or unsymmetrically substituted species. On the basis of the phosphanylidene complex addition reaction[6], it might be possible to introduce suitable functional groups at the phosphorus atoms. Corresponding precursor phosphanylide complexes have hitherto been reported for the alkoxy[8], alkoxycarbonyl[9], dialkylamino[10], and vinyl[11] substituents. Thus, our quantum chemical predictions should be amenable to experimental verification.

Scheme 1

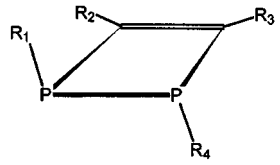

1

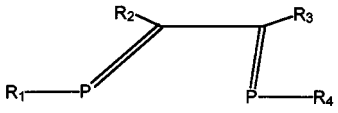

2

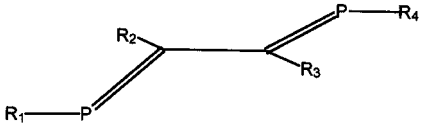

3

Methodology

Previous investigations[12] demonstrate that the barriers for valence isomerization as well as the equilibrium geometries of the various stationary points on the electronic hypersurface are strongly sensitive to explicit treatment of electron correlation in the wavefunction. Within this line we have chosen for the present investigations the MP2 level of optimization, conducted by analytically determined gradients[13]. As a basis set we have used a double-ζ basis set

 © WILEY-VCH Verlag GmbH, D-69451 Weinheim, 1998 1434−1948/98/0707−0951 $ 17.50+.50/0

augmented by polarization functions at the heavy atoms [6-31g(d)][14]. In addition for the anions one set of diffuse s,p functions was added. All details are provided in the discussion. The calculations were performed with the GAUSSIAN-94[15] set of programs.

Results and Discussion

a. Qualitative Considerations

We begin our discussion with an analysis of the electronic hypersurface for the ring-opening reaction of parent **1** (R^1 to R^4 = H) to its valence isomer, the *cis*-diphosphabutadiene **2**. It is valence-isoelectronic to cyclobutene, which undergoes a conrotatory ring opening ($\pi^2 + \sigma^2$) reaction to *cis*-butadiene according to the Woodward-Hoffmann rules[16]. Thus, one expects a similar reaction mode for the case at hand. However, there is an essential difference in bonding between cyclobutene and the 1,2-diphosphete. It becomes apparent by an inspection of bond energies (Table 1).

Table 1. Bond energies (in kcal/mol)

Type	*E* [kcal/mol]	Ref.
σ C−C	83	[a]
π C−C	65	[b]
σ P−P	50	[a]
π P−P	34	[b]
σ P−C	71	[c]
π P−C	43	[b]

[a] K. F. Purcell, J. C. Kotz, *Inorganic Chemistry*, Holt-Saunders International Editions, Honkong, **1977**. − [b] M. W. Schmidt, P. N. Truong, M. S. Gordon, *J. Am. Chem. Soc.* **1987**, *109*, 5217; W. W. Schoeller, C. Begemann, U. Tubbesing, J. Strutwolf, *J. Chem. Soc., Faraday Trans. 2* **1997**, *93*, 2957. − [c] Estimated by the Pauling relationship for heteropolar bonds, see: W. W. Schoeller, R. Schneider, *Chem. Ber.* **1997**, *130*, 1013; see Appendix.

A P−P σ bond is essentially weaker than a C−C σ bond. An estimate for the bond energy from (parent) **1** (R^1 to R^4 = H) to **2** results endothermic in $-E_\sigma^{PP} + 2\,E_\pi^{PC} - E_\pi^{CC} = -29$ kcal/mol, with the energy values given in Table 1. This estimate neglects (a) possible ring strain which would be released upon ring opening and (b) rehybridization effects. Since factor (a) is small in phosphorus ring systems[17] it does not contribute significantly to the energy balance. In comparison with, a corresponding energy balance for ring opening in cyclobutene, based on the consideration of bond transformations, results also endothermic ($E_\sigma^{CC} + 2\,E_\pi^{CC} - E_\pi^{CC} = -18$ kcal/mol). However, in cyclobutene the ring strain is large (65 kcal/mol[18]). It has to be added to the energy balance and makes the ring-opening reaction for this case exothermic, in accord with experiment[19] as well as theory[20]. A further consequence of these considerations may be noticed here, schematically shown in Scheme 2.

In cyclobutene the C−C π (π*) orbitals are higher (lower) in energy than the C−C σ (σ*) orbitals. In (parent) **1** the situation is different. The corresponding orbitals σ and π (σ* and π*) are similar in energy. It is in accord with the result of the quantum chemical calculations (not recorded here). As a consequence of the weaker P −P σ bond (in reference to the C−C σ bond) the energy barrier for an electrocyclic reaction from **1** to **2** should be smaller than in cyclobutene and the P−P σ bond sensitive to donating and/or σ-accepting substitutents attached to the phosphorus atoms. Regarding the ring-opening reaction, experimental investigations on parent **1** are not available, since the structures have to be synthesized with bulky substituents, in order to protect these compounds kinetically.

Scheme 2

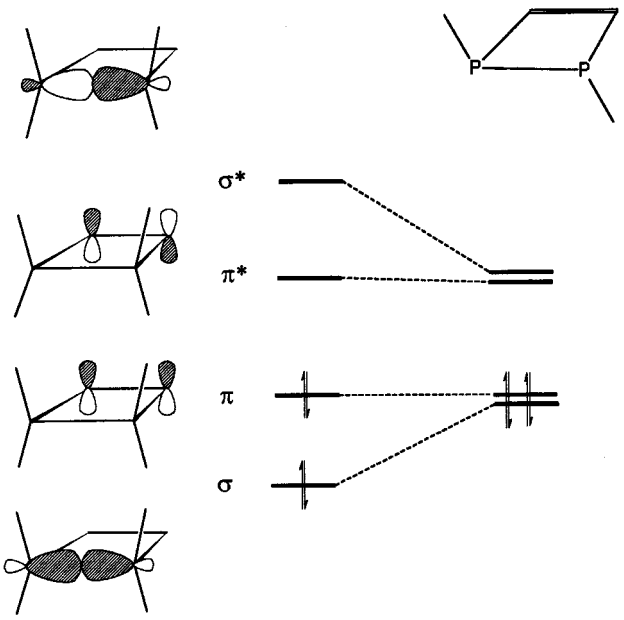

b. Valence Isomerization of Parent 1 to 2

According to recent quantum chemical calculations[12] the ring opening of the 1,2-diphosphete occurs with an energy barrier of 16.9 kcal/mol, a value comparable with an estimate at an RHF level of quantum chemical sophistication[21]. The energy balance to the *trans*-1,4-diphosphabutadiene **3** is endothermic by 2.9 kcal/mol[12]. The primary product in the ring-opening reaction of **1** is the *cis*-1,4-diphosphabutadiene **2**. It is less stable by 5.1 kcal/mol than its *trans* isomer **3**. It must be noted that the rotational barrier from **2** (C_2 symmetry) to **3** (C_{2h} symmetry) is fairly small[21]. Experimentally only the *trans* isomers are known[22][23] which is the most favoured butadiene structure because of the low-energy barrier for rotation. Overall these investigations indicate that the 1,2-diphosphete is the most stable species, but separated by a relatively small barrier from the butadiene derivatives.

c. Substituent Effects on 1

The conclusion that the P−P σ bond is weaker than a C−C σ bond raises the question about the magnitude of substituent effects on the geometries of 1,2-diphosphetes. To evaluate this aspect in more detail we first performed calculations on a variety of mono-substituted 1,2-diphosphetes, the substituents attached to one phosphorus center.

All geometries were determined at the MP2(fc)/6-31g(d). No symmetry restrictions were imposed in the structural energy optimizations.

Table 2. Relevant structural parameters (bond lengths in Å, bond angles in degrees) in mono-P-substituted 1,2-diphosphetes, at MP2 (fc)/6-31g(d) level, anions calculated at MP2(fc)/6-31+g(d) level

R^{1}[a]	P−P	P−C[b]	∠ P−C−C−P	∠ R−P−C−C (∠ H−P−C−C)
H	2.252	1.831	−16.1	110.8 (110.8)
CH_3	2.254	1.859	−15.3	112.5 (111.1)
SiH_3	2.260	1.831	−12.9	107.8 (107.8)
F	2.254	1.801	−25.9	124.2 (120.3)
Cl	2.260	1.827	−22.6	121.6 (116.9)
NH_2	2.291	1.822	−20.5	124.6 (118.0)
PH_2	2.264	1.829	−15.7	118.4 (111.8)
$O^{(-)}$	2.512	1.801	−26.8	131.8 (128.6)
$NH^{(-)}$	3.554	1.741	−20.2	174.1 (172.2)
$NSiH_3^{(-)}$	2.490	1.834	−25.1	131.4 (126.6)
$PH^{(-)}$	2.399	1.817	−16.8	126.4 (117.8)
$PSiH_3^{(-)}$	2.348	1.824	−13.7	127.9 (114.8)

[a] $R^2 = R^3 = R^4 = H$. − [b] P−C bond in vicinity to the the substituent R.

A typical spectrum of substituents at phosphorus were chosen. For the calculations of the anions one set of diffuse s,p functions was added to the heavy atoms.

A sizable lengthening of the P−P bond is already observed to R(P) = NH_2 (P−P = 2.291 Å), in reference to the parent compound (R = H; P−P = 2.252 Å). It is in conformity with the result of recent experimental findings[24]. An even stronger elongation of the P−P bond results for the substituents which carry a negative charge, $PH^{(-)}$ (2.399 Å), $PSiH_3^{(-)}$ (2.348 Å). The investigations indicate that π donors strongly elongate the P−P bond. Finally, for R = $NH^{(-)}$ the butadiene structure is already more stable than the diphosphete. Evidently the ring-opening reaction within the latter occurs without an energy barrier. Strong electronegative substituents, e.g., R = F do not exert considerable changes in the P−P bond lengths. Similarly operates a typical electron-accepting substituent, e.g., SiH_3. There is, however, a strong effect on the torsional angle ∠ R−P−C−C and the folding angle ∠ P−C−C−P of the ring moiety. In comparison to the parent compound, **1** (R^1 to R^4 = H), electronegative substituents (e.g., F) tend to increase and electropositive substituents (e.g., SiH_3) to decrease these torsional angles. A plot of both quantities (Figure 1) affirms an approximate relationship between both types of torsional angles (for a related discussion on torsional angles in cyclobutenes, see ref.[25]).

A rationale for the substituent effects can be given in an interaction diagram, as follows. For the case of simplicity we analyze these effects for the case of di-substitution at phosphorus, invoking simple symmetry arguments (Figure 2).

Two π donors at the phosphorus atoms (**B**) form a positive (p^+, *a* within C_2 symmetry) or negative (p^-, *b* within C_2 symmetry) combination of p orbitals, suitable for interaction with the bonding (σ, π) or antibonding (σ*, π*) orbitals of the ring moiety (**A**). Mutual interaction occurs in either of two ways. (i) Interaction among the *a* set of orbitals (<σ/p^+>) is overall four-electron destabilizing (type I). (ii) In comparison, the mingling of the *b* set of orbitals (<σ*/p^->) results in an overall stabilization (type II), since it involves donation of electron density of a doubly occupied orbital (p^- at **B**) into the empty (σ*) orbital (at **A**). With increasing donor capability (lower ionization potential) the stabilizing interaction (type II) comes to the fore. It will cause a weakening of the P−P bond with concomitant

Figure 1. Plot of torsional angles ∠ RPCC vs. ∠ PCCP, for mono-substituted 1,2-diphosphetes (angles in degrees)

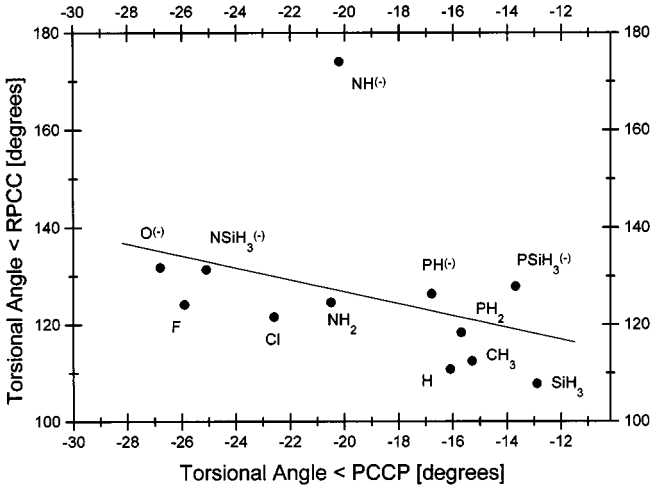

Figure 2. Interaction diagram of two donor p orbitals (**A**) with the σ (σ*) of the P−P bond (**B**)

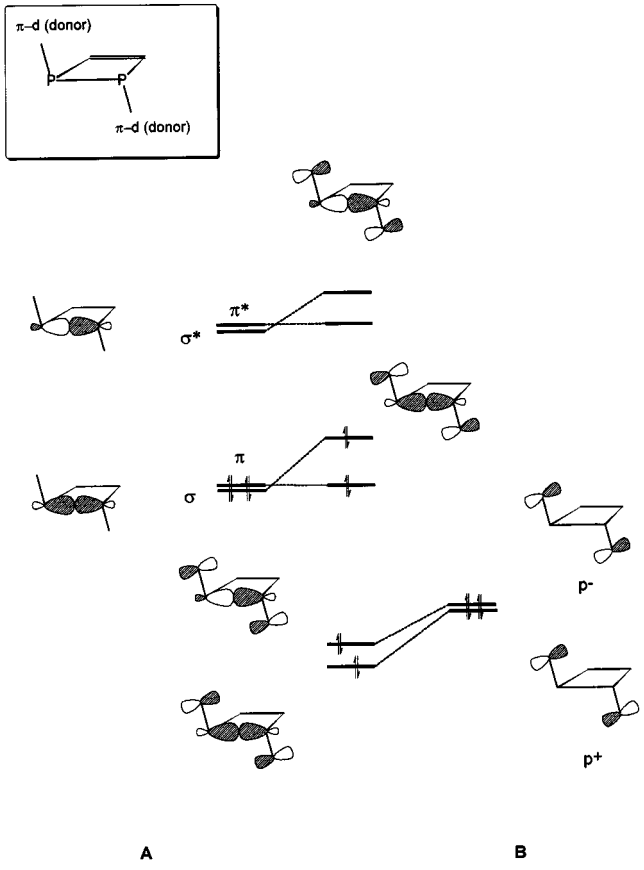

lengthening. Alternatively, if the donor p orbitals at R are low in energy, which refers to the case of electronegative substituents (with a high ionization potential, e.g., R = F) the type-II interaction will be weak and the P−P bond length almost unchanged. This tendency is reflected also for the case of the mono-substitution at phosphorus (see Table 2). We note that within this simplified picture the interactions of the donor orbitals (p^+, p^-, at P) with the π (π*) orbitals are not included in the discussion. To a first order the latter molecular orbitals are not effected, since they are in 1,3-position to the p-set of donor orbitals.

A variety of substituents were also calculated for the cases of di-substitution (a) at phosphorus and/or (b) at the carbon atoms. In contrast to phosphorus substitution, the various carbon-substituted 1,2-diphosphetes do not show considerable changes in the structures. Thus, the unusual bonding properties are only obtained for the case of phosphorus substitution. The di-substitution at phosphorus exerts additive trends on the P−P bond lengths. Corresponding investigations will not be reported here in detail. However, the most important results for the cases (a) and (b) are listed in the Appendix (Table 3).

One important point deserves further discussion. Following our analysis electron-donating substituents weaken the P−P bond. What is its effect on the energy barrier of the conrotatory ring opening reaction? We have examined this aspect in detail for the case of amino di-substitution at the diphosphete **1** ($R^1 = R^4 = NH_2$; $R^2 = R^3 = H$). The energy barrier disappears in fact [at a MP2(fc)/6-31g(d) level, plus additional MP4SDTQ(fc) and zero-point vibrational corrections]. In other words the description of **1** and **2** as two species in equilibrium, **C**, which implies separation by an energy barrier[7], is not valid for the case at hand, i.e., with a strong π-donor substitution at the phosphorus atom(s).

Scheme 3

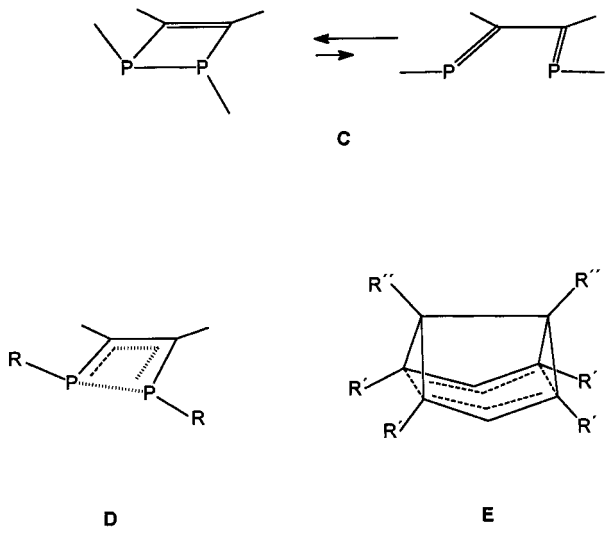

Consequently, **1** can be considered as a structure with pericyclic electron delocalization. Such a species, **D**, with 4 delocalized electrons may be described as a Möbius aromatic system[26][27].

We note that the discussion presented here is reminescent to the analysis of substituents for the design of a "frozen-in" transition-state geometry in semibullvalene[28][29], **E**. There, a structure with $[\sigma^2 + \pi^2 + \pi^2]$ delocalization is promoted for the cases R′ = σ acceptor, R′′ = σ donor. It refers to a delocalized Hückel aromatic system. In comparison, our investigations indicate that such a delocalized system may also exist for a Möbius-type arrangement, which involves 4 electrons in pericyclic delocalization $[\sigma^2 + \pi^2]$. This view does, however, imply that the phosphorus lone pairs are not included in the delocalization. It results in unusual structures for the 1,2-diphosphetes. The experimental verification of the concept of 1,2-diphosphete structures with strongly elongated P−P bonds remains, however, a challenge to the experimentalist. In addition, the validity of the presented concept of delocalized Möbius-type structures has to be analyzed for the related cases, such as the mono- and triphosphetes. The bonding situation in the diphosphetes may also be compared with that in the dithietes[33][34]. There, the ring structure (dithiete) and the corresponding open structures (dithioglyoxal) are similar in energy and their mutual energy differences are a balance of delicate substituent effects.

This work has been supported by the *Deutsche Forschungsgemeinschaft* and the *Fonds der Chemischen Industrie.*

Appendix

While the case of mono-substitution at phosphorus in the 1,2-diphosphetes was studied at the MP2(fc)/6-31g(d) or for the anions at the MP2(fc)/6-31+g(d) level, for the heterosubstituted cases (at phosphorus and carbon) we employed the less costly 3-21g(d) basis set[30], accounting within the density functional formalism[31][32] [B3LYP/3-21g(d)] for the importance for electron correlation. The results of these investigations are summarized in Table 3.

Table 3. Relevant geometrical parameters (bond lengths in A, angles in degrees) for disubstituted 1,2-diphosphetes, obtained at B3LYP/3-21g(d) level of sophistication

$R^1 = R^4$	$R^2 = R^3$	P−P	P−C	C−C	∠ P−C−C−P	∠ R−P−C−C
H	H	2.279	1.851	1.346	−11.5	104.4
F	H	2.292	1.805	1.365	−30.3	129.0
Cl	H	2.307	1.822	1.357	−22.9	120.2
CH_3	H	2.276	1.846	1.350	−11.8	109.3
SiH_3	H	2.290	1.850	1.350	−8.0	102.0
PH_2	H	2.297	1.842	1.351	−11.6	113.8
NH_2	H	2.349	1.817	1.360	−20.5	124.8
NH_2	CN	2.338	1.824	1.379	−22.0	126.1
NH_2	NH_2	2.304	1.824	1.471	−17.0	120.3
NH_2	F	2.323	1.823	1.350	−15.1	117.8
Ph	H	2.307	1.838	1.353	−15.0	113.7
CN	H	2.295	1.846	1.347	−15.4	110.3
H	CN	2.269	1.855	1.364	−12.3	105.6
CN	CN	2.289	1.856	1.364	−15.7	110.6
CN	NH_2	2.268	1.839	1.369	−14.5	109.8
F	F	2.282	1.811	1.351	−23.2	120.0

The results, although obtained at a lower level of sophistication, yield similar trends. In addition they indicate that substituents at the carbon position(s) do not exert strong substituent effects at the P−P bond length. As shown for the case of the mono-substitution electronegative substituents at phosphorus tend to increase the

folding angle of the four-membered ring. Full details of the obtained equilibrium geometries are available on request.

[☆] In memoriam to Professor *M. J. S. Dewar*.

[1] W. Mahler, *J. Am. Chem. Soc*. **1964**, *86*, 2306; A. Ecker, U. Schmidt, *Chem. Ber*. **1973**, *106*, 1453; C. Charrier, J. Guilhelm, F. Mathey, *J. Org. Chem*. **1981**, *46*, 3; C. Charrier, N. Maigrot, F. Mathey, F. Robert, Y. Jeannin, *Organometallics* **1986**, *5*, 623; I. G. Philipps, R. G. Ball, R. B. Cavell, *Inorg. Chem*. **1988**, *27*, 2269.

[2] N. H. Tran Huy, Y. Inubushi, L. Ricard, F. Mathey, *Organometallics* **1997**, 16, 2506.

[3] L. Ricard, N. Maigrot, C. Charrier, F. Mathey, *Angew. Chem*. **1987**, *99*, 590; *Angew. Chem. Int. Ed. Engl*. **1987**, *26*, 548.

[4] M. Linck, E. Niecke, M. Nieger, *Chem. Ber*. **1994**, *127*, 313.

[5] T. L. Breen, D. W. Stephan, *Organometallics* **1997**, *16*, 365.

[6] N. H. Tran Huy, L. Ricard, F. Mathey, *Organometallics* **1997**, *16*, 4501.

[7] F. Mathey, C. Charrier, N. Maigrot, A. Marinetti, L. Ricard, N. H. Tran Huy, *Comments Inorg. Chem*. **1992**, *13*, 61; S. Kummer, U. Zenneck, in *Comprehensive Heterocyclic Chemistry II* (Eds.: A. R. Katritzky, C. W. Rees, E. F. V. Scriven), Pergamon, Oxford, **1996**. vol. 1b, pp. 1157.

[8] J.-M. Alcarez, J. Svara, F. Mathey, *Nouv. J. Chim*. **1986**, *10*, 321.

[9] S. Holand, F. Mathey, *Organometallics* **1988**, *87*, 1796.

[10] B. Deschamps, L. Ricard, F. Mathey, *Polyhedron* **1989**, *8*, 2671. B. Deschamps, F. Mathey, *Synthesis* **1995**, 941.

[11] N. H. Tran Huy, L. Ricard, F. Mathey, *Organometallics* **1991**, *10*, 3958.

[12] W. W. Schoeller, U. Tubbesing, *Chem. Ber*. **1996**, *129*, 419.

[13] N. C. Handy, H. F. Schaefer, III, *J. Chem. Phys*. **1984**, *81*, 5031; J. A. Pople, R. Krishnan, H. B. Schlegel, J. S. Binkley, *Intern. J. Quant. Chem. Symp*. **1979**, *13*, 325; M. J. Frisch, M. Head-Gordon, J. A. Pople, *Chem. Phys. Lett*. **1990**, *166*, 275; M. J. Frisch, M. Head-Gordon, J. A. Pople, *Chem. Phys. Lett*. **1990**, *166*, 281.

[14] R. Ditchfield, W. J. Hehre, J. A. Pople, *J. Chem. Phys*. **1971**, *54*, 724; W. J. Hehre, R. Ditchfield, J. A. Pople, *J. Chem. Phys*. **1972**, *56*, 2257; P. C. Hariharan, J. A. Pople, *Mol. Phys*. **1974**, *27*, 209; P. C. Hariharan, J. A. Pople, *Theor. Chim. Acta* **1973**, *28*, 213.

[15] M. J. Frisch, G. W. Trucks, H. B. Schlegel, P. M. W. Gill, B. G. Johnson, M. A. Robb, J. R. Cheeseman, T. A. Keith, G. A. Petersson, J. A. Montgomery, K. Raghavachari, M. A. Al-Laham, V. G. Zakrewski, J. V. Ortiz, J. B. Foresman, J. Cioslowski, B. B. Stefanov, A. Nanayakkara, M. Challacombe, C. Y. Peng, P. Y. Avala, W. Chen, M. W. Wong, J. L. Andres, E. S. Replogle, R. Gomperts, R. L. Martin, D. J. Fox, J. S. Binkley, D. J. Defrees, J. Baker, J. P. Stewart, M. Head-Gordon, C. Gonzalez, J. A. Pople, *Gaussian 94* (Revision A.1), Gaussian, Inc., Pittsburgh, PA, **1995**.

[16] R. B. Woodward, R. Hoffmann, *The Conservation of Orbital Symmetry*, Verlag Chemie, Weinheim/Bergstraße, **1970**.

[17] W. W. Schoeller, *J. Mol. Struct. (THEOCHEM)* **1993**, *284*, 61.

[18] J. D. Cox, G. Pilcher, *Thermochemistry of Organic and Organometallic Compounds*, Academic Press, New York, **1970**.

[19] The experimentally measured energy barrier for the ring opening of cyclobutene results to 32.0 kcal/mol [W. Cooper, W. D. Walter, *J. Am. Chem. Soc*. **1958**, *80*, 4220; R. W. Carr, Jr., W. D. Walter, *J. Phys. Chem*. **1965**, *69*, 1073], 36 kcal/mol [H. M. Frey, R. F. Skinner, *J. Chem. Soc., Trans. Faraday Soc*. **1965**, *61*, 1918] with −11.4 kcal/mol for the heats of the reaction [K. B. Wiberg, R. A. Fenoglio, *J. Am. Chem. Soc*. **1968**, *90*, 3395].

[20] H. Yu, W.-T. Chan, J. D. Goddard, *J. Am. Chem. Soc*. **1990**, *112*, 7529; for further references see therein.

[21] S. M. Bachrach, M. Liu, *J. Org. Chem*. **1992**, *57*, 2040.

[22] R. Appel, J. Hünerbein, N. Siabalis, *Angew. Chem*. **1987**, *99*, 810; *Angew. Chem. Int. Ed. Engl*. **1987**, *26*, 779.

[23] S. Ito, K. Toyota, M. Yoshifuji, *Chem. Lett*. **1995**, 747.

[24] O. Schmidt, A. Fuchs, D. Gudat, M. Nieger, W. Hoffbauer, E. Niecke, W. W. Schoeller, *Angew. Chem*. **1998**, *110*, 995; *Angew. Chem. Int. Ed. Engl*. **1998**, *37*, 949.

[25] S. Niwayama, E. A. Kallel, D. C. Spellmeyer, C. Sheu, K. N. Houk, *J. Org. Chem*. **1996**, *61*, 2813.

[26] E. Heilbronner, *Tetrahedron Lett*. **1964**, 1923.

[27] M. J. S. Dewar, *Angew. Chem*. **1971**, *83*, 859; *Angew. Chem. Int. Ed. Engl*. **1971**, *10*, 761.

[28] M. J. S. Dewar, W. W. Schoeller, *J. Am. Chem. Soc*. **1971**, *93*, 1481.

[29] R. Hoffmann, W. D. Stohrer, *J. Am. Chem. Soc*. **1971**, *93*, 6941.

[30] J. S. Binkley, J. A. Pople, W. J. Hehre, *J. Am. Chem. Soc*. **1980**, *102*, 939; M. S. Gordon, J. S. Binkley, J. A. Pople, W. J. Pietro, W. J. Hehre, *J. Am. Chem. Soc*. **1982**, *104*, 2797; W. J. Pietro, M. M. Francl, W. J. Hehre, D. J. DeFrees, J. A. Pople, J. S. Binkley, *J. Am. Chem. Soc*. **1982**, *104*, 5039.

[31] A. D. Becke, *Phys. Rev*. **1988**, *A38*, 3098. A. D. Becke, *J. Chem. Phys*. **1993**, *98*, 5648.

[32] C. Lee, W. Yang, R. G. Parr, *Phys. Rev*. **1988**, *B37*, 785.

[33] J. D. Goddard, *J. Comput. Chem*. **1987**, *8*, 389.

[34] H. E. R. Simmons, R. D. Vest, D. C. Blomstrom, J. R. Roland, T. L. Cairns, *J. Am. Chem. Soc*. **1962**, *84*, 4746. H. E. R. Simmons, D. C. Blomstrom, R. D. Vest, *J. Am. Chem. Soc*. **1962**, *84*, 4756.

[97307]

Intramolecular Luminescence Quenching in Amino Acid Bridged Ruthenium(II)-Copper(II) Complexes with Negligible Ground-State Coupling

Bernd Geißer and Ralf Alsfasser*

Institut für Anorganische Chemie der Universität Erlangen-Nürnberg,
Egerlandstraße 1, D-91058 Erlangen, Germany
Fax: (internat.) + 49(0)9131/857387
E-mail: alsfassr@anorganik.chemie.uni-erlangen.de

Received December 16, 1997

Keywords: Amino acids / Bioinorganic chemistry / Copper / Luminescence / Ruthenium

A series of heterobimetallic complexes [{Ru(bipy)$_2$}m-AA{Cu(phen)(H$_2$O)}](PF$_6$)$_3$ (m-AA = N^{ω}-(4-carbonyl-4′-methyl-2,2′-bipyridyl)-L-α,ω-diamino acid; diamino acid (AA): **1b**, L-2,3-diaminopropionic acid; **2b**, L-2,4-diaminobutyric acid; **3b**, L-ornithine, **4b**, L-lysine) has been synthesized and characterized starting from the 2,2′-bipyridineruthenium(II)-substituted amino acids [{Ru(bipy)$_2$}m-AA-$^{\alpha}N$-^{t}Boc]$^{2+}$ ($^{\alpha}N$-^{t}Boc-**1a–4a**, $^{\alpha}N$-^{t}Boc = N^{α}-*tert*-butoxycarbonyl). The metal centers in **1b–4b** are bridged by insulating alkyl chains. Consequently, spectroscopic and electrochemical investigations confirmed the absence of any appreciable ground-state coupling between ruthenium(II) and copper(II). However, the luminescence of **1b–4b** is significantly quenched compared to that of the parent compounds **1a–4a**. Quenching was found to proceed only intramolecularly and to be most efficient in **1b** with the shortest alkyl spacer. Equilibrium constants for the formation of **1b–4b** were determined from luminescence titrations of the respective ruthenium-substituted amino acid with [Cu(phen)(NO$_3$)$_2$]. The complexes **2b–4b** (K = 1.61–2.08 × 10^7 M^{-1}) were found to be significantly more stable than **1b** (K = 5.7 × 10^6 M^{-1}). This is explained by a stronger electrostatic repulsion between the two metal centers in the latter compound.

Introduction

Owing to their fundamental importance in biological photosynthesis, photoinduced electron- and energy-transfer processes have attracted much attention in the context of supramolecular chemistry.[1][2][3][4] A particularly interesting challenge for synthetic chemists is the design of redox-active devices in which a photoinduced electron-transfer process triggers a chemical reaction. The light-dependent reduction of CO_2 by macrocyclic Ni^{II} complexes which have been covalently tethered to a polypyridineruthenium moiety may illustrate this goal.[5][6] In these compounds the electron-accepting nickel complex functions as a catalytically active site for substrate turnover, whereas the ruthenium chromophore serves the purpose of converting light into chemical energy.

Work in our laboratories has focussed on the design and synthesis of modified amino acids with well-defined binding sites for transition-metal complexes.[7] Our aim is to use these ligands as building blocks for the construction of polyfunctional supramolecular systems. Here we report the synthesis and characterization of novel dinuclear Ru^{II}-Cu^{II} complexes [{Ru(bipy)$_2$}m-AA{Cu(phen)(H$_2$O)}](PF$_6$)$_3$, **1b**−**4b** (Figure 1), with bridging bipyridyl-substituted α,ω-diamino acids (m-AA). The photoredox active [Ru(bipy)$_3$] subunit in **1b**−**4b** is thought to be suitable for the photochemical generation of phenanthrolinecopper(I).

It has been known for twenty years that phenanthrolinecopper(I) complexes can function as efficient chemical nucleases, catalysing the oxidative cleavage of ribose links of DNA in the presence of oxygen and a reducing agent.[8] This has stimulated considerable interest in using these systems as chemical probes for DNA structures.[9] DNA-strand scission occurs through a series of reactions starting with hydrogen-atom abstraction from a ribose unit.[9] The active agent is probably a metal-oxo or metal-hydroxyl intermediate formed upon reaction of hydrogen peroxide with a [Cu(phen)$_2$]$^+$ molecule bound to the surface of DNA within the minor groove.[9][10]

An interesting approach to the in situ generation of active Cu^{I} species has been reported by Strekas et al.[11] The authors have synthesized and characterized heterobimetallic complexes containing Cu^{I} and Cu^{II} fragments, and a bis(diimine)ruthenium(II) complex. It was shown that the compounds interact with DNA and that oxidative strand cleavage occurs in the presence of reducing agents. The combination of [Cu(phen)]$^{2+}$ fragments with photoredox-active polypyridineruthenium(II) complexes thus seems to be a promising route to bimetallic DNA-cleavage reagents. Photoinduced electron transfer should be possible between the ruthenium and the copper centers in dinuclear complexes, triggering oxidative strand-scission reactions upon irradiation with visible light.

Furthermore, both metal fragments are expected to interact with DNA with different affinities and selectivities. Polypyridineruthenium compounds typically intercalate into the base stacks of DNA,[12][13] whereas bis(phenanthroline-)copper(I) predominantly binds to the minor groove.[9][14] The combination of metal fragments with different DNA

 © WILEY-VCH Verlag GmbH, D-69451 Weinheim, 1998 1434−1948/98/0707−0957 $ 17.50+.50/0

Figure 1. Synthesis of the Ru^{II}-Cu^{II} complexes **1b**−**4b**[a]

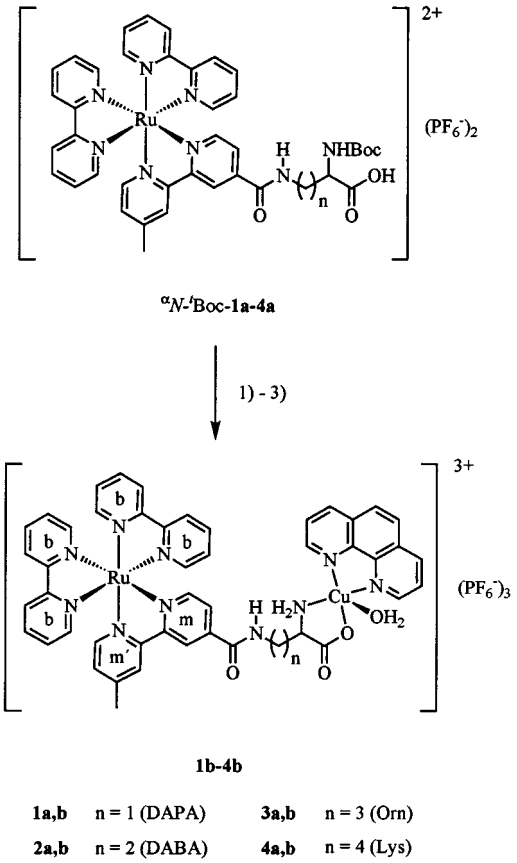

[a] 1) 4 N HCl/dioxane, 1 h, 0°C. − 2) 1 equiv. $[Cu(phen)(NO_3)_2]$/methanol. − 3) NH_4PF_6/H_2O.

binding patterns has been exploited by Brewer and co-workers for the synthesis of Ru^{II}-Pt^{II} and Os^{II}-Pt^{II} heterobimetallic complexes.[15] These compounds can interact with DNA by intercalation and/or covalent bonding.

It was first the aim of our studies on **1b**−**4b** to establish fundamental structure-function relationships in order to provide a basis for the applications described above. The compounds were investigated structurally by NMR and EPR spectroscopy. UV/Vis spectroscopy and cyclic voltammetry were used to confirm the absence of an efficient electronic coupling between the two metal centers. Finally, luminescence spectroscopy was applied as a tool to determine the effects of bridge structures on quenching efficiencies and complex stability constants.

Synthesis and Characterization of the Complexes

Synthesis

Our synthesis of the dinuclear Ru^{II}-Cu^{II} complexes **1b**−**4b** started from the $^{\alpha}N$-^{t}Boc-protected (amino acid)ruthenium(II) complexes $[\{Ru(bipy)_2\}m\text{-AA-}^{\alpha}N\text{-}^{t}Boc](PF_6)_2$ [$^{\alpha}N$-^{t}Boc-**1a**−**4a**; AA = L-2,3-diaminopropionic acid; L-2,4-diaminobutyric acid; L-ornithine; L-lysine (Figure 1)]. The latter compounds were prepared by coupling the succinimido ester $[Ru(bipy)_2(m\text{-OSu})](PF_6)_2$ with the appropriate $^{\alpha}N$-^{t}Boc-protected α,ω-amino acid according to a procedure reported earlier for the lysine derivative $^{\alpha}N$-^{t}Boc-**4a**.[16] Full experimental details will be published elsewhere.[17]

The ^{t}Boc protecting groups of $^{\alpha}N$-^{t}Boc-**1a**−**4a** were removed by acid deprotection in dioxane/HCl.[18] Deprotonation of the amine hydrochloride and subsequent reaction with one equivalent of commercially available $[Cu(phen)(NO_3)_2]$ in methanol yielded the desired complexes **1b**−**4b** (Figure 1). The compounds were isolated as PF_6^- salts from water in approximately 70% yield. Coprecipitated salts can be removed by stirring the complexes with water for one day. However, it is advantageous to use only a small excess (< 5 times) of NH_4PF_6 in order to prevent coprecipitation of ammonium hexafluorophosphate.

^{1}H NMR

Proton-NMR spectroscopy proved to be a valuable tool for structural investigations of the Ru^{II}-Cu^{II} mixed-metal complexes **1b**−**4b**. Binding of the paramagnetic $[Cu](phen)^{2+}$ fragment is easily confirmed by the disappearance of all signals related to the $^{\alpha}CH$ and $^{\beta-\omega}CH_2$ protons of the amino acid moieties.[19][20] In contrast, the resonances of the $[Ru(bipy)_2m]^{2+}$ fragments in **1b**−**4b** are broader than those of the parent compounds **1a**−**4a** but readily observable. This is a consequence of the $1/r^6$ dependence of longitudinal relaxation rates, $1/T_1$, on the distance between protons and paramagnetic centers such as Cu^{2+}.[19]

Most interesting are changes of the signals assigned to the m3 protons of **1b**−**4b** at $\delta \approx 8.96$ (notation see Figure 1). A clear dependence on the Ru−Cu distance is evident as the intensities decrease with the number of methylene spacers, *n*. Assuming fully extended hydrocarbon chains, the Ru−Cu distances can be calculated to range from ca. 13 Å in **4b** to ca. 9 Å in **1b**. We think this model is justified because of the electrostatic repulsion between the positively charged metal centers.

EPR

The EPR spectra of **1b**−**4b** in frozen methanol solutions at 77 K are anisotropic with $g_{||} > g_{\perp} > 2.04$ and large parallel hyperfine splittings ($A_{||} \approx 180 \times 10^{-4}$ cm^{-1}). These values are typical for copper(II) complexes with a $d_{x^2-y^2}$ (or d_{xy}) ground state.[21]

No significant differences are observed between the spectra of **1b**−**4b** (Table 1). This is expected since the copper centers possess identical local environments in these compounds. The spectrum of **3b** is shown in Figure 2 as an example.

Our data compare well with others reported in the literature for copper(II) complexes with square-pyramidal or elongated octahedral coordination geometries.[22] Particularly relevant examples are several ternary phenanthroline-copper(II) dipeptide complexes ($g_{||} \approx 2.24$, $A_{||} \approx 170 \times 10^{-4}$ cm^{-1}).[23] Slightly lower $g_{||}$ values (< 2.20) were found for square-planar complexes.[22] One or two solvent molecules may thus be coordinated to the copper centers of **1b**−**4b** in solution. Elemental analysis data confirm the

Table 1. EPR data of complexes **1b**−**4b** (frozen methanol, DPPH as internal reference)

Complex	$g_{\parallel}$	$g_{\perp}$	$A_{\parallel}$ [10^{-4} cm^{-1}]
1b	2.271	2.043	177
2b	2.268	2.046	179
3b	2.276	2.046	177
4b	2.274	2.049	179

Figure 2. EPR spectrum of complex **3b** in frozen methanol solution at 77 K (DPPH as internal reference)

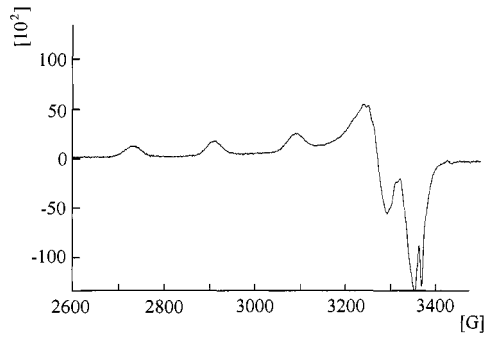

presence of at least one water molecule in the solid state. The water contents vary from 1−3.5 equiv. after several days under vacuum at elevated temperatures. We propose the solid-state structures shown in Figure 1 with water occupying the apical positions of square pyramidal coordination environments around the copper centers in our complexes. However, the presence of two weakly bound solvent molecules in solution cannot be ruled out and seems likely.

Absorption Spectra

The absorption spectra of **1b**−**4b** in methanol are dominated by the typical features of polypyridineruthenium(II) complexes.[24][25] Most significant is an MLCT band with a maximum at 455 nm and a shoulder at 427 nm. A weak absorption at around 340 nm may be assigned to either an MC[24][25] or an MLCT[26] transition. In the UV region a strong intraligand π-π* band is centered at 288 nm.

The presence of the $[Cu(phen)]^{2+}$ subunit is apparent from a shoulder at 274 nm due to a phenanthroline-based intraligand π-π* transition. A comparison of the absorption spectra in methanol obtained for **3a**, **3b**, and $[Cu(phen)(NO_3)_2]$ is shown in Figure 3. The spectrum of **3b** appears as the sum of the spectra of its constituents, consistent with the absence of any significant ground-state electronic coupling between the two metal centers. In addition, no intervalence charge-transfer absorption bands were observed for **1b**−**4b** in the near-infrared region (ε < 10 for the IT transition). According to the Hush theory[27][28][29] this is further evidence for weak electronic coupling in polynuclear complexes with noninteracting redox centers (class I according to the Robin−Day classification[30][31]).

Similar results were reported in the literature for dinuclear Ru^{II}-Ru^{II} and Ru^{II}-Pt^{II} compounds with bridging alkyl spacers.[32] The amino acid bridges in **1b**−**4b** evidently act as insulators between Ru^{II} and Cu^{II} and thus may be

Figure 3. Absorption spectra of 1.5×10^{-5} M solutions of **3a** [------, λ_{max} (lg ε) = 457 nm (4.24), 287 (4.89), 246 (4.53)], **3b** [——, λ_{max} (lg ε) = 455 nm (4.22), 287 (4.94), 256 (4.64)], and $[Cu(phen)(NO_3)_2]$ [·····, λ_{max} (lg ε) = 294 (4.38), 272 (4.79)] in methanol

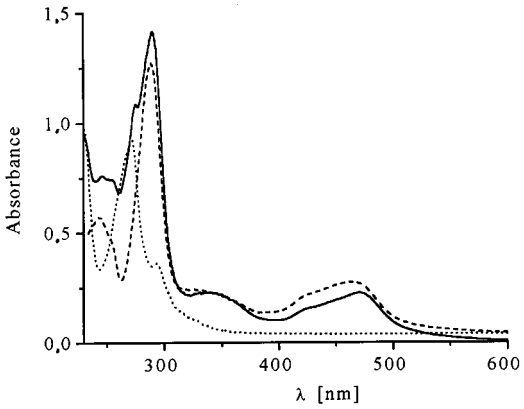

considered to play only a structural role. Each complex fragment is therefore expected to keep its essential individual properties. This condition has been discussed to be important for the definition of supramolecular systems[33] and is crucial for the prediction of properties such as DNA binding and cleavage abilities.

Cyclic Voltammetry

The weak coupling between ruthenium(II) and copper(II) in **1b**−**4b** is also evident from electrochemical data (Table 2). Figure 4 shows the cyclic voltammogram (2nd cycle) of **2b** as an example. Two redox couples are observed. One reversible at a half-wave potential of 1.30 V ($\Delta E_P \approx 80$ mV) is typical for the $Ru^{II/III}$ transition in $[Ru(bipy)_3]^{2+}$ derivatives[24][25] and similar to those observed for the mononuclear precursor complexes **1a**−**4a**. The other couple is irreversible and occurs at $E_{1/2} = 0.1$ V ($\Delta E_P \approx 280$ mV). This value is in good agreement with data reported in the literature for other phenanthrolinecopper complexes.[34][36]

Table 2. Electrochemical data of complexes **1b**−**4b** as measured by cyclic voltammetry[a]

Complex	$E_{1/2}$ [V] (ΔE_P [mV])		
	metal oxidation		ligand reduction
	$Ru^{II/III}$	$Cu^{I/II}$	
1b	1.31 (80)	0.14 (290)	−1.23 (120), −1.45, −1.68 (70)
2b	1.31 (80)	0.10 (280)	−1.23 (100), −1.39, −1.69 (130)
3b	1.30 (90)	0.08 (285)	−1.25 (90), −1.44, −1.66 (130)
4b	1.29 (80)	0.10 (285)	−1.23 (110), −1.44, −1.66 (130)

[a] All measurements were recorded against an Ag/AgCl reference electrode: $E_{1/2,\ Ag/AgCl} = E_{1/2,\ NHE} - 0.222$ V.

The irreversibility of the $Cu^{I/II}$ couple is most likely due to a change in coordination number and stereochemistry upon reduction of Cu^{2+} to Cu^{+}.[22][37][38] This is important since it may impose a kinetic barrier on electron-transfer reactions. It is interesting to note that relatively slow self-exchange rates of 1.5×10^4 M^{-1} s^{-1} have been reported for phenanthrolinecopper complexes.[39] However, an excited-state electron transfer from Ru^{*II} to Cu^{II} in our complexes is possible based on thermodynamic consideration.

Figure 4. Cyclic voltammograms of **2a** (------) and **2b** (——) in CH_3CN

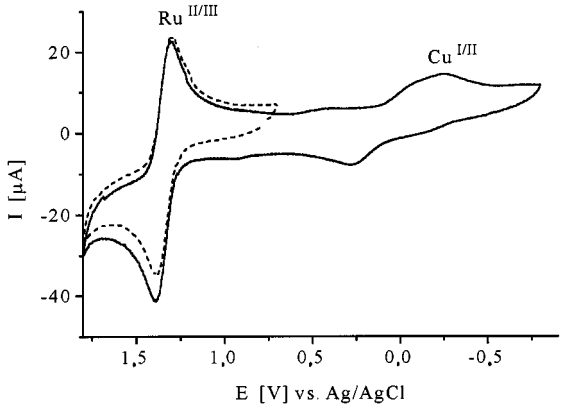

A negative driving force ΔG^0 of -80 kJ mol^{-1} is calculated from the reduction potential E^0_{Red} for $Cu^{I/II}$ (0.10 V), and the excited-state oxidation potential E^{*0}_{Ox} for $Ru^{*II/III}$ (-0.90 V). E^{*0}_{Ox} was obtained according to Equation (1).[40]

$$E^{*0}_{Ox}([M]/[M]^+) = E^0_{Ox}([M]/[M]^+) + E_{0\text{-}0} \quad (1)$$

$E^0_{Ox}([M]/[M]^+)$ is the oxidation potential of the ground-state molecule and E_{0-0} is the one-electron potential corresponding to the energy of the zero-zero transition (2.26 eV). They were determined from the cyclic voltammograms and the intersection between absorption and emission spectra, respectively.

Another characteristic feature of the $Cu^{I/II}$ redox couple is the broad reduction wave at -0.25 V which appears to consist of two unresolved contributions. This is typical for $[(phen)Cu]^{2+/+}$ complexes and has been ascribed to adsorption processes at the glassy carbon electrode.[36] Similar observations have also been reported for several polynuclear ruthenium complexes.[41]

Cyclic voltammetry and absorption spectroscopy both confirm that the individual properties of the two metal fragments are retained in our Ru^{II}-Cu^{II} complexes. No indication for efficient ground-state electronic coupling between the two metal ions was found. The amino acid bridge acts as an insulator and serves only the purpose of connecting the independent constituents. This observation is important for the following discussion of luminescence properties.

Luminescence Quenching Studies

The $[Ru(bipy)_3]^{2+}$-based emission of **1a−4a** is significantly quenched in the presence of $[Cu(phen)]^{2+}$. This is evident from the emission titration curves shown in Figure 5a. Stern−Volmer plots of the data are found to be non linear (Figure 5b). Saturation is observed at higher copper concentrations. It is therefore concluded that luminescence quenching occurs by intramolecular rather than intermolecular mechanisms.[42][43] This was further supported by titration of $[Ru(bipy)_3]^{2+}$ with $[Cu(phen)(NO_3)_2]$ under similar conditions, where no significant luminescence quenching was detectable. As has been discussed in the previous sections the alkyl bridges in **1b−4b** do not mediate efficient electronic interactions between the metal centers. We therefore propose that a bridged outer-sphere quenching mechanism without direct participation of the bridge in either electron- or energy-transfer processes seems most likely. The alkyl bridge is important for keeping the two metal centers together in a "precursor complex" and is therefore crucial for excited-state interactions even though it does not directly facilitate electronic exchange.

It is obvious from Figure 5a that the titration curves have not reached their minima at a Cu/Ru ratio of 1:1. An excess of copper is necessary to achieve maximum luminescence quenching. Since bimolecular processes have been shown to be negligible this must be a consequence of complex dissociation according to the equilibrium shown below.

$$\textbf{1a - 4a} + [Cu(phen)]^{2+} \overset{K}{\rightleftharpoons} \textbf{1b - 4b}$$

Luminescence-quenching studies have been employed earlier for the determination of equilibrium constants, K.[44][45][46] Two requirements have to be met for this approach to be valid. The first is that bimolecular processes do not contribute significantly to the observed quenching, as we have already demonstrated for our compounds. The second is a linear dependence of the observed emission intensities on complex concentrations as shown in Equation (2),

$$I_{obs} = I_{[Ru]} + I_{[Ru\text{-}Cu]} = i_{Ru}\,[Ru] + i_{Ru\text{-}Cu}\,[Ru\text{-}Cu] \quad (2)$$

where I_{obs} is the observed emission intensity, i_{Ru} and $i_{Ru\text{-}Cu}$ are the molar intensities of the mono- and bimetallic species, respectively, and [Ru] and [Ru-Cu] are the concentrations of the respective complexes in solution. The simple equation (2) generally applies if the absorbance of the solution is smaller than 0.05 at the excitation wavelength, λ_{exc}. This was the case in our studies at ruthenium concentrations of 2.5×10^{-6} M or lower. However, we repeated our experiments at several concentrations ranging from 2.5×10^{-6} M to 1.0×10^{-4} M and found no significant deviations for the obtained K values.

The validity of Equation (2) allows emission intensities to be treated similar to absorbances. Thus, Equation (3) can be derived which relates log K and the equilibrium concentration of free $[Cu(phen)]^{2+}$ to experimentally accessible luminescence data.

I_0 and I_∞ are the luminescence intensities at [Cu] = 0 and [Cu] = ∞, respectively. Computer programs have been developed for the treatment of absorbance data. We have employed the program PSEQUAD[47] for our evaluation of equilibrium constants. Emission intensities have been used instead of absorbances. The results are summarized in Table 3. Most significant is the observed lower stability of the diaminopropionic acid derivative **1b** compared to the three other compounds with increased spacer lengths. The obtained log K values follow the order **1b** < **2b** ≈ **3b** ≈ **4b** and are smaller than those reported in the literature for binary

Figure 5. a)Titrations of **1a** (□), **2a** (○), **3a** (△), and **4a** (▽) (2.5×10^{-6} M, 3 equiv. NaOMe, methanol) with $[Cu(phen)(NO_3)_2]$ (2.5×10^{-4} M); intensities are relative to the values obtained at [Cu] = 0. – b) Stern–Volmer plot of the titration curves

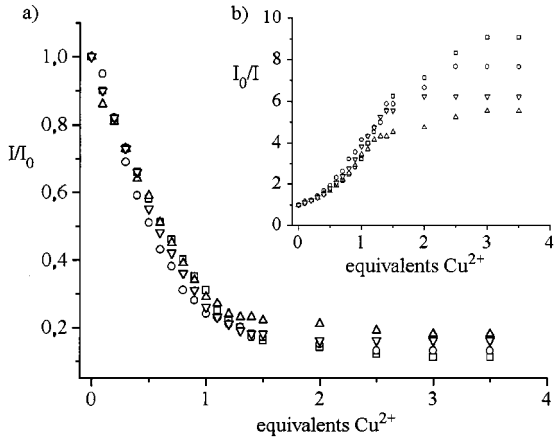

$$\log K + \log [Cu]_{eq} = \log \left(\frac{I_{obs} - I_0}{I_\infty - I_{obs}} \right) \qquad (3)$$

copper complexes of amino acids with uncharged side chains such as $[Cu(Ala)]^+$ (log K = 8.15) or $[Cu(Ile)]^+$ (log K = 8.45).[48]

The electrostatic repulsion between the two positively charged metal ions in our compounds apparently results in a destabilization of the complexes. This explains why **1b** is the least stable derivative in the series since it possesses the shortest alkyl spacer. The differences in stability between the other three compounds are insignificantly small within the experimental errors. This may in part be due to the increased flexibility of the bridges allowing the metal fragments to get closer in space. However, the following discussion of quenching efficiencies in **1b–4b** will support the view that the electrostatic repulsion results in a preference of structures with fully extended alkyl chains.

Table 3. Stability constants of complexes **1b–4b** obtained from luminescence spectra in methanol (c[Ru] = 2.5×10^{-6} M) using the program PSEQUAD[47]

Complex	log K
1b	6.76 ± 0.10
2b	7.30 ± 0.15
3b	7.21 ± 0.25
4b	7.32 ± 0.05

Two factors determine the experimentally observed steady-state luminescence intensities at different copper concentrations. The effect of complex stabilities has been discussed in the previous section. The other factor is how efficiently the ruthenium-based emission is quenched in the dinuclear complexes **1b–4b**. Table 4 shows the fraction of **1b–4b**, $x_{Ru\text{-}Cu}$, present in solution at a Ru/Cu ratio of 1:1, together with the corresponding relative luminescence intensities I/I_0 and $(I/I_0)_{100}$ (I = observed steady state emission intensities, I_0 = emission intensity at [Cu] = 0, $(I/I_0)_{100} = I/I_0$ for $x_{Ru\text{-}Cu} = 1$). The relative intensities $(I/I_0)_{100}$ have been calculated from $x_{Ru\text{-}Cu}$ and I/I_0 according to Equation (4).

$$\left(\frac{I}{I_0} \right)_{100} = \frac{\left(\frac{I}{I_0} \right) - (1 - x_{Ru-Cu})}{x_{Ru-Cu}} \qquad (4)$$

Table 4. Luminescence quenching data of complexes **1b–4b**

Complex	x_{Ru-Cu}[a]	I/I_0[b]	$(I/I_0)_{100}$[c]
1b	0.77	0.31	0.10
2b	0.87	0.24	0.13
3b	0.85	0.29	0.16
4b	0.87	0.26	0.15

[a] Fractions of **1b–4b** in solution at [Ru] = [Cu] = 2.5×10^{-6} M. – [b] I = observed emission intensity, I_0 = observed emission intensity at [Cu] = 0. – [c] Calculated value for I/I_0 at $x_{Ru\text{-}Cu} = 1$.

The data shown in Table 4 confirm a dependence of luminescence intensities on the bridge lengths in **1b–4b**. As would be expected intuitively, quenching is most efficient in compound **1b** with the shortest alkyl chain. $(I/I_0)_{100}$ follows the order **1b** < **2b** < **3b** ≈ **4b**. A slightly smaller number is found for **4b** than for **3b**, but the difference is not significant. Interesting in this context are observations made by Osman and Vogler.[49] These authors studied a series of alkyl-bridged naphthalene-Co^{III} complexes. In contrast to our results, photoinduced electron transfer from naphthalene to Co^{III} was reported to be most efficient in compounds with longer alkyl chains. This has been explained by an increased flexibility of the bridges resulting in reduced donor-acceptor distances. The opposite bridge-length dependence in our complexes therefore supports the statement made above that electrostatic repulsion between Ru^{II} and Cu^{II} forces the alkyl chains in **1b–4b** to adopt a fully extended conformation.

Conclusions

We have designed and synthesized the amino acid bridged heterobimetallic Ru^{II}-Cu^{II} complexes **1b–4b** as potential photoredox-active DNA-binding and -cleaving reagents. The studies described in this report served to clarify several important questions concerning fundamental structure-function relationships in the complexes.

We were able to demonstrate that **1b–4b** are typical supramolecular systems, i.e. the metal fragments retain their individual ground-state properties. This is important for the prediction of DNA-binding properties since the two functional sites are expected to follow different patterns. Luminescence quenching in our systems was shown to occur only intramolecularly indicating that the bridge efficiently mediates special interactions between the metal centers. A marked dependence of the stability constants and quenching efficiencies on the amino acid bridge structures of **1b–4b** was found. The data suggest that the electrostatic repulsion between Ru^{II} and Cu^{II} forces the bridges to adopt a fully extended configuration in solution. These results

provide valuable insight into the structural and functional roles of our amino acid ligands in solution.

Further mechanistic investigations will focus on photoinduced electron- or energy-transfer processes, as well as DNA binding and cleavage studies.

The authors gratefully acknowledge financial support from the *Deutsche Volkswagenstiftung* and the *Deutsche Forschungsgemeinschaft* (Habilitandenstipendium for R. A.). We thank Prof. *R. van Eldik* who generously let us share his equipment, laboratory space, and funding. We also thank Prof. *U. Zenneck* and Prof. *H. Kisch*, Universität Erlangen-Nürnberg, for offering EPR and luminescence-spectrometer capacities.

Experimental Section

General Methods: Spectra were recorded with the following instruments: UV/Vis: Shimadzu UV-2101PC. − NIR (acetonitrile solutions): Cary 5G. − IR (KBr pellets): Mattson Polaris FT IR. − Emission: Perkin Elmer LS 50B. − ^{1}H NMR: Bruker Avance DPX 300. All chemical shifts are referenced to residual solvent signals as internal standards previously referenced to TMS, with high-frequency shifts recorded as positive. − ESR: Bruker ESP 300 E. All spectra were recorded at 77 K in frozen methanol. DPPH radical (g = 2.0036) was used to standardize the klystron frequency. − Elemental analysis: Carlo Erba EA 1106. − Cyclic voltammetry was performed with a PAR potentiostat 263 using a three-electrodes cell with glassy carbon working, Ag/AgCl reference and Pt counter electrodes. Acetonitrile solutions of the complexes containing $TBAPF_6$ (10^{-1} M) as supporting electrolyte were used. $E_{1/2}$ values were calculated from half the difference between E_P values for the anodic and cathodic waves from cyclic voltammograms. The ferrocene-ferrocenium couple was observed at 0.45 V (ΔE_P = 88 mV) in acetonitrile under the measurement conditions. − $RuCl_3$ was a donation from Degussa. The synthesis of the $^{\alpha}N$-^{t}Boc-protected (amino acid)ruthenium(II) complexes [{Ru(bipy)$_2$}m-AA-$^{\alpha}N$-^{t}Boc](PF$_6$)$_2$ ($^{\alpha}N$-^{t}Boc-**1a**−**4a**, AA = DAPA, DABA, Orn, Lys) and [{Ru(bipy)$_2$}m-AA] (PF$_6$)$_3$ is described elsewhere.[17] Reagent-grade solvents were obtained from Roth NMR solvents, and all other chemicals, including [Cu(phen)(NO$_3$)$_2$], from Aldrich. Water for preparations was demineralized.

[{Ru(bipy)$_2$}m-AA{Cu(phen)(H$_2$O)}](PF$_6$)$_3$ (AA = DAPA **1b**, DABA **2b**, Orn **3b**, Lys **4b**). − *General Procedure:* A solution of the respective $^{\alpha}N$-protected (amino acid)ruthenium(II) complex [{Ru(bipy)$_2$}m-AA-$^{\alpha}N$-^{t}Boc](PF$_6$)$_2$ in 4 N HCl/dioxane (10 ml) was stirred at 0°C for 1 h. All solvent and excess HCl were removed by rotary evaporation and the residue dried in vacuo overnight. The resulting amine hydrochloride was dissolved in 15 ml of methanol and deprotonated with a solution of NaOMe (1.5 equiv.) in methanol (c = 10^{-1} M). Solid [Cu(phen)(NO$_3$)$_2$] (1.0 equiv.) was added and the suspension stirred at room temperature for 2 h. After the methanol was removed by rotary evaporation, the product was dissolved in 10 ml of water and precipitated with a 1.5-fold excess of NH_4PF_6 in 1 ml of water. The brown-orange suspension was stirred for 2 h and then the precipitate was isolated by filtration, washed three times with small amounts of water and dried in a desiccator over silica gel. The so obtained products contained varying amounts of water.

[{Ru(bipy)$_2$}m-DAPA{Cu(phen)(H$_2$O)}](PF$_6$)$_3$ (**1b**): Yield: 219 mg (78%). − $C_{47}H_{41}CuF_{18}N_{10}O_4P_3Ru \cdot H_2O$ (1409.4·H$_2$O): calcd. C 39.55, H 3.04, N 9.81; found C 39.66, H 3.17, N 9.53. − ^{1}H NMR (300 MHz, CD_3OD, all signals broad): δ = 2.59 (s, 3 H, m4′-CH_3); 7.35 (s, 1 H, m5′); 7.47 (s, 4 H, b5); 7.62 (d, 1 H, m5); 7.79−7.94 (m, 6 H, 4 × b6, m6, m6′); 8.09 (m, 4 H, b4); 8.63 (m, 5 H, 4 × b3, m3′). − IR (KBr): ν = 3115 cm^{-1} (m), 3087 (m), 2930 (m), 1650 (s, COO$^-$), 1542 (m), 1465 (m), 1431 (m), 1312 (m), 1270 (m), 1239 (m), 1107 (m), 843 (vs, PF_6^-), 766 (s), 727 (m), 558 (s). − UV/Vis (CH_3OH): λ_{max} (lg ε) = 455 nm (4.22), 288 (4.96), 256 (4.66).

[{Ru(bipy)$_2$}m-DABA{Cu(phen)(H$_2$O)}](PF$_6$)$_3$ (**2b**): Yield: 225 mg (79%). − $C_{48}H_{43}CuF_{18}N_{10}O_4P_3Ru \cdot 0.5\ H_2O$ (1423.4·0.5 H$_2$O): calcd. C 40.25, H 3.09, N 9.78; found C 40.28, H 2.80, N 9.67. − ^{1}H NMR (300 MHz, CD_3OD, all signals broad): δ = 2.59 (s, 3 H, m4′-CH_3); 7.36 (s, 1 H, m5′); 7.48 (s, 4 H, b5); 7.62 (s, 1 H, m5); 7.80 (d, 5 H, 4 × b6, m6′); 7.92 (m, 1 H, m6); 8.11 (s, 4 H, b4); 8.64 (t, 5 H, 4 × b3, m3′); 8.97 (d, 1 H, m3). − IR (KBr): ν = 3084 cm^{-1} (m), 2928 (m), 2862 (m), 1650 (s, COO$^-$), 1541 (m), 1463 (m), 1432 (m), 1400 (m), 1313 (m), 1270 (m), 1239 (m), 1107 (m), 842 (vs, PF_6^-), 766 (s), 727 (m), 558 (s). − UV/Vis (CH_3OH): λ_{max} (lg ε) = 455 nm (4.17), 288 (4.90), 256 (4.61).

[{Ru(bipy)$_2$}m-Orn{Cu(phen)(H$_2$O)}](PF$_6$)$_3$ (**3b**): Yield: 232 mg (81%). − $C_{49}H_{45}CuF_{18}N_{10}O_4P_3Ru$ (1437.5): calcd. C 40.97, H 3.09, N 9.74; found C 41.18, H 3.09, N 9.57. − ^{1}H NMR (300 MHz, CD_3OD, all signals broad): δ = 2.59 (s, 3 H, m4′-CH_3); 7.35 (d, 1 H, m5′); 7.47 (m, 4 H, b5); 7.61 (m, 1 H, m5); 7.79 (m, 5 H, 4 × b6, m6′); 7.92 (m, 1 H, m6); 8.09 (m, 4 H, b4); 8.64 (t, 5 H, 4 × b3, m3′); 8.95 (s, 1 H, m3). − IR (KBr): ν = 3086 cm^{-1} (m), 2930 (m), 2869 (m), 2862 (m), 1650 (s, COO$^-$), 1542 (m), 1465 (m), 1444 (m), 1431 (m), 1392 (m), 1312 (m), 1270 (m), 1239 (m), 1107 (m), 844 (vs, PF_6^-), 766 (s), 727 (m), 558 (s). − UV/Vis (CH_3OH): λ_{max} (lg ε) = 455 nm (4.22), 287 (4.94), 256 (4.64).

[{Ru(bipy)$_2$}m-Lys{Cu(phen)(H$_2$O)}](PF$_6$)$_3$ (**4b**): Yield: 296 mg (68%). − $C_{50}H_{47}CuF_{18}N_{10}O_4P_3Ru \cdot 2.5\ H_2O$ (1451.5·2.5 H$_2$O): calcd. C 40.13, H 3.50, N 9.36; found C 40.05, H 3.26, N 9.21. − ^{1}H NMR (300 MHz, CD_3OD, all signals broad): δ = 2.59 (s, 3 H, m4′-CH_3); 7.34 (s, 1 H, m5′); 7.47 (s, 4 H, b5); 7.60 (s, 1 H, m5); 7.79 (s, 5 H, 4 × b6, m6′); 7.91 (s, 1 H, m6); 8.10 (s, 4 H, b4); 8.66 (s, 5 H, 4 × b3, m3′); 8.95 (d, 1 H, m3). − IR (KBr): ν = 3080 cm^{-1} (m), 2930 (m), 2869 (m), 1650 (s, COO$^-$), 1542 (m), 1465 (m), 1445 (m), 1432 (m), 1312 (m), 1271 (m), 1239 (m), 1107 (m), 842 (vs, PF_6^-), 766 (s), 728 (m), 558 (s). − UV/Vis (CH_3OH): λ_{max} (lg ε) = 455 nm (4.25), 288 (4.96), 255 (4.64).

Titration Curves: Emission titration curves were followed by uncorrected luminescence spectra obtained with a Perkin Elmer LS 50B spectrophotometer (λ_{exc} = 400 nm, λ_{obs} = 500−690 nm). 25 ml of 2.5−10 × 10^{-6} M solutions of the complexes [{Ru(bipy)$_2$}m-AA](PF$_6$)$_3$ in methanol, containing 3.0 equiv. of NaOMe to yield the deprotonated complex form, were titrated with 2.5−10 × 10^{-4} M solutions of [Cu(phen)(NO$_3$)$_2$] in methanol. The solutions were deaerated by bubbling with dry nitrogen for at least 10 min prior to each measurement. The results were evaluated using the program PSEQUAD.[47]

[1] A. J. Bard, M. A. Fox, *Acc. Chem. Res.* **1995**, *28*, 141−145.
[2] T. J. Meyer, *Acc. Chem. Res.* **1989**, *22*, 163−170.
[3] V. Balzani, A. Juris, M. Venturi, S. Campagna, S. Serroni, *Chem. Rev.* **1996**, *96*, 759−833.
[4] M. A. Fox, M. Chanon, *Photoinduced Electron Transfer Reactions*, Elsevier, Amsterdam, **1988**, part D.
[5] E. Kimura, X. Bu, M. Shionoya, S. Wada, S. Maruyama, *Inorg. Chem.* **1992**, *31*, 4542−4546.
[6] E. Kimura, S. Wada, M. Shionoya, Y. Okazaki, *Inorg. Chem.* **1994**, *33*, 770−778.
[7] R. Alsfasser, R. van Eldik, *Inorg. Chem.* **1996**, *35*, 628−636.
[8] D. S. Sigman, D. R. Graham, V. D′Aurora, A. M. Stern, *J. Biol. Chem.* **1979**, *254*, 12269−12272.
[9] D. S. Sigman, *Acc. Chem. Res.* **1986**, *19*, 180−186.

[10] T. B. Therderahn, M. D. Kuwabara, T. A. Larsen, D. S. Sigman, *J. Am. Chem. Soc.* **1989**, *111*, 4941−4946.
[11] T. C. Strekas, A. D. Baker, O. Harripersad-Morgan, *J. Coord. Chem.* **1997**, *34*, 77−85.
[12] A. M. Pyle, J. P. Rehmann, R. Meshoyrer, C. V. Kumar, N. J. Turro, J. K. Barton, *J. Am. Chem. Soc.* **1989**, *111*, 3051−3058.
[13] A. Kirsch-De Mesmaeker, J.-P. Lecomte, J. M. Kelly, *Top. Curr. Chem.* **1995**, *177*, 25−76.
[14] R. Tamilarasan, D. R. McMillin, *Inorg. Chem.* **1990**, *29*, 2798−2802.
[15] M. Milkevitch, H. Storrie, E. Brauns, K. J. Brewer, B. W. Shirley, *Inorg. Chem.* **1997**, *36*, 4534−4538.
[16] B. M. Peek, G. T. Ross, S. W. Edwards, G. J. Meyer, T. J. Meyer, B. W. Erickson, *Int. J. Pept. Protein Res.* **1991**, *38*, 114−123.
[17] B. Geißer, A. Ponce, J. R. Winkler, R. Alsfasser, manuscript in preparation.
[18] S. L. Mecklenburg, D. G. McCafferty, J. R. Schoonover, B. M. Peek, B. W. Erickson, T. J. Meyer, *Inorg. Chem.* **1994**, *33*, 2974−2983.
[19] R. S. Drago, *Physical Methods for Chemists*, 2nd ed., Saunders College Publishing, Ft. Worth, **1977**, chapter 12.
[20] R. J. Abraham, J. Fisher, P. Loftus, *Introduction to NMR Spectroscopy*, 2nd ed., John Wiley and Sons, Chichester, New York, Brisbane, Toronto, Singapore, **1993**.
[21] B. J. Hathaway, A. A. G. Tomlinson, *Coord. Chem. Rev.* **1970**, *5*, 1.
[22] B. J. Hathaway in *Comprehensive Coordination Chemistry* (Eds.: S. G. Wilkinson, R. D. Gillard, J. A. McCleverty), Pergamon Press, Oxford, **1987**, vol. 5, chapter 53.
[23] S. V. Deshpande, T. S. Srivastava, *Inorg. Chim. Acta* **1983**, *78*, 75−80.
[24] K. Kalyanasundaram, *Coord. Chem. Rev.* **1982**, *46*, 159−244.
[25] A. Juris, V. Balzani, F. Barigelletti, S. Campagna, P. Belser, A. von Zelewsky, *Coord. Chem. Rev.* **1988**, *84*, 85−277.
[26] M. J. Root, B. P. Sullivan, T. J. Meyer, E. Deutsch, *Inorg. Chem.* **1985**, *24*, 2731−2739.
[27] N. Sutin, *Prog. Inorg. Chem.* **1983**, *30*, 441.
[28] N. S. Hush, *Electrochim. Acta* **1968**, *13*, 1005.
[29] C. Creutz, *Prog. Inorg. Chem.* **1983**, *30*, 1.
[30] It should be noted out that one of the referees suggested that the intervalence bands for our compounds may appear at higher energies in the visible range of the spectrum where they could be obscured by other absorptions. This is possible since the reorganization energies should be large, as will be discussed in the following section. The compounds would then belong to the Robin−Day class II.
[31] M. B. Robin, P. Day, *Adv. Inorg. Chem. Radiochem.* **1967**, *10*, 247−422.
[32] R. Sahai, D. A. Baucom, D. P. Rillema, *Inorg. Chem.* **1986**, *25*, 3843−3845.
[33] F. Scandola, C. A. Bignozzi, M. T. Indelli in *Photosensitization and Photocatalysis Using Inorganic and Organometallic Compounds* (Eds.: K. Kalyanasundaram, M. Grätzel), Kluwer Academic Publishers, Dordrecht, Boston, London, **1993**, vol. 14, p. 161−216.
[34] Y. Yao, M. W. Perkovic, D. P. Rillema, C. Woods, *Inorg. Chem.* **1992**, *31*, 3956−3962.
[35] M. A. Masood, D. J. Hodgson, *Inorg. Chem.* **1993**, *32*, 4839−4844.
[36] C.-W. Lee, F. C. Anson, *Inorg. Chem.* **1984**, *23*, 837−844.
[37] M. A. Augustin, J. K. Yandell, *Inorg. Chem.* **1979**, *18*, 577−583.
[38] K. M. Davies, *Inorg. Chem.* **1983**, *22*, 615−619.
[39] C.-W. Lee, F. C. Anson, *J. Phys. Chem.* **1983**, *87*, 3360−3362.
[40] K. Kalyanasundaram in *Photosensitization and Photocatalysis Using Inorganic and Organometallic Compounds* (Eds.: K. Kalyanasundaram, M. Grätzel), Kluwer Academic Publishers, Dordrecht, Boston, London, **1993**, vol. 14, p. 113−160.
[41] W. F. Wacholtz, R. A. Auerbach, R. H. Schmehl, *Inorg. Chem.* **1987**, *26*, 2989−2994.
[42] H. G. O. Becker, *Einführung in die Photochemie*, 3. Auflage, Deutscher Verlag der Wissenschaften, Berlin, **1991**, chapter 4.3.
[43] V. Balzani, M. Meastri in *Photosensitization and Photocatalysis Using Inorganic and Organometallic Compounds* (Eds.: K. Kalyanasundaram, M. Grätzel), Kluwer Academic Publishers, Dordrecht, Boston, London, **1993**, vol. 14, p. 15−70.
[44] R. H. Schmehl, R. A. Auerbach, W. F. Wacholtz, C. M. Elliott, R. A. Freitag, J. W. Merkert, *Inorg. Chem.* **1986**, *25*, 2440−2445.
[45] J. Polster, H. Lachmann, *Spectrometric Titrations*, VCH, Weinheim, **1989**, p. 344.
[46] A. M. Josceanu, P. Moore, S. C. Rawle, P. Sheldon, S. M. Smith, *Inorg. Chim. Acta* **1995**, *240*, 159−168.
[47] L. Zekany, I. Nagypal, G. Peintler, *PSEQUAD*, University Szeged, **1990**.
[48] S. H. Laurie in *Comprehensive Coordination Chemistry* (Eds.: S. G. Wilkinson, R. D. Gillard, J. A. McCleverty), Pergamon Press, Oxford, **1987**, vol. 2, chapter 20.2.
[49] A. H. Osman, A. Vogler in *Photochemistry and Photophysics of Coordination Compounds* (Eds.: H. Yersin, A. Vogler), Springer Verlag, Berlin, Heidelberg, **1997**, p. 197−203.

[97308]

Substituted Cyclopentadienides of Magnesium from the Reaction of Dialkyl Magnesium with Fulvenes

Matthias Westerhausen*, Nikolaos Makropoulos, Birgit Wieneke, Konstantin Karaghiosoff, Heinrich Nöth[+], Holger Schwenk-Kircher[+], Jörg Knizek[+], and Thomas Seifert[+]

Institut für Anorganische Chemie der Ludwig-Maximilians-Universität,
Meiserstr. 1, D-80333 München, Germany
Fax: +49 (0)89 / 5902 578
E-mail: maw@anorg.chemie.uni-muenchen.de

Received January 30, 1997

Keywords: Cyclopentadienes / Magnesium / Metalations / NMR spectroscopy / Sandwich complexes

The reaction of *n*/*sec*-dibutyl magnesium with 6-methyl-6-phenyl- and 6,6-dicyclopropylfulvene gives the β-hydride transfer products 1,1′-bis(1-phenylethyl)- and 1,1′-bis-(dicyclopropylmethyl)magnesocene, respectively. The latter crystallizes in the eclipsed conformation, whereas the first one shows an *anti* conformation in the solid state. Dimethylmagnesium deprotonates 6-methyl-6-phenylfulvene with formation of 1,1′-bis(1-phenylethen-1-yl)magnesocene, which decomposes upon isolation. The deprotonation of 6,6-dicyclopropylfulvene with $MgMe_2$ in thf solution yields [bis(tetrahydrofuran-*O*)]iro{cyclopropane-1,2′(1′-η^5-cyclopentadienyl-1′,3′,3′-tricyclopropyl-1′,2′,3′,3a′-tetrahydropenalene)}-3a′-6′-η^2-enyl]magnesium. In the absence of β-hydrogen atoms at the organometallic reagent as well as at the fulvene the addition reaction is the only possible reaction pathway. Thus, one Mg−C bond of $MgMe_2$ adds to tetramethylfulvene to give quantitatively dimeric methylmagnesium ethyltetramethylcyclopentadienide. The bridging methyl groups are sterically shielded against further attack of the fulvene.

The metalation of 6-methyl-6-phenylfulvene with calcium bis[bis(trimethylsilyl)amide] in tetrahydrofuran yields the bis(thf) complex of 1,1′-bis(1-phenyl-1-ethenyl)calcocene.[1] The bis(trimethylsilyl)amides of strontium and barium react in the same manner.[2] Enhancement of the ring strain leads to extended reaction periods. Therefore, the reaction of $(thf)_2Ca[N(SiMe_3)_2]_2$ with two equivalents of 6,6-dicyclopropylfulvene according to Eq. (1) needs several days even at elevated temperatures,[3] however, the yield of 1,1′-bis-(cyclopropylcyclopropylidenemethyl)calcocene is only moderate. The cyclopentadienide fragments and the alkenyl groups show no electronic interaction, free rotation around the C−C bond between these moieties is observed. An addition of the Ca−N bond to the fulvene has never been observed. In contrast to these findings, the addition of methyl lithium to 6,6-dimethylfulvene gives tert.-butylcyclopentadienyllithium,[4] whereas sterically demanding nucleophiles favor the metalation reaction. For example, lithium diisopropylamide metalates (α-deprotonates) fulvenes in tetrahydrofuran to alkenylcyclopentadienyllithium.[5] Erker and coworkers[5g] investigated the dependency of this reaction on the solvent and observed in diethylether a β-hydride transfer from alkyl lithium to the fulvenes. Based on the investigations of Fischer and coworkers[6a] addition reactions of anionic nucleophiles such as methyllithium, potassium diphenylphosphanide or sodium cyclopentadienide to 6,6-dimethylfulvene as well as the corresponding chromium tri(carbonyl) complex were reported by Edelmann et al.[6b][6c]

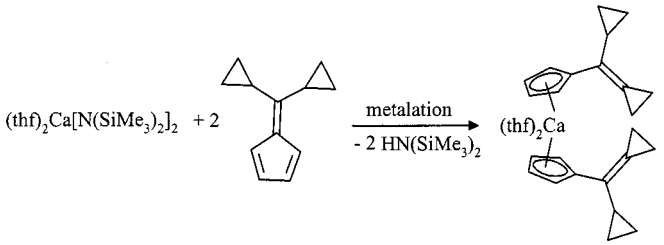

We were interested in the synthesis of magnesocenes by the reaction of halogen-free magnesium compounds with fulvenes to compare the magnesocenes with the heavier homologues. In contrast to calcium bis[bis(trimethylsilyl)-amide], the homologous magnesium bis(amide)[7] does not react with fulvenes. Although a monomer-dimer equilibrium is observed for $Mg[N(SiMe_3)_2]_2$ in toluene solution,[8a] the X-ray structure reveals the steric shielding of the Mg−N bonds of the dimer in the solid state.[8b] Due to a large cone angle of the bis(trimethylsilyl)amide substituent,[9] even in the monomer the metal center is not accessible to fulvenes. Therefore, we investigated the reactivity of dimethylmagnesium as well as commercially available *n*/*sec*-dibutylmagnesium towards 6-methyl-6-phenyl- and 6,6-dicyclopropylfulvene. The reductive coupling of 6,6-dimethylfulvene with magnesium, calcium or strontium in the presence of a catalytic amount of $HgCl_2$ gives the corresponding *ansa*-alkaline earth metallocenes in a good yield,[10] however, our interest was centered on protonation and deprotonation reactions with fulvenes and we could show that not only the substituents at the fulvene and the

[+] X-ray structure determinations.

 © WILEY-VCH Verlag GmbH, D-69451 Weinheim, 1998 1434−1948/98/0707−0965 $ 17.50+.50/0

metal led to different reaction products but that the size of the alkaline earth metal influenced the reaction pathway.

Synthesis

The reaction of dimethylmagnesium[11] with 6-methyl-6-phenylfulvene yields nearly quantitatively the metalation product 1,1′-bis(1-phenyl-1-ethenyl)magnesocene **1** according to Eq. (2). The ^{1}H- and ^{13}C{^{1}H}-NMR spectra are very similar to those of the heavier homologous alkaline earth metallocenes of calcium,[1] strontium and barium.[2] In Table 1 characteristic resonances are listed in comparison to the corresponding calcocene[1] and lithium derivative.[6] An isolation of **1** failed due to decomposition upon isolation. The use of butyl ligands instead of methyl groups leads to a β-hydride transfer from *n*/*sec*-dibutyl magnesium to 6-methyl-6-phenylfulvene and to the elimination of butene in a good yield. Butene was collected during the reaction and identified by IR spectroscopy. 1,1′-Bis(1-phenyl-1-ethyl)magnesocene **2** is a colorless, moisture-sensitive solid. Freshly prepared magnesium dihydride does not react with fulvenes to give 1,1′-dialkylmagnesocenes, therefore, β-hydride transfer reactions of *n*/*sec*-dibutyl magnesium with cyclic transition states as already known[12] are proposed.

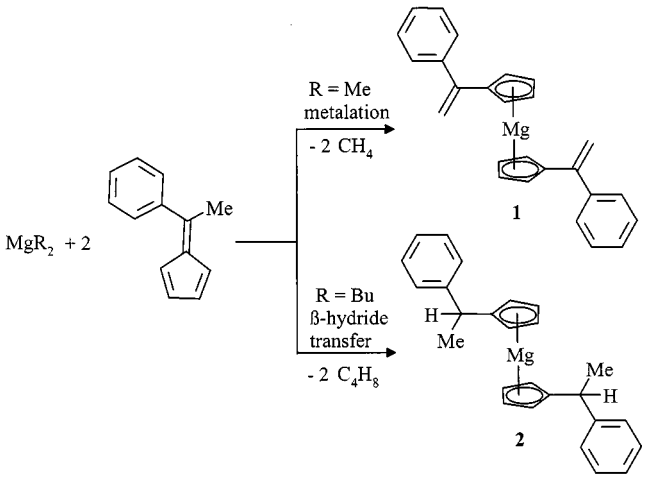

Table 1. Comparison of the NMR parameters of the homoleptic 1-phenylethen-1-ylcyclopentadienides of lithium, magnesium (**1**), and calcium (Cp′ = H_4C_5-C(=CH_2)Ph)

	LiCp′[5g]	$MgCp'_2$ (**1**)	$(thf)_2CaCp'_2$[1]
^{1}H NMR			
δ(=CH_2)	4.71, 5.30	4.92, 5.47	4.73, 5.23
^2J(H,H)	2.7	2.4	2.3
δ(C_5H_4)	5.94, 6.07	6.03, 6.28	5.79, 5.95
δ(Ph)	7.10−7.30, 7.65	7.6−7.7	7.2−7.5
^{13}C NMR			
δ(=CH_2)	101.9	105.03	104.57
^1J(C,H)	155	156	156.4
δ(C=CH_2)	149.5	147.74	148.54
δ(*i*-C/Cp)	120.5	122.13	123.13
δ(CH, Cp)	105.0, 105.1	103.69, 106.26	108.52, 108.70
δ(Ph)	126.6	126.64	127.32
δ(Ph)	127.6	127.52	128.06
δ(Ph)	129.2	128.83	129.30
δ(*i*-C, Ph)	146.1	144.78	145.21

These different reaction behaviors of dimethyl- and dibutylmagnesium allows the synthesis of two different compounds **1** and **2** without impurities stemming from the other reaction type.

To compare the reactivity of dimethyl- and dibutylmagnesium with the reactivity of $(thf)_2Ca[N(SiMe_3)_2]_2$ both the dialkylmagnesium compounds were reacted with 6,6-dicyclopropylfulvene. The calcium derivative metalates the fulvene and 1,1′-bis(cyclopropylcyclopropylidenmethyl)calcocene was isolated.[3] The use of *n*/*sec*-dibutylmagnesium gives quantitatively the β-hydride transfer product 1,1′-bis(dicyclopropylmethyl)magnesocene **3** [Eq. (3)]. Dimethylmagnesium on the other hand reacts with dicyclopropylfulvene in a completely different and unexpected manner. During the reaction methane is eliminated, however, the NMR parameters showed no similarities to the product obtained from the metalation with the above mentioned calcium bis(amide).

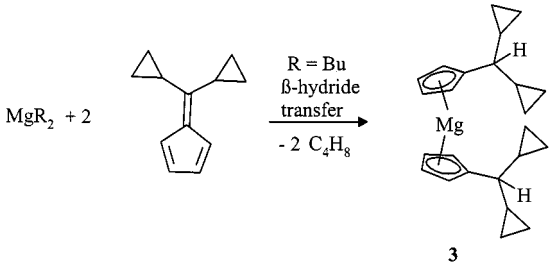

Eq. (4) describes the formation of [bis(tetrahydrofuran-*O*)]spiro{cyclopropane-1,2′(1′-η^5-cyclopentadienyl-1′,3′,3′-tricyclopropyl-1′,2′,3′,3a′-tetrahydropentalene)}-3a′-6′-η^2-enyl]magnesium **4** and proposes a reaction mechanism. The first step is the metalation of 6,6-dicyclopropylfulvene as also observed for the reaction of calcium bis[bis(trimethylsilyl)amide] according to Eq. (1).[3] This step is supported by the solvent-dependent studies of Erker and coworkers[5g] who found in tetrahydrofuran a favoring of the α-deprotonation against a β-hydride transfer. The ring strain of the thus formed cyclopropylidene fragment is released by the reaction with another molecule of 6,6-dicyclopropylfulvene. The second methyl nucleophil at the magnesium atom metalates the cyclopentadienyl moiety, a ring closure follows and a bis(cyclopentadienyl)magnesium derivative forms. Due to the enforced orientation of the cyclopentadienyl groups to each other, the aromatic fragments are not coplanar and two thf molecules occupy the coordination gap at the alkaline earth metal center. A rather similar mechanism was suggested to explain the reaction of sodium cyclopentadienide with 6,6-dimethylfulvene.[13]

Further enhancement of ring strain during the formation of an alkenyl substituted magnesocene prevents a metalation (α-deprotonation) of the fulvene. Therefore, dimethylmagnesium shows no reaction with cyclopentadienylideneadamantane.[14] The absence of α-CH moieties in the fulvene molecule would enforce another reaction mechanism, because the formation of an alkenylcyclopentadienyl substituent as an intermediate is impossible. Consequently, also 6,6-diphenylfulvene[15] does not react with $MgMe_2$. An-

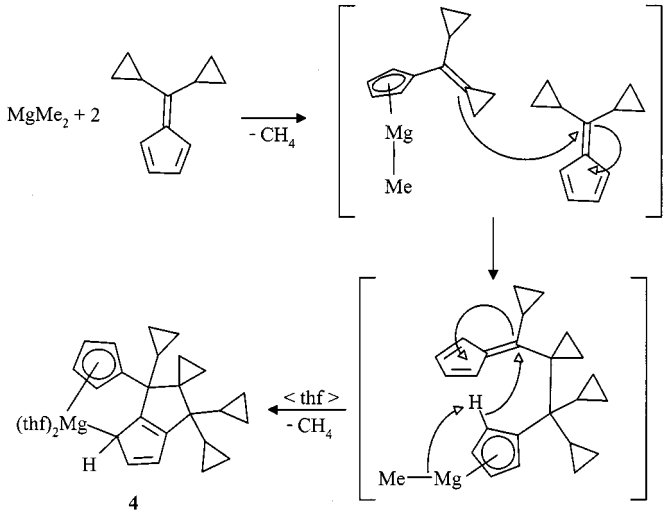

4

other conceivable reaction pathway would be the addition of a Mg-Me bond to the exocyclic C=C double bond of 6,6-diphenylfulvene, however, this reaction was not observed, probably due to steric reasons.

The reaction of dimethylmagnesium with tetramethylfulvene only allows the addition reaction, because the requirements for a β-hydride transfer reaction as well as for a α-deprotonation of the fulvene are not given. In the presence of Lewis bases such as thf and 1,4-dioxane the addition of one methyl substituent to tetramethylfulvene yields the tetrahydrofuran complex of bis(η^5-ethyltetramethylcyclopentadienyl)dimethyldimagnesium **5**. Due to the coordination of a thf molecule to the metal center and the formation of a four-membered Mg_2C_2 cycle the methylmagnesium moiety is sterically too shielded for an addition reaction to an additional molecule of tetramethylfulvene.

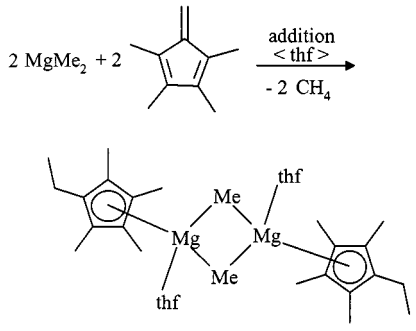

5

Heteroleptic cyclopentadienylmagnesium derivatives are well known since decades. The diethylether and tetrahydrofuran adducts of the halides RMgX are dimeric with a central Mg_2X_2 cycle[16][17] whereas the addition of tmeda yields monomeric complexes.[18] The Schlenk equilibrium interconverts Cp′MgX into magnesium dihalides and magnesocens.[19] Methylmagnesium cyclopentadienide is dimeric via methyl bridges as confirmed by IR spectroscopy,[20] however, diethyl ether leads to a partial cleavage of the dimer, whereas thf and tmeda cleave the methyl bridges completely.[20][21] In contrast to these findings neither the reaction of compound **5** with additional tetramethylfulvene occurs nor redistribution reactions to the homoleptic dimethylmagnesium and the substituted magnesocene are observable even in the presence of Lewis bases such as thf.

Molecular Structures

The alkaline earth metallocenes gained interest not only for their synthetic potential but moreover quite unusual solid state structures[22] led to theoretical investigations.[23] Although numerous magnesocenes are characterized by X-ray structure determinations we describe the molecular structures of **2** to **5**, however, only **2** and **3** show the characteristic sandwich structure. Figure 1 und 2 show the molecular structures and numbering schemes of **2** and **3**, respectively. The crystallographic inversion center in the structure of **2** lies on the magnesium atom and therefore, a *anti*-configuration of the alkyl substituents is enforced (Figure 3). The Mg−C bond lengths differ between 230.0 and 231.6 pm and the distance between Mg and the center Z of the cyclopentadienyl moiety lies at 198 pm. The molecular structure of **3** shows an eclipsed-conformation (Figure 3). This arrangement leads to steric repulsion between the dicyclopropylmethyl groups. As a consequence, the Z1−Mg−Z2 angle of 176.3° shows a small deviation from linearity and furthermore, the deviation from coplanarity of the cyclopentadienyl ligands amounts 4.4°.

Figure 1. Molecular structure and numbering scheme of **2**; symmetry-related atoms are marked by an apostrophe. Thermal ellipsoids are drawn at a 40% probability level[a]

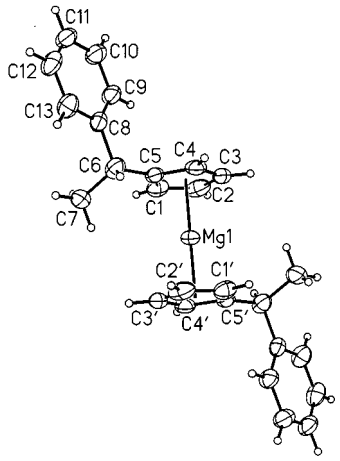

[a] Selected bond lengths [pm]: Mg1−C1 230.8(2), Mg1−C2 231.5(2), Mg1−C3 231.0(2), Mg1−C4 230.0(2), Mg1−C5 231.6(2), C1−C2 140.5(4), C1−C5 140.8(3), C2−C3 137.9(4), C3−C4 139.0(3), C4−C5 140.0(3), C5−C6 151.3(3), C6−C7 151.2(4), C6−C8 153.1(3).

Magnesocene $Mg(C_5H_5)_2$ shows Mg−C distances of 230.4[24] and 233.9 pm[25] in the solid state and the gas phase, respectively. In contrast to the antiprismatic (staggered) conformation in the crystalline state an eclipsed (prismatic) structure is found in the gas phase. A linear arrangement is also observed for 1,1′-di-*tert*-butylmagnesocene[26] with an average Mg−C bond length of 233.6 pm. Intramolecular steric repulsion leads to a bending of hexakis(trimethylsilyl)magnesocene.[27] In contrast to these

Figure 2. Molecular structure and numbering scheme of **3**; thermal ellipsoids are drawn at a 40% probability level[a]

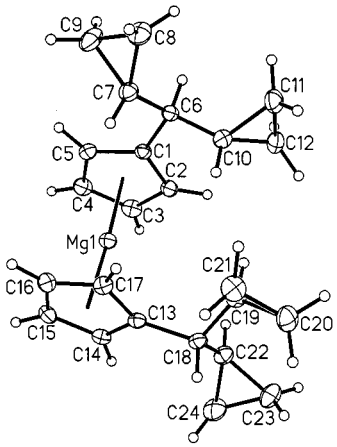

[a] Selected bond lengths [pm]: Mg1−C1 235.7(2), Mg1−C2 232.2(2), Mg1−C3 231.8(2), Mg1−C4 233.1(2), Mg1−C5 234.6(2), Mg1−C13 235.8(2), Mg1−C14 233.9(2), Mg1−C15 231.8(2), Mg1−C16 230.9(2), Mg1−C17 231.8(2), C1−C2 142.7(2), C1−C5 142.4(2), C1−C6 151.5(3), C2−C3 141.3(3), C3−C4 141.0(3), C4−C5 141.1(3), C13−C14 141.7(3), C13−C17 142.6(2), C13−C18 152.2(2), C14−C15 141.4(2), C15−C16 140.2(3), C16−C17 141.9(3).

Figure 3. Comparison of the conformations of **2** (left) and **3** (right) with a view perpendicular to the cyclopentadienide ligands; the carbon atoms are drawn with arbitrary radii and the hydrogen atoms omitted for clarity. The magnesium atoms are drawn at a 40% probability level.

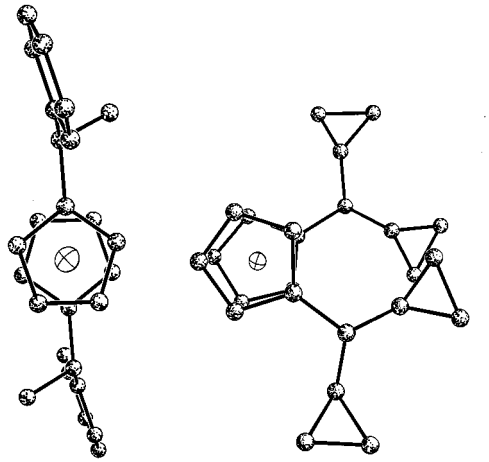

monomeric magnesocenes bis(indenyl)magnesium exhibits infinite chains with bridging and terminal indenyl substituents[28] bonded in η^1, η^2, or η^5 fashion.

The asymmetric unit of the crystal structure of **4** consists of two independent molecules. These two molecules are distinguished by the first number $n = 1$ or 2 following the element symbol. Due to the similar constitution the discussion of the molecular structure is limited to the molecule with $n = 1$ shown in Figure 4. The magnesium atom is η^5-bonded to the cyclopentadienyl fragment and the magnesium−carbon distances vary between 237.4 and 252.2 pm. Due to the rather unflexible backbone of the carbdianionic ligand the tetrahydropentalene unit acts as a η^2-bonded substituent with a short Mg1−C192 bond length of 227.2 pm, whereas the distance to the neighboring atom C191 is approximately 40 pm larger. Nevertheless, a delocalization of the double bonds within this five-membered cycle exists because the bonds C19−C191 (137.2 pm) and C193−C194 (139.1 pm) are only approximately 4 pm shorter than the other endocyclic C−C bonds with values of 141.0, 141.8, and 143.7 pm. In this molecule there are three neighboring quarternary carbon atoms C16, C17, and C18. Due to the steric repulsion, the C−C distances of these carbon atoms are unusual large (157.0 and 158.2 pm).

Figure 4. Molecular structure und numbering scheme of **4**; thermal ellipsoids are drawn at a 40% probability level. The hydrogen atoms are omitted for clarity[a]

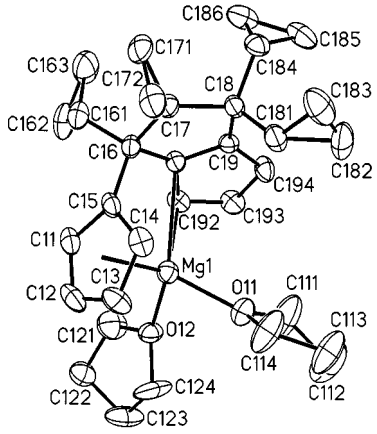

[a] Selected bond lengths [pm]: Mg1−O11 203.7(3), Mg1−O12 204.5(3), Mg1−C11 246.5(5), Mg1−C12 252.2(5), Mg1−C13 247.4(5), Mg1−C14 237.4(4), Mg1−C15 238.7(4), Mg1−C191 265.8(4), Mg1−C192 227.2(4).

The Mg−O bond lengths of 204 pm to the coordinated tetrahydrofuran molecules lie within the characteristic range and depend on the degree of steric strain. They are also influenced by the coordination number of the metal center; a comparison with published data[29] account for four to five-fold coordinated magnesium centers. Moreover, the Mg1−C192 bond length lies in the characteristic range for Mg−C σ bonds of a four or five-fold coordinated metal center[29] as for example in $(Et_2O)_2Mg(Br)CPh_3$ (225 pm[30]) and the anthracenyl derivatives $(thf)_3Mg(An)_2$ (229 pm[30]).

The molecular structure of **5** as well as the numbering scheme is represented in Figure 5. Symmetry related atoms are marked with an apostroph. The isotropic refinement of the methyl hydrogen atoms was successful and therefore, these H atoms are included in Figure 5. Bridging methyl substituents were also found in solvent-free dimethylmagnesium.[31]

Figure 5 shows the dimeric molecule of ethyltetramethylcyclopentadienylmagnesium methanide **5**. The methyl group bridges the magnesium atoms, the Mg−C bonds amount 227.0 and 228.5 pm. In polymeric dimethyl-[31] and diethylmagnesium[32] similar Mg−C distances of 224 and 226 pm were observed by Weiss. The magnesate anion

Figure 5. Molecular structure und numbering scheme of **5**; thermal ellipsoids are drawn at a 40% probability level. Only the hydrogen atoms of the bridging methyl substituents are represented[a]

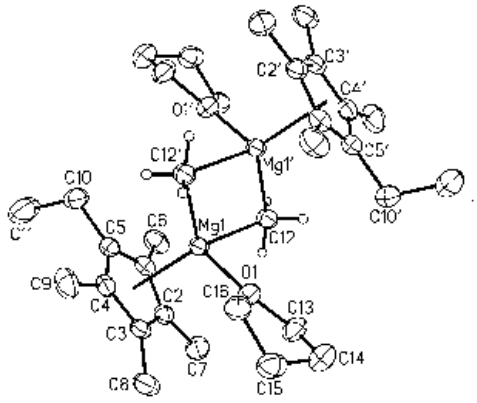

[a] Selected bond lengths [pm] and angles [°]: Mg1−O1 209.2(2), Mg1−C1 242.7(2), Mg1−C2 246.9(2), Mg1−C3 251.2(2), Mg1−C4 248.4(2), Mg1−C5 243.8(2), Mg1−C12 228.5(2), Mg1···Mg1′ 280.96(12), O1−Mg1−C12 94.22(8), O1−Mg1−C12′ 96.02(8), C12−Mg1−C12′ 103.82(7), Mg1−C12−Mg1′ 76.18(7).

$[Mg_3Me_8]^{2-}$ is best described as a tetramethylmagnesate dianion, where two methyl groups are bridged by $MgMe_2$ units.[33] The central Mg−C bond lengths lie in the expected region of approximately 224 pm, whereas the bonds between the outer magnesium atoms and the bridging methyl groups are more than 10 pm longer. Terminally bonded methyl groups show approximately 10 pm shorter Mg−C bond lengths.[21]

NMR Spectroscopic Characterization

The comparison of the NMR data of **1** with those of 1-phenylethen-1-ylcyclopentadienyllithium[6] and bis(tetrahydrofuran-*O*)calcium bis(1-phenylethen-1-ylcyclopentadienide)[1] shows nearly no dependency on the nature of the metal atom. On the other hand the composition of **1** can be proven by these NMR data which are listed in Table 1. Similar findings also hold for **2** and the corresponding lithium derivative.[6]

A different situation is observed for **4**. Whereas the aromatic CH protons of the cyclopentadienyl moiety of the lithium derivative show an AA′XX′coupling pattern, the ^{1}H-NMR spectrum of **4** is more complicated due to the fixed geometry of this fragment in regard of the rotation around the C−C bond between the cyclopentadienyl and the tetrahydropentalene units. Furthermore, large differences in the chemical shifts of the CH groups of the pentalene fragment are observed. This can be explained by the mainly η^2-coordination of the pentalene unit to magnesium in **4** whereas lithium forms a η^5-complex. The chemical $^{13}C\{^1H\}$ and ^{1}H shifts of the magnesium-bonded fragment (C192 in Figure 4) are δ = 75.1 and 4.6, respectively. The other CH fragments show values of approximately δ = 110 for the carbon (C193 and C194 in Figure 4) and δ = 6 for the ^{1}H nuclei.

The characteristic feature in the NMR spectra of **5** is the high field shift of the bridging methyl groups at δ = −2.1 for the ^{1}H and δ = −18.1 for the ^{13}C nuclei. The dimeric, but thf-free molecule is even present in the gas phase as shown by mass spectroscopy. Regarding the dimeric nature of this compound in solution as well as in the gas phase it is not surprising that the bridging methyl groups cannot add to another equivalent of tetramethylfulvene.

Conclusion

Erker and coworkers[5g] demonstrated the solvent dependency on the reaction of organyl lithiums whether a protonation (β-hydride transfer from alkyl lithium) or a deprotonation (metalation) of the fulvene is favored. Due to the absence of β-hydrogen atoms the alkaline earth metal bis-[bis(trimethylsilyl)amides] of calcium, strontium and barium deprotonate the fulvenes to give alkenyl substituted alkaline earth metallocenes. The corresponding magnesium derivative is not reactive enough to interact with fulvenes. If β-hydrogen atoms are present in dialkylmagnesium as for example in *n*/*sec*-dibutylmagnesium only the β-hydride transfer to the fulvene is observed. Dimethylmagnesium always deprotonates the fulvene, however, the reaction with 6,6-dicyclopropylfulvene proceeds different than the reaction with 6-phenyl-6-methylfulvene, which yields 1,1′-bis(1-phenylethen-1-yl)magnesocene. One of the fulvene molecules is not metalated at the alkyl substituent but in *ortho*-position at the cyclopentadienyl fragment. Thus, the ring strain induced by the formation of a cyclopropylidene moiety is avoided. Now a ring closure reaction gives [bis(tetrahydrofuran-*O*)]spiro{cyclopropane-1,2′(1′-η^5-cyclopentadienyl-1′,3′,3′-tricyclopropyl-1′,2′,3′,3a′-tetrahydropentalene)}-3a′-6′-η^2-enyl]magnesium. Thus far, an addition of an alkyl magnesium moiety to a fulvene is only observed when both the β-hydride transfer to and the deprotonation (metalation) of a fulvene is impossible.

This research was supported by the *Deutsche Forschungsgemeinschaft*, Bonn, and the *Fonds der Chemischen Industrie*, Frankfurt/Main.

Experimental Section

All experiments and manipulations were carried out under argon purified by passage through BTS catalyst and P_4O_{10}. Reactions were performed by using standard Schlenk techniques and dried, thoroughly deoxygenated solvents. The starting materials 6-methyl-6-phenylfulvene,[34] 6,6-dicyclopropylfulvene,[35] and dimethylmagnesium[11] were prepared by literature procedures. − NMR spectra were recorded on the Bruker spectrometers AM200, AC250, and AM400 or Jeol spectrometers GSX270 and EX400. − A Perkin-Elmer Paragon 1000 PC spectrophotometer was used to record the IR spectra; solid substances were measured in nujol between CsBr windows (vs very strong, s strong, m medium strong, w weak, vw very weak, sh shoulder). The frequencies in the region of the nujol vibrations were not listed. − The sensitivity towards moisture and oxygen during the handling of the compounds and the formation of carbides during combustion lead to low carbon values in the elemental analysis. Due to the moisture and air sensitivity of **4** and **5** the elemental analysis gave no reasonable results, even though if crystalline material was used. During handling of these compounds they turned dark and became waxy.

1,1′-Bis(1-phenyl-1-ethenyl)magnesocene (**1**). At 0°C 4.5 ml of 6-methyl-6-phenylfulvene were added to 13.8 mmol of dimethylmag-

nesium dissolved in 20 ml of the solvent mixture of thf, diethyl ether, and 1,4-dioxane. Stirring at r.t. for a few days led to quantitative formation of **1** as could be shown by NMR spectroscopy. The addition of 30 ml of pentane and cooling to 5°C yielded a precipitation of **1**. The nearly colorless precipitate turns dark upon removal of the mother liquor and drying in vacuum. Therefore, we used this solution without further purification or isolation of **1**. The NMR data is summarized in Table 1.

1,1′-Bis(1-phenyl-1-ethyl)magnesocene (**2**). At −30°C 3.3 ml (20.0 mmol) of 6-methyl-6-phenylfulvene were dropped to 10.0 ml of a 1 M solution of dibutylmagnesium in heptane. After complete addition the reaction mixture was stirred for 2 days, till the color changed from orange to bright yellow. The solution was decanted from the precipitate and reduced in vacuum. 2.6 g of compound **2** crystallized as colorless cuboids (72%), m.p. 47−48°C. − ^{1}H NMR (C_6D_6): δ = 1.48 [d, ^3J(H,H) = 7 Hz, Me], 3.85 [q, ^3J(H,H) = 7 Hz, CpC*H*], 5.7−5.9 [m, Cp], 7.0−7.2 [m, Ph]. − ^{13}C{^{1}H} NMR (C_6D_6): δ = 22.92 [Me], 40.05 [Cp-*C*H], 104.95, 105.08, 105.70, 106.56 [*C*H of Cp], 126.20 [*para*-C of Ph], 127.30, 128.58 [*meta* and *ortho*-C of Ph], 129.50 [*ipso*-C of Ph], 147.40 [*ipso*-C of Cp]. − IR (nujol): ν = 1688 cm^{-1} w, 1601 m, 1296 w, 1271 w, 1236 w, 1201 w, 1182 w, 1156 w, 1066 m, 1051 m, 1026 s, 1003 w, 978 m, 917 m, 895 sh, 862 w, 825 s, 768 s, 703 s, 632 w, 617 w, 584 w, 529 m, 504 sh, 452 w. − MS (70 eV); *m/z* (%): 169 (100) [CpCHMePh$^+$], 154 (99) [CpCHPh$^+$], 105 (95) [PhCHMe$^+$], 77 (42) [Ph$^+$]. − $C_{26}H_{26}Mg$ (362.78): calcd. C 86.07, H 7.22; found C 83.88, H 7.20.

1,1′-Bis(dicyclopropylmethyl)magnesocene (**3**). 5.0 ml (30 mmol) of 6,6-dicyclopropylfulvene were added to a cooled solution of 15.0 ml of 1 M dibutylmagnesium in heptane. After stirring for 2 days at r.t. the solution was reduced in vacuum. At 5°C 4.8 g of slightly yellow crystals of **3** precipitated (93%), m.p. 53−54°C. − ^{1}H NMR (C_6D_6): δ = 0.14−0.28 and 0.39−0.54 [m, CH_2], 0.92−1.01 [m, CH of ^{c}Pr], 1.22 [t, ^3J(H,H) = 9 Hz, CpC*H*^{c}Pr$_2$], 6.06 [s, Cp]. − ^{13}C{^{1}H} NMR (C_6D_6): δ = 3.80, 4.15 [CH_2], 17.45 [CH of ^{c}Pr], 47.90 [Cp*C*H^{c}Pr$_2$], 105.53 and 106.04 [CH of Cp], 128.72 [*ipso*-C of Cp]. − IR (nujol): $\tilde{\nu}$ = 1271 cm^{-1} s, 1261 sh, 1216 w, 1201 w, 1163 w, 1110 w, 1057 w, 1043 s, 1030 s, 1019 s, 1011 s, 973 m, 933 s, 916 m, 899 m, 855 sh, 829 s, 778 sh, 769 s, 750 s, 676 w, 530 w, 496 m, 453 m, 426 w, 321 w. − MS (70 ev); *m/z* (%): 158 (31) [Cp-C(C$_3$H$_5$)$_2^+$], 131 (100), 117 (63) [Cp-CH(C$_3$H$_5$)$^+$], 95 (28) [CH(C$_3$H$_5$)$_2^+$]. − $C_{24}H_{30}Mg$ (342.81): calcd. C 84.09, H 8.82; found C 83.43, H 8.64.

[Bis(tetrahydrofuran-O)]spiro{cyclopropane-1,2′(1′-η^5-cyclopentadienyl-1′,3′,3′-tricyclopropyl-1′,2′,3′,3a′-tetrahydropentalene)}-3a′-6′-η^2-enyl]magnesium (**4**). 1.6 ml (10.0 mmol) of 6,6-dicyclopropylfulvene was added at 0°C to 5.0 mmol of dimethylmagnesium dissolved in 7.1 ml of a mixture of thf, diethyl ether and 1,4-dioxane. Within 12 days the orange solution turned yellow. The addition of 10 ml of pentane led to the precipitation of 0.8 g of a reddish oil **4**, which crystallized at −5°C in the shape of yellowish cuboids (35%), m.p. 218°C (dec.). − ^{1}H NMR (C_6D_6, assignment with $^{1\ H,1}$H-COSY45 NMR experiments): δ = 0.4−0.48 [m], 0.64−0.68 [m], 0.82−0.84 [m], 0.98−1.07 [m], 1.27−1.33 [m], 1.40−1.48 [m], 1.51−1.60 [m], 1.72−1.82 [m], 4.60 [dd, ^3J(H,H) = 1.3 Hz], 5.95 [dd], 5.96 [m, Cp], 6.11 [m, Cp], 6.14 [m, Cp], 6.17 [dd], 6.76 [m, Cp]. − ^{13}C NMR (C_6D_6, assignment with means of DEPT, ^{1}H-*J*-resolved 2D-NMR and ^{1}H,^{13}C-HMQC experiments[36]): δ = 0.01, 1.07, 2.50, 2.74, 3.89, 6.71, 13.26, 13.43 [CH_2 of ^{c}Pr]; 17.88, 19.89, 22.47 [CH of ^{c}Pr]; 46.24, 47.34, 54.25 [quart. C]; 75.06, 105.28 116.40 [CH of pentalene fragment]; 97.80, 100.66, 104.18, 106.41 [CH of Cp]; 129.96, 134.44, 140.63 [quart. aromatic C]. − IR (nujol): ν = 1309 cm^{-1} vs, 1242 vs br, 1184 vs, 1129 vs br, 1045 m, 1020 s, 998 sh, 985 vs, 933 w, 918 w, 901 w, 871 w, 845 w, 828 w, 810 w, 760 sh, 745 w, 719 sh, 702 w, 675 w, 646 w, 625 w, 532 w br, 467 w, 438 w, 405 w, 370 w. MS (70 eV); *m/z* (%): 316 (24), 275 (45), 209 (39), 193 (55), 165 (71), 158 (100), 128 (96), 115 (98), 91 (87).

Bis(tetrahydrofuran-O)dimethyl-bis(η^5-ethyltetramethylcyclopentadienyl)dimagnesium (**5**). At 0°C 3.8 mmol of dimethylmagnesium dissolved in thf, dioxane, and diethyl ether were added to

Table 2. Crystallographic data of **2**, **3**, **4**, and **5** as well as details of the structure solution and refinement procedures

compound	**2**	**3**	**4**	**5**
formula	$C_{26}H_{26}Mg$	$C_{24}H_{30}Mg$	$C_{32}H_{42}MgO_2$	$C_{16}H_{28}MgO$
fw [g·mol^{-1}]	362.78	342.79	482.97	260.69
T [K]	193	193	193	193
space group[38]	$P2_1/c$ (No. 14)	$P1$ (No. 2)	$P2_1/c$ (No. 14)	$P2_1/n$ (No. 14)
a [pm]	1181.7(4)	853.8(4)	1268.6(3)	900.35(1)
b [pm]	803.1(3)	983.2(5)	2315.5(7)	1348.23(1)
c [pm]	1155.2(5)	1236.6(4)	18.41.9(5)	1297.14(2)
α [°]	90	82.442(7)	90	90
β [°]	109.24(1)	78.92(1)	97.55(1)	93.26(1)
γ [°]	90	73.347(7)	90	90
V [nm^3]	1.0352(6)	0.9729(7)	5.364(3)	1.57201(3)
Z	2	2	8	4
d_{calcd} [g·cm^3]	1.164	1.170	1.196	1.101
μ [mm^{-1}]	0.093	0.095	0.093	0.102
F(000)	388	372	2096	576
scan range [°]	1.7 ≤ θ ≤ 24.7	1.7 ≤ θ ≤ 29.3	1.4 ≤ θ ≤ 24.0	2.2≤ θ ≤ 29.4
measured data	4888	5505	17538	8768
unique data (R_{int})	1666 (0.0255)	2958 (0.0192)	7643 (0.0377)	2979 (0.0193)
parameters	129	227	735	180
wR_2[a] (all data)	0.1282	0.0900	0.2699	0.1516
R_1[a] (all data)	0.0570	0.0473	0.1192	0.0639
data [$I>2\sigma(I)$]	1567	2696	5647	2470
R_1 [$I>2\sigma(I)$]	0.0538	0.0416	0.0883	0.0519
goof σ[b] on F^2	1.052	1.159	1.108	1.068
residual dens [e·nm^{-3}]	561; −0.219	193; −158	599; −288	355; −325

[a] Definition of the *R* values: $R_1 = (\Sigma||F_o| - |F_c||)/\Sigma|F_o|$; $wR_2 = \{\Sigma[w(F_o^2 - F_c^2)^2]/\Sigma[w(F_o^2)^2]\}^{1/2}$ with $w^{-1} = \sigma^2(F_o^2) + (aP)^2$. − [b] $\sigma = \{\Sigma[w(F_o^2 - F_c^2)^2]/(N_o - N_p)\}^{1/2}$.

1.02 g of 1,2,3,4-tetramethylfulvene in *n*-pentane. Stirring at r.t. for 4 d resulted in a yellow solution. Recrystallization from pentane yielded 0.74 g of colorless **5** (75%), m.p. 124°C. – ^{1}H NMR ([D$_8$]THF): δ = −2.08 [s, Mg-Me], 0.90 [t, ^3J(H,H) = 7.6 Hz, CH$_3$ of Et], 1.76 [m, THF], 1.91 [Cp-Me], 1.94 [Cp-Me], 2.42 [q, ^3J(H,H) = 7.6 Hz], 3.60 [m, THF]. – ^{13}C{^{1}H} NMR ([D$_8$]THF): δ = −18.13 [Mg-Me], 10.41 [Cp*C*H$_3$], 10.56 [Cp*C*H$_3$], 15.75 [CH$_3$ of Et], 19.55 [CH$_2$ of Et], 25.44 [THF], 67.35 [THF], 106.70 [Cp], 107.45 [Cp], 114.23 [Cp]. – IR (nujol): ν = 1363 cm^{-1} m, 1339 m, 1310 w, 1293 w, 1242 m, 1182 vs, 1138 sh, 1126 w, 1105 w, 1070 w, 1053 w, 1025 vs, 985 w, 956 w, 944 sh, 927 m, 912 w, 870 vs, 844 m, 675 m, 637 sh, 564 s, 494 s, 429 s, 404 s, 390 sh, 353 sh, 330 s, 295 sh. – MS (70 eV); *m/z* (%): 377 (8) [M$^+$ − 2 THF], 299 (74) [M$^+$ − Cp′ − 2 THF], 285 (91), 269 (92), 149 (100) [Cp′$^+$], 134 (99) [Cp′$^+$-CH$_4$].

X-ray Crystallography.[37] The single crystals were covered with nujol, sealed in thin-walled capillaries and mounted on a diffractometer with graphite monochromated Mo-K_α radiation (λ = 71.073 pm). A Siemens SMART-CCD area detector was used to monitor the reflections. Crystallographic parameters and details of data collection performed at −80°C are summarized in Table 2.

All structures were solved by direct methods with the software package SHELXTL Plus[39] and refined with the program SHELXL-93.[40] Neutral atom scattering factors were taken from Cromer and Mann[41] and for the hydrogen atoms from Stewart et al.[42] The non-hydrogen atoms were refined anisotropically. The H-atoms were refined with a riding model under restriction of ideal symmetry at the corresponding carbon atom. The hydrogen atoms of the bridging methyl substituents of **5** were refined isotropically.

[1] M. Westerhausen, M. Hartmann, W. Schwarz, *J. Organomet. Chem.* **1995**, *501*, 359.
[2] M. Westerhausen, M. Hartmann, N. Makropoulos, B. Wieneke, M. Wieneke, W. Schwarz, D. Stalke, *Z. Naturforsch.* **1998**, *53b*, 117.
[3] M. Westerhausen, M. Hartmann, G. Heckmann, W. Schwarz, *J. Organomet. Chem.* **1997**, *541*, 261.
[4] Examples see: [4a] P. Renaut, G. Tainturier, B. Gautheron, *J. Organomet. Chem.* **1978**, *148*, 35. – [4b] S. T. Abu-Orabi, P. Jutzi, *J. Organomet. Chem.* **1987**, *329*, 169. – [4c] J. Okuda, *Chem. Ber.* **1989**, *122*, 1075. – [4d] S. Chen, *Gaodeng Xuexiao Huaxue Xuebao* **1988**, *9*, 342; *Chem. Abstr.* **1989**, *111*, 5745. – [4e] R. L. Haltermann, *Cem. Rev.* **1992**, *92*, 965.
[5] Examples see: [5a] S, Chen, Y. Chen, J. Wang, *Sci. China* **1990**, *B33*, 769. – [5b] M. Ogasa, D. T. Mallin, D. W. Macomber, M. D. Rausch, R. D. Rogers, A. N. Rollins, *J. Organomet. Chem.* **1991**, *405*, 41. – [5c] G. Erker, R. Aul, *Chem. Ber.* **1991**, *124*, 1301. – [5d] G. Erker, S. Wilker, C. Krüger, M. Nolte, *Organometallics* **1993**, *12*, 2140. – [5e] J. Wang, S. Chen, X. Wang, *Gaodeng Xuexiao Huaxue Xuebao* **1993**, *14*, 495; *Chem. Abstr.* **1994**, *120*, 164434. – [5f] S. Chen, Z. Lei, J. Wang, R. Wang, H. Wang, *Sci. China* **1994**, *B37*, 788. – [5g] G. Erker, R. Nolte, R. Aul, S. Wilker, C. Krüger, R. Noe, *J. Am. Chem. Soc.* **1991**, *113*, 7594.
[6] [6a] R. L. Cooper, E. O. Fischer, W. Semmlinger, *J. Organomet. Chem.* **1967**, *9*, 333. – [6b] F. Edelmann, U. Behrens, *J. Organomet. Chem.* **1977**, *134*, 31. – [6c] F. Edelmann, P. Behrens, S. Behrens, U. Behrens, *J. Organomet. Chem.* **1986**, *310*, 333.
[7] [7a] U. Wannagat, H. Kuckertz, *Angew. Chem.* **1963**, *75*, 95. – [7b] U. Wannagat, H. Autzen, H.-J. Wismar, *Z. Anorg. Allg. Chem.* **1972**, *394*, 254. – [7c] L. M. Engelhardt, B. S. Jolly, P. C. Junk, C. L. Raston, B. W. Skelton, A. H. White, *Aust. J. Chem.* **1986**, *39*, 1337.
[8] [8a] M. Westerhausen, *Inorg. Chem.* **1991**, *30*, 96. – [8b] M. Westerhausen, W. Schwarz, *Z. Anorg. Allg. Chem.* **1992**, *609*, 39.
[9] D. Dou, M. Westerhausen, G. L. Wood, G. Linti, E. N. Duesler, H. Nöth, R. T. Paine, *Chem. Ber.* **1993**, *126*, 379.
[10] [10a] S. Guttmann, P. Burger, H.-U. Hund, J. Hofmann, H.-H. Brintzinger, *J. Organomet. Chem.* **1989**, *369*, 343. – [10b] M. Rieckhoff, U. Pieper, D. Stalke, F. T. Edelmann, *Angew. Chem.* **1993**, *105*, 1102; *Angew. Chem. Int. Ed. Engl.* **1993**, *32*, 1079.
[11] W. Strohmeier, F. Seifert, *Chem. Ber.* **1961**, *94*, 2356.
[12] K. W. Henderson, J. F. Allan, A. R. Kennedy, *Chem. Commun.* **1997**, 1149.
[13] P. Kronig, M. Slongo, M. Neuenschwander, *Makromol. Chem.* **1982**, *183*, 359.
[14] S. Landa, J. Burkhardt, J. Vais, *Z. Chem.* **1967**, *7*, 388.
[15] G. Kresze, S. Rau, G. Sabelus, H. Goetz, *Liebigs Ann. Chem.* **1961**, *648*, 57.
[16] R. E. Cramer, P. N. Richmann, J. W. Gilje, *J. Organomet. Chem.* **1991**, *408*, 131.
[17] C. Dohmeier, D. Loos, C. Robl, H. Schnöckel, D. Fenske, *J. Organomet. Chem.* **1993**, *448*, 5.
[18] C. Johnson, J. Toney, G. D. Stucky, *J. Organomet. Chem.* **1972**, *40*, C11.
[19] [19a] W. T. Ford, *J. Organomet. Chem.* **1971**, *32*, 27. – [19b] W. T. Ford, J. B. Grutzner, *J. Org. Chem.* **1972**, *37*, 2561.
[20] G. E. Parris, E. C. Ashby, *J. Organomet. Chem.* **1974**, *72*, 1.
[21] [21a] H. O. House, R. A. Latham, G. M. Whitesides, *J. Org. Chem.* **1967**, *32*, 2481. – [21b] H. Viebrock, D. Abeln, E. Weiss, *Z. Naturforsch.* **1994**, *49b*, 89.
[22] [22a] P. Jutzi, *Adv. Organomet. Chem.* **1986**, *26*, 217. – [22b] P. Jutzi, *Chem. Rev.* **1986**, *86*, 894. – [22c] P. Jutzi, *Pure Appl. Chem.* **1989**, *61*, 1731. – [22d] P. Jutzi, *Pure Appl. Chem.* **1990**, *62*, 1035. – [22e] P. Jutzi, *J. Organomet. Chem.* **1990**, *400*, 1. – [22f] D. J. Burkey, T. P. Hanusa, *Comments Inorg. Chem.* **1995**, *17*, 41.
[23] A. J. Bridgeman, *J. Chem. Soc., Dalton Trans.* **1997**, 2887.
[24] W. Bünder, E. Weiss, *J. Organomet. Chem.* **1975**, *92*, 1.
[25] A. Haaland, J. Lusztyk, *J. Organomet. Chem.* **1975**, *85*, 279.
[26] M. G. Gardiner, C. L. Raston, C. H. L. Kennard, *Organometallics* **1991**, *10*, 3680.
[27] C. P. Morley, P. Jutzi, C. Krüger, J. M. Wallis, *Organometallics* **1987**, *6*, 1084.
[28] J. L. Atwood, K. D. Smith, *J. Am. Chem. Soc.* **1974**, *96*, 994.
[29] [29a] P. R. Markies, O. S. Akkerman, F. Bickelhaupt, W. J. J. Smeets, A. L. Spek, *Adv. Organomet. Chem.* **1991**, *32*, 147. – [29b] C. E. Holloway, M. Melnik, *J. Organomet. Chem.* **1994**, *465*, 1.
[30] L. M. Engelhardt, S. Harvey, C. L. Raston, A. H. White, *J. Organomet. Chem.* **1988**, *341*, 39.
[31] E. Weiss, *J. Organomet. Chem.* **1964**, *2*, 314; see also the review: E. Weiss, *Angew. Chem.* **1993**, *105*, 1565; *Angew. Chem. Int. Ed. Engl.* **1993**, *32*, 1501.
[32] E. Weiss, *J. Organomet. Chem.* **1965**, *4*, 101.
[33] H. Viebrock, U. Behrens, E. Weiss, *Angew. Chem.* **1994**, *106*, 1364; *Angew. Chem. Int. Ed. Engl.* **1994**, *33*, 1257.
[34] [34a] G. Kresze, H. Goetz, *Chem. Ber.* **1957**, *90*, 2161. – [34b] D. J. Sardella, C. M. Keane, P. Lemonias, *J. Am. Chem. Soc.* **1984**, *106*, 4962.
[35] [35a] M. Hanack, H. Eggensperger, *Liebigs Ann. Chem.* **1963**, 663. – [35b] R. C. Kerber, H. G. Linde, *J. Org. Chem.* **1966**, *31*, 4321. – [35c] L. Knothe, H. Prinzbach, H. Fritz, *Liebigs Ann. Chem.* **1977**, 687.
[36] A. Bax, S. Subramanian, *J. Magn. Reson.* **1986**, *67*, 565; for examples see: [36a] A. Bax, A. Aszalos, Z. Dinya, K. Sudo, *J. Am. Chem. Soc.* **1986**, *108*, 8056. – [36b] V. Skeluar, A. Bax, *J. Magn. Reson.* **1987**, *71*, 379.
[37] Crystallographic data (excluding structure factors) for the structures of **2**, **3**, **4**, and **5** have been deposited with the Cambridge Crystallographic Data Centre as supplementary publication no. CCDC-101070. Copies of the data can be obtained on application to CCDC, 12 Union Road, Cambridge CB2 1EZ, UK [Fax: +44(1223)336-033; E-mail: deposit@ccdc.cam.ac.uk].
[38] T. Hahn (Ed.), *International Tables for Crystallography*, Vol. A, *Space Group Symmetry*, 2nd Ed., D. Reidel, Dordrecht, **1984**.
[39] *SHELXTL Plus*, PC version, Siemens Analytical X-Ray Instruments, Inc., Madison/WI **1980**.
[40] G. M. Sheldrick, *SHELXL-93*, Universität Göttingen, **1993**.
[41] D. T. Cromer, J. B. Mann, *Acta Crystallogr.* **1968**, *24*, 321.
[42] R. F. Stewart, E. R. Davidson, W. T. Simpson, *J. Chem. Phys.* **1965**, *42*, 3175.

[98017]

Cyclopentadienone Cyclopentadienediyl Diselenoketals

Georg Thaler, Klaus Wurst, and Fritz Sladky*

Institut für Allgemeine, Anorganische und Theoretische Chemie der Universität Innsbruck,
A-6020 Innsbruck, Innrain 52a, Austria
Fax: (internat.) + 43(0)512/507-2934
E.mail: fritz.sladky@uibk.ac.at

Received February 5, 1998

Keywords: Cyclopentadiene / Selenium / Ketal

Reaction of di-*tert*-butylcyclopentadiene with excess potassium *tert*-butoxide in the presence of elemental selenium leads to cyclopentadienes bridged by two or three selenium atoms through one or two diselenoketal functionalities. 2,5,4′,6′-Tetra-*tert*-butyl-5′*H*-spirocyclopentane-1,2′-cyclopenta[*b*][1,3]diselena-2,4-diene (**1**) and 1,3,5,7-tetra-*tert*-butyl-3a,7a-dihydro-3a,7a-*epi*-selenodicyclopenta[*b,e*][1,4]diselenine (**2**) have been characterized by single-crystal X-ray diffraction.

Introduction

We have recently reported that lithium cyclopentadienides substituted by *t*Bu or Me_3Si groups, obtained by deprotonation of the corresponding cyclopentadiene with *n*-butyllithium, insert several equivalents of elemental selenium with formation of lithium cyclopentadienylpolyselenolates[1]. Subsequent in situ disproportionation leads to substituted bis(cyclopentadienyl)selanes, cp'_2Se_n ($n = 1-5$). If *n*-butyllithium is replaced by potassium *tert*-butoxide, a base of low nucleophilicity which itself reacts with elemental selenium and is able to cleave C−Se and Se−Se bonds if present in excess, the reaction pathway changes drastically. The hitherto unknown doubly and triply selenium-bridged cyclopentadienes **1** and **2** are obtained in moderate to good yield in a one-pot reaction. Bridging occurs through a previously unknown cyclopentadiene-centered diselenoketal functionality. Other identified products are labile and could not be isolated, e.g. $(tBu_2C_5H_3)_2Se$[2], which is formed primarily in the initial stages of the reaction, while a small amount of tetra-*tert*-butylpentafulvalene[3] was obtained as deep-red crystals (Scheme 1).

Scheme 1. Synthesis of compounds **1** and **2**

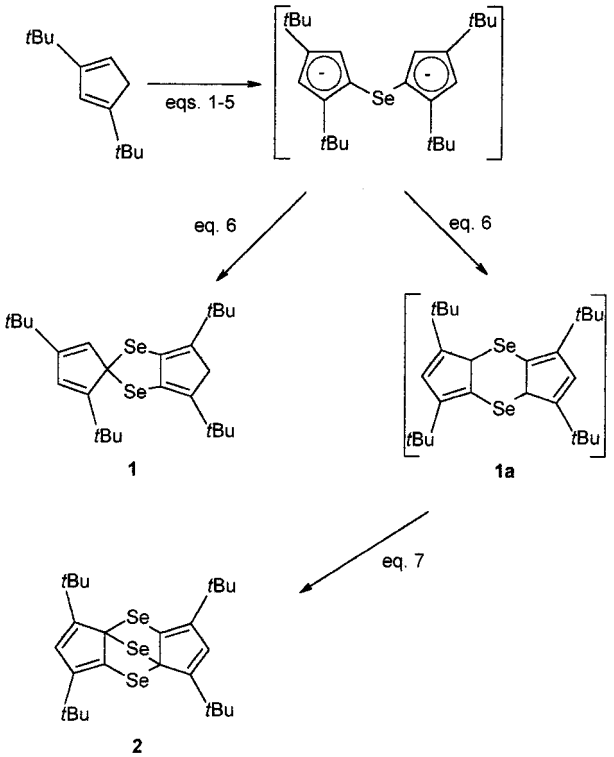

Results and Discussion

The formation of **1** and **2**, although entirely unexpected, can be understood in terms of a sequence of established reactions (Scheme 2).

The main driving force is the successive deprotonation of cyclopentadiene and subsequent insertion of elemental selenium into the formed cyclopentadienide anions (Eqs. 1 and 2). These processes are accelerated in a cascade-like manner owing to the increased acidity of the cyclopentadiene protons that results from the increasing selenium substitution of the cyclopentadiene. Disproportionation of the intermediate cyclopentadienylpolyselenolates leads to selenium-bridged cyclopentadiene species (Eq. 3). Bridges containing more than one selenium atom are known to be increasingly unstable and are degraded by lithium cyclopentadienide (Eq. 4). Repetition of these steps finally affords **1** and **2** (Eqs. 5−7). **1** is generated if bridging occurs with formation of a 1,3-diselenolane heterocycle. If, on the other hand, the postulated heterocyclic intermediate 1,4-diselenane **1a** is formed, an additional deprotonation−insertion−disproportionation sequence leads to **2**. The two *t*Bu groups serve to control the above reactions and thus prevent extensive oxidation and/or polymerization of cyclopentadiene.

The molecular structure of **1** consists of a 1,3-diselenolane heterocycle, which spans between an allylic spiro car-

 © WILEY-VCH Verlag GmbH, D-69451 Weinheim, 1998 1434−1948/98/0707−0973 $ 17.50+.50/0

Scheme 2. Proposed reaction steps leading to **1** and **2**

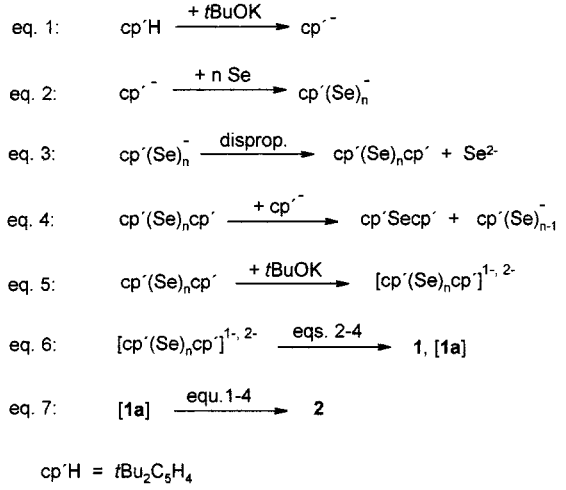

bon atom of the cyclopentadiene bearing the diselenoketal functionality, and the other cyclopentadiene, which is annelated via vicinal vinylic carbon atoms (Figure 1). This results in an almost mutually perpendicular orientation of the two cyclopentadiene rings [interplane angle: 87.7(3)°] and consequently to an optimal staggering of all the *t*Bu groups. The angle at the selenium atoms of 92.5(3)° is comparable to that found in other diorganylselanes such as $[(Me_3Si)_2C_5H_3]_2Se$ (97.9°)[2] and Me_2Se (96.3°)[4] and indicates negligible ring strain. However, the difference between the C(sp²)−Se and C(sp³)−Se bond lengths [1.914 A compared to 1.986 A (mean values)] is striking. The extreme shortening of the former represents a further example of a strong electronic interaction between selenium bound in a vinylic position and the π system of cyclopentadiene[1][2][5][6] (Table 1).

Figure 1. Molecular structure of **1**; anisotropic displacement parameters depicting 50% probability; hydrogen atoms of methyl groups have been omitted for clarity[a]

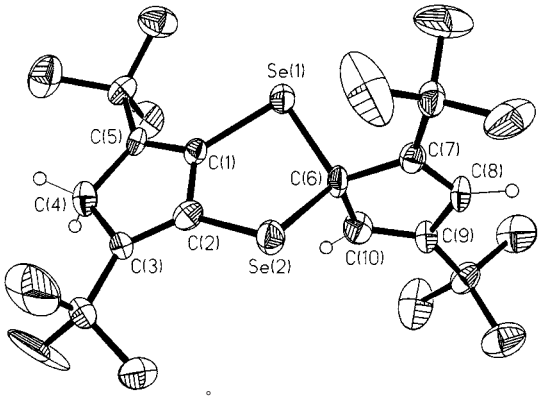

[a]Selected bond lengths [A] and angles [°]: Se(1)−C(1) 1.915(7), Se(1)−C(6) 1.992(7), Se(2)−C(2) 1.913(7), Se(2)−C(6) 1.980(7); C(1)−Se(1)−C(6) 92.5(3), C(2)−Se(2)−C(6) 92.5(3); interplane angle 87.7(3).

The molecular structure of **2** can be described as a kind of hexagonal pyramid, based on a 1,4-diselenane heterocycle in boat conformation (Figure 2). The unique Se(1) atom is at the top of the pyramid and is common to two 1,3-diselenolane heterocycles, which each bridge the two cyclopentadiene moieties in a similar manner as in **1**. The molecule possesses a twofold symmetry axis which passes through Se(1) and bisects the Se(2)−Se(2a) vector. The key difference between **1** and **2** is that in **2** the allylic positions of both cyclopentadienes are substituted by a diselenoketal functionality. Also in contrast to **1**, there appears to be considerable strain within the heterocyclic framework, as indicated by the extremely acute C−Se(1)−C angle of 82.6(2)°. Nevertheless, the striking difference in the C(sp²)−Se and C(sp³)−Se bond lengths seen in **1** is also seen in **2** [1.888 A compared to 1.985 A (mean values)]. In fact, these are amongst the shortest and longest C−Se bonds ever reported [e.g. 1.879(5) A in TMTSF[7] and 2.018(5) A in 3,3,5,5-tetrakis(trimethylsilyl)-1,2,4-triselenolane[8]] (Table 1). Whereas other cyclopentadienylselenium compounds form $W(CO)_5$ complexes[2][5][9], the multisubstitution of cyclopentadiene with selenium reduces the donor capacity of each selenium and no interaction of **2** with $[(CO)_5W(THF)]$ occurs.

Table 1. Crystal structure data of compounds **1** and **2**

	1	**2**
formula	$C_{26}H_{40}Se_2$	$C_{26}H_{38}Se_3$
M_r	510.50	587.44
cryst. size [mm]	0.60 × 0.50 × 0.20	0.51 × 0.18 × 0.13
T [K]	213(2)	293(2)
crystal system	monoclinic	monoclinic
space group	$P2_1/c$ (no. 14)	$P2/c$ (no. 13)
a [A]	9.681(2)	11.969(1)
b [A]	11.267(2)	6.177(1)
c [A]	24.366(4)	18.573(1)
β [°]	99.66(1)	106.12(1)
V [A³]	2620.1(8)	1319.2(3)
Z	4	2
$\rho_{calcd.}$ [g cm^{-3}]	1.294	1.479
μ [mm^{-1}]	2.831	4.192
F(000)	1056	592
2 θ_{max} [°]	45.00	55.00
reflections collected	4570	6227
independent reflections	3380	2954
reflections [$I > 2\ \sigma(I)$]	2429	2110
absorption correction	ψ scan	ψ scan
T_{min}, T_{max}	0.524, 1.000	0.565, 1.000
parameters	294	132
*R*1 [$I > 2\ \sigma(I)$][a]	0.0534	0.0374
*wR*2 [$I > 2\sigma(I)$][b]	01325	0.0748
largest diff. peak/hole [eA^{-3}]	1.884, −0.352	0.677, −0.337

[a] $R1 = \Sigma\|F_o| - |F_c\|/\Sigma|F_o|$. − [b] $wR2 = \{\Sigma[w(F_o^2 - F_c^2)^2]/\Sigma[w(F_o^2)^2]\}^{1/2}$.

The packing of **2** shows a highly oriented stacking along the *y* axis (Figure 3). This is accomplished by Se−Se interactions between the unique Se(1) of one molecule and Se(2) and Se(2a) of the neighbouring molecule. The former fits into a cavity formed by the latter (Figure 4). The intrastack Se(1)−Se(2, 2a) distances of 3.978 A are almost identical to the Se−Se intrastack distances in selenium-based organic metal superconductors $(TMTSF)_2X$[10]. In contrast to these materials, however, there are no Se−Se interstack interactions in **2**. Attempts at chemical doping have to date been unsuccessful. TCNQ does not interact, while nitrosyl salts react too vigorously with extrusion of elemental selenium.

Figure 2. Molecular structure of **2**; anisotropic displacement parameters depicting 50% probability; hydrogen atoms of methyl groups have been omitted for clarity[a]

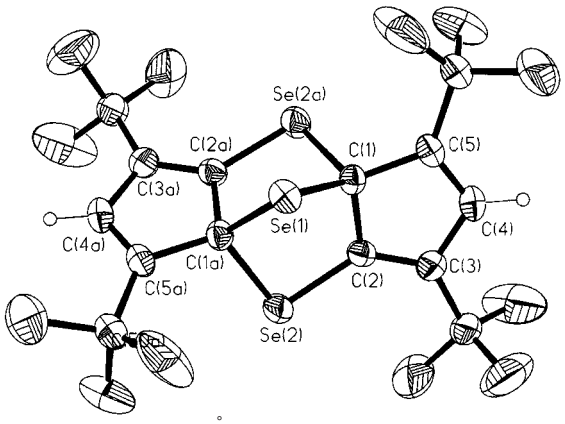

[a]Selected bond lengths [A] and angles [°]: Se(1)−C(1) 1.979(3), Se(2)−C(2) 1.888(3), Se(2)−Se(1a) 1.990(3); C(1)−Se(1)−C(1a) 82.6(2), C(2)−Se(2)−C(1a) 89.56(13); interplane angle 57.6(1).

Figure 3. Packing plot of **2** along the *y* axis

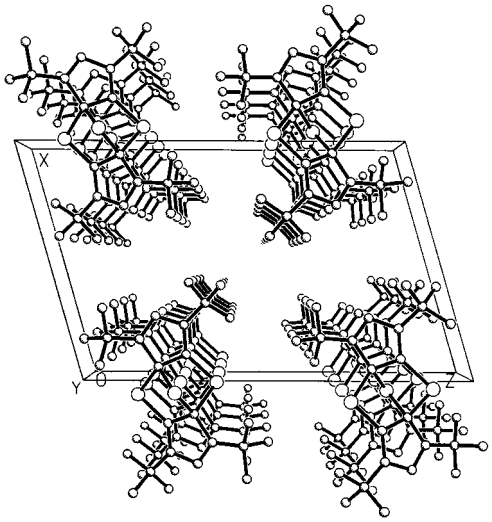

Figure 4. Intrastack Se−Se interactions in **2**

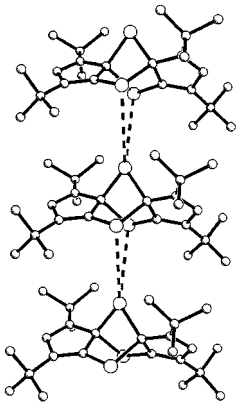

We thank Dr. *L. Call,* Institut für Organische Chemie der Universität Innsbruck, for his assistance in naming **1** and **2** according to the latest IUPAC proposals for the nomenclature of fused and bridged fused ring systems and of spiro compounds.

Experimental Section

General: All reactions were performed under argon by using standard Schlenk techniques. THF was purified and dried according to standard methods. KO*t*Bu and elemental grey selenium were obtained from Aldrich and Fluka, respectively. $t\mathrm{Bu_2C_5H_4}$[11] was prepared as described previously. Flash chromatography was performed on Merck silica gel (Type 60, 230−400 mesh ASTM) with petroleum ether as eluent. − ^{1}H- and ^{13}C-NMR spectra were recorded with a Bruker AC 200 spectrometer. ^{1}H and ^{13}C chemical shifts are referred to solvent signals [$CDCl_3$: (residual $CHCl_3$): $\delta_H = 7.26$; $\delta_C = 77.7$]. − Mass spectra were recorded with a Varian CH-7 instrument.

Preparation of Compounds **1** *and* **2**: KO*t*Bu (3.72 g, 33.1 mmol) was added to a solution of $t\mathrm{Bu_2C_5H_4}$ (1.97 g, 11.1 mmol) in THF (50 ml) at −30°C. After stirring the resulting suspension for 1 h at ambient temp., 2.63 g of grey selenium (33.3 mmol) was added and stirring was continued for a further 12 h. The solvent was then removed in vacuo, 100 ml of petroleum ether was added, and the resulting suspension was filtered through silica gel. Chromatography afforded 0.13 g of tetra-*tert*-butylpentafulvalene (7%) as deep-red crystals, 0.13 g of **1** (5%) as yellow crystals, and 1.28 g of **2** (39%) as yellow crystals. Single crystals of the air-stable compounds **1** and **2** were obtained from Et_2O/MeOH.

1: M.p. 190−191°C. − ^{1}H NMR (200 MHz, $CDCl_3$): δ = 1.11 (s, 9 H, 9-*t*Bu), 1.22 (s, 18 H, 3,5-*t*Bu), 1.37 (s, 9 H, 7-*t*Bu), 3.27 (s, 2 H, 4,4-H), 5.94 [d, $^4J_{HH}$ = 1.82 Hz, 1 H, 8-H], 6.28 [d, $^4J_{HH}$ = 1.82 Hz, 2 H, 10-H]. − ^{13}C NMR (50 MHz, $CDCl_3$): δ = 29.9 [9-C(CH_3)$_3$], 30.7 [3,5-C(CH_3)$_3$], 31.5 [3,5-*C*(CH_3)$_3$], 32.4 [7-C(CH_3)$_3$], 33.7 [9-*C*(CH_3)$_3$], 47.5 (4-C), 86.5 (6-C), 127 (8-C), 135 (10-C), 140 (3,5-C), 146 (1,2-C), 148 (9-C), 158 (7-C); 7-*C*(CH_3)$_3$ not observed. − EI MS (70 eV): *m/z* (%): 510 (100) [M^+], 495 (10) [M^+ − Me]. − $C_{26}H_{40}Se_2$ (510.50): calcd. C 61.17, H 7.90; found C 61.06, H 7.99.

2: M.p. 211−213°C. − ^{1}H NMR (200 MHz, $CDCl_3$): δ = 1.19 (s, $^1J_{CH}$ = 18 Hz, 9 H, *t*Bu), 1.40 (s, $^1J_{CH}$ = 18 Hz, 9 H, *t*Bu), 6.56 (s, $^1J_{CH}$ = 18 Hz, 1 H, 4-H). − ^{13}C NMR (50 MHz, $CDCl_3$): δ = 29.9 [C(CH_3)$_3$], 32.6 [C(CH_3)$_3$], 35.1 [*C*(CH_3)$_3$], 92.1 (1-C), 131 (4-C), 138 (5-C), 147 (2-C), 154 (3-C). − EI MS (70 eV): *m/z* (%): 588 (100) [M^+], 573 (26) [M^+ − Me], 512 (21) [M^+ − Se]. − $C_{26}H_{38}Se_3$ (587.44): calcd. C 53.16, H 6.52; found C 53.31, H 6.59.

Solution and Refinement of Structures **1** *and* **2**: Crystal data for structures **1** and **2** are given in Table 1. Data were collected with a Siemens P4 diffractometer with Mo-K_α (λ = 0.71073 A) radiation (graphite monochromator) using ω scans and were corrected for Lorentz and polarization effects. An empirical absorption correction based on a series of ψ scans was applied. The structures were solved by direct methods using SHELXS-86[12], and refined by a full-matrix least-squares procedure on F^2 using SHELXL-93[13]. The positions of the hydrogen atoms were calculated and were included in the refinement with isotropic temperature parameters 1.2 or 1.5 times higher than U_{eq} of the carbon atom to which they were attached. The methyl groups of *t*Bu at C(3) and C(7) of **1** are disordered by a rotation of 60° about the C−C(CH_3)$_3$ bond. The ratios of the two possible orientations are almost 5:3 at C(3) and 4:1 at C(7). Figure 2 shows the methyl groups in the major position. Crystallographic data (excluding structure factors) for the structures reported in this paper have been deposited with the Cambridge Crystallographic Data Centre as supplementary publication no. CCDC-101066. Copies of the data can be obtained free of

charge on application to CCDC, 12 Union Road, Cambridge CB2 1EZ, U.K. [Fax: (internat.) + 44(0)1223-336033; E-mail: deposit@-ccdc.cam.ac.uk].

[1] G. Thaler, W. Fimml, H. Schütz, K. Wurst, F. Sladky, *J. Organomet. Chem.*, submitted.
[2] G. Thaler, W. Fimml, K. Wurst, F. Sladky, *J. Organomet. Chem.*, submitted.
[3] R. Brand, H.-P. Krimmer, H.-J. Lindner, V. Sturm, K. Hafner, *Tetrahedron Lett.* **1982**, *23*, 5131−5134.
[4] G. K. Pandey, H. Dreizler, *Z. Naturforsch.* **1977**, *32a*, 482−484.
[5] G. Thaler, K. Wurst, F. Sladky, *Organometallics* **1996**, *15*, 4639−4641.
[6] G. Thaler, K. Wurst, F. Sladky, *Chem. Ber.* **1996**, *129*, 69−71.
[7] T. J. Kistenmacher, T. J. Emge, P. Shu, D. O. Cowan, *Acta Crystallogr.* **1979**, *B35*, 772−774.
[8] I. Wagner, W.-W. du Mont, S. Pohl, W. Saak, *Chem. Ber.* **1990**, *123*, 2325−2327.
[9] C. M. Bates, C. P. Morley, M. Di Vaira, *J. Chem. Soc., Chem. Commun*. **1994**, 2621−2622.
[10] J. M. Williams, *Progr. Inorg. Chem*. **1985**, *33*, 183−220.
[11] C. G. Vernier, E. W. Casserly, *J. Am. Chem. Soc*. **1990**, *112*, 2808−2809.
[12] G. M. Sheldrick, *SHELXS-86, Program for Crystal Structure Solutions*, University of Göttingen, Germany, **1986**.
[13] G. M. Sheldrick, *SHELXL-93, Program for the Refinement of Structures*, University of Göttingen, Germany, **1993**.

[98022]

Synthesis and Properties of Silver(I) and Copper(I) Helicates with Imine-Bridged Oligobipyridine Ligands

Regine Stiller[+] and Jean-Marie Lehn*

Institut Le Bel, Université Louis Pasteur,
4, rue Blaise Pascal, F-67000 Strasbourg, France

Received February 12, 1998

Keywords: Helicates / Oligobipyridine ligands / Self-recognition / NMR titration / Self-assembly

Oligobipyridine ligands containing one or two imine bridges were found to form double helicates by treatment with copper(I) or silver(I). The properties of the complexes are similar to those of oxapropylene-bridged oligobipyridines. Titration of a mixture of the bis(bipyridine) and the tris(bipyridine) ligands with silver(I) hexafluorophosphate showed that helicates formed with strict self-recognition.

In recent years, the design and study of properties of double and triple helical complexes organized by self-assembly of two or three ligand strands and metal ions to the so-called helicates have been subject to detailed investigations.[1][2][3][4][5][6][7][8] The architectural information is found in the matching between the ligand binding sites and the stereochemical preferences of the metal ion. Complexation of oligo-bidentate strands with tetrahedrally or octahedrally coordinating ions leads respectively to double or triple helices[1][2][3][4][5][][7][8][9]. On the other hand, oligotridentate strands give double or triple helices with octahedrally or nine coordinated ions[2][3][10][11]. The helicate formation with oligobipyridine ligands was found to occur with positive cooperativity[12], self-recognition and self/non-self-discrimination.[1][9] In the case of oligobipyridine ligands, spacers are introduced which separate the different metal-binding centers and dispose them in a suitable way for formation of multinuclear complexes. The features (length, flexibility, constitution) of the spacer separating the 2,2′-bipyridines (bpy) should be such as to allow the helical arrangement around metal ions but hinder the coordination of several binding units to the same metal ion by back-folding of the strand. Several spacers have been tested so far, of which the oxapropylene bridge (CH_2-O-CH_2) was the most studied.[1][2][5] The analogous bridge (CH_2-S-CH_2) did not allow helicate formation perhaps due to the competition of sulfur for Cu^I binding.[13] The ethylene bridge (CH_2-CH_2) permits helicate formation with Cu^I[14][15] whereas the unsaturated bridge (CH=CH) does not because of its rigidity.[16] In continuation of these studies, we report here on the syntheses of two novel oligobipyridine strands **1** and **2** with imine bridges. These ligands contain a rigid double bond and a nitrogen atom as potentially competing binding site, so that it has first to be shown whether helicate formation does occur. This −CH=N− bridge can easily be formed from monomer bpy units bearing amine and aldehyde functional groups in a reversible reaction, thus opening the way to the design of a system which might display self-generation and self-replicating properties.

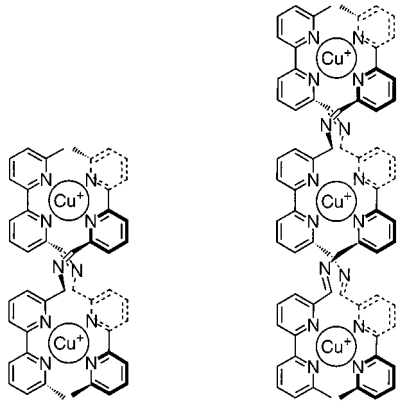

1-H **2-H**

Synthesis of the Oligobipyridine Ligands 1 and 2

The synthetic precursors for the formation of ligands **1** and **2** were all obtained from 6,6′-dimethyl-2,2′-bipyridine **3** (Scheme 1). After radical NBS bromination to **4** followed by amination with hexamethylene tetramine[17][18] the symmetrical diamine **5** was obtained. For the monosubstituted precursors **10** and **11**, another strategy proved to be more practical. Compound **3** was unsymmetrically functionalized by *N*-oxidation with *meta*-chloroperbenzoic acid[19] followed by rearrangement to acetate **6** and hydrolysis to monoalcohol **7**, which, after activation as monomesylate **8**, was converted into monobromide **9**.[5] The monobromide **9** was then converted into the monoamine **10** with hexamethylene tetramine. Alcohol **7** was also oxidized to monoaldehyde **11** under Swern conditions. The ligand synthesis was completed by Schiff base formation between the

[+] Present address: Biochemisches Institut der Universität Kiel, Olshausenstr. 40, D-24098 Kiel.

 © WILEY-VCH Verlag GmbH, D-69451 Weinheim, 1998 1434−1948/98/0707−0977 $ 17.50+.50/0

monoaldehyde **11** and either monoamine **10** or diamine **5** to form the dimer **1** or the trimer **2**, respectively.

Scheme 1. Synthesis of the oligobipyridine ligands **1** and **2**

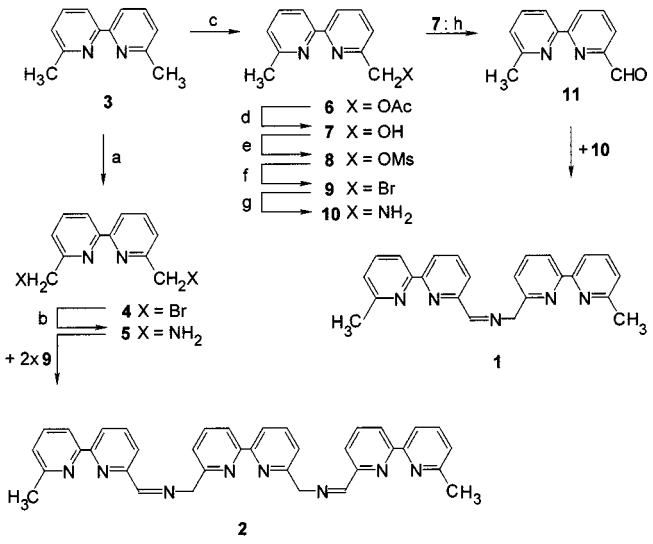

Formation of the Helicates 1-H and 2-H with Ag^I

The helicate complexes of ligands **1** and **2** were formed in situ by stoichiometric addition of the Ag^I salt to the ligands dissolved in CD_2Cl_2 with a minimal amount of CD_3CN. Their helical structure was proved by 500-MHz NMR and 2-dimensional H,H-correlated ^{1}H-NMR spectroscopy (COSY). In line with earlier observations[1][5] helicate formation results in characteristic changes in the NMR spectrum compared to that of the free ligands **1** and **2**. Shifts to lower δ values are observed for the methylene, imine, and methyl protons in the range of $\delta = 0.6-0.8$. As a result of helicate formation, the singlet for the methylene protons of the free ligand is split into an AB system ($J \approx 18$ Hz) because these protons are no longer equivalent in the complex. Furthermore, the singlet for the imine proton is also shifted to smaller δ values and now overlaps with the signals of the aromatic ring protons (compare Figure 3).

The self-assembly of the silver(I) helicates **1-H** and **2-H** was investigated by NMR titration experiments, which were performed by progressively adding a solution of $AgPF_6$ in CD_2Cl_2/CD_3CN (1:1) to a solution of the ligand in CD_2Cl_2 (spectra not shown, compare Figure 3). For trimer **2**, the following changes in the NMR spectrum were observed. Immediately after addition of only 0.28 equiv. of Ag^I with respect to binding sites, the A_2 system of the methylene protons splits into an AB system typical for helicity. Also, the aromatic peaks are significantly shifted up-field. With further addition of Ag^I, the AB pattern is still present, and even with an excess of Ag^I the helix is not destroyed. The dimer helicate is not as stable as the trimer helicate. Titrations of dimer **1** with $AgPF_6$ solution show that in the range of 0.2−0.9 equiv. of Ag^I added, the spectrum only consists of broad signals resulting from fast exchanges. The AB system only appears after addition of exactly one equiv. of Ag^I. On further titration, this signal rapidly converges into an A_2 signal which is shifted upfield (ca 0.7 ppm) compared to the free ligand, indicating that a species different from the helicate or the free ligand is formed. These observations can be explained by dissociation of the helicate structure and fast ligand exchange with the complex(es) formed. This agrees with the following observations: (1) in the new species, the methylene protons give again only an A_2 signal; (2) the imine proton is no longer shielded by the pyridine rings of the second strand, indeed a singlet at $\delta = 8.35$ appears which can be assigned to the imine proton; (3) on further addition of Ag^I the spectrum does not change.

Spectral and Thermodynamic Properties of the Copper(I) Helicates

The UV spectra of the colorless ligands **1** and **2** in dichloromethane as well as their monomers **5**, **10**, and **11** display two intense absorptions around 240 nm and 300 nm attributed to $\pi_2 \rightarrow \pi^*$ and $\pi_1 \rightarrow \pi^*$ by comparison with 2,2′-bipyridine.[20] Upon complexation with Cu^I ions, the $\pi_2 \rightarrow \pi^*$ band is split into several bands and the $\pi_1 \rightarrow \pi^*$ band is slightly red-shifted. Most significant is the appearance of a new band near 450 nm, which is responsible for the red color of the complexes. It can be assigned to MLCT ($Cu^I \rightarrow \pi^*$) transitions typical for pseudotetrahedral $[Cu(a,a'\text{-diimine})_2]^+$ chromophores.[21]

Figure 1. UV spectra for the titration of the bis(bipyridine) ligand **1** with $[Cu(CH_3CN)_4](PF_6)$ in dichloromethane; the amount of salt added increases from 1 to 19

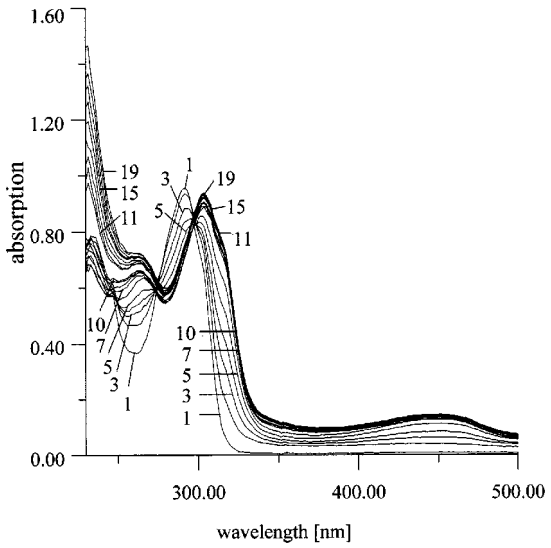

Figure 1 displays the UV spectra of the titration of dimer **1** with $[Cu(CH_3CN)_4](PF_6)$. Two isosbestic points can be distinguished at 299 nm and 273 nm. This indicates that either only two main products exist in solution or that eventual intermediates have the same molar extinction coefficient ε. With increasing Cu^I concentration, the bands for the $\pi \rightarrow \pi^*$ transitions are red-shifted because of complex formation. The absorbance diagram (not shown) for the MLCT band indicates that the final level is reached at a

ratio $c_M/c_L = 1$, which corresponds to equivalency for helicate formation.

The data obtained from the titration spectra were used for the determination of the binding constants with the LETAGROP-SPEFO program.[12a] This program allows the calculation of the binding constants β_{ml} for each species M_mL_l of a proposed model in a non-linear best fit of spectrophotometric data. For the dimer, the following equilibria should be considered:

$$M + L \rightleftharpoons ML$$
$$ML + L \rightleftharpoons ML_2$$
$$ML_2 + M \rightleftharpoons M_2L_2$$

The first equilibrium was neglected as its inclusion did not yield satisfactory results. This is reasonable since the formation of a 1:1 complex is unlikely for steric reasons. The log β_{ml} values calculated are in good agreement with those determined for a 4,4′-substituted dimer:[22]

$$\log \beta_{12} = 9.1 \qquad M + 2\,L \rightleftharpoons ML_2$$
$$\log \beta_{22} = 13.05 \qquad 2\,M + 2\,L \rightleftharpoons M_2L_2$$

Titration spectra for the trimer **2** are given in Figure 2. An isosbestic point is found at 273 nm. It should be noted that the absorbance at 450 nm first increases with the concentration of Cu^I as the trimer helicate is formed, but with an excess of more than 1.35 equiv. of Cu^I, it sinks again indicating the destruction of the helicate. This differs from the results obtained for NMR titrations with Ag^I (see above) and may be related to the higher stability of Cu^I versus Ag^I helicates. The ε value of the $\pi_1 \rightarrow \pi^*$ transition decreases much more than in the case of the dimer, and a shoulder develops at 313 nm.

Figure 2. UV spectra for the titration of the tris(bipyridine) ligand **2** with $[Cu(CH_3CN)_4](PF_6)$ in dichloromethane; the amount of salt added increases from 1 to 19

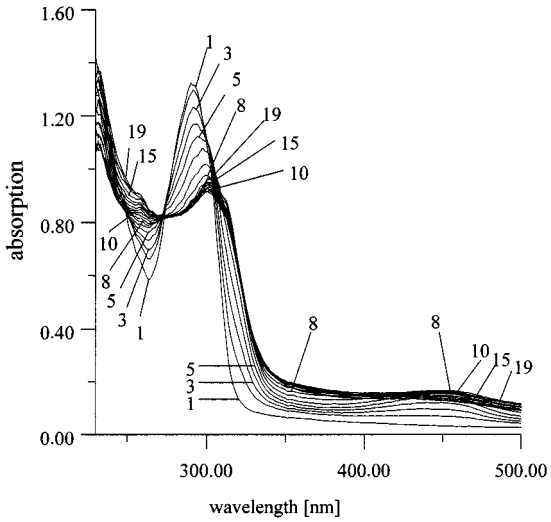

Self-Recognition in the Self-Assembly of the Helicates 1-H and 2-H

It has been found earlier that helicate formation from mixtures of oligobipyridine ligands occurs with self-recog-

Figure 3. 200-MHz ^{1}H-NMR spectra for the titration of ligands **1** and **2** in CD_2Cl_2 with $AgPF_6$ in CD_2Cl_2/CD_3CN (1:1); signals ascribed to the dimer are identified by **1**, those of the trimer by **2**; the following equivalents of Ag^I were added: A−E: 0, 0.2, 0.61, 0.75, 1 equiv. with respect to bipyridine binding sites

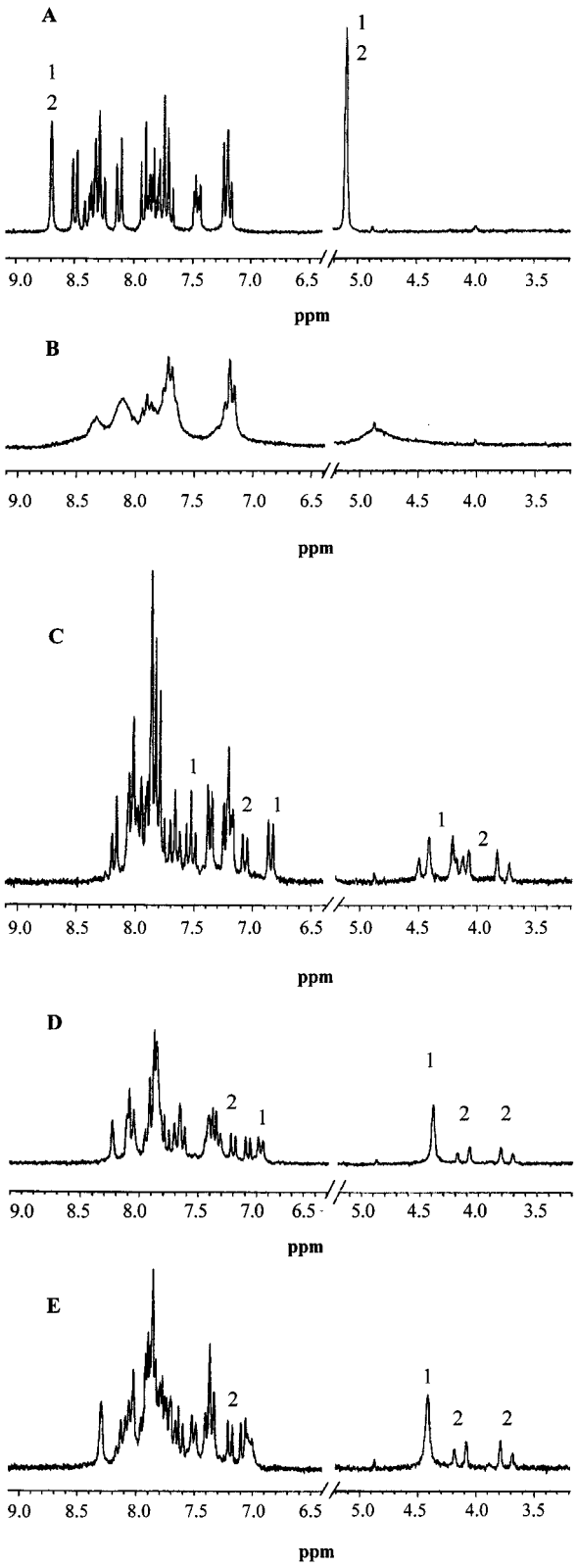

nition, each strand assembling with an identical partner.[9] In order to investigate whether this was also the case with the present ligands **1** and **2**, we performed a competition experiment by titrating mixtures of the two compounds. In a vernier mechanism[9][23], two complementary components differing in length aggregate to give linear side-by-side adducts; growth may then continue until the tips of the adjacent aggregates are in register. According to this model, an aggregate of 2 trimers, 3 dimers, and 6 Ag^I ions would form, whereas self-recognition of identical ligands leads to two individual helicate species. A mixture of 1.5 equiv. of dimer **1** and 1 equiv. of trimer **2** in CD_2Cl_2 was titrated with a solution of $AgPF_6$ in CD_2Cl_2/CD_3CN (1:1) and the titration was followed by recording the 200-MHz ^{1}H-NMR spectra (Figure 3). In agreement with titrations of the individual ligands, the singlet for the methylene protons collapsed to a broad signal immediately after addition of Ag^I. At low salt concentration, all signals were broad and badly resolved due to fast exchange. After addition of ca. 0.5 equiv. Ag^I per binding site, helicate formation can be anticipated, and indeed with 0.6 equiv. Ag^I added, two individual AB systems corresponding to the dimer and trimer helicates were clearly resolved. These titration NMR spectra (Figure 3) combine the features of the individual titration spectra indicating strict self-recognition as no new species are found. A polymer resulting from the vernier mechanism would be destabilised by steric interaction in the center of the structure between the methyl groups. On the other hand, its formation is entropically disfavored as the number of particles formed is smaller than in the case of a mixture of helicates. This agrees with the previous results where self-recognition in helicate formation with (CH_2-O-CH_2)-bridged oligobipyridine ligands was observed.[9] The ability to form helicates as well as to perform self-recognition make imine-bridged oligobipyridine strands potential candidates for setting up systems displaying self-generation and self-replication processes.[29]

We thank the *Alexander von Humboldt Stiftung* for a *Feodor Lynen* stipend to R. S. as well as the *CNRS* (URA422) and the *College de France* for financial support. We are also grateful to Dr. *Annie Marquis* for her help in some experiments and measurements and for the binding constants computations.

Experimental Section

General: All solvents were freshly distilled: chloroform from $CaCl_2$; acetonitrile and DMSO from CaH_2; dichloromethane, CCl_4 and TEA from P_2O_5; toluene from Na; THF from Na/benzophenone. Ethyl acetate and solvents used for imine syntheses and UV experiments were filtered through basic alumina before use. Reagents were used without further purification unless otherwise noted. $AgPF_6$ was obtained from Merck. $[Cu(CH_3CN)_4]PF_6$, $[Cu(CH_3CN)_4]BF_4$ and $[Cu(CH_3CN)_4]ClO_4$ were prepared according to a literature procedure.[24] − M.p. (uncorrected): Digital melting-point apparatus (Electrothermal). − UV/Vis: Cary 13 spectrometer. − NMR: Bruker AC-200 and Bruker ARX 500; chemical shifts in ppm rel. to TMS ($\delta = 0$). − 6-Bromo-2-picoline[25], 6,6′-dimethyl-2,2′-bipyridine[26] (**3**), 6,6′-bis(bromomethyl)-2,2′-bipyridine (**4**)[27], 6,6′-bis(aminomethyl)-2,2′-bipyridine (**5**)[18], 6-(hydroxymethyl)-6′-methyl-2,2′-bipyridine (**7**)[19], 6-(bromomethyl)-6′-methyl-2,2′-bipyridine (**9**)[28] were prepared according to literature procedures. Crude monoalcohol **7** was further purified by chromatography [alumina; A: dichloromethane; B: dichloromethane/2% methanol; elution procedure: 700 ml of A, followed by 400 ml of A/B (3:1), followed by 300 ml of A/B (2:1)]. In some cases, crude **7** was partitioned between water (pH = 2−3) and chloroform/hexane (1:1). The water phase containing **7** was neutralized with $NaHCO_3$ and extracted with chloroform. The organic layer was then dried with Na_2SO_4 and concentrated.

Bis(bipyridine) Ligand **1**: 30 mg (0.15 mmol) of monoamine **10** was suspended in 1 ml of acetonitrile. A solution of 30 mg (0.15 mmol) of monoaldehyde **11** in 1 ml of acetonitrile was added slowly. Immediately, a white precipitate formed. The mixture was stirred at room temp. under argon for 2 h. The white precipitate was centrifuged off, washed with acetonitrile, again centrifuged, and dried under vacuum yielding 46 mg of **1** (0.12 mmol, 80%) as a white solid, m.p. 181−182°C. − $C_{24}H_{21}N_5$ (379.18): calcd. C 75.97, H 5.58, N 18.46; found C 76.22, H 5.83. − FAB-MS: *m/z* calcd. for M^+: 379.18; found for MH^+: 380.1; EI-MS: M^+: 379.2. − ^{1}H NMR (500 MHz, CD_2Cl_2): δ = 8.69 (s, 1 H, imine-*H*), 8.48 (d, 1 H, aromatic-3^{II}), 8.33 (d, 1 H, aromatic-3^{III}), 8.30 (d, 1 H, aromatic-3^{I}), 8.26 (d, 1 H, aromatic-3^{IV}) 8.11 (d, 1 H, aromatic-5^{II}), 7.89 (t, 1 H, aromatic-4^{II}), 7.82 (t, 1 H, aromatic-4^{III}), 7.73 (t, 1 H, aromatic-4^{I}), 7.70 (t, 1 H, aromatic-4^{IV}), 7.44 (d, 1 H, aromatic-5^{III}), 7.21 (d, 1 H, aromatic-5^{I}), 7.18 (d, 1 H, aromatic-5^{IV}), 5.09 (s, 2 H, C*H*$_2$), 2.61 (s, 3 H, C*H*$_3$), 2.60 (s, 3 H, C*H*′$_3$). − ^{13}C NMR (50.3 MHz, $CDCl_3$): δ = 164.64 (imine-*C*), 158.38, 158.11, 157.95, 156.30, 156.12, 155.27, 154.13, (8 C-C); 137.55, 137.49, 137.21, 137.11, 123.55, 123.29, 122.41, 122.16, 121.02, 119.62, 118.40, 118.26 (12 *C*-H); 66.78 (*C*H$_2$); 24.76 (*C*H$_3$). − UV/Vis dichloromethane/acetonitrile (2:1)]: λ_{max} (lg ε) = 290 nm (4.55), 233 (4.46); shoulder (lg ε) = 301 nm (4.41), 246 nm (4.30).

Tris(bipyridine) Ligand **2**: 50 mg (0.23 mmol) of diamine **5** was suspended in 2 ml of acetonitrile. A solution of 93 mg (0.47 mmol) of monoaldehyde **11**, dissolved in 3 ml of acetonitrile, was added. The mixture was stirred for 2 h under argon at room temp. The white precipitate was centrifuged off, washed with acetonitrile, again centrifuged and dried under vacuum yielding 96 mg of **2** (0.17 mmol, 72%) as a white solid, m.p. 186−188°C. − $C_{36}H_{30}N_8$ (574.69): calcd. C 75.24, H 5.26, N 19.50; found C 74.21, H 5.25, N 19.50. − FAB-MS: *m/z* calcd. for M^+: 574.3; found for MH^+: 575.1. − ^{1}H NMR (500 MHz, CD_2Cl_2): δ = 8.70 (s, 2 H, imine-*H*), 8.49 (dd, 2 H, aromatic-3^{II}), 8.39 (d, 2 H, aromatic-3^{III}), 8.31 (d, 2 H, aromatic-3^{I}), 8.12 (dd, 2 H, aromatic-5^{II}), 7.90 (t, 2 H, aromatic-4^{II}), 7.84 (t, 2 H, aromatic-4^{III}), 7.74 (t, 2 H, aromatic-4^{I}), 7.47 (d, 2 H, aromatic-5^{III}), 7.21 (d, 2 H, aromatic-5^{I}), 5.11 (d, 4 H, C*H*$_2$), 2.62 (s, 6 H, C*H*$_3$). − ^{13}C NMR (50.3 MHz, $CDCl_3$): δ = 164.67 (imine-*C*), 158.34 (C-C), 137.49, 137.18, 123.52, 122.41, 122.29, 121.00, 119.72, 118.25 (C-H), 66.74 (*C*H$_2$), 24.72 (*C*H$_3$). UV/Vis (dichloromethane): λ_{max} (lg ε) = 291 nm (4.68); shoulder (lg ε) = 303 nm (4.55), 247 (4.50).

6-Aminomethyl-6′-methyl-2,2′-bipyridine (**10**): 0.81 g (5.8 mmol) of hexamethylenetetramine was stirred at 40°C in 12 ml of chloroform until everything was dissolved. A solution of 1.32 g (5.6 mmol) of 6-(bromomethyl)-6′-methyl-2,2′-bipyridine (**9**) in 10 ml of chloroform was added slowly. A white precipitate formed immediately. The addition funnel was washed with 3 ml of chloroform and the mixture was refluxed for 2 h. After cooling to room temp., the precipitate was filtered and dried. The solid was refluxed for 2 h at 70°C with a mixture of 11 ml of ethanol, 1.5 ml of water, and 1.5 ml of conc. HCl. The solution was left in a refrigerator overnight. The precipitate was filtered off, the filtrate was concentrated

to give more precipitate. The solids were dried under vacuum, redissolved in a minimal amount of water and adjusted to pH = 13 with 6 N NaOH. The water phase was extracted with dichloromethane (3 × 50 ml), the organic phase was dried with Na_2SO_4, concentrated and dried under vacuum yielding 0.33 g **10** (1.7 mmol, 30%) as a yellow solid. − TLC (Al_2O_3; dichloromethane/2% methanol): R_f = 0.10. − ^{1}H NMR (200 MHz, $CDCl_3$): δ = 8.28 (d, 1 H, aromatic H), 8.24 (d, 1 H, aromatic H), 7.76 (t, 1 H, aromatic H), 7.69 (t, 1 H, aromatic H), 7.25 (d, 1 H, aromatic H) 7.16 (d, 1 H, aromatic H), 4.04 (s, 2 H, CH_2), 2.63 (s, 3 H, CH_3), 1.73 (*s*, NH_2). − UV/Vis (dichloromethane): λ_{max} (lg ε) = 239 nm (4.13), 292 (4.34); shoulder (lg ε) = 245 nm (4.11), 283 (4.27), 301 (4.20).

6-Methyl-2,2′-bipyridine-6′-carbaldehyde (**11**): A solution of 2.5 ml of freshly distilled oxalyl chloride in 30 ml of dichloromethane was cooled to −60°C. A mixture of 1.5 ml of DMSO in 6 ml of dichloromethane was added in 10 min and it was stirred for another 10 min at −60°C. A solution of 1.48 g of highly purified 6-hydroxymethyl-6′-methyl-2,2′-bipyridine (**7**) in 12 ml of dichloromethane was added slowly, keeping the temperature at −60°C. The mixture was stirred for 30 min at that temperature. Then, 7.5 ml of TEA was added slowly. After the addition was complete, the mixture was warmed up to room temp. and 30 min later 60 ml of water was added. The organic phase was separated and the water was extracted with dichloromethane (2 × 40 ml). The combined organic phases were washed with 50 ml of brine, dried with Na_2SO_4, and concentrated. The residue was chromatographed [silica gel (2 × 14 cm); A: dichloromethane; B: dichloromethane/2% TEA/2% methanol; elution procedure: 300 ml of A followed by 200 ml of A/B (9:1)]. Recrystallization from ethanol gave 0.31 g of **11** (1.56 mmol, 21%), cream colored solid, m.p. 135−136°C. − TLC (Al_2O_3; dichloromethane/1% methanol): R_f = 0.66. − ^{1}H NMR (200 MHz, $CDCl_3$): δ = 10.16 (s, 1 H, C*H*O), 8.68 (dd, 1 H, aromatic H), 8.34 (d, 1 H, aromatic H), 7.98 (m, 2 H, aromatic H), 7.75 (t, 1 H, aromatic H), 7.22 (d, 1 H, aromatic H), 2.66 (s, 3 H, CH_3). − UV/Vis (dichloromethane): λ_{max} (lg ε) = 287 nm (4.08), 229 (4.15); shoulder (lg ε) = 299 nm (3.92), 253 (3.86).

General Procedure for the Preparation of the Helicate Complexes: Solvents were freshly distilled and filtered through a column of basic alumina and molcular sieves (4 A) before use. Copper(I) salts and silver(I) salts were dissolved in dichloromethane/acetonitrile (1:1). They were stable in solution for several weeks. Complexes were prepared by mixing a solution of the ligand in dichloromethane and adding the proper amount of salt solution (usually 0.5 equivalents per binding site). The complexes were characterized by UV and NMR.

Complexes of the Bis(bipyridine) Ligand **1**

*[Cu_2(**1**)$_2$](ClO_4)$_2$*: UV/Vis (dichloromethane): λ_{max} (lg ε) = 450 nm (3.81), 302 (4.74), 263 (4.62); shoulder (lg ε) = 317 nm (4.62). − FAB-MS: calcd. for $C_{48}H_{42}ClCu_2N_{10}O_4$: 983.17; found for $\{[Cu_2(\mathbf{1})_2](ClO_4)\}^+$: 985.2. − ^{1}H NMR (200 MHz, CD_2Cl_2): δ = 8.55 (d, 1 H, aromatic H), 8.47 (d, 1 H, aromatic H), 8.41 (d, 1 H, aromatic H), 8.24 (d, 1 H, aromatic H), 8.19 (t, 1 H, aromatic H), 8.08 (t, 1 H, aromatic H), 7.96 (t, 1 H, aromatic H), 7.62 (m, 2 H, aromatic H), 7.49 (t, 1 H, aromatic H), 7.36 (d, 1 H, aromatic H), 6.90 (d, 1 H, aromatic H), 4.57 (dd, 1 H, CH_2), 4.32 (dd, 1 H, CH'_2), 2.15 (s, 3 H, CH_3), 1.88 (s, 3 H, CH'_3).

*[Cu_2(**1**)$_2$](PF_6)$_2$*: UV/Vis (dichloromethane): λ_{max} (lg ε) = 451 nm (4.01), 301 (4.84), 267 (4.68), 231 (4.77); shoulder (lg ε) = 317 nm (4.66).

*[Ag_2(**1**)$_2$](PF_6)$_2$*: ^{1}H NMR (500 MHz, CD_2Cl_2): δ = 8.19 (d, 1 H, aromatic-3^{IV}), 8.01 (s, 1 H, imine-*H*), ca. 8.01 (t, 1 H, aromatic-4^{IV}), 7.99 (d, 1 H, aromatic-3^{I}), ca. 7.90 (d, 1 H, aromatic-3^{II}), ca. 7.87 (t, 1 H, aromatic-4^{II}), ca. 7.82 (d, 1 H, aromatic-3^{III}), ca. 7.81 (t, 1 H, aromatic-4^{I}), 7.52 (t, 1 H, aromatic-4^{III}), 7.36 (d, 1 H, aromatic-5^{II}), 7.21 (d, 1 H, aromatic-5^{I}), 7.16 (d, 1 H, aromatic-5^{IV}), 6.84 (d, 1 H, aromatic-5^{III}), 4.46 (d, 1 H, CH_2), 4.17 (d, 1 H, CH'_2), 2.33 (s, 6 H, CH_3). − FAB-MS: calcd. for $[Ag_2(\mathbf{1})_2](PF_6)^+$: 1117.1; found: 1118.7; calcd. for $[Ag_2(\mathbf{1})_2]^{2+}$: 972.1; found: 973.8.

*[Ag_2(**1**)$_2$](*Tf*)$_2$*: ^{1}H NMR (200 MHz, CD_2Cl_2): δ = 8.20 (d, 1 H, aromatic-3^{IV}), ca. 8.01 (m, 3 H, aromatic H/imine-*H*), ca. 7.87 (m, 4 H, aromatic H), 7.52 (t, 1 H, aromatic-4^{III}), 7.42 (d, 1 H, aromatic-5^{II}), 7.20 (d, 1 H, aromatic-5^{I}), 7.15 (d, 1 H, aromatic-5^{IV}), 6.84 (d, 1 H, aromatic-5^{III}), 4.47 (d, 1 H, CH_2), 4.15 (d, 1 H, CH'_2), 2.34 (s, 6 H, CH_3).

Complexes of the Tris(bipyridine) Ligand **2**

*[Cu_3(**2**)$_2$](ClO_4)$_3$*: UV/Vis (dichloromethane): λ_{max} (lg ε) = 450 nm (3.78), 302 (4.71); shoulder (lg ε) = 313 nm (4.66), 260 (4.68). − FAB-MS: calcd. for M^+ ($C_{72}H_{60}Cl_3Cu_3N_{16}O_8$): 1634.15; found 1638.2. − ^{1}H NMR [200 MHz, CD_2Cl_2/CD_3CN (1:1)]: δ = ca. 8.49 (d, aromatic H), ca. 8.14 (m, aromatic H), ca. 8.00 (m, aromatic H), ca. 7.88 (m, aromatic H), 7.62 (t, aromatic H) 7.51 (m, aromatic H), 7.32 (t, aromatic H), 7.16 (d, aromatic H), 7.00 (d, aromatic H), 6.81 (d, aromatic H), 4.12 (d, CH_2), 3.98 (d, CH'_2), 1.95 (s, CH_3).

*[Cu_3(**2**)$_2$](PF_6)$_3$*: UV/Vis (dichloromethane): λ_{max} (lg ε) = 451 nm (4.03)ł 302 (4.80), 231 (4.87); shoulder (lg ε) = 313 nm (4.75), 260 (4.74).

*[Ag_3(**2**)$_2$](PF_6)$_3$*: ^{1}H NMR (500 MHz, CD_2Cl_2): 8.07 (d, 1 H, aromatic-3^{I}), 7.93 (s, 1 H, imine-*H*), ca. 7.88 (t, 1 H, aromatic-4^{I}), 7.86 (d, 1 H, aromatic-3^{II}), 7.65 (t, 1 H, aromatic-4^{II}), ca. 7.61 (d, 1 H, aromatic-3^{III}), 7.47 (t, 1 H, aromatic-4^{III}), 7.13 (d, 1 H, aromatic-5^{II}), 7.02 (d, 1 H, aromatic-5^{I}), 6.74 (d, 1 H, aromatic-5^{III}), 4.44 (d, 1 H, CH_2), 4.32 (dd, 1 H, CH'_2), ca. 1.96 (s, 6 H, CH_3,). − FAB-MS: calcd. for $[Ag_3(\mathbf{2})_2](PF_6)_2^+$: 1762.9, found: 1763.1; calcd. for $\{[Ag_3(\mathbf{2})_2](PF_6)\}^{2+}$: 1614.2, found: 1617.2; calcd. for $[Ag_3(\mathbf{2})_2]^{3+}$: 1469.2, found: 1471.2.

Titration of Ligand **1** *with Ag^I:* 2 mg of dimer **1** (5.3 μmol) was weighed into an NMR tube and dissolved in 0.5 ml of CD_2Cl_2. The solution was then titrated with a 0.125 M $AgPF_6$ solution. NMR spectra were recorded with 70 scans after addition of 7 μl (0.17 equiv.), 14 μl (0.33 equiv.), 19 μl (0.45 equiv.), 24 μl (0.57 equiv.), 31 μl (0.74 equiv.), 37 μl (0.88 equiv.), 42 μl (1 equiv.), 47 μl (1.12 equiv.), 52 μl (1.24 equiv.), 57 μl (1.36 equiv.) 63 μl (1.5 equiv.), 70 μl (1.67 equiv.), 80 μl (1.91 equiv.), 90 μl (2.15 equiv.), 100 μl (2.39 equiv.), 110 μl (2.63 equiv.) and 130 μl (3.11 equiv.) of the Ag^I solution. Equivalents refer to mols of binding site.

Titration of Ligand **2** *with Ag^I:* 4.8 mg of trimer **2** (8.4 μmol) was weighed into an NMR tube and dissolved in 0.5 ml CD_2Cl_2. A solution of AgTf in CD_3CN (78 mM) was prepared. NMR spectra (200 MHz) were recorded with 50 scans after addition of 30 μl (0.28 equiv.), 45 μl (0.42 equiv.), 60 μl (0.56 equiv.), 75 μl (0.7 equiv.), 100 μl (0.84 equiv.), 130 μl (1.12 equiv.), 150 μl (1.31 equiv.), 170 μl (1.50 equiv.), 185 μl (1.64 equiv.) and 205 μl (1.83 equiv.) of the Ag^I solution. Equivalents refer to mols of binding site.

Competition Experiment: 2 mg of dimer **1** (5.3 μmol) and 2 mg of trimer **2** (3.5 μmol) corresponding to 21.1 μmol binding sites were given into an NMR tube and dissolved in 0.75 ml of CD_2Cl_2. The solution was then titrated with a 0.125 M $AgPF_6$ solution. NMR spectra were recorded with 70 scans after addition of successive amounts of Ag^I solution from 7 μl (0.042 equiv.) to 207 μl (1.23 equiv.) in 7−10 μl aliquots. Equivalents refer to mols of binding site, so helicity should be complete after addition of 0.5 equiv.

UV Titration of Ligand **1** *with* Cu^{I}*:* A stock solution of 23.5 μM dimer **1** in dichloromethane was prepared. 1 ml of this solution containing 23.5 nmol of dimer was titrated with a 0.43 mM solution of $[Cu(CH_3CN)_4](PF_6)$ in dichloromethane/acetonitrile (1:1). UV spectra were recorded after addition of successive amounts of Cu^{I} solution from 10 μl (0.18 equiv.) to 260 μl (4.76 equiv.) in 10−15-μl aliquots. Equivalents refer to mols of binding site. Absorption values and spectra were automatically corrected for dilution by an internal ADL program of the Cary spectrophotometer.

UV Titration of Ligand **2** *with* Cu^{I}*:* A stock solution of 28.7 μM of trimer **2** in dichloromethane was prepared. 1 ml of this solution containing 28.7 nmol of the trimer was titrated with a 0.43 mM solution of $[Cu(CH_3CN)_4](PF_6)$ in dichloromethane/acetonitrile (1:1). UV spectra were recorded after addition successive amounts of Cu^{I} solution from 10 μl (0.15 equiv.) to 180 μl (2.69 equiv.) in 10-μl aliquots. Equivalents refer to mols of binding site. Absorption values and spectra were automatically corrected for dilution by an internal ADL program of the Cary spectrophotometer.

[1] J.-M. Lehn, A. Rigault, J. Siegel, J. Harrowfield, B. Chevrier, D. Moras, *Proc. Natl. Acad. Sci. U.S.A.* **1987**, *84*, 2565−2569.
[2] E. C. Constable, *Tetrahedron* **1992**, *48*, 10013−10059; C. Piguet, G. Bernardinelli, G. Hopfgartner, *Chem. Rev.* **1997**, *97*, 2005.
[3] J.-M. Lehn, *Supramolcular Chemistry*, VCH, Weinheim, **1995**, chapter 9.
[4] J.-M. Lehn, A. Rigault, *Angew. Chem.* **1988**, *100*, 1121−1122; *Angew. Chem. Int. Ed. Engl* **1988**, *27*, 1059−1060.
[5] [5a] R. F. Carina, G. Bernardinelli, A. F. Williams, *Angew. Chem.* **1993**, *105*, 1483−1485; *Angew. Chem. Int. Ed. Engl.* **1993**, *32*, 1463−1465. − [5b] C. Piguet, J. C. G. Bünzli, G. Bernardinelli, G. Hopfgartner, A. F. Williams, *J. Am. Chem. Soc.* **1993**, *115*, 8197−8206.
[6] R. Krämer, J.-M. Lehn, A. DeCian, J. Fischer, *Angew. Chem.* **1993**, *105*, 764−767; *Angew. Chem. Int. Ed. Engl.* **1993**, *32*, 703−706.
[7] [7a] T. M. Garrett, U. Koert, J.-M. Lehn, A. Rigault, D. Meyer, J. Fischer, *J. Chem. Soc., Chem. Commun.* **1990**, 557−558. − [7b] U. Koert, M. M. Harding, J.-M. Lehn, *Nature* **1990**, *346*, 339−342.
[8] W. Zarges, J. Hall. J.-M. Lehn, C. Bolm, *Helv. Chim. Acta* **1991, 74**, 1843−1852.
[9] R. Krämer, J.-M. Lehn, A. Marquis-Rigault, *Proc. Natl. Acad. Sci. U.S.A.* **1993**, *90*, 5394−5398.
[10] C. Piguet, G. Bernardinelli, B. Bocquet, A. Quattropani, A. F. Williams, *J. Am. Chem. Soc.* **1992**, *114*, 7440−7451.
[11] B. Hasenknopf, J.-M. Lehn, *Helv. Chim. Acta* **1996**, *79*, 1643−1650.
[12] [12a] A. Pfeil, J.-M. Lehn, *J. Chem. Soc., Chem. Commun.* **1992**, 838−840. − [12b] T. M. Garrett, U. Koert, J.-M. Lehn, *J. Phys. Org. Chem.* **1992**, *5*, 529−532.
[13] U. Koert, J.-M. Lehn, unpublished work, ULP Strasbourg, **1990**.
[14] J.-M. Lehn, R. Ziessel, *Helv. Chim. Acta* **1988**, *71*, 1511−1516.
[15] M.-T. Youinou, R. Ziessel, J.-M. Lehn, *Inorg. Chem.* **1991**, *30*, 2144−2148.
[16] [16a] Y. He, J.-M. Lehn, *Chem. J. Chinese Univ.* **1990**, *6*, 183−188. − [16b] D.-P. Funeriu, Y. He, H.-J. Biester, J.-M. Lehn, *Bull. Soc. Chim. Fr.* **1996**, *133*, 673−678.
[17] N. Blazevic, D. Kolbah, B. Belin, V. Sunjic, F. Kajfez, *Synthesis* **1979**, 161−176.
[18] B. Alpha, E. Anklam, R. Deschenaux, J.-M. Lehn, M. Pietraskiewicz, *Helv. Chim. Acta* **1988**, *71*, 1042−1052.
[19] G. R. Newkome, W. E. Puckett, G. E. Kiefer, V. K. Gupta, Y. Xia, M. Coreil, M. A. Hackney, *J. Org. Chem.* **1982**, *47*, 4116−4120.
[20] K. Nakamoto, *J. Phys. Chem.* **1960**, *64*, 1420−1425.
[21] E. Müller, C. Piguet, G. Bernardinelli, A. F. Williams, *Inorg. Chem.* **1988**, *27*, 849−855.
[22] A. Pfeil, J.-M. Lehn, unpublished work, ULP Strasbourg, **1991**.
[23] J. S. Lindsey, *New J. Chem.* **1991**, *15*, 133−180.
[24] [24a] G. J. Kubas, *Inorg. Synth.* **1979**, *19*, 90−92. − [24b] B.J. Hathaway, D. G. Holah, J. D. Postlethwaite, *J. Chem. Soc.* **1961**, 3215−3218.
[25] G. R. Newkome, D. C. Pantaleo, W. E. Puckett, P. L. Ziefle, W. A. Deutsch, *J. Inorg. Nucl. Chem.* **1981**, *43*, 1529−1531.
[26] T. Rode, E. Breitmeier, *Synthesis* **1987**, 574−576.
[27] J.-C. Rodriguez-Ubis, B. Alpha, D. Plancherel, J.-M. Lehn, *Helv. Chim. Acta* **1984**, *67*, 2264−2269.
[28] G. R. Newkome, V. K. Gupta, F. R. Fronzcek, *Inorg. Chem.* **1983**, *22*, 171−174.
[29] A. Marquis, J.-M. Lehn, work in progress.

[98028]

Generation of 1,3-Dithia-, 1-Selena-3-thia-, and 1,3-Diselena-2-tellurole by Neutralization-Reionization Mass Spectrometry☆

Detlef Schröder[a], Helmut Schwarz*[a], Björn Löbrecht[a], Wolfram Koch[a], and Satoshi Ogawa[b]

Institut für Organische Chemie der Technischen Universität Berlin[a],
D-10623 Berlin, Germany

Department of Applied Chemistry and Molecular Science, Faculty of Engineering, Iwate University[b],
Morioka 020-8551, Japan

Received February 16, 1998

Keywords: Telluroles / Neutralization−reionization mass spectrometry / DFT calculations

2,2-Dichloro-1,3-dichalcogena-2-telluroles of sulfur and selenium, $C_6H_4[XTe(Cl)_2Y]$ with X, Y = S, Se, serve as precursors to generate the cation radicals of 1,3-dichalcogena-2-telluroles $C_6H_4[XTeY]^{+\bullet}$ as well as the corresponding neutral counterparts by means of neutralization-reionization mass spectrometry. These neutral 2-telluroles are intrinsically stable for at least 1 μs in the gas phase. The most abundant fragmentation channel at the neutral and cationic stages is due to loss of atomic tellurium to afford the corresponding benzo-1,2-dichalcogena-cyclobutenes. For the latter, partial isomerization to the related dichalcogena-*ortho*-quinones is indicated by the mass-spectrometric fragmentation pattern.

Fused aromatic ring systems comprise a huge body of heterocyclic chemistry including several natural products, e.g. indole derivatives. Heterocycles containing chalcogens are of particular relevance in redox processes, but knowledge about heteroindenes with several chalcogenes directly attached to each other is limited[1]. In particular, benzodichalcogena-2-telluroles, viz. 1,3-dichalcogena-2-telluraindenes, have not been isolated so far.

Scheme 1

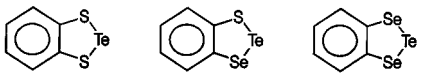

In this contribution, we describe the generation of the ionized and neutral 1,3-dichalcogena-2-telluroles **1**−**3** (Scheme 1) by means of neutralization-reionization mass spectrometry (NR)[2].

Results and Discussion

The cation radicals of the 1,3-dichalcogena-2-telluroles **1**−**3** are readily formed upon electron ionization (EI) of the corresponding 2,2-dichlorides, as shown in Scheme 2 for the dithia compound. The ease of one-electron oxidation of 1,2,3-trichalcogenoles has been demonstrated previously,[1] but the mass spectra do not reveal whether two chlorine atoms or molecular chlorine is lost from the precursors upon ionization. Thermal dechlorination appears unlikely, however, because $Cl_2^{+\bullet}$ is hardly observed in the EI mass spectra. None of the precursors yields a significant signal for the respective molecular ion of the corresponding dichloride, while weak isotope patterns for the monochloro derivatives were observed.

Scheme 2

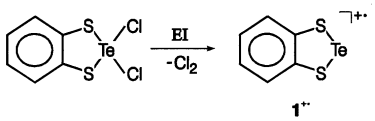

The metastable ion (MI) and collisional activation (CA) mass spectra of the cation radicals $\mathbf{1}^{+\bullet}$−$\mathbf{3}^{+\bullet}$ (Table 1) are dominated by loss of atomic tellurium (Δm = 130) yielding the corresponding $C_6H_4XY^{+\bullet}$ cations (X, Y = S, Se), while loss of neutral C_6H_4XY concomitant with $Te^{+\bullet}$ is hardly observed. Location of the positive charge on the organic fragment can be accounted for by the fact that already the dithiete $C_6H_4S_2$ has an ionization energy (IE) of ca. 8.2 eV[3] which is significantly lower than that of atomic Te (IE = 9.0 eV)[4]; thiaselenete C_6H_4SSe and diselenete $C_6H_4Se_2$ are expected to have IEs even lower than 8.2 eV. Additional fragmentation channels of the cation radicals are due to bond cleavages involving the other chalcogene atoms, while degradation of the hydrocarbon backbone is negligible. Interestingly, also losses of the chalcogene dimers S_2, SeS, Se_2, TeS, and TeSe, respectively, are observed to some extent. The three former of these fragments indicate the possible occurrence of some rearrangements prior to fragmentation because the connectivities of these diatomic entities are not contained in the precursor molecules (see below).

In neutralization-reionization (NR) mass spectrometry, fast-moving ions are subjected to a double-collision event in which first the ion is neutralized, then any remaining ions are deflected, and subsequently the neutrals are reionized

 © WILEY-VCH Verlag GmbH, D-69451 Weinheim, 1998 1434−1948/98/0707−0983 $ 17.50+.50/0

Table 1. Mass differences (Δm in amu) in metastable ion (MI) and collisional activation (CA) mass spectra of $\mathbf{1}^{+\bullet}-\mathbf{3}^{+\bullet}$ (data are given as percentages of the base peak)[a]

Δm (amu)[b] neutral lost[c]		−32 S	−64 S_2	−80 Se	−108 C_6H_4S	−112 SeS	−130 Te	−156 C_6H_4Se	−160 Se_2	−162 TeS	−194 TeS_2
$\mathbf{1}^{+\bullet}$	MI		3				100				
	CA	3	10		5		100		8	2	1
$\mathbf{2}^{+\bullet}$	MI			4			100			1	
	CA	2		12	15	8	100	3		4	
$\mathbf{3}^{+\bullet}$	MI			10			100		3		
	CA			15			100	8	3		

[a] For the sake of clarity in the MI spectra intensities of less than 1% are omitted, and for the CA spectra only the leading fragments are given. − [b] All data refer to the most abundant isotopes ^{32}S, ^{80}Se, and ^{130}Te, respectively. − [c] Some of the neutrals may also arise from multiple fragmentations, e.g. $\Delta m = 206$ may either correspond to loss of intact C_6H_4Te or to consecutive losses of Te and C_6H_4.

to allow for conventional mass-spectrometric detection[2]. Often, xenon is used as a collision gas for the neutralization of cations having kinetic energies in the keV range. For $\mathbf{1}^{+\bullet}-\mathbf{3}^{+\bullet}$, however, no recovery signals due to the reionized neutrals **1**−**3** are detectable when xenon is used for neutralization of the cation radicals, while recovery signals are observed when other collision gases are used. Target gas effects in NR mass spectrometry have been analyzed by Holmes[5] and have been associated with the thermochemistry of the neutralization step. In analogy to other heteroindenes, we can certainly estimate that the ionization energies of **1**−**3** are below 8 eV. Thus, due to the high ionization energy (IE) of xenon (12.1 eV), electron transfer from xenon to the cation radicals $\mathbf{1}^{+\bullet}-\mathbf{3}^{+\bullet}$ is highly endothermic and requires a large amount of energy transfer in the collision. As a consequence, the Franck−Condon factors for neutralization are unfavorable and fragments prevail the NR mass spectra instead. Therefore, we have examined some other collision gases for which electron transfer to the cation radicals $\mathbf{1}^{+\bullet}-\mathbf{3}^{+\bullet}$ is less endothermic, and the best results were obtained using cyclopropane (IE = 9.9 eV) and trimethylamine (IE = 7.8 eV), respectively.

The NR spectrum of $\mathbf{1}^{+\bullet}$ is dominated by signals due to $Te^{+\bullet}$ and $TeS^{+\bullet}$ (Figure 1a), but an unambiguous signal due to the reionized neutral parent is also detected. Similarly, recovery signals for the reionized neutral counterparts are present in the NR spectra of $\mathbf{2}^{+\bullet}$ and $\mathbf{3}^{+\bullet}$ along with $Te^{+\bullet}$, $TeS^{+\bullet}$, and $TeSe^{+\bullet}$ fragments (Figures 1b and 1c). The mere observation of the recovery signals implies that in the gas phase the neutral 1,3-dichalcogena-2-telluroles **1**−**3** correspond to stable species which can survive the flight time between the neutralization and the reionization events (about 1 μs). Although this time interval appears to be short, these telluroles can be considered as being long-lived as far as unimolecular processes are concerned, because the microsecond range is likely to allow for energy distribution over all internal modes. In addition to the recovery signals, several fragment ions are observed which are in accord with the structures **1**−**3** as deduced from the connectivities of the corresponding 2,2-dichlorides used as precursors. Note that the weak, but yet significant loss of atomic Se in Figure 1c points toward the formation of the hitherto unknown benzoselenatellurete, C_6H_4SeTe, from **3**.

Figure 1. NR mass-spectra (trimethylamine/O_2, both 80% *T*) of *B*(1)-mass-selected $C_6H_4\{XTeY\}^{+\bullet}$ cation radicals generated by electron ionization of (a) $C_6H_4\{STe(Cl)_2S\}$, (b) $C_6H_4\{STe(Cl)_2Se\}$, and (c) $C_6H_4\{SeTe(Cl)_2Se\}$

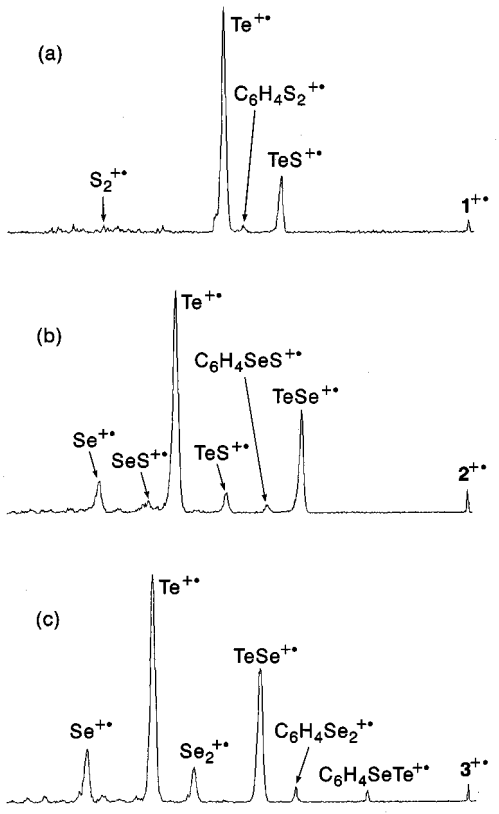

One particular series of fragments in the NR spectra should, however, be discussed in some more detail. Thus, the CA and NR spectra of $\mathbf{1}^{+\bullet}-\mathbf{3}^{+\bullet}$ show weak, but yet distinct signals due to the $S_2^{+\bullet}$, $SeS^{+\bullet}$, and $Se_2^{+\bullet}$, respectively, which are *not* in keeping with the proposed connectivities, because these do not contain S−S, Se−S, and Se−Se bonds, respectively. The most pronounced signal in this respect is the $Se_2^{+\bullet}$ fragment in the NR spectrum of $\mathbf{3}_3^{+\bullet}$ (Figure 1c).

Conceptually, there exist at least two possible scenarios − occurring either at the cationic or the neutral stage − which can account for this result. Route ⓐ involves re-

arrangement of the 2-telluroles (X, Y = S, Se) to the corresponding 1-telluroles **4** and subsequent formation of XY. In contrast, route ⓑ involves a stepwise fragmentation in which first atomic tellurium is lost to yield the dichalcogeno-*ortho*-quinones **5** which may rearrange via X−Y bond formation to bicyclic **6** from which XY can subsequently be formed. In order to get a handle for the distinction of these routes, we have examined the $C_6H_4XY^{+\bullet}$ cation radicals (X, Y = S, Se) which are also formed upon electron ionization of the dichloro telluroles used as precursors for $\mathbf{1}^{+\bullet}$−$\mathbf{3}^{+\bullet}$.

Scheme 3

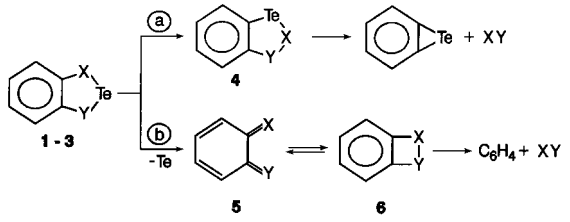

Figure 2. NR mass-spectra (cyclopropane/O_2, both 80% *T*) of *B*(1)-mass-selected $C_6H_4XY^{+\bullet}$ cation radicals generated by electron ionization of (a) $C_6H_4\{STe(Cl)_2S\}$, (b) $C_6H_4\{STe(Cl)_2Se\}$, and (c) $C_6H_4\{SeTe(Cl)_2Se\}$

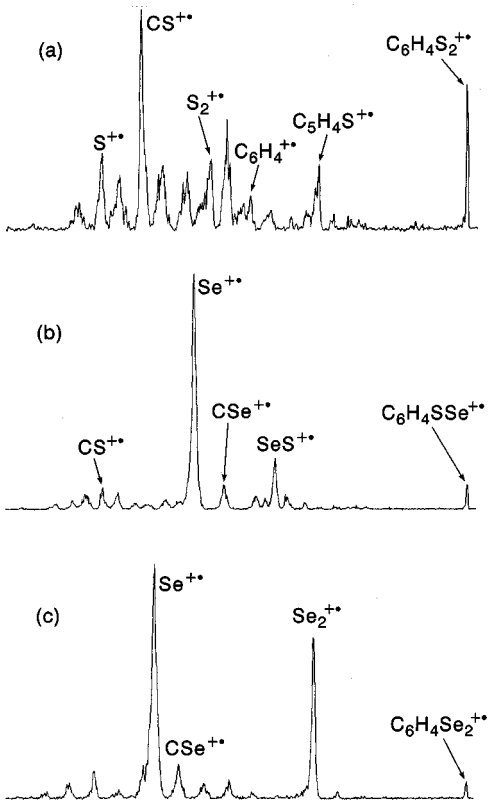

Besides sizable recovery signals, the NR spectra of these $C_6H_4XY^{+\bullet}$ ions show numerous fragments. In fact, the particularly rich fragmentation pattern in the NR spectrum of $C_6H_4S_2^{+\bullet}$ (Figure 2a) can account for the seemingly noisy low-mass region in the NR spectrum of $\mathbf{1}^{+\bullet}$ (Figure 1a) in that this is due to the many fragments formed upon reionization of neutral $C_6H_4S_2^{+\bullet}$. Notwithstanding, all three ions give rise to the corresponding signals due to formation of XY according to route ⓑ in Scheme 3.

Neutral benzodithiete $C_6H_4S_2$ has previously been examined by matrix isolation methods as well as photoelectron spectroscopy[3][6]. These studies have provided strong evidence for the existence of benzodithiete (**6**; X, Y = S), whereas contribution of the dithioquinone structure **5** (X, Y = S) was excluded[7]. Similarly, several substituted 1,2-dichalcogenacyclobutenes of sulfur and/or selenium have been characterized by various means[8][9]. Nevertheless, trapping reactions of dithiete with appropriate dienophiles led to cycloaddition products consistent with the formation of transient **5** (X, Y = S)[3].

Qualitatively, the NR spectra lead to a similar conclusion in that formation of the dichalcogenes XY is consistent with **6**, while the signals due to CS and/or CSe losses point towards **5**. Thus, for $C_6H_4S_2^{+\bullet}$ (Figure 2a), the loss of neutral CS and the complementary signal due to reionized CS can be considered to be indicative for the quinone structure **5** (X, Y = S), while the $S_2^{+\bullet}$ fragment is in keeping with structure **6**. The ratios of the corresponding (CX + CY) versus XY fragments decrease from ca. 3:1 for X, Y = S (Figure 2a), to about 1:1 for X = S, Y = Se (Figure 2b) and ca. 1:8 for X, Y = Se (Figure 2c). This trend can be interpreted in the sense that the bicyclic structure **6** is favored over **5** the more Se is incorporated. Moreover, the increasing abundance of the XY fragments going from X, Y = S to X, Y = Se provides a rationale for the $XY^{+\bullet}$ signals in the NR spectra of $\mathbf{1}^{+\bullet}$−$\mathbf{3}^{+\bullet}$ by involving route in Scheme 3. In fact, the low-mass parts of the NR spectra shown in Figure 1 can by and large be represented by a superposition of the NR spectra of the C_6H_4XY fragments with that of atomic Te.

In order to distinguish at which stage of the experiment formation of XY from C_6H_4XY takes place, we subjected $C_6H_4Se_2$ to some additional experiments because the corresponding fragment $Se_2^{+\bullet}$ is most pronounced in Figure 1c. In the MI spectrum of $C_6H_4Se_2^{+\bullet}$, loss of atomic Se leading to $C_6H_4Se^{+\bullet}$ is observed almost exclusively (100%). Formation of $Se_2^{+\bullet}$, as the only other fragment, is very minor (3%) and may be due to collisional activation with residual gas in the high-vacuum device. In fact, the 100:3 ratio of $C_6H_4Se^{+\bullet}$ and $Se_2^{+\bullet}$ becomes 100:30 upon collisional activation; in addition, a series of other fragments is formed among which $C_6H_4^{+\bullet}$ is most intense (8%). Accordingly, the fragmentation of the cation via route ⓑ in Scheme 3 can in part account for the $Se_2^{+\bullet}$ signal in the NR spectrum of $\mathbf{3}^{+\bullet}$, but nevertheless, the cation route cannot be a major route because otherwise also $C_6H_4Se^{+\bullet}$ must be much more intense. Accordingly, isomerization via route ⓐ of Scheme 3 can only be neglected, if Se_2 can be formed at the neutral stage. Conventional mass spectrometry cannot provide distinct information about the neutral's reactivity, but some variants of the NR method can be applied[10d]. One of the most sensitive and also straightforward approaches in this respect represents the NIDD method[10] which is based on the comparison of two different ways to accomplish two-

electron transfer either from an anion to a cation or vice versa. To this end, charge reversal (CR)[11] and NR mass spectra are compared with each other. In brief, the resulting NIDD spectra reflect the reactivity of the neutral species, and the scheme is defined as such that reactions occurring at the neutral stage appear as positive peaks, while processes

Figure 3. NIDD mass spectrum of *B*(1)-mass-selected $C_6H_4Se_2^{-\bullet}$ anion radicals generated by electron ionization of $C_6H_4\{SeTe(Cl)_2Se\}$ in the negative mode; note that reionization leads to cations; the NIDD spectrum was obtained by subtracting the normalized ion intensities in the CR mass spectrum (O_2, 80% *T*) of $C_6H_4Se_2^{-\bullet}$ from those in the corresponding NR mass spectrum (O_2/O_2, each 80% *T*); for further details of the NIDD method, see ref.[10]

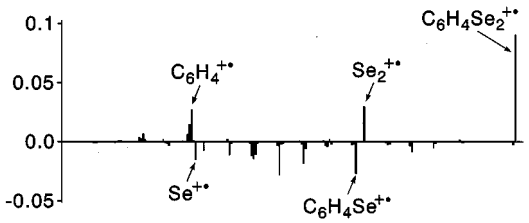

taking place in the ionic stage give rise to negative signals.

The NIDD spectrum of the $C_6H_4Se_2^{-\bullet}$ anion radical (Figure 3) shows three prominent signals at the positive scale, i.e. an intense recovery signal due to neutral counterpart reionized to the cation radical and signals due to reionized Se_2 and C_6H_4. As the latter two fragments are complementary to each other and appear on the positive scale, this observation identifies the occurrence of the reaction $C_6H_4Se_2 \rightarrow C_6H_4 + Se_2$ at the neutral stage. Accordingly, route ⓑ in Scheme 3 can account for the observation of $Se_2^{+\bullet}$ in the NR spectrum of $\mathbf{3}^{+\bullet}$, and although we cannot definitively rule out the isomerization to **4**, there is no need to invoke it. Further, we may assume that the anion radical $C_6H_4Se_2^{-\bullet}$ has an open structure similar to **5** (X, Y = Se), such that the formation of the Se_2 fragment indicates rearrangement to the bicyclic benzodiselenete at the neutral stage.

Figure 4. Calculated structures of C_{2v}-symmetrical **1** and **6** (X, Y = S) using the B3LYP method (bond lengths in A); for the sake of clarity, the hydrogen atoms are left out (all C−H bond lengths are close to 1.085 A)

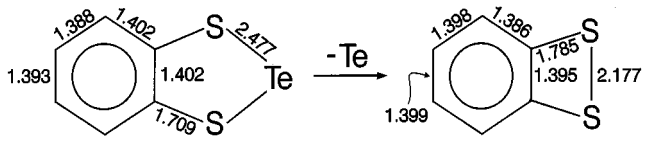

In order to assess the stability of the neutral 2-telluroles, we briefly examined the thermochemistry of the reaction **1** → Te + **6** (X, Y = S) by ab initio methods using the B3LYP method (Figure 4). The calculated structures are consistent with the description of **1** as 1,3-dithia-2-tellurole and formation of benzodithiete upon loss of tellurium. Both species exhibit singlet ground states and the similarity of the C−C bond lengths in the carbon skeleton suggest that these systems maintain aromaticity without any tendency for bond localization. At the B3LYP level of theory we could not locate **5** (X, Y = S) on the singlet surface, but a low-lying triplet state of **5** (X, Y = S) was found which is only about 15 kcal/mol less stable than singlet **6** (X, Y = S). Interestingly, the endothermicity associated with loss of tellurium from neutral **1** is predicted to be as small as 43 kcal/mol. This rather low value is consistent with loss of atomic Te as a low-lying fragmentation channel at the neutral stage and thus can account for the intense signals due to atomic Te present in the NR spectra. As we may expect that the reactions **1** → Te + **6** are even less endothermic when selenium is involved, the computational results add further confidence to the assignment of route ⓑ as the origin for the formation of $S_2^{+\bullet}$, $SeS^{+\bullet}$, and $Se_2^{+\bullet}$ under the experimental conditions.

Conclusions

Neutral 1,3-dithia-, 1-selena-3-thia-, and 1,3-diselena-2-telluroles can be generated by one-electron reduction of the corresponding cation radicals by means of neutralization-reionization mass spectrometry. In this respect, it is, however, of prime importance to choose appropriate neutralization agents, because otherwise long-lived neutrals cannot be assessed and dissociation by loss of atomic tellurium prevails. Thus, this study indicates that target-gas effects are particularly important in the neutralization of heavy, polyatomic ions. Finally, the present experimental results provide evidence for the formation of 3,4-benzo-1,2-dichalcogenacyclobutenes of sulfur, selenium, and tellurium.

Financial support by the *Deutsche Forschungsgemeinschaft*, the *Volkswagen-Stiftung*, the *Fonds der Chemischen Industrie*, and the *Gesellschaft von Freunden der Technischen Universität Berlin* is gratefully acknowledged. S. O. acknowledges a travel support by the *Iwate Network System*. We thank *R. Steudel* for initiating the contact between the German and Japanese research groups.

Experimental Section

The experiments were performed with a modified VG ZAB/HF/AMD 604 four-sector mass spectrometer of *BEBE* configuration (*B* stands for magnetic and *E* for electric sectors), which has been described elsewhere[12]. The cation radicals of the 1,3-dichalcogena-2-telluroles were generated by electron ionization (EI, 70 eV) of the corresponding 2,2-dichlorides. After acceleration to a kinetic energy of 8 keV, the ions of interest were mass-selected using the magnetic and electric sectors as indicated further below. Metastable ion (MI) and collisional activation (CA) spectra of *B*(1)/*E*(1)-mass-selected ions were obtained by monitoring the fragments formed in the field-free region preceding *B*(2) by scanning *B*(2); for CA, helium (80% transmission, *T*) was used as a collision gas. NR experiments were performed by colliding *B*(1)-mass-selected cations with either xenon, cyclopropane, or trimethylamine (80% *T*), deflecting the remaining ions by applying a potential of 1 kV, reionizing the fast neutrals by collision with oxygen (80% *T*), and scanning *E*(1) to monitor the cations formed. The NR spectra recorded for *B*(1)/*E*(1)-mass-selected ions show similar fragmentation pattern, but somewhat poor signal-to-noise ratios. All spectra were accumulated and on-line processed with the AMD/Intectra data system; 5−40 scans were averaged to improve the signal-to-noise ratio. The natural abundances (I_{nat}) of the chalcogenides' isotopes pose quite some restrictions for the mass selection of isotopically pure ion[13]. Accordingly, from the clusters of isotope patterns those ions were

chosen which contain the most abundant isotopes, i.e. ^{32}S (I_{nat} = 95%), ^{80}Se (I_{nat} = 50%), and ^{130}Te (I_{nat} = 34%), respectively. Nevertheless, the correspondingly mass-selected ions are not isotopically pure, e.g. the combination $^{80}Se^{130}Te$ is always accompanied by about 20% of $^{82}Se^{128}Te$. The intensities tabulated further below were corrected according to the natural isotope distributions. Charge reversal (CR)[11] and NR experiments were also performed with $C_6H_4Se_2^{-\bullet}$ anion radicals using oxygen as collision gas in all cases. The CR and NR spectra can be used to assess the unimolecular reactivity of the neutral species by converting them to neutral and ion decomposition difference (NIDD) spectra; for details of the NIDD approach, see ref.[10].

The 2,2-dichloro-1,3-dichalcogena-2-telluroles were prepared in analogy to a previously described method for substituted derivatives[14], and the synthesis of the compounds as well as their spectroscopic characterization will be published elsewhere.

Some quantum-chemical calculations employing the B3LYP density functional were performed using Gaussian94[15]. For tellurium, a relativistic effective core potential with a valence basis set of DZP quality was used[16], while all other atoms were described by the standard 6-311G* basis sets included in Gaussian94.

☆ Dedicated to Professor *Achim Müller*, Bielefeld, on the occasion of his 60th birthday.

[1] [1a] S. Ogawa, T. Kikuchi, S. Niizuma, R. Sato, *J. Chem. Soc., Chem. Commun.* **1994**, 1593. – [1b] S. Ogawa, T. Kikuchi, A. Sasaki, S. Chida, R. Sato, *Tetrahedron Lett.* **1994**, *35*, 5469. – [1c] S. Ogawa, S. Nobuta, R. Nakayama, Y. Kawai, S. Niizuma, R. Sato, *Chem. Lett.* **1996**, 757. – [1d] S. Ogawa, T. Ohmiya, T. Kikuchi, Y. Kawai, S. Niizuma, R. Sato, *Heterocycles* **1996**, *43*, 1843. – [1e] See also: T. M. Barclay, A. W. Cordes, J. D. Goddard, R. C. Mawhinney, R. T. Oakley, K. E. Preuss, R. W. Reed, *J. Am. Chem. Soc.* **1997**, *119*, 12136.

[2] Review: N. Goldberg, H. Schwarz, *Acc. Chem. Res.* **1994**, *27*, 347.

[3] P. de Mayo, A. C. Weedon, G. S. K. Wong, *J. Org. Chem.* **1979**, *44*, 1977.

[4] If not mentioned otherwise, all auxiliary thermochemical data were taken from: S. G. Lias, J. E. Bartmess, J. F. Liebman, J. L. Holmes, R. D. Levin, W. G. Mallard, *Gas Phase Ion and Neutral Thermochemistry, J. Phys. Chem. Ref. Data, Suppl. 1*, **1988, 17**.

[5] J. L. Holmes, *Mass Spectrom. Rev.* **1989**, *8*, 513.

[6] For surveys, see: [6a] J. Voss, in *Methoden der Organischen Chemie (Houben-Weyl)*, vol. E11 (Ed.: D. Klamann), Thieme, Stuttgart **1984**, p. 224. – [6b] H. Meier, N. Hanold, in *Methoden der Organischen Chemie (Houben-Weyl)*, vol. E11 (Ed.: D. Klamann), Thieme, Stuttgart **1984**, p. 1581.

[7] For a similar situation in C_6S_6, see: [7a] D. Sülzle, N. Beye, E. Fanghänel, H. Schwarz, *Chem. Ber.* **1989**, *122*, 2411. – [7b] G. Frenking, *Angew. Chem.* **1990**, *102*, 1516; *Angew. Chem. Int. Ed. Engl.* **1990**, *29*, 1410.

[8] Thiaselenetes: [8a] F. Diehl, A. Schweig, *Angew. Chem.* **1987**, *99*, 348; *Angew. Chem. Int. Ed. Engl.* **1987**, *26*, 343. – [8b] N. Tokitoh, H. Ishizuka, A. Yabe, W. Ando, *Tetrahedron Lett.* **1989**, *30*, 2955.

[9] Diselenetes: [9a] See ref.[8b]. – [9b] K. B. Borisenko, M. Broschag, I. Hargittai, T. M. Klapötke, D. Schröder, H. Schwarz, I. C. Tornieporth-Oetting, P. S. White, *J. Chem. Soc., Dalton Trans.* **1994**, 2705.

[10] [10a] D. Schröder, N. Goldberg, W. Zummack, H. Schwarz, J. C. Poutsma, R. R. Squires, *Int. J. Mass Spectrom. Ion Processes* **1997**, *165/166*, 71. – [10b] J. N. Harvey, D. Schröder, H. Schwarz, *Bull. Soc. Chim. Belg.* **1997**, *106*, 447. – [10c] C. A. Schalley, G. Hornung, D. Schröder, H. Schwarz, *Int. J. Mass Spectrom. Ion Processes* **1998**, *172*, 181. – [10d] C. A. Schalley, G. Hornung, D. Schröder, H. Schwarz, *J. Chem. Soc. Rev.* **1998**, *27*, 91.

[11] M. M. Bursey, *Mass Spectrom. Rev.* **1990**, *9*, 555.

[12] [12a] R. Srinivas, D. Sülzle, T. Weiske, H. Schwarz, *Int. J. Mass Spectrom. Ion Processes* **1991**, *107*, 368. – [12b] R. Srinivas, D. Sülzle, W. Koch, C. H. DePuy, H. Schwarz, *J. Am. Chem. Soc.* **1991**, *113*, 5970. – [12c] C. A. Schalley, D. Schröder, H. Schwarz, *Int. J. Mass Spectrom. Ion Processes* **1996**, *153*, 173.

[13] The isotope patterns were calculated using the Sheffield Chem-Puter which is available via the Internet: http://www.shef.ac.uk/chem/chemputer/isotopes.html (© M. Winter, **1997**).

[14] S. Ogawa, M. Yamashita, R. Sato, *Tetrahedron Lett.* **1995**, *36*, 587.

[15] Revision B.3, M. J. Frisch, G. W. Trucks, H. B. Schlegel, P. M. W. Gill, B. G. Johnson, M. A. Robb, J. R. Cheeseman, T. Keith, G. A. Petersson, J. A. Montgomery, K. Raghavachari, M. A. Al-Laham, V. G. Zakrzewski, J. V. Ortiz, J. B. Foresman, C. Y. Peng, P. Y. Ayala, W. Chen, M. W. Wong, J. L. Andres, E. S. Replogle, R. Gomperts, R. L. Martin, D. J. Fox, J. S. Binkley, D. J. Defrees, J. Baker, J. P. Stewart, M. Head-Gordon, C. Gonzalez, J. A. Pople, *Gaussian 94*, Gaussian, Inc., Pittsburgh, PA, **1995**.

[16] A. Bergner, M. Dolg, W. Küchle, H. Stoll, *Mol. Phys.* **1993**, *80*, 1431.

[98031]

Synthesis of Gold(I) and Gold(II) Complexes with Diphenyl(trimethylsilylmethyl)phosphane

Manuel Bardají[a], Peter G. Jones[b], and Antonio Laguna*[a]

Departamento de Química Inorganica, Instituto de Ciencia de Materiales de Aragón, Universidad de Zaragoza-CSIC[a], E-50009 Zaragoza, Spain

Institut für Anorganische und Analytische Chemie, Technische Universität Braunschweig[b], Postfach 3329, D-38023 Braunschweig, Germany

Received February 16, 1998

Keywords: Gold(I) / Gold(II) / Diphenyl(trimethylsilylmethyl)phosphane / Ligand effects

The reaction of diphenyl(trimethylsilylmethyl)phosphane with [AuCl(tht)] affords the gold(I) complexes [AuCl($PPh_2CH_2SiMe_3$)] (**1**) or [Au($PPh_2CH_2SiMe_3$)$_2$]Cl (**2**). An X-ray study of **1** does not reveal any Au···Au interaction. Treatment of [Au(tht)$_2$](CF_3SO_3) or [Au(tht)(PPh_3)](CF_3SO_3) with diphenyl(trimethylsilylmethyl)phosphane results in the displacement of the thioether ligands to give the ionic complexes [Au($PPh_2CH_2SiMe_3$)$_2$](CF_3SO_3) (**3**) or [Au($PPh_2CH_2SiMe_3$)(PPh_3)](CF_3SO_3) (**4**), the latter mixed with the symmetrical derivatives [Au(PPh_2R)$_2$](CF_3SO_3) (R = Ph, CH_2SiMe_3). The molecular structure of complex **3** has been established by X-ray diffraction and shows an antiperiplanar arrangement of the two PR_2R' rotors in the solid state. The reaction of the phosphane ligand with [Au$_2${μ-$(CH_2)_2PPh_2$}$_2$(tht)$_2$](ClO_4)$_2$ affords the dinuclear gold(II) complex [Au$_2${μ-$(CH_2)_2PPh_2$}$_2$($PPh_2CH_2SiMe_3$)$_2$](ClO_4)$_2$ (**5**).

Introduction

The supramolecular aggregates of gold(I) complexes of type L−Au−X (X = halide or pseudohalide) include dimers, trimers, higher oligomers, and polymers. The degree of oligomerization is determined by several factors, the steric requirement of the ligands being the most clear.[1][2][3]

Gold(I) complexes with silanes attracted particular attention after it was found that auration reactions of silanes or silylated alkylgold complexes afford gold(I) clusters with hypercoordinated carbon or nitrogen centers.[4][5][6][7] Gold complexes containing a silicon unit via a bridging O, S, Se, Te, or As donor atom are also known.[8][9][10][11][12] In contrast, no gold complexes with (silylmethyl)phosphanes have been described so far.

In this paper we describe the synthesis of gold(I) and gold(II) complexes with diphenyl(trimethylsilylmethyl)-phosphane. The crystal structures of [AuCl($PPh_2CH_2SiMe_3$)] and [Au($PPh_2CH_2SiMe_3$)$_2$](CF_3SO_3) have been solved by X-ray diffraction studies.

Results

The reaction of diphenyl(trimethylsilylmethyl)phosphane with [AuCl(tht)] (tht = tetrahydrothiophene), in molar ratio 1:1, proceeds by displacing the tht ligand to give complex **1**, which by reaction with another $PPh_2CH_2SiMe_3$ affords complex **2** (see Scheme 1). The latter can be also synthesised by reaction of $PPh_2CH_2SiMe_3$ and [AuCl(tht)] (molar ratio 2:1). Treatment of [Au(tht)$_2$](CF_3SO_3) with $PPh_2CH_2SiMe_3$ in a 1:2 molar ratio gives complex **3**, containing two phosphane ligands. Treatment of this phosphane with [Au(tht)(PPh_3)](CF_3SO_3) or [Au(thf)(PPh_3)](CF_3SO_3) (thf = tetrahydrofuran) leads to a mixture of **4** and the corresponding symmetric complexes, **3** and [Au(PPh_3)$_2$](CF_3SO_3), as shown in the $^{31}P\{^1H\}$-NMR spectra (Scheme 1).

Scheme 1. (i) [AuCl(tht)]; (ii) 2 [AuCl(tht)]; (iii) [AuCl(tht)]; (iv) [Au(tht)$_2$](CF_3SO_3); (v) [Au(tht)(PPh_3)](CF_3SO_3) or [Au(thf)(PPh_3)](CF_3SO_3)

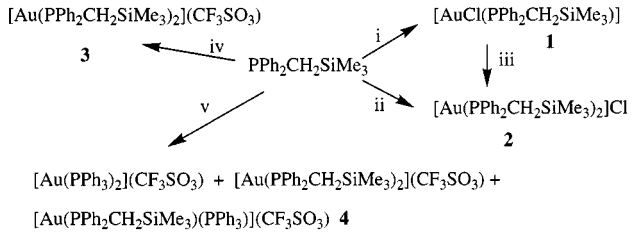

These complexes are air- and moisture-stable white solids at room temperature. They were readily characterised by ^1H and $^{31}P\{^1H\}$ NMR. Their $^{31}P\{^1H\}$-NMR spectra show a singlet at δ = 21.6 (**1**), 27.6 (**2**), and 36.4 (**3**); an AB spin system is observed for **4** (δ_A = 46.7, δ_B = 36.5, $^2J_{AB}$ = 331 Hz), besides two singlets corresponding to symmetric phosphane complexes. In the ^1H-NMR spectra the resonance of the CH_2 is observed at δ ≈ 2: a doublet for **1**−**2** [$^2J_{HP}$ = 15.3 (**1**) and 14.3 (**2**) Hz], a pseudotriplet for **3** (part A of an $A_2XX'A'_2$ system, N = 5.9 Hz) and a doublet of doublets for **4** ($^2J_{HP}$ = 13.7 Hz and $^4J_{HP}$ = 3.5 Hz). Their IR spectra show absorptions at 338 (**1**, medium) and 331 (**2**, very weak) cm^{-1} due to ν(Au−Cl)[13] and to 1264 (br., s) and 636 (m) from triflate[14] (**3**). The LSI-MS mass spectra show peaks at *m/z* (complex, abundance in%) 469 (**1**, 55), 741 (**2**, 100), 741 (**3**, 100), and 731 (**4**, 85) corresponding to $[M - X]^+$ (X = Cl or CF_3SO_3).

The crystal structures of **1** and **3** have been determined by means of X-ray diffraction studies. Complex **1** crystallises

 © WILEY-VCH Verlag GmbH, D-69451 Weinheim, 1998 1434−1948/98/0707−0989 $ 17.50+.50/0

with two independent molecules (Figure 1), of which one is disordered over two positions for all atoms except Au and Cl; a suitably restrained refinement proved successful, but the molecular dimensions of the disordered molecule should be interpreted with caution. Here we discuss only the ordered molecule. The gold(I) center displays an almost linear coordination with Cl−Au−P 176.86(6)°. The Au−P distance is 2.236(2) A, similar to that found in other chlorophosphanegold(I) complexes, 2.235(3) A in [AuCl(PPh$_3$)],[15] 2.236(6) A in [AuCl(PPhMe$_2$)],[16] 2.232(9) A in [AuCl(PEt$_3$)],[17] but somewhat longer than in [AuCl(PPh$_2$CH$_2$CONHMe)] [2.221(1) A].[18] The Au−Cl distance is 2.292(2) A, similar to that found in [AuCl(PEt$_3$)] [2.305(8) A], longer than in [AuCl(PPh$_2$CH$_2$CONHMe)] [2.275(2) A] or in [AuCl(PPh$_3$)] [2.279(3) A], and marginally shorter than in [AuCl(PPhMe$_2$)] [2.316(6) A].

Figure 1. The two independent molecules of compound **1** in the crystal: (a) the ordered molecule; (b) the disordered molecule showing both alternative sites (see text); H atoms omitted for clarity

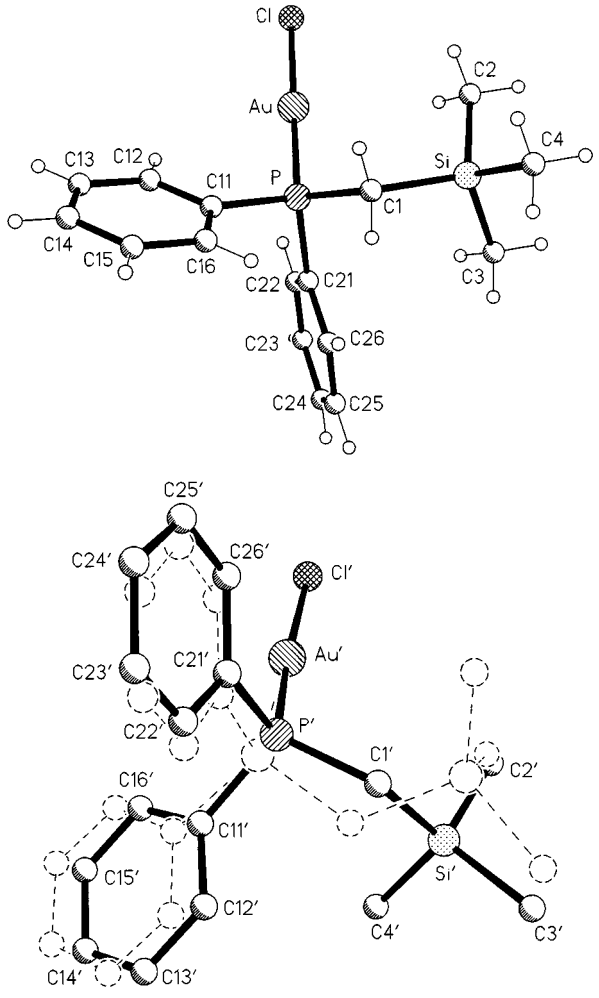

There are no short gold···gold contacts, the shortest Au−Au distance being 6.6 A. This long distance can be rationalised in terms of the steric bulk of the ligand, but it contrasts with other cases, as the 2.881 (1) A found in [Au(PPhMe$_2$)$_2$][Au(GeCl$_3$)$_2$][3], ca. 3.1 A in [AuX(PPhMe$_2$)] [X = Cl, 3.091(2) and 3.230(2) A; Br, 3.119(2) A; and I 3.104(2) A] or even the 5.916(1) A found in [AuCl(AsPh$_3$)][19]. There are no other contacts that could compete with gold−gold interactions, such as the Au···Cl found in [Au{P(*o*-Tol)$_3$}(GeCl$_3$)][3] or the hydrogen bonds in [AuCl(PPh$_2$CH$_2$CONHMe)].

The crystal structure of cation of **3** is shown in Figure 2. The geometry around the gold atom is distorted linear, P(1)−Au−P(2) = 172.12(4)°. The Au−P bond lengths are 2.3080(10) and 2.3149(10) A, similar to that found in other [Au(PR$_2$R′)$_2$]$^+$ complexes, 2.309(3) in [Au(PPh$_2$Me)$_2$][3,4-S$_2$C$_6$H$_3$CH$_3$)$_2$][20], and 2.316(4) A in [Au(PPh$_2$Me)$_2$]PF$_6$,[21] but longer than in [AuCl(PPh$_2$CH$_2$CONHMe)] [2.221(1) A][18] and in **1** [2.236(2) A] probably as a consequence of the lesser *trans* influence of Cl. The PR$_2$R′ ligands adopt an approximately antiperiplanar arrangement, with the torsion angle C1−P1···P2−C5 166°.

Figure 2. The cation of compound **3** in the crystal; H atoms omitted for clarity

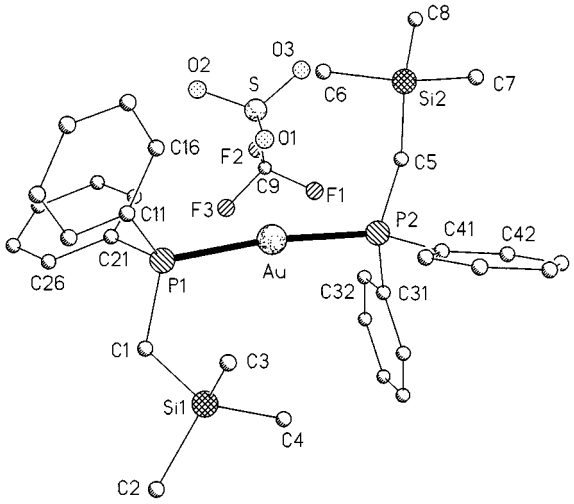

As in the similar complexes [Au(PPh$_2$Me)$_2$]$^+$,[20][21][22] there are no short gold−gold contacts, the shortest Au−Au distance being 9.1 A.

The presence of a pseudotriplet (which can be attributed to two superposed doublets) in the ^{1}H-NMR spectrum instead of the expected doublet could indicate a case of propeller isomerism. Schmidbaur and coworkers[23] reported recently that *ortho*-substituted triarylphosphanes can induce this kind of isomerism in complexes with a coordination number of two, even at room temperature, by hindered rotation of the aryl groups about the P−C$_{ipso}$ axes. The variable-temperature ^{1}H-NMR spectrum of **3** shows a triplet for the CH$_2$ resonance and the ^{31}P{^{1}H} spectrum a singlet from −60 to +20°C in CDCl$_3$ solution; when a ^{1}H{^{31}P}-NMR experiment is carried out at −60°C only one singlet (rather than two) is found, which confirms that there is no propeller isomerism but only two magnetically inequivalent CH$_2$ units (as the parts A of an A$_2$XX′A′$_2$ spin system).

We have also prepared gold(II) complexes by displacement of tht from [Au$_2${μ-(CH$_2$)$_2$PPh$_2$}$_2$(tht)$_2$](ClO$_4$)$_2$ [see Eq. (1)]. Complex **5** is a green solid, air- and moisture-stable

at room temperature. We were unable to obtain single crystals of **5** but expect its structure to be similar to that of $[Au_2(CH_2PPh_2CH_2)(PPh_3)_2](ClO_4)_2$[24]. The IR spectrum shows absorptions at 1092 (br., s) and 623 (m) cm^{-1} from the perchlorate anion[25] and at 568 (m) from ν(Au−C_{ylide})[26]. The $^{31}P\{^1H\}$-NMR spectrum shows two triplets at δ = 46.7 and 23.6 ($^3J_{PP}$ = 38.8 Hz) as expected for an A_2X_2 spin system. In the ^1H-NMR spectra the resonance of the CH_2−Si unit appears as a pseudotriplet (*N* = 5.4 Hz) at δ = 1.98 whilst a doublet at δ = 1.61 ($^2J_{HP}$ = 11.5 Hz) is observed for CH_2−Au; again when a $^1H\{^{31}P\}$-NMR experiment is carried out only a singlet is found for the CH_2−Si unit. The LSI-MS mass spectrum show peaks at *m/z* (abundance in%) 1463 (25) from $[M - ClO_4]^+$ whilst the base peak appears at 741, corresponding to $[Au(PPh_2CH_2SiMe_3)_2]^+$.

$$[Au_2\{\mu\text{-}(CH_2)_2PPh_2\}_2(tht)_2](ClO_4)_2 + 2\ PPh_2CH_2SiMe_3 \rightarrow [Au_2\{\mu\text{-}(CH_2)_2PPh_2\}_2(PPh_2CH_2SiMe_3)_2](ClO_4)_2 + 2\ tht \quad (1)$$

5

We thank the *Direccion General de Investigacion Cientifica y Tecnica* (Project PB94-0079) and the *Fonds der Chemischen Industrie* for financial support.

Experimental Section

General: All the reactions were carried out under argon at room temperature. $[Au(tht)_2](CF_3SO_3)$, $[Au(tht)(PPh_3)](CF_3SO_3)$ and $[Au(thf)(PPh_3)](CF_3SO_3)$ were prepared in situ by reaction of [AuCl(tht)] or $[AuCl(PPh_3)]$ with $[Ag(CF_3SO_3)(tht)]$ or $[Ag(CF_3SO_3)]$ according to a standard procedure: [AuCl(tht)][27], $PPh_2CH_2SiMe_3$[28], and $[Au_2\{\mu\text{-}(CH_2)_2PPh_2\}_2(tht)_2](ClO_4)_2$[24] were prepared according to literature procedures. − IR spectra were recorded on a Perkin-Elmer 883 spectrophotometer, over the range 4000−200 cm^{-1}, by using Nujol mulls between polyethylene sheets. − ^1H- and ^{31}P-NMR spectra were recorded with a Bruker ARX·300 or GEMINI 2000 apparatus in $CDCl_3$ solutions; chemical shifts are quoted relative to $SiMe_4$ (external, ^1H) and H_3PO_4 (external, ^{31}P). − C, H, and N analyses were performed with a Perkin-Elmer 2400 microanalyser. − Melting points were measured with a Büchi apparatus and are uncorrected. − Mass spectra were recorded with a VG Autospec using LSI-MS^+ techniques (with Cs gun) and 3-nitrobenzyl alcohol as matrix.

Caution: Perchlorate salts or derivatives must be manipulated with caution, mainly by avoiding evaporation to dryness.

[AuCl(PPh$_2$CH$_2$SiMe$_3$)] (**1**): To a dichloromethane solution (15 ml) of [AuCl(tht)] (96 mg, 0.3 mmol) was added $PPh_2CH_2SiMe_3$ (82 mg, 0.3 mmol). After stirring for 3 h, the solution was concentrated to ca. 2 ml and hexane (15 ml) was added to obtain **1** as a white solid. **1** was washed with hexane (2 × 5 ml). Yield: 70%, m.p. 118°C. − ^1H NMR: δ = 7.7−7.4 (m, 10 H, Ph), 1.83 (d, 2 H, $^2J_{HP}$ = 15.3 Hz, CH_2−P), 0.08 (s, 9 H, Me). − $C_{16}H_{21}AuClPSi$ (504.82): calcd. C 38.05, H 4.2; found C 37.75, H 3.85.

[Au(PPh$_2$CH$_2$SiMe$_3$)$_2$]Cl (**2**): This product can be synthesised by two different routes: a) To a solution of [AuCl(tht)] (0.064 g, 0.2 mmol) in dichloromethane (10 ml) was added $PPh_2CH_2SiMe_3$ (109 mg, 0.4 mmol). After stirring for 1 h, the solution was concentrated to ca. 2 ml and hexane (15 ml) was added. **2** appeared as a white solid which was washed with hexane (2 × 5 ml). Yield: 70%. b) To a dichloromethane solution (15 ml) of **1** (50 mg, 0.1 mmol) was added $PPh_2CH_2SiMe_3$ (27 mg, 0.1 mmol). After stirring for 1 h, the solution was concentrated to ca. 2 ml and hexane (15 ml) was added. **2** appeared as a white solid which was washed with hexane (2 × 5 ml). Yield: 80%, m.p. 125°C. − ^1H NMR: δ = 7.8−7.3 (m, 10 H, Ph), 2.00 (d, 2 H, $^2J_{HP}$ = 14.3 Hz, CH_2−P), −0.03 (s, 9 H, Me). − $C_{32}H_{42}AuClP_2Si_2$ (777.22) : calcd. C 49.45, H 5.45; found C 49.25, H 5.55.

[Au(PPh$_2$CH$_2$SiMe$_3$)$_2$](CF$_3$SO$_3$) (**3**): To a dichloromethane solution (20 ml) of $[Au(tht)_2](CF_3SO_3)$ (0.15 mmol, prepared "in situ") was added $PPh_2CH_2SiMe_3$ (82 mg, 0.3 mmol). After stirring for 2 h, the solution was concentrated to ca. 2 ml and diethyl ether (15 ml) was added to obtain **3** as a white solid. **3** was washed with diethyl ether. Yield: 70%, m.p. 136°C. − ^1H NMR: δ = 7.7−7.5 (m, 10 H, Ph), 2.08 (t, 2 H, $^2J_{HP}$ = 5.9 Hz, CH_2−P), −0.02 (s, 9 H, Me). − ^1H NMR (−60°C): δ = 7.7−7.5 (m, 10 H, Ph), 2.01 (t, 2 H, $^2J_{HP}$ = 5.7 Hz, CH_2−P), −0.01 (s, 9 H, Me). − $^{31}P\{^1H\}$ NMR (−60°C): δ = 35.8 (s). − $^1H\{^{31}P\}$ NMR (−60°C): δ = 7.8−7.5 (m, 10 H, Ph), 2.01 (s, 2 H, CH_2−P), −0.02 (s, 9 H, Me).− $C_{33}H_{42}AuF_3O_3P_2SSi_2$ (890.84) : calcd. C 44.5, H 4.75, S 3.6; found C 44.4, H 4.65, S 3.8.

[Au(PPh$_2$CH$_2$SiMe$_3$)(PPh$_3$)](CF$_3$SO$_3$) (**4**): This complex, mixed with the corresponding symmetric $[Au(PPh_2R)_2](CF_3SO_3)$ (R = Ph, CH_2SiMe_3), was prepared by two different ways. a) To a dichloromethane solution (20 ml) of $[Au(tht)(PPh_3)](CF_3SO_3)$ (0.15 mmol, prepared "in situ") was added $PPh_2CH_2SiMe_3$ (41 mg, 0.15 mmol). After stirring for 2 h, the solution was concentrated to ca. 2 ml and diethyl ether (15 ml) was added. The white solid was washed with diethyl ether. b) As for a) but using $[Au(thf)(PPh_3)](CF_3SO_3)$, prepared in situ in thf.

[Au$_2${μ-(CH$_2$)$_2$PPh$_2$}$_2$(PPh$_2$CH$_2$SiMe$_3$)$_2$](ClO$_4$)$_2$ (**5**): To a dichloromethane solution (10 ml) of $[Au_2\{\mu\text{-}(CH_2)_2PPh_2\}_2(tht)_2](ClO_4)_2$ (60 mg, 0.05 mmol) was added $PPh_2CH_2SiMe_3$ (27 mg, 0.1 mmol). After stirring for 2 h, the solution was concentrated to ca. 1 ml and diethyl ether (15 ml) was added to obtain **5** as a green solid. **5** was washed with diethyl ether. Yield: 85%, m.p. 120°C (decomp.). − ^1H NMR: δ = 7.5−7.0 (m, 40 H, Ph), 1.98 (t, 4 H, $^2J_{HP}$ = 5.4 Hz, P−CH_2−Si), 1.61 (d, 8 H, $^2J_{HP}$ = 11.5 Hz, Au−CH_2−P), −0.20 (s, 18 H, Me). − $^1H\{^{31}P\}$ NMR: δ = 7.5−7.0 (m, 40 H, Ph), 1.95 (s, 4 H, P−CH_2−Si), 1.60 (s, 8 H, Au−CH_2−P), −0.20 (s, 18 H, Me). − $C_{60}H_{70}Au_2Cl_2O_8P_4Si_2$ (1564.11) : calcd. C 46.05, H 4.5; found C 45.75, H 4.15.

Crystal Structure Determinations: Crystal data and refinement details are given in Table 1. Crystals of **1** were obtained by slow evaporation of a dichloromethane/ethanol slution; crystals of **3** were obtained by slow diffusion at −18°C of diethyl ether into a dichloromethane solution. − *Data collection:* Crystals were mounted in inert oil and transferred to the cold gas stream of a Siemens P4 diffractometer. Intensity measurements were performed using Mo-K_α radiation. Absorption corrections were based on ψ scans. − *Structure solution and refinement:* Solution by the heavy-atom method, anisotropic refinement on F^2 (program SHELXL-93, G.M. Sheldrick, University of Göttingen). H atoms with riding model or as rigid methyl groups. − *Special features*: For **1**, the second independent molecule is disordered, all atoms except Au and Cl occupying two alternative orientations. Nevertheless, the use of appropriate similarity restraints enabled a satisfactorily stable refinement to be performed. Disordered C and Si atoms were refined isotropically. − Full details of the crystal structures (except structure factors) have been deposited at the Cambridge Crystallo-

Table 1. Details of data collection and structure refinement for complexes **1** and **3**

Compound	**1**	**3**
Chemical Formula	$C_{16}H_{21}AuClPSi$	$C_{33}H_{42}AuF_3O_3P_2SSi_2$
Crystal habit	colourless prism	colourless tablet
Crystal size [mm]	0.55×0.20×0.10	0.60×0.30×0.15
Crystal system	triclinic	monoclinic
Space group	$P(-1)$	$P2_1/c$
a [A]	9.9920(12)	11.378(2)
b [A]	10.746(2)	18.880(2)
c [A]	17.707(3)	17.993(2)
α [°]	94.99(2)	90
β [°]	104.97(2)	99.43(1)
γ [°]	94.34(2)	90
V [A^3]	1820.4(5)	3813.2(9)
Z[a]	4	4
D_c [Mg m^{-3}]	1.842	1.552
M	504.80	890.81
F(000)	968	1776
T [°C]	−100	−100
$2\theta_{max}$ [°]	50	50
μ(Mo-K_α) [mm^{-1}]	8.37	4.11
Transmissions	0.49−1.00	0.63−0.96
No. of reflections measured	8494	7220
No. of unique reflections	6389	6714
R_{int}	0.020	0.022
R[a] [F, $F > 4\sigma(F)$]	0.029	0.026
wR[b] (F^2, all refl.)	0.058	0.047
No. of parameters	276	412
No. of restraints	244	280
S[c]	0.90	0.84
Max. Δρ [eA^{-3}]	0.6	0.63

[a] $R(F) = \Sigma||F_o| - |F_c||/\Sigma|F_o|$. – [b] $wR(F^2) = [\Sigma\{w(F_o^2 - F_c^2)^2\}/\Sigma\{w(F_o^2)^2\}]^{0.5}$; $w^{-1} = \sigma^2(F_o^2) + (aP)^2 + bP$, where $P = [F_o^2 + 2F_c^2]/3$ and a and b are constants adjusted by the program. – [c] $S = [\Sigma\{w(F_o^2 - F_c^2)^2\}/(n - p)]^{0.5}$, where n is the number of data and p the number of parameters.

graphic Data Centre, and can be obtained free of charge from CCDC, 12 Union Road, Cambridge CB2 1EZ, England [Fax: (internat.) + 44(0)1223/336033; E-mail: deposit@ccdc.cam.ac.uk] on quoting the reference number CCDC-101120.

[1] P. Pyykkö, N. Runeberg, F. Mendizabal, *Chem. Eur. J.* **1997**, *3*, 1451.
[2] W. Schneider, K. Angermaier, A. Sladek, H. Schmidbaur, *Z. Naturfosch* **1996**, *51b*, 790.
[3] A. Bauer, H. Schmidbaur, *J. Am. Chem. Soc.* **1996**, *118*, 5324.
[4] F.P. Gabbaı, A. Schier, J. Riede, H. Schmidbaur, *Chem. Ber.* **1997**, *130*, 111.
[5] H. Schmidbaur, F.P. Gabbaı, A. Schier, J. Riede, *Organometallics* **1995**, *14*, 4969.
[6] K. Angermaier, H. Schmidbaur, *Chem. Ber.* **1995**, *128*, 817.
[7] S. Bommers, H. Beruda, N. Dufour, M. Paul, A. Schier, H. Schmidbaur, *Chem. Ber.* **1995**, *128*, 137.
[8] A. Bauer, W. Schneider, K. Angermaier, A. Schier, H. Schmidbaur, *Inorg. Chim. Acta* **1996**, *251*, 249.
[9] W. Wojnowski, B. Becker, J. Sassmannhausen, E. M. Peters, K. Peters, H. G. von Schnering, *Z. Anorg. Allg. Chem.* **1994**, *620*, 1417.
[10] P. J. Bonasia, D. E. Gindelberger, J. Arnold, *Inorg. Chem.* **1993**, *32*, 5126.
[11] W. Eikens, P. G. Jones, C. Thone, *Z. Anorg. Allg. Chem.* **1997**, *623*, 735.
[12] D. Fenske, F. Simon, *Z. Anorg. Allg. Chem.* **1996**, *622*, 45.
[13] R. Uson, A. Laguna, M. Laguna, M. N. Fraile, P. G. Jones, G. M. Sheldrick, *J. Chem. Soc., Dalton Trans.* **1986**, 291.
[14] P. J. Stang, Y. Huang, A. M. Arif, *Organometallics* **1992**, *11*, 231.
[15] N.C. Baenziguer, W. E. Bennett, D. M. Soboroff, *Acta Crystallogr., Sect. B* **1976**, *32*, 962.
[16] D. Toronto, B. Weissbart, D. Tinti, A. Balch, *Inorg. Chem.* **1996**, *35*, 2484.
[17] E. R. T. Tiekink, *Acta Crystallogr.* **1989**, *C45*, 1233.
[18] P. Lange, A. Schier, H. Schmidbaur, *Inorg. Chim. Acta* **1995**, *235*, 263.
[19] B. Weissbart, L. J. Larson, M. M. Olmstead, C.P. Nash, D.S. Tinti, *Inorg. Chem.* **1995**, *34*, 393.
[20] M. C. Gimeno, P. G. Jones, A. Laguna, M. Laguna, R. Terroba, *Inorg. Chem.* **1994**, *33*, 3932.
[21] J. J. Guy, P. G. Jones, G. M. Sheldrick, *Acta Crystallogr., Sect. B* **1976**, *32*, 1937.
[22] S. M. Draper, C. E. Housecroft, J. E. Rees, M. S. Shongwe, B. S. Haggerty, A. L. Rheingold, *Organometallics* **1992**, *11*, 2356.
[23] A. Bayler, G. A. Bowmaker , H. Schmidbaur, *Inorg. Chem.* **1996**, *35*, 5959.
[24] R. Uson, A. Laguna, M. Laguna, J. Jimenez, P. G. Jones, *J. Chem. Soc., Dalton Trans.* **1991**, 1361.
[25] M. N. Gowda, S. B. Naikar, G. K. N. Reddy, *Adv. Inorg. Chem. Radiochem.* **1984**, *28*, 255.
[26] H. Schmidbaur, R. Franke, *Chem. Ber.* **1975**, *108*, 1321.
[27] R. Uson, A. Laguna, M. Laguna, *Inorg. Synth.* **1989**, *26*, 85.
[28] B. E. Cooper, W. J. Owen, *J. Organomet. Chem.* **1970**, *21*, 329.

[98033]

Transition Metal Complexes in Organic Synthesis, 41[◇]

Synthesis, Molecular Structure, Fluxional Behavior, and Tricarbonyliron Transfer Reactions of (η^4-1-Azabuta-1,3-diene)tricarbonyliron Complexes

Hans-Joachim Knölker*[a], Gerhard Baum[b], Norbert Foitzik[a], Helmut Goesmann[b], Peter Gonser[a], Peter G. Jones[c], and Herbert Röttele[a]

Institut für Organische Chemie der Universität Karlsruhe[a],
Richard-Willstätter-Allee, D-76131 Karlsruhe, Germany
Fax: +49 (0) 721/698529
E-mail: knoe@ochhades.chemie.uni-karlsruhe.de

Institut für Anorganische Chemie der Universität Karlsruhe[b],
Engesserstraße, D-76128 Karlsruhe, Germany

Institut für Anorganische und Analytische Chemie der Technischen Universität Braunschweig[c],
Hagenring 30, D-38106 Braunschweig, Germany

Received February 27, 1998

Keywords: Azabutadienes / Tricarbonyliron complexes / Transfer reagents / Molecular structure / Fluxionality

The (η^4-1-azabuta-1,3-diene)tricarbonyliron complexes **10** are easily prepared in high yield by condensation of the corresponding arylamines **7** with the cinnamaldehydes **8** and subsequent ultrasound-promoted complexation of the resulting 1-azabuta-1,3-dienes **9** with nonacarbonyldiiron. The complexes **10** are shown to represent excellent reagents for the transfer of the tricarbonyliron fragment onto cyclohexa-1,3-diene (**1a**). The structural characterization for the complexes **10** is achieved by IR, ^{1}H-NMR, and ^{13}C-NMR spectroscopy, as well as X-ray crystallography of **10b**, **10c**, and **10l**. Using variable temperature ^{13}C-NMR spectroscopy the fluxionality of the complexes **10a**, **10b**, **10c**, **10e**, and **2** is investigated and the activation barrier for the turnstile rotation of the tricarbonyliron fragment is determined. The transfer reaction and the structural factors influencing the transfer of the tricarbonyliron fragment are extensively investigated.

Introduction

Tricarbonyl(η^4-cyclohexa-1,3-diene)iron complexes have found many useful applications in synthetic organic chemistry and have been shown to represent excellent starting materials for the stereoselective synthesis of natural products.[1] The parent complex, tricarbonyl(η^4-cyclohexa-1,3-diene)iron (**2**), was prepared first in 1958 by Pauson via complexation of cyclohexa-1,3-diene (**1a**) with pentacarbonyliron under thermal reaction conditions (yield: 21%).[2] The yield of this complexation was later improved by photolytic reaction of cyclohexa-1,4-diene (**1b**) with pentacarbonyliron in benzene (yield: 56%),[3] by reaction of cyclohexa-1,4-diene (**1b**) with pentacarbonyliron in di-*n*-butyl ether at reflux (yield: 46%),[4] by reaction of cyclohexa-1,3-diene (**1a**) with nonacarbonyldiiron in tetrahydrofuran at reflux (yield: 43%),[5] and by photolytic reaction of cyclohexa-1,3-diene (**1a**) with pentacarbonyliron in hexane (yield: 77%)[5] (Scheme 1).

The high synthetic potential of tricarbonyl(η^4-cyclohexa-1,3-diene)iron (**2**) became evident in 1960, when E. O. Fischer found the possibility of hydride abstraction using triphenylmethyl tetrafluoroborate.[6] The reactivity of the resulting tricarbonyl(η^5-cyclohexadienylium)iron tetrafluoroborate (**3**) can be utilized for regio- and stereoselective bond formation with a broad range of nucleophiles.[1] Projected synthetic applications of the complex salt **3** require an access to the iron complex **2** in large scale and high yield. However, the methods described above, involving either thermally or photochemically induced direct complexation of the cyclohexadienes **1a** or **1b** with pentacarbonyliron or nonacarbonyldiiron, afford complex **2** in only 21−77% yield. Moreover, these procedures lead to the formation of pyrophoric iron which is hazardous during

Scheme 1. Complexation of cyclohexa-1,3-diene (**1a**) and cyclohexa-1,4-diene (**1b**) with $Fe(CO)_5$ or $Fe_2(CO)_9$ and preparation of the complex salt **3**

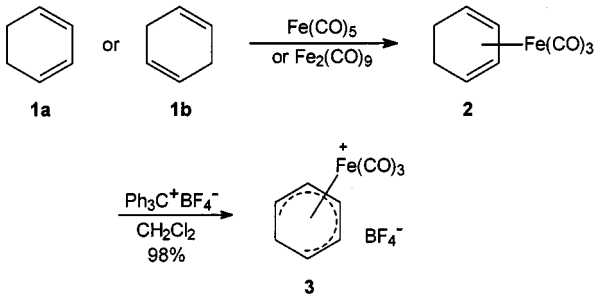

[◇] Part 40: H.-J. Knölker, E. Baum, M. Heininger, *Tetrahedron Lett.* **1997**, *38*, 8021.

 © WILEY-VCH Verlag GmbH, D-69451 Weinheim, 1998 1434−1948/98/0707−0993 $ 17.50+.50/0

workup, especially on large scale complexations. This problem can be circumvented by using labile tricarbonyliron complexes in order to transfer the tricarbonyliron fragment from the weakly bound ligand to cyclohexa-1,3-dienes or buta-1,3-dienes under mild reaction conditions. The development of such tricarbonyliron transfer reagents for the efficient complexation of 1,3-dienes has been extensively investigated over the last 25 years.[7]

The ability of tricarbonyl(η^4-1-oxabuta-1,3-diene)iron complexes to serve as a mild source of the tricarbonyliron fragment was first described by Lewis in 1972.[8] The (η^4-benzylideneacetone)tricarbonyliron (**4**) was found to represent an especially efficient transfer reagent. Brookhart reported the transfer of the tricarbonyliron fragment of **4** to cyclohexa-1,3-diene (**1a**) in a thermal reaction that affords the iron complex **2** in over 95% yield (Scheme 2).[9]

Scheme 2. Complexation of benzylideneacetone to **4** and tricarbonyliron transfer to cyclohexa-1,3-diene (**1a**) using the complex **4**

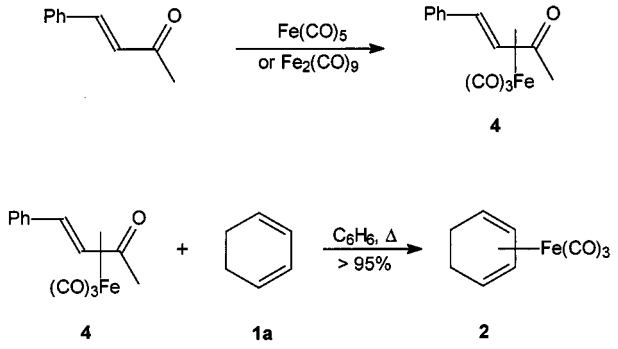

However, the problematic step of this reaction sequence is the preparation of the transfer reagent **4**. The original procedure described by Lewis involved complexation of benzylideneacetone with 1 equivalent of nonacarbonyldiiron in toluene at 60°C and afforded complex **4** in only 32% yield.[8] Brookhart improved this yield to 60% by a photolytic and subsequent thermal reaction of benzylideneacetone with pentacarbonyliron.[9] Only by heating a solution of benzylideneacetone with an excess of nonacarbonyldiiron in diethyl ether at reflux, as reported by Thomas, the tricarbonyliron complex **4** was obtained in reasonable yields (74–81%).[10]

Scheme 3. Complexation of cyclohexa-1,4-diene (**1b**) to **2** using Grevels′ reagent **6**

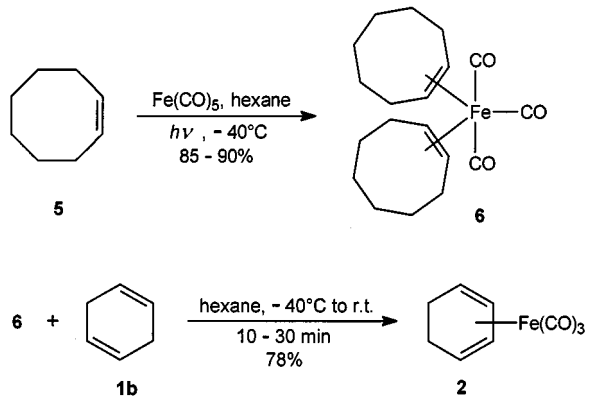

A further tricarbonyliron transfer reagent was developed by Grevels in 1984. Photolytic reaction of pentacarbonyliron with an excess of *cis*-cyclooctene (**5**) in hexane at −40°C afforded tricarbonylbis(η^2-*cis*-cyclooctene)iron (*Grevels′ reagent*) (**6**), which can be isolated as yellow crystals in 85–90% yield (Scheme 3).[11] While the solid compound can be handled at room temperature, complex **6** is labile in solution at temperatures above −35°C. The advantage of Grevels′ reagent is that the transfer of the tricarbonyliron fragment to 1,3-dienes occurs under extremely mild reaction conditions at temperatures below 0°C. Moreover, using Grevels′ reagent **6** also non-conjugated 1,4-dienes can be complexed with concomitant migration of the double bond, e.g. the transfer of the tricarbonyliron fragment of Grevels′ reagent **6** to cyclohexa-1,4-diene (**1b**) provides tricarbonyl(η^4-cyclohexa-1,3-diene)iron (**2**) in 78% yield (Scheme 3).

The high lability of the tricarbonyl(η^4-1-oxabuta-1,3-diene)iron complex **4** and the Grevels′ reagent **6** in solution at room temperature and in the air induced our search for alternative tricarbonyliron transfer reagents, whose higher stability should make them useful for a wider range of applications in synthetic organometallic chemistry.

Results and Discussion

Our investigations led us to the (η^4-1-azabuta-1,3-diene)-tricarbonyliron complexes **10** as efficient and selective tricarbonyliron transfer reagents of high stability (Scheme 4).[12][13] (η^4-1-Azabuta-1,3-diene)tricarbonyliron complexes were first described by Otsuka[14] and Lewis[15] and have been applied to the synthesis of dicarbonyl(η^4-styrene)iron carbene complexes,[16] substituted pyrroles,[17] and to the preparation of labile Schiff bases in the form of their metal complexes.[18] The following methods were previously used for the preparation of the complexes **10**: 1. condensation of amines with tetracarbonyl(η^2-1-oxabuta-1,3-diene)-iron complexes;[14a][18] 2. thermal reaction of the 1-azabuta-1,3-dienes **9** with nonacarbonyldiiron;[14][17] and 3. aza-Wittig reaction of tetracarbonyl(η^2-1-oxabuta-1,3-diene)iron complexes.[19] We found that the yields of the (η^4-1-azabuta-1,3-diene)tricarbonyliron complexes **10** are considerably improved by an ultrasound-promoted complexation[20] of 1-azabuta-1,3-dienes **9** with nonacarbonyldiiron at room temperature.[12][13] In the present paper we describe an extensive investigation of the transfer reaction of the tricarbonyliron fragment from the complexes **10** to cyclohexa-1,3-diene (**1a**) as well as the structural factors influencing the transfer of the metal fragment.

The synthesis of the 1-azabuta-1,3-dienes **9** was achieved by adaptation of standard literature procedures for the imine condensation of the arylamines **7** with the cinnamaldehydes **8**. Reaction of 1 equivalent of the freshly distilled or sublimated arylamine **7** and 1 equivalent of the cinnamaldehyde **8** in an inert solvent, generally with addition of a drying agent, afforded the 1-azabuta-1,3-dienes **9** in high yields (Scheme 4, Table 1). Most of the arylamines **7** and the cinnamaldehydes **8** are commercially available. 2,4,6-Trimethoxyaniline (**7i**) was prepared in 88% yield by hydrogen-

Scheme 4. Synthesis of the azadienes **9**, complexation of **9** to the iron complexes **10** with nonacarbonyldiiron, and the tricarbonyliron transfer to cyclohexa-1,3-diene (**1a**)

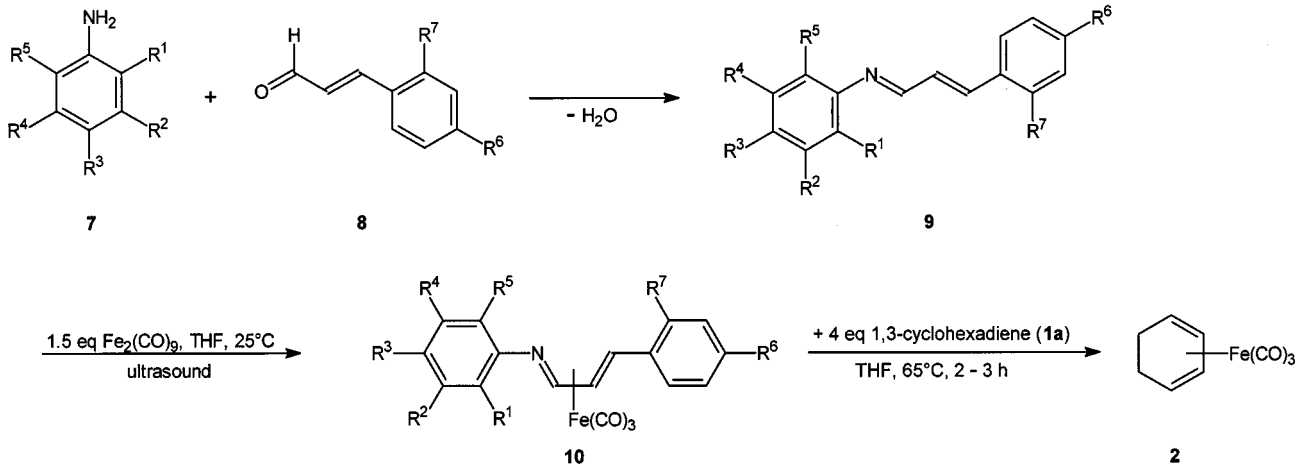

Table 1. Synthesis and characteristic ^{1}H-NMR data of the 1-azabuta-1,3-dienes **9** and their iron complexes **10** and transfer of the tricarbonyliron fragment to cyclohexa-1,3-diene (**1a**)

	R^1	R^2	R^3	R^4	R^5	R^6	R^7	**9**, Yield [%]	δ [ppm][a]	**10**, Yield [%]	δ [ppm][a]	**2**, Yield [%]
a	H	H	H	H	H	H	H	82	8.27	82	6.95	88
b	H	H	OMe	H	H	H	H	100	8.30	88	6.99	95
c	OMe	H	H	H	H	H	H	87	8.28	80	7.10	74
d	H	H	NMe_2	H	H	H	H	40	8.35	55	7.06	45
e	H	H	CF_3	H	H	H	H	72	8.24	59	6.84	78
f	H	NO_2	H	H	H	H	H	56	8.30	0	–	–
g	OMe	H	OMe	H	H	H	H	81	8.31	43	7.15	80
h	H	OMe	OMe	OMe	H	H	H	79	8.30	40	6.97	87
i	OMe	H	OMe	H	OMe	H	H	73	8.51	56	7.94	74
j	H	H	H	H	H	OMe	H	88	8.21	73	–[b]	93
k	H	H	OMe	H	H	OMe	H	95	8.26	41	6.95	90
l	OMe	H	H	H	H	OMe	H	79	8.24	82	–[b]	83
m	H	H	CF_3	H	H	OMe	H	59	8.20	64	6.83	88
n	OMe	H	OMe	H	H	OMe	H	80	8.26	79	7.10	78
o	H	H	OMe	H	H	H	OMe	86	8.31	81	6.95	92
p	H	H	H	H	H	CN	H	78	8.47	57	7.04	69
q	OMe	H	OMe	H	H	CN	H	99	8.36	61	7.23	60
r	H	H	OMe	H	H	NMe_2	H	85	8.24	62	6.89	74
s	H	H	OMe	H	H	NO_2	H	75	8.34	0	–	–

[a] Chemical shift of the H-C2 signal in the ^{1}H-NMR spectrum. – [b] No assignment possible, due to coincidental overlap of signals.

ation of 2,4,6-trimethoxynitrobenzene.[21] The synthesis of 4-cyanocinnamaldehyde (**8p** = **8q**; R^6 = CN, R^7 = H) was achieved in 78% yield by Wittig reaction of 4-cyanobenzaldehyde and (formylmethylene)triphenylphosphorane in toluene at reflux.

As shown below, the electron density at the nitrogen of the 1-azabuta-1,3-dienes **9** is crucial for the efficiency of the tricarbonyliron transfer from the corresponding complexes **10** and for the catalytic complexation[12][13] of cyclohexa-1,3-diene (**1a**) using **9** and nonacarbonyldiiron or pentacarbonyliron. The chemical shift of the imine proton (H-C2) in the ^{1}H-NMR spectra of the 1-azabuta-1,3-dienes **9** is a measure of the electron density at the imine nitrogen atom. A larger downfield shift of H-C2 correlates with a higher electron density at the nitrogen. Thus, this value can be used to estimate the activity of the 1-azabuta-1,3-dienes **9** for catalytic complexations and the transfer ability of the corresponding complexes **10**. Donor substituents in the *ortho* and *para* positions of the 1-aryl ring (R^1, R^3, R^5) cause a downfield shift of the signal of the imine proton relative to the value obtained for the parent compound **9a** (δ = 8.27). The maximum is observed for the 2,4,6-trimethoxy derivative **9i** with a chemical shift of δ = 8.51, which can be at least partly ascribed to the influence of the anisotropy of the oxygen atoms. In contrast, a highfield shift is found with donor substituents in the *para* position of the 4-aryl ring (R^6). Exactly the opposite effects on the chemical shift of H-C2 are observed with acceptor substituents in these positions. In a few cases steric effects are overriding, since substituents in the *ortho* positions of the aryl ring cause larger torsion angles between the aryl ring and the 1-azabuta-1,3-diene plane, resulting in decreased π-overlap.

The complexation of the 1-azabuta-1,3-dienes **9** to the (η^4-1-azabuta-1,3-diene)tricarbonyliron complexes **10** was conveniently achieved by reaction with nonacarbonyldiiron under sonication in tetrahydrofuran at room temperature

(Scheme 4, Table 1). The ultrasound-promoted tricarbonyliron complexation, previously applied by Ley and coworkers to buta-1,3-dienes and cyclohexa-1,3-dienes,[20] was found to be superior to the thermal complexation of the 1-azabuta-1,3-dienes **9**. With respect to the diastereoselectivity of the complexation of chiral 1-azabuta-1,3-dienes,[22] the ultrasound procedure also provides better results than the thermal reaction, since it does not require elevated temperatures, which were shown to cause epimerization of the planar chirality.[23]

The red crystalline (η^4-1-azabuta-1,3-diene)tricarbonyliron complexes **10** are stable in the air for months and therefore appeared to represent appropriate potential transfer reagents for our purposes. The IR spectra of the iron complexes **10** in KBr exhibit intense broad bands in the region of 1960−2060 cm^{-1}, which are typical of carbonyl ligands of tricarbonyliron−diene complexes (Table 2). The wave number of the CO stretching vibration represents an indirect measure of the strength of the bonding between the metal and the organic ligand. A shift to lower wave numbers relative to the value for the parent compound **10a** is observed by donor substituents in the *para* position of the 1-aryl ring (e.g. **10b**: R^3 = OMe, **10d**: R^3 = NMe_2) indicating a reduced back bonding from the iron atom to the azadiene ligand in these complexes, which is explained by an increase in energy of the π* orbitals of the 1-azabutadiene.

The ^{1}H-NMR spectra of the η^4-tricarbonyliron-complexed 1-azabuta-1,3-dienes **10** exhibit the characteristic high field shifts for the protons at the carbon atoms which are coordinated to the metal (C2 to C4). A closer inspection of the chemical shifts which are found for the signals of the imine protons (H-C2) of the complexes **10** reveals that generally a highfield shift of about 1.3−1.4 ppm relative to the value for the corresponding free ligand **9** is observed (Table 1). For those derivatives of **10** having one methoxy substituent in the *ortho* position of the 1-aryl ring (R^1 = OMe; **10c**, **10g**, **10n**, and **10q**) this highfield shift relative to **9** is decreased to 1.13−1.18 ppm, which is ascribed partly to a steric effect of the *ortho* substituent (increase of the torsion angle) leading to reduced π-overlap and partly to the anisotropy of the oxygen atom. For complex **10i** with two *ortho* methoxy substituents in the 1-aryl ring (R^1 = R^5 = OMe) the highfield shift of the imine proton relative to the value observed for **9i** drops to 0.57 ppm.

Almost all of the (η^4-1-azabuta-1,3-diene)tricarbonyliron complexes **10** described in this paper show no or at best three very broad signals for the carbon atoms of the carbonyl ligands in their ^{13}C-NMR spectra when taken in deuterochloroform at room temperature, although the IR spectra in KBr exhibit the typical three bands for the carbonyl ligands at 1960−2060 cm^{-1}. The trifluoromethyl-substituted compounds **10e** and **10m** are exceptions and exhibit three only slightly broadened signals in their ^{13}C-NMR spectra under these conditions (**10e**: δ = 204.77, 208.30, 211.49; **10m**: δ = 205.07, 208.94, 211.97). The ^{13}C-NMR spectra of (η^4-carba-1,3-diene)tricarbonyliron complexes show in most cases only one singlet at δ = 210−213 for the three carbonyl ligands at room temperature. The fluxionality of these complexes leading to equivalency of the three carbonyl ligands is caused by the turnstile rotation of the tricarbonyliron fragment. This dynamic process is sufficiently slow on the NMR time scale at low temperatures to allow the observation of two peaks for the three carbonyl ligands with an intensity ratio of 2:1 in the case of symmetrical diene ligands or three peaks of equal height for unsymmetrical diene ligands.[24] Previous investigations of the fluxional behavior of tricarbonyliron-diene complexes have demonstrated that the activation barriers for this intramolecular basal-apical exchange of the carbonyl groups for complexes with carbadiene ligands are significantly lower than those of 1-heterodiene ligands.[25] Takats concluded that the variations in the activation barrier for the turnstile rotation of the tricarbonyliron fragment can be rationalized by the metal-carbonyl back bonding, however steric factors also contribute to this value.[25c]

We determined precisely the activation barrier for the intramolecular carbonyl ligand exchange of four (η^4-1-azabuta-1,3-diene)tricarbonyliron complexes (**10a−c** and **10e**) and for tricarbonyl(η^4-cyclohexa-1,3-diene)iron (**2**) by dynamic ^{13}C-NMR spectroscopy at 125 MHz in deuterated toluene (Figure 1a−e, Table 2). The stepwise increase of the temperature up to 373 K during the measurement of the ^{13}C-NMR spectra of the complexes **10** provided a single signal for the three carbonyl ligands, which still showed some line broadening. As expected the low temperature spectra of the 1-azadiene complexes **10** at 233 K exhibited three sharp singlets for the carbonyl ligands. The coalescence temperature T_C of the dynamic process was clearly above room temperature for all four cases investigated. This was already indicated by the fact that the signals for the carbonyl ligands were missing in the ^{13}C-NMR spectra in deuterochloroform at room temperature for most of the 1-azadiene complexes **10** prepared in the present work. For the cyclohexadiene complex **2** one sharp singlet for the three carbonyl ligands is observed at room temperature, while the ^{13}C-NMR spectrum at 185 K exhibits two singlets at δ = 211.32 and 216.05 in a ratio of 2:1. The coalescence temperatures could be determined with a tolerance of ±5 K. With the value for δν taken from the low temperature spectrum, the free enthalpy of activation for the intramolecular exchange of carbonyl ligands could be calculated in good approximation by using the formula $\Delta G^{\neq} = R \cdot T_C [22.96 + \ln(T_C/\delta\nu)]$.[26] The activation barrier for this turnstile rotation of the tricarbonyliron fragment in the 1-*p*-anisyl-substituted 1-azadiene complex **10b** is 13.5 ± 0.3 kcal/mol. For the other 1-azadiene complexes that were investigated by dynamic ^{13}C-NMR spectroscopy (**10a**, **10c**, and **10e**), the value was found to be increased by about 1 kcal/mol (Table 2). Thus the intramolecular ligand exchange of the carbonyl groups is facilitated by a donor substituent in the *para* position of the 1-aryl ring (complex **10b**) as compared to the parent compound **10a**. This finding is again in agreement with the assumption of reduced back bonding from the iron atom to the 1-azadiene ligand in complex **10b** relative to **10a**. The opposite effect is observed with an acceptor group in this position (complex **10e**) and also with

Figure 1a. Dynamic ^{13}C-NMR spectra of complex **10a** in the metal carbonyl region (125 MHz, [D$_8$]toluene)

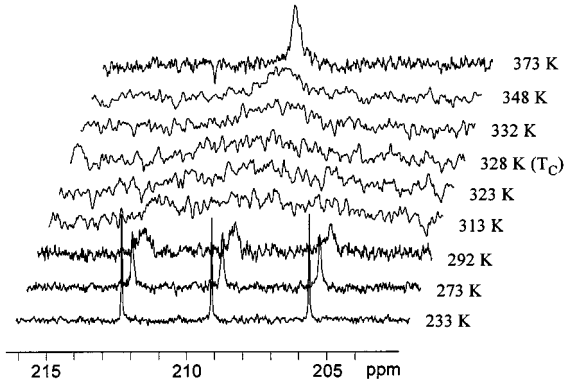

Figure 1b. Dynamic ^{13}C-NMR spectra of complex **10b** in the metal carbonyl region (125 MHz, [D$_8$]toluene)

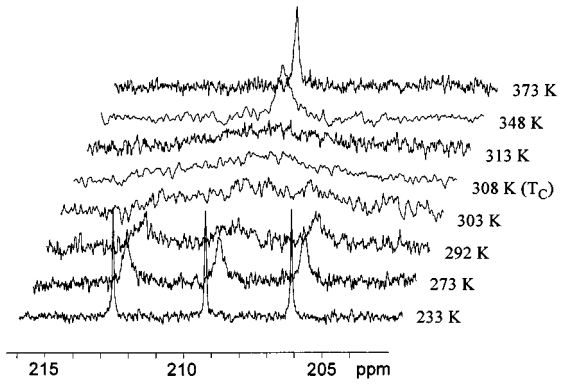

Figure 1c. Dynamic ^{13}C-NMR spectra of complex **10c** in the metal carbonyl region (125 MHz, [D$_8$]toluene)

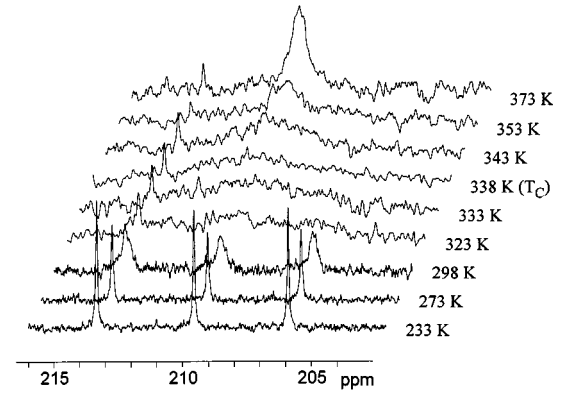

Figure 1d. Dynamic ^{13}C-NMR spectra of complex **10e** in the metal carbonyl region (125 MHz, [D$_8$]toluene)

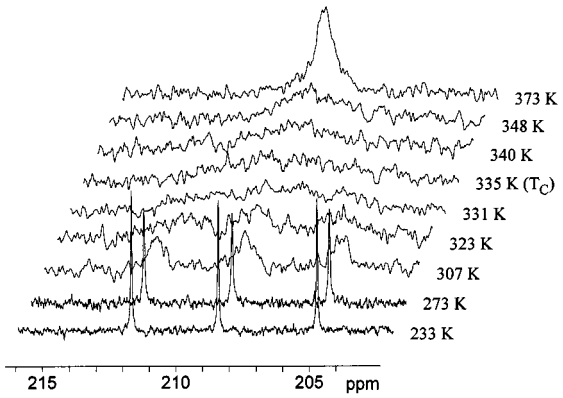

Figure 1e. Dynamic ^{13}C-NMR spectra of complex **2** in the metal carbonyl region (125 MHz, [D$_8$]toluene)

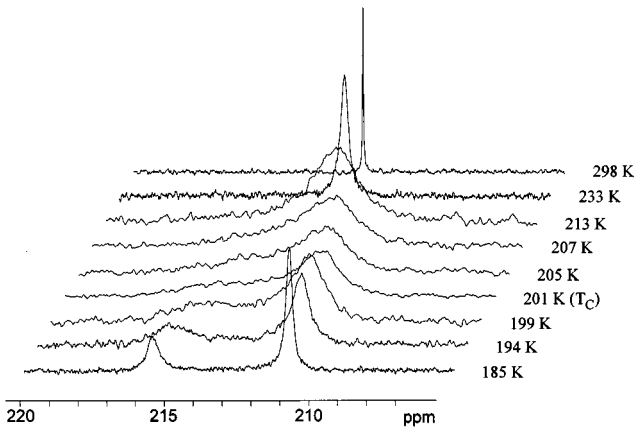

a donor group in the *ortho* position of the 1-aryl ring, because of the increased torsion angle (compound **10c**). For the cyclohexa-1,3-diene complex **2** the activation barrier for the rotation of the tricarbonyliron fragment has been determined as 8.7 ± 0.3 kcal/mol, which is in good agreement with the value of 8.8 ± 0.5 kcal/mol obtained earlier by Takats et al. in [D$_6$]DMSO/CS$_2$.[25c] For the related (η^4-buta-1,3-diene)tricarbonyliron complex activation barriers of 9.5 kcal/mol[24] and 10.5 ± 0.5 kcal/mol[25c] have been reported. These findings emphasize that the free enthalpy of activation for the turnstile rotation of the tricarbonyliron fragment for the complexes of 1-hetero-1,3-dienes is generally about 4−5 kcal/mol higher than for the corresponding complexes of carba-1,3-dienes, no matter whether they are cyclic or acyclic. The data are in agreement with decreased back donation of electrons from filled iron d-orbitals into the LUMO of the carbonyl group for the tricarbonyliron

Table 2. Characteristic IR and ^{13}C-NMR data for the carbonyl ligands of selected tricarbonyliron complexes[a]

	$\tilde{\nu}_{CO}$ [cm^{-1}]	δ_{CO} (233 K) [ppm]	δ_{CO} (373 K) [ppm]	T_C [K]	$\delta\nu$ [Hz]	$\Delta G^{\neq}$ [kcal/mol]
10a	2055, 1988, 1977	206.02, 209.49, 212.70	209.53	328 ± 5	840.79	14.3 ± 0.3
10b	2049, 1987, 1963	206.60, 209.71, 213.03	209.81	308 ± 5	809.65	13.5 ± 0.3
10c	2058, 2000, 1970	206.41, 210.06, 213.84	210.02	338 ± 5	934.21	14.7 ± 0.3
10e	2059, 2002, 1983	205.19, 208.90, 212.16	208.79	335 ± 5	876.08	14.6 ± 0.3
2	2042, 1957	211.32, 216.05[b]	212.56[c]	201 ± 5	594.79	8.7 ± 0.3

[a] IR spectra: Drift at room temp.; ^{13}C-NMR spectra: 125 MHz in [D$_8$]toluene. − [b] This spectrum was recorded at 185 K. − [c] This spectrum was recorded at 298 K.

complexes of 1-hetero-1,3-dienes, as compared to 1-carba-1,3-dienes. This is confirmed by the higher stretching frequencies for the carbonyl bands in the IR spectra of 1-hetero-1,3-diene complexes. In consequence the averaged chemical shifts in the ^{13}C-NMR spectra observed at high temperatures are shifted to higher field and the activation barrier for the rotation of the tricarbonyliron fragment is higher for the 1-heterodiene complexes.

Figure 2. Molecular structure of **10b** in the crystal (SCHAKAL representation; arbitrary numbering). Selected bond lengths [A]: Fe−N 2.075(3), Fe−C2 2.074(4), Fe−C3 2.068(4), Fe−C4 2.167(4). Torsion angle: C2,N−C11,C16: 10.8°

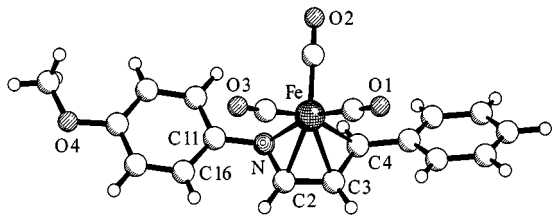

Figure 3. Molecular structure of **10c** in the crystal (SCHAKAL representation; arbitrary numbering). Selected bond lengths [A]: Fe−N 2.074(2), Fe−C2 2.064(2), Fe−C3 2.050(2), Fe−C4 2.132(3). Torsion angle: C2,N−C11,C16: 13.4°. Distance Fe−O4: 3.62 A

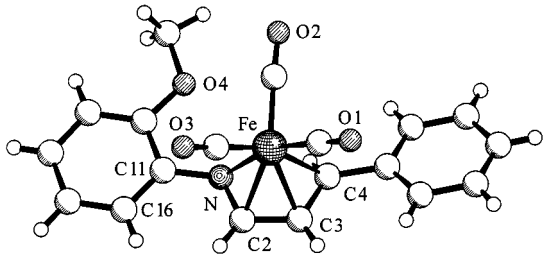

Figure 4. Molecular structure of **10l** in the crystal (SCHAKAL representation; arbitrary numbering). Selected bond lengths [A]: Fe−N 2.070(2), Fe−C2 2.068(2), Fe−C3 2.062(2), Fe−C4 2.155(2). Torsion angle: C2,N−C11,C16: 37.4°. Distance Fe−O4: 3.35 A

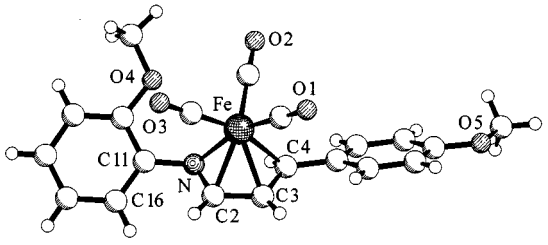

The X-ray crystal structure determinations of the (η^4-1-azabuta-1,3-diene)tricarbonyliron complexes **10b**, **10c**, and **10l** confirm the tetragonal pyramidal coordination of the iron atom (Figure 2−4, Table 4). Two basal positions are occupied by the two π bonds, the two others by carbonyl ligands. The third carbonyl ligand adopts the apical position of these complexes. Similar arrangements were previously found for tricarbonyliron complexes of buta-1,3-dienes and cyclohexa-1,3-dienes and also for the parent complex **10a**.[14b] The bond lengths found in the tricarbonyliron complexes of 1-azabuta-1,3-dienes, compared to those of cyclohexa-1,3-dienes and buta-1,3-dienes, correlate very well with the concept of increased back bonding from the filled iron d-orbitals into the π* orbitals of the organic ligand for the heterodiene complexes. This is emphasized by the IR, ^{1}H-NMR, and ^{13}C-NMR data described above. Some anomalies in the spectral data of the 1-azabuta-1,3-diene complexes presented above were ascribed to steric factors, especially for those cases of 1-azabuta-1,3-dienes resulting from an *ortho*-substituted arylamine. The X-ray crystal structures reveal an increased torsion angle for the complexes with an *ortho*-methoxy substituent. It is noteworthy that the out-of-plane arrangement of the 1-aryl ring relative to the 1-azabuta-1,3-diene plane in these complexes proceeds in a way that the oxygen atom of the methoxy group is oriented towards the iron atom. For electronic reasons this arrangement becomes most evident for complex **10l** with an *ortho*-methoxy substituent in the 1-aryl ring and a *para*-methoxy substituent in the 4-aryl ring. The torsional angle between the 1-aryl ring and the 1-azabuta-1,3-diene plane of **10l** is 37.4° and the distance Fe−O4 is only 3.35 A, suggesting the possibility of chelation of the tricarbonyliron fragment by coordination of the oxygen to the iron atom on haptotropic $\eta^4 \rightarrow \eta^1$ migration during the transfer of the metal fragment (see below).

The transfer of the tricarbonyliron fragment from the (1-azabuta-1,3-diene)tricarbonyliron complexes **10** to cyclohexa-1,3-diene (**1a**) was extensively investigated. It was shown that a smooth transfer of the metal fragment from all 1-azabuta-1,3-diene complexes described in this study was achieved simply by heating the reaction mixture of complex **10** and **1a** in tetrahydrofuran at reflux (Scheme 4, Table 1). The variation of the reaction time for the transfer of the tricarbonyliron fragment to cyclohexa-1,3-diene (**1a**) was investigated for the complexes **10b**, **10c**, and **10g** (Table 3). At all three different reaction times the transfer reagent **10b** was superior. Complex **10b** transfers the metal fragment faster and provides the best yield after 2 h. With increasing turnover, the transfer of the tricarbonyliron fragment from complex **10** to already generated corresponding free 1-azabuta-1,3-diene ligand **9** can compete with the desired transfer to **1a** and finally becomes dominant if only a 1:1 ratio

Table 3. Variation of the reaction time for the tricarbonyliron transfer to **1a** using the complexes **10b**, **c**, **g**

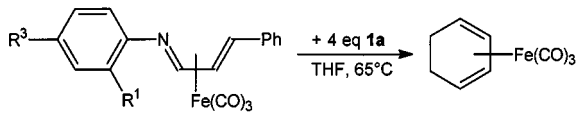

10b, c, g **2**

Transfer Reagent	R^1	R^3	Reaction Time **2**, Yield (%) 30 min	60 min	120 min
10b	H	OCH_3	61	83	95
10c	OCH_3	H	31	47	74
10g	OCH_3	OCH_3	50	67	80

of complex **10** and **1a** is employed. Therefore, an excess of cyclohexa-1,3-diene (**1a**) is used in order to bring the reaction to completion.

Using a standard set of reaction conditions, the transfer of the metal fragment to cyclohexa-1,3-diene (**1a**) was compared for the various (1-azabuta-1,3-diene)tricarbonyliron complexes **10** (Table 1, Scheme 4). By far the best overall result was achieved using tricarbonyl[(1-4-η)-1-(4-methoxyphenyl)-4-phenyl-1-azabuta-1,3-diene]iron (**10b**) as transfer reagent. First, the free 1-azabuta-1,3-diene **9b** can be prepared quantitatively and crystallizes very easily. Secondly, the complexation of **9b** with nonacarbonyldiiron promoted by ultrasound provided the tricarbonyliron complex **10b** in a yield of 88%. Thirdly, the reaction of **10b** with cyclohexa-1,3-diene (**1a**) afforded tricarbonyl(η^4-cyclohexa-1,3-diene)iron (**2**) in 95% yield. Thus, the complexation of **1a** using this 3-step sequence could be realized in an overall yield of 84%. Moreover, the free 1-azadiene **9b** can be recovered from the reaction mixture by simple crystallization in more than 95% yield.

Scheme 5. Transfer of the tricarbonyliron fragment from the 4-methoxybenzylideneacetone complex **11** to cyclohexa-1,3-diene (**1a**)

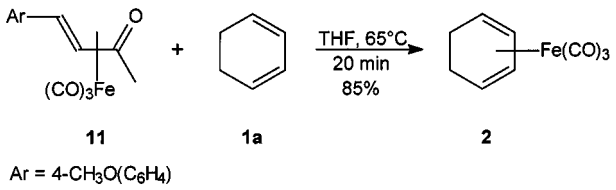

Some information on the relative reactivities of various tricarbonyliron transfer reagents was provided by competition experiments. For this purpose we prepared the tricarbonyliron complex **11** containing the more electron-rich 4-methoxybenzylideneacetone ligand. Complex **11** was reported to be more reactive in transfer reactions than the tricarbonyliron complex **4** with unsubstituted benzylideneacetone as ligand.[27] A smooth transfer of the metal fragment was observed on reaction of complex **11** with cyclohexa-1,3-diene (**1a**) in tetrahydrofuran at reflux and afforded the iron complex **2** after 20 min in 85% yield (Scheme 5). Thus, the required reaction time for comparable yields of **2** with the 1-oxabuta-1,3-diene complex **11** as transfer reagent is significantly shorter than with the 1-azabuta-1,3-diene complexes **10** (cf. Table 3). On direct comparison of the transfer reagents **11** and **10b** this difference in reactivity becomes even more evident (Scheme 6). The transfer of the tricarbonyliron fragment from the tricarbonyl(4-methoxybenzylideneacetone)iron complex **11** to the free 1-azadiene **9b** by heating in benzene at reflux for 20 min afforded exclusively the (1-azabuta-1,3-diene)tricarbonyliron complex **10b** along with the free 1-oxabuta-1,3-diene **12**. However, a transfer of the metal fragment from complex **10b** to the free ligand **12** could not be achieved. This result confirmed the higher reactivity of the 1-oxabuta-1,3-diene complexes for the transfer of the tricarbonyliron fragment.

A direct comparison of the (η^4-1-azabuta-1,3-diene)-tricarbonyliron complexes **10a** and **10b** demonstrated the higher transfer reactivity of the latter reagent. Reaction of either equimolar amounts of the free 1-azabuta-1,3-diene **9a** with the iron complex **10b** of the free ligand **9b** with the iron complex **10a** in tetrahydrofuran at reflux led within 4 h to an equilibrium with a 2:1 ratio of the iron complexes **10a** and **10b**. This result confirms again that the transfer of the tricarbonyliron fragment is facilitated by the donor substituent in the *para* position of the 1-aryl ring.

Based on previous kinetic studies on ligand exchange reactions at complex **10a**[28] and our own mechanistic investigations,[23][29] the following mechanism is proposed for the transfer of the tricarbonyliron fragment using (η^4-1-azabuta-1,3-diene)tricarbonyliron complexes **10** (Scheme 7). Complex **10** generates, by a thermally induced haptotropic migration, the 16-electron tricarbonyl(η^1-imine)iron complex **13**. This type of 16-electron η^1-imine complex is also considered as the intermediate in the thermal epimerization of tricarbonyliron complexes of chiral 1-azabuta-1,3-dienes[23] and was obtained on matrix photolysis studies of (η^4-1-azabuta-1,3-diene)tricarbonyliron complexes.[30] The vacant coordination site of complex **13** is filled by η^2-coor-

Scheme 6. Competition experiments between various tricarbonyliron transfer reagents

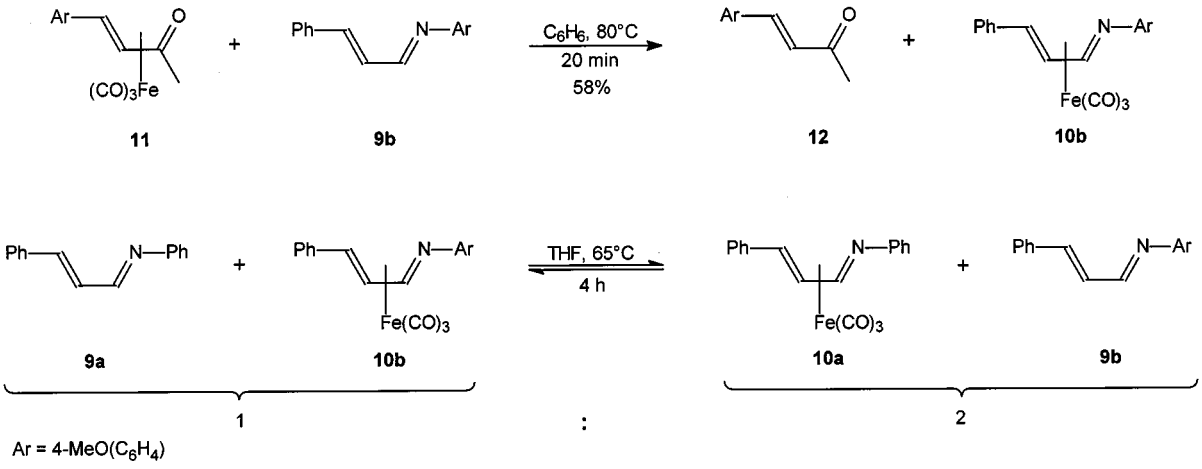

Scheme 7. Proposed mechanism of the tricarbonyliron transfer from 1,4-diaryl-1-azabuta-1,3-diene complexes **10** to cyclohexa-1,3-diene (**1a**)

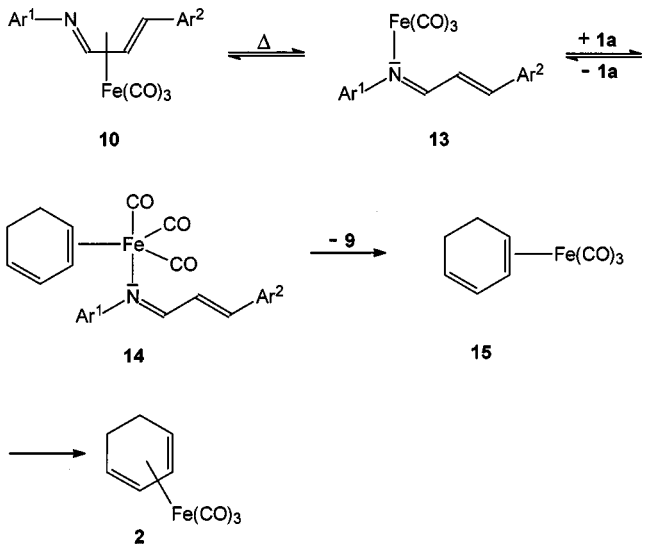

dination of cyclohexa-1,3-diene (**1a**) to provide complex **14**. This 18-electron complex, which could not be isolated, represents the crucial intermediate of the transfer reaction. Based on X-ray crystal structure determinations of (η^1-1-azabuta-1,3-diene)tetracarbonyliron complexes[29][31] and additional experimental evidence,[29][32] complex **14** is proposed to have a trigonal-bipyramidal structure with the η^2-coordinated 1,3-diene in equatorial and the η^1-coordinated α,β-unsaturated imine in an axial position. Disengagement of the 1-azabuta-1,3-diene **9** from complex **14** leads to the 16-electron complex **15**, which affords the tricarbonyliron complex **2** by haptotropic ($\eta^2 \rightarrow \eta^4$) migration of the metal fragment.

Conclusion

We have shown that the tricarbonyliron complexes of 1,4-diaryl-substituted 1-azabuta-1,3-dienes serve as highly efficient tricarbonyliron transfer reagents for the complexation of cyclohexa-1,3-diene. Complexation using these transfer reagents can also be applied to a broad range of other 1,3-dienes.[12] After the transfer of the metal fragment the 1-azabuta-1,3-dienes **9** are recovered almost quantitatively by simple crystallization. This fact has been exploited for the development of a complexation of 1,3-dienes using only catalytic amounts of the 1-azabuta-1,3-dienes **9**.[12][13] Most importantly, it has been demonstrated that high asymmetric inductions are achieved on the catalytic complexation of prochiral 1,3-dienes using chiral 1-azabuta-1,3-dienes.[32]

This work was supported by the *Deutsche Forschungsgemeinschaft* (Gerhard-Hess award) and the *Fonds der Chemischen Industrie*.

Experimental Section

General: All reactions were carried out using anhydrous and degassed solvents under an argon atmosphere. − Flash chromatography: Baker or Merck silica gel (0.03−0.06 mm). − Ultrasound: Bandelin Sonorex-TK52H cleaning bath; frequency: 35 kHz, used at 50% power. − Melting points: Leitz hot stage and Büchi 535. − IR spectra: Bruker IFS-88, Perkin-Elmer 882 and 1710. − ^{1}H-NMR and ^{13}C-NMR spectra: Bruker WP-200, AC-250, AM-400, and DRX-500; internal standard: tetramethylsilane or the signal of the deuterated solvent; coupling constants in Hz. − Mass spectra: Finnigan MAT-312 and MAT-90: ionization potential: 70 eV. − Elemental analysis: Heraeus CHN-Rapid. Bulb-to-bulb distillation: Büchi glass tube oven GKR-51. − X-ray analyses: The data were collected on a STOE STADI-4 diffractometer using Mo-K_α radiation. The structures were solved by direct methods (SHELXS-86) and refined anisotropically by full-matrix least squares based on all unique F^2 (SHELXL-93); the program SCHAKAL-92 was used for the graphical representation of the crystal structures (E. Keller, a computer program for the graphic representation of molecular and crystallographic models, Universität Freiburg, Germany, 1992).

2,4,6-Trimethoxyaniline (**7i**): A mixture of 2,4,6-trimethoxynitrobenzene[21] (500 mg, 2.35 mmol) and Pd/C (100 mg) in EtOH (30 ml) was stirred under a hydrogen atmosphere (1.1 bar) for 20 h. The reaction mixture was filtered through a short path of Celite/Alox B and the solvent was removed under reduced pressure. Bulb-to-bulb distillation (120°C, 0.1 mbar) of the residue afforded **7i** (380 mg, 88%). Pale yellow solid. M.p. 33−35°C. − IR (drift): ν = 3449, 3362, 2939, 2837, 1611, 1512, 1164 cm^{-1}. − ^{1}H NMR (400 MHz, $CDCl_3$): δ = 3.48 (br s, 2 H), 3.74 (s, 3 H), 3.81 (s, 6 H), 6.15 (s, 2 H). − ^{13}C NMR and DEPT (100 MHz, $CDCl_3$): δ = 55.91 (3 CH_3), 91.40 (2 CH), 118.97 (C), 148.13 (2 C), 152.62 (C). − MS (30°C): *m/z* (%) = 183 (100) [M$^+$], 168 (87), 140 (39), 125 (28); HRMS: 183.0910 ($C_9H_{13}NO_3$, calcd. 183.0895).

4-Cyanocinnamaldehyde (**8**; R^6 = CN, R^7 = H): A solution of 4-cyanobenzaldehyde (823 mg, 6.28 mmol) and (formylmethylene)triphenylphosphorane (2.10 g, 6.90 mmol) in toluene (40 ml) was stirred at 80°C for 24 h. The solvent was evaporated in vacuo and the residue was subjected to flash chromatography (gradient elution, first with Et_2O/pentane, 1:3 and then elution with Et_2O) on silica gel. Evaporation of the solvent afforded a crude product, which was dissolved in Et_2O (30 ml). Recrystallization at −30°C provided the aldehyde **8** (R^6 = CN, R^7 = H) as a mixture of diastereoisomers (771 mg, 78%, (*E*)/(*Z*) ≥ 10:1). Yellow solid. M.p. 132°C. − IR (drift): ν = 2228, 1685, 1627, 1420, 1293, 1129, 987, 817 cm^{-1}. − ^{1}H NMR (250 MHz, $CDCl_3$) [(*E*)-isomer]: δ = 6.78 (dd, *J* = 16.1, 7.5 Hz, 1 H), 7.49 (d, *J* = 16.1 Hz, 1 H), 7.67 (d, *J* = 8.5 Hz, 2 H), 7.74 (d, *J* = 8.5 Hz, 2 H), 9.78 (d, *J* = 7.5 Hz, 1 H). − MS (25°C): *m/z* (%) = 157 (100) [M$^+$], 156 (92), 129 (57), 128 (46), 103 (14), 102 (20), 101 (17); HRMS: 157.0516 ($C_{10}H_7NO$, calcd. 157.0528).

1,4-Diphenyl-1-azabuta-1,3-diene (**9a**): Na_2SO_4 (3 g) was added to a solution of cinnamaldehyde (**8**; R^6 = R^7 = H) (1.91 ml, 2.00 g, 15.1 mmol) and freshly distilled aniline (**7a**) (1.38 ml, 1.41 g, 15.1 mmol) in Et_2O (30 ml). The reaction mixture was stirred at room temp. for 1 h, then filtered, and the residue was washed with Et_2O (20 ml). Crystallization from the filtrate at −20°C afforded the product **9a** (2.56 g, 82%). Pale yellow needles. − IR (drift): ν = 2958, 2839, 1630, 1605, 1505, 1295, 1251, 1032, 986, 720 cm^{-1}. − ^{1}H NMR (400 MHz, $CDCl_3$): δ = 7.17 (m, 5 H), 7.38 (m, 5 H), 7.54 (m, 2 H), 8.27 (dd, *J* = 7.2, 1.0 Hz, 1 H). − ^{13}C NMR and DEPT (63 MHz, $CDCl_3$): δ = 120.87 (2 CH), 126.07 (CH), 127.44 (2 CH), 128.52 (CH), 128.87 (2 CH), 129.13 (2 CH), 129.55 (CH), 135.50 (C), 143.98 (CH), 151.64 (C), 161.60 (CH). − MS (35°C): *m/z* (%) = 207 (40) [M$^+$], 206 (100), 130 (3), 115 (7), 77 (22); HRMS: 207.1062 ($C_{15}H_{13}N$, calcd. 207.1048).

Table 4. Crystallographic data, summary of data collection, and refinement of **10b**, **10c**, and **10l**

	10b	**10c**	**10l**
empirical formula	$C_{19}H_{15}FeNO_4$	$C_{19}H_{15}FeNO_4$	$C_{20}H_{17}FeNO_5$
formula weight	377.17	377.17	407.20
crystal color	red	red	red
crystal size [mm]	0.54 x 0.12 x 0.12	0.4 × 0.3 × 0.3	0.80 × 0.60 × 0.55
crystal system	monoclinic	orthorhombic	triclinic
space group	$P2_1/c$	*Pbca*	*P*1
a [A]	11.975(5)	18.5970(10)	6.549(3)
b [A]	15.735(8)	7.938(3)	10.400(5)
c [A]	9.439(4)	23.483(3)	14.618(6)
α [°]	90	90	106.71(3)
β [°]	101.07(3)	90	96.30(3)
γ [°]	90	90	103.07(3)
V [A^3]	1745.5(14)	3466.6(14)	912.4(7)
Z	4	8	2
$\rho_{calcd.}$ [g cm^{-3}]	1.435	1.445	1.482
absorption coefficient [mm^{-1}]	0.862	0.893	0.858
F (θ00)	776	1552	420
λ [A]	0.71073	0.71073	0.71073
T [K]	293(2)	200(2)	173(2)
θ range [°]	5.20−28.15	1.73−25.03	3.04−25.00
reflections collected	9737	6121	3202
independent reflections	4111	3063	3202
refinement method	full-matrix least squares on F^2	full-matrix least squares on F^2	full-matrix least squares on F^2
data / restraints / parameters	4106 / 0 / 251	3062 / 0 / 286	3200 / 3 / 255
final *R* indices [$I>2\sigma(I)$]	$R_1 = 0.0583$; w$R_2 = 0.1376$	$R_1 = 0.0317$; w$R_2 = 0.0772$	$R_1 = 0.0317$; w$R_2 = 0.0805$
max. residual electron density [e A^{-3}]	0.467	0.274	0.395
CSD number[a]	59410	408182	58301

[a] Further details of the crystal structure investigations may be obtained from the Fachinformationszentrum Karlsruhe D-76344 Eggenstein-Leopoldshafen on quoting the CSD numbers given.

1-(4-Methoxyphenyl)-4-phenyl-1-azabuta-1,3-diene (**9b**): Cinnamaldehyde (**8**; $R^6 = R^7 = H$) (10 ml, 10.5 g, 79.3 mmol) was added to a solution of freshly sublimated *p*-anisidine (**7b**) (9.77 g, 79.3 mmol) in EtOAc (150 ml). $MgSO_4$ (4 g) was added and the mixture was stirred for 1 h at room temp. The solution was separated and the residue was washed with EtOAc. The solutions were combined and the solvent was evaporated slowly at 40°C until crystallization could be observed. Then pentane (100 ml) was added to the warm solution. Recrystallization at −20°C afforded the azadiene **9b** (18.8 g, 100%). Yellow-green crystals. M.p. 122°C. − IR (drift): ν = 3060, 1625, 1600, 1576, 1150, 999, 994, 753 cm^{-1}. − ^{1}H NMR (400 MHz, $CDCl_3$): δ = 3.83 (s, 3 H), 6.92 (br d, *J* = 9.0 Hz, 2 H), 7.11 (m, 2 H), 7.21 (br d, *J* = 9.0 Hz, 2 H), 7.38 (m, 3 H), 7.53 (m, 2 H), 8.30 (dd, *J* = 4.5, 3.8 Hz, 1 H). − ^{13}C NMR and DEPT (63 MHz, $CDCl_3$): δ = 55.29 (CH_3), 114.27 (2 CH), 122.11 (2 CH), 127.24 (2 CH), 128.61 (CH), 128.75 (2 CH), 129.23 (CH), 135.60 (C), 142.85 (CH), 144.37 (C), 158.25 (C), 159.29 (CH). − MS (55°C): *m/z* (%) = 237 (63) [M$^+$], 236 (100), 115 (17); HRMS: 237.1137 ($C_{16}H_{15}NO$, calcd. 237.1154). − $C_{16}H_{15}NO$: C 80.98, H 6.37, N 5.90; found: C 81.14, H 6.35, N 6.35.

1-(2-Methoxyphenyl)-4-phenyl-1-azabuta-1,3-diene (**9c**): Na_2SO_4 (1.5 g) was added to a solution of cinnamaldehyde (**8**; $R^6 = R^7 =$ H) (1.91 ml, 2.00 g, 15.1 mmol) and freshly distilled *o*-anisidine (**7c**) (1.70 ml, 1.86 g, 15.1 mmol) in Et_2O (30 ml). The reaction mixture was stirred at room temp. for 3 h. The solution was separated and the residue was washed with Et_2O. The solution of the combined organic layers was evaporated in vacuo to a volume of 5 ml. Crystallization from the filtrate at −20°C provided the product **9c** (3.11 g, 87%). Yellow crystals. M.p. 67°C. − IR (drift): ν = 1627, 1602, 1581, 1493, 1447, 1296, 1247, 1115, 1027, 1001, 754, 747 cm^{-1}. − ^{1}H NMR (400 MHz, $CDCl_3$): δ = 3.90 (s, 3 H), 6.95 (m, 2 H), 7.00 (dd, *J* = 7.7, 2.0 Hz, 1 H), 7.12 (d, *J* = 16.0 Hz, 1 H), 7.19 (m, 1 H), 7.23 (dd, *J* = 16.0, 8.7 Hz, 1 H), 7.33−7.41 (m, 3 H), 7.53 (m, 2 H), 8.28 (d, *J* = 8.7 Hz, 1 H). − ^{13}C NMR and DEPT (100 MHz, $CDCl_3$): δ = 55.75 (CH_3), 111.22 (CH), 119.41 (CH), 120.93 (CH), 126.99 (CH), 127.47 (2 CH), 128.89 (2 CH), 129.06 (CH), 129.47 (CH), 135.66 (C), 141.21 (C), 143.66 (CH), 152.73 (C), 162.01 (CH). − MS (45°C): *m/z* (%) = 237 (100) [M$^+$], 236 (81), 220 (21), 130 (12), 115 (17); HRMS: 237.1140 ($C_{16}H_{15}NO$, calcd. 237.1154). −$C_{16}H_{15}NO$: C 80.98, H 6.37, N 5.90; found: C 80.46, H 6.37, N 6.30.

1-(4-N,N-Dimethylaminophenyl)-4-phenyl-1-azabuta-1,3-diene (**9d**): A solution of cinnamaldehyde (**8**; $R^6 = R^7 =$ H) (0.95 ml, 1.00 g, 7.57 mmol) and freshly sublimated 4-*N*,*N*-dimethylaminoaniline (**7d**) (1.03 g, 7.57 mmol) in Et_2O (30 ml) was stirred at room temp. for 1 h. Na_2SO_4 (2 g) was added and the reaction mixture was stirred at room temp. for additionally 2 h. The solution was separated and evaporated in vacuo to a volume of 15 ml. Crystallization at −20°C provided the product **9d** (760 mg, 40%). Yellow crystals. M.p. 146°C. − IR (drift): ν = 1625, 1605, 1512, 1448, 1349, 1220, 1169, 955, 821, 752, 693 cm^{-1}. − ^{1}H NMR (400 MHz, $CDCl_3$): δ = 2.99 (s, 6 H), 6.75 (br d, *J* = 9.0 Hz, 2 H), 7.07 (d, *J* = 15.9 Hz, 1 H), 7.14 (dd, *J* = 15.9, 8.2 Hz, 1 H), 7.25 (br d, *J* = 9.0 Hz, 2 H), 7.33 (m, 1 H), 7.39 (m, 2 H), 7.53 (m, 2 H), 8.35 (d, *J* = 8.2 Hz, 1 H). − ^{13}C NMR and DEPT (100 MHz, $CDCl_3$): δ = 40.68 (2 CH_3), 112.76 (2 CH), 122.33 (2 CH), 127.25 (2 CH), 128.86 (2 CH), 129.07 (CH), 129.15 (CH), 136.03 (C), 140.31 (C), 141.63 (CH), 149.58 (C), 156.94 (CH). − MS (65°C): *m/z* (%) = 250 (84) [M$^+$], 249 (100), 233 (12), 124 (4); HRMS: 250.1450 ($C_{17}H_{18}N_2$, calcd. 250.1470).

1-(4-Trifluoromethylphenyl)-4-phenyl-1-azabuta-1,3-diene (**9e**): A solution of cinnamaldehyde (**8**; $R^6 = R^7 =$ H) (1.26 ml, 1.32 g, 10.0 mmol) and freshly sublimated 4-trifluoromethylaniline (**7e**) (1.61 g,

10.0 mmol) in Et_2O (30 ml) was stirred at room temp. for 2 h. The mixture was subsequently dried over Na_2SO_4. The solution was separated and the residue was washed with Et_2O. The solution of the combined organic layers was evaporated to a volume of 20 ml. Crystallization at −20°C provided a crude product, which was washed with a mixture of cold Et_2O/pentane (1:7) to afford **9e** (1.97 g, 72%). Yellow crystals. − IR (drift): ν = 1628, 1611, 1586, 1333, 1313, 1156, 1109, 1073, 841, 753 cm^{-1}. − ^1H NMR (400 MHz, $CDCl_3$): δ = 7.11 (dd, *J* = 15.9, 8.7 Hz, 1 H), 7.22 (d, *J* = 15.9 Hz, 1 H), 7.22 (d, *J* = 8.2 Hz, 2 H), 7.40 (m, 3 H), 7.56 (m, 2 H), 7.64 (d, *J* = 8.2 Hz, 2 H), 8.24 (d, *J* = 8.7 Hz, 1 H). − ^{13}C NMR and DEPT (100 MHz, $CDCl_3$): δ = 121.03 (2 CH), 124.51 (CF_3, q, $^1J_{CF}$ = 276 Hz), 126.38 (2 CH, q, $^3J_{CF}$ = 3.4 Hz), 127.67 (2 CH), 128.08 (CH), 129.00 (2 CH), 129.99 (CH), 135.25 (C), 145.51 (CH), 154.87 (C), 163.30 (CH), the signal of one carbon atom is missing. − MS (35°C): *m/z* (%) = 275 (34) [M^+], 274 (100), 145 (7), 115 (4); HRMS: 275.0907 ($C_{16}H_{12}F_3N$, calcd. 275.0922).

1-(3-Nitrophenyl)-4-phenyl-1-azabuta-1,3-diene (**9f**): A solution of cinnamaldehyde (**8**; $R^6 = R^7$ = H) (0.95 ml, 1.00 g, 7.57 mmol) and freshly sublimated 3-nitroaniline (**7f**) (1.05 g, 7.57 mmol) in C_6H_6 (30 ml) was stirred with activated molecular sieves (4 A, 5 g) at room temp. for 17 h. The reaction mixture was filtered over a short path of Celite. The solvent was evaporated and the residue dissolved in EtOAc (15 ml). The crude product was crystallized by addition of pentane (80 ml). The solid was recrystallized twice from EtOAc/pentane (1:10) to afford the product **9f** (1.07 g, 56%). Yellow needles. − ^1H NMR (200 MHz, $CDCl_3$): δ = 7.11 (dd, *J* = 16.0, 8.4 Hz, 1 H), 7.27 (d, *J* = 16.0 Hz, 1 H), 7.38−7.59 (m, 7 H), 8.00 (m, 1 H), 8.07 (dt, *J* = 7.2, 2.1 Hz, 1 H), 8.30 (d, *J* = 8.4 Hz, 1 H).

1-(2,4-Dimethoxyphenyl)-4-phenyl-1-azabuta-1,3-diene (**9g**): Na_2SO_4 (5 g) was added to a solution of cinnamaldehyde (**8**; $R^6 = R^7$ = H) (2.86 ml, 3.00 g, 22.7 mmol) and freshly distilled 2,4-dimethoxyaniline (**7g**) (3.24 ml, 3.48 g, 22.7 mmol) in Et_2O (50 ml) and the reaction mixture was stirred at room temp. for 2 h. The mixture was filtered and the residue was washed with Et_2O. The solution of the combined ethereal layers was evaporated in vacuo to a volume of 25 ml. Crystallization at −20°C provided the product **9g** (4.91 g, 81%). Yellow crystals. M.p. 75°C. − IR (drift): ν = 1628, 1602, 1588, 1497, 1280, 1259, 1206, 1157, 966, 824, 754 cm^{-1}. − ^1H NMR (250 MHz, $CDCl_3$): δ = 3.82 (s, 3 H), 3.89 (s, 3 H), 6.48 (dd, *J* = 8.5, 2.6 Hz, 1 H), 6.53 (d, *J* = 2.6 Hz, 1 H), 7.01 (d, *J* = 8.5 Hz, 1 H), 7.07 (d, *J* = 16.0 Hz, 1 H), 7.22 (dd, *J* = 16.0, 8.6 Hz, 1 H), 7.35 (m, 3 H), 7.50 (m, 2 H), 8.31 (d, *J* = 8.6 Hz, 1 H). − ^{13}C NMR and DEPT (63 MHz, $CDCl_3$): δ = 55.50 (CH_3), 55.82 (CH_3), 99.24 (CH), 104.33 (CH), 119.53 (CH), 127.36 (2 CH), 128.87 (2 CH), 129.25 (CH), 129.39 (CH), 134.50 (C), 135.90 (C), 142.59 (CH), 154.21 (C), 159.37 (C), 159.90 (CH). − MS (50°C): *m/z* (%) = 267 (93) [M^+], 266 (100), 130 (6), 115 (13); HRMS: 267.1254 ($C_{17}H_{17}NO_2$, calcd. 267.1259).

1-(3,4,5-Trimethoxyphenyl)-4-phenyl-1-azabuta-1,3-diene (**9h**): Na_2SO_4 (5 g) was added to a solution of cinnamaldehyde (**8**; $R^6 = R^7$ = H) (2.86 ml, 3.00 g, 22.7 mmol) and freshly sublimated 3,4,5-trimethoxyaniline (**7h**) (4.16 g, 22.7 mmol) in Et_2O (50 ml) and the reaction mixture was stirred at room temp. for 2 h. The mixture was filtered and the residue was washed with Et_2O. The solution of the combined organic layers was evaporated in vacuo to a volume of 25 ml. Crystallization at −20°C provided the product **9h** (5.33 g, 79%). Yellow needles. M.p. 88−91°C. − IR (drift): ν = 1627, 1584, 1503, 1446, 1417, 1243, 1232, 1008, 991, 838, 753, 693 cm^{-1}. − ^1H NMR (250 MHz, $CDCl_3$): δ = 3.87 (s, 3 H), 3.90 (s, 6 H), 6.48 (s, 2 H), 7.09 (dd, *J* = 15.9, 7.9 Hz, 1 H), 7.19 (d, *J* = 15.9 Hz, 1 H), 7.39 (m, 3 H), 7.55 (m, 2 H), 8.30 (d, *J* = 7.9 Hz, 1 H). − ^{13}C NMR and DEPT (100 MHz, $CDCl_3$): δ = 56.09 (2 CH_3), 60.97 (CH_3), 98.29 (2 CH), 127.46 (2 CH), 128.41 (CH), 128.93 (2 CH), 129.60 (CH), 135.57 (C), 136.67 (C), 143.97 (CH), 147.42 (C), 153.58 (2 C), 160.70 (CH). − MS (70°C): *m/z* (%) = 297 (100) [M^+], 296 (84), 282 (52), 115 (19), 74 (68), 59 (91); HRMS: 297.1347 ($C_{18}H_{19}NO_3$, calcd. 297.1365).

1-(2,4,6-Trimethoxyphenyl)-4-phenyl-1-azabuta-1,3-diene (**9i**): A solution of cinnamaldehyde (**8**; $R^6 = R^7$ = H) (195 µl, 204 mg, 1.54 mmol) and freshly sublimated 2,4,6-trimethoxyaniline (**7i**) (282 mg, 1.54 mmol) in Et_2O (20 ml) was stirred at room temp. for 2 h. The solvent was evaporated and the residue was dissolved in Et_2O (5 ml). Crystallization at −20°C provided the product **9i** (336 mg, 73%). Yellow crystals. M.p. 114°C. − IR (drift): ν = 1628, 1607, 1579, 1468, 1449, 1334, 1228, 1201, 1149, 1121, 812 cm^{-1}. − ^1H NMR (400 MHz, $CDCl_3$): δ = 3.82 (s, 3 H), 3.83 (s, 6 H), 6.21 (s, 2 H), 7.02 (d, *J* = 16.0 Hz, 1 H), 7.20 (dd, *J* = 16.0, 8.9 Hz, 1 H), 7.35 (m, 3 H), 7.51 (m, 2 H), 8.51 (d, *J* = 8.9 Hz, 1 H). − ^{13}C NMR and DEPT (100 MHz, $CDCl_3$): δ = 55.45 (CH_3), 56.12 (2 CH_3), 91.43 (2 CH), 123.64 (C), 127.34 (2 CH), 128.81 (2 CH), 129.02 (CH), 130.19 (CH), 136.15 (C), 142.04 (CH), 153.22 (2 C), 158.09 (C), 165.18 (CH). − MS (75°C): *m/z* (%) = 297 (100) [M^+], 296 (99.7), 266 (9), 130 (12), 115 (17); HRMS: 297.1351 ($C_{18}H_{19}NO_3$, calcd. 297.1365).

4-(4-Methoxyphenyl)-1-phenyl-1-azabuta-1,3-diene (**9j**): Na_2SO_4 (3 g) was added to a solution of 4-methoxycinnamaldehyde (**8**; R^6 = OMe, R^7 = H) (2.00 g, 12.3 mmol) and freshly distilled aniline (**7j**) (1.12 ml, 1.15 g, 12.3 mmol) in Et_2O (30 ml). The mixture was stirred for 3 h at room temp. and then filtered. The residue was washed with Et_2O and the solvent of the combined organic layers was evaporated. The crude product was dissolved in a mixture of Et_2O (80 ml) and EtOAc (10 ml). Recrystallization afforded the azadiene **9j** (2.58 g, 88%). Light yellow crystals. − ^1H NMR (400 MHz, $CDCl_3$): δ = 3.80 (s, 3 H), 6.90 (d, *J* = 8.4 Hz, 2 H), 6.98 (dd, *J* = 15.9, 8.5 Hz, 1 H), 7.07 (d, *J* = 15.9 Hz, 1 H), 7.18 (m, 3 H), 7.36 (t, *J* = 7.5 Hz, 2 H), 7.46 (d, *J* = 8.4 Hz, 2 H), 8.21 (d, *J* = 8.5 Hz, 1 H). − ^{13}C NMR and DEPT (100 MHz, $CDCl_3$): δ = 55.37 (CH_3), 114.40 (2 CH), 120.95 (2 CH), 125.91 (CH), 126.46 (CH), 128.40 (C), 129.07 (2 CH), 129.18 (2 CH), 143.85 (CH), 151.90 (C), 160.86 (C), 161.92 (CH).

1,4-Di-(4-methoxyphenyl)-1-azabuta-1,3-diene (**9k**): 4-Methoxycinnamaldehyde (**8**; R^6 = OMe, R^7 = H) (1.62 g, 10.0 mmol) and freshly sublimated *p*-anisidine (**7k**) (1.23 g, 10.0 mmol) were dissolved in a mixture of Et_2O (30 ml) and THF (15 ml). On cooling the reaction mixture to 5°C for 15 h, the azadiene **9k** crystallized (1.03 g, 39%). The solvent of the mother liquor was evaporated and the residue was dissolved in EtOAc (200 ml) at 65°C. Recrystallization at −20°C afforded **9k** (1.50 g, 56%). Total yield of the azadiene **9k**: 2.53 g (95%). Light yellow crystals. M.p. 182°C. − IR (drift): ν = 1900, 1627, 1602, 1576, 1504, 1441, 1307, 1290, 1245, 1178, 1031, 864, 816 cm^{-1}. − ^1H NMR (400 MHz, $CDCl_3$): δ = 3.82 (s, 3 H), 3.84 (s, 3 H), 6.91 (br d, *J* = 8.8 Hz, 4 H), 6.98 (dd, *J* = 15.9, 8.4 Hz, 1 H), 7.07 (d, *J* = 15.9 Hz, 1 H), 7.19 (br d, *J* = 8.8 Hz, 2 H), 7.47 (br d, *J* = 8.8 Hz, 2 H), 8.26 (d, *J* = 8.4 Hz, 1 H). − ^{13}C NMR and DEPT (63 MHz, $CDCl_3$): δ = 55.74 (CH_3), 55.86 (CH_3), 114.75 (2 CH), 114.78 (2 CH), 122.53 (2 CH), 127.08 (CH), 128.99 (C), 129.28 (2 CH), 143.19 (CH), 145.17 (C), 158.59 (C), 160.24 (CH), 161.07 (C). − MS (80°C): *m/z* (%) = 267 (34) [M^+], 266 (100), 252 (12), 145 (6); HRMS: 267.1264 ($C_{17}H_{17}NO_2$, calcd. 267.1259).

1-(2-Methoxyphenyl)-4-(4-methoxyphenyl)-1-azabuta-1,3-diene (**9l**): A solution of 4-methoxycinnamaldehyde (**8**; R^6 = OMe, R^7 =

H) (1.62 g, 10.0 mmol) and freshly distilled *o*-anisidine (**7l**) (1.13 ml, 1.23 g, 10.0 mmol) in Et_2O (30 ml) was stirred at room temp. for 2 h. Subsequently, the reaction mixture was dried over Na_2SO_4. The solution was separated and the residue was washed with Et_2O. The solution of the combined organic layers was evaporated in vacuo to a volume of 20 ml. Crystallization at −30°C afforded **9l** (2.11 g, 79%). Light yellow needles. M.p. 105°C. − IR (drift): ν = 1626, 1580, 1492, 1307, 1246, 1025, 810, 754 cm^{-1}. − ^1H NMR (400 MHz, $CDCl_3$): δ = 3.82 (s, 3 H), 3.90 (s, 3 H), 6.90−7.00 (m, 5 H), 7.04−7.20 (m, 3 H), 7.47 (br d, *J* = 8.8 Hz, 2 H), 8.24 (dd, *J* = 7.5, 0.8 Hz, 1 H). − ^{13}C NMR and DEPT (100 MHz, $CDCl_3$): δ = 55.30 (CH_3), 55.70 (CH_3), 111.12 (CH), 114.30 (2 CH), 119.34 (CH), 120.88 (CH), 126.69 (CH), 126.95 (CH), 128.46 (C), 128.96 (2 CH), 141.38 (C), 143.40 (CH), 152.69 (C), 160.69 (C), 162.21 (CH). − MS (50°C): *m/z* (%) = 267 (40) [M^+], 266 (100), 252 (24), 250 (8), 236 (6); HRMS: 267.1249 ($C_{17}H_{17}NO_2$, calcd. 267.1259).

1-(4-Trifluoromethylphenyl)-4-(4-methoxyphenyl)-1-azabuta-1,3-diene (**9m**): 4-Methoxycinnamaldehyde (**8**; R^6 = OMe, R^7 = H) (1.62 g, 10.0 mmol) and freshly distilled 4-trifluoromethylaniline (**7m**) (1.25 ml, 1.61 g, 10.0 mmol) were dissolved in a mixture of Et_2O (50 ml) and THF (15 ml). The reaction mixture was cooled to 5°C for 15 h and was dried over Na_2SO_4. After filtration the solvent was evaporated and the residue was crystallized from Et_2O/EtOAc (3:1, 80 ml) to afford the azadiene **9m** (1.81 g, 59%). Yellow crystals. M.p. 121°C. − IR (drift): ν = 1628, 1588, 1513, 1330, 1270, 1130, 1011, 850 cm^{-1}. − ^1H NMR (400 MHz, $CDCl_3$): δ = 3.85 (s, 3 H), 6.94 (br d, *J* = 8.8 Hz, 2 H), 6.99 (dd, *J* = 15.9, 8.9 Hz, 1 H), 7.16 (d, *J* = 15.9 Hz, 1 H), 7.21 (d, *J* = 8.4 Hz, 2 H), 7.50 (br d, *J* = 8.8 Hz, 2 H), 7.62 (d, *J* = 8.4 Hz, 2 H), 8.20 (d, *J* = 8.9 Hz, 1 H). − ^{13}C NMR and DEPT (100 MHz, $CDCl_3$): δ = 55.39 (CH_3), 114.44 (2 CH), 121.02 (2 CH), 124.30 (CF_3, q, $^1J_{CF}$ = 272 Hz), 125.93 (CH), 126.35 (2 CH, q, $^3J_{CF}$ = 3.5 Hz), 127.53 (C, q, $^2J_{CF}$ = 32.5 Hz), 128.06 (C), 129.27 (2 CH), 145.33 (CH), 155.04 (C), 161.15 (C), 163.54 (CH). − MS (40°C): *m/z* (%) = 305 (25) [M^+], 304 (100), 290 (13), 261 (7), 145 (7); HRMS: 305.1006 ($C_{17}H_{14}F_3NO$, calcd. 305.1027).

1-(2,4-Dimethoxyphenyl)-4-(4-methoxyphenyl)-1-azabuta-1,3-diene (**9n**): A solution of 4-methoxycinnamaldehyde (**8**; R^6 = OMe, R^7 = H) (1.00 g, 6.17 mmol) and freshly distilled 2,4-dimethoxyaniline (**7n**) (0.88 ml, 945 mg, 6.17 mmol) in THF (30 ml) was stirred at 40°C for 1 h. The solvent was evaporated and the residue was crystallized from a mixture of Et_2O (200 ml) and EtOAc (30 ml) at −20°C to provide the product **9n** (1.46 g, 80%). Yellow solid. M.p. 123°C. − IR (drift): ν = 1625, 1603, 1587, 1509, 1497, 1259, 1246, 1206, 1176, 1157, 1128, 1025, 824 cm^{-1}. − ^1H NMR (400 MHz, $CDCl_3$): δ = 3.80 (s, 3 H), 3.81 (s, 3 H), 3.88 (s, 3 H), 6.46 (dd, *J* = 8.6, 2.5 Hz, 1 H), 6.52 (d, *J* = 2.5 Hz, 1 H), 6.89 (d, *J* = 8.7 Hz, 2 H), 6.98 (d, *J* = 8.6 Hz, 1 H), 7.02 (d, *J* = 15.9 Hz, 1 H), 7.09 (dd, *J* = 15.9, 8.3 Hz, 1 H), 7.45 (d, *J* = 8.7 Hz, 2 H), 8.26 (d, *J* = 8.3 Hz, 1 H). − ^{13}C NMR and DEPT (100 MHz, $CDCl_3$): δ = 55.33 (CH_3), 55.49 (CH_3), 55.80 (CH_3), 99.20 (CH), 104.26 (CH), 114.33 (2 CH), 119.41 (CH), 127.30 (CH), 128.72 (C), 128.85 (2 CH), 134.72 (C), 142.40 (CH), 154.13 (C), 159.14 (C), 160.22 (CH), 160.57 (C). − MS (85°C): *m/z* (%) = 297 (56) [M^+], 296 (100), 282 (22), 145 (5); HRMS: 297.1354 ($C_{18}H_{19}NO_3$, calcd. 297.1365).

1-(4-Methoxyphenyl)-4-(2-methoxyphenyl)-1-azabuta-1,3-diene (**9o**): Na_2SO_4 (5 g) was added to a solution of 2-methoxycinnamaldehyde (**8**; R^6 = H, R^7 = OMe) (2.00 g, 12.3 mmol) and freshly sublimated *p*-anisidine (**7o**) (1.52 g, 12.3 mmol) in Et_2O (100 ml). The reaction mixture was stirred at room temp. for 2 h. The solution was separated and the residue was washed with Et_2O. The solvent of the combined organic solutions was evaporated and the residue was dissolved in Et_2O/pentane (2:1, 100 ml). Precipitation of the product was completed by cooling this solution to −78°C and subsequent warming to 40°C. Repetition of this procedure several times afforded the product **9o** (2.82 g, 86%). Yellow solid. M.p. 62°C. − IR (drift): ν = 2839, 1620, 1596, 1504, 1484, 1467, 1244, 1028, 990, 956, 756 cm^{-1}. − ^1H NMR (250 MHz, $CDCl_3$): δ = 3.82 (s, 3 H), 3.89 (s, 3 H), 6.88−7.01 (m, 2 H), 6.91 (br d, *J* = 8.9 Hz, 2 H), 7.11−7.23 (m, 2 H), 7.17 (dd, *J* = 16.1, 9.0 Hz, 1 H), 7.32 (m, 1 H), 7.48 (d, *J* = 16.1 Hz, 1 H), 7.57 (dd, *J* = 7.7, 1.6 Hz, 1 H), 8.31 (d, *J* = 9.0 Hz, 1 H). − ^{13}C NMR and DEPT (63 MHz, $CDCl_3$): δ = 56.13 (2 CH_3), 111.72 (CH), 115.04 (2 CH), 121.51 (CH), 122.85 (2 CH), 125.38 (C), 128.30 (CH), 129.90 (CH), 131.24 (CH), 138.96 (CH), 145.43 (C), 158.12 (C), 158.90 (C), 161.24 (CH). − MS (70°C): *m/z* (%) = 267 (32) [M^+], 266 (24), 252 (16), 237 (16), 236 (100), 115 (6); HRMS: 267.1237 ($C_{17}H_{17}NO_2$, calcd. 267.1259).

4-(4-Cyanophenyl)-1-phenyl-1-azabuta-1,3-diene (**9p**): A solution of 4-cyanocinnamaldehyde (**8**; R^6 = CN, R^7 = H) (157 mg, 1.00 mmol) and freshly distilled aniline (**7p**) (182 µl, 186 mg, 2.00 mmol) in THF (10 ml) was stirred at room temp. for 1.5 h. After addition of pentane (30 ml) the product was crystallized at −30°C to afford the azadiene **9p** (181 mg, 78%). Yellow crystals. M.p. 104°C. − IR (drift): ν = 3049, 2221, 1627, 1608, 1583, 1488, 1413, 1156, 983, 954, 816, 764 cm^{-1}. − ^1H NMR (250 MHz, $CDCl_3$): δ = 7.32−7.47 (m, 5 H), 7.58 (m, 2 H), 7.77 (d, *J* = 7.9 Hz, 2 H), 7.83 (d, *J* = 7.9 Hz, 2 H), 8.47 (d, *J* = 7.0 Hz, 1 H). − ^{13}C NMR and DEPT (63 MHz, $CDCl_3$): δ = 112.93 (C), 119.11 (C≡N), 121.48 (2 CH), 127.22 (CH), 128.27 (2 CH), 129.79 (2 CH), 132.27 (CH), 133.14 (2 CH), 140.35 (C), 141.68 (CH), 151.70 (C), 161.00 (CH). − MS (60°C): *m/z* (%) = 232 (53) [M^+], 231 (100), 77 (21); HRMS: 232.1015 ($C_{16}H_{12}N_2$, calcd. 232.1000).

4-(4-Cyanophenyl)-1-(2,4-dimethoxyphenyl)-1-azabuta-1,3-diene (**9q**): A solution of freshly distilled 2,4-dimethoxyaniline (**7q**) (141 µl, 153 mg, 1.00 mmol) in Et_2O (14 ml) was added to a solution of 4-cyanocinnamaldehyde (**8**; R^6 = CN, R^7 = H) (157 mg, 1.00 mmol) in Et_2O (20 ml). The reaction mixture was stirred for 10 min at room temp. and then cooled to −20°C for 15 h without stirring. Evaporation of the solvent afforded the product **9q** (289 mg, 99%). Orange solid. M.p. 121°C. − IR (drift): ν = 2223, 1623, 1604, 1585, 1498, 1311, 1258, 1210, 1161, 1130, 1047, 843, 827 cm^{-1}. − ^1H NMR (400 MHz, $CDCl_3$): δ = 3.83 (s, 3 H), 3.90 (s, 3 H), 6.49 (dd, *J* = 8.6, 2.6 Hz, 1 H), 6.54 (d, *J* = 2.6 Hz, 1 H), 7.05 (d, *J* = 8.6 Hz, 1 H), 7.06 (d, *J* = 16.0 Hz, 1 H), 7.28 (dd, *J* = 16.0, 8.9 Hz, 1 H), 7.58 (br d, *J* = 8.4 Hz, 2 H), 7.65 (br d, *J* = 8.4 Hz, 2 H), 8.36 (d, *J* = 8.9 Hz, 1 H). − ^{13}C NMR and DEPT (100 MHz, $CDCl_3$): δ = 55.54 (CH_3), 55.86 (CH_3), 99.23 (CH), 104.49 (CH), 112.06 (C), 118.69 (C≡N), 119.73 (CH), 127.59 (2 CH), 132.63 (2 CH), 132.69 (CH), 133.80 (C), 139.62 (CH), 140.27 (C), 154.45 (C), 158.43 (CH), 159.92 (C). − MS (85°C): *m/z* (%) = 292 (43) [M^+], 291 (42), 157 (100), 156 (82), 153 (25), 138 (28), 129 (51), 128 (43); HRMS: 292.1203 ($C_{18}H_{16}N_2$, calcd. 292.1212).

1-(4-Methoxyphenyl)-4-(4-N,N-dimethylaminophenyl)-1-azabuta-1,3-diene (**9r**): A solution of 4-*N*,*N*-dimethylaminocinnamaldehyde (**8**; R^6 = NMe_2, R^7 = H) (1.00 g, 5.71 mmol) and freshly sublimated *p*-anisidine (**7r**) (703 mg, 5.71 mmol) in CH_2Cl_2 (30 ml) was stirred at room temp. for 1 h. Na_2SO_4 (2 g) was added and the reaction mixture was stirred at room temp. for an additional 2 h. The solution was separated and by addition of Et_2O/pentane (1:7, 50 ml) the product **9r** was precipitated (1.36 g, 85%). Green crystals. M.p. 146−150°C. − IR (drift): ν = 2540, 2057, 2006, 1887,

1609, 1575, 1503, 1248, 1156, 836, 810 cm^{-1}. − ^1H NMR (250 MHz, $CDCl_3$): δ = 3.01 (s, 6 H), 3.82 (s, 3 H), 6.63−6.76 (m, 2 H), 6.87−6.94 (m, 2 H), 6.92 (dd, *J* = 15.7, 8.5 Hz, 1 H), 7.05 (d, *J* = 15.7 Hz, 1 H), 7.18 (br d, *J* = 8.9 Hz, 2 H), 7.42 (br d, *J* = 8.9 Hz, 2 H), 8.24 (d, *J* = 8.5 Hz, 1 H). − ^{13}C NMR and DEPT (125 MHz, $CDCl_3$): δ = 40.11 (2 CH_3), 55.40 (CH_3), 111.96 (2 CH), 114.30 (2 CH), 122.02 (2 CH), 123.74 (C), 124.08 (CH), 128.87 (2 CH), 143.90 (CH), 145.05 (C), 151.11 (C), 157.86 (C), 160.35 (CH). − MS (110°C): *m/z* (%) = 280 (45) [M^+], 279 (100), 265 (3), 158 (7); HRMS: 280.1563 ($C_{18}H_{20}N_2O$, calcd. 280.1576).

1-(4-Methoxyphenyl)-4-(4-nitrophenyl)-1-azabuta-1,3-diene (**9s**): A solution of 4-nitrocinnamaldehyde (**8**; R^6 = NO_2, R^7 = H) (713 mg, 4.02 mmol) in THF (20 ml) was added to a solution of freshly sublimated *p*-anisidine (**7s**) (495 mg, 4.02 mmol) in THF (20 ml). The reaction mixture was stirred at room temp. for 1 h. The solvent was evaporated and the residue was recrystallized from EtOAc (60 ml) to afford the azadiene **9s** (848 mg, 75%). Yellow needles. M.p. 164°C. − IR (drift): ν = 1622, 1608, 1595, 1441, 1415, 1300, 953, 758 cm^{-1}. − ^1H NMR (250 MHz, $CDCl_3$): δ = 3.84 (s, 3 H), 6.94 (br d, *J* = 8.9 Hz, 2 H), 7.14 (d, *J* = 16.1 Hz, 1 H), 7.23 (dd, *J* = 16.1, 8.3 Hz, 1 H), 7.24 (br d, *J* = 8.9 Hz, 2 H), 7.66 (br d, *J* = 8.8 Hz, 2 H), 8.25 (br d, *J* = 8.8 Hz, 2 H), 8.34 (d, *J* = 8.3 Hz, 1 H). − ^{13}C NMR and DEPT (100 MHz, $CDCl_3$): δ = 55.51 (CH_3), 114.52 (2 CH), 122.46 (2 CH), 124.25 (2 CH), 127.78 (2 CH), 132.86 (CH), 139.45 (CH), 142.02 (C), 143.95 (C), 147.76 (C), 157.90 (CH), 158.98 (C). − MS (100°C): *m/z* (%) = 282 (100) [M^+], 281 (74), 235 (65), 192 (9); HRMS: 282.0998 ($C_{16}H_{14}N_2O_3$, calcd. 282.1004).

Preparation of the (η⁴-1-Azabuta-1,3-diene)tricarbonyliron Complexes **10** *by Sonochemical Reaction of the 1-Azabuta-1,3-dienes* **9** *with Nonacarbonyldiiron at Room Temperature − General Procedure:* A solution of the 1-azabuta-1,3-dienes **9** (1 eq.) and $Fe_2(CO)_9$ (1.5 eq.) in THF (15 ml) was sonicated at room temp. for 16 h. Removal of the solvent by evaporation and flash chromatography (Et_2O/pentane) of the residue on silica gel afforded the tricarbonyliron complexes **10** as red crystals (Table 5).

Table 5. Sonochemical complexation of the 1-azabuta-1,3-dienes **9** and yield of the iron complexes **10**

Entry	**9**		$Fe_2(CO)_9$		Eluent[b]	Yield **10**	
	[g]	[mmol]	[g]	[mmol]	Et_2O/pentane	[g]	[%]
a	0.500	2.41	1.10	3.03[a]	1:10	0.682	82
b	0.500	2.11	0.960	2.64[a]	1:10	0.701	88
c	1.78	7.50	4.11	11.3	1:10	2.25	80
d	0.500	2.00	1.09	3.00	1:7 to 1:3	0.428	55
e[c]	1.00	3.63	1.98	5.45	1:10	0.882	59
g	1.50	5.61	3.06	8.42	1:10	0.990	43
h	1.50	5.04	2.75	7.56	1:10	0.890	40
i	1.00	3.36	1.83	5.04	10:1 to 5:1	0.819	56
j[c]	1.00	4.21	2.30	6.32	0:1 to 1:4	1.16	73
k	1.00	3.74	2.04	5.61	1:10 to 1:2	0.626	41
l	1.50	5.61	3.06	8.42	1:7	1.88	82
m	1.00	3.28	1.79	4.92	0:1 to 1:3	0.935	64
n	0.500	1.68	0.917	2.52	1:10 to 1:5	0.578	79
o	1.00	3.74	2.04	5.61	1:10	1.24	81
p	0.450	1.94	1.06	2.91	1:7 to 1:1	0.410	57
q	0.846	2.89	1.58	4.34	1:10 to 2:1	0.760	61
r	0.500	1.78	0.971	2.67	1:7 to 1:0	0.463	62

[a] 1.25 Equivalents of $Fe_2(CO)_9$. − [b] Gradient elution by entry **d**, **i**, **j**, **k**, **m**, **n**, **p**, and **q**. − [c] Reaction time (sonication) of entry **e** was 18 h and of entry **j** 17 h.

Tricarbonyl[(1-4-η)-1,4-diphenyl-1-azabuta-1,3-diene]iron (**10a**): Mp ≥ 132°C (dec). − IR (drift): ν = 2055, 1988, 1977, 1593, 1486, 1450, 1290, 1155, 761 cm^{-1}. − ^1H NMR (400 MHz, $CDCl_3$): δ = 3.38 (d, *J* = 9.4 Hz, 1 H), 5.72 (dd, *J* = 9.4, 2.8 Hz, 1 H), 6.92 (m, 3 H), 6.95 (d, *J* = 2.8 Hz, 1 H), 7.19 (m, 3 H), 7.30 (m, 4 H). − ^{13}C NMR and DEPT (100 MHz, $CDCl_3$): δ (*T* = 298 K) = 62.17 (CH), 74.45 (CH), 103.86 (CH), 121.86 (2 CH), 122.56 (CH), 126.61 (2 CH), 126.93 (CH), 128.80 (2 CH), 128.99 (2 CH), 138.81 (C), 153.38 (C), 205.79 (CO, very br), 208.77 (CO, very br), 211.90 (CO, very br); ^{13}C NMR (125 MHz, [D_8]toluene): δ (*T* = 233 K) = 62.31 (CH), 74.20 (CH), 104.37 (CH), 122.09 (2 CH), 122.63 (CH), 126.67 (2 CH), 127.08 (CH), 128.93 (2 CH), 129.16 (2 CH), 138.91 (C), 153.90 (C), 206.02 (CO), 209.49 (CO), 212.70 (CO); δ (*T* = 292 K) = 62.63 (CH), 74.29 (CH), 104.43 (CH), 122.16 (2 CH), 122.79 (CH), 126.81 (2 CH), 127.12 (CH), 128.96 (2 CH), 129.19 (2 CH), 138.13 (C), 153.96 (C), 206.04 (CO, br), 209.42 (CO, br), 212.66 (CO, br); δ (*T* = 373 K) = 63.21 (CH), 74.51 (CH), 104.75 (CH), 122.37 (2 CH), 123.13 (CH), 127.15 (2 CH), 127.30 (CH), 129.11 (2 CH), 129.34 (2 CH), 139.61 (C), 154.15 (C), 209.53 (3 CO, br). − MS (75°C): *m/z* (%) = 347 (3) [M^+], 319 (8), 291 (12), 263 (100), 207 (10), 206 (31), 56 (18); HRMS: 347.0217 ($C_{18}H_{13}FeNO_3$, calcd. 347.0245). − $C_{18}H_{13}FeNO_3$: C 62.28, H 3.77, N 4.03; found: C 62.33, H 4.08, N 4.22.

Tricarbonyl[(1-4-η)-1-(4-methoxyphenyl)-4-phenyl-1-azabuta-1,3-diene]iron (**10b**): Mp ≥ 140°C (dec). − IR (drift): ν = 2049, 1987, 1963, 1507, 1250, 1040, 832 cm^{-1}. − ^1H NMR (200 MHz, $CDCl_3$): δ = 3.37 (d, *J* = 9.4 Hz, 1 H), 3.75 (s, 3 H), 5.68 (dd, *J* = 9.4, 2.9 Hz, 1 H), 6.73 (d, *J* = 8.9 Hz, 2 H), 6.91 (d, *J* = 8.9 Hz, 2 H), 6.99 (d, *J* = 2.9 Hz, 1 H), 7.19−7.34 (m, 5 H). − ^{13}C NMR and DEPT (100 MHz, $CDCl_3$): δ (*T* = 298 K) = 55.42 (CH_3), 61.89 (CH), 73.95 (CH), 104.28 (CH), 114.28 (2 CH), 122.55 (2 CH), 126.59 (2 CH), 126.84 (CH), 128.77 (2 CH), 138.97 (C), 146.55 (C), 155.37 (C); ^{13}C NMR (125 MHz, [D_8]toluene): δ (*T* = 233 K) = 54.44 (CH_3), 62.10 (CH), 73.71 (CH), 104.82 (CH), 114.20 (2 CH), 122.76 (2 CH), 126.69 (2 CH), 127.00 (CH), 128.93 (2 CH), 139.12 (C), 146.74 (C), 155.59 (C), 206.60 (CO), 209.71 (CO), 213.03 (CO); δ (*T* = 298 K) = 54.85 (CH_3), 62.48 (CH), 73.81 (CH), 105.03 (CH), 114.65 (2 CH), 122.94 (2 CH), 126.92 (2 CH), 127.12 (CH), 129.03 (2 CH), 139.46 (C), 147.00 (C), 156.17 (C), 206.91 (CO, very br), 209.80 (CO, very br), 212.84 (CO, very br); δ (*T* = 373 K) = 55.31 (CH_3), 62.89 (CH), 73.90 (CH), 105.32 (CH), 115.17 (2 CH), 123.09 (2 CH), 127.15 (2 CH), 127.19 (CH), 129.08 (2 CH), 139.80 (C), 147.27 (C), 156.75 (C), 209.81 (3 CO). − MS (90°C): *m/z* (%) = 377 (3) [M^+], 349 (6), 321 (8), 293 (100), 237 (29), 236 (54), 115 (16); HRMS: 377.0339 ($C_{19}H_{15}FeNO_4$, calcd. 377.0350). − $C_{19}H_{15}FeNO_4$: C 60.50, H 4.01, N 3.71; found: C 60.51, H 4.05, N 3.94.

Tricarbonyl[(1-4-η)-1-(2-methoxyphenyl)-4-phenyl-1-azabuta-1,3-diene]iron (**10c**): Mp ≥ 123°C (dec). − IR (drift): ν = 2058, 2000, 1970, 1497, 1455, 1297, 1245, 1031, 749, 695 cm^{-1}. − ^1H NMR (400 MHz, $CDCl_3$): δ = 3.33 (d, *J* = 9.5 Hz, 1 H), 3.97 (s, 3 H), 5.80 (dd, *J* = 9.5, 3.0 Hz, 1 H), 6.81 (m, 2 H), 6.98 (br dt, *J* = 1.5, 7.8 Hz, 1 H), 7.04 (m, 1 H), 7.10 (br d, *J* = 3.0 Hz, 1 H), 7.19 (m, 1 H), 7.28 (m, 2 H), 7.34 (m, 2 H). − ^{13}C NMR and DEPT (100 MHz, $CDCl_3$): δ (*T* = 298 K) = 54.79 (CH_3), 62.08 (CH), 76.09 (CH), 101.99 (CH), 110.99 (CH), 118.96 (CH), 120.51 (CH), 123.57 (CH), 126.53 (2 CH), 126.75 (CH), 128.76 (2 CH), 139.11 (C), 141.38 (C), 150.88 (C), 205.70 (CO, very br), 209.33 (CO, very br), 212.82 (CO, very br); ^{13}C NMR (125 MHz, [D_8]toluene): δ (*T* = 233 K) = 53.90 (CH_3), 62.58 (CH), 76.24 (CH), 101.97 (CH), 110.90 (CH), 118.41 (CH), 120.39 (CH), 123.59 (CH), 126.61 (2 CH), 126.86 (CH), 128.91 (2 CH), 139.33 (C), 141.70 (C), 150.86 (C), 206.41 (CO), 210.06 (CO), 213.84 (CO); δ (*T* = 298 K) = 54.33 (CH_3), 62.85 (CH), 76.00 (CH), 102.71 (CH), 111.47 (CH), 119.17 (CH), 120.73 (CH), 123.64 (CH), 126.79 (2 CH),

126.93 (CH), 128.93 (2 CH), 139.54 (C), 142.14 (C), 151.44 (C), 206.46 (CO, br), 210.04 (CO, br), 213.75 (CO, br); δ (T = 373 K) = 55.01 (CH_3), 63.27 (CH), 75.85 (CH), 103.64 (CH), 112.50 (CH), 120.21 (CH), 121.27 (CH), 123.82 (CH), 127.10 (3 CH), 129.05 (2 CH), 139.93 (C), 142.73 (C), 152.26 (C), 210.02 (3 CO, br). − MS (75°C): *m/z* (%) = 377 (3) [M^+], 349 (12), 321 (23), 293 (58), 278 (100), 237 (11), 236 (11), 139 (12), 56 (6).

Tricarbonyl[(1-4-η)-1-(4-N,N-dimethylaminophenyl)-4-phenyl-1-azabuta-1,3-diene]iron (**10d**): Mp ≥ 136°C (dec). − IR (drift): ν = 2047, 1987, 1965, 1607, 1515, 1283, 1154, 822, 765, 698 cm^{-1}. − ^1H NMR (250 MHz, $CDCl_3$): δ = 2.88 (s, 6 H), 3.37 (d, J = 9.3 Hz, 1 H), 5.63 (dd, J = 9.3, 2.9 Hz, 1 H), 6.58 (br d, J = 9.0 Hz, 2 H), 6.93 (br d, J = 9.0 Hz, 2 H), 7.06 (dd, J = 2.9, 0.8 Hz, 1 H), 7.17−7.34 (m, 5 H). − ^{13}C NMR and DEPT (63 MHz, $CDCl_3$): δ = 40.91 (2 CH_3), 61.34 (CH), 73.43 (CH), 104.40 (CH), 113.28 (2 CH), 122.45 (2 CH), 126.56 (2 CH), 126.64 (CH), 128.69 (2 CH), 139.29 (C), 143.14 (C), 146.96 (C). − MS (105°C): *m/z* (%) = 390 (5) [M^+], 362 (1), 334 (7), 306 (100), 250 (69), 249 (89), 233 (15); HRMS: 390.0671 ($C_{20}H_{18}FeN_2O_3$, calcd. 390.0667).

Tricarbonyl[(1-4-η)-1-(4-trifluoromethylphenyl)-4-phenyl-1-azabuta-1,3-diene]iron (**10e**): Mp ≥ 151°C (dec). − IR (drift): ν = 3061, 2059, 2002, 1983, 1611, 1329, 1288, 1166, 1123, 1110, 842, 768, 698 cm^{-1}. − ^1H NMR (400 MHz, $CDCl_3$): δ = 3.41 (d, J = 9.5 Hz, 1 H), 5.75 (dd, J = 9.5, 2.9 Hz, 1 H), 6.84 (dd, J = 2.9, 0.7 Hz, 1 H), 6.92 (d, J = 8.3 Hz, 2 H), 7.22 (m, 1 H), 7.31 (m, 4 H), 7.41 (d, J = 8.3 Hz, 2 H). − ^{13}C NMR and DEPT (100 MHz, $CDCl_3$): δ (T = 298 K) = 63.04 (CH), 75.65 (CH), 102.01 (CH), 121.77 (2 CH), 123.98 (C, q, $^2J_{CF}$ = 32.6 Hz), 124.45 (CF_3, q, $^1J_{CF}$ = 271 Hz), 126.24 (2 CH, q, $^3J_{CF}$ = 3.5 Hz), 126.67 (2 CH), 127.26 (CH), 128.93 (2 CH), 138.34 (C), 156.70 (C), 204.77 (CO, br), 208.30 (CO, br), 211.49 (CO, br); ^{13}C NMR (125 MHz, [D_8]toluene): δ (T = 233 K) = 62.95 (CH), 75.33 (CH), 102.36 (CH), 121.94 (2 CH), 123.56 (C, q, $^2J_{CF}$ = 32.2 Hz), 125.22 (CF_3, q, $^1J_{CF}$ = 271 Hz), 126.32 (2 CH, br), 126.68 (2 CH), 127.41 (CH), 129.04 (2 CH), 138.38 (C), 156.97 (C), 205.19 (CO), 208.90 (CO), 212.16 (CO); δ (T = 307 K) = 63.49 (CH), 75.54 (CH), 102.50 (CH), 122.05 (2 CH), 124.31 (C, q, $^2J_{CF}$ = 33 Hz), 126.46 (2 CH, br), 126.89 (2 CH), 127.51 (CH), 129.08 (2 CH), 138.66 (C), 157.10 (C), 205.44 (CO, br), 208.89 (CO, br), 212.16 (CO, br), the signal of the CF_3 carbon atom is missing due to overlapping; δ (T = 373 K) = 64.02 (CH), 75.80 (CH), 102.74 (CH), 122.22 (2 CH), 125.35 (CF_3, q, $^1J_{CF}$ = 273 Hz), 126.63 (2 CH, br), 127.16 (2 CH), 127.66 (CH), 129.20 (2 CH), 139.01 (C), 157.25 (C), 208.79 (3 CO, br), the signal of the aromatic carbon atom α to the CF_3 group is missing due to overlapping. − MS (90°C): *m/z* (%) = 415 (1) [M^+], 387 (6), 359 (7), 331 (73), 275 (24), 274 (100), 256 (17), 145 (13), 115 (29); HRMS: 415.0085 ($C_{19}H_{12}F_3FeNO_3$, calcd. 415.0119).

Tricarbonyl[(1-4-η)-1-(2,4-dimethoxyphenyl)-4-phenyl-1-azabuta-1,3-diene]iron (**10g**): Mp ≥95°C (dec). − IR (drift): ν = 2048, 1994, 1970, 1503, 1456, 1285, 1259, 1205, 1030, 823 cm^{-1}. − ^1H NMR (400 MHz, $CDCl_3$): δ = 3.30 (d, J = 9.4 Hz, 1 H), 3.77 (s, 3 H), 3.96 (s, 3 H), 5.77 (dd, J = 9.4, 2.9 Hz, 1 H), 6.34 (dd, J = 8.7, 2.6 Hz, 1 H), 6.41 (d, J = 2.6 Hz, 1 H), 6.99 (d, J = 8.7 Hz, 1 H), 7.15 (d, J = 2.9 Hz, 1 H), 7.19 (m, 1 H), 7.28 (t, J = 7.4 Hz, 2 H), 7.34 (m, 2 H). − ^{13}C NMR and DEPT (100 MHz, $CDCl_3$): δ = 54.93 (CH_3), 55.43 (CH_3), 61.66 (CH), 75.59 (CH), 99.25 (CH), 102.30 (CH), 103.60 (CH), 118.53 (CH), 126.53 (2 CH), 126.66 (CH), 128.74 (2 CH), 135.03 (C), 139.29 (C), 152.27 (C), 156.67 (C). − MS (70°C): *m/z* (%) = 407 (1) [M^+], 379 (5), 351 (18), 323 (78), 308 (100), 267 (74), 266 (82), 154 (15), 115 (16); HRMS: 407.0447 ($C_{20}H_{17}FeNO_5$, calcd. 407.0456).

Tricarbonyl[(1-4-η)-1-(3,4,5-trimethoxyphenyl)-4-phenyl-1-azabuta-1,3-diene]iron (**10h**): Mp ≥ 147°C (dec). − IR (drift): ν = 2054, 1995, 1980, 1580, 1501, 1451, 1251, 1128, 1011, 770 cm^{-1}. − ^1H NMR (250 MHz, $CDCl_3$): δ = 3.38 (d, J = 9.4 Hz, 1 H), 3.78 (s, 3 H), 3.86 (s, 6 H), 5.70 (dd, J = 9.4, 2.9 Hz, 1 H), 6.18 (s, 2 H), 6.97 (dd, J = 2.9, 0.8 Hz, 1 H), 7.17−7.35 (m, 5 H). − ^{13}C NMR and DEPT (100 MHz, $CDCl_3$): δ = 56.00 (2 CH_3), 60.92 (CH_3), 62.30 (CH), 74.11 (CH), 99.26 (2 CH), 103.91 (CH), 126.61 (2 CH), 126.99 (CH), 128.81 (2 CH), 134.03 (C), 138.74 (C), 149.43 (C), 153.22 (2 C). − MS (90°C): *m/z* (%) = 437 (3) [M^+], 409 (9), 381 (6), 353 (100), 297 (51), 296 (45), 282 (28), 177 (8); HRMS: 437.0575 ($C_{21}H_{19}FeNO_6$, calcd. 437.0562).

Tricarbonyl[(1-4-η)-1-(2,4,6-trimethoxyphenyl)-4-phenyl-1-azabuta-1,3-diene]iron (**10i**): Mp ≥103°C (dec). − IR (drift): ν = 2052, 2038, 1992, 1978, 1968, 1597, 1578, 1465, 1337, 1205, 1131 cm^{-1}. − ^1H NMR (250 MHz, $CDCl_3$): δ = 3.23 (d, J = 9.4 Hz, 1 H), 3.77 (s, 3 H), 3.91 (s, 6 H), 5.65 (dd, J = 9.4, 3.0 Hz, 1 H), 6.09 (s, 2 H), 7.17 (m, 1 H), 7.30 (m, 4 H), 7.94 (dd, J = 3.0, 0.8 Hz, 1 H). − ^{13}C NMR and DEPT (63 MHz, $CDCl_3$): δ = 55.25 (CH_3), 55.44 (2 CH_3), 60.79 (CH), 74.06 (CH), 91.18 (2 CH), 106.17 (CH), 122.93 (C), 126.33 (CH), 126.43 (2 CH), 128.56 (2 CH), 139.62 (C), 153.60 (2 C), 156.00 (C). − MS (120°C): *m/z* (%) = 437 (0.2) [M^+], 409 (2), 381 (9), 353 (72), 338 (100), 297 (43), 296 (31), 115 (20); HRMS: 437.0546 ($C_{21}H_{19}FeNO_6$, calcd. 437.0562).

Tricarbonyl[(1-4-η)-4-(4-methoxyphenyl)-1-phenyl-1-azabuta-1,3-diene]iron (**10j**): Mp ≥136°C (dec). − IR (drift): ν = 2054, 1981, 1607, 1515, 1485, 1475, 1278, 1249, 1032, 835, 762 cm^{-1}. − ^1H NMR (400 MHz, $CDCl_3$): δ = 3.43 (d, J = 9.5 Hz, 1 H), 3.80 (s, 3 H), 5.65 (dd , J = 9.5, 2.9 Hz, 1 H), 6.84 (br d, J = 8.8 Hz, 2 H), 6.92 (m, 4 H), 7.17 (m, 2 H), 7.27 (br d, J = 8.8 Hz, 2 H). − ^{13}C NMR and DEPT (100 MHz, $CDCl_3$): δ = 55.27 (CH_3), 63.15 (CH), 74.28 (CH), 103.03 (CH), 114.31 (2 CH), 121.86 (2 CH), 122.44 (CH), 127.83 (2 CH), 128.96 (2 CH), 130.89 (C), 153.51 (C), 158.71 (C). − MS (85°C): *m/z* (%) = 377 (2) [M^+], 349 (7), 321 (11), 293 (100), 237 (19), 236 (73), 222 (12); HRMS: 377.0360 ($C_{19}H_{15}FeNO_4$, calcd. 377.0350).

Tricarbonyl[(1-4-η)-1,4-di-(4-methoxyphenyl)-1-azabuta-1,3-diene]iron (**10k**): Mp ≥132°C (dec). − IR (drift): ν = 2049, 1985, 1974, 1607, 1518, 1506, 1274, 1252, 1179, 1031, 839 cm^{-1}. − ^1H NMR (400 MHz, $CDCl_3$): δ = 3.41 (d, J = 9.5 Hz, 1 H), 3.75 (s, 3 H), 3.79 (s, 3 H), 5.61 (dd, J = 9.5, 2.9 Hz, 1 H), 6.72 (br d, J = 8.9 Hz, 2 H), 6.83 (br d, J = 8.8 Hz, 2 H), 6.90 (br d, J = 8.9 Hz, 2 H), 6.95 (br d, J = 2.9 Hz, 1 H), 7.26 (br d, J = 8.8 Hz, 2 H). − ^{13}C NMR and DEPT (100 MHz, $CDCl_3$): δ = 55.27 (CH_3), 55.42 (CH_3), 62.83 (CH), 73.77 (CH), 103.48 (CH), 114.23 (2 CH), 114.27 (2 CH), 122.52 (2 CH), 127.79 (2 CH), 131.05 (C), 146.68 (C), 155.27 (C), 158.64 (C). − MS (115°C): *m/z* (%) = 407 (0.4) [M^+], 379 (1), 351 (2), 323 (32), 267 (20), 266 (100), 252 (14), 145 (10); HRMS: 407.0473 ($C_{20}H_{17}FeNO_5$, calcd. 407.0456).

Tricarbonyl[(1-4-η)-1-(2-methoxyphenyl)-4-(4-methoxyphenyl)-1-azabuta-1,3-diene]iron (**10l**): Mp ≥ 134−136°C (dec). − IR (drift): ν = 2054, 1989, 1972, 1516, 1495, 1274, 1253, 1023, 831 cm^{-1}. − ^1H NMR (250 MHz, $CDCl_3$): δ = 3.38 (d, J = 9.5 Hz, 1 H), 3.80 (s, 3 H), 3.98 (s, 3 H), 5.74 (dd, J = 9.5, 3.0 Hz, 1 H), 6.78−6.87 (m, 2 H), 6.84 (br d, J = 8.8 Hz, 2 H), 6.95−7.07 (m, 3 H), 7.29 (br d, J = 8.8 Hz, 2 H). − ^{13}C NMR and DEPT (100 MHz, $CDCl_3$): δ = 54.80 (CH_3), 55.28 (CH_3), 63.00 (CH), 75.88 (CH), 101.18 (CH), 110.92 (CH), 114.27 (2 CH), 118.94 (CH), 120.48 (CH), 123.44 (CH), 127.72 (2 CH), 131.21 (C), 141.50 (C), 150.86 (C), 158.57 (C). − MS (110°C): *m/z* (%) = 379 (2) [M^+ − 28), 351 (13), 323 (42), 308 (100), 267 (11), 266 (28), 252 (10), 56 (11); HRMS: 379.0484 ($C_{19}H_{17}FeNO_4$ [M^+ − CO]), calcd. 379.0507).

Tricarbonyl[(1-4-η)-1-(4-trifluoromethylphenyl)-4-(4-methoxyphenyl)-1-azabuta-1,3-diene]iron (**10m**): Mp 124°C. − IR (drift): ν = 2066, 2001, 1982, 1610, 1517, 1443, 1325, 1312, 1172, 1129, 831 cm^{-1}. − ^1H NMR (400 MHz, $CDCl_3$): δ = 3.46 (d, *J* = 9.6 Hz, 1 H), 3.81 (s, 3 H), 5.71 (dd, *J* = 9.6, 2.9 Hz, 1 H), 6.83 (dd, *J* = 2.9, 0.8 Hz, 1 H), 6.85 (br d, *J* = 8.8 Hz, 2 H), 6.93 (d, *J* = 8.4 Hz, 2 H), 7.29 (br d, *J* = 8.8 Hz, 2 H), 7.42 (d, *J* = 8.4 Hz, 2 H). − ^{13}C NMR and DEPT (100 MHz, $CDCl_3$): δ = 55.33 (CH_3), 64.14 (CH), 75.49 (CH), 101.19 (CH), 114.48 (2 CH), 121.80 (2 CH), 123.86 (C, q, $^2J_{CF}$ = 32.6 Hz), 124.49 (CF_3, q, $^1J_{CF}$ = 271 Hz), 126.24 (2 CH, q, $^3J_{CF}$ = 3.8 Hz), 127.97 (2 CH), 130.42 (C), 156.87 (C), 159.01 (C), 205.07 (CO, br), 208.94 (CO, br), 211.97 (CO, br). − MS (90°C): *m/z* (%) = 445 (2) [M^+], 417 (6), 389 (11), 361 (100), 304 (52), 286 (16), 145 (17); HRMS: 445.0214 ($C_{20}H_{14}F_3FeNO_4$, calcd. 445.0224).

Tricarbonyl[(1-4-η)-1-(2,4-dimethoxyphenyl)-4-(4-methoxyphenyl)-1-azabuta-1,3-diene]iron (**10n**): Mp ≥116°C (dec). − IR (drift): ν = 2051, 2043, 1992, 1984, 1964, 1518, 1443, 1285, 1255, 1034, 837 cm^{-1}. − ^1H NMR (400 MHz, $CDCl_3$): δ = 3.34 (d, *J* = 9.5 Hz, 1 H), 3.76 (s, 3 H), 3.79 (s, 3 H), 3.96 (s, 3 H), 5.70 (dd, *J* = 9.5, 2.8 Hz, 1 H), 6.33 (dd, *J* = 8.6, 2.5 Hz, 1 H), 6.41 (d, *J* = 2.5 Hz, 1 H), 6.83 (d, *J* = 8.7 Hz, 2 H), 6.99 (d, *J* = 8.6 Hz, 1 H), 7.10 (d, *J* = 2.8 Hz, 1 H), 7.28 (d, *J* = 8.7 Hz, 2 H). − ^{13}C NMR and DEPT (100 MHz, $CDCl_3$): δ = 54.91 (CH_3), 55.28 (CH_3), 55.40 (CH_3), 62.52 (CH), 75.40 (CH), 99.14 (CH), 101.42 (CH), 103.44 (CH), 114.22 (2 CH), 118.39 (CH), 127.69 (2 CH), 131.35 (C), 135.10 (C), 152.18 (C), 156.52 (C), 158.48 (C). − MS (135°C): *m/z* (%) = 437 (0.2) [M^+], 409 (2), 381 (13), 353 (49), 338 (81), 310 (11), 299 (16), 297 (59), 296 (100), 282 (28), 153 (35), 138 (40), 84 (30), 56 (28); HRMS: 437.0583 ($C_{21}H_{19}FeNO_6$, calcd. 437.0562).

Tricarbonyl[(1-4-η)-1-(4-methoxyphenyl)-4-(2-methoxyphenyl)-1-azabuta-1,3-diene]iron (**10o**): Mp ≥121°C (dec). − IR (drift): ν = 2049, 1994, 1975, 1604, 1595, 1503, 1441, 1293, 1242, 1100, 1031, 1024, 836, 754 cm^{-1}. − ^1H NMR (250 MHz, $CDCl_3$): δ = 3.71 (d, *J* = 9.8 Hz, 1 H), 3.75 (s, 3 H), 3.92 (s, 3 H), 5.81 (dd, *J* = 9.8, 3.0 Hz, 1 H), 6.72 (br d, *J* = 8.9 Hz, 2 H), 6.85 (d, *J* = 7.9 Hz, 2 H), 6.92 (br d, *J* = 8.9 Hz, 2 H), 6.95 (br d, *J* = 3.0 Hz, 1 H), 7.15−7.24 (m, 2 H). − ^{13}C NMR and DEPT (100 MHz, $CDCl_3$): δ = 55.11 (CH_3), 55.44 (CH_3), 56.33 (CH), 73.73 (CH), 104.51 (CH), 110.46 (CH), 114.18 (2 CH), 120.30 (CH), 122.57 (2 CH), 125.27 (CH), 127.37 (C), 127.81 (CH), 147.01 (C), 155.14 (C), 157.14 (C). − MS (100°C): *m/z* (%) = 407 (1) [M^+], 379 (1), 351 (5), 323 (32), 267 (21), 266 (16), 252 (11), 236 (100); HRMS: 407.0455 ($C_{20}H_{17}FeNO_5$, calcd. 407.0456). − $C_{20}H_{17}FeNO_5$: C 58.99, H 4.21, N 3.44; found: C 58.80, H 4.26, N 3.65.

Tricarbonyl[(1-4-η)-4-(4-cyanophenyl)-1-phenyl-1-azabuta-1,3-diene]iron (**10p**): Mp ≥143°C (dec). − IR (drift): ν = 2224, 2057, 1997, 1991, 1485, 1439, 1295, 836, 764 cm^{-1}. − ^1H NMR (400 MHz, $CDCl_3$): δ = 3.24 (d, *J* = 9.2 Hz, 1 H), 5.70 (dd, *J* = 9.2, 2.9 Hz, 1 H), 6.94 (m, 3 H), 7.04 (dd, *J* = 2.9, 0.8 Hz, 1 H), 7.20 (m, 2 H), 7.37 (br d, *J* = 8.4 Hz, 2 H), 7.56 (br d, *J* = 8.4 Hz, 2 H). − ^{13}C NMR and DEPT (100 MHz, $CDCl_3$): δ = 58.69 (CH), 73.70 (CH), 105.71 (CH), 109.80 (C), 118.95 (C≡N), 121.82 (2 CH), 123.04 (CH), 126.85 (2 CH), 129.12 (2 CH), 132.57 (2 CH), 144.86 (C), 152.81 (C). − MS (95°C): *m/z* (%) = 372 (1) [M^+], 344 (2), 316 (5), 288 (32), 232 (51), 231 (100), 77 (24); HRMS: 372.0204 ($C_{19}H_{12}FeN_2O_3$, calcd. 372.0197).

Tricarbonyl[(1-4-η)-4-(4-cyanophenyl)-1-(2,4-dimethoxyphenyl)-1-azabuta-1,3-diene]iron (**10q**): Mp ≥118°C (dec). − IR (drift): ν = 2226, 2057, 2004, 1995, 1970, 1602, 1503, 1311, 1214, 843, 791 cm^{-1}. − ^1H NMR (400 MHz, $CDCl_3$): δ = 3.15 (d, *J* = 9.2 Hz, 1 H), 3.77 (s, 3 H), 3.97 (s, 3 H), 5.74 (dd, *J* = 9.2, 3.0 Hz, 1 H), 6.35 (dd, *J* = 8.7, 2.6 Hz, 1 H), 6.43 (d, *J* = 2.6 Hz, 1 H), 7.01 (d, *J* = 8.7 Hz, 1 H), 7.23 (br d, *J* = 3.0 Hz, 1 H), 7.37 (d, *J* = 8.4 Hz, 2 H), 7.55 (d, *J* = 8.4 Hz, 2 H). − ^{13}C NMR and DEPT (100 MHz, $CDCl_3$): δ = 54.91 (CH_3), 55.43 (CH_3), 58.19 (CH), 74.87 (CH), 99.27 (CH), 103.70 (CH), 103.93 (CH), 109.43 (C), 118.54 (CH), 119.10 (C≡N), 126.72 (2 CH), 132.51 (2 CH), 134.37 (C), 145.36 (C), 152.30 (C), 157.04 (C).

Tricarbonyl[(1-4-η)-1-(4-methoxyphenyl)-4-(4-N,N-dimethylaminophenyl)-1-azabuta-1,3-diene]iron (**10r**): Mp ≥125°C (dec). − IR (drift): ν = 2045, 2041, 1989, 1971, 1964, 1605, 1502, 1243, 1035, 836, 823 cm^{-1}. − ^1H NMR (250 MHz, $CDCl_3$): δ = 2.95 (s, 6 H), 3.50 (d, *J* = 9.6 Hz, 1 H), 3.75 (s, 3 H), 5.61 (dd, *J* = 9.6, 2.9 Hz, 1 H), 6.63 (d, *J* = 8.8 Hz, 2 H), 6.71 (d, *J* = 8.8 Hz, 2 H), 6.89 (br d, *J* = 2.9 Hz, 1 H), 6.89 (d, *J* = 8.8 Hz, 2 H), 7.22 (d, *J* = 8.8 Hz, 2 H). − ^{13}C NMR and DEPT (63 MHz, $CDCl_3$): δ = 40.36 (2 CH_3), 55.44 (CH_3), 65.36 (CH), 73.60 (CH), 102.53 (CH), 112.46 (2 CH), 114.22 (2 CH), 122.53 (2 CH), 126.06 (C), 127.80 (2 CH), 147.01 (C), 149.52 (C), 155.15 (C). − MS (130°C): *m/z* (%) = 420 (0.1) [M^+], 392 (0.2), 364 (1), 336 (9), 280 (43), 279 (100), 158 (10); HRMS: 420.0795 ($C_{21}H_{20}FeN_2O_4$, calcd. 420.0772).

Preparation of Tricarbonyl(η⁴-cyclohexa-1,3-diene)iron (**2**) *by Transfer of the Fe(CO)₃-Fragment of the (η⁴-1-Azabuta-1,3-diene)-tricarbonyliron Complexes* **10** *to Cyclohexa-1,3-diene* (**1a**) − *General Procedure:* Dry THF (10 ml) and cyclohexa-1,3-diene (**1a**) (0.37 ml, 3.88 mmol) were added to the azadiene complex **10** (1.00 mmol) and the reaction mixture was stirred at reflux (reaction time, see Table 6). The mixture was cooled to room temp. and the solvent was evaporated in vacuo to a volume of 1 ml. The residue was subjected to flash chromatography (pentane) on silica gel and afforded the iron complex **2** as a yellow oil (Table 6).

Table 6. Transfer reagent **10**, reaction time, and yield of the iron complex **2**

Entry	Iron Complex **10** [mg]	Reaction time [min]	**2**, Yield [mg]	[%]
a[a]	250	180	140	88
b	377	30	134	61
	377	60	183	83
[b]	200	120	111	95
c	377	30	68	31
	377	60	103	47
	377	120	163	74
d[c]	200	120	98	45
e	415	120	171	78
g	407	30	109	50
	407	60	148	67
	407	120	177	80
h	437	120	192	87
i	437	120	163	74
j	377	120	205	93
k	407	120	199	90
l	407	120	183	83
m	445	120	194	88
n	437	120	172	78
o	407	120	203	92
p	372	120	152	69
q	432	120	131	60
r	420	120	162	74

The following reactions were run on a different scale: [a] Cyclohexa-1,3-diene **1a** (0.20 ml, 168 mg, 2.10 mmol) and azadiene complex **10a** (250 mg, 0.720 mmol). − [b] Cyclohexa-1,3-diene **1a** (0.20 ml, 168 mg, 2.10 mmol) and azadiene complex **10b** (200 mg, 0.531 mmol). − [c] Cyclohexa-1,3-diene **1a** (0.25 ml, 210 mg, 2.62 mmol) and azadiene complex **10d** (200 mg, 0.513 mmol).

Preparation of Tricarbonyl(η^4-cyclohexa-1,3-diene)iron (**2**) *by Direct Complexation of Cyclohexa-1,3-diene* (**1a**) *with Nonacarbonyldiiron:* Cyclohexa-1,3-diene (**1a**) (13.9 ml, 146 mmol) was added to a suspension of nonacarbonyldiiron (44.2 g, 121.5 mmol) in THF (250 ml) and the heterogeneous mixture was stirred at reflux for 6 h. The mixture was cooled to room temp., filtered through a short path of Celite, and the solvent was removed. The residue was dissolved in light petroleum and filtered through a short path of Alox B. Evaporation of the solvent in vacuo afforded the iron complex **2** (11.5 g, 43%), which could be subjected directly to hydride abstraction. Yellow oil. − IR (film): ν = 3009, 2926, 2907, 2887, 2850, 2042, 1957, 1467, 1333, 1180, 1029, 1007, 938, 879, 865, 642, 623 cm^{-1}. − ^1H NMR (400 MHz, C_6D_6): δ = 1.18 (br d, *J* = 12 Hz, 2 H), 1.45 (br dt, *J* = 12, 2 Hz, 2 H), 2.74 (dd, *J* = 5, 2 Hz, 2 H), 4.63 (dd, *J* = 5, 3 Hz, 2 H). − ^{13}C NMR and DEPT (100 MHz, C_6D_6): δ (*T* = 298 K) = 23.82 (2 CH_2), 62.52 (2 CH), 85.37 (2 CH), 212.63 (3 CO); ^{13}C NMR (125 MHz, [D_8]toluene): δ (*T* = 185 K) = 23.45 (2 CH_2), 62.30 (2 CH), 85.09 (2 CH), 211.32 (2 CO), 216.05 (CO); δ (*T* = 298 K) = 23.89 (2 CH_2), 62.47 (2 CH), 85.41 (2 CH), 212.56 (3 CO). − MS (20°C): *m*/*z* (%) = 220 (9) [M^+], 192 (32), 164 (5), 162 (10), 134 (100), 56 (33); HRMS: 219.9834 ($C_9H_8FeO_3$, calcd. 219.9823).

Synthesis of the Tricarbonyl(η^5-cyclohexadienylium)iron Tetrafluoroborate (**3**) *by Hydride Abstraction of the Iron Complex* **2**: A solution of tricarbonyl(η^4-cyclohexa-1,3-diene)iron (**2**) (11.5 g, 52.4 mmol) in CH_2Cl_2 (70 ml) was added to a solution of triphenylmethyl tetrafluoroborate (20.8 g, 62.9 mmol) in CH_2Cl_2 (70 ml). The reaction mixture was stirred for 40 min at room temp. and then poured into wet Et_2O (700 ml). The resulting yellow precipitate was washed twice with Et_2O (150 ml) and dried in vacuo to provide pure tricarbonyl(η^5-cyclohexadienylium)iron tetrafluoroborate (**3**) (15.7 g, 98%). Yellow crystals. − IR (KBr): ν = 2118, 2060, 1455, 1410, 1311, 1062, 603, 589, 558 cm^{-1}. − ^1H NMR (200 MHz, CD_3CN): δ = 1.91 (d, *J* = 15.7 Hz, 1 H), 2.92 (dt, *J* = 15.7, 6.3 Hz, 1 H), 4.24 (t, *J* = 6.3 Hz, 2 H), 5.83 (t, *J* = 6.3 Hz, 2 H), 7.16 (t, *J* = 6.3 Hz, 1 H).

[1] For reviews, see: A. J. Pearson, *Acc. Chem. Res.* **1980**, *13*, 463; A. J. Pearson, in *Comprehensive Organometallic Chemistry*, *Vol. 8* (Eds.: G. Wilkinson, F. G. A. Stone, E. W. Abel), Pergamon Press, Oxford, **1982**, chap. 58; A. J. Pearson, *Metallo-organic Chemistry*, Wiley, Chichester, **1985**, chap. 7 and 8; H.-J. Knölker, in *Organic Synthesis via Organometallics* (Eds.: K. H. Dötz, R. W. Hoffmann), Vieweg, Braunschweig, **1991**, p. 119; H.-J. Knölker, *Synlett* **1992**, 371; A. J. Pearson, *Iron Compounds in Organic Synthesis*, Academic Press, London, **1994**, chap. 4 and 5; H.-J. Knölker, in *Advances in Nitrogen Heterocycles*, *Vol. 1* (Ed.: C. J. Moody), JAI Press, Greenwich, CT, **1995**, p. 173.

[2] B. F. Hallam, P. L. Pauson, *J. Chem. Soc.* **1958**, 642.

[3] A. J. Birch, P. E. Cross, J. Lewis, D. A. White, S. B. Wild, *J. Chem. Soc. A* **1968**, 332.

[4] A. J. Birch, K. B. Chamberlain, M. A. Haas, D. J. Thompson, *J. Chem. Soc., Perkin Trans. 1* **1973**, 1882.

[5] H.-J. Knölker, H. Hermann, J.-B. Pannek, unpublished results; J.-B. Pannek, Diplomarbeit, Universität Hannover, **1989**, p. 46; H.-J. Knölker, Habilitationsschrift, Universität Hannover, **1989**, p. 59; H. Hermann, Diplomarbeit, Universität Karlsruhe, **1994**, p. 28.

[6] E. O. Fischer, R. D. Fischer, *Angew. Chem.* **1960**, *72*, 919.

[7] For a brief review on tricarbonyliron transfer reagents, see: H.-J. Knölker, in *Encyclopedia of Reagents for Organic Synthesis*, *Vol. 1* (Ed.: L. A. Paquette), Wiley, Chichester, **1995**, p. 333.

[8] J. A. S. Howell, B. F. G. Johnson, P. L. Josty, J. Lewis, *J. Organomet. Chem.* **1972**, *39*, 329; A. J. P. Domingos, J. A. S. Howell, B. F. G. Johnson, J. Lewis, *Inorg. Synth.* **1976**, *16*, 103.

[9] C. R. Graham, G. Scholes, M. Brookhart, *J. Am. Chem. Soc.* **1977**, *99*, 1180; M. Brookhart, G. O. Nelson, *J. Organomet. Chem.* **1979**, *164*, 193.

[10] S. E. Thomas, T. N. Danks, D. Rakshit, *Philos. Trans. R. Soc. London A* **1988**, *326*, 611; N. W. Alcock, C. J. Richards, S. E. Thomas, *Organometallics* **1991**, *10*, 231.

[11] H. Fleckner, F.-W. Grevels, D. Hess, *J. Am. Chem. Soc.* **1984**, *106*, 2027.

[12] H.-J. Knölker, P. Gonser, *Synlett* **1992**, 517.

[13] H.-J. Knölker, P. Gonser, P. G. Jones, *Synlett* **1994**, 405.

[14] [14a] S. Otsuka, T. Yoshida, A. Nakamura, *Inorg. Chem.* **1967**, *6*, 20. − [14b] A. De Cian, R. Weiss, *J. Chem. Soc. Chem. Commun.* **1968**, 348; A. De Cian, R. Weiss, *Acta Cryst. B* **1972**, *28*, 3264.

[15] A. M. Brodie, B. F. G. Johnson, P. L. Josty, J. Lewis, *J. Chem. Soc. Dalton Trans.* **1972**, 2031.

[16] J. Yin, J. Chen, W. Xu, Z. Zhang, Y. Tang, *Organometallics* **1988**, *7*, 21.

[17] T. N. Danks, S. E. Thomas, *Tetrahedron Lett.* **1988**, *29*, 1425; T. N. Danks, S. E. Thomas, *J. Chem. Soc. Perkin Trans. 1* **1990**, 761.

[18] M. F. Semmelhack, C. H. Cheng, *J. Organomet. Chem.* **1990**, *393*, 237.

[19] H. Cherkaoui, J. Martelli, R. Gree, *Tetrahedron Lett.* **1994**, *35*, 4781.

[20] S. V. Ley, C. M. R. Low, A. D. White, *J. Organomet. Chem.* **1986**, *302*, C13; S. V. Ley, C. M. R. Low, *Ultrasound in Organic Synthesis*, Springer Verlag, Berlin, **1989**, chap. 14.

[21] M. Geisert, H. Oelschläger, *J. Prakt. Chem.* **1967**, *35*, 110.

[22] K. G. Morris, S. E. Thomas, *J. Chem. Soc. Perkin Trans. 1* **1991**, 97; A. J. Pearson, K. Chang, D. B. McConville, W. J. Youngs, *Organometallics* **1994**, *13*, 4.

[23] H.-J. Knölker, G. Baum, P. Gonser, *Tetrahedron Lett.* **1995**, *36*, 8191.

[24] A. J. Pearson, *Metallo-organic Chemistry*, Wiley, Chichester, **1985**, chap. 2.

[25] [25a] J.-Y. Lallemand, P. Laszlo, C. Muzette, A. Stockis, *J. Organomet. Chem.* **1975**, *91*, 71. − [25b] D. Leibfritz, H. tom Dieck, *J. Organomet. Chem.* **1976**, *105*, 255. − [25c] L. Kruczynski, J. Takats, *Inorg. Chem.* **1976**, *15*, 3140.

[26] H. Günther, *NMR-Spektroskopie*, 3rd ed., Thieme Verlag, Stuttgart, **1992**, p. 310.

[27] D. H. R. Barton, A. A. L. Gunatilaka, T. Nakanishi, H. Patin, D. A. Widdowson, B. R. Worth, *J. Chem. Soc. Perkin Trans. 1* **1976**, 821.

[28] G. Bellachioma, G. Cardaci, *J. Chem. Soc. Dalton Trans.* **1977**, 909; G. Bellachioma, G. Cardaci, *J. Chem. Soc. Dalton Trans.* **1977**, 2181; G. Bellachioma, G. Reichenbach, G. Cardaci, *J. Chem. Soc. Dalton Trans.* **1980**, 634.

[29] H.-J. Knölker, P. Gonser, H. Hermann, P. G. Jones, G. Rohde, unpublished results.

[30] M. W. Kokkes, P. C. J. Beentjes, D. J. Stufkens, A. Oskam, *J. Organomet. Chem.* **1986**, *306*, 77.

[31] A. N. Nesmeyanov, L. V. Rybin, N. A. Stelzer, Y. T. Struchkov, A. S. Batsanov, M. I. Rybinskaya, *J. Organomet. Chem.* **1979**, *182*, 399.

[32] H.-J. Knölker, H. Hermann, *Angew. Chem.* **1996**, *108*, 363; *Angew. Chem. Int. Ed. Engl.* **1996**, *35*, 341.

[98045]

Synthesis and Structural Characterization of Rare Earth Metal Disulfonamide Complexes☆

Hans W. Görlitzer, Michael Spiegler, and Reiner Anwander*

Anorganisch-chemisches Institut der Technischen Universität München,
Lichtenbergstraße 4, D-85747 Garching, Germany
Fax: (internat.) +49 (0)89/289-13473
E-mail: anwander@arthur.anorg.chemie.tu-muenchen.de

Received March 2, 1998

Keywords: Rare earth metals / Lanthanides / Chelating sulfonamides / Silylamide route / C_2 symmetry

The reaction of rare earth silylamides $Ln[N(SiHMe_2)_2]_3(thf)_n$ [n = 1 for Sc (**1a**); n = 2 for Y (**1b**), La (**1c**), Nd (**1d**)] with *trans*-1,2-bis(2,4,6-triisopropylbenzenesulfonamido)cyclohexane (H_2L, *rac*-**2**) in toluene at ambient temperature proceeds via an extended silylamide route, affording highly soluble complexes $Sc(L)[N(SiHMe_2)_2]$ (**3**) and $Ln(L)[N(SiHMe_2)_2](thf)$ (**4a–c**) in excellent yields. An X-ray crystallographic study performed on the solvent-free, dinuclear yttrium derivative **5** revealed an unusual $\mu_2,\eta^4:\eta^1$-coordination of the disulfonamide ligand, involving bridging S=O groups. In solution, equilibria between dimeric and monomeric forms, dependent on the presence of a donor molecule, were observed by NMR techniques.

In the last decade rare earth metals have gained considerable interest as highly efficient catalysts for a variety of organic transformations.[1] Dicyclopentadienyl complexes, e.g., *ansa*-lanthanidocenes as depicted in Figure 1, represent key compounds in precatalyst design. Although the cyclopentadienyl backbone imposes a unique electronic and steric situation including complex chirality, broader application of these systems is hampered by their pronounced sensibility towards moisture. Recently, alternative ligands were successfully introduced to cope with the peculiarities of organolanthanide chemistry, e.g., lanthanide binaphthol derivatives in Lewis acid catalysis.[2] Our current research interests put main emphasis on the replacement of the dicyclopentadienyl backbone by other divalent auxiliary ligands, which are prone to fine-tuning in the sense of solubility, chirality and steric and electronic factors. In the course of these studies we found synthetic access to the first monomeric salen complexes of the lanthanide elements via an extended silylamide route (Figure 1).[3] Encouraged by these results we anticipated application of this synthetic route to other catalytically relevant ligand systems. Disulfonamides constitute a class of ligands well established in the coordination chemistry of strongly Lewis acidic metal centers such as boron(III),[4] aluminum(III),[5] and titanium(IV).[6][7] These complexes are of significant importance in several catalytic transformations such as the Diels-Alder reaction or the alkylation of carbonyl groups.[8] Analogous lanthanide complexes, though postulated once,[9] have never been characterized. Here, we report the synthesis and characterization of the first soluble rare earth complexes derived from chelating disulfonamides.

[*] The use of $Ln[N(SiMe_3)_2]_3$ as a synthetic precursor is hampered by partial product oligomerization.

Results and Discussion

The synthesis of the novel disulfonamide complexes **3** and **4a–c** was achieved by an extended silylamide route,[3][10][11] utilizing $Ln[N(SiHMe_2)_2]_3(thf)_n$ as synthetic precursors as shown in Scheme 1. The ligand *trans*-1,2-bis(2,4,6-triisopropylbenzenesulfonamido)cyclohexane (*rac*-**2**) was chosen according to the following considerations: (i) *trans*-1,2-diaminocyclohexane provides a relatively rigid backbone. Additionally, it offers easy access to enantiomerically pure ligands, which should lead to enantioselective precatalysts.[12] (ii) The sterically demanding triisopropylphenyl groups should favor monomeric complexes, and (iii) induce increased solubility in non-polar solvents. The rare earth elements Sc, Y, and La were selected to cover the entire range of cation radii and in the case of Nd to visually follow the reaction by color effects. Our examinations on rare earth salen derivatives revealed that cation size and ligand bite angle are important factors to direct the formation of monomeric complexes.[3b]

The disulfonamide complexes **3** and **4a–c** are formed by the subsequent aminolysis of two rare earth bis(dimethylsilyl)amide bonds[*] by the more acidic sulfonamide (pK_a ca. 10–11, measured in water).[13] The remaining third bis(dimethylsilyl)amide ligand was characterized by a sharp Si–H vibration at ca. 2065 cm^{-1}. Interestingly, the reaction is accompanied by the loss of one molecule THF (GC-MS analysis). Compounds **3** and **4a–c** are obtained in yields > 90% after evaporation of the volatiles. Their excellent solubility even in non-polar solvents such as toluene or *n*-hexane indicates the formation of non-oligomerized products for the differently sized cations. Although the enhanced solubility hampered further purification by recrystallization, satisfying elemental analyses were obtained in most

 © WILEY-VCH Verlag GmbH, D-69451 Weinheim, 1998 1434–1948/98/0707–1009 $ 17.50+.50/0

Figure 1. Conceptional design of divalent auxiliary ligands

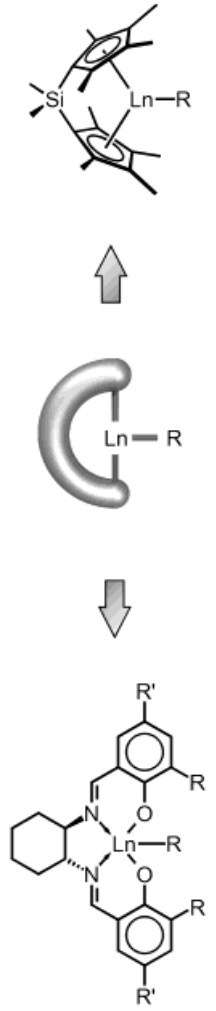

Scheme 1. Synthesis of the complexes **3** and **4a-c** via an extended silylamide route

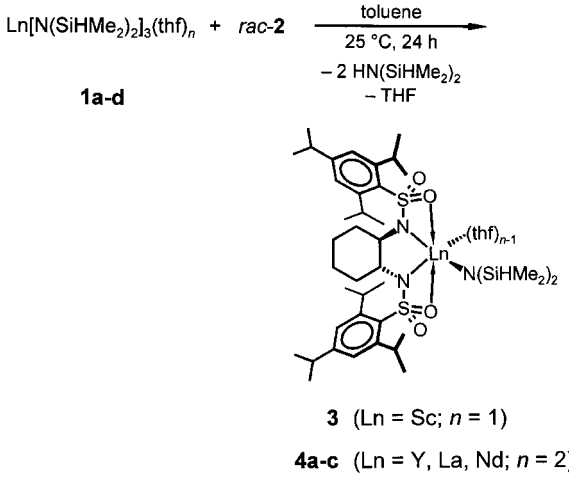

3 (Ln = Sc; n = 1)

4a-c (Ln = Y, La, Nd; n = 2)

cases, indicating a very clean reaction under mild conditions. Elemental analysis revealed that one THF solvent molecule coordinates to the larger lanthanide cations while scandium can accomodate no THF molecule. This finding could also be confirmed by ^{1}H-NMR spectroscopy. The yttrium derivative **4a** could be further desolvated by prolonged exposure to high vacuum to yield the less soluble compound **5**, crystals of which could be grown from hot *n*-hexane.

First NMR spectroscopic examinations of compounds **3**–**5** in C_6D_6 revealed spectra rather difficult to understand with broad, poorly resolved, overlapping signals. We assume two major effects to be responsible for this behavior. Firstly, sulfonyl moieties are known to serve as electron donors capable of forming Lewis acid-base adducts with metal cations. Depending on geometric and electronic factors Lewis acid-base adduct formation can occur in both an intra- and intermolecular fashion. As shown previously for aluminum (**6**)[5a] and indium (**7**)[14] sulfonamides, organization to dimers leads to extended heterocyclic ring systems (Figure 2).

Figure 2. Intermolecular bridging of sulfonamide ligands via S=O donor interactions; for **7**, even intramolecular interactions are discussed

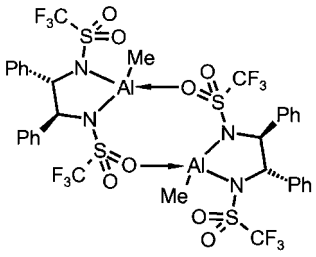

6

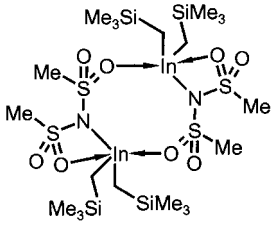

7

A monomer-dimer equilibrium in solution is supposed to partly contribute to the poor NMR spectra observed in C_6D_6. The second reason can be found in an unusually strong *intramolecular* coordination of the sulfonamido group. Very recently, Walsh and Gagne independently reported a η^2-coordination of the sulfonamido group in titanium complexes, resembling strongly our lanthanide derivatives.[6][7] Although these monomeric complexes do not show similar solution behavior, we postulate *cis*/*trans* isomers observable on NMR time scale, resulting from a hindered rotation around the S–N bond (Scheme 2). Evidence for both of these assumptions is given by an X-ray diffraction study performed on the yttrium complex **5** (vide infra).

Consequently, the NMR spectra simplified remarkably when recorded in a donor solvent like [D_8]THF. THF coor-

Scheme 2. Dynamic equilibrium between *trans*- and *cis*-rotamers (coordinated THF has been omitted for clarity)

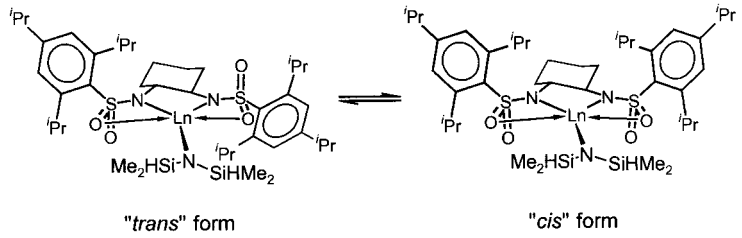

dination reduces the Lewis acidity of the metal center and thus lowers the rotation barrier around the S−N bond. Furthermore, THF coordination counteracts dimerization by replacing *intermolecular* sulfonyl bridging. The observed set of resonances is in agreement with a C_2-symmetric structure on the NMR time scale. As expected, ^{1}H-, ^{13}C-, and ^{29}Si-NMR spectra of **3**−**5** are very similar to each other. Moreover, addition of only one equivalent of a strong donor, e.g., triphenylphosphane oxide, is sufficient to achieve the same result, proven in case of the ^{1}H-NMR spectrum of THF-free **5** in C_6D_6. Trends within the series cannot be determined easily, except the rising high field shift of the ^{29}Si resonance from $\delta = -23.4$ to $\delta = -26.1$ which correlates to the decreasing Lewis acidity from Sc to La. No fluxional behavior could be observed by variable temperature NMR studies in the range of −80 to 110°C in [D_8]toluene.

Figure 3. Solid-state structure of dimeric complex **5** (PLATON[16] plot). Thermal ellipsoids are drawn at the 50% probability level. 2,4,6-Triisopropylphenyl groups at the sulfur atoms and all carbon bonded hydrogen atoms are omitted for clarity[a]

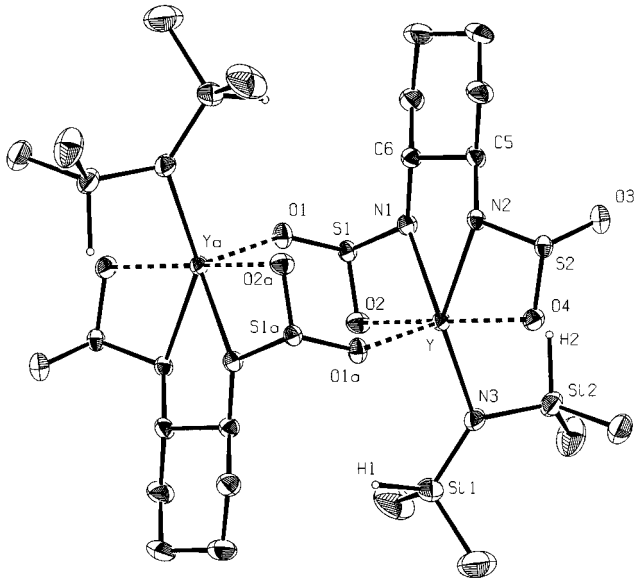

[a] Selected bond lengths [A] and angles [°]: Y−N(1) 2.365(2), Y−N(2) 2.403(2), Y−N(3) 2.239(2), Y−O(1)a 2.234(2), Y−O(2) 2.600(2), Y−O(4) 2.358(2), S(1)−O(1) 1.482(2), S(1)−O(2) 1.463(2), S(2)−O(3) 1.438(2), S(2)−O(4) 1.491(2), S(1)−N(1) 1.546(2), S(2)−N(2) 1.563(2), Y−Si(1) 3.5401(3), Y−Si(2) 3.1058(7), Y−H(1) 3.573(9), Y−H(2) 2.619(1); N(1)−Y−N(2) 66.41(6), Y−N(1)−S(1) 101.64(9), Y−N(2)−S(2) 96.45(8), O(2)−S(1)−N(1) 103.11(9), O(4)−S(2)−N(2) 100.87(9), Y−O(2)−S(1) 94.25(7), Y−O(4)−S(2) 100.45(7), O(2)−Y−N(1) 56.45(5), O(4)−Y−N(2) 59.29(5), Y−N(3)−Si(1) 127.6(1), Y−N(3)−Si(2) 103.57(9), Si(1)−N(3)−Si(2) 128.4(1).

The X-ray structure determination of **5** (triclinic, space group *P*1) both revealed its dimeric nature and an unusual coordination of the formally bidentate disulfonamide ligand. Complex **5** consists of the two enantiomers located on a crystallographic inversion center, forming a structure which could be described as a "racemic dimer" (Figure 3). The sulfonyl oxygen bridging results in the formation of an eight-membered chair-shaped ring system comparable to those in **6** and **7**.[5][14] A similar structural motif is also found in μ,η^2-SO_3CF_3 bridged lanthanidocene triflate complexes (cf. $[(C_5H_5)_2Yb(\mu\text{-}O_2SOCF_3)]_2$).[15] The resulting coordination polyhedron of the central yttrium is best considered as a bi-capped tetrahedron with the intramolecularly coordinating O(2) and O(4) in the capping positions.

In the solid state complex **5** adopts a *trans* configuration, which is fixed via intramolecular coordination of two sulfonyl oxygen atoms, as depicted in Figure 4. The detection of the *trans* form gives additional evidence of the solution behavior of compound **5** (Scheme 2).

Closer inspection of the yttrium disulfonamide bonding reveals an unprecedented $\mu_2,\eta^4{:}\eta^1$-coordination mode of this ligand system. The η^4-coordination results from two $Y-N^{(sulfonamide)}$ and two intramolecular $Y-O^{(sulfonyl)}$ bonds. The $Y-N^{(sulfonamide)}$ bond distances of 2.365(2) A and 2.403(2) A are longer than $Y-N^{(dialkylamide)}$ or $Y-N^{(silylamide)}$ bond lengths and are comparable to Y−N bonds containing delocalized charge density within the organic amide ligand. Representative examples include benzamidinate $[\{p\text{-}MeOC_6H_4C(NSiMe_3)_2\}_2YCH(SiMe_3)_2]$

Figure 4. Structure of the mononuclear unit of **5** (PLATON[16] plot). Thermal ellipsoids are drawn at the 50% probability level. All carbon bonded hydrogen atoms are omitted for clarity

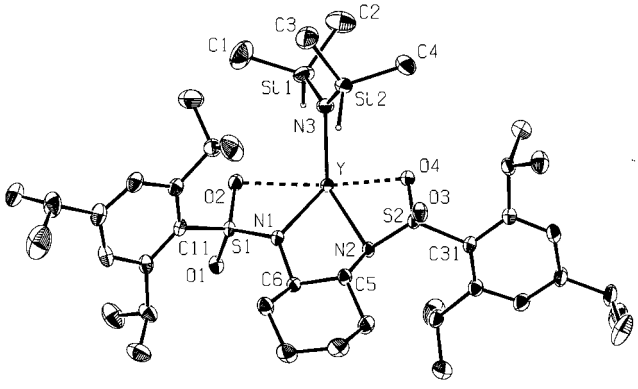

[Y−N 2.325(4)−2.345(4) A],[17] aminotroponiminate (ATI) [(*i*Pr$_2$ATI)YCl$_2$(thf)$_2$]$_2$ [2.331(5), 2.430(5) A],[18] phthalocyanine (Pc) [Y(Pc^{2-})(Pc$^-$)]·CH$_2$Cl$_2$ [2.395(3)−2.406(4) A],[19] or alkoxydimethylsilylamide [{Me$_2$Si(N*t*Bu)(O*t*Bu)}$_2$YCH(SiMe$_3$)$_2$] [2.20(2), 2.32(1) A].[20] The Y−O distances range between 2.234(2)−2.600(2) A. The Y−O(4) distance of 2.358(2) A of the non-bridging sulfonyl moiety together with the adjacent Y−N(2) bond of similar length resemble the bonding in η^2-coordinating carboxylates, e.g., [Cp$_2$Y{η^2-O$_2$C(CH$_2$)$_3$NMe$_2$}] [2.390(3), 2.406(3) A].[21] The bridging sulfonyl moiety forms a long intramolecular contact of 2.600(2) A [Y(1)−O(2)] which lies in the long range order of Y−O$^{(donor)}$ bonds and a relatively short Y−O(1a) contact which approaches bridging Y−O$^{(alkoxide)}$ bond lengths.[22] The marked differences in the Y−O bond distances arise from two effects: While the attractive interaction in Y−O(4) is affected by ring tension of the four-membered Y−N−S−O cycle [cf. Y−N(1)−S(1) 101.64(9)°, Y−N(2)−S(2) 96.45(8)°], reduced partial charge of the doubly coordinating SO$_2$ moiety additionally weakens the Y−O(2) interaction. The Y−O(1a) displays the unperturbed case and hence shows the shortest contact.

The charge delocalization in the disulfonamide ligand is also clear from the S=O and S−N bonding. The S=O bonds of the Y-bonded oxygen atoms average 1.479(2) A, whereas the bond distance of S(2)=O(3) [1.434(2) A] lies in the typical non-interacting range (1.423−1.444 A).[23] The S−N distances amount to an average of 1.555(2) A, clearly indicating a partial double bond character (cf. RNH−SO$_2$R′ 1.600-1.623 A).[23] The special mode of coordination is best understood by a charge delocalized model, as shown in Scheme 3. While **I** represents the classic case of a deprotonated sulfonamide, **II** displays a sulfonate type coordination, resulting in elongated S=O distances and shortened S−N bonds.

Scheme 3. Charge delocalized description of a η^2-coordinating sulfonamido group

I **II**

In contrast, the metal sulfonyl interactions in similar titanium complexes are weak and ascribed to crystal packing forces.[6] In fact, all Ti−O contacts are by far longer (0.17−0.38 A) than the Ti−N bonds.[6][7] In compound **5** the Y−N and Y−O bonds approximately equal each other which is consistent with strong metal oxygen interaction. The different metal oxygen bonding in the titanium and lanthanide complexes is also reflected in the different solution behavior described above.

The Y−N(3) bond length [2.239(2) A] of the silylamide ligand is comparable to that of the precursor silylamide [2.229(4)−2.276(4) A].[11] Interestingly, the N(SiHMe$_2$)$_2$ moiety coordinates asymmetrically to the yttrium center, featuring structural details previously ascribed to β-SiH agostic interactions.[24] The Y−N−Si angles differ significantly [103.57(9), 127.6(1)°] and the H(2) of one SiHMe$_2$ group could be localized relatively close to the yttrium center [Y−Si(2) 3.1058(7) A]. However, the sharp Si−H stretch frequencies in complexes **3**−**5** clearly range in the area of non-interacting Si−H groups,[25] although shoulders often termed as agostic could be detected at ca. 1950 cm^{-1}. If electronically forced, e.g., agostic, the Y···(Si−H) interaction in **5** would indicate electron deficiency at the metal center, which is highly desirable for the anticipated catalytic applications.

In conclusion, we have synthesized highly soluble rare earth complexes with formally bidentate disulfonamide ligands according to an extended silylamide route. The obtained heteroleptic complexes of type "(L)Ln^{III}R" bearing the disulfonamide ligand as a divalent auxiliary ligand L and the silylamide ligand R as a reactive, readily exchangeable moiety are potential candidates for rare earth mediated catalysis. The complexes show unprecedented ligand coordination, as evidenced by a $\mu_2,\eta^4{:}\eta^1$-coordination of a desolvated dinuclear complex in the solid state. The presence of a strong metal sulfonyl coordination is further suggested by the solution behavior (NMR experiments). The asymmetric coordination of the bis(dimethylsilyl)amide ligand appears to be sterically forced, albeit the metal···(Si−H) coordination might qualify as a sensitive probe to evaluate the electronic situation at early transition metal centers. Current studies concentrate on ligand variations and examinations of the resulting complexes in Lewis acid catalysis.

We thank the *Deutsche Forschungsgemeinschaft (DFG)* and *Degussa AG* for financial support of this research. R. A. thanks the *DFG* for the award of a fellowship. Generous support from Prof. *Wolfgang A. Herrmann* is gratefully acknowledged.

Experimental Section

General: All rare earth complexes were synthesized and manipulated under an argon atmosphere using either standard high-vacuum techniques or a glovebox (MBraun MB150B; O_2 < 2 ppm, H_2O < 1 ppm). Toluene and *n*-hexane were distilled from Na/K/benzophenone and stored under argon. Deuterated THF was dried by stirring over Na/K alloy. All starting materials were purchased from Aldrich Chemical Co. and used without further purification. The synthesis of the disulfonamide *rac*-**2** is described in detail, because slight modifications of the established synthesis procedures were applied.[26] The bis(dimethylsilyl)amides of Sc, Y, La, and Nd (**1a**−**d**) were prepared according to the literature procedure.[27] − NMR: Jeol JNM-GX-400 (399.80, 100.51, and 79.43 MHz for ^{1}H, ^{13}C, and ^{29}Si, respectively). Spectra were referenced internally using the residual solvent resonances (^{1}H, ^{13}C) or referenced externally to TMS (^{29}Si; δ = 0). [D$_8$]THF as solvent δ_H = 3.58/1.73, δ_C = 67.7/25.5. − FTIR: Perkin-Elmer 1650. − Elemental analyses: Mikroanalytisches Laboratorium at the department of inorganic chemistry of the Technische Universität München.

trans-1,2-Bis(2,4,6-triisopropylbenzenesulfonamido)cyclohexane (*rac*-**2**): Racemic **2** was prepared by addition of a pre-cooled solution of 6.36 g (21.0 mmol) of 2,4,6-triisopropylbenzene sulfonyl chloride in 30 ml of CH_2Cl_2 to an ice-cold, stirred solution of 1.14 g (10.0 mmol) of *trans*-1,2-diaminocyclohexane and 2.13 g (21.0 mmol) of triethyl amine in 50 ml of CH_2Cl_2. The mixture was

stirred overnight while it was allowed to warm up to room temperature. The solution was washed successively with 50 ml of hydrochloric acid (1 N), saturated $NaHCO_3$ solution, and brine. Drying of the organic phase over Na_2SO_4 and evaporation of the solvent gave a crude product which was purified by column chromatography (silica, CH_2Cl_2/EtOAc, 40:1 v/v, R_f = 0.32) to yield 5.96 g of *rac*-**2** (92%) as a white solid, m.p. 206−207°C. NMR and IR spectroscopic data and elemental analysis are in agreement with the data reported for (1*R*,2*R*)-1,2-bis(2,4,6-triisopropylbenzenesulfonamido)cyclohexane.[26]

General Procedure for the Preparation of the Rare Earth Metal Disulfonamide Complexes (**3** *and* **4a−c**): To a stirred solution of 0.50 mmol of the rare earth bis(dimethylsilyl)amide Ln[N(SiHMe$_2$)$_2$]$_3$(thf)$_n$ (Y, La, Nd: n = 2; Sc: n = 1) in 15 ml of toluene an equimolar amount (0.50 mmol) of *rac*-**2** was added slowly. The ligand dissolved within a few minutes (Sc: 1 h). To ensure complete reaction the mixture was stirred for further 24 h. Then the solvent and volatile products were evaporated in vacuo to yield the complexes **3** and **4a−c**.

[trans-1,2-Bis(2,4,6-triisopropylbenzenesulfonamidato)cyclohexane-N,N′][bis(dimethylsilyl)amido]scandium(III) (**3**): 385 mg (94%), colorless, amorphous solid. The compound starts to decompose at 130°C to yield a material that forms a homogeneous melt at 230°C. − ^{1}H NMR ([D$_8$]THF, 25°C): δ = 7.14 (s, 4 H, -C$_6$H$_2$*i*Pr$_3$), 4.58 [sept, ^3J = 6.8 Hz, 4 H, *o*-C*H*(CH$_3$)$_2$], 4.47 [sept, ^3J = 3.0 Hz, 2 H, -Si(CH$_3$)$_2$*H*], 3.48 [m, 2 H, -C*H*$_\alpha$(N−Sc)-], 2.86 [sept, ^3J = 6.9 Hz, 2 H, *p*-C*H*(CH$_3$)$_2$], 1.86 (m, 2 H, CH*H*$_\beta$), 1.60 (m, 2 H, C*H*H$_\beta$), 1.24 [d, ^3J = 6.8 Hz, 24 H, *o*-CH(C*H*$_3$)$_2$], 1.23 [d, ^3J = 6.9 Hz, 12 H, *p*-CH(C*H*$_3$)$_2$], 0.86 (m, 4 H, C*H*$_{2,\gamma}$), 0.12 [d, ^3J = 3.0 Hz, 12 H, -Si(C*H*$_3$)$_2$H]. − ^{13}C{^{1}H} NMR ([D$_8$]THF, 25°C): δ = 151.8 (*C*-4), 148.9 (*C*-2,6), 124.1 (*C*-3,5), 66.2 [-*C*H$_\alpha$(N−Sc)-], 35.0 (*C*H$_{2,\beta}$), 34.5 [*p*-*C*H(CH$_3$)$_2$], 30.6 [*o*-*C*H(CH$_3$)$_2$], 26.1 [*o*-CH(*C*H$_3$)$_2$], 24.0 [*p*-CH(*C*H$_3$)$_2$], 1.4 [-Si(*C*H$_3$)$_2$H]; *C*-1 not detected; *C*H$_{2,\gamma}$ might be hidden by the residual solvent signal. − ^{29}Si{^{1}H} NMR ([D$_8$]THF, 25°C): δ = −23.4. − IR (Nujol): ν = 2068 m [ν(Si−H)], 1601 m, 1565 w, 1423 m, 1363 m, 1315 w, 1243 s [ν(S=O)], 1207 w, 1167 s, 1150 m, 1133 m, 1106 s, 1064 m, 1046 m [ν(S=O)], 1019 m, 1007 m, 987 m, 971 m, 938 m, 900 s, 842 m, 802 w, 783 w, 699 w, 676 m, 660 m, 630 w, 586 w, 552 w cm^{-1}. − C$_{40}$H$_{70}$N$_3$O$_4$S$_2$ScSi$_2$ (822.3): calcd. C 58.43, H 8.58, N 5.11, S 7.80; found C 58.5, H 8.8, N 4.4, S 7.2.

(Tetrahydrofurane)[trans-1,2-bis(2,4,6-triisopropylbenzenesulfonamidato)cyclohexane-N,N′][bis(dimethylsilyl)amido]yttrium(III) (**4a**): 455 mg (97%), colorless, brittle solid. − ^{1}H NMR ([D$_8$]THF, 25°C): δ = 7.15 (s, 4 H, -C$_6$H$_2$*i*Pr$_3$), 4.66 [sept, ^3J = 3.0 Hz, 2 H, -Si(CH$_3$)$_2$*H*], 4.49 [sept, ^3J = 6.7 Hz, 4 H, *o*-C*H*(CH$_3$)$_2$], 3.41 [m, 2 H, -C*H*$_\alpha$(N−Y)-], 2.87 [sept, ^3J = 6.9 Hz, 2 H, *p*-C*H*(CH$_3$)$_2$], 1.84 (m, 2 H, CH*H*$_\beta$), 1.57 (m, 2 H, C*H*H$_\beta$), 1.25 [d, ^3J = 6.9 Hz, 12 H, *p*-CH(C*H*$_3$)$_2$], 1.23 [d, ^3J = 6.7 Hz, 24 H, *o*-CH(C*H*$_3$)$_2$], 0.89 (m, 4 H, C*H*$_{2,\gamma}$), 0.11 [d, ^3J = 3.0 Hz, 12 H, -Si(C*H*$_3$)$_2$H]. − ^{13}C{^{1}H} NMR ([D$_8$]THF, 25°C): δ = 151.3 (*C*-4), 149.2 (*C*-2,6), 142.1 (*C*-1), 124.2 (*C*-3,5), 64.0 [-*C*H$_\alpha$(N−Y)-], 35.7 [*p*-*C*H(CH$_3$)$_2$], 34.9 (*C*H$_{2,\beta}$), 30.0 [*o*-*C*H(CH$_3$)$_2$], 26.0 [*o*-CH(*C*H$_3$)$_2$], 25.7 (*C*H$_{2,\gamma}$), 24.0 [*p*-CH(*C*H$_3$)$_2$], 3.7 [-Si(*C*H$_3$)$_2$H]. − ^{29}Si{^{1}H} NMR ([D$_8$]THF, 25°C): δ = −25.7. − IR (Nujol): ν = 2069 m [ν(Si−H)], 1948 w sh, 1601 m, 1564 w, 1423 m, 1364 m, 1317 w, 1241 s [ν(S=O)], 1164 s, 1106 m, 1076 m, 1048 s [ν(S=O)], 1022 m, 984 s, 939 m, 899 s, 842 m, 813 w, 795 w, 777 w, 759 w, 673 s, 658 m, 587 m, 555 w cm^{-1}. − C$_{44}$H$_{78}$N$_3$O$_5$S$_2$Si$_2$Y (938.3): calcd. C 56.32, H 8.38, N 4.48, S 6.83; found C 55.9, H 7.3, N 4.2, S 7.0.

(Tetrahydrofurane)[trans-1,2-bis(2,4,6-triisopropylbenzenesulfonamidato)cyclohexane-N,N′][bis(dimethylsilyl)amido]lanthanum(III) (**4b**): 450 mg (91%), colorless, brittle solid. − ^{1}H NMR ([D$_8$]THF, 25°C): δ = 7.13 (s, 4 H, -C$_6$H$_2$*i*Pr$_3$), 4.75 [sept, ^3J = 3.0 Hz, 2 H, -Si(CH$_3$)$_2$*H*], 4.63 [sept, ^3J = 6.8 Hz, 4 H, *o*-C*H*(CH$_3$)$_2$], 3.39 [m, 2 H, -C*H*$_\alpha$(N−La)-], 2.88 [sept, ^3J = 6.8 Hz, 2 H, *p*-C*H*(CH$_3$)$_2$], 1.73 (m, 2 H, CH*H*$_\beta$), 1.47 (m, 2 H, C*H*H$_\beta$), 1.27 [d, ^3J = 6.8 Hz, 12 H, *p*-CH(C*H*$_3$)$_2$], 1.23 [d, ^3J = 6.8 Hz, 24 H, *o*-CH(C*H*$_3$)$_2$], 1.01 (m, 4 H, C*H*$_{2,\gamma}$), 0.11 [d, ^3J = 3.0 Hz, 12 H, -Si(C*H*$_3$)$_2$H]. − ^{13}C{^{1}H} NMR ([D$_8$]THF, 25°C): δ = 151.1 (*C*-4), 149.4 (*C*-2,6), 142.5 (*C*-1), 123.7 (*C*-3,5), 64.8 [-*C*H$_\alpha$(N−La)-], 35.0 (*C*H$_{2,\beta}$), 34.6 [*p*-*C*H(CH$_3$)$_2$], 29.8 [*o*-*C*H(CH$_3$)$_2$], 26.0 [*o*-CH(*C*H$_3$)$_2$], 25.4 (*C*H$_{2,\gamma}$), 24.1 [*p*-CH(*C*H$_3$)$_2$], 3.2 [-Si(*C*H$_3$)$_2$H]. − ^{29}Si{^{1}H} NMR ([D$_8$]THF, 25°C): δ = −26.1. − IR (Nujol): ν = 2062 m [ν(Si−H)], 1945 w sh, 1601 m, 1563 w, 1241 s [ν(S=O)], 1219 m, 1195 m, 1163 s, 1126 m, 1074 m, 1063 m, 1046 s [ν(S=O)], 1012 m, 980 m, 940 m, 896 s, 879 m, 842 m, 810 m, 789 w, 764 w, 671 s, 629 w, 596 m, 578 w, 492 w cm^{-1}. − C$_{44}$H$_{78}$LaN$_3$O$_5$S$_2$Si$_2$ (988.3): calcd. C 53.47, H 7.95, N 4.25, S 6.49; found C 53.9, H 7.7, N 4.3, S 6.7.

(Tetrahydrofurane)[trans-1,2-bis(2,4,6-triisopropylbenzenesulfonamidato)cyclohexane-N,N′][bis(dimethylsilyl)amido]neodymium(III) (**4c**): 421 mg (85%), pale blue, brittle solid. − IR (Nujol): ν = 2071 m [ν(Si−H)], 1951 w sh, 1601 m, 1563 w, 1314 w, 1241 s [ν(S=O)], 1219 s, 1193 m, 1163 s, 1130 m, 1106 m, 1064 m, 1046 s [(S=O)], 1013 s, 980 s, 940 m, 897 vs, 842 m, 810 m, 764 w, 671 s, 630 w, 586 m, 557 w cm^{-1}. − C$_{44}$H$_{78}$N$_3$NdO$_5$S$_2$Si$_2$ (993.7): calcd. C 53.19, H 7.91, N 4.23, S 6.45; found C 52.7, H 7.5, N 4.0, S 5.7.

Bis{[trans-1,2-bis(2,4,6-triisopropylbenzenesulfonamidato)cyclohexane-N,N′][bis(dimethylsilyl)amido]yttrium(III)} (**5**): In a Schlenk tube 1.877 g (2.00 mmol) of finely powdered **4a** was exposed to high vacuum (p < 10^{-5} mbar) for 24 h. Afterwards 25 ml of *n*-hexane was added in the cold, leading to an insoluble residue and a clear solution, which was separated. Recrystallization of the white residue from hot *n*-hexane yielded 534 mg of **5** (31%) as colorless crystals suitable for X-ray structure determination. − ^{1}H NMR ([D$_8$]THF, 25°C): δ = 7.15 (s, 4 H, -C$_6$H$_2$*i*Pr$_3$), 4.66 [sept, ^3J = 3.0 Hz, 2 H, -Si(CH$_3$)$_2$*H*], 4.49 [sept, ^3J = 6.7 Hz, 4 H, *o*-C*H*(CH$_3$)$_2$], 3.41 [m, 2 H, -C*H*$_\alpha$(N−Y)-], 2.87 [sept, ^3J = 6.9 Hz, 2 H, *p*-C*H*(CH$_3$)$_2$], 1.84 (m, 2 H, CH*H*$_\beta$), 1.57 (m, 2 H, C*H*H$_\beta$), 1.25 [d, ^3J = 6.9 Hz, 12 H, *p*-CH(C*H*$_3$)$_2$], 1.23 [d, ^3J = 6.7 Hz, 24 H, *o*-CH(C*H*$_3$)$_2$], 0.89 (m, 4 H, C*H*$_{2,\gamma}$), 0.11 [d, ^3J = 3.0 Hz, 12 H, -Si(C*H*$_3$)$_2$H]. − ^{13}C{^{1}H} NMR ([D$_8$]THF, 25°C): δ = 151.3 (*C*-4), 149.2 (*C*-2,6), 142.1 (*C*-1), 124.2 (*C*-3,5), 64.0 [-*C*H$_\alpha$(N−Y)-], 35.7 [*p*-*C*H(CH$_3$)$_2$], 34.9 (*C*H$_{2,\beta}$), 30.0 [*o*-*C*H(CH$_3$)$_2$], 26.0 [*o*-CH(*C*H$_3$)$_2$], 25.7 (*C*H$_{2,\gamma}$), 24.0 [*p*-CH(*C*H$_3$)$_2$], 3.7 [-Si(*C*H$_3$)$_2$H]. − ^{29}Si{^{1}H} NMR ([D$_8$]THF, 25°C): δ = −25.7. − IR (Nujol): ν = 2088 m [ν(Si−H)], 1917 w sh, 1602 m, 1566 w, 1423 m, 1365 s, 1314 w, 1296 w, 1239 s [ν(S=O)], 1206 m, 1182 s, 1160 s, 1146 m, 1128 m, 1079 s, 1067 s [ν(S=O)], 1042 m, 1019 m, 988 m, 965 m, 940 m, 903 s, 882 s, 838 m, 820 m, 792 m, 762 m, 674 s, 652 w, 633 w, 621 w, 594 w, 587 m, 564 w, 556 m, 495 w, 485 w, 411 w cm^{-1}. − C$_{80}$H$_{140}$N$_6$O$_8$S$_4$Si$_4$Y$_2$ (1732.4): calcd. C 55.46, H 8.15, N 4.85, S 7.40; found C 55.6, H 8.1, N 4.7, S 8.5.

X-ray Crystal Structure Analysis of **5**: C$_{80}$H$_{140}$N$_6$O$_8$S$_4$Si$_4$Y$_2$; M_r = 1732.44; a = 12.3022(5), b = 13.4696(8), c = 14.8607(9) Å, α = 74.823(6), β = 79.688(5), γ = 78.454(5)°; triclinic, *P*1 (Int. Table Nr.: 2); V = 2307.6(2) Å^3; Z = 1; D_{calc} = 1.247 g cm^{-3}; μ = 1.45 mm^{-1} (Mo-K_α); F(000) = 924; A colorless crystal was mounted on a STOE IPDS[28] diffractometer (graphite-monochromated Mo-K_α radiation). 32070 reflections (Θ range: 1.65°−26.05°; −13 < h < 13, −16 < k < 16, −18 < l < 18) were collected at 193 K and corrected for Lorentz, polarization and X-ray absorption

effects (program FACEIT[28]: T_{min} = 0.6779; T_{max} = 0.8307). Preliminary positions of heavy atoms were found by direct methods,[29] while positions of the other non-hydrogen atoms were determined from successive Fourier difference maps coupled with initial isotropic least square refinement.[30] All none-H atoms were refined anisotropically. The hydrogen atoms, except for Si−H, were placed in calculated positions. They were included in the structure factor calculation but not refined. The final refinement (on F_o^2) of 477 parameters with 8176 independent reflections (R_{merge} = 0.049) converged at R_1 = 0.0399, wR_2 = 0.0660 and GOF = 0.931. The final weighting scheme was calculated to $w^{-1} = \sigma^2(F_o^2)+(0.0392\cdot P)^2$ with $P = (F_o^2+2\cdot F_c^2)/3$. Crystallographic data (excluding structure factors) for the structures reported in this paper have been deposited with the Cambridge Crystallographic Data Centre as supplementary publication no. CCDC 101422. Copies of the data can be obtained free of charge on application to The Director, CCDC, 12 Union Road, Cambridge CB2 1EZ, UK [fax: int. code +44(0)1223/ 336-033, e-mail: teched@chemcrys.cam.ac.uk].

☆ Dedicated to Professor *William J. Evans* on the occasion of his 50th birthday.

[1] [1a] R. Anwander in *Applied Homogeneous Catalysis with Organometallic Compounds* (Eds.: W. A. Herrmann, B. Cornils), *Vol. 2: Developments*, VCH Verlagsgesellschaft, Weinheim, **1996**, pp. 866−892. − [1b] F. T. Edelmann, *Top. Curr. Chem.* **1996**, *179*, 247−276.

[2] [2a] M. Shibasaki, H. Sasai, T. Arai, *Angew. Chem.* **1997**, *109*, 1290−1310; *Angew. Chem. Int. Ed. Engl.* **1997**, *36*, 1236−1256. − [2b] C. J. Schaverien, N. Meijboom, A. G. Orpen, *J. Chem. Soc., Chem. Commun.* **1992**, 124−126.

[3] [3a] O. Runte, T. Priermeier, R. Anwander, *J. Chem. Soc., Chem. Commun.* **1996**, 1385−1386. − [3b] O. Runte, H. W. Görlitzer, R. Anwander, unpublished results.

[4] E. J. Corey, C.-M. Yu, S. S. Kim, *J. Am. Chem. Soc.* **1989**, *111*, 5495−5496.

[5] [5a] E. J. Corey, S. Sarshar, J. Bordner, *J. Am. Chem. Soc.* **1992**, *114*, 7938−7939. − [5b] E. J. Corey, S. Sarshar, D.-H. Lee, *J. Am. Chem. Soc.* **1994**, *116*, 12089−12090.

[6] S. Pritchett, P. Gantzel, P. J. Walsh, *Organometallics* **1997**, *16*, 5130−5132.

[7] L. T. Armistead, P. S. White, M. R. Gagne, *Organometallics* **1998**, *17*, 216−220.

[8] For a review see: A. Togni, L. M. Venanzi, *Angew. Chem.* **1994**, *106*, 517−547; *Angew. Chem. Int. Ed. Engl.* **1994**, *33*, 497−526 and references cited therein.

[9] K. Uotsu, H. Sasai, M. Shibasaki, *Tetrahedron: Asymmetry* **1995**, *6*, 71−74.

[10] W. A. Herrmann, J. Eppinger, M. Spiegler, O. Runte, R. Anwander, *Organometallics* **1997**, *16*, 1813−1815.

[11] W. A. Herrmann, R. Anwander, F. C. Munck, W. Scherer, V. Dufaud, N. W. Huber, G. R. J. Artus, *Z. Naturforsch., Teil B* **1994**, *B49*, 1789−1797.

[12] Y. L. Bennani, S. Hanessian, *Chem. Rev.* **1997**, *97*, 3161−3195.

[13] J. F. King in *The chemistry of sulfonic acids, esters and their derivatives* (Eds.: S. Patai, Z. Rappoport), John Wiley & Sons, New York, **1991**, pp. 249−260.

[14] A. Blaschette, A. Michalides, P. G. Jones, *J. Organomet. Chem.* **1991**, *411*, 57−68.

[15] J. Stehr, R. D. Fischer, *J. Organomet. Chem.* **1992**, *430*, C1−C4.

[16] A. L. Spek, *Acta Crystallogr., Sect. A* **1990**, *46*, C34.

[17] R. Duchateau, C. T. van Wee, A. Meetsma, P. T. van Duijnen, J. H. Teuben, *Organometallics* **1996**, *15*, 2279−2290.

[18] P. W. Roesky, *Chem. Ber./Recueil* **1997**, *130*, 859−862.

[19] J. L. Paillaud, M. Drillon, A. Decian, J. Fischer, R. Weiss, R. Poinsot, A. Herr, *Physica B* **1991**, *B175*, 337−348.

[20] R. Duchateau, T. Tuinstra, E. A. C. Brussee, A. Meetsma, P. T. van Duijnen, J. H. Teuben, *Organometallics* **1997**, *16*, 3511−3522.

[21] H. Schumann, J. A. Meese-Marktscheffel, A. Dietrich, F. H. Görlitz, *J. Organomet. Chem.* **1992**, *430*, 299−315.

[22] R. Anwander, *Top. Curr. Chem.* **1996**, *179*, 149−245.

[23] [23a] A.-M. Häkkinen, P. Ruostesuo, R. Kivekäs, *J. Chem. Soc., Perkin Trans. 2* **1988**, 815−820. − [23b] G. J. Gainsford, C. Lensink, *Acta Crystallogr., Sect. C* **1996**, *C52*, 472−474. − [23c] M. K. Urtiaga, M. I. Arriortua, D. Badıa, E. Domınguez, A. M. G. Cameno, X. Solans, *Acta Crystallogr., Sect. C* **1994**, *C50*, 1604−1608. − [23d] M. I. Arriortua, M. K. Urtiaga, D. Badıa, E. Domınguez, A. M. G. Cameno, X. Solans, *Acta Crystallogr., Sect. C* **1995**, *C51*, 109−112.

[24] [24a] L. J. Procopio, P. J. Carroll, D. H. Berry, *J. Am. Chem. Soc.* **1994**, *116*, 177−185. − [24b] W. S. Rees, O. Just, H. Schumann, R. Weimann, *Angew. Chem.* **1996**, *108*, 481−483; *Angew. Chem. Int. Ed. Engl.* **1996**, *35*, 419−422.

[25] X. L. Luo, G. J. Kubas, C. J. Burns, J. C. Bryan, C. J. Unkefer, *Book of Abstracts*, 209th ACS National Meeting, Anaheim, Division of Inorganic Chemistry, **1995**, #082.

[26] H. Takahashi, T. Kawakita, M. Ohno, M. Yoshioka, S. Kobayashi, *Tetrahedron* **1992**, *48*, 5691−5700.

[27] R. Anwander, O. Runte, J. Eppinger, G. Gerstberger, E. Herdtweck, M. Spiegler, *J. Chem. Soc., Dalton Trans.* **1998**, 847−858.

[28] STOE&Cie. GmbH, *IPDS Operating System Version 2.6.* **1995**, Darmstadt, Germany.

[29] A. Altomare, G. Cascarano, C. Giacovazzo, A. Guagliardi, *J. Appl. Cryst.* **1993**, *26*, 343−350.

[30] G. M. Sheldrick, *SHELXL 93* **1993**, Universität Göttingen, Germany.

[98046]

π-Bond vs. Agostic Interaction in Three-Coordinated Alkoxy and Thiolate Derivatives of Aluminium, Boron and Cationic Carbon – An ab initio Study of H_2X–YR Systems (X = Al, B, C^+; Y = O, S; R = H, CH_3)

Isabelle Demachy and François Volatron*

Laboratoire de Chimie Théorique (URA 506, IPCM), Bât. 490,
Université de Paris-Sud, F-91405, Orsay Cedex, France,
Fax: (internat.) +33/1 69 15 44 47
E-mail: volatron@cth.u-psud.fr

Received March 9, 1998

Keywords: Ab initio calculations / π interactions / Agostic interactions / Electronic structure

Rotational barriers and π conjugation effects have been studied in H_2X–YR systems (X = Al, B; Y = O, S; R = H, CH_3) by means of ab initio calculations at the MP4/6–311G**//MP2/6–311G** level. In non-substituted systems H_2X–YH, it is shown that the rotational barrier depends on three factors: (i) π conjugation strength between the X vacant p orbital and the Y p-lone pair; (ii) the opening ability of the Y-valence angle and (iii) a possible direct interaction between X and the Y hydrogen substituent. The conjugation stabilization has been estimated through Valence Bond calculations and is found to decrease in the order BO (22.6 kcal/mol), BS (16.6 kcal/mol), AlO (10.2 kcal/mol), and AlS (8.1 kcal/mol). Study of the methylated systems confirm the results found in unsubstituted species. The most important feature is the location of a deconjugated secondary minimum for H_2B–SCH_3 species. An acute B–S–C angle (69.6°) is found, thus evidencing a direct H···B agostic interaction with a four-membered (BSCH) heterocycle. To further evidence our analysis, additional calculations have been performed on carbocationic species H_2C^+–YR (Y = O, S; R = H, CH_3) for which the H_2C^+ moiety is a strong π acceptor. As expected, the C^+–O and C^+–S conjugation are strong (about 60 kcal/mol). Only two minima have been located for the H_2C^+–OCH_3 species. In the sulfur case, the Potential Energy Surface (PES) is more complicated and six stationary points have been characterized. A strong agostic interaction is found for a secondary deconjugated minimum for which an hydrogen symmetrically bridges the two carbon atoms. A schematic energy profile connecting the various extrema is given for this cationic species.

Introduction

The question of π conjugation between Al and O in alkoxy derivative of aluminium has not received a definite answer until now although much theoretical and experimental work has been devoted to the problem. Following Brothers and Powell,[1] the conjugation in 3-coordinated species is expected to be weak: for instance, the rotational barrier around the Al−O bond has been shown to have an upper limit of 8 kcal/mol. In addition, the Al−O bond length in 3-coordinated species is found to decrease in the series R_2Al-OR', $RAl(OR')_2$, $Al(OR')_3$, a trend which seems to be in contradiction with a strong π Al−O bonding. Different conclusions concerning the π Al−O bonding have been reached by Barron:[2] a noticeable π Al−O conjugation should be responsible for short Al−O bond lengths in 3-coordinated aluminium alkoxides. The lack of rotational barrier in these compounds is expected to have the same origin as in transition metal alkoxides where no rotational barrier is found although π-bonding in these complexes is not doubtful. In addition, similar π Al−O conjugation is also proposed in 4-coordinated alkoxy aluminium compounds.

Theoretical calculations by Barron, Dobbs and Francl[3] indicate that π Al−O conjugation in 3- and 4- coordinated systems may explain the geometrical distortions observed in these compounds. On the opposite, recent calculations by Fink, Power and Allen[4] give a low rotational barrier in both model compounds, H_2Al-OH (3.5 kcal/mol) and $(CH_3)_2Al-OCH_3$ (1.7 kcal/mol). However, large geometric distortions in the deconjugated conformer do not allow a definite conclusion regarding the π bonding in these 3-coordinated aluminium alkoxides.

To shed some light on this problem, we have undertaken ab initio calculations on H_2Al-OR model molecules (R = H, CH_3) in order to get a more detailed description of Al−O π bonding; the results are compared to those obtained when oxygen is replaced by sulfur. In order to calibrate our results, additional calculations where performed on boron systems H_2B-YR (Y = O, S; R = H, CH_3) for which B−O B−S π conjugation is well etablished. These calculations are expected to check our previous conclusions for $H_2X-Y-XH_2$ species[5] (X = Al, B; Y = O, S) where it was found that X−Y π conjugation is a determining factor for understanding the geometrical structure of these compounds.

The results will be presented as follows: first, calculations on model species H_2X-YH at a conventional MO level of theory will be followed by Valence-Bond (VB) calculations. Secondly, the effect of Y substitution by a methyl group will be studied. Finally, the conclusions drawn from these

 © WILEY-VCH Verlag GmbH, D-69451 Weinheim, 1998 1434−1948/98/0707−1015 $ 17.50+.50/0

two sets of results will be checked with systems in which X is replaced by a strong π acceptor: C^+. Both model systems H_2C-YH^+ and $H_2X-YCH_3^+$ (Y = O, S) will be analyzed.

Method of Calculation

The 6−311G** basis set was used throughout the paper. All geometries were optimized at the MP2 level with the help of an analytical gradient method. Characterization of the extrema were made by analytical frequencies calculations at this level. The stationary points may be minima (Min, no imaginary frequency) or transition states (TS, only one imaginary frequency) or *n*-order saddle points (*n*-SP, *n* imaginary frequencies). In this last case ($n > 1$), the stationary point has no chemical significance. Subsequent calculation of the correlation energy was made at the MP4(SDTQ) level on the geometries optimized at the MP2 level. Our level of calculation is therefore MP4/6−311G**//MP2/6−311G**. In the simplest model systems (H_2X-YH) we have tested the influence of improving the correlation energy by optimizing the geometries at the MP4 level. The GAUSSIAN 92 set of programs[6] was used. Valence-Bond calculations were made with the help of the Turtle program.[7]

Results

A. Unsubstituted Systems

Energetical Analysis

For each system (referred as BS, BO, AlS and AlO in the following), three geometries [planar (**1**), perpendicular (**2**) and linear (**3**)] have been optimized and fully characterized by analytical frequencies calculations.

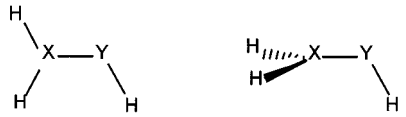

1

2

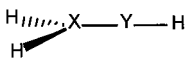

3

All twelve structures are found to be stationary points on the various potential energy surfaces. In each case, the planar geometry is a real minimum while the perpendicular geometry is a transition state (TS, one imaginary frequency). Following the transition vector associated with the imaginary frequency leads to the planar minimum. The linear structure is found to be a second-order saddle point (2-SP, two imaginary frequencies) and the two associated transition vectors lead to the planar minimum or to the perpendicular transition state. The geometrical parameters of the optimized structures (MP2/6−311G** level) are given in Figure 1 and the corresponding relative energies in Table 1.

Figure 1. Geometrical optimized parameters of the H_2X-YH species (bonds in A and angles in degrees)

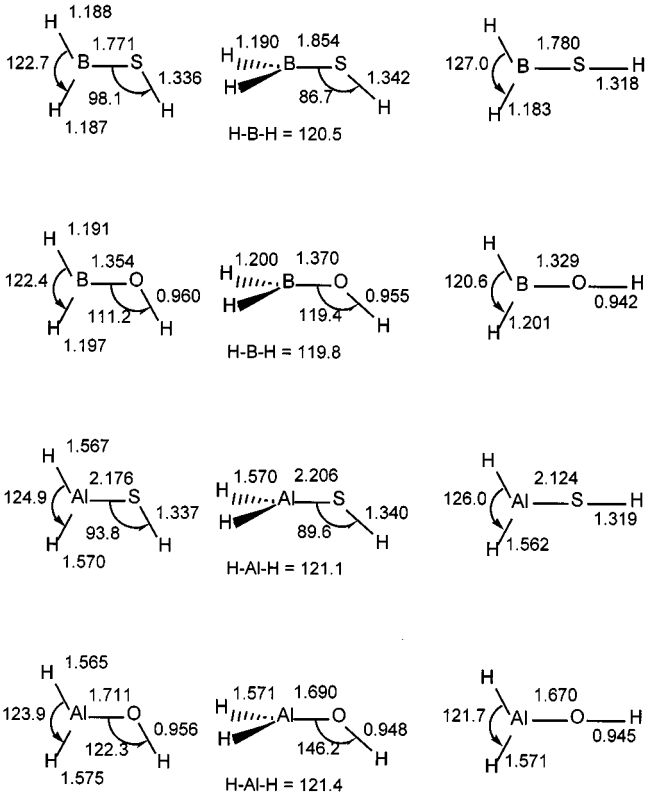

Table 1. Relative energies (in kcal/mol) of the three geometries for each species at the MP2/MP2 level of calculation.

	BS	BO	AlS	AlO
planar	0	0	0	0
perpendicular	20.5	16.9	7.6	3.6
linear	54.4	20.5	31.7	3.9

All the extrema have been recalculated at the MP4 level at the MP2 optimized geometries. The relative energies at the MP4/6−311G**//MP2/6−311G** level are given in Table 2.

Table 2. Relative energies (in kcal/mol) of the three geometries for each species at the MP4/MP2 level of calculation

	BS	BO	AlS	AlO
planar	0	0	0	0
perpendicular	20.6	17.1	7.8	3.9
linear	54.4	21.0	32.0	4.2

The results at MP2/MP2 and MP4/MP2 levels are very similar: improving the correlation energy calculation increases the energy differences by less than 0.5 kcal/mol. However, to be sure that improvement of the correlation energy calculation does not affect the optimized parameters, the planar and perpendicular geometries have been reoptimized at the MP4 level. The rotational barriers

[*E*(perp)−*E*(planar)] are exactly the same as that found at the MP4/MP2 level. In addition, the geometrical changes are less than 0.007 A for bond lengths and 1.5° for bond angles (except for the Al−O−H bond angle whose change is 3° in the perpendicular structure). Therefore, our calculation level can be considered as satisfactory. Note finally that our results agree well with those previously published: 18.0, 14.3, 7.3, and 3.5 kcal/mol for BS, BO,[8] AlS, and AlO[4] systems respectively. Similar values (19, 14, 8, and 4 kcal/mol) have been obtained by Zyubina and Charkin.[9]

The evolution of the rotational barrier should well illustrate the basic concept of conjugation in such compounds. In the planar structure, the vacant p orbital on aluminium or boron conjugates with the π-doubly occupied lone pair of sulfur or oxygen, leading to a 2-electron stabilization. A 90° rotation of the Y−H group destroy this conjugation and the rotational barrier could be a measure of the strength of the π X−Y bond. It is indeed found that the rotational barrier is very low when X and Y electronegativities are different (X = Al and Y = O) and becomes higher as the X and Y electronegativities become closer. As a result, the highest barrier is found when X = B and Y = S. In fact this interpretation of the barrier evolution is somewhat oversimplified as shown below.

Geometrical Analysis

The X−Y bond lengths and X−Y−H angles for each system are reported in Table 3. To our knowledge only the unsubstituted H_2BOH species has been experimentally characterized (Microwave Spectrum).[10] Our optimized parameters (B−O = 1.354 A; O−H = 0.960 A; B−O−H = 111.2°; O−B−Hc = 120.9°; O−B−Ht = 116.7°; BHc = 1.197 A; BHt = 1.191 A) are in excellent agreement with the experimental ones (B−O = 1.352 A; O−H = 0.967 A; B−O−H = 112.0°; O−B−Hc = 121.8°; O−B−Ht = 117.2°, the B−H bond length being assumed to be 1.200 A).

Table 3. X−Y bond lengths (in A) and X−Y−H bond angles (in degrees) in the various optimized extrema

X−Y Bond lengths	BS	BO	AlS	AlO
planar	1.771	1.354	2.176	1.711
perpendicular	1.854	1.370	2.206	1.690
linear	1.780	1.329	2.124	1.670
X−Y−H Bond angles				
planar	98.1	111.2	93.8	122.3
perpendicular	86.7	119.4	89.6	146.2

Let us first compare the X−Y bond lengths in planar and linear structures: in both structures π conjugation is at work between the p orbitals of X and Y (Scheme 1).

Scheme 1

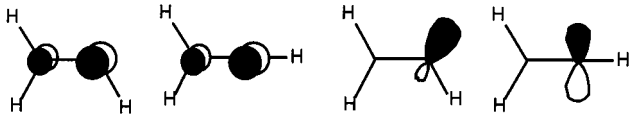

The main electronic difference between the two geometries comes from the interaction of the second Y lone pair with the H_2X moiety. The lone pair is expected to be strongly hybridized in the planar structure while it is a pure p orbital in the linear geometry (Scheme 1). In each case except H_2BSH, the X−Y bond length shortens from the planar to the linear geometry (Table 3). This shortening may come from a negative hyperconjugation interaction between this Y lone pair and the symmetry adapted H_2X antibonding orbitals (see below).

The geometrical evolutions from planar to perpendicular geometries are different for oxygen and sulfur systems and will be discussed separately. In *oxygen compounds*, the perpendicular structure is reminiscent of the linear geometry. The X−Y−H angle opens when going from the planar to the perpendicular geometries (by 8.2 and 23.9° in boron and aluminium cases respectively) which allows the dehybridization of the in-plane lone pair and therefore ensures a better conjugation with the p vacant orbital on the H_2X moiety. This effect is rather small in the boron compound and the BO bond length increases upon OH rotation (from 1.354 to 1.370 A). On the other hand, the Al−O−H angle dramatically increases by 23.9° upon rotation and that leads to a strong residual conjugation in the perpendicular geometry. This is illustrated by an Al−O bond length (1.690 A) which is intermediate between those of the planar (1.711 A) and linear (1.670 A) geometries. Consequently, the rotational barrier in H_2AlOH is not a measure of the π Al−O conjugation since a noticeable conjugation still remains in the perpendicular structure. A similar interaction (although attenuated) exists in H_2BOH, as previously pointed out by Ashby and Sheshtawy;[8] following these authors, the hydroxy group should be considered as a double-faced π-donor. Thus, the oxygen's ability to conjugate in both the planar and perpendicular geometries is further illustrated by the small energy differences between the perpendicular and linear geometries: it is 3.9 and only 0.3 kcal/mol for H_2BOH and H_2AlOH respectively (Table 2). These low values indicate that the energetical cost of dehybridization of the oxygen second lone pair is almost compensated by the additional conjugation interaction. This result gives an insight in the mechanism of aluminum alkoxides isomerization. Since the two (perpendicular and linear) structures are almost isoenergetic, this reaction may proceed by rotation or linearization of the alkoxide moiety (Scheme 2). As previously noted by Ashby,[8] the competition between the two mechanisms should be in favor the intermediacy of a perpendicular structure for H_2BOH because of the larger energy difference.

Fo the *sulfur derivatives*, linearization of the X−S−H arrangment costs much more energy (54.4 and 32.0 kcal/mol for H_2BSH and H_2AlSH respectively, Table 2). As a result, no dehybridization occurs in the perpendicular structure that is well illustrated by an X−S−H angle which is roughly equal to 90° in both planar and perpendicular geometries. The π residual conjugation is expected to be small in the rotated structure and, consequently, both Al−S and B−S bond lengths increase upon rotation (Table 3). A surprising

Scheme 2

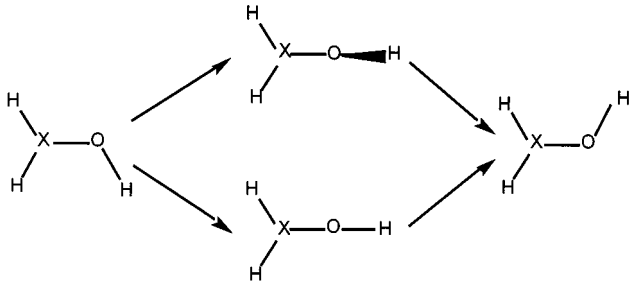

point is the decrease of the X−S−H angle in the planar → perpendicular interconversion: this variation is small in H_2AlSH (4.2°) and becomes rather large (11.4°) in H_2BSH. It allows a shortening of the X···H distance (**4**) and we attribute this geometrical change (which is opposite to that found in oxygenated systems) to a direct interaction between the H_2X p vacant orbital and the hydrogen atom. Such interactions are well-known in organometallic chemistry and have been called "agostic" by Brookhart and Green.[11] Similar interactions will be analyzed in more details in the study of substituted species. Note that, following Ashby,[8] this angle decrease may be attributed to a relief of Pauli repulsion.

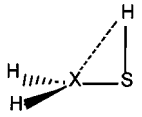

4

π-Conjugation in H_2X-YH Species?

Since the rotational barrier cannot be a good measure of X−Y conjugation in these species, additional VB calculations have been performed on planar and linear structures at the MP2 optimized geometries. In a first step, the total energy is recalculated in a "normal" manner i.e. all the interaction are taken into account. In a second step, the π interaction in both geometries is set to zero by forbiding any delocalization of the π lone pair of the Y atom on the XH_2 moiety in both planar and linear geometries. The energy differences between the two sets of results give a reasonable estimation of the π interaction in those systems. (Note that a more accurate calculation of the conjugation interaction should require a full geometry reoptimization in the deconjugated species that is not possible with our VB program.) Similar calculations have been performed in the linear geometry by cancelling the delocalization of the in-plane Y p-lone pair in order to get a measure of the hyperconjugation (HC) with the XH_2 moiety. Finally, in the linear geometry, both conjugation and hyperconjugation have been cancelled. The results of these calculations are given in Table 4 for each system under study.

For each species the conjugation stabilizations are not identical for the planar and linear geometries since the X−Y bond lengths are not the same in both geometries (Table 3). However the two sets of values are rather close to each others and the results obtained in the planar geometry are expected to correctly reflect the stabilization due to conjugation in H_2X-YH species. The lowest value (8.1 kcal/mol) is found in the Al−S case, confirming that the π bonds are weak between two second-row atoms.[12] The X−Y conjugation is still weak in H_2Al-OH (10.2 kcal/mol) and becomes stronger in the boron compounds (16.6 and 22.6 kcal/mol for H_2B-SH and H_2B-OH respectively, Table 4). As expected the highest stabilization is found for H_2B-OH in which conjugation develops between two first-row atoms.

Table 4. Stabilization (in kcal/mol) due to conjugation (planar and linear structures) and to hyperconjugation (linear structure only)

	BS	BO	AlS	AlO
planar conjugation	16.6	22.6	8.1	10.2
linear conjugation	19.0	21.1	9.6	9.6
linear HC	7.0	7.9	6.0	6.6
linear conjugation + HC	27.0	30.6	16.6	17.3

In the four linear structures, the hyperconjugation of the in-plane Y lone pair with the H_2X moiety is found to be stabilizing and almost constant (between 6 and 8 kcal/mol) whatever the nature of the X and Y atoms. Finally, it is worth noting that the two contributions (conjugation and hyperconjugation) are fairly additive in the linear structure: adding the stabilization due to conjugation (entrie 2) and to hyperconjugation (entrie 3) in Table 4, gives (within about 2 kcal/mol) the total stabilization (entrie 4) obtained when both lone pairs are allowed to delocalize.

In Table 5 are brought together the values of conjugation stabilization (Table 4) and rotational barrier (energy difference between planar and perpendicular geometries, Table 2).

Table 5. Conjugation stabilization and rotational barrier for the various systems; all quantities are in kcal/mol.

	BS	BO	AlS	AlO
planar conjugation	16.6	22.6	8.1	10.2
rotational barrier	20.6	17.1	7.8	3.9

The values are reasonably close in the sulfur-substituted systems but differ notably in the oxygenated cases. In these cases, the rotational barrier is systematically lower than the conjugation interaction (by 5.5 and 6.3 kcal/mol in boron and aluminium cases respectively) which indicates the reminiscent conjugation in the rotated structure as shown above. The two values notably differ in the H_2Al-OH case where the Al−O−H angle dramatically increases in the perpendicular geometry (Table 3).

B. Methyl-Substituted Systems

Energetical Analysis

Calculations on substituted systems H_2X-YCH_3 have been made in order to get more detailed informations on the various interactions in these species. As shown previously,[13] the eclipsed conformer (**5**) is the most stable in the planar geometry. Two rotamers have been fully optim-

ized and characterized in the perpendicular geometry. In the first one (**6**), a CH methyl bond eclipses the X−Y bond while in the second one (**7**), the CH methyl bonds are staggered with respect to the X−Y bond. The energetical results are reported in Table 6 together with the characterization of the various structures. The rotational energy barriers in unsubstituted species have also been reported for sake of comparison.

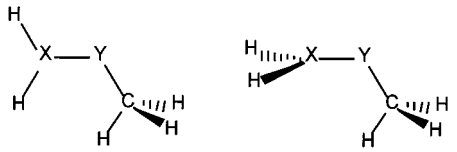

5

6

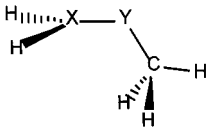

7

Table 6. Relative energies (in kcal/mol) at the MP4/MP2 level of the planar (**5**) and perpendicular (**6** and **7**) geometries in H_2X-YCH_3 species; the rotational barrier in unsubstituted species is also given for sake or comparison

	BS	BO	AlS	AlO
planar **5**	0 (Min)	0 (Min)	0 (Min)	0 (Min)
perpendicular **6**	22.2 (Min)	18.6 (2-SP)	9.2 (2-SP)	-[a]
perpendicular **7**	22.3 (TS)	17.2 (TS)	8.7 (TS)	3.0 (TS)
unsubst. R.B.	20.6	17.1	7.8	3.9

[a] No stationary point found, see text.

All the planar structures (**5**) are found to be real minima on the Potential Energy Surface (PES). Staggered perpendicular geometries (**7**) are found to be transition states (one imaginary frequency) and we have verified that they belong to the isomerization reaction path depicted in Scheme 3.

Scheme 3

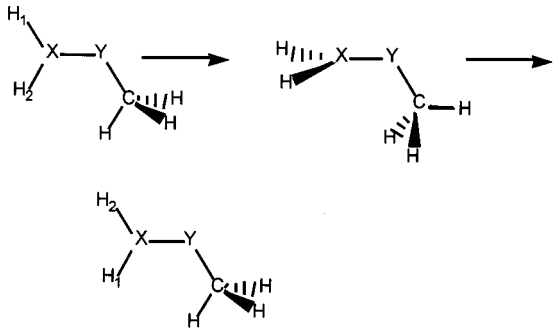

The rotational barriers in the methylated species are therefore equal to the energies differences between structures **5** and **7**. They are found to be very close to that of the hydrogenated systems: for each molecule, the barrier in methylated and unsubstituted systems are the same within 1.7 kcal/mol (Table 6). It is worth to compare our calculated barriers on methyl-substituted species to those experimentally determined. In BS and BO cases, the theoretical values (22.3 and 17.2 kcal/mol) are larger than the experimental values (18.2−19.7 kcal/mol (BS)[14][15] and 11.2−13.9 kcal/mol (BO)[15][16]. The presence of bulky substituents may well be at the origin of this discrepancy since steric repulsion should be smaller in the perpendicular structure that lowers the rotational barrier. In aluminium compounds, there are few experimentally determined values: it is found to be less than 8 kcal/mol in Al−O case[17] and between 8 and 9 kcal/mol in AlS case.[18] (This last value is obtained in bisthiolate derivative of aluminium. To our knowledge, no data on monosubstituted compound are available). Both these values are in agreement with our theoretical values.

In the perpendicular geometries, the methyl group bonded to the Y atom does not seem to exhibit strong conformational preference: the energy differences between structures **6** (eclipsed) and **7** (staggered) are about 0.5 kcal/mol for BS, and AlS and increases up to 1.4 kcal/mol in H_2B-OCH_3 system. However these small energy differences originate from very different interaction as shown below. More puzzling, the characterization of this structure depends on the nature of X and Y atoms. In BO and AlS cases, the eclipsed geometries are 2-order saddle points as expected. The transition vector associated with one imaginary frequency essentially develops on the twist angle between H_2X and XYC planes and corresponds to the **6** → **5** motion. The second transition vector involves the in-block rotation of the methyl substituent and corresponds to the **6** → **7** motion. For Al−O, we did not find any stationary point corresponding to the eclipsed perpendicular conformer **6**. Optimization of this geometry leads to an opening of the Al−O−C angle beyond 180° and this structure collapses to the conformer **7** which is a transition state located 3.0 kcal/mol above the planar structure. More puzzling is the fact that in BS case, the eclipsed perpendicular structure is found to be a secondary minimum on the PES.

Geometrical Analysis

The main optimized geometrical parameters are given in Figure 2. For each structure, the X−Y bond length is slightly shorter than that found in the unsubstituted species: for instance, B−O = 1.345 A in H_2B-OCH_3 and 1.354 A in H_2B-OH for the planar structures. Our optimized parameters (X−Y and Y−C bond lengths and X−Y−C angles are in reasonable agreement (Table 7) with the experimental data available on monosubstituted compounds (except in Al−S case where only bis-thiolate derivative has been characterized). It should be noted that we find a large X−Y−C angle only in Al−O−C case, in accordance with the experimental data.

Partial deconjugation (**5** → **6** or **7**) leads in each case to a lengthening of the X−Y bond, except in $H_2Al-OCH_3$. In this case, the shortening of the Al−O bond length may be explained (as in the unsubstituted species) by the quasi-linear geometry of the rotated structure (Al−O−C = 170.9°, Figure 2).

Table 7. Comparison between theoretical and experimental parameters determined on monosubstituted species; bonds are in A and angles in degrees

B−S	S−C	B−S−C	ref.
1.758	1.818	104.4	this work
1.787	1.815	109.8	[8]
1.790	1.773	107.0	[19]
1.779	1.825	107.2	[20]
B−O	O−C	B−O−C	ref.
1.345	1.427	120.5	this work
1.352	1.438	123.6	[8]
1.361	1.421	124.4	[21]
Al−S	S−C	Al−S−C	ref.
2.166	1.828	102.4	this work
2.184−2.197	1.803−1.814	95.9−102.7	[18][a]
Al−O	O−C	Al−O−C	ref.
1.706	1.411	131.6	this work
1.709/1.710	−	129.4/135.2	[17]

[a] Bis-thiolate derivative.

Figure 2. Geometrical optimized parameters of the H_2X-YCH_3 species (bonds in A and angles in degrees)

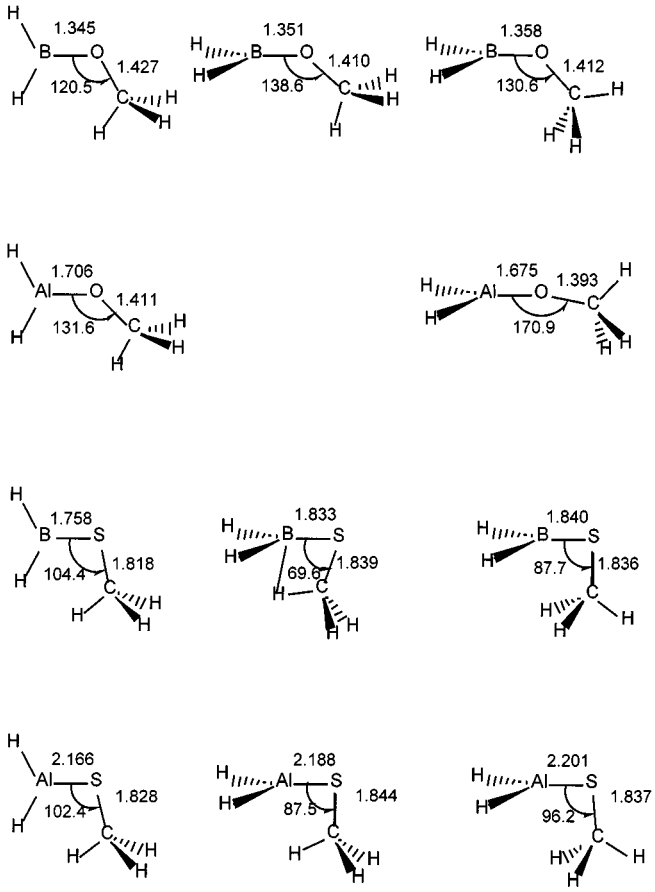

In oxygenated compounds, the 90° rotation of the X−O−C plane relative to the H_2X plane leads to an opening of the oxygen valence angle as already noted in the unsubstituted species. In sulfur compounds, we find a smaller X−S−C angle in perpendicular **7** geometry than in the planar **5** one. The angular variations are in the same range as in unsubstituted species (6.2 vs. 4.2° in Al compounds and 16.7 vs. 11.4° in B compounds).

A dramatic change occurs in H_2B-SCH_3 perpendicular geometry **6**: the B-S-C angle is found to be very acute (69.6°), about 35° smaller than in the planar geometry. This very small sulfur valence angle may be attributed to a direct interaction between the eclipsing methyl hydrogen and the boron atom. A short distance (B···H = 1.764 A) is indeed found and is accompanied with a noticeable lengthening of the C−H bond (C−H = 1.102 A which may be compared to the standard value (1.09 A) found in H_2B-OCH_3). As a result of this stabilizing agostic interaction, the eclipsed geometry **6** is found to be a secondary minimum on the PES. A similar interaction − although attenuated − is found in $H_2Al-SCH_3$: the Al−S−C angle is small (87.5°) and the eclipsing C−H bond lengthens to 1.10 A. However, the Al···H distance remains large (2.50 A) and leads to a rather weak interaction. As a consequence, the eclipsed perpendicular structure **6** is a 2-order saddle point which may be stabilized by a 90° rotation of the methyl group (**6** → **7**). The difference between these two molecules ($H_2Al-SCH_3$ and H_2B-SCH_3) may be attributed to the lower π-acceptor ability of the aluminium relative to the boron due to its lower electronegativity.

In summary of the study of these methylated and hydrogenated systems, the rotational energy barrier in H_2X-YR (R = H, CH_3) depends on three factors: (i) the strength of π-conjugation between X and Y; (ii) the plasticity of the Y valence angle and (iii) possible agostic iteraction with the unsaturated H_2X moiety. Note that a similar direct interaction between the deficient central atom and a non bonded hydrogen has already been shown in aluminium[17][22][23] and gallium[18][22][24][25] derivatives. In order to check these conclusions, we have performed additional calculations on similar systems obtained by taking a strong π-acceptor X atom: C^+.

C. Carbocationic Systems

Unsubstituted Compounds

The unsubstituted cationic species H_2C-OH^+ and H_2C-SH^+ have been fully optimized in planar (**1**), perpendicular (**2**) and linear (**3**) geometries. The energetic results and main optimized parameters are given in Tables 8 and 9. Our optimized parameters are very close to that found by Suarez and Sordo[26] in their recent study of the H_2 elimination from these cations.

Table 8. Relative energies (in kcal/mol, MP4/MP2 level) and characterization of the various extrema for the H_2C-OH^+ and H_2C-SH^+ systems

	1 (planar)	**2** (perpendicular)	**3** (linear)
Y = O	0 (Min)	-[a]	25.4 (TS)
Y = S	0 (Min)	50.3 (Min)	76.3 (2-SP)

[a] No stationary point found.

Since the H_2C^+ moiety is a strong π-acceptor, a strong π conjugation is expected between the C^+ and the Y atoms. VB calculations of the same type as presented before indeed give a C^+-O π-bond strength of 59.5 kcal/mol (planar geo-

Table 9. Main optimized parameters of the two cations H_2C-OH^+ and H_2C-SH^+; bond lengths are in A and angles in degrees

	CS	CO	COH	CSH
planar	1.617	1.354	114.1	98.0
perpendicular	1.680	—[a]	—[a]	50.3
linear	1.619	1.227		

[a] No stationary point found.

metry) and 57.3 kcal/mol (linear geometry). This π bond is therefore much stronger than that found between B and O (22.6 kcal/mol) or Al and O (10.2 kcal/mol). Similarly, the C^+-S π bond is calculated to be of 59.0 kcal/mol (planar) and 66.6 kcal/mol (linear);[27] as in the oxygen case, it is stronger than B−S (16.6 kcal/mol) or Al−S (8.1 kcal/mol) π bonds (Table 4).

Rotation of the Y−H moiety about the C^+-Y bond destroys this strong conjugation that is energetically much unfavorable. Geometrical deformations therefore occur in order to diminish this energetical cost. In H_2C-OH^+, the C−O−H angle opens up to 180° and the dehybridization of the perpendicular lone pair allows a favorable π interaction. As a result, no stationary point corresponding to a perpendicular geometry is found. The linear structure is then the transition state allowing the isomerization of this species with a 25.4 kcal/mol activation energy (Table 8). In H_2C-SH^+, similar linearization of the C−S−H angle is too much expansive: the linear structure is located 76.3 kcal/mol above the planar geometry. It is a 2-order saddle point, the two transition vectors associated with the imaginary frequencies leading to the planar or perpendicular structures. However, a diminution of the C−S−H angle to 50.3° allows a noticeable interaction between the H atom and the cationic carbon. As a result, the S−H bond lengthens (from 1.346 A in the planar geometry to 1.519 A in the perpendicular structure) and the $C^+\cdots H$ distance is only 1.368 A. This bridged structure is located 50.3 kcal/mol above the planar geometry and is found to be a real minimum (Table 8). We did not try to locate the transition state connecting these two minima. This has been previously done by Suarez and Sordo[26] who found the transition state only 0.2 kcal/mol above the secondary minimum.

Methylated Compounds

The potential energy surfaces associated with the methylated species $H_2C-OCH_3^+$ and $H_2C-SCH_3^+$ have also been investigated. The $H_2C-OCH_3^+$ cation behaves as its unsubstituted analog: the planar structure is found to be a real minimum and no stationary point corresponding to a perpendicular geometry has been found. A quasi-linear (C−O−C = 178.6°) transition state has been located 22.5 kcal/mol (MP4/MP2 level) above the minimum. The main geometrical parameters are depicted in Figure 3.

The PES associated with the $H_2C-SCH_3^+$ cation is more complicated. As in boron and aluminium systems, a planar (**5**) conformation and two perpendicular geometries (eclipsed **6** and staggered **7**) have been optimized.

Figure 3. Main geometrical parameters [A,°] and relative energies (kcal/mol, MP4/MP2 level) of the optimized structures of $H_2C-OCH_3^+$

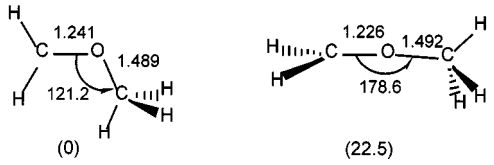

The planar structure **5** is a real minimum and we have verified that the conformation where a C−H bond eclipses the C−S bond is the most stable (by 0.6 kcal/mol with respect to the staggered conformation). The eclipsed perpendicular conformation **6** is also a real minimum located 41.3 kcal/mol above the planar geometry. In this structure, the $C^+\cdots H$ agostic interaction is strong and a C_{2v} geometry is found: the methyl hydrogen symmetrically bridges the two carbon atoms, both C−H distances being equal to 1.279 A (Figure 4). The sulfur valence angle is acute (58.9°) and the two S−C bond are lengthened to 1.780 A. The transition state connecting these two minima (**TS1**) has been located. Its geometry ressembles that of the secondary minimum **6** (Figure 4) and is located 3.5 kcal/mol above it.

Figure 4. Main geometrical parameters [A,°] and relative energies (kcal/mol, MP4/MP2 level) of the optimized isomers of $H_2C-SCH_3^+$

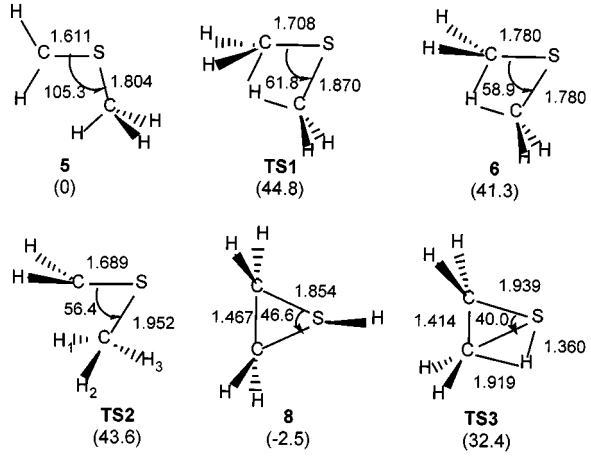

Optimization of the staggered conformation **7** leads to the location of two stationary points. Both of them are characterized to be transition states, **TS2** and **TS3**. The highest one, **TS2** is located 43.6 kcal/mol above the minimum **5**. It is of C_1 symmetry and its geometry is rather close to that of the secondary minimum **6** (C^+-S = 1.689

Scheme 4

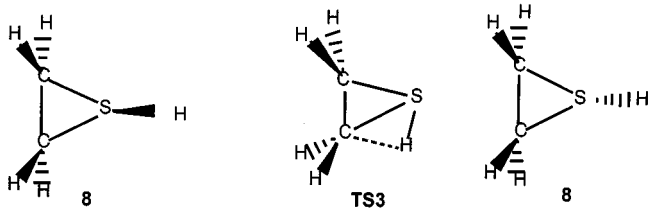

Scheme 5

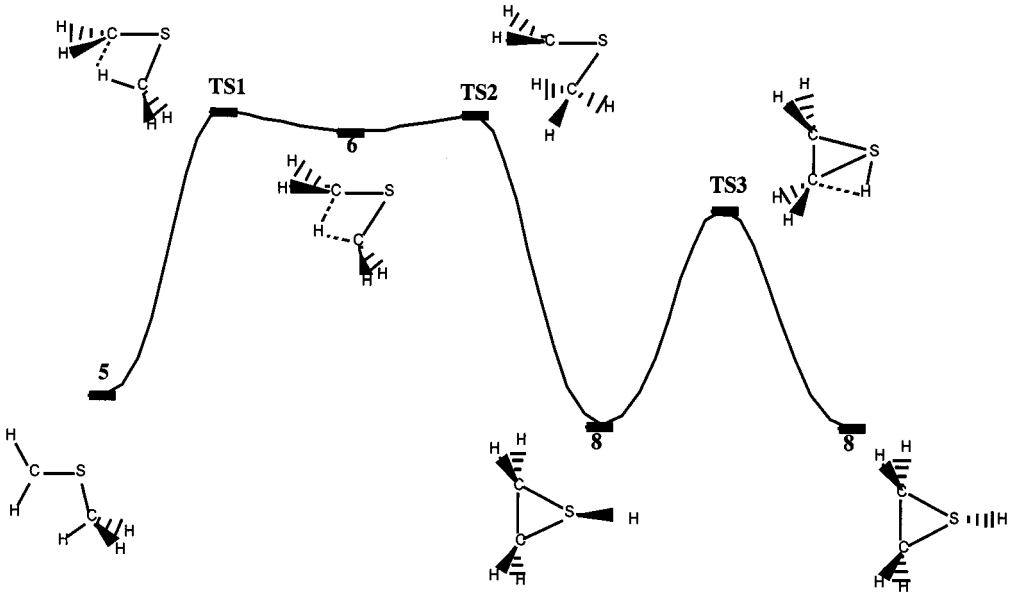

Å; C−S = 1.952 Å; C−S−C = 56.4°, Figure 4). Two C−H bonds of the methyl group are elongated (C−H_2 = 1.108 Å; C−H_3 = 1.104 Å). Following the transition vector associated with the imaginary frequency leads to a cyclic minimum which is the protonated thiooxirane **8**. This minimum is located 2.5 kcal/mol below the planar structure **5** (Figure 4). The structure **TS2** is therefore the transition state allowing the interconversion of the secondary minimum **6** into the protonated thiooxirane **8**. From a geometrical point of view, it should be noted that the migration of the hydrogen from carbon to sulfur is possible because the C_S symmetry plane has been removed in the **TS2** geometry. The second transition state (**TS3**) is of C_S symmetry and is located 32.4 kcal/mol above the minimum **5**. Formally, it is a conformer of the $H_2C-SCH_3^+$ cation, but severe distortions appear in this geometry: the C−C distance is very short (1.414 Å) indicating the presence of a C−C bond (Figure 4). In addition, the S−H (1.360 Å) and C−H (1.919 Å) distances indicate that a S−H bond is formed whereas a C−H bond is broken. With respect to the $H_2C-SCH_3^+$ cation, an hydrogen atom has moved from carbon to sulfur. The transition vector associated to the imaginary frequency almost only develops on the out-of-plane motion of the hydrogen atom bound to sulfur. This transition state is therefore thought to connect the two enantiomeric forms of the protonated thiooxirane (Scheme 4).

A schematic representation of the connection between these different extrema is given in Scheme 5.

Summary and Conclusion

Our theoretical study of H_2X-YR systems (X = Al, B, C^+; Y = O, S; R = H, CH_3) sheds some lights on π bonding in such compounds. π bonding is strong when X = C^+ (from 57 to 67 kcal/mol), intermediate for X = B (from 16 to 23 kcal/mol) and weak for X = Al (from 8 to 10 kcal/mol). The nature of the Y atom (Y = O or S) does not seem to strongly affect the strength of the X−Y π bond. The value of the rotational barrier is not a measure of the π conjugation because important geometrical deformations occur in the deconjugated perpendicular structure in order to compensate for -at least in part- the loss of the stabilization interaction. When Y = O, the X−O−R angle opens so that a X−O π conjugation still exists between the p(X) vacant orbital and the second oxygen lone pair which is partly dehybridized. The linearization of the X−O−R arrangment is more pronounced in methylated than in the unsubstituted systems. When Y = S, the opposite deformation is found, probably because of the reluctance of sulfur for obtuse valence angles. The X−S−R angle becomes more obtuse in the perpendicular geometry and a direct agostic interaction takes place between the X atom and the Y substituent R (R = H, CH_3). For R = H, as the π-acceptor capability of X increases, the X−S−H angle decreases [89.6° (Al); 86.7° (B); 50.3° (C^+)]. In methylated systems, the four-membered (X−S−C−H) ring seems to be particularly favorable and, provided that the agostic interaction is strong enough, the bridged structure is a secondary minimum on the PES (X = B, C^+). For X = C^+, this interaction is found to be rather strong and the bridging hydrogen is equally shared between the two carbon atoms.

[1] P. J. Brothers, P. P. Power *Advances in Organometallic Chemistry* **1996**, *39*, 1.
[2] A. R. Barron, *Polyhedron* **1995**, *14*, 3197.
[3] A. R. Barron, K. D. Dobbs, M. M. Francl, *J. Am. Chem. Soc.* **1991**, *113*, 39.
[4] W. H. Fink, P. P. Power, T. L. Allen, *Inorg. Chem.* **1997**, *36*, 1431.
[5] L. Boiteau, I. Demachy, F. Volatron, *Chem. Eur. J.* **1997**, *3*, 1852.
[6] Gaussian 92/DFT, Revision F.4, M. J. Frisch, G. W. Trucks, H. B. Schlegel, P. M. W. Gill, B. J. Johnson, M. W. Wong, J. B. Foresman, M. A. Robb, M. Head-Gordon, E. S. Reploge, R.

Gomperts, J. L. Andres, K. Raghavachari, J. S. Binkley, C. Gonzalez, R. L. Martin, D. J. Fox, D. J. Defrees, J. Baker, J. J. P. Stewart, J. A. Pople, Gaussian, Inc., Pittsburgh PA, 1993.
[7] J. Verbeek, J. H. Langenberg, J. H. van Lenthe, C. P. Byrman Turtle-an ab initio VB/VBSCF/VBCI program, Utrecht (1993).
[8] M. T. Ashby, N. A. Sheshtawy, *Organometallics* **1994**, *13*, 236.
[9] T. S. Zyubina, O. N. Charkin, *Russ. J. Inorg. Chem.* **1992**, *37*, 434.
[10] Y. Kawashima, H. Takeo, C. Matsumura, *J. Chem. Phys.* **1981**, *74*, 5430.
[11] M. Brookhart, M. L. H. Green, *J. Organomet. Chem.* **1983**, *250*, 395.
[12] W. Kutzelnig, *Ang. Chem. Int. Ed. Engl.* **1984**, *23*, 272.
[13] E. D. Jemmis, G. Subramanian, *J. Phys. Chem.* **1994**, *98*, 8937.
[14] F. Davidson, J. W. Wilson, *J. Organomet. Chem.* **1981**, *204*, 47.
[15] N. M. D. Brown, F. Davidson, J. W. Wilson, *J. Organomet. Chem.* **1981**, *210*, 1.
[16] P. Finocchiaro, D. Gust, K. Mislow, *J. Am. Chem. Soc.* **1973**, *95*, 7029.
[17] M. A. Petrie, M. M. Olmstead, P. P. Power, *J. Am. Chem. Soc.* **1991**, *113*, 8704.
[18] R. J. Wehmschulte, K. Ruhlandt-Senge, P. P. Power, *Inorg. Chem.* **1995**, *34*, 2593.
[19] R. J. Wehmschulte, K. Ruhlandt-Senge, M. M. Olmstead, M. A. Petrie, P. P. Power, *J Chem. Soc. Dalton Trans.* **1994**, 2113.
[20] K. Brendhaugen, E. Wisloff Nilssen, H. M. Seip, *Acta Chem. Scand.* **1973**, *27*, 2965.
[21] G. Gundersen, T. Jonvik, R. Seip, *Acta Chem. Scand.* **1981**, *A35*, 325.
[22] M. A. Petrie, P. P. Power, H. V. Rasika Dias, K. Ruhlandt-Senge, K. M. Waggoner, R. J. Wehmschulte, *Organometallics* **1993**, *12*, 1086.
[23] A. P. Shreve, R. Mulhaupt, W. Fultz, J. Calabrese, W. Robbins, S. D. Ittel, *Organometallics* **1988**, *7*, 409.
[24] K. Ruhlandt-Senge, P. P. Power, *Inorg. Chem.* **1991**, *30*, 2633.
[25] K. Ruhlandt-Senge, P. P. Power, *Inorg. Chem.* **1991**, *30*, 3683.
[26] D. Suarez, T. L. Sordo, *J. Phys. Chem. A* **1997**, *101*, 1561.
[27] We did not find any satisfactory explanation of the 7.6 kcal/mol difference between the two values of this π conjugation. However, it should be noted that in sulfur compounds, conjugation is always found to be larger in the linear geometry than in the planar geometry. The reverse tendency is found in oxygenated species.

[98053]

Formation of a Stable Adduct of Ethoxycarbonyldithiocarbamic Acid and a Dimer of Ethoxycarbonyl Isothiocyanate

Richard D. Adams* and Mingsheng Huang

Department of Chemistry and Biochemistry, University of South Carolina,
Columbia, SC 29208, USA
E-mail: ADAMS@psc.sc.edu

Received February 23, 1998

Keywords: Sulfur heterocycles / Hydrolyses / Isothiocyanate / Dithiocarbamic acids

The reaction of ethoxyxcarbonyl isothiocyanate with water in the absence of a solvent has yielded the new compound $[EtO_2CN{=}CS_2C\{N(H)CO_2Et\}\{S_2CN(H)CO_2Et\}]$ (**1**) in 76% yield that has been isolated in a crystalline form that contains one equivalent of ethoxyxcarbonyl isothiocyanate. Compound **1** can be viewed as an adduct of a dimer of $EtO_2CN{=}C{=}S$ and the dithiocarbamic acid **2**. Compound **1** dissociates in solution to yield **2** and free ethoxyxcarbonyl isothiocyanate. Compound **2** can be isolated chromatographically, but it is slowly oxidized when allowed to stand in the open air to form the thiuram disulfide **3**. Compounds **1** and **3** were characterized crystallographically. Compound **1** contains an imino-substituted dithietane ring with a dithiocarbamate substitutent bonded to one of the ring carbon atoms. Compound **3** is a thiuram disulfide which has C_2 crystallographic symmetry.

Introduction

Organic isothiocyanates have been used for the synthesis of a variety of new heterocycles.[1] They are also effective ligands for transition metals.[2][3] There are claims that isothiocyanates with electron withdrawing substitutents couple to form dimers **A**,[4] and there is an example of a coupled form **B** of two isothiocyanates coordinated to a transition metal atom that has been verified crystallographically[5]

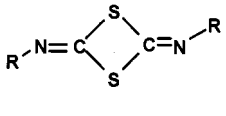

A

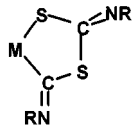

B

Organic isothiocyanates readily react with water to form amines with a release of CO_2 and H_2S (eq. 1).[6] H_2S is known to add to organic isothiocyanates to yield dithiocarbamic acids (eq. 2).[6]

$$RN{=}C{=}S + 2\ H_2O \rightarrow RNH_2 + H_2S + CO_2 \quad (1)$$

$$RN{=}C{=}S + H_2S \rightarrow RNHCS_2H \quad (2)$$

Dithiocarbamic acids are generally unstable, but the dithiocarbamate anions are a good ligands for transition metals and a large number of complexes have been made with them.[7] In this report we describe a reaction of the ethoxycarbonyl isothiocyanate with water. We have isolated and structurally characterized the new compound **1** which can be viewed as an adduct of the dimer **A**, and the ethoxycarbonyl dithiocarbamic acid (**2**).

Results and Discussion

When small amounts of water are allowed to mix with pure ethoxycarbonyl isothiocyanate, pale yellow crystals of compound **1** with one equiv. ethoxycarbonyl isothiocyanate are formed in up to 75% yield. The product actually forms crystals suitable for analysis by single crystal X-ray diffraction methods in the reaction mixture. Accordingly, a single crystal X-ray diffraction analysis of **1** was performed. An ORTEP diagram of the molecular structure of **1** is shown in Figure 1.

Figure 1. An ORTEP diagram of $\{EtO_2CN{=}CS_2C[N(H)CO_2Et]$-$[S_2CN(H)CO_2Et]\}$ (**1**) found in the crystal of **1**·$EtO_2CN{=}C{=}S$[a]

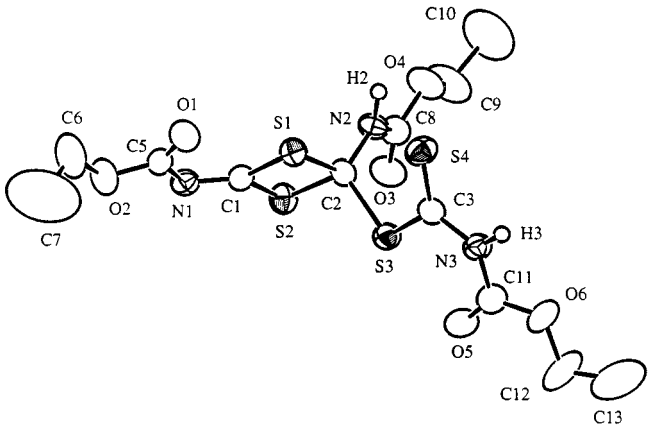

[a] Selected interatomic distances (A) and angles (°): S(1)−C(1) 1.755(8), S(2)−C(1) 1.715(9), S(1)−C(2) 1.831(8), S(2)−C(2) 1.870(7), S(3)−C(2) 1.824(8), S(3)−C(3) 1.762(8), S(4)−C(3) 1.630(8), S(5)−C(4) 1.51(2), C(1)−N(1) 1.28(1), C(2)−N(2) 1.41(1), C(3)−N(3) 1.39(1); S(1)−C(1)−S(2) 102.3(5), S(1)−C(2)−S(2) 93.8(4), S(2)−C(2)−S(3) 103.8(4), S(1)−C(2)−S(3) 115.5(5), N(2)−C(2)−S(1) 113.1(6), N(2)−C(2)−S(2) 112.5(6), N(2)−C(2)−S(3) 115.5(6).

Compound **1** can be viewed as an adduct of the dimer **A** of ethoxycarbonyl isothiocyanate and ethoxycarbonyldithiocarbamic acid. The dimeric ethoxycarbonyl isothiocyanate portion of the molecule is distinguished by a dithiet-

 © WILEY-VCH Verlag GmbH, D-69451 Weinheim, 1998 1434−1948/98/0707−1025 $ 17.50+.50/0

ane ring. One of the sulfur atoms of the ethoxycarbonyldithiocarbamyl grouping S(3) is bonded to one of the imino carbon atoms of the EtO_2CNCS dimer at C(2) atom. Thus, C(2) has three sulfur atoms, S(1), S(2), and S(3) bonded to it with bond lengths typical of C−S single bonds, S(1)−C(2) 1.831(8), S(2)−C(2) 1.870(8), S(3)−C(2) 1.824(8) A. The C−S bonds to C(1) are shorter, S(1)−C(1) 1.755(8) A, S(2)−C(1) 1.715(9) A due to partial multiple bonding character to C(1). A line drawing of the structure is shown below.

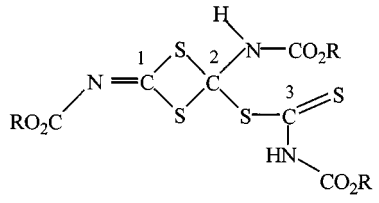

1

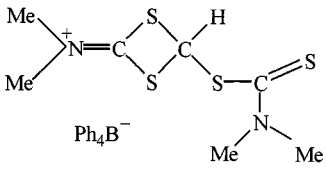

4

The molecule contains an imino-substituted four-membered dithietane ring which imposes a highly distorted tetrahedral structure around atom C(2). There are few molecules that are structurally similar to **1**. Perhaps, its closest relative is the cation of the compound $[Me_2N{=}CS_2C(H)S_2CNMe_2]BPh_4$ (**4**) which contains an amino-substituted dithietane ring.[8] The ^{1}H-NMR spectrum of **1** shows the presence of three ethyl groups, as expected, and two slightly broadened, deshielded resonances of intensity one at δ = 9.02 and 7.23. The latter are attributed to hydrogen atoms that have been assigned to sites on N(2) and N(3) since the C(1)−N(1) bond length is indicative a double bond, C(1)−N(1) 1.283(9) A while the lengths of other two, C(2)−N(2) and C(3)−N(3), 1.41(1) and 1.386(9), respectively, are more consistent with single bond lengths. One equivalent of ethoxycarbonyl isothiocyanate is crystallized with **1** in the same crystal lattice. There are no significant bonding interactions between **1** and the ethoxycarbonyl isothiocyanate solvate.

In solution compound **1** slowly dissociates to form the dithiocarbamic acid **2** and ethoxycarbonyl isothiocyanate as shown by ^{1}H-NMR analysis. Separation of the reaction mixture by column chromatography yielded pale yellow **2** in 85%. Compound **2** was characterized by IR and ^{1}H-NMR spectroscopy. The S−H vibration is observed at 2476 cm^{-1} in the region that is characteristic of this group.[9] Efforts to obtain crystals of **2** suitable for X-ray analysis have been unsuccessful.

Compound **2** decomposes when allowed to stand in the open air, and is converted to a dimer **3** of the dithiocarbamic acid **2**. Crystals of **3** suitable for single crystal X-ray diffraction analysis were obtained and the analysis has been completed. An ORTEP diagram of the molecular structure of **3** is shown in Figure 2.

Figure 2. ORTEP diagram of $[EtO_2CN(H)CS_2]_2$ (**3**)[a]

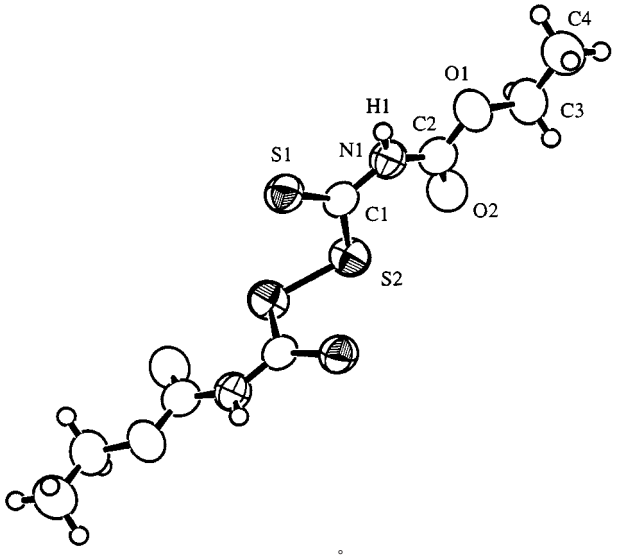

[a] Selected interatomic distances (A) and angles (°): S(2)−S(2′) 2.034(3), S(2)−C(1) 1.780(4), S(1)−C(1) 1.631(4), C(1)−N(1) 1.364(6), C(2)−O(1) 1.330(5), C(2)−O(2) 1.200(5); S(1)−C(1)−S(2) 125.3(3), N(1)−C(1)−S(1) 120.9(3), N(1)−C(1)−S(2) 113.8(3), C(1)−N(1)−C(2) 128.1(5).

Due to crystal symmetry only half of the molecule is present in the asymmetric unit. The two halves are related by a C_2 rotation. A similar situation was observed in both the structure of tetramethylthiuram disulfide and the structure of dipyrrolidylthiuram disulfide (space group *C*2/*c*).[10a][10b][10c] Compound **3** is a bis(ethoxycarbonyl)thiuram disulfide formed by the oxidation and coupling of two molecules of **2**. The geometry about C(1) of the S_2CN group is essentially planar. These two groups are connected by a S−S single bond with a C−S−S−C torsion angle of −86.2(3)°. The configuration about the S−S bond is similar to that found in the structures of other thiuram disulfides $(S_2CNR_2)_2$ [R_2 = Me_2, Et_2, $(CH_2)_4$, $(CH_2)_5$, Et, cyclo-C_6H_{11}].[10] The S−S bond distance 2.034(2) A, is slightly longer than that found for other thiuram disulfides 1.995−2.009.[11] However, an even longer S−S bond distance, 2.069(1) A, with a *trans*-C−S−S−C torsion angle has been found in a centric thiuram disulfide, tetraisopropylthiuram disulfide.[11] The ^{1}H-NMR spectrum of **3** shows only one set of resonances for the ethyl group and only one deshielded resonance for the hydrogen atoms bonded to nitrogen atoms at δ = 9.23 (s, br, 2 H, NH). This is consistent with the fact that the two halves of the molecule are symmetry equivalent.

The formation of **1** can be explained by the combination of one equivalent of **2** [formed by the series of reactions (1) and (2) of the isothiocyanate with water and H_2S] with two equiv. of the isothiocyanate. Mechanistically, this could occur by either of two mechanisms shown in Scheme 1: (1) The addition of the S−H bond to one of the two C−N double bonds of a dimer such as **A** formed by the combi-

nation of two equiv. of the ethoxycarbonyl isothiocyanate. The hydrogen atom is added to the nitrogen atom and the sulfur atom is added to the carbon atom. While there have been several well documented examples of adducts containing four membered rings formed by the addition of carbodiimides to isothiocyanates,[12] the isothiocyanate dimers are not yet well characterized[4]; (2) alternatively the dithiocarbamic acid could combine with the isothiocyanates in a sequential fashion. The combination of **2** with one equiv. of the ethoxycarbonyl isothiocyanate could yield a thiuram monosulfide **C**. A variety of stable thiuram monosulfide derivatives have been characterized.[13]

Scheme 1

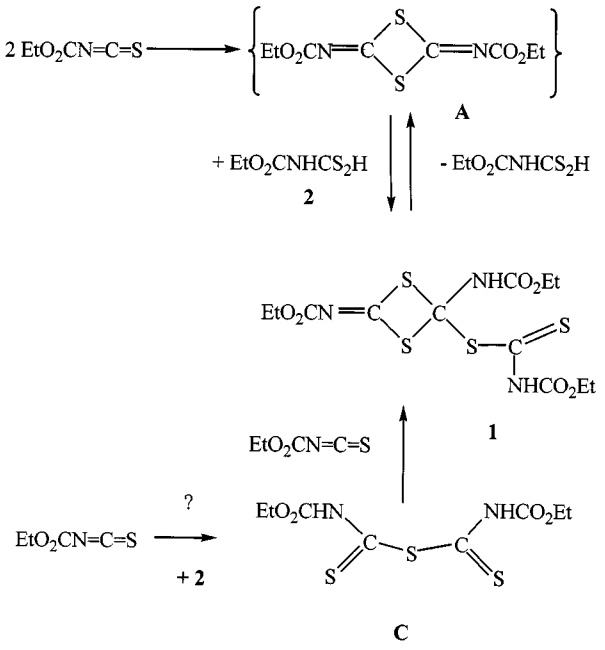

The addition of an equivalent of the ethoxycarbonyl isothiocyanate across one of the C=S double bonds in the thiuram monosulfide **C** could give the product **1**. Complex **1** is stable in the solid state, but it is readily dissociated into compound **2** and free isothiocyanate when dissolved in chloroform. This fact would support the first mechanism (microscopic reverse of the dissociation) as the mechanism of the formation of **1**.

Compound **2** can be obtained in a pure form when **1** is passed over a silica gel chromatography column. However, like most dithiocarbamic acids,[9][11][14] it is slowly oxidized upon standing in air to yield the corresponding thiuram disulfide **3**.

These studies were supported by the *Division of Chemical Sciences of the Office of Basic Energy Sciences of the U. S. Department of Energy*. Support for an upgrade of the NMR facilities at the University of South Carolina was provided by an *NSF ARI grant*, Grant No. CHE-9601723.

Experimental Section

General: Unless specified otherwise, all reactions were performed under an atmosphere of nitrogen. All solvents were appropriately dried and degassed prior to use. Ethoxycarbonyl isothiocyanate were purchased from Aldrich and freshly distilled prior to use. – TLC separations were performed in air by using silica gel (60 A, F_{254}) on plates (whatman, 0.25 mm). – Elemental analyses were performed by Desert Analytics, Tucson, AZ. – Mass spectra were obtained with a VG Model 70SQ mass spectrometer (direct inlet, electron impact ionization).

Preparation of [EtO$_2$CN=CS$_2$C{N(H)CO$_2$Et}{S$_2$CN(H)CO$_2$Et}] (**1**): A 60.0-µl amount (3.34 mmol) of distilled H_2O was added to a 200-µl amount (1.70 mmol) of $EtO_2CN=C=S$ in a small capped vial, and the mixture was simply allowed to stand at room temp. for 2 d. Pale yellow crystals formed and were separated. The crystals were washed with 10 × 1 ml of hexane and dried in vacuo. This yielded 175.6 mg (75%) of **1** with one equiv. of ethoxycarbonyl isothiocyanate. – ^{1}H NMR ($CDCl_3$): δ = 9.02(s, 1 H, NH), 7.23 (s, 1 H, NH), 4.27(q, $^3J_{H-H}$ = 7.1 Hz, 2 H, O*CH*$_2$Me), 4.24 (q, $^3J_{H-H}$ = 7.1 Hz, 2 H, O*CH*$_2$Me), 4.15 (q, $^3J_{H-H}$ = 7.1 Hz, 2 H, O*CH*$_2$Me), 4.10(q, $^3J_{H-H}$ = 7.1 Hz, 2 H, O*CH*$_2$Me), 1.32(t, $^3J_{H-H}$ = 7.1 Hz, 3 H, *CH*$_3$), 1.31(t, $^3J_{H-H}$ = 7.1 Hz, 3 H, *CH*$_3$), 1.25(t, $^3J_{H-H}$ = 7.1 Hz, 3 H, *CH*$_3$), 1.24(t, $^3J_{H-H}$ = 7.1 Hz, 3 H, *CH*$_3$). – $C_{16}H_{22}N_4O_8S_5$ (558.67): calcd. (found): C 33.71 (33.16), H 4.01 (4.12), N 9.83 (9.89).

Transformation of **1** *to EtO$_2$CNHCS$_2$H* (**2**): (a) A 400.0 mg amount (0.72 mmol) of **1**·(EtO_2CNCS) was dissolved in a minimum amount of CH_2Cl_2. The solution was transferred to a silica gel column and was eluted with a CH_2Cl_2/ethylacetate (6:1) solvent mixture to yield an orange band of EtO_2CNHCS_2H (**2**) (140 mg, 85% yield). – IR (CH_2Cl_2): ν = 3365 cm^{-1} (N–H), 2476(S–H), 1755(C=O). – ^{1}H NMR ($CDCl_3$): δ = 8.98 (s, br, 1 H, NH), 6.56 (s, br, 1 H, SH), 4.29 (q, $^3J_{H-H}$ = 7.1 Hz, 2 H, O*CH*$_2$Me), 1.33 (t, $^3J_{H-H}$ = 7.1 Hz, 3 H, *CH*$_3$).

(b) A 5.0 mg amount of **1**·($EtO_2CN=C=S$) was dissolved in 0.6 ml of $CDCl_3$ and placed in a 5-mm NMR tube at 25°C. The transformation of **1** was followed by ^{1}H-NMR spectroscopy. After 24 h, compound **1** was converted to **2** and $EtO_2CN=C=S$ completely.

Transformation of **2** *to (EtO$_2$CNHCS$_2$)$_2$* (**3**): A 15.0 mg amount (0.091 mmol) of **2** was dissolved in 5 ml of CH_2Cl_2. The solution was stirred at room temp. in open air for 48 h. After the solvent was removed, the residue was redissolved in a CH_2Cl_2/C_6H_6 (3:1) solvent mixture at room temp. Colorless crystals formed were collected and washed with 5 × 0.5 ml of hexane. This yield 9.2 mg (62%) of $[EtO_2CN(H)CS_2]_2$ (**3**). – ^{1}H NMR ($CDCl_3$): δ = 9.23 (s, br, 2 H, NH), 4.31 (q, $^3J_{H-H}$ = 7.1 Hz, 4 H, O*CH*$_2$Me), 1.35 (t, $^3J_{H-H}$ = 7.1 Hz, 6 H, *CH*$_3$). – $C_8H_{12}N_2O_4S_4$ (328.43): calcd. (found): C 29.26 (29.40), H 3.68 (3.44), N 8.53 (8.25).

X-ray Structural Analyses of **1** *and* **3**: Crystals of **1** suitable for X-ray diffraction analysis were obtained by crystallization of an $EtO_2CN=C=S$ solution at −4°C. Crystals of **3** suitable for X-ray diffraction analysis were obtained by slow evaporation of solvent from a CH_2Cl_2/benzene (3:1) solution at 25°C. The crystals used in intensity measurements were mounted in thin-walled glass capillaries. Diffraction measurements for **1** and **3** were made on a Rigaku AFC6S fully automated four-circle diffractometer using graphite-monochromated Mo-K_α radiation. The unit cells were determined and refined from 15 randomly selected reflections obtained by using the AFC6S or AFC5R automatic search, center, index, and least-squares routines. All data processing was performed on a Silicon Graphics Indigo2 computer by using the TEXSAN structure solving program library obtained from the Molecular Structure Corp., The Woodlands, TX. Neutral atom scattering factors were calculated by the standard procedures.[15a] Anomalous dispersion corrections were applied to all non-hydro-

gen atoms.[15b] Lorentz-polarization (*Lp*) and absorption corrections were applied in each analysis. Both structures were solved by a combination of direct methods (MITHRIL) and difference Fourier syntheses, and all nonhydrogen atoms were refined with anisotropic thermal parameters. Full matrix least-squares refinements minimized the function: $\Sigma_{hkl}w(|F_o| - |F_c|)^2$, where $w = 1/\sigma(F)^2$, $\sigma(F) = \sigma(F_o^2)/2F_o$, and $\sigma(F_o^2) = [\sigma(I_{raw})^2 + (0.02 \cdot I_{net})^2]^{1/2}/Lp$.

Compound **1** crystallized in the triclinic crystal system. The space group *P*1bar was assumed and confirmed by the successful solution and refinement of the structure. One equiv. of $EtO_2CN{=}C{=}S$ (unreacted reagent) cocrystallized with the product in the lattice. This was included in the calculations employing anisotropic thermal parameters for the sulfur atom S(5), a fixed thermal parameter for the carbon atom C(14) and isotropic thermal parameters for the other nonhydrogen atoms. In all cases, the positions of all hydrogen atoms were calculated by assuming idealized geometries with all C−H distances at 0.95 A. The scattering contributions of calculated hydrogen atoms were added to the structure factor calculations, but their positions were not refined.

Table 1. Crystal data for compounds **1** and **3**

Compound	**1**	**3**
Empirical formula	$S_5O_8N_4C_{16}H_{22}$	$S_4O_4N_2C_8H_{12}$
Molecular mass	558.67	328.43
Crystal system	triclinic	monoclinic
Lattice parameters:		
a (A)	10.168(2)	18.182(5)
b (A)	14.148(3)	5.484(2)
c (A)	9.431(2)	14.211(4)
α (°)	90.84(2)	90.00
β (°)	93.21(2)	90.84(2)
γ (°)	74.53(2)	90.00
V (A^3)	1305.5(5)	1416.7(6)
Space group	*P*1bar(no. 2)	*C2/c* (no. 15)
Z value	2	4
ρ_{calc} (g/cm^3)	1.42	1.54
μ(Mo-K_α) (cm^{-1})	4.89	6.76
$2\Theta_{max}$ (°)	45	50
No. obs. ($I>3\sigma$)	2096	640
No. variables	260	106
Goodness of fit (GOF[a])	3.53	1.40
Max shift in final cycle	0.01	0.01
Residuals*: *R*; R_w	0.066; 0.075	0.037; 0.032
Abs. Cor.	Difabs	Difabs
Transmis coeff max/min	1.29/0.76	1.00/0.53
Largest residual Pk (e/A^3)	0.70	0.20

[a] $R = \Sigma_{hkl}(||F_{obs}| - |F_{calc}||)/\Sigma_{hkl}|F_{obs}|$; $R_w = [\Sigma_{hkl}w(|F_{obs}| - |F_{calc}|)^2/\Sigma_{hkl}wF_{obs}^2]^{1/2}$, $w = 1/\sigma^2(F_{obs})$; GOF = $[\Sigma_{hkl}(w(|F_{obs}| - |F_{calc}|)^2)/(n_{data} - n_{vari})]^{1/2}$.

Compound **3** crystallized in the monoclinic crystal system. The systematic absences were consistent with either of the space groups *C2/c* or *Cc*. This structure was solved and refined in the higher symmetry centrosymmetric space group *C2/c*. The hydrogen atom H(1) on the nitrogen atom N(1) was located and the positions of other hydrogen atoms were calculated by assuming idealized geometries. These hydrogen atoms were successfully refined with isotropic thermal parameters.[16]

[1] A. K. Mukerjee, R. Ashare, *Chem. Rev.* **1991**, *91*, 1.
[2] [2a] H. Werner, *Coord. Chem. Rev.* **1982**, *43*, 165. – [2b] W. Bertleff, H. Werner, *Chem. Ber.* **1982**, *115*, 1012. – [2c] K. Itoh, L. Matsuda, F. Ueda, Y. Ishii, J. A. Ibers, *J. Am. Chem. Soc.* **1977**, *99,* 2118. – [2d] C. Bianchini, D. Masi, A. Meli, *J. Organomet. Chem.* **1983**, *247*, C29.
[3] R. D. Adams, M. Huang, *Organometallics.* **1996**, *15*, 3644.
[4] [4a] K. Dickore, E. Kühle, *Angew. Chem.* **1965**, *77*, 429−430; *Angew. Chem. int. Ed. Engl.* **1965**, *4*, 430. – [4b] J. Goerdeler, *Quart. Rep. Sulphur Chem.* **1970**, *5*, 169.
[5] [5a] M. Cowie, J. A. Ibers, Y. Ishii, K. Itoh, I. Matsuda, F. Ueda, *J. Am. Chem. Soc*. **1975**, *97,* 4748. – [5b] M. Cowie, J. Ibers, A. *Inorg. Chem.* **1976**, *15*, 552.
[6] Assony, in *Organic Sulfur Compounds*, (Ed.: N. Kharasch, Pergamon Press Inc., New York. **1961**, vol. 1, Ch. 28, p 326.
[7] D. Coucouvanis, *Prog. Inorg. Chem.* **1979**, *26*, 301; D. Coucouvanis, *Prog. Inorg. Chem.* **1970**, *11*, 233.
[8] R. R. Schumaker, M. Inoue, M. B. Inoue, M. A. Bruck, Q. Fernando, *J. Chem. Soc. Chem. Commun.* **1991**, 719.
[9] M. Sato, N. Fukada, M. Kurauchi, T. Takeshima, *Synthesis* **1981**, 554.
[10] [10a] Y. Wang, J. Liao C. H. Ueng, *Acta Cryst.* **1986**, *C42*, 1420. – [10b] G. A. Williams, J. R. Statham, A. H. White, *Aust J. Chem.* **1983**, *36*, 1371. – [10c] I. Ymen, *Acta Chem. Scand., Ser. B* **1983**, *37*, 707. – [10d] I. L. Karle, J. A. Estlin, K. Britts, *Acta Cryst.* **1967**, *22*, 273. – [10e] V. J. Hall, E. R. T. Tiekink, *Z. Kristallogr.* **1995**, *210*, 701.
[11] V. Kumar, G. Aravamudan, M. Seshasayee, *Acta Cryst.* **1990**, *C46,* 674.
[12] [12a] H. Ulrich, R. Richter, B. Tucker, *Chem. Ber.* **1987**, *120*, 849. – [12b] H. Ulrich, B. Tucker, A. A. R. Sayigh, *J. Am. Chem. Soc.* **1972**, *94*, 3484. – [12c] I. Ojima, N. Inamoto, *Chem. Commun.* **1970**, 1629. – [12d] A. Dondoni, A. Battaglia, *J. Chem Soc., Perkin II*, **1975**, 1475. – [12e] H. Ulrich, B. Tucker, A. A. R. Sayigh, *Tetrahedron* **1996**, *22*, 1565.
[13] P. L. Johnson, I. C. Paul, *J. Chem. Soc. A* **1970**, 1296. – [13b] B. W. Skelton, A. H. White, *Aust. J. Chem.* **1977**, *30*, 1693. – [13c] M. Colapietro, A. Domenicano, A. Vaciago, *Acta Cryst.* **1976**, *B32* 2581.
[14] E. E. Reid, in *Organic Chemistry of Bivalent Sulfur*, Chemical Publishing, New York. **1963**, vol. 1, Ch. 1, and vol. 4, Ch. 2.
[15] [15a] *International Tables for X-ray Crystallography,* Kynoch Press, Birmingham, England, **1975**, Vol. IV, Table 2.2b, pp99−101. – [15b] *Ibid.*, Table 2.3.1, pp 149−150.
[16] Crystallographic data (excluding structure factors) for the structures reported in this paper have been deposited with the Cambridge Crystallographic Data Centre as supplementary publication no. CCDC-101126 (**1**) and CCDC-101149 (**3**). Copies of the data can be obtained free of charge on application to The Director, CCDC, 12 Union Road, Cambridge CB2 1EZ, UK [Fax: (int. code) +44(1223)336-033, E-mail: deposit@chemcrys.cam.ac.uk, www: http://www.ccdc.cam.ac.uk].

[98072]

Water-Soluble Phosphanes, 10[◇]

Novel Syntheses of Mono- and Bisphosphonated Aromatic Phosphanes by Consecutive Pd-Catalyzed P–C Coupling Reactions and Nucleophilic Phosphanylation – X-ray Structure of $Ph_2P–C_6H_4–m\text{-}PO_3Na_2 \cdot 5.5\ H_2O \cdot$ *i*PrOH

Peter Machnitzki[a], Thomas Nickel[a], Othmar Stelzer*[a], and Claudia Landgrafe[b]

Fachbereich 9, Anorganische Chemie, Bergische Universität–GH Wuppertal[a],
Gaußstraße 20, D-42097 Wuppertal, Germany

Fakultät für Chemie, Lehrstuhl für Analytische Chemie, Ruhr-Universität Bochum[b],
Universitätsstraße 150, D-44780 Bochum, Germany

Received November 14, 1997

Keywords: Pd-catalyzed P–C coupling / Nucleophilic phosphanylation / Mono- and bisphosphonated phosphanes / Monoesters / Water solubility

The triphenylphosphane derivatives **2a** and **5**, bearing one and two phosphonic ester groups, are accessible in high yields by consecutive Pd-catalyzed P–C coupling reactions of *p*-bromoiodobenzene with Ph_2PH and $PhPH_2$, respectively, and then with diethyl phosphite. Ester hydrolysis yields the highly water-soluble sodium salts of mono- and bisphosphonated triphenylphosphane, **3a** and **6**, respectively. On reaction of the *p*- and *m*-fluorophenylphosphonic diethyl esters **7a**, **7b** with Ph_2PK and subsequent ester hydrolysis the isomeric disodium (diphenylphosphano)phenylphosphonates **3a**, **3b** were obtained. The X-ray structure of $Ph_2P(C_6H_4–m\text{-}PO_3Na_2) \cdot 5.5\ H_2O \cdot$ *i*PrOH (space group $Cmc2_1$) has been determined. In the solid state, it forms a layer structure with hydrophilic (PO_3^{2-}, H_2O, *i*PrOH) and hydrophobic (Ph_2P) compartments, in which the PO_3^{2-} anionic groups are not engaged in coordination of the sodium cations.

The introduction of the aqueous two-phase technique may be considered as a cornerstone in the development of homogeneous catalysis over the last two decades. The environmental benefits of using water instead of organic solvents and the ease with which the water soluble catalyst may be separated from the products are the principal advantages of this technique. Water solubility of the complex catalysts is achieved by incorporation of phosphanes bearing cationic[2], anionic[3], or non-charged hydrophilic[4] groups, respectively. The phosphonate group has been employed only very recently as a polar functionality to enhance the solubility of aliphatic and aromatic phosphanes in aqueous media. Thus, DuBois et al.[5] have reported the syntheses of tridentate phosphane ligands bearing $(EtO)_2(O)PCH_2CH_2$ side chains. Köckritz et al.[6] and Schull, Fettinger, and Knight[7] have developed a multistep synthesis for the sodium salts of monophosphonated triphenylphosphane, moderate yields being achieved in both cases. Phosphanorbornadiene monophosphonates are formed by addition of (phenylethynyl)phosphonates to 1-phenyl-3,4-dimethylphosphole[8].

The great potential of phosphonated and phosphinated derivatives of triphenylphosphane as catalyst ligands in two-phase catalysis has been demonstrated by the Pd-catalyzed carbonylation of benzyl chloride[7] and by Suzuki-type C−C coupling reactions[9].

[◇] Part 9: Ref.[1].

Syntheses of Mono- and Bisphosphonated Aromatic Phosphanes Using Consecutive Pd-Catalyzed P−C Coupling Reactions

Previously, we reported a novel synthetic route to multifunctional phosphanes by cross-coupling of aryl halides with primary or secondary phosphanes in the presence of a base and catalytic amounts of a palladium catalyst[10]. Using this method, *p*-bromophenyldiphenylphosphane[11] (**1a**) and bis(*p*-bromophenyl)phenylphosphane[12] (**4**) were obtained in high yields by reaction of *p*-bromoiodobenzene with diphenylphosphane and phenylphosphane, respectively in the presence of 0.1 mol-% $Pd(Ph_3P)_4$ (Eq. 1a, 2a). The *m* and *o* isomers **1b** and **1c** are also accessible by this synthetic procedure.

The final steps in the syntheses of the mixed-ligand phosphanophosphonates required the introduction of the phosphonic ester groups into **1a** and **4**. This was achieved by Pd-catalyzed P−C coupling reactions with diethyl phosphite, $HP(O)(OEt)_2$. The mono- (**2a**)[7] and bisphosphonated (**5**) *p* isomers were formed in high yields (Eq. 1b, 2b). The anionic derivatives **3a** and **6** were obtained by transesterification of **2a** and **5** using Me_3SiBr[14], followed by hydrolysis of the intermediate silyl esters and subsequent neutrali-

 © WILEY-VCH Verlag GmbH, D-69451 Weinheim, 1998 1434−1948/98/0707−1029 $ 17.50+.50/0

Scheme 1

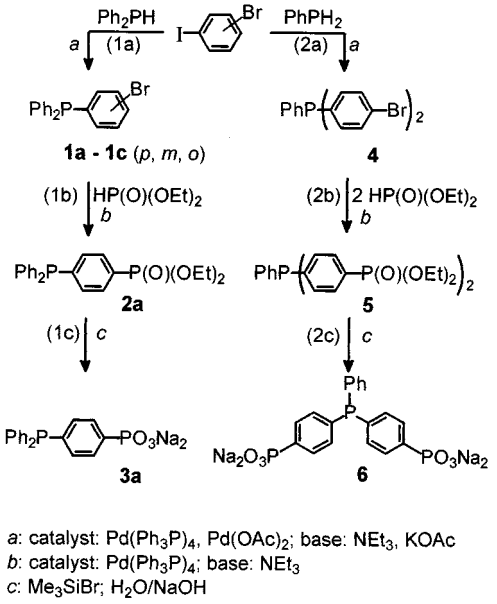

Scheme 2

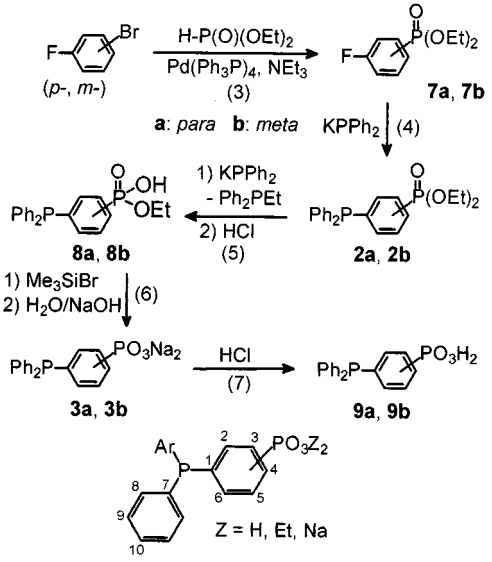

zation of the phosphonic acids with aqueous NaOH (Eq. 1c, 2c). As expected, the solubility of **6**, bearing two polar groups, was much higher (1000−1100 g/kg water, 20°C) than that of **3a** (300−400 g/kg water, 20°C).

Syntheses of *m*- and *p*-Phosphonated Aromatic Phosphanes by a Combination of Pd-Catalyzed P−C Coupling and Nucleophilic Substitution

Nucleophilic phosphanylation of fluorobenzene derivatives bearing electron-withdrawing substituents[1][3b][15] may be employed for the synthesis of a great variety of water-soluble phosphanes. In combination with the Pd-catalyzed coupling[10], the reaction has many attractive features as a general P−C bond-formation method. This is illustrated by the syntheses of the *p* and *m* isomers **2a**, **2b** of monophosphonated triphenylphosphane (Eq. 4). The starting materials, **7a**[16a], **7b**[16b], were obtained by P−C coupling reactions of *p*- and *m*-bromofluorobenzene with diethyl phosphite using catalytic amounts of $Pd(Ph_3P)_4$ in the presence of NEt_3 as the base (Eq. 3). This method was found to be more efficient than the multistep syntheses reported in the literature for **7a**[16a] and **7b**[16b].

Upon treatment of **7a** with Ph_2PK, a mixture of the expected diester **2a** and the potassium salt of the monoester **8a** was formed (Eq. 4, 5). The diester **2a** is formed initially until about half an equivalent of Ph_2PK has been added. The addition of further Ph_2PK yields Ph_2PEt and the potassium salt of **8a** as a result of dealkylation of the ester group in **2a** or **7a**. This indicates that in the initial stages of the reaction nucleophilic phosphanylation is faster than dealkylation. In contrast to our results, from a similar reaction of the *p* isomer **7a**, using Ph_2PLi instead of Ph_2PK, Köckritz et al.[6] obtained only the diester **2a** and, surprisingly, no dealkylation products were detected. However, the diester **2a** was formed only in moderate yields and no experimental details were given. Phosphanylation of diethyl *m*-fluorophenylphosphonate (**7b**) with Ph_2PK in THF solution proceeded much more slowly than that of the corresponding *p* isomer **7a**, the anion of **8b** being formed exclusively.

After acidification of the reaction mixtures, the monoesters **8a**, **8b** were precipitated as colorless crystals (Eq. 4, 5). Transesterification of **8a**, **8b** with Me_3SiBr and subsequent reaction of the intermediate silyl esters with NaOH gave the disodium salts **3a** and **3b**, respectively (Eq. 6), in overall yields much higher than those reported previously in the literature[7]. The free phosphonic acids **9a**, **9b** were precipitated from aqueous solutions of **3a**, **3b** on acidification with HCl (Eq. 7).

NMR-Spectroscopic Identification of 1a−11b

The $\delta P(P^{III})$ values of the phosphonated phosphanes differ only marginally from that of Ph_3P[11][17a] ($\delta P = -5.9$ to -8.0), with $\delta P(P^V)$ values (20.0−8.9) falling in the range typical for aromatic phosphonic acids and their esters[17b]. Assignment of all $^{13}C\{^1H\}$-NMR signals of **1a**−**1c**, **2a**, **3a**, **3b**, **4**, **5**, **6** and **7a**, **7b**, **9a**, **9b** was achieved with the aid of DEPT experiments[18a] and by comparison of the δC values and P−C coupling constants with the relevant data for Ph_3P[18b]. Further support was gained from the relative magnitude of the coupling constants $^nJ(PC)$, which decrease in the order $^2J(PC) > {}^3J(PC) > {}^4J(PC)$, with $^1J(PC)$ being smaller than $^2J(PC)$[18c]. Large coupling constants (160−190 Hz) are observed for the signals of the carbon atoms (C3 or C4, respectively) bound to P^V[18d] (for the numbering of the carbon atoms in the Experimental Section see Scheme 2).

The protons of the CH_2 groups of the $P(O)(OEt)_2$ substituents in **2a**, **7a**, and **7b** are diastereotopic[19] (Figure 1a, **7a**). In the ^{1}H-NMR spectra, complicated multiplet patterns are observed, representing the AB parts of ABM_3X spin systems [A, B = $H_{a,b}(CH_2)$, M = $H(CH_3)$, X = ^{31}P]. Analysis of these line patterns (Figure 1b) could be ac-

complished in the case of **7a** using $^1H\{^1H(CH_3)\}$ homo nuclei decoupling experiments (Figure 1c).

Figure 1. (a) Newman projection along the P···(O)···$C(H_2)$ axis. – (b) ^{1}H-NMR spectrum of **7a** (experimental/calculated); δH_a = 4.06, δH_b = −4.12, $^2J(H_aH_b)$ = 10.2, $^3J(H_aP)$ = 8.2, $^3J(H_bP)$ = 7.8, $^3J(HH)$ = 7.1 Hz. – (c) $^1H\{^1H(CH_3)\}$-NMR spectrum of **7a**, P(O)(O−CH_2−CH_3)$_2$ group

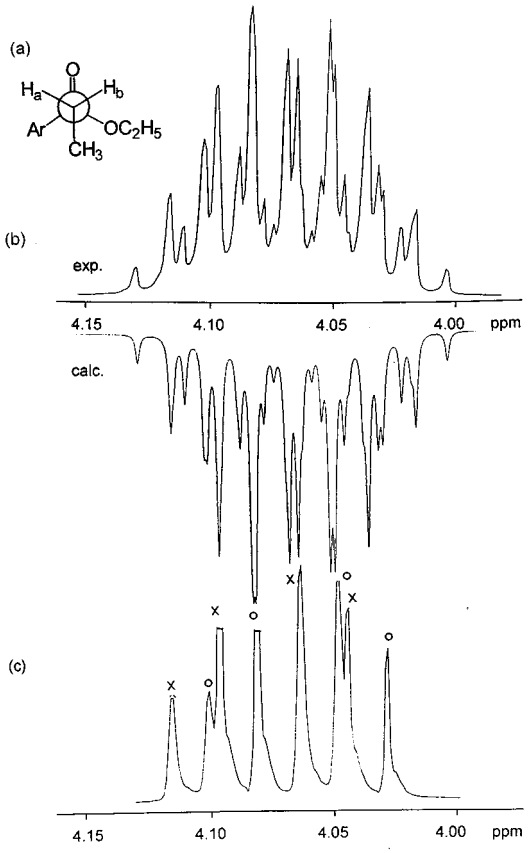

X-ray Structure of $Ph_2P(C_6H_4-m\text{-}PO_3Na_2)\cdot 5.5\ H_2O\cdot i$PrOH

Colorless crystals of the composition $Ph_2P(C_6H_4-m\text{-}PO_3Na_2)\cdot 5.5\ H_2O\cdot i$PrOH were formed at the interface between the two layers obtained on addition of 2-propanol to a concentrated aqueous solution of **3b**. The results of an X-ray structural analysis are shown in Figures 2 and 3, crystallographic data are collected in Table 1, and selected bond lengths and angles are given in the caption to Figure 2. A comparison of the structural parameters of triphenylphosphane[20] with those of the isolated diphenylphosphanophenyl-*m*-phosphonate dianion of **3b** and its *p* isomer **3a**[7], reveals that the PO_3^{2-} group in the *p* or *m* position of the aromatic ring system has only marginal influence on the geometry of the triarylphosphane subunit. The propeller-like arrangement of the phenyl rings (Figure 2), which are each rotated in the same sense, is found in all three structures. In contrast to $Na_2[Ph_2P(C_6H_4-p\text{-}PO_3)(H_2O)_3(CH_3OH)](CH_3OH)$[7], which is dimeric and contains two formula units in the unit cell, the phosphorus atom in the phosphonate group of $Na_2[Ph_2P(C_6H_4-m\text{-}PO_3)\cdot 5.5\ H_2O\cdot i$PrOH] displays only a slightly distorted tetrahedral geometry. The O−P−O bond angles and P−O bond lengths are identical within experimental standard deviation, and the P−O distances fall within the typical range[21][22].

Figure 2. Structure of the anion of **3b**[a]

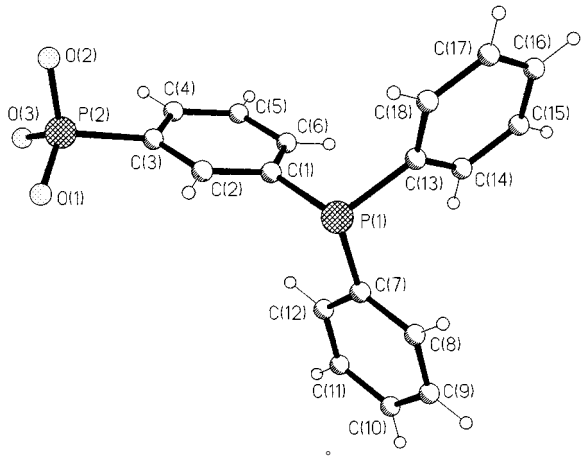

[a] Selected interatomic distances [A] and angles [°]: P(1)−C(1) 1.843(5), P(1)−C(7) 1.836(8), P(1)−C(13) 1.842(8), P(2)−C(3) 1.823(5), P(2)−O(1) 1.522(6), P(2)−O(2) 1.520(7), P(2)−O(3) 1.521(7); C(1)−P(1)−C(7) 103.7(4), C(7)−P(1)−C(13) 101.9(4), C(1)−P(1)−C(13) 102.6(4), C(2)−C(1)−P(1) 116.6(4), C(6)−C(1)−P(1) 123.3(4), O(1)−P(2)−O(2) 111.9(4), O(1)−P(2)−O(3) 111.6(4), O(2)−P(2)−O(3) 110.9(4).

Within the unit cell, the sodium cations are solvated by water and 2-propanol, thus forming a three-dimensional network supported by O···H−O hydrogen bonding (Figure 3). The shortest distance between the oxygen atoms of the $Ph_2P(C_6H_4-m\text{-}PO_3^{2-})$ dianions and the sodium atoms is 2.987(6) A [O(1)−Na(1)]. This is around 0.45−0.60 A larger than that of other Na−O interactions in the structure, implying that the phosphonate groups are not engaged in the primary coordination sphere of the sodium. The Na···O(P) distances found in $Na_2[Ph_2P(C_6H_4-p\text{-}PO_3)(H_2O)_3(CH_3OH)](CH_3OH)$[7] [Na(1)−O(2) 2.448(3), Na(2)−O(1) 2.249(3) A] are shorter than the closest Na−O contact in $Na_2[Ph_2P(C_6H_4-m\text{-}PO_3)\cdot 5.5\ H_2O\cdot i$PrOH] [Na(1)−O(1) 2.987(6) A]. Interestingly, the structure contains sodium cations in three different environments. Na(1) is coordinated to five water molecules in a trigonal-bipyramidal arrangement (Na···O distances 2.30−2.58 A), two of the water molecules [O(13), O(14)] form bridges to the hexacoordinate Na(2) (Na···O distances 2.36−2.46 A), which in turn is connected to Na(3) and symmetry-equivalent Na(3a) via two water molecules [O(21a), O(21)] in axial positions. Na(3a) is pentacoordinated, with the two axial positions in a strongly distorted trigonal-bipyramid being occupied by bridging oxygen atoms [O(21a) and O(12c)]. 2-Propanol and two water oxygen atoms lie in the equatorial plane of Na(3), with one of the latter [O(22)] bridging the symmetry-related Na cations [Na(3) and Na(3a)]. The closest cation−cation contact is 3.314(6) A [Na(2)···Na(3)].

This work was supported by the *Bundesministerium für Bildung, Wissenschaft, Forschung und Technologie* and the *Fonds der Chemischen Industrie*. The *Hoechst AG* is thanked for financial support and generous gifts of chemicals

Figure 3. Solid-state structure of **3b**·5.5 H_2O·*i*PrOH

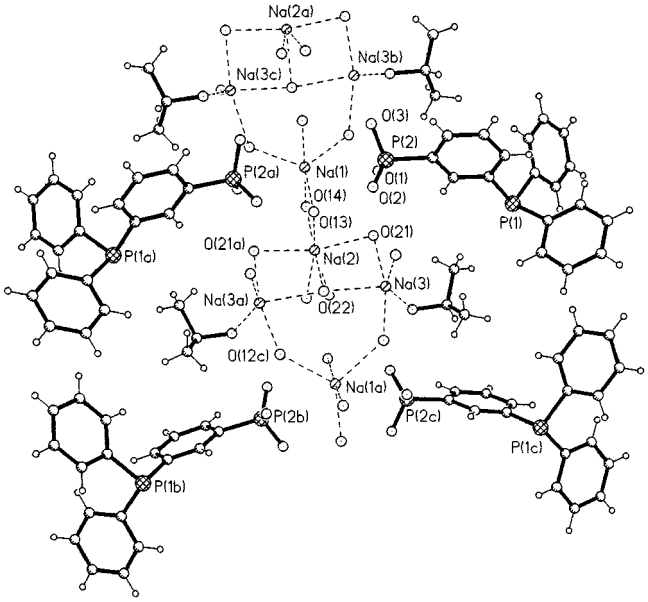

Experimental Section

For experimental details see Part 9 of this series[1]. Phenylphosphane, diphenylphosphane[23], and $Pd(Ph_3P)_4$[13] were prepared according to literature methods. Ph_2PK, 2-, 3-, and 4-bromoiodobenzene, 3- and 4-bromofluorobenzene, as well as bromotrimethylsilane were purchased from Aldrich Chemical Co. and used without further purification.

Preparation of **1a**−**1c** *by Palladium-Catalyzed Coupling of 2-, 3-, and 4-Bromoiodobenzene with Ph_2PH:* A mixture of 20.0 g (70.8 mmol) of the appropriate bromoiodobenzene, 7.64 g (78.0 mmol) of potassium acetate, and 28.4 ml of a $5.0 \cdot 10^{-3}$ M solution of palladium(II) acetate in dimethylacetamide was dissolved in 120 ml of dimethylacetamide. To this solution, 13.16 g (70.8 mmol) Ph_2PH was added and the mixture was heated for 5 d at 130°C. The reaction mixture was then poured into 200 ml of deoxygenated water and the resulting suspension was extracted with 200 ml of dichloromethane. The organic phase was separated, washed with 100 ml of saturated aqueous KCl solution, and dried with magnesium sulfate. After removal of the solvent under reduced pressure (20°C, 10 mbar), the residue was distilled in vacuo (0.1 mbar) at 200−300°C. Yields: 15.0 g (62%) **1a**, 18.4 g (76%) **1b**, 18.0 g (75%) **1c**. For further purification, **1a**−**1c** were recrystallized from water/ethanol.

1a: $C_{18}H_{14}BrP$ (341.2): calcd. C 63.36, H 4.14; found C 63.32, H 4.18. − MS: $[M^+]$: *m/z* = 342 (^{81}Br), 340 (^{79}Br). − $^{31}P\{^1H\}$ NMR (C_6D_6): δP = −4.8. − $^{13}C\{^1H\}$ NMR (C_6D_6): δC (C1−C10) = 137.0 (14.2), 135.4 (20.3), 131.8 (7.1), 123.5, 131.8 (7.1), 135.4 (20.3), 137.2 (12.2), 133.9 (19.3), 128.7 (7.1), 128.9. − **1b**: $C_{18}H_{14}BrP$ (341.2): calcd. C 63.36, H 4.14; found C 63.40, H 4.21. − MS: $[M^+]$: *m/z* = 342 (^{81}Br), 340 (^{79}Br). − $^{31}P\{^1H\}$ NMR (C_6D_6): δP = −3.3. − $^{13}C\{^1H\}$ NMR ($CDCl_3$): δC (C1−C10) = 141.4 (16.3), 136.4 (20.3), 123.6 (7.1), 132.1, 123.6 (7.1), 136.4 (19.3), 136.8 (12.2), 134.2 (19.3), 129.1 (7.1), 129.5. − **1c**: $C_{18}H_{14}BrP$ (341.2): calcd. C 63.36, H 4.14; found C 63.30, H 4.22. − MS: $[M^+]$: *m/z* = 342 (^{81}Br), 340 (^{79}Br). − $^{31}P\{^1H\}$ NMR (C_6D_6): δP = −3.3. − $^{13}C\{^1H\}$ NMR (C_6D_6): δC (C1−C10) = 139.7 (13.2), 130.5 (30.0), 133.2 (2.0), 130.1, 127.4, 134.7, 136.6 (12.2), 134.3 (21.4), 128.8 (7.1), 129.0.

Preparation of **4** *by Pd-Catalyzed Coupling of 4-Bromoiodobenzene with $PhPH_2$:* A Schlenk flask was charged with 250 ml of acetonitrile, 7.91 g (71.8 mmol) of phenylphosphane, 40.65 g (143.7 mmol) of 4-bromoiodobenzene, and 16.00 g (158.1 mmol) of triethylamine. The mixture was deoxygenated and 1.66 g (1.43 mmol, 1 mol-%) of $Pd(Ph_3P)_4$ was added. After heating the reaction mixture under reflux for 24 h, the solvent was removed in vacuo, and the residue was dissolved in 200 ml of dichloromethane. The resulting solution was washed with three 100-ml aliquots of water. The organic phase was separated and dried with magnesium sulfate. After removal of the solvent under reduced pressure (30°C, 10 mbar), the residue was distilled in vacuo (0.1 mbar) at 200−300°C. Yield: 19.03 g (63%). − **4**: $C_{18}H_{13}Br_2P$ (420.1): calcd. C 51.47, H 3.12; found C 51.12, H 3.25. − MS: $[M^+]$: *m/z* = 418 (^{79}Br), 420 (^{81}Br,^{79}Br), 422 (^{81}Br). − $^{31}P\{^1H\}$ NMR ($CDCl_3$): δP = −6.0; $^{13}C\{^1H\}$ NMR ($CDCl_3$): δC (C1−C10) = 135.9 (12.2), 135.1 (20.3), 131.7 (7.1), 123.6, 131.7 (7.1), 135.1 (20.3), 136.0 (10.2), 133.6 (19.3), 128.7 (7.1), 129.2.

Preparation of **2a**/**3a** *and* **5**/**6**: To a solution of 2.0 g (5.9 mmol) of **1a** or 4.26 g (10.1 mmol) of **4** in 40 or 80 ml of toluene, 0.89 g (6.45 mmol) or 3.08 g (22.3 mmol) of $HP(O)(OEt)_2$ and 0.65 g (6.45 mmol) or 2.26 g (22.3 mmol) of NEt_3 were added. After deoxygenation in vacuo, 68 mg (0.06 mmol, 1 mol-%) or 0.23 g (0.2 mmol, 1 mol-%) of $Pd(Ph_3P)_4$ was added. The reaction mixtures were then heated to 80°C for 50 h or 72 h. After cooling to ambient temperature and washing with three 25- or 50-ml aliquots of water, the toluene phases were collected and dried with $MgSO_4$. Evaporation of the solvent in vacuo left **2a** and **5** as yellow, viscous oils. Yields: 1.46 g (62%) **2a**, 3.78 g (70%) **5**. − **2a**: $^{31}P\{^1H\}$ NMR ($CDCl_3$): δP = −3.8 (P^{III}), 19.4 (P^V). − **5**: MS: $[M^+]$: *m/z* = 534. − $^{31}P\{^1H\}$NMR ($CDCl_3$): δP = −3.4 (P^{III}), 19.3 (P^V).

To a solution of 3.79 g (7.1 mmol) of **5** in 50 ml of dichloromethane at room temperature 6.5 g (42.4 mmol) of Me_3SiBr were added with stirring. After 12 h, all volatiles were removed in vacuo (60°C, 0.01 mbar) and the residual oily liquid was taken up in 50 ml of acetone. To the resulting solution 1.02 g (56.7 mmol) of water was added and the mixture was stirred at ambient temperature for 2 h. Thereafter, all volatiles were removed in vacuo (20°C, 0.01 mbar), and the pale-yellow solid (the free phosphonic acid) thus obtained was redissolved in 20 ml of conc. NaOH solution. On pouring this solution into 200 ml of ethanol, **6** was precipitated as pale-yellow crystals, which were separated by suction using a fritted Buchner funnel. The residue was washed with two 10-ml aliquots of ethanol and dried in vacuo (60°C, 0.01 mbar). Yield: 2.58 g (71.2%) **6**.

3a was obtained in high yield by the analogous procedure using **2a** as the starting material.

3a: $^{31}P\{^1H\}$ NMR (D_2O): δP = −5.5 (P^{III}), 12.0 (P^V). − **6**: $C_{18}H_{13}O_6Na_4P_3 \cdot 1.5\ H_2O$ (537.2): calcd. C 40.25, H 3.00; found C 40.19, H 3.24. − $^{31}P\{^1H\}$ NMR (D_2O): δP = −6.0 (P^{III}), 12.0 (P^V). − $^{13}C\{^1H\}$-NMR (D_2O): δC (C1−C10) = 138.5 (5.1, 3.1), 135.1 (18.8, 13.2), 132.8 (8.1, 8.1), 144.3 (165.8), 132.8 (8.1, 8.1), 135.1 (18.8, 13.2), 138.3 (5.1), 136.0 (19.3),131.2 (7.1), 131.7.

Preparation of **7a**, **7b**: A Schlenk flask was charged with 200 ml of toluene, 20.0 g (114.3 mmol) of 4-bromofluorobenzene or 25.0 g (142.8 mmol) of 3-bromofluorobenzene, 17.3 g (125.7 mmol) or 21.7 g (157.1 mmol) of $HP(O)(OEt)_2$, and 12.7 g (125.7 mmol) or 15.9 g (157.1 mmol) of NEt_3. Dissolved oxygen was removed by freeze-thaw cycles and after addition of 5.3 g (4.6 mmol, 4 mol-%) or 6.6 g (5.7 mmol, 4 mol-%) of $Pd(Ph_3P)_4$ the reaction mixture was heated to 70−80°C for 24 h. Thereafter, the mixture was washed with three 200-ml aliquots of water. The toluene phase was

dried with $MgSO_4$. The liquid obtained after removal of the solvent in vacuo was fractionated. Yields: 21.5 g (81%) **7a**, 28.0 g (84%) **7b**.

7a: $C_{10}H_{14}FO_3P$ (232.2): calcd. C 51.73, H 6.08, P 13.34; found C 51.94, H 6.18, P 13.13. – B.p. 96°C, 0.4 mbar. – $^{31}P\{^1H\}$ NMR ($CDCl_3$): δP = 18.9 [^5J(PF) = 1.4]. – $^{13}C\{^1H\}$ NMR ($CDCl_3$): δC (C1–C6) = 165.4 [4.1, 253.8 ^1J(CF)], 115.8 (16.3, 21.4), 134.4 (11.2, 8.6), 124.7 (192.8, 3.6), 134.4 (11.2, 8.6), 115.8 (16.3, 21.4), 62.2 (5.6, CH_2), 16.3 (6.6, CH_3). – **7b**: $C_{10}H_{14}FO_3P$ (232.2): calcd. C 51.73, H 6.08; found C 51.64, H 6.13. – B.p. 96°C, 0.4 mbar. – $^{31}P\{^1H\}$ NMR ($CDCl_3$): δP = 17.4 [^4J(PF) = 8.6]. – $^{13}C\{^1H\}$ NMR ($CDCl_3$): δC (C1–C6) = 162.3 (21.2, 249.2), 118.3 (10.2, 22.4), 131.2 (188.2, 6.1), 127.3 (9.2, 3.1), 130.4 (17.3, 8.1), 119.3 (3.1, 21.4), 62.2 (6.1, CH_2), 16.1 (6.1, CH_3).

Nucleophilic Phosphination of **7a** *with Ph_2PK in a 1:1 Molar Ratio:* To the solution of 1.63 g (7.0 mmol) **7a** in 20 ml of THF 17 ml of a 0.5 M solution of Ph_2PK in THF (8.5 mmol) was added at room temp. After completion of the addition, the solvent was evaporated under reduced pressure. From the oily residue Ph_2PEt formed during the reaction was removed at 100°C, 0.01 mbar using a short-path distillation apparatus. The remaining solid was extracted with a mixture of 20 ml of water and CH_2Cl_2. The organic phase was separated and dried with magnesium sulfate. After removal of the solvent in vacuo, **2a** was obtained as a colorless oil. Yield: 1.52 g (54.5%).

2a: $C_{22}H_{24}O_3P_2$ (398.4): calcd. C 66.33, H 6.07, P 15.55; found C 65.49, H 6.29 P 14.60. – MS: [M^+]: *m/z* = 398. – $^{31}P\{^1H\}$ NMR ($CDCl_3$): δP = –3.8 (P^{III}), 19.4 (P^V). – $^{13}C\{^1H\}$ NMR ($CDCl_3$): δC (C1–C10) = 143.6 (15.3, 3.1), 133.2 (18.3, 14.2), 131.6 (6.1, 12.2), 128.7 (188.2), 131.6 (6.1, 12.2), 133.2 (18.3, 14.2), 136.2 (10.2), 134.0 (20.3), 128.8 (7.1), 129.3, 62.2 (5.1, CH_2), 16.5 (6.1, CH_3).

Synthesis of **8a** *and* **8b**: A 0.5 M solution of Ph_2PK (250 mmol) in 500 ml of THF was added to 27.86 g (120 mmol) of **7a** dissolved in 500 ml of THF over a period of 3 h at 20°C. After completion of the addition, the reaction mixture was stirred for a further 1 h. Thereafter, the solvent was distilled off under normal pressure and the remaining residue was partitioned between 500 ml of water and 500 ml of dichloromethane. The organic phase was separated and dried with magnesium sulfate. The residue obtained after evaporation of the solvent at normal pressure was fractionated in vacuo (0.1 mbar) to afford 11.10 g of Ph_2PEt (b.p. 102°C, 0.1 mbar, yield 43%). The aforementioned aqueous phase was treated with HCl until a pH value of 2 was reached, and then extracted with three 150-ml aliquots of dichloromethane. The combined extracts were dried with magnesium sulfate. Removal of the solvent in vacuo left a colorless solid. Yield: 36.50 g (82%) **8a**.

8b was obtained in an analogous manner starting from 6.82 g (29.4 mmol) of **7b**, dissolved in 100 ml of THF, and 130 ml of a 0.5 M solution of Ph_2PK (65.0 mmol) in THF. Due to the lower reactivity of **7b**, a longer reaction time was needed, even at reflux temperature (72 h). Yield: 8.80 g (81%).

8a: $C_{20}H_{20}O_3P_2$ (370.3): calcd. C 64.87, H 5.44, P 16.73; found C 64.72, H 5.38, P 16.56. – MS: [M^+]: *m/z* = 370. – $^{31}P\{^1H\}$ NMR ($CDCl_3$): δP = –3.6 (P^{III}), 20.0 (P^V). – **8b**: $C_{20}H_{20}O_3P_2$ (370.3): calcd. C 64.87, H 5.44, P 16.73; found C 64.19, H 5.32, P 16.14. – MS: [M^+]: *m/z* = 370. – $^{31}P\{^1H\}$ NMR ($CDCl_3$): δP = –3.9 (P^{III}), 19.9 (P^V).

Preparation of **3a** *and* **3b**: To the solutions of 35.54 g (96.0 mmol) of **8a** or 8.11 g (21.9 mmol) of **8b** in 300 ml or 100 ml of dichloromethane 44.08 g (287.9 mmol) or 10.1 g (66.0 mmol) of Me_3SiBr was added. After stirring the reaction mixtures for 12 h at ambient temperature, all volatiles were removed in vacuo (60°C, 0.01 mbar). The intermediate silyl esters formed were obtained as very moisture-sensitive colorless oils. They were dissolved in acetone (300 ml or 100 ml, respectively), 4.13 g (229.4 mmol) or 1.44 g (80.0 mmol) of water was added and the reaction mixture was stirred at ambient temperature for 2 h. After removal of all volatiles in vacuo (20°C, 0.01 mbar), the respective diphenylphosphanophenylphosphonic acid was obtained as a colorless solid. The product was redissolved in 150 ml or 50 ml of conc. NaOH and the resulting solution was poured into 4.0 l or 400 ml of ethanol, whereupon the disodium salt of the diphenylphosphanophenylphosphonic acid was precipitated as colorless crystals. The product was filtered off using a Buchner funnel, washed with ethanol, and dried in vacuo (60°C, 0.01 mbar). Yields: 30.5 g (76%) **3a**, 5.81 g (63%) **3b**.

3a: $C_{18}H_{14}Na_2O_3P_2 \cdot 2\ H_2O$ (422.2): calcd. C 51.20, H 4.30; found C 51.43, H 4.34. – $^{31}P\{^1H\}$ NMR (D_2O): δP = –5.5 (P^{III}), 12.0 (P^V). – $^{13}C\{^1H\}$ NMR (D_2O): δC (C1–C10) = 136.8 (9.2, 2.0), 132.9 (19.3, 13.2), 130.7 (7.1, 8.1), 142.2 (166.8), 130.7 (7.1, 8.1), 132.9 (19.3, 13.2), 136.2 (6.1), 133.8 (19.3), 129.0 (7.1), 129.4. – **3b**: $C_{18}H_{14}Na_2O_3P_2 \cdot 2\ H_2O$ (422.2): calcd. C 51.20, H 4.30; found C 51.34, H 4.39. – $^{31}P\{^1H\}$ NMR (D_2O): δP = –5.1 (P^{III}), 11.8 (P^V). – $^{13}C\{^1H\}$ NMR (D_2O): δC (C1–C10) = 135.3 (12.2, 7.1), 136.1 (29.6, 9.5), 141.8 (9.2, 165.8), 133.2 (9.2), 128.4 (4.1, 12.2), 131.5 (9.2), 136.3 (6.1), 133.7 (18.3), 129.0 (8.1), 129.3.

The diphenylphosphanophenylphosphonic acids **9a** and **9b** were obtained as oily liquids in quantitative yields by acidification of aqueous solutions of the disodium salts **3a** and **3b** with HCl. The crude products were extracted with dichloromethane, and the combined extracts were dried with magnesium sulfate. After evaporation of the solvent, the diphenylphosphanophenylphosphonic acids **9a** and **9b** were obtained as colorless solids. The products were characterized by $^{31}P\{^1H\}$-NMR spectroscopy and APCI mass spectrometry. **9a**, **9b**: APCI-MS: [MH^+]: *m/z* = 343; [MH^+ – PO_2H]: *m/z* = 279; [MH^+ – PO_3H]: *m/z* = 263.

Crystal-Structure Analysis of $Na_2[Ph_2P(C_6H_4$–m-$PO_3) \cdot 5.5\ H_2O \cdot i$PrOH]: Experimental data for the X-ray structural analysis are collected in Table 1. Unit-cell constants were determined from a least-squares fit to the settings of 25 reflections centred on a Siemens P4 diffractometer. Intensity data were collected with the

Table 1. Experimental data for the X-ray structure of **3b**·5.5 $H_2O \cdot i$PrOH

formula weight	533.30
temperature	293(2) K
crystal system	orthorhombic
space group	$Cmc2_1$
unit cell dimensions	a = 48.462(10) Å b = 6.3360(10) Å c = 17.509(4) Å α = β = γ = 90°
V	5376(2) Å^3
Z	8
$D_{calcd.}$	1.318 Mg/m^3
absorption coefficient	0.240 mm^{-1}
F(000)	2200
crystal size	0.46 × 0.4 × 0.06 mm
θ range	2.33 to 25.01
reflections collected	2482
independent reflections	2482
absorption correction	semiempirical
max. and min. transmission	0.589 and 0.536
data/restraints/parameters	2479/1/291
final R indices [$I > 2\sigma(I)$]	$R1$ = 0.0694, $wR2$ = 0.1339
R indices all data	$R1$ = 0.1408, $wR2$ = 0.1691
largest diff. peak and hole	0.382/–0.315 eÅ^{-3}

diffractometer in the ω-mode (Mo-K_α radiation) and were corrected for absorptions on the basis of ψ-scan information for selected reflections. The structure was solved by direct methods (SHELXS) and refined against F^2 by full-matrix least squares (SHELXL) to $R = 0.069$ [for $I > 2\sigma(I)$] and $wR2 = 0.169$ for all independent reflections. Non-hydrogen atoms were refined anisotropically. H atoms of *i*PrOH were included at geometrical positions using the riding model (C−H = 0.96 A)[24].

[1] M. Hingst, M. Tepper, O. Stelzer, *Eur. J. Inorg. Chem.* **1998**, 73.
[2] R. T. Smith, R. K. Ungar, L. J. Sanderson, M. C. Baird, *Organometallics* **1983**, *2*, 1138; F. Bitterer, S. Kucken, O. Stelzer, *Chem. Ber*. **1995**, *128*, 275; A. Heßler, O. Stelzer, H. Dibowski, K. Worm, F. P. Schmidtchen, *J. Org. Chem*. **1997**, *62*, 2362; H. Dibowski, F. P. Schmidtchen, *Tetrahedron* **1995**, *51*, 2325.
[3] [3a] E. Kuntz, *Chemtech.* **1987**, 570; E. Kuntz, *Fr. Pat.* 2.314.910, **1975** (Rhone-Poulenc Recherche). – [3b] F. Bitterer, O. Herd, A. Heßler, M. Kühnel, K. Rettig, O. Stelzer, W. S. Sheldrick, S. Nagel, N. Rösch, *Inorg. Chem*. **1996**, *35*, 4103; O. Herd, A. Heßler, K. P. Langhans, O. Stelzer, W. S. Sheldrick, N. Weferling, *J. Organomet. Chem*. **1994**, *475*, 99. – [3c] W. Keim, R. P. Schulz, *J. Mol. Catal*. **1994**, *92*, 21; V. Ravindar, H. Hemling, H. Schumann, J. Blum, *Synth. Commun*. **1992**, *22*, 841.
[4] D. E. Bergbreiter, L Zhang, V. Mariagnanam, *J. Am. Chem. Soc*. **1993**, *115*, 9295; M. Beller, J. G. E. Krauter, A. Zapf, *Angew. Chem*. **1997**, *109*, 793; *Angew. Chem. Int. Ed. Engl*. **1997**, *36*, 793.
[5] A. Miedaner, C. J. Curtis, R. M. Barkley, D. L. DuBois, *Inorg. Chem*. **1994**, *33*, 5482.
[6] A. Köckritz, A. Weigt, M. Kant, *Phosphorus Sulfur Silicon* **1996**, *117*, 287.
[7] T. L. Schull, J. C. Fettinger, D. A. Knight, *Inorg. Chem*. **1996**, *35*, 6717.
[8] S. Lelievre, F. Mercier, F. Mathey, *J. Org. Chem*. **1996**, *61*, 3531.
[9] S. Haber, H. J. Kleiner, WO 97/05104 (Hoechst AG), 13. 2. **1997**.
[10] O. Herd, A. Heßler, M. Hingst, M. Tepper, O. Stelzer, *J. Organomet. Chem.* **1996**, *522*, 69.
[11] L. Maier in *Organic Phosphorus Compounds*, vol. 1 (Eds.: G. M. Kosolapoff, L. Maier), Wiley-Interscience, New York, London, Sydney, Toronto, **1972**, p. 1.
[12] M. Kumada, K. Noda, *Mem. Fac. Eng. Osakke City Univ.* **1962**, *4*, 173; *Chem. Abstr*. **1963**, *59*, 8782.
[13] C. A. Tolman, W. C. Seidel, D. H. Gerlach, *J. Am. Chem. Soc*. **1972**, *94*, 2669; D. R. Coulson, *Inorg. Synth.* **1972**, *13*, 121.
[14] C. E. McKenna, J. Schmidhauser, *J. Chem. Soc., Chem. Commun*. **1979**, 739; C. J. Salomon, E. Breuer, *Tetrahedron Lett.* **1995**, *36*, 6759.
[15] M. Tepper, O. Stelzer, T. Häusler, W. S. Sheldrick, *Tetrahedron Lett.* **1997**, *38*, 2257.
[16] [16a] H. Schindlbauer, *Chem. Ber.* **1967**, *100*, 3432. – [16b] R. C. Grabiak, J. A. Miles, G. M. Schwenzer, *Phosphorus Sulfur* **1980**, *9*, 197; H. Schindlbauer, W. Prikoszovich, *Chem. Ber.* **1969**, *102*, 2914.
[17] [17a] S. Berger, S. Braun, H. O. Kalinowski, *NMR-Spektroskopie von Nichtmetallen*, vol. 3 ("^{31}P-NMR Spektroskopie"), Georg Thieme Verlag, Stuttgart, New York, **1993**, p. 4. – [17b] K. Worms, M. Schmidt-Dunker in *Organic Phosphorus Compounds*, vol. 7 (Eds.: G. M. Kosolapoff, L. Maier), Wiley-Interscience, New York, London, Sydney, Toronto, **1976**, p. 6.
[18] [18a] D. P. Burum, R. R. Ernst, *J. Magn. Reson*. **1980**, *39*, 163; M. R. Bendall, D. M. Doddrell, D. T. Pegg, *J. Am. Chem. Soc*. **1981**, *103*, 4603. – [18b] H. O. Kalinowski, S. Berger, S. Braun, *^{13}*C-NMR Spectroscopy, Georg Thieme Verlag, Stuttgart, New York, **1984**, p. 424. – [18c] L. D. Quin in *Phosphorus-31 NMR Spectroscopy in Stereochemical Analysis* (Eds.: J. G. Verkade, L. D. Quin), VCH Publishers, Deerfield Beach, FL, **1987**, p. 391. – [18d] G. A. Gray, *J. Am. Chem. Soc.* **1971**, *93*, 2132.
[19] T. H. Siddall, W. E. Stewart in *Progress in Nuclear Magnetic Resonance Spectroscopy*, vol. 5 (Eds.: J. W. Emsley, J. Feeney, L. H. Sutcliffe), Pergamon Press, Ltd., Oxford, London, Edinburgh, New York, Toronto, Sydney, Paris, Braunschweig, **1969**, p.33.
[20] B. J. Dunne, A. G. Orpen, *Acta Crystallogr.* **1991**, *C47*, 345.
[21] G. Cao, V. M. Lynch, J. S. Swinnea, T. E. Mallouk, *Inorg. Chem*. **1990**, *29*, 2112.
[22] C. Bhardwaj, H. Hu, A. Clearfield, *Inorg. Chem*. **1993**, *32,* 4294.
[23] M. Baudler, A. Zarkadas, *Chem. Ber.* **1971**, *104*, 3519; G. U. Spiegel, O. Stelzer, *Chem. Ber*. 1990, *123*, 989; W. Gee, R. A. Shaw, B. C. Smith, *Inorg. Synth*. **1967**, *9*, 19.
[24] Further details of the crystal structure investigation are available from the Fachinformationszentrum Karlsruhe, D-76344 Eggenstein-Leopoldshafen (Germany), on quoting the depository number CSD 407786.

[97265]

1,2-Bis[trifluorosulfur(IV)]tetrafluoroethane $F_3S–CF_2–CF_2–SF_3$: A Bifunctional Molecule with Two Fluoroamphoteric Sulfur Centers☆

Detlef Viets[a], Werner Heilemann[a], Enno Lork[a], Rüdiger Mews*[a], Wolf-Dieter Stohrer[b], and Tobias Borrmann[b]

Institut für Anorganische und Physikalische Chemie der Universität Bremen[a],
Postfach 330440, Leobener Straße NW2, D-28334 Bremen, Germany
Fax: (internat.) + 49(0)421/218-4267
E-mail: Mews@chemie.uni-bremen.de

Institut für Organische Chemie der Universität Bremen[b],
Postfach 330440, Leobener Straße NW2, D-28334 Bremen, Germany
Fax: (internat.) + 49(0)421/218-4264
E-mail: Stohrer@chemie.uni-bremen.de

Received November 26, 1997

Keywords: α,ω-Bis(trifluorosulfur)perfluoroalkanes / α,ω-Bis(fluorosulfinyl)alkanes / Fluorosulfur anions / Fluorosulfur cations / Ab initio calculations

The title compound $(–CF_2–SF_3)_2$ (**2**) is prepared from $(–CF_2–SCl)_2$ (**1**) and F_2 at –90 °C in 83 % yield. Reaction of **2** with CsF and TASF yields $Cs[(–CF_2–SF_3)_2F]$ (**8**), TAS $[(–CF_2SF_3)_2F]$ (**9**) and $(TAS)_2[(–CF_2–SF_4)_2]$ (**10**). Fluoride-ion abstraction yields $[(–CF_2SF_2)_2F]$ $[AsF_6]$ (**6**), BF_3-catalysed solvolysis in SO_2 gives $[–CF_2–S(O)F]_2$ (**4**), and CsF-catalysed oxidation with F_2 leads to the previously reported $(–CF_2–SF_5)_2$ (**11**). Ab initio calculations of the molecular structures of **2** and the related methane derivative $F_2C(SF_3)_2$ are reported.

Introduction

α,ω-Bis(trifluorosulfur)perfluoroalkanes, $SF_3–(CF_2)_n–SF_3$, should show a rich and interesting chemistry as a result of the bifunctionality and high reactivity of the SF_3 groups. The only compound of this class known to date is $F_2C(SF_3)_2$, which is prepared by the direct fluorination of CS_2[1][2][3]. As well as the chemistry of this compound and its reaction product $CF_2[S(O)F]_2$[4], the gas-phase structure of bis(trifluorosulfur)difluoromethane has been studied by electron diffraction[5]. There is an intramolecular interaction between the two SF_3 groups in the gas phase; one of the axial fluorine atoms of the pseudo-trigonal bipyramidal sulfur atom interacts equatorially with the other sulfur center and vice versa.

We thought it would be interesting to observe the effect that increasing the length of the perfluoroalkane chain would have on the interaction between the sulfur centers, the stability and the reactivity. We report here the synthesis of 1,2-bis(trifluorosulfur)tetrafluoroethane and illustrate the diverse reaction possibilities with some examples. The structures of $SF_3(CF_2)_nSF_3$ (n = 1, 2) calculated by ab initio methods are compared to that of $CF_2(SF_3)_2$[5] determined by electron diffraction.

Results and Discussion

Synthesis of 1,2-Bis(trifluorosulfur)-1,1,2,2-tetrafluoroethane ($F_3S–CF_2–CF_2–SF_3$)

The bis(trifluorosulfur)ethane derivative **2** was prepared in high yield by low-temperature fluorination of the corresponding chlorosulfenyl derivative **1**[6].

$$\underset{\mathbf{1}}{ClS–CF_2–CF_2–SCl} + 3\,F_2 \xrightarrow{-\,90°C} \underset{\mathbf{2}}{F_3S–CF_2–CF_2–SF_3} + Cl_2 \qquad (1)$$

Fluorine was expanded through a metal vacuum line under reduced pressure into a cooled nickel reactor containing compound **1** as a thin film on the inner surface. Decomposition products and the resulting chlorine were periodically removed on reaching a pressure of approximately 100 mbar. The reaction was taken as complete when no more fluorine uptake was observed, i.e. a subsequent oxidation of compound **2** to the respective sulfur(VI) derivative **11** does not occur under these conditions.

Compound **2** was prepared by this reaction on a preparative scale with a yield of 83%. **2** is a colourless, hydrolysis-sensitive liquid, as is the corresponding methane derivative $CF_2(SF_3)_2$.

In an analogous way to $CF_2(SF_3)_2$, which was described in the Introduction, α,ω-bis(trifluorosulfur)perfluoroalkanes display intramolecular donor-acceptor properties as a result of the acid-base amphoteric behaviour of the SF_3 groups, a phenomenon that leads to a chemical stabilization of the SF_3 groups. Evidence for such an interaction was also obtained by NMR spectroscopy. The ^{19}F-NMR spectra of SF_4 and CF_3SF_3 show only one signal for the sulfur-bonded fluorine atoms as a result of Berry pseudorotation at room temperature. However, the fluorine atoms do become non-equivalent at −20 °C. In the ^{19}F-NMR spectrum of **2** [and also of $CF_2(SF_3)_2$], no inequivalence of the sulfur-bonded fluorine atoms is observed even at −80 °C. We assume that, in addition to Berry pseudorotation, fast intra-

 © WILEY-VCH Verlag GmbH, D-69451 Weinheim, 1998 1434–1948/98/0707–1035 $ 17.50+.50/0

molecular fluorine exchange between the two SF_3 groups is responsible for this behaviour.

NMR measurements of **2** and $CF_2(SF_3)_2$ at −30°C show that **2** is less stable to hydrolysis than $CF_2(SF_3)_2$ and forms the sulfinyl products $F_3S-CF_2-CF_2-S(O)F$ (**3**) and $[-CF_2-S(O)F]_2$ (**4**), while $F_2C(SF_3)_2$ is stable under these conditions.

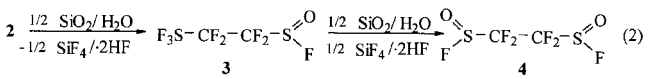

(2)

3 **4**

While **4** can be synthesized simply by BF_3-catalysed solvolysis of **2** in SO_2, **3** has only been observed as an intermediate (see Eq. 2). The ^{19}F-NMR spectrum of **3** shows a complex AA′BB′MX_3 splitting pattern with $\delta(SF_3) = +8.0$ (s, br.), δ[S(O)F] = −13.1 (m), $\delta(CF_2SF_3) = -102.2$ and $\delta[CF_2S(O)F] = -118.1$ (m).

The intramolecular interaction between the two SF_3 groups in **2** appears to be weaker than in $CF_2(SF_3)_2$ and the reactivity higher as a result of the longer perfluoroalkane chain. Evidence for this hypothesis through structural analysis of **2** has not yet been obtained.

Reaction of $(-CF_2SF_3)_2$ with BF_3 and AsF_5 in SO_2: Synthesis of $[-CF_2S(O)F]_2$ and $[(-CF_2SF_2)_2F][AsF_6]$

Perfluoroalkanesulfinyl fluorides can be obtained by two synthetic routes: (i) from perfluoroalkenes and SOF_2[7] or SO_2[8] and (ii) by hydrolysis of perfluoroalkylsulfur trifluorides[7]. The second route is particularly unsatisfactory due to the difficulty in controlling the reaction. As a result of our attempt to synthesize sulfonium salts $R_FSF_2^+BF_4^-$ from the corresponding perfluoroalkylsulfur trifluorides by fluoride abstraction using BF_3 in SO_2, we observed the quantitative formation of $R_FS(O)F$[4]. On addition of BF_3 to a solution of **2** in SO_2 at −40°C, a colourless solid precipitated. This precipitate disappeared on slow warming to room temperature and was not observed again on cooling.

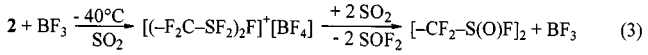

(3)

5 **4**

It is likely that the colourless precipitate is salt **5**. As discussed previously[4], the FSO_2^- ions resulting from the SO_2/BF_4^- equilibrium attack the cations of **5** leading to the formation of **4**. Compound **4** is isolated as a colourless liquid in > 90% yield.

The ^{19}F-NMR spectrum of compound **4** shows two AA′BB′XX′ spin patterns (see Experimental Section), demonstrating the presence of two isomers in a 1:1 ratio, which can be assigned to the *meso* and D,L compounds as a result of the two chiral sulfinyl centers.

If reaction (3) is performed with AsF_5 as a Lewis acid, the salt **6** is isolated in almost quantitative yield.

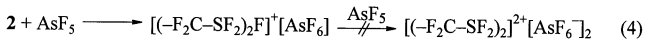

(4)

6 **7**

The formation of the dicationic compound **7** is not observed, even with a large excess of AsF_5. We assume that the abstraction is prevented due to the mutual interaction of both sulfonium centers. In the ^{19}F-NMR spectrum of **6** only one signal is observed for the *C*- and *S*-bonded fluorine atoms, even at low temperature [δ(CF) = −98.3 (s), δ(SF) = −37.2 (s, br.)]. This equivalence suggests a fast intramolecular fluoride exchange between the two sulfonium centers via a cyclic transition state in which the sulfur centers have pseudo-trigonal bipyramidal coordination through bridging over axially bonded fluoride. Single crystals of **6** suitable for an X-ray-structural analysis have not been obtained to date. In comparison with other sulfonium salts $R_FSF_2^+AsF_6^-$ ($R_F = CF_3$, C_2F_5, C_3F_7)[9][10][11], **6** is not very stable; **6** can only be stored satisfactorily at room temperature in Kel-F or Teflon vessels.

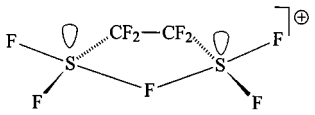

Reactions of $F_3SCF_2CF_2SF_3$ with Fluoride Ions

$R_FSF_4^-$ anions can be prepared by fluoride-ion addition to R_FSF_3 derivatives [$R_F = CF_3$, $(CF_3)_2CF$][12]. Spectroscopic studies show that the sulfur atom has a pseudo-octahedral geometry in these complexes, with the four fluorine atoms in the basal and the perfluoroalkyl groups in the apical positions. These anions correspond to the transition state of a nucleophilic S_N2 substitution at pseudo-pentacoordinated sulfur.

As we showed recently, fluoride-ion addition to $F_2C(SF_3)_2$ leads to a stable four-membered cyclic anion with a symmetrical S−F−S′ bridge[13]. Similarly, fluoride-ion addition to **2** with CsF and TASF [$(Me_2N)_3S^+Me_3SiF_2^-$] leads to the stable salts **8** and **9**.

(5)

8

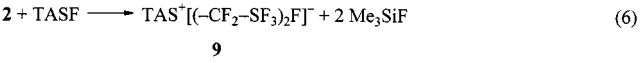

(6)

9

In contrast to the neutral starting material **2**, the salts **8** and **9** are much more stable. They can be stored in glass vessels at room temperature under an inert atmosphere for several weeks. The attack by nucleophiles (e.g. H_2O) is impeded through anion formation.

The ^{19}F-NMR spectra of the salts **8** and **9** each show two signals, and these have been assigned to the sulfur- and carbon-bonded fluorine atoms, respectively. Although only broad singlets are observed for the Cs salt **8** [δ(CF) = −96.0 (s), δ(SF) = +12.0 (s, br.)], the S*F* signal in the TAS salt **9** [δ(CF) = −95.6 (s, br.), δ(SF) = +12.5 (quint)] is split into a quintuplet (^3J = 15.6 Hz). The equivalence of all S*F* and C*F* atoms deduced from the ^{19}F-NMR spectra can be explained by a fast intramolecular exchange between the two sulfur centers and a rotation around the C−S bonds.

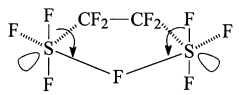

Although it was not possible to add a second fluoride ion to $CF_2(SF_3)_2$, the reaction of **2** with an excess of TASF led quantitatively to **10**, a salt containing a dianion with two pseudo-octahedrally coordinated sulfur centers.

$$\mathbf{2} + 2\ TASF \longrightarrow (TAS^+)_2[(-CF_2-SF_4)_2]^{2-} + 2\ Me_3SiF \quad (7)$$

10

These reactions show, on the one hand, that the interaction between the two sulfur centers in α,ω-bis(trifluorosulfur) derivatives of the type $F_3S-(CF_2-)_nSF_3$ seems to decrease with increasing chain length and, on the other hand, that the S−F−S′ bridge in **8** and **9** can only be broken by using "naked" or nearly naked, highly reactive fluoride ions such as those in TASF. The colourless stable salt **10** (mp 132°C, decomp.) was characterized by elemental analysis and IR spectroscopy (Experimental Section). Due to the high charge on the anion of **10** it is very insoluble in acetonitrile, the most convenient solvent for reactions with TASF, and, as a result, neither NMR-spectroscopic investigation nor recrystallization of the salt was possible.

CsF-Catalysed Oxidative Fluorination of $SF_3-CF_2-CF_2-SF_3$ to $SF_5-CF_2-CF_2-SF_5$ (11)

CsF-catalysed oxidative fluorinations have found wide use in fluorine chemistry. The oxidation is made easier through intermediate anion formation, as shown by numerous examples in the chemical behaviour of the elements of groups 15−18. Compound **2** can be oxidized to the corresponding sulfur(VI) oxidation state in a way similar to the conversion of $CF_2(SF_3)_2$ to $CF_2(SF_5)_2$[3].

$$\mathbf{2} + 2\ F_2 \xrightarrow[-196° \longrightarrow r.t.]{CsF} F_5S-CF_2-CF_2-SF_5\ (21.5\ \%) \quad (8)$$

11

11 was first observed as a by-product in the electrofluorination of 3-oxapentane-1,5-dithiol[14]. The ^{19}F-chemical shifts of the fluorine atoms of our product differ only slightly from the literature values. For the *C*-bonded fluorine atoms we observe a nonuplet of triplets, since $^3J(CF-SF_4) = {}^4J(CF-SF_4) = 14.6$ Hz and $^3J(CF-SF_{apical}) = {}^4J(CF-SF_{apical}) = 3.0$ Hz. The fine splitting of the A and B_4 parts of the SF_5 groups ($^2J = 152.3$ Hz) indicates a spin system of type $AA'B_4B_4'X_2X_2'$. From the splitting of the ^{13}C signal (δ = 119.9, ttq) we determined the following coupling constants: $^1J(C-F) = 314.2$ Hz, $^2J(C-F) = 35.5$ Hz and $^2J(C-SF_4) = 28.4$ Hz.

Structure and Bonding in $F_3S(CF_2)_nSF_3$ (n = 1, 2)

The gas-phase structure of the methane derivative $F_2C(SF_3)_2$ has been determined by electron diffraction[5]. However, our attempts to determine the structure of the ethane derivative **2** have been fruitless to date due to the extreme moisture sensitivity of this species. Figure 1 shows the RHF/6-311+G*-calculated[15] structure for $F_2C(SF_3)_2$, with the experimentally determined bond lengths and angles given for comparison. The conformation as well as the angles and distances are in good agreement. The experimentally observed interaction between the two SF_3 groups is also clearly seen in the calculated structure. The calculated distance between the axial fluoride F(2) and the neighbouring sulfur center S(1a) [or F(2a)−S(1)] of 263 pm lies well below the sum of the van der Waals radii of S and F (320 pm). The experimentally found value is 266 pm. The averaged S−F bond lengths of 163.6 pm (calculated) and 163.0(3) pm (experimental) are identical, although the individual values differ substantially.

Figure 1. Fully optimized structure of $F_3S-CF_2-SF_3$[a]

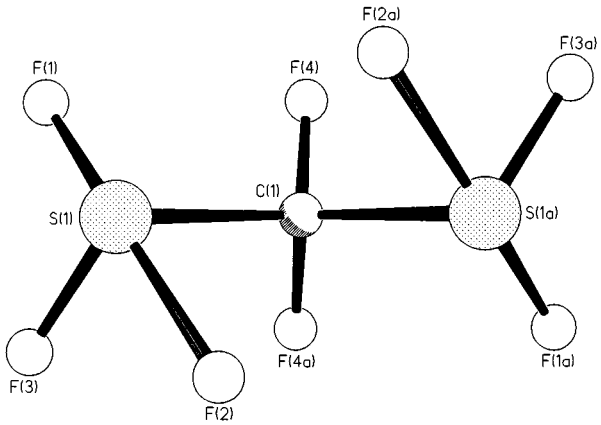

[a] Calculated [and experimental[5]] bond lengths [pm] and bond angles [°]: C(1)−S(1) 187.6 [188.8(7)], C(1)−F(4) 129.1 [131.8(5)], S(1)−F(1) 164.1 [166.4(4)], S(1)−F(2) 172.0 [166.6(4)], S(1)−F(3) 154.7 [156.2(6)], S(1)···F(2a) 263 [266]; S(1)−C(1)−S(1a) 108.6 [108.2(5)], F(4)−C(1)−F(4a) 110.1 [109.8(18)], F(4)−C(1)−S(1) 111.8 [109.7(5)], F(4a)−C(1)−S(1) 107.2, F(1)−S(1)−F(2) 167.7 [173.1(15)], F(1)−S(1)−F(3) 87.6 [88.1(13)], F(2)−S(1)−F(3) 85.8 [88.1(3)], F(1)−S(1)−C(1) 89.0 [89.1(8)], F(2)−S(1)−C(1) 82.0 [85.1(8)], F(3)−S(1)−C(1) 101.2 [97.2(11)].

An average S−F bond length and the difference Δ = $(S-F_a) - (S-F_e)$ were obtained experimentally, equally large $S-F_a$ distances were assumed. From these data the bond lengths $S-F_a$ and $S-F_e$ were derived. However, it is expected that the interaction of the axial 3c-4e$^-$ bond system with the neighbouring centers will lead to a stretching of the bridging SF and a corresponding shortening of the non-bridging fluoride. For example, this phenomenon is observed in the structure of SF_3-SF[16]. In this case the two $S-F_a$ bonds of the pseudo-pentacoordinated sulfur center differ by approximately 10 pm, and a difference of 7.9 pm was calculated for $F_2C(SF_3)_2$ (172.0 and 164.1 pm).

The influence of the interaction between the two SF_3 groups on the geometrical configuration of the substituents at the sulfur centers is minimal. Through the lengthening of the one axial S−F bond we would expect a distortion of the pseudo-trigonal bipyramid towards a pseudo-tetrahedron and through the interaction of this bridging fluoride with the neighbouring sulfur center we would expect an increase in sulfur coordination towards a pseudo-octahedron. These interactions have little influence, as shown by a comparison with the experimentally determined structure of CF_3SF_3[17]. Deviations from ideal pseudo-trigonal bipyramidal geometry can be explained by the influence of the lone pair of electrons in accordance with VSEPR theory[18].

The RHF/6-311 + G*-calculated[15] structure of $F_3S-CF_2-CF_2-SF_3$ (**2**) with bond lengths and angles is

shown in Figure 2. Interaction of the two SF_3 groups is also clearly seen here. The distances between the non-bonded atoms S(1)F(2a) and S(1a)F(2) of 283 pm are also significantly longer than those in the methane derivative. This is in agreement with the conclusions drawn from the experimental results, i.e. that the interaction of the SF_3 groups leads to a stabilization and that the lesser interaction in **2**, compared to that in $F_2C(SF_3)_2$, is responsible for its higher reactivity towards nucleophiles.

Figure 2. Fully optimized structure of compound **2**[a]

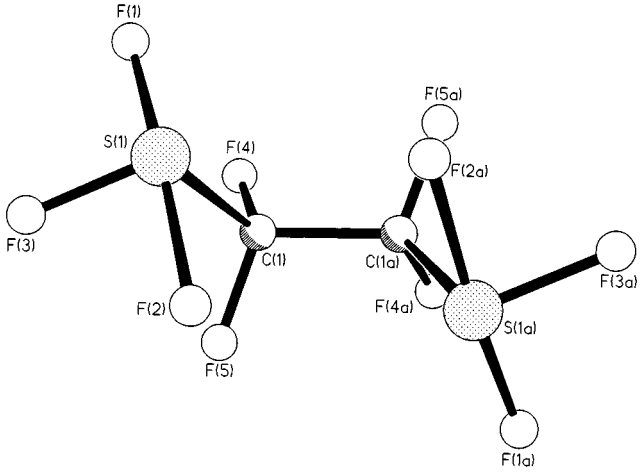

[a] Calculated bond lengths [pm] and bond angles [°]: C(1)−C(1a) 155.8, C(1)−S(1) 188.9, C(1)−F(4) 130.2, C(1)−F(5) 130.6, S(1)−F(1) 164.3, S(1)−F(2) 170.2, S(1)−F(3) 155.0, S(1)···F(2a) 283; F(1)−S(1)−F(2) 170.9, F(1)−S(1)−F(3) 88.1, F(1)−S(1)−C(1) 89.9, F(2)−S(1)−F(3) 86.7, F(2)−S(1)−C(1) 83.6, F(3)−S(1)−C(1) 99.2, S(1)−C(1)−C(1a) 115.4, S(1)−C(1)−F(4) 110.0.

As expected, the S−C and averaged S−F bonds, as well as the bond angles in the C−SF_3 groups of **2** and $CF_2(SF_3)_2$, differ only slightly. The weaker interaction of the two SF_3 groups in **2** corresponds to the lesser stretching of the axial S−F bonds [170.2 pm compared to 172.0 pm in $CF_2(SF_3)_2$] towards bridging fluorides S(1)F(2a) and S(1a)F(2). The terminal S−F bonds are only slightly longer.

Conclusions

In α,ω-bis(trifluorosulfur)perfluoroalkanes, $F_3S(CF_2)_n$-SF_3 (n = 1, 2), the intramolecular interaction between the two SF_3 groups decreases with increasing chain length, as shown unequivocally by experimental results and ab initio calculations. In both cases fluoride-ion addition and abstraction gives intramolecular fluoride-bridged anions and cations. With excess "naked" fluoride (e.g. from TASF) only the ethane derivative forms a dianion on ring cleavage. The synthesis of dications, even with a large excess of a strong fluoro Lewis acid (e.g. AsF_5), was unsuccessful. It will be interesting to perform further investigations to assess the chain length necessary in order that the SF_3 groups have no influence on each other.

We thank the *Fonds der Chemischen Industrie* and the *Deutsche Forschungsgemeinschaft* for financial support and the *Deutsche Solvay Fluor and Derivate GmbH* for the donation of elemental fluorine. We thank Dr. *A. Waterfeld* for the preparation of $(-CF_2SCl)_2$ and Dr. *P. G. Watson* for the translation of the manuscript.

Experimental Section

All reactions were performed with rigorous exclusion of moisture in thick-walled glass reactors with Teflon valves, or in nickel vessels previously passivated with ClF_5. Work involving aggressive gases was undertaken in a metal vacuum manifold. Volatile reagents were condensed in vacuum lines and solids transferred in a glove box under argon or nitrogen. The starting materials $(-CF_2-SCl)_2$[6], TASF[19] and AsF_5[20] were prepared using literature methods. − IR: Biorad FTS-7-FT-IR. − MS: Finnigan MAT 8222, EI 70 eV. − NMR: Bruker AC 80 and WH 360. − Elemental analyses were performed by the Mikroanalytisches Labor Beller (Göttingen).

$F_3S-CF_2-CF_2-SF_3$ (**2**): In a vacuum line, 3.0 g of F_2 (79 mmol) from a reservoir was added to 5.2 g of $(-CF_2-SCl)_2$ (**1**, 22 mmol), previously condensed onto the inner surface of a 1-l nickel vessel, over a period of 10 h at −90°C. The resulting chlorine and decomposition products were removed as soon as the pressure exceeded 100 mbar. The reaction was complete when uptake of fluorine was no longer observed. Fractional condensation at 10^{-3} mbar (−78 and −196°C) led to 5.1 g of **2** as a colourless solid in the −78°C trap, yield 83%. − IR (gas, cm^{-1}): ν = 1280 m, 1261 m, 1222 vs, 1149 m, 932 s, 850 vs, 680 vs, 637 m, 583 m, 564 s, 521 m, 455 w. − ^{19}F NMR: δ = −100.5 (s, CF), 8.0 (s, br., SF). − EI MS; *m/z* (%): 259(1) [M^+], 189(5) [$M^+ - SF_3$], 119(100) [$CF_3CF_2^+$].

$FS(O)CF_2-CF_2S(O)F$ (**4**): 3.0 g of **2** (10.8 mmol), approximately 10 ml of SO_2 and 0.2 g of BF_3 (2.9 mmol) were condensed into a glass reactor fitted with a Teflon valve at −196°C. A colourless solid formed on warming the mixture to −40°C, and this solid disappeared on stirring for 3 h at ambient temperature. BF_3 was then removed by condensation onto 5 g of NaF and subsequent stirring at ambient temperature for 6 h. Fractional condensation under vacuum (−78 and −196°C) resulted in 2.3 g of **4** in the −78°C trap, yield 91%. − IR (gas, cm^{-1}): ν = 1281 sh, 1255 vs, 1234 s, 1184 s, 1129 s, 745 s, 603 w, 481 w. − ^{19}F NMR ($CDCl_3$/$CFCl_3$, 307 K): Two AA′BB′XX′ spin patterns were observed in the ratio 1:1; δ = −17.75 (m, SF), −18.1 (m, SF), −119.5 (m, CF_2, center point of the AA′BB′ part). − ^{13}C NMR: δ = 117.0 (dddddd, $^1J_{CF}$ = 309.6 Hz, $^1J_{CF}$ = 306.0 Hz, $^2J_{CCF}$ = 32.5 Hz, $^2J_{CCF}$ = 32.0 Hz, $^2J_{C\text{-}SF}$ = 16.4 Hz, $^3J_{C\text{-}SF}$ = 2.0 Hz). − EI MS; *m/z* (%): 167(24) [M^+ − SOF], 148(2) [$CF_2CF_2SO^+$], 67(100) [SOF^+]. − $C_2F_6O_2S_2$ (234.1): calcd. F 48.7, S 37.4; found F 48.7, S 37.3.

$[(-CF_2-SF_2)F]AsF_6$ (**7**): 1.9 g of **2** (6.8 mmol), 2.0 g of AsF_5 (11.8 mmol) and approximately 10 ml of SO_2 as solvent were condensed into a glass reactor fitted with a Teflon valve at −196°C. The mixture was stirred for 1 h at −40°C and the volatile materials were subsequently removed at this temperature under dynamic vacuum. 3.0 g of **7** (quantitative) remained as a colourless solid, mp. 97°C. − IR: Due to the sensitivity of the compound we have been unable to obtain satisfactory IR spectra. − ^{19}F NMR: δ = −37.2 (s, br., SF), −57.2 (s, br., AsF), −98.3 (s, CF). − $C_2AsF_{15}S_2$ (448.0): calcd. As 16.7, F 63.6; found As 17.4, F 61.8.

$Cs[(-CF_2-SF_3)_2F]$ (**8**): 1.3 g of **2** (4.7 mmol) and 10 ml of CH_3CN were condensed onto 0.6 g of CsF (4.0 mmol), previously dried at 140°C under vacuum. The mixture was stirred for 3 h at −30°C and all volatile products were subsequently removed at this temperature and for a short time at ambient temperature under dynamic vacuum. 1.7 g of **8** (quantitative) was obtained as a colourless non-volatile solid, mp. 105°C (decomp.). − IR (nujol,

cm^{-1}): $\tilde{\nu}$ = 1247 s, 1203 s, 1184 vs, 1168 sh, 1127 m, 1113 sh, 1027s, 902s, 846 m, 778 sh, 741 sh, 722 vs (br.), 655 s. − ^{19}F NMR ($CD_3CN/CFCl_3$, 307 K): δ = +12.0 (s, br., SF), −96.0 (s, br., CF).

TAS[(−CF$_2$−SF$_3$)$_2$F] (**9**): 0.80 g of **2** (2.9 mmol) was condensed on to 0.67 g of TASF (2.4 mmol) in 5 ml of CH_3CN in a glass reactor fitted with a Teflon valve at −196°C. After stirring for 15 min at −40°C, approximately 20 ml of diethyl ether was condensed onto the reaction mixture at −80°C. The resulting oily product was then washed several times with diethyl ether. 1.13 g of **9** (quantitative) remained as a colourless solid after removal of the volatile materials under vacuum, mp 96°C. − IR (nujol, cm^{-1}): ν = 1282 m (br.), 1229 s, 1200 sh, 1168 m, 1153 sh, 1112 w, 1062 w, 1027 m, 970 m, 945 m, 901 s (br.), 766 sh, 736 vs, 722 vs, 605 s (br.), 579 s (br.), 482 m. − ^{19}F NMR (CD_3CN, $CFCl_3$, 173 K): δ = 12.5 (quint, SF, $^3J_{CF-SF}$ = 15.6 Hz), −95.6 (s, br., CF). − $C_8H_{18}F_{11}N_3S_3$ (461.4): calcd. C 20.8, H 3.93, F 45.3; found C 21.3, H 4.1, F 44.0.

(TAS)$_2$(−CF$_2$SF$_4$)$_2$ (**10**): 0.45 g of **2** (1.6 mmol) was stirred with 0.93 g TASF (3.4 mmol) in approximately 5 ml of CH_3CN at −40°C for 15 min in a way similar to the synthesis of **9**. A colourless solid precipitated and was washed twice with CH_3CN at −40°C. 1.09 g of **9** (quantitative) remained after removal of the volatile materials in vacuo, mp. 132°C (decomp.). − IR (nujol, cm^{-1}); ν = 1282 m, 1197 s, 1169 m, 1152 m, 1132 s, 1113 sh, 1065 m, 1032 m, 968 s, 950 s, 899 s, 768 m, 722 vs, 689 m, 676 w, 617 s, 550 vs (br.), 426 m. − $C_{14}H_{36}F_{12}N_6S_4$ (644.7): calcd. C 26.1, H 5.63, F 35.4; found C 26.7, H 6.39, F 33.7.

SF$_5$−CF$_2$−CF$_2$−SF$_5$ (**11**): 2.2 g of **2** (7.9 mmol) and 0.3 g of F_2 (7.9 mmol) were condensed onto 5.3 g of CsF (35 mmol) in a 1-l nickel reactor. The reaction mixture was allowed to warm up to ambient temperature over 12 h and subsequently left to stand for 48 h at this temperature. Fractional condensation (−78 and −196°C) gave 0.30 g of **11** in the −78°C trap, yield 21% (based on F_2).

[☆] Dedicated to Professor Dr. *Walter Siebert* on the occasion of his 60th birthday.

[1] A. Clifford, H. K. El-Shamy, H. J. Emeleus, R. N. Haszeldine, *J. Chem. Soc*. **1953**, 2372.
[2] L. A. Shimp, R. Lagow, *Inorg. Chem*. **1977**, *16*, 2974.
[3] A. Waterfeld, R. Mews, *J. Fluorine Chem.* **1983**, *23*, 325.
[4] D. Viets, R. Mews, M. Noltemeyer, H. G. Schmidt, A. Waterfeld, *Chem. Ber*. **1991**, *124*, 1353.
[5] I. Weiss, H. Oberhammer, D. Viets, R. Mews, A. Waterfeld, *J. Mol. Struct.* **1991**, *248*, 407.
[6] C. G. Krespan (E.I. du Pont), U.S. Pat. 3099688, **1960/63**; *Chem. Abstr*. **1964**, *60*, 1597.
[7] C. T. Ratcliffe, J. M. Shreeve, *J. Am. Chem. Soc*. **1968**, *90*, 5403.
[8] D. Sianesi, G. C. Bernardi, G. Moggi, *Tetrahedron Lett*. **1970**, 1313.
[9] M. Kramar, L. C. Duncan, *Inorg. Chem*. **1971**, *10*, 647; F. Pauer, M. Erhard, R. Mews, D. Stalke, *Z. Naturforsch*. **1990**, *45b*, 271.
[10] D. Viets, E. Lork, R. Mews, unpublished results; Dissertation D. Viets, Bremen, **1992**.
[11] Dissertation M. Erhart, Bremen, **1990**.
[12] W. Heilemann, R. Mews, S. Pohl, W. Saak, *Chem. Ber*. **1989**, *122*, 1613.
[13] D. Viets, W. Heilemann, A. Waterfeld, R. Mews, S. Besser, R. Herbst-Irmer, G. M. Sheldrick, W.-D. Stohrer, *J. Chem. Soc., Chem. Commun*. **1992**, 1017.
[14] T. Abe, S. Nagase, H. Baba, *Bull. Chem. Soc. Jpn*. **1973**, *46*, 3845.
[15] M. J. Frisch, G. W. Trucks, M. Head-Gordon, P. M. W. Gill, M. W. Wong, J. B. Foresman, B. G. Johnson, H. B. Schlegel, M. A. Robb, E. S. Replogle, R. Gomperts, J. L. Andres, K. Raghavachari, J. S. Binkley, C. Gonzalez, R. L. Martin, D. J. Fox, D. J. Defrees, J. Baker, J. P. Stewart, and J. A. Pople, *Gaussian 92*, Revision G.3, Gaussian Inc., Pittsburgh PA, **1992**. Frequency analyses confirm that the calculated structures are minima on the corresponding Born−Oppenheimer surface.
[16] M. v. Carlowitz, H. Oberhammer, H. Willner, J. E. Boggs, *J. Mol. Struct*. **1983**, *100*, 161.
[17] R. Minkwitz, W. Molsbeck, H. Oberhammer, *Inorg. Chem.* **1992**, *31*, 2104.
[18] R. J. Gillespie, *Molecular Geometry*, Van Nostrand-Reinhold, London, **1972**.
[19] W. J. Middleton, *Org. Synth*. **1985**, *64*, 221.
[20] O. Ruff. A. Braida, O. Bretschneider, W. Menzel, H. Plaut, *Z. Anorg. Allg. Chem.* **1932**, *206*, 59.

[97282]

Pseudoelement Compounds, XIII[◇]

On the Ambident Behaviour of Dicyanmethanidonitrite; Syntheses and Characterization of Complexes of the Type $[M\{N(O)C(CN)_2\}(PPh_3)_n]$ ($M = Cu^I, Ag^I$; $n = 2, 3$)

Lothar Jäger*[a], Carola Tretner[a], Helmut Hartung[b], and Matthias Biedermann[b]

Martin Luther University Halle-Wittenberg, Institute of Inorganic Chemistry[a],
D-06099 Halle/Saale, Germany

Martin Luther University Halle-Wittenberg, Institute of Physical Chemistry[b],
D-06099 Halle/Saale, Germany

Received September 22, 1997

Keywords: Silver / Copper / Dicyanmethanidonitrite / Coordination modes

Complexes of the type $[M\{N(O)C(CN)_2\}(PPh_3)_n]$ (M = Cu^I, Ag^I, n = 2, 3) were synthesized by metathesis of $K[N(O)C(CN)_2]$ and $[M(NO_3)(PPh_3)_n]$. The complexes were characterized by ^{13}C-, ^{31}P-NMR and IR spectroscopy and elemental analyses. The crystal structures of $[M\{N(O)C(CN)_2\}(PPh_3)_2]_2$ (M = Cu^I, Ag^I) have been determined by X-ray diffraction. Depending on the metal atom in the complexes $[M\{N(O)C(CN)_2\}(PPh_3)_3]$ the ionic ligand is coordinated via the central nitrogen (copper) or the oxygen atom (silver). In addition the two copper and silver complexes $[M\{N(O)C(CN)_2\}(PPh_3)_2]_2$ are not isostructural but have quite different structures. For M = Cu the two copper atoms are doubly bridged by two NCCN sequences, forming an approximately planar $Cu(NCCN)_2Cu$ ring. On the other hand, in the homologous silver derivative the metal atoms are also doubly bridged, but by two NO groups, thus forming a planar six-membered ring.

Considering the fragment $C(CN)_2$ as an oxygen homologous functional group, the anions $[N(O)C(CN)_2]^-$ (dicyanmethanidonitrite) and $[N\{C(CN)_2\}_2]^-$ [bis(dicyanmethanido)nitrite] appear as pseudochalcogenonitrites[2]. The strength of this approach is emphasized by the fact that, like $[NO_2]^-$, $[N(O)C(CN)_2]^-$ also behaves ambidentately towards metal ions. In both species oxygen and the middle nitrogen atoms should be comparable from the electronic point of view[3]. According to the soft-soft and hard-hard orientation, exceptionally soft metal ions coordinate unidentately to these ligands via the central nitrogen (Re^I [4], Ir^I [5], Pt^{II} [6]) whilst more hard 3d-metal ions (Ni^{II} [7], Cu^{II} [8], Co^{III} [8], Fe^{III} [5]) coordinate via the oxygen atom. In contrast to this finding the ion $[N\{C(CN)_2\}_2]^-$ is preferentially linked through an end-on nitrile group (Pt^{II}). However, in solution a linkage isomerization can be assumed[6].

To our knowledge, no complexes with dicyanmethanidonitrite in bidentate function were crystallographically characterized up to now. Several bonding motifs can be expected because apart from oxygen and the central nitrogen, end-on nitrile groups can also be discussed as potential donor atoms. In the past compounds of the type $[M\{N(O)C(CN)_2\}_2L_2]$ have been synthesized; some of them have indeed proved to be addition products of the expected complex and a protic solvent such as $[Cu\{ONC(CN)C(NH)OEt\}_2(H_2O)_2]$[8]. In this context the silver salt $Ag[N(O)C(CN)_2]$[9] is also worth mentioning. Its crystal structure shows ligand-metal contacts via oxygen and both types of nitrogen atoms.

Results and Discussion

In order to study the ambidentate behaviour of dicyanmethanidonitrite, depending on the hard/soft nature of metal ions in complexes with this ligand (in a uni- and especially in a bidentate function) we prepared compounds of copper(I) and silver(I) of the types $[MX(PPh_3)_3]$ and $[MX(PPh_3)_2]_2$. The syntheses were carried out in boiling $CHCl_3$ or CH_2Cl_2.

$$\underset{\mathbf{1}}{K[N(O)C(CN)_2]} + \underset{\mathbf{2}}{[M(NO_3)(PPh_3)_3]} \longrightarrow \underset{\mathbf{3}}{[M\{N(O)C(CN)_2\}(PPh_3)_3]} + KNO_3 \quad (1)$$

$$2\,\mathbf{1} + 2\,[M(NO_3)(PPh_3)_2] \longrightarrow \underset{\mathbf{5}}{[M\{N(O)C(CN)_2\}(PPh_3)_2]_2} + 2\,KNO_3 \quad (2)$$

(**4**)

2, **3**, **4**, **5**	M
a	Cu^I
b	Ag^I

$$\mathbf{1} + \mathbf{4a} + MeOH \longrightarrow \underset{\mathbf{6}}{[Cu\{ONC(CN)C(NH)OMe\}(PPh_3)_2]} + KNO_3 \quad (3)$$

[◇] Part XII: Ref.[1].

 © WILEY-VCH Verlag GmbH, D-69451 Weinheim, 1998 1434–1948/98/0707–1051 $ 17.50+.50/0

Dicyanmethanidonitrite tends to add protic agents[7] such as methanol or water. If $K[N(O)C(CN)_2]$ is treated with $[Cu(NO_3)(PPh_3)_2]$ in the presence of methanol the monomeric complex **6** is formed. In **6** $[ONC(CN)C(NH)OMe]^-$ acts as a chelating ligand which is coordinated through the nitrogen atoms of the NO and the NH groups, forming a five-membered ring (Figure 1)[10].

Figure 1. Schematic view of the molecular structure of **6**

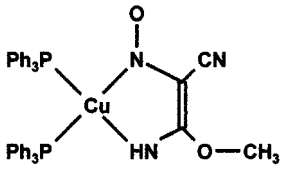

The new compounds were characterized by ^{13}C-NMR, ^{31}P-NMR and IR spectroscopy. Surprisingly, in contrast to **1,** the vibrations $\nu_{as}(CNO)$ and $\nu(CC)$ of **3a** and **3b** are shifted in opposite directions (Table 1). The shift of $\nu_{as}(CNO)$ to higher wavenumbers characterizes $[N(O)C(CN)_2]^-$ as centrally *N*-bonded (3a)[6]. On the other hand, the decrease of the N−O bond order corresponds to coordination via the oxygen atom. The IR spectra of the species **5** are in agreement with the results of the crystal structure analyses. In contrast to **5b** the complex **5a** shows three ν(CN) bands indicating a stronger differentiation of the nitrile groups. In comparison to $K[N(O)C(CN)_2]$ the shifts of the vibrations $\nu_{as}(CNO)$, $\nu_s(CNO)$, and ν(CC) of **5a** and **5b** are opposite in direction.

Table 1. Characteristic infrared absorptions (KBr [cm^{-1}]) of potassium dicyanmethanidonitrite and corresponding complexes **3a**, **3b**, **5a**, **5b**, and **6**

Compound	ν(CN)	$\nu_{as}(CNO)$	$\nu_s(CNO)$	ν(CC)	Mode
1	2236 vs, 2225 s	1325 vs	1275 vs	1236 vs	ionic
3a	2212 m, 2193 w	1345 m	1329 m	1208 s	unidentate
3b	2204 m	1306 s	1262 s	1275 vs	unidentate
5a	2216 m, 2207 m, 2188 w	1339 s	1253 w	1214 vs	bidentate
5b	2207 s	1326 vs	1288 vs	1245 vs	bidentate
6	2212 s, 2202 m	1359 vs	1330 vs	1313 vs	

Comparing the ^{13}C-NMR spectra of **1** with those of **3** and **5** very slight shifts, with no clear trend, can be observed. The ^{31}P-NMR chemical shifts of triphenylphosphane depend on the central metal atom. So the copper complexes show one resonance at about 0 ppm; the chemical shifts of **3b** or **5b** are δ 7.93 and 11.85 respectively.

According to the structure of the anionic ligand the infrared spectrum of **6** shows bands at 1606 (vs) and 1412 (vs) cm^{-1} which can be assigned to $\nu_{as}(C{=}N)$ and $\nu_s(C{=}N)$ vibrations. The (CN) vibration indicates an uncoordinated nitrile group. As expected for *N*O coordination the bands $\nu_{as}(CNO)$ and $\nu_s(CNO)$ are shifted to higher wavenumbers. In the ^{13}C-NMR spectrum resonances at δ 61.1 and 165.1 appear, confirming the assumed structure.

Crystal Structures of 5a and 5b

As a common feature, the homologous copper and silver complexes $[M\{N(O)C(CN)_2\}(PPh_3)_2]_2$ both exist in the crystal in form of discrete dimers in which the metal atoms are doubly bridged by two dicyanmethanidonitrite ligands $[N(O)C(CN)_2]^-$. But surprisingly, **5a** and **5b** are not isostructural and differ markedly with regard to the coordination mode of the ionic ligand. Depending on the central atom, the donor atoms are N(cyano) and N(central) in the copper complex **5a**, and O and N(central) in the silver complex **5b**.

The molecular structure of **5a** is shown in Figure 2. Two copper atoms are bridged by two ionic ligands $[N(O)C(CN)_2]^-$ coordinating the metal through the central and one cyano nitrogen atom. In this way a ten-membered ring, with a weakly pronounced chair conformation around a crystallographic inversion centre, is formed. The ligand itself is, to a good approximation, planar with significant deviations from planarity only for N1 [0.027(3) A] and O1 [0.016(3) A]. The copper atoms are at a distance of ±0.5188(4) A from the plane defined by the two NCCN fragments of the ring. The coordination geometry around Cu can be described as a distorted tetrahedron. The strongest deviation from the tetrahedral geometry is shown by the angle P1−Cu1−P2 with 122.62(3)°. The Cu−P bond lengths, being Cu1−P1 = 2.2853(8) A and Cu1−P2 = 2.2935(8) A, are in good agreement with the average value of 2.252(44) A established for Cu^I-PPh_3 complexes[11]. Surprisingly, the bond lengths between Cu and the two chemically non-equivalent N atoms are nearly the same [Cu1−N1 = 2.080(3) A, Cu1−N2a = 2.042(3) A]. In contrast to this finding, in the structurally analogous complex $[Cu(NCNNO_2)(PPh_3)_2]_2$[12], significantly different Cu−N bond lengths were found (Δ = 0.138 A). These relations are similar in the following complexes with trigonal-planar configured copper(I): $[Cu\{\mu\text{-}NCNC(NH_2)_2\}\{NCNC(NH_2)_2\}]_2A\cdot 2H_2O$ with A = SO_4 [Cu−N1 = 1.868(9) and 1.883(9) A, Cu−N2 = 2.25(1) and 2.250(9) A] and A = S_2O_6 [Cu−N1 = 1.874(4) A, Cu−N2 = 2.246(4) A][13]. On the other hand, for $[Cu(NCNC_6H_4Me\text{-}4)(PPh_3)_2]_2$ rather similar metal nitrogen bonds were found [Cu−N1 = 2.045(2) A and Cu−N2 = 2.095(2) A][14].

The molecular structure of **5b** is shown in Figure 3. The two silver atoms are doubly bridged by the NO groups of two dicyanmethanidonitrite ligands, and a centrosymmetric six-membered ring is formed in this way. A comparable bridging function is known for $[NO_2]^-$, and this is proved by X-ray analysis for $[(H_3N)_4Co(NH_2)ON(O)Co(NH_3)_4]^{4+}$[15]. The $Ag(NO)_2Ag$ ring is planar to a good approximation, the maximum deviation from the best plane shown by the O atoms [±0.083(4) A]. The coordination geometry around Ag is that of a strongly distorted tetrahedron; the greatest deviations from the ideal value shown by the bond angles P1−Ag1−P2 with 132.83(4)° and N1−Ag1−O1a with 89.7(1)°. The two Ag−P bond lengths [Ag1−P1 = 2.444(1) A, Ag1−P2 = 2.447(1) A] are equal within experimental error and agree well with experience

Figure 2. Molecular structure of **5a**[a]

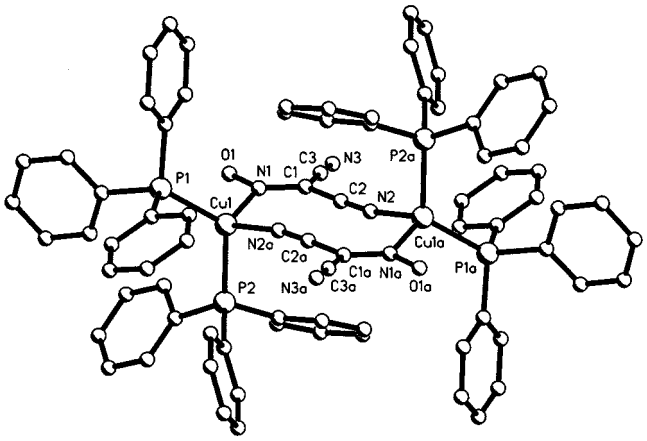

[a] Selected bond lengths [A] and angles [°]: Cu1−N1 2.080(3), Cu1−N2a 2.042(3), Cu1−P1 2.2853(8), Cu1−P2 2.2935(8), O1−N1−Cu1 113.4(2), C1−N1−Cu1 129.1(2), C2−N2−Cu1a 169.6(3), P1−Cu1−P2 122.62(3), N1−Cu1−N2a 104.98(10).

[2.419(46) A as average of 27 $Ag^{I}-PPh_3$ complexes][11]. The Ag1−N1 distance of 2.413(3) A is quite normal compared with the values of 2.400(4) and 2.416(4) A in $[Ag(NCNNO_2)(PPh_3)_2]_2$[12] but longer than the range from 2.28(1) to 2.332(5) A observed in a series of compounds $[Ag(NCS)L_n]$ (L = py-Me-2, py-Me-3, py-Me_2−2,6, quin)[16]. The Ag1−O1a distance of 2.504(3) A is just in the middle of the wide range observed for Ag−O bond lengths, which depend on the coordination mode and are illustrated by the following examples: NO_2^- chelating in $AgNO_2$ [2.441(3) A][17], NO_3^- terminal in $[AgONO_2$(1-Me-cytosine)] [2.469(3) A][18] or chelating in $[AgNO_3$(2-pyridyleneaniline)] [2,259(3) A][19] or bridging in $[AgNO_3$(cyclosarcosylsarcosine)$_2$] [2.612(8) and 2.679(7) A][20].

Figure 3. Molecular structure of **5b**[a]

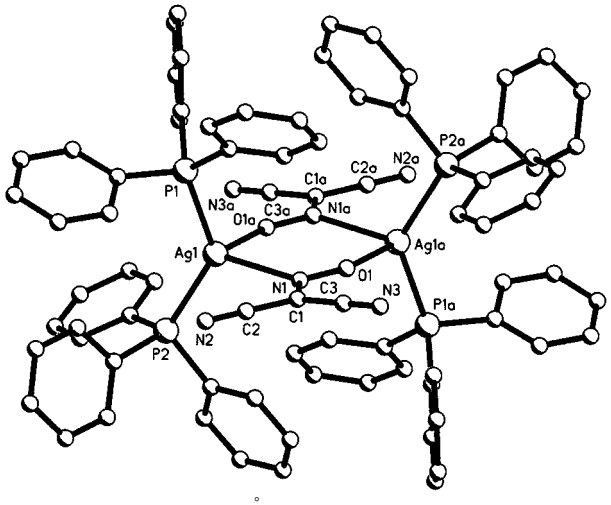

[a] Selected bond lengths [A] and angles [°]: Ag1−N1 2.413(3), Ag1−O1a 2.504(3), Ag1−P1 2.444(1), Ag1−P2 2.447(1), O1−N1−Ag1 125.4(3), C1−N1−Ag1 117.1(3), P1−Ag1−P2 132.83(4), N1−Ag1−O1a 89.7(1).

A survey of the bond lengths and angles characterizing the geometry of the ambidentate dicyanmethanidonitrite X in its ionic (**1** = KX)[21], bidentate (**5a**, **5b**) and unidentately *N*-bonded (*trans*-$[Pt(H)X(PPh_3)_2]$)[6] or *O*-bonded function ($[Co(X)Cl(en)_2]X$)[22] is given in Table 2. A comparison of the listed values reveals no significant, or only slight to moderate, differences, depending on the coordination modes. Even **5a** and **5b** agree completely within experimental error. For both compounds, within their ONC fragments, the N−O bond is slightly shortened and the N−C bond is slightly lengthened with respect to the uncoordinated anion X^- in **1**. The N−O bond lengths in **5a** and **5b** are a little bit longer than the value of 1.240(3) or 1.248(3) A found for the nitrite ion in the sodium[24] and the silver salt[17], respectively. All other bond lengths agree well with standard values[23]. The rigidity of the dicyanmethanidonitrite skeleton and its structural insensibility to variations in the coordination mode is also manifested by the small differences between the corresponding bond angles (Table 2). The maximum ranges of variation are shown by the angles C−C−C (Δ = 1.4°) and O−N−C (Δ = 3.9°).

Table 2. Geometric parameters [A, °] of $[N(O)C(CN)_2]^-$ in **1**, **5a**, **5b**, *trans*-$[Pt(H)N(O)C(CN)_2(PPh_3)_2]$ (**7a**), and $[Co(Cl)ONC(CN)_2(en)_2][ONC(CN)_2]$ (**7b**)

Distance/angle	1	5a	5b	7a	7b[a]
O1−N1	1.287(1)	1.266(3)	1.260(4)	1.260(3)	1.310(2)
N1−C1	1.324(2)	1.338(4)	1.329(5)	1.333(4)	1.299(3)
C1−C2	1.431(2)	1.418(4)	1.400(7)	1.421(5)	1.432(4)
C1−C3	1.422(2)	1.423(5)	1.411(8)	1.417(5)	1.424(4)
N2−C2	1.135(2)	1.135(4)	1.127(7)	1.134(5)	1.130(4)
N3−C3	1.143(2)	1.128(4)	1.143(8)	1.148(4)	1.130(4)
N2−C2−C1	179.1(2)	177.3(3)	178.2(6)	178.0(4)	177.4(4)
N3−C3−C1	177.3(1)	178.3(5)	178.5(10)	178.1(4)	179.2(3)
C2−C1−C3	119.8(1)	118.8(3)	118.6(4)	119.8(3)	118.4(2)
O1−N1−C1	115.9(1)	115.7(3)	116.0(4)	118.1(3)	114.2(2)

[a] *O*-coordinated.

This work is supported by the *Deutsche Forschungsgemeinschaft* and the *Fonds der Chemischen Industrie*.

Experimental Section

IR (KBr): Mattson 5000 FTIR. − ^{13}C NMR (TMS as reference): WP 200. − ^{31}P NMR (85% H_3PO_4 as reference, down-field shift positive): AC 80. The compounds **2a**[25], and **4a**[25] were prepared as described previously. For the synthesis of **2b** and **4b** known procedures were modified by using triphenylphosphane and silver nitrate[26][27].

General Method for the Syntheses of **3** *and* **5**: 2 mmol of **2a**, **4a** or **4b** were dissolved in 15 ml of $CHCl_3$, or 2 mmol of **2b** in 30 ml of CH_2Cl_2. While stirring the resulting mixture was treated with a solution of 2 mmol (0.25 g) of **1** in 20 ml of methanol or ethanol (synthesis of **3a**) and heated to reflux for 6 h in a water bath with exclusion of light. Afterwards the mixture was stirred at room temp. for 3 h. After filtration and evaporation of the solvent in vacuo the resulting solid was washed with methanol and dissolved in a small amount of $CHCl_3$ (**3a** in ethanol). A quantity of *n*-pentane was added until the onset of turbidity was observed and the solution kept at about 0°C. After some hours a microcrystalline solid was formed which was filtered off and dried in vacuo.

For the preparation of single crystals 0.010 g of **5a** or **5b** were dissolved in 2 ml of $CHCl_3$ and overlayed with 6 ml of petroleum ether.

Tris(triphenylphosphane)copper(I)dicyanmethanidonitrite (**3a**): slightly brown crystals, yield 80%, m.p. 143°C (dec). − IR (KBr): ν = 2212 s cm^{-1} [ν(CN)], 2193 w [ν(CN)], 1345 s [ν_{as}(CNO)], 1329 s [ν_s(CNO)], 1209 vs [ν(CC)], 694 vs (Ph), 742 vs (Ph), 1092 vs (Ph), 1434 vs (Ph), 1479 s (Ph), 3049 s (Ph). − ^{13}C NMR ($CDCl_3$): δ = 112.9 (s, CN), 119.0 (s, CN), 107.9 (s, methanide-C), 128.4, 128.5 [t, P−C-3,5, $^1J(^{31}P,^{13}C)$ = 8 Hz), 129.6 (s, P−C-4), 132.8, 133.0 [t, P−C1, $^1J(^{31}P,^{13}C)$ = 22.9 Hz], 133.6, 133.7 [t, P−C-2,6, $^1J(^{31}P,^{13}C)$ = 15.0 Hz]. − ^{31}P NMR ($CDCl_3$): δ = −0.27 (s, PPh_3). − $C_{57}H_{45}CuN_3OP_3$ (944.47): calcd. C 72.49, H 4.80, N 4.45; found C 70.70, H 4.67, N 4.04.

Tris(triphenylphosphane)silver(I)dicyanmethanidonitrite (**3b**): yellow crystals, yield 78%, m.p. 167.5°C. − IR (KBr): ν = 2204 s cm^{-1} [ν(CN)], 1306 s [ν_{as}(CNO)], 1262 s [ν_s(CNO)], 1226 vs [ν(CC)], 693 vs (Ph), 743 vs (Ph), 1093 vs (Ph), 1433 vs (Ph), 1479 vs (Ph), 3052 w (Ph). − ^{13}C NMR ($CDCl_3$): δ = 112.5 (s, CN), 118.6 (s, CN), 108.4 (s, methanide-C), 128.7, 128.8 [t, P−C-3,5, $^1J(^{31}P,^{13}C)$ = 10 Hz], 130.0 (s, P−C-4), 132.2, 132.4 [t, P−C1, $^1J(^{31}P,^{13}C)$ = 21.9 Hz], 133.7, 133.8 [t, P−C-2,6, $^1J(^{31}P,^{13}C)$ = 16.8 Hz]. − ^{31}P NMR ($CHCl_3$, capillary containing D_2O): δ = 6.98 (s, PPh_3), ^{31}P NMR ($CDCl_3$): δ = 7.93 (s, PPh_3). − $C_{57}H_{45}AgN_3OP_3$ (988.79): calcd. C 69.24 H 4.59 N 4.25; found C 68.74, H 4.50, N 4.28.

Bis(triphenylphosphane)copper(I)dicyanmethanidonitrite (**5a**): yellow crystals, yield 78%, m.p. 182−183°C. − IR (KBr): ν = 2216 s cm^{-1} [ν(CN)], 2207 m [ν(CN)], 2188 w [ν(CN)], 1339 s [ν_{as}(CNO)], 1253 m [ν_s(CNO)], 1214 vs [ν(CC)], 692 vs (Ph), 744 vs (Ph), 1091 vs (Ph), 1433 vs (Ph), 1479 vs (Ph), 3050 m (Ph). − ^{13}C NMR ($CDCl_3$): δ = 113.9 (s, CN), 108.3 (s, methanide-C), 128.4, 128.6 [t, P-C3,5, $^1J(^{31}P,^{13}C)$ = 8.4 Hz], 129.7 (s, P-C4), 132.7, 133.2 [t, P-C-1, $^1J(^{31}P,^{13}C)$ = 23.1 Hz], 133.6, 133.9 [t, P-C-2,6, $^1J(^{31}P,^{13}C)$ = 15.4 Hz]. − ^{31}P NMR ($CHCl_3$, capillary containing D_2O): δ = −0.95 (s, PPh_3). − ^{31}P NMR ($CDCl_3$): δ = 0.17 (s, PPh_3). − $C_{78}H_{60}Cu_2N_6O_2P_4$ (1364.36): calcd. C 68.67, H 4.43, N 6.16; found C 68.24, H 4.96, N 5.77.

Bis(triphenylphosphane)silver(I)dicyanmethanidonitrite (**5b**): slightly yellow crystals, yield 77%, m.p. 155°C. − IR (KBr): ν = 2208 vs cm^{-1} [ν(CN)], 1326 vs [ν_{as}(CNO)], 1287 vs [ν_s(CNO)], 1244 vs [ν(CC)], 693 vs (Ph), 744 vs (Ph), 1095 s (Ph), 1434 vs (Ph), 1479 vs (Ph), 3051 w (Ph). − ^{13}C NMR ($CDCl_3$): δ = 111.6 (s, CN), 116.9 (s, CN), 108.7 (s, methanide-C), 129.0, 129.1 [t, P-C-3,5, $^1J(^{31}P,^{13}C)$ = 10 Hz], 130.6 (s, P-C-4), 130.6, 130.8 [t, P-C-1, $^1J(^{31}P,^{13}C)$ = 30.9 Hz], 133.6, 133.7 [t, P-C-2,6, $^1J(^{31}P,^{13}C)$ = 17.0 Hz]. − ^{31}P NMR ($CHCl_3$, capillary containing D_2O): δ = 11.05 (s, PPh_3), ^{31}P NMR ($CDCl_3$): δ = 11.85 (s, PPh_3). − $C_{78}H_{60}Ag_2N_6O_2P_4$ (1453.02) calcd. C 64.48, H 4.16, N 5.78; found C 60.14, H 4.00, N 5.25.

Bis(triphenylphosphane)copper(I)-2-cyano-1-metoxy-2-nitroso-vinylamide (**6**): After addition of 0.25 g (2 mmol) of **1** in 20 ml of methanol to a solution of 1.3 g (2 mmol) of **4a** in 20 ml of $CHCl_3$ the resulting mixture was heated to reflux in a water bath for 6 h. After filtration at room temp. the solvent was evaporated to dryness. The remaining solid was washed with methanol (2 × 10 ml) and dissolved in about 10 ml of $CHCl_3$. A quantity of *n*-pentane was added until the onset of turbidity was observed and the solu-

Table 3. Crystal data and experimental details of X-ray structure determination of **5a** and **5b**

	5a	**5b**·$CHCl_3$
Empirical formula	$C_{39}H_{30}CuN_3OP_2$	$C_{39}H_{30}AgN_3OP_2 \cdot 0.5\ CHCl_3$
Molecular mass [g·mol^{-1}]	682.14	786.15
Crystal system	triclinic	monoclinic
Space group	*P*1	*C*2/c
Lattice parameters:		
a [A]	12.216(1)	24.712(1)
b [A]	12.958(1)	14.284(1)
c [A]	13.475(1)	24.834(2)
α [°]	66.908(6)	90.0
β [°]	64.859(5)	121.401(4)
γ [°]	67.490(5)	90.0
V [A^3]	1715.4(2)	7482.3(7)
Z	2	8
F(000)	704	3192
$D_{calc.}$ [g·cm^{-3}]	1.321	1.396
μ (MoK_α) [cm^{-1}]	7.65	7.66
Crystal dimensions [mm]	0.46 × 0.35 × 0.21	0.46 × 0.34 × 0.17
Check reflections	(555), (516), (431)	(800), (040), (067)
Intensity variations [%]	9.8	10.0
$2\Theta_{max.}$ [°]	50.0	50.0
hkl range	±14, ±15, ±15	±29, ±16, ±29
Measured reflections	12046	13118
Unique reflections	6023	6559
$R_{int.}$	0.0380	0.0285
Obs. Reflections [$I > 2\sigma(I)$]	4443	4931
Refined parameters	415	438
Weighting coefficients a/b [a]	0.0310/0.4660	0.0431/11.5720
Absorption correction	empirical (Psi scans)	empirical (Psi scans)
$T_{min}/T_{max.}$	0.6566/0.7898	0.6718/0.7709
*R*1/*wR2*/*S* (all data)	0.0706/0.0955/1.121	0.0661/0.1120/1.126
*R*1/*wR2*/*S* [$I > 2\sigma$(I)]	0.0392/0.0790/1.113	0.0408/0.0939/1.120
$(\Delta/\sigma)_{max.}$ in last l.s. cycle	0.000	−0.001
$\Delta\rho_{fin.}$ (min./max.) [e·A^{-3}]	−0.231/0.263	−0.677/0.722

[a] $w = [\sigma^2(F_o^2) + (a \cdot P)^2 + b \cdot P]^{-1}$ where $P = 1/3\ (F_o^2) + 2\ _c^2)$

tion kept at about 0°C for 12 h. The resulting microcrystalline precipitate was filtered off and dried in vacuo. Orange crystals, yield 48%, m.p. 182−183°C. − IR (KBr): ν = 2212 s cm^{-1} [ν(CN)], 2202 s [ν(CN)], 1358 vs [ν_{as}(CNO)], 1330 vs [ν_s(CNO)], 1312 vs [ν(CC)], 695 vs (Ph), 744 vs (Ph), 1095 vs (Ph), 1434 vs (Ph), 1479 vs (Ph), 3052 w (Ph), 1606 vs [ν_{as}(OCN)], 1412 vs [ν_s(OCN)], 1385 vs [ν_s(OCN)]. − ^{13}C NMR ($CDCl_3$): δ = 113.4 (s, CN), 61.1 [s, *C*(NO)CN)], 126.4, 128.5, 129.6, 133.4 (s, Ph), 165.1 [s, C(NH)O], 13.8 (O−CH_3). − ^{31}P NMR ($CDCl_3$): δ = −0.02 (s, PPh_3). − $C_{40}H_{34}CuN_3O_2P_2$ (714.22) calcd. C 67.27, H 4.80, N 5.88; found C 66.98, H 4.69, N 5.72.

X-ray Crystal Structure Determination: A summary of crystal data along with details of the structure determination is given in Table 3[28]. All measurements were performed with a STOE-STADI4 diffractometer using graphite-monochromatized Mo-K_α radiation (λ = 0.71069 A) in the ω-2θ scanning mode at room temp.. For structure solution and refinement programs SHELXS-86[29] and SHELXL-93[30] were used. The molecular structures in Figures 2 and 3 were plotted by use of the program XP/PC[31].

[1] L. Jäger, C. Tretner, K. Sünkel, J. Kozısek, *Z. Anorg. Allg. Chem.* **1998**, 6243, in the press.
[2] L. Jäger, H. Köhler, *Sulfur Reports* **1992**, *12*, 159−212.
[3] L. Jäger, H.-D. Schädler, U. Grobe, H. Köhler, V. I. Nefedov, *Z. Anorg. Allg. Chem.* **1992**, *617*, 123−126.
[4] E. Fritsch, K. Polborn, K. Sünkel, W. Beck, H. Köhler, L. Jäger, *Z. Anorg. Allg. Chem.* **1992**, *617*, 110−116.
[5] D. S. Bohle, B. J. Conklin, C.-H. Hung, *Inorg. Chem.* **1995**, *34*, 2569−2581.
[6] L. Jäger, C. Tretner, H. Hartung, M. Biedermann, *Chem. Ber.* **1997**, *130*, 1007−1012.
[7] M. Hvastijova, J. Kohout, J. Kozısek, L. Jäger, I. Svoboda, *Progress in Coordination and Organometallic Chemistry*, Slovak Technical University Press, Bratislava **1997**, 159−164.
[8] M. Hvastijova, J. Kozısek, J. Kohout, J. Mrozinski, L. Jäger, I. Svoboda, *Polyhedron* **1997**, *16*, 463−471.
[9] Y. M. Chow, D. Britton, *Acta Crystallogr.* **1974**, *30B* 1117−1118.
[10] L. Jäger, C. Tretner, C. Wagner, will be published.
[11] A. G. Orpen, G. Brammer, F. H. Allen, O. Kennard, D. G. Watson, R. Taylor, *J. Chem. Soc., Dalton Trans.* **1989**, S1−S83.
[12] L. Jäger, C. Tretner, H. Hartung, M. Biedermann, *Z. Anorg. Allg. Chem.* **1997**, *623*, 1299−1305.
[13] M. J. Begley, P. Hubberstey, P. H. Walton, *J. Chem. Soc., Dalton Trans.* **1995**, 957−962.
[14] E. W. Ainscough, E. N. Baker, M. L. Brader, A. M. Brodie, S. L. Ingham, J. M. Waters, J. V. Hanna, P. C. Healy, *J. Chem. Soc., Dalton Trans.* **1991**, 1243−1249.
[15] U. Thewalt, R. E. Marsh, *Inorg. Chem.* **1970**, *9*, 1604−1610.
[16] N. K. Mills, A. H. White, *J. Chem. Soc., Dalton Trans.* **1984**, 229−237.
[17] S. Ohba, Y. Saito, *Acta Crystallogr.* **1981**, *B37*, 1911−1913.
[18] T. J. Kistenmacher, M. Rossi, L. G. Marzilli, *Inorg. Chem.* **1979**, *18*, 240−244.
[19] A. Perez Salzar, F. H. Cano, S. Garcia-Blanco, *Z. Kristallogr.* **1980**, *152*, 253−258.
[20] E. Benedetti, A. Bavoso, B. di Blasio, V. Pavone, C. Pedone, F. Rossi, *Inorg. Chim. Acta* **1986**, *116*, 31−35.
[21] V. V. Skopenko, Yu. L. Zub, M. A. Porai-Koshitz, G. G. Sadikov, *Ukr. Khim. Zh.* **1979**, *45*, 811−816 [*Chem. Abstr.* **1979**, *91,* 202606s].
[22] L. Jäger, A. Dvorsky, H. Hartung, M. Biedermann, to be published.
[23] P. Rademacher, *Strukturen organischer Moleküle*, VCH, Weinheim, **1987**, p. 56.
[24] M. I. Kay, B. C. Frazer, *Acta Crystallogr.* **1961**, *14*, 56−57.
[25] F. H. Jardine, A. G. Vohra, F. J. Young, *J. Inorg. Nucl. Chem.* **1971**, *33*, 2941−2945 and H. J. Gysling, G. J. Kubas, *Inorg. Synth.* **1979**, *19*, 92−97.
[26] E. L. Muetterties, C. W. Alegranti, *J. Am. Chem. Soc.* **1972**, *94*, 6386−6391.
[27] D. V. Sanghani, P. J. Smith, D. W. Allen, B. F. Taylor, *Inorg. Chim. Acta* **1982**, *59*, 203−206.
[28] Further details of the crystal structure determination are available from the Fachinformationszentrum Karlsruhe, D76344 Eggenstein-Leopoldshafen, Germany, quoting the depository numbers CSD-407349 (**5a**) and CSD-407348 (**5b**).
[29] G. M. Sheldrick, SHELXS-86, *Acta Crystallogr.* **1990**, *A46*, 467−473.
[30] G. M. Sheldrick, *SHELXL-93, Program for the Crystal Structure Refinement*, University of Göttingen, **1993**.
[31] *XP/PC, Molecular Graphics Program Package for Display and Analysis of Stereochemical Data*, Version 4.2 for MS-DOS, Siemens Analytical X-Ray Instruments, Inc., Madison, Wisconsin, USA, **1990**.

[97212]

The 1,3-Sn_2O_2-Heterocycle as a Ligand in Organometallic Compounds – Dimerization of the Inidene Species $[\{(CO)_5M\}_2SnOR]^-$ (M = Cr, W)☆

Peter Kircher, Gottfried Huttner*, Katja Heinze, and Laszlo Zsolnai

Anorganisch-Chemisches Institut der Universität Heidelberg,
Im Neuenheimer Feld 270, D-69120 Heidelberg, Germany
Fax: (internat.) + 49(0)6221/545707

Received March 5, 1998

Keywords: Pentacarbonylmetal–tin bonding / Alkoxytin compounds / Inidene compounds / ^{119}Sn NMR / Bonding

Dimerized inidene complexes $[(CO)_5M{=}Sn(OR){=}M(CO)_5]_2^{2-}$ (M = Cr, W; R = Et, *i*Pr), **1**, are obtained from $[\{(CO)_5M\}_2SnCl_2]^{2-}$ by different routes. Dimerization occurs via alkoxy-donor tin-acceptor bonding by which a planar Sn_2O_2 ring is formed. The Sn–$\{M(CO)_5\}$ bonds are made in a plane vertical to this ring such that, with the R–O groups being almost coplanar with the Sn_2O_2 ring, the overall geometry of the compounds shows idealized D_{2h} symmetry. – The ^{119}Sn-NMR resonances of **1** are found at rather low fields (M = Cr: $\delta \approx 1400$; M = W: $\delta \approx 1170$) indicating a low-lying tin-centered orbital in the LUMO range. Correspondingly EHT analyses show that the 3-center-4π system, which characterizes monomeric inidene species $[L_nM{=}E(X){=}ML_n]^n$, is still prevalent in the dimeric species **1**. The low-lying π*-type LUMOs of **1** are the rationale for the observed ^{119}Sn-NMR low-field shifts of **1**. The dimeric compounds **1** react with 2,4-pentanedione to form chelate compounds of the same type as those characteristically obtained from monomeric inidene complexes: $[\{(CO)_5Cr\}_2SnOEt]_2^{2-}$ (**1a**) reacts to give $[\{(CO)_5Cr\}_2Sn(acac)]^-$ (**2**). The experimental results are verified by X-ray analyses in addition to the usual spectroscopic and analytical investigations.

Trigonal planar coordination around a tin center has so far only been achieved in a few types of compounds: stannylene complexes $[\{(CO)_5M\}SnR_2]$ (M = Cr, Mo, W)[1] which are isolobal analogues of olefins, the star-type compound $[\{(CO)_5Cr\}_3Sn]^{2-}$[2] which is isolobal to the carbonate anion, $[\{L_nM\}_2Sn{=}ML_n]$ (L_nM = $W(CO)_5$, $Cp^R(CO)_2Mn$; Cp^R = Cp, Cp′, Cp*)[3] which are analogues of the methylenecyclopropane system, and inidene compounds $[L_nM{=}Sn(X){=}ML_n]^-$ (ML_n = $MnCp'(CO)_2$, R = Cl, Br, S*t*Bu)[4] which are analogues of the allylic anion, represent the few types of compounds for which trigonal-planar coordination of tin is known. For the inidene series of compounds there is strong evidence that the species $[L_nM{=}Sn(X){=}ML_n]^-$ are only stable, as such, if the L_nM fragment is a potent d-π donor such as $[Cp^R(CO)_2Mn]$, while L_nM groups such as $[(CO)_5M]$ (M = Cr, Mo, W) with their reduced π-donor capabilities[5] will not sufficiently stabilize the allylic-type 3-center-4π system characteristic of these compounds.[6][7] Inidene compounds $[(CO)_5M{=}Sn(X){=}M(CO)_5]^-$ are obviously strongly Lewis-acidic at their unsaturated tin center, such that in any attempt to prepare them the base adducts, $[(CO)_5M{-}Sn(X)(B){-}M(CO)_5]^n$, appear to be inevitably formed. Quite a number of such base adducts have now been characterized,[8][9] while no unprotected compound $[(CO)_5M{=}Sn(X){=}M(CO)_5]^-$ has so far been obtained. In order to prepare such compounds it appears natural to try to compensate for the reduced d-π-donor capabilities of the $[(CO)_5M]$ entities by introducing a p-π donor as the substituent X at the tin center. As potentially π-donating substituents R–O or R–S entities are a straightforward choice. While an R–S substituent would be preferable due to its soft sulfur donor, hitherto uncontrollable side reactions have precluded the successful synthesis of $[(CO)_5M{=}Sn(SR){=}M(CO)_5]^-$ compounds.[8b] With the R–O substituent, which is decidedly less soft when compared to the R–S entity, the working hypothesis met with partial success: $[(CO)_5M{=}Sn(OR){=}M(CO)_5]^-$ entities are in fact formed, albeit not as monomeric species but as dimers $[\{(CO)_5M\}_2Sn(\mu_2\text{-}OR)_2Sn\{M(CO)_5\}_2]^{2-}$ (**1**) (Table 1). The Lewis acidity at the tin centers is still large enough to call for compensation by an oxygen "lone pair" of a second inidene species.

Table 1. Complexes of type **1**

	no.	M	R	cation
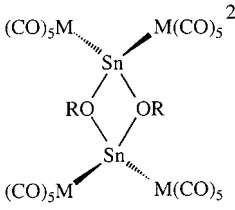	$[n\text{Bu}_4\text{N}]_2\cdot$ **1a**	Cr	Et	$[n\text{Bu}_4\text{N}]$
	$[\text{Ph}_4\text{P}]_2\cdot$ **1a**	Cr	Et	$[\text{Ph}_4\text{P}]$
	$[n\text{Bu}_4\text{N}]_2\cdot$ **1b**	Cr	*i*Pr	$[n\text{Bu}_4\text{N}]$
	$[n\text{Bu}_4\text{N}]_2\cdot$ **1c**	W	Et	$[n\text{Bu}_4\text{N}]$
	$[\text{Ph}_4\text{P}]_2\cdot$ **1d**	W	Et	$[\text{Ph}_4\text{P}]$

This type of dimerization is similar to that observed for $[\{Cp(CO)_2Mn\}_2BiCl]$.[7j][10] The dimeric entities have a strong relation to the well-characterized main-group ring species $[R{-}Sn(\mu_2\text{-}OR)_2Sn{-}R]$[11] as well as to the theoretically well-understood species $[Sn_2H_4]$ and $[Sn_2H_6]^{2+}$.[12] They are also closely related to genuine inidene compounds.

 © WILEY-VCH Verlag GmbH, D-69451 Weinheim, 1998 1434–1948/98/0808–1057 $ 17.50+.50/0

In this paper we describe the syntheses, structure, spectroscopy, and reactivity of type-**1** compounds, as well as the specific bonding situation pertaining to them.

Results and Discussion

Synthesis and Reactivity

When the dichlorostannate compounds **A**, $[\{(CO)_5M\}_2SnCl_2]^{2-}$ (M = Cr, W)[8], are treated with $[nBu_4N][BH_4]$ in an alcoholic solution the alkoxy-bridged dimers $[nBu_4N]_2 \cdot \mathbf{1}$ are obtained (Scheme 1) instead of the desired hydridotin species.

Scheme 1. Reaction of $[\{(CO)_5M\}_2SnCl_2]^{2-}$ (M = Cr, W) (**A**) with $[nBu_4N][BH_4]$ in alcoholic solution

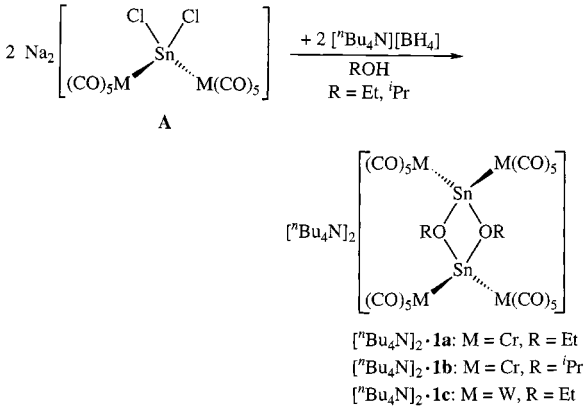

$[^nBu_4N]_2 \cdot \mathbf{1a}$: M = Cr, R = Et
$[^nBu_4N]_2 \cdot \mathbf{1b}$: M = Cr, R = ^{i}Pr
$[^nBu_4N]_2 \cdot \mathbf{1c}$: M = W, R = Et

The yellow compounds $[nBu_4N]_2 \cdot \mathbf{1}$ are obtained as microcrystalline solids, the constitution of which is documented by the usual spectroscopic and analytical techniques as well as by a series of X-ray analyses (Tables 3, 4, and 5). It is observed that under the reaction conditions described addition of $[nBu_4N][BH_4]$ to the solutions of **A** is accompanied by a rapid evolution of gas. It might therefore be assumed that the primary product, and hence intermediate in the formation of $[nBu_4N]_2 \cdot \mathbf{1}$, is a hydridotin species.

While this hypothesis can not be completely ruled out, it appears more probable that the hydridoborate is merely active as a base, deprotonating the alcohol which is used as the solvent; no hydridoborate is needed for the transformation of **A** into **1** if sodium ethoxide, NaOEt, is used as the reagent (Scheme 2).

Scheme 2. Reaction of $[\{(CO)_5M\}_2SnCl_2]^{2-}$ (M = Cr, W) (**A**) with NaOEt

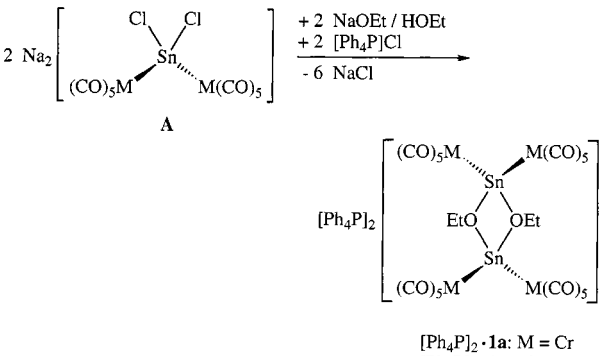

$[Ph_4P]_2 \cdot \mathbf{1a}$: M = Cr
$[Ph_4P]_2 \cdot \mathbf{1c}$: M = W

Under these conditions the dimeric dianions are immediately formed (IR control), and the salts $[Ph_4P]_2 \cdot \mathbf{1a}$ and $[Ph_4P]_2 \cdot \mathbf{1c}$ are precipitated, by the addition of $[Ph_4P]Cl$, in the form of microcrystalline yellow powders. Since solutions of **A** in alcohols are stable as such, it is evident that basic conditions are necessary to induce the transformation of **A** into **1**.

This fact is also inferred from the observation that treating THF solutions of $Na_2[\{(CO)_5W\}_2SnCl_2]$ with pyridine (py), which leads to the formation of the pyridine adduct **B**, $[\{(CO)_5W\}_2Sn(py)_2]$ as the major product[9], will also produce minor amounts of $[Ph_4P]_2 \cdot \mathbf{1c}$ when ethanol is used as the eluent during the chromatographic workup (Scheme 3). In this case pyridine obviously acts as the HCl scavenger.

Scheme 3. Reaction of $Na_2[\{(CO)_5W\}_2SnCl_2]$ with an excess of pyridine

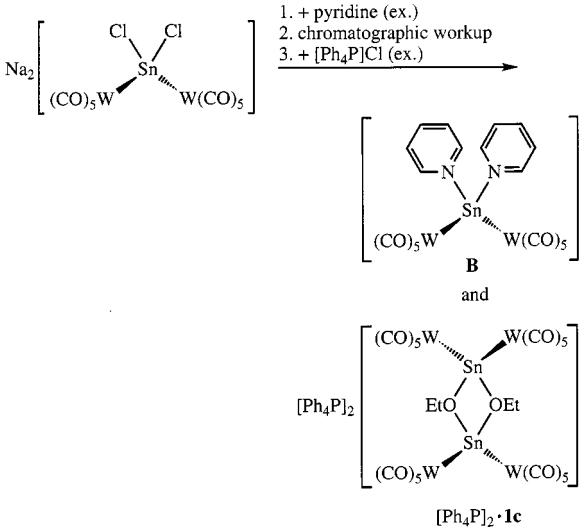

$[Ph_4P]_2 \cdot \mathbf{1c}$

Yet another way to produce $[Ph_4P]_2 \cdot \mathbf{1c}$ relies upon the basisity of the $[W_2(CO)_{10}]^{2-}$ anion (Scheme 4): when **A** is allowed to react with $Na_2[W_2(CO)_{10}]$ in ethanol an immediate color change from yellow to dark red is observed.

Scheme 4. Reaction of $Na_2[\{(CO)_5W\}_2SnCl_2]$ with $Na_2[W_2(CO)_{10}]$ in ethanol

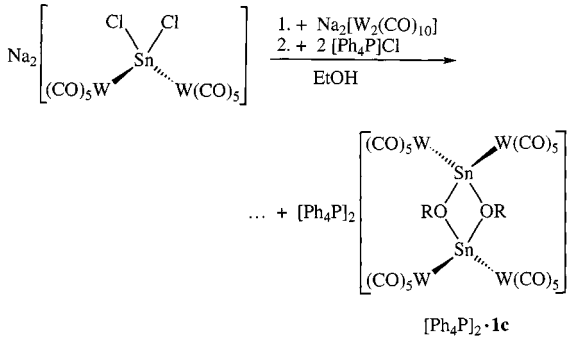

$[Ph_4P]_2 \cdot \mathbf{1c}$

^{119}Sn-NMR spectroscopy shows that a mixture of at least 5 species is formed, one of them being $[Ph_4P]_2 \cdot \mathbf{1c}$ which may be precipitated by addition of $[Ph_4P]Cl$.

As far as the reactivity of **1** is concerned the compounds behave similarly to dimerized inidene species; it is a charac-

teristic of $[L_nM{=}E(X){=}ML_n]^n$ (E = group 15 element, n = 0; E = group 14 element, $n = -1$; X = leaving group: e.g. Cl, etc.) to undergo substitution and addition with monovalent chelate bases to form chelate derivatives.[13] Correspondingly, $[n\mathrm{Bu_4N}]_2 \cdot$ **1a** reacts with 2,4-pentanedione (Hacac) to give **2** as its $[n\mathrm{Bu_4N}]$ salt (Scheme 5).

Scheme 5. Reaction of $[n\mathrm{Bu_4N}]_2 \cdot$ **1a** with 2,4-pentanedione

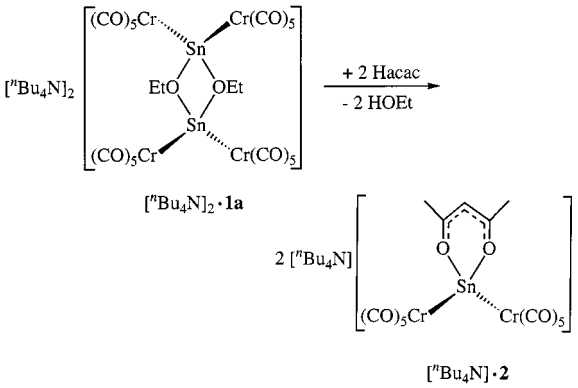

No external base is needed to promote this reaction. The reaction itself is monitored by NMR spectroscopy, either by observing the disappearance of the ^{1}H-NMR resonance of the diketo tautomer of 2,4-pentanedione in acetone solution or by observing the disappearance of the ^{119}Sn-NMR signal of $[n\mathrm{Bu_4N}]_2 \cdot$ **1a** (δ = 1445) and the appearance of the signal at δ = 1205 characterizing $[n\mathrm{Bu_4N}] \cdot$ **2** (Table 3). The spectroscopic data leave no doubt about the consitution of $[n\mathrm{Bu_4N}] \cdot$ **2**. Its solid-state structure could, however, not be analyzed since $[n\mathrm{Bu_4N}] \cdot$ **2** is (even after the chromatographic workup) an oil with no tendency to crystallize. Since the $[\mathrm{Ph_4P}]$ salt of **2** was also found to be an oil, the γ-pyronate analogue **3** of **2** was synthesized (Scheme 6) with the hope of obtaining a crystalline compound showing a bonding situation closely related to that in **2**. As an easy access to chelate compounds of this type the reaction of **A** with chelate bases had been described.[8b][9] Following this route **3** was prepared from $Na_2[\{(CO)_5Cr\}_2SnCl_2]$ and the sodium salt of 3-hydroxy-2-methyl-γ-pyrone (pyro) (Scheme 6).

Scheme 6. Reaction of $Na_2[\{(CO)_5Cr\}_2SnCl_2]$ with the sodium salt of 3-hydroxy-2-methyl-γ-pyrone

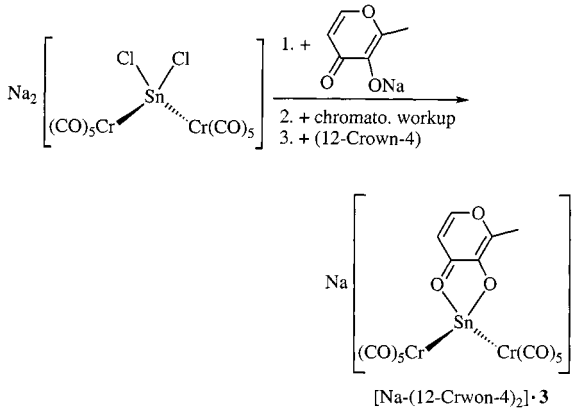

$[\mathrm{Na(12\text{-}Crown\text{-}4)_2}] \cdot$ **3** was prepared as a crystalline salt. The structure of the anion of this salt, as obtained by X-ray analysis, is shown in Figure 1. The accuracy of the structure determination is rather low due to insufficient crystal quality and the notorious disorder of the 12-Crown-4 entities.

Figure 1. Molecular strucutre of the anion of $[\mathrm{Na(12\text{-}Crown\text{-}4)_2}] \cdot$ **3**[a]

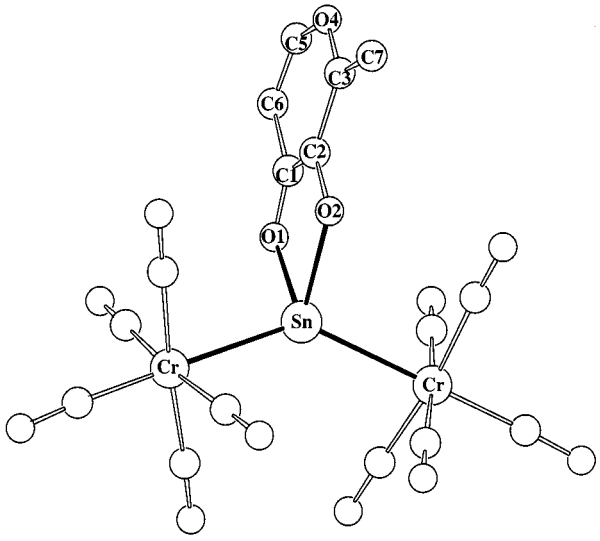

[a] The numbering system chosen does not correspond to the one adopted in the data deposited.

Even though the overall geometry of the chelate compound is established beyond doubt (Table 2), comparison of the spectrocopic properties of $[\mathrm{Na(12\text{-}Crown\text{-}4)_2}] \cdot$ **3** with those observed for $[n\mathrm{Bu_4N}] \cdot$ **2** (Table 3) shows that the general structural and electronic features of both compounds are very similar.

Table 2. Selected bond lenghts [pm], angles [°], and torsion angles [°] for the anion **3** of $[\mathrm{Na(12\text{-}Crown\text{-}4)_2}] \cdot$ **3**[a]

Cr−Sn	262.6(2)	Cr−Sn−Cr	137.17(6)
	262.8(2)	O−Sn−O	76.9(4)
Sn−O1	217.8(8)	Cr−Sn−O	107.8(2)
Sn−O2	216.5(8)		105.1(2)
O1−C1	120(1)		105.7(2)
O2−C2	151(1)		107.8(2)
C1−C2	129(2)	Sn−O−C	102.6(6)/118(1)
C2−C3	146(2)	Sn−Cr−C_{COax}	178.1(4)/178.8(4)
C3−O4	130(1)	Sn−Cr−C_{COeq}	85.7(3)−89.5(3)
O4−C5	146(2)	C_{COax}−Cr−C_{COeq}	90.7(5)−94.3(6)
C5−C6	123(2)	C_{COeq}−Cr−C_{COeq}	86.6(5)−92.2(5)
C6−C1	156(2)		172.3(5)−176.2(5)
C3−C7	136(2)	Cr−C−O	176.1(9)−179.5(9)
Cr−C_{COax}	184(1)		
Cr−C_{COeq}	184(1)−190(1)	torsion angle α[b]	11

[a] Estimated standard deviations in units of the least significant figures given in each case are quoted in parentheses. − [b] α is defined elsewhere in the text.

The integrity of the ligand is in both cases (**2** and **3**) supported by the ^{1}H- and ^{13}C-NMR spectra (see Experimental Section). The symmetrical binding of the acac ligand of **2** (averaged over time at least) is also apparent from these spectra.

Table 3. $\tilde{\nu}_{CO}$-IR and $^{119}Sn\{^1H\}$-NMR-spectroscopic data for the compounds **1**−**3**

	IR in CH_2Cl_2 ν [cm^{-1}]				$^{119}Sn\{^1H\}$ δ [ppm]
$[n\mathrm{Bu_4N}]_2\cdot$**1a**	2032 (w)	2007 (s)	1917 (vs)	1886 (s)	1445[a]
$[\mathrm{Ph_4P}]_2\cdot$**1a**	2033 (w)	2007 (s)	1918 (vs)	1880 (s)	1460[b]
$[n\mathrm{Bu_4N}]_2\cdot$**1b**[c]	2032 (w)	2005 (s)	1918 (vs)	1884 (s)	1379[a]
$[n\mathrm{Bu_4N}]_2\cdot$**1c**	2045 (w)	2026 (s)	1925 (vs)	1881 (s)	1169[b][d]
$[\mathrm{Ph_4P}]_2\cdot$**1c**	2044 (w)	2025 (s)	1923 (vs)	1878 (s)	1169[b][e]
$[n\mathrm{Bu_4N}]\cdot$**2**[c]	2039 (w)	2004 (s)	1919 (vs)	1891 (s)	1205[b]
$[\mathrm{Na(12C4)_2}]\cdot$**3**[c]	2037 (w)	2001 (s)	1917 (vs)	1889 (s)	1361[b]

[a] In CD_2Cl_2, 25°C. − [b] In [D_6]acetone, 25°C. − [c] In THF. − [d] $^1J(^{183}W,^{119}Sn)$ = 540 Hz; intensity ratio of peaks 17:100:17. − [e] $^1J(^{183}W,^{119}Sn)$ = 523 Hz; intensity ratio of peaks 15:100:17.

Structure and Bonding

X-ray analyses have been performed for the salts of $[n\mathrm{Bu_4N}]_2\cdot$**1a**, $[\mathrm{Ph_4P}]_2\cdot$**1a**, and $[\mathrm{Ph_4P}]_2\cdot$**1c**. The analysis of $[n\mathrm{Bu_4N}]_2\cdot$**1a** was hampered by the instability of the crystal, even at 173 K. Data were finally collected at 200 K (Table 5). Even when applying a rather high scan speed only the range up to $2\Theta = 28°$ could be covered . The phosphonium salts $[\mathrm{Ph_4P}]_2\cdot$**1a** and $[\mathrm{Ph_4P}]_2\cdot$**1c** did not pose these problems and data sets of good quality could be obtained up to $2\Theta \approx 50°$ for the two isotypic crystals (Table 5). The results of these three structure analyses are qualitatively similar for all three compounds (Table 4).

Only the structure of $[\mathrm{Ph_4P}]_2\cdot$**1c** is, therefore, shown in Figure 2. The structures of $[\mathrm{Ph_4P}]_2\cdot$**1a** and $[\mathrm{Ph_4P}]_2\cdot$**1c** have crystallographic inversion symmetry while the structure of $[n\mathrm{Bu_4N}]_2\cdot$**1a** has no crystallographic symmetry constraint (Table 4). The distances and angles, which by chemical reasoning should be equivalent in each case, are in fact very similar within each compound and, where appropriate, also for the whole class of compounds (Table 4).

Even the rotational position of the $[(CO)_5M]$ groups with respect to the Sn−M axes are almost identical in all three compounds; the angle α given in Table 4 (see also Table 2) refers to the pseudo torsion angle $C_{COeq}-M-M'-C_{COeq}'$ were M, C_{COeq} and M′, C_{COeq}' belong to $[(CO)_5M]$ groups bonded to one and the same tin center.[8b][9]

A characteristic feature of all three compounds $[n\mathrm{Bu_4N}]_2\cdot$**1a**, $[\mathrm{Ph_4P}]_2\cdot$**1a**, and $[\mathrm{Ph_4P}]_2\cdot$**1c** is a planar four-membered Sn_2O_2 ring (Table 4). Coordination of the $[(CO)_5M]$ groups occurs in a plane vertical to this cycle. The α-carbon atoms of the (μ_2-OEt) groups do not gener-

Table 4. Selected bond lenghts [pm], angles [°], torsion angles [°], and devitations of individual atoms from the Sn_2O_2 plane [pm] for the complex anions **1** in $[n\mathrm{Bu_4N}]_2\cdot$**1a**, $[\mathrm{Ph_4P}]_2\cdot$**1a**, and $[\mathrm{Ph_4P}]_2\cdot$**1c**[a]

	$[n\mathrm{Bu_4N}]_2\cdot$**1a** M = Cr	$[\mathrm{Ph_4P}]_2\cdot$**1a** M = Cr	$[\mathrm{Ph_4P}]_2\cdot$**1c** M = W
M−Sn	265.4(2)	265.3(1)	278.8(1)
	262.5(3)	265.4(1)	279.4(1)
	263.5(3)	−	−
	264.7(2)	−	−
Sn−O	216.6(9)	216.1(3)	214(1)
	215(1)	214.7(3)	215(1)
	214(1)	−	−
	215.2(9)	−	−
O−C_α	142(2)	144.2(5)	142(2)
	140(2)	−	−
C−C	145(2)	151.0(7)	151(2)
	148(2)	−	−
M−C_{COax}	178(2)−181(2)	183.0(5)/185.4(5)	196(2)/198(2)
M−C_{COeq}	180(2)−189(2)	187.5(5)−190.6(5)	199(2)/208(2)
M−Sn−M	125.22(8)	124.52(2)	125.52(5)
	124.40(8)	−	−
O−Sn−O	70.8(4)	72.8(1)	73.5(4)
	71.2(4)	−	−
Sn−O−Sn	108.8(4)	107.2(1)	106.5(4)
	109.1(5)	−	−
M−Sn−O	109.0(3)−117.4(3)	110.6(8)−113.4(8)	110.3(3)−113.7(3)
Sn−O−C_α	121.5(9)−125.1(8)	122.0(3)/123.3(3)	121.6(9)/123.2(9)
Sn−M−C_{COax}	174.3(5)−178.3(5)	170.1(2)/171.9(2)	167.6(6)/170.5(6)
Sn−M−C_{COeq}	81.9(4)−93.4(4)	82.4(2)−100.7(1)	82.3(5)−100.4(5)
C_{COax}−M−C_{COeq}	87.5(6)−96.3(6)	82.2(2)−97.9(2)	81.3(7)−96.1(8)
C_{COeq}−M−C_{COeq}	84.6(6)−94.9(6)	86.3(2)−94.1(2)	87.4(7)−92.5(7)
	168.6(6)−178.1(6)	166.0(2)−177.7(2)	168.1(7)−177.9(8)
M−C−O	175(1)−179(1)	173.1(4)−177.5(5)	172(2)−179(2)
O−C_α−C_β	115(1)/117(1)	110.3(4)	113(1)
α[b]	43	37	39
C_α−O−Sn−O	13.7−21.7	29.4/29.9	31.6/32.2
deviation of Sn	−2/−2	0/0	0/0
deviation of O	2/2	0/0	0/0
deviation of C_α	−26/−41	±63	±60

[a] Estimated standard deviations in units of the least significant figures given in each case are quoted in parentheses. − [b] Average values.

Table 5. Crystal structure data for $[n\mathrm{Bu_4N}]_2 \cdot$ **1a**, $[\mathrm{Ph_4P}]_2 \cdot$ **1a**, $[\mathrm{Ph_4P}]_2 \cdot$ **1c**, and [Na-(12-Crown-4)$_2$] · **3**

compound	$[n\mathrm{Bu_4N}]_2$·**1a**	$[\mathrm{Ph_4P}]_2$·**1a**	$[\mathrm{Ph_4P}]_2$·**1c**	[Na-(12-Crown-4)$_2$] ·**3**
formula	$C_{56}H_{43}Cr_4N_2O_{22}Sn_2$	$C_{72}H_{50}Cr_4O_{22}P_2Sn_2$	$C_{72}H_{50}O_{22}P_2Sn_2W_4$	$C_{32}H_{37}Cr_2NaO_{21}Sn$
molecular mass [g]	1541.300	1774.440	2301.840	1003.300
crystal dimensions [mm]	0.30 × 0.30 × 0.40	0.50 × 0.40 × 0.30	0.20 × 0.20 × 0.25	0.30 × 0.30 × 0.20
crystal system	triclinic	monoclinic	monoclinic	monoclinic
space group (No.)	$P\bar{1}$ (2)	$P2_1/c$ (14)	$P2_1/c$ (14)	$P2_1/c$ (14)
a [pm]	1145.8 (2)	947.3 (1)	965.4 (2)	1061.6 (8)
b [pm]	1361.7 (3)	2447.3 (3)	2473.0 (5)	1934.8 (9)
c [pm]	2262.3 (4)	1594.2 (2)	1588.5 (3)	2005.6 (8)
α [°]	85.45 (1)	90.00 (0)	90.00 (0)	90.00 (0)
β [°]	88.40 (1)	99.66 (1)	98.61 (1)	86.90 (4)
γ [°]	86.35 (2)	90.00 (0)	90.00 (0)	90.00 (0)
cell volume [10^6 pm^3]	3511 (1)	3643.5 (7)	3750 (1)	4113 (4)
molecular units / cell	2	2	2	4
density (calculated) [g cm^{-3}]	1.458	1.617	2.039	1.620
absorption coefficient [cm^{-1}]	13.65	13.69	68.81	12.12
temperature [K]	200	200	200	180
no. rflns. for cell parameter refinement	39	36	31	25
scan range	4.5° ≤ 2Θ ≤ 28.0°	4.2° ≤ 2Θ ≤ 56.0°	4.2° ≤ 2Θ ≤ 45.0°	3.8° ≤ 2Θ ≤ 60.0°
scan speed [° min^{-1}]	$\dot{\omega}$ = 15	$\dot{\omega}$ = 11	$\dot{\omega}$ = 13	8.0 ≤ $\dot{\omega}$ ≤ 60.0
no. rflns. measured	3120	9306	5175	6787
no. unique rflns.	2666	8796	4696	6467
no. rflns. observed	2443	7441	3245	3918
observation criterion	2 σ (*I*)	2 σ (*I*)	2 σ (*I*)	2 σ (*I*)
no. parameters refined	476	560	401	512
residual electron density [· 10^{-6} e pm^{-3}]	0.38 / - 0.38	1.27 / - 1.92	1.26 / - 1.32	1.36 / - 0.99
R_1 / R_W [%] (refinement on F^2)	4.2 / 11.1	4.2 / 15.2	5.6 / 14.0	6.8 / 19.7

Figure 2. Molecular structure of the anion of $[\mathrm{Ph_4P}]_2 \cdot$ **1c**

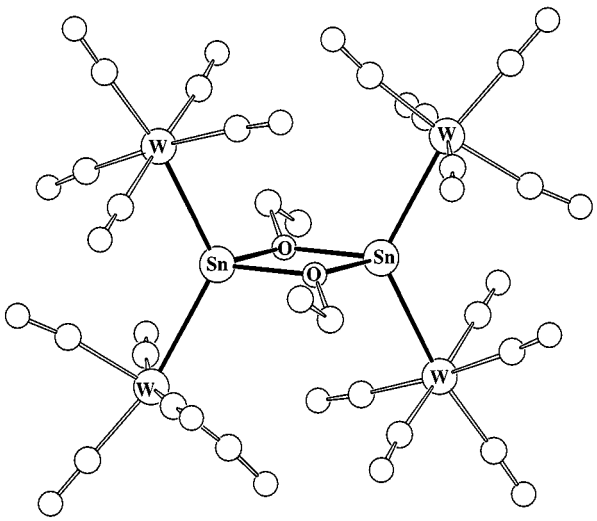

ally deviate too much from coplanarity with the heterocyclic plane (Table 4). The valence angles at the bridging oxygen atoms (Table 4) show that their coordination is more appropriately idealized as trigonal planar as compared to pseudo tetrahedral. Consequently, the torsion angles $C_\alpha-O-Sn-O$ (Table 4) are small.[11] The idealized symmetry of the core of the compounds, including the metal atoms, the tin centers and the $O-CH_2$ fragments, is close to D_{2h} (Figure 2).

As far as the bonding situation is concerned compounds **1** may be considered as composed of two $[(CO)_5M{=}Sn(OR){=}M(CO)_5]^-$ species which, due to the electron deficiency at the tin centers in these inidene-type entities, dimerize by oxygen-donor−tin-acceptor bonding (Figure 2).

On the other hand, the planar $Sn_2(OR)_2$ ring forming the central ligand entity in compounds **1** has a strong resemblance to the corresponding entities in $[RSn(OR)]_2$ (**a** in Figure 3). These species, which may be seen as dimerized stannylenes RSnOR, have been thoroughly analyzed by M. Veith and his group.[11]

Figure 3. Realtionship between **1** and some $Sn_2(OR)_2$- and Sn_2H_2-heterocycles

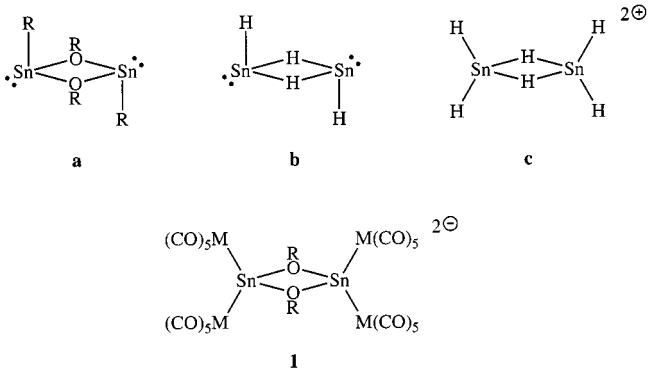

a **b** **c**

1

This kind of view is well born out by theoretical reasoning which makes clear that the most stable dimerized form

of H_2Sn does correspond to the cyclic structure of **b**[12] which is mutatis mutandis the same as that for the well-characterized compounds **a** (Figure 3). Protonation of the "lone pairs" in **b** leads to the dication **c** (Figure 3) which, as will be discussed later, is a close relative to the anions **1**. A structure corresponding to **c** is established as a true minimum on the potential surface for the isoelectronic $C_2H_6^{2+}$ cation and is a global minimum for B_2H_6 which is also an isoelectronic analogue.[14] The relationship of **c** to the anions **1** is the following:

1. Bridging hydrogen atoms may be replaced by bridging R−O groups without much change being caused by the three additional p-valence orbitals at the oxygen atom, as is seen by comparing **a** and **b**. The major change in bonding is the replacement of the 3-center-2-electron Sn−H−Sn bridges by 3-center-4-electron Sn−(OR)−Sn bridges, both referring to σ-bonding. The disturbance by potential π-interactions between the relevant oxygen and tin p orbitals will only be slight, due to the misfit of these two types of p orbitals in size as well as in energy. So far to the similarity of the Sn_2H_2 core in **b** and **c** and the $Sn_2(OR)_2$ core in **a** and **1**.

2. The analogy of **c** and **1** is immediately apparent by comparing the σ-bonding properties of H and $[(CO)_5Cr]^-$. Both species have just one orbital filled with one electron in each case for this type of interaction. They are "isoelectronic" in the sense that a seventeen-electron organometallic species $[(CO)_5Cr]^-$ is an analogue of a seven electron main-group species [R] or of hydrogen [H] with all three of them being short by one electron with respect to the noble-gas electronic configuration.

Many of the ideas worked out for **a**−**c** may therefore be applied to **1** as well. With compounds **a** it is observed that the O−Sn−O angles are without exception considerably smaller than 90° with the Sn−O−Sn angles being correspondingly larger.[11] This type of angle distribution has been analyzed for **b** as the model compound.[12a] It has been rationalized in terms of the charge distribution within compounds of this type with both the bridging hydrogen atoms and the terminal hydrogen atoms being rather negatively charged.[12a] A merely electrostatic model built on these grounds will reproduce structures as well as energies. Similar reasoning will apply to **1**.

The approach of looking at **1** as an analogue of **c** by replacing the terminal hydrogen atoms in **c** by negatively charged "isoelectronic" $[(CO)_5M]^-$ groups in **1** does appear somewhat less arbitrary with the ν(CO)-IR data of **1** (Table 3) in mind: these ν(CO)-IR absorptions occur at wavelengths which are characteristic for negatively charged $[(CO)_5M]$ groups.[15] The R−O groups should bear δ^- charges by simple electronegativity arguments.

When the bonding in **1** is rationalized in these terms, the structural properties of **1** are not astonishing. What is, however, astonishing at first glance is that the ^{119}Sn-NMR shift of **1** is far more on the low-field side than is usually observed for tin in pseudo-tetrahedral four-coordination (R_2SnCl_2).[16] From the observations made with inidene-type compounds there is convincing evidence that the low-field shifts observed for the central main-group elements in these compounds are intimately connected to the presence of a low-energy π* orbital of these 3-center-4π systems.[17] The theory of NMR shifts predicts that the presence of such a low-lying main-group-centered orbital will strongly contribute to the paramagnetic (low-field) term of the shift observed for this element.[18] Since the symmetry of **1** would allow for such a low-lying orbital in **1** an EHT-MO analysis of **1** was performed as well. As a simplified model of **1**, following common practice, its "isoelectronic" analogue $[\{H_5Cr\}_2Sn(\mu_2\text{-}OH)_2Sn\{CrH_5\}_2]^{22-}$ with R−O replaced by H−O and $[(CO)_5Cr]$ replaced by $[H_5Cr]^{5-}$ was chosen.[19]

3-center-4π systems, only slightly disturbed by the interaction with oxygen p orbitals localized at the Cr−Sn−Cr entities, make up an essential part of the orbital pattern.

The totally bonding combinations of the 3-center-4π-parts are found at the HOMO-10 and HOMO-12 positions (Figure 4). Due to the D_{2h} symmetry of **1** and the model compound as well, orbitals must occur in pairs, one with *gerade* (*g*) symmetry and the other one with *ungerade* (*u*) symmetry with respect to the phases characterizing the contributions of the two Cr_2Sn parts (Figure 4). Due to a modulation by minor contributions from the oxygen valence orbitals these pairs may be at slightly different energies in those cases where this interaction is allowed by symmetry (Figure 4). The energy differences calculated for these pairs are smaller than 0.1 eV for the bonding orbitals (Figure 4) but are significant for some of the unoccupied ones (Figure 4).

The non-bonding orbital of each 3-center-4π constituent will have a zero coefficient for the tin p_x orbital and will be composed by an anti-phase combination of the d orbitals which might by symmetry maximally interact with the tin p_x orbital as individuals. The relevant orbitals are found at the positions HOMO-2 to HOMO-5 (Figure 4). Due to the coordinate system chosen the relevant d orbitals are a combination of d_{xy} and d_{xz}. These orbitals transform in groups as a_u and b_{2g}. A linear combination of the a_u pair as well as the b_{2g} pair are the representatives of the *u* and *g* combination of the terminal orbitals of the two 3-center-4π systems characterizing the compound.

The HOMOs of the compound correspond to *g* und *u* combinations of mainly Cr−Sn σ-bonding orbitals with a significant Sn-p_z contribution (Figure 4). The LUMOs of the model compound are σ-anti-bonding with an almost negligible tin contribution (Figure 4).

The totally antibonding combinations of the 3-center-4π systems are found at the positions LUMO+2 and LUMO+7. These orbitals have large Sn-p_x contributions and comparatively small contributions from the relevant d orbitals. They are modified by contributions of the oxygen p orbitals and are thus at different energies.

The essence of this analysis is the following: the 3-center-(M−E−M)-4π system, which is characteristic for inidene compounds, is as well a characteristic ingredient to the bonding situation in **1**: non-bonding contributions of the relevant d orbitals make up MOs in the HOMO range. Anti-bonding combinations of the relevant metal d and

Figure 4. Characteristic orbitals of $[\{L_5Cr\}_2Sn(\mu_2\text{-}OR)_2Sn\{CrL_5\}_2]^{2-}$[a,b]

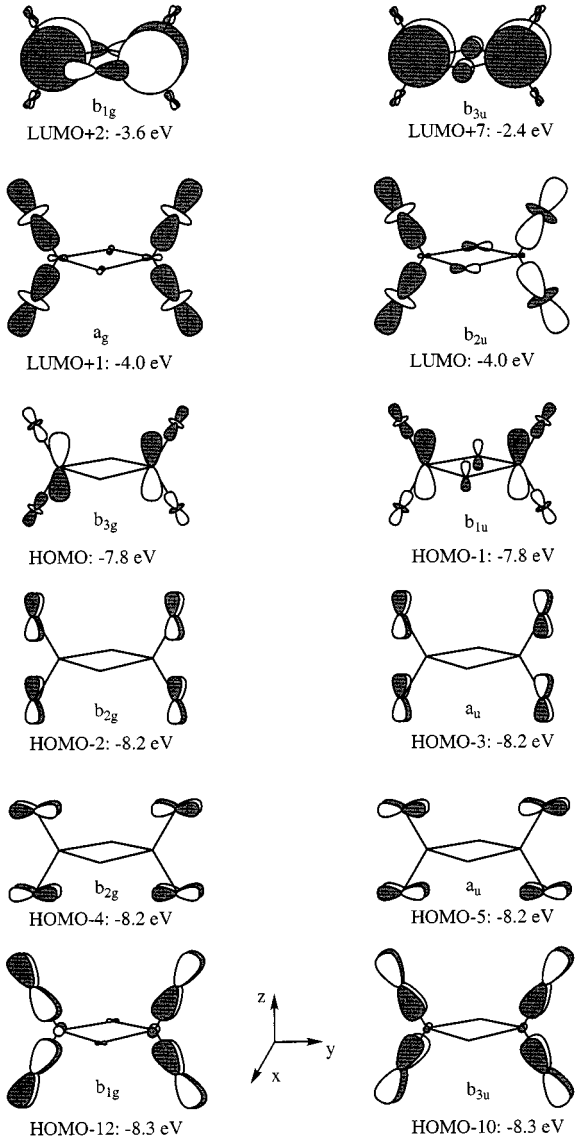

[a] The actual calculations were performed with $[CrH_5]^{5-}$ templates instead of $[L_5Cr]$. The R−O groups were replaced by H−O entities.− [b] The bottom three pairs of orbitals refer to the bonding and non-bonding sets of the (Cr−Sn−Cr) 3-center-4π-systems. The top pair corresponds to the LUMOs of these systems. The σ-type HOMO pairs and LUMO pairs of the model compound are given as well.

main-group p orbitals are found in the LUMO range. This situation is typically the one giving rise to large low-field shifts[2][8b][9][17][20] in the NMR spectra of the bridging elements as is also observed for **1**.[21]

It has been argued that real inidene-type compounds $[(CO)_5M{=}Sn(X){=}M(CO)_5]^-$ should have their ^{119}Sn-NMR shifts close to δ = 3000.[9] This argument was inferred in part from the observation that base adducts of these compounds $[(CO)_5M-Sn(X)(B)-M(CO)_5]^n$ show strong temperature dependence of their ^{119}Sn-NMR resonances. Equilibria of the type $[(CO)_5M-Sn(X)(B)-M(CO)_5]^n \rightleftarrows [(CO)_5M{=}Sn(X){=}M(CO)_5]^- + B$ have been put forward as an explanation.[9] Based on the same type of arguments the temperature dependence of the ^{119}Sn-NMR resonance of $[Ph_4P]_2\cdot$**1c** may be interpreted in terms of a ring-opening/ring-closing equilibrium (Figure 5). Upon cooling from 298 K to 198 K the ^{119}Sn-NMR signal of $[Ph_4P]_2\cdot$**1c** shifts to lower fields (from δ = 1158 to δ = 1135).

Figure 5. Ring-opening/ring-closing equilibrium

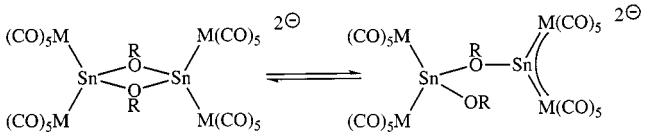

1

The shift difference observed for 10 K temperature difference is thus only 2 ppm in the case of $[Ph_4P]_2\cdot$**1c** while in other cases shifts of up to 20 ppm/10 K have been observed.[9]

Under the hypothesis that the temperature-induced shift is due to an equilibrium between three- and four-coordinated tin species the relatively small temperature dependence observed for $[Ph_4P]_2\cdot$**1c** indicates a high intrinsic stability of the four-membered Sn_2O_2 heterocycle.

Financial support by the *Fond der Chemischen Industrie* is gratefully acknowledged. The work had formerly been supported by the *Deutsche Forschungsgemeinschaft* (SFB 247).

Experimental Section

General: All manipulations were carried out under an argon atmosphere by means of standard Schlenk techniques at 25°C unless mentioned otherwise. All solvents were dried by standard methods and distilled under argon. [D$_6$]acetone and CD_2Cl_2 used for the NMR-spectroscopic measurements were degassed by three successive "freeze-pump-thaw" cycles and dried over 4-A molecular sieves. Silica gel (Kieselgel z. A., 0.06−0.2 mm, J. T. Baker Chemicals B. V.) used for chromatography and Kieselgur (Kieselgur, gereinigt, geglüht, Erg. B.6, Riedel-de Haen AG) used for filtration were degassed at 1 mbar at 180°C for 12 h and saturated with argon. − NMR: Bruker Avance DPX 200 at 200.13 MHz (^{1}H), 50.323 MHz (^{13}C{^{1}H}), 74.631 MHz (^{119}Sn{^{1}H}), 81.015 MHz (^{31}P{^{1}H}); chemical shifts (δ) in ppm with respect to [D$_6$]acetone (^{1}H: δ = 2.04, ^{13}C: δ = 29.8) and CD_2Cl_2 (^{1}H: δ = 5.32, ^{13}C: δ = 53.5) as internal standards; chemical shifts (δ) in ppm with respect to $SnMe_4$ (^{119}Sn: δ = 0, at 25°C) and to 85% H_3PO_4 (^{31}P: δ = 0) as external standard. − IR: Bruker FT-IR IFS-66; CaF_2 cells. − UV/Vis/NIR: Perkin Elmer Lambda 19; cells (0.2 cm; Hellma 110 suprasil). − MS (FAB or EI): Finnigan MAT 8400; TEA (triethanolamine) matrix. − Elemental analyses: Microanalytical laboratory of the Organisch-Chemisches Institut, Universität Heidelberg. − Melting points: Gallenkamp MFB-595 010; values not corrected. − The dinuclear sodium salts of the composition $Na_2[\{(CO)_5M\}_2SnCl_2]$ (M = Cr, W) were prepared by salt metathesis from the corresponding stable phosphonium salts $[Ph_4P]_2[\{(CO)_5M\}_2SnCl_2]$ as described[8b]. All other chemicals were commercially obtained and used without further purification.

$[nBu_4N]_2[\{(CO)_5Cr\}_2Sn(\mu_2\text{-}OEt)_2Sn\{Cr(CO)_5\}_2]$ ($[nBu_4N]_2\cdot$**1a**): $Na_2[\{(CO)_5Cr\}_2SnCl_2]$ (310 mg; 0.5 mmol) was dissolved in ethanol (50 ml). At 0°C solid $[nBu_4N][BH_4]$ (257 mg; 1 mmol) was added in portions under spontaneous evolution of gas as well as precipitation of $[nBu_4N]_2\cdot$**1a** as a yellow microcrystalline powder.

The reaction mixture was stirred until no further evolution of gas was observed. The yellow solid of $[n\mathrm{Bu_4N}]_2\cdot$ **1a** was seperated from the reaction mixture by filtration, washed with ethanol (3 × 10 ml) and diethyl ether (2 × 10 ml) and dried in vacuo. Yield: 670 mg, 85%. For growing single crystals of $[n\mathrm{Bu_4N}]_2\cdot$ **1a** the yellow powder was dissolved in dichloromethane (10 ml) and overlayered with ethanol (100 ml). Within 7 d yellow single crystals suitable for X-ray structure analysis were obtained. M.p. 65°C (dec.). − IR (CH_2Cl_2): ν_{CO} = 2032 cm^{-1} (w), 2007 (s), 1917 (vs), 1886 (s). − UV/Vis (THF): λ (lg ε) = 430 nm (3.41). − ^{1}H NMR (CD_2Cl_2, 25°C): δ = 4.30 (q, 4 H, OCH_2), 3.14 (m, 16 H, 1-H_N), 1.64 (m, 16 H, 2-H_N), 1.48 (m, 16 H, 3-H_N), 1.44 (t, 6 H, OCH_2CH_3), 1.09 (t, 24 H, 4-H_N). − ^{13}C NMR (CD_2Cl_2, 25°C): δ = 230.5 (s, C_{COax}), 222.9 (s, C_{COeq}), 61.6 (s, OCH_2), 59.2 (s, C_N-1), 24.1 (s, C_N-2), 20.0 (s, C_N-3), 19.5 (s, OCH_2CH_3), 13.6 (s, C_N-4). − ^{119}Sn NMR (CD_2Cl_2, 25°C): δ = 1445. − MS (neg.-FAB, TEA); *m/z* (%): 547 (30) $[\{(CO)_5Cr\}_2SnOEt]^-$.

[nBu4N]2[{(CO)5Cr}2Sn(μ2-iOPr)2Sn{Cr(CO)5}2] ($[n\mathrm{Bu_4N}]_2\cdot$ **1b**): In an analogous procedure to that for $[n\mathrm{Bu_4N}]_2\cdot$ **1a**, $Na_2[\{(CO)_5Cr\}_2SnCl_2]$ (310 mg; 0.5 mmol) was dissolved in 2-propanol (50 ml) and treated with $[n\mathrm{Bu_4N}][BH_4]$ (257 mg; 1 mmol) at 0°C. The workup and crystal growth followed the methods described above. Even at 200 K, the obtained yellow single crystals of $[n\mathrm{Bu_4N}]_2\cdot$ **1b**, were not stable enough to allow for the collection of high-quality X-ray diffraction data set. Yield: 280 mg, 35%. − M.p. 65°C (dec.). − IR (THF): ν_{CO} = 2032 cm^{-1} (w), 2005 (s), 1918 (vs), 1884 (s). − ^{1}H NMR (CD_2Cl_2, 25°C): δ = 5.00 (sept, 2 H, OC*H*), 3.16 (m, 16 H, 1-H_N), 1.66 (m, 16 H, 2-H_N), 1.51 (d+m, 12+16 H, $OCH(CH_3)_2$ + 3-H_N), 1.09 (t, 24 H, 4-H_N). − ^{13}C NMR (CD_2Cl_2, 25°C): δ = 230.1 (s, C_{COax}), 223.2 (s, C_{COeq}), 68.9 (s, O*C*H), 59.1 (s, C_N-1), 26.5 [s, $OCH(CH_3)_2$], 24.0 (s, C_N-2), 19.9 (s, C_N-3), 13.6 (s, C_N-4). − ^{119}Sn NMR (CD_2Cl_2, 25°C): δ = 1379.

[nBu4N]2[{(CO)5W}2Sn(μ2-OEt)2Sn{W(CO)5}2] ($[n\mathrm{Bu_4N}]_2\cdot$ **1c**): At 0°C $Na_2[\{(CO)_5W\}_2SnCl_2]$ (442 mg; 0.5 mmol) in ethanol (50 ml) was treated with $[n\mathrm{Bu_4N}][BH_4]$ (257 mg; 1 mmol) in an analogous procedure. The further workup and single-crystal growth followed the methods described for $[n\mathrm{Bu_4N}]_2\cdot$ **1a**. Yield: 830 mg, 72%. − IR (CH_2Cl_2): ν_{CO} = 2045 cm^{-1} (w), 2026 (s), 1925 (vs), 1881 (s). − ^{1}H NMR ([D$_6$]acetone, 25°C): δ = 4.24 (q, 4 H, OCH_2), 3.45 (m, 16 H, 1-H_N), 1.85 (m, 16 H, 2-H_N), 1.49 (m, 16 H, 3-H_N), 1.44 (t, 6 H, OCH_2CH_3), 1.02 (t, 24 H, 4-H_N). − ^{13}C NMR ([D$_6$]acetone, 25°C): δ = 209.2 (s, C_{COax}), 204.7 (s, C_{COeq}), 62.7 (s, OCH_2), 59.4 (s, C_N-1), 24.4 (s, C_N-2), 20.4 (s, C_N-3), 19.5 (s, OCH_2CH_3), 13.9 (s, C_N-4). − ^{119}Sn NMR ([D$_6$]acetone, 25°C): δ = 1169 ($^1J_{W,Sn}$ = 540 Hz).

[Ph4P]2[{(CO)5Cr}2Sn(μ2-OEt)2Sn{Cr(CO)5}2] ($[Ph_4P]_2\cdot$ **1a**): A yellow solution of $Na_2[\{(CO)_5Cr\}_2SnCl_2]$ (310 mg; 0.5 mmol) in ethanol (50 ml) was added to a solution of NaH (25 mg; 1 mmol) in ethanol (20 ml), with no color change observed. After stirring for 30 min, the yellow solution was filtered through Kieselgur (3 cm). By addition of solid [Ph$_4$P]Cl (375 mg; 1 mmol) in one portion the phosphonium salt $[Ph_4P]_2\cdot$ **1a** precipitated immediatly as a yellow solid. After stirring for another 1 h, the yellow microcrystalline powder was separated from the mother liquor by filtration, washed with ethanol (3 × 10 ml) and diethyl ether (2 × 10 ml) and dried in vacuo. Yield: 660 mg, 75%. For growing single crystals of $[Ph_4P]_2\cdot$ **1a** suitable for X-ray structure analysis the same procedure as described for $[n\mathrm{Bu_4N}]_2\cdot$ **1a** was performed. M.p. 182°C (slow dec.). − IR (CH_2Cl_2): ν_{CO} = 2033 cm^{-1} (w), 2007 (s), 1918 (vs), 1880 (s). − UV/Vis (THF): λ (lg ε) = 340 nm (4.32, sh), 392 (3.93, sh). − ^{1}H NMR ([D$_6$]acetone, 25°C): δ = 8.02−7.87 (m, 40 H, aromatic H), 4.35 (q, 4 H, OCH_2), 1.45 (t, 6 H, OCH_2CH_3). − ^{13}C NMR ([D$_6$]acetone, 25°C): δ = 230.6 (s, C_{COax}), 223.2 (s, C_{COeq}), 136.4 (s, C_{para}), 135.6 (d, $^2J_{P,C}$ = 11 Hz, C_{ortho}), 131.3 (d, $^3J_{P,C}$ = 13 Hz, C_{meta}), 118.9 (d, $^1J_{P,C}$ = 90 Hz, C_{ipso}), 61.9 (OCH_2), 19.8 (OCH_2CH_3). − ^{119}Sn NMR ([D$_6$]acetone, 25°C): δ = 1460. − ^{31}P NMR ([D$_6$]acetone, 25°C): δ = 24.3 ($^1J_{C,P}$ = 89 Hz). − $C_{72}H_{50}Cr_4O_{22}P_2Sn_2$ (1774.4): calcd. C 48.74, H 2.96; found C 47.90, H 2.84.

[Ph4P]2[{(CO)5W}2Sn(μ2-OEt)2Sn{W(CO)5}2] ($[Ph_4P]_2\cdot$ **1c**): In an analogous procedure $Na_2[\{(CO)_5W\}_2SnCl_2]$ (442 mg; 0.5 mmol) in ethanol (50 ml) was treated with a solution of NaH (25 mg; 1 mmol) in ethanol (20 ml). The workup and crystal growth followed the methods described above. Yield: 780 mg, 68%. − M.p. 203°C (dec.). − IR (CH_2Cl_2): ν_{CO} = 2044 cm^{-1} (w), 2025 (s), 1923 (vs), 1878 (s). − UV/Vis (THF): λ (lg ε) = 318 nm (4.21), 369 (3.86, sh), 417 (3.62). − ^{1}H NMR ([D$_6$]acetone, 25°C): δ = 8.04−7.86 (m, 40 H, aromatic H), 4.24 (q, *J* = 6.8 Hz, 4 H, OCH_2), 1.41 (t, *J* = 6.8 Hz, 6 H, OCH_2CH_3). − ^{13}C NMR ([D$_6$]acetone, 25°C): δ = 209.1 (s, C_{COax}), 204.7 (s, C_{COeq}), 136.4 (d, $^4J_{P,C}$ = 3 Hz, C_{para}), 135.7 (d, $^2J_{P,C}$ = 11 Hz, C_{ortho}), 131.5 (d, $^3J_{P,C}$ = 13 Hz, C_{meta}), 119.1 (d, $^1J_{P,C}$ = 90 Hz, C_{ipso}), 62.7 (OCH_2), 19.5 (OCH_2CH_3). − ^{119}Sn NMR ([D$_6$]acetone, 25°C): δ = 1169 ($^1J_{W,Sn}$ = 523 Hz). − ^{31}P NMR ([D$_6$]acetone, 25°C): δ = 24.3. − $C_{72}H_{50}O_{22}P_2Sn_2W_4$ (2301.9): calcd. C 37.57, H 2.19; found C 37.18, H 2.60.

[nBu4N][{(CO)5Cr}2Sn(acac)] ($[n\mathrm{Bu_4N}]_2\cdot$ **2**): 2,4-Pentandione (50 mg; 0.5 mmol) was added in one portion to a solution of $[n\mathrm{Bu_4N}]_2[\{(CO)_5Cr\}_2Sn(\mu_2\text{-}OEt)_2Sn\{Cr(CO)_5\}_2]$ ($[n\mathrm{Bu_4N}]_2\cdot$ **1a**) (790 mg; 0.5 mmol) in THF (30 ml). The reaction mixture was stirred for 2 h, filtered through Kieselgur (3 cm) and dried. The oily yellow residue was dissolved in THF (3 ml) and chromatographed on silica gel (10 cm; Ø = 3cm; diethyl ether). Elution with diethyl ether gave a yellow band which was found, by IR-spectroscopic comparison, to consist mainly of $[Cr(CO)_6]$.[22] An orange band which contained $[n\mathrm{Bu_4N}]_2\cdot$ **2** was eluted with THF. This THF solution was dried in vacuo leaving a yellow orange oil which could not be crystallized. Yield: 350 mg; 42%. − IR (THF): ν_{CO} = 2039 (w), 2004 (s), 1919 (vs), 1891 (s) cm^{-1}. − ^{1}H NMR ([D$_6$]acetone, 25°C): δ = 5.58 (s, 1 H, C*H*), 3.42 (m, 16 H, 1-H_N), 2.05 (s, 6 H, CH_3), 1.82 (m, 16 H, 2-H_N), 1.47 (m, 16 H, 3-H_N), 1.04 (t, 24 H, 4-H_N). − ^{13}C NMR ([D$_6$]acetone, 25°C): δ = 229.7 (s, C_{COax}), 222.7 (s, C_{COeq}), 192.8 (C_{C-O}), 101.4 ($C_{C=C}$), 59.5 (s, C_N-1), 27.7 (C_{Me}), 24.4 (s, C_N-2), 20.4 (s, C_N-3), 13.9 (s, C_N-4). − ^{119}Sn NMR ([D$_6$]acetone, 25°C): δ = 1205.

[Na(12-Crown-4)2][{(CO)5Cr}2Sn(pyro)] ([Na(12-Crown-4)$_2$]$\cdot$ **3**): 3-Hydroxy-2-methyl-γ-pyrone (63 mg; 0.5 mmol) was deprotonated with NaH (12 mg; 0.5 mmol) at −70°C in THF (20 ml). The solution was allowed to warm up slowly to 25°C and was poured into a yellow solution of the disodium salt $Na_2[\{(CO)_5Cr\}_2SnCl_2]$ (310 mg; 0.5 mmol) in THF (30 ml). The reaction mixture was stirred for 2 h, filtered through Kieselgur (3 cm) and dried. The oily orange residue was dissolved in diethyl ether (3 ml) and chromatographed on silica gel (15 cm; Ø = 3 cm; diethyl ether). Elution with diethyl ether gave a yellow band which contained $[Cr(CO)_6]$ and another unidentified product (by IR-spectroscopic comparison with $[\{(CO)_5Cr\}Sn(oxinato)_2]$ (oxinato = 8-oxoquinolato)[8b] it appears probable that the product is $[\{(CO)_5Cr\}Sn(pyro)_2]$). An orange band which contains $[Na(THF)_x]\cdot$ **3** could be eluted with THF. This THF fraction was concentrated to 5 ml and 12-Crown-4 (36 mg; 0.2 mmol) was added.

For growing single crystals of [Na(12-Crown-4)$_2$]$\cdot$ **3** the following procedure was carried out: A concentrated THF solution (5 ml) of [Na(12-Crown-4)$_2$]$\cdot$ **3** was shared out between three test-tubes (Ø =

1 cm) which were brought into a Schlenk tube (250 ml). Diethyl ether (30 ml), within the tube, was allowed to diffuse through the gas phase into the THF solution (3 h). After this period of time the diethyl ether was replaced by petroleum ether (boiling range 40−60°C) (50 ml). Vapor diffusion of the petroleum ether (10 d) yielded yellow single crystals suitable for X-ray structure analysis. Crystalline yield: 110 mg; 11%. M.p. 166°C (dec.). − IR (THF): ν_{CO} = 2037 (w), 2001 (s), 1917 (vs), 1889 (s) cm^{-1}. − UV/Vis (THF): λ (lg ε) = 309 (4.45), 357 (3.98). − ^1H NMR for $[Na(solv)_x]\cdot$**3** ([D$_6$]acetone, 25°C): δ = 8.04 (d, 1 H, H5), 6.73 (d, 1 H, H6), 2.44 (s, 3 H, H7) (numbers refer to Figure 1). − ^{13}C NMR for $[Na(solv)_x]\cdot$**3** ([D$_6$]acetone, 25°C): δ = 229.8 (s, C_{COax}), 222.6 (s, C_{COeq}), 177.6 (C1), 156.0 (C_5), 155.3 (C2), 153.7 (C3), 111.5 (C6), 15.3 (C7) (numbers as given in Figure 1). − ^{119}Sn NMR for $[Na(solv)_x]\cdot$**3** ([D$_6$]acetone, 25°C): δ = 1361. − [Na(12-Crown-4)$_2$]·**3**, $C_{32}H_{37}Cr_2NaO_{21}Sn$ (1003.3): calcd. C 38.31, H 3.72; found C 38.37, H 3.85.

X-ray Structure Determinations: The measurements for $[n\mathrm{Bu_4N}]_2\cdot$**1a**, $[Ph_4P]_2\cdot$**1a**, $[Ph_4P]_2\cdot$**1c**, and [Na(12-Crown-4)$_2$]·**3** were carried out with a Siemens P4 four-circle diffractometer with graphite-monochromated Mo-K_α radiation. The intensities of three check reflections (measured every 100 reflections) remained constant (except for $[n\mathrm{Bu_4N}]\cdot$**1a**) throughout the data collection, thus indicating crystal and electronic stability. All calculations were performed using the SHELXT PLUS software package. Structures were solved by direct methods with the SHELXS-86 program and refined with the SHELX93 program.[23] The program XPMA[24] was used for graphical handling of the data. Absorption corrections (ψ scan, Δψ = 10°) were applied to the data. The structures were refined in fully or partially anisotropic models by full-matrix least-squares calculations. Hydrogen atoms were introduced at calculated positions. Table 5 compiles the data for the structure determinations. Peculiarities about the structure of [Na(12-Crown-4)$_2$]·**3** are the following: One of the crown ether molecules shows disorder and could only be refined isotropically.

Further details of the crystal structure investigations may be obtained from the Fachinformationszentrum Karlsruhe, D-76344 Eggenstein-Leopoldshafen (Germany), on quoting the depository numbers CSD-408368 ($[n\mathrm{Bu_4N}]_2\cdot$**1a**), -408369 ($[Ph_4P]_2\cdot$**1a**), -408367 ($[Ph_4P]_2\cdot$**1c**), -408370 ([Na(12-Crown-4)$_2$]·**3**).

☆ Dedicated to Professor *Warren Roper* on the occasion of his 60th birthday.

[1] [1a] J. D. Cotton, P. J. Davidson, D. E. Goldberg, M. F. Lappert, K. M Thomas, *J. Chem. Soc., Chem. Commun*. **1974**, 893−895. − [1b] J. D. Cotton, P. J. Davidson, H. F. Lappert, *J. Chem. Soc., Dalton Trans.* **1976**, 2275−2286. − [1c] A. B. Cornwell, P. G. Harrison, J. A. Richards, *J. Organomet. Chem.* **1976**, *108*, 47−60. − [1d] M. Weidenbruch, A. Stilter, J. Schlaefke, K. Peters, H. G. von Schnering, *J. Organomet. Chem.* **1995**, *501*, 67−70. − [1e] M. Weidenbruch, A. Stilter, K. Peters, H. G. von Schnering, *Z. Anorg. Allg. Chem.* **1996**, *622*, 534−538. − [1f] S. L. Ellis, P. B. Hitchcock, S. A. Holmes, M. F. Lappert, M. J. Slade, *J. Organomet. Chem.* **1993**, *444*, 95−99.

[2] P. Kircher, G. Huttner, K. Heinze, *J. Organomet. Chem.*, in press.

[3] [3a] G. Huttner, U. Weber, B. Sigwarth, O. Scheidsteger, H. Lang, L. Zsolnai, *J. Organomet. Chem.* **1985**, *282*, 331−348. − [3b] W. A. Herrmann, H.-J. Kneuper, E. Herdtweck, *Chem. Ber.* **1989**, *122*, 437−444.

[4] [4a] F. Ettel, G. Huttner, L. Zsolnai, C. Emmerich, *J. Organomet. Chem.* **1991**, *414*, 71−87. − [4b] F. Ettel, M. Schollenberger, B. Schiemenz, W. Imhof, G. Huttner, L. Zsolnai, *J. Organomet. Chem.* **1994**, *476*, 207−214.

[5] [5a] W. Strohmeier, *Angew. Chem.* **1964**, *76*, 873−881; *Angew. Chem. Int. Ed. Engl.* **1964**, *3*, 730−738. − [5b] U. Honrath, H. Vahrenkamp, *Z. Naturforsch. B* **1979**, *34*, 1190−1194. − [5c] T. Madach, H. Vahrenkamp, *Z. Naturforsch. B* **1979**, *34*, 1195−1198.

[6] For reviews see: [6a] G. Huttner, *Pure Appl. Chem.* **1986**, *58*, 585−596. − [6b] G. Huttner, K. Evertz, *Acc. Chem. Res.* **1986**, *19*, 406−413.

[7] For more recent publications on "inidene" compounds $[L_nM{=}E(X){=}ML_n]^n$ see also: E = In, Tl: [7a] O. J. Curnow, B. Schiemenz, G. Huttner, L. Zsolnai, *J. Organomet. Chem.* **1993**, *459*, 17−20. − E = Ge: [7b] B. Schiemenz, G. Huttner, *Chem. Ber.* **1994**, *127*, 2129−2133. − E = Sn: See ref.[4]. − E = Pb: [7c] F. Ettel, G. Huttner, L. Zsolnai, *Angew. Chem.* **1989**, *101*, 1525−1527; *Angew. Chem. Int. Ed. Engl.* **1989**, *28*, 1496−1498. − E = P: [7d] R. A. Bartlett, H. V. R. Dias, K. M. Flynn, H. Hope, B. D. Murray, M. M. Olmstead, P. P. Power, *J. Am. Chem. Soc.* **1987**, *109*, 5693−5698. − [7e] J. Borm, G. Huttner, L. Zsolnai, K. Evertz, H. Berke, *J. Organomet. Chem.* **1987**, *327*, 223−235. − [7f] M. Scheer, K. Schuster, A. Krug, H. Hartung, *Chem. Ber.* **1996**, *129*, 973−979. − E = As: [7g] A. Strube, G. Huttner, L. Zsolnai, W. Imhof, *J. Organomet. Chem.* **1990**, *399*, 281−290. − [7h] C. Emmerich, G. Huttner, *J. Organomet. Chem.* **1993**, *447*, 81−89. − E = Sb: [7i] F. Bringewski, G. Huttner, W. Imhof, L. Zsolnai, *J. Organomet. Chem.* **1992**, *439*, 33−44. − E = Bi: [7j] S. J. Davies, N. A. Compton, G. Huttner, L. Zsolnai, S. E. Garner, *Chem. Ber.* **1991**, *124*, 2731−2738. − E = S: [7k] H. Braunwarth, G. Huttner, L. Zsolnai, *Angew. Chem.* **1988**, *100*, 731−732; *Angew. Chem. Int. Ed. Engl.* **1988**, *27*, 698−699. − [7l] P. Lau, H. Braunwarth, G. Huttner, D. Günauer, K. Evertz, W. Imhof, C. Emmerich, L. Zsolnai, *Organometallics* **1991**, *10*, 3861−3873. − E = Se: [7m] H. Braunwarth, F. Ettel, G. Huttner, *J. Organomet. Chem.* **1988**, *355*, 281−288. − [7n] P. Lau, G. Huttner, L. Zsolnai, *Z. Naturforsch. B* **1991**, *46*, 719−728. − E = Te: [7o] G. Huttner, S. Schuler, L. Zsolnai, M. Gottlieb, H. Braunwarth, M. Minelli, *J. Organomet. Chem.* **1986**, *299*, C4−C6. − [7p] P. Lau, G. Huttner, L. Zsolnai, *J. Organomet. Chem.* **1992**, *440*, 41−46.

[8] [8a] B. Schiemenz, B. Antelmann, G. Huttner, L. Zsolnai, *Z. Anorg. Allg. Chem.* **1994**, *620*, 1760−1767. − [8b] P. Kircher, G. Huttner, B. Schiemenz, K. Heinze, L. Zsolnai, O. Walter, A. Jacobi, A. Driess, *Chem. Ber.* **1997**, *130*, 687−699.

[9] P. Kircher, G. Huttner, K. Heinze, B. Schiemenz, L. Zsolnai, M. Büchner, A. Driess, *Eur. J. Inorg. Chem.* **1998**, 703−720.

[10] J. von Seyerl, G. Huttner, *J. Organomet. Chem.* **1980**, *195*, 207−212.

[11] See e.g.: [11a] T. Fjeldberg, P. B. Hitchcock, M. F. Lappert, S. J. Smith, A. J. Thorne, *J. Chem. Soc., Chem. Commun.* **1985**, 939−941. − [11b] M. Veith, P. Hobein, R. Rösler, *Z. Naturforsch. B* **1989**, *44*, 1067−1081. − [11c] W. A. Herrmann, N. W. Huber, O. Runte, *Angew. Chem.* **1995**, *107*, 2371−2390; *Angew. Chem. Int. Ed. Engl.* **1995**, *34*, 2187−2206. − [11d] M. Veith, C. Mathur, V. Huch, *Organometallics* **1996**, *15*, 2858−2859.

[12] [12a] G. Trinquir, *J. Am. Chem. Soc.* **1990**, *112*, 2130−2137. − [12b] G. Trinquir, *J. Am. Chem. Soc.* **1991**, *113*, 144−151.

[13] [13a] J. von Seyerl, B. Sigwarth, G. Huttner, *Chem. Ber.* **1981**, *114*, 1407−1412. − [13b] B. Sigwarth, L. Zsolnai, O. Scheidsteger, G. Huttner, *J. Organomet. Chem.* **1982**, *235*, 43−58. − [13c] H. Lang, L. Zsolnai, G. Huttner, *Z. Naturforsch. B* **1985**, *40*, 500−506. − [13d] A. Lombard, G. Huttner, *J. Organomet. Chem.* **1988**, *352*, 303−306. − [13e] F. Ettel, M. Schollenberger, B. Schiemenz, G. Huttner, L. Zsolnai, *J. Organomet. Chem.* **1994**, *476*, 153−162.

[14] [14a] G. A. Olah, M. Simonetta, *J. Am. Chem. Soc.* **1982**, *104*, 330−331. − [14b] P. v. R. Schleyer, A. J. Kos, J. A. Pople, A. T. Balaban, *J. Am. Chem. Soc.* **1982**, *104*, 3771−3773.

[15] C. Elschenbroich, A. Salzer, *Organometallchemie*, 3rd ed., Teubner, Stuttgart, **1990**, p.277.

[16] B. Wrackmeyer, *Annu. Rep. NMR Spec.* **1985**, *16*, 73−186.

[17] G. Huttner, *J. Organomet. Chem.* **1986**, *308*, C11−C13.

[18] R. S. Drago, *Physical Methods in Chemistry*, W. B. Saunders Company, Philadelphia, Eastbourne, Toronto, **1977**.

[19] CAChe, Extended Hückel, Release 3.6 with given parameters for Cr and Sn, basis STO-6G. The Sn−Cr and Sn−O distance refer to the structure of $[Ph_4P]_2\cdot$**1a** while Cr−H and O−H distances are used as set by the program.

[20] B. Schiemenz, G. Huttner, L. Zsolnai, P. Kircher, T. Diercks, *Chem. Ber.* **1995**, *128*, 187−191.

[21] With compounds **1** as well as with compounds **a** (Figure 3) it is generally observed that the bonds to the substituents R at the bridging oxygen atoms are made in the directions approximately coplanar with the four-membered cycle with a resulting

trigonal-planar coordination around the oxygen atom (see ref.[11]). While Sn−O π-bonding might be a reason for this this π contribution is found to be small. In an EHT analysis the model as used above was compared with a model in which the hydrogen atoms of the H−O groups were deliberately set at positions 40° away from the *x* direction in the *xz* plane (Figure 4) in a mutually anti-sense. Only a minor change in the total energy was observed; the "in-plane" model being about 0.1 eV more stable than the "out-of-plane" model. Bonding and antibonding effects of this bending must therefore almost compensate each other within the set of occupied orbitals. An analogous model calculation was done for $[HSnOH]_2$ as a prototype of the species **a**. Here as well bending did not cause dramatic change in the total energy (the "in-plane" model is about 0.01 eV more stable). It appears therefore that the potential describing this bending motion is quite soft and that neither the coplanarity nor the distortion from coplanarity of the R−O-bonds has any specific and easy to interpret meaning. It is observed that the compounds $[RGe(\mu_2\text{-}SR)_2GeR]$, isoelectronic to **a**, show distinctively pyramidal coordination around sulfur (see ref.[11]).

[22] F. A. Cotton, C. S. Kraihanzel, *J. Am. Chem. Soc.* **1962**, *84*, 4432−4438.
[23] G. M. Sheldrick, *SHELX86*, University of Göttingen, **1986**; G. M. Sheldrick, *SHELX93*, University of Göttingen, **1993**.
[24] L. Zsolnai, G. Huttner, *XPMA*, University of Heidelberg, **1998**; http://www.rzuser.uni-heidelberg.de/v54/xpm.html.

[98048]

Synthesis and Reactivity of Low-Coordinate Compounds, 7[◇]

Reaction of a Stable Silylene with Divalent Group 14 Compounds☆

Michael K. Denk*, Ken Hatano, and Alan J. Lough

Department of Chemistry, University of Toronto,
Mississauga, Ontario L5L 1C6, Canada
Fax: (internat.) 001-905-828-5335
E-mail: mdenk@credit.erin.utoronto.ca
Internet: http://mdenk.erin.utoronto.ca

Received March 20, 1998

Keywords: Silylene / N Heterocycles / Carbene analogs / Tin / Subvalent compounds

The reaction of the stable silylene **1** (L′Si:) with CO, $SnCl_2$, $PbCl_2$, the stable carbene L′C: (**2**) and the stable germylene L′Ge: (**3**) was investigated as a possible approach for the synthesis of *hetero*-polysilanes (*poly*-carbosilanes, *poly*-germasilanes, *poly*-stannasilanes). The silylene **1** was found to be inert towards all substrates except $SnCl_2$ and $PbCl_2$. Reaction with $SnCl_2$ led to the formation of the yellow, tris(silyl)stannane [(L′SiCl)$_3$SnCl] (**5**) and elemental tin. The photolabile (**5**) was characterized by multinuclear NMR (^{1}H, ^{13}C, ^{29}Si, ^{119}Sn) and single crystal X-ray diffraction: $C_{30}H_{60}Cl_4N_6Si_3Sn$, M = 849.60, orthorhombic, space group $Pca2_1$. The bond angles of 115.89 ° (ave. Si–Sn–Si) and 101.87 ° (ave. Cl–Sn–Si) show a slightly flattened tetrahedral geometry around the tin atom. – Thermolysis of **5** at 100 °C led to the deposition of thin films of tin; photolysis resulted in the formation of tin powder. All thermolysis products could be isolated and were characterized as $SnCl_2$, elemental tin, L′Si: (**1**), L′$SiCl_2$ (**6**) and the new disilane L′Si(Cl)-(Cl)SiL′ (**7**). Photolysis led to a reduced product spectrum (formation of Sn + $SnCl_2$ + **7**). Reaction of **1** with $PbCl_2$ gave elemental lead and L′$SiCl_2$ as the only products.

The heavy analogs of carbenes R_2E: (E = Si, Ge, Sn, Pb) are attractive building blocks for the synthesis of inorganic polymers $[R_2E]_n$. *Homo*-polymers of silicon, germanium, and tin are typically obtained by the reduction of the dihalides R_2SiCl_2,[1] R_2GeCl_2,[2] or R_2SnCl_2.[3] These reactions may proceed through the intermediacy of free silylenes, germylenes or stannylenes as reactive intermediates. The unique electronic structure of *poly*-silanes[1], *poly*-germanes[2], and *poly*-stannanes[3] has prompted detailed investigations of their physical properties. The partial replacement of silicon in *poly*-silanes by germanium or tin is of special interest as a 1-dimensional model for Si−Ge and Si−Sn alloys. The dehalogenation of mixtures of dichlorides R_2ECl_2 has been used to obtain copolymers of type $[R_2Si]_n[R'_2Si]_k$[4] and $[R_2Si]_n[R_2Ge]_k$,[4] but the very different susceptibility of the SiCl, GeCl, and SnCl bonds towards reduction limits the scope of the dehalogenation approach.

The recent synthesis of a number of stable carbenes[5][6] and silylenes[7][8] presents a new possible strategy to obtain group 14 polymers by copolymerization of these reactive molecules. We now report preliminary results on the reaction of the stable silylene L′Si (**1**)[7] with the stable divalent group 14 compounds: CO, $SnCl_2$, $PbCl_2$, L′C: (**2**)[9] and L′Ge: (**3**)[10] (Scheme 1).

Scheme 1

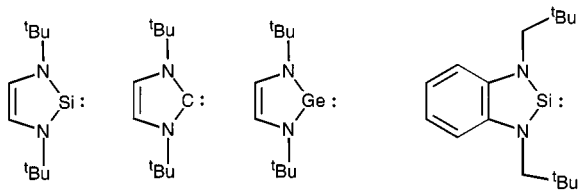

1 **2** **3** **4**

The reaction of the stable silylene **4** with the germylenes, stannylenes, and plumbylenes M[N(SiMe$_3$)$_2$]$_2$ (M = Ge, Sn and Pb) was investigated by Gehrhus, Hitchcock, and Lappert and was shown to proceed by insertion of the silylene **4** into the MN bond rather than formation of Si,Ge-, Si,Sn- or Si,Pb copolymers.[8a][8b] Similar MN insertion products were obtained by Weidenbruch et al. from the reaction of a stable diaminogermylene with a stable diaminosilylene.[8c]

No reaction was observed between the silylene **1** (L′Si:) and CO, L′C: or L′Ge: or any other combination of these compounds even after prolonged heating to 150 °C in sealed NMR tubes. Rapid reaction occurred between **1** and tin(II) chloride, however, to give the tris(silyl)stannane **5**.[11]

Compound **5** was characterized by multinuclear NMR (^{1}H, ^{13}C, ^{29}Si, and ^{119}Sn)[11], CI-MS[11] and single crystal X-ray diffraction[12][19] as a tris(silyl)stannane with Sn^{IV} and Si^{IV} centers. The oxidation of both divalent silicon and

[◇] Part 6: Ref.[6].

 © WILEY-VCH Verlag GmbH, D-69451 Weinheim, 1998 1434−1948/98/0808−1067 $ 17.50+.50/0

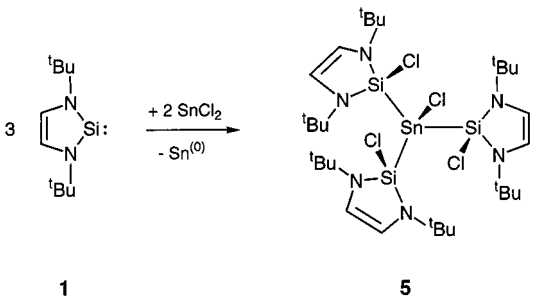

tin in the course of the reaction is balanced by the formation of a stoichiometric amount of metallic tin. Compound **5** can be stored at −10°C in the dark for months, but slowly decompose to give deposits of metallic tin at r. t. especially if exposed to light.

The decomposition of **5** under thermolytic[13] or photolytic[14] conditions follows different pathways. Both reactions lead to a fragmentation of the Si_3Sn framework and the formation of the disilane **7**.[15] Elemental tin is deposited as film (thermolysis) or powder (photolysis). Under thermolytic conditions, the silylene **1**,[7a] and the silane **6**[7a] are formed as additional products. The thermolytic decomposition pathway of **5** matches the CI-MS fragmentation pattern[11] (high abundance of the fragments $[L'Si:]^{+\bullet}$ and $[L'SiCl_2]^{+\bullet}$).

The crystal structure of **5**[12][19] (Figure 1) shows the tin atom in a distorted tetrahedral environment. The Si−Sn−Si bond angles (114.60−116.70°) and Si−Sn−Cl bond angles (100.07−102.96°) deviate from the ideal tetrahedral geometry. Few structural data are available on silyl-stannanes, but the Si-Sn bond distances in **5** (263.0−264.2 pm) closely

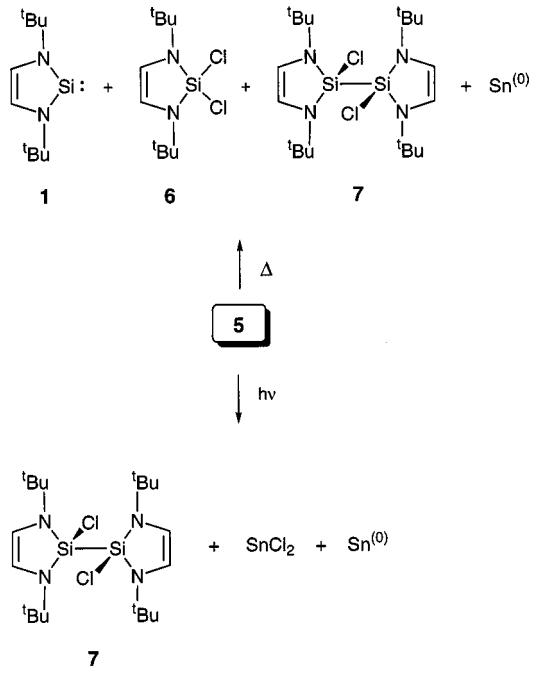

Figure 1. Molecular structure of **5** (ORTEP plot, 50% probability level, hydrogen atoms have been omitted for clarity)[a]

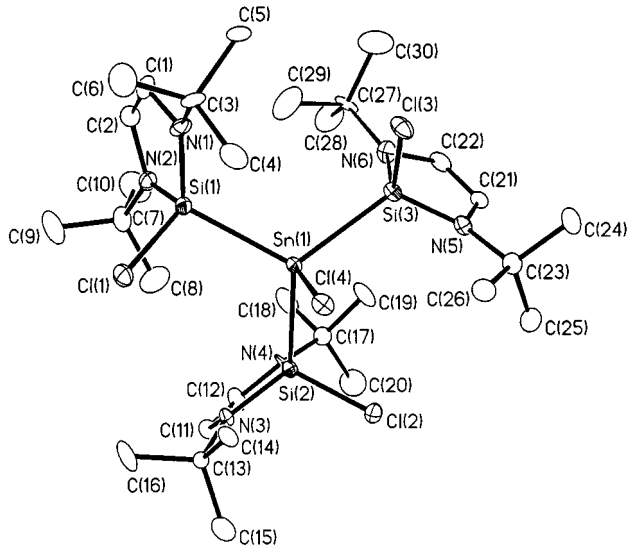

[a] Selected bond lengths [pm] and angles [°]: Sn(1)−Cl(4) 238.8(3), Sn(1)−Si(1) 263.0(4), Sn(1)−Si(2) 264.2(4), Sn(1)−Si(3) 264.0(3), Cl(1)−Si(1) 211.2(5), Cl(2)−Si(2) 209.3(5), Cl(3)−Si(3) 211.6(4); Cl(4)−Sn(1)−Si(1) 102.96(11), Cl(4)−Sn(1)−Si(2) 102.57(13), Cl(4)−Sn(1)−Si(3) 100.07(12), Si(1)−Sn(1)−Si(2) 116.38(11), Si(1)−Sn(1)−Si(3) 116.7(2), Si(2)−Sn(1)−Si(3) 114.60(12); Torsional angles: Cl(4)−Sn(1)−Si(1)−Cl(1) −50.15(0.18), Cl(4)−Sn(1)−Si(3)−Cl(3) −50.50(0.23), Cl(4)−Sn(1)−Si(2)−Cl(2) −47.95(0.17)

match those reported for the recently characterized silyl-stannanes $[(Me_3Si)_3Si]_2SnCl_2$ (259.7−260.4 pm)[16] and $[(Me_3Si)_3Sn]_2$ (260.9−261.1 pm).[17]

The normal Si−Sn bond distances, and especially the fact that the Si−Sn bonds of **5** are freely rotating in solution (equivalence of 6 *t*Bu groups and 6 ring protons in the ^1H NMR at r.t.), show that **5** is free of strong steric congestion. By contrast, the disilane L′Si(Cl)−(Cl)SiL′ (**7**, vide infra) shows hindered rotation of the *t*Bu-groups at r.t, as evidenced by the broad signals found for the methyl groups in the ^1H- and ^{13}C-spectrum. The $(SiCl)_3Sn-Cl$ framework has the idealized symmetry C_3, with Cl−Sn−Si−Cl torsional angles ranging from −47.95 to −50.15.

The reaction of **1** with $PbCl_2$ leads to the clean formation of elemental lead (powder) and $L'SiCl_2$ (**6**) as the only products.

Stable silylenes of type **1** can at present only be obtained by reduction of the corresponding dihalosilanes R_2SiCl_2 with potassium at elevated temperatures[7a]. The thermolytic generation of **1** from a stannylsilane such as **5** presents a potential alternative synthetic approach. The stannylsilanes $L'Si(SnR_3)(Cl)$ and $L'Si(SnR_3)_2$ are now under investigation as new precursors for stable silylenes.

The authors thank the *Natural Sciences and Engineering Research Council of Canada* (*NSERC*) and the *Connaught Fund of the University of Toronto* for support of this research, Dr. *Juris Strautmanis* (Toronto) for many helpful discussions and *Avinash Thadani* for preliminary experiments.

Experimental Section

General: All reactions were carried out under argon (99.994% purity) with usual Schlenk equipment or inside an inert-gas glovebox (O_2 and H_2O < 1 ppm). Solvents were purified by distillation over benzophenone/potassium (THF, hexanes, benzene) or by 30 minute sonication with CaH_2. – IR: Nicolet. – NMR: Varian Gemini 200, Unity 400 and 500. – The starting materials L′Si (**1**)[7a] L′C: (**2**)[9] and L′Ge: (**3**)[10] were obtained according to published procedures. The compounds **1**–**3** were purified by sublimation under exclusion of air and moisture. Anhydrous $SnCl_2$ was used as received (Aldrich). Reactions of **1** with CO, L′C: and L′Ge: were studied in ca. 5 wt.-% solutions in C_6D_6. Flame sealed samples were heated to 150°C for 4 weeks in 5-mm NMR tubes. For the synthesis and characterization of **6** see reference[7a].

Synthesis of **5**: $SnCl_2$ (10.0 mmol, 1.896 g) is added to a solution of the silylene **1** (20.0 mmol, 3.927 g) in 15 ml of THF at −10°C. The reaction mixture turns red and the starting material is completely consumed after 60 min. The crude reaction mixture contains **5** (> 85%) and small amounts (ca. 5%) of **6** and **7**. Analytically pure $(L'SiCl)_3SnCl$ (**5**) is isolated from the crude reaction mixture by chromatography on Celite (hexane as eluent), followed by recrystallization from toluene as orange crystals (46%) that decompose at 172°C without melting.

☆) Dedicated to Professor *Heinrich Nöth* on the occasion of his 70th birthday.

[1] [1a] D. Miller, J. Michl, *Chem. Rev.* **1989**, 89, 1359−1410. – [1b] R. West, *Comprehensive Organometallic Chemistry*, Vol. 2, Chapter 3, 77−110, (Eds.: E. W. Abel, F. G. A. Stone, G. Wilkinson), Pergamon Press, New York, **1995** and references therein. – [1c] H. Sakurai, *Synthesis and Applications of Polysilanes*, CMC, Tokyo, **1989**.

[2] [2a] P. Trefonas, R. West, *J. Polym. Sci., Polym. Chem. Ed.* **1985**, *23*, 2099−2017. – [2b] R. D. Miller, R. Sooriyakumaran, *J. Polym. Sci., Polym. Chem. Ed.* **1987**, *25*, 111−125. – [2c] W. J. Szymanski, G. T. Visscher, B. A. Bianconi, *Macromolecules* **1993**, *26*, 869−871. – [2d] K. Mochida, T. Ohkawa, H. Kawata, A. Watanabe, O. Ito, M. Matsuda, *Bull. Chem. Soc. Jpn.* **1996**, *69*, 2993−2998. – [2e] K. Mochida, S. Nagano, S. Maeyama, T. Kodaira, A. Watanabe, O. Ito, M. Matsuda, *Bull. Chem. Soc. Jpn*. **1997**, *70*, 713−716.

[3] [3a] L. R. Sita, *Adv. in Organomet. Chem*. **1995**, *38*, 189−243. – [3b] K. Mochida, M. Hayakawa, T. Tsuchikawa, Y. Yokoyama, M. Wakasa, H. Hayashi, *Chem. Lett.* **1998**, 91−92.

[4] [4a] P. A. Bianconi, F. C. Schilling, T. W. Weidman, *Macromolecules* **1989**, *22*, 1697−1704. – [4b] K. Furukawa, M. Fujino, N. Matsumoto, *Macromolecules* **1990**, *23*, 3423−3426. – [4c] W. L. Wilson, T. W. Weidman, *J. Phys. Chem.* **1991**, *95*, 4568−4572. – [4d] T. Shono, S. Kashimura, H. Murase, *J. Chem. Soc., Chem. Commun.* **1992**, 896−897. – [4e] A. Watanabe, H. Miike, Y. Tsutumi, M. Matsuda, *Macromolecules* **1993**, *26*, 2111−2116. – [4f] H. Kishida, H. Tachibana, M. Matsumoto, Y. Tokura, *Appl. Phys. Lett.* **1994**, *65*, 1358−1360. – [4g] K. Mochida, H. Chiba, *J. Organomet. Chem*. **1994**, *473*, 45−54. – [4h] A. Watanabe, T. Komatsubara, M. Matsuda, Y. Yoshida, S. Tagawa, *Macromol. Chem. Phys.* **1995**, *196*, 1229−1240. – [4i] K. Huang, L. A. Vermeulen, *J. Chem. Soc. Chem. Commun.* **1998**, 247−248.

[5] [5a] A. J. Arduengo, R. L. Harlow, M. Kline, *J. Am. Chem. Soc.* **1991**, *113*, 361−363. – [5b] M. Regitz, *Angew. Chem.* **1991**, *103*, 691−693; *Angew. Chem. Int. Ed. Engl.* **1991**, *30*, 674−676. – [5c] A. J. Arduengo, H. V. Rasika-Dias, R. L. Harlow, M. Kline, *J. Am. Chem. Soc.* **1992**, *114*, 5530−5534. – [5d] A. J. Arduengo, H. V. Rasika-Dias, D. A. Dixon, R. L. Harlow, W. T. Klooster, T. F. Koetzle, *J. Am. Chem. Soc.* **1994**, *116*, 6812−6822. – [5e] W. A. Herrmann, L. J. Goossen, C. Köcher, G. J. Artus, *Angew. Chem.* **1996**, *108*, 2980−2982; *Angew. Chem. Int. Ed. Engl.* **1996**, *35*, 2805−2807. – [5f] M. Regitz, *Angew. Chem.* **1996**, *108*, 791−794; *Angew. Chem. Int. Ed. Engl.* **1996**, *35*, 725−728. – [5g] R. W. Alder, P. R. Allen, M. Murray, A. G. Orpen, *Angew. Chem.* **1996**, *108*, 1211−1213; *Angew. Chem. Int. Ed. Engl.* **1996**, *35*, 1121−1122. – [5h] A. J. Arduengo, J. R. Goerlich, W. J. Marshall, *J. Am. Chem. Soc.* **1996**, *118*, 11027−11028. – [5i] T. A. Taton, P. Chen, *Angew. Chem.* **1996**, *108*, 1098−1100; *Angew. Chem. Int. Ed. Engl.* **1996**, *35*, 1011−1013.

[6] M. K. Denk, A. Thadani, K. Hatano, A. J. Lough, *Angew. Chem. Int. Ed. Engl.* **1997**, *36*, 2607−2609; *Angew. Chem.* **1997**, *109*, 2719−2721.

[7] [7a] M. Denk, R. Lennon, R. Hayashi, R. West, R. V. Belyakov, H. P. Verne, A. Haaland, M. Wagner, N. Metzler, *J. Am. Chem. Soc.* **1994**, *116*, 2691−2692. – [7b] M. Denk, R. Hayashi, R. West, *J. Chem. Soc., Chem. Commun.* **1994**, 33−34. – [7c] M. Denk, J. Green, N. Metzler, M. Wagner, *J. Chem. Soc., Dalton Trans.* **1994**, 2405−2410. – [7d] N. Metzler, M. Denk, *J. Chem. Soc., Chem. Commun.* **1996**, 2657−2658.

[8] [8a] B. Gehrhus, P. B. Hitchcock, M. F. Lappert, *Angew. Chem. Int. Ed. Engl.* **1997**, *36*, 2514−2516; *Angew. Chem.* **1997**, *109*, 2624−2626. – [8b] C. Drost, B. Gehrhus, P. B. Hitchcock, M. F. Lappert, *J. Chem. Soc., Chem. Commun.* **1997**, 1845−1846. – [8c] A. Schäfer, W. Saak, M. Weidenbruch, H. Marsmann, G. Henkel, *Chem. Ber.* **1997**, *130*, 1733 − 1737.

[9] Obtained from the imidazolium salt by deprotonation as described in: A. J. Arduengo, *J. Am. Chem. Soc.* **1992**, *114*, 5530−5534.

[10] W. A. Herrmann, M. Denk, J. Behm, W. Scherer, F.-R. Klingan, H. Bock, B. Solouki, M. Wagner, *Angew. Chem.* **1992**, *104*, 1489−1492; *Angew. Chem. Int. Ed. Engl.* **1992**, *31*, 1485−1488.

[11] $(L'SiCl)_3SnCl$ (**5**): ^1H NMR (200 MHz, C_6D_6): δ 1.45 (s, 54 H, CH_3), 5.83 [s, 6 H, =C*H*, tin satellites corresponding to $^4J(^1H, ^{117/119}Sn)$ = 7.8 Hz]. – ^{13}C NMR (100 MHz, C_6D_6): δ 31.43 [q, $^1J(C,H)$ = 121.5 Hz, CH_3], 53.13 [s, $C(CH_3)_3$], 115.33 [dd, $^1J(C,H)$ = 181.6 Hz, $^2J(C,H)$ = 8.8 Hz, =*C*H]. – ^{29}Si NMR (79.0 MHz, C_6D_6): δ −20.08 [$^1J(^{29}Si,^{117}Sn)$ = 881 Hz, $^1J(^{29}Si,^{119}Sn)$ = 923 Hz]. – ^{119}Sn NMR (186.0 MHz, C_6D_6): −222.6 ppm [$^1J(^{29}Si,^{119}Sn)$ = 922 Hz]. – CI-MS (+, *iso*-butane) *m/z* (rel. int.): 849 $[M + 1]^+$ (1), 582 $[M^{+\bullet}$ − L′Si:] (2), 462 (11), 266 $[L'SiCl_2]^{+\bullet}$ (90), 196 $[L'Si]^{+\bullet}$ (100). – IR (nujol): ν = cm^{-1}: 3107 w, 1639 m, 1598 m, 1393 m, 1368 s, 1343 m, 1270 s, 1212 s, 1196 s, 1122 s, 1106 s, 1089 s, 1048 s, 999 s, 810 m, 744 s, 663 s, 647 s.

[12] *X-ray Crystallographic* Study[19]: $C_{30}H_{60}Cl_4N_6Si_3Sn$, **5**, ◦*M* = 849.60, orthorhombic, space group $Pca2_1$, *a* = 11.365(3) A, *b* = 18.999(4) A, *c* = 19.808(5) A, *V* = 4277(2) A^3, *Z* = 4, *D(calc.)* = 1.319 g/cm^3, μ = 0.959 mm^{-1}. Data were collected on an Siemens P4 diffractometer using graphite monochromator, λ (Mo-K_α) = 0.71073 A. The intensities of standard reflections measured every 97 reflections showed no decay. The data were corrected for Lorentz and polarization effects and semi-empirical absorption correction was applied using ψ-scans. Minimum and maximum absorption corrections were 0.5712 and 0.5276. The structure were solved and refined using the SHELXTL\PC[18] package. Refinement was by full-matrix least-squares on F^2 using all data (negative intensities included). The weighting scheme was $w = 1/[\sigma^2(F_o^2) + (0.00295P)^2 + 4.7P]$ where $P = (F_o^2 + F_c^2)/3$. Hydrogen atoms were included in fixed positions and treated as riding atoms. Maximum residual electron densities were +0.875 and −0.557 e/A^3.

[13] Sealed NMR samples of **5** in C_6D_6 were monitored by ^1H, ^{13}C, and ^{29}Si NMR. After 3 h at 100°C, the decomposition was complete and L′Si: (**1**), $L'SiCl_2$ (**6**) and L′Si(Cl)−(Cl)SiL′ (**7**) were formed in the molar ratio 2:6:3 (^1H NMR). The NMR tubes were stored "upside down" during the thermolysis to prevent the formation of a tin film in the bottom part of the NMR tube.

[14] Irradiation of **5** (5% in hexanes) in a quartz tube for 6 days resulted in 60% conversion of **5** to L′Si(Cl)−(Cl)SiL′ (**7**), $SnCl_2$ and tin powder as sole products.

[15] The disilane **7** has been obtained earlier in our group from reactions of **1** with different chlorinating agents. L′Si(Cl)−(Cl)SiL′ (**7**): ^1H NMR (200 MHz, C_6D_6): δ 1.25−1.50 (br, 36 H, CH_3), 5.8 (s, 4 H, =C*H*). – ^{13}C NMR (100 MHz, C_6D_6): δ 30.25−31.50 (br, CH_3), 52.88 [s, $C(CH_3)_3$], 114.08 (=*C*H). – ^{29}Si NMR (79.0 MHz, C_6D_6): δ −33.18. EI-MS (40 eV) *m/z* (rel. int.): 466 (4), 465 (5), 464 (14), 463 (7), 462 (20), 295 (6), 294 (3), 293 (9), 270 (7), 269 (6), 268 (39), 267 (10), 266 (55) $L'SiCl_2$ = $[M - L'Si:]^{+\bullet}$, 253 (2), 251 (3), 239 (11), 238 (7), 237 (15), 236 (5), 233 (8), 232 (4), 231 (22) $[L'Si\text{-}Cl]^+$, 222 (3), 214 (7), 213 (6), 212 (36), 211 (12), 210 (51), 209 (7), 198 (6), 197 (20), 196 (100) $[L'Si]^{+\bullet}$, 195 (5), 158 (9), 156 (7), 156 (41), 155 (12), 154 (62), 153 (7), 140 (21), 133 (3), 125 (16), 121 (32), 120 (12), 119 (87), 99 (5), 94 (4), 92 (10), 85 (14), 84 (53), 83 (3), 57

(8). The identity of the compound has also been confirmed by single crystal X-ray diffraction (M. Denk, unpublished results).
[16] S. P. Mallela, R. A. Geanangel, *Inorg. Chem*., **1990**, *29*, 3525−3528.
[17] S. P. Mallela, R. A. Geanangel, *Inorg. Chem.*, **1993**, *32*, 5623−5625.
[18] Sheldrick, G. M., *SHELXTL\PC*, Siemens Analytical X-ray Instruments Inc., Madison, Wisconsin, U. S. A. (**1994**).
[19] Crystallographic data (excluding structure factors) for the structure of **5** have been deposited with the Cambridge Crystallographic Data Centre as supplementary publication no. CCDC-101272. Copies of the data can be obtained free of charge on applications to the Director, CCDC, 12 Union Road, Cambridge CB2 1EZ, UK (fax: Int. Code +44(0)1223/ 336-033. E-mail: deposit@chemcrys.cam.ac.uk).

[98072]

Preparation, Structures, and Properties of Dinuclear Ni and Pd Complexes of Tridentate Amine-Chalcogenolate Ligands

Berthold Kersting

Institut für Anorganische und Analytische Chemie, Universität Freiburg,
Albertstrasse 21, D-79104 Freiburg, Germany
Fax: (internat.) + 49(0)761/203-6001
E-mail: kerstber@sun2.ruf.uni-freiburg.de

Received March 27, 1998

Keywords: Dinuclear complexes / Nickel / Palladium / Amine-thiolate ligands/ Amine-selenolate ligands

The preparation and characterization of dinuclear Ni^{II} and Pd^{II} complexes of the tridentate amine-chalcogenolate ligands 4-*tert*-butyl-2,6-di(aminomethyl)thiophenol (**4a**) and 4-*tert*-butyl-2,6-di(aminomethyl)selenophenol (**4b**) are reported. Reaction of **4a**,**b** with $Ni(ClO_4)_2 \cdot 6\,H_2O$ or $(COD)PdCl_2$ in a 1:1 molar ratio yields 1:1 complexes of composition $[M_2(L)_2][BPh_4]_2 \cdot CH_3CN \cdot CH_3OH$ [M = Ni, L = **4a**,**b** (**5a**,**b**); M = Pd, L = **4a,b** (**6a**,**b**)]. The palladium complex **6a** is isomorphous with **5a** as shown by X-ray crystal structure analysis. NMR studies reveal that both complexes retain their solid-state structure in solution and that the selenolate complexes are isostructural with the thiolate complexes. All complexes undergo electrochemically reversible one-electron transfer processes in the potential range –1.0 to –0.8 V vs. SCE ascribed to metal-centered reductions with formation of mixed-valent $M^{I,II}$ species $[M_2(L)_2]^+$. Further reduction at more negative potentials then leads to the neutral $[M_2(L)_2]$ species, which are not stable on the time scale of the CV experiment. The spectroscopic properties of the thiolate and selenolate complexes are very similar indicating electronically similar properties of the tridentate amine-chalcogenolate ligands.

Introduction

The coordination chemistry of transition-metal thiolate, selenolate, and tellurolate complexes has been actively pursued in the past several years, motivated primarily by the bonding diversity[1][2], potential use as precursors to new solid-state materials[3], and the relevance of such complexes to biomimetic chemistry[4][5]. Monodentate chalcogenolate ligands, which have been studied most, form complexes with most of the elements, however, their inherent tendency to form bridges between transition-metal ions limits their use in the preparation of complexes of well-defined nuclearity[6]. Furthermore, an investigation of chemical reactivities is often hampered by ligand-centered redox reactions and the fact that such species can be notoriously labile[7].

More recently, multidentate nitrogen/sulfur-based ligands have been employed as spectator ligands in various mononuclear[8][9][10] and dinuclear transition-metal complexes[11][12] and have been shown to offer some unique properties in coordination chemistry. The notable feature of such complexes is their enormous stability that has enabled the preparation of complexes with metal ions in unusual high formal oxidation states[13][14] and has allowed for studies on their chemical reactivity[15]. However, while mononuclear complexes have been extensively studied, dinuclear complexes have been considered less often, and very little information is available on their reactivity[16][17]. This is true in particular for complexes with polydentate nitrogen/selenium-based ligands[18].

Scheme 1. Structures of amine-chalcogenolate ligands **4a**,**b** and the binding mode of **4a** in the dinuclear $[Ni_2(\mathbf{4a})_2]^{2+}$ dication in $[Ni_2(\mathbf{4a})_2][BPh_4]_2$ (**5a**)[20]

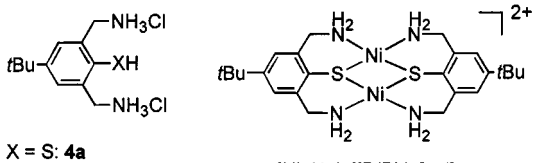

Our work on thiolate-bridged dimetal complexes[19] has shown that the dinickel complex **5a** of the tridentate N_2S ligand **4a** is quite robust, tolerating binding of exogenous ligands without affecting the dinuclear structure[20]. Complex **5a** also serves as a versatile starting agent in the preparation of novel face-sharing bioctahedral nickel complexes. This prompted us to investigate the possibility of synthesizing related complexes with the amine-selenolate ligand **4b**.

This article describes the syntheses and characterization of dinuclear nickel and palladium complexes of the analogous ligands 2,6-bis(aminomethyl)-4-*tert*-butylthiophenol (**4a**) and 2,6-bis(aminomethyl)-4-*tert*-butylselenophenol (**4b**).

Results and Discussion

Syntheses

Compounds **4a**,**b** were prepared in 3 steps starting from **1**, as is shown in Scheme 2. In the first step, compound **1** was treated with potassium benzylthiolate in dimethylformamide to afford benzyl [4-*tert*-butyl-2,6-diformylphe-

 © WILEY-VCH Verlag GmbH, D-69451 Weinheim, 1998 1434–1948/98/0808–1071 $ 17.50+.50/0

nyl]sulfide in nearly quantitative yield. The dialdehyde **2a** was subsequently converted to the corresponding dioxime **3a** by reaction with hydroxylamine. In the last step, reduction of compound **3a** was accomplished with sodium in liquid ammonia. The amine-thiolate compound **4a** was isolated as the hydrochloride salt **4a**·$(HCl)_2$ in 55% overall yield. A similar reaction sequence was employed to prepare the selenium analogue **4b**.

Scheme 2. Preparation of amine-chalcogenolate ligands **4a**,**b**

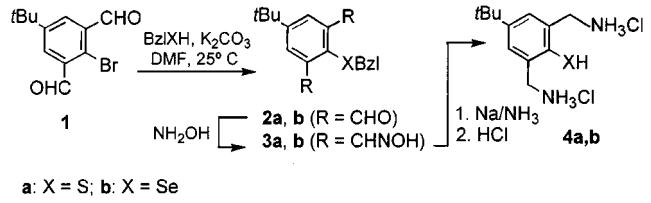

a: X = S; **b**: X = Se

Metal Complex Syntheses

The hydrochloride salts of the chalcogenolate ligands **4a**,**b** react with equimolar quantities of $Ni(ClO_4)_2 \cdot 6H_2O$ in the presence of base to give the air-stable dications $[Ni_2(\mathbf{4a})_2]^{2+}$ and $[Ni_2(\mathbf{4b})_2]^{2+}$, respectively (eq. 1). These cationic species were isolated as the tetraphenyl borate salts $[Ni_2(\mathbf{4a})_2][BPh_4]_2$ (**5a**) and $[Ni_2(\mathbf{4a})_2][BPh_4]_2$ (**5b**). Complexes **5a**,**b** are dark-red crystalline solids, soluble in polar aprotic solvents like acetonitrile, dichloromethane, dimethyl sulfoxide, and dimethylformamide. Similarly, reaction of **4a**,**b** with $(COD)PdCl_2$ and NaOMe in methanol produced, upon addition of $NaBPh_4$, yellow crystals of the palladium analogs of **5a**,**b** in good yields {$[Pd_2(\mathbf{4a})_2][BPh_4]_2$ (**6a**), 82%; $[Pd_2(\mathbf{4b})_2][BPh_4]_2$ (**6b**), 63%}.

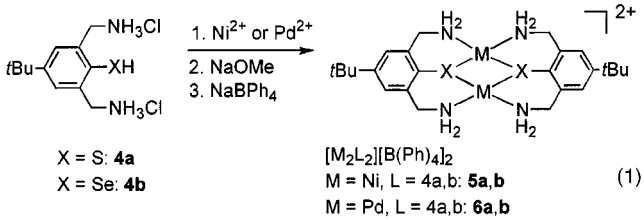

X = S: **4a**
X = Se: **4b**

$[M_2L_2][B(Ph)_4]_2$
M = Ni, L = 4a,b: **5a**,**b**
M = Pd, L = 4a,b: **6a**,**b**

(1)

When recrystallized from acetonitrile/methanol solution, the complexes crystallize with a solvent molecule of acetonitrile and a solvent molecule of methanol per dication. The dinuclear nature of the complexes was confirmed by X-ray crystal structure determination of the palladium complex **6a** · CH_3CN · CH_3OH. The structure of **5a** · CH_3CN · CH_3OH has been determined previously[20].

Crystal Structure of 6a·CH_3CN·CH_3OH

The X-ray crystal structure determination of **6a** ·CH_3CN·CH_3OH revealed the structure to consist of well-separated molecules of the dipalladium complex and two tetraphenylborate anions. The two solvent molecules of crystallization form hydrogen bonds with nitrogen atoms [N(1), N(3)] of the dication [N(1)−H(1B)···O(1) 2.892 A, N(3)−H(3A)···N(5) 3.307 A], but feature no bonding interactions with the palladium ions. **6a**·CH_3CN·CH_3OH is isomorphous and isostructural with **5a**·CH_3CN·CH_3OH. Although the dication does not possess crystallographically imposed symmetry, its idealized symmetry is C_{2v}. A perspective view of the molecular structure of the dipalladium complex with the atomic numbering scheme is shown in Figure 1.

Figure 1. Molecular structure of the $[Pd_2(\mathbf{4a})_2]^{2+}$ cation in **6a** (50% probability thermal ellipsoids)[a]

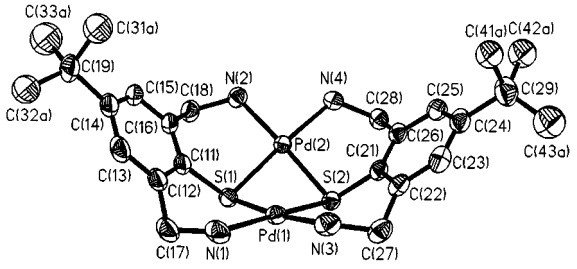

[a] Selected bond lengths [A] and angles [°]: Pd(1)−S(1) 2.3057(9), Pd(1)−S(2) 2.3020(11), Pd(1)−N(1) 2.076(3), Pd(1)−N(3) 2.076(3), Pd(2)−S(1) 2.3009(8), Pd(2)−S(2) 2.2951(9), Pd(2)−N(2) 2.069(2), Pd(2)−N(4) 2.084(2), Pd(1)···Pd(2) 3.0847(6); S(1)−Pd(1)−S(2) 81.79(3), S(1)−Pd(1)−N(1) 94.24(9), S(1)−Pd(1)−N(3) 173.56(8), S(2)−Pd(1)−N(1) 174.98(8), S(2)−Pd(1)−N(3) 94.34(8), N(1)−Pd(1)−N(3) 89.88(11), S(1)−Pd(2)−S(2) 82.05(3), S(1)−Pd(2)−N(2) 94.70(7), S(1)−Pd(2)−N(4) 175.48(7), S(2)−Pd(2)−N(2) 176.27(7), S(2)−Pd(2)−N(4) 93.78(7), N(2)−Pd(2)−N(4) 89.40(10).

As in the dinickel complex **5a**, the coordination of each Pd atom by two nitrogen and two bridging thiolate sulfur atoms is approximately planar. Maximum deviations from the least-squares planes defined by the atoms Pd(1), S(1), S(2), N(1), N(3) and Pd(2), S(1), S(2), N(2), N(4) are 0.078 and 0.028 A, respectively. The two planar PdN_2S_2 units are joined via two bridging thiolate atoms with a folding angle of 123.3° between the two planes. While this angle is only marginally smaller than the corresponding value in **5a** (124.6°), a larger difference is found for the angle between the two least-squares planes defined by the atoms of the phenyl rings of the two ligands (91.9° in **6a**, 96.1° in **5a**). The average Pd−N and Pd−S bond lengths are 2.076 and 2.301 A. In **5a**, the corresponding values were found to be 1.936 and 2.182 A, respectively. It is noted that the difference between Ni−N and Pd−N bond lengths (0.140 A) is larger than the difference in Ni−S and Pd−S bond lengths (0.119 A). Due to the longer Pd−S bonds in **6a**, the M···M distance within the dinuclear cations has increased from 2.973 A in **5a** to 3.085 A in **6a**.

In essence, the molecular structures of **6a** and **5a** show only slight differences. The most important information, however, is that both complexes are isomorphous and isostructural. The similar analytical and spectroscopic data of the complexes **5b** and **6b** (below) suggest that the selenolate complexes are also isomorphous and isostructural with the thiolate complexes.

NMR Spectroscopy

Complexes **5a**−**6b** have been examined by ^{1}H-NMR, $^{13}C\{^1H\}$-NMR, and, where appropriate, by ^{77}Se-NMR

spectroscopy. ^{1}H- and ^{13}C-chemical shifts and assignments according to Chart 1 are collected in Table 1.

Chart 1. ^{1}H-NMR labeling scheme

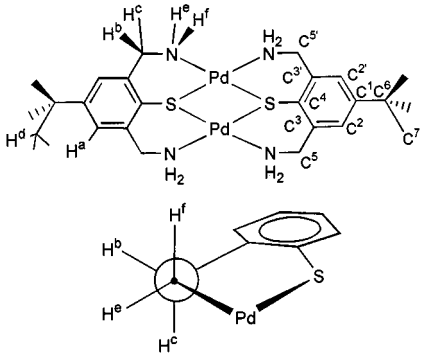

The ^{1}H-NMR spectrum of a solution of **6a** in CD_2Cl_2 is representative for all homodinuclear complexes **5a**−**6b**. Characteristic features are a singlet for the hydrogen atoms of the *tert*-butyl groups (H^d) at δ = 1.32 and a singlet for the hydrogen atoms bonded to the *meta*-carbon atoms of the phenyl ring (H^a) at δ = 7.24 (for **5a**,**b** this singlet is obscured by resonances of the anion). The signals of the methylene (H^b, H^c) and amine hydrogen atoms (H^e, H^f) of the aminomethyl groups appear as four multiplets centered at δ = 3.49, 3.11, 1.88, and 1.02. These form an ABCD spin system as evidenced by H,H-COSY spectroscopy, and this ABCD spin system in the alkane region is characteristic for all compounds (see Figure 2 for the spectrum of **5b**).

The vicinal coupling constants $|^3J_{b,f}|$, $|^3J_{b,e}|$, and $|^3J_{c,e}|$ were estimated (by graphical evaluation) to be less than 2 Hz, while $|^3J_{c,f}|$ was estimated to be ca. 12 Hz. Assignment of the amine hydrogen atoms was unambiguously achieved by an NH/ND-exchange experiment. Thus, addition of a few drops of a CD_3OD/D_2O (95:5) solution caused the two multiplets observed for H_e and H_f to disappear. Under these conditions the two multiplets observed for H_b and H_c now form an AB spin system (doublet of doublets). This allowed the geminal coupling constant of the methylene hydrogen atoms $^2J_{b,c}$ to be determined ($|^2J_{b,c}| \approx 12$ Hz). The two sets of vicinal coupling constants indicate a staggered conformation of the methylene and amine hydrogen atoms within the six-membered chelate ring similar to that observed in the solid state.

Figure 2. 200-MHz ^{1}H-NMR spectrum of **5b** in CD_2Cl_2 showing the four multiplets of the protons of the CH_2NH_2 groups in the region δ = 4.0−0.5 (*: resonances due to H_2O traces of the deuterated solvent)

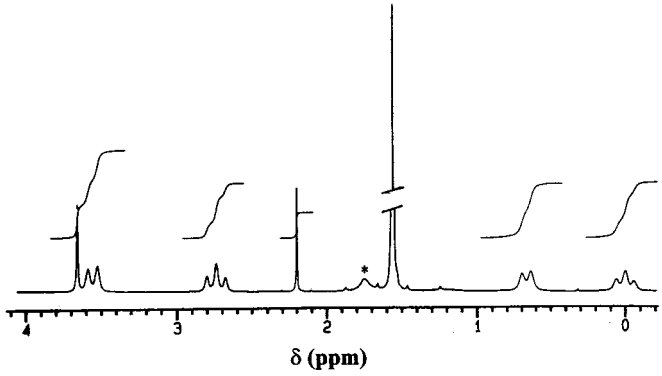

Table 1. ^{1}H- and ^{13}C{^{1}H}-NMR spectroscopic data and assignments of complexes **5a**−**6b**[a]

	5a	**5b**	**6a**	**6b**
^{1}H NMR[b]				
H^a	[c]	[c]	7.24 (s, 4 H)	7.27 (s, 4 H)
H^b	3.19 (d, 4 H)	3.32 (d, 4 H)	3.49 (d, 4 H)	3.56 (d, 4 H)
H^c	2.62 (t, 4 H)	2.50 (t, 4 H)	3.11 (t, 4 H)	3.06 (t, 4 H)
H^d	1.31 (s, 18 H)	1.32 (s, 18 H)	1.32 (s, 18 H)	1.34 (s, 18 H)
H^e	0.51 (d, 4 H)	0.43 (d, 4 H)	1.88 (d, 4 H)	1.71 (d, 4 H)
H^f	−0.03 (t, 4 H)	−0.23 (t, 4 H)	1.02 (t, 4 H)	0.91 (t, 4 H)
$[BPh_4]^-$	7.57 (br. s, 16 H)	7.57 (br. s, 16 H)	7.57 (br. s, 16 H)	7.59 (br. s, 16 H)
	7.10 (m, 28 H)	7.10 (m, 28 H)	7.05 (t, 16 H)	7.06 (t, 16 H)
			6.90 (t, 8 H)	6.89 (t, 8 H)
CH_3OH[d]	3.37 (s, 3 H)	3.37 (s, 3 H)	3.37 (s, 3 H)	3.37 (s, 3 H)
CH_3CN[d]	1.97 (s, 3 H)	1.97 (s, 3 H)	1.97 (s, 3 H)	1.97 (s, 3 H)
^{13}C NMR				
C^1	152.7	153.3	152.5	151.1
C^2	135.2	137.4	136.2	140.4
C^3	128.3	128.3	129.5	128.6
C^4	121.9	118.3	125.6	123.2
C^5	45.8	47.9	48.1	48.8
C^6	34.9	34.9	34.8	34.5
C^7	30.8	30.9	30.8	31.0
$[BPh_4]^-$	164.0	164.1	164.2	162.0
	135.6	135.6	135.6	135.7
	126.9	126.9	126.8	125.5
	123.1	123.1	123.0	121.7
CH_3OH	50.1	49.9	50.0	50.1
CH_3CN	117.7	117.7	117.6	117.5
CH_3CN	1.7	1.7	1.6	1.3

[a] See Chart 1 for atom labeling; data are δ values. − [b] δ values for solutions of complexes in CD_2Cl_2. − [c] Obscured by resonances of $[BPh_4]^-$. − [d] Crystals of **5a**−**6b** slowly lose the acetonitrile and methanol molecules of crystallization upon storage in air at 298 K.

In the $^{13}C\{^1H\}$-NMR spectrum of **6a**, the $[Pd_2(\mathbf{4a})]^{2+}$ dication gives rise to four signals in the aromatic region and three signals in the aliphatic region again consistent with local C_{2v} symmetry of the dication in solution. The four signals in the aromatic region correspond to the *para*- (C^1), the *ipso*- (C^4), the *ortho*- (C^3, $C^{3\prime}$), and the *meta*-carbon atoms (C^2, $C^{2\prime}$) of the phenyl ring, whereas the singlets in the aliphatic region correspond to the quaternary carbon atom of the *tert*-butyl group (C^6), the three equivalent methyl carbon atoms of the *tert*-butyl group (C^7), and the methylene carbon atoms (C^5, $C^{5\prime}$).

Although the chemical shifts of the protons of the aminomethyl groups of the nickel complex **5a** are upfield from the corresponding resonances in the palladium complex **6a**, the otherwise identical ^1H-NMR and $^{13}C\{^1H\}$-NMR data clearly reveal that **6a** and **5a** retain their solid-state structure in solution. Furthermore, the similar ^1H-NMR and ^{13}C-NMR data of the selenolate complexes suggest that these are isostructural with the thiolate complexes. The singlet ^{77}Se resonance observed for **6b** at $\delta = 24.5$ also supports this assumption, however, for reasons unclear no ^{77}Se resonance was observed for **5b**.

It should also be noted that no exchange occurs between these dinuclear complexes in solution. When pure compounds were mixed in a ca. 1:1 ratio and investigated by ^1H-NMR spectroscopy, the spectra of such solutions resemble just superpositions of the spectra of the pure compounds. These spectra remained unchanged even after one week at room temperature. If exchange had occurred under these conditions, one would expect new signals due to mixed species such as $[Ni_2(\mathbf{4a})(\mathbf{4b})]^{2+}$ or $[NiPd(\mathbf{4a})_2]^{2+}$. These results demonstrate the stability of complexes **5a**−**6b**. The same conclusions can be drawn from the electrochemical studies presented below.

Infrared and UV/Vis Spectroscopy

Complexes **5a**−**6a** exhibit very similar IR spectra which are all dominated by two strong absorptions in the region 3350−3200 cm^{-1} (Table 2). These latter absorptions were assigned to $\nu_s(NH_2)$ and $\nu_{as}(NH_2)$ stretching vibrations of the CH_2NH_2 groups[21]. As is expected, the replacement of sulfur in **5a** or **6a** by selenium in **5b** or **6b** produces no shifts in $\nu(NH_2)$ stretching frequencies. However, the $\nu(NH_2)$ stretching modes in palladium complexes **6a**,**b** appear at higher frequencies than in nickel complexes **5a**,**b**. The increase in N−H stretching frequencies in Pd complexes **6a**,**b** reflects a stronger N−H bond consistent with longer Pd−N bonds and, therefore, less polarized N−H bonds in **6a**,**b**.

The UV/Vis spectra are also very similar. In each case two features appear in the region 320−380 nm, which are assigned to π-π* transitions of the ligands. The red color of the nickel complexes is due to the absorption maxima at 499 nm in **5a** and 509 nm in **5b**, which are assigned to chalcogenolate-to-Ni charge-transfer transitions. These bands are shifted to 426 nm in **6a** and 430 nm in **6b**. Relative to the positions of the charge-transfer transitions of the thiolate complexes, those of the selenolate complexes are slightly shifted to lower energy. This is in agreement with the principle of hard and soft acids and bases that classifies selenolate selenium atoms easier to polarize than thiolate sulfur atoms[22].

Table 2. Electrochemical, IR-spectroscopic, and UV/Vis data of complexes **5a**−**6b**

	5a	**5b**	**6a**	**6b**
Electrochemical data, $E^x_{1/2}$ [V][a]				
$E^1_{1/2}$	−0.97	−0.83	−1.02	−0.98
$E^2_{1/2}$	−1.48 (irr.)	−1.34 (irr.)	−1.51 (irr.)	−1.44 (irr.)
Infrared spectroscopic data, ν [cm^{-1}][b]				
$\nu_{as}(NH_2)$	3250 s	3248 s	3262 s	3263 s
$\nu_s(NH_2)$	3193 s	3197 s	3200 s	3201 s
UV/Vis data, λ_{max} [nm] (ε [$M^{-1}\cdot cm^{-1}$])[c]				
	320 (5629)	327 (5043)	318 (9593)	320 (10537)
	380 (7157)	389 (6741)	354 (8272)	354 (7210)
	499 (1713)	509 (1069)	426 (744)	430 (873)

[a] Experiments were carried out using DMF as the solvent with 0.1 M n-Bu_4NPF_6 as the supporting electrolyte, Pt disc working electrode and Pt wire auxiliary electrodes. All half-cell potentials were calibrated against an internal ferrocenium/ferrocene (Fc^+/Fc) standard; $E^x_{1/2} = (E^{ox}_p + E^{red}_p)/2$ for reversible one-electron transfer processes; oxidation (E^{ox}_p) or reduction peak potentials (E^{red}_p) are given for irreversible (irr.) processes. Reported values are referenced vs. SCE. − [b] As KBr pellets. − [c] Data recorded for solutions of **5a**,**b** in CH_2Cl_2 and **6a**,**b** in CH_3CN.

Electrochemistry

Cyclic voltammograms (CVs) of complexes **5a**−**6b** have been recorded in dimethylformamide solution containing 0.10 M tetra-*n*-butylammonium hexafluorophosphate as supporting electrolyte. All potentials are referenced to the SCE. The CV of **5b** is representative for all homodinuclear complexes **5a**−**6a** (Figure 3). The complex undergoes two irreversible reduction processes with cathodic peak potentials at −0.87 and −1.38 V vs. SCE (Table 2). However, when the scan is reversed at −1.2 V vs. SCE, the first reduction process becomes quasi-reversible with the appear-

Figure 3. Cyclic voltammogram of **5b** in DMF with 0.1 M n-Bu_4NPF_6 as supporting electrolyte, Pt disc working electrode, Pt wire auxiliary electrode, and Ag wire pseudo reference electrode; scan rate 200 $mV\cdot s^{-1}$

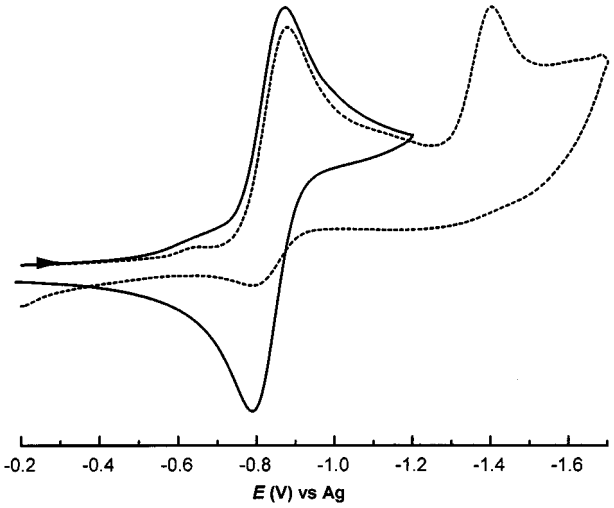

ance of an anodic peak at −0.76 V (ΔE^1 = 84 mV). Reduction of **5b** at a constant potential of −1.2 V vs. SCE consumed 0.94 e^-/complex indicative of a one-electron transfer process. A similar electrochemical behaviour is observed for the other dinuclear complexes (Table 2).

Since the ligands in complexes **5a**−**6b** are unlikely to undergo ligand-centered redox reactions, it is concluded that all complexes undergo metal-centered redox reactions with the initial formation of mixed-valent $M^{II,I}$ monocations $[M_2(L)_2]^+$ (eq. 2). This is also supported by the electrochemical behaviour of related Ni and Pd complexes with planar $N_2(\mu_2\text{-}SR)_2$ coordination environments. The thiolate-bridged Ni^{II} complex $[Ni(pdmt)]_2$ (H_2pdmt = pyridine-2,6-dimethanethiol), for example, undergoes a one-electron reduction at $E_{1/2}$ = −1.21 V vs. SCE ascribed to the formation of the mixed-valence $Ni^{II,I}$ complex $[Ni(pdmt)]_2^-$[23], while the trimetallic compounds $[(NiL')_2Ni]^{2+}$ and $[(NiL')_2Pd]^{2+}$ [L′ = 1,5-bis(mercaptoethyl)-1,5-diazacyclooctane] are reduced at −0.77 and −0.88 V vs. SCE, respectively[24]. It is noted that complexes **5a**−**6b** are readily reduced by $NaBH_4$ in THF to afford dark-brown solutions. These solutions are assumed to contain the respective mixed-valent $M^{I,II}$ monocations $[M_2(L)_2]^+$. However, any attempts to isolate the $M^{I,II}$ species have not yet been successful.

$$[M_2(L)_2]^{2+} + e^- \rightleftharpoons [M_2(L)_2]^+ \quad (2)$$
(L = **4a**,**b**; M = Ni, Pd) $E^1_{1/2}$

Figure 4. Top: cyclic voltammogram of a solution containing **5a** and **6a** in a 1:1 molar ratio (solid line); bottom: square-wave voltammograms of a solution containing **5a** and **6a** in a 1:1 molar ratio (solid line) and of the same solution containing a slight excess of **6a** (dashed line)

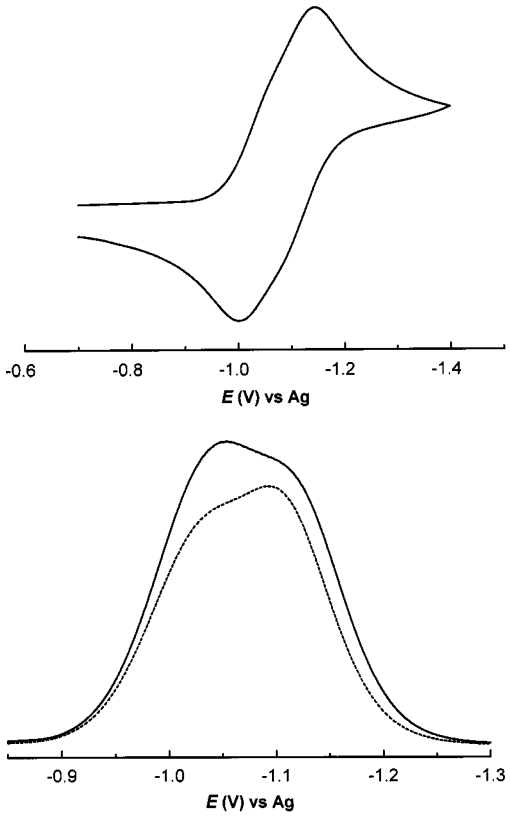

Table 2 shows that the redox potentials of the palladium complexes **6a**,**b** are only slightly shifted to more negative potentials when compared with those of the nickel complexes **5a**,**b**. Replacement of sulfur by selenium also does not dramatically shift the redox potentials, albeit both selenolate complexes are reduced at slightly less negative potentials than the thiolate complexes. It follows that the reduced species are equally well stabilized irrespective of the choice of N_2S_2 or N_2Se_2 coordination.

As previously established by NMR spectroscopy, the dinuclear complexes are quite stable in solution. These results are further confirmed by cyclic voltammetry. In Figure 4 (top), for example, is displayed the cyclic voltammogram of a mixture of complexes **5a** and **6a** in a 1:1 molar ratio in DMF solution. The CV reveals two overlapping reduction waves which correspond to independent reductions of **5a** and **6a**. Both reduction waves are clearly discernible in the corresponding square-wave voltammogram shown in Figure 4 (bottom).

In the present study it was shown that the tridentate amine-chalcogenolate ligands **4a**,**b** form dinuclear complexes with nickel and palladium. In contrast to many monodentate thiolate (or selenolate) ligands, the formation of complexes of higher or lower nuclearity was not observed. All complexes retain their solid-state structure in solution, where they do not undergo any exchange reactions. Furthermore, the existence as chalcogenolate-bridged dinuclear species in solution has allowed for reactivity studies. For example, all complexes undergo metal-centered electron-transfer reactions at potentials (−1.0 to −0.8 V vs. SCE) which are far more positive than those of mononuclear nickel or palladium complexes with N_2S_2 coordination environments ($E \approx -2.0$ V)[24]. Further studies will focus on the isolation, characterization, and an investigation of the chemical reactivity of these reduced species.

This work was supported by the *Deutsche Forschungsgemeinschaft*. The author thanks Prof. Dr. *H. Vahrenkamp* for his continuous and generous support and is grateful to Dipl.-Chem. *A. Trösch* for collecting the X-ray data.

Experimental Section

General: Dichloro(1,5-cyclooctadiene)palladium(II)[25], benzylselenol[26], and compound **5a**[20] were prepared according to literature procedures. Compound **1** was prepared by oxidation of 2-bromo-1,3-dimethyl-5-(1,1-dimethylethyl)benzene with CrO_3 in acetic anhydride[27]. All other chemicals were commercially available. The solvents were predried with molecular sieves and freshly distilled from appropriate drying agents. All reactions were carried out under dry nitrogen with standard Schlenk techniques. − CHN analyses: Perkin Elmer Elemental Analyzer 240. − IR: Bruker IFS25 spectrophotometer (KBr pellets). − ^{1}H NMR, $^{13}C\{^1H\}$ NMR: Bruker AC 200 spectrometer. − ^{77}Se NMR: Varian Unity 300 spectrometer. Dibenzyl diselenide was used as external standard. ^{77}Se NMR chemical shifts are referenced to Me_2Se_2[28]. − Absorption spectra: Jasco V-750 UV/VIS/NIR spectrometer. − Cyclic voltammetry: EG&G Princeton Applied Research Potentiostat/Galvanostat Model 263 A. The cell contained a Pt working electrode, a Pt wire auxiliary electrode, and an Ag wire pseudo reference electrode. Concentration of solutions were 0.1 M in supporting

electrolyte (nBu$_4$NPF$_6$) and ca 1×10^{-3} M in sample. All potentials were scaled to ferrocenium/ferrocene as internal standard and converted to the SCE reference[29].

Benzyl (4-tert-Butyl-2,6-diformylphenyl)sulfide (**2a**): To a suspension of phenylmethanethiol (6.58 g, 53.0 mmol) and K_2CO_3 (8.29 g, 60.0 mmol) in DMF (80 ml) was added solid 1-bromo-4-*tert*-butyl-2,6-diformylbenzene (14.3 g, 53.0 mmol). After stirring the reaction mixture for 12 h, the crude product solidified upon dropwise addition of water (200 ml). The solid was isolated by filtration, washed with 100 ml of water, and dried in vacuum. The crude product was used without further purification, yield 15.4 g (93%), m.p. 78−80°C. − IR (KBr pellet): ν = 1720 cm^{-1} (CO). − ^{1}H NMR ($CDCl_3$): δ = 10.57 (s, 2 H, C*H*O), 8.13 (s, 2 H, aromatic H), 7.20-7.16 (m, 3 H, aromatic H), 6.86 (m, 2 H, aromatic *H*), 3.91 (s, 2 H, SCH_2), 1.35 (s, 9 H, CH_3). − ^{13}C{^{1}H} NMR ($CDCl_3$): δ = 191.3 (*C*HO), 153.5, 138.8, 137.4, 135.8, 130.4, 128.7, 128.6, 127.7, 43.7, 35.1, 30.8.

Benzyl (4-tert-Butyl-2,6-diformylphenyl)selenide (**2b**): Analogously to the preparation of **2a**, compound **2b** was prepared from phenylmethaneselenol (9.07 g, 53.0 mmol), K_2CO_3 (8.29 g, 60.0 mmol), and 1-bromo-4-*tert*-butyl-2,6-diformylbenzene (14.3 g, 53.0 mmol). The crude product was used without further purification, yield 16.6 g (87%), m.p. 79−81°C. − ^{1}H NMR ($CDCl_3$): δ = 10.51 (s, 2 H, C*H*O), 8.13 (s, 2 H, aromatic H), 7.16 (m, 3 H, aromatic H), 6.87 (m, 2 H, aromatic H), 3.93 (s, $^2J_{Se,H}$ = 16 Hz, 2 H, SeCH_2), 1.36 (s, 9 H, CH_3). − ^{13}C{^{1}H} NMR ($CDCl_3$): δ = 193.0 (*C*HO), 153.3, 138.4, 136.6, 133.1, 130.3, 128.4, 128.3, 127.2, 35.2, 34.9, 30.7.

Benzyl [4-tert-Butyl-2,6-di(hydroximinoformyl)phenyl]sulfide (**3a**): To a suspension of $NH_2OH \cdot HCl$ (2.78 g, 40.0 mmol) in $CHCl_3$ (100 ml) was added a solution of NEt_3 (4.05 g, 40.0 mmol) in $CHCl_3$ (50 ml). A solution of compound **2a** (6.25 g, 20.0 mmol) in $CHCl_3$ (100 ml) was added, and stirring was continued for 12 h. The organic phase was washed with 200 ml of water, separated, and dried with $MgSO_4$. The solvent was removed in vacuum to afford a pale yellow crystalline residue. This material was recrystallized from benzene, colorless crystals, 5.96 g (87%). − ^{1}H NMR ([D$_6$]DMSO): δ = 11.41 (s, 2 H, O*H*), 8.55 (s, 2 H, C*H*), 7.82 (s, 2 H, aromatic H), 7.20 (m, 3 H, aromatic H), 7.02 (m, 2 H, aromatic H), 3.85 (s, 2 H, SCH_2), 1.29 (s, 9 H, CH_3). − ^{13}C{^{1}H} NMR ([D$_6$]DMSO): δ = 151.6, 146.9, 137.1, 136.9, 128.9, 128.7, 128.3, 127.2, 123.6, 41.3, 34.5, 30.8.

Benzyl [4-tert-Butyl-2,6-di(hydroximinoformyl)phenyl]selenide (**3b**): Analogously to the preparation of **3a**, compound **3b** was prepared from **2b** (7.19 g, 20.0 mmol), $NH_2OH \cdot HCl$ (2.78 g, 40.0 mmol), and NEt_3 (4.05 g, 40.0 mmol) in $CHCl_3$, colorless crystals, 6.62 g (85%). − ^{1}H NMR ([D$_6$]DMSO): δ = 11.37 (s, 2 H, O*H*), 8.52 (s, 2 H, C*H*), 7.79 (s, 2 H, aromatic H), 7.16 (m, 3 H, aromatic H), 7.00 (m, 2 H, aromatic H), 3.89 (s, $^2J_{Se,H}$ = 16 Hz, 2 H, SeCH_2), 1.30 (s, 9 H, CH_3). − ^{13}C{^{1}H} NMR ([D$_6$]DMSO): δ = 151.5, 149.0, 138.0, 137.3, 128.4, 128.2, 126.8, 126.4, 123.6, 34.4, 33.4, 30.8.

2,6-Bis(aminomethyl)-4-tert-butylthiophenol (**4a**): A solution of **3a** (6.85 g, 20.0 mmol) in THF (50 ml) was added dropwise to a solution of sodium (6.05 g, 28.3 mmol) in liquid ammonia (100 ml). During addition the temp. was kept below −60°C by cooling with a dry ice/2-propanol bath. After the deep blue reaction mixture was stirred for further 3 h at −50°C, solid ammonium chloride was added to destroy excess reducing equivalents. After the ammonia was allowed to evaporate at atmospheric pressure, the remaining THF was evaporated in vacuum. The pale yellow solid was dissolved in 30 ml of water and the pH of the solution adjusted to 1 by addition of 1 M HCl. After stirring for 30 min, the precipitate was collected by filtration, and recrystallized from 1 M HCl to give 4.04 g (68%) of **4a**·2HCl as pale yellow needles. − ^{1}H NMR (CD_3OD): δ = 7.65 (s, 2 H, aromatic H), 4.44 (s, 4 H, CH_2), 1.37 (s, 9 H, CH_3). − ^{13}C{^{1}H} NMR (CD_3OD): δ = 153.6, 138.1, 129.6, 127.6, 43.7, 36.1, 31.6.

2,6-Bis(aminomethyl)-4-tert-butylselenophenol (**4b**): Analogously to the preparation of **4a**, compound **4b** was prepared by reduction of **3b** (7.79 g, 20.0 mmol) with sodium in liquid ammonia. Recrystallization from 1 M HCl afforded 3.98 g (58%) of **4b**·2HCl as yellow needles. − ^{1}H NMR (CD_3OD): δ = 7.68 (s, 2 H, aromatic H), 3.92 (s, 4 H, CH_2), 1.42 (s, 9 H, CH_3). − ^{13}C{^{1}H} NMR (CD_3OD): δ = 156.8, 139.6, 130.9, 129.9, 45.3, 36.2, 31.6.

Bis[2,6-bis(aminomethyl)-4-tert-butylselenophenolato]-dinickel(II) Tetraphenylborate·Acetonitrile·Methanol (**5b**): A solution of $Ni(ClO_4)_2 \cdot 6H_2O$ (731 mg, 2.00 mmol) in methanol (10 ml) was added to a solution of **4b**·$(HCl)_2$ (688 mg, 2.00 mmol) in methanol (10 ml). After the pale yellow solution was stirred for 10 min, 12.0 ml of a 0.5 M solution of NaOMe in methanol (6.00 mmol) was added. To the dark red solution was added a solution of $NaBPh_4$ (856 mg, 2.50 mmol) in methanol (2 ml). After the mixture was allowed to stand overnight, the microcrystalline residue was collected by filtration, washed with methanol (3 × 5 ml), and dried in air. The crude product was recrystallized from CH_3CN/MeOH (1:1), dark-red crystals, 1.07 g (78%), m.p. 206−209°C (decomp.). − $C_{72}H_{78}B_2N_4Ni_2Se_2 \cdot CH_3CN \cdot CH_3OH$ (1369.45): calcd. C 65.78, H 6.26, N 5.11; found C 65.46, H 6.30, N 4.84.

Bis[2,6-bis(aminomethyl)-4-tert-butylthiophenolato]-dipalladium(II) Tetraphenylborate·Acetonitrile·Methanol (**6a**): A solution of (COD)$PdCl_2$ (571 mg, 2.00 mmol) in methanol (10 ml) was added to a solution of **4a**·$(HCl)_2$ (595 mg, 2.00 mmol) in methanol (10 ml). After the pale yellow solution was stirred for 10 min, 12.0 ml of a 0.5 M solution of NaOMe in methanol (6.00 mmol) was added. To the dark-yellow solution was added a solution of $NaBPh_4$ (856 mg, 2.50 mmol) in methanol (2 ml). After the mixture was allowed to stand overnight, the microcrystalline residue was collected by filtration, washed with methanol (3 × 5 ml), and dried in air. The crude product was recrystallized from CH_3CN/MeOH (1:1), yellow crystals, 1.12 g (82%), m.p. 207−209°C (decomp.). − $C_{72}H_{78}B_2N_4Pd_2S_2 \cdot CH_3CN \cdot CH_3OH$ (1371.11): calcd. C 65.70, H 6.25, N 5.11; found C 65.39, H 6.27, N 5.02.

Bis[2,6-bis(aminomethyl)-4-tert-butylselenophenolato]-dipalladium(II) Tetraphenylborate·Acetonitrile·Methanol (**6b**): Analogously to the preparation of **6a**, compound **6b** was prepared from **4b** (688 mg, 2.00 mmol), (COD)$PdCl_2$ (571 mg, 2.00 mmol), 0.5 M NaOMe (12.0 ml, 6.00 mmol), and $NaBPh_4$ (855 mg, 2.50 mmol) in MeOH. The crude product was recrystallized from CH_3CN/MeOH (1:1), yellow crystals, 0.93 g (63%), m.p. 208−210°C (decomp.). − ^{77}Se NMR ([D$_6$]DMSO, 200 MHz): δ = 24.5. − $C_{72}H_{78}B_2N_4Pd_2Se_2 \cdot CH_3CN \cdot CH_3OH$ (1464.91): calcd. C 61.49, H 5.85, N 4.78; found C 61.43, H 6.03, N 4.72.

Crystal-Structure Determination: Crystals of **6a** suitable for X-ray structure analysis were obtained by recrystallization from an acetonitrile/methanol (1:1) solution. A yellow crystal of approximate dimensions 0.30 × 0.30 × 0.40 mm was selected and mounted on a glass fibre with a small amount of perfluoroether oil. After optical alignment at 193 K on an Enraf Nonius CAD4 diffractometer, the unit cell was determined from a least-squares fit of the setting angles of 25 carefully centered high-angle reflections. Crystal data and refinement details: $C_{75}H_{85}B_2N_5Pd_2OS_2$, M_r = 1371.11, monoclinic, space group $P2_1/n$, a = 22.130(4), b = 13.806(3), c = 23.672(5) A, β = 109.81(3)°, V = 6804.4 A^3, Z =

4, $\rho_{calcd.} = 1.34\ g\cdot cm^{-3}$, $\mu(Mo\text{-}K_\alpha) = 0.64\ mm^{-1}$, empirical absorption correction, transmission factors 0.89−0.98, 14383 reflections collected, 13297 unique reflections ($R_{int} = 0.0233$), 11448 observed reflections [$I > 2\sigma(I)$]. The structure was solved by direct methods (SHELXS-86)[30] and refined by full-matrix least-squares techniques against F^2 (SHELX-93). All non-hydrogen atoms were refined anisotropically except for the methyl carbon atoms of the disordered *tert*-butyl groups, which were refined isotropically. Hydrogen atoms were placed at calculated positions and were refined using a riding model with isotropic thermal parameters fixed at 1.2 times the equivalent isotropic U of the atom to which they were bonded. An isotropic split-atom model was applied for the disordered methyl carbon atoms. The multiplicities of the respective orientations C(31A)−C(33A), C(31B)−C(33B), C(41A)−C(43A), C(41B)−C(43B) were refined as follows: 0.58, 0.42, 0.51, 0.49. Final residuals: $R1$, $wR2$ [$F_o > 4\sigma(F_o)$]: 0.0369, 0.0955, $R1$, $wR2$ (all data): 0.0473, 0.1047, goodness-of-fit on F^2: 1.07, residual electron density: 0.771/−0.836 eA^{-3}. Crystallographic data (excluding structure factors) for the structure reported in this paper have been deposited with the Cambridge Crystallographic Data Centre as supplementary publication no. CCDC-101312. Copies of the data can be obtained free of charge on application to CCDC, 12 Union Road, Cambridge CB2 1EZ, UK [Fax: int. code + 44(1223)336-033; E-mail: deposit@cam.ac.uk].

[1] B. Krebs, G. Henkel, *Angew. Chem.* **1991**, *105*, 785−804; *Angew. Chem. Int. Ed. Engl*. **1991**, *30*, 769−788.
[2] J. Arnold, *Prog. Inorg. Chem.*, **1995**, *43*, 353−417.
[3] M. G. Kanatzidis, S. Huang, *Coord. Chem. Rev.* **1994**, *130*, 509−621.
[4] A. Volbeda, E. Garcin, C. Piras, A. L. de Lacey, V. M. Fernandez, E. C. Hatchikian, M. Frey, J. C. Fontecilla-Camps, *J. Am. Chem. Soc.* **1996**, *118*, 12989−12996.
[5] M. K. Eidsness, R. A. Scott, B. C. Prickril, D. V. DerVartanian, J. LeGall, I. Moura, J. J. G. Moura, H. D. Peck, *Proc. Natl. Acad. Sci. USA*, **1989**, *86*, 147−151.
[6] I. G. Dance, *Polyhedron* **1986**, *5*, 1037−1104.
[7] M. Kumar, R. O. Day, G. J. Colpas, M. J. Maroney, *J. Am. Chem. Soc.* **1989**, *111*, 5974−5976.
[8] D. Sellmann, W. Prechtel, F. Knoch, M. Moll, *Z. Naturforsch.* **1992**, *47b*, 1411−1423.
[9] T. Beissel, K. S. Bürger, G. Voigt, K. Wieghardt, C. Butzlaff, A. X. Trautwein, *Inorg. Chem.* **1993**, *32*, 124−126.
[10] D. K. Mills, J. H. Reibenspies, M. Y. Darensbourg, *Inorg. Chem.* **1990**, *29*, 4364−4366.
[11] T. Beissel, T. Glaser, F. Kesting, K. Wieghardt, B. Nuber, *Inorg. Chem.* **1996**, *35*, 3936−3947.
[12] [12a] A. J. Atkins, A. J. Blake, M. Schröder, *J. Chem. Soc., Chem. Commun.* **1993**, 1662−1665. − [12b] A. J. Atkins, D. Black, A. J. Blake, A. Marin-Becerra, S. Parsons, L. Ruiz-Ramirez, M. Schröder, *J. Chem. Soc., Chem. Commun.* **1996**, 457−464.
[13] [13a] D. Sellmann, S. Emig, F. W. Heinemann, *Angew. Chem.* **1997**, *109*, 1808−1810; *Angew. Chem. Int. Ed. Engl.* **1997**, *36*, 1734−1736. − [13b] D. Sellmann, S. Emig, F. W. Heinemann, F. Knoch, *Angew. Chem.* **1997**, *109*, 1250−1252; *Angew. Chem. Int. Ed. Engl*. **1997**, *36*, 1201−1203.
[14] [14a] J. Hanss, H.-J. Krüger, *Angew. Chem.* **1996**, *108*, 2989−2991; *Angew. Chem. Int. Ed. Engl*. **1996**, *35*, 2827−2830. − [14b] J. Hanss, H.-J. Krüger, *Angew. Chem.* **1998**, *110*, 366−369; *Angew. Chem. Int. Ed.* **1998**, *37*, 360−363.
[15] D. Sellmann, M. Hannakam, F. Knoch, M. Moll, *Z. Naturforsch.* **1992**, *47b*, 1545−1550.
[16] D. Sellmann, W. Soglowek, F. Knoch, M. Moll, *Angew. Chem.* **1989**, *101*, 1244−1245; *Angew. Chem. Int. Ed. Engl.* **1989**, *28*, 1271−1272.
[17] S. Brooker, P. D. Croucher, *J. Chem. Soc., Chem. Commun.* **1997**, 459−460.
[18] C. M. Goldman, M. M. Olmstead, P. K. Mascharak, *Inorg. Chem.* **1996**, *35*, 2752−2757.
[19] B. Kersting, M. J. Kolm, C. Janiak, *Z. Anorg. Allg. Chem.* **1998**, *624*, 775−780.
[20] B. Kersting, D. Siebert, *Inorg. Chem.*, in press.
[21] K. Nakamoto, *Infrared and Raman Spectra of Inorganic and Coordination Compounds*, Wiley, New York, **1978**.
[22] R. G. Pearson, *Survey Prog. Chem.* **1969**, *5*, 1−52.
[23] H.-J. Krüger, R. H. Holm, *Inorg. Chem.* **1989**, *28*, 1148−1155.
[24] G. Musie, P. J. Farmer, T. Tuntulani, J. H. Reibenspies, M. Y. Darensbourg, *Inorg. Chem.* **1996**, *35*, 2176−2183.
[25] D. Drew, J. R. Doyle, *Inorg. Synth.* **1972**, *13*, 47−55.
[26] H. J. Reich, C. P. Jasperse, J. M. Renga, *J. Org. Chem.* **1986**, *51*, 2981−2988.
[27] M. Tashiro, T. Yamato, *J. Chem. Soc., Perkin Trans. 1* **1979**, 176−179.
[28] R. K. Harris, B. E. Mann, *NMR and the Periodic Table*, Academic Press, London, **1978**.
[29] For formal potentials of the ferrocenium/ferrocene couple vs. SCE, see: N. G. Connelly, W. E. Geiger, *Chem. Rev.* **1996**, *96*, 877−910. Under our experimental conditions, the couple ferrocenium/ferrocene (Fc^+/Fc) is at $E_{1/2} = 0.45$ V (DMF, CH_2Cl_2) and $E_{1/2} = 0.40$ V (CH_3CN) vs. Ag.
[30] G. M. Sheldrick, *SHELXS-86*, University of Göttingen, Germany, **1990**; G. M. Sheldrick, *SHELXL-93,* University of Göttingen, Germany, **1993**.

[98084]

Complexes of Azaphospholes: Synthesis and Structure of Pentacarbonyl-(η^1)-2-phosphaindolizine)chromium(0), -molybdenum(0), and -tungsten(0)

Neelima Gupta[a][+], Chandra B. Jain[a][+], Joachim Heinicke*[a], Raj K. Bansal*[b], and Peter G. Jones[c]

Institut für Anorganische Chemie, EMA-Universität Greifswald[a],
17487 Greifswald, Germany
Fax (internat.) +49 (0)3834/ 864319
E-mail: heinicke@rz.uni-greifswald.de

Department of Chemistry, University of Rajasthan[b],
Jaipur 302004, India
Fax: (internat.) +91(0)141/652784

Institut für Anorganische und Analytische Chemie, Technische Universität Braunschweig[c],
Postfach 3329, D-38023 Braunschweig, Germany
E-mail: p.jones@tu-bs.de

Received March 30, 1998

Keywords: Phosphorus heterocycles / P ligands / Transition metals / Carbonyl complexes

The complex chemical behaviour of 2-phosphaindolizines **1** (1,3-azaphospholo[1,5-*a*]pyridines) towards metal carbonyl compounds was studied. (η^1-2-Phosphaindolizine)$M(CO)_5$ complexes **2–4** (M = Cr, Mo, W) were formed from **1** and [(THF)$M(CO)_5$], the *cis*-$L_2Cr(CO)_4$ complex **5f** from **1f** and tetracarbonyl(norbornadiene) chromium(0). The reaction of 2-phosphaindolizines **1e**, **1f**, or **1g** with tricarbonyl(cycloheptatriene)molybdenum(0) or tricarbonyl(mesitylene)-tungsten(0) yielded σ-complexes of the types $L_2M(CO)_4$ or $L_3M(CO)_3$ rather than isolable π-complexes. In one case a strong upfield signal ($\delta^{31}P$ = 6.1) was observed with a coordination shift of $\Delta\delta$ = –161.7, which is typical for π-coordination. Prolonged reaction or work-up led, however, to dismutation yielding **1g** and the *fac*-$L_3Mo(CO)_3$ complex **6g**. X-ray structure analysis of **2a** indicates an increased 10π-delocalization compared with **1a** and a changed conformation of the acyl substituent. The influence of substituents and metals on the ^{31}P and ^{13}C complexation chemical shifts and coupling constants is discussed.

Introduction

The coordination behaviour of five-membered π-excess heterocycles has found considerable interest[1][2][3][4][5]. Mono-, di-, and triphosphole anions exhibit different coordination modes but, like cyclopentadienyl anions, they preferably form η^5-complexes[1][2][6] emphasizing the similarities of P=C and C=C structural units[7]. Pyrroles and pyrrole anions also form various types of complexes with π- and σ-coordination. Simple sandwich or η^5-coordinate (tricarbonyl)transition metal(0) complexes of pyrroles or pyrrole anions, however, need sterical stabilization by suitable substituents[4]. Thus, tricarbonyl(η^5-pyrrole)chromium(0) complexes belong to the most labile π-complexes with benzene-like ligands, reacting even with THF or benzene by ligand substitution[8], in sharp contrast to the η^5-phosphole or η^5-arsole complexes. 1*H*-1,3-azaphospholes and their anions, contain both two-coordinate phosphorus and three-coordinate nitrogen; they are aromatic 6π-systems even in the neutral state and, according to the P=C/C=C-similarity principle, should resemble the pyrroles[9][10]. There are several studies on azaphospholes and annelated azaphospholes[10][11][12] but very little is known about their behaviour in complex formation. Only two η^1-$LCr(CO)_5$ complexes with the ligands 2-phenyl-1,3-benzazaphosphole[13] and 2-phosphaindolizine[14] have been reported, which exhibit even lower ^{31}P-coordination shifts than related η^1-di- and -triazaphosphole[11][15] and η^1-phosphabenzene complexes[16] with $sp^2(p_\pi)$ hybridized phosphorus. This may be viewed in association with the reduced σ- and the increased π-charge density at phosphorus[10][14] in these π-excess heterocycles. These various aspects prompted us to investigate complexation reactions of neutral and anionic 1,3-azaphospholes or more easily accessible annelated representatives thereof and to study the preferred coordination mode and possible alternatives. We report here on reactions of 2-phosphaindolizines[14][17][18] with group VI metal carbonyl complexes and the characterization of the complexes by NMR and, for **2a**, by X-ray structural analysis.

Results and Discussion

Synthesis of Phosphaindolizine Carbonyl Complexes

Various substituted 2-phosphaindolizines **1** bearing an electron-withdrawing substituent R^2 such as acyl, carbalk-

[+] Present Address: University of Rajasthan.

 © WILEY-VCH Verlag GmbH, D-69451 Weinheim, 1998 1434–1948/98/0808–1079 $ 17.50+.50/0

oxy or *p*-nitrophenyl in 3-position and a further substituent (Me, *n*Bu or Ph) in position 1, 6, or 7 were treated at room temperature with [(THF)M(CO)$_5$] (M = Cr, Mo, W). This led to selective formation of (η^1-2-phosphaindolizine)M(CO)$_5$ complexes **2**–**4**. The carbonyl or nitro groups did not interfere. Extractive purification or recrystallization of the crude products with hexane afforded powdery or crystalline, analytically pure, pale to dark yellow complexes. They were characterized by ^{31}P (Table 1), ^{1}H (Table 2), and ^{13}C NMR (Table 3) as well as by infrared spectroscopy (Table 4) and (for **2a**) by X-ray structural analysis (Figure 1). The spectroscopic data and structure are discussed below.

The reaction of **1e** with [(THF)Cr(CO)$_5$] to **2e** (δ^{31}P = 190.6) was accompanied by formation of a smaller amount of the tetracarbonyl bis(phosphaindolizine) complex **5e** (δ^{31}P = 201.5). Recrystallization of the crude product afforded, however, only pure **2e**. The synthesis of tetracarbonyl bis(phosphaindolizine) complexes can be achieved by refluxing **1** with tetracarbonyl(norbornadiene)chromium(0) in petroleum ether. In this way, **1f** gave an orange-yellow mixture of two complexes, **2f** (δ^{31}P = 190.8) and **5f** (δ^{31}P = 202.3). Recrystallization from hexane gave **5f**. Structure elucidation is based on ^{13}C and ^{1}H NMR investigations. The appearance of two triplets of equal intensity in the ^{13}C-NMR spectrum at δ = 217.0 [$^2J(^{31}P\text{-}^{13}C)$ = 17.2 Hz, *cis* CO] and δ = 224.0 ($J_{AX} + J_{A'X}$ = 20.2 Hz, *trans* CO) besides the signals for the ligand indicates the presence of two equally populated types of carbonyl groups and thus proves **5f** to be the tetracarbonyl-*cis*-bis(η^1-2-phosphaindolizine)chromium(0) complex. It should be mentioned that the *cis*-L$_2$M(CO)$_4$ isomers were also formed preferentially in the reaction of triphenylphosphabenzene with tetracarbonyl(norbornadiene) complexes of group VI[16a] whereas thermal reactions of phosphanes and the metal hexacarbonyls provide mixtures of *cis* and *trans* complexes[19].

Scheme 1

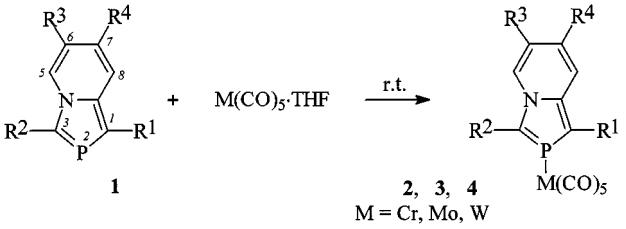

1 **2, 3, 4** M = Cr, Mo, W

In view of the existence of σ- and π-coordination modes in carbonyl complexes of phosphabenzene[16][20][21], phosphole anions[1][2], and π-excess heterocycles such as pyrrole[3][4][5], we tried to obtain η^5-2-phosphaindolizine π-complexes. However, isolable π-complexes were obtained neither on prolonged irradiation by a high-pressure mercury lamp, e.g. of **4b** in hexane, nor on heating, nor from the reactions of 2-phosphaindolizines **1e**, **1f**, or **1g** with tricarbonyl(cycloheptatriene)molybdenum(0) or tricarbonyl(mesitylene)tungsten(0). Instead, a variety of σ-complexes of the types L$_2$M(CO)$_4$ or L$_3$M(CO)$_3$ were formed.

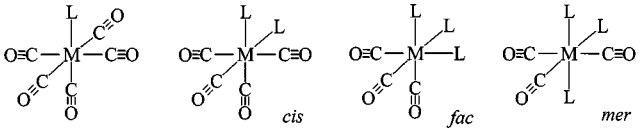

2, 3, 4 **5e, f** (M = Cr) **6e** (M = W) **6f, g** (M = Mo) **7g** (M = Mo)

Solely during the reaction of excess **1g** with tricarbonyl(cycloheptatriene)molybdenum(0) in tetrahydrofuran at room temperature could a strong upfield signal at δ^{31}P = 6.1 with a coordination shift of $\Delta\delta$ = −161.7 be observed, which is close to the phosphorus resonance δ^{31}P = 4.3 and $\Delta\delta$ = −173.9 of tricarbonyl-η^3-(2,4,6-triphenylphosphabenzene)chromium(0)[20]. On prolonged reaction or attempted isolation this signal disappeared, however, and only **1g** and the *fac*-L$_3$Mo(CO)$_3$ complex **6g** (δ^{31}P = 181.2) were detected. This suggests formation of a little stable π-complex that underwent dismutation. Curiously, if the reaction was performed in a 1:1 ratio using the same solvent and reaction conditions, the isomeric *mer*-L$_3$Mo(CO)$_3$ complex **7g** [δ^{31}P = 196.3, d, 2 P$_{trans}$; 203.8, t, 1 P$_{cis}$; $^2J(^{31}P\text{-}^{31}P_{cis})$ = 9.3 Hz] was obtained. Formation of **7g** was also observed if CDCl$_3$ was used as solvent. Attempts at extractive purification or reaction in refluxing ether/hexane furnished a mixture of **6g** and **7g**. The structure assignment is supported by proton-coupled phosphorus spectra. In **6g** the proton coupling with the initial phosphorus singlet led to a symmetric multiplet with seven resolved lines, lines 1 and 7 being weak, lines 3 and 5 broad. A calculated spectrum[22] with δ^{31}P = 173.13, $^2J(^{31}P\text{-}^{31}P)$ = 30 Hz and ^2J(PH1) = 30.8 Hz is in good accordance with the experimental coupling pattern. It consists of 9 inner lines, two pairs of which lie close together to form the experimental lines 3 and 5. Weak outer lines are hinted at in the spectrum by a raised base line. In **7g** the P$_c$ triplet becomes a double triplet by coupling with the H-1 proton within the ligand, while the doublet corresponding to the P$_{trans}$ ligands is split into a multiplet with five strong lines. A simulation using $\delta^{31}P(C_6D_6)$ = 193.34, 200.90, $^2J(^{31}P\text{-}^{31}P_{cis})$ = 9.3 Hz, $^2J(^{31}P\text{-}^{31}P_{trans})$ = 41 Hz and ^2J(PH1) = 30.8 Hz (δ_{H1} = 6.38) fits with the experimental spectrum (Figure 1). Since ^2J(PH1) is similar to the respective coupling in **3g** (31.5 Hz) and $^2J(^{31}P\text{-}^{31}P)$ generally larger in *trans* than in *cis* complexes these values seem reasonable.

In the reaction of **1f** with tricarbonyl(cycloheptatriene)-molybdenum(0), initial formation of probably **6f** was observed by a singlet at δ^{31}P = 178.9 and a line form of the proton-coupled phosphorus multiplet resembling rather a *fac*-L$_3$Mo(CO)$_3$ than a *trans*-L$_2$Mo(CO)$_4$ coupling pattern. However, this complex proved to be unstable in extractive work-up and subsequently underwent dismutation yielding the LMo(CO)$_5$ complex **3f** (δ^{31}P = 169.3), which could be isolated in spectroscopically and analytically pure form (Tables 1–4). Prolonged heating of **1e** with tricarbonyl(mesitylene)tungsten(0) in THF afforded a mixture of **6e** [δ^{31}P = 149.6, $^1J(^{31}P\text{-}^{183}W)$ = 265 Hz, multiplet with five

Figure 1. Proton-coupled phosphorus spectra of **6f** (left) and **7f** (middle and right)

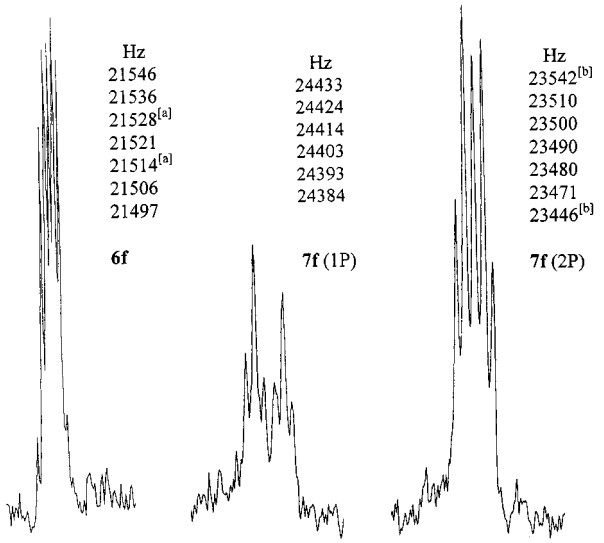

[a]Each two unresolved lines (calculated 21528, 21530; 21514, 21512), of which only the stronger one is seen. – [b] Small lines (calculated 23541, 23532; 23440, 23449) are superimposed by noise.

broad lines by ^{31}P-^{1}H coupling] and **4e** (δ = 140.2, quartet by ^{31}P-^{1}H coupling).

The phosphaindolizine carbonyl complexes are less stable than phosphane carbonyl complexes and are attacked by water and by air, slowly in the solid state and more rapidly in solution. In a moist $CDCl_3$ solution of **4a** we observed the phosphorus resonance of **1a**. After four days, signals of **1a** and an addition product ($\delta^{31}P$ = 128.5) are exhibited (intensity 1:2) and after a further day all of **1a** and a part of the addition product was decomposed to give a hydrolysis product with $\delta^{31}P$ = 21.8. The volatility is low but sufficient to record EI mass spectra of the complexes $LM(CO)_5$. For **2f**, **3f**, **4e** and **4h** the molecular ion peaks M^+ were observed. The appearance of $[M - CO]^{+\cdot}$, $[M - 2\ CO]^{+\cdot}$, $[M - 3\ CO]^{+\cdot}$, $[M - 4\ CO]^{+\cdot}$ and $[M - 5\ CO]^{+\cdot}$ peaks indicates primary decomposition by the successive loss of carbon monoxide molecules from the $LM(CO)_5$ moieties. Further fragmentation follows similar pathways as for the free ligand[18].

Spectra of Phosphaindolizine $M(CO)_5$ Complexes and Structural Aspects

Phosphorus NMR: Preliminary reports of two $Cr(CO)_5$ complexes of annelated 1,3-azaphospholes, 2-phenyl-1,3-benzazaphosphole[13], and a 2-phosphaindolizine[14], had indicated small ^{31}P-coordination shifts of $\Delta\delta$ = 4.4 and 7.5, respectively. The larger body of data for **2–4** (Table 1) now reveals a much broader range of $\Delta\delta^{31}P$ and allows a comparison with $LM^{VI}(CO)_5$ complexes of phosphane and heterocyclic σ^2-phosphorus ligands. The coordination shift in complexes $R_3PM^{VI}(CO)_5$ becomes smaller with increasing group electronegativity of R, for $Hal_3PM^{VI}(CO)_5$ even negative[23][24][25][26]. η^1-Complexes of σ^2-phosphorus compounds possessing a higher s-character at phosphorus (sp^2 hybridization) may be compared with complexes of electron-poor phosphanes, which are weak σ-donor but more efficient π-acceptor ligands. In fact, $\Delta\delta^{31}P$ of the 2-phosphaindolizine complexes **2–4** is somewhat lower than $\Delta\delta^{31}P$ of $(MeO)_3PM^{VI}(CO)_5$[26][27] and similar to the η^1-phosphabenzene complexes 2,4,6-$Ph_3C_5H_2PM^{VI}(CO)_5$[16]. The electron-withdrawing effect of nitrogen and -M groups in α-position to phosphorus is partly compensated by the π-excess character of the 1,3-azaphosphole ring. The stronger upfield coordination shifts of the pivaloyl and phenacyl derivatives **a**-**d** may be attributed to the changed conformations with increased anisotropy and reduced –M effects on phosphorus as compared to the free ligand. The one-bond ^{31}P-^{183}W couplings of **4** (253–268 Hz) are larger than those in (triorganophosphane)$W(CO)_5$ complexes which, however, increase with the group electronegativity of R in $R_3PW(CO)_5$[23][24][25][26].

Proton NMR: The chemical shifts and almost all coupling constants of free ligands **1a–h**[14][17][18] and their complexes (Table 2) in $CDCl_3$ are very similar. Thus the differences of respective δ values of the complex **2e** and the ligand **1e** in $CDCl_3$ are less than 0.13. However, a strong influence on the proton resonance is exerted by deuterobenzene. Almost all signals of phosphaindolizine protons in **2–4** are upfield shifted by $\Delta\delta$ = 0.6 to 1.1 in C_6D_6 as compared to the ligands in $CDCl_3$. Methyl groups in position 7 and 1 are also affected, but to a lower extent. Phenyl groups are at most slightly influenced, indicating stacking interactions between C_6D_6 and the phosphaindolizine ring. The lack of an upfield shift of H-5 in the 3-carbalkoxy derivatives **3e**, **4e**, **2f**, and **3f** can be attributed to a superimposed deshielding anisotropy effect of the carbonyl group of COOR (R = Me, Et). Another exception, the extreme increase of δ(H-5) in **2**a ($\Delta\delta$ = 2.75), **4a** ($\Delta\delta$ = 2.34), and **5a** ($\Delta\delta$ = 2.58) compared to **1a** in $CDCl_3$, is associated with a change in conformation of the 3-pivaloyl substituent which is also found for the solid state. In crystalline **1a**, the acyl group is arranged nearly coplanar to the ring system (torsion angle P–C1–C=O 178°) with the *tert*-butyl group at the P-side, whereas in the chromium complex **2a** the latter is oriented to the N-side of the azaphosphole ring, adopting a staggered conformation (see below). This arrangement shields the proton in position 5. Concerning proton couplings, the only marked changes between **1** and **2–4** are the solvent-independent increase of the magnitude of ^3J(PH) involving the 1-methyl protons by ΔJ = 3.7 to 5.3 Hz, slightly increasing from chromium to tungsten and from the 3-pivaloyl to the 3-carbalkoxy derivatives, and the decrease of the magnitude of $^2J(^{31}P$-$^{1}H)$ of the protons in 1-position of **2b**, **4b**, **4d**, and **3g** relative to the respective ligands by 7–8 Hz.

Carbon NMR: In contrast to organometallic compounds, phosphane complexes have not been extensively investigated with respect to the impact of coordination on carbon chemical shifts and couplings in the ligands[23][24][25]. In the ^{13}C NMR spectra of **2–4** (Table 3) we observed *trans* ^{13}CO (δ = 197-225) at lower field than *cis* carbonyls (δ = 194–215) and for both an increasing shielding in the series

Table 1. ^{31}P-NMR chemical shifts (δ) of **1**−**4** and coordination shifts (Δδ)

	R^1	R^2	R^3	R^4	δ **1**	δ **2** M = Cr	Δδ (**2**−**1**)	δ **3** M = Mo	Δδ (**3**−**1**)	δ **4** ($^1J_{PW}$, Hz) M = W	Δδ (**4**−**1**)
a	CH_3	$COC(CH_3)_3$	H	H	172.1	155.4	−16.7	135.3	−36.8	108.2 (258.2)	−63.9
b	H	COC_6H_5	*n*Bu	H	179.9	184.6	+4.7			133.4 (253.7)	−46.4
c	CH_3	COC_6H_5	H	H	183.6			164.3	−19.3		
d	H	COC_6H_5	H	CH_3	182.5					137.1 (264.2)	−45.4
e	CH_3	$COOC_2H_5$	H	H	165.5	190.6	+25.1	167.5	+2.0	140.2 (268.1)	−25.3
f	CH_3	$COOCH_3$	H	H	165.8	190.8	+25.0	169.3	+3.5		
g	H	CN	H	CH_3	164.5			169.9	+5.4		
h	C_6H_5	C_6H_4-NO_2(*p*)	H	H	130.6					105.2 (262.4)	−25.4

Table 2. ^{1}H-NMR data of the complexes **2**−**4**[a]

δ *J* [Hz]	**2a**	**2b**	**2e**	**2f**	**3a**	**3c**	**3e**	**3f**	**3g**	**4a**	**4b**	**4d**	**4e**	**4h**	**5e**	**5f**
1-H		7.09							6.38		6.95	6.85				
^2J(P,H)		28.3							31.5		27.8	28.3				
5-H	7.49	9.51	9.95	9.80	7.90	9.48	9.87	9.81	7.48	7.66	9.57	9.55	9.86	7.21	9.91	9.90
^4J(P,H)						1.8	1.9	1.9		1.6	1.5		1.9	1.4		
^3J(5-H,6-H)	7.1		7.3	7.3	7.3	7.2	7.3	7.3	7.2	7.3		7.4	7.3	6.8	7.3	7.2
^4J(5-H,7-H)			0.9	0.8		0.9	1.1	0.9		1.3	0.8		0.9	1.1		
6-H	5.87	[b]	6.89	6.12	5.98	6.05	6.16	6.14	5.70	5.91	[c]	5.96	6.14	5.95	6.82	6.09
^5J(P,H)	1.1		1.3	1.2		1.4	1.3	1.3	1.2	1.3		1.5	1.3	0.6		
^3J(6-H,7-H)	7.0		7.0	7.1	7.0	6.4	6.7	6.9		7.0			6.8	6.6	6.9	6.8
^4J(6-H,8-H)	1.1		1.4			1.3	1.3	1.0		1.3		1.0	1.5			
7-H	6.24	6.71	7.22	6.41	6.30	6.41	6.43	6.40	[d]	6.27	6.45	[e]	6.41	6.30	7.15	6.36
^5J(P,H)	1.2		1.4	1.4		1.3	1.5	1.5		1.3	1.3		1.6	1.3		
^3J(7-H,8-H)	9.1	9.0	8.9	8.9	9.1	9.3	8.9	8.9		9.0	9.0		8.9	9.1	8.9	8.9
8-H	6.58	6.47	7.43	6.54	6.66	6.63	6.60	6.57	6.29	6.58	6.70	6.41	6.55	7.08	7.32	6.53
^4J(P,H)	1.1		2.5			2.5	2.5	2.5	1.2	2.4		1.9	2.6	1.1		
R^1:																
CH_3	2.21		2.58	2.12	2.25	2.22	2.13	2.10		2.15			2.07	[f]	2.35	2.15
^3J(P,H)	16.0		16.7	16.7	16.2	16.8	16.9	16.9		16.6			17.3		(m)	(m)
R^2:																
OCH_2/OCH_3			4.47	3.65			4.28	3.64					4.28		4.26	3.61
CH_3			1.46				1.26						1.25		1.22	
^3J(H,H)			7.1				7.1						7.1		7.0	
$COC(CH_3)_3$	1.19				1.30					1.23						
o-H		7.83				7.82					7.86			7.43		
m-, *p*-H		7.17−7.19				7.20					7.16−7.21			7.94		

[a] **2e** and **5e** in $CDCl_3$, others in C_6D_6. − [b] 6-Bu: α-CH_2: δ = 2.12; β-CH_2: δ = 1.35; γ-CH_2: δ = 1.30; δ-CH_3: δ = 0.83. − [c] 6-Bu: α-CH_2: δ = 2.11; β-CH_2: δ = 1.28; γ-CH_2: δ = 1.14; δ-CH_3: δ = 0.80. − [d] 7-CH_3: δ = 1.66. − [e] 7-CH_3: δ = 1.74. − [f] 1-C_6H_5: *o*-H: δ = 6.88; *m*-H: δ = 7.37; *p*-H: δ = 7.18.

Cr, Mo, W. This can be seen e.g. for the series **2e**, **3e**, **4e** where each Δδ is about 10. The magnitude of the two-bond coupling with the phosphorus decreases for *cis* carbonyls in the order Cr, Mo, W pentacarbonyl (ca. 17, 12, 9 Hz, respectively) and increases with the metal radii for the respective *trans* carbonyls (ca. 4 << 32 , 32 Hz), causing small *trans* couplings in chromium carbonyl P-complexes. Marked differences in some carbon chemical shifts and coupling constants occur also between free and coordinate phosphaindolizines and can be attributed to steric and electronic effects. The solvent influence, in contrast to proton NMR data, is essentially negligible as can be seen, e.g., by the very small differences of $\delta^{13}C$ (< 0.6) and $J(^{31}P\text{-}^{13}C)$ (≤1) of **4b** in $CDCl_3$ and C_6D_6. The upfield coordination shift for C-5 and the opposite change for C-3 and the 3-carbonyl groups in **2a** and **4a**, not observed in other derivatives, are attributed to the distortion of the 3-pivaloyl group, causing enhanced shielding of C-5 by the *tert*-butyl group and reduced π-charge density at C-CO by loss of delocalization compared to the coplanar free ligand. Marked coordination shifts for C-5 are found in the phenacyl derivatives, nearly no effect for **3c**, shielding for **4b** and deshielding for **4d**, whereas δ(3-CO) is slightly influenced by the coordination, suggesting a torsion of the phenyl ring around the C−C(O) axis to give the minimum energy arrangement. A general upfield shift on coordination for C-1 and, except for **2a** and **4a**, also for C-3, with a slight increase from chromium to tungsten, may be assigned to electronic as well as steric influences, viz. the change in hybridization of phosphorus, back-bonding and steric shielding by the $M(CO)_5$ group. The same holds to an reduced extent for the α-C atoms of the substituents at C1 and C3, reflecting inductive effects. The lack of noticeable shift differences for C6 to C9 in free and coordinated ligands suggests that back donation, ascribed to $(d_M\text{-}\pi^*)\pi$ bonding[25], has a rather localized effect. Indeed, according to PM3 cal-

culations[28] phosphorus has the highest coefficient in the LUMO (π*-orbital) of 2-phosphaindolizine (ε = −0.77 eV, c^2 = 0.50) and is separated by nodal planes from C1 and C3.

A strong decrease in $^1J(^{31}P\text{-}^{13}C)$ coupling constants is observed by complexation. For C1 and C3 one-bond $^{31}P\text{-}^{13}C$ coupling constants are in the range 18−30 Hz and 10−37 Hz as compared to 38−44 and 45−59 Hz, respectively, in the free ligands[14][17][18]. The absolute magnitude of $^1J(^{31}P\text{-}^{13}C3)$ increases with the electron-withdrawing effect of the 3-substituent R^2 in the order C_6H_4-4-NO_2 << COOEt < COOMe ≈ or < COPh ≈ CO*t*Bu. The much lower one-bond couplings in the complexes may be attributed to the participation of the s-orbital in the hydridization of phosphorus. The smaller differences between $^1J(^{31}P\text{-}^{13}C1)$ and $^1J(^{31}P\text{-}^{13}C3)$ in the complexes reflect a higher degree of delocalization and aromaticity than in the ligands themselves. This is consistent with nearly equal P−C bond lengths in **2a**, whereas they differ in **1a**. In rounding off this section it should be mentioned that two-bond couplings are also reduced on complexation, $^2J(^{31}P\text{-}1\text{-}^{13}CH_3)$ larger than $^2J(^{31}P\text{-}^{13}C9)$ and $^2J(^{31}P\text{-}3\text{-}^{13}CO)$, whereas $^3J(^{31}P\text{-}^{13}C8)$ are usually increased.

X-ray Analysis of 2a

X-ray structure analysis of the $Cr(CO)_5$ complex **2a** (Figure 2) shows a planar ring system (mean deviation 3 pm) with trigonal planar coordination at phosphorus; the metal lies only slightly outside the plane (12 pm). The endocyclic angle at phosphorus in the rigid five-membered ring is not greatly affected by the steric requirements and thus only slightly opened, from 91.9(2)° in **1a**[18] to 93.5(1)° in **2a**. The P−C bond lengths become more equal [172.4, 171.7(2) pm] on complexation than in the free ligand [174.7(3), 170.8(4) pm] and on average shorter (172.1 versus 172.8 pm) indicating more effective delocalization. The rotation of the pivaloyl group from a coplanar arrangement (dihedral angle P−C1−C=O 178°) in **1a** to a staggered conformation with ϑ(P−C1−C9−O1) = 45.5° in **2a** prevents the strong -M interactions possible in **1a** and is certainly an important factor in the increase in aromaticity. Another factor may be the change in hybridization from p^2 to sp^2

Table 3. ^{13}C-NMR data of the complexes **2**−**4**[a]

δ *J* in Hz	**2a**	**2e**	**2f**	**3c**	**3e**	**3f**	**3g**	**4a**	**4b**	**4d**	**4e**	**4h**	**5f**[b]
C-1	130.3	132.5	132.2	[c]	131.7	132.4	129.7	128.6	121.6	120.3	130.8	134.4	132.0
^1J(CP)	18.3	22.9	23.0		22.2	22.3	22.5	25.1	28.3	28.6	29.4	25.5	23.3
C-3	147.0	130.0	130.1	133.2	129.5	129.6	145.4	143.4	139.7	139.4	127.4	145.1	129.3
^1J(CP)	10.0	18.3	18.4	19.3	19.1	19.7	14.7	17.0	12.7	13.5	28.2	36.9	12.1
C-5	126.7	129.6	129.1	130.0	129.6	130.1	127.2	127.1	128.2	137.1	129.8	123.8	128.3
^3J(CP)	–	2.3	–	2.0	2.4	2.3	–	–	1.7	2.3	7.8	–	8.0
C-6	112.0	113.2	113.3	113.3	113.7	113.8	116.8	112.6	125.7	116.2	113.7	112.9	112.7
^4J(CP)	4.0	4.8	4.7	–	4.7	4.9	4.7	4.4	–	4.5	5.1	3.8	<1.0
C-7	120.7	124.1	124.2	124.7	123.4	124.0	122.5	121.2	127.9	129.5	124.3	121.3	123.9
^4J(CP)	3.0	3.2	3.0	3.2	2.9	3.0	2.9	2.6	2.0	–	3.0	1.8	<1.0
C-8	116.2	115.3	115.3	115.9	115.7	116.4	117.9	116.8	118.0	117.1	116.0	118.0	115.1
^3J(CP)	17.0	11.3	11.3	–	11.7	11.2	11.8	11.2	12.4	12.4	11.7	9.5	11.4
C-9	140.6	143.6	143.7	143.7	143.3	144.0	147.6	140.6	145.6	147.0	143.6	140.3	143.6
^2J(CP)	4.0	5.7	5.7	5.8	5.7	5.7	–	2.9	8.4	8.3	4.6	–	7.3
R^1: CH_3	10.9	11.3	11.3	11.8	11.4	11.9	[d]	11.3	[e]	[f]	11.6	[g]	11.5
^2J(CP)	14.9	14.4	14.5	15.3	15.6	16.0		15.3			14.9		14.4
R^2: CO/CN	204.9	163.0	163.1	186.8	162.8	163.6	117.5	204.9	186.6	186.3	163.0		163.6
^2J(CP)	12.0	17.7	17.4	20.5	16.8	17.0	19.7	12.1	20.6	20.6	17.4		19.6
OCH_2/OCH_3		60.7	50.6		60.6	51.3					60.8		50.9
CH_3	27.5	14.4	14.4		14.4			27.1			14.5		
^4J(CP)								1.6					
$C(CH_3)_3$	45.7							45.7					
C-*i*				140.8					140.5	140.6		137.4	
$^{2/3}J$(CP)				1.8					1.8	1.8		13.6	
C-*o*				130.8					131.3	131.3		137.3	
$^{3/4}J$(CP)				2.9					2.9	3.0		7.4	
C-*m*				129.0					129.0	129.0		129.4	
C-*p*				132.5					132.7	132.6		148.2	
^5J(CP)												1.6	
$M(CO)_5$:													
CO(*cis*)	215.2	214.6	214.6	203.6	204.3	204.9	208.8	194.9	194.5	194.6	194.4	194.2	217.0
^1J(CW)								125.2	125.7	125.6	125.5	128.9	
^2J(CP)	16.0	17.2	17.3	10.7	11.7	11.8	11.9	8.7	8.7	8.8	9.4	8.7	17.2
CO(*para*)	221.1	220.9	220.9	209.6	210.0	210.6	225.1	198.4	198.2	198.3	198.7	197.8	224.0
^1J(CW)								151.4	148.8	[h]	151.6	145.2	
^2J(CP)	5.0	3.9	3.8	[i]	31.9	31.9	33.0	30.7	32.2	32.2	32.0	31.0	20.2

[a] **4e** in $CDCl_3$, others in C_6D_6. − [b] Coupling constants are not *J* values but $N = |J_{AX} - J_{A'X}|$ values. − [c] Merged in C_6D_6 peak. − [d] 7-CH_3: δ = 20.9. − [e] α-C: δ = 32.7; β-C: δ = 32.5; γ-C: δ = 22.4; δ−C: δ = 13.9. − [f] 7-CH_3: δ = 20.4. − [g] 1-C_6H_5: *i*-C: δ = 133.6 (J_{PC} = 12.8); *o*-C: δ = 130.9 (J_{PC} = 6.9); *m*-C: δ = 124.5; *p*-C: δ = 129.2. − [h] Not observed due to small intensity of signal. − [i] Not resolved.

Figure 2. Structure of **2a** in the crystal. Ellipsoids represent 50% probability levels. H atom radii are arbitrary[a]

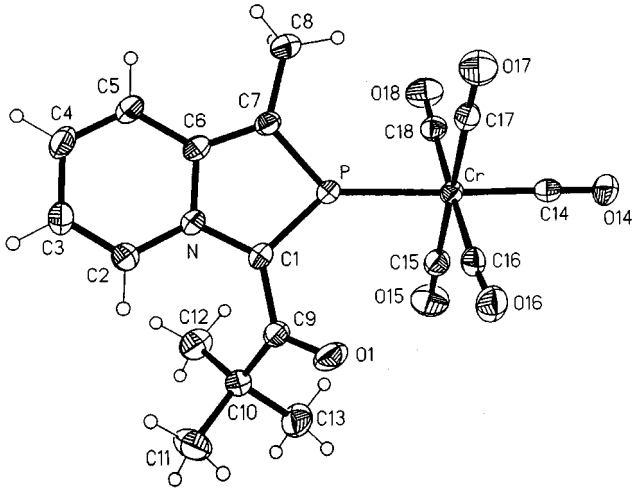

[a] Selected bond lengths [pm] and angles: Cr−C(14) 187.0(3), Cr−C(16) 189.8(3), Cr−C(15) 190.0(3), Cr−C(18) 190.3(3), Cr−C(17) 190.6(3), Cr−P 232.50(14), P−C(7) 171.7(2), P−C(1) 172.4 (2), C(1)−N 138.2(3), N−C(6) 140.4(3), C(6)−C(7) 138.7(3); C(1)−P−Cr 135.95(8), C(7)−P−Cr 130.47(8), C(7)−P−C(1) 93.51(11), N−C(1)−P 109.6(2), C(1)−N−C(6) 113.7(2), C(7)−C(6)−N 113.2(2), C(6)−C(7)−P 109.9(2).

which makes the phosphorus more similar to carbon. In **2a** the Cr−P bond [232.50(14) pm] is slightly shortened compared to a variety of $R_3PCr(CO)_5$ and phosphaalkene $Cr(CO)_5$ complexes (235-245 pm)[29] and also the Cr−C bond of *trans*-CO [187.0(3) pm] is shorter (*trans* effect) by 3 pm than those of *cis*-CO (average 190.2 pm). Finally, it should be mentioned that the averaged P−Cr−C angles of *cis*-and *trans*-carbonyls are 90.2° and 178.4°, respectively, corresponding closely to ideal octahedral geometry around chromium.

Funding by the *Deutsche Forschungsgemeinschaft* and financial support by the *Fonds der Chemischen Industrie*, Germany, is gratefully acknowledged. Furthermore, we appreciate the help by Dr. *M. K. Kindermann* and *B. Witt* for numerous NMR measurements, I. *Stoldt* for IR and Dr. *A. Müller* for mass spectra.

Experimental Section

General Comments: All reactions were carried out under a dry argon atmosphere using the Schlenk technique. − NMR spectra were recorded on Bruker ARX 300 (^{31}P-NMR at 121.5 MHz, ^{1}H-NMR at 300.1 MHz and ^{13}C-NMR at 75.5 MHz). The chemical shifts refer to 85% H_3PO_4 (external) or TMS (internal). − Mass spectra were recorded on AMD 40(intectra), IR spectra on System 2000 of Perkin-Elmer. − The synthesis of the 2-phosphaindolizines **1a-h** was recently reported[14][17][18]. [(THF)M(CO)$_5$] were freshly prepared before use[30], tetracarbonyl(norbornadiene)chromium(0) was synthesized by refluxing chromium hexacarbonyl with norbornadiene in light petroleum[31]. Tricarbonyl(cycloheptatriene)molybdenum(0) and tricarbonyl(mesitylene)tungsten(0) were commercially available and used without further treatment. Melting points of complexes are uncorrected and were determined in a capillary under argon.

Reaction of 2-Phosphaindolizines **1** *with THF·M(CO)$_5$* (**2**, **3**, **4**) − *General Procedure:* A solution of 2.0 mmol of metal hexacarbonyl [440 mg of $Cr(CO)_6$; 704 mg of $W(CO)_6$ or 528 mg of $Mo(CO)_6$] in 200 ml of oxygen-free THF was irradiated using a high-pressure mercury photo lamp with continuous stirring and monitoring of the volume of CO evolved. [If with $Mo(CO)_6$ the reaction became slower, the irradiation was interrupted and argon was bubbled through the solution to diminish the CO concentration, using a separate outlet.] After evolution of 2 mmol (44.8 ml) of CO the irradiation was stopped. The [(THF)M(CO)$_5$] solution was added to a solution of the respective 2-phosphaindolizine **1** (2.0 mmol) in THF and stirred overnight at room temperature. The solvent was removed in vacuo and the residue extracted with hexane (2 × 50 ml). Shining crystals were obtained on leaving the concentrated hexane extract (10−15 ml) in a refrigerator (−20°C). If no crystals separated, the solvent was removed completely to obtain yellow to orange powdery complexes. **2a**, **b**, **e**, **3a**, **c**, **e**, **g**, **4a**, **b**, **d**, **e** and **h** were synthesized in this manner. In case of the reaction of **1e** with [(THF)Cr(CO)$_5$], formation of some **5e** was observed in addition to **2e**. On recrystallization from hexane pure **2e** was obtained. NMR-spectroscopic data are given in Tables 1-3, substance and IR data in Table 4.

Reaction of **1f** *with Tetracarbonyl(norbornadiene)chromium(0)* (**2f** *and* **5f**): 207 mg (1.0 mmol) of **1f** was refluxed with 256 mg (1.0 mmol) of tetracarbonyl(norbornadiene)chromium(0) in petroleum ether (50 ml, b.p. 100−120°C) for three hours. The colour of the solution changed from yellow to orange. The reaction mixture was filtered, and the filtrate placed in a refrigerator (ca. −20°C). Yellow-orange crystals consisting of **2f** (δ^{31}P = 190.8) and **5f** (δ^{31}P = 202.3) precipitated. For ^{1}H- and ^{13}C-NMR data see Tables 2 and 3. Extraction of the mixture with hexane afforded spectroscopically pure **5f**, yield 18%, m.p. 135−137°C.

Reactions of **1g** *with Tricarbonyl(cycloheptatriene)molybdenum(0)* (**6g** *and* **7g**) − *A*: 236 mg of **1g** (1.35 mmol) and 123 mg (0.45 mmol) of (cycloheptatriene)Mo(CO)$_3$ were dissolved in THF. ^{31}P NMR (THF/[D$_8$]THF) spectra were recorded (i) after 18 hours and (ii) after 2 days at room temperature. In the first case we observed signals at δ (rel.int.) = 6.1 (65), 11.4 (12), 167.8 (85) **1g** and 181 (8) **6g**, in the second case only at δ (rel.int.) = 167.8 (110) and 181.2 (20).

B: 130 mg (0.75 mmol) of **1g** was stirred for 2 days with 203 mg (0.75 mmol) of (cycloheptatriene)Mo(CO)$_3$ in THF (40 ml) at room temperature. ^{31}P NMR (THF/[D$_8$]THF) control showed only signals of **7g**, δ = 196.3, d; 203.8, t; $^{2}J(^{31}P\text{-}^{31}P)$ = 9 Hz, intensity ratio 2:1. Similarly, **7g** is formed preferentially in $CDCl_3$.

C: 120 mg (0.69 mmol) of **1g** was refluxed for 2 days with 188 mg (0.69 mmol) of (cycloheptatriene)Mo(CO)$_3$ in ether/hexane (1:2). The precipitate was separated and washed with little hexane. The ^{31}P-NMR spectra of the solid, dissolved in C_6D_6, showed it to be a mixture of **7g** (δ = 193.3, d; δ = 200.9, t; $^{2}J(^{31}P\text{-}^{31}P)$ = 9.3 Hz) and **6g** (δ = 177.1, s); proton-coupled ^{31}P-NMR: **7g** δ = 193.3, dt, $^{2}J(^{31}P\text{-}^{1}H)$ = 30.5 Hz, δ = 200.8, multiplet; **6g** δ = 177.1, multiplet.

Reaction of **3f** *with Tricarbonyl(cycloheptatriene)molybdenum(0)* (**3f** *and* **6f**): 207 mg (1.0 mmol) of **1f** and 272 mg of (cycloheptatriene)Mo(CO)$_3$ was stirred in THF (50 ml) for two days. ^{31}P-NMR of the reaction mixture indicated **6f** (δ = 178.9) as major product, along with **3f** (δ = 169.3). THF was removed and the residue extracted with hexane. On concentrating the filtrate, analytically and spectroscopically pure **3f** was obtained as a yellow solid. For ^{1}H- and ^{13}C-NMR see Table 2 and 3, for substance data see Table 4.

Reaction of **1e** *with Tricarbonyl(mesitylene)tungsten(0)* (**4e** *and* **6e**): 111 mg (0.5 mmol) of **1e** was heated with 194 mg (0.5 mmol)

Table 4. Substance and IR data of the complexes **2**–**4**

	IR ν (CO) [cm^{-1}]	mp [°C]	yield [%]	mol. formula [m. wt.]	analysis found / calc. (%) C	H	N
2a	2071 m, 2004 w, 1954 s, 1940 s, 1915 sh	90–92	77	$C_{18}H_{16}O_6NPCr$ (425.29)	50.93 50.83	4.02 3.79	3.34 3.29
2b	–	68–69	78	$C_{23}H_{18}O_6NPCr$ (487.35)	56.21 56.68	3.44 3.72	2.61 2.87
2e	2069 m, 1995 sh, 1956 s, 1929 s,	164–65	82	$C_{16}H_{12}O_7NPCr$ (413.24)	46.15 46.50	2.67 2.93	3.29 3.39
3a	–	89–90	72	$C_{18}H_{16}O_6NPMo$ (469.23)	46.26 46.07	3.28 3.44	2.75 2.99
3c	2079 w, 1987 s, 1964 m, 1953 s, 1936 s	124–25	65	$C_{20}H_{12}O_6NPMo$ (489.22)	49.34 49.09	2.73 2.47	2.93 2.86
3e	2075 m, 2035 w, 1986 m, 1961s, 1926 s	146–47	77	$C_{16}H_{12}O_7NPMo$ (457.18)	42.53 42.03	2.72 2.65	3.04 3.06
3f	2075 m, 1987 m, 1961 s, 1948 s, 1926 s	115–16	51	$C_{15}H_{10}O_7NPMo$ (443.15)	40.49 40.65	2.43 2.28	3.28 3.16
3g	2072 w, 986 s, 1950 s	135–38	64	$C_{14}H_7O_5N_2PMo$ (410.1)	40.16 40.99	1.81 1.72	6.98 6.83
4a	2077 m, 1995 w, 1970 sh, 1953 s, 1920 s	74–76	68	$C_{18}H_{16}O_6NPW$ (557.14)	39.08 38.80	2.83 2.90	2.37 2.51
4b	2078 m, 1999 w, 1952 s, 1920 sh	66–67	75	$C_{23}H_{18}O_6NPW$ (619.20)	45.61 44.61	3.14 2.93	2.23 2.26
4d	2079 m, 2007 m, 1970 s,1943 s, 1908 s	166–68	70	$C_{20}H_{12}O_6NPW$ (577.13)	42.13 41.62	2.13 2.10	2.39 2.43
4e	2074 m, 1993 m, 1954 s, 1935 s, 1917 s	179–81	81	$C_{16}H_{12}O_7NPW$ (545.09)	36.16 35.25	2.54 2.22	2.24 2.57
4h	2075 m, 1994 w, 1961 s, 1930 s, 1918 sh	170–71	66	$C_{24}H_{13}O_7N_2PW$ (656.18)	43.12 43.93	2.16 2.00	4.32 4.27

of tricarbonyl(mesitylene)tungsten(0) in THF (40 ml) for 20 hours at 45–50°C. ^{31}P NMR presents signals of **1e**, **4e**, and **6e** in an intensity ratio of 14:8:78. After removal of THF, the residue was extracted with hexane and filtered. Removal of the solvent in vacuo afforded a yellow solid that proved to be a mixture (m.p. 110–118°C) of **6e** as major product with some **4e**. Proton-coupled ^{31}P NMR: **6e** δ = 149.6, multiplet, $^1J(^{31}P\text{-}^{183}W)$ = 263 Hz; **4e** δ = 140.2, q, $^3J(^{31}P\text{-}^1H)$ = 17 Hz.

X-ray Structure Analysis of **2a** – *Crystal Data*: $C_{18}H_{16}CrNO_6P$, triclinic, *P*1, *a* = 905.9(3), *b* = 977.8(4), *c* = 1238.0(4) pm, α = 94.13(3), β = 97.52(3), γ = 116.72(3)°, *V* = 0.9604 nm^3, *Z* = 2, μ = 0.71 mm^{-1}, D_x = 1.471 Mg m^{-3}, λ(Mo-*K*α) = 71.073 pm, *T* = −130°C. *Data Collection*: Yellow tablet 0.7 × 0.5 × 0.15 mm, Stoe STADI-4 diffractometer, $2\theta_{max}$ 50°; 3622 intensities, absorption correction with ψ-scans (transmissions 0.82–0.96), 3387 unique reflections (R_{int} 0.021). *Structure Solution and Refinement*: Direct methods, refined on F^2 using SHELXL-93[32]. Hydrogen atoms: riding model or rigid methyls. Final $wR(F^2)$ 0.077 for all reflections, conventional *R*(*F*) 0.032 for 248 parameters; *S* 1.06, max. Δρ 295 e nm^{-3}.

Crystallographic data (excluding structure factors) have been deposited at the Cambridge Crystallographic Data Centre under the number CSD 101226. Copies may be obtained free of charge from: The Director, CCDC, 12 Union Road, Cambridge CB2 1EZ (Fax internat.: +44-1223-336033; e-mail: deposit@ccdc.cam.ac.uk).

[1] J. F. Nixon, *Chem. Rev.* **1988**, *88*, 1327–1362.
[2] J. H. Nelson, F. Mathey in *Methods in Stereochemical Analysis 8: 31P NMR in Stereochemical Analysis* (Eds.: J. G. Verkade, L. D. Quin), VCH, **1987**, p. 665–694.
[3] A. P. Sadimenko, A. D. Garnovskii, N. Retta, *Coord. Chem. Rev.* **1993**, *127*, 237–318.
[4] Ch. Janiak, N. Kuhn, *Adv. Nitrogen Heterocycl.* **1996**, *2*, 179–210.
[5] M. O. Senge, *Angew. Chem.***1996**, *108*, 2051–2053; *Angew. Chem. Int. Ed. Engl*. **1996**, *35*, 1923–1925.
[6] V. Caliman, P. B. Hitchcock, J. F. Nixon, L. Nyulaszi, N. Sakarya, *J. Chem. Soc., Chem. Commun.* **1997**, 1305.
[7] L. Nyulaszi, T. Veszpremi, J. Reffy, *J. Phys. Chem.* **1993**, *97*, 4011–4015.
[8] [8a] K. Öfele, E. Dotzauer, *J. Organometal. Chem*. **1971**, *30*, 211–220. – [8b] N. Kuhn, J. Kreutzberg, E. M. Lampe, D. Blaser, R. Boese, *J. Organomet. Chem.* **1993**, *458*, 125–129.
[9] T. Veszpremi, L. Nyulaszi, J. Reffy, J. Heinicke, *J. Phys. Chem.* **1992**, *96*, 623–626.
[10] J. Heinicke, *Trends Organometal. Chem*. **1994**, *1*, 307–322.
[11] A. Schmidpeter, K. Karaghiosoff in *Multiple Bonds and Low Coordination in Phosphorus Chemistry* (Eds.: M. Regitz, O. J. Scherer), Thieme, Stuttgart, **1990**, p. 258–286.
[12] R. K. Bansal, K. Karaghiosoff, A. Schmidpeter, *Tetrahedron* **1994**, *50*, 7675–7745.
[13] K. Issleib, R, Vollmer, *Z. Allg. Anorg. Chem.* **1981**, *481*, 22–32.
[14] R. K. Bansal, K. Karaghiosoff, N. Gupta, A. Schmidpeter, C. Spindler, *Chem. Ber*. **1991**, *124*, 475–480.
[15] [15a] K. Karaghiosoff, A. Schmidpeter, *Phosphorus Sulfur* **1988**, *36*, 217. – [15b] J. H. Weinmaier, H. Tautz, A. Schmidpeter, S. Pohl, *J. Organometal. Chem*. **1980**, *185*, 53–68.
[16] [16a] J. Deberitz, H. Nöth, *J. Organomet. Chem*. **1973**, *49*, 453–468. – [16b] G. Märkl, H.-J. Beckh, *Tetrahedron Lett.* **1987**, *28*, 3475.
[17] R. K. Bansal, V. Kabra, N. Gupta, K. Karaghiosoff, *Indian J. Chem*. **1992**, *31B*, 254.
[18] N. Gupta, C. B. Jain, J. Heinicke, N. Bhartiya, R. K. Bansal, P. G. Jones, *Heteroatom Chem.* **1998**, *9*, 333–339.
[19] S. O. Grim, D. A. Wheatland, *Inorg. Che*m. **1969**, *8*, 1716–1719.
[20] [20a] J. Deberitz, H. Nöth, *Chem. Ber. 103*, **1970**, 2541–2547. – [20b] H. Vahrenkamp, H. Nöth, *Chem. Ber. 105*, **1972**, 1148–1157.
[21] D. Böhm, H. Geiger, F. Knoch, F. Kremer, S. Kummer, P. LeFloch, F. Mathey, U. Schmidt, U. Zennek, *Phosphorus Sulfur Silicon Relat. Elem*. **1996**, *109–110*, 173–176.
[22] The program *gNMR* from Cherwell Scientific Publishing was used.
[23] J. G. Verkade, *Coord. Chem. Rev.* **1972**, *9*, 1–106;
[24] P. S. Pregosin , R.W. Kunz in *NMR Basic Principles, Progress* (Eds.: P. Diehl, E. Flock, R. Kosfeld), Springer, Berlin, **1979**, vol. 16.
[25] C. A. McAuliffe in *Comprehensive Coordination Chemistry*

(Eds.: G. Wilkinson, R. D. Gillard, J. A. McCleverty, Pergamon, Oxford, **1987**, vol. 2, chapter 14.
[26] S. Berger, S. Braun, H.-O. Kalinowski, *NMR-Spektroskopie von Nichtmetallen*, Band 3, ^{31}P-NMR Spektroskopie, Thieme, Stuttgart **1993**.
[27] R. Mathieu, M. Lenzi, R. Poilblanc, *C.R. Acad. Sci., Paris* **1968**, *266*, 806.
[28] Calculated by the PM3 method using *MOPAC 6.0*: J. J. P. Steward, QCPE 455, **1990**.
[29] S. Woodward, in *Comprehensive Organometallic Chemistry* (Eds.: E. W. Abel, F. G. A. Stone, G. Wilkinson), Pergamon, **1995**, vol.5, (Vol.eds.: J. A. Labinger, M. J. Winter), chapter 4.
[30] H. L. Krauss in *Synthetic Methods of Organometallic and Inorganic Chemistry* (Ed.: W. A. Herrmann), Thieme, Stuttgart, **1996**, vol. 1 (Eds.: W. A. Herrmann, A. Salzer), p 117.
[31] N. A. Bennet, L. Pratt, G. Wilkinson, *J. Chem. Soc.* **1961**, 2037.
[32] G. M. Sheldrick, University of Göttingen.

[98085]

Cation Stabilities, Electrophilicities, and "Carbene Analogue" Character of Low Coordinate Phosphorus Cations

Dietrich Gudat

Anorganisch Chemisches Institut der Universität Bonn
Gerhard-Domagk-Straße 1, D-53121 Bonn
Fax: (internat.) +49(0)228/73-5327
E-mail: dgudat@uni-bonn.de

Received September 2, 1997

Keywords: Phosphenium cations / Cation stabilities / Electrophilicity / Carbene homologues / Computer Chemistry

The stabilities of low coordinated phosphorus cations can be expressed in the frame of the HSAB concept by the transferred charge density Δq(N) which a cation receives upon formation of a donor-acceptor adduct with a Lewis base N. This concept allows to differentiate between relative stabilities towards different reaction partners, and to compare the electrophilicities of phosphenium ions to those of isoelectronic carbenes and silylenes. An analysis of substituent influences on Δq(H) in cations $[P(R)_2]^+$ suggests an increasing stabilizing power of substituents in the series R = Cl < CH_3 < OH, SH < NH_2. The same ordering was derived from isodesmic hydride transfer reactions. Interpretation of population analyses suggests that the individual substituent contributions to cation stabilities result from a balance between π-donation into the empty p(P) orbital and electrostatic stabilization by polar P–R σ-bonds. A further stabilizing effect, which is of similar magnitude as in isoelectronic carbenes or silylenes, may arise from cyclic π-conjugation between a diaminophosphenium fragment and an adjacent double bond. Substituent effects influence further the nature of the frontier orbitals of phosphenium ions, resulting in orbital sequences which resemble those of carbenes, allyl anions, or phospholides, respectively. The absence of frontier orbital related changes in reactivity patterns suggests that in all reactions, including metal complex formation, phosphenium ions behave as purely *electrophilic* rather than *ambiphilic* species.

Introduction

Belonging to the first isolable compounds with (p-p)π bonding to phosphorus, amino-phosphenium ions, $[P(NR_2)(R')]^+$, and phosphanetriyl-ammonium ions, $[P{\equiv}N{-}R]^+$, have received continuous attention during the last 25 years and are still objects of current interest.[1] The results of extensive studies of chemical reactivities have coined the opinion that the cations are ambiphiles which have both nucleophilic and electrophilic properties. The electrophilic character comes to the fore in C−H- and C−C bond insertion reactions, cycloadditions, and complex formation with Lewis bases, while the nucleophilic properties are considered responsible for the formation of transition metal complexes.[1]

In contrast to the wealth of experimental studies, theoretical investigations of these cations are rare. Earlier ab-initio calculations on simple model systems ($[P(H)_2]^+$, $[P(H)(NH_2)]^+$, $[P(NH_2)_2]^+$) confirmed singlet ground states and revealed the stabilizing effect of conjugation between nitrogen lone-pairs and the empty p-orbital at phosphorus which resulted in a heteroallylic frontier orbital sequence for $[P(NH_2)_2]^+$.[1a][2] For selected cyclic cations, the issue of conjugation between amino(thioxo)phosphenium fragments and adjacent double bond systems to form "aromatic" π-systems was discussed.[3] Only recently, Schoeller et al. reported a first attempt to establish a relative scale of gas phase stabilities for selected cations from a comparison of hydride transfer reaction energies.[4] In addition, a discussion of molecular structures and frontier orbitals was presented which substantiated the isolobal relationship between phosphenium ions and carbenes, and between phosphanetriyl-ammonium ions (and the isolelectronic PO^+ and PS^+ cations) and (iso)cyanides.

Regarding that low coordinate phosphorus cations engage frequently in donor-acceptor interactions with nucleophilic counter ions or solvents,[1c] it becomes clear that in condensed phases their stability and electrophilicity are closely connected. It is the primary objective of this work to attempt an analysis of cation stabilities which not only covers a wider range of molecular structures, but also takes this effect explicitly into consideration. For this purpose, a concept is proposed which is based on a discussion of stability and electrophilicity in the frame of the extended HSAB concept.[5][6] The pivotal idea is to use the amount of charge transfer which a cation receives in the formation of a donor-acceptor adduct as a measure of its stability. In order to elucidate the origin of the stability differences, a discussion of population analyses is presented which suggests an interplay between mesomeric effects and electrostatic contributions associated with high P−R bond polarities. To highlight further the connection between electronic structure and reactivity, some comments on frontier orbital sequences and the "carbenic" nature of phosphenium ions will be made.

 © WILEY-VCH Verlag GmbH, D-69451 Weinheim, 1998 1434−1948/98/0808−1087 $ 17.50+.50/0

Results and Discussion

Stability and Electrophilicity of Low Coordinate Phosphorus Cations

Relative gas phase stabilities of phosphenium ions $[P(R^1)(R^2)]^+$ can be determined according to Schoeller et al. by comparing the energies ΔE_{GT} of the hydride transfer reaction of Eq. (1) (Scheme 1).[4] Formally, this reaction can be separated into two steps as described by Eq. (2a) and (2b). Since Eq. (2a) and ΔE_1 remain the same for different cations, ΔE_{GT} essentially quantifies the variation in hydride affinities, ΔE_2. In view of the fact that the stability of phosphenium ions in condensed phases is often limited by their tendency to form Lewis acid-base adducts with solvent molecules or counter ions [Eq. (3)],[1] of which the reaction with a hydride is just a special case, Schoeller's definition may easily be put in a more general form: relative stabilities of cations ***E*** (in condensed phases) are reflected in different energies ΔE_{Add} associated with the formation of covalent donor-acceptor adducts ***E*–*N*** with a given nucleophile ***N*** (counter ion or solvent).

Scheme 1

$$[P(R^1)(R^2)]^+ + PH_3 \longrightarrow HP(R^1)(R^2) + [P(H)_2]^+ + \Delta E_{GT} \quad \text{(Eq. (1))}$$

$$PH_3 \longrightarrow [P(H)_2]^+ + H^- + \Delta E_1 \quad \text{(Eq. (2a))}$$

$$[P(R^1)(R^2)]^+ + H^- \longrightarrow HP(R^1)(R^2) + \Delta E_2 \quad \text{(Eq. (2b))}$$

$$[P(R^1)(R^2)]^+ + |Nu \longrightarrow [Nu{\rightarrow}P(R^1)(R^2)]^+ + \Delta E_{Add}$$

E ***N*** ***E-N*** (Eq. (3))

On a first glance, this approach seems to offer no obvious advantage, since a concise evaluation of hydride or nucleophile affinities imposes more severe computational problems than calculation of the energies of isodesmic hydride transfer reactions.[7] However, as an estimation of *relative* stabilities requires only the correct evaluation of trends in adduct formation energies ΔE_{Add} rather than their true values, an approximate solution to the problem can be obtained on a much simpler level.

Thus, the formation of a donor–acceptor bond in the adduct ***E*–*N*** [Eq. (3)] induces a charge transfer Δq(N) from ***N*** to the phosphorus cation. Using the principle of electronegativity equalization,[5][8] Δq(N) can be approximated as $\Delta q(N) = (\chi^e - \chi^n)/(\eta^e + \eta^n)$. Here, $\chi^{e(n)}$ and $\eta^{e(n)}$ denote the absolute electronegativity and absolute hardness of the cation (nucleophile), whose operational definitions are $\chi = -(I + E)/2$ and $\eta = (E - I)/2$ (I = ionization potential, E = electron affinity) in the frame of the extended HSAB concept.[5] Within Hartree-Fock theory, χ and η may be approximated as $\chi = -(\varepsilon_{HOMO} + \varepsilon_{LUMO})/2$ and $\eta = (\varepsilon_{LUMO} - \varepsilon_{HOMO})/2$ by using Koopman's theorem.[6] It may be noted that, despite the severe deficiencies of this approximation,[9][10] qualitative trends in χ and η between related molecules are reproduced at this level with sufficient accuracy.[10][11]

If we compare the interactions of two cations with an arbitrary nucleophile (e.g. ***N*** = H^-), the less stable cation will receive a larger charge transfer and form a stronger bond. Presuming a monotonous relation between the transferred charge density Δq(N) and the donor–acceptor bond strength ΔE_{Add},[12] an increase in Δq(N) corresponds to an increase in ΔE_{Add} and thus a lower cation stability, and vice versa, so that Δq(N) values can in principle be used directly as indicators of relative stabilities.

In order to apply this concept we computed transferred charge densities Δq(H) for some 30 model cations with low coordinate phosphorus atoms, using hydride as an archetypal nucleophile. The studied systems (Scheme 2) include cyclic and acyclic phosphenium ions $[P(R^1)(R^2)]^+$ (R^1, R^2 = H, Ph, Cl, alkyl, alkoxy, thioxo, amino), the 1.3-bisphosphanyl-phosphapropenides and -phospholides **12**, **25** which are isolobal and isoelectronic to the diaminophosphenium ions **11**, **24**,[13] and the phosphanetriyl-ammonium ions **30–32**. Details on the calculations are given in the experimental section; the resulting values of Δq(H) are listed in Table 1, together with frontier orbital energies and the values of χ and η.

Scheme 2. (* = Ph-group orientation parallel (**17**) and orthogonal (**17′**) with respect to P–NH_2–plane)

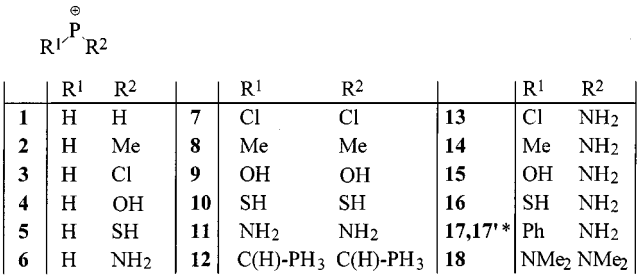

	R^1	R^2		R^1	R^2		R^1	R^2
1	H	H	**7**	Cl	Cl	**13**	Cl	NH_2
2	H	Me	**8**	Me	Me	**14**	Me	NH_2
3	H	Cl	**9**	OH	OH	**15**	OH	NH_2
4	H	OH	**10**	SH	SH	**16**	SH	NH_2
5	H	SH	**11**	NH_2	NH_2	**17,17′***	Ph	NH_2
6	H	NH_2	**12**	C(H)-PH_3	C(H)-PH_3	**18**	NMe_2	NMe_2

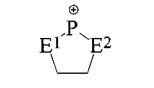

	E^1	E^2
19	S	S
20	NH	NH

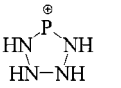

21

	E^1	E^2
22	S	S
23	NH	S
24	NH	NH
25	C(H)-PH_3	C(H)-PH_3

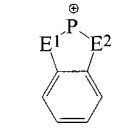

	E^1	E^2
26	S	S
27	NH	NH

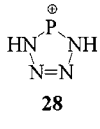

28

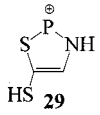

29

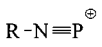

	R
30	H
31	Me
32	Ph

Inspection of the computed Δq(H) values reveals an increasing stabilizing effect of the substituents R^1, R^2 in a

Table 1. Frontier orbital energies, absolute electronegativities and hardness, transferred charge densities Δq(H), and cation stabilization energies ΔE_{GT} at MP2/6-31+g(d) level for **1**−**32**

[a]	ε_{HOMO} [eV]	[b]	ε_{LUMO} [eV]	[b]	χ [eV]	η [eV]	Δq(H) [c]	ΔE_{GT} [kcal/mol]
1 (C_{2v})	−19.79	a_1(n)	−8.56	b_1(p*)	14.17	5.62	1.08	0.0
2 (C_s)	−18.30	a′(n)	−7.40	a″(π*)	12.85	5.45	0.99	−22.2
3 (C_s)	−18.57	a′(n)	−8.04	a″(π*)	13.30	5.26	1.04	−18.9
4 (C_s)	−19.08	a′(n)	−7.18	a″(π*)	13.13	5.95	0.97	−39.5
5 (C_s)	−18.13	a′(n)	−7.11	a″(π*)	12.62	5.51	0.96	−45.6
6 (C_s)	−18.69	a′(n)	−6.11	a″(π*)	12.40	6.29	0.89	−66.3
7 (C_{2v})	−18.60	a_1(n)	−7.71	b_1(π*)	13.15	5.45	1.01	−32.8
8 (C_2)	−17.20	a′(n)	−6.50	a″(π*)	11.82	5.39	0.91	−40.6
9 (C_{2v})	−19.46	a_1(n)	−5.99	b_1(π*)	12.72	6.74	0.89	−63.3
10 (C_{2v})	−16.36	a_2(π_2)	−6.38	b_1(π*)	11.37	4.99	0.90	−62.3
11 (C_{2v})	−17.63	a_2(π_2)	−4.40	b_1(π*)	11.02	6.62	0.77	−93.8
12 (C_{2v})	−12.05	a_2(π_2)	−2.17	b_1(π*)	7.11	4.94	0.54	−145.7
13 (C_s)	−18.32	a′(n)	−6.00	a″(π*)	12.16	6.16	0.88	−63.9
14 (C_s)	−17.50	a′(n)	−5.41	a″(π*)	11.45	6.05	0.83	−77.3
15 (C_s)	−18.90	a′(n)	−5.18	a″(π*)	12.04	6.86	0.83	−80.2
16 (C_s)	−16.67	a″(π_2)	−5.44	a″(π*)	11.06	5.61	0.83	−76.7
17 (C_s)	−13.76	a″(π_2)	−4.77	a″(π*)	9.27	4.49	0.76	−97.2
17′ (C_s)	−13.42	a″(π_2)	−4.98	a″(π*)	9.20	4.22	0.77	−86.3
18 (C_2)	−14.80	a(π_2)	−3.60	b(π*)	9.20	5.60	0.68	−107.5
19 (C_2)	−15.50	a(π_2)	−5.85	b(π*)	10.67	4.82	0.85	−76.9
20 (C_2)	−15.85	a(π_2)	−4.15	b(π*)	10.00	5.85	0.73	−107.9
21 (C_2)	−16.25	a(π_2)	−4.91	b(π*)	10.58	5.67	0.79	−85.7
22 (C_{2v})	−15.07	b_1(π_3)	−5.82	b_1(π*)	10.44	4.62	0.85	−90.8
23 (C_s)	−14.59	a″(π_3)	−5.07	a″(π*)	9.83	4.76	0.79	−107.9
24 (C_{2v})	−14.10	b_1(π_3)	−4.17	b_1(π*)	9.13	4.97	0.71	−129.0
25 (C_{2v})	−11.31	b_1(π_3)	−1.85	b_1(π*)	6.58	4.73	0.51	−173.1
26 (C_{2v})	−13.52	b_1(π_3)	−5.52	b_1(π*)	9.52	4.00	0.81	−86.9
27 (C_{2v})	−12.90	b_1(π_3)	−4.24	b_1(π*)	8.57	4.33	0.70	−120.9
28 (C_{2v})	−17.09	b_1(π_3)	−5.39	b_1(π*)	11.24	5.85	0.83	−97.3
29 (C_s)	−14.15	a″(π_3)	−5.41	a″(π*)	9.78	4.37	0.81	−94.8
30 ($C_{\infty v}$)	−20.37		−6.09		13.23	7.14	0.90	−78.3
31 (C_{3v})	−18.47		−5.42		11.94	6.52	0.84	−94.8
32 (C_{2v})	−13.26		−5.13		9.20	4.06	0.78	−99.5

[a] Symbols in parentheses denote the molecular point group. − [b] Symmetry race and type of the orbital (in parentheses); n = phosphorus lone-pair, π_2 = heteroallylic π_2-orbital, π_3 = "phospholide" type orbital (see text), p* = unoccupied phosphorus p-orbital, π^* = π^*-orbital with P−X antibonding character. − [c] $\Delta q(H) = -[\chi - \chi(H)]/[\eta + \eta(H)]$; values of χ(H) and η(H) taken from ref.[6]

cation $[P(R^1)(R^2)]^+$ in the series R^1, R^2 = H < Cl < Me < SH, OH < Ph < NH_2 < C(H)PH_3. A general increase in stability is further observed upon replacement of hydrogens at an adjacent element E in EH_n-fragments by alkyl groups, and of $-CH_2CH_2-$ moieties in the five membered rings of cyclic cations by ethylene or phenylene units. On the whole, the order of relative stabilities of the model systems is in accord with interpretations of physical and chemical properties of experimentally known cations.[1]

Transferred charge densities for the interaction of phosphenium ions with a variety of anionic (e.g. halides) and neutral nucleophiles (NMe_3, PMe_3) can be computed straightforwardly. The results, which are not included here for the sake of shortness, give on the whole a similar account of relative cation stabilities as Δq(H) values. A detailed inspection reveals, however, some characteristic deviations which mirror a preference for "hard-hard" or "soft-soft" over "hard-soft" interactions in the sense of the HSAB concept.[5] Some examples involving the interaction of selected phosphenium ions with a hard (F^-) and soft nucleophile (I^-) are illustrated in Scheme 3. Thus, the similarity of Δq(F) for **14**−**16**, **19**, **22**, **28** suggests nearly identical stabilities towards F^-, whereas towards I^-, the softer cations with sulfur substituents receive a larger charge transfer Δq(I) (and are hence considered less stable) than cations with oxygen or nitrogen substituents. Still more pronounced variations are noted for **10**, **13** and **11**, **17′**, which display a reversed order of relative stabilities depending on whether the interaction of the cations with F^- or I^- is considered.

Extension of the concept to other species than phosphenium ions should further allow to compare the Lewis acid/base behavior of different types of electrophiles. As an example, the interaction of trimethylamine and -phosphane with cyclic diaminophosphenium ions and isoelectronic carbenes and silylenes was considered, (Scheme 4). The magnitude of Δq for the cations **22**, **24** reflects their electrophilicity and is in accord with the known tendency of phosphenium ions to form stable donor adducts.[1] In contrast, Δq values for the carbenes and silylenes **33**−**36** are close to zero, or even negative,[14] indicating that the electrophilic character is negligible. This is in line with experimental evidence for low π-acceptor capabilities and classification of these systems as *nucleophilic* carbenes (silylenes).[1c][15]

In order to compare relative stabilities derived from transferred charge densities with hydride transfer energies, we have also computed stabilization energies ΔE_{GT} for **1**−**32** at the MP2/6-31+g(d) level. The results are included in Table 1. According to a regression analysis, ΔE_{GT} and Δq(H) are connected by a linear relation (correlation coef-

Scheme 3. Comparison of transferred charge densities for the interaction of selected phosphenium ions with fluoride [$\Delta q(F^-)$] and iodide [$\Delta q(I^-)$] anions. Values of χ and η employed in the calculation of Δq were taken from table 1 for the cations; for the halide anions, the corresponding data of the neutral atoms given in ref.[5] were used

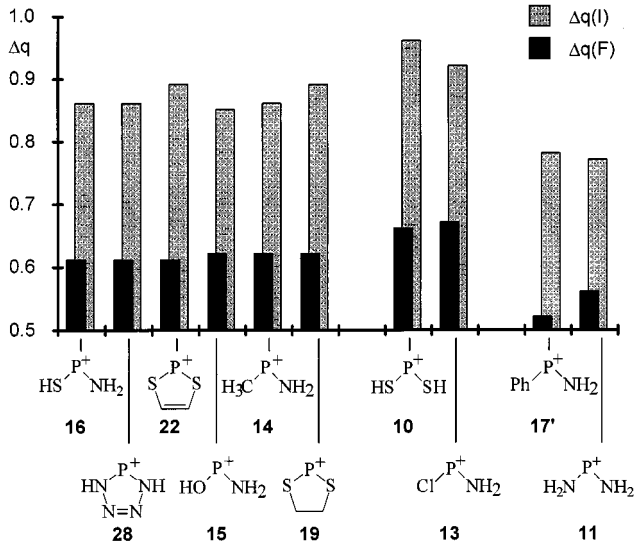

Scheme 4. Comparison of transferred charge densities $\Delta q(NMe_3)$ and $\Delta q(PMe_3)$ for isoelectronic diaminophosphenium cations and neutral diaminocarbenes and -silylenes. All values of χ and η employed in the calculation of Δq were taken from MP2/6-31+g(d) orbital energies of MP2 optimized molecular structures

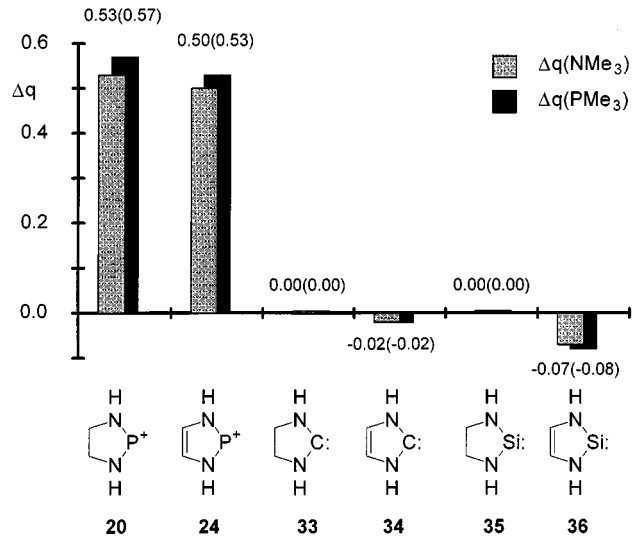

ficient $r = 0.96$, Figure 1). This suggests that despite some discrepancies in the assessment of the stability of individual cations, which are reflected in the scatter of the data, both scales give a similar account of the general trends which govern the stability of low coordinate phosphorus cations.

Electronic Origin of the Stability of Phosphenium Cations

Appealing features of the application of $\Delta q(N)$ to predict relative stabilities (and reactivities) are the use of a minimum number of parameters, and the possibility to distinguish between stabilities towards different reaction partners according to the HSAB concept. However, since the pivotally important quantities χ and η are molecular and not orbital properties, the origin of the stability differences remains obscure. In order to obtain further insight in the bonding situation of low coordinate phosphorus cations, we have attempted a more detailed analysis of the electronic structure based on the results of natural population analyses (NPA).[16]

Figure 1. Plot of $\Delta q(H)$ vs. ΔE_{GT} for **1**−**32** (solid circles) and result of a linear regression analysis [solid line, $\Delta q(H)_{regr} = 3.30 \cdot 10^{-3}$ $\Delta E_{GT} + 1.10$, correlation coefficient $r = 0.96$]

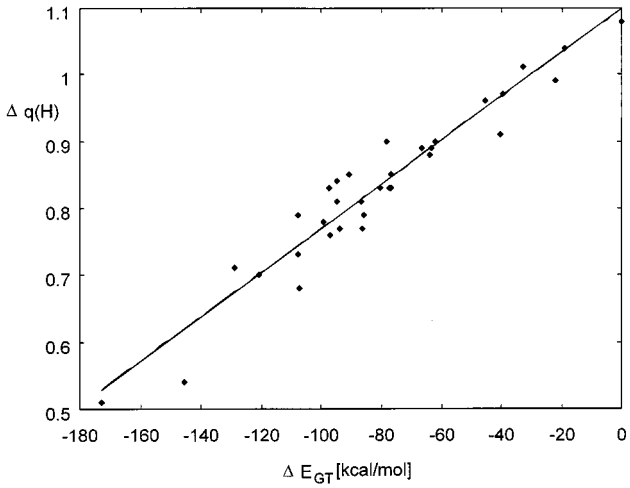

π-Interactions vs. σ-Bond Polarization: Most discussions on the origin of the stabilization of phosphenium ions focus on mesomeric interactions of the formally empty p-orbital at phosphorus with adjacent π-donors.[2][3][4] The varying extent of this π-donation in different cations may be estimated in a straightforward manner by comparing either the electron populations in the phosphorus p-orbital, $n_\pi(P)$, or the bond orders in the P−X bonds. A listing of the values of $n_\pi(P)$ as well as Wiberg bond indexes[16] for the phosphenium ions **1**−**29** is given in Table 2. For the simplest case, $[P(H)_2]^+$, $n_\pi(P)$ is nearly zero, indicating vanishing π-stabilization. Introduction of ER_n-groups at phosphorus induces partial population of the p-orbital via dative (E−P)-π-interactions (ER_n = Cl, OR, SR, NR_2), or hyperconjugation ($ER_n = CR_3$), and $n_\pi(P)$ increases in the order $ER_n = CR_3 < OR < Cl < NR_2 < SR$. The same order of increasing π-stabilizing capabilities emerges also from the comparison of Wiberg bond indexes.

Interestingly, the above mentioned ordering according to increasing degree of E−P π-stabilization differs markedly from the order of overall cation stabilities. Here, regardless if one refers to a comparison of $\Delta q(N)$ or ΔE_{GT} values, cations with NR_2- and OR groups should be more stable than analogous derivatives with SR- or Cl substituents, respectively. This discrepancy suggests that further influences beside mesomeric stabilization have a significant effect on cation stability. In order to understand the underlying mechanisms, a comparison of the bonding situation in phosphenium ions and carbenium ions of the type $[C(EH)_3]^+$ (E = chalcogen) appears useful. For the latter it

Table 2. Electron population in the phosphorus p(π)-orbital [n_π(P)], "electrostatic factors" $\varepsilon = 1/2\ \Sigma\ [q(P)\ q(X_i)]/[r(PX_i)]$, and P−X Wiberg bond indices for the phosphenium cations **1−29**. Natural charges q(P, X_i), orbital populations n_π(P), and Wiberg bond indices were computed from NPA analyses of MP2/6-31+g* electron densities

	n_π(P)	Wiberg Indices		ε
1	0.02	P−H 0.96		−0.02
2	0.12	P−C 1.02	P−H 0.95	−0.42
3	0.37	P−Cl 1.40	P−H 0.94	0.00
4	0.31	P−O 1.08	P−H 0.94	−0.39
5	0.58	P−S 1.66	P−H 0.94	0.02
6	0.46	P−N 1.34	P−H 0.93	−0.37
7	0.55	P−Cl 1.25		−0.01
8	0.18	P−C 0.98		−0.91
9	0.42	P−O 0.94		−1.04
10	0.75	P−S 1.35		−0.01
11	0.56	P−N 1.08		−1.06
12	0.80	P−C 1.26		−0.63
13	0.57	P−Cl 1.11	P−N 1.20	−0.47
14	0.45	P−C 0.93	P−N 1.26	−0.87
15	0.51	P−O 0.87	P−N 1.16	−1.04
16	0.64	P−S 1.29	P−N 1.14	−0.40
17	0.55	P−C 1.01	P−N 1.15	−0.61
17′	0.46	P−C 0.89	P−N 1.27	−0.64
18	0.70	P−N 1.05		−0.64
19	0.78	P−S 1.32		0.06
20	0.61	P−N 1.06		−0.83
21	0.63	P−N 1.06		−0.68
22	1.04	P−S 1.21		0.08
23	0.98	P−N 0.95	P−S 1.19	−0.12
24	0.94	P−N 0.95		−0.55
25	1.06	P−C 1.10		−0.34
26	1.02	P−S 1.21		0.08
27	0.90	P−N 0.96		−0.57
28	0.78	P−N 0.99		−0.50
29	0.95	P−N 1.01		−0.09

was shown recently,[17] that beside (E−C) π-donation also the polarity of the C−E bonds may add substantially to the stabilization energy. The effect is most pronounced for E = O, where the high σ bond polarity [$C^{(+)}-O^{(-)}$] overcompensates the O→C-π-electron shift. This leads to a net increase of charge separation in the C−O bond and results in a marked contribution of the Coulomb-term to the bond energy.

The assessment of a similar contribution to the stability of phosphenium ions $[P(E^1R_n)(E^2R_n)]^+$ becomes feasible from a comparison of the "electrostatic factors"

$$\varepsilon = 1/2 \sum_{i=1}^{2} \frac{q(P)\ q(E^i)}{r(PE^i)}$$

which characterize the average Coulomb stabilization associated with the presence of polar P−E bonds based on a simple point-charge model. A comparison of the listed values of ε in Table 2 reveals an increasing Coulomb stabilization in the order X = S ≈ Cl << N < O. If we assume that the overall cation stability is influenced by both Coulomb and π-donor contributions (which increase with n_π(P) in the order OH < Cl < NH_2 < SH), the higher stabilizing power of NH_2- with respect to OH- (which exert stronger Coulomb stabilization) or SH-groups (which are better π-donors) is consistently explained as the consequence of a balance of both effects. Likewise, the slightly higher stabilizing effect of a CH_3- as compared to a Cl-substituent is attributable to overcompensation of the lower π-donor capability of the former by a larger Coulomb stabilization.

A heuristic confirmation of this concept can be derived from a correlation analysis involving n_π(P), ε, and ΔE_{GT} as an indicator of overall cation stabilities. While a regression analysis between n_π(P) and ΔE_{GT} for the phosphenium ions **1−11**, **13−24**, **26−29** yielded a linear relation with a correlation coefficient $r = 0.77$, a nonlinear fit using both n_π(P) and ε as independent variables furnished the equation $E_{GT,regr} = -3(10) + 92(15)\ n_\pi(P) - 89(15)\ \varepsilon - 49(16)\ \varepsilon^2$, with a correlation coefficient $r = 0.88$. Despite the still substantial scatter of the data, it is apparent that the two parameter model gives a more concise account on phosphenium ion stabilities than the consideration of mesomeric effects alone.

Cyclic π-Conjugation: An issue which attracted considerable interest and was debated rather controversially is the formation of delocalized 6(10)π-systems in cyclic cations such as **22−29**.[3][18][19][20] Positive evidence for the presence of conjugation of this type is provided both by the increase of n_π(P) and the decrease of Δq(H) (or increase of ΔE_{GT}, respectively) for **22 - 29** relative to their CC-saturated analogues **19−21** (cf. Table 1). The net energetic gain [e.g. $\Delta(\Delta E_{GT})$ 21.1 and 13.9 kcal/mol for **20/24** and **19/22**, respectively] is, however, much lower than the inherent mesomeric stabilization in the PE_2 fragment {E = N, S; $\Delta(\Delta E_{GT})$ 93.8 and 62.3 kcal/mol between $[P(H)_2]^+$ and $[P(NH_2)_2]^+$ or $[P(SH)_2]^+$}; it may rather be compared to the inductive stabilization which results from replacement of H in EH_n-moieties by alkyl groups {e.g. $\Delta(\Delta E_{GT})$ 13.7 kcal/mol for $[P(NH_2)_2]^+$ and $[P(NMe_2)_2]^+$}.

As we have demonstrated earlier for **25**, the energetic effects of cyclic π-conjugation may also be analyzed in terms of the reaction energy of the homodesmotic reaction of Scheme 5.[13] This approach is easily extended to a comparison of the π-electron structures in the isoelectronic carbene analogues **24**, **33**, and **35**. The value of ΔE_{deloc} in the cation **24** is higher (4−5 kcal/mol) than in **33** or **35**, but still notably lower than in **25** or the isolobal[13] phospholide anion **37** (Scheme 5). Without attempting to establish a quantitative scale, these results indicate that all three carbene analogues exhibit only weak aromatic character, even if cyclic conjugation in the cation **24** is somewhat more effective than in the neutral species **33, 35**.[21] Natural population analyses indicate further that the increase in n_π(P) in **24** relative to **20** results from a shift of π-electron density within the N_2P-unit, and not from a net transfer from the C_2 to the N_2P fragment. In a simple orbital picture, this corresponds to mixing of occupied and empty N_2P-π orbitals under perturbation by the additional double bond.

Frontier Orbital Considerations

Phosphenium ions are with regard to their reactivity generally considered as carbene analogues.[1][2] The justification for this hypothesis was derived from the similarity of the HOMO (phosphorus lone pair) and LUMO (empty p-orbital) in $[P(H)_2]^+$ (Figure 2a) and the parent carbene,

Scheme 5. Isodesmic reactions describing the interaction of heteroallylic $N_2E(C_2E)$-fragments in cyclic phosphenium ions, carbenes, silylenes, and phospholide anions with an adjacent double bond. Reaction energies ΔE_{deloc} were calculated at the MP2/6-31+g(d) + ZPE level. The value for **25** was taken from ref.[13]

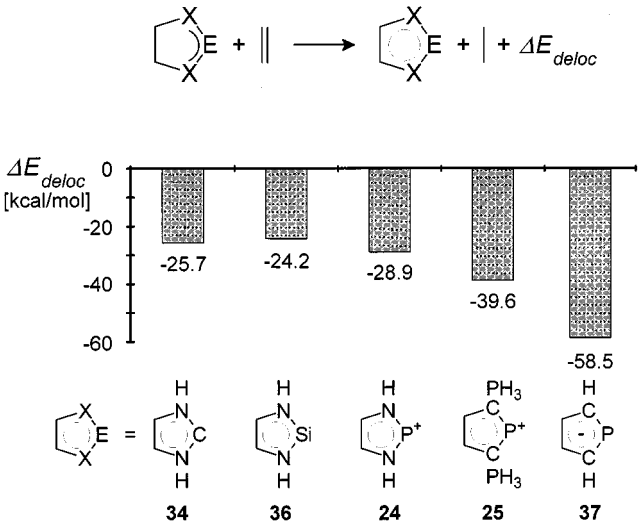

CH_2, which makes the two systems both isolobal and isoelectronic.[1][2]

Inspection of the frontier orbitals of cations **1**−**29** (Table 1) reveals that this analogy is not preserved in all cases. A true carbene analogue frontier orbital sequence is confined to cations with small to moderate E→P-π stabilization such as $[P(H)(X)]^+$ (X = any substituent) or $[P(NH_2)(Y)]^+$ (Y = Cl, CH_3, OH). The frontier orbitals of cations $[P(ER_n)_2]^+$ with two strong π-donor groups (ER_n = NH_2, NMe_2, SH) resemble in accord with earlier studies[2][4] those of an allyl anion (Figure 2b): the HOMO is an antisymmetric combination of p_π(E)-orbitals with a node at phosphorus, and the LUMO an antibonding π_3*-orbital. The "lone pair" at phosphorus corresponds to the HOMO-1 and lies 0.5−2.4 eV below the HOMO. The LUMO of the cyclic conjugated cations **22**−**29** is similar to the previous case, but the HOMO resembles now the highest occupied π-orbital of a phospholide anion[13] and has a large coefficient at phosphorus (Figure 2c). The highest σ-orbital with significant "lone-pair"-character lies 1.8−4.9 eV below the HOMO.

In the frame of frontier orbital theory, one can expect that such significant variations in the type of frontier orbitals imply concomitant changes in reactivity patterns. That this is actually not observed may be explained on the basis of a closer inspection of frontier orbital interactions for individual reactions. In the majority of known reactions which comprise oxidative additions and cycloadditions, phosphenium ions act as electrophiles,[1] and the dominant frontier orbital interaction involves the LUMO of the cation and the HOMO of the reaction partner. Since the largest lobe in the LUMO is always centered at the phosphorus-p-orbital, no changes in frontier orbital interactions or reactivity patterns are expected.

The most prominent reaction which supposedly reflects the nucleophilic character of phosphenium ions is the formation of transition metal complexes. The phosphorus-metal bonding can in this case be described as superposition of a dative P→M σ- and a retrodative P←M π-bond.[1c][22] An analysis of frontier orbital interactions must therefore consider both the HOMO(cation)-LUMO(metal) and LUMO(cation)-HOMO(metal) interactions, and the reactivity of the cation will be directed by the electron densities in *both* of its frontier orbitals.

Figure 2. MOLDEN[29] plot of the LUMO (top row) and HOMO (bottom row) of (a) $[P(H)_2]^+$ (**1**), (b) $[P(NH_2)_2]^+$ (**11**), and (c) [cyclo-$P(NH)_2(CH)_2]^+$ (**24**). The shown surfaces correspond to electron densities of (a) 0.14, (b) 0.10, and (c) 0.09, respectively

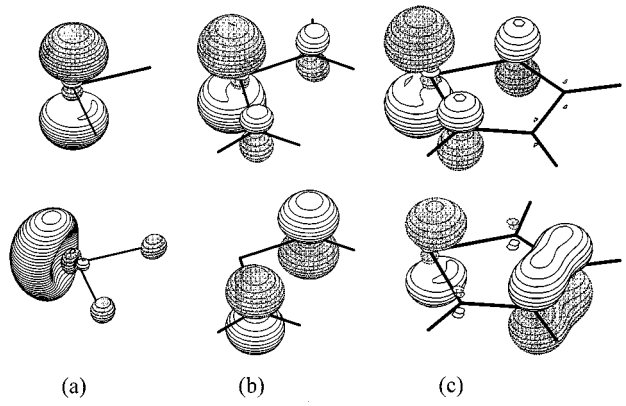

For "carbene analogue" cations such as **1** where the maximum electron density in both HOMO and LUMO occurs at phosphorus, the formation of dative P→M-σ- and P←M-π-bonds is straightforward. For "heteroallylic" cations such as **11**, the shapes of the frontier orbitals imply that a nucleophilic attack of the ligand at a transition metal should occur via the nitrogen,[23] and an electrophilic attack via the phosphorus. The observed formation of P-coordinated complexes[1] suggests therefore that the metal-ligand interaction is dominated by the LUMO(cation)-HOMO-(metal) contribution. Since the HOMO of the cation has a node at phosphorus, secondary interactions between LUMO(metal) and HOMO-1 (phosphorus lone pair) become important, leading to the same bonding description as before. It should be noted that, even if the results of this analysis agree with the generally acknowledged picture of phosphorus-metal bonding in phosphenium complexes[1], they suggest a different weighting of the two contributions: the dominant interaction is here the P←M π- rather than the P→M σ-contribution, and the electrophilic character of phosphenium cations commands even the reaction with transition metal substrates.[24][25]

In the cyclic cations **22**−**29**, the shapes of HOMO and HOMO-1 (which likewise resembles the HOMO-1 of a phospholide[13] and is very close in energy) suggest that a nucleophilic attack at a metal should favor side-on coordination via the π-electron system, while for an electrophilic attack a similar situation as in the previous examples prevails. So far, stable complexes of diazaphospholenium ions of either type are unknown, but the preference of bis-phosphonio-benzophospholides to form σ-complexes[1c] suggests

that the coordination properties may still reflect the electrophilic character of these cations.[26]

Conclusions

The results of the presented studies may be summarized as follows:

(1) Transferred charge densities Δq(N), which describe the shift of electron density upon formation of a dative bond between a low coordinate phosphorus cation and a nucleophile N, are an alternative to hydride transfer energies for the classification of relative cation stabilities. The evaluation of Δq(N) requires less computational effort, since an energy optimization of neutral reaction products in each single case is avoided. Further appealing prospects are the possibilities to discriminate between stabilities towards different nucleophiles which should allow to develop a more distinguished view on stabilities/reactivities in condensed phases, and to compare the electrophilicity of phosphenium ions with isoelectronic carbenes or silylenes.

(2) In addition to mesomeric E→P π-interactions, also the polarity of P−E σ-bonds exerts a relevant influence on the stabilities of phosphenium ions. In particular, the higher stabilizing effect of R_2N- as compared to RS-groups may be related to a balance of both contributions. The stabilities of heterocyclic cations with formal 6π-electron systems are further enhanced by cyclic conjugation. The energetic effect of this interaction is slightly higher than in the carbene or silylene system, but still significantly lower than the effect of N→P-π-interaction, or the electron delocalization energy in aromatic phospholide anions. As in aminocarbenes,[21] cyclic π-conjugation in aminophosphenium ions therefore amplifies the energetic stabilization by N→P-π-interaction, but is not the primary stabilizing factor.

(3) Depending on the substituent pattern at phosphorus, phosphenium ions exhibit different frontier orbital sequences which resemble those of carbenes, heteroallyl anions, or phospholide anions. The failure to observe any changes in reaction patterns suggests that the reactivity is in all cases determined by the LUMO of the cation. In other words: phosphenium ions that are isolobal to heteroallyl or phospholide anions exhibit carbene analogue reactivity patterns because they always react as electrophiles rather than as nucleophiles (or ambiphiles), even in the complexation of transition metals. This implies that despite the isoelectronic and isolobal relationship between diaminophosphenium ions and *nucleophilic* diaminocarbenes, the observed reactivity patterns are better comparable to those of *electrophilic* carbenes

Experimental Section

All calculations were made with the Gaussian 94 package of programs.[27] Molecular geometries of cations **1−32**, the corresponding hydrogen substituted neutral compounds, carbenes and silylenes **33−36**, and the nucleophiles Me_3P and Me_3N were first energy optimized at the HF/6-31+g* level. Frequency analyses at this stage of optimization revealed that all structures except **17′** represent local minima on the energy hypersurface. Starting from these geometries, further energy optimizations were then carried out at the MP2/6-31+g(d) level. The resulting final geometries were used for all subsequent calculations. The absolute electronegativity χ and absolute hardness η of **1−32**, Me_3P, and Me_3N were computed from orbital energies obtained with 6-31+g(d) basis sets. Because of the conceptual difficulties associated with the determination of electron affinities for anions,[5][28] the values of χ and η for the neutral atoms from ref.[5] were used for H^-, F^-, and I^-. Transferred charge densities Δq(N) were then computed as described in the text. Values of ΔE_{GT} and ΔE_{deloc} were computed according to Eq. (1) and (3) at the MP2/6-31+g(d) and MP2/6-31+g(d)+ZPE level, respectively (zero point corrections were derived from additional frequency analyses at the MP2/6-31+g(d) level). The values of orbital populations and Wiberg indexes for **1−29**, and the atomic charges required for the calculation of ε were obtained from natural population analyses[16] of MP2 electron densities. Electrostatic factors ε were calculated as described. Representations of frontier orbitals were generated with the program MOLDEN.[29]

[1] [1a] A. H. Cowley, R. Kemp, *Chem. Rev.* **1985**, *85*, 367. − [1b] M. Sanchez, M. R. Mazieres, L. Lamande, R. Wolf, *Multiple Bonds and Low Coordination Chemistry in Phosphorus Chemistry* (Eds.: M. Regitz, O. Scherer), Georg Thieme Verlag, Stuttgart, **1990**, D1, pp. 129ff. − [1c] D. Gudat, *Coord. Chem. Rev.* **1997**, *173*, 71, and references cited therein.

[2] [2a] A. H. Cowley, M. C. Cushner, M. Lattman, M. L. McKee, J. S. Szobota, J. C. Wilburn, *Pure Appl. Chem.***1980**, *52*, 789. − [2b] G. Trinquier, M. R. Marre, *J. Phys. Chem*, **1983**, *87*, 1903.

[3] [3a] N. Burford, B. W. Royan, A. Linden, T. S. Cameron, *Inorg. Chem.* **1989**, *28,* 144. − [3b] N. Burford, A. I. Dipchand, B. W. Royan, P. S. White, *Inorg. Chem.* **1990**, *29*, 4938. − [3c] G. David, E. Niecke, M. Nieger, V. von der Gönna, W. W. Schoeller, *Chem. Ber.* **1993**, *126*, 1513. − [3d] C.-J. Zhang, C.-G. Zhan, T.-B. Huang, *J. Mol. Struct. (Theochem)* **1995**, *357*, 9.

[4] W. W. Schoeller, U. Tubbesing, *J. Mol. Struct. (Theochem)* **1995**, *343*, 49.

[5] R. G. Pearson, *J. Am. Chem. Soc.* **1985**, *107*, 6801, and cited lit.

[6] R. G. Pearson, *Proc. Natl. Acad. Sci. USA* **1986**, *89*, 1827.

[7] W. J. Hehre, L. Radom, P. v. R. Schleyer, J. A. Pople, *Ab Initio Molecular Orbital Theory*, J. Wiley&Sons, New York **1986**, pp 270ff.

[8] D. Bergmann, J. Hinze, *Angew. Chem.* **1996**, *108*, 162; *Angew. Chem. Int. Ed. Engl.* **1996**, *35*, 150.

[9] J. Cioslowski, S. T. Mixon, *J. Am. Chem. Soc.* **1993**, *115*, 1084.

[10] P. K. Chattaraj, P. v. R. Schleyer, *J. Am. Chem. Soc.* **1994**, *116*, 1067.

[11] D. Datta, *Inorg. Chem.* **1992**, *31*, 2797.

[12] A relation of this kind was e. g. shown to hold for the mean MC-bond energies in metal carbonyl complexes, R. G. Pearson, *Inorg. Chem.* **1984**, *23*, 4675.

[13] D. Gudat, V. Bajorat, M. Nieger, *Bull. Soc. Chim. Fr.*, **1995**, *132*, 280.

[14] Negative values of Δq for **36** indicate the formation of adducts in which the silylene acts as a donor rather than an acceptor. The formation of such species is in accord with studies on the interaction of **36** with NH_3. Energy optimization at MP2/6-31+g(d) level revealed that a structure with a dative H_3N→Si interaction does not correspond to a minimum on the electronic hypersurface; the result of the optimization can be described as an adduct with a weak interaction between one NH moiety and the silylene π-system.

[15] [15a] M. Regitz, *Angew. Chem.* **1996**, *108*, 317; *Angew. Chem. Int. Ed. Engl.* **1996**, *35*, 791. − [15b] W. A. Herrmann, C. Köcher, *Angew. Chem.* **1997**, *109*, 2256; *Angew. Chem. Int. Ed. Engl.* **1997**, *36*, 2162

[16] [16a] J. P. Foster, F. Weinhold, *J. Am. Chem. Soc.* **1980**, *102*, 7211. − [16b] A. E. Reed, F. Weinhold, *J. Chem. Phys.***1985**, *83*, 1736. − [16c] J. F. Carpenter, F. J. Weinhold, *J. Mol. Struct. (Theochem)* **1988**, *169*, 41.

[17] D. Ohlman, C. M. Marchand, H. Grützmacher, G. S. Chen, D. Farmer, R. Glaser, A. Currao, R. Nesper, H. Pritzkow, *Angew. Chem.* **1996**, *108*, 317; *Angew. Chem. Int. Ed. Engl.* **1996**, *35*, 300, and cit. lit.

[18] T. S. Cameron, B. Borecka, A. Linden, *Phosphor. Sulfur Silicon Relat. Elem*. **1992**, *65,* 131.
[19] [19a] I. A. Litvinov, V. A. Naumov, T. V. Gryaznova, A. N. Pudovik, A. M. Kibardin, *Dokl. Akad. Nauk SSSR* **1990**, *312*, 623. – [19b] V. V. Zverev, T. V. Gryaznova, A. M. Kibardin, *Zh. Obshch. Khim.* **1991**, *61*, 2690.
[20] M. K. Denk, S. Gupta, R. Ramachandran, *Tetrahedr. Lett.* **1996**, *37*, 9025.
[21] This is in accord with earlier studies on **33**, **35**; see:
[21a] C. Heinemann, T. Müller, Y. Apeloig, H. Schwarz, *J. Am. Chem. Soc.* **1996**, *118*, 2023. – [21b] C. Boehme, G. Frenking, *J. Am. Chem. Soc.* **1996**, *118*, 2039.
[22] [22a] H. Nakazawa, M. Ohta, K. Miyoshi, H. Yoneda, *Organometallics* **1989**, *8*, 638. – [22b] D. Gudat A. W. Holderberg, S. Kotila, M. Nieger, *Chem. Ber.* **1996**, *129*, 465.
[23] A nucleophilic attack of this type is represented by the dimerization of homologous diaminoarsenium cations where the observed formation of intermolecular As···N contacts may be rationalized in terms of interaction of the HOMO of one with the LUMO of a second cation; see: N. Burford, T. M. Parks, B. W. Royan, B. Borecka, T. S. Cameron, J. F. Richardson, E. J. Gabe, R. Hynes, *J. Am. Chem. Soc.* **1992**, *114*, 8147.
[24] A similar dominance of L←M π-back donation over L→M σ-bonding had also been suggested for metal carbonyl complexes, see ref.[12].
[25] The dominance of the P←M π- over the P→M σ-contribution is supported by the results of a preliminary study of the complex $[(H_2N)_2P\text{-}Fe(CO)_4]^+$. According to a natural population analysis of the MP2 electron density (LANL2dz basis set, molecular geometry optimized at the MP2/LAN2dz-level), the coordination is accompanied by a reduction of the positive charge on the $(H_2N)_2P$-moiety from a value of +1.00 for the free ligand to +0.88 in the complex, thus implying a net transfer of electron density from the metal to the ligand. Further studies of the metal-phosphorus bonding in phosphenium complexes are in progress.
[26] It should be noted that for reactions of soft acids the influence of electron correlation becomes important and these reactions are in some cases described incorrectly at the SCF-level (see ref.[10]). One should therefore bear in mind that different predictions of the reactivities of phosphenium ions may result when correlation effects are included.
[27] *Gaussian 94*, Rev. B.3, M. J. Frisch, G. W. Trucks, H. B. Schlegel, P. M. W. Gill, B. G. Johnson, M. A. Robb, J. R. Cheeseman, T. Keith, G. A. Petersson, J. A. Montgomery, K. Raghavachari, M. A. Al-Laham, V. G. Zakrzewski, J. V. Ortiz, J. B. Foresman, C. Y. Peng, P. Y. Ayala, W. Chen, M. W. Wong, J. L. Andres, E. S. Replogle, R. Gomperts, R. L. Martin, D. J. Fox, J. S. Binkley, D. J. Defrees, J. Baker, J. P. Stewart, M. Head-Gordon, C. Gonzalez, J. A. Pople, Gaussian, Inc., Pittsburgh PA, **1995**.
[28] Pearson, *J. Chem. Educ.* **1987**, *64*, 561.
[29] *MOLDEN3.2*, a pre- and post processing program of molecular and electronic structure, written by G. Schaftenaar, CAOS/CAMM Center, University of Nijmegen.

[97203]

The Aluminum–Nitrogen Bond in Monomeric Bis(amino)alanes: A Systematic Experimental Study of Bis(tetramethylpiperidino)alanes and Quantum Mechanical Calculations on the Model System $(H_2N)_2AlY$

Klaus Knabel, Ingo Krossing[1], Heinrich Nöth*, Holger Schwenk-Kircher[2], Martin Schmidt-Amelunxen[2], and Thomas Seifert[2]

Institute of Inorganic Chemistry, University of Munich,
Meiserstraße 1, D-80333 Munich, Germany

Received November 10, 1997

Keywords: Aminoalanes / Alanes / Ab initio calculations / ^{27}Al-NMR spectroscopy / Structure elucidation / Substituent effects

Reactions of metallated nucleophiles M^IY [Y = OR, SR, NR_2, PR_2, AsR_2, CR_3, $Si(SiMe_3)_3$, R = organyl, H] with bis(2,2,6,6-tetramethylpiperidino)aluminum halides [tmp_2AlX, (X = Cl, Br, I)] offer facile access to a variety of bis(amino)alanes of the type tmp_2AlY. As indicated by ^{27}Al-NMR spectroscopy, mass spectrometry and X-ray crystal structure determinations, all of these compounds are monomeric in the solid state, in solution, and in the gas phase. Even Al–E single bonds (E = Si, P, As etc.) that are not commonly encountered are stabilized by the supporting tmp fragments. The results of a systematic analysis of the bonding parameters determined for the tmp_2AlY compounds, combined with a quantum mechanical study on model compounds $(H_2N)_2AlY$, not only reveal the presence of a highly polar Al–N bond, but at the same time rule out AlN-pp(π) bonding, in contrast to the situation in the analogous tmp_2BY compounds. It is shown that the Al–N bond length depends on the acidic character of the protic species HY: the shorter *d*(Al–N), the less basic is Y.

Introduction

Homo- and heteroatomic multiple bonding, especially involving heavier main-group elements, has been a major field of interest in the last decade. Thus, many compounds with element−element double bonds, kinetically stabilized by using bulky substituents attached to the element atom in question, have been produced. Application of this principle has led to the synthesis and characterization of Si=Si, Ge=Ge, Sn=Sn[3][4][5] and III−V (B=N, B=P, B=As)[6][7][8] doubly bonded systems. In the latter species, bond shortening and small twist angles between the planes at boron and the group-V elements are reported, indicative of pp(π) interactions. By means of variable-temperature ^{1}H-NMR spectroscopy[9] and quantum mechanical calculations[10], activation barriers for rotation about the B−E bond (E = N, P, As) as high as 33 kcal/mol have been determined.

Considering the heavier homologues of boron, i.e. aluminum and gallium, these might also be capable of adopting such bonding arrangements. However, no compounds containing Al=P or Al=As double bonds have yet been characterized. Thus, the gallyl phosphide $tBu_2GaP(Mes)(SiPh_3)$ exhibits a barrier to rotation about the Ga−P bond of only 12.7 kcal/mol[11]. Taking this result, together with an almost planar (sum of bond angles 346.2°) geometry at the phosphorus atom and a short Ga−P bond length, the authors concluded that a small pp(π) contribution might be present[11]. In the case of aluminum amides, pp(π) interaction, well established for the homologous aminoboranes[6][9], has been used to explain short bond lengths in monomeric aminoalanes {e.g. 1.78(2) Å in $Al[N(SiMe_3)_2]_3$ and 1.782(2) Å in $(MeAlNdipp)_3$ (dipp = 2,6-$iPr_2C_6H_3$)}[12][13]. Moreover, a barrier to rotation about the Al−N bond in $tBu_2AlN(dipp)(SiPh_3)$ of 9.9 kcal/mol has been determined, indicative of weak pp(π) interactions[14]. However, Al−N bond lengths in tricoordinated aluminum amides vary considerably from 1.78 to 1.88 Å. An analysis of structural data and rotational barriers in tricoordinated Al−N compounds lead to the conclusion that the bonding is primarily determined by Al−N bond polarity[15]. However, no systematic analysis on the variation of Al−N bonding parameters in a family of compounds has so far been performed. We found that bis(tetramethylpiperidino)alanes represent such a family.

Recently, we published the synthesis and structures of the monomeric bis(2,2,6,6-tetramethylpiperidino)aluminum halides {tmp_2AlX [X = Cl (**1a**), Br (**1b**), I (**1c**)]}[16], which allow even the synthesis of transition-metal compounds such as $[tmp_2Al-Fe(cp)(CO)_2,]$ (**2**)[17]. Here, we report on a variety of additional derivatives of bis(tmp)alanes. The compounds **1a−c**, **2**, and of the type tmp_2AlY **3−6** {Y = OR, SR, NR_2, PPh_2, $AsPh_2$, CR_3, $Si[Si(Me)_3]_3$, R = organyl, H} possess tricoordinated aluminum and nitrogen centers. To allow a distinction to be made between possible pp(π) interactions, N(p)AlX(σ*) interactions and a highly polar bonding situation at the aluminum center [χ(N) = 3.1; χ(Al) = 1.6; Pauling electronegativity], the structures of these compounds were determined in the solid state. Systematic variation of the group Y not only changes the electronic situation at the aluminum atom, but − since the am-

 © WILEY-VCH Verlag GmbH, D-69451 Weinheim, 1998 1434−1948/98/0808−1095 $ 17.50+.50/0

ino ligands remain constant − this allows quantification of the effect of various substituents at the Al−N unit.

Although most of the tmp_2AlY compounds are sterically severely crowded, we expected to obtain supporting evidence from ab initio calculations (MP2/6-31+G*) on systematically varied model compounds $(H_2N)_2Al-Y$ (**7a−h**) [Y = Cl, OH, SH, NH_2, PH_2, CH_3, SiH_3, $Al(NH_2)_2$], including NBO analysis for interpretation of their bonding situation in the LMBO picture (= Lewis picture)[18].

Synthesis and Reactions

In order to delineate the effects of a systematic change of the group Y in tmp_2AlY, the following results describe tmp_2AlY compounds in which the substituent Y is varied across the main-group elements from right to left. All bis(tmp)alanes were obtained by the metathesis of tmp_2AlX (X = Cl, Br, I) with nucleophiles Y^-. The reactions proceeded well in aliphatic organic solvents. Monitoring of the reactions by ^{1}H-NMR spectroscopy indicated the exclusive formation of compounds tmp_2AlY (**3−6**). Competing reactions, which commonly hamper aluminum chemistry (e.g. dismutation leading to mixtures), were not observed.

(i) Main Group VI Nucleophiles

When mixtures of tmp_2AlX **1a−c** with the freshly prepared lithium compounds PhOLi, dippOLi, PhSLi, and *t*BuSLi were refluxed in *n*-hexane solution for about three hours, the monomeric bis(tmp)aluminum phenolates and thiolates $tmp_2Al-OPh$ **3a**, $tmp_2Al-Odipp$ **3b**, $tmp_2Al-SPh$ **3c**, and $tmp_2Al-StBu$ **3d** were obtained in 54−87% yield. The relatively weak nucleophilic character of the lithium aryloxides and thiolates necessitates heating in this case to make reaction times suitably short.

$$tmp_2AlX + LiY \xrightarrow[-LiX]{\text{n-hexane}} tmp_2AlY \quad (1)$$

X = Cl, Br, I Y = OPh **3a**, Odipp **3b**

Y = SPh **3c**, StBu **3d**

(ii) Main Group V Nucleophiles

Powdered LiN(H)R (R = *t*Bu, Ph) and $LiEPh_2$ (E = P, As) react with tmp_2AlX (**1a−c**) in *n*-hexane solution at ambient temperature to give $tmp_2Al-N(H)tBu$ (**4a**), $tmp_2Al-N(H)Ph$ (**4b**), $tmp_2Al-PPh_2$ (**4c**), and $tmp_2Al-AsPh_2$ (**4d**) in 42−65% yield. To verify the donor properties of the phosphorus atom in **4c**, one equivalent of AlI_3 was added to a solution of the compound in benzene. From the resulting solution, crystals separated on cooling, which proved to be the trimeric I_2AlPPh_2 (**4e**). The supernatant solution was found to contain tmp_2AlI (**1c**), which was characterized by its NMR spectra[15].

(iii) Main Group IV Nucleophiles

PhLi (Bu_2O solution), *n*BuLi (*n*-hexane solution), freshly prepared *p*-$MeOC_6H_4MgBr$ (THF), $H_{10}B_{10}C_2Li_2$ (= 1,2-dilithio-1,2-dicarba-*closo*-dodecaborane) and the tmeda adduct of $FecLi_2$ (Fec = ferrocene) each reacted smoothly with tmp_2AlX (**1a−c**) (within minutes to one hour) to give the organylalanes tmp_2Al-Ph (**5a**), tmp_2Al-Bu (**5b**), $tmp_2Al-C_6H_4OMe$ (**5c**), $(tmp_2Al)_2C_2B_{10}H_{10}$ (**5d**), and $(tmp_2Al)_2Fec$ (**5e**) in 48−79% yield. Reaction with $(Me_3Si)_3Si-Li(thf)_3$ afforded the silylalane $tmp_2Al-Si(SiMe_3)_3$ (**5f**) in 65% yield, whereas addition of freshly prepared $Me_3SnLi(thf)_x$ ($x \approx 3$) led only to the transient formation of $tmp_2Al-SnMe_3$ (**5g**), which quickly decomposed by stannylene elimination $(SnMe_2)_n$ to give tmp_2Al-Me (**5h**) as the sole isolated species. On leaving the latter compound to stand for several weeks in CO_2 at −78°C, quantitative insertion of CO_2 into the Al−N bonds occurred, resulting in the methylaluminum bis(carbaminate) $[MeAl(O_2Ctmp)_2]_2$ (**5i**).

The silylalane **5f** was subjected to a series of solvolysis reactions. Treatment with stoichiometric amounts of EtOH, PhOH, and HCl led exclusively to the products of Al−N cleavage $[(Me_3Si)_3SiAl(OEt)_2]_2$ (**5j**) and $[(Me_3Si)_3SiAlZ_3]tmpH_2$ [Z = OPh (**5k**), Cl (**5l**)] in 65−85% yield. Use of bulkier alcohols such as *t*BuOH, MesOH and dippOH led to inseparable mixtures, whereas 2,4,6-$tBu_3C_6H_2OH$ did not react.

$$tmp_2AlPPh_2 + AlI_3 \xrightarrow{\text{benzene}} [\,tmp_2AlPPh_2{*}AlI_3\,] \quad (2a)$$

4c

tmp_2AlI + $I_2Al(PPh_2)(AlI_2)PPh_2$

1c **4e**

(iv) Main Group III Nucleophiles

Suspensions of $LiBH_4$ or $Li(H_29\text{-BBN})$ (9-BBN = 9-borabicyclononane) in *n*-hexane reacted with tmp_2AlX compounds (X = Cl, Br, I) to afford the highly soluble compounds $tmp_2AlH_2BH_2$ (**6a**) (42%) and tmp_2AlH_2(9-BBN) (**6b**) (74%).

Characterization

Monomeric Bis(tmp)alanes

The chemical shift of the ^{27}Al-NMR signals of **1−6** is a function of the electron density at the aluminum nucleus (see Table 1). Strong σ- and possible π-donors such as the aryloxides, phosphanides, and arsanides **3a−b** and **4c−d** induce an upfield shift of the ^{27}Al signal up to δ = 65 [compared to tmp_2AlX (X = Cl, Br, I), $\delta^{27}Al = 130$][15]. Organyl or silyl substituents cause a deshielding, which reaches its maximum for $tmp_2Al-Si(SiMe_3)_3$ (**5f**) ($\delta^{27}Al = 186$). How-

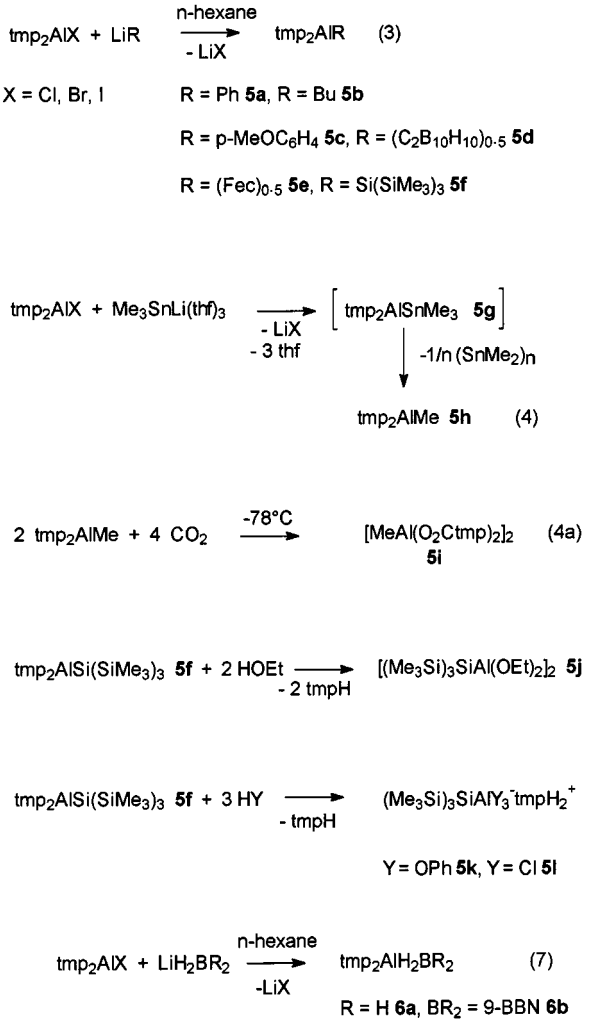

ever, there is one exception: δ^{27}Al of $(tmp_2Al)_2Fec$ (**5e**), possibly as a result of an anisotropic effect of the iron atom, exhibits a remarkable high-field shift (δ^{27}Al = 59). Due to the low local symmetry at the aluminum center, signals with half-widths as broad as 19400 Hz are a characteristic feature of the tricoordinated aminoalanes **2**−**6**[18][19]. The halides **1a**−**c** were shown to be monomeric by cryoscopic molar-mass determinations and, therefore, the signals in the ^{27}Al-NMR spectrum exhibit very broad half-widths of 9100−13700 Hz[15]. Since all other tmp_2AlY compounds possess the same local symmetry at the aluminum atom and exhibit signal half-widths similar to those observed in **1a**−**c**, it can be assumed that **2**−**6** do not form associates in solution.

In agreement with this assumption is the observation that in the ^{1}H- and ^{13}C-NMR spectra, only one set of resonances is observed for the tmp ligand, indicating free rotation about the Al−N bond and rapid inversion of the piperidinyl ring. In the case of the phosphanide **4c**, a long-range coupling [$^4J(^{31}P,^{13}C)$ = 4.1 Hz] of the tmp methyl carbon atoms and the phosphorus atom is characteristic. At ambient temperature, **5f**, probably the sterically most crowded molecule of this series, shows a set of broad ^{1}H-NMR and ^{13}C-NMR signals for the tmp methyl groups. Upon cooling to −70°C, these separate into two distinct lines (depicted in Figure 1). As the free activation enthalpy for this process has been determined to be about 54 kJ/mol (using the Eyring equation)[21], we take this as evidence for hindered inversion of the piperidinyl ring (cf. for example, the inversion barrier of cyclohexane: 46 kJ/mol)[22], while we assume free rotation about the Al−N bond even at a temperature of −70°C (if there was hindered rotation about the Al−N bond, one should observe four signals for the then magnetically inequivalent tmp methyl groups).

Table 1. Chemical shifts δ^{27}Al and line width of tmp_2 AlY compounds

tmp_2AlY compd.	**3a**	**3b**	**3c**	**3d**	**4a**	**4b**	**4c**	**4d**
R =	OPh	Odipp	SPh	S*t*Bu	N(H)*t*Bu	N(H)Ph	PPh_2	$AsPh_2$
δ^{27}Al[a]	75	85	153	152	129	124	110	74
$h_{1/2}$[b]	8800	9000	14000	9500	8700	9600	13400	18300

tmp_2AlY compd.	**5a**	**5b**	**5c**	**5d**	**5e**	**5f**	**5h**	**6b**
R =	Ph	Bu	[c]	[d]	$(Fec)_2$	$(Me_3Si)_3Si$	Me	H_29-BBN
δ^{27}Al[a]	153	164	160	164	59	186	173	115
$h_{1/2}$[b]	12300	13400	19400	12400	7400	12400	–	10700

[a] In ppm. − [b] In Hz. − [c] *p*-$MeOC_6H_4$.− [d] $(C_2B_{10}H_{10})_2$.

In the ^{11}B-NMR spectrum of the tetrahydroborate **6a** ($\delta^{11}B$ = −24.4), a $^1J(^{11}B,^1H)$ coupling constant of 85 Hz is found. This lies well within the range found for other aminoaluminum tetrahydroborates [e.g. $H_2B(\mu\text{-}NMe_2)\text{-}Al(BH_4)_2$, $^1J(^{11}B,^1H)$ = 89 Hz][23]. In contrast, the proton-coupled ^{11}B-NMR spectrum of **6b** exhibits only a broad, unresolved signal, which narrows on proton decoupling from 247 Hz to 207 Hz. From the IR spectra, a bidentate coordination of the BH_4 group to the aluminum atom can be deduced.

To investigate their gas-phase behavior, **3d**, **5a**−**b**, **h**, and **6a** were subjected to mass spectrometry (70 eV). No fragments of higher *m*/*z* ratios than the molecular ions of the monomers (15−20% relative intensity) were observed, confirming the unassociated nature of these species in the vapour phase. Due to the low Al−C and Al−H bond strengths[24], the bis(tmp)aluminum cation tmp_2Al^+, *m*/*z* = 307, is formed as the major fragment with 18−100% relative intensity. Since these compounds contain eight methyl groups, the (M − 15) fragment is formed very readily (31−100% relative intensity). It is noteworthy that the phosphanide **4c**, the arsanide **4d**, and the silylalane **5f** decomposed upon vaporization; only fragments of low *m*/*z* ratio were detected.

^{1}H- and ^{13}C-NMR spectroscopic analysis of the crystals and the supernatant solution obtained according to equation 2a revealed Al−P bond cleavage of the presumably formed adduct $tmp_2AlPPh_2{*}AlI_3$. The crystals only gave rise to signals in the aromatic region, while the solution

Figure 1. ^{1}H-NMR and ^{13}C-NMR spectra of **5f** in [D_8]toluene recorded at various temperatures

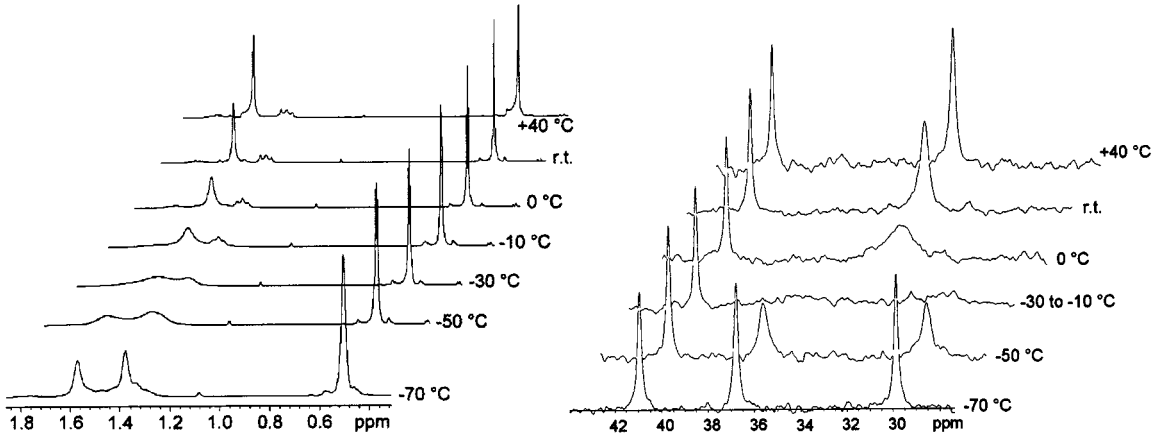

exhibited signals attributable to tmp_2AlI (**1c**)[15]. The ^{31}P-NMR signal of **4e** is shifted downfield compared to **4c**, appearing at $\delta^{31}P = -42.9$, thus indicating a tetracoordinated phosphorus atom. Since **4e** is trimeric in the solid state, as ascertained by X-ray crystal structure determination, it is most likely that the phosphanide retains this degree of oligomerization in solution. This would correspond to the behavior of $(Me_2AlPMe_2)_3$[25].

The ^{27}Al-NMR spectrum of the aluminum carbaminate **5i** shows two sharp signals in the region typical of pentacoordinated species [$d^{27}Al = 21$ ($\Delta_{1/2} = 1.120$ Hz); $d^{27}Al = 9$ ($\Delta_{1/2} = 980$ Hz)] {cf. $[(Me_2NCS_2)_2AlCl]_2$: $d^{27}Al = 14$}[26], indicating that the dimeric compound found in the solid state (vide infra) dissociates in solution partly into monomers . This is confirmed by ^{1}H- and ^{13}C-NMR spectroscopy. Two sets of signals are observed for the tmp ligands, those assigned to the dimer having twice the intensity (see Figure 2).

Figure 2. Possible bonding patterns of the carbaminate **5i**

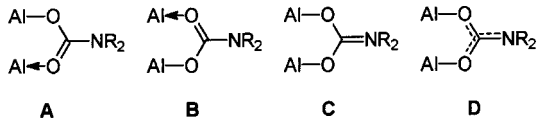

Considering the IR spectrum, formula **D** is consistent with the strong absorption at 1582 cm^{-1}. Thus, the partial C−N double bond, as indicated by the rather short C−N bond length (vide infra), results in hindered rotation about this bond and makes inversion of the ring more difficult, rendering pairs of atoms in the tmp ligand magnetically inequivalent.

The presence of tetracoordinated aluminum centers in the silylalane **5j** and the silylaluminates **5k−l** is evident from the dramatically decreased line widths in the ^{27}Al-NMR spectra ($\Delta_{1/2} = 1000-3000$ Hz vs. 12400 Hz in **5f**)[18]. A double set of lines for the ethoxy groups in **5j** indicates its dimeric nature (terminal and bridging EtO resonances) and rules out the possibility that a mixture of *cis* and *trans* isomers is present, since only one signal for the bridging ethoxy group is found. Most probably, the terminal EtO groups are oriented *trans* to one another, as this isomer crystallizes from the solution (the *trans* isomer is favoured by about 6 kcal/mol according to a semiempirical AM1 calculation). Aluminate formation in the case of **5k−l** is deduced from the ^{13}C-NMR signals of the $tmpH_2^+$ cation, which differ markedly compared to those observed when a tricoordinated nitrogen atom is present in the piperidino ligand [e.g. $\delta^{13}C$ (N−*C*) = 57−58 vs. 51−53 in tmp_2AlY], and from the presence of an NH_2 stretching band in the IR spectrum. The ^{29}Si-NMR signals of the $Me_3{}^{29}Si$ groups of **5j−l** fall in the small range of $\delta = -8$ to -10, well within the range of reported values for the homologous gallium compounds prepared by Linti et al.[27]. Compared to **5f**, the ^{1}H-NMR signals for the Me_3Si groups are shifted by 0.3−0.4 ppm to higher field. We attribute this to the reduced steric crowding that results from the replacement of the tmp ligands with less bulky substituents.

Crystal Structures

Monomeric Bis(tmp)alanes tmp_2AlY (3−6)

Structural parameters are presented in Table 2, additional values are given in the caption of each ORTEP representation. Hydrogen atoms are omitted for clarity in the figures except in the plots of **4b** and **6b** where selected hydrogen atoms are depicted. All molecules **3−6** possess tricoordinated aluminium atoms residing in a planar envirnonment [sum of bond angles $\Sigma(Al) = 360.0°$]. The nitrogen atoms of the tmp ligands, which exhibit the chair conformation, seem to have sp^2 character, as their sum of bond angles range from 359.4 to 360.0°.

$tmp_2AlOdipp$ (3b)

The structure of **3b** is depicted in Figure 3. The molecule shows a rather long Al−O distance of 1.696(2) A, compared to that in the electronically similar tris(aryloxides) [e.g. $Al(OAr)_3$, OAr = 2,6-tBu$_2$-4-Me-C_6H_2, d(Al−O) = 1.647 A (av.)][28] investigated by Barron et al. Due to the steric requirements of the bulky substituents, the Al−O−C angle, 158.4(2)°, is rather large a feature commonly observed for monomeric aluminum aryloxides. This can be

Table 2. Some characteristic bonding parameters of tmp_2AlY compounds

tmp_2AlY Y =	d(Al−N) [Å]	d(Al−E) [Å]	N−Al−N [°]	C−N1−Al−E [°]	C−N2−Al−E [°]	Σ(N) [°]	Σ(Al) [°]
Cl[a] (**1a**)	1.785(4)	2.144(2)	130.1(2)	66.2	30.8	357.6	360.0
	1.810(4)			84.3	52.1	356.7	
Br[a] (**1b**)	1.782(6)	2.309(2)	130.4(3)	66.0	31.1	357.5	359.8
	1.812(6)			88.7	46.9	356.9	
I[a] (**1c**)	1.788(3)	2.571(1)	129.5(1)	65.2	35.6	357.9	359.9
	1.803(3)			89.3	48.8	357.1	
Odipp (**3b**)	1.807(2)	1.696(2)	128.9(1)	59.5	57.4	359.8	360.0
	1.809(2)			59.4	62.7	360.0	
SPh (**3c**)	1.800(2)	2.225(1)	128.2(1)	−141.0	59.6	360.0	360.0
	1.807(2)			37.8	−106.9	358.9	
	1.798(2)	2.233(1)	130.8(1)	119.4	110.3	358.6	360.0
	1.813(2)			−44.1	−60.3	359.5	
S*t*Bu (**3d**)	1.817(2)	2.200(1)	128.6(1)	−73.5	−70.6	359.9	360.0
	1.820(2)			109.9	116.1	359.8	
N(H)Ph (**4b**)	1.813(2)	1.790(2)	131.8(1)	66.2	67.2	359.9	360.0
	1.822(2)			70.4	70.2	359.9	
PPh_2 (**4c**)	1.819(2)	2.377(1)	128.8(1)	65.3	65.1	359.9	360.0
	1.819(2)			66.7	68.7	360.0	
$AsPh_2$ (**4d**)	1.816(3)	2.485(2)	129.1(1)	65.5	64.9	359.9	360.0
	1.822(3)			69.6	66.1	360.0	
Ph (**5a**)	1.826(2)	1.971(3)	128.9(1)	67.7	−	359.8	359.9
				73.2			
$(Fec)_{0.5}$ (**5e**)	1.824(3)	1.952(3)	126.1(1)	69.7	61.6	359.8	360.0
	1.825(3)			74.0	62.0	359.9	
$(Me_3Si)_3Si$ (**5f**)	1.844(2)	2.514(1)	123.8(1)	76.5	59.9	359.6	360.0
	1.848(2)			82.9	66.8	359.6	
H_2(9-BBN)[d] (**6b**)	1.814(4)	2.223(7)	132.4(2)	67.1	−	359.4	360.0[d]
				75.9			
$Altmp_2$[b] (**8**)	1.849(1)	2.640(2)	121.8(1)	64.1	68.1	359.9	360.0
	1.851(2)			67.6	69.7	359.9	
$Fecp(CO)_2$ (**2**)[c]	1.847(4)	2.450(1)	121.9(2)	72.2	64.6	359.3	360.0
	1.862(4)			73.8	74.5	359.9	

[a] See ref.[15]. – [b] See ref.[49i]. – [c] See ref.[16]. – [d] Al···B distance.

taken as an indication of a strong polar Al−O bond, which should lead to a short Al−O bond[15].

tmp_2AlSPh (3c) (Figure 4) and $tmp_2AlStBu$ (3d) (Figure 5)

The asymmetric unit of **3c** contains two independent, slightly different molecules. Compared to the published structure of monomeric aluminum thiolates $(mes^*S)_3Al$ [mes* = 2,4,6-tBu$_3$C$_6$H$_2$, d(Al−S) = 2.185(2) Å][29], Bu-Al(Smes*)$_2$ [d(Al−S) = 2.188(9) Å] and tBuAl(Smes*)$_2$ [d(Al−S) = 2.196(3) Å][30], the Al−S distances found in **3c−d** are elongated [**3c**: 2.225(1), 2.233(1) Å; **3d**: 2.200(1) Å]. This is consistent with the lower basicity of PhS^- (compared to tBuS$^-$), since d(Al−S) in **3c** is longer, and d(Al−N) is shorter than in **3d**, and vice versa. The C−S−Al angles are 105.7(1)° and 106.5(1)° for **3c**, and 118.9(1)° for **3d** and, as expected, are smaller than the C−O−Al angles observed in **3b** [158.4(2)°] or $R_xAl(OAr)_{3-x}$ (R = organo, up to 171°)[27].

$tmp_2AlN(H)Ph$ (4b)

As the anilide **4b** (depicted in Figure 6) is the derivative of the primary amine $PhNH_2$, it belongs to the rare class of kinetically stabilized, hydrogen-bearing aluminum amides[15]. These are normally unstable with respect to intramolecular amine elimination and formation of oligomeric iminoalanes $(RAl-NR)_n$ (n = 2−8)[31][32]. The anilide

Figure 3. Molecular structure of $tmp_2AlOdipp$ (**3b**) in the solid state; thermal ellipsoids are shown at a 25% probability level[a]

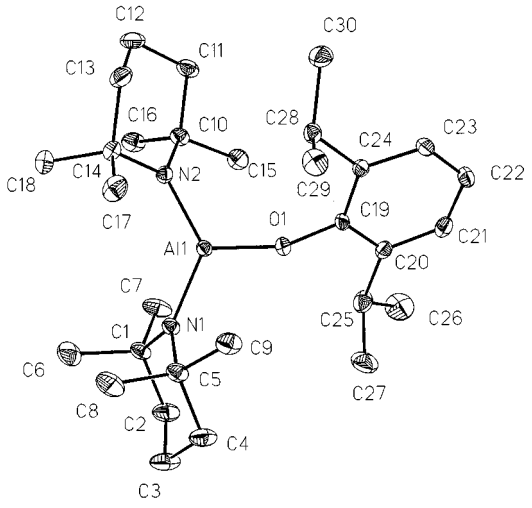

[a] Additional bond angles [°]: Al(1)−O(1)−C(19) 158.4(2), N(1)−Al(1)−O(1) 113.3(1), N(2)−Al(2)−O(1) 117.8(1).

Al−N bond [1.790(2) Å] is shorter than the Al−N bonds to the piperidino ligand [1.813(2) and 1.822(2) Å], presumably due to the reduced steric requirement of the ligand. However, in the monomeric tris(amides) $Al[N(SiMe_3)]_3$[12] and $Al(NiPr_2)_3$[33] similar or even shorter Al−N bond

Figure 4. Molecular structure of one of the two independent species of tmp_2AlSPh (**3c**) in the solid state; thermal ellipsoids are shown at a 25% probability level[a]

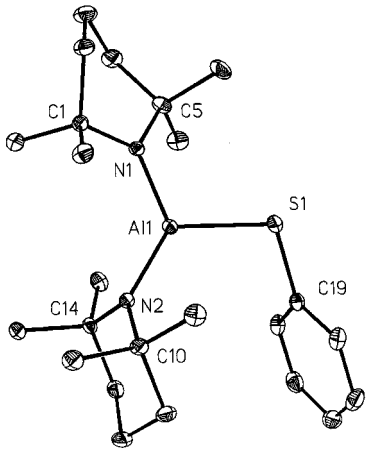

[a] Bond lengths [A] and bond angles [°]: Al(1)−S(1) 2.225(1), Al(2)−S(2) 2.233(1); C(19)−S(1)−Al(1) 105.7, C(43)−S(2)−Al(2) 106.5, N(1)−Al(1)−S(1) 110.1(1), N(2)−Al(1)−S(1) 121.7(1), N(3)−Al(2)−S(2) 109.4(1), N(4)−Al(2)−S(2) 119.6(1).

Figure 5. Molecular structure of $tmp_2AlStBu$ (**3d**) in the solid state; thermal ellipsoids are shown at a 25% probability level[a]

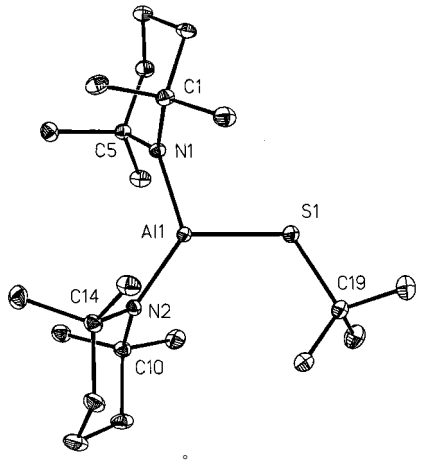

[a] Additional bond lengths [A] and bond angles [°]: Al(1)−S(1) 2.220(1); C(19)−S(1)−Al(1) 118.9(1), N(1)−Al(1)−S(1) 107.0(1), N(2)−Al(1)−S(1) 124.4(1).

lengths are reported [1.78(2) A for the silylamide and 1.791(4)−1.801(4) A for the isopropylamide]. The anilide N atom resides in a distorted trigonal-planar environment (sum of bond angles at the anilide nitrogen atom: 359.9°), with a large Al−N−C angle [138.9(2)°] and small Al−N−H and C−N−H angles [110.9(2) and 110.1(2)°].

tmp_2AlPPh_2 (4c) (Figure 7) and $tmp_2AlAsPh_2$ (4d) (Figure 8)

4c−d are isotypic. The most important structural parameter of these compounds is the Al−E bond length [E = P: 2.377(1) A; E = As: 2.485(2) A]. Only a few bonding parameters of this kind are known at the present time.[15] Compared to the recently published tricoordinated aluminum phosphanide $trip_2Al-P(Ada)(SiPh_3)$ [d(Al−P) = 2.342(2) A; trip = 2,4,6-iPr$_3$C$_6$H$_2$; Ada = adamantyl][34] and to the sum of the relevant covalent radii [1.25 A (Al) + 1.10 A (P) = 2.35 A][35], the Al−P bond in **4c** is elongated. The arsanide **4d** represents a acyclic compound featuring an aluminum−arsenic σ-bond, although two molecules, the trimeric (mes*Al−AsPh)$_3$ [d(Al−As) = 2.43 A][36] and the cp*$_3$Al$_3$As$_2$ cluster [d(Al−As) = 2.48 A][37], have previously been subjected to crystal structure analyses. The latter compound may be viewed as a subvalent species, and thus it is inappropriate to compare its Al−As bond length with that in **4d**. Considering the sum of the covalent radii [1.25 A (Al) + 1.21 A (As) = 2.46 A][33], the Al−As single bond in **4d** seems to be slightly lengthened. The phosphorus and arsenic atoms in **4c−d** reside in pyramidal environments [sum of bond angles: 316.2° (P) and 308.1° (As)]. Due to its position in the main-group V, the geometry at the arsenic atom is more pyramidalized than that at the phosphorus atom [cf. for example, the sum of bond angles in PCl_3 (300.9°) and $AsCl_3$ (296.1°)]. The pyramidal P and As atoms, as well as the geometric orientations of the EPh_2 fragments relative to the N_2Al planes, prevent the formation of Al−E pp(π) bonds.

Figure 6. Molecular structure of $tmp_2AlN(H)Ph$ (**4b**) in the solid state; thermal ellipsoids are shown at a 25% probability level[a]

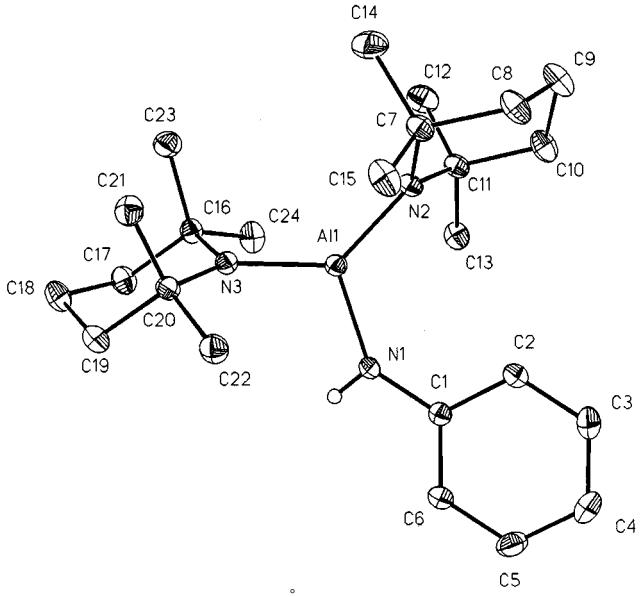

[a] Additional bond lengths [A] and bond angles [°]: Al(1)−N(1) 1.790(2); Al(1)−N(1)−C(1) 138.9(2), N(2)−Al(1)−N(1) 118.57(9), N(3)−Al(1)−N(1) 109.7(1), Al(1)−N(1)−H(1) 110.9(2), C(1)−N(1)−H(1) 110.1(2).

tmp_2AlPh (5a) (Figure 9) and $(tmp_2Al)_2Fec$ (5e) (Figure 10)

Colorless needles of **5a** are monoclinic, space group $C2/c$. There are four molecules in the unit cell, which suggests crystallographically imposed C_2 symmetry. The Al−C distances of 1.971(3) A (**5a**) and 1.952(3) A (**5e**) fall well within the range of published Al−C bond lengths for organylbis(amino)alanes [e.g. 1.970(3) A for Mes−Al[N(SiMe$_3$)$_2$]$_2$][15][38]. Due to the higher electronegativity of the ferrocenyl ligand, which is associated with more contracted orbitals, the Al−C bond in this compound is slightly shorter. The C−Al−N−C torsion angles are very

Figure 7. Molecular structure of tmp_2AlPPh_2 (**4c**) in the solid state; thermal ellipsoids are shown at a 25% probability level[a]

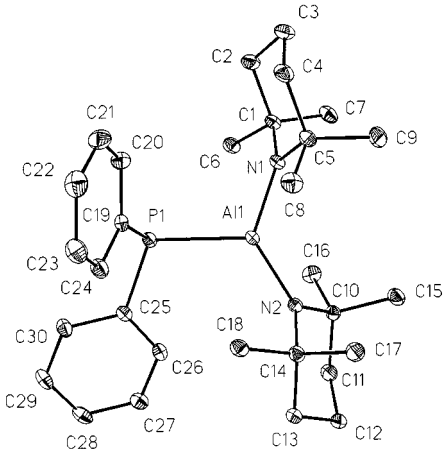

[a] Additional bond angles [°]: Al(1)−P(1) 2.377(1); Al(1)−P(1)−C(19) 100.55(8), Al(1)−P(1)−C(25) 110.90(9), N(1)−Al(1)−P(1) 109.35(7), N(2)−Al(1)−P(1) 121.76(7).

Figure 8. Molecular structure of $tmp_2AlAsPh_2$ (**4d**) in the solid state; thermal ellipsoids are shown at a 25% probability level[a]

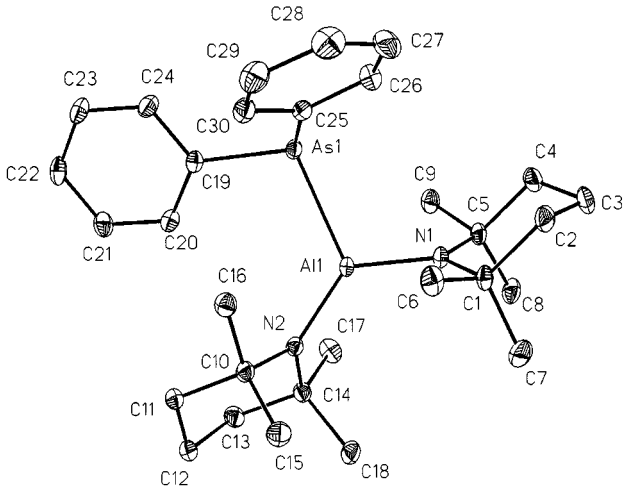

[a] Additional bond angles [°]: Al(1)−As(1) 2.485(2); Al(1)−As(1)−C(19) 108.3(1), Al(1)−As(1)−C(25) 97.6(1), N(1)−Al(1)−As(1) 108.8(1), N(2)−Al(1)−As(1) 122.1(1).

small (**5a**: 18.0°; **5e**: 7.2−15.8°), facilitating Al−C double bonding. However, closer examination of the reported Al−C distances in tetracoordinated alanes, which are not capable of bond shortening due to pp(π) interactions, is indicative of σ-bonding. Values of *d*(Al−C) similar to those in **5a** and **5e** are found in the tetracoordinated aminoalanes $(Me_2AlNC_6H_{12})_2$ [*d*(Al−C) = 1.963(6) and 1.986(7) A] and $(i\text{Bu}_2AlNMe_2)_2$ [*d*(Al−C) = 1.956(8) and 1.982(8) A][15][39]. In contrast to the crystal structures of the borylated ferrocenes $(Hal_2B)_nFec$ (Hal = Br, I; $n = 1-4$)[40], no Al−Fe interaction is apparent, which might have resulted from an interaction of the electron-deficient aluminum atom (with respect to an eight-electron system) and the electron-rich iron atom. The C−C−C−Al torsion angles of 12.5−12.9° reveal a bending of the $Altmp_2$ fragment away from the iron atom.

Figure 9. Molecular structure of tmp_2AlPh (**5a**) in the solid state; thermal ellipsoids are shown at a 25% probability level[a]

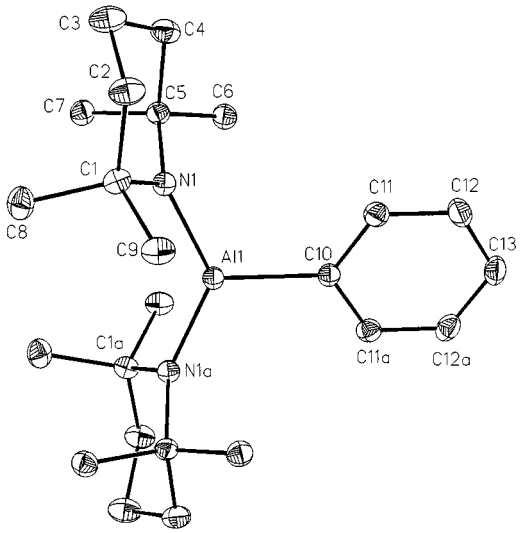

[a] Additional bond angles [°] and torsion angles [°]: Al(1)−C(10) 1.971(3); N(1)−Al(1)−C(10) 115.5(1); N(1)−Al(1)−C(10)−C(11) 18.0.

$tmp_2AlSi(SiMe_3)_3$ (5f)

The molecular structure of **5f** is depicted in Figure 11. Compared to a series of tetracoordinated silylalanes, which exhibit Al−Si distances of around 2.47 A[41], the bond length of 2.514(1) A found in **5f** is rather long, but is nevertheless in accordance with the steric demand of the ligands attached to the aluminum atom. Moreover, Linti et al. have prepared the homologous compound $tmp_2GaSi(SiMe_3)_3$, which, according to its crystal structure, exhibits the same structural features (e.g. long Ga−Si and Ga−N distances)[26] as **5f**. The decreased Si−Si−Si bond angles (av. 103.5°) may be attributable to steric factors, but could also be taken as an indication of a polar Al−Si bond (strong repulsion between the Al−Si σ-electrons and the Me_3Si groups due to the negative charge), since comparable angles have been found in the lithium silanides $(Me_3Si)_3SiLi^*(thf)_3$ and $(Me_3Si)_3SiLi(DME)_{1.5}$ (av. 102.4 and 104.0°)[42]. In the more relaxed $(Me_3Si)_3SiAlCl_3^-$, prepared by Stalke et al.[43], the Si−Si−Si bond angles are on average 110.0°.

$tmp_2AlH_2(9\text{-BBN})$ (6b)

6b forms colorless monoclinic crystals, space group *C*2/*c*, $Z = 4$ and possesses crystallographically imposed C_2 point group symmetry. The core of the structure consists of a four-membered AlH_2B ring. Since a twofold axis runs through Al1 and B1, this ring must be planar. The Al−H (1.738 A) and B−H (1.208 A) bond lengths are shorter than those found in aluminum tris(tetrahydroborate) $Al(BH_4)_3$ (1.80 A and 1.28 A). Moreover, *d*(Al−B) [2.223(7) A] is only 9 pm longer than the sum of their covalent radii (1.25 + 0.88 = 2.13 A)[33]. Assuming a bonding pattern as illustrated in Figure 13, the aluminum and boron atoms can be described as sp^2-hybridized, in accord with the large N−Al−N and C−B−C angles.

Figure 10. Molecular structure of $(tmp_2Al)_2Fec$ (**5e**) in the solid state; thermal ellipsoids are shown at a 25% probability level[a]

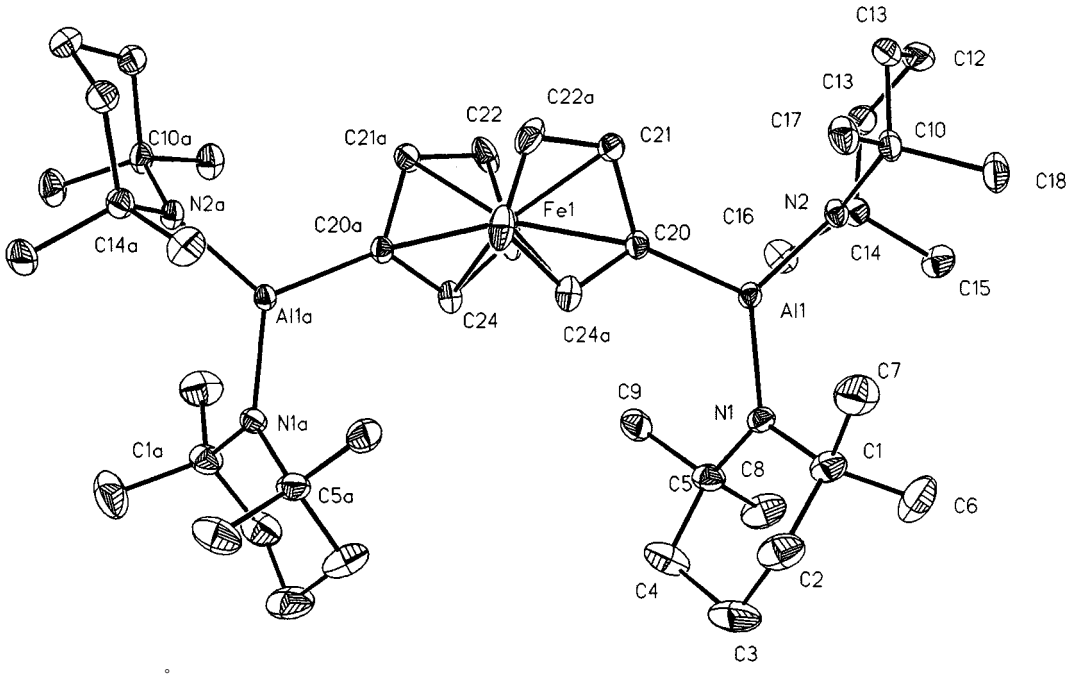

[a] Additional bond lengths [A] and bond angles [°] and torsion angles [°]: Al(1)−C(20) 1.952(3), Fe(1)−C(20) 2.103(3), Fe(1)−C(21) 2.036(3), Fe(1)−C(22) 2.028(3), Fe(1)−C(23) 2.049(3), Fe(1)−C(24) 2.065(3); N(1)−Al(1)−C(20) 117.4(1), N(2)−Al(1)−C(20) 116.1(1); C(21)−C(20)−Al(1)−N(2) 7.2, C(24A)−C(20)−Al(1)−N(1) 15.8.

Figure 11. Molecular structure of $tmp_2AlSi(SiMe_3)_3$ (**5f**) in the solid state; thermal ellipsoids are shown at a 25% probability level[a]

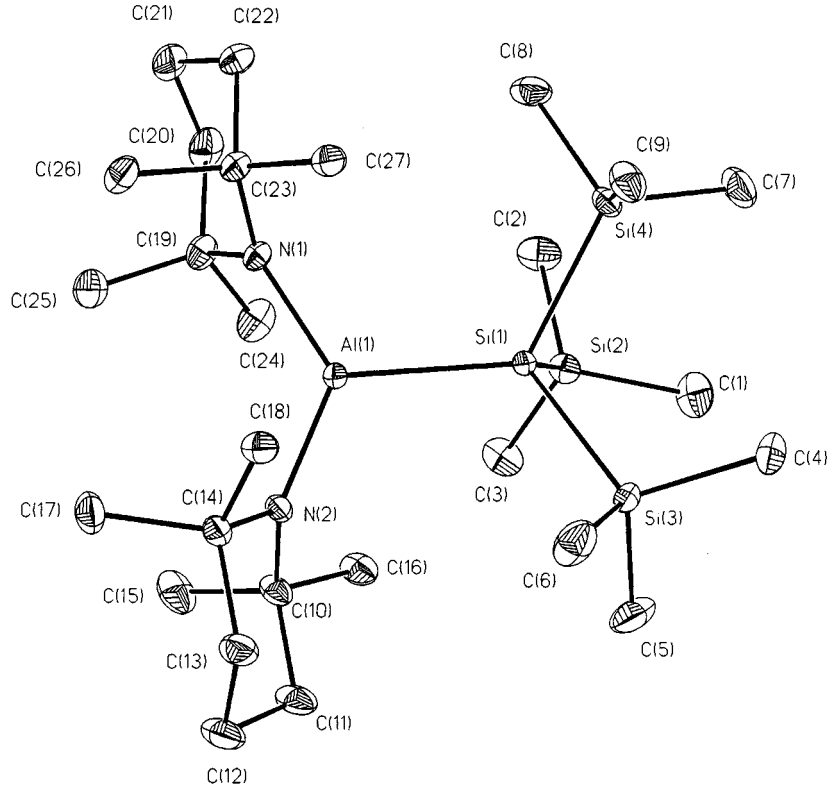

[a] Additional bond lengths [A] and bond angles [°]: Al(1)−Si(1) 2.5136(9), Si(1)−Si(2) 2.375(1), Si(1)−Si(3) 2.3703(9), Si(1)−Si(4) 2.3745(8); N(2)−Al(1)−Si(1) 117.81(6), N(1)−Al(1)−Si(1) 118.41(7), Si(3)−Si(1)−Al(1) 112.58(3), Si(4)−Si(1)−Al(1) 115.24(3), Si(3)−Si(1)−Si(4) 104.70(3), Si(3)−Si(1)−Si(2) 106.04(3), Si(4)−Si(1)−Si(2) 99.80(3), Si(2)−Si(1)−Al(1) 116.98(3).

Figure 12. Molecular structure of tmp_2AlH_2(9-BBN) (**6b**) in the solid state; thermal ellipsoids are shown at a 25% probability level[a]

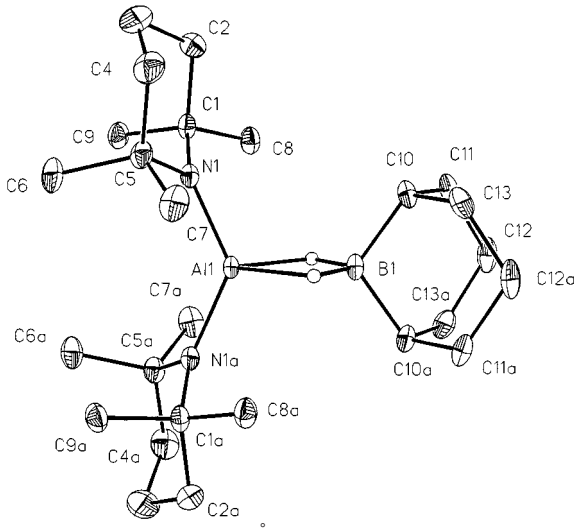

[a] Additional bond lengths [A] and bond angles [°]: Al(1)−B(1) 2.223(7), Al(1)−H(1) 1.738, B(1)−H(1) 1.208; N(1)−Al(1)−B(1) 113.8(1), H(1)−Al(1)−H(1A) 65.4, Al(1)−H(1)−B(1) 96.3, H(1)−B(1)−H(1A) 112.4.

Figure 13. Possible bonding pattern in **6b**

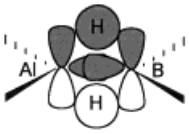

Whereas the N−Al−N angle in **6b** is as wide as 132.4°, and thus exceeds the 120° ideal by 12.4°, the C−B−C angle is only 110.2(6)°. Thus, the description of the bonding in **6b** is reminiscent of that of diborane[42]. A large exocyclic H−B−H angle of 121.8° and a short B−B distance of 1.71 A have been reported for this compound[42].

$(Ph_2PAlI_2)_3$ (4e)

Colorless prisms of **4e** crystallize in the trigonal space group $R\bar{3}$ with $Z = 24$ monomeric units. The six-membered ring is present in a chair conformation, (see Figure 14). The environment around each of the tetracoordinated Al and P atoms can be described as distorted tetrahedral, with maximum deviations of −8.2°/+4.6° from 109.5°. Values of d(Al−P) vary only slightly within the range from 2.435(2) to 2.461(3) A, and thus are very similar to the structural data of the trimeric phosphanylalane $(Me_2PAlMe_2)_3$ [d(Al−P) = 2.434(3) A], as determined by an electron diffraction study[24]. In contrast, the Al−P−Al [131.7(8)°] and P−Al−P [96.4(7)°] angles in $(Me_2PAlMe_2)_3$ differ considerably from those found in **4e** [114.8(1)−115.6(1)° and 108.2(1)−110.3(1)°]. Due to steric effects and bond polarity ($Al^{\delta+}-P^{\delta-}$), the Al−P−Al angles are widened compared to those in the cyclohexane ring. A siimilar behavior is observed in the homologous aminoalane trimers: Whereas in $(H_2Al-NMe_2)_3$ the Al−N−Al and N−Al−N angles are 114.9 and 108.8°, in $[Me_2Al-N(H)Me]_3$ these angles are 122.3 and 102.1°, respectively[24]. There is only a slight variation in the distance d(Al−I), the average being 2.532(2) A, which is in good agreement with the Schomaker-Stevenson corrected sum of the relevant sum of covalent radii (2.51 A)[33]. Moreover, for the compound $I_4Al_4(\mu\text{-}S)_2(\mu\text{-}SMe)_4$, which crystallizes in an adamantane-like Al_4S_6 framework bearing terminal iodine atoms, a similar bond length of 2.50 A has been reported[46].

Figure 14. Molecular structure of **4e** in the solid state; thermal ellipsoids are shown at a 25% probability level[a]

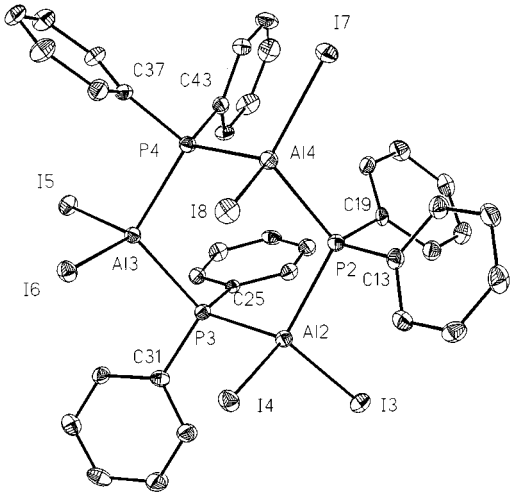

[a] Selected bond lengths [A] and bond angles [°]: Al(2)−P(2) 2.470(3), Al(2)−P(3) 2.461(3), Al(2)−I(3) 2.538(2), Al(2)−I(4) 2.541(2), Al(3)−P(3) 2.452(3), Al(3)−P(4) 2.438(3), Al(3)−I(5) 2.544(2), Al(3)−I(6) 2.525(2), Al(4)−P(4) 2.461(3), Al(4)−P(2) 2.444(3), Al(4)−I(7) 2.536(2), Al(4)−I(8) 2.521(2); Al(2)−P(3)−Al(3) 115.1(1), P(3)−Al(3)−P(4) 110.3(1), Al(3)−P(4)−Al(4) 114.8(1), P(4)−Al(4)−P(2) 108.2(1), Al(4)−P(2)−Al(2) 115.5(1), P(2)−Al(2)−P(3) 109.1(1), I(3)−Al(2)−I(4) 111.15(8), I(5)−Al(3)−I(6) 111.00(8), I(7)−Al(4)−I(8) 112.81(9).

$[MeAl(O_2Ctmp)_2]_2$ (5i)

Crystals of **5i** are very sensitive to warming and disintegrate when exposed to temperatures above −10°C (possibly due to a change of the modification?). The low-temperature phase is found to be monoclinic, space group $P2_1/c$, and contains two molecules in the unit cell (see Figure 15). The skeleton of **5i** is formed by two orthogonally linked, planar, eight-membered $C_2Al_2O_4$ rings, which meet at the pentacoordinated aluminum atoms. A C_4 axis (neglecting the Al−Me hydrogen atoms) passes through the Me−Al−Al−Me vector. The aluminum atoms reside in the center of a tetragonal pyramid, of which the four oxygen atoms form the base. The Al−Me groups are coordinated in an *exo* fashion, with short Al−C distances of 1.952(4) A to the pentacoordinated aluminum center. Longer Al−C bond lengths, up to 1.974(5) and 1.981(5) A, have been found for $\{AlMe_2[N(H)CH_2\text{-}2\text{-}Py]\}_2$[47]. The short Al−C bond in **5i** is due to the coordination of the Al center to four strongly electronegative oxygen atoms, which induce a positive charge at the Al atoms center, thereby reducing its effective radius due to coulombic interactions. The C30/31−N distances are consistent with a partial pp(π) double bond [d(C30/31−N) = 1.355(5) and 1.358(5) A]; the planes

through C_3N stand almost coplanar with those formed by the eight-membered rings. As indicated by the C−N−C−O torsion angles of 6.2 to 12.8°, C30 and C31 reside in planar environments, the O−C−O and N−C−O angles showing only very slight deviation from the 120° ideal (+/−0.5°). Coordination of the oxygen atoms to the aluminum nuclei is electrostatic, since the C−O−Al angles are found to be 133.4(3) to 136.4(3)°, and not of 115°, as would be expected for the appropriate hybridization of the oxygen atoms (intermediate between sp^2 and sp^3). In accordance with this description are quite long Al−O bonds, found in the range of 1.863(3) to 1.880(3) A, which adhere to the steric requirements of the carbaminate ligands.

Figure 15. Molecular structure of **5i** in the solid state; thermal ellipsoids are shown at a 25% probability level[a]

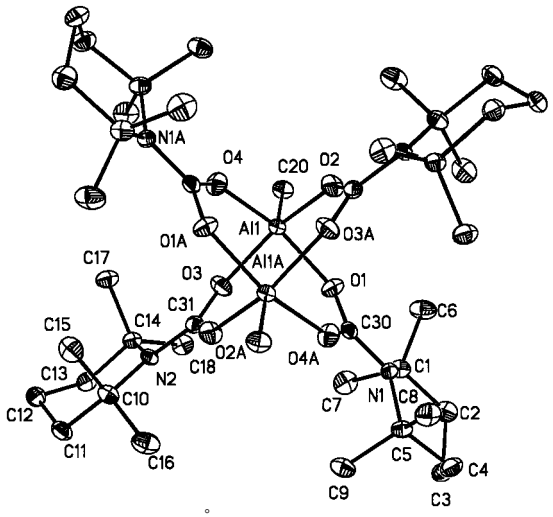

[a] Selected bond lengths [A] and bond angles [°] and torsion angles [°]: Al(1)−O(2) 1.863(3), Al(1)−O(3) 1.866(3), Al(1)−O(1) 1.873(3), Al(1)−O(4) 1.880(3), Al(1)−C(20) 1.952(4), O(1)−C(30) 1.271(5), O(2)−C(31A) 1.273(5), O(3)−C(31) 1.279(5), O(4)−C(30A) 1.270(4), N(1)−C(30) 1.358(5), N(1)−C(1) 1.524(5), N(1)−C(5) 1.527(4), N(2)−C(31) 1.355(5), N(2)−C(14) 1.516(5), N(2)−C(10) 1.520(4); O(2)−Al(1)−O(3) 149.2(1), O(2)−Al(1)−O(1) 85.6(1), O(3)−Al(1)−O(1) 86.1(1), O(2)−Al(1)−O(4) 86.3(13), O(3)−Al(1)−O(4) 86.0(1), O(1)−Al(1)−O(4) 149.4(1), O(2)−Al(1)−C(20) 105.3(2), O(3)−Al(1)−C(20) 105.5(2), O(1)−Al(1)−C(20) 105.1(2), O(4)−Al(1)−C(20) 105.5(2), C(30)−O(1)−Al(1) 133.4(3), C(31A)−O(2)−Al(1) 136.4(3), C(31)−O(3)−Al(1) 133.7(3), C(30A)−O(4)−Al(1) 136.1(3), C(30)−N(1)−C(1) 117.3(3), C(30)−N(1)−C(5) 117.2(3), C(1)−N(1)−C(5) 121.6(3), C(31)−N(2)−C(14) 117.1(3), C(31)−N(2)−C(10) 116.5(3), C(14)−N(2)−C(10) 123.4(3), O(4A)−C(30)−O(1) 120.8(3), O(4A)−C(30)−N(1) 119.7(3), O(1)−C(30)−N(1) 119.5(3), O(2A)−C(31)−O(3) 120.2(3), O(2A)−C(31)−N(2) 120.2(3), O(3)−C(31)−N(2) 119.7(3); C(5)−N(1)−C(30)−O(4A) 10.12, C(1)−N(1)−C(30)−O(1) 12.48, C(14A)−N(2A)−C(31A)−O(3A) 6.24, C(10A)−N(2A)−C(31A)−O(2) 12.82.

$[(Me_3Si)_3SiAl(OEt)_2]_2$ (5j)

The silylalane **5j** crystallizes in the monoclinic space group $P2_1/c$, with $Z = 2$ (see Figure 16). The central structural feature is, therefore, a four-membered, planar and crystallographically centrosymmetric Al_2O_2 ring [*d*(Al−O) = 1.833(4) A, O−Al−O = 80.7(2)°] with $(Me_3Si)_3Si$ and OEt ligands in *trans* positions. This is reminiscent of the recently published structure of $[tmp(Br)AlOEt]_2$, where these parameters are 1.827(6) A and 81.3(2)°, respectively[15]. The terminal Al−O distance [1.676(6) A] in **5j**, about 16 pm shorter than that of the Al−O bridge, is very similar to that found in $[H(OtBu)AlOtBu]_2$ [1.675(3) A][47]. The distance *d*(Al−Si) [2.444(2) A] is about 6 pm shorter than that in the starting material **5f** and other tetracoordinated silylalanes which show an average Al−Si distance of 2.47 A[39]. This lies at the lower end of the range of known Al−Si bond lengths, and indicates a relaxation in the steric strain on going from the tmp ligands to the EtO groups. Moreover, short Si−Si distances (2 pm shorter than that in **5f**) and acute Al−Si−Si angles are observed, which deviate up to 4.0° from the ideal angle of 109.5° (7.5° in **5f**).

Figure 16. Molecular structure of **5j** in the solid state; thermal ellipsoids are shown at a 25% probability level[a]

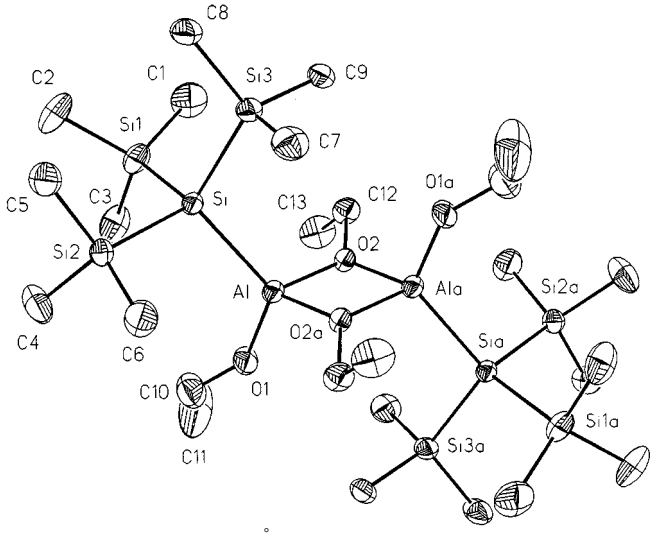

[a] Selected bond lengths [A] and bond angles [°]: Al−Si 2.444(2), Al−O(2A) 1.833(4), Al−O(1) 1.676(6), Al−O(2) 1.836(4), O(2)−Al(A) 1.833(4), Al−Al(A) 2.797(3), Si−Si(1) 2.350(2), Si−Si(2) 2.353(2), Si−Si(3) 2.353(2); O(1)−Al−O(2A) 106.0(2), O(1)−Al−O(2) 110.2(2), O(2A)−Al−O(2) 80.7 (2), O(1)−Al−Si 120.1(2), O(2)−Al−Si 115.3(1), Al(A)−O(2)−Al 99.3(2), Si(1)−Si−Si(3) 109.08(9), Si(3)−Si−Si(2) 107.94(9), Si(1)−Si−Si(2) 106.01(9), Si(3)−Si−Al 110.62 (8), Si(2)−Si−Al 109.86(8), Si(1)−Si−Al 113.11(9).

$[(Me_3Si)_3SiAl(OPh)_3]tmpH_2$ (5k) and $[(Me_3Si)_3SiAlCl_3]tmpH_2$ (5l)

Crystals of the triphenoxyaluminate **5h** are found to be monoclinic, space group $P2_1/n$. However, **5l** forms mixed crystals with $[tmpH_2]Cl$, a by-product of the reaction, without intermolecular contacts between the two species. Thus, the composition of compound **5l** corresponds to $[(Me_3Si)_3SiAlCl_3]tmpH_2*[tmpH_2]Cl$. The crystals are of the monoclinic space group $P2_1/c$, $Z = 4$. The aluminum atoms in **5k**, **l** reside in the centers of "tetrahedra" formed by three oxygen or chlorine atoms and one silicon atom (see Figures 17 and 18). Due to the steric demand of the phenoxy group, the angles in **5k** show larger deviation from the ideal value of 109.5° [97.4(1) to 117.1(1)°] than those in the trichloro derivative **5l** [104.7(1) to 113.0(1)°]. Both aluminate anions are linked to the $tmpH_2^+$ cations by hydrogen bonds. Whereas the triphenoxyaluminate **5k** forms two hydrogen

bonds to oxygen atoms incorporated in a six-membered, almost planar AlO_2H_2N ring, only one chlorine atom is coordinated by a hydrogen bond in **5l**. These atoms exhibit longer bond lengths to the aluminum center than their non-coordinated counterparts [**5k**: *d*(Al−O) = 1.775(3), 1.784(3) A vs. 1.736(3) A; **5l**: *d*(Al−Cl) = 2.187(3) A vs. 2.160(3), 2.166(3) A]. While the Al−Si distance in **5k** [2.468(3) A] corresponds to the average value[39] of 2.47 A, in the trichloro derivative **5l** it is only 2.420(3) A, which is even shorter than the Al−Si bond length found in the very similar compound $[(Me_3Si)_3SiAlCl_3]Li(thf)_4$ [2.446(1) A][41].

Figure 17. Molecular structure of **5k** in the solid state; thermal ellipsoids are shown at a 25% probability level[a]

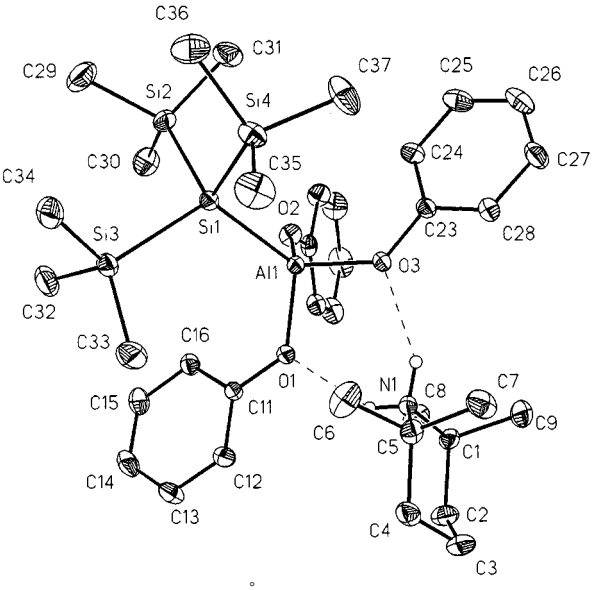

[a] Selected bond lengths [A] and bond angles [°]: Al(1)−O(1) 1.775(3), Al(1)−O(2) 1.736(3), Al(1)−O(3) 1.784(3), Al(1)−Si(1) 2.468(3), Si(1)−Si(2) 2.344(3), Si(1)−Si(3) 2.359(3), Si(1)−Si(4) 2.346(4); O(2)−Al(1)−O(1) 112.2(1), O(2)−Al(1)−O(3) 109.4(1), O(1)−Al(1)−O(3) 97.4(1), O(2)−Al(1)−Si(1) 107.2(1), O(1)−Al(1)−Si(1) 113.6(1), O(3)−Al(1)−Si(1) 117.1(1), Si(2)−Si(1)−Si(4) 106.6(1), Si(2)−Si(1)−Si(3) 104.24(9), Si(4)−Si(1)−Si(3) 105.41(9), Si(2)−Si(1)−Al(1) 107.0(1), Si(4)−Si(1)−Al(1) 115.2(1), Si(3)−Si(1)−Al(1) 117.4(1).

Al−N Bond Lengths and Related Structural Parameters

Although in the tricoordinated tmp_2AlY species **1−6** the tmp ligand is not changed, and thus little influence on *d*(Al−N) can therefore be expected, the observed Al−N bond lengths nevertheless vary from 1.782(6) to 1.862(4) A (see Table 2). These values are close to the shortest and longest Al−N distances reported for tricoordinated aminoalanes [e.g. 1.78(2) A for $Al[N(SiMe_3)_2]_3$, 1.782(4) A for $(MeAlNdipp)_3$, (dipp = 2,6-*i*Pr_2-C_6H_3) and 1.880(4) A for $tBu_2AlN(SiPh_3)_2$][12][13][14]. Moreover, an elongation of the Al−N bonds is observed when the ligand Y is varied from main-group VII (strongly electronegative ligands) to main-group III (electropositive ligands), reaching maximum values in the dialane(4)[48] [1.851(2) A] and the ferrioalane[16] [1.862(4) A]. An analysis of the structural parameters reveal a relationship between the N−Al−N bond angle and the Al−N bond lengths. For short Al−N bonds, a wide angle (> 130°) is noted, whereas compounds with long Al−N bonds exhibit smaller angles [down to 121.8(1)°]. This relationship cannot be associated with the steric effect of the attached ligands, since the sterically crowded aryloxide $tmp_2AlOdipp$ (**3b**) shows a large angle of 128.9(1)°, while the undemanding substituted ferrioalane **2** has a value of only 121.9(2)°. The orientation of perpendiculars through the nitrogen atoms in relation to the respective aluminum atoms indicates a strongly twisted orientation of the tmp ligands, with the relevant C−N−Al−E torsion angles (E = element) in **2−6** lying in the range of 57.4−82.9°.

Figure 18. Molecular structure of **5l** in the solid state; thermal ellipsoids are shown at a 25% probability level[a]

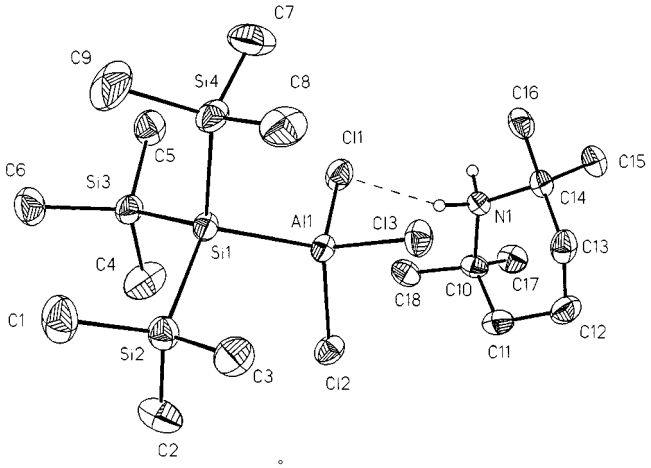

[a] Selected bond lengths [A] and bond angles [°]: Al(1)−Cl(3) 2.160(2), Al(1)−Cl(1) 2.187(3), Si(1)−Si(4) 2.331(3), Si(1)−Si(3) 2.342(3), Al(1)−Cl(2) 2.166(3), Al(1)−Si(1) 2.420(3), Si(1)−Si(2) 2.340(3), Si(2)−C(2) 1.858(5); Cl(3)−Al(1)−Cl(2) 106.48(7), Cl(2)−Al(1)−Cl(1) 104.66(1), Cl(2)−Al(1)−Si(1) 112.99(6), Si(4)−Si(1)−Si(2) 109.8(1), Si(2)−Si(1)−Si(3) 109.88(9), Si(2)−Si(1)−Al(1) 110.87(6), Cl(3)−Al(1)−Cl(1) 105.7(1), Cl(3)−Al(1)−Si(1) 115.5(1), Cl(1)−Al(1)−Si(1) 110.62(6), Si(4)−Si(1)−Si(3) 111.28(7), Si(4)−Si(1)−Al(1) 108.03(6), Si(3)−Si(1)−Al(1) 106.9(1).

Ab Initio Calculations of Model Compounds $(H_2N)_2AlY$

To gain an insight into the relationship between *d*(Al−N) and the N−Al−N bond angle, a series of ab initio calculations (MP2/6-31+G*)[17] has been performed on model compounds $(H_2N)_2AlY$, in which Y is systematically varied [Y = Cl (**7a**), OH (**7b**), SH (**7c**), NH_2 (**7d**), PH_2 (**7e**), CH_3 (**7f**), SiH_3 (**7g**), $Al(NH_2)_2$ (**7h**)]. The 6-31+G* basis set was chosen in order to provide a better approximation for the nitrogen lone pair and of the potentially highly polar Al−N bond. In this basis set, diffuse functions are implemented, which adequately describe electron density even far away from the nuclei. The structural parameters of the minimum structures are given in Table 3.

To understand the bonding situation in **7a−h**, natural bonding orbital analyses (NBO analyses) have been performed on the minimum energy structures. The results are listed in Table 3, and will be discussed later. It is apparent that the results of the calculations for the model compounds **7a−h** show the same trends as those observed in the crystal structures of **1−6**. The shortest Al−N bonds (1.782 A), are

Table 3. Calculated bonding parameters for bis(amino)alanes $(H_2N)_2AlY$ in their most stable configuration

Compound[a]	Sym.	d(Al−N) [A]	d(Al−E) [A]	N−Al−N [°]	q(Al) [e]	q(N) [e]	q(E) [e]	B.O. Al−N	LP[b] (Al)
$(H_2N)_2Al-Cl$ (**7a**)	C_{2v}	1.782	2.100	123.18	1.96	−1.53	−0.59	0.56	0.19
$(H_2N)_2Al-OH$ (**7b**)	C_s	1.786, 1.793	1.730	121.39	2.15	−1.54	−1.27	0.54, 0.55	0.17
$(H_2N)_2Al-SH$ (**7c**)	C_s	1.788, 1.791	2.192	121.39	1.89	−1.53	−0.66	0.55, 0.55	0.21
$(H_2N)_2Al-NH_2$ (**7d**)	D_{3h}	1.796	−	120.00	2.10	−1.53	−	0.53	0.19
$(H_2N)_2Al-PH_2$ (**7e**)	C_s	1.794	2.331	119.82	1.79	−1.53	−0.38	0.55	0.18
$(H_2N)_2Al-CH_3$ (**7f**)	C_s	1.799	1.962	117.91	2.00	−1.52	−1.33	0.54	0.15
$(H_2N)_2Al-SiH_3$ (**7g**)	C_s	1.797	2.451	119.09	1.67	−1.53	0.27	0.55	0.16
$(H_2N)_2Al-Al(NH_2)_2$ (**7h**)	D_2	1.804	2.579	116.71	1.40	−1.53	−	0.54	0.16

[a] All calculations MP2/6-31+G*.– [b] Number of electrons in $3p_z$ orbital of Al.

observed for the chloride **7a** and the longest for the dialane(4) **7h** (1.804 A); there is an inverse proportionality of d(Al−N) and the bond angle N−Al−N (large angles associated with short bond lengths). Moreover, the calculated Al−E bond lengths are in good agreement with the experimental values. Comparison with the crystal structures reveals that the observed correlation is not due to the steric requirements of the substituents, but is a consequence of the electronic situation (see Tables 2 and 3).

Discussion of Al−N Bonding

First of all, there is the paradox of the Al−N bonds: the shortest distances d(Al−N) ever found have been reported for compounds with tetracoordinated aluminum atoms [e.g. 1.767(3)−1.771(3) A in **9a**, 1.770(1) A in **9b**][49][50]. Therefore, the reason for the short bonds cannot be due to Al−N pp(π) interaction.

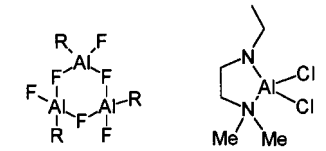

As all monomeric aminoalanes tmp_2AlX (**1**−**6**) contain planar tricoordinated nitrogen atoms in the tmp ligands, three Al−N bonding patterns (depicted in Figure 19) are possible to explain the trends in the Al−N bond lengths, namely pp(π) interaction (**D**), N(p)AlX(σ*) interaction (**E**), or a highly polar bonding situation (**F**).

Figure 19. Possible Al−N bonding patterns for the monomeric tmp_2AlY species **1**−**6**

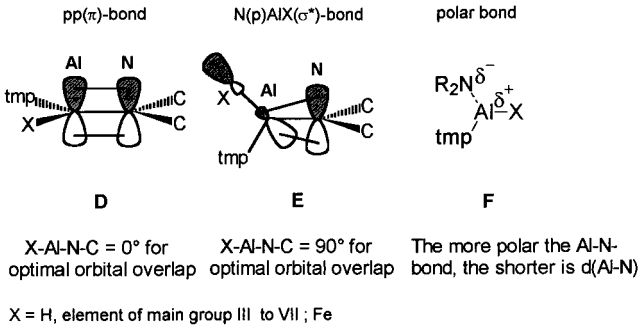

If pp(π) or N(p)AlX(σ*) interactions are responsible for the short Al−N distances, the tmp ligands should show a preference for a parallel orientation of the nitrogen lone pairs with respect to the free p_z orbital of the aluminum atom. Optimal orbital overlap for a pp(π) bond would be achieved with a C−N−Al−X torsion angle of 0°. For an N(p)AlX(σ*) bond, however, the corresponding C−N−Al−X torsion angle should be close to 90° (see Figure 19). If the Al−N bond is to be described as highly polar, these torsion angles should be a compromise between coulombic attraction ($Al^{\delta+}-N^{\delta-}$) and the steric requirements of the ligands. These three possibilities may be distinguished from a plot of d(Al−N) versus the C−N−Al−X torsion angle. Such a plot of 35 bond lengths versus the corresponding torsion angles for monomeric aminoalanes, (see Table 5) is depicted in Figure 20.

Figure 20. Plot of 35 Al−N bond lengths against the C−N−Al−X torsion angles

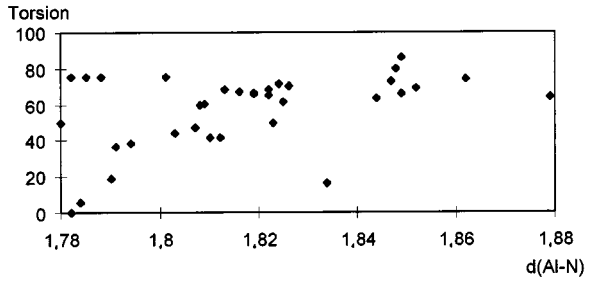

The C−N−Al−X torsion angles of short Al−N bonds reveal *no* preferential orientation of the attached ligands. Values between 0 and 80° are found for short d(Al−N) (< 1.80 A) values, indicating an absence of double bond contributions. Thus, a highly polar bonding situation for the Al−N bond is clearly the best description. Taking the geometry of the bis(tmp)borinium cation (**10a**) (linear; N−B−N angle: 180°) as the limiting case of an ideal bis(tmp)aluminum cation (**10b**), (a semiempirical AM1 calculation led to an N−Al−N angle of 171° for the tmp_2Al^+ cation)[51], for the present tmp_2AlY species **1**−**6**, the N−Al−N angle can be taken as an indicator of the extent of polarity of the Al−N bond (see Figure 21). Compounds tmp_2AlY with short, highly polar Al−N bonds, associated with loosely bound ligands R of low basicity, exhibit large N−Al−N angles, and vice versa. Figure 22 gives a graphical representation of the data collected for **1**−**6**. It can be

Table 4. Al−N distances and torsion angles of tmp_2AlY compounds

Compound	Ref.	d(Al−N) [Å]	Torsion angle [°]
tmp_2AlCl (**1a**)	[15]	1.785	75.2
		1.810	41.45
tmp_2AlBr (**1b**)	[15]	1.782	75.25
		1.812	41.23
tmp_2AlI (**1c**)	[15]	1.788	75.17
		1.803	44.2
$tmp_2AlOdipp$ (**3b**)	–	1.809	60.09
		1.808	59.45
tmp_2AlSPh (**3c**)	–	1.800	
		1.807	
		1.798	
		1.813	
tmp_2AlS*t*Bu (**3d**)	–	1.820	
		1.817	
$tmp_2AlN(H)Ph$ (**4b**)	–	1.790	18.79
		1.813	68.25
		1.822	68.7
tmp_2AlPPh_2 (**4c**)	–	1.819	65.97
		1.819	66.94
$tmp_2AlAsPh_2$ (**4d**)	–	1.816	67.55
		1.822	65.46
tmp_2AlPh (**5a**)	–	1.826	70.42
$(tmp_2Al)_2Fec$ (**5e**)	–	1.824	71.83
		1.825	61.79
$tmp_2AlSi(SiMe_3)_3$ (**5f**)	–	1.844	63.38
		1.848	79.68
$tmp_2Al-Altmp_2$ (**8**)	[48]	1.849	65.88
		1.852	68.9
$tmp_2AlFe(cp)(CO)_2$ (**2**)	[16]	1.847	73.03
		1.862	74.51
$Al[N(SiMe_3)_2]_3$	[12]	1.78	50
$trip_2AlN(H)dipp$	[56]	1.784	5.5
$tBu_2AlNMes_2$	[14]	1.823	49.5
$tBu_2AlN(dipp)(SiPh_3)$	[14]	1.834	16.1
$tBu_2AlN(Ad)(SiPh)_3$	[14]	1.849	86.3
$tBu_2AlN(SiPh_3)_2$	[14]	1.879	64.3
$MesAl[N(SiMe_3)_2]_2$	[36]	1.807	47.1
$(MeAlNdipp)_3$	[13]	1.782	0
$Al(NiPr_2)_3$	[31]	1.791	36.6
		1.794	38.3
		1.801	75.5

seen that d(Al−N) depends on the basicity of the substituent Y. Stabilized, weakly basic anions (like the halides) lead to strongly polar, short Al−N bonds, and vice versa. To obtain some appraisal of the influence of the basicity of the conjugate acid YH, the pK_a values of the Brønsted acids YH are plotted against d(Al−N) (Figure 23).

Figure 21. The N−Al−N angle as an indicator for a polar Al−N bonding situation

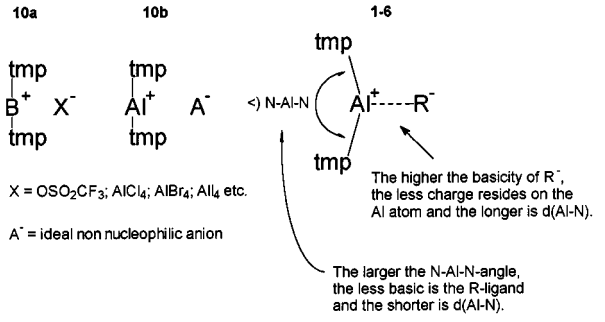

This representation reveals a good agreement with the experimental data. The insertion reaction of CO_2 with **5h** also supports the presence of a highly polar Al−N bond, as tmp_2AlMe (**5h**) possesses two reactive sites (Al−N and Al−C), of which the Al−Me site is undoubtedly also very polar. Even in the presence of excess CO_2, only the Al−N bond reacted to produce the carbaminate **5i**, leaving the Al−C bond intact. Moreover, solvolysis reactions of $tmp_2AlSi(SiMe_3)_3$ (**5f**) also support this assumption. Both the Al−N and Al−Si bonds are labile[23], but stoichiometric solvolysis reactions gave only the products of deamination, even though the Al−N bond is sterically more shielded than the Al−Si bond [cf. e.g. d(Al−N) = 1.846 Å vs. d(Al−Si) = 2.514 Å; d(C−N) = 1.50 Å vs. d(Si−Si) = 2.37 Å]. Thus, we conclude that the Al−N bonds in the present series of sterically encumbered, monomeric tmp_2AlY compounds **1**−**6** are best described as being highly polar. The degree of polarity, and thus d(Al−N), is governed by the third ligand Y.

Figure 22. Graphical representation of the dependence of d(Al−N) on the N−Al−N angles

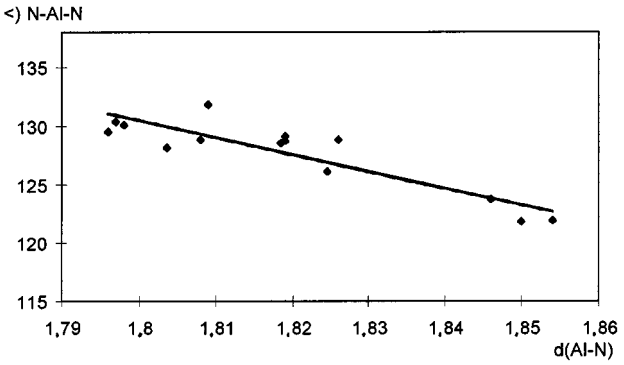

Figure 23. Plot of d(Al−N) of compounds tmp_2AlY versus the pK_a value of the corresponding Brønsted acid YH as a measure of its basicity

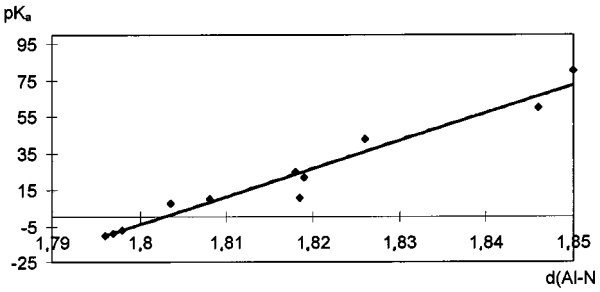

To evaluate the contributions from pp(π), N(p)AlX(σ*) and electrostatic interactions in small aminoalanes, ab initio calculations of some model compounds have been performed[17]. To understand their behavior, some results pertaining to the homologous aminoboranes are cited[10]. In the latter species, pp(π) interactions provide an additional stabilization enthalpy of up to 33 kcal/mol per B−N bond (cf. 65 kcal/mol found for the homoatomic and isoelectronic C=C double bond in ethylene)[10]. The planes around the boron and the nitrogen atoms of aminoboranes R_2NBX_2 are coplanar. In the coplanar ground state of $H_2B=NH_2$ (C_{2v}), d(B−N) is as short as 1.378 Å (calcd.). However, in the orthogonal transition state (C_s), the B−N distance is

elongated considerably (by about 9 pm) to 1.469 Å (calcd.). Due to saturation of the electron-deficient boron center, pp(π) contributions decrease with the attachment of an increasing number of π-donors. Applying this principle to aminoalanes, we will first discuss the results of ab initio calculations on H_2AlNH_2 (Figure 24: planar: **11a**; orthogonal: **11b**) and $Al(NH_2)_3$ (Figure 25: planar: **7d**; orthogonal: **12a**).

Figure 24. Structural parameters and results of the NBO analysis of **11a−b**

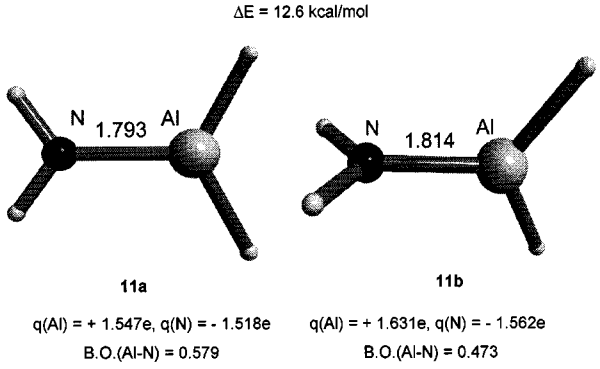

In contrast to the calculated structures for H_2BNH_2, the calculated C_{2v} structures of the planar ground state **11a** and the orthogonal transition state **11b** do not show marked differences in the values of *d*(Al−N) (1.793 vs. 1.814 Å), *d*(Al−H) (1.586 vs. 1.591 Å), Wiberg Al−N bond order (0.579 vs. 0.473) and NBO charges [*q*(Al): 1.547 vs. 1.631 e; *q*(N): −1.518 vs. −1.562 e]. Moreover, the NBO analysis reveals that in **11a** only 0.096 electrons are transferred from the N(p_z) orbital (populated with 1.905 electrons) to the 3p_z orbital of the aluminum atom. Thus, no effective pp(π) bond is formed, as is evident from the small energy difference on going to the orthogonal transition state **11b**. The pp(π) contribution amounts at most to 12.6 kcal/mol. In the transition state **11b**, which exhibits the requisite geometry for N(p)AlH(σ*) bonding, only 0.035 electrons are transferred from the N(p_z) orbital (containing 1.959 electrons) to the AlH(σ*) orbitals. Moreover, the Al−H bond is only very slightly lengthened (by 0.5 pm). These results are wholly consistent with a highly polar bonding situation, but not with effective pp(π) or N(p)AlH(σ*) bonding.

The tris(amide) $Al(NH_2)_3$ (D_{3h}) has been subjected to the same analysis in order to evaluate saturation effects, i.e. when more potential π-donors are bonded to the aluminum center (see Figure 25).

Here, the energy differences between the planar ground state **7d** and the orthogonal transition state **12a** are even smaller than those between **11a** and **11b**, even though three electronegative nitrogen atoms are present in the tris(amide), further supporting the argument for a polar bonding situation. Thus, the differences between the data for **7d** and **12a** amount to only 2.1 pm [*d*(Al−N)], 0.107 e [*q*(Al)], 0.029 e [*q*(N)] and 0.076 (Wiberg Al−N bond order). In **7d**, 0.189 electrons are transferred into the 3p_z(Al) orbital, while in **12a** only 0.043 electrons are transferred into the Al−N σ* orbital. Moreover, the pp(π) contribution per Al−N bond,

Figure 25. Structural parameters and results of the NBO analysis of **12a** and **7d**

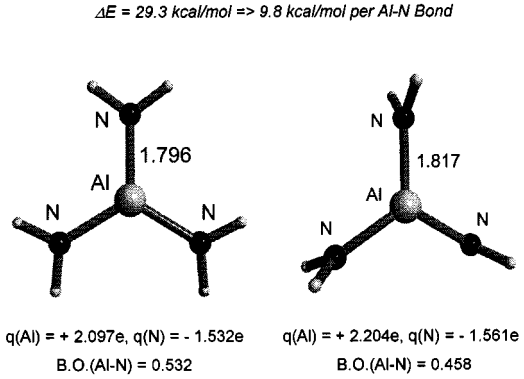

calculated by dividing the energy difference between **7d** and **12a** by three, decreases to 9.8 kcal/mol.

In the minimum energy structures of the bis(amino)alanes $(H_2N)_2AlY$ (**7a−h**) short Al−N bond lengths are associated with highly charged aluminum centers (see Table 3), and vice versa. Since only 0.15 to 0.21 electrons are transferred to the aluminum 3p_z orbitals [which negates the presence of strong pp(π) bonding] and the NBO charge on the nitrogen atoms remains essentially constant (−1.52 e to −1.54 e), the differences in the Al−N distances must be attributed to the influence of the third substituent Y. So Y has a significant effect on the charge at the aluminum atom (varying from +1.40 to +2.15 e), and, therefore, influences the coulombic interaction between Al and N, and consequently determines the Al−N bond lengths.

Conclusion

Bis(tmp)aluminum halides **1a−c** have been subjected to a series of nucleophilic substitution reactions in order to generate a systematically varied series of compounds tmp_2AlY (**2−6**). The tmp_2Al fragment not only prevents dimerization, but is also effective in stabilizing even and as yet "unusual" Al−E σ bonds (E = P, As, Si, Al, Fe). The distances *d*(Al−N) in these compounds vary from 1.782(6) to 1.862(4) Å. There is an inverse proportionality between the Al−N bond lengths and the N−Al−N bond angles. Ab initio calculations revealed the presence of very weak dative pp(π) bonding in hypothetical sterically non-demanding aminoalanes, which becomes weaker as the number of π-donors attached to the aluminum center increases. However, these pp(π) contributions (about 10 kcal/mol) are too weak to enforce on tmp_2AlY compounds geometric restrictions required to achieve optimal π-orbital overlap. Experimental and quantum mechanical results best describe the Al−N bond as being highly polar. The orientation of the tmp ligands is a compromise between the electrostatic attraction of the charged aluminum and nitrogen centers and the steric requirements of the tmp ligand. Moreover, in the tmp_2AlY system, *d*(Al−N) is a function of the pK_a value of the conjugate Brønsted acid Y−H: the stronger the acid Y−H, the higher the Al−N bond polarity and the shorter the Al−N bond lengths. Ab initio calculations reveal that

this effect can be attributed to the considerable influence that the ligand Y exerts on the charge at the aluminum atoms (variation from +1.40 to +2.15 e). Since the charge on the nitrogen atoms remains almost constant (−1.52 to −1.54 e), the differing Al−N distances can be rationalized in terms of the changing electrostatic attraction between the nitrogen and aluminum atoms, as influenced by the inductive effect of the third substitutent Y. These results not only reinforce the qualitative analysis of Al−N and Al−X bond lengths as summarized by P. J. Brothers and P. P. Power[15] but provide a much more systematic approach supported by ab initio calculations.

Investigations into the Lewis acidity of compounds tmp_2AlX (**1a−c**) and their potential to form adducts of the type tmp_2AlX*Do have been performed also. For example, the abstraction of the halide ion by strong halide abstractors with formation of ionic species $[tmp_2AlDo^+]Y^-$ (Y^- = non-nucleophilic anion) has been studied. These results will be part of forthcoming publications.

We thank the *Fonds der Chemischen Industrie* and the *Chemetall mbH* for support of our research. Moreover, we thank Mrs. *Käser* and Mrs. *Ullmann* for carrying out the C/H/N analyses, Mr. *P. Mayr*, Mr. *R. Waldhör* and Mr. *C. Miller* for recording many NMR spectra, Mrs. *D. Ewald* for mass spectra and Mrs. *E. Kiesewetter* for IR spectra.

Experimental Section

All manipulations were performed using Schlenk techniques under dinitrogen or argon. All solvents were rigorously dried prior to use and stored under N_2 or Ar. Due to insufficient protection against oxidation and hydrolysis of the air- and moisture-sensitive compounds while weighing for microanalysis, the C/H/N data are often not very accurate; Al^{3+} was determined by EDTA titration. NMR: Bruker ACP 200, Jeol GSX400 and Jeol GSX270. − IR: Nicolet FT-IR spectrometer model 6000; CsI plates, Nujol. − MS: Varian Atlas CH7 spectrometer.

tmp_2AlOPh (**3a**): Lithiation of PhOH (0.80 g, 8.5 mmol) was performed at ambient temperature in 20 ml of *n*-hexane by the addition of a solution of *n*BuLi (5.3 ml, 1.6 M, 8.5 mmol). Then, a solution of tmp_2AlBr in *n*-hexane (47.8 ml, 0.178 M, 8.5 mmol) was added at 25°C. The mixture was heated to reflux for 3−4 h. After removal of the insoluble material by filtration (0.86 g, calcd. LiBr 0.74 g), the yellowish filtrate was reduced to one-third of its original volume in vacuo and stored overnight at −20°C. 2.96 g (87%) of yellowish crystals was recovered, m.p. 80−85°C. − ^{1}H NMR (C_6D_6) (270 MHz): δ = 1.31 (t, 8 H, tmp-β-CH_2), 1.40 (s, 24 H, tmp-CH_3), 1.55 (m, 4 H, tmp-γ-CH_2), 6.8−7.4 (m, Ph-*H*, 5 H). − ^{13}C NMR (C_6D_6) (100 MHz): δ = 18.5 (tmp-γ-*C*H_2), 34.1 (tmp-*C*H_3), 39.7 (tmp-β-*C*H_2), 51.9 (N−*C*), 119.7 (Ph-*C*), 120.5 (Ph-*C*), 129.7 (Ph-*C*), 157.4 (Ph-*C*). − ^{27}Al NMR (C_6D_6) (70 MHz): δ = 75 ($\Delta_{1/2}$ = 8800 Hz). − $C_{24}H_{41}AlN_2O$ (400.59): calcd. C 71.96, H 10.00, Al 6.7, N 6.99; found C 67.99, H 10.12, Al 6.6, N 6.11.

$tmp_2AlOdipp$ (**3b**): dippOH (0.93 ml, 5.0 mmol), dissolved in 20 ml of *n*-hexane, was lithiated at ambient temperature by addition of *n*BuLi (3.2 ml, 1.6 M, 5.0 mmol) in *n*-hexane. To this solution, tmp_2AlCl in *n*-hexane (25 ml, 0.20 M, 5.0 mmol) was added and the mixture was heated for 3 h under reflux. Removal of the insoluble material by filtration yielded a yellowish solution. After reducing its volume to one-third and cooling to −78°C, yellowish crystals of **3b** (1.30 g, 54%) were formed and isolated, m.p. 97−99°C. − ^{1}H NMR (C_6D_6) (270 MHz): δ = 1.26 (t, 8 H, tmp-β-CH_2), 1.34 (s, 24 H, tmp-CH_3), 1.57 (m, 4 H, tmp-γ-CH_2), 1.27 (d, 12 H, *i*Pr-CH_3), 3.65 (sept, 2 H, Me_2C-*H*), 6.95 (dd, 1 H, Ar-*H*), 7.12 (d, Ar-*H*). − ^{13}C NMR (C_6D_6) (100 MHz): δ = 18.6 (tmp-γ-*C*H_2), 33.9, (tmp-*C*H_3), 40.2 (tmp-β-*C*H_2), 51.8 (N−*C*), 23.9 [(H)C(*C*H_3)$_2$], 26.9 [(H)*C*(CH_3)$_2$], 120.1 (Ar-*C*), 123.7 (Ar-*C*), 137.4 (Ar-*C*). − ^{27}Al NMR (C_6D_6) (70 MHz): δ = 85 ($\Delta_{1/2}$ = 9400 Hz). − $C_{30}H_{53}AlN_2O$ (484.75): calcd. C 74.33, H 11.02, Al 5.6, N 5.78; found C 71.56, H 11.27, Al 5.8, N 5.63.

tmp_2AlSPh (**3c**): Thiophenol (0.54 g, 4.9 mmol) was metallated with BuLi (4.9 mmol, 3.1 ml, 1.6 M) by stirring in hexane at −30°C. Then, tmp_2 AlBr (4.9 mmol, 25 ml of a 0.196 M solution in hexane) was added at 20°C. Stirring was continued for 14 h, and the solid material was removed by filtration. The yellow solution was then reduced in vacuo to one-third of its original volume. Cooling the solution to −78°C furnished crystals of **3c**, yield 1.0 g (49%). − ^{1}H NMR (C_6D_6) (270 MHz): δ = 1.30 (t, 8 H, tmp-β-CH_2), 1.45 (s, 24 H, tmp-CH_3), 7.00 (m, 3 H, *m*-*H*, *p*-*H*), 7.41 (m, 2 H, *o*-*H*), the tmp-γ-CH_2 protons are represented by an unresolved, very broad signal. − ^{13}C NMR (C_6D_6) (67.9 MHz): δ = 18.0 (tmp-γ-*C*H_2), 34.1 (tmp-*C*H_3), 39.2 (tmp-β-*C*H_2), 52.0 (N−*C*), 125.4 (*p*-*C*), 128.3 (*m*-*C*), 135.0 (*o*-*C*), 135.9 (1-*C*). − ^{27}Al: δ = 153 ($\Delta_{1/2}$ = 14000 Hz).

$tmp_2AlS(tBu)$ (**3d**): Prepared analogously to **3c** from *t*BuSH (0.41 g, 4.4 mmol), BuLi (2.8 ml, 1.6 M), tmp_2AlCl (4.4 mmol, 19.5 ml of a 0.228 M hexane solution). Yield 1.0 g of **3d** (58%), m.p. 87°C. − ^{1}H NMR (C_6D_6) (270 MHz): δ = 1.32 (t, 8 H, tmp-β-CH_2), 1.52 (s, 24 H, tmp-CH_3), 1.61 (s, 9 H, *t*Bu-CH_3). − ^{13}C NMR (C_6D_6) (100 MHz): δ = 18.5 (tmp-γ-*C*H_2), 34.3 (tmp-*C*H_3), 36.9 (C*Me*$_3$), 40.3 (tmp-β-*C*H_2), 44.4 (*C*Me$_3$), 52.3 (N−*C*). − ^{27}Al (C_6D_6) (70.4 MHz): δ = 152 ($\Delta_{1/2}$ = 8000 Hz). − $C_{22}H_{45}AlN_2S$ (396.65): calcd. C 66.62, H 11.43, N 7.06; found C 62.78, H 11.33, N 6.59.

$tmp_2AlNHtBu$ (**4a**): *t*BuN(H)Li (0.62 g, 7.8 mmol) was suspended in 20 ml of *n*-hexane. A solution of tmp_2AlBr (3.0 g, 7.8 mmol) in 45 ml of *n*-hexane was then added at ambient temperature. After heating the sample for 3 h under reflux, the insoluble material (0.86 g, calcd. LiBr 0.68 g) was filtered off and the filtrate reduced to one-third of its original volume and the solution stored overnight at −20°C. 1.46 g of **4a** (3.8 mmol, 49%) was recovered as a yellowish precipitate, m.p. 148−152°C. − ^{1}H NMR (C_6D_6) (400 MHz): δ = 1.45 (s, 24 H, tmp-CH_3), 1.32 (s, 9 H, *t*Bu-CH_3), 1.31 (t, 8 H, tmp-β-CH_2), 1.65 (m, 4 H, tmp-γ-CH_2). − ^{13}C NMR (C_6D_6) (100 MHz): δ = 18.7 (C2,C6), 34.3 (tmp-Me), 35.2 [C(*C*H_3)$_3$], 40.6 (C3,C5), 50.0 [*C*(CH_3)$_3$], 51.8 (C4). − ^{27}Al NMR (C_6D_6) (70 MHz): δ = 129 ($\Delta_{1/2}$ = 8900 Hz). − $C_{22}H_{46}AlN_3$ (379.61): calcd. Al 7.1; found 7.4.

$tmp_2AlNHPh$ (**4b**): Prepared as described for **4a**. PhNHLi (0.53 g, 5.3 mmol), tmp_2AlBr (48.2 ml, 0.11 M solution in *n*-hexane, 5.3 mmol). − Yield 1.32 g of **4b** (62%); m.p. 134−137°C. − ^{1}H NMR (C_6D_6) (400 MHz): δ = 1.38 (s, 24 H, tmp-CH_3), 1.31 (t, 8 H, tmp-β-CH_2), 1.65 (m, 4 H, tmp-γ-CH_2), 6.75 (t, 1 H, *p*-Ph-*H*), 7.00 (d, 2 H, *o*-Ph-*H*), 7.17 (t, 2 H, *m*-Ph-*H*). − ^{13}C NMR (C_6D_6) (100 MHz): δ = 18.8 (C2,C6), 33.9 (tmp-Me), 40.2 (C3,C5), 52.0 (C4), 117.5 (Ph-*C*), 118.7 (Ph-*C*), 129.2 (Ph-*C*), 150.3 (Ph-*C*-N). − ^{27}Al NMR (C_6D_6) (70 MHz): δ = 124 ($\Delta_{1/2}$ = 9600 Hz). − $C_{24}H_{42}AlN_3$ (399.60): calcd. Al 6.8; found 6.7.

tmp_2AlPPh_2 (**4c**): To a suspension of $LiPPh_2$ (1.19 g, 7.4 mmol) in 15 ml of *n*-hexane, a solution of tmp_2AlBr in *n*-hexane (50 ml, 0.11 M, 5.5 mmol) was added at ambient temperature and the mixture was kept for 4 h under reflux. A clear, yellow solution was removed from insoluble material by means of a syringe and reduced

in vacuo to one-third of its original volume. Storing the solution overnight at −20°C afforded 1.14 g (42%) of colorless crystals of **4c** [m.p. > 278°C (decomp.)]. − ^{1}H NMR ($CDCl_3$) (400 MHz): δ = 1.10 (t, 8 H, tmp-β-CH_2), 1.31 (s, 24 H, tmp-CH_3), 1.54 (m, 4 H, tmp-γ-CH_2), 7.10 (d, 4 H, Ar-*H*), 7.18 (t, 4 H, Ar-*H*), 7.52 (t, 2 H, Ar-*H*). − ^{13}C NMR ($CDCl_3$) (100 MHz): δ = 18.8 (tmp-γ-*C*H$_2$), 33.5 [d, ^4J(P,C) = 4.1 Hz, tmp-*C*H$_3$], 39.5 (tmp-β-*C*H$_2$), 52.0 (N-*C*), 126.2 (s, C_6H_5), 128.1 [d, ^3J(P,C) = 6.8 Hz, C_6H_5], 133.7 [d, ^2J(P,C) = 15.5 Hz, C_6H_5], 137.8 [d, ^1J(P,C) = 15.0 Hz, C_6H_5]. − ^{27}Al NMR ($CDCl_3$) (70 MHz): δ = 110 ($\Delta_{1/2}$ = 13400 Hz). − $C_{30}H_{46}AlN_2P$ (492.66): calcd. C 73.14, H 9.41, Al 5.5, N 5.69; found C 69.30, H 8.59, Al 5.5, N 4.85 (C/H/N: calcd. 15:23:1; found 16.7:24.6:1).

tmp$_2$AlAsPh$_2$ (**4d**): $LiAsPh_2$ (0.75 g, 3.2 mmol) was suspended in 20 ml of *n*-hexane and tmp$_2$AlBr (27.3 ml, 0.11 M, 3.0 mmol) in *n*-hexane was added at ambient temperature. Stirring overnight produced a yellow suspension (insoluble material as mentioned above), which was filtered off. The filtrate was reduced to one-third of its original volume and left for 4 d at −20°C. Colorless crystals of **4d** (0.93 g, 58%) separated; m.p. > 254°C (decomp.). − ^{1}H NMR ($CDCl_3$) (400 MHz): δ = 1.13 (t, 8 H, tmp-β-CH_2), 1.30 (s, 24 H, tmp-CH_3), 1.55 (m, 4 H, tmp-γ-CH_2), 7.14 (t, 4 H, Ar-*H*), 7.19 (t, 4 H, Ar-*H*), 7.54 (d, 2 H, Ar-*H*). − ^{27}Al NMR ($CDCl_3$) (70 MHz): δ = 74 ($\Delta_{1/2}$ = 18300 Hz). − $C_{30}H_{46}AlAsN_2$ (536.61): calcd. C 67.15, H 8.84, Al 5.0, N 5.22; found C 63.22, H 6.79, Al 4.9, N 5.25.

(Ph$_2$PAlI$_2$)$_3$ (**4e**): To a solution of tmp$_2$AlPPh$_2$ (0.52 g, 1.05 mmol) in 20 ml of benzene, AlI_3 (12.2 ml, 0.086 M, 1.05 mmol) in benzene was added at ambient temperature. Addition of 20 ml of *n*-pentane and cooling to 5°C led to the precipitation of 0.40 g (27%) of colorless crystals of **4e**, m.p. > 314°C (decomp.). − ^{1}H NMR (C_6D_6) (400 MHz): δ = 6.95 (m, C_6H_5, 12 H), 7.42 (t, C_6H_5, 6 H), 7.55 (t, C_6H_5, 12 H). − ^{13}C NMR (C_6D_6) (100 MHz): δ = 129.35 [d, ^3J(P,C) = 9.6 Hz], 131.35 [d, ^4J(P,C) = 11.1 Hz], 134.30 [d, ^2J(P,C) = 12.3 Hz, C_6H_5], 134.89 [d, ^1J(P,C) = 12.3 Hz, C_6H_5], 135.01 [d, ^1J(P,C) = 12.2 Hz, C_6H_5]. − ^{31}P NMR (C_6D_6) (81 MHz): δ = −42.9. − $C_{36}H_{30}Al_3I_6P_3$ (1397.89): calcd. Al 5.8, I 54.5; found Al 6.0, I 54.1.

tmp$_2$AlPh (**5a**): To a solution of tmp$_2$AlBr in *n*-hexane (50 ml, 0.11 M, 5.5 mmol), PhLi (2.42 ml, 2.27 M, 5.5 mmol) in *n*Bu$_2$O was added at ambient temperature, resulting in the immediate formation of a colorless precipitate. After stirring for 1/2 h, the suspension was allowed to settle. The clear, yellow supernatant solution was removed by means of a syringe reduced to one-third of its original volume and stored overnight at 8°C, resulting in the deposition of 1.54 g (73%) of colorless crystals of **5a**; m.p. 85−88°C. − ^{1}H NMR ($CDCl_3$) (400 MHz): δ = 1.32 (t, 8 H, tmp-β-CH_2), 1.29 (s, 24 H, tmp-CH_3), 1.66 (m, 4 H, tmp-γ-CH_2), 7.20 (d, 2 H, Ar-*H*), 7.23 (m, 1 H, Ar-*H*), 7.72 (dd, 2 H, Ar-*H*). − ^{13}C NMR ($CDCl_3$) (100 MHz): δ = 18.5 (tmp-γ-*C*H$_2$), 34.0 (tmp-*C*H$_3$), 40.6 (tmp-β-*C*H$_2$), 51.8 (N-*C*), 127.2 (s, C_6H_5), 127.8 (C_6H_5), 137.4 (C_6H_5), Al−C signal not observed. − ^{27}Al NMR ($CDCl_3$) (70 MHz): δ = 153 ($\Delta_{1/2}$ = 12300 Hz). − $C_{23}H_{41}AlN_2$ (384.43): calcd. C 74.98, H 10.75, Al 7.0, N 7.29; found C 73.19, H 9.88, Al 7.3, N 6.39.

tmp$_2$Al(nBu) (**5b**): To a solution of tmp$_2$AlBr (5.73 g, 14.8 mmol) in 80 ml of *n*-hexane, *n*BuLi (9.25 ml, 1.6 M, 14.8 mmol) in *n*-hexane was added dropwise at ambient temperature. To complete the reaction, the mixture was stirred for 1 h at ambient temperature. After removal of the insoluble material, the solvent of the yellow filtrate was removed in vacuo providing **5b** as a viscous oil, which could not be crystallized from various solvents. Yield 5.23 g (97%). − ^{1}H NMR ($CDCl_3$) (270 MHz): δ = 1.31 (t, 8 H, tmp-β-CH_2), 1.36 [s, 24 H, tmp-C(CH_3)$_2$], 1.65 (m, 4 H, tmp-γ-CH_2), 0.39 (t, 2 H, Bu-α-CH_2), 1.10 (t, 3 H, Bu-CH_3), 1.23 and 1.47 (2 m, each 2 H, β- and γ-CH_2). − ^{13}C NMR (C_6D_6) (100 MHz): δ = 18.7 (tmp-*C*4), 34.1 (tmp-*C*7−10), 40.5 (tmp-*C*3/5), 51.9 (tmp-*C*2/6), 14.1 (Bu-*C*4), 28.4 (Bu-*C*3), 29.1 (Bu-*C*2), Al−C signal not observed. − ^{27}Al NMR ($CDCl_3$) (70 MHz): δ = 164 ($\Delta_{1/2}$ = 13400 Hz). − MS: *m*/*z* = 364 [tmp$_2$AlnBu$^+$].

tmp$_2$AlC$_6$H$_4$OCH$_3$ (**5c**): A solution of *p*-bromoanisole (0.63 ml, 5.0 mmol) in 20 ml of THF was refluxed for 1 h with 0.13 g of Mg and then cooled to ambient temperature. To this Grignard solution (assuming 100% conversion), tmp$_2$AlBr (18.7 ml, 0.268 M, 5.0 mmol) in *n*-hexane was added and the mixture was refluxed overnight. After filtration, the collected precipitate (1.67 g) was extracted with 20 ml of CH_2Cl_2 (the insoluble material subsequently weighed 0.93 g). The combined filtrates were reduced to one-third of the original volume and then stored overnight at −20°C to yield 1.61 g (79%) of **5c** as a microcrystalline precipitate, m.p. > 100°C (decomp.). − ^{1}H NMR ($CDCl_3$) (400 MHz): δ = 1.36 (t, 8 H, tmp-β-CH_2), 1.34 [s, 24 H, tmp-C(CH_3)$_2$], 1.70 (m, 4 H, tmp-γ-CH_2), 3.79 (s, 3 H, O-CH_3), 6.85 (d, 2 H, Ar-*H*), 7.70 (d, 2 H, Ar-*H*). − ^{13}C NMR ($CDCl_3$) (100 MHz): δ = 18.6 (tmp-*C*4), 33.8 (tmp-*C*7−10), 40.6 (tmp-*C*3/5), 51.6 (tmp-*C*2/6), 54.6 (O-*C*H$_3$), 113.0, 139.1, 159.9 (Ar-*C*), Al−C signal not observed. − ^{27}Al NMR ($CDCl_3$) (70 MHz): δ = 160 ($\Delta_{1/2}$ = 19400 Hz). − $C_{25}H_{43}AlN_2O$ (414.61): calcd. Al 6.5; found Al 6.7.

(tmp$_2$Al)$_2$C$_2$B$_{10}$H$_{10}$ (**5d**): To a solution of 1,2-dicarba-*closo*-dodecaborane(12) (1.0 g, 6.9 mmol) in 20 ml of toluene, *n*BuLi in *n*-hexane (40.6 ml, 1.6 M, 64.9 mmol) (cooled to 0°C) was added dropwise over a period of 20 min. After 5 min, a colorless precipitate of 1,2-dilithio-1,2-dicarba-*closo*-dodecaborane started to separate. The mixture was then stirred for a further 1.5 h to ensure completion of the reaction. The precipitate was isolated by filtration, washed with two 20-ml portions of *n*-pentane, and dried in vacuo. The resulting colorless, pyrophoric powder was suspended in 40 ml of *n*-pentane and treated at −78°C with a solution of tmp$_2$AlI (6.1 g, 14 mmol, in 50 ml of *n*-hexane). The mixture was allowed to warm to room temperature, and stirring was continued for 2 d. Removal of the insoluble material by filtration left a yellow solution, from which the solvent was removed in vacuo. The nonvolatile, yellow-brownish oil was rigorously dried in vacuo and then subjected to analysis. Yield 2.57 g of **5d** (3.4 mmol, 49%). − ^{1}H NMR ($CDCl_3$) (270 MHz): δ = 1.29 (t, 8 H, tmp-β-CH_2), 1.32 [s, 24 H, tmp-C(CH_3)$_2$], 1.64 (m, 4 H, γ-CH_2). − ^{13}C NMR ($CDCl_3$) (100 MHz): δ = 18.3 (tmp-*C*4), 33.9 (tmp-*C*7−10), 40.2 (tmp-*C*3/5), 51.7 (tmp-*C*2/6), Al−C signal not observed. − ^{27}Al NMR ($CDCl_3$) (70 MHz): δ = 164 ($\Delta_{1/2}$ = 12300 Hz). − ^{11}B NMR ($CDCl_3$) (86.4 MHz): δ = −15.0 [(^1J(B,H) = 173.3 Hz], −13.8 [^1J(B,H) = 169.2 Hz], −11.7 [^1J(B,H) not resolved], −9.4 [^1J(B,H) = 161.8 Hz], −7.1 [^1J(B,H) = 187.3 Hz], −2.6 [^1J(B,H) = 145.0 Hz]. − $C_{38}H_{82}Al_2B_{10}N_4$ (757.16): calcd. C 60.28, H 10.92, N 7.40; found C 59.35, H 10.87, N 7.64.

(tmp$_2$Al)$_2$Fec (**5e**): $FecLi_2$ (1.1 g, 5.5 mmol) was suspended in 20 ml of *n*-hexane and tmp$_2$AlCl in *n*-hexane (50 ml, 0.20 M, 5.0 mmol) was added at ambient temperature. After stirring overnight, the insoluble material was removed by filtration and the resulting red filtrate was reduced to one-third of its original volume. Storage of the solution overnight at −20°C led to the deposition of red crystals of **5e** (2.10 g, 48%), m.p. 176−179°C. − ^{1}H NMR (C_6D_6) (400 MHz): δ = 1.45 (t, 8 H, tmp-β-CH_2), 1.57 (s, 24 H, tmp-CH_3), 1.73 (m, 4 H, tmp-γ-CH_2), 4.47 (t, 4 H, cp-*H*), 4.55 (t, 4 H, cp-*H*). − ^{13}C NMR (C_6D_6) (100 MHz): δ = 18.6 (tmp-γ-*C*H$_2$), 34.3 (tmp-*C*H$_3$), 40.6 (tmp-β-*C*H$_2$), 52.0 (N-*C*), 71.9 (C_5H_4Al), 79.1

Table 5. Crystallographic data and relevant data referring to the structure solution and refinement

Compound	$tmp_2AlOdipp$ (**3b**)	tmp_2AlSPh (**3c**)	$tmp_2AlStBu$ (**3d**)	$tmp_2AlN(H)Ph$ (**4b**)tmp_2AlPPh_2 (**4c**)	$tmp_2AlAsPh_2$ (**4d**)	$(I_2AlPPh_2)_3$ (**4e**)
Code	Kros31	Knab7	Knabe8	Kros16	Ingo10	Ingo13	Kros22
Chem. formula	$C_{30}H_{53}AlN_2O$	$C_{24}H_{41}AlN_2S$	$C_{22}H_{45}AlN_2S$	$C_{36}H_{72}Al_2N_4$	$C_{30}H_{46}AlN_2P$	$C_{30}H_{46}AlAsN_2$	$C_{15}H_{13}AlI_2P$
Formula weight	484.72	416.63	396.64	614.94	492.64	536.59	505.02
Cryst. size [mm]	0.2 × 0.2 × 0.3	0.4 × 0.5 × 0.5	0.2 × 0.3 × 0.4	0.2 × 0.32 × 0.6	0.3 × 0.3 × 0.4	0.5 × 0.5 × 0.6	0.12 × 0.2 × 0.4
Cryst. system	monoclinic	monoclinic	monoclinic	monoclinic	triclinic	triclinic	trigonal
Space group	$P2_1/c$	$P2(1)/n$	$P2(1)/n$	$C2/c$	$P1$	$P1$	$R3$
a [A]	17.008(1)	8.3000(14)	10.5638(2)	21.264(9)	10.1560(1)	10.156(3)	23.45920(1)
b [A]	10.760(8)	41.673(8)	14.66050(10)	7.876(4)	10.5220(1)	10.652(6)	23.45920(1)
c [A]	17.449(1)	14.044(2)	15.5048(2)	24.426(9)	15.154(7)	15.239(9)	23.45920(1)
α [°]	90	90.00	90.00	90	98.98(2)	98.93(5)	106.47
β [°]	110.462(1)	96.120(7)	96.84(1)	114.058(8)	90.51(2)	90.80(4)	106.47
γ [°]	90	90.00	90.00	90	117.980(1)	118.10(4)	106.47
V [A^3]	2991.8(4)	4829.9(14)	2384.15(6)	3735.5(3)	1406.3(7)	1429.4(1)	10902.49(8)
Z	4	8	4	4	2	2	24
$\rho_{calcd.}$ [Mg/m^3]	1.076	1.146	1.105	1.093	1.163	1.247	1.846
μ [mm^{-1}]	0.091	0.182	0.181	0.094	0.150	1.240	3.584
F(000)	1072	1824	880	1368	536	572	5688
Index range	$-21 \le h \le 21$	$-10 \le h \le 10$	$-13 \le h \le 13$	$-26 \le h \le 24$	$-3 \le h \le 11$	$0 \le h \le 11$	$-26 \le h \le 24$
Index range	$-13 \le k \le 13$	$-51 \le k \le 47$	$-18 \le k \le 16$	$-10 \le k \le 10$	$-11 \le k \le 10$	$-12 \le k \le 10$	$-25 \le k \le 25$
Index range	$-21 \le l \le 21$	$-16 \le l \le 15$	$-19 \le l \le 20$	$-33 \le l \le 25$	$-17 \le l \le 17$	$-18 \le l \le 18$	$-25 \le l \le 25$
2θ [°]	54.72	55.44	58.26	58.16	47.98	50.10	46.50
T [K]	193	183	193	213	223	233	193
Refl. collected	13267	21001	13292	9285	4611	4688	46312
Refl. unique	5691	7098	4779	3772	4335	4386	10154
Refl. observed (4σ)	3170	6131	2626	2794	3249	3633	7757
R_{int}	0.0474	0.0553	0.0513	0.0881	0.0213	0.0259	0.0890
No. of variables	319	521	246	199	315	315	685
Weighting scheme[a] x/y	0.0075/2.6126	0.0250/4.9687	0.0187/2.1682	0.0560/6.0270	0.0383/0.5694	0.0510/1.2191	0.0254/44.7300
GooF	1.163	1.214	1.186	1.193	1.030	1.038	1.186
Final R (4σ)	0.0543	0.0508	0.0476	0.0668	0.0405	0.0399	0.0427
Final $wR2$	0.0995	0.1151	0.0919	0.1473	0.0879	0.0934	0.0791
Larg. res. peak [e/A^3]	0.301	0.488	0.216	0.325	0.220	0.521	0.989

[a] $w^{-1} = \sigma^2 F_o^2 + (xP)^2 + yP$; $P = (F_o^2 + 2F_c^2)/3$.

(C_5H_4Al), Al−C signal not observed. − ^{27}Al NMR (C_6D_6) (70 MHz): δ = 59 ($\Delta_{1/2}$ = 7400 Hz). − $C_{46}H_{80}Al_2FeN_4$ (798.98): calcd. C 69.15, H 10.09, Al 6.8, N 7.01; found C 63.59, H 9.04, Al 6.5, N 6.27 (C/H/N: calcd. 11.50:20:1; found 11.77:19.93:1).

$tmp_2AlSi(SiMe_3)_3$ (**5f**): To a stirred solution of $(Me_3Si)_3SiLi{\cdot}3$ thf[52] (1.01 g, 2.14 mmol) in 30 ml of *n*-hexane, was added a solution of tmp_2AlBr (0.83 g, 2.14 mmol) in 12 ml of *n*-hexane. After stirring overnight, the solvent was evaporated in vacuo. The residue was extracted with 20 ml of *n*-pentane, filtered, and the filtrate reduced to one-third of its original volume. Cooling of the yellow solution overnight at −20°C led to the deposition of 0.76 g (65%) of colorless crystals of **5f**, m.p. 203−206°C. (^{1}H-NMR and ^{13}C-NMR spectra at various temperatures are depicted in the text). − ^{1}H NMR (C_6D_6) (270 MHz): δ = 0.44 [s, 27 H, $Si(CH_3)_3$], 1.36 (t, 8 H, tmp-β-CH_2), 1.49 [s, 24 H, tmp-$C(CH_3)_2$], 1.63 (m, 4 H, tmp-γ-CH_2). − ^{13}C NMR (C_6D_6) (100 MHz): δ = 5.3 [$Si(CH_3)_3$], 18.6 (tmp-*C*4), 33.8 (tmp-*C*7−10), 41.4 (tmp-*C*3/5), 53.1 (tmp-*C*2/6). − ^{27}Al NMR (C_6D_6) (70 MHz): δ = 186 ($\Delta_{1/2}$ = 12400 Hz). − ^{29}Si NMR (C_6D_6) (55 MHz): δ = −7.9. − $C_{27}H_{63}AlN_2Si_4$ (555.13): calcd. C 58.42, H 11.44, Al 4.9, N 5.05; found C 55.99, H 11.52, Al 5.0, N 4.92 (C/H/N: calcd. 13.50:31.50:1; found 13.27:32.54:1).

tmp_2AlMe (**5h**) *and $[(tmpCO_2)_2AlMe]_2$* (**5i**): To a solution of tmp_2AlCl (40 ml, 0.20 M, 8.0 mmol) in *n*-hexane, 10 ml of a freshly prepared solution of $LiSnMe_3$ (1.0 M, 10.0 mmol) in THF was added over a period of 30 min. After stirring the mixture overnight, all volatile materials were removed in vacuo and the residue was extracted with 30 ml of *n*-pentane. From a portion of this solution all volatiles were removed in vacuo and the maining oil was subjected to analysis by NMR and mass spectrometry and proved to be **5h**. − ^{1}H NMR (C_6D_6) (60 MHz): δ = −0.24 (s, 3 H, Al-CH_3), 1.45 (s, 24 H, tmp-CH_3), 1.40 (t, 8 H, tmp-β-CH_2), 1.70 (m, 4 H, tmp-γ-CH_2). − ^{13}C NMR (C_6D_6) (100 MHz): δ = −1.0 [Al(*C*H_3)], 18.5 (tmp-*C*4), 34.3 (tmp-*C*7−10), 40.4 (tmp-*C*3/5), 52.0 (tmp-*C*2/6). − ^{27}Al NMR (C_6D_6) (70 MHz): δ = 173. − MS (70 eV, 30°C): *m*/*z* (%) = 322 (41) [$tmp_2AlMe^{+\cdot}$].

Since crystals of **5h** could not be obtained from the *n*-pentane solution, 5 ml of diethyl ether was added. The solution was then cooled to −78°C (dry-ice). During the course of several weeks, CO_2 slowly diffused into the vessel and underwent insertion into the Al−N bonds, resulting in the deposition of colorless crystals of **5i** (1.93 g, 29%), m.p. 140−142°C. − ^{1}H NMR (C_6D_6) (400 MHz): (monomer): δ = −0.24 (br. s, Al-CH_3), 1.30 (t, 8 H, tmp-β-CH_2), 1.56 (s, 24 H, tmp-CH_3); (dimer): δ = −0.24 (br. s, Al-CH_3), 1.41, 1.44 (2 t, each 8 H, tmp-β-CH_2), 1.61, 1.64 (2 s, each 24 H, tmp-CH_3). − ^{13}C NMR (C_6D_6) (100 MHz): (monomer): δ = 16.2 (tmp-γ-*C*H_2), 29.3 (tmp-*C*H_3), 42.0 (tmp-β-*C*H_2), 57.3 (N-*C*), 170.1 (N-*C*O_2), Al−C signal not observed; (dimer): δ = 15.3, 16.5 (tmp-γ-*C*H_2), 29.7, 29.9 (tmp-*C*H_3), 39.4, 42.7 (tmp-β-*C*H_2), 57.0, 57.2 (N−*C*), 160.9 (N−*C*O_2), Al−C signal not observed. − ^{27}Al NMR (C_6D_6) (70 MHz): (monomer): δ = 21 ($\Delta_{1/2}$ = 1120 Hz); (dimer): δ = 9 ($\Delta_{1/2}$ = 980 Hz). − IR (Nujol): ν = 1582 cm^{-1}, ν(C=N)].

Table 5 *(Continued)*

Compound	tmp_2AlPh (**5a**)	$(tmp_2Al)_2Fec$ (**5e**)	Carbaminate (**5i**)	$tmp_2AlSi(SiMe_3)_3$ (**5f**)
Code	Kros21	Kros32	Kros33	Kros11
Chem. formula	$C_{24}H_{41}AlN_2$	$C_{46}H_{80}Al_2FeN_4$	$C_{45.33}H_{86}Al_2N_4O_8$	$C_{27}H_{63}AlN_2Si_4$
Formula weight	384.57	798.95	869.16	555.13
Cryst. size [mm]	0.5 × 0.5 × 0.7	0.15 × 0.2 × 0.3	0.1 × 0.2 × 0.2	0.25 × 0.25 × 0.45
Cryst. system	monoclinic	orthorhombic	monoclinic	triclinic
Space group	*C*2/*c*	*Pbcn*	*P*2(1)/*c*	*P*1
a [A]	11.256(6)	25.07(2)	11.61950(10)	11.418(1)
b [A]	20.869(1)	18.67(1)	11.299	11.915(1)
c [A]	10.672(5)	9.805(6)	20.827	16.129(2)
α [°]	90	90	90.00	93.17(1)
β [°]	113.11(1)	90	93.5030(10	109.08(1)
γ [°]	90	90	90.00	118.48(1)
V [A^3]	2305.7(2)	4589(5)	2729.11(2)	1762.9(3)
Z	4	4	2	2
$\rho_{calcd.}$ [Mg/m^3]	1.108	1.156	1.058	1.046
μ [mm^{-1}]	0.099	0.401	0.101	0.211
F(000)	848	1744	952	616
Index range	$-14 \le h \le 14$	$-32 \le h \le 32$	$-14 \le h \le 14$	$-11 \le h \le 9$
Index range	$-25 \le k \le 25$	$-23 \le k \le 24$	$-14 \le k \le 14$	$-13 \le k \le 12$
Index range	$-13 \le l \le 13$	$-11 \le l \le 12$	$-22 \le l \le 26$	$-18 \le l \le 18$
2θ [°]	57.50	55.10	58.40	49.00
Temp, [K]	193(3)	193	173	198
Refl. collected	6410	18335	15176	8085
Refl. unique	1956	4756	5308	5661
Refl. observed (4σ)	1235	3097	3231	4600
R_{int}	0.0565	0.0473	0.1065	0.0466
No. of variables	128	248	282	324
Weighting scheme[a] x/y	0.0564/3.2577	0.0249/5.6830	0.0980/4.2353	0.0411/0.7067
GooF	1.165	1.190	1.122	1.051
Final *R* (4σ)	0.0557	0.0537	0.0793	0.0393
Final *wR*2 °	0.1278	0.1062	0.2070	0.0950
Larg. res. peak [e/A^3]	0.227	0.356	0.901	0.308

− $C_{42}H_{78}Al_2N_4O_8$ (821.07): calcd. C 61.44, H 9.58, Al 5.1, N 6.82; found C 60.60, H 9.36, Al 5.0, N 6.72.

[(Me$_3$Si)$_3$Si(OEt)Al(μ-OEt)]$_2$ (**5j**): To a stirred solution of $tmp_2AlSi(SiMe_3)_3$ (0.78 g, 1.8 mmol) in 25 ml of *n*-hexane, was added 10 ml (3.5 mmol) of a 2% EtOH solution in *n*-hexane. The turbid mixture was exposed to ultrasound for 24 h and then filtered. The yellow filtrate thus obtained was reduced in vacuo to a volume of 5 ml and stored at −20°C, resulting in the deposition of 0.56 g (85%) of colorless crystals of **5j**. − ^{1}H NMR (C_6D_6) (270 MHz): δ = 0.17 [s, 54 H, Si(C*H*$_3$)$_3$], 1.20 (t, 6 H, OCH$_2$C*H*$_3$), 1.28 (t, 6 H, μ-OCH$_2$C*H*$_3$), 4.13 (q, 4 H, μ-OC*H*$_2$), 3.86 (q, 4 H, OC*H*$_2$). − ^{27}Al NMR (C_6D_6) (70 MHz): δ = 42.2 ($\Delta_{1/2}$ = 1660 Hz). − $C_{26}H_{74}Al_2O_4Si_8$ (729.53): calcd. Al 7.4; found 7.1.

[(PhO)$_3$AlSi(SiMe$_3$)$_3$]tmpH$_2$ (**5k**): To a stirred solution of $tmp_2AlSi(SiMe_3)_3$ (0.87 g, 2.0 mmol) in 25 ml of diethyl ether and 25 ml of *n*-hexane powdered phenol (0.37 g, 4.0 mmol) was added. The resulting suspension was stirred overnight, insoluble material filtered off, and the filtrate reduced in vacuo to a volume of 20 ml. Crystals of **5k** separated: yield 1.05 g (76%), m.p. 145−147°C. − ^{1}H NMR ($CDCl_3$) (400 MHz): δ = −0.04 [s, 27 H, Si(C*H*$_3$)$_3$], 1.36 (s, 12 H, tmp-C*H*$_3$), 1.45 [t, 4 H, ^{3}*J*(H,H) = 5.5 Hz, tmp-β-C*H*$_2$], 1.57 (m, 2 H, tmp-γ-C*H*$_2$), 6.78 [t, 3 H, ^{3}*J*(H,H) = 7.4 Hz, OPh-δ-C*H*], 6.97 [d, 6 H, ^{3}*J*(H,H) = 7.1 Hz, OPh-γ-C*H*], 7.17 [t, 6 H, ^{3}*J*(H,H) = 7.7 Hz, OPh-β-C*H*]. − ^{13}C NMR ($CDCl_3$) (100 MHz): δ = 3.4 [Si(*C*H$_3$)$_3$], 16.2 (tmp-*C*4), 28.3 (tmp-*C*H$_3$), 36.2 (tmp-*C*3/5), 57.4 (tmp-*C*2/6), 118.4 (OPh-β-*C*H), 120.5 (OPh-γ-*C*H), 129.5 (OPh-δ-*C*H), 158.7 (OPh-α-*C*H). − ^{27}Al NMR ($CDCl_3$) (70 MHz): δ = 91 ($\Delta_{1/2}$ = 1000 Hz). − ^{29}Si NMR ($CDCl_3$) (55 MHz): δ = −8.7. − IR (Nujol): ν = 3076 cm^{-1} [ν(N−H)]. − $C_{36}H_{62}AlNO_3Si_4$ (694.20): calcd. C 62.11, H 8.98, N 2.01; found C 60.57, H 8.80, N 2.1 (C/H: calcd. 1:1.72; found 1:1.73).

[(Me$_3$Si)$_3$SiAlCl$_3$][tmpH$_2$] (**5l**): To a stirred solution of $tmp_2AlSi(SiMe_3)_3$ (0.55 g, 1.25 mmol) in 40 ml of *n*-hexane at −70°C, was added HCl (21.9 ml of a 0.225 M solution of HCl in diethyl ether, 5.0 mmol). The mixture was then allowed to warm to ambient temperature and stirring was continued overnight. The insoluble material was filtered off, all volatiles from the solution were removed in vacuo, and the residue was dissolved in 15 ml of CH_2Cl_2. Cooling of this solution overnight at −20°C afforded colorless crystals of **5l**. Yield 0.41 g (65%), m.p. 154−155°C. − ^{1}H NMR ($CDCl_3$) (400 MHz): δ = 0.16 [s, 27 H, Si(C*H*$_3$)$_3$], 1.25 (m, 4 H, tmp-γ-C*H*$_2$), 1.52 (s, 24 H, tmp-C*H*$_3$), 1.67 (m, 8 H, tmp-β-C*H*$_2$). − ^{13}C NMR ($CDCl_3$) (100 MHz): δ = 0.9 [Si(*C*H$_3$)$_3$], 22.9 (tmp-*C*4), 35.0 (tmp-*C*7−10), 38.6 (tmp-*C*3/5), 58.0 (tmp-*C*2/6). − ^{27}Al NMR ($CDCl_3$) (70 MHz): δ = 133 ($\Delta_{1/2}$ = 3000 Hz). − ^{29}Si NMR ($CDCl_3$) (55 MHz): δ = −8.5. − $C_{18}H_{47}AlCl_3NSi_4$ (523.26): calcd. C 46.27, H 9.63, N 4.00; found C 45.79, H 9.50, N 3.64. − Crystal structure analysis was carried out with a crystal of the composition $[(Me_3Si)_3SiAlCl_3][tmpH_2][tmpH_2]Cl \cdot 0.25\ OEt_2$.

tmp$_2$AlH$_2$BH$_2$ (**6a**): A suspension of $LiBH_4$ (0.070 g, 3.3 mmol) in 20 ml of *n*-hexane was cooled to −78° C, and a solution of tmp_2AlBr (0.64 g, 1.7 mmol) in 5 ml of *n*-hexane was added dropwise. The mixture was then allowed to warm to ambient temperature and stirred overnight. Removal of the insoluble material by filtration yielded a yellow solution, which was reduced to a volume of 15 ml and stored overnight at −20°C. The resulting precipitate of **6a** (0.23 g, 42%) melted with decomposition at $T > 316$°C. − ^{1}H NMR (C_6D_6) (270 MHz): δ = 1.37 (s, 24 H, tmp-C*H*$_3$), 1.25 (t, 8 H, tmp-β-C*H*$_2$), 1.57 (m, 4 H, tmp-γ-C*H*$_2$). − ^{13}C NMR (C_6D_6) (100 MHz): δ = 52.5 (tmp-*C*2,6), 40.5 (tmp-β-*C*H$_2$), 34.0 (tmp-*C*H$_3$), 18.5 (tmp-γ-*C*H$_2$). − ^{11}B NMR (C_6D_6) (64 MHz): δ = −24.4 (quint) [^{1}*J*(B−H) = 85 Hz]. − ^{27}Al NMR (C_6D_6) (70 MHz):

Table 5 *(Continued)*

Compound	$Cl_3AlSi(SiMe_3)_3^-$ (**5l**)	$(Me_3Si)_3SiAl(OPh)_3^-$ (**5k**)	$[(Me_3Si)_3SiAlOEt_2]_2$ (**5j**)	tmp_2AlH_2(9-BBN) (**6b**)
Code	Kros17	Kros15	Kros19	Kros20
Chem. formula	$C_{28}H_{69.50}AlCl_4N_2Si_4O_{0.25}$	$C_{36}H_{62}AlNO_3Si_4$	$C_{13}H_{37}AlO_2Si_4$	$C_{26}H_{52}AlBN_2$
Formula weight	715.50	696.21	364.77	430.49
Cryst. size [mm]	0.2 × 0.1 × 0.1	0.3 × 9.3 × 0.2	0.24 × 0.3 × 0.6	0.2 × 0.3 × 0.4
Cryst. system	monoclinic	monoclinic	monoclinic	monoclinic
Space group	$P2_1/c$	$P2_1/n$	$P2_1/c$	$C2/c$
a [A]	17.59(2)	19.76(3)	9.2471(6)	13.2641(3)
b [A]	11.10(1)	12.05(2)	17.294(1)	19.7133(3)
c [A]	24.88(3)	20.35(3)	15.492(1)	10.9173(2)
α [°]	90	90	90	90
β [°]	108.7(3)	118.95(4)	106.891(1)	107.0650(1)
γ [°]	90	90	90	90
V [A^3]	4601(1)	4240(1)	2370.7(3)	2728.88(6)
Z	4	4	4	4
$\rho_{calcd.}$ [Mg/m^3]	1.033	1.091	1.022	1.048
μ [mm^{-1}]	0.399	0.192	0.288	0.089
F(000)	1554	1512	800	960
Index range	$-19 \le h \le 19$	$-25 \le h \le 25$	$-10 \le h \le 12$	$-25 \le k \le 25$
Index range	$-12 \le k \le 11$	$-15 \le k \le 15$	$-21 \le k \le 22$	$-25 \le k \le 25$
Index range	$-27 \le l \le 26$	$-25 \le l \le 24$	$-19 \le l \le 19$	$-13 \le l \le 11$
2θ [°]	46.5	58.22	57.44	57.08
T [K]	293(2)	293(2)	213	193
Refl. collected	17137	20920	11446	7410
Refl. unique	6411	8896	4797	2524
Refl. observed (4σ)	4878	5993	1934	1242
R_{int}	0.0500	0.0571	0.1124	0.1337
No. Variables	367	425	191	146
Weighting scheme[a] x/y	0.0765/4.8394	0.0374/3.7774	0.0330/5.2990	0.1397/8.4413
GooF	1.106	1.076	1.089	1.245
Final R (4σ)	0.0598	0.0471	0.0671	0.0802
Final $wR2$	0.1535	0.1026	0.1280	0.2517
Larg. res. peak [e/A^3]	0.315	0.636	0.346	0.299

[a] $w^{-1} = \sigma^2F_o^2 + (xP)^2 + yP$; $P = (F_o^2 + 2F_c^2)/3$.

δ = 125 ($\Delta_{1/2}$ = 7040 Hz). − IR (Nujol): $\tilde{\nu}$ [ν(B−H) region] = 2289 cm^{-1} vs, 2317 vs, 2341 vs, 2403 vs, 2455 m. − MS: m/z = 322 [$tmp_2AlH_2BH_2^+$]. − $C_{18}H_{40}AlBN_2$ (322.32): calcd. Al 8.4; found Al 8.9.

tmp_2AlH_2(9-BBN) (**6b**): LiH_2(9-BBN) (1.52 g, 6.25 mmol) was suspended in 20 ml of *n*-hexane. At ambient temperature, 25 ml of a 0.20 M *n*-hexane solution of tmp_2AlCl (5.0 mmol) was added and the mixture was stirred overnight. The clear, yellow solution was then reduced to one-third of its original volume. Cooling of the solution overnight at −20°C afforded 1.59 g (74%) of colorless crystals of **6b**, m.p. > 288°C (decomp.). − ^1H NMR (C_6D_6) (400 MHz): δ = 1.39 (s, 24 H, tmp-CH_3), 1.23 (t, 8 H, tmp-β-CH_2), 1.58 (m, 4 H, tmp-γ-CH_2), 1.60−2.20 (m, 14 H, 9-BBN-CH_2). − ^{13}C NMR (C_6D_6) (100 MHz): δ = 52.2 (tmp-*C*2,6), 41.1 (tmp-β-*C*H_2), 33.6 (tmp-*C*H_3), 18.4 (tmp-γ-*C*H_2), 24.6 (9-BBN-*C*H_2), 34.6 (9-BBN-*C*H_2), B−C signal not observed. − ^{11}B NMR (C_6D_6) (64 MHz): δ = −3.0 (s, $\Delta_{1/2}$ = 207.4 Hz ^1H-decoupled; $\Delta_{1/2}$ = 246.7 Hz ^1H-coupled). − ^{27}Al NMR (C_6D_6) (70 MHz): δ = 115 ($\Delta_{1/2}$ = 10700 Hz). − IR (Nujol): ν [ν(B−H) region] = 1706 cm^{-1} w, 1753 w, 1788 w, 1824 m, 1859 m, 1895 s, 1911 vs, 1955 vs, 1997 vs, 2057 s, 2200 w. − $C_{26}H_{52}AlBN_2$ (430.51): calcd. C 72.54, H 12.18, Al 6.3, N 6.51; found C 67.86, H 11.55, Al 6.4, N 5.54 (C/H/N: calcd. 13:26:1; found 14.28:28.97:1; C/H: calcd. 1:2; found 1:2.02).

X-ray Crystal Structure Determinations: Data collection for X-ray structure determinations was performed with a Syntex P4 or a Syntex R3 four-circle diffractometer, using graphite-monochromated Mo-K_α (0.71073 A) radiation. Single crystals were mounted in Lindemann capillaries and sealed under argon. Other data collections for X-ray structure determinations were performed with a Syntex P4 four-circle diffractometer equipped with a CCD area detector[53]. Single crystals were mounted in polyfluoroether oil and fixed on top of a glass fibre. Data collections were carried out at −80 to −100°C. All calculations were performed on PCs and workstations using the Siemens SHELXTL-Plus[54] or SHELX-93[55] software packages. The structures were solved by direct or heavy-atom methods and successive interpretation of the difference Fourier maps, followed by least-squares refinement. All non-hydrogen atoms were refined anisotropically. Hydrogen atoms were included in the final refinement in calculated positions by a riding model using fixed isotropic parameters. Relevant data relating to the crystallography, data collection and refinement are compiled in Table 4. Further details on the crystal structure determinations have been deposited with the Cambridge Crystallographic Data Centre and may requested by quoting the depository number CCDC-101483, the names of the authors, and the full journal citation.

[1] I. Krossing, Dissertation, University of Munich, **1997**.
[2] X-ray structure determinations.
[3] R. West, *Angew. Chem.* **1987**, *99*, 1231−1245; *Angew. Chem. Int. Ed. Engl.* **1987**, *26*, 1201.
[4] S. Masamune, *Angew. Chem.* **1991**, *103*, 916−937; *Angew. Chem. Int. Ed. Engl.* **1991**, *30*, 902.
[5] L. F. Guselnikov, N. S. Nametkin, *Chem. Rev.* **1979**, *79*, 529−577.
[6] H. Nöth, *Angew. Chem.* **1988**, *100,* 1664−1684; *Angew. Chem. Int. Ed. Engl.* **1988**, *27*, 1603.
[7] [7a] R. T. Paine, H. Nöth, *Chem. Rev.* **1995**, *95*, 343−379. − [7b] G. Linti, H. Nöth, R.T. Paine, *Chem. Ber.* **1993**, *126*, 875−887.
[8] H. G. von Schnering, M. Somer, M. Hartweg, K. Peters, *Angew. Chem.* **1990**, *102*, 6364; *Angew. Chem. Int. Ed. Engl.* **1990**, *29*, 5758.
[9] M. F. Lappert, P. P. Power, A. R. Sanger, R. C. Srivastava, *Me-*

tal and Metalloid Amides, Synthesis, Structures, Physical and Chemical Properties, Ellis Horwood Publishers, New York, **1980**.
[10] A. Haaland, *Angew. Chem.* **1989**, *101*, 1017–1032; *Angew. Chem. Int. Ed. Engl.* **1989**, *28*, 968.
[11] R. J. Wehmschulte, K. Ruhlandt-Senge, P. P. Power, *Inorg. Chem.* **1994**, *33*, 3205–3207.
[12] G. M. Sheldrick, W. S. Sheldrick, *J. Chem. Soc. A* **1969**, 2279–2282.
[13] K. M. Waggoner, H. Hope, P. P. Power, *Angew. Chem.* **1988**, *100*, 1765–1766; *Angew. Chem. Int. Ed. Engl.* **1988**, *27*, 1699–1705.
[14] M. A. Petrie, P. P. Power, K. Ruhlandt-Senge, *Inorg. Chem.* **1993**, *32*, 1135–41.
[15] P. J. Brothers, P. P. Power, *Adv. Organomet. Chem.* **1996**, *39*, 1–69. Particularly relevant to the present paper is the discussion of tricoordinate Al compounds with a $AlNC_2$, $AlN_{2\,C,}$ and AlN_3 core (p. 15 ff.).
[16] I. Krossing, H. Nöth, C. Tacke, M. Schmidt, H. Schwenk, *Chem. Ber.* **1997**, *130*, 1047–1052.
[17] I. Krossing, H. Nöth, B. N. Anand, *Inorg. Chem.* **1997**, *36*, 1979–1981.
[18] M. J. Frisch, G. W. Trucks, H. B. Schlegel, P. M. W. Gill, B. G. Johnson, M. A. Robb, J. R. Cheeseman, T. Keith, G. A. Petersson, J. A. Montgomery, K. Raghavachari, M. A. Al-Laham, V. G. Zakrzewski, J. V. Ortiz, J. B. Foresman, C. Y. Peng, P. Y. Ayala, W. Chen, M. W. Wong, J. L. Andres, E. S. Replogle, R. Gomperts, R. L. Martin, D. J. Fox, J. S. Binkley, D. J. Defrees, J. Baker, J. P. Stewart, M. Head-Gordon, C. Gonzalez, J. A. Pople, *Gaussian 94, Revision B.2*, Gaussian, Inc., Pittsburgh PA, **1995**.
[19] J. Mason, *Multinuclear NMR*, Plenum Press, New York and London, **1987**, 259–278.
[20] H. Lehmkuhl, *J. Organomet. Chem.* **1991**, *411*, 37–55.
[21] M. Hesse, H. Meier, B. Zeeh, *Spektroskopische Methoden in der organischen Chemie*, 4th ed., Georg Thieme Verlag, Stuttgart, New York, **1991**.
[22] R. T. Morrison, R. N. Boyd, *Lehrbuch der organischen Chemie*, 2nd ed., Verlag Chemie, Weinheim, New York, **1978**.
[23] P. C. Keller, *Inorg. Chem.* **1974**, *96*, 3073–3077.
[24] A. J. Downs (Ed.), *Chemistry of Aluminium, Gallium, Indium and Thallium*, Blackie Academic and Professional, London, **1993**, p. 3.
[25] A. Haaland, J. Hougen, H. V. Volden, G. Hanika, H. H. Karsch, *J. Organomet. Chem.* **1987**, *322*, C24.
[26] H. Nöth, *Chem. Ber.* **1983**, *116*, 3552–3557.
[27] G. Linti, R. Frey, W. Köstler, H. Urban, *Chem. Ber.* **1996**, *129*, 561–569.
[28] M. D. Healy, A. R. Barron, *Angew. Chem.* **1992**, *104*, 939–941; *Angew. Chem. Int. Ed. Engl.* **1992**, *31*, 921–928.
[29] K. Ruhlandt-Senge, P. P. Power, *Inorg. Chem.* **1991**, *30*, 2633–2637
[30] R. J. Wehmschulte, K. Ruhlandt-Senger, P. P. Power, *Inorg. Chem.* **1998**, *34*, 2593..
[31] M. Cesari, S. Cucinella, in *The Chemistry of Inorganic Homo- and Heterocycle* (Eds.: I. Haiduc, D. B. Sowerby), Academic Press, London, **1987**, vol.1, p.176–190.
[32] S. Schulz, A. Voigt, H. W. Roesky, L. Häming, R. Herbst-Irmer, *Organometallics* **1996**, *15*, 5252–5253.
[33] J. K. Ruff, *J. Am. Chem. Soc.* **1961**, *83*, 2835–2839.
[34] R. J. Wehmschulte, K. Ruhlandt-Senge, P. P. Power, *Inorg. Chem.* **1994**, *33*, 3205–3207.
[35] V. Shomaker, D. P. Stevenson, *J. Am. Chem. Soc.* **1941**, 63, 37–40.
[36] R. J. Wehmschulte. P. P. Power, *J. Am. Chem. Soc.* **1996**, *118*, 791–795.
[37] C. K. F. von Hänisch, C. Üffing, M. A. Junker, A. Ecker, B. O. Kneisel, H. G. Schnöckel, *Angew. Chem.* **1996**, *108*, 3003–3005; *Angew. Chem. Int. Ed. Engl.* **1996**, *35*, 108, 2875–2877.
[38] P. J. Brothers, R. J. Wehmschulte, M. M. Olmstead, K. Ruhlandt-Senge, S. R. Parkin, P. P. Power, *Organometallics* **1994**, *13*, 2792–2799.
[39] C. B. Lagrone, S. J. Schauer, C. J. Thomas, G. M. Gray, C. L. Watkins, L. K. Krannich, *Organometallics* **1996**, *15*, 2458–2464.
[40] A. Appel, PhD Thesis, University of Munich, **1996**; B. Wrackmeyer, U. Dörfler, M. Herberhold, *Z. Naturforsch., B* **1993**, *48*, 121–123; B. Wrackmeyer, U. Dörfler, W. Milius, M. Herberhold, *Polyhedron* **1995**, *14*, 1425-1431, 2683–2689.
[42] $Al(SiMe_3)_3{\cdot}OEt_2$, $Na[Al(SiMe_3)_4]$, $[Al(SiMe_3)_3]_2{\cdot}$tmeda, $[(Me_3Si)_2Al(NH_2)]_2$, $(Me_3Si)_3SiAl(C_6H_5)_2{\cdot}$thf, $Na[Al(SiMe_3)_4]{\cdot}2$ toluene in: M. L. Sierra, V. S. J. de Mel, J. P. Oliver, *Organometallics* **1989**, *8*, 2312–2316.
[43] G. Becker, H. M. Hartman, A. Münch, H. Riffel, *Z. Anorg. Allg. Chem.* **1985**, *530*, 29–42.
[44] A. Heine, D. Stalke, *Angew. Chem.* **1993**, *105*, 90–92; *Angew. Chem. Int. Ed. Eng.* **1993**, *32*, 121–123.
[45] H. F. Holleman, E. Wiberg, N. Wiberg, *Lehrbuch der anorganischen Chemie*, Walter de Gruyter, Berlin, New York, 101st ed., **1995**.
[46] S. J. Schauer, G. H. Robinson, *J. Coord. Chem.* **1993**, *30*, 197–214.
[47] A. Boardman, R. W. H. Small, I. J. Worall, *Inorg. Chim. Acta* **1986**, *120*, L23.
[48] S. J. Trepanier, S. Wang, *Organometallics* **1996**, *15*, 760–765.
[49] M. Veith, S. Faber, H. Wolfanger, V. Huch, *Chem. Ber.* **1996**, *129*, 381–384.
[50] I. Krossing, H. Nöth, unpublished results, publication in progress; see: I. Krossing, PhD Thesis, University of Munich, **1997**.
[51] H. W. Roesky, *Organometallics* **1997**, *16*, 1260–64.
[52] M. J. Zaworotko, J. L. Atwood, *Inorg. Chem.* **1980**, *19*, 268–271.
[53] Performed with the program: *Hyperchem*, V3.0, Autodesk, **1993**.
[54] [54a] H. Gilman, C. L. Smith, *J. Organomet. Chem.* **1968**, *14*, 91–101. – [54b] G. Gutekunst, A. G. Brook, *J. Organomet. Chem.* **1982**, *225*, 1–3. – [54c] A. Heine, R. Herbst-Irmer, G. M. Sheldrick, D. Stalke, *Inorg. Chem.* **1993**, *32*, 2694–2698.
[55] Siemens Industrial Automation, **1995**.
[56] *PC SHELXTL Rel. 5.03*, Siemens Analytical Instruments, Version 4.1, **1994**.
[57] G. M. Sheldrick, *SHELX-93*, University of Göttingen, **1993**.
[58] K. M. Waggoner, P. P. Power, R. J. Wehmschulte, K. Ruhlandt-Senge, M. M. Olmstead, M. He, M. M. Power, *Inorg. Chem.* **1993**, *32*, 2557–2564.

[97260]

Hydrolysis and Condensation Reactions of Transition Metal Alkoxides: Calorimetric Study and Evaluation of the Extent of Reaction

Juliette Blanchard, Martin In, Barbara Schaudel, and Clément Sanchez*

Laboratoire de Chimie de la Matière Condensée, Université Pierre et Marie Curie,
URA CNRS 1466, 4, Place Jussieu, F-75252 Paris Cedex 05, France
Fax: (internat.) +33 (0)1/ 44 27 47 69
E-mail: clems@ccr.jussieu.fr

Received January 5, 1998

Keywords: Sol-gel process / Polymers, inorganic / Transition metal alkoxides / ^{17}O-NMR spectroscopy

The behavior of titanium and zirconium alkoxides towards complexation and water addition is analyzed through water titration and calorimetric experiments. A simple model is presented, which allows evaluation of the mean hydrolysis and condensation constants, K_h and K_c, of both pure and complexed transition metal alkoxides in the sol state, through the analysis of consumed water versus initial hydrolysis ratio curves. These constants allow comparison of the extents of the hydrolysis and condensation reactions for sols obtained from several alkoxide precursors. The complexation ratio only affects the condensation constant K_c, whereas the hydrolysis constant K_h remains unchanged. Analysis of the K_h/K_c ratios has shown that in the sol state, silanol Si–OH groups are more stable than the Ti–OH or Zr–OH groups. Moreover, this study has shown that the proton concentration not only affects the kinetics, but also the final composition of the system. Calorimetric studies of the complexation and hydrolysis/condensation reactions have highlighted the role of coordination unsaturation of the transition metal alkoxides in the exothermicity of these reactions, clearly demonstrating that coordination unsaturation is the driving force behind the reactivity of these alkoxides towards nucleophilic species (e.g. water, complexing ligands, polar solvents).

Introduction

Sol-gel processes are a means of preparing dispersed materials through the growth of metal oxo-polymers in a solvent[1][2][3]. Indeed, sol-gel chemistry is based on inorganic polymerization reactions. Metal oxo-polymers can be obtained through hydrolysis and condensation of molecular precursors such as metal alkoxides $M(OR)_n$ (where M = Si, Ti, Zr, Al, Sn, Ce; OR is an alkoxy group, and n is the valence or the oxidation state of the metal). In the case of silicon alkoxides, these reactions are known to be equilibrium processes[4]. The present work demonstrates, through the use of ^{17}O-NMR spectroscopy, that, in the sol state, the hydrolysis and condensation reactions of titanium alkoxides also exhibit reversible behavior. These reactions start with the nucleophilic addition of hydroxylated groups to the electrophilic metal atom M, which leads to an increase of the coordination number of the metal atom in the transition state[3]. Consequently, the chemical reactivity of metal alkoxides toward nucleophilic reactions largely depends on the electrophilic character of the metal and its ability to increase its coordination number.

Silicon has a low electrophilicity and it remains tetracoordinated in the $Si(OR)_4$ alkoxide precursors, as well as in its oxide. Thus, silicon alkoxides are not very reactive and gelation times range from hours to several days. On the other hand, many non-silicate metal alkoxides including transition metal alkoxides, lanthanides, aluminum, tin alkoxides, etc. are coordinatively unsaturated and in most cases the metallic center exhibits a higher electrophilicity than silicon[5]. These alkoxides are consequently very reactive towards nucleophilic reagents. Both the higher electrophilicity and the coordination unsaturation of the metallic center can be invoked in explaining this higher reactivity of non-silicate alkoxides. However, coordination unsaturation seems to be the key parameter: titanium (χ = 1.32), zirconium (χ = 1.29), and cerium (χ = 1.17) have electronegativities χ lower than that of silicon (χ = 1.74), whereas the value for tin (χ = 1.89) is higher. Thus, the difference in electrophilicities of the metal atoms does not seem to be the key parameter to account fully for the much higher reactivity of these non-silicate tetravalent alkoxides. In the work described herein, we confirm experimentally that coordination unsaturation is the main driving force behind the reactivity of transition metal alkoxides.

Hydrolysis/condensation reactions of silicon alkoxides are rather slow, and consequently they can be monitored using many analytical techniques (e.g. chromatography, infrared spectroscopy[6]). Moreover, silicon has an isotope with a nuclear spin I = 1/2, so that ^{29}Si-NMR experiments offer the possibility of accurately characterizing the different species (monomers, oligomers, etc.) generated by hydrolysis and condensation[1][7][8][9][10]. This accurate NMR speciation allows the determination of kinetic and thermodynamic constants for the different reactions occurring during the formation of silica-based sol-gel materials (hydrolysis, condensation, transalcoholysis, esterification).

 © WILEY-VCH Verlag GmbH, D-69451 Weinheim, 1998 1434–1948/98/0808–1115 $ 17.50+.50/0

Hydrolysis and condensation reactions of non-silicate metal alkoxides must, on the other hand, be controlled by using inhibitors such as high proton concentration[8] or complexing ligands[9]. However, even in the presence of inhibitors, the kinetics are too fast to be monitored by the usual techniques employed for the characterization of silicon-based systems. Moreover, many of the most interesting systems, as far as the field of material science is concerned[1][2][3][4][5][6][7][8][9][10][11][12], are not amenable to study by NMR because they are paramagnetic (Fe^{III}, $Mn^{II,III}$, Co^{II}, etc.) or because they possess a strong quadrupolar moment ($^{47}Ti^{IV}$, $^{49}Ti^{IV}$, $^{91}Zr^{IV}$, $^{93}Nb^{V}$, etc.). Since it is extremely difficult to get detailed and specific information on the hydrolysis/condensation reactions of transition metal alkoxides, an alternative approach is to collect macroscopic information and to rely upon a model to estimate the chemical composition of the polycondensates. This approach has been very successful with regard to organic polymers. Preferentially, the analysis of the polycondensates should be done in the wet state, before any drying process that can result in further condensation reactions and therefore modify the chemical composition of the system. The development of new tools could be especially helpful in classifying the behavior of metal alkoxides towards complexation, hydrolysis, and condensation reactions. A better knowledge of the extent of these reactions is of paramount importance because the structures and morphologies of the resulting networks are strongly dependent on their relative contributions. Control of the growth of transition metal oxo-polymers can be achieved through changes in the chemical reactivity of each component. The hydrolysis ratio ($H = H_2O/M$), the use of a catalyst[8], of complexing ligands[11], or of a templating medium[12][13] are the main factors that must be mastered by the sol-gel chemist in order to achieve this control.

Taking titanium and zirconium alkoxides as examples, two main points will be discussed in this article: (i) the calorimetric behavior of transition metal alkoxides towards complexation and hydrolysis, and (ii) a model leading to an evaluation of mean hydrolysis and condensation pseudo-equilibrium (metastable equilibrium) constants of transition metal alkoxides through the analysis of water titration curves. This simple model, based on constants evaluated from a mean polymer formula, leads to a pertinent classification of the alkoxides, and allows determination of the extents of the hydrolysis and condensation reactions. However, because this model is simple, it necessarily involves certain approximations, which, of course, imply limitations. These limitations will be discussed in the context of the evolution of silica-based systems, for which hydrolysis and condensation constants have been evaluated using both the model and the speciation provided by ^{29}Si-NMR experiments.

Results and Discussion

Evidence of the Reversibility of Hydrolysis/Condensation Reactions

The ^{17}O-NMR spectrum of sample ① was recorded just before the second hydrolysis (a), 5 min. after the second hydrolysis (b), and after 24 h of ageing (c); the ^{17}O-NMR spectrum of sample ② was recorded 5 min. after the second hydrolysis (d), and after 24 h of ageing (e). The spectra obtained are presented in Figure 1.

Figure 1. (Left:) ^{17}O-NMR spectra of sample ①, just before the second hydrolysis (a), 5 min. after the second hydrolysis (b), and 24 h after (c). (Right:) ^{17}O-NMR spectra of sample ②, 5 min. after the second hydrolysis (d), and 24 h after (e).[a]

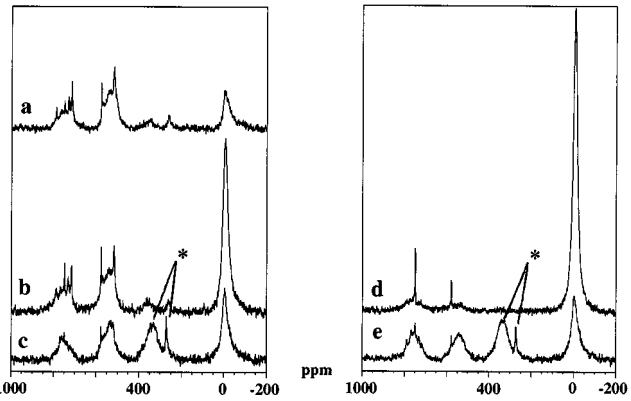

[a] For sample ①, the water used for the first and second hydrolyses was 5%-enriched in oxygen-17. – For sample ②, the first hydrolysis was performed with unenriched water and the second hydrolysis with 10%-enriched water. The total hydrolysis ratio of the sample was equal to 2. – The two peaks (see *) at $\delta = 273$ (enol form of free acetylacetone) and at about $\delta = 340$ (acetylacetone bonded to titanium) result from the isotopic ^{17}O exchange between H_2O and acacH (ketolization).

Spectrum (a) has already been described in a previous report[28]. Five signals are observed, which can be assigned as follows:

$\delta = 800-650$	μ_2O oxo-bridges
$\delta = 600-450$	μ_3O oxo-bridges
$\delta = 400-300$	μ_4O oxo-bridges
$\delta = 300-200$	μ_5O oxo-bridges
$\delta \approx 0$	H_2O

A second addition of water to sample ① resulted, after a short time spectrum (b)], in a significant increase in the intensity of the H_2O signal ($\delta = -50$ to 50), and in a slight increase in the intensity of the signals of the μ_2O and μ_3O oxo bridges (see Table 1); the intensities of the μ_4O and μ_5O oxo bridge signals remained the same, within an experimental error of ±10%. The ratio of residual water to oxo bridges, H_2O/Σ_{oxo}, was around 1:1. After 24 h of ageing, the intensities of the μ_2O and μ_3O oxo-bridge signals decreased slightly. The main evolution of the spectrum was seen in the $\delta = 200-400$ region, where a significant increase of the intensities was observed. In this chemical shift region, two kinds of signals can be observed:

- the signals of the μ_4O and μ_5O oxo bridges, which have been previously observed in the spectra (a) and (b);
- the signals of free and titanium-bound acac ($\delta = 273$ and 300–400, respectively).

The chemical shift and the width of the narrow peak ($\delta = 272$, $w = 370$ Hz) correspond exactly to those of free acac, and make the assignment of this peak to the free ligand unambiguous. The signal in the range $\delta = 300-400$ can be

Table 1. Intensities of the peaks of the spectra of Figure 1. For sample ①, the water used for the first and second hydrolyses was 5%-enriched in oxygen-17. For sample ②, the first hydrolysis was performed with unenriched water and the second hydrolysis with 10%-enriched water. The total hydrolysis ratio of the sample was equal to 2

		μ_2O (δ = 800−650)	μ_3O (δ = 600−400)	μ_4O or bonded acac (δ = 400−300)	μ_5O or free acac (δ = 300−200)	water (δ ca. 0)	sum of the intensities[a]
	before the 2nd hydrolysis (a)	4	7	1	<1	4	16
sample ①	5 min. after (b)	5	8	1	<1	14	28
	24 hours ageing (c)	4	7	5	1	9	26
sample ②	5 min. after (d)	2	3	–	–	25	30
	24 hours ageing (e)	7	6	5	1	10	29

[a] The sum of the intensities of the spectra of samples ① and ② after the second addition of water and after 24 hours of ageing are equal within an experimental error of ±10% and the sum of the intensities of sample ① before the second hydrolysis is about half of that of sample ② after the second hydrolysis, within an experimental error of ±15%.

assigned to both μ_4O oxo bridges (which are also observed in the spectrum recorded 5 min after the second hydrolysis) and to acac bonded to titanium. However, previous studies performed on acac-complexed and uncomplexed titanium butoxide have all shown a decrease in the intensity of the signal of the μ_4O bridges with time[28]. The significant increase of intensity observed in this chemical shift region after 24 h of ageing can therefore be mainly assigned to the enrichment of acac in oxygen-17, according to the reaction described in Scheme 1.

Scheme 1. Reaction leading to ^{17}O enrichment of the ketones

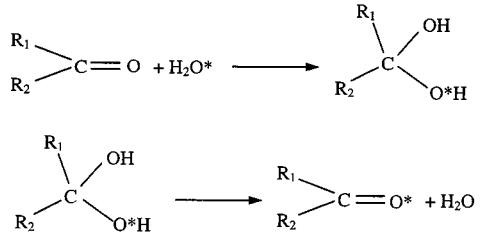

Just after the second addition of water, the spectrum of sample ② was very different to that of sample ①. In spectrum (d), the signals due to the μ_2O and μ_3O oxo-bridges are weak, and the ratio of residual water to oxo bridges, H_2O/Σ_{oxo}, is around 6:1. The evolution of the spectrum of sample ② over a period of 24 h was drastic spectrum 2, (e)]. In fact, after 24 h of ageing, it became very similar to that of sample ① (see Table 1 for the intensities of the oxo bridge signals and the water signal). One could also observe the appearance of two signals in the 200−400 region, which can be assigned to free and titanium-bonded acac, respectively.

For these two samples, when the second hydrolysis takes place, many oxo-bridges are already present following the addition of the first mole of water. The difference between these two samples is the as follows: in the case of sample ①, these pre-formed oxo-polymers are 5%-enriched in oxygen-17, whereas in the case of sample ②, these oxo-polymers are initially unenriched. The second addition of water leads to a further hydrolysis of the pre-formed oxo-polymers, which results in the formation of new oxo-bridges. This second mole of water is only partially consumed by the hydrolysis reaction and some water remains in solution. In the case of sample ①, the enrichment of the pre-formed polymers, of the new oxo bridges, and of the residual water is the same (5% in oxygen-17), whereas in sample ②, the unenriched pre-formed polymers are, after the second hydrolysis, in the presence of 10%-enriched water. The slight increase in the intensities of the μ_2O and μ_3O signals in spectrum (b) of sample ①, as well as the two weak μ_2O and μ_3O signals observed in spectrum (d) of sample ②, can be assigned to this further hydrolysis. On the other hand, the oxo-bridges that appear in the spectrum of sample ② after 24 h of ageing cannot be assigned to such a reaction because the intensities of these two peaks are only weakly modified after 24 h of ageing in the case of sample ①. This further modification of the spectrum of sample ② can therefore be attributed to ^{17}O exchange between the enriched water and the unenriched oxo-polymers. The pre-formed oxo-core is consequently accessible to nucleophilic species, and depolymerization/repolymerization reactions can occur. The depolymerization reactions imply the nucleophilic attack of a water molecule at the metallic center, and, therefore, an increase of its coordination. A mechanism can be proposed, in which the first step is the change of coordination of the acetylacetonate group from bidentate to monodentate; the water molecule can then occupy the empty coordination site and subsequently be incorporated into the network by intramolecular rearrangements[14].

This experiment highlights the equilibrium behavior of the hydrolysis and condensation processes. It was performed at a low hydrolysis ratio (H = 2) in order to avoid any quantitativity problems: at a higher initial hydrolysis ratio, part of the oxo signal is lost due to the formation of large titanium oxo-polymers that cannot be detected using solution ^{17}O-NMR[28]. However SAXS experiments[15][16] have shown that the titanium oxo-polymer sols and gels synthesized under these conditions are tenuous (the fractal dimension of the titanium oxo-polymers varies between 1.5 and 2.5, depending on the hydrolysis, complexation, or proton ratio). The fact that the structure of the oxo-polymers is non-dense indicates a high surface-to-volume ratio, which will favor the equilibria between the polymers and the water and alcohol molecules present in the solution. In the sol state, the swollen titanium oxo-polymers are not kinetically "locked-in".

Evaluation of Hydrolysis/Condensation Constants Through Water Titration Data

Curves showing the consumed water h as a function of the initial hydrolysis ratio H of the various alkoxides are shown in Figures 2−4. These curves have been fitted using Equation 5 and the values of K_h and K_c obtained are reported in Table 2 (See Experimental Section).

Figure 2. Hydrolysis of Ti(O*n*Bu)$_4$: variation of the consumed water h with the initial hydrolysis ratio H at different complexation ratios r

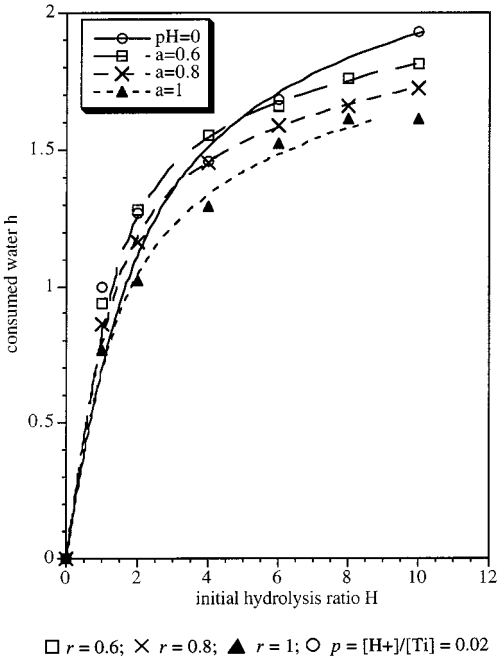

Figure 3. Hydrolysis of Zr(O*n*Pr)$_4$: variation of the consumed water h with the initial hydrolysis ratio H at different complexation ratios r

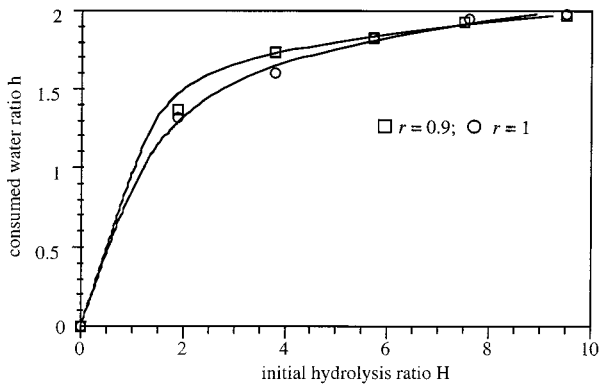

Titanium Oxide Based Sols

The curves $h = f(H)$ of Ti(O*n*Bu)$_4$ are presented in Figure 2. At low initial hydrolysis ratios ($H \leq 1$), the consumption of water is almost complete. At higher initial hydrolysis ratios, the water is only partially consumed and its consumption tends toward a limiting value that depends on the complexation ratio. The values of K_h and K_c calculated for this

Figure 4. Hydrolysis of Si(OEt)$_4$: variation of the consumed water h with the initial hydrolysis ratio H at different pH values of the hydrolysis solution

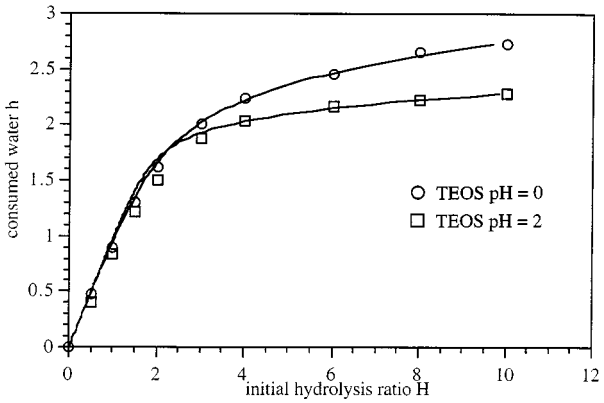

Table 2. Hydrolysis constants K_h and condensation constants K_c for reactions of Ti(O*n*Bu)$_4$, Zr(O*n*Pr)$_4$, Si(OEt)$_4$, calculated using Equation 5

Sample	Hydrolysis constant K_h	Condensation constant K_c
Ti(O*n*Bu)$_4$ $r = 0.6$	0.51 ± 0.01	16 ± 2
Ti(O*n*Bu)$_4$ $r = 0.8$	0.52 ± 0.01	15 ± 1
Ti(O*n*Bu)$_4$ $r = 1$	0.52 ± 0.1	8 ± 4
Ti(O*n*Bu)$_4$ $p = [H^+]/[Ti] = 0.02$	0.55 ± 0.04	16 ± 5
Zr(O*n*Pr)$_4$ $r = 0.9$	3 ± 1	30 ± 10
Zr(O*n*Pr)$_4$ $r = 1$	1.8 ± 0.5	7 ± 3
Si(OEt)$_4$ pH = 0	2.1 ± 0.2	6 ± 1
Si(OEt)$_4$ pH = 2	1.2 ± 0.1	26 ± 6

alkoxide do not depend strongly on the experimental conditions: K_h is equal to 0.5 in all cases (hydrolysis of acac-modified precursors or acidic hydrolysis). However, the value of K_c seems to depend slightly on the complexation ratio, increasing marginally as the complexation ratio decreases. The ratio $K_o = K_c/K_h$ is always very high (between 16 and 32), indicating that the majority of Ti−OH groups are engaged in forming oxo bridges. It is possible to calculate the theoretical values of $k = [M-O-M]/[M(OR)_4]$, h, $(h - k) = [M-OH]/[M(OR)_4]$, and $(4 - r - h - k) = [M-OR]/[M(OR)_4]$ from the values of K_h and K_c using Equations 5 and 6. Figure 5 shows the calculated consumed water ratio h, the condensation ratio k, the titanium hydroxyl ratio $(h - k)$ and the alkoxy ratio $(4 - r - h - k)$ as functions of the initial hydrolysis ratio H for $K_h = 0.51$ and $K_c = 16$ (i.e., for the complexation ratio $r = 0.6$). This simulation shows that the alkoxy ratio decreases very quickly: for an initial hydrolysis ratio $H = 10$, 90% of the alkoxy groups have been hydrolyzed. This simulation also shows that the Ti−OH ratio is very small at a low initial hydrolysis ratio; at higher initial hydrolysis ratios, however, the Ti−OH/Ti ratio becomes rather significant: at $H = 10$ it has a value of 0.5. This simulation is therefore an indirect proof of the presence in solution of such groups, the number of which increases with increasing initial hydrolysis ratio. The mean formula for the titanium oxo-polymers can be calculated from the fitted values of h, k, and r. As an

example, the mean formulae of the polymers obtained through hydrolysis ($0.5 < H < 10$) of one of the acac-modified samples ($r = 0.6$) are reported in Table 3. The self-consistency of this simple model can be checked by comparing the calculated Ti−OH/Ti ratio to that estimated from Karl-Fischer titrations. This estimation can be performed by carrying out the titration in two different solvents. The first one, 2-chloroethanol, is quite inert to the presence of M−OH groups, while the second one, methanol, reacts with M−OH groups to form M−O−Me groups with elimination of water. As a matter of fact, as shown in Figure 6 for the same sample (for example $r = 0.6$, $H = 2$), the measured consumption of water versus time in methanol solution is less than that measured in 2-chloroethanol. The difference between the two curves permits an evaluation of the M−OH/M ratio. This ratio was found to be 0.15, which is quite close to that calculated from the fitted K_h and K_c constants, and which leads to the following mean formula $[TiO_{1.09}acac_{0.6}(OH)_{0.16}(OR)_{1.06}]$.

Figure 5. Simulation of the curves h, k, $(h - k)$, $(4 - r - h - k) = f(H)$ for $K_h = 0.51$ and $K = 16$

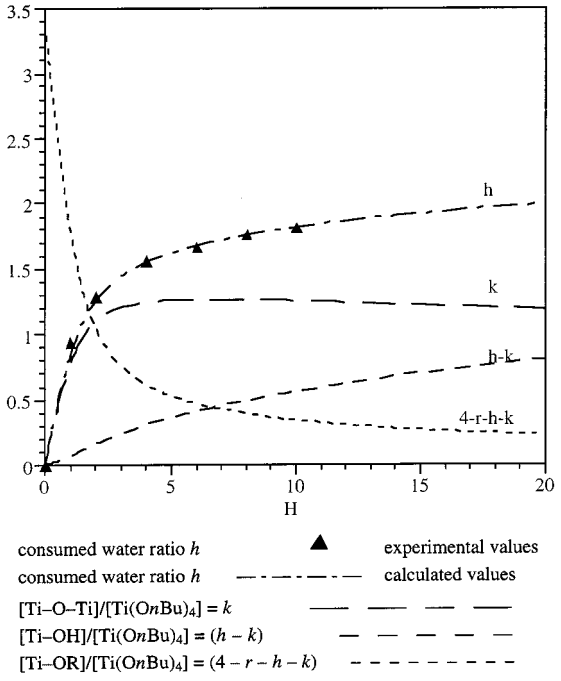

Figure 6. Comparison of the evolution of the residual water ratio $(H - h)$ *versus* time in two different solvents[a]

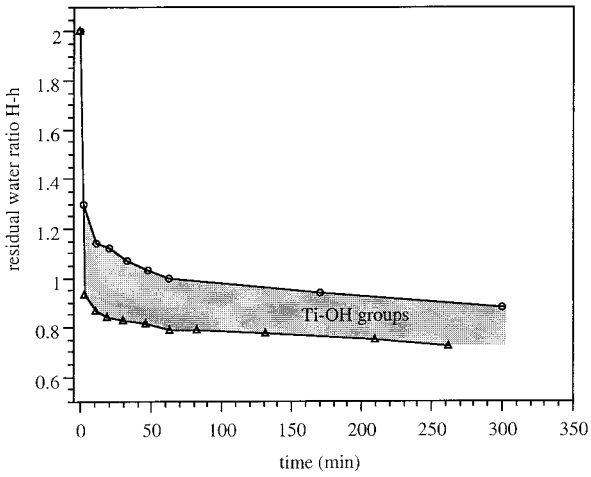

[a] ○ methanol, Δ 2-chloroethanol/chloroform for the system $Ti(OnBu)_4$; $r = 0.6$, $H = 2$

Zirconium Oxide Based Sols

The measured values of h as a function of H for $Zr(OnPr)_4$ complexed by acetylacetone ($r = 0.9$; $r = 1$) are plotted in Figure 3. The curves $h = f(H)$ have a shape similar to those for $Ti(OnBu)_4$: the consumption of water increases as H increases. At a low initial hydrolysis, ratio most of the water is consumed. At higher initial hydrolysis ratios, the $h = f(H)$ curves show marked deviations from linearity; the h values are invariably below 2, even at $H = 10$. These results underline the fact that the hydrolysis/condensation reactions are incomplete. The curves have been fitted using Equation 5 and the values of K_h and K_c obtained for these systems are reported in Table 2. The hydrolysis constants of the two systems are rather similar, but the condensation constant seems, as in the case of $Ti(OnBu)_4$, to increase as the complexation ratio decreases. These results allow quantification of the inhibitory effect towards condensation of complexing ligands such as acac.

Silicon Oxide Based Sols

Karl-Fischer titrations were performed for the two series of samples. The values of K_h and K_c are reported in Table 2 and the curves $h = f(H)$ are plotted in Figure 4. They are

Table 3. Mean formula of titanium oxo-polymers calculated from K_h and K_c values at different hydrolysis ratios and $r = [acac]/[Ti(OnBu)_4] = 0.6$. H is the $[H_2O]/[Ti]$ ratio, h is the consumed water ratio, Ti−O−Ti is the ratio of oxo bridges per titanium, Ti−OH is the ratio of hydroxo groups per titanium, and H_2O is the ratio of unconsumed water molecules per titanium

H	h	Ti−O−Ti	Ti−OH	Ti−OR	H_2O	structural unit
0	0	0	0	3.4	0	$Ti\ (acac)_{0.6}(OR)_{3.4}$
0.5	0.45	0.42	0.02	2.52	0.05	$TiO_{0.42}(acac)_{0.6}(OH)_{0.02}(OR)_{2.52}$
1	0.85	0.78	0.07	1.77	0.19	$TiO_{0.78}(acac)_{0.6}(OH)_{0.07}(OR)_{1.77}$
2	1.25	1.09	0.16	1.06	0.73	$TiO_{1.09}(acac)_{0.6}(OH)_{0.16}(OR)_{1.06}$
4	1.55	1.24	0.31	0.61	2.50	$TiO_{1.24}(acac)_{0.6}(OH)_{0.31}(OR)_{0.61}$
6	1.67	1.26	0.41	0.47	4.29	$TiO_{1.26}(acac)_{0.6}(OH)_{0.41}(OR)_{0.47}$
8	1.75	1.26	0.49	0.39	6.19	$TiO_{1.26}(acac)_{0.6}(OH)_{0.49}(OR)_{0.39}$
10	1.81	1.25	0.56	0.33	8.31	$TiO_{1.25}(acac)_{0.6}(OH)_{0.56}(OR)_{0.33}$

similar to those of the titanium and zirconium alkoxides. At low hydrolysis ratios, most of the water is consumed; at higher initial hydrolysis ratios, the consumed water ratio h remains below 3.

The curves $h = f(H)$ of $Si(OEt)_4$ hydrolyzed at pH 0 and pH 2 are quite different. The two curves are in fact similar up to $H = 2$, but at higher initial hydrolysis ratios, the pH 2 curve stays below the pH 0 curve. The hydrolysis constants of these two systems are close, but the condensation constant at pH 2 is 4 times as high as that at pH 0. This result is consistent with the fact that the condensation is more complete at pH 2 than at pH 0[1]. Protons are usually considered as catalysts for hydrolysis/condensation reactions[8][15]. The above result shows that the proton concentration will also change the final composition of the system, and thus the effect of the protons is not merely kinetic. Protonation of the oxo- or hydroxo-bridges is likely to assist the redissolution-polymerization processes occurring during the formation of the transition metal oxo-polymers[17].

For titanium and zirconium alkoxides, the only experimental value that can be measured is the consumed water h. The measurement of the condensation ratio k should however give relevant information for the determination of the hydrolysis and condensation constants. With the values of h and k, it is indeed possible to calculate K_h and K_c, for each value of H, directly from Equations 3 and 4. The condensation ratio k can be measured for silicon alkoxides by means of ^{29}Si-NMR spectroscopy, which distinguishes the silicon atoms according to their chemical environments. The chemical shifts of the species $SiO_n(OR,OH)_{4-2n}$ ($0 < n < 4$) are reported in Table 4. We have used the commonly accepted notation to describe these species: a silicon Q^n is a silicon having n −OSi neighbors and $(4 - n)$ −OR (−OH) neighbors.

The NMR spectra of the systems {$Si(OEt)_4 + H\ H_2O$, pH = 0; $0.5 < h < 10$ } are presented in Figure 7; they have been fitted in order to derive the percentages of the atoms Q^n, as given in Table 4. The condensation ratios were calculated by using the formula:

$k = (\%Q^1 + 2 \times \%Q^2 + 3 \times \%Q^3 + 4 \times \%Q^4)/(2 \times 100)$,

where $\%Q^n$ is the percentage of the silicon atoms Q^n.

The k values are reported in Table 5, together with the consumed water ratio measured by a Karl-Fischer titration, and the values of K_h and K_c. K_h and K_c were calculated only between $H = 1.5$ and $H = 4$; at higher values of H, the Si−OR/Si ratio is too small to obtain relevant values of K_h and K_c; on the other hand, at lower values of H, the Si−OH/Si ratio is too small.

K_h and K_c values calculated for these samples using Equation 5 are reported in Table 2. The values of K_h obtained by the two methods are quite similar; however, the K_c values are different (from NMR the mean K_c is 10−12, while the mean K_c is 6−7 from water titration). These differences are especially noticeable at higher hydrolysis ratios. This discrepancy between the values of K_c obtained from ^{29}Si-NMR data and from the modelling of water titration curves, gives an indication of the limitations of the model. Such differences can have several sources:

Figure 7. ^{29}Si-NMR spectra of the systems [$Si(OEt)_4 + H\ H_2O$, pH = 0; $0.5 < H < 10$]

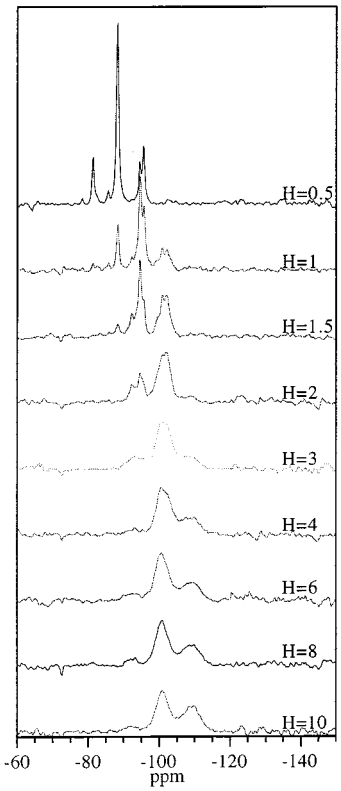

Table 4. Silicon-29 NMR chemical shifts [ppm] and percentage of Q^n species

	Q^0	Q^1	Q^2	Q^3	Q^4
chemical shift	−73 to −78	−80 to −89	−91 to −95	−99 to −103	−110 (broad)
$H = 0.5$	13	55	3		
$H = 1$		16	57	27	
$H = 1.5$		5	45	50	
$H = 2$			34	58	8
$H = 3$			17	63	21
$H = 4$			8	59	33
$H = 6$			10	57	33
$H = 8$			9	52	39
$H = 10$			8	49	44

Table 5. Values of the consumed water ratio h (Karl-Fischer titration) and the oxo bridge ratio k (^{29}Si NMR) of TEOS hydrolyzed at pH = 0, as a function of the initial water ratio H; hydrolysis and condensation constants calculated using Eq. 3 and Eq. 4

H	h	k	K_h	K_c
0.5	0.5	0.5		
1	0.98	1		
1.5	1.37	1.2	1.9	8.7
2	1.82	1.3	1.9	6.5
3	2.14	1.5	1.7	11.1
4	2.33	1.6	2.8	24
6	2.40	1.6		
8	2.64	1.6		
10	2.99	1.7		

(i) The ^{29}Si resonances in the highly hydrolyzed samples ($H \geq 3$) are broad, indicating that some polymers have become so large that their mobility is restricted. This broadening of the NMR resonances is expected to reduce the precision of the NMR data. An accuracy of about ±15% in the integration of the NMR data would be sufficient to account for the differences observed between the two approaches.

(ii) some M−OH groups might have been partially titrated during Karl-Fischer titration, thus decreasing the accuracy of the estimation of the consumed water h.

Comparison of the Hydrolysis and Condensation Constants of Titanium, Zirconium, and Silicon Alkoxides

The curves $h = f(H)$ of these three alkoxides are similar: at low hydrolysis ratios, the hydrolysis reaction is almost complete, whereas at higher initial hydrolysis ratios, the consumed water tends towards a plateau. The titanium alkoxide has the lowest hydrolysis constant. The condensation constants of the titanium and zirconium species are similar. For these two alkoxides, the condensation constants are about 10 times higher than their respective hydrolysis constants. These results indicate that the condensation of M−OH groups is important and that the M−OH/M ratio is low. The influence of the complexation ratio on these two alkoxides is also the same: an increase of r results in a decrease of K_c, whereas K_h remains unchanged. The pH of the hydrolyzing solution does not seem to change K_h and K_c: their values are very close to those of the modified precursors. For silicon alkoxides, however, the condensation constant is strongly dependent on the pH of the hydrolyzing solution: at pH = 2, K_c is high, indicating that the condensation is almost complete. At pH = 0, K_c is low, the condensation reaction is in equilibrium, and the ratio [Si−OH]/[Si] is high. The silanol Si−OH groups seem to be more stable than the Ti−OH or Zr−OH groups. This result is consistent with previous ^{17}O-NMR studies: Ti−OH and Zr−OH have never been observed by liquid-state ^{17}O-NMR, whereas Si−OH groups give rise to readily detectable signals[16][18].

Calorimetric Study of the Complexation Reaction

The enthalpy of complexation of tetravalent transition metal alkoxides by acetylacetone provides a relevant insight into this reaction. Four alkoxides have been studied: three titanium alkoxides (ethoxide, butoxide, isopropoxide) and one zirconium alkoxide (*n*-propoxide). The curves of the enthalpy of complexation versus the complexation ratio r = [acac]/[M] are shown in Figure 8. These curves show that the complexation reaction is always exothermic ($\Delta H < 0$), but that it reaches a plateau at $r \geq 2$ for titanium alkoxides or at $r \geq 4$ for zirconium propoxide. The complexation enthalpies of these four alkoxides are reported in Table 6.

Moreover, the entropy change associated with complexation by chelating ligands is always positive[19], so that the free enthalpy $\Delta G = \Delta H - T\Delta S$ should be negative. Consequently, the equilibrium of complexation should be strongly shifted toward the formation of the chelated precursor up to $r = 2$ for titanium alkoxides or up to $r = 4$ for zirconium propoxide.

Figure 8. Variation of the enthalpies of complexation of several metal alkoxides by acetylacetone

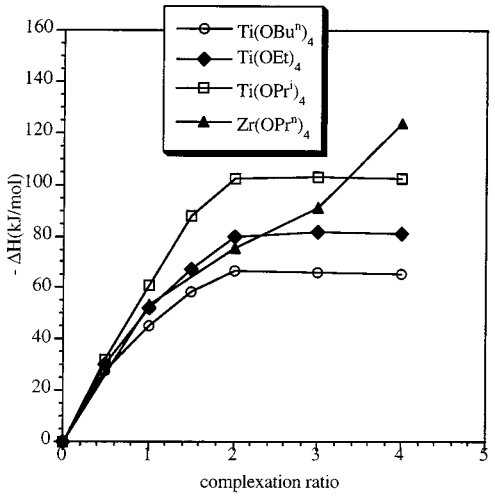

Table 6. Enthalpies (kJ·mol^{-1}) of the complexation reactions of Ti(O*n*Bu)$_4$, Ti(OEt)$_4$, Ti(O*i*Pr)$_4$, and Zr(O*n*Pr)$_4$. Gap [kJ·mol^{-1}] is the gap of enthalpy of complexation, taking Ti(O*i*Pr)$_4$ as reference

	Ti(O*n*Bu)$_4$	Ti(OEt)$_4$	Ti(O*i*Pr)$_4$	Zr(O*n*Pr)$_4$
Enthalpy of complexation	−67	−82	−102	−75 (2 acacH) −125 (4 acacH)
Energy of Ti−OR bond	−439	−422	−430	−
Gap (exp. value)	35	20	0	−
Gap (theoretical value)	18	−16	0	−

These results are in good agreement with previous observations, which have shown that, in the case of titanium alkoxides, substitution of the two first alkoxy groups by acetylacetone ligands occurs readily, but that the further replacement of a third alkoxy substituent by acetylacetone requires a large excess of the ligand[5]. Zirconium alkoxides, on the other hand, react readily with four acetylacetone ligands, thus forming the Zr(acac)$_4$ complex.

The complexation of the metallic center by acetylacetone results in an increase of its coordination number. For titanium, the most stable coordination number is 6; this is its usual coordination number in metallic oxides (rutile and anatase). The coordination number for titanium in the alkoxide precursor depends on the nature of the alkoxy group and on the solvent. For neat alkoxides, or in non-polar solvents such as benzene, the coordination number of titanium is 4 when the alkoxy is secondary or tertiary, or 5 with primary alkoxy groups. Primary alkoxides show a general tendency to form solvated dimers in alcoholic solution[5]. In the bis-complexed precursor Ti(OR)$_2$acac$_2$, however, the coordination number of the metallic center is 6. This increase in coordination number is the main reason for the exothermicity of the complexation reaction.

On the other hand, the most stable coordination numbers of zirconium are 7 and 8. Hence, zirconium propoxide can react with up to four acac ligands, forming the complex $Zr(acac)_4$, in which eightfold zirconium coordination is attained[20].

The complexation enthalpies of the various alkoxides are reported in Table 6. The enthalpies of the reactions involving $Ti(OnBu)_4$ and $Ti(OEt)_4$ are smaller than that with $Ti(OiPr)_4$. These enthalpies can be calculated from the bond energies:

$$\Delta H[Ti(OR)_4] = 2E(Ti-acac) + 2\,E(ROH) - 2E(Ti-OR) - 2E(acacH) \quad (1)$$

The bond energy values for the three titanium alkoxides are reported in Table 6. The energy of the RO−H bond depends only slightly on the nature of the R group[21].

Using Equation 1, we are able to calculate the gap between the enthalpies of two alkoxides. The calculated and experimental values of these gaps are also reported in Table 6. The reference point ($E = 0$) was taken as the value for $Ti(OiPr)_4$. The experimental and calculated values are at variance, both for $Ti(OnBu)_4$ and $Ti(OEt)_4$. In order to explain these differences, we have to take into account the structure of the alkoxides in solution in their parent alcohols. $Ti(OiPr)_4$ is monomeric, but $Ti(OEt)_4$ and $Ti(OnBu)_4$ are partially oligomerized via μ_2-OR bridges. The energies of these bridges have been previously calculated to be about 40 kJ·mol^{-1}, both for the ethoxy bridge[22] and for the butoxy bridge[23]. The enthalpy of the complexation reaction is therefore:

$$\Delta H[Ti(OR)_4] = 2E(Ti-acac) + 2E(RO-H) - 2E(Ti-OR) - 2E(acacH) - x\cdot E(alkoxo) \quad (2)$$

where x is the ratio bridges/titanium [$x = 0$ in the case of $Ti(OiPr)_4$].

Using Equation 2, we were are able to estimate the values of x for each alkoxide: $x_{Ti(OBu)4} = 0.9$ and $x_{Ti(OEt)4} = 1.8$. Of course, these values are only approximate, but they provide an interesting way of calculating the degree of oligomerization of the primary alkoxides in solution in their parent alcohols.

Calorimetric Study of Hydrolysis/Condensation Reactions

The enthalpies of hydrolysis were determined as described in the Experimental Section. The variations of the heats of hydrolysis of $Ti(OiPr)_4$, $Ti(OnBu)_4$, $Ti(OEt)_4$, and $Zr(OnPr)_4$ with the initial hydrolysis ratio, $H = H_2O$/metal, are plotted in Figure 9. The enthalpies of hydrolysis of these four alkoxides are reported in Table 7. The hydrolysis reaction is, in all cases, exothermic, which is in line with previous observations[5]. The curves $\Delta H = f(H)$ of the three titanium alkoxides show similar behavior: the hydrolysis reaction is exothermic up to $H = 1$ and reaches a plateau for $H > 1$. These results can be compared with those of the Karl-Fischer titrations, which show that at low initial hydrolysis ratios, the consumption of water is complete, while at higher initial hydrolysis ratios, the hydrolysis and condensation reactions are incomplete. These results can also be compared with those of XANES experiments, which have indicated that at low initial hydrolysis ratios, most of the titanium atoms become hexacoordinated[24]. We conclude from these results that the hydrolysis and condensation reactions are governed by the coordination unsaturation of the metallic center, which results in rapid reactions with any nucleophiles, and especially with water. However, the hydrolysis, oxolation, and alkoxolation reactions do not lead to an increase of coordination, since they correspond to nucleophilic substitution reactions. As a consequence, these results suggest that for transition metal alkoxides, the early stages of hydrolysis and condensation are driven by nucleophilic addition reactions. Among the two possible addition reactions, olation (creation of hydroxy bridges) or alkoxy bridging, olation is probably the driving force responsible for the high reactivity towards water of the transition metal alkoxides.

Figure 9. Variation of the enthalpy of hydrolysis/condensation of non-complexed alkoxides with the initial hydrolysis ratio; influence of the complexation ratio

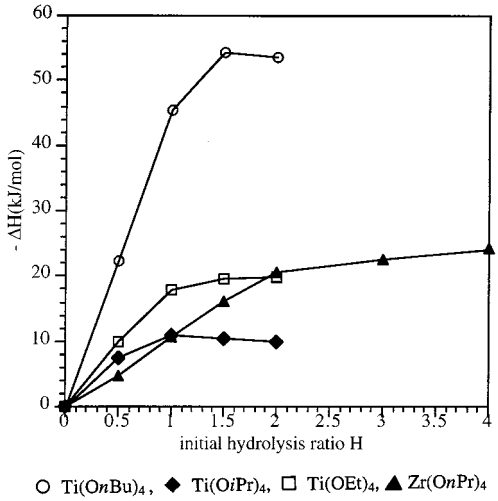

Table 7. Enthalpies of the hydrolysis reactions of: $Ti(OnBu)_4$, $Ti(OEt)_4$, $Ti(OiPr)_4$, and $Zr(OnPr)_4$

substrate	ratio	enthalpy [kJ·mol^{-1}]
$Ti(OnBu)_4$	r = [acac]/[Ti] = 0	−19.6
	r = [acac]/[Ti] = 1	−8.4
	r = [acac]/[Ti] = 2	−0.8
$Ti(OiPr)_4$	$r = 0$	−54.3
	$r = 1$	−32.6
	$r = 2$	−0.2
$Ti(OEt)_4$		−10.7
$Zr(OnPr)_4$		−20.5

The hydrolysis reaction of $Zr(OnPr)_4$ is exothermic until higher values of the initial hydrolysis ratio are reached ($H = 2$ and even $H = 4$). This result can be attributed to the previously mentioned fact[2][3][9] that the coordination unsaturation (the coordination number of the metal in the oxide minus the metal valency) is higher for zirconium alkoxides (8 − 4 = 4) than for titanium alkoxides (6 − 4 =

2). Again, the enthalpies of reactions between nucleophilic species (e.g., organic ligands, water, hydroxy groups) and transition metal alkoxide precursors are mainly due to the increase in the coordination of the metallic center. As a consequence, the enthalpies of hydrolysis/condensation should strongly depend on the complexation ratio. Indeed, the hydrolysis reaction of the precursor solution obtained from $Ti(OnBu)_4$ and acacH with a complexation ratio $r = 2$ is barely exothermic, while at lower complexation ratios, it is decidedly exothermic. Moreover, at a complexation ratio $r = 1$, the enthalpy of hydrolysis is about half of that of the non-complexed precursor (see Figure 10 and Table 7). These results confirm the importance of the coordination unsaturation in the hydrolysis/condensation reactions, since at a complexation ratio $r = 2$, the coordination of all the titanium atoms is 6. At $r = 1$, the system reacts as an equimolar mixture of non-complexed and bis-complexed precursors. The hydrolysis of acac-modified ($r = 1$; $r = 2$) $Ti(OiPr)_4$ leads to similar results (see Table 7).

Figure 10. Variation of the enthalpy of hydrolysis/condensation of pure or complexed titanium butoxide with the initial hydrolysis ratio: influence of the complexation ratio

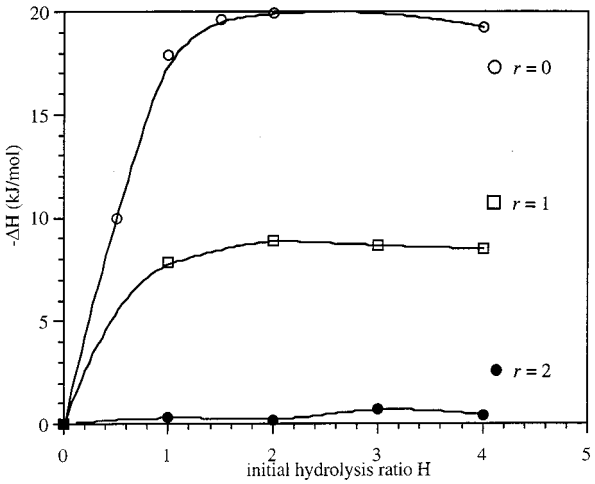

Conclusions

This work has shown that mean hydrolysis and condensation constants calculated from water titration curves offer a useful means of quantifying the influence of parameters such as the complexation or proton ratio on the behavior of titanium alkoxides towards hydrolysis. In addition, this approach allows comparisons to be made between metal alkoxides of different metals, particularly those of transition metals, for which NMR speciation and quantitative spectroscopic analysis cannot as yet be realized.

This work has also given an indication of the limitations of the proposed model. The assumptions that were invoked to determine mean constants will benefit from further refinement. These include:

− the postulate that the polymers can all be represented by a mean structural unit;

− the assumption that the system reaches, after ageing, a metastable equilibrium state, which results in residual OR groups. We have shown using ^{17}O-NMR spectroscopy that hydrolysis and condensation reactions are equilibrium processes. It is important to point out that another interpretation can be proposed for incomplete hydrolysis of OR groups, namely the lower reactivity of OR groups of large clusters compared to those of monomers[17]. It is probable that both these phenomena (reversibility of hydrolysis/condensation reactions and decrease of the reactivity of OR groups with increasing cluster size) contribute to the presence of residual OR groups.

− for the acac-modified precursor, it was considered that acac was a non-hydrolyzable ligand. At high initial hydrolysis ratios and/or high acac ratios, however, some acac ligands can be partially hydrolyzed[28][28]. The stability of the metal−acac bond toward hydrolysis/condensation reactions strongly depends on the nature of the metallic center. From the literature, it is known that for tetravalent metals, this stability can be classified according to the sequence Ce, Zr > Ti >> Sn[3][11][25].

This work has also incorporated key thermodynamic data, which are consistent with the conclusions obtained. Estimates of the enthalpies for the complexation and hydrolysis/condensation reactions indicate that the increase of coordination number of the transition metal alkoxide is of paramount importance. The tendency of the metallic center to attain the coordination that it usually has in naturally-occurring crystalline oxide networks is the driving force of all the reactions of transition metal alkoxides that take place in sol-gel processes. Hydrolysis and oxolation are nucleophilic substitutions and, therefore, do not modify the coordination of the metallic center. As a consequence, it is addition reactions (e.g. olation and alkoxy bridging) that are responsible for the high reactivity of titanium and zirconium alkoxides. These should correspond to the consumption of the first molecules of water ($H_2O/Ti \leq 1$), for which the reaction is complete and highly exothermic. However, only a small number of M−OH groups is observed when the metastable equilibrium state is reached. This phenomenon can be explained by the high acidity of the protons of the μ_2-OH and μ_3-OH groups bonded to titanium atoms, which leads to deprotonation of these groups[26].

Experimental Section

Synthesis

Titanium Oxide Based sols and gels were prepared using two different methods:

(i) Hydrolysis of acac-Modified Precursors: $Ti(OnBu)_4$ was diluted with *n*-butanol and acetylacetone (acacH) was added dropwise under magnetic stirring, resulting in a yellow solution. Hydrolysis was performed by the dropwise addition of a solution of water in *n*-butanol. The complexation ratio [acac]/[Ti] was varied from 0.6 to 1. The hydrolysis ratio $[H_2O]/[Ti]$ was varied from 1 to 10. The titanium concentration of the resulting sols was 0.4 $mol \cdot l^{-1}$.

(ii) Hydrolysis with Water Acidified with 35% (w/w) HCl: $Ti(OnBu)_4$ was diluted with *n*-butanol as above. Hydrolysis was performed by the dropwise addition of a solution of acidified water

in *n*-butanol. The ratio $[H^+]/[Ti]$ was kept at 0.02, while the hydrolysis ratio was varied from 1 to 10. The concentration of the resulting sol was 0.18 mol·l^{-1}.

The samples used for recording ^{17}O-NMR spectra were prepared as follows:

Sample ① was prepared following procedure (i) with both the [acac]/[Ti] and $[H_2O]/[Ti]$ ratios equal to 1. The water used for this first hydrolysis was 5%-enriched with oxygen-17. After 1 h at room temperature, the sample was further hydrolyzed with a solution of 5% enriched water in *n*-butanol. The total hydrolysis ratio of the sample was thus equal to 2.

Sample ② was prepared according to the same procedure as sample ①, but the first hydrolysis was performed with unenriched water and the second hydrolysis with 10%-enriched water. Thus, after the second hydrolysis, the two systems have the same chemical composition and the same enrichment in oxygen-17.

Zirconium Oxide Based sols and gels were prepared according to a procedure analogous to (i) above: $Zr(OnPr)_4$ was first diluted with *n*-propanol, and then acetylacetone was added. The [acac]/[Zr] ratio was either 0.9 or 1. Hydrolysis was performed by the dropwise addition of a solution of water in *n*-propanol. The $[H_2O]/[Zr]$ ratio was varied from 1 to 10. The concentration of the resulting sols was 0.44 mol·l^{-1}.

Silicon Oxide Based sols and gels were prepared following procedure (ii): $Si(OEt)_4$ was first diluted with ethanol. A solution of water acidified with HCl (pH 0 or pH 2) in ethanol was then added dropwise. The hydrolysis ratio was varied from 0.5 to 10 and the concentration of the resulting sol was 0.54 mol·l^{-1}.

Characterizations

Water Titrations were performed by the Karl-Fischer method using a 701 KF Titrino apparatus. The solvent used for the titrations was Hydranal Solvent K, rather than methanol, in order to prevent side reactions of ketones and metal hydroxyls[27]. The reagent was Hydranal-composite 5K (Riedel-de-Haen).

The ^{29}Si-NMR spectra were recorded on a Bruker MSL 400 spectrometer operating at 79.48 MHz. The sample solution was placed in an 8 mm tube, which was placed inside a 10 mm tube containing C_6D_6 as a lock solvent. Tetramethylsilane was used as reference ($\delta = 0$).

Silicon-29 is a spin 1/2 nucleus with a natural abundance of 4.7%. A disadvantage of this nucleus is its high spin lattice relaxation time T_1, which results in a long recycle delay. Thus, the relaxation agent chromium acetylacetonate $Cr(acac)_3$ was added in order to reduce this delay. $Cr(acac)_3$ has previously been used in similar systems, where it was shown that it does not interfere with the polymerization process[7].

A second disadvantage of this nucleus is the presence of background Q^4 silicon units present in the silica tube, which result in a large peak at about $\delta = 110$. In order to suppress this peak, we used a $\pi.2-\tau-\pi$ echo sequence.The experimental NMR conditions were as follows: first pulse 12.8 μs; $\tau = 40$ ms; second pulse 25.6 μs; recycle delay 30 s.

The ^{17}O-NMR spectra were recorded on a Bruker MSL 400 spectrometer operating at 54.2 MHz. Again, the sample solutions were placed in an 8 mm tube, which was immersed in C_6D_6, as a lock solvent, in a 10 mm tube. H_2O was used as reference ($\delta = 0$). The experimental NMR conditions were as follows: pulse 19.6 μs; pre-acquisition delay (time between the end of the RF pulse and the beginning of the acquisition) 24 μs; recycle delay 0.2 s, number of scans 1000.

The ^{17}O spectra of ^{17}O-enriched titanium oxo-polymers have been reported previously[28]. They are characterized by four broad bands, which can be assigned, on the basis of the published literature[29][30], as follows:

- $\delta = 650-850$: μ_2O oxo-bridges
- $\delta = 450-600$: μ_3O oxo-bridges
- $\delta = 300-400$: μ_4O oxo-bridges
- $\delta = 200-300$: μ_5O oxo-bridges

- the signal appearing at around $\delta = 0$ corresponds to the residual water.

Two additional peaks can be observed in the presence of acetylacetone[28]:

- one broad peak at $\delta = 300-400$, attributable to acac bonded to titanium

- one narrow peak at $\delta = 273$, attributable to the enol form of free acetylacetone.

These two peaks appear a few hours after hydrolysis, and are only observed at complexation ratios higher than 1 and with a hydrolysis ratio higher than 2[16]. They result from the isotopic ^{17}O-exchange between enriched H_2O and the free acetylacetone released by the hydrolysis of the acac ligands[28].

$$Ti-acac + H_2O \rightarrow Ti-OH + acacH$$
$$acacH + H_2O^* \rightarrow acac^*H + H_2O$$
$$Ti-OH + acac^*H \rightarrow Ti-acac^* + H_2O$$

(the reaction leading to enrichment of the acetylacetone in oxygen-17 is described in Scheme 1).

The recording of oxygen-17 NMR spectra necessitates a pre-acquisition delay in order to eliminate the trailing edge of the high-power pulse. This delay gives rise to a rolling baseline of sin *x*/*x* shape. A baseline correction is then performed, using a cubic splines baseline function (WinNMR 1D). The total intensity of the NMR signal has been measured for all the spectra reported herein, in order to check that this area does not vary with the ageing and the preparation of the sample solution. The areas of the spectra of all the samples after the second hydrolysis are equal, within an experimental error of ±10%. A calibration has also been performed using a solution of 10%-enriched water in *n*-butanol, at the same concentration as in the samples of oxo-polymers. The total intensities of the spectra of the oxo-polymer samples before the second hydrolysis, after the second hydrolysis, and after 24 hours of ageing are all consistent with the intensity of the water peak of the calibration solution, within an experimental error of ±10%. This result indicates that the formation of large polymers, which would result in the partial loss of the signal of the oxo-polymers and, therefore, in quantitativity problems, is negligible.

Calorimetric Study of the Complexation and Hydrolysis Reactions: Four alkoxides were studied: $Ti(OnBu)_4$, $Ti(OEt)_4$, $Ti(OiPr)_4$, $Zr(OnPr)_4$.

First, m_1 g of the alkoxide (or acac-modified alkoxide) was diluted with m'_1 g of its parent alcohol. This solution was placed in a Dewar vessel and its temperature T was measured. A solution of m_2 g of acetylacetone in m'_2 g of the parent alcohol (or the hydrolysis solution of water in parent alcohol) at temperature T_2 was then added. The final temperature T_f was measured about 1 min. after the addition of acetylacetone (or water). The [acac]/[M] ratio of the resulting solution was varied from 0.5 to 2 [or to 4 for $Zr(OnPr)_4$]. The hydrolysis ratio was varied from 0.5 to 4. The molar enthalpy ΔH of the reaction was calculated using the equation:

$$(m_1\Delta H)/M + Cp(M_a + m_1 + m'_1)(T_f - T_1) + Cp(m_2 + m'_2)(T_f - T_2) = 0$$

(adiabatic reaction), where M is the molar mass of the alkoxide (or of the acac-modified alkoxide), $Cp_{alcohol}$ is the heat capacity of the alcohol, M_a is defined as $M_d \times Cp_d = M_a \times Cp_{alcohol}$, where Cp_d is the heat capacity of the Dewar vessel and M_d the mass of the Dewar vessel.

This measurement of the enthalpy is very simple, but it is only intended to give approximate data. Two assumptions are made to estimate the enthalpy of the reaction: first, we assume that the complexation occurs during the first minute after the addition of acetylacetone. This hypothesis is supported by infra-red experiments, which have shown that no free acac can be detected 1 min. after addition of the ligand[18][31]. Secondly, we have assumed that all the reactants and products have the same heat capacity of the solvent, i.e. the parent alcohol. In order to minimize the error introduced by this approximation, the concentrations of reactants were kept below 5% (*w*/*w*).

Modelling of the h = f(H) Water Titration Curves

Evaluation of Hydrolysis/Condensation Mean Equilibrium Constants: Hydrolysis and condensation reactions of metal alkoxides do not generally reach completion, showing reversible character in the sol state, as demonstrated by the ^{17}O-NMR experiments. Complete hydrolysis and condensation of a metal alkoxide $M(OR)_n$ would result in the consumption of all the added water, up to a hydrolysis ratio $H = [H_2O]/[Ti] = n/2$, and, for hydrolysis ratios H higher than $n/2$, a plateau at $h = n/2$ (h being the consumed water ratio), according to the equation:

$$M(OR)_n + H\ H_2O \rightleftharpoons MO_{n/2} + n\ ROH + (H - n/2)\ H_2O$$

For a tetravalent metal alkoxide [$Ti(OR)_4$, $Si(OR)_4$, etc.)] this equation becomes:

$$M(OR)_4 + H\ H_2O \rightleftharpoons MO_2 + 4\ ROH + (H - 2)\ H_2O$$

This behavior is only rarely observed. For all the alkoxides studied in the present paper, we have observed that the consumption of water does not follow this law. Two hypotheses can be made to explain this difference: the first one is that hydrolysis and condensation reactions are kinetically controlled, so that the system never reaches an equilibrium state. This hypothesis effectively rules out any possibility of evaluating the extent of reaction. The second hypothesis that can be made is that the system reaches a metastable equilibrium state, which represents a steady state where the reactants are no longer being consumed, but because of their high surface/volume ratio, the solvent-swollen oxo-polymers are still in equilibrium with free water and alcohol molecules. This steady state is not the lower minimum of the system (i.e. the crystalline oxide), but it is well known that chemical pathways can possess several minima of different depth. This second assumption is confirmed by ^{17}O-NMR experiments presented in the Results and Discussion section (vide infra). These experiments show that the hydrolysis and condensation reactions are equilibrium processes. Moreover, this hypothesis has the advantage that it allows one to study the extent of the hydrolysis and condensation reactions through to the determination of a mean chemical formula for the oxo-polymers.

The transition metal oxo-polymers that are formed by the sol-gel process are generally polydisperse in size and composition and it is therefore impossible to perform a straightforward calculation of the pseudo-equilibrium constants of each of these polymers. In order to circumvent this problem, we have defined a mean structural unit that has the mean composition of the polymers. This mean structural unit has the following approximate formula: $MO_k(OH)_{h-k}(OR)_{4-r-h-k}(acac)_r$, where h is the consumed water ratio, k is the ratio of oxo bridges, and r is the initial complexation ratio. Details of the calculation of the chemical composition of the mean structural unit are presented in Appendix 1.

It is possible to define two constants K_h and K_c in order to describe the hydrolysis and condensation pseudo-equilibrium:

hydrolysis:

$$\cdots M\text{–}OR + H_2O \rightleftharpoons \cdots M\text{–}OH + ROH$$

$$K_h = \frac{[\cdots M\text{–}OH]}{[\cdots M\text{–}OR][H_2O]}$$

condensation (alkoxolation):

$$\cdots M\text{–}OH + \cdots M\text{–}OR \rightleftharpoons \cdots M\text{–}O\text{–}M\cdots + ROH$$

$$K_c = \frac{[\cdots M\text{–}O\text{–}M\cdots]}{[\cdots M\text{–}OH][\cdots M\text{–}OR]}$$

condensation (oxolation):

$$\cdots M\text{–}OH + \cdots M\text{–}OH \rightleftharpoons \cdots M\text{–}O\text{–}M\cdots + H_2O$$

$$K_o = \frac{[\cdots M\text{–}O\text{–}M\cdots][H_2O]}{[\cdots M\text{–}OH][\cdots M\text{–}OR]}$$

where M is a metal and R an alkyl group

The pseudo-equilibrium oxolation constant K_o can be directly deduced from K_h and K_c, as follows: $K_o = K_c/K_h$. The formula of the mean structural unit does not depend on the kind of condensation reaction (oxolation or alkoxolation) that occurs (see Appendix 1).

It is possible to express K_h and K_c as a function of k, the mean number of oxo groups, h the water effectively consumed (expressed as the ratio water/metal), r the complexation ratio, and H the initial hydrolysis ratio $H = [H_2O]/[M(OR)_4]$:

An expression for the initial hydrolysis ratio H as a function of the water/metal ratio corresponding to the water effectively consumed can be obtained using Equations 3 and 4:

$$K_h = \frac{(h-k)}{(4-r-h-k)\cdot(H-h)\cdot[M(OR)_4]} \quad (3)$$

$$K_c = \frac{k}{(4-r-h-k)\cdot(H-h)\cdot[M(OR)_4]} \quad (4)$$

$$H = h + \frac{4-r+K'_c(4-r-2h)^2-(4-r-2h)\sqrt{K'^2_c(4-r-2h)^2+2K''_c(4-r)+1}}{2K'_h(4-r-h)} \quad (5)$$

The details of the determination of this equation are presented in Appendix 2.

where $K'_c = K_c*[M(OR)_n]$; $K'_h = K_h*[M(OR)_n]$.

It is also possible to express k, the mean degree of oxo condensation, as a function of h and H:

$$k = \frac{K'_h(4-r-h)(H-h)}{K'_h(H-h)-1} \quad (6)$$

Figure 11. Examples of simulation of water titration curves: (a) $K_h = 1$, $K_c = 100$; (b) $K_h = 100$, $K_c = 1$; (c) $K_h = 0.1$; $K_c = 0.1$; K_h is the hydrolysis constant and K_c the condensation constant

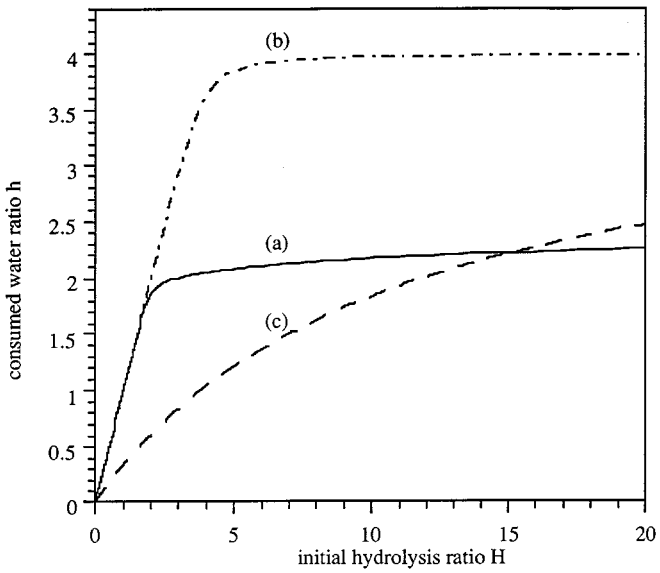

The water consumed during the hydrolysis/condensation reactions was measured once the metastable equilibrium state had been reached. These measurements were performed after ageing of the sols of the various metal alkoxides for several weeks or months. The time of ageing was fixed once the consumption of water was negligible. The initial hydrolysis ratio was varied between 0.5 and 10, while the other parameters (acac/metal ratio, H^+/metal ratio and concentration) were kept constant.

Examples of Simulation

Figure 11 depicts "extreme" behavior of the $h = f(H)$ curves:

• when the condensation constant is higher than the hydrolysis constant ($K_h = 1$; $K_c = 100$; Figure 11-a), the consumption of water is complete up to $H = 2$, and for H higher than 2 it reaches a plateau. All the M−OH groups that are formed in the hydrolysis reaction are consumed in the condensation reaction, and the final composition of the system corresponds to the oxide MO_2. The shift of the equilibria toward the formation of the oxide is due to the high value of K_c.

• When the hydrolysis constant is higher than the condensation constant ($K_h = 100$; $K_c = 1$; Figure 11-b), the consumption of water is almost complete up to $H = 4$, and then reaches a plateau at higher values of H. This limiting case corresponds to the formation of $M(OH)_4$ units, which do not polymerize.

• If the hydrolysis and condensation constants are both low ($K_h = 0.1$; $K_c = 0.1$; Figure 11-c), i.e. when both hydrolysis and condensation are incomplete, the consumption of water is not complete, even at low values of H, and the number of residual alkoxy groups is high.

Appendix 1: Determination of the formula of the mean structural unit

The parameters that determine the formula of the mean structural unit are:

- H the initial hydrolysis ratio
- h the consumed water ratio
- k the ratio of oxo bridges
- r the initial complexation ratio.

Hydrolysis:

$$M(OR)_{4-r}acac_r + H\,H_2O \rightleftharpoons M(OR)_{4-r-a}acac_r(OH)_a + (H-a)\,H_2O + a\,ROH$$

considering that *oxolation* is the only condensation reaction

$$2\,M(OR)_{4-r-a}acac_r(OH)_a \rightleftharpoons 2\,M(OR)_{4-r-a}acac_r(OH)_{a-b}O_{b/2} + b/2\,H_2O$$

where b is the proportion of M–OH groups that have reacted with an M–OH group to form oxo bridges

$$\frac{n(H_2O)}{n(M)} = H - a + b/2 = H - h$$
$$\frac{n(M\text{–}O\text{–}M)}{n(M)} = b/2 = k$$
$$\frac{n(M\text{–}OR)}{n(M)} = 4 - r - a = 4 - r - h - k$$
$$\frac{n(M\text{–}OH)}{n(M)} = a - b = h - k$$

mean structural unit $M(OR)_{4-r-h-k}acac_r(OH)_{h-k}O_k$

considering that *alkoxolation* is the only condensation reaction

$$2\,M(OR)_{4-r-a}acac_r(OH)_a \rightleftharpoons 2\,M(OR)_{4-r-a-c}acac_r(OH)_{a-c}O_c + 2c\,ROH$$

where c is the proportion of M–OH groups that have reacted with an M–OR group to form oxo bridges

$$\frac{n(H_2O)}{n(M)} = H - a = H - h$$
$$\frac{n(M\text{–}O\text{–}M)}{n(M)} = c = k$$
$$\frac{n(M\text{–}OR)}{n(M)} = 4 - r - a - c = 4 - r - h - k$$
$$\frac{n(M\text{–}OH)}{n(M)} = a - c = h - k$$

mean structural unit $M(OR)_{4-r-h-k}acac_rOH)_{h-k}O_k$

The mean structural units calculated by assuming that condensation occurs via alkoxolation or oxolation are the same.

Appendix 2: Determination of the equation of H as a function of h

from Equation 3: $k = \dfrac{K'_h(4-r-h)(H-h)}{K'_h(H-h)-1}$ (3')

from Eq. 4 and Eq. 3':

$$[K'_h(4-r-h)(H-h)-h][K'_h(H-h)-1] = K'_c\,K'_h(H-h)\,(2h-4+r)^2$$

this equation can be expressed as a polynomial of degree 2 in $(H-h)$:

$$(4-r-h)K'^2_h(H-h)^2 - K'_h[4-r+K'_c(2h-4+r)^2](H-h) + h = 0$$

the discriminant of the polynomial is:

$$\Delta = K'^2_h(4-r-2h)[K'^2_h(4-r-2h)^2 + 2(4-r)K'_c + 1]$$

the root of this equation is:

$$H = h + \frac{4-r+K'_c(4-r-2h)^2-(4-r-2h)\sqrt{K'^2_c(4-r-2h)^2+2K''_c(4-r)+1}}{2K'_h(4-r-h)} \quad (5)$$

[1] C. J. Brinker; G. W. Scherrer, *Sol-Gel Science, the Physics and Chemistry of Sol-Gel Processing*, Academic Press, San Diego, **1990**.
[2] J. Livage, M. Henry, C. Sanchez, *Prog. in Solid-State Chem.* **1988**, *18*, 259−341.
[3] C. Sanchez, F. Ribot, *New J. Chem.* **1994**, *18*, 1007−1047.
[4] C. J. Brinker, G. W. Scherrer, *Sol-Gel Science, the Physics and Chemistry of Sol-Gel Processing*, Academic Press, San Diego, **1990**, 109−108; 136−137; 150−152.
[5] D. C. Bradley, R. C. Mehrotra, D. P. Gaur, *Metal Alkoxides*, Academic Press, London-New-York-San Francisco, **1978**.
[6] L. C. Klein, Ed., *Sol-Gel Technology*, Noyes Publications, New Jersey, **1988**.
[7] L. W. Kelts, N. J. Effinger, S. M. Melpolder, *J. Non-Cryst. Solids* **1989**, 83, 354−374.
[8] B. E. Yoldas, *J. Mater. Sci.* **1986**, *21*, 1086−1092.

[9] C. Sanchez, J. Livage, M. Henry, F. Babonneau, *J. Non-Cryst. Solids* **1988**, *100*, 65−76.
[10] B. K. Coltrain, C. Sanchez, D. W. Schaefer, G. L Wilkes, Eds., *Better Ceramics Through Chemistry VII: Organic/Inorganic Hybrid Materials*, Materials Research Society, Pittsburg, **1996**, *435.*
[11] F. Ribot, P. Toledano, C. Sanchez, *Chem. Mater.* **1991**, *3*, 759−764.
[12] D. M. Antonelli, J. Y. Ying, *Angew. Chem. Int. Ed. Engl.* **1995**, *34*, 2014−2017.
[13] D. M. Antonelli, J. Y. Ying, *Chem. Mater.* **1996**, *8*, 874−881.
[14] U. Schubert, Private communication.
[15] M. Kallala, C. Sanchez, B. Cabane, *Phys. Rev. E* **1993**, *48*, 3692−3704.
[16] [19a] J. Blanchard, These de l′Universite Pierre et Marie Curie, (Chimie Inorganique), **1997**. [19b] J. Blanchard, C. Sanchez, forthcoming papers.
[17] J. R. Bartlett, J. L. Woolfrey, *Chemical Processing of Advanced Materials* (Eds.: L. L. Hench, J. K. West), Wiley, New York, **1992**, 247−256.
[18] F. Babonneau, *Better Ceramics Through Chemistry VI* (Eds.: A. K. Cheetham, C. J. Brinker, M. L. Mecartney, C. Sanchez), Materials Research Society, Pittsburg, **1994**, *346*, 949−960.
[19] S. Chabarek, A. E. Martell, *Organic Sequestering Agents*, Wiley, New York, **1959**.
[20] J. V. Silverton, J. L. Hoard, *Inorg. Chem.* **1963**, *2*, 243−249.
[21] J. D. Cox, G. Pilcher, *Thermochemistry of Organic and Inorganic Compounds*, Academic Press, London, **1965**.
[22] H. Weingarten, J. R. Van Wazer, *J. Am. Chem. Soc.* **1965**, *87*, 724−730.
[23] R. L. Martin, G. Winter, *J. Chem. Soc.* **1961**, 2947−2952.
[24] M. Kallala, C. Sanchez, Private communication: XANES experiments have been performed at the titanium K-edge on hydrolyzed titanium butoxide under acidic conditions and at low hydrolytic ratios $H = 1$ and 2. The XANES pre-peak exhibits a low intensity triplet centered at about 4968 eV, which is characteristic of a titanium atom in an octahedral oxygen ligand field.
[25] L. Armelao, F. O. Ribot, C. Sanchez, *Better Ceramics Through Chemistry VII: Organic/Inorganic Hybrid Materials* (Eds.: B. K. Coltrain, C. Sanchez, D. W. Schaefer, G. L. Wilkes), Materials Research Society, Pittsburg, **1996**, *435*, 387−393.
[26] T. Hiemtra, W. H. Van Riemsdjik, G. H. Bolt, *J. Coll. Interf. Sci.* **1989**, *133*, 91, 104.
[27] R. Aelion, A. Loebel, F. Eirich, *J. Am. Chem. Soc.* **1950**, *72*, 5705.
[28] J. Blanchard, S. Barboux-Doeuff, J. Maquet, C. Sanchez, *New J. Chem.* **1995**, *19*, 929−941.
[29] V. W. Day, T. A. Eberspacher, W. G. Klemperer, C. W. Park, F. S. Rosenberg, *J. Am. Chem. Soc.* **1991**, *113*, 8190−8192.
[30] T. J. Bastow, S. N. Stuart, *Chem. Phys.* **1990**, *143*, 459−467.
[31] A. Leaustic, F. Babonneau, J. Livage, *Chem. Mater.* **1989**, *1−2*, 240−247.

[98001]

Insertion Reactions into Palladium–Carbon Bonds of Complexes Containing Terdentate Nitrogen Ligands; Experimental and Ab initio MO Studies[+]

Johannes H. Groen[a], Annemieke de Zwart[a], Mark J. M. Vlaar[a], Jan M. Ernsting[a], Piet W. N. M. van Leeuwen[a], Kees Vrieze*[a], Huub Kooijman[b], Wilberth J. J. Smeets[b], Anthony L. Spek[b][++], Peter H. M. Budzelaar[c], Qin Xiang[d], and Randolph P. Thummel[d]

Anorganisch Chemisch Laboratorium, J.H. van't Hoff Research Instituut, Universiteit van Amsterdam[a],
Nieuwe Achtergracht 166, NL-1018 WV Amsterdam, The Netherlands
Fax: (internat.) + 31(0)20/5256456
E-mail: vrieze@anorg.chem.uva.nl

Bijvoet Center for Biomolecular Research, Kristal- en Structuurchemie, Universiteit Utrecht[b],
Padualaan 8, NL-3584 CH Utrecht, The Netherlands

Vakgroep Anorganische Chemie, Katholieke Universiteit Nijmegen[c],
Toernooiveld 1, NL-6525 ED Nijmegen, The Netherlands

Department of Chemistry, University of Houston[d],
Houston, Texas 77204-5641, USA

Received January 26, 1998

Keywords: Insertion / N ligands / Terdentate ligands / Rigid ligands / Palladium

Novel methyl complexes [Pd(Me)(N-N-N)]X (N-N-N = flexible or rigid terdentate nitrogen ligand, X = Cl, SO_3CF_3, BAr'_4) have been synthesized and fully characterized. All complexes readily underwent insertion of carbon monoxide resulting in the quantitative formation of complexes [Pd{C(O)Me}(N-N-N)]X [X = Cl (**1d–6d**), BAr'_4 (**1e–6e**)]. Subsequently, complexes **2e–6e** underwent quantitative insertion of norbornadiene, resulting in complexes [Pd{C_7H_8C(O)Me}(N-N-N)]BAr'_4 (**2f–6f**). Unexpectedly, these complexes, including even those containing rigid terdentate nitrogen ligands, possess a structure in which the nitrogen ligand is coordinated in a bidentate fashion. A kinetic study of the reaction of norbornadiene with complexes **1e–6e** revealed that the reactivity of complexes **1e–6e** toward norbornadiene increases with increasing rigidity of the terdentate ligand, i.e. with increasing strain in the PdN_3 moiety, which indicates that insertion very likely occurs via a mechanism involving nitrogen dissociation. This is fully supported by ab initio MO calculations on CO and ethylene insertion into carbon–palladium bonds of cationic model systems containing a rigid terdentate nitrogen ligand, which showed that the lowest-energy pathway for both insertion reactions consists of substitution of one of the distal nitrogen atoms of the rigid terdentate nitrogen ligand by the substrate, followed by a rate-determining migratory insertion of the substrate into the carbon–palladium bond.

In many transition-metal-catalyzed reactions the insertion of an unsaturated molecule into a carbon−metal bond is a key step.[1][2] A recent example is the palladium-catalyzed copolymerization of carbon monoxide and alkenes, leading to the formation of polyketones, which process involves the perfectly alternating insertion of CO and alkenes into carbon−palladium bonds.[3][4][5][6][7] We[8][9][10][11][12][13][14][15] and others[16][17][18][19][20][21][22][23][24] have extensively studied CO and alkene insertion reactions in model complexes of the type Pd(R)X(L-L) {R = Me, C(O)Me; X = Cl, Br, I, SO_3CF_3, BF_4, [3,5-$(CF_3)_2C_6H_3)_4$B]; L-L = P-P, P-N, N-N} mimicking the intimate steps of the catalytic cycle of polyketone formation.[25] From these studies it is clear that the mechanism of CO and alkene insertion reactions is highly dependent on the nature of the ligands. In the case of ionic complexes [Pd(R)(solv)(L-L)]X {R = Me, C(O)Me; solv = Et_2O, MeCN; L-L = P-P, P-N, N-N; X = SO_3CF_3, BF_4, [3,5-$(CF_3)_2C_6H_3)_4$B} it has been shown that precoordination of CO and alkenes occurs via dissociation of the weakly coordinated solvent molecule. Both CO and alkene precoordinated complexes of the type [Pd(Me)(CO)(L-L)]X[10][19][23] and [Pd{C(O)Me}(η^2-alkene)(N-N)]X[23], respectively, have been characterized as intermediates. Studies of the insertion reactions of CO into the methyl−palladium bond of complexes Pd(Me)X(P-P) (X = Cl, PPh_3, MeCN; P-P = bidentate phosphorus ligand) showed that the reactions were enhanced by flexible bidentate phosphorus ligands, which are able to coordinate with a large bite angle, thereby lowering the energy of the transition state.[8] Furthermore, the reactions were strongly dependent on the coordinating capability of the X ligand, which indicates that insertion occurs mainly by X dissociation. Unexpectedly, insertion reactions in complexes containing flexible and rigid bidentate nitrogen ligands with a small bite angle were much faster than those in complexes containing

[+] Netherlands Institute for Research in Catalysis (NIOK) publication UvA 98-3-04.
[++] Correspondence address concerning crystallographic data.

 © WILEY-VCH Verlag GmbH, D-69451 Weinheim, 1998 1434−1948/98/0808−1129 $ 17.50+.50/0

bidentate phosphorus ligands.[11][12][26] Mechanistic studies provided strong evidence that insertion reactions in neutral complexes containing bidentate nitrogen ligands occur via intermediates in which these ligands are coordinated in a unidentate fashion.[12][13][14][15]

Although most experimental studies indicate that insertion by a mechanism involving four-coordinate intermediates is more favorable than insertion by a mechanism involving five-coordinate intermediates, for a few insertion reactions a mechanism involving five-coordinate species has been suggested. For example, both intra-[27] and intermolecular[28] alkene insertions into hydride−platinum bonds and also CO insertions into aryl−[29] and alkyl−palladium[30] bonds have been proposed to occur from five-coordinate intermediates. Recently, we reported the high reactivity toward CO of the ionic complex [Pd(Me)(tpy)]Cl, containing a terdentate 2,2′:6′,2′′-terpyridine ligand.[31][32] At first, insertion was proposed to occur via five-coordinate species, as creation of a free coordination site was assumed to be rather difficult due to the favorable terdentate coordination of the tpy ligand.[31] However, Orrell et al.[33][34][35][36][37] and also others[38][39][40][41][42][43] have reported on the ability of tpy to coordinate in a bidentate fashion, which suggests that the CO insertion reaction in [Pd(Me)(tpy)]Cl may occur by a mechanism involving four-coordinate intermediates, which contain a bidentate coordinated tpy ligand. Therefore, we turned our attention to complexes containing rigid terdentate nitrogen ligands, in which dissociation of one of the distal nitrogen atoms was expected to be unlikely. We have used the novel rigid ligand **1** and the known ligands **2**[44], **3**[45], **4**[45], **5**[46], and **6** (Figure 1). In this series ligands **3** and **4** can be considered as rigid analogs of **5** and tpy (**6**).

Figure 1. Terdentate nitrogen ligands **1**−**6** with the adopted numbering schemes

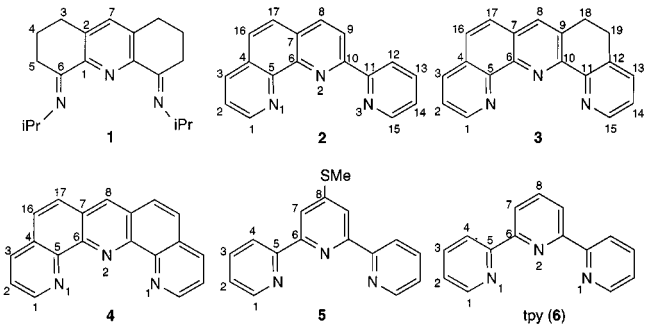

We report here the results of our study of the palladium coordination chemistry of ligands **1**−**6**. Furthermore, we present the results of an extensive kinetic study of the norbornadiene insertion in acetylpalladium complexes containing the ligands **1**−**6** and the results of ab initio MO calculations of CO and ethylene insertion reactions into carbon−palladium bonds of model complexes containing a rigid terdentate nitrogen ligand, which lead to a novel view of the role and behavior of rigid terdentate ligands in CO and alkene insertion reactions.

Results and Discussion

Synthesis and Characterization of Compound 1 and Methylpalladium Complexes 1a−5a, 1b, and 1c−6c

The novel compound 4,5-bis(isopropylimino)-1,2,3,4,5,6,7,8-octahydroacridine (**1**) was synthesized by a condensation reaction of 1,2,3,4,5,6,7,8-octahydroacridine-4,5-dione with isopropylamine in the presence of an excess $MgSO_4$ and a catalytic amount of formic acid (Equation 1). Compound **1** was obtained as a yellow oil. In this form or in solution at 20°C, compound **1** is rather unstable and decomposes into several uncharacterized products within a few hours. At −80°C compound **1** can be stored for several days without decomposition. As reported for 1,2-bis(isopropylimino)cyclohexane[47], (5,6-dihydro[1]pyrindin-7-ylidene)isopropylamine[15], and isopropyl-(5*H*-[1]pyrindin-7-yl)amine[15], compound **1** exists predominantly in the tautomeric form **1′**. Formation of this tautomer was revealed by NMR where a two-proton resonance at δ = 4.85 in the ^{1}H-NMR spectrum and a resonance at δ = 74.7 in the ^{13}C-NMR spectrum were observed, both characteristic of a = CH fragment. Furthermore, the IR spectrum of **1** revealed an NH stretching frequency at 3390 cm^{-1}. The instantaneous disappearance of the 5-H NMR resonance upon addition of a drop of D_2O to a solution of **1** in $CDCl_3$ indicates the presence of a rapid equilibrium between enamine and imine forms.

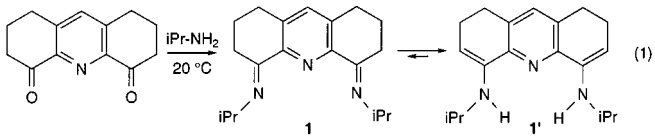

The chloro(methyl)palladium complexes **1a**−**5a** were synthesized by substitution of COD (= 1,5-cyclooctadiene) in Pd(Me)Cl(COD) by ligands **1**−**5** (Equation 2), similar to what is reported for methylpalladium complexes containing bidentate N-N,[11][12] N-S[48][49], P-N[10], P-P[8], and terdentate N-N-N[31][32], P-N-N[50], P-N-S[51], and N-N-S[51] ligands. Analogously to [Pd(Me)(**6**)]Cl (**6a**)[32], complexes **2a**−**5a** were obtained as yellow, air-stable solids, which are only moderately soluble in polar solvents such as methanol, ethanol, and water. In contrast, complex **1a** readily dissolves in dichloromethane and chloroform.

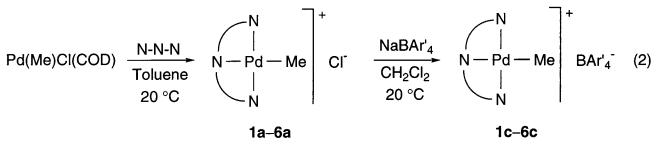

The complexes of the type [Pd(N-N-N)(Me)]X [N-N-N = terdentate nitrogen ligands **1**−**6**; X = SO_3CF_3 (**b**), BAr'_4 (**c**)] were obtained by the reaction the complexes **1a**−**6a** with silver trifluoromethanesulfonate and sodium tetrakis[3,5-bis(trifluoromethyl)phenyl]borate (Equation 2). Complexes **1b**−**6b**, however, except for **1b**, are insoluble in

common solvents and could not be characterized. In contrast, complexes **1c**−**6c** are soluble in dichloromethane, chloroform, and even in diethyl ether. Complexes **1a**,**c**−**6a**,**c** and **1b** were isolated and fully characterized. Crystals of **1b** and **4c**, suitable for X-ray analyses, were obtained by recrystallization from dichloromethane/hexane at 4°C (vide infra).

All methylpalladium complexes show a characteristic *Me*−Pd resonance at $\delta \approx 1$ in the ^{1}H-NMR spectra and at $\delta \approx 0$ in the ^{13}C-NMR spectra.[11][12][15][32][52][53][54] At 20°C, as well as at −60°C, the ^{1}H-NMR spectra of complexes **1a**, **4a**, and **5a**, show a symmetrically bonded nitrogen ligand, indicating that these ligands are coordinated in the expected terdentate fashion to the palladium center and that the chloride is present as a counter anion. The observed high equivalent conductivities for **1a**−**5a** in methanol at 20°C of 51−70 Ω^{-1} cm^2 mol^{-1} are also in agreement with an ionic complex, whereas that of the neutral precursor Pd(Me)Cl(COD) is 2.3 Ω^{-1} cm^2 mol^{-1}.

Interestingly, addition of a drop of D_2O to a solution of **1a** in $CDCl_3$ led to a complete disappearance of the 5-H NMR resonance due to H/D exchange. This result can be explained by dissociation of one of the distal nitrogen atoms of the ligand, caused by coordination of the chloride (Scheme 1). This mechanism is supported by the absence of H/D exchange for **1a** in CD_3OD, which efficiently solvates the chloride ion, hereby preventing chloride-initiated dissociation of one of the distal nitrogen atoms. Furthermore, it is in agreement with the absence of H/D exchange for **1b** and **1c**, which contain weakly coordinating anions.

Scheme 1

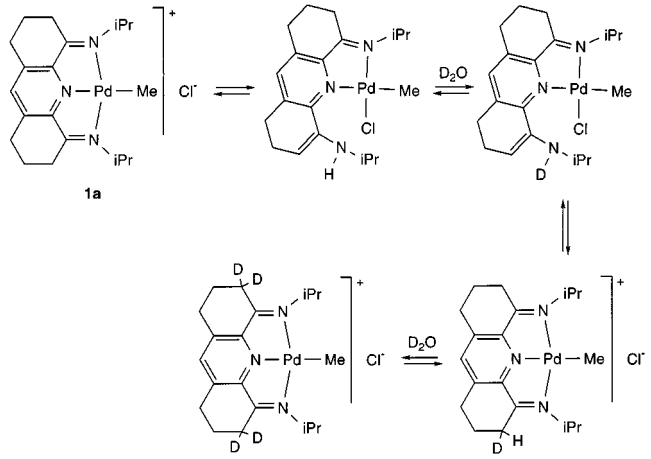

1a

In order to investigate the relative coordinating capabilities of the terdentate nitrogen ligands **2**−**6**, competition experiments were carried out. Addition of an equimolar amount of free **6** to a solution of complex **5c** in $CDCl_3$ at 20°C resulted in a mixture of complexes **5c** and **6c** and the free ligands **5** and **6** in a ratio **5c**/**6c** (= **6**/**5**) = 1:2. A mixture with the same **5c**/**6c** ratio was obtained upon addition of an equimolar amount of free **6** to a solution of complex **5**. These experiments and similar competition experiments with the other nitrogen ligands show that the coordinating capabilities of **2**, **3**, **4**, and **6** are comparable, but higher than that of **5**.

Molecular Structures of [Pd(Me)(1)]SO_3CF_3 (1b) and [Pd(Me)(4)]BAr'_4 (4c)

The molecular structures of **1b** and **4c** are shown in Figures 2 and 3. Selected bond lengths and bond angles of the non-hydrogen atoms are listed in Tables 1 and 2. The molecular structures of **1b** and **4c** both show a square-planar geometry with the three nitrogen atoms of the terdentate nitrogen ligand and a methyl ligand coordinated to the palladium(II) center. The relatively short Pd−N(2) bond lengths of 1.959(5) A for **1b** and 1.993(3) A for **4c** and the small *trans*-N(1)−Pd−N(3) bond angles of 155.50(19)° for **1b** and 156.95(11)° for **4c** have been observed also for **6a**[32] and for other palladium complexes containing comparable symmetric terdentate nitrogen ligands.[43][55][56][57][58][59][60][61] Interestingly, the Pd−N(1) and Pd−N(3) bond lengths in **4c** [2.103(4) and 2.116(4) A, respectively] are longer than those in [Pd(Me)(**6**)]Cl (**6a**) [Pd−N(1) = 2.048(9) A; Pd−N(3) = 2.057(8) A][32] and the angles Pd−N(1)−C(1) and Pd−N(3)−C(19) in **4c** [132.4(3) and 132.1(3)°] show a larger deviation from the ideal 120° than to those in **6a** [Pd−N(1)−C(1) = 128.8(7)°; Pd−N(3)−C(19) = 128.4(7)°].[32] These data indicate that the more rigid terdentate ligand **4** coordinates less strongly to the palladium center than the more flexible tpy ligand **6**. Whereas the four donor atoms and the palladium atom are confined to one plane in **4c** [maximum deviation from the least-squares plane is 0.005(3) A], the methyl ligand in complex **1b** is bent out of the coordination plane with an angle of 12.4(3)° between the methyl−palladium bond and the plane defined by N(1), N(2), and N(3). As a result, the methyl−palladium bond length of 2.189(4) A is large as compared to those of other palladium complexes containing a methyl ligand *trans*-positioned to a nitrogen atom (2.00−2.09 A).[10][11][12][32][47][48][50][52][53][54][58][61][62][63][65][66] The distances between C20 and the nearest hydrogen atoms on C15 and C18 of 2.67 A and 2.59 A, which are 0.23 A and 0.31 A shorter than the sum of the Van der Waals radii, clearly show that the distortion from planarity in **1b** is caused by steric interaction between the methyl ligand and the isopropyl groups. Recently, a similar observation has been made for a series of chlororhodium(I) complexes containing a terdentate nitrogen ligand. In these complexes, substituents on the side arms of the terdentate nitrogen ligand were found to force the chloride ligand out of the coordination plane.[61]

Carbon Monoxide Insertion

The methylpalladium complexes **1a**−**5a** and **1c**−**6c** reacted within 1 minute with carbon monoxide to give the corresponding acetylpalladium complexes **1d**−**5d** and **1e**−**6e**, respectively (Equation 3).

The acetylpalladium complexes **1e**−**6e** were isolated and characterized by ^{1}H NMR, ^{13}C NMR, and IR spectroscopy. In contrast, complexes **1d**−**5d** could not be iso-

Figure 2. ORTEP drawing (50% probability level) and adopted numbering scheme of [Pd(Me)(**1**)]SO_3CF_3 (**1b**); hydrogen atoms and SO_3CF_3 anion have been omitted for clarity

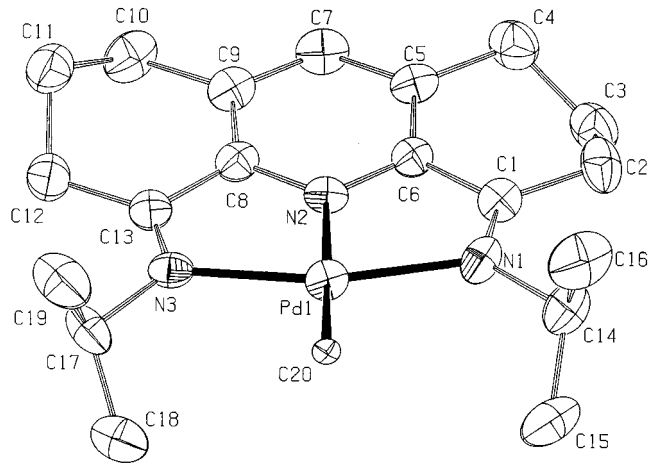

Figure 3. ORTEP drawing (50% probability level) and adopted numbering scheme of [Pd(Me)(**4**)]SO_3CF_3 (**4c**); hydrogen atoms and BAr'_4 anion have been omitted for clarity

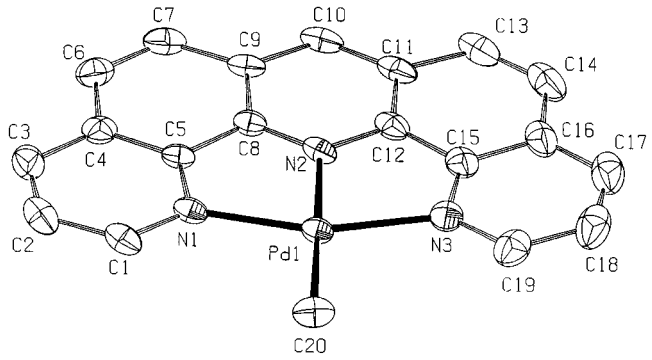

Table 1. Selected bond lengths [A] and angles [°] for [Pd(Me)(**1**)]SO_3CF_3 (**1b**) (with esd's in parentheses)

Bond lengths			
Pd(1)−N(1)	2.111(6)	N(2)−C(6)	1.333(8)
Pd(1)−N(2)	1.959(5)	N(2)−C(8)	1.341(9)
Pd(1)−N(3)	2.116(6)	N(3)−C(13)	1.262(9)
Pd(1)−C(20)	2.189(4)	N(3)−C(17)	1.490(9)
N(1)−C(1)	1.285(9)	C(1)−C(6)	1.474(9)
N(1)−C(14)	1.485(9)	C(8)−C(13)	1.488(9)
Bond angles			
N(1)−Pd(1)−N(2)	78.1(2)	Pd(1)−N(1)−C(1)	113.5(5)
N(1)−Pd(1)−N(3)	155.50(19)	Pd(1)−N(1)−C(14)	127.7(4)
N(1)−Pd(1)−C(20)	102.2(2)	Pd(1)−N(2)−C(6)	118.6(4)
N(2)−Pd(1)−N(3)	77.7(2)	Pd(1)−N(2)−C(8)	118.8(4)
N(2)−Pd(1)−C(20)	170.28(18)	Pd(1)−N(3)−C(13)	114.0(5)
N(3)−Pd(1)−C(20)	102.30(19)	Pd(1)−N(3)−C(17)	127.0(4)

lated, since these complexes, except for **1d**, are only soluble in alcohols, in which decomposition occurs within a few minutes, resulting in palladium black and an organic compound. This organic product was analyzed for **4d** and **6d** by ^{1}H NMR and GC-MS, and proved to be methyl acetate, methyl [D_3]acetate, ethyl acetate, and ethyl [D_5]acetate for decomposition in methanol, [D_4]methanol, ethanol, and

Table 2. Selected bond lengths [A] and angles [°] for [Pd(Me)(**4**)]BAr'_4 (**4c**) (with esd's in parentheses)

Bond lengths			
Pd(1)−N(1)	2.103(4)	N(2)−C(8)	1.309(5)
Pd(1)−N(2)	1.993(3)	N(2)−C(12)	1.323(6)
Pd(1)−N(3)	2.116(4)	N(3)−C(15)	1.373(5)
Pd(1)−C(20)	2.025(4)	N(3)−C(19)	1.334(5)
N(1)−C(1)	1.320(6)	C(5)−C(8)	1.431(5)
N(1)−C(5)	1.379(4)	C(12)−C(15)	1.429(6)
Bond angles			
N(1)−Pd(1)−N(2)	78.68(13)	Pd(1)−N(1)−C(1)	132.4(3)
N(1)−Pd(1)−N(3)	156.95(11)	Pd(1)−N(1)−C(5)	110.9(3)
N(1)−Pd(1)−C(20)	100.50(16)	Pd(1)−N(2)−C(8)	119.1(3)
N(2)−Pd(1)−N(3)	78.28(13)	Pd(1)−N(2)−C(12)	119.3(3)
N(2)−Pd(1)−C(20)	179.18(17)	Pd(1)−N(3)−C(15)	111.2(3)
N(3)−Pd(1)−C(20)	102.54(16)	Pd(1)−N(3)−C(19)	132.1(3)

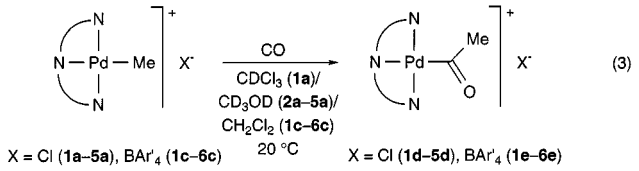

[D_6]ethanol respectively, indicating that the instability of complexes **1d**−**5d** in alcohols is caused by alcoholysis of the acetyl−palladium bond. A mechanism of this degradation process might involve dissociation of one of the distal nitrogen atoms of the terdentate ligand caused by coordination of the chloride counter anion,[67][68] followed by methanol coordination and reductive elimination of methyl acetate. This mechanism is supported by the observation that decomposition in alcohols proceeds much more slowly for complexes **2e**−**6e**, which contain the weakly coordinating tetrakis[3,5-bis(trifluoromethyl)phenyl]borate anion.[69]

The insertion of CO into the methyl−palladium bond of **1c**−**6c** is a reversible reaction. In solution decarbonylation of **1e**−**6e** occurs, resulting in reformation of the methylpalladium complexes **1c**−**6c**, without formation of any palladium black. For example, after 1 h of bubbling N_2 through a solution of **4e** in dichloromethane, 80% of decarbonylated [Pd(Me)(**4**)]BAr'_4 (**4c**) and 20% unreacted **4e** were present, whereas complete decarbonylation took place within 1 h in refluxing dichloromethane. Interestingly, complexes **1e**−**6e** also undergo decarbonylation in the solid state. Drying in vacuo for several hours or storage at 20°C for several days resulted in formation of the methylpalladium complexes **1c**−**6c**, without any other decomposition.

Alkene Insertion

(a) *Synthesis and Characterization of Alkylpalladium Complexes* **1f**−**6f**: Whereas insertion of ethylene, styrene, maleic anhydride, and cyclopentene does not occur, the acetylpalladium complexes **2e**−**6e**, but not **1e**, do react with the strained alkenes norbornene, norbornadiene, and dicyclopentadiene. Because of their complex NMR spectra, the products obtained after insertion of norbornene and dicyclopentadiene were difficult to characterize. However, the insertion of norbornadiene into the acetyl−palladium bond

of complexes **2e**−**6e** yielded the novel characterizable alkylpalladium complexes [Pd{$C_7H_8C(O)Me$}(N-N-N)]BAr'_4 (**2f**−**6f**) (Equation 4).

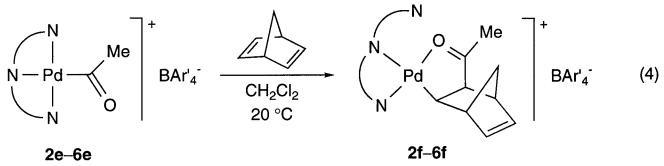

2e–6e **2f–6f** (4)

The reactions were completed within 30 minutes for **2e**−**6e** showing rates comparable to those found for the neutral complexes Pd{C(O)Me}Cl(Ar-BIAN) containing the rigid bidentate nitrogen ligands bis(arylimino)acenaphthene,[11][13] but the rates were slower than those observed for the ionic complexes [Pd{C(O)Me}(solv)(N-N)]SO_3CF_3 (solv = solvent; N-N = Ar-BIAN, bpy).[11][22] Complexes **2f**−**6f** were isolated and characterized by spectroscopic techniques. The ^{1}H-NMR spectra of **2f**−**6f** show the typical pattern of an inserted norbornadiene moiety and a coupling constant between the former olefinic protons of about 6 Hz, which indicates the expected *cis* addition of the carbon−palladium bond to the *exo* face of the norbornadiene.[9][11][13][16][22][32][70] Furthermore, the spectral data of **2f**−**6f** show the following interesting features: (i) In the IR spectra a low CO stretching frequency at ca. 1600 cm^{-1} is observed; (ii) In the ^{13}C-NMR spectra a low-field CO resonance appears at $\delta \approx 235$; (iii) In the ^{1}H-NMR spectra of **4f**−**6f** at −70°C separate signals for the two arms of the nitrogen ligands are observed; (iv) In the ^{15}N-NMR spectra of **2f**, **4f**, and **6f**, which will be discussed in detail separately,[71] a signal representing one distal nitrogen atom appears at $\delta \approx -150$, which is characteristic of a coordinated pyridine nitrogen atom.[72] In the case of **2f**, the signal of the other distal nitrogen atom is observed at $\delta = -68$, which is characteristic of a noncoordinated pyridine moiety[72] and can be compared to the distal nitrogen resonances of $\delta \approx -75$ for the free ligands **2**, **4**, and **6**.[71] Unfortunately, in the case of **4f** and **6f**, the signal of the noncoordinated nitrogen atom could not be observed, most probably due to the absence of a sufficiently large N-H coupling constant.

From these spectroscopic data, we conclude that the acyl oxygen atom is coordinated to the palladium center forming a C,O chelate and that, unexpectedly, the nitrogen ligand is coordinated in a bidentate fashion. In the case of flexible terdentate ligands such as **5** and **6**, the noncoordinated pyridyl moiety is most probably in a position perpendicular with regard to the palladium coordination plane, as observed in molecular structures of $Pd(C_6F_5)_2$(tpy)[36] and [Pd(η^3-C_3H_5)(tpy)]ClO_4[43], which contain a bidentate tpy ligand. In the case of rigid terdentate nitrogen ligands such as **4**, an asymmetrically bidentate coordination mode of the nitrogen ligand, i.e. with a relatively long Pd−N(central) bond and a relatively short Pd−N(distal) bond, may result in a long distance between palladium and the dissociated nitrogen atom (ca. 3.5 A, vide infra), which enables C,O chelate formation.

Complexes **4f**−**6f** show fluxional behavior on the ^{1}H-NMR time scale, as both sides of the terdentate ligand become magnetically equivalent in the temperature range of −50 to 20°C. The mechanism probably proceeds by site exchange of the distal nitrogen atoms involving a species in which the nitrogen ligand is coordinated in a terdentate fashion.

(b) *Kinetic Study of Norbornadiene Insertion:* To study the kinetics of the norbornadiene insertion into the carbon−palladium bond of complexes **1e**−**6e**, the reactions were carried out under pseudo-first-order conditions and were recorded by means of UV/Vis spectroscopy. In all cases, plotting the observed rate constants k_{obsd} versus time led to straight lines with a zero intercept, within experimental error, indicating that the rate law $k_{obsd} = k_2$[nbd] is obeyed. The experimental values of k_2 are independent of the presence of free terdentate nitrogen ligand and are listed with the respective activation parameters in Table 3.

Table 3. Rate constants k_2 and the enthalpy and entropy of activation of the reaction of complexes **1e**, **2e**, **4e**−**6e**, and **5d** with norbornadiene (standard deviations in parentheses)[a]

Compound	T [°C]	$10^2 k_2$ [s^{-1} м$^{-1}$]	$\Delta H^{\neq}$ [kJ mol^{-1}]	$\Delta S^{\neq}$ [J mol^{-1} K^{-1}]
1e	10.0(5)	0.11(1)	58(4)	−96(13)
	20.5(5)	0.24(1)		
	31.0(5)	0.65(1)		
2e	6.0(5)	120(5)	31(1)	−132(5)
	11.0(5)	150(6)		
	20.5(5)	251(12)		
	29.0(5)	350(9)		
4e	6.0(5)	17.7(3)	39(2)	−119(7)
	13.0(5)	25.1(4)		
	20.5(5)	40(2)		
	30.0(5)	72(3)		
5d	7.5(5)	655(28)		
5e	7.5(5)	16(1)	32(2)	−144(8)
	13.5(5)	25(1)		
	20.5(5)	33(2)		
	30.5(5)	52(2)		
6e	6.0(5)	1.86(3)	51(1)	−95(1)
	13.0(5)	3.22(3)		
	20.5(5)	5.8(1)		
	30.0(5)	11.5(3)		

[a] Conditions: dichloromethane as solvent, [Pd] = 0.19 мм.

The activation enthalpy (31−58 kJ mol^{-1}) and the large negative activation entropy (−144 to −95 J mol^{-1} K^{-1}) are comparable with those of the k_2 pathway of reaction of norbornadiene with Pd{C(O)Me}Cl(*p*-An-BIAN) containing the rigid bidentate nitrogen ligand bis(*p*-anisylimino)acenaphthene ($\Delta H^{\neq}$ = 48.4(18) kJ mol^{-1}; $\Delta S^{\neq}$ = −126(6) J mol^{-1} K^{-1}).[13] The rate constant k_2 is highly dependent on the terdentate nitrogen ligand in [Pd{C(O)Me}(N-N-N)]BAr'_4 (**1e**−**6e**) and increases in the order N-N-N = **1** << **6** << **5** < **4** << **2** (Figure 4). The reaction of norbornadiene with **1e** proceeded very slowly and an extremely large excess of norbornadiene (800−4000 equiv.) was required in order to ensure relatively fast norbornadiene insertion as compared to decarbonylation. Due to the absence of isosbestic points for the reaction of **3e**

with norbornadiene, no rate constants were determined for this reaction.

Figure 4. Pseudo-first-order rate constants (k_{obsd}) of the reaction of [Pd{C(O)Me}(N-N-N)]BAr'_4 (**1e**, **2e**, and **4e**−**6e**) with nbd as a function of the concentration of nbd; conditions: dichloromethane as solvent, 20.5°C, [Pd] = 0.19 mM

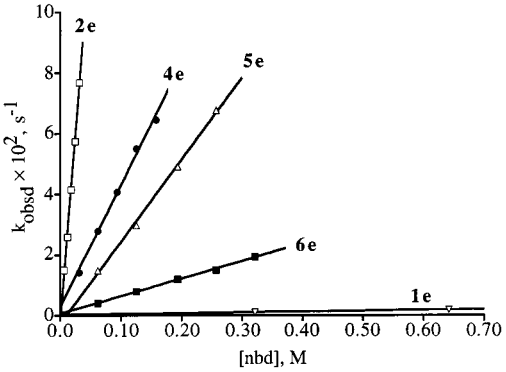

The influence of the counter anion X of [Pd{C(O)Me}(N-N-N)]X on the reaction with nbd was studied for the rigid ligand **4** and the flexible ligands **5** and **6**. In order to prevent decomposition of the unstable acetylchloropalladium complexes **4d**−**6d**, the reactions were carried out at 7.5°C. Unfortunately, a rate constant could be determined only in the case of **5d**, as isosbestic points were not obtained for **4d** or **6d**. From Figure 5 it is clear that the k_2 value of the reaction of [Pd{C(O)Me}(**5**)]X [X = Cl (**5d**), BAr'_4 (**5e**)] with nbd is highly dependent on the nature of the counter anion X; the k_2 rate constant increases from 0.16(1) s^{-1} M^{-1} for **5e** to 6.55(28) s^{-1} M^{-1} for **5d**.

Figure 5. Pseudo-first-order rate constants (k_{obsd}) of the reaction of [Pd{C(O)Me}(**5**)]X [X = Cl (**5d**), BAr'_4 (**5e**)] with nbd as a function of the concentration of nbd; conditions: dichloromethane as solvent, 7.5°C, [Pd] = 0.19 mM

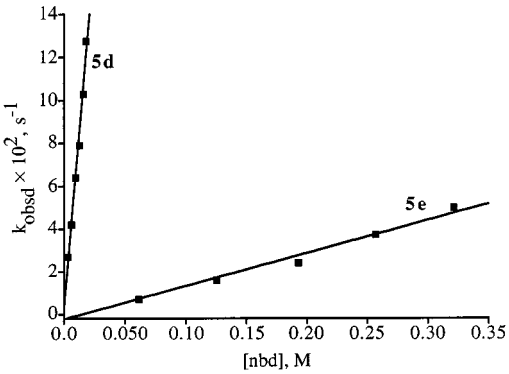

Ab Initio MO Calculations

To obtain more insight into the mechanism of insertion reactions of CO and alkenes into the carbon−palladium bond of complexes containing rigid terdentate nitrogen ligands, we have carried out for the first time ab initio MO calculations of the cationic model systems [Pd(Me)(N-N-N)]$^+$ (**I**) + CO and [Pd{C(O)Me}(N-N-N)]$^+$ + ethylene.

(a) *Carbon Monoxide Insertion:* The optimized geometries and selected bond lengths and bond angles of the starting methylpalladium complex **I**, the intermediate **III**, the transition states **II** and **IV**, and the acetylpalladium product **V** are shown in Scheme 2. The relative RHF and MP2 energies have been collected in Table 4 and the potential energy profile at the MP2 level is shown in Figure 6. The calculated bond angles N(1)−Pd−N(2) and N(2)−Pd−N(3) and nitrogen−palladium bond lengths for starting complex **I** and product **V** are in good agreement with those observed experimentally for the terdentate nitrogen ligand containing methylpalladium complexes **1b** (vide supra), **4c** (vide supra), and **6a**.[32] The calculated carbon−palladium distances in structures **I** (2.05 A) and **V** (1.97 A) are as expected for methyl-[12][32][47][50][52][53][62][73][74] and acetylpalladium[12][15][23][50][52][53][75] complexes, respectively. The Pd−CO bond lengths in CO-coordination transition state **II** (2.10 A) and CO-containing complex **III** (2.10 A) are very close to that calculated for *cis*-[Pd(Me)$(NH_3)_2$(CO)]$^+$ (2.106 A)[59], but somewhat longer than that calculated for [Pd(Me)$(NH_2CH_2CH_2NH_2)$(CO)]$^+$ (1.922 A)[76] and that experimentally observed for [Pd{C(O)Me}(phen)(CO)]BAr'_4 [1.922(11) A].[23] The geometry of the CO-containing species **III** can be considered to be square-planar, in which the four coordination sites are occupied by two nitrogen atoms of the terdentate nitrogen ligand, a CO and a methyl group. At the RHF level there is a small barrier (E_a = +13 kJ mol^{-1}) for formation of species **III**, but at the MP2 level formation of species **III** appears to be barrierless (E_a = −3 kJ mol^{-1}). The formation of species **III** is much less exothermic (−64 kJ mol^{-1}, MP2 value), however, than in the case of [Pd(Me)(**8**)]$^+$ containing the rigid bidentate model ligand HN=$CHCH_2$N=CH_2 (**8**) (−170 kJ mol^{-1}, MP2 value), as expected. The CO insertion is found to proceed via a three-centered insertion transition state **IV**, which is rather close to those reported for CO insertion into the carbon−palladium bond of the complexes Pd(Me)H(PH_3)(CO)[77], *cis*-[Pd(Me)$(NH_3)_2$(CO)]$^+$[59], and [Pd(Me)$(NH_2CH_2CH_2NH_2)$(CO)]$^+$[76]. The geometry of the acetyl species **V** suggests that the reaction occurs by CO insertion into the carbon−palladium bond. The geometry of species **IV**, however, clearly shows that it is the methyl group, not the carbonyl group, that migrates during the reaction, as experimentally demonstrated for platinum and palladium complexes with bidentate phosphorus ligands by van Leeuwen et al.[20][21] The formation of the transition state for CO insertion, **IV**, appears to be the rate-determining step for acetyl formation. The transition state **IV** lies 48 kJ mol^{-1} (MP2 value) above **III**. This activation barrier is slightly lower than those found for systems containing the bidentate ligands **8** (+59 kJ mol^{-1}, MP2 value) and $NH_2CH_2CH_2NH_2$ (+62 kJ mol^{-1}, B3LYP/I value)[76], presumably because of the stronger steric repulsion in the case of species **III**. The energy of the acetyl species **V** lies only 10 kJ mol^{-1} below that of **III**, which is completely in agreement with the experimentally observed reversibility of the CO insertion in complexes **1c**−**6c** (vide supra).

Scheme 2

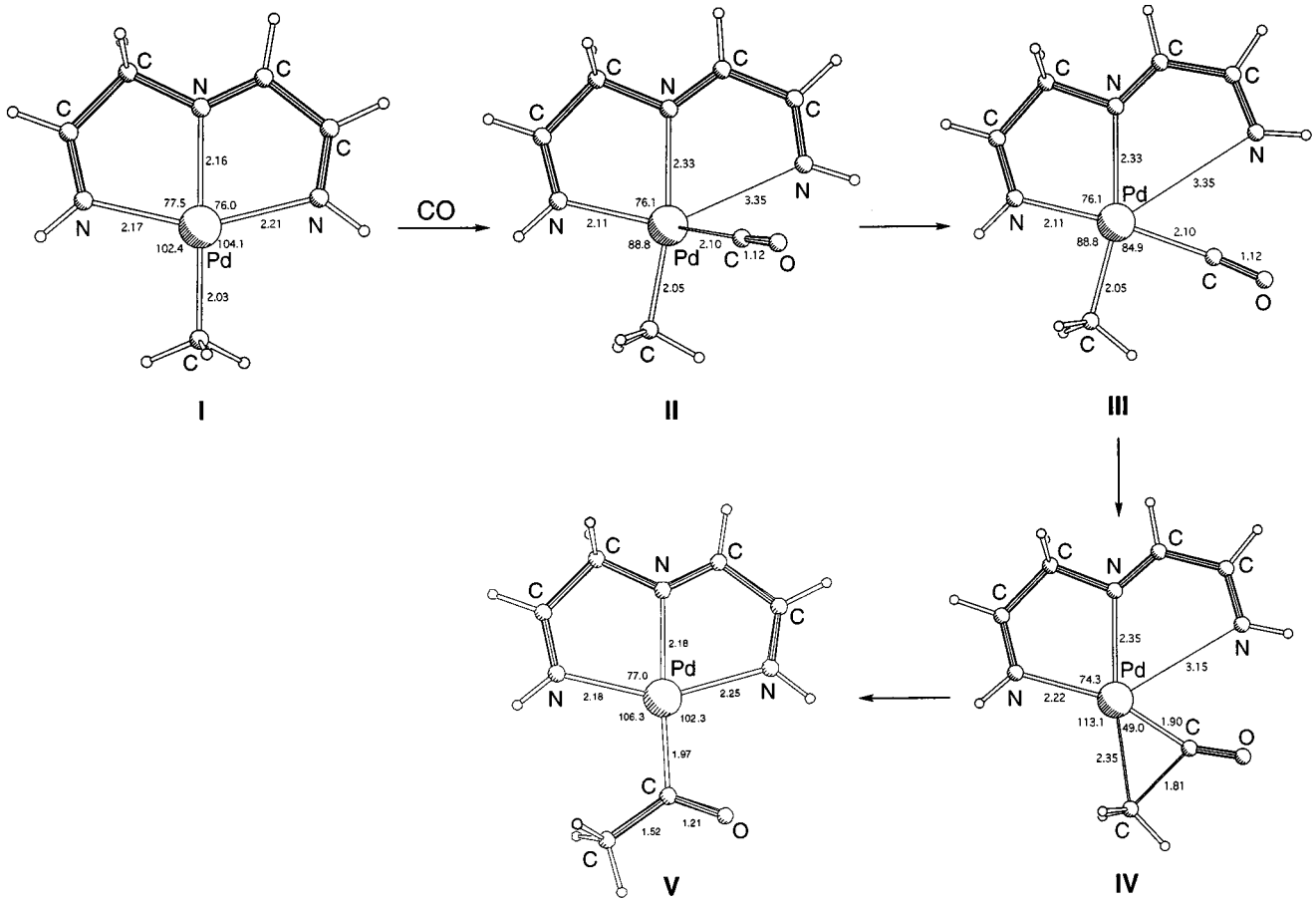

Table 4. Relative energies [kJ mol^{-1}] for stages of the CO and ethylene insertion in model systems with the ter- and bidentate nitrogen ligands **7** and **8**, respectively

Species[a]	L = **7** RHF	L = **7** MP2	L = **8** RHF	L = **8** MP2
$[Pd(Me)(L)]^+$ (**I**)	0.0	0.0	−0.0	3
CO coordination TS (**II**)	13	−3	[b]	[b]
$[Pd(Me)(CO)(L)]^+$ (**III**)	−16	−64	−93	−167
CO insertion TS (**IV**)	107	−16	15	−108
$[Pd\{C(O)Me\}(L)]^+$ (**V**)	−34	−74	−72	−137
$[Pd\{C(O)Me\}(C_2H_4)(L)]^+$	[c]	[c]	−110	−220
C_2H_4 insertion TS (**VI**)	77	−43	−34	−174
$[Pd\{\kappa^2\text{-}CH_2CH_2C(O)Me\}(L)]^+$ (**VII**)	−122	−114	−260	−278
$[Pd\{\kappa^1\text{-}CH_2CH_2C(O)Me\}(L)]^+$ (**VIII**)	−148	−156	[c]	[c]
$[Pd\{\kappa^2\text{-}CH_2CH_2C(O)Me\}(L)]^+$ (**IX**)	−149	−150	–	–

[a] Numbers of species with L = **7** are given in parentheses. – [b] Formation of $[Pd(Me)(CO)(\mathbf{8})]^+$ from $[Pd(Me)(\mathbf{8})]^+$ and CO appears to be barrierless. – [c] No minimum was found for this structure.

Figure 6. Potential-energy profile of CO and subsequent ethylene insertion in $[Pd(Me)(\mathbf{7})]^+$ (**I**), in kJ mol^{-1} at the MP2 level, relative to **I** + CO

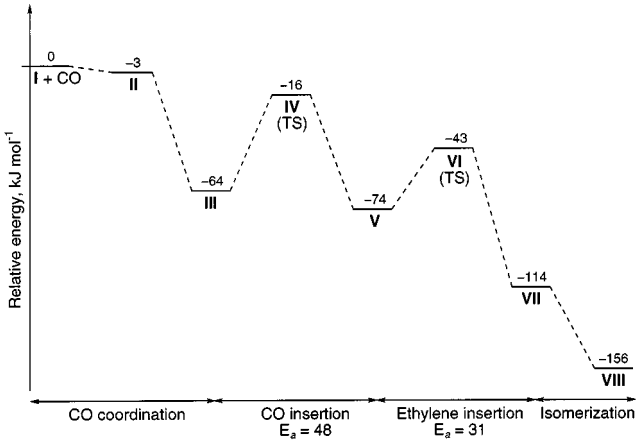

(b) *Ethylene Insertion:* The optimized geometries and selected bond lengths and bond angles of the starting complex, the transition state, and the initial and final product are shown in Scheme 3. The relative RHF and MP2 energies have been collected in Table 4 and the potential energy profile at the MP2 level is shown in Figure 6. Analogously to the CO insertion reaction in $[Pd(Me)(\mathbf{7})]^+$, the ethylene insertion into the acetyl−palladium bond of $[Pd\{C(O)Me\}(\mathbf{7})]^+$ is found to proceed via a four-coordinate transition state (species **VI**), in which two nitrogen atoms, the inserting ethylene molecule and the acetyl ligand occupy the four coordination sites. The ethylene insertion is found to pass through a four-centered transition state, similar to those found by others in systems which contain

Scheme 3

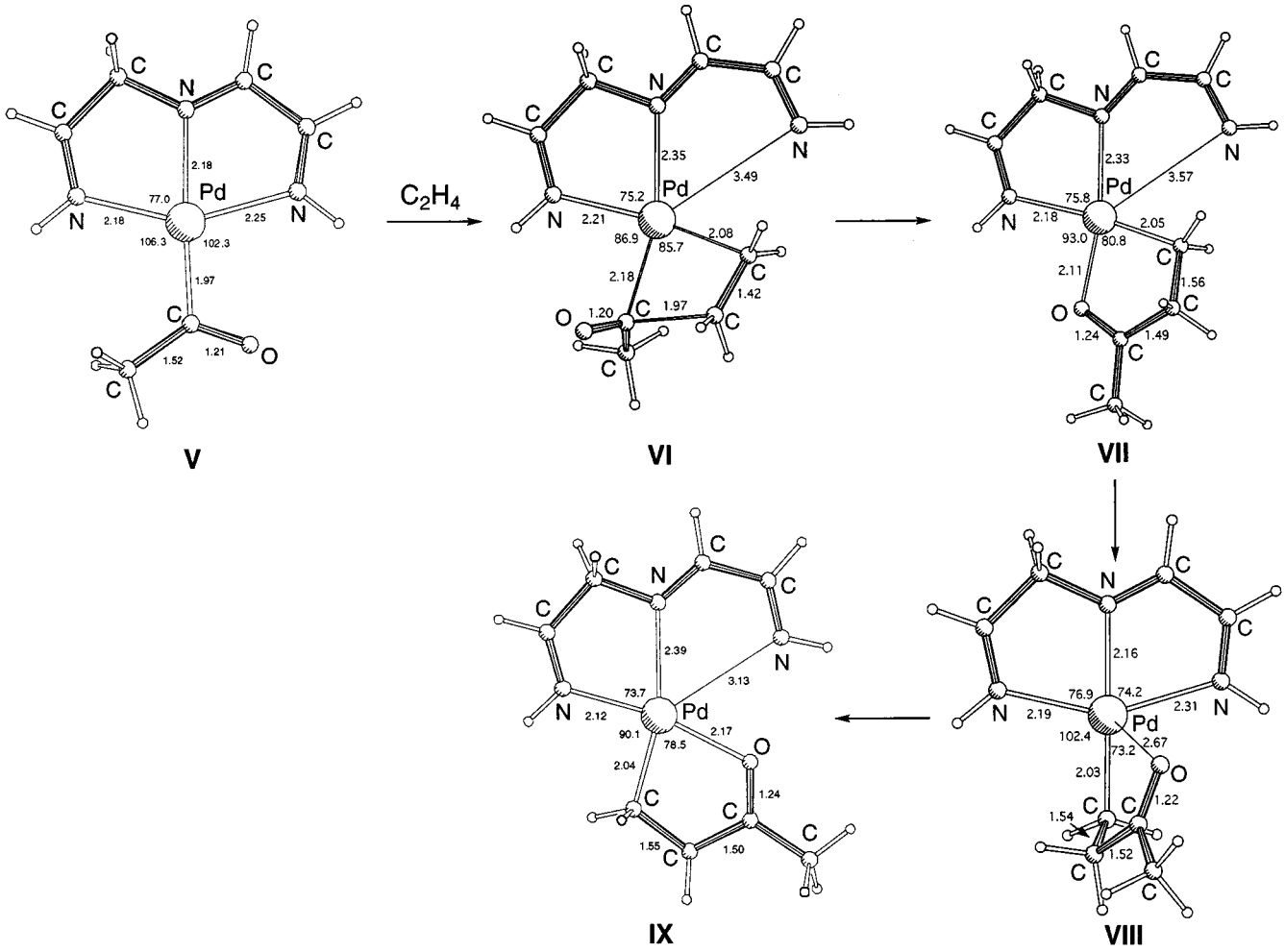

a bidentate ligand.[76][78][79][80] At the RHF level, we did not find a minimum for a structure containing a coordinated alkene and a nitrogen ligand coordinated in a bidentate fashion; therefore, the activation energy has been calculated relative to the acetyl species and free ethylene. Since complexation energies are much higher at the MP2 level, there might be a shallow local minimum at this level, which would result in a slightly higher activation energy. In any case, the calculated activation energy of 31 kJ mol^{-1} (MP2 value) is fairly low and comparable to that of the system, which contains the bidentate ligand **8** (E_a = 37 kJ mol^{-1} at MP2 level), despite the obvious crowding in structure **VI**. In the structure of the initial product **VII**, the acyl oxygen atom interacts strongly with the palladium center, which results in a relatively long C−O bond of 1.24 A and a short Pd−O distance of 2.11 A. These values agree well with that theoretically observed in [Pd{$C_2H_4C(O)Me$}($NH_2CH_2CH_2NH_2$)]$^+$ (C−O = 1.28 A; Pd−O = 2.07 A)[76] and those experimentally observed for [Pd{$C_7H_{10}C(O)Me$}(PPh_3)$_2$]BF_4[16] (C−O = 1.240(10) A; Pd−O = 2.114(6) A) and [Pd{$C_{10}H_{12}C(O)Me$}(bpy)]SO_3CF_3[22] (C−O = 1.249(6) A; Pd−O = 2.026(3) A). In the calculations, the chelate structure **VII** isomerizes to species **VIII**, in which the nitrogen ligand is coordinated in a terdentate fashion. The carbonyl group now occupies an apical position, as theoretically observed in [Pd($C_2H_4C(O)Et$)(PH_2CH=$CHPH_2$)(CO)]$^+$[79]. Our experiments show that for complexes **2f**−**6f**, obtained after norbornadiene insertion, species **IX** is more stable than structure **VIII**. On both the RHF and MP2 level, the energies of species **IX** and **VIII** are similar. This is completely in agreement with the experimentally observed fluxional behavior on the ^{1}H-NMR time scale for complexes **4f**−**6f**, which process is proposed to proceed via species of type **VIII**.

Comparison Between Theoretical and Experimental Results

The results of the ab initio MO calculations are fully in agreement with our experimental results. The observed H/D exchange in **1a** in the presence of D_2O, the fast alcoholysis of the acetylchloropalladium complexes **1d**−**6d**, and the structure of complexes **1f**−**6f** show the ability of ligands **1**−**6** to coordinate in a bidentate fashion. Furthermore, a mechanism by substitution of one of the distal nitrogen donor atoms by the substrate followed by rate-determining migratory insertion explains the following observations.

(i) Strained alkenes undergo facile insertion in complexes **2e**−**6e**, whereas simple unstrained alkenes failed to react. Strained alkenes are known to coordinate more strongly to palladium than unstrained alkenes[9][32], so it seems reasonable to assume that unstrained alkenes are unable to compete with the distal nitrogen atoms of the nitrogen ligand for coordination to the palladium.

(ii) Complex **1e** reacts very slowly with nbd, as the two bulky isopropyl groups in **1e** will hinder alkene association significantly.

(iii) The nbd insertion rate increases in the order **6e** < **5e**, with decreasing coordinating capability of the nitrogen ligand (vide supra).[81] Consequently, the distal nitrogen atoms will dissociate more easily, resulting in a more facile substitution by the alkene.

(iv) The nbd insertion rate increases in the order **5e** << **5d**. The chloride counter anion in **5d** may initiate nitrogen dissociation by coordination to the palladium.[32][67][68]

Interestingly, the nbd insertion rate increases in the order **6e** < **4e** < **2e**, whereas on the basis of the rigidity of nitrogen ligands **2**, **4**, and **6** an insertion rate for **2e** in between those of **4e** and **6e** would be expected. Both from calculations and from the molecular structures of **1b**, **4c**, and **6a**[32], it appears that considerable deformations of the ligand skeleton are needed to achieve terdentate coordination with acceptable nitrogen−palladium distances.[82] Even so, the coordination environment is distorted, with *trans* N−Pd−N angles deviating significantly from the ideal value of 180°. In that sense, these complexes can be considered to be strained. Dissociation of one of the arms of the nitrogen ligand, relieving the strain, can be expected to be a low-energy process, which indeed is observed in the experimental and theoretical studies. The strain in the ligand backbone in the terdentate coordinated situations obviously increases in the order **6** < **2** < **4**, reflecting the tendency of the ligand to coordinate in a bidentate fashion. However, ligands **6** and **2** can both create space with the same ease by rotating the dangling pyridyl group, whereas creation of space is much more difficult in the case of ligand **4**. Thus, we believe that the higher insertion rate for **2e** and **4e** relative to **6e** reflects the higher strain in **2e** and **4e**. Furthermore, the higher insertion rate for **2e** relative to **4e** is most probably caused by more facile creation of a free coordination site.

Complexes **2f**−**6f** showed further reactivity toward CO and nbd, but the complexity of the ^{1}H-NMR spectra made assignment difficult. Furthermore, further insertions are expected to proceed alike, and our results have demonstrated that not only complexes containing flexible terdentate nitrogen ligands, but also complexes containing rigid terdentate nitrogen ligands are useful in studying the intimate steps of the catalytic cycle of polyketone formation.

Conclusion

We have shown that ionic methyl- and acetylpalladium complexes containing flexible and rigid terdentate nitrogen ligands undergo sequential insertion of carbon monoxide and strained alkenes. Although nitrogen dissociation was expected to be difficult for complexes containing rigid terdentate nitrogen ligands, ab initio MO calculations show that the mechanism of both insertion reactions unexpectedly proceeds by substitution of one of the distal nitrogen atoms of the terdentate nitrogen ligand, followed by a rate-determining migratory insertion reaction. These theoretical results, which indicate that even rigid terdentate nitrogen ligands may coordinate in a bidentate fashion, are fully supported by the experimentally observed bidentate coordination mode of both flexible and rigid terdentate nitrogen ligands in alkylpalladium complexes, obtained after norbornadiene insertion and the kinetic study of this insertion reaction. In our attempt to prevent nitrogen dissociation by employing rigid terdentate nitrogen ligands, the opposite effect has been observed, as the increasing rigidity of this particular set of terdentate nitrogen ligands leads to increasing strain, *facilitating* nitrogen dissociation.

This work was supported by the *Netherlands Foundation for Chemical Research (SON)* with financial aid from the *Netherlands Organization for Scientific Research (NWO)*. P. H. M. B. thanks Dr. *J.H. van Lenthe* (Utrecht University) for generous amounts of computer time. Q. X. and R. P. T. thank the *Robert A. Welch Foundation* and the *National Science Foundation* (Grant CHE-9224686) for the financial support. We thank Dr. *R. E. Rülke* for helpful discussions and for the GC-MS measurements, and *J. W. H. Peeters* for the mass-spectrometry measurements.

Experimental Section

General: All manipulations were carried out in purified dry nitrogen by using standard Schlenk techniques. Solvents were dried and stored under nitrogen. Carbon monoxide 99.5% was purchased from HoekLoos and was used without further purification. The compounds 1,2,3,4,5,6,7,8-octahydroacridine-4,5-dione[83], 2-(2′-pyridyl)-1,10-phenanthroline (**2**)[44], 1,2-dihydrodipyrido[4,3-*b*;5,6-*b*]-acridine (**3**)[45], dipyrido[4,3-*b*;5,6-*b*]acridine (**4**)[45], 4′-methylthio-2,2′:6′,2′′-terpyridine (**5**)[46], Pd(Me)Cl(COD)[72] (COD = 1,5-cyclooctadiene), [Pd(Me)(**6**)]Cl (**6a**)[32], [Pd{C(O)Me}(**6**)]Cl (**6d**)[32], and sodium tetrakis[3,5-bis(trifluoromethyl)phenyl]borate (NaBAr′$_4$)[84] were prepared according to the literature. All other starting chemicals were used as commercially obtained. Silver trifluoromethanesulfonate was stored under nitrogen in the dark. − ^{1}H- and ^{13}C-NMR spectra (300.13 and 75.48 MHz, respectively) were recorded with a Bruker AMX 300 spectrometer at 20°C, unless noted otherwise. Chemical shifts are in ppm relative to TMS as external standard (s = singlet, d = doublet, dd = doublet of doublets, t = triplet, q = quadruplet, qq = quadruplet of quadruplet, sept = septuplet, m = multiplet, br. = broad). ^{15}N chemical shifts, which are in ppm relative to nitromethane as external standard, were extracted from gradient-selected (^{1}H,^{15}N)-HMQC experiments[85][86][87] with a Bruker DRX 300 spectrometer. For adopted numbering schemes see Figure 1. − IR spectra were obtained with a Bio-Rad FTS-7 spectrophotometer and mass spectra were obtained with a JEOL JMS SX/SX102A four-sector mass spectrometer, coupled to a JEOL MS-MP7000 data system. GC-MS spectra were obtained with a Hewlett-Packard 5890 series II gas chromatograph with a Gerstel CIS III temperature-controllable injector, an HP 5971A mass-selective detector with electron-impact ionization at 70 eV, and an HP Ultra-2 column (25 m, 0.20 mm inner diameter, 0.33 μm film thickness).

4,5-Bis(isopropylimino)-1,2,3,4,5,6,7,8-octahydroacridine (**1**): A solution of 1,2,3,4,5,6,7,8-octahydroacridine-4,5-dione (1.04 g, 4.84

mmol) in 20 ml of isopropylamine, to which formic acid (2 drops) and $MgSO_4$ (2 g) were added, was stirred at 20°C. After 5 h, the solution was filtered and the isopropylamine was evaporated in vacuo, which resulted in a red oil. Purification by chromatography on neutral alumina with hexane/diethyl ether (4:1) as eluent, resulted in **1** as a yellow oil (704 mg, 49%). – ^{1}H NMR ($CDCl_3$): δ = 7.16 (s, 7-H), 4.85 (d, *J* = 4.8 Hz, 5-H), 4.80 (br., NH), 3.48 (sept, *J* = 6.3 Hz, C*H*Me$_2$), 2.76 (t, *J* = 7.6 Hz, 3-H), 2.35 (m, 4 H, 4-H), 1.24 (d, *J* = 6.3 Hz, CH*Me*$_2$). – ^{13}C NMR ($CDCl_3$): δ = 146.1 (C-1), 139.0 (C-2), 133.8 (C-7), 130.5 (C-6), 94.7 (C-5), 43.5 (*C*HMe$_2$), 27.5, 21.5 (C-3 and C-4), 22.6 (CH*Me*$_2$). – IR (KBr): ν = 3390 cm^{-1} (NH). – MS (EI): calcd. for $C_{19}H_{27}N_3$ 297.2205; found 297.2202.

Chloro(methyl)palladium Complexes **1a–5a**: 4,5-Bis(isopropylimino)-1,2,3,4,5,6,7,8-octahydroacridine (**1**) (714 mg, 2.38 mmol) was added to a solution of Pd(Me)Cl(COD) (431 mg, 1.63 mmol) in 20 ml of toluene. The yellow precipitate, which was formed instantaneously, was separated from the toluene and was washed with diethyl ether (2 × 20 ml). This resulted in **1a** as a yellow solid (577 mg, 78%).

By following the procedure for **1a**, complexes **2a–5a** were synthesized in yields varying from 83 to 95%.

*[Pd(Me)(**1**)]Cl* (**1a**): ^{1}H NMR ($CDCl_3$): δ = 8.03 (s, 7-H), 4.28 (sept, *J* = 6.5 Hz, C*H*Me$_2$), 3.14 (t, *J* = 5.9 Hz, 3-H), 3.09 (t, *J* = 6.4 Hz, 5-H), 2.14 (m, 4 H, 4-H), 1.33 (d, *J* = 6.5 Hz, CH*Me*$_2$), 0.86 (s, Pd–Me). – ^{13}C NMR ($CDCl_3$): δ = 175.6 (C-6), 146.3 (C-1), 142.9 (C-2), 138.9 (C-7), 55.1 (*C*HMe$_2$), 29.9 (C-5), 26.9 (C-3), 22.2 (C-4), 21.5 (CH*Me*$_2$), –6.0 (Pd–Me). – MS (FAB): calcd. for $[C_{20}H_{30}N_3Pd]^+$ 418; found 418. – $C_{20}H_{30}ClN_3Pd \cdot H_2O$: calcd. C 50.85, H 6.83, N 8.90; found C 50.67, H 6.44, N 8.57.

*[Pd(Me)(**2**)]Cl* (**2a**): ^{1}H NMR (CD_3OD): δ = 8.69 (m, 3 H, 1-H, 8-H, and 9-H), 8.50 (d, *J* = 4.7 Hz, 15-H), 8.43 (m, 2 H, 3-H and 12-H), 8.29 (m, 1 H, 13-H), 8.08 (d, *J* = 9.0 Hz, 16-H or 17-H), 8.04 (d, *J* = 9.0 Hz, 16-H or 17-H), 7.92 (dd, *J* = 8.2, 5.2 Hz, 2-H), 7.74 (m, 1 H, 14-H), 0.85 (s, Pd–Me). – ^{13}C NMR (CD_3OD): δ = 157.6, 152.7, 152.1, 149.8, 149.2, 141.8, 140.8, 140.1, 139.3, 131.6, 129.8, 129.5, 129.4, 127.5, 127.2, 125.9, 122.0 (C-1–C-17), 5.3 (Pd–Me). – MS (FAB): calcd. for $[C_{18}H_{14}N_3Pd]^+$ 378.0222; found 378.0242. – $C_{18}H_{14}ClN_3Pd \cdot 1.5\ H_2O$: calcd. C 49.00, H 3.89, N 9.52; found C 49.23, H 4.00 , N 9.60.

*[Pd(Me)(**3**)]Cl* (**3a**): ^{1}H NMR (CD_3OD): δ = 8.38 (d, *J* = 8.1 Hz, 3-H), 8.26 (d, *J* = 5.1 Hz, 1-H), 8.18 (s, 8-H), 7.93 (m, 2 H, 13-H and 15-H), 7.70 (m, 2 H, 16-H and 17-H), 7.63 (dd, *J* = 8.1, 5.1 Hz, 2-H), 7.49 (dd, *J* = 7.8, 5.4 Hz, 14-H), 3.23 (m, 4 H, 18-H and 19-H), 0.47 (s, Pd–Me). – ^{13}C NMR (CD_3OD, –20°C): δ = 153.6, 152.5, 150.7, 148.8, 146.5, 141.2, 139.7, 139.1, 138.5, 136.0, 135.5, 130.7, 130.0, 129.4, 129.0, 126.9, (C-1–C-17), 26.0, 24.4, (C-18 and C-19), 3.3 (Pd–Me). – MS (FAB): calcd. for $[C_{20}H_{16}N_3Pd]^+$ 404.0379; found 404.0391. – $C_{20}H_{16}ClN_3Pd \cdot 2\ H_2O$: calcd. C 50.44, H 4.24, N 8.82; found C 50.37, H 4.51, N 8.69.

*[Pd(Me)(**4**)]Cl* (**4a**): ^{1}H NMR (CD_3OD): δ = 8.85 (s, 8-H), 8.54 (d, *J* = 7.9 Hz, 3-H), 8.42 (d, *J* = 4.7 Hz, 1-H), 7.85 (m, 6 H, 2-H, 16-H, and 17-H), 0.79 (s, Pd–Me). – ^{13}C NMR (CD_3OD): δ = 152.5 (C-1), 148.0, 139.2 (C-5 and C-6), 139.8 (C-3), 135.3 (C-8), 131.1, 128.0 (C-4 and C-7), 128.7, 128.2, 127.2 (C-2, C-16 and C-17), 3.7 (Pd–Me). – MS (FAB): calcd. for $[C_{20}H_{14}N_3Pd]^+$ 402.0222; found 402.0200. – $C_{20}H_{14}ClN_3Pd \cdot 2.5\ H_2O$: calcd. C 49.71, H 3.97, N 8.70; found C 50.36, H 4.13, N 8.70.

*[Pd(Me)(**5**)]Cl* (**5a**): ^{1}H NMR (CD_3OD): δ = 8.11 (d, *J* = 6.0 Hz, 1-H), 8.03 (pst, 2-H), 7.96 (d, *J* = 5.0 Hz, 4-H), 7.59 (s, 7-H), 7.48 (pst, 3-H), 2.58 (s, SMe), 0.20 (s, Pd–Me). – ^{13}C NMR (CD_3OD): δ = 159.6 (C-8), 156.1, 150.2 (C-5 and C-6), 151.8 (C-1), 141.6 (C-3), 129.0 (C-2), 125.4 (C-4), 118.9 (C-7), 14.5 (SMe), 6.6 (Pd–Me). – MS (FAB): calcd. for $[C_{17}H_{16}N_3PdS]^+$, 400; found 400. – $C_{17}H_{16}ClN_3PdS \cdot 1.5\ H_2O$: calcd. C 44.07, H 4.14, N 9.07; found C 43.83, H 4.02, N 8.90.

*[Pd(Me)(**1**)]SO$_3$CF$_3$* (**1b**): To a solution of [Pd(Me)(**1**)]Cl (**1a**) (56.9 mg, 0.12 mmol) in a mixture of 20 ml of dichloromethane and 0.5 ml of acetonitrile was added $AgSO_3CF_3$ (34.6 mg, 0.13 mmol), and the mixture was stirred in the dark at 20°C. After 10 min, the mixture was evaporated to dryness and 20 ml of dichloromethane were added. After filtering the solution through Celite and extracting the residue with dichloromethane (5 ml), the combined filtrates were evaporated to dryness. Washing the residue with diethyl ether (2 × 20 ml) and drying in vacuo, yielded **1b** as a yellow solid (62.5 mg, 89%). – ^{1}H NMR ($CDCl_3$): δ = 7.84 (s, 7-H), 4.28 (sept, *J* = 6.6 Hz, C*H*Me$_2$), 3.01 (m, 8 H, 3-H and 5-H), 2.12 (m, 4 H, 4-H), 1.34 (d, *J* = 6.6 Hz, CH*Me*$_2$), 0.88 (s, Pd–Me). – ^{13}C NMR ($CDCl_3$): δ = 175.5 (C-6), 146.3 (C-1), 142.8 (C-2), 138.7 (C-7), 55.3 (*C*HMe$_2$), 29.7 (C-5), 26.6 (C-3), 22.1 (C-4), 21.4 (CH*Me*$_2$), –5.9 (Pd–Me). – MS (FAB): calcd. for $[C_{20}H_{30}N_3Pd]^+$ 418; found 418. – $C_{21}H_{30}F_3N_3O_3PdS$: calcd. C 44.41, H 5.33, N 7.40; found C 44.49, H 5.21, N 7.24.

Methylpalladium Tetrakis[3,5-bis(trifluoromethyl)phenyl]borate Complexes **1c–6c**: To a solution of [Pd(Me)(**1**)]Cl (**1a**) (69.6 mg, 0.15 mmol) in 20 ml of dichloromethane, $NaBAr'_4$ (123.3 mg, 0.14 mmol) was added. After stirring for 15 min at 20°C the solution was concentrated to dryness. After addition of 20 ml of diethyl ether, the solution was filtered and concentrated to dryness. The resulting yellow solid was washed with hexane (2 × 20 ml) and dried in vacuo, yielding complex **1c** (148.7 mg, 83%).

By following the procedure for **1c**, complexes **2c–6c** were obtained from the corresponding chloro(methyl)palladium complexes **2a–6a** in yields varying from 78 to 95%.

*[Pd(Me)(**1**)]BAr′$_4$* (**1c**): ^{1}H NMR ($CDCl_3$): δ = 7.70 (s, Ar′ H$_{ortho}$), 7.52 (s, Ar′ H$_{para}$), 7.48 (s, 7-H), 4.23 (sept, *J* = 6.6 Hz, C*H*Me$_2$), 2.87 (t, *J* = 6.5 Hz, 5-H), 2.76 (t, *J* = 6.0 Hz, 3-H), 1.99 (m, 4 H, 4-H), 1.31 (d, *J* = 6.6 Hz, CH*Me*$_2$), 0.97 (s, Pd–Me). – ^{13}C NMR ($CDCl_3$): δ = 174.4 (C-6), 161.5 (q, *J* = 50 Hz, Ar′ C$_{ipso}$), 146.3 (C-1), 142.2 (C-2), 137.9 (C-7), 134.6 (Ar′ C$_{ortho}$), 128.7 (qq, *J* = 31, 3 Hz, Ar′ C$_{meta}$), 124.3 (q, *J* = 273 Hz, Ar′ CF$_3$), 117.3 (Ar′ C$_{para}$), 55.4 (*C*HMe$_2$), 29.5, 26.5 (C-3 and C-5), 21.8 (C-4), 21.3 (CH*Me*$_2$), –4.8 (Pd–Me). – MS (FAB): calcd. for $[C_{20}H_{30}N_3Pd]^+$ 418.1474; found 418.1435. – $C_{52}H_{42}BF_{24}N_3Pd$: calcd. C 48.71, H 3.30, N 3.28; found C 48.35, H 3.33, N 3.13.

*[Pd(Me)(**2**)]BAr′$_4$* (**2c**): ^{1}H NMR ($CDCl_3$): δ = 8.81 (dd, *J* = 5.0, 0.9 Hz, 1-H), 8.65 (d, *J* = 5.1 Hz, 15-H), 8.49 (dd, *J* = 8.3, 0.9 Hz, 3-H), 8.41 (d, *J* = 8.6 Hz, 12-H), 8.05 (m, 3 H, 8-H, 9-H, and 13-H), 7.92 (d, *J* = 8.9 Hz, 16-H or 17-H), 7.86 (d, *J* = 8.9 Hz, 16-H or 17-H), 7.86 (dd, *J* = 8.3, 5.0 Hz, 2-H), 7.74 (s, Ar′ H$_{ortho}$), 7.64 (m, 1 H, 14-H), 7.48 (s, Ar′ H$_{para}$), 1.11 (s, Pd–Me). – ^{13}C NMR ($CDCl_3$): δ = 161.5 (q, *J* = 50 Hz, Ar′ C$_{ipso}$), 134.5 (Ar′ C$_{ortho}$), 128.7 (qq, *J* = 31, 3 Hz, Ar′ C$_{meta}$), 124.2 (q, *J* = 273 Hz, Ar′ CF$_3$), 117.3 (Ar′ C$_{para}$), 157.6, 152.3, 151.3, 150.0, 149.5, 141.7, 140.4, 139.0, 138.2, 131.2, 129.3, 129.0, 128.1, 126.4, 123.9, 120.4 (C-1–C-17), 5.6 (Pd–Me). – MS (FAB): calcd. for $[C_{18}H_{14}N_3Pd]^+$ 378; found 378. – $C_{50}H_{26}BF_{24}N_3Pd$: calcd. C 48.36, H 2.11, N 3.38; found C 48.51, H 2.16, N 3.37.

*[Pd(Me)(**3**)]BAr′$_4$* (**3c**): ^{1}H NMR ($CDCl_3$): δ = 8.76 (dd, *J* = 5.0, 1.0 Hz, 1-H), 8.44 (dd, *J* = 8.3, 1.2 Hz, 3-H), 8.39 (d, *J* = 5.2 Hz, 15-H), 8.17 (s, 8-H), 7.84 (d, *J* = 8.9 Hz, 16-H or 17-H), 7.79

(d, J = 8.9 Hz, 16-H or 17-H), 7.71 (s, Ar′ H_{ortho}), 7.52 (dd, J = 8.0, 5.2 Hz, 14-H), 7.47 (s, Ar′ H_{para}), 3.30 (m, 4 H, 18-H and 19-H), 1.09 (s, Pd−Me), signals of 2-H, 3-H, and 13-H are overlapping with signals of protons from $BAr'_4{}^-$. − ^{13}C NMR ($CDCl_3$): δ = 161.5 (q, J = 51 Hz, Ar′ C_{ipso}), 134.5 (Ar′ C_{ortho}), 128.7 (qq, J = 31, 3 Hz, Ar′ C_{meta}), 124.2 (q, J = 273 Hz, Ar′ CF_3), 117.3 (Ar′ C_{para}), 154.4, 151.7, 150.2, 149.8, 147.0, 140.5, 140.3, 139.7, 138.8, 137.2, 134.7, 134.6, 130.6, 129.9, 128.4, 126.3, 126.0 (C-1−C-17), 26.0, 24.5 (C-18 and C-19), 3.4 (Pd−Me). − MS (FAB): calcd. for $[C_{20}H_{16}N_3Pd]^+$ 404; found, 404. − $C_{52}H_{28}BF_{24}N_3Pd$: calcd. C 49.26, H 2.23, N 3.31; found C 49.27, H 2.62, N 3.31.

*[Pd(Me)(**4**)]BAr′$_4$* (**4c**): ^1H NMR ($CDCl_3$): δ = 8.90 (s, 8-H), 8.86 (dd, J = 4.9, 0.9 Hz, 1-H), 8.52 (dd, J = 8.4, 0.9 Hz, 3-H), 8.01 (d, J = 9.2 Hz, 16-H or 17-H), 7.90 (d, J = 9.2 Hz, 16-H or 17-H), 7.93 (dd, J = 8.4, 4.9 Hz, 2-H), 7.72 (s, Ar′ H_{ortho}), 7.46 (s, Ar′ H_{para}), 1.26 (s, Pd−Me). − ^{13}C NMR ($CDCl_3$): δ = 161.5 (q, J = 50 Hz, Ar′ C_{ipso}), 151.9 (C-1), 150.0, 141.3 (C-5 and C-6), 138.9 (C-3), 134.5 (Ar′ C_{ortho}), 131.3, 128.7 (C-4 and C-7), 128.7 (qq, J = 31, 3 Hz, Ar′ C_{meta}), 128.2, 127.0, 126.9 (C-2, C-16, and C-17), 124.2 (q, J = 273 Hz, Ar′ CF_3), 117.2 (Ar′ C_{para}), 3.4 (Pd−Me), signal of C-8 is overlapping with signal of Ar′ C_{ortho}. − MS (FAB): calcd. for $[C_{20}H_{14}N_3Pd]^+$ 402; found 402. − $C_{52}H_{26}BF_{24}N_3Pd$: calcd. C 49.34, H 2.07, N 3.32; found C 49.73; H 2.06, N 3.18.

*[Pd(Me)(**5**)]BAr′$_4$* (**5c**): ^1H NMR ($CDCl_3$): δ = 8.58 (d, J = 5.4 Hz, 1-H), 8.00 (m, 4 H, 3-H and 4-H), 7.72 (m, 10 H, Ar′ H_{ortho} and 7-H), 7.59 (m, 2 H, 2-H), 7.51 (s, Ar′ H_{para}), 2.60 (s, SMe), 0.94 (s, Pd−Me). − ^{13}C NMR ($CDCl_3$): δ = 161.5 (q, J = 50 Hz, Ar′ C_{ipso}), 158.8 (C-8), 157.6, 149.9 (C-5 and C-6), 151.4 (C-1), 140.1 (C-3), 134.6 (Ar′ C_{ortho}), 128.7 (qq, J = 32, 3 Hz, Ar′ C_{meta}), 127.8 (C-2), 124.3 (q, J = 273 Hz, Ar′ CF_3), 123.3 (C-4), 117.2 (Ar′ C_{para}), 117.1 (C-7), 14.0 (SMe), 7.0 (Pd−Me). − MS (FAB): calcd. for $[C_{17}H_{16}N_3SPd]^+$ 400; found 400. − $C_{49}H_{28}BF_{24}N_3PdS$: calcd. C 46.56, H 2.23, N 3.32; found C 46.65, H 2.28, N 3.30.

*[Pd(Me)(**6**)]BAr′$_4$* (**6c**): ^1H NMR ($CDCl_3$): δ = 8.60 (d, J = 5.1 Hz, 1-H), 8.08 (m, 2 H, 3-H), 7.97 (d, J = 8.1 Hz, 4-H), 7.91 (m, 1 H, 8-H), 7.85 (m, 2 H, 7-H), 7.73 (s, Ar′ H_{ortho}), 7.64 (m, 2 H, 2-H), 7.50 (s, Ar′ H_{para}), 0.99 (s, Pd−Me). − ^{13}C NMR ($CDCl_3$): δ = 161.5 (q, J = 50 Hz, Ar′ C_{ipso}), 157.6, 150.9 (C-5 and C-6), 151.4 (C-1), 140.7 (C-8), 140.3 (C-3), 134.5 (Ar′ C_{ortho}), 128.8 (qq, J = 32, 3 Hz, Ar′ C_{meta}), 127.9 (C-2), 124.2 (q, J = 273 Hz, Ar′ CF_3), 123.6 (C-4), 122.1 (C-7), 117.2 (Ar′ C_{para}), 8.1 (Pd−Me). − MS (FAB): calcd. for $[C_{16}H_{14}N_3Pd]^+$, 354; found 354. − $C_{48}H_{26}BF_{24}N_3Pd$: C 47.34, H 2.15, N 3.45; found C 46.82, H 2.28, N 3.42.

Acetylchloropalladium Complexes **1d−5d**: Carbon monoxide was bubbled through a glass capillary into a solution of ca. 5 mg of the methylpalladium complexes **1a−5a** in 0.5 ml of solvent (**1a**, $CDCl_3$, **2a−5a**, CD_3OD). After 0.5 min, the products were identified by ^1H-NMR spectroscopy. Complexes **1d−5d** could not be isolated due to rapid decomposition.

*[Pd{C(O)Me}(**1**)]Cl* (**1d**): ^1H NMR ($CDCl_3$, −35°C): δ = 7.95 (s, 7-H), 4.15 (sept, J = 6.2 Hz, C*H*Me_2), 3.03 (m, 8 H, 3-H and 5-H), 2.67 [s, C(O)Me], 2.11 (m, 4 H, 4-H), 1.16 (d, J = 6.2 Hz, CH*Me*$_2$).

*[Pd{C(O)Me}(**2**)]Cl* (**2d**): ^1H NMR (CD_3OD): δ = 8.83 (1 H, m), 8.66 (2 H, m), 8.47 (3 H, m), 8.20 (1 H, m), 8.03 (2 H, m), 7.95 (1 H, m), 7.70 (1 H, m), 2.72 [s, C(O)Me].

*[Pd{C(O)Me}(**3**)]Cl* (**3d**): ^1H NMR (CD_3OD): δ = 9.13 (d, J = 5.4 Hz, 1-H), 8.89 (s, 8-H), 8.84 (dd, J = 8.1, 1.5 Hz, 3-H), 8.38 (d, J = 8.9 Hz, 16-H or 17-H), 8.34 (d, J = 8.9 Hz, 16-H or 17-H), 7.98 (m, 2 H, 13-H and 15-H), 7.69 (dd, J = 8.1, 5.4 Hz, 2-H), 7.33 (dd, J = 7.9, 5.4 Hz, 14-H), 1.62 [s, C(O)Me], signals of 18-H and 19-H are overlapping with signals of the solvent.

*[Pd{C(O)Me}(**4**)]Cl* (**4d**): ^1H NMR (CD_3OD): δ = 8.60 (s, 8-H), 8.58 (d, J = 4.7 Hz, 1-H), 8.36 (d, J = 8.1 Hz, 3-H), 7.73 (m, 6 H, 2-H, 16-H, and 17-H), 2.75 [s, C(O)Me].

*[Pd{C(O)Me}(**5**)]Cl* (**5d**): ^1H NMR (CD_3OD): δ = 8.50 (d, J = 7.8 Hz, 4-H), 8.42 (d, J = 5.4 Hz, 1-H), 8.26 (m, 2 H, 3-H), 8.15 (s, 7-H), 7.73 (m, 2 H, 2-H), 2.77 [s, C(O)Me], 2.64 (s, SMe).

Acetylpalladium Tetrakis[3,5-bis(trifluoromethyl)phenyl]borate Complexes **1e−6e**: A solution of [Pd(Me)(**1**)]BAr′$_4$ (**1c**) (20.3 mg, 0.016 mmol) in 20 ml of dichloromethane was stirred at 20°C in CO. After 10 min, the solution was filtered through Celite and the residue was extracted with dichoromethane (5 ml). The combined filtrates were concentrated to dryness and the product was washed with hexane (2 × 20 ml), giving **1e** as a yellow solid (18.3 mg, 86%).

By following the procedure for **1e**, complexes **2e−6e** were obtained from **2c−6c** in yields of 85−97%. Analytical data and mass spectra for **1e−6e** could not be obtained due to decarbonylation in the solid state.

*[Pd{C(O)Me}(**1**)]BAr′$_4$* (**1e**): ^1H NMR ($CDCl_3$): δ = 7.70 (s, Ar′ H_{ortho}), 7.52 (s, Ar′ H_{para}), 7.47 (s, 7-H), 4.13 (sept, J = 6.6 Hz, C*H*Me_2), 2.86 (t, J = 6.6 Hz, 5-H), 2.75 (t, J = 6.0 Hz, 3-H), 2.63 [s, C(O)Me], 1.98 (m, 4 H, 4-H), 1.17 (d, J = 6.6 Hz, CH*Me*$_2$). − ^{13}C NMR ($CDCl_3$): δ = 171.8 (C-6), 161.4 (q, J = 50 Hz, Ar′ C_{ipso}), 145.6 (C-1), 141.9 (C-2), 139.2 (C-7), 134.5 (Ar′ C_{ortho}), 128.7 (qq, J = 31, 3 Hz, Ar′ C_{meta}), 124.3 (q, J = 273 Hz, Ar′ CF_3), 117.3 (Ar′ C_{para}), 54.8 (*C*HMe_2), 34.5 [C(O)*Me*], 29.2, 26.6 (C-3 and C-5), 22.0 (CH*Me*$_2$), 21.5 (C-4), signal of *C*(O)Me was not observed. − IR (KBr): ν = 1689 cm^{-1} (CO).

*[Pd{C(O)Me}(**2**)]BAr′$_4$* (**2e**): ^1H NMR ($CDCl_3$): δ = 8.83 (d, J = 5.0 Hz, 1-H), 8.63 (d, J = 5.2 Hz, 15-H), 8.51 (d, J = 8.2 Hz, 3-H), 8.38 (d, J = 8.6 Hz, 12-H), 8.06 (m, 3 H, 8-H, 9-H, and 13-H), 7.92 (d, J = 9.0 Hz, 16-H or 17-H), 7.85 (d, J = 9.0 Hz, 16-H or 17-H), 7.89 (dd, J = 8.2, 5.0 Hz, 2-H), 7.72 (s, Ar′ H_{ortho}), 7.70 (m, 1 H, 14-H), 7.47 (s, Ar′ H_{para}), 2.74 [s, C(O)Me]. − ^{13}C NMR ($CDCl_3$): δ = 161.5 (q, J = 50 Hz, Ar′ C_{ipso}), 134.5 (Ar′ C_{ortho}), 128.7 (qq, J = 31, 3 Hz, Ar′ C_{meta}), 124.2 (q, J = 272 Hz, Ar′ CF_3), 117.3 (Ar′ C_{para}), 154.8, 152.9, 152.3, 149.9, 147.4, 141.5, 140.8, 139.6, 139.4, 131.0, 129.0, 128.9, 128.3, 126.5, 123.8, 120.3 (C-1−C-17), 29.2 [C(O)*Me*], signal of *C*(O)Me was not observed. − IR (KBr): ν = 1695 cm^{-1} (CO).

*[Pd{C(O)Me}(**3**)]BAr′$_4$* (**3e**): ^1H NMR ($CDCl_3$): δ = 8.84 (d, J = 5.1 Hz, 1-H), 8.46 (m, 2 H, 3-H and 15-H), 8.16 (s, 8-H), 7.85 (m, 2 H, 16-H/17-H and 13-H), 7.78 (d, J = 9.0 Hz, 16-H or 17-H), 7.70 (s, Ar′ H_{ortho}), 7.56 (dd, J = 7.8, 5.4 Hz, 14-H), 7.46 (s, Ar′ H_{para}), 3.26 (m, 4 H, 18-H and 19-H), 2.71 [s, C(O)Me], signal of 2-H is overlapping with signals from $BAr'_4{}^-$. − ^{13}C NMR ($CDCl_3$): δ = 161.5 (q, J = 50 Hz, Ar′ C_{ipso}), 134.5 (Ar′ C_{ortho}), 128.7 (qq, J = 32, 3 Hz, Ar′ C_{meta}), 124.2 (q, J = 272 Hz, Ar′ CF_3), 117.3 (Ar′ C_{para}), 152.2, 151.6, 150.7, 149.5, 147.0, 140.2, 139.4, 138.8, 137.1, 136.1, 134.4, 130.5, 130.3, 128.4, 126.3, 126.0 (C-1−C-17), 27.3 [C(O)*Me*], 26.0, 24.5 (C-18 and C-19), signal of *C*(O)Me was not observed. − IR (KBr): ν = 1698 cm^{-1} (CO).

*[Pd{C(O)Me}(**4**)]BAr′$_4$* (**4e**): ^1H NMR ($CDCl_3$): δ = 8.98 (d, J = 5.1 Hz, 1-H), 8.87 (s, 8-H), 8.50 (d, J = 8.1 Hz, 3-H), 7.99 (d, J = 9.1 Hz, 16-H or 17-H), 7.90 (d, J = 9.1 Hz, 16-H or 17-H), 7.95 (dd, J = 8.1, 5.1 Hz, 2-H), 7.71 (s, Ar′ H_{ortho}), 7.46 (s, Ar′ H_{para}), 2.81 [s, Pd−C(O)Me]. − ^{13}C NMR ($CDCl_3$): δ = 161.5 (q, J = 50 Hz, Ar′ C_{ipso}), 152.1 (C-1), 147.1, 141.4 (C-5 and C-6),

139.4 (C-3), 136.0 (C-8), 134.5 (Ar′ C_{ortho}), 131.0, 128.3 (C-4 and C-7), 128.7 (qq, J = 32, 3 Hz, Ar′ C_{meta}), 128.1, 127.0, 126.8 (C-2, C-16, and C-17), 124.2 (q, J = 272 Hz, Ar′ CF_3), 117.3 (Ar′ C_{para}), 26.4 [C(O)*Me*], signal of *C*(O)Me was not observed. − IR (KBr): ν = 1703 cm^{-1} (CO).

*[Pd{C(O)Me}(**5**)]BAr′*$_4$ (**5e**): ^{1}H NMR ($CDCl_3$): δ = 8.47 (d, J = 4.8 Hz, 1-H), 8.02 (m, 6 H, 3-H, 4-H, and 7-H) 7.72 (s, Ar′ H_{ortho}), 7.61 (m, 2 H, 2-H), 7.50 (s, Ar′ H_{para}), 2.64 [s, C(O)Me], 2.59 (s, SMe). − ^{13}C NMR ($CDCl_3$): δ = 231.8 [*C*(O)Me], 161.5 (q, J = 50 Hz, Ar′ C_{ipso}), 160.1 (C-8), 155.2, 149.9 (C-5 and C-6), 152.5 (C-1), 140.5 (C-3), 134.5 (Ar′ C_{ortho}), 128.7 (qq, J = 32, 3 Hz, Ar′ C_{meta}), 128.0 (C-2), 124.3 (q, J = 273 Hz, Ar′ CF_3), 123.3 (C-4), 117.2 (Ar′ C_{para}), 30.7 [C(O)*Me*], 13.9 (SMe), signal of C-7 is overlapping with signal of Ar′ C_{para}. − IR (KBr): ν = 1685 cm^{-1} (CO).

*[Pd{C(O)Me}(**6**)]BAr′*$_4$ (**6e**): ^{1}H NMR ($CDCl_3$): δ = 8.47 (d, J = 4.3 Hz, 1-H), 8.05 (m, 2 H, 3-H), 7.96 (d, J = 6.9 Hz, 4-H), 7.91 (m, 1 H, 8-H), 7.83 (m, 2 H, 7-H), 7.72 (s, Ar′ H_{ortho}), 7.64 (m, 2 H, 2-H), 7.49 (s, Ar′ H_{para}), 2.66 [s, C(O)Me]. − ^{13}C NMR ($CDCl_3$): δ = 161.5 (q, J = 50 Hz, Ar′ C_{ipso}), 156.7, 150.9 (C-5 and C-6), 152.5 (C-1), 141.8 (C-8), 140.8 (C-3), 134.5 (Ar′ C_{ortho}), 128.7 (qq, J = 32, 3 Hz, Ar′ C_{meta}), 128.1 (C-2), 124.2 (q, J = 273 Hz, Ar′ CF_3), 123.5 (C-4), 122.0 (C-7), 117.3 (Ar′ C_{para}), 30.8 [C(O)*Me*], signal of *C*(O)Me was not observed. − IR (KBr): ν = 1689 cm^{-1} (CO).

Alkylpalladium Tetrakis[3,5-bis(trifluoromethyl)phenyl]borate Complexes **2f**−**6f**: Norbornadiene (30 µl, 0.28 mmol) was added to a solution of [Pd{C(O)Me}(**2**)]BAr'_4 (**2e**) (98.0 mg, 0.077 mmol) in 20 ml of dichloromethane. The solution was stirred at 20°C and after 30 min concentrated to dryness. The product was washed with hexane (2 × 20 ml) and dried in vacuo, yielding **2f** as a yellow oil (91.3 mg, 86%).

By following the procedure for **2f**, complexes **3f**−**6f** were synthesized from complexes **3e**−**6e** in yields of 88−91%. Since the complexes **2f**−**6f** were isolated as oils, correct analytical data could not be obtained.

*[Pd{C$_7$H$_8$C(O)Me}(**2**)]BAr′*$_4$ (**2f**): ^{1}H NMR ($CDCl_3$): δ = 8.78 (m, 2 H, 1-H and 15-H), 8.61 (d, J = 8.4 Hz, 8-H), 8.52 (dd, J = 8.1, 1.5 Hz, 3-H), 8.30 (d, J = 8.4 Hz, 9-H), 8.02 (d, J = 9.0 Hz, 16-H or 17-H), 7.92 (d, J = 9.0 Hz, 16-H or 17-H), 7.84 (m, 3 H, 2-H, 12-H, and 13-H), 7.73 (s, Ar′ H_{ortho}), 7.50 (s, Ar′ H_{para}), 7.45 (dd, J = 4.5, 1.2 Hz, 14-H), 6.22 (dd, J = 5.5, 3.0 Hz, =CH), 6.15 (dd, J = 5.5, 3.0 Hz, =CH), 3.03 (br., CHC=), 2.97 (br., CHC=), 2.52 (dd, J = 6.0, 2.1 Hz, PdCH), 2.42 [d, J = 6.0 Hz, C*H*C(O)Me], 1.96 [s, C(O)Me], 1.71 (d, J = 9.3 Hz, CH_2), 1.42 (d, J = 9.3 Hz, CH_2). − ^{13}C NMR ($CDCl_3$): δ = 235.3 [*C*(O)Me], 161.5 (q, J = 50 Hz, Ar′ C_{ipso}), 134.6 (Ar′ C_{ortho}), 128.7 (qq, J = 32, 3 Hz, Ar′ C_{meta}), 124.3 (q, J = 272 Hz, Ar′ CF_3), 117.2 (Ar′ C_{para}), 159.5, 154.9, 149.7, 149.5, 147.4, 143.6, 139.3, 138.8, 136.3, 135.3, 133.9, 130.6, 129.1, 127.7, 127.1, 126.5, 125.2, 124.5, 124.3 (C-1−C-17 and 2× =CH), 62.2 [*C*HC(O)Me], 48.2, 47.9, 47.8 (PdCH and 2 × *C*HC=), 45.2 (CH_2), 26.2 [C(O)*Me*]. − ^{15}N NMR ($CDCl_3$, −60°C): δ = −68.0, −158.4 (N1 and N3), signal of N2 was not observed due to the absence of a hydrogen atom with a sufficiently large N-H coupling constant. − IR (KBr): ν = 1612 cm^{-1} (CO). − MS (FAB): calcd. for $[C_{26}H_{22}N_3OPd]^+$ 498.0798; found 498.0779.

*[Pd{C$_7$H$_8$C(O)Me}(**3**)]BAr′*$_4$ (**3f**): ^{1}H NMR ($CDCl_3$): δ = 8.79 (d, J = 4.8 Hz, 1-H), 8.59 (d, J = 4.8 Hz, 15-H), 8.47 (d, J = 7.8 Hz, 3-H), 8.33 s (8-H), 7.89 (d, J = 9.0 Hz, 16-H or 17-H), 7.85 (d, J = 9.0 Hz, 16-H or 17-H), 7.82 (dd, J = 7.8, 4.8 Hz, 2-H), 7.73 (m, 9 H, Ar′ H_{ortho} and 13-H), 7.51 (s, Ar′ H_{para}), 7.37 (dd, J = 7.8, 4.8 Hz, 14-H), 6.26 (dd, J = 5.1, 3.0 Hz, =CH), 6.20 (dd, J = 5.1, 3.0 Hz, =CH), 3.26 (m, 2 H, 18-H or 19-H), 3.15 (m, 2 H, 18-H or 19-H), 3.08 (m, 2 H, 2 × CHC=), 2.52 (dd, J = 6.0, 2.1 Hz, PdCH), 2.46 [d, J = 6.0 Hz, C*H*C(O)Me], 2.05 [s, C(O)Me], 1.98 (d, J = 9.0 Hz, CH_2), 1.58 (d, J = 9.0 Hz, CH_2). − ^{13}C NMR ($CDCl_3$): δ = 233.0 [*C*(O)Me], 161.5 (q, J = 50 Hz, Ar′ C_{ipso}), 134.6 (Ar′ C_{ortho}), 128.7 (qq, J = 32, 3 Hz, Ar′ C_{meta}), 124.3 (q, J = 272 Hz, Ar′ CF_3), 117.2 (Ar′ C_{para}), 153.4, 149.3, 149.1, 148.2, 147.4, 143.4, 138.7, 137.7, 136.4, 136.3, 136.0, 135.3, 134.0, 129.9, 129.5, 127.1, 126.9, 125.2, 124.7 (C-1−C-17 and 2 × =CH), 62.2 [*C*HC(O)Me], 48.2, 47.9, 46.7 (PdCH and 2 × *C*HC=), 45.3 (CH_2), 27.5, 26.8 (C-18 and C-19), 26.4 [C(O)*Me*]. − IR (KBr): ν = 1624 cm^{-1} (CO). − MS (FAB): calcd. for $[C_{28}H_{24}N_3OPd]^+$ 524.0954; found 524.0921.

*[Pd{C$_7$H$_8$C(O)Me}(**4**)]BAr′*$_4$ (**4f**): ^{1}H NMR ($CDCl_3$): δ = 9.03 (s, 8-H), 8.92 (dd, J = 4.8, 1.2 Hz, 1-H), 8.43 (dd, J = 8.0, 1.2 Hz, 3-H), 8.05 (d, J = 9.0 Hz, 16-H or 17-H), 7.92 (d, J = 9.0 Hz, 16-H or 17-H), 7.84 (dd, J = 8.0, 4.8 Hz, 2-H), 7.74 (s, Ar′ H_{ortho}), 7.50 (s, Ar′ H_{para}), 6.30 (dd, J = 5.4, 3.0 Hz, =CH), 6.26 (dd, J = 5.4, 3.0 Hz, =CH), 3.23 (br., CHC=), 3.17 (br., CHC=), 2.58 (dd, J = 6.0, 2.1 Hz, PdCH), 2.52 [d, J = 6.0 Hz, C*H*C(O)Me], 2.22 (d, J = 9.0 Hz, CH_2), 1.72 (d, J = 9.0 Hz, CH_2), 2.15 [s, C(O)Me]. − ^{13}C NMR ($CDCl_3$): δ = 231.2 [*C*(O)Me], 161.5 (q, J = 50 Hz, Ar′ C_{ipso}), 148.8 (C-1), 146.2, 144.8 (C-5 and C-6), 137.5, 135.2, 134.3 (C-8 and 2 × =CH), 137.4 (C-3), 134.6 (Ar′ C_{ortho}), 130.6, 128.9 (C-4 and C-7), 128.7 (qq, J = 32, 3 Hz, Ar′ C_{meta}), 127.7, 126.7, 125.3 (C-2, C-16, and C-17), 124.3 (q, J = 272 Hz, Ar′ CF_3), 117.2 (Ar′ C_{para}), 62.1 [*C*HC(O)Me], 48.3, 47.9, 46.4 (PdCH and 2 × *C*HC=), 45.4 (CH_2), 26.5 [C(O)*Me*]. − ^{15}N NMR ($CDCl_3$, −60°C): δ = −130.1 (coordinated N1), signals of N2 and noncoordinated N1 were not observed due to the absence of a hydrogen atom with a sufficiently large N-H coupling constant. − IR (KBr): ν = 1624 cm^{-1} (CO). − MS (FAB): calcd. for $[C_{28}H_{22}N_3OPd]^+$ 522.0797; found 522.0781.

*[Pd{C$_7$H$_8$C(O)Me}(**5**)]BAr′*$_4$ (**5f**): ^{1}H NMR ($CDCl_3$): δ = 8.57 (d, J = 4.5 Hz, 1-H), 8.00 (d, J = 7.5 Hz, 4-H), 7.89 (m, 2 H, 3-H), 7.82 (s, 7-H), 7.71 (s, Ar′ H_{ortho}), 7.52 (s, Ar′ H_{para}), 7.48 (m, 2 H, 2-H), 6.14 (dd, J = 5.5, 3.0 Hz, =CH), 6.10 (dd, J = 5.5, 3.0 Hz, =CH), 2.95 (br., CHC=), 2.82 (br., CHC=), 2.65 (s, SMe), 2.32 [d, J = 6.1 Hz, C*H*C(O)Me], 2.28 (dd, J = 6.1, 2.2 Hz, PdCH), 1.87 [s, C(O)Me], 1.57 (d, J = 9.6 Hz, CH_2), 1.42 (d, J = 9.6 Hz, CH_2). − ^{13}C NMR ($CDCl_3$): δ = 235.0 [*C*(O)Me], 161.5 (q, J = 50 Hz, Ar′ C_{ipso}), 157.6 (C-8), 155.9, 150.5 (C-5 and C-6), 149.5 (C-1), 139.8 (C-3), 134.6 (Ar′ C_{ortho}), 135.2 (=CH), 133.8 (=CH), 128.7 (qq, J = 32, 3 Hz, Ar′ C_{meta}), 125.6 (C-2), 124.3 (q, J = 272 Hz, Ar′ CF_3), 123.6 (C-4), 117.2 (Ar′ C_{para}), 62.1 [*C*HC(O)Me], 48.1, 48.0, 47.5 (PdCH and 2× *C*HC=), 45.2 (CH_2), 26.1 [C(O)*Me*], 13.9 (SMe), signal of C-7 is overlapping with signal of Ar′ C_{para}. − IR (KBr): ν = 1610 cm^{-1} (CO). − MS (FAB): calcd. for $[C_{25}H_{25}N_3OPdS]^+$ 520.0675; found 520.0647.

*[Pd{C$_7$H$_8$C(O)Me}(**6**)]BAr′*$_4$ (**6f**): ^{1}H NMR ($CDCl_3$): δ = 8.58 (d, J = 5.1 Hz, 1-H), 8.14 (m, 1 H, 8-H), 8.05 (m, 2 H, 7-H), 7.97 (d, J = 7.8 Hz, 4-H), 7.90 (m, 2 H, 3-H), 7.72 (s, Ar′ H_{ortho}), 7.50 (s, Ar′ H_{para}), 6.15 (dd, J = 5.4, 3.0 Hz, =CH), 6.11 (dd, J = 5.4, 3.0 Hz, =CH), 2.96 (br., CHC=), 2.85 (br., CHC=), 2.33 [m, 2 H, C*H*C(O)Me and PdCH], 1.88 [s, C(O)Me], 1.60 (d, J = 9.3 Hz, CH_2), 1.44 (d, J = 9.3 Hz, CH_2), signal of 2-H is overlapping with signal of Ar′ C_{para}. − ^{13}C NMR ($CDCl_3$): δ = 234.4 [*C*(O)Me], 161.5 (q, J = 50 Hz, Ar′ C_{ipso}), 155.9 (C-5 or C-6), 149.6 (C-1), 140.2, 138.2 (C-3 and C-8), 135.3 (=CH), 133.9 (=CH), 134.5 (Ar′ C_{ortho}), 128.7 (qq, J = 32, 3 Hz, Ar′ C_{meta}), 128.7, 126.1, 123.6 (C-2, C-4, and C-7), 124.2 (q, J = 272 Hz, Ar′ CF_3), 117.2 (Ar′ C_{para}),

61.9 [*C*HC(O)Me], 48.1, 48.0, 47.5 (PdCH and 2× *C*HC=), 45.2 (CH_2), 26.2 [C(O)*Me*], signal of C-5 or C-6 is overlapping with signal of Ar′ C_{para}. − ^{15}N NMR ($CDCl_3$, −60°C): δ = −155.0 (coordinated N1), signals of N2 and noncoordinated N1 were not observed due to the absence of a hydrogen atom with a sufficiently large N-H coupling constant. − IR (KBr): ν = 1610 cm^{-1} (CO). − MS (FAB): calcd. for $[C_{24}H_{22}N_3OPd]^+$ 474.0798; found 474.0801.

Kinetics: The rates of the reactions of norbornadiene with complexes **1e**−**6e**, resulting in complexes **1f**−**6f**, were followed spectrophotometrically by repetitive scanning of the spectrum at suitable time intervals at a fixed wavelength, at which the difference between absorbance of educt and product was largest. The reactions were started by addition of norbornadiene to a $1.9\cdot10^{-4}$ M solution of the acetylpalladium complex in a quartz cell, which was placed in the thermostated cell compartment of a Perkin-Elmer Lambda 5 spectrophotometer, with a temperature accuracy of ± 0.5°C. The use of at least a 10-fold excess of norbornadiene over acetylpalladium complex ensured pseudo-first-order kinetics in all runs. All reactions, except for the reaction of **3e** with nbd, were clean and quantitative, and in all cases isosbestic points were obtained. Furthermore, the reactions obeyed a first-order rate law for at least four half-lives of the reaction. The rate constants k_{obsd} were calculated from the slopes of plots of $\ln\{(A_t - A_\infty)/(A_0 - A_\infty)\}$ vs time (A_0 = absorbance after mixing of the reagents, A_∞ = absorbance at completion of the reaction). The activation parameters $\Delta S^{\neq}$ and $\Delta H^{\neq}$ were obtained from an Eyring plot.

X-ray Structure Determinations of **1b** *and* **4c**[88]: Crystals suitable for X-ray structure determination were mounted on a Lindemann-glass capillary and transferred to an Enraf-Nonius CAD4-Turbo diffractometer on rotating anode. Accurate unit-cell parameters and an orientation matrix were determined by least-squares fitting of the setting angles of a set of well-centered reflections (SET4).[89] Reduced-cell calculations did not indicate higher lattice symmetry.[90] Crystal data and some details on data collection are given in Table 5. Reflection data were collected at 150 K in ω-scan mode, using graphite-monochromated Mo-K_α radiation (λ = 0.71073A). Data were corrected for Lp effects and for the linear instability of the reference reflections, but not for absorption. The structure of **1b** was solved by automated direct methods (SHELXS96)[91]; the structure of **4c** was solved by automated Patterson methods (SHELXS86)[92]. Refinement on F^2 was carried out by full-matrix least-squares techniques (SHELXL-96);[93] no observance criterion was applied during refinement. Hydrogen atoms were included in the refinement on calculated positions riding on their carrier atoms. In complex **4c** two CF_3 groups of the counterion displayed conformational disorder. A two-site model was introduced to describe this disorder. Severely disordered solvent molecules occupy two of the crystallographic inversion centers of structure **4c**. Since no discrete solvent model could be refined, this electron density was taken into account using the SQUEEZE/BYPASS procedure[94], as implemented in PLATON[95]. The two solvent areas were found to have a volume of 100.5 and 80.5 A^3, containing 38.9 and 24.7 e, respectively. Non-hydrogen atoms were refined with anisotropic thermal parameters, with exception of the minor component of the disordered atoms. The hydrogen atoms were refined with a fixed isotropic displacement parameter related to the value of the equivalent isotropic displacement parameter of their carrier atoms. Neutral atom scattering factors and anomalous dispersion corrections were taken from the International Tables for Crystallography[96]. Geometrical calculations and illustrations were performed with PLATON[95].

Ab initio MO Calculations on the Insertion Reactions: The split-valence 3-21G basis was used for C, N, O, and H atoms.[97] The Pd basis was based on the (18s,11p,9d)→[6s,5p,3d] basis of Godbout[98], but the (9d)→[3d] contraction was replaced by a (9d)→[4d] contraction by releasing the most diffuse d primitive of the middle d shell. In order to save computational time, ligand HN=CHCH$_2$N=CHCH=NH (**7**) was used as a model and solvation and counter anions were left out. To simulate the enforced planarity of the rigid ligands used in the experimental study, the structure of **7** was forced to keep a horizontal mirror plane (local C_s symmetry). Apart from this restriction, all structures were fully optimized (in particular, the metal atom and remaining fragments were allowed to move out of the ligand plane). All structures were optimized at the restricted Hartree-Fock (RHF) level; improved single-point energies were then obtained from second-order Møller-Plesset perturbation (MP2) calculations at the RHF optimized geometries. To enable comparison with bidentate systems, a similar set of calculations was performed on ligand HN=CHCH$_2$N=CH$_2$ (**8**), which was again forced to have local C_s symmetry. All calculations were carried out using the GAMESS[99] and Gaussian[100] packages.

Table 5. Crystallographic data for **1b** and **4c**

Complex	**1b**	**4c**
Formula	$[C_{20}H_{30}N_3Pd]^+$ $[CF_3SO_3]^-$	$[C_{20}H_{14}N_3Pd]^+$ $[C_{32}H_{12}BF_{24}]^-$[a]
Molecular weight	567.97	1265.99[a]
Crystal system	monoclinic	triclinic
Space group	$P2_1/c$ (No. 14)	$P\bar{1}$ (No. 2)
a [A]	13.521(6)	12.3298(14)
b [A]	8.791(6)	15.1874(19)
c [A]	21.507(7)	15.443(3)
α [°]	−	66.060(12)
β [°]	115.13(3)	71.132(11)
γ [°]	−	84.576(9)
V [A^3]	2314(2)	2498.8(7)
$D_{calcd.}$ [$g\cdot cm^{-3}$]	1.630(1)	1.6826(5)[a]
Z	4	2
F(000)	1160	1252[a]
μ [Mo-K_α] [$^{-1}$]	9.4	5.0
Crystal color	yellow	yellow
Crystal size [mm]	0.08×0.23×0.53	0.4×0.4×0.5
θ_{min}, θ_{max} [°]	1.05, 27.50	1.47, 27.50
Total, unique data	14444, 5316	13732, 11429
Final R[b]	0.0634 [3395 $F_o > 4\sigma(F_o)$]	0.0552 [9467 $F_o > 4\sigma(F_o)$]
Final $wR2$[c]	0.1628	0.1493
Goodness of fit	1.018	1.027
Min. and max. residual density [e A^{-3}]	−1.42, 1.23	−1.63, 1.11

[a] Without disordered solvent contribution. − [b] $R = \Sigma||F_o - F_c| / \Sigma F_o$. − [c] $wR2 = \{\Sigma[w(F_o^2 - F_c^2)^2]/\Sigma[w(F_o^2)^2]\}^{1/2}$.

[1] A. Yamamoto, *Organotransition Metal Chemistry*; Wiley, New York, **1986**.
[2] J. P. Collman, L. S. Hegedus, J. R. Norton, R. G. Finke, *Principles and Applications of Organotransition Metal Chemistry*, University Science Books, Mill Valley, **1987**.
[3] A. Sen, *Chemtech* **1986**, 48.
[4] E. Drent, J. A. M. van Broekhoven, M. J. Doyle, *J. Organomet. Chem.* **1991**, *417*, 235.
[5] A. Sen, *Acc. Chem. Res.* **1993**, *26*, 303.
[6] E. Drent, P. H. M. Budzelaar, *Chem. Rev.* **1996**, *96*, 663.
[7] E. Drent, J. A. M. van Broekhoven, P. H. M. Budzelaar, *Recl. Trav. Chim. Pays-Bas* **1996**, *115*, 263.
[8] G. P. C. M. Dekker, C. J. Elsevier, K. Vrieze, P. W. N. M. van Leeuwen, *Organometallics* **1992**, *11*, 1598.
[9] G. P. C. M. Dekker, C. J. Elsevier, K. Vrieze, P. W. N. M. van Leeuwen, C. F. Roobeek, *J. Organomet. Chem.* **1992**, *430*, 357.
[10] G. P. C. M. Dekker, A. Buijs, C. J. Elsevier, K. Vrieze, P. W. N.

M. van Leeuwen, W. J. J. Smeets, A. L. Spek, Y. F. Wang, C. H. Stam, *Organometallics* **1992**, *11*, 1937.
[11] R. van Asselt, E. E. C. G. Gielens, R. E. Rülke, K. Vrieze, C. J. Elsevier, *J. Am. Chem. Soc.* **1994**, *116*, 977.
[12] R. E. Rülke, J. G. P. Delis, A. M. Groot, C. J. Elsevier, P. W. N. M. van Leeuwen, K. Vrieze, K. Goubitz, H. Schenk, *J. Organomet. Chem.* **1996**, *508*, 109.
[13] J. H. Groen, J. G. P. Delis, P. W. N. M. van Leeuwen, K. Vrieze, *Organometallics* **1997**, *16*, 68.
[14] J. G. P. Delis, J. H. Groen, K. Vrieze, P. W. N. M. van Leeuwen, N. Veldman, A. L. Spek, *Organometallics* **1997**, *16*, 551.
[15] J. H. Groen, M. J. M. Vlaar, P. W. M. N. van Leeuwen, K. Vrieze, H. Kooijman, A. L. Spek, *J. Organomet. Chem.*, in press.
[16] J. S. Brumbaugh, R. R. Whittle, M. Parvez, A. Sen, *Organometallics* **1990**, *9*, 1735.
[17] F. Ozawa, T. Hayashi, H. Koide, A. Yamamoto, *J. Chem. Soc., Chem. Commun.* **1991**, 1469.
[18] M. Brookhart, F. C. Rix, J. M. DeSimone, J. C. Barborak, *J. Am. Chem. Soc.* **1992**, *114*, 5894.
[19] I. Toth, C. J. Elsevier, *J. Am. Chem. Soc.* **1993**, *115*, 10388.
[20] P. W. N. M. van Leeuwen, C. F. Roobeek, H. van der Heijden, *J. Am. Chem. Soc.* **1994**, *116*, 12117.
[21] P. W. N. M. van Leeuwen, K. F. Roobeek, *Recl. Trav. Chim. Pays-Bas* **1995**, *114*, 73.
[22] B. A. Markies, D. Kruis, M. H. P. Rietveld, K. A. N. Verkerk, J. Boersma, H. Kooijman, M. T. Lakin, A. L. Spek, G. van Koten, *J. Am. Chem. Soc.* **1995**, *117*, 5263.
[23] F. C. Rix, M. Brookhart, P. S. White, *J. Am. Chem. Soc.* **1996**, *118*, 4746.
[24] Y. Kayaki, I. Shimizu, A. Yamamoto, *Bull. Chem. Soc. Jpn.* **1997**, *70*, 917.
[25] See for a review: K. J. Cavell, *Coord. Chem. Rev.* **1996**, *155*, 209.
[26] W. de Graaf, J. Boersma, G. van Koten, *Organometallics* **1990**, *9*, 1479.
[27] P. W. N. M. van Leeuwen, C. F. Roobeek, J. H. G. Frijns, A. G. Orpen, *Organometallics* **1990**, *9*, 1211.
[28] H. C. Clark, C. R. Jablonski, J. Halpern, T. A. Weil, A. Matovani, *Inorg. Chem.* **1974**, *13*, 1541.
[29] B. A. Markies, P. Wijkens, J. Boersma, A. L. Spek, G. van Koten, *Recl. Trav. Chim. Pays-Bas* **1991**, *110*, 133.
[30] K. Frankcombe, K. J. Cavell, R. Knott, B. Yates, *J. Chem. Soc., Chem. Commun.* **1996**, 781.
[31] R. E. Rülke, I. M. Han, C. J. Elsevier, K. Vrieze, P. W. N. M. van Leeuwen, C. F. Roobeek, M. C. Zoutberg, Y. F. Wang, C. H. Stam, *Inorg. Chim. Acta* **1990**, *169*, 5.
[32] R. E. Rülke, V. E. Kaasjager, D. Kliphuis, C. J. Elsevier, P. W. N. M. van Leeuwen, K. Vrieze, K. Goubitz, *Organometallics* **1996**, *15*, 668.
[33] E. W. Abel, V. S. Dimitrov, N. J. Long, K. G. Orrell, A. G. Osborne, V. Sik, M. B. Hursthouse, M. A. Mazid, *J. Chem. Soc., Dalton Trans.* **1993**, 291.
[34] E. W. Abel, V. S. Dimitrov, N. J. Long, K. G. Orrell, A. G. Osborne, H. M. Pain, V. Sik, *J. Chem. Soc., Dalton Trans.* **1993**, 597.
[35] E. W. Abel, K. G. Orrell, A. G. Osborne, H. M. Pain, V. Sik, *J. Chem. Soc., Dalton Trans.* **1994**, 111.
[36] E. W. Abel, K. G. Orrell, A. G. Osborne, H. M. Pain, V. Sik, M. B. Hursthouse, M. A. Mazid, *J. Chem. Soc., Dalton Trans.* **1994**, 3441.
[37] A. Gelling, K. G. Orrell, A. G. Osborne, V. Sik, *J. Chem. Soc., Chem. Commun.* **1996**, 2329.
[38] G. B. Deacon, J. M. Patrick, B. W. Skelton, N. C. Thomas, A. H. White, *Aust. J. Chem.* **1984**, *37*, 929.
[39] P. A. Anderson, F. R. Keene, E. Horn, E. R. T. Tiekink, *Appl. Organomet. Chem.* **1990**, *21*, 119.
[40] N. C. Thomas, J. Fischer, *J. Coord. Chem.* **1990**, *21*, 119.
[41] E. C. Constable, M. J. Hannon, A. M. W. Cargill Thompson, D. A. Tocher, J. Walker, *Supramol. Chem.* **1993**, *2*, 243.
[42] E. R. Civitello, P. S. Dragovitch, T. B. Karpishin, S. G. Novick, G. Bierach, J. F. O′Connell, T. D. Westmoreland, *Inorg. Chem.* **1993**, *32*, 237.
[43] S. Ramdeehul, L. Barloy, J. A. Osborn, A. De Cian, J. Fischer, *Organometallics* **1996**, *15*, 5442.
[44] C.-Y. Hung, T.-L. Wang, Z. Shi, R. P. Thummel, *Tetrahedron* **1994**, *50*, 10685.
[45] C.-Y. Hung, T.-L. Wang, Y. Jang, W. Y. Kim, R. H. Schmehl, R. P. Thummel, *Inorg. Chem.* **1996**, *35*, 5953.
[46] K. T. Potts, D. A. Usifer, A. Guadalupe, H. D. Abruna, *J. Am. Chem. Soc.* **1987**, *109*, 3961.
[47] R. van Asselt, C. J. Elsevier, W. J. J. Smeets, A. L. Spek, R. Benedix, *Recl. Trav. Chim. Pays-Bas* **1994**, *113*, 88.
[48] H. A. Ankersmit, N. Veldman, A. L. Spek, K. Eriksen, K. Goubitz, K. Vrieze, G. van Koten, *Inorg. Chim. Acta* **1996**, *252*, 203.
[49] H. A. Ankersmit, P. T. Witte, H. Kooijman, M. T. Lakin, A. L. Spek, K. Goubitz, K. Vrieze, G. van Koten, *Inorg. Chem.* **1996**, *35*, 6053.
[50] R. E. Rülke, V. E. Kaasjager, P. Wehman, C. J. Elsevier, P. W. N. M. van Leeuwen, K. Vrieze, J. Fraanje, K. Goubitz, A. L. Spek, *Organometallics* **1996**, *15*, 3022.
[51] H. A. Ankersmit, N. Veldman, A. L. Spek, K. Vrieze, G. van Koten, *Inorg. Chim. Acta* **1996**, *252*, 339.
[52] J. G. P. Delis, P. W. N. M. van Leeuwen, K. Vrieze, N. Veldman, A. L. Spek, J. Fraanje, K. Goubitz, *J. Organomet. Chem.* **1996**, *514*, 125.
[53] J. G. P. Delis, M. Rep, R. E. Rülke, P. W. N. M. van Leeuwen, K. Vrieze, J. Fraanje, K. Goubitz, *Inorg. Chim. Acta* **1996**, *250*, 87.
[54] J. G. P. Delis, M. Rep, M. Kranenburg, P. W. N. M. van Leeuwen, K. Vrieze, N. Veldman, A. L. Spek, K. Goubitz, J. Fraanje, to be published.
[55] G. M. Intille, C. E. Pfluger, W. A. Baker Jr, *J. Cryst. Mol. Struct.* **1973**, *3*, 47.
[56] P. Castan, F. Dahan, S. Wimmer, F. L. Wimmer, *J. Chem. Soc, Dalton Trans.* **1990**, 2679.
[57] B. A. Markies, P. Wijkens, H. Kooijman, A. L. Spek, J. Boersma, G. van Koten, *J. Chem. Soc., Chem. Commun.* **1992**, 1420.
[58] B. A. Markies, P. Wijkens, J. Boersma, H. Kooijman, N. Veldman, A. L. Spek, G. van Koten, *Organometallics* **1994**, *13*, 3244.
[59] B. A. Markies, P. Wijkens, A. Dedieu, J. Boersma, A. L. Spek, G. van Koten, *Organometallics* **1995**, *14*, 5628.
[60] R. Nesper, P. Pregosin, K. Püntener, M. Wörle, A. Albinati, *J. Organomet. Chem.* **1996**, *507*, 85.
[61] H. F. Haarman, J. M. Ernsting, M. Kranenburg, H. Kooijman, N. Veldman, A. L. Spek, P. W. N. M. van Leeuwen, K. Vrieze, *Organometallics* **1997**, *16*, 887.
[62] V. De Felice, V. G. Albano, C. Castellari, M. E. Cucciolito, A. De Renzi, *J. Organomet. Chem.* **1991**, *403*, 269.
[63] H. A. Ankersmit, B. H. Løken, H. Kooijman, A. L. Spek, K. Vrieze, G. van Koten, *Inorg. Chim. Acta* **1996**, *252*, 141.
[64] R. A. Klein, R. Belzen, K. Vrieze, C. J. Elsevier, R. P. Thummel, J. Fraanje, K. Goubitz, *Collect. Czech. Chem. Commun.* **1997**, *62*, 238.
[65] P. K. Byers, A. J. Canty, B. W. Skelton, A. H. White, *J. Organomet. Chem.* **1990**, *393*, 299.
[66] W. de Graaf, J. Boersma, W. J. J. Smeets, A. L. Spek, G. van Koten, *Organometallics* **1989**, *8*, 2907.
[67] H. F. Haarman, F. R. Bregman, J. M. Ernsting, N. Veldman, A. L. Spek, K. Vrieze, *Organometallics* **1997**, *16*, 54.
[68] J. H. Groen, P. W. N. M. van Leeuwen, K. Vrieze, *J. Chem. Soc., Dalton Trans.* **1998**, 113.
[69] The high stability of complexes containing the BAr'_4 counterion has been reported earlier. See e.g. ref.[84].
[70] J. H. Groen, C. J. Elsevier, K. Vrieze, W. J. J. Smeets, A. L. Spek, *Organometallics* **1996**, *15*, 3445.
[71] J. M. Ernsting, J. H. Groen, C. J. Elsevier, to be published.
[72] R. E. Rülke, J. M. Ernsting, C. J. Elsevier, A. L. Spek, P. W. N. M. van Leeuwen, K. Vrieze, *Inorg. Chem.* **1993**, *32*, 5769.
[73] J. L. Hoare, K. J. Cavell, R. Hecker, B. W. Skelton, A. H. White, *J. Chem. Soc., Dalton Trans.* **1996**, 2197.
[74] J. H. Groen, B. J. de Jong, J. M. Ernsting, P. W. N. M. van Leeuwen, K. Vrieze, W. J. J. Smeets, A. L. Spek, *J. Organomet. Chem.*, in press.
[75] H. Jin, K. J. Cavell, B. W. Skelton, A. H. White, *J. Chem. Soc., Dalton Trans.* **1995**, 2159.
[76] M. Svensson, T. Matsubara, K. Morokuma, *Organometallics* **1996**, *15*, 5568.
[77] N. Koga, K. Morokuma, *J. Am. Chem. Soc.* **1986**, *108*, 6136.
[78] P. E. M. Siegbahn, S. Stroemberg, K. Zetterberg, *Organometallics* **1996**, *15*, 5542.
[79] P. Margl, T. Ziegler, *Organometallics* **1996**, *15*, 5519.
[80] P. Margl, T. Ziegler, *J. Am. Chem. Soc.* **1996**, *118*, 7337.
[81] It should be noted that the higher rate constant for **5e** than that for **6e** is not caused by inter- or intramolecular coordination of the sulfur donor atom in the nitrogen ligand of **5e**, as addition of 1−100 equiv. of free C_6H_5SMe did not influence the rate constant for **6e**.
[82] One may think that trinitrogen ligands containing three instead

of two carbon atoms between the nitrogen atoms exhibit a more favorable terdentate coordination fashion. However, it is known that this type of terdentate ligands coordinate less strongly to a palladium center.[50]
[83] U. Westerwelle, A. Esser, N. Risch *Chem. Ber.* **1991**, *124*, 571.
[84] M. Brookhart, B. Grant, A. F. Volpe, Jr., *Organometallics* **1992**, *11*, 3920.
[85] R. E. Hurd, B. K. John, *J. Magn. Reson.* **1991**, *91*, 648.
[86] J. Ruiz-Cabello, G. W. Vuister, C. T. W. Moonen, P. van Gelderen, J. S. Cohen, P. C. M. van Zijl, *J. Magn. Reson.* **1992**, *100*, 282.
[87] W. Wilker, D. Leibfritz, W. Kerssebaum, W. Bermel, *Magn. Reson. Chem.* **1993**, *31*, 287.
[88] Crystallographic data (excluding structure factors) for the structures reported in this paper have been deposited with the Cambridge Crystallographic Data Centre as supplementary publication no. CCDC-101040. Copies of the data can be obtained free from charge on application to CCDC, 12 Union Road, Cambridge CB2 1EZ, UK [Fax: int. code + 44(1223)336-033; E-mail: deposit@ccdc.cam.ac.uk].
[89] J. L. de Boer, A. J. M. Duisenberg, *Acta Crystallogr.* **1984**, *A40*, C410.
[90] A. L. Spek, *J. Appl. Crystallogr.* **1988**, *21*, 578.
[91] G. M. Sheldrick, *SHELXS96, Program for Crystal Structure Determination*, University of Göttingen, Germany, **1996**.
[92] G. M. Sheldrick, *SHELXS86, Program for Crystal Structure Determination*, University of Göttingen, Germany, **1986**.
[93] G. M. Sheldrick, *SHELXL-96, Program for Crystal Structure Refinement*, University of Göttingen, Germany, **1996**.
[94] P. van der Sluis, A. L. Spek, *Acta Crystallogr.* **1990**, *A46*, 194.
[95] A. L. Spek, *Acta Crystallogr.* **1990**, *A46*, C34.
[96] *International Tables for Crystallography* (Eds.: A. J. C. Wilson), Kluwer Academic Publishers, Dordrecht, The Netherlands, **1992**, vol. C.
[97] J. S. Binkley, J. A. Pople, W. J. Hehre, *J. Am. Chem. Soc.* **1980**, *102*, 939.
[98] N. Godbout, D. R. Salahub, J. Andzelm, E. Wimmer, *Can. J. Chem.* **1992**, *70*, 560.
[99] *GAMESS-UK V5.2:* GAMESS-UK is a package of ab initio programs written by M. F. Guest, J. H. Van Lenthe, J. Kendrick, K. Schoffel, P. Sherwood, R. J. Harrison, with contributions from R. D. Amos, R. J. Buenker, M. Dupuis, N. C. Handy, I. H. Hillier, P. J. Knowles, V. Bonacic-Koutecky, W. Von Niessen, V. R. Saunders, A. J. Stone. The package is derived from the original GAMESS code due to M. Dupuis, D. Spangler, J. Wendoloski: NRCC Software Catalog, vol. 1, Program No. QG01 (GAMESS), **1980**. MP2 implementation: J. E. Rice, R. D. Amos, N. C. Handy, T. J. Lee, H. F. Schaefer, *J. Chem. Phys.* **1986**, *85*, 963; J. D. Watts, M. Dupuis, *J. Comput. Chem.* **1988**, *9*, 158.
[100] *Gaussian 94 Revision E.1:* M. J. Frisch, G. W. Trucks, H. B. Schlegel, P. M. W. Gill, B. G. Johnson, M. A. Robb, J. R. Cheeseman, T. A. Keith, G. A. Petersson, J. A. Montgomery, K. Raghavachari, M. A. Al-Lahan, V. G. Zakrewski, J. V. Ortiz, J. B. Foresman, J. Cioslowski, B. B. Stefanov, A. Nanayakkara, M. Challacombe, C. Y. Peng, P. Y. Ayala, W. Chen, M. W. Wong, J. L. Andres, E. S. Reploge, R. Gomperts, R. L. Martin, D. J. Fox, J. S. Binkley, D. J. DeFrees, J. Baker, J. P. Stewart, M. Head-Gordon, C. Gonzalez, J. A. Pople, Gaussian, Inc., Pittsburgh, PA, **1995**.

[98016]

Preparation, Structure and Reactivity of 2-Chloro-, 2-Fluoro- and 2-Iodo-2,3-dihydro-1*H*-1,3,2-diazaboroles☆

Lothar Weber*[a], Eckhard Dobbert[a], Roland Boese[b], Michael T. Kirchner[b], and Dieter Bläser[b]

Fakultät für Chemie der Universität Bielefeld[a],
Universitätsstraße 25, D-33615 Bielefeld, Germany,
Fax: (internat.) +49(0)5201-106-6146
E-mail: lothar.weber@uni-bielefeld.de

Institut für Anorganische Chemie der Universität-Gesamthochschule Essen[b],
Universitätsstraße 5−7, D-45117 Essen, Germany

Received March 3, 1998

Keywords: Boron / Diazaboroles / Halogens / Isocyanides / Heterocycles

A series of differently substituted 2-chloro-, 2-fluoro- and 2-iodo-2,3-dihydro-1*H*-1,3,2-diazaboroles have been prepared by various methods. 1,3-Di-*tert*-butyl-2-fluoro-2,3-dihydro-1*H*-1,3,2-diazaborole (**3a**), 1,3-di-*tert*-butyl-2-chloro-2,3-dihydro-1*H*-1,3,2-diazaborole (**5a**), 1,3-bis(2,6-dimethylphenyl)-2-chloro-2,3-dihydro-1*H*-1,3,2-diazaborole (**5b**), 2-chloro-4,5-dimethyl-1,3-dineopentyl-2,3-dihydro-1*H*-1,3,2-diazaborole (**5c**), and 1,3-di-*tert*-butyl-2-iodo-2,3-dihydro-1*H*-1,3,2-diazaborole (**6a**) were formed from the corresponding lithiated Z-1,2-diaminoethenes, by treatment with $BF_3{\cdot}OEt_2$, BCl_3, or BI_3 in *n*-hexane. Compounds **3a**, **5a**, and **5b** are also available by sodium amalgam reduction of the adduct (*t*Bu)(BF_3)N=CH–CH=N(BF_3)(*t*Bu) (**2a**), and the borolium salts [RN^a=CH–CH=N^b(R)BCl_2]X (N^a–B) (**4a**: R = *t*Bu, X = BCl_4 and **4b**: R = 2,6-$Me_2C_6H_2$, X = Cl) respectively. The iodo derivative (2,6-$Me_2C_6H_2$)–N^a–CH=CH–N^b(2,6-$Me_2C_6H_2$)BI (N^a–B) (**6b**) was synthesized in a redox reaction between the 1,4-diazabutadiene **1b** and BI_3. The novel compounds were characterized by ^{1}H-, ^{11}B- and ^{13}C-NMR spectroscopy, as well as by an X-ray structure analysis of **6b**.

The formal replacement of a C=C fragment in pyrrole **I** by a B−N unit affords 2,3-dihydro-1*H*-1,3,2-diazaboroles **II**.

I **II**

The first reports on heterocycles of the type **II** date back to the early 1970s[1][2]. Meanwhile, a series of papers concerned with the synthesis, structure, and bonding of such molecules has been published.[3][4] Apart from the synthesis of [$Cr(CO)_3$] complexes with η^5-1,3,2-diazaborole ligands[5][6] and the cleavage of the N−Si bond in *N*-silylated derivatives by metal amides or alcoholates to yield the corresponding alkali metal 1,3,2-diazaborolides,[7] the chemistry of heterocycles **II** has remained largely unexplored. The lack of functional groups in the 2,3-dihydro-1*H*-1,3,2-diazaboroles examined to date may account for this situation.

Recently we launched a program for the synthesis of 2-halo-2,3-dihydro-1*H*-1,3,2-diazaboroles as precursors for a variety of chemical transformations. In a first account we described the preparation of 2-bromo-2,3-dihydro-1*H*-1,3,2-diazaboroles **III** and their reactions with water and imidazol-2-ylidenes. The resulting salts such as **V** contain the first borylated carbenium ions.[8]

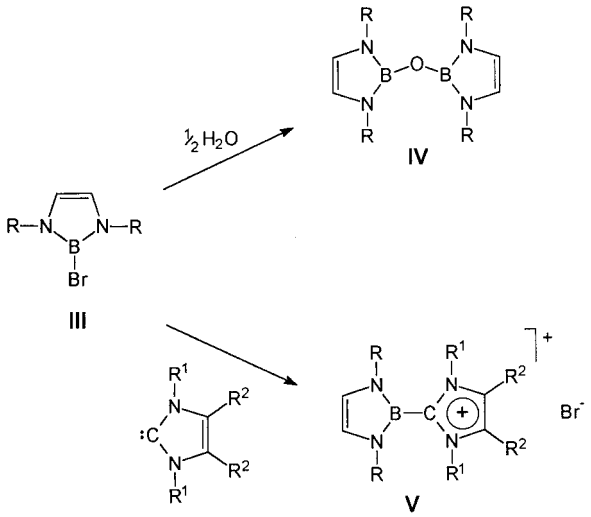

III **IV** **V**

The intention of the work described herein is to provide efficient syntheses for 2-fluoro-, 2-chloro- and 2-iodo-2,3-dihydro-1*H*-1,3,2-diazaboroles.

Results and Discussion

For the preparation of 2-bromo-2,3-dihydro-1*H*-1,3,2-diazaboroles, as well as the corresponding fluoro, chloro and iodo derivatives, two synthetic approaches are generally available. The first pathway [Scheme 1 (a)], involves the gen-

☆ Supporting information for this article is available on the WWW under http://www.wiley-vch.de/home/eurjic or from the author.

 © WILEY-VCH Verlag GmbH, D-69451 Weinheim, 1998 1434−1948/98/0808−1145 $ 17.50+.50/0

eration of the bis(trifluoroborane) adduct **2a**, by the combination of 1,4-diazabutadiene **1a** with two molar equivalents of $BF_3{\cdot}Et_2O$ in *n*-hexane.

Scheme 1

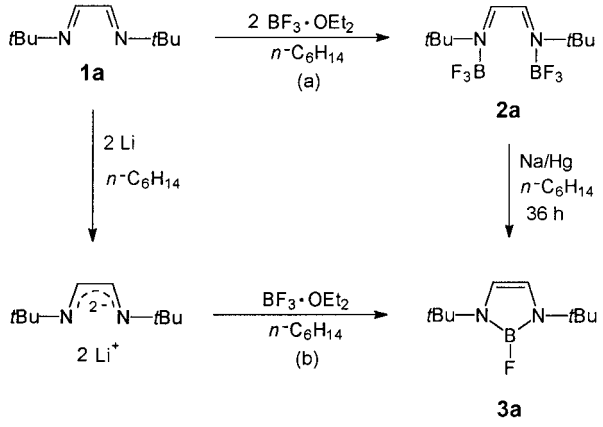

The adduct was obtained as a yellow amorphous solid in 74% yield. Its $^{11}B\{^1H\}$-NMR spectrum in CD_3CN shows only one singlet (at $\delta = 0.4$) for the two chemically and magnetically equivalent boron atoms. Similarly, only one resonance was observed in the $^{19}F\{^1H\}$-NMR spectrum of **2a** (at $\delta = 73.0$) for the six fluorine atoms. The synthesis of 2-fluoro-1,3,2-diazaborole (**3a**) was accomplished by the reduction of **2a** with an excess of sodium amalgam in an *n*-hexane slurry (Scheme 1). After 36 h, the ^{11}B-NMR spectrum only showed the resonance for **3a** at $\delta^{11}B = 20.8$. The crude yellow **3a** was purified by fractional condensation at 40°C and 0.01 Torr to give colorless crystals. At temperatures above 40°C the 2-fluoro-1,3,2-diazaborole decomposed with liberation of **1a**. Compound **3a** is soluble in common aprotic organic solvents. In solution complete decomposition of the heterocycle occurred within 2 days.

A second approach to **3a** [Scheme 1 (b)] made use of the reduction of **1a** by two equivalents of lithium in hexane, prior to the condensation with $BF_3{\cdot}Et_2O$.

In contrast to the symmetrical adduct **2a**, the treatment of **1a** with two molar equivalents of BCl_3 in *n*-hexane at −30°C afforded the colorless amorphous borolium tetrachloroborate **4a** in 71% yield. Accordingly, the ^{11}B-NMR spectrum of the salt gave rise to two singlets for the BCl_4^- ion[9] and the boron atom of the ring at $\delta = 1.6$ and 7.7 respectively. The analogous borolium chloride, described in the literature, gave a boron resonance at $\delta = 7.2$ (in $CDCl_3$).[3] The reduction of **4a** with sodium amalgam in *n*-hexane led to the formation of 2-chloro-1,3,2-diazaborole (**5a**) as a colorless solid after sublimation (40−60°C, 0.01 Torr, 91%). The course of the reduction was followed by ^{11}B-NMR spectroscopy. After 5 h, the spectrum of the supernatant solution showed signals at $\delta = 32.3$ and 21.0 in a ratio of 2:1. A small resonance at $\delta = 47.0$ was assigned to BCl_3. After 14 h, the spectrum was dominated by two intense singlets at $\delta = 21.1$ and 47.0, in addition to a weak singlet at $\delta = 31.8$. This observation may be rationalized by the initial formation of the intermediate acyclic aminoborane $(tBu)N(BCl_2)-CH=CH-N(BCl_2)(tBu)$ (**A**)[10] which subsequently disproportionated into **5a** and BCl_3 (Scheme 2). The synthesis of **5a** can also be effected by the reaction of the lithiated diazabutadiene with BCl_3 [Scheme 2 (b)].

Scheme 2

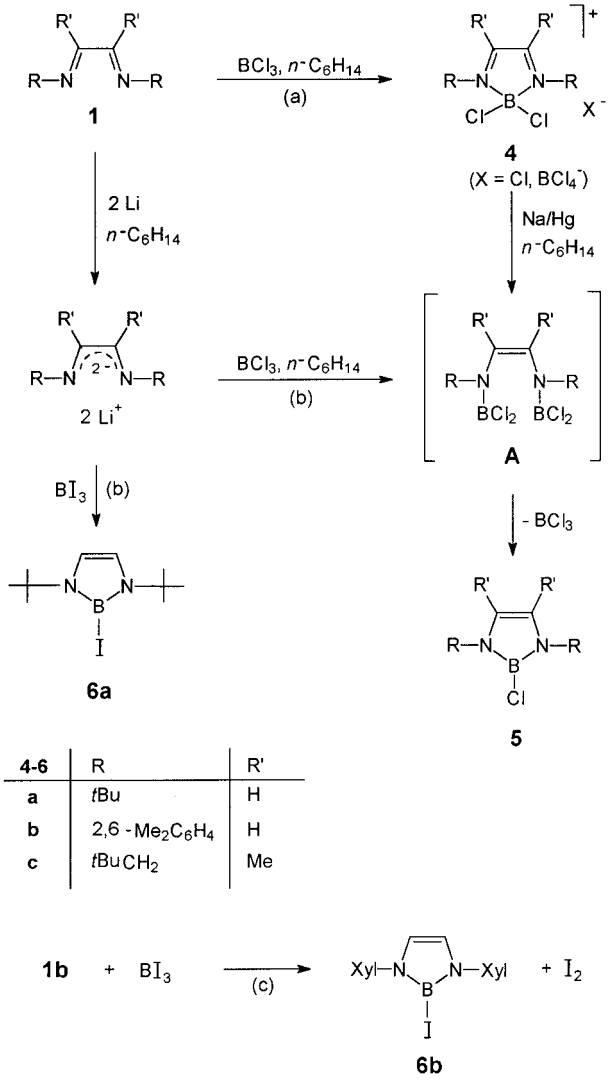

The reaction of 1,4-diazabutadiene **1b** with an equimolar amount of BCl_3 in a hexane/dichloromethane mixture, led to the violet borolium chloride **4b** (38%) and the corresponding black tetrachloroborate **4b′** (7%). The ^{11}B-NMR spectra of the salts displayed signals at $\delta = 7.2$ for **4b**, and at $\delta = 7.7$ and 1.5 for **4b′**.

Reduction of **4b** by an excess of sodium amalgam in *n*-hexane afforded the 2-chloro-1,3,2-diazaborole **5b** (55% yield). Treatment of 1,4-diazabutadiene **1b** with lithium sand and condensation of the lithium derivative with BCl_3 gave 1,3,2-diazaborole **5b** (53%) as the final product after 3 d. After 1 h, the ^{11}B-NMR spectrum of the yellow solution showed a resonance at $\delta = 32.5$ for an intermediate. Minor resonances at $\delta = 22.0$ and 47.0 were attributed to **5b** and BCl_3, respectively. After 14 h, a spectrum of the same sample displayed only the singlets of **5b** and BCl_3. In an

additional experiment, the reaction mixture was filtered after 1 h of stirring at ambient temperature and the concentrated hexane solution was stored overnight at −80°C to give a tan precipitate. The ^{11}B-NMR spectrum of the tan precipitate in $CDCl_3$ showed a major resonance at δ = 32.6 and an impurity of **5b** at δ = 21.8. The ^{1}H-NMR spectrum of the tan solid in C_6D_6 was dominated by singlets at δ = 1.99 (s, 12 H, CH_3), 6.40 (s, 2 H, N=CH), and 6.93 (m, 6 H, aryl-H), in addition to the resonances of **5b**. A 2:1 ratio of the intermediate to **5b** was determined. Based on the spectroscopic data and its good solubility in non-polar solvents, we attributed the formula (Xyl)(Cl_2B)N−CH=CH−N(BCl_2)(Xyl) to this intermediate (Scheme 2).

Lithium reduction of 1,4-diazabutadiene **1c** for 10 d in *n*-hexane, and the subsequent quenching of the lithium derivative with BCl_3 furnished 1,3,2-diazaborole **5c** as a dark brown oil, which slowly solidified to a tan wax (60%).

The synthesis of the 2-iodo-1,3,2-diazaborole (*t*Bu)-N^a−CH=CH−N^b(*t*Bu)BI(*N*^{a}−B) (**6a**) was achieved by allowing Li_2[(*t*Bu)NCH=CHN(*t*Bu)] to react with an equimolar amount of BI_3 to give a colorless, light-sensitive oil (83%), which completely decomposed within 5 h at room temperature. In contrast, 2-iodo-1,3,2-diazaborole **6b**, accessible by the redox reaction between **1b** and BI_3, was sublimed at 380°C/0.01 Torr without significant decomposition.

As previously shown, 2-bromo-2,3-dihydro-1*H*-1,3,2-diazaborole (**7a**) can be brought to reaction with imidazolylidenes to give borylated imidazolium salts (eq. 1). In the light of these data, an analogous synthesis of borylated nitrilium salts seemed possible, by reaction of compounds **5**−**7** with organic isocyanides.

Treatment of **5a**, **6a**, and **7a** with an equimolar amount of *tert*-butyl isocyanide in *n*-hexane, led to the formation of the 2-cyano-1,3,2-diazaborole (**8a**). The expected nitrilium salt could not be detected spectroscopically. The formation of *tert*-butylbromide as a byproduct was proven by ^{1}H-NMR spectroscopy (δ = 1.78) and by comparison with an authentic sample.

The corresponding reaction of **7a** with cyclohexyl isocyanide afforded **8a** in 38% yield after 5 days. No intermediates were observed spectroscopically. Similarly, **5b** and **6b** were converted into **8b** by *tert*-butyl isocyanide in 70% and 55% yield, respectively (Scheme 3).

No reaction was observed between 2-halo-1,3,2-diazaboroles **5**−**7** and 2,6-$Me_2C_6H_3$N≡C. The cyano compound **8a** was also synthesized in high yield by treatment of the diazaboroles **5a** or **7a** with a slight excess of silver cyanide in acetonitrile at room temperature. The 2-bromo compound was found to be more reactive than the 2-chloro analogue. Similarly, compound **8b** was obtained by treatment of **6b** with AgCN over a period of 2 days (79%).

In line with the synthetic approach to isocyanatoboranes and isothiocyanatoboranes devised by Lappert et al.,[11] diazaborole **5a** was converted by silver cyanate in acetonitrile into the isocyanato diazaborole **9a**, which was isolated after 30 min as a colorless thermolabile oil in 78% yield. The analogous reaction between **7a** and AgOCN to afford **9a**

Scheme 3

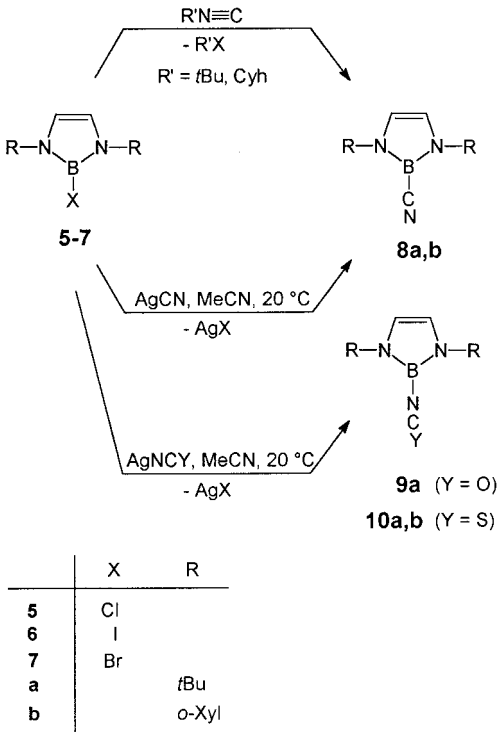

was complete after 5 min (83%). The corresponding isothiocyanato diazaborole **10a**, resulted from the reaction of **5a** or **7a** with AgSCN under similar conditions. Again, the reactivity of **7a** exceeded that of **5a**. Derivative **10b** was synthesized from **6b**, **5b**, or (2,6-$Me_2C_6H_3$)N^a−CH=CH−N^b(2,6-$Me_2C_6H_3$)BBr(*N*^{a}−B) (**7b**) (78−93% yield). The reactivity of the 2-halo-1,3,2-diazaboroles was found to be: **7b** > **5b** > **6b**.

It was not possible to unambiguously identify the B−X stretching frequencies in the IR-spectra of the 2-halo-1,3,2-diazaboroles **3**, **5**, **6**, and **7**. In the IR spectra (KBr) of **8a** and **8b**, weak bands at ν = 2207 and 2218 cm^{-1} are attributed to the stretching frequency of the C≡N group. In the IR spectra of MeN^a−CH_2−CH_2−N^b(Me)BCN(*N*^{a}−B)[12] and MeN^a−N^b=N^c−N^d(Me)BCN(*N*^{a}−B)[13] the ν(CN) mode was observed as weak bands at 2225 and 2239 cm^{-1}, respectively. A very intense band in the IR spectrum of **9a** at ν = 2317 cm^{-1} was assigned to the asymmetric stretching frequency of the isocyanato group, which is consistent with the data for compounds (R_2N)$_2$B−N=C=O [ν_{as}(NCO) = 2290 ± 15 cm^{-1}],[11c] and the IR spectrum of Me_2B−N=C=O [ν_{as}(NCO) = 2285 cm^{-1} vs].[14] These frequencies also underline the presence of an isocyanatoborane R_2BN=C=O, and disfavor the isomeric cyanatoborane structure R_2BOC≡N. Similar arguments support an isothiocyanatoborane structure in the 1,3,2-diazaboroles **10a** and **10b**, where very strong bands at 2121 and 2114 cm^{-1}, respectively, are assigned to the ν_{as}(NCS) mode. Intense bands at 871 and 856 cm^{-1} are due to the symmetric stretching frequency of the NCS group. The ν_{as}(NCS) of a series of isothiocyanatoboranes occurs in the range 2089 ± 31 cm^{-1}.[11]

The $^{11}B\{^1H\}$-NMR spectra of the halo- and pseudohalodiazaboroles display an increased shielding as follows: **3a** ≈ **5a** (δ = 20.2) > **7a** (16.2) > **9a** ≈ **10a** (14.7) > **8a** (12.0) > **6a** (6.5). Similarly, the ^{11}B-NMR signals of **5b**, **7b**, **10b**, **8b**, and **6b** range from δ = 21.1 to 11.8. The significant high-field shift of **8a** relative to the saturated analogue Me-$N^a-CH_2CH_2-N^b$(Me)BCN(*N*^{a}−B) (δ = 21.0)[12] sustains the heteroaromatic nature of the rings under discussion. The ring protons in **3a** and **5a**−**10a** are observed at δ = 5.99−6.40, whereas in the dixylyl-substituted derivatives **5b**−**8b** and **10b**, singlets at δ = 5.71−5.99 are assigned to these protons. In the $^{13}C\{^1H\}$-NMR spectra of **3a** and **5a**−**10a**, singlets at δ = 109.9−114.6 were assigned to the C=C group of the rings. The respective ^{13}C-nuclei of **5b**−**8b**, and **10b** gave rise to resonances at δ = 117.2−120.0.

X-ray Structural Analysis of 6b

The molecular structure of **6b** (Figure 1) features a planar 1,3,2-diazaborole ring with two nearly orthogonally oriented *ortho*-xylyl substituents at the nitrogen atoms (interplanar angle between the heterocycle and an arene ring ψ = 85.6°). A C_2 axis bisects the molecule along the B(1)−I(1) vector. The bond length B(1)−I(1) [2.119(5) A] is close to the sum of the covalent radii of boron (0.81 A) and iodine (1.33 A)[15] and compares well with the atomic distance between the tricoordinate boron and an iodine atom in the dimer of $IB^a-C(Et)=C(Et)-B^b(I)S$(*B*^{a}−S) [2.13(2) A][16]. B−I bond lengths involving sp^2-hybridized boron atoms range from 2.10(4) A in BI_3[17] to 2.237(6) A in the triborane $[(Me_2N)(I)B]_2BNMe_2$[18]. Atomic distances and valence angles within the diazaborole ring are in good agreement with the respective data for $EtN^a-CH=CH-N^b$(Et)BMe(*N*^{a}−B).[4] In **6b**, the B−N bond length [1.418(4) A] indicates multiple-bond character. In a series of diazaboroles the B−N bond lengths range from 1.407(3) to 1.450(2) A. The atomic distance C(1)−C(1′) [1.362(8) A], and the N−C(sp^2) bond length [1.401(4) A] also indicate multiple bonding. For the N(sp^2)−C(sp^2) single bond, N(1)−C(2) bond lenghths of 1.438(4) A were measured. The endocyclic angles in **6b**: N(1)−B(1)−N(1)′ [106.9(4)°], B(1)−N(1)−C(1) [107.5(3)°], and N(1)−C(1)−C(1)′ [109.1(2)°] resemble those in the borylimidazolium cation **V** [107.1(6), 105.9(4), and 110.5(3)°, respectively].[1] This also applies to the exocyclic angle N(1)−B(1)−I(1) [126.6(2)°] in **6b**, and the corresponding angle N(1)−B(1)−C(6) in **V** [126.5(3)°].

The packing of **6b** shows some interesting features. The molecules are arranged in a pattern with the iodine atoms pointing to the centers of the carbon−carbon double bonds (distance from the iodine atom to the center of the bond 3.17 A), such that each iodine atom is in contact with two hydrogen atoms (distance from iodine to hydrogen 3.093 A, with a normalized 1.08 A distance for C−H). This linkage produces chains of molecules with adjacent chains running in opposite directions, and with the phenyl groups interlocked (Figure 2).

In the layer depicted in Figure 2, one of the methyl groups is oriented so that a hydrogen atom points towards

Figure 1. Crystal molecular structure of **6b**[a]

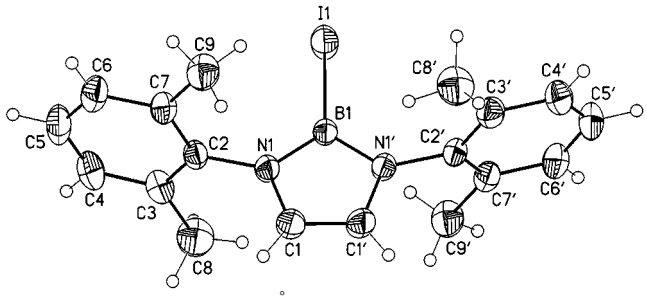

[a] Selected bond lengths [A] and bond angles [°]: B(1)−I(1) 2.119(5), B(1)−N(1) 1.418(4), N(1)−C(1) 1.401(4), C(1)−C(1′) 1.362(8), N(1)−C(2) 1.438(4); N(1)−B(1)-N(1′) 106.9(4), N(1)−B(1)−I(1) 126.6(2), B(1)−N(1)−C(1) 107.5(3), B(1)−N(1)−C(2) 130.0(3), C(1)−N(1)−C(2) 122.5(3), N(1)−C(1)−C(1′) 109.1(2). [B(1), N(1),C(1)−C(1′)−N(1′)−C(2), C(3), C(4), C(5), C(6), C(7)] 85.6.

Figure 2. View of the crystal structure of **6b** along the *c* axis; depicted are two adjacent chains with three molecules each

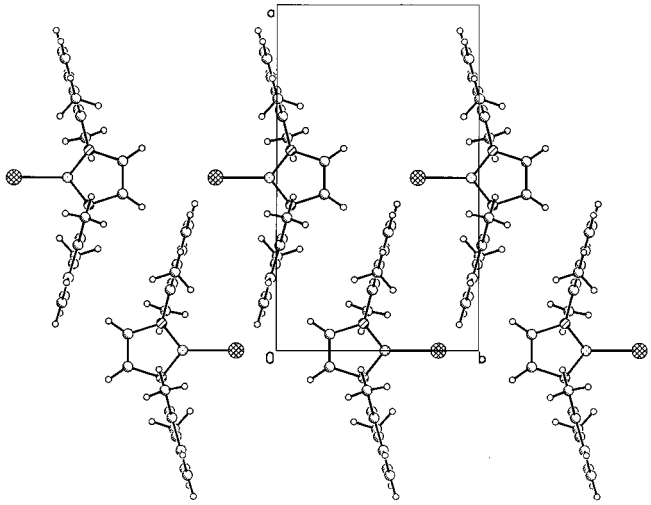

the aromatic ring system of the adjacent chain. A cheletropic intermolecular interaction of iodine with two hydrogen atoms bonded to sp^2-carbon atoms is expected to be mostly electrostatic in nature, and seems to dominate the molecular packing of **6b**. An analysis of specific packing motifs is possible with the help of a statistical approach which involves plots of intermolecular distances and angles for groups of crystals structures that contain the motif under investigation (scatter-plots). The more frequent certain short contacts with reasonable angles occur, the more likely it is that this represents a "supramolecular synthon".[19] Therefore we performed a search in the CSD,[20] which revealed 5703 structures that possess: (1) a *cis*-1,2-dihydro group, attached to a double or aromatic bond of two carbon atoms, and (2) an uncharged halogen (not fluorine) atom with a single bond. Amongst these, 426 structures and 1079 fragments have an intermolecular distance from the halogen atom to the hydrogen atoms of less than the sum of van der Waals radii plus 1 A (H···Cl 3.95 A; H···Br 4.05 A; H···I 4.18 A). A characteristic cheletropic interaction is evident from the polar scatter diagrams, given in Figures 3

and 4. Figure 3 represents the positions of the halogen atoms relative to the aromatic carbon−carbon double bond, with this bond at the equator, and the *cis*-oriented hydrogen atoms situated in the northern hemisphere. An accumulation of structures at a distance of 4 A from the center of the aromatic C=C bond and perpendicular to this bond axis demonstrates that the halogen atoms prefer to be located in the same manner as we found for **6b**. In our case, the intermolecular distance with iodine, and even with bromine, is amongst the smallest found for all the given fragments.

Figure 3. Polar scatter plot of the distance from the halogen to the center of the carbon−carbon double bond, the angle between the carbon−carbon double bond, and the projection of the intermolecular vector to the plane for 1079 fragments in the Cambridge Data Base that contain the halogen···HC=CH motif as defined

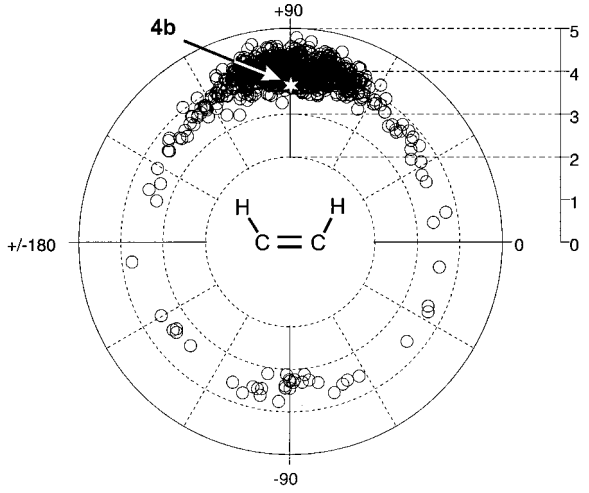

Figure 4. Polar scatter plot of the distance from the halogen to the center of the carbon−carbon double bond and the angle between the molecular plane and the intermolecular vector (section perpendicular to Figure 3)

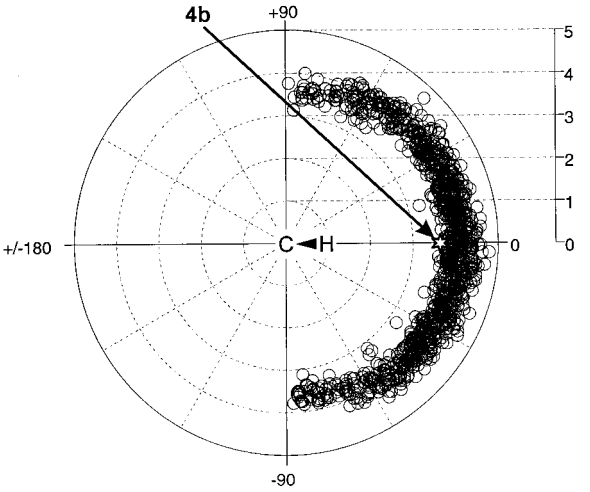

The distribution of halogen positions below and above the one in Figure 3 is shown in Figure 4. Here the equator of the pole scatter diagram intercepts the center of the double (aromatic) C=C bond, with the hydrogen atoms below and above the plane of the diagram. An accumulation, albeit not so pronounced, of halogen atoms in the plane of the carbon and hydrogen atoms (at 0°) again demonstrates the cheletropic character of the interaction in **6b**. The angles used in Figures 3 and 4 were obtained from the *LP2 method in Quest3D[21], where the positions of one hydrogen atom, the nearest carbon atom, the center of the carbon−carbon bond, and the halogen atom were used as the parameters. The scatter plot was produced by the distance between the halogen atom and the center of the carbon−carbon double bond. Equivalent scatter plots produced for iodine, bromine, and chlorine are available as supporting information on the WWW or from the author.

This work was financially supported by the *Fonds der Chemischen Industrie*, Frankfurt/Main, and the *Deutsche Forschungsgemeinschaft*, Bonn, which are gratefully acknowledged.

Experimental Section

General: All manipulations were performed under dry argon. Solvents were rigorously dried with an appropriate drying agent and distilled before use. − The following compounds were prepared as described in the literature: *t*BuN=CH−CH=N*t*Bu (**1a**),[22] 2,6-$Me_2C_6H_3N$=CH−CH=$NC_6H_3Me_2$-2,6 (**1b**),[23] *t*$BuCH_2N$=C(Me)−C(Me)=NCH_2*t*Bu (**1c**),[24] and BI_3.[25] Boron trichloride, boron trifluoride−diethyl ether, *t*BuNC, cyclohexyl isocyanide, AgCN, AgOCN, and AgSCN were purchased. − IR spectra: Bruker FTIR IFS66. − ^{1}H-, ^{11}B-, ^{13}C-, and ^{19}F-NMR spectra: Bruker AC 100 (^{1}H, 100.13 MHz; ^{13}C, 25.18 MHz), and Bruker AM Avance DRX 500 (^{1}H, 500.13 MHz; ^{11}B, 160.46 MHz; ^{13}C, 125.75 MHz; ^{19}F, 470.60 MHz). References: $SiMe_4$ (^{1}H, ^{13}C), $BF_3{\cdot}OEt_2$ (^{11}B), $CFCl_3$ (^{19}F). − Mass spectra (EI): VG Autospec sector-field mass spectrometer (Micromass) 70 eV.

(tBu)(BF_3*)N=CH−CH=N(tBu)(*BF_3*)* (**2a**): A solution of *t*BuN=CH−CH=N*t*Bu (**1a**) (10.0 g, 59.0 mmol) in 200 ml of *n*-hexane, and an emulsion of $BF_3{\cdot}OEt_2$ (18.6 g, 118.0 mmol) in 200 ml of *n*-hexane were added separately, dropwise, into a flask filled with chilled *n*-hexane (1000 ml, −10°C). After 24 h of stirring at room temp., a yellow solid was filtered off and washed with *n*-hexane (4 × 30 ml). Drying at 0.01 Torr for 2 h gave **2a** as a bright yellow powder (13.2 g, 74%). − IR (KBr): ν = 3206cm^{-1} w, 3102 w, 2984 vs, 2892 s, 2796 m, 2695 m, 2585 m, 2486 m, 2034 m, 1950 w, 1608 w, 1509 m, 1476 w, 1404 m, 1378 m, 1299 m, 1214 m, 1055 vs, br. [ν(BF)], 534 m, 522 m, 444 m, 419 w. − ^{1}H NMR (CD_3CN): δ = 1.48 (s, 18 H, *t*Bu), 8.90 (s, 2 H, CH). − ^{13}C{^{1}H} NMR (CD_3CN): δ = 28.5 [s, C(CH_3)$_3$], 66.3 [s, C(CH_3)$_3$], 163.2 (s, CH). − ^{11}B{^{1}H} NMR (CD_3CN): δ = 0.4 (s). − ^{19}F{^{1}H} NMR (CD_3CN): δ = 73.0 (s). − $C_{10}H_{20}B_2F_6N_2$ (303.86): calcd. C 39.52, H 6.65, N 9.21; found C 39.40, H 6.83, N 9.23.

(tBu)N^a*−CH=CH−*N^b*(tBu)BF(*N^a*−B)* (**3a**). − *Path (a):* A slurry of adduct **2a** (5.0 g, 16.5 mmol) in *n*-hexane (100 ml) was treated at 20°C with sodium amalgam prepared from 3.8 g (165.2 mmol) of sodium and 500 g of mercury. After 36 h of stirring, the yellow hexane phase was decanted. Solvent and volatile components were removed in vacuo (0.1 Torr, 10°C) to give a yellow solid residue. Purification of crude **3a** was achieved by fractional condensation at 40°C and 0.01 Torr (yield 2.38 g, 73%).

Path (b): 1.4-Diazabutadiene **1a** (1.67 g, 10.0 mmol) was reduced with lithium sand (0.139 g, 20.0 mmol) in 70 ml of *n*-hexane for 7 d at 20°C. The yellow slurry obtained was treated with 1.58 g (10.0 mmol) of $BF_3{\cdot}Et_2O$, and the mixture was stirred for 10 min. The red solution was filtered, concentrated to ca. 10 ml, and stored

overnight at −78°C to afford 1.1 g (56%) of colorless crystalline **3a**. − IR (nujol): ν = 1631cm^{-1} w, 1489 sh, 1428 s, 1395 sh, 1366 s, 1293 m, 1273 w, 1244 s, 1224 m, 1211 m, 1136 s, 1062 w, 1028 w, 951 w, 933 w, 879 w, 822 w, 746 w, 658 w, 623 s. − ^{1}H NMR (C_6D_6): δ = 1.26 (d, $^5J_{FH}$ = 1.1 Hz, 18 H, *t*Bu), 5.99 (d, $^4J_{FH}$ = 2.3 Hz, 2 H, CH). − ^{13}C{^{1}H} NMR (C_6D_6): δ = 30.9 [s, C(*C*H$_3$)$_3$], 51.6 [s, *C*(CH$_3$)$_3$], 109.9 (s, CH). − ^{11}B{^{1}H} NMR (C_6D_6): δ = 20.3 (s). − ^{19}F{^{1}H} NMR (C_6D_6): δ = 57.9 (s). − MS/EI (70 eV); *m*/*z*: 199 [M$^+$]. − $C_{10}H_{20}BFN_2$ (198.09): calcd. C 60.63, H 10.18, N 14.14; found C 60.44, H 10.59, N 14.17.

[tBuN^a=CH−CH=N^b(tBu)BCl$_2$]$^+$BCl$_4^-$(N^a−B) (**4a**): A three-necked 2-l flask was filled with 900 ml of *n*-hexane and cooled to −30°C. Solutions of **1a** (8.10 g, 48.0 mmol) in 200 ml of *n*-hexane and BCl_3 (11.30 g, 96.0 mmol) in 200 ml of *n*-hexane were added dropwise at a similar rate into the well-stirred *n*-hexane. The resulting mixture was stirred overnight. The colorless precipitate was filtered off and washed with *n*-hexane (2 × 50 ml) and *n*-pentane (2 × 50 ml) before drying in vacuo to give 13.7 g (71%) of **4a**. − IR (KBr): ν = 2985 cm^{-1} m, 2360 w, 1580 m, 1465 s, br., 1405 s, 1385 s, 1232 m, 1191 s, 1119 w, 1071 m, 1036 w, 920 w, 898 m, 821 s, 804 s, 711 m, 657 m, 547 w, 481 w. − ^{1}H NMR (CD_3CN): δ = 1.70 (s, 18 H, *t*Bu), 8.90 (s, br., 2 H, CH). − ^{13}C{^{1}H} NMR (CD_3CN): δ = 30.0 [s, C(*C*H$_3$)$_3$], 67.3 [s, *C*(CH$_3$)$_3$], 162.7 (s, CH). − ^{11}B{^{1}H} NMR (CH_3CN): δ = 1.6 (s, BCl_4^-), 7.7 (s, N_2BCl_2). − $C_{10}H_{20}B_2Cl_6N_2$ (402.62): calcd. C 29.83, H 5.01, N 6.96; found C 29.91, H 5.00, N 6.80.

[2,6-Me$_2$C$_6$H$_3$N^a=CH−CH=N^b(2,6-Me$_2$C$_6$H$_3$)BCl$_2$]$^+$Cl$^-$(N^a−B) (**4b**) *and [2,6-Me$_2$C$_6$H$_3$N^a=CH−CH=N^b(2,6-Me$_2$C$_6$H$_3$)BCl$_2$]$^+$BCl$_4^-$(N^a−B)* (**4b′**): A three-necked 2-l flask was charged with 1200 ml of *n*-hexane and chilled to −20°C. As described before the solutions of BCl_3 (5.90 g, 50.0 mmol) in 200 ml of *n*-hexane and **1b** (13.2 g, 50.0 mmol) in a mixture of *n*-hexane (150 ml) and CH_2Cl_2 (50 ml) were added dropwise into the flask. After warming up to ambient temp., a violet precipitate was filtered off, washed with *n*-hexane (3 × 30 ml) and dried in vacuo to give 7.2 g (38%) of **4b**. The mother liquor was concentrated to ca 500 ml and stored at 5°C overnight to yield 1.7 g (7%) of black crystalline **4b′**.

4b: IR (KBr): $\tilde{\nu}$ = 2567 cm^{-1} w, 1585 w, 1473 s, br., 1197 m, 1095 w, 884 w, 821 m, 775 m, 656 w, 548 w. − Due to the poor solubility and due to decomposition no reliable ^{1}H- and ^{13}C-NMR spectra were available. − ^{11}B{^{1}H} NMR ($CDCl_3$): δ = 7.2 (s). − $C_{18}H_{20}BCl_3N_2$ (381.54): calcd. C 56.66, H 5.28, N 7.34; found C 57.87, H 5.20, N 6.95.

4b′: IR (KBr): $\tilde{\nu}$ = 2963 cm^{-1} w, 2922 w, 1608 sh, 1535 sh, 1473 s, 1444 s, 1374 s, 1252 sh, 1227 m, 1094 s, 1000 s, 933 m, 908 w, 771 s, 722 w, 668w, 542 w. − ^{11}B{^{1}H} NMR (CD_3CN): δ 7.7 (s, BN_2), 1.5 (s, BCl_4^-). − $C_{18}H_{20}B_2Cl_6N_2$ (498.71): calcd. C 43.35, H 4.04, N 5.62; found C 38.6, H 4.31, N 4.77. − Repeated attempts to purify the crude product by recrystallization failed.

(tBu)N^a−CH=CH−N^b(tBu)BCl(N^a−B) (**5a**). − *Path (a):* A sample of 4.46 g (11.0 mmol) of borolium salt **4a** was stirred overnight with 305.2 g of sodium amalgam (96.0 mmol sodium) in 120 ml of hexane. The reaction mixture was protected from light. The slightly yellow solution was decanted from a yellow precipitate. Filtration and removal of volatile components in vacuo afforded an orange-yellow oil, which slowly solidified to give orange crystalline **5a**. The crude material was sublimed at 40−60°C (0.01 Torr) to yield 2.18 g (91%) of colorless product.

Path (b): A sample of 1,4-diazabutadiene **1a** (2.50 g, 14.8 mmol) was stirred with lithium sand (0.21 g, 29.6 mmol) in 70 ml of *n*-hexane for 7 d at 20°C. A solution of 1.75 g (14.8 mmol) of BCl_3 in 30 ml of *n*-hexane was added dropwise to the chilled yellow slurry (−50°C). The mixture was allowed to warm up to room temp., and stirring was continued overnight. Filtration and removal of solvent from the filtrate in vacuo gave 1.74 g (55%) of **5a**. − IR (CsI, film): ν = 1515 cm^{-1} w, 1464 m, 1399 s, 1367 s, 1347 sh, 1327 s, 1285 m, 1237 s, 1209 m, 1136 m, 1030 w, 987 m, 943 w, 893 w, 822 w, 696 w, 662 m. − ^{1}H NMR (C_6D_6): δ = 1.35 (s, 18 H, *t*Bu), 6.19 (s, 2 H, CH). − ^{13}C{^{1}H} NMR (C_6D_6: δ = 30.9 [s, C(*C*H$_3$)$_3$], 53.2 [s, *C*(CH$_3$)$_3$], 112.0 (s, CH). − ^{11}B{^{1}H} NMR (C_6D_6): δ = 20.2 (s). − MS/EI; *m*/*z* (%): 214 (20) [M$^+$], 158 (8.5) [M$^+$ − C$_4$H$_8$], 143 (13) [M$^+$ − C$_4$H$_8$ − CH$_3$], 102 (100) [M$^+$ − 2 C$_4$H$_8$]. − $C_{10}H_{20}BClN_2$ (214.55): calcd. C 55.99, H 9.39, N 13.05; found C 55.11, H 9.42, N 12.85.

2,6-Me$_2$C$_6$H$_3$N^a−CH=CH−N^b(2,6-Me$_2$C$_6$H$_3$)BCl(N^a−B) (**5b**). − *Path (a):* A slurry of 4.00 g of **4b** (10.5 mmol) in 150 ml of *n*-hexane was treated with sodium amalgam obtained from 1.38 g of Na (60.0 mmol) and 200 g of mercury. Stirring at ambient temp. was maintained for 5 d. The solution was decanted from the metal, and volatile components were removed in vacuo to yield 1.80 g (55%) of **5b** as a colorless solid.

Path (b): A solution of the 1,4-diazabutadiene **1b** (4.00 g, 15.0 mmol) in 80 ml of *n*-hexane was reduced by 0.21 g (30.0 mmol) of lithium sand during 7 d at 20°C. The resulting brown slurry was chilled to −30°C and a solution of 1.76 g (15.0 mmol) of BCl_3 in 50 ml of *n*-hexane was added dropwise. Stirring at room temp. was continued for 3 d. Filtration was followed by removing volatile components in vacuo to afford a colorless solid. Recrystallization from *n*-hexane gave 2.48 g (53%) of pure **5b**. − ^{1}H NMR (C_6D_6): δ = 2.17 (s, 12 H, CH_3), 5.86 (s, 2 H, HC=N), 6.99 (m, 6 H, aryl-H). − ^{13}C{^{1}H} NMR (C_6D_6): δ = 18.1 (s, CH_3), 117.7 (s, HC=N), 127.3 (s, *p*-C aryl), 135.8 (s, *o*-C aryl), 139.9 (*i*-C aryl). − ^{11}B{^{1}H} NMR (C_6D_6): δ = 21.1 (s). − MS/EI; *m*/*z*: 310 [M$^+$]. − $C_{18}H_{20}BClN_2$ (310.63): calcd. C 69.60, H 6.49, N 9.02; found C 68.78, H 6.45 N 8.87.

(tBuCH$_2$)N^a−C(Me)=C(Me)−N^b(CH$_2$tBu)BCl(N^a−B) (**5c**): Lithium sand (0.32 g, 46.8 mmol) was added to a solution of 3.50 g (15.0 mmol) of 1,4-diazabutadiene (**1c**) in 100 ml of *n*-hexane. After stirring the mixture for 10 d at room temp., the resulting green slurry was chilled to −30°C, and a solution of 1.76 g (15.0 mmol) of BCl_3 in 50 ml of *n*-hexane was added dropwise. After 2 h of stirring, the slurry was filtered, and the solvent was removed in vacuo to afford 2.53 g (60%) of **5c** as a dark brown oil, which solidified to a tan wax. − Due to the lability of the product no reliable IR spectrum was available. − ^{1}H NMR (C_6D_6): δ = 0.89 (s, 18 H, *t*Bu), 1.77 (s, 6 H, CH_3), 3.21 (s, 4 H, CH_2). − ^{13}C{^{1}H} NMR (C_6D_6): δ = 10.9 (s, =C−*C*H$_3$), 28.4 [s, C(*C*H$_3$)$_3$], 34.3 (s, CH_2), 53.7 [s, *C*(CH$_3$)$_3$], 118.9 (s, C=C). − ^{11}B{^{1}H} NMR (C_6D_6): δ = 22.7 (s). − MS/EI; *m*/*z*: 270 [M$^+$ in relation to ^{11}B and ^{35}Cl]. − $C_{14}H_{28}BClN_2$ (270.65): calcd. C 62.13, H 10.43, N 10.35; found C 62.02, H 10.56, N 10.31.

(tBu)N^a−CH=CH−N^b(tBu)BI(N^a−B) (**6a**): A slurry of 2.50 g (14.8 mmol) of 1,4-diazabutadiene **1a** in 100 ml of *n*-hexane was allowed to react with lithium sand (0.21 g, 29.6 mmol) for 7 d at 20°C. A solution of 5.83 g (14.9 mmol) of BI_3 in 50 ml of *n*-hexane was added dropwise to the chilled slurry (−20°C). Stirring for 2 h was followed by filtration. The filtrate was liberated from volatile components in vacuo to afford 3.78 g (83%) of **6a** as a colorless oil. At room temp. the pure compound decomposed completely within 5 d, whereas in the dark at −30°C a *n*-hexane solution of **6a** remained unaffected. − Due to decomposition a reliable IR spectrum was not available. − ^{1}H NMR (C_6D_6): δ = 1.45 (s, 18 H, *t*Bu), 6.40 (s, 2 H, CH). − ^{13}C{^{1}H} NMR (C_6D_6): δ = 31.7 [s,

C(CH_3)$_3$], 54.2 [s, C(CH$_3$)$_3$], 114.6 (s, C=C). − ^{11}B{^{1}H} NMR (C_6D_6): δ = 6.5 (s). − MS /EI; *m/z*: 306 (27) [M$^+$], 250 (11) [M$^+$ − C_4H_8], 194 (100) [M$^+$ − 2 C_4H_8], 178 (3) [M$^+$ − I]. − $C_{10}H_{20}BIN_2$ (305.99): calcd. C 39.21, H 6.59, N 9.15; found C 39.35, H 6.48, N 8.99.

(2,6-Me$_2$C$_6$H$_3$)N^a−CH=CH−N^b(2,6-Me$_2$C$_6$H$_3$)BI(N^a−B) (**6b**): A mixture of CH_2Cl_2 (600 ml) and *n*-hexane (400 ml) was cooled to −10°C and two separate solutions of 6.00 g (22.7 mmol) of 1,4-diazabutadiene **1b** in CH_2Cl_2 (250 ml) and 8.89 g (22.7 mmol) of BI_3 in *n*-hexane (200 ml) were added dropwise. The reaction was filtered after warming up to room temp. and stirring for 5d. The filtrate was concentrated to dryness. The brown-black residue was extracted with 150 ml of *n*-hexane, and the red *n*-hexane solution was decanted from insoluble components. Storing the concentrated filtrate (ca 20 ml) at −4°C for 3 d afforded 2.43 g (26%) of colorless crystalline **6b**. The compound was purified by sublimation at 0.01 Torr and 380°C. − IR (KBr): ν = 1554 cm^{-1} w, 1551 w, 1475 vs, 1439 m, 1397 s, 1340 m, 1279 s, 1263 s, 1244 m, 1197 m, 1162 w, 1105 s, 1032 w, 908 s, 772 vs, 688 s, 621 s, 569 w, 530 w. − ^{1}H NMR (C_6D_6): δ = 2.16 (s, 6 H, CH_3), 5.99 (s, 2 H, HC=N), 6.98 (m, 6 H, arylH). − ^{13}C{^{1}H} NMR (C_6D_6): δ = 18.3 (s, CH_3), 120.0 (s, HC=N), 126.2 (s, *p*-C-aryl), 135.7 (s, *o*-C-aryl), 140.7(s, *i*-C-aryl), − ^{11}B{^{1}H} NMR (C_6D_6): δ = 11.8 (s). − MS/EI; *m/z*: 402 (96) [M$^+$], 275 (100) [M$^+$ − I]. − $C_{18}H_{20}BIN_2$(402.08): calcd. C 53.72, H 5.01, I 31.56, N 6.97; found C 53.56, H 5.16, I 31.44, N 6.99.

(tBu)N^a−CH=CH−N^b(tBu)BCN(N^a−B) (**8a**). − *From Isocyanides:* A solution of **5a** (1.07 g, 5.00 mmol) in 50 ml of *n*-hexane was treated at room temp. with 0.43 g (5.0 mmol) of *tert*-butyl isocyanide. After 4 h of stirring it was filtered, and the volatile components removed from the filtrate in vacuo (0.01 Torr) to give crude **8a** as a colorless solid. Purification was achieved either by recrystallization from *n*-hexane or by sublimation at 0.03 Torr and 55°C, yield 0.61 g (60%). Similarly, 1.30 g (5.00 mmol) of (*t*Bu)N^a−CH=CH−N^b(*t*Bu)BBr(N^a−B) (**7a**) was converted into 0.66 g (64%) of **8a**. Starting from **6a** (1.53 g, 5.0 mmol) 0.41 g of **8a** (41%) was obtained analogously. The reaction of 0.78 g (3.0 mmol) of **7a** with 0.33 g (3.0 mmol) of cyclohexyl isocyanide in 50 ml of *n*-hexane at 20°C for 5 d also afforded **8a** (0.23 g, 38%).

From AgCN: A mixture of **5a** (0.43 g, 2.0 mmol) and silver cyanide (0.32 g, 2.4 mmol) was stirred in acetonitrile (50 ml) for 1 h at room temp. After concentration to dryness, the residue was extracted with *n*-hexane (3 × 50 ml) and the combined extracts were filtered. Repeated concentration to dryness gave analytically pure **8a** (0.35 g, 84%). The analogous reaction of **7a** (0.52 g, 2.0 mmol) with AgCN (0.32 g, 2.4 mmol) in 50 ml of CH_3CN for 20 min afforded 0.46 (89%) of **8a**. − IR (KBr): ν = 2207 cm^{-1} w [ν(C≡N)], 1501 w, 1467 m, 1405 s, 1368 s, 1344 m, 1295 m, 1261 m, 1234 s, 1207 m, 1147 s, 1100 w, 1032 w, 953 w, 824 s, 804 s, 694 s, 660 sh, 649 s, 500 m. − ^{1}H NMR (C_6D_6): δ = 1.29 (s, 18 H, *t*Bu), 6.14 (s, 2 H, CH). − ^{13}C{^{1}H} NMR (C_6D_6): δ = 31.5 [s, C(CH_3)$_3$], 53.7 [s, C(CH$_3$)$_3$], 114.6 (s, C=C). − ^{11}B{^{1}H} NMR (C_6D_6): δ = 12.0 (s). − MS/EI; *m/z* (%): 205 (27) [M$^+$], 149 (10) [M$^+$ − C_4H_8], 93 (100) [M$^+$ − 2 C_4H_8]. − $C_{11}H_{20}BN_3$ (205.12): calcd. C 64.40, H 9.85, N 20.48; found C 63.72, H 9.45, N 19.45.

(2,6-Me$_2$C$_6$H$_3$)N^a−CH=CH−N^b(2,6-Me$_2$C$_6$H$_3$)BCN(N^a−B) (**8b**). − *From Isocyanides:* Equimolar amounts of **5b** (0.62 g, 2.0 mmol) and *tert*-butyl isocyanide (0.17 g, 2.0 mmol) were allowed to react in 40 ml of *n*-hexane for 8 h at room temp. The solution was filtered and the colorless filtrate was concentrated to dryness. The remaining yellow solid was sublimed at 0.001 Torr and ca. 400°C to give 0.42 g (70%) of **8b**. Similarly, a sample of 0.80 g (2.0 mmol) of **6b** was converted into 0.33 g of **8b** by treatment with 0.17 g (2.0 mmol) of *tert*-butyl isocyanide.

From AgCN: A mixture of **6b** (0.80 g, 2.0 mmol) and AgCN (0.32 g, 2.4 mmol) was stirred in 50 ml of CH_3CN for 2 d at room temp. Concentration to dryness, extraction with *n*-hexane, filtration and removal of volatile components from the filtrate yielded 0.47 g (79%) of **8b**. − IR (KBr): ν = 2218 cm^{-1} w [ν(C≡N)], 1949 w, 1868 w, 1791 w, 1647 w, 1594 w, 1541 w, 1479 s, 1441 m, 1399 m, 1368 w, 1282 m, 1207 m, 1109 m, 915 m, 775 s, 717 m, 658 m, 421 w. − ^{1}H NMR (C_6D_6): δ = 2.06 (s, 12 H, CH_3), 5.75 (s, 2 H, CH), 6.95 (m, 6 H, H-aryl). − ^{13}C{^{1}H} NMR (C_6D_6): δ = 17.8 (s, CH_3), 119.4 (s, C=C), 128.6 (s, *p*C-aryl). − ^{11}B{^{1}H} NMR (C_6D_6): δ = 13.5 (s). − MS/EI; *m/z* (%): 301 (100) [M$^+$]. − $C_{19}H_{20}BN_3$ (301.18): calcd. C 75.70 , H 6.69, N 13.95; found C 75.30, H 7.25, N 13.61.

(tBu)N^a−CH=CH−N^b(tBu)BNCO(N^a−B) (**9a**): Analogously, the treatment of **5a** (0.43 g, 2.0 mmol) with AgOCN (0.53 g, 2.4 mmol) in 50 ml of CH_3CN for 30 min at 20°C afforded 0.35 g (78%) of **9a** as a colorless viscous oil. Complete decomposition of **9a** occurred within 2 d. Heterocycle **9a** was also prepared from **7a** and AgOCN in CH_3CN (50 ml) for 5 min (83% yield). − IR (CsI): ν = 2972 cm^{-1} s, 2317 vs [ν_{as}(NCO)], 1699 m, 1684 m, 1527 w, 1474 m, 1458 m, 1404 s, 1367 s, 1322 s, 1288 w, 1240 s, 1138 m, 1033 w, 1001 w, 822 w, 807 w, 632 m [ν_{sym}(NCO)], 596 w. − ^{1}H NMR (C_6D_6): δ = 1.21 (s, 18 H. *t*Bu), 6.04 (s, 2 H, =CH). − ^{11}B{^{1}H} NMR (C_6D_6): δ = 14.7 (s). − ^{13}C{^{1}H} NMR (C_6D_6): δ = 31.0 [s, C(CH_3)$_3$], 52.5 [s, C(CH$_3$)$_3$], 111.6 (s, =CH), 123.9 (s, br., N=C=O). − MS/EI (70 eV); *m/z* (%): 221 (20) [M$^+$]. − $C_{11}H_{20}BN_3O$ (221.12): calcd. C 59.74, H 9.13, N 18.99; found C 59.30, H 9.33, N 18.63.

(tBu)N^a−CH=CH−N^b(tBu)BNCS(N^a−B) (**10a**): Compound **10a** was prepared analogously from **5a** (0.43 g, 2.0 mmol) and AgSCN (0.40 g, 2.4 mmol) in CH_3CN (50 ml, 20°C, 1 h), yield: 0.42 g (74%). The corresponding reaction of **7a** and AgSCN took place within 10 min to give a 76% yield of **10a**. − IR (CsI): ν = 3133 cm^{-1} w, 2975 s, 2936 sh, 2910 sh, 2875 sh, 2122 vs, br. [ν_{as}(NCS)], 1475 m, 1406 s, 1375 s, 1291 m, 1241 s, 1205 m, 1141 s, 1029 w, 948 w, 871 s [ν_{sym}(NCS)], 822 w, 802 m, 683 w, 632 s. − ^{1}H NMR (C_6D_6): δ = 1.20 (s, 18 H, *t*Bu), 5.99 (s, 2 H, =CH); ($CDCl_3$): δ = 1.42 (s, 18 H, *t*Bu), 6.16 (s, 2 H, =CH). − ^{11}B{^{1}H} NMR (C_6D_6): δ 14.7 (s). − ^{13}C{^{1}H} NMR ($CDCl_3$): δ = 31.1 [s, C(CH_3)$_3$], 53.0 [s, C(CH$_3$)$_3$], 111.8 (s, =CH), 140.5 (s, NCS), (C_6D_6): δ = 31.0 [s, C(CH$_3$)$_3$], 52.9 [s, C(CH$_3$)$_3$], 112.1 (s, =CH). − MS/EI (70 eV); *m/z* (%): 237 (70) [M$^+$], 125 (100) [M$^+$ − 2 *t*Bu]. − $C_{11}H_{20}BN_3S$ (237.17): calcd. C 55.71, H 8.50, N 17.72; found C 54.89, H 8.78, N 17.24.

(2,6-Me$_2$C$_6$H$_3$)N^a−CH=CH−N^b(2,6-Me$_2$C$_6$H$_3$)BNCS-(N^a−B) (**10b**): A sample of solid AgSCN (0.41 g, 3.0 mmol) was added to a slurry of **6b** (1.00 g, 2.5 mmol) in CH_3CN (40 ml) and stirred for 5 h at 20°C. The slurry was filtered, and the filtrate concentrated to dryness. The residue was extracted with *n*-hexane (3 × 50 ml) and the combined extracts were filtered. The volatile components were removed from the filtrate to give pure **10b** (0.77 g, 93%) as a waxy solid. Analogously, **5b** was converted into **10b** within 3 h in 78% yield. The corresponding bromide gave **10b** after 1 h in 87% yield. − IR (KBr): ν = 2918 cm^{-1} w, 2177 sh, 2114 vs [ν_{as}(NCS)], 2038 sh, 1516 w, 1479 s, 1441 s, 1402 s, 1390 s, 1303 w, 1285 m, 1201 w, 1111 s, 1032 w, 992 w, 909 m, 856 s [ν_{sym}(NCS)], 768 s, 702 w, 656 w, 643 s. − ^{1}H NMR (C_6D_6): δ = 2.10 (s, 12 H, CH_3), 5.71 (s, 2 H, =CHN), 6.97 (m, 6 H, aryl-H). − ^{11}B{^{1}H} NMR (C_6D_6): δ = 14.5 (s). −^{13}C{^{1}H} NMR (C_6D_6): δ = 17.9 (s, CH_3), 117.2 (s, =CHN), 127.3 (s, *p*-aryl-C), 128.6 (s, *m*-aryl-C), 135.2 (s, *o*-aryl-C), 139.2 (s, *i*-aryl-C). − MS/EI (70 eV); *m/z* (%):

333 (100) [M^+]. – $C_{19}H_{20}BN_3S$ (333.15): calcd. C 68.44, H 6.05, N 12.61; found C 68.38, H 6.30, N 12.38.

X-ray Structural Analysis of **6b**: Colorless single crystals from *n*-hexane; 0.42 × 0.37 × 0.32 mm; T = 293 K; Siemens P4 four-circle diffractometer; Mo-K_α (graphite monochromator, λ = 0.71073 A), empirical formula $C_{18}H_{20}BIN_2$, monoclinic space group $C2/c$; unit cell dimensions: a = 14.911(2), b = 7.9706(8), c = 16.9105(12) A; β = 114.360(6)°; V = 1830.9(3) A^3, $d_{calcd.}$ = 1.459 g cm^{-3}, Z = 4; μ(Mo-K_α) = 1.747 mm^{-1}; range for data collection: 5.3° ≤ 2Θ ≤ 60.1°; ω-scan, index ranges: $-20 \le h \le 0$, $-11 \le k \le 0$, $-21 \le l \le 23$; reflections collected 2769 (R_{int} = 0.017); independent reflections 2675; parameters 102; absorption correction: empirical φ-scans, min/max transmission 0.94/0.79 [R_{merg}(before/after) = 0.0333/0.0136]. Program used: Siemens SHELXTL Ver. 5.03. Structure solution: Direct Methods; structure refinement: Full-matrix least-squares on F^2, $R1$ = 0.042, $wR2$ = 0.1043 based on 1884 reflections with $I > 2\sigma(I)$, $wR2$ (all data) = 0.1189 with $w = 1/[\sigma^2(F_o^2) + (0.0484P)^2 + 3.11P]$, where $P = (F_o^2 + 2F_c^2)/3$; GOOF (F^2) = 1.029, maximum residual electron density 0.922 eA^{-3}, hydrogen atoms treated as riding groups with the 1.2-fold isotropic U value of the corresponding C atom and 1.5-fold for methyl groups.[26]

☆ Dedicated to Professor *Heinrich Nöth* on the occasion of his 70th birthday.

[1] [1a] K. Niedenzu, J. S. Merriam, *J. Organomet. Chem.* **1973**, *51*, C1–C2. – [1b] K. Niedenzu, J. S. Merriam, *Z. Anorg. Allg. Chem.* **1974**, *406*, 251–259.
[2] L. Weber, G. Schmid, *Angew. Chem.* **1974**, *86*, 519; *Angew. Chem. Int. Ed. Engl.* **1974**, *13*, 467.
[3] G. Schmid, J. Schulze, *Chem. Ber.* **1977**, *110*, 2744–2750.
[4] G. Schmid, M. Polk, R. Boese, *Inorg. Chem.* **1990**, *29*, 4421-4429.
[5] G. Schmid, J. Schulze, *Angew. Chem.* **1977**, *89*, 258-259; *Angew. Chem. Int. Ed. Engl.* **1977**, *16*, 249.
[6] G. Schmid, J. Schulze, *Chem. Ber.* **1981**, *114*, 495–504.
[7] G. Schmid., J. Lehr, M. Polk, R. Boese, *Angew. Chem.* **1991**, *103*, 1029–1031; *Angew. Chem. Int. Ed. Engl.* **1991**, *30*, 1015.
[8] L. Weber, E. Dobbert, H.-G. Stammler, B. Neumann, R. Boese, D. Bläser, *Chem. Ber.* **1997**, *130*, 705–710.
[9] K. M. Harmon, F. E. Cummings, *J. Am. Chem. Soc.* **1962**, *84*, 1751.
[10] [10a] In Cl_2BNMe_2 and Cl_2BNEt_2 chemical shifts $\delta^{11}B$ = 30.8 and 30.6 were measured: A. J. Banister, N. N. Greenwood, B. P. Straughan, J. Walker, *J. Chem. Soc.* **1964**, 995–1000. – [10b] H. Nöth, H. Vahrenkamp, *Chem. Ber.* **1966**, *99*, 1049–1067.
[11] [11a] M. F. Lappert, H. Pyszora, *J. Chem. Soc.* **1963**, 1744–1750. – [11b] M. F. Lappert, H. Pyszora, M. Rieber, *J. Chem. Soc.* **1965**, 4256–4264. – [11c] M. F. Lappert, H. Pyszora, *J. Chem. Soc. A* **1967**, 854–860.
[12] A. Meller, W. Maringgele, U. Sicker, *J. Organomet. Chem.* **1977**, *141*, 249–255.
[13] B. Hessett, J. B. Leach, J. H. Morris, P. G. Perkins, *J. Chem. Soc., Dalton Trans.* **1972**, 131–134.
[14] J. Goubeau, H. Gräbner, *Chem. Ber.* **1960**, *93*, 1379–1387.
[15] Holleman-Wiberg, *Lehrbuch der Anorganischen Chemie*, vol. 91–100, de Gruyter, Berlin **1985**, p. 133.
[16] F. Zettler, H. Hess, W. Siebert, R. Full, *Z. Anorg. Allg. Chem.* **1976**, *420*, 285–291.
[17] M. A. Ring, J. D. H. Donnay, W. S. Korski, *Inorg. Chem.* **1962**, *1*, 109–111.
[18] G. Linti, D. Loderer, H. Nöth, K. Polborn, W. Rattay, *Chem. Ber.* **1994**, *127*, 1909–1922.
[19] G. R. Desiraju, *Angew. Chem.* **1995**, *107*, 2540–2558; *Angew. Chem. Int. Ed. Engl.* **1995**, *34*, 2311–2329.
[20] October **1997** release of CSD with 175093 entries.
[21] F. H. Allen, O. Kennard *Chem. Design Automation News* **1993**, *8*, 31–37.
[22] J. M. Klugman, R. K. Barnes, *Tetrahedron* **1970**, *26*, 2555–2560.
[23] H. tom Dieck, M. Svoboda, T. Greiser, *Z. Naturforsch., B* **1981**, *36*, 823–832.
[24] M. Svoboda, H. tom Dieck, C. Krüger, Y. H. Tsay, *Z. Naturforsch., B* **1981**, *36*, 814–822.
[25] F. Klanberg, H. W. Kohlschütter, *Chem. Ber.* **1961**, *94*, 786–789.
[26] Further details of the crystal structure investigation are available on request from Fachinformationszentrum Karlsruhe, D-76344 Eggenstein-Leopoldshafen, on quoting the depository number CSD-408392, the names of the authors, and the journal citation.

[98047]

Formation of a Constrained-Geometry Ziegler Catalyst System Containing a C_1 Instead of the Usual Si_1 Connection Between the Cyclopentadienyl and Amido Ligand Components☆

Lothar Duda, Gerhard Erker*, Roland Fröhlich, and Frank Zippel

Organisch-Chemisches Institut der Universität Münster,
Corrensstraße 40, D-48149 Münster
Fax: (internat.) + 49 (0)251/83-36503
E-mail: erker@uni-muenster.de

Received March 9, 1998

Keywords: "Constrained-geometry" Ziegler catalysts / Cp/amido zirconium complex / 6-Aminofulvene deprotonation / Ethene polymerization

6-Amino-6-methylfulvene (**4**) is cleanly *N*-acylated by treatment with pivaloylchloride/triethylamine to give the fulvene (C_5H_4)=C(CH_3)NHCOCMe_3 (**5c**). Treatment of **4** with trimethylchlorosilane similarly yields the mono-*N*-silylated fulvene (C_5H_4)=C(CH_3)NHSiMe_3 (**7**). Both **5c** and **7** are cleanly doubly deprotonated e.g. by treatment with LDA to give ligand systems $[(C_5H_4)C(=CH_2)NR]Li_2$ [**8a** (R = COCMe_3) and **8b** (R = SiMe_3), respectively]. Their treatment with $MCl_4 \cdot 2$ THF (M = Ti, Zr) yield the *spiro*-metallocenes $[(C_5H_4)C(=CH_2)NR]_2M$ (**9**, **10**). Complex **10a** (M = Zr, R = COCMe_3) was characterized by X-ray diffraction. The reaction of **8a** with $(Et_2N)_2ZrCl_2$ in THF gives rise to the formation of $[(C_5H_4)C(=CH_2)NCOCMe_3]Zr(NEt_2)_2$ (**11**) (70 % isolated), and the reaction of **8b** with $(Et_2N)_2ZrCl_2$ yields $[(C_5H_4)C(=CH_2)NSiMe_3]Zr(NEt_2)_2$ (**12**) (76 % isolated). Treatment of complex **12** with an excess of methylalumoxane (MAO) in toluene solution results in the generation of an active homogeneous Ziegler catalyst for the polymerization of ethene. A comparison with the usually employed $[(Me_5C_4)SiMe_2NCMe_3]ZrCl_2$/MAO "constrained-geometry" Ziegler catalyst system reveals a similar catalyst activity and performance of this novel type of a C_1-bridged "constrained-geometry" catalyst as it is exemplified by the $[(C_5H_4)C(=CH_2)NSiMe_3]ZrX_2$ (**12**)/MAO combination.

Introduction

Homogeneous Ziegler catalysts on the basis of group-4 bent metallocenes have become of enormous importance in metal-catalyzed α-olefin polymerization and related processes.[1] Variation of the ligand systems and the development of novel types of catalyst precursors have been of great interest recently in order to expand the scope of the application of this general type of very active and at the same time often extremely selective catalyst systems.[2] In this context the "constrained-geometry catalysts" have recently found a special attention. They are catalyst systems that are formally derived from the dimethylsilylene-bridged ansa-metallocenes in which one of the Cp units is replaced by an amido-nitrogen atom. The most frequently employed ligand system was introduced by J. E. Bercaw et al. at a group-3 metal complex.[3] It is comprized by a tetramethylcyclopentadienyl moiety that is connected with a *tert*-butylamido building block by means of a bridging Me_2Si group. The scandium complex **1a** (ML_n = Sc−Cl) is a typical early example. The corresponding titanium and zirconium complexes (**2b**, **c**) were prepared consecutively and used as Ziegler catalyst precursors. These systems have achieved a great interest with regard to the practical application of ligand-controlled Ziegler catalysts in α-olefin polymerization processes.[4]

The use of the silylene bridge for connecting the Cp and amido subunits has appeared to be essential for these organometallic systems for quite some time. The presence of the silylene group prevents the elimination reaction to the corresponding fulvene system and additional fragmentation reactions to occur at some intermediate stages of the synthesis, reaction alternatives that are very favourable and have been observed in previous attempts to prepare the corresponding C_1-bridged constrained-geometry Ziegler systems.[5] These facile alternative reactions have probably favoured the design of hydrocarbyl-bridged $Cp(CR_2)_n-NR'$ systems with longer bridging chains ($n > 1$).[6] Practically feasible synthetic pathways to C_1-bridged constrained Ziegler catalyst systems to the best of our knowledge appear not to have been reported on so far with one potential exception.[7] We have now developed a simple synthetic entry to such organometallic complexes of the group-4 metals and shown that homogeneous Ziegler catalysts can be derived from examples of such $[Cp-C_1(R)-NR']ML_n$ systems that

Scheme 1

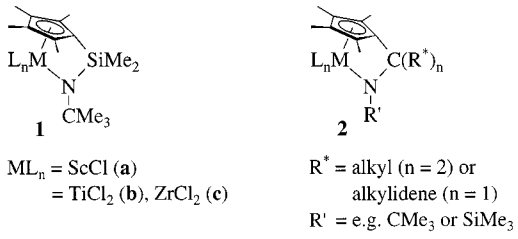

 © WILEY-VCH Verlag GmbH, D-69451 Weinheim, 1998 1434−1948/98/0808−1153 $ 17.50+.50/0

are of at least equal catalyst quality as compared to the commonly employed [Cp*−SiR_2−NR′]MCl_2 derived systems.

Results and Discussion

Starting material for our synthesis is 6-dimethylamino-6-methylfulvene (**3**), which is readily available by treatment of cyclopentadienide with *O*-methylated *N,N*-dimethylacetamide. As also described by K. Hafner et al.[8] **3** was treated with excess NH_3 to give 6-amino-6-methylfulvene (**4**). We have then acylated the aminofulvene system. Here the general problem arises that in **4** two positions are amenable to electrophilic attack, namely the amino group and the α-carbon center (C-2) at the five-membered carbocyclic ring.[9]

Scheme 2

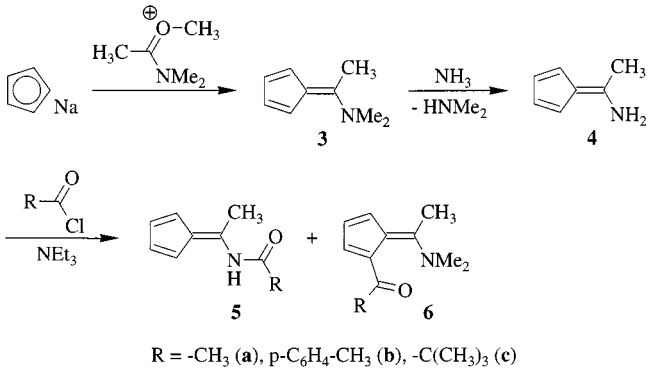

Treatment of the aminofulvene **4** with acetyl chloride indeed furnished a mixture of the regioisomers **5a**, resulting from *N*-acylation, and **6a**, resulting from *C*-acylation at the fulvene α-carbon center C-2, respectively. The isomers **5a** (major) and **6a** (minor) were separated by column chromatography and isolated in ca. 70 and 5% yield, respectively. The spectral appearance of the two regioisomeric acetylation products is quite different. The four fulvene CH groups in the major product **5a** are just marginally differentiated [^{1}H NMR ($CDCl_3$): δ = 6.58−6.35 (m, 4 H); ^{13}C NMR: δ = 129.2, 128.3, 122.2, 116.8], whereas a clearly separated AMX system is characterized for the ^{1}H NMR fulvene section of **6a** (δ = 7.56, 7.27, 6.42; coupling constants: J_{HH} = 1.9, 3.2, 4.8 Hz). The situation is even less favourable for the aroylation of **4** with *p*-methylbenzoyl chloride. In this case a mixture of products was obtained from which the required *N*-aroylated product **5b** was isolated only in ca. 20% yield after chromatographic workup. In contrast, the acylation reaction with the bulky pivaloyl chloride reagent was very clean and selectively resulted in the formation of the *N*-pivaloylfulvene system **5c**, which was obtained in 80% yield as a yellow crystalline material after recrystallization from ether.

Single crystals were obtained from the three *N*-acylated fulvenes **5a−c** that allowed their characterization by X-ray crystal structure analyses. As a typical example, a view of the molecular structure of the *N*-acetylated fulvene **5a** is depicted in Figure 1. It can be seen from Table 1 that all three fulvenes exhibit the typical carbon−carbon bond length alternation in their frameworks and a transoidal connection of fulvene and carboxamide structural subunits with conformer **B** being favoured over **A** (see Scheme 3).

Scheme 3

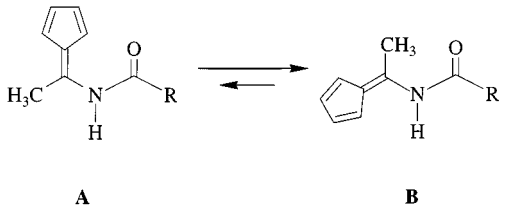

Table 1. Compilation of typical bond lengths, bond angles, and torsional angles of the *N*-acylated fulvenes **5a−c**

	5a	**5b**	**5c**[a]
C1−C2	1.447(5)	1.447(3)	1.458(2)
C2−C3	1.348(5)	1.345(3)	1.348(2)
C3−C4	1.428(6)	1.435(4)	1.442(3)
C4−C5	1.339(5)	1.352(4)	1.346(2)
C1−C5	1.462(5)	1.456(3)	1.457(2)
C1−C6	1.359(5)	1.354(3)	1.358(2)
C6−C7	1.487(5)	1.489(3)	1.491(2)
C6−N	1.395(5)	1.404(3)	1.399(2)
N−C8	1.380(5)	1.365(3)	1.370(2)
C8−O	1.207(4)	1.228(2)	1.219(1)
C8−C9	1.504(5)	1.483(3)	1.533(2)
C1−C6−N	118.6(3)	117.9(2)	118.5(1)
C6−N−C8	127.9(3)	129.0(2)	128.4(1)
N−C8−O	124.0(4)	123.4(2)	122.3(1)
N−C8−C9	113.6(3)	115.0(2)	115.2(1)
C7−C6−N−H	171(3)	152(2)	154(1)
C7−C6−N−C8	12.3(6)	28.4(3)	25.9(2)
C6−N−C8−O	6.9(7)	7.2(4)	2.0(2)
C6−N−C8−C9	−173.3(4)	−172.9(2)	177.5(1)
O−C8−N−H	−170(3)	−173(2)	179(1)

[a] Averaged absolute values of the three independent molecules in the unit cell of **5c**.

The fulvenes **5** are not monomeric in the crystal but connected by intermolecular hydrogen bonds, that link the carbonyl and NH functionalities of the amide groups,[10] to form oligomeric chain-type structures. In the resulting supra-structure the core atoms of the individual amide groups of **5a** and **5b** are oriented in a single plane, giving rise to elongated narrow sheet-like structures. The two-dimensional arrangement of the self-assembled associate of **5a** is depicted in Figure 1. It is probably due to the steric bulk of the *tert*-butyl substituent that a related but spatially different supra-structure is found for **5c**. Again a linear arrangement of fulv−NHCO−R units is found, with the individual carboxamide functionalities being connected via intermolecular N−H···O=C−NHR hydrogen bonds, only in this case are the individual −NH−CO− planes rotated substantially [angle between the planes O1−C8−N1/O2−C18−N2: 8.8(2)°; O1−C8−N1/O3−C28−N3: 54.5(2)°; O2−C18−N2/O3−C28−N3: 58.8(2)°]. A projection of the resulting three-dimensional arrangement is given in Figure 2.

Treatment of **4** with chlorotrimethylsilane in the presence of excess triethylamine results in the selective *N*-silylation

Figure 1. A view of the hydrogen-bonded associated structure of **5a** (**5b** exhibits a similar two-dimensional supramolecular core structure in the crystal)

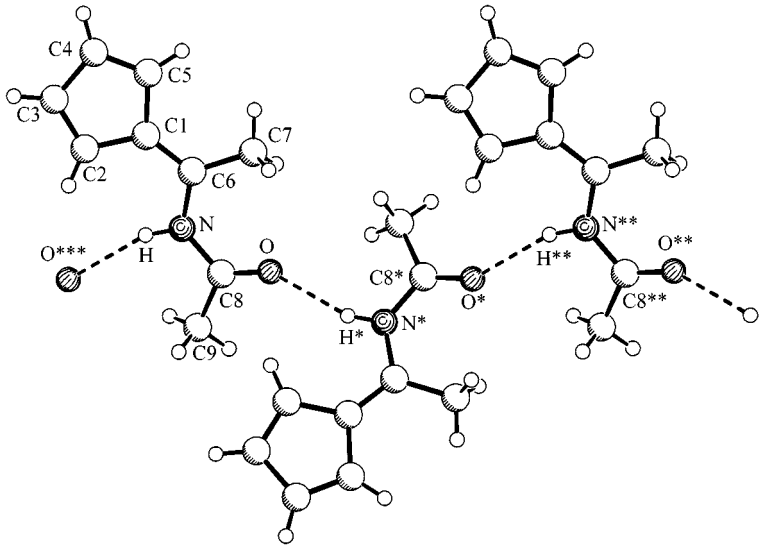

Figure 2. The three-dimensional assembled supramolecular solid-state structure of the *N*-pivaloylfulvene **5c**

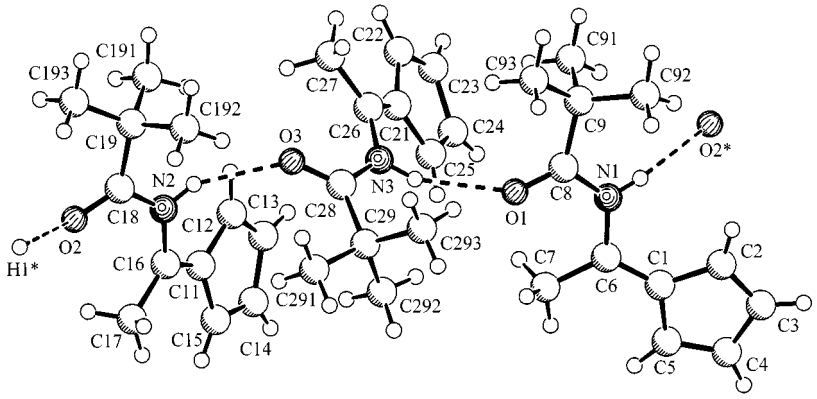

of the aminofulvene. Only mono-silylation is achieved under these conditions to give the product **7** which was isolated in near-to-quantitative yield. Compound **7** shows a very characteristic ^{13}C-NMR spectrum with the electrophilic fulvene carbon center C-6 (δ = 154.7) being spectroscopically clearly differentiated from the remaining sp^2-carbon atoms of the ring system (C-1: δ = 117.9; C2−C5: δ = 124.6, 122.1, 119.7, 112.3).

Scheme 4

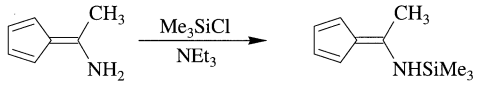

4 **7**

Our experiments had thus shown that 6-methyl-6-(pivaloylamino)fulvene (**5c**) and 6-methyl-6-(trimethylsilylamino)fulvene (**7**) among the investigated series of compounds were the easiest and most selective to be synthesized on a preparative scale,[11] and we consequently have decided to use these two compounds as the starting materials for the preparation of the anticipated Cp−C(R)$_n$−NR′ dianion-type ligands and the corresponding C$_1$-bridged constrained-geometry group-4 metal complex systems.

Principally, fulvene systems can be converted to cyclopentadienides by either the addition of a suitable nucleophile to the electrophilic C-6 carbon center[12] or by a deprotonation reaction at the alkyl carbon atom directly adjacent to the C-6 fulvene center.[13] For this study we have briefly tested the former procedure. We found out that a sufficiently soft nucleophile can be added to the C-6 carbon atom of the systems **5**. Thus the reaction of **5c** with two molar equivalents of lithium dimethylcuprate[14] eventually leads to the formation of the $[Cp-CMe_2-N(COCMe_3)]^{2-}$ ligand system that can be transmetallated with $Cl_2Zr(NEt_2)_2$. However, the resulting ansa-metallocene-like system was never obtained free of sizable amounts of as yet unidentified contaminants. For practical purposes it has thus turned out to be advantageous to rely on the second alternative methode and deprotonate the fulvenes at the C^6-CH_3 group (in addition to the kinetically rapid NH deprotonation) to generate the required C$_1$-bridged ligand system. This route has turned out to be very convenient and

successful. It can easily be applied to all the *N*-monosubstituted fulvene systems described above. The outcome of the reactions starting from **5c** and **7** will be described in the following as very typical examples.

Treatment of 6-methyl-6-(pivaloylamino)fulvene (**5c**) with two molar equivalents of methyllithium or even better with the less nucleophilic bases lithium hexamethyldisilazide or lithium diisopropylamide cleanly furnished the corresponding ligand system $[Cp-C(=CH_2)-N(COCMe_3)]^{2-}$ as the dilithio compound **8a** [$^1H/^{13}C$ NMR ([D_8]THF, 200.1 MHz): δ = 5.82, 5.89/118.2 (*ipso*-C), 106.3, 103.2 (C_5H_4); 4.47, 3.66 (^2J = 2.4 Hz)/155.4, 87.5 ($C=CH_2$), 1.08/179.3, 39.0, 29.5 ($COCMe_3$)]. Analogously, treatment of 6-methyl-6-(trimethylsilylamino)fulvene (**7**) with these bases gave the corresponding ligand system $[Cp-C(=CH_2)-NSiMe_3]^{2-}$ (obtained and isolated as the dilithio compound **8b**).

Scheme 5

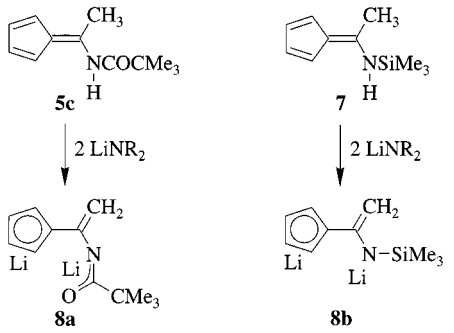

The reaction of **8b** with zirconium tetrachloride results, under all reaction conditions tested by us, in a rapid substitution of all four halogen atoms[7b][15] to yield the organometallic *spiro*-metallocene complex **10b**. The product **10b** was isolated in close to 80% yield. It shows typical $^1H/^{13}C$-NMR spectra {in [D_6]benzene: C_5H_4 resonances at δ = 6.36, 6.00, 5.41, 5.36/118.4 (*ipso*-C), 116.3, 114.4, 112.6, 109.1; ($C=CH_2$): δ = 4.22, 4.18/144.7, 88.7; $SiMe_3$: δ = 0.24/1.75}. The analogous reaction of the dilithio ligand system **8b** with $TiCl_4$ gives the corresponding *spiro*-titanocenebisamido complex **9b** (isolated in 81% yield). Treatment of the *N*-acylated ligand system employed as the dilithiated reagent **8a** with $TiCl_4$ or $ZrCl_4$ proceeds quite analogously. In these cases the corresponding chiral *spiro*-metallocene complexes **9a** (M = Ti, 58% yield) and **10a** (M = Zr, isolated in 74% yield) were obtained (see Scheme 6).

The *spiro*-metallocene complex **10a** was characterized by an X-ray crystal structure analysis. Single crystals of **10a** suitable for X-ray diffraction were obtained by crystallization from pentane/toluene. The central zirconium atom in complex **10a** is coordinated to two cyclopentadienyl units and the acylamido groups of the pair of near-to-symmetry-equivalent $[Cp-C(=CH_2)-NC(CMe_3)O]$ ligand systems in an overall pseudotetrahedral coordination geometry [D1−Zr1−D2 = 131.0° (D1 and D2 denote the centroids of the Cp ring systems), O14−Zr1−O34 = 99.95(13)°]. Complex **10a** is chiral; in the crystal it is chemically, but not strictly crystallographically, to be regarded as C_2-symmetric (see Figure 3).

The C6=C7 double bond of **10a** [1.332(6) Å; accordingly C26−C27: 1.341(6) Å] is oriented approximately coplanar with the adjacent cyclopentadienyl ring system. The dihedral angle θ C4−C5−C6−C7 amounts to −31.9(7)°; the corresponding value of θ C21−C25−C26−C27 is −29.4(7)°. The adjacent nitrogen atom N8 is also oriented in this substituent plane [dihedral angles θ C1−C5−C6−N8 −19.2(6)°, and correspondingly C24−C25−C26−N28 −15.6(6)°]. The N8−C9 bond is short [1.278(5) Å; N28−C29 1.289(5) Å] and must be regarded as an N=C double bond. Consequently, the C9−O14 linkage is elongated [1.338(5) Å; C29−O34 1.334(5) Å]. Apparently the ambidentate *N*-acylamido functional group is present as the imino tautomer in complex **10a**. Coordination of this group to the group-4 metal takes place exclusively by means of the oxygen atom [O14−Zr1 2.026(2) Å; O34−Zr1 2.038(3) Å] and not through the nitrogen center [the N8···Zr1 separation is 3.682(4) Å; N28···Zr1 3.666(4) Å]. Consequently, the individual ligand systems in **10a** are not planar but the two sections used for coordinating to the transition-metal center are segregated by a strong rotation about the C6−N8 vector [dihedral angles θ C5−C6−N8−C9 −52.1(5)°, C25−C26−N28−C29 −52.9(5)°, C7−C6−N8−C9 130.5(5)°, C27−C26−N28−C29 129.6(4)°, C6−N8−C9−O14 −5.4(6)°, C26−N28−C29−O34 −6.6(6)°] to allow for the thermodynamically favourable coordination of the ligand system to the zirconium center through the carboxamido oxygen atom. The bond angles at these oxygen atoms are substantially enlarged at 136.5(3)° (C9−O14−Zr1) and 136.0(2)° (C29−O34−Zr1), respectively. This probably indicates a tendency to form a stabilizing Zr−O π interaction, similar as it has been observed in a variety of Zr−O linkages in metallacyclic systems of ring sizes of 6 and larger.[16] The remaining angles inside the metallacyclic framework of **10a** are in a normal and expected range [C6−N8−C9 117.9(4)°, C26−N28−C29 118.3(3)°, N8−C9−O14 125.2(4)°, N28−C29−O34 124.8(4)°].

We have then treated the dilithio compound **8a** with the dichlorobis(diethylamido)zirconium reagent, employed as its bis(tetrahydrofuran) adduct.[17] This results in a clean reaction that takes place by a selective displacement of the two chloride ligands by the $[Cp-C(=CH_2)-N(CMe_3)O]^{2-}$ ligand system. The $Zr(NEt_2)_2$ moiety is retained during this transformation.[18] The resulting zirconium complex **11** was obtained in 70% yield. The spectroscopic data of the newly introduced $[Cp-C=CH_2)-N(CMe_3)O]$ ligand in **11** are quite similar as previously observed for the *spiro* complexes **9a** and **10a** {**11**: $^1H/^{13}C$ NMR in [D_8]THF: δ = 6.60, 5.95/111.3, 110.5 (C_5H_4), 4.77, 4.72 ($^2J_{HH}$ = 1.8 Hz)/147.6, 102.4 ($C=CH_2$), 171.4 (NCO)}. Therefore, we assume that the $[Cp-C(=CH_2)N(CMe_3)O]$ ligand system in **11** is coordinated by means of the Cp ring and the carboxamido oxygen, and not the nitrogen center, just analogously as it was previously observed for the *spiro*-metal complexes **9a** and **10a** (see above).

Scheme 6

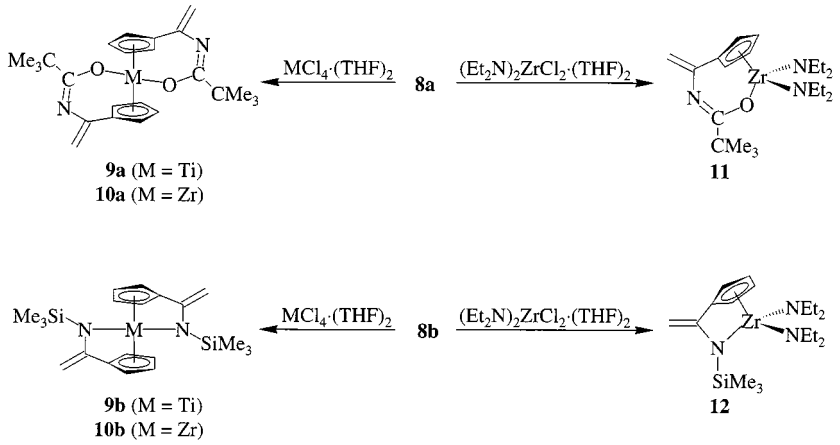

Figure 3. Molecular structure of **10a**[a]

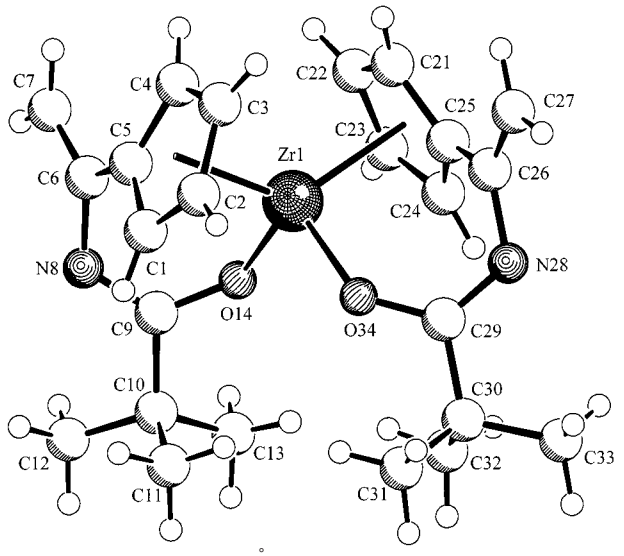

[a] Selected bond lengths [A] and angles [°]: Zr1−O14 2.026(2), Zr1−O34 2.038(3), Zr1−N8 3.682(4), Zr1−N28 3.666(4), Zr1−C_{Cp} 2.511(5), C5−C6 1.474(6), C25−C26 1.466(6), C6−C7 1.332(6), C26−C27 1.341(6), C6−N8 1.418(5), C26−N28 1.414(5), N8−C9 1.278(5), N28−C29 1.289(5), C9−O14 1.338(5), C29−O34 1.334(5), C9−C10 1.523(6), C29−C30 1.524(6); O14−Zr1−O34 99.95(13), Zr1−O14−C9 136.5(3), Zr1−O34−C29 136.0(2), C5−C6−C7 122.2(4), C25−C26−C27 123.5(4), C5−C6−N8 116.5(4), C25−C26−N28 116.0(3), C7−C6−N8 121.3(4), C27−C26−N28 120.5(4), N8−C9−O14 125.2(4), N28−C29−O34 124.8(4), N8−C9−C10 120.8(4), N28−C29−C30 120.0(4), O14−C9−C10 113.9(4), O34−C29−C30 115.2(3); see text for additional values.

As expected, the $[Cp-C(=CH_2)-NSiMe_3]^{2-}$ ligand, employed as the respective dilithio reagent **8b**, reacts analogously with the $(Et_2N)_2ZrCl_2(THF)_2$ reagent very cleanly and in good yield to give the C_1-bridged constrained-geometry metal-complex system $[Cp-C(=CH_2)-NSiMe_3]Zr(NEt_2)_2$ (**12**). Exclusive metathetical exchange of the chloride ligands takes place, and the C_1-bridged Cp/amido-zirconium complex **12** was isolated in 76% yield. It shows very typical $^1H/^{13}C$-NMR spectra {in [D_6]benzene: δ = 6.03, 5.92/112.2 (*ipso*-C), 115.4, 111.3 (C_5H_4), 4.36, 4.34/150.9, 87.9 ($C=CH_2$), 0.39/0.8 ($SiMe_3$), 3.13, 0.90/43.2, 15.6 (NEt_2)}.

We have employed the $[Cp-C(=CH_2)-NSiMe_3]Zr(NEt_2)_2$ complex **12** as a starting material for generating a homogeneous Ziegler catalyst system and used it for carrying out a small series of preliminary ethene polymerization experiments. These few and as yet unoptimized polymerization reactions have revealed that the Ziegler catalysts, based on the C_1-bridged constrained-geometry framework, are at least comparable in activity and performance to the commonly used and studied Si_1-bridged "parent" system. This lets us hope that future variations of our here described $[Cp-C(R^*)NR']MX_2$ complexes will indeed lead to an even better catalyst performance and open ways to novel and advanced catalytic applications.

For the series of catalytic experiments carried out in the course of this study we have activated the zirconium complex **12** by treatment with a large excess of methylalumoxane (employed as a standard toluene solution).[19] In a typical experiment a solution of 19.4 mg (47.0 μmol) of **12** was activated by treatment with 10 ml of a 10% solution of methylalumoxane in toluene (Al/Zr = 340) at ambient temperature under an initial ethene pressure of 37 bar. After a short induction period a rapid temperature increase took place (up to 87°C) and the pressure dropped due to rapid consumption of the monomer. Ethene pressure was reestablished and the monomer constantly fed into the reactor for a time period of ca. 10 min. The reaction was stopped by ceasing the monomer fed. Opening of the reactor revealed that the interior of the reaction vessel was almost filled with an amorphous lump of polymer. Workup, as described in the Experimental Section, gave 16.6 g of polyethylene (mp 129°C, DSC), which corresponds to an overall catalyst activity of ca. 57 g polymer/mmol [Zr]·bar·h under these unoptimized non-isothermal conditions. A number of similar experiments, which gave comparable results, are listed in the Experimental Section.

For a direct comparison we have carried out a few ethene polymerization experiments under analogous reaction conditions using the Si_1-bridged "Bercaw/Exxon/Dow" system $[Me_4C_5-SiMe_2-NCMe_3]ZrCl_2$ (**1c**, see Scheme 1)[4] as the Ziegler catalyst precursor. In a typical experiment under very similar conditions as described above a sample of **1c**

(8.6 mg, 20.9 μmol) was activated by treatment with methylalumoxane (Al/Zr = 1530) in toluene under ethene (40 bar) in an autoclave. Rapid polymerization set in at once; the contents of the autoclave increased its temperature up to 103°C. A yield of 14.4 g of polyethylene was obtained under these conditions (mp 135°C, by DSC), corresponding to an overall catalyst activity of ca. 52 g polymer/mmol [Zr]·h·bar under these non-isothermal conditions.

We have also carried out the ethene polymerization reaction in a thermostated glass autoclave employing the **12**/methylalumoxane system in toluene (Al/Zr = 700) at 25°C and a constant pressure of 2.2 bar and obtained polyethylene (mp 137°C) with a slightly lower activity of a = 23 g polymer/mmol [Zr]·h·bar.

Conclusions

We had recently shown that the C_1-bridged fluorenyl/amido system $[Flu-CH_2-NCMe_3]^{2-}$ (generated and studied as the corresponding lithiated compound) is kinetically and thermodynamically rather stable, but, of course, difficult to handle because of its high basicity.[5] Much more problematic seems to be a prediction of the chemistry of related systems on the mono-anionic stage. For the examples $[Flu(H)-CH_2-NCMe_3]^-$/$[Flu-CH_2-NHCMe_3]^-$ (Flu = fluorenylidene) we had in a detailed study been able to characterize a number of readily available competing reaction pathways, involving e.g. fulvene formation and fragmentation pathways.[5] It appears, that similar multiple reaction pathways are getting involved when such dianions are treated with early transition-metal reagents that, due to the highly covalent character of e.g. the N−Zr or C−Zr bonds, can lead to very reactive intermediates, that then are prone to enter into the manifold of the competing pathways that are so typical for the respective $[Cp-CR_2-NR']^-$ mono-anion systems. This effect does not generally preclude the successful synthesis of such $[Cp-CR_2-NR']MX_2$-type systems,[7] but will in very many cases lead to complicated organometallic mixtures of products and will make the handling of such systems probably rather difficult. This is very likely to be the reason why reports on such C_1-bridged constrained-geometry systems are extremely sparse, in contrast to their Si_1- or their elongated C_n-bridged analogues.[3][4][6][7] The system developed by us and described with some first examples in this article seems to provide a useful and generally easily accessible alternative. Introduction of the sp^2-carbon center in the system adjacent to the Cp-ring as a bridging atom between the C_5H_4 and N−R′ moieties appears very effectively to make all the usually encountered reactive alternatives and diversions on the intermediate stages of the overall reaction sequence to the final group-4 metal complexes sufficiently unfavourable to allow for a straightforward and easily performed synthesis of the respective $[Cp-C(=CH_2)-NR]ML_n$-type systems. Our preliminary ethene polymerization experiments have shown that the first examples of the thus derived C_1-bridged constrained-geometry Ziegler catalysts are at least equally effective, very active polymerization catalysts as the commonly employed $[Cp^*-SiMe_2-NCMe_3]ZrCl_2$ system.

Our entry into the novel class of the $[Cp-C(=CH_2)-NR']ZrX_2$-type catalyst precursors should allow for the synthesis of a large number of easily accessible variations of such systems. We are confident that this will lead to a significant extension and further development of the scope of application of such interesting catalyst types in polymerization reactions and in organic synthesis.[20] The further development of the C_1-bridged "constrained-geometry catalysts" is, therefore, actively pursued in our laboratory.

Financial support from the *Fonds der Chemischen Industrie*, the *Bundesminister für Bildung, Wissenschaft, Forschung und Technologie (BMBF),* and the *Ministerium für Wissenschaft und Forschung des Landes Nordrhein-Westfalen* is gratefully acknowledged.

Experimental Section

General Information: All reactions with organometallic reagents or substrates were carried out under argon using Schlenk-type glassware or in a glove-box. Solvents (including deuterated solvents used for NMR spectroscopy) were dried and distilled under argon prior to use. − The following instruments were used for spectroscopic and physical characterization of the compounds: Bruker AC 200P (^{1}H: 200.13, ^{13}C: 50.3 MHz), Bruker ARX 300, and Varian Unity Plus (^{1}H: 599.2, ^{13}C: 150.8 MHz) NMR spectrometers (spectral assignments were usually secured by GCOSY, GHSQC and GHMBC experiments[21]); Nicolet 5 DXC FT-IR spectrometer; melting points: DSC 2910 (Thermo Analysis/DuPont); elemental analyses: Foss-Heraeus CHN-Rapid; X-ray crystal structure analyses: Enraf-Nonius CAD4 and MACH3 diffractometers (programs used: data reduction MolEN, structure solution SHELXS-86, structure refinement SHELXL-93, graphics SCHAKAL-92). − The reagent $(Et_2N)_2ZrCl_2(THF)_2$ was prepared according to a literature procedure.[17] The aminofulvenes were synthesized by variations of the procedures previously described by K. Hafner et al.[8]

Crystallographic data (excluding structure factors) for the structures reported in this paper have been deposited with the Cambridge Crystallographic Data Centre as supplementary publication no. CCDC-101213. Copies of the data can be obtained free of charge on application to CCDC, 12 Union Road, Cambridge CB2 1EZ, UK [fax: int. code + 44(1223)336-033, e-mail: deposit@ccdc.cam.ac.uk].

6-Dimethylamino-6-methylfulvene (**3**): Dimethyl sulfate (49 ml, 62 g, 0.49 mol) was added dropwise with gentle heating in such a way to 49 ml (43 g, 0.49 mol) of freshly distilled *N,N*-dimethylacetamide that the temperature was maintained at 50−60°C. Then the solution was kept at 70−80°C for 2 h. The viscous oil was added with stirring to a solution of 44 g (0.50 mol) of sodium cyclopentadienide in 300 ml of tetrahydrofuran with external cooling at a rate that the reaction temperature was kept between −5 and −10°C. The precipitated sodium methyl sulfate was filtered off and the solvent removed from the filtrate in vacuo. The dark brown oil was treated with 2 g of active charcoal in 400 ml of hot cyclohexane and filtered. The product **3** crystallizes upon cooling. The mother liquor was concentrated and treated again with charcoal to give a combined yield of 59.5 g (88%) of **3**, mp 90°C. − $C_9H_{13}N$ (135.2): calcd. C 79.95, H 9.69, N 10.36; found C 79.81, H 9.90, N 10.18. − ^{1}H NMR (200.1 MHz, [D$_1$]chloroform): δ = 6.83−6.44 (m, 4 H, C_5H_4), 3.48 (s, 6 H, NCH_3), 2.62 (s, 3 H, 6-CH_3). − ^{13}C NMR (50.3 MHz, [D$_1$]chloroform): δ = 158.5 (C-6), 121.4, 120.1, 118.5, 116.5 (Cp, C-2−5), 117.3 (C-1), 43.4 (NCH_3), 20.5 (6-CH_3).

6-Amino-6-methylfulvene (**4**): A 300-ml autoclave, containing an internal glass vessel, was charged with 59.7 g (400 mmol) of **3** and ca. 150 ml condensed NH_3 at −78°C. The closed system was left for 7 d at 40°C (at 10 bar pressure). The system was then cooled (< −33°C) and the autoclave opened. NH_3 was allowed to evaporate and the yellow product dried in vacuo to give 41.6 g (97%) of **4**, mp. 85°C. − C_7H_9N (107.1): calcd. C 78.46, H 8.47, N 13.07; found C 78.33, H 8.72, N 12.68. − ^{1}H NMR (200.1 MHz, [D$_1$]chloroform): δ = 6.56−6.27 (m, 4 H, C_5H_4), 5.13 (br., 2 H, NH_2), 2.31 (s, 3 H, 6-CH_3). − ^{13}C NMR (50.3 MHz, [D$_1$]chloroform): δ = 154.7 (C-6), 117.9 (C-1), 124.6, 122.1, 119.7, 112.3 (Cp, C-2−5), 19.5 (6-CH_3).

6-Acetylamino-6-methylfulvene (**5a**) *and 2-Acetyl-6-amino-6-methylfulvene* (**6a**): A solution of acetyl chloride (314 mg, 4.03 mmol) in 15 ml of ether was added dropwise to a solution of 599 mg (4.00 mmol) of the fulvene **4** in 30 ml of ether containing 3 ml of triethylamine at 0°C. The mixture was stirred overnight and was then concentrated to one half of its volume in vacuo. Triethylammonium chloride was removed by filtration. The product was precipitated by cooling to −20°C. The resulting crude product was purified by column chromatography (silica gel, 60 mesh, diethyl ether/triethylamine, 50:1). Compound **6a** (30 mg, 5% yield) was recovered from the first eluate, compound **5a** (406 mg, 68%) was collected from the third fraction. **5a**: mp 119°C (DSC). − $C_9H_{11}NO$ (149.2): calcd. C 72.46, H 7.43, N 9.39; found C 70.98, H 7.38, N 8.75. − ^{1}H NMR (200.1 MHz, [D$_1$]chloroform): δ = 7.78 (br., NH), 6.58−6.35 (m, 4 H, C_5H_4), 2.68 (s, 3H), 2.17 (s, 3 H, COCH_3). − ^{13}C NMR (50.3 MHz, [D$_8$]tetrahydrofuran): δ = 169.5 (C=O), 146.8 (C-6), 129.4 (C-1), 129.0, 128.3, 122.2, 116.8 (Cp, C-2−5), 24.3 (COCH_3), 19.2 (C-7).

X-ray Crystal Structure Analysis of **5a**: Formula $C_9H_{11}NO$, M = 149.19, 0.25 × 0.20 × 0.10 mm, a = 7.265(2), b = 11.576(3), c = 9.729(1) A, β = 104.84(2)°, V = 790.9(3) A^3, $\rho_{calcd.}$ = 1.253 g cm^{-3}, μ = 0.82 cm^{-1}, no absorption correction, Z = 4, monoclinic, space group $P2_1/c$ (No. 14), λ = 0.71073 A, T = 223 K, ω/2θ scans, 1721 reflections collected (−h, +k, ±l), [(sinθ)/λ] = 0.62 A^{-1}, 1596 independent and 733 observed reflections [$I \geq 2\ \sigma(I)$], 105 refined parameters, R = 0.063, wR^2 = 0.158, max. residual electron density 0.28 (−0.33) e A^{-3}, hydrogen atom at N from difference Fourier, others calculated and all refined as riding atoms.

6a: ^{1}H NMR (200.1 MHz, [D$_1$]chloroform): δ = 14.6 (br., 2 H, NH), 7.56 (1 H), 7.27 (1 H), and 6.42 (1 H, ABX, C_5H_3, J_{HH} = 1.9, 3.2, and 4.8 Hz), 2.87, 2.56 (s, each 3 H, CH_3).

6-Methyl-6-[(p-methylbenzoyl)amino]fulvene (**5b**): Triethylamine (7 ml) was added to a solution of 4.14 g (38.7 mmol) of the aminofulvene **4** in 150 ml of ether. *p*-Methylbenzoyl chloride (5.40 ml, 41.0 mmol) was very slowly added by syringe to the vigorously stirred solution at 0°C. After 24 h, the mixture was concentrated to half its volume in vacuo and the precipitated triethylammonium chloride removed by filtration. The remaining solvent was then removed in vacuo. The resulting crude product (5.6 g, ca. 60%) was purified by column chromatography at a deactivated (by treatment with 5% triethylamine in pentane/ether, 8:1) silica gel column (60 mesh). Elution with pentane/ether (8:1) gave the product **5b** as the third fraction, yield 1.8 g (21%). Single crystals suited for the X-ray crystal structure analysis were obtained from ether at 0°C; mp 104°C (DSC). − $C_{15}H_{15}NO$ (225.3): calcd. C 79.97, H 6.71, N 6.22; found C 78.62, H 7.05, N 6.10. − ^{1}H NMR (200.1 MHz, [D$_8$]tetrahydrofuran): δ = 9.32 (br., 1 H, NH), 7.83 (m, 2 H), 7.29 (m, 2 H, *o*,*m*-Ph), 6.66−6.54 (m, 2 H), 6.32−6.28 (m, 2 H, C_5H_4), 2.73 (s, 3 H, 6-CH_3), 2.40 (s, 3 H, Ph-CH_3). − ^{13}C NMR (150.8 MHz, [D$_1$]chloroform): δ = 165.1 (C=O), 145.9 (C-6), 143.4 (*p*-C, Ph), 131.3 (*ipso*-C, Ph), 130.2 (C-5), 129.7 (*m*-C, Ph), 128.9 (C-1), 128.7 (C-3), 127.1 (*o*-C, Ph), 121.8 (C-2), 113.9 (C-4), 21.5 (Ph-CH_3), 18.6 (6-CH_3). − IR (KBr): ν = 3335, 1662, 1622 cm^{-1}.

X-ray Crystal Structure Analysis of **5b**: Formula $C_{15}H_{15}NO$, M = 225.28, 0.50 × 0.30 × 0.10 mm, a = 7.169(1), b = 24.276(2), c = 7.289(1) A, β = 97.99(1)°, V = 1256.2(3) A^3, $\rho_{calcd.}$ = 1.191 g cm^{-3}, μ = 5.84 cm^{-1}, no absorption correction, Z = 4, monoclinic, space group $P2_1/n$ (No. 14), λ = 1.54178 A, T = 223 K, ω/2θ scans, 2743 reflections collected (±h, −k, +l), [(sinθ)/λ] = 0.62 A^{-1}, 2547 independent and 1673 observed reflections [$I \geq 2\ \sigma(I)$], 160 refined parameters, R = 0.056, wR^2 = 0.146, max. residual electron density 0.20 (−0.20) e A^{-3}, hydrogen atom at N from difference Fourier, others calculated and all refined as riding atoms.

6-Methyl-6-(pivaloylamino)fulvene (**5c**): Pivaloyl chloride (5.60 g, 46.7 mmol) was added at 0°C to a solution of 5.00 g (46.7 mmol) of **4** and 3 ml of triethylamine in 30 ml of tetrahydrofuran. After warming and stirring overnight at room temperature, the emulsion was filtered. The solvent was removed in vacuo. The residue was taken up in ether, filtered and the product crystallized from the clear ethereal solution at −30°C. Some of the thus obtained crystals were suitable for X-ray diffraction. Yield of **5c**: 7.14 g (80%), mp 82°C (DSC). − $C_{12}H_{17}NO$ (191.3): calcd. C 75.35, H 8.96, N 7.32; found C 75.14, H 9.08, N 7.25. − ^{1}H NMR (200.1 MHz, [D$_1$]chloroform): δ = 8.17 (br., 1 H, NH), 6.60−6.34 (m, 4 H, C_5H_4), 2.70 (s, 3 H, 6-CH_3), 1.29 [s, 9 H, C(CH_3)$_3$]. − ^{13}C NMR (50.3 MHz, [D$_1$]chloroform): δ = 176.5 (C=O), 146.3 (C-6), 128.3 (C-1), 130.1, 128.5, 121.8, 113.6 (Cp, C-2−5), 40.4 [C(CH$_3$)$_3$], 27.4 [C(CH_3)$_3$], 18.6 (6-CH_3). − IR (KBr): ν = 3342, 1683, 1620 cm^{-1}. − HRMS (70eV); $C_{12}H_{17}NO$: calcd. 191.13101; found 191.13054; *m*/*z* (%): 191 [M$^+$] (38), 134 [M$^+$ − C_4H_9] (10), 107 [M$^+$ − COC_4H_8] (9), 57 [$C_4H_9^+$] (100).

X-ray Crystal Structure Analysis of **5c**: Formula $C_{12}H_{17}NO$, M = 191.27, 0.60 × 0.30 × 0.10 mm, a = 14.076(1), b = 8.474(1), c = 28.982(3) A, β = 91.16(1)°, V = 3456.3(6) A^3, $\rho_{calcd.}$ = 1.103 g cm^{-3}, μ = 5.44 cm^{-1}, empirical absorption correction with ψ scan data (0.945 ≤ C ≤ 0.999), Z = 12, monoclinic, space group $P2_1/c$ (No. 14), λ = 1.54178 A, T = 223 K, ω/2θ scans, 7207 reflections collected (±h, +k, −l), [(sinθ)/λ] = 0.62 A^{-1}, 7057 independent and 5847 observed reflections [$I \geq 2\ \sigma(I)$], 401 refined parameters, R = 0.040, wR^2 = 0.116, max. residual electron density 0.21 (−0.15) e A^{-3}, hydrogen atom at N from difference Fourier, others calculated and all refined as riding atoms.

6-Methyl-6-[(trimethylsilyl)amino]fulvene (**7**): To a cold solution (0°C) of 702 mg (6.55 mmol) of the aminofulvene **4** in 100 ml of ether, containing three molar equivalents of triethylamine (2.0 g) was slowly added with stirring 1.5 molar equivalents (1.25 ml, 1.07 g, 9.83 mmol) of chlorotrimethylsilane. After 8 h at ambient temperature, the mixture was filtered and the solvent removed in vacuo to give the product **7** as a viscous oil. Yield of **7**: 1.15 g (98%), mp 12°C (DSC). − $C_{10}H_{17}NSi$ (179.3): calcd. C 66.97, H 9.55, N 7.81; found C 66.83, H 9.50, N 8.03. − ^{1}H NMR (200.1 MHz, [D$_1$]chloroform): δ = 6.57−6.28 (m, 4 H, C_5H_4), 5.4 (br., 1 H, NH), 2.39 (s, 3 H, 6-CH_3), 0.35 (s, 9 H, SiCH_3). − ^{13}C NMR (50.3 MHz, [D$_1$]chloroform): δ = 158.8 (C-6), 125.0, 122.4, 119.5, 111.9 (C-2−5), 122.1 (C-1), 19.3 (6-CH_3), 0.8 [Si(CH$_3$)$_3$]. − IR (NaCl): ν = 3353, 1616 cm^{-1}. − MS (70eV); *m*/*z* (%): 179 [M$^+$] (84), 164 [M$^+$ − CH_3] (100), 73 [$SiMe_3^+$] (71).

Lithium [1-(Lithio-N-pivaloylamido)ethenyl]cyclopentadienide (**8a**): A solution of the fulvene **5c** (380 mg, 1.99 mmol) in 30 ml of ether was treated at −20°C with two molar equivalents of lithium hexamethyldisilazide (675 mg, 4.04 mmol), dissolved in 20 ml of ether. The mixture was warmed to room temperature and stirred

for 4 h. The resulting precipitate of **8a** was collected by filtration, washed with ether (10 ml), then with pentane (20 ml), and dried in vacuo to give 363 mg (81%) of **8a** (· 0.3 Et_2O). – ^1H NMR (200.1 MHz, [D_8]tetrahydrofuran): δ = 5.82 (m, 2 H), 5.69 (m, 2 H, Cp), 4.47 (1 H), and 3.66 (1 H, AB system, $^2J_{HH}$ = 2.3 Hz, C=CH_2), 1.08 [s, 9 H, C(CH_3)$_3$]. – ^{13}C NMR (50.3 MHz, [D_8]tetrahydrofuran): δ = 179.3 (C=O), 155.4 (*C*=CH_2), 118.2 (*ipso*-C, Cp), 106.3, 103.2 (Cp), 87.5 (C=*C*H_2), 39.0 [*C*(CH_3)$_3$], 29.5 [C(*C*H_3)$_3$].

Lithium [1-(Lithio-N-trimethylsilylamido)ethenyl]cyclopentadienide (**8b**): A solution of lithium diisopropylamide (LDA, 2.1 g, 20 mmol) in 5 ml of tetrahydrofuran was added to a solution of 1.81 g (10 mmol) of the fulvene **7** in 30 ml of ether at 0°C. The mixture was stirred for 20 h at ambient temperature, then the solvent was removed in vacuo. The residue was suspended in pentane and the solid product collected by filtration, washed with pentane and dried in vacuo to yield 3.10 g (89%) of **8b** (· 1.5 THF). – ^1H NMR (200.1 MHz, [D_8]tetrahydrofuran): δ = 5.81 (m, 2 H) and 5.66 (m, 2 H, Cp), 3.61 (1 H) and 3.17 (1 H, AB system, $^2J_{HH}$ = 2.6 Hz, C=CH_2), −0.01 [s, 9 H, Si-CH_3)$_3$]. – ^{13}C NMR (50.3 MHz, [D_8]tetrahydrofuran): δ = 130.0 (*C*=CH_2), 119.1 (*ipso*-C of Cp), 104.5, 101.3 (Cp), 73.3 (C=*C*H_2), 2.4 [Si(*C*H_3)$_3$].

Reaction of **8a** *with Titanium Tetrachloride, Preparation of Bis{η⁵:κ-O-[1-(pivaloylamido)ethenyl]cyclopentadienyl}titanium* (**9a**): A suspension of the dilithium compound **8a**, generated by treatment of 191 mg (1.00 mmol) of the fulvene **5c** with 220 mg (2.06 mmol) of LDA in 50 ml of THF at −20°C (24 h), was slowly added at −20°C to a solution of 167 mg (502 μmol) $TiCl_4$ · 2 THF in 50 ml of THF. The dark red mixture was warmed to room temperature and then stirred for 3 h. The solvent was removed in vacuo and the residue extracted with 80 ml of pentane. Removal of the solvent in vacuo gave the product **9a** as a red, microcrystalline solid, yield 124 mg (58%), mp 123°C (DSC, decomp.), that was characterized spectroscopically. – ^1H NMR ([D_2]dichloromethane): δ = 6.21, 6.12, 6.07, 5.82 (m, each 2 H, Cp), 5.32, 4.89 (d, ^2J = 0.96 Hz, each 1 H, C=CH_2), 1.13 [s, 18 H, C(CH_3)$_3$]. – ^{13}C NMR (CD_2Cl_2): δ = 176.9 (N*C*O), 146.0 (*C*=CH_2), 124.5 (*ipso*-C, Cp), 126.3, 117.3, 109.9, 107.3 (Cp), 105.3 (C=*C*H_2), 39.1, 28.6 [C(CH_3)$_3$]. – IR (KBr): ν = 1619, 1566, 1557 cm^{-1}.

Preparation of Bis(η⁵:κ-N-{1-[(trimethylsilyl)amido]ethenyl}-cyclopentadienyl)titanium (**9b**): Analogously as described above, treatment of 688 mg (3.84 mmol) of the fulvene **7** with 822 mg (7.68 mmol) of LDA followed by reaction with 641 mg (1.92 mmol) of $TiCl_4$ · 2 THF gave **9b**, yield 626 mg (81%), mp 135°C (DSC, decomp.). – ^1H NMR ([D_6]benzene): δ = 6.55, 6.91, 5.28, 5.11 (m, each 2 H, Cp), 4.07, 3.95 (d, each 1 H, =CH_2), 0.27 [s, 18 H, Si(CH_3)$_3$]. – ^{13}C NMR ([D_8]tetrahydrofuran): δ = 151.3 (*C*=CH_2), 122.3 (*ipso*-C, Cp), 117.7, 116.6, 115.4, 114.0 (Cp), 84.3 (C=*C*H_2), 2.65 ($SiMe_3$). – IR (KBr): ν = 1623 cm^{-1}.

Synthesis of Bis{η⁵:κ-O-[1-(pivaloylamido)ethenyl]cyclopentadienyl}zirconium (**10a**): 546 mg (2.86 mmol) of the fulvene **5c** was doubly deprotonated by treatment with 614 mg (5.74 mmol) of LDA in 50 ml of THF, analogously as described above. A solution of $ZrCl_4$ · 2 THF (539 mg, 1.43 mmol) in 50 ml of THF was added at ambient temperature. After stirring for 20 h at room temperature, the solvent was removed in vacuo. Extraction with pentane yielded 739 mg (74%) of the product **10a**, mp 111°C (DSC, decomp.). – $C_{24}H_{30}N_2O_2Zr$ (469.8): calcd. C 61.37, H 6.44, N 5.96; found C 59.84, H 6.63, N 5.96. – ^1H NMR ([D_8]tetrahydrofuran, 600 MHz): δ = 6.40, 6.35, 6.17, 5.82 (m, each 2 H, Cp), 4.80, 4.73 (d, ^2J = 1.4 Hz, each 2 H, =CH_2), 1.12 [s, 18 H, C(CH_3)$_3$]. – ^{13}C NMR ([D_2]dichloromethane, 50 MHz): δ = 174.1 (N*C*O), 145.9 (*C*=CH_2), 125.8 (*ipso*-C, Cp), 120.9, 113.0, 108.3, 106.0 (Cp), 103.9 (C=*C*H_2), 38.7, 28.4 (CMe_3). – IR (KBr): $\tilde{\nu}$ = 1621, 1589, 1502 cm^{-1}.

X-ray Crystal Structure Analysis of **10a**: Formula $C_{24}H_{30}N_2O_2Zr$, *M* = 469.72, 0.40 × 0.40 × 0.10 mm, *a* = 13.301(1), *b* = 14.968(1), *c* = 11.099(1) A, *V* = 2209.7(3) A^3, $\rho_{calcd.}$ = 1.412 g cm^{-3}, μ = 5.19 cm^{-1}, no absorption correction, *Z* = 4, orthorhombic, space group $Pna2_1$ (No. 33), λ = 0.71073 A, *T* = 223 K, ω/2θ scans, 2364 reflections collected (−*h*, +*k*, −*l*), [(sinθ)/λ] = 0.62 A^{-1}, 2364 independent and 1960 observed reflections [$I \geq 2\sigma(I)$], 268 refined parameters, R = 0.025, wR^2 = 0.061, Flack parameter 0.00(6), max. residual electron density 0.27 (−0.34) e A^{-3}, hydrogen atoms calculated and refined as riding atoms.

Synthesis of Bis(η⁵:κ-N-{1-[(trimethylsilyl)amido]ethenyl}cyclopentadienyl)zirconium (**10b**): 362 mg (2.62 mmol) of the fulvene **7** was doubly deprotonated by treatment with 566 mg (5.28 mmol) of LDA in 50 ml of THF. This solution was then added dropwise at −20°C to a solution of 489 mg (1.30 mmol) of $ZrCl_4$ · 2 THF in 40 ml of THF. The reaction mixture was warmed to room temperature and stirred for 2 h. The solvent was then removed in vacuo and the product extracted from the residue with 100 ml of pentane to yield 446 mg (77%) of **10b**, mp 117°C (DSC, decomp.). – $C_{20}H_{30}N_2Si_2Zr$ (445.9): calcd. C 53.88, H 6.78, N 6.28, found C 53.42, H 7.35, N 6.18. – ^1H NMR ([D_2]dichloromethane): δ = 6.36 (m, 4 H), 6.20, 5.80 (m, each 2 H, Cp), 3.95, 3.90 (AB, each 2 H, =CH_2), 0.16 [s, 18 H, Si(CH_3)$_3$]. – ^{13}C NMR ([D_2]dichloromethane): δ = 150.1 (*C*=CH_2), 118.2 (*ipso*-C, Cp), 116.3, 114.7, 122.9, 109.6 (Cp), 87.6 (=*C*H_2), 1.6 ($SiMe_3$). – IR (KBr): ν = 1591 cm^{-1}.

Synthesis of Bis(diethylamido){η⁵:κ-O-[1-(pivaloylamido)ethenyl]cyclopentadienyl}zirconium (**11**): A suspension of the dilithium reagent **8a**, generated by treatment of the fulvene **5c** (339 mg, 1.78 mmol) with 381 mg (3.56 mmol) of LDA in 50 ml of THF, was combined with a suspension of 794 mg (1.77 mmol) of $(Et_2N)_2ZrCl_2$ · 2 THF in 50 ml of THF at 0°C. After stirring for 2 h at room temperature, the solvent was removed in vacuo and the product isolated from the residue by extraction with 50 ml of pentane. Yield of **11**: 528 mg (70%) as a red viscous oil. – $C_{20}H_{35}N_3OZr$ (424.7): calcd. C 56.56, H 8.31, N 9.89, found C 55.66, H 8.54, N 9.71. – ^1H NMR ([D_6]benzene): δ = 5.97, 5.90 (m, each 2 H, Cp), 5.25, 5.00 (d, ^2J = 1.6 Hz, each 1 H, C=CH_2), 3.12 (q, ^3J = 7.4 Hz, 8 H, NCH_2), 1.38 [s, 9 H, C(CH_3)$_3$], 0.88 (t, ^3J = 7.4 Hz, 12 H, NCH_2CH_3). – ^{13}C NMR ([D_8]THF): δ = 171.4 (N*C*O), 147.6 (*C*=CH_2), 125.3 (*ipso*-C, Cp), 111.3, 110.5 (Cp), 102.4 (C=*C*H_2), 44.3 (N*C*H_2), 38.8, 28.6 (CMe_3), 15.6 (NCH_2*C*H_3). – IR (NaCl): ν = 1590 cm^{-1}.

Synthesis of Bis(diethylamido)(η⁵:κ-N-{1-[(trimethylsilyl)amido]ethenyl}cyclopentadienyl)zirconium (**12**): Analogously as described above, the fulvene **7** (100 mg, 55.9 mmol) was doubly deprotonated by treatment with 120 mg (112 mmol) of LDA in 50 ml of THF. The resulting solution of **8b** was then allowed to react with a solution of 253 mg (561 μmol) of $(Et_2N)_2ZrCl_2$ · 2 THF in 50 ml of THF. After workup of the mixture as described above and extraction with pentane, complex **12** was obtained as a dark colored viscous oil, yield 176 mg (76%). – $C_{18}H_{35}N_3SiZr$ (412.8): calcd. C 52.37, H 8.55, N 10.18; found C 52.39, H 7.98, N 9.85. – ^1H NMR ([D_6]benzene): δ = 6.03, 5.92 (m, each 2 H, Cp), 4.36, 4.34 (AB, each 1 H, =CH_2), 3.13 (q, ^3J = 6.9 Hz, 8 H, NCH_2), 0.90 (t, ^3J = 6.9 Hz, 12 H, NCH_2CH_3), 0.39 [s, 9 H, Si(CH_3)$_3$]. – ^{13}C NMR ([D_6]benzene): δ = 150.9 (*C*=CH_2), 112.2 (*ipso*-C, Cp), 115.4, 111.3 (Cp), 87.9 (=*C*H_2), 43.3 (N*C*H_2), 15.6 (NCH_2*C*H_3), 0.8 [Si(CH_3)$_3$]. – IR (NaCl): ν = 1626 cm^{-1}.

Ethene Polymerization Reactions: For the high-pressure polymerization reactions [p(ethene) ≈ 40 bar] a steel autoclave was used that was equipped with a connected steel dropping funnel that could be kept under the same pressure. This 100-ml autoclave was charged through the dropping funnel under argon with 20 ml of a 10% methylalumoxane solution in toluene. The dropping funnel was rinsed with 20 ml of toluene which was added to the contents of the autoclave. Ethene pressure (ca. 40 bar) was applied to the reaction vessel, and the system was allowed to equilibrate for 0.5 h with stirring. 10 ml of a toluene solution of the organometallic catalyst precursor (**12** or **1c**, respectively) was added under pressure. The temperature of the reaction mixture raised rapidly, in a specific case (see Table 2, entry 2) to 141°C. After a typical reaction time of e.g. 20 min the monomer feed was stopped which resulted in a rapid termination of the polymerization reaction. The autoclave was vented and its contents hydrolyzed by treatment with 20 ml of a 1:1 volume mixture of methanol and 2 N aqueous hydrochloric acid. The polymer was collected by filtration, extracted with toluene and then washed 3 × consecutively with half conc. HCl, H_2O, and then with acetone. The resulting polyethylene samples were then dried for 24 h at 70°C. Details of the respective polymerization experiments carried out according to this general procedure are compiled in Table 2. In a number of experiments (Table 2, entries 4, 5, and 7) the starting materials **12** and **1c** were pretreated with trimethylaluminum in toluene before they were given into the reactor.

Table 2. Details of the ethene polymerization reactions employing the C_1-(**12**-) and Si_1-(**1c**-)bridged constrained-geometry Ziegler catalyst systems

Entry	Precursor (mg/μmol)	ml MAO[a]	Al/Zr	p[b]	t[c]	T[d]	PE[e]	mp [°C]	act[f]
1	**12** (19.4/47.0)	10	340	37	10	87	16.6	129	57.7
2	**12** (11.0/26.7)	20	1200	42	25	141	15.2	145	32.5
3	**12** (9.8/23.8)	20	1340	42	20	78	10.1	137	30.3
4	**12** (5.9/14.3)	20[g]	2590	40	25	53	3.8	132	15.9
5	**12** (5.6/13.6)	20[g]	2730	40	25	70	7.0	138	30.9
6	**1c** (8.6/20.9)	20	1530	40	20	103	14.4	135	51.7
7	**1c** (7.1/17.2)	20[g]	2150	40	20	81	11.5	137	50.1

[a] Ca. 1.6 M methylalumoxane solution in toluene. – [b] Ethene pressure [bar]. – [c] Reaction time [min]. – [d] Final temperature [°C] reached under the employed non-isothermal conditions. – [e] Polyethylene isolated [g]. – [f] Catalyst activity in g polymer/mmol [Zr]·bar·h. – [g] 5 ml of ca. 1 M $AlMe_3$ solution in toluene added for in situ methylation.

Ethene Polymerization at Low Pressure: A thermostated Büchi glass autoclave (25°C) was charged with 200 ml of toluene and 20 ml of a 10% MAO solution in toluene. Ethene was introduced at a pressure of 2.2 bar. After 0.5 h, a solution of 18.9 mg of **12** in 10 ml of toluene was added and the polymerization reaction allowed to proceed for 1.5 h. The system was then vented and its contents quenched by treatment with aqueous HCl/CH_3OH. Workup analogously as described above gave 3.6 g polyethylene [mp 137°C, DSC (after premelting)].

☆ Dedicated to Professor *Carl Krüger* on the occasion of his 65th birthday.

[1] H.-H. Brintzinger, D. Fischer, R. Mülhaupt, B. Rieger, R. Waymouth, *Angew. Chem.* **1995**, *107*, 1255; *Angew. Chem. Int. Ed. Engl*. **1995**, *34*, 1143.

[2] T. J. Marks, *Acc. Chem. Res.* **1992**, *25*, 57. M. Aulbach, F. Küber *Chem. Unserer Zeit* **1994**, *28*, 197, and references cited therein. M. J. Bochmann, *J. Chem. Soc., Dalton Trans.* **1996**, 255.

[3] P. J. Shapiro, W. D. Cotter, W. P. Schaefer, J. A. Labinger, J. E. Bercaw, *J. Am. Chem. Soc.* **1994**, *116*, 4623. W. E. Piers, P. J. Shapiro, E. E. Bunel, J. E. Bercaw, *Synlett* **1990**, *2*, 74. E. E. Bunel, B. J. Burger, J. E. Bercaw, *J. Am. Chem. Soc.* **1988**, *110*, 976. P. J. Shapiro, E. E. Bunel, W. P. Schaefer, J. E. Bercaw, *Organometallics* **1990**, *9*, 867.

[4] [4a] J. C. Stevens, F. J. Timmers, D. R. Wilson, G. F. Schmidt, P. N. Nickias, R. K. Rosen, G. W. Knight, S. Lai, Eur. Patent Appl. EP 416815-A2, **1991** (Dow Chemical Co.) (*Chem. Abstr.* **1991**, *115*, 93163m); J. M. Canich, Eur. Patent Appl. EP 420436-A1, **1991** (Exxon Chemical Co.) (*Chem. Abstr.* **1991**, *115*, 184145y); J. M. Canich, G. G. Hlatky, H. W. Turner, PCT Appl. WO 92-00333, **1992** (*Chem. Abstr.* **1992**, *116*, 174967z). – [4b] J. Okuda, F. J. Schattenmann, S. Wocaldo, W. Massa, *Organometallics* **1995**, *14*, 789. K. E. du Plooy, U. Rose, H.-C. Kang, J. Okuda, W. Massa, *Chem. Ber.* **1996**, *129*, 275. D. D. Devore, F. J. Timmers, D. L. Hasha, R. K. Rosen, T. J. Marks, P. A. Deck, C. L. Stern, *Organometallics* **1995**, *14*, 3132. Y.-X. Chen, C. L. Stern, S. Yang, T. J. Marks, *J. Am. Chem. Soc.* **1996**, *118*, 12451. T. K. Woo, P. M. Margl, J. C. W. Lohrenz, P. E. Blochl, T. Ziegler, *J. Am. Chem. Soc.* **1996**, *118*, 13021. – [4c] W. A. Herrmann, M. J. A. Morawietz, *J. Organomet. Chem*. **1994**, *482*, 169. D. W. Carpinetti, L. Kloppenburg, J. T. Kupec, J. L. Petersen, *Organometallics* **1996**, *15*, 1572. L. Kloppenburg, J. L. Petersen, *Organometallics* **1996**, *15*, 7. – [4d] A. L. McKnight, Md. A. Masood, R. M. Waymouth, D. A. Straus, *Organometallics* **1997**, *16*, 2879. Y.-X. Chen, T. J. Marks, *Organometallics* **1997**, *16*, 3649. F. Amor, T. P. Spaniol, J. Okuda, *Organometallics* **1997**, *16*, 4765; and references cited in these articles.

[5] M. Könemann, G. Erker, R. Fröhlich, E.-U. Würthwein, *J. Am. Chem. Soc.* **1997**, *119*, 11155, and references cited therein.

[6] B. Rieger, *J. Organomet. Chem*. **1991**, *420*, C17. I. M. Ewen, P. Ahlberg, *J. Am. Chem. Soc.* **1992**, *114*, 10869. H. V. R. Dias, Z. Wang, S. G. Bott, *J. Organomet. Chem*. **1996**, *508*, 91. H. V. R. Dias, Z. Wang, *J. Organomet. Chem*. **1997**, *539*, 77. P.-J. Sinnema, L. van der Veen, A. L. Spek, N. Veldman, J. H. Teuben, *Organometallics* **1997**, *16*, 4245. P. T. Witte, A. Meetsma, B. Hessen, P. H. M. Budzelaar, *J. Am. Chem. Soc.* **1997**, *119*, 10561. L. Schwink, P. Knochel, T. Eberle, J. Okuda, *Organometallics* **1998**, *17*, 7.

[7] The possible industrial use of a $[(Me_4C_5)CH_2NR)]TiCl_2$ system was mentioned in the literature; cited in: [7a] A. D. Horton, *Trends Poly. Sci*. **1994**, *2*, 153; [7b] P. B. Hitchcock, J. Hu, M. F. Lappert, *J. Chem. Soc., Chem. Commun.* **1998**, 143.

[8] K. Hafner, K. H. Vöpel, G. Ploss, C. König, *Org. Synth. Coll. Vol. 5*, **1973**, 431. K. Hafner, G. Schultz, K. Wagner, *Chem. Ber.* **1964**, *768*, 539.

[9] W. J. Linn, W. H. Sharkey, *J. Am. Chem. Soc.* **1957**, *79*, 4970. D. Peters, *J. Chem. Soc.* **1959**, 1757. L. M. Jackman, J. C. Trewella, R. C. Haddon, *J. Am. Chem. Soc.* **1980**, *102*, 2519. K. Hartke, A. Kohl, T. Kämpchen, *Chem. Ber.* **1983**, *116*, 2653. M. I. Bruce, J. K. Walton, M. L. Williams, S. R. Hall, B. W. Skelton, A. H. White, *J. Chem. Soc., Dalton Trans.* **1982**, 2209; **1983**, 2183. M. I. Bruce, P. A. Humphrey, J. M. Patrick, B. W. Skelton, W. H. White, M. L. Williams, *Aust. J. Chem*. **1985**, *38*, 1441. M. I. Bruce, P. A. Humphrey, B. W. Skelton, A. H. White, *J. Organomet. Chem*. **1989**, *361*, 369. L. B. Kool, G. J. Kotora, *Macromolecules* **1992**, *25*, 2582, and references cited in these articles.

[10] Reviews: J. Bernstein, R. E. Davis, L. Shimoni, N.-L. Chang, *Angew. Chem.* **1995**, *107*, 1689; *Angew. Chem., Int. Ed. Engl*. **1995**, *34*, 1545. G. R. Desiraju, *Angew. Chem.* **1995**, *107*, 2541; *Angew. Chem., Int. Ed. Engl*. **1995**, *34*, 2328. See also: M. Berlekamp, G. Erker, R. Fröhlich, *Z. Naturforsch*. **1996**, *51b*, 1649. H. C. Strauch, G. Erker, R. Fröhlich, *Chem. Ber*. **1996**, *129*, 1029.

[11] See for a comparison: M. Oberhoff, L. Duda, J. Karl, R. Mohr, G. Erker, R. Fröhlich, M. Grehl, *Organometallics* **1996**, *15*, 4005.

[12] G. R. Knox, P. C. Pauson, *J. Chem. Soc.* **1961**, 4610. F. Le-Moigne, A. Dormond, J. C. Leblanc, C. Moise, J. Tirouflet, *J. Organomet. Chem*. **1975**, *97*, 6272. J. Leblanc, C. Moise, *J. Organomet. Chem*. **1976**, *120*, 65; **1977**, *131*, 35. P. Renaut, G. Tainturier, B. Gautheron, *ibid*. **1978**, *148*, 35.

[13] G. Erker, S. Wilker, C. Krüger, M. Nolte, *Organometallics* **1993**, *12*, 2140. G. Erker, S. Wilker, C. Krüger, R. Goddard, *J. Am. Chem. Soc*. **1992**, *114*, 10983.

[14] For a successful application of this route see e.g.: M. Köne-

mann, G. Erker, R. Fröhlich, S. Kotila, *Organometallics* **1997**, *16*, 2900.

[15] See for a comparison: W. A. Herrmann, M. J. A. Morawietz, T. Priermeir, *Angew. Chem.* **1994**, *106*, 2025; *Angew. Chem. Int. Ed. Engl.* **1994**, *33*, 11946. U. Böhme, K.-H. Thiele, *J. Organomet. Chem*. **1994**, *472*, 39. For structurally related systems see also: J. Christoffers, R. G. Bergman, *Angew. Chem.* **1995**, *107*, 2423; *Angew. Chem., Int. Ed. Engl*. **1995**, *34*, 2266. G. A. Molander, H. Schumann, E. C. E. Rosenthal, J. Demtschuk, *Organometallics* **1996**, *15*, 3817. Y.-X. Chen, P.-F. Fu, C. L. Stern, T. J. Marks, *Organometallics* **1997**, *16*, 5958. B. E. Bosch, G. Erker, R. Fröhlich, O. Meyer, *Organometallics* **1997**, *16*, 5449.

[16] I. D. Williams, S. F. Pedersen, K. B. Sharpless, S. J. Lippard, *J. Am. Chem. Soc.* **1984**, *106*, 6430. M. G. Finn, K. B. Sharpless, in J. D. Morrison (Ed.), *Asymmetric Synthesis*, vol. 5, Academic Press, New York, **1985**, p. 247. S. F. Pedersen, J. C. Dewan, R. R. Eckman, K. B. Sharpless, *J. Am. Chem. Soc.* **1987**, *109*, 1279. P. G. Potvin, P. C. C. Kwong, M. A. Brook, *J. Chem. Soc., Chem. Commun*. **1988**, 773. P. G. Potvin, P. C. C. Kwong, R. Gau, S. Bianchet, *Can. J. Chem*. **1989**, *67*, 1523. D. W. Stephan, *Organometallics* **1990**, *9*, 2718. T. T. Nadiski, D. W. Stephan, *Can. J. Chem.* **1991**, *69*, 167. S. S. Woddard, M. G. Finn, K. B. Sharpless, *J. Am. Chem. Soc.* **1991**, *113*, 106. M. G. Finn, K. B. Sharpless, *J. Am. Chem. Soc.* **1991**, *113*, 113. G. Erker, S. Dehnicke, M. Rump, C. Krüger, S. Werner, M. Nolte, *Angew. Chem*. **1991**, *103*, 1371, *Angew. Chem. Int. Ed. Engl*. **1991**, *30*, 1349. G. Erker, R. Petrenz, C. Krüger, M. Nolte, *J. Organomet. Chem*. **1992**, *431*, 297. G. Erker, R. Petrenz, C. Krüger, F. Lutz, A. Weiß, S. Werner, *Organometallics* **1992**, *11*, 1646. R. Noe, D. Wingbermühle, G. Erker, C. Krüger, J. Bruckmann, *Organometallics* **1993**, *12*, 4993. W. Spaether, M. Rump, G. Erker, R. Fröhlich, J. Hecht, C. Krüger, J. Kuhnigk, *An. Quim. Int. Ed*. **1997**, *93*, 394.

[17] R. Kempe, S. Brenner, P. Arndt, *Z. Anorg. Allg. Chem.* **1995**, *621*, 2021.

[18] For an alternative application of (dialkylamido)zirconium complexes in the preparation of metallocenes and related complexes by a deprotonation route of the neutral Cp-ligand precursors see e.g.: G. Chandra, M. F. Lappert, *J. Chem. Soc. A* **1968**, 1940; A. K. Hughes, A. Meetsma, J. H. Teuben, *Organometallics* **1993**, *12*, 1936; G. M. Diamond, S. Rhodewald, R. F. Jordan, *Organometallics* **1995**, *14*, 5; G. M. Diamond, J. L. Petersen, R. F. Jordan, *Organometallics* **1996**, *15*, 4030. See also ref.[4c].

[19] H. Sinn, W. Kaminsky, *Adv. Organomet. Chem*. **1980**, *18*, 99. R. F. Jordan, *Adv. Organomet. Chem*. **1991**, *32*, 325, and references cited therein.

[20] J. Christoffers, R. G. Bergman, *J. Am. Chem. Soc.* **1996**, *118*, 4715. S. Thiele, G. Erker, *Chem. Ber*. **1997**, *130*, 201, and references cited therein.

[21] S. Braun, H. Kalinowski, S. Berger, in *100 and More Basic NMR Experiments*, VCH, Weinheim, 1996, and references cited therein.

[98050]

New *P,N*-Chelate Ligands Based on Pyridyl-Substituted Phosphaferrocenes

Christian Ganter*, Corinna Glinsböckel, and Beate Ganter

Institut für Anorganische Chemie, Technische Hochschule Aachen,
Prof.-Pirlet-Straße 1, D-52056 Aachen, Germany
Fax: (internat.) + 49(0)241/8888-288
E-mail: christian.ganter@ac.rwth-aachen.de

Received March 24, 1998

Keywords: Chelates / P,N ligands / Phosphaferrocene / Catalysis / Heterocycles

The new pyridyl-substituted phosphaferrocene ligands **3** and **6** are prepared by addition of lithiated pyridine or α-picoline to 2-formyl-3,4-dimethylphosphaferrocene (**1**). The ligands **3** and **6** react with $[Cp^*RuCl]_4$ in THF to give the *P,N*-chelate complexes $[Cp^*RuCl\cdot\mathbf{3}]$ (**9**) and $[Cp^*RuCl\cdot\mathbf{6}]$ (**10**) with high diastereoselectivity. Addition of monodentate ligands like CO or PPh_3 to the complexes leads by displacement of the Ru-bound pyridyl group to the respective carbonyl or phosphane complexes with monodentate *P*-coordinated phospha-ferrocene ligands. Reaction of the ligand **6** with $[(C_3H_5)PdCl]_2$ and NH_4PF_6 gives the seven-membered chelate complex $[(C_3H_5)Pd\cdot\mathbf{6}]PF_6$ (**13**) which was characterized by X-ray diffraction. The ligands **3** and **6** were tested in the palladium-catalyzed asymmetric alkylation of 1,3-diphenylallyl acetate.

Chiral chelate ligands continue to be of interest in coordination chemistry and asymmetric catalysis. Recently, we reported a new concept for chelate ligands with planar chirality based on substituted phosphaferrocenes. Meanwhile, we have prepared a variety of *P,P* and *P,N* compounds comprising, inter alia, those with aminoalkyl, phosphanylalkyl and phosphinite donor substituents attached to the phosphaferrocene nucleus.[1][2] In this contribution we wish to report the syntheses of pyridyl-substituted phosphaferrocenes as well as the coordination behaviour of the new ligands toward transition-metal fragments. Furthermore, preliminary results obtained with the new ligands in the Pd-catalyzed asymmetric alkylation of 1,3-diphenylallyl acetate are reported.

Results

Ligand Synthesis

As depicted in Scheme 1, the synthesis of the pyridyl ligands **3** and **6** can be carried out in one-pot procedures starting from 2-formyl-3,4-dimethylphosphaferrocene (**1**) which has already proven to be a versatile building block for the synthesis of phosphaferrocene ligands before.[1][2] Treatment of the aldehyde **1** with 2-lithiopyridine − prepared in situ from 2-bromopyridine and *n*BuLi − leads to the alcohol **2** (de 83%) which can be deoxygenated with $NaBH_4$ and trifluoroacetic acid to yield the pyridylmethyl ligand **3** as a brown oil which crystallizes on standing. The homologous pyridylethyl ligand **6** with a backbone extended by one CH_2 unit is obtained in an analogous reaction sequence when 2-(lithiomethyl)pyridine − prepared from 2-methylpyridine by deprotonation with *n*BuLi − is employed as the nucleophilic reagent.

If the work-up procedure of the preliminarily formed alcohol **4** (de 60%) is carried out under slightly acidic conditions, the formation of the olefin **5** (as a mixture of *E* and *Z* isomers) is observed by elimination of water. However, the olefin can successfully be transformed into the desired saturated ligand **6** by treatment with $NaBH_4$ and trifluoroacetic acid. The ligands **3** and **6** are obtained in good yield in analytically pure form after chromatography on deactivated alumina and exhibit resonances in the ^{31}P-NMR spectra in the expected range [δ = −77.1 (**3**) and −80.2 (**6**)]. Recently, Mathey and coworkers reported the synthesis of the 2-(2′-pyridyl)phosphaferrocene ligand **8** by combining the [1,5]-sigmatropic rearrangement of the *P*-pyridyl-substituted phosphole **7** with the complexation reaction with $[CpFe(CO)_2]_2$ in a one-pot procedure.[3]

Scheme 1. Preparation of ligands **3** and **6**[a]

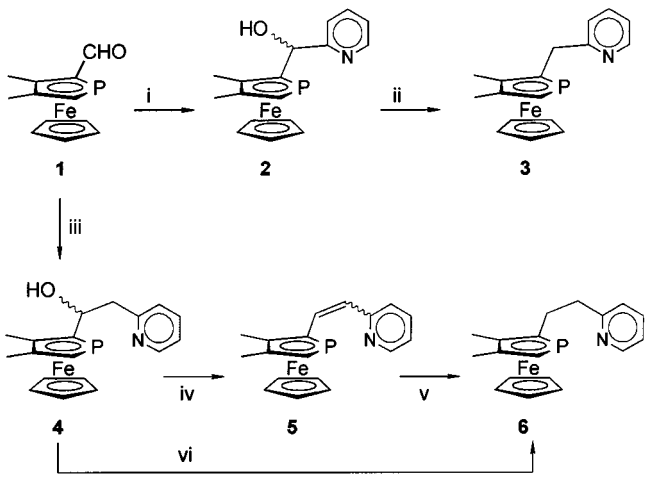

[a] Reagents: i: 2-Lithiopyridine, Et_2O, 55%. − ii: $NaBH_4$, CF_3CO_2H, CH_2Cl_2, 64%. − iii: 2-(lithiomethyl)pyridine, THF, 77%. − iv: Aqueous acidic conditions. − v, vi: $NaBH_4$, CF_3CO_2H, CH_2Cl_2, 80%.

 © WILEY-VCH Verlag GmbH, D-69451 Weinheim, 1998 1434−1948/98/0808−1163 $ 17.50+.50/0

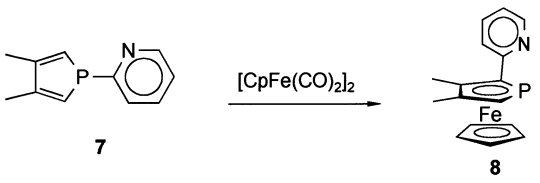

7 8

However, since Mathey's synthesis is carried out under non-stereoselective conditions the racemate of ligand **8** was obtained, whereas our approach allows the synthesis of the enantiomerically pure ligands **3** and **6**, starting from the enantiomerically pure aldehyde **1** which is readily available on a preparative scale.[4]

Complexation Experiments

*Cp*Ru Complexes:* Reaction of the ligands **3** and **6** with appropriate metal fragments should lead to six- and seven-membered chelate complexes, respectively. First, experiments were carried out with $[Cp^*RuCl]_4$ as a source of Cp*RuCl fragments with two vacant coordination sites.[1][5] If the reactants are mixed in a metal-to-ligand ratio of 1:1 in THF the quantitative formation of the anticipated chelate complexes [Cp*RuCl·**3**] (**9**) and [Cp*RuCl·**6**] (**10**) is observed within a few moments by NMR spectroscopy. The complexes **9** and **10** are isolated in analytically pure form as yellow and orange microcrystalline solids in 95 and 93% yield, respectively. In the ^{31}P-NMR spectra a characteristic downfield shift of ca. 95 ppm is observed for the phospholyl P atom on going from the free ligands to the complexes. Whereas the typical reduction of the ^2J(HP) coupling constant for the α-phospholyl proton from 36 Hz to 33 Hz is observed for the complexation of ligand **3**, an unprecedented increase of that coupling constant to 40 Hz was observed for the transformation of the ligand **6** to the complex **10**. The *N*-coordination of the pyridyl group to the Ru centre in that complex leads to a downfield shift for the pyridine 6-H from δ = 8.47 to 9.70. As a result of the chelate formation reaction with the Cp*Ru fragment the Ru atom becomes a stereogenic centre in the complexes. Only one set of signals is observed in the NMR spectra of the six-membered chelate complex **9** indicating the stereoselective formation of only one diastereomer (dr > 99:1). The more flexible seven-membered chelate complex **10** is also formed with high, but significantly decreased selectivity (dr = 95:5). The high diastereoselectivity observed in the reaction of the ligands **3** and **6** with $[Cp^*RuCl]_4$ is in contrast to the findings of Consiglio et al. who observed the formation of almost 1:1 mixtures of diastereomers in the reaction of chiral bidentate *P,P*-chelate ligands with the tetrameric ruthenium complex.[6]

Addition of monodentate ligands such as CO or PPh_3 to THF solutions of the chelate complexes **9** and **10** leads under selective rupture of the Ru−N bond to the formation of the respective carbonyl or PPh_3 complexes **11** and **12** in which the ligands **3** and **6** behave as monodentate *P* ligands (Scheme 2). The reactions were monitored by IR and multinuclear NMR spectroscopy. The diastereomeric ratios of

Scheme 2. Synthesis of complexes

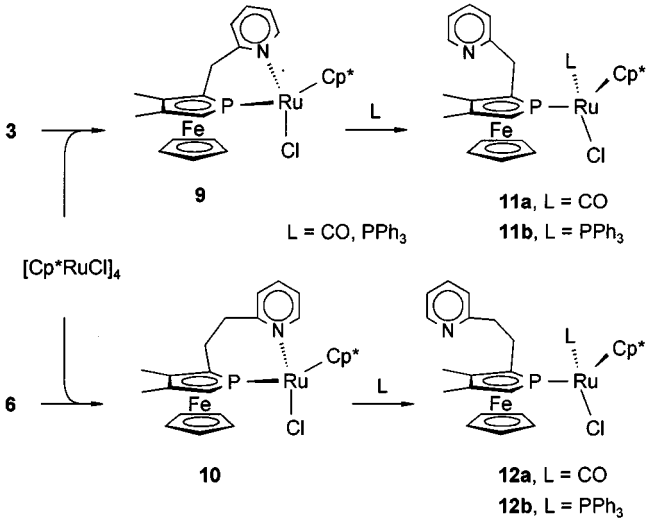

the reaction products are easily obtained from the integrated ^{31}P-NMR spectra. Interestingly, the reactions with CO lead to almost complete epimerization at the Ru centre (dr < 60:40), whereas the additions of PPh_3 proceed with diastereoselectivities of dr = 92:8 and 86:14; thus, the stereochemical integrity is at least partially preserved in the latter case. The carbonyl complex [Cp*RuCl(CO)·**3**] (**11a**) now exhibits a coupling constant of ^2J(HP) = 31 Hz in the expected range and the resonance for the pyridyl 6-H at δ = 8.50 is characteristic for an uncoordinated pyridyl group. The carbonyl C signal appears as a doublet with ^2J(CP) = 36 Hz, comparable to the value reported by Kirchner et al. for the complex $[Cp^*RuCl(CO)(Ph_2PCH_2CH_2NMe_2)]$.[7] In the PPh_3 complexes **11b** and **12b** the resonances of the P nuclei appear as doublets with ^2J(PP) coupling constants in the range of 55 to 68 Hz (see Experimental Section).

(Allyl)palladium Complexes: (Allyl)palladium complexes with *P,N*-chelate ligands have been intensively studied in view of their superior performance in catalytic asymmetric allylic substitutions.[8] The reaction of the ligands **3** and **6** with $[(C_3H_5)PdCl]_2$ in ethanol proceeds smoothely and is accompanied by a color change from orange to deep red. The complexes were precipitated by addition of NH_4PF_6 and isolated by filtration. The complex formed with ligand **3** turned out to be insoluble in common organic solvents which precluded further characterization. We anticipate the formation of a polymeric structure with the ligand **3** acting in a bridging rather than a chelating manner. In contrast, the complex $[(C_3H_5)Pd\cdot\mathbf{6}]PF_6$ (**13**) is soluble in polar solvents and can be recrystallized from ethanol to give orange needles which were suited for X-ray diffraction analysis.

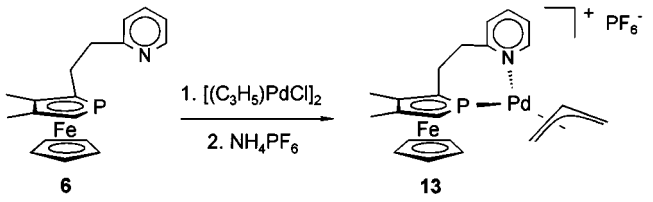

6 13

A PLATON plot of the molecular structure of the cation of complex **13** is depicted in Figure 1, selected bond lenghts and angles are compiled in Table 1. The structure features the typical parameters for a Pd centre in a distorted square-planar coordination geometry with a bite angle P1−Pd−N of 93.6(3)°.

Figure 1. Molecular structure (PLATON) of the cation of complex **13**; hydrogen atoms have been omitted for clarity

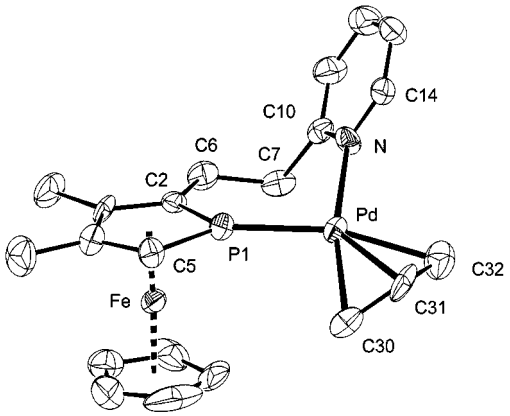

Table 1. Selected bond lengths [A] and angles [°] of complex **13**

Pd−P1	2.274(3)	P1−Pd−N	93.6(3)
Pd−N	2.13(1)	P1−Pd−C30	99.0(5)
Pd−C30	2.12(1)	P1−Pd−C31	134.2(7)
Pd−C31	2.09(1)	N−Pd−C31	130.6(7)
Pd−C32	2.18(2)	N−Pd−C32	99.1(6)
P1−C2	1.75(1)	Pd−P1−C2	126.7(5)
P1−C5	1.71(1)	Pd−P1−C5	141.2(5)
C30−C31	1.39(2)	C2−P1−C5	91.4(7)
C31−C32	1.34(2)	C10−N−C14	120(1)
N−C10	1.33(2)	Pd−C30−C31	69.5(8)
N−C14	1.34(2)	Pd−C32−C31	68(1)
C2−C3	1.41(2)	C30−C31−C32	123(2)
C4−C5	1.39(2)		

As is usually observed for palladium complexes with *P,N* ligands the distance Pd−P1 [2.274(3) A] is significantly longer than the corresponding bond to the nitrogen donor [Pd−N: 2.13(1) A], although the differences tend to be more pronounced for *P,N* ligands with phosphane donor groups.[9][10] The high π-acceptor character of the phospholyl P atom leads to the rather short Pd−P distance. This π acidity has another consequence involving the Pd−C bond lenghts: the distances Pd−C30 [2.12(1) A] and Pd−C32 [2.18(2) A] are not very different if compared to (allyl)Pd complexes with softer *P* donors, where the Pd−C bond *trans* to the phosphorus atom is often found to be roughly 10 pm longer than the Pd−C bond *trans* to the sp^2 nitrogen donor atom.[9][10] The allyl ligand adopts an almost symmetrical orientation with respect to the coordination plane of the palladium centre as is evident from the virtually identical angles between the plane (P1,Pd,N) and the planes (Pd,C30,C31) (27.8°) and (Pd,C31,C32) (28.4°), respectively. In contrast, a pronounced rotation of the 1,3-diphenylallyl moiety about the (allyl)Pd axis by ca. 15−20° was observed in complexes with ferrocene-derived *P,N* ligands.[9] This rotation seems to be the consequence of the sterically more demanding 1,3-diphenyl substitution on the allyl ligand. In complex **13** the Pd−P1 vector is only slightly tilted out of the phospholyl mean plane away from the CpFe fragment [tilt angle: 3.7(4)°]. The coordination plane about the Pd atom forms an angle with the allyl plane of 112.3(9)°.

The ^{31}P-NMR spectrum of complex **13** shows one broad signal (δ = −42.6) at room temperature. On cooling to −20°C four baseline-separated signals are observed in the range from δ = −39 to −44 in the ratio of 15:16:39:30. We assume, that these signals are due to the presence of two isomers with *exo* and *endo* orientation of the allyl ligand, which both exist in two different chelate ring conformations. Such conformational isomers of seven-membered (allyl)Pd-*P,N*-chelate complexes have been observed by Togni et al.[9b]

Reaction of the pyridine ligand **6** with $[(1,3\text{-}Ph_2C_3H_3)PdCl]_2$ under the same conditions as above leads to the analogous chelate complex **14** with a (diphenylallyl)palladium fragment which was recrystallized from CH_2Cl_2/hexane. At room temperature 3 broad signals are found in the ^{31}P-NMR spectrum in CD_2Cl_2, which split into 4 resonances at −20°C. Obviously, the activation enthalpy for the dynamic interconversion of the isomers is higher in the 1,3-diphenylallyl case.

Preliminary experiments were carried out with ligands **3** and **6** to test their applicability in asymmetric allylic substitutions. 1,3-Diphenylallyl acetate was treated with sodium malonate as *C*-nucleophile in the presence of $[(C_3H_5)PdCl]_2$ and the enantiomerically pure ligands **3** or **6** (5 mol-%) in THF. The substitution reaction is complete after 3 h at room temperature and the product **15** was isolated in 65−80% yield. However, the enantiomeric purity was only 19 and 11%, respectively.

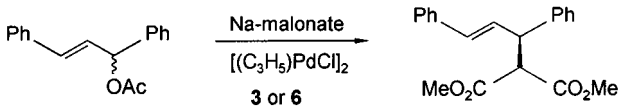

15

We are currently modifying the ligands in order to obtain higher selectivity in catalysis. Furthermore, we are looking for other catalytic reactions for which the ligand type described here might be better suited.

Support of this work by the *Deutsche Forschungsgemeinschaft* (SFB 380) is greatfully acknowledged.

Experimental Section

General: All manipulations were carried out under dry N_2 in Schlenk glassware. Solvents were dried and purified by standard methods and were stored under N_2. − NMR: Varian Unity 500 (499.843 MHz, ^{1}H, int. TMS; 125.639 MHz, ^{13}C{^{1}H}, APT, int. TMS; 202.265 MHz, ^{31}P{^{1}H}, ext. 85% H_3PO_4). − MS: Finnigan MAT 95. − Elemental analysis (C, H, N): Carlo-Erba elemental analyzer, Modell 1106. − IR: Perkin-Elmer 1720 X FTIR. − 2-Formyl-3,4-dimethylphosphaferrocene (**1**),[11] $[Cp^*RuCl]_4$,[5] $[(C_3H_5)PdCl]_2$[12] and di-μ-chlorobis(1,3-diphenyl-π-allyl)dipalladium[13] were prepared as described in the literature.

(3,4-Dimethylphosphaferrocene-2-yl)(pyridin-2-yl)methanol (**2**): 2-Bromopyridine (0.83 ml, 8.71 mmol) was dissolved in 5 ml of Et_2O, cooled to −78°C and *n*BuLi (5.4 ml of a 1.6 M solution in hexane, 8.71 mmol) was added. After stirring for 30 min at −78°C, a solution of 2-formyl-3,4-dimethylphosphaferrocene (**1**) (1.75 g, 6.3 mmol) in 10 ml Et_2O was added, the cooling bath was removed and the mixture was stirred for additional 3 h. The reaction was quenched by 10 ml of H_2O and the phases were seperated. The aqueous phase was washed twice with Et_2O, the combined organic phases were washed with H_2O and brine and dried with Na_2SO_4. Filtration and concentration gave the crude product as a brown oil which was further purified by chromatography on alumina (eluent: THF). **2** was isolated as brown crystals (1.25 g, 3.5 mmol, 55%) after removal of the solvent in vacuo, de 83%. − ^{1}H NMR ($CDCl_3$, major isomer): δ = 2.21 (s, 3 H, CH_3), 2.28 (s, 3 H, CH_3), 3.77 (d, $^2J_{PH}$ = 36 Hz, 1 H, α-C*H*), 4.17 (s, 1 H, O*H*), 4.29 (s, 5 H, Cp), 5.43 (br. s, 1 H, C*H*OH), 7.30−8.60 (4 H, pydidine H). − ^{13}C NMR ($CDCl_3$, major isomer): δ = 14.4 (s, 1 C, *C*H_3), 16.6 (s, 1 C, *C*H_3), 72.1 (s, 5 C, Cp), 73.2 (d, *J* = 12.5 Hz, 1 C, *C*HOH), 76.4 (d, *J* = 59.1 Hz, 1 C, α-*C*H), 92.6 (s, 1 C, *C*CH_3), 96.3 (s, 1 C, *C*CH_3), 104.9 (d, *J* = 57.6 Hz, 1 C, α-*C*CHOH), 120.7 (s, 1 C, *C*H), 122.2 (s, 1 C, *C*H), 136.4 (s, 1 C, *C*H), 147.8 (s, 1 C, N*C*H), 162.3 (s, 1 C, N*C*CHOH). − ^{31}P NMR ($CDCl_3$): δ = −86.1 (major isomer), −77.9 (minor isomer). − MS (70 eV); *m*/*z* (%): 339.0 (100) [M^+], 322.8 (10) [$(M - O)^+$], 274.1 (45) [$(M - Cp)^+$], 232.0 (20) [$(M - CHOHC_5H_4N)^+$]. − $C_{17}H_{18}{}^{56}$FeNOP (339.3): calcd. C 339.047539; found 339.047502 (HRMS).

2-[(3,4-Dimethylphosphaferrocene-2-yl)methyl]pyridine (**3**): 5 ml of CF_3COOH was cooled to 0°C and 1/2 of an $NaBH_4$ tablet was added. A solution of **2** (0.52 g, 1.48 mmol) in 10 ml of CH_2Cl_2 was slowly added and the reaction mixture was stirred over night at room temp. Solvents were evaporated in vacuo and 10 ml of H_2O and 10 ml of CH_2Cl_2 were added. Phases were separated, the aqueous phase was washed twice with CH_2Cl_2, the combined organic layers were washed with water and brine and dried with Na_2SO_4. Filtation and evaporation of the solvent gave the crude product. Chromatography on alumina with hexane/Et_2O (4:1) as eluent gave **3** (0.32 g, 0.95 mmol, 64%) as brown oil, which crystallized within 24 h. − ^{1}H NMR ($CDCl_3$): δ = 2.11 (s, 3 H, CH_3), 2.18 (s, 3 H, CH_3), 3.70 (m, 2 H, CH_2), 3.73 (d, *J* = 36.0 Hz, 1 H, α-C*H*), 4.14 (s, 5 H, Cp), 7.05 (m, 2 H, C*H*), 7.51(m, 1 H, C*H*), 8.47 (br. s, 1 H, NC*H*). − ^{13}C NMR ($CDCl_3$): δ = 13.7 (s, 1 C, *C*H_3), 16.9 (s, 1 C, *C*H_3), 39.9 (d, *J* = 6.0 Hz, 1 C, *C*H_2), 72.1 (s, 5 C, Cp), 76.0 (d, *J* = 57.0 Hz, 1 C, α-*C*H), 93.7 (d, *J* = 3.9 Hz, 1 C, *C*CH_3), 95.8 (d, *J* = 6.8 Hz, 1 C, *C*CH_3), 96.3 (d, *J* = 57.4 Hz, 1 C, α-*C*CH_2), 121.2 (s, 1 C, CH), 122.6 (s, 1 C, *C*H), 136.1 (s, 1 C, *C*H), 148.7 (s, 1 C, N*C*H), 161.6 (s, 1 C, N*C*CH_2). − ^{31}P NMR ($CDCl_3$): δ = −77.1 . − MS (70 eV); *m*/*z* (%): 322.9 (100) [M^+], 258.0 (60) [$(M - Cp)^+$]. − $C_{17}H_{18}$FeNP (323.2): calcd. C 63.18, H 5.61, N 4.33; found C 62.93, H 5.71, N 4.28.

1-(3,4-Dimethylphosphaferrocene-2-yl)-2-(pyridin-2-yl)ethanol (**4**): To a solution of α-picoline (0.72 ml, 7.27 mmol) in 10 ml of THF at −40°C was added a solution of *n*BuLi in hexane (4.5 ml, 1.6 M solution of *n*BuLi, 1.51 mmol). After warming up to room temp. and stirring for 15 min, the orange solution was again cooled to −40°C and 2-formyl-3,4-dimethylphosphaferrocene (**1**) (1.27 g, 4.85 mmol), dissolved in 10 ml of THF, was added. The reaction mixture was stirred at room temp. for 3 h, then 10 ml of H_2O was added and the organic solvent was evaporated in vacuo. After addition of 10 ml of CH_2Cl_2, the phases were separated, the aqueous phase was extracted twice with CH_2Cl_2, the combined organic phases were washed with water and brine and dried with Na_2SO_4. Filtration and evaporation of the solvent yielded the crude product which was further purified by chomatography on alumina. Elution with Et_2O/THF (1:1) and evaporation of solvents gave **3** (1.32 g, 3.73 mmol, 77%) as orange powder, de 60%. − ^{1}H NMR ($CDCl_3$, major isomer): δ = 2.12 (s, 3 H, CH_3), 2.19 (s, 3 H, CH_3), 2.80−3.00 (m, 2 H, CH_2), 3.70 (d, *J* = 36.6 Hz, 1 H, α-C*H*), 4.19 (s, 5 H, Cp), 4.57 (s, 1 H, O*H*), 4.68 (m, 1 H, C*H*OH), 7.10−7.60 (m, 3 H, C*H*), 8.50 (d, *J* = 4.9 Hz, 1 H, NC*H*). − ^{13}C NMR ($CDCl_3$, major isomer): δ =.13.9 (s, 1 C, *C*H_3), 16.6 (s, 1 C, *C*H_3), 47.1 (s, 1 C, *C*H_2), 71.6 (d, *J* = 12,0 Hz, 1 C, *C*HOH), 72.0 (s, 5 C, Cp), 75.5 (d, *J* = 60.0 Hz, 1 C, α-*C*H), 91.7 (s, 1 C, *C*CH_3), 96.2 (s, 1 C, *C*CH_3), 105.5 (d, *J* = 60.6 Hz,1 C, α-*C*CHOH), 121.7 (s, 1 C, *C*H), 124.2 (s, 1 C, *C*H), 136.4 (s, 1 C, *C*H), 148.4 (s, 1 C, N*C*H), 159.5 (s, 1 C, N*C*CH_2). − ^{31}P NMR ($CDCl_3$): δ = −86.5 (major isomer), −85.0 (minor isomer). − MS (70 eV); *m*/*z* (%): 353.1 (50) [M^+], 335.2 (55) [$(M - H_2O)^+$], 232 (70) [$(M - CHOHCH_2C_5H_4N)^+$]. − $C_{18}H_{20}$FeNOP (353.2): calcd. C 61.21, H 5.71, N 3.96; found C 61.53, H 6.12, N 4.14.

2-[(3,4-Dimethylphosphaferrocene-2-yl)ethyl]pyridine (**6**): **4** (1.32 g, 3.72 mmol) was treated as described above for the preparation of **3**. The product **6** (0.98 g, 2.91 mmol, 80%) was isolated as a brown oil. − ^{1}H NMR ($CDCl_3$): δ = 2.10 (s, 3 H, CH_3), 2.18 (s, 3 H, CH_3), 2.58 (m, 2 H, CH_2), 2.87 (m, 2 H, CH_2). 3.67 (d, *J* = 35.7 Hz, 1 H, α-C*H*), 4.07 (s, 5 H, Cp), 7.10 (m, 2 H, C*H*), 7.55 (m 1 H, C*H*), 8.55 (s, 1 H, NC*H*). − ^{13}C NMR ($CDCl_3$): δ = 13.4 (s, 1 C, *C*H_3), 16.8 (s, 1 C, *C*H_3), 31.0 (s, 1 C, *C*H_2), 41.2 (s, 1 C, *C*H_2), 71.8 (s, 5 C, Cp), 75.3 (d, *J* = 58.7 Hz, 1 C, α-*C*H), 93.0 (s, 1 C, *C*CH_3), 95.4 (s, 1 C, *C*CH_3), 99.1 (d, *J* = 58.6 Hz, 1 C, α-*C*CH_2), 121.0 (s, 1 C, *C*H), 123.0 (s, 1 C, *C*H), 136 (s, 1 C, *C*H), 149.1 (s, 1 C, N*C*H), 161.5 (s, 1 C, N*C*CH_2). − ^{31}P NMR ($CDCl_3$): δ = −80.2 . − MS (70 eV); *m*/*z* (%): 337.2 (100) [M^+], 272.3 (60) [$(M - Cp)^+$], 245.1 (20) [$(M - CH_2C_5H_4N)^+$]. − $C_{18}H_{20}$FeNP (337.2): calcd. C 64.12, H 5.98, N 4.15; found C 63.46, H 5.87, N 4.01.

*[Cp*RuCl·**3**]* (**9**): **3** (38,0 mg, 0.12 mmol) was dissolved in 3 ml of THF and added to a suspension of $[Cp^*RuCl]_4$ (31.9 mg, 0.029 mmol) in 2 ml of THF. The resulting clear red solution was stirred for 30 min, filtered and the solvent was evaporated. The yellow powder was washed with a small portion of hexane and dried in vacuo to give spectroscopically pure **9** (67.8 mg, 0.11 mmol, 95%), dr > 99:1. − ^{1}H NMR ([D_8]THF): δ = 1.53 (d, *J* = 2.9 Hz, 15 H, Cp*), 2.20 (s, 3 H, CH_3), 2.22 (s, 3 H, CH_3), 3.38 (m, 2 H, CH_2), 3.58 (d, *J* = 40 Hz, 1 H, α-C*H*), 3.79 (s, 5 H, Cp), 7.10 (m, 1 H, C*H*), 7.18 (m, 1 H, C*H*), 7.59 (m, 1 H, C*H*), 9.70 (d, *J* = 4.9 Hz, 1 H, NC*H*). − ^{13}C NMR ([D_8]THF): δ = 8.5 (s, 5 C, *C*H_3-Cp*), 11.5 (s, 1 C, *C*H_3), 14.9 (s, 1 C, *C*H_3), 36.3 (d, *J* = 13.8 Hz, 1 C, *C*H_2), 65.1 (d, *J* = 30 Hz, 1 C, α-*C*H), 71.0 (s, 5 C, Cp), 79.6 (s, 1 C, *C*CH_3), 81.2 (d, *J* = 3.1 Hz, 5 C, *C*CH_3-Cp*), 87.5 (d, *J* = 35 Hz, 1 C, α-*C*CH_2), 120.1 (s, 1 C, *C*H), 123.9 (s, 1 C, *C*H), 134.5 (s, 1 C, *C*H), 158.2 (s, 1 C, N*C*H), 162.1 (d, *J* = 4.9 Hz, 1 C, N*C*CH_2). − ^{31}P NMR ([D_8]THF): δ = 14.9 . − SIMS (70 eV); *m*/*z* (%): 560.3 (100) [$(M - Cl)^+$]. − $C_{27}H_{33}$ClFeNPRu (594.9): calcd. C 54.51, H 5.59, N 2.35; found C 54.57, H 5.74, N 2.36.

*[Cp*RuCl·**6**]* (**10**): **6** (56.2 mg, 0.16 mmol) was dissolved in 3 ml of THF and added to a suspension of $[Cp^*RuCl]_4$ (45.2 mg, 0.041 mmol) in 2 ml of THF. The resulting clear red solution was stirred for 30 min, filtered and the solvent was evaporated. The orange powder was washed with a small portion of hexane and dried in vacuo to give spectroscopically pure **10** (94.4 mg, 0.15 mmol, 93%). dr = 95:5. − ^{1}H NMR ([D_8]THF, major isomer): δ = 1.56 (d, *J* = 2.64 Hz, 15 H, Cp*), 2.09 (s, 3 H, CH_3), 2.15 (s, 3 H, CH_3), 2.90 (m, 2 H, CH_2), 3.10 (m, 2 H, CH_2), 3.43 (d, *J* = 33 Hz, 1 H, α-C*H*), 3.62 (s, 5 C, Cp), 7.09 (m, 1 H, C*H*), 7.32 (m, 1 H, C*H*), 7.64

(m, 1 H, C*H*), 9.80 (d, J = 5.18 Hz, 1 H, NC*H*). − ^{13}C NMR ([D$_8$]THF, major isomer): δ = 10.3 (s, 5 C, *C*H$_3$-Cp*), 13.3 (d, J = 3.0 Hz, 1 C, *C*H$_3$), 16.8 (d, J = 3.2 Hz, 1 C, *C*H$_3$), 33.3 (d, J = 12.4 Hz, 1 C, *C*H$_2$), 39.3 (d, J = 13.2 Hz, 1 C, *C*H$_2$), 67.6 (d, J = 22.0 Hz, 1C, α-CH), 73.9 (s, 5 C, Cp), 83.1 (d, J = 3.0 Hz, 5 C, *C*CH$_3$-Cp*), 87.0 (d, J = 11.2 Hz, 1 C, α*C*), 88.5 (s, 1 C, *C*CH$_3$), 91.1 (s, 1 C, *C*CH$_3$), 121.9 (s, 1 C, *C*H), 124.2 (s, 1 C, *C*H), 136.3 (s, 1 C, *C*H), 158.2 (s, 1 C, N*C*H), 168.8 (s, 1 C, N*C*CH$_2$). − ^{31}P NMR ([D$_8$]THF): δ = 17.5 (major isomer), 21.8 (minor isomer). − MS (70 eV); *m*/*z* (%): 609.6 (1) [M$^+$], 544.3 (2) [(M − Cp)$^+$], 337.3 (100) [**5**$^+$]. − $C_{28}H_{35}ClFeNPRu$ (608.9): calcd. C 55.23, H 5.79, N 2.30; found C 55.21, H 5.98, N 2.18.

NMR Experiments: For the substitution reaction of the pyridine moiety with CO about 30 mg of the complex [Cp*RuCl·**3**/**6**] was prepared in situ by dissolving ligand **3** or **6** and [Cp*RuCl]$_4$ in [D$_8$]THF. Purity was proven by NMR and 10 ml of CO was bubbled through the solution by syringe. Then the NMR spectra were recorded. For the substitution with triphenylphosphane, the complexes **9** and **10** were prepared as described and the stoichiometric amount of PPh_3 was added. The resulting clear red solution was analyzed by NMR spectroscopy.

*[Cp*RuCl(CO)·**3**]* (**11a**): dr = 50:50. − ^{1}H NMR ([D$_8$]THF): δ = 1.64 (br. s, 15 H, Cp*), 2.20 (br. s, 6 H, C*H*$_3$), 3.46 (d, J = 30.5 Hz, 1 H, α-C*H*, isomer I), 3.70 (d, J = 30.8 Hz, 1 H, α-C*H*, isomer II), 3.84 (br. s, 2 H, C*H*$_2$), 4.31 (s, 5 H, Cp), 7.07 (br. s, 2 H, C*H*), 7.49 (br. s, 1 H, C*H*), 8.49 (s, 1 H, NC*H*). − ^{13}C NMR ([D$_8$]THF): δ = 9.7 (d, J = 5.8 Hz, 5 C, C*C*H$_3$-Cp*), 13.8 (s, 1 C, *C*H$_3$), 16.4 (s, 1 C, *C*H$_3$), 37.5 (s, 1 C, *C*H$_2$), 74.0 + 74.1 (s, 1 C, Cp), 85.2 (s, 1 C, *C*CH$_3$), 88.1 (s, 1 C, *C*CH$_3$), 91.5 (d, J = 47.8 Hz, 1 C, α-*C*CH$_2$), 96.1 (s, 5 C, *C*CH$_3$-Cp*), 122.0 (br. s, 2 C, *C*H), 135.7 (br. s, 1 C, *C*H), 148.5 (br. s, 1 C, N*C*H), 162.0 (br. s, 1 C, N*C*CH$_2$), 203.7 (d, J = 36 Hz, 1 C, *C*O). − ^{31}P NMR ([D$_8$]THF): δ = 10.3 (isomer I), 22.0 (isomer II). − IR ([D$_8$]THF): ν = 1940 cm^{-1}.

*[Cp*RuCl(CO)·**6**]* (**12a**): dr = 60:40. − ^{1}H NMR ([D$_8$]THF): δ = 1.81 (d, J = 2.8 Hz, 15 H, Cp*), 2.00−2.20 (br. s, 6 H, C*H*$_3$), 2.60−3.00 (br. m, 4 H, C*H*$_2$), 3.43 and 3.52 (d, J = 32 Hz, 1 C, α-C*H*), 4.18 and 4.25 (s, 5 H, Cp), 7.00−7.60 (br. m, 3 H, C*H*), 8.46 (br. s, 1 H, NC*H*). − ^{13}C NMR ([D$_8$]THF): δ = 10.0 (d, J = 4.1 Hz, 5 C, C*C*H$_3$-Cp*), 13.4 (s, 1 C, *C*H$_3$), 16.5 (s, 1 C, *C*H$_3$), 30.0 (d, J = 14.8 Hz, 1 C, *C*H$_2$), 41.5 (br. s, 1 C, *C*H$_2$), 73.9 (s, 5 C, Cp), 91.2 (d, J = 55 8 Hz, 1 C, *C*CH$_3$) 96.2 (s, 5 C, *C*CH$_3$-Cp*), 121.0 (s, 1 C, *C*H), 123.5 (s, 1 C, *C*H), 136.4 (s, 1 C, *C*H), 148.5 (s, 1 C, N*C*H), 163.0 (s, 1 C, N*C*CH$_2$), 204.0 (d, J = 26 Hz, 1 C, *C*O). − ^{31}P NMR ([D$_8$]THF): δ = 9.7 (major isomer), 18.8 (minor isomer). − IR ([D$_8$]THF): ν = 1940 cm^{-1}.

*[Cp*RuCl(PPh$_3$)·**3**]* (**11b**): dr = 92:8. − ^{1}H NMR ([D$_8$]THF, major isomer): δ = 1.22 (d/d, 15 H, Cp*), 2.16 (s, 3 H, C*H*$_3$), 2.27 (s, 3 H, C*H*$_3$), 2.53 (br. s, 2H, CH$_2$), 3.03 (d, J = 29.6 Hz, 1 H, α-C*H*), 3.46 (s, 5 H, Cp), 7.00−7.80 (m, 18 H, aromatic H), 8.40 (br. s, 1 H, NC*H*). − ^{31}P NMR ([D$_8$]THF): major isomer: δ = 21.6 (d, ^3J = 65.9 Hz, cycl. P), 51.7 (d, J = 65.9 Hz, PPh$_3$); minor isomer: δ = 28.0 (d, J = 51.3 Hz, cycl. P), 48.6 (d, J = 51.3 Hz, PPh$_3$).

*[Cp*RuCl(PPh$_3$)·**6**]* (**12b**): dr = 86:14. − ^{1}H NMR ([D$_8$]THF, major isomer): δ = 1.29 (d/d, 15 H, Cp*), 2.22 (s, 3 H, C*H*$_3$), 2.25 (s, 3 H, C*H*$_3$), 2.50−3.20 (m, 4 H, C*H*$_2$), 3.51 (s, 5 H, Cp), 7.00−8.00 (m, 18 H, aromatic H), 8.40 (d, 1 H, NC*H*). − ^{31}P NMR ([D$_8$]THF): major isomer: δ = 18.5 (d, J = 67.8 Hz, cycl. P), 51.8 (d, J = 67.8 Hz, PPh$_3$); minor isomer: δ = 29.3 (d, J = 55.0 Hz, cycl. P), 50.5 (d, J = 55.0 Hz, PPh$_3$).

*[(C$_3$H$_5$)Pd·**6**][PF$_6$]* (**13**): [(C$_3$H$_5$)PdCl]$_2$ (28.2 mg, 0,077 mmol) was suspended in 10 ml of EtOH and **6**, (52.0 mg, 0.154 mmol) dissolved in 10 ml of EtOH, was added and the mixture was stirred for 30 min. The clear orange-red solution was treated with NH_4PF_6 (25.1 mg, 0.154 mmol) and cooled to 0°C until an orange precipitate formed. The orange powder was filtered off, washed with EtOH and dried in vacuo. Recrystallization from hot EtOH gave pure **13** (85.3 mg, 88%) as orange needles. − ^{1}H NMR (CD_2Cl_2, room temp.): δ = 2.14 (s, 3 H, C*H*$_3$), 2.20 (s, 3 H, C*H*$_3$), 2.75 (m, 2 H, C*H*$_2$), 3.15−3.25 (m, 2 H, C*H*$_2$), 3.40 (br. m, 1 H, allyl-H), 3.86 (s, 5 H, Cp), 3.9−4.2 (br. m, 2 H, allyl-H), 5.08 (br. m, 1 H, allyl-H), 6.05 (2 br. m, 1 H, 2-allyl-H), 7.45 (s, 1 H, C*H*), 7.61 (s, 1 H, C*H*), 7.97 (s, 1 H, C*H*), 8.71 (s, 1 H, NC*H*). − ^{13}C NMR (CD_2Cl_2, room temp.): δ = 13.5 (s, 1 C, *C*H$_3$), 16.5 (s, 1 C, *C*H$_3$), 32.0 (s, 1 C, *C*H$_2$), 39.5 (s, 1 C, *C*H$_2$), 56.7 (d, J = 57.0 Hz, 1 C, α-*C*H), 74.3 (s, 5 C, Cp), 83.0 (d, J = 30.1 Hz, 1 C, allyl-C), 83.6 (d, J = 32.7 Hz, 1 C, allyl-C), 120.8 (d, J = 19.7 Hz, 1 C, 2-allyl-C), 124.5 (s, 1 C, *C*H), 126.8 (s, 1 C, *C*H), 140.0 (s, 1 C, *C*H), 152.7 (s, 1 C, N*C*H), 165.0 (s, 1 C, N*C*CH$_2$). − ^{31}P NMR (CD_2Cl_2), room temp.: δ = −42.6 (br. s, cycl. P), −144.7 (sept, J = 708 Hz, PF_6), −20°C: δ = −43.6, −42.9, −40.6, −39.5 (30:39:16:15) (cycl. P). − SIMS (70 eV); *m*/*z* (%): 483.3 (5) [(M − PF_6)$^+$], 338.3 (100) [(**5** + H)$^+$]. − $C_{21}H_{25}F_6FeNP_2Pd$ (629.6): calcd. C 40.03, H 3.97, N 2.22; found C 39.67, H 3.87, N 2.24.

*[(C$_{13}$H$_{13}$)Pd·**6**][PF$_6$]* (**14**): The complex was prepared from [(C$_{13}$H$_{13}$)PdCl]$_2$ as described above for **13**. Recrystallisation from CH_2Cl_2/hexane (1:1) afforded orange-red crystals in 54% yield. − ^{1}H NMR (CD_2Cl_2, −20°C): δ = 1.93 (s, 3 H, C*H*$_3$), 2.03 (s, 3 H, C*H*$_3$), 2.35−2.44 (m, 2 H, C*H*$_2$), 2.78−2.91 (m, 2 H, C*H*$_2$), 3.34−3.53 (m, 1 H, α-C*H*), 3.50−4.25 (4 s, 5 H, Cp), 5.40 (2 d, 1 H, 2-allyl-H), 5.84−5.95 (m, 1 H, allylic H), 6.79−7.07 (m, 1 H, allylic H), 7.30−7.80 (m, 14 H, aromatic H). − ^{13}C NMR (CD_2Cl_2, +23°C): δ = 13.4 (s, 1 C, *C*H$_3$), 16.6 (s, 1 C, *C*H$_3$), 32.2 (s, 1 C, *C*H$_2$), 38.7 (s, 1 C, *C*H$_2$), 63.4 (br. m, 1 C, α-*C*H), 73.5−76.7 (4 s, 5 C, Cp), 93.8 (m, 3 C, quat. phospholyl-C), 97.0 (d, J = 26.3 Hz, 1 C, allylic C), 109.5 (d, J = 7.2 Hz, 1 C, allylic C), 110.4 (br. s, 1 C, allylic C), 124.3−130.2 (m, 13 C, aromatic C), 138.2−139.4 (m, 3 C, aromatic *ipso*-C), 150.4 (s, 1 C, N*C*H), 164.5 (s, 1 C, N*C*CH$_2$). − ^{31}P NMR (CD_2Cl_2, +24°C): δ = −19.7, −29.4, −37.1 (8:42:50), (3 br. s, 1 P, cycl. P), −144.6 (sept, J = 708 Hz, 1 P, PF_6), (CD_2Cl_2, −20°C): δ = −18.8, −28.8, −36.4, −38.0 (7:46:38:8), (4 s, 1 P, cycl. P), 144.6 (sept, J = 708 Hz, PF_6). − SIMS (70 eV); *m*/*z* (%): 636.5 (4)[(M − PF_6)$^+$], 338.3 (100) [(**5** + H)$^+$]. − $C_{33}H_{33}F_6FeNP_2Pd \cdot 0.5\ CH_2Cl_2$ (824.3): calcd. C 48.85, H 4.13, N 1.70; found C 48.80, H 4.24, N 1.77.

General Procedure for the Catalytic Allylic Alkylation: [(C$_3$H$_5$)PdCl]$_2$ (0.012 mmol, 4.6 mg), the ligand (**3** or **6**, 0.025 mmol) and 1,3-diphenyl-2-propenyl acetate (126.1 mg, 0.5 mmol) were dissolved in 5 ml of THF to give a clear orange solution. NaH (24 mg, 1.0 mmol) and dimethyl malonate (132.1 mg, 1 mmol) were dissolved in 5 ml of THF and added to the orange solution by syringe. The solution was stirred for 13−19 h, then 1 ml of acetic acid was added and the solvent was removed in vacuo. 10 ml of water was added to the mixture, followed by extraction with Et_2O. Then the organic layers were washed with water and brine, dried with Na_2SO_4 and the solvent was removed in vacuo. The resulting yellow oil was further purified by chromatography on silica gel with hexane/ethyl acetate (5:1) to yield pure product **15**. The enantiomeric excess of **15** was determined by polarimetry, the NMR data are consistent with those reported in the literature.[14]

X-ray Structural Analysis of **13**: $C_{21}H_{25}F_6FeNP_2Pd$, M = 629.63 g mol^{-1}, orthorhombic space group *Pna*2$_1$ (no. 33), a = 8.978(1), b = 29.010(4), c = 9.102(2) A, V = 2370(1) A^3, Z = 4, $d_{calcd.}$ = 1.76 g cm^{-3}, μ(Mo-K_α) = 15.49 cm^{-1}, F(000) = 1256. ENRAF-

Nonius CAD4, ω-2θ scan, Mo-K_α radiation (0.71073 Å), graphite monochromator, 7865 reflections at 298 K with $2° \leq \theta \leq 30°$, crystal size 0.04 × 0.30 × 0.60 mm. Structure solution with Patterson methods. Refinement[15] with anisotropic thermal parameters for all non-hydrogen atoms converged at $R = 0.067$, $R_w = 0.049$ for 288 parameters and 2609 independent observations with $I > 1.5\ \sigma(I)$. Hydrogen atoms were treated as riding atoms. A final difference Fourier synthesis showed a residual density of 2.31 (0.51 Å from Pd)/−0.62 eA^{-3}. Crystallographic data (excluding structure factors) for the structure reported in this paper have been deposited with the Cambridge Crystallographic Data Centre as supplementary publication no. CCDC-101282. Copies of the data can be obtained free of charge on application to CCDC, 12 Union Road, Cambridge CB2 1EZ (Fax: int. code + 1223/336-033; E-mail: deposit@ccdc.cam.ac.uk).

[1] C. Ganter, L. Brassat, C. Glinsböckel, B. Ganter, *Organometallics* **1997**, *16*, 2862−2867.
[2] C. Ganter, L. Brassat, B. Ganter, *Chem. Ber.* **1997**, *130*, 1771−1776.
[3] B. Deschamps, L. Ricard, F. Mathey, *J. Organomet. Chem.* **1997**, *548*, 17−22.
[4] C. Ganter, L. Brassat, B. Ganter, *Tetrahedron: Asymmetry* **1997**, *8*, 2607−2611.
[5] P. J. Fagan, W. S. Mahoney, J. C. Calabrese, I. D. Williams, *Organometallics* **1990**, *9*, 1843−1852.
[6] [6a] F. Morandini, G. Consiglio, B. Straub, G. Ciani, A. Sironi, A. *J. Chem. Soc., Dalton Trans.* **1983**, 2293−2298. − [6b] G. Consiglio, F. Morandini, *Chem. Rev.* **1987**, *87*, 761−778. − [6c] G. Consiglio, F. Morandini, F. Bangerter, *Inorg. Chem.* **1982**, *21*, 455−457. − [6d] See also: C. White, E. Cesarotti, *J. Organomet. Chem.* **1985**, *287*, 123.
[7] K. Mauthner, C. Slugovc, K. Mereiter, R. Schmid, K. Kirchner, *Organometallics* **1997**, *16*, 1956−1961.
[8] For leading reviews on asymmetric allylic substitutions see for example: [8a] B.Trost, D. L. Van Vranken, *Chem. Rev.* **1996**, *96*, 395−422. − [8b] G. Consiglio, R. M. Waymouth, *Chem. Rev.* **1989**, *89*, 257−276.
[9] [9a] A. Togni, U. Burckhardt, V. Gramlich, P. S. Pregosin, R. Salzmann, *J. Am. Chem. Soc.* **1996**, *118*, 1031−1037. − [9b] U. Burckhardt, V. Gramlich, P. Hofmann, R. Nesper, P. S. Pregosin, R. Salzmann, A. Togni, *Organometallics* **1996**, *15*, 3496−3503. − [9c] P. E. Blöchl, A. Togni, *Organometallics* **1996**, *15*, 4125−4132.
[10] N. Baltzer, L. Macko, S. Schaffner, M. Zehnder, *Helv. Chim. Acta* **1996**, *79*, 803−812.
[11] G. de Lauzon, B. Deschamps, J. Fischer, F. Mathey, A. Mitschler, *J. Am. Chem. Soc.* **1980**, *102*, 994−1000.
[12] W. T. Dent, R. Long, A. J. Wilkinson, *J. Chem. Soc.* **1964**, 1585−1588.
[13] T. Hayashi, A. Yamamoto, Y. Ito, E. Nishioka, H. Miura, K. Yanagi, *J. Am. Chem. Soc.* **1989**, *111*, 6301−6311.
[14] M. Yamaguchi, T. Shima, T. Yamagishi, M. Hida, *Tetrahedron: Asymmetry* **1991**, *2*, 663−666.
[15] *MolEN, An Interactive Structure Solution Procedure*, ENRAF-Nonius, Delft, The Netherlands, **1990**.

[98076]

Heterobimetallic *d*−*f* Metal Complexes as Potential Single-Source Precursors for MOCVD: Structure and Thermodynamic Study of the Sublimation of [Ni(salen)Ln(hfa)$_3$], Ln = Y, Gd

Alain Gleizes*[a], Miguel Julve[b], Natalia Kuzmina[c], Andrei Alikhanyan[c], Francesc Lloret[b], Irina Malkerova[c], Jose Luis Sanz[b], and François Senocq[a]

Ecole Nationale Superieure de Chimie de Toulouse, Laboratoire des Materiaux de l'I.N.P.T. (UPRESA 5071)[a],
118 route de Narbonne, F-31077 Toulouse cedex 4, France
E-mail: agleizes@ensct.fr

Universitat de Valencia, Departament de Quimica Inorganica de la Facultat de Quimica[b],
Dr Moliner 50, E-46100 Burjassot, Valencia, Spain
E-mail: miguel.julve@uv.es

Moscow State University, Department of Inorganic Chemistry[c],
Leninskie Gory, 119899 Moscow, Russia
E-mail: kuzmina@inorg.chem.msu.ru

Received March 30, 1998

Keywords: Heterobimetallic complexes / Lanthanides / Nickel / Mass spectrometry / Thermochemistry

Heterobimetallic [Ni(salen)Ln(hfa)$_3$] species [H$_2$salen and Hhfa being *N,N′*-ethylenebis(salicylideneimine) and hexafluoroacetylacetone respectively], where Ni(salen) acts as a neutral chelating ligand towards Ln^{III}, form a series of isostructural compounds for Ln = Y^{III} and any lanthanide^{III} cation from La to Yb. They are also isostructural with some of the [Cu(salen)Ln(hfa)$_3$] compounds. They sublime without decomposition under vacuum which makes them potential single-source precursors in MOCVD. Sublimation, thermal behaviour, pressure and composition of the vapour phase versus temperature have been studied for the yttrium derivative, by means of thermal analyses, and mass spectrometry using a Knudsen cell. The dissociation process [Ni(salen)Y(hfa)$_3$] = Ni(salen) + Y(hfa)$_3$ has been thermodynamically investigated. Information on the solid-state intermolecular interactions in relation with volatility was obtained through the crystal structure determination of the gadolinium derivative. A comparative structural study of [Ni(salen)Gd(hfa)$_3$] and [Cu(saloph)Y(hfa)$_3$], [H$_2$saloph is *N,N′*-*o*-phenylenebis(salicylideneimine)], allows to understand why the latter is less volatile than the former despite similar molecular and solid-state structures.

Introduction

Many materials for high technology applications are heterometallic compounds in which at least two different metal elements are associated ($BaTiO_3$, $NaNbO_3$, $YBa_2Cu_3O_7$, AsGa, NiAl, ...). Their preparation as thin films using the technique of CVD requires as much precursors as metal elements to deposit. The idea of using single-source precursors is somewhat attractive since it allows a simplification of the reactor design and processing conditions, and a good control of the gas phase composition up to the deposition zone[1]. It has initiated a quest for volatile heterometallic compounds which is by itself a chemical challenge. Pioneering works include the growth of AsGa films from compounds such as $R_3As-GaR'_3$[2]. More recently, intermetallic films associating a p^3 element (Ga, In) and a *d* element (Ni, Co, Pt) have been grown from complexes with non-bridged[3][4][5] or bridged[6][7] $d-p^3$ bond. This approach was boosted up when the technique of CVD started to be used to grow thin films of heterotrimetallic $YBa_2Cu_3O_7$ for which not only there are three metals to deposit, but also arises a difficulty inherent to the CVD of barium.

To make a volatile complex associating two elements having different chemistries, such as a *d* and a *s* or a *f* element, is somewhat challenging. Surprisingly, the first reported volatile heterobimetallic complex was ionic Cs[Y(hfa)$_4$], which Lippard sublimed without decomposition both in air and in vacuum[8]. More recently, Purdy et al. reported the synthesis of heterometallic alkoxides among which NaCu(OCMe$_3$)$_3$ and Na$_2$Cu[OCH(CF$_3$)$_2$]$_4$ start to sublime without decomposition in dynamic vacuum at temperatures as low as 70°C and 90°C respectively, and Ba[Cu(OCMe$_3$)$_3$]$_2$ sublimes at 133−160°C with partial decomposition[9].

A strategy based on the use of alkoxides as bridging ligands and β-diketonates as terminal ligands allowed Hubert-Pfalzgraf et al. to prepare $YBa_3(OtBu)_6(thd)_3$ which sublimes at 190°C/10^{-3} torr[10], BaY$_2$[OCH(CF$_3$)$_2$]$_4$(thd)$_4$, BaCu$_2$[OCH(CF$_3$)$_2$]$_4$(thd)$_2$, and YCu[OCH(CF$_3$)$_2$]$_2$(thd)$_3$ which sublime without decomposition at 150°C/10^{-3} torr, 170°C/10^{-3} torr, 160°C/10^{-3} torr respectively[11]. A $LaNb_3$ complex, [La{OC$_2$H$_4$)$_3$N}$_2${Nb(OPr^i)$_4$}$_3$], which sublimes at about 180−250°C/10^{-1} torr, was obtained using triethanolamine as a bridging ligand and isopropoxide as a terminal ligand[12].

 © WILEY-VCH Verlag GmbH, D-69451 Weinheim, 1998 1434−1948/98/0808−1169 $ 17.50+.50/0

We present here a thourough study of a new kind of volatile heterobimetallic complexes made from two complexes, Ni(salen) and $Ln(hfa)_3$, which add to form [Ni(salen)-$Ln(hfa)_3$] in which Ni(salen) acts as a bidentate ligand and coordinatively saturates $Ln(hfa)_3$ as confirmed by the crystal structure determination of the gadolinium derivative. This structure determination was part of an investigation of the magnetism of heterobimetallic compounds of general formula [M(salen)$Ln(hfa)_3$] and [M(saloph)$Ln(hfa)_3$], M being Ni or Cu[13]. We observed that [Ni(salen)$Gd(hfa)_3$] could be transported in the vapour phase at 180°C/10^{-2} torr, without decomposition as checked by infra-red and powder X-ray diffraction analyses. We have also established that yttrium and lanthanide derivatives are isostructural. As a preliminary study for qualification as a precursor for MOCVD, we decided to further investigate the thermal behaviour of the yttrium derivative, both in the solid state and in the vapour phase, through thermal analyses (TGA, DTG, DTA), and mass-spectrometry using single-cell and double-cell Knudsen chambers. Thermodynamical parameters relative to sublimation and partial dissociation have been derived. This presentation will be completed with a description of the intermolecular interactions in the solid state, and a brief comparative study with [Cu(saloph)$Gd(hfa)_3$] which proved less easy to sublime despite an alike solid-state structure.

This work is part of an INTAS program on synthesis and application of heterobimetallic complexes as precursors for the preparation of thin film materials by the technique of MOCVD.

Results and Discussion

Crystal and Molecular Structure of [Ni(salen)$Gd(hfa)_3$]

From single crystal studies run for the Gd, Yb and Y derivatives in this work, and the La derivative in a previous work[14], it may be inferred that [Ni(salen)$Y(hfa)_3$] and [Ni-(salen)$Ln(hfa)_3$] for Ln going from La to Yb are isostructural (the Lu derivative was not investigated). They crystallize in the monoclinic system, space group $P2_1/n$, with the following unit-cell constants: a = 17.2(1), b = 22.41(6) A, c = 19.7(3) A, β = 90.4(9)° for La[14]; a = 17.153(1), b = 22.296(2), c = 19.454(2) A, β = 90.36(1)° for Gd; a = 17.29(1), b = 22.349(6), c = 19.59(1) A, β = 90.12(6)° for Y; a = 17.191(3), b = 22.056(6), c = 19.563(4) A, β = 90.18(2)° for Yb. They are isostructural with [Cu(salen)$Gd(hfa)_3$] whose structure has been described in ref.[14] but was not published at the time of this study. Crystal and molecular structures of [Ni(salen)$Gd(hfa)_3$] have been determined as part of an investigation of the magnetic behaviour[13] and of the volatility (this study) of compounds of the [M(salen)$Ln(hfa)_3$] (M = Cu, Ni) series.

The asymmetric unit is made of two symmetrically independent [Ni(salen)$Gd(hfa)_3$] molecules, namely mol__1 and mol__2, paired up into a pseudo-centrosymmetrical dimeric entity in which Ni(salen) moieties overlap, as shown in Figure 1. There are four such dimers per unit-cell. The Ni__1−Ni__2 distance is equal to 3.583(1) A, and the Gd−Ni distances are equal to 3.165(1) A in mol__1 and 3.225(1) A in mol__2. Ni(salen) chelates gadolinium through its oxygen atoms. It is almost planar with atom-to-plane deviations ranging from −0.24 to 0.33 A in mol__1, and −0.40 to 0.24 A in mol__2. The folding angles of the NiO(1)O(2)Gd bridging parts about O(1)O(2) are 52.2(2)° in mol__1 and 47.4(2)° in mol__2. In both molecules, the gadolinium atom is bound to eight oxygen atoms forming a pseudo square antiprism.

A screening of van der Waals contacts gave results shown in Table 1. The shortest contacts between fluorine atoms are larger than 2.8 A, that is more than twice their van der Waals radius of 1.35 A[15]. Examination of H···H distances and C−H···H angles revealed no van der Waals contacts between −CH or $-CH_2$ groups. No π-interactions was no-

Figure 1. Pseudo-centrosymmetrical pairing of molecule__1 and molecule__2 in [Ni(salen)$Gd(hfa)_3$] (letters a, b and c number *hfa* ligands in either molecules)

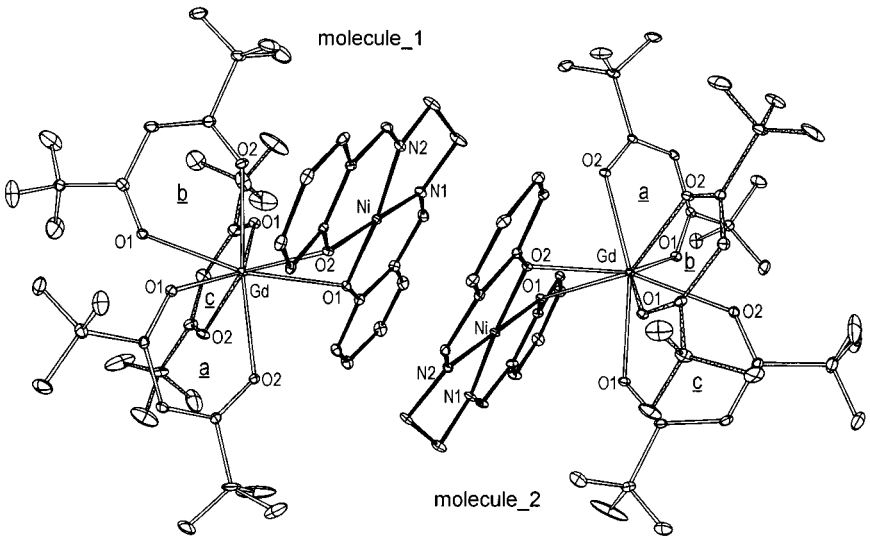

Table 1. Tentative comparison of van der Waals interactions in [Ni(salen)Gd(hfa)$_3$] and [Cu(saloph)Y(hfa)$_3$] (distances in A and angles in deg.). Van der Waals radii are those of Pauling[15]: F, 1.35 A; H, 1.20 A; half-thickness of an aromatic molecule, 1.70 A

	[Ni(salen)Gd(hfa)$_3$]	[Cu(saloph)Y(hfa)$_3$]
Distance between mean planes	3.354(9)	3.291(2) or 3.149(2)[a]
Angle between mean planes	1.1(1)	0
Shortest F···F contacts	none less than 2.82	none less than 2.82
Shortest H···F contacts	none less than 2.61	H19···F31a[i][b]: 2.57(2) H3a···F31c[ii]: 2.55(3)
Shortest −CH···HC− contacts	none less than 2.45	none less than 2.45
−CH···phenyl ring contacts,	H42···C(8−13)1 2.74	none
Contacts between π systems of ajacent M(sal*) entities	none	C(14)···C(18)[i]: 3.55(1) C(17)···C(17)[i]: 3.58(1)

[a] See text. − [b] Code of symmetry operations: [i] $-1-x, -y, -z$; [ii] $-x, -y, 1-z$.

ticed between six-membered rings of ajacent molecules. The main significant interactions occur in the dimers between overlaping Ni(salen) entities. The overlaping scheme of two Ni(salen) entities in a dimer is shown in Figure 2. The mean planes make an angle of 1.1(1)° and are 3.354(8) A apart. This value is slightly less than twice the van der Waals half-thickness of a planar cycle with delocalized π-electrons (1.70 A[15]).

Figure 2. Overlap scheme of two pseudo-centrosymmetrically related Ni(salen) entities in [Ni(salen)Gd(hfa)$_3$] (top), and of two centrosymmetrically related Cu(saloph) entities in [Cu(saloph)Y(hfa)$_3$] (bottom)

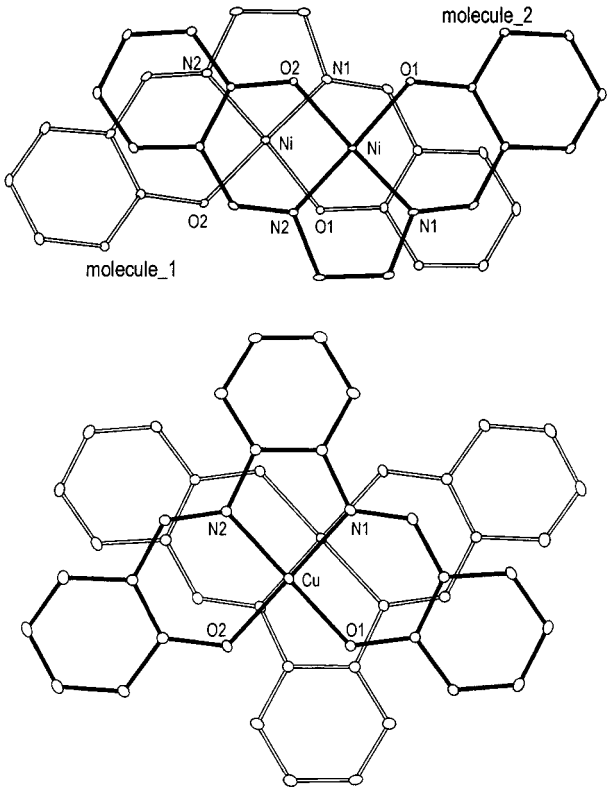

Thermal Analyses and Vacuum Sublimation

Thermogravimetric (TGA) curve recorded at 1 atmosphere under nitrogen [Figure 3 (a)] shows that [Ni(salen)Y(hfa)$_3$] is thermally stable up to 210°C, and decomposes in the 210−510°C temperature range. The total loss of weight is about 85% which is consistent with the formation of a 1:1 mixture of YF_3 and NiO. Corresponding DTG-curve showed a six-step process with the main effect occuring at 460°C. Figure 3 (b) shows the thermogravimetric curve recorded under vacuum (0.01 torr). A single-stepped and quasi total (>99%) weight loss occurs in the 220−340°C range. The DTA curve showed a single endothermic peak at about 300°C. This corresponds to sublimation exclusively.

Figure 3. Thermal gravimetric analyses of [Ni(salen)Y(hfa)$_3$] at 1 atm; (a) and under vacuum (b)

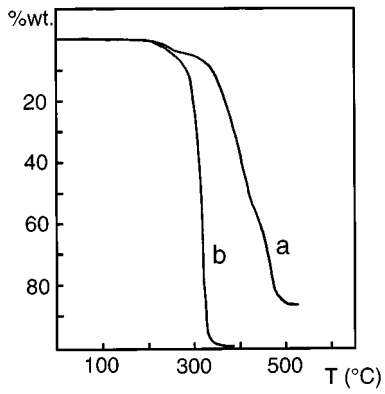

Several samples of [Ni(salen)Y(hfa)$_3$] were submitted to isothemal vacuum sublimation (0.01 torr). Freshly prepared product could be totally sublimed at 240°C without decomposition, and an X-ray powder diffraction analysis showed that the sublimate was isostructural with the starting material. A sublimed sample could be sublimed again more than once in the 240−300°C temperature range without decomposition. Air storing over 6 months proved not to affect the sublimation process.

In order to determine whether [Ni(salen)Y(hfa)$_3$] exists in the vapour phase, or if the solid dissociates into gaseous Y(hfa)$_3$ and Ni(salen) which recombine in the cold part of the reactor, mass-spectrometry experiments were carried out, not only for the heterobimetallic complex but also for the component monometallic complexes Y(hfa)$_3$ and Ni(salen).

Table 2. Intensities of main ion currents (relative units) in mass spectra of $Y(hfa)_3$, Ni(salen), and $[Ni(salen)Y(hfa)_3]$ (U = 80 eV)

$Y(hfa)_3$ (341 K)		Ni(salen) (515 K)		$[Ni(salen)Y(hfa)_3]$ (450 K)	
$[Y(hfa) - CF]^+$	0.98	$Ni(salen)^+$	1.00	$[Y(hfa)_3Ni(salen)]^+$	1.00
$Y(hfa)O^+$	0.33	$NiO(C_6H_4)CHNCH_2^+$	0.56	$[Y(hfa)CONi(salen)]^+$	0.75
$[Y(hfa) - 3\ F]^+$	0.17	$NiO(C_6H_4)CH^+$	0.55	$[Y(OH)_2Ni(salen)]^+$	2.4
$[Y(hfa)_2 - 3\ F]^+$	1.00	$Ni(C_6H_4)^+$	0.34	$[Y(hfa)_3 - 3\ F]^+$	1.4
$Y(hfa)_2^+$	0.65	$NiO(C_6H_4)NCH_2^+$	0.29	$Y(hfa)_3^+$	0.18
$[Y(hfa)_3 - 3\ F]^+$	0.30	NiO^+	0.06	$Ni(salen)^+$	19.9
$Y(hfa)_3^+$	0.18			$NiO(C_6H_4)CHNCH_2^+$	2.75
$[Y_2(hfa)_3 - 3\ F]^+$	0.08			$[Y(hfa) - CF]^+$	0.52
$[Y_2(hfa)_5 - 3\ F]^+$	0.13			$NiO(C_6H_4)CH^+$	2.6

Mass Spectrometry Study of $[Ni(salen)Y(hfa)_3]$, $Y(hfa)_3$, and Ni(salen)

The results are displayed in Table 2.

$Y(hfa)_3$: The mass spectrum of $Y(hfa)_3$ shows that the major species are three yttrium-containing ions with m/z of 446 ($[Y(hfa)_2 - 3\ F]^+$), 265 ($[Y(hfa) - CF]^+$), and 503 amu ($[Y(hfa)_2]^+$). Therefore, the saturated vapour over anhydrous $Y(hfa)_3$ mainly consists of monomeric molecules $Y(hfa)_3$. Ions including two yttrium atoms are present as minor species, thus indicating that the vapour phase contains dimeric $[Y(hfa)_3]_2$ molecules too. At 341 K, the respective vapour pressures are $3.9\cdot10^{-3}$ torr ($5.13\cdot10^{-6}$ atm) for $Y(hfa)_3$, and $3.8\cdot10^{-4}$ torr ($5.0\cdot10^{-7}$ atm) for $[Y(hfa)_3]_2$. The enthalpy of dissociation of $[Y(hfa)_3]_2$ in the gas phase according to the equation $[Y(hfa)_3]_{2\ (g)} = 2\ [Y(hfa)_3]_{(g)}$ (*1*) was determined in the 312−365 K temperature range: $\Delta_D H°_T$ = 78.0 kJ/mol. The enthalpy of sublimation of monomeric $Y(hfa)_3$ was also calculated (Table 3).

Table 3. Temperature dependence of saturated vapour pressures of $Y(hfa)_3$, Ni(salen), and $[Ni(salen)Y(hfa)_3]$

Complex	A[a]	B[a]	T range [K]	$\Delta_s H°_T$ [kJ/mol]
$Y(hfa)_3$	4786±500	8.75±0.2	312−365	91.6±8.5
Ni(salen)	7823±350	9.74±0.15	459−545	149.8±7
$[Ni(salen)Y(hfa)_3]$	8894±1000	13.4±0.2	420−471	170.3

[a] A and B are the coefficients of the equation $\log P_{atm} = -A/T + B$.

Ni(salen): Peaks assigned to monomeric species only were detected in the mass spectrum of Ni(salen). At 501 K, the vapour pressure of Ni(salen) is equal to $7.82\cdot10^{-4}$ torr ($1.03\cdot10^{-6}$ atm). The enthalpy of sublimation was calculated (Table 3).

[Ni(salen)Y(hfa)$_3$]: The mass spectrum shows that the vapour phase over $[Ni(salen)Y(hfa)_3]$ contains the heterobimetallic ions $[Y(hfa)_3Ni(salen)]^+$, $[Y(hfa)(CO)Ni(salen)]^+$, $[Y(OH)_2Ni(salen)]^+$, thus indicating that molecules $[Ni(salen)Y(hfa)_3]$ are present in the saturated vapour. However, ion currents corresponding to monometallic species were also detected. A *LAMMA* analysis of the solid residue after sublimation of 50% of the starting material showed the Y/Ni ratio to be still 1:1, from what it may be deduced that $[Ni(salen)Y(hfa)_3]$ sublimes congruously. It may be inferred that monomeric species originate by dissociation of gaseous $[Ni(salen)Y(hfa)_3]$.

$$[Ni(salen)Y(hfa)_3]_{(s)} \rightleftharpoons [Ni(salen)Y(hfa)_3]_{(g)} \quad (2)$$

$$[Ni(salen)Y(hfa)_3]_{(g)} \rightleftharpoons Y(hfa)_{3\ (g)} + Ni(salen)]_{(g)} \quad (3)$$

One notices that the intensities for monometallic Ni species are higher (relative intensity of 19.9 in Table 2) than the ones for bimetallic species. In our opinion, such an unbalanced distribution of relative intensities might result from a dissociative mechanism during the ionization process of $[Ni(salen)Y(hfa)_3]$ (under electron impact) with predominant formation of Ni-containing cationic species. Similar distributions of ion current intensities were observed for volatile $M[Ln(hfa)_4]$ (M = alkaline element)[8] and for complex halogenides of alkaline elements[16].

The temperature dependencies of ion current intensities were studied for heterobimetallic and monometallic species in the mass spectra of $[Ni(salen)Y(hfa)_3]$ in the 420−471 K range. A two-temperature Knudsen chamber was used to study the composition of the unsaturated overheated vapour. It was found that the dissociation process *3* took place in the top part of the chamber. Using these results and assuming a congruent sublimation for $[Ni(salen)Y(hfa)_3]$ − $(P_{[Ni(salen)Y(hfa)3]} + P_{Ni(salen)})/(P_{[Ni(salen)Y(hfa)3]} + P_{Y(hfa)3}) = 1$ and $P_{Ni(salen)} = P_{Y(hfa)3}$ − we calculated the enthalpies for processes *2* and *3*: $\Delta_s H°_T$ = 170.3 ± 21.0 kJ/mole for *2*; $\Delta_D H°_T$ = 127.2 ± 9.0 kJ/mol for *3* (Table 3). A comparison of the latter value with the enthalpy of process *1* shows that $[Ni(salen)Y(hfa)_3]$ is more stable than $[Y(hfa)_3]_2$.

The variation of the equilibrium constant versus temperature for process *3* was determined in the 487−581 K range:

$$\log K_{patm} = -(6643\pm500)/T + (6.33\pm0.3)$$

Table 4 shows partial pressures and vapour phase compositions calculated at 420 and 520 K. In the working tem-

Table 4. Partial pressures [torr] and composition [%] of the vapour phase of $[Ni(salen)Y(hfa)_3]$ at 420 and 520 K

T [K]	$[Ni(salen)Y(hfa)_3]$		Ni(salen)		$Y(hfa)_3$	
420	78%	$1.2\cdot10^{-5}$	11%	$1.7\cdot10^{-6}$	11%	$1.7\cdot10^{-6}$
520	54%	$1.4\cdot10^{-1}$	23%	$6.0\cdot10^{-2}$	23%	$6.0\cdot10^{-2}$

perature range of the present study (420−471 K), the vapour phase over solid [Ni(salen)Y(hfa)$_3$] contains [Ni(salen)-Y(hfa)$_3$] molecules as its main species. However, the partial pressures of the dissociation products, Y(hfa)$_3$ and Ni-(salen), increase rapidly with temperature.

Comparison with [Cu(saloph)Y(hfa)$_3$]: The solid-state structure of [Ni(salen)Ln(hfa)$_3$] shows that part of intermolecular forces to be overcome for vaporization originates with non bonded contacts between Ni(salen) moieties in the pseudo dimers (Figure 1). To discuss this point, it is interesting to make a comparison with [Cu(saloph)Y(hfa)$_3$]. This compound has a structure[13] closely related to the one of [Ni(salen)Gd(hfa)$_3$], but proved less volatile[17]. The *saloph* ligand possesses one more peripheral phenyl ring than *salen*. Like [Ni(salen)Gd(hfa)$_3$], [Cu(saloph)Y(hfa)$_3$] molecules form dimers in which the Cu(saloph) entities overlap. The presence of an extra phenyl ring results in a different overlapping scheme as shown in Figure 2. The molecules are centrosymmetrically related so that the overlapping entities have their mean planes strictly parallel, which is not the case for [Ni(salen)Gd(hfa)$_3$]. The interplanar distance is equal to 3.149(1) A, that is 0.20 A shorter than for the Ni(salen). However, to be more correct it should be noticed that in [Ni(salen)Gd(hfa)$_3$], the phenyl rings are involved in the overlapping scheme, which is not the case for [Cu(saloph)Y(hfa)$_3$]. In this compound, only the three cycles comprising the metal atom overlap while the peripheral phenyl cycles do not. The plane-to-plane distance for the overlapping parts is equal to 3.291(1) A. This is still shorter (by 0.06 A) than for [Ni(salen)Gd(hfa)$_3$]. This shortening most likely results from slightly stronger intermolecular interactions in the *saloph* derivative with respect to the *salen* one. These interactions are all the more efficient that the planes are strictly parallel. They mainly account for the lesser volatility of [Cu(saloph)Y(hfa)$_3$]. Van der Waals contacts between fluorine atoms are very similar in both compounds (Table 1).

Conclusion

[Ni(salen)Ln(hfa)$_3$], which results from the coordination of Ni(salen) to Ln(hfa)$_3$, has proved to sublime congruently. In the working temperature range of this study (420−471 K), the vapour phase contains [Ni(salen)Y(hfa)$_3$] molecules as its main species. At higher temperature, dissociation of gaseous [Ni(salen)Y(hfa)$_3$] into Y(hfa)$_3$ and Ni(salen) increases rapidly with temperature. Therefore, dissociation might play a more or less important role in a MOCVD experiment depending on substrate temperature. It could influence the process of deposition, and it has to be taken into account for a practical use of [Ni(salen)Y(hfa)$_3$] and related complexes in a MOCVD process.

MOCVD experiments are in progress. Since substitution of copper for nickel and/or of one lanthanide for an other one does not change the crystal structure, this kind of complex is expected to be precursors of materials containing both Ni or Cu and Y or a lanthanide element.

Examination of the crystal structure clearly suggests to modify the ligand around Ni in order to prevent dimerization hence increase volatility. This is under current investigation. Complexes of formula [(Ni$_{1-y}$Cu$_y$)(salen)-(Ln$_{1-x}$Ln′$_x$)(hfa)$_3$], which would allow transportation of more than two metal elements in the vapour phase, are being studied too.

Financial support from *INTAS* (contract # 95-118) and the *Russian Fundation for Basic Research* (RFBR) is acknowledged.

Experimental Section

Preparation and Characterization of the Complexes [Ni(salen)Ln(hfa)$_3$], [M = Y (1) and Gd (2)]: Ni(salen) was prepared according to a literature method[18]. For Ln(hfa)$_3$(H$_2$O)$_2$ (Ln = Y, Gd), a procedure adapted from the one described in ref.[19] was used. Elemental analyses (C, H, N) were carried out by the Microanalytical Service of the Universidad Autonoma de Madrid (Spain). IR spectra were taken on a Perkin-Elmer 1750 FTIR spectrophotometer for KBr disks in the 4000−300 cm^{-1} region. Magnetic susceptibility measurements of polycrystalline samples at room temperature were performed with a pendulum-type susceptometer.

Compounds **1** and **2** were synthesized by reaction of Ni(salen) with Ln(hfa)$_3$(H$_2$O)$_2$ in chloroform. A typical preparation is as follows: 0.5 mmol of Ln(hfa)$_3$(H$_2$O)$_2$ dissolved in a minimum amount of chloroform was slowly added under continuous stirring to a hot chloroform solution (50 ml) containing 0.5 mmol of Ni(salen). The orange solution was heated under reflux for 1 hr. Slow evaporation of the resulting solution in a refrigerator yields orange single crystals. − $C_{31}H_{17}F_{18}N_2NiO_8Y$ (**1**) (1035.1): calcd. C 35.93, H 1.65, N 2.70; found C 36.10, H 1.51, N 2.69. − $C_{31}H_{17}F_{18}GdN_2NiO_8$ (**2**) (1103.4): calcd. C 33.59, H 1.54, N 2.53; found C 33.60, H 1.47, N 2.87.

Compound **1** was found diamagnetic whereas a C_MT value (X_M = molar magnetic susceptibility) of 7.90 cm^{3}mol^{-1}K was measured for compound **2** at room temperature. This is consistent with the occurrence of diamagnetic Ni(salen) with a diamagnetic Y^{III} containing unit in **1** and a paramagnetic Gd^{III} containing unit in **2**. IR data for **1** and **2** clearly support the coordination of Ni-(salen) to Ln(hfa)$_3$: shifting towards higher wavenumbers of the C=N stretching vibration and out-of-plane aromatic C−H bend of the *salen* ligand (1622 and 736 cm^{-1} for Ni(salen) to be compared with 1630 and 760 cm^{-1} for **1** and **2**) as well as a splitting of the C=O stretching vibration of the *hfa* ligand (a strong sharp peak at 1647 cm^{-1} for Ln(hfa)$_3$(H$_2$O)$_2$, but two strong sharp peaks at 1663 and 1645 cm^{-1} for **1** and **2**).

X-ray Structure Studies: Gadolinium, ytterbium, and yttrium derivatives of the series [Ni(salen)Ln(hfa)$_3$] were shown to be isomorphous by measuring unit-cell constants from single crystals mounted on an Enraf-Nonius CAD4 diffractometer using Mo-*K*α radiation. The structure of [Ni(salen)Gd(hfa)$_3$] was determined from a single crystal mounted on a Stoe Imaging Plate Diffraction System (IPDS). The structure of [Cu(saloph)Y(hfa)$_3$] was determined from a single crystal mounted on an Enraf-Nonius CAD4 diffractometer. Experimental conditions and structure determinations are reported elsewhere[13].

Thermal Analyses: Samples of [Ni(salen)Y(hfa)$_3$] were submitted to thermal analyses. Thermogravimetric and differential thermogravimetric analyses at the atmospheric pressure were performed in a nitrogen stream, at a heating rate of 5°/min, on a 1500-Q MOM derivatograph. Thermogravimetric and differential thermal analyses under vacuum (0.01 torr) were carried out on a Sinuki-Riko TGD-700 thermal analyzer, at a heating rate of 10°/min. Iso-

thermal dynamic sublimation experiments were run with samples (100 mg) placed in glass test tubes for periods of 30 min. at a pressure of 0.01 torr. Weight losses were determined by gravimetric and complexometric analyses.

Mass Spectrometry and Study of the Vapour Phase: The mass spectra of [Ni(salen)Y(hfa)$_3$], Y(hfa)$_3$, and Ni(salen) were recorded on a MS 1301 spectrometer having a 50−1500 amu mass range, and using 80 eV ionizing electrons. The complexes were vaporized from a Knudsen effusion cell. The ratio of surface of evaporation to surface of the effusion hole was about 600. The cell temperature was measured with a Pt/Pt(Rh) thermocouple (±0.1 K). The experiments were carried out in ranges 312−365 K for Y(hfa)$_3$, 459−545 K for Ni(salen) and 420−471 K for [Ni(salen)Y(hfa)$_3$]. The main molecular ion peaks in mass spectra of Y(hfa)$_3$, Ni(salen), and [Ni(salen)Y(hfa)$_3$] are given in Table 2.

Vapour pressures versus temperature were determined by means of isothermal vaporization experiments and use of the Herz-Knudsen equation. Enthalpies of sublimation were calculated from the temperature dependences of ion current intensities by using Clausius-Clapeyron equation and a least-squares method.

A two-temperature Knudsen cell was used to determine the composition of overheated unsaturated vapour of [Ni(salen)Y(hfa)$_3$]. The saturated vapour was passed from the lower part of a double Knudsen cell to the top part. The temperature of the top part was varied from 487 to 581 K.

Crystallographic data (excluding the structure factor tables) for the structures reported in this paper have been deposited with the Cambridge Crystallographic Data Centre as supplementary publication CCDC-101159. Copies of the data can be obtained free of charge on application to CCDC, 12 Union Road, Cambridge CB2 1EZ, UK [Fax (internat): +44(0)1223/336-033; E-mail: deposit@ccdc.cam.ac.uk].

[1] F. Maury, *J. Phys. IV* **1995**, *C5*, 449−463.
[2] F. Maury, *Adv. Mater.* **1991**, *3*, 542−548.
[3] R. A. Fischer, H. D. Kaesz, unpublished observations; R. A. Fischer, H. D. Kaesz, S. I. Khan, H.-J. Müller, *Inorg. Chem.* **1990**, *29*, 1601−1602.
[4] F. Maury, L. Brandt, H. D. Kaesz, *J. Organomet. Chem.* **1993**, *449*, 159−165.
[5] R. A. Fischer, E. Herdtweck, T. Priermeier, *Inorg. Chem.* **1994**, *33*, 934−943, and references therein.
[6] Y. J. Chen, H. D. Kaesz, Y. K. Kim, H.-J. Müller, R. S. Williams, Z. Xue, *Appl. Phys. Lett.* **1989**, *55*, 2760−2761.
[7] B. Fraser, L. Brandt, W. K. Stovall, H. D. Kaesz, S. I. Khan, F. Maury, *J. Organomet. Chem.* **1994**, *472*, 317−328.
[8] S. J. Lippard, *J. Am. Chem. Soc.* **1966**, 88, 4300−4301.
[9] A. P. Purdy, C. F. George, J. F. Callahan, *Inorg. Chem.* **1991**, *30*, 2812−2819.
[10] F. Labrize, L. G. Hubert-Pfalzgraf, J. Vaissermann, C. B. Knobler, *Polyhedron* **1996**, *15*, 577−589.
[11] F. Labrize, L. G. Hubert-Pfalzgraf, J.-C. Daran, S. Halut, P. Tobaly, *Polyhedron* **1996**, *15*, 2707−2718.
[12] V. G. Kessler, LK. G. Hubert-Pfalzgraf, S. Halut, J.-C. Daran, *J. Chem. Soc., Chem. Commun.* **1994**, 705−706.
[13] J. L. Sanz, F. Lloret, M. Julve, A. Gleizes, to be published.
[14] I. Ramade, O. Kahn, Y. Jeannin, F. Robert, *Inorg. Chem.* **1997**, *36*, 930−936.
[15] L. Pauling, *Nature of the Chemical Bond*, 3rd ed., Cornell University Press, Ithaca (NY), **1960**.
[16] K. A. Kingerich in *Current Topics in Material Science* (Ed.: E. Kaldis), New-York, **1980**, *6*, p. 345.
[17] A. Gleizes, F. Senocq, unpublished observations.
[18] R. H. Bailes, M. Calvin, *J. Am. Chem. Soc.* **1947**, *69*, 1886−1893.
[19] M. F. Richardson, W. F. Wagner, D. E. Dands, *J. Inorg. Nucl. Chem.* **1968**, *30*, 1275−1289.

[98087]

Coordination Modes of 2,5-Di(*tert*-butyl)pyrrolide – Crystal Structures of HPyr*, Pyr*H·thf, $(thf)_2$LiPyr*, and $[(Me_3Si)_3C\text{-}Zn]_2(\mu\text{-}Cl)(\mu\text{-}Pyr^*)$ (Pyr* = 2,5-tBu$_2$NC$_4$H$_2$)

Matthias Westerhausen*[a], Michael Wieneke[a], Heinrich Nöth[a][+], Thomas Seifert[a][+], Arno Pfitzner[b],[+] Wolfgang Schwarz[c][+], Oliver Schwarz[c], and Johann Weidlein*[c]

Institut für Anorganische Chemie der Ludwig-Maximilians-Universität München[a],
Meiserstraße 1, D-80333 München, Germany
Fax: (internat.) + 49(0)89/5902-578
E-mail: maw@anorg.chemie.uni-muenchen.de

Institut für Anorganische Chemie der Universität Siegen[b],
Adolf-Reichwein-Straße, D-57068 Siegen, Germany

Institut für Anorganische Chemie der Universität Stuttgart[c],
Pfaffenwaldring 55, D-70569 Stuttgart, Germany
Fax: (internat.) +49(0)711/685-4241

Received March 30, 1998

Keywords: Hydrogen bonds / Indium / Lithium / Nitrogen heterocycles / Zinc

The lithiation of 2,5-di(*tert*-butyl)pyrrole (**1**) yields bis(tetrahydrofuran)lithium 2,5-di(*tert*-butyl)pyrrolide (**2**), which is monomeric in solution as well as in the solid state. Due to the coordination number of three for the lithium atom, short Li–O and Li–N bond lengths of 193 pm are observed. The metathesis reaction of **2** with tris(trimethylsilyl)-methylzinc chloride (**3**) gives colorless bis[tris(trimethylsilyl)methylzinc] chloride 2,5-di(*tert*-butyl)pyrrolide (**4**). The pyrrolide ligand and the chlorine atom bridge the zinc atoms. One of the zinc atoms is bonded to the nitrogen atom of the pyrrolide substituent, while the other bonds to the opposite C–C bond. At 215 pm, the Zn–N bond is very long compared to those in alkylzinc amides, whereas the Zn–C distances lie in the range of Zn–C bond lengths found between zinc and η^5-bonded cyclopentadienide ligands. The molecular structures of **1** and of the low-melting THF adduct **1**·thf show a similar 2,5-di(*tert*-butyl)pyrrole molecule, but in the latter case a weak N–H···O bond is observed (N–H 97 pm, O···H 199 pm).

The pyrrolide substituent $[NC_4H_4]^-$ is isoelectronic with the cyclopentadienide anion, and since it possesses 6π electrons can be regarded as a Hückel aromatic system. In contrast to this (formal) analogy of these ligands, the substitution of a cyclopentadienide ligand of the well-known ferrocene by a pyrrolide substituent to yield an azaferrocene was first reported in 1963.[1] The significantly lower tendency of the $NC_4H_4^-$ anion to coordinate as a π ligand and the enhanced tendency to form M−N σ bonds is a consequence of the high electronegativity of the heteroatom. On the other hand, the bonding properties depend on the substitution pattern on the pyrrolide ring. In 2,2′,5,5′-tetramethyl-1,1′-diazaplumbocene, η^1 bonding to the 2,5-dimethylpyrrolide is observed,[2] whereas the corresponding 2,5-di-*tert*-butyl-substituted pyrrolide crystallizes with an η^5-bonded ring.[3] In contrast to these findings, the group-13 metals (boron group, triels) form derivatives of the type $Me_2M^{III}NC_4H_{4-x}R_x$ with σ(M−N) bonds (η^1 coordination), although in the solid state the M^{III} metal centers are also bonded to the π-system of a pyrrolide ligand of a neighboring molecule, thus forming π associates.[4]

Here, we describe three different coordination modes of the 2,5-di(*tert*-butyl)pyrrolide anion Pyr*$^-$. This ligand forms Li−N σ bonds, but the reaction of LiPyr* with InCl[5] yields the indium(I) derivative with a η^5-bonded Pyr* anion. The unusual bridging mode is found to be adopted in bis[tris(trimethylsilyl)methylzinc] chloride 2,5-di(*tert*-butyl)pyrrolide. For the sake of comparison, the molecular structures of 2,5-di(*tert*-butyl)pyrrole and of its tetrahydrofuran complex are also included.

Results

Preparation

The starting material 2,5-di(*tert*-butyl)pyrrole[6] (H−Pyr*, **1**), which crystallizes from a concentrated tetrahydrofuran solution as a THF solvate (**1**·thf), has been well known for more than 30 years. With *n*-butyllithium, **1** is lithiated according to eq. 1 to give quantitatively bis(tetrahydrofuran-*O*)lithium 2,5-di(*tert*-butyl)pyrrolide (**2**).

$$\underset{\mathbf{1}}{\text{HPyr*}} + n\text{BuLi} \rightarrow \underset{\mathbf{2}}{\text{Li–Pyr*}} + n\text{BuH} \quad (1)$$

Meanwhile, the reaction of lithium tris(trimethylsilyl)-methanide with anhydrous $ZnCl_2$ yields $[(thf)_4Li][(Me_3Si)_3$-

[+] X-ray structure analysis.

 © WILEY-VCH Verlag GmbH, D-69451 Weinheim, 1998 1434−1948/98/0808−1175 $ 17.50+.50/0

$CZn]_2(\mu\text{-}Cl)_3$. In order to obtain a product free from lithium halide and THF, tris(trimethylsilyl)methylzinc chloride (**3**) was purified by sublimation. Reactions of **3** with alkyl- and phenyllithium compounds yield the heteroleptic compounds $(Me_3Si)_3C-Zn-R$, which have in part been characterized by X-ray crystallography.[7] All these derivatives are monomeric and contain solely σ(Zn−C) bonds. The metathesis reaction of **3** with $(thf)_2$LiPyr* (**2**) (eq. 2) yields bis[tris(trimethylsilyl)methylzinc] chloride 2,5-di(*tert*-butyl)pyrrolide (**4**) as a colorless and moisture-sensitive solid with a melting point of 74−75°C.

$$\underset{\mathbf{3}}{2\,(Me_3Si)_3C\text{–}ZnCl} + \underset{\mathbf{2}}{Li\text{–}Pyr^*} \rightarrow \underset{\mathbf{4}}{[(Me_3Si)_3C\text{–}Zn]_2(\mu\text{-}Cl)(\mu\text{-}Pyr^*)} + LiCl \qquad (2)$$

The stoichiometry of this metathesis reaction obeys a 2:1 ratio, irrespective of the molar ratio of the reactants. Stirring or refluxing of a 1:1 mixture of the starting materials does not lead to the formation of a halogen-free derivative, as is known for the metathesis reactions with lithium alkanides.[7] The cryoscopically determined molecular mass of **4** is consistent with the proposed structure shown in eq. 2. Dissociation into **3** and mononuclear, heteroleptic tris(trimethylsilyl)methylzinc 2,5-di(*tert*-butyl)pyrrolide does not occur under these conditions.

Indium(I) chloride reacts with lithiated 2,5-dimethyl-, 2,3,4,5-tetramethyl- as well as 2,5-di-*tert*-butylpyrrole in toluene, hexane, or tetrahydrofuran at low temperatures. However, the expected products of the methyl-substituted species are not isolable, since decomposition occurs even at temperatures of −90°C and −30°C, respectively, and precipitation of indium metal is observed. In contrast to this instability, indium(I) 2,5-di(*tert*-butyl)pyrrolide $In^I[Pyr^*]$ (**5**), which forms in tetrahydrofuran at low temperatures according to eq. 3, can be isolated and purified by distillation or sublimation in vacuo. During the melting of **5** at 77−78°C, the compound turns grey. The volatility of In[Pyr*] (**5**) is comparable to that of hexameric (pentamethylcyclopentadienyl)indium [pentamethylindocene(I)].[8] The sensitivities of these compounds towards oxygen are also similar, since In[Pyr*] (**5**) decomposes immediately with precipitation of metallic indium.

$$\underset{\mathbf{2}}{InCl} + \underset{}{Li\text{–}Pyr^*} \rightarrow \underset{\mathbf{5}}{In[Pyr^*]} + LiCl \qquad (3)$$

Molecular Structures

For comparison purposes, the molecular structure of HPyr* (**1**) is briefly described. Suitable single crystals form during the sublimation of **1** at 35°C in vacuo. The molecular structure is shown in Figure 1. The asymmetric unit contains three crystallographically independent molecules, which are distinguished by the first digit n = 1, 2 and 3 following the element symbol. The delocalization within the five-membered ring is disturbed, as is evident from the bond lengths of 137 pm for C(n1)−C(n2) and C(n3)−C(n4), and the value of 142 pm for C(n2)−C(n3). The bond lengths N(n)−H(n) fall in the narrow range from 83 to 91 pm.

The molecular structure of the tetrahydrofuran complex **1**·thf is depicted in Figure 2. This adduct shows a crystallographically imposed C_{2v} symmetry. The bond lengths in the pyrrole ring are not affected by coordination of a tetrahydrofuran molecule to the N1−H1 group. Even the N1−H1 distance of 97 pm differs only by 3 times the esd. On the other hand, the O2···H1 contact of 199 pm is quite long (cf. the O−H distances in ice, which vary between 99 and 176 pm). This weak interaction explains the low melting point of **1**·thf (below 0°C).

The molecular structure of lithium 2,5-di(*tert*-butyl)pyrrolide (**2**) is shown in Figure 3. To date, only one related molecule has been described in the literature, namely an *N*-lithiocarbazole dimer. Compound **2** crystallizes as a monomer due to the steric shielding of the lithium atom by the *tert*-butyl groups. The lithium atom is in a trigonal-planar coordination sphere, with a short Li−N bond length of 193 pm. The low coordination number of the alkali metal is also the reason for the short Li−O distances of 193 pm. In comparison to **1**, the endocyclic C−C bond lengths in the pyrrolide ligand of **2** are 138 and 140 pm for C1−C2 and C2−C2′, respectively, and are therefore very similar.

The molecular structure of **4** is depicted in Figure 4. The molecule contains a crystallographic mirror plane, although this symmetry element does not indicate the molecular symmetry, but rather leads to a two-site disorder of the 2,5-di(*tert*-butyl)pyrrolide ligand. However, only one orientation is shown in Figure 4. The atoms generated by the crystallographic mirror plane are marked with apostrophes. The two zinc atoms of the isomer shown in Figure 4 are in different environments; Zn has a coordination number of four, whereas Zn′ is threefold coordinated by the atoms C1′, Cl and N2.

The chlorine atom bridges the two zinc atoms with Zn−Cl bond lengths of 241 pm and a Zn−Cl−Zn′ bond angle of 110.3°. Terminal Zn−Cl bond lengths, as for example in $(bpy)ZnCl_2$[10] or (tmeda)Zn(Cl)R[11] are typically around 225 pm, and similar values are observed for various zinc(II) chloride modifications.[12] The Zn−Cl distances in dimeric $(Me_2PhSi)_3C-Zn-Cl$[13] as well as in dimeric $F_3C-CCl_2-Zn(OEt_2)Cl$[14] are distinctly shorter (average 233 pm) than those in **4**. Moreover, the endocyclic Zn−Cl−Zn angle is approximately 18° smaller than the corresponding angle in **4**. This distortion of the $(RZn)_2Cl$ moiety is due to the 2,5-di-*tert*-butylpyrrolide ligand, which also bridges the two zinc atoms. The planes Cl/Zn/Zn′ and N2/C21/C22/C23/C24 are oriented almost perpendicular to one another, with an angle between their normals of 93.5°.

Sterically uncrowded cyclopentadienyl complexes of zinc tend to form polymers. Whereas methyl(cyclopentadienyl)zinc is monomeric in the gaseous phase, it polymerizes in the solid state to form a structure with bridging $C_5H_5^-$ ligands and the metal atoms on opposite sides of the aromatic rings.[15] Analogous behavior is observed for bis(cyclopentadienyl)zinc with a bridging and a terminal η^1-bonded ligand.[16] In the gas phase, monomeric decamethyl-

Figure 1. Molecular structure and numbering scheme of the asymmetric unit of HPyr* (**1**); the ellipsoids represent a probability of 40%; the hydrogen atoms of the *tert*-butyl groups are omitted for clarity; those of the azacyclopentadiene unit are drawn with arbitrary radii[a]

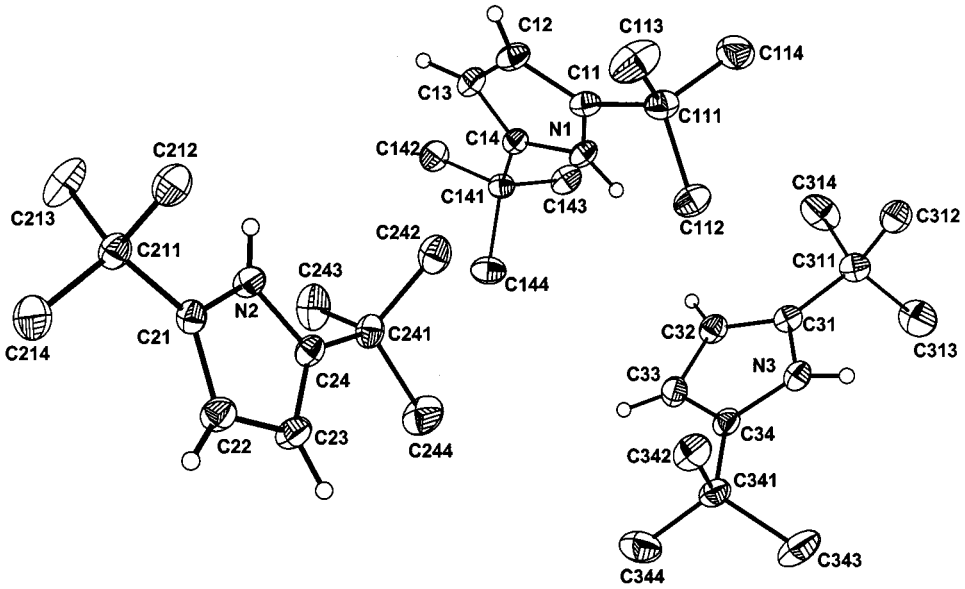

[a] Selected bond lengths [pm]: N1−H1 85(2), N1−C11 137.2(3), N1−C14 138.3(3), C11−C12 136.4(3), C12−C13 141.8(4), C13−C14 137.1(3), N2−H2 83(3), N2−C21 137.5(3), N2−C24 137.8(3), C21−C22 136.5(3), C22−C23 142.4(3), C23−C24 136.3(3), N3−H3 91(3), N3−C31 139.0(3), N3−C34 136.3(3), C31−C32 135.7(4), C32−C33 141.8(4), C33−C34 137.0(3).

Figure 2. Molecular structure and numbering scheme of **1**·thf; the ellipsoids represent a probability of 40% and the H atoms are drawn with arbitrary radii; the hydrogen bond is shown by a dotted line; symmetry-related atoms are marked with an apostrophe[a]

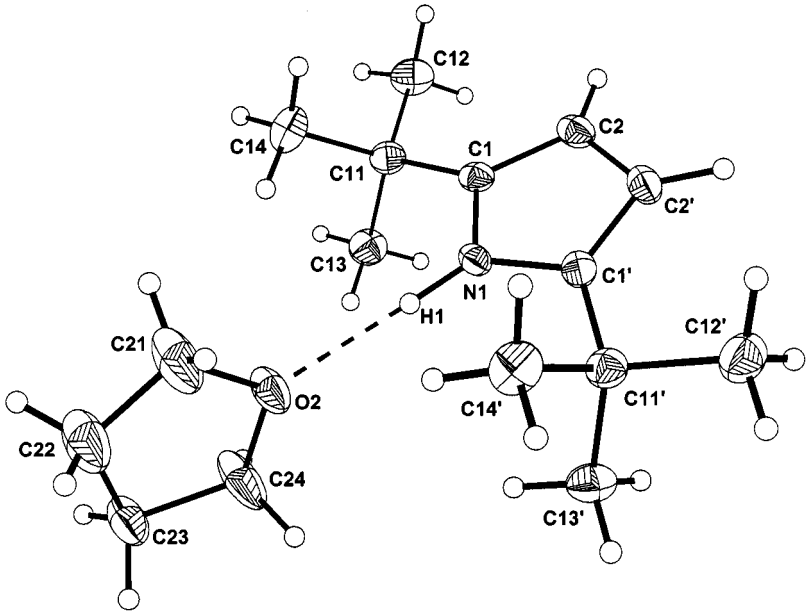

[a] Selected bond lengths [pm]: N1−H1 97(3), N1−C1 138.1(3), C1−C2 137.1(3), C2−C2′ 141.1(5), O2−H1 199(3).

zincocene [bis(pentamethylcyclopentadienyl)zinc] has a structure of the type $(\eta^1\text{-}C_5Me_5)(\eta^5\text{-}C_5Me_5)Zn$.[17] The pyrrolide substituent in **3** is planar and shows a different coordination behavior. Both the zinc atoms coordinate at the same side of the ligand, but one zinc atom bonds via a σ(Zn−N2) bond whereas the other metal center shows an η^2 coordination to the C22−C23 bond. The Zn−N2 bond length of 215 pm is very long compared to the values in [tris(trimethylsilyl)methyl]zinc bis(trimethylsilyl)amide[11] (185 pm), in monomeric zinc bis(amides)[18] (characteristic value 182 pm), or even in bridging μ-bonded bis(trimethylsilyl)amide substituents, where Zn−N distances of approximately 200 pm are found.[19] The Zn−N2 vector shows a deviation of 40.6° from an imaginary in-plane vector; the

Figure 3. Molecular structure and numbering scheme of $(thf)_2$Li-Pyr* (**2**); the ellipsoids represent a probability of 40%; the hydrogen atoms are drawn with arbitrary radii; symmetry-related atoms are marked with an apostrophe; agostic interactions between Li and the methyl groups are indicated with dotted lines[a]

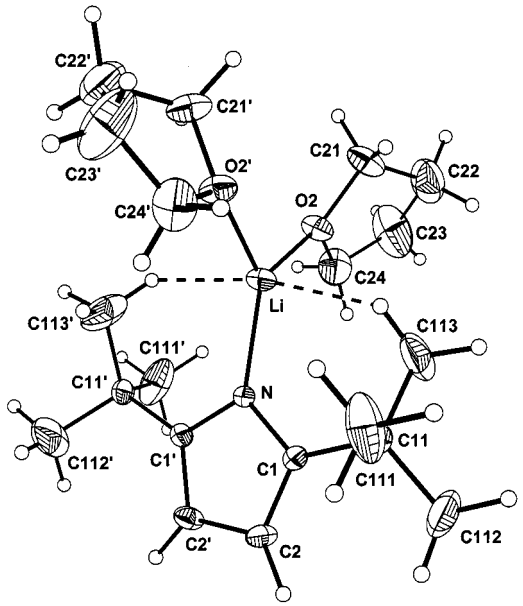

[a] Selected bond lengths [pm] and bond angles [°]: Li−N 193.2(7), Li−O2 192.6(4), N−C1 137.7(3), C1−C2 138.4(4), C2−C2′ 140.4(5); N−Li−O2 127.4(2), O2−Li−O2′ 105.3(3), Li−N−C1 127.0(1), C1−N−C1′ 106.0(3).

Figure 4. Molecular structure and numbering scheme of $[(Me_3Si)_3CZn]_2$(μ-Cl)(μ-Pyr*) (**4**); the ellipsoids represent a probability of 40%; the disordering of the Pyr* ligand is not shown (see text); all hydrogen atoms are omitted for clarity; symmetry-related atoms are marked with an apostrophe[a]

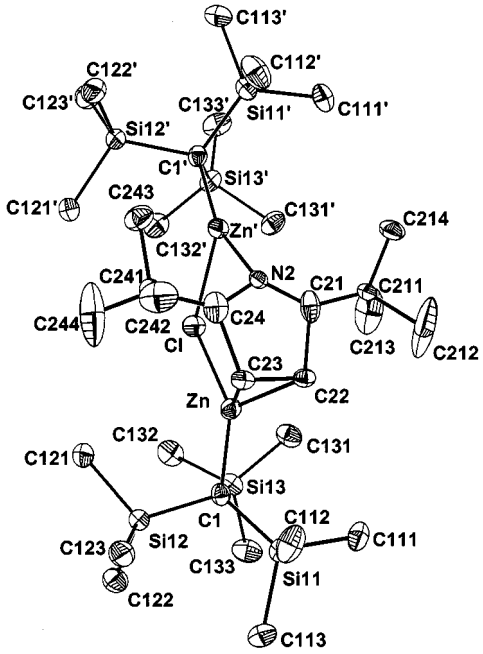

[a] Selected bond lengths [pm] and bond angles [°]: Zn−C1 201.3(4), Zn−Cl 241.0(1), Zn′−N2 215.1(6), N2−C21 126.1(7), N2−C24 127.5(8), Zn−C22 219.0(7), Zn−C23 219.4(7), C1−Si11 188.6(4), C1−Si12 188.8(4), C1−Si13 188.9(4); C1−Zn−Cl 120.2(1), C1′−Zn′−N2 155.1(2), Cl−Zn′−N2 84.7(2), Zn−Cl−Zn′ 110.32(6).

Scheme 1. Selected bond lengths [pm] in tris(cyclopentadienyl)dizinc μ-bis(trimethylsilyl)amide (**A**)

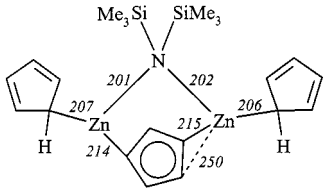

A

N2-bonded zinc atom lies 143 pm above the calculated plane containing the atoms N2, C21, C22, C23, and C24.

The Zn−C22 and Zn−C23 distances of 219.0 and 219.4 pm fall within the broad range of values found for multihapto-bonded cyclopentadienide ligands. The chain-like zincocene[16] has Zn−C bond lengths between 204 and 241 pm, whereas in the zig-zag chain of methylzinc cyclopentadienide[15] Zn−C distances of 222 to 241 pm are observed. In both these molecules, the cyclopentadienide substituents bridge zinc atoms on opposite sides of the aromatic ring. Monomeric zincocenes such as decamethyl-, 1,1′-diphenyl- and 1,1′-bis(trimethylsilyl)zincocene[17] display one η^1-bonded (Zn−C 204−209 pm) and one η^5-coordinated cyclopentadienide ligand (217−230 pm). A similar bonding situation as in **4** is observed for dizinc tris(cyclopentadienide) bis(trimethylsilyl)amide (**A**)[19b] (Scheme 1), although the bridging ligand in this case is doubly η^1-coordinated; the third Zn−C distance of 250 pm is clearly too long to be considered as a bond.

The bridging mode of the ligand Pyr* is not very common, however, there are some other examples.[20] To the σ-bonded nitrogen heterocycles of tricarbonyl(diphenylacetato)manganese dipyrrolide a tricarbonylmanganese fragment is bonded side-on.[20a] Dicarbonylrhodium 2,5-dimethylpyrrolide dimerizes via an unsymmetric heterocycle bridge.[20b] The bridging mode of the pyrrolide anion in this molecule is quite similar to the geometry observed for **4** since the rhodium atoms do not lie above the center of the NC_5 cycle. Solvent-free sodium tetramethylpyrrolide crystallizes as a polymer with a similar bridging pattern of the pyrrolide substituent.[20d] Kuhn et al.[20c] linked two octamethyl-1,1′-diazaferrocene molecules via silver cations σ-bonded to the nitrogen atoms.

The Zn−C1 bond length in **4** exceeds the Zn−C bond lengths in [tris(trimethylsilyl)methyl]zinc derivatives $(Me_3Si)_3C-Zn-R$ with R as phenyl[7] (196 pm), bis(trimethylsilyl)methyl[7] (197 pm), and tris(trimethylsilyl)methyl[7][21] (198 pm); Zn−C bond lengths of sterically unstrained molecules are even shorter. All these findings are indicative of the steric strain within the molecule. The shielding of the $ClZn_2$ moiety by the bulky substituents, which is illustrated in Figure 5, accounts for the fact that this molecule cannot react with a further equivalent of lithium 2,5-di(*tert*-butyl)-pyrrolide (**2**).

Figure 5. Space-filling model of **4** viewed from the chlorine atom, showing the steric shielding of the Zn_2Cl fragment

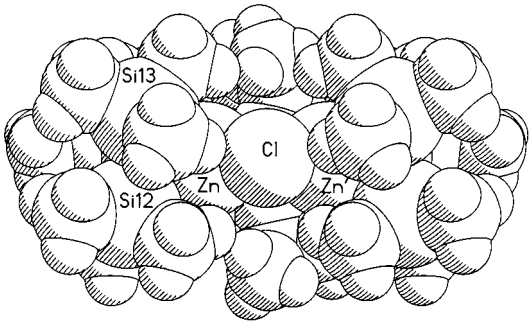

Figure 6 gives a stereoscopic view of the arrangement of **4**, together with the incorporated pentane. There are no significant intermolecular contacts; the pentane molecules lead to an additional separation of the molecules of **4**.

$Me_3Sn-Pyr^*$, the resonances of these nuclei are shifted to higher field by approximately 20 ppm.

Considering the molecular structure of the zinc derivative **2**, the magnetic equivalence of the tris(trimethylsilyl)methyl groups was not expected. However, the long distances between the zinc atoms and the pyrrolide substituent and the shape of the coordination gap allow a tilting motion, leading to a dynamic equilibrium through a Zn−N−Zn-bonded intermediate, in which the pyrrolide is rotated through approximately 90°. This situation is depicted in eq. 4.

The mass spectrum of **4** shows the dissociation products **3** and [tris(trimethylsilyl)methyl]zinc 2,5-di(*tert*-butyl)pyrrolide if the sample is heated above the melting point. At 425 K, the mass peaks of these compounds are the signals of highest intensity, besides that at *m/z* 179 for H−Pyr*. At 460 K, even fragments containing two zinc atoms and one chlorine atom are detected. Products of a dismutation reaction such as $Zn[C(SiMe_3)_3]_2$ or Cl−Zn−Pyr* were not observed.

Figure 6. Stereoscopic representation of the molecular packing of **4** in the unit cell; the atoms are drawn with arbitrary radii and H atoms are omitted for clarity; the *n*-pentane molecules were refined with a fixed population factor of 0.67; the disordering of the 2,5-di(*tert*-butyl)pyrrolide ligand is not shown

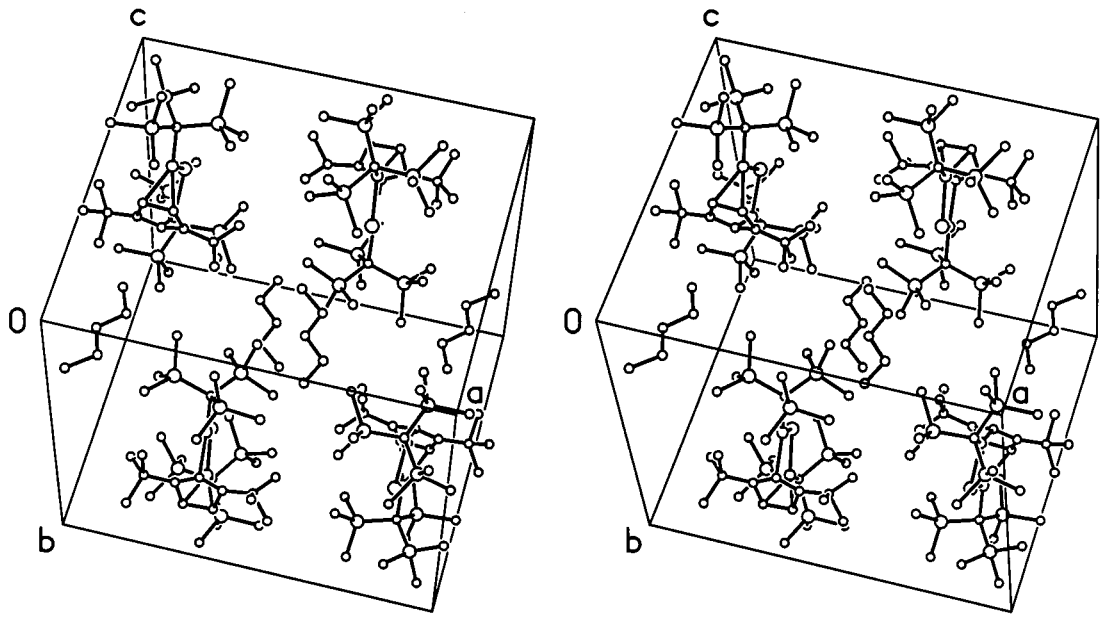

Spectroscopic Characterization

The NMR parameters of the 2,5-di-*tert*-butylpyrrolide ligands of **1**−**5** are compared in Table 1, along with data for $Me_2Ga-Pyr^*$,[2] $Me_3Sn-Pyr^*$,[2] $Sn^{II}[Pyr^*]_2$,[22] and $Pb^{II}[Pyr^*]_2$.[3] The coordination mode of Pyr* does not affect the NMR parameters of the *tert*-butyl groups. The influence of the hapticity of the pyrrolide ligand on the chemical shifts of the carbon atoms in the 2- and 5-positions is small, although η^5 coordination leads to a low-field shift of the ^{13}C resonances. The δ values of the carbon atoms in the 3- and 4-positions show no dependency on the coordination mode, except that in the case of the Sn^{IV} derivative

Due to the insensitivity of the NMR parameters to the hapticity of the Pyr* ligand, the characterization of the In^I derivative **5** is limited. In this case, the most significant results were obtained from Raman spectroscopy, although the In^I derivative **5** decomposes during laser irradiation. For σ(M−N)- and σ(H−N)-bonded derivatives such as H−Pyr*, $Me_2Ga-Pyr^*$, and $Me_3Sn-Pyr^*$, a characteristic polarized high-intensity band at approximately 1560 cm^{-1} is observed. For the compounds $In^I[Pyr^*]$ (**5**) and $Sn^{II}[Pyr^*]_2$, this band is shifted to lower energies, appearing in the region 1500−1510 cm^{-1}. On the other hand, other vibrations of the ring at lower frequencies are shifted to higher values [for example, 1124 (η^1) → 1165 (η^5) cm^{-1}],

Table 1. NMR parameters of the 2,5-di(*tert*-butyl)pyrrolide ligand in HPyr* (**1**), $(thf)_2LiPyr^*$ (**2**), $[(Me_3Si)_3CZn]_2(\mu\text{-}Cl)(\mu\text{-}Pyr^*)$ (**4**), and $In^I\{Pyr\}^*$ (**5**) compared with data for $Sn\{Pyr^*\}_2$[22], $Pb\{Pyr^*\}_2$[3], $Me_2Ga-Pyr^*$[2] and $Me_3Sn-Pyr^*$[2] (M{Pyr*} symbolizes an η^5-bonded, M−Pyr* a σ_N-bonded azacyclopentadienide moiety)

		1	**2**	**4**	**5**	$Me_2Ga-Pyr^*$	$Sn^{II}\{Pyr^*\}_2$	$Me_3Sn-Pyr^*$	$Pb^{II}\{Pyr^*\}_2$
	Solvent	C_6D_6	$[D_8]THF$	C_6D_6	C_6D_6	C_6D_6	C_6D_6	C_6D_6	C_6D
^1H NMR	CH_3(M), (H^1-N)	7.53	−	−	−	0.19	−	0.02	−
	CH_3 (*t*Bu)	1.17	1.22	1.40	1.40	1.24	1.39	1.26	1.39
	$H^{3,4}$	5.93	5.59	6.22	5.96	6.23	5.47	4.86	5.51
	$^3J(H^{3,4}, H^1)$	2.8	−	−	−	−	−	−	−
^{13}C NMR	C(M−Me)	−	−	−	−	0.95	−	−5.86	−
	^1J(C,H)	−	−	−	−	124.3	−	129.8	−
	CH_3(*t*Bu)	30.67	32.77	34.63	32.44	32.9	32.01	30.57	32.69
	^1J(C,H)	125.5	123.9	−	125.45	124.9	−	125.6	−
	C(*t*Bu)	31.24	33.47	[a]	32.73	32.5	33.78	34.59	33.31
	^2J(C,H)	3.75	3.71		3.85			3.8	
	$C^{3,4}$	102.53	100.13	104.60	103.34	105.5	100.51	81.40	105.19
	$^1J(C^{3,4},H)$	166.47	157.03		167.0	163.8		157.8	
	$^2J(C^{3,4},H^{4,3})$	7.0	5.49		6.2	−		−	
	$^3J(C^{3,4},H^1)$	7.05	−		−	−		−	
	$C^{2,5}$	139.46	146.72	148.57	153.55	145.3	162.30	173.33	161.71

[a] Signal not detected.

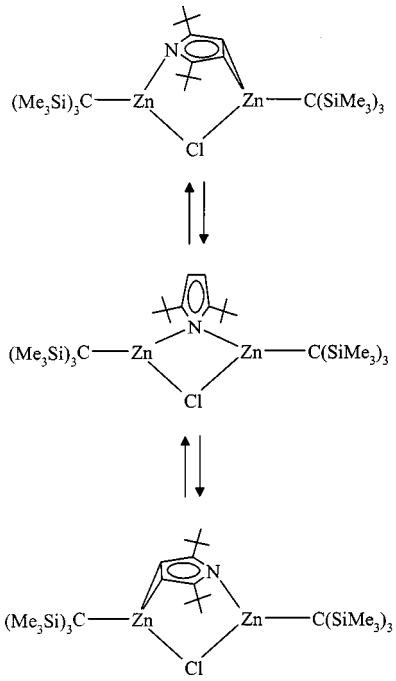

(4)

which has to be interpreted in terms of a change of the π-system of the nitrogen heterocycle. Characteristic for the In^I derivative **5** is the vibration In Pyr* at 170 cm^{-1}, which is lower in energy by 60 cm^{-1} compared to the In C_5 mode of the simple, unsubstituted indocene.[23]

Finally, it should be mentioned that theoretical investigations on a monomeric (hypothetical) 2,5-dimethylazaindocene $In^I(NC_4H_2Me_2\text{-}2,5)$ predict a very short distance of 238 pm between the indium atom and the heterocycle.[24] Such a bond length is only comparable with the values determined for the permethylated indocenes $In^I(C_5R_5)$.[8][25]

Conclusion

The diverse coordination modes adopted by the 2,5-di(*tert*-butyl)pyrrolide ligand have been illustrated by an η^5 coordination to an indium(I) atom as well as bridging between two zinc atoms. Whereas the properties of 2,5-di(*tert*-butyl)azaindocene (**5**) are approximately as one would expect by analogy with pentamethylindocene, the zinc derivative **4** shows a unique structure as well as surprisingly low reactivity. Not even treatment with excess lithium 2,5-di(*tert*-butyl)pyrrolide (**2**) leads to substitution of the chloride ligand by a pyrrolide anion. The reason for this lack of reactivity is the steric shielding of the central $ClZn_2$ moiety by two tris(trimethylsilyl)methyl and two *tert*-butyl groups. These demanding substituents also lead to an extension of the Zn−Cl, Zn−N and Zn−C distances.

This work has been generously supported by the *Deutsche Forschungsgemeinschaft* (DFG) and the *Fonds der Chemischen Industrie*.

Experimental Section

General: All experiments and manipulations were carried out under argon purified by passage through BTS catalyst and P_4O_{10}. Reactions were performed in dried, thoroughly deoxygenated solvents using standard Schlenk techniques. The starting materials 2,5-di(*tert*-butyl)pyrrole (**1**),[6] indium(I) chloride,[5] and [tris(trimethylsilyl)methyl]lithium[26] were prepared by literature procedures. The extreme sensitivity of **5** has thwarted all attempts to prove its purity by elemental analysis.

Bis(tetrahydrofuran-O)lithium 2,5-Di(tert-butyl)pyrrolide (**2**): At −78°C, a solution of *n*-butyllithium (15% in hexane, 9.4 ml) was added dropwise to a solution of 2,5-di(*tert*-butyl)pyrrole (2.70 g, 15.1 mmol) in 50 ml of *n*-hexane. On warming to room temp., a colorless solid precipitated, which was collected. Washing with two portions of *n*-hexane and subsequent drying in vacuo gave lithium 2,5-di(*tert*-butyl)pyrrolide (2.65 g, 14.3 mmol, 95%, dec. at 197°C; lithium analysis for $C_{12}H_{20}NLi$: calcd. 3.75; found 3.7). Carrying

out this reaction in a solvent mixture of diethyl ether and tetrahydrofuran yielded colorless **2** after recrystallization from tetrahydrofuran at −30°C (4.71 g, 14.3 mmol, 95%). Loss of THF at 60°C, m.p. of the residue 348°C. − ^{1}H NMR ([D$_8$]THF): δ = 5.59 [CH(Pyr*)], 1.22 [CMe$_3$(Pyr*)]. − ^{13}C NMR ([D$_8$]THF): δ = 146.72 [C-2,5(Pyr*)], 100.13 [dd, C-3,4(Pyr*), ^1J(C^{3,4}H) = 157.03 Hz, ^2J(C^{3,4}H^{4,3}) = 5.5 Hz], 33.47 (*C*Me$_3$), 32.77 (C*Me*$_3$). − ^{7}Li NMR ([D$_8$]THF): δ = 3.60. − IR (Nujol, CsBr): ν = 1584 cm^{-1} w, 1560 w, 1487 m, 1459 m, 1450 sh, 1392 w, 1388 m, 1381 w, 1348 s, 1299 m, 1265 w, 1248 s, 1200 s, 1139 w, 1051 sh, 1040 vs, 983 m, 954 sh, 949 w, 910 m, 886 s, 848 w, 822 w, 764 w, 732 vs, 713 vs, 674 w, 622 w, 574 m, 519 s, 515 sh, 429 m, 405 w, 337 w. − MS (70 eV, sample temp. 293 K); *m*/*z* (%): 185 (4) [LiPyr*$^+$], 179 (15) [HPyr*$^+$], 164 (83) [HPyr*$^+$ − Me], 149 (18) [HPyr*$^+$ − 2Me], 115 (73), 72 (100) [thf$^+$], 57 (21) [*t*Bu$^+$].

[Tris(trimethylsilyl)methyl]zinc Chloride (**3**): Tris(trimethylsilyl)-methane (8.47 g, 36.4 mmol) was dissolved in a mixture of tetrahydrofuran (45 ml) and diethyl ether (8.5 ml). At 0°C, a solution of methyllithium in diethyl ether (27.7 ml, 1.6 M, 44.3 mmol) was added. After stirring for 8 h at room temp., the solution was heated under reflux for an additional 6 h to destroy the remaining methyllithium. At room temp., anhydrous ZnCl$_2$ (4.96 g) was added in small portions and the mixture was stirred for 8 h. All volatile materials were then removed in vacuo and the residue was redissolved in diethyl ether. The insoluble part of the residue (LiCl) was filtered off, and the ethereal solution was dried and concentrated. The solid material was sublimed at 110°C in vacuo to afford LiCl-free **3** (3.1 g, 9.3 mmol, 26%), m.p. 211°C. − ^{1}H NMR ([D$_8$]THF): δ = 0.19. − ^{13}C NMR ([D$_8$]THF): δ = 6.38 [SiMe$_3$, ^1J(SiC) = 49.8 Hz]. − ^{29}Si NMR ([D$_8$]THF): δ = −2.75. − IR: ν = 1462 cm^{-1} m, 1377 m, 1262 s, 1250 s, 861 vs, 842 vs, 784 w, 725 w, 673 m, 661 m, 630 w, 614 w. − MS (70 eV, sample temp. 360 K, source temp. 470 K); *m*/*z* (%): 315 (12.8) [M$^+$ − Me], 201 (100) [C(SiMe$_3$)$_3^+$ − 2Me], 73 (27) [SiMe$_3^+$]. − C$_{10}$H$_{27}$ClSi$_3$Zn: calcd. C 36.13, H 8.19; found C 34.57, H 8.19.

Bis[tris(trimethylsilyl)methyl]zinc Chloride 2,5-Di(tert-butyl)-pyrrolide (**4**): At 0°C, a solution of *n*-butyllithium (2.5 M in hexane) was added dropwise to a solution of **1** (0.65 g, 3.62 mmol) in 20 ml diethyl ether, so as to give a colorless suspension of **2**. Sublimed **3** (2.4 g, 7.2 mmol), dissolved in 20 ml of diethyl ether, was then slowly added to this suspension. Once a clear solution had been obtained, all volatile materials were removed in vacuo. The residue was redissolved in *n*-pentane and insoluble LiCl was filtered off. At −20°C, colorless **4** co-crystallized with a stoichiometric amount of *n*-pentane (1.85 g, 2.1 mmol, 58%); dec. at 75°C. − ^{1}H NMR (C$_6$D$_6$): δ = 6.22 [CH(Pyr*)], 1.40 [CMe$_3$(Pyr*)], 0.32 [SiMe$_3$]. − ^{13}C NMR (C$_6$D$_6$): δ = 148.57 [C-2,5(Pyr*)], 104.60 [C-3,4(Pyr*)], 34.63 [C*Me*$_3$], 7.13 [SiMe$_3$]. − IR (Nujol, CsBr): ν = 1364 cm^{-1} m, 1349 m, 1283 m, 1259 vs, 1248 vs, 1207 m, 1154 w, 1148 sh, 1077 w, 1047 m, 1021 m, 982 w, 860 vs, 850 sh, 797 s, 782 s, 749 m, 723 m, 673 s, 660 s, 621 m, 550 w, 529 w, 471 m, 442 w, 362 w. − MS (70 eV, sample temp. 425 K, source temp. 460 K); *m*/*z* (%): 611 (4.5) {[(Me$_3$Si)$_3$CZn]$_2$Cl − CH$_2^+$}, 473 (49.5) [(Me$_3$Si)$_3$-CZnPyr*$^+$], 458 (7.9) [(Me$_3$Si)$_3$CZnPyr*$^+$ − Me], 315 (54.9) [(Me$_3$Si)$_3$CZnCl$^+$ − Me], 295 (17.3) [(Me$_3$Si)$_3$CZn$^+$], 216 (7.4) [(Me$_3$Si)$_3$C$^+$ − Me], 201 (30.5) [(Me$_3$Si)$_3$C$^+$ − 2Me], 179 (100) [HPyr*$^+$]. − MS (70 eV, sample temp. 460 K, source temp. 460 K); *m*/*z* (%): 626 (1.3) [M$^+$ − 2SiMe$_3$ − 2MeH], 611 (15.3) {[(Me$_3$Si)$_3$CZn]$_2$Cl − CH$_2^+$}, 593 (100) [M$^+$ − Me − 2SiMe$_3$ − CH$_2$], 315 (20.6) [(Me$_3$Si)$_3$CZnCl$^+$ − Me], 295 (98.1) [(Me$_3$Si)$_3$CZn$^+$], 216 (8.7) [(Me$_3$Si)$_3$C$^+$ − Me], 201 (23.3) [(Me$_3$Si)$_3$C$^+$ − 2Me]. − C$_{32}$H$_{74}$ClNSi$_6$Zn$_2$: calcd. C 47.58, H 9.24, N 1.73; found C 47.65, H 9.23, N 1.44.

Indium(I) 2,5-Di(tert-butyl)pyrrolide (**5**): As described above, a suspension of LiPyr* was prepared from HPyr* (2.7 g, 15 mmol) and a stoichiometric amount of *n*BuLi in 50 ml of THF. At −110°C, In$^{\mathrm{I}}$Cl powder (2.2 g, 14.6 mmol) was added. During warming to room temp., the orange color of InCl disappeared. Thereafter, the reaction mixture was stirred for an additional 10 h. The solution was then concentrated to a volume of approximately

Table 2. Crystallographic data of **1**, **1**·thf, **2**, and **4**, as well as details of the structure solution and refinement procedures

Compound	**1**	**1**·thf	**2**	**4**·0.67pentane
Formula	C$_{12}$H$_{21}$N	C$_{16}$H$_{25}$NO	C$_{20}$H$_{36}$LiNO$_2$	C$_{35.33}$H$_{81.99}$ClNSi$_6$Zn$_2$
formula mass [g·mol^{-1}]	179.30	247.37	329.44	855.70
T [K]	163(2)	163(2)	193(2)	193(3)
Space group[28]	*P*1 (No. 2)	*P*2$_1$/*m* (No. 11)	*Pnna* (No. 52)	*Pnma* (No. 62)
a [pm]	944.28(5)	642.55(2)	1001.3(1)	1793.0(3)
b [pm]	1333.07(8)	1603.21(5)	1759.8(2)	1780.8(3)
c [pm]	1494.61(9)	802.46(2)	1177.7(2)	1575.6(2)
α [°]	83.516(1)	90	90	90
β [°]	77.668(1)	98.194(2)	90	90
γ [°]	80.239(1)	90	90	90
V [nm^3]	1.8056(2)	0.81821(4)	2.0752(5)	5.031(1)
Z	6	2	4	4
$d_{calcd.}$ [g·cm^3]	0.989	1.004	1.054	1.130
μ [mm^{-1}]	0.057	0.062	0.065	1.172
F(000)	600	272	728	1848
Scan range [°]	1.4 < θ < 25	6.8 < θ < 26.4	2.7 < θ < 24.0	1.7 < θ < 26.0
Measured data	9291	4471	14180	5118
Unique data (R_{int})	4903 (0.025)	1357	1596 (0.055)	5118
Parameters	382	97	128	406
*wR*2[a] (all data)	0.1437	0.1842	0.2760	0.1773
*R*1[a] (all data)	0.0806	0.0883	0.1015	0.0843
Data [*I* > 2σ(*I*)]	3551	1075	1362	3867
R_1[a] [*I* > 2σ(*I*)]	0.0537	0.0703	0.0925	0.0599
Goof[b] on *F*^{2}	1.021	1.090	1.125	1.084
Residual density [e·A^{-3}]	0.19/−0.28	0.38/−0.21	0.63/−0.26	1.10/−0.67

[a] Definition of the *R* values: $R_1 = (\Sigma||F_o| - |F_c||)/\Sigma|F_o|$; $wR_2 = \{\Sigma[w(F_o^2 - F_c^2)^2]/\Sigma[w(F_o^2)^2]\}^{1/2}$ with $w^{-1} = \sigma^2(F_o^2) + (aP)^2$. − [b] $s = \{\Sigma[w(F_o^2 - F_c^2)^2]/(N_o - N_p)\}^{1/2}$.

20 ml and the precipitated LiCl was filtered off. All volatiles were then removed in vacuo. Subsequent sublimation at 80°C and 5×10^{-3} Torr yielded a fraction of InPyr* still contaminated with traces of THF. A second sublimation gave colorless cuboids of InPyr* (4.5 mmol, 31%). These crystals were found to be composed of very thin plates and proved unsuitable for an X-ray structure determination. For NMR data, see Table 1; for discussion of relevant IR/Raman data, see text. – $C_{12}H_{20}NIn$ (293.12): calcd. In 39.17; found In 38.3 (complexometric titration), 38.9 (ICP).

X-ray Crystallographic Studies:[27] Suitable single crystals of **1**, **1**·thf, and **4** were covered with Nujol, mounted on a Siemens P4 diffractometer, and examined with graphite-monochromated Mo-K_α radiation (λ = 71.073 pm). For the collection of data sets for **1** and **1**·thf, the diffractometer was equipped with a Siemens SMART-CCD area detector. Due to its low melting point, compound **1**·thf was kept at temperatures below −30°C during handling and mounting on the diffractometer. For the data collection of **2**, a STOE-IPDS diffractometer was used. Crystallographic parameters and details of the data collection are summarized in Table 2.

All structures were solved by direct methods with the software package SHELXTL-Plus[29] and refined with the program SHELXL-93.[30] Neutral atom scattering factors were taken from Cromer and Mann[31] and for the hydrogen atoms from Stewart et al.[32] The non-hydrogen atoms were refined anisotropically. The H atoms of **1** and **1**·thf were refined as a riding model with restriction of ideal geometry at the corresponding carbon atoms, whereas the nitrogen-bonded hydrogen atoms were refined isotropically. The H atoms of **2** were refined group by group to a common C–H bond length while maintaining ideal geometry at the corresponding C atoms, whereas the azacyclopentadienide-bonded hydrogen atoms were refined isotropically. The hydrogen atoms of **4** were refined isotropically, with the exception of those of the *tert*-butyl groups and of the *n*-pentane molecule, which were calculated in ideal positions with a C–H distance of 96 pm. The *n*-pentane molecules located between the molecules of **4** (Figure 6) were considered to have an occupancy factor of 0.67.

[1] R. King, M. Bisnette, *Inorg. Chem.* **1964**, *3*, 796.
[2] O. Schwarz, Ph.D. Thesis, University Stuttgart, in preparation.
[3] N. Kuhn, G. Henkel, S. Stubenrauch, *Angew. Chem.* **1992**, *104*, 766; *Angew. Chem. Int. Ed. Engl.* **1992**, *31*, 778.
[4] [4a] M. Porchia, F. Benetollo, N. Brianese, G. Rosetto, P. Zanella, G. Bombieri, *J. Organomet. Chem.* **1992**, *424*, 1. – [4b] J. Tödtmann, W. Schwarz, J. Weidlein, A. Haaland, *Z. Naturforsch.* **1993**, *48b*, 1437. – [4c] H.-D. Hausen, J. Tödtmann, J. Weidlein, *J. Organomet. Chem.* **1994**, *466*, C1. – [4d] H.-D. Hausen, J. Tödtmann, J. Weidlein, *Z. Naturforsch.* **1994**, *49b*, 430.
[5] F. Smith, R. Barrow, *J. Chem. Soc., Faraday Trans.* **1958**, *54*, 826.
[6] [6a] R. Ramasseul, A. Rassat, *Bull. Soc. Chim. Fr.* **1965**, 3136. – [6b] G. Gragnaire, R. Ramasseul, A. Rassat, *Bull. Soc. Chim. Fr.* **1969**, 415.
[7] M. Westerhausen, B. Rademacher, W. Schwarz, J. Weidlein, S. Henkel, *J. Organomet. Chem.* **1994**, *469*, 135 and references cited therein.
[8] O. T. Beachley Jr., R. Blom, M. R. Churchill, K. Faegri Jr., J. C. Fettinger, J. C. Pazik, L. Victoriano, *Organometallics* **1989**, *8*, 346.
[9] R. Hacker, E. Kaufmann, P. v. R. Schleyer, W. Mahdi, H. Diedrich, *Chem. Ber.* **1987**, *120*, 1533.
[10] [10a] M. A. Khan, D. G. Tuck, *Acta Crystallogr.* **1984**, *C40*, 60. – [10b] R. Gregorzik, H. Vahrenkamp, *Chem. Ber.* **1994**, *127*, 1857.
[11] M. Westerhausen, M. Wieneke, W. Schwarz, *J. Organomet. Chem.* **1996**, *522*, 137.
[12] *Struct. Rep.* **1960**, *25*, 283; *ibid.* **1961**, *26*, 319; *ibid.* **1978**, *43a*, 154.
[13] S. S. Al-Juaid, C. Eaborn, A. Habtemariam, P. B. Hitchcock, J. D. Smith, K. Tavakkoli, A. D. Webb, *J. Organomet. Chem.* **1993**, *462*, 45. See also the review: C. Eaborn, J. D. Smith, *Coord. Chem. Rev.* **1996**, *154*, 125.
[14] J. Behm, S. D. Lotz, W. A. Herrmann, *Z. Anorg. Allg. Chem.* **1993**, *619*, 849.
[15] T. Aoyagi, H. M. M. Shearer, K. Wade, G. Whitehead, *J. Organomet. Chem.* **1978**, *146*, C29.
[16] P. H. M. Budzelaar, J. Boersma, G. J. M. van der Kerk, A. L. Spek, A. J. M. Duisenberg, *J. Organomet. Chem.* **1985**, *281*, 123. See also the review: J. Boersma in *Comprehensive Organometallic Chemistry*, vol. 2 (Eds.: G. Wilkinson, F. G. A. Stone, E. W. Abel), Pergamon, Oxford, **1982**, chapter 16, p. 823.
[17] [17a] R. Blom, J. Boersma, P. H. M. Budzelaar, B. Fischer, A. Haaland, H. V. Volden, J. Weidlein, *Acta Chem. Scand.* **1986**, *A40*, 113. – [17b] B. Fischer, P. Wijkens, J. Boersma, G. van Koten, W. J. J. Smeets, A. L. Spek, P. H. M. Budzelaar, *J. Organomet. Chem.* **1989**, *376*, 223.
[18] [18a] A. Haaland, K. Hedberg, P. P. Power, *Inorg. Chem.* **1984**, *23*, 1972. – [18b] P. P. Power, K. Ruhlandt-Senge, S. C. Shoner, *Inorg. Chem.* **1991**, *30*, 5013. – [18c] W. S. Rees, D. M. Green, W. Hesse, *Polyhedron* **1992**, *11*, 1667.
[19] [19a] H. Grützmacher, M. Steiner, H. Pritzkow, L. Zsolnai, G. Huttner, A. Sebald, *Chem. Ber.* **1992**, *125*, 2199. – [19b] P. H. M. Budzelaar, J. Boersma, G. J. M. van der Kerk, A. L. Spek, *Organometallics* **1984**, *3*, 1187.
[20] [20a] W. A. Herrmann, I. Schweitzer, P. S. Skell, M. L. Ziegler, K. Weidenhammer, B. Nuber, *Chem. Ber.* **1979**, *112*, 2423. – [20b] K. Yünlü, F. Basolo, A. L. Rheingold, *J. Organomet. Chem.* **1987**, *330*, 221. – [20c] N. Kuhn, E.-M. Horn, R. Boese, D. Bläser, *Chem. Ber.* **1989**, *122*, 2275. – [20d] N. Kuhn, G. Henkel, J. Kreutzberg, *Angew. Chem.* **1990**, *102*, 1179; *Angew. Chem. Int. Ed. Engl.* **1990**, *29*, 1143.
[21] [21a] F. Glockling, N. S. Hosmane, V. B. Mahale, J. J. Swindall, L. Magos, T. J. King, *J. Chem. Res. (S)* **1977**, 116; *J. Chem. Res. (R)* **1977**, 1201. – [21b] C. Eaborn, N. Retta, J. D. Smith, *J. Organomet. Chem.* **1980**, *190*, 101. – [21c] M. Westerhausen, B. Rademacher, W. Poll, *J. Organomet. Chem.* **1991**, *421*, 175.
[22] N. Kuhn, G. Henkel, S. Stubenrauch, *J. Chem. Soc., Chem. Commun.* **1992**, 760.
[23] O. G. Garkusha, B. V. Lokshin, R. B. Materikova, L. M. Golubinskaya, V. I. Bregadze, A. P. Kurbakova, *J. Organomet. Chem.* **1988**, *342*, 282.
[24] A. Haaland, private communication, **1997**.
[25] H. Schumann, C. Janiak, F. Görlitz, J. Loebel, A. Diedrich, *J. Organomet. Chem.* **1989**, *363*, 243.
[26] [26a] A. H. Cowley, N. C. Norman, M. Pakulski, *Inorg. Synth.* **1990**, *27*, 235. – [26b] F. Schaller, W. Schwarz, H.-D. Hausen, K. W. Klinkhammer, J. Weidlein, *Z. Anorg. Allg. Chem.* **1997**, *623*, 1455.
[27] Crystallographic data (excluding structure factors) for the structures of **1**, **1**·thf, **2**, and **4** have been deposited with the Cambridge Crystallographic Data Centre as supplementary publication no. CCDC-101239. Copies of the data can be obtained on application to CCDC, 12 Union Road, Cambridge, CB2 1EZ, U.K. [Fax: (internat.) + 44(0)1223/336033; E-mail: deposit@ccdc.cam.ac.uk].
[28] T. Hahn (Ed.), *International Tables for Crystallography*, vol. A ("Space Group Symmetry"), 2nd ed., D. Reidel, Dordrecht, **1984**.
[29] SHELXTL Plus, PC version, Siemens Analytical X-ray Instruments, Inc., **1980**.
[30] G. M. Sheldrick, *SHELXL-93*, Universität Göttingen, **1993**.
[31] D. T. Cromer, J. B. Mann, *Acta Crystallogr.* **1968**, *24*, 321.
[32] R. F. Stewart, E. R. Davidson, W. T. Simpson, *J. Chem. Phys.* **1965**, *42*, 3175.

[98090]

On the Geometry of the Fulleride Dianion C_{60}^{2-} in Crystalline Fullerides – Syntheses and Crystal Structures of $[M(NH_3)_6]C_{60} \cdot 6\ NH_3$ ($M = Mn^{2+}$, Cd^{2+})☆

Klaus Himmel[a] and Martin Jansen*[b]

Institut für Anorganische Chemie der Rheinischen Friedrich-Wilhelms-Universität[a],
Gerhard-Domagk-Straße 1, D-53121 Bonn, Germany

Max-Planck-Institut für Festkörperforschung[b],
Heisenbergstraße 1, D-70569 Stuttgart, Germany
Fax: (internat.) +49(0)711/6891502
E-mail: hamilton@vsibl.mpi-stuttgart.mpg.de

Received April 16, 1998

Keywords: Fullerides / Crystal structure analysis / Jahn-Teller effect

The fullerides $[M(NH_3)_6]C_{60}$ ($M = Mn^{2+}$, Cd^{2+}) have been synthesized by ion exchange in liquid ammonia and analyzed by X-ray single-crystal diffraction. With both complex cations the C_{60}^{2-} units are in fixed orientations, and their geometries have been determined with good accuracy. An inspection of the fulleride dianions with respect to geometric deformations in the title compounds and three further independent determinations has led to the conclusion that no significant static Jahn-Teller distortion is present.

Introduction

Due to the high symmetry of icosahedral C_{60} its LUMO is triply degenerate (t_{1u}). In accordance with the Jahn-Teller theorem[1] partial filling of the LUMO with one to five electrons should remove this degeneracy and possibly cause a structural distortion in the carbon cage. The nature and the degree of this distortion, however, are difficult to determine experimentally since in most cases structure determinations suffer from orientational disorder of the almost spheric fullerides. Jahn-Teller distortion could reduce the symmetry to D_{5d}, D_{3d}, D_{2h}, C_{2h}, or C_i, all of which are subgroups of I_h. From linear approximation D_{5d} and D_{3d} structures have been derived as possible minima, and the D_{2h} structure as a saddle point of the associated potential energy surface[2]. For the monoanion C_{60}^- the relative energies of these configurations have been calculated as roughly equal[3]. Thus, rearrangement among different Jahn-Teller distorted structures on the potential energy surface would be an easy process. Density functional calculations[4] have yielded D_{2h} symmetry for the singlet and D_{3d} symmetry for the triplet ground state of the dianion C_{60}^{2-}. All theoretical approaches end up with the result that structural changes due to a Jahn-Teller splitting of the formerly degenerate t_{1u} LUMO should be very small. Only modest static Jahn-Teller energy gains of approximately 0.1 eV are predicted which fall in the range of typical vibrational frequencies. Thus, C_{60}^{2-} anions could well be subject to a dynamic exchange between several Jahn-Teller distorted structures[5][6][7]. In the superposition of, e.g., the six degenerate D_{5d} configurations the higher symmetry I_h would be restored. In order to be able to investigate the degree of distortion and to decide, whether those distortions are static or dynamic in nature, precise X-ray crystal structure data are desirable.

In our earlier work we have introduced bulky organic cations into the structure to stabilize fulleride anions in a fixed orientation[8][9]. Other groups have used different organic or organometallic cations, or cryptates of alkali metals[10][11][12][13][14]. Nevertheless, many of the structures still exhibit disorder in the anionic or cationic parts of the structure, thereby reducing the accuracy of the information gained from structure determinations. By the synthesis of $[Ba(NH_3)_7]C_{60} \cdot NH_3$[15] we have demonstrated that complex ammines are well suited to fix the orientation of the fulleride cages. More recently we have exemplified with the preparation of $[Ni(NH_3)_6]C_{60} \cdot 6\ NH_3$ that a broad variety of fulleride salts with different counterions is accessible by ion exchange in liquid ammonia[16]. Here we present the synthesis and characterization of two new fullerides, $[M(NH_3)_6]C_{60} \cdot 6\ NH_3$ ($M = Mn^{2+}$, Cd^{2+}). Both compounds are sufficiently well determined to allow for an inspection of geometrical distortions in the C_{60}^{2-} cage. The results are discussed with respect to the Jahn-Teller effect and compared to those obtained in the crystal-structure investigations of $[Ba(NH_3)_7]C_{60} \cdot NH_3$, $[Ni(NH_3)_6]C_{60} \cdot 6\ NH_3$ and $(PPN)_2C_{60}$ [PPN^+ = bis(triphenylphosphanyl)iminium cation][12].

Results and Discussion

Like isostructural $[Ni(NH_3)_6]C_{60} \cdot 6\ NH_3$ the title compounds crystallize in a distorted rock salt type of structure (Figure 1). The fulleride dianions form a distorted *fcc* sublattice where hexaammine complexes of the metal ions occupy the octahedral sites.

 © WILEY-VCH Verlag GmbH, D-69451 Weinheim, 1998 1434–1948/98/0808–1183 $ 17.50+.50/0

Figure 1. Rock salt type arrangement of fulleride anions and transition metal ammine complexes

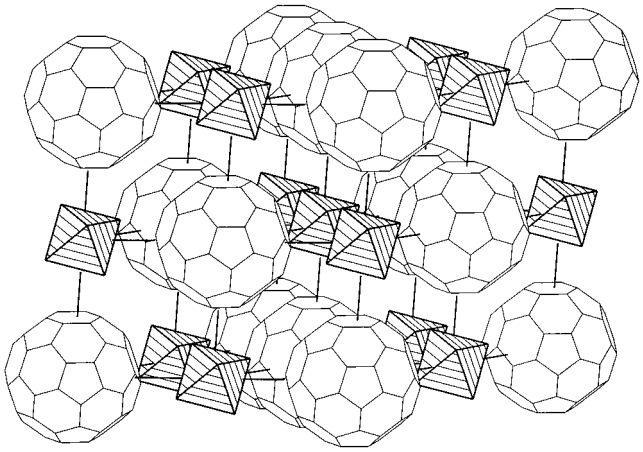

Each molecule of ammonia of solvation is coordinated via a hydrogen bond to one of the ammonia molecules in the ligand sphere of the ammine complex. This extended coordination sphere (Figure 2) can change its shape flexibly to meet the needs of the octahedral site of the C_{60}^{2-} sublattice, at the same time absorbing differences in the size of the cations [$r(Ni^{2+})$ = 69 pm, $r(Mn^{2+})$ = 83 pm (high spin), $r(Cd^{2+})$ = 95 pm[17]] and fixing the orientation of the fulleride anion.

Figure 2. ORTEP plot[24] of the fulleride dianion in $[Mn(NH_3)_6]C_{60}\cdot 6\ NH_3$ (50% probability ellipsoids)

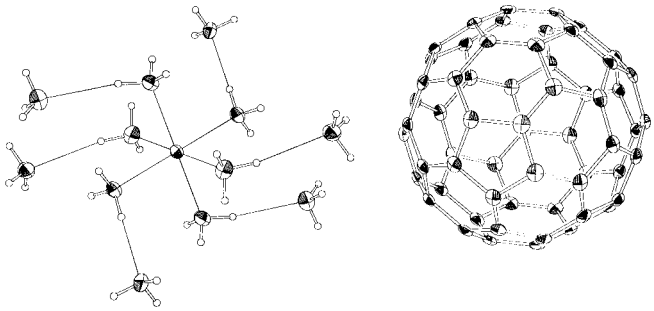

The obvious relationship between the structures presented here and the NaCl-type structure implies Coulomb interactions mainly to determine the crystal structure. However, the deviation from cubic symmetry indicates the presence of other forces which affect the structure at the same time. Short distances of hydrogen atoms to the fulleride carbon atoms suggest interactions between the $N^{\delta-}-H^{\delta+}$ dipoles and electron density on the surface of the dianion. The hydrogen atoms are located above the centres of the 6:6 and 6:5 ring junctures where the majority of π-electron density is located. Similar interactions between $C^{\delta-}-H^{\delta+}$ dipoles and fullerides have been reported previously and are assumed to be responsible for the stabilization of the dianion in a fixed orientation[12].

In all fullerides of complex ammoniates thermal displacement parameters of the carbon atoms are physically reasonable and do not indicate any static or rotational disorder. Thus, the structures seem to be of sufficient accuracy to allow for an inspection of geometric distortions of C_{60}^{2-}, e.g. of Jahn-Teller type. In an earlier investigation of $(PPN)_2C_{60}$ [PPN^+ = bis(triphenylphosphanyl)iminium cation][12] such distortions have been reported to be present. The authors have observed a change in point symmetry of the fullerene moiety from I_h to C_i and have interpreted this distortion as due principally to the Jahn-Teller effect.

For an evaluation of the degree of ellipsoidal distortion from the ideal sphere we have considered the longest and shortest carbon-to-carbon diameters. In Table 1 such diameters of the title compounds, of $[Ni(NH_3)_6]C_{60}\cdot 6\ NH_3$, $[Ba(NH_3)_7]C_{60}\cdot NH_3$, $(PPN)_2C_{60}$, and of neutral C_{60} as determined in two different investigations[18][19] are given. The variation in diameters is largest for $(PPN)_2C_{60}$ and very small for $[Ba(NH_3)_7]C_{60}\cdot NH_3$, while all other compounds fall in between. Remarkably, even in the most reliable determinations neutral C_{60} exhibits a small deviation from the ideal shape of a sphere.

In order to reveal any particular pattern in the arrangement of atoms with an elongated or shortened radial distance to the centre of the fullerene cage, the distances between the carbon atoms and the centre of the fulleride dianion have been calculated with the program package PARST97[20]. The calculations were based on the lattice parameters, the atom coordinates and their respective standard deviations as determined in the different crystal-structure analyses.

For each fulleride the individual distances (d_i) of the carbon atoms from the centre have been compared to the mean radius r. All differences $d_i - r$ that are larger than three times the standard deviation of the individual radial distances have been treated as significant.

The results of the calculations are visualized in Figure 3. For the fulleride moieties in the different crystal structure analyses those atoms with a significantly elongated radial distance to the centre are plotted with a crossed hatching, those with a shortened radial distance are plotted with a simple hatching.

Three of the triclinic structures {$[Mn(NH_3)_6]C_{60}\cdot 6\ NH_3$, $[Ni(NH_3)_6]C_{60}\cdot 6\ NH_3$, and $(PPN)_2C_{60}$} seem to exhibit similarities in the pattern. Elongated atoms form a closed pentagon, suggesting a symmetry reduction to D_{5d} which has been discussed previously[7] as the most probable distortion caused by the Jahn-Teller effect. However, the elongations discussed here are as small as 0.01 A and in addition to experimental error might be caused by crystal packing effects. As some of the dianions, e.g. in $[Ba(NH_3)_7]C_{60}\cdot NH_3$, are not significantly distorted at all, the present experimental data give no conclusive evidence for an intrinsic distortion of C_{60}^{2-} due to a static Jahn Teller effect.

In order to check our approach, the deviation from ideal I_h symmetry was determined using a procedure which has been described previously[4]: First, the dianion was oriented in a fixed Cartesian frame, with x, y, and z directions coinciding with C_2 symmetry axes. For each atom, the Cartesian displacements from the icosahedral position (i.e., from the position of that atom in a C_{60} cage of I_h symmetry

Figure 3. Geometry of fulleride anions as determined in different crystal structure analyses; atoms with an elongated distance to the centre are plotted with a cross-hatched pattern, those with a shortened distance relative to the mean radius are plotted as hatched spheres

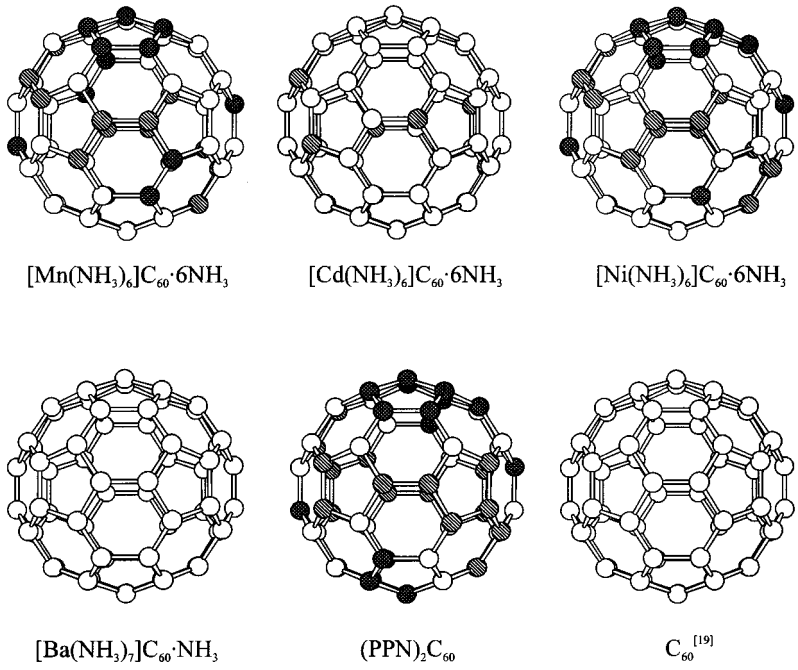

with the same average single and double bond lengths as found for the anion) were calculated and the root mean squares (r.m.s.) value for the distances between corresponding atoms was determined. To put these values into an appropriate context we have applied the same formalism to neutral C_{60} and have included the results in Table 1.

as a result of experimental error, even at very favourable experimental conditions.

The considerations presented here have led us to the conclusion that at the present state of knowledge there is no experimental evidence for a static deviation from icosahedral symmetry of the dianion C_{60}^{2-}. As an alternative a dynamic Jahn-Teller effect could be discussed. The related "breathing" movement of the fullerene cage should lead to enlarged thermal parameters of the carbon atoms in radial direction with respect to the centre of the fulleride. However, the thermal displacement parameters as determined reflect the rigid body librational motion of the fulleride rather well and do not show any significant enlargement in radial direction (Figure 2). Thus, the amplitudes of vibrations caused by a dynamic Jahn-Teller effect must be smaller than or equal to the thermal displacement parameters in radial direction, as determined by X-ray crystal-

Table 1. Geometry of the fullerides: largest and shortest carbon-to-carbon distances ($Ø_{max.}$, $Ø_{min.}$) and their difference ΔØ are given; r.m.s values were calculated as described in the text

Compound	$Ø_{max.}$ [A]	$Ø_{min.}$ [A]	ΔØ [A]	r.m.s. value [A]
$[Ni(NH_3)_6]C_{60}\cdot 6\ NH_3$ (triclinic)	7.1106 (C13−C13′)	7.0408 (C16−C16′)	0.0698	0.0118
$[Mn(NH_3)_6]C_{60}\cdot 6\ NH_3$ (triclinic)	7.1132 (C4−C4′)	7.0484 (C9−C9′)	0.0648	0.0110
$[Cd(NH_3)_6]C_{60}\cdot 6\ NH_3$ (triclinic)	7.1034 (C14−C14′)	7.0286 (C13−C13′)	0.0748	0.0144
$[Ba(NH_3)_7]C_{60}\cdot NH_3$ (trigonal)	7.0923 (C5−C10)	7.0781 (C3−C11)	0.0142	0.0075
$[PPN]_2C_{60}$ (triclinic)	7.1264 (C15−C15′)	7.0394 (C9−C9′)	0.087	0.0155
C_{60} (cubic)[19]	7.0926 (C8−C8′)	7.0678 (C2−C2′)	0.0248	0.031
C_{60} (cubic)[18]	7.112 (C8−C8′)	7.0824 (C4−C4′)	0.0296	0.0171

Again the dianion in $[Ba(NH_3)_7]C_{60}\cdot NH_3$ shows the smallest variation from ideal atom positions, while this time the deviation from I_h is strongest for neutral C_{60}. Even for $(PPN)_2C_{60}$, which has shown the greatest ellipsoidal distortion, the deviation from icosahedral atom positions is modest. Neutral C_{60} clearly can not be subject to a Jahn-Teller distortion. Thus, the observed deviations can only reflect experimental error and perhaps effects of crystal packing. Since in a crystalline environment not all symmetry elements of point group I_h can agree with a given site symmetry, small deviations from the ideal have to be expected

lography. Based on theoretical calculations only very small deviations from an ideal icosahedron have been predicted upon filling the formerly degenerate LUMO of neutral C_{60}. In this paper we present experimental evidence that in a crystalline environment I_h symmetry of anionic C_{60}^{2-} units can be retained. Any deviation found is in the range of or smaller than the experimental error.

We are grateful to *Hoechst AG*, Frankfurt, for providing C_{60}.

Experimental Section

$[M(NH_3)_6]C_{60}\cdot 6\ NH_3$ (M = Mn^{2+}, Cd^{2+}) has been synthesized by ion exchange in liquid ammonia. All reactions were carried out under dry argon, either in all-glass reaction and handling vessels that were dried in vacuo, or in a glove box. Liquid ammonia (Bayer AG, purity 2.8) was first distilled from sodium, then from potassium, and was stored as a potassium/ammonia solution at 195 K. Buckminsterfullerene C_{60} (Hoechst AG, gold grade) was dried before use for 12 h at 300°C in vacuo. A thoroughly dried exchange resin (Amberlyst 15, Fluka) was loaded with M^{2+} (M = Mn^{2+}, Cd^{2+}) and placed on one side of an H-type glass vessel equipped with a glass sieve (porosity 3). K_2C_{60} was placed on the other side of the sieve. After cooling (ethanol/dry-ice slush) ammonia was condensed into the vessel until the glass sieve was completely covered. The reaction mixture was stored at 230 K for about 3 weeks. During this period K_2C_{60} slowly diffused onto the ion-exchange resin where $[M(NH_3)_6]C_{60}\cdot 6\ NH_3$ precipitated as shiny black platelets that are sensitive to air, moisture and elevated temperatures. Crystals were transferred from liquid ammonia into a mixture of inert oils (1:1 Perfluorpolyether 216, Riedel-de Haen/Perfluorpolyether Fomblin Y HVAC 40/11, Aldrich) which was cooled with a nitrogen stream to 230 K, and picked up on the tip of a glass capillary mounted on a goniometer head[21].

Table 2. Crystallographic data

	$[Mn(NH_3)_6]C_{60}\cdot 6\ NH_3$	$[Cd(NH_3)_6]C_{60}\cdot 6\ NH_3$
Formula	$C_{60}H_{36}N_{12}Mn$	$C_{60}H_{36}N_{12}Cd$
M_r [g/mol]	938.72	1037.41
Crystal system	triclinic	triclinic
Space group	*P*1	*P*1
a[pm]	996.7(1)	999.2(3)
b [pm]	1023.0(1)	1024.4(3)
c [pm]	1055.4(1)	1055.5(2)
α [°]	77.60(1)	77.49(2)
β [°]	79.56(1)	79.34(3)
γ [°]	79.13(1)	78.96(3)
V [nm^3]	1.0210(2)	1.0235(5)
Z	1	1
$\rho_{calcd.}$ [g cm^{-3}]	1.619	1.683
μ(Mo-K_α) [mm^{-1}]	0.55	0.599
Measured reflns.	6495	4715
Independent reflns.	3993	3598
Observed reflns. [$I > 2\sigma(I)$]	3201	2904
θ_{max} [°]	26	25
Parameters	385	361
*R*1 [$F > 4\sigma(F)$]	0.035	0.047
*wR*2 [F^2, all data]	0.102	0.118

Structure Determination: Diffraction data were collected with an Enraf-Nonius CAD4 diffractometer with graphite-monochromated Mo-K_α radiation (λ = 71.069 pm) at 113(2) K. The structures were solved by the Patterson method[22] and refined on F^2 using all independent reflections[23]. Hydrogen atoms of the ammonia molecules were located by difference Fourier synthesis. Details of the crystal structure determinations for $[M(NH_3)_6]C_{60}\cdot 6\ NH_3$ (M = Mn, Cd) are given in Table 2.

Further details of the crystal structure investigations may be obtained from the Fachinformationszentrum Karlsruhe, D-76344 Eggenstein-Leopoldshafen, on quoting the depository numbers CSD-408601 (Mn) and -408602 (Cd).

☆ Dedicated to Professor *Heinrich Nöth* on the occasion of his 70th birthday.

[1] H. A. Jahn, E. Teller, *Proc. R. Soc. London A* **1937**, *161*, 220−235.
[2] A. Ceulemans, *J. Chem. Phys.* **1987**, *87*, 5374−5385.
[3] N. Koga, K. Morokuma, *Chem. Phys. Lett.* **1992**, *196*, 191−196.
[4] W. H. Green, Jr., S. M. Gorun, G. Fitzgerald, P. W. Fowler, A. Ceulemans, B. C. Titeca, *J. Phys. Chem.* **1996**, *100*, 14892−14898.
[5] W. Z. Wang, C. L. Wang, A. R. Bishop, L. Yu, z. B. Su, *Phys. Rev. B* **1995**, *51*, 10209−10212.
[6] E. Tosatti, N. Manini, O. Gunnarsson, *Phys. Rev. B* **1996**, *54*, 17184−17190.
[7] W. Z. Wang, C. L. Wang, A. R. Bishop, L. Yu, z. B. Su, *Synth. Met.* **1997**, *86*, 2365−2368.
[8] U. Bilow, M. Jansen, *J. Chem. Soc., Chem. Commun.* **1994**, 403−404.
[9] K. Himmel, M. Jansen, *Z. Anorg. Allg. Chem.* **1998**, *624*, 1−3.
[10] A. Penicaud, A. Perez-Benitez, R. Gleason V., E. Munoz P., R. Escudero, *J. Am. Chem. Soc.* **1993**, *115*, 10392−10393.
[11] W. C. Wan, X. Liu, G. M. Sweeney, W. E. Broderick, *J. Am. Chem. Soc.* **1995**, *117*, 9580−9581.
[12] P. Paul, Z. Xie, R. Bau, P. D. W. Boyd, C. A. Reed, *J. Am. Chem. Soc.* **1994**, *116*, 4145−4146.
[13] C. Janiak, S. Mühle, H. Hemling, K. Köhler, *Polyhedron* **1996**, *15*, 1559−1563
[14] T. F. Fässler, A. Spiekermann, M. E. Spahr, R. Nesper, *Angew. Chem.* **1997**, *109*, 502−504; *Angew. Chem. Int. Ed. Engl.* **1997**, *36*, 486−488.
[15] K. Himmel, M. Jansen, *Inorg. Chem.*, in press
[16] K. Himmel, M. Jansen, *J. Chem. Soc., Chem. Commun.*, in press
[17] R. D. Shannon, *Acta Crystallogr., Sect. A* **1976**, *32*, 751−767.
[18] W. I. F. David, R. M. Ibberson, J. C. Matthewman, K. Prassides, T. J. S. Dennis, J. P. Hare, H. W. Kroto, R. Taylor, D. R. M. Walton, *Nature* **1991**, *353*, 147−149.
[19] H.-B. Bürgi, E. Blanc, D. Schwarzenbach, S. Liu, Y.-J. Lu, M. M. Kappes, J. A. Ibers, *Angew. Chem.* **1992**, *104*, 667−669; *Angew. Chem. Int. Ed. Engl.* **1992**, *31*, 640−642.
[20] M. Nardelli, *PARST97*, University of Parma, Italy, **1997**; *J. Appl. Crystallogr.* **1995**, *28*, 659−660.
[21] T. Kottke, D. Stalke, *J. Appl. Crystallogr.* **1993**, *26*, 615−619; the method was modified to the needs of the preparation in liquid ammonia.
[22] G. M. Sheldrick, *SHELXS 86, Program for Crystal Structure Determination*, University of Göttingen, Germany, **1986**
[23] G. M. Sheldrick, *SHELXL 93, Program for the refinement of Structures*, University of Göttingen, Germany, **1993**
[24] C. K. Johnson, *ORTEP, A Fortran Thermal Ellipsoids Program for Structure Illustrations*, Oak Ridge, Tennessee, **1965** (modified by R. Hundt, University of Bonn, **1970**)

[98112]

Heterobimetallic and Mixed-Valence Chloro-Bridged Complexes with Orthometalated Rhodium(III) and Iridium(III) Fragments☆

Kurt Polborn and Kay Severin*

Institut für Anorganische Chemie der Ludwig-Maximilians-Universität,
Meiserstraße 1, D-80333 München, Germany
Fax.: (internat.) + 49(0)89/5902–214
E-mail: kse@anorg.chemie.uni-muenchen.de

Received February 20, 1998

Keywords: Iridium / Rhodium / Chloro-bridged complexes / Heterobimetallic complexes

The synthesis and characterization of heterobimetallic and mixed-valence complexes in which orthometalated $[(ppy)_2MCl]$ (M = Rh, Ir; ppy = 2-phenylpyridine anion) and $[(bzq)_2RhCl]$ (bzq = benzo[*h*]quinoline anion) fragments are linked via chloro-bridges with rhodium(I), iridium(I), palladium(II), and platinum(II) fragments is reported. These complexes are formed in nearly quantitative yields by metathesis reactions from the respective homodimeric compounds. The structures of $[(ppy)_2Rh(\mu\text{-}Cl)_2Rh(cod)]$ (cod = η^4-1,5-cyclooctadiene) and $[(ppy)_2Rh(\mu\text{-}Cl)_2Pt(PBu_3)\text{-}Cl]$ were determined by X-ray structure analyses.

Introduction

Dichloro-bridged complexes of rhodium and iridium play an important role as starting materials in organometallic chemistry and catalysis. Subsequent functionalization of these complexes is easily possible through bridge-splitting reactions with various donor ligands.[1] Generally, the two metal fragments are symmetrically linked by halide ligands. Dinuclear complexes in which rhodium or iridium complexes are *asymmetrically joined* with a different transition metal fragment, on the other hand, are rare.[2][3][4][5][6][7] Among the more prominent examples are the mixed-valence hydrido complexes shown below. They are produced in catalytic hydrogenation[3] and dehydrogenation[4] reactions with rhodium(I) phosphine complexes. At present there is no general methodology available for the synthesis of such heterodimeric or mixed-valence complexes. Furthermore the reactivity of these compounds is virtually unexplored.

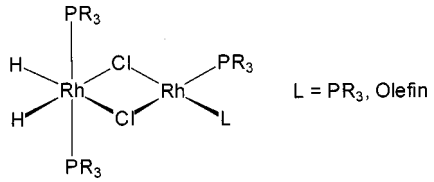

L = PR_3, Olefin

Here we describe the synthesis and characterization of new dinuclear, chloro-bridged complexes containing Rh^{III} or Ir^{III} fragments together with Rh^{I}, Ir^{I}, Pd^{II}, and Pt^{II} fragments. They are obtained by metathesis reactions of $[(cod)MCl]_2$ (M = Rh, Ir) or $[(R_3P)MCl_2]_2$ (M = Pd, Pt; R = Et, *n*-Bu) with the orthometalated Rh^{III} and Ir^{III} complexes $[(bzq)_2RhCl]_2$ or $[(ppy)_2MCl]_2$ (M = Rh, Ir). The latter compounds have found considerable attention since they are powerful photoreducing agents.[8][9]

Dinuclear Rh^{III}-Rh^{I}, Rh^{III}-Ir^{I}, and Ir^{III}-Ir^{I} Complexes

The dinuclear complexes **1**–**3** were obtained in nearly quatitative yield when a suspension of $[(ppy)_2MCl]_2$ (M = Rh, Ir) in dichloromethane was stirred with equivalent amounts of $[(cod)MCl]_2$ (M = Rh, Ir) (Scheme 1). Upon completion of the reactions clear yellow solutions were formed indicating a strongly enhanced solubility of the heterodimeric products with respect to the homodimeric Rh^{III} and Ir^{III} complexes. Yellow powders were obtained after removal of the solvent. Other Rh^{III}-Rh^{I} complexes containing Rh^{III} fragments with orthometalated ligands (e.g. the tridentate *o*,*o*′-$(Me_2NCH_2)C_6H_3$) were described by van Koten[5], Bruce[6], and Mills.[7]

Scheme 1

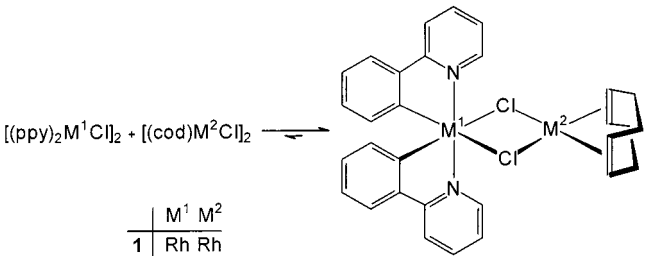

	M^1	M^2
1	Rh	Rh
2	Rh	Ir
3	Ir	Ir

1–**3**

The ^1H and ^{13}C NMR spectra ($CDCl_3$) of racemic **1**–**3** are in accordance with the structures shown in Scheme 1. For the two phenylpyridyl ligands one set of signals is observed. The ^1H NMR spectra of the cyclooctadiene ligand reflect the reduced symmetry of **1**–**3** as compared to $[(cod)MCl]_2$: the vinylic proton signals appear as two well separated groups at δ 3.8 and 4.0.

Minor amounts of starting material can be detected in the ^1H NMR spectra of **1**–**3** indicating a dynamic equilib-

 © WILEY-VCH Verlag GmbH, D-69451 Weinheim, 1998 1434–1948/98/0808–1187 $ 17.50+.50/0

rium between homo- and heterodimeric complexes (K_{eq} > 100). Similar equilibria were observed in solutions of $[(R_3P)PtCl_2]_2$ together with $[(R_3P)PdCl_2]_2$.[10] In these cases, however, the amount of heterodinuclear Pd-Pt complexes present in solution were close to what is expected for a statistical distribution. Quantitative formation of heterodimeric complexes, on the other hand, was also observed in reactions of $[(\eta^3{:}\eta^3\text{-}C_{10}H_{16})RuCl_2]_2$ with various chloro-bridged complexes.[11]

The molecular structure of **1** was confirmed by single crystal X-ray analysis (Figure 1). The Rh^{III} center is coordinated in a slightly distorted octahedral fashion with the two N-donor groups adopting a *trans* configuration. The Rh(μ-Cl)$_2$Rh unit is markedly non-planar with a dihedral angle between the normals to the planes defined by Rh1, Cl1, Cl2 and Rh2, Cl1, Cl2, of 24.14°. Folded Rh(μ-Cl)$_2$Rh units are also found for $[(CO)_2RhCl]_2$,[12] $[(PMe_2Ph)(CO)RhCl]_2$,[13] $[(C_6H_{10})_2RhCl]_2$,[14] $[(PhN{=}NC_6H_4)_2(CO)_2Rh_2]$,[7] $[(CO)_2(cod)Rh_2]$,[2a] and for **5** (Figure 2). According to a recent theoretical and structural analysis of square-planar complexes of the general formula $[L_2M(\mu\text{-}Cl)_2ML_2]$ the main driving force for bending are attractive metal−metal interactions[15] but for **1** direct Rh−Rh interactions are unlikely due to a Rh−Rh bond length of 3.60 A. The Rh2−Cl bond lengths are very close to that in the homodimeric complex $[(cod)RhCl]_2$.[16] Significantly longer are the Rh1−Cl bond lengths (2.55 and 2.57 A), presumably due to the strong σ-donor character of the coordinating carbons in *trans* position.

Figure 1. Molecular structure of complex **1**. Selected bond lengths [A] and angles [°]: Rh2−C26 2.104(4), Rh2−C27 2.120(4), Rh2−Cl2 2.407(1), Rh2−Cl1 2.410(2), Rh1−C11 1.980(4), Rh1−C22 1.982(4), Rh1−N2 2.046(3), Rh1−N1 2.043(4), Rh1−Cl1 2.553(1), Rh1−Cl2 2.569(2), N1−Rh1−Cl1 95.56(11), N1−Rh1−Cl2 86.42(11), Cl1−Rh1−Cl2 81.36(5), N1−Rh1−N2 174.66(14), Cl2−Rh2−Cl1 87.74(5)

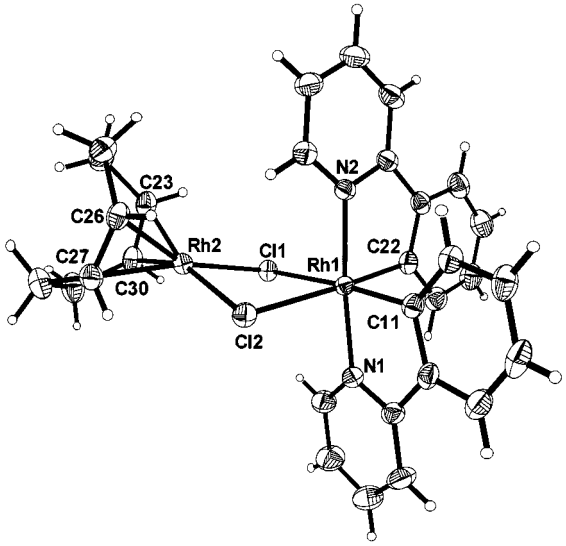

Dinuclear Rh^{III}-Pd^{II}, Rh^{III}-Pt^{II}, and Ir^{III}-Pt^{II} Complexes

Similar as for **1**−**3** the heterobimetallic complexes **4**−**8** are obtained by metathesis reactions of $[(ppy)_2MCl]_2$ (M = Rh, Ir) with the respective chloro-bridged palladium or platinum phosphine complex (Scheme 2). The yields are quantitative for the platinum complexes **5**, **7**, and **8**. ^{1}H NMR spectra ($CDCl_3$) of the palladium complexes **4** and **6** show very small amounts of homodimeric starting material (K_{eq} > 100). The dynamic nature of these metathesis reactions as well as the higher stability of Rh^{III}-Pt^{II} complexes in comparison to the corresponding Rh^{III}-Pd^{II} complexes was confirmed by a direct competition experiment: if one equivalent of $[(ppy)_2Rh(\mu\text{-}Cl)_2Pd(PBu_3)Cl]_2$ (**4**) was mixed with 0.5 equivalents of $[(Bu_3P)PtCl_2]_2$ in dichloromethane the immediate formation of $[(ppy)_2Rh(\mu\text{-}Cl)_2Pt(PBu_3)Cl]_2$ (**5**) together with $[(Bu_3P)PdCl_2]_2$ was observed by ^{31}P NMR spectroscopy. The ratio between **5** and **4**, which was estimated by integration of the respective ^{31}P NMR signals, was 3:1.

Scheme 2

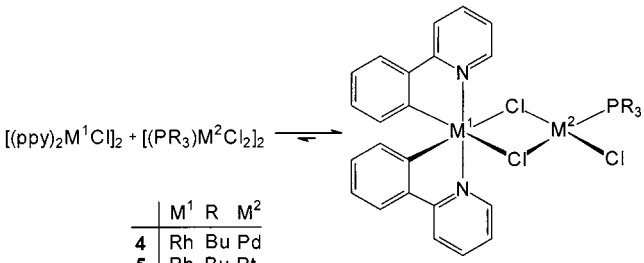

	M^1	R	M^2
4	Rh	Bu	Pd
5	Rh	Bu	Pt
6	Rh	Et	Pd
7	Ir	Bu	Pt
8	Ir	Et	Pt

The ^{1}H- and ^{13}C-NMR spectra ($CDCl_3$) of **4**−**6** are strongly temperature dependent. At temperatures below 250 K the phenylpyridyl ligands show two distinct sets of signals in accordance with the structure depicted in Scheme 2. At room temperature, however, only one set of signals can be observed (Figure 2).

Figure 2. Aromatic region of the ^{1}H NMR spectra of complex **5** at 233 K (top) and at 328 K (bottom) in $CDCl_3$

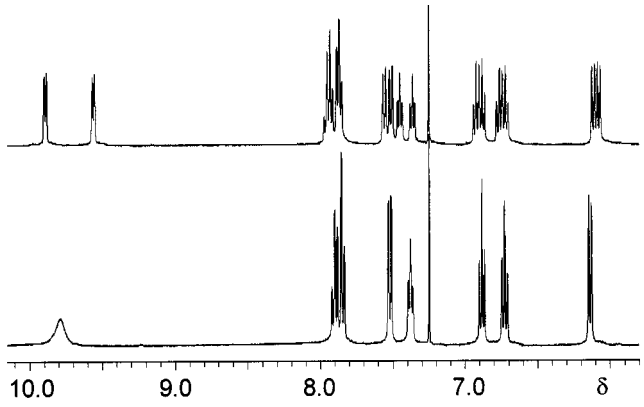

The fluctional process most probably consists of a "*cis-trans*" isomerisation as shown in Scheme 3. Plausible intermediates are solvent stabilized complexes with only one chloride bridge. From the coalescence temperature T_c and the difference in chemical shift Δν of selected signals a $\Delta G^{\#}$ value of 59 (±1) kJ mol^{-1} was calculated for **5**.[17] A similar

dynamic behaviour was previously observed for mixtures of *cis*- and *trans*-$[(Ph_3P)(CO)RhCl]_2$.[18] In contrast to the rhodium complexes **4**−**6** the iridium complexes **7** and **8** exhibit no fluxional behavior at room temperature. Coalescence effects are observed at temperatures above 325 K. For **7** a $\Delta G^{\#}$ value of 69 (±1) kJ mol^{-1} was calculated.

When the ^{1}H NMR spectra of **5** and **7** are recorded in $CDCl_3$ containing 20% CD_3OD only minor changes in the coalescence temperature can be observed. Interestingly this more polar solvent mixture disfavors the formation of the heterobimetallic complexes: significant amounts ($K_{eq} \approx 10$) of the homodimeric starting materials are present in solution as judged by integration of selected ^{1}H NMR signals. NMR experiments in neat CD_3OD were not performed due to the very low solubility of the complexes in this solvent. Other polar solvents like dimethyl sulfoxide or acetonitrile were likewise omitted because they are known to react with chloro-bridged complexes to yield the respective monomeric species.

Scheme 3

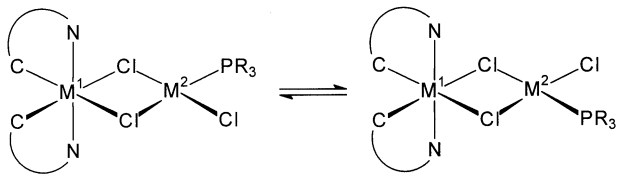

In analogy to **4**−**8** the Rh^{III}-Pd^{II} complex **9** and the Rh^{III}-Pt^{II} complex **10** containing two metalated benzoquinoline ligands were synthesized. Again, the NMR spectra ($CDCl_3$) exhibit dynamic behavior with a coalescence temperature close to what was observed for the rhodium complexes **4**−**6**.

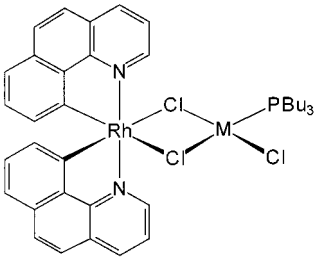

	M
9	Pd
10	Pt

The structural assignments for **4**−**10** are supported by a single crystal X-ray analysis of **5** (Figure 3). There are two independent molecules in the unit cell, the metric parameters of which are very similar. As in **1**, the two metal centers are bridged by a slightly bent dichloro-bridge with the dihedral angle of the folded Rh(μ-Cl)$_2$Pt unit beeing 13.2°. Furthermore, the dichloro bridge is highly asymmetric with four distinct M−Cl bond lengths between 2.31 (Pt1−Cl2) and 2.54 A (Rh1−Cl2). Metal-metal interactions are unlikely due to a Rh−Pt bond length of 3.61 A. The configuration and the bond lengths of the octahedral Rh^{III} fragment are similar to that observed for **1**.

Figure 3. Molecular structure of complex **5**. Selected bond lengths [A] and angles [°]: Pt1−P1 2.216(3), Pt1−Cl1 2.407(2), Pt1−Cl2 2.313(2), Pt1−Cl3 2.270(3), Rh1−C11 1.975(9), Rh1−C22 1.995(11), Rh1−N2 2.036(8), Rh1−N1 2.038(8), Rh1−Cl1 2.528(3), Rh1−Cl2 2.540(2); N1−Rh1−Cl1 85.8(2), N1−Rh1−Cl2 96.8(2), Cl1−Rh1−Cl2 80.52(8), N1−Rh1−N2 175.2(3), Cl1−Pt1−Cl2 87.85(8), Cl3−Pt1−Cl2 174.70(10)

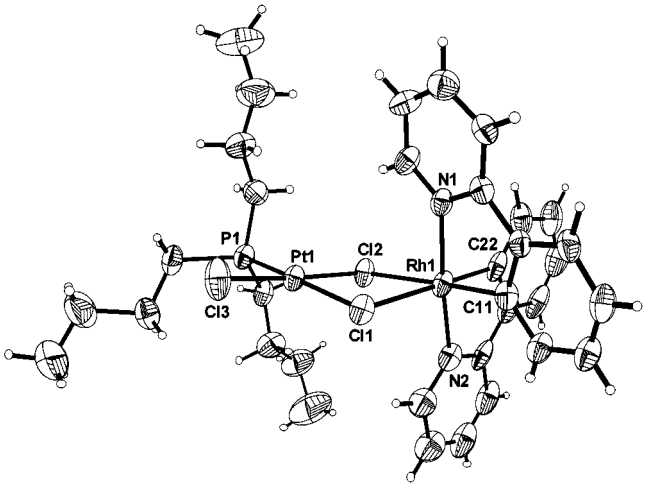

Conclusions

The present study establishes that heterobimetallic and mixed-valence complexes containing orthometalated Rh^{III} and Ir^{III} fragments can be obtained in nearly quantitative yields by metathesis reactions of $[(N-C)_2MCl]_2$ (M = Rh, Ir) with various dichloro-bridged complexes of the late transition metals. It is conceivable that this synthetic scheme is not restricted to the cyclooctadiene and phosphine complexes described here. Indeed, preliminary experiments have shown that chloro-bridged, orthometalated Pd^{II} and Pt^{II} complexes undergo similar disproportion reactions. It remains to be seen, how general the concept of chloro-bridge metathesis is appliciable for the synthesis of new, heterometallic complexes. Studies along these lines will be reported shortly.

We thank Prof. Dr. *W. Beck* (LMU München) for his generous support. Financial funding from the *Bayerischer Habilitations-Förderpreis* is gratefully acknowledged.

Experimental Section

General: All solvents were of analytical grade quality, obtained commercially and used without further purification. Reactions with $[(cod)IrCl]_2$ were performed with degassed solvents under an inert atmosphere. The complexes $[(R_3P)MCl_2]_2$ (M = Pd, Pt; R = Et, *n*-Bu),[18] $[(ppy)_2MCl]_2$ (M = Rh, Ir),[8b] $[(bzq)_2RhCl]_2$,[8b] $[(cod)RhCl]_2$,[20] and $[(cod)IrCl]_2$[21] were prepared as described in the literature. − IR: Perkin-Elmer 841, Nicolet 520. − NMR: JEOL EX 400,GSX 270. The NMR spectra were recorded at room temperature − exceptions are indicated. Due to the low solubility of **6** and **8** ^{13}C NMR spectra were not recorded.

General Procedure for the Synthesis of **1**−**10**: 10 ml of dichloromethane were added to 0.1 mmol of $[(ppy)_2MCl]_2$ (M = Rh, Ir) or

$[(bzq)_2RhCl]_2$ and 0.1 mmol of the respective chloro-bridged complex $[(cod)RhCl]_2$ (M = Rh, Ir) or $[(R_3P)MCl_2]_2$ (M = Pd, Pt). After 1 h clear yellow or orange solutions were observed. The products were isolated after evaporation of the solvent under reduced pressure and dried in vacuo at 50°C.

[(ppy)$_2$Rh(μ-Cl)$_2$Rh(cod)] (**1**): Yellow powder. Crystals can be obtained by slow diffusion of diethyl ether in a solution of **1** in chloroform. M. p. 255−258°C (dec.). − ^{1}H NMR (270 MHz, $CDCl_3$): δ = 1.61−1.74 (m, 4 H, CH_2, cod), 2.27−2.53 (m, 4 H, CH_2, cod), 3.98−4.03 (m, 2 H, CH, cod), 4.14−4.19 (m, 2 H, CH, cod), 6.14 (d, ^3J = 8.0 Hz, 2 H, CH, ppy), 6.72 (t, ^3J = 7.4 Hz, 2 H, CH, ppy), 6.85 (t, ^3J = 7.4 Hz, 2 H, CH, ppy), 7.43 (t, ^3J = 7.4 Hz, 2 H, CH, ppy), 7.51 (d, ^3J = 7.7 Hz, 2 H, CH, ppy), 7.83−7.94 (m, 4 H, CH, ppy), 9.94 (d, ^3J = 5.6 Hz, 2 H, NCH, ppy). − ^{13}C NMR (68 MHz, $CDCl_3$): δ = 30.81, 31.07 (CH_2, cod), 78.13, 78.33, 78.55, 78.75 (CH, cod), 118.83, 122.12, 122.62, 123.81, 129.37, 132.65, 137.39, 143.73, 151.87, 164.71 (CH, ppy), 164.64 (d, $^1J_{RhC}$ = 37.4 Hz, RhC). − $C_{30}H_{28}Cl_2N_2Rh_2{\cdot}CHCl_3$ (812.67): calcd. C 45.82, H 3.59, N 3.45; found C 45.16, H 3.82, N 3.14.

[(ppy)$_2$Rh(μ-Cl)$_2$Ir(cod)] (**2**): Yellow powder, m.p. 209−213°C (dec.). − ^{1}H NMR (270 MHz, $CDCl_3$): δ = 1.22−1.35 (m, 4 H, CH_2, cod), 2.02−2.24 (m, 4 H, CH_2, cod), 3.75−3.81 (m, 2 H, CH, cod), 3.90−3.96 (m, 2 H, CH, cod), 6.13 (d, ^3J = 8.0 Hz, 2 H, CH, ppy), 6.72 (t, ^3J = 7.4 Hz, 2 H, CH, ppy), 6.87 (t, ^3J = 7.5 Hz, 2 H, CH, ppy), 7.39 (t, ^3J = 7.4 Hz, 2 H, CH, ppy), 7.51 (d, ^3J = 7.7 Hz, 2 H, CH, ppy), 7.82−7.94 (m, 4 H, CH, ppy), 9.77 (d, ^3J = 5.6 Hz, 2 H, NCH, ppy). − ^{13}C NMR (68 MHz, $CDCl_3$): δ = 31.62, 31.82 (CH_2, cod), 61.35, 61.79 (CH, cod), 118.82, 122.18, 122.84, 123.87, 129.45, 132.67, 137.54, 143.73, 151.92, 164.48 (CH, ppy), 163.99 (d, $^1J_{RhC}$ = 37.7 Hz, RhC). − $C_{30}H_{28}Cl_2IrN_2Rh{\cdot}CH_2Cl_2$ (867.54): calcd. C 42.92, H 3.49, N 3.23; found C 43.25, H 3.55, N 3.23.

[(ppy)$_2$Ir(μ-Cl)$_2$Ir(cod)] (**3**): Orange powder, m.p. 194−197°C (dec.). − ^{1}H NMR (270 MHz, CD_2Cl_2): δ = 1.21−1.34 (m, 4 H, CH_2, cod), 1.99−2.23 (m, 4 H, CH_2, cod), 3.68−3.74 (m, 2 H, CH, cod), 3.88−3.94 (m, 2 H, CH, cod), 6.06 (d, ^3J = 7.7 Hz, 2 H, CH, ppy), 6.62 (t, ^3J = 7.7 Hz, 2 H, CH, ppy), 6.79 (t, ^3J = 7.4 Hz, 2 H, CH, ppy), 7.36−7.52 (m, 4 H, CH, ppy), 7.83−7.90 (m, 4 H, CH, ppy), 9.76 (d, ^3J = 5.9 Hz, 2 H, NCH, ppy). − ^{13}C NMR (68 MHz, CD_2Cl_2): δ = 37.21, 37.55 (CH_2, cod), 62.06, 62.35 (CH, cod), 118.72, 121.86, 122.50, 123.93, 129.34, 131.45, 137.76, 142.79, 144.13, 151.37, 167.34 (CH, ppy). − $C_{30}H_{28}Cl_2Ir_2N_2{\cdot}1/2\ CH_2Cl_2$ (914.38): calcd. C 40.06, H 3.20, N 3.06; found C 39.58, H 2.86, N 2.96.

[(ppy)$_2$Rh(μ-Cl)$_2$Pd(PBu$_3$)Cl] (**4**): Orange powder, m.p. 265−268°C (dec.). − ^{1}H NMR (270 MHz, $CDCl_3$, 35°C): δ = 0.90 (t, ^3J = 7.3 Hz, 9 H, CH_3, PBu_3), 1.35−1.79 (m, 18 H, CH_2, PBu_3), 6.13 (d, ^3J = 7.8 Hz, 2 H, CH, ppy), 6.72 (dt, ^3J = 7.4 Hz, ^5J = 1.3 Hz, 2 H, CH, ppy), 6.86 (dt, ^3J = 7.5 Hz, ^5J = 1.3 Hz, 2 H, CH, ppy), 7.37 (t, br, ^3J = 5.6 Hz, 2 H, CH, ppy), 7.51 (dd, ^3J = 7.7 Hz, ^5J = 1.0 Hz, 2 H, CH, ppy), 7.82−7.93 (m, 4 H, CH, ppy), 9.81 (s, br, 2 H, NCH, ppy). − ^{13}C NMR (68 MHz, $CDCl_3$, 35°C): δ = 13.72 (CH_3, PBu_3), 23.32 (d, $^1J_{PC}$ = 32.0 Hz, PCH_2), 24.11 (d, $^2J_{PC}$ = 14.8 Hz, PCH_2CH_2), 26.04 (d, $^3J_{PC}$ = 2.8 Hz, $PCH_2CH_2CH_2$), 118.81, 122.23, 122.72, 123.74, 129.37, 132.64, 137.56, 143.75, 151.68, 164.75 (CH, ppy), 164.77 (d, $^1J_{RhC}$ = 37.0 Hz, RhC). − ^{31}P NMR (109 MHz, CH_2Cl_2): δ = 33.51. − $C_{34}H_{43}Cl_3N_2PPdRh{\cdot}1/3\ CH_2Cl_2$ (854.71): calcd. C 48.25, H 5.15, N 3.28; found C 48.27, H 5.17, N 3.24.

[(ppy)$_2$Rh(μ-Cl)$_2$Pt(PBu$_3$)Cl] (**5**): Yellow powder. Crystals can be obatined by slow diffusion of diethyl ether in a solution of **5** in dichloromethane. M.p. 255−257°C (dec.). − ^{1}H NMR (400 MHz, $CDCl_3$): δ = 0.90 (t, ^3J = 7.4 Hz, 9 H, CH_3, PBu_3), 1.33−1.74 (m, 18 H, CH_2, PBu_3), 6.12 (d, ^3J = 7.7 Hz, 2 H, CH, ppy), 6.73 (t, ^3J = 7.1 Hz, 2 H, CH, ppy), 6.89 (t, ^3J = 7.7 Hz, 2 H, CH, ppy), 7.39 (s, br, 2 H, CH, ppy), 7.52 (d, ^3J = 7.4 Hz, 2 H, CH, ppy), 7.85−7.94 (m, 4 H, CH, ppy), 9.75 (d, br, 2 H, NCH, ppy). − ^{13}C NMR (101 MHz, $CDCl_3$): δ = 13.87 (CH_3, PBu_3), 21.50 (d, $^1J_{PC}$ = 39.6 Hz, PCH_2), 24.05 (d, $^2J_{PC}$ = 14.3 Hz, PCH_2CH_2), 25.72 (d, $^3J_{PC}$ = 2.8 Hz, $PCH_2CH_2CH_2$), 118.94, 122.42, 122.94, 123.87, 129.47, 132.61, 137.60, 143.83, 151.80, 164.45 (CH, ppy), 164.51 (d, $^1J_{RhC}$ = 37.8 Hz, RhC). − ^{31}P NMR (162 MHz, $CDCl_3$): δ = −2.80 ($^1J_{PtP}$ = 3489 Hz). − $C_{34}H_{43}Cl_3N_2PPtRh$ (915.06): calcd. C 44.63, H 4.74, N 3.06; found C 44.23, H 4.57, N 2.96.

[(ppy)$_2$Rh(μ-Cl)$_2$Pd(PEt$_3$)Cl] (**6**): Yellow powder, m.p. 288−291°C (dec.). − ^{1}H NMR (400 MHz, $CDCl_3$): δ = 1.15 (dt, $^3J_{HH}$ = 7.8 Hz, $^3J_{PH}$ = 18.0 Hz, 9 H, CH_3, PEt_3), 1.75−1.84 (m, 6 H, CH_2, PEt_3), 6.14 (d, ^3J = 8.2 Hz, 2 H, CH, ppy), 6.73 (t, ^3J = 7.4 Hz, 2 H, CH, ppy), 6.87 (t, ^3J = 7.5 Hz, 2 H, CH, ppy), 7.40 (s, br, 2 H, CH, ppy), 7.53 (d, ^3J = 6.7 Hz, 2 H, CH, ppy), 7.85−7.94 (m, 4 H, CH, ppy), 9.81 (s, br, 2 H, NCH, ppy). − ^{31}P NMR (109 MHz, CH_2Cl_2): δ = 40.43. − $C_{28}H_{31}Cl_3N_2PPdRh$ (742.23): calcd. C 45.31, H 4.21, N 3.77; found C 45.31, H 3.86, N 3.76.

[(ppy)$_2$Ir(μ-Cl)$_2$Pt(PBu$_3$)Cl] (**7**): Yellow powder; m.p. 253−255°C (dec.). − ^{1}H NMR (400 MHz, $CDCl_3$): δ = 0.90 (t, ^3J = 6.7 Hz, 9 H, CH_3, PBu_3), 1.34−1.72 (m, 18 H, CH_2, PBu_3), 6.08 (d, ^3J = 7.3 Hz, 1 H, CH, ppy), 6.11 (d, ^3J = 8.0 Hz, 1 H, CH, ppy), 6.63 (t, ^3J = 7.2 Hz, 1 H, CH, ppy), 6.66 (t, ^3J = 7.5 Hz, 1 H, CH, ppy), 6.78 (t, ^3J = 7.3 Hz, 1 H, CH, ppy), 6.81 (t, ^3J = 7.5 Hz, 1 H, CH, ppy), 7.31 (t, ^3J = 6.4 Hz, 1 H, CH, ppy), 7.41 (t, ^3J = 5.5 Hz, 1 H, CH, ppy), 7.45 (d, ^3J = 8.2 Hz, 1 H, CH, ppy), 7.49 (d, ^3J = 7.5 Hz, 1 H, CH, ppy), 7.78−7.87 (m, 4 H, CH, ppy), 9.63 (d, ^3J = 5.5 Hz, 1 H, NCH, ppy), 10.05 (d, ^3J = 5.6 Hz, 1 H, NCH, ppy). − ^{13}C NMR (101 MHz, $CDCl_3$): δ = 13.84 (CH_3, PBu_3), 21.43 (d, $^1J_{PC}$ = 39.3 Hz, PCH_2), 24.03 (d, $^2J_{PC}$ = 14.6 Hz, PCH_2CH_2), 25.68 (d, $^3J_{PC}$ = 3.1 Hz, $PCH_2CH_2CH_2$), 118.41, 118.75, 121.89, 122.29, 122.44, 123.85, 129.42, 129.53, 131.34, 131.74, 137.43, 137.47, 143.12, 143.68, 143.95, 144.22, 150.61, 151.77, 167.65, 167.78 (CH, ppy). − ^{31}P NMR (109 MHz, CH_2Cl_2): δ = −1.49 ($^1J_{PtP}$ = 3602 Hz). − $C_{34}H_{43}Cl_3N_2PPtIr$ (1004.37): calcd. C 40.66, H 4.32, N 2.79; found C 40.95, H 4.09, N 2.85.

[(ppy)$_2$Ir(μ-Cl)$_2$Pt(PEt$_3$)Cl] (**8**): Yellow powder, m.p. 275−277°C (dec.). − ^{1}H NMR (270 MHz, $CDCl_3$): δ = 1.10 (dt, $^3J_{HH}$ = 7.7 Hz, $^3J_{PH}$ = 17.5 Hz, 9 H, CH_3, PEt_3), 1.64−1.80 (m, 6 H, CH_2, PEt_3), 6.09 (pt, ^3J = 5.7 Hz, 2 H, CH, ppy), 6.63 (pq, ^3J = 6.9 Hz, 2 H, CH, ppy), 6.78 (pq, ^3J = 6.2 Hz, 2 H, CH, ppy), 7.29−7.49 (m, 4 H, CH, ppy), 7.84 (m, 4 H, CH, ppy), 9.62 (d, ^3J = 5.7 Hz, 1 H, CH, ppy), 10.02 (d, ^3J = 5.2 Hz, 1 H, CH, ppy). − ^{31}P NMR (109 MHz, $CDCl_3$): δ = 5.98 ($^1J_{PtP}$ = 3722 Hz). − $C_{28}H_{31}Cl_3N_2PPtIr$ (920.20): calcd. C 36.55, H 3.40, N 3.04; found C 36.50, H 3.24, N 2.97.

[(bzq)$_2$Rh(μ-Cl)$_2$Pd(PBu$_3$)Cl] (**9**): Orange powder; m.p. 250−253°C (dec.). − ^{1}H NMR (400 MHz, $CDCl_3$, 35°C): δ = 0.87 (t, ^3J = 7.2 Hz, 9 H, CH_3, PBu_3), 1.34−1.77 (m, 18 H, CH_2, PBu_3), 6.11 (d, ^3J = 7.4 Hz, 2 H, CH, bzq), 6.95 (t, ^3J = 7.8 Hz, 2 H, CH, bzq), 7.30 (d, ^3J = 7.7 Hz, 2 H, CH, bzq), 7.66−7.79 (m, 6 H, CH, bzq), 8.41 (d, ^3J = 6.7 Hz, 2 H, CH, bzq), 10.10 (d, br, 2 H, NCH, bzq). − ^{13}C NMR (101 MHz, $CDCl_3$, 35°C): δ = 13.68 (CH_3, PBu_3), 23.33 (d, $^1J_{PC}$ = 31.9 Hz, PCH_2), 24.09 (d, $^2J_{PC}$ = 14.4 Hz, PCH_2CH_2), 26.02 (d, $^3J_{PC}$ = 2.5 Hz, $PCH_2CH_2CH_2$), 120.77, 121.62, 123.18, 126.85, 128.64, 129.30, 129.48, 133.55, 135.94, 140.07, 151.12, 154.77 (CH, bzq), RhC: not observed. −

Table 1. Crystal data for complexes **1** and **5**

	1	**5**
Empirical formula	$C_{67}H_{69}Cl_{13}N_4Rh_4$	$C_{34.5}H_{44}Cl_4N_2PPtRh$
Molecular mass [g mol^{-1}]	1818.75	957.49
Crystal size	0.53 × 0.47 × 0.27	0.47 × 0.37 × 0.27
Crystal system	monoclinic	triclinic
Space group	*C*2/*c*	*P*-1
a [A]	23.100(9)	11.950(2)
b [A]	12.161(5)	17.517(3)
c [A]	26.498(9)	20.294(3)
α [°]	90.00(3)	66.40(2)
β [°]	104.81(3)	86.53(2)
γ [°] °	90.00(3)	75.318(14)
Volume [A^3]	7197(5)	3761.8(11)
Z	4	4
Density [g cm^{-3}]	1.679	1.691
Absorption coefficient [mm^{-1}]	1.428	4.506
Θ range [°]	2.33 to 23.98	2.56 to 23.97
Index ranges	−26 → 0, −13 → 0, −29 → 30	−13 → 13, −20 → 0, −23 → 21
Reflections collected	5772	12203
Independent reflections	5620 (R_{int} = 0.0166)	11763 (R_{int} = 0.0202)
Absorption correction	semi-empirical	semi-empirical
Max. and min. transmission	0.9999 and 0.6810	0.9999 and 0.6848
Weights	$w = 1/(\sigma^2(F_0^2)+(0.0319\ P)^2 +23.5103P]$; $P = (F_0^2+2F_c^2)/3$	$w = 1/(\sigma^2(F_0^2)+(0.0376\ P)^2 +9.7166P]$; $P = (F_0^2+2F_c^2)/3$
Data / restraints / parameters	5620 / 12 / 418	11763 / 20 / 791
Goodness-of-fit on F^2	1.079	1.110
Final *R* indices [$I>2\sigma(I)$]	$R1$ = 0.0316, $wR2$ = 0.0726	$R1$ = 0.0463, $wR2$ = 0.0896
R indices (all data) °	$R1$ = 0.0403, $wR2$ = 0.0786	$R1$ = 0.0787, $wR2$ = 0.1043
Largest diff. peak/hole [eA^{-3}]	0.643/−0.720	1.064/−0.906

^{31}P NMR (162 MHz, CH_2Cl_2): δ = 32.34. − $C_{38}H_{43}Cl_3N_2PPdRh{\cdot}1/4\ CH_2Cl_2$ (895.67): calcd. C 51.31, H 4.90, N 3.13; found C 51.45, H 5.05, N 3.07.

[(bzq)$_2$Rh(μ-Cl)$_2$Pt(PBu$_3$)Cl] (**10**): Yellow powder; m.p. 280−283°C (dec.). − ^{1}H NMR (400 MHz, $CDCl_3$): δ = 0.87 (t, ^3J = 8.0 Hz, 9 H, CH_3, PBu_3), 1.35−1.73 (m, 18 H, CH_2, PBu_3), 6.10 (d, ^3J = 7.4 Hz, 2 H, CH, bzq), 6.95 (t, ^3J = 8.1 Hz, 2 H, CH, bzq), 7.33 (d, ^3J = 7.3 Hz, ^5J = 1.3 Hz, 2 H, CH, bzq), 7.67−7.80 (m, 6 H, CH, bzq), 8.42 (d, ^3J = 6.7 Hz, 2 H, CH, bzq), 10.05 (d, br, 2 H, NCH, bzq). − ^{13}C NMR (68 MHz, $CDCl_3$, 35°C): δ = 13.70 (CH_3, PBu_3), 21.54 (d, $^1J_{PC}$ = 39.0 Hz, PCH_2), 23.94 (d, $^2J_{PC}$ = 14.7 Hz, PCH_2CH_2), 25.67 (d, $^3J_{PC}$ = 2.2 Hz, $PCH_2CH_2CH_2$), 120.88, 121.67, 123.23, 126.83, 128.65, 129.23, 130.06, 133.55, 136.02, 139.94, 150.56, 154.56 (CH, bzq), 160.93 (d, $^1J_{RhC}$ = 37.5 Hz, RhC). − ^{31}P NMR (109 MHz, CH_2Cl_2): δ = −2.64 ($^1J_{PtP}$ = 3704 Hz). − $C_{38}H_{43}Cl_3N_2PPtRh$ (963.10): calcd. C 47.39, H 4.50, N 2.91; found C 46.89, H 4.49, N 2.84.

X-ray Crystallographic Investigations: An Enraf Nonius CAD 4 diffractometer was employed for data collection using Mo-K_α radiation (T = 295 K). The structures were solved by direct methods (SHELXS86) and were refined by means of the full-matrix least squares procedures using SHELXL93 (Table 1). All non-hydrogen atoms were refined anisotropically. For the hydrogen atoms a riding model was employed. **1** crystallizes with 1.5 molecules of chloroform and 0.5 molecules of diethyl ether, all of which are disordered (restraints were used for $CHCl_3$). **5** crystallizes with 0.5 molecules of dichloromethane. The *n*-butyl groups as well as the solvent molecule are disordered (restraints were used for CH_2Cl_2).[21]

☆ Dedicated to Professor *Heinrich Nöth* on the occasion of his 70th birthday.

[1] R. P. Hughes in *Comprehensive Organometallic Chemistry* (Eds.: G. Wilkinson, F. G. A. Stone, E. W. Abel), vol. 5, Pergamon, Oxford, **1982**, p. 277 ff. − G. J. Leigh, R. L. Richards in *Comprehensive Organometallic Chemistry* (Eds.: G. Wilkinson, F. G. A. Stone, E. W. Abel), vol. 5, Pergamon, Oxford, **1982**, p. 541 ff.

[2] [2a] E. Corradi, N. Masciocchi, G. Palyi, R. Ugo, A. Vizi-Orosz, C. Zucchi, A. Sironi, *J. Chem. Soc., Dalton Trans.* **1997**, 4651−4655. − [2b] S. B. Duckett, R. Eisenberg, *J. Am. Chem. Soc.* **1993**, *115*, 5292−5293. − M. Onishi, K. Isagawa, *Inorg. Chim. Acta* **1991**, *179*, 155−156. − J. W. Suggs, M. J. Wovkulich, P. G. Willard, K. S. Lee, *J. Organomet. Chem*. **1986**, *307*, 71−82. − A. Albinati, H. Lehner, L. M. Venanzi, *Inorg. Chem.* **1985**, *24*, 1483−1488. − L. Dahlenburg, A. Yardimcioglu, *J. Organomet. Chem.* **1985**, *291*, 371−386. − C. E. Briant, K. A. Rowland, C. T. Webber, D. M. P. Mingos, *J. Chem. Soc., Dalton Trans.* **1981**, 1515−1519. − R. Huis, C. Masters, *J. Chem. Soc., Dalton Trans.* **1976**, 1796−1799. − J. Coetzer, G. Gafner, *Acta. Cryst*. **1970**, *B26*, 985−991. − J. W. Kang, K. Moseley, P. M. Maitlis, *J. Am. Chem. Soc.* **1969**, *91*, 5970−5977. − L. M. Haines, *Inorg. Nucl. Chem. Letters* **1969**, *5*, 399−403.

[3] E. Lindner, T. Schneller, F. Auer, P. Wegner, H. A. Mayer, *Chem. Eur. J.* **1997**, *3*, 1833−1845. − S. B. Duckett, C. L. Newell, R. Eisenberg, *J. Am. Chem. Soc.* **1994**, *116*, 10548−10556. − C. A. Tolman, P. Z. Meakin, D. L. Lindner, J. P. Jesson, *J. Am. Chem. Soc.* **1997**, *96*, 2762−2774.

[4] K.-C. Shih, A. S. Goldman, *Organometallics* **1993**, *12*, 3390−3392.

[5] A. A. H. van der Zeijden, G. van Koten, R. Luijk, K. Vrieze, C. Slob, H. Krabbendam, A. L. Spek, *Inorg. Chem.* **1988**, *27*, 1014−1019.

[6] R. L. Bennett, M. I. Bruce, B. L. Goodall, M. Z. Iqbal, F. G. A. Stone, *J. Chem. Soc., Dalton Trans.* **1972**, 1787−1791. − M. I. Bruce, M. Z. Iqbal, F. G. A. Stone, *J. Organomet. Chem*. **1972**, *40*, 393−401.

[7] R. J. Hoare, O. S. Mills, *J. Chem. Soc., Dalton Trans.* **1972**, 2141−2145.

[8] [8a] R. Urban, R. Krämer, S. Mihan, K. Polborn, B. Wagner, W. Beck, *J. Organomet. Chem.* **1996**, *517*, 191−200. − G. Calogero, G. Guiffrida, S. Serroni, V. Ricevuto, S. Campagna, *Inorg. Chem*. **1995**, *34*, 541−545. − B. Schmid, F. O. Garces, R. J. Watts; *Inorg. Chem*. **1994**, *33*, 9−14. − G. A. Carlson, P. I. Djurovich, R. J. Watts, *Inorg. Chem*. **1993**, *32*, 4483−4484. − F. O. Garces, K. A. King, R. J. Watts, *Inorg. Chem*. **1988**, *27*, 3464−3471. − [8b] S. Sprouse; K. A. King, P. J. Spellane, R. J. Watts, *J. Am. Chem. Soc.* **1984**, *106*, 6647−6653.

[9] The incorporation of $[(ppy)_2M]^+$ (M = Rh, Ir) fragments into multimetallic molecular ensembles is expected to alter their photophysical properties and therefore of special interest: I. Ortmans, P. Didier, A. Kirsch-De Mesmaeker, *Inorg. Chem.* **1995**, *34*, 3695−3704. − S. Serroni, A. Juris, S. Campagna, M. Venturi, G. Denti, V. Balzani, *J. Am. Chem. Soc.* **1994**, *116*, 9086−9091. − P. Didier, L. Jacquet, A. Kirsch-De Mesmaecker, R. Hueber, A. van Dorsselaer, *Inorg. Chem*. **1992**, *31*, 4803−4809. − J. H. van Diemen, R. Hage, J. G. Haasnoot, H. E. B. Lempers, J. Reedijk, J. G. Vos, L. De Cola, F. Barigelletti, V. Balzani, *Inorg. Chem*. **1992**, *31*, 3518−3522.

[10] H. C. Clark, G. Ferguson, V. K. Jain, M. Parvez, *Inorg. Chem*. **1986**, *25*, 3808−3811. − H. C. Clark, G. Ferguson, V. K. Jain, M. Parvez, *Inorg. Chem.* **1985**, *24*, 1477−1482. − A. A. Kiffen, C. Masters, J. P. Visser, *J. Chem. Soc., Dalton Trans.* **1975**, 1311−1315. − C. Masters, J. P. Visser, *Chem. Commun*. **1974**, 932−933.

[11] K. Severin, S. Mihan, W. Beck, *Inorg. Chim. Acta* **1995**, *240*, 339−346.

[12] L. Walz, P. Scheer, *Acta Cryst*. **1991**, *C47*, 640−641.

[13] J. J. Bonnet, Y. Jeannin, P. Kalck, A. Maisonnat, R. Poilblanc, *Inorg. Chem*. **1975**, *14*, 743−747.

[14] M. G. B. Drew, S. M. Nelson, M. Sloan, *J. Chem. Soc., Dalton Trans.* **1973**, 1485−1489.

[15] G. Aullon, G. Ujaque, A. Lledos, S. Alvarez, P. Alemany, *Inorg. Chem.* **1998**, *37*, 804−813.

[16] D. J. A. Ridder, P. Imhoff, *Acta Cryst.* **1994**, *C50*, 1569−1572.

[17] H. Friebolin, *Ein- und zweidimensionale NMR-Spekroskopie*, Verlag Chemie, Weinheim, **1992**, pp. 285−312.

[18] G. Giordano, E. Rotondo, *Polyhedron* **1994**, *13*, 2507−2511.

[19] a) W. Baratta, P. S. Pregosin, *Inorg. Chim. Acta* **1993**, *209*, 85−87; b) F. R. Hartley, *Organomet. Chem. Rev. A* **1970**, *6*, 119−137.

[20] G. Giordano, R. H. Crabtree, *Inorg. Synth.* **1990**, *28*, 88−90.

[21] J. L. Herde, J. C. Lambert, C. V. Senoff, *Inorg. Synth.* **1974**, *15*,18−19.

[22] Further details of the crystal structure determination may be obtained from Fachinformationszentrum Karlsruhe, 76344 Eggenstein-Leopoldshafen. Any request for this material should quote the full literature citation and the reference numbers CSD-408186 for **1** and -408187 for **5**.

[98039]

Direct Evidence of Solvent-Peroxovanadium Clusters by Electrospray Ionization Mass Spectrometry

Olga Bortolini*[b], Valeria Conte*[a], Fulvio Di Furia[a†], and Stefano Moro[c]

Centro Studi Meccanismi Reazioni Organiche del CNR, Dipartimento di Chimica Organica Università di Padova[a],
via Marzolo 1, I-35131 Padova, Italy
Fax: (internat.) + 39(0)49/8275239
E-mail: CONTE@CHOR.UNIPD.IT

Dipartimento di Chimica, Università di Ferrara[b],
via Borsari 46, I-44100 Ferrara, Italy
Fax: (internat.) + 39(0)532/240709
E-mail: BRL@DNS.UNIFE.IT

Departimento di Scienze Farmaceutiche, Università di Padova[c],
via Marzolo 5, I-35131 Padova, Italy

Received February 12, 1998

Keywords: Peroxo complexes / Vanadium / Mass spectrometry / Ion-molecule reactions / Ab initio calculations

Electrospray Ionization Mass Spectrometry (ESI-MS) measurements and *ab initio* calculations on $[OV(O_2)(H_2O)_m(CH_3OH)_n]^+$ (*m*,*n*: 0–4) peroxo cations have been carried out. This experimental technique allowed the direct observation of the above mentioned species for the first time. The results obtained clearly indicate that the exchange reactions between water and methanol molecules, within the coordination sphere of monoperoxo-vanadium complexes, is a conceivable and fast process.

Introduction

The peroxo species formed in aqueous acid solutions by interaction of vanadates with hydrogen peroxide have been studied by several techniques, including heteronuclear NMR[1][2], Raman spectroscopy[3] and ab initio calculations.[4][5] In spite of all these studies, however, a fundamental aspect of these systems, i.e. the nature of the first coordination sphere of the peroxovanadium derivatives present in solution, is still a matter of debate.[1][2] As an example recent ab initio calculations indicate that the oxo(monoperoxo)vanadium cation likely binds three H_2O molecules to form a species whose structure is a distorted octahedron,[5] whereas in the solid state peroxovanadium complexes prefer the pentagonal bipyramid geometry.[6][7]

In order to obtain direct experimental information on the solution structure of peroxovanadium species, we have undertaken an electrospray ionization mass spectrometry (ESI-MS)[8][9] analysis of water/methanol acid solutions of vanadates in the presence of hydrogen peroxide. The electrospray technique is a gentle ionization method of transferring ions from solution to the gas phase with no apparent fragmentation, and has been successfully applied to the analysis of many inorganic and organometallic systems.[10] In our case the direct observation of $[OV(O_2)(H_2O)_m(CH_3OH)_n]^+$ (m, n = 0−4) peroxo cations has been achieved for the first time. Ab initio calculations were also carried out, whose results appear to rationalize most of the experimental behaviors observed.

Results and Discussion

Preliminary data, reported in Table 1, were obtained for solutions containing weighted amounts of ammonium vanadate in CH_3OH/H_2O (1:1; pH = 1, $HClO_4$). The electrospray mass spectrum of this solution, obtained by direct infusion into the ESI source, showed the occurrence of different species[11][12][13] identified as monomeric homo ions $[OV(OH)_3H]^+$ (*m*/*z* 119) and $[OV(OCH_3)_3H]^+$ (*m*/*z* 161), and mixed ions $[OV(OH)_2(OCH_3)H]^+$ and $[OV(OH)(OCH_3)_2H]^+$ (centered at *m*/*z* 133 and 147, respectively). The base peak of the spectrum is associated with the formation of the dimeric species[14] $[OV-O-VO(OH)_4H]^+$ at *m*/*z* 219. Other significant peaks, related to dimeric complexes and formally having the composition reported in Table 1, were found at *m*/*z* 237, 247 and 279.

As expected, addition of an equimolar amount of H_2O_2 to the vanadate solutions produces significant changes in the electrospray mass spectrum. Besides the above-mentioned ions at *m*/*z* 147 and 161, new ionic monoperoxo species at *m*/*z* 117, 131, 135, 181 and 195 were detected (see Table 1). Signals corresponding to the tetraaquo complex $[OV(O_2)(H_2O)_4]^+$ at *m*/*z* 171 and to the mixed $[OV(O_2)(H_2O)_m(CH_3OH)_n]^+$ ($m + n = 4$) cations at *m*/*z* 199 and 213 are also observed, although in low relative intensity.

Acid catalysis appears to play a fundamental role in the chemistry of peroxovanadium species, particularly when they are involved in the catalytic cycle of bromoperoxidase

 © WILEY-VCH Verlag GmbH, D-69451 Weinheim, 1998 1434−1948/98/0808−1193 $ 17.50+.50/0

Table 1. Percentage of ion abundances in Electrospray Ionization Mass Spectra of vanadates and peroxovanadates in water methanol acid solutions[a]

ion	*m/z*	rel. abund. (%)
vanadates		
$[OV(OH)_3H]^+$	119	14
$[OV(OH)_2(OCH_3)H]^+$	133	5
$[OV(OH)(OCH_3)_2H]^+$	147	2
$[OV(OCH_3)_3H]^+$	161	20
$[OV-O-VO(OH)_4H]^+$	219	100
$[OV-O-VO(H_2O)(OH)_4H]^+$	237	12
$[OV-O-VO(OCH_3)_2(OH)_2H]^+$	247	7
$[OV-O-VO(OCH_3)_3(H_2O)(OH)H]^+$	279	85
peroxo vanadates		
$[OV(O_2)]^+$	99	24
$[OV(O_2)(H_2O)]^+$	117	100
$[OV(O_2)(CH_3OH)]^+$	131	60
$[OV(O_2)(H_2O)_2]^+$	135	18
$[OV(O_2)(H_2O)(CH_3OH)]^+$	149	25
$[OV(O_2)(H_2O)_3]^+$	153	10
$[OV(O_2)(CH_3OH)_2]^+$	163	[b]
$[OV(O_2)(H_2O)_4]^+$	171	2
$[OV(O_2)(H_2O)(CH_3OH)_2]^+$	181	20
$[OV(O_2)(CH_3OH)_3]^+$	195	25
$[OV(O_2)(H_2O)_2(CH_3OH)_2]^+$	199	[b]
$[OV(O_2)(H_2O)(CH_3OH)_3]^+$	213	5

[a] NH_4VO_3 (0.0005 M), in CH_3OH/H_2O (1:1; pH = 1, $HClO_4$), and NH_4VO_3 (0.0005 M), H_2O_2 (0.0005 M), in CH_3OH/H_2O (1:1; pH = 1, $HClO_4$). – [b] Relative peak intensity less than 2%.

enzymes.[15] In that respect the knowledge of the protonation site of peroxovanadium complexes is an important piece of information. In the present work, where cationic peroxovanadium species are studied in acid solutions, we have addressed such a problem by carrying out ab initio calculations on the oxoperoxo complexes $[OV(O_2)(H_2O)]^+$ and $[OV(O_2)(CH_3OH)]^+$. The calculations have been made by using two different levels of theory, i.e. Hartree-Fock with a small all-electron basis set (HF/3-21G(*))[16] and density functional theory (DFT) with effective core potentials (B3LYP/LANL2DZ),[17][18] and are shown in a pictorial way in Figure 1. As it can be seen, the differences in energies of the three possible protonation sites, i.e. the oxo oxygen atom , the peroxo oxygen atom and solvent molecule, for both peroxo complexes are rather small, thus suggesting the occurrence of equilibria among them. Details on the calculations are reported in the experimental section.[19]

Although in the case of vanadium derivatives a comparison between the theoretically calculated and experimentally found isotopic cluster in ESI-MS spectra is hampered by the lack of vanadium isotopes, further support to the identification of the ions reported in Table 1 was obtained with tandem (MS^2) analysis and deuteration experiments.

The preferential decomposition patterns of the peroxidic species, as obtained by MS^2 experiments, are the loss of

Figure 1. Relative-energy diagrams for the gas-phase proton-migration reactions of species $[OV(O_2)(H_2O)]^+$ (**A**) and $[OV(O_2)(CH_3OH)]^+$ (**B**); energy values are given in kcal/mol

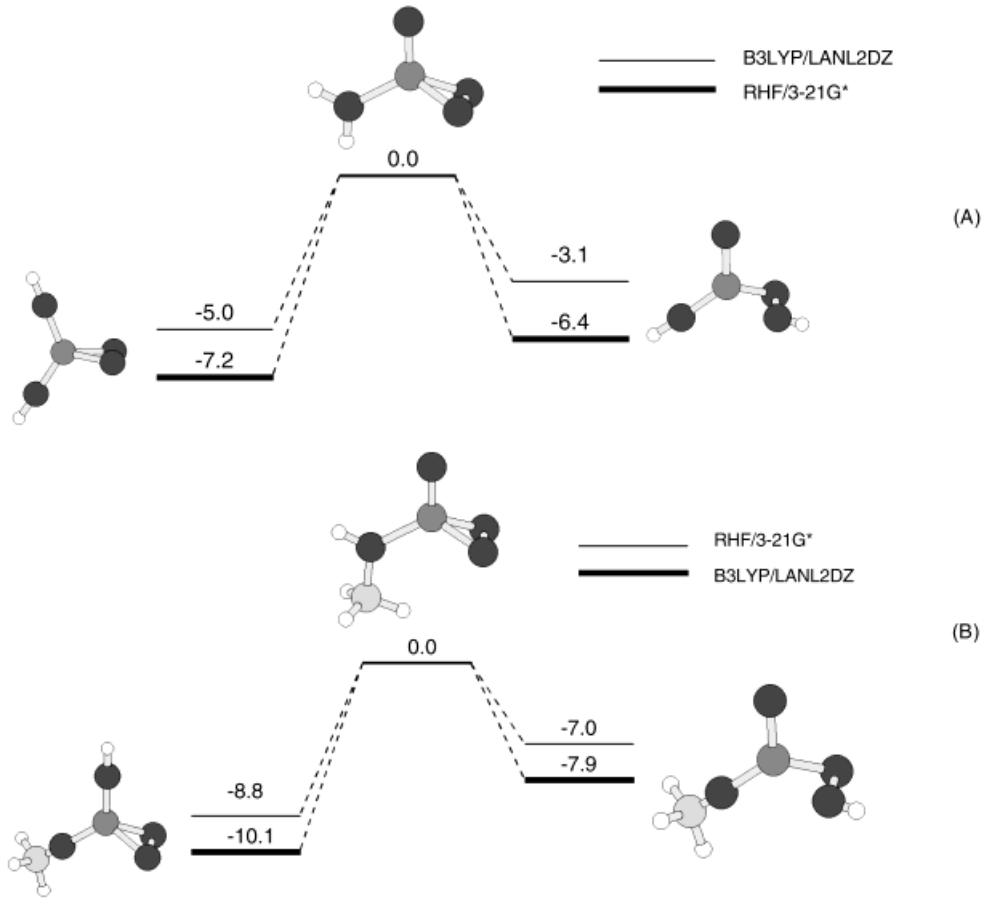

Figure 2. MS/MS mass spectrum of $[OV(O_2)(H_2O)(CH_3OH)_2]^+$ (*m*/*z* 181) using 2 V tickling voltage

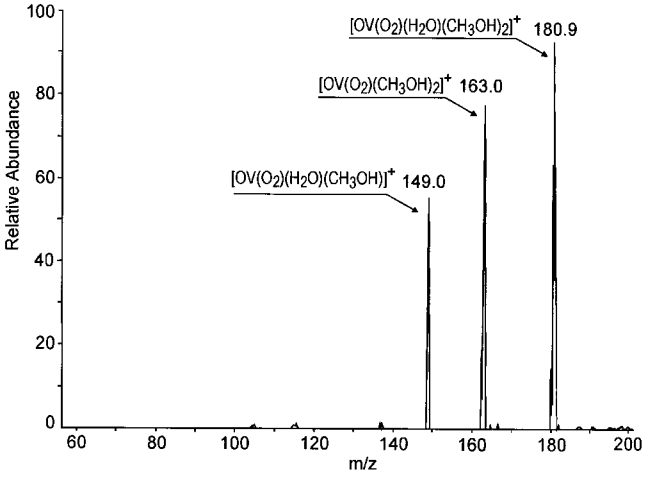

Figure 3. MS/MS mass spectra of $[OV(O_2)(H_2O)]^+$ using tickling voltages of: 3 V (**A**), 1 V (**B**) and 15 mV (**C**), respectively

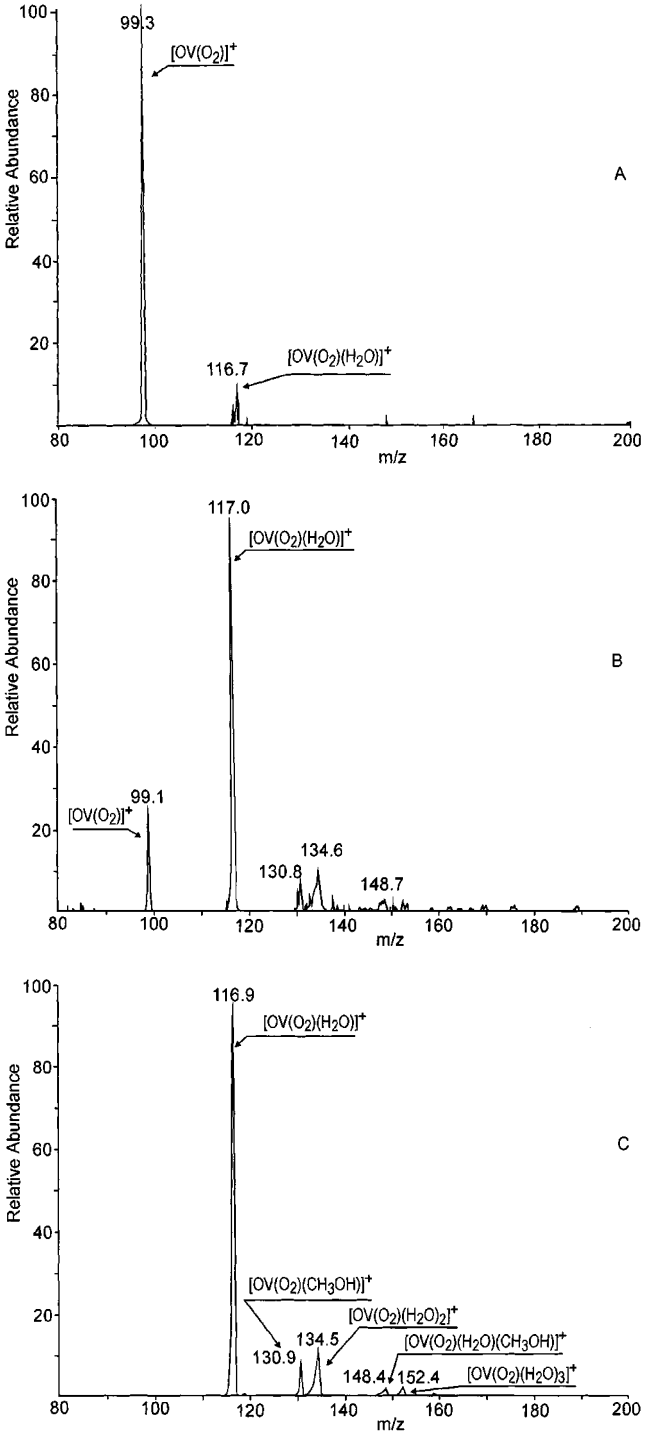

H_2O and/or CH_3OH molecules. As an example, at 2 V tickling voltage, the mixed species $[OV(O_2)(H_2O)(CH_3OH)_2]^+$ (*m*/*z* 181) fragments through expulsion of H_2O and CH_3OH, affording the ions at *m*/*z* 163 and 149, respectively (see Figure 2). On the other hand, the aquo(oxo)peroxovanadium cation $[OV(O_2)(H_2O)]^+$ (*m*/*z* 117) decomposes to the "naked" ion $[OV(O_2)]^+$ (*m*/*z* 99) by using 3 V tickling voltage (Figure 3A). Most noteworthy however, ionic species at higher mass-over-charge values are detected upon isolation of the ion under analysis. This is shown for ion $[OV(O_2)(H_2O)]^+$ (*m*/*z* 117), which has been isolated and trapped within the ion-trap analyzer in the presence of relatively small tickling voltages (10−15 mV), for times of about 0.1 ms. Under these conditions (Figure 3C) no fragmentation products, but formation of ions at *m*/*z* 131, 135, 149, 153 is observed. A likely explanation for such a result is the reaction of the ion $[OV(O_2)(H_2O)]^+$ with solvent molecules present in the ion trap (see Scheme 1), i.e. exchange between H_2O and CH_3OH (eq. 1), coordination of water [eq. 2 (n = 1, 2)] or coordination of methanol (eq. 3). At intermediate tickling voltage (1 V) formation of these ions is reduced and collision-induced decomposition product ions prevail (Figure 3B). An analogous behavior has been recently reported for (allyl)Pt^{II} compounds.[20]

The same ion-molecule reactions have been observed with the corresponding deuterated ion $[OV(O_2)(D_2O)]^+$ (*m*/*z* 119) and with other oxoperoxo species with different coordination-sphere composition. Thus, after the isolation of the ion $[OV(O_2)(H_2O)_2]^+$ (*m*/*z* 135), the ionic species at *m*/*z* 167 (addition of methanol) and 185 (addition of water and methanol) are formed, whereas the complex $[OV(O_2)(H_2O)(CH_3OH)]^+$ (*m*/*z* 149) gives rise to ions at *m*/*z* 163 (exchange water/methanol), 167 (addition of water) and 181 (addition of methanol). Furthermore, the occurrence of these ion-molecule reactions upon trapping the selected ions in the ion trap and the high tickling voltages that must be used (up to 3 V, see Figures 2 and 3C) to have complete collision-induced decomposition of peroxovanadium compounds $[OV(O_2)(H_2O)_m(CH_3OH)_n]^+$ (m, n = 0−4), likely suggest[20] the binding of water and/or methanol to the vanadium center.

^{51}V-NMR studies in mixed H_2O/CH_3OH solvents, revealed for oxo(monoperoxo)vanadium species the presence of a single broad peak ($\delta \approx -540$, ca. 1200 Hz at half width),[1b] thus suggesting the occurrence of fast equilibria, on the ^{51}V-NMR time scale, between water and methanol molecules for complexation to the metal center. A direct observation of the rapidly exchanging species by lowering

Scheme 1

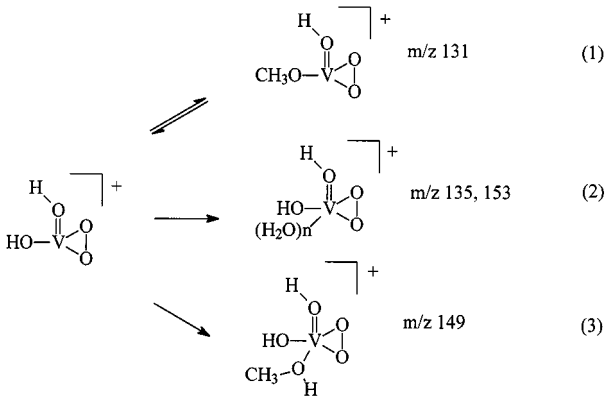

the temperature is hampered by the simultaneous increase of the line width due to the increase of the correlation time. The ESI-MS results here reported, however, show that the substitution of water molecules with methanol, and vice versa, in the coordination sphere of monoperoxovanadium complexes, is a conceivable and detectable process which leads to several peroxo complexes. The tandem use of ESI-MS and low-temperature NMR spectroscopy in the investigation of rapidly exchanging organometallic systems has been recently reported.[21]

In order to obtain further support to the occurrence of exchange process between water and methanol molecules in the coordination sphere of oxo(monoperoxo)vanadium complexes, ab initio calculations were also carried out. The reactions taken into consideration are the addition to the "naked" ion $[OV(O_2)]^+$ of either H_2O or CH_3OH molecule. As in the calculations reported above, two different levels of theory were used[16][17][18] and the relevant results are collected in Table 2.

The binding of a methanol molecule to the "naked" oxo(peroxo) ion involves a larger degree of stabilization as compared with that observed in the binding of a water molecule [99.6 kcal/mol against 86.4 kcal/mol with RHF/3-21G(*) calculation]. Such a result, supported also by the good agreement with that obtained with the DFT level of theory (see Table 2), may indeed substantiate the evidence that exchange between water and methanol molecules in the coordination sphere of oxo(monoperoxo)vanadium complexes is a likely process. If this were not the case, the exchange reaction between water and methanol detected upon isolation in the ion trap of the previously reported cations, could not be observed (see eq. 1, Scheme 1).

The higher affinity of methanol molecules for peroxovanadium center as compared with that of water is also confirmed by various experiments such as that shown in Figure 2. In particular, the relative abundance of ion $[OV(O_2)(CH_3OH)_2]^+$ at *m/z* 163, corresponding to the expulsion of a water molecule from $[OV(O_2)(H_2O)(CH_3OH)_2]^+$ (*m/z* 181), is higher than that of the ion at *m/z* 149, $[OV(O_2)(H_2O)(CH_3OH)]^+$, corresponding to the loss of methanol, despite of the statistical factor of 2 which would favor the latter process. The use of closely related

Table 2. Calculated reaction energies for the addition of water and methanol molecules to $OV(O_2)^+$ ion (**1**)[a]

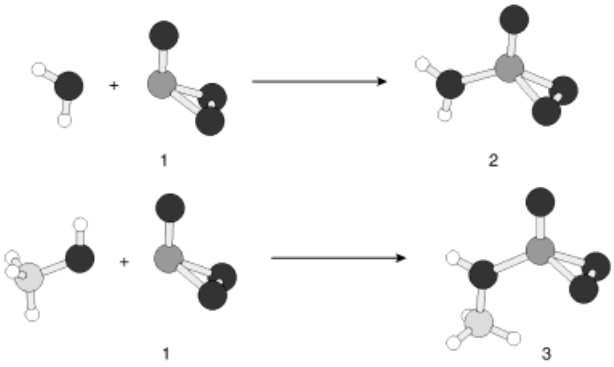

Species	RHF/3−21G(*)		B3LYP/LANL2DZ
	Energy[a]	ZPE[b]	Energy[a]
H_2O	−75.585959	0.019391	−76.4143166
CH_3OH	−114.398019	0.048494	−115.705434
1	−1161.196492	0.009055	−296.581537
2	−1236.925096	0.033333	−373.116073
3	−1275.750310	0.060562	−412.423621
$\Delta E_{(2-1-H2O)}$[c]		−86.4	−75.4
$\Delta E_{(3-1-CH3OH)}$[c]		−99.6	−83.9

[a] Energies in atomic units (1 au = 627.5 kcal/mol). − [b] Zero-point vibrational energy (ZPE) scaled by 0.89. − [c] Reaction energies in kcal/mol.

experiments for measuring the relative affinities toward cationic species has been recently reviewed.[22]

Conclusion

In conclusion the possibility to select and trap ions in a defined region of space with relatively simple devices (ITMS), together with the development of electrospray ionization, has added interesting new perspectives to the study of inorganic and organometallic compounds for the possibility to perform collisional experiments and/or gas-phase ion-molecule reactions on the isolated ionic species. Furthermore, this technique is particularly useful in the analysis of highly labile and reactive intermediates, such as peroxidic species[23] and of rapidly exchanging systems.[21]

We would like to thank the *Servizio Spettrometria di Massa CNR Area di Ricerca di Padova* for the use of their instrumentation and for stimulating discussion. We are indebted to the referees for their very helpful comments and suggestions. Financial support from the *Italian Research Council* (CNR) and from the *Italian Ministry of the University and of the Scientific Research* (MURST) is gratefully acknowledged.

Experimental Section

General Remarks: The ESI-MS measurements were obtained using a Finnigan MAT LCQ instrument (San Jose, CA). The samples were introduced by direct injection of NH_4VO_3 (0.0005 M), dissolved in CH_3OH/H_2O (1:1; pH = 1, $HClO_4$), in the absence or in the presence of an equimolar amount of H_2O_2. The same experiments were also performed using perdeuterated solvents, in

the presence of $DClO_4$. Solution flow rate 8 μl min^{-1}, capillary temperature 145°C, spray voltage 2.4 kV, capillary voltage 14 V, nebulizing gas N_2 (40 units flow rate). The parameters related to octapoles and detector were those achieved by the automatic set-up procedure. Collision-induced decompositions of selected ions were obtained by applying a supplementary r.f. voltage (tickling voltage) to the end-cap electrodes of the ion trap (resonance activation). Typical V_{tickle} values for fragmentation were up to 3 V. For ion-molecule reaction studies, a tickling voltage of 15 mV was employed. − All calculations were carried out with *Spartan* v. 4[24] and *Gaussian 94*,[25] running on IBM RS/6000 workstations. Hartree-Fock calculations were run with the 3-21G(*) basis set.[16] Density functional theory (DFT) calculations were carried out with Becke′s hybrid 3-parameter functional with Lee-Yang-Parr non-local correlation (B3LYP);[17][26] these calculations had to be run with the (99,302) numerical integration grid[25] and full accuracy at all stages in order to achieve SCF convergence. Hay and Wadt′s effective core potentials (ECP)[18][26] for vanadium were employed in DFT calculations. However, V^V compounds have a $3d^0$ configuration, and therefore ECP′s incorporating up to the outermost core orbitals ($3s^23p^6$) will not give satisfactory results. Accordingly, the ECP′s developed specifically for these cases[26] (i.e., explicitly treating $3s^23p^6$ electrons), were employed; this basis set is denoted as LANL2DZ in *Gaussian 9x*. Atomic charges were calculated by fitting to electrostatic potential maps (CHELPG method).[27] NMR experiments were carried out as already described.[1]

[1] [1a] V. Conte, F. Di Furia, S. Moro, *J. Mol. Catal.* **1995**, *104*, 159. − [1b] V. Conte, F. Di Furia, S. Moro, *Inorg. Chim. Acta* **1998**, *272*, 62.

[2] O. W. Howarth, J. R. Hunt, *J. Chem. Soc., Dalton Trans.* **1979**, 1388. − O. W. Howarth, A. T. Harrison, *J. Chem. Soc., Dalton Trans.* **1985**, 1173. − J. S. Jaswal, A. S. Tracey, *Inorg. Chem.* **1991**, *30*, 3718.

[3] N. S. Campbell, A. C. Dengel, W. P. Griffith, *Polyhedron* **1989**, *8*, 1379.

[4] V. Conte, F. Di Furia, S. Moro, S. Rabbolini, *J. Mol. Catal.* **1996**, *113*, 175.

[5] A. Bagno, V. Conte, F. Di Furia, S. Moro, *J. Phys. Chem. A* **1997**, *101*, 4637.

[6] H. Mimoun, *The Chemistry of Peroxides* (Ed.: S. Patai), Wiley, Chichester, U.K., **1983**, chapter 15.

[7] V. Conte, F. Di Furia, G. Modena, In *Organic Peroxides* (Ed.: W. Ando), Wiley, Chichester, U.K., **1992**, ,hapter 11.2.

[8] C. M. Whitehouse, R. N. Dreyer, M. Yamashita, J. B. Fenn, J. B. *Anal. Chem.* **1985**, *57*, 675.

[9] J. B. Fenn, M. Mann, C. K. Meng, S. F. Wong, C. M. Whitehouse, *Mass Spectrom. Rev.* **1990**, *10*, 37.

[10] R. Colton, A. D′Agostino, J. C. Traeger, *Mass Spectrom. Rev.* **1995**, *14*, 79.

[11] *Metal Ions in Biological Systems*, vol. 31 (“Vanadium and its Role in Life”) (Ed.: H. Sigel), Marcel Dekker, Inc., New York, NY, **1995**.

[12] D. C. Crans, R. A. Felty, M.M. Miller, *J. Am. Chem. Soc*. **1991**, *113*, 265.

[13] D. C. Crans, R. W. Marshman, M.S. Gottlieb, O. P. Anderson, M. M. Miller, *Inorg. Chem*. **1992**, *31*, 4939.

[14] Dimeric vanadates in water solution are known species at higher pH values. See as an example: N. D. Chasteen, *Vanadium in Biological Systems*, Kluwer Academic Publishers, Dordrecht, **1990**.

[15] B. J.Hamstra G. J. Colpas, V. L. Pecoraro, *Inorg. Chem*. **1998**, *37*, 949.

[16] K. D. Dobbs, W. J. Hehre, *J. Comp. Chem.* **1987**, *8*, 861.

[17] A. D. Becke, *J. Chem. Phys.* **1993**, *98*, 5648.

[18] P. J. Hay, W. R. Wadt, *J. Chem. Phys.* **1985**, *82*, 270.

[19] Coordinate files for molecular models are available from the authors.

[20] S. Favaro, L. Pandolfo, P. Traldi, *Rapid Commun. Mass Spectrom.* **1997**, *11*, 1859.

[21] T. Lover, W. Henderson, G. A Bowmaker, J. Seakins, R. P. Cooney, *Inorg. Chem*. **1997**, *36*, 3711. − R. Colton, K. L. Harrison, Y. A. Mah, J. C. Traeger, *Inorg. Chim. Acta* **1995**, *231*, 65. − R. Colton, B. D. James, I. D. Potter, J. C. Traeger, *Inorg. Chem*. **1993**, *32*, 2626.

[22] R. Cooks, J. S. Patrick, T. Kotiaho, S. A. McLuckey, *Mass Spectrom. Rev.* **1994**, *13*, 287 and refs. cited therein.

[23] J. W. Sam, X. J. Tang, J. Peisach, *J. Am. Chem. Soc.* **1994**, *116*, 5250. − C. W. Fenwick, A. M. English, *J. Am. Chem. Soc.* **1996**, *118*, 12236. − M. Bonchio, G. Licini, G. Modena, S. Moro, O. Bortolini, P. Traldi, W. A. Nugent, *J. Chem. Soc., Chem. Commun.* **1997**, 869. − D. Feichtinger, D. A. Plattner, *Angew. Chem.* **1997**, *109*, 1796; *Angew. Chem. Int. Ed. Engl*. **1997**, *36*, 1718.

[24] *Spartan, v. 4.0*, Wavefunction, Inc., 18401 von Karman Ave. #370, Irvine, CA 92715, USA, **1995**.

[25] *Gaussian 94, Revision C.2*, M. J. Frisch, G. W. Trucks, H. B. Schlegel, P. M. W. Gill, B. G. Johnson, M. A. Robb, J. R. Cheeseman, T. Keith, G. A. Petersson, J. A. Montgomery, K. Raghavachari, M. A. Al-Laham, W. G. Zakrzewski, J. V. Ortiz, J. B. Foresman, J. Cioslowski, B. B. Stefanov, A. Nanayakkara, M. Challacombe, C. Y. Peng, P. Y. Ayala, W. Chen, M. W. Wong, J. L. Andres, E. S. Replogle, R. Gomperts, R. L. Martin, D. J. Fox, J. S. Binkley, D. Defrees, J. J. Baker, J. P. Stewart, M. Head-Gordon, C. Gonzalez, J. A. Pople, Gaussian, Inc., Pittsburgh, **1995**.

[26] P. J. Hay, W.R. Wadt, *J. Chem. Phys.* **1985**, *82*, 299.

[27] C. M. Breneman, K. B. Wiberg, *J. Comp. Chem.* **1990**, *11*, 361.

[98040]

Synthesis of Homo- and Hetero-Bimetallic Complexes Containing the $Ni(C_6F_5)_2$ Moiety – Crystal Structure of $[(C_6F_5)_2Ni(\mu\text{-}SPh)_2Pd(dppe)]$

Gregorio Sánchez[a], Francisca Momblona[a], Mateo Sánchez[a], Jose Pérez[a], Gregorio López*[a], Jaume Casabó[b], Elies Molins[c], and Carles Miravitlles[c]

Departamento de Química Inorgánica, Universidad de Murcia, Facultad de Química[a],
Campus Universitario de Espinardo, E-30071 Murcia, Spain

Departament de Química, Universitat Autònoma de Barcelona[b],
Campus Universitari de Bellaterra, E-08193 Cerdanyola (Barcelona), Spain

Institut de Ciència de Marerials de Barcelona − CSIC[c],
Campus Universitari de Bellaterra, E-08193 Cerdanyola (Barcelona), Spain

Received November 25, 1997

Keywords: Organometallic compounds / Nickel complexes / Crystal structures

The compound *cis*-$[Ni(C_6F_5)_2(PhCN)_2]$ has been used as the starting material for the preparation of the bimetallic complexes $[(C_6F_5)_2Ni(\mu\text{-}X)_2Ni(C_6F_5)_2]^{2-}$ (X = SCN, OCN, N_3), $[(C_6F_5)_2Ni(\mu\text{-}SCN)_2Pd(C_6F_5)_2]^{2-}$, $[(C_6F_5)_2Ni(\mu\text{-}NCS)_2Pd(dppe)]$ [dppe = 1,2-bis(diphenylphosphanyl)ethane], and the trimetallic$[(C_6F_5)_2Ni(\mu\text{-}NCS)_2Pd(\mu\text{-}SCN)_2Ni(C_6F_5)_2]^{2-}$. The mononuclear compounds $[(C_6F_5)_2NiLX]$ (L = PPh_3, $P(C_6H_4MeO\text{-}p)_3$; X = SCN, OCN) are obtained by reaction between $[(C_6F_5)_2Ni(\&\mu\text{-}X)_2Ni\text{-}(C_6F_5)_2]^{2-}$ and L. The treatment of *cis*-$[Ni(C_6F_5)_2(PhCN)_2]$ with $[M(SAr)_2(dppe)]$ leads to the formation of the arylthiolate complexes $[(C_6F_5)_2Ni(\mu\text{-}SAr)_2M(dppe)]$ (Ar = Ph, $C_6H_4Me\text{-}p$, $C_6H_4NO_2\text{-}p$; M = Ni, Pd, Pt). The X-ray diffraction study of $[(C_6F_5)_2Ni(\mu\text{-}SPh)_2Pd(dppe)]$ shows that both metal atoms, Ni and Pd, are coordinated in a slightly distorted square-planar geometry and the μ-thiolato groups are in the *syn* conformation.

Introduction

Anionic complexes of the group-10 elements of the type $[M_2R_4(\mu\text{-}X)_2]^{2-}$ (M = Ni, R = C_6F_5, X = F or Cl; M = Pd or Pt, R = C_6F_5, X = Cl, Br, I or SCN; M = Pd, R = $C_6F_3H_2$-2,4,6, X = Cl, Br, I, SCN) have been reported[1][2][3][4]. Labile complexes such as $[MR_2(tht)_2]$ (M = Pd or Pt; R = C_6F_5)[5] and $[PdR_2(PhCN)_2]$ (R = C_6F_5, $C_6F_3H_2$-2,4,6)[6] have shown to be excellent precursors for the synthesis of asymmetric homo- and hetero-bimetallic complexes with halide bridges.

Symmetric or antisymmetric binuclear complexes can be obtained by treating the labile complex R_2ML_2 with the appropriate reagent [Eq. (1) and (2)]. The reaction represented by Eq. (1) was used for the preparation of bis(μ-hydroxo) complexes of nickel[7] and palladium[8] $[(C_6F_5)_2M(\mu\text{-}OH)_2M(C_6F_5)_2]^{2-}$ from the reaction between *cis*-$[M(C_6F_5)_2(PhCN)_2]$ and OH^-, but the platinum anologue[9] could not be prepared by this method because the nucleophilic attack of coordinated PhCN by OH^- was competitive. The process represented by Eq. (2) was used for the preparation of bimetallic (Pd−Ni, Pd−Pd, or Pd−Pt) palladium complexes[6]. We report here the preparation and study of a number of new bimetallic pseudohalide-bridged complexes derived from the $Ni(C_6F_5)_2$ starting from the labile complex *cis*-$[Ni(C_6F_5)_2(PhCN)_2]$.

$$2\ R_2ML_2 + 2\ X^- \rightarrow R_2M(\mu\text{-}X)_2M'R_2 + 4\ L \quad (1)$$

$$R_2ML_2 + X_2M'L'_2 \rightarrow R_2M(\mu\text{-}X)_2M'L'_2 + 2\ L \quad (2)$$

The above method has been extended to the preparation of some bimetallic arylthiolate-bridged complexes of nickel. The relevance of transition-metal complexes with aliphatic thiolate ligands as models of biologically redox-active metalloproteins[10] has stimulated interest in the chemistry of metal thiolates[11]. Nickel(II) thiolates are generally square-planar species with a strong tendency to form dimers and oligomers[12][13][14][15]. We have prepared a number of di- and trinuclear nickel(II) complexes with bridging thiolate groups by reaction of $[(C_6F_5)_2Ni(\mu OH)_2Ni(C_6F_5)_2]^{2-}$ with thiols[16]. Now we report the preparation of asymmetric bimetallic complexes of the type $[(C_6F_5)_2Ni(\mu\text{-}SAr)M(dppe)]$ [dppe = 1,2-bis(diphenylphosphanyl)ethane] starting from the precursor *cis*-$[Ni(C_6F_5)_2(PhCN)_2]$.

Results and Discussion

1. Pseudohalide Complexes

The reaction (1:1 molar ratio) between $[Ni(C_6F_5)_2(PhCN)_2]$ and the pseudohalides SCN^-, OCN^-, and N_3^- gives the pseudohalide-bridged complexes **1−3** (Scheme 1) in 60−85% yields. The new complexes are air-stable solids and their acetone solutions exhibit conductances in the range 207−217 S cm^2 mol^{-1}, corresponding to 2:1 electrolytes[17]. The infrared spectra of the complexes show bands attributed to the C_6F_5 group[18] at ca. 1630 m, 1495 vs, 1460 vs, 1050 vs, 950 vs, and 780 br., s cm^{-1}. Complex **1** gives a ν(CN) band at 2158 cm^{-1} consistent with the presence of bridged thiocyanate[19] and the ^{19}F-NMR spectrum indicates that there are two sorts of C_6F_5 rings, so the sym-

 © WILEY-VCH Verlag GmbH, D-69451 Weinheim, 1998 1434−1948/98/0808−1199 $ 17.50+.50/0

metric structure Ni(SCN)(NCS)Ni is proposed for this complex. The infrared spectrum of the cyanate complex **2** shows a band at 2168 cm^{-1} supporting the bridging character of the cyanate group by means of the nitrogen atom[20]. The ^{19}F-NMR spectrum is consistent with the presence of four equivalent pentafluophenyl groups. The IR[21] and NMR data of complex **3** are consistent with a binuclear structure contaning two azide bridges. The electronic spectra of complexes **1**−**3** show an absorption band which may be assigned to the $^1A_{1g} \rightarrow {}^1A_{2g}$ transition in a square-planar ligand field[22].

Scheme 1. Pseudohalide complexes (R = C_6F_5)

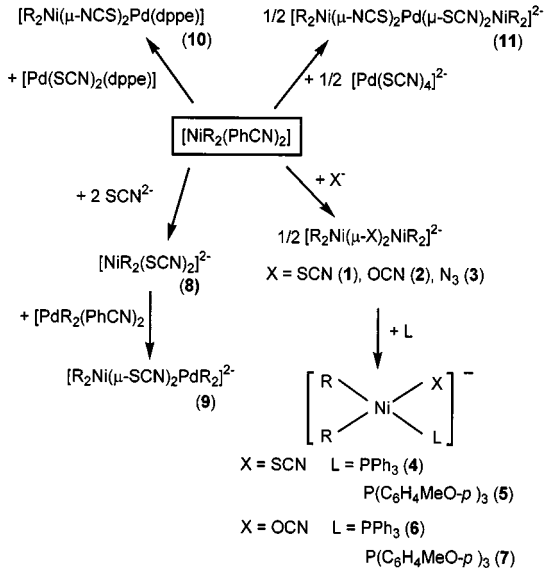

Complexes **1** and **2** react with triphenylphophane and tris(*p*-methoxyphenyl)phosphane to give the mononuclear complexes $(PPh_4)[Ni(C_6F_5)_2XL]$ [X = SCN, OCN; L = PPh_3, $P(C_6H_4MeO\text{-}p)_3$] (**4**-**7**) (Scheme 1). However, similar reactions with pyridine or triethylphosphane give a mixture of $[Ni(C_6F_5)_2(SCN)_2]^{2-}$ and $[Ni(C_6F_5)_2L_2]$. The azide-bridged complex **3** does not react with neutral ligands. The IR data of the mononuclear complexes **4**−**7** are consistent with terminal S-thiocyanate or N-cyanate. The ^{19}F-NMR spectra exhibit six signals corresponding to two inequivalent C_6F_5 rings, one *trans* to the pseudohalide and the other *trans* to the neutral ligand. Their acetone solutions show conductance values (83−95 S cm^2 mol^{-1}) corresponding to 1:1 electrolytes[17]. The elemental analyses of complexes $(PPh_4)[Ni(C_6F_5)_2XL]$ (**4**−**7**) showed no significant variation when the crystals were twice recrystallized from acetone/diethyl ether and the spectroscopic data also supported that a mixture of $[Ni(C_6F_5)_2L_2]$ and $(PPh_4)_2[Ni(C_6F_5)_2X_2]^{2-}$ should be discarded. For example, $(PPh_4)[Ni(C_6F_5)_2(SCN)(PPh_3)]$ gives a single IR band for the ν(CN) vibration (at 2102 cm^{-1}) while $(PPh_4)_2[Ni(C_6F_5)_2(SCN)_2]$ gives a split band for the same vibrational mode (2112 and 2124 cm^{-1}).

The reaction between $[Ni(C_6F_5)_2(PhCN)_2]$ and SCN^- (molar ratio 1:2) gives the corresponding mononuclear complex $(PPh_4)_2[Ni(C_6F_5)_2(SCN)_2]$ (**8**). However, similar complexes with cyanate and azide anions could not be obtained. Complex **8** behaves as a 2:1 electrolyte in acetone solution (molar conductance 224 S cm^2 mol^{-1}) and the infrared band observed at 2112 cm^{-1} indicates that the thiocyanate ligand is S-bonded[19]. The expected three signals (4 F_o/2 F_p/4 F_m) of two equivalent C_6F_5 groups are observed in the ^{19}F-NMR spectrum. In dichloromethane, complex **8** reacts with the labile *cis*-$[Pd(C_6F_5)_2(PhCN)_2]$ to give the binuclear heterobimetallic complex $[(C_6F_5)_2Ni(\mu\text{-}SCN)(\mu\text{-}NCS)Pd(C_6F_5)_2]^{2-}$ (**9**). The IR spectrum shows a band at 2144 cm^{-1} which is consistent with a bridging thiocyanate[19] and four signals observed in the ^{19}F-NMR spectrum for the pentafluorophenyl *ortho*-fluorine atoms indicate that there are four different C_6F_5 rings, in accordance with the structure proposed above.

The asymmetric binuclear complex **10** (Scheme 1) is prepared by reaction between the labile nickel complex $[Ni(C_6F_5)_2(PhCN)_2]$ and the thiocyanate palladium complex $[Pd(SCN)_2(dppe)]$. The infrared absorption found at 2158 cm^{-1} for complex **10** is consistent with the presence of bridging thiocyanate[19] and the ^{19}F-NMR spectrum exhibits two signals in the *ortho*-fluorine region attributed to the structure $[(C_6F_5)_2Ni(\mu\text{-}SCN)(\mu\text{-}NCS)Pd(dppe)]$, i.e., one C_6F_5 ring *trans* to N and one C_6F_5 ring *trans* to S.

The trinuclear complex **11** (Scheme 1) is obtained by reaction of *cis*-$[Ni(C_6F_5)_2(PhCN)_2]$ with the thiocyanate complex $[Pd(SCN)_4]^{2-}$. The absorption found at 2146 cm^{-1} for complex **11** indicates the presence of bridging thiocyanate[27]. The ^{19}F-NMR spectrum shows three signals (intensity ratio of 2:1:2) corresponding to the *ortho*-, *para*-, and *meta*-fluorine atoms of four equivalent C_6F_5 rings, in accord with the structure $[(C_6F_5)_2Ni(\mu\text{-}NCS)_2Pd(\mu\text{-}SCN)_2Ni(C_6F_5)_2]^{2-}$.

2. Thiolate Complexes

In methanol, *cis*-$[Ni(C_6F_5)_2(PhCN)_2]$ reacts with $[M(SAr)_2(dppe)]$ (M = Ni, Pd, Pt; Ar = Ph, $C_6H_4Me\text{-}p$, $C_6H_4NO_2\text{-}p$) to give the corresponding asymmetric binuclear thiolate complexes shown in Scheme 2. They are orange or red, air-stable solids which in acetone solution behave as non-electrolytes.

Scheme 2. Arylthiolate complexes (R = C_6F_5)

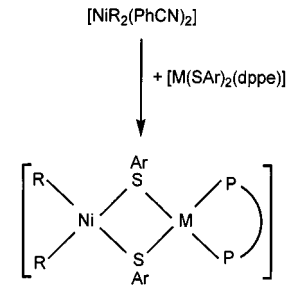

	M = Ni	Pd	Pt
Ar = Ph	(12)	(13)	(14)
$C_6H_4Me\text{-}p$	(15)	(16)	(17)
$C_6H_4NO_2\text{-}p$	(18)	(19)	(20)

The infrared spectra of these *gem* derivatives show the bands attributed to the C_6F_5 group[18] at ca. 1630 m, 1490 vs, 1050 vs, and 950 vs cm^{-1}, as well as a broad or split band at 780 cm^{-1} for the so-called "X-sensitive" mode of C_6F_5 which is characteristic of the *cis*-$M(C_6F_5)_2$ fragment[23][24]. The ^1H-, ^{19}F-, and $^{31}P\{^1H\}$-NMR data for the binuclear complexes are in agreement with the formula $[(C_6F_5)_2Ni(\mu\text{-}SAr)_2M(dppe)]$. As expected, the ^{31}P-NMR spectra show a single resonance and that of the platinum complexes are flanked by the satellites by coupling to ^{195}Pt, the coupling constant being in the range 2900−3100 Hz. The three signals observed in the ^{19}F NMR correspond to the A_2MX_2 spin system of two equivalent pentafluorophenyl groups freely rotating around the Ni−C bond and with the coupling constant $J_{AX} = 0$. The ^1H-NMR data also give evidence of free rotation of the thiolate aryl group around the C−S bond, although in complexes **18** and **19** the resonance signals of the $C_6H_4NO_2$-*p* substituent are overlapped with the dppe phenyl resonances.

3. Crystal Structure of $[(C_6F_5)_2Ni(\mu\text{-}SPh)_2Pd(dppe)]\cdot Me_2CO$

Figure 1 represents an ORTEP[25] projection of the molecular structure with the atom numbering and Table 1 shows some selected bond lengths and bond angles. Both metal atoms, Ni and Pd, are coordinated in a slightly distorted square-planar geometry and the μ-thiolato groups are in the *syn* conformation.

Figure 1. Molecular structure of compound **13**

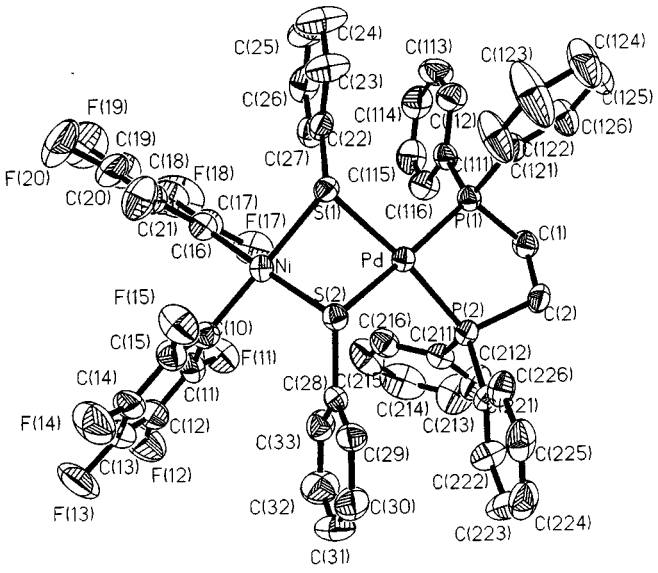

The main distortion of the square-planar coordination is a slight twist of de PdS_2 plane relative to the PdP_2 plane, by 9.4°. The Ni−C and Ni−S distances are similar to values reported in the literature[16][26]. The Ni−S and Pd−S distances are also similar to values found in other homonuclear complexes[27][28]. The distortion of the square-planar coordination in the Ni atom is a slight twist of the NiS_2 plane relative to the NiC_2 plane, by 9.6°.

The phosphane has a strong *trans* influence, lengthening the Pd−S bonds. So, the Pd−S distances are 2.356(2) and 2.360(2) A giving a weighted mean distance of 2.358(2) A, significantly longer than distances with other ligands[27][28].

Table 1. Selected intramolecular distances [A] and angles [°] for **13**

a) Distances		b) Angles	
Pd−P(2)	2.2720(14)	P(2)−Pd−P(1)	84.27(5)
Pd−P(1)	2.2973(14)	P(2)−Pd−S(2)	99.76(5)
Pd−S(2)	2.3564(13	P(1)−Pd−S(2)	171.10(4)
Pd−S(1)	2.3597(13)	P(2)−Pd−S(1)	173.40(4)
Pd···Ni	3.1157(10)	P(1)−Pd−S(1)	101.73(5)
Ni−C(10)	1.900(5)	S(2)−Pd−S(1)	74.70(4)
Ni−C(16)	1.906(5)	C(10)−Ni−C(16)	87.0(2)
Ni−S(2)	2.214(2)	C(10)−Ni−S(2)	95.05(14)
Ni−S(1)	2.2509(14)	C(16)−Ni−S(2)	177.82(14)
		C(16)−Ni−S(2)	177.82(14)
		C(10)−Ni−S(1)	169.3(2)
		C(16)−Ni−S(1)	98.46(14)
		S(2)−Ni−S(1)	79.69(5)
		C(10)−Ni−Pd	132.91(14)

The Ni···Pd distance is 3.116(2) A, showing no significant metal-metal interaction. The NiSPdS ring adopts a hinged square-planar geometry with a dihedral angle of 120.4° along the S···S line.

As expected, the two carbon atoms of the aliphatic chain of dppe ligand lie on each side of the PdP_2 plane. Thus, C(1) lies 0.067 to one side, while C(2) lies 0.640 A to the other side of the plane, the PdP_2C_2 chelate ring adopting a twist conformation. The non-planarity of the PdP_2C_2 ring is a consequence of the tetrahedral geometry at the carbon and phosphorus atoms and the square-planar coordination of the metal center.

The two pentafluorophenyl rings are planar and rotated 83.5° with respect to each other. The rings present distortions as indicated by the values of the C−C−C angles which range from 112.5(4) to 125.5(5). This type of distortion has already been observed in other fluorophenyl rings[29].

This work was supported by the *Direccion General de Investigacion Cientifica y Tecnica* (project PB94−1157), Spain. F. M. and J. P. thank the *Ministerio de Educacion y Ciencia*, Spain, for grants.

Experimental Section

General Methods: C, H, N, and S analyses were carried out with a Carlo Erba instrument. − Infrared spectra were recorded with a Perkin-Elmer 1430 spectrophotometer using Nujol mulls between polyethylene sheets. − ^1H-, ^{19}F-, and ^{31}P-NMR spectra were recorded with a Bruker AC 200E or a Varian 300 spectrometer. − Conductance measurements were performed with a Crison 525 conductimeter (in acetone, $c \approx 5\cdot10^{-4}$ mol dm^{-3}). − Decomposition temperatures were determined with a Reichert microscope. − All solvents were dried by conventional methods. − The compounds $[Ni(C_6F_5)_2(PhCN)_2]$[7], $(PPh_4)SCN$[30], KN_3[31], $Pd(dppe)(SCN)_2$[32], $(NBu_4)_2[Pd(SCN)_4]$[33], $[Ni(SAr)_2(dppe)]$[34] and $[M(SAr)_2(dppe)]$ (M = Pd, Pt)[35] were prepared as described elsewhere.

$(PPh_4)_2[Ni_2(C_6F_5)_4(\mu\text{-}SCN)_2]$ (**1**) *and $(PPh_4)_2[Ni(C_6F_5)_2(SCN)_2]$* (**8**): A solution of $(PPh_4)SCN$ (1.33 mmol for **1** and 2.66 mmol for **8**) in dichloromethane (10 ml) was added to a solution of $[Ni(C_6F_5)_2(PhCN)_2]$ (0.8 g, 1.33 mmol) in dichloromethane (15 ml) and the mixture was stirred (**1**) or boiled under reflux (**8**) for

30 min. The solution was then concentrated under reduced pressure to half the original volume. Addition of diethyl ether caused the precipitation of a yellow solid which was filtered off, washed with diethyl ether and air-dried.

1: Yield 84%. − $C_{74}H_{40}F_{20}N_2Ni_2P_2S_2$ (1580.58): calcd. C 56.2, H 2.6, N 1.8, S 4.1; found C 56.7, H 2.3, N 1.8, S 3.7. − M.p. 211°C (dec.). − Λ_M = 193 S cm^2 mol^{-1}. − IR (Nujol): ν = 2158 cm^{-1} (CN str). − UV/Vis (acetone): λ_{max} [cm^{-1} × 10^{-3}] (ε) = 22.6 (1088). − ^{19}F NMR ([D$_6$]acetone, $CFCl_3$): δ = −115.4 (m, 4 F$_o$), −116.9 (m, 4 F$_o$), −165.2 (t, 2 F$_p$, J_{pm} = 19.7), −165.6 (t, 2 F$_p$, J_{pm} = 21.7 Hz), −167.3 (m, 4 F$_m$), −167.5 (m, 4 F$_m$). − ^{31}P NMR ([D$_6$]acetone, H_3PO_4): δ = 24.6.

8: Yield 58%. − $C_{62}H_{40}F_{10}N_2NiP_2S_2$ (1187.77): calcd. C 62.7, H 3.4, N 2.4, S 5.4; found C 62.6, H 3.6, N 2.5, S 5.3. − M.p. 189°C (dec.). − Λ_M = 224 S cm^2 mol^{-1}. − IR (Nujol): ν = 2112 cm^{-1}, 2124 (sh) (CN str). − UV/Vis (acetone): λ_{max} [cm^{-1} × 10^{-3}] (ε) = 23.4 (752). − ^{19}F NMR ([D$_6$]acetone, $CFCl_3$): δ = −115.9 (d, 4 F$_o$, J_{om} = 29.9 Hz), −166.9 (t, 2 F$_p$, J_{pm} = 20.3 Hz), −167.9 (m, 4 F$_m$). − ^{31}P NMR ([D$_6$]acetone, H_3PO_4): δ = 24.6.

(PPh$_4$)$_2$[Ni$_2$(C$_6$F$_5$)$_4$(μ-NCO)$_2$]; X = NCO (**2**) *or N$_3$* (**3**): An acetone (20 ml) solution containing [Ni(C$_6$F$_5$)$_2$(PhCN)$_2$] (100 mg, 0.17 mmol) and KNCO or KN_3 (0.17 mmol) was stirred at room temperature for 15 min and then a solution of $(PPh_4)Cl$ (62.6 mg, 0.17 mmol) in hot acetone (15 ml) was added. The mixture was stirred at room temperature for 30 min. The KCl formed during the reaction was removed by filtration, and the resulting solution was then concentrated under reduced pressure to ca. 10 ml. Addition of diethyl ether (for **2**) or hexane (for **3**) resulted in the precipitation of an orange solid. This was filtered off, washed with water and diethyl ether (**2**) or ethanol and hexane (**3**) and air-dried. Complexes **2** and **3** were recrystallized from acetone/diethyl ether and acetone/hexane respectively.

2: Yield 61%. − $C_{74}H_{40}F_{20}N_2Ni_2O_2P_2$ (1548.45): calcd. C 57.4, H 2.6, N 1.8; found C 57.5, H 2.7, N 1.8. − M.p. 187°C (dec.). − Λ_M = 207 S cm^2 mol^{-1}. − IR (Nujol): ν = 2168 cm^{-1} (CN str). − UV/Vis (acetone): λ_{max} [cm^{-1} × 10^{-3}] (ε) = 21.6 (798). − ^{19}F NMR ([D$_6$]acetone, $CFCl_3$): δ = −115.4 (d, 8 F$_o$, J_{om} 29.1 Hz), −165.9 (t, 4 F$_p$, J_{pm} 20.0), −167.7 (m, 4 F$_m$). − ^{31}P NMR ([D$_6$]acetone, H_3PO_4): δ = 24.6.

3: Yield 79%. − $C_{72}H_{40}F_{20}N_6Ni_2P_2$ (1548.45): calcd. C 55.9, H 2.6, N 5.4; found C 55.9, H 2.9, N 5.5. − M.p. 196°C (dec.). − Λ_M = 217 S cm^2 mol^{-1}. − IR (Nujol): ν = 2063 cm^{-1} (CN str). − UV/Vis (acetone): λ_{max} [cm^{-1} × 10^{-3}] (ε) = 21.7 (1165). − ^{19}F NMR ([D$_6$]acetone, $CFCl_3$): δ = −115.3 (d, 8 F$_o$, J_{om} = 29.1), −165.1 (t, 4 F$_p$, J_{pm} = 19.2 Hz), −167.2 (m, 8 F$_m$). − ^{31}P NMR ([D$_6$]acetone, H_3PO_4): δ = 24.6.

(PPh$_4$)[Ni(C$_6$F$_5$)$_2$XL]; X = SCN, L = PPh$_3$ (**4**) *or P(C$_6$H$_4$CH$_3$O-p)$_3$* (**5**); *X = NCO, L = PPh$_3$* (**6**) *or P(C$_6$H$_4$CH$_3$-O-p)$_3$* (**7**): A solution of $(PPh_4)_2[Ni_2(C_6F_5)_4(\mu\text{-}X)_2]$ (X = SCN or NCO; 0.094 mmol) and the corresponding neutral ligand (PPh_3 or $P(C_6H_4CH_3O\text{-}p)_3$; 0.22 mmol) in dichloromethane (15 ml) was stirred at room temperature for 30 min. The resulting solution was concentrated under reduced pressure to half the original volume. Addition of diethyl ether precipitated a yellow solid which was filtered off, washed with diethyl ether and air-dried.

4: Yield 79%. − $C_{55}H_{35}F_{10}NNiP_2S$ (1052.58): calcd. C 62.8, H 3.4, N 1.3, S 3.1; found C 62.9, H 3.4, N 1.5, S 3.2. − M.p. 190°C (dec.). − Λ_M = 91 S cm^2 mol^{-1}. − IR (Nujol): ν = 2102 cm^{-1} (CN str). − UV/Vis (acetone): λ_{max} [cm^{-1} × 10^{-3}] (ε) = 24.9 (868). − ^{19}F NMR ([D$_6$]acetone, $CFCl_3$): δ = −116.2 (m, 2 F$_o$), −117.7 (m, 2 F$_o$), −166.2 (t, 1 F$_p$, J_{pm} = 19.7 Hz), −166.9 (m, 1 F$_p$ + 2 F$_m$), −167.4 (m, 2 F$_m$). − ^{31}P NMR ([D$_6$]acetone, H_3PO_4): δ = 24.6, 23.1.

5: Yield 77%. − $C_{58}H_{41}F_{10}NNiO_3P_2S$ (1141.69): calcd. C 61.0, H 3.6, N 1.2, S 2.8; found C 61.3, H 3.4, N 1.4, S 2.9. − M.p. 171°C (dec.). − Λ_M = 94 S cm^2 mol^{-1}. − IR (Nujol): ν = 2106 cm^{-1} (CN str). − UV/Vis (acetone): λ_{max} [cm^{-1} × 10^{-3}] (ε) = 25.0 (931). − ^{19}F NMR ([D$_6$]acetone, $CFCl_3$): δ = −115.6 (m, 2 F$_o$), −116.9 (m, 2 F$_o$), −165.8 (t, 1 F$_p$, J_{pm} = 22.6 Hz), −166.4 (m, 1 F$_p$ + 2 F$_m$), −166.8 (m, 2 F$_m$). − ^{31}P NMR ([D$_6$]acetone, H_3PO_4): δ = 24.6, 19.5.

6: Yield 75%. − $C_{55}H_{35}F_{10}NNiOP_2$ (1036.51): calcd. C 63.7, H 3.4, N 1.4; found C 63.6, H 3.6, N 1.3. − M.p. 175°C (dec.). − Λ_M = 95 S cm^2 mol^{-1}. − IR (Nujol): ν = 2222 cm^{-1} (CN str). − UV/Vis (acetone): λ_{max} [cm^{-1} × 10^{-3}] (ε) = 24.2 (572). − ^{19}F NMR ([D$_6$]acetone, $CFCl_3$): δ = −115.6 (m, 2 F$_o$), −117.1 (m, 2 F$_o$), −167.1 (m, 2 F$_p$ + 2 F$_m$), −167.7 (m, 2 F$_m$). − ^{31}P NMR ([D$_6$]acetone, H_3PO_4): δ = 24.6, 22.7.

7: Yield 65%. − $C_{58}H_{41}F_{10}NNiO_4P_2$ (1126.59): calcd. C 61.8, H 3.7, N 1.2; found C 61.6, H 3.5, N 1.3. − M.p. 98°C (dec.). − Λ_M = 83 S cm^2 mol^{-1}. − IR (Nujol): ν = 2218 cm^{-1} (CN str). − UV/Vis (acetone): λ_{max} [cm^{-1} × 10^{-3}] (ε) = 24.5 (663). − ^{19}F NMR ([D$_6$]acetone, $CFCl_3$): δ = −115.6 (m, 2 F$_o$), −116.9 (m, 2 F$_o$), −167.1 (m, 2 F$_p$), −167.7 (m, 4 F$_m$). − ^{31}P NMR ([D$_6$]acetone, H_3PO_4): δ = 24.6, 18.9.

(PPh$_4$)$_2$[(C$_6$F$_5$)$_2$Ni(μ-SCN)$_2$Pd(C$_6$F$_5$)$_2$] (**9**): A solution of (**8**) (0.15 g, 0.126 mmol) and [Pd(C$_6$F$_5$)$_2$(PhCN)$_2$] (81.6 mg, 0.126 mmol) in dichloromethane (15 ml) was stirred at room temperature for 30 min. The resulting solution was concentrated under reduced pressure to half the original volume. Addition of hexane precipitated a yellow solid which was filtered off, washed with hexane and air-dried. The compound was recrystallized from dichloromethane/hexane. − Yield 84%. − $C_{74}H_{40}F_{20}N_2NiP_2PdS_2$ (1628.31): calcd. C 54.6, H 2.5, N 1.7, S 3.9; found C 54.3, H 2.2, N 1.7, S 3.8. − M.p. 221°C (dec.). − Λ_M = 197 S cm^2 mol^{-1}. − IR (Nujol): ν = 2144 cm^{-1} (CN str). − UV/Vis (acetone): λ_{max} [cm^{-1} × 10^{-3}] (ε) = 22.8 (731). − ^{19}F NMR ([D$_6$]acetone, $CFCl_3$): δ = −113.2 (d, 2 F$_o$, J_{om} = 29.6 Hz), −114.4 (m, 2 F$_o$), −114.8 (m, 2 F$_o$), −116.3 (m, 2 F$_o$), −164.2 (m, 2 F$_p$), −164.7 (t, 1 F$_{p,\,Jpm}$ = 19.2 Hz), −165.1 (t, 1 F$_p$, J_{pm} = 19.7 Hz), −165.7 (m, 1 F$_m$), −166.2 (m, 1 F$_m$), −166.7 (m, 1 F$_m$), −167.0 (m, 1 F$_m$). − ^{31}P NMR ([D$_6$]acetone, H_3PO_4): δ = 24.6.

[(C$_6$F$_5$)$_2$Ni(μ-SCN)$_2$Pd(dppe)] (**10**): A solution of [Pd(SCN)$_2$(dppe)] (0.134 g, 0.21 mmol) and [Ni(C$_6$F$_5$)$_2$(PhCN)$_2$] (0.129 g, 0.21 mmol) in dichloromethane (20 ml) was stirred at room temperature for 20 min. The resulting solution was concentrated under reduced pressure to half the original volume. Addition of diethyl ether precipitated a yellow solid which was filtered off, washed with diethyl ether and air-dried. The compound was recrystallized from dichloromethane/diethyl ether. − Yield 73%. − $C_{40}H_{24}F_{10}N_2NiP_2PdS_2$ (1013.82): calcd. C 47.4, H 2.4, N 2.8, S 6.3; found C 47.1, H 2.5, N 2.9, S 6.2. − M.p. 177°C (dec.). − Λ_M = 6 S cm^2 mol^{-1}. − IR (Nujol): ν = 2158 cm^{-1} (CN str). − UV/Vis (acetone): λ_{max} [cm^{-1} × 10^{-3}] (ε) = 29.7 (7564). − ^{19}F NMR ([D$_6$]acetone, $CFCl_3$): δ = −116.2 (m, 2 F$_o$), −117.6 (m, 2 F$_o$), −164.3 (t, 1 F$_p$, J = 19.7 Hz), −164.8 (t, 1 F$_p$, J = 19.7 Hz), −167.0 (m, 4 F$_m$). − ^{31}P NMR ([D$_6$]acetone, H_3PO_4): δ = 71.5 (br.).

[NBu$_4$]$_2$[(C$_6$F$_5$)$_2$Ni(μ-SCN)$_2$Pd(μ-SCN)$_2$Ni(C$_6$F$_5$)$_2$] (**11**): A solution of $[NBu_4]_2[Pd(SCN)_4]$ (0.130 g, 0.15 mmol) and [Ni(C$_6$F$_5$)$_2$(PhCN)$_2$] (0.2 g, 0.33 mmol) (molar ratio 1:2.2) in acetone (10 ml) was stirred at room temperature for 20 min. The re-

sulting solution was concentrated under reduced pressure to half the original volume. Addition of diethyl ether precipitated a red solid which was filtered off, washed with diethyl ether and air-dried. The compound was recrystallized from dichloromethane/diethyl ether. – Yield 54%. – $C_{60}H_{72}F_{20}N_6Ni_2PdS_4$ (1609.31): calcd. C 44.8, H 4.5, N 5.2, S 8.0; found C 45.1, H 4.7, N 5.4, S 7.7. – M.p. 180°C (dec.). – Λ_M = 164 S cm^2 mol^{-1}. – IR (Nujol): ν· = 2146 cm^{-1} (CN str). – UV/Vis (acetone): λ_{max} [cm^{-1} × 10^{-3}] (ε) = 29.7 (10320). – ^{19}F NMR ([D$_6$]acetone, $CFCl_3$): δ = −117.4 (m, 8 F$_o$), −164.9 (m, 4 F$_p$), −167.1 (m, 8 F$_m$).

[(dppe)M(μ-SAr)$_2$Ni(C$_6$F$_5$)$_2$] (**12–20**) (see Scheme 2): Complexes **12–20** were obtained by treating *cis*-[Ni(C$_6$F$_5$)$_2$(PhCN)$_2$] with [M(SAr)$_2$(dppe)] (molar ratio 1:1) in MeOH according to the following general method. To a MeOH (10 ml) solution of the *cis*-[Ni(C$_6$F$_5$)$_2$(PhCN)$_2$] (0.174 mmol) was added [M(SAr)$_2$(dppe)] (0.174 mmol), and the solution was stirred at room temperature for 30 min. It was concentrated under reduced pressure to ca. one fifth of the initial volume obtaining an orange or red precipitate, which was filtered off, washed with hexane and air-dried.

12: Yield 75%. – $C_{50}H_{34}F_{10}Ni_2P_2S_2$ (1068.27): calcd. C 56.2, H 3.2, S 6.0; found C 55.9, H 3.1, S 5.8. – M.p. 215°C (dec.). – ^{1}H NMR ([D$_6$]acetone, TMS): δ = 2.5 (d, 4 H, dppe), 6.7 (t, 4 H, Ph), 6.9 (t, 2 H, Ph), 7.3 (d, 4 H, Ph), 7.5 (m, 12 H, dppe), 7.9 (m,8 H, dppe). – ^{19}F NMR ([D$_6$]acetone, $CFCl_3$): δ = −115.2 (d, 4 F$_o$, J_{om} = 28.8 Hz), −165.3 (t, 2 F$_p$, J_{pm} = 19.7 Hz), −166.6 (m, 4 F$_m$). – ^{31}P NMR ([D$_6$]acetone, H_3PO_4): δ = 58.7.

13: Yield 68%. – $C_{50}H_{34}F_{10}NiP_2PdS_2$ (1116): calcd. C 53.8, H 3.1, S 5.8; found C 53.5, H 3.3, S 5.6. – M.p. 119°C (dec). – ^{1}H NMR ([D$_6$]acetone, TMS): δ = 2.6 (d, 4 H, dppe), 6.7 (t, 4 H, Ph), 6.9 (t, 2 H, Ph), 7.3 (d, 4 H, Ph), 7.5 (m, 12 H, dppe), 7.9 (m, 8 H, dppe). –^{19}F NMR ([D$_6$]acetone, $CFCl_3$): δ = −115.3 (d, 4 F$_o$, J_{om} = 28.3), −165.6 (t, 2 F$_p$, J_{pm} = 19.8), −166.8 (m, 4 F$_m$). – ^{31}P NMR ([D$_6$]acetone, H_3PO_4): δ = 58.6.

14: Yield 65%. – $C_{50}H_{34}F_{10}NiP_2PtS_2$ (1204.66): calcd. C 49.9, H 2.8, S 5.3; found C 49.8, H 3.0, S 5.2. – M.p. 235°C (dec.). – ^{1}H NMR ([D$_6$]acetone, TMS): δ = 2.7 (d, H, dppe), 6.6 (t, 4 H, Ph), 6.8 (t, 2 H, Ph), 7.2 (d, 4 H, Ph), 7.5 (m, 12 H, dppe), 7.8 (m, 8 H, dppe). – ^{19}F NMR ([D$_6$]acetone, $CFCl_3$): δ = −116.9 (d, 4 F$_o$, J_{om} = 24.5 Hz), −164.4 (m, 2 F$_p$), −166.2 (m, 2 F$_m$). – ^{31}P NMR ([D$_6$]acetone, H_3PO_4): δ = 43.3 [J(PPt) = 3076.5 Hz].

15: Yield 73%. – $C_{52}H_{38}F_{10}Ni_2P_2S_2$ (1096.32): calcd. C 57.0, H 3.5, S 5.9; found C 56.7, H 3.4, S 5.7. – M.p. 213°C (dec.). – ^{1}H NMR ([D$_6$]acetone, TMS): δ = 2.1 (s, 6 H, C$_6$H$_4$Me-*p*), 2.4 (d, 4 H, dppe), 6.5 (d, 4 H, C$_6$H$_4$Me-*p*), 7.2 (d, 4 H, C$_6$H$_4$Me-*p*), 7.5 (m, 8 H, dppe). –^{19}F NMR ([D$_6$]acetone, $CFCl_3$): δ = −115.4 (d, 4 F$_o$, J_{om} = 28.8 Hz), −166.0 (t, 2 F$_p$, J_{pm} = 19.7 Hz), −167.1 (m, 4 F$_m$). – ^{31}P NMR ([D$_6$]acetone, H_3PO_4): δ = 57.9.

16: Yield 89%. – $C_{52}H_{38}F_{10}NiP_2PdS_2$ (1144.05): calcd. C 54.6, H 3.4, S 5.6; found C 54.5, H 3.3, S 5.5. – M.p. 224°C (dec.). – ^{1}H NMR ($CDCl_3$, TMS): δ = 2.1 (s, 6 H, C$_6$H$_4$Me-*p*), 2.3 (d, 4 H, dppe), 6.4 (d, 4 H, C$_6$H$_4$Me-*p*), 7.2 (d, 4 H, C$_6$H$_4$Me-*p*), 7.4 (m, 12 H, dppe), 7.6 (m, 8 H, dppe). – ^{19}F NMR ($CDCl_3$, $CFCl_3$): δ = −115.6 (d, 4 F$_o$, J_{om} = 28.8 Hz), −166.2 (t, 2 F$_p$, J_{pm} = 20.0 Hz), −167.3 (m, 4 F$_m$). – ^{31}P NMR ($CDCl_3$, H_3PO_4): δ = 57.8.

17: Yield 81%. – $C_{52}H_{38}F_{10}NiP_2PtS_2$ (1232.71): calcd. C 50.7, H 3.1, S 5.2; found C 50.8, H 3.3, S 5.1. – M.p. 205°C (dec.). – ^{1}H NMR ($CDCl_3$, TMS): δ = 1.5 (s, 6 H, C$_6$H$_4$Me-*p*), 2.2 (d, 4 H, dppe), 6.4 (d, 4 H, C$_6$H$_4$Me-*p*), 7.1 (d, 4 H, C$_6$H$_4$Me-*p*), 7.4 (m, 12 H, dppe), 7.6 (m, 8 H, dppe). – ^{19}F NMR ($CDCl_3$, $CFCl_3$): δ = −116.9 (d, 4 F$_o$, J_{om} = 29.1 Hz), −164.6 (t, 2 F$_p$, J_{pm} = 19.7 Hz), −166.3 (m, 4 F$_m$). – ^{31}P NMR ($CDCl_3$, H_3PO_4): δ = 46.3 [J(PPt) = 2899.2 Hz].

18: Yield 88%. – $C_{50}H_{32}F_{10}N_2Ni_2O_4P_2S_2$ (1158.27): calcd. C 51.9, H 2.8, N 2.4, S 5.5; found C 51.7, H 3.1, N 2.6, S 5.4. – M.p. 184°C (dec.). – ^{1}H NMR ($CDCl_3$, TMS): δ = 2.1 (d, 4 H, dppe), 7.4 (m, 20 H, dppe + C$_6$H$_4$NO$_2$-*p*), 7.8 (m, 8 H, dppe). – ^{19}F NMR ($CDCl_3$, $CFCl_3$): δ = −116.9 (d, 4 F$_o$, J_{om} = 27.6 Hz), −162.5 (t, 2 F$_p$, J_{pm} = 19.7 Hz), −165.0 (m, 4 F$_m$). – ^{31}P NMR ($CDCl_3$, H_3PO_4): δ = 59.0.

19: Yield 70%. – $C_{50}H_{32}F_{10}N_2NiO_4P_2PdS_2$ (1205.99): calcd. C 49.8, H 2.7, N 2.3, S 5.3; found C 49.9, H 2.5, N 2.4, S 5.1. – M.p. 180°C (dec.). – ^{1}H NMR ($CDCl_3$, TMS): δ = 2.4 (d, 4 H, dppe), 7.4 (m, 28 H, dppe + C$_6$H$_4$NO$_2$-*p*). – ^{19}F NMR ($CDCl_3$, $CFCl_3$): δ = −117.1 (d, 4 F$_o$, J_{om} = 27.3 Hz), −162.7 (t, 2 F$_p$, J_{pm} = 19.7 Hz), −165.1 (m, 4 F$_m$). – ^{31}P NMR ($CDCl_3$, H_3PO_4): δ = 58.9.

20: Yield 70%. –$C_{50}H_{32}F_{10}N_2NiO_4P_2PtS_2$ (1294.65): calcd. C 46.4, H 2.5, N 2.2, S 5.0; found C46.3, H 2.7, N 2.4, S 4.9. – M.p. 207°C (dec.). – ^{1}H NMR ($CDCl_3$, TMS): δ = 2.4 (d, 4 H, dppe), 7.2 (d, 4 H, C$_6$H$_4$NO$_2$-*p*), 7.3 (d, 4 H, C$_6$H$_4$NO$_2$-*p*), 7.5 (m, 12 H, dppe), 7.6 (m, 8 H, dppe). – ^{19}F NMR ($CDCl_3$, $CFCl_3$): δ = −117.2 (d, 4 F$_o$, J_{om} = 27.3 Hz), −162.5 (t, 2 F$_p$, J_{pm} = 19.6 Hz), −165.0 (m, 4 F$_m$). – ^{31}P NMR ($CDCl_3$, H_3PO_4): δ = 45.4 [J (PPt) = 3103.2 Hz].

Determination of the X-ray Crystal Structure of **13**: A single crystal of complex **13** (approximate dimensions 0.42 × 0.35 × 0.20 mm) was mounted on an Enraf-Nonius CAD4 diffractometer equipped with a graphite monochromator for Mo-K_α radiation. The crystallographic data are shown in Table 2. Accurate cell parameters were determined by least-squares fitting of 25 high-angle reflections. The scan method was ω-2Θ with the range of *hkl* (−16 ≤ h ≤ 16, −19 ≤ k ≤ 19, 0 ≤ l ≤ 22) corresponding to $2\Theta_{max}$ = 60.88°. Empirical ψ-scan mode absorption was made. The structure was solved by heavy-atom methods SHELXS-86[36] and refined by full-matrix least-squares techniques using anisotropic thermal parameters for non-H atoms. Hydrogen atoms were introduced in calculated positions and were refined during the last stages of the refinement. The final R factor was 0.0539 [R_w = 0.0984, where w = $1/\sigma^2(F_o^2)$ + (0.0465 P)^2 and P = (F_o^2 + 2 F_c^2)/3] over 5879 ob-

Table 2. Crystal data and structure refinement for complex **13**

Empirical formula	$C_{50}H_{34}F_{10}NiP_2$ PdS2·C3H6O
Formula weight	1174.02
Temperature	293(2) K°
Wavelength (Mo-*Kα*)	0.71073 A
Crystal system	Triclinic
Space group	*P*1 °
Unit cell dimensions	*a* = 11.803(2) A; α = 95.86(3)°
	b = 13.541(3) A; β = 93.86(3)°
	c = 15.739(3) A; γ = 94.05(3)°
Volume, *Z*	2489.0(9) A^3, 2
Density (calculated)	1.566 Mg/m^3
Absorption coefficient	0.964 mm^{-1}
F(000)	1184
h range for data collection	2.39–30.44°
Limiting indices	−16 ≤ h ≤ 16, −19 ≤ k ≤ 19, 0 ≤ l ≤ 22
Reflections collected	15576
Observed reflections	5879
Independent reflections	15074 (R_{int} = 0.0681)
Refinement method	Full-matrix least squares on F^2
Data/restraints/parameters	15074/0/635
Goodness-of-fit on F^2	0.833
Final R indices [$I > 2\sigma(I)$]	$R1$ = 0.0539, $wR2$ = 0.0984
R indices (all data)	$R1$ = 0.2690, $wR2$ = 0.1231
Largest diff. peak and hole	0.708 and −1.921 eA^{-3}

served reflections [$I > 2\sigma(I)$]. The residual peaks in the final Fourier difference synthesis were located close to the metal atoms. Scattering factors were taken from the literature[37]. Crystallographic data (excluding structure factors) for the structure reported in this paper have been deposited with the Cambridge Crystallographic Data Centre as supplementary publication no. CCDC-100812. Copies of the data can be obtained free of charge on application to CCDC, 12 Union Road, Cambridge CB2 1EZ, UK [fax: int. code + 44(0)1223/336-033, e-mail: deposit@ccdc.cam.ac.uk].

[1] M. M. Brezinski, J. Schneider, L. J. Radonovich, K. J. Klabunde, *Inorg. Chem.* **1989**, *28*, 2414.
[2] R. Uson, J. Fornies, F. Martınez, M. Tomas, *J. Chem. Soc., Dalton Trans.* **1980**, 888.
[3] G. Lopez, G. Garcıa, M. D. Santana, G. Sanchez, J. Ruiz, J. A. Hermoso, A. Vegas, M. Martınez-Ripoll, *J. Chem. Soc., Dalton Trans.* **1990**, 1621.
[4] R. Uson, J. Fornies, P. Espinet, F. Martınez, M. Tomas, *J. Chem. Soc., Dalton Trans.* **1981**, 463.
[5] R. Uson, J. Fornies, M. Tomas, B. Menjon, A. J. Welch, *Organometallics* **1988**, *7*, 1318.
[6] G. Lopez, G. Garcıa, G. Sanchez, C. de Haro, M. D. Santana, J. Casabo, M. Caldes, M. Mejıas, E. Molins, C. Miravitlles, *J. Chem. Soc., Dalton Trans.* **1991**, *3311*.
[7] G. Lopez, G. Garcıa, G. Sanchez, J. Garcıa, J. Ruiz, J. A. Hermoso, A. Vegas, M. Martınez-Ripoll, *Inorg. Chem.* **1992**, *31*, 1518.
[8] G. Lopez, J. Ruiz, G. Garcıa, C. Vicente, J. Casabo, E. Molins, C. Miravitlles, *Inorg. Chem.* **1991**, *30*, 2605.
[9] G. Lopez, J. Ruiz, G. Garcıa, C. Vicente, J. M. Martı, J. A. Hermoso, A. Vegas, M. Martınez−Ripoll, *J. Chem. Soc., Dalton Trans.* **1992**, 53.
[10] P. P. Power, S. C. Shoner, *Angew. Chem. Int. Ed. Engl.* **1991**, *30*, 330; *Angew. Chem.* **1991**, *103*, 308.
[11] P.G. Blower, J.R. Dilworth, *Coord. Chem. Rev.* **1987**, *76*, 121.
[12] A. D. Watson, Ch. P. Rao, J. R. Dorfman, R. H. Holm, *Inorg. Chem.* **1985**, *24* , 2820.
[13] W. Tremel, M. Kriege, B. Krebs, G. Henkel, *Inorg. Chem.* **1988**, *27*, 3886.
[14] G. S. White, D. W. Stephan, *Organometallics* **1988**, *7*, 903.
[15] T. A. Wark, D. W. Stephan, *Organometallics* **1989**, *8*, 2836.
[16] G. Sanchez, F. Ruiz, M. D. Santana, G. Garcıa, G. Lopez, J. A. Hermoso, M. Martınez-Ripoll, *J. Chem. Soc., Dalton Trans.* **1994**, 19.
[17] W. J. Geary, *Coord. Chem. Rev.* **1971**, *7*, 81.
[18] D. A. Long, D. Steele, *Spectrochim. Acta* **1963**, *19*, 1955.
[19] P. P. Singh, *Coord. Chem. Rev.* **1980**, *32*, 33.
[20] J. Nelson, S. M. Nelson, *J. Chem. Soc. (A)* **1969**, 1597.
[21] K. Nakamoto, *Vibrational Spectra of Inorganic and Coordination Compounds*, Wiley, New York, **1978**, p. 278.
[22] A. B. P. Lever, *Inorganic Electronic Spectroscopy,* Elsevier, New York, **1986**, p. 534.
[23] G. B. Deacon, J. H. S. Green, *Spectrochim. Acta* **1968**, *24* , 1125.
[24] E. Maslowiski, *Vibrational Spectra of Organometallic Compounds*, Wiley, New York, **1977**, p. 437.
[25] C. K. Johnson, *ORTEP, Report ORNL−3794*, Oak Ridge, National Laboratory, TN, **1965**.
[26] G. Lopez, G. Sanchez, G. Garcıa, J. Garcıa, A. Martınez, J. A. Hermoso, M. Martınez-Ripoll, *J. Organomet. Chem.* **1992**, *435*, 193.
[27] I. Nakanishi, S. Tanaka, K. Matsumoto, S. Ooi, *Acta Crystallogr. C* **1994**, *13* , 667.
[28] E. M. Padilla, J. A. Golen, P. N. Richmann, C. M. Jensen, *Polyhedron* **1994**, *13*, 667.
[29] P. G. Jones, *J. Organomet. Chem.* **1988**, *345*, 405.
[30] D. Forster, D. M. L. Goodgame, *Inorg. Chem.* **1965**, *4*, 823.
[31] M. W. Miller, L. F. Audrieth, *Inorganic Synth.* **1946**, *2*, 139.
[32] A. D. Westland, *J. Chem. Soc.* **1965**, 3060.
[33] H. Isci, O. Dag, W. R. Mason, *Inorg. Chem.* **1993**, *32*, 3909.
[34] R. G. Hayter, F. S. Humiec, *J. Inorg. Nucl. Chem.* **1964**, *26*, 807.
[35] Ch. Xu, J. W. Siria, K. G. Anderson, *Inorg. Chim. Acta* **1993**, *206*, 123.
[36] G. M. Sheldrick, *Crystallogr. Comp.* **1991**, *5*, 145−157.
[37] *International Tables for X-Ray Crystallography*, Kynoch Press, Birmingham, **1974**, vol. 4, pp. 99 and 149.

[97281]

4′-Nitro-2,2′:6′,2′′-terpyridine, 4′-Amino-2,2′:6′,2′′-terpyridine and Their Homo- and Heteroleptic Iron(II) and Ruthenium(II) Complexes

Reza-Ali Fallahpour

Institut für Anorganische Chemie, Universität Basel,
Spitalstrasse 51, CH-4056 Basel, Switzerland

Received March 19, 1998

Keywords: Terpyridine / Stille coupling reaction / Microwave

The new ligands 4′-nitro-2,2′:6′,2′′-terpyridine and 4′-amino-2,2′:6′,2′′-terpyridine and their homoleptic and heteroleptic iron(II) and ruthenium(II) complexes have been prepared and the electrochemistry of the complexes has been investigated.

2,2′:6′,2′′-Terpyridine (tpy) is a versatile ligand for complex formation with transition metals. Particular interest rests in 4′-substituted tpy ligands and many substituents can be directly inserted by the Kröhnke methodology[1]. Some of these substituents may then be further derivatised. Some functionalised 2,2′:6′,2′′-terpyridines, such as 5,5′′-dimethyl-4′-hydroxy-2,2′:6′,2′′-terpyridine (Me_2-HO-tpy)[2], 4′-hydroxy-2,2′:6′,2′′-terpyridine (HO-tpy)[3] and 4′-chloro-2,2′:6′,2′′-terpyridine (Cl-tpy),[3] in which the functional groups are directly linked to C-4′, have also been reported. The placing of electron-withdrawing or electron-donating substituents in the 4′-position of 2,2′:6′,2′′-terpyridine alters the electronic properties of the whole ligand. A nitro substituent is electron-withdrawing with respect to hydrogen, whilst the amino group is electron-donating.

To the best of my knowledge, only one synthesis of a nitrogen substituent directly attached to C-4′ of tpy, 4′-dimethylamino-2,2′:6′,2′′-terpyridine (Me_2N-tpy), has been reported[4]. Dimethylamine and Cl-tpy were allowed to react in the presence of iron(II) salts to give the iron(II) complex of Me_2N-tpy, which was then oxidised with hydrogen peroxide under basic conditions to yield the free ligand Me_2N-tpy. In this communication the synthesis of 4′-nitro-2,2′:6′,2′′-terpyridine (O_2N-tpy) and 4′-amino-2,2′:6′,2′′-terpyridine (H_2N-tpy) is reported. These compounds are precursors for new ligands and complexes.

Although electrophilic reactions on pyridine rings do not normally occur, oxidation of the ring nitrogen atom to form pyridine *N*-oxide facilitates electrophilic attack at C-4 of the pyridine ring. By utilising standard methods, commercially available 2,6-dibromopyridine was converted to 2,6-dibromopyridine *N*-oxide, which was then treated with nitric acid in sulphuric acid to give 2,6-dibromo-4-nitropyridine *N*-oxide[5]. Subsequent deoxygenation with phosphorus trichloride in chloroform produced 2,6-dibromo-4-nitropyridine (**1**) in 43% overall yield.

Compound **1** was then used in a Stille coupling reaction[6] with 2 equivalents of tributyl(pyridin-2-yl)stannane (**2**)[7] in the presence of 1 mol-% of $Pd(PPh_3)_4$ to give O_2N-tpy (**3**) in 50% yield as a pale yellow microcrystalline solid (Scheme 1).

Scheme 1. a) 1 mol-% of $Pd(PPh_3)_4$, toluene, 110°C, 16 h, 50%

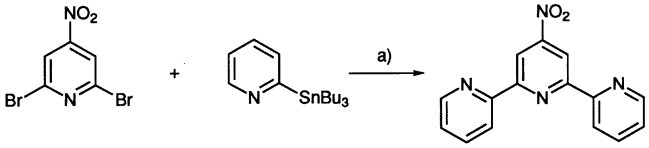

1 2 3

This is the first example of a tpy with such a strong electron-withdrawing group directly linked to C-4′. The withdrawing effect of this group can be observed in the deshielding of protons at C-3′ in the ^{1}H-NMR spectrum, and this is consistent with the known σ values[8]. The shifts of the signals of protons at C-3′ of this new tpy may be compared with two related ligands with electron-withdrawing groups at C-4′ (Table 1).

Table 1. Shifts of protons at C-3′ of tpy in $CDCl_3$ solution

tpy	σ	δ	ref.
Cl-tpy	0.24	8.48	[3]
$MeSO_2$-tpy	0.73	8.97	[9]
O_2N-tpy	0.81	9.16	

The homoleptic complex $[Fe(O_2N\text{-tpy})_2][PF_6]_2$ (**4**) (95%) was obtained as a blue microcrystalline solid from the reaction of **3** with $FeCl_2 \cdot 4\ H_2O$ in ethanol, followed by precipitation with $[NH_4][PF_6]$ (Scheme 2).

All spectroscopic data (^{1}H NMR, IR, UV, MS), as well as elemental analysis, confirmed the formation of this homoleptic iron(II) complex. Complex **4** exhibits the expected MLCT absorption at 605 nm in the electronic spectrum and, as a consequence of the strong electron-withdrawing effect of the nitro group, the compound appears blue.

 © WILEY-VCH Verlag GmbH, D-69451 Weinheim, 1998 1434–1948/98/0909–1205 $ 17.50+.50/0

Scheme 2. a) $FeCl_2 \cdot 4\ H_2O$, ethanol, 25°C, 30 min, 95%. – b) Fe/HCl, ethanol, 78°C, 30 min, 96%. – c) **5**, NaOH, H_2O_2, 25°C, 70%. – d) $RuCl_3 \cdot 3\ H_2O$, ethylene glycol, microwave, 30 min, 95%. – e) $RuCl_3 \cdot 3\ H_2O$, ethanol, 78°C, 1 h, 95%. – f) ethanol, *N*-ethylmorpholine, 1 h; **7** → **10** (10%); **8** → **11** (20%). – g) as (e), 95%

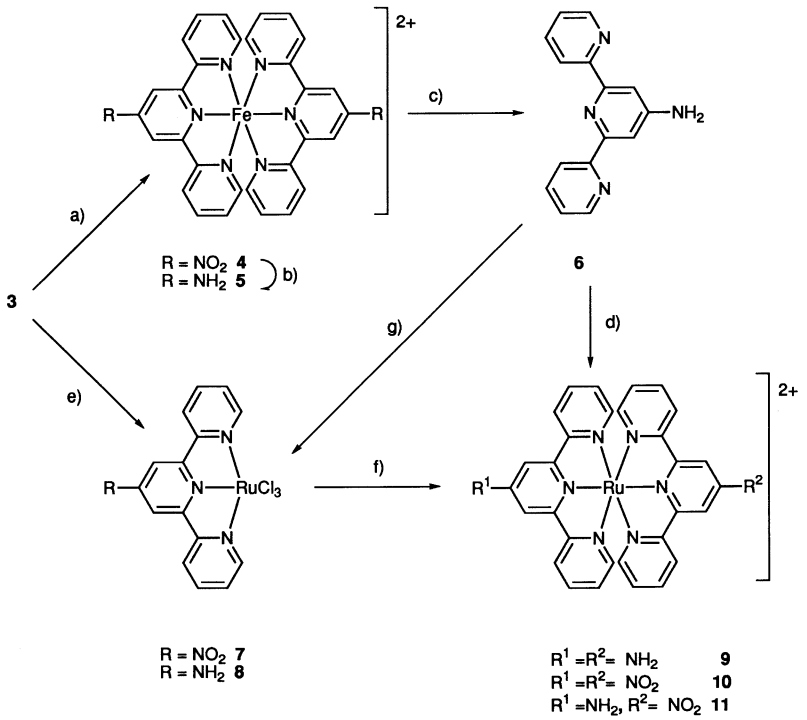

When coordinated, ligand **3** may be reduced with metallic iron and hydrochloric acid in ethanol. Reduction of the blue iron(II) complex **4** gave the purple amino complex **5** in 96% yield. All data are consistent with the assigned structure. This complex exhibits an MLCT absorption at 566 nm in the electronic spectrum due to the presence of the electron-releasing group.

The iron(II) complex **5** was cleaved with hydrogen peroxide under basic conditions to give H_2N-tpy (**6**) as yellow monoclinic crystals in 70% yield. All data are consistent with the proposed structure of this free tpy ligand. Ligand **6** was also prepared directly, in 90% yield, by selective reduction of the nitro group of **3** in refluxing ethanol over palladium on charcoal in the presence of hydrazine hydrate[10].

Ruthenium(II) complexes of tpy ligands have always been of interest to chemists due to their photochemical and photophysical properties[11][12]. The formation of kinetically inert ruthenium(II) complexes of these ligands, i.e. $[Ru(H_2N\text{-}tpy)_2][PF_6]_2$ (**9**), $[Ru(O_2N\text{-}tpy)_2][PF_6]_2$ (**10**), and $[(H_2N\text{-}tpy)Ru(O_2N\text{-}tpy)][PF_6]_2$ (**11**), was also investigated. The synthesis of the three ruthenium(II) complexes was carried out in two stages to allow for the synthesis of heteroleptic species[4].

Alternatively, the homoleptic complexes **9** and **10** could also be obtained by direct reaction of the ligands **3** and **6** with $RuCl_3 \cdot 3\ H_2O$ in ethylene glycol in a microwave oven for 10 min. The resulting ruthenium(II) complexes were precipitated as their hexafluorophosphate salts. While the amino complex **9** can be prepared without any side reactions, some reduction of the nitro groups of **3** was observed in this protic solvent.

In the ^{1}H-NMR spectra of ruthenium(II) complexes **9**, **10**, and **11** in CD_3CN solution, the chemical shifts of the 3′-H protons are of interest. These protons were observed as a singlet [$\delta = 7.91$ (**9**), $\delta = 9.47$ (**10**)] in the homoleptic complexes. The protons of the amino groups in **9** were observed as broad singlets at $\delta = 5.84$. The situation, however, changed in the heteroleptic complex **11**. While the signals of the 3′-H protons of the nitro-substituted ligand were shifted to higher field and observed at $\delta = 9.40$, those of the 3′-H protons of the amino-substituted ligand were shifted to lower field, appearing at $\delta = 7.97$. More dramatically, the signals of the amino protons were shifted to lower field in this electron-donating/accepting complex and were observed at $\delta = 6.06$.

All five complexes are electrochemically active in acetonitrile solution, exhibiting waves corresponding to the iron(II)/iron(III) or ruthenium(II)/ruthenium(III) processes. As expected, the introduction of the electron-releasing amino and the strongly electron-withdrawing nitro substituents has a dramatic influence on these redox processes. The iron(II) complex **5** has a potential of 0.356 V (versus ferrocene/ferrocenium) while **4** exhibits a potential of 0.963 V, shifted by about 60 mV with respect to $[Fe(MeSO_2\text{-}tpy)_2][PF_6]_2$ ($E^0 = 0.904$ V). This effect is in accord with the strength of the electron-withdrawing nitro group (cf.

Table 1). This means that this ligand is the strongest electron-withdrawing tpy ligand yet synthesised. The potential difference between the electron-acceptor and electron-donor iron complexes **4** and **5**, respectively, is 0.607 V.

The homoleptic ruthenium(II) complex **9** showed a potential of 0.474 V, which is shifted by 32 mV with respect to $[Ru(Me_2N\text{-}tpy)_2][PF_6]_2$[4]. This is consistent with the electron-donating effect of the two methyl groups in the latter complex. The potential of the homoleptic complex **10** was 1.114 V in comparison to $[Ru(MeSO_2\text{-}tpy)_2][PF_6]_2$ (E^0 = 1.10 V)[4]. In the donor/acceptor complex **11** the potential was shifted by 266 mV and 374 mV with respect to the ruthenium(II) complexes **9** and **10**, respectively, and was observed at 0.740 V. The potential difference between the electron-donor and electron-acceptor complexes **9** and **10** is 0.640 V.

In conclusion, a new method has been established for the synthesis of novel 4′-nitro-2,2′:6′,2′′-terpyridine and 4′-amino-2,2′:6′,2′′-terpyridine, which are precursors for new heterocycles and oligopyridines. These new tpy ligands may be incorporated in metal complexes, which are under current investigation.

I would like to thank Prof. *Edwin C. Constable* for his generous support and Dr. *Carol Pohl-Ferry* for critical reading of the manuscript. I should also like to thank the *Schweizerischer Nationalfonds zur Förderung der wissenschaftlichen Forschung* and the *University of Basel* for support.

Experimental Section

Palladium-Catalysed Coupling Reaction. − General Procedure: Compound **1** (1 mol) or **2** (2 mol) and $Pd(PPh_3)_4$ (1 mol-%) were heated under nitrogen in 50 ml of toluene for 16 h. Upon cooling to room temperature 10 ml of saturated ammonium chloride was added and the organic phase separated. The aqueous phase was extracted with toluene (3 × 20 ml). The combined organic phases were dried ($MgSO_4$) and the solvent was removed. Concentrated hydrochloric acid (30 ml) was added to the residue and this was extracted with dichloromethane (3 × 30 ml). The aqueous phase was cautiously neutralised by the addition of solid sodium hydroxide. The ligand **3** was then filtered off and purified by chromatography on silica gel with dichloromethane to give 50% yield.

3: m.p. 177°C. − IR (KBr): $\tilde{\nu}$ = 1531, 1359 cm^{-1}. − UV (CH_3CN): λ_{max} = 279, 345 nm; λ_{min} = 305 nm. − ^1H NMR ($CDCl_3$): δ = 9.16 (s, 3′-H, 2 H), 8.76 (d, 6-H, *J* = 7.80 Hz, 2 H), 8.64 (d, 3-H, *J* = 7.80 Hz, 2 H), 7.91 (ddd, 4-H, *J* = 8.30, 7.80, 1.95 Hz, 2 H), 7.42 (ddd, 5-H, *J* = 8.30, 7.80, 1.95 Hz, 2 H). − ^{13}C NMR ($CDCl_3$): δ = 158.44, 156.33, 154.05, 149.47, 136.97, 124.77, 121.33, 113.33. − MS (Maldi-TOF); *m*/*z*: 278. − $C_{11}H_{10}N_4O_2$ (278.273): calcd. C 64.74, H 3.62, N 20.13; found C 64.51, H 3.58, N 20.09.

6: m.p. 179−180°C. − IR (KBr): $\tilde{\nu}$ = 3226 cm^{-1}. − ^1H NMR ($CDCl_3$): δ = 8.67 (d, 6-H, *J* = 7.80 Hz, 2 H), 8.60 (d, 3-H, *J* = 7.80 Hz, 2 H), 7.84 (ddd, 4-H, *J* = 8.30, 7.80, 1.95 Hz, 2 H), 7.75 (s, 3′-H, 2 H), 7.32 (ddd, 5-H, *J* = 8.30, 7.80, 1.95 Hz, 2 H), 4.33 (br. s, NH_2, 2 H). − ^{13}C NMR ($CDCl_3$): δ = 156.52, 156.23, 154.55, 148.89, 136.76, 123.61, 121.30, 106.77. − MS (Maldi-TOF); *m*/*z*: 248. − $C_{15}H_{12}N_4$ (248.21): calcd. C 72.56, H 4.87, N 22.57; found C 72.01, H 4.93, N 22.55.

Synthesis of the Homoleptic Ruthenium(II) Complexes in a Microwave Oven. − General Procedure: A suspension of tpy **3** or **6** (1 mol) and $RuCl_3 \cdot 3\ H_2O$ (0.5 mol) in ethylene glycol (5 ml) was heated in a microwave oven at 600 W during 10 min. In each case the red solution was then poured into water (40 ml). Upon adding $[NH_4][PF_6]$ the desired complexes were isolated and purified by chromatography on silica gel followed by recrystallisation by diffusion of diethyl ether into the acetonitrile solution.

9: ^1H NMR (CD_3CN): δ = 9.47 (s, 3′-H, 4 H), 8.73 (d, 3-H, *J* = 7.80 Hz, 4 H), 7.98 (ddd, 4-H, *J* = 8.30, 7.80, 1.95 Hz, 4 H), 7.37 (d, 6-H, *J* = 7.80 Hz, 4 H), 7.24 (ddd, 5-H, *J* = 8.30, 7.80, 1.95 Hz, 4 H). − MS (Maldi-TOF); *m*/*z*: 657.

10: ^1H NMR (CD_3CN): δ = 8.24 (d, 3-H, *J* = 7.80 Hz, 4 H), 7.91 (s, 3′-H, 4 H), 7.83 (ddd, 4-H, *J* = 8.30, 7.80, 1.95 Hz, 4 H), 7.40 (d, 6-H, *J* = 7.80 Hz, 4 H), 7.11 (ddd, 5-H, *J* = 8.30, 7.80, 1.95 Hz, 4 H), 5.84 (br. s, NH_2, 4 H). − MS (Maldi-TOF); *m*/*z*: 627.

Synthesis of the Heteroleptic Ruthenium(II) Complex: Compounds **3** and **6** (1 mol) were hated separately with $RuCl_3 \cdot 3\ H_2O$ (1 mol) in ethanol at reflux during 1 h. The insoluble dark solids **7** and **8** were filtered off in yields of 95%. These salts (1 mol) were treated with 1 mol of tpy **6** and **3**, respectively, in ethanol for 1 h to yield complex **11**. This compound was purified by the addition of water (50 ml) as described above.

Alternatively, the reaction of the salts **7** and **8** with tpy ligands **3** and **6**, respectively, gave the homoleptic complexes **9** and **10** under the same conditions.

11: − ^1H NMR (CD_3CN): δ = 9.40 (s, 3′′′-H, 4 H), 8.70 (d, 3′′-H, *J* = 7.80 Hz, 4 H), 8.27 (d, 3-H, *J* = 7.80 Hz, 4 H), 7.99 (ddd, 4′′-H, *J* = 8.30, 7.80, 1.95 Hz, 4 H), 7.96 (s, 3′-H, 4 H), 7.86 (ddd, 4-H, *J* = 8.30, 7.80, 1.95 Hz, 4 H), 7.60 (d, 6-H, *J* = 7.80 Hz, 4 H), 7.33 (ddd, 5′′-H, *J* = 8.30, 7.80, 1.95 Hz, 4 H), 7.13 (d, 6′′-H, *J* = 7.80 Hz, 4 H), 7.03 (ddd, 5-H, *J* = 8.30, 7.80, 1.95 Hz, 4 H), 6.06 (br. s, NH_2, 2 H). − MS (Maldi-TOF); *m*/*z*: 597.

[1] F. Kröhnke, *Synthesis* **1976**, 1−24.
[2] R.-A. Fallahpour, E. C. Constable, *J. Chem. Soc., Perkin Trans. 1* **1997**, 2263−2264.
[3] E. C. Constable, M. D. Ward, *J. Chem. Soc., Dalton Trans.* **1990**, 1405−1409.
[4] E. C. Constable, A. M. W. Cargill Thompson, D. A. Tocher, M. A. M. Daniels, *New J. Chem.* **1992**, *16*, 855−867.
[5] U. Neumann, F. Vögtle, *Chem. Ber.* **1989**, *122*, 589−891.
[6] V. Farina, V. Krishnamurthy, W. J. Scott, *Org. React.* **1997**, *50*, 1−652.
[7] C. Bolm, M. Ewald, M. Felder, G. Schlingloff, *Chem. Ber.* **1992**, *125*, 1169−1190.
[8] J. March in *Advanced Organic Chemistry*, Wiley, Chichester, **1985**, p. 244.
[9] K. Potts, *Bull. Soc. Chim. Belg.* **1990**, *99*, 741−767.
[10] D. S. C. Black, N. E. Rothnie, *Aust. J. Chem.* **1983**, *36*, 1141−1147.
[11] V. Balzani, A. Juris, M. Venturi, S. Campagna, S. Serroni, *Chem. Rev.* **1996**, *96*, 759−833.
[12] J.-P. Collin, P. Gaviña, V. Heitz, J.-P. Sauvage, *Eur. J. Inorg. Chem.* **1998**, 1−14.

[98069]

Thermodynamic and Multinuclear NMR Study of Beryllium(II) Hydrolysis and Beryllium(II) Complex Formation with Oxalate, Malonate, and Succinate Anions in Aqueous Solution

Lucia Alderighi[a], Antonio Bianchi[a], Alfredo Mederos[b], Stefano Midollini[c], Agustin Rodriguez[b], and Alberto Vacca*[a]

Dipartimento di Chimica, Università degli Studi di Firenze[a],
Via Maragliano 77, I-50144 Firenze, Italy
Fax: (internat.) + 39-055/354845
E-mail: vacsab@chim1.unifi.it

Departamento de Química Inorgánica, Universidad de La Laguna[b],
E-38200 La Laguna, Tenerefe, Canary Islands
Fax: (internat.) +34-22/603634
E-mail: amederos@ull.es

I.S.S.E.C.C., Consiglio Nazionale delle Ricerche[c],
Via J. Nardi 39, I-50132 Firenze, Italy
Fax: (internat.) +39-055/2478366
E-mail: midolla@cacao.issecc.fi.cnr.it

Received March 10, 1998

Keywords: Beryllium(II) hydrolysis / Beryllium(II) complexes / Carboxylate ligands / Thermodynamics of complex formation / ^{9}Be-NMR spectra

The hydrolysis of beryllium(II) and its complexation by oxalate, malonate, and succinate in 0.5 mol dm^{-3} $NaClO_4$ aqueous solution at 298 K has been studied by means of potentiometric (pH-metric), microcalorimetric, and multinuclear NMR-spectroscopic measurements. The protonation properties of the three ligands have also been investigated by potentiometry and microcalorimetry under the same experimental conditions. Thermodynamic results are consistent with a previously proposed chemical model for beryllium(II) hydrolysis, involving the species $[Be_2OH]^{3+}$, $[Be_3(OH)_3]^{3+}$, $[Be_5(OH)_6]^{4+}$, $[Be_6(OH)_8]^{4+}$, and $Be(OH)_2$. Complex formation of beryllium(II) with the dicarboxylate ligands is invariably promoted by favourable entropic contributions ($\Delta S^\circ > 0$), while the enthalpic terms are always unfavourable ($\Delta H^\circ > 0$). Malonate forms by far the most stable complexes owing to a more favourable (less endothermic) enthalpic contribution. These data reflect the fitting of the "bites" of the ligands with the stereochemically required tetrahedral coordination geometry about the metal ion, as well as the ligand preorganization.

Introduction

Beryllium is the most toxic non-radioactive element[1][2]. However, in spite of its particular toxicity, which to a large extent prevents the expansion of its applications, there is an increasing demand for beryllium, principally associated with the major use of this light metal in the nuclear, aerospace, and electronics industries[1][2][3]. The most notable biochemical effects resulting from beryllium contamination in mammalians include permanent cell modification, alteration of DNA replication, interference in enzymatic reactions, and impairment of cell division[1][2][3]. Nevertheless, there is not yet a clear rationalization of the relationships between beryllium toxicity and the chemical species formed in biological and environmental systems, principally because this depends very much on the particular tissue or cell type exposed to contamination, and because the actual speciation of the poisoned systems is still rather an obscure area.

The solution chemistry of Be^{2+} coordination compounds has been the subject of a limited number of studies, which have been included in two recent chemical databases[4]. The paucity of data is most likely attributable to the high toxicity exhibited by the metal ion and its complexes. In several cases, the results obtained appear to be inconsistent because of the different experimental conditions employed and, where considered, the disparate chemical models proposed for Be^{2+} hydrolysis[4].

Recently, some of us commenced a re-examination of Be^{2+} hydrolysis and Be^{2+} interaction with naturally occurring ligands by means of pH-metric measurements and NMR spectroscopy[5][6][7][8]. In one of these studies, which was concerned with the determination of equilibrium constants for the coordination of oxalate and malonate anions[8], a rational approach to the synthesis of beryllium complexes in water was also developed, leading to the isolation of crystalline $K_3[Be_3(OH)_3(oxalate)_3]\cdot 3\ H_2O$ and $K_3[Be_3(OH)_3(malonate)_3]\cdot 6\ H_2O$ and, furthermore, to the determination of the crystal structure of the latter compound.

In the present paper, we complete a first set of thermodynamic data for the coordination chemistry of beryllium

 © WILEY-VCH Verlag GmbH, D-69451 Weinheim, 1998 1434–1948/98/0909–1209 $ 17.50+.50/0

ion with dicarboxylate ligands in aqueous solution, integrating the previously determined equilibrium constants for oxalate and malonate complexes[8] with new stability data for succinate and the enthalpy changes determined microcalorimetrically for the formation of beryllium complexes with the three ligands. Naturally, the hydrolysis of Be^{2+} and the protonation of the ligands have also been the subject of microcalorimetric investigations.

Results and Discussion

Be^{2+} Hydrolysis

The microcalorimetric determination of the complexation enthalpies of beryllium(II) in aqueous solution necessarily requires knowledge of the enthalpy changes associated with formation of the species produced upon Be^{2+} hydrolysis. Hence, the complexation experiments were preceded by a calorimetric study of beryllium(II) hydrolysis.

The $[Be(H_2O)_4]^{2+}$ cation exists only in very acidic solutions. In less acidic media, several polynuclear hydrolytic species are formed: in the most recent investigations (performed in 3.0 mol dm^{-3} $NaClO_4$[9] and in 0.5 mol dm^{-3} $NaClO_4$[6]) the species $[Be(OH)_2]$, $[Be_2OH]^{3+}$, $[Be_3(OH)_3]^{3+}$, $[Be_5(OH)_6]^{4+}$, and $[Be_6(OH)_8]^{4+}$ were identified, with the $[Be_3(OH)_3]^{3+}$ cation predominating over almost all of the pH range up to the precipitation of $Be(OH)_2$, which takes place at pH > 5. In solution, tetracoordination of Be^{2+} is preserved by coordinated water molecules, and tetrahedral arrangements are also to be expected for the species formed upon hydrolysis. Tentative structures for these polynuclear hydrolytic species have been suggested previously[9]; in particular, a cyclic structure for $[Be_3(OH)_3(H_2O)_6]^{3+}$, already indicated by a ^{1}H-NMR study[10], has been corroborated by a recent X-ray investigation[11]. The cyclic arrangement of this trimeric unit, where water molecules are replaced by bidentate ligands, has also been found in some crystalline complexes[8][12][13].

The equilibrium model and the values of the equilibrium constants for the hydrolysis of beryllium(II) were taken from a previous work[6]. The species formed in appreciable amounts in 0.5 mol dm^{-3} $NaClO_4$ solution at 298 K and the relevant thermodynamic data are listed in Table 1. In spite of various experimental modifications, it was not possible to obtain appreciable formation of the soluble species $[Be(OH)_2]$ in the microcalorimetric experiments. Therefore, the corresponding formation enthalpy was not determined.

Scheme 1

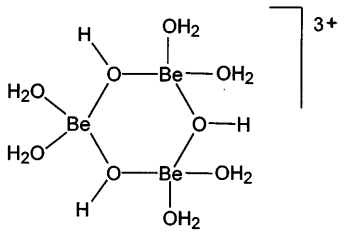

The enthalpy changes determined in the present study for $[Be_2OH]^{3+}$, $[Be_3(OH)_3]^{3+}$, and $[Be_6(OH)_8]^{4+}$ are in good agreement with those quoted in previous reports[14], while no reference values could be found in the literature for $[Be_5(OH)_6]^{4+}$[4].

It is worthy to note that the formation of these species is promoted by both favourable enthalpic and entropic contributions. The thermodynamic data reported in Table 1 can be interpreted in terms of metal-to-OH^- bonding interactions and solvation/desolvation equilibria. The reaction between Be^{2+} and OH^--solvated ions gives rise to considerable charge neutralization, resulting in the release of water molecules from the interacting species. This desolvation process is accompanied by an entropy gain, due to the increasing number of species, and by an enthalpy loss, owing to the cleavage of $Be^{2+}-OH_2$ bonds. This entropy gain seems to be the main contribution to the favourable entropic terms observed in the formation of the hydrolytic species, while the favourable formation enthalpies are most likely attributable to contributions deriving from strong covalent bonding interactions between Be^{2+} and OH^- ions, which are only partly cancelled out by the desolvation enthalpy loss.

The balance of these opposing contributions leads to almost constant increments per OH^- group in the enthalpic and entropic terms ($-\Delta H^\circ$ = 31 ± 4 kJ mol^{-1}, ΔS° = 97 ± 10 J K^{-1} mol^{-1}) for the formation of the hydrolytic species, which is reflected by the almost steady increase of the species stability ($-\Delta G^\circ$) with the number of bonded OH^- groups (Figure 1).

Protonation of the Ligands

Table 2 reports the thermodynamic functions for the protonation of the three ligands investigated. There is a good

Table 1. Thermodynamic parameters for the formation of hydrolytic Be^{2+} species, determined in 0.50 mol dm^{-3} $NaClO_4$ at 298.1 ± 0.1 K[a]

reaction	log K[b]	$-\Delta G^\circ$[b] [kJ mol^{-1}]	$-\Delta H^\circ$ [kJ mol^{-1}]	ΔS° [J K^{-1} mol^{-1}]
$2\ Be^{2+} + OH^- \rightarrow [Be_2(OH)]^{3+}$	10.49(1)	59.87(8)	27(2)	111(7)
$3\ Be^{2+} + 3\ OH^- \rightarrow [Be_3(OH)_3]^{3+}$	32.39(3)	184.9(2)	100.8(4)	282(1)
$5\ Be^{2+} + 6\ OH^- \rightarrow [Be_5(OH)_6]^{4+}$	63.83(5)	364.3(3)	208(3)	523(10)
$6\ Be^{2+} + 8\ OH^- \rightarrow [Be_6(OH)_8]^{4+}$	83.75(5)	478.0(3)	239(2)	802(7)
$Be^{2+} + 2\ OH^- \rightarrow Be(OH)_2$	15.70(6)	89.6(3)	–	–

[a] Values in parentheses are standard deviations in the last significant figure. – [b] Values taken from ref.[6].

Figure 1. Thermodynamic functions for the formation of hydrolytic species as a function of the number of hydroxide groups bonded to Be^{2+}; the dashed lines are obtained by linear least-squares regression of the reported values, the correlation coefficients being > 0.99

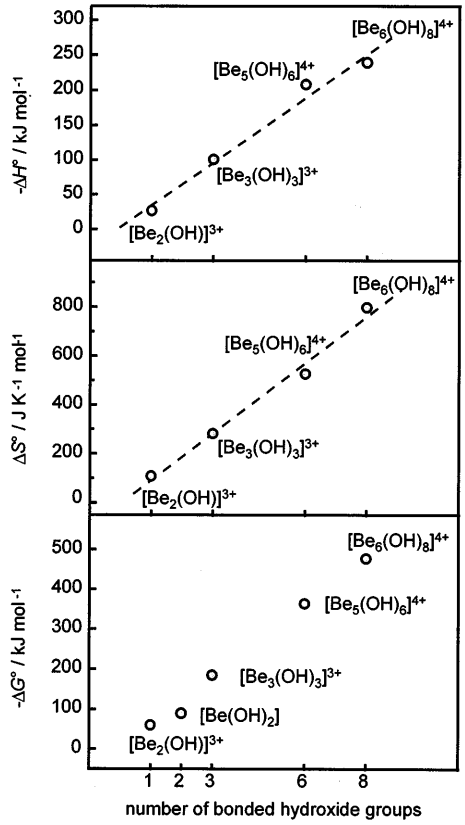

general agreement with previously reported values[4], in spite of the rather different conditions of temperature and/or ionic strength used in the various investigations. The well-known increase in basicity observed in the series oxalate < malonate < succinate, as a consequence of the increasing length of the aliphatic chain, appears to be accompanied by a corresponding increase of the enthalpic contribution, while the entropic terms do not show any particularly evident trend.

Complex Formation

The thermodynamic parameters for the complexation of Be^{2+} by oxalate, malonate, and succinate are listed in Table 3.

In a previous paper, dealing with the determination of the stability constants of beryllium(II) complexes with oxalate and malonate[8] under the same experimental conditions as in the present study, it was noted that malonate complexes are significantly more stable than their oxalate counterparts. This enhanced stability can be ascribed to the formation of 6-membered chelate rings in the malonate complexes, which, compared to the 5-membered chelate rings formed by oxalate, produce less distortion in the preferred tetrahedral coordination geometry around the beryllium ion. As a matter of fact, in the molecular structures of the complexes $[Be(malonate)_2]^{2-}$[15], $[Be_3(OH)_3(malonate)_3]^{3-}$[8], $[Be(salicylate)_2]^{2-}$[16], and $[Be(acac)_2]$[17], which all feature 6-membered chelate rings, the O−Be−O bite angles imposed by the ligands range between 104.3(7) and 109.3(2)°, comparing well with the angles in an ideal tetrahedron (109.5°), while the corresponding bite angles in the 5-membered chelate rings formed by oxalate in the crystal structure of $[Be(oxalate)_2]^{2-}$ [99.6(2) and 99.7(2)°][18] deviate considerably from this value. More recently, it has been shown that the bite angles [109.1(1), 110(1)°] in the unique example of 7-membered chelate rings seen in the crystal structure of $[Be(o\text{-phthalate})_2]^{2-}$ are also very similar to the ideal tetrahedral angle, with the Be−O distances falling within the range exhibited by related compounds, and the phthalate anion not showing any structural anomalies[19]. Furthermore, in an earlier paper, it was noted that phthalate and oxalate have comparable abilities in forming [BeL] and $[BeL_2]^{2-}$ complexes[20]. On the other hand, the complexes formed by Be^{2+} with succinate, which can in principle involve 7-membered chelate rings, are largely less stable than the corresponding species formed with malonate and oxalate (Table 3), although the difference in stability between the [BeL] complexes of oxalate and succinate is not as large as in the case of the $[BeL_2]$ and $[Be_3(OH)_3L]^+$ species. Probably as a result of this reduced stability, in the case of succinate the $[Be_3(OH)_3L_3]^{3-}$ (L = dicarboxylate ligand)

Table 2. Thermodynamic parameters for the protonation of oxalate, malonate, and succinate, determined in 0.50 mol dm^{-3} $NaClO_4$ at 298.1 ± 0.1 K[a]

reaction	log K	$-\Delta G°$ [kJ mol^{-1}]	$-\Delta H°$ [kJ mol^{-1}]	$\Delta S°$ [J K^{-1} mol^{-1}]
L = oxalate				
$L^{2-} + H^+ \rightarrow HL^-$	3.64(1)[b]	20.76(6)[b]	−4.7(1)	85.3(6)
$HL^- + H^+ \rightarrow H_2L$	1.00(1)[b]	5.7(6)[b]	−4.6(1)	35(7)
L = malonate				
$L^{2-} + H^+ \rightarrow HL^-$	5.054(2)[b]	28.84(1)[b]	−2.3(2)	104.5(6)
$HL^- + H^+ \rightarrow H_2L$	2.51(2)[b]	14.3(1)[b]	1.7(3)	42(2)
L = succinate				
$L^{2-} + H^+ \rightarrow HL^-$	5.041(3)	28.77(2)	1.5(8)	91(3)
$HL^- + H^+ \rightarrow H_2L$	3.908(3)	22.30(2)	6.2(8)	54(3)

[a] Values in parentheses are standard deviations in the last significant figure. − [b] Values taken from ref.[8].

Table 3. Thermodynamic parameters for the complexation of Be^{2+} by oxalate, malonate, and succinate anions, determined in 0.50 mol dm^{-3} $NaClO_4$ at 298.1 ± 0.1 K[a]

reaction	log *K*	$-\Delta G°$ [kJ mol^{-1}]	$-\Delta H°$ [kJ mol^{-1}]	$\Delta S°$ [J K^{-1} mol^{-1}]
L = oxalate				
$Be^{2+} + L^{2-} \rightarrow [BeL]$	3.47(2)[b]	19.8(1)[b]	−19.5(3)	132(1)
$[BeL] + L^{2-} \rightarrow [BeL_2]^{2-}$	1.77(7)[b]	10.1(4)[b]	−31(1)	138(3)
$Be^{2+} + 2L^{2-} \rightarrow [BeL_2]^{2-}$	5.24(7)[b]	29.9(4)[b]	−49(2)	263(6)
$[Be_3(OH)_3]^{3+} + L^{2-} \rightarrow [Be_3(OH)_3L]^{+}$	3.78(7)[b]	21.7(4)[b]	−10.9(8)	109(3)
$[Be_3(OH)_3]^{3+} + 3L^{2-} \rightarrow [Be_3(OH)_3L_3]^{3-}$	8.3(1)[b]	47.7(8)[b]	−28(1)	254(6)
L = malonate				
$Be^{2+} + L^{2-} \rightarrow [BeL]$	5.36(2)[b]	30.6(1)[b]	−10.53(6)	138.0(5)
$[BeL] + L^{2-} \rightarrow [BeL_2]^{2-}$	3.85(1)[b]	21.91(5)[b]	−5.19(8)	91.2(4)
$Be^{2+} + 2L^{2-} \rightarrow [BeL_2]^{2-}$	9.21(2)[b]	52.50(8)[b]	−15.82(8)	229.2(5)
$[Be_3(OH)_3]^{3+} + L^{2-} \rightarrow [Be_3(OH)_3L]^{+}$	5.26(7)[b]	30.1(4)[b]	−8.4(8)	129(3)
$[Be_3(OH)_3]^{3+} + 3L^{2-} \rightarrow [Be_3(OH)_3L_3]^{3-}$	12.84(6)[b]	73.3(3)[b]	−18.8(8)	309(3)
L = succinate				
$Be^{2+} + L^{2-} \rightarrow [BeL]$	3.04(1)	17.34(4)	−21.1(1)	129(5)
$[BeL] + L^{2-} \rightarrow [BeL_2]^{2-}$	1.0(2)	6(1)	−15(1)	69(5)
$Be^{2+} + 2L^{2-} \rightarrow [BeL_2]^{2-}$	4.1(2)	23.1(1)	−36(1)	198(5)
$[Be_3(OH)_3]^{3+} + L^{2-} \rightarrow [Be_3(OH)_3L]^{+}$	2.03(6)	11.6(3)	−42(1)	181(3)

[a] Values in parentheses are standard deviations in the last significant figure. − [b] Values taken from ref.[8].

complex is not formed in appreciable amounts, at least under our experimental conditions, and its presence was not detected by means of the techniques employed in this study. Conversely, in a previous paper[21], the stability constant of this species was reported, together with that for the formation of the complex $[Be_3(OH)_3(HL)]^{2+}$ (L = succinate), containing the monoprotonated form of the ligand. In view of this report, we performed some experimental work aimed at identifying these two species in our systems, but no evidence of their formation was obtained.

Considering the low stability of the Be^{2+} complexes with succinate, a doubt arose concerning the possible monodentate coordination of the dicarboxylate anion. Nevertheless, this type of coordination should, in principle, favour the formation of complexes with the monoprotonated form of the ligand, although as mentioned above, such complexes were not detected in our experiments. In order to assess the ability of dicarboxylate ligands to bind Be^{2+} through a single carboxylate group, we also investigated the Be^{2+}/acetate system by both potentiometric and NMR techniques. The results indicated that, at least under our experimental conditions, the formation of acetate complexes is not appreciable. As a matter of fact, the ^{9}Be-NMR spectra of aqueous solutions of the system $BeSO_4/CH_3COOH$ (molar ratio 1:4) at various pH values fully resemble those of $BeSO_4$[22], indicating that acetate does not significantly coordinate the Be^{2+} ion.

On the basis of this evidence, it seems reasonable to assume that, in accordance with the behaviour of oxalate and malonate, succinate also acts as bidentate ligand towards Be^{2+}, and consequently its complexes can be formulated as Be(succinate)$(H_2O)_2$, $[Be(succinate)_2]^{2-}$, and $[Be_3(OH)_3$-(succinate)$(H_2O)_4]^{+}$, where water molecules preserve the Be^{2+} tetrahedral coordination geometry.

Evidence of a weak coordination of Be^{2+} by succinate comes from ^{9}Be-NMR spectra. Indeed, the ^{9}Be spectra of aqueous solutions containing $BeSO_4$ and succinic acid in a molar ratio of 1:2 in the pH range of 4−6, before the occurrence of $Be(OH)_2$ precipitation, show a signal at δ = 1.05 overlapping the broad resonance due to $[Be_3(OH)_3(H_2O)_6]^{3+}$ at δ = 0.7 (Figure 2). The new resonance must be attributed to a succinate−beryllium complex, probably the [Be(succinate)$(H_2O)_2$] species. Accordingly, the corresponding $^{13}C\{^{1}H\}$ spectrum shows in both the CH_2 and COO regions a signal due to the uncoordinated ligand (these bands have been assigned by comparison with the spectra of free succinic acid under the same pH conditions) and a less intense resonance attributable to coordinated succinate (Figure 3).

Figure 2. $^{9}Be\{^{1}H\}$-NMR spectrum of an aqueous solution containing 0.2 mol dm^{-3} $BeSO_4$ and 0.4 mol dm^{-3} succinate at pH = 5.90

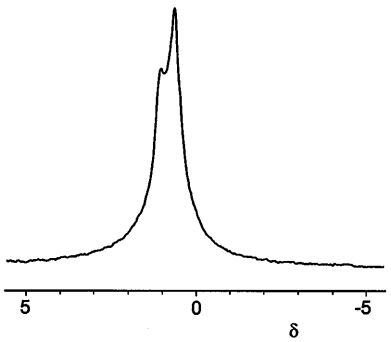

Therefore, assuming the bidentate coordination of succinate, in the absence of direct structural information on Be^{2+} derivatives with this ligand, it seems reasonable to assume that no special strain is accumulated in the 7-membered chelate rings of such complexes compared to the analogous chelate rings in $[Be(o\text{-phthalate})_2]^{2-}$. The principal reason for the lower stability of the succinate complexes might have its origins in the greater flexibility of this rather long ligand, which necessitates a considerable organization to achieve the coordinative conformation. Similar structural changes

Figure 3. $^{13}C\{^1H\}$-NMR spectrum of an aqueous solution containing 0.2 mol dm^{-3} $BeSO_4$ and 0.4 mol dm^{-3} succinate at pH = 5.90

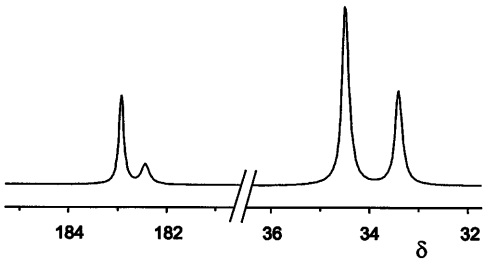

are not necessary for the rigid and preorganized *o*-phthalate ligand.

Considering the thermodynamic results reported here, different reasons can be advanced to account for the lower stability of beryllium complexes with oxalate and succinate compared to those with malonate: inadequate ligand-binding bite in the case of oxalate and considerable reorganization of ligand structure upon coordination of succinate.

As shown in Table 3, the stability of the Be^{2+} complexes with oxalate, malonate, and succinate is invariably determined by favourable entropic contributions, with the enthalpic terms always being unfavourable. This behaviour is typical of reactions between oppositely charged partners, in which charge neutralization and associated desolvation effects are of major importance. Nevertheless, energetic effects due to non-optimal matching between the stereochemical requirements of the ligand and metal ion and ligand conformational changes required for coordination also have to be taken into account. Considering the $-\Delta G°$ values obtained for [BeL] and $[BeL_2]^{2-}$, it appears that malonate forms by far the most stable complexes, as depicted in Figure 4a, as a consequence of the most favourable enthalpic contribution (less endothermic) shown in Figure 4b. The entropic contributions are very similar for the three [BeL] complexes, while in the case of $[BeL_2]^{2-}$ a greater $\Delta S°$ value favours the formation of the bis(oxalate) complex (Figure 4c).

It is noteworthy that the equilibrium constants for the binding of oxalate to Be^{2+} and $[Be_3(OH)_3]^{3+}$ are very similar, as is also the case for malonate. This is de facto due to a compensation between the enthalpic and entropic terms (Table 3), the reaction of these ligands with the trinuclear $[Be_3(OH)_3]^{3+}$ species being less endothermic than the analogous reaction with Be^{2+}. The presence of OH^- anions in $[Be_3(OH)_3]^{3+}$ produces a partial neutralization of charge on the metal ion, weakening the $Be-OH_2$ bonds, and hence the replacement of these coordinated water molecules by the ligands becomes less expensive from an enthalpic point of view. On the other hand, similar features are not operative in the succinate complexes, where a very unfavourable enthalpic contribution reduces the stability of the $[Be_3(OH)_3(succinate)]^+$ species, the formation of which is accompanied by the largest entropic gain for this type of reaction.

Since no anomalies are observed in the thermodynamic parameters for the formation of [BeL] (L = oxalate, malonate, succinate) complexes, it seems that the peculiar enthalpic and entropic terms for the formation of $[Be_3(OH)_3(succinate)]^+$ are not attributable to a special binding mode of succinate, but most likely to a loosening of the complex structure, which might originate from the hindrance brought about by the bulkier ligand, producing weakening of the binding interaction within the complex and increasing the disorder of its structure. As a matter of fact, we did not observe the addition of more than one dicarboxylate ligand in the case of succinate.

Figure 4. Plot of the thermodynamic functions $\Delta G°$ (a), $\Delta H°$ (b), and $\Delta S°$ (c) in relation to the cumulative formation of [BeL] and $[BeL_2]^{2-}$, where L = oxalate, malonate, and succinate

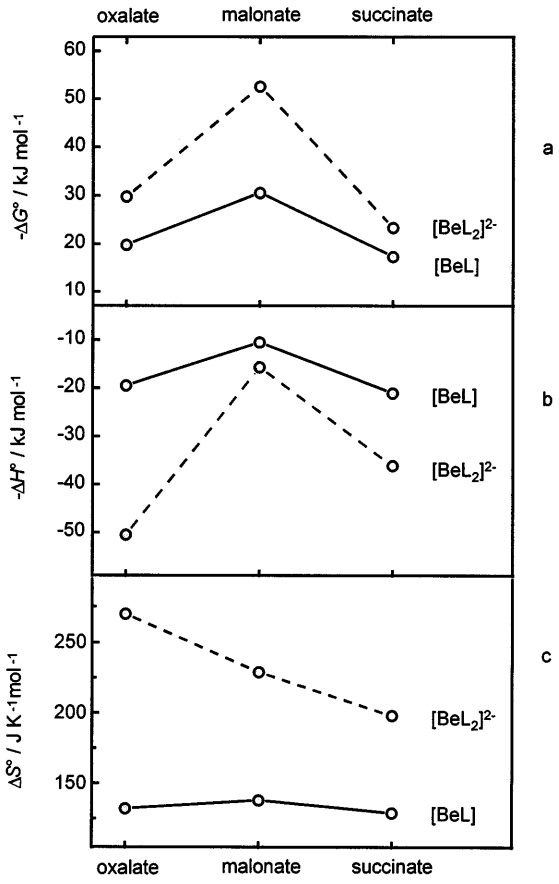

Conclusion

On the basis of the thermodynamic data obtained in this work concerning the solution chemistry of Be^{2+}, including metal ion hydrolysis and coordination equilibria with oxalate, malonate, and succinate ligands, the following points can be made:

1. Calorimetric data are consistent with a chemical model for Be^{2+} hydrolysis involving the species $[Be_2OH]^{3+}$, $[Be_3(OH)_3]^{3+}$, $[Be_5(OH)_6]^{4+}$, and $[Be_6(OH)_8]^{4+}$.

2. Considering a homogeneous series of chelating ligands containing the same binding groups, such as that constituted by oxalate, malonate, and succinate as investigated here, there is a distinct selectivity for the binding of Be^{2+} species by those ligands capable of forming 6-membered chelate rings.

3. Chelation of Be^{2+} ions is promoted by favourable entropic terms ($\Delta S° > 0$), the unfavourable enthalpic contributions ($\Delta H° > 0$) reflecting the fitting of ligand binding bites with the stereochemically required tetrahedral coordination geometry about the metal ion, as well as ligand preorganization.

Financial support from the *EU* (HCM program "Metals and Environmental Problems" 1995−1998, Grant ERBCHRHX-CT94-0632), the *Ministero dell'Ambiente* (Italy, Contract PR/1/C), and *MURST* (Italy, quota 60%) is gratefully acknowledged. We are indebted to Mr. *Franco Cecconi* for technical assistance.

Experimental Section

Caution: In view of the extreme toxicity of beryllium compounds all experimental work was carried out in a well-ventilated fume cupboard used exclusively for this work. Established procedures for handling dangerous materials were followed rigorously at all stages of the preparations and measurements.

General Remarks: High-purity oxalic, malonic, and succinic acids were purchased from Merck. Be^{2+} stock solutions (0.02 mol dm^{-3}) were prepared by reacting metallic Be (Aldrich, 99.99% purity) with a slight excess of $HClO_4$. Be^{2+} and free acid concentrations were checked periodically by means of standard methods.

All potentiometric (pH-metric) measurements ($pH = -\log[H^+]$) used for the determination of ligand protonation and metal ion complexation constants were performed in 0.5 mol dm^{-3} $NaClO_4$ at 298.1 ± 0.1 K using the apparatus described previously[8]. The combined Ingold 405 S7/120 electrode was calibrated as a hydrogen concentration probe by titrating known amounts of HCl with CO_2-free NaOH solutions and determining the equivalent point by Gran's method[23]. This allows one to determine the standard potential $E°$ and the ionic product of water [pK_w = 13.69(1) at 298 K in 0.5 mol dm^{-3} $NaClO_4$]. In the complex formation experiments care was taken to verify the attainment of equilibrium after each titrant addition: a few minutes were necessary to reach constant emf readings. The potentiometric data were analysed using the computer program HYPERQUAD[24]. Experimental details of the potentiometric measurements are given in Table 4.

Table 4. Summary of experimental conditions for the beryllium−succinate system

Solution composition	
$[T_L]$ range [mol dm^{-3}]	0.003−0.010
$[T_M]$ range [mol dm^{-3}]	0.003−0.004
I [mol dm^{-3}], electrolyte	0.50, $NaClO_4$
pH range	3.0−6.0
Experimental method	pH titration, calibrated in concentration
T [°C]	25
Total number of data points	
Protonation	103 (2 titrations)
Beryllium complexation	387 (5 titrations)
Method of calculation	HYPERQUAD[24]
Protonation constants	
(ligand = H_2L, errors as σ)	
log β (HL)	5.041 ± 0.003
log β (H_2L)	8.950 ± 0.003
Stability constants	
log β ([BeL])	3.04 ± 0.01
log β ($[BeL_2]^{2-}$)	4.1 ± 0.2
log β ($[Be_3(OH)_3L]^+$)	−6.65 ± 0.06

The enthalpies of reaction were determined in 0.5 mol dm^{-3} $NaClO_4$ solution by means of an automated system consisting of a Thermometric AB thermal activity monitor (model 2277) equipped with perfusion-titration device and a Hamilton pump (model Microlab M) coupled with a 0.250-cm^3 gas-tight Hamilton syringe (model 1750 LT). The measuring vessel was housed in a 25-dm^3 thermostatted water bath, which was maintained at the chosen temperature within $\pm 2 \cdot 10^{-4}$ K. The microcalorimeter was checked by determining the enthalpy of reaction of strong base (NaOH) with strong acid (HCl) solutions. The value of −56.7(2) kJ mol^{-1} obtained was in agreement with literature values[4]. The protonation enthalpies of the ligands were determined as previously reported for other compounds[25]. In a typical complexation experiment, a solution containing the disodium salt of the ligand (0.08 mol dm^{-3}, ionic strength adjusted to 0.5 mol dm^{-3} by $NaClO_4$) was added in successive steps (15 μl) to acidic solutions of Be^{2+} (0.02 mol dm^{-3}, ionic strength adjusted to 0.50 mol dm^{-3} by $NaClO_4$, 1.5 cm^3) until a 1:1 metal-to-ligand molar ratio was reached. The complexation experiments were set up in such a way so as to produce a change of solution pH in the calculated range of ca. 3.7−5.0. Corrections for the heats of dilution were applied. At least three titrations (about 110 data points) were performed for each system. The corresponding enthalpies of reaction were determined from the calorimetric data by means of the AAAL program[26].

^{9}Be- and ^{13}C-NMR spectra were recorded with a Bruker AC 200 spectrometer at 28.18 MHz and 50.32 MHz, respectively. Chemical shifts are quoted with respect to external 0.10 mol dm^{-3} $BeSO_4$ in H_2O for ^{9}Be and external TMS for ^{13}C. All measurements were carried out in aqueous solutions, in the pH range of 2.3−6.0, using a coaxial inner tube containing D_2O to provide a lock signal.

[1] D. N. Skilleter, *Chem. Br.* **1990**, *26*, 26−30.
[2] O. Kumberger, H. Schmidbaur, *Chem. Unserer Zeit* **1993**, *6*, 310−316.
[3] C. Y. Wong, J. D. Woollins, *Coord. Chem. Rev.* **1994**, *130*, 243−273 and references therein.
[4] K. J. Powell, L. D. Pettit, *IUPAC Stability Constants Database − SC-Database*, Academic Software, Otley (U.K.), **1997**. − R. M. Smith, A. E. Martell, *NIST Critically Selected Stability Constants of Metal Complexes Database*, Version 4.0, U.S. Department of Commerce, National Institute of Standards and Technology, Gaithersburg, MD 20899 (U.S.A.), **1997**.
[5] E. Chinea, S. Dominguez, A. Mederos, F. Brito, J. M. Arrieta, A. Sánchez, G. Germain, *Inorg. Chem.* **1995**, *34*, 1579−1587.
[6] E. Chinea, S. Dominguez, A. Mederos, F. Brito, A. Sánchez, A. Ienco, A. Vacca, *Main Group Met. Chem.* **1997**, *20*, 11−17.
[7] A. Mederos, S. Dominguez, E. Chinea, F. Brito, S. Midollini, A. Vacca, *Bull. Soc. Chil. Quím.* **1997**, *42*, 281−295.
[8] P. Barbaro, F. Cecconi, C. A. Ghilardi, S. Midollini, A. Orlandini, L. Alderighi, D. Peters, A. Vacca, E. Chinea, A. Mederos, *Inorg. Chim. Acta* **1997**, *262*, 187−194.
[9] J. Bruno, *J. Chem. Soc., Dalton Trans.* **1987**, 2431−2437.
[10] J. W. Akitt, R. H. Duncan, *J. Chem. Soc., Faraday Trans. 1* **1980**, *76*, 2212−2220.
[11] F. Cecconi, C. A. Ghilardi, S. Midollini, A. Orlandini, A. Mederos, *Inorg. Chem.* **1998**, *37*, 146−148.
[12] P. R. Faure, F. Bertin, H. Loiseleur, T. D. Germaine, *Acta Crystallogr.* **1974**, *B30*, 462−467.
[13] Y. Sohrin, M. Matsui, Y. Hata, H. Hasegawa, H. Kokusen, *Inorg. Chem.* **1994**, *33*, 4376−4383.
[14] B. Carell, A. Olin, *Acta Chem. Scand.* **1962**, *16*, 2357−2364. − R. E. Mesmer, C. F. Baes, *Inorg. Chem.* **1967**, *6*, 1951−1960.
[15] G. Duc, R. Faure, H. Loiseleur, *Acta Crystallogr.* **1978**, *B34*, 2115−2118.
[16] H. Schmidbaur, O. Kumberger, *Chem. Ber.* **1993**, *126*, 3−9.
[17] S. Onuma, S. Shibata, *Acta Crystallogr.* **1985**, *C41*, 1181−1183.
[18] M. Jaber, R. Faure, H. Loiseleur, *Acta Crystallogr.* **1978**, *B34*, 429−431.
[19] M. Schmidt, A. Bauer, H. Schmidbaur, *Inorg. Chem.* **1997**, *36*, 2040−2043.

[20] H. J. De Bruin, D. Kairaitis, R. B. Temple, *Aust. J. Chem.* **1962**, *15*, 457−466.
[21] G. Duc, F. Bertin, G. Thomas-David, *Bull. Soc. Chim. Fr.* **1977**, 645−648.
[22] S. Midollini, unpublished results.
[23] G. Gran, *Analyst* **1952**, *77*, 661−671.
[24] P. Gans, A. Sabatini, A. Vacca, *Talanta* **1996**, *43*, 1739−1753.
[25] A. Bianchi, B. Escuder, E. Garcia-España, S. V. Luis, V. Marcelino, J. F. Miravet, J. A. Ramírez, *J. Chem. Soc., Perkin Trans. 2* **1994**, 1253−1259. − R. Cini, G. Giorgi, D. Masi, A. Sabatini, A. Vacca, *J. Chem. Soc., Perkin Trans. 2* **1991**, 765−771.
[26] A. Vacca, *AAAL program*, University of Florence, **1996**.
[98052]

Vinylidene Transition-Metal Complexes, 46[◇]

Di- and Trinuclear Alkyne- and Vinylidenerhodium(I) Complexes Including the X-ray Crystal Structure of a Dendrimer-Like Rh_3 Compound☆

Helmut Werner*, Petra Bachmann, Matthias Laubender, and Olaf Gevert

Institut für Anorganische Chemie der Universität Würzburg,
Am Hubland, D-97074 Würzburg, Germany

Received April 21, 1998

Keywords: Rhodium / Alkyne complexes / Alkynyl(hydrido) complexes / Vinylidene complexes / Dendrimer-like structure

The dimer $[RhClL_2]_2$ (**1**; L = P*i*Pr$_3$) reacts with 1,3,5-$C_6H_3(C{\equiv}CH)_3$ to give in the initial step the tris(alkyne)trirhodium compound **2**, which rearranges in toluene at 60 °C to yield the isomeric tris(vinylidene) complex **3**. Treatment of either **2** or **3** with pyridine affords the trinuclear tris(alkynyl)trihydridorhodium(III) complex **4**. The trisilyl derivative 1,3,5-$C_6H_3(C{\equiv}CSiMe_3)_3$ reacts with **1** to form the mononuclear compound **5**, in which only one of the C≡C bonds is coordinated to Rh. The diynes 1,3- and 1,2-$C_6H_4(C{\equiv}CH)_2$ behave analogously to 1,3,5-$C_6H_3(C{\equiv}CH)_3$ and upon treatment with **1** yield initially the bis(alkyne)dirhodium complexes **6** and **7** and subsequently the bis(vinylidene)dirhodium isomers **8** and **9**. The reactions of 1,2-, 1,3-, and 1,4-$C_6H_4(C{\equiv}CSiMe_3)_2$ with **1** take a similar course and give the bis(alkyne) and bis(vinylidene) compounds **10**–**12** and **13**–**15**, respectively. In the same way, the dinuclear bis(alkyne) and bis(vinylidene) complexes **16** and **17** have been prepared from **1** and the naphthalene derivative 1,5-$C_{10}H_6(C{\equiv}CH)_2$. The molecular structures of **17** and of the dendrimer-like Rh_3 compound **3** have been determined by X-ray crystallography.

We have recently shown that terminal alkynes HC≡CR are easily converted to the isomeric vinylidenes :C=CHR in the coordination sphere of rhodium(I).[1][2] This process is thermodynamically preferred,[3] and based on ab initio MO studies its mechanism is quite well understood.[4] Besides acetylene and monosubstituted derivatives HC≡CR with R = alkyl, aryl, vinyl, SiR_3 or CO_2R, also butadiyne[5] and 1,4-bis(ethynyl)benzene[6] have been used as substrates and, in the presence of $[RhCl(PiPr_3)_2]$ as the template, transformed to the isomeric bridge-forming bis(vinylidenes).

The present paper reports that likewise to 1,4-$C_6H_4(C{\equiv}CH)_2$ not only the 1,3- and 1,2-bis(ethynyl)benzene isomers but also the trisubstituted benzene derivative 1,3,5-$C_6H_3(C{\equiv}CH)_3$ forms alkyne- and vinylidenerhodium(I) complexes upon treatment with $[RhClL_2]_2$ (**1**; L = P*i*Pr$_3$). An interesting facet of this work is that while the disilylated compounds 1,3- and 1,2-$C_6H_4(C{\equiv}CSiMe_3)_2$ behave similarly to the parent diynes and yield dinuclear rhodium complexes, the trisilylated triyne 1,3,5-$C_6H_3(C{\equiv}CSiMe_3)_3$ reacts with **1** to give a mononuclear alkynerhodium(I) compound, leaving two of the three triple bonds of 1,3,5-$C_6H_3(C{\equiv}CSiMe_3)_3$ uncoordinated.

Rhodium Complexes from 1,3,5-$C_6H_3(C{\equiv}CH)_3$ and the Trisilylated Derivative

Treatment of a solution of the reactive dimer **1**[7] with 1,3,5-tris(ethynyl)benzene in pentane leads even at −60°C to a rapid change of colour and, after warming to room temperature and removal of the solvent, gives the triyne complex **2** in ca. 80% yield. The yellow microcrystalline solid is moderately air-sensitive and easily soluble in most organic solvents.

The proposed structure of **2** (see Scheme 1) is fully supported by the spectroscopic data. The IR spectrum displays only one strong C≡C stretch at 1795 cm^{-1} indicating that all three triple bonds are involved in the coordination to the rhodium center. In agreement with this, the ^{1}H-NMR spectrum of **2** shows one signal for the ≡CH protons at δ = 4.02, which due to Rh-H coupling is split into a doublet. For the CH_3 protons of the P*i*Pr$_3$ units a doublet of virtual triplets appears being consistent with the *trans* disposition of the two phosphane ligands at each metal center.[8]

Although **2** is stable both in the solid state and in solution at room temperature, on warming in toluene at 60°C it slowly rearranges to the tris(vinylidene) complex **3**. In contrast to **2**, the isomer **3** is a dark green solid, the NMR spectra of which indicate a symmetrical structure as shown in Scheme 1. There is only one resonance for the P*i*Pr$_3$ phosphorus atoms in the ^{31}P-NMR and only one set of signals for the phosphanyl CH_3 protons in the ^{1}H-NMR spectrum. The most characteristic feature in the ^{13}C-NMR spectrum of **3** is the position of the signal of the α-C atom of the vinylidene ligands which appears at δ = 292.9 as a doublet of triplets. Both the Rh-C and P-C couplings are significantly larger than those of the resonance for the vinylidene β-C atom at δ = 111.1.

[◇] Part 45: J. Gil-Rubio, M. Laubender, H. Werner, *Organometallics* **1989**, *17*, 1202−1207.

 © WILEY-VCH Verlag GmbH, D-69451 Weinheim, 1998 1434−1948/98/0909−1217 $ 17.50+.50/0

Scheme 1. L = P*i*Pr$_3$

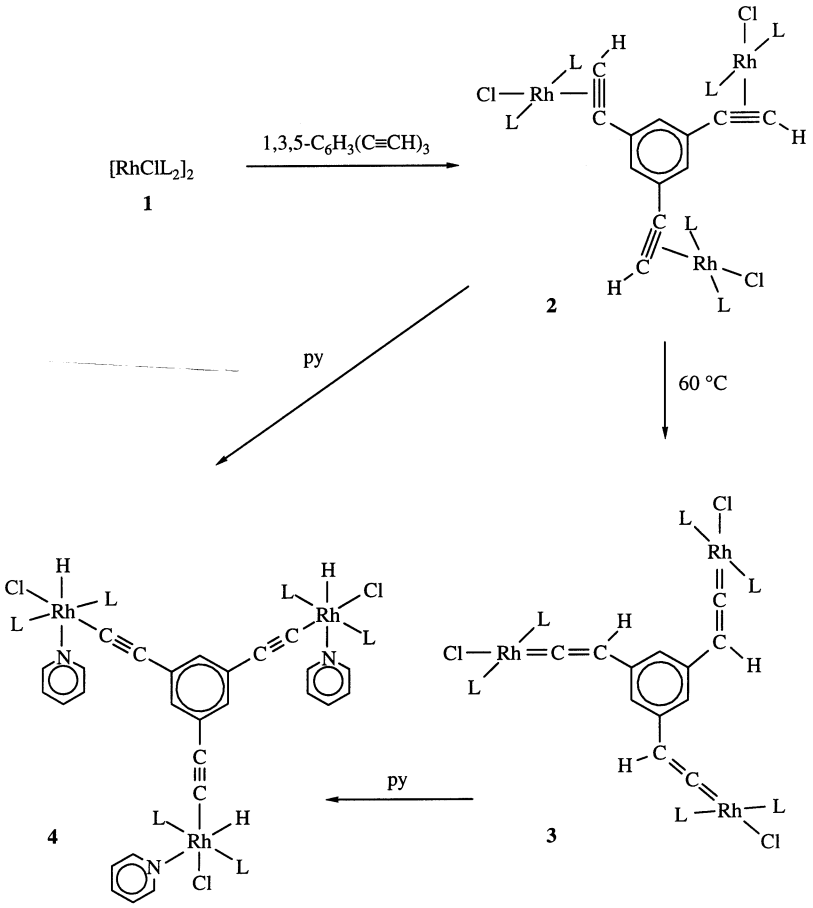

The result of the X-ray crystal structure analysis of **3** is shown in Figure 1. The coordination geometry around the three rhodium centers is square-planar with bond angles (mean values) P−Rh−C of 89.9° and P−Rh−Cl of 90.3°. The axes Cl−Rh−C and P−Rh−P are not exactly linear, the bond angles lying between 166.5° and 177.4° (for Cl−Rh−C) and between 171.09° and 173.61° (for P−Rh−P), respectively. The Rh−C and C−C distances of the vinylidenemetal units are in the expected range, i.e., they are almost identical to the corresponding bond lengths in *trans*-[RhCl(=C=CHMe)(P*i*Pr$_3$)$_2$] and *trans*-[RhCl(=C=CHC(Me)=CH$_2$)(P*i*Pr$_3$)$_2$].[9][10] An unexpected result is that the planes formed by each rhodium center, the α- and β-carbon atoms of the vinylidene ligand and the *ipso*-C atom of the substituted benzene are not coplanar with the central six-membered ring; the respective dihedral angles are between 10° and 15°. The plane of the C$_6$ ring is not exactly perpendicular to the three [Rh,P,P,Cl,α-C] planes, in this case the dihedral angles being 81−89°. The molecule of **3** as a whole can be described as a dendrimer-like species (zero-order dendrimer) with three branched organometallic moieties around the planar C$_6$ core.

The mechanism of the isomerization of **2** to **3** is not clear as yet. Due to theoretical studies[4] it is conceivable that in the initial step an intramolecular oxidative addition occurs and a tris(alkynyl)trishydridotrirhodium complex is generated. In the second step, this intermediate could rearrange to the vinylidene isomer **3**. The assumed stepwise mechanism is supported by the observation that on treatment of **2** with pyridine the trinuclear compound **4** containing three rhodium(III) centers is formed. The same product is also obtained from **3** and excess pyridine. The ^{1}H-NMR spectrum of **4** displays in the high-field region a signal at δ = −17.64 (with the intensity of 3 H) which is consistent with the proposed structure.

In contrast to 1,3,5-C$_6$H$_3$(C≡CH)$_3$, the trisilylated derivative 1,3,5-C$_6$H$_3$(C≡CSiMe$_3$)$_3$ reacts with **1** to afford the mononuclear alkyne complex **5** (Scheme 2). The IR spectrum of the bright orange solid shows besides the expected band at ca. 1800 cm^{-1} for the C≡C stretching frequency of a metal-bonded alkyne, another absorption at 2140 cm^{-1} which is typical for non-coordinated C≡C bonds. In agreement with this result, the ^{13}C-NMR spectrum of **5** displays two signals at δ = 103.7 and 95.9 for the carbon atoms of the uncoordinated and two signals at δ = 86.4 and 82.2 for those of the coordinated triple bonds. Owing to the Rh-C coupling, the latter resonances are split into doublets with *J*(RhC) of 13.5 Hz.

Figure 1. Molecular structure (ORTEP plot) of **3**[a]; the methyl groups of the isopropyl units are omitted for clarity

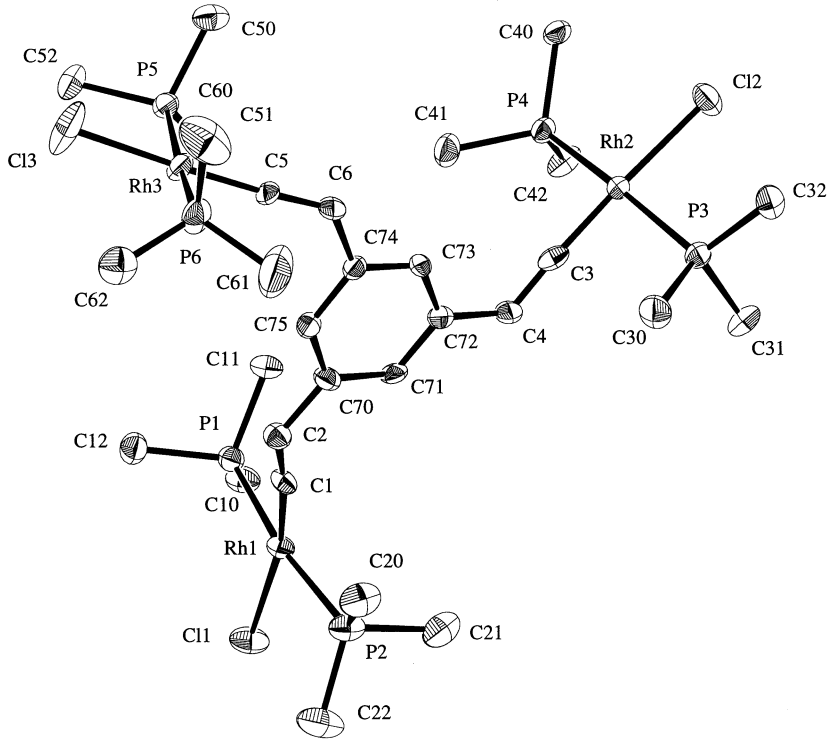

[a] Selected bond lengths [Å] and angles [°]: Rh1−Cl1 2.381(2), Rh1−P1 2.348(2), Rh1−P2 2.357(2), Rh1−C1 1.790(6), C1−C2 1.319(9), C2−C70 1.471(9), Rh2−Cl2 2.394(2), Rh2−P3 2.345(2), Rh2−P4 2.346(2), Rh2−C3 1.809(6), C3−C4 1.323(9), C4−C72 1.503(9), Rh3−Cl3 2.399(2), Rh3−P5 2.362(2), Rh3−P6 2.357(2), Rh3−C5 1.820(6), C5−C6 1.327(9), C6−C74 1.483(8); P1−Rh1−P2 171.09(7), Cl1−Rh1−C1 166.5(2), P1−Rh1−Cl1 91.10(6), P1−Rh1−C1 89.0(2), P2−Rh1−Cl1 92.15(7), P2−Rh1−C1 89.8(2), Rh1−C1−C2 172.1(6), C1−C2−C70 125.5(6), P3−Rh2−P4 171.97(6), Cl2−Rh2−C3 175.9(2), P3−Rh2−Cl2 90.20(6), P3−Rh2−C3 89.4(2), P4−Rh2−Cl2 90.32(6), P4−Rh2−C3 89.5(2), Rh2−C3−C4 175.8(5), C3−C4−C72 129.2(6), P5−Rh3−P6 173.61(7), Cl3−Rh3−C5 177.4(2), P5−Rh3−Cl3 92.31(7), P5−Rh3−C5 87.9(2), P6−Rh3−Cl3 85.95(7), P6−Rh3−C5 93.6(2), Rh3−C5−C6 176.6(5), C5−C6−C74 128.5(6).

Scheme 2. L = P*i*Pr$_3$

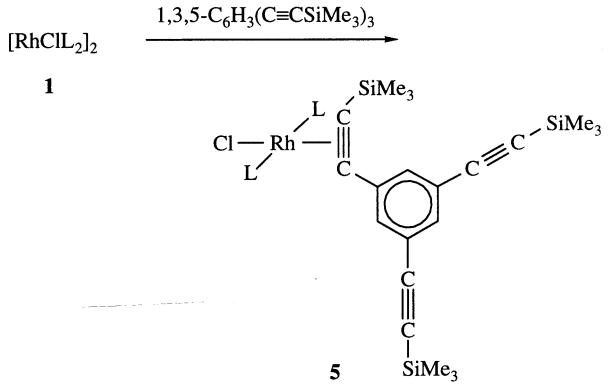

Dinuclear Complexes from Bis(ethynyl)benzene and -naphthalene Derivatives

Likewise to 1,3,5-$C_6H_3(C{\equiv}CH)_3$, the isomers 1,3- and 1,2-$C_6H_4(C{\equiv}CH)_2$ also react with **1** at low temperatures to give the bis(alkyne) complexes **6** and **7** as orange-yellow or yellow microcrystalline solids. The position of the ν(C≡C) stretches in the IR and the chemical shift of the single resonance for the P*i*Pr$_3$ phosphorus nuclei in the ^{31}P-NMR spectra of **6** and **7** are almost identical to those of **2** and thus the proposed structure as shown in Scheme 3 seems to be correct. When heated in toluene, compounds **6** and **7** behave analogously to **2** and afford by an intramolecular rearrangement the isomeric bis(vinylidene) complexes **8** and **9** in excellent yield. Again the spectroscopic data of **8** and **9** are very similar to those of **3** and deserve no further comments.

While 1,3,5-$C_6H_3(C{\equiv}CH)_3$ and 1,3,5-$C_6H_3(C{\equiv}CSiMe_3)_3$ behave differently toward the starting material **1**, the disilyl derivatives 1,2-, 1,3-, and 1,4-$C_6H_4(C{\equiv}CSiMe_3)_2$ react in the same way as the parent diynes 1,2-, 1,3-, and 1,4-$C_6H_4(C{\equiv}CH)_2$. In the presence of **1**, they afford the dinuclear dirhodium compounds **10**−**12**, respectively. Since the spectroscopic data of **6**, **7**, and [1,4-$C_6H_4(C{\equiv}CH)_2\{RhCl(P{i}Pr_3)_2\}_2$][6] on one hand and those of **10**−**12** on the other are quite similar, a related structure can be assumed (Scheme 4).

In contrast to compound **5**, which is rather inert, the dinuclear complexes **10**−**12** smoothly rearrange to the vinylidenerhodium compounds **13**−**15** (Scheme 4). The isomerization can be performed either thermally (in toluene at 60 °C) or photochemically and leads to the dark-red moisture-sensitive solids in 60−70% yield. Compounds **13**−**15** were identified by IR, NMR, and UV/Vis spectroscopy as well as by satisfactory microanalyses. In analogy to the re-

Scheme 3. L = P*i*Pr$_3$

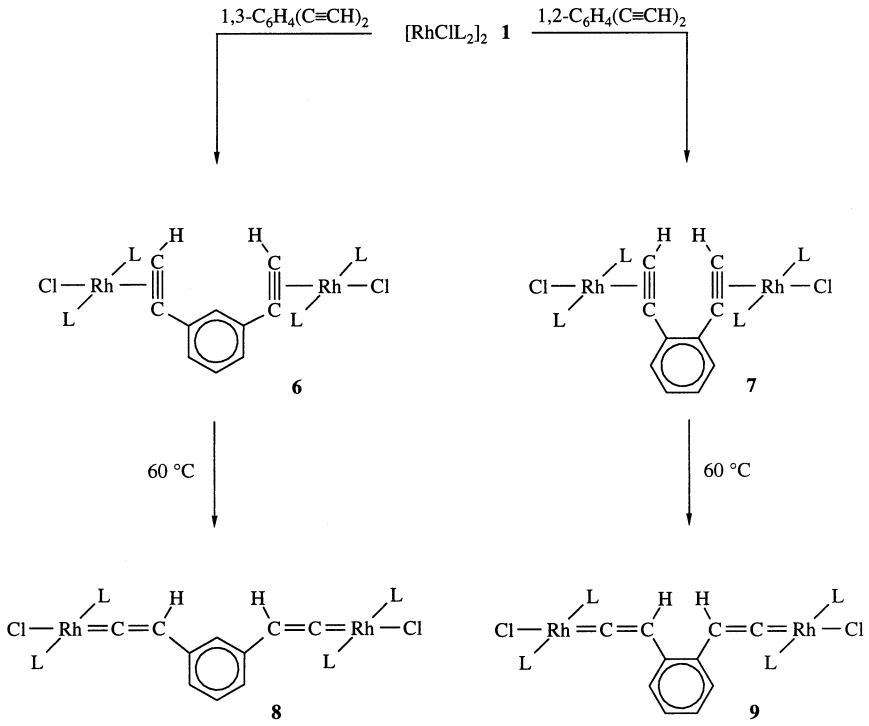

Scheme 4. A = $C_6H_4(C{\equiv}CSiMe_3)_2$; L = P*i*Pr$_3$

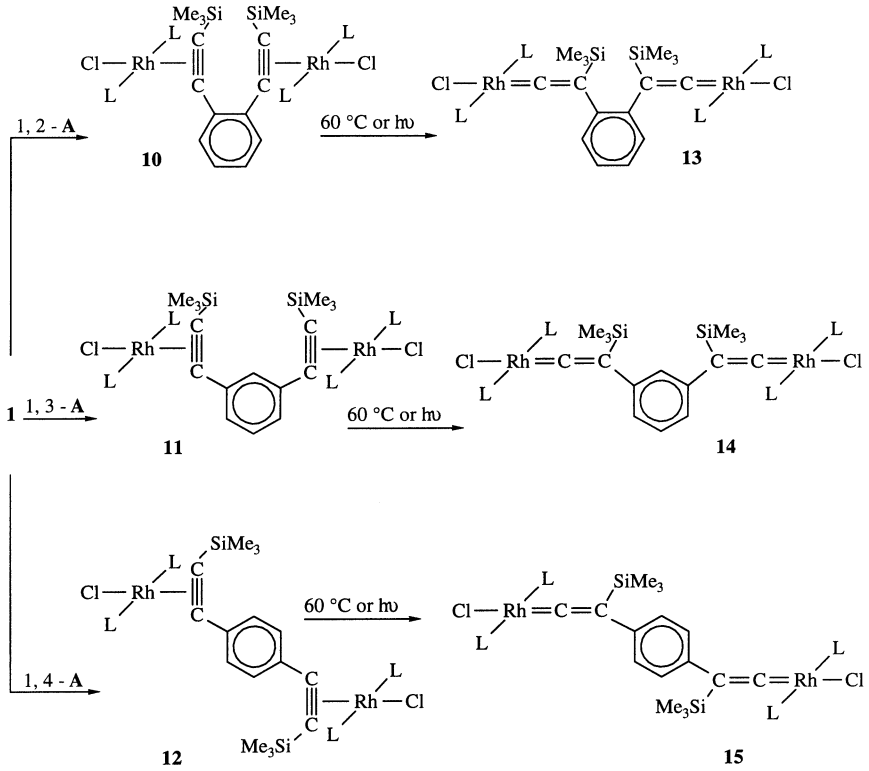

arrangement of the mononuclear complexes *trans*-[RhCl(RC≡CSiR′$_3$)(P*i*Pr$_3$)$_2$] to *trans*-[RhCl{=C=C(SiR′$_3$)R}(P*i*Pr$_3$)$_2$],[11] there is no evidence that the isomerization of **10**–**12** to **13**–**15** occurs stepwise and thus a concerted mechanism is most likely.[4][12] Although there might be some steric hinderance between the two bulky RhCl(alkyne)(P*i*Pr$_3$)$_2$ units, particularly in compounds **10** and **11**, the reaction of the bis(alkyne) to the bis(vinylidene)

complexes proceeds very cleanly and is not accompanied by the formation of oligomeric or polymeric by-products.

Scheme 5. L = P*i*Pr$_3$

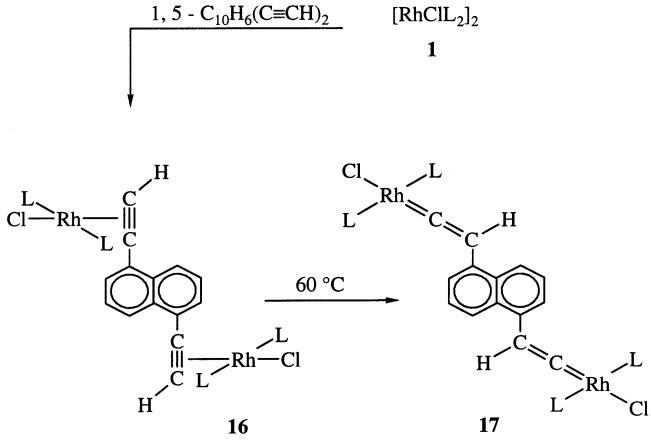

Not only 1,2-, 1,3-, and 1,4-bis(ethynyl)benzene but also 1,5-bis(ethynyl)naphthalene reacts with the starting material **1** in a stepwise manner to give initially the bis(alkyne) and then the bis(vinylidene) compounds **16** and **17**, respectively (Scheme 5). Both have been isolated as red-violet or violet solids in good yield. Single crystals of **17** could be grown from toluene and the molecular structure was determined by X-ray crystallography. As is shown in Figure 2, the dinuclear complex contains a center of inversion which is the midpoint of the C4−C4′ bond. Both rhodium atoms possess a square-planar coordination sphere with axes P1−Rh−P2 and Cl−Rh−C1 that deviate slightly from linearity. The distances Rh−C1 and C1−C2 are almost the same as in the tris(vinylidene) complex **3** and agree with the cumulene-like arrangement. A characteristic structural feature of **17** in the crystal is that the dihedral angle between the planes [Rh,P1,P2,Cl] and [C3,C4,C5,C6,C7] is 78.8(3)° and the torsional angle C1−C2−C3−C4 is 137(1)°. In order to explain these unexpected values, we assume that the non-perpendicular arrangement between the coordination planes [ClRhP$_2$C] and the naphthalene minimizes the steric repulsion between the two space-filling [RhCl(P*i*Pr$_3$)$_2$] units.

This work was supported by the *Deutsche Forschungsgemeinschaft* (SFB 347) and the *Fonds der Chemischen Industrie*. We are grateful to Dr. *B. Stempfle* and Dr. *C. Grünwald* for NMR spectra, to Mrs. *R. Schedl* and Mr. *C. P. Kneis* for performing the elemental analyses and DTA measurements, and to the *Degussa AG* for the gifts of chemicals.

Experimental Section

All operations were carried out under argon using Schlenk techniques. The starting materials **1**,[7a] the diynes 1,2-C$_6$H$_4$(C≡CH)$_2$, 1,3-C$_6$H$_4$(C≡CH)$_2$, and 1,5-C$_{10}$H$_6$(C≡CH)$_2$, the triyne 1,3,5-C$_6$H$_3$(C≡CH)$_3$, and the trimethylsilyl derivatives 1,2-C$_6$H$_4$(C≡CSiMe$_3$)$_2$ and 1,3,5-C$_6$H$_3$(C≡CSiMe$_3$)$_3$ were prepared analogously as described in the literature.[13] 1,3- and 1,4-C$_6$H$_4$(C≡CSiMe$_3$)$_2$ were commercial products from ABCR. − IR: Perkin-Elmer 1420. − UV/Vis: Hewlett Packard 8452 A. − NMR: Bruker AC 200 and AMX 400 [dvt = doublet of virtual triplets; $N = {}^3J(\mathrm{PH}) + {}^5J(\mathrm{PH})$ or ${}^2J(\mathrm{PC}) + {}^4J(\mathrm{PC})$, respectively]. − Melting points determined by DTA.

Figure 2. Molecular structure (ORTEP plot) of **17**[a]

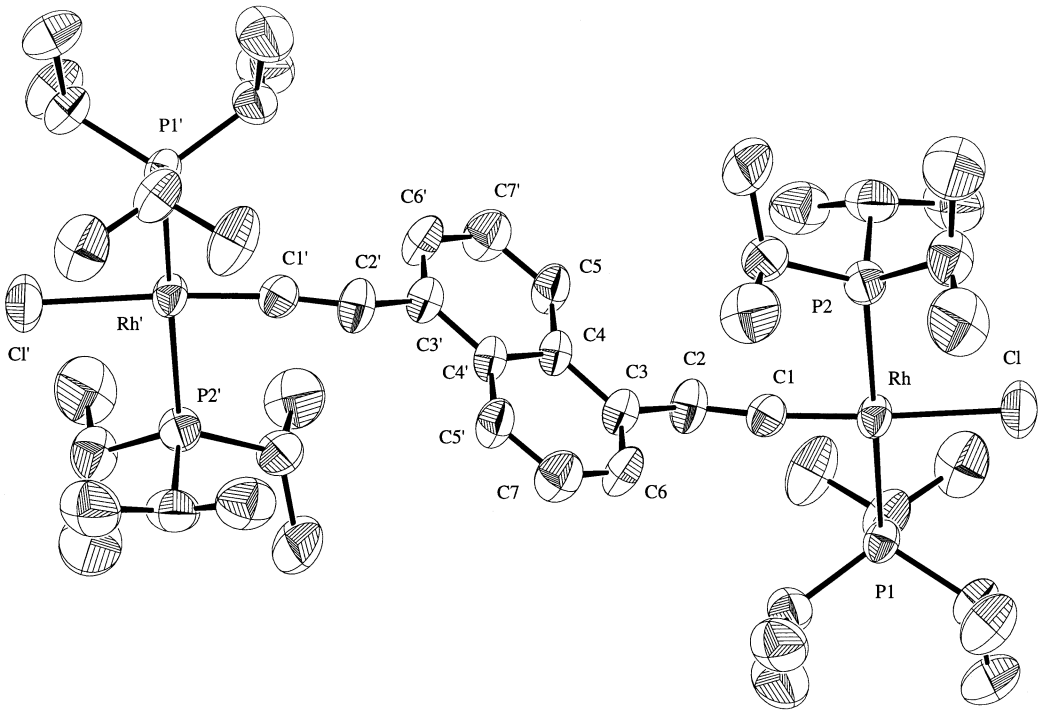

[a] Selected bond lengths [Å] and angles [°]: Rh−Cl 2.374(2), Rh−P1 2.360(2), Rh−P2 2.359(2), Rh−C1 1.780(8), C1−C2 1.30(1), C2−C3 1.48(1), C3−C4 1.42(1), C4−C5 1.42(1), C6−C7 1.41(1), C4−C4′ 1.42(1); P1−Rh−P2 172.30(8), Cl−Rh−C1 174.2(3), P1−Rh−Cl 90.96(8), P1−Rh−C1 89.3(2), P2−Rh−Cl 90.28(8), P2−Rh−C1 88.7(2), Rh−C1−C2 173.1(7), C1−C2−C3 126.9(8).

1. Preparation of [1,3,5-C_6H_3(C≡CH)$_3${RhCl($PiPr_3$)$_2$}$_3$] (**2**): A solution of 126 mg (0.14 mmol) of **1** in 20 ml of pentane was treated dropwise at −60°C with a solution of 14 mg (0.09 mmol) of 1,3,5-C_6H_3(C≡CH)$_3$ in 3 ml of pentane. A fairly rapid change of colour from dark red to orange occurred. After the solution was warmed to room temperature, it was stirred for 10 min and then the solvent was removed in vacuo. The yellow microcrystalline residue was repeatedly washed with small portions (1−2 ml) of pentane (0°C) and dried; yield 106 mg (77%); m. p. 125°C (dec.). − IR (KBr): $\tilde{\nu}$ = 3070 cm^{-1} (≡CH), 1795 (C≡C). − ^{1}H NMR (200 MHz, C_6D_6): δ = 8.70 (s, 3 H, C_6H_3), 4.02 [d, J(RhH) = 2.4 Hz, 3 H, ≡CH], 2.36 (m, 18 H, PCHCH$_3$), 1.27 [dvt, N = 12.8, J(HH) = 6.1 Hz, 54 H, PCHCH_3], 0.98 [dvt, N = 13.9, J(HH) = 7.0 Hz, 54 H, PCHCH_3]. − ^{31}P NMR (81.0 MHz, C_6D_6): δ = 33.3 [d, J(RhP) = 117.0 Hz]. − $C_{66}H_{132}Cl_3P_6Rh_3$ (1526.7): calcd. C 51.92, H 8.71; found C 51.80, H 8.91.

2. Preparation of [1,3,5-C_6H_3{CH=C=RhCl($PiPr_3$)$_2$}$_3$] (**3**): A solution of 106 mg (0.07 mmol) of **2** in 10 ml of toluene was stirred for 2 h at 60°C, which led to a change of colour from orange-yellow to dark green. After cooling to room temperature, the solvent was removed in vacuo. The residue was dissolved in ca. 2 ml of toluene, and the solution was chromatographed on Al_2O_3 (neutral, activity grade V, height of column 6 cm). With toluene, a blue-green fraction was eluted which was brought to dryness in vacuo. The remaining green solid was washed twice with 2-ml portions of pentane (0°C) and dried; yield 78 mg (73%); m. p. 159°C (dec.). − IR (CH_2Cl_2): $\tilde{\nu}$ = 1620 cm^{-1} (C=C). − UV (hexane): λ_{max} = 580, 438, 294, 242, 224 nm. − ^{1}H NMR (200 MHz, C_6D_6): δ = 6.77 (s, 3 H, C_6H_3), 2.74 (m, 18 H, PCHCH$_3$), 1.31 [dvt, N = 13.4, J(HH) = 7.0 Hz, PCHCH_3], signal of =CH protons partially covered by signal of PCHCH_3 protons. − ^{13}C NMR (50.3 MHz, C_6D_6): δ = 292.9 [dt, J(RhC) = 59.8, J(PC) = 15.8 Hz, Rh=C], 133.2, 129.7 (both s, C_6H_3), 111.1 [dt, J(RhC) = 15.2, J(PC) = 6.3 Hz, Rh=C=C], 23.8 (vt, N = 20.2 Hz, PCHCH$_3$), 20.2 (s, PCHCH$_3$). − ^{31}P NMR (81.0 MHz, C_6D_6): δ = 43.1 [d, J(RhP) = 135.1 Hz]. − $C_{66}H_{132}Cl_3P_6Rh_3$ (1526.7): calcd. C 51.92, H 8.71; found C 51.25, H 8.79.

3. Reaction of Compounds **2** *and* **3** *with Pyridine: a)* A mixture of 115 mg (0.08 mmol) of **2** and 0.1 ml (1.22 mmol) of pyridine was heated for 10 min at ca. 100°C, which led to a change of colour from yellow to off-white. After the reaction mixture was cooled to room temperature, 2 ml of pentane was added, and the solution was stored for 12 h at −78°C. A white solid precipitated which was separated from the mother liquor, washed twice with 2-ml portions of pentane (0°C) and dried; yield 82 mg (58%). Although the ^{1}H- and ^{31}P-NMR spectra confirmed that the isolated sample was pure, no reliable elemental analysis of **4** could be obtained. − *b)* Analogously as described for a), by using 102 mg (0.07 mmol) of **3** and 0.1 ml (1.22 mmol) of pyridine as the starting materials. White solid; yield 99 mg (80%). − IR (KBr): $\tilde{\nu}$ = 2150 cm^{-1} (RhH), 2080 (C≡C). − ^{1}H NMR (200 MHz, $CDCl_3$): δ = 9.51, 7.68−6.50 (both m, 18 H, C_6H_3 and NC_5H_5), 2.71 (m, 18 H, PCHCH$_3$), 1.26 [dvt, N = 13.0, J(HH) = 6.2 Hz, 54 H, PCHCH_3], 1.11 [dvt, N = 13.2, J(HH) = 6.3 Hz, 54 H, PCHCH_3], −17.64 [dt, J(RhH) = 13.8, J(PH) = 13.7 Hz, 3 H, RhH]. − ^{31}P NMR (81.0 MHz, $CDCl_3$): δ = 37.7 [d, J(RhP) = 97.4 Hz].

4. Preparation of trans-[RhCl{η^2-Me_3SiC≡CC_6H_3-3,5-(C≡$CSiMe_3$)$_2$}($PiPr_3$)$_2$] (**5**): A solution of 200 mg (0.22 mmol) of **1** in 20 ml of pentane was treated dropwise at −60°C with a solution of 144 mg (0.44 mmol) of 1,3,5-C_6H_3(C≡$CSiMe_3$)$_3$ in 3 ml of pentane. After the solution was worked up as described for **2** a bright orange solid was obtained; yield 222 mg (61%); m. p. 66°C (dec.). − IR (KBr): $\tilde{\nu}$ = 2140 cm^{-1} (C≡C)$_{uncoord}$, 1795 (C≡C)$_{coord}$. − ^{1}H NMR (200 MHz, C_6D_6): δ = 7.68−7.38 (m, 3 H, C_6H_3), 2.28 (m, 6 H, PCHCH$_3$), 1.29 [dvt, N = 13.5, J(HH) = 6.7 Hz, 18 H, PCHCH_3], 1.01 [dvt, N = 12.8, J(HH) = 6.3 Hz, 18 H, PCHCH_3], 0.27 (s, 9 H, $SiMe_3$), 0.17 (s, 18 H, $SiMe_3$). − ^{13}C NMR (100.6 MHz, C_6D_6): δ = 135.3, 134.8, 125.6, 124.3 (all s, C_6H_3), 103.7, 95.9 (both s, C≡C$_{uncoord}$), 86.4, 82.2 [both d, J(RhC) = 13.5 Hz, C≡C$_{coord}$], 22.6 (vt, N = 17.1 Hz, PCHCH$_3$), 21.0, 19.5, (both s, PCHCH$_3$], 1.0, 0.5 (both s, $SiMe_3$). − ^{31}P NMR (81.0 MHz, C_6D_6): δ = 33.1 [d, J(RhP) = 116.3 Hz].

5. Preparation of [1,3-C_6H_4(C≡CH)$_2${RhCl($PiPr_3$)$_2$}$_2$] (**6**): Analogously as described for **2**, by using 147 mg (0.16 mmol) of **1** and 20 mg (0.16 mmol) of 1,3-C_6H_4(C≡CH)$_2$ as starting materials. Orange-yellow solid; yield 128 mg (77%); m. p. 118°C (dec.). − IR (KBr): $\tilde{\nu}$ = 3070 cm^{-1} (≡CH), 1790 (C≡C). − ^{1}H NMR (200 MHz, C_6D_6): δ = 7.08−6.42 (m, 4 H, C_6H_4), 3.73 [d, J(RhH) = 2.8 Hz, 2 H, ≡CH], 2.06 (m, 12 H, PCHCH$_3$), 1.03 [dvt, N = 13.8, J(HH) = 7.3 Hz, 36 H, PCHCH_3], 0.87 [dvt, N = 13.1, J(HH) = 7.3 Hz, 36 H, PCHCH_3]. − ^{31}P NMR (81.0 MHz, C_6D_6): δ = 33.8 [d, J(RhP) = 116.3 Hz]. − $C_{46}H_{90}Cl_2P_4Rh_2$ (1043.8): calcd. C 52.93, H 8.69; found C 53.02, H 8.94.

6. Preparation of [1,2-C_6H_4(C≡CH)$_2${RhCl($PiPr_3$)$_2$}$_2$] (**7**): Analogously as described for **2**, by using 117 mg (0.13 mmol) of **1** and 16 mg (0.13 mmol) of 1,2-C_6H_4(C≡CH)$_2$ as starting materials. Yellow solid; yield 88 mg (65%); m. p. 135°C (dec.). − IR (KBr): $\tilde{\nu}$ = 3070 cm^{-1} (≡CH), 1790 (C≡C). − ^{1}H NMR (200 MHz, C_6D_6): δ = 8.73−7.29 (m, 4 H, C_6H_4), 4.53 [d, J(RhH) = 2.2 Hz, 2 H, ≡CH], 2.25 (m, 12 H, PCHCH$_3$), 1.21 [dvt, N = 13.1, J(HH) = 6.9 Hz, 36 H, PCHCH_3], 1.07 [dvt, N = 12.6, J(HH) = 6.4 Hz, 36 H, PCHCH_3]. − ^{13}C NMR (100.6 MHz, C_6D_6): δ = 131.8, 127.4, 127.0 (all s, C_6H_4), 88.3, 85.2 [both d, J(RhC) = 17.8 Hz, C≡C], 22.9 (vt, N = 17.6 Hz, PCHCH$_3$), 20.5, 20.3 (both s, PCHCH$_3$). − ^{31}P NMR (81.0 MHz, C_6D_6): δ = 34.0 [d, J(RhP) = 116.3 Hz]. − $C_{46}H_{90}Cl_2P_4Rh_2$ (1043.8): calcd. C 52.93, H 8.69; found C 53.13, H 8.63.

7. Preparation of [1,3-C_6H_4{CH=C=RhCl($PiPr_3$)$_2$}$_2$] (**8**): Analogously as described for **3**, by using 134 mg (0.13 mmol) of **6** as starting material. Blue-green solid; yield 102 mg (75%), m. p. 82°C (dec.). − IR (pentane): $\tilde{\nu}$ = 1620 cm^{-1} (C=C). − UV (hexane): λ_{max} = 580, 446, 282, 240, 224, 210 nm. − ^{1}H NMR (200 MHz, C_6D_6): δ = 7.29−6.54 (m, 4 H, C_6H_4), 2.63 (m, 12 H, PCHCH$_3$), 1.16 [dvt, N = 13.7, J(HH) = 6.7 Hz, PCHCH_3], signal of =CH protons partially covered by signal of PCHCH_3 protons. − ^{13}C NMR (50.3 MHz, C_6D_6): δ = 293.1 [dt, J(RhC) = 60.0, J(PC) = 15.9 Hz, Rh=C], 135.7, 132.2, 125.6, 122.5 (all s, C_6H_4), 111.3 [dt, J(RhC) = 15.3, J(PC) = 6.4 Hz, Rh=C=C], 23.7 (vt, N = 20.3 Hz, PCHCH$_3$), 20.1 (s, PCHCH$_3$). − ^{31}P NMR (81.0 MHz, C_6D_6): δ = 43.2 [d, J(RhP) = 133.9 Hz]. − $C_{46}H_{90}Cl_2P_4Rh_2$ (1043.8): calcd. C 52.93, H 8.69; found C 53.29, H 9.08.

8. Preparation of [1,2-C_6H_4{CH=C=RhCl($PiPr_3$)$_2$}$_2$] (**9**): Analogously as described for **3**, by using 121 mg (0.12 mmol) of **7** as starting material. Bright green solid; yield 84 mg (67%); m. p. 128°C (dec.). − IR (KBr): $\tilde{\nu}$ = 1620 cm^{-1} (C=C). − UV (hexane): λ_{max} = 574, 436, 280, 240, 222 nm. − ^{1}H NMR (200 MHz, C_6D_6): δ = 7.80−6.48 (m, 4 H, C_6H_4), 2.70 (m, 12 H, PCHCH$_3$), 2.25 [dt, J(PH) = 3.1, J(RhH) = 1.0 Hz, 2 H, =CH], 1.29 [dvt, N = 13.0, J(HH) = 6.2 Hz, 72 H, PCHCH_3]. − ^{13}C NMR (100.6 MHz, C_6D_6): δ = 292.2 [dt, J(RhC) = 59.6, J(PC) = 15.3 Hz, Rh=C], 132.9, 128.9, 127.1 (all s, C_6H_4), 110.3 [dt, J(RhC) = 15.5, J(PC) = 5.7 Hz, Rh=C=C], 24.0 (vt, N = 20.2 Hz, PCHCH$_3$), 20.3 (s, PCHCH$_3$). − ^{31}P NMR (81.0 MHz, C_6D_6): δ = 43.6 [d, J(RhP) =

133.7 Hz]. − $C_{46}H_{90}Cl_2P_4Rh_2$ (1043.8): calcd. C 52.93, H 8.69; found C 52.72, H 8.29.

9. Preparation of [1,2-C_6H_4(C≡$CSiMe_3$)$_2${RhCl($PiPr_3$)$_2$}$_2$] (**10**): Analogously as described for **2**, by using 157 mg (0.17 mmol) of **1** and 46 mg (0.17 mmol) of 1,2-C_6H_4(C≡$CSiMe_3$)$_2$ as starting materials. Light orange solid; yield 156 mg (77%); m. p. 112°C (dec.). − IR (KBr): $\tilde{\nu}$ = 1810 cm^{-1} (C≡C). − ^{1}H NMR (400 MHz, C_6D_6): δ = 9.93−6.64 (m, 4 H, C_6H_4), 2.98 (m, 12 H, PC*H*CH_3), 1.33 [dvt, *N* = 13.9, *J*(HH) = 7.0 Hz, 36 H, PCHC*H*$_3$], 1.08 [dvt, *N* = 11.7, *J*(HH) = 6.1 Hz, 36 H, PCHC*H*$_3$], 0.6 (s, 18 H, $SiMe_3$). − ^{13}C NMR (100.6 MHz, C_6D_6): δ = 138.2, 132.2, 126.5 (all s, C_6H_4), 109.2 [d, *J*(RhC) = 18.8 Hz, *C*≡C], 85.1 [d, *J*(RhC) = 12.5 Hz, C≡*C*], 22.9 (vt, *N* = 15.6 Hz, P*C*HCH$_3$), 21.3, 19.6 (both s, PCH*C*H$_3$], 0.7 (s, $SiMe_3$). − ^{31}P NMR (162.0 MHz, C_6D_6): δ = 29.5 [d, *J*(RhP) = 117.7 Hz]. − $C_{52}H_{106}Cl_2P_4Rh_2Si_2$ (1188.2): calcd. C 52.56, H 8.99; found C 52.84, H 9.02.

10. Preparation of [1,3-C_6H_4(C≡$CSiMe_3$)$_2${RhCl($PiPr_3$)$_2$}$_2$] (**11**): Analogously as described for **2**, using 121 mg (0.13 mmol) of **1** and 36 mg (0.13 mmol) of 1,3-C_6H_4(C≡$CSiMe_3$)$_2$ as starting materials. Light orange solid; yield 114 mg (74%); m. p. 106°C (dec.). − IR (KBr): $\tilde{\nu}$ = 1800 cm^{-1} (C≡C). − ^{1}H NMR (200 MHz, C_6D_6): δ = 7.54−6.75 (m, 4 H, C_6H_4), 2.40 (m, 12 H, PC*H*CH_3), 1.37 [dvt, *N* = 13.5, *J*(HH) = 6.8 Hz, 36 H, PCHC*H*$_3$], 1.10 [dvt, *N* = 12.4, *J*(HH) = 6.2 Hz, 36 H, PCHC*H*$_3$], 0.46 (s, 18 H, $SiMe_3$). − ^{13}C NMR (100.6 MHz, C_6D_6): δ = 134.2, 130.8, 126.3, 125.8 (all s, C_6H_4), 105.8 [d, *J*(RhC) = 19.8 Hz, *C*≡C], 80.6 [d, *J*(RhC) = 16.8 Hz, C≡*C*], 22.5 (vt, *N* = 16.0 Hz, P*C*HCH$_3$), 21.3, 19.5 (both s, PCH*C*H$_3$), 0.9 (s, $SiMe_3$). − ^{31}P NMR (81.0 MHz, C_6D_6): δ = 33.2 [d, *J*(RhP) = 117.9 Hz]. − $C_{52}H_{106}Cl_2P_4Rh_2Si_2$ (1188.2): calcd. C 52.56, H 8.99; found C 52.75, H 8.93.

11. Preparation of [1,4-C_6H_4(C≡$CSiMe_3$)$_2${RhCl($PiPr_3$)$_2$}$_2$] (**12**): Analogously as described for **2**, by using 139 mg (0.15 mmol) of **1** and 41 mg (0.15 mmol) of 1,4-C_6H_4(C≡$CSiMe_3$)$_2$ as starting materials. Yellow solid; yield 128 mg (72%); m. p. 108°C (dec.). − IR (KBr): $\tilde{\nu}$ = 1790 cm^{-1} (C≡C). − ^{1}H NMR (200 MHz, C_6D_6): δ = 8.65−6.51 (m, 4 H, C_6H_4), 2.40 (m, 12 H, PC*H*CH_3), 1.38 [dvt, *N* = 13.6, *J*(HH) = 6.9 Hz, 36 H, PCHC*H*$_3$], 1.08 [dvt, *N* = 12.8, *J*(HH) = 6.2 Hz, 36 H, PCHC*H*$_3$], 0.37 (s, 18 H, $SiMe_3$). − ^{13}C NMR (100.6 MHz, C_6D_6): δ = 132.1, 122.3 (both s, C_6H_4), 106.4 [d, *J*(RhC) = 18.7 Hz, *C*≡C], 80.6 [d, *J*(RhC) = 14.4 Hz, C≡*C*], 22.4 (vt, *N* = 17.1 Hz, P*C*HCH$_3$), 21.0, 19.4 (both s, PCH*C*H$_3$), 0.8 (s, $SiMe_3$). − ^{31}P NMR (81.0 MHz, C_6D_6): δ = 33.1 [d, *J*(RhP) = 116.9 Hz]. − $C_{52}H_{106}Cl_2P_4Rh_2Si_2$ (1188.2): calcd. C 52.56, H 8.99; found C 52.14, H 8.68.

12. Preparation of [1,2-C_6H_4{C($SiMe_3$)=C=RhCl($PiPr_3$)$_2$}$_2$] (**13**): *a)* A solution of 134 mg (0.11 mmol) of **10** in 10 ml of toluene was stirred for 1.5 h at 60°C. A change of colour from orange-red to dark brown occurred. After the solution was cooled to room temperature, it was concentrated to ca. 2 ml in vacuo and then 5 ml of pentane was added. A redbrown solid precipitated which was filtered, washed twice with 2-ml portions of pentane and dried; yield 81 mg (62%). − *b)* A solution of 106 mg (0.09 mmol) of **10** in 10 ml of benzene was irradiated for 2 h at room temperature with a UV lamp (500-W mercury arc). After the solvent was removed, the remaining residue was recrystallized from pentane (20°C to −60°C). Dark red crystals; yield 69 mg (65%); m. p. 109°C (dec.). − IR (KBr): $\tilde{\nu}$ = 1610 cm^{-1} (C=C). − UV (hexane): λ_{max} = 568, 440, 280, 240, 222, 206 nm. − ^{1}H NMR (400 MHz, C_6D_6): δ = 7.82−6.48 (m, 4 H, C_6H_4), 2.71 (m, 12 H, PC*H*CH_3), 1.27 [dvt, *N* = 13.6, *J*(HH) = 6.9 Hz, 36 H, PCHC*H*$_3$], 0.87 [dvt, *N* = 13.5, *J*(HH) = 6.8 Hz, 36 H, PCHC*H*$_3$], 0.25 (s, 18 H, $SiMe_3$). − ^{13}C NMR (100.6 MHz, C_6D_6): δ = 286.4 [dt, *J*(RhC) = 60.3, *J*(PC) = 15.9 Hz, Rh=C], 131.6, 126.7, 124.7 (all s, C_6H_4), 110.7 [dt, *J*(RhC) = 10.5, *J*(PC) = 3.8 Hz, Rh=C=*C*], 22.6 (vt, *N* = 20.1 Hz, P*C*HCH$_3$), 21.3 (s, PCH*C*H$_3$), 0.7 (s, $SiMe_3$). − ^{31}P NMR (81.0 MHz, C_6D_6): δ = 43.6 [d, *J*(RhP) = 133.7 Hz]. − $C_{52}H_{106}Cl_2P_4Rh_2Si_2$ (1188.2): calcd. C 52.56, H 8.99; found C 52.11, H 8.96.

13. Preparation of [1,3-C_6H_4{C($SiMe_3$)=C=RhCl($PiPr_3$)$_2$}$_2$] (**14**): *a)* A solution of 132 mg (0.11 mmol) of **11** in 10 ml of toluene was stirred for 2.5 h at 60°C. A change of colour from orange-red to dark brown occurred. After the solution was worked up as described for **13**, a dark red solid was obtained; yield 85 mg (65%). − *b)* A solution of 118 mg (0.10 mmol) of **11** in 10 ml of benzene was irradiated for 2 h at room temperature with a UV lamp (500-W mercury arc). The work-up procedure was the same as for **13**. Dark red crystals; yield 72 mg (61%); m. p. 81°C (dec.). − IR (KBr): $\tilde{\nu}$ = 1620 cm^{-1} (C=C). − UV (hexane): λ_{max} = 502, 358, 240, 222, 204 nm. − ^{1}H NMR (200 MHz, C_6D_6): δ = 7.67−6.72 (m, 4 H, C_6H_4), 2.71 (m, 12 H, PC*H*CH_3), 1.33 [dvt, *N* = 13.4, *J*(HH) = 6.4 Hz, 36 H, PCHC*H*$_3$], 0.86 [dvt, *N* = 13.2, *J*(HH) = 6.2 Hz, 36 H, PCHC*H*$_3$], 0.27 (s, 18 H, $SiMe_3$). − ^{13}C NMR (100.6 MHz, C_6D_6): δ = 291.3 [dt, *J*(RhC) = 60.2, *J*(PC) = 15.8 Hz, Rh=C], 133.4, 130.2, 126.5, 125.0 (all s, C_6H_4), 110.2 [dt, *J*(RhC) = 9.8, *J*(PC) = 3.7 Hz, Rh=C=*C*], 22.1 (vt, *N* = 19.9 Hz, P*C*HCH$_3$), 21.1 (s, PCH*C*H$_3$), 0.9 (s, $SiMe_3$). − ^{31}P NMR (81.0 MHz, C_6D_6): δ = 42.5 [d, *J*(RhP) = 135.2 Hz]. − $C_{52}H_{106}Cl_2P_4Rh_2Si_2$ (1188.2): calcd. C 52.56, H 8.99, Rh 17.32; found C 52.09, H 8.94, Rh 17.15.

14. Preparation of [1,4-C_6H_4{C($SiMe_3$)=C=RhCl($PiPr_3$)$_2$}$_2$] (**15**): *a)* A solution of 137 mg (0.12 mmol) of **12** in 10 ml of toluene was stirred for 3 h at 60°C. A change of colour from orange-red to dark brown occurred. After the solution was worked up as described for **13**, a dark brown solid was obtained; yield 91 mg (64%). − *b)* A solution of 121 mg (0.10 mmol) of **12** in 10 ml of benzene was irradiated for 2 h at room temperature with a UV lamp (500-W mercury arc). After the solvent was removed, the remaining residue was recrystallized from pentane (20°C to −60°C). Dark red crystals; yield 75 mg (63%); m. p. 60°C (dec.). − IR (KBr): $\tilde{\nu}$ = 1620 cm^{-1} (C=C). − UV (hexane): λ_{max} = 536, 346, 248, 222, 202 nm. − ^{1}H NMR (400 MHz, C_6D_6): δ = 7.62−6.95 (m, 4 H, C_6H_4), 2.75 (m, 12 H, PC*H*CH_3), 1.31 [dvt, *N* = 13.0, *J*(HH) = 6.5 Hz, 36 H, PCHC*H*$_3$], 0.85 [dvt, *N* = 13.4, *J*(HH) = 6.6 Hz, 36 H, PCHC*H*$_3$], 0.28 (s, 18 H, $SiMe_3$). − ^{31}P NMR (81.0 MHz, C_6D_6): δ = 43.2 [d, *J*(RhP) = 135.1 Hz]. − $C_{52}H_{106}Cl_2P_4Rh_2Si_2$ (1188.2): calcd. C 52.56, H 8.99; found C 52.14, H 9.23.

15. Preparation of [1,5-$C_{10}H_6$(C≡$CH)_2${RhCl($PiPr_3$)$_2$}$_2$] (**16**): Analogously as described for **2**, by using 123 mg (0.13 mmol) of **1** and 23 mg (0.13 mmol) of 1,5-$C_{10}H_6$(C≡$CH)_2$ as starting materials. Red-violet solid; yield 95 mg (67%); m. p. 122°C (dec.). − IR (KBr): $\tilde{\nu}$ = 3070 cm^{-1} (≡CH), 1795 (C≡C). − ^{1}H NMR (400 MHz, C_6D_6): δ = 9.17 [d, *J*(H_cH_b) = 6.8 Hz, 2 H, H_c and $H_{c'}$], 8.44 [d, *J*(H_aH_b) = 8.4 Hz, 2 H, H_a and $H_{a'}$], 7.61 {dd, *J*(H_bH_a) = *J*(H_bH_c) = 1/2 [*J*(H_bH_a) + *J*(H_bH_c)] = 7.6 Hz, 2 H, H_b and $H_{b'}$}, 4.37 [d, *J*(RhH) = 2.4 Hz, 2 H, ≡CH], 2.34 (m, 12 H, PC*H*CH_3), 1.29 [dvt, *N* = 13.2, *J*(HH) = 6.7 Hz, 36 H, PCHC*H*$_3$], 1.28 [dvt, *N* = 13.4, *J*(HH) = 6.8 Hz, 36 H, PCHC*H*$_3$]. − ^{31}P NMR (81.0 MHz, C_6D_6): δ = 33.9 [d, *J*(RhP) = 117.7 Hz]. − $C_{50}H_{92}Cl_2P_4Rh_2$ (1093.9): calcd. C 54.90, H 8.48, Rh 18.82; found C 54.73, H 8.88, Rh 18.48.

16. Preparation of [1,5-$C_{10}H_6${CH=C=RhCl($PiPr_3$)$_2$}$_2$] (**17**): Analogously as described for **3**, by using 132 mg (0.12 mmol) of **16** as starting material. Violet solid; yield 96 mg (73%); m. p. 196°C (dec.). − IR (KBr): $\tilde{\nu}$ = 1620 cm^{-1} (C=C). − ^{1}H NMR (400 MHz, C_6D_6): δ = 7.82 [dd, *J*(H_bH_a) = *J*(H_bH_c) = 7.6 Hz, 2 H, H_b and

Figure 3. Numbering scheme in **16** and **17** for NMR assignments

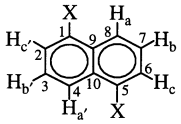

X = (C≡CH){RhCl(P*i*Pr$_3$)$_2$}

or (CH=C){RhCl(P*i*Pr$_3$)$_2$}

$H_{b'}$], 7.11 [d, J(HH$_b$) = 7.6 Hz, 2 H, H_a or H_c], 7.01 [d, J(HH$_b$) = 7.6 Hz, 2 H, H_a or H_c], 2.72 (m, 12 H, PC*H*CH$_3$), 2.27 [t, J(PH) = 3.2 Hz, 2 H, =CH], 1.28 [dvt, N = 13.6, J(HH) = 6.9 Hz, 72 H, PCHC*H*$_3$]. – ^{13}C NMR (100.6 MHz, C_6D_6): δ = 137.8 (s, C^1 and C^5), 130.3 (s, C^9 and C^{10}), 129.3, 128.5, 125.6 (all s, C^2 and C^6, C^3 and C^7, C^4 and C^8), 107.6 [dt, J(RhC) = 15.3, J(PC) = 5.8 Hz, Rh=C=*C*], 24.1 (dvt, N = 20.0 Hz, P*C*HCH$_3$), 20.4 (s, PCH*C*H$_3$), signal of Rh=C could not be observed. – ^{31}P NMR (81.0 MHz, C_6D_6): δ = 43.4 [d, J(RhP) = 135.1 Hz]. – $C_{50}H_{92}Cl_2P_4Rh_2$ (1093.9): calcd. C 54.90, H 8.48, Rh 18.82; found C 54.51, H 8.30, Rh 19.17.

17. Determination of the X-ray Crystal Structure of **3**[14]: Single crystals were grown upon cooling of a saturated solution of **3** in acetone from 50°C to 25°C. Crystal data (from 25 reflections, 10° < Θ < 15°): monoclinic; space group $P\,2_1/c$ (No. 14); a = 29.729(5), b = 11.2733(9), c = 26.579(5) Å, β = 114.406(8)°; V = 8112(2) Å^3, Z = 4; $d_{calcd.}$ = 1.250 gcm^{-3}; μ(Mo-K_α) = 0.853 mm^{-1}; crystal size 0.72 × 0.44 × 0.40 mm; Enraf-Nonius CAD-4 diffractometer, Mo-K_α radiation (λ = 0.71073 Å), graphite monochromator, zirconium filter (factor 16.4); T = 173(2) K; ω-2θ scan, max. 2θ = 48°; 13712 reflections measured, 12400 independent ($R_{int.}$ = 0.0395), 8211 with $I > 2\sigma(I)$. Intensity data were corrected for Lorentz and polarization effects and an empirical absorption correction (Ψ scan method) was applied (min. transmission 82.49%). The structure was solved by direct methods (SHELXS-86)[15]. Atomic coordinates and the anisotropic thermal parameters of non-hydrogen atoms were refined by full-matrix least squares on F^2 (SHELXL-93)[16]. The positions of all hydrogen atoms except H(2), H(4), H(6), H(71), H(73), and H(75) were calculated according to ideal geometry and were refined by using the riding method. The positions of H(2), H(4), H(6), H(71), H(73), and H(75) could be located in a final difference Fourier synthesis and refined without restrictions. Conventional R = 0.0505 [for 8211 reflections with $I > 2\sigma(I)$], and weighted wR_2 = 0.1218 for all 12400 located reflections; reflection/parameter ratio 16.2; residual electron density +0.869/−0.842 eÅ^{-3}.

18. Determination of the X-ray Crystal Structure of **17**[14]: Single crystals were grown upon cooling of a saturated solution of **17** in toluene from 80°C to 25°C. Crystal data (from 25 reflections, 10° < Θ < 15°): triclinic; space group $P\bar{1}$ (No. 2); a = 8.843(2), b = 12.093(3), c = 15.496(3) Å, α = 107.45(1), β = 96.65(1), γ = 94.51(1)°; V = 1559.1(6) Å^3, Z = 2; $d_{calcd.}$ = 1.267 gcm^{-3}; μ(Mo-K_α) = 0.744 mm^{-1}; crystal size 0.2 × 0.3 × 0.45 mm; Enraf-Nonius CAD-4 diffractometer, Mo-K_α radiation (λ = 0.7093 Å), graphite monochromator, zirconium filter (factor 15.4); T = 293(2) K; ω-θ scan, max. 2θ = 60°; 6930 reflections measured, 6500 independent ($R_{int.}$ = 0.0243), 4675 with $I > 2\sigma(I)$. Intensity data were corrected for Lorentz and polarization effects. The structure was solved by direct methods (SHELXS-86)[15]. Atomic coordinates and the anisotropic thermal parameters of non-hydrogen atoms were refined by full-matrix least squares on F^2 (SHELXL-93)[16]. The positions of all hydrogen atoms were calculated according to ideal geometry and were refined by using the riding method. One half of multi-disordered toluene is present in the asymmetric unit. Though two alternative positions were found and refined anisotropically (with occupation factor of 0.5 each), bond lengths and angles within this molecule could not be refined properly. Conventional R = 0.0775 [for 4675 reflections with $I > 2\sigma(I)$], and weighted wR_2 = 0.4229 for all 6500 located reflections; reflection/parameter ratio 16.2; residual electron density +1.473/−0.860 eÅ^{-3}.

☆ Dedicated to Professor *Heinrich Nöth* on the occasion of his 70th birthday.

[1] [1a] J. Wolf, H. Werner, D. Serhadli, M. L. Ziegler, *Angew. Chem.* **1983**, *95*, 428–429; *Angew. Chem. Int. Ed. Engl.* **1983**, *22*, 414–416. – [1b] F. J. Garcia Alonso, A. Höhn, J. Wolf, H. Otto, H. Werner, *Angew. Chem.* **1985**, *97*, 401–402; *Angew. Chem. Int. Ed. Engl.* **1985**, *24*, 406–408.

[2] Summarizing articles: [2a] H. Werner, *Nachr. Chem. Tech. Lab.* **1992**, *40*, 435–444. – [2b] H. Werner, *J. Organomet. Chem.* **1994**, *475*, 45–55.

[3] [3a] B. E. R. Schilling, R. Hoffmann, D. L. Lichtenberger, *J. Am. Chem. Soc.* **1979**, *101*, 585–591. – [3b] N. M. Kostic, R. F. Fenske, *Organometallics* **1982**, *1*, 974–982.

[4] Y. Wakatsuki, N. Koga, H. Werner, K. Morokuma, *J. Am. Chem. Soc.* **1997**, *119*, 360–366.

[5] T. Rappert, O. Nürnberg, H. Werner, *Organometallics* **1993**, *12*, 1359–1364.

[6] H. Werner, T. Rappert, J. Wolf, *Isr. J. Chem.* **1990**, *30*, 377–384.

[7] [7a] Isolation: H. Werner, J. Wolf, A. Höhn, *J. Organomet. Chem.* **1985**, *287*, 395–407. – [7b] Molecular structure: P. Binger, J. Haas, G. Glaser, R. Goddard, C. Krüger; *Chem. Ber.* **1994**, *127*, 1927–1929.

[8] R. K. Harris, *Can. J. Chem.* **1964**, *42*, 2275–2281.

[9] H. Werner, F. J. Garcia Alonso, H. Otto, J. Wolf, *Z. Naturforsch., B* **1988**, *43*, 722–726.

[10] T. Rappert, O. Nürnberg, N. Mahr, J. Wolf, H. Werner, *Organometallics* **1992**, *11*, 4156–4164.

[11] [11a] D. Schneider, H. Werner, *Angew. Chem.* **1991**, *103*, 710–712; *Angew. Chem. Int. Ed. Engl.* **1991**, *30*, 700–702. – [11b] H. Werner, M. Baum, D. Schneider, B. Windmüller, *Organometallics* **1994**, *13*, 1089–1097. – [11c] M. Baum, B. Windmüller, H. Werner, *Z. Naturforsch., B* **1994**, *49*, 859–869.

[12] J. Silvestre, R. Hoffmann, *Helv. Chim. Acta* **1985**, *68*, 1461–1506.

[13] [13a] R. Diercks, J. C. Armstrong, R. Boese, K. P. C. Vollhardt, *Angew. Chem.* **1986**, *98*, 270–271; *Angew. Chem. Int. Ed. Engl.* **1986**, *25*, 268–269. – [13b] B. C. Berris, G. H. Hovakeemian, Y.-H. Lai, H. Mestdagh, K. P. C. Vollhardt, *J. Am. Chem. Soc.* **1985**, *107*, 5670–5687.

[14] Crystallographic data (excluding structure factors) for the structures reported in this paper have been deposited with the Cambridge Crystallographic Data Centre as supplementary publication no. CCDC-101424. Copies of the data can be obtained free of charge on application to CCDC, 12 Union Road, Cambridge CB2 1EZ, UK (Fax: internat. + 44-1223/336-033; E-mail: deposit@ccdc.cam.ac.uk).

[15] G. M. Sheldrick, *Acta Crystallogr., Sect. A* **1990**, *46*, 467.

[16] G. M. Sheldrick, *A program for crystal structure refinement*, University of Göttingen, **1993**.

[98121]

Di-, Tri-, and Tetranuclear Cyclobutenylidene Complexes☆

Frédéric Leroux, Rüdiger Stumpf, and Helmut Fischer*

Fakultät für Chemie, Universität Konstanz, Fach M727,
D-78457 Konstanz, Germany
Fax: (internat.) + 49(0)7531/88-2783
E-mail: hfischer@dg6.chemie.uni-konstanz.de

Received April 24, 1998

Keywords: Vinylidene complexes / Cyclobutenylidene complexes / Bridging ligands / Cycloadditions / Cross-coupling

Pentacarbonyl(dimethylvinylidene)chromium, $[(CO)_5Cr{=}C{=}CMe_2]$ (**1**), reacts with the butadiynyl complexes $[Cp(CO)_2FeC{\equiv}CC{\equiv}CR]$ [**2**; R = $SiMe_3$ (**a**), *n*Bu (**b**), Ph (**c**)] and $[Cp(CO)(PPh_3)FeC{\equiv}CC{\equiv}CSiMe_3]$ (**3a**) by regiospecific cycloaddition of the $C^{\alpha}{\equiv}C^{\beta}$ bond of the butadiynyl complexes to the C=C bond of **1** to form the 1,3-*hetero*binuclear cyclobutenylidene complexes **4a–c** and **5a** with an alkynyl substituent at C-2 of the bridging ring. Desilylation of the 2-$C{\equiv}CSiMe_3$ substituent in **4a** and **5a** with tetrabutylammonium fluoride affords the 2-$C{\equiv}CH$-substituted complexes **6** and **7**. Complex **4a** reacts with $HNMe_2$ and $HN(CH_2)_5$ by substitution of NR_2 for the 3-$Fe(CO)_2Cp$ fragment to form the corresponding 3-aminocyclobutenylidene complexes **10** and **11**. Sequential reactions of **4a** with $[n Bu_4N]F$ and $n Bu_3SnNEt_2$ give the trinuclear 2-$C{\equiv}CSn n Bu_3$-substituted complex **12**. Coupling of **12** with $C_6H_4I_2$-*p* yields the 2-$C{\equiv}CC_6H_4I$-*p*-substituted complex **13**. Coupling of **7** with $C_6H_4I_2$-*p* yields a mixture of the mono-coupling product **14** and the tetranuclear $C{\equiv}C{-}C_6H_4{-}C{\equiv}C$-bridged bis(cyclobutenylidene) complex **15**. Coupling of **7** with *trans*-$[(Et_3P)_2MCl_2]$ in the presence of CuI/$[Pd(PPh_3)_4]$ gives the trinuclear 2-$C{\equiv}C{-}M(PEt_3)_2X$-substituted complexes **16** (M = Pd, X = I) and **17** (M = Pt, X = Cl). The spectroscopic data as well as the results of the X-ray-structural analysis of **5a** indicate strong electronic communication between the metal centers. In the solid state, **5a** exhibits a "butterfly" conformation.

Introduction

Electronic communication between the metal centers in bi- and polynuclear transition-metal complexes containing unsaturated carbon bridges should lead to unusual physical and chemical properties[1]. For example, carbon-bridged bimetallic π-conjugated complexes of the type $[L_nMC_mM'(L')_{n'}]$ have been proposed as a new class of one-dimensional molecular wires[2]. Rigid-rod polymers like $[L_nMC{\equiv}CXC{\equiv}C]_m$ (X = aryl) can exhibit both liquid-crystalline[3] and nonlinear optical properties[4] similar to certain metal acetylides[5]. Binuclear complexes with different L_nM end groups at a conjugated π system should exhibit second-order nonlinear optical (NLO) properties.

Related to linear C_n bridges are rigid cyclic bridges with a delocalized π system. We recently reported on the syntheses of 1,3-*hetero*binuclear complexes with a cyclic C_4R_3 bridging ligand (cyclobutenylidene complexes)[6]. By variation of the substituents at the bridging ligand a fine-tuning of the magnetic, electronic, and spectroscopic properties of such binuclear complexes should be possible. Until now, 1,3-*hetero*binuclear cyclobutenylidene complexes with alkyl and aryl substituents as well as with functional groups at the bridging ligand, and with various metal-ligand fragments in 1- and 3-position of the ring have been prepared by reaction of suitable vinylidene complexes of chromium and tungsten, $[(CO)_5M{=}C{=}CR^1{}_2]$, with alkynyl complexes, $[L_nM'{-}C{\equiv}CR^2]$ (Scheme 1)[6a].

Cyclobutenylidene complexes with an exocyclic C=C bond were accessible by a regiospecific cycloaddition of alkynyl complexes to the $C^{\alpha}{=}C^{\beta}$ bond of allenylidene(pentacarbonyl)chromium and -tungsten complexes[6b]. The properties of these 1,3-*hetero*binuclear complexes are strongly influenced by the substituents at both non-metal-bonded ring atoms.

Scheme 1

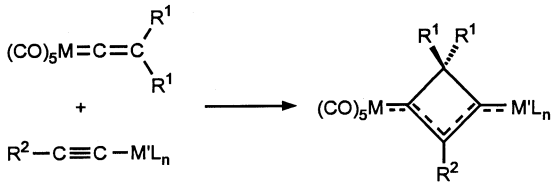

Transition-metal butadiynyl complexes, $[L_nMC^{\alpha}{\equiv}C^{\beta}C^{\gamma}{\equiv}C^{\delta}R]$, are related to alkynyl complexes $[L_nMC{\equiv}CR]$. In alkynyl complexes the HOMO is mainly localized at the terminal C atom. Therefore, electrophiles add to this carbon atom. Spectroscopic investigations of butadiynyl complexes indicate a strong communication between the metal center and the butadiynyl ligand[7][8]. In contrast to alkynyl complexes, two pathways are conceivable for the reactions of butadiynyl with vinylidene complexes as electrophiles depending on whether initial electrophilic attack of the vinylidene C^{α} atom in $[L_nM{=}C^{\alpha}{=}C^{\beta}R^1{}_2]$ is directed towards the C^{β} or the C^{δ} atom of the butadiynyl ligand. Attack at the C^{β} atom and subsequent ring closure would lead to 1,3-*hetero*binuclear cyclobutenylidene complexes with an alkynyl functionality at C-2 of the ring (**A**; Scheme 2). Such complexes should constitute inter-

 © WILEY-VCH Verlag GmbH, D-69451 Weinheim, 1998 1434−1948/98/0909−1225 $ 17.50+.50/0

esting starting compounds for further derivatization by coupling reactions. An attack at the butadiynyl C^{δ} atom followed by ring closure would lead to complexes of type **B** (Scheme 2) thus extending the conjugated system between the metal centers in cyclobutenylidene complexes.

Scheme 2

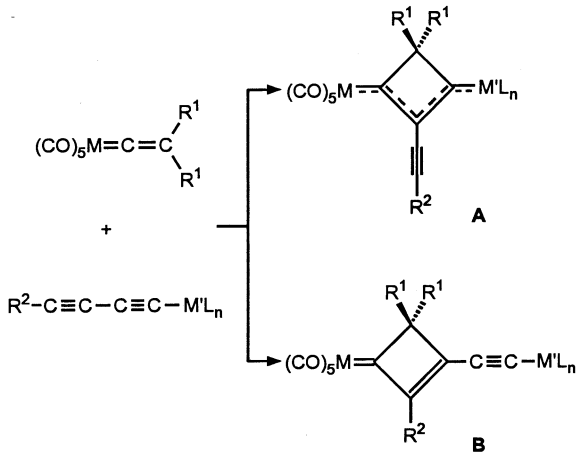

In this paper we report on the syntheses of the first 1,3-*hetero*binuclear cyclobutenylidene complexes with an alkynyl substituent at the bridging ring and on coupling reactions of these complexes leading to new di-, tri-, and tetrametallic systems.

Results and Discussion

The vinylidene complex $[(CO)_5Cr{=}C{=}CMe_2]$ (**1**)[6a] was chosen as the starting compound. Complex **1** was generated by the reaction sequence shown in Scheme 3.

Scheme 3

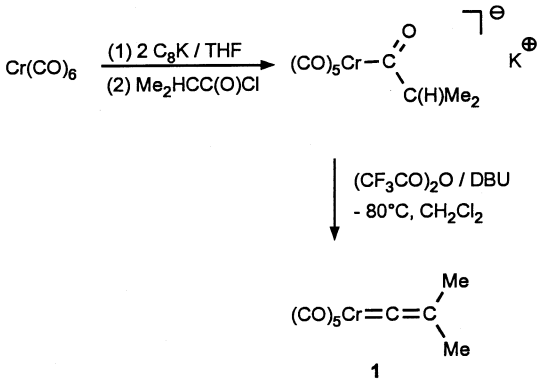

Reduction of $Cr(CO)_6$ with potassium-graphite (C_8K) laminate in tetrahydrofuran at 0°C followed by reaction with isobutyryl chloride afforded pentacarbonyl(isobutyryl) chromate by a method described by M. F. Semmelhack et al.[9]. Treatment of the chromate with trifluoroacetic anhydride/DBU finally gave the vinylidene complex **1**. Compound **1** is thermally very labile. Therefore, **1** was not isolated and its solutions were immediately employed in the subsequent reactions with butadiynyl complexes.

The dicarbonyl-butadiynyl complex $[Cp(CO)_2FeC{\equiv}CC{\equiv}CSiMe_3]$ (**2a**) was prepared in analogy to a previously published procedure[7a] by reaction of $[Cp(CO)_2FeI]$ with $Li[(C{\equiv}C)_2SiMe_3]$, obtained by monodesilylation of 1,4-bis(trimethylsilyl)-1,3-butadiyne with MeLi·LiBr (Scheme 4)[10]. The corresponding phenyl- and *n*-butyl-substituted butadiynyl complexes [**2b** (R = *n*Bu) and **2c** (R = Ph)] were accessible by coupling of $[Cp(CO)_2FeI]$ with $nBu_3Sn{-}C{\equiv}CC{\equiv}C{-}R$ (R = *n*Bu, Ph) in THF with CuI/$[Pd(PPh_3)_4]$ as the catalyst (Scheme 4).

Scheme 4

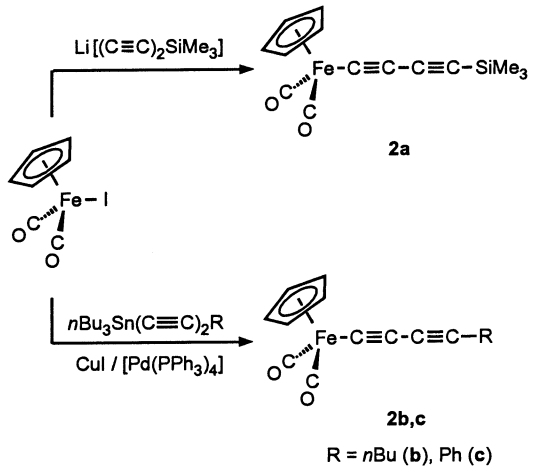

Thermal decarbonylation of **2a** by refluxing in toluene in the presence of PPh_3 yielded the monocarbonyl-butadiynyl complex $[Cp(CO)(PPh_3)FeC{\equiv}CC{\equiv}CSiMe_3]$ (**3a**)[7a] albeit in rather low yield (about 30%). Significantly higher yields were achieved by oxidative decarbonylation of **2a** with trimethylamine *N*-oxide in the presence of PPh_3 at room temperature. By this procedure, complex **3a** was obtained in 63% yield (Scheme 5). The lower yield in the former route is presumably due to competition between formation and decomposition of **3a** at the temperature of boiling toluene.

Scheme 5

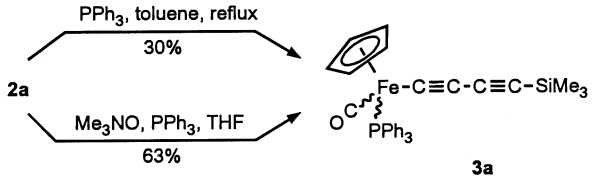

When solutions of the vinylidene complex **1** and the butadiynyl complexes **2a−c** or **3a** in CH_2Cl_2 were combined at −60°C and then warmed to room temperature, the color of the solutions changed within about 30 minutes from green to red. Chromatographic workup of the reaction mixtures afforded the novel 2-alkynyl-substituted 1,3-*hetero*binuclear cyclobutenylidene complexes **4a−c** and **5a** (Scheme 6) in 45−65% yield. Alternatively, complex **5a** was also formed

when **4a** was oxidatively decarbonylated with trimethylamine *N*-oxide in the presence of PPh_3.

Scheme 6

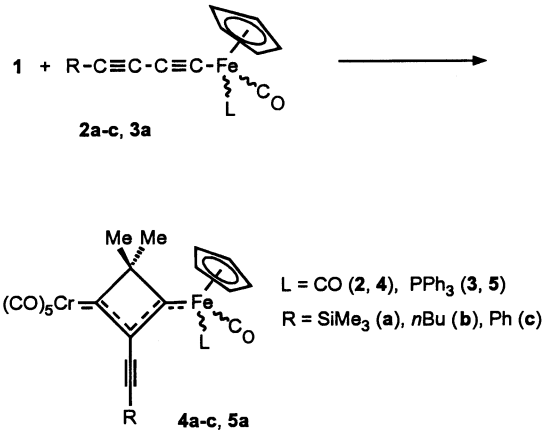

The addition of the butadiynyl complexes $[L_nM-C^{\alpha}\equiv C^{\beta}-C^{\gamma}\equiv C^{\delta}-R]$ to the vinylidene ligand in **1** is highly regioselective. In each case, only the product of cycloaddition of the $C^{\alpha}\equiv C^{\beta}$ bond to the C=C bond of the vinylidene ligand was obtained (complex type **A**; Scheme 2). The formation of isomers derived from cycloaddition of the $C^{\gamma}\equiv C^{\delta}$ bond to the C=C bond of the vinylidene ligand (complex type **B**; Scheme 2) was not detected. Likewise, 1,2-dimetallated cyclobutenylidenes, derived from the inverse regiochemistry of the cycloaddition of either the $C^{\alpha}\equiv C^{\beta}$ or the $C^{\gamma}\equiv C^{\delta}$ bond of the butadiynyl ligand to the C=C bond of the vinylidene ligand, were not observed.

Desilylation of **4a** and **5a** with tetrabutylammonium fluoride (TBAF) in THF afforded the 2-ethynylcyclobutenylidene complexes **6** and **7** after chromatographic workup in 67% and 57% yield, respectively (Scheme 7). The highest yields were obtained when 0.4 equivalents of TBAF was used instead of the stoichiometric amount. Similar observations have been reported for the desilylation of other compounds with TBAF[7a].

Scheme 7

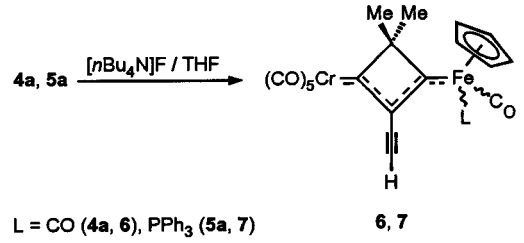

The complexes **4a**, **5a**, **6**, and **7** should constitute convenient starting compounds for the synthesis of tri- and tetranuclear complexes by coupling reactions. In coupling reactions, often amines are employed as the solvent. Therefore, we investigated the reactivity of these 2-alkynyl-substituted cyclobutenylidene complexes towards amines with the example of **4a** and **5a**. In earlier experiments it was observed that a cationic 1,3-*homo*binuclear cyclobutenylidene complex **8** reacts with aqueous Et_3N yielding the iron complex **9** by a formal substitution of "O" for $[Cp(CO)_2Fe]^+$ (Scheme 8)[11]. In contrast, 2-*alkyl*-substituted 1,3-*hetero*binuclear cyclobutenylidene complexes are inert towards amines.

Scheme 8

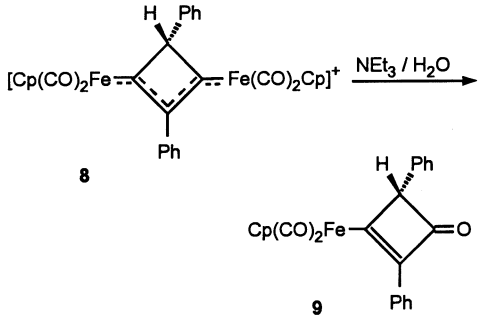

The dicarbonyl complex **4a** reacted rapidly at room temperature in THF with aqueous dimethylamine or with piperidine by substitution of NR_2 for the 3-dicarbonyl(cyclopentadienyl)iron fragment to form the 3-aminocyclobutenylidene complexes **10** and **11** (Scheme 9).

3-Alkoxy-substituted cyclobutenylidene complexes of chromium analogously react with secondary amines HNR_2 by displacement of OR by NR_2 to form 3-aminocyclobutenylidene complexes[12]. These substitution reactions are reminiscent of the aminolysis of alkoxycarbene complexes[13] and emphasize the close relationship of these cyclobutenylidene complexes with π-donor-substituted carbene complexes. Thus, cyclobutenylidene complexes can be regarded as a novel type of vinylogous heteroatom-stabilized carbene complexes. However, the ready displacement of the substituent in 3-position of the cyclobutenylidene complex by amines excludes the use of primary and secondary amines as solvents in coupling reactions with **4a** and **6**. Therefore, palladium-catalyzed C−C coupling reactions require the use of the corresponding *C*-stannylated compound (Stille coupling)[14].

The heterotrinuclear tributyltin-substituted compound **12** was obtained as a red oil by transformation of **4a** with $[nBu_4N]F$ in THF into **6** and subsequent reaction of **6** with nBu_3SnNEt_2 in toluene[15] (Scheme 9). The palladium-catalyzed coupling of **12** with half an equivalent of 1,4-diiodobenzene in the presence of CuI[16] afforded only the monocoupling product **13** (Scheme 9). The formation of a tetranuclear complex by coupling of two molecules of **12** with one molecule of 1,4-diiodobenzene was not observed.

In contrast to **4a**, the triphenylphosphane-substituted cyclobutenylidene complex **5a** did not react with amines to give 3-aminocyclobutenylidene complexes but was inert towards amines presumably due to the better back-bonding properties of $Cp(CO)(PPh_3)Fe$ compared to $Cp(CO)_2Fe$ and thus the reduced electrophilicity of 3-C in **5a**. Therefore, coupling reactions of 3-$Cp(CO)(PPh_3)$Fe-substituted cyclobutenylidene complexes in amines as the solvent should be possible.

This was confirmed by the reaction of **7** with half an equivalent of 1,4-diiodobenzene in $HNEt_2$ and $[Pd(PPh_3)_4]$/

Scheme 9

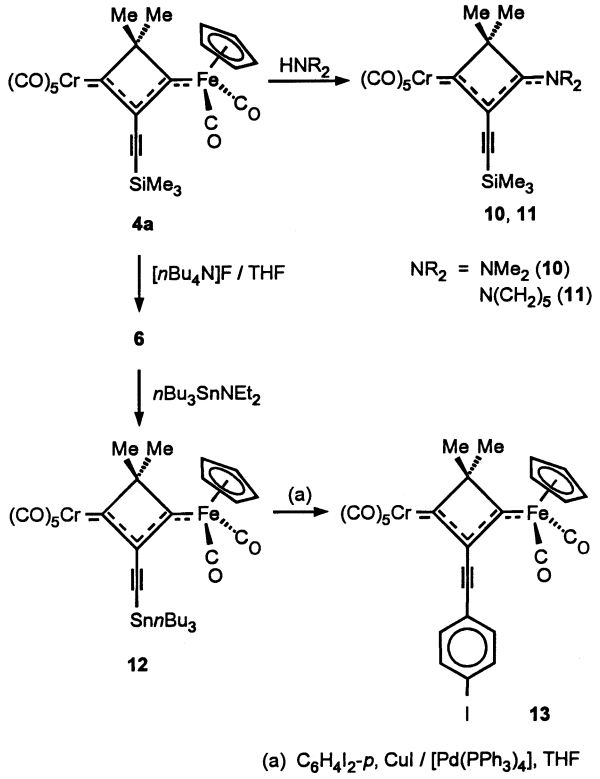

CuI as the catalyst. The mono-coupling product **14** as well as the tetranuclear complex **15** were formed within several hours (Scheme 10) and, after chromatographic workup, obtained in 35% (**14**) and 10% (**15**) yield. Complex **15** was isolated in form of a single diastereomer (*meso* or *R*/*S*).

Scheme 10

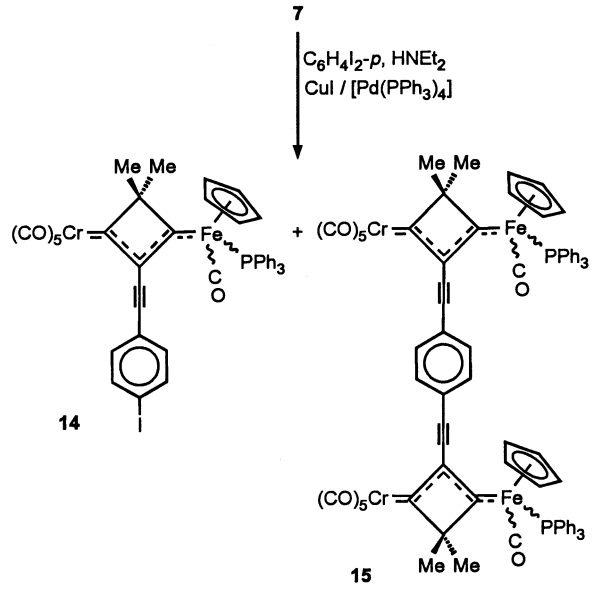

The $[Pd(PPh_3)_4]$/CuI-catalyzed reaction of **7** with *trans*-$[(PEt_3)_2PdCl_2]$ in $HNEt_2$ afforded the mono-coupling product **16** in 23% yield (Scheme 11). In addition to the coupling of both complexes, Pd-coordinated chloride was replaced by iodide from CuI. Presumably, the substitution took place in the trinuclear complex initially formed from **7** and *trans*-$[(PEt_3)_2PdCl_2]$. The displacement of Cl^- for X^- in *trans*-$[(PEt_3)_2Pd(C{\equiv}CR)Cl]$ complexes in the presence of NaX (X = Br, I) has been observed several times[17]. Although a threefold excess of **7** over *trans*-$[(PEt_3)_2PdCl_2]$ was used, the formation of a pentanuclear complex by coupling of *trans*-$[(PEt_3)_2PdCl_2]$ with two molecules of **7** was not detected.

The trimetallic *trans*-chloroplatinum complex **17** was obtained by initial *C*-stannylation of **7** with nBu_3SnNEt_2 in toluene followed by $[Pd(PPh_3)_4]$/CuI-catalyzed coupling of the product with *trans*-$[(PEt_3)_2PtCl_2]$ in THF. A halide exchange was not observed in these reactions. Presumably, free iodide was trapped as nBu_3SnI (Scheme 11). A pentanuclear complex was likewise not detected.

Scheme 11

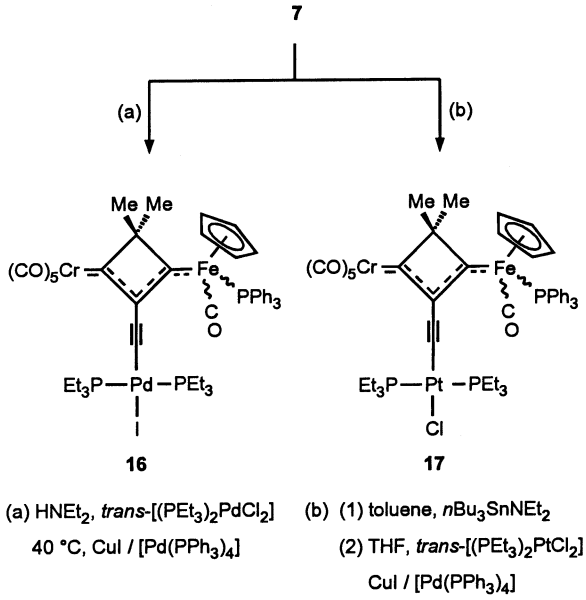

When **11** was stannylated in situ and the resulting derivative then coupled with iodobenzene under Stille conditions complex **5c** was obtained (see Scheme 6).

Spectroscopic Investigations and Molecular Structure of 5a

All new compounds were stable at room temperature and fully characterized by spectroscopic means and by elemental analyses.

The $\tilde{\nu}$(CO) absorptions of the pentacarbonyl chromium moiety in **4**–**7** and **10**–**17** are at rather low wave numbers indicating considerable transfer of electron density from C_4R_3–FeCO(L)Cp to $(CO)_5Cr$. The $\tilde{\nu}$(CO) spectra are similar to those of aminocarbene complexes (e. g. $[(CO)_5Cr{=}C(NHMe)Me]$)[18] and 3-amino-substituted cyclobutenylidene complexes[19] as well as to those of the previously described 1,3-*hetero*binuclear[6] cyclobutenylidene complexes. The positions of the absorptions are strongly influenced by the donor capacity of the substituent in 3-position and shift in the series $Fe(CO)_2Cp$, NR_2, $Fe(CO)(PPh_3)Cp$ towards smaller wave numbers. In contrast, the influence of the substituent in 2-position (alkyl,

C≡C−R) is only small. With increasing donor capacity of R the $\tilde{\nu}$(C≡C) absorption shifts towards smaller wave numbers [R = $SiMe_3$: $\tilde{\nu}$(C≡C) = 2141 cm^{-1} (**5a**); R = *trans*-$(PEt_3)_2PdI$: $\tilde{\nu}$(C≡C) = 2092 cm^{-1} (**16**)].

The ^{13}C resonances of both the chromium- (1-C) and the iron-bound (3-C) ring carbon atoms appear at low field. The 1-C resonance is in the range usually observed for alkoxycarbene complexes (δ = 290−320)[20]. The resonance of the 3-C atom is in the region characteristic for alkenyliron complexes[21]. Increasing the ability of the alkynyl group C≡C−R at 2-C to donate electron density {R = Ph (**4c**) → $SiMe_3$ (**5a**) → *trans*-[$(PEt_3)_2PdI$] (**16**)} leads to an upfield shift of the 1-C and 3-C resonances and to a downfield shift of the 2-C resonance. These results are consistent with earlier observations with 1,3-*hetero*binuclear cyclobutenylidene complexes[6].

In general, the UV/Vis spectra of these cyclobutenylidene complexes are solvent-dependent. The UV/Vis absorption at lowest energy is shifted to shorter wavelength when a nonpolar solvent like pentane is replaced by a more polar one (DMF). However, whereas the solvent dependence of the 3-aminocyclobutenylidene complexes **10** and **11** is pronounced [$\Delta\tilde{\nu}$ = 1930 (**10**), 1820 cm^{-1} (**11**)] that of the 3-Fe(CO)LCp-substituted complexes **5a**, **7**, **14**, and **15** is rather small [$\Delta\tilde{\nu}$ = 80−300 cm^{-1}].

The structure of the complex **5a** was additionally established by an X-ray-structural analysis (Table 1, Figure 1). The C(6)−C(9) [1.401(4) Å] and the C(8)−C(9) distance [1.410(5) Å] are almost equal in length indicating that the resonance structures **C** and **D** (Scheme 12) contribute to almost the same extent to the overall bonding description. The distances are in between the characteristic bond lengths of a $C(sp^2)-C(sp^2)$ single bond (1.46 Å)[22] and a $C(sp^2)=C(sp^2)$ double bond (1.32 Å)[22]. The Cr(1)−C(6) distance [2.054(4) Å] is typical for heteroatom-stabilized carbene complexes[13].

Scheme 12

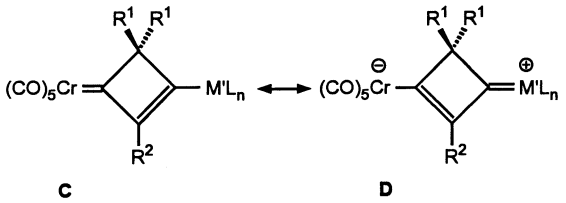

The Fe−C(8) distance is comparable to that in cyclobut-1-en-3-one complexes[21a][21c]. The Fe−C(36) axis in **5a** is almost coplanar with the plane formed by the atoms C(7), C(8), C(9) [torsion angle C(9)−C(8)−Fe(1)−C(36) = 170.9°]. This conformation allows for maximal Fe→C(8) backdonation.

The most striking feature is the nonplanarity of the bridging ligand in **5a**. The puckering angle [angle between the planes formed by the atoms C(7), C(6), C(9) and C(7), C(8), C(9)] is 148.2°. A similar puckering has been observed with other 1,3-*hetero*binuclear cyclobutenylidene complexes[6], however, usually the four-membered ring in 3-amino- and 3-ethoxy-substituted cyclobutenylidene complexes[19], (cyclobut-1-en-3-one)iron complexes[21a][21c], free cyclobut-1-en-3-ones[23], and 1,3-*homo*binuclear cyclobutenylidene complexes[24] is nearly planar. As a consequence of the puckering, the transannular distance C(6)−C(8) in **5a** is small (1.986 Å) and the distance is well below the sum of the van der Waals radii. Therefore, direct electronic exchange cannot be excluded.

Figure 1. Molecular structure of complex **5a** in the crystal (hydrogen atoms are omitted for clarity)[a]

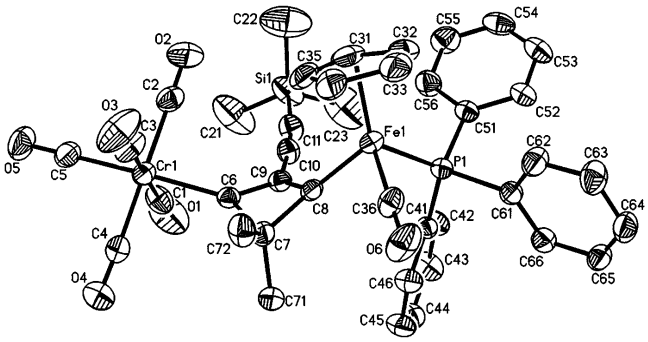

[a] Selected bond lengths [Å], bond angles, and torsion angles [°]: Cr(1)−C(6) 2.054(4), C(6)−C(9) 1.401(4), C(8)−C(9) 1.410(5), C(9)−C(10) 1.428(4), C(10)−C(11) 1.199(5), C(8)−Fe(1) 1.910(4); C(6)−C(9)−C(8) 89.9(3), C(7)−C(6)−C(9) 91.3(3), C(7)−C(8)−C(9) 91.0(3); C(7)−C(6)−C(9)−C(8) 22.7(2).

Conclusion

Our results demonstrate that an alkynyl functionality is readily introduced into the 2-position of 1,3-*hetero*binuclear cyclobutenylidene complexes by [2+2] cycloaddition of butadiynyl complexes to vinylidene complexes. These cyclobutenylidene complexes offer an easy access to a wide range of di-, tri-, and tetranuclear cyclobutenylidene complexes by derivatization of the alkynyl group and coupling reactions. In addition, the substituents in 4- and 3-position can be modified by use of other vinylidene complexes and by variation of the starting butadiynyl complexes.

By substitution of amines for the $Fe(CO)_2Cp$ fragment in **5a** a large variety of amines such as chiral amines can be introduced into the 3-position which is crucial for the nonlinear optical properties of these compounds. Thus, the synthesis of butadiynes $R-C{\equiv}CC{\equiv}C-NR_2$[25], which are rather difficult to prepare, can be avoided.

The nonplanarity of the cyclobutenylidene ring in **5a** decreases the symmetry of the molecule. Thus, taking into account the chirality of the iron center the existence of two diastereomers might be expected. However, only one isomer of **5a** could be isolated and the NMR spectra of **5a** exhibit only one set of signals. Obviously, in solution a rapid inversion of the four-membered ring occurs. For the analogous compound with an *n*Bu substituent at 2-C and a $Cp(PEt_3)Ni$ fragment at 3-C this dynamic process is still fast even at −80 °C[6a].

The geometry of the complexes **7** and **15** is similarly flexible. However, for the diastereoselective coupling of **7** to **15** a second effect has to be considered. Probably due to the steric demand of the bulky PPh_3 substituent, only one isomer of **15** (*meso* or *R*/*S*) was formed. A similar selectivity

has been reported by Gladysz et al. for the formation of comparable cyclobutenylidene complexes[24a].

Support of this work by the *Deutsche Forschungsgemeinschaft* and the *Fonds der Chemischen Industrie* is gratefully acknowledged. We also thank *B. Weibert* for collecting the data set for the X-ray-structural analysis.

Experimental Section

General: All operations were performed under either nitrogen or argon by using standard Schlenk techniques. Solvents were dried by refluxing over CaH_2 (CH_2Cl_2) or sodium/benzophenone ketyl (pentane, Et_2O, THF) and were freshly distilled prior to use. Silica gel (Fa. J. T. Baker; silica gel for flash chromatography) and alumina (Fa. Fluka) used for chromatography were nitrogen-saturated. Flash chromatography was performed at a nitrogen pressure of 1.4 bar. The complexes **1**[6a], **2a**[7a], **3a**[7a], $[Cp(CO)_2FeI]$[26], and $[Pd(PPh_3)_4]$[26] as well as R−C≡C−C≡C−Sn*n*Bu$_3$ (R = *n*Bu, Ph)[27] and *n*Bu$_3$SnNEt$_2$[28] were prepared according to literature procedures. − NMR: Bruker AC 250 (^{1}H and ^{13}C) and Jeol JNX 400 (^{1}H, ^{13}C, and ^{31}P); chemical shifts are reported relative to internal TMS (^{1}H and ^{13}C) or external H_3PO_4 (^{31}P). Unless mentioned otherwise, NMR spectra were recorded in $CDCl_3$ at room temperature. − IR: Biorad FTS 60. − MS: Finnigan MAT 312, modified either for EI or FAB (NBOH or NBOE used as solvent for FAB). − UV/Vis: Hewlett-Packard diode-array spectrophotometer 8452A. − Elemental analyses: Heraeus CHN-O-RAPID.

Dicarbonyl(η^5-cyclopentadienyl)(octa-1,3-diynyl)iron (**2b**): 9.9 g (25.0 mmol) of *n*Bu$_3$Sn−C≡C−C≡C−*n*Bu, 0.3 g (2.0 mmol) of CuI, and 2.5 g (2.0 mmol) of $[Pd(PPh_3)_4]$ were added to a solution of 6.1 g (20.0 mmol) of $[Cp(CO)_2FeI]$ in 150 ml of THF. The reaction mixture was stirred at room temp. for about 1 h. The solvent was evaporated in vacuo and the residue was chromatographed at −20°C first two times with pentane/CH_2Cl_2 (ratio decreasing from 1:0 to 4:1) on alumina and then two times with pentane/CH_2Cl_2 (ratio decreasing from 1:0 to 3:2) on silica gel. The solvent was evaporated in vacuo. The residue was recrystallized from 40 ml of pentane/CH_2Cl_2 (3:2) to give **2b** as a yellow powder. Yield: 2.3 g (32%, based on $[Cp(CO)_2FeI]$), m.p. 45°C. − IR (CH_2Cl_2): $\tilde{\nu}$(CO) = 2040 cm^{-1} vs, 1997 vs; $\tilde{\nu}$(C≡C) = 2203 cm^{-1} vw. − ^{1}H NMR (250 MHz): δ = 0.88 (t, $^3J_{HH}$ = 7.0 Hz, 3 H, CH_3), 1.32−1.51 (m, 4 H, CH_2), 2.24 (t, $^3J_{HH}$ = 6.7 Hz, 2 H, CH_2), 5.06 (s, 5 H, C_5H_5). − ^{13}C NMR (250 MHz): δ = 13.5 (CH_3), 18.7, 21.9, 30.9 (CH_2), 67.1, 67.9, 83.8 (C≡C), 85.2 (C_5H_5), 97.4 (C≡C), 211.4 (CO). − $C_{15}H_{14}FeO_2 \cdot CH_2Cl_2$ (367.0): calcd. C 52.36, H 4.39; found C 51.86, H 3.97.

Dicarbonyl(η^5-cyclopentadienyl)(phenylbuta-1,3-diynyl)iron (**2c**): The synthesis of **2c** from 6.1 g (20.0 mmol) of $[Cp(CO)_2FeI]$, 10.4 g (25.0 mmol) of *n*Bu$_3$Sn−C≡C−C≡C−Ph, 0.3 g (2.0 mmol) of CuI, and 2.5 g (2.0 mmol) of $[Pd(PPh_3)_4]$ in 150 ml of THF and the purification of the product by chromatography first with pentane/CH_2Cl_2 (ratio decreasing from 1:0 to 3:1) on alumina and then with pentane/CH_2Cl_2 (ratio slowly decreasing from 1:0 to 1:1) on silica gel] were carried out similarly to that of **2b**. Recrystallization from 40 ml of pentane/CH_2Cl_2 (1:1) gave **2c**. Yellow powder. Yield: 2.7 g (45%, based on $[Cp(CO)_2FeI]$), m.p. 91°C. − IR (CH_2Cl_2): $\tilde{\nu}$(CO) = 2042 cm^{-1} vs, 1994 vs; $\tilde{\nu}$(C≡C) = 2184 cm^{-1} m. − ^{1}H NMR (250 MHz): δ = 5.06 (s, 5 H, C_5H_5), 7.24, 7.39 (m, br., 5 H, C_6H_4). − ^{13}C NMR (250 MHz): δ = 64.8, 77.3 (C≡C), 85.4 (C_5H_5), 96.2, 97.3 (C≡C), 123.6, 127.5, 128.1, 132.4 (C_6H_5), 211.1 (CO). − MS (EI, 70 eV); *m/z* (%): 302 (38) [M$^+$], 274 (23), 246 (100) [M$^+$ − *n* CO; *n* = 1, 2]. − Although the product was chromatographed several times, it still contained small amounts of tin compounds. Therefore, a satisfactory elemental analysis could not be obtained.

Carbonyl(η^5-cyclopentadienyl)(trimethylsilyl-1,3-diynyl)(triphenylphosphane)iron (**3a**): A THF solution (50 ml) of 3.0 g (10.0 mmol) of **2a**, 0.8 g (10.0 mmol) of Me_3NO, and 4.0 g (15.0 mmol) of PPh_3 was stirred at room temp. The reaction was monitored by IR spectroscopy. After ca. 2 h, the solvent was removed in vacuo, the residue dissolved in 30 ml of CH_2Cl_2 and transferred to a column packed with silica gel. Gradient elution at 0°C with a mixture of pentane/CH_2Cl_2 (ratio slowly decreasing from 1:0 to 3:7) yielded the product as an orange band. After evaporation of the solvent in vacuo, the product was obtained as an orange oil. Yield: 3.4 g (63%, based on **2a**). The product was identified by comparison with literature data.[7a]

Pentacarbonyl{3-dicarbonyl(η^5-cyclopentadienyl)ferrio]-4,4-dimethyl-2-(trimethylsilylethynyl)cyclobut-2-en-1-ylidene}chromium (**4a**): At −60°C, a solution of 1.49 g (5.0 mmol) of **2a** in 50 ml of CH_2Cl_2 was added to a solution of **1**[6a]. The reaction mixture was allowed to slowly warm up to room temp. Then, 50 ml of pentane was added. The resulting suspension was filtered through a 2-cm layer of alumina and the alumina was eluted with CH_2Cl_2. The solvent was removed in vacuo and the residue was chromatographed at −30°C on silica gel. Elution with pentane/CH_2Cl_2 (ratio decreasing from 1:0 to 4:1) gave a red solution. The solvent was removed in vacuo and the residue recrystallized from 20 ml of pentane/CH_2Cl_2 (3:1). Red crystals of **4a**. Yield: 1.79 g (65%, based on $[Cr(CO)_6]$), m.p. 84°C. − IR (CH_2Cl_2): $\tilde{\nu}$(CO) = 2053 cm^{-1} s, 2034 s, 1990 s, 1939 vs; $\tilde{\nu}$(C≡C) = 2148 cm^{-1} vw. − UV/Vis (pentane): λ_{max} (lg ε) = 494 nm (4.212); (DMF): λ_{max} (lg ε) = 492 nm (4.178). − ^{1}H NMR (250 MHz): δ = 0.25 (s, 9 H, $SiMe_3$), 1.33 (s, 6 H, CH_3), 5.25 (s, 5 H, C_5H_5). − ^{13}C NMR (CD_2Cl_2, 250 MHz): δ = −0.4 ($SiMe_3$), 26.4 (CH_3), 74.3 (4-C), 87.1 (C_5H_5), 100.2, 104.4 (C≡C), 180.6 (2-C), 211.9 (Fe−CO), 217.9 (*cis*-CO), 229.2 (*trans*-CO), 251.5 (3-C), 313.3 (1-C). − $C_{23}H_{20}CrFeO_7Si$ (544.3): calcd. C 50.75, H 3.70; found C 50.52, H 3.88.

Pentacarbonyl{3-dicarbonyl(η^5-cyclopentadienyl)ferrio]-4,4-dimethyl-2-(hexa-1-ynyl)cyclobut-2-en-1-ylidene}chromium (**4b**): The synthesis of **4b** from **1** and 1.4 g (5.0 mmol) of **2b** in 50 ml of CH_2Cl_2 at −60°C and the purification of the product with pentane/CH_2Cl_2 (ratio decreasing from 1:0 to 2:1) were carried out analogously to that of **4a**. Red oil. Yield: 1.19 g (45%, based on $[Cr(CO)_6]$). − IR (CH_2Cl_2): $\tilde{\nu}$(CO) = 2051 cm^{-1} m, 2031 s, 1981 vs, 1935 vs; $\tilde{\nu}$(C≡C) = 2142 cm^{-1} vw. − UV/Vis (solvent): λ_{max} (lg ε) = (pentane) 490 nm (4.116), (DMF) 486 nm (4.161). − ^{1}H NMR (CD_2Cl_2, 250 MHz): δ = 0.86 (t, $^3J_{HH}$ = 7.1 Hz, 3 H, CH_3), 1.27 (s, 6 H, CH_3), 1.39−1.54 (m, 4 H, CH_2), 2.41 (t, $^3J_{HH}$ = 6.9 Hz, 2 H, CH_2), 5.14 (s, 5 H, C_5H_5). − ^{13}C NMR (CD_2Cl_2, 250 MHz): δ = 13.8 (CH_3), 19.8, 22.5 (CH_2), 26.8 (CH_3), 30.9 (CH_2), 74.3 (4-C), 75.9 (C≡C), 86.9 (C_5H_5), 100.6 (C≡C), 182.7 (2-C), 212.1 (Fe−CO), 218.3 (*cis*-CO), 228.9 (*trans*-CO), 245.3 (3-C), 304.8 (1-C). − $C_{24}H_{20}CrFeO_7$ (528.0): calcd. C 54.55, H 3.82; found C 54.29, H 4.11. − MS (FAB); *m/z* (%): 528 (22) [M$^+$], 500 (14), 472 (38), 444 (10), 416 (100), 388 (50), 360 (10), 332 (12) [M$^+$ − *n* CO; *n* = 1−7].

Pentacarbonyl{3-dicarbonyl(η^5-cyclopentadienyl)ferrio]-4,4-dimethyl-2-(phenylethynyl)cyclobut-2-en-1-ylidene}chromium (**4c**): The synthesis of **4c** from **1** and 1.5 g (5.0 mmol) of **2c** and the purification of the product were carried out analogously to **4b**. Recrystallization from 20 ml of pentane/CH_2Cl_2 (3:1) gave red crystals of **4c**. Yield: 1.65 g (60%, based on $[Cr(CO)_6]$), m.p. 84°C. − IR (CH_2Cl_2): $\tilde{\nu}$(CO) = 2052 cm^{-1} m, 2033 m, 1989 m, 1937 vs; $\tilde{\nu}$(C≡C) = 2146 cm^{-1} vw. − UV/Vis (pentane): λ_{max} (lg ε) = 494

nm (4.062); (DMF): λ_{max} (lg ε) = 492 nm (4.183). − ^{1}H NMR (CD_2Cl_2, 250 MHz): δ = 1.40 (s, 6 H, CH_3), 5.29 (s, 5 H, C_5H_5), 7.38−7.56 (m, 5 H, C_6H_5). − ^{13}C NMR (CD_2Cl_2, 250 MHz): δ = 26.6 (CH_3), 74.8 (4-C), 84.8 (C≡C), 87.0 (C_5H_5), 98.0 (C≡C), 123.3, 128.9, 131.5, 132.3 (C_6H_5), 180.7 (2-C), 211.9 (Fe−CO), 218.1 (*cis*-CO), 229.0 (*trans*-CO), 250.6 (3-C), 311.5 (1-C). − $C_{26}H_{16}CrFeO_7$ (548.3): calcd. C 56.96, H 2.94; found C 57.12, H 3.06. − MS (FAB); *m/z* (%): 548 (38) [M^+], 520 (22), 492 (40), 464 (10), 436 (100), 408 (52), 380 (10), 352 (30) [$M^+ - n$ CO; n = 1−7].

Pentacarbonyl{3-[carbonyl(η^5-cyclopentadienyl)(triphenylphosphane)ferrio]-4,4-dimethyl-2-(trimethylsilylethynyl)cyclobut-2-en-1-ylidene}chromium (**5a**): The synthesis of **5a** from **1** and 2.7 g (5.0 mmol) of **3a** in 50 ml of CH_2Cl_2 at −60°C, the purification, and the chromatography of the product were carried out analogously to that of **4a**. The red fraction was eluted with pentane/CH_2Cl_2 (ratio decreasing from 1:0 to 1:1). Recrystallization from 20 ml of pentane/CH_2Cl_2 (3:1) gave red crystals of **5a**. Yield: 2.53 g (65%, based on [$Cr(CO)_6$]), m.p. 152°C. − IR (CH_2Cl_2): $\tilde{\nu}$(CO) = 2043 cm^{-1} m, 1950 sh, 1927 vs; $\tilde{\nu}$(C≡C) = 2141 cm^{-1} vw. − UV/Vis (pentane): λ_{max} (lg ε) = 520 nm (4.246); (DMF): λ_{max} (lg ε) = 512 nm (3.889). − ^{1}H NMR (CD_2Cl_2, 250 MHz): δ = 0.26 (s, 9 H, $SiMe_3$), 0.49 (s, 3 H, CH_3), 1.25 (s, 3 H, CH_3), 4.82 (d, $^3J_{PH}$ = 1.5 Hz, 5 H, C_5H_5), 7.41−7.56 (m, 15 H, Ph). − ^{13}C NMR (CD_2Cl_2, 250 MHz): δ = −0.1 ($SiMe_3$), 25.8, 27.9 (CH_3), 76.2 (4-C), 87.2 (C_5H_5), 102.9, 104.1 (C≡C), 128.9, 129.0, 130.8, 130.9, 133.7, 133.9, 135.2, 135.9 (C_6H_5), 183.2 (2-C), 218.4 (d, $^2J_{PC}$ = 30 Hz, Fe−CO), 219.1 (*cis*-CO), 228.6 (*trans*-CO), 276.5 (d, $^2J_{PC}$ = 19 Hz, 3-C), 288.5 (1-C). − $C_{40}H_{35}CrFeO_6PSi$ (778.6): calcd. C 61.69, H 4.53; found C 61.91, H 4.63.

Decarbonylation of **4a** *with Me_3NO in the Presence of PPh_3:* A solution of 1.6 g (3.0 mmol) of **4a**, 0.3 g (3.0 mmol) of Me_3NO, and 1.6 g (6.0 mmol) of PPh_3 in 30 ml of THF was stirred at room temp. The progress of the reaction was monitored by IR spectroscopy. After about 1 h, the solvent was removed in vacuo, the residue dissolved in 15 ml of CH_2Cl_2, and the solution transferred to a chromatography column packed with silica gel. Gradient elution at −20°C with pentane/CH_2Cl_2 (ratio slowly decreasing from 1:0 to 1:1) yielded 1.71 g (72%, based on **4a**) of **5a**.

Pentacarbonyl{3-[carbonyl(η^5-cyclopentadienyl)(triphenylphosphane)ferrio]-4,4-dimethyl-2-(phenylethynyl)cyclobut-2-en-1-ylidene}chromium (**5c**): A solution of 1.4 g (2.0 mmol) of **7** in 5 ml of toluene was treated at room temp. with 0.5 g (2.5 mmol) of Me_3SnNMe_2. The reaction was followed by thin-layer chomatography. After 30 min, the solvent was removed in vacuo. The remaining oil was dissolved in THF (30 ml) and 0.5 g (2.5 mmol) of iodobenzene, 30 mg (0.2 mmol) of CuI, and 280 mg (0.2 mmol) of [$Pd(PPh_3)_4$] were added. The reaction mixture was stirred for 30 min at 40°C. The solvent was removed in vacuo, the residue dissolved in 15 ml of CH_2Cl_2 and chromatographed at −30°C with pentane/CH_2Cl_2 (ratio decreasing from 1:0 to 3:2) on silica gel. A red band was eluted. Recrystallization from 20 ml of pentane/CH_2Cl_2 (1:1) gave red crystals of **5c**. Yield: 1.25 g (76%, based on **7**), m.p. 95°C (dec.). − IR (CH_2Cl_2): $\tilde{\nu}$(CO) = 2043 cm^{-1} m, 1950 sh, 1925 vs, 1901 sh. − UV/Vis (pentane): λ_{max} (lg ε) = 522 nm (3.891); (DMF): λ_{max} (lg ε) = 516 nm (4.122). − ^{1}H NMR (250 MHz): δ = 0.56 (s, 3 H, CH_3), 1.27 (s, 3 H, CH_3), 4.80 (d, $^3J_{PH}$ = 1.5 Hz, 5 H, C_5H_5), 7.28−7.57 (m, 20 H, C_6H_5, PPh_3). − ^{13}C NMR (250 MHz): δ = 25.5, 27.7 (CH_3), 76.0 (4-C), 86.5 (C_5H_5), 97.5, 123.6 (C≡C), 128.2, 128.4, 128.6, 129.5, 130.5, 131.1, 132.8, 133.2, 134.1, 134.4, 134.8, 135.5 (C_6H_5, PPh_3), 182.0 (2-C), 217.8 (d, $^2J_{PC}$ = 29 Hz, Fe−CO), 218.7 (*cis*-CO), 228.1 (*trans*-CO), 275.8 (d, $^2J_{PC}$ = 17 Hz, 3-C), 291.8 (1-C). − ^{31}P NMR: δ = 68.8 (s). − $C_{43}H_{31}CrFeO_6P \cdot 1/2\ CH_2Cl_2$ (824.6): calcd. C 63.35, H 3.91; found C 63.51, H 4.40. − MS (FAB); *m/z* (%): 782 (16) [M^+], 754 (2), 698 (2), 670 (16), 642 (30), 614 (46) [$M^+ - n$ CO; n = 1, 3−6].

Pentacarbonyl{3-dicarbonyl(η^5-cyclopentadienyl)ferrio]-4,4-dimethyl-2-(ethynyl)cyclobut-2-en-1-ylidene}chromium (**6**): At −90°C, 0.4 equiv. of tetrabutylammonium fluoride (1 M solution in THF) was added to a solution of **4a** (5.4 g, 10.0 mmol) in 100 ml of THF. The mixture was warmed to room temp. and stirred for ca. 3 h at room temp. The progress of the reaction was monitored by thin-layer chromatography. The solvent was removed in vacuo and the residue dissolved in 30 ml of CH_2Cl_2. Chromatography at −40°C with pentane/CH_2Cl_2 (ratio decreasing from 1:0 to 1:1) and recrystallization from 20 ml of pentane/CH_2Cl_2 (1:1) afforded red crystals of **6**. Yield: 3.16 g (67%, based on **4a**), m.p. 68°C. − IR (CH_2Cl_2): $\tilde{\nu}$(CO) = 2054 cm^{-1} s, 2033 s, 1990 m, 1938 vs; $\tilde{\nu}$(C≡C) = 2139 cm^{-1} vw, br. − UV/Vis (pentane): λ_{max} (lg ε) = 492 nm (4.206); (DMF): λ_{max} (lg ε) = 486 nm (4.238). − ^{1}H NMR (CD_2Cl_2, 250 MHz): δ = 1.35 (s, 6 H, CH_3), 3.68 (s, 1 H, C≡CH), 5.25 (s, 5 H, C_5H_5). − ^{13}C NMR (CD_2Cl_2, 250 MHz): δ = 26.3 (CH_3), 74.2 (4-C), 79.0, 86.3 (C≡C), 87.0 (C_5H_5), 179.5 (2-C), 211.8 (Fe−CO), 217.8 (*cis*-CO), 229.1 (*trans*-CO), 253.7 (3-C), 315.1 (1-C). − $C_{20}H_{12}CrFeO_7$ (472.2): calcd. C 50.88, H 2.52; found C 50.80, H 2.61.

Pentacarbonyl{3-[carbonyl(η^5-cyclopentadienyl)-(triphenylphosphane)ferrio]-4,4-dimethyl-2-(ethynyl)-cyclobut-2-en-1-ylidene}chromium (**7**): The synthesis of **7** by reaction of **5a** (7.8 g, 10.0 mmol) with 0.4 equiv of tetrabutylammonium fluoride and the purification were performed analogously to **6**. Red crystals of **7**. Yield: 4.24 g (57%, based on **5a**), m.p. 72°C. − IR (CH_2Cl_2): $\tilde{\nu}$(CO) = 2043 cm^{-1} s, 1950 sh, 1927 vs, 1888 sh; $\tilde{\nu}$(C≡C) = 2143 cm^{-1} vw, br. − UV/Vis (pentane): λ_{max} (lg ε) = 518 nm (4.030); (DMF): λ_{max} (lg ε) = 512 nm (4.166). − ^{1}H NMR (CD_2Cl_2, 250 MHz): δ = 0.62 (s, 3 H, CH_3), 1.24 (s, 3 H, CH_3), 3.58 (s, 1 H, C≡C-H), 4.80 (d, $^3J_{PH}$ = 1.5 Hz, 5 H, C_5H_5), 7.39−7.54 (m, 15 H, Ph). − ^{13}C NMR (CD_2Cl_2, 250 MHz): δ = 25.9, 27.4 (CH_3), 76.3 (4-C), 81.3, 86.1 (C≡C), 86.9 (C_5H_5), 128.4, 128.6, 129.0, 129.7, 130.9, 133.2, 133.7, 133.9, 135.1, 135.8 (C_6H_5), 181.8 (2-C), 218.1 (d, $^2J_{PC}$ = 29 Hz, Fe−CO), 219.0 (*cis*-CO), 228.4 (*trans*-CO), 280.7 (d, $^2J_{PC}$ = 17 Hz, 3-C), 289.9 (1-C). − ^{31}P NMR: δ = 68.8 (s). − $C_{37}H_{27}CrFeO_6P \cdot 1/2\ C_5H_{12}$ (742.5): calcd. C 63.98, H 4.35; found C 63.95, H, 4.51. − MS (FAB); *m/z* (%): 706 (8) [M^+], 594 (15), 566 (20), 538 (35) [$M^+ - n$ CO; n = 4, 5, 6], 263 (100) [$HPPh_3^+$].

Pentacarbonyl[3-dimethylamino-4,4-dimethyl-2-(trimethylsilylethynyl)cyclobut-2-en-1-ylidene]chromium (**10**): An aqueous solution of $HNMe_2$ (40%, 0.25 ml, 2.0 mmol) was added at room temp. to a solution of 0.5 g (1.0 mmol) of **4a** in 10 ml of THF. The color of the solution changed within a few minutes from red to yellow. The solvent was removed in vacuo and the residue chromatographed at −20°C on silica gel. With pentane/CH_2Cl_2 (ratio decreasing from 1:0 to 1:1) a yellow band was eluted. Recrystallization from 5 ml of pentane/CH_2Cl_2 (3:1) gave yellow crystals of **10**. Yield: 0.35 g (83%, based on **4a**), m.p. 113°C. − IR (CH_2Cl_2): $\tilde{\nu}$(CO) = 2046 cm^{-1} m, 1971 vw, 1929 vs, 1893 sh; $\tilde{\nu}$(C≡C) = 2146 cm^{-1} w. − UV/Vis (pentane): λ_{max} (lg ε) = 450 nm (4.383); (DMF): λ_{max} (lg ε) = 414 nm (4.290). − ^{1}H NMR (CD_2Cl_2, 250 MHz): δ = 0.20 (s, 9 H, $SiMe_3$), 1.41 (s, 6 H, CH_3), 3.06, 3.42 (s, 6 H, NMe_2). − ^{13}C NMR (CD_2Cl_2, 250 MHz): δ = −0.4 ($SiMe_3$), 23.8 (CH_3), 39.8, 49.9 (NMe_2), 60.7 (4-C), 98.4, 102.0 (C≡C), 134.2 (2-C), 176.1 (3-C), 219.1 (*cis*-CO), 227.2 (*trans*-CO), 307.1 (1-C). − $C_{18}H_{21}CrNO_5Si \cdot 1/10\ CH_2Cl_2$ (420.0): calcd. C 51.82, H 5.08, N,

3.88; found C 51.78, H 5.09, N 3.34. − MS (EI, 70 eV); *m/z* (%): 411 (9) [M^+], 355 (4), 299 (20), 271 (100) [$M^+ - n$ CO; $n = 2, 4, 5$].

Pentacarbonyl[4,4-dimethyl-3-piperidino-2-(trimethylsilylethynyl)cyclobut-2-en-1-ylidene]chromium (**11**): The synthesis of **11** from 0.5 g (1.0 mmol) of **4a** and 1.5 equiv. of piperidine in 10 ml of THF and the purification of the product were carried out similarly to **10**. On chromatography, pentane/CH_2Cl_2 (ratio decreasing from 1:0 to 7:1) was used as the eluant. Recrystallization from 5 ml of pentane/CH_2Cl_2 (6:1) afforded yellow crystals of **11**. Yield: 0.18 g (40%, based on **4a**), m.p. 120°C. − IR (CH_2Cl_2): $\tilde{\nu}$(CO) = 2046 cm^{-1} m, 1970 w, 1926 vs, 1896 sh; $\tilde{\nu}$(C≡C) = 2145 cm^{-1} w. − UV/Vis (pentane): λ_{max} (lg ε) = 450 nm (4.325); (DMF): λ_{max} (lg ε) = 416 nm (4.360). − ^{1}H NMR (CD_2Cl_2, 250 MHz): δ = 0.20 (s, 9 H, $SiMe_3$), 1.40 (s, 6 H, CH_3), 1.77, 3.40, 3.94 (m, br., 10 H, $N(CH_2)_5$). − ^{13}C NMR (CD_2Cl_2, 250 MHz): δ = −0.3 ($SiMe_3$), 23.6 (CH_2), 23.8 (CH_3), 26.3, 26.7, 49.0, 49.9 (CH_2), 60.6 (4-C), 98.5, 102.1 (C≡C), 133.3 (2-C), 173.6 (3-C), 219.2 (*cis*-CO), 227.1 (*trans*-CO), 305.3 (1-C). − $C_{21}H_{25}CrNO_5Si$ (451.5): calcd. C 55.86, H 5.58, N 3.10; found C 55.80, H 5.59, N 3.37. − MS (FAB); *m/z* (%): 451 (45) [M^+], 423 (8), 395 (42), 367 (18), 339 (100), 311 (82) [$M^+ - n$ CO; $n = 1-5$], 260 (50) [$(C_{16}H_{25}NSi)^+$].

Pentacarbonyl{3-dicarbonyl(η^5-cyclopentadienyl)ferrio]-4,4-dimethyl-2-(tri-n-butylstannylethynyl)cyclobut-2-en-1-ylidene}chromium (**12**): At room temp., 0.9 g (2.5 mmol) of nBu_3SnNEt_2 was added to a solution of 0.9 g (2.0 mmol) of **6** in 5 ml of toluene. The progress of the reaction was monitored by thin-layer chomatography. After ca. 5 min, the solvent was removed in vacuo, the residue dissolved in 10 ml of CH_2Cl_2, and chromatographed at −20°C on silica gel with pentane/CH_2Cl_2 (ratio decreasing from 1:0 to 1:1). Complex **12** was obtained as a red oil. Yield: 1.29 g (85%, based on **6**). − IR (pentane): $\tilde{\nu}$(CO) = 2054 cm^{-1} m, 2033 s, 1990 s, 1951 vs, 1938 sh; $\tilde{\nu}$(C≡C) = 2131 cm^{-1} vw, br. − ^{1}H NMR (250 MHz): δ = 0.91 (t, $^3J_{HH}$ = 7.3 Hz, 9 H, CH_3), 1.03−1.09 (m, 6 H, CH_2), 1.29−1.43 (m, 6 H, CH_2), 1.34 (s, 6 H, CH_3), 1.55−1.68 (m, 6 H, CH_2), 5.24 (s, 5 H, C_5H_5). − ^{13}C NMR (250 MHz): δ = 11.1 (CH_3), 13.6, 26.4, 27.0 (CH_2), 28.9 (CH_3), 73.7 (4-C), 86.4 (C_5H_5), 104.2, 105.0 (C≡C), 181.6 (2-C), 211.4 (Fe−CO), 217.5 (*cis*-CO), 228.6 (*trans*-CO), 243.9 (3-C), 308.1 (1-C). −It was not possible to completely remove small amounts of tin compounds. Therefore, a satisfactory elemental analysis was not obtained.

Pentacarbonyl{3-dicarbonyl(η^5-cyclopentadienyl)ferrio]-2-(p-iodophenylethynyl)-4,4-(dimethyl)cyclobut-2-en-1-ylidene}chromium (**13**): Compound **12** was generated in situ from 2.8 g (6.0 mmol) of **6** and 2.2 g (6.0 mmol) of nBu_3SnNEt_2 in 10 ml of toluene as described above. After changing the solvent to THF (100 ml), 1.0 g (3.0 mmol) of $C_6H_4I_2$-*p*, 30 mg (0.2 mmol) of CuI, and 280 mg (0.2 mmol) of [$Pd(PPh_3)_4$] were added. The reaction mixture was stirred for 30 min at 40°C. The solvent was removed in vacuo, the residue dissolved in 20 ml of CH_2Cl_2, and chromatographed at −30°C with pentane/CH_2Cl_2 (ratio decreasing from 1:0 to 2:1) on silica gel. A red band was eluted. Recrystallization from 20 ml of pentane/CH_2Cl_2 (1:1) gave red crystals of **13**. Yield: 0.41 g (20%, based on $C_6H_5I_2$-*p*), m.p. 77°C. − IR (CH_2Cl_2): $\tilde{\nu}$(CO) = 2053 cm^{-1} m, 2033 m, 1984 m, 1937 vs; $\tilde{\nu}$(C≡C) = 2197 cm^{-1} vw. − UV/Vis (pentane): λ_{max} (lg ε) = 494 nm (3.900); (DMF): λ_{max} (lg ε) = 492 nm (4.187). − ^{1}H NMR (CD_2Cl_2, 400 MHz): δ = 1.39 (s, 6 H, CH_3), 5.28 (s, 5 H, C_5H_5), 7.26−7.28, 7.72−7.74 (m, 4 H, C_6H_4I). − ^{13}C NMR (CD_2Cl_2, 400 MHz): δ = 26.2 (CH_3), 74.6 (4-C), 86.8 (C_5H_5), 94.6, 96.7 (C≡C), 122.6, 132.7, 133.5, 137.8 (C_6H_4I), 179.8 (2-C), 211.5 (Fe−CO), 217.7 (*cis*-CO), 228.7 (*trans*-CO), 251.6 (3-C), 313.2 (1-C). − $C_{27}H_{15}CrFeIO_7$ (686.2): calcd. C 47.26, H 2.20; found C 47.36, H 2.29.

Pentacarbonyl{3-[carbonyl(η^5-cyclopentadienyl)-(triphenylphosphane)ferrio]-2-(p-iodophenyl)ethynyl-4,4-(dimethyl)cyclobut-2-en-1-ylidene}chromium (**14**) *and 1,4-Bis({4-pentacarbonylchromium-2-[carbonyl(η^5-cyclopentadienyl)-(triphenylphosphane)ferrio]-3,3-(dimethyl)cyclobut-1-en-4-ylidene}ethynyl)benzene* (**15**): 0.2 g (0.5 mmol) of $C_6H_4I_2$-*p*, 20 mg (0.1 mmol) of CuI, and 120 mg (0.1 mmol) of [$Pd(PPh_3)_4$] were added to a solution of 0.7 g (1.0 mmol) of **7** in 30 ml of $HNEt_2$. The reaction mixture was stirred for 5 h at 40°C. The solvent was removed in vacuo, the residue dissolved in 4 ml of CH_2Cl_2 and then chromatographed at −20°C with pentane/CH_2Cl_2 (ratio decreasing from 1:0 to 4:1) on silica gel. Two slightly different red bands were eluted. The first band contained **14**, the second one **15**.

14: Yield: 0.18 g (38%, based on $C_6H_4I_2$-*p*), m.p. 87°C. − IR (CH_2Cl_2): $\tilde{\nu}$(CO) = 2042 cm^{-1} m, 1948 sh, 1926 vs, 1901 sh. − UV/Vis (pentane): λ_{max} (lg ε) = 522 nm (4.213); (DMF): λ_{max} (lg ε) = 516 nm (4.216). − ^{1}H NMR (400 MHz): δ = 0.58 (s, 3 H, CH_3), 1.25 (s, 3 H, CH_3), 4.79 (s, 5 H, C_5H_5), 7.14−7.69 (m, 19 H, C_6H_4, C_6H_5). − ^{13}C NMR (400 MHz): δ = 25.4, 27.8 (CH_3), 86.5 (C_5H_5), 88.9 (4-C), 94.0, 96.5 (C≡C), 123.2, 128.1, 128.5, 128.6, 128.8, 129.2, 130.5, 132.5, 133.0, 133.3, 133.5, 133.7, 134.9, 135.4, 137.6 (C_6H_4, C_6H_5), 181.5 (2-C), 217.7 (d, $^2J_{PC}$ = 29 Hz, Fe−CO), 218.6 (*cis*-CO), 228.1 (*trans*-CO), 277.3 (d, $^2J_{PC}$ = 17 Hz, 3-C), 294.2 (1-C). − ^{31}P NMR: δ = 68.5 (s). − $C_{43}H_{30}CrFeIO_6P \cdot 1/2\ C_5H_{12}$ (944.1): calcd. C 57.88, H 3.84; found C 57.74, H 3.74. − MS (FAB); *m/z* (%): 908 (6) [M^+], 796 (12), 768 (26), 740 (52) [$M^+ - n$ CO; $n = 4, 5, 6$], 478 (30) [$M^+ - 6$ CO − PPh_3], 383 (100) [$(CpFePPh_3)^+$].

15: Yield: 0.07 g (10%, based on $C_6H_4I_2$-*p*), m.p. 72°C. − IR (CH_2Cl_2): $\tilde{\nu}$(CO) = 2043 cm^{-1} s, 1947 sh, 1925 vs; $\tilde{\nu}$(C≡C) = 2067 cm^{-1} vw. − UV/Vis (pentane): λ_{max} (lg ε) = 522 nm (3.890); (DMF): λ_{max} (lg ε) = 516 nm (4.348). − ^{1}H NMR (CD_2Cl_2, 250 MHz): δ = 0.61 (s, 6 H, CH_3), 1.28 (s, 6 H, CH_3), 4.86 (d, $^3J_{PH}$ = 1.2 Hz, 10 H, C_5H_5), 7.30−7.57 (m, 34 H, C_6H_4, C_6H_5). − ^{13}C NMR (CD_2Cl_2, 250 MHz): δ = 25.9, 27.9 (CH_3), 76.6 (4-C), 87.1 (C_5H_5), 89.7, 97.6 (C≡C), 123.7, 128.9, 129.1, 130.9, 131.4, 133.7, 133.8, 135.2, 135.9 (C_6H_4, C_6H_5), 182.1 (2-C), 218.3 (d, $^2J_{PC}$ = 29 Hz, Fe−CO), 219.2 (*cis*-CO), 228.6 (*trans*-CO), 280.0 (d, $^2J_{PC}$ = 18 Hz, 3-C), 291.1 (1-C). − ^{31}P NMR: δ = 68.5 (s). − $C_{80}H_{56}Cr_2Fe_2O_{12}P_2$ (1487.0): calcd. C 64.62, H 3.80; found C 64.90, H 4.52. − MS (FAB); *m/z* (%): 1487 (25) [M^+], 1402 (4), 1374 (15), 1347 (40), 1319 (88) [$M^+ - n$ CO; $n = 3-6$], 944 (38), 916 (58), 888 (60) [$M^+ - HPPh_3 - n$ CO; $n = 10-12$].

Pentacarbonyl{3-[carbonyl(η^5-cyclopentadienyl)(triphenylphosphane)ferrio]-2-[trans-iodobis(triethylphosphane)palladio]-ethynyl-4,4-(dimethyl)cyclobut-2-en-1-ylidene}]chromium (**16**): 0.4 g (1.0 mmol) of *trans*-[$(PEt_3)_2PdCl_2$], 60 mg (0.3 mmol) of CuI, and 350 mg (0.3 mmol) of [$Pd(PPh_3)_4$] were added to a solution of 2.1 g (3.0 mmol) of **7** in 30 ml of $HNEt_2$. The reaction mixture was stirred for 1 d at 40°C. The solvent was removed in vacuo, the residue dissolved in 15 ml of CH_2Cl_2, and chromatographed at −20°C with pentane/CH_2Cl_2 (ratio decreasing from 1:0 to 1:1) on alumina. An orange band was eluted which was then chromatographed two times at −20°C with pentane/CH_2Cl_2 (ratio decreasing from 1:0 to 1:1) on silica gel. Recrystallization yielded **16** as an orange powder. Yield: 0.27 g (22%, based on *trans*-[$(PEt_3)_2PdCl_2$]), m.p. 82°C. − IR (CH_2Cl_2): $\tilde{\nu}$(CO) = 2042 cm^{-1} m, 1965 sh, 1942 sh, 1919 vs, 1888 sh; $\tilde{\nu}$(C≡C) = 2092 cm^{-1} vw. − ^{1}H NMR (250 MHz): δ = 0.84 (s, 3 H, CH_3), 1.29 (s, 3 H, CH_3), 0.88−1.29 (m, br., 18 H, CH_2CH_3), 2.00−2.30 (m, br., 12 H, CH_2), 4.63 (s, 5 H, C_5H_5), 7.21−7.56 (m, 15 H, C_6H_5). − ^{13}C NMR (250 MHz): δ = 8.4 (PEt_3), 17.5 (m, PEt_3), 27.1, 30.7 (CH_3), 78.2 (4-C), 86.3 (C_5H_5),

103.4 (t, $^3J_{PC}$ = 5 Hz, C≡C), 117.5 (t, $^2J_{PC}$ = 14 Hz, C≡C), 128.0, 128.4, 128.8, 129.4, 130.5, 130.8, 132.9, 133.2, 133.4, 133.6, 135.2, 135.9 (C_6H_5), 192.2 (2-C), 218.7 (d, $^2J_{PC}$ = 32 Hz, Fe−CO), 219.7 (*cis*-CO), 226.3 (*trans*-CO), 236.2 (d, $^2J_{PC}$ = 18 Hz, 3-C), 241.4 (1-C). − ^{31}P NMR: δ = 72.8 (s, PPh_3), 13.8 (s, PEt_3). − $C_{49}H_{56}CrFeIO_6P_3Pd \cdot C_5H_{12}$ (1246.2): calcd. C 52.09, H 5.35; found C 52.20, H 5.06. − MS (FAB); *m/z* (%): 1174 (28) [M^+], 1062 (25), 1034 (10), 1006 (5) [$M^+ - n$ CO; n = 4−6], 916 (10), 888 (12) [$M^+ - n$ CO − PEt_3; n = 5, 6], 800 (10), 772 (15), 744 (15) [$M^+ - PPh_3 - n$ CO; n = 4−6], 383 (100) [$CpFePPh_3^+$].

Pentacarbonyl{3-[carbonyl(η^5-cyclopentadienyl)(triphenylphosphane)ferrio]-2-[trans-chlorobis(triethylphosphane)-platinio]ethynyl-4,4-(dimethyl)cyclobut-2-en-1-ylidene}-chromium (**17**): 1.1 g (3.0 mmol) of nBu_3SnNEt_2 was added at room temp. to a solution of 2.1 g (3.0 mmol) of **7** in 5 ml of toluene. The progress of the reaction was followed by thin-layer chomatography. After 30 min, the solvent was removed in vacuo and the remaining oil dissolved in THF (50 ml). This solution was treated with 0.5 g (1.0 mmol) of *trans*-[$(PEt_3)_2PtCl_2$], 57 mg (0.3 mmol) of CuI, and 350 mg (0.3 mmol) of [$Pd(PPh_3)_4$]. The reaction mixture was stirred for 12 h at room temp. The solvent was removed in vacuo, the residue dissolved in 15 ml of CH_2Cl_2 and chromatographed at −30°C with pentane/acetone (ratio decreasing from 1:0 to 7:3) on silica gel. An orange fraction was eluted. Recrystallization from 20 ml of pentane/CH_2Cl_2 (1:1) yielded **17** as an orange powder. Yield: 0.42 g (36%, based on *trans*-[$(PEt_3)_2PtCl_2$]), m.p. 78°C. − IR (CH_2Cl_2): $\tilde{\nu}$(CO) = 2041 cm^{-1} m, 1963 sh, 1940 sh, 1918 vs , 1889 sh; $\tilde{\nu}$(C≡C) = 2096 cm^{-1} vw. − ^{1}H NMR (CD_2Cl_2, 400 MHz): δ = 0.80 (s, 3 H, CH_3), 1.28 (s, 3 H, CH_3), 1.09−1.26 (m, br., 18 H, CH_2CH_3), 1.85−2.10 (m, br., 12 H, CH_2), 4.62 (s, 5 H, C_5H_5), 7.42−7.59 (m, 15 H, C_6H_5). − ^{13}C NMR (400 MHz): δ = 7.9 (PEt_3), 14.1−14.6 (m, PEt_3), 25.5, 26.8 (CH_3), 77.6 (4-C), 86.3 (C_5H_5), 99.9 (m, C≡C), 128.5, 128.6, 130.3, 133.5, 133.6, 135.4, 135.8 (C_6H_5), 193.2 (2-C), 218.9 (d, $^2J_{PC}$ = 32 Hz, Fe−CO), 219.8 (*cis*-CO), 226.4 (*trans*-CO), 233.9 (3-C), 239.9 (1-C). − ^{31}P NMR: δ = 72.9 (s, PPh_3), 14.1 (s and d, $^1J_{PtP}$ = 2371 Hz, PEt_3). − $C_{49}H_{56}ClCrFeO_6P_3Pt$ (1172.3): calcd. C 50.20, H 4.81; found C 50.00, H 5.06. − MS (FAB); *m/z* (%): 1172 (2) [M^+], 1060 (16), 1032 (38), 1004 (38) [$M^+ - 6$ CO; n = 4−6], 886 (34) [$M^+ - 6$ CO − PEt_3], 769 (26) [$M^+ - 6$ CO − 2 PEt_3 + H], 742 (92) [$M^+ - 6$ CO − PPh_3], 624 (100) [$M^+ - 6$ CO − PPh_3 − PEt_3].

X-ray-Structural Analysis of **5a**: $C_{40}H_{35}CrFeO_6PSi$ (778.6), crystal size 0.3 × 0.3 × 0.3 mm (obtained from pentane/CH_2Cl_2, 3:1), triclinic, $P\bar{1}$, a = 11.555(2), b = 12.599(2), c = 15.382(2) Å, α = 83.83(2), β = 75.10(1), γ = 63.62(1)°, V = 1937.4(5) Å^3, Z = 2, $d_{calcd.}$ = 1.335 g cm^{-3}, μ(Mo-K_α) = 0.760 mm^{-1}, F(000) = 804, Wyckoff scan 4° < 2Θ < 54°, scan rate variable 4.00−30.00° min^{-1} in ω; Δω = 1.40°, T = 244 K, 8873 reflections collected, 8446 independent reflections, 6373 reflections with $F > 4.0\ \sigma(F)$; 451 refined parameters; R = 0.047, R_w = 0.051. Largest difference peak (hole): +0.45 e Å^{-3} (−0.38 e Å^{-3}). Data were collected with a crystal mounted in a glass capillary on a Siemens P4 diffractometer (graphite monochromator, Mo-K_α radiation, λ = 0.71073 Å). The structure was solved by Patterson methods and refined by full-matrix least-squares techniques (Siemens SHELXTL PLUS program package). The positions of the hydrogen atoms were calculated by assuming ideal geometries (d_{C-H} = 0.96 Å) and their coordinates were refined together with the attached C atoms as "riding models". Complete lists of atom coordinates and their thermal parameters have been deposited[29].

☆ Dedicated to Professor *Ernst Otto Fischer* on the occasion of his 80th birthday.

[1] For example: [1a] E. A. Maatta, D. D. Devore, *Angew. Chem.* **1988**, *100*, 583−585; *Angew. Chem. Int. Ed. Engl.* **1988**, *27*, 569−571. − [1b] M. H. Chisholm, *Angew. Chem.* **1991**, *103*, 690−691; *Angew. Chem. Int. Ed. Engl.* **1991**, *103*, 673−674. − [1c] F. Diederich, Y. Rubin, *Angew. Chem.* **1992**, *104*, 1123−1146; *Angew. Chem. Int. Ed. Engl.* **1992**, *31*, 1101−1123. − [1d] W. Beck, B. Niemer, M. Wieser, *Angew. Chem.* **1993**, *105*, 969−996; *Angew. Chem. Int. Ed. Engl.* **1993**, *32*, 923−949. − [1e] H. Lang, *Angew. Chem.* **1994**, *106*, 569−572; *Angew. Chem. Int. Ed. Engl.* **1994**, *33*, 547−550. − [1f] M. J. Irwin, G. Jia, N. C. Payne, R. J. Puddephatt, *Organometallics* **1996**, *15*, 51−57. − [1g] U. H. F. Bunz, *Angew. Chem.* **1996**, *108*, 1047−1049; *Angew. Chem. Int. Ed. Engl.* **1996**, *35*, 968−971. − [1h] W. Weng, T. Bartik, J. A. Gladysz, *Angew. Chem.* **1994**, *106*, 2269−2272; *Angew. Chem. Int. Ed. Engl.* **1994**, *33*, 2199−22021 and literature cited therein.

[2] [2a] J. S. Schumm, D. L. Pearson, J. M. Tour, *Angew. Chem.* **1994**, *106*, 1445−1448; *Angew. Chem. Int. Ed. Engl.* **1994**, *33*, 1360−1363. − [2b] T. Bartik, B. Bartik, M. Brady, R. Dembinski, J. A. Gladysz, *Angew. Chem.* **1996**, *108*, 467−469; *Angew. Chem. Int. Ed. Engl.* **1996**, *35*, 414−417.

[3] A.-M. Giroud-Godquin, P. M. Maitlis, *Angew. Chem.* **1991**, *103*, 370−398; *Angew. Chem. Int. Ed. Engl.* **1991**, *30*, 375−402.

[4] See e.g.: [4a] *Inorganic Materials* (Eds.: D. W. Bruce, D. O'Hare), Wiley, Chichester, **1992**. − [4b] "Inorganic and Organometallic Polymers II: Advanced Materials and Intermediates", *ACS Symp. Ser. 572* (Eds.: P. Wisian-Neilson, H. R. Allcock, K. J. Wynne), American Chemical Society, Washington, DC, **1994**.

[5] H. B. Fyfe, M. Mlekuz, D. Zargarian, N. J. Taylor, T. B. Marder, *J. Chem. Soc., Chem. Commun.* **1991**, 188−190.

[6] [6a] H. Fischer, F. Leroux, G. Roth, R. Stumpf, *Organometallics* **1996**, *15*, 3723−3731. − [6b] H. Fischer, F. Leroux, R. Stumpf, G. Roth, *Chem. Ber.* **1996**, *129*, 1475−1482.

[7] [7a] A. Wong, P. C. W. Kang, C. D. Tagge, D. R. Leon, *Organometallics* **1990**, *9*, 1992−1994. − [7b] R. Crescenzi, C. Lo Sterzo, *Organometallics* **1992**, *11*, 4301−4305. − [7c] P. J. Stang, R. Tykwinski, *J. Am. Chem. Soc.* **1992**, *114*, 4411−4412. − [7d] Y. Sun, N. J. Taylor, A. J. Carty, *Organometallics* **1992**, *11*, 4293−4300. − [7e] P. J. Kim, H. Masai, K. Sonogashira, N. Hagihara, *Inorg. Nucl. Chem. Lett.* **1970**, *6*, 181−185. − [7f] Y. Sun, N. J. Taylor, A. J. Carty, *J. Organomet. Chem.* **1992**, *423*, C43−C47. − [7g] A. Romero, D. Peron, P. H. Dixneuf, *J. Chem. Soc., Chem. Commun.* **1990**, 1410−1412. − [7h] L. D. Field, A. V. George, E. Y. Malouf, I. H. M. Slip, T. W. Hambley, *Organometallics* **1991**, *10*, 3842−3848. − [7i] G. H. Worth, B. H. Robinson, J. Simpson, *Organometallics* **1992**, *11*, 501−513.

[8] D. L. Lichtenberger, S. K. Renshaw, A. Wong, C. D. Tagge, *Organometallics* **1993**, *12*, 3522−3526.

[9] M. F. Semmelhack, G. R. Lee, *Organometallics* **1987**, *6*, 1839−1844.

[10] [10a] A. B. Holmes, G. E. Jones, *Tetrahedron Lett.* **1980**, *21*, 3111−3112. − [10b] A. B. Holmes, C. L. D. Jennings-White, A. H. Schulthess, *J. Chem. Soc., Chem. Commun.* **1979**, 840−842.

[11] [11a] Yu. L. Slovokhotov, A. I. Yanovskyi, V. G. Andrianov, Yu. T. Struchkov, *J. Organomet. Chem.* **1980**, *184*, C57−C60. − [11b] N. E. Kolobova, T. V. Rozantseva, Yu. T. Struchkov, A. S. Batsanov, V. I. Bakhmutov, *J. Organomet. Chem.* **1985**, *292*, 247−256.

[12] C. C. Karl, H. Fischer, unpublished results.

[13] *Transition Metal Carbene Complexes* (Eds.: K. H. Dötz, H. Fischer, P. Hofmann, F. R. Kreissl, U. Schubert, K. Weiss), Verlag Chemie, Weinheim, **1983**.

[14] [14a] C. Lo Sterzo, M. M. Miller, J. K. Stille, *Organometallics* **1989**, *8*, 2331−2337. − [14b] J. K. Stille, *Angew. Chem.* **1986**, *98*, 504−519; *Angew. Chem. Int. Ed. Engl.* **1986**, *25*, 508−523. − [14c] C. Lo Sterzo, J. K. Stille, *Organometallics* **1990**, *9*, 687−694.

[15] [15a] C. Cauletti, C. Furlani, A. Sebald, *Gazz. Chim. Ital.* **1988**, *118*, 1−23. − [15b] K. Jones, M. F. Lappert, *J. Organomet. Chem.* **1965**, *3*, 295−307.

[16] V. Farina, *Pure Appl. Chem.* **1996**, *68*, 73−78.

[17] H.-F. Klein, B. D. Zettel, *Chem. Ber.* **1995**, *128*, 343−350.

[18] E. Moser, E. O. Fischer, *J. Organomet. Chem.* **1969**, *16*, 275−282.

[19] H. Fischer, O. Podschadly, A. Früh, C. Troll, R. Stumpf, A. Schlageter, *Chem. Ber.* **1992**, *125*, 2667−2673.

[20] B. E. Mann, B. F. Taylor, *^{13}C NMR Data for Organometallic Compounds*, Academic Press, London, **1981**.

[21] [21a] A. G. M. Barrett, N. E. Carpenter, J. Mortier, M. Sabat, *Organometallics* **1990**, *9*, 151−156. − [21b] L. S. Chen, D. W. Lichtenberg, P. W. Robinson, Y. Yamamoto, A. Wojcicki, *Inorg. Chim. Acta* **1977**, *25*, 165−172. − [21c] G. G. Alexandrov, V. V. Skripkin, N. E. Kolobova, Yu. T. Struchkov, *Koord. Khim.* **1979**, *5*, 453−458 (*Chem. Abstr.* **1979**, *90*: 178495m).
[22] F. H. Allen, O. Kennard, D. G. Watson, L. Brammer, A. G. Orpen, R. Taylor, *J. Chem. Soc., Perkin Trans. 2* **1987**, S1−S19.
[23] [23a] L. S. Trifonov, A. S. Orahovats, R. Prewo, J. H. Bieri, H. Heimgartner, *J. Chem. Soc., Chem. Commun.* **1986**, 708−709. − [23b] S. Hirokami, T. Takahashi, M. Nagata, T. Yamazaki, *J. Org. Chem.* **1987**, *52*, 2455−2468.
[24] [24a] W. Weng, T. Bartik, M. T. Johnson, A. M. Arif, J. A. Gladysz, *Organometallics* **1995**, *14*, 889−897. − [24b] Yu. L. Slovokhotov, A. I. Yanovskyi, V. G. Andrianov, Yu. T. Struchkov, *J. Organomet. Chem.* **1980**, *184*, C57−C60.
[25] J.-L. Dumont, W. Chodkiewicz, P. Cadiot, *Bull. Soc. Chim. Fr.* **1967**, 1197−1203.
[26] *Handbuch der präparativen Anorganischen Chemie* (Ed.: G. Brauer), Ferdinand Enke Verlag, Stuttgart, **1978**, vol. 2.
[27] G. Himbert, H. Umbach, M. Barz, *Z. Naturforsch.* **1984**, *39b*, 661−667.
[28] K. Sisido, S. Kozima, *J. Org. Chem.* **1962**, *27*, 4051−4052.
[29] Crystallographic data (excluding structure factors) for the structure reported in this paper have been deposited with the Cambridge Crystallographic Data Centre as supplementary publication no. CCDC-101439. Copies of the data can be obtained free of charge on application to CCDC, 12 Union Road, Cambridge CB2 1EZ, UK [fax: int. code + 44(1223)336-033, e-mail: deposit@ccdc.cam.ac.uk].

[98127]

Mesogenic Dinuclear Cyclopalladated Derivatives with Mixed Bridges − Crystal Structure of *cis*-[Bis({4,4′-di-*n*-butoxy}benzylideneaniline-C^2,*N*)-(μ-*n*-butylthiolato)(μ-chloro)dipalladium(II)]

Julio Buey[a], Gustavo A. Díez[b], Pablo Espinet*[a], Santiago García-Granda[c], and Enrique Pérez-Carreño[c]

Departamento de Química Inorgánica, Facultad de Ciencias, Universidad de Valladolid[a],
E-47005 Valladolid, Spain
E-mail: espinet@cpd.uva.es

Laboratorio de Química Inorgánica, Facultad de Químicas, Universidad de Burgos[b],
E-09002 Burgos, Spain

Departamento de Química Física y Analítica, Facultad de Química, Universidad de Oviedo[c],
E-33006 Oviedo, Spain

Received May 14, 1998

Keywords: Liquid crystals / Palladium / Metallomesogens / Orthometallated imine / Thiolate

The dinuclear cyclopalladated compounds $[Pd(\mu\text{-}Cl)Ln]_2$ (**2**) [HLn = *p*-$C_nH_{2n+1}OC_6H_4CH{=}NC_6H_4OC_nH_{2n+1}$-*p* (*n* = 6, 8, and 10)] react with silver thiolates AgSRm (Rm = C_mH_{2m+1}, *m* = 6, 8, 10, and 18) to give dinuclear derivatives with mixed bridges $[Pd_2(\mu\text{-}Cl)(\mu\text{-}SRm)Ln_2]$ (**3**). Treatment of derivatives **2** with silver acetate (Pd/AgOAc = 2:1) or treatment of $[Pd(\mu\text{-}OAc)Ln]_2$ (**1**) with thiols HSRm (Pd/thiol = 2:1) affords acetato-thiolato bridged complexes $[Pd_2(\mu\text{-}OAc)(\mu\text{-}SRm)Ln_2]$ (**4**). In addition to their mesogenic behavior, the most interesting feature of these complexes is the *cis* disposition of the palladium-imine moieties, that can be inferred from their ^{1}H-NMR spectra. The *cis* structure as well as the disposition of the bridges was confirmed by the X-ray diffraction study of **3** (*n* = *m* = 4).

The synthesis of metal-containing liquid crystals is an area of research which has seen a fast development in the last two decades[1]. Cyclometallated compounds of Pd^{II} with imines and related groups have received much attention due to: i) their thermal stability; ii) the variety of ligands useful for orthometallation leading either to calamitic or to discotic mesogens; and iii) the possibility of tuning the mesogenic properties not only by varying the nature or the length of the chains, but also the nature of the bridges in dinuclear complexes. The imine moiety provides the rigid core and flexible chains needed for liquid-crystal behavior, and two of these moieties are fused together upon orthometallation to give a X-bridged dinuclear complex (Figure 1). We have reported in the last years several types of cyclopalladated imine complexes and studied the structure-mesogenic activity relationships[2][3]. It seems from these studies that the acetato-bridged derivatives $[Pd(\mu\text{-}OAc)Ln]_2$ (**1**) are rigid non-planar dimers ("open book" or "butterfly" shaped), both in the solid state and in solution. Because of this unfavorable molecular shape the compounds do not display mesogenic behavior (there are, however, a few exceptions: some chiral-carboxylate derivatives[3], as well as certain carboxylate complexes using azine instead of imine as ligand[4], are mesomorphic). Their NMR spectra show that the acetato-bridged complexes are in fact a mixture of two isomers, depending on the relative arrangement of the two imine moieties (ca. 96% *trans* versus 4% *cis*). On the contrary, planar ("H" shaped) chloro-bridged dimers $[Pd(\mu\text{-}Cl)Ln]_2$ (**2**) contain only the *trans* isomer, and show the widest mesophase ranges (compared to other derivatives with azobenzene or azine as ligands)[5], although both the melting and the clearing points are quite high, above 100 and 200°C respectively. In both structures the separation between the two imine fragments leaves a wide empty space in the central part of the dimer, which could be filled using bridges that contained long alkyl chains. This should have a noticeable effect on the thermal properties of the material.

Figure 1. Sketch of the different space-filling efficiencies for complexes having bridges without or with long alkyl chains

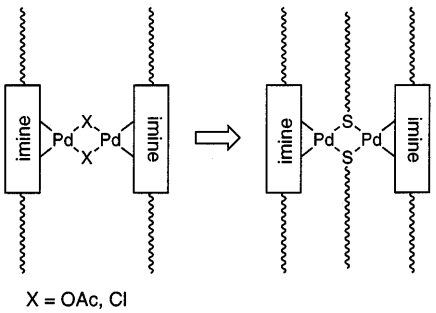

In this paper we report on the attempt of replacing the chloro or acetato groups by thiolates bearing long alkyl chains. They were chosen taking advantage of the tendency of such ligands to form very stable Pd^{II}- or Pt^{II}-bridged complexes[6]. Furthermore, they could be expected to produce a basically planar dimer[7]. The results have shown that using silver thiolates only one of the chloro bridges is displaced, leading to mixed-bridged derivatives.

 © WILEY-VCH Verlag GmbH, D-69451 Weinheim, 1998 1434−1948/98/0909−1235 $ 17.50+.50/0

Scheme 1

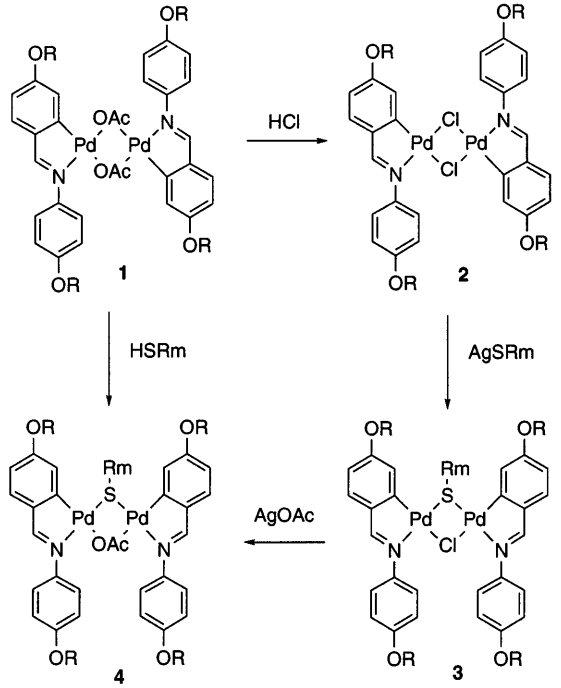

Results and Discussion

Synthesis of the Complexes

Mixed-bridged chloro-thiolate or acetato-thiolate complexes were prepared as shown in Scheme 1. The syntheses of the precursors **1** and **2** have been recently described by our group[3]. Treatment of $[Pd(\mu\text{-Cl})Ln]_2$ (**2**) with the appropriate silver thiolate (AgSRm) in CH_2Cl_2 (Pd/thiolate = 2:1.1) afforded $[Pd_2(\mu\text{-Cl})(\mu\text{-SRm})Ln_2]$ (**3**) in good yields (73−91%). It should be noted that, regardless of the reaction conditions or the ratio Pd/AgSRm used, only monosubstitution was obtained. The replacement of the second chloro bridge yielding $[Pd_2(\mu\text{-OAc})(\mu\text{-SRm})Ln_2]$ (**4**) was achieved by treating derivatives **3** with silver acetate in CH_2Cl_2 (Pd/acetate = 2:1, method A). This kind of complexes could also be obtained by displacement of one acetato bridge in complexes **1** using the corresponding thiol (Pd/thiol = 2:1, method B). Yields were similar (64−86%) in both cases.

All the complexes gave satisfactory elemental analyses, and were characterized by IR and ^{1}H-NMR spectroscopy. The latter is very informative, because both the iminic proton and H^3 are very sensitive to changes in the molecular structure, and the reactions can be monitored using these signals. These ^{1}H-NMR parameters are summarized in Table 2 only for complexes **3** and **4** with $n = m = 6$; the rest of complexes show little variation, within ± 0.03 ppm for the chemical shifts, and unnoticeable for the coupling constants.

Characterization of Complexes 3

The ^{1}H-NMR spectra of these complexes indicate that there is only one thiolato group in the dinuclear molecule. Three isomers are possible (Figure 2), but only one is formed since only one set of signals is observed in the aromatic region.

Figure 2. Sketch of the three possible isomers in mixed-bridged complexes **3** and **4**

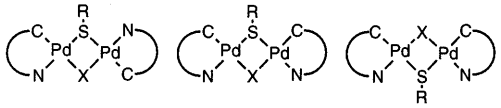

The *trans*-I structure can be discounted since the different environment of the two imines should give rise to two sets of signals. Thus, the disposition of the palladium-imine moieties must be *cis*. The *cis*-II structure is favored because the antisymbiotic behavior of the palladium atom should place the thiolate group *cis* to the metallated carbon

Table 1. ^{1}H-NMR parameters for complexes **3** and **4**[a]

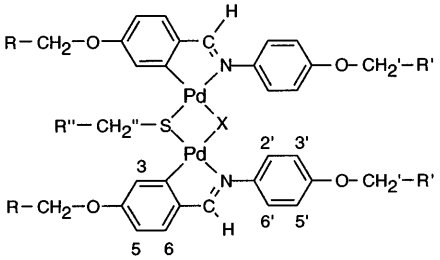

X	H	H^3	H^5	H^6	$H^{2',6'}$[b]	$H^{3',5'}$[b]	O−CH_2/O−CH'_2[c]	S-CH_2''[c]	OTHERS[d]
Cl	7.93 s	7.39 d [2.3]	6.58 dd [8.2, 2.4]	7.28 d [8.3]	7.21 [8.9]	6.80 [8.9]	4.04 t/3.94 t	2.96 t	–
OAc	7.89 s	7.49 d [2.3]	6.48 dd [8.3, 2.3]	7.21 d [8.3]	7.19 [8.9]	6.81 [8.9]	4.00 m/3.88 t	2.46 t	1.62 s $MeCO_2^-$

[a] In $CDCl_3$ at 300.13 MHz; δ values and [*J* in Hz]; key: s, singlet; d, doublet; t, triplet; dd, doublet of doublets; m, multiplet. – [b] Apparent AB system. – [c] Broad signals. – [d] Aliphatic proton signals (R, R′, and R′′) appear in the range δ = 2.0−0.8.

atom[8]. In fact, this structure has been observed in complexes $[M_2(\mu\text{-Cl})(\mu\text{-SR})Cl_2(PR_3)_2]$ (M = Pd or Pt)[9]: for M = Pd only the *cis* isomer was obtained, whereas for M = Pt a mixture of *cis* and *trans* isomers was found. On the contrary, cycloplatinated complexes similar to **3** lead only to the *cis* isomer[10]. Complexes **3** are expected to be basically planar both in solution and in the solid state and the comparable sizes of the chloro- and sulfur-bridging atoms should lead to an approximately parallel arrangement of the two imines.

Bridged dimers with orthopalladated ligands either have *trans* structure, or are mixtures of *cis*/*trans* isomers (*cis* being the minor isomer). Thus, these complexes are interesting for they afford isomerically pure *cis*-cyclopalladated derivatives in high yields. The *cis* arrangement is particularly interesting in view of possible application where a net dipolar moment on the material is required. The proposed structure was confirmed by the X-ray crystal analysis of the complex with $n = m = 4$. This is one of the few X-ray crystal structures of a cyclopalladated mesogen[11], probably due to the difficulty to obtain crystals suitable for X-ray analysis when long aliphatic chains are present. This complex displays an S_A mesophase between 175 and 235°C on heating.

The crystal structure consists of four molecules per unit cell, grouped in pairs. There are two different molecules in each pair (labelled as M1 and M2) in a disposition perpendicular to one another, and parallel to the molecules of the other pair. A perspective ORTEP view of these independent molecules is given in Figure 3. Selected bond lengths and angles are listed in Table 2.

Figure 3. ORTEP view of the two independent molecules, M1 and M2, of complex **3** ($n = m = 4$) showing the atom-labelling scheme

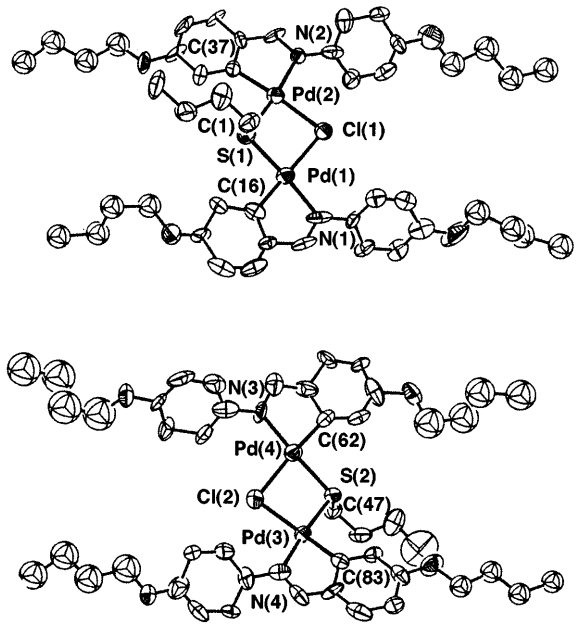

The coordination at each palladium atom is approximately square planar, with maximum deviations from the mean plane of 0.019 (Pd1) and 0.053 (Pd2) Å on M1 and 0.017 (Pd3) and 0.028 (Pd4) Å on M2. The Pd−C bond lengths in the two molecules are slightly different: 2.03(2) and 1.99(2) Å in M1 and 1.93(2) and 1.98(2) Å in M2. They are in good agreement with those described for $[Pd_2(\mu\text{-Cl})_2(\text{imine})_2]$ 1.97 Å[11]. The distances Pd−Cl and Pd−S are also quite similar to those found in complexes of the type $[Pd_2(\mu\text{-Cl})(\mu\text{-SR})Cl_2(PR'_3)_2]$ (R = alkyl or aryl; R′ = Me, Et, Ph)[12]. The small bite of the bidentate imine ligands produces the deviation of the angles around the palladium atoms from the ideal square disposition, 84.2(6) and 79.3(8)° in M1, and 77.8(7) and 83.1(6)° in M2. The angle between the two palladium-imine moieties is small, 16.5(2)° in M1 and 9.1(2)° in M2. The non-bonding Pd−Pd distances within each molecule are 3.443 Å in M1 and 3.437 Å in M2. Due to the tetrahedral coordination of the sulfur atom the first methylene of the thiolate group lies out of the mean Pd−S−Pd plane. The CH_2−S bond makes an angle with this Pd−S−Pd plane of 106° in M1 and 105.2° in M2. However, in both molecules the thiolato chains align themselves in the direction of the long molecular axis.

Table 2. Selected bond lengths [Å] and angles [°] for complex **3** ($n = m = 4$)

M1		M2	
Pd(1)−C(16)	2.03(2)	Pd(4)−C(62)	1.98(2)
Pd(1)−N(1)	2.11(2)	Pd(4)−N(3)	2.065(13)
Pd(1)−S(1)	2.300(6)	Pd(4)−S(2)	2.307(5)
Pd(1)−Cl(1)	2.483(5)	Pd(4)−Cl(2)	2.464(6)
Pd(2)−C(37)	1.99(2)	Pd(3)−C(83)	1.93(2)
Pd(2)−N(2)	2.142(14)	Pd(3)−N(4)	2.13(2)
Pd(2)−S(1)	2.261(6)	Pd(3)−S(2)	2.266(5)
Pd(2)−Cl(1)	2.444(6)	Pd(3)−Cl(2)	2.444(5)
S(1)−C(1)	1.73(2)	S(2)−C(47)	1.90(2)
C(16)−Pd(1)−N(1)	84.2(6)	C(62)−Pd(4)−N(3)	83.1(6)
C(16)−Pd(1)−S(1)	90.3(5)	C(62)−Pd(4)−S(2)	92.4(5)
C(16)−Pd(1)−Cl(1)	172.9(5)	C(62)−Pd(4)−Cl(2)	174.8(5)
N(1)−Pd(1)−S(1)	174.1(4)	N(3)−Pd(4)−S(2)	175.4(4)
N(1)−Pd(1)−Cl(1)	102.4(4)	N(3)−Pd(4)−Cl(2)	100.6(4)
S(1)−Pd(1)−Cl(1)	83.0(2)	S(2)−Pd(4)−Cl(2)	83.8(2)
C(37)−Pd(2)−N(2)	79.3(8)	C(83)−Pd(3)−N(4)	77.8(7)
C(37)−Pd(2)−S(1)	95.2(6)	C(83)−Pd(3)−S(2)	96.2(5)
C(37)−Pd(2)−Cl(1)	173.2(6)	C(83)−Pd(3)−Cl(2)	177.3(6)
N(2)−Pd(2)−S(1)	174.2(5)	N(4)−Pd(3)−S(2)	173.8(5)
N(2)−Pd(2)−Cl(1)	100.6(4)	N(4)−Pd(3)−Cl(2)	100.8(5)
S(1)−Pd(2)−Cl(1)	84.7(2)	S(2)−Pd(3)−Cl(2)	85.1(2)
Pd(1)−S(1)−Pd(2)	98.1(2)	Pd(3)−S(2)−Pd(4)	97.5(2)

Figure 4a shows the crystal packing viewed perpendicular to the long molecular axis. A layer structure can be easily recognized where the molecular long axis is tilted respect to the layer plane, reminiscent of the S_C packing. The molecular arrangement within the layers is better seen in Figure 4b, which shows a view approximately along the molecular axis. It consists in arrays of pairs of molecules in alternate (zig-zag) directions. The minimun Pd−Pd distance between the antiparallel molecules making a pair is Pd(2)−Pd(4) = 4.024 Å. Some other non-bonding distances between the palladium atom and the carbon atoms of the other antiparallel molecule are quite short [e.g. Pd(2)−C(62) = 3.34 Å]. One of the rings linked to the nitrogen atom lies close to the empty space between the cyclopalladated moieties (Figure 4c), thus filling this space. The angles between the free-to-rotate phenyl ring linked to the

nitrogen atom and the cyclometallated ring are quite different 38.7(4)° and 47.2(5)° in M1 and 21.5(4)° and 57.6(5)° in M2, indicating poor conjugation along the imine ligands.

Figure 4. Crystal packing viewed (a) perpendicular to, and (b) approximately along the major molecular axis, (c) Chem3D view of the closest perpendicular molecules; hydrogen atoms are omitted for clarity

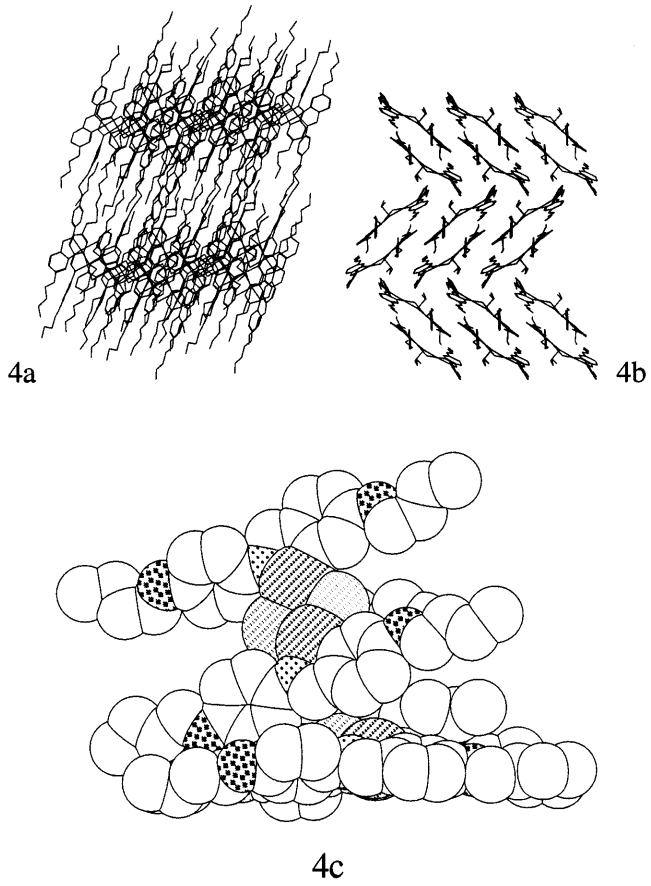

Characterization of Complexes 4

As for **3**, there is only one set of signals in the aromatic region of the ^{1}H-NMR spectra of complexes **4**, indicating the presence of only one isomer. It is assigned the structure *cis*-II (Figure 2) for the same reasons discussed for complexes **3**, and for the previously reported mixed-bridged thiolate-chiral carboxylate derivatives[13]. Both the signal of the first methylene group of the thiolate (δ = 2.47) and the methyl group of the acetato bridge (δ = 1.60) appear upfield with respect to their parent complexes **3** and **1**, respectively. The proposed disposition of the ligands is in agreement with the X-ray structures of similar orthopalladated complexes $[Pd_2(\mu\text{-OAc})(\mu\text{-SR})(\text{imine})_2]$[14] or $[Pd_2(\mu\text{-}CF_3CO_2)(\mu\text{-}t\text{BuS})(\text{C-N})_2]$[15], (C-N = cyclopalladated 8-methylquinoline). According to these structures complexes **4** are not planar in the solid state, showing a folded structure with an average angle of 98° between the two moieties of the molecule in the acetate-thiolate complex above mentioned. In solution the NMR spectra observed are those expected for a planar complex, due to a fast inversion at the sulfur atom[17]. Furthermore, the different size of the two bridges leads to a non-parallel arrangement of the long axes of the imine ligands.

Mesogenic Behavior

All the complexes display liquid-crystal behavior. Their mesophases, nematic (N) and smectic A (S_A), and/or smectic C (S_C) have been identified by their characteristic textures, noticeably more viscous than in organic mesogens[18]. The transition temperatures, as well as the corresponding enthalpies were determined by differential scanning calorimetry and are given in Tables 3 and 4 (in a few cases the transitions could not be detected by DSC and microscope data are given). Figure 5 shows this mesogenic behavior compared to that of the parent dinuclear complexes **2** (for complexes **3**) or **1** (for complexes **4**).

Table 3. Optical, thermal, and thermodynamic data for the complexes **3**[a]

n/*m*	transition	*T* [°C]	ΔH [kJ mol^{-1}]
6/6	C-S_C	129.0	8.0
	S_C-S_A[b]	164.0	–
	S_A-I	210.1[c]	7.3
6/8	C-S_C	126.6	26.8
	S_C-S_A[b]	136.0	–
	S_A-I	189.4[c]	3.2
6/10	C-S_C	102.9	24.3
	S_C-S_A[b]	132.0	–
	S_A-I	196.5[c]	1.5
6/18	C-S_C	103.5	32.0
	S_C-S_A[b]	108.0	–
	S_A-I	192.7[c]	6.1
8/6	C-S_C	115.7	17.7
	S_C-S_A[b]	129.0	–
	S_A-I	193.1[c]	1.9
8/8	C-S_C	101.9	8.9
	S_C-S_A[b]	126.2	–
	S_A-I	192.4[c]	4.9
8/10	C-C′	66.5	−12.7
	C′-S_C	94.5	2.9
	S_C-S_A[b]	129.0	
	S_A-I	192.4[c]	4.2
8/18	C-S_A	111.8	35.5
	S_A-I	187.2[c]	6.2
10/6	C-S_A	115.8	18.7
	S_A-I	196.2[c]	7.0
10/8	C-S_A	118.4	19.9
	S_A-I	179.8[c]	8.8
10/10	C-S_C	108.2	20.5
	S_C-S_A[b]	112.0	–
	S_A-I	184.2[c]	8.6
10/18	C-S_C	114.7	39.8
	S_C-S_A[b]	117.0	
	S_A-I	181.8[c]	

[a] C, C′ = crystal; N = nematic; S_A = smectic A; S_C = smectic C. – [b] Optical microscopy data. – [c] Decomposition.

Complexes **3** show lower melting and clearing temperatures than the chloro complexes **2**. In all cases there is some decomposition at the clearing point. In complexes **4** the improvement of the mesogenic properties is clear, since the acetato complexes **1** are not mesogenic. Furthermore, compared to **1** these complexes display nematic phases for short

Table 4. Optical, thermal, and thermodynamic data for the complexes **4**[a]

n/*m*	transition	T [°C]	ΔH [kJ mol^{-1}]
6/6	C-S_A	154.4	13.7
	S_A-N	168.9	2.5[b]
	N-I	173.2	
6/8	C-S_A	130.8	16.5
	S_A-N	158.0	2.8[b]
	N-I	161.8	
6/10	C-S_A	120.0	19.5
	S_A-I	161.3	3.2
6/18	C-S_A	96.7	13.8
	S_A-N	144.6	2.8[b]
	N-I	146.4	
8/6	C-S_A	126.4	11.4
	S_A-I	172.1	3.8
8/8	C-S_A	124.0	28.5
	S_A-I	156.9	3.3
8/10	C-S_A	112.7	23.5
	S_A-I	146.9	3.0
8/18	C-S_A	81.0	6.4
	S_A-I	145.6	3.6
10/6	C-S_A	106.9	21.4
	S_A-I	163.4	4.2
10/8	C-S_A	114.1	28.2
	S_A-I	149.2	3.6
10/10	C-S_A	116.3	33.7
	S_A-I	141.7	3.5
10/18	C-S_A	67.0	19.1
	S_A-I	136.9	3.7

[a] C = crystal; N = nematic; S_A = smectic A. – [b] Combined enthalpies.

chains in the imines and the thiolate. This phase is not usual in dinuclear cyclopalladated imine mesogens. It is also remarkable that complexes **4** are able to display lyotropic behavior on mixing with linear alkanes or chiral solvents. The derivatives with $n = m = 6$ display broad ranges of nematic (or chiral nematic) lyomesophases, which are maintained until room temperature[16].

Figure 5. Thermotropic behavior of complexes **3** and **4**; *n* and *m* represent the number of carbon atoms in the imine and thiolate, respectively; the left bar on each group corresponds to the chloro-brigded derivative in complexes **3**, and to the acetato-brigded derivative in complexes **4**

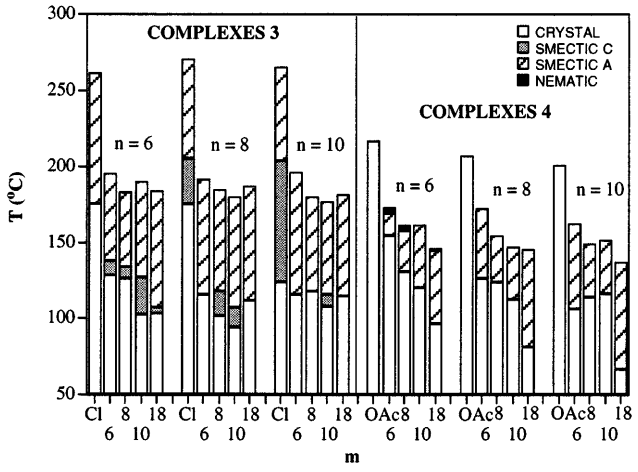

Comparing the properties of compounds **3** and **4**, the influence of the structure on the liquid crystal behavior appears clearly. Planar complexes **3** display quite high transition temperatures as a consequence of the strong intermolecular interactions as well as a good packing of molecules leading to ordered smectic mesophases (S_A, S_C). Changing to the folded structure in complexes **4**, a less efficient packing of molecules leads to lower molecular interactions, less ordered mesophases (appearance of nematic phases), and lower transition temperatures. The stronger molecular interactions in complexes **3** can be also verified looking at the enthalpy figures of the same transition in both families: The crystal to smectic A mesophase gives a value of 21.4 and 18.7 kJ mol^{-1} for the complexes **3** and **4** ($n = 10$, $m = 6$), respectively.

Conclusions

i) Isomerically pure dinuclear complexes with mixed bridges leading to a *cis* structure can be easily prepared. ii) These complexes improve the mesogenic properties of the starting materials, either by decreasing the transition temperatures or by generating new mesophases . iii) The mesogenic properties of this kind of compounds can be doubly tuned, either by varying the nature of the thiolato bridge, or by replacing the second bridge with other bridging groups.

We thank the *Comisión Interministerial de Ciencia y Tecnología* (project MAT96-0708), the *Dirección General de Enseñanza Superior* (project PB96-0556), and the *Junta de Castilla y León* (project VA41/96) for financial support.

Experimental Section

General Procedures and Measurements:. ^{1}H-NMR spectra: Bruker AC-80 or AC-300 MHz spectrometers using $CDCl_3$. – Elemental analyses: Perkin-Elmer 2400 microanalyzer. – IR spectra: Perkin-Elmer 843 spectrophotometer using KBr pellets, unless otherwise noted. – The textures of the mesophases were studied with a Leitz Laborlux-D polarizing microscope, equipped with a Leitz 350 hot stage. – Transition temperatures and enthalpies were measured by differential scanning calorimetry, with a Perkin-Elmer DSC-7 operated at a scanning rate of 5°C min^{-1} on heating, using aluminium crucibles and N_2 as inert gas. The apparatus was calibrated with indium (156.6°C, 28.5 J g^{-1}) as standard.

Materials: CH_2Cl_2 was distilled from CaH_2. Literature procedures were used to synthesize the silver thiolates (AgSRm)[19], [Pd(μ-OAc)Ln]$_2$ (**1**) and [Pd(μ-Cl)Ln]$_2$ (**2**)[3]. AgOAc and aliphatic thiols (HSRm) were obtained from commercial sources and were used without further purification.

Preparation of [Pd_2(μ-Cl)(μ-SRm)Ln_2] (**3**): A solution of **2** (0.2 mmol) in 25 ml of CH_2Cl_2 was treated with a slight excess of the correspondig silver thiolate (Pd/AgSRm = 1:1.1), and the mixture was stirred in the dark for 5 h. The AgCl formed, as well as the excess thiolate, were filtered off and ethanol was added to the solution. Evaporation of the CH_2Cl_2 gave complexes **3** as yellow crystalline solids, which were filtered, washed with ethanol and air-dried. Yields were in the range 75–92%. – IR (KBr): $\tilde{\nu}$ = 1603 s (C=N), 1247 s 1028 m (C–O–C), 1574 s 829 m (Ar) cm^{-1}. – Analysis (%) for each *n*/*m* compound: **6/6**: calcd. C, 59.70; H, 7.24; N, 2.49; found C, 59.64; H, 7.10; N, 2.53. **6/8**: calcd. C, 60.33; H, 7.42; N, 2.43; found: C 60.07, H 7.28, N 2.64. **6/10**: calcd. C 60.93,

H 7.58, N 2.37; found C 61.34, H 7.50, N 2.38. **6/18**: calcd. C 63.07, H 8.17, N 2.16; found C 63.13, H 8.11, N 2.09. **8/6**: calcd. C 62.05, H 7.89, N 2.26; found C 62.44, H 7.71, N 2.30. **8/8**: calcd. C 62.57, H 8.03, N 2.21; found C 62.35, H 7.55, N 2.41. **8/10**: calcd. C 63.07, H 8.17, N 2.16; found C 62.86, H 8.11, N 2.12. **8/18**: calcd. C 64.87, H 8.66, N 1.99; found C 64.66, H 8.37, N 1.92. **10/6**: calcd. C 64.01, H 8.43, N 2.07; found: C 64.11, H 8.19, N 2.09. **10/8**: calcd. C 64.41, H 8.55, N 2.03; found C 64.58, H 8.35, N 1.92. **10/10**: calcd. C 64.87, H 8.66, N 1.99; found C 64.89, H 8.53, N 1.79. **10/18**: calcd. C 66.40, H 9.08, N 1.84; found C 65.97, H 8.79, N 1.94.

Preparation of [Pd_2(μ-OAc)(μ-SRm)Ln_2] (**4**). − *Method A:* AgOAc (0.1 mmol) was added to a solution of **3** (0.1 mmol) in 25 ml of CH_2Cl_2 (Pd/AgOAc = 2:1), and the mixture was stirred in the dark for 1 h. After removal of the AgCl formed, ethanol was added to the solution and the CH_2Cl_2 was removed in vacuo, yielding complexes **4** as yellow crystalline solids, which were filtered, washed with ethanol and air-dried. − *Method B:* To a red solution of **1** (0.1mmol) in 25 ml of CH_2Cl_2 was added the corresponding amount of thiol (0.1 mmol, Pd/HSRm = 2:1). The solution became orange-yellow, and was stirred for 2 h. After addition of ethanol, the solution was worked up as in method A. − Yields were in the range 65−86%. − IR (KBr): $\tilde{\nu}$ = 1605 s (C=N), 1245 s 1028 m (C−O−C), 1574 s 829 m (Ar) cm^{-1}. − Analysis (%) for each *n/m* compound: **6/6**: calcd. C 60.57, H 7.36, N 2.43; found C 60.51, H 7.22, N 2.48. **6/8**: calcd. C 61.16, H 7.52, N 2.37; found C 60.99, H 7.22, N 2.06. **6/10**: calcd. C 61.73, H 7.68, N 2.32; found C 61.66, H 7.53, N 2.25. **6/18**: calcd. C 63.76, H 8.25, N 2.12; found C 63.70, H 8.00, N 2.05. **8/6**: calcd. C 62.79, H 7.98, N 2.22; found C 62.73, H 7.83, N 2.63. **8/8**: calcd. C 63.29, H 8.12, N 2.17; found C 63.25, H 7.91, N 2.25. **8/10**: calcd. C 63.76, H 8.25, N 2.12; found C 63.07, H 8.00, N 1.91. **8/18**: calcd. C 65.48, H 8.73, N 1.95; found C 65.71, H 8.54, N 1.81. **10/6**: calcd. C 64.66, H 8.50, N 2.09; found C 64.61, H 8.01, N 2.37. **10/8**: calcd. C 65.08, H 8.62, N 2.00; found C 65.32, H 8.50, N 1.85. **10/10**: calcd. C 65.48, H 8.73, N 1.96; found C 65.53, H 8.55, N 1.61. **10/18**: calcd. C 66.95, H 9.14, N 1.81; found C 67.04, H 8.94, N 1.55.

Crystal-Structure Determination of **3** (*n* = *m* = 4)[20]: Details of the crystal and refinement data for the structure are given in Table 5.

Suitable yellow single crystals were grown by slow diffusion of a $CHCl_3$ solution of the complex into ethanol at room temperature. All diffraction measurements were made with an Enraf-Nonius CAD-4 single-crystal diffractometer. The unit-cell dimensions were determined from the angular settings of 25 reflections in the range 15° < θ < 22°. The intensity data of 8915 reflections were measured, using the ω-2θ scan technique and a variable scan rate with a maximum scan time of 60 s per reflection. The intensity of the primary beam was checked throughout the data collection by monitoring three standard reflections every 60 min. The final drift correction factors were between 0.96 and 1.09. On all reflections profile analysis was performed[21][22]. 8230 reflections were "observed" with $I > 2\sigma(I)$. Lorentz and polarization corrections were applied and the data were reduced to F_o values. The structure was solved by Patterson methods using the program DIRDIF[23]. After isotropic least-squares refinement, using SHELXL93[24], an empirical absorption correction was applied using DIFABS[25]. The maximum and minimum absorption correction factors were 0.48 and 0.41, respectively. During the final stages of the refinement on F^2, the positional parameters and the anisotropic thermal parameters of the non-H atoms were refined, except the carbon atoms of the *n*-butoxy groups, which were refined isotropically as a rigid group with a common thermal parameter for each group. Hydrogen atoms were isotropically refined riding on their parent atoms with a common thermal parameter. The final conventional agreement factors were $R = 0.042$ and $wR^2 = 0.115$ for the 8230 "observed" reflections and 775 variables. The function minimized was $\Sigma w(F_o - F_c)^2$, $w = 1/[\sigma^2(F_o^2) + 0.0868 \cdot P)^2]$ with $\sigma(F_o)$ from counting statistics and $P = [\max(F_o^2,0) + 2 \cdot F_c^2]/3$. The maximum shift/e.s.d. ratio in the last full-matrix least-squares cycle was 0.019. Atomic scattering factors were taken from International Tables for X-ray Crystallography[26]. Geometrical calculations were made with PARST[27]. The figure showing the coordination and the atomic numbering scheme was drawn by EUCLID package[28]. All calculations were made with VAX computers at the Scientific Computer Center of the University of Oviedo.

Table 5. Crystal data and structure refinement for complex **3** (*n* = *m* = 4)

crystal data	
formula	$C_{46}H_{61}ClN_2O_4Pd_2S$
mol weight	986.28
crystal system	monoclinic
space group	P21
a [Å]	10.275(5)
b [Å]	23.713(7)
c [Å]	18.780(13)
β [°]	93.52(5)
V [Å]^3	4566(4)
Z	4
$D_{calcd.}$ [g cm^{-3}]	1.435
F(000)	2032
μ [$^{-1}$]	0.934
crystal size [mm]	0.36 × 0.25 × 0.20
data collection and refinement	
T [K]	293
θ_{max} [°]	25
radiation, λ [Å]	Mo-K_α ⊥ft parenthesis-graphite), 0.71073
scan type	ω-2θ
data set	*h* −12:12, *k* −28:0, *l* −22:0
total no. of data	8915
obsd. data [$I > 2\sigma(I)$]	8230
no. of refined parameters	775
weighting scheme	$w = 1/[\sigma^2(F_o^2) + (0.0868 \cdot P)^2]$
final *R*, *wR2*	0.042, 0.115
min and max residual density [e Å^{-3}]	−0.57, 0.71

[1] Reviews: A. M. Giroud-Godquin, P. M. Maitlis, *Angew. Chem. Int. Ed. Engl.* **1991**, *30*, 375; P. Espinet, M. A. Esteruelas, L. A. Oro, J. L. Serrano, E. Sola, *Coord. Chem. Rev.* **1992**, *117*, 215; *Inorganic Materials* (Eds.: D. Bruce, D. O'Hare), John Wiley and Sons, Chichester (England), **1992**; S. A. Hudson, P. M. Maitlis, *Chem. Rev.* **1993**, *93*, 861; *Metallomesogens*, J. L. Serrano (Ed.), VCH, Weinheim, Germany, **1996**.

[2] J. Barberá, P. Espinet, E. Lalinde, M. Marcos, J. L. Serrano, *Liq. Cryst.* **1987**, *2*, 833; M. A. Ciriano, P. Espinet, E. Lalinde, M. B. Ros, J. L. Serrano, *J. Mol. Struct.* **1989**, *196*, 327; M. J. Baena, P. Espinet, M. B. Ros, J. L. Serrano, *Angew. Chem. Int. Ed. Engl.* **1991**, *30*, 711; M. J. Baena, P. Espinet, M. B. Ros, J. L. Serrano, A. Ezcurra, *Angew. Chem. Int. Ed. Engl.* **1993**, *32*, 1203; M. J. Baena, J. Barberá, P. Espinet, A. Ezcurra, M. B. Ros, J. L. Serrano, *J. Am. Chem. Soc.* **1994**, *116*, 1899; M. J. Baena, P. Espinet, M. B. Ros, J. L. Serrano, *J. Mater. Chem.* **1996**, *6*, 1291.

[3] J. Buey, P. Espinet, *J. Organomet. Chem.* **1996**, *507*, 137.

[4] P. Espinet, J. Etxebarría, M. Marcos, J. Pérez, A. Remón, J. L. Serrano, *Angew. Chem. Int. Ed. Engl.* **1989**, *28*, 1065; P. Espinet, E. Lalinde, M. Marcos, J. L. Serrano, *Organometallics* **1990**, *9*, 555; P. Espinet, M. Marcos, J. Pérez, M. B. Ros, J. L. Serrano, J. Barberá, A. M. Levelut, *Organometallics* **1990**, *9*, 2028.

[5] M. Ghedini, D. Pucci, G. de Munno, D. Viterbo, S., Armentano, *Chem. Mater.* **1991**, *3*, 65.
[6] P. J. Blower, J. R. Dilworth, *Coord. Chem. Rev.* **1992**, *117*, 215.
[7] M. Capdevila, W. Clegg, P. González-Duarte, B. Harris, I. Mira, J. Sola, I. C. Taylor, *J. Chem. Soc., Dalton Trans.* **1992**, 2817.
[8] F. R. Hartley, *Chem. Soc. Rev.* **1973**, *2*, 163.
[9] J. Chatt, F. G. Mann, *J. Chem. Soc., Dalton Trans.* **1938**, 1949; J. Chatt, F. A. Hart, *J. Chem. Soc., Dalton Trans.* **1953**, 2363.
[10] J. Buey, L. Díez, P. Espinet, H. S. Kitzerow, J. A. Miguel, *Chem. Mater.* **1996**, *8*, 2375.
[11] M. Ghedini, S. Armentano, G. de Munno, A. Crispini, F. Neve, *Liq. Cryst.* **1990**, *8*, 739.
[12] J. H. Yamamoto, G. P. A. Yap, C. M. Jensen, *J. Am. Chem. Soc.* **1992**, *113*, 5060; E. M. Padilla, J. A. Golen, P. N. Richmann, C. M. Jensen, *Polyhedron* **1991**, *10*, 1343; V. K. Jain, R. P. Patel, K. V. Muralidharan, R. Bohra, *Polyhedron* **1989**, *8*, 2151.
[13] M. J. Baena, J. Buey, P. Espinet, G. Heppke, H. S. Kitzerow, *Angew. Chem. Int. Ed. Engl.* **1993**, *32*, 1201.
[14] J. Buey, S. Coco, L. Díez, P. Espinet, J. M. Martín, J. A. Miguel, S. García-Granda, A. Tesouro, I. Ledoux, J. Zyss, *Organometallics* **1998**, *17*, 1750.
[15] J. Ruiz, N. Cutillas, J. Torregosa, G. García, G. López, P. Chaloner, P. B. Hitchcock, R. M. Harrison, *J. Chem. Soc., Dalton Trans.* **1994**, 2353.
[16] N. Usol′tseva, P. Espinet, J. Buey, J. L. Serrano, *J. Mater. Chem.* **1997**, *7*, 215.
[17] M. P. Brown, R. J. Puddephatt, C. E. E. Upton, *J. Chem. Soc., Dalton Trans.* **1976**, 2490; I. G. Dance, *Polyhedron* **1986**, *5*, 1037.
[18] *Textures of Liquid Crystals* (Eds.: D. Demus, L. Ritcher), Verlag Chemie, Weinheim, Germany, **1978**.
[19] M. J. Baena, P. Espinet, M. C. Lequerica, A. M. Levelut, *J. Am. Chem. Soc.* **1992**, *114*, 4182.
[20] Crystallographic data (excluding structure factors) for the structures reported in this paper have been deposited with the Cambridge Crystallographic Data Centre as supplementary publication no. CCDC-101499. Copies of the data can be obtained free of charge on application to CCDC, 12 union Road, Cambridge CB2 1EZ, UK [Fax: int. code + 44(1223)336-033; E-mail: deposit@ccdc.cam.ac.uk].
[21] D. F. Grant, E. J. Gabe, *J. Appl. Crystallogr.* **1978**, *11*, 114.
[22] M. S. Lehman, F. K. Larsen, *Acta Crystallogr.* **1974**, *A30*, 580.
[23] P. T. Beurskens, G. Admiraall, G. Beurskens, W. P. Bosman, S. García-Granda, R. O. Gould, J. M. M. Smits, C. Smykalla, *DIRDIF User's Guide*, Technical Report of the Crystallography Laboratory, University of Nijmegen, The Nederlands, **1992**.
[24] G. M. Sheldrick, "SHELXL93" in *Crystallographic Computing 6* (Eds.: H. D. Flack, P. Parkanyi, K. Simon), IUCr, Oxford University Press, Oxford, England, **1993**.
[25] N. Walker, D. Stuart, *Acta Crystallogr.* **1983**, *A39*, 158.
[26] *International Tables for X-ray Crystallography*, Kynoch Press, Birmingham, England, **1974**, vol. IV (present distributor: Kluwer Academic Publishers, Dordrecht, The Netherlands).
[27] M. Nardelli, *Comput. Chem.* **1983**, *7*, 95.
[28] A. L. Spek, "The EUCLID Package" in *Computational Crystallography* (Ed.: D. Sayre), Clarendon Press, Oxford, England, **1985**, p 528.

[98148]

Syntheses, Structures, and Spectroscopic Properties of *cis,cis*- and *trans,cis*-[Ru(I)(Me)(CO)$_2$(α-diimine)] Complexes

Cornelis J. Kleverlaan[a], Derk J. Stufkens*[a], Jan Fraanje[b], and Kees Goubitz[b]

Anorganisch Chemisch Laboratorium, Institute of Molecular Chemistry, Universiteit van Amsterdam[a], Nieuwe Achtergracht 166, NL-1018 WV Amsterdam, The Netherlands

Laboratorium voor Kristallografie, Institute of Molecular Chemistry, Unmiversiteit van Amsterdam[b], Nieuwe Achtergracht 166, NL-1018 WV Amsterdam, The Netherlands

Received March 20, 1998

Keywords: Ruthenium / α-Diimine ligand / Carbonylmetal compounds / Isomers /X-ray structure / Resonance Raman spectra

The syntheses, structures, and spectroscopic properties are reported for *trans,cis* and *cis,cis* isomers of [Ru(I)(Me)(CO)$_2$(α-diimine)] [α-diimine = *N,N′*-diisopropyl-1,4-diazabutadiene (*i*Pr-DAB), pyridine-2-carbaldehyde *N*-isopropylimine (*i*Pr-PyCa), 4,4′-dimethyl-2,2′-bipyridine (dmb)] which differ in their photochemical behaviour. The structures of *trans,cis*- and *cis,cis*-[Ru(I)(Me)(CO)$_2$(*i*Pr-DAB)] have been determined by a single-crystal X-ray diffraction study. The crystals of both isomers are monoclinic and belong to the same $P2_1/n$ space group with $Z = 4$. Refinement converged to $R = 0.043$ for the *trans,cis* isomer and to $R = 0.065$ for the *cis,cis* isomer. Both complexes have a distorted octahedral geometry, in the *cis,cis* isomer the methyl ligand is located in an equatorial, the iodide in an axial position. According to the ^{1}H- and ^{13}C-NMR and resonance Raman spectra the imine groups of the *i*Pr-DAB ligand are inequivalent in the *cis,cis* isomer. The absorption spectra vary with the α-diimine, not so much with the isomeric structure of the complex. Both isomers possess two visible absorption bands, which, according to the resonance Raman spectra, belong to charge transfer transitions from mixed metal-halide orbitals to the α-diimine. The resonance Raman spectra show that this charge transfer excitation is accompanied, for both isomers, with an angular distortion of the methyl ligand. These spectral data show that the difference in photochemical behaviour of the two isomers is not due to a change in the excited state character.

Introduction

Many transition metal complexes having a lowest metal-to-ligand charge transfer (MLCT) excited state undergo efficient energy and electron transfer processes. Best studied in this respect are the complexes $[Ru(bpy)_3]^{2+}$[1][2][3] and $[Re(L')(CO)_3(bpy)]^{n+}$ ($n = 0$, 1; bpy = 2,2′-bipyridine; L′ = halide, O- or N-donor ligand)[4][5][6][7][8], and their derivatives. The $[Re(L')(CO)_3(\alpha\text{-diimine})]^{n+}$ complexes have the special property that variation of L′ not only influences the energy and character of the lowest excited state but may also change its reactivity. For instance, the metal−metal-bonded complexes [(L$_n$M)Re(CO)$_3$(α-diimine) [L$_n$M = (CO)$_5$Mn, (CO)$_5$Re, (CO)$_4$Co, Cp(CO)$_2$Fe] show a homolytic splitting of the Re−metal bond on irradiation with visible light.[4][9][10][11][12][13][14][14][15][16][17][18][19][20][21][22][23] Such homolysis reactions have also been observed for the Mn complexes [(CO)$_5$Mn−Mn(CO)$_3$(α-diimine)][13][18] and the Ru compounds [(L$_n$M)Ru(Me)(CO)$_2$(α-diimine)] [L$_n$M = (CO)$_5$Mn, (CO)$_5$Re, (CO)$_4$Co][24][25] and [Ru(SnPh$_3$)$_2$(CO)$_2$(α-diimine).[25][26] Similar photoreactions occur for the metal−alkyl (R) complexes [M(R)(CO)$_3$(α-diimine)] (M = Mn, Re)[27][28][29][30][31], [Ru(X)(R)(CO)$_2$(α-diimine)] (X = halide)[31][32], [Ir(R)(CO)(PAr$_3$)$_2$(mnt)][33], [Pt(Me)$_4$(α-diimine)][34], and [Zn(R)$_2$(α-diimine)][35], and even for the metal−halide complexes *mer*-[Mn(X)(CO)$_3$(α-diimine)].[36][37] These homolysis reactions are assumed to occur from a reactive $^3\sigma\pi^*$ state in which σ represents the high-lying σ-bonding orbital, and π* the lowest unoccupied orbital of the α-diimine ligand. Nearly all metal−metal-bonded complexes show at room temperature an efficient homolysis reaction, whereas the reactivity of the metal−alkyl complexes strongly depends on the nature of the alkyl group. For instance, the complexes [Re(R)(CO)$_3$(α-diimine)] (R = Et, Bzl) photodecompose into radicals with high quantum yield ($\Phi > 0.8$), whereas the quantum yield is only 0.05 for the corresponding [Re(Me)(CO)$_3$(*i*Pr-DAB)] complex.[27] Similarly, in the case of [Ru(X)(R)(CO)$_2$(*i*Pr-DAB)] (X = halide; R = Me, Et, *i*Pr, Bzl), the isopropyl and benzyl complexes show a high efficiency for their homolysis reaction, whereas the methyl and ethyl complexes do not undergo such a reaction.[32] A preliminary study showed that the complex *trans,cis*-[Ru(I)(Me)(CO)$_2$(dmb)] does not undergo a homolysis reaction, but is yet photolabile. It photoisomerises from its thermally stable *trans*(I,Me),*cis*(CO,CO) conformation into one of the two *cis,cis* isomeric forms. This photoproduct is photostable but thermally regenerates the parent *trans,cis* complex. In order to understand this remarkable behaviour, we have undertaken a structural and spectroscopic study of the *trans,cis* and *cis,cis* isomers. The results of this study are presented in this article.

The syntheses and molecular structures of several of these complexes have been first described by tom Dieck and

 © WILEY-VCH Verlag GmbH, D-69451 Weinheim, 1998 1434−1948/98/0909−1243 $ 17.50+.50/0

co-workers[38][39], while the complexes have been used for an acylation reaction by Vrieze and co-workers.[40][41] The related complexes $[Ru(Cl)_2(CO)_2(\alpha\text{-diimine})]$ are known to form selectively stereoisomers.[42] It will be shown that in the case of the complexes under study only one of the possible four stereoisomers presented in Figure 1 [structure **IIb**] is formed.

Figure 1. General molecular structures of the different isomers of $[Ru(I)(Me)(CO)_2(\alpha\text{-diimine})]$ and of the α-diimine ligands used

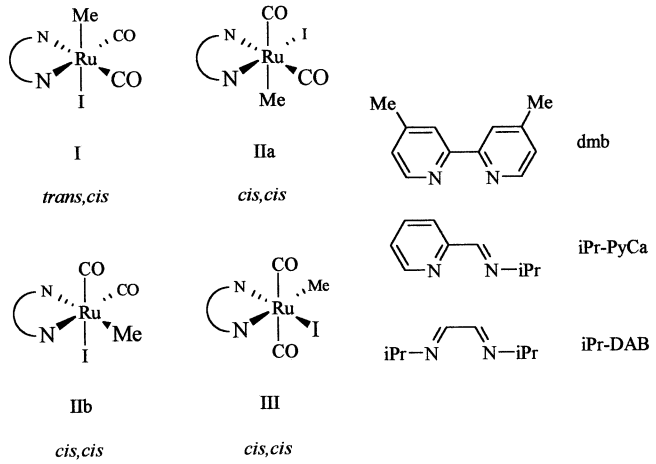

Results and Discussion

From the various *trans,cis*- and *cis,cis*-$[Ru(I)(Me)(CO)_2(\alpha\text{-diimine})]$ complexes which were synthesised, two isomers are structurally characterised by X-ray diffraction, the others by spectroscopic means. After presentation of the X-ray data, attention will be paid to several aspects of the synthesis procedure, in particular to the identity of the intermediates **1** and **2** of this reaction. Finally, the spectroscopic data of the complexes will be reported and discussed.

Crystal Structure of *trans,cis*-[Ru(I)(Me)(CO)$_2$(*i*Pr-DAB)]

Table 1 presents the bond lengths and bond angles of the non-hydrogen atoms of the complex. The ORTEP drawing of Figure 2 shows its *trans,cis* geometry.

Figure 2. Molecular structure and selected atom numbering of the non-hydrogen atoms (ORTEP drawing at 50% probability) of *trans,cis*-$[Ru(I)(Me)(CO)_2(i\text{Pr-DAB})]$

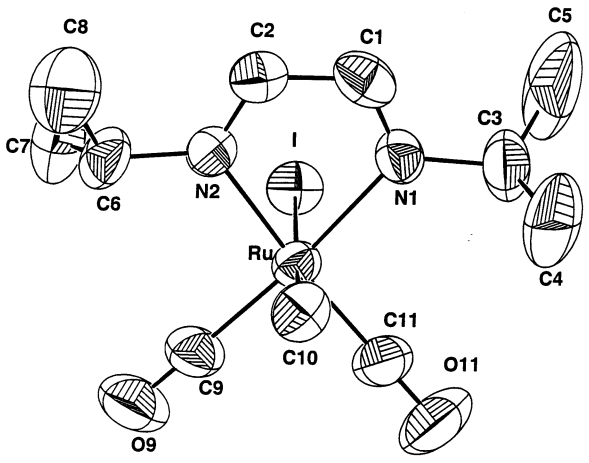

The *i*Pr-DAB ligand is σ(N1)−σ(N2)-bonded to the ruthenium centre, just as in the case of $[Ru(Me)(CO)_2(i\text{Pr-DAB})]^+OTf^-$[43], [Ru(I){C(O)Me}(CO)$_2$(*i*Pr-DAB)][43] and [Ru(I)(Me)(*i*Pr-DAB)(nbd)].[44] The bite angle of 76.8(2)°, which causes the deviation from a regular octahedral structure, has also been found for these complexes. The Ru−Me bond length [2.183(9) Å] is comparable with those of the Ru−C bonds in the complexes $[Ru(Me)(CO)_2(i\text{Pr-DAB})]^+OTf^-$ [2.122(9) Å][43], [Ru(Me)(Mn(CO)$_5$)(CO)$_2$(*i*Pr-PyCa)] [2.148(5) Å][45], $[Ru(Me)(CO)_2(i\text{Pr-DAB})]_2$ [2.152(5) Å][39] and [Ru(I)(Me)(*i*Pr-DAB)(nbd)] [2.222(13) Å].[44] The Ru−I bond length [2.7998(9) Å] is comparable with that of the same bond in $[Ru(I)(Si(Me)_2Ph)(CO)_2(NH_2CH_2C_6H_5)_2]$ [2.848(1) Å][46], [Ru(I){C(O)Me}(CO)$_2$(*i*Pr-DAB)] [2.811(9) Å][43] and [Ru(I)(Me)(*i*Pr-DAB)(nbd)] [2.878(1) Å].[44] It is somewhat larger than found for this bond in $[Ru(I)_2(CO)_2(i\text{Pr-DAB})]$ [2.711(8) Å][32] and $[Ru(I)_2(CO)_2(\text{pTol-DAB})]$ [2.708(1) Å][47] due to the much larger *trans* influence of the methyl group compared to I^-. The Ru−CO bonds (ca. 1.870 Å) are slightly longer than those of $[Ru(Me)(CO)_2(i\text{Pr-DAB})]^+OTf^-$ [1.847(9) Å][43], but comparable in length with those of [Ru(I){C(O)Me}(CO)$_2$(*i*Pr-DAB)] [1.874(7) Å].[43]

Crystal Structure of *cis,cis*-[Ru(I)(Me)(CO)$_2$(*i*Pr-DAB)]

The bond lengths and angles are collected in Table 2, while the ORTEP drawing of the complex is presented in Figure 3.

Figure 3 confirms the *cis,cis* conformation of the complex with the methyl ligand in the equatorial plane and the iodide in an axial position. The structural data agree well with those of the *trans,cis* isomer discussed above and with those of the related complexes [Ru(I){C(O)Me}(CO)$_2$(*i*Pr-DAB)][43], $[Ru(Me)(CO)_2(i\text{Pr-DAB})]^+OTf^-$[43], $[Ru(I)_2(CO)_2(\text{pTol-DAB})]$[47], $[Ru(I)_2(CO)_2(i\text{Pr-DAB})]$[32], and [Ru(I)(Me)(*i*Pr-DAB)(nbd)].[44] The complex has a distorted octahedral geometry [I−Ru−C(10) 176.8(7)°]. The *i*Pr-DAB ligand has a bite angle of 75.7(5)°, which is slightly smaller than found for the corresponding *trans,cis* complex [76.8(2)°]. Since the CO ligand has a smaller *trans* influence than the methyl group, the Ru−I bond is shorter [2.754(2) Å] than in the case of *trans,cis*-[Ru(I)(Me)(CO)$_2$(*i*Pr-DAB)] [2.7998(9) Å]. The bond lengths given in Table 2 for Ru−C(9) and Ru−C(11) are not very accurate. In the complex O(9) is divided in such a way that the CO and Me ligand are both equally distributed over the two possible positions, resulting in the introduction of two half O positions [O(9) and O(11)].

Mechanism of the Complex Formation

The reactions leading to the formation of the two isomers are presented in Scheme 1. The reaction of $[Ru_3(CO)_{12}]$ with MeI in acetonitrile (MeCN) results in the formation of an unknown product **1a**, which has ν(CO) vibrations at 2058(s), 1996(s), and 1637 cm^{-1}, and which is converted thermally into a second species **2a** having ν(CO) bands at 2041(s) and 1974(s) cm^{-1}. Both **1a** and **2a** react with an α-

Table 1. Bond lengths and angles of the non-hydrogen atoms of *trans,cis*-[Ru(I)(Me)(CO)$_2$(*i*Pr-DAB)] with standard deviations in parentheses

bond	length [Å]	bond	length [Å]	bond	length [Å]
Ru−I	2.7998(9)	C(1)−C(2)	1.48(1)	C(6)−C(7)	1.50(2)
Ru−C(9)	1.870(8)	C(1)−N(1)	1.25(1)	C(6)−C(8)	1.52(2)
Ru−C(10)	2.183(9)	C(2)−N(2)	1.26(1)	C(6)−N(2)	1.49(1)
Ru−C(11)	1.869(9)	C(3)−C(4)	1.52(2)	C(9)−O(9)	1.12(1)
Ru−N(1)	2.111(6)	C(3)−C(5)	1.37(2)	C(11)−O(11)	1.14(1)
Ru−N(2)	2.105(6)	C(3)−N(1)	1.51(1)		
bonds	**angle [°]**	**bonds**	**angle [°]**	**bonds**	**angle [°]**
I−Ru−C(9)	93.9(3)	C(10)−Ru−N(2)	85.1(3)	C(7)−C(6)−N(2)	109.2(8)
I−Ru−C(10)	175.4(2)	C(11)−Ru−N(1)	97.7(3)	C(8)−C(6)−N(2)	113.6(9)
I−Ru−C(11)	92.4(3)	C(11)−Ru−N(2)	172.8(3)	Ru−C(9)−O(9)	178.3(8)
I−Ru−N(1)	86.6(2)	N(1)−Ru−N(2)	76.8(2)	Ru−C(11)−O(11)	176.1(8)
C(9)−Ru−C(10)	89.9(4)	C(2)−C(1)−N(1)	117.2(7)	Ru−N(1)−C(1)	114.5(5)
C(9)−Ru−C(11)	88.5(4)	C(1)−C(2)−N(2)	116.6(8)	Ru−N(1)−C(3)	123.4(6)
C(9)−Ru−N(1)	173.8(3)	C(4)−C(3)−C(5)	120(1)	C(1)−N(1)−C(3)	122.0(7)
C(9)−Ru−N(2)	97.1(3)	C(4)−C(3)−N(1)	109.7(9)	Ru−N(2)−C(2)	114.9(5)
C(10)−Ru−C(11)	90.4(4)	C(5)−C(3)−N(1)	116(1)	Ru−N(2)−C(6)	123.9(5)
C(10)−Ru−N(1)	89.4(3)	C(7)−C(6)−C(8)	111.9(9)	C(2)−N(2)−C(6)	121.2(7)

Figure 3. Molecular structure and selected atom numbering of the non-hydrogen atoms (ORTEP drawing at 50% probability) of *cis,cis*-[Ru(I)(Me)(CO)$_2$(*i*Pr-DAB)]

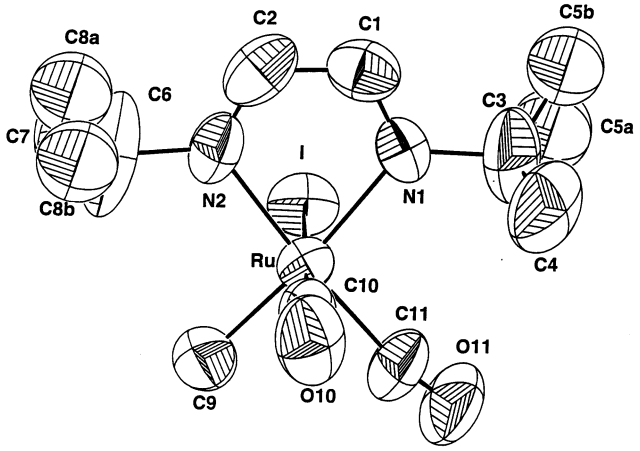

diimine ligand. Thus, adding one equivalent of the α-diimine to a solution of **2a** results in the formation of *cis,cis*-[Ru(I)(Me)(CO)$_2$(α-diimine)], which has been structurally characterised with X-ray diffraction for α-diimine = *i*Pr-DAB (vide supra). The *cis,cis* isomers transform thermally within 3−7 days into the *trans,cis* isomers. On reaction of a *cis,cis* isomer with AgOTf, the halide (I^-) is replaced by OTf^-. This OTf complex can easily be converted into the *trans,cis* isomer by adding an excess of (nBu)$_4$NI.

In order to elucidate the structure of the first product in the reaction sequence, **1a**, the reaction between [Ru$_3$(CO)$_{12}$] and MeI was first brought to completion with formation of product **2a**. This solution was then put under 1 atm of CO and after 2 h **2a** was completely converted into **1a**. On addition of one equivalent of *i*Pr-DAB, **1a** produced a mixture of two complexes in a 4:1 ratio, which are assigned to *cis, cis*- and *trans,cis*-[Ru(I){C(O)Me}(CO)$_2$(*i*Pr-DAB)], respectively, with the use of their ^{1}H-NMR spectra.[48] Attempts to separate the two isomers failed. From the formation of these products by reaction of **1a** with *i*Pr-DAB it is tentatively concluded that **1a** is the acyl derivative of **2a**.

The structure of intermediate **2a** could not be determined by ^{1}H-NMR spectroscopy because of its low solubility and dynamic behaviour on the NMR time scale. Because of this, [Ru$_3$(CO)$_{12}$] was allowed to react with benzyl bromide (BzlBr) instead of with MeI. Intermediate **2b** is then formed as a major product with ν(CO) bands at 2042(s) and 1979(s) cm^{-1}, very similar to those of product **2a**. On addition of one equivalent of *i*Pr-DAB to **2b**, *cis,cis*-[Ru(Br)(Bzl)(CO)$_2$-(*i*Pr-DAB)] is formed, which in turn transforms within 30 min into the thermodynamically more stable *trans,cis* isomer. As **2a** and **2b** selectively produce the *cis,cis* isomers, these intermediates will neither represent *trans,cis,cis*-[Ru(X)(R)(CO)$_2$(MeCN)$_2$], analogous to *trans,cis,cis*-[Ru(Cl)$_2$(CO)$_2$(C$_6$H$_5$CN)$_2$][49] and *trans,cis,cis*-[Ru(Cl)$_2$-(CO)$_2$(pyridine)$_2$][50], nor the thermodynamically unfavourable all-*cis*-[Ru(I)(Me)(CO)$_2$(MeCN)$_2$]. The ^{1}H-NMR spectrum of **2b** shows that the complex possesses one equivalent of both the Bzl and acetonitrile (MeCN) ligands. Intermediates **2** are therefore proposed to be the dimeric species [Ru(X)(R)(CO)$_2$(MeCN)]$_2$ [X = I, R = Me (**2a**); X = Br, R = Bzl (**2b**)]. Figure 4 presents four possible structures of this dimer. The ^{1}H-NMR spectrum of **2b** clearly shows a diastereotopic effect on the CH_2 group of the benzyl ligand. Since a similar effect is observed for *cis,cis*-[Ru(Br)(Bzl)(CO)$_2$(*i*Pr-DAB)] it is concluded that structures **2.II** of Figure 4 are the most likely ones of **2**. For, if **2** had one of the **2.I** structures, a single resonance would have been observed for the CH_2 group, just as in the case of *trans,cis*-[Ru(Br)(Bzl)(CO)$_2$(*i*Pr-DAB)]. The formation of the *cis,cis*-[Ru(X)(R)(CO)$_2$(α-diimine)] complexes from the dimeric intermediates [Ru(X)(R)(CO)$_2$(MeCN)]$_2$ (**2**) is then straightforward. The α-diimine substitutes MeCN (L) and chelation of this ligand occurs after rupture of an Ru−X bond. As the weaker Ru−X bond *trans* to R will preferably be broken, this celation reaction leads to the formation of

Table 2. Bond lengths and angles of the non-hydrogen atoms of *cis,cis*-[Ru(I)(Me)(CO)$_2$(*i*Pr-DAB)] with standard deviations in parentheses

bond	length [Å]	bond	length [Å]	bond	length [Å]
Ru−I	2.754(2)	C(1)−N(1)	1.28(3)	C(6)−N(2)	1.51(2)
Ru−C(9)	1.97(2)	C(2)−N(2)	1.27(3)	C(6)−C(8a)	1.46(8)
Ru−C(10)	1.88(2)	C(3)−C(4)	1.50(4)	C(6)−C(8b)	1.40(5)
Ru−C(11)	2.01(2)	C(3)−N(1)	1.55(2)	C(9)−O(9)	0.99(3)
Ru−N(1)	2.15(1)	C(3)−C(5a)	1.29(8)	C(10)−O(10)	1.03(3)
Ru−N(2)	2.15(1)	C(3)−C(5b)	1.48(4)	C(11)−O(11)	0.97(3)
C(1)−C(2)	1.45(3)	C(6)−C(7)	1.50(4)		
bonds	**angle [°]**	**bonds**	**angle [°]**	**bonds**	**angle [°]**
I−Ru−C(9)	89.8(6)	C(11)−Ru−N(2)	174.5(7)	N(2) -C(6)−C(8a)	116(3)
I−Ru−C(10)	176.8(7)	N(1)−Ru−N(2)	75.7(5)	N(2)−C(6)−C(8b)	117(2)
I−Ru−C(11)	89.3(6)	C(2)−C(1)−N(1)	118(2)	C(8a)−C(6)−C(8b)	41(4)
I−Ru−N(1)	86.6(3)	C(1)−C(2)−N(2)	118(2)	Ru−C(9)−O(9)	175(2)
I−Ru−N(2)	88.3(4)	C(4)−C(3)−N(1)	105(1)	Ru−C(10)−O(10)	178(2)
C(9)−Ru−C(10)	88.1(8)	C(4)−C(3)−C(5a)	135(4)	Ru−C(11)−O(11)	169(2)
C(9)−Ru−C(11)	86.7(8)	C(4)−C(3)−C(5b)	113(2)	Ru−N(1)−C(1)	114(1)
C(9)−Ru−N(1)	173.0(7)	N(1)−C(3)−C(5a)	120(4)	Ru−N(1)−C(3)	124(1)
C(9)−Ru−N(2)	98.2(7)	N(1)−C(3)−C(5b)	118(2)	C(1)−N(1)−C(3)	121(1)
C(10)−Ru−C(11)	88.2(9)	C(5a)−C(3)−C(5b)	54(4)	Ru−N(2)−C(2)	115(1)
C(10)−Ru−N(1)	95.7(7)	C(7)−C(6)−N(2)	107(2)	Ru−N(2)−C(6)	125(1)
C(10)−Ru−N(2)	94.4(7)	C(7)−C(6)−C(8a)	115(3)	C(2)−N(2)−C(6)	119(2)
C(11)−Ru−N(1)	99.3(6)	C(7)−C(6)−C(8b)	136(2)		

Scheme 1. Proposed mechanism for the reaction of [Ru$_3$(CO)$_{12}$] with RX and α-diimine

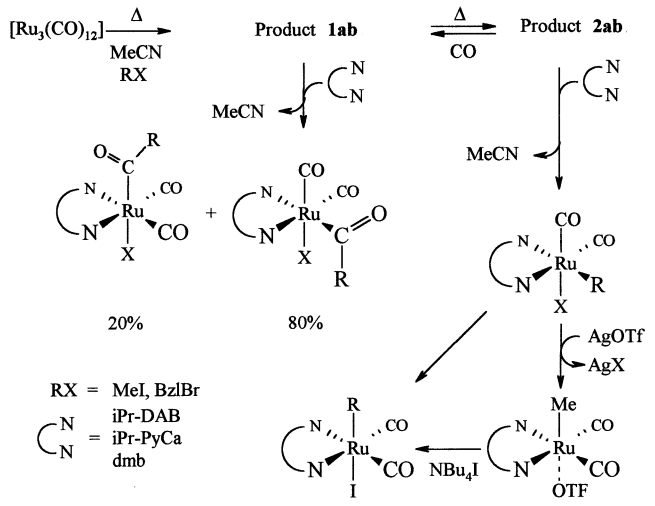

a *cis,cis* isomer in which R occupies an equatorial position and the remaining halide an axial one.

Figure 4. Relevant structures of [Ru(X)(R)(CO)$_2$(MeCN)]$_2$

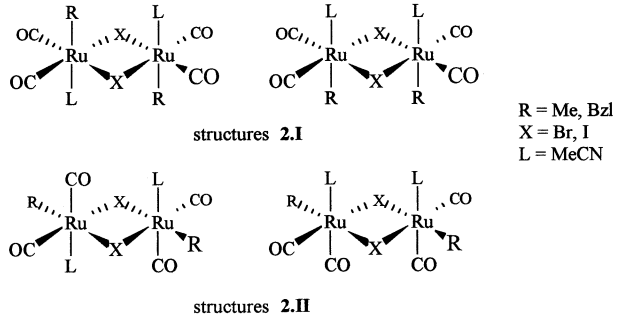

^{1}H- and ^{13}C-NMR Spectra

The structures of the *cis,cis* and *trans,cis* isomers of the *i*Pr-PyCa and dmb complexes were not determined by X-ray diffraction but were instead deduced from their ^{1}H- and ^{13}C-NMR spectra. The *trans,cis*-[Ru(I)(Me)(CO)$_2$(*i*Pr-DAB)] complex has C_s symmetry, and in agreement with this a simple pattern for the ^{1}H and ^{13}C resonances is observed.[40] The corresponding *cis,cis* complex has no symmetry anymore and two sets of proton and carbon signals are therefore expected for the coordinated *i*Pr-DAB ligand. These sets are indeed observed (see Experimental Section). However, due to the small difference in resonance frequencies in both the ^{1}H- and ^{13}C-NMR spectra, the sets of signals can not be assigned separately to the two imine parts of the *i*Pr-DAB ligand positioned *trans* to the methyl and CO ligand, respectively.

For the complex *trans,cis*-[Ru(I)(Me)(CO)$_2$(dmb)] only one set of signals is observed in the NMR spectra, just as for *trans,cis*-[Ru(I)(Me)(CO)$_2$(bpy)].[51] The *cis,cis* isomer shows again two sets of resonances in the ^{1}H- and ^{13}C-NMR spectra, with small shifts comparable to those observed for the *i*Pr-DAB complex. These ^{1}H-NMR data exclude the formation of the *cis*(I,Me),*cis*(CO,CO) complex, with the iodide equatorial and the methyl group axial. The ^{1}H-NMR spectrum of *cis,cis*-[Ru(Cl)$_2$(CO)$_2$(R-PyCa)], with the chloride *trans* to the imine moiety, shows a resonance for H^6, which is shifted down field by approximately 0.5 ppm with respect to that of H^6 in the *trans,cis*-[Ru(Cl)$_2$(CO)$_2$(R-PyCa)] complex.[42] This shift is not found for *cis,cis*-[Ru(I)(Me)(CO)$_2$(dmb)], and these signals are accordingly assigned to the latter conformation, with the methyl in an equatorial and the iodide in an axial position.

The complexes of the asymmetric ligand *i*Pr-PyCa can in principle form two diastereoisomers (Figure 5), both con-

Figure 5. General molecular structures of the diastereoisomers of *cis,cis*-[Ru(I)(Me)(CO)$_2$(*i*Pr-PyCa)]

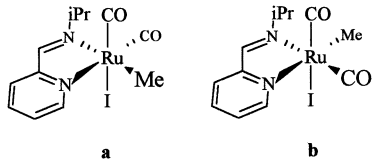

a **b**

sisting of two enantiomers. ^{1}H- and ^{13}C-NMR data reveal that only one diastereoisomer of *cis,cis*-[Ru(I)(Me)(CO)$_2$-(*i*Pr-PyCa)] is formed, since only one set of resonances is observed for the pyridine and imine moieties of the *i*Pr-PyCa ligand. This diastereoisomer is proposed to have structure **a** (see Figure 5) with a carbonyl ligand *trans* to the strongly σ-donating and weakly π-accepting pyridine moiety and the methyl *trans* to the more weakly σ-donating and more strongly π-accepting imine part of the *i*Pr-PyCa ligand. A similar structure had been found for *cis,cis*-[Ru(Cl)$_2$(CO)$_2$(R-PyCa)], which has the chloride in a *trans* position with respect to the imine moiety.[42] Based on the ^{1}H- and ^{13}C-NMR data alone, it is not possible to assign the position of the halide ligand. In order to confirm this proposal and prove the structure, an NOE-difference experiment was performed. These spectra show that an interaction exists between the methyl ligand and H^6 of the pyridine moiety. Thus, the methyl ligand coordinates selectively *trans* with respect to the imine group, which confirms that the complex has the structure (**a**) of Figure 5.

It has been shown above that replacement of the methyl ligand by CO has hardly any influence on the NMR resonances of the *trans*-positioned α-diimine ligand. In contrast with this, changing the position of the methyl ligand from axial (*trans* to I$^-$) to equatorial (*trans* to the α-diimine) on going from the *trans,cis* isomer to the *cis,cis* isomer, has a pronounced effect on the NMR signals of the methyl group. The methyl signals of the *cis,cis* complexes are observed in the region δ = 0.78−0.93, and those of the *trans,cis* complexes in the region δ = 0.08−0.10 (^{1}H NMR).[40][41] This shift is most probably due to through-space interaction between the methyl and the iodide, when these ligands are in a *cis* position.[42]

Electronic Absorption Spectra

The absorption spectral data of the complexes are collected in Table 3. Figure 6 (left) presents the spectra of the complexes *cis,cis*-[Ru(I)(Me)(CO)$_2$(L)] (L = dmb, *i*Pr-PyCa, and *i*Pr-DAB) in toluene. For comparison the spectra of both *trans,cis*- and *cis,cis*-[Ru(I)(Me)(CO)$_2$(*i*Pr-DAB)] in toluene are depicted in Figure 6 (right).

In a previous article it was shown that the *trans,cis*-[Ru(X)(Me)(CO)$_2$(α-diimine)] (X = halide) complexes possess two visible absorption bands, the relative intensities of which depend on the halide used.[51] In accordance with a similar behaviour observed for the corresponding *fac*- and *mer*-[Mn(X)(CO)$_3$(bpy)] complexes[36], these two bands were then assigned to charge transfer transitions to the α-diimine ligand from two sets of orbitals having metal (d$_\pi$)−halide (p$_\pi$) bonding and anti-bonding character, respectively. In the case of the iodide complexes one of the iodide p$_\pi$ orbitals has the largest contribution to the HOMO and the lowest-energy transition of *trans,cis*-[Ru(I)-(Me)(CO)$_2$(α-diimine)] has therefore predominant halide to α-diimine (XLCT) character. The transitions of the higher energy band have mainly MLCT character.[51]

Table 3. Absorption maxima [nm] and solvatochromism [Δ is σ_{max}(MeCN) − σ_{max}(toluene) in cm^{-1}] of *trans,cis*- and *cis,cis*-[Ru-(I)(Me)(CO)$_2$(α-diimine)]

Compound	λ_{max} (MeCN)	λ_{max} (THF)	λ_{max} (toluene)	Δ
cis,cis-[Ru(I)(Me)(CO)$_2$(dmb)]	384; 344	405; 363	416; 374	2003; 2331
trans,cis-[Ru(I)(Me)(CO)$_2$(dmb)]	372	397	410	2491
cis,cis-[Ru(I)(Me)(CO)$_2$(*i*Pr-PyCa)]	420; 378	438; 394	470; 403	2533; 1641
trans,cis-[Ru(I)(Me)(CO)$_2$(*i*Pr-PyCa)][a]		427; 350		
cis,cis-[Ru(I)(Me)(CO)$_2$(*i*Pr-DAB)]	460; 383	478; 395	505; 416	1937; 2071
trans,cis-[Ru(I)(Me)(CO)$_2$(*i*Pr-DAB)][a]	436; 360	463; 374	485; 386	2320; 1870

[a] From ref.[51].

Figure 6. Left: Electronic absorption spectra of *cis,cis*-[Ru-(I)(Me)(CO)$_2$(α-diimine)] (dmb = ——, *i*Pr-PyCa = ----- and *i*Pr-DAB = ·····) in toluene; right: electronic absorption spectra of *trans,cis*- (-----) and *cis,cis*-[Ru(I)(Me)(CO)$_2$(*i*Pr-DAB)] (——) in toluene

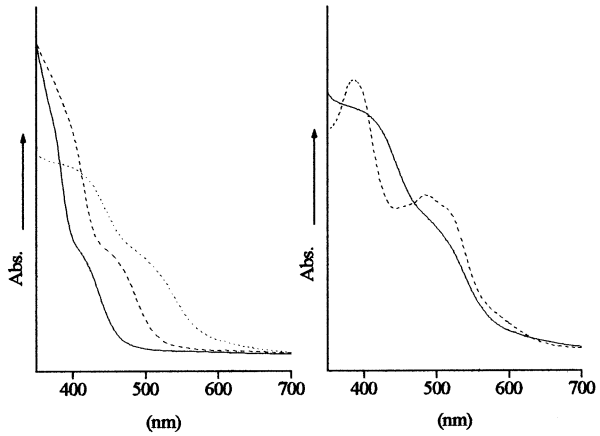

A similar two-band system is observed in the spectra of the complexes *cis,cis*-[Ru(Me)(I)(CO)$_2$(α-diimine)]. Varying the α-diimine ligand from *i*Pr-DAB to *i*Pr-PyCa and dmb causes a shift of both absorption bands to higher energy (Figure 6). The shifts are closely related to the changes in energy of the lowest π* orbital of the α-diimine ligand.[15][52] In the case of the dmb complex these shifts are so large, that the second absorption band has almost completely disappeared under the much stronger absorptions at higher energy. In agreement with its CT character, the lowest-energy band is solvatochromic, shifting to lower energy

by ca. 2000 cm^{-1} on going from acetonitrile to toluene (Table 3).

Resonance Raman Spectra

Resonance Raman (rR) spectroscopy is a very valuable technique for the assignment and characterisation of allowed electronic transitions.[53][54][55][56] Since only those vibrations are normally resonance-enhanced, which are vibronically coupled to the electronic transitions, these transitions can be characterised by the observed resonance effects. From the three *cis,cis* isomers rR spectra could only be recorded for the *cis,cis*-[Ru(I)(Me)$(CO)_2$(*i*Pr-DAB)] and *cis,cis*-[Ru(I)(Me)$(CO)_2$(*i*Pr-PyCa)] complexes. The corresponding dmb complex is too photolabile to provide reliable spectra. Spectra were obtained by excitation with the 488.0-nm line of an argon ion laser into the lowest-energy absorption band of the complexes. The resonantly enhanced Raman bands of the complexes are collected in Table 4. Figure 7 shows the rR spectra of *trans,cis*-[Ru(I)(R)$(CO)_2$(*i*Pr-DAB)] (R = CD_3, CH_3) and *cis,cis*-[Ru(I)$(CH_3)(CO)_2$(α-diimine)] (α-diimine = *i*Pr-DAB, *i*Pr-PyCa), respectively. The spectra of *trans,cis*-[Ru(I)(R)$(CO)_2$(*i*Pr-DAB)] (R = CD_3, CH_3) show a strong rR effect for a band at approximately 1555 cm^{-1}, which belongs to ν_s(CN), the symmetrical stretching mode of the imine groups of the *i*Pr-DAB ligand. This band is split in the rR spectra of the *cis,cis* isomer, indicating that the two imine groups of the *i*Pr-DAB ligand are inequivalent due to the different *trans* influences of the Me and CO groups. This effect is not evident from the X-ray structures, but is also observed in the ^1H- and ^{13}C-NMR spectra (vide supra). The Raman spectrum of *cis,cis*-[Ru(I)(Me)$(CO)_2$(*i*Pr-PyCa)] is very similar to that of its *trans,cis* isomer.[51]

Table 4. Resonantly enhanced Raman bands of *trans,cis*- and *cis,cis*-[Ru(I)(R)$(CO)_2$(α-diimine)] (R = CH_3, CD_3; α-diimine = *i*Pr-DAB, *i*Pr-PyCa), measured at 80 K in KNO_3 ⊥ft parenthesisλ_{exc} = 488.0 nm)

Compound	Raman shift [cm^{-1}]
trans,cis-[Ru(I)$(CD_3)(CO)_2$(*i*Pr-DAB)]	1555, 1328, 1287, 1132, 909, 615, 599, 475
trans,cis-[Ru(I)(Me)$(CO)_2$(*i*Pr-DAB)]	2010, 1553, 1328, 1287, 1194, 806, 475
cis,cis-[Ru(I)(Me)$(CO)_2$(*i*Pr-DAB)]	2022, 1568, 1550, 1293, 1198, 806, 486, 395
cis,cis-[Ru(I)(Me)$(CO)_2$(*i*Pr-PyCa)]	1620, 1560, 1471, 1291, 1254, 1230, 1194, 1151, 1021, 801, 500, 395

The rather strong rR effect of ν_s(CN) confirms the charge transfer character of the electronic transition in which excitation takes place. For both isomers there is hardly any rR effect for ν_s(CO). This means that their charge transfer transitions do not originate from a central metal orbital since this would involve a change of metal-to-CO π backbonding and invoke an rR effect for ν_s(CO). Instead, the transition takes place from an orbital having mainly halide character just as for the *trans,cis* isomer.[51] In addition, the rR spectra of *trans,cis*- and *cis,cis*-[Ru(I)(Me)$(CO)_2$(*i*Pr-DAB)] show weaker rR effects for bands at 1328, 1194, 806, and 475 cm^{-1}. Replacement of CH_3 by CD_3 in the *trans,cis* isomer causes a shift of the 1194 cm^{-1} band to 909 cm^{-1}, while the 806 cm^{-1} band is both shifted and split, giving rise to two new bands at 615 and 599 cm^{-1}, respectively. The positions of the other bands are not affected.

Figure 7. Resonance Raman spectra of (A) *trans,cis*-[Ru(I)(CD_3)-$(CO)_2$(*i*Pr-DAB)], (B) *trans,cis*-[Ru(I)(Me)$(CO)_2$(*i*Pr-DAB)], (C) *cis,cis*-[Ru(I)(Me)$(CO)_2$(*i*Pr-DAB)], (D) *cis,cis*-[Ru(I)(Me)$(CO)_2$(*i*Pr-PyCa)] in KNO_3 at 80 K, λ_{exc} = 488.0 nm (* = NO_3^-)

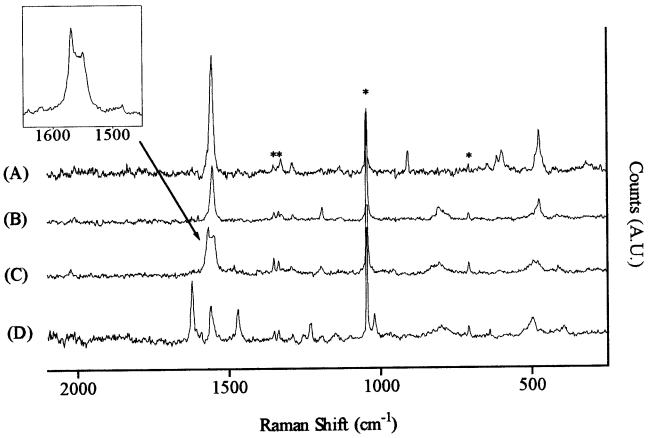

In agreement with the vibrational spectra of [M$(CH_3)(CO)_5$] and [M$(CD_3)(CO)_5$] (M = Mn, Re)[57], the bands at 1194/909 cm^{-1} are assigned to $\delta_s(CH_3/CD_3)$ and those at 806/615;599 cm^{-1} to $\rho(CH_3/CD_3)$. The doublet spacing of the $\rho(CD_3)$ band in [Ru(I)$(CD_3)(CO)_2$(*i*Pr-DAB)] (16 cm^{-1}) is rather small compared with that observed for [Re$(CH_3)(CO)_5$] (44 cm^{-1})[57] and [Re$(CD_3)(CO)_3$(dmb)] (51 cm^{-1}).[58] The rR effect of the two methyl vibrations is clearly an electronic effect and not the result of a coupling to other vibrations since the deuteration does not affect the frequencies of other Raman bands. The observation of these CH_3/CD_3 bands implies that the charge transfer transition influences the bond angles of these ligands, most probably as a result of a change of the hybridisation of the C atom of the CH_3 ligand due to a charge redistribution during the charge transfer transition.

The observation that deuteration of the methyl ligand does not affect the frequency of any Raman bands below 800 cm^{-1}, leads to the following conclusions. First of all, the Raman band at approximately 500 cm^{-1} does not belong to ν(Ru−CH_3) and is assigned to ν_s(Ru−CO), expected in this frequency region. Secondly, the absence of a rR effect for ν(Ru−CH_3) implies that the electronic transition, in which the excitation takes place, does not influence the Ru−methyl σ bond, although it affects the bond angles of the methyl ligand. This result agrees with the proposed XLCT character of the transition and excludes the possibility that the lowest-energy absorption band belongs to an allowed σ(Ru-methyl)→π*(α-diimine) transition instead.

According to the rR spectra, the *trans,cis* and *cis,cis* isomers of the [Ru(I)(Me)$(CO)_2$(*i*Pr-DAB)] complexes have very similar low-energy transitions. The difference in photo-

chemistry between *trans,cis*- and *cis,cis*-[Ru(I)(Me)-(CO)$_2$(dmb)], viz. photoisomerization of the *trans,cis* into the *cis,cis* isomer and no apparent product formation of the *cis,cis* isomer, can therefore not be ascribed to a different character of the lowest excited state. This difference in photochemical behaviour is the subject of a detailed photochemical study of these complexes, the results of which will be published in a forthcoming article.

Prof. *A. Oskam* is gratefully acknowledged for advice and for critical reading of the manuscript. Mr *J. M. Ernsting* is thanked for measuring the NOE-difference spectrum. Thanks are due to the *Netherlands Foundation for Chemical Research* (SON) and the *Netherlands Organisation for the Advancement of Pure Research* (NWO) for financial support.

Experimental Section

Materials, Apparatus and Preparations: [Ru$_3$(CO)$_{12}$], MeI, BzlBr, silver triflate (AgOTf), (*n*Bu)$_4$NI, and 4,4′-dimethyl-2,2′-bipyridine (dmb) were used without further purification. Silica gel for column chromatography (Kieselgel 60, 70−230 mesh, Merck) was activated by heating overnight in vacuo at 160°C. Solvents for synthetic purposes were of reagent grade and carefully dried over sodium wire (THF, *n*-hexane, diethyl ether) or $CaCl_2$ (CH_2Cl_2) and freshly distilled under nitrogen prior to use. Acetonitrile was used without further purification. Solvents for spectroscopic measurements were of analytical grade, dried over sodium and distilled under N_2 before use. *i*Pr-DAB and *i*Pr-PyCa were synthesised according to literature procedures.[59] Electronic absorption spectra were measured with a Varian Cary 4E spectrophotometer, infrared spectra with an FTS-60A FTIR spectrometer equipped with a liquid-nitrogen-cooled MCT detector. − The ^{1}H-, NOE-difference, and ^{13}C-NMR spectra were recorded with a Bruker AMX 300 spectrometer (300.13, 75.46 MHz, respectively) at 293K. Resonance Raman measurements were performed with a Dilor XY spectrometer, using an SP Model 2016 argon ion laser as excitation source. To avoid photodecomposition the spectra of the complexes (dispersed in a KNO_3 pellet) were measured at 80K. Typical concentrations were 30 mg of complex and 150 mg of KNO_3.

Synthesis of cis,cis-[Ru(I)(Me)(CO)$_2$(L)] (L = iPr-DAB, iPr-PyCa, dmb): Ru$_3$(CO)$_{12}$ (300 mg, 0.46 mmol) and MeI (1.5 ml, excess) were refluxed in 20 ml of acetonitrile at 100°C. After 10 min, a product with CO-stretching frequencies at 2058 (s), 1996 (s) and 1637 (w) was obtained. The reaction was brought to completion within ca. 1 h; a yellow solution was then obtained which contained product **2a** with CO-stretching frequencies of 2041 (s) and 1974 (s) cm^{-1}. After evaporating the solvent, product **2a** was dissolved in 10 ml of diethyl ether together with 0.5 mmol of the α-diimine ligand. After stirring for 1 h, the solution was filtered off and the residue was washed with hexane (2 × 10 ml). The complex was purified by column chromatography on silica gel using gradient elution with CH_2Cl_2/THF. Yield 80−90%.

cis,cis-[Ru(I)(Me)(CO)$_2$(iPr-DAB)]: ^{1}H NMR ($CDCl_3$): δ = 8.26/8.20 (s, 1 H, H_{im}), 4.64/4.20 [sept, *J* = 6.6 Hz, 1 H, C*H*(CH$_3$)$_2$], 1.63/1.55/1.49/1.40 [d, *J* = 6.6 Hz, 3 H, CH(C*H*$_3$)$_2$], 0.78 (s, 3 H, Ru−Me). − ^{13}C NMR APT ($CDCl_3$): δ = 200.8 (Ru-*C*O$_{eq}$), 193.3 (Ru-*C*O$_{ax}$), 160.1/157.7 (*C*H$_{im}$), 65.6/57.2 [*C*H(CH$_3$)$_2$], 24.8/23.5/23.3/22.2 [CH(*C*H$_3$)$_2$], −14.7 (Ru-*C*H$_3$). − IR (CH_2Cl_2): ν(CO) = 2028 (s), 1958 (s) cm^{-1}. − MS (FAB$^+$): M(calcd.) 439.95, M(found) 439.95.

cis,cis-[Ru(I)(Me)(CO)$_2$(iPr-PyCa)]: ^{1}H NMR ($CDCl_3$): δ = 9.01 (d, *J* = 5.1 Hz, 1 H, py-H^6), 8.48 (s, 1 H, H_{im}), 8.05 (t, *J* = 7.7 Hz, 1 H, py-H^4), 7.85 (d, *J* = 7.7 Hz, 1 H, py-H^3), 7.61 (t, *J* = 5.1 Hz, 1 H, py-H^5), 4.20 [sept, 6.3 Hz, 1 H, C*H*(CH$_3$)$_2$], 1.64/1.52 [d , 6.3 Hz, 6 H, CH(C*H*$_3$)$_2$], 0.93 (s, 3 H, Ru-Me). − ^{13}C NMR APT ($CDCl_3$): δ = 201.1 (Ru-CO$_{eq}$), 194.0 (Ru-CO$_{ax}$), 160.2 (H_{im}), 155.5 (py-C^2), 149.7 (py-C^6), 138.8 (py-C^3), 127.7 (py-C^5), 126.6 (py-C^4), 65.3 [*C*H(CH$_3$)$_2$], 24.6/23.7 [CH(*C*H$_3$)$_2$]. −13.4 (Ru-*C*H$_3$). − IR (CH_2Cl_2): ν(CO) = 2027 (s), 1956 (s) cm^{-1}. − MS (FAB$^+$): M(calcd.) 449.92, M(found) 449.92.

cis,cis-[Ru(I)(Me)(CO)$_2$(dmb)]: ^{1}H NMR ($CDCl_3$): δ = 8.85 (d, *J* = 5.6 Hz, 2 H, py-H^6), 7.99/7.96 (s, 2 H, py-H^3/py-H$^{3'}$), 7.38/7.27 (d, *J* = 5.6 Hz, 1 H, py-H^5/py-H$^{5'}$), 2.58/2.55 (s, 6 H, py-Me/py-Me′), 0.89 (s, 3 H, Ru-Me). − ^{13}C NMR APT ($CDCl_3$): δ = 200.7 (Ru-CO$_{eq}$), 195.6 (Ru-CO$_{ax}$), 156.0/153.5(py-C^2/py-C$^{2'}$), 153.0/148.8 (py-C^6/py-C$^{6'}$), 150.2/149.8 (py-C^4/py-C$^{4'}$), 127.1/126.7 (py-C^3/py-C$^{3'}$), 123.4/123.2 (py-C^5/py-C$^{5'}$), 21.2 (py-*C*H$_3$), −14.3 (Ru-*C*H$_3$). − IR (CH_2Cl_2): ν(CO) = 2025 (s), 1952 (s) cm^{-1}. −MS (FAB$^+$): M(calcd.) 483.92, M(found) 483.92.

Synthesis of trans,cis-[Ru(I)(Me)(CO)$_2$(L)] (L = iPr-DAB, dmb): The complexes *trans,cis*-[Ru(I)(R)(CO)$_2$(*i*Pr-DAB)] (R = CH_3, CD_3), which were used for X-ray structure analysis and Raman spectroscopic measurements, were prepared by the procedure described by Kraakman et al.[40] The corresponding dmb complex was prepared from its *cis,cis* isomer according to the following procedure. One equivalent of AgOTf was added to a solution of *cis,cis*-[Ru(I)(Me)(CO)$_2$(dmb)] in CH_2Cl_2, which was then stirred for 2 h. The residue, AgI, was filtered off and 1 g (excess) of (*n*Bu)$_4$NI was added while light was excluded to prevent photodecomposition. This solution was stirred for 3 h. The excess of (*n*Bu)$_4$NI and (*n*Bu)$_4$NOTf was filtered off and the solvent was evaporated. The complex was purified by column chromatography on silica gel using gradient elution with CH_2Cl_2/THF. Yield 80−90%.

trans,cis-[Ru(I)(Me)(CO)$_2$(dmb)]: ^{1}H NMR ($CDCl_3$): δ = 8.83 (d, *J* = 5.7 Hz, 2 H, py-H^6), 7.96 (s, 2 H, py-H^3), 7.30 (d, *J* = 5.7 Hz, 2 H, py-H^5), 2.56 (s, 6 H, py-Me), 0.10 (s, 3 H, Ru-Me). − ^{13}C NMR APT ($CDCl_3$): δ = 202.2 (Ru-CO), 153.4 (py-C^2), 151.6 (py-C^6), 150.2 (py-C^4), 127.2 (py-C^3), 123.5 (py-C^5), 21.3 (py-*C*H$_3$), −4.8 (Ru-*C*H$_3$). − IR (CH_2Cl_2): ν(CO) = 2030 (s), 1962 (s) cm^{-1}.

Synthesis of cis,cis-[Ru(I){C(O)Me}(CO)$_2$(iPr-DAB)]: Ru$_3$-(CO)$_{12}$ (300 mg, 0.46 mmol) and MeI (1.5 ml, excess) were refluxed in 20 ml of acetonitrile at 100°C. The reaction was completed after ca. 1 h; a yellow solution was then obtained containing product **2a** with ν(CO) frequencies of 2041(s) and 1974(s) cm^{-1}. The solution was pressurised with CO (1 atm) and stirred for 2 h. Product **1a** was obtained with ν(CO) of 2058(s) and 1996(s) cm^{-1}. After evaporation of the solvent, product **1a** and 75 mg (0.5 mmol) of *i*Pr-DAB were dissolved in 10 ml of diethyl ether. After stirring for 1 h, the solution was filtered and the residue was washed with hexane (2 × 10 ml). The complex was purified by column chromatography on silica gel using gradient elution with CH_2Cl_2/THF. Total yield 75% {the ^{1}H-NMR spectrum shows that *trans,cis*-[Ru(I){C(O)Me}(CO)$_2$(*i*Pr-DAB)] and *cis,cis*-[Ru(I){C(O)Me}(CO)$_2$(*i*Pr-DAB)] are formed in a 1:4 ratio}.

trans,cis-[Ru(I){C(O)Me}(CO)$_2$(iPr-DAB)]: ^{1}H NMR ($CDCl_3$): δ = 8.20 (s, 2 H, H_{im}), 4.24 [sept, *J* = 6.6 Hz, 2 H, C*H*(CH$_3$)$_2$], 2.53 [s, 3 H, Ru-C(O)Me], 1.43/1.38 [d, *J* = 6.6 Hz, 6 H, CH(C*H*$_3$)$_2$]. − IR (CH_2Cl_2): ν(CO) = 2040 (s), 1974 (s), 1640 (w) cm^{-1}.

cis,cis-[Ru(I){C(O)Me}(CO)$_2$(iPr-DAB)]: ^{1}H NMR ($CDCl_3$): δ = 8.20/8.18 (1 H, s, H_{im}), 5.15/4.17 [sept, *J* = 6.6 Hz, 2 H, C*H*(CH$_3$)$_2$], 2.81 [s, 3 H, Ru-C(O)Me], 1.69−1.38 [m, *J* = 6.6 Hz, 12 H, CH(C*H*$_3$)$_2$]. − IR (CH_2Cl_2): ν(CO) = 2040 (s), 1974 (s), 1640 (w) cm^{-1}.

Synthesis of Product **2b**: $Ru_3(CO)_{12}$ (300 mg, 0.46 mmol) and BzlBr (0.5 ml, excess) were refluxed in 20 ml of acetonitrile at 100°C. After completion of the reaction (ca. 0.5 h), a yellow solution was obtained with product **2b** having ν(CO) frequencies of 2042(s) and 1976(s) cm^{-1} and a product with ν(CO) bands at 2077(s) and 2020(s), in a 2:1 ratio. After evaporation of the solvent, the complex was washed with diethyl ether (2 × 10 ml). Yield 30%.

Product **2b**: ^1H NMR ($CDCl_3$): δ = 7.25−7.15 (m, 4 H, H_{Ph}), 7.01 (m, 1 H, H_{Ph}), 2.96/2.89 (d, ^2J = 8.5 Hz, 2 H, PhCH_2), 2.29/2.26 (s, 3 H, CH_3CN). − IR (MeCN): ν(CO) = 2042 (s), 1976 (s) cm^{-1}.

Synthesis of cis,cis-[Ru(Br)(Bzl)(CO)$_2$(iPr-DyAB)]: Product **2b** was prepared in acetonitrile. After evaporation of the solvent, complex **2b** and 0.5 mmol of *i*Pr-DAB were dissolved in 10 ml of diethyl ether. After stirring for 0.5 h, the solution was filtered off and the residue was washed with hexane (2 × 10 ml). Yield 50%.

cis,cis-[Ru(Br)(Bzl)(CO)$_2$(iPr-DAB)]: ^1H NMR ($CDCl_3$): δ = 8.26/8.24 (s, 1 H, H_{im}), 7.37 (d, *J* = 7.5 Hz, 2 H, H_{Ph}), 7.17 (t, *J* = 7.5 Hz, 2 H, H_{Ph}), 6.95 (t, *J* = 7.5 Hz, 1 H, H_{Ph}), 4.64/4.11 [sept, *J* = 6.6 Hz, 1 H, C*H*(CH_3)$_2$], 3.57 (d, ^2J = 7.8 Hz, 1 H, PhCH_2), 2.98 (d, ^2J = 7.8 Hz, 1 H, PhCH_2), 1.56−1.41 [m, 12 H, CH(CH_3)$_2$]. − IR (CH_2Cl_2): ν(CO) = 2030 (s), 1962 (s) cm^{-1}.

Synthesis of trans,cis-[Ru(Br)(Bzl)(CO)$_2$(iPr-DAB)]: This complex was prepared by the procedure of Kraakman et al.[40]

trans,cis-[Ru(Br)(Bzl)(CO)$_2$(iPr-DAB)]: ^1H NMR ($CDCl_3$): δ = 8.16 (s, 2 H, H_{im}), 7.10 (t, *J* = 7.6 Hz, 2 H, H_{Ph}), 7.02 (t, *J* = 7.5 Hz, 1 H, H_{Ph}), 6.88 (d, *J* = 7.5 Hz, 2 H, H_{Ph}), 4.22 [sept, *J* = 6.6 Hz, 2 H, C*H*(CH_3)$_2$], 2.36 (s, 2 H, PhCH_2), 1.61/1.38 [d, 12 H, CH(CH_3)$_2$]. − IR (CH_2Cl_2): ν(CO) = 2033 (s), 1969 (s) cm^{-1}.

Crystal Structure Determination of trans,cis-[Ru(I)(Me)(CO)$_2$-(iPr-DAB)] and cis,cis-[Ru(I)(Me)(CO)$_2$(iPr-DAB)]: Crystals of both compounds were grown from a saturated CH_2Cl_2 solution at 293 K. Crystals with approximate dimensions 0.20 × 0.30 × 0.40 mm (0.15 × 0.20 × 0.60 mm) were used for data collection with an Enraf-Nonius CAD-4 diffractometer with graphite-monochromated Mo-K_α radiation and ω-2θ scan. Totals of 4661 (4819) unique reflections were measured. Of these, 3168 (1931) were above the significance level of 2.5 σ(*I*). The maximum value of (sinθ)/λ was 0.70 $Å^{-1}$. Unit-cell parameters were refined by a least-squares fitting procedure using 23 reflections with 40° < 2θ < 41° (40° < 2θ < 42°). Corrections for Lorentz and polarization effects were applied. The structures were solved by the PATTY option of the DIRDIF-94 program system.[60] Hydrogen atom positions were calculated. Full-matrix least-squares refinement of *F*, anisotropic for the non-hydrogen atoms and isotropic for the hydrogen atoms, with a fixed temperature factor of $U = 0.15$ $Å^2$ and restraining the latter in such a way that the distance to their carrier remained constant at approximately 1.0 Å, converged to $R = 0.043$ (0.065), R_w = 0.045 (0.063), $(\Delta.\sigma)_{max} = 0.45$ (0.61), $S = 0.81$ (1.49). An empirical absorption correction (DIFABS[61]) was applied, with coefficients in the range of 0.68−1.22 (0.40−1.53). A final difference Fourier map revealed a residual electron density between −0.7 and 0.7 e$Å^{-3}$ (−1.2 and 1.0 e$Å^{-3}$) in the vicinity of the heavy atoms. Scattering factors were taken from Cromer and Mann.[62][63] The anomalous scattering of Ru and I was taken into account.[64] All calculations were performed with XTAL[65], unless stated otherwise. Both isomers were refined in the same way but after isotropic refinement of the starting model of the *cis,cis* isomer some atoms had a rather high temperature factor (C5, C8 and O9). C5 and C8 could be split into two positions a and b with occupancy factors for a = 0.35 and for b = 0.65. O9 was divided in such a way that the CO and CH_3 were both equally distributed over the two possible positions and thus resulting in the introduction of two half occupied O positions (O9 and O11). The disordered C atoms were kept isotropic during refinement. No attempts were made to calculate the H atoms for C5a, C5b, C8a and C8b and the H atoms for C3 and C6 were divided into separate positions and kept fixed entirely at their calculated position. The experimental data for the crystal structure determinations and refinements are listed in Table 5.

Table 5. Crystallographic data and details of the structure determinations of *trans,cis*-[Ru(I)(Me)(CO)$_2$(*i*Pr-DAB)] (**A**) and *cis,cis*-[Ru(I)(Me)(CO)$_2$(*i*Pr-DAB)] (**B**)

	A	**B**
Crystal data		
Chemical formula	$C_{11}H_{19}IN_2O_2Ru$	$C_{11}H_{19}IN_2O_2Ru$
Formula weight	439.3	439.3
Lattice type	monoclinic	monoclinic
Space group	$P2_1/n$	$P2_1/n$
Z	4	4
a [Å]	7.389(2)	7.409(1)
b [Å]	22.880(3)	22.434(8)
c [Å]	10.540(2)	10.140(3)
β [°]	98.41(1)	99.31(2)
V [$Å^3$]	1608.7(6)	1663.2(9)
Crystal size [mm]	0.20 × 0.30 × 0.40	0.15 × 0.20 × 0.60
D_x [g cm^{-3}]	1.81	1.75
F(000)	848	848
μ (Mo-K_α) [cm^{-1}]	28.5	27.57
Data collection		
T [K]	293	293
λ (Mo-K_α) [Å]	0.71069	0.71069
θ_{min}, θ_{max} [°]	2.0, 29.9	1.8, 29.9
Monochromator	graphite	graphite
Δω [°]	1.20 + 0.35tan θ	1.30 + 0.35tan θ
Aperture [mm]	3.0 + 1.0tan θ	3.0 + 1.0tan θ
Exposure time [h]	65	60
Linear instability [%]	−	−
Reference reflections	121, 210	$\bar{1}61$, $\bar{1}22$
Dataset	0/10, 0/29, −14/14	−10/0, 0/31, −13/14
Total unique data	4661	4819
Observed data	3168 ($I > 2.5\sigma_I$)	1931 ($I > 2.5\sigma_I$)
DIFABS	0.68−1.22	0.40−1.53
Refinement		
R	0.043	0.065
R_w	0.045	0.063
w^{-1}	$6.0 + 0.012[\sigma(F_\sigma)]^2$	$4.0 + 0.015[\sigma(F_\sigma)]^2$
$(\Delta/\sigma)_{max}$	0.45	0.61
Min., max. resd. dens. [e$Å^3$]	−0.7, 0.7	−1.2, 1.0

[1] K. Kalyanasundaram, *Coord. Chem. Rev.* **1982**, *46,* 159.
[2] R. J. Watts, *J. Chem. Educ.* **1983**, *60,* 834.
[3] H. Riesen, Y. Gao, E. Krausz, *Chem. Phys. Lett.* **1994**, *228,* 610.
[4] D. J. Stufkens, *Comments Inorg. Chem.* **1992**, *13,* 359.
[5] T. A. Perkins, W. Humer, T. L. Netzel, K. S. Schanze, *J. Phys. Chem.* **1990**, *94,* 2229.
[6] P. Chen, T. D. Westmoreland, E. Danielson, K. S. Schanze, D. Anthon, P. E. Neveux, Jr., T. J. Meyer, *Inorg. Chem.* **1987**, *26,* 1116.
[7] K. S. Schanze, D. B. MacQueen, T. A. Perkins, L. A. Cabana, *Coord. Chem. Rev.* **1993**, *122,* 63.
[8] L. A. Worl, R. Duesing, P. Chen, L. D. Ciana, T. J. Meyer, *J. Chem. Soc., Dalton Trans.* **1991**, 849.
[9] J. C. Luong, R. A. Faltynek, M. S. Wrighton, *J. Am. Chem. Soc.* **1980**, *102,* 7892.
[10] J. C. Luong, R. A. Faltynek, M. S. Wrighton, *J. Am. Chem. Soc.* **1979**, *101,* 1597.
[11] D. L. Morse, M. S. Wrighton, *J. Am. Chem. Soc.* **1976**, *98,* 3931.
[12] M. W. Kokkes, D. J. Stufkens, A. Oskam, *Inorg. Chem.* **1985**, *24,* 2934.
[13] M. W. Kokkes, W. G. J. de Lange, D. J. Stufkens, A. Oskam, *J. Organomet. Chem.* **1985**, *294,* 59.

[14] M. W. Kokkes, D. J. Stufkens, A. Oskam, *Inorg. Chem.* **1985**, *24,* 4411.
[15] D. J. Stufkens, *Coord. Chem. Rev.* **1990**, *104,* 39.
[16] R. R. Andréa, W. G. J. de Lange, D. J. Stufkens, A. Oskam, *Inorg. Chem.* **1989**, *28,* 318.
[17] H. K. van Dijk, J. van der Haar, D. J. Stufkens, A. Oskam, *Inorg. Chem.* **1989**, *28,* 75.
[18] T. van der Graaf, D. J. Stufkens, A. Oskam, K. Goubitz, *Inorg. Chem.* **1991**, *30,* 599.
[19] T. van der Graaf, A. van Rooy, D. J. Stufkens, A. Oskam, *Inorg. Chim. Acta* **1991**, *187,* 133.
[20] J. W. M. van Outersterp, D. J. Stufkens, A. Vlček, Jr., *Inorg. Chem.* **1995**, *34,* 5183.
[21] B. D. Rossenaar, T. van der Graaf, R. van Eldik, C. H. Langford, D. J. Stufkens, A. Vlček, Jr., *Inorg. Chem.* **1994**, *33,* 2865.
[22] B. D. Rossenaar, E. Lindsay, D. J. Stufkens, A. Vlček, Jr., *Inorg. Chim. Acta* **1996**, *250,* 5.
[23] P. C. Servaas, G. J. Stor, D. J. Stufkens, A. Oskam, *Inorg. Chim. Acta* **1990**, *178,* 185.
[24] H. A. Nieuwenhuis, A. van Loon, M. A. Moraal, D. J. Stufkens, A. Oskam, K. Goubitz, *J. Organomet. Chem.* **1995**, *492,* 165.
[25] M. P. Aarnts, D. J. Stufkens, A. Vlček, Jr., *Inorg. Chim. Acta*, **1997**, *226*, 37.
[26] M. P. Aarnts, D. J. Stufkens, M. P. Wilms, E. J. Baerends, A. Vlček, Jr., I. P. Clark, M. W. George, J. J. Turner, *Chem. Eur. J.* **1996**, *2,* 1556.
[27] B. D. Rossenaar, C. J. Kleverlaan, M. C. E. van de Ven, D. J. Stufkens, A. Vlček, Jr., *Chem. Eur. J.* **1996**, *2,* 228.
[28] B. D. Rossenaar, D. J. Stufkens, A. Oskam, J. Fraanje, K. Goubitz, *Inorg. Chim. Acta* **1996**, *247,* 215.
[29] B. D. Rossenaar, C. J. Kleverlaan, M. C. E. van de Ven, D. J. Stufkens, A. Oskam, J. Fraanje, K. Goubitz, *J. Organomet. Chem.* **1995**, *493,* 153.
[30] B. D. Rossenaar, M. W. George, F. P. A. Johnson, D. J. Stufkens, J. J. Turner, A. Vlček, Jr., *J. Am. Chem. Soc.* **1995**, *117,* 11582.
[31] C. J. Kleverlaan, D. M. Martino, H. v. Willigen, D. J. Stufkens, A. Oskam, *J. Phys. Chem.* **1996**, *100,* 18607.
[32] H. A. Nieuwenhuis, M. C. E. van de Ven, D. J. Stufkens, A. Oskam, K. Goubitz, *Organometallics* **1995**, *14,* 780.
[33] P. Bradley, G. Suardi, A. P. Zipp, R. Eisenberg, *J. Am. Chem. Soc.* **1994**, *116,* 2859.
[34] J. E. Hux, R. J. Puddephat, *J. Organomet. Chem.* **1992**, *437,* 251.
[35] K. Kaupp, H. Stoll, W. Kaim, T. Stahl, G. van Koten, E. Wissing, W. J. Smeets, A. L. Spek, *J. Am. Chem. Soc.* **1991**, *113,* 5606.
[36] G. J. Stor, S. L. Morrison, D. J. Stufkens, A. Oskam, *Organometallics* **1994**, *13,* 2641.
[37] C. J. Kleverlaan, F. Hartl, D. J. Stufkens, *J. Photochem. Photobiol.* **1997**, *203,* 231.
[38] W. Rohde, H. tom Dieck, *J. Organomet. Chem.* **1987**, *328,* 209.
[39] H. tom Dieck, W. Rohde, U. Behrens, *Z. Naturforsch.* **1989**, *44b,* 158.
[40] M. J. A. Kraakman, K. Vrieze, H. Kooijman, A. L. Spek, *Organometallics* **1992**, *11,* 3760.
[41] B. de Klerk-Engels, J. H. Groen, J. M. A. Kraakman, J.-M. Ernsting, K. Vrieze, K. Goubitz, J. Fraanje, *Organometallics* **1994**, *13,* 3279.
[42] B. de Klerk-Engels, H.-W. Frühauf, K. Vrieze, H. Kooijman, A. L. Spek, *Inorg. Chem.* **1993**, *32,* 5528.
[43] M. J. A. Kraakman, B. de Klerk-Engels, P. P. M. de Lange, K. Vrieze, W. J. J. Smeets, A. L. Spek, *Organometallics* **1992**, *11,* 3774.
[44] W. Rohde, H. tom Dieck, *J. Organomet. Chem.* **1990**, *385,* 101.
[45] H. A. Nieuwenhuis, A. van Loon, M. A. Moraal, D. J. Stufkens, A. Oskam, K. Goubitz, *Inorg. Chim. Acta* **1995**, *232,* 19.
[46] B. J. Rappoli, K. J. McGrath, C. F. George, J. C. Cooper, *J. Organomet. Chem.* **1993**, *450,* 85.
[47] H. tom Dieck, W. Kollvitz, I. Kleinwachter, W. Rohde, L. Stamp, *Transition Met. Chem.* **1986**, *11,* 361.
[48] J. M. A. Kraakman, K. Vrieze, H. Kooijman, A. L. Spek, *Organometallics* **1992**, *11,* 3774.
[49] J.-C. Daran, Y. Jeannin, C. Rigault, *Acta Crystallogr.* **1984**, *C40,* 249.
[50] E. Alessio, B. Milani, M. Bolle, G. Mestroni, P. Faleschini, F. Tonone, S. Geremia, M. Calligaris, *Inorg. Chem.* **1995**, *34,* 4722.
[51] H. A. Nieuwenhuis, D. J. Stufkens, A.Oskam, *Inorg. Chem.* **1994**, *33,* 3212.
[52] J. Reinhold, R. Benedix, P. Birner, H. H., *Inorg. Chim. Acta* **1979**, *33,* 209.
[53] R. J. H. Clark, T. J. Dines, *Angew. Chem. Int. Ed. Engl.* **1986**, *25,* 131.
[54] J. I. Zink, K.-S. Kim Shin, *Adv. Photochem.* **1991**, *16,* 119.
[55] R. W. Balk, D. J. Stufkens, A. Oskam, *J. Chem. Soc., Dalton Trans.* **1981**, 1124.
[56] R. W. Balk, T. Snoeck, D. J. Stufkens, A. Oskam, *Inorg. Chem.* **1980**, *19,* 3015.
[57] G. P. McQuillan, D. C. McKean, C. Long, A. R. Morrisson, I. Torto, *J. Am. Chem. Soc.* **1986**, *108,* 863.
[58] C. J. Kleverlaan, D.J. Stufkens, *Inorg. Chim. Acta*, in press.
[59] H. Bock, H. tom Dieck, *Chem. Ber.* **1967**, *100,* 228.
[60] P. T. Beurskens, G. Admiraal, G. Beurskens, W. P. Bosman, R. de Gelder, R. Israel, J. M. M. Smits, *The DIRDIF-94 program system*, University of Nijmegen, Netherlands, **1994**.
[61] N. Walker, D. Stuart, *Acta Crystallogr.* **1983**, *A39,* 158.
[62] *International Tables for X-Ray Crystallography*Birmingham, Kynoch Press, **1974**, vol. IV, p. 55.
[63] D. T. Cromer, J. B. Mann, *Acta Crystallogr.* **1986**, *A24,* 321.
[64] D. T. Cromer, J. B. Liberman, *J. Chem. Phys.* **1970**, *53,* 1891.
[65] S. R. Hall, H. D. Flack, J. M. Stewart, *Eds. XTAL3.2 Reference Manual, Universities of Western Australia, Geneva and Maryland*, **1992**.

[98071]

Novel Nine-Membered Titanaheterocycles – Structure, ab initio Calculations, and Preparative Use towards the Selective Synthesis of Substituted Cyclopentanols

Frank Hampel[a], Nico van Eikema Hommes*[b], Sven Hoops[a], Faramarz Maaref[a], and Rainer Schobert*[a]

Institut für Organische Chemie der Universität Erlangen-Nürnberg[a],
Henkestr. 42, D-91054 Erlangen, Germany
Fax: (internat.) + 49(0)9131/856864
E-mail: schobert@organik.uni-erlangen.de

Computer-Chemie-Centrum der Universität Erlangen-Nürnberg[b],
Nägelsbachstr. 25, D-91052 Erlangen, Germany
Fax: (internat.) + 49(0)9131/856566
E-mail: hommes@ccc.uni-erlangen.de

Received March 24, 1998

Keywords: Cyclizations / Cross-coupling / Ab initio calculations / Titanium / Metallacycles

Reactions of $Cp_2Ti(CO)_2$ (**3**) with two equivalents of α,β-unsaturated ketones **4** yield the novel titana-2,9-dioxacyclonona-3,7-dienes **5**. Cross-coupling of **3** with two different ketones **4** and **6** to give **7** can be achieved under certain reaction conditions. Hydrolysis of **5** or **7** may generate diketones **9**, cyclopentanols **10/11**, or cyclopentenes **12/13**, depending on substituents and conditions. The X-ray crystal structure of **5a**, the first nine-membered bis(η^5-cyclopentadienyl)-substituted titanaheterocycle containing carbon, is presented. Ab initio calculations were performed for **5a** and for titana-2-oxacyclopentene **1**, a conceivable intermediate in the coupling reaction.

Introduction

Titanaheterocycles are known with ring sizes ranging from three to ten and with different degrees of "unsaturation". Whereas most of the publications focussed on systems featuring four-[1], six-[2][3][4], eight-[4][5] or ten-membered[5] rings, we were interested in the chemistry of the odd-numbered chelate complexes, like titanaheterocyclopropanes,[3] titanaheterocyclopentanes and -pentenes,[4][5][6][7][8][9][10][11] or titana-2,7-dioxacyclohepta-3,5-dienes.[6][11][12] Structurally characterized nine-membered titanacycles are known as well, but most of them lack carbon in their metallacycle, as for instance TiS_8 systems.[4][13] We reported[14] on the synthesis of "carbon-rich" bis(η^5-cyclopentadienyl)titanadioxacyclononadienes **5** by a novel coupling of two α,β-unsaturated ketones with $Cp_2Ti(CO)_2$, and recently Okuda[15] published the X-ray structures of nine-membered titanacycles built up from a 2,2′-ethylenebisphenol and simple TiR_4 precursors. We now present the structure and preparative use of the titanacycles **5**, as well as cross-coupling variants of our reaction with two different ketones. We also took a closer look at the mechanism of the coupling process and performed ab initio calculations on the title complexes **5** and on conceivable intermediates like titana-2-oxacyclopent-3-enes **1**, which are hitherto unknown[16] in contrast to their zirconium analogues[17] and their isomers, the titanacyclopent-4-enes **2**.[9][10]

Figure 1. Unknown (**1**) and stable (**2**) 1-titana-2-oxacyclopentenes

Results and Discussion

Synthesis of "Symmetric" Titana-2,9-dioxacyclonona-3,7-dienes 5; Scope and Limits

We have recently shown that α,β-unsaturated arylketones (e.g. **4a**) readily react under mild, non-basic conditions with dicarbonyltitanocenes **3**[18] to furnish the corresponding nine-membered bis-unsaturated metallacycles **5** right away without five-membered species of type **1** being detectable intermediates[14]. Oxidative addition of two ketone units, loss of two equivalents of CO and exclusive *trans*-β,β coupling are the features of this reaction, which at first seemed to be restricted to bis(aryl)-substituted ketones, though.

Scheme 1

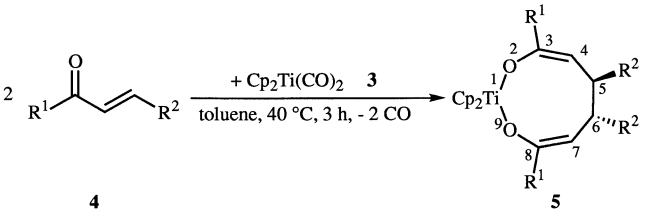

4 5

4/5	a	b	c	d	e
R^1	Ph	Ph	^{t}Bu	Ph	PhCH=CHCH=CH
R^2	Ph	Me	Ph	PhCH=CH	Ph

 © WILEY-VCH Verlag GmbH, D-69451 Weinheim, 1998 1434–1948/98/0909–1253 $ 17.50+.50/0

We now found, that the residues R^2 may also be aliphatic to give equally high yields of **5** (**5b**), whereas R^1 adjacent to the carbonyl function is more crucial to the course of the reaction. Aryl groups, alkyl systems not bearing an α-hydrogen atom, like *tert*-butyl (**5c**), or vinyl units are compatible as R^1. Ketones **4** with methyl or saturated primary or secondary alkyl groups next to the carbonyl function do usually not give any metallacycles **5** on reaction with **3** in isolable yields.

α,β;γ,δ-Bis(unsaturated) ketones (**4d**) do not give metallacycles with larger rings but merely the corresponding vinyl-substituted cyclononadienes (**5d**). Remarkably, reaction of **3** with the tris(unsaturated) ketone **4e** yields exclusively the symmetric 5,6-diphenyl-substituted derivative **5e** by a β,β-C−C coupling at the "short ends" of the trienones. This pathway may be preferred due to kinetic reasons or due to the highest degree of olefinic conjugation of the product compared with 11- or 13-membered metallacycles, which would result from β,δ-C−C and δ,δ-C−C coupling reactions, respectively. Reactions of **3** with carbocyclic ketones like **4f** also give rise to the corresponding metallacycles like **5f** without providing evidence for the intermediacy of − now bicyclic and thus in principle more stable − species of type **1**. **5f** is also the first derivative carrying substituents at each ring carbon atom.

Scheme 2

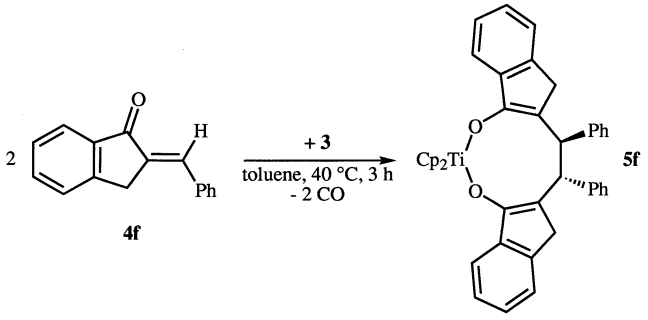

The most attractive extension of this basic reaction would be cross-coupling variants of **3** with two different unsaturated carbonyl moieties. *Intra*molecular cross-coupling does not take place, however, with ketones bearing a second unsaturated keto or ester group at an appropriate distance. Reaction of **3** with the keto ester **4g**, for instance, proceeds with 1:2 stoichiometry and with formation of titanacycle **5g** in low yield. Although bearing an α-hydrogen atom at a saturated residue R^1, complex **5g** is as stable as more typical derivatives of **5** bearing vinyl, aryl or *tert*-butyl residues at C3 and C8. **5g** is the only example of a titanacycle with this structural feature.

Table 1 shows a representative collection of new "symmetric" titanadioxacyclononadienes prepared from **4** and **3** in a 2:1 stoichiometry.

X-ray Crystal Structure of Complex 5a

So far, only a few titanaheterocycles with ring sizes larger than six have been characterized by X-ray analysis[5][13]. Single crystals of **5a** suitable for an X-ray crystal structure analysis could be obtained from a solution in toluene kept in the dark at room temperature for twenty days. To our knowledge, the structure obtained from these crystals is the first one of an unsaturated nine-membered titanacycle except for the non-cyclopentadienyl systems Ti[2,2′-ethylenebis(6-*tert*-butyl-4-methylphenolato)]X_2[15] [X = Br, O*i*Pr, $CH_2(SiMe_3)_2$].

Scheme 3

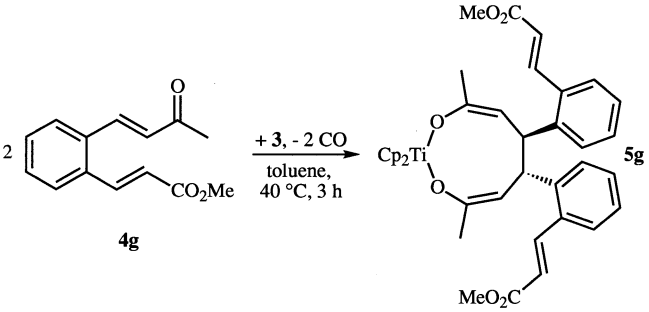

Table 1. Symmetric titanadioxacyclononadienes **5** from **3** and ketones **4**[a]

5	R^1	R^2	Yield[b]	m.p.[c]
a	Ph	Ph	52	204
b	Ph	Me	63	170
c	*t*Bu	Ph	70	181
d	Ph	PhCH=CH	85	125
e	PhCH=CHCH=CH	Ph	55	135
f	*see Scheme 2*	Ph	93	125
g	Me	*see Scheme 3*	12	170

[a] Conditions: 24 h, room temperature, 1 mmol of **3**, 2 mmol of **4**. − [b] Isolated yield in [%] based on **4**. − [c] M. p. in [°C].

Figure 2. Molecular structure of **5a**; hydrogen atoms are omitted[a]

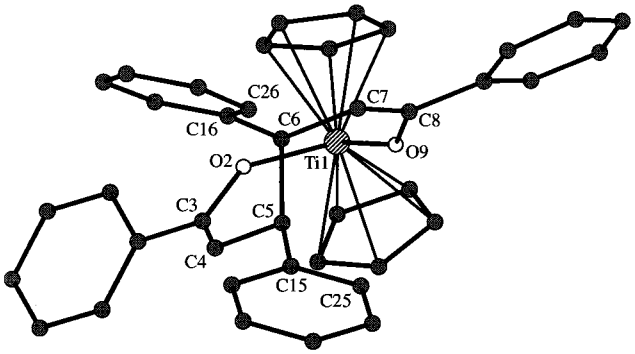

[a] Selected bond lengths [Å], angles [°] and dihedral angles [°]: Ti1−O2 1.885, Ti1−O9 1.892, O2−C3 1.359, O9−C8 1.356, C3−C4 1.344, C4−C5 1.494, C5−C6 1.587, C6−C7 1.506, C7−C8 1.346; Ti1−O2−C3 144.7, Ti1−O9−C8 143.1, O2−Ti1−O9 101.8, O2−C3−C4 121.0, O9−C8−C7 121.7, C3−C4−C5 124.3, C4−C5−C6 110.8, C5−C6−C7 111.5, C6−C7−C8 123.1; Ti1−O2−C3−C4 −67.9, Ti1−O9−C8−C7 −63.6, O2−Ti1−O9−C8 68.6, O2−C3−C4−C5 5.0, O9−Ti1−O2−C3 68.0, C3−C4−C5−C6 −58.1, C3−C4−C5−C15 174.2, C4−C5−C6−C7 150.8, C4−C5−C6−C16 −78.6, C5−C6−C7−C8 −62.0, C5−C6−C16−C26 −90.9, C6−C5−C15−C25 93.4, C6−C7−C8−O9 2.9, C15−C5−C6−C7 −79.3, C15−C5−C6−C16 51.3, C16−C6−C7−C8 167.9.

Scheme 4

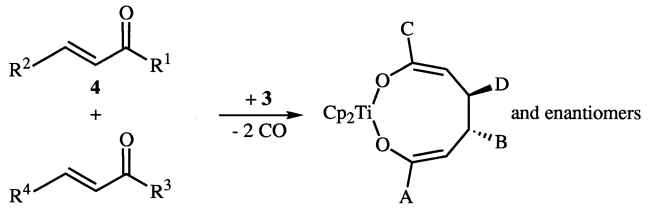

6	R^3	R^4
a	Ph	Ph
b	*o,p*-$(MeO)_2C_6H_3$	Ph
c	*p*-$(MeO)C_6H_4$	Ph
d	*p*-$(MeO)C_6H_4$	*p*-$(MeO)C_6H_4$

5: A = C = R^1, B = D = R^2
7: A = R^1, B = R^2, C = R^3, D = R^4
8: A = C = R^3, B = D = R^4

5a features roughly C_2 symmetry about an axis through the titanium atom and the opposite ring bond between C5 and C6. All bonds of the chelate have lengths as expected, with only small differences for the pairs of corresponding bonds. Only the C5−C6 bond (1.59 Å) is slightly longer than an average carbon−carbon single bond (1.55 Å).The adjoining bonds (C4−C5 and C6−C7) are both roughly 1.50 Å long. The C=C bonds C3−C4 and C7−C8 have lengths of 1.34 and 1.35 Å. Both C−O bonds have very similar lengths (1.36 Å), as have the Ti−O bonds (1.89 Å). The cyclopentadienyl rings in **5a** are staggered by an angle of 132°. In contrast, the few other published nine-membered Cp_2Ti-chelates all show eclipsed Cp ligands.[13] The titanium atom is coordinated pseudo-tetrahedrally, with the angle O−Ti−O being 102°, which is in the typical range. The metallacyclic system is puckered about the C_2 axis, the angle between the O−Ti−O plane and the opposite C5−C6 bond is roughly 90°, both C=C bonds are *cis* configured. In **5a**, the angles Ti−O−C are 143° and 145°, which are common values for unstrained cycles. All four dihedral angles including Ti−O segments are close to 70°, the dihedral angles C3−C4−C5−C6 and C5−C6−C7−C8 are ca. 60°, and the angle C4−C5−C6−C7 is 151°. This results in coplanarity of the phenyl groups at C5 and C6, which are oriented formally *trans* to each other. Crystals of **5a** pertinaciously contain half an equivalent of toluene per molecule.

Synthesis of Cross-Coupled Nine-Membered Metallacycles 7

"Unsymmetric" cross-coupled titanacycles **7** can be prepared in special cases from two unsaturated ketones **4** and **6** of sufficiently different reactivity towards **3**. In principle, three distinct products could result from reactions of a mixture of **3**, **4**, and **6**. Formation of complex **8** from **3** and two equivalents of the more reactive ketone **6** can be supressed by dropwise addition of **6** to a mixture of **4** (lower reactivity) and **3**. The ratio of chelate complexes **5** and **7** is strongly influenced by the reaction temperature. The yields of the cross-coupled products **7** increase markedly with increasing temperature. Best results are obtained by preparing a mixture of **3** and **4** at 50°C, followed immediately by dropwise addition of **6**. Only cases where **7** is formed exclusively are of synthetic interest, as separation of mixtures of **5**, **7**, and **8** is cumbersome due to their lack of air-stability and to similar chromatographic behaviour. Table 2 shows a couple of such well-defined examples.

Hydrolysis of Titanadioxacyclononadienes 5 and 7

Acidic hydrolysis of the "symmetric" titanacycles **5** leads to only one racemic pair of highly substituted cyclopentanols **10**, bearing four stereocentres, by a selective aldol reaction.[14] In most cases some diketone **9** and/or cyclopentene **12** is formed as well but can be easily removed by column chromatography. The *trans* orientation of the substituents at C3 (B) and C4 (D) is defined in the course of the β-β coupling leading to **5**. The keto function at C2 then is oriented *trans* to B and the hydroxy group at C1 is finally formed *cis* to this keto group due to favourable hydrogen bond interactions. The unambiguous assignment of the relative stereochemistry of **10** and proof of the absence of further diastereomers (or epimers) is based on NMR spectra. Table 3 shows some new examples for the formation of cyclopentanols **10** from titanacycles **5** to illustrate the widened scope and the limits of the method and the influence of the solvent used for hydrolysis. As a rule of thumb, low temperatures and the use of ethereal instead of aqueous solutions of hydrogen chloride favour the formation of cyclopentanols **10** over that of diketones **9**. Hydrolysis of the unusual titanacycle **5f** gives rise to the interesting spiro compound **10b** (besides minor amounts of diketone **9b**) featuring five stereocentres about the central cyclopentane core, although rather unselectively. All possible eight isomers (plus enantiomers), when a *trans* orientation of the phenyl groups is assumed, are found in rather arbitrary ratios and can be separated by HPLC. Hydrolyses of the "un-

Table 2. Titanadioxacyclononadienes **7** from two different ketones **4/6**[a]

7	R^1	R^2	R^3	R^4	Yield[b]	m.p.[c]	starting compounds
a	*p*-$(MeO)C_6H_4$	CH=CHPh	Ph	Ph	69	101	**4h**, **6a**[e]
b	*p*-$(MeO)C_6H_4$	CH=CHPh	*o,p*-$(MeO)_2C_6H_3$	Ph	60	115	**4h**, **6b**
c	*p*-$(MeO)C_6H_4$	CH=CHPh	*p*-$(MeO)C_6H_4$	Ph	65	114	**4h**, **6c**
d	Ph	CH=CHPh	*p*-$(MeO)C_6H_4$	*p*-$(MeO)C_6H_4$	68	–	**4e**, **6d**
e[d]	Ph	CH=CHPh	*o,p*-$(MeO)_2C_6H_3$	Ph	66	160	**4e**, **6b**
f	Ph	CH=CHPh	*p*-$(MeO)C_6H_4$	Ph	81	152	**4e**, **6c**
g	Ph	CH=CHPh	Ph	Ph	65	79	**4e**, **6a**[e]

[a] Conditions: 1 h, 50°C, 1 mmol of **3**, 1 mmol of **4**, 1 mmol of **6**, dropwise addition of **6**. – [b] Isolated yield in [%] based on **4** and **6**. – [c] M.p. in [°C]. – [d] Additionally, 7% of **5d** was obtained. – [e] Identical to **4a**.

Table 3. Hydrolysis of titanacycles **5** and **7** with ethereal (C) and aqueous (D) hydrogen chloride

9–13	method[a]	**9** yield[b]	**10** yield[b]	**11** yield[b]	**12** yield[b]	**13** yield[b]	starting compound
a	D	89	9	[c]			**5d**
a	C	35	42	[c]			**5d**
b	C	13	80	[c]			**5f**
c	D		45	[c]			**5g**
d	D	56	10	7			**7d**
e	D	55	11	8			**7e**
e	C				35	25	**7e**
f	C				38	27	**7f**

[a] Method C: excess HCl in Et_2O, 3 h, −10°C; method D: excess HCl in H_2O, 3 h, room temperature. – [b] Isolated yield in [%] based on **4** and **6**. – [c] **11** identical to **10**.

Scheme 5. Hydrolysis of titanadioxacyclononadienes **5**[a] and **7**

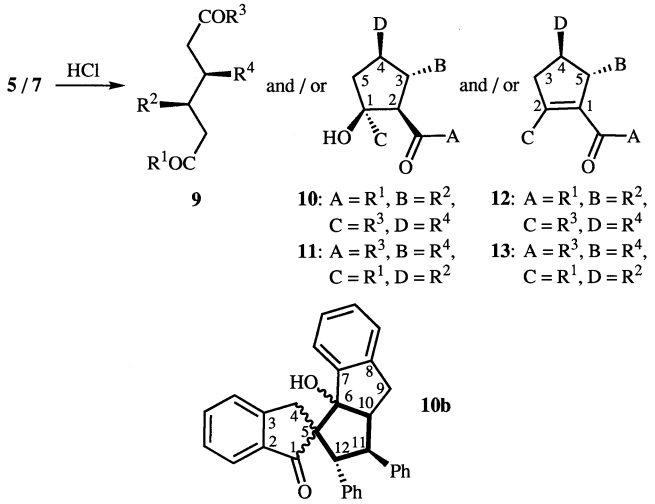

[a] If **5** is involved instead of **7**, for all compounds applies $R^1 = R^3$ and $R^2 = R^4$; only one regioisomer of cyclopentanol (designated **10** in Table 3) or cyclopentene is possible.

symmetric" titanacycles **7** are of little synthetic use, as leading merely to mixtures of alcohols **10/11** and of cyclopentenes **12/13**. Two typical examples are enclosed in Table 3.

Ab Initio Calculations on Five- and Nine-Membered Metallacycles

As mentioned above, all our attempts to obtain even trace amounts of the expected intermediate titana-2-oxacyclopent-3-enes **1** instead of the exclusively formed corresponding nine-membered titanacycles **5** were unsuccessful. On the other hand, stable examples of the isomeric titana-2-oxacyclopent-4-ene **2** have been reported by several research groups. In order to understand this difference, we performed ab initio (MP2) and hybrid density functional (B3LYP) calculations on **1**, **2**, **5**, and some related species.[19][20][21][22][23] With one exception (see below), both methods yield essentially the same results. The calculated geometries are in good agreement with available experimental data. Figure 3 shows the MP2-optimized structures of **1** and **2**.

Titana-2-oxacyclopent-3-ene **1** is computed to be 10 kcal/mol more stable than its isomer **2**. The five-membered ring in **2** is planar, with bond lengths and angles indicating regular C–C single and double bonds (bond lengths are 1.506 and 1.343 Å, respectively). The computed values agree well with those obtained in the crystal structure determination of the diphenyl derivative, the main difference being a slight folding of the five-membered ring in the experimental structure.[9][10] In the computed structure of **1**, however, the ring is strongly folded, with significant delocalization (C–C bond lengths are 1.446 and 1.394 Å for the formal single and double bonds, respectively). As far as we know, no bis(cyclopentadienyl)-substituted five-membered titanacycles with structures deviating significantly from planarity are published. Thus, instead of a titanacyclopentene with a Ti–C σ bond, our calculations predict a strong interaction of the titanium centre with the CH_2 moiety and the C–C double bond in a π-allylic fashion. While unusual in organotitanium compounds, π-allylic bonding is common for the later transition metals. With 2.267 Å, the computed Ti–CH_2 distance is roughly 0.1 Å longer than a regular Ti–C single bond. The distances to the double bond carbon atoms are 2.451 and 2.520 Å. Due to the short distance between the metal centre and the double bond, an exceptionally small value of 94° results for the Ti–O–C angle. Analysis of the electronic structure reveals a strong donation from the π-bond to the metal centre and an increased polarity of the Ti–CH_2 σ bond. Thus, **1** is best described as a C-nucleophilic electron-rich (18 valence electrons) allyl complex.

Figure 3. MP2-optimized structures of titana-2-oxacyclopentenes **1** ($R^{1,2}$ = H), left, and **2** ($R^{1,2}$ = H), right[a]

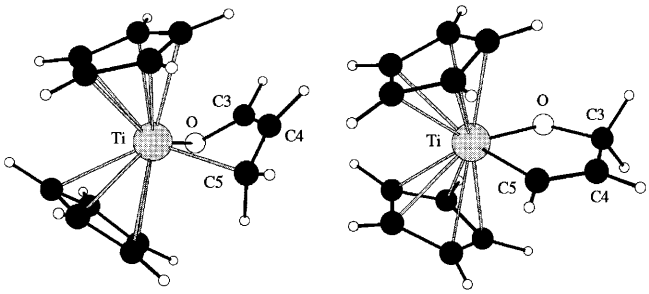

[a] Selected bond lengths [Å] and angles [°]: **1**: Ti–O 1.9734, Ti–C3 2.4512, Ti–C4 2.5199, Ti–C5 2.2670, C3–C4 1.3942, C4–C5 1.4461; Ti–O–C3 93.8; **2**: Ti–O 1.8280, Ti–C5 2.1638, C3–C4 1.5031, C4–C5 1.3524; Ti–O–C3 125.2.

Two conformations are possible for **5**, which differ in the orientation of the organic fragment with respect to the Cp_2TiO_2 moiety. The geometric data of the experimental conformer are in good agreement with the X-ray structure. The relative stability of the two conformers is predicted differently by the MP2 and B3LYP methods, although the actual difference is small. At MP2/TZ2p, the experimental conformer is 1.2 kcal/mol more stable, whereas B3LYP/TZ2p predicts it to be less stable by 1.1 kcal/mol.

A possible route to **5** involves addition of **1** to propenal. This reaction is calculated to be 49 kcal/mol exothermic. The activation barrier appears to be very low: several attempts, with different starting geometries, were made to compute the structure of the initial complex for the addition but in all cases, the structure collapsed to **5** during the optimization. We believe the combination of the unusual bonding features in **1**, in particular the lengthening and corresponding weakening of the $Ti-CH_2$ bond, and the significant exothermicity of the reaction to be responsible for this behaviour.

We probed alternative mechanisms via complexes of titanocene and two propenal moieties. These gave the same result as above (optimization leads to **5** without activation barrier), but in all cases, high-energy intermediates must be involved. Hence, we consider these alternatives less probable than reaction via **1**.

Conclusions

By careful choice of conditions, novel nine-membered titanadioxacycles **5** and **7** can be prepared from α,β-unsaturated ketones with a broad variety of substituents. The X-ray analysis of the tetraphenyl derivative **5a** revealed a C_2-symmetric puckered structure with two *Z*-configured C=C bonds and a *trans* orientation of residues about the newly formed C−C bond. Acidic hydrolysis of these chelate complexes is synthetically useful in case of "symmetrically" substituted derivatives **5**, where highly substituted cyclopentanes **10** are obtained as one racemic pair of stereoisomers out of eight possible ones, due to selectivity in the C−C bond formation process and to steric restraints and preferences. Ab initio calculations on the nine-membered rings **5** and on conceivable five-membered intermediates were performed. For the expected intermediate complex **1** of our coupling reaction, an unusual structure of high reactivity of the Ti−C σ bond due to an interaction of the titanium centre with the CH_2 moiety and the C−C double bond in a π-allylic fashion was calculated, thus providing an explanation for its elusive character. Further work is in progress now to prepare titanacycles with even larger rings by similar C−C coupling reactions or by Cope rearrangement of aptly substituted nine-membered systems like **5d**.

Financial support from the *Volkswagen-Stiftung* and the *Fonds der Chemischen Industrie e. V.* is gratefully acknowledged.

Experimental Section

General Information: All reactions involving organometallic compounds were carried out in an inert atmosphere (argon) using Schlenk-type glassware. Solvents were dried and distilled under argon prior to use according to standard procedures. The starting complex **3**[18] as well as most of the unsaturated ketones were prepared as published [**4b**[24] by Wittig reaction, **4c−e**[25], **4f**[26], **4h** [1-(*p*-methoxyphenyl)-5-phenylpentadien-1-one][25], **6b−d**[25] by aldol condensation]. Compound **4a** (= **6a**) is commercially available (Fluka). − Melting points are not corrected, boiling points quoted for Kugelrohr distillations refer to the temperature of the air bath. − NMR: Jeol JNMX GX-400 and PMX-60; δ given in ppm; TMS as internal standard. − IR: Bruker IFS 48, Beckmann Acculab A1, A3. − MS: Varian MAT CH-4B (EFO-4B-source), Varian MAT 311A (EI/FD source). − MA: Heraeus Mikromat C-H-N. − HPLC: Shimadzu LC-10 AT, SIL-10 A, CBM 10 A, SPD-10 M A, FCV-10 AL; column: Macherey-Nagel Nucleosil ET 200/4. − Isomeric ratios were determined from the relative intensities of the pertaining ^{1}H-NMR signals or by analytic HPLC.

1. *Synthesis of Ketone* **4g**. − *Synthesis of Methyl (o-Formyl-trans-cinnamate):* 2.24 g (16.7 mmol) of phthaldialdehyde were dissolved in 40 ml of THF and stirred at 60°C. A solution of 4.95 g (16.7 mmol) of (methoxycarbonylmethylene)triphenylphosphorane[27] in 100 ml of THF was added dropwise over a period of 1 h and the mixture was then stirred overnight. The solvent was then removed in vacuo and most of the PPh_3O by repeated chromatography over silica gel using neat CH_2Cl_2 as the eluent. GC analysis of the eluate showed 58% of product, 17% of starting dialdehyde, 10% of double-olefination product, and 8% of PPh_3O. Final purification by Kugelrohr distillation (110−120°C, 0.5 mbar) gave 1.54 g (8.0 mmol; 48%) of the cinnamate as a bright yellow viscous oil. − ^{1}H NMR (60 MHz, $CDCl_3$): δ = 3.8 (s, 3 H, CH_3), 6.3 (d, ^3J = 16 Hz, 1 H, CH=C*H*C=O), 7.4−7.9 (m, 4 H, H^{ar}), 8.5 (d, ^3J = 16 Hz, 1 H, C*H*=CHC=O), 10.2 (s, 1 H, CHO). − $C_{11}H_{10}O_3$ (190.20): calcd. C 69.47, H 5.30; found C 69.11, H 5.63. − *Synthesis of Methyl [(o-3′-Oxobutenyl)-trans-cinnamate]* (**4g**): 1.54 g (8.08 mmol) of methyl (*o*-formyl-*trans*-cinnamate) was dissolved in 30 ml of THF and stirred at 40°C. A solution of 2.37 g (8.08 mmol) of (2-oxopropylene)triphenylphosphorane[28] in 50 ml of THF was added dropwise and the resulting mixture was stirred at 50°C overnight. The solvent was then removed to leave a crude product which was purified by CC (silica gel; CH_2Cl_2): 1.15 g (4.99 mmol; 62%); pale solid; m.p. 46°C. − ^{1}H NMR (60 MHz, $CDCl_3$): δ = 2.4 (s, 3 H, CH_3CO), 3.8 (s, 3 H, OCH_3), 6.30 (d, ^3J = 16 Hz, 1 H, CH=C*H*CO_2CH_3), 6.55 (d, ^3J = 16 Hz, 1 H, CH=C*H*$COCH_3$), 7.2−7.65 (m, 4 H, H^{ar}), 7.85 (d, ^3J = 16 Hz, 1 H, C*H*=CHCOCH_3), 8.0 (d, ^3J = 16 Hz, 1 H, C*H*=CHCOOCH_3) .− $C_{14}H_{14}O_3$ (230.27): calcd. C 73.03, H 6.13; found C 73.14, H 5.90.

2. *Synthesis of* **5**. − *General Procedure (A):* The respective α,β-unsaturated ketone **4** (2 mmol) was added to a solution of **3** (234 mg; 1 mmol) in toluene (15 ml) and the resulting mixture stirred at 40°C for 3 h. Once the starting materials were completely consumed, 5 ml of hexane was added to give a precipitate which was collected on a sinter funnel, washed twice with hexane and dried in vacuo. For analytical purposes samples of **5** were recrystallized from CH_2Cl_2/hexane (2:1).

(±)-(5,6-threo-3Z,7Z)-1,1-Bis(η^5-cyclopentadienyl)-3,5,6,8-tetraphenyl-1-titana-2,9-dioxacyclonona-3,7-diene (**5a**)[29]: 3.50 g (5.89 mmol; 52%) from 2.65 g of **3** and 4.71 g of **4a**; dark red air-sensitive crystals from toluene; m.p. 204°C. − IR (KBr): $\tilde{\nu}$ = 3040 cm^{-1}, 3030, 3020, 1600, 1490, 1450, 1330, 810, 750, 700. − ^{1}H NMR (400 MHz, C_6D_6)[30]: δ = 5.03 (d, ^3J = 5.50 Hz, 2 H, 5-H, 6-H), 5.89 (d, ^3J = 5.50 Hz, 2 H, 4-H, 7-H), 5.95 (s, 10 H, Cp), 7.07 (m, 10 H, H^{ar}), 7.21 (t, ^3J = 7.15 Hz, 2 H, H^{ar}), 7.31 (t, ^3J = 7.15 Hz, 4 H, H^{ar}), 7.59 (d, ^3J = 7.15 Hz, 4 H, H^{ar}). − ^{13}C NMR

(100.4 MHz, C_6D_6): δ = 48.1 (C-5, C-6), 106.8 (C-4, C-7), 116.2 (Cp), 125.0, 126.1, 127.4, 128.1, 128.7, 129.9 (CH^{ar}), 140.6, 143.2 (*ipso*-C), 163.8 (C-3, C-8). − MS (70 eV); *m/z* (%): 386 (6) [M^+ − PhCH=CHCOPh], 207 (96) [PhCOCH=CPh^+], 178 (49) [Cp_2Ti^+], 105 (61) [$PhCO^+$], 77 (100) [Ph^+]. − $C_{40}H_{34}O_2Ti$ (594.34): calcd. C 80.83, H 5.72; found C 80.68, H 5.78.

X-ray Crystal Structure Analysis of **5a**[31][32]: Clear, dark red single crystals of **5a** × toluene were obtained directly from the reaction mixture upon standing 2 d in the dark. Formula $C_{44}H_{34}O_2Ti$, molar mass 642.61 g mol^{-1}, crystal size 0.5 × 0.3 × 0.1 mm, a = 15.924(3), b = 8.347(2), c = 24.558(5) Å, β = 99.34(3)°, V = 3221.1(11) $Å^3$, T = 173(2) K; $d_{calcd.}$ = 1.325 g cm^{-3}, μ = 3.05 cm^{-1}, Z = 4, monoclinic, space group $P2(1)/c$, Nonius MACH3 diffractometer, λ = 0.71037 Å, Θ range 2.58−24.98°; ω/Θ scans, index ranges $-18 \le h \le 18$, $-9 \le k \le 0$, $-29 \le l \le 0$, 5794 collected reflections, 2625 reflections [$I > 2\sigma(I)$], 428 refined parameters, absorption correction with Ψ scans. Structure solution: direct methods (SHELXS86); structure refinement: full-matrix least squares on F^2 (SHELXL93), H atoms calculated and not included into least-squares refinement. In the unit cell two additional strongly disordered toluene molecules were found. $R1$ = 0.0746, $wR2$ = 0.2265 (all data), largest diff. peak and hole 0.552 and −0.747 $eÅ^{-3}$ with $R1 = \Sigma|F_o - F_c|/\Sigma F_o$ and $wR2 = \{\Sigma w(F_o^2 - F_c^2)^2/\Sigma[w(F_o^2)^2\}^{0.5}$.

(±)-(5,6-threo-3Z,7Z)-1,1-Bis(η⁵-cyclopentadienyl)-5,6-dimethyl-1-titana-2,9-dioxa-3,8-diphenylcyclonona-3,7-diene (**5b**): 296 mg (0.63 mmol; 63%) from 234 mg of **3** and 444 mg of **4b**; dark red air-sensitive needles from toluene; m.p. 170°C. − IR (KBr): $\tilde{\nu}$ = 3058 cm^{-1}, 2961, 1680, 1447, 1271, 803. − ^{1}H NMR (400 MHz, C_6D_6)[30]: δ = 1.18 (d, ^3J = 7.14 Hz, 6 H, CH_3), 3.36 (m, 2 H, 5-H, 6-H), 5.49 (d, ^3J = 5.50 Hz, 2 H, 4-H, 7-H), 5.90 (s, 10 H, Cp), 7.16−7.57 (m, 10 H, H^{ar}). − ^{13}C NMR (100.4 MHz, C_6D_6): δ = 15.7 (5-C, 6-C), 33.5 (C-5, C-6), 109.8 (C-4, C-7), 115.8 (Cp), 125.3, 126.1, 127.1 (CH^{ar}), 140.1 (3-C, 8-C), 163.8 (C-3, C-8). − MS (70 eV); *m/z* (%): 276 (10), 178 (65) [Cp_2Ti], 171 (25), 105 (100) [$C_6H_5CO^+$]. − $C_{30}H_{30}O_2Ti$ (470.47): calcd. C 76.59, H 6.38; found C 76.20, H 5.97.

(±)-(5,6-threo-3Z,7Z)-1,1-Bis(η⁵-cyclopentadienyl)-3,8-di-tert-butyl-1-titana-2,9-dioxa-5,6-diphenylcyclonona-3,7-diene (**5c**): 390 mg (0.7 mmol; 70%) from 234 mg of **3** and 528 mg of **4c**; dark red air-sensitive needles from toluene; m.p. 181°C. − IR (KBr): $\tilde{\nu}$ = 3058 cm^{-1}, 2952, 1604, 1452, 1306, 1079, 806. − ^{1}H NMR (400 MHz, C_6D_6)[30]: δ = 1.21 (s, 18 H, CH_3), 4.22 (d, ^3J = 6.05 Hz, 2 H, 5-H, 6-H), 5.00 (d, ^3J = 6.05 Hz, 2 H, 4-H, 7-H), 6.01 (s, 10 H, Cp), 7.89−7.93 (m, 10 H, H^{ar}). − ^{13}C NMR (100.4 MHz, C_6D_6): δ = 29.5 (CH_3), 37.6 (3-C, 8-C), 47.8 (C-5, C-6), 101.7 (C-4, C-7), 116.3 (Cp), 127.8, 128.4, 128.9 (CH^{ar}), 145.2 (5-C, 6-C), 173.2 (C-3, C-8). − MS (70 eV); *m/z* (%): 378 (10), 321 (90), 278 (60), 189 (50), 131 (100). − $C_{36}H_{42}O_2Ti$ (554.63): calcd. C 77.97, H 7.58; found C 78.22, H 7.40.

(±)-(5,6-threo-3Z,7Z)-1,1-Bis(η⁵-cyclopentadienyl)-5,6-bis-β-(trans-phenylethenyl)-1-titana-2,9-dioxa-3,8-diphenylcyclonona-3,7-diene (**5d**): 549 mg (0.85 mmol; 85%) from 234 mg of **3** and 468 mg of **4d**; dark red air-sensitive needles from toluene; m.p. 125°C. − IR (KBr): $\tilde{\nu}$ = 2850 cm^{-1}, 1600, 1100, 800. − ^{1}H NMR (400MHz, C_6D_6)[30]: δ = 4.46 (dd, ^3J = 4.94, 5.50 Hz, 2 H, 5-H, 6-H), 5.98 (d, ^3J = 5.50 Hz, 2 H, 4-H, 7-H), 6.06 (s, 10 H, Cp), 6.80 (dd, ^3J = 4.98, 15.95 Hz, 2 H, C*H*=CHPh), 6.98 (d, ^3J = 15.95 Hz, 2 H, CHPh), 7.11−8.07 (m, 20 H, H^{ar}). − ^{13}C NMR (100.4 MHz, C_6D_6): δ = 45.1 (C-5, C-6), 92.1, 92.7 (*C*H=*C*HPh), 102.2 (C-4, C-7), 116.2 (Cp), 126.4, 126.7, 127.9, 128.6, 129.7, 130.1 (CH^{ar}), 145.2, 146.4 (*ipso*-C), 163.5 (C-3, C-8). − MS (70 eV); *m/z* (%): 542 (7), 348 (7), 382 (38), 234 (45), 105 (100). − $C_{44}H_{38}O_2Ti$ (646.69): calcd. C 81.73, H 5.88; found C 81.87, H 6.02.

(±)-(5,6-threo-3Z,7Z)-1,1-Bis(η⁵-cyclopentadienyl)-3,8-bis-δ-(phenyl-trans,trans-butadienyl)-1-titana-2,9-dioxa-5,6-diphenylcyclonona-3,7-diene (**5e**): 384 mg (0.55 mmol; 55%) from 234 mg of **3** and 520 mg of **4e**; dark red air-sensitive needles from toluene; m.p. 135°C. − IR (KBr): $\tilde{\nu}$ = 3065−3024 cm^{-1}, 1580, 1565, 1490, 785, 750. − ^{1}H NMR (400 MHz, C_6D_6)[30]: δ = 4.92 (d, ^3J = 5.61 Hz, 2 H, 5-H, 6-H), 5.35 (d, ^3J = 5.61 Hz, 2 H, 4-H, 7-H), 5.98 (s, 10 H, Cp), 6.22−7.52 (m, 28 H, CH=CH-CH=CH and H^{ar}). − ^{13}C NMR (100.4 MHz, C_6D_6), δ = 48.6 (C-5, C-6), 114.9 (C-4, C-7), 115.8 (Cp), 125.6, 126.1, 126.6, 126.7 (CH=CHCH=CH), 129.1, 129.7, 129.8 (CH^{ar}), 138.2, 144.2 (*ipso*-C), 163.6 (C-3, C-8). − MS (70 eV); *m/z* (%): 488 (15), 448 (35), 460 (65), 260 (100), 178 (76) [Cp_2Ti^+]. − $C_{48}H_{42}O_2Ti$ (698.77): calcd. C 82.52, H 6.01; found C 82.71, H 6.16.

(±)-(5,6-threo)-1,1-Bis(η⁵-cyclopentadienyl)-5,6-diphenylbis-indeno[3,2-c;2′,3′-g]-1-titana-2,9-dioxa-cyclonona-3,7-diene (**5f**): 380 mg (0.6 mmol; 93%) from 154 mg of **3** and 440 mg of **4f**; dark red air-sensitive needles from toluene; m.p. 125°C (decomp.). − IR ($CDCl_3$): $\tilde{\nu}$ = 3068 cm^{-1}, 2961, 2878,1572, 1559. − ^{1}H NMR (400 MHz, $CDCl_3$)[30]: δ = 3.11 (d, ^2J = 22.10 Hz, 2 H, C*H*H′), 3.24 (d, ^2J = 22.10 Hz, 2 H, CH*H*′), 5.10 (s, 2 H, 5-H, 6-H), 6.47 (s, 10 H, Cp), 7.01 (m, 4 H, H^{ar} of C_6H_5), 7.04 (m, 2 H, H^{ar} of C_6H_5), 7.04 (dd, ^3J = 7.44, 7.44 Hz, 2 H, H^{ar} of C_6H_4), 7.08 (m, 4 H, H^{ar} of C_6H_5), 7.16 (d, ^3J = 7.44 Hz, 2 H, H^{ar} of C_6H_4), 7.23 (d, ^3J = 7.44 Hz, 2 H, H^{ar} of C_6H_4), 7.26 (dd, ^3J = 7.44, 7.44 Hz, 2 H, H^{ar} of C_6H_4). − ^{13}C NMR (100.4 MHz, $CDCl_3$): δ = 36.2 (4-C, 7-C), 49.7 (C-5, C-6), 116.7 (Cp), 117.0 (CH^{ar}), 119.7 (C-4, C-7), 123.7, 123.8, 125.5, 125.7, 127.4, 129.8 (CH^{ar}), 142.0, 143.2, 143.7 (*ipso*-C), 162.0 (C-3, C-8). − MS (70 eV); *m/z* (%): 406 (60) [M^+ − $Cp_2Ti(OH)_2$], 333 (93), 219 (40), 66 (100) [CpH^+]. − $C_{42}H_{34}O_2Ti$ (618.64): calcd. C 81.55, H 5.50; found C 81.63, H 5.44.

(±)-(5,6-threo-3Z,7Z)-1,1-Bis(η⁵-cyclopentadienyl)-3,8-dimethyl-5,6-bis(o-methyl-trans-cinnamoyl)-1-titana-2,9-dioxa-cyclonona-3,7-diene (**5g**): 95 mg (0.15 mmol; 12%) from 567 mg **3** and 460 mg **4g**; dark red air-sensitive needles from toluene; m.p. 170°C (decomp.). − IR (CH_2Cl_2): $\tilde{\nu}$ = 1710 cm^{-1}, 1625, 1310, 1165. − ^{1}H NMR (400 MHz, $CDCl_3$)[30]: δ = 1.82 (s, 6 H, CCH_3), 3.82 (s, 6 H, OCH_3), 4.31 (d, ^3J = 5.70 Hz, 2 H, 5-H, 6-H), 4.92 (d, ^3J = 5.70 Hz, 2 H, 4-H, 7-H), 6.07 (d, ^3J = 8.10 Hz, 2 H, H^{ar}), 6.35 (d, ^3J = 15.70 Hz, 2 H, CH=C*H*CO), 6.40 (s, 10 H, Cp), 6.88 (dd, ^3J = 7.10, 8.10 Hz, 2 H, H^{ar}), 7.09 (dd, ^3J = 7.10, 8.10 Hz, 2 H, H^{ar}), 7.56 (d, ^3J = 8.10 Hz, 2 H, H^{ar}), 8.32 (d, ^3J = 15.70 Hz, 2 H, C*H*=CHCO). − ^{13}C NMR (100.4 MHz, $CDCl_3$): δ = 23.0 (3-C, 8-C), 42.2 (C-5, C-6), 51.4 (OCH_3), 103.9 (C-4, C-7), 115.7 (Cp), 117.9 (CH=*C*HCO), 125.8, 125.8, 128.4, 131.7 (CH^{ar}), 133.9 (*C*CH=CHCO), 143.0 (5-C, 6-C), 145.3 (*C*H=CHCO), 164.4 (C-3, C-8), 167.7 (CO_2CH_3). − MS (70 eV); *m/z* (%): 638 (2) [M^+], 408 (11) [$M^+ - C_{14}H_{14}O_3$], 278 (16) [408 − 2 Cp], 219 (35) [$Cp_2TiOCCH^+$], 178 (87) [Cp_2Ti^+], 128 (99), 43 (100). − $C_{38}H_{38}O_6Ti$ (638.62): calcd. C 71.47, H 6.00; found C 71.42, H 5.81.

3. *Synthesis of* **7**. − *General Procedure (B):* The respective α,β-unsaturated ketone **4** (1 mmol) was added at once to a solution of **3** (234 mg; 1 mmol) in toluene (15 ml) at 50°C. Immediately thereafter, a solution of 1 mmol of the second ketone **6** in toluene (20 ml) was added dropwise over a period of 30 min. Once the starting materials were completely consumed (NMR monitoring, typically 1 h), the solution was filtered at ambient temperature, 5 ml of hexane was added and the resulting precipitate was collected on a sinter funnel, washed twice with hexane and dried in vacuo. For ana-

lytical purposes samples of **7** were recrystallized from CH_2Cl_2/hexane (2:1).

(5,6-threo-3Z,7Z)-3-(p-Anisyl)-1,1-bis(η^5-cyclopentadienyl)-6,8-diphenyl-5-(β-trans-phenylethenyl)-1-titana-2,9-dioxacyclonona-3,7-diene (**7a**): 448 mg (0.69 mmol; 69%) from 234 mg of **3**, 264 mg of **4h** and 208 mg of **4a** (as the more reactive component); dark red air-sensitive needles from toluene; m.p. 101°C. − IR (KBr): $\tilde{\nu}$ = 3025 cm^{-1}, 2834, 1598, 1506, 1284, 811. − ^1H NMR (400 MHz, C_6D_6)[30][33]: δ = 3.42 (s, 3 H, CH_3), 4.46 (dd, ^3J = 5.62, 5.86 Hz, 1 H, 5-H), 4.84 (d, ^3J = 5.86 Hz, 1 H, 6-H), 5.49 (d, ^3J = 5.62 Hz, 1 H, 4-H), 5.97 (s, 5 H, Cp), 6.02 (s, 5 H, Cp), 6.04 (d, ^3J = 5.86 Hz, 1 H, 7-H), 6.15 (dd, ^3J = 5.86, 15.63 Hz, 1 H, C*H*=CHPh), 6.63 (d, ^3J = 15.63 Hz, 1 H, CH=C*H*Ph), 6.92−7.62 (m, 19 H, H^{ar}). − ^{13}C NMR (100.4 MHz, C_6D_6): δ = 45.2, 47.5 (C-5, C-6), 55.1 (CH_3), 110.2, 112.9 (C-4, C-7), 116.1 (Cp), 125.1, 126.9 (*C*H=*C*HPh), 129.1, 129.7, 130.1, 130.7, 130.9, 134.1, 135.7, 137.2, 138.5, 138.9 (CH^{ar}), 141.2, 143.8, 144.3, 144.8 (*ipso*-C), 159.1 (*C*OCH_3), 163.1, 163.9 (C-3, C-8). − MS (70 eV); *m/z* (%): 512 (10), 456 (60), 365 (22), 295 (25), 208 (18) [PhCH=CHCOPh$^+$], 105 (100). − $C_{43}H_{38}O_3Ti$ (650.68): calcd. C 79.38, H 5.38; found C 79.52, H 5.48.

(5,6-threo-3Z,7Z)-8-(p-Anisyl)-1,1-bis(η^5-cyclopentadienyl)-3-(o,p-dimethoxyphenyl)-5-phenyl-6-β-(trans-phenylethenyl)-1-titana-2,9-dioxacyclonona-3,7-diene (**7b**): 426 mg (0.6 mmol; 60%) from 234 mg of **3**, 264 mg of **4h** and 268 mg of **6b**; dark red air-sensitive needles from toluene; m.p. 115°C. − IR (KBr): $\tilde{\nu}$ = 3025 cm^{-1}, 2934, 2836, 1600, 1254, 808. − ^1H NMR (400 MHz, C_6D_6)[30][33]: δ = 3.35 (s, 3 H, CH_3), 3.43 (s, 6 H, CH_3), 4.58 (dd, ^3J = 5.86, 5.86 Hz, 1 H, 6-H), 4.89 (d, ^3J = 5.86 Hz, 1 H, 5-H), 5.53 (d, ^3J = 5.86 Hz, 1 H, 7-H), 6.03 (d, ^3J = 5.86 Hz, 1 H, 4-H), 6.07 (s, 5 H, Cp), 6.08 (s, 5 H, Cp), 6.18 (dd, ^3J = 5.86, 15.86 Hz, 1 H, C*H*=CHPh), 6.76 (d, ^3J = 15.86 Hz, 1 H, CH=C*H*Ph), 6.90−7.68 (m, 17 H, H^{ar}). − ^{13}C NMR (100.4 MHz, C_6D_6): δ = 46.0, 48.1 (C-5, C-6), 54.7, 54.8, 54.9 (CH_3), 113.9, 114.2 (C-4, C-7), 116.1 (Cp), 124.2, 126.7 (*C*H=*C*HPh), 126.2, 126.9, 127.3, 127.8, 129.4, 132.3, 133.7, 134.5, 136.1, 137.8, 138.2 (CH^{ar}), 142.2, 142.9, 144.1, 144.8 (*ipso*-C), 158.5, 159.6, 160.6 (*C*OCH_3), 162.2, 162.9 (C-3, C-8). − MS (70 eV); *m/z* (%): 486 (42), 460 (10), 395 (15), 351 (30), 264 (17) [$C_{18}H_{16}O_2^+$], 238 (20). − $C_{45}H_{42}O_5Ti$ (710.73): calcd. C 76.05, H 5.92; found C 75.94, H 5.88.

(5,6-threo-3Z,7Z)-3,8-Bis(p-anisyl)-1,1-bis(η^5-cyclopentadienyl)-5-phenyl-6-β-(trans-phenylethenyl)-1-titana-2,9-dioxacyclonona-3,7-diene (**7c**): 442 mg (0.65 mmol; 65%) from 234 mg of **3**, 264 mg of **4h** and 238 mg of **6c**; dark red air-sensitive needles from toluene; m.p. 114°C.− IR (KBr): $\tilde{\nu}$ = 3026 cm^{-1}, 2960, 1600, 1251, 810. − ^1H NMR (400 MHz, C_6D_6)[30][33]: δ = 3.21 (s, 3 H, CH_3), 3.23 (s, 3 H, CH_3), 4.50 (dd, ^3J = 5.71, 5.71 Hz, 1 H, 6-H), 4.86 (d, ^3J = 5.86 Hz, 1 H, 5-H), 5.51 (d, ^3J = 5.71 Hz, 1 H, 7-H), 5.96 (d, ^3J = 5.86 Hz, 1 H, 4-H), 6.02 (s, 5 H, Cp), 6.04 (s, 5 H, Cp), 6.18 (dd, ^3J = 5.71, 15.86 Hz, 1 H, C*H*=CHPh), 6.53 (d, ^3J = 15.86 Hz, 1 H, CH=C*H*Ph), 6.71−7.85 (m, 18 H, H^{ar}). − ^{13}C NMR (100.4 MHz, C_6D_6): δ = 46.5, 48.3 (C-5, C-6), 54.5, 54.8 (CH_3), 113.5, 114.0 (C-4, C-7), 115.7 (Cp), 124.5, 127.2 (*C*H=*C*H), 126.4, 126.7, 127.3, 127.7, 129.5, 132.7, 134.7, 135.5, 136.5, 137.5, 138.1, 138.9 (CH^{ar}), 142.2, 142.5, 144.4, 145.2 (*ipso*-C), 156.5, 156.9 (*C*OCH_3), 163.1, 163.5 (C-3, C-8). − MS (70 eV); *m/z* (%): 516 (20), 381 (25), 264 (22) [$C_{18}H_{16}O_2^+$], 165 (100). − $C_{44}H_{40}O_4Ti$ (680.71): calcd. C 77.67, H 5.88; found C 76.50, H 5.75.

(5,6-threo-3Z,7Z)-3,5-Bis(p-anisyl)-1,1-bis(η^5-cyclopentadienyl)-8-phenyl-6-β-(trans-phenylethenyl)-1-titana-2,9-dioxacyclonona-3,7-diene (**7d**): 462 mg (0.68 mmol; 68%) from 234 mg of **3**, 234 mg of **4d** and 268 mg of **6d**; dark red air-sensitive needles from toluene. − IR (KBr): $\tilde{\nu}$ = 3008−2800 cm^{-1}, 1595, 1480, 1245, 1070, 805. − ^1H NMR (400 MHz, C_6D_6)[30][33]: δ = 3.03 (s, 3 H, CH_3), 3.12 (s, 3 H, CH_3), 4.16 (dd, ^3J = 5.62, 5.86 Hz, 1 H, 6-H), 4.70 (d, ^3J = 5.62 Hz, 1 H, 5-H), 5.33 (d, ^3J = 5.62 Hz, 1 H, 7-H), 5.67 (s, 5 H, Cp), 5.70 (s, 5 H, Cp), 5.80 (d, ^3J = 5.62 Hz, 1 H, 4-H), 5.90 (dd, ^3J = 5.86, 15.62 Hz, 1 H, C*H*=CHPh), 6.34 (d, ^3J = 15.62 Hz, 1 H, CH=C*H*Ph), 6.35−7.82 (m, 18 H, H^{ar}). − ^{13}C NMR (100.4 MHz, C_6D_6): δ = 45.2, 47.2 (C-5, C-6), 54.61, 54.67 (CH_3), 112.2, 112.4 (C-4, C-7), 116.2 (Cp), 122.2, 123.1 (*C*H=*C*HPh), 125.8, 126.3, 127.1, 127.9, 132.8, 134.5, 135.3, 136.8, 139.1, 139.9 (CH^{ar}), 142.1, 142.7 (*ipso*-C of C_6H_5), 150.2, 150.8 (*ipso*-C of $C_6H_4OCH_3$), 159.4, 159.9 (*C*OCH_3), 163.0, 163.8 (C-3, C-8). − MS (70 eV); *m/z* (%): 444 (20), 324 (18), 178 (65) [Cp2Ti$^+$],105 (100) [PhCO$^+$]. − $C_{44}H_{40}O_4Ti$ (680.7): calcd. C 77.64, H 6.15; found C 77.62, H 5.98.

(5,6-threo-3Z,7Z)-1,1-Bis(η^5-cyclopentadienyl)-3-(o,p-dimethoxyphenyl)-5,8-diphenyl-6-β-(trans-phenylethenyl)-1-titana-2,9-dioxacyclonona-3,7-diene (**7e**): A mixture of 449 mg of **7e** (0.66 mmol; 66%) and **5d** (0.07 mmol; 7%) from 234 mg of **3**, 234 mg of **4d**, and 268 mg of **6b**; ratio **7e/5d** determined by NMR; **7e** purified by crystallization from CH_2Cl_2/hexane (2:1); dark red air-sensitive needles from toluene, m.p. 160°C. − IR (KBr): $\tilde{\nu}$ = 3030−2820 cm^{-1}, 1600, 1430, 1240, 1020, 810. − ^1H NMR (400 MHz, C_6D_6)[30][33]: δ = 3.36 (s, 3 H, CH_3), 3.44 (s, 3 H, CH_3), 4.56 (dd, ^3J = 5.71, 5.86 Hz, 1 H, 6-H), 4.86 (d, ^3J = 5.86 Hz, 1 H, 5-H), 5.51 (d, ^3J = 5.71 Hz, 1 H, 7-H), 5.96 (d, ^3J = 5.86 Hz, 1 H, 4-H), 6.05 (s, 5 H, Cp), 6.06 (s, 5 H, Cp), 6.19 (dd, ^3J = 5.86, 15.62 Hz, 1 H, C*H*=CHPh), 6.67 (d, ^3J = 15.62 Hz, 1 H, CH=C*H*Ph), 6.70−7.92 (m, 18 H, H^{ar}). − ^{13}C NMR (100.4 MHz, C_6D_6): δ = 46.4, 48.1 (C-5, C-6), 55.3, 57.1 (CH_3), 105.7, 107,2 (C-4, C-7), 117.1 (Cp),122.2, 122.9 (*C*H=*C*HPh), 126.1, 128.4, 128.9, 129.2, 130.1, 132.2, 133.1, 133.7, 134.1, 135.8, 137.1, 141.9 (CH^{ar}), 142.5, 143.1, 143.9, 145.2 (*ipso*-C), 159.1, 160.1 (*C*OCH_3), 163.2, 165.1 (C-3, C-8). − MS (70 eV); *m/z* (%): 405 (20), 377 (35), 342 (30), 178 (55), 77 (100). − $C_{44}H_{40}O_4Ti$ (680.71): calcd. C 77.64, H 5.88; found C 76.47, H 5.78.

(5,6-threo-3Z,7Z)-3-(p-Anisyl)-1,1-bis(η^5-cyclopentadienyl)-5,8-diphenyl-6-β-(trans-phenylethenyl)-1-titana-2,9-dioxacyclonona-3,7-diene (**7f**): 527 mg (0.81 mmol; 81%) from 234 mg of **3**, 234 mg of **4d** and 238 mg of **6c**; dark red air-sensitive needles from toluene; m.p. 152°C. − IR (KBr): $\tilde{\nu}$ = 3040−2800 cm^{-1}, 1610, 1450, 1250, 1100, 1030, 800. − ^1H NMR (400 MHz, C_6D_6)[30][33]: δ = 3.42 (s, 3 H, CH_3), 4.48 (dd, ^3J = 5.62, 5.87 Hz, 1 H, 6-H), 4.84 (d, ^3J = 5.62 Hz, 1 H, 5-H), 5.60 (d, ^3J = 5.62 Hz, 1 H, 7-H), 5.95 (d, ^3J = 5.62 Hz, 1 H, 4-H), 6.01 (s, 5 H, Cp), 6.03 (s, 5 H, Cp), 6.17 (dd, ^3J = 5.87, 15.62 Hz, 1 H, C*H*=CHPh), 6.64 (d, ^3J = 15.62 Hz, 1 H, CH=C*H*Ph), 6.68−7.82 (m, 19 H, H^{ar}). − ^{13}C NMR (100.4 MHz, C_6D_6): δ = 46.7, 48.1 (C-5, C-6), 55.2 (CH_3), 105.7, 107.1 (C-4, C-7), 117.2 (Cp), 120.1, 122.2 (*C*H=*C*HPh), 125.1, 125.7, 126.4, 126.2, 131.6, 132.6, 134.1, 135.1, 135.8, 137.2, 138.1 (CH^{ar}), 141.1, 142.1, 142.9, 145.4 (*ipso*-C), 159.7 (*C*OCH_3), 163.2, 163.3 (C-3, C-8). − MS (70 eV); *m/z* (%): 412 (9), 349 (22), 131 (55), 66 (100). − $C_{43}H_{38}O_3Ti$ (650.68): calcd. C 79.38, H 5.84; found C 78.49, H 6.05.

(5,6-threo-3Z,7Z)-1,1-Bis(η^5-cyclopentadienyl)-3,5,8-triphenyl-6-β-(trans-phenylethenyl)-1-titana-2,9-dioxacyclonona-3,7-diene (**7g**): 403 mg (0.65 mmol; 65%) from 234 mg of **3**, 234 mg of **4d** and 208 mg of **4a** (as the more reactive component); dark red air-sensitive needles from toluene; m.p. 79°C. − IR (KBr): $\tilde{\nu}$ = 3060−2800 cm^{-1}, 1579, 1448, 1261, 1020, 807. − ^1H NMR (400 MHz, C_6D_6)[30][33]: δ = 4.46 (dd, ^3J = 5.50, 5.50 Hz, 1 H, 6-H), 4.84 (d, ^3J = 5.50 Hz, 1 H, 5-H), 5.59 (d, ^3J = 5.50 Hz, 1 H, 7-

H), 5.94 (s, 5 H, Cp), 5.98 (s, 5 H, Cp), 6.03 (d, ^3J = 5.50 Hz, 1 H, 4-H), 6.16 (dd, ^3J = 5.50, 15.40 Hz, 1 H, C*H*=CHPh), 6.50 (d, ^3J = 15.40 Hz, 1 H, CH=C*H*Ph), 6.81−7.98 (m, 20 H, H^{ar}). − ^{13}C NMR (100.4 MHz, C_6D_6): δ = 45.5, 45.6 (C-5, C-6), 106.1, 106.7 (C-4, C-7), 116.1, 116.2 (Cp), 125.2, 125,9 (*C*H=*C*HPh), 127.0, 127.9, 128.2, 128.9, 129.3, 130.1, 130.9, 132.1, 134.1, 137.2, 138.1, 139.1 (CH^{ar}), 141.1, 141.9, 143.9, 145.1 (*ipso*-C), 163.2, 164.0 (C-3, C-8). − MS (70 eV); *m/z* (%): 450 (10), 386 (15) [Cp_2Ti-OCPhCH=CHPh$^+$], 221 (45), 178 (55) [Cp_2Ti^+], 77 (100). − $C_{42}H_{36}O_2Ti$ (620.65): calcd. C 81.28, H 5.80; found C 81.12, H 5.69.

4. *Synthesis of* **9**, **10**, **11**, **12**, *and* **13**. − *General Procedure (C):* Complex **5** or **7** (1 mmol) was dissolved in CH_2Cl_2 (10 ml). 5 mmol of HCl in 5 ml of diethyl ether was added at −10°C and the mixture was then stirred for 5 h, whereupon the colour turned from dark red to bright red. The solvent and excess HCl were removed at reduced pressure, Cp_2TiCl_2 was removed by CC on silica gel (CH_2Cl_2). The eluate was concentrated and the products **9**−**13** were separated by using preparative TLC (silica gel, CH_2Cl_2). Separation of the respective diastereomers was done by TLC (silica gel 60, diethyl ether/petroleum ether, 1:2) or by HPLC (silica gel 60, heptane/ethyl acetate, 9:1). For analytical purposes samples were recrystallized from chloroform or CH_2Cl_2/hexane, 3:1. − *General Procedure (D):* Complex **7** or **5** (1 mmol) was dissolved in CH_2Cl_2 (10 ml). At ambient temperature 5 ml of aqueous HCl (6%) was added. After stirring this mixture for 3 h, the layers were separated, the aqueous one was washed twice with 5 ml of CH_2Cl_2 and the combined organic extracts thus obtained were dried with sodium sulphate. Separation of the products **9**−**13** and Cp_2TiCl_2 was accomplished as described in General Procedure (C).

1,6-Diphenyl-3,4-bis-β-(trans-phenylethenyl)hexan-1,6-dione (**9a**): According to general procedure D: 418 mg (0.89 mmol; 89%) from 646 mg of **5d**; yellow needles from chloroform; m.p. 140°C. − IR (film): $\tilde{\nu}$ = 3050 cm^{-1}, 2980, 2960, 1680, 1650, 1490. − ^1H NMR (400 HMz, $CDCl_3$): δ = 3.09−3.27 (m, 6 H, 2-H, 3-H, 4-H, 5-H), 6.16 (dd, ^3J = 15.62/8.97 Hz, 2 H, C*H*=CHPh), 6.42 (d, ^3J = 15.62 Hz, 2 H, CH=C*H*Ph), 7.21−7.93 (m, 20 H, H^{ar}). − ^{13}C NMR (100.4 MHz, $CDCl_3$): δ = 42.2 (C-2, C-5), 43.0 (C-3, C-4), 124.0, 126.2 (*C*H=*C*HPh), 128.5, 128.9, 132.9, 132.1, 137.0, 137.2 (CH^{ar}), 137.8, 138.2 (*ipso*-C), 198.8 (C-1, C-6). − MS (70 eV); *m/z* (%): 470 (7) [M^+], 350 (80), 235 (92), 105 (100). − $C_{34}H_{30}O_2$ (470.62): calcd. C 86.80, H 6.38; found C 86.72, H 6.47.

1,2-Bis[2′-(1′-oxoindanyl)]-1,2-diphenylethane (**9b**): According to general procedure C: 90 mg (0.2 mmol; 13%) from 944 mg of **5f** as a separable 22:55:24 mixture of diastereomers; yellow needles from chloroform; a sample of the major isomer was separated by TLC; m.p. 200°C. − IR (film): $\tilde{\nu}$ = 1963 cm^{-1}, 1714, 1694. − ^1H NMR (400 MHz, $CDCl_3$): δ = 2.82 (dd, ^2J = 17.00, ^3J = 4.40 Hz, 2 H, C*H*H′), 3.45 (dd, ^2J = 17.00, ^3J = 8.00 Hz, 2 H, CH*H*′), 4.07 (m, 2 H, CHC=O), 4.28 (m, 2 H, 1-H, 2-H), 6.85 (t, ^3J = 7.70 Hz, 4 H, H^{ar}), 6.86 (t, ^3J = 7.70 Hz, 2 H, H^{ar}), 6.92 (d, ^3J = 7.70 Hz, 4 H, H^{ar}), 7.24 (d, ^3J = 7.70 Hz, 2 H, H^{ar}), 7.28 (t, ^3J = 7.70 Hz, 2 H, H^{ar}), 7.44 (t, ^3J = 7.70 Hz, 2 H, H^{ar}), 7.73 (d, ^3J = 7.70 Hz, 2 H, H^{ar}). − ^{13}C NMR (100.4 MHz, $CDCl_3$): δ = 31.7 (CH_2), 48.3 (*C*HC=O), 51.0 (C-1, C-2), 123.2, 126.1, 126.3, 127.0, 127.7, 129.2, 134.5 (CH^{ar}), 138.1, 140.5 (*ipso*-C), 154.3 [*C*(C=O)CH], 209.8 (C=O). − MS (70 eV); *m/z* (%): 442 (6) [M^+], 310 (68) [$M^+ - C_9H_8O$], 221 (100) [$M/2^+$], 132 (20) [$C_9H_8O^+$], 91 (48) [$PhCH_2^+$]. − $C_{32}H_{26}O_2$ (442.56): calcd. C 86.85, H 5.92; found C 86.77, H 5.82.

1,3-Bis(p-anisyl)-6-phenyl-4-β-(trans-phenylethenyl)hexan-1,6-dione (**9d**): According to general procedure D: 281 mg (0.56 mmol; 56%) from 680 mg **7d**; yellow needles from chloroform; m.p. 149°C. − IR (film): $\tilde{\nu}$ = 3095−2790 cm^{-1}, 1680, 1590, 1510, 1250. − ^1H NMR (400 MHz, $CDCl_3$): δ = 2.90 (m, 1 H, 5-H), 3.12 (m, 1 H, 5-H′), 3.25 (m, 1 H, 4-H), 3.30 (m, 1 H, 2-H), 3.33 (m, 1 H, 2-H′), 3.67 (m, 1 H, 3-H), 3.79 (s, 3 H, CH_3), 3.80 (s, 3 H, CH_3), 5.93 (dd, ^3J = 9.35, 15.40 Hz, 1 H, C*H*=CHPh), 6.36 (d, ^3J = 15.40 Hz, 1 H, C*H*Ph), 6.82−7.82 (m, 18 H, H^{ar}). − MS (70 eV); *m/z* (%): 504 (30) [M^+], 359 (45), 331 (55), 281 (100), 145 (70). − $C_{34}H_{32}O_4$ (504.63): calcd. C 80.95, H 6.35; found C 80.75, H 6.47.

1-(o,p-Dimethoxyphenyl)-3,6-diphenyl-4-β-(trans-phenylethenyl)hexan-1,6-dione (**9e**): According to general procedure D: 282 mg (0.56 mmol; 55%) from 680 mg of **7e**; yellow needles from cloroform; m.p. 145°C. − IR (film): $\tilde{\nu}$ = 3150−2800 cm^{-1}, 1680, 1600, 1255. − ^1H NMR (400 MHz, $CDCl_3$): δ = 2.92 (m, 1 H, 5-H), 3.14 (m, 1 H, 5-H′), 3.25 (m, 1 H, 4-H), 3.30 (m, 1 H, 2-H), 3.33 (m, 1 H, 2-H′), 3.68 (m, 1 H, 3-H), 3.78 (s, 3 H, CH_3), 3.79 (s, 3 H, CH_3), 5.93 (dd, ^3J = 9.35, 15.40 Hz, 1 H, C*H*=CHPh), 6.36 (d, ^3J = 15.40 Hz, 1 H, CH=C*H*Ph), 6.82−7.82 (m, 18 H, H^{ar}). − MS (70 eV); *m/z* (%): 504 (40) [M^+], 390 (53), 354 (45), 135 (100). − $C_{34}H_{32}O_4$ (504.63): calcd. C 80.95, H 6.34; found C 80.90, H 6.40.

(±)-2-Benzoyl-1-hydroxy-1-phenyl-3,4-bis-β-(trans-phenylethenyl)cyclopentane (**10a**)[34]: According to general procedure C: 197 mg (0.42 mmol: 42%) from 646 mg of **5d**; white needles from chloroform; m.p. 140°C. − IR (film): $\tilde{\nu}$ = 3090 cm^{-1}, 2780, 1675, 1590, 1515, 1250. − ^1H NMR (400 MHz, $CDCl_3$): δ = 2.17 (dd, ^3J = 5.50, ^2J = 14.30 Hz, 1 H, 5-H), 2.59 (dd, ^3J = 10.45 Hz, ^2J = 14.30 Hz, 1 H, 5-H′), 2.92 (m, 1 H, 3-H or 4-H), 3.39 (m, 1 H, 4-H or 3-H), 4.18 (d, ^3J = 11.55 Hz, 1 H, 2-H), 5.04 (s, 1 H, OH), 6.02 (dd, ^3J = 15.94 Hz and 8.79 Hz, 2 H, C*H*=CHPh), 6.48 (d, ^3J = 15.94 Hz, 2 H, CH=C*H*Ph), 6.91−7.68 (m, 20 H, H^{ar}). − MS (70 eV); *m/z* (%): 470 (10) [M^+], 452 (20) [$M^+ - H_2O$], 345 (20) [$M^+ -$ PhCO], 105 (100) [$PhCO^+$]. − $C_{34}H_{30}O_2$ (470.62): calcd. C 86.80, H 6.38; found C 86.81, H 6.35.

Spiroketone **10b**: According to general procedure C: 538 mg (1.22 mmol; 80%) from 944 mg of **5f** as a 8:7:3:26:5:14:17:21 mixture of 8 stereoisomers; white needles from chloroform; separation of a sample of the major diastereomer (26%) for analytical purposes by TLC; m.p. 199°C. − IR (KBr): $\tilde{\nu}$ = 3429 cm^{-1}, 1705, 1682, 1605. − ^1H NMR (400 MHz, $CDCl_3$): δ = 1.96 (s, 1 H, OH), 2.74 (d, ^3J = 8.0 Hz, ^2J not observed, 2 H, 9-H), 2.80 (d, ^2J = 16.5 Hz, 1 H, 4-H), 3.26 (ddd, ^3J = 8.0, 8.0, 8.0 Hz, 1 H, 10-H), 3.98 (d, ^2J = 16.5 Hz, 1 H, 4-H′), 4.27 (d, ^3J = 13.5 Hz, 1 H, 12-H), 4.38 (dd, ^3J = 8.0, 13.5 Hz, 1 H, 11-H), 6.64 (m, 1 H, H^{ar}), 7.03 (m, 2 H, H^{ar}), 7.07 (m, 2 H, H^{ar}), 7.11 (m, 2 H, H^{ar}), 7.14 (m, 1 H, H^{ar}), 7.16 (m, 2 H, H^{ar}), 7.22 (m, 2 H, H^{ar}), 7.32 (m, 2 H, H^{ar}), 7.39 (m, 1 H, H^{ar}), 7.50 (m, 1 H, H^{ar}), 7.52 (m, 1 H, H^{ar}), 7.68 (m, 1 H, H^{ar}). − ^{13}C NMR (100.4 MHz, $CDCl_3$): δ = 31.4, 33.4 (C-4, C-9), 46.7 (C-11), 49.3 (C-10), 57.4 (C-12), 71.1 (C-5), 94.6 (C-6), 123.5, 124.4, 124.7, 125.9, 126.1, 126.4, 126.6, 127.0, 128.1, 128.2, 128.8, 129.0, 129.3, 134.7 (CH^{ar}), 137.8, 138.0, 139.6, 143.5, 144.7, 154.3 (C-2, C-3, C-7, C-8, 11-C, 12-C), 207.0 (C-1). − MS (70 eV); *m/z* (%): 442 (10) [M^+], 424 (2) [$M^+ - H_2O$], 310 (15) [$M^+ - C_9H_8O$], 221 (100) [$M/2^+$]. − $C_{32}H_{26}O_2$ (442.56): calcd. C 86.85, H 5.92; found C 86.77, H 5.87.

(±)-(3,4-threo)-2-Acetyl-1-hydroxy-1-methyl-3,4-bis-o-(methyl-trans-cinnamoyl)cyclopentane (**10c**)[34]: According to general procedure D: 31 mg (0.07 mmol; 45%) from 95 mg of **5g**; white needles from chloroform; m.p. 101°C. − IR (CH_2Cl_2): $\tilde{\nu}$ = 1697 cm^{-1}, 1660, 1618, 1342, 1300, 1178, 1155. − ^1H NMR (400 MHz, $CDCl_3$): δ = 1.58 (s, 3 H, 1-CH_3), 1.76 (s, 1 H, OH), 1.93 [s, 3 H, (CO)CH_3], 2.27 (dd, ^2J = 14.3, ^3J = 6.5 Hz, 1 H, 5-H), 2.43 (dd, ^2J = 14.3, ^3J = 11.0 Hz, 1 H, 5-H′), 3.59 (m, 1 H, 4-H), 3.71 (s, 3

H, OCH_3), 3.72 (s, 3 H, OCH_3), 3.72 (hidden, 1 H, 3-H), 4.00 (d, ^3J = 11.50 Hz, 1 H, 2-H), 5.74 (d, ^3J = 15.00 Hz, 2 H, CH=C*H*CO), 7.11 (m, 1 H, H^{ar}), 7.15 (m, 1 H, H^{ar}), 7.18 (m, 1 H, H^{ar}), 7.35 (m, 1 H, H^{ar}), 7.38 (m, 1 H, H^{ar}), 7.43 (m, 1 H, H^{ar}), 7.55 (m, 1 H, H^{ar}), 7.60 (m, 1 H, H^{ar}), 7.87 (d, ^3J = 15.00 Hz, 1 H, C*H*=CHCO), 7.88 (d, ^3J = 15.00 Hz, 1 H, C*H*=CHCO). − ^{13}C NMR (100.4 MHz, $CDCl_3$): 28.1 [(CO)*C*H_3], 33.1 (1-C), 47.8 (C-4), 48.2 (C-5), 51.4, 51.5 (OCH_3), 53.5 (C-3), 66.0 (C-2), 80.1 (C-1), 118.9, 119.9 (CH=*C*HCO), 126.2, 126.7, 127.3, 127.4, 127.8, 128.1, 130.3, 130.7 (8 C, CH^{ar}), 133.5, 134.5 (*C*CH=CHC=O), 134.9, 138.9 (3-C, 4-C), 141.3, 142.1 (*C*H=CHCO), 166.5, 166.9 (COO), 212.1 (2-C). − MS (70 eV); *m/z* (%): 462 (9) [M^+], 369 (9), 337 (6), 277 (51), 232 (19) [$C_{14}H_{16}O_3^+$], 199 (68), 171 (75), 157 (99), 129 (94), 115 (70), 43 (100). − $C_{28}H_{30}O_6$ (462.54): calcd. C 72.71, H 6.54; found C 72.82, H 6.59.

(±)-1,4-Bis(p-anisyl)-2-benzoyl-1-hydroxy-3-β-(trans-phenylethenyl)cyclopentane (**10d**)[34]: According to general procedure D: 52 mg (0.1 mmol; 10%) from 680 mg of **7d**; white needles from chloroform. − IR (film): $\tilde{\nu}$ = 3059−2805 cm^{-1}, 1675, 1600, 1510, 1450, 1260. − ^{1}H NMR (400 MHz, $CDCl_3$): δ = 2.33 (dd, ^3J = 5.50 Hz, ^2J = 14.30 Hz, 1 H, 5-H), 2.77 (dd, ^3J = 11.00 Hz, ^2J = 14.30 Hz, 1 H, 5-H′), 3.25 (m, 1 H, 3-H), 3.60 (m, 1 H, 4-H), 3.76 (s, 3 H, CH_3), 3.80 (s, 3 H, CH_3), 4.37 (d, ^3J = 12.09 Hz, 1 H, 2-H), 4.93 (s, 1 H, OH), 5.96 (dd, ^3J = 9.35, 15.95 Hz, 1 H, C*H*=CHPh), 6.20 (d, ^3J = 15.95 Hz, 1 H, C*H*Ph), 6.45−7.82 (m, 18 H, H^{ar}). − MS (70 eV); *m/z* (%): 504 (4) [M^+], 486 (10) [$M^+ - H_2O$], 389 (40), 269 (100), 135 (20). − $C_{34}H_{32}O_4$ (504.63): calcd. C 80.93, H 6.39; found C 80.85, H 6.44.

(±)-2-Benzoyl-1-(o,p-dimethoxyphenyl)-1-hydroxy-4-phenyl-3-β-(trans-phenylethenyl)cyclopentane (**10e**)[34]: According to general procedure D: 57 mg (0.11 mmol; 11%) from 680 mg of **7e**; white needles from chloroform. − IR (film): $\tilde{\nu}$ = 3059−2850 cm^{-1}, 1676, 1598, 1512, 1450, 1260, 1027. − ^{1}H NMR (400 MHz, $CDCl_3$): δ = 2.30 (dd, ^3J = 5.50, ^2J = 14.30 Hz, 1 H, 5-H), 2.75 (dd, ^3J = 11.10, ^2J = 14.30 Hz, 1 H, 5-H′), 3.26 (m, 1 H, 3-H), 3.52 (m, 1 H, 4-H), 3.78 (s, 3 H, CH_3), 3.80 (s, 3 H, CH_3), 4.39 (d, ^3J = 12.11 Hz, 1 H, 2-H), 4.90 (s, 1 H, OH), 6.04 (dd, ^3J = 9.35, 15.95 Hz,1 H, C*H*=CHPh), 6.44 (d, ^3J = 15.95 Hz, 1 H, CH=C*H*Ph), 6.90−7.80 (m, 18 H, H^{ar}). − MS (70 eV); *m/z* (%): 504 (6) [M^+], 486 (10) [$M^+ - H_2O$], 381 (100), 135 (70). − $C_{34}H_{32}O_4$ (504.63): calcd. C 80.93, H 6.39; found C 80.87, H 6.40.

3-(p-Anisyl)-1-hydroxy-2-(p-methoxybenzoyl)-1-phenyl-4-β-(trans-phenylethenyl)cyclopentane (**11d**)[34]: According to general procedure D: 35 mg (0.07 mmol; 7%) from 680 mg of **7d**; white needles from chloroform. − IR (film): $\tilde{\nu}$ = 3060−2800 cm^{-1}, 1690, 1510, 1500, 1450, 1260, 1100. − ^{1}H NMR (400 MHz, $CDCl_3$): δ = 2.30 (dd, ^3J = 5.50, ^2J = 14.30 Hz, 1 H, 5-H), 2.78 (dd, ^3J = 11.00, ^2J = 14.30 Hz, 1 H, 5-H′), 2.96 (m, 1 H, 4-H), 3.63 (s, 3 H, CH_3), 3.67 (s, 3 H, CH_3), 3.80 (m, 1 H, 3-H), 4.32 (d, ^3J = 11.60 Hz, 1 H, 2-H), 4.95 (s, 1 H, OH), 5.96 (dd, ^3J = 9.35, 15.95 Hz, 1 H, C*H*=CHPh), 6.20 (d, ^3J = 15.95 Hz, 1 H, C*H*Ph), 6.45−7.82 (m, 18 H, H^{ar}). − MS (70 eV); *m/z* (%): 504 (5) [M^+], 486 (9) [$M^+ - H_2O$], 360 (35), 269 (100). − $C_{34}H_{32}O_4$ (504.63): calcd. C 80.93, H 6.39; found C 80.85, H 6.34.

2-(o,p-Dimethoxybenzoyl)-1-hydroxy-1,3-diphenyl-4-β-(trans-phenylethenyl)cyclopentane (**11e**)[34]: According to general procedure D: 40 mg (0.08 mmol; 8%) from 680 mg of **7e**; white needles from chloroform. − IR (film): $\tilde{\nu}$ = 3059−2850 cm^{-1}, 2850, 1679, 1598, 1512, 1450, 1260, 1027. − ^{1}H NMR (400 MHz, $CDCl_3$): δ = 2.27 (dd, ^3J = 5.50, ^2J = 14.30 Hz, 1 H, 5-H), 2.75 (dd, ^3J = 11.01, ^2J = 14.30 Hz, 1 H, 5-H′), 3.02 (m, 1 H, 4-H), 3.76 (s, 3 H, CH_3), 3.78 (s, 3 H, CH_3), 3.82 (m, 1 H, 3-H), 4.37 (d, ^3J = 12.11 Hz, 1 H, 2-H), 4.91 (s, 1 H, OH), 6.04 (dd, ^3J = 9.35, 15.95 Hz, 1 H, C*H*=CHPh), 6.44 (d, ^3J = 15.95 Hz, 1 H, CH=C*H*Ph), 6.90−7.80 (m, 18 H, H^{ar}). − MS (70 eV); *m/z* (%): 504 (6) [M^+], 486 (10) [$M^+ - H_2O$]. − $C_{34}H_{32}O_4$ (504.63): calcld. C 80.93, H 6.39; found C 80.78, H 6.29.

1-Benzoyl-2-(o,p-dimethoxyphenyl)-4-phenyl-5-β-(trans-phenylethenyl)cyclopent-1-ene (**12e**): According to general procedure C: 170 mg (0.35 mmol; 35%) from 681 mg of **7e**; white needles from chloroform. − IR (film): $\tilde{\nu}$ = 2962 cm^{-1}, 1721, 1677, 1604, 1450, 1261. − ^{1}H NMR (400 MHz, C_6D_6): δ = 3.00 (m, 1 H, 4-H), 3.62 (m, 2 H, 3-H), 3.63 (s, 3 H, CH_3), 3.72 (s, 3 H, CH_3), 4.26 (dd, ^3J = 6.10, 9.36 Hz, 1 H, 5-H), 6.12 (dd, ^3J = 9.36, 15.95 Hz, 1 H, C*H*=CHPh), 6.42 (d, ^3J = 15.95 Hz, 1 H, CH=C*H*Ph), 7.02−7.92 (m, 18 H, H^{ar}). − MS (70 eV); *m/z* (%): 486 (28) [M^+], 455 (15) [$M^+ - OCH_3$], 381 (28) [$M^+ -$ PhCO], 149 (100). − $C_{34}H_{30}O_3$ (486.62): calcd. C 83.92, H 6.21; found C 83.83, H 6.18.

2-(p-Anisyl)-1-benzoyl-4-phenyl-5-β-(trans-phenylethenyl)-cyclopent-1-ene (**12f**): According to general procedure C: 173 mg (0.38 mmol; 38%) from 650 mg of **7f**; white needles from cloroform. − IR (film): $\tilde{\nu}$ = 3090−2800 cm^{-1}, 1660, 1600, 1510, 1450, 1260. − ^{1}H NMR (400 MHz, $CDCl_3$): δ = 3.01 (m, 1 H, 4-H), 3.45 (s, 3 H, CH_3), 3.63 (m, 2 H, 3-H), 4.24 (dd, ^3J = 6.05, 9.35 Hz, 1 H, 5-H), 6.03 (dd, ^3J = 9.35, 15.95 Hz, 1 H, C*H*=CHPh), 6.33 (d, ^3J = 15.95 Hz, 1 H, CH=C*H*Ph), 6.91−7.79 (m, 19 H, H^{ar}). − MS (70 eV); *m/z* (%): 456 (72) [M^+], 365 (20), 351 (100) [$M - C_6H_5CO$], 105 (75). − $C_{33}H_{28}O_2$ (456.59): calcd. C 86.40, H 6.14; found C 86.47, H 6.11.

1-(o,p-Dimethoxybenzoyl)-2,5-diphenyl-4-β-(trans-phenylethenyl)cyclopent-1-ene (**13e**): According to general procedure C: 122 mg (0.25 mmol; 25%) from 681 mg of **7e**; white needles from chloroform. − IR (film): $\tilde{\nu}$ = 2925 cm^{-1}, 2854, 1736, 1677, 1601, 1450, 1261. − ^{1}H NMR (400 MHz, C_6D_6): δ = 2.91 (m, 1 H, 4-H), 3.39 (s, 3 H, CH_3), 3.47 (m, 2 H, 3-H), 3.75 (s, 3 H, CH_3), 4.45 (d, ^3J = 7.82 Hz, 1 H, 5-H), 6.14 (dd, ^3J = 9.35, 15.95 Hz, 1 H, C*H*=CHPh), 6.45 (d, ^3J = 15.95 Hz, 1 H, CH=C*H*Ph), 7.05−7.92 (m, 18 H, H^{ar}). − MS (70 eV); *m/z* (%): 486 (16) [M^+], 322 (16) [$M^+ - C_6H_3(OCH_3)_2CO$], 280 (45), 149 (100).− $C_{34}H_{30}O_3$ (486.62): calcd. C 83.92, H 6.21; found C 83.81, H 6.30.

Ab initio Calculations: The ab initio and density functional calculations were performed with the Gaussian 94 suite of programs.[19] Structures were optimzed with no constraints other than symmetry at the B3LYP/SVp level, i.e. using the B3LYP[20] density functional and a split valence basis set[21], augmented with standard polarization functions on the non-hydrogen atoms.[22] Vibrational frequencies and zero-point energy corrections, scaled by 0.98[23], were computed at this level. Refinement of the structures was performed at the MP2/SVp level. Energy calculations were done at MP2/TZ2p level (i.e., using a triple-zeta basis set[21] and split polarization functions).

---

[1] For 4-membered titanaheterocycles see: [1a] R. Beckhaus, *J. Chem. Soc., Dalton Trans.* **1997**, 1991−2001. − [1b] R. Beckhaus, J. Oster, J. Sang, I. Strauß, T. Wagner, *Synlett* **1997** 241−249. − [1c] S. C. Ho, S. Hentges, R. H. Grubbs, *Organometallics* **1988**, *7*, 780−782. − [1d] R. Beckhaus, *Angew. Chem.* **1997**, *109*, 694−722; *Angew. Chem. Int. Ed. Engl.* **1997**, *36*, 686−713. − [1e] K. M. Doxsee, J. J. J. Juliette, J. K. M. Mauser, K. Zientara, *Organometallics* **1993**, *12*, 4742−4744. − [1f] D. Seyferth, T. Wang, W. M. Davis, *Organometallics* **1994**, *13*, 4134−4136. − [1g] R. Gómez, R. Duchateau, A. N. Chernega, J. H. Teuben, F. T. Edelmann, M. L. H. Green, *J. Organomet. Chem.* **1995**, *491*, 153−158.

[2] For 6-membered titanaheterocycles see ref.[1d] and: [2a] R. Beckhaus, T. Wagner, C. Zimmermann, E. Herdtweck, *J. Organomet.*

Chem. **1993**, *460*, 181−189. − [2b] N. M. Kablaoui, F. A. Hicks, S. L. Buchwald, *J. Am. Chem. Soc.* **1997**, *119*, 4424−4431. − [2c] P. Veya, C. Floriani, A. Chiesi−Villa, C. Rizzoli, *Organometallics* **1993**, *12*, 4892−4898. − [2d] K. Mashima, K. Jyodoi, A. Ohyoshi, H. Takaya, *J. Chem. Soc., Chem. Commun.* **1986**, 1145−1146 and *Organometallics* **1987**, *6*, 885−887. − [2e] K. M. Doxsee, J. J. J. Juliette, T. J. R. Weakley, K. Zientara, *Inorg. Chim. Acta* **1994**, *222*, 305−313. − [2f] K. M. Doxsee, J. B. Farahi, H. Hope, *J. Am. Chem. Soc.* **1991**, *113*, 8889−8898. − [2g] K. Mashima, H. Haraguchi, A. Ohyoshi, N. Sakai, H. Takaya, *Organometallics* **1991**, *10*, 2731−2736.

[3] A. V. Firth, D. W. Stephan, *Organometallics* **1997**, *16*, 2183−2188.

[4] R. Steudel, M. Kustos, V. Münchow, U. Westphal, *Chem. Ber.* **1997**, *130*, 757−764.

[5] T. E. Waldman, A. M. Wilson, A. L. Rheingold, E. Melendez, R. D. Ernst, *Organometallics* **1992**, *11*, 3201−3209.

[6] K. Andrä, *J. Organomet. Chem.* **1968**, *11*, 567−570.

[7] [7a] M. Pasquali, C. Floriani, A. Chiesi-Villa, C. Guastini, *Inorg. Chem.* **1981**, *20*, 349−355. − [7b] J. Scholz, M. Dlikan, K. Thiele, *J. Prakt. Chem.* **1988**, *330*, 808.

[8] For 5-membered titanaheterocycles see: [8a] G. Doyle, R. S. Tobias, *Inorg. Chem.* **1968**, *7*, 2484−2488. − [8b] C. Floriani, G. Fachinetti, *J. Chem. Soc., Chem. Commun.* **1972**, 790−791. − [8c] M. Pasquali, C. Floriani, A. Chiesi−Villa, C. Guastini, *J. Am. Chem. Soc.* **1979**, *101*, 4740−4742. − [8d] J. Scholz, M. Dlikan, D. Ströhl, A. Dietrich, H. Schumann, K. H. Thiele, *Chem. Ber.* **1990**, *123*, 2279−2285. − [8e] N. M. Kablaoui, F. A. Hicks, S. L. Buchwald, *J. Am. Chem. Soc.* **1996**, *118*, 5818−5819. − [8f] R. Beckhaus, J. Oster, R. Kempe, A. Spannenberg, *Angew. Chem.* **1996**, *108*, 1636−1638; *Angew. Chem. Int. Ed. Engl.* **1996**, *35*, 1565−1567. − [8g] B. Tsuie, D. C. Swenson, R. F. Jordan, *Organometallics* **1997**, *16*, 1392−1400. − [8h] S. Gambarotta, C. Floriani, A, Chiesi-Villa, C. Guastini, *J. Am. Chem. Soc.* **1982**, *104*, 1918−1924. − [8i] P. Binger, F. Sandmeyer, C. Krüger, *Organometallics* **1995**, *14*, 2969−2976.

[9] V. B. Shur, V. V. Burlakov, A. I. Yanovsky, P. V. Petrovsky, Y. T. Struchkov, M. E. Vol′pin, *J. Organomet. Chem.* **1985**, *297*, 51−59.

[10] C. Lefeber, A. Ohff, A. Tillack, W. Baumann, R. Kempe, V. V. Burlakov, U. Rosenthal, H. Görls, *J. Organomet. Chem.* **1995**, *501*, 179−188.

[11] S. Dürr, U. Höhlein, R. Schobert, *J. Organomet. Chem.* **1993**, *458*, 89−96.

[12] For other 7-membered titanaheterocycles see: [12a] R. O. Duthaler, A. Hafner, M. Riediker, *Pure Appl. Chem.* **1990**, 62−63. − [12b] R. O. Duthaler, A. Hafner, M. Riediker, "Asymmetric C−C bond formation with Ti-, Zr-, and Hf-carbohydrate complexes" in *Organic Synthesis via Organometallics* (Eds.: K. H. Dötz, R. W. Hoffmann), Vieweg, Braunschweig, **1991**, p. 285−309.

[13] K. Bergemann, M. Kustos, P. Krüger, R. Steudel, *Angew. Chem.* **1995**, *107*, 1481−1483; *Angew. Chem. Int. Ed. Engl.* **1995**, *34*, 1330−1331.

[14] R. Schobert, F. Maaref, S. Dürr, *Synlett* **1995**, 83−84.

[15] [15a] S. Fokken, T. P. Spaniol, J. Okuda, F. G. Sernetz, R. Mülhaupt, *Organometallics* **1997**, *16*, 4240−4242. − [15b] S. Fokken, Ph. D. Thesis, University of Marburg, **1997**.

[16] For a brief note lacking any further data see: J. M. Davis, R. J. Whitby, A. Jaxa-Chamiec, *J. Chem. Soc. Chem. Commun.* **1991**, 1743−1745.

[17] M. J. Carney, P. J. Walsh, F. J. Hollander, R. G. Bergman, *J. Am. Chem. Soc.* **1989**, *111*, 8751−8753 and *Organometallics* **1992**, *11*, 761−777.

[18] B. Demerseman, G. Bouquet, M. Bigorgne, *J. Organomet. Chem.* **1975**, *101*, C24−C26.

[19] M. J. Frisch, G. W. Trucks, H. B. Schlegel, P. M. W. Gill, B. G. Johnson, M. A. Robb, J. R. Cheeseman, T. Keith, G. A. Petersson, J. A. Montgomery, K. Raghavachari, M. A. Al-Laham, V. G. Zakrzewski, J. V. Ortiz, J. B. Foresman, J. Cioslowski, B. B. Stefanov, A. Nanayakkara, M. Challacombe, C. Y. Peng, P. Y. Ayala, W. Chen, M. W. Wong, J. L. Andres, E. S. Replogle, R. Gomperts, R. L. Martin, D. J. Fox, J. S. Binkley, D. J. Defrees, J. Baker, J. P. Stewart, M. Head-Gordon, C. Gonzalez, J. A. Pople, *Gaussian 94 Revision E.2*, Gaussian, Inc., Pittsburgh PA, **1995**.

[20] [20a] A. D. Becke, *J. Chem. Phys.* **1993**, *98*, 5648−5652, and references therein. − [20b] P. J. Stevens, F. J. Devlin, C. F. Chablowski, M. J. Frisch, *J. Phys. Chem.* **1994**, *98*, 11623−11627.

[21] A. Schaefer, H. Horn, R. Ahlrichs, *J. Chem. Phys.* **1992**, *97*, 2571−2577.

[22] S. Huzinaga (Ed.), *Gaussian Basis Sets for Molecular Calculations*, Elsevier, Amsterdam, **1984**.

[23] C. W. Bauschlicher, Jr., H. Partridge, *J. Chem. Phys.* **1995**, *103*, 1788−1791.

[24] K. R. Bharucha, *J. Chem. Soc.* **1956**, 2446−2447.

[25] R. Cornubert, C. H. R. Borrel, *Bull. Soc. Chim. Fr.* **1929**, *45*, 1148−1161.

[26] A. Hassner, T. C. Mead, *Tetrahedron* **1964**, *20*, 2201−2210.

[27] O. Isler, H. Gutmann, M. Montavon, R. Rüegg, P. Zeller, *Helv. Chim. Acta* **1957**, *40*, 1242−1249.

[28] [28a] F. Ramirez, S. Dershowitz, *J. Org. Chem.* **1957**, *22*, 41−45. − [28b] A. Groß, Ph. D. Thesis, University of Erlangen-Nürnberg, **1994**, p. 75.

[29] S. Dürr, Ph. D. Thesis, University of Erlangen-Nürnberg **1997**, p. 102.

[30] ^3J coupling constants between 5-H und 6-H in compounds **5** und **7** are below 1 Hz and not clearly determinable (broad signals for 5-H and 6-H).

[31] Crystallographic data (excluding structure factors) for the structure reported in this paper have been deposited with the Cambridge Crystallographic Data Centre (CCDC-100857). Copies of the data can be obtained free of charge on application to CCDC, 12 Union Road, Cambridge CB2 1EZ, UK (fax: int. code + 44-1223/336-033; e-mail: deposit@ccdc.cam.ac.uk).

[32] The moderate *R* value is due to the fact, that **5a** is a poorly reflecting compound. Unfortunately, it was only possible to solve the strong disorder of the toluene solvent molecules in a very rough way.

[33] Assignment of NMR signals by comparison with spectra of similarly substituted "symmetric" derivatives of type **5**.

[34] Characterization of **10**/**11** by comparison with spectral data of analogous "symmetric" alcohols. The stereochemistry of the hydroxy function of **10** was determined by comparing NMR and IR data of similar compounds characterized by other groups, as for example: [34a] H. Olivier, Y. Chauvin, L. Saussine, *Tetrahedron* **1989**, *45*, 165−169. − [34b] K. Takaki, F. Beppu, I. Nakagawa, Y. Fujiwara, *Chem. Lett.* **1992**, 535−538. − [34c] K. Takaki, F. Beppu, S. Tanaka, Y. Tsubaki, T. Jintoku, Y. Fujiwara, *J. Chem. Soc., Chem. Commun.* **1990**, 516−517. − [34d] K. Takaki, K. Nagase, F. Beppu, Y. Fujiwara, *Chem. Lett.* **1991**, 1665−1668. − [34e] S. Falicki, H. Alper, *Organometallics* **1988**, *7*, 2548−2552. − [34f] F. Fournier, J. Berthelot, J.-J. Basselier, *Tetrahedron* **1985**, *41*, 5667−5676.

[98077]

Carbonyl Transition Metal Complexes of a Silaborate Ligand☆

Lars Wesemann*[a][+], Yves Ramjoie[a], Michael Trinkaus[a], and Thomas P. Spaniol[b]

Institut für Anorganische Chemie der Technischen Hochschule Aachen[a],
Prof.-Pirlet-Str. 1, D-52056 Aachen, Germany
Fax: (internat.) + 49(0)241/888-8288
E-mail: lars.wesemann@ac.rwth-aachen.de

Institut für Anorganische Chemie und Analytische Chemie, Johannes Gutenberg-Universität Mainz[b],
J.-J.-Becher-Weg 24, D-55099 Mainz, Germany

Received April 3, 1998

Keywords: Cluster chemistry / Silaborane clusters / Carbonyl complexes / Silicon coordination / Ruthenium complexes

Reaction between three equivalents of the silaborate $[NEt_4][MeSiB_{10}H_{12}]$ (**2**) and one equivalent of $[Ru_3(CO)_{12}]$ resulted in almost quantitative formation of the mononuclear transition metal complex $[NEt_4][Ru(CO)_3(\eta^5\text{-}MeSiB_{10}H_{10})]$ (**5**), which was characterized by X-ray structure analysis. The trinuclear ruthenium complex $[NEt_4][Ru_3(CO)_8(\eta^5\text{-}MeSiB_{10}H_{10})]$ (**7**) was synthesized in high yield from the reaction of one equivalent of **2** and $[Ru_3(CO)_{12}]$. The cluster **7** reacts with two equivalents of PMe_2Ph with substitution of two carbonyl groups to give the substitution product $[NEt_4][Ru_3(CO)_6(PMe_2Ph)_2(\eta^5\text{-}MeSiB_{10}H_{10})]$ (**8**).

The coordination chemistry of the dicarbollide ligand $[C_2B_9H_{11}]^{2-}$ has been investigated for almost 35 years. Metallocene-like complexes, mixed cyclopentadienyl dicarbollide sandwich species, and carbonyl dicarbollide transition metal complexes are described in the literature[1]. Many of these metallacarboranes have compositions and structures which are related to their cyclopentadienyl counterparts. One of the most surprising properties of the dicarbollide coordination products is their remarkable stability towards air oxidation and hydrolysis. After 35 years of research in the field of metallacarborane chemistry a dicarbollide coordination product of almost every transition metal is known. In 1969 Hawthorne described for the first time the synthesis of a carbonyliron dicarbollide complex[2] and 20 years later he developed an organometallic chemistry based on the dimeric dicarbonyliron carborane [*closo*-3-CO-3,3′-(μ-CO)-3,1,2-$FeC_2B_9H_{11}]_2^{2-}$[3]. In the case of ruthenium Siedle[4] reported for the first time on the successful preparation of *closo*-3,3,3-$(CO)_3$-3,1,2-$RuC_2B_9H_{11}$ (**1**) (Figure 1). From the reaction between $[Ru(CO)_3Cl_2]_2$ and $[7,8\text{-}C_2B_9H_{11}]^{2-}$ in refluxing THF 7% of **1** has been isolated.

The yield of dicarbaruthena-*closo*-dodecaborane was improved nine years later by Hawthorne[5] to 65% by treating $[7,8\text{-}C_2B_9H_{11}]^{2-}$ with $[Ru(CO)_3Cl_2(THF)]$ in THF at 0°C. In 1995 Stone[6] published a further improvement of the yield to 80% with $[Ru_3(CO)_{12}]$ as a starting material. Reaction between $[C_2B_9H_{13}]$ and $[Ru_3(CO)_{12}]$ results exclusively in the formation of the mononuclear complex **1**. Whereas the carborane with methyl groups attached to the carbon atoms produces in the corresponding reaction a 1:2 mixture of mononuclear complex $[Ru(CO)_3(\eta^5\text{-}7,8\text{-}Me_2\text{-}7,8\text{-}C_2B_9H_{11})]$ and trinuclear cluster $[Ru_3(CO)_8(\eta^5\text{-}7,8\text{-}Me_2\text{-}7,8\text{-}C_2B_9H_{11})]$.[7] The trinuclear ruthenium and osmium clusters $[M_3(CO)_8(\eta^5\text{-}7\text{-}NMe_3\text{-}7\text{-}CB_{10}H_{10}]$ (M = Os[8] and Ru[9]) were synthesized from the reaction of the zwitterionic monocarborane $7\text{-}NR_3\text{-}7\text{-}CB_{10}H_{10}$ and the respective carbonylmetal complexes. In both cases no mononuclear transition metal complex is known.

Figure 1. Syntheses of the tricarbonylruthenium dicarbollide complex

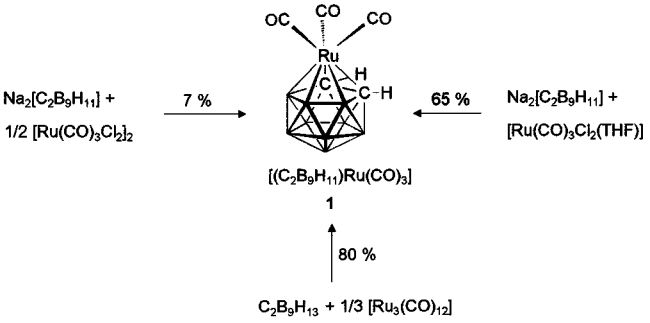

We have recently presented the first examples of transition metal complexes of the 7-sila-*nido*-undecaborate(1−) (**2**) cluster.[10] In the reaction of the deprotonated silaborate with iron(II) bromide we found with **3** (Figure 2) an unprecedented structural motif for cluster coordination chemistry.[11] The coordination of the silaborate cluster trianion is realized in the series of the cyclopentadienyl complexes of cobalt, rhodium **4** (Figure 2) and iridium.[12]

In this paper we report on the formation of silaborate ruthenium complexes. These complexes can be either mononuclear or trinuclear in dependency of the chosen stoichiometry between $[Ru_3(CO)_{12}]$ and $[MeSiB_{10}H_{12}]^-$.

[+] Present address: Institut für Anorganische Chemie II, Universität Karlsruhe, Engesserstrasse, Gebäude 30.45, D-76128 Karlsruhe, Germany.

 © WILEY-VCH Verlag GmbH, D-69451 Weinheim, 1998 1434−1948/98/0909−1263 $ 17.50+.50/0

Figure 2. Transition metal silaborate complexes

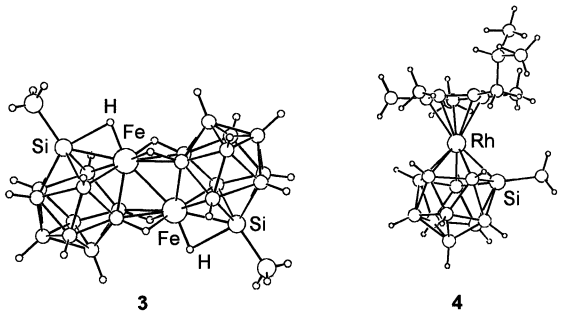

3 4

Results

Mononuclear Complexes

The mononuclear tricarbonylruthenium complex is readily formed by heating a suspension of three equivalents of $[NEt_4][MeSiB_{10}H_{12}]$ with one equivalent of $[Ru_3(CO)_{12}]$ in heptane for 15 h at 110°C (Scheme 1). The resulting dark brown oil was recrystallized by slow diffusion of Et_2O into a CH_2Cl_2 solution of the reaction mixture to give colourless crystals of $[NEt_4][Ru(CO)_3(MeSiB_{10}H_{10})]$ (**5**) in 92% yield.

Scheme 1. Synthesis of **5**

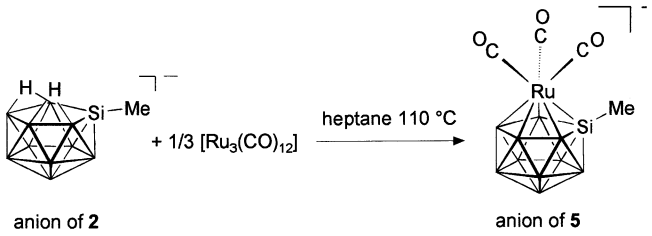

anion of **2** anion of **5**

The metallasilaborate **5** was characterized by elemental analyses, NMR spectroscopy, mass spectrometry, and single crystal X-ray structure analysis. Six signals in the ^{11}B-NMR spectrum for ten boron atoms with an intensity ratio of 1:2:2:1:2:2 are consistent with C_s symmetry of the cluster anion of **5** in solution. In the two-dimensional $^{11}B\{^1H\}$-$^{11}B\{^1H\}$ COSY-NMR spectrum the cross peak between B3/6 and B4/5 is missing due to bridging by the silicon atom. The effect, that connections between boron atoms, which are bridged by hetero atoms, are not visible in the two-dimensional COSY ^{11}B-NMR spectrum, is known from other heteroboranes like carboranes[13].

The ^{11}B-NMR chemical shifts in heteroborane clusters are governed by the antipodal effect[14]. Substitution of a heteroatom in a borane cluster is equivalent to changes of the electronic structure of the cage compound, with the strongest variations at the antipodal atom. In the anion of **5** the two heteroatoms Ru and Si are opposite to the boron atoms B9 and B12. As expected the chemical shift for B12 opposite to the silicon atom appears at high field ($\delta = -9.7$) in the range of values which are known from other metallasilaboranes ($\delta = -5.3$ to -19.4)[11][12] (Figure 3). In comparison to B12 the resonance for B9, the boron atom opposite to the transition metal center, appears at lower field ($\delta = +4.1$ to -0.1; M = Fe, Co, Rh, Ir)[12]. In the presented complex for B9 a value of $\delta = 12.2$ was determined. This chemical shift represents the resonance at lowest field in the series of the so far known metallasilaboranes. It can be interpreted as an indicator for the electron-withdrawing ability of the tricarbonylruthenium group.

The stretching frequencies for the terminal carbonyl substituents of 2075 and 2002 cm^{-1} are smaller than the comparable values in **1** (2114, 2058 cm^{-1}). Obviously, π-back bonding in MCO is not as much reduced in **5** as in **1**, which could be attributed to stronger σ-donation by the silaborate ligand.

A perspective view of the anion of **5** is presented as the result of the X-ray crystal structure analysis in Figure 4 and selected interatomic distances are listed in the Table. The structural study confirms the prediction of the spectroscopic analyses, a *closo* structure for the ruthenasilaborate. The $Ru(CO)_3$ fragment is η^5-coordinated at the silaborate ligand. As a common structural motif for transition metal coordination on the silaborate ligand the distances to B7/11 [2.292(6), 2.300(6) Å] are shorter than to B3/6 [2.372(6), 2.377(6) Å][11][12].

The short Ru−Si distance of 2.396(2) Å can be compared with distances in silyl complexes[15]. The short Ru−B7/11 and Ru−Si distances indicate a major contribution to these atoms of the pentagonal open face of the ligand for transition metal coordination. Tilley described in 1994 the synthesis of $(\eta^5\text{-}C_5Me_5)Ru[\eta^5\text{-}Me_4C_4SiSi(SiMe_3)_3]$ a stable silacyclopentadienyl complex of ruthenium[16]. In the case of the protonated derivative $[Cp^*Ru(H)\{\eta^5\text{-}Me_4C_4SiSi(SiMe_3)_3\}][BPh_4]$ a Ru−Si distance of 2.441(3) Å was determined by X-ray structure analysis.

Based on the isolobal analogy the $Ru(CO)_3$ fragment donates two electrons to the cluster electron count. Summation over the complete skeleton gives a total of 26 electrons, which corresponds to $2n+2$ electrons for a *closo* cluster with 12 edges.

The degradation product of *o*-silaborane **2** reacts with the trinuclear dodecacarbonyltriiron to give the tricarbonyliron silaborate cluster **6** in quantitative yield based on the ^{11}B-NMR spectra. The pattern in the two-dimensional $^{11}B\{^1H\}$-$^{11}B\{^1H\}$ COSY-NMR spectrum (Figure 5) and the ^{11}B chemical shifts of the iron derivative are strongly related to the ruthenium complex **5**.

6 was also characterized by mass spectrometry and IR spectroscopy. Unfortunately, the elemental analyses failed due to carbonyliron impurities.

Trinuclear Metallasilaborates

The *nido*-silaborate **2** reacts with $[Ru_3(CO)_{12}]$ in heptane at reflux temperatures to give the trinuclear rutheniumsilaborate cluster **7** (Scheme 2). The cluster was obtained in almost quantitative yield as yellow crystals by slow diffusion of Et_2O into a CH_2Cl_2 solution of the reaction mixture.

As with **5**, **7** was characterized by elemental analyses, mass spectrometry, IR spectroscopy, and NMR spec-

Figure 3. ^{11}B-NMR chemical shifts

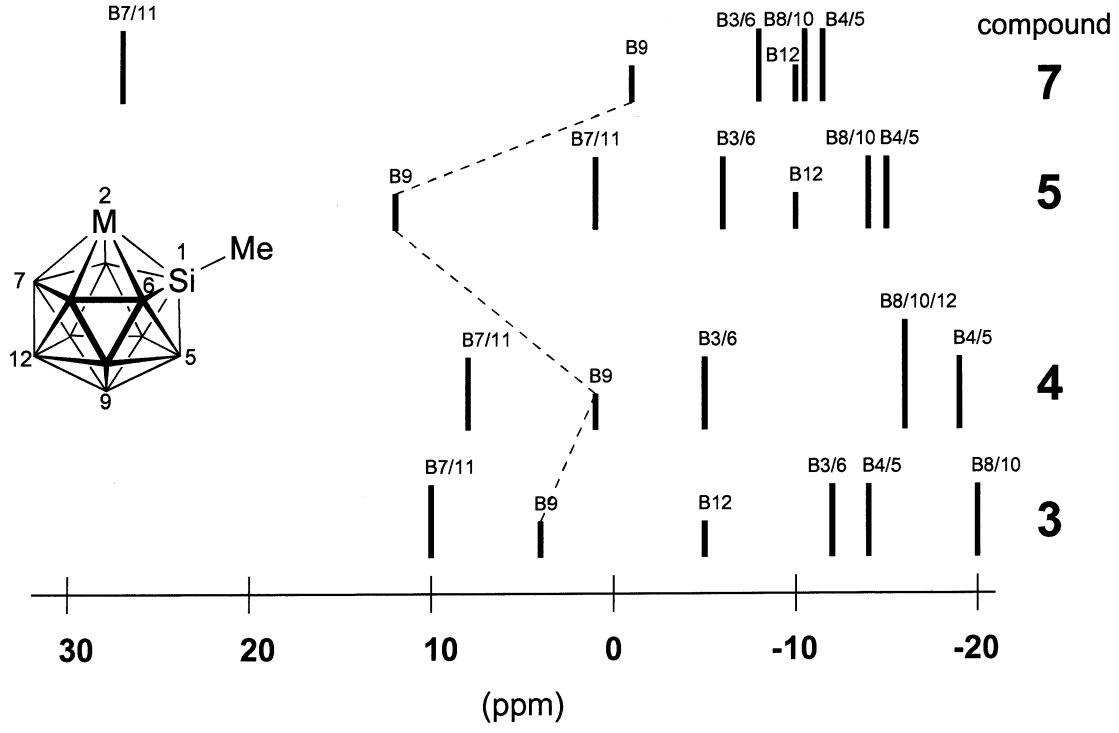

Figure 4. Molecular structure for the anion of **5**

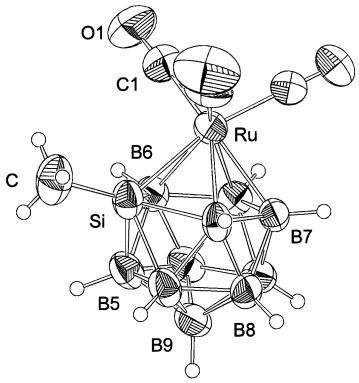

Table 1. Selected interatomic distances [Å] in **5**

Ru−C1	1.919(7)	B3−B4	1.834(9)
Ru−C2	1.937(6)	B3−B7	1.815(8)
Ru−C3	1.901(7)	B3−B8	1.764(9)
Ru−Si	2.396(2)	B4−B5	1.854(9)
Ru−B3	2.372(6)	B4−B8	1.765(9)
Ru−B6	2.377(6)	B4−B9	1.766(11)
Ru−B7	2.292(6)	B5−B6	1.822(10)
Ru−B11	2.300(6)	B5−B9	1.763(10)
Si−C4	1.859(6)	B5−B10	1.750(10)
Si−B3	2.091(6)	B6−B10	1.751(10)
Si−B4	2.027(7)	B6−B11	1.793(9)
Si−B5	2.033(7)	B7−B8	1.791(9)
B7−B12	1.781(9)	B10−B11	1.779(9)
B8−B9	1.775(9)	B10−B12	1.765(9)
B8−B12	1.781(9)	B11−B12	1.782(9)
B9−B10	1.758(10)	B7−B11	1.865(8)
B9−B12	1.764(9)	Si−B6	2.104(7)

troscopy. On the basis of these spectroscopical data the constitution of **7** was unequivocally determined. The silaborate ligand is η^5-coordinated at one ruthenium atom replacing two carbonyl substituents. Two BH units coordinate at the other two ruthenium atoms of the Ru_3 cluster, replacing each one carbonyl substituent. Coordination of the BH units of B7/11 is proven by the reduced coupling constant of $^1J_{BH}$ = 67 Hz, the shift to low field in the ^{11}B-NMR spectrum for the resonances of B7/11 (Figure 3), and the cross peak in the two dimensional HMQC $^1H\{^{11}B\}$-$^{11}B\{^1H\}$ NMR spectrum between the resonances for B7/11 and a broad quadruplet in the ^{1}H-NMR spectrum at $\delta = -10$. Longer reaction times resulted in the decomposition of **7** and the isolation of the mononuclear cluster **5** together with the formation of a tetranuclear ruthenium cluster anion $[NEt_4][(\mu\text{-}H)_3Ru_4(CO)_{12}]$[17]. In contrast to the inertness of **5** towards nucleophiles **7** reacts readily with phosphanes (Scheme 2) to give the disubstituted derivative **8**. Carbonyl substitution at the ruthenium cluster skeleton is known from the dicarbollide analogues. **7** reacts with two equivalents of PMe_2Ph under substitution of one carbonyl group at each $Ru(CO)_3$ unit. In contrast to the analogue reaction of $[Ru_3(CO)_8(C_2B_9H_{11})]$ leading to oxidative addition of one coordinated BH unit at a ruthenium centre in the silaborane case the coordinated BH units of B7/11 remain unchanged. The constitution of **8** was deduced from the spectroscopical data together with elemental analysis and mass spectrometry. As in **7** a reduced coupling constant ($^1J_{BH}$ = 83 Hz) for the BH units of B7/11, a low-field chemical shift in the ^{11}B NMR for B7/11 and a cross peak in the HMQC $^1H\{^{11}B\}$-$^{11}B\{^1H\}$ between the resonances for B7/11 and a signal at $\delta = -10.6$ indicates the coordination

Figure 5. $^{11}B\{^1H\}$-$^{11}B\{^1H\}$ COSY-NMR spectrum of the anion of **6**

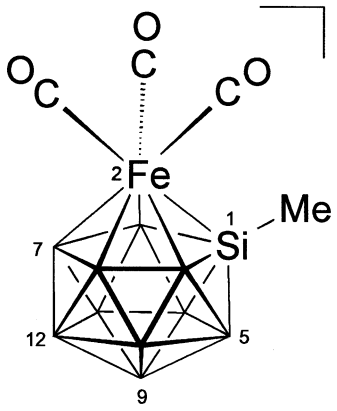

anion of **6**

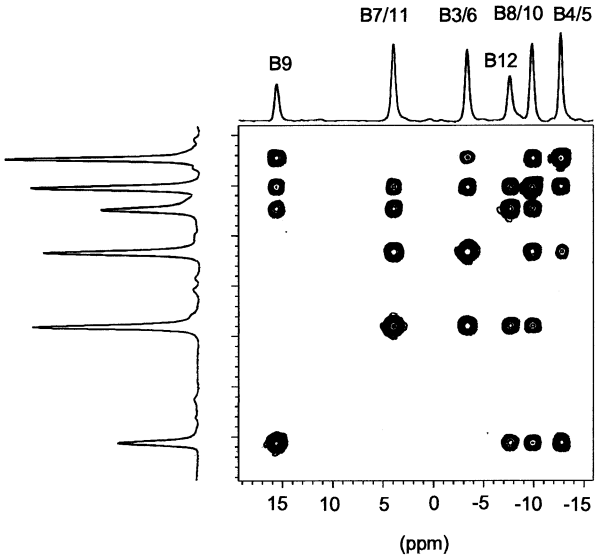

of these BH units at the ruthenium centres. The C_s symmetry of the cluster anion in solution is proven by five signals in the ^{11}B NMR for ten boron atoms, the resonances for B3/6 and B9 are accidentily isochronic, and one ^{31}P-NMR resonance for the two phosphane ligands. **8** crystallizes with one equivalent of dichloromethane in the space group $P2_1/a$ with a = 13.881(3), b = 12.773(7), c = 27.2800(9) Å, and β = 97.99(2)°. Due to an immediate loss of cocrystallized CH_2Cl_2 after isolation from the solution, no crystals of good quality could be obtained. Reflections were broad and of relative low intensity. In addition the atoms of the CH_2Cl_2 show large displacement parameters. Therefore no geometric details of the structure will be discussed but the constitution of **8** was confirmed.

Conclusion

The anionic degradation product of *o*-silaborane reacts with dodecacarbonyltriruthenium to give the first carbonyl transition metal complexes with a silaborate ligand. In contrast to the syntheses of the carbonylruthenium dicarbollide and monocarbollide complexes the formation of the mononuclear or trinuclear ruthenium complex is determined by the stoichiometry of silaborate and carbonylruthenium.

Scheme 2. Syntheses of **7** and **8**

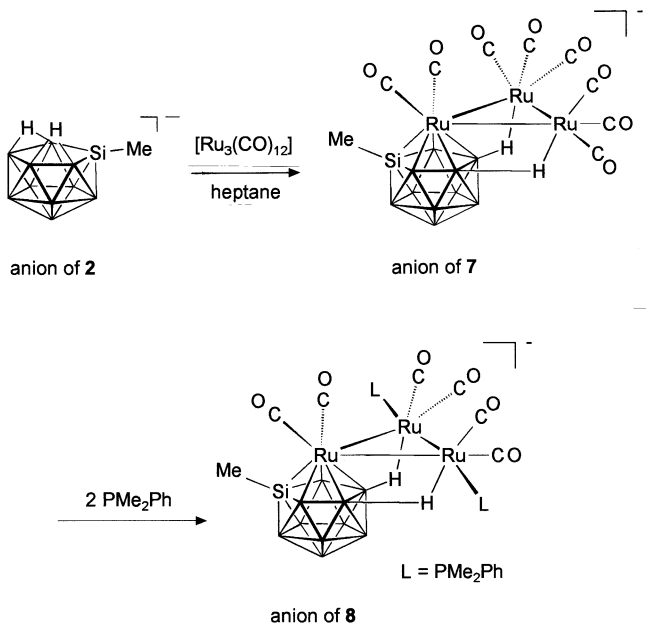

Support of this work by the *Deutsche Forschungsgemeinschaft (Schwerpunktprogramm Polyeder, Heisenberg fellowship)* and the *Fonds der Chemischen Industrie* is gratefully acknowledged.

Experimental Section

General: All manipulations were carried out under dry N_2 in Schlenk glassware. Solvents were dried and purified by standard methods and were stored under N_2. – NMR: Varian Unity 500 (500 MHz, ^1H, int. TMS; 126 MHz, $^{13}C\{^1H\}$, int. TMS; 202 MHz, ^{31}P, ext. H_3PO_4; 160 MHz, ^{11}B, ext. BF_3OEt_2; 100 MHz, ^{29}Si, ext. TMS). – MS: Finnigan MAT 95. – Elemental analysis: Institut für Anorganische Chemie RWTH Aachen, Carlo-Erba elemental analyzer, Modell 1106; Mikroanalytisches Labor Pascher, Remagen.

[NEt$_4$][Ru(CO)$_3$(η^5-MeSiB$_{10}$H$_{10}$)] (**5**): Tetraethylammonium dodecahydro-7-methyl-7-sila-*nido*-undecaborate(1–) (**2**; 250 mg, 0.85 mmol) was suspended with 25 ml of heptane and dodecacarbonyltriruthenium (181 mg, 639.3 g/mol, 0.28 mmol). The mixture was refluxed for 15 h and the solvent was evaporated in vacuum to give a red oily residue. Recrystallization was carried out by slow diffusion of diethyl ether into a solution of dichloromethane at −30°C to give 376 mg (93% yield) of **5** as colourless crystals. – IR (KBr) $\tilde{\nu}$ = 2075 cm^{-1} (CO), 2002 (CO). – $^1H\{^{11}B\}$ NMR (CD_2Cl_2): δ = 3.67 (s, 1 H, H9), 2.14 (s, 2 H, H7/11), 2.00 (s, 2 H, H3/6), 1.92 (s, 1 H, H12), 1.84 (s, 2 H, H4/5), 1.37 (s, 2 H, H8/10), 0.84 (s, 3 H, $SiCH_3$). – $^{13}C\{^1H\}$ NMR (CD_2Cl_2): δ = 196.4 (s, 3 C, CO), −4.8 (s, 1 C, $SiCH_3$). – ^{11}B NMR (CD_2Cl_2): δ = 12.2 (d, ^1J = 134 Hz, 1 B, B9), 0.7 (d, ^1J = 134 Hz, 2 B, B7/11), −6.2 (d,

^1J = 134 Hz, 2 B, B3/6), −9.7 (d, ^1J = 134 Hz, 1 B, B12), −13.8 (d, ^1J = 158 Hz, 2 B, B8/10), −15.1 (d, ^1J = 146 Hz, 2 B, B4/5). − ^{29}Si NMR (CD_2Cl_2): δ = 28.2 (s, MeSi). − MS (70 eV) SIMS; *m/z* (%): 347.2 (100) [M$^-$]. − $C_{12}H_{33}B_{10}NO_3RuSi$ (476.66): calcd. C 30.24, H 6.98; found C 29.41, H 5.90.

X-ray Crystallographic Study of **5**: $C_{12}H_{33}B_{10}NO_3RuSi$; formula mass 476.66 g mol^{-1}; monoclinic space group *C*2/*c* (no. 15); *a* = 32.641(5), *b* = 8.451(3), *c* = 21.489(3) Å, β = 125.73(2)°, *V* = 4812(2), *Z* = 8, $d_{calcd.}$ = 1.316 g cm^{-3}; $\mu_{lin.}$ = 0.714 mm^{-1}. Enraf-Nonius CAD4 diffractometer; Mo-K_α radiation (λ = 0.71070 Å); graphite monochromator. Data collection at room temperature on a crystal of about 1.1 × 0.2 × 0.2 mm using ω-scans (6° ≤ 2θ ≤ 60°) yielded 7093 reflections, which after merging the symmetry equivalents gave 6983 independent reflections with 3888 observations [$I > 2\sigma(I)$]. Intensity data were corrected for Lorentz and polarization effects, and a semi-empirical absorption correction (using ψ-scans)[18] was applied with the program system MolEN.[19] After solving the structure by direct and Difference Fourier methods[20], the structure was refined against F^2 using SHELXL-93[21] with anisotropic parameters for the non hydrogen atoms. This resulted in *wR*2 = 0.134 and *R* = 0.061 (observed reflections only) for 289 variables (GOF = 1.169). The hydrogen atoms attached to boron atoms were refined in their positions; the remaining hydogen atoms were included into calculated positions. A final difference Fourier map gave min./max. residual electron densities of 0.940/−1.361 eA^{-3}[22].

[NEt$_4$][Fe(CO)$_3$(η^5-MeSiB$_{10}$H$_{10}$)] (**6**): Tetraethylammonium dodecahydro-7-methyl-7-sila-*nido*-undecaborate(1−) (**2**; 250 mg 0.85 mmol) was suspended with 25 ml of heptane and dodecacarbonyltriruthenium (429 mg, 503.7 g/mol, 0.85 mmol). The mixture was refluxed for 15 h and the solvent was evaporated in vacuum to give a red oily residue, which could not be purified by recrystallization. − IR (KBr) $\tilde{\nu}$ = 2081 cm^{-1} (CO), 2009 (CO). − ^{1}H{^{11}B} NMR (CD_2Cl_2): δ = 3.57 (s, 1 H, H9), 2.35 (s, 2 H, H7/11), 2.11 (s, 1 H, H12), 1.94 (s, 4 H, H3/6, 4/5), 1.91 (s, 2 H, H8/10), 0.81 (s, 3 H, $SiCH_3$). − ^{13}C{^{1}H} NMR (CD_2Cl_2): δ = 208.6 (s, 3 C, CO), −7.1 (s, 1 C, $SiCH_3$). − ^{11}B NMR (CD_2Cl_2): δ = 13.9 (d, ^1J = 134 Hz, 1 B, B9), 3.1 (d, ^1J = 122 Hz, 2 B, B7/11), −3.8 (d, ^1J = 134 Hz, 2 B, B3/6), −8.4 (d, ^1J = 134 Hz, 1 B, B12), −10.6 (d, ^1J = 134 Hz, 2 B, B8/10), −12.9 (d, ^1J = 146 Hz, 2B, B4/5). − ^{29}Si NMR (CD_2Cl_2): δ = 38.9 (s, MeSi). − MS (70 eV) SIMS; *m/z* (%): 301.2 (100) [M$^-$], 272.3 (23, M$^-$ − CO), 245.1 (22, M$^-$ − 2CO).

[NEt$_4$][Ru$_3$(CO)$_8$(η^5-MeSiB$_{10}$H$_{10}$)] (**7**): Tetraethylammonium dodecahydro-7-methyl-7-sila-*nido*-undecaborate(1−) (**2**, 250 mg 0.85 mmol) was suspended with 25 ml of heptane and dodecacarbonyltriruthenium (544.4 mg, 639.3 g/mol, 0.85 mmol). The mixture was refluxed for 15 h and the solvent was evaporated in vacuum to give a red oily residue. Recrystallization was carried out by slow diffusion of diethyl ether into a solution of dichloromethane at −30°C to give 697 mg (91% yield) of **7** as yellow crystals. − IR (KBr) $\tilde{\nu}$ = 2071 cm^{-1} (CO), 2029 (CO), 1994 (CO), 1972 (CO). − ^{1}H{^{11}B} NMR (CD_2Cl_2): δ = 2.83 (s, 1 H, H9), 2.18 (s, 1 H, H12), 1.97 (s, 4 H, H4/5/8/10), 1.86 (s, 2 H, H3/6), 0.83 (s, 3 H, $SiCH_3$), −10.25 (s, 2 H, H7/11). − ^{13}C{^{1}H} NMR (CD_2Cl_2): δ = 211.8 (s, 1 C, CO), 206.1 (s, 1 C, CO), 200.3 (s, 1 C, CO), 199.5 (s, 1 C, CO), 197.2 (s, 1 C, CO), 196.4 (s, 1 C, CO), 194.2 (s, 1 C, CO), 191.3 (s, 1 C, CO), 53.6 (s, 4 C, N*C*H$_2$CH$_3$), 8.0 (s, 4 C, NCH$_2$*C*H$_3$) −4.5 (s, 1 C, $SiCH_3$). − ^{11}B NMR (CD_2Cl_2): δ = 27.1 (d, ^1J = 67 Hz, 2 B, B7/11), −0.9 (d, ^1J = 140 Hz, 1 B, B9), −8.1 (d, ^1J = 134 Hz, 2 B, B3/6), −9.8 (d, ^1J = 153 Hz, 1 B, B12), −10.8 (d, ^1J = 116 Hz, 2 B, B8/10), −11.3 (d, ^1J = 104 Hz, 2 B, B4/5). − ^{29}Si NMR (CD_2Cl_2): δ = 6.7 (s, MeSi). − MS (70 eV) SIMS; *m/z* (%): 690.6 (18) [M$^-$ − 2CO], 662.8 (64) [M$^-$ − CO], 634.8 (100) [M$^-$ − 2CO]. − $C_{17}H_{31}B_{10}NO_8Ru_3Si$ (816.83): calcd. C 25.00, H 3.83, N 1.72; found C 24.66, H 4.01, N 1.69.

[NEt$_4$][Ru$_3$(CO)$_6$(PMe$_2$Ph)$_2$(η^5-MeSiB$_{10}$H$_{10}$)] (**8**): 200 mg (*M* = 818.8 g/mol, 0.24 mmol) of **7**, dissolved in 20 ml of THF, was treated with 71 µl of PMe_2Ph (*M* = 138.2 g/mol, 0.50 mmol) at room temperature. After heating for 2 h under reflux, the solution was concentrated to dryness and the resulting orange solid was recrystallized from 20 ml of CH_2Cl_2 by slow diffusion of hexane at −30°C to give 233 mg (91% yield) of **8** as red crystals. − IR (dioxane) $\tilde{\nu}$ = 2050 cm^{-1} (CO), 1962 (CO). − ^{1}H{^{11}B} NMR ([D$_8$]THF): δ = 7.44−7.22 (m, 10 H, PPh), 2.62, 1.87, 1.78, 1.69 (s, br., BH), 1.71 (s, br., 12 H, PMe_2), 0.69 (s, 3 H, $SiCH_3$), −10.55 (q, br., 2 H, BHRu). − ^{13}C{^{1}H} NMR ([D$_8$]THF): δ = 211.1, 204.3, 201.2 (s, 2 C, CO), 142.4 (s, br., 2 C, PC), 129.2, 128.6, 128.3 (s, Ph), 52.9 (s, 4 C, N*C*H$_2$CH$_3$), 7.8 (s, 4 C, NCH$_2$*C*H$_3$), −4.0 (s, 1 C, $SiCH_3$). − ^{11}B NMR ([D$_8$]THF): δ = 26.0 (d, ^1J = 83 Hz, 2 B, B7/11), −3.0 (d, ^1J = 140 Hz, 3 B, B3/6/9), −10.2 (d, ^1J = 134 Hz, 2 B, B4/5), −11.7 (d, ^1J = 109 Hz, 1 B, B12), −12.5 (d, ^1J = 141 Hz, 2 B, B8/10). − ^{29}Si NMR ([D$_8$]THF): δ = −29.8 (s, MeSi). − ^{31}P NMR ([D$_8$]THF): δ = −4.3 (s, 2 P, PMe_2Ph). − MS (70 eV) SIMS; *m/z* (%): 910.2 (100) [M$^-$ − 10]. − $C_{31}H_{55}B_{10}NO_6P_2Ru_3Si$·($CH_2Cl_2$) (1124.06): calcd. C 34.19, H 5.11; found C 33.85, H 4.93.

☆ Dedicated to Prof. Dr. *Heinrich Nöth* on the occasion of his 70th birthday.

[1] [1a] M. F. Hawthorne, *Acc. Chem. Res.* **1968**, *1*, 281−288. − [1b] A. K. Saxena, N. S. Hosmane, *Chem. Rev.* **1993**, *93*, 1081−1124.
[2] M. F. Hawthorne, H. W. Ruhle, *Inorg. Chem.* **1969**, *8*, 176−178.
[3] [3a] S. S. Lee, C. B. Knobler, M. F. Hawthorne, *Organometallics* **1991**, *10*, 670−677. − [3b] S. S. Lee, C. B. Knobler, M. F. Hawthorne, *Organometallics* **1991**, *10*, 1054−1062.
[4] A. R. Siedle, *J. Organomet. Chem.* **1975**, *90*, 249−256.
[5] P. E. Behnken, M. F. Hawthorne, *Inorg. Chem.* **1984**, *23*, 3420−3423.
[6] S. Anderson, D. F. Mullica, E. L. Sappenfield, F. G. A. Stone, *Organometallics* **1995**, *14*, 3516−3526.
[7] Y.-H. Liao, D. F. Mullica, E. L. Sappenfield, F. G. A. Stone, *Organometallics* **1996**, *15*, 5102−5111.
[8] V. N. Lebedev, D. F. Mullica, E. L. Sappenfield, F. G. A. Stone, *J. Organomet. Chem.* **1997**, *536−537*, 537−539.
[9] V. N. Lebedev, D. F. Mullica, E. L. Sappenfield, F. G. A. Stone, *Organometallics* **1996**, *15*, 1669−1675.
[10] L. Wesemann, U. Englert, D. Seyferth, *Angew. Chem.* **1995**, *107*, 2435−2436; *Angew. Chem. Int. Ed. Engl.* **1995**, *34*, 2236−2238.
[11] L. Wesemann, Y. Ramjoie, B. Ganter, B. Wrackmeyer, *Angew. Chem.* **1997**, *109*, 902−904; *Angew. Chem. Int. Ed. Engl.* **1997**, *36*, 888−890.
[12] L. Wesemann, Y. Ramjoie, M. Trinkaus, B. Ganter, *Inorg. Chem.* **1997**, *36*, 5192−5197.
[13] T. L. Venable, W. C. Hutton, R. N. Grimes, *J. Am. Chem. Soc.* **1984**, *106*, 29−37.
[14] [14a] M. Bühl, P. v. R. Schleyer, Z. Havlas, D. Hynk, S. Hermanek, *Inorg. Chem.* **1991**, *30*, 3107−3111. − [14b] S. Hermanek, *Chem. Rev.* **1992**, *92*, 325−362.
[15] D. A. Straus, T. D. Tilley, A. L. Rheingold, S. J. Geib, *J. Am. Chem. Soc.* **1987**, *109*, 5872−5873.
[16] W. P. Freeman, T. D. Tilley, A. L. Rheingold, *J. Am. Chem. Soc.* **1994**, *116*, 8428−8429.
[17] J. W. Koepke, J. R. Johnson, S. A. R. Knox, H. D. Kaesz, *J. Am. Chem. Soc.* **1975**, *97*, 3947−3952.
[18] A. C. T. North, D. C. Phillips, F. C. Mathews, *Acta Crystallogr.* **1968**, *A24*, 351.
[19] C. K. Fair, *MolEN, An Interactive Structure Solution Procedure*,

Enraf-Nonius, Delft, The Netherlands, **1990**.
[20] G. M. Sheldrick, SHELXS-86, *Acta Crystallogr.* **1990**, *A46,* 467.
[21] G. M. Sheldrick, *Program for the refinement of Crystal Structures*, Universität Göttingen, **1993**.
[22] Further details of the crystal structure investigations are available on request from the Fachinformationszentrum Karlsruhe, D-76344 Eggenstein-Leopoldshafen, on quoting the depository number CSD-408509, the names of the authors, and the journal citation.

[98096]

Oxidation of Polycyclic Aromatic Hydrocarbons Catalyzed by Iron Tetrasulfophthalocyanine FePcS: Inverse Isotope Effects and Oxygen Labeling Studies

Alexander Sorokin and Bernard Meunier*

Laboratoire de Chimie de Coordination du CNRS,
205 route de Narbonne, F-31077 Toulouse cedex 4, France
Fax: (internat.) + 33-5/61553003
E-mail: bmeunier@lcc-toulouse.fr

Received April 24, 1998

Keywords: Oxidation / Catalysis / Phthalocyanine / Iron / Anthracene

Iron(III) tetrasulfophthalocyanine (FePcS) was shown to catalyze the oxidation of polycyclic aromatic hydrocarbons by H_2O_2. Benzo[*a*]pyrene and anthracene were converted to the corresponding quinones while biphenyl-2,2′-dicarboxylic acid was the main product of phenanthrene oxidation. The mechanism of the anthracene oxidation by H_2O_2 in the presence of FePcS or by $KHSO_5$ with iron(III) *meso*-tetrakis(3,5-disulfonatomesityl)porphyrin (FeTMPS) (see Figure 1 for catalyst structures) has been investigated in details by using kinetic isotope effects (KIEs) and ^{18}O labeling studies. KIEs measured on the substrate consumption in the competitive oxidation of [H_{10}]anthracene and [D_{10}]anthracene by FePcS/H_2O_2 and FeTMPS/$KHSO_5$ were essentially the same, 0.75 ± 0.02 and 0.76 ± 0.06, respectively. These inverse KIEs on the first oxidation step can be explained by the sp^2-to-sp^3 hybridization change during the addition of an electrophilic oxoiron complex to the sp^2 carbon center of anthracene to form a σ adduct (this inverse KIE being enhanced by stronger stacking interactions between the perdeuterated substrate with the macrocyclic catalyst). Although the first oxidation step seems to be the same, different distribution of the oxidation products of anthracene and very different ^{18}O incorporation into anthrone and anthraquinone in catalytic oxidations performed in the presence of $H_2{}^{18}O$ suggested that different active species should be responsible for anthracene oxidation in both catalytic systems. All the results obtained are compatible with an involvement of $TMPSFe^{V}=O$ (or $TMPS^{+}Fe^{IV}=O$), having two redox equivalents above the iron(III) state of the metalloporphyrin precursor, while $PcSFe^{IV}=O$ (one redox equivalent above Fe^{III} state of FePcS) was proposed to be the active species in the metallophthalocyanine-based system.

Introduction

Polycyclic aromatic hydrocarbons (PAH) belong to environmental pollutants because of their rather slow biodegradation. PAHs can be metabolized by bacteria, fungi or algae. Three main degradation pathways have been identified for the microbial catabolism of polycyclic aromatic hydrocarbons[1]. Cytochrome P-450 monooxygenases catalyze the formation of arene oxides, which are then transformed to phenol or epoxy-diol derivatives. Ligninases are capable of oxidizing PAH to quinones followed by ring cleavage[2]. For example, benzo[*a*]pyrene was oxidized to a mixture of 1,6-, 3,6- and 6,12-quinones[3], pyrene to 1,6- and 1,8-quinones[4] and anthracene to 9,10-anthraquinone[2]. The third enzymatic degradation process involves dioxygenase enzymes to incorporate both atoms of molecular oxygen into the aromatic ring to form *cis*-dihydrodiols. After a dehydrogenase-catalyzed rearomatization to produce catechols, a subsequent enzymatic cleavage by intradiol or extradiol dioxygenases gives *cis,cis*-muconic acid or 2-hydroxymuconic semialdehyde as products of aromatic cycle cleavage, respectively[5]. Although biodegradation of PAHs is the major decontamination process, along with photochemical oxidation with dioxygen[6], microorganisms capable of rapidly and efficiently mineralizing recalcitrant and potentially carcinogenic PAHs needs to be found[1]. Chemical oxidation of PAH[7] needs elevated temperatures and/or powerful oxidants, e.g. chromium compounds which constitute environmental problems. For example, phenanthrene has been oxidized to phenanthrenequinone by CrO_3 at 55°C (yield 80%)[8], by the system $Ce^{IV}/H_2SO_4/(NH_4)_2SO_4$ at 50°C (yield 42%)[9], by $KMnO_4/Al_2O_3/H_5IO_6$ (yield 25%)[10]. Arenes can be oxidized to quinones by H_2O_2/hexafluoroacetone at 70°C[11]. In this latter case, biphenyl-2,2′-dicarboxylic acid was the only isolated oxidation product of phenanthrene[11]. Obviously, there is a need for environmental-friendly chemical catalysts to oxidize PAH. An alternative approach using biomimetic metalloporphyrin catalysts[12] has been shown to be useful in the oxidation of 2-methylnaphthalene[12a]. Phenanthrene and naphthalene were oxidized by a porphyrinruthenium/2,6-dichloropyridine *N*-oxide system to give the corresponding quinones with 40% and 29% yields, respectively[13]. Recently, the oxidation of naphthalene and methylnaphthalenes by peracetic

 © WILEY-VCH Verlag GmbH, D-69451 Weinheim, 1998 1434–1948/98/0909–1269 $ 17.50+.50/0

acid catalyzed by octanitrophthalocyanine Mn^{III} and Fe^{II} complexes has been reported[14].

We recently developed a new efficient catalytic system for the oxidative degradation of polychlorinated phenols based on the association of iron(III) or manganese(III) complexes of tetrasulfophthalocyanine (FePcS, MnPcS) and the rather inexpensive and "green" oxidant H_2O_2[15][16]. This biomimetic system is able to cleave the aromatic cycle of 2,4,6-trichlorophenol with the formation of chloromaleic acid as the main product[15]. Besides FePcS and MnPcS, CoPcS is also highly efficient in the oxidation of catechols[17]. Having on hands these efficient catalysts for the oxidation of recalcitrant pollutants such as chlorinated phenols, we decided to investigate the activity of these catalysts in the oxidation of other poorly biodegradable molecules. Here we report the catalytic oxidation of polycondensed aromatics (mainly anthracene, but also phenanthrene and benzo[*a*]pyrene) by hydrogen peroxide or potassium monopersulfate ($KHSO_5$) and FePcS as catalyst [FeTMPS, a water-soluble iron(III) porphyrin, was also used for comparison]. Detailed mechanistic studies involving kinetic isotope effects (KIEs) and ^{18}O labeling experiments are also reported.

Figure 1. Structures of iron(III) complexes of tetrasulfophthalocyanine (FePcS) and *meso*-tetrakis(3,5-disulfonatomesityl)porphyrin

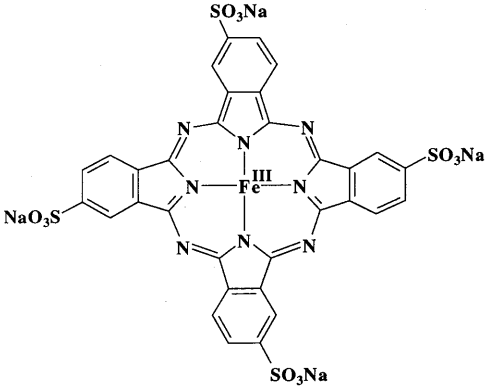

Iron tetrasulfophthalocyanine (FePcS)

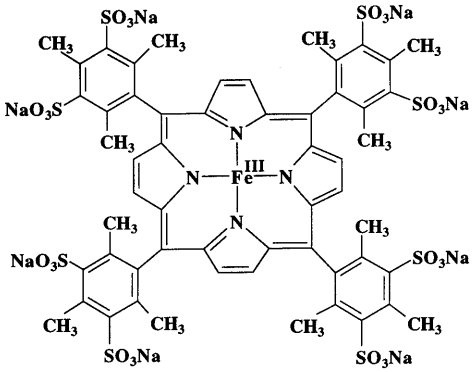

Iron meso-tetrakis(3,5-disulfonatomesityl)porphyrin (FeTMPS)

Results

Products and Reactivity Order in PAH Oxidations by FePcS/H_2O_2

We checked the oxidations of benzo[*a*]pyrene, phenanthrene and anthracene, performed in a MeCN/H_2O mixture (3:1, v/v) using $KHSO_5$ and H_2O_2 as oxidants. The final concentrations of oxidant and substrate were 5 mM and 1 mM, respectively. The catalyst concentrations were 10 μM, 37 μM and 100 μM corresponding to 1, 3.7 and 10% catalyst/substrate ratios, respectively. The data of Table 1 indicated that FePcS was also an efficient catalyst for the oxidation of these polyaromatic hydrocarbons. The oxidation of benzo[*a*]pyrene by FePcS/$KHSO_5$ (run 1) and by FePcS/H_2O_2 (run 4) at pH = 7 was complete within in a few minutes leading to an orange material isolated by precipitation with water. DCI-CH_4 mass spectrometry analysis gave peaks at 282 (M^+, 100), 254 [$(M - CO)^+$, 17.4], 226 [$(M - 2\ CO)^+$, 17.4] indicating the final product was a quinone (or a mixture of quinone isomers) with a molecular weight equal to 282. Three components were isolated by dry column chromatography (neutral Al_2O_3, benzene) after oxidation of benzo[*a*]pyrene in conditions used for run 4 of Table 1 and characterized by UV spectroscopy according to ref.[18] (Scheme 1). The UV/Vis spectra for all three quinones were in an excellent agreement with the data previously published[18]. Based on reported extinction coefficients, the distribution of quinones was as follows: 6,12-benzo[*a*]pyrenedione (32%, first eluted product from column), 1,6- benzo[*a*]pyrenedione (44%, second eluted product) and 3,6- benzo[*a*]pyrenedione (24%, third eluted product). The total yield for all three quinones was quantitative

Table 1. Oxidation of polyaromatic hydrocarbons PAH by H_2O_2 and $KHSO_5$ catalyzed by sulfonated phthalocyanineiron(III) FePcS[a]

Run	Oxidant	pH	% Cat./Sub.	Conversion [%]		
				1 min	5 min	60 min
		Benzo[*a*]pyrene oxidation				
1	$KHSO_5$	2	1	50	97	100
2	$KHSO_5$	7	1	14	41	70
3	H_2O_2	7	1	11	20	20
4	H_2O_2	7	3.7	43	100	100
		Anthracene oxidation				
5	H_2O_2	4.4	10	12	40	96
6	H_2O_2	7	10	100		
7	H_2O_2	7	3.7	57	74	86
8	H_2O_2	7	1	15	28	32
		Anthracene oxidation by FeTMPS/$KHSO_5$				
9	$KHSO_5$	7	3.7	11	33	100
		Phenanthrene oxidation				
10	$KHSO_5$	7	3.7	28	40	64
11	H_2O_2	5.3	3.7	10	24	35
12	H_2O_2	5.3	10	n.d.	n.d.	66
13	H_2O_2	5.5	10	32	46	64
14	H_2O_2	5.9	10	n.d.	45	60
15	H_2O_2	4.4	10	n.d.	24	80

[a] n.d.: not determined.

The H_2O_2 oxidation of phenanthrene is pH-dependent. Using a 10% catalyst/substrate ratio the highest conversion of phenanthrene was obtained at pH = 4.4 (conversion be-

Scheme 1. Oxidation products of benzo[*a*]pyrene by $FePcS/H_2O_2$

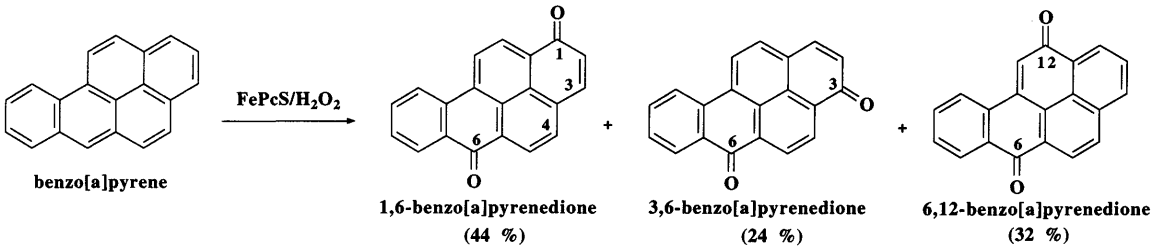

ing rather low at pH = 7) (Figure 2). But it should be noted that anthracene was quickly and completely oxidized within 1 min at pH = 7 (Table 1, run 6) while 1 hour was necessary to reach 96% conversion at pH = 4.4 (the pH optimum for phenanthrene). At pH = 7 the order of substrate reactivity was in agreement with oxidation potentials: benzo[*a*]pyrene > anthracene > phenanthrene (the ionization potentials being 7.2, 7.4 and 8.1 eV, respectively[2]).

Figure 2. pH dependence of phenanthrene oxidation by FePcS/H_2O_2[a]

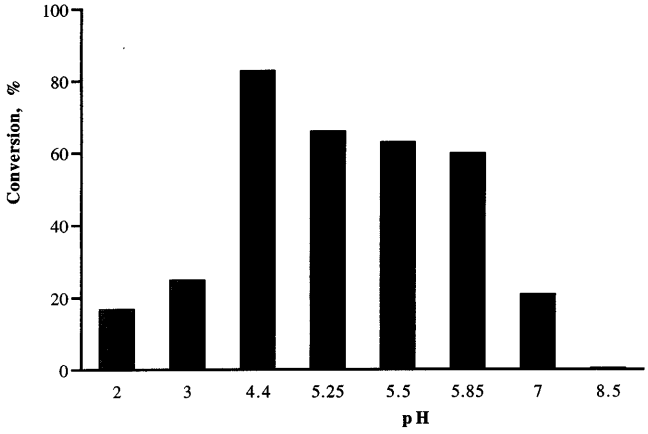

[a] Reaction conditions: [catalyst] = 0.1 mM, [oxidant] = 5 mM, [substrate] = 1 mM, acetonitrile/50 mM phosphate buffer at pH = 7 (3:1, v/v). Reaction time 60 min.

The FePcS-catalyzed oxidation of anthracene by H_2O_2 resulted in the formation of anthrone (tautomeric form of 9-hydroxyanthracene), oxanthrone (tautomeric form of anthrahydroquinone) and anthraquinone (Scheme 2). The yields of oxanthrone (5%) and anthraquinone (25%) were determined after 1 h by HPLC using calibration curve and molar extintion coefficients obtained with authentic samples.

Biphenyl-2,2′-dicarboxylic acid (product of cleavage of one aromatic cycle) was the main oxidation product of phenanthrene, 9,10-phenanthrenequinone being the second main product. Three other minor products of the oxidative degradation of phenanthrene were also identified by GC-MS analysis: 2-formyl-2′-hydroxybiphenyl, 2-carboxy-2′-hydroxybiphenyl and 2,2′-biphenylcarbolactone (Scheme 3). So, the $FePcS/H_2O_2$ system is able to cleave the aromatic cycle of phenanthrene and to perform oxidative decarboxylation.

Oxidation of Anthracene by $FeTMPS/KHSO_5$

We also checked the oxidation of anthracene by $FeTMPS/KHSO_5$ performed in an MeCN/25 mM phosphate buffer mixture (3:1, v/v) at pH = 7. The concentrations of oxidant, substrate and catalyst were 5 mM, 1 mM and 37 μM, respectively. The anthracene conversion was complete after 60 min (run 9, Table 1). The yields of oxanthrone and anthraquinone were determined by HPLC. Differing from the $FePcS/H_2O_2$ mediated oxidation, the main product with $FeTMPS/KHSO_5$ was oxanthrone (yield by HPLC = 60%), while only 3% of anthraquinone were found. Isolation of reaction products from a large scale anthracene oxidation by $FeTMPS/KHSO_5$ followed by NMR analysis gave 43% yield for oxanthrone, 16% yield for anthraquinone and 14% yield of non-identified compounds (probably coupling products). A partial oxidation of oxanthrone to anthraquinone might have occured during the sample preparation for NMR analysis, explaining the discrepancy with the HPLC analysis of the reaction mixture. This rather unexpected result, oxanthrone, an easily oxidizable compound, as main reaction product in the presence of strong oxidants, stimulated us for a detailed mechanistic study of anthracene oxidation by both catalytic systems, $FePcS/H_2O_2$ and $FeTMPS/KHSO_5$.

Scheme 2. Oxidation products of anthracene by $FePcS/H_2O_2$ or $FeTMPS/KHSO_5$

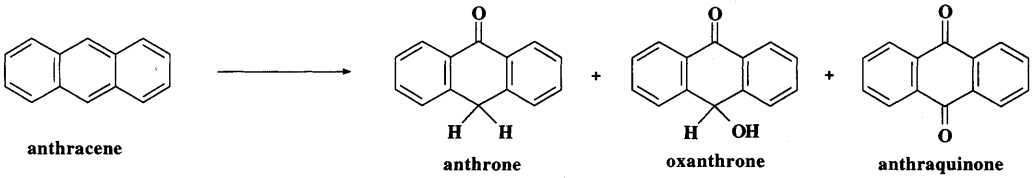

Conversion: 79 % (30 min)	**$FePcS/H_2O_2$**	**< 5 %**	**5 %**	**21 %**
Conversion: 100 % (30 min)	**$FeTMPS/KHSO_5$**	**< 5 %**	**43 %**	**16 %**

Scheme 3. Oxidation products of phenanthrene by $FePcS/H_2O_2$

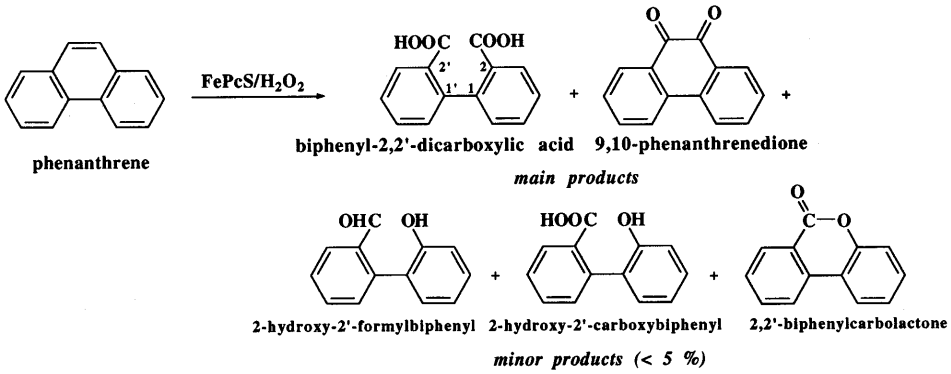

Stability of Anthrone, Oxanthrone and Anthraquinone in the Presence of $FePcS/H_2O_2$ and $FeTMPS/KHSO_5$

In these experiments we used the same reaction conditions as those for anthracene oxidation: a MeCN/50 mM phosphate buffer pH = 7 reaction medium (3:1, v/v), [catalyst] = 37 μM, [oxidant] = 5 mM, [substrate] = 1 mM, except for anthraquinone (its concentration was reduced to 0.5 mM because of its low solubility in the reaction mixture). Under these reaction conditions the conversions of anthrone in the presence of $FePcS/H_2O_2$ and $FeTMPS/KHSO_5$ were 23% and 38%, respectively, after 1 h, indicating that anthrone oxidation was slightly faster with $FePcS/KHSO_5$. Oxanthrone was easily oxidized to anthraquinone by $FePcS/H_2O_2$: the conversion was 90% after only 5 min. Again, oxanthrone was relatively stable with $FeTMPS/KHSO_5$: the conversions were only 18 and 23% after 30 and 60 min, respectively. Finally, we checked that anthraquinone was stable in both catalytic systems. There was no observable conversion after 60 min with $FeTMPS/KHSO_5$ and only 10% with $FePcS/H_2O_2$. These results on stability of products of anthracene oxidation were in good agreement with the composition of the reaction products for both catalytic systems.

Method of Determination of Kinetic Isotope Effects

Kinetic isotope effects (KIEs) can be determined in intra- or intermolecular competitive experiments by the analysis of the ratios of reaction products resulting from C−H versus C−D bond transformations. Such analyses are reliable when the oxidation products, different only in their isotopic substitution, are primary oxidation products and are stable in the reaction conditions. Since this is not a case in PAH oxidations by $FePcS/H_2O_2$ system we decided to determine the KIE values by analyzing of the competitive consumption of the deuterated versus the non-deuterated substrate. In this case intermolecular KIE values of the initial oxidation reaction can be obtained. In order to determine these KIEs concentrations of labeled and unlabeled substrates should be determined before and after the oxidation reaction by monitoring the isotopic composition of the initial reaction mixture, the substrate conversion and the isotopic composition of the remaining substrate after reaction. Isotopic compositions of substrates were determined by GC-MS analyses and substrate conversions were obtained by HPLC analyses (see Experimental Section). Equations to calculate KIEs depend on a reaction order in substrate[19]. When the reaction is first order in substrate KIEs can be determined from equation (1) where a_H°, a_D° and a_H, a_D denote initial and current substrate concentrations of H-labeled and D-labeled substrates, respectively.

$$k_H/k_D = \log (a_H/a_H^\circ) / \log (a_D/a_D^\circ) \quad (1)$$

Determination of the Reaction Order for the Substrate in Anthracene Oxidation by $FePcS/H_2O_2$

The reaction order in anthracene was determined with concentrations of H_2O_2, anthracene and FePcS being 5 mM, 1 mM and 37 μM, respectively. The reactions were carried out in an MeCN/50 mM phosphate buffer mixture at pH = 7 (3:1, v/v). Under these conditions the catalytic reaction follows a first-order kinetic in substrate at least for 2 times the reaction half-time and KIEs could be then determined according to equation (1).

KIEs in Anthracene and Phenanthrene Oxidation by $FePcS/H_2O_2$ and $FeTMPS/KHSO_5$

Analysis of the reaction mixture after 3−5 min of reaction (conversions being 40−60%) indicated a preferential consumption of $[D_{10}]$anthracene corresponding to an inverse isotope effect. The kinetic isotope effect in anthracene oxidation by the $FePcS/H_2O_2$ system was determined to be equal to 0.75 ± 0.02. Oxidation of anthracene by $FeTMPS/KHSO_5$ presented the same isotope effect of 0.76 ± 0.06 (Table 2). In contrast, oxidation of phenanthrene by both catalytic systems proceeds with no significant isotope effect: 0.96 ± 0.04 and 1.02 ± 0.01 for $FePcS/H_2O_2$ and $FeTMPS/KHSO_5$, respectively (Table 2).

In order to find the origin of this inverse isotope effects we prepared 9,10-dideuterioanthracene and determined the KIE value in the competitive oxidation of the mixture of 9,10-dideuterioanthracene and $[H_{10}]$anthracene. In this latter case the KIE value were 0.90 ± 0.05 and 0.95 ± 0.01 with the $FePcS/H_2O_2$ and $FeTMPS/KHSO_5$ systems, respectively.

Table 2. Kinetic isotope effect[a] in anthracene and phenanthrene oxidation by $FePcS/H_2O_2$ and $FeTMPS/KHSO_5$ at 20°C

Catalytic system	KIE in the competitive oxidation of [H_{10}]anthracene/[D_{10}]anthracene[b] ([H_{10}]anthracene/9,10-[D_2]anthracene)	[H_{10}]phenanthrene/[D_{10}]phenanthrene[c]
$FePcS/H_2O_2$	0.75 ± 0.02 (0.90 ± 0.05)	0.96 ± 0.04
FeTMPS/$KHSO_5$	0.76 ± 0.06 (0.95 ± 0.01)	1.02 ± 0.01

[a] These data are the mean values obtained from 3 independent oxidation reactions. – [b] Reaction conditions: [catalyst] = 37 μM, [oxidant] = 5 mM, [substrate] = 1 mM, MeCN/50 mM phosphate buffer pH = 7 (3:1, v/v). – [c] Reaction conditions: [catalyst] = 100 μM, [oxidant] = 5 mM, [substrate] = 1 mM, MeCN/33.3 mM phosphate buffer pH = 4.6 (1:1, v/v).

Analysis of Isotopic Composition of Products of Anthracene Oxidation

Anthrone, oxanthrone and anthraquinone were identified as oxidation products of anthracene by NMR and GC-MS techniques. GC-MS analysis of the reaction mixture indicated that anthrone, the primary oxidation product, was enriched in the deuterated derivative as expected from the inverse isotope effect on the first step of anthracene oxidation. In contrast, anthraquinone, a second oxidation product, was enriched in unlabeled product indicating a KIE value > 1 during the oxidation of anthrone to this quinone. Oxanthrone was unstable under GC-MS analysis conditions and its isotopic composition could not be determined. The molecular peak of deuterated anthrone formed after 3 min of reaction was 202 corresponding to a [D_8]-containing molecule, not a [D_9]-molecule as expected for 9-hydroxyanthracene. This result suggested that the equilibrium between the two tautomeric forms, anthrone and 9-hydroxyanthracene, was rather fast (Scheme 4). Consequently, a putative σ adduct with a Fe–O–arene bond, which should stabilize the 9-hydroxyanthracene tautomer, could not be a long-lived intermediate as previously observed in the metalloporphyrin-catalyzed oxidation of 2-methylnapthalene[12a].

^{18}O-Labeling Experiments

Oxidations of organic substrates catalyzed by metalloporphyrin[12][20][21] and metallophthalocyanine[16] complexes in the presence of ^{18}O-labeled water or dioxygen provided valueable mechanistic information. In order to investigate the mechanism of these catalytic PAH oxidations we performed the oxidation of anthracene by $FePcS/H_2O_2$ and $FeTMPS/KHSO_5$ in reaction mixtures containing ^{18}O-labeled water. In control experiments we checked that light oxygen atoms of anthraquinone did not exchange with heavy oxygen atoms of ^{18}O-labeled water under the used reaction conditions, i.e. a mixture of acetonitrile/50mM phosphate buffer (3:1, v/v) at pH = 7. Also, $KHSO_5$ itself does not exchange its oxygen atoms with water[20c]. FePcS-mediated oxidations of anthracene were performed under standard conditions (run 7 of Table 1) either under air or under nitrogen, using a 50:50 mixture of [H_{10}]anthracene and [D_{10}]anthracene. The oxygen atom distribution was analyzed in both deuterated and non-deuterated products for each experiment. In all cases, the oxygen atom distribution for a defined product was exactly the same. For example, the ^{18}O incorporation into anthraquinone was followed by determination of the molecular ion percentages at 208/216 [M], 210/218 [M + 2] and 212/220 [M + 4] corresponding to the incorporation of none, one or two ^{18}O oxygen atoms in [H_8]anthraquinone and [D_8]anthraquinone, respectively. In both cases, under air or under nitrogen, anthrone, the primary oxidation product, contained only a light oxygen atom. This result indicates that this oxygen atom originated from H_2O_2, the non-labeled oxidant. In contrast, both ^{16}O and ^{18}O atoms were incorporated into anthraquinone. When the reaction was performed under air, the molecular cluster consisted of M (68%) and M + 2 (32%) peaks, meaning that the ^{18}O atom was unambiguously only located in one carbonyl group of this quinone. If ^{18}O would occupied both carbonyl positions, the molecular cluster would have consisted on three peaks: M, M + 2 and M + 4. So, anthraquinone contained 100% of ^{16}O in one carbonyl position, 36% of ^{16}O and 64% of ^{18}O in another one (Figure 3). When the reaction was performed under nitrogen, again, only two peaks were found in the molecular cluster: M (56%) and M + 2 (44%). Consequently, ^{16}O incorporation in one carbonyl position was complete, another carbonyl position was enriched with heavy oxygen: 12% of ^{16}O and 88% of ^{18}O (Figure 3). This more significant incorporation of ^{18}O at the second carbonyl position produced in the absence of dioxygen suggests a possibility of O_2 involvement into oxidation pathway from anthrone to anthraquinone.

We also studied the ^{18}O incorporation from labeled water into the oxidation products of anthracene mediated by $FeTMPS/KHSO_5$. In this latter case, the mass spectrum of anthrone indicated the incorporation of ^{18}O atom, unlike with the $FePcS/H_2O_2$ oxidation. The percentage of ^{18}O found in anthrone was 63%, ^{16}O incorporation being only 37% (Figure 3). The MS molecular cluster of anthraquinone consisted of 3 peaks: M (16%), M + 2 (59%) and M

Scheme 4. Deuterium exchange during the formation of anthrone in aqueous medium

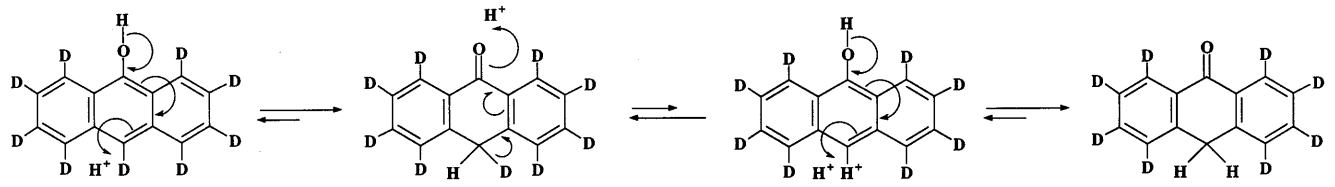

Figure 3. ^{18}O incorporation into anthrone and anthraquinone during the oxidation of anthracene by $FePcS/H_2O_2$ and $FeTMPS/KHSO_5$ in the presence of $H_2{}^{18}O$

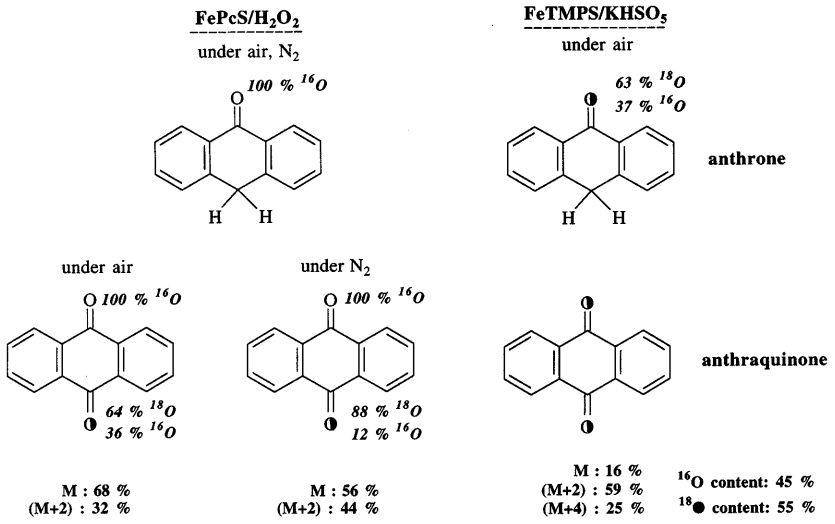

+ 4 (25%), indicating that ^{18}O was incorporated in both carbonyl groups of the quinone (the amount of ^{16}O and ^{18}O being 45 and 55%, respectively) (Figure 3). From these labeled water experiments we concluded that active species involved in the oxidation of anthracene by $FePcS/H_2O_2$ or by $FeTMPS/KHSO_5$ must be different.

Discussion

We found that FePcS associated with H_2O_2 can be useful in oxidation of polycyclic aromatic compounds. Anthracene was used as substrate to perform kinetic isotope studies and oxygen labeling experiments. Then we compared the results of the catalytic oxidations of anthracene by $FePcS/H_2O_2$ with those obtained with $FeTMPS/KHSO_5$ in order to gain a more complete view on the mechanisms of these oxidation reactions catalyzed by two related iron macrocyclic complexes. High-valent oxometal complexes have been proposed as active intermediates in hydrocarbon oxygenations (hydroxylations and epoxidations) using $KHSO_5$, NaOCl or *m*CPBA as oxidants and porphyriniron or -manganese compounds as catalysts[20][21][22]. We recently proposed a nucleophilic peroxoiron(III) complex of tetrasulfophthalocyanine, $PcSFe^{III}OOH$, as active species responsible for the oxidative cleavage of quinones generated during the oxidation of 2,4,6-trichlorophenol by $FePcS/H_2O_2$[15][16].

In the present work, several important differences must be noted in anthracene oxidations performed by $FePcS/H_2O_2$ or $FeTMPS/KHSO_5$. These differences are (i) a different composition of oxidation products depending on the oxidation system used (Scheme 2), (ii) a different reactivity of oxanthrone, which is relatively stable in the presence of $FeTMPS/KHSO_5$, but very quickly oxidized by $FePcS/H_2O_2$, (iii) and very different ^{18}O incorporations into anthrone and anthraquinone in experiments performed in the presence of $H_2{}^{18}O$ (Figure 3). On the other side, both catalytic systems, $FePcS/H_2O_2$ and $FeTMPS/KHSO_5$, showed essentially the same KIE values in the oxidation of anthracene (KIE = 0.75 and 0.76, respectively) or phenanthrene (KIE = 0.96 and 1.02, respectively) (Table 2).

Mechanistic Significance of Inverse Isotope Effects

The observation of a significant inverse isotope effect in the anthracene oxidation by $FePcS/H_2O_2$ or $FeTMPS/KHSO_5$ indicated that these KIEs could not be interpreted as primary KIEs involving a C−H(D) bond cleavage in the rate determining step of the initial step of the oxidation reaction. Consequently, these inverse KIEs precluded an oxygen rebound mechanism which involves a hydrogen atom abstraction from substrate by an electrophilic high-valent oxoiron complex to give a short-life radical intermediate followed by rapid recombination step[23]. Inverse KIEs are usually associated with secondary KIEs when no C−H(D) bond is cleaved or formed, but this bond should modify some parameters in the transition state (TS). This is usually the case when a C−H(D) bond is located at the reaction site itself, containing the leaving group (α secondary KIE) or at the adjacent carbon atom (β secondary KIE). In the case of the intermolecular $[H_{10}]$anthracene/$[D_{10}]$anthracene competitive oxidation an α secondary KIE is observed. Generally, the magnitude of an α-secondary KIE is determined by an inverse stretching and a normal bending contribution to the KIE value[24][25]. For example, in S_N2 reactions, a tighter TS, with short nucleophile α-carbon and/or α-carbon leaving group bond lengths, the KIE values would be inverse or normal and small[24]. Based on calculations with model systems, the α-secondary KIEs have been interpreted as reflecting the changes in the out-of-plane bending motion, i.e. hybridization changes or differences in the loose/tight character of the TS[26]. The activation energy for $sp^2 \rightarrow sp^3$ change in hybridization is lower for the deuterated substrate compared to the non-deuterated analogue, creating then an inverse KIE[27]. When the TS of the reaction occurs very late along the reaction coordinate, i.e. the TS exhibits essentially a fully sp^3-hybridized

carbon atom like in the reaction product, the k_H/k_D value will be more pronounced, the maximum KIE expected for a $sp^2 \rightarrow sp^3$ rehybridization will be 0.71[27]. Values of k_H/k_D ranging from 0.8 to 0.9 correspond to TS geometries somewhere between sp^2 and sp^3 and are more frequently observed. Inverse secondary KIEs have been measured for the addition of a variety of electrophilic reagents to olefins and aromatics, e.g. for the reaction of 1-naphthylcarbene to toluene ($k_H/k_D = 0.52$)[28]. An other example of an inverse α-secondary k_H/k_D equal to 0.83 has been recently observed during of the [2 + 2] photocycloaddition of arylalkenes to C_{60}[29]. Inverse KIEs have been reported for styrene epoxidations catalyzed by cytochrome P-450 ($k_H/k_D = 0.93$) or performed with *m*-chloroperbenzoic acid ($k_H/k_D = 0.82$)[27a] or by hexacyanoferrate(III) in acid medium ($k_H/k_D = 0.80$)[27b]. The cytochrome P-450 catalyzed oxidation of isotopically labeled chlorobenzenes provides also an inverse KIE (0.95)[30]. This result has been explained by an initial attack of an activated triplet-like oxygen atom on the π-system of substrate to generate a tetrahedral intermediate followed by rearrangement to phenol directly or via epoxide or ketone intermediates[30]. The aromatic hydroxylation of *o*- and *p*-xylene, catalyzed by cytochrome P-450, showed also an inverse α-secondary isotope effects (0.83−0.94) which were consistent with an addition reaction of a oxoiron species onto an sp^2-hybridized carbon atom[31]. The inverse nature of KIEs was anticipated for sp^2-to-sp^3 rehybridization during the covalent modification of human 5α-reductases by finasteride (a specific inhibitor) by a nucleophilic N addition to the double bond of this steroid-type molecule[32]. The reaction of the nitroethane anion (the α-carbon atom is sp^2-hybridized) with D-amino acid oxidase proceeds with an inverse $k_H/k_D = 0.84$ which was indicative of significant sp^2-to-sp^3 rehybridization in the TS[33]. Apart from the sp^2-to-sp^3 rehybridization, inverse isotope effects can be due to the difference in C−H and C−D distances, C−D bond being slightly shorter than corresponding C−H bond (d = 1.112 and 1.107 Å, respectively)[34]. The racemization of 2,2′-dibromo-4,4′-dicarboxybiphenyl[35] and 9,10-dihydro-4,5-dimethylphenanthrene[36] showed inverse KIEs of 0.85 and 0.88, respectively. The origin of a large inverse secondary KIE in the bromination of a sterically congested olefin (0.36−0.65) has been attributed to the fact that C−D bonds are shorter and less sterically demanding[37]. Large inverse equilibrium isotope effects have also been observed for the oxidative addition of H_2 to *trans*-$W(PMe_3)_4I_2$ ($K^H_{eq}/K^D_{eq} = 0.63$)[38a] and cyclohexane to $CpRh(CO)_2$ ($K^H_{eq}/K^D_{eq} = 0.1$, at 163−193 K)[38b]. Recently, a substantial inverse isotope effect of $k_H/k_D = 0.48$ has also been published in Co^{III}-catalyzed polymerization of ethylene[39] and explained by the presence of a β-agostic Co···H···C (Co···D···C) interaction, the inverse KIE being associated with the release of the agostic bond. Related to this interpretation of an inverse KIE, it must be noted that complexation of *n*-heptane with double A-frame porphyriniron(III) has been recently observed in crystals[40]. An out-of-plane displacement of the iron center of 0.26 Å and an Fe···C distance of 2.5 Å strongly suggest moderate to weak agostic interactions between C−H bonds of the alkane and the metal center. *p*-Xylene can interact with the metal center of an porphyriniron(III), the smallest Fe−C distance was 2.94 Å and the iron atom was drawn 0.07 Å out of the mean plane of the porphyrin core indicating a possible weak agostic interaction[41].

In the present case of the oxidation of anthracene catalyzed by phthalocyanine- or porphyriniron complexes, anthracene, a polyaromatic substrate, should have a pronounced tendency to form a stacking complex with FePcS or FeTMPS. A rather polar reaction medium (an acetonitrile/water mixture) should favor stacking interactions between two large planar hydrophobic molecules. Then a question arises: can the difference in C−H/C−D substitution on anthracene generate different stacking interactions between $[H_{10}]$anthracene or $[D_{10}]$anthracene with the macrocyclic plane molecule of FePcS or FeTMPS? In other words, are the observed KIEs only related to hydrophobic interactions between the aromatic substrate and the macrocyclic catalyst? The differences observed on inverse KIEs during the $[H_{10}]$anthracene/$[D_{10}]$anthracene and $[H_{10}]$anthracene/$[D_2]$anthracene competitive oxidations (Table 2) could be due to possible differences in stacking interactions between $[D_{10}]$anthracene and $[D_2]$anthracene with the macrocycle of the catalyst resulting from a slight difference of the nature of C−H bonds compared to C−D bonds. So, the stacking interactions should increased with the deuterium content of anthracene. This is the case with both catalytic systems: the KIE is 0.90 for $[D_2]$anthracene and 0.75 with $[D_{10}]$anthracene with $FePcS/H_2O_2$ (0.95 and 0.76 with $FeTMPS/KHSO_5$, respectively) (Table 2). Consequently, the value of the inverse KIE due to the sp^2-to-sp^3 hybridization change should be enhanced in a highly stacked substrate-catalyst intermediate during the addition of an electrophilic oxoiron complex to the sp^2-carbon atom of anthracene to give a σ adduct. The data on ^{18}O labeling experiments are also consistent with this proposal (see below).

The quasi-absence of KIE observed in the phenanthrene oxidation by $FePcS/H_2O_2$ or by $FeTMPS/KHSO_5$ (0.96 and 1.02, respectively) can be due to the reduction of stacking interactions compared to anthracene and also to the different nature of C9−H and C10−H bonds in phenanthrene. The C9−C10 bond of phenanthrene exhibits a relatively high bond order, indicating that it possesses a considerable degree of double bond character (K region bonds of polyaromatics), while anthracene bonds show essentially an aromatic character (*meso* region bonds)[42]. As a result, the main product of phenanthrene oxidation was biphenyl-2,2′-dicarboxylic acid. A similar cleavage of the double bond of styrene was observed when oxidized by $FePcS/H_2O_2$[16].

Mechanistic Significance of ^{18}O Labeling Experiments

In aqueous media oxo(porphyrin)metal(V) complexes have an axial hydroxo ligand. In order to explain the observed 50% ^{18}O incorporation from $H_2{}^{18}O$ in epoxides during olefin epoxidations by a metalloporphyrin/$KHSO_5$ system[20a][21b][21c], hydroxylation of DNA deoxyriboses[20b] or

C−H bond hydroxylation of 4-isopropylbenzoic acid[20c] it was proposed that the active hydroxo(oxo)(porphyrin)metal(V) complex undergoes a "redox tautomerism" (Figure 4). The ^{18}O incorporation depends on the reaction conditions[21b], primarily on relative kinetics of oxidation step and ligand exchange processes between the hydroxo ligand and bulk water and the nature of the catalyst. The rate of the oxo-hydroxo interchange in the oxo(porphyrin)manganese(V) complex was estimated to be about 10^3 s^{-1}[21c].

Figure 4. Redox tautomerism in a hydroxo(oxo)metal(V) species having a water-soluble porphyrin ligand (O = ^{16}O, black O = ^{18}O)

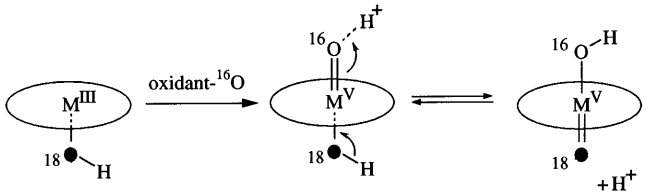

The large ^{18}O incorporation into anthrone (63%) and anthraquinone (55%) observed during FeTMPS/KHS$^{16}O_5$ anthracene oxidation in the presence of $H_2{}^{18}O$ is consistent with the involvement of oxo(porphyrin)iron complex as active species. By contrast, the absence of ^{18}O incorporation into anthrone, produced in the oxidation by FePcS/H_2O_2, could be explained by the involvement of an active oxo-metal species unable to undergo such an oxo-hydroxo equilibrium (in particular if there is no hydroxo ligand in the axial position *trans* to the oxo group).

Tautomeric Equilibria in Oxidation Products of Anthracene

The sequence of anthracene oxidation to anthraquinone and the relation between tautomeric forms of products are depicted in Scheme 5. The first oxidation product, 9-hydroxyanthracene is in fast keto-enol equilibrium with anthrone, which is the predominant form. The anthrone/9-hydroxyanthracene ratio determined by NMR in $CDCl_3$ at 25°C was estimated to be 80:20[43]. 9,10-Dihydroxyanthracene exists in solution in equilibrium with oxanthrone (K_{eq} = 0.13) and is the major tautomer (89%)[44]. However, the equilibrium is reached very slowly. The rate constants for the 9,10-dihydroxyanthracene-oxanthrone interconversion were determined to be $k_{-2} = 3 \times 10^{-6}$ s^{-1} and $k_2 = 4 \times 10^{-7}$ s^{-1}[45]. It means that in 1 mM solution only 1% of oxanthrone will be transformed into 9,10-dihydroxyanthracene after 1 h at room temperature.

Mechanism of Anthracene Oxidation by FeTMPS/$KHSO_5$

The oxidation of anthracene by FeTMPS/$KHSO_5$ was significantly faster than those of anthrone and oxanthrone. Under the same conditions the conversions of anthracene, anthrone and oxanthrone after 30 min were 100, 38 and 18%, respectively. These data indicated that there was an oxidation pathway to give directly oxanthrone, the main oxidation product, without intermediate formation of anthrone.

An electrophilic attack of a high-valent oxo(porphyrin)-iron complex at a central sp^2-carbon atom of anthracene to give a σ complex is probably the initial oxidation step (Figure 5). The inverse isotope effect, indicative of an sp^2-to-sp^3 rehybridization in the TS containing both substrate and catalyst stacked and the observed ^{18}O incorporation into anthrone, the first oxidation product, typical for oxoiron complex mediated oxidation in aqueous medium strongly suggested the formation of a new carbon−oxygen bond to form a σ complex **A**. This intermediate **A** can be trapped by O_2 to produce oxanthrone and anthraquinone via an intermediate radical **B**. An intramolecular electron transfer in intermediate **A** can lead to an intermediate carbocation **C**, which can undergo either a proton elimination to give a σ complex **D** or a nucleophilic attack of water to produce an intermediate **E**, providing a reaction pathway for oxanthrone formation without intermediate formation of anthrone. The hydrolysis of the Fe^{III}−O−aromatic bond in both intermediates **D** and **E** gave 9-hydroxyanthracene (quickly tautomerized to anthrone) and 9,10-dihydro-9,10-dihydroxyanthracene **F**. Then **F** can be further oxidized by a $2e^-$ process with the release of $2H^+$, producing oxanthrone with an increased ^{18}O content, or by oxidation of a C−H bond by an oxygen rebound mechanism. The GC-MS analysis of [H_{10}]anthracene/[D_{10}]anthracene oxidation products after 6 min of reaction revealed that anthraquinone was enriched with nondeuterated material: 57% of [H_8]anthraquinone and 43% of [D_8]anthraquinone, indicating a KIE value > 1 on the anthrone-to-anthraquinone oxidation step. The ^{18}O content in anthraquinone (55%) was not increased compared to that in anthrone (63%). Both findings suggest that oxidation of intermediate **F** proceeds by an oxygen rebound mechanism followed by H_2O elimination to generate oxanthrone. The fact that the metallopor-

Scheme 5. Oxidation products of anthracene and tautomeric equilibria for anthrone and oxanthrone

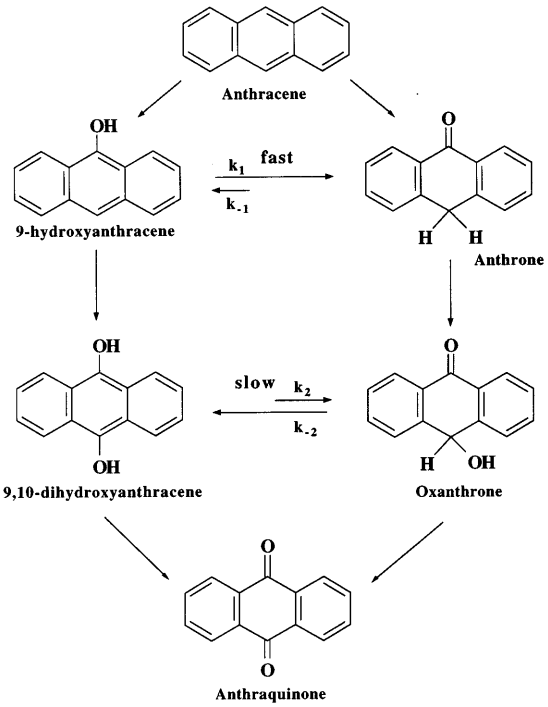

Figure 5. Proposed mechanism for anthracene oxidation by FeTMPS/$KHSO_5$ (O = ^{16}O, black ● = ^{18}O)

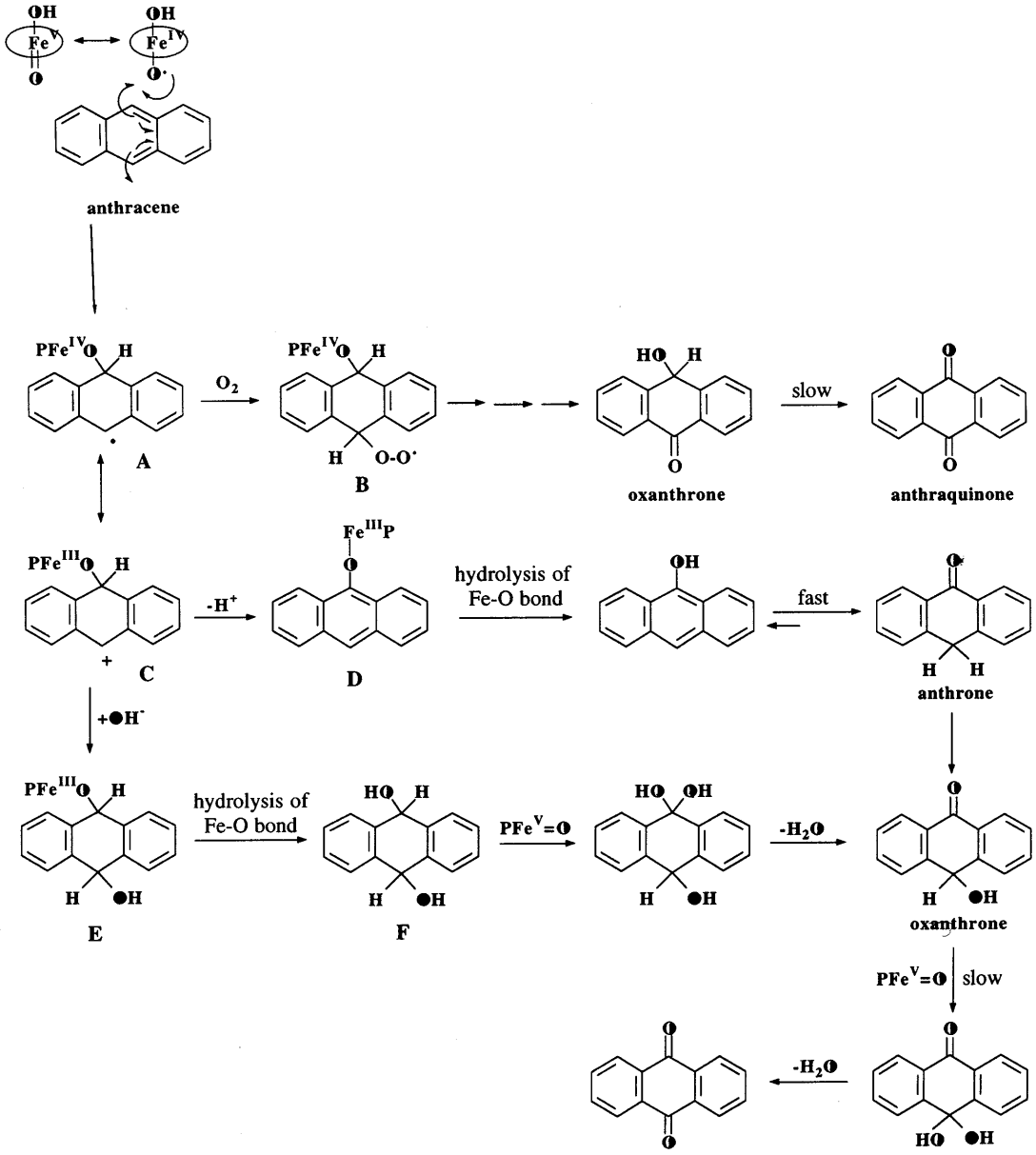

phyrin-catalyzed oxidation of anthracene gave oxanthrone, not the more oxidizable 9,10-hydroxyanthracene tautomeric form, explains the rather low yield of anthraquinone, since oxanthrone is relatively stable under the reaction conditions (oxanthrone conversion being only 23% after 60 min).

Active Species in FePcS/H_2O_2 Oxidations

In the FePcS/H_2O_2 mediated oxidation of trichlorophenol[15][17] a nucleophilic $PcSFe^{III}OO^-$ complex was proposed to be the active species, able to perform two key steps: (i) a nucleophilic addition to the electron-deficient double bond of intermediate quinones to provide epoxy quinones and (ii) a nucleophilic attack on the carbonyl group of the different quinones, leading to their ring cleavage[16]. Although the addition of nucleophiles to polyarenes, e.g. the addition of alkyllithium reagents to anthracene, has been published[46], such a peroxoiron(III) complex is probably not nucleophilic enough for a direct attack onto an sp^2-carbon atom of a PAH. Another possible active metal-oxygen species could be a high-valent oxoiron complex, having two redox equivalents above the Fe^{III} state. Several lines of evidence indicate that it is not the case for the FePcS/H_2O_2 system[15b]. The fact that the oxygen atom in anthrone originated from H_2O_2 (Figure 3) also indicated that an oxoiron(V) complex was not involved in anthracene oxidation by FePcS/H_2O_2. With such an oxoiron(V) complex we could expect both ^{16}O and ^{18}O incorporations due to redox tautomerism, as observed in anthracene oxidation by FeTMPS/$KHSO_5$. The other possible formulation of the active species involved in PAH oxidations by FePcS/H_2O_2 is a $PcSFe^{IV}=O$ species[15b]. It can be formed by a $1e^-$ oxi-

Figure 6. Generation of peroxoiron(III) and oxoiron(IV) species by activation of FePcS with hydrogen peroxide

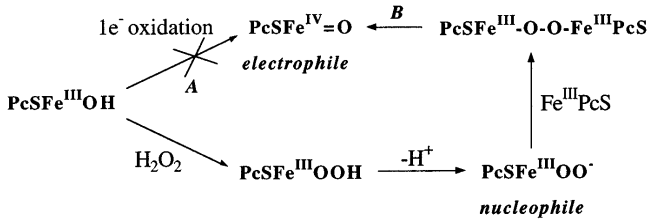

dation of $PcSFe^{III}OH$ complex (Figure 6, pathway *A*) or by the intermediate formation of a μ-peroxo dimer (pathway *B*). In the former case ^{18}O from water should be found in anthrone obtained in the presence of $H2^{18}O$. The absence of ^{18}O incorporation into anthrone during the oxidation of anthracene by $FePcS/H_2O_2$ in $H_2{}^{18}O$ eliminated this possibility. Consequently, $PcSFe^{IV}=O$ should be formed by pathway *B* by the homolytic cleavage of a μ-peroxo dimer (we proposed the pathway *A* in ref.[15b] before having on hands the data of these labeling studies). This $PcSFe^{IV}=O$ species is neutral and does not require the presence of an anionic axial anion ligand (e.g. HO^-) to compensate a charge. Consequently, no redox tautomerism is possible in the absence of HO^- ligand *trans* to the oxo entity. This absence of redox tautomerism for $PcSFe^{IV}=O$ explained the 100% incorporation of ^{16}O into anthrone during the $FePcS/H_2O_2$ oxidation of anthracene performed in heavy water.

Mechanism of Anthracene Oxidation by $FePcS/H_2O_2$

The first step of the $FePcS/H_2O_2$ mediated oxidation of anthracene resembles that described in the FeTMPS/$KHSO_5$ oxidation (Figure 7). The nearly identical inverse KIE (0.75) found for the first reaction step suggested also the formation of a σ complex, intermediate **A′** which can be trapped by O_2 to produce oxanthrone and anthraquinone via a radical intermediate **B′**. The significant ^{16}O incorporation in anthraquinone when the oxidation was performed under air compared to that obtained under nitrogen (Figure 3) was strongly indicative of this pathway 1. Hydrolysis of the $Fe^{III}-O-$aromatic bond followed by proton elimination and $1e^-$ oxidation generated 9-hydroxyanthracene which rapidly tautomerized to the thermodynamically favored anthrone. Successive $1e^-$ oxidation and proton elimination steps gives rise to carbocation **I′**, which can react with water (pathway 2) to produce oxanthrone and anthraquinone. $PcSFe^{IV}=O$ complex is not such a strong oxidant to perform the abstraction of an H atom of a aliphatic or aromatic C−H bond. However, $PcSFe^{IV}=O$ is

Figure 7. Proposed mechanism for anthracene oxidation by $FePcS/H_2O_2$ (O = ^{16}O, black ● = ^{18}O)

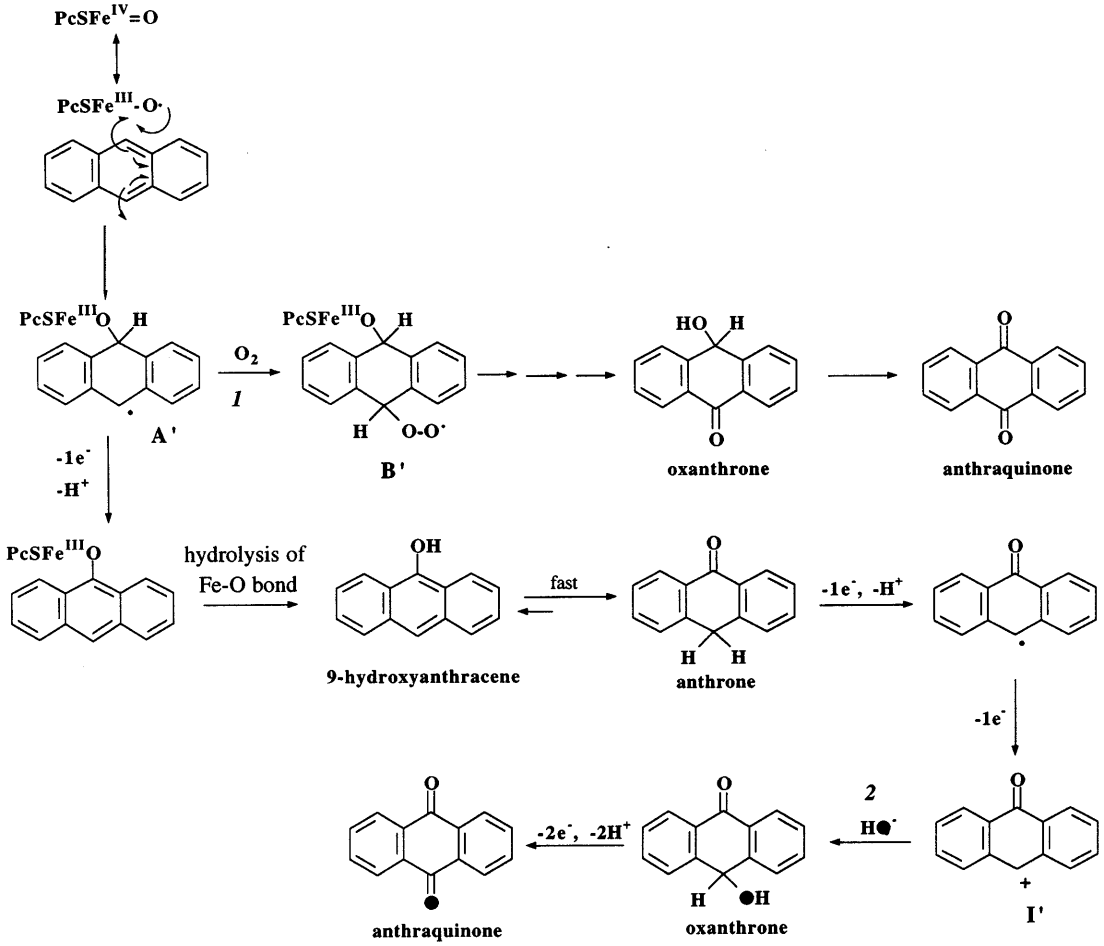

probably a sufficiently good $1e^-$ oxidant to perform $1e^-$ oxidations of intermediate products or of oxanthrone by successive $1e^-$ oxidations and proton eliminations to provide anthraquinone.

The rather low yields of anthrone and anthraquinone after 30 min (5 and 21%, respectively) might be due to radical intermediates capable of undergoing side reactions, e.g. coupling reactions. Accordingly, the presently proposed mechanism, the first oxygen atom incorporated into the different products originates from $PcSFe^{IV}=O$ (^{16}O in labeling experiments), and the value of ^{18}O incorporation of the second oxygen atom of anthraquinone from $H_2{}^{18}O$ will depend on the relative rates of the different pathways indicated on Figure 7. Very significant ^{18}O incorporation into the second oxygen position of anthraquinone under air (64%) and, especially under nitrogen (88%), strongly suggest that pathway 2 is the major reaction pathway.

Conclusion

The (tetrasulfophthalocyanine)iron/hydrogen peroxide oxidation system, based on an easy-to-prepare catalyst and a "clean" oxidant, is capable of oxidizing polycyclic aromatic hydrocarbons, like anthracene, phenanthrene and benzo[*a*]pyrene. Data obtained from product distribution, kinetic isotope effects and ^{18}O labeling studies, as well as a comparative study of anthracene oxidation by FeTMPS/$KHSO_5$ allowed us to propose that an oxo(phthalocyanine)iron(IV) complex, is probably responsible of these PAH oxidations. Consequently, taking in consideration the previously reported mechanistic studies on quinone cleavage by the same $FePcS/H_2O_2$ system, two kinds of the active species can be generated from FePcS in the presence of H_2O_2: (i) a nucleophilic peroxoiron complex $PcSFe^{III}OO^-$ responsible for double carbon−carbon bond cleavage in the deep oxidation of trichlorophenol[15][16] and (ii) an electrophilic $PcSFe^{IV}=O$ complex capable of oxidizing aromatic hydrocarbons by the formation of a σ adduct. This versatility makes (tetrasulfophthalocyanine)iron in association with hydrogen peroxide a suitable catalytic method for the chemical degradation of different pollutants.

A. S. is indebted to *ELF-Atochem* for a postdoctoral fellowship. The authors are grateful to *Jean-Louis Séris* (*ELF-Atochem*, Lacq) and Prof. *Jean Bernadou* (*LCC-CNRS*) for fruitful discussions.

Experimental Section

Instrumentation: Gas chromatography-mass spectrometry (GC-MS) was performed with a Hewlett-Packard 5890 instrument using electron-impact ionization at 70 eV. The carrier gas for GC-MS was He, and a 12 m × 0.2 mm HL-1 (Crosslinked Methyl Silicone Gum) capillary column was used. − High performance liquid chromatography (HPLC) analyses were performed with a Waters-486 Liquid Chromatograph equipped with a μ-Bondapak C18 column, eluent being a mixture of methanol and water (85:15, v/v) at a flow rate of 1 ml min^{-1}, detection at 242 nm for anthracene, 252 nm for phenanthrene and 280 nm for benzo[*a*]pyrene analyses. − UV/Vis spectra were recorded with a Hewlett-Packard 8452A diode array spectrophotometer. − ^1H NMR spectra were recorded with Bruker WM 250 spectrometer.

Materials: All chemicals used were of reagent grade. Potassium monopersulfate was a gift from Interox (Curox^R) and is the triple salt $2KHSO_5{\cdot}KHSO_4{\cdot}K_2SO_4$. Hydrogen peroxide was obtained from Janssen Chimica as a 35% aqueous solution. $H_2{}^{18}O$ (98 atom-%) was supplied by Eurisotop (Gif-sur-Yvette, France). Lithium aluminum deuteride was purchased from Fluka (minimum 99 atom-% D). (Tetrasulfophthalocyanine)iron (FePcS) was prepared according to the method of Weber and Busch.[47] The iron complex of octasodium *meso*-tetrakis(3,5-disulfonatomesityl)porphyrin (TMPS) was synthesized according to ref.[48]. Anthracene (97%), phenanthrene (98%), benzo[*a*]pyrene (98%), [D_{10}]anthracene (> 98 atom-% D), [D_{10}]phenanthrene (97 atom-% D), anthrone (96%), anthraquinone (97%), phenanthrenequinone (99%), 9,10-dibromoanthracene (98%) were purchased from Aldrich. Oxanthrone was prepared from anthrone via 10-bromoanthrone according to ref.[45]. NMR (CD_2Cl_2): δ = 2.47 (d, 1 H, *J* = 9.5 Hz, OH), 5.78 (d, 1 H, *J* = 9.5 Hz, H_{10}), 7.54 (td, 2 H, *J* = 7.5 and 0.7 Hz, H_3), 7.73 (td, 2 H, *J* = 7.5 and 1.5 Hz, H_2), 7.90 (dd, 2 H, *J* = 7.5 and 0.7 Hz, H_4), 8.25 (dd, 2 H, *J* = 7.5 and 1.5 Hz, H_1); (CD_2Cl_2 + small amount of D_2O): the same signals, except doublet at δ = 2.47 disappeared and the doublet at δ = 5.78 became a singlet.

Preparation of 9,10-Dideuterioanthracene: The procedure was adapted from ref.[49]. Dibromoanthracene (1.008 g, 3 mmol) and $LiAlD_4$ (504 mg, 12 mmol) were added under nitrogen to 15 ml of anhydrous dimethoxyethane. The reaction mixture, contained in a 50-ml round-bottom single-neck flask and maintained under nitrogen, was partly submerged in a ultrasonic laboratory cleaner Branson 2200 (working frequency 47 kHz, 205 W) at 35−40°C. The reaction was monitored by GC-MS. After 13 h, all dibromoanthracene was reduced and the reaction mixture contained 9,10-dideuterioanthracene accompanied by minor amount of 9-bromo[D_1]-anthracene.The reaction mixture was cooled at −40°C and 1 ml of D_2O (99%) was slowly added. The temperature was allowed to return to 20°C and hydrolysis of the excess of $LiAlD_4$ was performed for 30 min. Then the resulting mixture was pourred into 30 ml of water and extracted with diethyl ether (4 × 40 ml). The combined organic extracts were washed with saturated NaCl solution, dried with Na_2SO_4 and concentrated. The white precipitate was separated by filtration and recrystallized from diethyl ether to give 148 mg (27% yield) of the pure 9,10-dideuterioanthracene material. The isotopic purity was determined by NMR and GC-MS methods. The material contained 72.8% of 9,10-dideuterioanthracene and 27.2% of 9-deuterioanthracene.

General Catalytic Procedure for PAH Oxidation: Oxidation of anthracene was carried out in a mixture of acetonitrile/50 mM phosphate buffer at pH = 7 (3:1, v/v) at 20°C under aerobic conditions. Oxidations of phenanthrene and benzo[*a*]pyrene were performed in acetonitrile/33.3 mM phosphate buffer at pH = 4.6 (1:1, v/v). The reaction mixture (2 ml) contained 2 μmol of substrate introduced as a 4 mM acetonitrile solution and 0.074 or 0.1 μmol of catalyst, introduced as a 1.28 mM solution in water, and the required amounts of acetonitrile and stock buffer solution to obtaine the desired organic solvent/water ratios. Oxidations were started by addition of 10 μmol of oxidant (10 μl of 3.5% H_2O_2 solution or 3.1 mg of potassium monopersulfate). The final concentrations of the catalyst, substrate and oxidant were 37 (or 100) μM, 1 mM and 5 mM, respectively. The reactions were followed by HPLC and GC-MS techniques. Anthraquinone and anthrone were identified by comparison of its GC-MS behavior (retention time and mass spectrum) with those of an authentic sample. Oxanthrone was identified by comparison of its NMR spectrum with that of an authentic sample.

$H_2{}^{18}O$ Experiments: Reactions were carried out using $H_2{}^{18}O$ (98 atom-%) according to the following procedure. A mixture of 25 μl of 0.5 M phosphate buffer pH = 7 and 29 μl of catalyst stock solution (1.28 mM in water) was dried under vacuum. The dry residue was then dissolved in 250 μl of $H_2{}^{18}O$ and 250 μl of [H_{10}]anthracene and [D_{10}]anthracene stock solutions (50:50 mixture, 4 mM total concentration in MeCN) and 500 μl of MeCN were added. The oxidations were performed under air and under nitrogen. In the latter case the reaction mixture was submitted to 3 freeze-pump-thaw cycles and the reaction flask was filled up with nitrogen. The reaction was started by the addition of 5 μl of 3.5% H_2O_2 (for FePcS oxidation) or 1.6 mg of $KHSO_5$ (for FeTMPS oxidation). The substrate conversion was monitored by HPLC and isotopic compositions of products were analyzed by GC-MS.

Determination of Isotopic Composition of Substrates and Products: Mass spectra of [H_{10}]anthracene and [D_{10}]anthracene show very strong molecular peaks accompanied with little fragmentations. [H_{10}]anthracene: MS; *m/z* (%): 178 (100) [M^+], 176 (18) [M − 2 H]$^+$, 152 (8) [M − C_2H_2]$^+$, 89 (13) [M − C_7H_5]$^+$. [D_{10}]anthracene: MS; *m/z* (%): 188 (100) [M^+], 184 (13) [M − 2 D]$^+$, 160 (9) [M − C_2D_2]$^+$, 94 (17) [M − C_7D_5]$^+$. So, under conditions of GC-MS analysis, within experimental error, there is no isotope effect on fragmentation and isotopic compositions of [H_{10}]anthracene and [D_{10}]anthracene can be determined from the intensities of corresponding molecular peaks. The mass spectra of phenanthrene and products of oxidation of anthracene and phenanthrene showed the same features and their isotopic compositions were determined from the intensities of the molecular peaks of deuterated and non-deuterated compounds.

KIE determinations based on [H_{10}]anthracene/9,10-dideuterioanthracene oxidations were performed taking into account admixture of monodeuterated anthracene, the presence of [M + 1] peaks due to ^{13}C natural content and [M − 1] and [M − 2] fragmentations according to the following formalism:

$$I_{178} = [D_0]\text{-A} + F_{M-1}\cdot[D_1]\text{-A} + F_{M-2}\cdot[D_2]\text{-A} \quad (2)$$

$$I_{179} = [D_1]\text{-A} + F_{M+1}\cdot[D_0]\text{-A} + F_{M-1}\cdot[D_2]\text{-A} \quad (3)$$

$$I_{180} = [D_2]\text{-A} + F_{M+1}\cdot[D_1]\text{-A} \quad (4)$$

where I_{178}, I_{179}, I_{180} were intensities of peaks at *m/z* 178, 179 and 180, respectively; [D_0]-A, [D_1]-A, [D_2]-A were percentages of corresponding isotopomers of anthracene; F_{M+1}, F_{M-1}, F_{M-2} were relative intensities of [M + 1], [M − 1] and [M − 2] peaks. The latter intensities were determined in separate GC-MS experiments to be $F_{M+1\,=\,0}$.15, F_{M-1} = 0.11, F_{M-2} = 0.18. KIEs were calculated from the data obtained on conversions and the percentages of [H_{10}]anthracene and 9,10-dideuterioanthracene in an initial reaction mixture and after several minutes when the substrate conversion was near 50%.

[1] C. E. Cerniglia, *Biodegradation* **1992**, *3*, 351−368.
[2] K. E. Hammel in *Degradation of Environmental Pollutants by Microorganisms and their Metalloenzymes. Metal Ions in Biological Systems* (Eds.: H. Sigel, A. Sigel), Marcel Dekker, New York, **1992**, vol. 28, p. 41.
[3] S. D. Haemmerli, M. S. A. Leisola, D. Sanglard, A. Fiechter, *J. Biol. Chem.* **1986**, *261*, 6900−6903.
[4] K. E. Hammel, B. Kalyanaraman, T. K. Kirk, *J. Biol. Chem.* **1986**, *261*, 16948−16952.
[5] J. D. Lipscomb, A. M. Orville in *Degradation of Environmental Pollutants by Microorganisms and their Metalloenzymes. Metal Ions in Biological Systems* (Eds.: H. Sigel, A. Sigel), Marcel Dekker, New York, **1992**, vol. 28, p. 243.
[6] D. A. Lane in *Chemical Analysis of Polycyclic Aromatic Compounds* (Ed.: T. Vo-Dinh), Wiley, New York, **1989**, p. 31.
[7] For a review on chemistry of polyarenes see: R. G. Harvey, *Polycyclic Aromatic Compounds*, Wiley, New York, **1997**, p. 96.
[8] M. Juaristi, J. M. Aizpurua, B. Lecea, C. Palomo, *Can. J. Chem.* **1984**, *62*, 2941−2944.
[9] E. V. Dehmlov, J. K. Makrandi, *J. Chem. Research (S)* **1986**, 32−33.
[10] D. Villemin, M. Ricard, *Nouv. J. Chem.* **1984**, *8*, 185−189.
[11] W. Adam, P. A.Ganeshpure, *Synthesis* **1993**, 280−282.
[12] [12a] R. Song, A. Sorokin, J. Bernadou, B. Meunier, *J. Org. Chem.* **1997**, *62*, 673−678. − [12b] G. J. Harden, M. M. Coombs, *J. Chem. Soc., Perkin Trans. 1* **1995**, 3037−3042.
[13] T. Higuchi, C. Satake, M. Hirobe, *J. Am. Chem. Soc.* **1995**, *117*, 8879−8880.
[14] S. V. Barkanova, V. M. Derkacheva, O. V. Dolotova, V. D. Li, V. M. Negrimovsky, O. L. Kaliya, E. A. Luk′yanets, *Tetrahedron Lett.* **1996**, *37*, 1637−1640.
[15] [15a] A. Sorokin, J.-L. Séris, B. Meunier, *Science* **1995**, *268*, 1163−1166. − [15b] B. Meunier, A. Sorokin, *Acc. Chem. Soc.* **1997**, *30*, 470−476.
[16] [16a] A. Sorokin, B. Meunier, *Chem. Eur. J.* **1996**, *2*, 1308−1317. − [16b] A. Sorokin, S. De Suzzoni-Dezard, D. Poullain, J.-P. Noël, B. Meunier, *J. Am. Chem. Soc.* **1996**, *118*, 7410−7411. − [16c] A. Hadasch, A. Sorokin, A. Rabion, B. Meunier, *New J. Chem.* **1998**, 45−51.
[17] A. Sorokin, L. Fraisse, A. Rabion, B. Meunier, *J. Mol. Cat.* **1997**, *117,* 103−114.
[18] R. J. Lorentzen, J. Caspary, S. A. Lesko, P. O. Ts′o, *Biochemistry* **1975**, *14*, 3970−3977.
[19] L. Melander, J. M. Saunders, *Reaction Rates of Isotopic Molecules*, Wiley, New York, **1980**, p. 95.
[20] [20a] J. Bernadou, A.-S. Fabiano, A. Robert, B. Meunier, *J. Am. Chem. Soc*. **1994**, *116*, 9375−9376. − [20b] M. Pitié, J. Bernadou, B. Meunier, *J. Am. Chem. Soc*. **1995**, *117*, 2935−2936. − [20c] R. J. Balahura, A. Sorokin, J. Bernadou, B. Meunier, *Inorg. Chem.* **1997**, *36*, 3488−3492.
[21] [21a] W. Nam, J. S. Valentine, *J. Am. Chem. Soc*. **1993**, *115*, 1772−1778. − [21b] K. A. Lee, W. Nam, *J. Am. Chem. Soc*. **1997**, *119*, 1916−1922. − [21c] J. T. Groves, J. Lee, S. S. Marla, *J. Am. Chem. Soc*. **1997**, *119*, 6269−6273.
[22] B. Meunier, *Chem. Rev.* **1992**, *92*, 1411−1456.
[23] [23a] T. J. McMurry, J. T. Groves, In *Cytochrome P-450 Structure, Mechanism and Biochemistry* (Ed.: P. R. Ortiz de Montellano), Plenum, New York, **1986**; pp. 1−28. − [23b] M. Newcomb, M.-H. Le Tadic-Biadatti, D. L. Chestney, E. S. Roberts, P. F. Hollenberg, *J. Am. Chem. Soc*. **1995**, *117*, 12085−12091.
[24] R. A. Poirier, Y. Wang, K. C.Westaway, *J. Am. Chem. Soc.* **1994**, *116*, 2526−2533.
[25] S. Wolfe, C.-K. Kim, *J. Am. Chem. Soc.* **1991**, *113*, 8056−8061.
[26] [26a] P. A. Nielsen; S. S. Glad, F. Jensen, *J. Am. Chem. Soc.* **1996**, *118*, 10577−10583. − [26b] S. S. Glad, F. Jensen, *J. Am. Chem. Soc.* **1997**, *119*, 227−232.
[27] [27a] R. P. Hanzlik, G. O. Shearer, *Biochem. Pharm.* **1978**, *27*, 1441−1444 and references therein. − [27b] A. K. Bhattacharjee, M. K. Mahanti, *Gazz. Chim. Ital.* **1984**, *114*, 337−340.
[28] G. W. Griffin, K. A. Horn, *J. Am. Chem. Soc.* **1987**, *109*, 4919−4926 and references therein.
[29] G. Vassilikogiannakis, M. Orfanopoulos, *J. Am. Chem. Soc.* **1997**, *119*, 7394−7395.
[30] K. R. Korzekwa, D. C. Swinney, W. F. Trager, *Biochemistry* **1989**, *28*, 9019−9027.
[31] R. P. Hanzlik, K.-H. J. Ling, *J. Am. Chem. Soc.* **1993**, *115*, 9363−9370.
[32] G. Tian, S.-Y. Chen, K. L. Facchine, S. R. Prakash, *J. Am. Chem. Soc.* **1995**, *117*, 2369−2370.
[33] K. A. Kurtz, P. F. Fitzpatrick, *J. Am. Chem. Soc.* **1997**, *119*, 1155−1156.
[34] J. March, *Advanced Organic Chemistry: Reactions, Mechanisms and Structure*, 4th ed., Wiley, New York, **1992**, p. 20.
[35] L. Melander, R. E. Carter, *Acta Chem. Scand*. **1964**, *18*, 1138−1149.
[36] K. Mislow, R. Graeve, A. J. Gordon, G. H. Wahl, Jr., *J. Am. Chem. Soc.* **1963**, *85*, 1199−1200.
[37] R. W. Nagorski, H. Slebocka-Tilk, R. S. Brown, *J. Am. Chem. Soc.* **1994**, *116*, 419−420.
[38] [38a] D. Rabinovich, G. Parkin, *J. Am. Chem. Soc.* **1993**, *115*, 353−354. − [38b] R. H. Schultz, A. A. Bengali, M. J. Tauber, B. H. Weiller, E. P. Wasserman, K. R. Kyle, C. B. Moore, R. G. Bergman, *J. Am. Chem. Soc.* **1994**, *116*, 7369−7377.
[39] M. J. Tanner, M. Brookhart, J. M. DeSimone, *J. Am. Chem. Soc.* **1997**, *119*, 7617−7618.

[40] D. R. Evans, T. Drovetskaya, R. Bau, C. A. Reed, P. D. W. Boyd, *J. Am. Chem. Soc.* **1997**, *119*, 3633−3634.
[41] Z. Xie, R. Bau, C. A. Reed, *Angew. Chem. Int. Ed. Engl.* **1994**, *33*, 2433−2434.
[42] See ref.[7], p. 26.
[43] T. R. Criswell, B. H. Klanderman, *J. Org. Chem.* **1974**, *39*, 770−774.
[44] K. Brederesk, E. F. Sommermann, *Tetrahedron Lett.* **1966**, *41*, 5009−5014.
[45] S. A. Carlson, D. H. Hercules, *Anal. Chem.* **1973**, *45*, 1794−1799.
[46] P. P. Fu, R. G. Harvey, *Chem. Rev.* **1978**, *78*, 317−361.
[47] J. H. Weber, D. H. Busch, *Inorg. Chem.* **1965**, *4*, 469−471.
[48] P. Hoffmann, G. Labat, A. Robert, B. Meunier, *Tetrahedron Lett.* **1990**, *31*, 1991−1994.
[49] B. H. Han, P. Boudjouk, *Tetrahedron Lett.* **1982**, *23*, 1643−1646.

[98126]

Determination of the Prototropic Exchange Rate at the Water Molecule Coordinated to an Anionic Paramagnetic Gd^{III} Chelate

Silvio Aime*[a], Simonetta Geninatti Crich[a], Eliana Gianolio[a], Enzo Terreno[a], Andrea Beltrami[b], and Fulvio Uggeri[b]

Dipartimento di Chimica I.F.M.[a],
Via Pietro Giuria 7, I-10125 Torino

Bracco S.p.A.[b],
Via Egidio Folli 50, I-20134 Milano

Received March 19, 1998

Keywords: MRI Contrast agents / Gd^{III} complexes / Relaxometry / Water exchange / Prototropic exchange

A thorough investigation of the proton and oxygen-17 relaxation rates of water nuclei has been carried out for a solution containing an amphiphilic, paramagnetic Gd^{III} chelate of potential interest as a contrast agent for MRI. It has been found that at pH = 7, 298 K and 20 MHz (proton observation frequency), the contribution to the overall relaxation enhancement from the water molecule in the inner coordination sphere is dominated by the relaxation time (T_{1M}^H) of its protons. However, upon formation of a slowly tumbling adduct with β-cyclodextrin, the observed relaxation enhancement is also affected by the exchange lifetime (τ_M^H) of the coordinated water and by the transfer rate of its protons. This situation has been exploited to assess the prototropic exchange rate from the coordinated water to the bulk, which is base-catalyzed. In fact, under these experimental conditions, at basic pH, the proton transfer is faster than the exchange of the whole water molecule, and it becomes the factor determining the observed relaxation enhancement. The effect is further enhanced at low temperature as a consequence of the concomitant lengthening of either τ_R (which causes a reduction of T_{1M}^H) and/or the exchange lifetime of the coordinated water molecule.

Introduction

Recently, it has been shown that the exchange rate of the coordinated water molecule in Gd^{III} complexes of octadentate ligands may be markedly slower than in chelates with ligands of lower denticity.[1] The observed behaviour has been accounted for in terms of the occurrence of a dissociative exchange mechanism, the rate-determining step of which is determined by the energy difference between the nonacoordinated ground state and the octacoordinated activated state.[2] The actual value of the exchange rate of the water molecule coordinated at the paramagnetic metal site may be accurately evaluated by measuring the temperature dependence of the transverse relaxation rate of the ^{17}O-NMR water resonance of an aqueous solution containing the Gd^{III} chelate.[3]

Currently, the main interest in water-soluble Gd^{III} complexes stems from their use as contrast agents for MRI, owing to their remarkable ability to enhance the relaxation rate of water protons in the tissues in which they are distributed.[4] The contribution to the overall relaxation rate arising from the metal-bound water molecule in a Gd^{III} chelate may result either from the exchange of the whole water molecule or from the exchange of just its protons. At physiological pH, the latter process is much slower than the former,[5] making the assessment of the prototropic exchange rate for the protons of the metal-bound water molecule rather difficult.

Recently, we showed that the determination of the exchange rate for the protons of the water molecule in the inner coordination sphere of a Gd^{III} chelate may be successfully pursued by quantitative analysis of the pH dependence of the water ^1H-NMR longitudinal relaxivity, provided that the exchange lifetime of the whole metal-bound water molecule (τ_M^O) is longer than, or at least of the same order of magnitude as, the longitudinal relaxation time of its protons (T_{1M}^H).[6][7]

Until now, this behaviour has been observed only for Gd^{III} chelates endowed with a cationic or neutral residual charge. In the most commonly encountered anionic Gd^{III} complexes, τ_M^O is shorter than T_{1M}^H at ambient temperature. Thus, in such systems, the assessment of the prototropic exchange rate first requires a reduction of T_{1M}^H.

In principle, one may envisage several ways of shortening T_{1M}^H, e.g. by increasing the molecular correlation time through the formation of reversible adducts between the Gd^{III} chelate and a slowly tumbling substrate, or by lowering the temperature. In the latter case, besides the reduction of T_{1M}^H, a further advantage may be obtained by the decrease of τ_M^O as well.

In this work, we deal with the assessment of the prototropic exchange rate at the metal-bound water molecule in a derivative of $Gd(DTPA)^{2-}$, in which one acetate proton is replaced by a cyclohexyloxymethyl residue [$Gd(COPTA)^{2-}$; COPTA = 4-carboxy-5,8,11-tris(carboxymethyl)-1-cyclohexyl-2-oxa-5,8,11-triazatridecan-13-oic acid, Chart 1]. On the basis of the data collected to date for polyaminocarboxylate Gd^{III} chelates, we would expect the exchange lifetime at room temperature of the metal-bound water molecule in

 © WILEY-VCH Verlag GmbH, D-69451 Weinheim, 1998 1434–1948/98/0909–1283 $ 17.50+.50/0

this anionic complex to be lower than T_{1M}^H. However, the presence of the hydrophobic tail should allow this chelate to reversibly form an adduct with a slowly tumbling substrate such as β-cyclodextrin (β-CD). The consequent lengthening of the reorientational correlation time, τ_R, of the complex should result in a decrease of T_{1M}^H, allowing the prototropic exchange rate to be determined through its effect on the overall water proton relaxation rate.

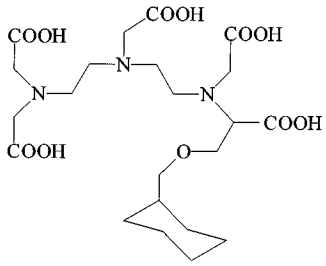

Results and Discussion

Determination of the Water Proton Exchange Lifetime τ_M^H

Analysis of the temperature dependence of the transverse relaxation rate for the ^{17}O water nuclei is the most accurate method for evaluating the exchange lifetime of the water molecule/s directly coordinated to the metal in a paramagnetic Gd^{III} chelate.

This approach allows assessment of the exchange lifetime of the metal-bound water oxygen nucleus which, at neutral pH and in non-buffered solutions, corresponds to the exchange lifetime of the metal-bound water protons, i.e. $\tau_M^H = \tau_M^O$.

The paramagnetic contribution (R_{2p}^O) to the observed transverse relaxation rate of water ^{17}O nuclei (R_{2obs}^O) is given by equation (1)

$$R_{2p}^O = R_{2obs}^O - R_{2d}^O \tag{1}$$

where R_{2d}^O is the transverse relaxation rate measured in a solution containing a diamagnetic chelate of the corresponding ligand at the same concentration.

According to the theory first proposed by Swift and Connick[8], R_{2p}^O depends on several parameters [equation (2)]

$$R_{2p}^O = P_M(\tau_M^O)\frac{R_{2M}^{O2} + (\tau_M^O)^{-1}R_{2M}^O + \Delta\omega_M^{O2}}{R_{2M}^{O2} + (\tau_M^O)^{-1})^2 + \Delta\omega_M^{O2}} \tag{2}$$

such as the chemical shift difference between the metal-bound and bulk water ^{17}O nuclei $\Delta\omega_M^O$, the molar fraction of the metal-bound water molecules P_M, their intrinsic ^{17}O transverse relaxation rate R_{2M}^O, and the exchange rate τ_M^O.

For quickly tumbling Gd^{III} chelates and at relatively low magnetic field strength (as used in this work), R_{2M}^O is dominated by the nucleus-electron scalar relaxation mechanism, which may be evaluated using equation (3).

$$R_{2M}^O = \frac{1}{3}\left(\frac{A}{\hbar}\right)^2 S(S+1)\left(\tau_{E1} + \frac{\tau_{E2}}{1+\omega_s^2\,\tau_{E2}}\right) \tag{3}$$

Here, S is the electronic spin quantum number [7/2 for Gd^{III}], $A/\hbar$ is the Gd-^{17}O scalar coupling constant, and τ_{Ei} (i = 1,2) are the correlation times for the dynamic processes modulating the scalar interaction. Both the longitudinal and the transverse electronic relaxation times (T_{1E} and T_{2E}), as well as the exchange lifetime of the metal-bound water molecule, may modulate the scalar interaction. The correlation time for this process is given by equation (4).

$$\tau_{Ei}^{-1} = \tau_M^{O^{-1}} + T_{iE}^{-1} \tag{4}$$

The scalar coupling constant is related to the unpaired electron spin density at the ^{17}O nucleus and it mainly depends on the distance between the metal ion and the metal-bound ^{17}O nucleus. Since for polyaminocarboxylate Gd^{III} chelates with a single inner-sphere water molecule this distance does not seem to vary significantly, for the $Gd(COPTA)^{2-}$ complex we used the same value as that reported for the closely related $Gd(DTPA)^{2-}$ chelate (-3.8×10^6 rad s^{-1}).[1]

For Gd^{III} complexes, T_{iE} values are basically related to the modulation of the transient zero-field splitting (ZFS) of the electronic spin states arising from the dynamic distortions of the ligand field caused by the solvent collision and, according to the Bloembergen-Morgan and Rubinstein theory,[9][10] they are expressed by equations (5) and (6)

$$T_{1E}^{-1} = \frac{1}{25}\Delta^2[4S(S+1)-3]\left[\frac{\tau_v}{1+\omega_s^2\,\tau_v^2} + \frac{4\tau_v}{1+4\omega_s^2\,\tau_v^2}\right] \tag{5}$$

$$T_{2E}^{-1} = \frac{1}{50}\Delta^2[4S(S+1)-3]\left[3\tau_v + \frac{5\tau_v}{1+\omega_s^2\,\tau_v^2} + \frac{2\tau_v}{1+4\omega_s^2\,\tau_v^2}\right] \tag{6}$$

where Δ^2 is related to the square of the mean transient ZFS energy, τ_v is the correlation time for the collision-related modulation of the ZFS hamiltonian, and ω_s is the electronic Larmor frequency.

The temperature dependence of R_{2M}^O is, therefore, expressed by the temperature effect on τ_M^O, τ_v, and $\Delta\omega_M^O$ according to equations (7) and (8)

$$\tau_j^{-1} = \frac{(\tau_j^{-1})^{298.15}\,T}{298.15}\exp\left[\frac{\Delta H_j}{R}\left(\frac{1}{298.15} - \frac{1}{T}\right)\right] \tag{7}$$

$$\Delta\omega_M^O = \frac{g_e\mu_B S(S+1)B}{3k_B T}\frac{A}{\hbar} \tag{8}$$

where the subscripts j refer to the two dynamic processes (j = M, v), ΔH_j is their activation enthalpy, B is the magnetic field strength, k_B is the Boltzmann constant, g_e is the free-electron Landè factor (2.0023), and μ_B is the Bohr magneton.

In Figure 1, we present a comparison between the temperature dependence of ^{17}O-R_{2p}^O for $Gd(COPTA)^{2-}$ and for the

parent Gd(DTPA)$^{2-}$, both recorded at 2.1 T, pH = 7 and at a concentration of 50 mM.

Figure 1. Temperature dependence of the transverse water ^{17}O relaxation rate at 2.1 T and pH = 7 for 50 mM solutions of Gd(COPTA)$^{2-}$(■) and Gd(DTPA)$^{2-}$ (□)

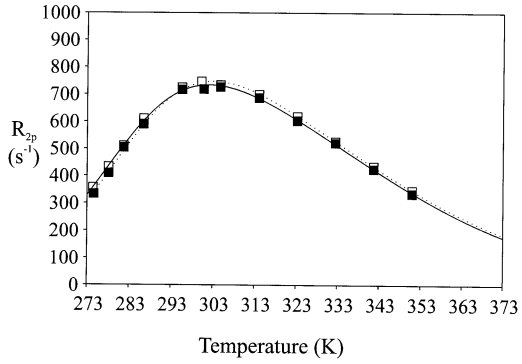

The two profiles appear to be superimposable, both being characterized by a relaxivity maximum centered at about 300 K. This means that the introduction of the hydrophobic substituent on one acetate arm of the Gd(DTPA)$^{2-}$ chelate does not significantly affect the exchange process of the metal-bound water molecule. An analogous observation has been recently reported by Muller et al. for the related Gd(EOB-DTPA)$^{2-}$ complex [EOB-DTPA = 3,6,9-triaza-3,6,9-tris(carboxymethyl)-4-(4-ethoxybenzyl)undecanedicarboxylic acid].[11] The fitting of the data afforded a τ_M^O value at 298 K for Gd(COPTA)$^{2-}$ of 290 ns, a value very close to those obtained for Gd(DTPA)$^{2-}$ (320 ns) and Gd(EOB-DTPA)$^{2-}$ (201 ns)[11] chelates.

Determination of the Longitudinal Water Proton Relaxation Time of the Coordinated Water Molecule τ_{1M}^H

In principle, the observed longitudinal relaxation rate of the water protons (R_{1obs}^H) of an aqueous solution containing a paramagnetic Gd^{III} chelate is given by the sum of three terms [equation (9)]

$$R_{1obs}^H = R_{1p}^{His} + R_{1p}^{Hos} + R_{1d}^H \quad (9)$$

where R_{1p}^{His} represents the paramagnetic contribution from the metal-bound water molecule, R_{1p}^{Hos} is the contribution from the water molecules that diffuse around the complex, and R_{1d}^H corresponds, in analogy to the ^{17}O approach, to the diamagnetic contribution measured in the presence of an equimolar amount of a diamagnetic analogue of the chelate.

The paramagnetic contribution to the observed relaxation rate ($R_{1p}^{His} + R_{1p}^{Hos}$) for a 1 mM solution of the paramagentic complex is called "relaxivity" and it is commonly indicated as r_{1p}.

According to the established theory,[12] R_{1p}^{His} for a 1 mM concentration of a Gd^{III} chelate with one exchanging metal-bound water molecule is given by equation (10)

$$R_{1p}^{His} = \frac{1.8 \cdot 10^{-5}}{T_{1M}^H + \tau_M^H} \quad (10)$$

where T_{1M}^H is the longitudinal relaxation time of the exchangeable metal-bound water protons.

This parameter is related to the dipolar interaction between the unpaired electrons of the metal and the inner-sphere water proton nuclei through equation (11)

$$(T_{1M}^H)^{-1} = \frac{2}{15}\frac{\gamma_I^2 g_e^2 \mu_B^2 S(S+1)}{r_H^6}\left[\frac{3\tau_{C1}}{1+\omega_I^2\tau_{C1}^2} + \frac{7\tau_{C2}}{1+\omega_S^2\tau_{C2}^2}\right] \quad (11)$$

where γ_I is the proton gyromagnetic ratio, r_H is the mean distance between the metal and the inner-sphere water protons, and ω_I and ω_S are the nuclear and electronic Larmor frequencies, respectively.

The two correlation times (τ_{ci}; i = 1,2) associated with the modulation of the proton-electron dipolar coupling are given by equation (12)

$$\tau_{ci}^{-1} = \tau_R^{-1} + (\tau_M^H)^{-1} + T_{iE}^{-1} \quad (12)$$

where τ_R is the reorientational correlation time for the Gd^{III} chelate. Since the rotational motion of the whole complex is assumed to be isotropic, τ_R may be simply related to its molecular size and, for relatively small Gd^{III} chelates, it usually dominates τ_{ci} at the magnetic field strengths routinely employed for MRI applications (0.2−1.5 T).

On the contrary, the outer-sphere contribution, R_{1p}^{Hos}, is not affected by the exchange process occurring at the metal site, since it basically depends, according to the model developed by Hwang and Freed,[13] on the distance of minimum approach between the metal and the diffusing water molecules a, the relative diffusion coefficient D, and the electronic relaxation times (T_{iE}) [equation (13)]

$$R_{1p}^{Hos} = C^{os}\left(\frac{1}{aD}\right)[7J(\omega_s) + 3J(\omega_I)] \quad (13)$$

where C^{os} is equal to 5.8×10^{-13} M^{-1} s^{-2} for a 1 mM concentration of the paramagnetic chelate and $J(\omega_i)$ represents the non-Lorentzian spectral density functions, including the dependence of T_{iE}, a and D.

The large number of parameters responsible for the water proton relaxation enhancement in the presence of a paramagnetic chelate makes their simultaneous and precise evaluation rather difficult. Nevertheless, this goal may be achieved by measuring the water proton relaxation rate over an extended range of magnetic field strengths.[14] The resulting plot of R_{1obs}^H vs. the proton Larmor frequency, called the NMRD profile (Nuclear Magnetic Relaxation Dispersion), is then fitted through eqs. 9−13 to obtain reliable values for the relaxation parameters. The possibility of fixing the values of some of the parameters involved makes the determination of others more accurate. The analysis of the NMRD profiles collected in recent years for a series of structurally similar Gd^{III} polyaminopolycarboxylate chelates provided us with reliable estimates for some relaxation parameters. In particular, values of 2.96 Å, 3.6 Å and 2.6×10^{-5} cm^2 s^{-1} (at 298 K) were obtained for $r_H a$ and D, respectively, from the fitting of the NMRD data for the strictly analogous Gd(BOPTA)$^{2-}$ chelate.[15] On this basis, we have assumed that these parameters do not change for the two complexes and, with these constraints, along with the values of q (1) and τ_M^H (290 ns as obtained from ^{17}O data), we carried out the fitting of the NMRD data for Gd(COPTA)$^{2-}$.

In Figure 2, the NMRD profile (25°C and pH = 7) of $Gd(COPTA)^{2-}$ is presented, along with the outer-sphere contribution to the relaxivity, while in Table 1 the best-fitting parameters are compared with those reported for $Gd(DTPA)^{2-}$.[15]

Figure 2. $1/T_1$ NMRD profile of a 1 mM aqueous solution of $Gd(COPTA)^{2-}$ at pH = 7 and 298 K. The dotted curve represents the outer-sphere contribution to the overall relaxivity

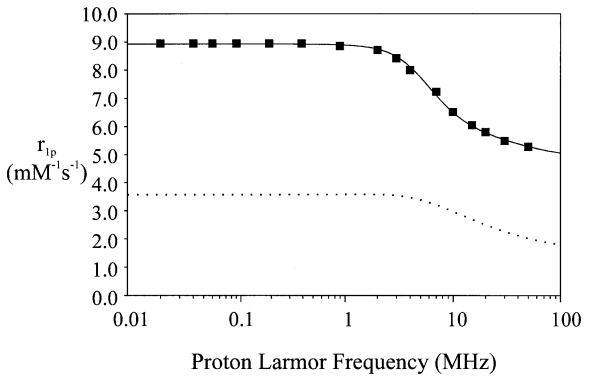

Table 1. Relaxation parameters calculated from NMRD data for $Gd(COPTA)^{2-}$ and $Gd(DTPA)^{2-}$ complexes at pH = 7 and 298 K[a]

Parameter	$Gd(DTPA)^{2-}$[b]	$Gd(COPTA)^{2-}$
Δ^2 ($/10^{19}$ s^{-2})	5.3 (0.3)	4.0 (0.2)
τ_V^{298} (ps)	19.0 (1.0)	25.0 (1.4)
τ_M^H (ns)	320[c]	290[c]
τ_V^{298} (ps)	73.0 (2.0)	80.1 (4.1)

[a] Numbers in parentheses represent standard deviations in mean parameter estimates on 1000 simulated relaxation rate data sets obtained by repeatedly introducing a random error of 1% into the experimental data set and estimating best parameters. – [b] From ref.[15]. – [c] The value was obtained in this work from the ^{17}O data and it has been kept fixed in the fitting of the NMRD profiles.

The main differences between the two sets of parameters lie in the higher τ_R value and the smaller r value obtained for $Gd(COPTA)^{2-}$. A longer reorientational correlation time may be easily accounted for in terms of a larger molecular size for this chelate and very similar τ_R values at 298 K have been reported for both $Gd(BOPTA)^{2-}$ (88.0 ps)[15] and Gd(EOB-DTPA)$^{2-}$ (84.0 ps)[11] complexes.

Once the relaxation parameters for the metal-bound water protons are known, it is possible to calculate their T_{1M}^H at 25°C. We obtained a value (5.3 μs) an order of magnitude larger than the water exchange lifetime (0.29 μs), indicating that for the $Gd(COPTA)^{2-}$ complex at 0.47 T, 298 K and pH = 7, the condition $T_{1M}^H > \tau_M^H$ is undoubtedly fulfilled.

Determination of the Prototropic Exchange Lifetime for the Metal-Bound Water Proton τ_M^{Hp}

The exchange lifetime of the protons of water molecules is strongly pH-dependent, being very long at neutral pH (of the order of ms) and significantly shorter (down to ns values) as the pH is adjusted to values either side of 7. The prototropic exchange process may be adequately treated as a pseudo-first-order mechanism, characterized by a rate constant k_p^i, the values of which for pure water at 301 K were reported to be in the range $4.1-7.1 \times 10^9$ M^{-1} s^{-1} and $2.2-4.3 \times 10^9$ M^{-1} s^{-1} for the acidic (k_p^a) and basic (k_p^b) catalysis, respectively.[5]

The prototropic exchange lifetime for the protons of a water molecule coordinated to a paramagnetic Gd^{III} chelate may be determined by analyzing the pH dependence of the water proton relaxivity. As it is well-known that the Gd^{III} chelates derived from the DTPA ligand are not sufficiently stable under very acidic conditions, we are forced, in the case of $Gd(COPTA)^{2-}$, to deal only with the base-catalysis of the prototropic exchange.

In order to account for the contribution arising from the prototropic exchange rate 1, the relaxation data are fitted to a modified version of equation 10, where τ_M^H is replaced by [equation (14)]

$$\tau_M^H = [(\tau_M^O)^{-1} + (\tau_M^{Hp})^{-1}]^{-1} \quad (14)$$

and [equation (15)]

$$\tau_M^{Hp} = \left(k^b \frac{Kw}{[H_3O^+]}\right)^{-1} \quad (15)$$

As it is reasonable to assume that the outer-sphere contribution to the observed relaxivity is unaffected by the pH of the solution, the reliability of the method is based on two main assumptions: (i) T_{1M}^H does not change over the investigated pH range, and (ii) at neutral pH the observed relaxivity has to be affected by the water exchange lifetime, i.e the condition $T_{1M}^H \approx \tau_M^H$ has to be fulfilled.

The temperature dependence of the water ^{17}O-R_{2p} is particularly sensitive to changes of the coordination cage of the chelate, thus allowing assessment of whether the pH of the solution causes either structural changes or variations in the exchange lifetime of the whole water molecule (τ_M^O). In Figure 3, the temperature dependence ^{17}O-R_{2p} profiles for $Gd(COPTA)^{2-}$ at pH = 7 and pH = 12 are shown.

Figure 3. Temperature dependence of the transverse water ^{17}O relaxation rate at 2.1 T and pH = 7 for 50 mM solution of $Gd(COPTA)^{2-}$ at pH = 7 (□) and pH = 12 (■)

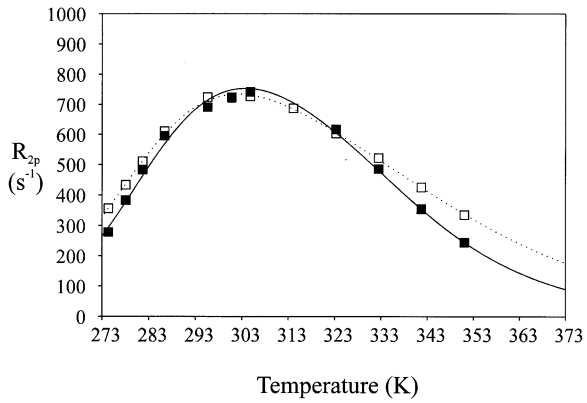

The two profiles are rather similar, being the differences observed in the best fitting parameters within experimental error. These findings support the view that the structure of this Gd^{III}

chelate, and consequently its T_{1M}^H value, is not affected by the pH of the solution.

On the contrary, as emphasized in the previous paragraph, the second condition is not valid for $Gd(COPTA)^{2-}$ at 298 K and 0.47 T and, therefore, the water proton relaxivity is not affected by the pH of the solution (Figure 4, bottom). Thus, this behaviour prevents the determination of the prototropic exchange rate for this chelate under these experimental conditions.

Figure 4. pH dependence of the longitudinal water proton relaxivity at 20 MHz and 298 K of $Gd(COPTA)^{2-}$ free (□) and bound to β-CD (■)

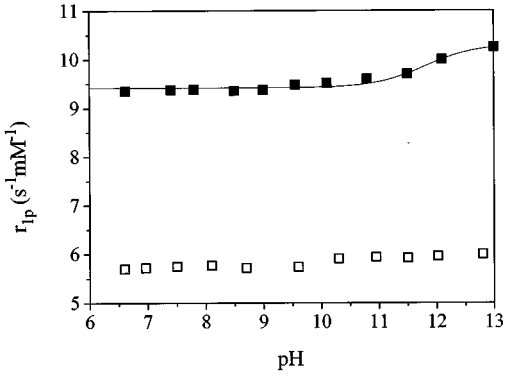

In order to meet the conditions under which the prototropic contribution to the overall relaxation rate can be expressed, we followed two different approaches: (i) formation of a paramagnetic adduct with a slowly tumbling substrate, such as β-cyclodextrin, in order to reduce T_{1M}^H, and (ii) decrease of the experimental temperature in order to either reduce T_{1M}^H or increase τ_M^H.

Reduction of T_{1M}^H Through Non-Covalent Interaction with β-Cyclodextrin

The increase of the relaxivity of a Gd^{III} chelate caused by the lengthening of its reorientational correlation time τ_R is a well-known phenomenon. In fact, it represents the most useful approach to enhance the effectiveness of a CA for MRI applications.[16] Usually, the increase of τ_R is pursued through the formation of adducts between the paramagnetic chelate and slowly tumbling substrates. For this purpose, it is necessary to have a complex endowed with a suitable substituent able to interact with the macromolecular substrate. The benzyloxymethyl residue has been reported to be an excellent recognition synthon that is able to interact with many substrates such as β-cyclodextrin, albumin and micelles.[17][18][19] As the interaction of this group is basically hydrophobic in origin, we expect that the replacement of the phenyl group by cyclohexyl should not significantly modify the interaction properties of the former substituent. Furthermore, in the context of this work, we have to choose a macromolecular substrate, the chelate adduct of which affects the exchange mechanism of the metal-coordinated water molecule as little as possible. For this reason, β-cyclodextrin is the best candidate, since in this case the non-covalent interaction should involve only the hydrophobic tail of the amphiphilic complex and its coordination cage should remain unchanged.

The increase of relaxivity resulting from this interaction may be also exploited for evaluating the affinity of the chelate for β-cyclodextrin. In fact, by measuring the longitudinal water proton relaxation rates of a solution of $Gd(COPTA)^{2-}$ in the presence of increasing amounts of β-CD, we obtained the saturation profile shown in Figure 5, fitting of which allows derivation of an association constant of $(1.5 \pm 0.1) \times 10^3\ M^{-1}$ and a relaxivity for the bound complex of $9.2 \pm 0.1\ s^{-1}mM^{-1}$ (25°C and pH = 7), i.e. 1.6 times larger compared to the unbound chelate.

Figure 5. Longitudinal water proton relaxation enhancement of a 0.11 mM solution of $Gd(COPTA)^{2-}$ upon addition of β-CD (20 MHz, pH = 7, 298 K)

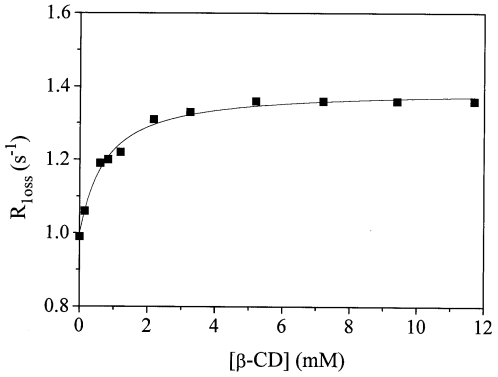

As the interaction with the β-CD essentially causes a lengthening of the reorientational correlation time of the Gd^{III} chelate, the outer-sphere contribution to the overall relaxivity of the bound complex is not expected to be significantly different compared to that of the unbound chelate. From the quantitative analysis of the NMRD profile of $Gd(COPTA)^{2-}$ shown in Figure 2, an R_{1p}^{Hos} value of $2.45\ s^{-1}mM^{-1}$ at 20 MHz and 25°C was obtained. Therefore, the inner-sphere contribution for the $Gd(COPTA)^{2-}$/β-CD adduct is $6.75\ s^{-1}mM^{-1}$ under the same experimental conditions.

In order to calculate the value of T_{1M}^H for the metal-bound water protons in the paramagnetic inclusion compound, it is also necessary to evaluate the value of their exchange lifetimes τ_M^H (equal to τ_M^O at neutral pH). The temperature dependence of the ^{17}O water transverse relaxation rate for the $Gd(COPTA)^{2-}$ chelate bound to β-CD is almost superimposable on the profile recorded for the unbound complex (Figure 6), confirming that τ_M^H does not vary appreciably upon interaction.

On this basis, a value of T_{1M}^H of 2.4 μs for the metal-bound water protons in the inclusion compound may be calculated through eqs. 9–10. This value is only 2.2 times lower than that for the unbound chelate and the condition $T_{1M}^H \approx \tau_M^H$ is not yet met. Nevertheless, the pH dependence of the longitudinal water proton relaxivity for the $Gd(COPTA)^{2-}$/β-CD adduct measured at 298 K (Figure 4, top) is characterized by a slight increase of relaxivity at pH > 11. As the binding with β-CD basically occurs through van der Waals' forces,[20] the affinity of the Gd^{III} chelate for the cyclic oligosaccharide should not

Figure 6. Temperature dependence of the transverse water ^{17}O relaxation rate at 2.1 T and pH = 7 for 50 mM solution of $Gd(COPTA)^{2-}$ free (■) and bound to β-CD (□)

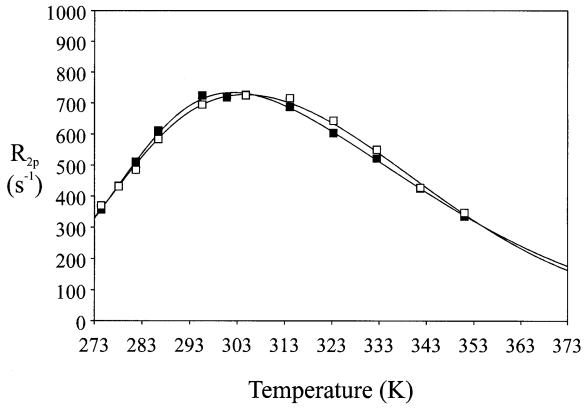

depend on the pH of the solution. Moreover, from the close similarity between the ^{17}O data for the free chelate and those of the adduct with β-CD (either at neutral or basic pH), we can safely rule out the possibility that the relaxation enhancement observed at basic pH is due to structural changes of the Gd^{III} complex. Therefore, the increase of relaxivity may be ascribed to the occurrence of a fast base-catalyzed prototropic exchange of the metal-bound water protons, which results in a reduction of τ_M^H at pH > 11. This hypothesis was further confirmed through a quantitative analysis of the data using equations 10, 14−15. The best fitting parameters (T_{1M}^H, τ_M^O and k_p^b) were in good agreement with the expected values at 298 K. In fact, values of 2.3 ± 0.02 μs and 0.29 μs were obtained for T_{1M}^H and τ_M^O, respectively. As far as the base-catalyzed prototropic exchange rate constant is concerned, we obtained a value of (7.3 ± 2.6) × 10^8 s^{-1} M^{-1}, which is lower than the value measured in pure water and similar to the value determined for the Gd(DTPA-BBA) chelate.[7]

In conclusion, the reduction of T_{1M}^H caused by the formation of an inclusion compound with β-CD allows detection of the effect on the relaxivity arising from the prototropic exchange at the metal-bound water molecule of the Gd^{III} chelate. Unfortunately, the effect of the interaction on R_{1M}^H is not particularly marked owing to the small increase of τ_R for the chelate bound to the β-CD. For this reason, the associated relaxivity enhancement observed at basic pH is relatively small and the error in the estimation of k^b is consequently rather large (ca. 36%).

Reduction of T_{1M}^H by Lowering the Temperature

Another possible approach to achieve the condition $T_{1M}^H \leq \tau_M^H$ is to exploit the opposite temperature dependence of these two parameters. In particular, at low temperature, one can expect a decrease of T_{1M}^H (due to the increase of τ_R) and a simultaneous lengthening of τ_M^H. The temperature dependence of the longitudinal water proton relaxivity for $Gd(COPTA)^{2-}$ complex is depicted in Figure 7.

The profile may be split in two regions: at temperatures higher than 288 K, the relaxivity decreases pseudo-exponentially owing to the increase of T_{1M}^H, whereas at lower temperature, the elongation of τ_M^H and the simultaneous decrease of R_{1p}^{Hos} causes a flattening of the profile. On the basis of these data, at a temperature lower than 288 K, the condition $R_{1M}^H \approx \tau_M^H$ can be expected to hold.

Figure 7. Temperature dependence of the water proton relaxivity of $Gd(COPTA)^{2-}$ at 20 MHz and pH = 7

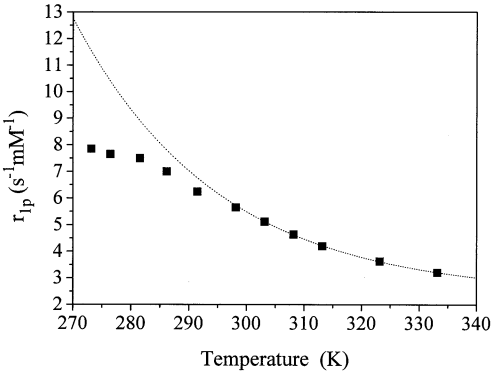

The pH dependence of the relaxivity of the $Gd(COPTA)^{2-}$ complex recorded at 278 K is shown in Figure 8.

Figure 8. pH dependence of the longitudinal water proton relaxivity at 20 MHz and 278 K of $Gd(COPTA)^{2-}$

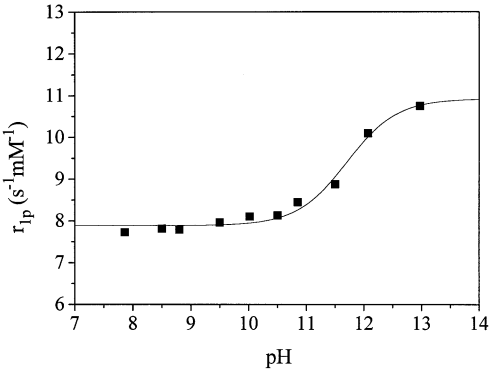

At this temperature, the relaxivity enhancement promoted by the activation of the prototropic exchange appears to be much more pronounced compared to the effect observed at room temperature for the same system. Before carrying out a quantitative analysis of the data reported in Figure 8, it was thought useful to gain more information about the relaxation parameters of the chelate at 278 K. In particular, by fixing a value of D of 1.1 × 10^{-5} cm^2 s^{-1},[21] the fitting of the NMRD data recorded at this temperature and at pH = 7 afforded a value of 4.4 s^{-1} mM^{-1} for the outer-sphere contribution to the relaxivity and values of 3.2 ± 0.2 μs and 2.4 ± 0.1 μs for T_{1M}^H and τ_M^H (equal to τ_M^O at neutral pH), respectively. Interestingly, we obtained very similar T_{1M}^H and τ_M^H values (2.8 ± 0.1 μs and 2.4 ± 0.1 μs) from the fitting of the data shown in Figure 8. Furthermore, it is noteworthy that the values obtained for the water proton exchange lifetime at pH = 7 ($\tau_M^H = \tau_M^O$) from the analysis of both magnetic field and pH dependence of the ^1H relaxivity are in good agreement with the value calculated at 278 K from the ^{17}O data (1.3 ± 0.1 μs). As expected, the value of the rate constant for the base-catalyzed prototropic ex-

change process is lower [$(1.5 \pm 0.3) \times 10^8$ s^{-1} M^{-1}], but more accurate (standard deviation ca. 20%), compared to the value obtained at room temperature in the case of the Gd^{III} complex incorporated into β-CD.

Conclusion

In this work, we have shown that NMR (^1H and ^{17}O) relaxometric methods provide a powerful tool for assessing the exchange rate of the coordinated water molecule, as well as the proton transfer rate, in a paramagnetic Gd^{III} complex.

This has been possible through the decrease of the relaxation time of the protons of the coordinated water (T_{1M}^H) upon formation of a paramagnetic adduct with the slowly tumbling β-cyclodextrin substrate.

When T_{1M}^H becomes smaller than the exchange lifetime of the coordinated water, the prototropic contribution to the overall proton relaxation enhancement may be evaluated, since, at basic pH, the proton transfer rate becomes faster than the exchange of the whole water molecule.

Support from *MURST* CNR is gratefully acknowledged.

Experimental Section

Synthesis: The COPTA ligand and its Gd^{III} chelate were prepared using a procedure analogous to that previously reported for the BOPTA ligand[15] starting from diethylenetriamine and 2-bromo-3-(cyclohexylmethoxy)propanoic acid, followed by peralkylation of the monoalkylated intermediate with sodium bromoacetate in water at pH = 10. 2-Bromo-3-(cyclohexylmethoxy)propanoic acid was obtained by alkaline hydrolysis of the corresponding methyl ester, which was prepared according to a reported procedure.[22]

^1H-NMR Measurements: Longitudinal water proton relaxation rates were measured at 25°C and 0.47 T with a Stelar Spinmaster spectrometer [Stelar, Mede (PV), Italy] by using the inversion recovery (180° − τ − 90°) pulse sequence. A phase cycle ($+x$, $-x$, $-x$, $+x$) was applied on the 90° observation pulse in order to cut off the y scale receiver offset. Each measurement consisted of 4 scans and the values of the magnetization were obtained in the time domain by averaging the first 128 points of the free induction decay. The reproducibility in T_1 measurements was ±0.4%. The temperature was controlled with a Stelar VTC-91 air-flow heater equipped with a copper-constantan thermocouple; the actual temperature was measured inside the probehead (uncertainty of ±0.1 °C) by using a Fluka 52 k/j digital thermometer.

The ^1H-NMRD profiles were recorded on a Koenig-Brown field-cycling relaxometer by measuring water proton longitudinal relaxation rates at magnetic field strengths in the range from 2.4×10^{-4} to 1.5 T (corresponding to 0.01−50 MHz proton Larmor frequencies) with a T_1 uncertainty of ±1%.

^{17}O-NMR Measurements: The measurement of the ^{17}O transverse relaxation rates was carried out with a JEOL EX-90 spectrometer operating at 2.1 T (corresponding to a ^{17}O Larmor frequency of 12.2 MHz) by using an external D_2O lock. The temperature calibration was performed following the same procedure described for the Stelar SpinMaster spectrometer.

The value of the transverse relaxation rate was obtained by evaluating the linewidth at half-height ($\Delta\nu_{1/2}$) of the water ^{17}O signal ($R_2 = \pi\Delta\nu_{1/2}$). Solutions containing 2.6% of the ^{17}O isotope were used. ^{17}O-enriched (10.4%) water was purchased from Yeda (R. & D. Co., Rehovot, Israel).

[1] D. H. Powell, O. M. Ni Dhubhghaill, D. Pubanz, L. Helm, Y. S. Lebedev, W. Schlaepfer, A. E. Merbach, *J. Am. Chem. Soc.* **1996**, *118*, 9333−9346.
[2] D. Pubanz, G. Gonzàlez, D. H. Powell, A. E. Merbach, *Inorg. Chem.* **1995**, *34*, 4447−4453.
[3] A. E. Merbach, D. H. Powell, U. Frey, *Dynamics of Solutions and Fluid Mixtures by NMR* (Ed.: J. J. Delpuech), John Wiley & Sons, New York, **1997**, ch. 6 ("Solvent Exchange on Metal Ions: A Variable Pressure NMR Approach"), p. 263−308.
[4] B. L. Engelstadt, G. L. Wolf, *Magnetic Resonance Imaging* (Eds.: D. D. Stark, W. G. Bradley, Jr.), Mosby, St. Louis, **1988**, ch. 9 ("Contrast Agents"), p. 161−81.
[5] B. Halle, G. Karlström, *J. Chem. Soc., Faraday Trans. 2* **1983**, *79*, 1031−1046 and references therein.
[6] S. Aime, A. Barge, M. Botta, D. Parker, A. S. De Sousa, *J. Am. Chem. Soc.* **1997**, *119*, 4767−4768.
[7] S. Aime, M. Botta, M. Fasano, S. Paoletti, E. Terreno, *Chem. Eur. J.* **1997**, *3*, 1499−1504.
[8] T. J. Swift, R. E. J. Connick, *J. Chem. Phys.* **1962**, *37*, 307.
[9] N. Bloembergen, L. O. Morgan, *J. Chem. Phys.* **1961**, *34*, 842−850.
[10] M. Rubenstein, A. Bararn, Z. Luz, *Molec. Phys.* **1971**, *20*, 67.
[11] L. Vander Elst, F. Maton, S. Laurent, F. Seghi, F. Chapelle, R. N. Muller, *Magn. Res. Med.* **1997**, *38*, 604−614.
[12] L. Banci, I. Bertini, C. Luchinat, *Nuclear and Electron Relaxation*, VCH, Weinheim, **1991**.
[13] L. P. Hwang, J. H. Freed, *J. Chem. Phys.* **1975**, *63*, 118−130.
[14] S. H. Koenig, R. D. Brown III, *Prog. Nucl. Magn. Reson. Spectrosc.* **1990**, *22*, 487−567.
[15] F. Uggeri, S. Aime, P. L. Anelli, M. Botta, M. Brochetta, C. de Haen, G. Ermondi, M. Grandi, P. Paoli, *Inorg. Chem.* **1995**, *34*, 633−642.
[16] S. Aime, M. Botta, M. Fasano, E. Terreno, *Chem. Soc. Rev.* **1998**, *27*, 19−29 and references therein.
[17] S. Aime, M. Botta, G. Ermondi, F. Fedeli, F. Uggeri, *Inorg. Chem.* **1992**, *31*, 1100−1103.
[18] S. Aime, M. Botta, M. Fasano, S. Geninatti Crich, E. Terreno, *J. Bioinorg. Chem.* **1996**, *1*, 312−319.
[19] S. Aime, L. Barbero, M. Botta, *Magn. Res. Chem.* **1991**, *9*, 843.
[20] M. L. Bender, M. Komiyama, *Cyclodextrin Chemistry*, Springer-Verlag, Berlin, **1978**.
[21] S. Aime, A. S. Batsanov, M. Botta, J. A. K. Howard, D. Parker, K. Senanayake, G. Williams, *Inorg. Chem.* **1994**, *33*, 4696−4706.
[22] P. L. Anelli, A. Beltrami, M. Lolli, F. Uggeri, *Synth. Commun.* **1993**, *23*, 2639−2645.

[98062]

Catalytic and Structural Features of Hydroxy and Methoxy Groups as Hemilabile Coordinating Ligands in Chiral (Diphosphane)rhodium(I) Hydrogenation Catalysts☆

Susanne Borns, Renat Kadyrov, Detlef Heller*, Wolfgang Baumann, Anke Spannenberg, Rhett Kempe, Jens Holz, and Armin Börner*

Institut für Organische Katalyseforschung an der Universität Rostock e.V.,
Buchbinderstr. 5/6, D-18055 Rostock, Germany
Fax: (internat.) + 49(0)381/4669324
E-mail: aboern@chemie1.uni-rostock.de

Received March 25, 1998

Keywords: Asymmetric catalysis / Hydrogenations / Hemilabile ligand / Hydroxy phosphane / Methoxy phosphane

The influence of two *threo*-arranged methoxy or hydroxy groups as hemilabile ligands in seven-membered (diphosphane)Rh^I chelates upon the asymmetric hydrogenation is studied. In comparison to the parent complex based on 1,4-bis(diphenylphosphanyl)butane (DPPB) a lowering of the reaction rate is caused by the hemilabile ligands. The catalyst bearing the hydroxy groups gives significantly higher enantioselectivities than the corresponding methoxy complex (by ca. 35 % ee). X-ray structural analysis reveals that the oxygen atom of the hydroxy group is by 0.9 Å closer to the metal center than that of the methyl ether. ^{31}P-NMR studies give evidence that the dihydroxy diphosphane ligand binds at low temperature exclusively in the η^3-coordination mode, whereas for the dimethoxy complex also an η^2-coordinated isomer can be found. These differences in complexation could be responsible for the superior enantioselectivities achieved with this and other hydroxy catalysts.

Introduction

(Alkoxyaryl and -alkyl)phosphanes have seen broad application in asymmetric hydrogenations[1] as well as in numerous other metal-catalyzed stereodifferentiating reactions.[2] For example, (*R*,*R*)-DIPAMP [(*R*,*R*)-1,2-bis(*o*-anisylphenylphosphanyl)ethane] was the first industrially applied ligand.[3] The unique role of the alkoxy and preferentially that of the methoxy group is attributed to their property to act as hemilabile ligands[4] or intramolecular solvent,[5] which may temporarily coordinate to the metal center in the course of the catalytic cycle.[6][7]

Despite this, much less information is available on the influence of the related hydroxy group,[8] although it deserves particular attention due to its potential to create secondary interactions with a suitable substrate and to enhance the solubility of the catalyst in water.[9][10]

In recent investigations with a (diphosphane)rhodium complex bearing a single methoxy group we could show that the replacement of the latter by the hydroxy group increased the enantioselectivity of the hydrogenation in methanol.[11] Simultaneously, a conspicuous loss of reactivity was observed. To date there is no explanation for this unique behaviour of this and other catalysts bearing hydroxy groups.[12]

Herein, we report on a study concerning the synthesis, catalytic properties, and structure elaboration of cationic Rh^I complexes based on the ligands (*R*,*R*)-1,4-bis(diphenylphosphanyl)butane-2,3-diol (**1-OH**)[13a] and its bis(methyl ether) **1-OMe**[14] which may have important implications to the aspects discussed above. Both ligands are related to 1,4-bis(diphenylphosphanyl)butane (DPPB) which forms with metals seven-membered chelate rings.

Scheme 1

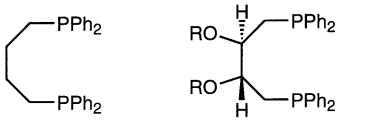

DPPB **1-OH** (R = H) **1-OMe** (R = Me) **1-OSiPh$_3$** (R = Ph_3Si)

In general, Rh catalysts based on such large and highly flexible chelates are more active in asymmetric hydrogenations than rigid five-membered chelates e.g. (DIPAMP)Rh^I, but require additional stabilization in order to provide for appreciable enantioselectivity. Due to the absence of any other stabilizing groups in our model complexes chosen catalytic effects can be clearly traced to the effect of the oxy functionalities.

Results and Discussion

The Rh^I complexes were synthesized by reaction of the C_2-symmetric diphosphanes with $[Rh(COD)_2]BF_4$ [COD = (*Z*,*Z*)-cycloocta-1,5-diene] (Scheme 2). The COD complex of **1-OH** was converted into the better crystallizing complex [Rh(NBD)(**1-OH**)]BF_4 by treatment with norbornadiene (NBD).[15]

The complexes obtained catalyze the hydrogenation of itaconic acid (ItH_2) and (*Z*)-2-*N*-acetylaminocinnamic acid (AH) in methanol (Table 1). The Rh complex of DPPB is

 © WILEY-VCH Verlag GmbH, D-69451 Weinheim, 1998 1434–1948/98/0909–1291 $ 17.50+.50/0

Scheme 2

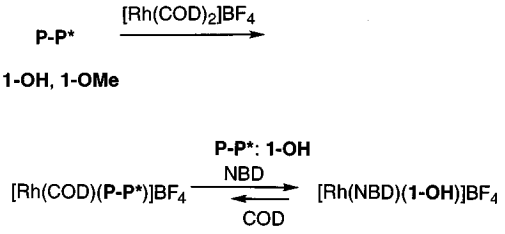

the most active catalyst in the series. It is remarkable that the incorporation of the methoxy groups diminishes seriously the rate of the reaction, however, the selectivity observed is low. This gives a clear indication that the ether groups are not able to stabilize certain conformations of the highly flexible seven-membered chelate. The exchange of the methoxy by the hydroxy groups gives rise to a further loss of reactivity, however, affords a significant gain in selectivity by approximately 35% ee.

Table 1. Asymmetric hydrogenation of prochiral olefins in methanol[a]

Precatalysts	Substrate	$t/2$ [min][b]	ee [%] (config.)
$[Rh(COD)(DPPB)]BF_4$	ItH_2	<2	–
$[Rh(COD)(\mathbf{1\text{-}OMe})]BF_4$	ItH_2	3.7	22.4 (*S*)
$[Rh(NBD)(\mathbf{1\text{-}OH})]BF_4$	ItH_2	6.0	56.8 (*S*)
$[Rh(COD)(DPPB)]BF_4$	AH	<2	–
$[Rh(COD)(\mathbf{1\text{-}OMe})]BF_4$	AH	145	0.6 (*S*)
$[Rh(NBD)(\mathbf{1\text{-}OH})]BF_4$	AH	190	36.3 (*R*)

[a] Conditions: 0.01 mmol of precatalysts, 1.0 mmol of substrate in 15 ml of MeOH at 25°C and at 0.1 MPa H_2 pressure. – [b] Corresponds to that time, when 50% of substrate is converted.

In order to explain these differences, X-ray structural analyses of the precatalysts were performed and their $^{31}P\{^1H\}$-NMR spectra recorded. Suitable crystals of $[Rh(NBD)(\mathbf{1\text{-}OH})]BF_4$ and $[Rh(COD)(\mathbf{1\text{-}OMe})]BF_4$ were obtained from methanol. The single-crystal X-ray structural analyses established the structures as shown in Figure 1a and 1b, respectively, along with selected bond lengths and interbond angles.[17] The inspection of the data shows some agreements but also striking differences.

In the complex $[Rh(NBD)(\mathbf{1\text{-}OH})]BF_4$[17a] both phosphorus atoms are differently bound to the rhodium center; the distances are 2.283 Å and 2.377 Å. One of the enantiotopic hydroxy groups interacts with the metal center (distance 2.396 Å) never before observed to such an extent in related (methyl phosphanylaryl ether)rhodium[6c] or -palladium complexes[1e]. The BF_4 anion binds via a hydrogen bond to the second hydroxy group. In the IR spectrum (KBr) appear two bands at 3508 and 3441 cm^{-1} also clearly indicating two different hydroxy groups.[18] One important force for the formation of the five-membered O–Rh–P ring is apparantly the pseudo-equatorial arrangement of the hydroxy group in the fused six-membered ring being fixed in a distorted chair conformation, since the interaction could not be found in the corresponding monohydroxy complex.[11] The dihedral angle formed by the two hydroxy groups is 157.3° which reveals a strong deviation from the *anti* arrangement.

Figure 1. Structures of $[Rh(NBD)(\mathbf{1\text{-}OH})]BF_4$ (Figure 1a) and $[Rh(COD)(\mathbf{1\text{-}OMe})]BF_4$ (Figure 1b) in the crystalline state; hydrogen atoms are omitted for clarity[a]

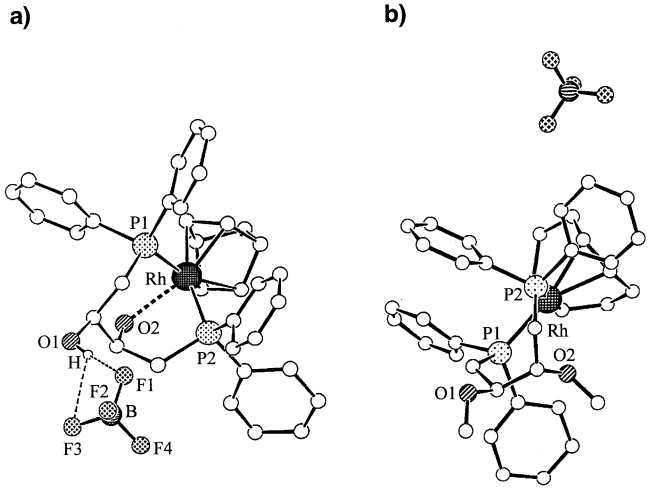

[a] Selected atomic distances [Å] and torsional angles [°]: $[Rh(NBD)(\mathbf{1\text{-}OH})]BF_4$: Rh(1)–P(1) 2.283(2), Rh(1)–P(2) 2.377(2), Rh(1)–O(2) 2.396, F(1)–O(1) 2.717; O(1)–C–C–O(2) 157.3; $[Rh(COD)(\mathbf{1\text{-}OMe})]BF_4$: Rh(1)–P(1) 2.320(2), Rh(1)–P(2) 2.333(2), Rh(1)–O(2) 3.282; O(1)–C–C–O(2) 169.1.

For the structure of $[Rh(COD)(\mathbf{1\text{-}OMe})]BF_4$ different features are noted.[17b] Thus, both phosphorus atoms are bound in approximately equal distances to the metal center. Due to the absence of a hydrogen-bond donor the BF_4 anion is located far away from the oxy groups. The most important difference in comparison to the hydroxy compound is the distance between the rhodium and the oxygen atom O(2) of the neighboured ether group (3.282 Å). This is a difference of more than 0.9 Å. The dihedral angle O(1)CCO(2) is widened to 169.1°.

In the $^{31}P\{^1H\}$-NMR spectra in CD_3OD also remarkable differences exist (Figure 2). $[Rh(NBD)(\mathbf{1\text{-}OH})]BF_4$ is characterized at 302 K by a doublet at $\delta = 18.1$. The decrease of the temperature caused the broadening of the signal. At 222 K the initial resonance had disappeared and two new signals could be observed at $\delta = 40$ and 0. Finally, the spectrum at 189 K displays two sets of well-separated double doublets at $\delta = 44.0$ ($J_{Rh\text{-}P} = 141.5$ Hz, $J_{P\text{-}P} = 41.4$ Hz) and $\delta = -2.7$ ($J_{Rh\text{-}P} = 129.1$ Hz, $J_{P\text{-}P} = 41.4$ Hz) produced by two nonequivalent phosphorus atoms. These results are consistent with one oxygen atom being attached to the metal center. The resonance at $\delta = 44.0$ has to be assigned to a phosphane which is involved in an O–P five-membered chelate.[19] Compared to related seven-membered chelate complexes {e.g. $[Rh(COD)(DPPB)]BF_4$} the downfield shift observed is caused by the increased ring strain in the newly formed five-membered ring. The fused O–P six-membered ring is characterized by a considerable shift of the concerned signal to higher field and the decrease of the ^{103}Rh-^{31}P coupling. The coordination of the oxygen atom causes the formation of the boat conformation (**B**) (Figure 2c). The typical change of the band shapes with

decreasing temperature gives clear evidence that the doublet observed at room temperature characterizes a rapid exchange of the phosphane signals. This exchange caused by the alternate coordination of the two oxygen atoms is not distinguishable on the NMR time scale at elevated temperatures.

ylsilyl ether) **1-OSiPh$_3$** (Scheme 1) recently published by Tamao.[20] In contrast to the complexes considered herein, [Rh(COD)(**1-OSiPh$_3$**)]SbF_6 is fixed in the C_2-symmetric conformation **A**.[21] This feature is explained by repulsive interactions between the bulky silyl groups and the phenyl rings of the phosphanyl moiety (Figure 2c). Clearly, these

Figure 2. $^{31}P\{^1H\}$-NMR spectra of the complexes [Rh(NBD)(**1-OH**)]BF_4 (Figure 2a; the small $J_{P\text{-}P}$ couplings of 41.4 Hz are not visible in the presentation) and [Rh(COD)(**1-OMe**)]BF_4 (Figure 2b) in CD_3OD at different temperatures; the relevant equilibrium of conformers is depicted in Figure 2c

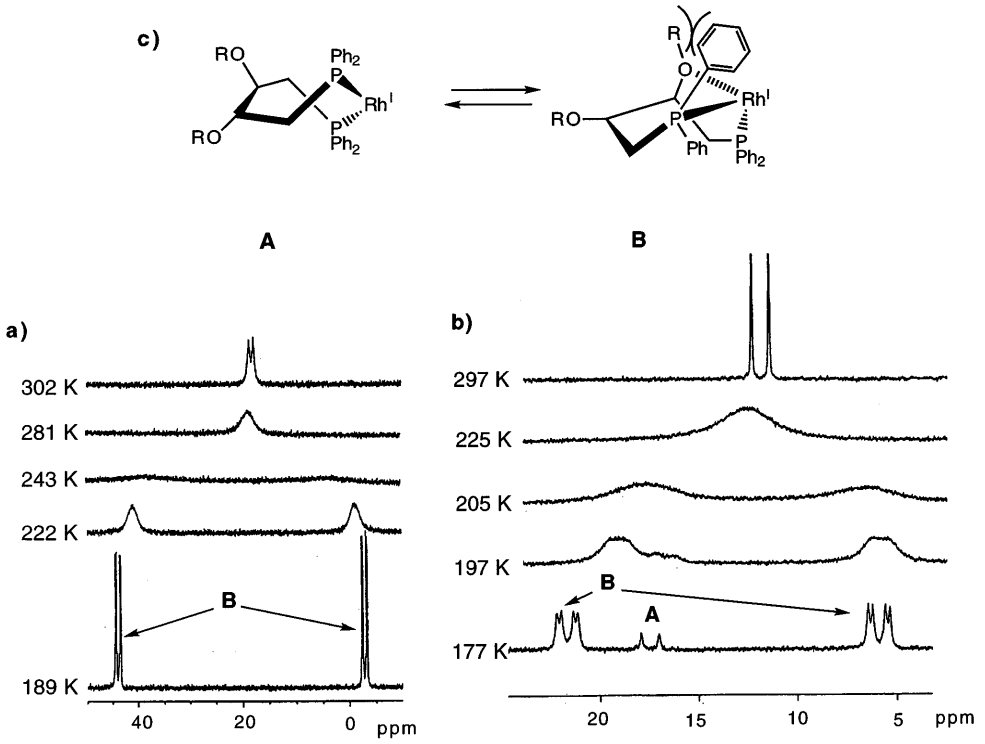

The methoxy complex [Rh(COD)(**1-OMe**)]BF_4 shows a different behaviour with decreasing temperature. Thus, in comparison to the hydroxy complex the coalescence temperature is 35 K lower. Even at 177 K the doublets of doublets are less separated. Additionally, at $\delta = 17.2$ a doublet can be observed which corresponds in shift and coupling to that of the Rh(DPPB) complex. The signal can be unambigeously attributed to a C_2-symmetric complex and gives proof that at low temperatures [Rh(COD)(**1-OMe**)]BF_4 exists also in a conformation where the oxygen atoms do not interact with the metal center (twisted chair conformation **A**).

Due to the temperature dependency of the coupling constants and the inaccessibility of the data of the twisted chair conformation of Rh(NBD)(**1-OH**)]BF_4 we were not able to calculate the concentrations of the conformers at room temperature. However, taking the differences in the low-temperature spectra and the coalescence temperatures into account considerable differences in the populations of the conformers **A** and **B** of hydroxy und methoxy complex can be concluded.

The observation of these differences between hydroxy and methoxy complex provoked the comparison with the structure of a Rh complex based on the related bis(triphen-

interactions are also responsible for the fact that none of the oxygen atoms approaches the rhodium center, as found in [Rh(NBD)(**1-OH**)]BF_4 and [Rh(COD)(**1-OMe**)]BF_4. Taking our and the results of Tamao into consideration the preference for the shift of the boat (**B**) into the twisted chair conformation (**A**) is in the order $Ph_3Si > Me > H$. In other words, large groups at the oxygen atom prevent by interactions with the phenylphosphanyl groups the ligand to bind in the η^3-coodination mode. The η^2-coordination mode is responsible for a high hydrogenation activity as seen for the $(DPPB)Rh^I$ complex. Apparently, the tripodal coordination hinders the hydrogenation. However, only by this arrangement the highly flexible seven-membered chelate can be sufficiently stabilized which is the precondition to achieve conspicuous enantioselectivity.[22][23]

Conclusion

The conformation of chiral, highly flexible rhodium diphosphane chelates can be stabilized by the incorporation of hemilabile oxy groups. Due to the additional interaction of the ligand with the metal center a deceleration of the rate of the asymmetric hydrogenation results. With the hydroxy group significant higher enantioselectivities were achieved in comparison to the usually applied methoxy group. This

observation can be rationalized by the stronger preference of the hydroxy diphosphane ligand to bind in the η^3-coordination mode. In the precatalysts investigated herein the tripodal coordination is forced by the interplay of two *erythro*-arranged functional groups. The interaction between the hemilabile ligand and the rhodium center is counterbalanced by the repulsive interaction of the substituent at the oxygen atom with one phenylphosphanyl unit, which is stronger for the methyl group than for the proton of the hydroxy group.

In extension of these conclusions we suggest that in the catalytic cycle also other interactions between the hydroxy group and the metal center become operative,[24] since a significant gain of selectivity could be also noted in the hydrogenation with complexes bearing only one hydroxy group.[11][12] In general, these results and preliminary investigations with catalyst−substrate complexes clearly show that the main differences between hydroxy and methoxy group are preserved during the asymmetric hydrogenation. In combination with other conformation-stabilizing features selectivities of ≥ 90% ee can be achieved.[8][25] Therefore, the assistance of hemilabile hydroxy groups should be recommended also in other stereoselective reactions.

This work was supported by the *BMBF* (Förderkennzeichen 03D0032D0) and the *Fonds der Chemischen Industrie*. We thank Mrs. *G. Voß* for skilled technical assistance. It is a pleasure to thank Prof. Dr. *K. Tamao* (Kyoto), Prof. Dr. *U. Rosenthal* und Prof. Dr. *R. Selke* (Rostock) for fruitful discussions.

Experimental Section

General: All reagents were obtained from Aldrich and Merck. Solvents were dried and freshly distilled under argon before use. Reactions were performed under argon by using standard Schlenk techniques. (*Z*,*Z*)-Cycloocta-1,5-diene (COD) and norborna-2,5-diene (NBD) were dried with CaH_2 and distilled under argon. (*R*,*R*)-1,4-bis(diphenylphosphanyl)butane-2,3-diol (**1-OH**) was synthesized by cleavage of the acetal group of (*R*,*R*)-3,4-bis(diphenylphosphanylmethylene)-2,3-dimethyl-1,3-dioxolane (DIOP) according to an already published procedure.[13a][13b] (*R*,*R*)-1,4-bis(diphenylphosphanyl)-2,3-dimethoxybutane (**1-OMe**) was prepared starting from (*R*,*R*)-tartaric acid as described in ref.[14]. Commercially available (*Z*)-2-(acetylamino)cinnamic acid (AH) and itaconic acid (ItH_2) were recrystallized under argon. − NMR: Bruker ARX 400 (400.13 MHz, 100.63 MHz, and 161.98 MHz for ^1H, ^{13}C and ^{31}P, respectively); for ^1H and ^{13}C NMR TMS as internal standard; for ^{31}P NMR H_3PO_4 as external standard. − X-ray: STOE-IPDS diffractometer. − IR: Nicolet Magna − IR 550 instrument. − MS: AMD 402 (Firma Intectra) − Elemental analysis: LECO CHNS-932. − The hydrogenation experiments were carried out under normal pressure and isobaric conditions with an automatically registrating gas-measuring device (1.0 atm overall pressure over the solution). The experiments were carried out under standard conditions with 0.01 mmol precatalyst, 1.0 mmol of prochiral olefin in 15 ml of solvent at 25°C. The conversion of the prochiral olefins was determined by GC. The acids were esterified with trimethylsilyldiazomethane before the GC measurements: GC 5890 Serie II; FID, carrier gas: argon: 1 ml/min. Methyl *N*-acetylphenylalaninate: fused silica; 10 m, XE-60-L-valin-*tert*-butylamide; ID 0.2 mm; oven temperature: 150°C. Dimethyl methylsuccinate: fused silica, Lipodex E (Machery and Nagel), 25 m, ID 0.25 mm; oven temperature: 85°C.

*[Rh(COD)(***1-OH***)]BF$_4$:* (*R*,*R*)-1,4-Bis(diphenylphosphanyl)butane-2,3-diol (120 mg, 0.262 mmol) and $[Rh(COD)_2]BF_4$ (106 mg, 0.262 mmol) were stirred in THF (2 ml) at ambient temperature for 1.5 h. After the addition of diethyl ether (8 ml), a precipitate formed which was filtered off and washed with a small quantity of diethyl ether to give 182 mg (92%) of the complex as a yellow-orange powder. − ^{31}P NMR ($CDCl_3$, 297 K): δ = 15.0 (d, *J* = 148.1 Hz). − ^{13}C NMR ($CDCl_3$, 297 K): δ = 133.9−128.5 (Ar), 95.9 (s, COD-*CH*), 95.5 (s, COD-*CH*), 71.7 (s, O*CH*), 33.0 (m, PCH_2), 28.7 (s, COD-CH_2). − ^1H NMR ($CDCl_3$, 297 K): δ = 7.70−7.34 (m, 20 H, Ar), 4.52 (m, 2 H, COD-*CH*), 4.17 (m, 2 H, COD-*CH*), 4.04 (m, 2 H, O*CH*), 2.84 (m, 2 H, H_b of PCH_2), 2.62−2.18 (m, 8 H, COD-CH_2), 2.01 (m, 2 H, H_a of PCH_2). − IR (KBr): $\tilde{\nu}$ = 3548, 3463, 3053, 2946, 2919, 2882, 2835, 2361, 1894, 1844, 1480 cm^{-1}. − FAB MS (3-nitrobenzyl alcohol matrix): *m*/*z* = 668.6 $[M - BF_4]^+$, 560.7 $[M - BF_4 - COD]^+$. − $C_{36}H_{40}BF_4O_2P_2Rh$ (756.37): C 57.17, H 5.33; found C 56.78, H 5.35.

*[Rh(NBD)(***1-OH***)]BF$_4$:* To a suspension of [Rh(COD)(**1-OH**)]BF_4 (151 mg, 0.2 mmol) in THF (45 ml) freshly distilled NBD (10 ml, 100 mmol) was added. Stirring over a period of 48 h yielded a dark orange solution. After the addition of diethyl ether (200 ml), an orange powder precipitated, which was filtered off and dried to give 133 mg (90%) of the desired NBD complex. − ^{31}P NMR (CD_2Cl_2, 297 K): δ = 18.1 (d, *J* = 146.2 Hz). − ^{13}C NMR (CD_2Cl_2, 297 K): δ = 134.3−129.2 (Ar), 72.2 (m, *CH*), 71.7 (m, *CH*), 70.6 (m, *CH*), 66.2 (s, *CH*), 31.9 [t, ^1J(P-C) = 12.3 Hz, PCH_2]. − ^1H NMR (CD_2Cl_2, 297 K): δ = 7.38−7.06 (m, 20 H, Ar), 3.97 (s, 2 H, *CH*), 3.85 (s, 2 H, *CH*), 3.76 (m, 2 H, *CH*), 3.62 (m, 2 H, *CH*), 2.65 (m, 2 H, H_a of PCH_2), 2.19 (m, 2 H, H_b of PCH_2), 1.23 (s, 2 H, NBD-CH_2). − IR (KBr): $\tilde{\nu}$ = 3508, 3441, 3056, 3003, 2952, 2920, 2848, 2681 cm^{-1}. − IR (CD_2Cl_2) $\tilde{\nu}$ = 3410, 3396 cm^{-1}. − FAB MS (3-nitrobenzyl alcohol matrix): *m*/*z* = 652.7 $[M - BF_4]^+$. − $C_{35}H_{36}BF_4O_2P_2Rh$ (740.33): C 56.78, H 4.90; found C 56.96, H 4.93.

*[Rh(COD)(***1-OMe***)]BF$_4$:* (*R*,*R*)-1,4-Bis(diphenylphosphanyl)-2,3-dimethoxybutane (290 mg, 0.6 mmol) and $[Rh(COD)_2]BF_4$ (243 mg, 0.6 mmol) were stirred in THF (2 ml) at ambient temperature for 2 h. After the addition of diethyl ether (8 ml), a precipitate formed which was filtered off and recrystallized from THF and diethyl ether to give 367 mg (78%) of the complex as a orange powder. − ^{31}P NMR ($CDCl_3$, 297 K): δ = 12.3 (d, *J* = 144.0 Hz). − ^{13}C NMR ($CDCl_3$, 297 K): δ = 134.5−128.9 (Ar), 99.4 (s, COD-*CH*), 95.0 (s, COD-*CH*), 78.0 (s, O*CH*), 58.5 (s, OCH_3), 31.8 [t, ^1J(P-C) = 13.2 Hz, PCH_2], 30.7 (s, COD-CH_2). − ^1H NMR ($CDCl_3$, 297 K): δ = 7.82−7.08 (m, 20 H, Ar), 4.38 (m, 2 H, *CH*), 4.25 (m, 2 H, *CH*), 3.46 (m, 2 H, *CH*), 3.27 (s, 6 H, OCH_3), 2.84−2.01 (m, 12 H, PCH_2 and COD-CH_2). − IR (KBr): $\tilde{\nu}$ = 3047, 2951, 2920, 2882, 2837, 1480, 1433 cm^{-1}. − FAB-MS (3-nitrobenzyl alcohol matrix): *m*/*z* = 696.6 $[M - BF_4]^+$, 588.6 $[(M - BF_4) - COD]^+$. − $C_{38}H_{44}BF_4O_2P_2Rh$ (784.42): C 58.19, H 5.65; found C 58.33, H 5.54.

☆ Dedicated to Professor *H. B. Kagan*.

[1] [1a] H. Brunner in *Applied Homogeneous Catalysis with Organometallic Compounds*, vol. 1 (Eds.: B. Cornils, W. A. Herrmann), VCH, Weinheim, **1996**, p. 201−216. − [1b] U. Nagel, T. Krink, *Chem. Ber.* **1995**, *128*, 309−316. − [1c] H. Yang, M. Alvarez, N. Lugan, R. Mathieu, *J. Chem. Soc., Chem. Commun.* **1995**, 1721−1722. − [1d] U. Nagel, T. Krink, *Angew. Chem.* **1993**, *105*, 1099−1101; *Angew. Chem. Int. Ed. Engl.* **1993**, *32*, 1052−1054. − [1e] U. Nagel, T. Krink, *Chem. Ber.* **1993**, *126*, 1091−1100. − [1f] K. Burgess, M. J. Ohlmeyer, K. H. Whitmire, *Organometallics* **1992**, *11*, 3588−3600. − [1g] C. R. Johnson, T. Imamoto, *J. Org. Chem.* **1987**, *52*, 2170−2174. − [1h] L. Horner,

H. Siegel, H. Büthe, *Angew. Chem.* 1968, *80*, 1034; *Angew. Chem. Int. Ed. Engl.* **1968**, *7*, 942.

[2] Recent publications: [2a] U. Nettekoven, M. Widhalm, P. C. J. Kamer, P. W. N. M. van Leeuwen, *Tetrahedron: Asymmetry* **1997**, *8*, 3185−3188. − [2b] U. Nagel, H. G. Nedden, *Chem. Ber.* **1997**, *130*, 989−1006. − [2c] J.-F. Marcoux, S. Wagaw, S. L. Buchwald, *J. Org. Chem.* **1997**, *62*, 1568−1569. − [2d] H. Yang, M. Alvarez-Gressier, N. Lugan, R. Mathieu, *Organometallics* **1997**, *16*, 1401−1409. − [2e] Y. Uozumi, K. Kitayama, T. Hayashi, K. Yanagi, E. Fukuyo, *Bull. Chem. Soc. Jpn.* **1995**, *68*, 713−722. − [2f] T. Hayashi, H. Iwamura, M. Naito, Y. Matsumoto, Y. Uozumi, *J. Am. Chem. Soc.* **1994**, *116*, 775−776. − [2g] T. Hayashi, H. Iwamura, Y. Uozumi, Y. Matsumoto, F. Ozawa, *Synthesis* **1994**, 526−532.

[3] [3a] W. S. Knowles, *Acc. Chem. Res.* **1983**, *16*, 106−112. − [3b] R. A. Sheldon, *Chirotechnology*, Marcel Dekker, New York, **1993**, pp. 271, 273.

[4] [4a] J. C. Jeffrey, T. B. Rauchfuss, *Inorg. Chem.* **1979**, *18*, 2658−2666. − [4b] A. Bader, E. Lindner, *Coord. Chem. Rev.* **1991**, *108*, 27−110.

[5] E. Lindner, S. Pautz, M. Haustein, *Coord. Chem. Rev.* **1996**, *155*, 145−162.

[6] [6a] J. A. Ramsden, T. D. W. Claridge, J. M. Brown, *J. Chem. Soc., Chem. Commun.* **1995**, 2469−2471. − [6b] A. M. Allgeier, E. T. Singewald, C. A. Mirkin, C. L. Stern, *Organometallics* **1994**, *13*, 2928−2930. − [6c] B. McCulloch, J. Halpern, M. R. Thompson, C. R. Landis, *Organometallics* **1990**, *9*, 1392−1395.

[7] Recently, Imamoto advocated the idea that the cooperative effect of the methoxy group in the (DIPAMP)Rh catalyst is based on purely steric grounds: T. Imamoto, H. Tsuruta, Y. Wada, H. Masuda, K. Yamaguchi, *Tetrahedron Lett.* **1995**, *36*, 8271−8274.

[8] Review on the synthesis of chiral hydroxy phosphanes and their application in asymmetric catalysis: J. Holz, M. Quirmbach, A. Börner, *Synthesis* **1997**, 983−1006.

[9] [9a] M. Beller, J. G. E. Krauter, A. Zapf, *Angew. Chem.* **1997**, *109*, 793−795; *Angew. Chem. Int. Ed. Engl.* **1997**, *36*, 793−795. − [9b] K. V. Katti, *Curr. Sci.* **1996**, *70*, 219−225. − [9c] W. A. Herrmann, C. W. Kohlpaintner, *Angew. Chem.* **1993**, *105*, 1588−1609; *Angew. Chem. Int. Ed. Engl.* **1993**, *32*, 1524−1544.

[10] Already one hydroxy group in a chiral (diphosphane)Rh complex is sufficient to achieve in the asymmetric hydrogenation in water in the presence of amphiphiles a dramatic increase of the enantioselectivity: R. Selke, J. Holz, A. Riepe, A. Börner, *Chem. Eur. J.* **1998**, *4*, 769−771.

[11] A. Börner, A. Kless, R. Kempe, D. Heller, J. Holz, W. Baumann, *Chem. Ber.* **1995**, *128*, 767−773.

[12] D. Heller, J. Holz, S. Borns, A. Spannenberg, R. Kempe, U. Schmidt, A. Börner, *Tetrahedron: Asymmetry* **1997**, *8*, 213−222 and ref. cited therein.

[13] [13a] A. Börner, J. Ward, K. Kortus, H. B. Kagan, *Tetrahedron: Asymmetry* **1993**, *4*, 2219−2228. − [13b] The amount of methanesulfonic acid (85 ml) given in the original paper for the cleavage of the acetal is to be corrected to 85 µl.

[14] H. B. Kagan, T.-P. Dang, *J. Am. Chem. Soc.* **1972**, *94*, 6429−6433.

[15] D. Heller, S. Borns, W. Baumann, R. Selke, *Chem. Ber.* **1996**, *129*, 85−89.

[16] The results of the hydrogenation were identical for the COD and the NBD complex.

[17] General methods for X-ray structural analyses: STOE-IPDS diffractometer, graphite-monochromated Mo-K_α radiation, structure solution with direct methods (SHELXS-86: G.M. Sheldrick, *Acta Crystallogr. Sect. A* **1990**, *46*, 467), refinement against F^2 (SHELXL-93: G.M. Sheldrick, unpublished), structure representation: Schakal-92 (E. Keller, Universität Freiburg, **1992**). − [17a] Crystal data of [Rh(NBD)(**1-OH**)]BF_4: 0.3 × 0.2 × 0.1 mm, orange-red prism, space group $P2_12_12_1$, orthorhombic, a = 9.783(2), b = 17.870(3), c = 21.334(3) A, V = 3730(1) A^3, Z = 4, $\rho_{calcd.}$ = 1.381 g cm^{-3}, 11214 collected, 5864 unique reflections, observed 3658 [$I = 2\sigma(I)$], $R1$ = 0.054, wR^2 (all data) = 0.143, 397 parameters. − [17b] Crystal data of [Rh(COD)(**1-OMe**)]BF_4: 0.4 × 0.3 × 0.3 mm, orange prism, space group $P2_1$, monoclinic, a = 9.240(2), b = 13.878(3), c = 15.159(4) A, β = 94.74(1)°, V = 1937.2(8) A^3, Z = 2, $\rho_{calcd.}$ = 1.345 g cm^{-3}, 5862 collected, 5862 unique reflections, observed 5005 [$I = 2\sigma(I)$], $R1$ = 0.052, wR^2 (all data) = 0.149, 401 parameters. − Crystallographic data (excluding structure factors) for the structures reported have been deposited with the Cambridge Crystallographic Centre as supplementary publication no. CCDC-100869. Copies of the data can be obtained free of charge on application to CCDC, 12 Union Road, Cambridge CB2 1EZ (Fax: int. code + 44-1223/336-033; E-mail: deposit@ccdc.cam.ac.uk).

[18] In the related (monohydroxy diphosphane)$RhBF_4$ complex the noncoordinating hydroxy group was characterized in the solid-state IR by a band at 3511 cm^{-1}[11]. Therefore, we tentatively attribute the band observed at the longer wavelength to the Rh-coordinated hydroxy group.

[19] A. Börner, A. Kless, J. Holz, W. Baumann, A. Tillack, R. Kadyrov, *J. Organomet. Chem.* **1995**, *490*, 213−219.

[20] [20a] K. Tamao, K. Nakamura, S. Yamaguchi, M. Shiro, S. Saito, *Chem. Lett.* **1996**, 1007−1008. − [20b] K. Tamao, K. Nakamura, H. Ishii, S. Yamaguchi, M. Shiro, *J. Am. Chem. Soc.* **1996**, *118*, 12469−12470.

[21] The distance between the oxygen and the rhodium atom is larger than 3.5 A.

[22] In the related (DIOP)Rh complex[14] the stablization of the seven-membered chelate is provided by the rigid 1,3-dioxolane ring. Simultaneously, due to this construction both oxygen atoms are not available for the interaction with the metal center.

[23] In case of the HO-bearing complex attractive interactions between hydroxy and carboxylic group of the substrate may contribute to the improved stereoselection, however, up to now all attempts to obtain spectroscopical evidence for these interactions in methanol failed.

[24] Due to the change from Rh^I to Rh^{III} during the catalytic cycle[6a] electrostatic interactions may become more dominant at certain steps.

[25] J. Ward, A. Börner, H. B. Kagan, *Tetrahedron: Asymmetry* **1992**, *3*, 849−852.

[98079]

Aminoindanes in Oxygen Transfer Reactions, 2[◇]

Copper Complexes as Functional Models for Dopamine β-Hydroxylase − Stereospecific Oxygen Atom Transfer

Ingrid Blain[a], Pascale Bruno[a], Michel Giorgi[a], Elisabeth Lojou[b], Doris Lexa[b], and Marius Réglier*[a]

Chimie, Biologie et Radicaux Libres, UMR-CNRS 6517[a],
Universités d'Aix-Marseille 1 et 3, Faculté des Sciences et Techniques de Saint Jérôme,
case 432, av. Escadrille Normandie-Niemen, F-13397 Marseille Cedex 20, France
Fax: (internat.) +33 (0)4/ 91 98 32 08
E-mail: marius.reglier@lbs.u-3mrs.fr

Laboratoire de Bioénergétique et d'Ingéniérie des Protéines, UPR CNRS 9036[b],
31, chemin de Joseph Aiguier, F-13009 Marseille, France

Received March 26, 1998

Keywords: Metalloenzymes / Copper / Copper-containing monooxygenase / Dopamine β-hydroxylase / Copper–oxygen radical species / RPY2 ligand / Oxygen atomtransfer

The stereochemistry of oxygen atom transfer mediated by copper–oxygen species has been studied through a substrate binding ligand approach. Copper(II) [(IndPY2)Cu]$(CF_3SO_3)_2$ (**2a**) and copper(I) [(IndPY2)Cu]PF_6 (**5a**) complexes were prepared and exposed to O_2 in media of benzoin/NEt_3/CH_2Cl_2 and CH_2Cl_2, respectively. In both cases, highly regio- and stereoselective oxygen atom transfer to the benzylicC–H bond of the indane ligand occurred. Using deuterium-labelled copper complexes **2b** and **5b**, we found that, in both cases, the oxygen atom transfer occurs with retention of configuration. The high deuterium kinetic isotope effects (7.6 and 11, respectively), determined by ^{13}C-NMR spectroscopy, strongly suggest the intermediacy of two different copper–oxygen reactive species.

Introduction

The mechanism of dioxygen activation by copper-containing monooxygenases such as dopamine β-hydroxylase (DBH)[1], peptidylglycine α-hydroxylating monooxygenase (PHM)[2], and particulate methane monooxygenase (pMMO)[3] is of current interest.[4] Given that these enzymatic processes involve the formation of highly reactive copper/oxygen radical species, which are responsible for hydrogen atom abstraction from the substrate, the Cu/O_2 chemistry has been the subject of recent investigations.[5] From these studies, it has become apparent that copper(I) complexes derived from tridentate ligands {RPY2[5a][6], $HB(3,5\text{-}i\text{Pr}_2\text{pz})_3$[5b][7], $P(2,4\text{-}i\text{Pr}_2\text{im})_3$[8], and $i\text{Pr}_3$tacn[9]} lead to side-on $[L_2Cu_2(\mu\text{-}\eta^2\text{:}\eta^2\text{-}O_2)]^{2+}$ species upon reaction with O_2. In some cases, these side-on peroxo species are capable of inserting an oxygen atom into a C−H bond of the ligand.[10] In earlier papers, we described the substrate binding ligand approach in the chemical modelling of the copper-containing monooxygenase active site.[11] This approach involves the study of copper complexes derived from RPY2-type ligands in which a "substrate" is covalently bound to the tertiary amino group of the ligand such that an intramolecular oxygen atom transfer from copper to the ligand is favoured. Using such complexes, both ourselves[11b] and Itho's group[12] have described hydroxylation at the β-position of the tertiary amino group (Scheme 1). Herein, we describe the study of new RPY2 ligands in which we chose to attach a 2-aminoindane group as the "substrate". This substituent possesses two stereogenic centres in benzylic positions, each bearing two hydrogen atoms, and thus the stereochemistry of aminoindanols obtained after hydroxylation can be regarded as indicating the stereoselectivity of the oxygen atom transfer.

Scheme 1. Substrate binding ligand approach

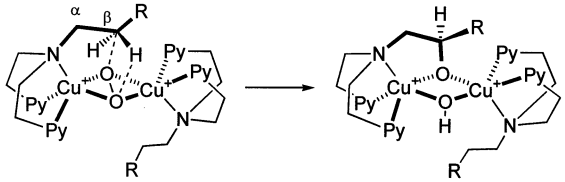

AmidPY2; R = —$CONHCH_2CH_2Ph$ [11b]
PhenPY2; R = —Ph [11a, 12]

Results and Discussion

Syntheses

Ligands **1a** and **1b** were obtained by Michael-type addition of 2-aminoindane and *cis*-1-deutero-2-aminoin-

[◇] For Part 1, see ref.[21].

 © WILEY-VCH Verlag GmbH, D-69451 Weinheim, 1998 1434−1948/98/0909−1297 $ 17.50+.50/0

dane[13], respectively, to freshly distilled vinylpyridine in a MeOH/AcOH mixture.[10a] The corresponding copper(II) complexes **2a** and **2b** were quantitatively prepared by reaction of **1a** and **1b**, respectively, with $Cu(CF_3SO_3)_2$ in MeOH. Crystallization of $[(IndPY2)Cu](CF_3SO_3)_2$ (**2a**) from CH_2Cl_2/Et_2O gave blue crystals suitable for X-ray analysis (Table 1, Figure 1).

Figure 1. Perspective view of copper(II) complex **2a** displaying the numbering scheme and selected bond distances and angles[a]

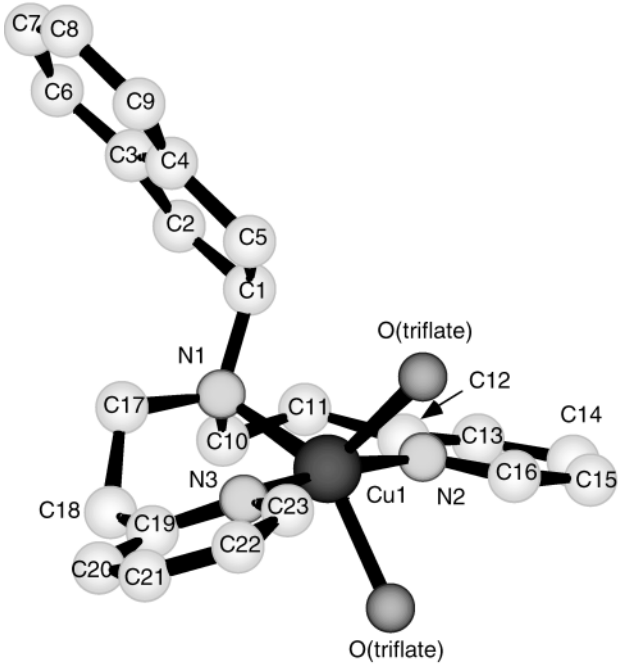

[a] Bond lengths in Å: Cu1−O2 2.108(7), Cu1−O4 2.210(7), Cu1−N1 2.019(7), Cu1−N2 2.042(6), Cu1−N3 1.977(8). Bond angles in°: O2−Cu1−O4 97.5(3), O2−Cu1−N1 148.4(3), O2−Cu1−N2 86.3(3), O2−Cu1−N3 85.0(3), O4−Cu1−N1 114.0(3), O4−Cu1−N2 88.7(3), O4−Cu1−N3 91.5(3), N1−Cu1−N2 92.1(3), N1−Cu1−N3 95.9(3), N2−Cu1−N3 171.2(3). Numbers in parentheses denote the estimated standard deviation in the least significant digits.

Reactions with Dioxygen

When the copper(II) complex **2a** was treated with 2 equiv. of benzoin/NEt_3 in CH_2Cl_2 at 25°C under Ar[14], reduction to a copper(I) complex occurred in less than one hour. This was clearly demonstrated by the complete disappearance of the *d-d* absorption at 671 nm in the electronic spectrum, which is characteristic for copper(II) complexes, and the silent EPR spectrum of the reaction mixture obtained after 40 min. Upon exposure to O_2 atmosphere, a new copper(II) complex **3a** was obtained in quantitative yield. Demetallation with 35% aqueous ammonia and analysis of the organic products indicated that complete conversion to the *cis*-2-amino-1-indanol derivative (**4a**) had occurred (Scheme 2). The stereochemistry of **4a** was assigned by comparison of its spectral data with those of an authentic sample prepared by Michael-type addition of *cis*-2-amino-1-indanol[15] to vinylpyridine, and was confirmed by X-ray analysis of the green crystals of complex **3a** obtained after recrystallization from CH_2Cl_2/MeOH (Table 1, Figure 2).

Scheme 2. Reactions with O_2 involving copper complexes **2a** and **5a**

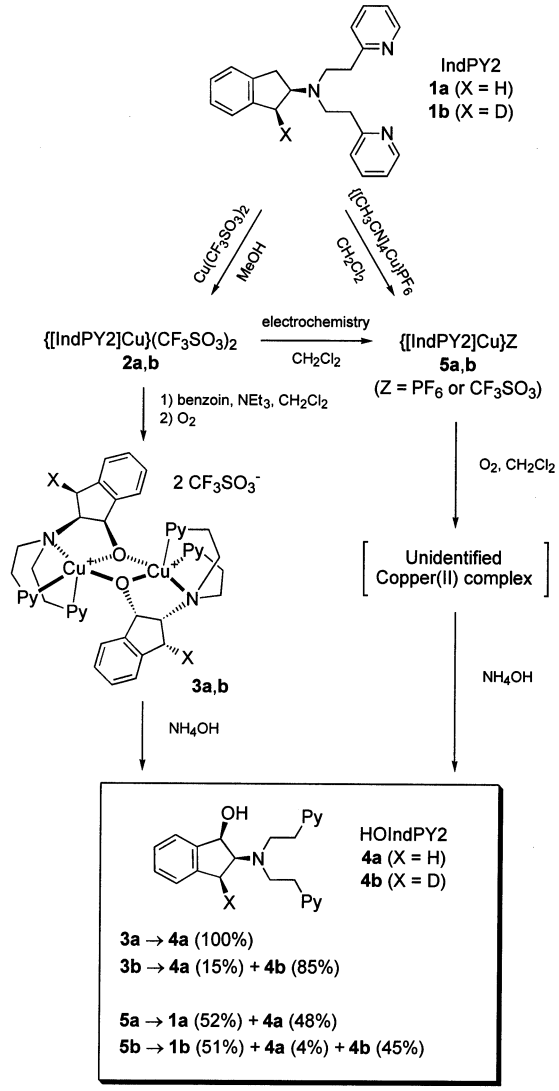

Since the first step in this reaction sequence is reduction to a copper(I) complex, we examined the reaction of the copper(I) complex [(IndPY2)Cu]Z (**5a**; Z = PF_6 or CF_3SO_3) with O_2 in CH_2Cl_2. Complex **5a** was either prepared in situ by reaction of ligand **1a** with $[(CH_3CN)_4Cu]PF_6$ in CH_2Cl_2, or by electrolysis of the copper(II) complex **2a**. The voltammetric behaviour of **2a** is depicted in Figure 3, which shows a single quasi-reversible process characteristic of the Cu^{II}/Cu^{I} transition. Upon electrolysis of **2a** under a constant potential of 0 V vs. SCE, the solution turned from blue to pale-yellow after an equivalent charge of 1 electron had been passed. As expected for a reversible electron transfer, the cyclic voltammetry (CV) curve relating to the Cu^{II}/Cu^{I} couple had not changed.

When copper(I) complex **5a** (Z = PF_6 or CF_3SO_3) was placed under an O_2 atmosphere, the pale-yellow solution rapidly turned green. A new copper(II) complex was quantitatively obtained. Demetallation with 35% aqueous am-

Figure 2. Perspective view of copper(II) complex **3a** displaying the numbering scheme and selected bond distances and angles[a]

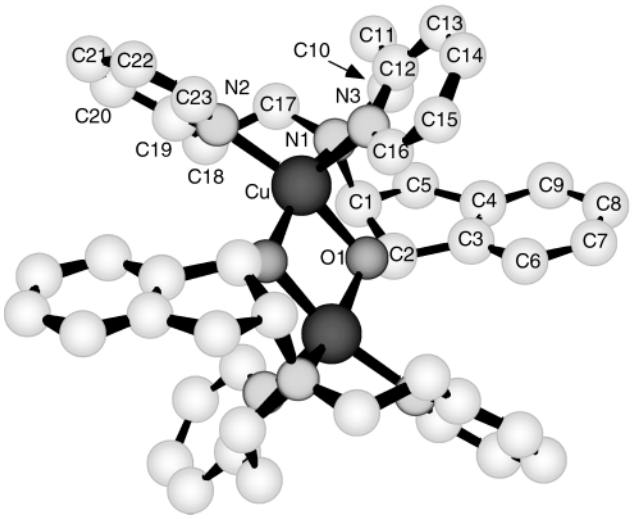

[a] Bond lengths in Å: Cu−O1 1.927(5), Cu−N1 2.057(7), Cu−N2 2.208(7), Cu−N3 1.984(7). Bond angles in°: O1−Cu−N1 85.7(2), O1−Cu−N2 96.5(2), O1−Cu−N3 165.0(3), N1−Cu−N2 99.0(2), N1−Cu−N3 94.5(3), N2−Cu−N3 98.3(3). Numbers in parentheses denote the estimated standard deviation in the least significant digits.

monia and analysis of the organic products revealed that 52% of unchanged ligand **1a** had been recovered, besides 48% of the *cis*-2-amino-1-indanol derivative **4a**. The reaction of **5a** (Z = CF_3SO_3) with O_2 was followed by CV. As can be seen in Figure 3, consumption of **5a** by O_2 progressively gives rise to a double-wave electrochemical signal. This result, as well as the smaller value of the peak currents, is consistent with either: (i) the formation of a dimeric complex with two non-equivalent copper(II) ions such as **A** (Scheme 5), or (ii) the formation of a mixture of symmetrical dimeric complexes such as **3a** and $[(IndPY2)_2Cu_2(\mu\text{-}OH)_2]^{2+}$ **B**. This second hypothesis is supported by the fact that two types of crystals (green and blue) are obtained after crystallization of the copper(II) complex from CH_2Cl_2/MeOH. Unfortunately, these crystals were not suitable for carrying out an X-ray structure analysis.

Stereoselectivity of Oxygen Atom Insertion

The aforementioned hydroxylations are highly stereoselective, and we propose, as is generally accepted, a process involving oxygen atom insertion into the benzylic C−H bond. The question then arises as to whether this insertion occurs with retention or inversion of configuration. Indeed, the hydroxylation can be envisaged as being either the result of a concerted mechanism in which oxygen atom insertion occurs at a *cis* C−H bond, or the result of a two-step process in which C−H bond scission and formation of the C−O bond occur at the same face (*cis* with respect to the amino group). In both cases, the product would be formed with retention of configuration at the benzylic carbon atom (Scheme 3). Another possibility is that the hydroxylation takes place via a two-step process involving *trans* C−H bond scission and *cis* formation of the C−O bond. If this

Figure 3. Cyclic voltammograms of **2a** after electrolysis at 0 V vs. SCE and reaction with O_2 in CH_2Cl_2, $nBu_4NCF_3SO_3$ 0.1 M at 50 mV s^{-1}: (*solid line*) **2a** or **5a**; (*dotted line*) **5a** after 1 min. O_2 bubbling and (*bold line*) **5a** after 45 min. O_2 bubbling (steady-state CV)

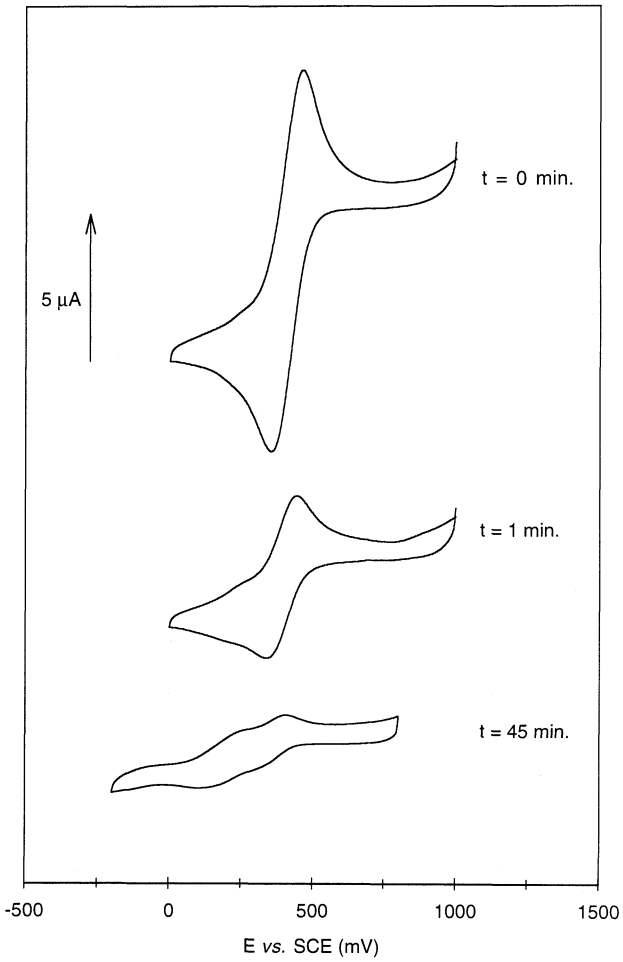

were the case, we should observe inversion of configuration. In order to decide in favour of one of these mechanisms, we studied the reaction of deuterium-labelled copper complexes **2b** and **5b**. If the stereochemical course were to proceed with inversion of configuration, we would expect the formation of a mixture of deuterated compounds **4b** and **4c**. However, if the configuration was retained, we would expect the formation of a mixture of non-deuterated **4a** and its deuterated analogue **4b**.

Under standard conditions (benzoin, NEt_3, CH_2Cl_2, 25°C), the copper(II) complex {(*cis*-[D]-IndPY2)Cu}$(CF_3SO_3)_2$ **2b** (D content of 99 ± 0.1% determined by FAB-MS) was quantitatively transformed into complex **3b** (D content of 87.57 ± 0.16%). Demetallation with 35% aqueous ammonia gave the deuterated hydroxy ligand **4b** as the main product of the reaction. This is clearly evident from the ^{1}H-NMR spectrum, which shows a doublet of doublets at δ = 3.41 ($^3J_{2\text{-H,3-H}cis}$ = 7 Hz and $^3J_{2\text{-H,1-H}cis}$ = 5 Hz) instead of the doublet of doublet of doublets ($^3J_{2\text{-H,3-H}trans}$ = 9 Hz, $^3J_{2\text{-H,3-H}cis}$ = 7 Hz and $^3J_{2\text{-H,1-H}cis}$ = 5 Hz} observed for the non-deuterated hydroxy ligand **4a**. The ^{13}C-NMR spectrum reveals the

Scheme 3

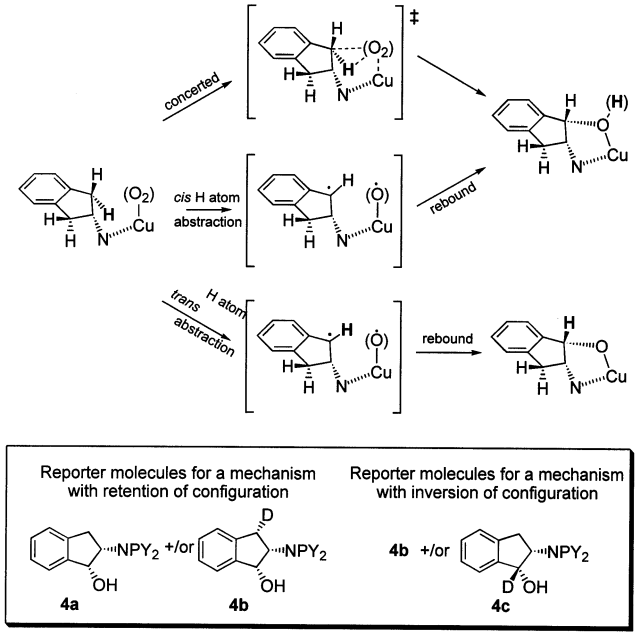

presence of a small amount of **4a** (singlet at δ = 34.14, C-3; Figure 4a) in addition to **4b** (triplet at δ = 33.72, $^1J_{13C,D}$ = 21 Hz, C-3; Figure 4b), but no signals corresponding to a hypothetical deuterated hydroxy ligand **4c**, which might have arisen from a mechanism involving inversion of configuration, were observed. Moreover, the ^{13}C-NMR spectrum shows a singlet at δ = 66.64 attributable to C-2 of compound **4b**, in addition to the corresponding signal of **4a** (δ = 66.74). Integration of these signals after a DEPTCH sequence led to a **4b**/**4a** ratio of 7.6 ± 0.5. This ratio was confirmed by mass spectrometry analysis (FAB-MS) of complex **3b**, for which an 87.57 ± 0.16% deuterium content was found [**4b**/**4a** = 87.57/(100 − 87.57) = 7.04 ± 0.02]. Using the same methodology under standard conditions (O_2, CH_2Cl_2, 25°C), the deutero-copper(I) complex **5b** was quantitatively transformed into a copper(II) complex, which, after demetallation with 35% aqueous ammonia, also gave a mixture of **4b** and **4a** (**4b**/**4a** = 11.0 ± 0.7).

In both reactions, ratios of non-deuterated **4a** to the deuterated compound **4b** are very large (7.6 and 11). These findings can be explained if we assume that the copper/oxygen species responsible for the observed hydroxylations exist as two conformers, **C1** and **C2**, which are in equilibrium (Scheme 4). It is clear that conformer **C2**, which exposes a deuterium atom to the copper−oxygen core, must react with a lower rate than conformer **C1**, which exposes a hydrogen atom. Since conformers **C1** and **C2** are in rapid equilibrium, the deuterium kinetic isotope effect (DKIE) expressed by the k_H/k_D ratio is directly related to the **4b**/**4a** ratio.[16] The large DKIEs (7.6 vs. 11) indicate that the hydroxylations occur with retention of configuration in a process in which the benzylic C−H bond is broken in the rate-determining step.[17]

Figure 4. Aliphatic region of ^{13}C-NMR spectra of aminoindanols **4a**, **b**: (*a*) reaction of **2a** with benzoin/NEt_3/O_2 or **5a** with O_2 in CH_2Cl_2; (*b*) reaction of **2b** with benzoin/NEt_3/O_2 or **5b** with O_2 in CH_2Cl_2

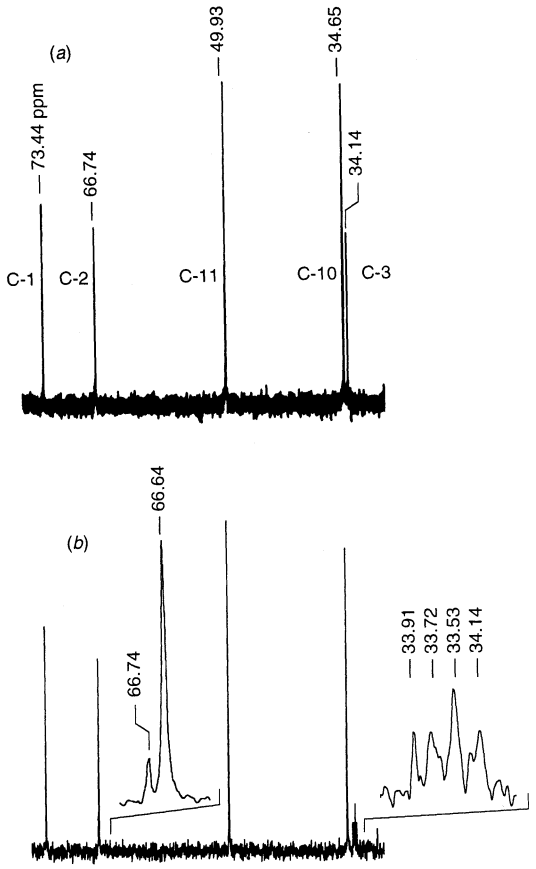

Scheme 4.

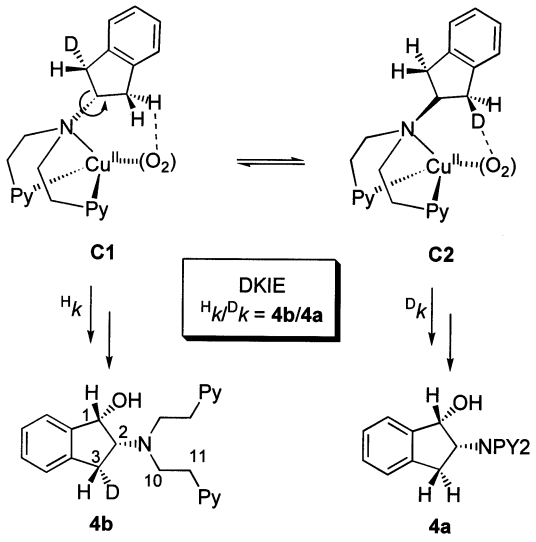

Dioxygen Adducts and Mechanistic Hypothesis

Finally, we turn to the question of the dioxygen adduct that may be involved in these hydroxylations. At present, for the reaction of the copper(I) complex **5a** with O_2 in CH_2Cl_2, it is difficult to obtain structural information con-

cerning copper/oxygen species, because, even at −80°C, such species are too reactive to be amenable to structural analysis, e.g. by UV/vis or X-ray spectroscopy. However, since copper(I) complexes derived from tridentate ligands are known to lead to $[L_2Cu_2(\mu\text{-}\eta^2\text{:}\eta^2\text{-}O_2)]^{2+}$ species by reaction with O_2[5a][6], we can reasonably expect the formation of this type of intermediate (**C**) upon reaction of **5a** with O_2 (Scheme 5). Kitajima has observed that the $\{[HB(3,5\text{-}Me_2pz)_3]_2Cu_2(\mu\text{-}\eta^2\text{:}\eta^2\text{-}O_2)\}$ complex is capable of oxidising cyclohexene to 2-cyclohexen-1-ol and 2-cyclohexen-1-one.[18] To account for this finding, a mechanism was proposed involving: (i) formation of the radical $\{[HB(3,5\text{-}Me_2pz)_3]Cu-O^{\bullet}\}$ by homolysis of the peroxo bond; (ii) abstraction of a hydrogen atom from cyclohexene, and (iii) subsequent reaction of these intermediates with O_2 to generate the observed products. Given that we did not observe any formation of an indanone derivative, and that the oxygen atom transfer proceeds with high DKIEs and high *cis* stereoselectivity, we can rule out the possibility that the hydroxylated ligand is formed by a mechanism akin to that postulated for Kitajima's cyclohexene oxidation. More recently, Tolman has reported that $[Cu^{II}_2(\mu\text{-}\eta^2\text{:}\eta^2\text{-}O_2)]^{2+}$ species exist in equilibrium with a bis(μ-oxo)dicopper species with a formal $[Cu^{III}_2(\mu\text{-}O)_2]^{2+}$ oxidation state, and it was demonstrated that these species behave like electrophilic radicals.[19] Considering these findings and the fact that oxidation of **5a** by O_2 results in stereospecific *cis*-hydroxylation in yields not exceeding 50%, Scheme 5 illustrates possible pathways whereby hydroxylation can occur via the $\{[IndPY2]_2Cu^{III}_2(\mu\text{-}O)_2\}^{2+}$ species (**D**): (i) by a concerted mechanism (pathway *a*), or (ii) by abstraction of a *cis* benzylic hydrogen atom forming a benzylic radical and a copper/oxygen radical species, which recombine at the same face to give the observed copper(II) complex in an overall mechanism with retention of configuration (pathway *b*).

Concerning the reaction of **2a** with benzoin/NEt_3, we have shown that under Ar the first step is the reduction to the cuprous state. Upon exposure to O_2, the next step could then be the formation of the peroxo complex **C** and/or its subsequent species **D**. As already described, this reaction sequence could lead to the observed compounds. As an explanation for the quantitative yield of oxidised complex **3a**, we can assume that a 1:1 mixture of complexes **3a** and **B** is obtained, and that only **B** is reduced to the copper(I) complex **2a** by excess benzoin/NEt_3 and is thus able to participate in the hydroxylation reaction once more (Scheme 6). We can effectively demonstrate that complex **3a** does not react with benzoin/NEt_3, even after several hours, but the higher DKIE observed for the reaction of **2a**/O_2 compared to that of **5a**/benzoin/NEt_3/O_2 (11 vs. 7.6) suggests the intermediacy of another reactive species, for which several structures can be proposed. As previously assumed for the active species in pMMO[3], a μ-oxo mixed-valence Cu^{II}/Cu^{III} species **E** derived from a one-electron reduction of species **C** or **D** could be responsible for the present ligand hydroxylation. However, as it is known that the reaction of copper salts with O_2 in the presence of a reducing agent leads to hydroperoxo species[20], another possibility could be the formation of the hydroperoxo species **F** or its subsequent (one-electron reduction) copper radical species **G**. Structural studies of the copper/oxygen species involved in these hydroxylations aimed at elucidating details of the reaction mechanism are currently in progress.

Scheme 5. Proposed mechanism for the ligand hydroxylation

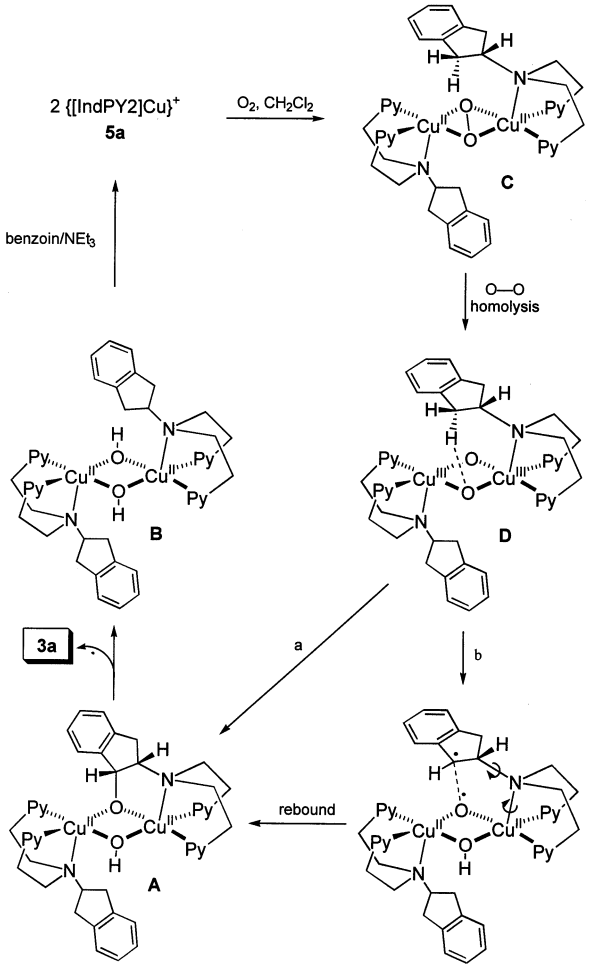

Scheme 6. Possible copper/oxygen intermediates in the reaction of copper(II) complex **2a** with O_2/benzoin/NEt_3

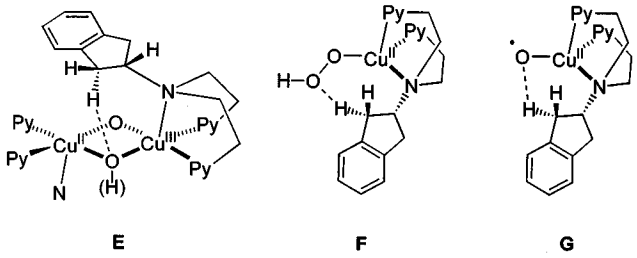

Conclusion

Once again, we have shown that a conformationally-restricted substrate approach can provide valuable information about the mechanism of oxygen atom transfer from copper to a ligand. On the basis of deuterium-labelling experiments, we have demonstrated that oxygen atom insertion into a C−H bond of the ligand occurs at a benzylic

position with retention of configuration. This is an important approach, which is of interest because of the possibility of performing parallel enzymatic studies. For example, we have recently found that the DBH-catalysed hydroxylation of 2-aminoindane produces exclusively *trans*-(1*S*,2*S*)-2-amino-1-indanol with 93% *ee*. Studies with stereospecifically deuterium-labelled 2-aminoindanes have further shown that the formation of (1*S*)-aminoindanol is the result of stereospecific *pro*-(*S*) hydrogen abstraction followed by oxygen binding, with overall retention of configuration.[21] Nevertheless, for modelling reactivity of the order of that of DBH, we have to admit that our approach needs to be improved and that we have to find a copper complex with catalytic properties towards an exogenous 2-aminoindane (oxygen atom transfer that does not involve the ligand). To achieve this goal, the problem of 2-aminoindane association in the copper coordination sphere still has to be solved.

This research was supported by the *CNRS* and the *French Ministry of Universities*. The authors are grateful to Dr. *A. Heumann* for a number of enlightening discussions.

Experimental Section

General: Solvents were freshly distilled under Ar (MeOH/Mg, Et_2O/Na-benzophenone ketyl, CH_3CN/CaH_2, and CH_2Cl_2/P_2O_5). Deoxygenation of solvents and solutions was carried out by 3 vacuum/purge cycles. Preparation and handling of air-sensitive compounds was carried out by using standard Schlenk techniques. Commercial starting materials were used without further purification, except for 2-vinylpyridine, which was distilled prior to use; *cis*-1-deutero-2-aminoindane was obtained by $LiAlD_4$ reduction of *trans*-2-azido-1-bromoindane.[13] – $^1H\{^{13}C\}$-NMR spectra were recorded at 25°C on a Bruker AC-400 spectrometer. Chemical shifts are reported in ppm as δ values downfield from an internal standard of TMS. – IR spectra were recorded on a Nicolet MX 5 spectrometer. – Elemental analyses were obtained with a CHN Technicon microanalyser. – FAB-MS were obtained by the LSIMS ionization technique in thioglycerol (TG) or nitrobenzyl alcohol (NB) lattices.

Ligands **1a** *and* **1b**: To absolute MeOH (8 ml) were added 2-vinylpyridine (3.785 g, 36 mmol), 2-aminoindane (798 mg, 6 mmol) and acetic acid (900 mg, 15 mmol). After refluxing for 5 days, the MeOH was evaporated and 15% NaOH (10 ml) was added. The product was extracted with CH_2Cl_2 (3 × 20 ml) and the combined organic layers were dried over Na_2SO_4. Evaporation of the CH_2Cl_2 under reduced pressure (18 mmHg) left the crude product. Flash chromatography (SiO_2, CH_2Cl_2/MeOH, 90:10) afforded ligand **1a** (**1b**). – **1a**: Yield: 800 mg (2.3 mmol, 40%). – ^1H NMR ($CDCl_3$): δ = 8.51 (ddd, *J* = 5, 2 and 1 Hz, 2 CH-pyr), 7.55 (td, *J* = 8 and 2 Hz, 2 CH-pyr), 7.15–7.07 (m, 8 CH-aryl), 3.74 (qt, *J* = 9 Hz, 2 2-H), 3.07–2.95 (m, 10 H), 2.83 (dd, *J* = 15 and 9 Hz, 2 1-H_{cis}). – ^{13}C NMR ($CDCl_3$): δ = 160.65 (2 C-pyr), 149.25 (2 CH-pyr), 141.75 (2 C-ind), 136.15 (2 CH-pyr), 126.26 (2 CH-ind), 124.42 (2 CH-pyr), 123.36 (2 CH-pyr), 121.07 (2 CH-pyr), 63.25 (C-2), 51.50 (2 C-10), 36.93 (2 C-11), 36.11 (2 C-1). – IR (neat): $\tilde{\nu}$ = 1595 cm^{-1} (C=N), $\tilde{\nu}$ = 1570, 1480, 1440 cm^{-1} (C=C). – **1b**: Yield: 930 mg (2.7 mmol, 45%). – ^1H NMR ($CDCl_3$): δ = 8.50 (ddd, *J* = 5, 2 and 1 Hz, 2 H), 7.53 (td, *J* = 8 and 2 Hz, 2 H), 7.15–7.05 (m, 8 H), 3.74 (q, *J* = 9 Hz, 1 H), 3.07–2.96 (m, 10 H), 2.85 (dd, *J* = 15 and 9 Hz, 1 H). – ^{13}C NMR ($CDCl_3$): δ = 160.70 (2 C-pyr), 149.30 (2 CH-pyr), 141.84 (2 CH-pyr), 141.75 (2 C-ind), 136.19 (2 CH-pyr), 126.32 (CH-ind), 126.35 (CH-ind), 124.49 (CH-ind), 124.46 (CH-ind), 123.41 (2 CH-pyr), 121.11 (2 CH-pyr), 63.21 (C-2), 51.55 (2 C-10), 36.96 (2 C-11), 36.62 (t, $^1J_{13\,C,D}$ = 21 Hz, C-1), 36.17 (C-3).

Complexes **2a** *and* **2b**: To a solution of $Cu(CF_3SO_3)_2$ (362 mg, 1 mmol) in MeOH (15 ml), a solution of **1a** (**1b**) (344 mg, 1 mmol) in MeOH (15 ml) was added dropwise and the mixture was stirred for 30 min. The MeOH was then evaporated in vacuo and Et_2O (50 ml) was added. The resulting precipitate was filtered off, washed with further Et_2O, and dried in vacuo to give complex **2a** (**2b**) as a blue solid. – **2a**: Yield: 634 mg (0.9 mmol, 90%). Recrystallization from CH_2Cl_2/Et_2O gave blue crystals suitable for X-ray analysis. – $C_{25}H_{25}CuF_6N_3O_6S_2$ (705.15): calcd. C 42.58, H 3.57, N 5.96; found C 42.98, H 3.52, N 6.05. – MS (FAB); *m*/*z* (%): 344 (100) [IndPY2 + H]$^+$, 345 (27) [*p* + 1], 343 (2.6) [*p* – 1]. – **2b**: Yield: 635 mg (0.9 mmol, 90%). – MS (FAB); *m*/*z* (%): 345 (100) [*d*-IndPY2 + H]$^+$, 346 (26.54) [*p* + 1], 344 (3.44) [*p* – 1]; deuterium content 99 ± 0.1%.

Complexes **3a** *and* **3b**: To a solution of **2a** (**2b**) (70 mg, 0.1 mmol) in degassed CH_2Cl_2 (6 ml) were added benzoin (42 mg, 0.2 mmol) and NEt_3 (20 mg, 0.2 mmol). This mixture was stirred under Ar for 2 h and then exposed to an O_2 atmosphere for 24 h. The CH_2Cl_2 was subsequently evaporated in vacuo and Et_2O (20 ml) was added. The precipitate thus obtained was filtered off, washed with Et_2O, and dried in vacuo to give complex **3a** (**3b**). – **3a**: Yield: 49 mg (86 μmol, 86%). Recrystallization from CH_2Cl_2/MeOH gave green crystals suitable for X-ray analysis. – $C_{24}H_{24}CuF_3N_3O_4S$ (571.08): calcd. C 50.48, H 4.24, N 7.36; found C 50.55, H 4.27, N 7.56. – MS (FAB); *m*/*z* (%): 360 (100) [IndOHPY2 + H]$^+$, 361 (27.7) [*p* + 1], 359 (1.7) [*p* – 1]. – **3b**: Yield: 48 mg (85 μmol, 85%). – MS (FAB); *m*/*z* (%): 361 (100) [*d*-IndOHPY2 + H]$^+$, 362 (29.7) [*p* + 1], 360 (14.0) [*p* – 1]; deuterium content 87.57 ± 0.16%.

In situ Preparation and Oxidation of Complexes **5a** *and* **5b**: To a solution of $[CH_3CN]_4CuPF_6$ (37.3 mg, 0.1 mmol) in degassed CH_2Cl_2 (50 ml), a solution of **1a** (**1b**) (34.4 mg, 0.1 mmol) in CH_2Cl_2 (50 ml) was added dropwise. The mixture was stirred under Ar for 1 h, and then exposed to an O_2 atmosphere for 24 h. The CH_2Cl_2 was subsequently evaporated in vacuo, Et_2O (50 ml) was added, and the precipitate thus obtained was filtered off, washed with Et_2O, and dried in vacuo to give a mixture of copper(II) complexes. This mixture was redissolved in CH_2Cl_2 (20 ml), washed with 35% NH_4OH (5 ml) and brine (3 × 5 ml), and dried over Na_2SO_4. Evaporation of the CH_2Cl_2 under reduced pressure (18 mmHg) gave the crude product. Flash chromatography (SiO_2, CH_2Cl_2/MeOH, 90:10) afforded ligands **1a** (**1b**) and **4a** (**4b**). – **4a**: Yield: 17.3 mg (48 μmol, 48%). – ^1H NMR ($CDCl_3$): δ = 8.51 (ddd, *J* = 4, 2 and 1 Hz, 2 H-pyr), 7.54 (td, *J* = 8 and 2 Hz, 2 H-pyr), 7.43 (d, *J* = 6 Hz, 1 H-ind), 7.49–7.17 (m, 3 H-ind), 7.11–7.06 (m, 4 H-pyr), 4.97 (d, *J* = 5 Hz, 1-H), 3.41 (ddd, *J* = 9, 7 and 5 Hz, 2-H), 3.24–3.09 (m, 4 H), 3.07–2.95 (m, 6 H). – ^{13}C NMR ($CDCl_3$): δ = 160.05 (2 C-pyr), 149.34 (2 CH-pyr), 143.28 (C-ind), 141.77 (C-ind), 136.50 (2 CH-pyr), 128.70 (CH-ind), 126.95 (CH-ind), 125.52 (CH-ind), 124.81 (CH-ind), 123.57 (2 CH-pyr), 121.39 (2 CH-pyr), 73.44 (C-1), 66.74 (C-2), 49.93 (2 C-10), 34.65 (2 C-11), 34.14 (C-3). – **4b**: Yield: 17.4 mg (48 μmol, 48%). – ^1H NMR ($CDCl_3$): δ = 8.50 (d, *J* = 5 Hz, 2 H-pyr), 7.54 (td, *J* = 8 and 2 Hz, 2 H-pyr), 7.44 (d, *J* = 7 Hz, H-ind), 7.24–7.17 (m, 3 H-ind), 7.11–7.06 (m, 4 H-pyr), 4.96 (d, *J* = 5 Hz, 1-H), 3.41 (dd, *J* = 7 and 5 Hz, 2-H), 3.23–3.10 (m, 4 H), 3.05–2.94 (m, 5.28 H). – ^{13}C NMR ($CDCl_3$): δ = 160.05 (2 C-pyr), 149.26 (2 CH-pyr), 143.30 (C-ind), 141.65 (C-ind), 136.34 (2 CH-pyr), 128.56 (CH-ind), 126.84 (CH-ind), 125.40 (CH-ind), 124.72 (CH-ind),

Table 1. Crystallographic data for copper(II) complexes **2a** and **3a**

Complexes	**2a**	**3a**
Crystal data		
formula	$C_{50}H_{50}Cu_2F_{12}N_6O_{12}S_4$	$C_{24}H_{24}CuF_3N_3O_4S$
M_r	1410.30	571.08
crystal system	triclinic	orthorhombic
space group	$P\bar{1}$	*Pbca*
a [Å]	9.858(1)	13.787(3)
b [Å]	13.023(2)	15.083(3)
c [Å]	27.465(3)	22.935(4)
α [°]	98.85(23)	90.00
β [°]	94.72(29)	90.00
γ [°]	92.19(34)	90.00
V [Å^3]	3467.4	4769(3)
D_{calc} [g cm^{-3}]	1.35	1.59
Z	2	8
F(000) [e]	1432	2344
μ (Mo-K_α) [cm^{-1}]	8.13	10.60
Data collection		
T [K]	294	294
scan mode	ω−2θ	ω−2θ
scan width [°]	0.9 + 0.35 tanθ	0.8 + 0.35 tanθ
$2\theta_{max}$ [°]	48	48
measured refl.	10760	4193
unique refl.	6359	4051
refl. used for refinement	5660	1977
absorption correction	no	no
extinction correction	no	isotropic[25]
extinction coefficient	−	4.19×10^{-8}
Structure refinement		
refined parameters	775	326
H atoms	included, not refined	
R	0.075	0.06
R_w	0.104	0.073
w	$4\,F_0^2/[\sigma^2(F_0^2) + 0.0025\,F_0^4]$	$4\,F_0^2/[\sigma^2(F_0^2) + 0.0016\,F_0^4]$
$(\text{shift/e.s.d.})_{max}$	0.11	0.62
goodness of fit	2.807	2.22
$\Delta\rho_{fin}$(max./min.) [e Å^{-3}]	0.61/0.54	0.606/0.452

123.42 (2 CH-pyr), 121.25 (2 CH-pyr), 73.38 (C-1), 66.64 (C-2), 49.96 (2 C-10), 34.75 (2 C-11), 33.72 (t, $^1J_{13\,C,D}$ = 21 Hz, C-3).

X-ray Structure Analysis: Crystals of complexes **2a** and **3a** of suitable quality and size were mounted in glass capillaries and examined on an Enraf-Nonius CAD4 diffractometer [Mo-K_α radiation, λ(Mo-K_α) = 0.71073 Å]. During data collection, three standard reflections were measured periodically as a general check of crystal and instrument stability. The data reduction was performed with Begin in SDP-Plus.[22] The structures were solved by the Patterson method for **2a** and by direct methods with MULTAN80[23] for **3a**, and were refined with LSFM-Plus. The scattering factors were taken from the International Tables for X-ray Crystallography.[24]

Crystallographic data for the structure(s) reported in this paper have been deposited with the Cambridge Crystallographic Data Centre as supplementary publication no. CCDC-101037. Copies of the data can be obtained free of charge on application to The Director, CCDC, 12 Union Road, Cambridge CB2 1EZ, UK [fax: int. code +44(0)1223/ 336-033, e-mail: deposit@chemcrys.cam.ac. uk].

Electrochemical Measurements: Cyclic voltammetric (CV) experiments were carried out using an EG&G 263A potentiostat with EG&G M270 software. CV curves were obtained at a scan rate of 50 mVs^{-1}. A three-electrode system consisting of a saturated calomel reference electrode, a platinum wire auxiliary electrode, and a gold microelectrode (surface area: 7.8×10^{-3} cm^2) was used throughout. Both the reference and auxiliary electrodes were connected to the solution through porous bridges. Coulometric measurements were made using an EG&G 379 coulometer. Electrolyses were performed using a gold grid (geometric surface: 7 cm^2) under a constant potential.

[1] J. J. Villafranca, *Metal Ions in Biology* (Ed.: T. G. Spiro), John Wiley and Sons, New York, **1981**, Vol 3, pp. 263−290; L. C. Stewart, J. P. Klinman, *Ann. Rev. Biochem.* **1988**, *57*, 551−592.

[2] S. T. Pridge, A. S. Kolhenar, B. A. Eipper, R. E. Mains, L. M. Amzel, *Science* **1997**, *278*, 1300−1305.

[3] S. J. Eliot, M. Zhu, L. Tso, H.-H. T. Nguyen, J. H.-K. Yip, S. I. Chan, *J. Am. Chem. Soc.* **1997**, *119*, 9949−9955.

[4] J. P. Klinman, *Chem. Rev.* **1996**, *96*, 2541−2561; W. Kaim, J. Rall, *Angew. Chem.* **1996**, *108*, 47−64; *Angew. Chem. Int. Ed. Engl.* **1996**, *35*, 43−60.

[5] [5a] K. D. Karlin, S. Kaderli, A. D. Zuberbühler, *Acc. Chem. Res.* **1997**, *30*, 139−147. − [5b] N. Kitajima, Y. Moro-Oka, *Chem. Rev.* **1994**, *94*, 737−757.

[6] I. Sanyal, M. Mahroof-Tahir, S. Nasir, P. Ghosh, B. I. Cohen, Y. Gultneh, R. Cruse, A. Farooq, K. D. Karlin, S. Liu, J. Zubieta, *Inorg. Chem.* **1992**, *31*, 4322−4332.

[7] N. Kitajima, K. Fujisawa, Y. Moro-Oka, K. Toriumi, *J. Am. Chem. Soc.* **1989**, *111*, 8975−8976.

[8] T. N. Sorrel, W. E. Allen, P. S. White, *Inorg. Chem.* **1995**, *34*, 952−960.

[9] S. Mahapatra, J. A. Halfen, E. C. Wilkinson, L. Que Jr., W. B. Tolman, *J. Am. Chem. Soc.* **1994**, 116, 9785−9786.

[10] [10a] K. D. Karlin, J. C. Hayes, Y. Gultneh, R. W. Cruse, J. W. McKown, J. P. Hutchinson, J. Zubieta, *J. Am. Chem. Soc.* **1984**, *106*, 2121−2128. − [10b] S. Mahapatra, J. A. Halfen, E. C. Wilkinson, G. Pan, C. J. Cramer, L. Que Jr., W. B. Tolman, *J. Am. Chem. Soc.* **1995**, *117*, 8865−8866; J. A. Halfen, V. G. Young Jr., W. B. Tolman, *J. Am. Chem. Soc.* **1996**, *118*, 10920−10921. − [10c] W. E. Allen, T. N. Sorrell, *Inorg. Chem.* **1997**, *36*, 1732−1734.

[11] [11a] M. Réglier, E. Amadéi, R. Tadayoni, B. Waegell, *J. Chem. Soc., Chem. Commun.* **1989**, 447−450. − [11b] E. Amadéi, E. H. Alilou, F. Eydoux, M. Pierrot, M. Réglier, B. Waegell, *J. Chem. Soc., Chem. Commun.* **1992**, 1782−1784. − [11c] M. Réglier, E. Amadéi, E. H. Alilou, F. Eydoux, M. Pierrot, B. Waegell, *Bioinorganic Chemistry of Copper* (Eds.: K. D. Karlin, Z. Tiecklar), Chapman and Hall, **1993**, 348−362.

[12] S. Itho, T. Kondo, M. Komatsu, Y. Ohshiro, C. Li, N. Kanehisa, Y. Kai, S. Fukuzumi, *J. Am. Chem. Soc.* **1995**, *117*, 4714−4715.

[13] A. A. Mitrochkine, I. Blain, C. Bit, C. Canlet, S. Pierre, J. Courtieu, M. Réglier, *J. Org. Chem.* **1997**, *62*, 6204−6209.

[14] With 1 equivalent, only 50% of **4a** was obtained besides 50% of recovered ligand **1a**.

[15] A. Mitrochkine, F. Eydoux, M. Martres, G. Gil, A. Heumann, M. Réglier, *Tetrahedron Asymmetry* **1995**, *6*, 59−62; A. Mitrochkine, G. Gil, M. Réglier, *Tetrahedron Asymmetry* **1995**, *6*, 1535−1538.

[16] The DKIEs are calculated on the basis of an equal concentration of the two conformers **C1** and **C2** ignoring possible secondary effects (steric and electronic) which are diffucult to evaluate.

[17] J. T. Groves, *Cytochrome P450* (Ed. P. R. Ortiz de Montellano), Plenum Press, **1995**, p. 11.

[18] N. Kitajima, T. Koda, Y. Iwata, Y. Moro-Oka, *J. Am. Chem. Soc.* **1990**, *112*, 8833−8839.

[19] [19a] J. A. Halfen, S. Mahapatra, E. C. Wilkinson, S. Kaderli, V. C. Young Jr., L. Que Jr., A. D. Zuberbühler, W. B. Tolman, *Science* **1996**, *271*, 1397−1400. − [19b] S. Mahapatra, J. A. Halfen, E. C. Wilkinson, G. Pan, X. Wang, V. G. Young Jr., C. J. Cramer, L. Que Jr., W. B. Tolman, *J. Am. Chem. Soc.* **1996**, *118*, 11555−11574. − [19c] S. Mahapatra, J. A. Halfen, W. B. Tolman, *J. Am. Chem. Soc.* **1996**, *118*, 11575−11586. − [19d] C. J. Cramer, B. A. Smith, W. B. Tolman, *J. Am. Chem. Soc.* **1996**, *118*, 11283−11287.

[20] R. A. Sheldon, J. K. Kochi, *Metal-Catalyzed Oxidations of Organic Compounds*, Academic Press, **1981**.

[21] A. A. Mitrochkine, F. Eydoux, G. Gil, M. Réglier, *Eur. J. Org.*

Chem. **1998**, 1171−1176
[22] B. A. Frenz, *Enraf-Nonius SDP-Plus Structure Determination Package,* Version 3.0, Enraf-Nonius, Delft, The Netherlands, **1985**.
[23] P. Main, S. J. Fiske, S. E. Hull, L. Lessiger, G. Germain, J. P. Declercq, M. M. Woolfson, *MULTAN80, A System of Computer Programs for the Automatic Solution of Crystal Structure from X-ray Diffraction Data*, Universities of York (England) and Louvain (Belgium), **1980**.
[24] *International Tables for X-ray Crystallography* (Eds.: J. Ibers, W. C. Hamilton), Kynoch Press, Birmingham, **1974**, vol. IV (Present distributor: Kluwer Academic Publishers, Dordecht).
[25] W. H. Zachariasen, *Acta Cryst.* **1963**, *16*, 1139−1144.
[98080]

Isomerism of Amides Coordinated to Platinum – X-ray Crystal Structure of *O*-Bonded Acetamide in a Platinum(II) Complex

Renzo Cini[a], Francesco P. Intini[b], Luciana Maresca[b], Concetta Pacifico[b], and Giovanni Natile*[b]

Dipartimento di Scienze e Tecnologie Chimiche e dei Biosistemi, Universitá di Siena[a],
Pian dei Mantellini 44, I-53100 Siena, Italy

Dipartimento Farmaco-Chimica, Universitá di Bari[b],
via E. Orabona 4, I-70125 Bari, Italy
Fax: (internat.) + 39-080/5442724
E-mail: natile@farmchim.uniba.it

Received March 27, 1998

Keywords: *O*-Coordinated amides / Platinum / *O*-to-*N* Isomerization / Atropisomers

O-bonded amide complexes of platinum(II), which are stable in acetone solution and which undergo solvolysis in neat water with a rate constant as slow as $8.7 \cdot 10^{-5}$ s^{-1}, are reported. The structure of a sample compound $[Pt(Me_5dien)\{O\text{-}MeC(O)NH_2\}](CF_3SO_3)_2$ has been solved by X-ray diffraction allowing comparison with related *N*-bonded (amide)platinum complexes. Isomerization from *O*-amide to *N*-amidate species takes place instantaneously under basic conditions. Protonation of the amidate species leads to the *N*-bonded amide. *N*-bonded amides, like the *N*-bonded amidates, represent the thermodynamically preferred species due to the higher affinity of platinum for nitrogen donors. In contrast *O*-bonded amides owe their stability to their kinetic inertness, where a high pH is required for deprotonation of the NH_2 moiety, the leading step in the isomerization process. In the case of the 2-pyridone complex, the *O*-bonded form is unstable and isomerizes spontaneously to the *N*-bonded form, due to the higher acidity of the protonated pyridine-like nitrogen atom. Two rotamers are present in both the *N*-pyridone and *N*-pyridonate species. Hindered rotation stems from the steric rigidity of both rotating moieties [(Me_5dien)Pt and pyridone/pyridonate].

Introduction

Amides of carboxylic acids can be either *O*- or *N*-donor ligands[1]. In the case of *N*-coordination, they can adopt different tautomeric forms {oxo amine $[RC(O)NH_2]$ and iminol $[RC(OH)NH]$}[2].

Changes in the metal center, the R group, or the solvent system can influence the mode of coordination. For complexes of metal ions which are considered to be "hard" Lewis acids, such as $[M(NH_3)_5(amide)^{3+}$ (M = Co[3], Cr[4], Ru[5], and Rh[6]), the *O*-bonded form was found to be thermodynamically as well as kinetically favored over the *N*-bonded form.

The "softer" platinum(II) species, on the other hand, usually exhibits only a weak affinity for *O*-donor ligands[7] and therefore a thermodynamic preference for *N*-bonded amides is expected. In accordance with this, all platinum compounds characterized by X-ray diffraction analysis[8] contained the amide ligands in the *N*-coordinated tautomeric iminol form. They were prepared by direct reaction with the preformed amide[9] or by hydrolysis of a coordinated nitrile[10][11][12][13][14][15]. However, since these ligands are known to protonate the carbonyl oxygen atom rather than the nitrogen atom[16], there could also be a kinetic preference for *O*-coordination in the case of platinum(II). This possibility has recently been demonstrated in a study showing that acetamide can displace a weakly coordinated water molecule from the $[Pt(dien)(OH_2)]^{2+}$ species (dien = diethylenetriamine) acting as an oxygen donor ligand[17][18] in solution. The kinetically preferred *O*-bonded complex can then undergo an intramolecular rearrangement to the thermodynamically more stable *N*-bonded iminol complex[18].

The $[Pt(dien)\{O\text{-}RC(O)NH_2\}]^{2+}$ complexes isomerize to the corresponding *N*-bonded form, as well as undergoing displacement of the *O*-bonded amide by weak nucleophiles such as water. This instability prevented their characterization by X-ray crystallography. In this paper we present the conditions for stabilization of such a species. It was found that using a substituted dien ligand, such as *N*,*N*,*N*′,*N*′′,*N*′′-pentamethylethylenediamine (Me_5dien), *O*-bonded amide complexes, which are infinitely stable in acetone solution and which undergo solvolysis in neat water with a rate constant as low as $8.7 \cdot 10^{-5}$ s^{-1}, can be prepared. The structure of the complex $[Pt(Me_5dien)\{O\text{-}MeC(O)NH_2\}](CF_3SO_3)_2$ (**4b**) has been solved by X-ray diffraction allowing comparison to *N*-bonded platinum amides. Furthermore this investigation has allowed a deeper insight into the mechanism of isomerization from *O*- to the *N*-bonded amides, and other conformational restraints within the coordination sphere.

Results and Discussion

Stereochemistry of the Me_5dien Ligand in Solution

The ^{1}H-NMR spectrum in D_2O solution of the aqua species $[Pt(Me_5dien)(H_2O)](CF_3SO_3)_2$ (**2**) shows three signals for the *N*-Me groups (relative intensities of 3:6:6) and four signals for the protons of the ethylene chains linking

 © WILEY-VCH Verlag GmbH, D-69451 Weinheim, 1998 1434–1948/98/0909–1305 $ 17.50+.50/0

Table 1. ^{1}H-NMR data (δ, downfield from $SiMe_4$; [D_6]acetone solvent) for complexes **1**−**7**[a]

	Me5dien[b] N(2)Me	Me5dien[b] N(1,3)Me_2	C(1,4)H_2 (ax, eq)	C(2,3)H_2 (ax, eq)	Amide R	$NH_{(1,2)}$	OH
1	3.37	3.28, 3.11	3.82[d]	4.20[d]			
2[c]	3.07	2.94, 2.77	3.51, 3.04	3.68, 2.96			
3a	3.34	3.26, 3.07	3.84, 3.25	4.08, 3.15	1.65		
3b	3.34	3.27, 3.08	3.82, 3.22	4.10, 3.15	2.87		
3c	3.40	3.18, 3.38	3.90, 3.30	4.17, 3.20	8.23(*o*) 7.74(*m*) 7.95(*p*)		
4a	3.24	3.09, 2.86	3.69, 3.21	4.04, 3.12	1.36	9.42, 8.92	
4b	3.26	3.10, 2.91	3.69, 3.21	4.03, 3.13	2.40	9.35, 9.23	
4c	3.31	3.16, 2.95	3.73, 3.28	4.11, 3.19	8.14(*o*) 7.59(*m*) 7.74(*p*)	9.74, 9.70	
5a	3.23	3.07, 2.84	3.71, 3.15	3.93, 3.09	1.37	8.45	11.92
5b	3.26	3.09, 2.86	3.73, 3.17	3.98, 3.12	2.47	8.61	12.27
5c	3.32	3.19, 2.95	3.80, 3.21	4.04, 3.17	8.04(*o*) 7.57(*m*) 7.69(*p*)	9.28	12.60
6	3.31	3.10, 2.80	3.69[d]	4.06[d]	8.08(C^6H) 7.08(C^5H) 8.16(C^4H) 7.86(C^3H)	13.20	
7	3.35	3.07, 2.72	3.85[d]	4.14[d]	9.04(C^6H) 7.27(C^5H) 8.06(C^4H) 7.27(C^3H)		
7′	3.36	2.98, 2.75	3.86[d]	4.04[d]	8.65(C^6H) 7.23(C^5H) 8.03(C^4H) 7.23(C^3H)		

[a] **1** [$Pt(Me_5dien)I]_2Pt_2I_6$, **2** [$Pt(Me_5dien)(H_2O)](CF_3SO_3)_2$, **3** [$Pt(Me_5dien)(N{\equiv}CR)](CF_3SO_3)_2$ [R = *t*Bu (**a**), Me (**b**), and Ph (**c**)], **4** [$Pt(Me_5dien)\{O\text{-}RC(O)NH_2\}](CF_3SO_3)_2$ [R = *t*Bu (**a**), Me (**b**), and Ph (**c**)], **5** [$Pt(Me_5dien)\{N\text{-}RC(OH)NH\}](CF_3SO_3)_2$ [R = *t*Bu (**a**), Me (**b**), and Ph (**c**)], **6** [$Pt(Me_5dien)\{O\text{-}HNC(O)C^3HC^4HC^5HC^6H\}(N-C^6)](CF_3SO_3)_2$, **7**/**7′** [$Pt(Me_5dien)\{N\text{-}NC(OH)C^3HC^4HC^5HC^6H\}(N-C^6)](CF_3SO_3)_2$. − [b] Numbering scheme of the Me_5dien ligand: $Me_2N(1)C(1)H_2C(2)H_2N(2)MeC(3)H_2C(4)H_2N(3)Me_2$. − [c] Solvent D_2O. − [d] The signal of the equatorial proton is obscured by overlap.

the central nitrogen atom with the terminal nitrogen atoms (each signal integrating for two protons) (Table 1).

There is a geminal coupling (13 Hz) between the signals at δ = 3.68 and 2.96 and between the signals at δ = 3.51 and 3.04, indicating that the two signals of each couple belong to the same methylene group. From the observation of distinct signals for the two protons of a given methylene group, it is possible to conclude that the two condensed rings have a fixed puckering[19][20]. Two vicinal protons (signals at δ = 3.68 and 3.51) are strongly coupled (ca. 13 Hz), therefore they are both axial (torsion angle of ca. 180°). The other two vicinal protons (δ = 3.04 and 2.96) are weakly coupled (3 Hz) and therefore they are both equatorial (forming a torsion angle of ca. 60°). It is also possible to assign the signals at δ = 3.51 and 3.04 to the methylene group adjacent to the terminal nitrogen atoms (corresponding to $C1H_2$ and $C4H_2$ in Scheme 1) because the axial protons (δ = 3.51) have NOE cross peaks with the central *N*-Me group (δ = 3.07) and two equivalent terminal *N*-Me groups (δ = 2.77). In contrast, the couple of signals at δ = 3.68 and 2.96 can be assigned to the methylene groups adjacent to the central nitrogen atoms (corresponding to $C2H_2$ and $C3H_2$ in Scheme 1) because the axial protons (δ = 3.68) have NOE cross-peaks only with terminal *N*-Me groups (δ = 2.94).

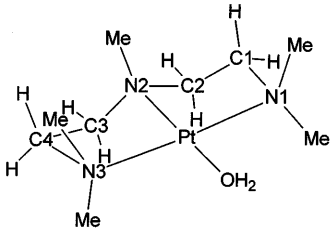

The *N*-Me signal at δ = 2.77, which has NOE cross-peaks with the axial protons of $C1H_2$ and $C4H_2$ methylene groups (δ = 3.51), must belong to the terminal *N*-Me groups which are on the same side of the coordination plane as the central methyl group. The *N*-Me signal at δ = 2.94, having NOE cross-peaks with the axial protons of the $C2H_2$ and $C3H_2$ methylene groups (δ = 3.68), must belong to the terminal *N*-Me groups which are on the opposite side of the coordination plane from the central methyl group.

O-Amide Complexes Formed in the Reaction of the Aqua Species 2 with Free Amide

Reaction of the aqua species **2** with free amide in acetone solution leads to displacement of the coordinated water molecule by the free amide, and formation of the $[Pt(Me_5dien)\{O\text{-}RC(O)NH_2\}]^{2+}$ complex [**4**; R = *t*Bu (**a**),

Me (**b**), or Ph (**d**)]. The reaction is rather slow (k_{obs} = $3.5 \cdot 10^{-5}$ s^{-1} for 0.1 M acetamide) and requires a slight excess of amide to go to completion. The isolated species, however, can be dissolved in pure water, where they undergo solvolysis at a very slow rate (k_{obs} = $8.7 \cdot 10^{-5}$ s^{-1} for **4b**). It has already been reported that the presence of *N*-substituents can reduce the reactivity of dien complexes by a factor of 300[20][21].

The ^{1}H-NMR spectral features of the Me_5dien ligand are very similar to those observed for the aqua species, indicating a similar structure with fixed puckering of the two condensed chelate rings. The *O*-coordination of the amide is deduced from the presence of two close NH_2 ^{1}H-NMR signals which are ca. 2 ppm downfield with respect to those of the free amide (in contrast, *N*-coordination is undoubtedly accompanied by a switch to the iminol tautomer with chemical shifts of the NH and OH protons ca. 2 and 4 ppm, respectively, downfield with respect to the NH_2 signals of the free ligand). The two NH_2 proton signals are rather sharp at low temperature (ca. −80°C) and both undergo broadening and a shift to higher field as the temperature is raised (Figure 1).

lead to the formation of two rotamers, differing in the relative position of the amide aminic group and the Me_5dien central *N*-Me group with respect to the platinum coordination plane (A and B in Scheme 2); (ii) ligand-coordination isomerism with the Pt atom either *cis* to NH_2 or *cis* to R with respect to the C=O double bond (C and D in Scheme 2). Observed similarities among the three complexes with R = *t*Bu (**a**), Me (**b**), or Ph (**d**) suggests that the first hypothesis is more correct.

Conversion of *O*-Bonded to *N*-Bonded Amides by Base Catalysis

The *O*-bonded amide complexes **4a−c** are stable for weeks in acetone solution under neutral conditions. Treatment with bases, however, leads to instant formation of the corresponding *N*-bonded amidate species. Alkaline bases can be used, but, since they are not soluble in acetone, they must be added in powdered form and with concomitant addition of a few drops of water. Organic nitrogen bases (such as triethylamine) can also be used but displacement of the *O*-bonded amide by the amine can also take place. Treatment of the amidate with an acid (such as triflic acid, CF_3SO_3H) restores the amide, but to the *N*-bonded form

Figure 1. ^{1}H-NMR spectrum (δ, downfield from $SiMe_4$; [D_6]acetone as solvent) of [Pt(Me_5dien){*O*-MeC(O)NH_2}](CF_3SO_3)$_2$ (**4b**); assignment of resonances as reported in Table 1; A: water moisture, B: [D_6]acetone

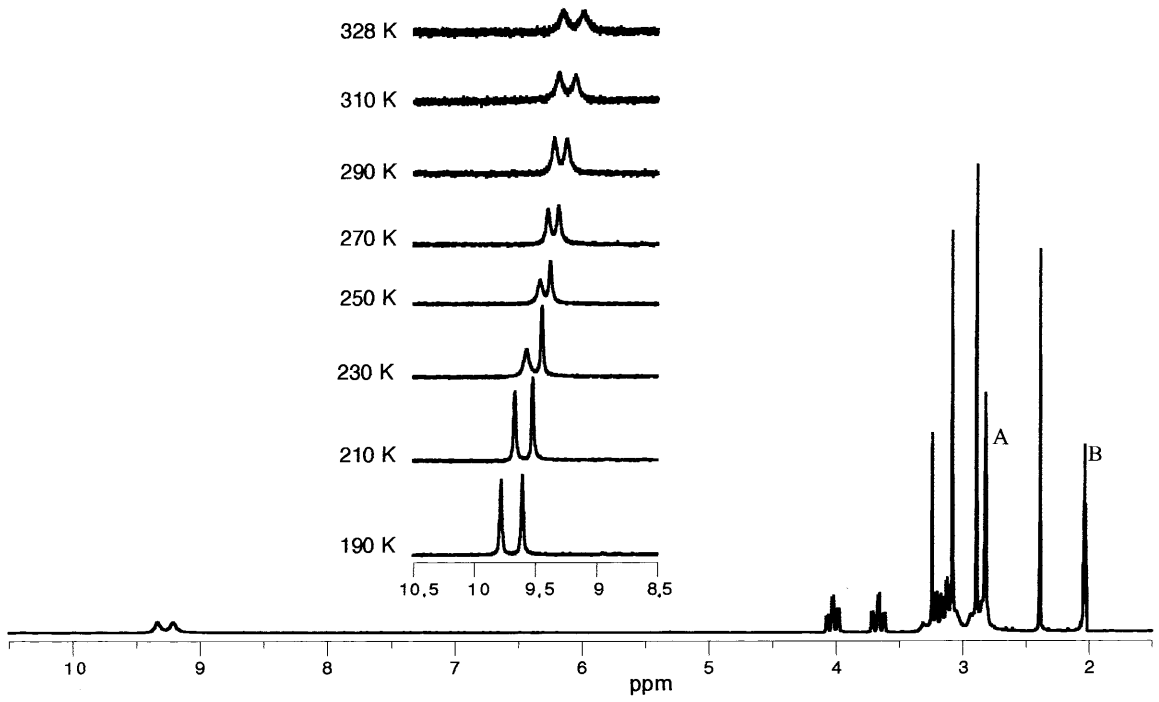

The shift in field and the broadening are more pronounced for one signal. The signal is found more downfield at −80°C and more upfield at +50°C. A possible explanation for this behavior is that at low temperature there is preference for a given isomer and that, as the temperature is raised, a second isomer contributes to the stereochemistry of the complex causing the observed spectral changes. There are two possible causes for isomerism: (i) Restricted rotation of the amide ligand about the Pt−O bond would

(compounds **5a−c**). The identification of the *N*-bonded amides was facilitated by the preparation of the same species by an alternative route, that is, by hydrolysis of the corresponding nitrile complexes as already reported[11]. The *N*-bonded amides invariably adopt the iminol form with two downfield signals at δ ≈ 12 and 8−9 assigned to the OH and NH protons, respectively. The OH proton generally gives a very broad signal because, being rather acidic ($pK_a \approx 3.7$), it exchanges rapidly with water. With time, the

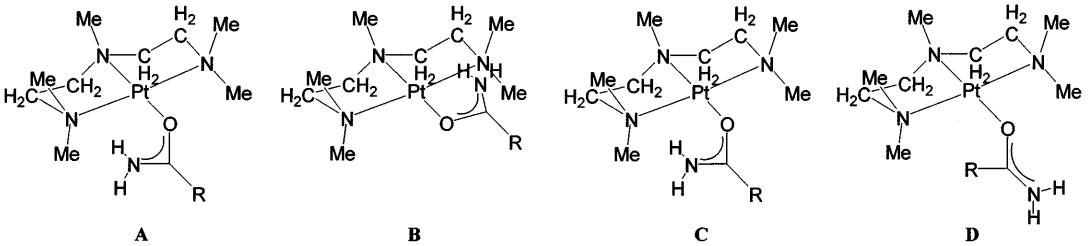

A B C D

intensities of the OH and H_2O peaks decrease and eventually disappear. However, the intensity of the partially deuterated acetone ([D_5]acetone) peaks increases. Although this type of reaction is not new, in the present case it is exceptionally fast ($k_{obs} = 1.0 \cdot 10^{-4}$ s^{-1} at 24°C).

Spontaneous Isomerization of *O*-Bonded to *N*-Bonded 2-Pyridone − Formation of *N*-Bonded Rotamers

The reaction of the aqua species **2** with pyridone leads initially to product **6** which is not stable but isomerizes over time to a new species (**7**) ($k_{obs} = 4.5 \cdot 10^{-5} s^{-1}$ for a pyridone concentration of 2.2 mM at 24°C) (Scheme 3). The NMR spectrum of **6** is in agreement with an *O*-bonded pyridone complex, analogous to the *O*-bonded species (**4a−c**) obtained with other amides. A broad signal at δ = 13.2 was identified as an *N*-bonded proton, the other signals at δ = 8.07, 7.08, 8.16, and 7.86 were easily identified as C^6H, C^5H, C^4H, and C^3H signals, respectively, on the basis of H,H coupling.

Me$_5$dien ligand. At equilibrium, the two species are present in comparable yields ([**7**]/[**7′**] ≈ 40:60). It is most likely that **7** and **7′** are rotamers resulting from the non-C_2 symmetry of the Me$_5$dien ligand. This hypothesis has been fully confirmed by an NOE experiment showing that the C^6H signals of the two isomers have cross peaks with different couples of terminal *N*-Me groups: isomer **7′** with the *N*-Me groups which are on the same side of the platinum coordination plane as the central *N*-Me group and isomer **7** with the *N*-Me groups which are on the opposite side of the platinum coordination plane from the central *N*-Me group. It is interesting to note that one of the two rotamers (**7**) is kinetically favored in the isomerization from *O*- to *N*-bonded form, while at equilibrium the two rotamers are nearly equally abundant.

Treatment with base also causes instant isomerization of the *O*-bonded amide complex **6** to the *N*-bonded amidate complex. Furthermore, the amidate species formed first, like the *N*-amide formed first, also isomerizes to a new

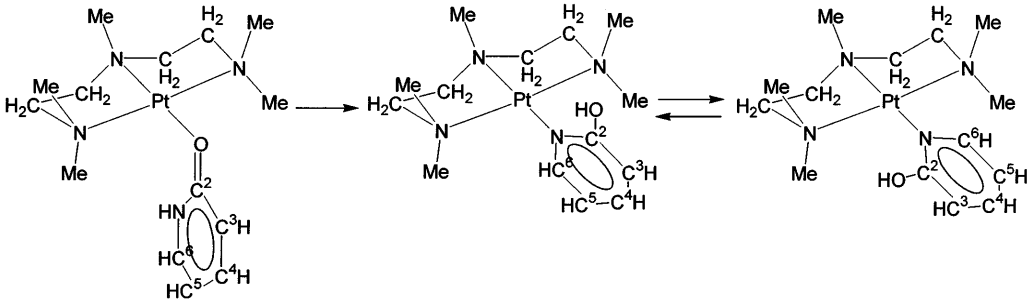

6 7 7′

In the isomerization from **6** to **7**, the signals assigned to C^5H and C^4H remain nearly unchanged (Δδ ≈ 0.2). In contrast, the signal of the C^6H proton undergoes a downfield shift of ca. 1 ppm (δ = 9.04) and couples to platinum (30 Hz), while the signal of the C^3H proton undergoes an upfield shift of ca. 0.6 ppm (δ = 7.26). The changes in chemical shifts and the coupling with platinum are in agreement with **7** being an *N*-bonded 2-hydroxypyridine complex (2-pyridone and 2-hydroxypyridine are the equivalents of the oxo amine and iminol tautomers of amides).

A peculiar feature of the *N*-bonded pyridone complex **7** is its slow isomerization to a new species (**7′**) (Scheme 3). The rate of isomerization of **7** to **7′** is much slower than the isomerization of **6** to **7**, occurring over several days as compared to a few hours. The new species (**7′**) has spectral features which are also in agreement with an *N*-bonded pyridone (C^6H coupled to platinum, 30 Hz) and a tricoordinate species (presumably a rotamer). At equilibrium, the ratio of the two rotamers is similar to that observed for the corresponding *N*-amides (**7** and **7′**). Obviously, starting from an equilibrium mixture of **7** and **7′**, treatment with base leads to the corresponding *N*-amidate in the equilibrium isomer composition.

Insight into the Mechanism of *O*- to *N*-Isomerization of Amides

The reason why the isomerization from the *O*- to the *N*-bonded form takes place for the pyridone and not for the other amide complexes under similar experimental conditions (acetone solution, in the absence of added base), deserves further discussion. It has been hypothesized that *O*- to *N*-isomerization of coordinated amides takes place intramolecularly through a transition state in which both N and O atoms of the amide are equally predisposed towards nucleophilic attack on Pt^{II}[18]. It is impossible for the *O*-

bonded amide ligand to adopt a conformation with lone pairs of electrons at the O and N atoms pointing towards the same metal center because of the π-electron delocalization of the nitrogen lone pair of electrons. Therefore the isomerization process ought to take place by deprotonation of the nitrogen atom and conversion of the amide to an amidate species. The latter species can have convergent lone-pairs of electrons at the O and N atoms and can promote a transition state in which both atoms donate a lone pair of electrons to the platinum center. Protonation of the amidate would revert it back to the amide, but in the isomerized *N*-bonded form. On this basis the slow isomerization from *O*- to *N*-coordination of the pyridone, even in the absence of added base, can be explained in terms of the higher acidity of the NH protons in 2-pyridone, as compared to that in acyclic amides.

X-ray Structure Analysis of the (*O*-Acetamide)platinum Complex 4b

An X-ray Structure analysis of complex **4b**, for which the *O*-coordination of the amide had already been established by NMR experiments, has been carried out in order to compare structural features of the amide functionality in the *O*- and *N*-coordinated linkage isomerism. An ORTEP drawing of **4b** is shown in Figure 2. Selected bond lengths and angles are given in Table 2. The crystals of **4b** consist of the complex cation $[Pt(Me_5dien)\{O\text{-}MeC(O)NH_2\}]^{2+}$ and triflate anions in a 1:2 molar ratio. The platinum atom has the usual square-planar ligand coordination sphere in which the three nitrogen atoms from Me_5dien and the oxygen atom from the acetamide act as donors.

Figure 2. ORTEP drawing of $[Pt(Me_5dien)\{O\text{-}MeC(O)NH_2\}](CF_3SO_3)_2$ (**4b**) with the labelling scheme; the ellipsoids enclose 30% probability

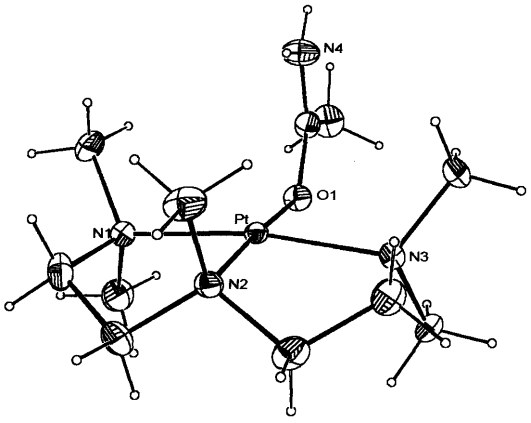

The Pt−N(1) and Pt−N(3) bonds (terminal aminic groups) have similar lengths [2.056(5) and 2.065(5) Å, respectively] and both are significantly longer than the Pt−N(2) bond [2.007(5) Å] (central aminic group). The N(1)−Pt−N(2) and N(2)−Pt−N(3) angles of the two condensed chelate rings are significantly smaller than 90° [86.3(2) and 86.5(2)°, respectively]. In contrast, the N(1)−Pt−O(1) and N(3)−Pt−O(1) angles are significantly larger than 90° [93.0(2) and 93.6(2)°, respectively]. The strain within the tridentate ligand appears to be responsible for the observed deviation from planarity of the (Me_5dien)Pt moiety, where the platinum atom is displaced by 0.140 Å above the plane of the three nitrogen donors)[23].

Table 2. Selected bond lengths [Å] and angles [°] of $[Pt(Me_5dien)\{O\text{-}MeC(O)NH_2\}](CF_3SO_3)_2$; standard deviations are in parentheses

Pt−N(1)	2.056(5)	N(3)−C(4)	1.504(8)
Pt−N(2)	2.007(5)	N(3)−C(8)	1.487(8)
Pt−N(3)	2.065(5)	N(3)−C(9)	1.485(7)
Pt−O(1)	2.038(4)	O(1)−C(10)	1.262(7)
N(1)−C(1)	1.509(10)	C(1)−C(2)	1.515(12)
N(1)−C(5)	1.493(10)	C(3)−C(4)	1.498(10)
N(1)−C(6)	1.488(9)	C(10)−N(4)	1.303(9)
N(2)−C(2)	1.496(9)	C(10)−C(11)	1.498(9)
N(2)−C(3)	1.499(8)	N(4)−H(a)	0.78(9)
N(2)−C(7)	1.482(8)	N(4)−H(b)	0.96(9)
N(1)−Pt−N(2)	86.3(2)	N(2)−C(3)−C(4)	108.0(5)
N(1)−Pt−N(3)	169.7(2)	N(3)−C(4)−C(3)	110.8(5)
N(1)−Pt−O(1)	93.0(2)	O(1)−C(10)−N(4)	123.4(6)
N(2)−Pt−N(3)	86.5(2)	O(1)−C(10)−C(11)	117.4(6)
N(2)−Pt−O(1)	175.4(2)	C(1)−N(1)−C(5)	108.0(6)
N(3)−Pt−O(1)	93.6(2)	C(1)−N(1)−C(6)	109.7(6)
Pt−N(1)−C(1)	107.2(4)	C(5)−N(1)−C(6)	108.4(6)
Pt−N(1)−C(5)	108.8(4)	C(2)−N(2)−C(3)	112.7(5)
Pt−N(1)−C(6)	114.7(4)	C(2)−N(2)−C(7)	110.6(6)
Pt−N(2)−C(2)	104.7(4)	C(3)−N(2)−C(7)	111.0(6)
Pt−N(2)−C(3)	104.9(4)	C(4)−N(3)−C(8)	108.7(5)
Pt−N(2)−C(7)	113.6(4)	C(4)−N(3)−C(9)	110.3(5)
Pt−N(3)−C(4)	106.1(4)	C(8)−N(3)−C(9)	108.0(5)
Pt−N(3)−C(8)	107.3(4)	N(4)−C(10)−C(11)	119.2(6)
Pt−N(3)−C(9)	116.2(4)	C(10)−N(4)−H(a)	119(7)
Pt−O(1)−C(10)	127.3(4)	C(10)−N(4)−H(b)	116(6)
N(1)−C(1)−C(2)	109.9(6)	H(a)−N(4)−H(b)	125(9)
N(2)−C(2)−C(1)	108.0(6)		

The Pt−O bond length [2.038(4) Å] is in agreement with the values of Pt−O lengths previously reported for *N,O*-2-pyridonate complexes $[Pt_2(en)_2(C_5H_4NO)_2]_2^{4+}$ [2.049(6) Å][24] and $[Pt_2(NH_3)_4(C_5H_4NO)_2]^{2+}$ [2.024(5) Å] (where C_5H_4NO = 2-pyridonate)[25].

The acetamide molecule is strictly planar, with deviations of the heavy atoms from the least-square plane of ca. 0.004(6) Å, and orthogonal to the coordination plane where the dihedral angle between the planes is 89.4(3)°. The C−O and C−N bond lengths within the acetamide ligand [1.262(7) and 1.303(9) Å, respectively] are very similar to those previously found for acetamide *O*-coordinated to nickel [1.248(3) and 1.311(4) Å, respectively][26] and for free amides [1.23(1) and 1.32(1) Å, respectively][27] and indicate an extensive π-bond delocalization over the O=C=N functionality. Compared to the *N*-coordinated (acetamide)platinum species, the trend in C−O and C−N bond lengths is reversed [1.321(14) and 1.275(13) Å, for C−O and C−N, respectively][13]. This is in agreement with the different tautomerism of the acetamide in the two cases (oxo amine in the *O*-bonded and iminol in the *N*-bonded forms). The platinum−donor distances are also comparable to *O*- and *N*-bonded acetamide (within 0.01 Å).

The NH_2 group of the amide ligand is *cis* to the platinum center with respect to the C=O double bond and comes close to it. The intramolecular distance between the platinum atom and one proton of the amide [H(a)] is 2.86(9) Å

(as compared to the sum of the van der Waals radii for Pt and H of 2.9−3.2 Å)[28] and the Pt···H(a)−N(4) angle is 114(7)°. These data indicate the existence of an attractive Pt···H(a) interaction. Similarly, an interaction between the hydroxy group and the platinum atom was observed in the *N*-bonded acetamide [Pt···HO = 2.56(2)Å, Pt···H−O = 124(8)°] and was believed to be responsible for the stabilization of the isomer with the OH group, instead of the isomer with the Me group *cis* to the Pt center across the C=N double bond. The same conclusion can be drawn in the present case, although the Pt···HN interaction appears to be slightly weaker than the Pt···HO interaction.

The N(2)−Pt−O axis is slightly bent [175.4(2)°] in the same direction as the N(1)−Pt−N(3) axis [169.6(2)°] and, as a consequence, the coordination sphere of the platinum center assumes a pyramidal distortion, with the Pt atom displaced by 0.104(1) Å above the average plane of the donor atoms. This distortion contrasts with the tetrahedral distortion observed in the related $[Pt(Me_5dien)I]^+$ complex[29].

The triflate anions are kept in the vicinity of the metal center by a hydrogen bond between a triflate oxygen atom and the NH_2 group of the amide. The hydrogen bonds have geometrical parameters: O(2)−N(4) 2.837(9) Å, O(2)−H(b) 2.02(9) Å, O(2)−H(b)−N(4) 175.9(9)°, and O(5)−N(4) 3.050(11) Å, O(5)−H(a) 2.35(9) Å, O(5)−H(a)−N(4) 149(9)°[22].

Conclusions

In spite of the higher affinity of platinum(II) for *N*- over *O*-donor ligands, suitable platinum substrates react preferentially with the oxygen terminus to give the *O*-bonded amide complexes. Although the *O*-bonded species are very labile, since the amide can be displaced by water, they are indefinitely stable in acetone solution under neutral conditions. In contrast, isomerization from *O*- to *N*-bonded species takes place instantly under basic conditions. Therefore, the deprotonation of the aminic group ($pK_a > 11$) is accompanied by the shift of the metal center from the *O*- to the *N*-atom, leading to the formation of *N*-bonded amidate species. The main factor leading to the isomerization is the higher affinity of platinum to the nitrogen over the oxygen donor atom.

Protonation of the amidate species under acidic conditions leads to the *N*-bonded amide. The *N*-bonded amides, like the *N*-bonded amidates, represent the thermodynamically preferred species due to the higher affinity of platinum to nitrogen donors. In contrast, *O*-bonded amides owe their stability to their kinetic inertness, where a high pH is required for deprotonation of the NH_2 functionality. In the case of the pyridone complex, the *O*-bonded form is unstable and isomerizes spontaneously to the *N*-bonded form. The isomerization from the *O*- to the *N*-bonded species can take place in the absence of added base because of the higher acidity of the protonated pyridine-like nitrogen atom.

Differently to dien, Me_5dien adopts a fixed puckering of the two condensed chelate rings. Due to the rigidity of the puckered ring, the methyl groups at the terminal nitrogen atoms are held in fixed positions and strongly hinder the rotation of the amide. The steric hindrance is expected to be particularly severe in the case of cyclic pyridone. In this case, we have convincing evidences for the presence of two rotamers in both the *N*-amide and the *N*-amidate species. Hindered rotation stems from the steric rigidity of both rotating fragments, namely the (Me_5dien)Pt moiety and the pyridone. Slow rotation (on the NMR time scale) of aryl[22], pyrimidine, and purine rings in $(Me_5dien)Pd^{2+}$ complexes has already been reported[20]. This, however, is the first case that such a rate has been measured and found to be exceptionally low.

Comparison of the X-ray structure analysis of *O*- and *N*-coordinated (acetamide)platinum complexes has confirmed that because of the change in the ligand tautomerism (oxo amine and iminol for *O*- and *N*-bonded amides, respectively), the two isomeric amide functionalities are nearly superimposable.

This work was financially supported by the *Ministero della Università e della Ricerca Scientifica e Tecnologica (MURST*; Contribution 40%), the *Consiglio Nazionale delle Ricerche (CNR)*, the *European Community* (EC, Contract BMH4-CT97-2485 and COST Chemistry project D8/0012/97) and the *University of Siena* (Contribution 60%). The data collections were carried out by Mr. *A. Laurita, Università della Basilicata*.

Experimental Section

Starting Materials: Commercial reagent-grade chemicals were used without further purification.

Preparation of the Complexes: $[Pt(Me_5dien)I]_2(Pt_2I_6)$ (**1**) was prepared by direct reaction of $K_2[PtI_4]$ with free amine. In a typical experiment K_2PtCl_4 (0.5 g, 1.2 mmol) was dissolved in water (5 ml) and treated with excess KI (0.82 g, 4.9 mmol). After 5 min of stirring at 50°C, a stoichiometric amount of Me_5dien (0.207 g, 1.2 mmol) was added and the reaction mixture was kept stirring at 50°C for 1 h. The yellow-green precipitate which formed was separated, washed with water, and dried in dry air. Yield: 0.55 g, 67%. − $C_{18}H_{46}I_8N_6Pt_4$ (**1**; 2141.5): calcd. C 10.1, H 2.2, N 3.9; found C 10.0, H 2.2, N 3.9.

$[Pt(Me_5dien)(H_2O)](CF_3SO_3)_2$ (**2**) was prepared from $[Pt(Me_5dien)I]_2(Pt_2I_6)$ (**1**) (0.3 g, 0.14 mmol), suspended in water (20 ml) and treated with silver triflate (0.15 g, 0.58 mmol). The reaction mixture was kept stirring for about 16 h at room temperature in the dark. The solution was then filtered through Celite and concentrated to dryness. The oily residue was triturated with diethyl ether to give a white hygroscopic solid. Yield: 0.150 g, 40%. − $C_{11}H_{27}F_6N_3O_8PtS_2$ (**2**; 702.1): calcd. C 18.8, H 3.9, N 6.0; found C 18.8, H 3.8, N 5.8.

The complexes $[Pt(Me_5dien)(N{\equiv}CR)](CF_3SO_3)_2$ (**3**) were prepared by reaction of the aqua species $[Pt(Me_5dien)(H_2O)](CF_3SO_3)_2$ (**2**) with free nitrile. In a typical experiment, $[Pt(Me_5dien)(H_2O)](CF_3SO_3)_2$ (**2**) was dissolved in the minimum amount of the appropriate nitrile [N≡CR, R = *t*Bu (**a**), Me (**b**), and Ph (**c**)] (ca. 1 mmol of complex in about 10 ml of nitrile) and then kept stirring for 1 h at room temperature. In the case of *tert*-butyl cyanide, the complex **3a** precipitated from the reaction solution and was recovered by filtration of the mother liquor. In the case of acetonitrile, the complex **3b** was recovered after evaporation of the solvent and trituration of the oily residue with diethyl ether. Finally, in the case of benzonitrile, an excess of *n*-hexane was added

Table 3. Selected crystallographic data of $[Pt(Me_5dien)\{O\text{-}MeC(O)NH_2\}](CF_3SO_3)_2$

Empirical formula	$C_{13}H_{28}F_6N_4O_7PtS_2$	$d_{calcd.}$ [Mg m^{-3}]	1.940
Formula mass	725.58	μ(Cu-K_α), [cm^{-1}]	129.17
Space group	$P21/n$	Crystal size [mm]	0.4 × 0.15 × 0.15
a [Å]	11.631(2)	θ range [°] for data collection	2 < 2Θ < 140
b [Å]	12.4217(9)	Independent reflections	4705 [R_{int} = 0.0163]
c [Å]	17.314(2)	Observed reflections [$F > 4\sigma(F)$] used for the final refinement	4690
β [°]	96.002(9)	Absorption correction	DIFABS
V [Å^3]	2487.8(4)	Refinement method	Full-matrix least-squares on F^2
Z	4	$R1$[a]	0.0378
Temperature [°C]	25	$wR2$[a]	0.0985
F(000)	1416	Parameters refined	311
Radiation (λ [Å])	1.5418		

[a] $R1 = \Sigma\|\|F_o| - |F_c\|\|/\Sigma|F_o|$. – [b] $wR2 = [\Sigma[w(F_o^2 - F_c^2)^2]/\Sigma[w(F_o^2)^2]]^{1/2}$; $w = 1/[\sigma^2(F_o^2) + (0.0631 \times P)^2 + 21.74 \times P]$ where $P = [\text{Max}(F_o^2,0) + 2 \times F_c^2]/3$.

to the solution and the mixture kept in the refrigerator for 1 d. The sticky precipitate which formed was washed three times with *n*-hexane and then treated with diethyl ether to give a solid product **3c**. In all cases the yields were above 75%. – $C_{16}H_{32}F_6N_4O_6PtS_2$ (**3a**; 749.1): calcd. C 25.6, H 4.3, N 7.5; found C 25.4, H 4.4, N 7.4. – $C_{13}H_{26}F_6N_4O_6PtS_2$ (**3b**; 707.1): calcd. C 22.1, H 3.7, N 7.9; found C 21.7, H 3.6, N 7.7. – $C_{18}H_{28}F_6N_4O_6PtS_2$ (**3c**; 769.1): calcd. C 28.1, H 3.7, N 7.3; found C 27.8, H 3.5, N 6.9.

The *O*-bonded amide complexes $[Pt(Me_5dien)\{O\text{-}RC(O)NH_2\}](CF_3SO_3)_2$ (**4**) [R = *t*Bu (**a**), Me (**b**), and Ph (**c**)] were prepared by reaction of the aqua species $[Pt(Me_5dien)(H_2O)](CF_3SO_3)_2$ (**2**) with the free amide according to a slight modification of the method of Woon and Fairlie[18]. In a typical experiment, compound **2** (0.07 g, 0.1 mmol) was dissolved in acetone (10 ml), treated with the free amide [$RC(O)NH_2$, R = *t*Bu (**a**), Me (**b**), and Ph (**c**)] (0.15 mmol) and then kept stirring for 16 h at room temperature. Addition of a large excess of diethyl ether induced complete precipitation of the compound. The white precipitate was collected and dried in a vacuum desiccator in the presence of KOH pellets as the drying agent, with the yields always above 90%. In the case of acetamide, suitable crystals for X-ray diffraction were obtained by slow crystallization from an acetone solution layered under diethyl ether. – $C_{16}H_{34}F_6N_4O_7PtS_2$ (**4a**·H_2O; 767.1): calcd. C 25.0, H 4.5, N 7.3; found C 24.9, H 4.6, N 7.1. – $C_{13}H_{28}F_6N_4O_7PtS_2$ (**4b**·H_2O; 725.1): calcd. C 21.5, H 3.9, N 7.7; found C 21.4, H 3.9, N 7.7. – $C_{18}H_{30}F_6N_4O_7PtS_2$ (**4c**·H_2O; 787.1): calcd. C 27.4, H 3.8, N 7.1; found C 26.8, H 3.9, N 7.1.

The *N*-bonded amide complexes $[Pt(Me_5dien)\{N\text{-}RC(OH)NH\}](CF_3SO_3)_2$ (**5**) [R = *t*Bu (**a**), Me (**b**), and Ph (**c**)] were prepared either by hydrolysis of the corresponding nitriles (procedure 1) or by isomerization of the *O*-bonded amides (procedure 2). – Procedure 1: In a typical experiment, the nitrile complex $[Pt(Me_5dien)(N{\equiv}CR)](CF_3SO_3)_2$ (0.1 mmol), dissolved in water (10 ml), was treated with a slight excess of KOH (0.12 mmol in 10 ml of water) with stirring, in an ice bath. After 1–2 h reaction time, the resulting solution was brought to pH = 2–3 with triflic acid, the solvent was evaporated, and the sticky residue crystallized from acetone/diethyl ether. The products **5a–c** are hygroscopic and must be stored under anhydrous conditions. Yields 70%. – Procedure 2: In a typical experiment, the *O*-bonded complex $[Pt(Me_5dien)\{O\text{-}RC(O)NH_2\}](CF_3SO_3)_2$ (**4**) (0.1 mmol), was dissolved in acetone (25 ml) and treated with powdered KOH (0.7 mmol). A few drops of water were added to the reaction mixture, which was kept stirring for about 5 min. The solution was filtered, acidified with triflic acid, and then treated with diethyl ether to allow precipitation of a white product which was recrystallized from acetone/diethyl ether. Yields 70%. – $C_{17}H_{34}F_9KN_4O_{10}PtS_3$ (**5a**·KCF_3SO_3·H_2O; 955.1): calcd. C 21.4, H 3.6, N 5.8; found C 21.3, H 3.8, N 5.7. – $C_{27}H_{56}F_{15}KN_8O_{17}Pt_2S_5$ (**5b**·KCF_3SO_3·2 H_2O; 1638.1): calcd. C 19.8, H 3.4, N 6.8; found C 19.5, H 3.5, N 6.6. – $C_{19}H_{30}F_9KN_4O_{10}PtS_3$ (**5c**·KCF_3SO_3·H_2O; 975.0): calcd. C 23.4, H 3.1, N 5.7; found C 23.3, H 3.5, N 5.6.

The reaction of the acqua species **2** with pyridone leading to a first reaction product (*O*-coordinated pyridone; **6**) which is not stable but isomerizes with time to a new species (*N*-coordinated pyridone; **7**) which, in turn, gives rise to formation of an equilibrium mixture of two rotamers (**7** and **7′**) was performed in the NMR tube and no attempt to isolate isomerically pure species was made.

Physical Measurements: IR spectra in the range 4000–400 cm^{-1} were recorded as KBr pellets; spectra in the range 400–200 cm^{-1} were recorded as polythene pellets with Perkin Elmer 283 and FT 1600 spectrophotometers. ^{1}H-NMR spectra were obtained with a Bruker AM 300 spectrometer and are collected in Table 1. Rate constants were calculated from plots of $\ln(C_t - C_{inf.})$ against time where C_t and $C_{inf.}$ are concentrations at time t and after at least six half-lives, respectively.

X-ray Crystallographic Study[30]: Colorless crystals of $[Pt(Me_5dien)\{O\text{-}RC(O)NH_2\}](CF_3SO_3)_2$ (**4b**) were obtained from acetone/diethyl ether solution. X-ray data were collected with an Enraf-Nonius CAD4 single-crystal diffractometer by using graphite-filtered Cu-K_α radiation (λ = 1.5418 Å). The unit-cell dimensions were refined by a least-squares algorithm using 25 automatically centered reflections. A total of 5101 reflections were collected in the range $-14 \le h \le 14$, $0 \le k \le 15$, $0 \le l \le 21$; 4705 independent reflections. Four reflections were monitored during data collection, no decay was observed. Crystallographic data are summarized in Table 3. The full data set was corrected for Lorentz and polarization effects. A correction for absorption effects was applied using the DIFABS package[31] at the isotropic stage of refinement.

The structure was solved using Patterson and Fourier techniques, in the $P21/n$ space group. The model was refined by full-matrix least-squares methods. Anisotropic thermal parameters were applied for all non-hydrogen atoms. The NH_2 hydrogen atoms of the amide were found in the final Fourier difference map, the other hydrogen atoms were placed at their geometrically calculated positions and included in the full-matrix least-square cycles with iso-

tropic thermal parameters (U) tied at 1.2 times the values of U of the relative carbon or nitrogen atoms.

All calculations were carried out with Vax 11/750 and AST Pentium 100 MHz computers using the SHELX-86[32], SHELXL-93[33], and PARST97 packages[34].

[1] H. Sigel, R. B. Martin, *Chem. Rev.* **1982**, *82*, 385.
[2] D. P. Fairlie, H. Taube, *Inorg. Chem.* **1985**, *24*, 3199.
[3] R. L. Angel, D. P. Fairlie, W. G. Jackson, *Inorg. Chem.* **1990**, *29*, 20.
[4] N. J. Curtis, G. A. Lawrence, A. M. Sargeson, *Aust. J. Chem.* **1983**, *36*, 1495.
[5] D. P. Fairlie, Y. Ilan, H. Taube, *Inorg. Chem.* **1997**, *38*, 1029.
[6] N. J. Curtis, N. E. Dixon, A. M. Sargeson, *J. Am. Chem. Soc.* **1983**, *105*, 5347.
[7] F. R. Hartley, *The Chemistry of Platinum and Palladium*, Applied Sciences Publishers, London, New York, **1973**.
[8] Our considerations will be restricted to monodentate amides and will not include bridging amide complexes for which the reader may refer to the following papers: J. K. Barton, H. N. Rabinowitz, D. J. Szulda, S. J. Lippard, *J. Am. Chem. Soc.* **1977**, *99*, 2827. − T. V. O'Halloran, P. K. Masharak, I. D. Williams, M. M. Roberts, S. J. Lippard, *Inorg. Chem.* **1987**, *26*, 1261. − F. D. Rochon, P. C. Kong, R. Melanson, *Inorg. Chem.* **1990**, *29*, 1352. B. Lippert, *Prog. Inorg. Chem.* **1989**, *37*, 1.
[9] D. B. Brown, M. B. Robin, R. D. Burbank, *J. Am. Chem. Soc.* **1968**, *90*, 5621. − D. B. Brown, R. D. Burbank, M. B. Robin, *J. Am. Chem. Soc.* **1969**, *91*, 2895.
[10] R. Cini, F. P. Fanizzi, F. P. Intini, G. Natile, *J. Am. Chem. Soc.* **1991**, *113*, 7805.
[11] R. Cini, F. P. Fanizzi, F. P. Intini, G. Natile, *J. Am. Chem. Soc.* **1993**, *115*, 5123.
[12] R. Cini, F. P. Intini, G. Natile, C. Pacifico, *J. Chem. Soc., Dalton Trans.* **1994**, 3753.
[13] R. Cini, F. P. Fanizzi, F. P. Intini, G. Natile, C. Pacifico, *Inorg. Chim. Acta* **1996**, *251*, 111.
[14] R. Cini, F. P. Fanizzi, F. P. Intini, C. Pacifico, G. Natile, *Inorg. Chim. Acta* **1997**, *264*, 279.
[15] A. Erxleben, I. Mutikainen, B. Lippert, *J. Chem. Soc., Dalton Trans.* **1994**, 3667.
[16] J. Zabicky, *The Chemistry of Amides*, J. Wiley-Interscience, New York, **1970**, chapter 1, p. 1.
[17] J. S. Kerrison, P. J. Sadler, *J. Chem. Soc., Chem. Commun.* **1981**, 61.
[18] T. C. Woon, D. P. Fairlie, *Inorg. Chem.* **1992**, *31*, 4069.
[19] T. P. Pitner, R. B. Martin, *J. Am. Chem. Soc.* **1971**, *93*, 4400.
[20] S.-H. Kim, R. B. Martin, *Inorg. Chim. Acta* **1984**, *91*, 11.
[21] W. H. Baddley, F. Basolo, *J. Am. Chem. Soc.* **1966**, *88*, 2944.
[22] B. A. Markies, P. Wijkens, J. Boersma, H. Kooijman, N. Veldman, A. L. Spak, G. van Koten, *Organometallics* **1994**, *13*, 3244.
[23] B. A. Markies, P. Wijkens, H. Kooijman, A. L. Spek, J. Boersma, G. van Koten, *J. Chem. Soc. Chem. Commun.* **1992**, 1420.
[24] L. S. Hollis, S. J. Lippard, *Inorg. Chem.* **1983**, *22*, 2600.
[25] L. S. Hollis, S. J. Lippard, *J. Am. Chem. Soc.* **1983**, *105*, 3494.
[26] M. E. Stone, B. E. Robertson, E. Stanley, *J. Chem. Soc. A* **1971**, 3632.
[27] F. H. Allen, O. Kennard, D. G. Watson, L. Brammer, G. Orpen, R. Taylor, *J. Chem. Soc., Perkin Trans. 2* **1987**, S1.
[28] A. Bondi, *J. Phys. Chem.* **1964**, *68*, 441.
[29] F. P. Intini, C. Pacifico, G. Natile, unpublished results.
[30] Crystallographic data (excluding structure factors) for the structure reported in this paper have been deposited with the Cambridge Crystallographic Data Center as supplementary publication no. CCDC-101247. Copies of the data may be obtained free of charge on application to CCDC, 12 Union Road, Cambridge CB2 1EZ, UK [fax: (internat.) + 44(0)1223/336033; e-mail: deposit@ccdc.cam.ac.uk].
[31] N. Walker, D. Stuart, "DIFABS", *Acta Crystallogr., Sect. A*. **1983**, *39*, 158.
[32] G. M. Sheldrick, *SHELXS-86*, University of Göttingen, **1986**.
[33] G. M. Sheldrick, *SHELXL-93*, University of Göttingen, **1993**.
[34] M. Nardelli, *PARST 97*, University of Parma, **1996**.

[98083]

Chelate Complexes, 13[◇]

Self-Assembly of {2}-Metallacryptands and {2}-Metallacryptates

Rolf W. Saalfrank*[a], Verena Seitz[a], Dana L. Caulder[b], Kenneth N. Raymond[b], Markus Teichert[c], and Dietmar Stalke[d]

Institut für Organische Chemie der Universität Erlangen-Nürnberg[a],
Henkestr. 42, D-91054 Erlangen, Germany
Fax: (internat.) + 49(0)9131/85-1165
E-mail: saalfrank@organik.uni-erlangen.de

Department of Chemistry, University of California[b],
Berkeley, CA 94720, USA

Institut für Anorganische Chemie der Universität Göttingen[c],
Tammannstr. 4, D-37077 Göttingen, Germany

Institut für Anorganische Chemie der Universität Würzburg[d],
Am Hubland, D-97074 Würzburg, Germany

Received March 30, 1998

Keywords: Metallacryptate / Supramolecular chemistry / Helical structures / Host–guest chemistry / Iron

Reaction of H_2L (**1**) with potassium or strontium hydride, or lanthanum(III) chloride, followed by iron(III) chloride, yielded the {2}-ironcryptates **2a–c**. The mono-, di-, and trivalent guest cations are endohedrally encapsulated. In contrast, the dinuclear trispyridinium ironcryptand **2d** was generated from the reaction of H_2L (**1**) with only iron(III) chloride. The potassium metallacryptate **2a′** was formed from the triple-helicate **2d** by addition of potassium carbonate. The new compounds **2b**, **2c**, and **2d** were unequivocally characterised by X-ray diffraction analyses.

Introduction

The selective complexation of guest molecules and metal cations is an essential prerequisite for the proper functioning of enzymes and biological receptors. In order to mimic the geometric and electronic requirements necessary for selective complexation as observed in nature, many different model compounds with cavities of variable size and electronic structure have been constructed[1]. Examples are the well-known crown ethers, cryptands, spherands and their inclusion complexes[1][2], along with the corresponding metallatopomers, which are easily accessible by self-organisation[3][4][5]. Recently, the bicyclic metallacryptate $[K\subset Fe_2L_3][PF_6]$ (**2a**) was synthesised and characterised by X-ray crystallographic analysis[6][7][8] (Scheme 1).

Results and Discussion

Herein we describe the formation of the bicyclic ironcryptates **2b** and **2c**, with endohedrally encapsulated divalent alkaline earth or trivalent rare earth metal ions, and the cation-free trispyridinium {2}-ironcryptand **2d** (Scheme 1). Upon reaction of H_2L (**1**)[9] in THF with strontium hydride or lanthanum(III) chloride, followed by iron(III) chloride, and subsequent workup with dichloromethane, a dark-red solid was isolated. The FAB-MS spectra (FAB-MS = Fast Atom Bombardment) of the solid materials showed peaks at *m*/*z* 1187 and 985, corresponding to the dication $[Sr\subset Fe_2L_3]^{2+}$ of **2b**, and the trication $[La\subset Fe_2L_3]^{3+}$ of **2c**, indicating the formation of strontium- and lanthanum-containing bicyclic metallacryptates, respectively. Ruby-red crystals of the strontium complex, suitable for X-ray analysis, were prepared by a slightly modified procedure. Strontium chloride was added to a solution of H_2L (**1**; R = *t*Bu) and iron(III) chloride in THF, and the crude material was crystallised from dichloromethane by diffusion of a mixture of diethyl ether and hexanes (1:5). The X-ray diffraction analysis of these crystals proved the formation of a strontium-containing bicyclic ironcryptate $[(Sr\cdot H_2O)\subset Fe_2L_3]$-$[FeCl_4]_2$ (**2b**) with two ferric tetrachloride counterions (Figure 1).

The encapsulated strontium dication does not lie perfectly on the iron−iron axis (Fe−Sr−Fe 174.39°). Strontium is deca-coordinated by six oxygen and three nitrogen atoms of the three ligands, and one molecule of water. In addition, water forms a hydrogen bond to a molecule of diethyl ether solvent. The ligands are approximately octahedrally coordinated to the iron center in a helical fashion. In the chiral complex of racemic **2b**, both iron centers are identically coordinated. Therefore, **2b** is either a (Δ,Δ)-*fac*- or (Λ,Λ)-*fac*-{2}-metallacryptate. The crystals obtained were composed of the homochiral {2}-metallacryptate **2b**. The iron−iron distance in **2b** (715 pm) is identical to the Fe−Fe distance observed in the potassium-containing ironcryptate **2a**.

[◇] Part 12: Ref.[5]

 © WILEY-VCH Verlag GmbH, D-69451 Weinheim, 1998 1434−1948/98/0909−1313 $ 17.50+.50/0

Scheme 1. Reaction scheme for the formation of $[M\subset Fe_2L_3]Y_n$ [**2a**: R = *t*Bu, M = K^+, $Y_n = PF_6^-$; **2a′**: R = *t*Bu, M = K^+, $Y_n = FeCl_4^-$; **2b**: R = *t*Bu, M = $(Sr^{2+}\cdot H_2O)$, $Y_n = (FeCl_4^-)_2$; **2c**: R = Me, M = $(La^{3+}\cdot H_2O\cdot THF)$, $Y_n = (FeCl_4^-)_3$] and $[Fe_2(LH^N)_3]Y_n$ [**2d**: $Y_n = (FeCl_4^-)_3$]

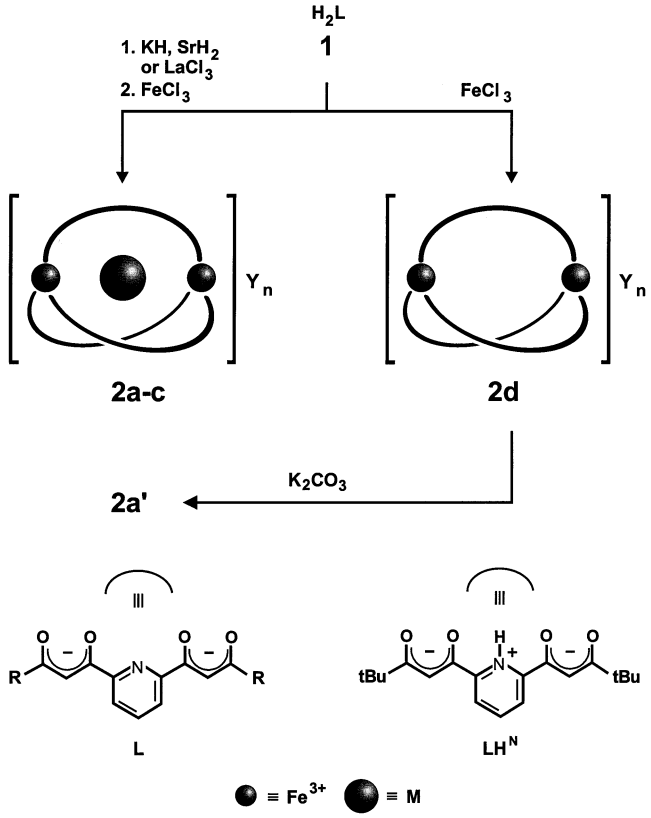

Figure 1. Molecular structure of the dication $[(Sr\cdot H_2O)\subset Fe_2L_3]^{2+}$ of {2}-ironcryptate **2b** (hydrogen atoms, counterions and solvent molecules omitted for clarity; O atoms black, C atoms shaded, N atoms net, Sr atoms segment, Fe atoms diagonal)

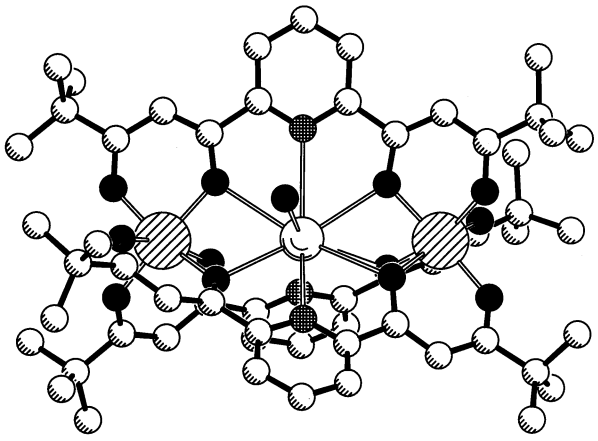

Single crystals suitable for an X-ray diffraction analysis of the chiral racemic lanthanum-containing compound were obtained by diffusion of diethyl ether into a dichloromethane solution of **2c**. There are two slightly different, independent, homochiral ironcryptates (Δ,Δ)- or (Λ,Λ)-$[(La\cdot THF\cdot H_2O)\subset Fe_2L_3][FeCl_4]_3$ (**2c**) of the same chirality present in the asymmetric unit (Figure 2).

Figure 2. Molecular structure of the trication $[(La\cdot H_2O\cdot THF)\subset Fe_2L_3]^{3+}$ of {2}-ironcryptate **2c**; top: stereo view; bottom: view along the Fe−Fe axis (hydrogen atoms, counterions and solvent molecules omitted for clarity; O atoms black, C atoms shaded, N atoms net, La atoms segment, Fe atoms diagonal)

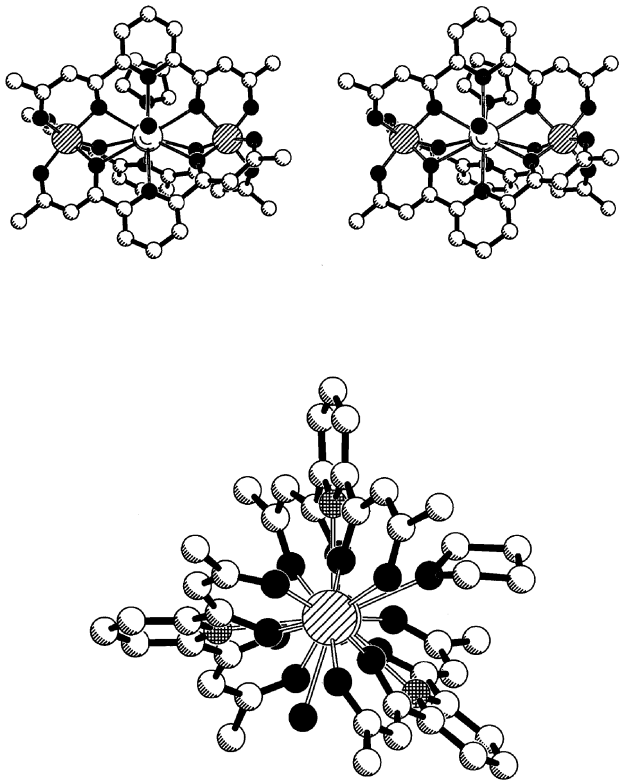

The two iron(III) cations (d_{Fe-Fe} = 719 pm) in the molecule are each approximately octahedrally coordinated by six oxygen atoms of three ligands. They are located on the idealised C_3 axis of the D_{3h}-symmetric molecule. The incorporated lanthanum(III) cation is eleven-coordinate. The six internal oxygen atoms of the ligands form a trigonal prismatic coordination sphere around the lanthanum center. The three nitrogen atoms of the ligands, a THF molecule, and a water molecule coordinate the lanthanum center equatorially in a near perfect plane. The lanthanum−iron distances are similar within each molecule ($\bar{d}_{Fe-La}$ = 360 pm). The encapsulated lanthanum trication lies almost on the Fe−Fe axis (Fe−La−Fe 176.93°). In contrast to the aforementioned potassium-containing (Δ,Λ)-*fac* (*meso*) ironcryptate **2a**, the lanthanum-containing analogue **2c** forms a racemic mixture of the homochiral (Δ,Δ)-*fac* and (Λ,Λ)-*fac* stereoisomers.

Upon addition of iron(III) chloride to a solution of H_2L (**1**; R = *t*Bu) in dry THF, followed by workup with dichloromethane, and crystallisation by diffusion of diethyl ether into a dichloromethane solution of the crude solid material, ruby crystals were obtained. The crystal structure determination revealed the formation of bicyclic metallacryptand $[Fe_2(LH^N)_3][FeCl_4]_3$ (**2d**). In **2d** the pyridine nitrogen atoms of the three ligands are protonated, and the re-

Figure 3. Molecular structure of the trication $[Fe_2(LH^N)_3]^{3+}$ of {2}-ironcryptand **2d**; top: stereo view; bottom: view along the Fe−Fe axis (pyridinium hydrogen atoms shown; counterions and solvent molecules omitted for clarity; H atoms void, O atoms black, C atoms shaded, N atoms net, Fe atoms diagonal)

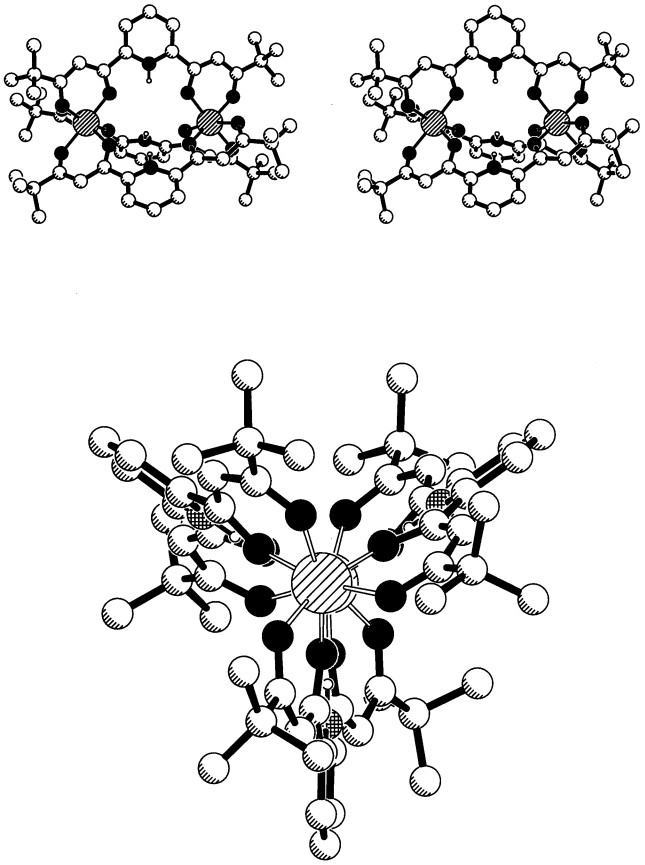

sulting charge of the complex is compensated by three $FeCl_4^-$ counterions. In addition to the two molecules of **2d** in the asymmetric unit, there are four dichloromethane molecules (Figure 3).

The mean Fe−Fe distance of **2d** (642 pm) is much smaller than those in the metallacryptates **2a**, **b**, and **c** (715 and 719 pm). Inclusion of a cation in **2a**, **b**, and **c** causes an expansion of the ligands of the metallacryptates, and an elongation of the iron−iron distances. The average N−N distance for **2d** (539 pm) is considerably larger than that of the ironcryptate **2c** (481 pm). In the chiral, racemic complex **2d**, both iron centers are identically coordinated to six oxygen atoms. Therefore, the {2}-metallacryptand **2d** is either a (Δ,Δ)-*fac* or (Λ,Λ)-*fac* dinuclear triple helicate. A racemic mixture of complex **2d** self-selectively sorts by chirality to generate an enantiomerically pure crystal. As only one crystal was analysed by X-ray, there possibly exists crystals of opposite chirality, forming a conglomerate.

The {2}-ironcryptand **2d** can be converted into the potassium {2}-ironcryptate $[K\subset Fe_2L_3][FeCl_4]$ (**2a′**) on addition of an excess of potassium carbonate to a solution of complex $[Fe_2(LH^N)_3][FeCl_4]_3$ (**2d**) in THF. After stirring of the reaction mixture for one day at room temperature and workup with dichloromethane, a red solid was obtained, which was characterised by FAB-MS, microanalysis, and IR to be **2a′**.

Conclusion

In summary, a series of bicyclic ironcryptates with encapsulated alkaline, alkaline earth, and rare earth metal cations was synthesised, as was a bicyclic metallacryptand with pyridinium units in the ligands. According to X-ray analyses, the strontium- and lanthanum-containing ironcryptates and the bicyclic pyridinium ironcryptand form helical structures, in contrast to the known *meso*-potassium ironcryptate. Future work will concentrate on possible interesting physical and chemical properties of rare earth metallacryptates and the potential use of the ironcryptates as selective complexation agents for certain cations.

This work was supported by a *NATO* grant (SRG 951516), by a *NSF/DAAD* grant, the *Deutsche Forschungsgemeinschaft*, the *Volkswagen-Stiftung* and the *Fonds der Chemischen Industrie*. V. S. thanks the *Freistaat Bayern* and the *Studienstiftung des Deutschen Volkes* for a postgraduate fellowship.

Experimental Section

General: The compounds H_2L (**1**) [1,1′-(2,6-pyridyl)bis-1,3-butanedione and 1,1′-(2,6-pyridyl)bis-4,4′-dimethyl-1,3-pentanedione] were prepared according to a literature procedure[9]. − IR: Bruker IFS 25. − FAB-MS: Micromass ZabSpec. − Microanalysis: Heraeus CHN-Mikroautomat; **2a−d** lose crystal solvent during drying.

General Procedure for the Synthesis of the Dinuclear Iron(III) Complexes **2b** *and* **2c**: To a solution of H_2L (**1**) (2 mmol) in 75 ml of dry THF, 359 mg (4 mmol) of strontium hydride, or 491 mg (4 mmol) of lanthanum(III) chloride was added. The mixture was stirred for 15 min at 20°C. Iron(III) chloride (216 mg, 1.33 mmol) was then added, and the dark red solution was stirred for 16 h at 20°C. The solvent was removed in vacuo, and the residue was suspended in 50 ml of dichloromethane. After standing for 16 h at 20°C, the red solution was filtered, the solvent removed, and the remaining crude product dried under vacuum (oil pump).

$[(Sr{\cdot}H_2O)\subset Fe_2L_3][FeCl_4]_2{\cdot}CH_2Cl_2{\cdot}Et_2O$ (**2b**): Ruby-coloured crystals were obtained according to the general procedure using 634 mg (4 mmol) of strontium chloride instead of strontium hydride and diffusion of a mixture of diethyl ether and hexanes into a dichloromethane solution. Yield 676 mg (76%), m. p. > 250°C (decomp.). − IR ($CHBr_3$): $\tilde{\nu}$ = 1721 cm^{-1} (C=O), 1553, 1515 (C=C). − FAB MS (3-nitrobenzyl alcohol matrix); *m/z*: 1222 ($Sr\subset Fe_2L_3{\cdot}2H_2O$), 1187 ($Sr\subset Fe_2L_3$). − $C_{63}H_{85}Cl_{12}Fe_4N_3O_{14}Sr$ (1844,77): calcd. C 41.02, H 4.64, N 2.28; found C 40.81, H 4.71, N 2.02.

$[(La{\cdot}THF{\cdot}H_2O)\subset Fe_2L_3][FeCl_4]_3{\cdot}2CH_2Cl_2$ (**2c**): Ruby-coloured tablets were obtained by diffusion of diethyl ether into a dichloromethane solution. Yield 898 mg (80%), m. p. > 250°C (decomp.). − IR ($CHBr_3$): $\tilde{\nu}$ = 1736 cm^{-1} (C=O), 1603, 1586 (C=C). − FAB MS (3-nitrobenzyl alcohol matrix); *m/z*: 1020 ($La\subset Fe_2L_3{\cdot}2H_2O$), 985 ($La\subset Fe_2L_3$), 757 ($La\subset Fe_2L_2{\cdot}H_2O$). − $C_{43}H_{45}Cl_{12}Fe_5LaN_3O_{14}$ (1687.41): calcd. C 30.61, H 2.69, N 2.49; found C 30.71, H 3.12, N 2.31.

$[Fe_2(LH^N)_3][FeCl_4]_3{\cdot}2CH_2Cl_2$ (**2d**): To a solution of 662 mg (2 mmol) of H_2L (**1**) in 75 ml of dry THF, 216 mg (1.33 mmol) of iron(III) chloride was added and the dark red solution was stirred

for 16 h at 20°C. The solvent was removed in vacuo and the residue was suspended in 50 ml of dichloromethane. After standing for 16 h at 20°C, the red solution was filtered, the solvent removed and the remaining crude product dried under vacuum (oil pump). Ruby-coloured crystals were obtained by diffusion of diethyl ether into a dichloromethane solution. Yield 1094 mg (97%), m. p. > 250°C (decomp.). – IR ($CHBr_3$): $\tilde{\nu}$ = 3217 cm^{-1} (N=H), 1587 (C=O), 1494 (C=C). – FAB MS (3-nitrobenzyl alcohol matrix); *m/z*: 1155 $[Fe_2(LH^N)_3 \cdot Fe]$, 1099 (Fe_2L_3), 771 (Fe_2L_2). – $C_{57}H_{72}Cl_{12}Fe_5N_3O_{12}$ (1695.88): calcd. C 40.37, H 4.28, N 2.48; found C 39.93, H 4.52, N 2.70.

[K⊂Fe$_2$L$_3$][FeCl$_4$] (**2a′**): To a solution of 102 mg (0.06 mmol) of $[Fe_2(LH^N)_3][FeCl_4]_3$ (**2d**) in 50 ml of dry THF, 24 mg (0.18 mmol) of potassium carbonate was added and the dark-red solution was stirred for 16 h at 20°C. The solvent was removed in vacuo, and the residue was suspended in 25 ml of dichloromethane. After standing for 16 h at 20°C, the red solution was filtered, the solvent removed, and the remaining crude product dried under vacuum (oil pump). Ruby-coloured microcrystals of **2a′** were obtained by diffusion of diisopropyl ether into a dichloromethane solution. Yield 67 mg (72%), m. p. > 250°C (decomp.). – IR ($CHBr_3$): $\tilde{\nu}$ = 1723 cm^{-1} (C=O), 1573, 1514 (C=C). – FAB MS (3-nitrobenzyl alcohol matrix); *m/z*: 1138 ($[K\subset Fe_2L_3]$), 809 ($[K\subset Fe_2L_2]$). – $C_{69}H_{93}Cl_5Fe_3KN_3O_{15}$ ($[K\subset Fe_2L_3][FeCl_4]\cdot 3THF$; 1552.96): calcd. C 53.37, H 6.04, N 2.71; found C 53.44, H 5.99, N 2.62.

Crystal Structure Determination of Compound **2b**: $C_{61}H_{81}Cl_8Fe_4N_3O_{14}Sr$, M = 1674.91, monoclinic, space group $P2_1/c$, a = 1735.6(4), b = 1925.7(4), c = 2299.6(5) pm, β = 98.35(3)°, V = 7.60(1) nm^3, Z = 4, $\rho_{calcd.}$ = 1.463 Mg/m^3, $F(000)$ = 3432, λ = 71.073 pm, T = 133 K, μ(Mo-K_α) = 1.781 mm^{-1}, min/max transmission: 0.470/0.776, crystal dimensions 0.50 × 0.28 × 0.15 mm; 3.48° ≤ 2Θ ≤ 50.00°; 110590 measured reflections of which 13252 were independent (R_{int} = 0.0672) and employed in the structure refinement (884 parameters, 492 restraints). The R values are $R1 = \Sigma|F_o - F_c|/|\Sigma F_o$ = 0.0465 [$I > 2\sigma(I)$] and $wR2 = [\Sigma w(F_o^2 - F_c^2)^2/\Sigma wF_o^4]^{1/2}$ = 0.0831 (all data); min/max residual electron density: −599 e nm^{-3}/602 e nm^{-3}. Two *tert*-butyl groups show two different rotameric conformations. One tetrachloroferrate anion is disordered over two sites[18].

Crystal Structure Determination of Compound **2c**: $C_{45}H_{47}Cl_{16}Fe_5LaN_3O_{14}$, M = 1839.27, triclinic, space group $P\bar{1}$, a = 1535.04(7), b = 2131.21(9), c = 2175.03(9) pm, α = 102.948(1), β = 91.732(1), γ = 97.320(1)°, V = 6.8654(5) nm^3, Z = 2, $\rho_{calcd.}$ = 1.78 g/cm^3, $F(000)$ = 3636.00, λ = 71.069 pm, T = 182 K, μ(Mo-K_α) = 0.2312 mm^{-1}, min/max transmission: 0.899/0.670, crystal dimensions 0.35 × 0.18 × 0.08 mm, 3.00° ≤ 2Θ ≤ 46.5°; 29795 collected reflections of which 19097 were independent (R_{int} = 0.046) and employed in the structure refinement (11762 parameters, 0 restraints). The R values are: $R1 = R = \Sigma\ F_o - F_c\ / \Sigma F_o$ = 0.057 [$I > 3\sigma(I)$] and $wR2 = R_w = [\Sigma w(F_o - F_c)^2 / \Sigma wF_o^2]^{1/2}$ = 0.065 (all data), where

$$w = \frac{1}{\sigma^2(F_o^2)} = \frac{4F_o^2}{\sigma^2(F_o^2)};$$

max/min residual electron density: 0.76 $e^-/Å^3$/−0.86 $e^-/Å^3$.

Crystal data were collected using a Siemens SMART diffractometer equipped with a CCD area detector. Data were integrated using SAINT and were corrected for Lorentz- and polarization effects. An empirical absorption correction was applied using XPREP (ellipsoidal model); equivalent reflections were merged. The structure was solved by direct methods and was refined on F using the teXsan crystallographic software package. The non-hydrogen atoms were refined anisotropically. Hydrogen atoms were included but not refined.

Crystal Structure Determination of Compound **2d**: $C_{59}H_{76}Cl_{16}Fe_5N_3O_{12}$, M = 1875.68, monoclinic, space group $P2_1$, a = 1467.8(3), b = 4000.1(8), c = 1511.4(3) pm, β = 111.20(3)°, V = 8.27(1) nm^3, Z = 4, $\rho_{calcd.}$ = 1.498 Mg/m^3, $F(000)$ = 3796, λ = 71.073 pm, T = 133 K, μ(Mo-K_α) = 1.4251 mm^{-1}, min/max transmission: 0.467/0.675, crystal dimensions 0.63 × 0.40 × 0.30 mm, 3.54° ≤ 2Θ ≤ 50.34°; 93692 measured reflections of which 23822 were independent (R_{int} = 0.0381) and employed in the structure refinement (1878 parameters, 1027 restraints). The R values are $R1$ = 0.0518 [$I > 2\sigma(I)$] and $wR2$ = 0.1136 (all data); min/max residual electron density: −752 e nm^{-3}/727 e nm^{-3}. Three *tert*-butyl groups and one tetrachloroferrate anion are disordered over two sites. Crystallographic data for **2b** and **2d** were collected with a Stoe-Siemens-Huber four-circle diffractometer with Siemens CCD area detector by using φ and ω scans on a shock-cooled crystal in an oil drop[15]. Data integration was performed with the program SAINT. A semi-empirical absorption correction was applied. The structures were solved by direct methods (SHELXS-97)[16]. Refinement of F^2 was accomplished by the least-squares method[17]. All non-hydrogen atoms were refined anisotropically. For the hydrogen atoms, the riding model was used. The hydrogen atoms attached to the nitrogen atoms in **2d** could be located in the difference Fourier synthesis. NH distances were restrained to a target value of 95 pm. All disordered components were refined anisotropically with the assistance of distance and ADP restraints[18].

[1] See for example: D. J. Cram, J. J. Cram, *Container Molecules and Their Guests*, in *Monographs in Supramolecular Chemistry*, The Royal Society of Chemistry, Cambridge, **1994**; F. Vögtle, *Supramolecular Chemistry: An Introduction*, J. Wiley and Sons, New York, **1993**; *Frontiers in Supramolecular Organic Chemistry and Photochemistry* (Eds.: H.-J. Schneider, H. Dürr), VCH, Weinheim, **1991**; J.-M. Lehn, *Supramolecular Chemistry*, VCH, Weinheim, **1995**; *Comprehensive Supramolecular Chemistry* (Eds.: J. L. Atwood, J. E. D. Davies, D. D. Macnicol, F. Vögtle, J.-M. Lehn), especially vol. 1 (Ed.: G. W. Gokel), *Molecular Recognition: Receptors for Cationic Guests*, vol. 9 (Eds.: J.-P. Sauvage, M. W. Hosseini), *Templating, Self-assembly and Self-organization*, 1st ed., Pergamon, Oxford, **1996**; S. J. Lippard, J. M. Berg, *Bioanorganische Chemie*, Spektrum Akademischer Verlag, Heidelberg, **1995**, chap. 5; C. Seel, F. Vögtle, *Angew. Chem.* **1992**, *104*, 542−563; *Angew. Chem. Int. Ed. Engl.* **1992**, *31*, 528−549; C. Moore, B. C. Pressman, *Biochem. Biophys. Res. Commun.* **1964**, *15*, 562; S. M. Gorun, G. C. Papaefthmiou, R. B. Frankel, S. J. Lippard, *J. Am. Chem. Soc.* **1987**, *109*, 4244−4255; S. J. Lippard, *Angew. Chem.* **1988**, *100*, 353−371; *Angew. Chem. Int. Ed. Engl.* **1988**, *27*, 344−361; K. Wieghardt, K. Pohl, I. Jibril, G. Huttner, *Angew. Chem.* **1984**, *96*, 66−67; *Angew. Chem. Int. Ed. Engl.* **1984**, *23*, 77−78; C. M. Flynn, Jr., *Chem. Rev.* **1984**, *84*, 31−41; and literature cited.

[2] G. W. Gokel, *Crown Ethers and Cryptands,* in *Monographs in Supramolecular Chemistry* (Ed.: J. Fraser Stoddart), The Royal Society of Chemistry, Cambridge, **1991**; C. J. Pedersen, *J. Am. Chem. Soc.* **1967**, *89*, 7017−7036; B. Dietrich, J.-M. Lehn, J.-P. Sauvage, *Tetrahedron Lett.* **1969**, 2885−2888; B. Dietrich, J.-M. Lehn, J.-P. Sauvage, *Tetrahedron Lett.* **1969,** 2889−2892; J.-M. Lehn, *Pure Appl. Chem.* **1978**, *50*, 871−892; J.-M. Lehn, *Pure Appl. Chem.* **1980**, *52*, 2442−2459;

[3] R. W. Saalfrank, A. Stark, K. Peters, H.-G. v. Schnering, *Angew. Chem.* **1988**, *100*, 878−880; *Angew. Chem. Int. Ed. Engl.* **1988**, *27*, 851−853; R. W. Saalfrank, R. Burak, A. Breit, D. Stalke, R. Herbst-Irmer, J. Daub, M. Porsch, E. Bill, M. Müther, A. X. Trautwein, *Angew. Chem.* **1994**, *106*, 1697−1699; *Angew. Chem. Int. Ed. Engl.* **1994**, *33*, 1621−1623; R. W. Saalfrank, R. Burak, S. Reihs, N. Löw, F. Hampel, H.-D. Stachel, J. Lentmeier, K. Peters, E. M. Peters, H.-G. v. Schnering, *Angew. Chem.* **1995**, *107*, 1085−1087; *Angew. Chem. Int. Ed. Engl.*

1995, *34*, 993−995; R. W. Saalfrank, N. Löw, F. Hampel, H.-D Stachel, *Angew. Chem.* **1996**, *108*, 2353−2354; *Angew. Chem. Int. Ed. Engl.* **1996**, *35*, 2209−2210; R. W. Saalfrank, N. Löw, S. Kareth, V. Seitz, F. Hampel, D. Stalke, M. Teichert, *Angew. Chem.* **1998**, *110*, 182−184; *Angew. Chem. Int. Ed. Engl.* **1998**, *37*, 172−174.

[4] D. Philp, J. F. Stoddart, *Angew. Chem.* **1996**, *108*, 1243-1286; *Angew. Chem. Int. Ed. Engl.* **1996**, *35*, 1154-1196; J.-M. Lehn, *Angew. Chem.* **1988**, *100*, 91−116; *Angew. Chem. Int. Ed. Engl.* **1988**, *27*, 89−112; J.-M. Lehn, *Angew. Chem.* **1990**, *102*, 1347−1362; *Angew. Chem. Int. Ed. Engl.* **1990**, *29*, 1304−1319.

[5] R. W. Saalfrank, N. Löw, B. Demleitner, D. Stalke, M. Teichert, *Chem. Eur. J.* **1998**, *4*, 1305−1311.

[6] R. W. Saalfrank, A. Dresel, V. Seitz, S. Trummer, F. Hampel, M. Teichert, D. Stalke, C. Stadler, J. Daub, V. Schünemann, A. X. Trautwein, *Chem. Eur. J.* **1997**, *3*, 2058−2062.

[7] For similar structures of metallacryptands c.f.: E. C. Constable, *Tetrahedron* **1992**, *48*, 10013−10059; E. C. Constable, *Angew. Chem.* **1991**, *103*, 1482−1483; *Angew. Chem. Int. Ed. Engl.* **1991**, *30*, 1450−1451; E. C. Constable, T. Kulke, M. Neuburger, M. Zehnder, *Chem. Commun.* **1997**, 489−490; E. J. Enemark, T. D. P. Stack, *Angew. Chem.* **1995**, *107*, 1082−1084; *Angew. Chem. Int. Ed. Engl.* **1995**, *34*, 996−998; R. Krämer, J.-M. Lehn, A. DeCian, J. Fischer, *Angew. Chem.* **1993**, *105*, 764−768; *Angew. Chem. Int. Ed. Engl.* **1993,** *32*, 703−706; R. C. Scarrow, D. L. White, K. N. Raymond, *J. Am. Chem. Soc.* **1985**, *107*, 6540−6546; C. J. Carrano, K. N. Raymond, *J. Am. Chem. Soc.* **1978**, *100*, 5371−5374; B. Kersting, M. Meyer, R. E. Powers, K. N. Raymond, *J. Am. Chem. Soc.* **1996**, *118*, 7221−7222; A. Williams, *Chem. Eur. J.* **1997**, *3*, 15−19; L. J. Charbonniere, A. F. Williams, U. Frey, A. E. Merbach, P. Kamalaprija, O. Schaad, *J. Am. Chem. Soc.* **1997**, *119*, 2488−2496; C. Piguet, G. Bernardinelli, A. F. Williams, B. Bocquet, *Angew. Chem.* **1995**, *107*, 618−621; *Angew. Chem. Int. Ed. Engl.* **1995**, *34*, 582−584.

[8] For similar structures of metallacryptates c.f.: E. J. Corey, C. L. Cywin, M. C. Noe, *Tetrahedron Lett.* **1994**, *35*, 69−72; C. Krebs, M. Winter, T. Weymüller, E. Bill. K. Wieghardt, P. Chaudhuri, *J. Chem. Soc., Chem. Commun.* **1995**, 1913−1915; P. Chaudhuri, M. Winter, P. Fleischhauer, W. Haase, U. Flörke, H.-J. Haupt, *J. Chem. Soc., Chem. Commun.* **1990**, 1728−1730; P. Chaudhuri, M. Winter, B. P. C. Della Vedova, P. Fleischbauer, W. Haase, U. Flörke, H.-J. Haupt, *Inorg. Chem.* **1991**, *30*, 4777−4783; P. Chaudhuri, M. Winter, F. Birkelbach, P. Fleischbauer, W. Haase, U. Flörke, H.-J. Haupt, *Inorg. Chem.* **1991**, *30*, 4291−4293; M. Albrecht, S. Kotila, *Angew. Chem.* **1996**, *108*, 1299−1300; *Angew. Chem. Int. Ed. Engl.* **1996**, *35*, 1208−1210.

[9] D. E. Fenton, J. R. Tate, *Inorg. Chim. Acta* **1984**, *83*, 23−31.

[10] *SMART, Area-Detector Software Package*, Siemens Industrial Automation, Inc., Madison, WI, **1995**.

[11] *SAINT, SAX Area-Detector Integration Program, V4.024*, Siemens Industrial Automation, Inc., Madison, WI, **1995**.

[12] *XPREP, v. 5.03*, Part of the *SHELXTL Crystal Structure Determination Package*, Siemens Industrial Automation, Inc., Madison,WI, **1995**.

[13] *SIR92*: A. Altomare, M. C. Burla, M. Camalli, M. Cascarano, C. Giacovazzo, A. Guagliardi, G. Polidori, *J. Appl. Crystallogr.* **1993**, *26*, 343.

[14] *teXsan, Crystal Structure Analysis Package*, Molecular Structure Corporation, **1985**, **1992**.

[15] T. Kottke, D. Stalke, *J. Appl.Crystallogr.* **1993**, *26*, 615.

[16] G. M. Sheldrick, "SHELXS-97, Program for structure solution", *Acta Crystallogr.* **1990**, *A46*, 467.

[17] G. M. Sheldrick, *SHELXL-97*, *Program for structure refinement*, University of Göttingen, **1997**.

[18] Crystallographic data (excluding structure factors) for the structures reported in this paper have been deposited with the Cambridge Crystallographic Data Centre as supplementary publication no. CCDC-101639 (**2b**), -101640 (**2d**) and -101280 (**2c**). Copies of the data can be obtained free of charge on application to CCDC, 12 Union Road. GB-Cambridge CB2 1EZ, UK (Fax: int. code + 44-1223/336-033; E-mail: deposit@ccdc.cam.ac.uk). A red-green stereo presentation of **2a** is available on the WWW under http://www.organik.uni-erlangen.de/saalfrank/index.html [98086]

Thermal Decomposition of (Pentamethylcyclopentadienyl)titanium(IV) Complexes Containing Dialkylamido Ligands – X-ray Structure of $[\{\eta^5:\eta^2\text{-}C_5Me_4CH_2CH_2N(Me)CN(C_6H_3Me_2)\}TiCl_2]$

Mikhail Galakhov, Pilar Gómez-Sal, Avelino Martín, Miguel Mena*, and Carlos Yélamos

Departamento de Química Inorgánica, Universidad de Alcalá, Campus Universitario,
E-28871 Alcalá de Henares, Spain
Fax: (internat) + 34-1/8854683
E.mail: mmena@inorg.alcala.es

Received March 30, 1998

Keywords: Titanium / C–H activation / Amido complexes / Bridging imide ligands / Bridging imine group

The new organometallic binuclear complexes $[\{Cp^*Ti(NEt_2)\}_2(\mu\text{-}NEt)_2]$ (**1**), $[(Cp^*Ti)_2(NMe_2)(NHMe_2)(\mu\text{-}NMe)(\mu\text{-}NCH_2)]$ (**2**), and $[(Cp^*TiCl)_2(\mu\text{-}NMe)_2]$ (**3**) have been obtained by heating the dialkylamido derivatives $[Cp^*Ti(NR_2)_nCl_{3-n}]$ (R = Et, n = 3; R = Me, n = 2, 3) ($Cp^* = \eta^5\text{-}C_5Me_5$) in solution and at different temperatures. The thermal decomposition of $[Cp^*Ti(NMe_2)Cl_2]$ at temperatures above 145 °C caused the activation of the pentamethylcyclo-pentadienyl ligand to give the new, geometrically constrained, complex $[\{\eta^5:\eta^1\text{-}C_5Me_4CH_2CH_2N(Me)\}TiCl_2]$ (**5**). Addition of the isocyanide 2,6-$Me_2C_6H_3NC$ to the solution obtained in this last process led to the isolation of the complex $[\{\eta^5:\eta^2\text{-}C_5Me_4CH_2CH_2N(Me)CN(C_6H_3Me_2)\}\text{-}TiCl_2]$ (**6**) by insertion of one isocyanide molecule into the titanium–nitrogen bond in **5**. The structure of **6** has been proved by an X-ray diffraction study which showed the organic ligand, $C_5Me_4CH_2CH_2N(Me)CN(C_6H_3Me_2)$, to be coordinated to the titanium atom via the cyclopentadienyl ring and a η^2-iminocarbamoyl fragment. Heating of the trinuclear oxo derivative $[\{Cp^*Ti(NMe_2)\}_3(\mu\text{-}O)_3]$ at 110 °C gave the complex $[\{Cp^*{}_3Ti_3(NMe_2)(\mu\text{-}\eta^2\text{-}CH_2NMe)\}(\mu\text{-}O)_3]$ (**4**) where an imine ligand bridges two of the three metallic centres.

Studies on the decomposition of inorganic or organometallic complexes and polymers is currently a fast emerging area in chemistry. The preparation of ceramic materials from precursor complexes is a fascinating challenge for inorganic or solid-state chemists involved in the design of routes to new or improved refractory metal oxides, carbides, and nitrides.[1]

For instance, titanium nitride possesses a number of useful properties, including extreme hardness, excellent chemical resistance, desirable optical properties, and good electrical conductivity.[2] The current trend to obtain this material in low-temperature processes necessitates the use of inorganic precursors, and in particular amido complexes $Ti(NR_2)_4$ have been extensively used.[3] Their thermal decomposition in vapour-phase CVD processes has been shown to lead to the incorporation of carbon and hydrogen in the desired nitride.[4] These impurities can be reduced by reaction with ammonia[5] but in all cases, the carbon percentage is significant, and attributed to the formation of metallacycles, as has been described in solution.[6]

In our research into the stability of mono(pentamethylcyclopentadienyl)titanium derivatives, we have recently reported on the formation of alkylidyne complexes by the thermal decomposition of the alkyl precursors[7] and we were interested in expanding these studies to other ligands attached to the metal centre. Here we describe the synthesis and characterisation of several organometallic derivatives obtained by heating the dialkylamido complexes of titanium, $[Cp^*Ti(NR_2)_nCl_{3-n}]$ and $[\{Cp^*Ti(NMe_2)\}_3(\mu\text{-}O)_3]$ in solution.[8]

Results and Discussion

A toluene solution of the complex $[Cp^*Ti(NEt_2)_3]$ was heated at 70°C for 20 d in a Carius tube (to guarantee the purity of the atmosphere); subsequent evacuation of the volatiles under vacuum and crystallisation from hexane allowed the isolation of $[\{Cp^*Ti(NEt_2)\}_2(\mu\text{-}NEt)_2]$ (**1**) as a pure complex (see Scheme 1).

The spectroscopic and analytical data (Experimental Section) are consistent with a dimeric structure of **1**, with two bridging ethylimide ligands. According to the ^{1}H-NMR data, this complex is characterised by a *cis* arrangement[9] of both the terminal diethylamido and pentamethylcyclopentadienyl ligands with respect to the central $Ti_2(\mu\text{-}NEt)_2$ core.

Complex $[Cp^*Ti(NMe_2)_3]$ decomposed between 120 and 150°C with elimination of $NHMe_2$ and formation of the organometallic derivative $\{[Cp^*Ti]_2(NMe_2)(NHMe_2)(\mu\text{-}NMe)(\mu\text{-}N{=}CH_2)\}$ (**2**) (see Scheme 1 and Experimental Section). Complex **2** was isolated in a yield of 64% as a dark-green crystalline solid. The ^{13}C-NMR spectrum of **2** shows one doublet of doublets at δ = 100.8 (^1J = 154.1 Hz, ^1J = 159.6 Hz) while its ^{1}H-NMR spectrum presents two signals at δ = 3.79 (1 H) and 3.81 (1 H) (^2J < 0.2 Hz), corresponding to the existence of a bridging $\mu\text{-}N{=}CH_2$ ligand.[10] Two broad signals for the methyl groups of the

 © WILEY-VCH Verlag GmbH, D-69451 Weinheim, 1998 1434–1948/98/0909–1319 $ 17.50+.50/0

Scheme 1. Thermolyses of the complexes $[Cp^*Ti(NEt_2)_3]$, $[Cp^*Ti(NMe_2)_3]$ and $[Cp^*Ti(NMe_2)_2Cl]$

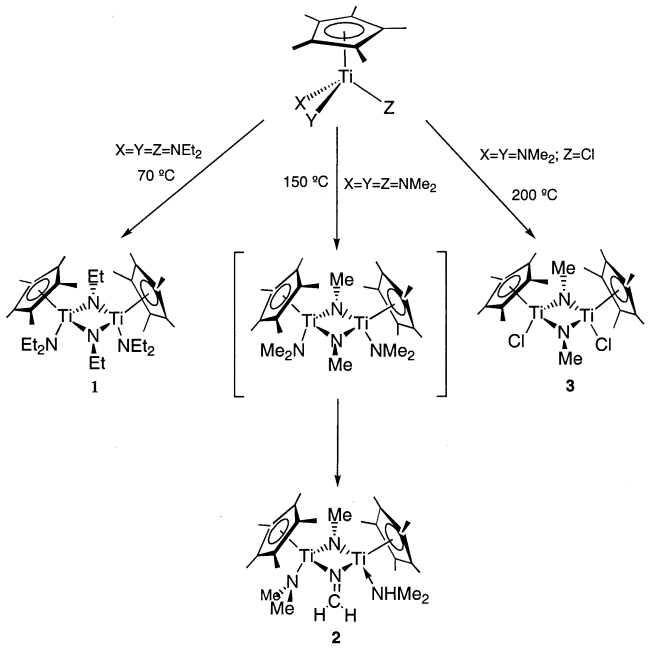

terminal NMe_2 ligands were also observed in the spectra at room temp., which collapsed together at 313 K ($\Delta G^{\#} \approx 63$ kJ/mol). This spectral behaviour is based on the slow rotation around the Ti−N bond, indicating π-donation of the nitrogen electron pair to the titanium centre. The value of the Gibbs free energy is similar to those reported for other dimethylamido complexes (46−100 kJ/mol).[11] Finally the ^{1}H-NMR spectrum exhibits two doublets at δ = 1.6 (^3J = 6.0 Hz) and 1.7 (^3J = 6.0 Hz) for the diastereotopic methyl groups, and one septuplet at δ = 4.01 for the amine proton of the coordinated $HNMe_2$ ligand. This ligand remains in the complex after several hours under vacuum (10^{-2} Torr) or even in THF solution. The formation of complex **2** might be explained by the activation of one C−H bond in a methylimide group[12] from a "$[\{Cp^*Ti(NMe_2)\}_2(\mu\text{-}NMe)_2]$" intermediate, similar to **1** (Scheme 1), and formation of one equivalent of $NHMe_2$ which is retained in the complex.

In an analogous procedure, heating a solution of $[Cp^*Ti(NMe_2)_2Cl]$ in toluene at 135−200°C afforded the compound $[(Cp^*TiCl)_2(\mu\text{-}NMe)_2]$ (**3**) in a yield of 63%. The analytical and spectroscopic data of **3** agree with a dimeric formulation where the Cp* rings appear in a *cis* arrangement, as proposed for **1** (Scheme 1).

In order to explain the formation of the complexes **1**−**3**, we suggest that the thermal decomposition of the compounds $[Cp^*Ti(NR_2)_nCl_{3-n}]$ (R = Et, n = 3; R = Me, n = 2, 3) produces azatitanacyclopropane or imine intermediates similar to those described in the literature for other dialkylamido derivatives.[6] The evolution of these intermediates at high temperatures would give rise to Ti=NR groups; processes which are well-documented for tantalum complexes.[6b][13] However, titanium derivatives with terminal imido ligands are only known in the presence of donor molecules,[14] and in their absence binuclear arrangements with $[Ti_2(\mu\text{-}NR)_2]$ cores are usually found.[15]

The proposed azatitanacyclopropane intermediates were not detected in the case of mononuclear precursors, but fortunately we could isolate and characterise the complex $[Cp^*_3Ti_3(NMe_2)(\mu\text{-}\eta^2\text{-}CH_2NMe)(\mu\text{-}O)_3]$ (**4**) with the imine group bridging two titanium centres, as mentioned above (see Scheme 2). This compound was obtained as a crystalline red solid (63% yield) by heating a toluene solution of the trinuclear oxo derivative $[Cp^*_3Ti_3(NMe_2)_3(\mu\text{-}O)_3]$.

Scheme 2. Thermal evolution of the trinuclear oxo compound $[\{Cp^*Ti(NMe_2)\}_3(\mu\text{-}O)_3]$

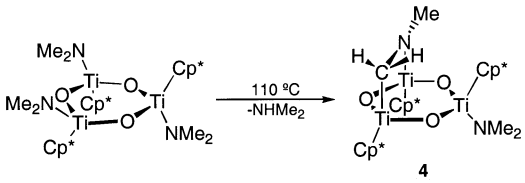

The ^{1}H- and ^{13}C-NMR data of **4** show three resonances for the Cp* ligands and one signal for the terminal NMe_2 group, while the signal of the CH_2 moiety of the bridging imine fragment appears as a triplet of quadruplets (δ = 87.9, ^1J = 149.5 Hz, ^3J = 3.7 Hz) in the ^{13}C-NMR spectrum and as an AB spin system (δ = 1.82, 2.86; J_{AB} = 5.9 Hz) in the ^{1}H-NMR spectrum. The formation of this kind of bridging imine groups from an amido ligand has been already reported by Chisholm et al. for the complex $[W_2Cl_3(NMe_2)_2L_2(\mu\text{-}CHCH_2)(\mu\text{-}CH_2NMe)]$.[6e]

Different results than those described above were observed when a [D$_6$]benzene solution of the $[Cp^*Ti(NMe_2)Cl_2]$ derivative was heated above 140°C. Not only did the activation of the amido group take place, but also the activation of the Cp* unit, yielding the compound $[\{\eta^5\text{:}\eta^1\text{-}C_5Me_4CH_2CH_2N(Me)\}TiCl_2]$ (**5**) (see Scheme 3).

Scheme 3. Thermal decomposition of the complex $[Cp^*Ti(NMe_2)Cl_2]$

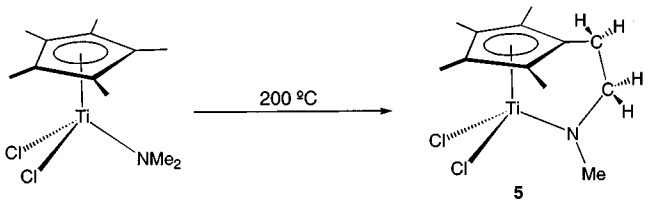

The ^{1}H-NMR spectrum of **5** in $CDCl_3$ shows two resonances for the α- and β-methyl groups of the C_5Me_4 ring [δ = 2.11 (6 H), 2.17 (6 H)] and an AA′BB′K$_3$ spin system [δ = 3.32 (2 H), 4.54 (2 H) and 3.55 (3 H)] assigned to the CH_2CH_2NMe moiety, supporting the hypothesis of C−H activation giving rise to the chelating ligand $[C_5Me_4(CH_2)_2NMe]$. This ligand is linked to the titanium atom via the cyclopentadienyl ring and the amido group in a similar fashion to those reported for the $\{[\eta^5\text{:}\eta^1\text{-}C_5H_4(CH_2)_nNR]MX_2\}$ (M = Ti, Zr) complexes.[16]

The most important features of the ^{13}C-NMR spectrum (see Experimental Section) are the downfield shift (Δδ =

11.3) of the $C_{ipso}CH_2$ resonance (δ = 139.7) with respect to the starting complex [Cp*Ti(NMe_2)Cl_2], and the observation of the CH_2NMe signal at δ = 79.4. These data are best accounted for if a high contribution of the constrained geometry resonance structure **II** depicted in Figure 1 is assumed.

Figure 1. Resonance structures proposed for compound **5**

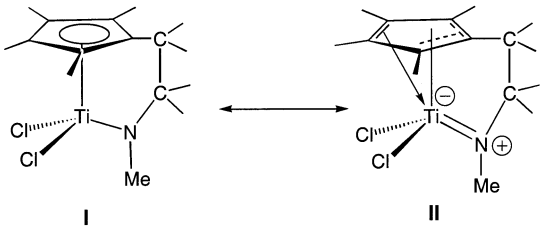

The addition of excess of 2,6-dimethylphenyl isocyanide to a solution of **5** causes the insertion of one molecule of isocyanide into the Ti−N bond affording the iminocarbamoyl derivative [{η^5:η^2-$C_5Me_4CH_2CH_2N(Me)CN(C_6H_3Me_2)$}$TiCl_2$] (**6**) (Scheme 4).

Scheme 4. Insertion reaction of isocyanide in complex **5**

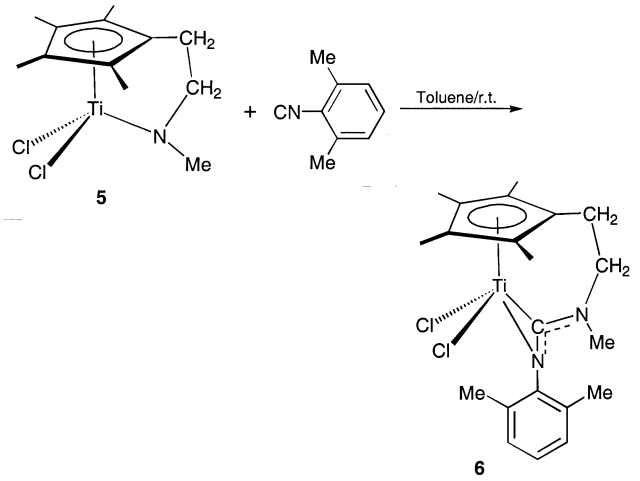

The complex **6** was obtained as an orange solid, insoluble in hexane, slightly soluble in benzene or toluene, and soluble in chloroform or dichloromethane. The most prominent band in the IR spectrum is the very intense ν_{CN} absorption at 1668 cm^{-1}, in agreement with the insertion of xylyl isocyanide.

In order to confirm the Cp* activation and assess its structural consequences, the molecular structure of this compound was determined by an X-ray diffraction study (see Figure 2). Selected bond lengths and angles of **6** can be found in Table 1. The compound is a monomer with the ligand [$C_5Me_4CH_2CH_2N(Me)CN(C_6H_3Me_2)$] linked to the metal centre through the cyclopentadienyl ring (η^5) and both the carbon and the nitrogen atoms (η^2) of the inserted isocyanide.

The molecule exhibits a four-legged stool geometry for the titanium atom [Cl(1), Cl(2), C(1), N(2)] where the N(2) atom lies down from, and C(1) is shifted up to, the cyclopentadienyl ring due to the side chain [N(1), C(3), C(16)]; this shows a zigzag disposition similar to those found in the complexes [{η^5:η^1-$C_5Me_4CH_2CH_2NMe_2$}CoI_2],[17] [{η^5:η^1-$C_5H_4CH_2CH_2NMe_2$}$Mo(CO)_2I$],[18] and [{η^5:η^2-$C_5H_4CH_2CH_2N(Me)CO$]Re(CO)SePh].[19] The carbon−carbon bond lengths in the cyclopentadienyl ring are in the normal range [1.395(12)−1.420(12) Å]. The methyl groups in the C_5Me_4 fragment are displaced with respect to the metal centre, in particular C(16), which is placed 0.23 Å above the cyclopentadienyl ring plane.

Figure 2. ORTEP drawing of [{η^5:η^2-$C_5Me_4CH_2CH_2N(Me)CN(C_6H_3Me_2)$}$TiCl_2$] (**6**); thermal ellipsoids at a 50% level are shown

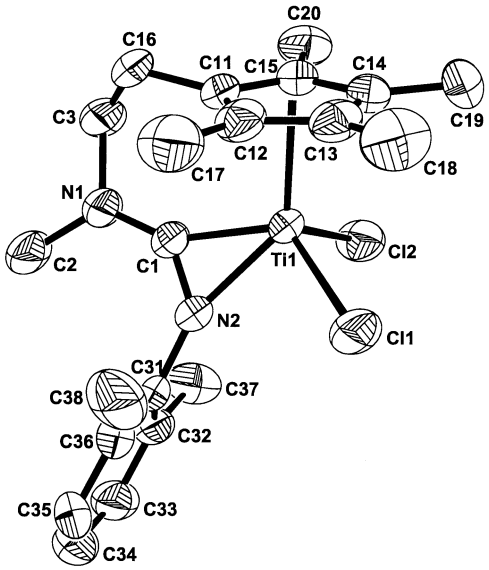

Table 1. Selected bond lengths [Å] and angles [°] for the compound [{η^5:η^2-$C_5Me_4CH_2CH_2N(Me)CN(C_6H_3Me_2)$}$TiCl_2$] (**6**); Cp* and E are the centroids of the cyclopentadienyl ring and the N(2)−C(1) bond, respectively

Ti(1)−C(1)	2.000(8)	N(2)−C(31)	1.421(10)
Ti(1)−N(2)	2.047(6)	N(1)−C(1)	1.316(10)
Ti(1)−Cl(1)	2.349(3)	N(1)−C(2)	1.457(11)
Ti(1)−Cl(2)	2.287(3)	N(1)−C(3)	1.476(11)
Ti(1)−C(11)	2.333(8)	C(3)−C(16)	1.513(14)
Ti(1)−C(12)	2.329(8)	C(16)−C(11)	1.504(12)
Ti(1)−C(13)	2.392(8)	C(11)−C(15)	1.399(11)
Ti(1)−C(14)	2.428(8)	C(11)−C(12)	1.420(12)
Ti(1)−C(15)	2.365(8)	C(12)−C(13)	1.403(13)
Ti(1)−Cp*	2.046	C(13)−C(14)	1.395(12)
Ti(1)−E	1.920	C(14)−C(15)	1.413(11)
N(2)−C(1)	1.284(9)		
C(1)−Ti(1)−N(2)	37.0(3)	N(2)−Ti(1)−Cl(1)	88.1(2)
C(1)−Ti(1)−Cl(2)	100.9(2)	Ti(1)−N(2)−C(31)	158.4(5)
C(1)−Ti(1)−Cl(1)	123.3(2)	Ti(1)−N(2)−C(1)	69.5(4)
Cl(1)−Ti(1)−Cl(2)	101.01(11)	C(1)−N(2)−C(31)	132.0(7)
E−Ti(1)−Cl(1)	105.6	Ti(1)−C(1)−N(1)	150.7(6)
E−Ti(1)−Cl(2)	100.7	Ti(1)−C(1)−N(2)	73.5(5)
Cp*−Ti(1)−Cl(1)	112.7	N(2)−C(1)−N(1)	135.5(8)
Cp*−Ti(1)−Cl(2)	112.5	C(1)−N(1)−C(2)	126.2(7)
Cp*−Ti(1)−N(2)	136.5	C(1)−N(1)−C(3)	115.5(7)
Cp*−Ti(1)−C(1)	105.7	C(2)−N(1)−C(3)	118.3(7)
Cp*−Ti(1)−E	121.8	N(1)−C(3)−C(16)	111.6(8)
N(2)−Ti(1)−Cl(2)	99.3(2)	C(3)−C(16)−C(11)	117.3(8)

The inserted isocyanide has an N(2)−C(1) bond length of 1.284(9) Å, which is consistent with a double bond,[20] while Ti(1)−N(2) [2.047(6) Å] is in agreement with the Ti−N distances found in η^2-iminoacyltitanium complexes,[20b][21] and is very similar to those of [Cp*$_2$Ti^{III}(NMePh)] [2.054(2) Å][22] and [(CO_5)W{C(NMe$_2$)O}TiCp*(NMe$_2$)$_2$] (av. 2.058 Å)[23] where a single bond with absence of multiple bonding is suggested. The Ti(1)−C(1) [2.000(8) Å] distance is not significantly different to that found in the comparable acyl complex [Cp*Ti(η^2-COMe)Cl$_2$] [2.021(6) Å].[24]

On the other hand, N(1)(sp^2) has a planar environment and its bond length with C(1)(sp^2) [1.316(10) Å] is only slightly longer than the double bond N(2)(sp^2)−C(1)(sp^2) and 0.1 Å shorter than the single bond N(2)(sp^2)−C(31)(sp^2) [1.421(10) Å]. All these data, together with the planarity of the C(3)C(2)N(1)C(1)N(2)C(31)Ti(1) system, are indicative of an extensive π delocalisation along the N(1)C(1)N(2) fragment, while the xylyl group is twisted 80.5(4)° with respect to this fragment. Analogous structural features have been reported in the literature for other η^2-iminocarbamoyl complexes, and are explained by the contribution of the three resonance forms shown in Figure 3.[25]

Figure 3. Resonance forms for the η^2-iminocarbamoyl group in complex **6**

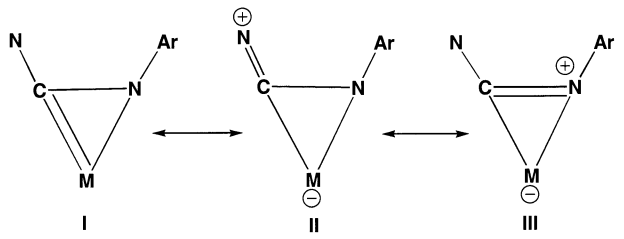

The ^{1}H-NMR spectrum indicates two signals for methyl groups of the C$_5$*Me*$_4$ ring and an AA′BB′K$_3$ spin system for the C*H*$_2$C*H*$_2$N*Me* fragment. The C_s symmetry observed in solution is due to a very fast exchange, on the NMR time scale and even at low temperature, between the two enantiomers present (Figure 4).

Figure 4. The two enantiomers of complex **6**

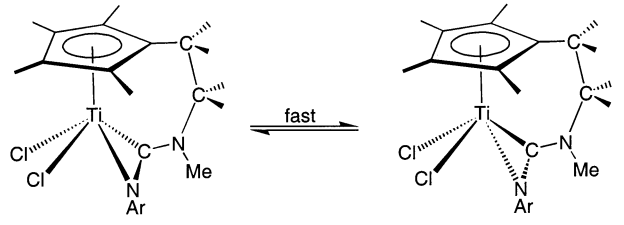

In the ^{13}C-NMR spectrum we observed a signal at δ = 197.2 associated with the (η^2-iminocarbamoyl)Ti entity and a considerable higher field displacement for the carbon resonances of C_{ipso}CH$_2$ [δ = 123.4, Δδ = δ(**5**) − δ(**6**) = 16.3], N*C*H$_2$ (δ = 56.3, Δδ = 23.1) and CH$_2$N*C*H$_3$ (δ = 35.9, Δδ = 9.8). This spectral behaviour is attributable to the isocyanide insertion into the titanium−nitrogen bond of **5**, the consequent backbone expansion and the π delocalisation proposed for the iminocarbamoyl fragment (structures **I** and **III** in Figure 3).

Conclusions

In our exploration of the thermal decomposition of the titanium complexes [Cp*Ti(NR$_2$)$_n$Cl$_{3-n}$] we have observed the formation of binuclear derivatives with [Ti$_2$(μ-NEt)$_2$] and [Ti(μ-NMe)(μ-N=CH$_2$)Ti] cores, and a mononuclear compound with the interesting methyl activation of the pentamethylcyclopentadienyl ligand. This last observation was definitely confirmed by the characterisation of the complex [{η^5:η^2-C$_5$Me$_4$CH$_2$CH$_2$N(Me)CN(C$_6$H$_3$Me$_2$)}TiCl$_2$], which is one of few examples known of isocyanide insertion into metal−nitrogen bonds. The thermal evolution of the trinuclear oxo compound [{Cp*Ti(NMe$_2$)}$_3$(μ-O)$_3$] seems to be facilitated by a cooperative effect between the metallic centres to form a bridging imine group [−CH$_2$−N(Me)−] supported on a TiO$_2$-like arrangement.

Financial support from the Spanish *DGICYT* (PB93-0476), *CAM* (C198/91) and the *Universidad de Alcalá* (E001/97) is gratefully acknowledged. C. Y. also thanks the *CAM* for a Predoctoral Fellowship.

Experimental Section

All reactions were carried out under argon by Schlenk techniques or in an M. Braun glovebox.[26] Hexane was refluxed over Na/K amalgam, toluene over sodium, and both distilled under argon prior to use. NMR solvents were dried with P_2O_5 (CDCl$_3$) or Na/K amalgam (C$_6$D$_6$) and vacuum-distilled from 4 Å molecular sieves. Oven-dried glassware was repeatedly evacuated with a pumping system (ca. 1×10^{-3} Torr) and subsequently filled with inert gas. 2,6-Me$_2$C$_6$H$_3$NC (FLUKA) was used as received. [Cp*Ti(NR$_2$)$_n$Cl$_{3-n}$] and [{Cp*Ti(NMe$_2$)}$_3$(μ-O)$_3$] were prepared by known procedures.[8] − IR (KBr): Perkin-Elmer 883 spectrophotometer. − ^{1}H and ^{13}C NMR: Varian Unity-300 and/or 500-Plus spectrometer, trace amounts of protonated solvents were used as references, and chemical shifts are reported relative to TMS. − EI MS: 70 eV with a Hewlett-Packard 5988 spectrometer. − Elemental analyses: Heraeus CHN-O-Rapid microanalyzer. − Thermolyses: Roth autoclave model III (300 ml), with heater model 30S (20−300°C) and temperature regulator model DR 500.

*Synthesis of [{Cp*Ti(NEt$_2$)}$_2$(μ-NEt)$_2$]* (**1**): A solution of [Cp*Ti(NEt$_2$)$_3$] (0.55 g, 1.38 mmol) in toluene (20 ml) was transferred via cannula into a Carius tube (40 ml capacity) ready to be sealed by flame in vacuum. This solution was heated at 70°C for 20 d. The Carius tube was opened in a glovebox and the volatiles were removed under vacuum. The oily red solid obtained was dissolved in 15 ml of hexane and cooled overnight at −40°C to afford a red solid which, after several hours under vacuum, was characterised as the complex **1** (0.14 g, 37%). − IR (KBr): $\tilde{\nu}$ = 1439 cm^{-1} s, 1372 s, 1322 m, 1142 m, 1118 s, 1000 s, 875 m, 787 s, 584 s, 508 s, 419 m. − ^{1}H NMR (C$_6$D$_6$, 20°C): δ = 3.85 [q, ^3J = 7.2 Hz, 8 H, N(C*H*$_2$CH$_3$)$_2$], 3.66 [q, ^3J = 7.2 Hz, 4 H, μ-N(C*H*$_2$CH$_3$)], 2.04 (s, 30 H, C$_5$*Me*$_5$), 1.15 [t, 12 H, N(CH$_2$C*H*$_3$)$_2$], 1.11 [t, 6 H, μ-N(CH$_2$C*H*$_3$)]. − ^{13}C{^{1}H} NMR (C$_6$D$_6$, 20°C): δ = 118.3 (*C*$_5$Me$_5$), 55.6 [μ-N(*C*H$_2$CH$_3$)], 50.5 [N(*C*H$_2$CH$_3$)$_2$], 20.3 [(μ-N(CH$_2$*C*H$_3$)], 16.1 [N(CH$_2$*C*H$_3$)$_2$], 12.3 (C$_5$*Me*$_5$). − EI MS (70 eV); *m/z* (%): 523 (3) [M$^+$ − NHEt$_2$], 448 (17) [M$^+$ − 2NHEt$_2$], 313 (7) [M$^+$ − 2 NHEt$_2$ − Cp*]. − C$_{32}$H$_{60}$N$_4$Ti$_2$ (596.65): calcd. C 64.42, H 10.14, N 9.39; found: C 64.00, H 10.24, N 8.42.

*Synthesis of [{Cp*Ti}$_2$(NMe$_2$)(NHMe$_2$)(μ-NMe)(μ-N=CH$_2$)]* (**2**): As for compound **1**, a hexane solution (40 ml) of 1.00 g (3.17 mmol) of [Cp*Ti(NMe$_2$)$_3$] was heated in an autoclave at 150°C for 8 d. The solution was cooled at −40°C for 1 d to yield dark-green crystals of **2**. After washing with hexane (20 ml) and drying under vacuum, 0.52 g (64%) of the complex **2** was isolated. − IR (KBr): $\tilde{\nu}$ = 1437 cm^{-1}s, 1373 s, 1304 m, 1233 m, 1131 s, 1023 m, 930 s, 902 m, 787 s, 638 m, 595 s, 518 s, 460 m, 350 m. − ^{1}H NMR (C$_6$D$_6$, 20°C): δ = 4.54 (s, 3 H, μ-N*Me*), 4.01 (spt, 1 H, N*H*Me$_2$), 3.81 (s, 1 H, NC*H*H), 3.79 (s, 1 H, NCH*H*), 2.22 (br., 3 H, N*Me*Me), 2.05 (br., 3 H, NMe*Me*), 2.04 (s, 15 H, C$_5$*Me*$_5$), 1.94 (s, 15 H, C$_5$*Me*$_5$), 1.70 (d, ^3J = 6.0 Hz, 3 H, NH*Me*Me), 1.61 (d, ^3J = 6.0 Hz, 3 H, NHMe*Me*). − ^{13}C{^{1}H} NMR (C$_6$D$_6$, 20°C): δ = 115.4 and 114.8 (*C*$_5$Me$_5$), 100.8 (N=*C*H$_2$), 50.6 (μ-N*Me*), 44.6 and 42.0 (br. s, N*Me*$_2$), 39.0 and 38.9 (NH*Me*$_2$), 11.5 and 11.3 (C$_5$*Me*$_5$). − EI MS (70 eV); *m/z* (%): 467 (51) [M$^+$ − NHMe$_2$], 448 (29) [M$^+$ − 2 NHMe$_2$]. − C$_{26}$H$_{48}$N$_4$Ti$_2$ (512.49): calcd. C 60.94, H 9.44, N 10.93; found C 61.18, H 9.34, N 10.87.

*Synthesis of [{Cp*TiCl}$_2$(μ-NMe)$_2$]* (**3**): After heating 1.06 g (3.46 mmol) of [Cp*Ti(NMe$_2$)$_2$Cl] in toluene (25 ml) at 200°C for 6 d, the resulting solution was left at room temp. affording a first portion of red crystals of **3**, which were collected by filtration. A second portion of crystals was obtained from the filtrate after cooling at −40°C. The combined yield of the imido complex **3** was 0.54 g (63%). − IR (KBr): $\tilde{\nu}$ = 1488 cm^{-1} m, 1427 s, 1377 s, 1107 vs, 1024 m, 785 vs, 730 m, 581 vs, 521 m, 444 s, 407 m, 357 m, 314 m. − ^{1}H NMR (C$_6$D$_6$, 20°C): δ = 3.41 (s, 6 H, μ-N*Me*), 1.98 (s, 30 H, C$_5$*Me*$_5$). − ^{13}C{^{1}H} NMR (C$_6$D$_6$, 20°C): δ = 124.1 (*C*$_5$Me$_5$), 48.6 (μ-N*Me*), 11.4 (C$_5$*Me*$_5$). − EI MS (70 eV); *m/z* (%): 495 (19) [M$^+$], 465 (100) [M$^+$ − 2 Me], 360 (37) [M$^+$ − Cp*], 330 (52) [M$^+$ − 2 Me − Cp*]. − C$_{22}$H$_{36}$Cl$_2$N$_2$Ti$_2$ (495.25): calcd. C 53.36, H 7.33, N 5.66; found C 53.10, H 7.42, N 5.71.

Synthesis of [{Cp$_3$Ti$_3$(NMe$_2$)(μ-η^2-CH$_2$NMe)}(μ-O)$_3$]* (**4**): In a similar procedure, 1.04 g (1.43 mmol) of [{Cp*Ti(NMe$_2$)}$_3$(μ-O)$_3$] in 70 ml of toluene was heated at 110°C for 17 d to give a dark solution. Red crystals of complex **4** were obtained when the solution was allowed to cool to room temp. Other fractions of the product were collected by concentration to half of the initial volume and cooling at −40°C for 5 d. The combined yield was 0.62 g (63%). − IR (KBr): $\tilde{\nu}$ = 1438 cm^{-1} s, 1372 s, 1235 s, 1172 m, 1074 m, 956 s, 717 vs, 681 s, 645 s, 617 s, 567 m, 402 vs. − ^{1}H NMR (C$_6$D$_6$, 20°C): δ = 2.97 (s, 6 H, N*Me*$_2$), 2.86 and 1.82 (AB spin system, ^2J = 5.9 Hz, 2 H, C*H*$_2$NMe), 2.71 (s, 3 H, CH$_2$N*Me*), 2.01 (s, 15 H, C$_5$*Me*$_5$), 1.98 (s, 15 H, C$_5$*Me*$_5$), 1.91 (s, 15 H, C$_5$*Me*$_5$). − ^{13}C{^{1}H} NMR (C$_6$D$_6$, 20°C): δ = 120.1, 118.7 and 118.5 (*C*$_5$Me$_5$), 87.9 (*C*H$_2$NMe), 48.5 (N*Me*$_2$), 48.2 (CH$_2$N*Me*), 11.7, 11.4 and 11.1 (C$_5$*Me*$_5$). − EI MS (70 eV); *m/z* (%): 639 (9) [M$^+$ − NHMe$_2$], 625 (67) [M$^+$ − NMe$_3$], 611 (90) [M$^+$ − NMe$_2$ − C$_2$H$_5$], 596 (76) [M$^+$ − NHMe$_2$ − NC$_2$H$_5$], 477 (84) [M$^+$ − NMe$_2$ − C$_2$H$_4$ − Cp*], 341 (63) [M$^+$ − NMe$_2$ − C$_2$H$_4$ − 2 Cp*], 206 (58) [M$^+$ − NMe$_2$ − C$_2$H$_4$ − 3 Cp*]. − C$_{34}$H$_{56}$N$_2$O$_3$Ti$_3$ (684.53): calcd. C 59.66, H 8.25, N 4.09; found C 58.83, H 8.19, N 4.09.

Synthesis of [{η^5:η^1-C$_5$Me$_4$CH$_2$CH$_2$NMe}TiCl$_2$] (**5**): Heating for 15 d at 200°C 2.06 g (6.91 mmol) of [Cp*Ti(NMe$_2$)Cl$_2$] in 50 ml of toluene afforded a dark-red solution. The volatiles were removed under vacuum to give a dark red solid. All attempts to obtain a pure fraction of **5** failed and it could be characterised only by NMR spectroscopy. − ^{1}H NMR (C$_6$D$_6$, 20°C): δ = 3.88 (m, 2 H, NC*H*$_2$), 3.37 (m, 3 H, N*Me*), 2.66 (m, 2 H, C$_5$Me$_4$C*H*$_2$), 1.97 (s, 6 H, C$_5$*Me*$_4$), 1.82 (s, 6 H, C$_5$*Me*$_4$). − ^{13}C{^{1}H} NMR (C$_6$D$_6$, 20°C): δ = 139.7, 133.9 and 125.6 (*C*$_5$Me$_4$), 79.4 (NCH$_2$), 45.7 (N*Me*), 24.4 (C$_5$Me$_4$*C*H$_2$), 12.9 and 12.6 (C$_5$*Me*$_4$).

Synthesis of [{η^5:η^2-C$_5$Me$_4$CH$_2$CH$_2$N(Me)CN(C$_6$H$_3$Me$_2$)}TiCl$_2$] (**6**): 0.45 g (3.43 mmol) of 2,6-Me$_2$C$_6$H$_3$NC was added to the solution obtained in the thermal decomposition of 1.00 g (3.35 mmol) of [Cp*Ti(NMe$_2$)Cl$_2$] in 40 ml of toluene. Strong magnetic stirring overnight at room temp., followed by slow deposition during 1 d, afforded an orange powder and a red solution. After filtration, the orange solid was washed with hexane (2 × 20 ml) and dried under vacuum to yield 0.40 g (28% with respect to the initial [Cp*Ti(NMe$_2$)Cl$_2$]) of compound **6**. − IR (KBr): $\tilde{\nu}$ = 3065 cm^{-1} w, 2952 m, 2917 s, 1668 vs, 1587 m, 1467 s, 1422 s, 1378 s, 1326 m, 1238 m, 1206 m, 814 m, 771 s, 679 m, 447 m, 405 m, 379 m, 298 m. − ^{1}H NMR (CDCl$_3$, 20°C): δ = 7.00 (m, 3 H, C$_6$*H*$_3$Me$_2$), 3.82 (m, 2 H, NC*H*$_2$), 3.05 (m, 2 H, C$_5$Me$_4$C*H*$_2$), 2.85 (m, 3 H, N*Me*), 2.18 (s, 6 H, C$_5$*Me*$_4$), 2.04 (s, 6 H, C$_6$H$_3$*Me*$_2$), 1.78 (s, 6 H, C$_5$*Me*$_4$). − ^{13}C{^{1}H} NMR (CDCl$_3$, 20°C): δ = 197.2 (*C*N), 142.9, 132.2, 128.0 and 125.5 (*C*$_6$H$_3$Me$_2$), 128.9, 125.4 and 123.4 (*C*$_5$Me$_4$), 56.3 (N*C*H$_2$), 35.9 (N*Me*), 25.4 (C$_5$Me$_4$*C*H$_2$), 19.5 (C$_6$H$_3$*Me*$_2$), 13.0 and 12.4 (C$_5$*Me*$_4$). − EI MS (70 eV); *m/z* (%): 426 (4) [M$^+$], 295 (17) [{(C$_5$Me$_4$CH$_2$CH$_2$NMe)TiCl$_2$}$^+$], 252 (100) [{(C$_5$Me$_4$CH$_2$)TiCl$_2$}$^+$], 216 (35) [{(C$_5$Me$_3$(CH$_2$)$_2$)TiCl}$^+$].− C$_{21}$H$_{28}$Cl$_2$N$_2$Ti (427.27): calcd. C 59.04, H 6.61, N 6.56; found C 59.20, H 6.37, N 6.93.

X-ray Structure Determination of **6**: An orange block of **6** crystallised from hexane at room temp. and was mounted in a glass capillary in a random orientation on an automatic Enraf-Nonius Cad-4 four-circle diffractometer with graphite-monochromated Mo-K_α radiation (λ = 0.71073 Å). Crystallographic and experimental details of **6** are summarised in Table 2. Intensities were corrected for Lorentz and polarisation effects in the usual manner. No absorption or extinction corrections were made. Intensity measurements were performed by ω-2θ scans in the range 6° < 2θ < 50°.

Table 2. Crystal and X-ray structural analysis data for the compound [{η^5:η^2-C$_5$Me$_4$CH$_2$CH$_2$N(Me)CN(C$_6$H$_3$Me$_2$)}TiCl$_2$] (**6**)

Empirical formula	$C_{21}H_{28}Cl_2N_2Ti$
Formula weight	427.25
Temperature	293(2) K
Crystal system	orthorhombic
Space group	*Pbca*
a, *b*, *c* [Å]	14.780(3), 16.059(3), 18.356(4)
V [Å^3], *Z*	4357(2), 8
Density (calculated)	1.303 g/cm^3
μ (Mo-K_α)	0.645 mm^{-1}
F(000)	1792
Crystal size	0.38 × 0.35 × 0.19 mm
Index ranges	$0 < h < 17, -19 < k < 0, 0 < l < 21$
Reflections collected	3904
Independent reflections	3834 (R_{int} = 0.0228)
Observed reflections [$I > 2\sigma(I)$]	1924
Data/restraints/parameters	3827/0/235
Goodness-of-fit on F^2	1.029
Final *R* indices [$I > 2\sigma(I)$]	*R*1 = 0.069, *wR*2 = 0.166
R indices (all data)	*R*1 = 0.200, *wR*2 = 0.260
Largest diff. peak and hole	0.382 and −0.377 eÅ^{-3}

The structure was solved by direct methods (SHELXS-90)[27] and refined by least squares against F^2 (SHELXL-93).[28] Of the 3904 measured reflections, 3834 were independent; *R1* = 0.069 and *wR2* = 0.166 [for 1924 reflections with $F > 4\sigma(F)$]. The values of *R1* and *wR2* are defined as $R1 = \Sigma||F_o| - |F_c||/[\Sigma|F_o|]$; $wR2 = \{[\Sigma w(F_o^2$

$- F_c^2)^2]/[\Sigma w(F_o^2)^2]\}^{1/2}$, where $w = 1/[\sigma^2(F_o^2) + (0.114P)^2 + 15.092P]$, $P = (F_o^2 + 2F_c^2)/3$ and σ was obtained from counting statistics. All non-hydrogen atoms were refined anisotropically, and the hydrogen atoms were introduced in the last cycle of refinement from geometrical calculations and refined using a riding model with thermal parameters fixed at $U = 0.08$ Å^2.

Crystallographic data (excluding structure factors) for the structure reported in this paper have been deposited with the Cambridge Crystallographic Data Centre as supplementary publication no. CCDC-101283. Copies of the data can be obtained free of charge on application to CCDC, 12 Union Road, Cambridge CB2 1EZ, UK [Fax: (internat.) + 44(0)1223/336-033; E-mail: deposit@ccdc.cam.ac.uk].

[1] [1a] R. M. Laine (Ed.), *Transformation of Organometallics into Common and Exotic Materials: Design and Activation*, Nijhoff Publishers, Dordrecht, Netherlands, **1988**. – [1b] D. Segal, *Chemical Synthesis of Advanced Ceramic Materials*, Cambridge University Press, Cambridge, **1989**. – [1c] B. I. Lee, E. J. A. Pope, *Chemical Processing of Ceramics*, Marcel Dekker, **1994**. – [1d] L. V. Interrante, L. A. Casper, A. B. Ellis (Eds.), *Materials Chemistry: An Emergent Discipline*, American Chemical Society, Washington, DC, **1995**. – [1e] H. P. Baldus, M. Jansen, *Angew. Chem., Int. Ed. Engl.* **1997**, *36*, 328–343; *Angew. Chem.* **1997**, *109*, 338–354.

[2] L. E. Toth, *Transition Metal Carbides and Nitrides*, vol.7, Academic Press, New York, **1971**.

[3] [3a] D. M. Hoffman, *Polyhedron* **1994**, *13*, 1169–1179. – [3b] L. H. Dubois, *Polyhedron* **1994**, *13*, 1329–1336.

[4] Often references to solution-chemistry studies are used to understand the intermediate stages and to explain the impurities present in the ceramic materials. See: [4a] K. C. Jayaratne, G. P. A.Yap, B. S. Haggerty, A. L. Rheingold, C. H. Winter, *Inorg. Chem.* **1996**, *35*, 4910–4920. – [4b] J. Cheon, D. M. Rogers, G. S. Girolami, *J. Am. Chem. Soc.* **1997**, *119*, 6804–6813. – [4c] J. Cheon, L. H. Dubois, G. S. Girolami, *J. Am. Chem. Soc.* **1997**, *119*, 6814–6820.

[5] [5a] J. A. Prybyla, C. M. Chiang, L. H. Dubois, *J. Electrochem. Soc.* **1993**, *140*, 2695–2702. – [5b] C. M. Truong, P. J. Chen, J. S. Corneille, W. S. Oh, D. W. Goodman, *J. Phys. Chem.* **1995**, *99*, 8831–8842. – [5c] G. Ruhl, R. Rehmet, M. Knizová, R. Merica, S. Veprek, *Chem. Mater.* **1996**, *8*, 2712–2720. – [5d] B. H. Weiller, *J. Am. Chem. Soc.* **1996**, *118*, 4975–4983.

[6] [6a] M. H. Chisholm, I. P. Rothwell in *Comprehensive Coordination Chemistry* (Eds.: G. Wilkinson, R. D. Gillard, J. A. McCleverty), Pergamon, Oxford, **1987**, vol. 2, p. 161–188. – [6b] Y. Takahashi, N. Onoyama, Y. Ishikawa, S. Motojima, K. Sugiyama, *Chem. Lett.* **1978**, 525–528. – [6c] W. A. Nugent, D. W. Ovenall, S. J. Holmes, *Organometallics* **1983**, *2*, 161–162. – [6d] J. M. Mayer, C. J. Curtis, J. E. Bercaw, *J. Am. Chem. Soc.* **1983**, *105*, 2651–2660. – [6e] K. J. Ahmed, M. H. Chisholm, K. Folting, J. C. Huffman, *J. Am. Chem. Soc.* **1986**, *108*, 989–999. – [6f] S. L. Buchwald, B. T. Watson, M. W. Wannamaker, J. C. Dewan, *J. Am. Chem. Soc.* **1989**, *111*, 4486–4494. – [6g] N. Coles, M. C. J. Harris, R. J. Whitby, J. Blagg, *Organometallics* **1994**, *13*, 190–199.

[7] [7a] R. Andrés, M. Galakhov, A. Martín, M. Mena, C. Santamaría, *Organometallics* **1994**, *13*, 2159–2163. – [7b] R. Andrés, M. Galakhov, A. Martín, M. Mena, C. Santamaría, *J. Chem. Soc., Chem. Commun.* **1995**, 551–552. – [7c] R. Andrés, P. Gómez-Sal, E. de Jesús, A. Martín, M. Mena, C. Yélamos, *Angew. Chem., Int. Ed. Engl.* **1997**, *36*, 115–117; *Angew. Chem.* **1997**, *109*, 72–74.

[8] A. Martín, M. Mena, P. R. Raithby, R. Serrano, C. Yélamos, *J. Organomet. Chem.* **1994**, *467*, 79–84.

[9] [9a] C. T. Vroegop, Ph. D. Thesis, Groningen University, Groningen, **1984**. – [9b] Y. Bai, H. W. Roesky, H. G. Schmidt, M. Noltemeyer, *Z. Naturforsch., B* **1992**, *47b*, 603–608. – [9c] F. Q. Liu, A. Herzog, H. W. Roesky, I. Usón, *Inorg. Chem.* **1996**, *35*, 741–744.

[10] The IR spectrum did not show any band in the range 1725–1525 cm^{-1}, reported for terminal alkylideneamido groups, but a bridging arrangement would shift this absorption to a lower frequency. [10a] B. F. G. Johnson, B. L. Haymore, J. R. Dilwoth, in *Comprehensive Coordination Chemistry* (Eds.: G. Wilkinson, R. D. Gillard, J. A. McCleverty), Pergamon, Oxford, **1987**, vol. 2, p. 128–129 and references therein. – [10b] I. A. Latham, G. J. Leigh, G. Huttner, I. Jibril, *J. Chem. Soc., Dalton Trans.* **1986**, 377–383. – [10c] G. Erker, W. Frömberg, C. Krüger, E. Raabe, *J. Am. Chem. Soc.* **1988**, *110*, 2400–2405. – [10d] C. Kreuder, R. F. Jordan, H. Zhang, *Organometallics* **1995**, *14*, 2993–3001. – [10e] C. Lefeber, P. Arndt, A. Tillack, W. Baumann, R. Kempe, V. V. Burlakov, U. Rosenthal, *Organometallics* **1995**, *14*, 3090–3093. – [10f] P. A. Shapley, J. M. Shusta, J. L. Hunt, *Organometallics* **1996**, *15*, 1622–1629.

[11] [11a] M. H. Chisholm, I. P. Rothwell in *Comprehensive Coordination Chemistry* (Eds.: G. Wilkinson, R. D. Gillard, J. A. McCleverty), Pergamon, Oxford, **1987**, vol. 2, p. 177–178. – [11b] W. E. Buhro, M. H. Chisholm, K. Folting, J. C. Huffman, *J. Am. Chem. Soc.* **1987**, *109*, 905–906. – [11c] I. de Castro, M. Galakhov, M. Gómez, P. Gómez-Sal, P. Royo, *Organometallics* **1996**, *15*, 1362–1368.

[12] Other examples see refs.[10f] and N. C. Mosch-Zanetti, R. R. Schrock, W. M. Davis, K. Wanninger, S. W. Seidel, M. B. O'Donoghue, *J. Am. Chem. Soc.* **1997**, *119*, 11037–11048.

[13] M. Galakhov, M. Gómez, G. Jiménez, M. A. Pellinghelli, P. Royo, A. Tiripicchio, *Organometallics* **1995**, *14*, 1901–1910.

[14] For selected examples, see: – [14a] D. E. Wigley in *Progress in Inorganic Chemistry* (Ed.: K. D. Karlin), John Wiley and Sons, New York, **1994**, *42*, 239–482. – [14b] K. M. Doxsee, L. C. Garner, J. J. J. Juliette, J. K. M. Mouser, J. R. Weakley, H. Hope, *Tetrahedron* **1995**, *51*, 4321–4332. – [14c] P. J. McKarns, G. P. A. Yap, A. L. Rheingold, C. H. Winter, *Inorg. Chem.* **1996**, *35*, 5968–5969. – [14d] S. D. Gray, J. L. Thorman, L. M. Berreau, L. K. Woo, *Inorg. Chem.* **1997**, *36*, 278–283. – [14e] J. L. Bennet, P. T. Wolczanski, *J. Am. Chem. Soc.* **1997**, *119*, 10696–10719. – [14f] P. E. Collier, A. J. Blake, P. Mountford, *J. Chem. Soc., Dalton Trans.* **1997**, 2911–2919. – [14g] E. Müller, J. Müller, F. Olbrich, W. Brüser, W. Knapp, D. Abeln, F. T. Edelmann, *Eur. J. Inorg. Chem.* **1998**, 87–91. – [14h] C. J. Carmalt, S. R. Whaley, P. S. Lall, A. H. Cowley, R. A. Jones, B. G. McBurnett, J. G. Ekerdt, *J. Chem. Soc., Dalton Trans.* **1998**, 553–557.

[15] [15a] C. C. Cummins, C. P. Schaller, G. D. Van Duyne, P. T. Wolczanski, A. W. Edith Chan, R. Hoffmann, *J. Am. Chem. Soc.* **1991**, *113*, 2985–2994. – [15b] Y. Bai, M. Noltemeyer, H. W. Roesky, *Z. Naturforsch., B* **1991**, *46b*, 1357–1363. – [15c] T. S. Lewkebandara, P. H. Sheridan, M. J. Heeg, A. L. Rheingold, C. H. Winter, *Inorg. Chem.* **1994**, *33*, 5879–5889. – [15d] J. L. Bennett, P. T. Wolczanski, *J. Am. Chem. Soc.* **1994**, *116*, 2179–2180. – [15e] F. Q. Liu, A. Herzog, H. W. Roesky, I. Usón, *Inorg. Chem.* **1996**, *35*, 741–744. – [15f] S. C. Dunn, P. Mountford, D. A. Robson, *J. Chem. Soc., Dalton Trans.* **1997**, 293–304. – [15g] P. Mountford, *Chem. Commun.* **1998**, 2127–2134.

[16] [16a] A. K. Hughes, A. Meetsma, J. H. Teuben, *Organometallics* **1993**, *12*, 1936–1945. – [16b] A. K. Hughes, S. M. B. Marsh, J. A. K. Howard, P. D. Ford, *J. Organomet. Chem.* **1997**, *528*, 195–198. – [16c] P. J. Sinnema, L. van der Veen, A. L. Spek, N. Veldman, J. H. Teuben, *Organometallics* **1997**, *16*, 4245–4247.

[17] P. Jutzi, M. O. Kristen, J. Dahlhaus, B. Neumann, H. G. Stammler, *Organometallics* **1993**, *12*, 2980–2985.

[18] T. F. Wang, T. Y. Lee, J. W. Chou, C. W. Ong, *J. Organomet. Chem.* **1992**, *423*, 31–38.

[19] T. F. Wang, Ch. Ch. Hwu, Ch. W. Tsai, Y. S. Wen, *Organometallics* **1998**, *17*, 131–138.

[20] [20a] J. March, *Advanced Organic Chemistry: Reactions, Mechanisms and Structure*, 3rd ed., John Wiley and Sons, New York, **1985**, p. 19. – [20b] L. D. Durfee, Y. P. Rothwell, *Chem. Rev.* **1988**, *88*, 1059–1079.

[21] [21a] J. E. Hill, G. Balaich, P. E. Fanwick, I. P. Rothwell, *Organometallics* **1993**, *12*, 2911–2924. – [21b] S. De Angelis, E. Solari, C. Floriani, A. Chiesi-Villa, C. Rizzoli, *Organometallics* **1995**, *14*, 4505–4512. – [21c] R. Andrés, M. Galakhov, M. Pilar Gómez-Sal, A. Martín, M. Mena, C. Santamaría, *Chem. Eur. J.*, in press.

[22] J. Feldman, J. C. Calabrese, *J. Chem. Soc., Chem. Commun.* **1991**, 1042–1044.

[23] M. V. Galakhov, A. Martín, M. Mena, F. Palacios, C. Yélamos, P. R. Raithby, *Organometallics* **1995**, *14*, 131–136.

[24] A. Martín, M. Mena, M. A. Pellinghelli, P. Royo, R. Serrano, A. Tiripicchio, J. *Chem. Soc., Dalton Trans.* **1993**, 2117–2122.

[25] [25a] A. Dormond, A. Aaliti, C. Moïse, *J. Chem. Soc., Chem. Commun*. **1985**, 1231−1233. − [25b] M. H. Chisholm, C. E. Hammond, D. Ho, J. C. Huffman, *J. Am. Chem. Soc*. **1986**, *108,* 7860−7861. − [25c] P. Zanella, N. Brianese, U. Casellato, F. Ossola, M. Porchia, G. Rossetto, R. Graziani, *J. Chem. Soc. Dalton Trans.* **1987**, 2039−2043.

[26] R. J. Errington, Advanced Practical Inorganic and Metalorganic Chemistry, Blackie A and P, an Imprint of Chapman and Hall, London, UK, **1997**.

[27] G. M. Sheldrick, *Acta Crystallogr., Sect. A* **1990**, *46*, 467.

[28] G. M. Sheldrick, *SHELXL 93*, Universität Göttingen, Germany, **1993**.

[98089]

Tuning Metal Stoichiometry in Heterometal Alkoxides: First Structurally Characterised Molecular Precursor to $BaZrO_3$ ☆

Michael Veith*, Sanjay Mathur*, Volker Huch, and Timo Decker

Institute of Inorganic Chemistry, University of Saarland,
D-66041 Saarbrücken, Germany
Fax: (internat.) + 49(0)681/302-3995
E-mail: veith@rz.uni-sb.de

Received April 3, 1998

Keywords: Barium / Zirconium / O ligand / Heterometal alkoxides

Manipulable metal ratios are accessible in a series of heterometal Ba-Zr alkoxides by changing the size and the charge of the ligands. The synthesis and characterisation of four mixed-metal Ba-Zr species $[BaZr_2(OtBu)_{10}]$ (**1**), $[Ba_2Zr(OtBu)_8(tBuOH)(THF)_2]$ (**2**), $[BaZr(OtBu)_6(THF)_2]$ (**3**) and $[BaZr(OH)(OiPr)_5(iPrOH)_3]_2$ (**4**), based on different Ba/Zr stoichiometries, are reported. The molecular structures of **1**, **2**, and **4** have been determined by single-crystal X-ray diffraction studies. **1** exhibits a bow-tie structural motif in which a trigonally distorted six-coordinate barium atom is chelated by two bipyramidal $\{Zr(OtBu)_5\}^-$ units. **2** reveals a triangular "$Ba_2Zr(\mu_3\text{-}OtBu)_2(\mu_2\text{-}OtBu)_3$" core structure formed by the fusion of three octahedra built about two Ba atoms and a Zr atom. The structure is unique in terms of the distribution of terminal ligands at each of the metal centers. One of the barium atoms possesses one –O*t*Bu and one *t*BuOH as terminal ligands, while the terminal ligands on the second barium atom are two THF molecules; the zirconium center bears –O*t*Bu groups as the terminal ligands. Hydrolysis of compound **3** with one equivalent of water, followed by alcoholysis (*i*PrOH) of the resulting product, gave **4**. The structure of **4** shows a planar tetrametallic Ba_2Zr_2 frame capped by two μ_3-hydroxo ligands. The coordination figure of the zirconium atoms resembles a distorted octahedron, whereas the geometry of the barium centers is best described as capped trigonal prisms. Both **3** and **4** are excellent precursors to morphologically pure $BaZrO_3$ ceramic by the sol-gel process.

Interest in metal alkoxides is stimulated by their suitability as useful reagents for chemical synthesis of high-purity oxides and metal oxide/metal composites.[1][2] The insoluble and polymeric nature of simple alkoxides of alkaline earth elements $[M(OR)_2]$[3] limits their direct application in sol-gel techniques, however, solubilisation can be achieved by the addition of transition metal alkoxides [e.g., $Ti(OR)_4$, $Zr(OR)_4$].[4] Although this strategy of forming soluble heterometallic preceramic aggregates is advantageous, particularly in view of the mixed-metal composition of most of the advanced ceramics [e.g., $YBa_2Cu_3O_{7-\delta}$, $MM'O_3$ (M^{IV} = Ti, Zr, Sn; M′ = Ca, Sr, Ba, Pb)], the nature (with regard to the metal stoichiometry) of product(s) formed in such "heterometal solutions" remains ambiguous or poorly characterised.[5] Furthermore, the equilibrium among various heterometal species existing in the solution, and the kinetics of their formation, complicate the precursor chemistry. Since various heterometal combinations are possible due to the structure potential (terminal, μ_2 or μ_3) of the alkoxo ligand,[6] the consequences (e.g., metal segregation, phase inhomogeneity) are encountered during the processing of ceramic material.[5] Of principal interest in this context are heterometal molecules, tailored to the need of the targeted ceramic which in turn requires (i) the development of synthetic and chemical approaches for a precise control over the metal stoichiometry, and (ii) the unequivocal characterisation of molecular precursors as well as the products obtained from their partial hydrolysis reactions (oxo-alkoxides) as they are the real intermediates of a sol-gel process and can therefore reveal how a molecular compound begins to form extended networks. A recent study on the solubility isotherms of $Ba(OR)_2$–$Zr(OR)_4$–ROH (R = Et, *i*Pr) ternary systems reports the formation of various heterobimetallic alkoxides with different Ba/Zr ratios. An oxo-alkoxide of composition $BaZrO(OR)_4 \cdot n(ROH)$ is reportedly formed in the equimolar alcoholic solution of barium and zirconium alkoxides.[2d] To the best of our knowledge, a synthetic approach for a rational control over the Ba/Zr metal stoichiometry has not been described so far.

Results and Discussion

Using $[Ba(OtBu)_2]_n$ and $Zr(OtBu)_4$ as building "bricks", we have synthesised a series of molecular alkoxides with different (1:2, 2:1, 1:1) Ba/Zr stoichiometries. The manipulation of metal ratios in well-defined molecular derivatives provides optimism when looking towards tailor-made molecules and demonstrates the governing role that ligands [alkoxo (OR), oxo (O^{2-}), or neutral (ROH, THF)] can play in anchoring stable mixed-metal clusters. The Ba/Zr derivatives based on 1:1 stoichiometry of the metals have proved to be excellent precursors for clean and selective synthesis (sol-gel) of $BaZrO_3$ ceramic at much lower sintering temperatures than are usually required for the solid-state synthesis.[7]

 © WILEY-VCH Verlag GmbH, D-69451 Weinheim, 1998 1434–1948/98/0909–1327 $ 17.50+.50/0

The reaction (1:2 molar ratio) of $[Ba(OtBu)_2]_n$ with $Zr(OtBu)_4$ in refluxing toluene (Eq. 1) produces a clear pale yellow solution which on cooling (0°C) offers $BaZr_2(OtBu)_{10}$ (**1**) as large transparent crystals (72% yield).

$$1/n\ [Ba(OtBu)_2]_n + 2\ Zr(OtBu)_4 \rightarrow \underset{\mathbf{1}}{BaZr_2(OtBu)_{10}} \quad (1)$$

The analytical data are compatible with the formulation of **1**, and the molecule is found to be monomeric in benzene (cryoscopy). The NMR data are deceptively simple and only a single set of ligand resonances is observed in the room-temperature ^{1}H- and ^{13}C-NMR spectra in contrast to the solid-state NMR spectrum (vide infra). The low-temperature NMR studies ([D_8]toluene) show **1** to be highly fluxional and the intramolecular ligand rearrangements or site exchange processes, causing equivalence (on an NMR time scale) of all 10 O*t*Bu groups could not be frozen out, even at −80°C. **1** is stable up to 200°C/10^{-2} Torr; at higher temperatures (> 230°C) partial decomposition was observed with $Zr(OtBu)_4$ as the only volatile material.

The result of the single crystal X-ray diffraction analysis of $BaZr_2(OtBu)_{10}$, including the numbering system, is shown in Figure 1a, and the pertinent bond lengths and angles are compiled in Table 1. The central barium atom, encapsulated by six bridging (μ_2-)O*t*Bu groups of two tridentate monoanionic $[Zr(OtBu)_5]^-$ units, is present in a trigonally distorted octahedral geometry. The crystallographically inequivalent Zr centers [Zr(1) and Zr(2)] are present in distorted trigonal bipyramidal environments. With respect to Ba−O distances (Table 1) in the molecule (Figure 1a), the two $[Zr(OtBu)_5]^-$ units are coordinated to Ba^{2+} in an asymmetric fashion. The Ba−O distances clearly fall in three ranges [Ba−O(1) = 2.651(3), Ba−O(6) = 2.656(3); Ba−O(8) = 2.768(3), Ba−O(3) = 2.806(3); Ba−O(2) = 2.947(3), Ba−O(7) = 2.965(3) Å] and the barium coordination sphere can be precisely defined as "2 + 2 + 2". The Ba−O(1) and Ba−O(6) distances are significantly shorter than the remaining four Ba−O contacts, and in a "building block" approach, the architecture of **1** can also be described as an interaction of two tetrahedral $Zr(OtBu)_4$ moieties with a bent O(1)−Ba−O(6) unit. The terminal (av. 1.951 Å) and bridging (av. 2.064 Å) Zr−O distances are comparable with those observed in $[KZr(OtBu)_5]_2$.[8] To our knowledge, **1** reveals a structural type unprecedented among metal alkoxides, however, the $BaZr_2O_6$ core in **1** is comparable with the molecular structures of $[M(\mu_2\text{-}OtBu)_3M'(\mu_2\text{-}OtBu)_3M]$ (M = Ge^{I}, Sn^{II}, Pb^{II}; M′ = Mg, Ca, Sr, Ba or Pb) alkoxide derivatives.[9] However, in contrast to the linear arrray of metallic elements in $M'M_2(OtBu)_6$ compounds, the Zr···Ba···Zr arrangement in **1** is bent (149.61°) due to the violation of the three-fold symmetry of $Zr(OtBu)_5^-$ units and as an effect of the two different orientations of the ZrO_5 bipyramids, with respect to the central BaO_6 unit. An interesting influence of the alkoxide steric profile on the structural type (resulting from same metal stoichiometry) is observed on comparing **1** with the corresponding isopropoxy derivative $[BaZr_2(OiPr)_{10}]_2$[4b]; whereas **1** is monomeric and displays a bow-tie structural motif with a slightly bent arrangement of metal atoms, $[BaZr_2(OiPr)_{10}]_2$ is dimeric and the metallic elements form a closed triangular structure. The relative and total intensities of the signals in the ^{13}C CP-MAS/NMR spectrum of **1** (Figure 1b) corroborates the observed solid-state structure. A line deconvolution experiment corresponds to the presence of 10 O*t*Bu groups and the observed spectral pattern arises from the accidental overlapping of some of the O*t*Bu groups.

Figure 1a. Ball-and-stick representaion of the molecular structure of **1** with selected atom labelling; hydrogen atoms of the *tert*-butyl moieties are omitted for clarity

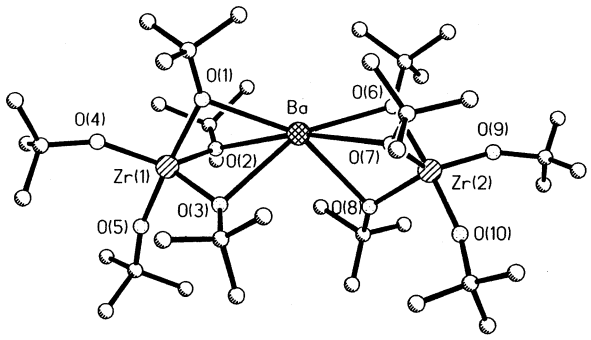

Figure 1b. Solid-state ^{13}C CP-MAS NMR spectrum of **1**

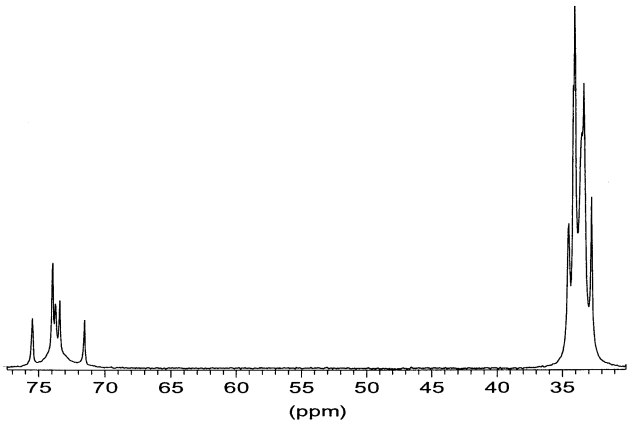

Table 1. Selected bond lengths [Å] and angles [°] of compound **1**

Ba−O(1)	2.651(3)	Ba−O(2)	2.947(3)
Ba−O(3)	2.806(3)	Ba−O(6)	2.656(3)
Ba−O(7)	2.965(3)	Ba−O(8)	2.768(3)
Zr−O(4)	1.952(3)	Zr−O(1)	2.149(3)
Zr−O(2)	2.020(3)	Zr−O(3)	2.017(3)
O(1)−Ba−O(6)	144.25(9)	O(8)−Ba−O(3)	95.10(8)
O(1)−Ba−O(3)	60.80(9)	O(1)−Ba−O(2)	57.50(10)
O(3)−Ba−O(2)	63.50(8)	O(4)−Zr(1)−O(2)	133.64(14)
O(4)−Zr(1)−O(3)	126.58(14)	O(3)−Zr(1)−O(2)	97.28(13)
O(1)−Zr(1)−O(5)	175.96(12)	Zr(1)−O(1)−Ba	93.78(10)
Zr(1)−O(2)−Ba	88.21(10)	Zr(1)−O(3)−Ba	92.30(10)

In order to investigate the nature of product formed by reversing the metal ratios in **1**, two equivalents of $[Ba(OtBu)_2]_n$, dissolved in a THF/*t*BuOH mixture were treated with $Zr(OtBu)_4$ (1 equiv.) to obtain $Ba_2Zr(OtBu)_8$(*t*-

BuOH)$(THF)_2$ (**2**) in a yield of 45% (Eq. 2). Compound **2** is readily soluble in benzene, toluene, and chloroform.

$$2/n\,[Ba(OtBu)_2]_n + Zr(OtBu)_4 + tBuOH + 2\,THF \rightarrow \underset{\mathbf{2}}{Ba_2Zr(OtBu)_8(tBuOH)(THF)_2} \quad (2)$$

The room-temperature ^{1}H-NMR spectrum exhibits two resonances for *tert*-butyl protons in a 4:5 integration ratio. The presence of the alcoholic proton is discerned from the NMR signal observed at $\delta = 4.31$ and a broad IR band at 3160 cm^{-1} (ν OH) indicating an R(M)−O···H−OR bonding.[10] The THF chemical shifts are observed in the region typical for THF molecules coordinated to metal centers. To probe the persistence of solid-state structure (Figure 2) in solution, low-temperature NMR studies were performed on a [D_8]toluene solution of **2**. The methyl signal intensities decoalesce on lowering the temperature and the best resolved spectrum at −30°C displays four sharp resonances in an intensity ratio of 4:2:1:2. This spectral pattern is characteristically observed for heterometal systems containing the triangulo-$MM'_2(OR)_9$ unit,[4][11] which in case of **2** can be assigned to the "$ZrBa_2(OtBu)_8(tBuOH)$" substructure, if the *tert*-butyl resonances of the alcohol ligand overlaps with the resonances of three terminal alkoxo ligands present at Ba and Zr centers. These findings are supported by the ^{13}C-NMR spectrum (−30°C) which exhibits four resonances each for methyl and tertiary carbon atoms.

Figure 2. Ball-and-stick drawing of the molecular structure of **2**; hydrogen atoms are not drawn for clarity; the dotted line represents the hydrogen bonding between O4 and O4′

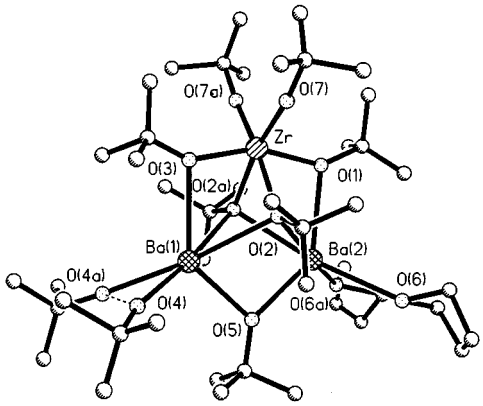

The X-ray study established compound **2** to be $Ba_2Zr(OtBu)_8(tBuOH)(THF)_2$ as depicted in Figure 2. The structure is comprised of a trimetallic framework which, although common among $MM'_2(OR)_x$ alkoxides[12], is worthy of special note due to the unique ligand (terminal) environments of the metal centers and the inequivalence of the two barium atoms. One of the barium atoms [Ba(1)] achieves an octahedral environment by adding an alcohol (*t*BuOH) ligand, whereas the coordination sphere of Ba(2) is completed by two THF molecules. In contrast to **1**, the zirconium atom in **2** is surrounded by six O*t*Bu groups. The molecule possesses a crystallographic mirror plane passing through the metal atoms and the three doubly bridging oxygen atoms [O(1), O(3), and O(5)]. Owing to the much larger size of Ba^{2+} (1.34 Å) compared to Zr^{IV}, the triangular Ba_2Zr core exhibits a long Ba···Ba [3.8617(15) Å] nonbonding contact; the Ba···Zr distances [3.7165(19) Å) and 3.7109(18) Å] are almost symmetrical. In view of the published data on other related compounds,[13] the terminal Ba−O bond lengths clearly allow the distinction of metal−ligand distances; the Ba−O(THF) distances (av. 2.831 Å) being significantly longer than the Ba−O(terminal) bond lengths involving alkoxo or alcohol ligands (av. 2.565 Å). Among the triply bridging (μ_3-)oxygen atoms, O(2) [O(2a)] binds strongly to Ba(2) center [2.687(8) Å] in comparison to Ba(1) [2.740(8) Å]. Although the hydroxylic hydrogen atom could not be located crystallographically, an intramolecular hydrogen bond is evident in the short O(4)···O(4a) (2.471 Å) contact [cf. O(6)···O(6a) = 3.589 Å; O(7)···O(7a) = 2.989 Å]. Furthermore, **2** shows no significant intermolecular contacts of oxygen atoms to other oxygen or metal atoms (> 4 Å) in the crystal as would be the case for intermolecular hydrogen bonding. The Zr−O distances (Table 2) follow the trend: Zr−OR(terminal) (av. = 1.998 Å) < Zr−μ_2-(OR) (av. = 2.105 Å) < Zr−μ_3-(OR) (av. = 2.245 Å). Curiously, the doubly bridging (μ_2-)Ba−O bond lengths (av. = 2.768 Å) are longer than the triply bridging (μ_3-)Ba−O distances (av. = 2.706 Å) which, in analogy to **1**, could lead to the conceptual fragmentation of **2** into neutral building units, $Zr(OtBu)_4$ and $(tBuOH)(OtBu)Ba(\mu_2\text{-}OtBu)_3Ba(THF)_2$. Apparently, the coordinating solvents employed in the synthesis of **2** effectively change the degree of aggregation of $[Ba(OtBu)_2]_n$ which seems to alter its Lewis acid-base reaction with $Zr(OtBu)_4$ to form **2** (Figure 2). Interestingly, the reaction (2:1 molar ratio) of Ba and Zr *tert*-butoxides in the absence of donor solvents produces only $BaZr_2(OtBu)_{10}$ (**1**) as the soluble species, leaving 1.5 equiv. of Ba alkoxide unreacted, which further supports the preceding argument.

Table 2. Selected interatomic distances [Å] and angles [°] of compound **2**

Ba(1)−O(3)	2.796(14)	Ba(1)−O(2)	2.740(8)
Ba(1)−O(4)	2.565(9)	Ba(1)−O(5)	2.611(15)
Ba(2)−O(1)	2.740(15)	Ba(2)−O(2)	2.673(8)
Ba(2)−O(6)	2.831(11)	Ba(2)−O(5)	2.487(14)
Zr−O(1)	2.123(13)	Zr−O(2)	2.245(8)
Zr−O(3)	2.088(14)	Zr−O(7)	1.998(9)
O(4)···O(4a)	2.471	O(7)···O(7a)	2.989
O(6)···O(6a)	3.589		
O(4)−Ba(1)−O(4a)	57.7(5)	O(6)−Ba(2)−O(6a)	79.0(6)
O(4)−Ba(1)−O(5)	110.9(5)	O(4)−Ba(1)−O(2)	121.7(3)
O(4)−Ba(1)−O(2a)	173.0(4)	O(5)−Ba(1)−O(2a)	76.0(3)
O(2)−Ba(1)−O(2a)	58.0(3)	O(4)−Ba(1)−O(3)	110.9(5)
O(5)−Ba(1)−O(3)	131.9(3)	O(3)−Ba(1)−O(2a)	62.4(3)
O(5)−Ba(2)−O(2)	79.3(3)	O(5)−Ba(2)−O(1)	135.3(5)
O(5)−Ba(2)−O(6)	106.4(4)	O(1)−Ba(2)−O(6)	107.8(4)
O(2)−Ba(2)−O(6a)	167.8(4)	O(2)−Ba(2)−O(1)	62.3(3)
O(7)−Zr−O(7a)	96.6(6)	O(3)−Zr−O(1)	158.3(6)
O(7)−Zr−O(3)	97.8(4)	O(7)−Zr−O(2)	95.4(4)
O(1)−Zr−O(2)	79.8(4)	O(3)−Zr−O(2)	82.7(4)
Ba(1)−O(5)−Ba(2)	98.5(4)	Ba(1)−O(3)−Zr	97.8(5)
Ba(1)−O(2)−Ba(2)	91.0(2)	Ba(1)−O(2)−Zr	95.7(2)

The successful switching of metal ratios from $BaZr_2$ (**1**) to Ba_2Zr (**2**) prompted us to explore a molecule with a Ba/

Zr stoichiometry of 1:1 which could act as a model precursor to $MM'O_3$ ceramics. A solution of $Ba(OtBu)_2$ in THF was treated with one equivalent of $Zr(OtBu)_4$ and the reaction mixture was heated. The clear solution was concentrated in vacuo and cooled (−30°C) to obtain colorless crystals of analytical composition $BaZr(OtBu)_6(THF)_2$ (**3**) in 65% yield (Eq. 3a). The ^{1}H-NMR spectrum of **3** displays at room temperature a single resonance for the methyl protons of O*t*Bu groups which integrates approximately 6:2 with the resonances corresponding to the two coordinated THF molecules. The ^{13}C-NMR spectrum also shows a single ligand environment. Structurally diagnostic spectra could not be obtained until −73°C. **3** rapidly looses the crystallinity upon removal of the mother liquor, even under a cold stream of nitrogen which precluded a single crystal X-ray diffraction study.

$$1/n\ [Ba(OtBu)_2]_n + Zr(OtBu)_4 + 2\ THF \rightarrow \underset{\mathbf{3}}{1/m\ [\{BaZr(OtBu)_6\}\cdot 2\ THF]_m} \quad (3a)$$

$$\mathbf{3} + H_2O + 6i\text{PrOH} \rightarrow \underset{\mathbf{4}}{[BaZr(OH)(OiPr)_5(i\text{PrOH})_3]_2} + 6\ t\text{BuOH} + 2\ THF \quad (3b)$$

Heterometal aggregates supported by oxo- or hydroxo-assembling ligands are intermediates to oxide ceramics and their characterisation is likely to feature the inital steps of sol-gel chemistry. The hydrolysis of **3** with one equivalent of water followed by alcoholysis with 2-propanol (see Experimental Section) offered $[BaZr(OH)(OiPr)_5(i\text{PrOH})_3]_2$ (**4**) in a high yield (70%) (Eq. 3b). The room-temperature spectra (^{1}H and ^{13}C NMR) of **4** are too complex to be diagnostic. The ^{1}H-NMR spectrum displays several closely associated doublets for the *gem*-dimethyl protons; the methine protons are observed as two multiplets formed by various overlapping septuplets. A similar spectral pattern is observed in the ^{13}C-NMR spectra (solution and solid-state CP MAS). The presence of hydroxylic groups in **4** is established by the intense ν(OH) band (3340 cm^{-1}) observed in both the solution ($CDCl_3$) and the solid-state IR spectra and is corroborated by the ^{1}H-NMR observation (δ = 4.65). The spectral pattern of **4** remains complex even at low temperature (−40°C), however, a downfield migration of −OH chemical shift is observed on decreasing the temperature. Thus, the fate of compound **4** in solution can not be discerned from the available data.

The solid-state structure of $[BaZr(OH)(OiPr)_5(i\text{PrOH})_3]_2$ (**4**) reveals a tetranuclear cluster (Figure 3) where the four metal atoms are coplanar due to the requirements of the crystallographic inversion center. The gross structural features of the oxo-metalate framework in **4** are comparable with other compounds adopting an M_4O_{16} edge-shared octahedral arrangement [e.g., $Ti_4(OEt)_{16}$,[14] $W_4(OEt)_{16}$[15]], however, the solvating 2-propanol molecules in **4** provide different coordination numbers to Ba and Zr centers. The Zr atoms are present at the center of slightly distorted octahedra, whereas Ba centers (being seven-coordinate) display a trigonal-prismatic face-capped geometry. The

Figure 3. Ball-and-stick drawing of the molecular structure of **4**; hydrogen atoms are not drawn for clarity

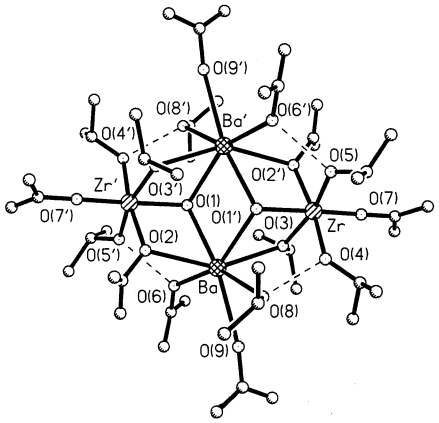

$Ba_2Zr_2O_6$ core is built up from two analogous *seco*-norcubane units fused along one face defined by two barium atoms and two oxygen atoms of the hydroxo groups. A similar face-capping arrangement of hydroxo ligand against a planar tetrametallic (M_4) frame has been observed in $[Eu_4(OC_6H_3iPr_2\text{-}2,6)_6(OH)_2(NCMe)_6]$[16] and $[Nd_4(\mu_3\text{-}OH)_2(\mu_2,\mu_1\text{-}acac)_6(acac)_4]$.[17] Whereas the doubly bridging oxygen atoms [O(2) and O(3)] are nearly planar (sum of angles = av. 356.61°), the angles around O(1) sum to 316.64° (see Table 3) accounting for a tetrahedral geometry (sp^3 hybridisation) that support the assignment of O(1) [O(1a)] as a μ_3-hydroxo ligand. The expected dispersion of metal−oxygen bond lengths [M−μ_3-OR > M−μ_2-OR > M−O(terminal)] is found in ZrO_6 polyhedron with Zr−O (terminal) distances (av. 2.048 Å) being the smallest [cf. Zr−O (terminal) in $Zr_2(OiPr)_8(i\text{PrOH})_2$ = 1.984 Å].[10b] On the contrary, all the terminal Ba−O distances in **4**, are extremely large (av. 2.836 Å) which can be understood in terms of much reduced donor capacity of the alcohol (ROH) in comparison to the alkoxo (RO^-) ligand. Out of the three terminal alcohol ligands at barium [O(6), O(8), and O(9)], O(6) and O(8) are involved in an intramolecular hydrogen bonding with the terminal alkoxo ligands [O(5) and O(4)] of neighbouring Zr atoms (Figure 3). The short O(5)···O(6′) (2.664 Å) and O(4)···O(8) (2.614 Å) separations, together with the bent orientation (away from the O···O vector) of −*i*Pr fragments, is in accord with the proposed hydrogen bonding.

The authors gratefully acknowledge the continuing support of the *Deutsche Forschungsgemeinschaft* under the framework of research programme SFB-277. Authors also thank Dr. *Michael Zimmer* for recording the solid-state ^{13}C CP-MAS NMR spectra. S. M. thanks the *Alexander von Humboldt Foundation* (Germany) for a research fellowship.

Experimental Section

General: All operations were carried out under a dry nitrogen with rigorous exclusion of oxygen and moisture. Tertiary butyl alcohol was dried by distillation from potassium metal and aluminium *tert*-butoxide. All other solvents were distilled from Na/K alloy or $LiAlH_4$, prior to use. $Ba(OtBu)_2$ was prepared by the reac-

Table 3. Selected interatomic distances [Å] and angles [°] of compound **4**

Ba−O(1)	2.718(3)	Ba−O(3)	2.671(3)
Ba−O(8)	2.892(4)	Ba−O(2)	2.679(3)
Ba−O(6)	2.780(3)	Ba−O(9)	2.836(4)
Zr−O(1′)	2.172(3)	Zr−O(5)	2.092(3)
Zr−O(4)	2.103(3)	Zr−O(7)	1.951(3)
Zr−O(3)	2.107(3)	Zr−O(2′)	2.107(3)
O(1)−Ba−O(1′)	74.13(9)	O(2)−Ba−O(1)	63.59(8)
O(1′)−Ba−O(3)	61.43(9)	O(1)−Ba−O(9)	160.78(12)
O(9)−Ba−O(6)	89.57(15)	O(9)−Ba−O(8)	57.81(16)
O(3)−Ba−O(2)	149.26(9)	O(3)−Ba−O(1)	87.65(9)
O(3)−Ba−O(6)	105.07(10)	O(2)−Ba−O(6)	77.06(10)
O(1′)−Ba−O(6)	143.38(9)	O(1)−Ba−O(6)	71.31(9)
O(3)−Ba−O(9)	95.72(14)	O(2)−Ba−O(9)	115.02(13)
O(1′)−Ba−O(9)	123.97(14)	O(3)−Ba−O(8)	87.93(12)
O(2)−Ba−O(8)	107.37(11)	O(1)−Ba−O(8)	141.37(10)
O(6)−Ba−O(8)	146.28(11)	O(1′)−Zr−O(7)	176.60(12)
O(7)−Zr−O(4)	94.07(14)	O(7)−Zr−O(5)	98.27(13)
O(7)−Zr−O(3)	97.15(13)	O(5)−Zr−O(4)	90.79(12)
O(5)−Zr−O(3)	164.43(12)	O(4)−Zr−O(3)	90.25(12)
Zr−O(3)−Ba	108.68(12)	Zr′−O(1)−Ba′	106.03(10)
Ba−O(1)−Ba′	105.87(8)	Zr′−O(1)−Ba	104.74(10)
O(4)−Zr−Ba	77.02(9)	O(6)−Ba−Zr′	69.26(8)
O(8)−Ba−Zr	70.15(9)	O(5)−Zr−Ba′	81.71(8)

tion of barium metal and alcohol in the presence of dry ammonia following a published procedure[18] ($C_8H_{18}BaO_2$: calcd. C 33.88, H 6.39, Ba 48.42; found C 33.01, H 6.43, Ba 48.52). $Zr(OtBu)_4$ was obtained by the alcoholysis of $Zr(NEt_2)_4$ which was synthesised following the literature method.[19] − ^1H and $^{13}C\{^1H\}$ NMR: Bruker AC-200 spectrometer and chemical shifts referenced to residual solvent peaks. − ^{13}C CP-MAS NMR: Bruker MSL 200S spectrometer. − IR: Bio-Rad FTS-165 spectrometer. − Elemental analyses: LECO CHN 900 elemental analyser. Established analytical procedures were used to determine the metal contents in the new derivatives.

Synthesis of [$BaZr_2(OtBu)_{10}$] (**1**): $Zr(OtBu)_4$ (4.45 g; 11.59 mmol) in toluene (15 ml) was added to a slurry of $Ba(OtBu)_2$ (1.64 g; 5.78 mmol) in toluene. The clear solution obtained after the dissolution of $Ba(OtBu)_2$ was refluxed (16 h) and cooled at 0°C for 24 h, whereupon colourless crystals of **1** were formed (4.36 g; 72%). − ^1H NMR (C_7D_8, 20°C): δ = 1.51 (CH_3). − ^{13}C NMR (C_7D_8, 20°C): δ = 32.88 (CH_3); 73.12 (CMe_3). − ^{13}C CP-MAS NMR: δ = 32.74, 33.32 33.50, 34.02 34.14, 34.49 (CH_3); 71.51, 73.37, 73.72, 73.89, 75.47 (CMe_3). − MW: calcd. 1069; found 1051. − $C_{40}H_{90}BaO_{10}Zr_2$: calcd. C 45.71, H 8.29, Ba 13.06, Zr 17.36; found C 45.37, H 8.29, Ba 12.95, Zr 17.05.

Synthesis of [$Ba_2Zr(OtBu)_8(tBuOH)(THF)_2$] (**2**): To $Ba(OtBu)_2$ (1.08 g; 3.80 mmol), dissolved in a mixture of *tert*-butyl alcohol (5 ml) and THF (30 ml), was added $Zr(OtBu)_4$ (0.74 g; 1.93 mmol) in 30 ml of hexane. The reaction mixture was stirred overnight at 50°C. The clear pale yellow solution obtained was reduced to one fourth and left at ambient temperature. Colourless cubes of $Ba_2Zr(OtBu)_8(tBuOH)(THF)_2$ (**2**) grew over a period of two weeks. Yield: 0.98 g [45% based on $Zr(OtBu)_4$]. − ^1H NMR (C_7D_8, 20°C): δ = 1.35 [$HOC(CH_3)_3$ + CH_3]; 1.56, 1.84 (CH_3); 1.47 (OCH_2CH_2); 3.57 (OCH_2CH_2); 3.35 (OH). − ^1H NMR (C_7D_8, −30°C): δ = 1.40, 1.66, 1.73, 1.75 (CH_3); 1.42 (OCH_2CH_2); 3.52 (OCH_2CH_2). − ^{13}C NMR (C_7D_8, −30°C): δ = 25.74 (OCH_2CH_2); 33.20, 34.72, 35.01, 35.57 (CH_3); 67.94 (OCH_2CH_2); 69.19, 70.76, 71.89, 75.18 (CMe_3). − $C_{44}H_{128}Ba_2O_{11}Zr$: calcd. C 45.39, H 11.07, Ba 23.59, Zr 7.83; found C 45.08, H 10.85, Ba 23.18, Zr 7.70.

Synthesis of [$BaZr(OtBu)_6(THF)_2$] (**3**): To $Ba(OtBu)_2$ (1.78 g; 6.27 mmol) in THF (40 ml) was added $Zr(OtBu)_4$ (2.42 g; 6.30 mmol) and the resulting mixture was stirred at 50°C for 16 h. The sticky solid obtained after the removal of volatiles in vacuo was dissolved in a minimum amount of THF and cooled (−30°C) to yield $BaZr(OtBu)_6(THF)_2$ (**3**) as a crystalline material which turned into a waxy solid, on removing the mother liquor. Yield: 3.22 g [63% based on $Zr(OtBu)_4$]. − ^1H NMR (C_7D_8, 20°C): δ = 1.48 (CH_3), 1.44 (OCH_2CH_2), 3.60 (OCH_2CH_2). − ^{13}C NMR (C_7D_8, 20° C): δ = 25.19 (OCH_2CH_2), 32.95 (CH_3), 67.61 (OCH_2CH_2), 73.08 (CMe_3). − $C_{32}H_{70}BaO_8Zr$: calcd. Ba 16.92, Zr 11.24; found Ba 16.47, Zr 11.30.

[$BaZr(OtBu)_6$]$_n$: Obtained by prolonged pumping of **3** in vacuo at 50°C. − ^1H NMR (C_6D_6, 20°C): δ = 1.50 (CH_3). − ^{13}C NMR (C_6D_6, 20°C): δ = 32.95 (CH_3), 73.08 (CMe_3).

Table 4. Crystal data and data collection parameters for the derivatives **1**, **2**, and **4**

	1	**2**	**4**
Empirical formula	$C_{40}H_{90}BaO_{10}Zr_2$	$C_{44}H_{128}Ba_2O_{11}Zr$	$C_{24}H_{60}BaO_9Zr$
Crystal system	Triclinic	Orthorhombic	Monoclinic
Space group	$P\bar{1}$	$Cmc2(1)$	$P2(1)/n$
a [Å]	10.508(2)	17.159(3)	11.060(2)
b [Å]	10.631(2)	20.749(4)	15.625(3)
c [Å]	28.500(6)	17.934(4)	21.648(4)
α [°]	81.70(3)	90	90
β [°]	89.59(3)	90	98.76(3)
γ [°]	61.84(3)	90	90
V [Å^3]	2770.7(9)	6385(2)	3697.4(12)
Z	2	4	4
Crystal size [mm]	0.45 × 0.30 × 0.26	0.30 × 0.25 × 0.10	0.40 × 0.30 × 0.25
D_c [Mgm^{-3}]	1.260	1.216	1.296
μ [mm^{-1}]	1.114	1.422	1.377
T [K]	293(2)	293(2)	293(2)
Independent reflections	7261	3018	5629
Observed reflections [with $I > 2\sigma(I)$]	6785	2661	4360
GOF on F^2	1.140	1.119	1.012
R	0.0349	0.0538	0.0336
R_w	0.0377	0.0640	0.0473
Max. residual [eÅ^{-3}]	0.797	0.794	0.582
Min. residual [eÅ^{-3}]	−0.817	−0.730	−0.342

Synthesis of [BaZr(OH)(OiPr)$_5$(iPrOH)$_3$]$_2$ (**4**): To a THF (50 ml) solution of 1.67 g (2.50 mmol) of [BaZr(O*t*Bu)$_6$]$_n$, 2.5 mmol solution of water in THF (20 ml) was added dropwise. The workup of the reaction mixture gave a pasty mass poorly soluble in non-polar solvents even on heating and in the presence of *t*BuOH, however, it readily dissolved in hot 2-propanol to give a clear solution. 2-Propanol was pumped off and the resulting solid was redissolved in a minimum amount of *i*PrOH. Large colourless cubes of [BaZr(OH)(O*i*Pr)$_5$(*i*PrOH)$_3$]$_2$ (**4**) were formed after 2 d. Yield: 1.26 g {70%, based on the initial amount of [BaZr(O*t*Bu)$_6$]$_n$}. – ^{1}H NMR ($CDCl_3$, 20°C): δ = 1.16, 1.17, 1.24, 1.27, 1.29, 1.43, 1.50 (C*H*$_3$); 4.43, 4.74 (C*H*); 4.65 (O*H*). – ^{13}C NMR ($CDCl_3$, 20°C): δ = 26.12, 27.10, 27.37, 27.49, 27.60, 27.75, 28.27, 28.38, 28.52 (*C*H$_3$); 66.66, 68.28, 68.78, 69.45, 70.03, 71.17, 71.33, 71.52, 71.76, 71.97 (*C*H). – ^{13}C CP-MAS NMR: δ = 27.22, 27.68, 28.15 (*C*H$_3$); 63.37, 63.60, 67.44, 68.43, 69.19, 69.60, 70.00, 70.82 (*C*H). – $C_{24}H_{60}BaO_9Zr$: calcd.C 39.96, H 8.37, Ba 19.04, Zr 12.64; found C 39.22, H 8.13, Ba 18.79, Zr 12.40.

Crystallography: Monocrystalline specimens were selected from the bulk samples of compounds **1**, **2**, and **4** and sealed in Lindemann capillaries of appropriate dimensions, under inert gas. Crystal data and structure refinement parameters are given in Table 4. Diffraction data were collected with Stoe AED 2 (**1** and **2**) and Stoe IPDS (**4**) diffractometers. The intensities were corrected for Lorentz and polarisation factors, and a semi-empirical absorption correction (ψ scans) was applied for **1** and **2**. The structures were solved by direct methods (SHELXS-86)[20a] and refined by full-matrix least-squares procedures on all F^2 values (SHELXS-97).[20b] All non-hydrogen atoms were refined anisotropically. The two hydroxylic protons in **4** were located by difference Fourier techniques and were refined together with the geometrically fixed hydrogen atoms. Crystallographic data for the structure(s) reported in this paper have been deposited with the Cambridge Crystallographic Data Centre as supplementary publication no CCDC-101435. Copies of the data can be obtained free of charge on application to CCDC, 12 Union Road, Cambridge CB2 1EZ, UK [Fax: int. code + 44(1223)336-033; E-mail: deposit@ccdc.cam.ac.uk].

☆ Dedicated to Professor *Heinrich Nöth* on his 70th birthday.

[1] For reviews see: [1a] D. C. Bradley, *Chem. Rev.* **1989**, *89*, 1317. – [1b] T. J. Boyle, R. W. Schwartz, *Comments Inorg. Chem.* **1994**, *16*, 243. – [1c] L. G. Hubert-Pfalzgraf, *Polyhedron* **1994**, *13*, 1181.

[2] [2a] M. Veith, S. Kneip, *J. Mater. Sci. Lett.* **1994**, *13*, 335. – [2b] M. Veith, S. Faber, R. Hempelmann, S. Janssen, J. Prewo, H. Eckerlde, *J. Mater. Sci.* **1996**, *31*, 2009. – [2c] M. Veith, S. J. Kneip, A. Jungmann, S. Hüfner, *Z. Anorg. Allg. Chem.* **1997**, *623*, 1507. – [2d] E. P. Turevskaya, D. V. Berdyev, N. Ya. Turova, *J. Sol-Gel Sci. Tech*. **1997**, *8*, 111. – [2e] L. G. Hubert-Pfalzgraf, S. Daniele, J. M. Decans, J. Vaissermann, *J. Sol-Gel Sci. Tech*. **1997**, *8*, 49. – [2f] H. Herrig, R. Hempelmann, *Mater. Lett*. **1996**, *27*, 287.

[3] D. C. Bradley, R. C. Mehrotra, D. P. Gaur, *Metal Alkoxides*, Academic Press, London, **1978**.

[4] [4a] M. Veith, S. Mathur, V. Huch, *Inorg. Chem.* **1997**, *36*, 2391. – [4b] B. A. Vaarstra, J. C. Huffman, W. E. Streib, K. G. Caulton *Inorg. Chem*. **1991**, *30*, 3068.

[5] C. D. Chandler, R. Christopher, M. J. Hampden-Smith, *Chem. Rev.* **1993**, *93*, 1205.

[6] [6a] R. C. Mehrotra, A. Singh, S. Sogani, *Chem. Rev.* **1994**, *94*, 1643. – [6b] R. C. Mehrotra, A. Singh, S. Sogani, *Chem. Soc. Revs.* **1994**, 215. – [6c] R. C. Mehrotra, A. Singh, U. M. Tripathi, *Chem. Rev.* **1991**, *91*, 1287.

[7] M. Veith, S. Mathur, T. Decker, H. P. Beck, Manuscript in preparation.

[8] D. J. Teff, J. C. Huffman, K. G. Caulton, *Inorg. Chem.* **1994**, *33*, 6289.

[9] [9a] M. Veith, *Chem. Rev.* **1990**, *3*, 1. – [9b] M. Veith, D. Kaefer, V. Huch, *Angew. Chem*. **1986**, *98*, 367; *Angew. Chem. Int. Ed. Engl.* **1986**, *25*, 375. – [9c] M. Veith, J. Hans, L. Stahl, P. May, V. Huch, *Z. Naturforsch.* **1991**, *46b*, 403.

[10] [10a] M. Veith, S. Mathur, C. Mathur, V. Huch, *J. Chem. Soc., Dalton Trans.* **1997**, 2101. – [10b] B. A. Vaartstra, J. C. Huffman, P. S. Gradeff, L. G. Hubert-Pfalzgraf, J. C. Daran, S. Parraud, K. Yunlu, K. G. Caulton, *Inorg. Chem.* **1990**, *29*, 3126.

[11] [11a] M. Veith, S. Mathur, V. Huch, *J. Am. Chem. Soc.* **1996**, *118*, 903. – [11b] M. Veith, S. Mathur, V. Huch, *Inorg. Chem.* **1996**, *35,* 7295. – [11c] M. Veith, S. Mathur, V. Huch, *J. Chem. Soc., Chem. Commun.* **1997**, 2197.

[12] [12a] M. Veith, S. Mathur, C. Mathur, *Polyhedron* **1998**, *17*, 1005. – [12b] M. Veith, E. C. Yu, V. Huch, *Eur. J. Chem*. **1995**, *1*, 26. – [12c] B. Borup, W. E. Streib, K. G. Caulton, *Chem. Ber*. **1996**, *129*, 1003. – [12d] S. Sogani, A.Singh, R. Bohra, M. Noltemeyer, R. C. Mehrotra, J. Chem. Soc., *Chem. Commun*. **1991**, 738. – [12e] W. J. Evans, M. A. Greci, M. A. Ansari, J. W. Ziller, *J. Chem. Soc., Dalton Trans.* **1997**, 4503.

[13] [13a] B. Borup, J. A. Samuels, W. E. Streib, K. G. Caulton, *Inorg. Chem.* **1994**, *33*, 994. – [13b] K. G. Caulton, M. H. Chisholm, S. R. Drake, W. E. Streib, *Angew. Chem.* **1990**, *102*, 1492; *Angew. Chem. Int. Ed. Engl.* **1990**, *29*, 1483.

[14] J. A. Ibers, *Nature* **1963**, 197, 686.

[15] M. H. Chisholm, J. C. Huffman, K. C. Kirkpatrick, J. Leonelli, K. Folting, *J. Am.Chem. Soc.* **1981**, *103*, 6093.

[16] W. J. Evans, M. A. Greci, J. W. Ziller, *J. Chem. Soc., Dalton Trans.* **1997**, 3035.

[17] O. Poncelet, L. G. Hubert-Pfalzgraf, *Polyhedron* **1989**, *8*, 2183

[18] F. Schmidt *Methoden Org. Chem. (Houben-Weyl)* **1971**, vol. 6/2.

[19] D. C. Bradley, I. M. Thomas, *J. Chem. Soc.* **1960**, 3857.

[20] [20a] G. M. Sheldrick, *SHELXS-86, Program for Crystal Structure Determination*, University of Göttingen, **1986**. – [20b] G. M. Sheldrick, *SHELXL-97, Program for Crystal Structure Refinement*, University of Göttingen, **1997**.

[98094]

Compounds of Germanium and Tin, 25[◇]

A Zwitterionic Distannene and Two $(RSnX)_4$ Cages with an Unusual Arrangement of the Sn_4X_4 Cluster Atoms (R = tBu$_3$Si, X = Se, Te)☆

Manfred Weidenbruch*[a], Artur Stilter[a], Heinrich Marsmann[b], Karl Peters[c], and Hans Georg von Schnering[c]

Fachbereich Chemie der Universität Oldenburg[a],
Carl-von-Ossietzky-Straße 9–11, D-26111 Oldenburg, Germany

Fachbereich Chemie der Universität (GH) Paderborn[b],
Warburger Straße 100, D-33095 Paderborn, Germany

Max-Planck-Institut für Festkörperforschung[c],
Heisenbergstraße 1, D-70506 Stuttgart, Germany

Received April 3, 1998

Keywords: Tin / Silicon / Chalcogens / Cluster compounds

Reaction of tin(II) chloride with RNa(THF)$_2$ (R = tBu$_3$Si) in THF at –30 °C led to a complex reaction mixture, from which the compounds $R_4Sn_4(THF)_2$, R_2SnSnR_2 (**5**), R–R (**7**), and a brownish black compound **6** were isolated. In toluene as solvent, the zwitterionic distannene **5** was obtained together with **7** and **6** which upon treatment with Et_3PX, furnished the cluster compounds $(RSnX)_4$ (**10**: X = Se; **11**: X = Te). The X-ray structure analyses of the isotypic compounds **10** and **11** revealed that the tin atoms occupy the corners of an undistorted tetrahedron with weak tin–tin interactions. The chalcogen atoms form a plane which bisects the Sn_4 tetrahedron.

Lappert's distannene **1** was the first molecule with a formal homonuclear double bond between the heavier elements of group 14 to be prepared.[2][3] Although compound **1** was prepared in 1976 and characterized by X-ray crystallography almost twenty years passed before the compounds **2**[4] and **3**[5] could be isolated as further examples of this class of compound.

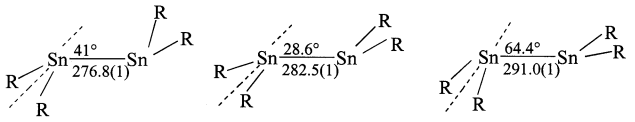

1, R = CH(SiMe$_3$)$_2$ **2**, R = Si(SiMe$_3$)$_3$ **3**, R = 2-tBu-4,5,6-Me$_3$C$_6$H

The three crystalline distannenes possess widely differing structures. While the centrosymmetrical compound **1** exhibits an undistorted *trans*-bent arrangement of its substituents with a fold angle of 41° – which closely approaches the theoretically predicted fold angles of 46–51° for the parent compound $[Sn_2H_4]$[3][5] – the sterically overloaded compound **2** avoids interactions between its substituents by adopting a twist angle of 63.2° and a fold angle of 28.6°.[4] The behavior of compound **3** is even more surprising. The markedly lengthened tin–tin bond length and the differing environments of the two tin atoms possibly suggest that merely an interaction between the fully occupied 5s orbital of one tin atom with the empty 5p orbital of the other tin atom is operative. The zwitterionic structure of **3** that could be deduced from this assumption, however, is not supported by the ^{119}Sn CP-MAS NMR spectrum in which only one signal at δ_{iso} = 819 is observed.[6] Similar to **1**, the recently described heteroleptic distannene RR′Sn=SnRR′ [R = Si(SiMe$_3$)$_3$, R′ = 2,4,6-(CF$_3$)$_3$C$_6$H$_2$] exhibits a centrosymmetric structure with an Sn–Sn bond length of 283.3(1) pm and a fold angle of 41.5°.[7]

The distannenes **1**–**3** decompose in solution to the respective stannylene molecules R_2Sn:. We have now examined whether a distannene that is stable both in the solid state and in solution can be obtained by use of other substituents R. Our first choice of substituent was the tri-*tert*-butylsilyl group with its extremely high steric requirements for which we reported a simple access more than 20 years ago[8] and which in the mean time has been used successfully by Wiberg et al. in the syntheses of many interesting compounds including the tetrahedral molecules $(RSi)_4$ and $(RGe)_4$.[9]

We now report on a zwitterionic distannene as well as a tin cluster compound for which, however, characterization was only possible on the basis of the products of subsequent reactions.

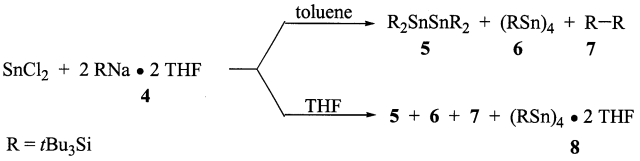

Reaction of tin(II) chloride with the tri-*tert*-butylsilylsodium · THF adduct **4**[10] in toluene furnished a black-brown

[◇] Part 24: Ref.[1].

 © WILEY-VCH Verlag GmbH, D-69451 Weinheim, 1998 1434–1948/98/0909–1333 $ 17.50+.50/0

solution from which three products were isolated by fractional crystallization. First of all, a black-brown, finely crystalline precipitate was obtained but its constitution could not be determined neither by analytical nor spectroscopic means, an account of its poor solubility and extreme sensitivity to air. Only the subsequent reactions described below allowed conclusions to be drawn about the structure of this compound **6**. Colorless needles of the known hexa-*tert*-butyldisilane (**7**)[11] were obtained as a second fraction. Finally, upon longer standing of the solution at −25°C, dark brown, fibrous crystals separated, complete elemental analysis data of which are indicative of the distannene **5** or the corresponding stannylene R_2Sn:.

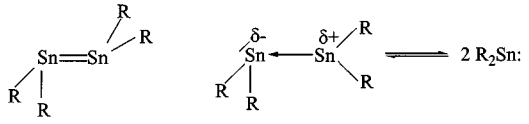

5a, R = *t*Bu$_3$Si **5b** **9**

Since we have not yet been able to obtain crystals of **5** suitable for X-ray diffraction analysis, its structural elucidation is based on NMR examinations of all nuclei present in **5** (C, H, Si, Sn). The presence of two singlet signals of equal intensity in the ^{1}H-NMR spectrum as well as the presence of two signals each for the primary and quaternary carbon atoms in the ^{13}C-NMR spectrum clearly show that two sorts of differently bonded *tert*-butyl groups are present. This is supported by the observation of two signals with different $^1J(^{29}Si,^{119}Sn)$ coupling constants in the ^{29}Si-NMR spectrum. Unambiguous information about the structure of **5** is provided by the ^{119}Sn-NMR spectrum in which two signals with chemical shifts of $\delta = -690$ and $+413$ and a coupling constant of $^1J(^{119}Sn,^{117}Sn) = 2135$ Hz demonstrate the presence of two tin atoms bonded to each other but having widely differing electronic environments.

It would seem that neither the stannylene **9** nor the centrosymmetric distannene **5a** exists in the solution. The data rather support the zwitterionic structure **5b** with the tin atom producing the ^{119}Sn signal shifted to low field acting as an electron donor from its doubly occupied 5s orbital to the unoccupied 5p orbital of the electron-accepting tin atom giving rise to the ^{119}Sn-NMR signal shifted to high field. An adduct of tin(II) chloride and a four-coordinated stannylene was recently reported;[12] the X-ray crystallographic analysis and ^{119}Sn-NMR spectrum of this adduct are, in spite of the different bonding partners and coordination numbers, suggestive of a bonding situation similar to that in **5b**.

The behavior of **5** as well as that of the $SnCl_2$ adduct is not self-evident since the distannenes **1**,[13] **2**,[4] and **3**[6] – which are stable in the solid state – do not give rise to any ^{119}Sn-NMR signals in solution at room temperature. This is assumed to be due in all cases to the rapid equilibrium distannene $\rightleftarrows$ stannylene. In order to determine whether **5** is also subject to a similar equilibrium the molecular mass of **5** was determined in dilute solution (dilution from 4 g/100 ml to 0.6 g/100 ml). The measured value of 520 g · mol^{-1} was in good agreement with the calculated value of 517.5 for the stannylene **9**. The appearance of only one ^{1}H-NMR signal at $\delta = 1.35$ and of two ^{13}C-NMR signals at $\delta = 27.74$ (C_p) and 32.12 (C_q) is a further indication for the equilibrium **5** $\rightleftarrows$ 2 **9**; ^{29}Si-and ^{119}Sn-NMR signals could not be recorded from this dilute solution.

When the reaction of tin(II) chloride with **4** was performed in THF instead of toluene a dark-blue, fine crystalline solid was isolated in addition to compounds **5**–**7**. The analytical and spectroscopic data of this solid are indicative of the THF adduct **8**. However, the broad signals in the ^{1}H-NMR spectrum and the failure to observe ^{29}Si- and ^{119}Sn-NMR signals suggest that, like compounds **1**, **2**, and **3**, rapid exchange processes are in operation. Spectroscopic measurements at lower temperatures did not furnish a different result.

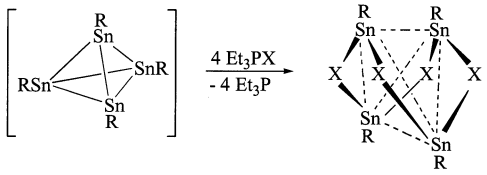

6, R = *t*Bu$_3$Si **10**, X = Se; **11**, X = Te

In order to obtain information about the structure of the practically insoluble and highly sensitive compound **6** we attempted to convert it to better characterizable products by treatment with the heavier chalcogenes. Although no rections with selenium or tellurium were observed, treatment of **6** with triethylphosphane selenide or telluride furnished the compounds **10** or **11**, respectively, in a smooth reaction. NMR data of these products indicate the existence of highly symmetrical molecules.

Figure 1. Molecular structure of **10** in the crystal (hydrogen atoms omitted)[a]

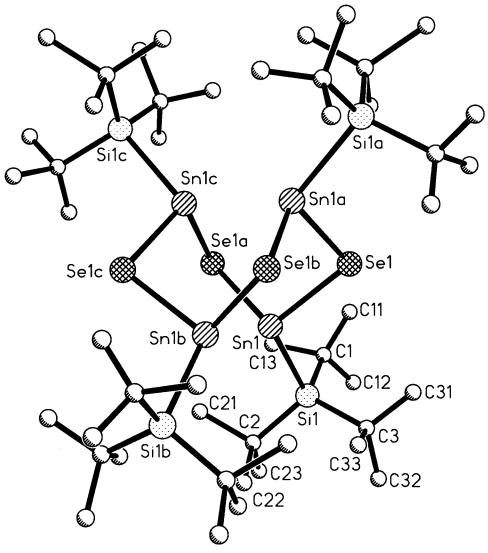

[a] Selected bond lengths [pm] and angles [°]: Sn–Se 255.2(2), Sn–Sn 301.8(3), Sn–Si 265.6(5); Sn–Se–Sn 94.8(1), Se–Sn–Se 101.5(1), Se–Sn–Si 108.0(1), Se–Sn–Sn 100.2(1).

The X-ray crystallographic analysis of **10** (Figure 1) confirmed the deductions from the NMR data and additionally

provided some noteworthy details. In the crystal the asymmetrical unit contains a quarter of the molecule. The equivalent positions are designated by the letters a, b, and c in the figure. Accordingly, the respective Sn−Se, Sn−Si, and also Sn−Sn bond lengths are the same. The structure of **10** is not only unusual but also without precedent in the chemistry of tin chalcogenides. The four tin atoms form an undistorted tetrahedron that is divided into two equal parts by a quadratic layer of selenium atoms. The structure resembles that of the arsenic sulfide mineral realgar in which the arsenic and chalcogen atoms have a similar arrangement.[14] The tin−tin separations of 301.8 pm markedly exceed the normal value of 278 pm for the single bond in the reference substance hexamethylditin.[15] The long tin−tin bonds become reasonable upon simple electron counting. Merely four electrons are available for a total of six Sn−Sn bonds (one from each tin atom) within the tetrahedron so that the existence of a delocalized electron system with bond orders of markedly less than one may be assumed.

Figure 2. Molecular structure of **11** in the crystal (hydrogen atoms omitted)[a]

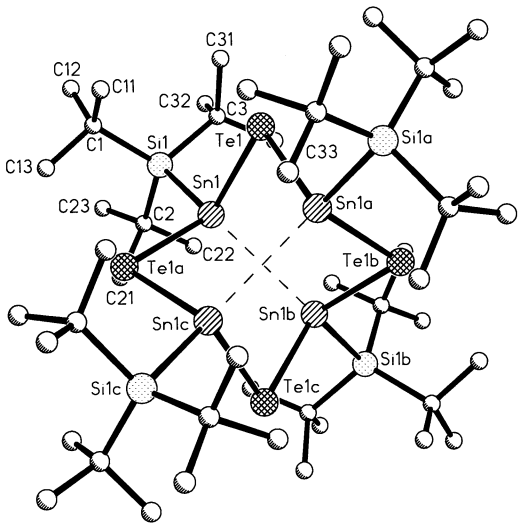

[a] Selected bond lengths [pm] and angles [°]: Sn−Te 274.2(1), Sn−Sn 328.1(2), Sn−Si 265.2(3); Sn−Te−Sn 95.1, Te−Sn−Te 101.8(1), Te−Sn−Si 109.1(1), Fe−Sn−Sn 100.3(1).

These structural peculiarities are even more pronounced in **11**, which is isotypical with **10** and is shown in a different perspective in Figure 2 in order to emphasize the unusual atomic arrangement. The tin−tin separation in **11** of 328.1(2) pm is even larger than that in **10** and again supports a low bond order for the Sn−Sn bonds.

The isolation of compounds **10** and **11** allows the conclusion, albeit with some reservations, that compound **6** could be a representative of the long sought *tetrahedro*-tetrastannane system and that chalcogen insertion into four of the six Sn−Sn bonds has given rise to these unequivocally characterized cage compounds. Wiberg et al. also obtained a product from similar reactions that they held to be **6** but which could not, on account of its above-mentioned properties, be characterized further.[9][16]

The various products arising from the action of **4** on tin(II) chloride can be most simply explained in terms of the primary formation of the stannylene **9** which either dimerizes to give the zwitterionic distannene **5** or reacts further with cleavage of tBu$_3$Si radicals[9] to furnish **7** and **6** (or **8** in THF). Hexaarylcyclotristannanes also behave similarly: their pyrolyses furnish, by suitable choice of the aryl groups, a wide variety of tin cluster compounds.[17]

Financial support of our work by the *Deutsche Forschungsgemeinschaft* and the *Fonds der Chemischen Industrie* is gratefully acknowledged.

Experimental Section

All manipulations were performed by using standard Schlenk techniques under dry argon. − ^{1}H and ^{13}C NMR: Bruker AM 300. − ^{29}Si and ^{119}Sn NMR (inverse gated, ^{1}H-decoupled, Me$_4$Sn external): Bruker AMX 300. − MS: Varian MAT 212. − Elemental analyses: Analytische Laboratorien, D-51789 Lindlar, Germany.

Reactions of Tin(II) Chloride with **4**: A solution of anhydrous tin(II) chloride (2.11 g, 11.8 mmol) in 25 ml of THF was added dropwise to a solution of **4** (7.70 g, 22.4 mmol) in 50 ml of toluene at −30°C over a period of 3 h with stirring. The brownish black reaction mixture was stirred for an additional 1 h at −20°C and the insoluble compound **6** (0.38 g, 11% yield), m.p. 182°C, was filtered off. The solvents were removed and the residue redissolved in 30 ml of *n*-hexane. Precipitated NaCl was filtered off and the solution cooled to −50°C. After 12 h at this temperature, colorless crystals of **7** (1.0 g, 24% yield) were isolated and identified by comparison with literature data.[11] Concentration of the solution to a volume of 20 ml and cooling at −24°C for 3 d yielded dark brown, fibrous crystals of **5** (1.2 g, 21% yield).

Tetrakis(tri-tert-butylsilyl)distannene (**5**): M.p. 104°C. − ^{1}H NMR (C_6D_6, 25°C): δ = 1.40 [s, 54 H, $^4J(^1H,^{119}Sn)$ = 17.7 Hz], 1.51 [s, 54 H, $^4J(^1H,^{119}Sn)$ = 17.9 Hz]. − ^{13}C NMR (C_6D_6, 25°C): δ = 26.27 (C_q), 28.90 (C_q), 32.42 (C_p), 34.54 (C_p); C_p and C_q refer to primary and quaternary carbon atoms. − ^{29}Si NMR (C_6D_6, 25°C): δ = 24.99 [s, $^1J(^{29}Si,^{13}C)$ = 35 Hz, $^1J(^{29}Si,^{119}Sn)$ = 85.5 Hz], 54.49 [s, $^1J(^{29}Si,^{13}C)$ = 42.1 Hz, $^1J(^{29}Si,^{119}Sn)$ = 11.6 Hz]. − ^{119}Sn NMR (C_6D_6, 25°C): δ = 412.6 [s, $^1J(^{119}Sn,^{117}Sn)$ = 2135 Hz], − 689.9. − MS (CI, isobutane); *m/z* (%): 1037 (1) [MH$^+$], 519 (16) [MH$^+$ − SnR$_2$]. − $C_{48}H_{108}Si_4Sn_2$ (1035.1): calcd. C 55.70, H 10.52, Sn 22.93; found C 55.34, H 10.36, Sn 23.20.

A similar reaction in which toluene was replaced by THF led to the same products in comparable yields. However, in addition to compounds **5**, **6**, and **7**, 0.29 g of the dark blue, microcrystalline compound **8**, m.p. 76°C was isolated.

(tBu$_3$Si)$_4$Sn$_4$(THF)$_2$ (**8**): ^{1}H NMR ([D$_8$]toluene, 243 K): δ = 1.31 (br. s, 54 H), 1.43 (br. s, 54 H), 1.89 (m, 8 H), 3.57 (m, 8 H). − ^{13}C NMR ([D$_8$]toluene, 243 K): δ = 25.84 (C_q), 26.09 (C_q), 31.89 (C_p), 33.16 (C_p). − The ^{29}Si- and ^{119}Sn-NMR signals could not be observed. − $C_{56}H_{124}O_2Si_4Sn_4$ (1179.1): calcd. C 47.48, H 8.82; found C 47.40, H 8.91.

Formation of the Cluster Compound **10**: A solution of triethylphosphane selenide (0.32 g, 1.62 mmol) in 10 ml of *n*-hexane was added dropwise to a suspension of **6** (0.51 g, 0.40 mmol) in 100 ml of toluene at ambient temperature over a period of 30 min. The reaction mixture was stirred for 3 d in the dark. All insoluble components were filtered off and the solvents removed. The residue was redissolved in 10 ml of DME. Cooling of the yellow, light-sensitive solution to −24°C afforded 0.42 g (66% yield) of pale yellow, rectangular crystals of **10**, m.p. 115°C. − ^{1}H NMR (C_6D_6, 25°C): δ = 1.38 (s). − ^{13} C NMR (C_6D_6, 25°C): δ = 31.87 (C_q),

32.48 (C_p). – ^{119}Sn-NMR (C_6D_6, 25°C): δ = 120.21. – MS (CI, isobutane); *m/z* (%): 1112 (8) [$tBu_3Sn_3Se_3$]. – $C_{48}H_{108}Se_4Si_4Sn_4 \cdot 2$ DME (1768.6): calcd. C 38.03, H 7.29; found C 38.80, H 7.43.

Formation of the Cluster Compound **11**: A solution of triethylphosphane telluride (0.98 g, 3.99 mmol) in 10 ml of *n*-hexane was added dropwise to a suspension of **6** (0.80 g, 0.63 mmol) in 60 ml of toluene over a period of 30 min. The reaction mixture was stirred in the dark for 3 d at room temperature. The solvents were removed and the residue was dissolved in 10 ml of *n*-hexane. All insoluble components were filtered off and the remaining red solution was stored for 4 d at 4°C. Excess triethylphosphane telluride was filtered off, the solvent removed and the residue redissolved in 8 ml of DME. Cooling to −24°C for 4 d furnished 0.64 g (57% yield) of air- and light-sensitive red crystals of **11**, m.p. 183°C. – ^{1}H NMR (C_6D_6, 25°C): δ = 1.37 (s). – ^{13}C NMR (C_6D_6, 25°C): δ = 32.03 (C_q), 34.02 (C_p). – ^{119}Sn NMR (C_6D_6, 25°C): between δ = +300 and −500 no signal could be observed. – $C_{48}H_{108}Si_4Sn_4Te_4$ (1782.9): calcd. C 32.34, H 6.11; found C 33.43, H 6.62.

X-ray Structure Analyses of **10 and 11**: Crystal data and numerical data of the structure determinations are given in Table 1. Crystals were obtained by cooling a solution of **10** in diethyl ether to −24°C (**10**) or by cooling a DME solution of **11** to 4°C. In each case, the crystal was mounted in a thin-walled glas capillary. The structures were solved by direct phase determination using the SHELXTL PLUS program system and refined by full-matrix least-squares techniques. Hydrogen atoms were placed in the calculated positions, and all other atoms were refined anisotropically.[18]

Table 1. Crystallographic data of **10** and **11**

	10	**11**
Formula	$C_{48}H_{108}Se_4Si_4Sn_4$	$C_{48}H_{108}Si_4Sn_4Te_4$
Mol. mass	1588.32	1782.88
Cryst. dimensions [mm]	0.45 × 0.55 × 0.30	0.4 × 0.45 × 1.35
Cryst. system	tetragonal	tetragonal
Space group	$I\bar{4}2d$	$I\bar{4}2d$
a [pm]	2371.1(1)	2388.0(3)
c [pm]	1420.3(1)	1455.8(2)
V [× 10^6 pm^3]	7958	8302
Z	16	16
$d_{calcd.}$ [g cm^{-3}]	1.982	2.140
Diffractometer	Siemens P4	Siemens P4
Radiation (graphite-monochromated) [pm]	Mo-K_α 71.073	Mo-K_α 71.073
T [K]	296(2)	296(2)
μ [mm^{-1}]	3.14	2.65
Scan method	ω	ω
$2\theta_{max}$ [°]	55	55
No. of unique reflections	2666	2767
No. of observed reflections	1702	2133
F_o/parameter ratio	12.51	14.03
R (R_w) [$F > 3\sigma$ (*F*)]	0.066 (0.060)	0.064 (0.065)

☆ Dedicated to Professor *Bernt Krebs* on the occasion of his 60th birthday.

[1] A. Schäfer, W. Saak, M. Weidenbruch, *Z. Anorg. Allg. Chem.*, in press.
[2] D. E. Goldberg, D. H. Harris, M. F. Lappert, K. M. Thomas, *J. Chem. Soc., Chem. Commun.* **1976**, 261–262.
[3] D. E. Goldberg, P. B. Hitchcock, M. F. Lappert, K. M. Thomas, T. Fjeldberg,A. Haaland, B. E. R. Schilling, *J. Chem. Soc., Dalton Trans.* **1986**, 2387–2394.
[4] K. W. Klinkhammer, W. Schwarz, *Angew. Chem.* **1995**, *107*, 1448–1450; *Angew. Chem. Int. Ed. Engl.* **1995**, *34*, 1334–1336.
[5] G. Trinquier, J. P. Malrieu, *J. Am. Chem. Soc.* **1987**, *109*, 5303–5315. – G. Trinquier, *J. Am. Chem. Soc*. **1990**, *112*, 2130–2137. – T. L. Windus, M. S. Gordon, *J. Am. Chem. Soc.* **1992**, *114*, 9559–9568. – H. Jacobsen, T. Ziegler, *J. Am. Chem. Soc.* **1994**, *116*, 3667–3679.
[6] M. A. Della Bona, M. C. Cassani, J. M. Keates, G. A. Lawless, M. F. Lappert, M. Stürmann, M. Weidenbruch, *J. Chem. Soc., Dalton Trans.* **1998**, 1187–1190.
[7] K. W. Klinkhammer, T. F. Fässler, H. Grützmacher, *Angew. Chem.* **1998**, *110*, 114–116; *Angew. Chem. Int. Ed.* **1998**, *27*, 124–126.
[8] M. Weidenbruch, W. Peter, *Angew. Chem.* **1975**, *87*, 670–671; *Angew. Chem. Int. Ed. Engl.* **1975**, *14*, 642–643.
[9] Review: N. Wiberg, *Coord. Chem. Rev.* **1997**, *163*, 217–252.
[10] N. Wiberg, G. Fischer, P. Karampatses, *Angew. Chem.* **1984**, *96*, 58–59; *Angew. Chem. Int. Engl.* **1984**, *23*, 59–60.
[11] N. Wiberg, H. Schuster, A. Simon, K. Peters, *Angew. Chem.* **1986**, *98*, 100–101; *Angew. Chem. Int. Ed. Engl.* **1986**, *25*, 79–80.
[12] W.-P. Leung, W.-H. Kwok, F. Xue, T. C. W. Mak, *J. Am. Chem. Soc.* **1997**, *119*, 1145–1146.
[13] K. W. Zilm, G. A. Lawless, R. M. Merrill, J. M. Millar, G. G. Webb, *J. Am. Chem. Soc.* **1987**, *109*, 7236–7238.
[14] D. J. E. Mullen, W. Nowacki, *Z. Kristallogr.* **1972**, *136*, 48–65.
[15] A. Haaland, A. Hammel, H. Thomassen, H. V. Volden, H. B. Singh, P. K. Khanna, *Z. Naturforsch*. **1990**, *45b*, 1143–1146; see also: N. Wiberg in *Progress im Organosilicon Chemistry* (Eds.: B. Marciniec, J. Chojnowski), London and Breach, Basel, **1995**, p. 19–39.
[16] N. Wiberg, personal communication; see also: N. Wiberg in *Progress in Organosilicon Chemistry* (Eds.: B. Marciniec, J. Chojnowski), Gordon and Breach, Basel, **1995**, p. 19–39.
[17] Review: L. R. Sita, *Acc. Chem. Res.* **1994**, *27*, 191–197.
[18] Crystallographic data (excluding structure factors) for the structures reported in this paper have been deposited with the Cambridge Crystallographic Data Centre as supplementary publication no. CCDC-101345. Copies of the data can be obtained free of charge on applications to CCDC, 12 Union Road, Cambridge CB2 1EZ, UK [Fax. (internat.) + 44(0)1223/336-093; E-mail: deposit@ccdc.cam.ac.uk].

[98095]

Synthesis, X-ray Crystal Structure and Magnetism of $[NiCl_2\{(bis(2\text{-benzimidazolyl})propane\}]_2 \cdot (C_2H_5OH)_2$ − A Second Example of a Ferromagnetically Coupled Five-Coordinated High-Spin Dichloro-Bridged Nickel(II) Dimer

Gerard A. van Albada[a], Jeroen J. A. Kolnaar[a], Wilberth J. J. Smeets[b], Anthony L. Spek[b], and Jan Reedijk*[a]

Leiden Institute of Chemistry, Gorlaeus Laboratories, Leiden University[a],
P. O. Box 9502, NL-2300 RA Leiden, Netherlands

Bijvoet Center for Biomolecular Research, Vakgroep Kristal-en Structuurchemie, Utrecht University[b],
Padualaan 8, NL-3584 CH Utrecht, Netherlands
E-mail: spea@chem.ruu.nl
E-mail: reedijk@chem.leidenuniv.nl

Received April 20, 1998

Keywords: Crystal structures / Nickel complexes / Dinuclear complexes / Magnetism / Far-infrared

The ligand bis(2-benzimidazolyl)propane coordinates to Ni^{II} with chloride as an anion, thereby forming a dinuclear compound with the formula: $[NiCl_2(tbz)_2]_2(C_2H_6O)_2$. This compound crystallizes in the space group $P2_1/c$. Each five-coordinated Ni^{II} ion has a distorted trigonal bipyramidal environment which consist of two asymmetrically bridging Cl anions with distances of 2.3556(17) and 2.4275(16) Å, a terminal Cl anion with a distance of 2.3496(17) Å and two nitrogen atoms of the ligand with distances of 2.022(4) and 2.000(4) Å. The Ni–Ni distance is 3.5891(12) Å, while the Ni–Cl–Ni angle is 97.23(6)°. The magnetic properties of the compound, as studied in the range 5–280 K, have been fitted with a zero-field splitting parameter D (–14.3 cm^{-1}) and a ferromagnetic exchange between the Ni ions in the dinuclear unit (J = +2.5 cm^{-1}). The title compound appears to be the second example for a five-coordinated ferromagnetic dinuclear Ni^{II} compound of this type, and its magnetic properties appear to correlate with the ligand structure. With the availability of an increasing number of examples of such species it appears that antiferromagnetic exchange is found for all cases with the chromophore $N_2ClNiCl_2NiClN_2$ where the MN_2 ring is 5-membered. In the case, where this ring is six-membered, the exchange is ferromagnetic.

During the last 2 decades only a few dichloro-bridged Ni^{II} dimers have been studied in detail both structurally and magnetically[1][6][7][8][9]. Such compounds all contain a sterically crowded didentate amine or imine ligand (NN) resulting in the centrosymmetric chromophore $(NN)ClNiCl_2NiCl(NN)$. The geometry of Ni^{II} in all cases is trigonal bipyrimidal with varying degrees of distortion to tetragonal pyramidal[1][6][7][8][9]. The $NiCl_2Ni$ rectangle has Ni−Cl−Ni angles of 97.5 ± 0.9° and the Ni−Cl distances vary from 2.296 to 2.456 Å, Ni−Ni varies from 3.56 to 3.65 Å.

Magnetically these compounds are very interesting as both Ni ions interact, albeit weakly, through the Cl bridges. In fact, this only leaves the chelating ligand (NN) as a possible synthetic variable. Most of the earlier antiferromagnetically coupled systems have a rigid N−C−C−N structure with a five-membered chelate ring. Only one system[1] has a flexible non-conjugated ligand with a six-membered chelate ring.

By using parameters for both the zero-field splitting (D) and the exchange J and zJ' (the latter being a parameter which describes lattice effects on the exchange), the low-T magnetic data can be fitted accurately. So far most compounds of this category $[\{Ni(NN)Cl_2\}_2]$ have shown the commonly observed antiferromagnetic exchange and only in one case[1] has ferromagnetic exchange been reported. No correlations with any structural parameter (Ni−Cl−Ni angle, Ni−Cl distances) could be found at the time, although the more recently developed parameter[2] to describe the degree of deviation from trigonal-bipyrimidal (τ) gave a clue that an increased distortion towards square pyrimidal could be the origin.

To investigate whether this hypothesis is useful, a new system had to be investigated. Bis(2-benzimidazoles) have been shown to be useful tools in the coordination chemistry of azoles which act as ligands in the context of mimicking biological systems[3]. The ligands bis(2-benzimidazolyl)propane and bis(2-benzimidazolyl)butane form dinuclear alkoxo-bridged compounds[4] with Cu^{II} and less strong anions, such as tetrafluoroborate, triflate, perchlorate, and nitrate. With strong anions, such as the halides, mononuclear Cu^{II} compounds are formed[5]. With Ni^{II} chloride, bis(2-benzimidazolyl)propane (abbreviated as tbz) yields a dinuclear chloride-bridged compound. As this compound has the flexible ligand chelate ring, it was expected to yield a ferromagnetically coupled system, if our hypothesis were true. Therefore the title compound was studied both structurally and magnetically in detail. The results which are described below, show that they indeed agree with our hypothesis.

 © WILEY-VCH Verlag GmbH, D-69451 Weinheim, 1998 1434−1948/98/0909−1337 $ 17.50+.50/0

Results and Discussion

Description of the Crystal Structure of $[NiCl_2(tbz)_2]_2(C_2H_6O)_2$

The dinuclear unit consists of two $NiCl_2(tbz)$ units, which are related by the crystallographic center of symmetry. Each unit consists of a five-coordinate Ni^{II} ion, surrounded by two N atoms of the ligand [Ni1−N13 2.022(4), Ni1−N23 2.000(4) Å], a terminal Cl ion [Ni1−Cl2 2.3496(17) Å], a bridging Cl ion [Ni1−Cl1 2.3556(17) Å], and a second bridging Cl ion [Ni1−Cl1a 2.4275(16) Å], belonging to the other half of the dimer, resulting in a slightly asymmetric bridge.

The structure is depicted in Figure 1. The Ni−Ni distance is 3.5891(12) Å, while the Ni−Cl−Ni angle is 97.23(6). The Ni−Cl distances and angles are comparable with those distances known for such Ni^{II} species[1b][6a][7a], while the distances and angles of the ligand are comparable with other structures known for this ligand[4].

Figure 1. ORTEP plot showing the structure $[NiCl_2(tbz)_2]_2$ with atom-labeling scheme; ethanol molecules are ommitted for clarity; atoms marked with an "a" are generated by an inversion centre

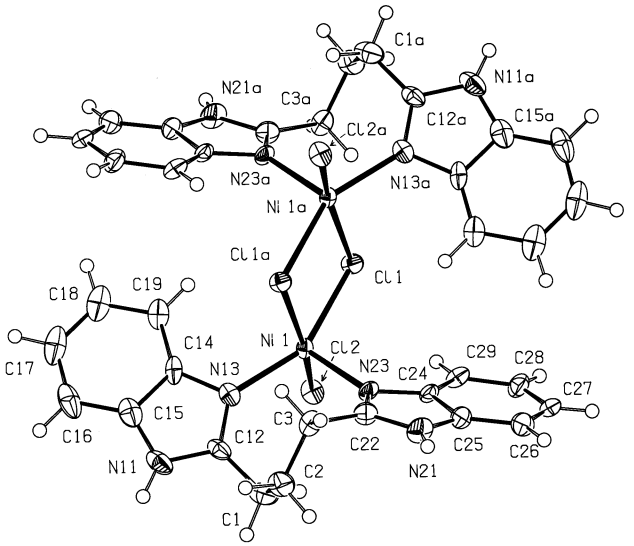

[a] Selected bond lengths [Å] and angles [°]: Ni(1)−Ni(1)a 3.5891(12), Ni(1)−Cl(1) 2.3556(17), Ni(1)−Cl(2) 2.3496(17), Ni(1)−N(13) 2.022(4), Ni(1)−N(23) 2.000(4), Ni(1)− Cl(1)a 2.4275(16); Cl(1)−Ni(1)−Cl(2) 88.45(6), Cl(1)−Ni(1)−N(13) 150.00(14), Cl(1)−Ni(1)−N(23) 104.31(13), Cl(1)−Ni(1)−Cl(1)a 82.77(6), Cl(2)−Ni(1)−N(13) 91.01(13), Cl(2)−Ni(1)−N(23) 102.05(12), Cl(1<9a−Ni(1)−Cl(2) 162.85(7), N(13)−Ni(1)−N(23) 105.13(18), Cl(1)a−Ni(1)−N(13) 98.33(12), Cl(19a)−Ni(1)−N(23) 94.40(12), Ni(1)−Cl(1)−Ni(1)a 97.23(6).

The coordination around the Ni ion can be best described as basically trigonal bipyramidal with a distortion towards square pyramidal. The two largest angles are 162.85(7)° and 150.00(14)°, yielding the structural parameter $\tau = 0.21$ (τ describes the relative amount of trigonality; $\tau = 0$ for square pyramid and $\tau = 1$ for trigonal bipyramid)[2].

When comparing the structural parameters to the other four five-coordinated structures listed in Table 2, the τ value is in fact closer to the structures **1**−**3** than to structure **4** from this table.

The crystal packing is dictated by van der Waals contacts and by a quite strong hydrogen bonding network with $N\cdots O_{ethanol}$ [N(11)−H(11)···O(1) 2.722(8) Å] and $O_{ethanol}\cdots Cl$ contacts [O(1) H(1)···Cl(2) 3.077(6) Å].

Ligand Field and Infrared Spectra

The ligand field and far-infrared spectra of the considered five-coordinated Ni^{II} compounds are given in Table 1. Comparing the ligand-field maxima of the present compound with other five-coordinated Ni^{II} compounds, it is shown that the d-d transitions fall all in the same range, with no significant differences between the various compounds (**1**−**5**).

As also shown in Table 1 the Ni−N far infrared vibrations are found at ca. 290 cm^{-1}, all in the range found in the literature[13]. The Ni−Cl stretch vibrations are found between 245 and 260 cm^{-1} and the Ni−Cl bridging vibrations in the range 198−218 cm^{-1}, which is also in agreement with the literature[13]. In fact, further evidence for this assignment is found with the Ni^{II}(bbdhp) compounds [in which bbdhp = 1,7-bis(benzimidazol-2-yl)-2,6-dithiaheptane][14]. The monomeric compound $[Ni(bbdhp)Cl_2]\cdot 4\ H_2O$ shows the Ni−Cl vibrations at 260 cm^{-1} and the Ni−N vibration at 320 cm^{-1}, while the dinuclear compound $[Ni_2(bbdhp)_2(\mu\text{-}Cl_2]Cl_2\cdot 5\ H_2O\cdot 2$ EtOH, which has only bridging chloride ions, has the Ni-μ-Cl−Ni vibration at 220 cm^{-1}, with the Ni−N vibrations at 315 cm^{-1}.

Magnetic Properties

Magnetic susceptibility data in the range 5−280 K were collected. The molar susceptibility data (corrected for diamagnetism) is plotted in Figure 2. In this figure the μ_{eff} values and the results of the fitting procedure are also included. The values listed are normal, as is the small value for zJ'.

The magnetic moment μ_{eff} was found to be 3.5 B.M. at 140 K, slightly increasing to a maximum 3.6 B.M. at 30 K and decreasing rapidly at lower temperatures, typical for a weak ferromagnetic interaction between the Ni^{2+} ions in the dinuclear unit, with a zero-field effect dominating at lower temperatures.

For the description of the susceptibility data the equation obtained by Ginsberg et al[10] using the Hamiltonianin

$$H = -2\cdot J\hat{S}_1\cdot\hat{S}_2 - D(\hat{S}1_z{}^2 + \hat{S}_{2z}{}^2) - 2\cdot ZJ'\hat{S}_i\langle\hat{S}_i\rangle - g_i\beta H\hat{S}_i$$

which the symbols have their usual meanings[10], was employed.

The J value of +2.5 cm^{-1} calculated from the best fit indeed shows the ferromagnetic exchange hypothised above. So far, such a ferromagnetic interaction has also been known to occur in dimeric chloride-bridged Ni^{II} compounds that have an octahedral geometry; in these case the J values vary from +4.8 to +9 cm^{-1}[1b][8][12]. To develop a magneto-structure relationship we have concentrated on the 5-coordinated cases.

As shown in Table 2 three chloride-bridged Ni compounds seem to have an antiferromagnetic behaviour (compounds **1**−**3**) with J values varying from −4.4 to −10.45

Table 1. Ligand field and far-infrared data of five-coordinated dimeric chloro-bridged Ni^{II} units

Compound	Ligand field [a] (10^3 cm^{-1})						FIR [cm^{-1}] Ni−N	Ni−Cl	Ni−$Cl_{(br)}$	
1. $[Ni(qnqn)Cl_2]_2$	6.5		13.0	19.6(sh)	22.8	[d]	285	228		[d]
2. $[Ni(dmp)Cl_2]_2$	6.4	10.6(w)	13.8	19.8(sh)	23.3	[b]	294	260	198	[b]
3. $[Ni(biq)Cl_2]_2$	6.3	10.5(w)	13.8	19.8(sh)	23.4	[c]	298	275	203	[c]
4. $[Ni(CH_2(dmpz)_2)Cl_2]_2$	7.0		12.5	19.2(sh)	21.7	[e]	290	267	210	[e]
5. $[Ni(tbz)Cl_2]_2(C_2H_6O)_2$	6.1		12.5(vbr)	19.6(sh)	22.0		289	245	218	

[a] Abbreviations: sh = shoulder, w = weak, vbr = very broad. − [b] Synthesized according to ref.[9] and re-measured. − [c] Synthesized according to ref.[7a] and re-measured, the bridging Ni−Cl vibration can be at 198 cm^{-1} or at 203 cm^{-1}, as a ligand vibration occurs in this area. − [d] Data from ref.[6b], assignement of the FIR vibrations is uncertain as the compound was measured in CsI to ca. 200 cm^{-1}. This compound could not be synthesized to be re-measured. − [e] Data from ref.[1a] and[1c].

Table 2. Comparison between structural and magnetic data of five-coordinated dimeric chloro-bridged Ni^{II} units

Compound[a]	Ni−Cl [Å]	Ni−Ni [Å]	Ni−Cl−Ni [°]	Largest angles [°] α ,β (τ)[b]	J [cm^{-1}]	D [cm^{-1}]	g	ref. (s = structure, m = magnetism)
$[Ni(qnqn)Cl_2]_2$ (**1**)	2.408(2) 2.422(2) 2.296(2)	3.652(1)	98.23(5)	160.55(6), 158.00(7) (τ = 0.04)	−4.4	−7.0	2.25	[8](m),[6a](s)
$[Ni(dmp)Cl_2]_2$ (**2**)	2.378(1) 2.414(1) 2.307(1)	3.600(1)	97.4(1)	168.5(1), 155.41(5) (τ = 0.21)	−5.1	−8.8	2.20	[7a](s)[c],[8](m)
					−10.45	−33.7	2.21	[7b](m)
$[Ni(biq)Cl_2]_2$ (**3**)	2.372(1) 2.400(1) 2.306(1)	3.563(1)	96.68(2)	164.03(2), 157.55(5) (τ = 0.10)	−7.74	−18.43	2.31	[7a](s),[7b](m)
$[Ni(CH_2(dmpz)_2)Cl_2]_2$ (**4**)	2.319(1) 2.318(1) 2.456(1)	3.587(2)	97.36(4)	144.2(1), 173.8(3) (τ = 0.49)	+2.58	2.17	2.31	[1b](s, m)
$[Ni(tbz)Cl_2]_2(C_2H_6O)_2$ (**5**)	2.3556(17) 2.3496(17) 2.4275(16)	3.5891(12)	97.23(6)	162.85(7), 150.00(14) (τ = 0.21)	+2.49	−14.3	2.14	this work

[a] Ligand abbreviations: qnqn = *trans*-2(2′-quinoly)methylene-3-quinuclidinone, dmp = 2,9-dimethyl-1,10-phenantroline (neocuproine), biq = 2,2′-biquinolyl, $CH_2(dmpz)_2$ = bis(3,5-dimethylpyrazolyl)methane. − [b] See ref.[2], τ = defined as α − β/60. − [c] Another crystal structure with this ligand was solved, i.e. $[Ni(dmp)Cl_2]_2 \cdot 2\ CHCl_3$;[9] some distances slightly differ from those from the $[Ni(dmp)Cl_2]_2$ compound.

Figure 2. Molar susceptibility (o) and effective magnetic moment per Ni^{II} ion (×) of $[NiCl_2(tbz)_2]_2(C_2H_6O)_4$ as a function of the temperature; the full curves represent the theoretical curves for J = +2.5 cm^{-1}, D = −14.3 cm^{-1}, zJ' = −0.36 cm^{-1} and g = 2.14 (see text), with an R value of $3.20 \cdot 10^{-3}$ (in which $R = \Sigma\ \chi_{obs} - \chi_{calc}{}^2 / \Sigma\ \chi_{obs}{}^2$)

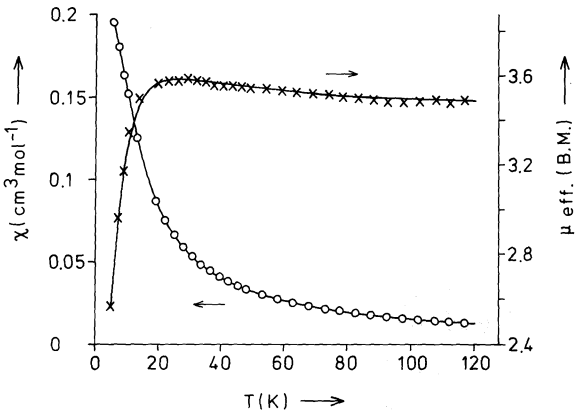

cm^{-1}. Compound **4**, however, shows a ferromagnetic behaviour, as is also the case in the title compound **5**. In fact, such a weak ferromagnetic interaction was also observed in another compound $[Ni(dae)Cl_2]_2$[11] {dae = *N,N′*-[2-(3,5-dimethyl-1-pyrazolyl)ethyl]ethylamine}, but in this case, the J value had not been reported.

For di-μ-hydroxo-bridged copper compounds a well-known correlation holds between the J vs. the bridging Cu−O−Cu angle and for a change of 1° a change of approx. 40 cm^{-1} is expected in the J value[12][15]. As seen from Table 2, for di-μ-chloride-bridged Ni^{II} compounds a quantitative correlation is not found. However, it appears that antiferromagnetic exchange is found for all cases with the chromophore $N_2ClNiCl_2NiClN_2$ where the MN_2 ring is 5-membered. In the case, where this ring is six-membered, the exchange is ferromagnetic. In general the variation in the extreme values of the exchange parameter J vary between −10 cm^{-1} and +19 cm^{-1}, the geometries of the Ni^{II} compounds are often difficult to compare, from hexacoordinate octahedral to pentacoordinate trigonal bipyramide intermediates. Different geometries usually result in different energies (and orientation) of the orbitals of the unpaired electrons. This in contrary to the di-μ-hydroxo-bridged copper compounds were the variation in the J value vary from +172 cm^{-1} to −509 cm^{-1}[15] and the geometries are mostly all square planar. It must also

be pointed out that the energy differences are very weak (ca. 10 cm^{-1}) and the J value itself must be regarded as an estimate of the exchange interaction, since the J value can be affected slightly by other parameters[12] (see compound **2** in Table 2 in ref.[1b]).

Although we did find, for the first time, a qualitative structure-magnetism relation for 5-coordinated di-μ-chloronickel(II) species, a quantitative conclusion about the magnetic behaviour in relation to the structural component for such Ni^{II} compounds cannot be drawn at this moment.

This work was supported in part (W. J. J. S. and A. L. S.) by the *Netherlands Foundation of Chemical Research* (SON) with financial aid from the *Netherlands Organization for Scientific Research* (NWO). The work described in the present paper has been supported by the *Leiden University Study Group WFMO* (Werkgroep Fundamenteel Materialen Onderzoek). The authors are indebted to the *EU* for a grant as Host Institute in the EU Programme Human Capital and Mobility (1994−1997). Use of the services and facilities of the *Dutch National NWO/SURF Expertise Center CAOS/CAMM*, under grant numbers SON 326-052 and STW NCH99.1751, is gratefully acknowledged.

Experimental Section

General: C, H, N, and Ni determinations: Microanalytical Laboratory of University College, Dublin, Ireland. − UV/Vis spectra: Perkin-Elmer 330 spectrophotometer using the diffuse reflectance technique, with MgO as a reference. − FTIR spectra: Bruker 113v infrared spectrophotometer, polyethylene mulls (600−100 cm^{-1}, mirror velocity 0.099 cm/s, resolution 2 cm^{-1}, Mylar 3.5 μ beam splitter). − Magnetic susceptibility: The title compound was measured in the temperature range 4.2−300 K with a fully automated Manics DSM-8 susceptometer equipped with a TBT continuous-flow cryostate and a Drusch EAF 16 NC electromagnet, operating at ca. 1.4 T. Data were corrected for magnetization of the sample holder and for diamagnetic contributions, which were estimated from the Pascal constants[16]. Magnetic data were fitted to a theoretical expression minimizing the function $R = \Sigma|\chi_{obs} - \chi_{calc}|^2/\Sigma|\chi_{obs}|^2$.

Synthesis of the Compound: The synthesis of the ligand bis(2-benzimidazolyl)propane has been described earlier[4c]. The nickel compound was prepared according to the following procedure: 1.2 mmol of Ni^{II} chloride and 1.2 mmol of the ligand were each dissolved in 10 ml of ethanol. The Ni^{II} salt solution was then added slowly to the ligand solution preventing any precipitation, filtered to remove any solids and after a few days the yellow-orange crystals separated. − $C_{19}H_{22}Cl_2N_4NiO$ (452.0): calcd. C 50.49, H 4.91, N 12.39, Ni 12.99; found C 50.25, H 4.60, N 12.80, Ni 13.80.

Crystal Structure Determination and Refinement of the Structure: The X-ray diffraction data were collected with an Enraf-Nonius CAD4T diffractometer at 150 K [rotating anode, 60 kV, 50 mA, graphite-monochromated Mo-K_α radiation, ω-scan mode]. Unit-cell parameters were checked for the presence of higher lattice symmetry[17]. The structure was solved by Direct Methods DIRDIF[18]. Neutral atom scattering factors and anomalous dispersion factors were taken from ref.[19]. Calculations were performed with programs SHELXL93[20] and PLATON[21] on a DEC-5000 cluster. The structure was refined on F^2 to $R1 = 0.0612$ for 2093 reflections for with $F_o > 4\ \sigma(F_o)$. ($wR2 = 0.105$ for 3562 unique reflections, $S = 0.968$, $-0.49 < \Delta\rho < 0.41$). A summary of the crystallographic data is given in Table 3. Anisotropic thermal parameters were used for all non-hydrogen atoms. Hydrogen atoms were included in the refinement cycle at calculated positions, riding on their carrier atoms except for the one on the ethanol molecule that was located from a difference map and its parameters refined.

Table 3. Crystal data and details of the structure determination

Compound	$C_{34}H_{32}Cl_4N_8Ni_2\cdot(C_2H_6O)_2$
Mol. wt.	904.02
Crystal system	monoclinic
Space group	$P2_1/c$ (No. 14)
a [Å]	13.0105(10)
b [Å]	8.3307(5)
c [Å]	19.6619(14)
β (°)	108.833(10)
V [Å^3]	2017.0(3)
Z	2
$D_{calcd.}$ [g cm^{-3}]	1.489
F[000]	936
μ [cm^{-1}]	12.4
Crystal size [mm], colour	0.12 × 0.18 × 0.17, red-orange
T [K]	150
θ_{max}	25
Δω [°]	0.66 + 0.35 tan
index ranges, h, k, l	−15/16, −10/0, −25/14
Total data, total unique data	5347, 3562
Observed data	2093 [$I > 2\ \sigma(I)$]
No. of refined refl. and params.	3562, 249
Final $R1$, $wR2$[a]	0.0612, 0.105
G.o.F.[b]	0.968
$(\Delta/\sigma)_{av}$ and $(\Delta/\sigma)_{max}$ in final cycle	< 0.001, < 0.001

[a] $R1 = \Sigma||F_o|-|F_c||/|F_o|$; $wR2 = \Sigma[w(F_o^2 - F_c^2)^2]/[w(F_o^2)^2]^{0.5}$. − [b] G.o.F. $= \{\Sigma[w(F_o^2 - F_c^2)^2]/(n-p)\}^{0.5}$.

Atomic positional and thermal parameters, lists of bond lengths and angles, and F_o/F_c values are available as supplementary material from one of the authors (A. L. S.). Crystallographic data (excluding structure factors) for the structure reported in this paper have been deposited with the Cambridge Crystallographic Data Centre as supplementary publication no. CCDC-101365. Copies of the data can be obtained free of charge on application to CCDC, 12 Union Road, Cambridge CB2 1EZ, UK [Fax: (internat.) + 44(1223)336-033, E-mail: deposit@ccdc.cam.ac.uk].

[1] [1a] J. Reedijk, J. Verbiest, *Transition Met. Chem.* **1978**, *3*, 51−52. − [1b] J. C. Jansen, H. van Koningsveld, J. A. C. van Ooijen, J. Reedijk, *Inorg. Chem.* **1980**, *19*, 170−174. − [1c] J. Reedijk, J. Verbiest, *Transition Met. Chem.* **1979**, *4*, 239−243.
[2] A. W. Addison, T. N. Rao, J. Reedijk, J. van Rijn, G. C. Verschoor, *J. Chem. Soc., Dalton Trans.* **1984**, 1349−1356.
[3] [3a] J. Reedijk, *Comprehensive Coordination Chemistry* (Ed.: Sir Geoffrey Wilkinson), Pergamon Press, London, **1987**, p. 73−98. − [3b] E. Bouwman, W. L. Driessen, J. Reedijk, *Coord. Chem. Rev.* **1990**, *104*, 143−172.
[4] [4a] G. Bernardinelli, A. Kübel-Pollak, S. Rüttimann, A. F. Williams, *Chimia* **1992**, *46*, 155−158. − [4b] G. Bernardinelli, A. Kübel-Pollak, S. Rüttimann, A. F. Williams, *Z. Kristallogr.* **1993**, *203*, 132−134. − [4c] G. A. van Albada, M. T. Lakin, N. Veldman, A. L. Spek, J. Reedijk, *Inorg. Chem.* **1995**, *34*, 4910−4917.
[5] [5a] M. A. Pujar, T. D. Bharamgoudar, *Transition Met. Chem.* **1988**, *13*, 423−425.− [5b] N. Donappa, S. B. Naikar, *Asian J. Chem.* **1993**, *5*, 995−997. − [5c] G. A. van Albada, unpublished results.
[6] [6a] G. J. Long, E. O. Schlemper, *Inorg. Chem.* **1974**, *13*, 279−285. − [6b] G. J. Long, D. L. Coffen, *Inorg. Chem.* **1974**, *13*, 270−278.
[7] [7a] R. J. Butcher, E. Sinn, *Inorg. Chem.* **1977**, *16*, 2334−2343. − [7b] R. J. Butcher, C. J. O′Connor, E. Sinn, *Inorg. Chem.* **1979**, *18*, 492−497.
[8] E. J. Laskowski, T. R. Felthouse, D. N. Hendrickson, G. J. Long, *Inorg. Chem.* **1976**, *15*, 2908−2911.

[9] H. S. Preston, C. H. L. Kennard, *J. Chem. Soc. A* **1969**, 2682−2685.
[10] A. P. Ginsberg, R. L. Martin, R. W. Brookes, R. C. Sherwood, *Inorg. Chem.* **1972**, *11*, 2884−2889.
[11] W. L. Driessen, R. M. de Vos, A. Etz, J. Reedijk, *Inorg. Chim. Acta* **1995**, *235,* 127−133.
[12] T. Bkouche-Waksman, Y.Journaux, O. Kahn, *Transition Met. Chem.* **1981**, *6*, 176−180 and references citied therein.
[13] J. R. Ferraro, *Low-Frequency vibrations of Inorganic and Coordination compounds*, Plenum Press, New York, **1971**.
[14] R. Carballo, A. Castiñeiras, W. Hiller, J. Strähle, *Polyhedron* **1993**, *12*, 1083−1092.
[15] O. Kahn, *Molecular Magnetism*, Chapter 8.6., VCH Publishers, New York, **1993**, and references citied therein.
[16] I. M. Kolthoff, P. J. Elving, *Treatise on Analytical Chemistry*, Interscience Publ., New York, **1963**, vol. 4, part 1.
[17] A. L. Spek, *J. Appl. Cryst.* **1988**, *21*, 578−579.
[18] P. T. Beurskens, G. Admiraal, G. Beurskens, W. P. Bosman, S. Garcia-Granda, R. O. Gould, J. M. M. Smits, C. Smykalla, C. *The DIRDIF program system*, Technical report of the Crystallography Laboratory. University of Nijmegen, The Netherlands, **1992**.
[19] A. J. C. Wilson (Ed.), *International Tables for Crystallography*, vol. C, Kluwer Academic Publ., Dordrecht, The Netherlands, **1992**.
[20] G. M. Sheldrick, *SHELXL93, Program for crystal structure refinement*, University of Göttingen, Germany, **1993**.
[21] A. L. Spek, *Acta Crystallogr.* **1990**, *A46*, C34.

[98119]

Monomeric *N*-Lithioaryl- and *N*-Lithioborylstannylamines from Distannylamines☆

Thomas Seifert[+], Wolfgang Storch*, and Martina Vosteen

Institute of Inorganic Chemistry, Ludwig-Maximilians-Universität München,
Meiserstraße 1–3, D-80333 Munich, Germany
E-mail: wst@anorg.chemie.uni-muenchen.de

Received May 4, 1998

Keywords: Distannylamines / *N*-Lithiostannylamines / *N*-Lithioborylamines / Amides / Structure elucidation

8-Aminoquinoline reacts with (dimethylamino)trimethylstannane in a 2:1 molar ratio, undergoing transamination to the distannylamine **1a**. The 9-[bis(trimethylstannyl)amino]-9-borabicyclo[3.3.1]nonane (**1b**) is obtained by the stannazane cleavage reaction of tris(trimethylstannyl)amine with 9-chloro-9-BBN. The cleavage of one Sn–N bond of the distannylamines **1a** and **1b** with MeLi yields the first two monomeric *N*-lithioaminostannanes, **2a** and **2b**, which can be stored at ambient temperature without decomposition. The molecular structures of **1a**, **1b**, **2a**, and **2b** have been determined by multinuclear magnetic resonance spectra in solution, as well as by X-ray structure analysis. Characteristic features are the intramolecular adduct formation of the quinoline ring nitrogen atom with one of the stannyl groups in **1a**, as well as with the lithium cation in **2a**, and the surprisingly short bonds between the central nitrogen atom and the adjacent elements [$d_{(NSn)}$: 2.02 Å, $d_{(NB)}$: 1.38 Å, $d_{(NC)}$: 1.34 Å, $d_{(NLi)}$: 1.95 Å] detected in the molecular structures of the lithium salts.

Introduction

Distannylamines have been shown to be useful precursors for the synthesis of novel main-group element nitrogen compounds[1]. Stannazane cleavage reactions, proceeding under mild conditions, may also serve for the preparation of doubly metallated alkali metal imides, RNM_2 (e.g. with M = Li, Na, K). Their molecular structures in solution as well as in the solid state are scarcely known, with the exception of the complex structure of dilithiated α-naphthylamine, which crystallizes as a cyclooligomeric aggregate containing ten molecular units with intermolecular Li−N bridging bonds[2]. Monometallated metal organostannylamides of the type $RN(SnMe_3)M$ (**2**) which, in contrast to some silylated homologues[3], have hitherto been unknown, should be accessible as intermediates en route to doubly metallated species.

Investigations of the stabilities, structures, and reactivities of the metal amides of primary amines, bearing one N−Li and one N−Sn bond instead of two N−H bonds, are of potential importance with regard to the synthesis of new main-group element nitrogen heterocycles, as well as of unsaturated Sn−N compounds under kinetically controlled conditions. Moreover, the influence of the electropositive lithium atom on the electron densities of the nitrogen atom and its adjacent bonds could be of particular interest.

We describe here the syntheses, structures, and spectroscopic properties of two distannylamines of the type $R-N(SnMe_3)_2$ (**1**) and of their *N*-lithiated derivatives **2**.

[+] X-ray structure analysis.

Results and Discussion

8-[Bis(trimethylstannyl)amino]quinoline (**1a**) was obtained by a well-established transamination reaction[4]. A 2:1 molar ratio of $Me_2N-SnMe_3$ and 8-aminoquinoline was heated at 80°C for 25 h, leading to reaction according to Eq. 1. No further purification was needed after removal of the volatile components in vacuo, since the reaction proceeded quantitatively. **1a** was recrystallized from hexane in good yield.

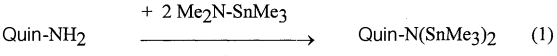

(1)

(2)

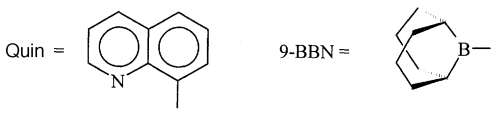

9-[Bis(trimethylstannyl)amino]-9-borabicyclo[3.3.1]nonane (**1b**) was formed in quantitative yield by mixing CH_2Cl_2 solutions of 9-chloro-9-BBN and $N(SnMe_3)_3$ at −40°C, according to Eq. 2. The distannylaminoborane **1b**, purified by crystallization from hexane at −20°C, is the only such compound yet to be characterized in the solid state.

The spectroscopic data of compounds **1a** and **1b** are listed in Table 1, and confirm the proposed structures. At room temperature, the ^{119}Sn-NMR signal of **1a** at δ = 26.4

 © WILEY-VCH Verlag GmbH, D-69451 Weinheim, 1998 1434−1948/98/0909−1343 $ 17.50+.50/0

indicates a remarkably better shielding of the tin nuclei relative to all known distannylamines. However, at −80°C, the ^{119}Sn-NMR spectrum shows two different signals at δ = 61.6 and −18.4, the latter falling in the range of pentacoordinated tin atoms. This is possibly due to the interaction of one tin atom with the lone-pair electrons of the quinoline nitrogen atom. At −60°C, the two signals collapse and only one fairly broad signal is observed. Furthermore, two resonance signals are detected in the ^{15}N-NMR spectrum at ambient temperature; the signal at δ = −318 can be assigned to the nitrogen atom of the exocyclic amino group, and that at δ = −89 to the nitrogen nucleus of the quinoline ring.

Table 1. ^{7}Li-, ^{11}B-, $^{14/15}$N-, and ^{119}Sn-NMR data of the distannylamines **1**, the lithioaminostannanes **2**, and another compound for comparison

	1a	**1b**	**2a**	**2b**	$Me_2BN(SnMe_3)_2$
δ^{7}Li			3.12	2.86	
δ^{11}B		56.2		48.6	53.4
$\delta^{(14)15}$N	−318.0[a]	−289.0	−214.2[a]	−228.0	(−272)
	−89.0[b]		−96.4[b]		
δ^{119}Sn	26.4	48.6	5.39	0.08	47.5

[a] Exocyclic nitrogen nucleus. − [b] Endocyclic nitrogen nucleus.

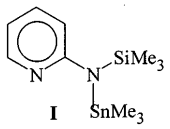

I

These findings are in good agreement with investigations on compounds of type **I**[5], which have been proposed to form an intramolecular Sn−N adduct. The NMR data and the X-ray structure analysis of **1a** (see below) also confirm this hypothesis. The ^{119}Sn- and ^{15}N-NMR data of the borylated distannylamines **1b** are in good agreement with the data of known compounds[6]. However, the ring strain of the bicyclic boryl group causes a deshielding of the boron nucleus (Δδ = 5 ppm), as well as a modest upfield shift of the nitrogen signal (Δδ = 17 ppm) relative, for example, to $Me_2BN(SnMe_3)_2$ (see Table 1). However, the data still indicate multiple bonding between the boron and the nitrogen atoms, in accordance with previous data[7].

The reaction of aryldistannylamines with R = C_6H_5 (**1c**), 2,4,6-$Me_3C_6H_2$ = Mes (**1d**), and 2,6-*i*$Pr_2C_6H_3$ = Dipp (**1e**), in the presence of L = 1,4,7-pentamethyldiethylenetriamine (pmdta), with organolithium compounds in a 1:1 molar ratio led to a mixture of products according to Eq. 4[8]. The monolithium salts **2c** to **2e**, which form even at −50°C, decompose at ambient temperatures, probably under dismutation into the distannylamines **1c** to **1e** and the dilithioamines **3** according to Eq. 4. The species **1c** to **1e** and the byproduct $SnMe_4$ (see Eq. 3) can be detected by NMR, but there is no spectroscopic evidence for the dilithioimines, which are thought to be the main components of the insoluble residue obtained.

$$\underset{\mathbf{1}}{R{-}N(SnMe_3)_2} \xrightarrow[-\ SnMe_4]{+\ MeLi/\ L\ /\ tBuOMe} \underset{\mathbf{2}}{R{-}N(SnMe_3)Li\cdot L} \qquad (3)$$

The following combinations of R and L have been investigated:

	1a/2a	**1b/2b**	**1c/2c**	**1d/2d**	**1e/2e**
R	Quin	9-BBN	Ph	Mes	Dipp
L	tmeda	pmdta	pmdta	pmdta	pmdta

$$\underset{\mathbf{2}}{2\ ArN(SnMe_3)Li\cdot L} \longrightarrow \underset{\mathbf{1}}{ArN(SnMe_3)_2} + \underset{\mathbf{3}}{[ArNLi_2]} + 2\,L \qquad (4)$$

$$\underset{\mathbf{3}}{[ArNLi_2]} + 2\ Me_3SiCl \longrightarrow \underset{\mathbf{4}}{ArN(SiMe_3)_2} + 2\,LiCl \qquad (5)$$

Treatment of this residue with Me_3SiCl according to Eq. 5 gave a mixture of products, which did not unambiguously confirm the presence of dilithioimides of type **3**. The disilazane derivatives **4** could only be detected in trace amounts, since silylstannylamines, $Ar{-}N(SiMe_3)SnMe_3$, are also formed under the chosen reaction conditions. Details of these investigations will be discussed elsewhere[9].

In contrast, the treatment of **1a** with LiMe·L (L = tmeda) in *tert*-butyl methyl ether (diveron) solution gave the lithium aryl(trimethylstannyl)amide **2a** in good yield under mild conditions (−30°C). This product is stabilized by complexation of the lithium cation by one equivalent of the diamine tmeda. It is very soluble in diveron, and moderately soluble in petroleum ether, benzene, and hexane. **2a** can be recrystallized from a hexane/diveron mixture by storing the solution at −20°C for 2 days. It can be stored for weeks at ambient temperature under argon without decomposition.

The NMR spectra in diveron solution show a sharp resonance signal of the ^{7}Li nuclei at δ = 3.12 and a broad signal of the ^{119}Sn nuclei at δ = 5.39. The ^{15}N-NMR spectrum shows two signals, one due to the amido nitrogen atom at δ = −214.2 and another due to the ring nitrogen atom at δ = −96.4. Compared to the starting material **1a**, the substitution of the stannyl group for the lithium cation causes a large downfield shift of the amido nitrogen signal (Δδ = 100 ppm) and a significant upfield shift of the ring nitrogen signal (Δδ = −7 ppm), due to the influence of the electropositive lithium atom on the paramagnetic term of the ^{15}N shielding[9]. In analogy to information obtained from a low-temperature ^{119}Sn-NMR study of the distannazane **1a** the ^{15}N-NMR data of **2a** clearly indicate a coordination of the lone-pair electrons of the quinoline nitrogen atom to the lithium cation, as well as high electron density concentrated at the amido nitrogen atom. Single-crystal structure determinations of the species **1a** and **2a** confirm the nature of the bonding, as deduced from the NMR data in solution. Clearly, the chelation of the lithium atom is responsible for the stability of the stannylated lithium amide **2a**.

The function of the amidoquinoline group as a chelate ligand presumably prevents the dismutation postulated for the derivatives **2c**, **2d**, and **2e** according to Eq. 4. The decomposition could probably proceed, with the formation of a dimer as an intermediate, under partial displacement of the chelate ligand pmdta by the amido nitrogen atom (Figure 1).

Figure 1. Postulated dimeric intermediate of $RN(SnMe_3)Li{\cdot}L$ (**2**)

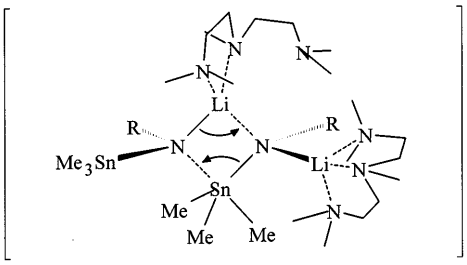

After the dismutation of **2**, the products **1** and **3** (see Eq. 4) can be formed by simultaneous 1,2-migration of a lithium atom and a stannyl group.

If the course of the dismutation reaction of compounds of type **2** is dependent on the basicity of the central nitrogen atom, then Lewis acidic substituents R that reduce the basicity of the nitrogen atom should be as significant as sterically hindering or chelating groups in controlling the reaction. Therefore, the introduction of dialkylboryl groups can be expected to reduce the bridging tendency of the nitrogen lone-pair electrons through π-bonding with boron.

In fact, the synthesis of the monomeric *N*-lithiostannylaminoborane **2b** from distannylaminoborane **1b** proceeds under mild conditions in the presence of pmdta, which stabilizes the Li cation by complexation according to Eq. 3. Product **2b** can be stored indefinitely at ambient temperatures and can even be warmed to 50°C in diveron solution without decomposition.

In all probability, effective (pp) π interaction of the lone-pair electrons at the nitrogen atom with the vacant p orbital of the B atom reduces the donor ability of the nitrogen atom, thereby preventing dimerization and subsequent decomposition of the lithium amide **2b**.

The metallation of the nitrogen atom leads to a large upfield shift of the boron signal of about $\Delta\delta = 8$ ppm compared to that in the distannylamine **1b**. One common explanation would be a strengthening of the B−N π bond[10], due to the high electron density concentrated at the nitrogen atom as a consequence of the polar Li−N bond. An alternative explanation might be the decreased polarity and increased s electron density of the B−N σ bond. However, the unexpectedly large downfield shift of the ^{15}N-NMR signal ($\delta = -228$, recorded at −50°C to depress quadrupolar relaxation with the boron nucleus) is supportive of the first explanation. Surprisingly though, the ^{119}Sn-NMR signal, like the boron NMR signal, is shifted upfield by $\Delta\delta \approx 50$ ppm ($\delta = 0.08$). This can only be due to a significant change in electron density in the Sn−N σ bond, since ab initio calculations rule out any significant Sn−N π interaction[11]. The increase of s electron density in the Sn−N single bond is also indicated by the small but negative $^1J(^{119}Sn^{15}N)$ coupling[1c]. Further conclusions can be drawn from the molecular structures in the solid state (see below).

Molecular Structures

The structures of the distannylamines and of the *N*-lithiostannylamines were determined by X-ray crystallography. Figures 2, 3, 4, and 5 show ORTEP plots of the molecules **1a**, **1b**, **2a**, and **2b**, respectively. Selected bonding parameters are listed in the caption of each figure. Contrary to the structural information implied by the NMR data in solution at ambient temperatures, the characteristic features of the molecular structure of **1a** (Figure 2) in the solid state are determined by an intramolecular donor−acceptor interaction between the quinoline nitrogen atom and the tin atom of one of the trimethylstannyl groups. Compared to the adduct $Me_3SnCl{\cdot}py$ (d_{SnN}: 2.26 Å)[12] and the distannylamine pyridine adduct **5** (d_{SnN}: 2.426 Å)[13], the Sn2−N2 bond of 2.531 Å is remarkably long, owing to the ring strain arising from the formation of the intramolecular adduct.

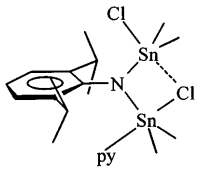

5

As a consequence of the relatively weak N2−Sn2 interaction, the trigonal-bipyramidal environment of the Sn2 center is considerably distorted, as shown by the 12° deviation of the angle N2−Sn2−C13 from 180°. Moreover, the sum of the angles of the trigonally coordinated ligands at the tin center is only 348° rather than 360°.

Figure 2. Molecular structure of $QuinN[Sn(CH_3)_3]_2$ (**1a**) with an ORTEP-type description; thermal ellipsoids represent a 25% probability; hydrogen atoms are omitted for the sake of clarity[a]

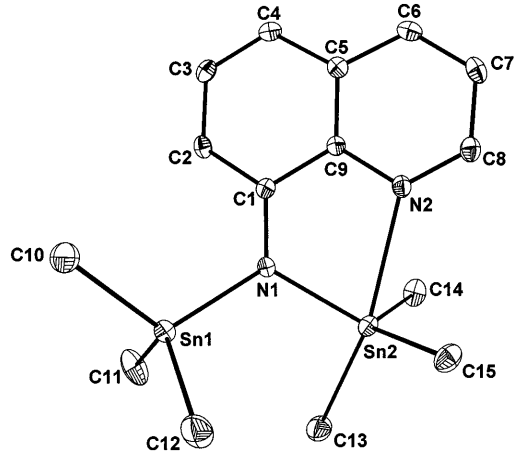

[a] Selected bond lengths [Å] and bond angles [°] (estimated standard deviations are given in parentheses as units in the last digit): Sn1−N1 2.064(3), Sn2−N1 2.099(3), Sn2−N2 2.531(3), N1−C1 1.381(4), Sn1−C10 2.144(4), Sn1−C12 2.142(4), Sn2−C13 2.177(4), Sn2−C14 2.146(4); Sn1−N1−Sn2 118.3(1), Sn1−N1−C1 121.8(2), Sn2−N1−C1 119.8(2), N1−Sn2−N2 71.3(1), N2−Sn2−C13 167.9(2), N1−Sn2−C13 98.2(1), C14−Sn2−C15 117.1(2), C14−Sn2−N1 116.6(1), C15−Sn2−N1 114.7.

Figure 3. Molecular structure of 9-BBN−N[Sn(CH_3)$_3$]$_2$ (**1b**) with an ORTEP-type description; thermal ellipsoids represent a 25% probability; hydrogen atoms are omitted for the sake of clarity[a]

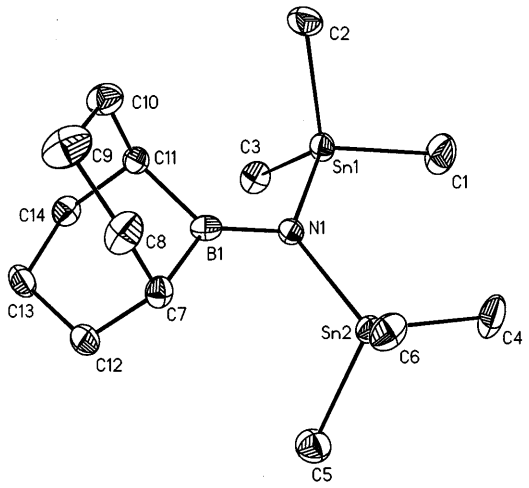

[a] Selected bond lengths [Å] and bond angles [°] (estimated standard deviations are given in parentheses as units in the last digit): Sn1−N1 2.071(6), Sn2−N1 2.059(6), N1−B1 1.42(1), C7−B1 1.58(1), C11−B1 1.66(1), Sn1−C1 2.13(1), Sn1−C2 2.15(1), Sn1−C3 2.13(1), Sn2−C4 2.150(9), Sn2−C5 2.145(10), Sn2−C6 2.14(1); Sn1−N1−Sn2 126.1(3), Sn1−N1−B1 117.0(5), Sn2−N1−B1 116.9(5), C7−B1−C11 107.8(7), N1−Sn1−C1 114.2(4), N1−Sn2−C4 111.0(3), N1−B1−C7 126.9(8), N1−B1−C11 125.3(8).

Figure 4. Molecular structure of QuinN(Li)Sn(CH_3)$_3$ (**2a**) with an ORTEP-type description; thermal ellipsoids represent a 25% probability; hydrogen atoms are omitted shown for the sake of clarity[a]

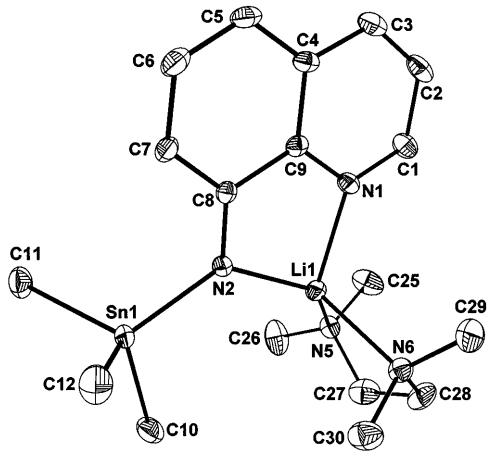

[a] Selected bond lengths [Å] and bond angles [°] (estimated standard deviations are given in parentheses as units in the last digit): Sn1−N2 2.031(3), C8−N2 1.351(5), Li1−N2 1.968(7), Li1−N1 2.035(8), Li1−N5 2.116(8), Li1−N6 2.115(8), Sn1−C10 2.149(5), Sn1−C11 2.154(5), Sn1−C12 2.147(5); Sn1−N2−Li1 130.0(3), Sn1−N2−C8 119.5(3), C8−N2−Li1 110.1(3), N1−Li1−N2 85.9(3), N2−Li1−N5 133.7(4), N1−Li1−N5 119.1(3), N1−Li1−N6 110.0(3), N5−Li1−N6 86.7(3), C10−Sn1−C11 108.4(2), C10−Sn1−N2 105.0(2), C11−Sn1−N2 114.3(2); second molecule: Sn2−N4 2.028(3), C20−N4 1.339(5), Li2−N4 1.957(7), Li2−N3 2.088(7), Li2−N7 2.160(7), Li2−N8 2.147(8), Sn2−C22 2.143(5), Sn2−C23 2.165(5), Sn2−C24 2.147(5); Sn2−N4−Li2 122.8(2), Sn2−N4−C20 123.1(3), C20−N4−Li2 112.7(3), N4−L1−N3 84.0(3), N4−Li2−N7 135.5(4), N4−Li2−N8 124.1(4), N7−Li2−N8 86.0(3), C22−Sn2−C23 109.4(2), C22−Sn2−C24 111.4(3), C22−Sn2−N4 99.9(2) C24−Sn2−N4 111.4(2).

Figure 5. Molecular structure of 9-BBN−N(Li)Sn(CH_3)$_3$ (**2b**) with an ORTEP-type description; thermal ellipsoids represent a 25% probability; hydrogen atoms are omitted for the sake of clarity[a]

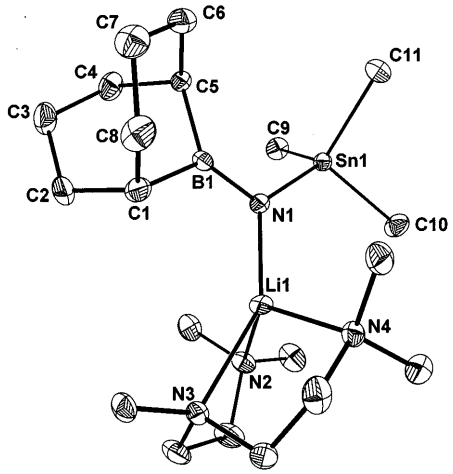

[a] Selected bond lengths [Å] and bond angles [°] (estimated standard deviations are given in parentheses as units in the last digit): Sn1−N1 2.020(3), B1−N1 1.381(6), Li1−N1 1.945(8), Li1−N2 2.144(8), Li1−N3 2.337(8), Li1−N4 2.149(8), B1−C1 1.623(6), B1−C5 1.608(6), Sn1−C9 2.159(5), Sn1−C10 2.161(5), Sn1−C11 2.154(5); Sn1−N1−Li1 126.7(3), Sn1−N1−B1 117.7(3), B1−N1−L1 115.6(3), N1−Li1−N2 111.4(4), N1−Li1−N3 147.7(4), N1−Li1−N4 112.1(4), C9−Sn1−C10 105.6(2), C9−Sn1−N1 113.1(2), C11−Sn1−N1 112.8(2).

Surprisingly, the Sn−C bond lengths are rather insensitive to the different coordination numbers of Sn1 and Sn2. The ring strain may also be responsible for the large N1−Sn2 distance of 2.099(3) Å, which represents the largest nitrogen−tin distance yet found in distannylamines[14]. The N1−Sn1 bond length of 2.064(3) Å is, however, in good accord with those found for other Sn−N−Sn units. The sum of the angles at the amino nitrogen atom of 360° confirms this to be a planar unit, as is usually the case. The fairly short N1−C1 distance of 1.381(4) Å can be explained by the strong σ-N−C bond, due to the large overlap of the sp^2-sp^2 bond orbitals of each atom.

The distannylamine **1b** (Figure 3), with a cyclic dialkylboryl group attached to the nitrogen atom, also shows planar coordination at the central nitrogen atom. It represents the first example of this class of compounds for which the molecular structure has been determined in the solid state. Characteristic features are the large Sn−N−Sn angle of 126.1°, as also found in aryldistannylamines[15], and the fairly small C−B−C angle of 107.8(7)° in the boryl group, probably due to the ring strain of the bicyclic substituent. Compared to the quinoline group in **1a**, the 9-borabicyclo[3.3.1]nonyl group is sterically less demanding. This might account for the larger Sn−N−Sn angle in **1b** (difference ca. 8°) compared to that in **1a**. Moreover, the stannylaminoborane **1b** shows a significant elongation of the Sn−N bonds [$d_{(SnN)}$ = 2.07 Å] compared to those in other distannazanes with bulkier groups R attached to the nitrogen atom [$d_{(SnN)}$ = 2.05 Å][15]. This is presumably due to the electron-withdrawing properties of the boryl group on the pair of electrons at the central nitrogen atom. There-

fore, the ^2J(Sn/Sn) coupling transmission, which has been thought to be dependent on the Sn−N−Sn angle[16] and on the Sn−N bond lengths[1c], seems to be particularly predominated by the position of the lone-pair electrons at the nitrogen atom (see NMR discussion).

The effective (pp) π interaction of the lone-pair electrons of the nitrogen atom with the vacant p orbital of the boron atom is indicated by the short B−N bond of 1.42(1) Å. The small torsion angle Sn1−N1−B1−C11 of about 2° additionally underlines the double bond character of this bond.

Instead of the associated structures usually found for R_2NLi compounds[17], the *N*-lithiostannylamines **2a** and **2b**, derivatives of the distannylamines **1a** and **1b**, crystallize as monomeric molecular units (shown in Figures 4 and 5). The unit cell in the crystal of compound **2a** contains two independent molecules, which show slightly different bond lengths and angles. Significant differences in bond lengths are only detectable in case of the N−Li distances (ca. 0.04 Å). The characteristic features of both lithioamines are the surprisingly short Sn−N bonds of 2.028(3) for **2a** and 2.020(3) Å for **2b**, respectively. The sum of the covalent radii of the elements is 2.033 Å[18]. Moreover, the N2−C8 distance of 1.339(5) Å in **2a** is considerably shorter than that in **1a** (see above), indicating a significant enhancement of the N−C double bond character. These findings can be explained in terms of the transfer of the high electron density, primarily located at the nitrogen atom of the amino group (as a consequence of the polar and indeed essentially ionic character of the Li−N bond[17]), into the adjacent bonds. Support for this explanation comes from the NMR studies, which indicate a remarkable high-field shift of the ^{119}Sn signals of **2a** and **2b** relative to those of the distannylamines **1a** and **1b**. The sum of the angles at the amine nitrogen atom, as well as at the quinoline nitrogen atom, is 360°, confirming the sp^2 hybridization of these centers. Therefore, two different Li−N bond lengths have been found, taking the lithium cation to be the center of a spirocyclic ring fragment. Short distances are present due to the typical sp^2-hybridized nitrogen atoms of the chelating aminoquinoline group acting as a donor ligand [$d_{(LiN)}$: ca. 1.97/2.03 Å]. Two long Li−N bonds are formed with the sp^3-hybridized nitrogen atoms [$d_{(LiN)}$: ca. 2.11 Å] of the chelating diamine tmeda. The tetrahedral symmetry around the metal cation is slightly distorted. There is no simple explanation for the deviation of the coordination of the lithium center from tetrahedral symmetry other than packing effects.

The structure of the *N*-lithiated stannylaminoborane **2b** is the third example of a monomeric *N*-lithioaminoborane[10][19], but it is the first one with essentially planar cores of $C_2BN(Li)Sn$ atoms with only small dihedral angles between the boron and nitrogen planes. The structure indicates the influence that the electropositive metal cation attached to the nitrogen atom exerts on the adjacent B−N and Sn−N bonds. Compared to the distannylborylamine **1b**, the B−N bond of **2b** [$d_{(BN)}$: 1.381(6) Å] is shortened by about 0.04 Å, and represents one of the shortest B−N double bonds yet found[10].

Short B−N bonds in aminoboranes are usually explained in terms of an enhancement of B−N π bonding. However, short B−N bonds are also present in lithioaminoboranes, such as tBu$_2$B−N(Li)tBu·OEt$_2$, although here there is a fairly large dihedral angle of 30.4° between the boron and nitrogen planes[19]. Moreover, the B−N bond length of 1.40 Å in the *N*-silylated lithioaminoborane 9-BBN−NLi−$SiMe_3$, which crystallizes as a trimer with pseudo-tetracoordinated nitrogen atoms, is indicative of B−N double bonds[1a]. Therefore, the short bonds are more likely to be attributable to the positive inductive effect of the lithium atom, which strengthens the σ bonds. This is also the case for the adjacent Sn−N bond, which is extremely short compared to that in the starting material **1b**. Taking into account that, on the basis of ab initio calculations, any π-bonding in Sn−N bonds is negligible, the electron-donating property of the lithium atom, as discussed above, is solely responsible for the strengthening of the σ bonds.

We gratefully acknowledge the support of this research by the *Deutsche Forschungsgemeinschaft*, the *Fonds der Chemischen Industrie*, and the *Chemetall GmbH*. We also thank Prof. Dr. *H. Nöth* for helpful discussions and comments, Prof. Dr. *W. Wrackmeyer* (low-temperature NMR measurements), and Mrs. *C. Neumann* (essential support of synthetic work).

Experimental Section

General: All operations were performed under dry argon. Glassware was dried prior to use by heating in vacuo. − NMR spectra were recorded with Bruker AC P 200 (^{11}B), Jeol GSX 270 (^{15}N, ^{119}Sn), and Jeol EX 400 (^{1}H, ^{7}Li, ^{13}C) instruments; standards: TMS (internal, ^{1}H, ^{13}C), ext. 1 M LiCl solution (^{7}Li), ext. $BF_3·Et_2O$ (^{11}B), ext. CH_3NO_2 (^{15}N), tetramethyltin (external ^{119}Sn). ^{15}N-NMR spectra were recorded by polarization transfer techniques: refocused INEPT pulse sequence based on the $^2J(^{15}N^1H)$ and the $^3J(^{15}N^1H)$ coupling constants of ca.12 Hz and ca.1.5−2 Hz, respectively, (assumed values). The notation $^nJ(^{119/117}Sn^mX)$ represents the coupling of both isotopomers with X if the coupling cannot be observed separately. Chemical shifts, δ, are given in ppm, coupling constants, *J*, in Hz. − Mass spectra: Varian CH7 instrument with electron impact ionization at 70 eV. The masses found refer to the isotopes ^{1}H, ^{7}Li, ^{12}C, ^{11}B, ^{14}N, ^{120}Sn. − Elemental analyses: Microchemical Laboratory of the Institute. − X-ray: Siemens P4 diffractometer, CCD area detector with Siemens LT 2 device; Mo-K_α radiation, λ = 0.71063 Å, graphite monochromator; single crystals, coated with perfluoro ether oil, were mounted on a glass fibre. Crystal data were determined and intensity data recorded at 173−193 K (see Table 2); data reduction was performed with the program SAINT, structure solution by Patterson method and refinement using the SHELXTL system[20]; final refinement was performed using the SHELX-97 programs[21]. All atoms except the hydrogen atoms were described with anisotropic temperature factors; all hydrogen positions were geometrically placed [d(CH) = 0.96 Å] and refined by using the riding model and fixed U_i. Details of the crystal structure determinations are available on request from Cambridge Crystallographic Data Centre (CCDC), 12 Union Road, Cambridge CB2 1EZ, U.K. [Fax: (internat.) + 44-1223/336033; E-mail: deposit@ccdc.cam.ac.uk] on quoting the depository numbers CSD-101616 (**1a**), -101617 (**1b**), -101618 (**2a**), -101619 (**2b**), the names of the authors, and the full journal citation.

Starting Materials: $N(SnMe_3)_3$[22] was prepared according to a modified literature procedure[23] from $NaNH_2/NH_3/OEt_2$/

Me_3SnCl; 9-chloro-BBN[24] and Me_2NSnMe_3[25] were prepared according to literature procedures. The MeLi solution (ca. 1.6 M in Et_2O) was supplied by Chemetall, Frankfurt.

8-[Bis(trimethylstannyl)amino]quinoline (**1a**): A mixture of 8-aminoquinoline (5.0 g, 35 mmol) and Me_2NSnMe_3 (20.8 g, 92 mmol) was stirred at room temp. A slighty exothermic reaction occurred, with evolution of Me_2NH. After heating the reaction mixture at 80°C for 25 h, so as to complete the elimination of Me_2NH, the excess Me_2NSnMe_3 was condensed at 10^{-3} Torr into a cold trap at −60°C. The residual orange, viscous liquid was dissolved in 40 ml of hexane and kept at 4°C for 4 d, yielding 14.1 g (86%) of **1a** as orange crystals suitable for X-ray analysis; m.p. ca. 12−15°C. − ^{1}H NMR (C_6D_6): δ = 0.38 [s, $^2J(^{119/117}Sn^1H)$ = 53.7 Hz, 18 H, $SnMe_3$], 6.74 (dd, 1 H, 7-H), 6.82 (m, 2 H, 5-H/6-H), 7.24 (dd, 1 H, 3-H), 7.61 (dd, 1 H, 4-H), 8.87 (dd, 1 H, 2-H). − ^{13}C NMR: δ = −0.75 [$^1J(^{119/117}Sn^{13}C)$ = 389.1 Hz, $SnMe_3$], 117.5 [$^3J(^{119/117}Sn^{13}C)$ = 35.1 Hz, C-7], 120.7 (C-5), 129.5 (C-3), 136.2 (C-10), 136.5 (C-6), 138.3 (C-9), 142.7 (C-4), 149.2 (C-8), 154.9 (C-2). − ^{15}N NMR: δ = −318.0 [$^1J(^{117/119}Sn^{15}N)$ = 28.8 Hz, Sn*N*Sn], −89.0 [$^1J(^{117/119}Sn^{15}N)$ = 35.0 Hz, C*N*C]. − ^{119}Sn NMR: δ = 26.2 [$^2J(^{119}Sn^{117}Sn)$ = 46.7 Hz]. − $C_{15}H_{24}N_2Sn_2$ (469.8): calcd. C 38.35, H 5.16, N 5.96; found C 40.10, H 5.15, N 6.74. − Mol. mass: 470 (MS).

9-[Bis(trimethylstannyl)amino]-9-borabicyclo[3.3.1]nonane (**1b**): $N(SnMe_3)_3$ (12.1 g, 24 mmol) was dissolved in 20 ml of CH_2Cl_2. At −40°C, this solution was added dropwise with stirring to a solution of 9-chloro-9-borabicyclo[3.3.1]nonane (3.7 g, 24 mmol) in 10 ml of CH_2Cl_2. After allowing the reaction mixture to slowly warm to ambient temp. (15 h), all volatile components were removed in vacuo (25−80°C/10^{-3} Torr). From a solution of the colourless non-volatile residue in 50 ml of hexane, 9.1 g (82%) of **1b** crystallized after storing the mixture at −20°C for 10 d; m.p. 60−62°C. The crystals were found to be suitable for X-ray analysis. − ^{1}H NMR (C_6D_6): δ = 0.24 [s, $^2J(^{119/117}Sn^1H)$ = 53.9 Hz, 18 H, $SnMe_3$], 1.21 (m, 4 H, BCCCH), 1.42−1.46 (m, 2 H, BCH), 1.78−1.86 (m, 8 H, BCCH). − ^{13}C NMR δ = −2.07 [$^1J(^{119/117}Sn^{13}C)$ = 363.5 Hz, $SnMe_3$], 23.7 (BCC*C*H), 31.4 (BCH), 34.2 (BC*C*H). − ^{11}B NMR: δ = 56.2. − ^{15}N NMR: δ = −289.0 [$^1J(^{117/119}Sn^{15}N)$ = 31.9 Hz, Sn*N*Sn]. − ^{119}Sn NMR: δ = 48.6. − $C_{14}H_{32}BNSn_2$ (462.6): calcd. C 36.35, H 6.97, N 3.03; found C 36.24, H 6.73, N 2.96. − Mol. mass: 463 (MS).

(8-Aminoquinolyl)(lithio)(trimethylstannyl)amine·tmeda (**2a**): To 5 ml of an MeLi solution (1.6 M in diethyl ether) at 25°C, tmeda (0.97 g, 8.33 mmol) was added dropwise, and then the solvent was removed in vacuo at 25°C/10^{-1} Torr. The colourless solid residue was dissolved in 30 ml of *tert*-butyl methyl ether, and to this solution 14.9 ml (8.33 mmol) of a solution of **1a** (0.56 M in *tert*-butyl methyl ether) was added dropwise at −30°C, resulting in a deep-red colouration. After stirring for 2.5 h, the reaction mixture was allowed to warm to ambient temp. Filtration of the slightly cloudy solution (G4), concentration of the filtrate to a volume of ca. 25 ml under reduced pressure, and storing the concentrate at −20°C for 20 d gave **2a** as dark-red crystals, suitable for X-ray analysis: yield 2.43 g (68%); m.p. 134−136°C. − ^{1}H NMR (C_6D_6): δ = −0.69 [s, $^2J(^{119/117}Sn^1H)$ = 53.9 Hz, 9 H, $SnMe_3$], 2.70 (s, 12 H, NCH_3), 2.89 (s, 4 H, NCH_2-), 6.70 (m, 2 H, 5-H, 6-H), 7.41 (t, 1 H, 3-H), 7.52 (dd, 1 H, 7-H), 8.28 (dd, 1 H, 4-H), 8.61 (dd, 1 H, 2-H). − ^{13}C NMR: δ = −1.32 ($SnMe_3$), 46.2 (N*C*H$_3$), 58.2 (N*C*H$_2$-), 114.2 [$^3J(^{119/117}Sn^{13}C)$ = 77.6 Hz, C-7], 120.0 (C-5), 130.2 (C-3), 136.8 (C-10), 137.2 (C-6), 141.4 (C-4), 155.2 (C-9), 163.6 (C-8),

Table 2. X-ray structure analysis data of **1a**, **1b**, **2a**, and **2b**

Compound	**1a**	**1b**	**2a**	**2b**
Chem. formula	$C_{15}H_{24}N_2Sn_2$	$C_{28}H_{64}B_2N_2Sn_4$	$C_{18}H_{31}LiN_4Sn$	$C_{20}H_{46}LiN_4Sn$
Formula weight	469.74	925.19	429.10	479.05
Cryst. size [mm]	0.2 × 0.3 × 0.4	0.1 × 0.2 × 0.3	0.3 × 0.3 × 0.4	0.2 × 0.2 × 0.3
Cryst. system	monoclinic	triclinic	monoclinic	monoclinic
Space group	*P*2(1)/*c*	*P*1̄	*P*2(1)/*c*	*P*2(1)/*c*
a [Å]	14.528(4)	9.70820(10)	13.89870(10)	13.29350(10)
b [Å]	10.028(3)	14.92160(10)	11.07780(10)	10.2085(2)
c [Å]	12.350(4)	15.4379(2)	27.8251(2)	18.87590(10)
α [°]	90.00	66.548(1)	90.00	90.00
β [°]	96.783(7)	73.685(1)	95.980(1)	91.025(1)
γ [°]	90.00	71.99	90.00	90.00
V [Å^3]	1786.8(9)	1918.94(3)	4260.83(6)	2561.18(6)
Z	4	2	8	4
ρ(calcd.) [Mg/m^3]	1.746	1.601	1.338	1.242
μ [mm^{-1}]	2.786	2.590	1.205	1.008
F(000)	912	912	1760	1008
Index range	$-15 \le h \le 18$	$-10 \le h \le 10$	$-17 \le h \le 18$	$-15 \le h \le 13$
	$-12 \le k \le 12$	$-16 \le k \le 16$	$-14 \le k \le 14$	$-12 \le k \le 12$
	$-15 \le l \le 15$	$-16 \le l \le 14$	$-37 \le l \le 34$	$-22 \le l \le 22$
2θ [°]	57.58	46.50	58.62	49.42
Temp. [K]	183	183	193	173(2)
Refl. collected	9913	8234	23832	12138
Refl. unique	3208	4328	8435	3644
Refl. observed (4σ)	2955	3963	5239	3435
R (int.)	0.0402	0.0195	0.0390	0.0278
No. of variables	202	338	447	252
Weighting scheme *x*/*y*[a]	0.0151/1.9239	0.0204/17.3145	0.0000/12.3307	0.0000/7.8454
GooF	1.197	1.135	1.129	1.234
Final *R* (4σ)	0.0227	0.0414	0.0339	0.0361
Final *wR*2	0.0540	0.0963	0.0746	0.0847
Larg. res. peak [e/Å^3]	0.553	0.873	2.173	0.905

[a] $w^{-1} = \sigma^2F_o^2 + (xP)^2 + yP$; $P = (F_o^2 + 2F_c^2)/3$.

166.4 (C-2). – ^{7}Li NMR: δ = 3.12. – ^{15}N NMR: δ = −214.2, −96.4. – ^{119}Sn NMR: δ = 5.18 (br.). – $C_{18}H_{31}LiN_4Sn$ (479.1): calcd. C 50.21, H 7.26, N 13.02; found C 48.60, H 6.73, N 11.86.

(9-Borabicyclo[3.3.1]nonyl)(lithio)(trimethylstannyl)-amine·pmdta (**2b**): To 2.4 ml of an MeLi solution (1.6 M in diethyl ether) at 25°C, pmdta (0.69 g, 4.0 mmol) was added dropwise, and then the solvent was removed in vacuo at 25°C/10^{-1} Torr. The colourless, oily residue was diluted with 20 ml of *tert*-butyl methyl ether. To this solution, a solution of **1b** (1.85 g, 4.00 mmol) in 15 ml of *tert*-butyl methyl ether was added dropwise at −50°C. After allowing the mixture to slowly warm to ambient temp. over a period of 15 h, and then storing the colourless solution at −20°C for 28 d, **2b** (1.19 g, 62%) crystallized as colourless prisms; m.p. 124−127°C. The crystals were found to be suitable for X-ray analysis. – ^{1}H NMR (C_6D_6): δ = 0.38 [s, $^{2}J(^{119/117}Sn^{1}H)$ = 48.4 Hz, 18 H, $SnMe_3$], 1.24 (m, 4 H, BCCCH), 1.44−1.50 (m, 2 H, BCH), 1.89−1.96 (m, 8 H, BCCH), 2.11 [s, 12 H, $MeN(C_2H_4NMe_2)_2$], 2.18 [s, 3 H, $MeN(C_2H_4NMe_2)_2$], 2.40−2.52 [m, 8 H, $MeN(C_2H_4NMe_2)_2$]. – ^{13}C NMR: δ = −3.06 [$^{1}J(^{119/117}Sn^{13}C)$ = 291.7 Hz, $SnMe_3$], 24.9 (BCCCH), 32.2 (BCH), 35.1 (BCCH), 45.7 [$MeN(C_2H_4NMe_2)_2$], 53.4 [$MeN(C_2H_4NMe_2)_2$], 56.7 + 57.8 [$MeN(C_2H_4NMe_2)_2$]. – ^{7}Li NMR: δ = 2.86. – ^{11}B NMR: δ = 48.5. – ^{15}N NMR: δ = −228.0 [$^{1}J(^{117/119}Sn^{15}N)$ = 10.4 Hz, Li*N*Sn]. – ^{119}Sn NMR: δ = 0.08 (br.). – $C_{20}H_{46}BLiN_4Sn$ (473.1): calcd. C 50.14, H 9.68, N 11.70; found C 53.30, H 10.18, N 12.54.

☆ Dedicated to Professor *Heinrich Nöth* on the occasion of his 70th birthday.

[1] [1a] W. Storch, H. Nöth, *Angew. Chem.* **1976**, *88*, 231; *Angew. Chem. Int. Ed. Engl.* **1976**, *15*, 235. – [1b] S. Diemer, H. Nöth, W. Storch, *Functionally Substituted Diborylamines*, in preparation. – [1c] A. Appel, C. Kober, C. Neumann, H. Nöth, M. Schmidt, W. Storch, *Chem. Ber.* **1996**, *129*, 175−189 and refs. quoted therein.

[2] D. R. Armstrong, D. Barr, R. Snaith, *Angew. Chem.* **1991**, *103*, 1702−1704; *Angew. Chem. Int. Ed. Engl.* **1991**, *30*, 1707−1709.

[3] [3a] B. Wrackmeyer, B. Schwarze, J. Weidinger, M. Milius, *Z. Naturforsch.* **1997**, *52b*, 431−433. – [3b] M. Westerhausen, W. Schwarz, *Z. Anorg. Allg. Chem.* **1993**, *619*, 1053−1063. – [3c] T. Fjeldberg, P. B. Hitchcock, M. F. Lappert, A. J. Thorne, *J. Chem. Soc., Chem. Commun.* **1984**, 822−826. – [3d] R. Köster, G. Seidel, *Angew. Chem.* **1981**, *93*, 1009−1010; *Angew. Chem. Int. Ed. Engl.* **1981**, *20*, 972−973.

[4] [4a] K. Jones, M. F. Lappert, *Proc. Chem. Soc.* **1962**, 358− 359. – [4b] K. Jones, M. F. Lappert, *J. Chem. Soc.* **1965**, 1944−1951.

[5] B. Wrackmeyer, G. Kehr, H. Zhuo, S. Ali, *Magn. Res. Chem.* **1996**, *34*, 921−928.

[6] W. Storch, H. Nöth, *Chem. Ber.* **1977**, *110*, 1636−1642.

[7] G. Schmid, R. Boese, D. Bläser, *Z. Naturforsch.* **1982**, *B37*, 1230−1236; H. Nöth, H. Prigge, A.-R. Rotsch, *Chem. Ber.* **1977**, *119*, 1361−1367.

[8] S. Lustig, Diplomarbeit, Universität München, **1994**.

[9] B. Wrackmeyer, W. Storch, M. Vosteen, *NMR Studies on Lithiostannylamines and -imines*, in preparation.

[10] H. Chen, R. A. Bartlett, M. M. Olmstead, P. P. Power, S. C. Shoner, *J. Am. Chem. Soc.* **1990**, *112*, 1048−1055.

[11] C. Kober, J. Kroner, W. Storch, *Angew. Chem.* **1993**, *105*, 1693−1695; *Angew. Chem. Int. Ed. Engl.* **1993**, *31*, 1608−1610.

[12] R. Hulme, *J. Chem. Soc.* **1963**, 1524−1527; V. G. Kumar Das, L. K. Mun, W. Chen, *Organometallics*, **1987**, *6*, 10−14.

[13] C. Kober, H. Nöth, W. Storch, *Chem. Ber.* **1997**, *130*, 765−769.

[14] C. Kober, H. Nöth, W. Storch, *Structure Investigations of Distannazanes*, in preparation.

[15] S. Diemer, H. Nöth, K. Polborn, W. Storch, *Chem. Ber.* **1992**, *125*, 389−400.

[16] W. Biffar, T. Gasparis-Ebeling, H. Nöth, W. Storch, B. Wrackmeyer, *J. Magn. Res.* **1981**, *44*, 54−61.

[17] K. Gregory, P. V. R. Schleyer, R. Snaith, *Adv. Inorg. Chem.* **1991**, *37*, 47−49; R. E. Mulvey, *Chem. Soc. Rev.* **1991**, *20*, 167−172.

[18] Calculated from the sum of the covalent radii by applying the Schomaker−Stevenson correction: A. F. Wells, *Structural Inorganic Chemistry*, 4th ed., Clarendon, Oxford University Press, **1979**, p. 236.

[19] [19a] P. Paetzold, C. Pelzer, R. Boese, *Chem. Ber.* **1988**, *121*, 51−59. – [19b] R. A. Bartlett, X. Feng, M. M. Olmstead, P. R. Power, K. J. Weese, *J. Am. Chem. Soc.* **1988**, *109*, 4851−4854.

[20] *SHELXTL-Plus*, *PC version*, Siemens Analytical X-ray Instruments, Inc., Madison, WI, **1980**.

[21] G. M. Sheldrick, *SHELXL-97, Program for the Refinement of Crystal Structures*, University of Göttingen, **1997**.

[22] K. Sisido, S. Kozima, *J. Org. Chem.* **1964**, *29*, 907−909.

[23] P. Otto, Ph. D. Thesis, University of Munich, **1986**.

[24] H. C. Brown, S. U. Kularni, *J. Organomet. Chem.* **1979**, *168*, 281−286.

[25] C. M. Wright, E. L. Muetterties, *Inorg. Synth.* **1976**, *10*, 137−139.

[98133]

Reactions of ε-Caprolactone with (Alkyne)zirconocene Complexes: Investigation of Elemental Steps in Catalytic Ring-Opening Polymerization of Lactones☆

Dominique Thomas, Perdita Arndt*, Normen Peulecke, Anke Spannenberg, Rhett Kempe, and Uwe Rosenthal

Abteilung "Komplexkatalyse", Institut für Organische Katalyseforschung an der Universität Rostock e.V., Buchbinderstraße 5–6, D-18055 Rostock, Germany

Received March 24, 1998

Keywords: ε-Caprolactone complexes / Zirconocene / Ring-opening polymerization

The reactions of $Cp_2Zr(L)(\eta^2\text{-}Me_3SiC_2SiMe_3)$ (L = THF, pyridine) with ε-caprolactone, cyclohexanone and cycloheptanone result in an insertion of the carbonyl group into the zirconacyclopropene ring system of the alkyne complexes to yield the five-membered metallacyclic spirozirconadihydrofurane complexes **1**, **3**, **4**. The product with ε-caprolactone is not stable at room temperature and was identified only by NMR spectra and chemical reactions. Starting from *rac*-(ebthi)$Zr(\eta^2\text{-}Me_3SiC_2SiMe_3)$ with ε-caprolactone and ethylene carbonate under analogous conditions more stable complexes (**2**, **5**) were obtained. Complexes **2** and **3** were characterized by X-ray crystal-structure analysis. Complexes **1** and **2** react with further ε-caprolactone in a catalytic ring-opening polymerization. The polymerization reactions were monitored by NMR spectroscopy.

Introduction

Group-4 transition-metal and lanthanide complexes containing one or two cyclopentadienyl ligands (metallocenes) have emerged as a new class of initiators of the polymerization of various polar monomers including methacrylate, epoxides, lactones.[1] The polymerization of lactones is known to give polyesters, which are becoming an increasingly important class of versatile biodegradable and biocompatible polymeric materials.[2] Since ε-caprolactone is rapidly polymerized by many metal complexes, little information is available on the details of the first steps in metal-mediated polymerization process. For example, only *mer*-YCl_3(ε-caprolactone)$_3$,[2b] in which the caprolactone is coordinated by a carbonyl oxygen atom, has been characterized by an X-ray structure analysis. Recently, we described how (alkyne)zirconocene and -titanocene complexes are capable of polymerizing ε-caprolactone with living characteristics and high yield.[3a] Lactams react with (alkyne)titanocene or -zirconocene complexes to yield different complexes, depending on the nature of the metal and the ring size. These complexes have been discussed as elemental steps in the ring-opening polymerization.[3b]

Here we report on reactions of (alkyne)zirconocene complexes with cyclic carbonyl compounds such as ε-caprolactone, giving cyclic acetals, postulated as intermediates in the well-established ring-opening polymerization reaction.

The reactions of (alkyne)zirconocene and olefin complexes with carbonyl compounds have been well investigated.[4] For the complexes $Cp_2Zr(L)(\eta^2\text{-}Me_3SiC_2SiMe_3)$ (L = THF,[6] pyridine[7]) the reaction with acetone, formaldehyde or benzaldehyde[5] leads to insertion products of the carbonyl unit into the zirconacyclopropene ring of the alkyne complex giving zirconadihydrofuranes $[Cp_2Zr\{-C(SiMe_3)=C(SiMe_3)-CRR'-O-\}]$, which, in the case of the aldehydes, were additionally stabilized by formation of a coordination dimer. Benzophenone reacted by apparent displacement of the alkyne by the ketone to give the complex $Cp_2Zr(THF)(\eta^2\text{-}O=CPh_2)$.

Results and Discussion

ε-Caprolactone (CL) reacts with $Cp_2Zr(L)(\eta^2\text{-}Me_3SiC_2SiMe_3)$ (L = THF, pyridine) and forms, comparable to the reaction with acetone[5a], in a single step, the five-membered metallacyclic spiroacetal **1** (Eq. 1).

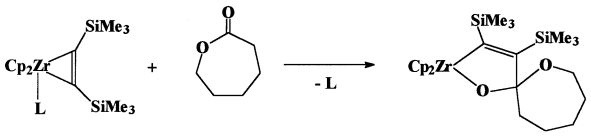

(1)

L = py, THF **1**

Complex **1** is an orange solid, which is not stable at room temperature and decomposes in toluene to poly-ε-caprolactone (PCL) and a mixture of as yet unidentified zirconocene complexes.

The reaction of *rac*-(ebthi)$Zr(\eta^2\text{-}Me_3SiC_2SiMe_3)$ with ε-caprolactone yields the analogous *ansa*-metallocene compounds **2a** and **2b** (Eq. 2).

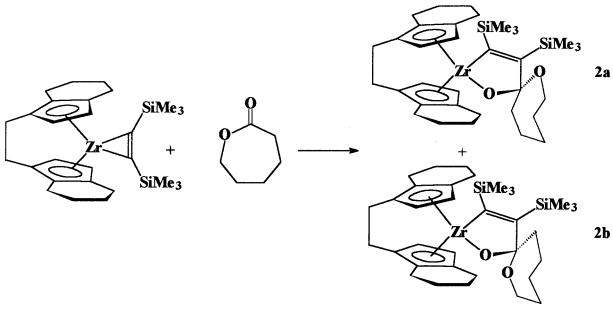

(2)

 © WILEY-VCH Verlag GmbH, D-69451 Weinheim, 1998 1434–1948/98/0909–1351 $ 17.50+.50/0

Complex **2a** crystallizes as orange yellow prisms, which, in contrast to complex **1**, are stable at room temperature under argon. It was therefore possible to obtain crystals for an X-ray structure analysis. The enhanced stability of complex **2** when compared to **1** seems to be a consequence of the steric shielding of the ebthi ligand system that has been found in other reactions, e.g., with substituted olefins[8] and with ethylene carbonate (see below). In solution complex **2** has C_1 symmetry, and both diastereomers (**2a**, **2b**) could be observed by NMR investigations. The ratio of the diastereomers formed is strongly influenced by temperature: for the product of this reaction, conducted at −10°C, we observed by NMR investigations at room temperature the stereoselective formation of the major complex **2a** (ratio **2a**/**2b** = 6:1), while running the same reaction at room temperature the ratio of the diastereomers formed was 1:1.

In a similar reaction a cycloreversion of the metallacycle formed was found by heating the coupling product of the nonsymmetrically substituted alkyne *t*BuC≡CSiMe$_3$ with acetone. The kinetically preferred zirconacycle with an SiMe$_3$ group in the β position rearranges at higher temperature to the thermodynamically more stable α-SiMe$_3$ product.[5b]

Heating of pure complex **2a**, up to 50°C, gave no inversion of the configuration at the acetal C and thus no complex **2b**, rather only decomposition products. It seems reasonable to assume that the ebthi ligand, in comparison to the sterically less demanding Cp ligand, prevents the cycloreversion by allowing less space for the ring-opening process. It therefore seems that there is no equilibrium between the two diastereomers and that the kinetically favoured product should be **2a**. The ratio of the formed diastereomers cannot be explained by the steric restriction coming from the ebthi ligand. The formation of **2a** as the major isomer indicates that there is no steric repulsion between the ebthi ligand and the seven-membered ring in the β position of the metallacycle due to the similarity of **2a** and **2b**. Investigations concerning coupling reactions with substituted olefins show the same stereochemical behaviour.[8]

Additionally, for comparison, other cyclic carbonyl compounds with a different number of oxygen atoms in the ring, such as ketones (no O atoms) and ethylene carbonate (two O atoms) were also investigated.

The reaction of Cp$_2$Zr(L)(η^2-Me$_3$SiC$_2$SiMe$_3$) (L = THF, pyridine) with cyclohexanone yields, by an insertion of the carbonyl compound into a Zr−C bond, the metallacyclic complex **3** (Eq. 3).

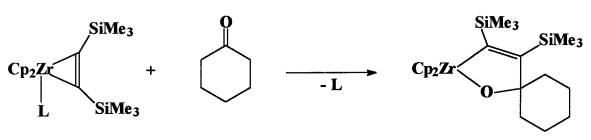

(3)

L = py, THF

3

In the reaction with cycloheptanone the analogous complex **4** was obtained. Both complexes are orange solids (**3**: m.p. 136°C; **4**: 138°C), which were characterized using NMR spectra (**3**, **4**) and X-ray crystal-structure analysis (**3**).

In addition, the reaction of *rac*-(ebthi)Zr(η^2-Me$_3$SiC$_2$SiMe$_3$) with ethylene carbonate results in an insertion of the carbonyl compound into a Zr−C bond of the zirconacyclopropene to yield the five-membered metallacyclic complex **5** (Eq. 4). Complex **5** is a yellow crystalline substance (m.p. 120°C).

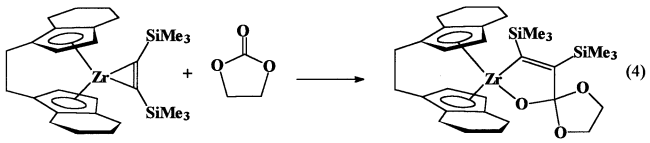

(4)

5

From reactions of Cp$_2$Zr(L)(η^2-Me$_3$SiC$_2$SiMe$_3$) (L = THF, pyridine) with ethylene carbonate no defined product could be isolated. The ^{1}H-NMR spectra showed within a mixture of products the formation of a small amount of a metallacyclic complex analogous to **5** and free ethylene carbonate; no polymeric product was obtained.

Spectroscopic Characteristics

The NMR spectra of complexes **1**−**5** are very similar to those reported earlier for such metallacycles, obtained from reactions of (alkyne)zirconocene complexes with acyclic carbonyl compounds such as aldehydes, ketones and esters.[5] Table 1 lists the relevant NMR data in comparison to the acetone metallacycle [Cp$_2$Zr{−C(SiMe$_3$)=C(SiMe$_3$)−CMe$_2$−O−}] (**6**).

Table 1. Selected NMR data of zirconacyclic complexes **1**, **2a**, **3**, **4** and **6**

	1	**2a**	**3**	**4**	**6**[5a]
^{1}H NMR					
Cp	6.07 6.16		6.32	6.11	6.12
SiMe$_3$	0.19 0.47	0.35 0.51	0.13 0.20	0.20 0.35	0.19 0.29
^{13}C NMR					
C$_\alpha$,C$_\beta$ (alkyne)	214.7 190.0	219.6 187.4	215.3 192.8	211.6 195.3	211.7 193.5
C(CO)	106.8	105.5	93.0	95.2	89.0

These data allow a clear distinction between the C_1- (**1**, **2**) and the C_s-symmetric (**3**, **4**, **6**) complexes to be made. While the coupling of Cp$_2$Zr(L)(η^2-Me$_3$SiC$_2$SiMe$_3$) with the prochiral carbonyl compound ε-caprolactone leads to a C_1-symmetric complex with two signals for the inequivalent Cp ligands (**1**: 2 s, each 5 H, δ = 6.07 and 6.16), the reaction product formed by the coupling with symmetrically substi-

tuted carbonyl compounds is C_s-symmetric and exhibits one signal for the two Cp rings (**3**, **4**, **6**, cf. Table 1).

Starting from the C_2-symmetric alkyne complex *rac*-(ebthi)Zr(η^2-$Me_3SiC_2SiMe_3$) we obtained as coupling products with the prochiral ε-caprolactone a mixture of two diastereomers (see above) for which each diastereomer shows four doublets for the Cp′ protons. By coupling the C_{2v}-symmetric ethylene carbonate with *rac*-(ebthi)Zr(η^2-$Me_3SiC_2SiMe_3$) the C_1-symmetric complex **5** is formed quantitatively, as shown by NMR investigations, and the spectra exhibit four characteristic doublets in the Cp region.

Structural Investigations

Complexes **2a** and **3** were investigated by an X-ray crystal structure analysis (Figure 1 and 2).

Figure 1. Molecular structure of complex **2a**, shown by an ORTEP plot at the 30% probability level[a]

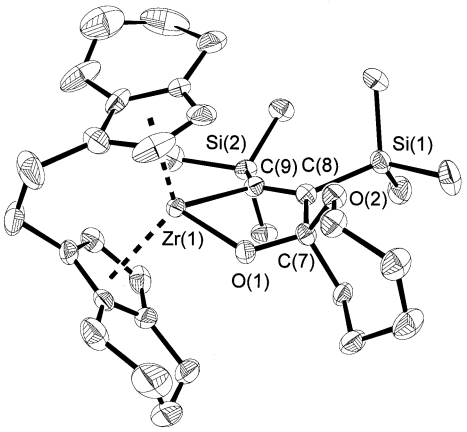

[a] Selected bond lengths [Å] and bond angles [°]: Zr1−C9 2.320(6), O1−C7 1.402(7), Zr1−O1 1.972(4), C7−C8 1.549(8), C8−C9 1.367(8), C9−Zr−O1 77.7(2), C7−O1−Zr 120.0(4), C8−C9−Zr 106.7(4).

Figure 2. Molecular structure of complex **3**, shown by an ORTEP plot at the 30% probability level[a]

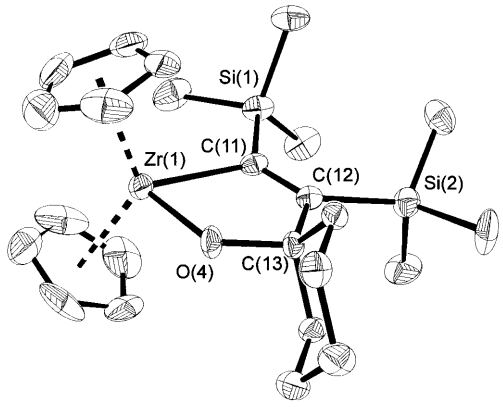

[a] Selected bond lengths [Å] and bond angles [°]: Zr1−C11 2.324(5), C11−C12 1.358(7), C12−C13 1.527(7), C13−O4 1.441(5), Zr−O4 1.922(3); C11−Zr1−O4 76.2(2), C12−C11−Zr1 110.1(4).

The obtained data for the five-membered zirconacyclic ring of complexes **2a** and **3** are listed in Table 2 and compared with those of complex **6**.

Table 2. Selected bond lengths [Å] and angles [°] for compounds **2a**, **3** and **6**

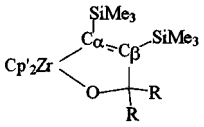

	2a	**3**	**6**[5a]
Bond lengths [Å]			
Zr−O	1.972(4)	1.922(3)	1.936(3)
Zr−C_α	2.320(6)	2.324(5)	2.324(5)
C_α−C_β	1.367(8)	1.358(7)	1.371(7)
C_β−CR_2	1.549(8)	1.527(7)	1.544(7)
O−CR_2	1.402(7)	1.441(5)	1.426(6)
Bond angles [°]			
O−Zr−C_α	77.7(2)	76.2(2)	76.4(2)
Si−C_α−Zr	125.8(2)	120.9(3)	121.6(2)
Si−C_α−C_β	127.4(5)	129.0(4)	128.4(4)
C_α−C_β−Si	126.6(5)	125.7(4)	125.6(4)
Si−C_β−CR_2	115.9(4)	115.3(4)	116.1(3)
O−CR_2−C_β	111.8(5)	108.2(4)	108.7(4)

Both structures correspond very well to that of the acetone product **6**[5a] and show as a result of a coupling of the alkyne with the carbonyl compound the metallacyclic ring substituted by an intact lactone or cyclohexane ring system. The C_α−C_β bond lengths [**2a**: 1.367(8); **3**: 1.358(7) Å] are in the expected range for C−C double bonds and the C−O distances [**2a**: 1.402(7); **3**: 1.441(5) Å] are in the C−O single-bond range. All bond lengths and angles of the five-membered zirconacycle in the three compounds compared are very similar.

Stoichiometric Reactions

The reaction behaviour of [Cp_2Zr{−C($SiMe_3$)=C($SiMe_3$)−CMe_2−O−}] (**6**) has been well studied.[5a] In solutions containing **6** and acetone an equilibrium with an "opened form" [$Cp_2Zr(Me_2CO)(\eta^2$-$Me_3SiC_2SiMe_3)$] was proposed, the latter paving the way to numerous ligand replacements. These reactions are reversible and degenerate, and were studied by NMR methods.[5c] With another alkyne, e.g. tolan, complex **6** reacts with substitution of the silylalkyne to yield the analogous thermodynamically more stable phenyl-substituted metallacyclic complex.

In reactions of **1**, **4** and **5** with carbonyl compounds similar behaviour was expected and the stability of the complexes depending on different carbonyl compounds was investigated.

In the reaction of **1** with equimolar amounts of cycloheptanone the ε-caprolactone (CL) part of the metallacycle is substituted by cycloheptanone, and **4**, as well as poly-ε-caprolactone (PCL), are formed. It is reasonable to assume that the substitution to give **4** is slow and the free CL can react quickly with unchanged **1** to give PCL. This substitution also proceeds very well with acetone to give the corresponding metallacycle **6**.

Complex **1** alone reacts with further CL under ring-opening polymerization to PCL. **1** is thermally unstable, and decomposes at room temperature to form PCL. In contrast, the cyloheptanone complex **4** is thermodynamically so

Scheme 1

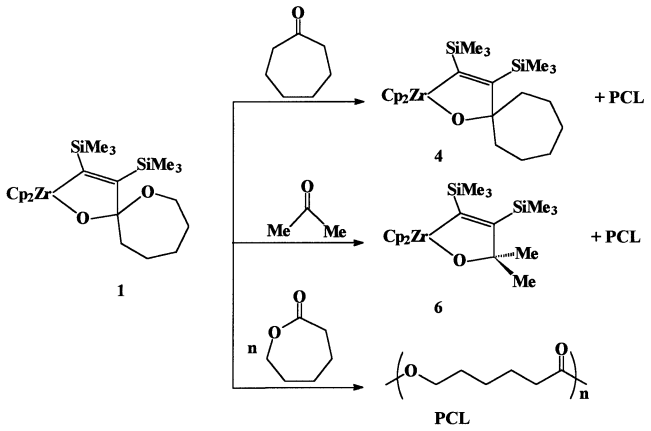

stable that it is unreactive toward ethylene carbonate (EC) or ε-caprolactone (toluene, 75°C, 1 h). It could be handled for a short time in air. The acetone complex **6** also forms compound **4** with cycloheptanone. The comparison of stabilities and reactivities thus shows the following trend: **4** > **6** > **1**. In this series, complex **4** is the most stable and complex **1** the most reactive compound.

The differences in the reaction behaviour, which were observed in spite of the accordance in structural parameters of the metallacycles, can be explained on the basis of steric and/or electronic factors of the substituents of the metallacyclic ring.

NMR Investigations of the Catalytic Ring-Opening Polymerization

The (alkyne)zirconocene complexes with additional ligands $Cp_2Zr(L)(\eta^2\text{-}Me_3SiC_2SiMe_3)$ (L = THF, pyridine) and the corresponding compound without stabilizing ligands *rac*-(ebthi)$Zr(\eta^2\text{-}Me_3SiC_2SiMe_3)$ are active in catalytic ring-opening polymerizations of ε-caprolactone. The poly-ε-caprolactone (PCL) produced was shown to possess a very high molecular weight (M_w = 73 000) and a narrow molecular weight distribution (M_w/M_n = 1.4) by GPC analysis.[3a] In order to learn about the polymerization mechanism, the ring-opening process was monitored directly by NMR spectroscopy (Figure 3). $Cp_2Zr(L)(\eta^2\text{-}Me_3SiC_2SiMe_3)$ (L= pyridine, THF) was treated with ε-caprolactone (1−10 equivalents) in an NMR tube. The ^{1}H- and ^{13}C-NMR spectra recorded immediately after the addition of CL showed at the initial stage the resonances arising from complex **1**, which is rapidly formed and indicated by

Figure 3. ^{13}C-NMR spectra of $Cp_2Zr(py)(\eta^2\text{-}Me_3SiC_2SiMe_3)$ with 10 equivalents of ε-caprolactone in C_6D_6; (CL = ε-caprolactone, PCL = poly-ε-caprolactone, complex **1**)

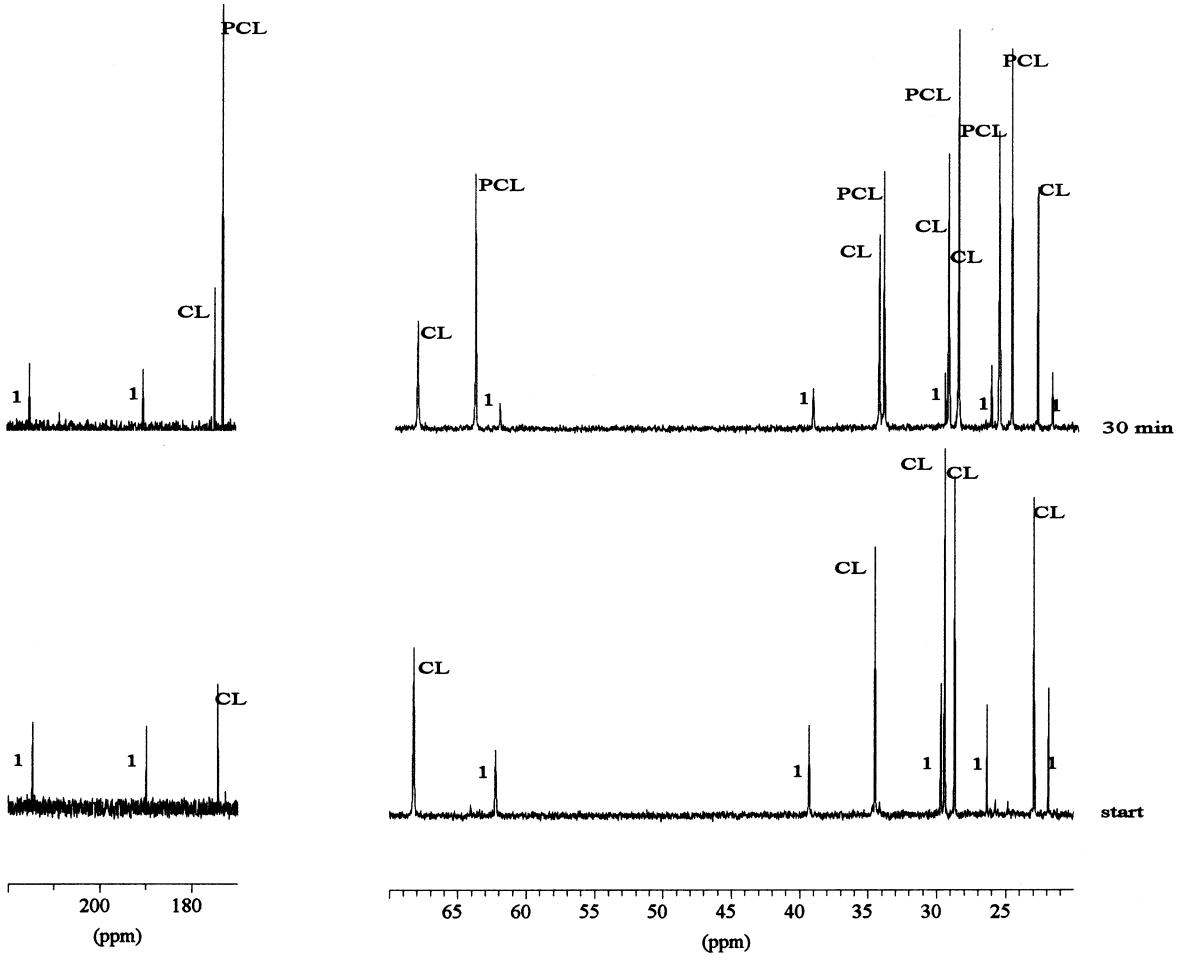

the shift of the CO signal from δ = 174.8 (free CL) to 106.8 (complex **1**). With an excess of the substrate free CL was also observed. NMR spectra taken 30 minutes after mixing showed signals arising from complex **1**, from free substrate (CL) and from poly-ε-caprolactone (PCL). The signals of monomeric ε-caprolactone (CL) disappeared within 1 h, the solution becoming highly viscous. No other species and unfortunately no end-group signals could be detected.

By combining ε-caprolactone with ethylene carbonate, polymers containing parts of PCL as well as polyethylenecarbonate (PEC) were indicated. The ^{13}C-NMR spectra of the copolymer exhibit, in addition to the carbonyl peaks of PCL (δ = 172.8), one of PEC (δ = 155.0). The amount of ethylene carbonate in the copolymer can be calculated from the ratio of the areas of these peaks and was in the range of about 8 mol-%. In contrast to this observation, ethylene carbonate is not homopolymerized in toluene or THF even at reflux (see above). Also $Cp^*_2Sm(THF)_2$ systems, which could not polymerize ethylene carbonate, form copolymers, derived from CL and EC.[9]

Based on the results discussed for the ring-opening polymerization of ε-caprolactone by Cp^*_2SmMe[1c] and $Cp^*_2LnOMe(THF)$,[1c] as well as our results mentioned above, we propose that at an early stage an exchange of the ligand L (L = THF or pyridine) takes place; ε-caprolactone approaches through the carbonyl oxygen atom. Examples of this interaction can be found in the crystallographically characterized complexes *mer*-YCl_3(ε-caprolactone)$_3$[2b] and $Cp_2Zr(Me_3SiC_2SiMe_3)$(Me-ε-caprolactam),[3b] or in the ^{1}H-NMR-spectroscopically identified initiator complex $Cp^*_2Y(OMe)$(ε-caprolactone).[1c] The next step is the insertion of the carbonyl group of the lactone into the zirconacyclopropene ring system to yield the five-membered metallacyclic complex **1**. On the basis of ^{13}C-NMR studies in the initiation of the ring-opening polymerization of ε-caprolactone and δ-valerolactone by Cp^*_2SmMe,[1c] the formation of an acetal has also been discussed.

The results of the NMR studies are disappointing. All subsequent steps of the catalytic cycles such as propagation and chain termination are very fast on the NMR time scale, and could not be detected. This is consistent with the results obtained by other groups in monitoring lactone polymerization by NMR.[1] Furthermore, no end-group signals were found. This has also been explained in some other works,[1b][1f] by the formation of a cyclic polymer as the termination step.

Conclusion

The present study demonstrated that in the reaction of the (alkyne)zirconocene complexes $Cp_2Zr(L)(\eta^2\text{-}Me_3SiC_2SiMe_3)$ (L= THF, pyridine) and *rac*-(ebthi)$Zr(\eta^2\text{-}Me_3SiC_2SiMe_3)$ with ε-caprolactone the five-membered spirocyclic zirconadihydrofuranes **1** and **2** are formed. Both complexes are intermediates in the catalytic ring-opening polymerization of ε-caprolactone. Complex **2** is the first well-characterized example for the formation of such an acetal, which was proposed as an elemental step of the ring-opening polymerization of lactones.[1] NMR studies showed that further steps of the catalytic cycle such as propagation and chain termination are very fast on the NMR time-scale and could not be detected.

The reaction of (alkyne)zirconocene complexes with other cyclic carbonyl compounds such as ketones or ethylene carbonate yields analogous metallacycles, but no polymerization was observed.

Work is in progress to expand the ring-opening capability to other heterocyclic substrates and to utilize the chiral initiator for stereoselective ring openings.

We thank the *Fonds der Chemischen Industrie* and the *Max-Planck-Gesellschaft* for financial support.

Experimental Section

General: All operations were carried out under argon using standard Schlenk techniques. Prior to use, solvents were freshly distilled from sodium tetraethylaluminate and stored under argon. Deuterated solvents were treated with sodium or sodium tetraethylaluminate, distilled and stored under argon. ε-Caprolactone (Aldrich) was dried over molecular sieves and degassed before use. − Mass spectra: AMD 402. − NMR spectra: Bruker ARX 400. Chemical shifts referenced to signals of the solvents used: [D_6]benzene (δ_H = 7.16; δ_C = 128.0). The spectra were assigned with the help of DEPT and COLOC experiments. − Melting points: sealed capillaries, Büchi 535 apparatus. − Elemental analyses: Leco CHNS-932 elemental analyzer.

Preparation of **1**: To a solution of 377 mg (0.80 mmol) of $Cp_2Zr(py)(\eta^2\text{-}Me_3SiC_2SiMe_3)$ in 10 ml of diethyl ether was added at −10°C 92 μl (0.80 mmol) of ε-caprolactone. The mixture was stirred for 30 min at this temperature and the colour changed to orange. After concentration to dryness, *n*-hexane was added. The solution was filtered, and after 12 h at −78°C orange crystals formed. The crystals were washed with cold *n*-hexane and dried in vacuo to give 210 mg (51%) of **1**. − ^{1}H NMR (C_6D_6): δ = 0.19, 0.47 (s, 2 × 9 H, $SiMe_3$), 1.4−2.1 (m, 6 H, CH_2), 3.5−3.6 (m, 2 H, CH_2), 3.83 (m, 2 H, CH_2), 6.07, 6.16 (s, 2 × 5 H, Cp). − ^{13}C{^{1}H} NMR (C_6D_6): δ = 4.4, 4.8 ($SiMe_3$), 21.9, 26.4, 29.7, 39.3, 62.3 (CH_2), 106.8 (CO), 113.1, 114.3 (Cp), 190.0 (β-*C*$SiMe_3$), 214.7(α-*C*$SiMe_3$). − MS (70 eV); *m/z* (%): 220 $[Cp_2Zr]^+$, 170 $[Me_3SiC_2SiMe_3]^+$, 114 [ε-caprolactone]$^+$. − $C_{24}H_{38}O_2Si_2Zr$ (505.96): calcd. C 56.97, H 7.57; found C 56.83, H 7.63.

Preparation of **2a and 2b**: To a solution of 140 mg (0.266 mmol) of *rac*-(ebthi)$Zr(\eta^2\text{-}Me_3SiC_2SiMe_3)$ in 10 ml of *n*-hexane, 28.1 μl (0.266 mmol) of ε-caprolactone was added. The colour of the reaction mixture changed from green to red-orange after a few seconds. After standing for two weeks at −78°C, red crystals separated which were suitable for X-ray structure analysis (crystals were the pure diastereomer **2a** as checked by NMR). Evaporation of the solvent at room temperature yielded 73 mg (43%) of an orange foam of **2a** and **2b**. − **2a** (major isomer): ^{1}H NMR (C_6D_6): δ = 0.35 (s, 9 H, $SiMe_3$), 0.51 (s, 9 H, $SiMe_3$), 1.4−3.2 (m, 28 H, CH_2), 3.57 (1 H, OCH_2), 3.90 (1 H, OCH_2), 5.12 (d, *J* = 2.8 Hz, 1 H, Cp′), 5.39 (d, *J* = 3.0 Hz, 1 H, Cp′), 6.58 (d, *J* = 3.0 Hz, 1 H, Cp′), 6.85 (d, *J* = 2.8 Hz, 1 H, Cp′). − ^{13}C{^{1}H} NMR (C_6D_6): δ = 4.6, 6.2 ($SiMe_3$), 21.2, 22.6, 23.0, 23.0, 23.2, 23.3, 23.5, 24.0, 24.0, 24.6, 25.5, 28.0, 28.1, 28.9 (CH_2), 44.0 [CH_2C(O)], 60.8 (CH_2O), 107.7, 109.5, 110.6, 114.7, 122.1, 122.9, 129.3, 129.4 (CH) 105.5 (CO), 187.4 (β-*C*$SiMe_3$), 219.6 (α-*C*$SiMe_3$). − $C_{34}H_{52}O_2Si_2Zr$ (640.2): calcd. C 63.79, H 8.19; found C 64.00, H 8.16. − **2b** (minor

Table 3. Crystal data, data collection and structure refinement for compounds **2a** and **3**

	2a	**3**
cryst. colour	orange	yellow
cryst. system	triclinic	monoclinic
space group	$P\bar{1}$	$P2_1/n$
a [Å]	9.900(2)	9.7050(12)
b [Å]	14.214(3)	18.887(3)
c [Å]	15.897(3)	13.902(2)
α[°]	99.38(2)	90
β [°]	107.07(2)	97.300(11)
γ [°]	95.01(2)	90
Z	2	4
F(000) [e]	747	1032
μ [mm^{-1}]	0.348	0.547
T [K]	200(2)	293(2)
no. of rflns. (indep.)	6284	4071
no. of rflns. (obsd.)	4686	1819
no. of parameters	390	253
$R1$ [($I \geq 2\sigma(I)$)]	0.074	0.046
$wR2$ (all data)	0.226	0.095

isomer, could only be obtained in a mixture with **2a**): ^{1}H NMR (C_6D_6): δ = 0.29 (s, 9 H, $SiMe_3$), 0.34 (s, 9 H, $SiMe_3$), 5.15 (d, J = 2.7 Hz, 1 H, Cp′), 5.33 (d, J = 3.2 Hz, 1 H, Cp′), 6.35 (d, J = 3.2 Hz, 1 H, Cp′), 6.76 (d, J = 2.7 Hz, 1 H, Cp′), further signals could not be assigned. – ^{13}C{^{1}H} NMR (C_6D_6): δ = 5.4, 6.2 ($SiMe_3$), 39.5 [CH_2C(O)], 61.2 (CH_2O), 106.7, 108.7, 112.1, 116.5, 123.1, 123.5, 126.2, 127.3, 130.0, 130.6 (CH-ebthi), 105.0 (CO), 191.4 (β-CSiMe$_3$), 216.6 (α-CSiMe$_3$).

Preparation of **3**: An amount of 250 mg (0.54 mmol) of $Cp_2Zr(THF)(\eta^2$-$Me_3SiC_2SiMe_3)$ was dissolved in 10 ml of THF, and cyclohexanone (56 μl, 0.54 mmol) was added to the solution. The mixture was stirred, whereupon the colour changed from orange to yellow. The solution was concentrated to dryness and the residue was dissolved in *n*-hexane. On standing at −78°C for 2 d, orange crystals deposited which were dried in vacuo to give 210 mg (79%) of **3**, m.p. 136°C. – ^{1}H NMR (C_6D_6): δ = 0.13, 0.20 (s, 2 × 9 H, $SiMe_3$), 0.90−1.0 (m, 2 H, CH_2), 1.30−1.41 (m, 4 H, CH_2), 1.61−1.70 (m, 4 H, CH_2), 6.32 (s, 10 H, Cp). – ^{13}C{^{1}H} NMR (C_6D_6): δ = 5.2, 5.4 ($SiMe_3$), 22.7, 26.1, 35.4 (CH_2), 93.0 (CO), 113.9 (Cp), 192.8 (β-CSiMe$_3$), 215.3 (α-CSiMe$_3$). – MS(70 eV); m/z (%): 220 Cp_2Zr^+, 170 $[Me_3SiC_2SiMe_3]^+$, 98 [cyclohexanone]$^+$. – $C_{24}H_{38}OSi_2Zr$ (489.94): calcd. C 58.83, H 7.82; found: C 58.53, H 8.13.

Preparation of **4**: The reaction was carried out in the same manner as described for complex **3** with an amount of 420 mg (0.89 mmol) of $Cp_2Zr(py)(\eta^2$-$Me_3SiC_2SiMe_3)$ and cycloheptanone (104 μl, 0.89 mmol) to give 330 mg of **4** (74%), orange crystals, m.p. 138°C. – ^{1}H NMR (C_6D_6): δ = 0.20, 0.35 (s, 2 × 9 H, $SiMe_3$), 1.51 (m, 4 H, CH_2), 1.66 (m, 4 H, CH_2), 1.83 (m, 2 H, CH_2), 2.03 (m, 2 H, CH_2), 6.11 (s, 10 H, Cp). – ^{13}C{^{1}H} NMR (C_6D_6): δ = 5.0, 5.2 ($SiMe_3$), 22.8, 27.6, 38.4 (CH_2), 95.2 (CO), 113.2 (Cp), 195.3 (β-CSiMe$_3$), 211.6 (α-CSiMe$_3$). – MS(70 eV); m/z (%): 220 Cp_2Zr^+, 170 $[Me_3SiC_2SiMe_3]^+$, 112 [cycloheptanone]$^+$. – $C_{25}H_{39}OSi_2Zr$ (489.94): calcd. C 59.70, H 7.82; found C 58.83, H 8.11.

Preparation of **5**: To a solution of 310 mg (0.589 mmol) of *rac*-(ebthi)$Zr(\eta^2$-$Me_3SiC_2SiMe_3)$ in 3 ml of diethyl ether, 52 mg (0.589 mmol) of ethylene carbonate was added . The colour of the reaction mixture changed from green to red-orange after stirring for 5 min. Addition of 3 ml of pentane and standing for 12 h at −40°C gave 310 mg of **5** (85%), yellow crystalline solid, m.p. 120°C. – ^{1}H NMR (C_6D_6): δ = 0.19, 0.27 (s, 2 × 9 H, $SiMe_3$), 1.1−3.4 (20 H, CH_2), 3.51(2 H, OCH_2), 3.59 (1 H, OCH_2), 4.91 (1 H, Cp′), 5.20 (d, 1 H, Cp′), 6.65 (d, 1 H,Cp′), 6.70 (d, 1 H, Cp′). – ^{13}C{^{1}H} NMR (C_6D_6): δ = 3.3 ($SiMe_3$), 5.6 ($SiMe_3$), 22.3, 22.9, 23.0, 23.1, 23.1, 23.6, 23.9, 24.6, 27.3, 27.6 (CH_2-ebthi), 62.3, 62.6 (CH_2O), 108.4, 109.4, 111.0, 118.2 (CH-ebthi) 119.0, 122.9, 123.7, 128.7, 129.5, 131.6 (C_q), 181.5 (β-CSiMe$_3$), 227.7 (α-CSiMe$_3$). – $C_{31}H_{46}O_3Si_2Zr$ (614.10): calcd. C 60.63, H 7.55; found C 60.59, H 7.47.

Polymerization of ε*-Caprolactone in an NMR Tube:* In a 5-mm NMR tube the catalyst (20−30 mg) was dissolved in C_6D_6 (0.6 ml). ε-Caprolactone (1−10 equivalents) was placed at the upper end of the tube to prevent early mixing. The NMR tube was closed and vigorously shaken just before running the spectra.

X-ray-Crystallographic Study of Complexes **2 and 3**: Diffraction data were collected on a STOE-IPDS diffractometer using graphite-monochromated Mo-K_α radiation. Crystal data, details of the data collections and structure refinement are compiled in Table 3. The structures were solved by direct methods (SHELXS-86: G. M. Sheldrick, *Acta Crystallogr., Sect. A* **1990**, *46*, 467) and refined by full-matrix least-squares techniques against F^2 (SHELXL-93: G. M. Sheldrick, University of Göttingen, Germany, **1993**). Further details of the crystal-structure investigations are available on request from the Cambridge Crystallographic Data Centre, on quoting the depository number CCDC-101309. Copies of the data can be obtained free of charge on application to CCDC, 12 Union Road, Cambridge CB2 1EZ, UK [Fax: (internat.) + 44(0)1223/336033; E-mail: deposit@ccdc.cam.ac.uk].

☆ Dedicated to Dr. habil. *Erhard Kurras* on the occasion of his 70th birthday.

[1a] J. Okuda, I. L. Rushkin, *Macromolecules* **1993**, *26*, 5530−5532. – [1b] J. Okuda, K. C. Hulitzsch, *Macromol. Rapid Commun.* **1997**, *18*, 809−815. – [1c] H. Yasuda, E. Ihara, *Bull. Chem. Soc. Jpn.* **1997**, *70*, 1745−1767 and references therein. – [1d] M. Hayakawa, M. Mitani, T. Yamada, T. Mukaiyama, *Macromol. Chem. Phys.* **1997**, *198*, 1305−1317. – [1e] T. Mukaiyama, M. Hayakawa, K. Oouchi, M. Mitani, T. Yamada, *Chem. Lett.* **1995**, 737−738 and references therein. – [1f] K. C. Hultzsch, T. P. Spaniol, J. Okuda, *Organometallics* **1997**, *16*, 4845−4856.

[2a] D. Seebach, H.-M. Müller, *Angew. Chem.* **1993**, *105*, 483−509; *Angew. Chem. Int. Ed. Engl.* **1993**, *32*, 457−476. – [2b] W. J. Evans, J. L. Shreeve, R. J. Doedens, *Inorg. Chem.* **1993**, *32*, 245−246.

[3a] P. Arndt, D. Thomas, U. Rosenthal, *Tetrahedron Lett.* **1997**, *38*, 5467−5468. – [3b] P. Arndt, C. Lefeber, R. Kempe, U. Rosenthal, *Chem. Ber.* **1996**, *129*, 1281−1285. –

[4a] G. Erker, F. Rosenfeldt, *J. Organomet. Chem.* **1982**, *224*, 29−42. – [4b] G. Erker, U. Dorf, P. Czisch, J. Petersen, *Organometallics* **1986**, *5*, 668−676. – [4c] S. Buchwald, R. Nielsen, *Chem. Rev.* **1988**, *88*, 1047−1058. – [4d] E. Negischi, T. Takahashi, *Synthesis* **1988**, 1−19. – [4e] H. Yasuda, T. Okamoto, K. Matsuoka, Y. Nakamura, Y. Kai, N. Kanehisa, N. Kasai, *Organometallics* **1989**, *8*, 1139−1152. – [4f] G. Erker, *Angew. Chem.* **1989**, *101*, 411−426; *Angew. Chem. Int. Ed. Engl.* **1989**, *28*, 397−412. – [4g] H. Alt, C. Denner, *J. Organomet. Chem.* **1990**, *390*, 53−60. – [4h] T. Takahashi, N. Suzuki, M. Hasegawa, Y. Nitto, K. Aoyagi, M. Saburi, *Chem. Lett.* **1992**, 331−334. – [4i] S. Buchwald, R. Broene, *Science* **1993**, *261*, 1696−1701. – [4k] E. Negishi, T. Takahashi, *Acc. Chem. Res.* **1994**, *27*, 124−130. – [4l] G. Erker, L. Lopez, M. Berlekamp, D. Kowalski, *Angew. Chem.* **1994**, *106*, 1168−1170; *Angew. Chem. Int. Ed. Engl.* **1994**, *33*, 1114−1116. – [4m] G. Erker, M. Berlekamp, L. Lopez, M. Grehl, B. Schönecker, R. Krieg, *Synthesis* **1994**, 214−222. – [4n] E. Hey-Hawkins, *Chem. Rev.* **1994**, *94*, 1661−1717. – [4o] M. Hasegawa, Y. Nitto, M. Saburi, *J. Organomet. Chem.* **1994**, *473*, 117−128. – [4p] M. Maier, T. Oost, *J. Organomet. Chem.* **1995**, *505*, 95−107.

[5a] U. Rosenthal, A. Ohff, W. Baumann, A. Tillack, V. V. Burlakov, V. B. Shur, *J. Organomet. Chem.* **1994**, *484*, 203−207. – [5b] C.

Lefeber, A. Ohff, A. Tillack, W. Baumann, R. Kempe, V. V. Burlakov, U. Rosenthal, *J. Organomet. Chem.* **1995**, *501*, 189−194. − [5c] W. Baumann, A. Ohff, M. Ebener, *Helv. Chim. Acta* **1996**, *79*, 454−460. − [5d] N. Peulecke, A. Ohff, A. Tillack, W. Baumann, R. Kempe, V. V. Burlakov, U. Rosenthal, *Organometallics* **1996**, *15*, 1340−1343.

[6] U. Rosenthal, A. Ohff, M. Michalik, H. Görls, V. V. Burlakov, V. B. Shur, *Angew. Chem.* **1993**, *105*, 1228−1230; *Angew. Chem. Int. Ed. Engl.* **1993**, *32*, 1193−1195.

[7] U. Rosenthal, A. Ohff, W. Baumann, A. Tillack, H. Görls, V. V. Burlakov, V. B. Shur, *Z. Anorg. Allg. Chem.* **1995**, *621*, 77−83.

[8] S. Mansel, D. Thomas, C. Lefeber, D. Heller, R. Kempe, W. Baumann, U. Rosenthal, *Organometallics* **1997**, *16*, 2886−2890.

[9] W. J. Evans, H. Katsumata, .*Macromolecules* **1994**, *27*, 4011−4013.

[98078]

Preparation of *P,N*-Heterodifunctional Ferrocene-Coordinating Ligands by Selective Functionalization of Polyphosphanes by the Staudinger Reaction – Crystal and Molecular Structure of a New Cyclometallaphosphoraniminophosphane of Palladium(II)

Pedro Molina*[a], Antonio Arques*[a], Alejandro García[a], and M. Carmen Ramírez de Arellano[b]

Departamento de Química Orgánica, Facultad de Química, Universidad de Murcia[a],
Campus de Espinardo, E-30071 Murcia, Spain
E-mail: pmolina@fcu.um.es; arques@fcu.um.es

Departamento de Química Inorgánica, Facultad de Química, Universidad de Murcia[b],
Campus de Espinardo, E-30071 Murcia, Spain

Received March 23, 1998

Keywords: β-Ferrocenylvinyl azide / Polyphosphanes / Iminophosphoranes / *P,N*-Difunctional ligands / Palladium

Staudinger reactions of the β-ferrocenylvinyl azide **1** with several diphosphanes in a 1:1 molar ratio afford the monoiminophosphorane derivatives **2**–**4**, whereas with a 2:1 stoichiometry these reactions afford the bis(iminophosphoranes) **5**–**7**. Similar results are obtained for the reactions of **1** with tris(diphenylphosphanylmethyl)ethane (*triphos*) and tris[2-(diphenylphosphanyl)ethyl]phosphane (*tetraphos*). Reaction of these *P,N*-difunctional ferrocene ligands with dichlorobis(benzonitrile)palladium(II) leads to the Pd^{II}-metallacycle derivatives **13** and **14**. The molecular structures of **5d** and **13** have been established by X-ray crystallography.

Ferrocene derivatives containing phosphane groups have proved to be very useful in coordination chemistry[1] and have found application in enantioselective transition-metal-catalyzed reactions[2]. In contrast to the large number of ferrocene-derived phosphanes and their complexes in which the phosphorus atom is directly bonded to a cyclopentadienyl ring, ligands with a tether connecting the two functionalities are less common[3], although chiral analogues have been attracting interest owing to their catalytic activity[4].

There is also a general interest in transition-metal complexes with heterodifunctional ligands because of their potential as catalysts[5] and their proven usefulness in the preparation of heterobimetallic species[6]. Heterodifunctional ligands provide versatile binding sites for metals, and thus effective catalysts may be generated from complexes of bifunctional chelate ligands in which one arm of the chelate is more loosely bound than the other, so that an equilibrium opening a coordinate site and thus providing access to a reactive intermediate can be established.

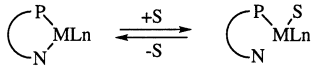

Since M−N π bonds are known to be more labile than M−P π bonds in some complexes[7], the use of bidentate ligands containing one phosphorus and one nitrogen donor can be expected to improve the catalytic activity. In this context, the preparations and catalytic activities of a number of rhodium, iridium, palladium and platinum *P,N* complexes, which contain a soft phosphorus(III) center at one end and a hard nitrogen center (amino, amido, imine or pyridine ring) at the other, have been reported[8].

Following our work on the preparation of new ferrocene derivatives by means of aza Wittig reactions[9], we now wish to report on the efficient synthesis of *P,N*-heterodifunctional ferrocene-based ligands. Our approach is based on the Staudinger imination[10] of trivalent phosphorus compounds with azides to produce an iminophosphorane function after nitrogen evolution. This method, which allows the partial oxidation of diphosphanes using the β-ferrocenylvinyl azide **1**, is applicable to diphosphanes of various alkene chain lengths, and even to tri- and tetraphosphanes.

Results and Discussion

Reaction of the starting β-ferrocenylvinyl azide **1**[9] with the appropriate diphosphane (1:1 molar ratio) in dry dichloromethane for 15 h at room temperature provides the corresponding monoiminophosphorane **2**, along with trace amounts of the bis(iminophosphorane) **5**. Compounds **2** could be isolated in yields ranging from 33 to 66% after purification by column chromatography and recrystallization. Similarly, reactions of **1** with (*E*)-1,2-bis(diphenylphosphanyl)ethene and 1,1′-bis(diphenylphosphanyl)ferrocene afford the monoiminophosphoranes **3** (46%) and **4** (21%), respectively. However, when reactions of azide **1** with diphosphanes (2:1 molar ratio) were carried out in diethyl ether at −15°C, the major product is the corresponding bis(iminophosphorane) **5** (45−89%), together with a small amount of the monoiminophosphorane **2**. Under these conditions, reaction with 1,1′-bis(diphenylphosphanyl)ferrocene provides the bis(iminophosphorane) **6**, while

 © WILEY-VCH Verlag GmbH, D-69451 Weinheim, 1998 1434−1948/98/0909−1359 $ 17.50+.50/0

that with (*E*)-1,2-bis(diphenylphosphanyl)ethene afforded **7**, albeit in very low yield (9%) (Scheme 1).

Scheme 1

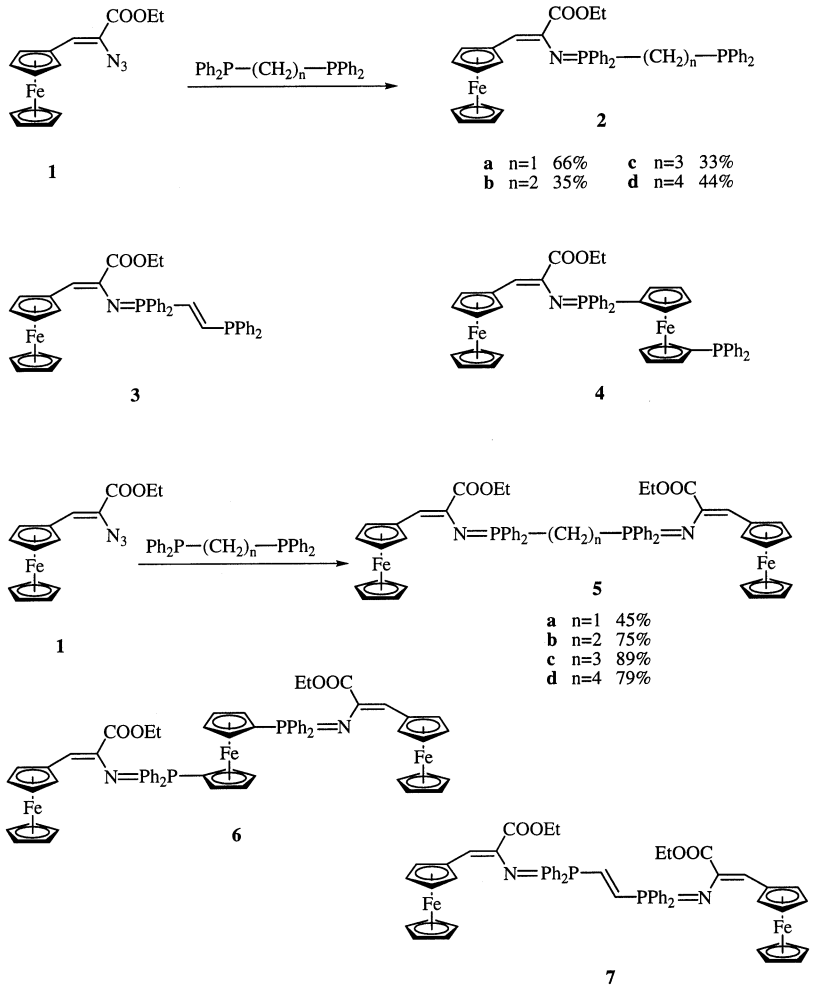

The ^{1}H-NMR spectra of compounds **2** and **5** show characteristic features: the ferrocenyl hydrogen atoms give a singlet at $\delta = 4.01-4.12$ for the unsubstituted cyclopentadienyl ring, and two pseudo triplets at $\delta = 4.17-4.59$ and $\delta = 4.90-5.06$, corresponding to an AA′MM′ pattern for the monosubstituted ring, while the vinylic proton signal appears as a doublet at $\delta = 6.14-6.53$ due to P^V coupling. The ^{13}C{^{1}H}-NMR spectra also exhibit the typical signals for monosubstituted ferrocenes. NOE experiments performed on compound **2b** allowed us to assign the α- and β-protons of the substituted cyclopentadienyl ring (Figure 1).

Figure 1. Selected NOE correlations for compound **2b**

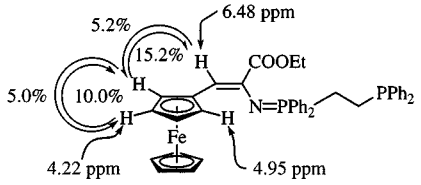

Some salient ^{13}C{^{1}H}- and ^{31}P{^{1}H}-NMR data for compounds **2** and **5** are compiled in Table 1. The ^{13}C-NMR spectrum of monoiminophosphorane **3** can be described as an AMX system, the ethylenic carbon atom $C-P^{III}$ signal appears at $\delta = 148.41$ as a doublet ($^1J_{P\text{-}C} = 23.4$ Hz), while the ethylenic $C-P^V$ signal appears at $\delta = 134.73$ as a doublet of doublet ($^1J_{P\text{-}C} = 87.2$ Hz, $^2J_{P\text{-}C} = 10.5$ Hz). In the bis(iminophosphorane) **7**, the two ferrocene subunits are equivalent; the C=O carbon atom signals appear as an apparent triplet and the ethylenic carbon atom signals $C-P^V$ appear at $\delta = 141.16$ as five-line multiplets. The ^{31}P{^{1}H}-NMR spectrum of **3** features two doublets centered at $\delta = 1.04$ and $\delta = -7.25$, attributable to the pentavalent and trivalent phosphorus atoms, respectively, whereas the spectrum of bis(iminophosphorane) **7** shows only one singlet at $\delta = 0.63$. In the ^{1}H- and ^{13}C-NMR spectra of compounds **4** and **6**, the characteristic signals of mono- and disubstituted ferrocenes are observed. In the ^{13}C-NMR spectrum of compound **4**, the disubstituted ferrocene ring signals appear as a set of six pairs of doublets, whereas in compound **6** it gives rise to a set of three pairs of doublets, besides only one set of signals for the two monosubstituted ferrocenes, indicating that they are equivalent. The ^{31}P-NMR spectrum of compound **4** shows two singlets at $\delta = 4.40$ and $\delta = -19.04$, assigned to the pentavalent and trivalent phosphorus atoms respectively, while that of compound **6** shows

Table 1. $^{13}C\{^1H\}$-NMR[a] and $^{31}P\{^1H\}$-NMR[b] data of the diphosphane framework in compounds **2** and **5**[c]

2 **5**

	C-1	C-2	C-3	C-4	P^V	P^{III}
2a	31.68 (dd, $^1J_{P(V)}$ = 59.5, $^1J_{P(III)}$ = 30.5)				3.36 (d, $^2J_{PP}$ = 53.8)	−29.49
2b	26.88 (dd, $^1J_{P(V)}$ = 66.2, $^2J_{P(III)}$ = 16.9)	19.37 (dd, ^1J = 13.9, ^2J = 4.0)			8.15 (d, $^3J_{PP}$ = 48.8)	−12.93
2c	31.39 (dd, $^1J_{P(V)}$ = 65.1, $^3J_{P(III)}$ = 12.5)	18.52 (dd, $^2J_{P(V)}$ = 17.0, $^2J_{P(III)}$ = 2.5)	29.37 (dd, $^1J_{P(III)}$ = 26.5, $^3J_{P(V)}$ = 14.5)		6.91	−18.87
2d	30.10 (d, $^1J_{P(V)}$ = 66.6)	23.06 (dd, $^2J_{P(V)}$ = 15.5, $^3J_{P(III)}$ = 3.5)	27.54 (dd, $^2J_{P(III)}$ = $^3J_{P(V)}$ = 14.5)	27.71 (d, $^1J_{P(III)}$ = 11.4)	7.32	−16.61
5a	31.43 (quint, $^1J+^1J$ = 108.0)				−2.64	
5b	23.13 (quint, $^1J+^2J$ = 130.2)				8.60	
5c	30.27 (dd, ^1J = 64.0, ^3J = 10.9)	15.22 (m)			6.73	
5d	30.07 (d, ^1J = 66.4)	23.05 (dd, ^2J = 16.0, ^3J = 3.1)			7.36	

[a] Chemical shift δ(^{13}C) relative to TMS; coupling constants in Hz. − [b] Chemical shift δ(^{31}P) relative to external 85% H_3PO_4; coupling constants in Hz. − [c] Solvent $CHCl_3$.

only one singlet at δ = 5.34. The constitution of compound **5d** was further corroborated by a single-crystal X-ray diffraction study. The molecular structure shows an inversion centre in the C17−C17a bond mid point. The P−N bond lenght [1.566(2) Å] is within the expected values. An ORTEP drawing of **5d** is shown in Figure 2; selected bond lengths and angles are given in the caption.

Figure 2. ORTEP plot of compound **5d**[a]

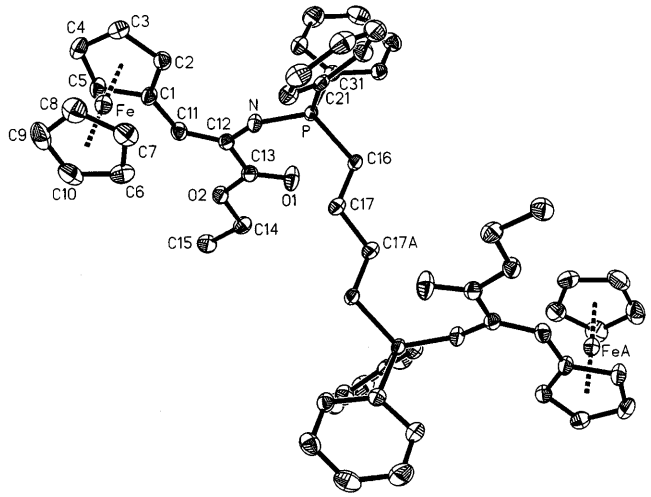

[a] 50% probability ellipsoids; selected bond lengths [Å] and angles [°]: P−N 1.566(2), N−C(12) 1.384(3), C(1)−C(11) 1.453(3), C(11)−C(12) 1.350(3); C(12)−N−P 131.6(2), C(12)−C(11)−C(1) 127.5(2), C(11)−C(12)−N 122.8(2).

Reaction of the β-ferrocenylvinyl azide **1** with tris(diphenylphosphanylmethyl)ethane (*triphos*) (1:1 molar ratio) in dry dichloromethane at room temperature afforded a mixture of the monoiminophosphorane **8** (21%) and the bis(iminophosphorane) **9** (7%), which were readily separated by column chromatography. However, when the reaction was carried out in diethyl ether at −15°C in a 3:1 molar ratio, the corresponding tris(iminophosphorane) **10** was obtained in good yield as the sole reaction product (77%) (Scheme 2).

The ^1H-NMR spectrum of the bis(iminophosphorane) **9** shows two sets of signals for the two ferrocene subunits, indicating that they are non-equivalent. ^1H-, ^{13}C- and ^{31}P-NMR data of the *triphos* framework in compounds **8**, **9** and **10** are compiled in Table 2.

Reaction of azide **1** with tris[2-(diphenylphosphanyl)-ethyl]phosphane (*tetraphos*) in a 1:1 molar ratio in dichloromethane at room temperature afforded the monoiminophosphorane **11** in 31% yield. However, when the reaction was carried out in a 4:1 molar ratio in diethyl ether at −15°C, the main product was found to be the tetra(iminophosphorane) **12** (28%) (Scheme 3). The ^1H- and ^{13}C-NMR spectra of compound **12**, which bears four ferrocene subunits, showed the non-equivalence of one ferrocene group.

At this point, it seemed interesting to assess the complexation behavior of these heterodifunctional ferrocene derivatives **2** and **8** with palladium(II) (Scheme 4), as these compounds possess a complex-forming diphenylphosphanyl group and an iminophosphorane function, which has also demonstrated its versatility in forming M−N σ bonds to transition metals[11].

Scheme 2

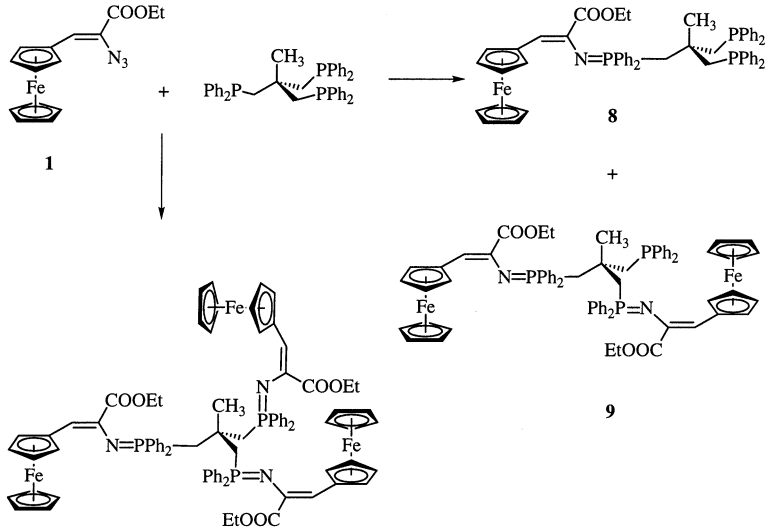

Scheme 3

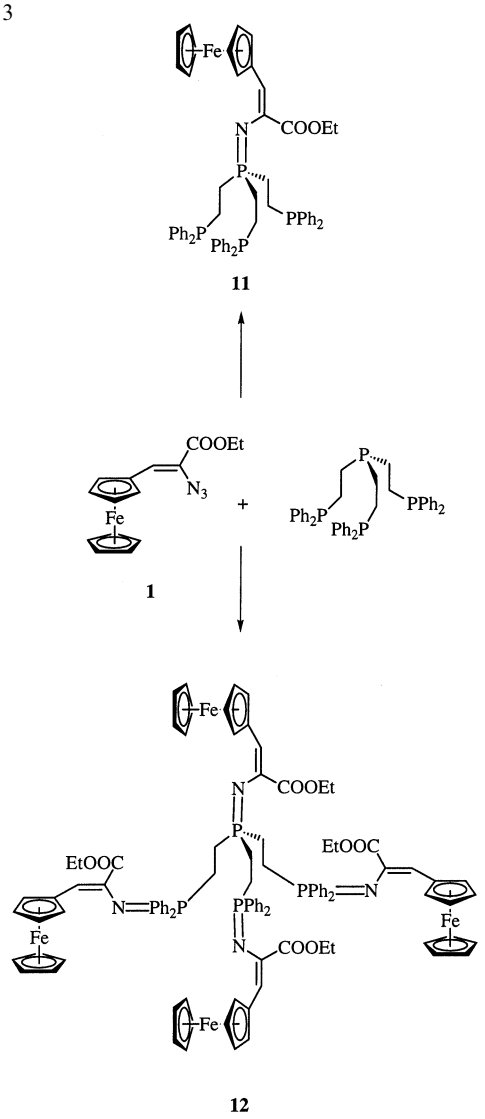

The ferrocene derivative **2a** was found to react cleanly with dichlorobis(benzonitrile)palladium(II) in toluene at −15°C affording the new *P,N*-chelate **13**, the structure of which has been determined by X-ray analysis (Figure 3). The ^{31}P-NMR spectrum of **13** features two doublets, with the iminophosphorane unit resonating at lower field (δ = 44.23) than the diphenylphosphanyl center (δ = 14.16).

Complex **13** represents the first example of a ferrocene derivative containing an iminophosphorane phosphane ligand. The palladium atom has a distorted square-planar coordination geometry. The large Pd−Cl1 bond length (2.3719 Å) compared to Pd−Cl2 (2.3133 Å) is consistent with the larger *trans* influence of P compared to N. The P−N bond length (1.628 Å) indicates that this bond is slightly elongated due to the coordination, since free iminophosphoranes show shorter P−N bond lengths (1.567 Å). The P^V atom geometry corresponds to a distorted tetrahedron, with the N−P−C angle [102.3(1)°] being the smallest. The distortion is probably due to the chelate ring stress.

The complexation behavior of **8** with Pd^{II} under the same reaction conditions was found to be different from that of **2a** and the *P,P*-chelate **14** was formed (Scheme 4). The ^{31}P-NMR spectrum showed this clearly, featuring only two singlets at δ = 0.1, characteristic of a non-coordinated iminophosphorane function, and at δ = 15.60, attributable to the coordinated diphenylphosphane groups.

The difference of 26.6 ppm between the chemical shifts of the P^{III} and P^V centers in **8** is reduced to 15.7 ppm in **14**. The ^{13}C-NMR spectrum of **14** shows two sets of signals for the aromatic rings of the diphenylphosphanyl groups and phosphorus-coupled resonances split into "a non 1:2:1 triplet". Such a triplet could be observed due to a ^{13}C nucleus and two ^{31}P nuclei forming an AXX′ spin system, as characteristic splitting clearly indicates that the two chemically equivalent phosphorus atoms are bound to palladium in a *cis* manner[12]. The differing complexation behavior of

Table 2. NMR data of the triphos framework in compounds **8**, **9** and **10**[c]

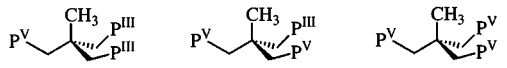

8 **9** **10**

	^{1}H NMR[a] CH_3	CH_2P^V	CH_2P^{III}	^{13}C NMR[a] CH_3	CH_2P^V	^{31}P NMR[b] CH_2P^{III}	CCH_2		
8	0.88−0.85 (m)	3.00 (d, $^2J_{P(V)}$ = 11.4)	2.62 (d, ^2J_H = 15.0), 2.42 (d, ^2J_H = 15.0)	28.08 (m)	40.90 (dt, $^1J_{P(V)}$ = 58.2, $^3J_{P(III)}$ = 8.2)	42.83 (dt, $^1J_{P(III)}$ = 9.0, $3J_{P(V)}$ = 9.0)	39.50 (dt, $^2J_{P(III)}$ = 13.8, $^2J_{P(V)}$ = 3.5)	0.20 (s)	−26.86 (s)
9	0.86 (m)	3.38 (dd, ^2J_H = 12.0, $^2JH_{P(V)}$ = 11.8), 3.19 (dd, ^2J_H = 12.0, $^2J_{HP(V)}$ = 11.8)	2.58 (d, $^2J_{P(III)}$ = 1.0)	26.76 (m)	41.00 (m)	42.77 (m)	40.10 (dt, $^2J_{P(III)}$ = 14.2, $^2J_{P(V)}$ = 3.8)	0.92 (s)	−26.97 (s)
10	0.70 (m)	3.20 (m)			40.16 (m)			1.89 (s)	

[a] Chemical shift δ(^{1}H and ^{13}C) relative to TMS; coupling constants in Hz. − [b] Chemical shift δ(^{31}P) relative to external 85% H_3PO_4. − [c] Solvent $CHCl_3$.

Scheme 4

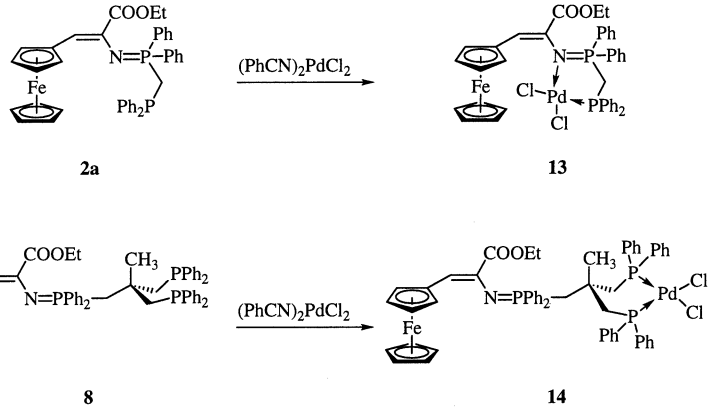

2a **13**

8 **14**

Figure 3. ORTEP plot of compound **13**[a]

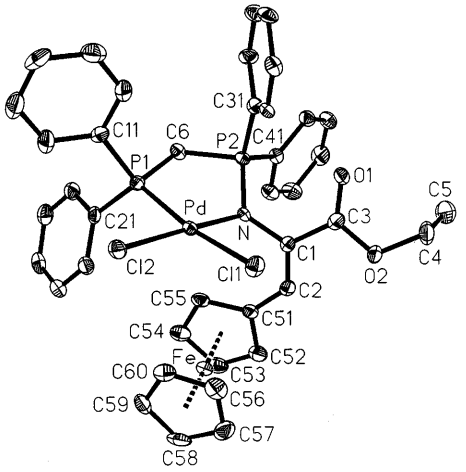

[a] 50% probability ellipsoids; selected bond lengths [Å] and angles [°]: Pd−N 2.062(3), Pd−P(1) 2.2259(11), Pd−Cl(2) 2.3133(9), Pd−Cl(1) 2.3719(11), P(2)−N 1.628(2); N−Pd−P(1) 87.35(8), P(1)−Pd−Cl(2) 88.71(4), N−Pd−Cl(1) 91.75(9), Cl(2)−Pd−Cl(1) 93.10(3), C(6)−P(1)−Pd 105.60(12), N−P(2)−C(6) 102.32(14), P(2)−N−Pd 112.5(2), P(2)−C(6)−P(1) 108.8(2).

2a and **8** may be due to their structural features, since the second diphenylphosphanyl group of **8** has stronger coordination ability toward Pd^{II} that the iminophosphorane group of **2a**.

A final word about the conformation of the ligand **8** and of its complex **14** is relevant. In triphos[13] the signal of the CH_3C protons exhibits a chemical shift of δ = 0.95, while in transition-metal complexes[14] these protons give rise to a signal in the range δ = 1.12−2.09. In the ^{13}C-NMR spectra, the signal of the CH_3C carbon atom appears at δ = 29.5 in the free ligand, while in complexes it appears at δ = 36−40. In all these cases, the triphos fragment adopts a "CH_3-*out*" conformation. The ^{1}H-NMR spectra of compounds **8** and **14** show the signal of the CH_3C protons at δ = 0.85 and δ = 0.14, respectively, while in the ^{13}C-NMR spectra the signal of this methyl carbon atom appears at δ = 28.08 and δ = 28.15, respectively. In view of the fact that in cyclic compounds with bridgehead 1,1,1-trisubstituted ethane fragments, the signal of the "CH_3C-*in*" group is shifted upfield relative to that of the "CH_3-*out*" group[15], the conformation of the triphos fragment in compounds **8** and **14** seems likely to be another than the "CH_3-*out*" one.

We gratefully acknowledge the financial support of the *Dirección General de Investigación Científica y Técnica*, project number PB95-1019.

Experimental Section

All experiments were carried out with the exclusion of air and moisture under nitrogen. Solvents were purified and dried according to standard methods. Compound **1** was prepared according to a literature procedure[9]. − NMR: Bruker AC200 or Varian Unity 300. − MS: Fisons Autospec 5000 VG. − IR: Nicolet Impact 400. − Elemental analyses: Perkin-Elmer 240c. − Melting points were determined with a Kofler hot-plate and are uncorrected.

Preparation of Monoiminophosphoranes **2** *and* **4**. − *General Procedure:* To a solution of the β-ferrocenylvinyl azide **1** (0.50 g, 1.53 mmol) in 10 ml of dry CH_2Cl_2, an equimolar amount of the appropriate diphosphane in 10 ml of dry CH_2Cl_2 was added at room temperature. The reaction mixture was stirred for 15 h. The solvent was then removed in vacuo and the remaining residue was chromatographed on a silica gel column using ethyl acetate/*n*-hexane (1:3) as eluent.

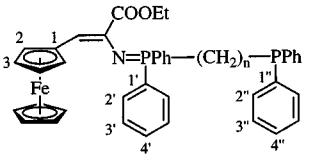

2

2a: 66%, red prisms, m.p. 143−144°C, R_f = 0.375. − IR (Nujol): ν = 1693, 1590, 1415, 1220, 1109, 806 cm^{-1}. − ^1H NMR ($CDCl_3$): δ = 7.87−7.70 (m, 4 H), 7.42−7.12 (m, 16 H), 6.37 (d, 1 H, ^4J_P = 8.2 Hz, CH=C), 4.96 (pseudo-t, 2 H, *J* = 1.8 Hz, 2-H/5-H), 4.21 (pseudo-t, 2 H, *J* = 1.8 Hz, 3-H/4-H), 4.12 (s, 5 H, Cp), 3.82 (q, 2 H, ^3J = 7.1 Hz, CH_2CH$_3$), 3.55 (dd, 2 H, *J* = 12.1, 1.0 Hz, CH_2P), 1.09 (t, 3 H, ^3J = 7.1 Hz, CH_2CH_3). − $^{13}C\{^1H\}$ NMR ($CDCl_3$): δ = 167.95 (d, ^3J = 8.0 Hz, CO), 138.33 (dd, ^1J = 15.5 Hz, ^3J = 7.5 Hz, C-1′′), 134.90 (dd, ^1J = 104.1 Hz, ^3J = 1.0 Hz, C-1′), 134.06 (d, ^2J = 7.5 Hz, CH=*C*), 132.92 (d, ^2J = 20.0 Hz, C-2′′), 131.15 (dd, ^2J = 9.0 Hz, ^4J = 1.5 Hz, C-2′), 130.42 (d, ^4J = 2.4 Hz, C-4′), 128.40 (C-4′′), 128.20 (d, ^3J = 6.4 Hz, C-3′′), 128.07 (d, ^3J = 12.0 Hz, C-3′), 115.65 (d, ^3J = 22.0 Hz, *C*H=C), 83.25 (C-1), 69.69 (C-2/C-5), 68.95 (Cp), 68.14 (C-3/C-4), 60.53 (*C*H_2CH$_3$), 31.68 (dd, $^1J_{P(V)}$ = 59.5 Hz, $^1J_{P(III)}$ = 30.5 Hz, CH_2P), 14.14 (CH_2*C*H$_3$). − $^{31}P\{^1H\}$ NMR ($CDCl_3$): δ = 3.36 (d, P^V), −29.49 (d, P^{III}), $^2J_{PP}$ = 53.8 Hz. − MS (EI, 70 eV); *m/z* (%): 681 (98) [M^+], 616 (81), 431 (35), 121 (100). − $C_{40}H_{37}FeNO_2P_2$ (681.54): calcd. C 70.49, H 5.47, N 2.06; found C 70.58, H 5.63, N 1.99.

2b: 35%, red prisms, m.p. 62−64°C, R_f = 0.393. − IR (Nujol): ν = 1695, 1590, 1416, 1210, 1109, 806 cm^{-1}. − ^1H NMR ($CDCl_3$): δ = 7.78−7.67 (m, 4 H, 2′′-H), 7.45−7.39 (m, 6 H, 4′-H, 3′-H), 7.27−7.24 (m, 10 H, 3′-H, 3′′-H, 4′′-H), 6.48 (d, 1 H, ^4J = 7.3 Hz, CH=C), 4.95 (pseudo-t, 2 H, *J* = 1.7 Hz, 2-H/5-H), 4.22 (pseudo-t, 2 H, *J* = 1.7 Hz, 3-H/4-H), 4.07 (s, 5 H, Cp), 3.90 (q, 2 H, ^3J = 7.1 Hz, CH_2CH$_3$), 2.75−2.58 (m, 2 H, CH_2-P^V), 2.27−2.12 (m, 2 H, CH_2P^{III}), 1.07 (t, 3 H, ^3J = 7.1 Hz, CH_2CH_3). − $^{13}C\{^1H\}$ NMR ($CDCl_3$): δ = 167.91 (d, ^3J = 6.9 Hz, CO), 137.62 (d, ^1J = 13.5 Hz, C-1′′), 134.05 (d, ^2J = 7.0 Hz, CH=*C*), 133.48 (d, ^1J = 98.9 Hz, C-1′), 132.59 (d, ^2J = 18.4 Hz, C-2′′), 131.17 (d, ^2J = 8.8 Hz, C-2′), 130.68 (d, ^4J = 2.7 Hz, C-4′), 128.65 (C-4′), 128.44 (d, ^3J = 6.5 Hz, C-3′′), 128.28 (d, ^3J = 10.7 Hz, C-3′), 116.24 (d, ^3J = 20.6 Hz, *C*H=C), 82.99 (C-1), 69.66 (C-2/C-5), 68.90 (Cp), 68.28 (C-3/C-4), 60.56 (*C*H_2CH$_3$), 26.88 (dd, $^1J_{P(V)}$ = 66.2 Hz, $^2J_{P(III)}$ = 16.9 Hz), 19.37 (dd, ^1J = 13.9 Hz, ^2J = 4.0 Hz), 14.13 (CH_2*C*H$_3$). − $^{31}P\{^1H\}$ NMR ($CDCl_3$): δ = 8.15 (d, P^V), −12.93 (d, P^{III}), $^3J_{PP}$ = 48.8 Hz. − MS (EI, 70 eV); *m/z* (%): 695 (100) [M^+], 183 (55), 121 (34). − $C_{41}H_{39}FeNO_2P_2$ (695.56): calcd. C 70.80, H 5.65, N 2.01; found C 70.55, H 5.80, N 2.12.

2c: 33%, red prisms, m.p. 49−51°C, R_f = 0.428. − IR (Nujol): ν = 1693, 1585, 1415, 1211, 1110, 806 cm^{-1}. − ^1H NMR ($CDCl_3$): δ = 7.82−7.70 (m, 4 H), 7.44−7.20 (m, 16 H), 6.44 (d, 1 H, ^4J = 7.5 Hz, CH=C), 4.91 (br. s, 2 H, 2-H/5-H), 4.18 (br. s, 2 H, 3-H/4-H), 4.05 (s, 5 H, Cp), 3.94 (q, 2 H, ^3J = 7.2 Hz, CH_2CH$_3$), 2.62−2.45 (m, 2 H, CH_2P^V), 2.10−1.95 (m, 2 H, CH_2P^{III}), 1.58−1.42 (m, 2 H, C$H_2CH_2P^{III}$), 1.09 (t, 3 H, ^3J = 7.2 Hz, CH_2CH_3). − $^{13}C\{^1H\}$ NMR ($CDCl_3$): δ = 168.04 (d, ^3J = 7.0 Hz, CO), 138.32 (d, ^1J = 12.5 Hz, C-1′′), 134.12 (d, ^2J = 6.4 Hz, CH=*C*), 134.13 (d, ^1J = 98.6 Hz, C-1′), 132.58 (d, ^2J = 18.5 Hz, C-2′′), 131.06 (d, ^2J = 9.0 Hz, C-2′), 130.50 (d, ^4J = 2.5 Hz, C-4′), 128.37 (C-4′), 128.28 (d, ^3J = 7.0 Hz, C-3′′), 128.18 (d, ^3J = 11.4 Hz, C-3′), 115.97 (d, ^3J = 21.0 Hz, *C*H=C), 83.07 (C-1), 69.60 (C-2/C-5), 68.88 (Cp), 68.18 (C-3/C-4), 60.50 (*C*H_2CH$_3$), 31.39 (dd, $^1J_{P(V)}$ = 65.1 Hz, $^3J_{P(III)}$ = 12.5 Hz, CH_2-P^V), 29.37 (dd, $^1J_{P(III)}$ = 26.5 Hz, $^3J_{P(V)}$ = 14.5 Hz, CH_2P^{III}), 18.52 (dd, $^2J_{P(V)}$ = 17.0 Hz, $^2J_{P(III)}$ = 2.5 Hz, *C*$H_2CH_2P^{III}$), 14.13 (CH_2*C*H$_3$). − ^{31}P NMR ($CDCl_3$): δ = 6.91 (s, P^V), −18.87 (s, P^{III}). − MS (EI, 70 eV); *m/z* (%): 709 (100) [M^+], 183 (25), 121 (31). − $C_{42}H_{41}FeNO_2P_2$ (709.59): calcd. C 71.09, H 5.82, N 1.97; found C 71.00, H 5.89, N 1.85.

2d: 44%, orange prisms, m.p. 88−90°C, R_f = 0.40. − IR (Nujol): ν = 1695, 1595, 1415, 1216, 1114, 806 cm^{-1}. − ^1H NMR ($CDCl_3$): δ = 7.80−7.65 (m, 4 H), 7.47−7.28 (m, 16 H), 6.41 (d, 1 H, ^4J = 7.2 Hz, CH=C), 4.91 (s, 2 H, 2-H/5-H), 4.20 (s, 2 H, 3-H/4-H), 4.08 (s, 5 H, Cp), 3.91 (q, 1.7 H, ^3J = 7.2 Hz, CH_2CH$_3$), 3.43 (q, 0.3 H, ^3J = 6.9 Hz, CH_2CH$_3$), 2.53 (br. s, 2 H, CH_2P^V), 2.02 (br. s, 2 H, CH_2P^{III}), 1.57 (br. s, 4 H, C$H_2CH_2CH_2P^{III}$), 1.20 (t, 0.4 H, ^3J = 6.9 Hz, CH_2CH_3), 1.07 (t, 2.6 H, ^3J = 7.2 Hz, CH_2CH_3). − $^{13}C\{^1H\}$ NMR ($CDCl_3$): δ = 168.01 (d, ^3J = 6.5 Hz, CO), 138.74 (d, ^1J = 13.5 Hz, C-1′′), 134.30 (d, ^2J = 6.9 Hz, CH=*C*), 133.96 (d, ^1J = 98.6 Hz, C-1′), 132.64 (d, ^2J = 18.5 Hz, C-2′′), 131.07 (d, ^2J = 9.0 Hz, C-2′), 130.55 (d, ^4J = 2.4 Hz, C-4′), 128.42 (C-4′), 128.32 (d, ^3J = 6.0 Hz, C-3′′), 128.21 (d, ^3J = 11.0 Hz, C-3′), 115.79 (d, ^3J = 20.5 Hz, *CH*=C), 83.14 (C-1), 69.60 (C-2/C-5), 68.90 (Cp), 68.26 (C-3/C-4), 60.50 (*C*H_2CH$_3$), 30.10 (d, $^1J_{P(V)}$ = 66.6 Hz, CH_2-P^V), 27.71 (d, $^1J_{P(III)}$ = 11.4 Hz, CH_2-P^{III}), 27.54 (dd, $^2J_{P(III)}$ = $^3J_{P(V)}$ = 14.5 Hz, *C*$H_2CH_2P^{III}$), 23.06 (dd, $^2J_{P(V)}$ = 15.5 Hz, $^3J_{P(III)}$ = 3.5 Hz, *C*$H_2CH_2P^V$), 14.13 (CH_2*C*H$_3$). − ^{31}P NMR ($CDCl_3$): δ = 7.32 (s, P^V), −16.61 (s, P^{III}). − MS (EI, 70 eV); *m/z* (%): 723 (30) [M^+], 606 (36), 241 (100), 183 (40), 121 (39). − $C_{43}H_{43}FeNO_2P_2$ (723.62): calcd. C 71.37, H 5.99, N 1.94; found C 71.51, H 6.08, N 1.85.

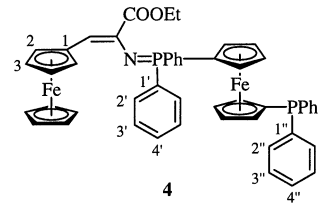

4

4: 21%, orange prisms, m.p. 78−80°C, R_f = 0.464. − IR (Nujol): ν = 1693, 1591, 1413, 1213, 1108, 807 cm^{-1}. − ^1H NMR ($CDCl_3$): δ = 7.64 (ddd, 4 H, ^3J_P = 12.0 Hz, ^3J = 8.1 Hz, ^4J = 1.5 Hz), 7.42−7.33 (m, 6 H), 7.28−7.23 (m, 10 H), 6.43 (d, 1 H, ^4J = 7.8 Hz, CH=C), 5.06 (pseudo-t, 2 H, *J* = 1.8 Hz, 2-H/5-H), 4.50

(pseudo-t, 2 H, J = 1.7 Hz, Cp′), 4.29−4.26 (m, 4 H, Cp′), 4.24 (pseudo-t, 2 H, J = 1.8 Hz, 3-H/4-H), 4.11 (s, 5 H, Cp), 3.98 (dd, 2 H, J = 3.0, 1.8 Hz, Cp′), 3.89 (q, 2 H, ^3J = 7.2 Hz, CH_2CH$_3$), 1.05 (t, 3 H, ^3J = 7.2 Hz, CH$_2$CH_3). − ^{13}C{^{1}H} NMR (CDCl$_3$): δ = 167.85 (d, ^3J = 7.9 Hz, CO), 138.65 (d, ^1J = 9.5 Hz, C-1′′), 134.37 (d, ^1J = 103.6 Hz, C-1′), 134.25 (d, ^2J = 6.5 Hz, CH=C), 133.34 (d, ^2J = 19.5 Hz, C-2′′), 131.72 (d, ^2J = 9.5 Hz, C-2′), 130.43 (d, ^4J = 3.0 Hz, C-4′), 128.45 (C-4′′), 128.08 (d, ^3J = 6.5 Hz, C-3′′), 127.73 (d, ^3J = 12.0 Hz, C-3′), 115.01 (d, ^3J = 22.0 Hz, CH=C), 83.43 (C-1), 77.14 (d, ^1J = 8.0 Hz, CP^{III}), 76.81 (d, ^1J = 115.6 Hz, CP^{V}), 74.39 (d, J = 12.0 Hz), 73.91 (d, ^2J = 14.5 Hz), 73.31 (d, ^3J = 3.6 Hz), 72.92 (dd, J = 10.5 Hz, J = 2.0 Hz), 69.61 (C-2/C-5), 68.96 (Cp), 68.10 (C-3/C-4), 60.46 (CH$_2$CH$_3$), 14.18 (CH$_2$$CH_3$). − ^{31}P NMR (CDCl$_3$): δ = 4.40 (s, P^V), −19.04 (s, P^{III}). − MS (EI, 70 eV); *m/z* (%): 851 (100) [M$^+$], 602 (59), 305 (54), 121 (28). − $C_{49}H_{43}Fe_2NO_2P_2$ (851.48): calcd. C 69.12, H 5.09, N 1.64; found C 69.25, H 5.23, N 1.53.

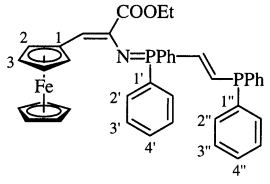

3

Reaction of β-Ferrocenylvinyl Azide **1** *with (E)-1,2-Bis(diphenylphosphanyl)ethene:* To a cooled (−15°C) solution of compound **1** (0.50 g, 1.53 mmol) in 10 ml of dry diethyl ether, a solution of (*E*)-1,2-bis(diphenylphosphanyl)ethene (0.61 g, 1.53 mmol) in 10 ml of dry CH_2Cl_2 was added dropwise under nitrogen, and the reaction mixture was stirred for 15 h at this temperature. The solvent was then removed in vacuo and the residue was chromatographed on a silica gel column using ethyl acetate/*n*-hexane (1:5) as eluent to give **3**: 46%, red prisms, m.p. 55−57°C, R_f = 0.41. − IR (Nujol): ν = 1695, 1588, 1430, 1105, 805 cm^{-1}. − ^{1}H NMR (CDCl$_3$): δ = 7.73 (ddd, 4 H, ^3J_P = 11.7 Hz, ^3J = 8.1 Hz, J = 2.1 Hz), 7.51−7.30 (m, 16 H), 7.10 (ddd, 1 H, J_P = 22.8 Hz, J_P = 21.3 Hz, ^3J = 18.6 Hz, =CH−P), 6.81 (ddd, 1 H, J_P = 21.6 Hz, J_P = 11.1 Hz, =CH−P), 6.49 (d, 1 H, ^4J_P = 7.5 Hz, CH=C−N), 4.90 (pseudo-t, 2 H, J = 1.8 Hz, 2-H/5-H), 4.17 (pseudo-t, 2 H, J = 1.8 Hz, 3-H/4-H), 4.06 (s, 5 H, Cp), 3.87 (q, 2 H, ^3J = 6.9 Hz, CH_2CH$_3$), 1.02 (t, 3 H, ^3J = 6.9 Hz, CH$_2$CH_3). − ^{13}C NMR{^{1}H} (CDCl$_3$): δ = 167.69 (d, ^3J = 7.5 Hz, CO), 148.41 (d, $^1J_{P(III)}$ = 23.4 Hz, =CHP^{III}), 135.53 (d, $^1J_{P(III)}$ = 10.0 Hz, C-1′′), 134.73 (dd, $^1J_{P(V)}$ = 87.0 Hz, $^2J_{P(III)}$ = 10.5 Hz, =CHP^V), 133.70 (d, ^2J = 19.5 Hz, C-2′′), 133.37 (d, $^1J_{P(V)}$ = 106.2 Hz, C-1′), 131.52 (d, $^2J_{P(V)}$ = 9.2, C-2′), 130.79 (d, $^4J_{P(V)}$ = 3.0 Hz, C-4′), 129.27 (C-4′′), 128.68 (d, $^3J_{P(III)}$ = 7.5 Hz, C-3′′), 128.23 (d, $^3J_{P(V)}$ = 12.0 Hz, C-3′), 116.60 (d, $^3J_{P(V)}$ = 21.5 Hz, CH=C−N), 82.93 (C-1), 69.72 (C-2/C-5), 68.94 (C$_p$), 68.34 (C-3/C-4), 60.57 (CH$_2$CH$_3$), 14.17 (CH$_2$$CH_3$), CH=$C$N signal overlapped. − ^{31}P NMR{^{1}H} (CDCl$_3$): δ = 1.04 (d, P^V), −7.27 (d, P^{III}), $^3J_{PP}$ = 20.0 Hz. − MS (EI, 70 eV); *m/z* (%): 693 (100) [M$^+$], 224 (35). − $C_{41}H_{37}FeNO_2P_2$ (693.55): calcd. C 71.00, H 5.38, N 2.02; found C 70.87, H 5.55, N 2.11.

Preparation of Bis(iminophosphoranes) **5** *and* **6**. − *General Procedure:* To a cooled (−15°C) solution of compound **1** (0.50 g, 1.53 mmol) in 10 ml of dry diethyl ether, a solution of the appropriate diphosphane (0.75 mmol) in 10 ml of dry diethyl ether was added under nitrogen, and the reaction mixture was stirred for 15 h at this temperature. The separated solid was collected by filtration, air-dried, and chromatographed on a silica gel column using ethyl acetate/*n*-hexane (1:3) as eluent.

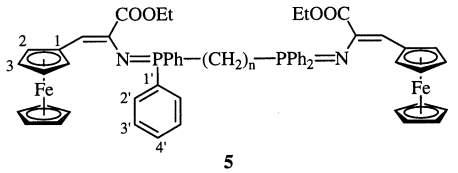

5

5a: 45%, red prisms, m.p. 180−182°C, R_f = 0.178. − IR (Nujol): ν = 1690, 1597, 1413, 1213, 1110, 807 cm^{-1}. − ^{1}H NMR (CDCl$_3$): δ = 7.70 (br. s, 8 H), 7.40−7.15 (m, 12 H), 6.39 (d, 0.6 H, ^4J_P = 7.5 Hz, CH=C), 6.14 (d, 1.4 H, ^4J_P = 7.7 Hz, CH=C), 4.92 (br. s, 4 H, 2-H/5-H), 4.54 (t, 2 H, ^2J = 13.9 Hz, CH$_2$P), 4.29 (br. s, 4 H, 3-H/4-H), 4.08 (s, 10 H, Cp), 3.84−3.42 (m, 4 H, CH_2CH$_3$), 1.20 (t, 2 H, ^3J = 7.0 Hz, CH$_2$CH_3), 1.05 (t, 4 H, ^3J = 6.9 Hz, CH$_2$CH_3). − ^{13}C{^{1}H} NMR (CDCl$_3$): δ = 167.32 (t, ^3J + ^5J = 8.4 Hz, CO), 135.18 (d, ^1J = 110.6 Hz, C-1′), 133.12 (d, ^2J = 7.5 Hz, CH=C), 131.22 (t, ^2J + ^4J = 9.8 Hz, C-2′), 130.02 (s, C-4′), 127.95 (t, ^3J + ^5J = 12.3 Hz, C-3′), 116.30 (m, CH=C), 83.12 (C-1), 69.63 (C-2/C-5), 68.83 (Cp), 68.17 (C-3/C-4), 60.22 (CH$_2$CH$_3$), 60.54 (CH$_2$CH$_3$), 31.43 (quint, ^1J + ^1J = 108.0 Hz, CH$_2$P), 15.26 (CH$_2$$CH_3$), 14.06 (CH$_2$$CH_3$). − ^{31}P NMR (CDCl$_3$): δ = −2.64 (s, P^V). − MS (FAB); *m/z* (%): 979 (100) [M$^+$ + 1], 978 (46) [M$^+$], 224 (21). − $C_{55}H_{52}Fe_2N_2O_4P_2$ (978.68): calcd. C 67.50, H 5.36, N 2.86; found C 67.44, H 5.50, N 2.70.

5b: 75%, red prisms, m.p. 228−231°C, R_f = 0.205. − IR (Nujol): ν = 1685, 1595, 1411, 1211, 1105, 805 cm^{-1}. − ^{1}H NMR (CDCl$_3$): δ = 7.71 (br. s, 4 H, 2′-H), 7.38 (br. s, 6 H, 3′-H/4′-H), 6.46 (br. s, 1 H, CH=C), 4.93 (s, 2 H, 2-H/5-H), 4.23 (s, 2 H, 3-H/4-H), 4.01 (s, 5 H, Cp), 3.78 (q, 1.6 H, ^3J = 6.9 Hz, CH_2CH$_3$), 3.47 (q, 0.4 H, ^3J = 6.9 Hz, CH_2CH$_3$), 2.76 (s, 2 H, CH$_2$P), 1.20 (t, 0.6 H, ^3J = 6.9 Hz, CH$_2$CH_3), 0.99 (t, 2.4 H, ^3J = 6.9 Hz, CH$_2$CH_3). − ^{13}C{^{1}H} NMR (CDCl$_3$): δ = 167.66 (t, ^3J + ^6J = 6.3 Hz, CO), 134.01 (t, ^2J + ^5J = 7.1 Hz, CH=C), 133.24 (quint, C-1′), 131.12 (t, ^2J + ^5J = 9.0 Hz, C-2′), 130.67 (s, C-4′), 128.26 (t, ^3J + ^6J = 11.5 Hz, C-3′), 116.24 (t, ^3J + ^6J = 20.5 Hz, CH=C), 82.96 (C-1), 69.65 (C-2/C-5), 68.91 (Cp), 68.29 (C-3/C-4), 65.80 (CH$_2$CH$_3$), 60.44 (CH$_2$CH$_3$), 23.13 (quint, ^1J + ^2J = 130.2 Hz, CH$_2$P), 15.24 (CH$_2$$CH_3$), 14.04 (CH$_2$$CH_3$). − ^{31}P NMR (CDCl$_3$): δ = 8.60 (s, P^V). − MS (FAB); *m/z* (%): 993 (71) [M$^+$ + 1], 992 (30) [M$^+$], 510 (100), 307 (59). − $C_{56}H_{54}Fe_2N_2O_4P_2$ (992.71): calcd. C 67.76, H 5.48, N 2.82; found C 67.60, H 5.45, N 2.57.

5c: 89%, red prisms, m.p. 62−65°C, R_f = 0.100. − IR (Nujol): ν = 1697, 1593, 1417, 1216, 1105, 805 cm^{-1}. − ^{1}H NMR (CDCl$_3$): δ = 7.64 (ddd, 8 H, ^3J_P = 11.1 Hz, ^3J = 6.9 Hz, ^4J = 1.2 Hz, 2′-H), 7.42−7.24 (m, 12 H, 3′-H/4′-H), 6.46 (d, 2 H, ^4J_P = 7.5 Hz, CH=C), 4.90 (pseudo-t, 4 H, J = 1.8 Hz, 2-H/5-H), 4.19 (pseudo-t, 4 H, J = 1.8 Hz, 3-H/4-H), 4.04 (s, 10 H, Cp), 3.93 (q, 3.2 H, ^3J = 7.2 Hz, CH_2CH$_3$), 3.46 (q, 0.8 H, ^3J = 6.9 Hz, CH_2CH$_3$), 2.73 (dd, 4 H, ^2J_P = 18.0 Hz, ^4J_P = 10.2 Hz, CH$_2$P), 1.73 (m, 2 H, CH$_2$CH$_2$P), 1.20 (t, 1.2 H, ^3J = 6.9 Hz, CH$_2$CH_3), 1.05 (t, 4.8 H, ^3J = 7.2 Hz, CH$_2$CH_3). − ^{13}C{^{1}H} NMR (CDCl$_3$): δ = 168.06 (d, ^3J = 6.8 Hz, CO), 134.06 (d, ^2J = 6.8 Hz, CH=C), 133.98 (d, ^1J = 101.1 Hz, C-1′), 130.97 (d, ^2J = 9.0 Hz, C-2′), 130.40 (d, ^4J = 2.4 Hz, C-4′), 128.23 (d, ^3J = 11.5 Hz, C-3′), 116.10 (d, ^3J = 21.0 Hz, CH=C), 83.10 (C-1), 69.67 (C-2/C-5), 68.90 (Cp), 68.20 (C-3/C-4), 65.82 (CH$_2$CH$_3$), 60.53 (CH$_2$CH$_3$), 30.27 (dd, ^1J = 64.0 Hz, ^3J = 10.9 Hz, CH$_2$P), 15.22 (m, CH$_2$CH$_2$P), 14.04 (CH$_2$$CH_3$). − ^{31}P NMR (CDCl$_3$): δ = 6.73 (s, P^V) − MS (FAB); *m/z* (%): 1006 (100) [M$^+$], 725 (38), 334 (25), 223 (64). − $C_{57}H_{56}Fe_2N_2O_4P_2$

(1006.73): calcd. C 68.01, H 5.61, N 2.78; found C 68.13, H 5.70, N 2.55.

5d: 79%, orange prisms, m.p. 160−163°C, R_f = 0.071. − IR (Nujol): ν = 1693, 1595, 1417, 1216, 1107, 808 cm^{-1}. − ^1H NMR ($CDCl_3$): δ = 7.80−7.65 (m, 4 H, 2′-H), 7.45−7.38 (m, 6 H, 3′-H + 4′-H), 6.42 (d, 1 H, ^4J_P = 7.2 Hz, CH=C), 4.91 (br. s, 2 H, 2-H/5-H), 4.20 (br. s, 2 H, 3-H/4-H), 4.08 (s, 5 H, Cp), 3.90 (q, 1.8 H, ^3J = 7.1 Hz, CH_2CH_3), 3.46 (q, 0.2 H, ^3J = 7.0 Hz, CH_2CH_3), 2.53 (br. s, 2 H, CH_2P), 1.57 (br. s, 2 H, CH_2CH_2P), 1.20 (t, 0.3 H, ^3J = 7.0 Hz, CH_2CH_3), 1.05 (t, 2.7 H, ^3J = 7.1 Hz, CH_2CH_3). − $^{13}C\{^1H\}$ NMR ($CDCl_3$): δ = 168.00 (d, ^3J = 7.1 Hz, CO), 134.26 (d, ^2J = 7.1 Hz, CH=*C*), 133.92 (d, ^1J = 99.5 Hz, C-1′), 131.05 (d, ^2J = 9.0 Hz, C-2′), 130.54 (d, ^4J = 2.5 Hz, C-4′), 128.31 (d, ^3J = 11.6 Hz, C-3′), 115.80 (d, ^3J = 20.8 Hz, *C*H=C), 83.11 (C-1), 69.58 (C-2/C-5), 68.89 (Cp), 68.17 (C-3/C-4), 65.80 (CH_2CH_3), 60.49 (CH_2CH_3), 30.07 (d, ^1J = 66.4 Hz, CH_2P), 23.05 (dd, ^2J = 16.0 Hz, ^3J = 3.1 Hz, CH_2CH_2P), 14.13 (CH_2CH_3). − ^{31}P NMR ($CDCl_3$): δ = 7.36 (s, P^V). − MS (FAB); *m/z* (%): 1021 (100) [M^+ + 1], 723 (15), 307 (18), 224 (30). − $C_{58}H_{58}Fe_2N_2O_4P_2$ (1020.76): calcd. C 68.25, H 5.73, N 2.74; found C 68.40, H 5.65, N 2.56.

6: 54%, orange prisms, m.p. 103−105°C, R_f = 0.054. − IR (Nujol): ν = 1700, 1590, 1410, 1213, 1105, 807 cm^{-1}. − ^1H NMR ($CDCl_3$): δ = 7.70−7.50 (m, 4 H, 2′-H), 7.40−7.24 (m, 6 H, 3′-H + 4′-H), 6.43 (d, 1 H, ^4J = 7.7 Hz, CH=C), 5.04 (s, 2 H, 2-H/5-H), 4.59 (s, 2 H, 3-H/4-H), 4.23 (s, 4 H, Cp′), 4.11 (s, 5 H, Cp), 3.85 (q, 1.2 H, ^3J = 7.0 Hz, CH_2CH_3), 3.46 (q, 0.8 H, ^3J = 7.0 Hz, CH_2CH_3), 1.20 (t, 1.2 H, ^3J = 7.0 Hz, CH_2CH_3), 1.01 (t, 1.8 H, ^3J = 7.0 Hz, CH_2CH_3). − $^{13}C\{^1H\}$ NMR ($CDCl_3$): δ = 167.77 (d, ^3J = 7.8 Hz, CO), 134.41 (d, ^1J = 104.0, C-1′), 134.14 (d, ^2J = 6.7 Hz, CH=*C*), 131.64 (d, ^2J = 9.6 Hz, C-2′), 130.45 (d, ^4J = 2.5 Hz, C-4′), 127.74 (d, ^3J = 12.0 Hz, C-3′), 115.04 (d, ^3J = 22.3 Hz, *C*H=C), 83.32 (C-1), 69.56 (C-2/C-5), 68.96 (Cp), 68.10 (C-3/C-4), 77.18 (d, ^1J = 115.9 Hz, CP^V), 74.57 (d, ^3J = 12.4 Hz), 73.75 (d, ^3J = 10.2 Hz), 65.79 (CH_2CH_3), 60.44 (CH_2CH_3), 15.25 (CH_2CH_3), 14.14 (CH_2CH_3). − ^{31}P NMR ($CDCl_3$): δ = 5.34 (s). − MS (FAB); *m/z* (%): 1149 (89) [M^+ + 1], 602 (100), 305 (58). − $C_{64}H_{58}Fe_3N_2O_4P_2$ (1148.67): calcd. C 66.92, H 5.09, N 2.44; found C 66.85, H 5.21, N 2.30.

(E)-1,2-Bis[(α-ethoxycarbonyl-β-ferrocenyl)vinylimino-diphenylphosphoranyl]ethene (**7**): To a cooled (−15°C) solution of compound **1** (0.50 g, 1.53 mmol) in 10 ml of dry diethyl ether, a solution of (*E*)-1,2-bis(diphenylphosphanyl)ethene (0.30 g, 0.77 mmol) in 10 ml of dry CH_2Cl_2 was added dropwise under nitrogen, and the mixture was stirred for 15 h at this temperature. The solvent was then removed in vacuo and the remaining solid was chromatographed on a silica gel column using ethyl acetate/*n*-hexane (2:7) as eluent to give **7**: 9%, red prisms, m.p. 175−178°C, R_f = 0.27. − IR (Nujol): ν = 1682, 1594, 1409, 1209, 1110, 1041 cm^{-1}. − ^1H NMR ($CDCl_3$): δ = 7.82−7.70 (m, 4 H), 7.54−7.30 (m, 7 H, aryl H + =CHP), 6.53 (quint, 1 H, *J* = 3.6 Hz, CH=CN), 4.92 (br. s, 2 H, 2-H/5-H), 4.21 (br. s, 2 H, 3-H/4-H), 4.08 (s, 5 H, Cp), 3.88 (q, 2 H, ^3J = 6.9 Hz, CH_2CH_3), 1.03 (t, 3 H, ^3J = 6.9 Hz, CH_2CH_3). − $^{13}C\{^1H\}$ NMR ($CDCl_3$): δ = 167.54 (t, ^3J_P + ^6J_P = 7.5 Hz, CO), 141.16 (quint, ^1J_P + ^2J_P = 131.1 Hz, $=CHP^V$), 132.64 (quint, ^1J_P + ^4J_P = 106.2 Hz, C-1′), 131.58 (t, ^2J_P + ^5J_P = 9.5 Hz, C-2′), 131.00 (br. s, C-4′), 128.30 (t, ^3J_P + ^6J_P = 12.0 Hz, C-3′), 116.93 (t, ^3J_P + ^6J_P = 21.6 Hz, *C*H=*C*), 82.62 (C-1), 69.70 (C-2/C-5), 68.91 (Cp), 68.37 (C-3/C-4), 60.60 (CH_2CH_3), 14.09 (CH_2CH_3), CH=*C*N signal overlapped. − ^{31}P NMR ($CDCl_3$): δ = 0.63 (s). − MS (FAB); *m/z* (%): 990 (40) [M^+], 693 (55). − $C_{56}H_{52}Fe_2N_2O_4P_2$ (990.69): calcd. C 67.89, H 5.29, N 2.83; found C 68.00, H 5.15, N 2.90.

Reaction of β-Ferrocenylvinyl Azide **1** *with Tris(diphenylphosphanylmethyl)ethane (triphos).* − *Procedure A:* To a solution of compound **1** (0.50 g, 1.53 mmol) in 10 ml of dry CH_2Cl_2, a solution of triphos (0.96 g, 1.53 mmol) in 10 ml of the same solvent was added dropwise under nitrogen. The reaction mixture was stirred at room temperature for 15 h. The solvent was then removed in vacuo and the residue was chromatographed on a silica gel column using ethyl acetate/*n*-hexane (1:3) as eluent.

8: 21%, red prisms, m.p. 79−82°C, R_f = 0.50. − IR (Nujol): ν = 1690, 1589, 1435, 1410, 1213, 1106, 816 cm^{-1}. − ^1H NMR ($CDCl_3$): δ = 7.68−7.61 (m, 4 H), 7.37−7.17 (m, 26 H), 6.48 (d, 1 H, ^4J_P = 8.7 Hz, CH=C), 5.00 (pseudo-t, 2 H, *J* = 1.6 Hz, 2-H/5-H), 4.25 (pseudo-t, 2 H, *J* = 1.6 Hz, 3-H/4-H), 4.10 (s, 5 H, Cp), 3.80 (q, 2 H, ^3J = 7.1 Hz, CH_2CH_3), 3.00 (d, 2 H, $^2J_{P(V)}$ = 11.4 Hz, CH_2P^V), 2.62 (d, 2 H, $^2J_{P(III)}$ = 15.0 Hz, CH_2P^{III}), 2.42 (d, 2 H, $^2J_{P(III)}$ = 15.0 Hz, CH_2P^{III}), 0.98 (t, 3 H, ^3J = 7.1 Hz, CH_2CH_3), 0.88−0.85 (m, 3 H, CH_3C). − $^{13}C\{^1H\}$ NMR ($CDCl_3$): δ = 167.92 (d, ^3J = 8.4 Hz, CO), 139.83 (quint, ^1J_P + ^5J_P = 29.5 Hz, C-1′′), 137.14 (d, ^1J = 103.3 Hz, C-1′), 134.28 (d, ^2J = 6.8 Hz, CH=*C*), 133.08 (d, ^2J = 20.5 Hz, C-2′′)*, 132.95 (d, ^2J = 20.4 Hz, C-2′′)*, 130.40 (d, ^2J = 8.6 Hz, C-2′), 129.90 (d, ^4J = 2.6 Hz, C-4′), 128.33 (C-4′′)**, 128.31 (C-4′′)**, 128.20 (d, ^3J = 7.0 Hz, 2 × C-3′′), 128.11 (d, ^3J = 11.5 Hz, C-3′), 115.83 (d, ^3J = 21.3 Hz, *CH*=C), 83.21 (C-1), 69.79 (C-2/C-5), 68.95 (Cp), 68.21 (C-3/C-4), 60.61 (CH_2CH_3), 42.83 (dt, $^1J_{P(III)}$ = 9.0 Hz, $^3J_{P(V)}$ = 9.0 Hz, 2 × CH_2P^{III}), 40.90 (dt, $^1J_{P(V)}$ = 58.2 Hz, $^3J_{P(III)}$ = 8.2 Hz, CH_2P^V), 39.50 (dt, $^2J_{P(III)}$ = 13.8 Hz, $^2J_{P(V)}$ = 3.5 Hz, CCH_3), 28.08 (m, CCH_3), 14.12 (CH_2CH_3). − ^{31}P NMR ($CDCl_3$): δ = 0.20 (s, P^V), −26.86 (s, P^{III}). − MS (FAB); *m/z* (%): 921 (100) [M^+], 547 (13). − $C_{56}H_{54}FeNO_2P_3$ (921.83): calcd. C 72.97, H 5.90, N 1.52; found C 73.10, H 5.78, N 1.65.

9: 7%, red prisms, m.p. 101−103°C, R_f = 0.44. − IR (Nujol): ν = 1687, 1587, 1410, 1209, 1105, 806 cm^{-1}. − ^1H NMR ($CDCl_3$): δ = 7.78−7.65 (m, 8 H), 7.35−7.10 (m, 22 H), 6.58 (d, 2 H, ^4J_P = 8.6 Hz, CH=C), 5.03 (br. s, 2 H, 2-H/5-H), 4.98 (br. s, 2 H, 2-H/5-H), 4.27 (br. s, 2 H, 3-H/4-H), 4.22 (br. s, 2 H, 3-H/4-H), 4.11 (s, 10 H, C_p), 3.96−3.86 (m, 4 H, 2 × CH_2CH_3), 3.38 (dd, ^2J_H = 12.0 Hz, $^2J_{P(V)}$ = 11.8 Hz, CH_2P^V), 3.19 (dd, ^2J_H = 12.0 Hz, $^2J_{P(V)}$ = 11.8 Hz, CH_2P^V), 2.58 (d, $^2J_{P(III)}$ = 1.0 Hz, CH_2P^{III}), 1.05 (t, 6 H, ^3J = 7.0 Hz, 2 × CH_2CH_3), 0.86 (m, 3 H, CH_3C). − $^{13}C\{^1H\}$ NMR ($CDCl_3$): δ = 167.95 (d, ^3J = 8.3 Hz, CO), 139.83 (d, $^1J_{P(III)}$ = 11.4 Hz, C-1′′), 137.12 (d, ^1J = 102.0 Hz, C-1′)*, 136.71 (d, ^1J = 103.8 Hz, C-1′)*, 134.25 (d, ^2J = 6.8 Hz, CH=*C*), 132.95 (d, ^2J = 19.9 Hz, C-2′′), 130.54 (d, ^2J = 8.9 Hz, C-2′)**, 130.42 (d, ^2J = 8.8 Hz, C-2′)**, 129.87 (d, ^4J = 2.3 Hz, 2 × C-4′), 128.38 (C-4′′), 128.31 (d, ^3J = 7.0 Hz, C-3′′), 116.43 (d, ^3J = 21.4 Hz, *C*H=C), 83.21 (C-1), 69.93 (C-2/C-5), 68.95 (Cp), 68.26 (C-3/C-4), 60.70 (CH_2CH_3), 42.77 (m, CH_2P^{III}), 41.00 (m, CH_2P^V), 40.10 (dt, $^2J_{P(III)}$ = 14.2 Hz, $^2J_{P(V)}$ = 3.8 Hz, C−CH_3), 26.76 (m, C−CH_3), 14.21 (CH_2CH_3), 2 × C-3′ signal overlapped. − ^{31}P NMR ($CDCl_3$): δ = 0.92 (s, P^V), −26.97 (s, P^{III}). − MS (FAB); *m/z* (%): 1218 (100) [M^+], 722 (56), 423 (21). − $C_{71}H_{69}Fe_2N_2O_4P_3$ (1218.97): calcd. C 69.96, H 5.71, N 2.30; found C 70.15, H 5.90, N 2.10.

Procedure B: To a cooled (−15°C) solution of compound **1** (0.50 g, 1.53 mmol) in 10 ml of dry diethyl ether, was added a solution of triphos (0.32 g, 0.51 mmol) in 10 ml of the same solvent. The reaction mixture was stirred at this temperature for 15 h. The precipitated solid was collected by filtration and chromatographed on a silica gel column using ethyl acetate/*n*-hexane (1:3) as eluent to give **10** (77%), red prisms, m.p. 107−109°C, R_f = 0.375. − IR (Nujol): ν = 1690, 1590, 1415, 1205, 1105, 806 cm^{-1}. − ^1H NMR ($CDCl_3$): δ = 8.00−7.48 (m, 12 H), 7.38−7.00 (m, 18 H), 6.70 (d,

2 H, ^4J_P = 8.4 Hz, 2 × CH=C), 6.57 (d, 1 H, ^4J_P = 8.4 Hz, CH=C), 5.56 (br. s, 6 H, 2-H/5-H), 4.48 (br. s, 6 H, 3-H/4-H), 4.15 (s, 15 H, Cp), 4.04−3.96 (m, 6 H, 3 × CH_2CH$_3$), 3.30−3.10 (m, 6 H, 3 × CHP^V), 1.12 (t, 9 H, ^3J = 7.2 Hz, 3 × CH$_2$CH_3), 0.70 (m, 3 H, CH$_3$C). − ^{13}C{^{1}H} NMR (CDCl$_3$): δ = 167.96 (d, ^3J = 7.9 Hz, CO), 134.57 (d, ^2J = 6.4 Hz, CH=*C*), 129.42 (C-4′), 128.09 (d, ^3J = 11.5 Hz, C-3′), 116.54 (d, ^3J = 21.5 Hz, *C*H=C), 83.18 (C-1), 70.01 (C-2/C-5), 68.99 (Cp), 68.22 (C-3/C-4), 60.72 (*C*H$_2$CH$_3$), 40.16 (m, CH$_2$P^V), 14.13 (CH$_2$*C*H$_3$), some signals are overlapped or absent. − ^{31}P NMR (CDCl$_3$): δ = 1.89 (s, P^V). − MS (FAB); *m/z* (%): 1517 (100) [M$^+$ + 1]. − C$_{86}$H$_{84}$Fe$_3$N$_3$O$_6$P$_3$ (1516.01): calcd. C 68.13, H 5.58, N 2.77; found C 68.25, H 5.49, N 2.65.

Reaction of β-Ferrocenylvinyl Azide **1** *with Tris[2-(diphenylphosphanyl)ethyl]phosphane (tetraphos). − Procedure A:* To a solution of compound **1** (0.25 g, 0.77 mmol) in 10 ml of dry CH$_2$Cl$_2$, a solution of tetraphos (0.5 g, 0.77 mmol) in 10 ml of the same solvent was added dropwise under nitrogen, and the reaction mixture was stirred at room temperature for 20 h. The solution was then concentrated to dryness and the residue was chromatographed on a silica gel column using ethyl acetate/*n*-hexane (2:7) as eluent to give **11** (31%), orange prisms, m.p. 120−122°C, R_f = 0.48. − IR (Nujol): ν = 1685, 1597, 1410, 1206, 1108, 1040, 810 cm^{-1}. − ^{1}H NMR (CDCl$_3$): δ = 7.42−7.20 (m, 30 H), 6.37 (d, 1 H, ^4J_P = 7.2 Hz, CH=C), 4.80 (pseudo-t, 2 H, *J* = 1.8 Hz, 2-H/5-H), 4.20 (pseudo-t, 2 H, *J* = 1.8 Hz, 3-H/4-H), 4.04 (q, 2 H, ^3J = 6.8 Hz, CH_2CH$_3$), 3.94 (s, 5 H, Cp), 2.10−1.93 (m, 12 H, P^{III}CH$_2$CH$_2$P^V), 1.25 (t, 3 H, ^3J = 6.8 Hz, CH$_2$CH_3). − ^{13}C{^{1}H} NMR (CDCl$_3$): δ = 168.33 (d, ^3J = 7.5 Hz, CO), 137.62 (d, $^1J_{P(III)}$ = 13.0 Hz, C-1′), 134.10 (d, $^2J_{P(V)}$ = 6.7 Hz, CH=*C*), 132.70 (d, $^2J_{P(III)}$ = 18.5 Hz, C-2′), 128.87 (C-4′), 128.55 (d, $^3J_{P(III)}$ = 7.0 Hz, C-3′), 115.58 (d, ^3J = 19.5 Hz, *C*H=C), 83.04 (C-1), 69.49 (C-2/C-5), 68.82 (Cp), 68.21 (C-3/C-4), 60.82 (*C*H$_2$CH$_3$), 24.28 (dd, $^1J_{P(V)}$ = 61.5 Hz, $^2J_{P(III)}$ = 16.5 Hz, 3 × CH$_2$P^V), 20.49 (dd, $^1J_{P(III)}$ = 14.4 Hz, $^2J_{P(V)}$ = 4.0 Hz, 3 × CH$_2$P^{III}), 14.44 (CH$_2$*C*H$_3$). − ^{31}P{^{1}H} NMR (CDCl$_3$): δ = 20.91 (q, P^V), −12.96 (d, P^{III}), $^3J_{PP}$ = 43.8 Hz. − MS (FAB); *m/z* (%): 968 (30) [M$^+$ + 1], 457 (22). − C$_{57}$H$_{57}$FeNO$_2$P$_4$ (967.84): calcd. C 74.28, H 6.06, N 1.22; found C 74.40, H 5.90, N 1.40.

Procedure B: To a cooled (−15°C) solution of compound **1** (0.50 g, 1.53 mmol) in 10 ml of dry diethyl ether, a solution of tetraphos (0.25 g, 0.38 mmol) in 10 ml of the same solvent was added dropwise under nitrogen. The resulting mixture was stirred for 15 h at this temperature. The precipitated solid was collected by filtration and chromatographed on a silica gel column using ethyl acetate/*n*-hexane (1:3) as eluent to give **12** (28%), orange prisms, m.p. 103−106°C, R_f = 0.125. − IR (Nujol): ν = 1682, 1599, 1410, 1210, 1112, 1039, 817 cm^{-1}. − ^{1}H NMR (CDCl$_3$): δ = 7.85−7.75 (m, 12 H), 7.52−7.20 (m, 18 H), 6.45 (br. s, 3 H, 3 × CH=C), 6.30 (br. s, 1 H, CH=C), 4.86 (br. s, 6 H, 3 × 2-H/5-H), 4.71 (br. s, 2 H, 2-H/5-H), 4.15 (br. s, 8 H, 3-H/4-H), 4.04 (s, 20 H, Cp), 3.74 (br. s, 8 H, CH_2CH$_3$), 2.66 (br. s, 6 H, CH$_2$P), 2.14−1.85 (m, 6 H, CH$_2$P^V), 0.97 (br. s, 12 H, CH$_2$CH_3). − ^{13}C{^{1}H} NMR (CDCl$_3$): δ = 168.06 (d, ^3J = 6.4 Hz, CO), 167.99 (d, ^3J = 7.0 Hz, 2 × CO), 167.67 (d, ^3J = 7.1 Hz, 1′′-CCC*CO*), 133.92 (d, ^2J = 6.8 Hz, *C*=CH), 133.61 (d, ^2J = 8.7 Hz, 1′′-CH=*C*), 132.91 (d, ^1J = 103.5 Hz, C-1′), 131.39 (d, ^2J = 9.2 Hz, C-2′), 130.73 (C-4′), 128.25 (d, ^3J = 11.6 Hz, C-3′), 117.09 (d, ^3J = 21.0 Hz, CH=*C*), 116.58 (d, ^3J = 20.5 Hz, 2 × *C*H=C), 115.21 (d, ^3J = 19.1 Hz, 1′′-*C*H=C), 83.02 (C-1), 82.85 (2 × C-1), 82.67 (C-1), 69.65 (C-2/C-5), 69.38 (C-2′′/C-5′′), 68.93 (Cp), 68.78 (Cp′′), 68.40 (C-3′′/C-4′′), 68.31 (C-3/C-4), 60.65 (*C*′H$_2$CH$_3$), 60.56 (*C*H$_2$CH$_3$), 23.92 (dm, $^1J_{P(V)}$ = 67.9 Hz, 3 × CH$_2$P^V), 20.74 (dm, $^1J_{P(V)}$ = 63.4 Hz, 3 × CH$_2$P^V). − ^{31}P{^{1}H} NMR (CDCl$_3$): δ = 21.61 (q, P^V), 7.30 (d, P^V), 6.62 (d, 2 × P^V), $^3J_{PP}$ = 50.5 Hz. − MS (FAB); *m/z* (%): 1854 (35), 510 (100). − C$_{102}$H$_{102}$Fe$_4$N$_4$O$_8$P$_4$ (1859.14): calcd. C 65.89, H 5.53, N 3.01; found C 66.05, H 5.39, N 3.13.

Synthesis Complexes **13** *and* **14**. − *General Procedure:* To a cooled (−15°C) solution of monoiminophosphorane **2a** or **8** (0.367 mmol) in 15 ml of dry toluene, a solution of dichlorobis(benzonitrile)palladium(II) (0.14 g, 0.367 mmol) in 10 ml of the same solvent was added dropwise. The resulting mixture was stirred at this temperature for 10 h. The precipitated solid was collected by filtration and recrystallized from chloroform.

13: 94%, red prisms, m.p. 170−172°C. − IR (Nujol): ν = 1688, 1613, 1412, 1259, 1149, 1034 cm^{-1}. − ^{1}H NMR (CD$_2$Cl$_2$): δ = 8.50−8.10 (m, 4 H), 7.75−6.88 (m, 16 H), 6.15 (d, 1 H, ^4J_P = 8.2 Hz, CH=C), 5.09 (br. s, 2 H, 2-H/5-H), 4.39 (s, 5 H, Cp), 4.18 (br. s, 2 H, 3-H/4-H), 3.82 (q, 2 H, ^3J = 7.1 Hz, CH_2CH$_3$), 3.55 (br. s, 2 H, CH$_2$P), 0.96 (t, 3 H, ^3J = 7.1 Hz, CH$_2$CH_3). − ^{31}P{^{1}H} NMR (CD$_2$Cl$_2$): δ = 44.23 (d), 14.16 (d), $^2J_{PP}$ = 29.6 Hz. − MS (FAB); *m/z* (%): 822 (37) [M$^+$ − Cl], 787 (100) [M$^+$ − 2 Cl], 681 (72), 666 (93). − C$_{40}$H$_{37}$Cl$_2$FeNO$_2$P$_2$Pd (859.15): calcd. C 55.94, H 4.34, N 1.63; found C 56.10, H 4.17, N 1.49.

14: 58%, orange prisms, m.p. 247−250°C. − IR (Nujol): ν = 1683, 1590, 1415 cm^{-1}. − ^{1}H NMR (CDCl$_3$): δ = 8.09−8.02 (m, 4 H), 7.77−7.67 (m, 4 H), 7.48−7.31 (m, 22 H), 6.47 (d, 1 H, ^4J_P = 8.7 Hz, CH=C), 5.06 (pseudo-t, 2 H, *J* = 1.6 Hz, 2-H/5-H), 4.96 (pseudo-t, 2 H, *J* = 1.6 Hz, 3-H/4-H), 4.16 (s, 5 H, Cp), 3.70 (q, 2 H, ^3J = 7.0 Hz, CH_2CH$_3$), 2.92 (d, 2 H, $^2J_{P(V)}$ = 10.7 Hz, CH$_2$P^V), 2.49 (d, 4 H, ^2J_P = 8.1 Hz, 2 × CH$_2$PPd), 2.42 (d, 2 H, $^2J_{P(III)}$ = 14.0 Hz, CH$_2$P^{III}), 0.91 (t, 3 H, ^3J = 7.0 Hz, CH$_2$CH_3), 0.14 (s, 3 H, CH$_3$C). − ^{13}C{^{1}H} NMR (CDCl$_3$): δ = 168.17 (d, ^3J = 8.3 Hz, CO), 137.14 (d, ^1J = 103.3 Hz, C-1′), 135.67 (t, ^2J + ^4J = 11.5 Hz, C-2′′)*, 132.97 (d, ^2J = 7.5 Hz, CH=C), 132.38 (t, ^2J + 4*J* = 10.3 Hz, C-2′′)*, 130.22 (d, ^2J = 9.1 Hz, C-2′), 130.50 (d, *J* = 2.4 Hz, C-4′), 131.88 (C-4′′), 128.75 (t, ^2J + ^5J = 11.1 Hz, C-3′′), 128.39 (t, ^3J = 11.7 Hz, C-3′), 128.16 (t, ^2J + ^5J = 10.6 Hz, C-3′′), 118.51 (d, ^3J = 21.4 Hz, *C*H=C), 82.33 (C-1), 69.92 (C-2/C-5), 68.99 (Cp), 68.21 (C-3/C-4), 60.81 (*C*H$_2$CH$_3$), 45.79 (dt, $^1J_{P(V)}$ = 57.6 Hz, ^3J + ^5J = 9.5 Hz, CH$_2$P^V), 37.24 (dt, ^1J + ^3J = 18.5 Hz, $^3J_{P(V)}$ = 9.0 Hz, 2 × CH$_2$P), 39.20 (d, $^2J_{P(V)}$ = 3.6 Hz, *C*−CH$_3$), 28.15 (m, C−*C*H$_3$), 13.72 (CH$_2$*C*H$_3$). − ^{31}P NMR (CDCl$_3$): δ = 0.10 (s, P^V), 15.60 (s, PPd). − MS (FAB); *m/z* (%): 1099 (11) [M$^+$], 1063 (43) [M$^+$ − Cl], 1027 (37), 906 (46). − C$_{56}$H$_{54}$Cl$_2$FeNO$_2$P$_3$Pd (1099.43): calcd. C 61.19, H 4.95, N 1.27; found C 61.31, H 5.07, N 1.04.

X-ray Crystallographic Studies: Crystal data are given in Table 3. Crystals of **5d** suitable for X-ray diffraction were prepared by slow difussion of *n*-hexane in a dichloromethane solution. Slow concentration of a solution of compound **13** in chlroform affords crystals suitable for X-ray diffraction studies. Crystals of **13** · 2 CHCl$_3$ and **5d** were mounted in inert oil on a glass fibre and transferred to the diffractometer (Siemens P4 with LT2 low-temperature attachment). Measurements were made at −100°C using monochromated Mo-K_α radiation (λ = 0.71073 Å). Unit-cell parameters were determined from a least-squares analysis of ca. 70 accurately centered reflections (10° < 2θ < 27°). Intensities were measured using ω scans. Absorption corrections were based on ψ scans. The structures were solved by direct methods (**13** · 2 CHCl$_3$) or by the heavy-atom method (**5d**) and refined anisotropically on F^2 (program SHELXL-93).[16] Hydrogen atoms were included using a riding model or as rigid methyl groups. Crystallographic data (excluding structure factors) for the structures reported in this paper have been deposited with the Cambridge Crystallographic Data Centre as supplementary publication no. CCDC-101187. Copies of the

Table 3. Crystal data for compounds **5d** and **13** · 2 $CHCl_3$

	5d	**13** · 2 $CHCl_3$
empirical formula	$C_{58}H_{58}Fe_2N_2O_4P_2$	$C_{42}H_{39}Cl_8FeNO_2P_2Pd$
M_r	1020.70	1097.53
a [Å]	10.401(1)	12.480(1)
b [Å]	11.327(2)	25.091(3)
c [Å]	11.199(2)	14.288(2)
α [°]	87.024(10)	90
β [°]	76.015(10)	93.776(10)
γ [°]	75.246(10)	90
Z	1	4
D [Mg/m^3]	1.369	1.633
crystal system	triclinic	monoclinic
space group	$P\bar{1}$	$P2_1/n$
crystal size [mm]	0.66 × 0.18 × 0.10	0.60 × 0.20 × 0.06
θ range [°]	3.12−25.00	3.22−25.00
reflections measured	5022	8805
independent reflections	4333	4453
μ [mm^{-1}]	0.701	1.316
max./min. transmission	0.746/0.793	0.792/0.699
parameters	308	514
F(000)	534	2208
max. Δρ [e Å^{-3}]	0.395	0.276
$R1$[a]	0.0338	0.0248
$wR2$[b]	0.0868	0.0462

[a] $R1 = \Sigma||F_o| - |F_c||/\Sigma|F_o|$ for reflections with $I > 2\sigma(I)$. − [b] $wR2 = [\Sigma[w(F_o^2 - F_c^2)^2]/\Sigma[w(F_o^2)^2]]^{0.5}$ for all reflections; $w^{-1} = \sigma^2(F^2) + (aP)^2 + bP$, where $P = (2F_c^2 + F_o^2)/3$ and a and b are constants set by the program.

data can be obtained free of charge on application to CCDC, 12 Union Road, Cambridge CB2 1EZ, U.K. [Fax: (internat.) + 44(0)1223 336033; E-mail: deposit@ccdc.cam.ac.uk].

[1] For selected recent references, see: K.-S. Gan, T. S. A. Hor, *Ferrocenes* (Eds.: A. Togni, T. Hayashi), VCH, Weinheim, **1995**, p 1.

[2] [2a] A. Yamaraki, T. Morimoto, K. Achiwa, *Tetrahedron: Asymmetry* **1993**, *4*, 2287−2290. − [2b] A. Mernyi, C. Kratky, W. Weissenteiner, M. Widhalm, *J. Organomet. Chem.* **1996**, *508*, 209−218.

[3] See for example: [3a] S. Hoppe, H. Weichmann, K. Jurkschat, C. Schneider-Koglin, M. Dräger, *J. Organomet. Chem.* **1995**, *505*, 63−72.

[3b] N. J. Goodwin, W. Henderson, J. K. Sarfo, *J. Chem. Soc., Chem. Commun.* **1996**, 1551−1552. − [3c] P. Barbaro, A. Togni, *Organometallics* **1995**, *14*, 3570−3573.

[4] [4a] H. C. L. Abbenhuis, U. Burckhardt, V. Gramlich, C. Köllner, P. S. Pregosin, R. Salzmann, A. Togni, *Organometallics* **1995**, *14*, 759−766. − [4b] M. Sawamura, H. Hamashima, M. Sugawara, R. Kuwano, Y. Ito, *Organometallics* **1995**, *14*, 4549−4558. − [4c] M. Sawamura, R. Kuwano, Y. Ito, *J. Am. Chem. Soc.* **1995**, *117*, 9602−9603. − [4d] N. C. Zanetti, F. Spindler, J. Spencer, A. Togni, G. Rihs, *Organometallics* **1996**, *15*, 860−866.

[5] [5a] T. B. Rauchfuss, J. L. Clements, S. F. Agnew, D. M. Roundhill, *Inorg. Chem.* **1977**, *16*, 775−778. − [5b] D. M. Roundhill, R. A. Bechtold, S. G. N. Roundhill, *Inorg. Chem.* **1980**, *19*, 284−289. − [5c] G. J. Organ, M. K. Cooper, K. Henrick, M. McPartlin, *J. Chem. Soc., Dalton Trans.* **1984**, 2377−2382. − [5d] M. C. Bonnet, B. Stitou, I. Tkatchenko, *J. Organomet. Chem.* **1985**, *279*, C1−C4. − [5e] H. Brunner, A. F. M. M. Rahman, *Chem. Ber.* **1984**, *117*, 710−724. − [5f] A. Breque, C. C. Santini, F. Mathey, J. Fischer, A. Mitschler, *Inorg. Chem.* **1984**, *23*, 3463−3467.

[6] [6a] J. P. Farr, M. M. Olmstead, F. E. Wood, A. L. Balch, *J. Am. Chem. Soc.* **1983**, *105*, 792−798. − [6b] J. P. Farr, M. M. Olmstead, A. L. Balch, *Inorg. Chem.* **1983**, *22*, 1229−1235. − [6c] A. L. Balch, *Homogeneous Catalysis with Metal Phosphine Complexes* (Ed: L. H. Pignolet), Plenum, New York, **1983**. − [6e] R. J. McNair, L. H. Pignolet, *Inorg. Chem.* **1986**, *25*, 4717−4723. − [6f] R. J. McNair, P. V. Nilsson, L. H. Pignolet, *Inorg. Chem.* **1985**, *24*, 1935−1939. − [7] [7a] W. J. Knebel, R. J. Angelici, *Inorg. Chem.* **1974**, *13*, 627−631 and 632−637. − [7b] W. J. Knebel, R. J. Angelici, O. A. Gansow, D. J. Darensbourg, *J. Organomet. Chem.* **1974**, *66*, C11−C13. − [7c] T. B. Rauchfuss, D. M. Roundhill, *J. Am. Chem. Soc.* **1974**, *96*, 3098−3105. − [7d] E. Drent, P. Arnoldy, P. H. M. Budzelaar, *J. Organomet. Chem.* **1993**, *455*, 247−253. − [7e] G. P. C. M. Dekker, A. Buijs, C. J. Elsevier, K. Vrieze, P. W. N. M. van Leeuwen, W. J. J. Smeets, A. L. Spek, Y. F. Wang, C. H. Stam, *Organometallics* **1992**, *11*, 1937−1948.

[8] [8a] T. D. Appleton, W. R. Cullen, S. V. Evans, T.-J. Kim, J. Trotter, *J. Organomet. Chem.* **1985**, *279*, 5−21. − [8b] S. Park, D. Hedden, A. L. Rheingold, D. M. Roundhill, *Organometallics* **1986**, *5*, 1305−1311. − [8c] H.-H. Wang, A. L. Casalnuovo, B. J. Johnson, A. M. Mueting, L. H. Pignolet, *Inorg. Chem.* **1988**, *27*, 325−331. − [8d] M. P. Anderson, A. L. Casalnuovo, B. J. Johnson, B. M. Mattson, A. M. Mueting, L. H. Pignolet, *Inorg. Chem.* **1988**, *27*, 1649−1658. − [8e] K. V. Katti, R. G. Cavell, *Organometallics* **1989**, *8*, 2147−2153. − [8f] K. V. Katti, R. J. Batchelor, F. W. B. Einstein, R. G. Cavell, *Inorg. Chem.* **1990**, *29*, 808−814. − [8g] E. Shirakawa, Y. Murota, Y. Nakao, T. Hiyama, *Synlett* **1997**, 1143−1144. − [8h] H. Brunner, I. Deml, W. Dirnberger, B. Nuber, W. Reißer, *Eur. J. Inorg. Chem.* **1998**, 43−54. − [8i] E. K. van den Beuken, W. J. J. Smeets, A. L. Spek, B. L. Feringa, *J. Chem. Soc., Chem. Commun.* **1998**, 223−224.

[9] [9a] P. Molina, A. Pastor, M. J. Vilaplana, M. C. Ramírez de Arellano, *Tetrahedron Lett.* **1996**, 7829−7832. − [9b] P. Molina, A. Pastor, M. J. Vilaplana, M. D. Velasco, M. C. Ramírez de Arellano, *Organometallics* **1997**, *16*, 5836−5843.

[10] [10a] H. Staudinger, J. Meyer, *Helv. Chim. Acta* **1919**, *2*, 635−646. − [10b] Y. G. Gololobov, I. N. Zhmurova, L. F. Kasukhin, *Tetrahedron* **1981**, *37*, 437−472.

[11] [11a] J. Kiji, A. Matsumura, T. Haishi, S. Okazaki, J. Fukukawa, *Bull. Chem. Soc. Jpn.* **1977**, *50*, 2731−2733. − [11b] K. W. Katti, R. G. Cavell, *Inorg. Chem.* **1989**, *28*, 3033−3036. − [11c] M. V. Avis, M. E. van der Boom, C. J. Elsevier, W. J. J. Smeets, A. L. Spek, *J. Organomet. Chem.* **1997**, *527*, 263−276.

[12] [12a] M. Sawamura, H. Hamashima, M. Sugawara, R. Kuwano, Y. Ito, *Organometallics* **1995**, *14*, 4549−4558. − [12b] D. A. Redfield, L. W. Cary, J. H. Nelson, *Inorg. Chem.* **1975**, *14*, 50−59. − [12c] A. W. Verstuyft, J. H. Nelson, L. W. Cary, *Inorg. Chem.* **1976**, *15*, 732−734.

[13] T. Seitz, A. Muth, G. Huttner, *Chem. Ber.* **1994**, *127*, 1837−1842.

[14] [14a] C. A. Ghilardi, P. Innocenti, S. Midollini, A. Orlandini, A. Vacca, *J. Chem. Soc., Dalton Trans.* **1995**, 1109−1113. − [14b] C. Bianchini, A. Marchi, L. Marvelli, M. Peruzzini, A. Romerosa, R. Rossi, A. Vacca, *Organometallics* **1995**, *14*, 3203−3215.

[15] M. Alajarín, P. Molina, A. López-Lázaro, C. Foces-Foces, *Angew. Chem.* **1997**, *109*, 147−150; *Angew. Chem. Int. Ed. Engl.* **1997**, *36*, 67−70.

[16] G. M. Sheldrick, *SHELXL-93*, University of Göttingen, **1993**.

[98075]

Stabilization of the New Antimonide $Zr_2V_6Sb_9$ by V–V and Sb–Sb Bonding

Holger Kleinke

Fb Chemie der Philipps-Universität Marburg,
Hans-Meerwein-Straße, D-35032 Marburg, Germany
Fax: (internat.) + 49(0)6421/28-8917
E-mail: kleinke@mailer.uni-marburg.de

Received April 8, 1998

Keywords: Cluster / Metal-rich antimonides / Magnetism / Sb–Sb bonds / Structure and bonding

The metal-rich antimonide $Zr_2V_6Sb_9$ has been prepared by arc-melting of stoichiometric mixtures of Zr, V, and VSb_2. $Zr_2V_6Sb_9$ is the first example of a ternary ordered (filled) variant of the unusual $V_{15}Sb_{18}$ structure type. In addition to strong metal–antimony bonding, the crystal structure is significantly stabilized by bonding V–V and Sb–Sb interactions, whereas the Zr atoms do not form short metal–metal bonds. Band structure calculations using the Extended Hückel approximation reveal $Zr_2V_6Sb_9$ being metallic, in agreement with the Pauli paramagnetism experimentally observed.

Introduction

Several different binary pnictides and chalcogenides of the valence-electron-poor ("early") transition elements with a metal/pnicogen ratio of ca. 1 or higher have been uncovered in the past[1]. Only very few antimonides and bismuthides form structures with short contacts between the pnicogen atoms Q, which are not found among the phosphides and arsenides or the chalcogenides. The fact that short Q−Q distances occur only in case of metal-rich antimonides and bismuthides can be explained with the relatively high electronegativities of phosphorus and arsenic, compared to the early transition-metal atoms. Similarly, the absence of chalcogen−chalcogen bonds in metal-rich chalcogenides can be deduced from the large differences in the electronegativities of the chalcogen atoms sulfur, selenium and tellurium on one hand and of the valence-electron-poor transition metals on the other hand. Especially the occurrence of Q−Q bonds in metal-rich antimonides appears to be somewhat special, because bismuth is classified as a metal, whereas antimony is rather a metalloid or nonmetal. From this point of view, the antimonides are the only metal-rich pnictides whose structures consist in part of nonmetal−nonmetal bonds and thus not completely reduced Q(−III) species.

The only known Bi-rich binary bismuthides of the early transition metals containing Bi−Bi bonds are $Ti_{8-x}Bi_9$ and Hf_8Bi_9[2] which crystallize in the $V_{15}Sb_{18}$ structure type[3]. As for the antimonides, ZrSb[4] and V_3Sb_2[5] both occur in structures consisting in part of hexagonal antimony layers with Sb−Sb distances between 320 pm and 325 pm. These distances are too short for van-der-Waals interactions, as a comparison with the bonding Sb−Sb contacts in the elemental form of antimony (3 × 290.8 pm and 3 × 335.5 pm) reveals[6]. It is worthwhile to note that both vanadium antimonides mentioned, i. e. $V_{15}Sb_{18}$ and V_3Sb_2, are low-temperature phases, and that no Sb−Sb contacts occur in the structure of the high-temperature form $V_{1+x}Sb$ (NiAs structure type)[7]. That leaves ZrSb and the isostructural HfSb[8] as the only binary metal-rich antimonides with Sb−Sb bonds being stable in an inert atmosphere above 1000°C with respect to disproportionation. This paper presents the synthesis, structure and properties of the new antimonide $Zr_2V_6Sb_9$. Furthermore, attempts to replace zirconium by titanium, hafnium and vanadium are discussed.

Experimental Details

The antimonides discussed below were prepared in a two-step synthesis. To avoid substantial loss of antimony during the process of arc-melting, VSb_2 was synthesized first in a fused silica tube at 650°C, starting from the elements in the stoichiometric 1:2 ratio (V: ABCR, powder, −45 micron, 99.7%, first cleaned in a 10% HCl solution, then washed with distilled water and acetone, finally dried under dynamic vacuum at approximately 500 K; Sb: MERCK, powdered, >99%). Second, stoichiometric mixtures of Zr, Ti, or Hf [Ti: VENTRON, powder, −325 mesh, 99%; Zr: ALFA, powder, 4−20 mesh, 99.6%; Hf: STREM, powder, 99.6% (including up to 2.2% Zr)], and V and VSb_2 were pressed into pellets using a force of 20 kN. The pellets were arc-melted twice after inversion under a dynamic flow of Argon (3 l/min) on a water-cooled copper hearth. The reactions of the starting compositions "$M_2V_6Sb_9$" (with M = Ti, Zr, Hf) led to homogenous products, according to the powder diagrams obtained with Cu-$K_{\alpha1}$ radiation (λ = 154.05 pm, using silicon as internal standard). The lattice dimensions as obtained from the powder diagrams are listed in Table 1. In addition to the fact that here the $V_{15}Sb_{18}$ structure type was found after the rapid cooling in the arc melter, the significant increase of the lattice dimensions in comparison to $V_{15}Sb_{18}$ prove the incorporation of the larger atoms of the titanium group.

Attempts to determine the phase range of $Zr_{2-x}V_{6+x}Sb_9$ did not result in homogenous samples when $x \neq 0$. The

 © WILEY-VCH Verlag GmbH, D-69451 Weinheim, 1998 1434−1948/98/0909−1369 $ 17.50+.50/0

Table 1. Comparison of lattice dimensions

Starting composition	Empirical formula[a]	Side products[b]	*a*/pm	*c*/pm	$V/10^6$pm^3
1V, 1Sb (ref.[3])[a]	$V_{7.46(3)}Sb_9$	?	958.66(5)	704.74(5)	647.68
1.2V, 1Sb[a]	$V_{7.49(1)}Sb_9$	V_3Sb_2	959.2(1)	705.46(7)	649.1
2Ti, 6V, 9Sb[b]			966.3(3)	709.9(3)	662.9
0.3 Zr, 7.7V, 9Sb[b]		$V_{1+x}Sb$	969.0(2)	713.2(3)	669.7
1Zr, 7V, 9Sb[b]		$V_{1+x}Sb$	973.6(4)	715.9(4)	678.6
1Zr, 7V, 9Sb[a]	$Zr_{1.61(6)}V_{6.41}Sb_9$[c]		973.2(1)	716.66(8)	678.8
2Zr, 6V, 9Sb[b]			973.4(6)	716.8(4)	679.2
2Zr, 6V, 9Sb[a]	$Zr_{1.80(4)}V_{6.20}Sb_9$[c]		973.7(2)	716.5(2)	679.3
3Zr, 5V, 9Sb[b]		ZrSb	977.7(1)	717.9(1)	686.2
3Zr, 5V, 9Sb[a]	$Zr_2V_6Sb_9$		978.3(1)	719.5(1)	688.6
2Hf, 6V, 9Sb[b]			975.7(2)	721.7(3)	687.1

[a] Single crystal data. – [b] Powder data. – [c] Obtained with the postulation of mixed Zr/V but full occupation of the "Zr1" and "Zr2" sites.

Zr-poor samples contained $V_{1+x}Sb$, and the Zr-rich phases ZrSb. EDX investigations of selected crystals showed only a minor phase range of $Zr_{2-x}V_{6+x}Sb_9$, i. e. the Zr content varied from 7 to 15 atom-%. These variations may in part be due to different orientations of the crystals to the incident beam. Indexing of the powder diagrams, however, led to different lattice dimensions of the $Zr_{2-x}V_{6+x}Sb_9$ phases, which increase with increasing x (see Table 1). This is a consequence of the larger atomic radius of zirconium, compared to vanadium. However, based on the fact that the V(1) site is not completely occupied in the structure of $V_{15}Sb_{18}$, it may be possible that comparable voids occur in the structures of the $Zr_{2-x}V_{6+x}Sb_9$ phases.

In order to determine the site preferences of the Zr atoms, plate-like single crystals were selected for structure investigations of the phases of the starting compositions "$Zr_1V_7Sb_9$", "$Zr_2V_6Sb_9$" and "$Zr_3V_5Sb_9$". In all three cases, the unit-cell dimensions obtained from the single-crystal diffractometer were in good agreement with those calculated from the powder diagrams of the corresponding bulk samples. In all cases, numerical absorption corrections were performed.

As a starting model, the atomic positions of the binary antimonide $V_{15}Sb_{18}$ were used. The V(1) and V(2) positions were tentatively assigned to Zr sites, because of the higher Sb coordination numbers [eight for V(1) and V(2), and six for V(3) and V(4)]. The refinements of the three different data sets (using SHELXL93[9]) converged smoothly to reasonable residual factors, i. e. conventional R values of $R(F) = 0.0316$ for "$Zr_1V_7Sb_9$", $R(F) = 0.0216$ for "$Zr_2V_6Sb_9$" and $R(F) = 0.0342$ for "$Zr_3V_5Sb_9$". Since the thermal displacement parameters of the Zr positions of the first two data sets were significantly higher than those of the V sites, and at least some mixed occupancies were expected because of the differences in the lattice dimensions, the occupancy factors of all metal sites were refined in order to check for deviations from the ideal stoichiometries. Only the occupancy factors of the Zr sites of the first two data sets differed more than 2% from 100%. Since these sites are completely filled in case of "$Zr_3V_5Sb_9$", corresponding to the formula $Zr_2V_6Sb_9$, they were refined as being statistically mixed occupied by Zr and V to 100% in cases of "$Zr_1V_7Sb_9$" and "$Zr_2V_6Sb_9$". This model led in both cases to more uniform displacement parameters and lower residual factors [R(F) = 0.0295 for "$Zr_1V_7Sb_9$" and $R(F) = 0.0210$ for "$Zr_2V_6Sb_9$"]. The formulas were finally refined to $Zr_{1.61(6)}V_{6.39}Sb_9$, $Zr_{1.80(4)}V_{6.20}Sb_9$, and $Zr_2V_6Sb_9$, respectively. More details about the structure determinations are given in Table 2[10], and atomic parameters are listed in Table 3. It should be noted, however, that two other models, based on the occurrence of voids, would also be in agreement with these experimental data. First, the assumption of no incorporation of V on the Zr sites would result in the formulas $Zr_{1.85(2)}V_6Sb_9$ and $Zr_{1.93(2)}V_6Sb_9$, and second, one might also assume voids, V and Zr atoms on the two Zr sites.

Results and Discussion

$Zr_2V_6Sb_9$ is the first ternary ordered substitution variant of the $V_{15}Sb_{18}$ structure type. For easier comparisons, the setting and the atomic labeling of $V_{15}Sb_{18}$ are used throughout this article, but, of course, V(1) and V(2) of $V_{15}Sb_{18}$ are replaced by Zr(1) and Zr(2). The structure of $Zr_2V_6Sb_9$ is shown in a projection along the crystallographic c axis in Figure 1.

The $Zr_2V_6Sb_9$ structure contains chains of face-sharing square Zr-centered Sb_8 antiprisms, which are surrounded by V layers, where the V atoms are situated in severely distorted Sb_6 octahedra. The Zr(1) and Zr(2) atoms, alternating in each chain along [001], have different distances to the eight surrounding Sb atoms, i. e. 4 × 305.1(2) pm and 4 × 309.2(2) pm for Zr(1), and 4 × 293.2(2) pm and 4 × 293.4(1) pm for Zr(2). The latter distances correspond to those found in the ternary ZrNiSb [TiNiSi-type, five Zr–Sb bonds per Zr atom between 291.44(7) pm and 296.65(6) pm][11]. The differences in the averaged bond lengths occur

Table 2. Crystallographic data for $Zr_{2-x}V_{6+x}Sb_9$

Empirical formula	$Zr_{1.61(6)}V_{6.39}Sb_9$[a]	$Zr_{1.80(4)}V_{6.20}Sb_9$[a]	$Zr_2V_6Sb_9$
Molar mass	1568.12 g/mol	1575.77 g/mol	1583.83
Temp. of data collection	295 K		
Crystal size/mm	0.14 × 0.04 × 0.003	0.08 × 0.02 × 0.007	0.12 × 0.10 × 0.07
Space group	*P4/nmm* (No. 129)		
a/pm	973.2(1)	973.7(2)	978.3(1)
c/pm	716.66(8)	716.5(2)	719.5(1)
V/(10^6 pm^3)	678.8(1)	679.3(2)	688.6(1)
Radiation	Mo-$K\alpha_1$, λ = 71.609 pm		
No. of formula units; *F*(000)	2; 1341	2; 1347	2; 1354
Calculated density	7.67 g/cm^3	7.70 g/cm^3	7.64 g/cm^3
Absorption coefficient	228.7 cm^{-1}	228.7 cm^{-1}	225.8 cm^{-1}
Range of 2θ		3°−60°	
No. of independent reflections	609 (R_{int} = 0.081)	593 (R_{int} = 0.045)	616 (R_{int} = 0.103)
No. of observed reflections [$I > 2\sigma(I)$]	457	453	434
No. of parameters	34	34	32
$R(F)$, $R_w(F^2)$, GOF	0.030, 0.059, 1.05	0.021, 0.036, 1.07	0.034, 0.064, 1.02
Extinction coefficient	0.0007(2)	0.0007(1)	0.0011(2)
Max., min. peak in final diff. map	3.05 e$^-$/(10^6 pm^3), −1.99 e$^-$/(10^6 pm^3)	1.43 e$^-$/(10^6 pm^3), −1.41 e$^-$/(10^6 pm^3)	2.20 e$^-$/(10^6 pm^3), −1.81 e$^-$/(10^6 pm^3)

[a] See Table 1.

Table 3. Positional parameters and equivalent displacement factors for $Zr_2V_6Sb_9$

Atom	site	*x*	*y*	*z*	U_{eq}/(10^4 pm^2)
Zr(1)	2c	1/4	1/4	0.9164(3)	0.0102(5)
Zr(2)	2c	1/4	1/4	0.4132(3)	0.0069(4)
V(3)	4d	0	0	0	0.0077(5)
V(4)	8i	3/4	0.3910(2)	0.1621(3)	0.0070(4)
Sb(1)	2c	3/4	1/4	1/2	0.0127(4)
Sb(2)	8j	0.92206(5)	0.92206(5)	0.3488(1)	0.0102(2)
Sb(3)	8i	3/4	0.99776(8)	0.81671(9)	0.0082(2)

Figure 1. Projection of the structure of $Zr_2V_6Sb_9$ along [001]; large, white circles: Zr; small, black: V; medium, gray: Sb; metal−Sb bonds omitted for clarity

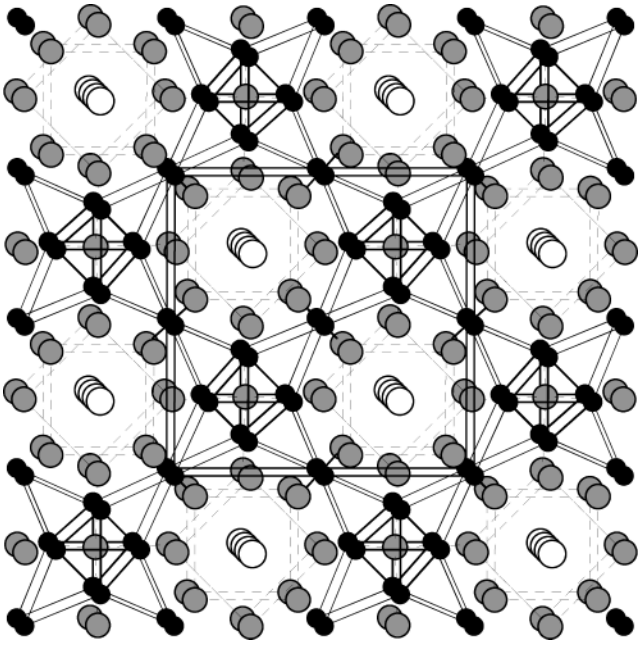

to a comparable extent in the structures of $V_{15}Sb_{18}$ and $Ti_{8-x}Bi_9$ (17.2 pm in both structures), also. The V(1) position, being the one which is occupied only to 50% in the structure of $V_{15}Sb_{18}$, shows very high displacement parameters. Similarly, the displacement parameters of that position in $Zr_2V_6Sb_9$ and $Ti_{8-x}Bi_9$ are approximately between 50% and 100% higher than those of the other metal sites, but the position is filled completely in both cases. The high displacement parameters can be understood as a consequence of the large metal−pnicogen distances, pointing to a "rattling" in a large Sb_8 (or Bi_8) cage, which might result in an unusually low thermal conductivity, as observed for the antimonides LnM_4Sb_{12} (M = Fe, Co, ...)[12].

Each V atom in $Zr_2V_6Sb_9$ is situated in a distorted Sb_6 octahedron with V−Sb distances between 271.3(2) pm and 283.1(1) pm. The averaged distances are slightly enlarged compared to the distances in $V_{15}Sb_{18}$ [between 272.3(4) pm and 279.2(2) pm]. The shorter V−Sb distances, compared to the Zr−Sb distances, most likely inhibit a significant incorporation of the larger Zr atoms on the V positions. The V layers (Figure 2) contain V(4) tetrahedra, which are interconnected via common V(3) atoms capping four edges of each V(4) tetrahedron.

The description based on V tetrahedra should not imply the existence of localized bonds within the tetrahedral units. In contrast, the V−V bonds between the tetrahedra and the bridging V(3) atoms are shorter than the edges capped by the V(3) atoms [291.2(1) pm vs. 304.2(3) pm]. The shortest V−V bond [275.9(4) pm] is situated at the edge of the tetrahedron capped by an Sb(1) atom. The lengths of these bonds are just between the two shortest distances observed in the body-centered cubic (*bcc*) element V (262 pm and 303 pm)[13].

The Sb_4 units of the $ZrSb_8$ square antiprisms are exactly planar squares with Sb−Sb distances of 336.65(9) pm in the $Sb(2)_4$ square and 342.76(8) pm in the $Sb(3)_4$ plane. These

Figure 2. Projection of the V layer along the slightly tilted *c* axis

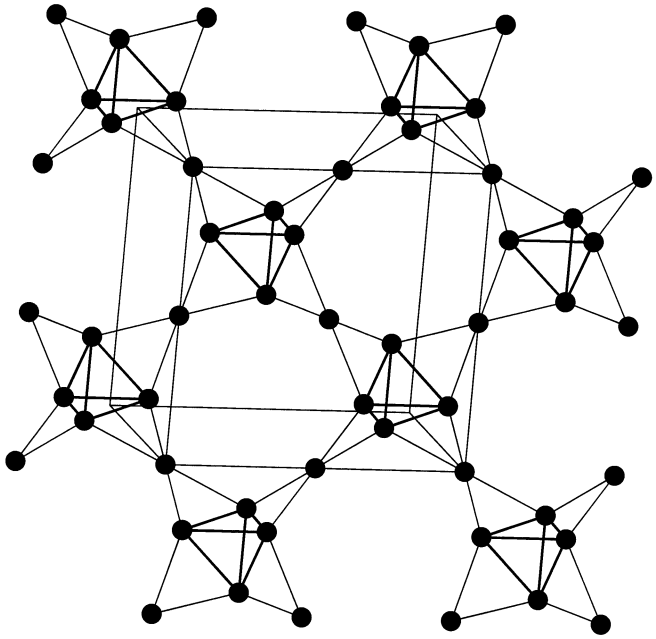

Figure 3. Projection of the puckered Sb(1),Sb(3) layer along the slightly tilted *c* axis

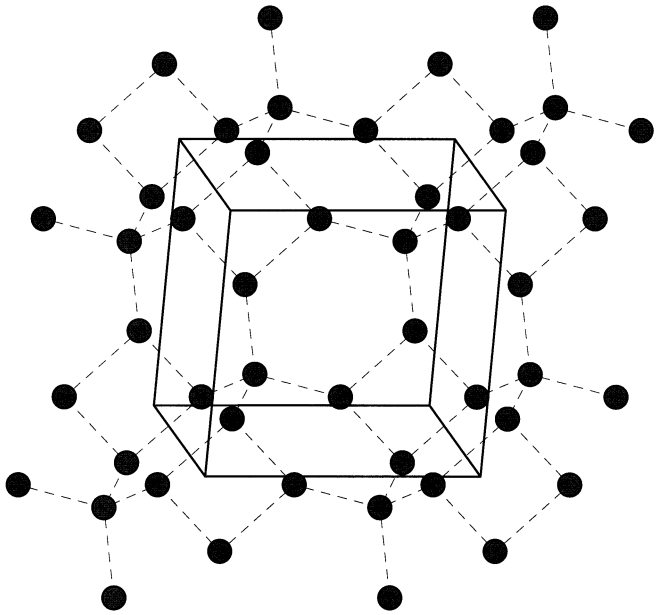

distances, being significantly larger than in the structure of $V_{15}Sb_{18}$ [319.0(1) pm and 322.9(1) pm], may be compared to the second shortest Sb−Sb bonds in elemental antimony of 335.5 pm. The latter, connecting the layers in the element, have to have bonding character because elemental antimony does not exhibit two-dimensional physical properties. The similar lengths in case of the structure of $Zr_2V_6Sb_9$ might occur with similar bond strengths, however, the shorter contacts of ca. 320 pm in $V_{15}Sb_{18}$ correspond most likely to stronger, but still somewhat weak, Sb−Sb bonds. Three causes complement each other: first, the larger size of Zr, compared to V, results in enlarged lattice parameters and therefore in longer Sb−Sb separations; second, the higher amount of valence electrons of the Zr phase (4.22 vs. 4.17 per Sb atom) and third the lower electronegativity of Zr, compared to V, both lead to higher negatively charged Sb atoms in case of $Zr_2V_6Sb_9$. As a consequence, more antibonding Sb−Sb states are filled in case of $Zr_2V_6Sb_9$, compared to $V_{15}Sb_{18}$, leading to weaker net bonding.

Additional Sb−Sb interactions between the Sb(1) and Sb(3) atoms of comparable length [335.89(7) pm] connect the $Sb(3)_4$ planes to infinite puckered layers consisting of planar Sb_4 and Sb_6 rings, as emphasized with dashed lines in Figure 3. The latter rings were also observed in the structure of the low-temperature phase V_3Sb_2 with shorter Sb−Sb distances of 320 pm.

On the other hand, the Sb(2) squares are interconnected via the shortest Sb−Sb contacts in this structure [306.3(2) pm] to puckered layers, which contain puckered eight-membered Sb(2) rings in addition to the $Sb(2)_4$ squares. The short Sb−Sb bonds are shown as bold lines in Figure 4, whereas the longer distances of 336.65(9) pm correspond to the dashed lines.

Figure 4. Projection of the puckered Sb(2) layer along the slightly tilted *c* axis

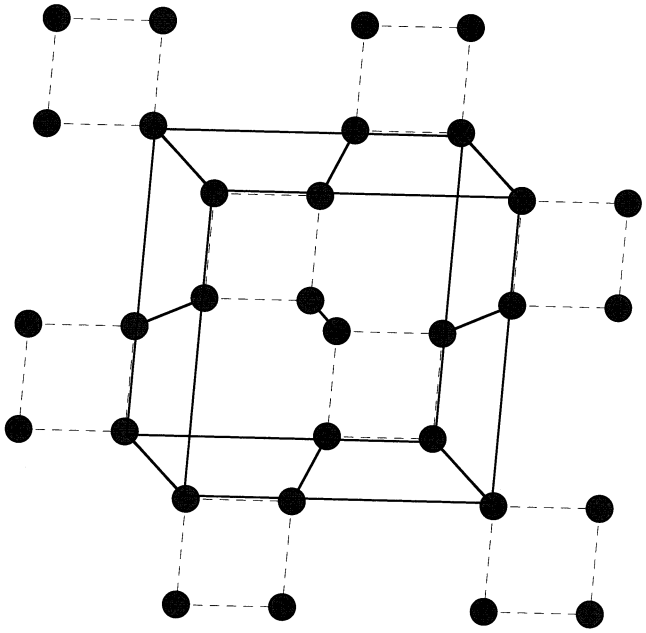

The Sb(2)−Sb(2) distance of 306.3(2) pm may be compared to other intermediate Sb−Sb distances in rather Sb-rich phases without metal−metal bonding, such as $LaCrSb_3$ with distances between 305.81(5) pm and 317.5(2) pm[14] and La_3TiSb_5 with a linear Sb chain consisting of Sb−Sb separations of 314.00(5) pm[15]. In both cases, it was concluded that all electrons from the metal atoms were transferred to the Sb atoms, leading to the tentative ionic formulations $(La^{3+})(Cr^{3+})(Sb^{2.5-})_2(Sb^{1-})$ and $(La^{3+})_3(Ti^{4+})(Sb^{3-})_3(Sb^{2-})_2$. These assignments are in agreement with a consideration of the above mentioned

Sb−Sb contacts as 1-electron-2-center bonds in a local view. In case of $Zr_2V_6Sb_9$, a comparable classification is less straightforward because of the different V−V bond lengths and the occurrence of the longer Sb−Sb distances > 330 pm. Neglecting the longer Sb−Sb distances and considering the shortest Sb−Sb bond as a one-electron bond would result in the formal ionic formulation $(Zr^{4+})_2(V^{2.83+})_6(Sb^{3-})_5(Sb^{2.5-})_4$, if one also ignores in a zeroth approximation the large Zr−Zr and Zr−V distances (> 350 pm). The ionic formulation is not meant to imply ionic character of $Zr_2V_6Sb_9$, but it may be helpful in understanding the bonding situation. According to this electron counting, 2.17/6 = 0.36 electrons remain available for V−V bonding per V atom, i. e. four V−V bonds per V(3) atom [291.2(1) pm] and five V−V bonds per V(4) atom [between 275.9(4) pm and 304.2(3) pm]. This very crude approximation gives an explanation for the occurrence of fractional bond orders of the V−V and Sb−Sb bonds. In case of $V_{15}Sb_{18}$, a similar discussion would result in the electron counting scheme $(V^{5+})_3(V^{2.92+})_{12}(Sb^{3-})_{10}(Sb^{2.5-})_8$, and therefore 0.35 electrons for each V(3) and V(4) atom to form V−V bonds. In the latter case, however, the Sb−Sb contacts of ca. 320 pm should not be neglected.

Calculations of the electronic structure using the Extended Hückel approximation (EH)[16,17,18] were performed in order to evaluate the bonding situation (and the physical properties) of the structure of $Zr_2V_6Sb_9$. Since the standard values of the metal parameters are usually energetically lower than the parameters in low-valent compounds, the metal parameters were optimized by charge iteration of vanadium in $V_{15}Sb_{18}$ with constant Sb parameters[19], followed by the optimization of zirconium in $Zr_2V_6Sb_9$. The parameters used are summarized in Table 4. The calculated densities of states (Figure 5) show a significant number of states at the Fermi level, which basically are centered at the vanadium atoms. The Zr orbitals are much less filled than the V orbitals, confirming the electron-counting scheme mentioned above. The *p* states of antimony are found in a wide peak between −10 eV and −15.5 eV, with a tail going up above the Fermi level. The latter is a hint to not completely reduced antimony ions, in agreement with the occurrence of rather small Sb−Sb distances. The fact that the Sb(2) atoms have shorter Sb−Sb contacts, compared to Sb(1) and Sb(3), expresses itself in smaller Mulliken gross populations calculated with the EH method [Sb(2): 5.23; Sb(3): 5.35; Sb(1): 5.53 electrons], supporting the trend implied but certainly overestimated by the electron-counting scheme $(Zr^{4+})_2(V^{2.83+})_6(Sb^{3-})_5(Sb^{2.5-})_4$. The differences between Sb(1) and Sb(3) also show the treatment of both atoms as Sb^{III} as being a crude approximation. Furthermore, the covalent mixing of the Sb states with the V and Zr states, as can be seen from the contribution of the *d* states of both different kinds of metal atoms to the Sb peak below −11 eV, imply $Zr_2V_6Sb_9$ being a compound with covalent Zr−Sb and V−Sb interactions.

The vanadium substructure with fractional V−V bonds should occur with metallic properties in the *a*,*b* plane, especially under consideration of the huge contribution of V states to the densities of states at the Fermi level. In addition, the occurrence of Zr states at the Fermi level and the somewhat long Zr−Zr distances parallel to the *c* axis might lead to metallic conductivity along the *c* direction, also. However, since the antimony atoms, having holes in the *sp* band, certainly contribute to the metallic properties, three-dimensional metallic properties are assumed. The temperature-independent Pauli paramagnetism experimentally obtained from the $Zr_2V_6Sb_9$ bulk sample (Figure 6) shows the presence of itinerant electrons, and thus metallic properties, but it provides no information on the dimensionality of the physical properties. Attempts to synthesize crystals suitable for direction dependent measurements were unsuccessful.

Table 4. Parameters used for EH calculations on $Zr_2V_6Sb_9$

Orbital	H_{ii}/eV	ζ_1	c_1	ζ_2	c_2
Zr, 5s	−8.204	1.82			
Zr, 5p	−4.593	1.78			
Zr, 4d	−8.117	3.84	0.6213	1.51	0.5798
V, 4s	−7.894	1.30			
V, 4p	−4.304	1.30			
V, 3d	−8.510	4.75	0.4755	1.70	0.5798
Sb, 5s	−18.80	2.32			
Sb, 5p	−11.70	2.00			

Figure 5. Calculated densities of states for $Zr_2V_6Sb_9$; horizontal line: Fermi level; solid line: total DOS; long dashes: Zr contribution; short dashes: V; dots: Sb

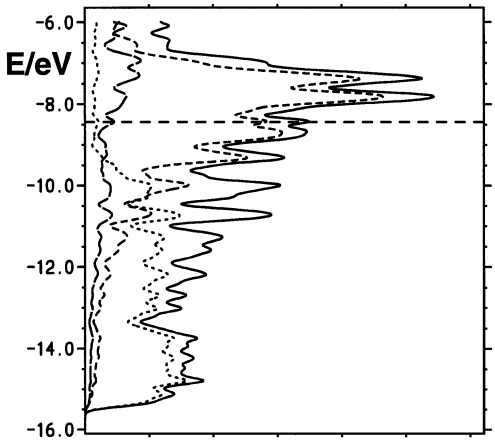

A discussion of the total crystal orbital overlap populations of all Zr−Sb, V−Sb and V−V interactions is instructive. These interactions are depicted in Figure 7, whereas the Zr−Zr states are neglected because of their small contributions. Mainly bonding interactions are found between −15.5 eV and the Fermi level at −8.44 eV, which are dominated by the V−Sb bonds. Only very few antibonding V−Sb states are filled below the Fermi level. Although the Zr−Sb peak area is roughly half as large as the V−Sb peak area, the Zr−Sb interactions play a similar role per bond, because 2 × 8 = 16 Zr−Sb bonds and 6 × 6 = 36 V−Sb bonds exist per formula unit. The V−V bonds are precisely optimized in the structure of $Zr_2V_6Sb_9$, according to the results of the EH calculations. Altogether,

Figure 6. Temperature dependence of the magnetic susceptibility of $Zr_2V_6Sb_9$

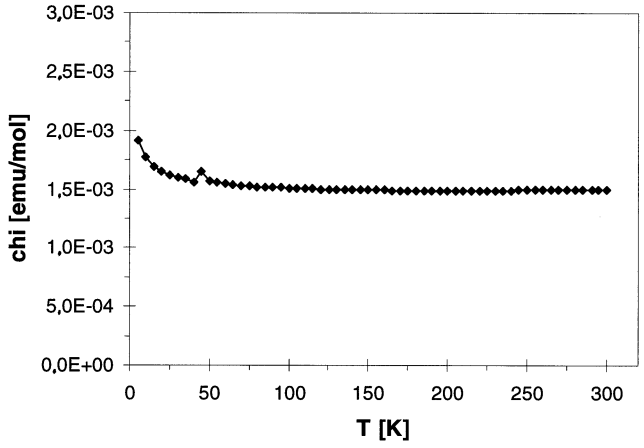

the V−V interactions play a minor but still significant role for the stability of $Zr_2V_6Sb_9$, compared to the Zr−Sb and V−Sb bonds. This can be taken from a rough optical estimation of the sizes of the different areas under the different COOP curves as shown in Figure 7, which reflect the different sums of the overlap populations. This simplistic view should be regarded cautiously, because a Zr−Sb bond may be a much stronger bond than a V−V bond of a comparable overlap population.

Figure 7. Selected total COOP curves for $Zr_2V_6Sb_9$; horizontal line: Fermi level; solid line: V−V interactions; long dashes: Zr−Sb; short dashes: V−Sb; right part of the diagram: bonding interactions (+); left: antibonding (−)

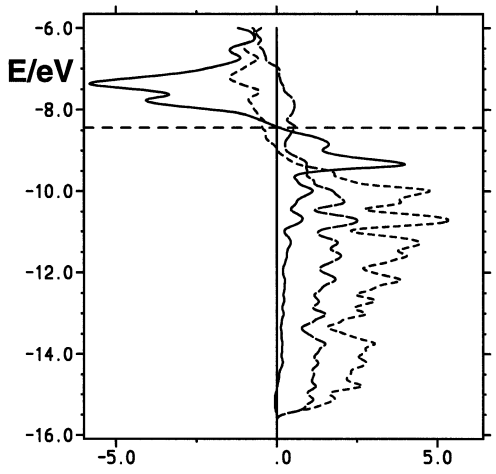

The concrete Mulliken overlap populations (MOPs) of selected interatomic interactions are listed in Table 5. The V−V interactions have significant positive MOP values, ranging from 0.184 and 0.096 within the tetrahedral units to 0.145 for every V(3)−V(4) bond. This may be compared to the values calculated for the shortest interaction of 262 pm (0.298) and for the longer ones of 303 pm (0.120) in elemental vanadium[20]. As proposed above, the Zr−Zr and Zr−V interactions have only weak bonding character, if any, with overlap populations between 0.029 and 0.065 electrons per bond. Similar values (i.e. between 0.025 and 0.048) also are found for the Sb−Sb interactions between 330 pm and 350 pm. The small positive net overlap populations are the result of the sum of bonding and antibonding Sb−Sb states, as shown in the averaged Sb−Sb COOP curves in Figure 8. The positive but small values point to weak bonding character for these interactions. The overlap population of 0.077 for the comparable Sb−Sb bond in elemental antimony (335.5 pm) is of the same magnitude.

Table 5. Selected interatomic distances and overlap populations of $Zr_2V_6Sb_9$

interaction	length/pm	MOP[a]
Zr(1)−1 Zr(2)	357.4(3)	0.041
Zr(1)−1 Zr(2)	362.1(3)	0.065
Zr(1)−4 V(3)	351.06(5)	0.053
Zr(1)−4 V(4)	355.7(2)	0.029
Zr(1)−4 Sb(2)	305.1(2)	0.234
Zr(1)−4 Sb(3)	309.2(2)	0.239
Zr(2)−4 Sb(2)	293.2(2)	0.422
Zr(2)−4 Sb(3)	293.4(1)	0.453
V(3)−4 V(4)	291.2(1)	0.145
V(3)−2 Sb(2)	273.2(1)	0.388
V(3)−4 Sb(3)	277.87(4)	0.302
V(4)−1 V(4)	275.9(4)	0.184
V(4)−2 V(4)	304.2(3)	0.096
V(4)−1 Sb(1)	279.5(2)	0.411
V(4)−2 Sb(2)	282.5(2)	0.348
V(4)−1 Sb(3)	271.3(2)	0.382
V(4)−2 Sb(3)	283.1(1)	0.245
Sb(1)−4 Sb(3)	335.89(7)	0.048
Sb(2)−1 Sb(2)	306.3(2)	0.339
Sb(2)−2 Sb(2)	336.65(9)	0.042
Sb(3)−2 Sb(3)	342.76(8)	0.025

[a] MOP = Mulliken Overlap Population [electrons per bond].

Figure 8. Selected averaged COOP curves for $Zr_2V_6Sb_9$; horizontal line: Fermi level; solid line: Sb−Sb interactions < 310 pm; dashed: Sb−Sb interactions between 310 pm and 350 pm; right part of the diagram: bonding interactions (+); left: antibonding (−)

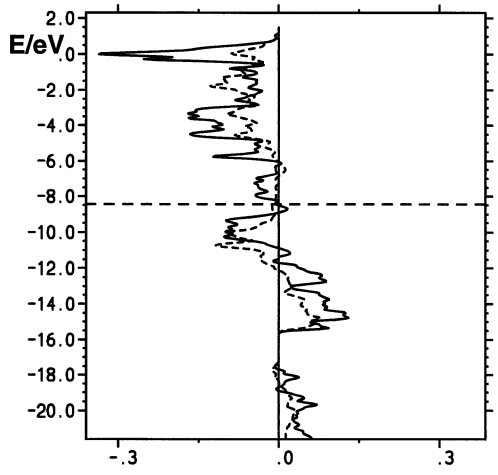

Fewer antibonding states are filled in case of the shortest Sb−Sb interaction in the structure of $Zr_2V_6Sb_9$ [d = 306.3(2) pm, MOP = 0.339]. The COOP curves also show the presence of antibonding Sb−Sb states above the Fermi level, supporting the model of not completely reduced Sb^{III}

anions. For an evaluation of the bond strength, the short Sb−Sb bond may be compared with shorter Sb−Sb bonds, i.e. in the element (d = 290.8 pm, MOP = 0.530[20]), with the Sb_2 pair in (α-)$ZrSb_2$ (d = 288 pm, MOP = 0.51[4]) or the $^1_\infty[Sb^{1-}]$ chain in KSb with $\bar{d}$ = 284 pm[21] and an averaged MOP of 0.645[20]. Since the latter bonds may be described to a first estimation as 2-electrons-2-center bonds (i. e. corresponding to a bond order of one), the crude approximation of a half bond order for the short Sb−Sb bond in $Zr_2V_6Sb_9$ is supported by the calculations of the electronic structure. It is thus concluded that the Sb−Sb interactions contribute significantly to the formation energy of $Zr_2V_6Sb_9$, although $Zr_2V_6Sb_9$ is to be considered a low-valent antimonide because of the V−V bonds.

[1] P. Villars, *Pearson's Handbook*, Materials Park, Ohio 44073, **1997**.
[2] C. G. Richter, W. Jeitschko, *J. Solid State Chem.* **1997**, *134*, 26−30.
[3] S. Furuseth, H. Fjellvåg, *Acta Chem. Scand.* **1995**, *49*, 417−422.
[4] E. Garcia, J. D. Corbett, *J. Solid State Chem.* **1988**, *73*, 452−467.
[5] J. Steinmetz, B. Malaman, B. Roques, *C. R. Acad. Sci., Ser C* **1977**, *284 C,* 499−502.
[6] C. S. Barrett, P. Cucka, K. Haefner, *Acta Crystallogr.* **1963**, *16*, 451−453.
[7] J. Bouwma, C. F. van Bruggen, C. Haas, *J. Solid State Chem.* **1973**, *7*, 255−261.
[8] W. Rossteutscher, K. Schubert, *Z. Metallk.* **1965**, *56*, 813−822.
[9] G. M. Sheldrick, *SHELX93*, University of Göttingen, **1993**.
[10] Further details of the crystal-structure investigations may be obtained from the Fachinformationszentrum Karlsruhe, D-76344 Eggenstein-Leopoldshafen, Germany, on quoting the depository numbers CSD-408567, -408566, and -408565.
[11] H. Kleinke, *Z. Anorg. Allg. Chem.*, in press.
[12] B. C. Sales, D. Mandrus, R. K. Williams, *Science* **1996**, *272*, 1325−1328.
[13] Y. N. Smirnov, V. A. Finkel, *Sov. Phys. − JETP (Engl. Transl.)* **1966**, *22*, 750−753; *Chem. Abstr.* **1966**, *64*, 4365.
[14] M. J. Ferguson, R. W. Hushagen, A. Mar, *J. Alloys Compd.* **1997**, *249*, 191−198.
[15] G. Bolloré, M. J. Ferguson, R. W. Hushagen, A. Mar, *Chem. Mater.* **1995**, *7*, 2229−2231.
[16] R. Hoffmann, *J. Chem. Phys.* **1963**, *39*, 1397−1412.
[17] M.-H. Whangbo, R. Hoffmann, *J. Am. Chem. Soc.* **1978**, *100*, 6093−6098.
[18] Program EHMACC, adapted for use on a PC by M. Köckerling, Gesamthochschule Duisburg, **1997**.
[19] E. Clementi, C. Roetti *At. Nucl. Data Tables* **1974**, *14*, 177.
[20] H. Kleinke, unpublished calculations.
[21] W. Hönle, H.-G. von Schnering, *Z. Kristallogr.* **1981**, *155*, 307−314.

[98082]

Photoelectron-Spectrum and Electronic Structure of Perfluoro(2,4-dimethyl-3-oxa-2,4-diazapentane) $(CF_3)_2N–O–N(CF_3)_2$

Stefan Reinemann[a], Rolf Minkwitz[a], Klaus Kowski[b], and Paul Rademacher*[b]

Institut für Anorganische Chemie,[a]
Universität Dortmund, D-44221 Dortmund, Germany

Institut für Organische Chemie,[b]
Universität Essen, D-45117 Essen, Germany
E-mail: paul.rademacher@uni-essen.de

Received April 6, 1998

Keywords: Ab initio calculations / Electronic structure / Photoelectron spectroscopy

The electronic structure of the title compound **1** has been investigated by UV photoelectron spectroscopy and quantum chemical calculations. **1** has two nearly degenerate n_N lone-pair orbitals which form the two highest occupied MOs. The third highest occupied MO is mainly localized at the oxygen atom (n_O). All calculations indicate that the molecule has a twisted C_2 conformation.

We have recently reported a synthesis and gas-phase electron-diffraction structure analysis of perfluoro(2,4-dimethyl-3-oxa-2,4-diazapentane), $(CF_3)_2N–O–N(CF_3)_2$ (**1**).[1] This compound consists of an N–O–N chain that is substituted by four CF_3 groups. The structure analysis indicated that the molecule has C_{2v} symmetry and an sp,sp conformation in which both nitrogen electron lone-pairs are synperiplanar to the vicinal N–O bond. The electronic structure of this molecule is characterized by electron lone-pairs on three neighbouring (directly bound) atoms which makes it an ideal candidate to study the mutual interactions of such orbitals. We have investigated the electronic structure of **1** by photoelectron (PE) spectroscopy and quantum chemical calculations. The measured ionization potentials are summarized in Table 1 together with the relevant results of the calculations. The PE spectrum of **1** is depicted in Figure 1. In Figure 2 plots of the three highest occupied molecular orbitals are shown.

The PE spectrum consists of two broad bands with minor intensities, centred at about 12.2 and 13.7 eV, and several broad bands with larger intensities between 15 and 21 eV. Since the intensity of the first band is somewhat larger than that of the second, two ionization events contribute to it although it is not possible to assign different *IP* values to them. For the first band beginning ionization corresponding to the adiabatic ionization energy can be localized at 11.0 eV while the vertical *IP* is at 12.15 eV. For the second band the adiabatic value can be estimated to 12.7 eV.

Figure 1. PE spectrum of $(CF_3)_2N–O–N(CF_3)_2$ (**1**)

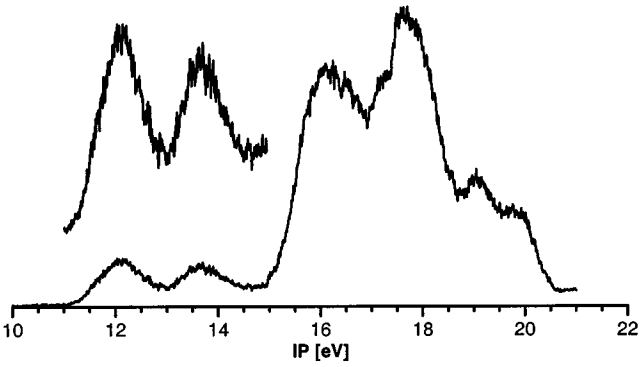

For analysis of the electronic structure of **1** and the interpretation of the PE spectrum quantum chemical calculations on different levels of theory were performed. Semi-empirical methods like AM1[2] and PM3[3] are known to be superior to simple ab initio methods, in particular for the

Table 1. Ionization potentials *IP* [eV] and orbital energies ε [eV] of $(CF_3)_2N–O–N(CF_3)_2$ (**1**)

		B3LYP/6–31+G*		B3LYP/ 3–21+G*	HF/ 6–31+G*	AM1	PM3	Assignment	
IP_v exp.	IP_v	IP_a	$-\varepsilon$	$-\varepsilon$	$-\varepsilon$	$-\varepsilon$	$-\varepsilon$		
12.15[a]	11.90	10.82	9.76	10.62	13.90	12.91	12.83	n_N^+	(A)
			9.74	10.79	14.26	12.99	12.92	n_N^-	(B)
13.70[b]			11.13	12.24	16.16	13.95	14.57	n_O	(B)
16.2			12.35	13.02	17.82	14.78	15.87	σ	(A)

[a] IP_a = 11.0 eV. – [b] IP_a = 12.7 eV.

 © WILEY-VCH Verlag GmbH, D-69451 Weinheim, 1998 1434–1948/98/1010–1377 $ 17.50+.50/0

Figure 2. Plots of the three highest occupied MOs of $(CF_3)_2N-O-N(CF_3)_2$ (**1**) (PM3 results)

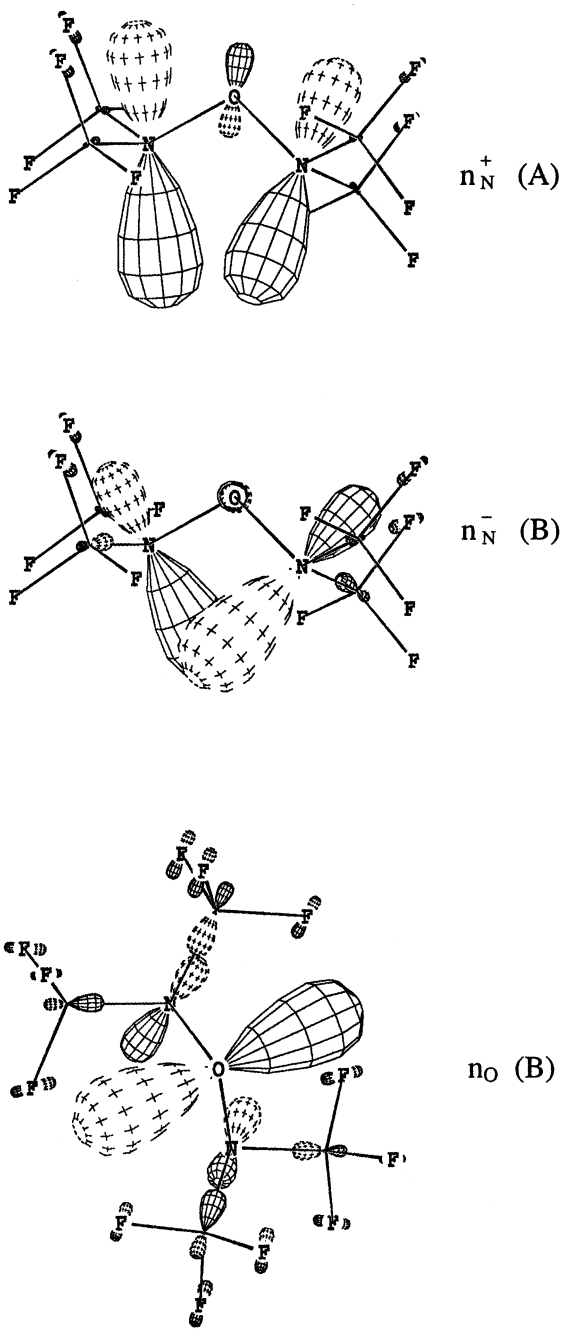

calculation of orbital energies ε_i which can be used to assign ionization potentials (IP_i) making use of the Koopmans theorem, $IP_i = -\varepsilon_i^{SCF}$.[4] These methods are, however, often of limited value for molecules like **1** with vicinal electron lone-pairs since their interaction is not correctly reproduced which often leads to wrong conformations. Good results have been obtained for a variety of molecules with the Becke3LYP (B3LYP) method,[5] a hybrid Hartree-Fock/density functional theory (HF/DFT) method.[6][7] This method also leads to excellent values for the first adiabatic ionization potential, $IP_{1,a}$, as the energy difference of the molecule and the radical cation. By performing single-point energy calculations for the radical cation on the molecule's geometry, i.e. without allowing for relaxation during ionization, the first vertical *IP*, $IP_{1,v}$, is accessible. Total energies from these calculations are given in Table 2; orbital energies and calculated *IP* values are listed in Table 1.

All theoretical methods lead to a C_2 structure as the most stable conformer of **1** that is twisted from the C_{2v} structure by about 30° as measured from the C−N···N−C dihedral angles. For the untwisted C_{2v} structure higher energy values of 1.0−5.8 kcal mol^{-1} were obtained. These results indicate that the molecule has a double minimum (W shaped) energy potential for its deformation, both C_2 minima are equally populated, and transition between the conformers through the C_{2v} conformation is rapid. This makes it difficult to distinguish experimentally between C_2 and C_{2v} symmetry. In Table 3 the structure parameters of **1** as obtained from electron diffraction,[1] from HF and from B3LYP calculations using the basis set 6−31+G* are compared. The agreement between experimental and theoretical data is generally not quite satisfactory. Deviations are smaller for the B3LYP than for the HF results and for C_2 than for C_{2v} symmetry. The latter observation may be considered as an additional indication for a twisted conformation of **1**.

The orbital energies given in Table 1 refer to the more stable C_2 conformer and correspond to the structure of minimum energy found by the respective method. All calculations lead to the same interpretation of the spectrum: The first two ionizations, which are nearly degenerate, are assigned to the two n_N MOs, and the third ionization is assigned to the $n_O{}^p$ MO. The strong bands centred at about 16.0 and 17.5 eV are mainly composed of n_F ionizations. When only the first three MOs are considered, the energies calculated for ε by the AM1 method show the best agreement with the *IP* values, but there is only a minor difference to the PM3 results, while − as expected − the orbital energies of the ab initio methods cannot be used equally well. Deviations from the Koopmans theorem[4] of 0.3−0.8 eV are found for the AM1 results, the PM3 values are more uniformly wrong by 0.7−0.9 eV, and the deviations of the ab initio methods range from −1.4−(−1.5) eV (B3LYP/6−31+G*) to 1.8−2.5 eV (HF/6−31+G*). Although it has to be admitted that caution is necessary, the AM1 and the PM3 method can be praised for their performance in the interpretation of the PE spectrum of **1**. In comparing the quality of the computational methods, not only the size of the deviations but also their uniformty has to be considered and according to this aspect the B3LYP/6−31+G* results rank first.

Leaving the limitations of the Koopmans theorem,[4] and calculating the first adiabatic and vertical *IP* from the energy difference of molecule and radical cation, the values obtained on the B3LYP/6−31+G* level of theory are in quite satisfactory agreement with the experimental ones (Table 1).

As is evident from Figure 2, there are coefficients on all atoms of the N−O−N chain in the three highest occupied

Table 2. Calculated total energy E [au] and enthalpy of formation ΔH_f [kcal mol^{-1}] of two conformers and the radical cation $M^{+\cdot}$ of $(CF_3)_2N-O-N(CF_3)_2$ (**1**)

	E B3LYP/6−31+G*	E HF/6−31+G*	ΔH_f AM1	ΔH_f PM3
sp,sp (C_2)	−1535.2127732	−1528.4542501	−521.46	−598.23
sp,sp (C_{2v})	−1535.2065303	−1528.4450707	−520.51	−595.74
$\Delta(C_{2v}-C_2)$ [a]	3.92	5.76	0.95	2.49
$M^{+\cdot}$ [b]	−1534.7755083			
$M^{+\cdot}$ [c]	−1534.8149655			

[a] kcal mol^{-1}. − [b] Single-point calculation on the molecule's structure. − [c] Optimized structure.

Table 3. Structure parameters [pm, °] of $(CF_3)_2N-O-N(CF_3)_2$ (**1**) from electron diffraction (ED), ab initio HF and B3LYP calculations

	ED[a] (C_{2v})	B3LYP[b] (C_{2v})	B3LYP[b] (C_2)	HF[b] (C_{2v})	HF[b] (C_2)
N−O	146.2(8)	143.8	142.4	139.2	138.1
N−C	143.5(4)	147.2	145.9, 146.1	145.2	144.0, 144.3
C−F	132.3(2)	132.9−134.6	133.2−135.0	130.0−131.4	130.3−131.7
N−O−N	105.2(2.6)	112.3	109.7	114.1	111.0
C−N−C	117.9(1.2)	114.9	117.2	115.0	117.3
O−N−C	109.3(8)	107.2	107.6, 109.2	107.6	108.0, 109.5
F−C−F	109.3(2)	108.1−108.5	108.0−109.2	108.2−108.6	108.2−109.2
C−N···N−C	0.0	0.0	30.8	0.0	32.8

[a] From ref.[1]. − [b] Basis set 6−31+G*.

MOs of **1** indicating mutual interaction of n_N and n_O orbitals. The nearly degenerate energy levels of the two n_N MOs are closely related to the sp,sp conformation of **1** in which both nitrogen electron lone-pairs are synperiplanar to the opposite N−O bonds;[1] $n_N{}^+$ and $n_N{}^-$ are the symmetric and antisymmetric linear combination of the two nitrogen lone-pair orbitals (n_1 and n_2), respectively, with reference to the relevant symmetry operation. The MOs depicted in Figure 2, which correspond to the C_2 structure obtained with the PM3 method (torsional angle 31.3°), should be considered as qualitative illustrations, since the shape of the MOs varies with the structure and the method used in the calculation.

The energy difference Δn_N of $n_N{}^+$ and $n_N{}^-$ is attributed to the interaction of n_1 and n_2 and is dependent on their mutual geometrical orientation.[8] In 1,3-diamines Δn_N values between 0 and more than 1 eV have been observed by PE spectroscopy.[9] The PE spectrum of 1,3-diazaadamantane[10] shows two well-separated n_N ionization bands at 7.75 ($n_N{}^-$) and 8.78 eV ($n_N{}^+$). The orientation of the lone-pairs in this compound corresponds to the ap,ap conformation of **1**,[1] in which the nitrogen electron lone-pairs are antiperiplanar to the vicinal N−O bonds, and the splitting is dominated by through-space interaction. On the other hand, 2-substituted 1,3-dimethylimidazolidines[11] have a single broad band, and the energies of the two n_N orbitals are split by only 0.0−0.3 eV indicating little interaction, which is consistent with envelope conformations of the five-membered ring and an axial-equatorial orientation of the two *N*-methyl groups.

For the sp,sp conformation of **1** one would expect good through-space interaction of the nitrogen lone-pair orbitals n_1 and n_2 leading to a sizeable Δn_N value and an energy sequence $n_N{}^- > n_N{}^+$. However, this interaction would have its maximum value in the undistorted C_{2v} conformation (see below), whereas the torsion in the C_2 form will reduce the overlap of n_1 and n_2 and thus result in a smaller Δn_N. The splitting is then obviously overcompensated by n_N/n_O interactions. The $n_O{}^p$ orbital is geometrically orthogonal to n_1 and n_2 in the C_{2v} form so that there will be some interaction only in twisted C_2 conformations. On the other hand, the $n_O{}^s$ orbital overlaps effectively with n_1 and n_2. However, only the linear combination $n_N{}^+$ has the same symmetry as $n_O{}^s$ so that this orbital is destabilized while $n_N{}^-$ remains unaffected. This vicinal n_N/n_O interaction is also conformation dependent having its maximum extent in the untwisted C_{2v} form. For this conformation the following MO energies are calculated with the B3LYP/6−31+G* method: −9.75 eV ($n_N{}^+$, A_1), −10.22 eV ($n_N{}^-$, B_2), −10.78 eV (n_O, B_1). In this case the two n_N MOs would no longer be nearly degenerate, and accordingly the first two *IP*s of the PE spectrum should be sufficiently split in order to be detected separately. The actual PE spectrum is thus an indication of the twisted C_2 form. Here the $n_N/n_O{}^s$ interaction is obviously approximately of the same magnitude as the 1,3-n_N/n_N interaction which explains the observed orbital degeneracy $n_N{}^+ \approx n_N{}^-$ of **1**.

That the conformational properties of **1** are mainly determined by the mutual interactions of the electron lone-pairs is also indicated by the large difference between adiabatic and vertical *IP* values of more than 1 eV for the first and the third *IP*. The ionizations reduce the electrostatic repulsion of the electron pairs and lead to a less twisted, i.e. more C_{2v} like, conformation of the radical cation than in the neutral molecule.

We thank the *Fonds der Chemischen Industrie*, Frankfurt am Main, for financial support.

Experimental Section

The PE spectrum of **1** was recorded with a Leybold-Heraeus UPG200 spectrometer equipped with an He(I) radiation source (21.21 eV). The spectrum was calibrated with the lines of xenon at 12.130 and 13.436 and of argon at 15.759 and 15.937 eV. The accuracy of the measurements was approximately ± 0.03 eV for ionization energies, for broad and overlapping signals it was only ± 0.1 eV.

Semi-empirical AM1[2] and PM3[3] calculations were performed with the MOPAC[12] program package (version 6.1, IBM version of MOPAC 6.00), ab initio HF[13] and Becke3LYP[5] calculations with the program GAUSSIAN 94.[14] Geometries were fully optimized at the respective levels of theory. In the AM1 and PM3 calculations the keyword "PRECISE" was used to tighten the convergence criteria. MOs were plotted by using the program PERVAL.[15]

[1] S. Reinemann, R. Minkwitz, H. Oberhammer, *Angew. Chem.* **1997**, *109*, 1579−1580; *Angew. Chem. Int. Ed. Engl.* **1997**, *36*, 1518−1519.
[2] M. J. S. Dewar, E. G. Zoebisch, H. F. Healy, J. J. P. Stewart, *J. Am. Chem. Soc.* **1985**, *107*, 3902−3909.
[3] J. J. P. Stewart, *J. Comput. Chem.* **1989**, *10*, 209−220, 221−264.
[4] T. Koopmans, *Physica* **1933**, *1*, 104−113.
[5] [5a] A. D. Becke, *J. Chem. Phys.* **1993**, *98*, 5648−5652. − [5b] C. Lee, W. Yang, R. G. Parr, *Phys. Rev. B* **1988**, *37*, 785−789.
[6] H. M. Muchall, P. Rademacher, *J. Mol. Struct.* **1997**, *435*, 157−167.
[7] H. M. Muchall, P. Rademacher, *J. Mol. Struct.*, in print.
[8] R. Hoffmann, *Acc. Chem. Res.* **1971**, *4*, 1−9.
[9] P. Rademacher, *Photoelectron spectra of amines, nitroso and nitro compounds*, in *The chemistry of amino, nitroso, nitro and related groups* (Ed.: S. Patai), Wiley, Chichester, **1996**, vol. suppl. F2, p. 159−204.
[10] R. Gleiter, M. Kobayashi, J. Kuthan, *Tetrahedron* **1976**, *32*, 2775−2781.
[11] P. Rademacher, U. Schüle, H.-D. Beckhaus, C. Rüchardt, *J. Chem. Res.* **1995**, *(S)* 20, *(M)* 274−281.
[12] J. J. P. Stewart, Quantum Chemistry Program Exchange No. 455, **1983**.
[13] W. J. Hehre, L. Radom, P. v. R. Schleyer and J. A. Pople, *Ab Initio Molecular Orbital Theory*, John Wiley & Sons, New York, **1986**.
[14] M. J. Frisch, G. W. Trucks, H. B. Schlegel, P. M. W. Gill, B. G. Johnson, M. A. Robb, J. R. Cheeseman, T. Keith, G. A. Petersson, J. A. Montgomery, K. Raghavachari, M. A. Al-Laham, V. G. Zakrzewski, J. V. Ortiz, J. B. Foresman, J. Cioslowski, B. B. Stefanov, A. Nanayakkara, M. Challacombe, C. Y. Peng, P. Y. Ayala, W. Chen, M. W. Wong, J. L. Andres, E. S. Replogle, R. Gomperts, R. L. Martin, D. J. Fox, J. S. Binkley, D. J. Defrees, J. Baker, J. P. Stewart, M. Head-Gordon, C. Gonzalez, J. A. Pople, *Gaussian 94, Revision E.2.*, Gaussian, Inc., Pittsburgh, PA, **1995**.
[15] R. Sustmann, W. Sicking, *Chem. Ber.* **1987**, *120*, 1323−1330.

[98098]

Tridentate Coordination Mode of *N*,*N*′-Dimethyl-2,11-diaza-[3.3](2,6)pyridinophane in a Tricarbonylmolybdenum(0) Complex

Harald Kelm and Hans-Jörg Krüger*

Institut für Anorganische und Angewandte Chemie der Universität Hamburg,
Martin-Luther-King-Platz 6, D-20146 Hamburg, Germany
Fax: (internat.) + 49(0)40/4123-2893
E-mail: krueger@xray.chemie.uni-hamburg.de

Received May 20, 1998

Keywords: Carbonyl complexes / Coordination modes / Fluxionality / Macrocyclic ligands / N ligands

Tridentate coordination of the potentially tetradentate ligand *N*,*N*′-dimethyl-2,11-diaza[3.3](2,6)pyridinophane (L–N_4Me_2) has been structurally established in the tricarbonylmolybdenum(0) complex [Mo(L–N_4Me_2)$(CO)_3$]. The fluxional behavior of the coordinated tetraazamacrocyclic ligand is demonstrated by a variable-temperature ^{1}H-NMR study. The relevance of the tridentate coordination mode of the ligand is discussed with respect to its intermediacy in the reaction mechanism for the formation of *cis* octahedral metal complexes containing tetradentate 2,11-diaza[3.3](2,6)-pyridinophane derivatives as ligands.

Introduction

The macrocyclic ligand 2,11-diaza[3.3](2,6)pyridinophane (L−N_4R_2) disposes of four potential nitrogen donor atoms for the complexation of metal ions. Due to its small ring size, the tetraazamacrocycle generally forms *cis* octahedral coordination geometries (**1**) with all nitrogen donor atoms bound to the metal ions.[1][2] With iron(II), iron(III), and cobalt(II) ions, eight-coordination has been observed in complexes of the composition $[M(L-N_4H_2)_2]^{n+}$ (**2**), in which both diazapyridinophane units act as tetradentate ligands.[3][4] In contrast, the nickel(II) ion in the complex $[Ni(L-N_4H_2)_2]^{2+}$ (**3**) is coordinated to all nitrogen donor atoms of one of the tetraazamacrocyclic ligands and to one each of the pyridine and amine nitrogen atoms of the second ligand.[4] Thus, in octahedral metal complexes only the tetra- and bidentate coordination modes have been structurally established with 2,11-diaza[3.3](2,6)pyridinophane ligands. Because we are interested in the general coordination chemistry of this type of ligand, we decided to explore the possibility of a tridentate coordination of the diazapyridinophane ligands in octahedral metal complexes. It is known that tricarbonylmolybdenum(0) fragments can sustain the tridentate coordination mode with the tetraazamacrocycles **4**−**7** which possess 12-, 14-, 15-, and 16-membered rings.[5][6] In one instance a structure analysis has been reported.[5] Tridentate coordination may, however, be more difficult to achieve with the macrocyclic ligand L−N_4R_2, since this type of ligand is, relative to the tetraazamacrocycles **4**−**7**, significantly more rigid due to the presence of two pyridine units in the ring and therefore has considerably fewer degrees of conformational freedom. The initial results of a study directed towards the feasibility of the tridentate coordination of 2,11-diaza[3.3](2,6)pyridinophane ligands are described here.

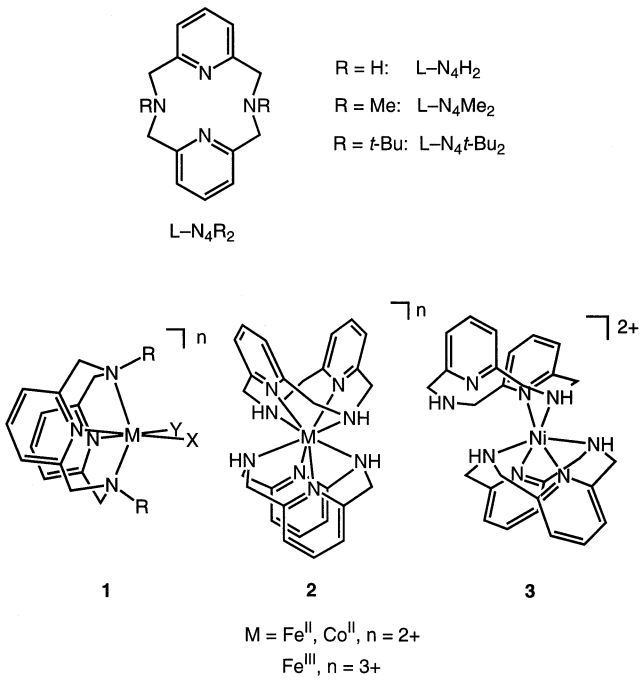

1 **2** **3**

Results and Discussion

The reaction of the ligand L−N_4Me_2 with an equivalent amount of $[Mo(CO)_6]$ in refluxing toluene yields a dark red complex whose elemental analysis is consistent with its formulation as [Mo(L−N_4Me_2)$(CO)_3$] (**8**). The IR spectrum of the compound is dominated by a very intense, narrow ($\Delta\nu_{1/2}$ = 30 cm^{-1}) band at 1893 cm^{-1} and an equally intense, rather broad ($\Delta\nu_{1/2}$ = 60 cm^{-1}) band at 1762 cm^{-1}; these bands are assigned to the two CO stretching vibrations (A_1 and E) expected for a *fac*-Mo$(CO)_3$ fragment with a local C_{3v}-symmetry. The ν(CO) frequencies for the

 © WILEY-VCH Verlag GmbH, D-69451 Weinheim, 1998 1434−1948/98/1010−1381 $ 17.50+.50/0

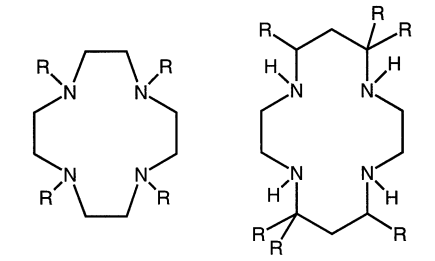

4
R = H or Me

5
R = H or Me

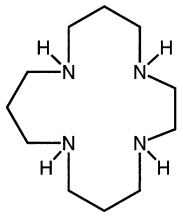

6

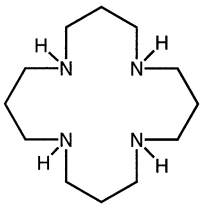

7

terminally bound carbonyl ligands lie in the same range as those observed for other octahedral tricarbonylmolybdenum(0) complexes with C_3N_3 coordination environments.[6][7][8] The relatively low energy of these ν(CO) frequencies, indicating strong π-back bondings between the metal and the carbon atoms, is attributed to the presence of strong σ-only donors with no or rather weak π-acceptor capabilities, such as amines and pyridines.

A perspective view of the structure of **8** is presented in Figure 1. The molecule possesses crystallographically imposed C_s symmetry. The most noteworthy structural aspect of complex **8** is the finding that the potentially tetradentate ligand $L-N_4Me_2$ acts only as a tridentate ligand here. Thus, the somewhat distorted octahedral coordination environment around the molybdenum atom is composed of three carbonyl ligands occupying one face of the octahedron and three nitrogen donor atoms of the macrocyclic ligand coordinated to the opposite face. By maintaining a *syn* chair-boat conformation, $L-N_4Me_2$ is bound to the metal ion only through the two pyridine and one of the amine nitrogen atoms. In contrast to previously discussed octahedral complexes where the tetraazamacrocyclic ligand is bound to a metal ion in a tetradentate fashion,[1][2] here the bond from the metal ion to the amine nitrogen atom ($Mo-N_{amine}$ bond, 2.306 Å) is considerably shorter than that to the pyridine nitrogen atoms ($Mo-N_{py}$ bond, 2.342 Å). Overall the lengths of the Mo^0-N bonds are similar to those observed in other six-coordinate molybdenum complexes with the same ligand donor set (2.242–2.407 Å with the mean at 2.314 Å).[5][8][9][10] Presumably due to steric interactions between the methylene protons next to the uncoordinated amine nitrogen atom and the axial carbonyl ligand [containing C(10) and O(1)], the coordination of the macrocycle to the metal ion is considerably distorted, as demonstrated, for example, by the rather small N–Mo–N angles of 68.7° and 75.5°. In agreement with the rather low ν(CO) frequencies, the Mo–C bond lengths of 1.933 and 1.943 Å indicate substantial Mo=C double bond character.[9] These bond lengths fall into the general range observed for Mo–CO bonds in complexes with an octahedral MoC_3N_3 coordination sphere (1.898–1.952 Å with the mean at 1.923 Å).[5][8][9][10]

Figure 1. Perspective view of the structure of $[Mo(L-N_4Me_2)(CO)_3]$ showing thermal ellipsoids at 50% probability and the atom-numbering scheme; the primed and unprimed atoms are related by a mirror plane[a]

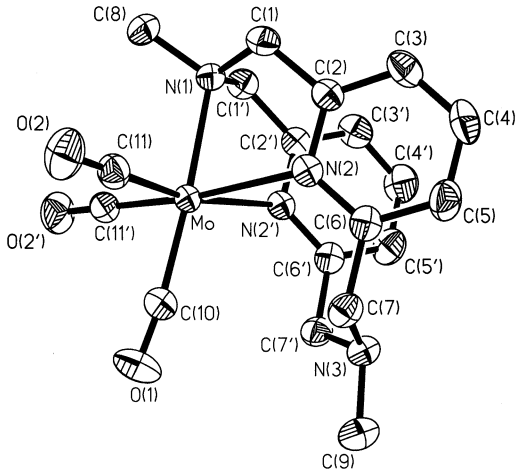

[a] Selected bond lengths [Å] and angles [°]: Mo–N(1) 2.306(3), Mo–N(2) 2.342(2), Mo–C(10) 1.943(4), Mo–C(11) 1.933(3), C(10)–O(1) 1.167(5), C(11)–O(2) 1.172(3); C(10)–Mo–C(11) 83.4(1), C(11)–Mo–C(11′) 88.0(2), N(1)–Mo–N(2) 75.49(8), N(1)–Mo–C(11) 94.3(1), N(1)–Mo–C(10) 176.7(1), N(2)–Mo–N(2′) 68.7(1), N(2)–Mo–C(10) 107.2(1), N(2)–Mo–C(11) 100.9(1), N(2)–Mo–C(11′) 166.79(9).

In solution, fluxional behavior is observed for the coordinated macrocyclic ligand by a variable-temperature ^{1}H-NMR study. Thus, at low temperatures (240 K), the methylene proton signals appear as two well separated AB systems in the ^{1}H-NMR spectrum (Figure 2). The first AB system occurs at $\delta = 4.02$ and 5.51 with a coupling constant $J_{AB} = 14$ Hz and the second at $\delta = 4.23$ and 4.51 with $J_{AB} = 15$ Hz. Raising the temperature causes the two AB systems to be replaced by a new AB system at $\delta = 4.1$ and 5.1 with $J_{AB} = 15$ Hz by coalescence of the signals at $\delta = 4.02$ and 4.23 and those at $\delta = 4.51$ and 5.51. In a similar way, the two signals corresponding to the protons of two methyl groups which are found at $\delta = 2.50$ and 3.23 at low temperatures coalesce to a singlet at $\delta = 2.9$. In analogy, the slightly different signals attributed to the 3-pyridine and 5-pyridine protons appear at higher temperatures as one signal. The dynamic NMR study clearly demonstrates that, when the complex is dissolved, an intramolecular substitution reaction takes place in which, as depicted in Scheme 1, the uncoordinated amine nitrogen donor replaces the bound one. Simulations of the NMR subspectra corresponding to the methylene protons at different temperatures yield the reaction velocities k for this process at each temperature; at room temperature, k and the free activation energy $\Delta G^{\neq}$ were determined to be 286 s^{-1} and 59.0 kJ mol^{-1},

respectively. From a plot of $\ln(k/T)$ vs $1/T$, the free activation parameters $\Delta H^{\neq} = 58.1$ kJ mol^{-1} and $\Delta S^{\neq} = -3.14$ J K^{-1} mol^{-1} were obtained. Since the experimental error in determining the value of the entropy of activation by NMR spectroscopy is inherently quite large, this rather small value for the entropy of activation prohibits its use in a discussion of the possible mechanism of the reaction. The reaction mechanism is currently being investigated with a series of tricarbonyl metal complexes $[M(L-N_4R_2)(CO)_3]$ (where M = Cr^0, Mo^0, or W^0 and R = H, Me, or *t*Bu). Preliminary results of this kinetic study suggest that the reaction proceeds either by an associative or an associative interchange mechanism.

Figure 2. ^{1}H-NMR signals of the methylene protons of $[Mo(L-N_4Me_2)(CO)_3]$ in deuterated dimethylformamide at different temperatures (360 MHz)

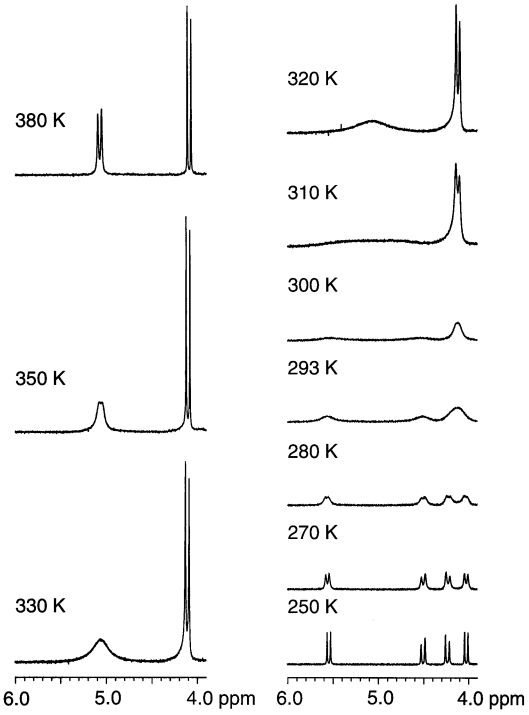

Scheme 1

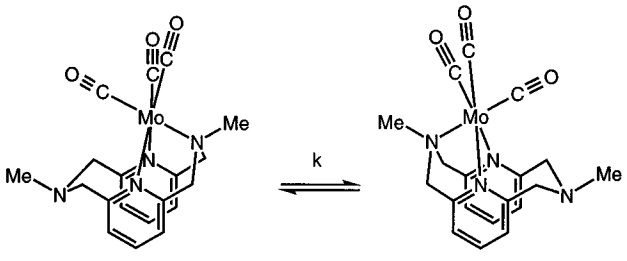

The tridentate coordination mode of the ligand $L-N_4Me_2$ has only been observed here because the tricarbonylmolybdenum(0) fragment is quite stable. Since adequate π-back-bonding from the metal ion to the carbonyl ligands is required to stabilize the molybdenum(0) atom, the presence of only two carbonyl ligands is apparently not sufficient to stabilize a molybdenum(0) atom if it is coordinated to four relatively strong σ-donors, such as amines or pyridines, with no or only rather weak π-acceptor capabilities. Therefore, the molybdenum(0) atom prefers the coordination of three carbonyl ligands and forfeits ligation of one of the four possible nitrogen donors of the macrocyclic ligands. However, it is interesting to point out that for all diamagnetic *cis* octahedral metal complexes investigated thus far the NMR spectra demonstrate that the tetraazamacrocycle, once coordinated as tetradentate ligand, stays bound to the metal ion through all its nitrogen donor atoms.

The structures of the complexes **3** and **8** provide some quite interesting insights into mechanistic aspects of the coordination of octahedral metal ions by diazapyridinophane ligands. Thus, the bidentate and tridentate coordination modes of the tetraazamacrocyclic ligands observed in these complexes can be viewed as intermediates in the formation of tetradentate chelation of the ligand. As uncoordinated macrocycle the dialkyl-substituted diazapyridinophane is present as *syn* chair-chair conformer. The reaction sequence depicted in Figure 3 starts with the coordination of just one nitrogen atom, most likely one of the amine nitrogen donors since these can be approached by the metal ion more easily because of steric considerations. Next, by changing the chair-chair conformation of the ligand to a boat-chair conformation, bidentate chelation over one amine and one pyridine nitrogen atom occurs, similar to that found in **3**. The macrocyclic ring slides further over the metal ion, and the second pyridine nitrogen atom forms a bond to the metal ion, yielding a facial coordination of the ligand like that observed in **8**. By converting the chair-boat conformation to a boat-boat conformation, the last amine nitrogen donor atom is then able to interact with the metal ion and, thus, tetradentate chelation of the ligand is completed.

Conclusion

Tridentate coordination has been structurally established for the ligand $L-N_4Me_2$ in a tricarbonylmolybdenum(0) complex. In solution, an intramolecular rearrangement of the ligand occurs where the uncoordinated amine nitrogen atom replaces the coordinated one at the molybdenum atom. In general, 2,11-diaza[3.3](2,6)pyridinophanes display a decisive tendency to form preferentially *cis* octahedral complexes; only in very specific cases, e.g. when the other ligands in the complex are very strongly bound as in $[Mo(L-N_4Me_2)(CO)_3]$ or when no further coordination sites are available in the octahedral complex as in $[Ni(L-N_4H_2)_2]^{2+}$, do these ligands relinquish tetradentate chelation and become tri- or bidentate chelators. Similar bi- and tridentate coordination modes of the macrocyclic ligand are proposed to occur in the intermediates in formation of *cis* octahedral complexes.

We thank the *Deutsche Forschungsgemeinschaft* for financial support.

Figure 3. Possible mechanism for the formation of octahedral metal complexes by reaction of hydrated metal ions (L = H_2O) with ligands of the type $L-N_4R_2$

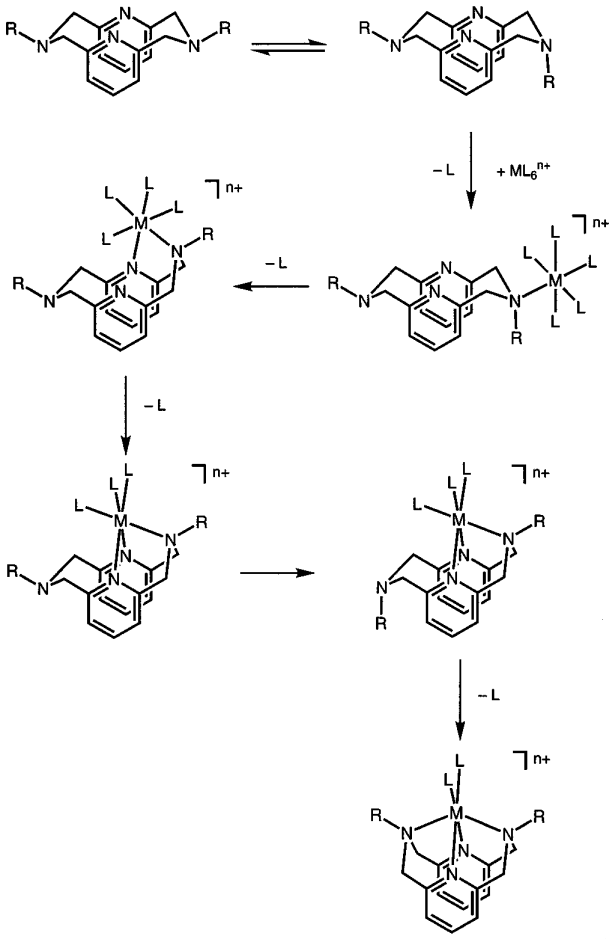

Experimental Section

Physical Methods: ^{1}H-NMR: Bruker AM 360, TMS as internal standard. The spectra of the dynamic NMR study were simulated using the program geNMR Version 3.4, IvorySoft, 1993. – UV/Vis: Varian Cary 5 E. – IR: Perkin-Elmer 1720 FT-IR.

Preparation of the Ligand: The tetraazamacrocyclic ligand $L-N_4Me_2$ was synthesized according to already published procedures, employing some slight modifications.[11]

[Mo(L−N$_4$Me$_2$)(CO)$_3$] (**8**): A solution of $[Mo(CO)_6]$ (134 mg, 0.5 mmol) and $L-N_4Me_2$ (134 mg, 0.5 mmol) in toluene (30 ml) was refluxed for 5 h under anaerobic conditions. The resulting red precipitate was collected by filtration, washed with toluene, and dried. Recrystallization by diffusion of ether into a solution of the solid in dimethylformamide (40 ml) afforded analytically pure product (127 mg, 57% yield) as a dark red crystalline material. – $C_{19}H_{20}N_4MoO_3$ (448.33): calcd. C 50.90, H 12.50, N 4.50; found C 50.72, H 12.45, N 4.57. – UV/Vis (dimethylformamide): λ_{max} (ε_M) = 407 (3090) and 315 (3610) nm. – IR (KBr): $\tilde{\nu}$ = 2933, 2898, 2766, 1893, 1762, 1604, 1570, 1464, 1449, 1431, 1374, 1163, 1093, 1020, 976, 819, 765 cm^{-1} (strong bands only).

Crystal Structure Analysis: Slow mixing by diffusion of two layers consisting of hexane and a solution of $[Mo(L-N_4Me_2)(CO)_3]$ in dimethylformamide afforded single crystals. Formula $C_{19}H_{20}N_4MoO_3$; M_r 448.33 g mol^{-1}; crystal dimensions 0.25 × 0.4 × 0.4 mm; crystal system monoclinic; space group $P2_1/m$ (No. 11); Z = 2; cell dimensions: a = 9.371(3), b = 11.780(3), c = 9.551(2) Å, β = 118.96(2)°; V = 922.5(4) Å^3; $\rho_{calcd.}$ = 1.614 g cm^{-3}; $F(000)$ = 456; graphite-monochromated Mo-K_α radiation (λ = 0.71073 Å); μ = 7.39 cm^{-1}; T = 293 K; Hilger & Watts diffractometer; ω-2Θ scans in the range 4.90° ≤ 2Θ ≤ 55.10°; 2167 unique reflections [1994 reflections with $F_o > 4\,\sigma(F_o)$]; 136 variables; GooF on F^2 [$F_o > 4\,\sigma(F_o)$] = 1.181; R [$F_o > 4\,\sigma(F_o)$] = 3.11% with $R = \Sigma\|F_o| - |F_c\|/\Sigma|F_o|$; wR^2 [$F_o > 4\,\sigma(F_o)$] = 7.05% with $wR^2 = \{\Sigma[w(F_o^2 - F_c^2)^2]/\Sigma[w(F_o^2)^2]\}^{1/2}$; largest peak (hole) = 0.58 (−0.92) e Å^{-3}. The positions of the non-hydrogen atoms were determined by SHELXS 86[12] and by Fourier difference maps using the program SHELXL-93.[12] The structural parameters were refined with the program SHELXL-93, using F^2 of all symmetry-independent reflections except those with very negative F^2 values. All non-hydrogen atoms were refined anisotropically. The complex is bisected by a crystallographical mirror plane passing through the molybdenum ion, one of the carbonyl ligands, the two amine nitrogen atoms, and the carbon atoms of the two methyl groups. Hydrogen atoms were assigned idealized locations and their isotropic temperature factors were refined.

Crystallographic data (excluding structure factors) for the structures reported in this paper have been deposited with the Cambridge Crystallographic Data Center as supplementary publication no. CCDC-101671. Copies of the data can be obtained free of charge on application to CCDC, 12 Union Road, Cambridge CB2 1EZ, UK (Fax: int. code + 44-1223/336-033; E-mail: deposit@ccdc.cam.ac.uk).

[1] [1a] H.-J. Krüger, *Chem. Ber.* **1995**, *128*, 531–539. – [1b] W. O. Koch, H.-J. Krüger, *Angew. Chem.* **1995**, *107*, 2928–2931; *Angew. Chem. Int. Ed. Engl.* **1995**, *34*, 2671–2674. – [1c] H. Kelm, H.-J. Krüger, *Inorg. Chem.* **1996**, *35*, 3533–3540. – [1d] W. O. Koch, V. Schünemann, M. Gerdan, A. X. Trautwein, H.-J. Krüger, *Chem. Eur. J.* **1998**, *4*, 686–691. – [1e] W. O. Koch, V. Schünemann, M. Gerdan, A. X. Trautwein, H.-J. Krüger, *Chem. Eur. J.* **1998**, *4*, 1255–1265.

[2] [2a] F. R. Fronczek, A. Mamo, S. Pappalardo, *Inorg. Chem.* **1989**, *28*, 1419–1422. – [2b] H. Sakaba, C. Kabuto, H. Horino, M. Arai, *Bull. Chem. Soc. Jpn.* **1990**, *63*, 1822–1824. – [2c] C.-M. Che, Z.-Y. Li, K.-Y. Wong, C.-K. Poon, T. C. W. Mak, S.-M. Peng, *Polyhedron* **1994**, *13*, 771–776.

[3] W. O. Koch, A. Barbieri, M. Grodzicki, V. Schünemann, A. X. Trautwein, H.-J. Krüger, *Angew. Chem.* **1996**, *108*, 484–486; *Angew. Chem. Int. Ed. Engl.* **1996**, *35*, 422–424.

[4] W. O. Koch, J. T. Kaiser, H.-J. Krüger, *J. Chem. Soc., Chem. Commun.* **1997**, 2237–2238.

[5] R. W. Hay, I. Fraser, G. Ferguson, *J. Chem. Soc., Dalton Trans.* **1989**, 2183–2186.

[6] V. Patinec, J.-J. Yaouanc, J. C. Clément, H. Handel, H. des Abbayes, M. M. Kubicki, *J. Organomet. Chem.* **1995**, *494*, 215–222.

[7] [7a] E. W. Abel, M. A. Bennett, G. Wilkinson, *J. Chem. Soc.* **1959**, 2323–2327. – [7b] L. W. Houk, G. R. Dobson, *J. Chem. Soc. A* **1966**, 317–319.

[8] G. Haselhorst, S. Stoetzel, A. Strassburger, W. Walz, K. Wieghardt, B. Nuber, *J. Chem. Soc., Dalton Trans.* **1993**, 83–90.

[9] F. A. Cotton, R.M. Wing, *Inorg. Chem.* **1965**, *4*, 314–317.

[10] [10a] S. E. Anslow, K. S. Chong, S. J. Rettig, A. Storr, J. Trotter, *Can. J. Chem.* **1981**, *59*, 3123–3135. – [10b] C. P. Marabella, J. H. Enemark, *J. Organomet. Chem.* **1982**, *226*, 57–62. – [10c] T. J. Desmond, F. J. Lalor, G. Ferguson, M. Parvez, *J. Organomet. Chem.* **1984**, *277*, 91–97. – [10d] R. A. Howie, G. P. McQuillan, *J. Chem. Soc., Dalton Trans.* **1986**, 759–764. – [10e] S. P. van Kouwenberg, E. H. Wong, G. R. Weisman, E. J. Gabe, F. L. Lee, P. Jackson, *Polyhedron* **1989**, *8*, 2333–2338. – [10f] T. M. Bockman, J. K. Kochi, *New J. Chem.* **1992**, *16*, 39–49. – [10g] K.-B. Shiu, J. Y. Lee, Y. Wang, M.-C. Cheng, S.-L. Wang, F.-

L. Liao, *J. Organomet. Chem.* **1993**, *453*, 211−219. − [10h] A. Chandrasekaran, S. S. Krishnamurthy, M. Nethaji, *J. Chem. Soc., Dalton Trans.* **1994**, 63−68.

[11] [11a] B. Alpha, E. Anklam, R. Deschenaux, J.-M. Lehn, M. Pietraskiewicz, *Helv. Chim. Acta* **1988**, *71*, 1042−1052. − [11b] F. Bottino, M. Di Grazia, P. Finocchiaro, F. R. Fronczek, A. Mamo, S. Pappalardo, *J. Org. Chem.* **1988**, *53*, 3521−3529.

[12] G. M. Sheldrick, *SHELXS-86: Crystal Structure Solution Program*, Göttingen, **1986**; G. M. Sheldrick in *Crystallographic Computing 3* (Eds.: G. M. Sheldrick, C. Krüger, R. Goddard) Oxford University Press, **1985**, pp. 175; G. M. Sheldrick, *SHELXL-93: Crystal Structure Refinement Program*, Göttingen, **1993**.

[98157]

Hemilabile Properties of Chelate Iron Complexes: Synthesis and Structure of Oxametallacycles

Géraldine Poignant, Sourisak Sinbandhit, Loïc Toupet, and Véronique Guerchais*

UMR 6509 CNRS – Université de Rennes 1, "Organométalliques et Catalyse", Université de Rennes 1, Beaulieu, F-35042 Rennes Cedex, France
Fax: (internat.) + 33-2/99281646
E-mail: guerchai@univ-rennes1.fr

Received April 22, 1998

Keywords: Carbene complexes / Aromatic substitution / Chelate iron complexes / Bond activation

Oxametallacycles $[Fe(C_5Me_5)(CO)\{C_3(C_6H_4\text{-}o\text{-}Cl)(CO_2Me)(R)O^a\}(Fe\text{–}O^a)]$ (**2**, R = OMe; **4**, R = Me) are accessible from the chelate (chloroaryl)carbene complex $[Fe(C_5Me_5)(CO)\{C(OMe)C_6H_4\text{-}o\text{-}Cl^a\}(Fe\text{–}Cl^a)][OTf]$ (**1**) upon treatment with the appropriate carbanions. Their formation arises from the lability of the chlorine atom. The related phosphonium salt $[Fe(C_5Me_5)(CO)\{C_3(C_6H_4\text{-}o\text{-}PMe_3)(CO_2Me)(OMe)O^a\}(Fe\text{–}O^a)][OTf]$ (**3**) is formed only for the bis(ester) derivative, via Ar–Cl bond activation. No reaction occurs for **4**, for which the coordination of the acetyl group has been supported by an X-ray analysis.

Aryl halides coordinating to metal centers are the focus of general interest especially for the functionalization of aromatic rings.[1] Halogenoarenes can be activated towards nucleophilic displacement by η^6 complexation to electron-deficient transition-metal centers.[2] We have previously reported that Ar−Cl bond cleavage can be achieved by complexation of the halide group.[3] Moreover, alkyl halide complexes $M(\eta^1\text{-}XR)$ have been shown to undergo nucleophilic attack at the α-carbon atom in the presence of Lewis bases.[4][5][6] This led us to investigate the reactivity of the electrophilic chelate (chloroaryl)carbene complex[7] $[Fe(C_5Me_5)(CO)\{C(OMe)C_6H_4\text{-}o\text{-}Cl^a\}(Fe-Cl^a)][OTf]$ (**1**) towards stabilized carbanions possessing coordinating carbonyl groups. Here, we report the access to new oxametallacycles, the lability of the chelated group, Cl versus C=O, involved in the formation of these species allows to induce nucleophilic aromatic substitution.

Complex **1** reacts at −80°C (1 h) with a THF solution of $NaCH(CO_2Me)_2$ affording the oxametallacycle $[Fe(C_5Me_5)(CO)\{C_3(C_6H_4\text{-}o\text{-}Cl)(CO_2Me)(OMe)O^a\}(Fe-O^a)]$ (**2**) which is isolated after chromatography as a green powder (Scheme 1). The complexation of the carbonyl group is evidenced by the ^{13}C-NMR spectrum ($CDCl_3$); the most characteristic features are the signals at δ = 262.4 ($Fe-C_\alpha$), 124.9 [$C(CO_2Me)$], and 177.3 ($C-O$) for the carbon atoms of the metallacycle. The low-field ^{13}C shift of the C_α resonance is intermediate between that of a carbene carbon atom and that of an alkenyl group, in agreement with two possible mesomeric forms. We assume that the formation of **2** results from an α attack by the nucleophile to give the C−C intermediate adduct, subsequent dissociation of the chlorine atom by the coordinating carbonyl group leads to the formation of a new five-membered ring (Scheme 2). Eventually, a spontaneous elimination of MeOH produces a more stable conjugated ring, i.e. the final product. Subsequent addition of PMe_3 to the reaction mixture affords the corresponding phosphonium salt $[Fe(C_5Me_5)(CO)\{C_3(C_6H_4\text{-}o\text{-}PMe_3)(CO_2Me)(OMe)O^a\}(Fe-O^a)][OTf]$ (**3**). The presence of the PMe_3 group is clearly established by NMR spectroscopy; its resonance is located at δ = 24.1 in the $^{31}P\{^1H\}$-NMR spectrum ($CDCl_3$). The $^3J(P-H_{Ar})$ and $^1J(P-C_{Ar})$ coupling constants of 15.6 Hz and 89 Hz, respectively, support the presence of the phosphorus atom on the aromatic ring. We assume that the formation of such species requires the activation of the Ar−Cl bond by the organo−iron fragment, the C=O group would be labile enough to be in equilibrium with the corresponding chloro-chelated species.

Scheme 1. Reagents and conditions: i) $NaCH(CO_2Me)_2$, THF, −80°C; ii) PMe_3

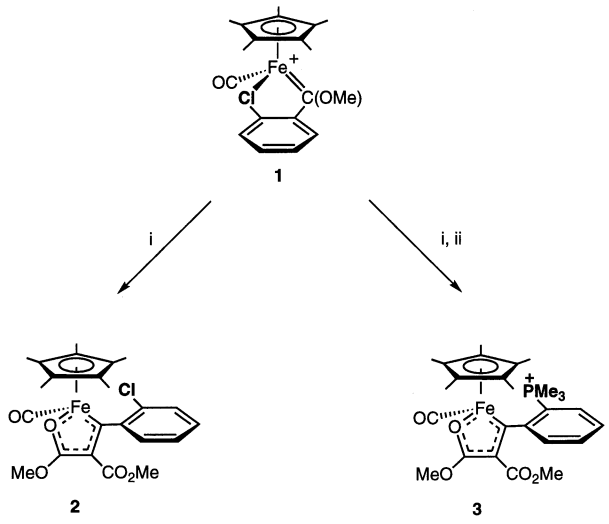

 © WILEY-VCH Verlag GmbH, D-69451 Weinheim, 1998 1434−1948/98/1010−1387 $ 17.50+.50/0

Scheme 2

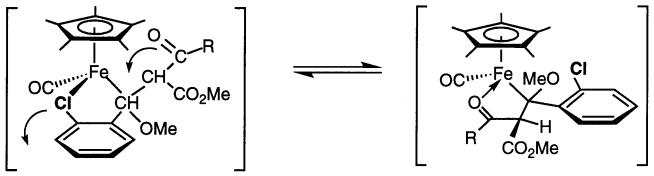

not dissociate in such conditions, the phosphorus-substituted derivative is only formed for the bis(ester)-containing complex.

In summary, oxametallacycles − depending on the labile character of the chelated group − allow Ar−Cl bond activation under mild conditions, a process which is mediated by the organo−iron fragment acting as a Lewis acid.[10] Studies on carbanions possessing other functional groups with different labile properties are under progress.

Figure 1. Molecular structure (ORTEP drawing) of **4**[a]

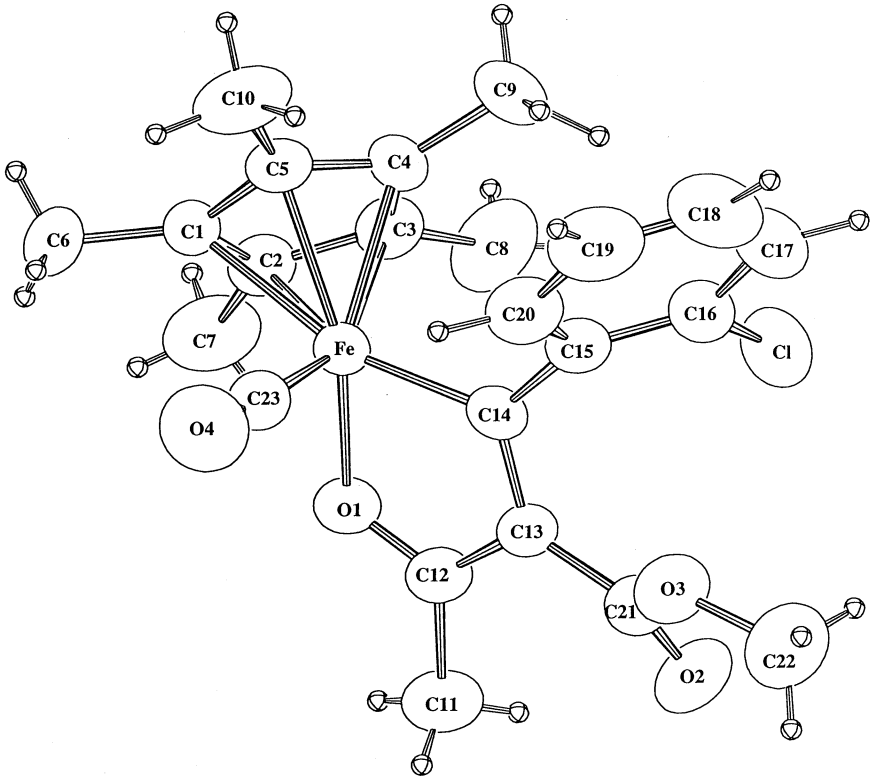

[a] Selected bond lengths [Å] and angles [°]: Fe−O1 1.951(3), O1−C12 1.254(6), C12−C13 1.429(6), C13−C14 1.387(6), Fe−C14 1.920(5); O1−Fe−C14 81.4(2), C14−Fe−C23 90.7(2), O1−Fe−C23 98.1(2), Fe−O1−C12 115.6(3), O1−C12−C13 116.9(4), C12−C13−C14 112.2(4), C13−C14−Fe 113.8(3).

Treatment of **1** with $NaCH(CO_2Me)(COMe)$, in which two different coordinating functions are present, gives $[Fe(C_5Me_5)(CO)\{C_3(C_6H_4\text{-}o\text{-}Cl)(CO_2Me)(Me)O^a\}(Fe-O^a)]$ (**4**) in which the acetyl group is complexed to the iron center. Green crystals are obtained in 50% yield after purification by chromatography. The ^{13}C resonances of the metallacycle [δ = 277.4 (Fe−C_α), 126.0 $C(CO_2Me)$, 207.6 (C−O)] are similar to those of **2**, the acetyl group giving rise to a lower field signal. The molecular structure[8] of **4** (Figure 1) confirms the proposed structure. The acetyl fragment coordinated to the iron center displays bond lengths which are closely similar to those of the chelate complex $[Fe(C_5H_5)(t\text{BuNC})[C_6F_4\text{-}o\text{-}C(O)Me](Fe-O^a)]$.[9] The bond lengths of the five-membered ring are in agreement with a delocalized system.

By contrast, no reaction with PMe_3 is observed in the case of complex **4**. This suggests that the acetyl group does

We thank the *Region Bretagne* for a grant to G. P., the *CNRS* and the *Université de Rennes 1* for financial support.

Experimental Section

A THF solution of **1** (520 mg, 1 mmol) was treated at −80°C with a freshly prepared THF solution of 2 equiv. of $NaCH(CO_2Me)(COR)$ (R = OMe, Me). After stirring for 3 h, the solution was concentrated to dryness. Compounds **2** and **4** were extracted with CH_2Cl_2 and chromatographed on alumina (eluent: pentane/Et_2O). Complex **2** (25%): ^1H NMR (200 MHz, $CDCl_3$): δ = 7.48 (dd, $^3J_{HH}$ = 7.8 Hz, $^4J_{HH}$ = 1.7 Hz, 1 H, Ar), 7.34 (dd, $^3J_{HH}$ = 8.8 Hz, $^4J_{HH}$ = 1.3 Hz, 1 H, Ar), 7.29 (td, $^3J_{HH}$ = 7.6 Hz, $^4J_{HH}$ = 1.3 Hz, 1 H, Ar), 7.11 (td, $^3J_{HH}$ = 7.5 Hz, $^4J_{HH}$ = 1.7 Hz, 1 H, Ar), 3.89 (s, 3 H, OMe), 3.49 (s, 3 H, OMe), 1.45 (s, 15 H, C_5Me_5). − $^{13}C\{^1H\}$ NMR (50.3 MHz, $CDCl_3$): δ = 262.4 (Fe−C_α), 218.2 (CO), 177.3 (C−O), 161.9 (C=O), 150.9 (Ar_{ipso}), 128.7 (Ar), 127.1 (Ar), 126.9 (Ar), 126.5 (Ar), 126.3 (Ar_{Cl}), 124.9 ($C$$CO_2Me$), 92.6

(C_5Me_5), 54.1 (OMe), 51.4 (OMe), 9.3 (C_5Me_5). − IR (pentane, cm^{-1}): $\tilde{\nu}$ = 1934 (s, ν_{CO}), 1724.8 (m, $\nu_{C=O}$). − HRMS for $C_{23}H_{25}ClFeO_5$; *m/z*: calcd. 472.0740 [M^+]; found 472.0738. − It is noteworthy that the disubstituted complex [Fe(C_5Me_5)(CO)-{$C_3(C_6H_4$-*o*-CH(CO_2Me)$_2$)(CO_2Me)(OMe)O^a}(*Fe*−*O*^{a})], in which the chloride has been replaced by the dimethylmalonate anion, is detected from the crude reaction mixture by HRMS (FAB) for $C_{29}H_{36}FeNaO_{10}$; *m/z*: calcd. 623.1556; found 623.1543 [M^+ + Na].

Complex **3** is obtained by addition of 3 ml of PMe_3 (1 M in toluene) at −80°C to the reaction mixture prepared as decribed above. Extraction with CH_2Cl_2 and crystallisation in CH_2Cl_2/Et_2O gave green microcrystals (17%). − ^{1}H NMR (300 MHz, $CDCl_3$): δ = 7.86 (dd, $^3J_{PH}$ = 15.6 Hz, $^3J_{HH}$ = 7.9 Hz, 1 H, Ar), 7.55 (m, 1 H, Ar), 7.45 (m, 2 H, Ar), 3.84 (s, 3 H, OMe), 3.49 (s, 3 H, OMe), 2.28 (d, $^2J_{PH}$ = 13.8 Hz, 9 H, PMe_3), 1.42 (s, 15 H, C_5Me_5). − ^{13}C{^{1}H} NMR (75.47 MHz, $CDCl_3$): δ = 261.5 (Fe−C_α), 218.3 (CO), 176.1 (C−O), 162.1 (C=O), 155.1 (d, $^2J_{PC}$ = 8.7 Hz, Ar_{ipso}), 132.5 (d, $^4J_{PC}$ = 3 Hz, Ar), 131.2 (d, $^2J_{PC}$ = 12 Hz, Ar), 127.1 (d, $^3J_{PC}$ = 13 Hz, Ar), 126.5 (*C*CO_2Me), 126.4 (d, $^3J_{PC}$ = 11 Hz, Ar), 115.6 (d, $^1J_{PC}$ = 89 Hz, Ar), 92.0 (C_5Me_5), 54.1 (OMe), 51.5 (OMe), 13.1 (d, $^1J_{PC}$ = 56.7 Hz, PMe_3), 9.4 (C_5Me_5). − ^{31}P {^{1}H} NMR (121.5 MHz, $CDCl_3$): δ = 24.11 (s, PMe_3). − IR (CH_2Cl_2, cm^{-1}): $\tilde{\nu}$ = 1938 (s, ν_{CO}), 1752 (m, $\nu_{C=O}$). − $C_{27}H_{34}FeF_3O_8PS$: calcd. C 48.96, H 5.17; found C 48.95, H 5.27.

Complex **4** (50%). − ^{1}H NMR (200 MHz, $CDCl_3$): δ = 7.43 (dd, $^3J_{HH}$ = 7.7 Hz, $^4J_{HH}$ = 1.8 Hz, 1 H, Ar), 7.36 (dd, $^3J_{HH}$ = 8 Hz, $^4J_{HH}$ = 1.3 Hz, 1 H, Ar), 7.29 (td, $^3J_{HH}$ = 7.8 Hz, $^4J_{HH}$ = 1.4 Hz, 1 H, Ar), 7.12 (td, $^3J_{HH}$ = 7.5 Hz, $^4J_{HH}$ = 1.7 Hz, 1 H, Ar), 3.50 (s, 3 H, OMe), 2.55 (s, 3 H, Me), 1.48 (s, 15 H, C_5Me_5). − ^{13}C{^{1}H} NMR (50.3 MHz, $CDCl_3$): δ = 277.4 (Fe−C_α), 217.3 (CO), 207.6 (C−O), 163.7 (C=O), 151.9 (Ar_{ipso}), 128.7 (Ar), 127.2 (Ar), 126.9 (Ar), 126.6 (Ar), 126.5 (Ar_{Cl}), 126.0 (*C*CO_2Me), 94.3 (C_5Me_5), 51.3 (OMe), 27.8 (Me), 9.3 (C_5Me_5). − IR (CH_2Cl_2, cm^{-1}): $\tilde{\nu}$ = 1930 (s, ν_{CO}), 1694 (m, $\nu_{C=O}$). − $C_{23}H_{25}ClFeO_4$: calcd. C 60.48, H 5.52; found C 60.43, H 5.47.

[1] V. V. Grushin, H. Alper, *Chem. Rev.* **1994**, *94*, 1047−1062 and references therein.

[2] For a review, see: L. Balas, D. Jurrhy, L. Latxague, S. Grelier, Y. Morel, M. Hamdani, N. Ardoin, D. Astruc, *Bull. Soc. Chim. Fr.* **1990**, *127*, 401−426.

[3] G. Poignant, S. Sinbandhit, L. Toupet, V. Guerchais, *Angew. Chem., Int. Ed. Engl.* **1998**, *37*, 963−965.

[4] R. J. Kulawiec, R. H. Crabtree, *Coord. Chem. Rev.* **1990**, *99*, 89−115.

[5] M. D. Butts, B. L. Scott, G. J. Kubas, *J. Am. Chem. Soc.* **1996**, *118,* 11831−11843.

[6] T.-S. Peng, C. H. Winter, J. A. Gladysz, *Inorg. Chem.* **1994**, *33*, 2534−2542.

[7] G. Poignant, S. Nlate, V. Guerchais, A. J. Edwards, P. R. Raithby, *Organometallics* **1997**, *16*, 124−132.

[8] Crystal structure of **4**: Enraf-Nonius CAD4 diffractometer, Mo-K_α radiation, μ = 8.16 cm^{-1}, *F*(000) = 1904, *T* = 294 K. Monoclinic *I*2/*a*, *a* = 16.071(8), *b* = 14.745(6), *c* = 19.558(9) Å, β = 104.81(6)°, *V* = 4481(6) $Å^{-3}$, Z = 8, ρ = 1.354 gcm^{-3}. 4227 reflections, 2179 with $I > 2\sigma(I)$ observed, ω/2θ = 1, *hkl*: −26.26, 0.17, 0.23. Lorentz and polarisation corrections (DEFLT 1990), *R* = 0.041, R_w = 0.043, $w = 1/\sigma(F_o)^2 = [\sigma^2(I) + (0.04F_o^2)^2]^{-1/2}$, S_w = 2.92 (residual $\Delta\rho < 0.48$ $eÅ^{-3}$). Crystallographic data (excluding structure factors) for the structure reported in this paper have been deposited with the Cambridge Crystallographic Data Centre as supplementary publication no CCDC-101876. Copies of the data can be obtained free of charge on application to CCDC, 12 Union Road, Cambridge CB2 1EZ, UK [Fax: int. code + 44(1223)366-033; E-mail: deposit@ccdc.cam.ac.uk].

[9] M. L. H. Green, J. Haggitt, C. P. Mehnert, *J. Chem. Soc. Chem. Commun.* **1995**, 1853−1854. A. N. Chernega, A. J. Graham, M. L. H. Green, J. Haggitt, J. Lloyd, C. P. Mehnert, N. Metzler, J. Souter, *J. Chem. Soc., Dalton Trans* **1997**, 2293−2303.

[10] The parent C_5H_5 complex was expected to be a better Lewis acid, however, attempts to synthesize the chelate complex [Fe(C_5H_5)(CO){C(OMe)C_6H_4-*o*-Cl^a}(*Fe*−*Cl*^{a})][OTf] was unsuccessful: C. Schulz, V. Guerchais, unpublished results.

[98122]

Chromium Sandwich Complexes of Polycyclic Aromatic Hydrocarbons: Triphenylene and Fluoranthene as η^6 Ligands

Christoph Elschenbroich*[1], Reinhart Möckel[A1], Alexander Vasil'kov[A2], Bernhard Metz[A1], and Klaus Harms[A1],

Fachbereich Chemie der Philipps-Universität Marburg[a],
Hans-Meerwein-Strasse, D-35032 Marburg, Germany
Fax: (internat.) + 49(0)6421/28-8917
E-mail: eb@ps1515.chemie.uni-marburg.de

A. N. Nesmeyanov Institute of Organoelement Compounds, Russian Academy of Sciences[b],
V-334 Vavilov st. 28, 117813 Moscow, Russia

Received March 10, 1998

Keywords: Polycycles / Sandwich complexes / Site preference / Cyclic voltammetry / NMR and EPR spectroscopy

The sandwich complexes bis(η^6-triphenylene)chromium (**12**) and bis(η^6-fluoranthene)chromium (**13**) have been prepared by means of metal atom/ligand vapor cocondensation. Whereas for triphenylene exclusive coordination to the peripheral rings is observed, the situation is more complicated for fluoranthene. According to NMR evidence initial metal coordination to the benzene (B) as well as to the naphthalene (N) section of the fluoranthene ligand occurs, leading to the isomers **13**(I) (η^6-B, η^6-B), **13**(II) (η^6-B, η^6-N) and **13**(III) (η^6-N, η^6-N). Since the substitutional lability of the chromium–naphthalene bond largely exceeds that of the chromium–benzene bond, the isomer distribution depends on the workup conditions; **13**(I) is clearly the most stable isomer. Crystal structure determinations performed for the salts [**12**][BPh_4] and [**13**][I] point to the preference for *syn* orientation of the polycyclic aromatic hydrocarbons and to a minute metal slippage in the peripheral direction. The triphenylene complex **12** features the electrochemically reversible redox couples **12** (+/0, metal-centered), **12** (0/–, ligand-centered) and **12** (–/2–, ligand-centered), the latter displaying a redox splitting of 300 mV. Conversely, for the fluoranthene complex **13**, secondary reduction **13** (–/2–) is irreversible. This finding is consistent with the larger redox splitting of ca. 480 mV which indicates more extensive interligand interaction in the dianion $\mathbf{13}^{2-}$, thereby favoring metal–ligand cleavage. While the radical cations $\mathbf{12}^{+\cdot}$ and $\mathbf{13}^{+\cdot}$ are amenable to EPR study, the radical anions $\mathbf{12}^{-\cdot}$ and $\mathbf{13}^{-\cdot}$ are too unstable. Instead, the radical anions of the free ligands are observed by EPR upon electrochemical reduction. In the case of **12**, the temporary existence of the radical anion $\mathbf{12}^{-\cdot}$ is indicated, however.

Introduction

Polycyclic aromatic hydrocarbons (PAHs)[2] have played an important role as potential ligands in sandwich complexes from the onset of bis(arene)metal chemistry. Fundamental questions deal with regioselectivity of coordination and the possibility of preparing oligonuclear complexes or even polymers with novel properties. PAHs as π ligands are encountered in a large number of carbonylmetal derivatives $[(PAH)metal(CO)_m]^{n+}$, in $[(PAH)metal(cyclopentadienyl)]^{n+}$ cations, in $[(PAH)metal(olefin)_m]^{n+}$ cations and in a few complexes of the type [(PAH)metal(phosphane)$_n$][3]. Conversely, the number of sandwich complexes (η^6-PAH)$_2$metal is very limited, the species $\mathbf{1}^{2-}$[4], $\mathbf{2}$[5a], $\mathbf{3}$[5], $\mathbf{4}$[6], $\mathbf{5}^{2+}$[7], $\mathbf{6}$[8], $\mathbf{7}^{+}$[9], $\mathbf{8}$[10] being the only examples characterized to date. The dianion $[(C_{10}H_8)_3Zr]^{2-}$ features bent naphthalene ligands and η^4 coordination[11]. The synthesis of binary complexes of transition metals and polycyclic hydrocarbons is desirable since it is only in the absence of auxiliary ligands that the basic questions addressed below may be studied unequivocally.

An ubiquitous feature of the coordination chemistry of polycyclic aromatic hydrocarbons is the ease of ligand hydrogenation during the course of wet chemical synthesis. Thus, early attempts to prepare bis(naphthalene)chromium by means of the Fischer−Hafner synthesis afforded bis(tetralene)chromium and the Nesmeyanov reaction was frequently accompanied by partial hydrogenation of the PAH. Therefore, metal atom/ligand vapor cocondensation techniques were originally used. Recently, the reaction of conventionally generated alkali metal naphthalenides with $MCl_3(THF)_3$ (M = V, Cr, Mo) and $MoCl_4(THF)_2$ has been introduced as a convenient method for the synthesis of bis(η^6-naphthalene)metal complexes[12]. Here we report on the binary chromium complexes of triphenylene **9** and fluoranthene **10**. These ligands are examples of the two types of condensation, triphenylene (**9**) representing the *kata* and fluoranthene (**10**) the *peri* principle. Furthermore, **9** is an alternant and **10** a nonalternant PAH. **9** and **10** may also be regarded as benzene rings with a biphenyl or a naphthalene unit, respectively, fused to them.

Fundamental questions in PAH coordination chemistry relate to site selectivity of bonding and to the possibility of

[◇] Part 51: Ref.[1].

 © WILEY-VCH Verlag GmbH, D-69451 Weinheim, 1998 1434−1948/98/1010−1391 $ 17.50+.50/0

Scheme 1

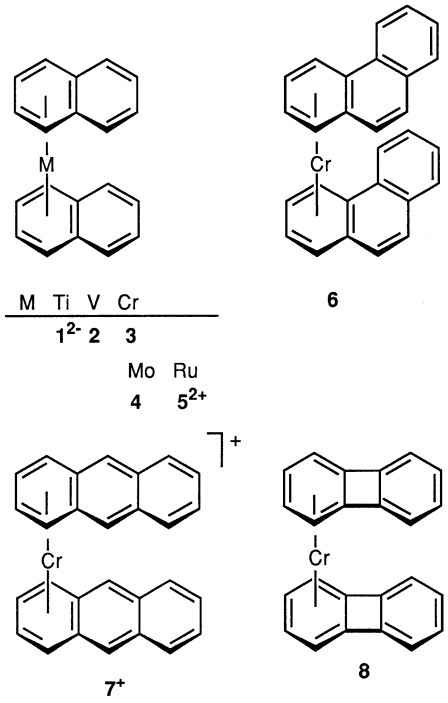

Scheme 2

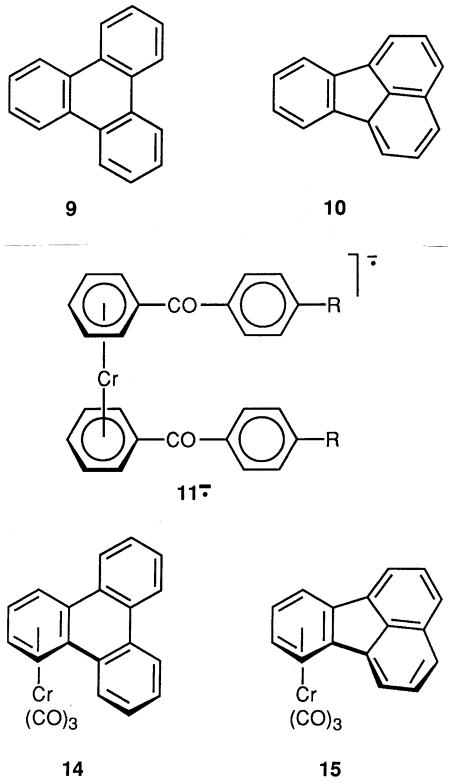

haptotropic shifts. Furthermore, in the case that in their η^6-coordinated state the ligands **9** and **10** maintain their ability to accept an additional electron forming radical anions, the question as to the rate of intramolecular electron transfer (ET) arises, since spin localization in one ligand as well as rapid interligand ET (delocalization) is conceivable. This dichotomy has previously been studied using EPR for benzoyl derivatives of bis(benzene)chromium ($\mathbf{11}^{-\cdot}$)[13]. Finally, interligand communication should also be apparent from an eventual redox splitting $\delta E_{1/2}$ exhibited by primary and secondary reduction of the complexes (η^6-PAH)$_2$Cr.

Results and Discussion

As has been demonstrated in the past for PAHs, metal atom/ligand vapor cocondensation techniques (CC) circumvent the problem of ligand hydrogenation and we therefore applied this method to the synthesis of bis(η^6-triphenylene)chromium (**12**) and bis(η^6-fluoranthene)chromium (**13**) (Scheme 3). The new complexes **12** and **13** were obtained in low yield as, respectively, brown or dark-violet air-sensitive solids which were only sparingly soluble in common organic solvents. The isomers **13**(II) and **13**(III) will be dealt with later. The separation of excess ligand from metal complex is a common problem in the metal-vapor technique of synthesis; it is particularly aggravating in the case of PAHs since the solubilities of the ligands and of the neutral complexes are often very similar. Conversion of the complex to its radical cation and extraction with water is not generally applicable since certain complex cations (η^6-PAH)$_2$Cr$^+$ are labile with respect to solvolysis (example: PAH = naphthalene[5]). However, the radical cations $\mathbf{12}^{+\cdot}$ and $\mathbf{13}^{+\cdot}$ are moderately inert in aqueous solution if kept in the dark; the photolability of $\mathbf{13}^{+\cdot}$ clearly exceeds that of $\mathbf{12}^{+\cdot}$. Thus, the redox cycle [**12** (**13**) $-$ e$^-$ $\rightarrow$ $\mathbf{12}^{+\cdot}$ ($\mathbf{13}^{+\cdot}$); extraction; $\mathbf{12}^{+\cdot}$ ($\mathbf{13}^{+\cdot}$) + e$^-$ $\rightarrow$ **12** (**13**)] can be utilized to effect separation of the complex from excess free ligand.

Single crystals suitable for X-ray diffraction could only be obtained for the complex cations $\mathbf{12}^{+\cdot}$ and $\mathbf{13}^{+\cdot}$ with BPh_4^- or I$^-$ serving as the counterion. Views of the structures are presented in Figures 1 and 2; bond lengths and bond angles are collected in the captions. Structural discussions of the class of compounds treated here should address the conformation in the solid state, ring slippage and the modification of ligand geometry induced by metal coordination. In **12**, as well as in **13**, chromium coordinates to the ring with the highest index of local aromaticity (ILA)[14] i.e. the ring which among the canonical forms most frequently appears with a Kekulé structure; this is a peripheral ring in **12** and the benzene (rather than the naphthalene) unit in **13**. The same site preference is adopted by the Cr(CO)$_3$ fragments in **14**[15] and **15**[16]. The complex cation in [**12**][BPh_4] adopts a conformation with regard to the sandwich axis which may be designated as synclinal, the torsional angle being 23.6°. This differs from the exact synperiplanar conformation which prevails in the related neutral complexes **3**[5b] and **8**[10]. Conceivably, the twisted disposition of the two ligands in $\mathbf{12}^+$, which is reminiscent of the graphite lattice, reduces interannular π-electron repulsion and is favored by the less dense packing in the complex salt [**12**][BPh_4] compared to the neutral complexes **3** and **8**.

For the salt [**13**][I], which contains the less bulky counterion I$^-$, the conformation with regard to the sandwich axis is synperiplanar. Interestingly, incorporation of solvent

Scheme 3

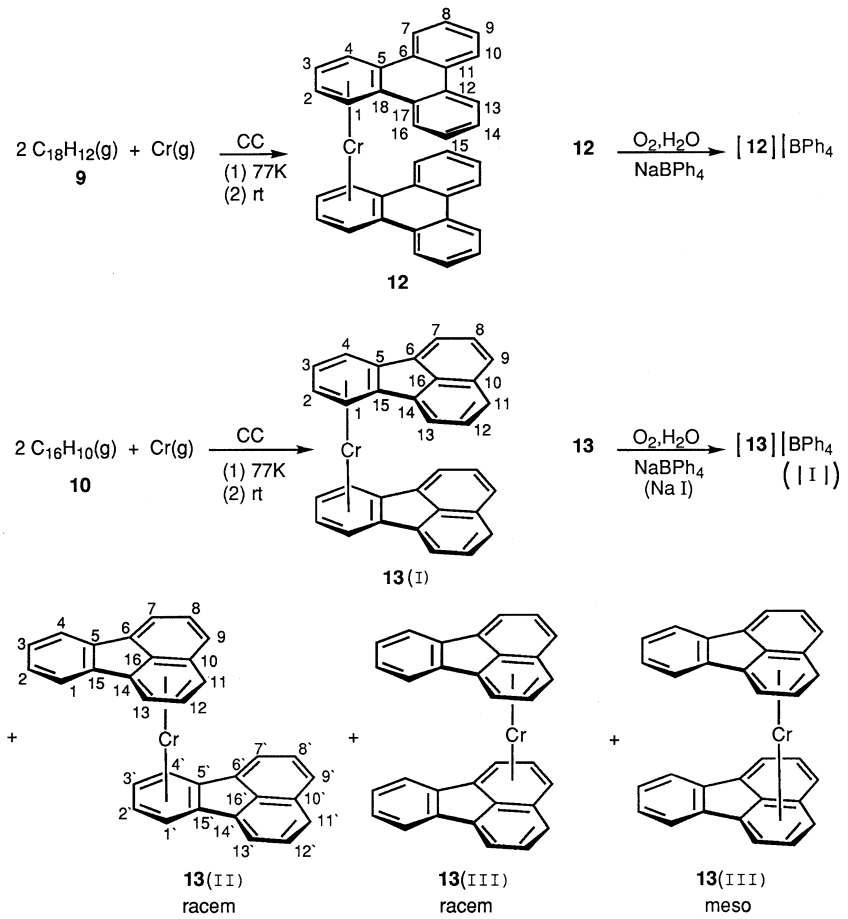

molecules in the lattice, as well as the use of a larger counterion, causes deviations of the conformation of $\mathbf{13}^{+\cdot}$ from exact synperiplanarity; for specimens of [**13**][I]·0.5 acetone and [**13**][BPh_4] torsional angles of 6.7° and 16.5° respectively were determined using X-ray diffraction[17]. Obviously, for sandwich complexes of PAHs packing forces are an important factor in the establishment of a certain ligand−metal−ligand disposition, probably overriding electronic factors. Ring slippage is minute in the structures of the cations $\mathbf{12}^{+\cdot}$ and $\mathbf{13}^{+\cdot}$; it is directed toward the ligand periphery and amounts to 3.9 pm ($\mathbf{12}^{+\cdot}$) and 5.2 pm ($\mathbf{13}^{+\cdot}$). A similar slippage has been reported for the half-sandwich complex (η^6-triphenylene)$Cr(CO)_3$[15]. Ring tilting is small as well, in that the deviations of the PAH ligands from a parallel disposition amount to 3.5° only for $\mathbf{12}^{+}$ and $\mathbf{13}^{+}$, the larger interplanar distance being encountered in the noncoordinated region; η^6 coordination renders the three peripheral rings of triphenylene structurally inequivalent in that the metal-bonded ring features significantly enlarged C−C bond lengths. Although the weighted average bond length of the free peripheral C rings amounts to 139 pm, that of the η^6-arene is 141 pm. The average C−C bond length for the central ring, which contributes two carbon centers to the coordinate bond, is 144 pm. This value exceeds the respective number for the free ligand triphenylene[18] by 1 pm and reflects the usual finding that in bis(arene)metal coordination δ backbonding M-δ→L is slightly more effective than σ, π donation M←σ,π-L. Bond length alternation in the central ring reflects the existence of three largely independent 6-π-electron systems in the peripheral rings and is, of course, also observed for the complex cation $\mathbf{12}^{+\cdot}$.

A similar trend is exhibited by the C−C bond lengths in (η^6-fluoranthene)$_2Cr^{+\cdot}$ ($\mathbf{13}^{+\cdot}$); the geometry of the naphthalene moiety is identical to that in the free ligand fluoranthene[19] while the η^6-benzene unit shows the typical increase of 2 pm for the C−C distances. The bonds C(5)−C(6), C(5′)−C(6′) and C(14)−C(15), C(14′)−C(15′) which connect the benzene and naphthalene moieties possess a mean length of 147 pm; thus, in the complex **13**, as well as in the free ligand **10**, naphthalene is linked to benzene by single bonds.

The site of chromium coordination in **12** and **13** follows, inter alia, from the ^{1}H-NMR spectra which in the case of the triphenylene complex **12** unambiguously demonstrate η^6 bonding to a peripheral ring. The relevant data are found

Figure 1. Molecular structure of compound [**12**][BPh_4]; top: SHELXTL/XP drawing with 50% probability ellipsoids; bottom: SHELXTL/XP drawing showing the ligand−metal−ligand torsion; C−*H* atoms omitted for clarity[a]

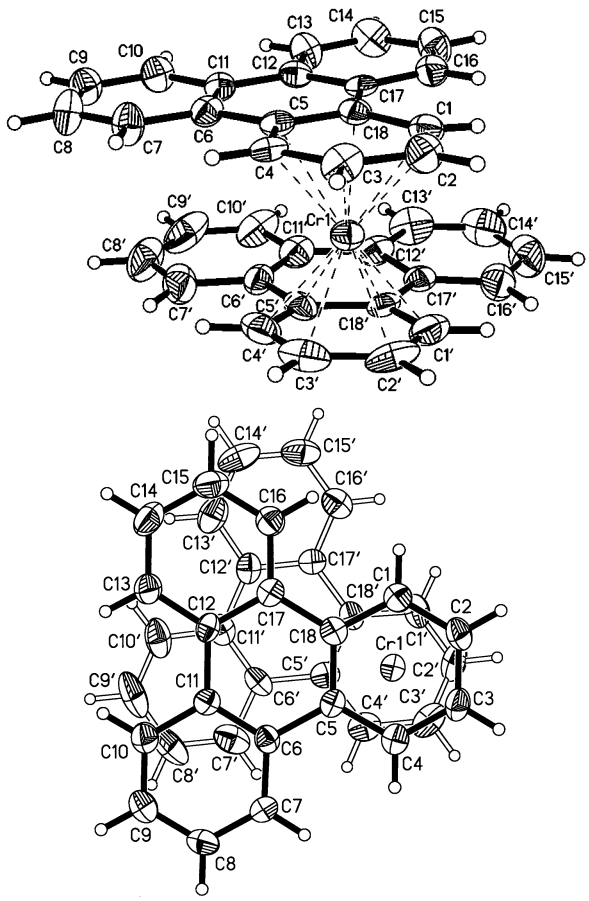

[a] Selected bond lengths [Å]: C1−C2 1.402(6), C2−C3 1.394(6), C3−C4 1.408(7), C4−C5 1.423(6), C5−C18 1.427(6), C1−C18 1.426(7), C5−C6 1.478(6), C6−C7 1.397(6), C7−C8 1.373(7), C8−C9 1.381(6), C9−C10 1.366(6), C10−C11 1.413(7), C11−C12 1.470(6), C12−C17 1.417(6), C12−C13 1.402(6), C13−C14 1.369(6), C14−C15 1.388(7), C15−C16 1.364(6), C16−C17 1.400(6), C17−C18 1.464(6), Cr1−C1 2.145(5), Cr1−C2 2.147(4), Cr1−C3 2.140(5), Cr1−C4 2.135(5), Cr1−C5 2.182(6), Cr1−C18 2.227(5); interplanar angle [°]: tilt of best ligand planes 3.50(7); torsional angle [°]: C1−C2−C2′−C1′ 23.6; ring slippage [A]: (Cr displacement toward ligand periphery) 0.037(2).

in Table 1. The spectrum initially obtained is unaffected by heating, therefore isomerization by haptotropic metal shifts is absent. Assignment of the chemical shifts δH(1, 4) and δH(2, 3) is based on their coordination shifts and on linewidth considerations; unresolved inter-ring coupling broadens the multiplet at lower field compared to that at higher field. Differentiation between δH(7, 16) and δH(10, 13) is achieved by means of selective homonuclear decoupling in that irradiation at δH(7) = 7.4 sharpens the signal δH(1, 4); differentiation between δH(8, 15) and δH(9, 14) follows from the effect of irradiation at δH(10) = 7.78 on the former two multiplets. It may be noted that apart from the usual, large coordination shifts Δδ*H* = −3.1 experienced by the protons H(1−4) which are directly bonded to an η-C atom, the protons H(7−10, 13−16) on the noncoordinated rings in **12** also display considerable upfield shifts.

Figure 2. Molecular structure of compound [**13**][I], SHELXTL/XP drawing viewed perpendicular and parallel to the sandwich axis; C−*H* atoms omitted for clarity[a]

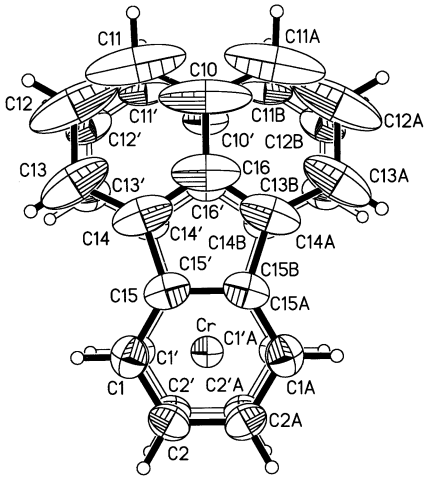

[a] Selected bond lengths [Å]: C1−C2 1.401(5), C2−C2A 1.407(7), C1−C15 1.393(5), C15−C15A 1.457(7), Cr−C1 2.149(3), Cr−C2 2.135(4), Cr−C2A 2.135(4), Cr−C1A 2.149(3), Cr−C15A 2.179(3), Cr−C15 2.179(3); interplanar angle [Å]: tilt of best ligand planes 3.70(8); torsional angle C1−C2−C1′−C2′ 0.2°; ring slippage [Å]: (Cr displacement toward ligand periphery) 0.036(6).

This probably reflects the temporary existence in solution of rotamers, which place one ligand in the shielding region (ring current) of the other. ^{13}C NMR of **12** suffers from low solubility; this calls for broad-band proton decoupling. A compilation of the chemical shifts and their provisional analysis is also given in Table 1. Whereas the differentiation between metal-coordinated and free positions is trivial in view of the large coordination shifts of the former, specific assignments are less secure. They are based on intensity criteria and on comparisons with the related complexes bis(naphthalene)chromium (**3**)[5c], bis(fluorene)chromium[20], and bis(9,10-dihydroanthracene)chromium[9] for which unequivocal analysis has been possible.

While NMR study of the *triphenylene* complex **12** was straightforward, essentially confirming the structural characteristics gleaned from X-ray diffraction, more complicated, albeit informative, NMR behavior is exhibited by the *fluoranthene* complex **13**. The complications arise from isomerism for which the spectra provide evidence; the additional information concerns the occurrence of haptotropic shifts which explain the spectral changes effected by modifying the workup conditions and upon thermal treatment of solutions of neutral **13**. As shown in Scheme 3, complex **13** may exist as an achiral bis(η^6-benzene) form (I), a pair of enantiomers featuring (η^6-benzene)(η^6-naphthalene) coordination (II) and a bis(η^6-naphthalene) variant (III) which should generate a pair of enantiomers and a *meso* form. Experimental evidence,[2][3][4] as well as local aromaticity (ILA) considerations,[14] suggest that coordination to a benzene ring is favored over bonding to a naphthalene unit, rendering isomer I the thermodynamically most stable product. Therefore, if the purification process, which consists of separating the water-soluble cation $\mathbf{13}^+$ from excess ligand is carried out at leisure, i.e. exposing $\mathbf{13}^+$

to the aqueous medium for one hour or more, the isomers featuring the labile (η^6-naphthalene) coordination are solvolytically cleaved and pure **13**(I) is isolated after reduction. The ^{1}H-NMR pattern in the η^6-arene region is depicted in Figure 3a; spectral parameters are collected in Table 2. Thermal treatment of this probe does not cause spectral changes, thereby confirming that in fact, **13**(I) is the most stable isomer.

Table 1. ^{1}H- and ^{13}C-NMR data for the ligand **9** and the complex **12**

Position	**9**[a]	**12**[a]	Δδ(**9**, **12**)[a]	**9**[b]	**12**[b]	Δδ(**9**, **12**)[b]
1, 4	8.42	5.39	−3.03	123.71	72.40	−51.31
2, 3	7.39	4.44	−2.95	127.38	78.23	−49.15
5, 18				130.35	84.41	−45.94
6, 17				130.35	135.02	+4.67
7, 16	8.42	7.40	−1.02	123.71	122.87	−0.84
8, 15	7.39	7.00	−0.39	127.38	125.26	−2.12
9, 14	7.39	7.19	−0.20	127.38	126.51	−0.87
10, 13	8.42	7.78	−0.64	123.71	123.22	−0.49
11, 12				130.35	130.11	−0.24

[a] δ^1H in C_6D_6 − [b] δ^{13}C in C_6D_6; coupling constants $J(^1H,^1H)$ [Hz]: **9**: J(1,2; 3,4; 7,8; 10,9; 13,14; 15,16) = 8.4, J(1,3; 2,4; 7,9; 8,10; 13,15; 14,16) = 1.3, J(1,4; 7,10; 13,16) = 0.5, J(2,3; 8,9; 14,15) = 6.8. − **12**: J(1,2; 3,4) = 5.5, J(1,3; 2,4) = 0.7, J(2,3) = 5.2, J(7,8; 15,16) = 7.5, J(7,9; 14,16) = 1.3, J(8,9; 14,15) = 7.3, J(8,10; 13,15) = 1.2, J(9,10; 13,14) = 7.9.

Table 2. ^{1}H-NMR data for the ligand **10**, the isomeric complexes **13**(I), **13**(II), **13**(III), and the complex **16**

Position	**10**[a]	**13**(I)[a]	**13**(II)[a]	**13**(III)[a]	**16**[a]
1 (1, 1′)[b]	7.73	4.86	(7.63, 5.13)	8.08	5.49
2 (2, 2′)	7.24	4.45	(7.34, 4.75)	7.40	4.67
3 (3, 3′)	7.24	4.45	(7.24, 4.52)	7.54	4.67
4 (4, 4′)	7.73	4.86	(7.55, 4.71)	8.03	5.49
7 (7, 7′)	7.64	6.83	(7.03, 6.75)	5.34	
8 (8, 8′)	7.37	7.08	(6.64, 7.20)	4.79	
9 (9, 9′)	7.61	7.35	(7.06, 7.44)	5.86	
11 (11, 11′)	7.61	7.35	(5.42, 7.42)	7.98	
12 (12, 12′)	7.37	7.08	(4.61, 7.37)	7.52	
13 (13, 13′)	7.64	6.83	(4.99, 7.05)	7.81	
17					3.76[c]

[a] δ^1H in C_6D_6; for the numbering see Scheme 3. − [b] In **13**(II). − [c] ^{2}H NMR in C_6H_6; coupling constants $J(^1H,^1H)$ [Hz]: **10**: J(7,8; 12,13) = 6.9, J(7,9; 11,13) = 0.5, J(8,9; 11,12) = 8.2, J(1,2; 3,4) = 7.6, J(1,3; 2,4) = 1.0, J(1; 4) = 0.7, J(2,3) = 7.5. − **13**(I): J(7,8; 12,13) = 6.9, J(7,9; 11,13) = 0.5, J(8,9; 11,12) = 8.2, J(1,2; 3,4) = 5.3, J(1,3; 2,4) = 0.7, J(1,4) = 0.8, J(2,3) = 5.2. − **13**(II): J(1′,2′; 3′,4′) = 5.5, J(2′,3′) = 5.2, J(11,12) = 5.3, J(12,13) = 5.5. − **13**(III): J(7,8) = 5.4, J(8,9) = 5.2. − **16**: J(1,2; 3,4) = 5.3, J(1,3; 2,4) = 0.6, J(1,4) = 0.6, J(3,2) = 5.0.

With the aim of identifying the less stable isomers, the redox procedure which effects the separation of unreacted excess ligand which is soluble in benzene from the water-soluble complex cation $\mathbf{13}^{+\cdot}$ was performed expeditiously, such that the mixture of primary cocondensation products was exposed to the aqueous medium for less than 10 minutes. After reduction to the neutral complex stage, ^{1}H NMR indicated the presence of two species A and B in a ratio of ca. 1:6. Attempts to isolate in pure form the species giving rise to spectrum B failed; however, after repeated crystallization of the product mixture, species B could be enriched to a composition A/B = 1:20 (Figure 3b). The ^{1}H-NMR spectrum of this sample was unchanged up to 80°C, whilst heating to 100°C led to the gradual disappearance of spectrum B and to the emergence of two new spectra C and D. During prolonged heating, spectrum D grew at the expense of spectrum C (Figures 3c−e). During all these manipulations the intensity of A remained approximately constant.

Table 3. ^{13}C-NMR data for the ligand **10**, the isomeric complexes **13**(I), **13**(II), **13**(III), and the complex **16**

Position	**10**[a]	**13**(I)[a]	**13**(II)[a]	**13**(III)[a]	**16**[a]
1 (1, 1′)[b]	121.91	76.27	(120.48, 77.05)	122.07	72.88
2 (2, 2′)	127.81	78.58	(127.66, 77.23)	124.58	74.26
3 (3, 3′)	127.81	78.58	(124.24, 76.48)	126.24	74.26
4 (4, 4′)	121.91	76.27	(121.74, 78.01)	120.79	72.88
7 (7, 7′)	120.35	117.19	(118.04, 117.59)	73.56	
8 (8, 8′)	128.22	128.00	(128.11, 128.29)	78.01	
9 (9, 9′)	126.89	123.14	(132.89, 123.08)	73.38	
11 (11, 11′)	126.89	123.14	(76.88, 123.04)	134.98	
12 (12, 12′)	128.22	128.00	(81.82, 127.91)	128.30	
13 (13, 13′)	120.35	117.19	(76.70, 117.47)	115.35	
17					80.29[c]

[a] δ^{13}C in C_6D_6; for the numbering see Scheme 3. − [b] In **13**(II). − [c] Triplet.

In order to interpret this evolution we start from the premise that the metal−ligand cocondensation process initially yields a mixture of isomers stemming from statistical, unspecific coordination of chromium atoms to all of the available benzenoid moieties. Extended exposure to an aqueous medium will lead to solvolytic cleavage of all of those species which contain either one or both sandwich ligands in an η^6-naphthalene coordination mode. Therefore, only **13**(I) survives in which both fluoranthene ligands bind to chromium via their benzene section. It is well known that in bis(naphthalene)chromium (**3**) the "first" naphthalene ligand is substitutionally more labile than the "second"[6a]. Thus, spectrum B, which is detected in addition to A after fast workup, should belong to isomer **13**(II). This suggestion is borne out by the observation of seven inequivalent proton signals, four doublets and three triplets, in the shift range characteristic for η-arene protons. The assignment given in Table 2 is based on HH-COESY and NOESY experiments. Spectrum C which dominates after thermal treatment points to isomer **13**(III) in which both ligands engage in coordination to chromium via a benzenoid system belonging to the naphthalene section. Apparently **13**(II) and **13**(III) exist in thermal equilibrium, the less stable isomer **13**(III) being formed at higher temperature, albeit at a small rate of interconversion. The room-temperature spectrum Figure 3d may therefore reflect a metastable state. Spectrum D which is also visible at this stage shows a simple AA′XX′ pattern, thereby indicating the presence of only *one* coordination mode, namely η^6 bonding via the benzene moiety. Since the chemical shifts in spectrum D differ from those observed for **13**(I) it must be assumed that

Figure 3. ^{1}H-NMR spectra (η^6-arene shift range, C_6D_6, room temperature) of the products from cocondensing fluoranthene vapor with chromium atoms; (a) after workup with extended (90 min) exposure to an aqueous medium; (b) after workup with short ($\leq$ 10 min) exposure to an aqueous medium and repeated recrystallization to enrich component B (A/B $\approx$ 1:20); (c) after subjecting probe b to 100°C for 8d; (d) after 16 d at 100°C; (e) after 42 d at 100°C

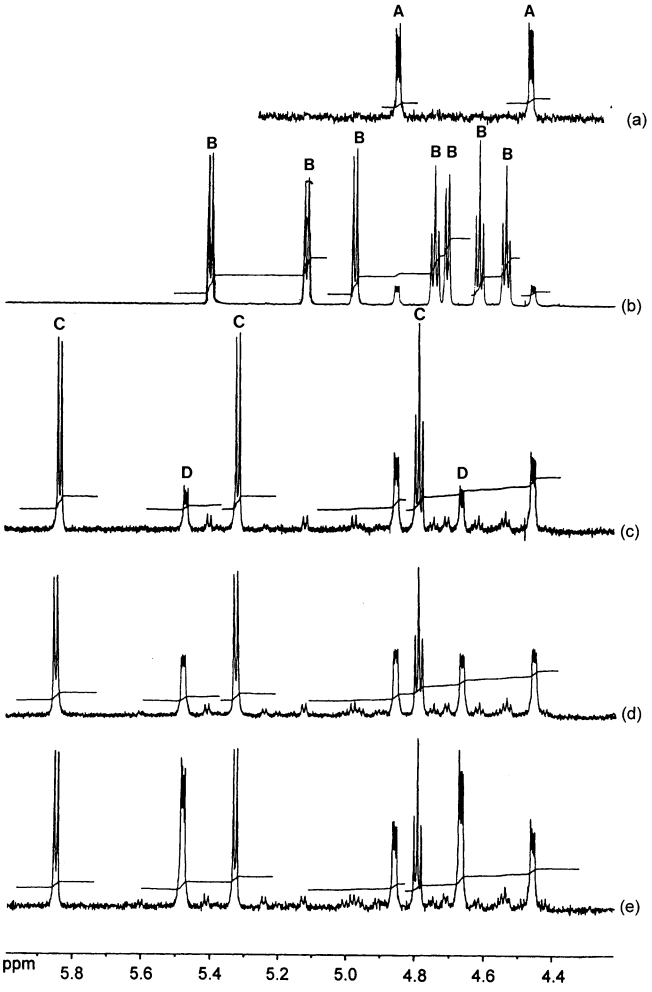

a second ^{1}H-NMR-silent ligand completes the coordination sphere. C_6D_6, the solvent molecule, could be a likely candidate, introduced by ligand substitution leading to (η^6-fluoranthene)(η^6-deuterobenzene)chromium (**16**). In order to test this hypothesis, thermal treatment of a mixture of **13**(I) and **13**(II), dissolved in C_6D_6, was repeated and at various time intervals, after having recorded the ^{1}H-NMR spectrum, the solvent C_6D_6 was removed in vacuo and replaced by C_6H_6. The solutions thus obtained were subjected to ^{2}H NMR. It was found that build-up of the ^{1}H-NMR spectrum C correlates with the observation in ^{2}H NMR of a singlet at δ = 3.76, the characteristic chemical shift for η^6-benzene. This attests to ligand substitution of fluoranthene by benzene. Based on the NMR observations, the course of events may therefore be sketched as shown in Scheme 4.

The redox behavior of the complexes **12** and **13**, not surprisingly, reflects the properties of the bis(η^6-arene)chromium core and those of the ligands triphenylene **9** and fluoranthene **10**. Cyclovoltammetric traces are depicted in Figures 4 and 5; the electrochemical parameters are given in

Scheme 4

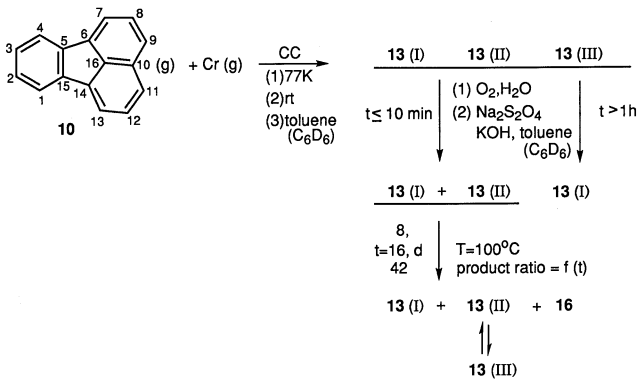

the captions. The redox couples $E_{1/2}$ ($\mathbf{12}^{+/0}$) = -0.62 V and $E_{1/2}$ ($\mathbf{13}^{+/0}$) = -0.64 V are reversible and deviations from the peak current ratio $p_c/p_a = 1$ are probably due to adsorption effects. The magnitudes of the potentials differ only marginally, which is plausible in view of the fact that the redox orbital is essentially metal centered[21]. Changes in the ligand periphery therefore exert only an indirect influence. Conversely, the reduction processes as gauged by the potentials $E_{1/2}$ ($\mathbf{12}^{0/-}$), E($\mathbf{12}^{-/2-}$) and E($\mathbf{13}^{0/-}$), E($\mathbf{13}^{-/2-}$), respectively, mirror the differing electron affinities of triphenylene and fluoranthene, again in accord with the electronic structure of bis(arene)chromium which assigns considerable ligand participation to the LUMO. Thus, compared to **12**, electron transfer to **13** occurs at a somewhat more positive potential. This gradation also applies to the free ligands **10** and **9**[22]. Relative to the free ligands **9** and **10**, reduction of the complexes **12** and **13** features cathodic shifts; this accords with the ligand-dominated nature of the LUMO in bis(arene)metal complexes and the fact that the η^6-arenes bear a negative partial charge[21b]. For the triphenylene complex, a second reduction step can be observed which, as judged from the peak separation, appears to be reversible too. The peak current ratio is difficult to assess at this negative potential near the cathodic limit imposed by the medium. It is worth mentioning that the cyclovoltammogram of **12** does not feature waves which indicate the presence of free ligand. Therefore, bis(triphenylene)-chromium must be fairly robust, at least in the oxidation states $\mathbf{12}^{+,0,-}$, although the potential separation δE(0/$-$, $-$/2$-$) = 300 mV between primary and secondary reduction demonstrates appreciable interligand interaction. For the fluoranthene complex **13** this interaction seems to be even more pronounced since δE(0/$-$, $-$/2$-$) = 480 mV is larger. Consequently, the second reduction step $\mathbf{13}^{-/2-}$ is irreversible and the cyclovoltammogram contains weak waves which point to the presence of free fluoranthene, generated through metal$-$ligand bond cleavage. Therefore, strictly speaking, the value $\delta E(\mathbf{13}^{0/-,\ -/2-})$ given above is only a rough estimate.

The differing robustness of **12** and **13** against solvolytic cleavage also emanates from the EPR spectra; these are depicted in Figures 6 and 7, with the EPR parameters listed

Figure 4. Cyclic voltammogram of complex **12** at −40°C in 1,2-dimethoxyethane/0.1 M tetrabutylammonium perchlorate: working electrode, glassy carbon; reference electrode, SCE; v = 100 mVs^{-1}. $E_{1/2}$(**12** +/0) = −0.62 V, ΔE_p = 44 mV, r = 0.7; $E_{1/2}$(**12** 0/−) = −2.31 V, ΔE_p = 90 mV, r = 1.0; $E_{1/2}$(**12** −/2−) = −2.61 V, $\Delta E_p \approx$ 80 mV, $r \approx 0.5$; E_{pa} = 0.85 V (irreversible secondary oxidation)

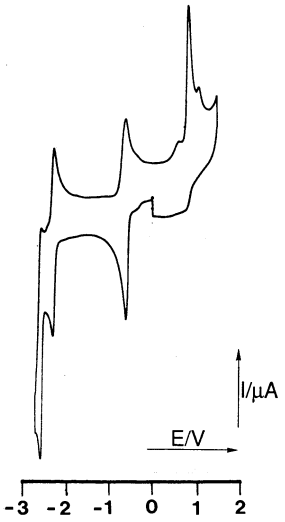

Figure 5. Cyclic voltammogram of complex **13** at −40°C in dimethoxyethane/0.1 M tetrabutylammonium perchlorate: working electrode, glassy carbon; reference electrode, SCE. v = 100 mVs^{-1}; $E_{1/2}$(**13** +/0) = −0.62 V, ΔE_p = 60 mV, r = 0.7; $E_{1/2}$(**13** 0/−) = −1.87 V, ΔE_p = 86 mV, $r \approx 1.1$ (cannot be measured accurately due to overlap with free ligand reduction); E_{pc} = −2.39 V (irreversible secondary reduction); E_{pa} = 0.65 (irreversible secondary oxidation); the shoulders marked L, are caused by first and second reduction of the free ligand **10**: $E_{1/2}$(**10** 0/−) = −1.73 V, ΔE_p = 54 mV, r = 0.76; E_{pc} = −2.21 V (irreversible secondary reduction); these data agree with those obtained from a control experiment with pure **10**

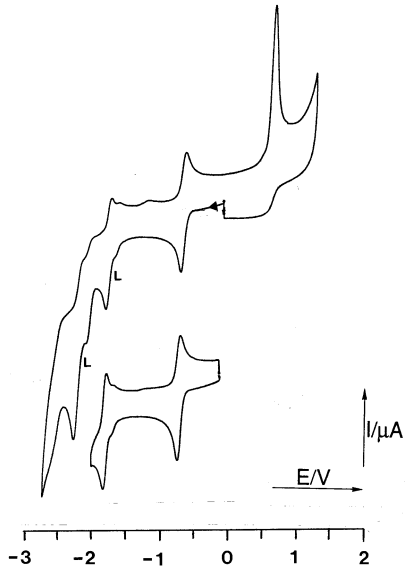

in the captions. The EPR spectra of the radical cations $\mathbf{12}^{+\cdot}$ and $\mathbf{13}^{+\cdot}$, generated either by air oxidation or electrochemically, differ in the extent to which chemically nonequivalent proton sites are resolved in the hyperfine structure. For $\mathbf{13}^{+\cdot}$ (Figure 7c) a pattern is observed which is consistent with eight equivalent protons, a(8 ^{1}H) = 0.34 mT, the difference between the coupling constants a(4 ^{1}H 1, 4) and a(4 ^{1}H 2, 3) not being resolved. Conversely, for $\mathbf{12}^{+\cdot}$ experiment and simulation yield the parameters a_1(4 ^{1}H) = 0.32 mT and a_2(4 ^{1}H) = 0.395 mT. Independent assignment of these coupling constants to positions at the ring cannot be made in the absence of specific deuteration. Thus, taking into consideration the aggregate nature of the mechanism of spin transfer from the central metal to ring protons in bis(arene)metal complexes[23], attempts to interpret in detail the 20% difference in the two experimental proton coupling constants for $\mathbf{12}^{+\cdot}$ would not be worthwhile. An aspect which should be addressed here, however, is the isomerism of the fluoranthene complex **13** which was discussed in the NMR section and which would be expected to manifest itself in the EPR spectra of the corresponding radical cations as well. As in the NMR study, we therefore varied the workup protocol in order to search for spectral differences. The results are depicted in Figure 7. A surprising observation is the detection of an EPR signal in the original cocondensation *before* oxidation to the radical cation (Figure 7a). While the basic features of this spectrum are characteristic of a bis(π-perimeter)chromium(d^5) species, the hyperfine pattern is unexpected since it shows coupling to *four* equivalent protons only. This can only be reconciled with a structure in which one of the fluoranthene ligands is η^6-bonded via its benzene moiety, the remainder of the coordination sphere being EPR silent. A possibility would be that the second fluoranthene ligand binds to chromium with the central, five-membered ring which is devoid of protons. Interestingly, the EPR parameters observed for this species [a(4 ^{1}H) = 4.38, a(^{53}Cr) = 15.4 G], apart from proton hyperfine multiplicity, differ significantly from the data typical for a bis(η^6-arene)Cr$^{+\cdot}$ radical cation such as $\mathbf{13}^{+\cdot}$ [a(8 ^{1}H) = 3.4, a(^{53}Cr) = 18.3 G]; they are very similar to the coupling constants reported for (η^5-C_5H_5)Cr(η^6-C_6H_6) [a(5 ^{1}H) = 2.35, a(6 ^{1}H) = 4.65, a(^{53}Cr) = 14.68 G[24]], however, thereby lending support to the proposal given above. On the other hand, coordination of chromium to the central five-membered ring is difficult to reconcile with the structural data of the ligand **9.** For this ligand the lengths of the bonds connecting the benzene and the naphthalene moieties are close to those of single bonds[18]. Furthermore, the presence of Cr(d^5), formally Cr^{1+}, would require a negatively charged ligand in the species under consideration, assuming that the latter is neutral. While in the parent complex (η^6-C_6H_6)Cr^{I}(η^5-C_5H_5) the negative charge of the cyclopentadienyl ligand results from deprotonation of C_5H_6, in the case of the primary radical complex in the cocondensation of chromium atoms with fluoranthene metal→ligand single-electron transfer could lead to an anionic ligand. This would, however, generate a biradical for which EPR fails to provide evidence. The nature of the species giving rise to the primary EPR signal cannot, therefore, be determined definitively.

In the NMR study, the critical factor leading to differences in the product distribution was the duration of exposure to an aqueous medium during the workup process.

Figure 6. EPR spectra of (a) the radical cation $\mathbf{12}^{+\cdot}$, (b) the radical anion $\mathbf{12}^{-\cdot}$ and (c) the radical anion $\mathbf{9}^{-\cdot}$ of the free ligand, generated electrochemically in situ (gold cathode, DME, nBu$_4$NPF$_6$, −40°C); the applied potential was gradually increased to 5 V; (d): $\mathbf{12}^{+\cdot}$ in CH_3OH at −30°C, second derivative trace and simulation; $\mathbf{12}^{+\cdot}$: $\langle g\rangle = 1.986$, $a_1(4\ ^1H) = 3.2$ G, $a_2(4\ ^1H) = 3.95$ G, $a(^{53}Cr) = 18.22$ G; $\mathbf{12}^{-\cdot}$: $\langle g\rangle = 1.991$, hyperfine pattern irregularly spaced; $\mathbf{9}^{-\cdot}$: $\langle g\rangle = 2.0037$; 1 G = 0.1 mT

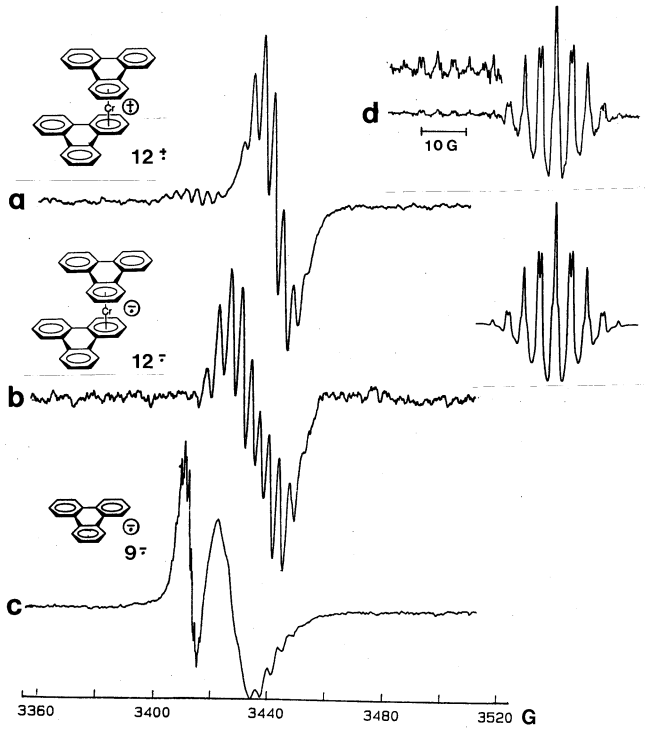

This parameter also governs the nature of the EPR spectra obtained. The fast workup variant led to a sample which gave rise to the ^{1}H-NMR spectrum shown in Figure 3b, which was assigned to isomer **13**(II). When this sample was oxidized in DME as a solvent to its radical cation, the EPR spectrum depicted as Figure 7b was observed. The hyperfine pattern points to seven protons which are equivalent within the resolution attained. The detection of an even number of lines clearly demonstrates that one ligand must coordinate to Cr(d^5) via benzene and the other via a naphthalene π subsystem [isomer $\mathbf{13}(II)^{+\cdot}$]. If, alternatively, the cocondensate is taken up in methanol and extensively oxidized with air, the spectrum shown in Figure 7c arises. This spectrum is also obtained from analytically pure [**13**][BPh_4]. The well-resolved nonuplet is in accord with the coordination mode of isomer $\mathbf{13}(I)^{+\cdot}$.

The reversible nature of the redox couples **12** (0/−) and **13** (0/−) suggested that intra muros reduction in the cavity of an EPR instrument[25] should yield spectra of the radical anions $\mathbf{12}^{-\cdot}$ and $\mathbf{13}^{-\cdot}$. However, experiments were frustrated by metal−ligand cleavage, possibly at the dianion stage, which could not be avoided due to insufficient control of the potential in the two-electrode set-up. A typical course of events is shown in Figure 6. Upon applying a negative potential to the gold spiral in the electrochemical cell the EPR spectrum due to $\mathbf{12}^{+\cdot}$ (a) becomes gradually superimposed by a new signal, shifted to a g factor which is closer

Figure 7. EPR spectra of products from the cocondensation of fluoranthene **10** with chromium atoms; (a) initial product mixture extracted with toluene, exclusion of oxygen $\langle g\rangle = 1.9892$, $a(4\ ^1H) = 4.38$ G, $a(^{53}Cr) = 15.4$ G, lower trace simulated; (b) spectrum observed after short exposure of the cocondensate to oxygen, reduction and reoxidation in an aprotic medium (DME), $\langle g\rangle = 1.9888$, $a(7\ ^1H) = 3.43$ G, $a(^{53}Cr) = 18.13$ G; (c) spectrum observed upon extraction of cocondensate with CH_3OH, access of oxygen, for 1 h, −40°C, $\langle g\rangle = 1.9871$, $a(8\ ^1H) = 3.40$ G, $a(^{53}Cr) = 18.3$ G; (d) spectral change caused by electrochemical intra muros reduction of probe b, applied potential −3.8 V; the well-resolved spectrum at low field belongs to the free ligand radical anion $\mathbf{10}^{-\cdot}$.

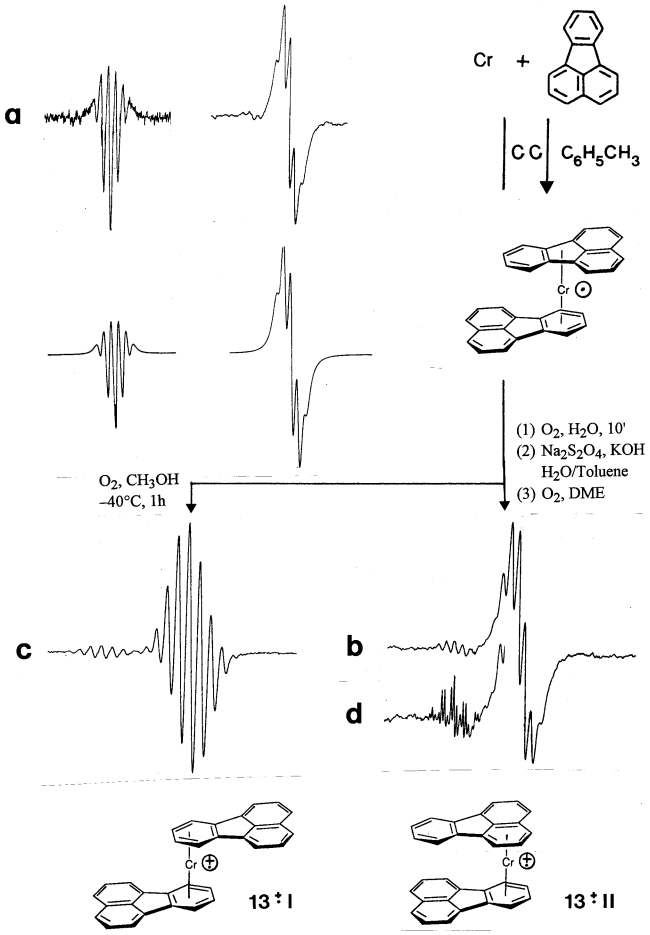

to the free spin value (b). This is in accord with the spectrum expected for the radical anion $\mathbf{12}^{-\cdot}$ since the metal contribution to the LUMO of bis(arene)chromium falls short of that which is contained in the HOMO. Before reaching the stage of reduction where $\mathbf{12}^{-\cdot}$ is the only species present, line broadening sets in which presumably stems from self exchange either of the $\mathbf{12}/\mathbf{12}^{-\cdot}$ or of the $\mathbf{12}^{-\cdot}/\mathbf{12}^{2-}$ type. Alternatively, line broadening could be caused by spin−spin interaction in a biradical dianion $\mathbf{12}^{2-\cdot\cdot}$ generated in the second reduction step. This dianion is very labile, however, since concurrently a signal with $g = 2.0037$ builds up which, upon expansion, is identified as being caused by $\mathbf{9}^{-\cdot}$, the radical anion of the free ligand[26] (c). Unequivocal analysis of the EPR spectrum of $\mathbf{12}^{-\cdot}$ is therefore prevented and the extent of electron delocalization cannot be determined. An analogous situation is encountered in the reduction of **13**; here, as demonstrated by the cyclovoltammetric results, the tendency toward metal−ligand cleavage

Table 4. Crystallographic data for compounds [**12**][BPh_4], [**13**][I]·acetone, and [**13**][I]

Cmpd.	[12][BPh_4]	[13][I]*0.5 acetone	[13][I]
Crystal size [mm]	0.4 x 0.4 x 1	0.3 x 0.3 x 0.1	0.25 x 0.20 x 0.05
Crystal system	monoclinic	orthorhombic	Orthorhombic
Space group	$P2_1/n$, Z= 4	Fdd2 , Z= 16	Pnma , Z= 4
Lattice constants (pm/°]	a = 1537.4(2)	a = 2163.7(1)	a = 2239.2(2)
	b = 1663.6(2) β = 107.1(1)	b = 2697.5(2)	b = 1018.1(1)
	c = 1672.1(4)	c = 1752.1(1)	c = 1044.8(1)
Volume (nm^3)	4.0869(12)	10.2263(11)	2.3818(4)
Formula sum	$C_{60}H_{44}BCr$	$C_{33.5}H_{23}CrIO_{0.5}$	$C_{32}H_{20}CrI$
Formula weight	827.76	612.42	583.38
Density (calc.) (Mg/m^3)	1.345	1.591	1.627
Absorpt. coefficient (mm^{-1})	0.323	1.678	1.795
F(000)	1732	4880	1156
Diffraktometer used	Enraf Nonius CAD4	Stoe IPDS	Stoe IPDS
Wave length	MoKα (71.073 pm)	MoKα (71.073 pm)	MoKα (71.073 pm)
T [K]	193(2)	293(2)	233(2)
Theta range[°]	2.45 to 21.95	2.41 to 25.93	2.15 to 25.90
Index range (h,k,l)	–16/0, 0/17, –16/7	–26/25, –33/33,–20/21	–27/23, –12/12, 12/12
Scan type	Omega	area detector	area detector
Program data collection	CAD4 EXPRESS	Stoe Expose	Stoe Expose
Data reduction	XCAD4 (Harms, 1993)	Stoe Integrate	Stoe Integrate
No. of collected refl.	3703	19778	13447
No. of unique refl.	3575 [R(int) = 0.0228]	4792 [R(int) = 0.0865]	2428 [R(int) = 0.0665]
No. of obs. refl. (>2σ(I))	2572	3550	1460
No. of used reflections	3575	4792	2428
Absorption correction	none	none	Analytical
Max. und min. transmission			0.916, 0.662
Structure solution	direct methods	direct methods	direct methods
Structure refinement	full matrix on F^2	full matrix on F^2	full matrix on F^2
Programs used	SHELXTL–PLUS (Siemens)	SHELXTL–PLUS	SHELXTL–PLUS
	SHELXS–96 (Sheldrick,1996)	SHELXS–96	SHELXS–97 (Sheldruck,1997)
	SHELXL–96 (Sheldrick,1996)	SHELXL–96	SHELXL–97 (Sheldrick, 1997)
Extinction coefficient	0.0010(3)		
Weighting param. q1,q2*	0.0629, 1.0397	0.0595, 0	0.0291, 0
"Goodness–of–fit" on F^2	1.053	0.945	0.833
e–max,min [e/nm^3]	177, –207	558, –360	736, –595
"Flack" parameter		–0.04(3)	
No. of refined parameters	560	327	163
R (observed reflections)	0.0456	0.0405	0.0341
wR2 (used reflections)	0.1166	0.1052	0.0642

* weighting scheme : $w=1/[\sigma^2(Fo^2)+(q1*P)^2+q2*P]$ with $P=(Fo^2+2Fc^2)/3$

of the anion is even more pronounced. As shown in Figure 7d, the EPR spectrum of the free fluoranthene radical anion $\mathbf{10}^{-\cdot}$[27] appears at a stage where the radical cation $\mathbf{13}^{+\cdot}$ is still present in large excess. While $\mathbf{10}^{-\cdot}$ would be expected to be removed instantaneously through electron transfer to $\mathbf{13}^{+\cdot}$, simultaneous observation of both paramagnetic species may be traced to the cell construction[25]. A high local concentration of electrochemical reduction products is generated in a region where EPR sensitivity is maximal, namely near the surface of the gold spiral which serves as the cathode.

We thank the *Deutsche Forschungsgemeinschaft* and the *Fonds der Chemischen Industrie* for support. This work is a part of cooperative project between Ch. E. and A. V. sponsored by the *Volkswagen Stiftung* which we gratefully acknowledge. We are indebted to Prof. *M. Zander* for a gift of triphenylene and for helpful comments.

Experimental Section

General: All manipulations were carried out with exclusion of air under dinitrogen or argon (CV) unless stated otherwise. Physical measurements were performed with the equipment specified previously[28].

Bis[η(1,2,3,4,5,18)triphenylene]chromium (**12**): 5 g (22 mmol) of triphenylene was evaporated from an electrically heated internal

glass vessel held at 10^{-4} Torr within a 6-l glass reactor which was cooled with liquid N_2. Simultaneously, 1.8 g (34.6 mmol) of chromium, contained in a spiral of tungsten wire (∅ 1 mm), was evaporated by a heating current of 40 A at 8 V. The brownish black cocondensate was warmed to room temperature and suspended in 100 ml of toluene. After the access of air, 200 ml of water was added and the red aqueous phase washed with two portions (50 ml) of toluene and one portion of petroleum ether. The aqueous phase was then layered with 150 ml of toluene, exclusion of air provided for and ca. 10 g of $Na_2S_2O_4$ and 10 g of KOH added. Stirring was continued for about 2 h, the aqueous phase then turned colorless and the organic phase brown. Toluene was removed in vacuo and the residue kept at 10^{-4} Torr for 6 h. **12** (280 mg, 1.6% referred to Cr evaporated) was obtained as a dark brown microcrystalline product. Recrystallization was effected by layering a solution of **12** in toluene with petroleum ether (boiling range 40−60°C) and cooling to −20°C. − MS (EI, 70 eV); *m/z* (%): 508 (3.2) [M^+], 280 (4.3) [$M^+ - C_{18}H_{12}$], 228 (100) [$C_{18}H_{12}^+$], 52 (10.9) [Cr^+]. − $C_{36}H_{24}Cr$ (508.58): calcd. C 85.04, H 4.72; found C 84.77, H 4.83.

Bis[η(1,2,3,4,5,18)triphenylene]chromium Tetraphenylborate ([**12**][BPh_4]): To the aqueous solution of $\mathbf{12}^{+\cdot}$ obtained from a cocondensation of chromium (1.2 g, 23 mmol) and triphenylene (2 g, 8.7 mmol) performed as described above was added, under stirring, 0.5 g (1.46 mmol) of $NaBPh_4$. The reddish brown precipitate was washed with water and dried in vacuo. − Yield 530 mg (2.8% referred to Cr evaporated). Crystals suitable for X-ray diffraction were obtained by layering of solution of [**12**][BPh_4] (100 mg in 40 ml of acetone) with 120 ml of diethyl ether at 0°C. − $C_{60}H_{44}BCr$ (827.81): calcd. C 87.06, H 5.32; found C 85.67, H 5.41.

Bis[η(1,2,3,4,5,15)fluoranthene]chromium (**13**, isomer I): Chromium (2.1 g, 40.4 mmol) and fluoranthene (8 g, 39.6 mmol) were cocondensed during 2 h at 77 K as described for **12**. The workup procedure followed that given for **12**; in order to generate the radical cation $\mathbf{13}^{+\cdot}$ a stream of air was applied for 1 h before phase separation and reduction. − Yield: 110 mg (0.24 mmol, 0.6% based on Cr evaporated) of **13** as a dark violet microcrystalline product. − ^{1}H- and ^{13}C-NMR: Tables 2 and 3. − MS (EI, 70 eV); *m/z* (%): 456 (2.0) [M^+], 254 (5.1) [$M^+ - C_{16}H_{10}$], 202 (100) [$C_{16}H_{10}^+$], 52 (10.0) [Cr^+]. − $C_{32}H_{20}Cr$ (456.51): calcd. C 84.21, H 4.39; found C 84.95, H 5.18.

Bis[η(1,2,3,4,5,15)fluoranthene]chromium Tetraphenylborate ([**13**][BPh_4], isomer I): The reaction mixture from a cocondensation of chromium (1.9 g, 36.5 mmol) and fluoranthene (8 g, 39.6 mmol) was air-oxidized for 1 h. Subsequent manipulations and precipitation of the salt [**13**][BPh_4] followed the instructions given for [**12**][BPh_4]. − Yield: 310 mg (0.40 mmol, 1.1%) of [**13**][BPh_4] as dark red material. Crystals suitable for X-ray diffraction were grown by layering a solution of 140 mg of [**13**][BPh_4] in 60 ml of acetone with 100 ml of diethyl ether at ambient temperature.

Bis[η(1,2,3,4,5,15)fluoranthene]chromium Iodide ([**13**][I], isomer I): Cocondensation of chromium (1.6 g, 30.7 mmol) with fluoranthene (8 g, 39.6 mmol) and subsequent air oxidation (1 h) in the two-phase system H_2O/toluene led to an aqueous solution of $\mathbf{13}^+$ from which dark red [**13**][I] was precipitated by addition of KI (1.0 g, 6.0 mmol). The product was dried in vacuo. − Yield: 470 mg (0.8 mmol, 2.6%). Crystalline material for X-ray diffraction was obtained by layering a solution of 200 mg of [**13**][I] in 80 ml of acetone with 120 ml of diethyl ether. − $C_{32}H_{20}CrI$ (583.41): calcd. C 65.87, H 3.43; found C 66.28, H 3.81.

[η(1',2',3',4',5',15')fluoranthene][η(10,11,12,13,14,16)fluoranthene]chromium (**13**, isomer II): The preparation followed the instructions given for isomer I apart from a shorter (10 min) duration of air oxidation. − Yield 380 mg (0.83 mmol, 2.4%) of a dark violet microcrystalline material. According to ^{1}H NMR, this product was a mixture of ca. 85% of **13**(II) and 15% of **13**(I), see Tables 2 and 3. − $C_{32}H_{20}Cr$ (456.41): calcd. C 84.21, H 4.39; found C 84.87, H 4.93. − The mother liquor of the initial crystallisation was enriched in the more soluble isomer **13**(II). Repeated recrystallisation of the contents of this solution led to a product with the isomer distribution **13**(II)/**13**(I) = 95:5 as gleaned from ^{1}H NMR (see Figure 3 and Tables 2 and 3).

X-ray Crystal Structure Analysis of [**12**][BPh_4] *and* [**13**][I]: The crystal structures were solved by direct methods. Non-hydrogen atoms were refined anisotropically, hydrogen atoms on calculated positions with isotropic temperature factors $U(H) = 1.2\ U_{eq}(C)$. An inspection of the thermal parameters of [**13**][I] indicated unresolved disorder with respect to the crystallographic mirror symmetry. A refinement in the space group $Pna2_1$ (without this mirror symmetry) was not successful. Further details of the crystal structure determinations are given in Table 4.

[1] Ch. Elschenbroich, E. Schmidt, R. Gondrum, B. Metz, O. Burghaus, W. Massa, S. Wocadlo, *Organometallics* **1997**, *16*, 4589.
[2] M. Zander, *Polycyclische Aromaten*, Teubner, Stuttgart, **1995**.
[3] G. Wilkinson, F. G. A. Stone, E. W. Abel, Eds., *Comprehensive Organometallic Chemistry*, Pergamon, Oxford, U.K., **1982**, **1995**.
[4] J. E. Ellis, D. W. Blackburn, P. Yuen, M. Jang, *J. Am. Chem. Soc.* **1993**, *115*, 11616.
[5] [5a] E. P. Kündig, P. L. Timms, *J. Chem. Soc., Chem. Commun.* **1977**, 912. − [5b] Ch. Elschenbroich, R. Möckel, *Angew. Chem. Int. Ed. Engl.* **1977**, *16*, 870; *Angew. Chem.* **1977**, *89*, 908. − [5c] Ch. Elschenbroich, R. Möckel, W. Massa, M. Birkhan, U. Zenneck, *Chem. Ber.* **1982**, *115*, 334.
[6] [6a] E. P. Kündig, C. Perret, S. Spichiger, G. Bernardinelli, *J. Organomet. Chem.* **1985**, *286*, 183. − [6b] N. P. Do Thi, S. Spichiger, P. Paglia, G. Bernardinelli, E. P. Kündig, P. L. Timms, *Helv. Chim. Acta* **1992**, *75*, 2593.
[7] [7a] E. O. Fischer, Ch. Elschenbroich, *J. Organomet. Chem.* **1967**, *7*, 481. − [7b] Evidence for the possible existence of $(\eta^6\text{-}C_{10}H_8)_2Fe$ has been derived from matrix isolation studies: P. D. Morand, C. G. Francis, *Organometallics* **1985**, *4*, 1653.
[8] Ch. Elschenbroich, E. Bilger, R. Möckel, *Z. Naturforsch., B* **1983**, *38*, 1357.
[9] Ch. Elschenbroich, R. Möckel, *Z. Naturforsch., B* **1984**, *39*, 375.
[10] Ch. Elschenbroich, J. Schneider, W. Massa, G. Baum, H. Mellinghoff, *J. Organomet. Chem.* **1988**, *355*, 163.
[11] M. Jang, J. E. Ellis, *Angew. Chem. Int. Ed. Engl.* **1994**, *33*, 1973; *Angew. Chem.* **1994**, *106*, 2036.
[12] M. K. Pomije, C. J. Kurth, J. E. Ellis, M. V. Barybin, *Organometallics* **1997**, *16*, 3582.
[13] Ch. Elschenbroich, J. Heck, F. Stohler, E. Bilger, *Chem. Ber.* **1984**, *117*, 23.
[14] M. Randic, *Tetrahedron* **1975**, *31*, 1477.
[15] R. D. Rodgers, J. L. Atwood, T. A. Albright, W. A. Lee, M. D. Rausch, *Organometallics* **1984**, *3*, 263.
[16] B. Deubzer, E. O. Fischer, H. P. Fritz, C. G. Kreiter, N. Kriebitzsch, H. D. Simmons, Jr., B. R. Willeford, Jr., *Chem. Ber.* **1967**, *100*, 3084.
[17] Apart from the torsional angle, the structural parameters of [**13**][I]·0.5 acetone differ insignificantly from those of the solvent-free sample. The crystal quality of [**13**][BPh_4] was insufficient for refinement.
[18] F. R. Ahmed, J. Trotter, *Acta Crystallogr.* **1963**, *16*, 503.
[19] A. C. Hazell, D. W. Jones, J. M. Sowden, *Acta Crystallogr.* **1977**, *B33*, 1516.
[20] F. G. N. Cloke, A. R. Dias, A. M. Galvão, J. L. Ferreira da Silva, *J. Organomet. Chem.* **1997**, *548*, 177.
[21] [21a] Ch. Elschenbroich, E. Bilger, B. Metz, *Organometallics*

1991, *10*, 2823 for further references. – [21b] H. Binder, Ch. Elschenbroich, *Angew. Chem. Int. Ed. Engl.* **1973**, *12*, 659; *Angew. Chem.* **1973**, *85*, 665.
[22] $E_{1/2}$(triphenylene$^{0/-}$) = −2.49 V; $E_{1/2}$(fluoranthene$^{0/-}$) = −1.77 V: A. Streitwieser, *Molecular Orbital Theory for Organic Chemists*, Wiley, New York, **1961**, p. 178.
[23] Ch. Elschenbroich, J. Koch, J. Schneider, B. Spangenberg, *J. Organomet. Chem.* **1986**, *317*, 41; Ch. Elschenbroich, R. Möckel, U. Zenneck, D. W. Clack, *Ber. Bunsenges. Phys. Chem.* **1979**, *83*, 1008 and papers cited therein.
[24] Ch. Elschenbroich, F. Gerson, *J. Organomet. Chem.* **1973**, *49*, 445.
[25] R. D. Allendoerfer, G. A. Martinchek and S. Bruckenstein, *Anal. Chem.* **1975**, *47*, 890.
[26] M. T. Jones, R. H. Ahmed, *J. Phys. Chem.* **1980**, *84*, 2913.
[27] F. Gerson, *Hochaufgelöste ESR-Spektroskopie*, VCH, Weinheim, **1967**, p. 108.
[28] Ch. Elschenbroich, P. Kühlkamp, A. Behrendt, K. Harms, *Chem. Ber.* **1996**, *129*, 859.

[98055]

Dimethylphosphanylethylcyclopentadienyl Complexes of Lanthanum and Yttrium

Hans H. Karsch*, Volker Graf, Manfred Reisky, and Eva Witt

Technische Universität München, Institut für Anorganische Chemie,
Lichtenbergstr. 4, D-85747 Garching, Germany
Fax: (internat.) + 49(0)89/2891-4421
E-mail: Hans.H.Karsch@lrz.tu-muenchen.de

Received May 26, 1998

Keywords: Rare earth metal complexes / Anionic phosphanes / Phosphanylethylcyclopentadienyl complexes

The reactions of $Li[C_5H_4(CH_2)_2P(CH_3)_2]$ (**1**) with $La(CF_3SO_3)_3$ and $Y(CF_3SO_3)_3$ are described. Three equivalents of **1** reacted with $La(CF_3SO_3)_3$ under formation of $La[C_5H_4(CH_2)_2P(CH_3)_2]_3$ (**2**). Two equivalents of **1** with one equivalent of $Y(CF_3SO_3)_3$ in the presence of LiBr yielded $BrY[C_5H_4(CH_2)_2P(CH_3)_2]_2$ (**3**). Both complexes **2** and **3** have been characterized by X-ray structure analysis. In both cases an intramolecular coordination of the phosphanoethyl chain is established in the solid state by X-ray crystallography as well as in solution by NMR spectroscopy.

In general, neutral phosphane ligands do not form stable donor complexes with rare earth metals. Only a few complexes with neutral phosphane ligands are found in the literature: $La[TeSi(SiMe_3)_3]_3(Me_2PCH_2CH_2PMe_2)_2$[1], $[(C_5Me_4SiMe_2N\mathit{t}Bu)Sc(PMe_3)\mu\text{-}H]_2$[2], $[N(SiMe_3)_2]_2Yb(Me_2PCH_2CH_2PMe_2)$[3], $(C_5Me_5)_2YbCl(Me_2PCH_2PMe_2)$[4], and $(C_5H_4Me)_3CePMe_3$[5]. Stable complexes are known with anionic phosphane ligands like phosphanides[6], phosphanomethanides[7], phosphanoalkoxides[8], and amidophosphanes[9]. Phosphanomethanides were found to stabilize even high phosphane coordination numbers (up to 8 P−Ln bonds).

Continuing our investigations on phosphane compounds of rare earth metals we now focus on phosphanoalkylcyclopentadienide ligands. The characteristic feature of this ligand system is the linkage of a cyclopentadienyl and a phosphane moiety by means of an alkyl chain. Similar cyclopentadienyl-based ligands with amino- or alkoxyalkyl side chains coordinated to lanthanoide centers have been described[10][11][12][13][14][15]. However, the strong coordination of the heteroatom to the metal center normally is irreversible in these cases.

The additional phosphane functionality, in contrast, should provide a more labile and hence reversible coordination to the metal center which should enable enhanced reactivity and in particular is of great interest for catalytic reactions.

Only a restricted number of phosphanylcyclopentadienyl complexes have been reported so far and only a few are characterized by X-ray structure determinations[16][17][18][19][20]. Several independent routes have been applied for the synthesis of phosphanoalkyl-substituted cyclopentadienyl ligands, depending on the length of the alkyl chain connecting the cyclopentadienyl and the phosphane functionality.[21][22][23][24][25]. Phosphanoethyl-substituted cyclopentadienides {$M[C_5H_4(CH_2)_2PR_2]$, M = Li, Na, K} best are prepared by reaction of the corresponding phosphanide with spiro[2.4]hepta-4,6-diene[26] and anionic ligands with R = Ph, *i*Pr, *t*Bu are known[18]. The ligand $Li[C_5H_4(CH_2)_2P(CH_3)_2]$ (**1**) was newly synthesized using this method (Eq. 1).

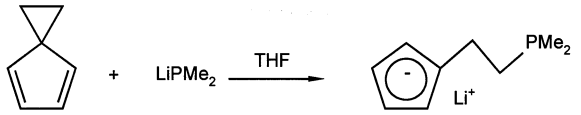

(1)

The reaction of three equivalents of $Li[C_5H_4(CH_2)_2P(CH_3)_2]$ with one equivalent of $La(CF_3SO_3)_3$ led to the homoleptic compound $La[C_5H_4(CH_2)_2P(CH_3)_2]_3$ (**2**) in good yield (Eq. 2).

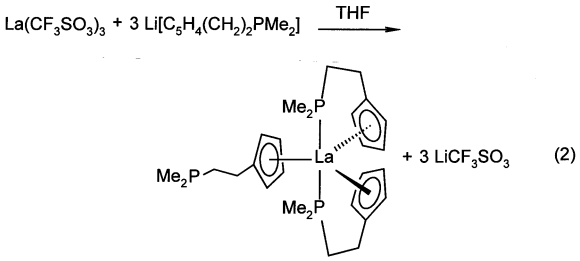

(2)

Colorless crystals were obtained from a concentrated solution of **2** in toluene. The complex is soluble in THF and aromatic hydrocarbons. At −90°C the $^{31}P\{^1H\}$-NMR shows two signals at δ = −39.91 and δ = −51.24 of intensity 2:1 which coalesce at −50°C, and at room temperature only one broad singlet at δ = −43.62 is observed. This is explained by a fast exchange of two coordinated and one "dangling" phosphano groups with the low-field signal being assigned to the coordinating phosphane ligands and the signal at δ = −51.24 being assigned to the noncoordinating phosphorus nucleus. This latter chemical shift corresponds to that of the neutral phosphane $[C_5H_5(CH_2)_2P(CH_3)_2]$

 © WILEY-VCH Verlag GmbH, D-69451 Weinheim, 1998 1434−1948/98/1010−1403 $ 17.50+.50/0

($\delta = -51.42$; -51.54). Careful analysis of the spectra at various temperatures led to the conclusion that two phosphano groups throughout remain coordinated to the metal center during the exchange process, i. e. a dissociative pathway is unlikely. The ^{139}La NMR ($I = 7/2$, 99.1%) resonance of **2** is observed at $\delta = -509.92$ (cf.: $Cp_3LaNCCH_3$, $\delta = -578$[27]) as a broad singlet. These spectroscopic findings are also consistent with the result of an X-ray structure determination (Figure 1).

Figure 1. Molecular structure of **2**

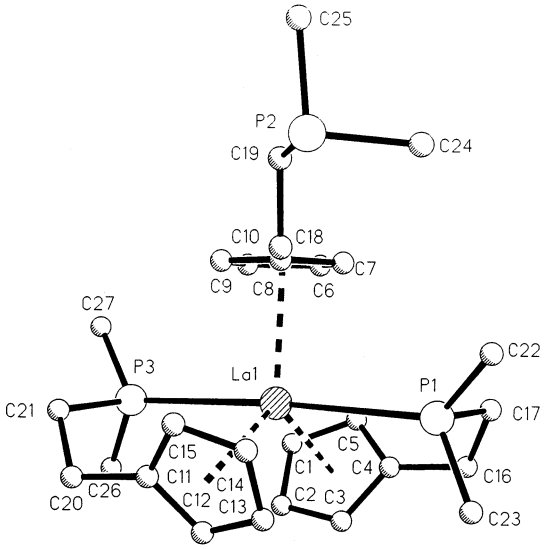

Lanthanum is trigonal planar, surrounded by three cyclopentadienyl rings, as it is the case in other cyclopentadienyllanthanum compounds[28]. Additionally, two phosphorus atoms complete the coordination sphere to a trigonal bipyramid by occupying the axial positions.

The lanthanum−phosphorus bond lengths [La−P1 = 3.211(5), La−P3 = 3.186(5) Å] are in the expected range for a lanthanum interaction with a phosphorus atom of covalency 3[1][7]. The molecular geometry and atom numbering scheme are shown in Figure 1, selected bond lengths [Å] and angles [°] are listed in Table 1.

Table 1. Selected bond lengths [Å] and angles [°] of compounds **2** and **3**

	1		**2**
La−X1a[a]	2.622(1)	Y−X1a[b]	2.386(1)
La−X1b	2.621(1)	Y−X1b	2.392(1)
La−X1c	2.621(1)	Y−P1	2.960(1)
La−P1	3.211(5)	Y−P2	2.933(1)
La−P3	3.186(5),	Y−Br	2.7939(5)
P1−La−P3	176.17(1)	X1a−Y−X1b	129.9(1)
X1a−La−X1c	118.7(1)	X1a−Y−Br	117.1(1)
X1b−La−X1a	121.6(1)	X1b−Y−Br	113.0(1)
X1c−La−X1a	119.7(1)	X1a−Y−P1	91.6(1)
X1a−La−P1	85.3(1)	X1a−Y−P2	99.9(1)
X1a−La−P3	91.6(1)		

[a] X1a, b, c: centroids of the Cp rings (C1 to C5, C6 to C10, C11 to C15). − [b] X1a, b: centroids of the Cp rings (C111 to C115 and C211 to C215).

The reaction of two equivalents of $Li[C_5H_4(CH_2)_2P(CH_3)_2]$ with one equivalent of $Y(CF_3SO_3)_3$ in the presence of LiBr proceeds under formation of the disubstituted yttrium bromide derivative **3** (Eq. 3).

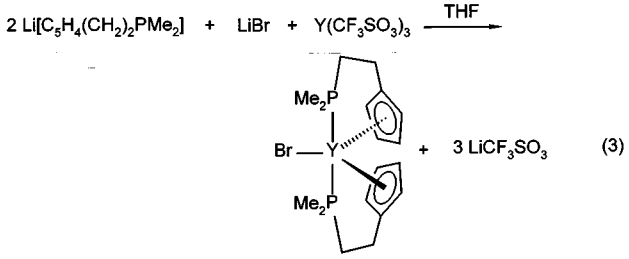

The product is obtained as colorless solid, soluble in aromatic solvents. The stabilisation by intramolecular coordination of the two phosphano functionalities is a dominant feature: this additional coordination prevents the dimerisation of the system and also the coordination of donor solvents, which otherwise are common features of bis(cyclopentadienyl)lanthanoid halides[29]. The $^{31}P\{^1H\}$-NMR spectrum shows a doublet at $\delta = -36.53$ with a $^1J_{PY}$ coupling constant of 72.8 Hz (^{89}Y, $I = 1/2$, 100%)[30] which remains unchanged over a temperature range from +30 to −100°C. This indicates that the system is not involved in dynamic processes.

Single crystals for an X-ray study were grown by slowly cooling a solution of **3** in toluene to low temperature. The compound crystallizes with one molecule of toluene in the formular unit. Both phosphano groups are bonded to the yttrium center (Figure 2) which confirms the spectroscopic findings. Similar to compound **2**, the two phosphorus atoms occupy the apical positions of a slightly distorted trigonal bipyramid. The Y−P bond lengths [2.960(1) and 2.933(1) Å] are only slightly longer than in $\{Y[N(SiMe_3CHPMe_2)(SiMe_2CH_2PMe_2)[N(SiMe_2CH_2PMe_2)_2]\}$ (2.817, 2.896, and 2.903 Å)[30]. Compound **3** represents the second hitherto known (and the first mononuclear) yttrium bromide featuring a terminal Y−Br bond, which is slightly longer [2.7939(5) Å] than that in $Y_3(OCMe_3)_7Br_2(THF)_2$ (Y−Br = 2.782 Å)[31]. Together with two cyclopentadienyl moieties of the $CpCH_2CH_2PMe_2$ ligands, the bromine completes the trigonal plane of the tbp molecular skeleton. With regard to the center of the Cp rings, the Cp(1)−Y−Cp(2) angle amounts to 129.9°, which gives an indication for the steric demand of the terminal bromine ligand. The average Y−Cp(center) distance (2.39 Å) agrees well with that found in other Y^{III} cyclopentadienyl complexes[32]. The molecular geometry and atom numbering scheme are shown in Figure 2, selected bond lengths [Å] and angles [°] are listed in Table 1.

Experimental Section

All operations were performed under dry, oxygen free nitrogen and with thoroughly dried solvents and glassware. Standard high-vacuum-line techniques were used. − Elemental analyses were ob-

Figure 2. Molecular structure of **3**

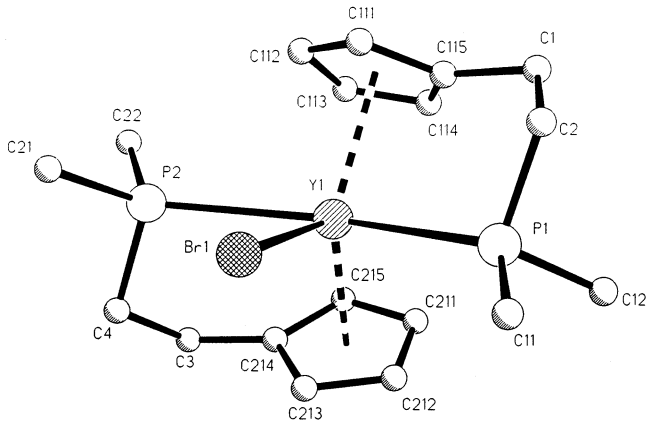

tained with a Vario EL CHN elemental analyzer of the microanalytical laboratory of the TU München. No attempts were made to further ameliorate the analytical data, which were not satisfying in all cases due to the high sensitivity of the compounds. – MS: Varian MAT 70 eV, CI. – NMR: Jeol GX 270 (^{1}H 270.17 MHz, ^{13}C 67.94 MHz, ^{31}P 109.4 MHz), Jeol GX 400 (^{1}H 399.65 MHz, ^{31}P 161.7 MHz, ^{13}C 100.40 MHz, ^{139}La 56.35 MHz), Jeol JNM Lambda 400 (^{7}Li 155.40 MHz). Chemical shifts (^{1}H, ^{13}C) refer to TMS ($\delta = 0$) as internal standard. For ^{31}P, 80% H_3PO_4, for ^{139}La, $LaCl_3$ (0.1 M in D_2O, $\delta = 0$) and for ^{7}Li, LiBr (20% in D_2O, $\delta = 0$) as external standards. All chemical shifts are reported in ppm and coupling constants J in Hz. In case of high-order spin systems, the distance "N" [Hz] between the two outermost lines of the multiplet is given. All measurements were carried out at 25°C in C_6D_6 as solvent. Temperature-dependent NMR spectra were recorded with [D_8]toluene as solvent. $LiPMe_2 \cdot 0.5\ Et_2O$[33], $La(CF_3SO_3)_3$, $Y(CF_3SO_3)_3$[34], and spiro[2.4]hepta-4,6-diene[26] were prepared according to literature procedures.

Li[$C_5H_4(CH_2)_2P(CH_3)_2$] (**1**): To a solution of 0.024 mol (2.5 g) of $LiPMe_2 \cdot 0.5\ Et_2O$ in 50 ml of THF, 0.024 mol (2.19 g) of spiro[2.4]hepta-4,6-diene in 20 ml of THF was added by pipette. After stirring the reaction mixture for 12 h at room temperature, the solvent was removed and the product was washed three times with pentane. After drying the residue, 3.15 g (82%) of a colorless solid was obtained. – ^{1}H NMR ([D_8]dioxane, 293 K): 1.06 [d, $^2J_{HP} = 1.24$, 6 H, $P(CH_3)_2$], 1.75 [dt, $^2J_{HP} = 1.95$, $^3J_{HH} = 7.32$, 2 H, $CpCH_2CH_2P(CH_3)_2$], 2.75 [dt, $^3J_{HP} = 12.21$, $^3J_{HH} = 7.32$, 2 H, $CpCH_2CH_2P(CH_3)_2$], 5.65 [A_2B_2: $\delta_A = 5.68$, $\delta_B = 5.61$, $J_{AB} = 2.44$, 4 H, $C_5H_4CH_2CH_2$]. – ^{13}C {^{1}H} NMR ([D_8]dioxane, 293 K): $\delta = 12.07$ (d, $^1J_{CP} = 2.59$, CH_3), 25.10 (d, $^2J_{CP} = 11.92$ CH_2P), 39.32 (s, $CpCH_2$), 101.62 (s, CH_2CCH), 101.90 (s, $CCHCH$), 119.84 (d, $^3J_{CP} = 9.33$, C-*ipso*). – ^{31}P{^{1}H} NMR ([D_8]dioxane, 293 K): $\delta = -56.34$ (s). – ^{7}Li NMR ([D_8]dioxane, 293 K): $\delta = -8.21$ (s). – $C_9H_{14}LiP$ (160.13): calcd. C 67.51, H 8.81, Li 4.33, P 19.35; found C 65.67, H 8.74, Li 4.35, P 18.37.

La[$C_5H_4(CH_2)_2P(CH_3)_2$]$_3$ (**2**): To a mixture of 6.2 mmol (1.0 g) of **1** and 2.05 mmol (1.2 g) of $La(CF_3SO_3)_3$, 40 ml of THF was added at –78°C. The reaction mixture was slowly warmed up to room temperature and stirred for another 12 h. The solvent was removed and the product was extracted with 40 ml of toluene. The toluene extract was concentrated and **2** was isolated as colorless crystals, 1.14 g, (92%), dec. 138°C. – ^{1}H NMR (C_6D_6, 293 K): $\delta = 0.92$ [s, 18 H, $P(CH_3)_2$], 1.56 ["t", $N = 14.29$, 6 H, $CpCH_2CH_2P(CH_3)_2$], 2.60 [m, $N = 30.27$, 6 H, $CpCH_2CH_2P(CH_3)_2$], 5.76 [A_2B_2 spin system, uncompletely resolved, $\delta_A = 5.72$, $\delta_B = 5.79$, 12 H, $C_5H_4CH_2CH_2$]. – ^{13}C{^{1}H} NMR (C_6D_6, 293 K): $\delta = 12.99$ (s, CH_3), 25.68 (s, CH_2P), 35.05 (s, $CpCH_2$), 109.03 (s, CH_2CCH), 110.12 (s, $CCHCH$), 128.90 (s, C-*ipso*). – ^{31}P{^{1}H} NMR (C_6D_6, 293 K): $\delta = -43.62$ (s, br). – ^{31}P{^{1}H} NMR ([D_8]toluene, 203 K): $\delta = -39.91$ (s, br, 2P, La-PMe_2), –51.24 [s, br 1P, $C_5H_4(CH_2)_2PMe_2$]. – ^{139}La NMR (C_6D_6 293 K): $\delta = -509.92$. – MS (70 eV); *m/z* (%): 445 (100) [$M^+ - C_5H_4(CH_2)_2P(CH_3)_2$], 384 (50) [$M^+ - C_5H_4(CH_2)_2P(CH_3)_2 - P(CH_3)_2$], 154 (13.9)

Table 2. Crystal data of compounds **2** and **3**

Empirical formula	$C_{27}H_{42}LaP_3$ (**2**)	$C_{25}H_{36}BrP_2Y$ (**3**)
Molecular mass	598.431 g/mol	567.301 g/mol
Crystal dimensions [mm]	0.11 × 0.45 × 0.5	0.5 × 0.4 × 0.3
Crystal System	monoclinic	monoclinic
Space group	$P2_1/n$	$P2_1/n$
a [Å]	8.555(1)	12.357(1)
b [Å]	25.003(1)	14.249(1)
c [Å]	13.080(1)	15.206(2)
β [°]	92.03(1)	101.48(1)
V [Å^3]	2796.1(4)	2623.8(4)
Z	4	4
Diffractometer	Enraf Nonius CAD4-Turbo	Enraf Nonius CAD4-Turbo
Radiation	Mo-K_α (λ = 0.71073 Å)	Mo-K_α (λ = 0.71073 Å)
Density (calculated) [Mg/m^3]	1.422	1.436
Absorption coefficient [mm^{-1}]	1.712	3.877
F (000)	1224	1160
θ range for data collection [°]	3 to 27	3 to 27
Limiting indices	$-10 \le h \le 10$, $0 \le k \le 31$, $0 \le l \le 16$	$-15 \le h \le 15$, $0 \le k \le 18$, $0 \le l \le 19$
Reflexions collected	6048	5901
Independent reflexions	6047	5697
Absorption correction	DIFABS[29]	Empir.
Data/restraints/parameters	5348/0/280	4134/0/267
Goodness-of-fit on F^2	1.054	1.007
Final R indices [$F_o > 4\ \sigma(F_o)$]	$R1 = 0.0185$, $wR2 = 0.0439$	$R1 = 0.0356$, $wR2 = 0.0788$
R indices (all data)	$R1 = 0.0258$, $wR2 = 0.0462$	$R1 = 0.0722$, $wR2 = 0.0906$
Largest diff. peak and hole	0.370 and −0.463 e × Å^{-3}	0.681 and −0.422 e × Å^{-3}

$[C_5H_5(CH_2)_2P(CH_3)_2]$. – $C_{27}H_{42}LaP_3$ (598.43): calcd. C 54.2, H 7.07; found C 51.56, H 7.13.

$BrY[C_5H_4(CH_2)_2P(CH_3)_2]_2$ (**3**): To a mixture of 3.73 mmol (0.6 g) of **1**, 1.86 mmol (1 g) of $Y(CF_3SO_3)_3$ and 1.86 mmol (0.16 g) of LiBr, 40 ml of THF was added at −78°C. The reaction mixture was slowly warmed up to room temperature and stirred for another 12 h. The solvent was removed and the product was extracted with 40 ml of toluene. The toluene extract was concentrated and **3** was isolated as colorless crystals 0.8 g, (75%), dec. 135°C. – ^{1}H NMR (C_6D_6, 293 K): δ = 0.91[s, 12 H, $P(CH_3)_2$], 1.65 [s, br, 4 H, $CpCH_2CH_2P(CH_3)_2$], 2.43 [m, 4 H, $CpCH_2CH_2P(CH_3)_2$], 5.80 [s, br, 8 H, $C_5H_4CH_2CH_2$]. – $^{13}C\{^1H\}$ NMR (C_6D_6, 293 K): δ = 10.73 (s, CH_3), 24.61 ("t", N = 12.12, CH_2PMe_2), 33.86 ("t", N = 12.67, $CpCH_2$), 107.81 [s, br, CH (Cp)], 131.85 ("t", N = 4.42 C-*ipso*). – $^{31}P\{^1H\}$ NMR (C_6D_6, 293 K): δ = −36.53 (d, $^1J_{P\text{-}Y}$ = 72.8). – MS (70 eV); *m/z* (%): 476 (40) [M^+ + 1], 395 (100) [M^+ − $C_5H_4(CH_2)_2P(CH_3)_2$], 154 (71) $[C_5H_5(CH_2)_2P(CH_3)_2]$. – $C_{18}H_{28}P_2BrY$ (475.19): calcd. C 45.50, H 5.94, Br 16.81; found C 44.81, H 6.0, Br 15.64.

Crystal Structure Determination: Suitable crystals of **2** and **3** were sealed into glass capillaries. The structures were solved by direct methods and refined by full-matrix least-squares calculations against F^2 (SHELXL-93)[35][36]. Crystal data and numerical data of the structure determinations are given in Table 2. The thermal motion of all non-hydrogen atoms was treated anisotropically. All hydrogen atoms were calculated in ideal positions. Further informations may be obtained from the Fachinformationszentrum Karlsruhe, D-76344 Eggenstein-Leopoldshafen (Germany), on quoting the depository numbers CSD-408608 (**2**) and CSD-408609 (**3**).

[1] D. R. Cary, G. E. Ball, J. Arnold, *J. Am. Chem. Soc.* **1995**, *117*, 3492.
[2] P. J. Shapiro, E. Bunel, W. P. Schaefer, J. E. Bercaw, *Organometallics* **1990**, *9*, 867.
[3] T. D. Tilley, R. A. Anderson, A. Zalkin, *J. Am. Chem. Soc.* **1982**, *104*, 3725.
[4] T. D. Tilley, R. A. Anderson, A. Zalkin, *Inorg. Chem.* **1983**, *22*, 856.
[5] S. Stults, A. Zalkin, *Acta Crystallogr., C* **1987**, *43*, 430.
[6] [6a] G. Bielang, R. D. Fischer, *J. Organomet. Chem.* **1978**, *161*, 335. – [6b] G. W. Rabe, J. W. Ziller, *Inorg. Chem.* **1995**, *34*, 5378.
[7] H. H. Karsch, G. Ferazin, O. Steigelmann, H. Kooijman, A. Schier, P. Bissinger, W. Hiller, *J. Organomet. Chem.* **1994**, *482* 151.
[8] P. B. Hitchcock, M. F. Lappert, J. A. Mckinnon, *J. Chem. Soc., Chem. Commun.* **1988**, 1557.
[9] M. D. Fryzuk, T. S. Haddad, *J. Am. Chem. Soc.* **1988**, *110*, 8263.
[10] W. A. Herrmann, R. Anwander, F. Munck, W. Scherer, *Chem. Ber.* **1993**, *126*, 331.
[11] C. Quian, X. Zheng, B. Wang, D. Deng, *J. Organomet. Chem.* **1994**, *446*, 101.
[12] P Jutzi, J. Dahlhaus, M. O. Kristen, *J. Organomet. Chem.* **1993**, *450*, C1.
[13] B. Wang, D. Deng, C. Quian, *New J. Chem.* **1995**, *19*, 515.
[14] P Jutzi, U. Siemeling, *J. Organomet. Chem.* **1995**, *500*, 175.
[15] R. Anwander, W. A. Herrmann, *Top. Curr. Chem.* **1996**, *179*, 1–32.
[16] A. H. Cowley, C. S. King, A. Decken, *Organometallics* **1995**, *14*, 20.
[17] J. C. Leblanc, C. Moise, A. Maisonnant, R. Poilblanc, C. Charrier, F. Mathey, *J. Organomet. Chem.* **1982**, *231*, C43.
[18] R. T. Kettenbach, W. Bonrath, H. Butenschön, *Chem. Ber.* **1993**, *126*, 1657.
[19] T. F. Wang, J. P. Juang, Y. S. Wen, *J. Organomet. Chem.* **1995**, *502*, 117.
[20] A. M. Slawin, D. L. Williams, J. Crosby, J. A. Ramsden, C. White, *J. Chem. Soc., Dalton Trans.* **1988**, 2491.
[21] T. Kauffmann, J. Ennen, H. Lhotak, A. Rensing, F. Steinseifer, A. Woltermann, *Angew. Chem.* **1980**, *92*, 321; *Angew. Chem. Int. Ed. Engl.* **1980**, *19*, 328.
[22] C. Charrier, F. Mathey, *J. Organomet. Chem.* **1979**, *170*, C41.
[23] C. Charrier, F. Mathey, *Tetrahedron Let.* **1978**, 2407.
[24] S. O. Grim, R. C. Barth, *J. Organomet. Chem.* **1975**, *94*, 327.
[25] R. Uriate, T. J. Mazanec, K. D. Tau, D. W. Meek, *Inorg. Chem.* **1980**, *19*, 79.
[26] C. F. Wilcox, R. R. Craig, *J. Am. Chem. Soc.* **1961**, *83*, 3866.
[27] S. H. Eggers, R. D. Fischer, *J. Organomet. Chem.* **1986**, *315*, C61.
[28] S. H. Eggers, J. Köpf, R. D. Fischer, *Organometallics* **1986**, *5*, 383.
[29] [[29a] R. E. Maginn, S. Manastyrskyj, M. Dubeck, *J. Am. Chem. Soc* **1963**, *85*, 672. – [29b] T. D. Tilley, R. A. Andersen, *Inorg. Chem.* **1981**, *20*, 3267. – [29c] A. L. Wayda, W. J. Evans, *Inorg. Chem.* **1980**, *19*, 2190.
[30] M. D. Fryzuk, T. S. Haddad, S. J. Rettig, *Organometallics* **1991**, *10*, 2026.
[31] J. Wu, T. J. Boyle, J. L. Shreeve, J. W. Ziller, W. J. Evans, *Inorg. Chem.* **1993**, *32*, 1130.
[32] C. Qian, X. Zheng, B. Wang, D. Deng, J. Sun, *J. Organomet. Chem.* **1994**, *466*, 101.
[33] K. L. Lundberg, R. J. Rowatt, W. E. Miller, *Inorg. Chem.* **1969**, *8* 1336.
[34a] H. M. Hamidi, J. L. Pascal, *Polyhedron* **1994**, *13*, 1787.
[34b] R. D. Howells, J. D. McCrow, *Chem. Rew.* **1977**, *77*, 69.
[35a] G. M. Sheldrick, C. Krüger, R. Goddard, *Oxford Univ. Press*, **1985**, p. 175.
[35b] G. M. Sheldrick, *Program for refinement of structures*, University of Göttingen, **1993**.
[36] N. Walker, D. Stuart, *Acta Crystallogr., A* **1983**, *39*, 1.

[98160]

Functionalized Ether Derivatives of $HOCH_2C(CH_2PPh_2)_3$ and Related Tripod Ligands – Synthesis and Coordination Chemistry☆

Peter Schober, Rainer Soltek, Gottfried Huttner*, Laszlo Zsolnai, and Katja Heinze

Anorganisch-Chemisches Institut der Universität Heidelberg,
Im Neuenheimer Feld 270, D-69120 Heidelberg, Germany
Fax: (internat.) + 49(0)6221/545707

Received March 16, 1998

Keywords: Functionalized tripod ligands / Mixed donor set ligands / Solubilized tripod ligands / Molybdenum / Iron /

Neopentane-derived tripod ligands of the general type $HOCH_2C(CH_2PPh_2)(CH_2Y)(CH_2Z)$ (**1**; Y, Z = PPh_2, SR) are notoriously resistant to ether formation at their hydroxy group. Two routes have been found, which allow the transformation of **1** into ether functionalized tripod ligands $ROCH_2C(CH_2PPh_2)(CH_2Y)(CH_2Z)$ (Y = Z = PPh_2: **5**, Y = Z = SR: **8**). One of these strategies relies upon the η^3 coordination of **1** in **1**·$Mo(CO)_3$ (**2**). By this way the donor groups are efficiently protected and the steric encumbrance of the CH_2OH group at the backbone of the ligands is greatly reduced by fixing three arms of the neopentane scaffolding to the metal center. After deprotonation, reaction with electrophiles will produce the corresponding ether derivatives $ROCH_2C(CH_2PPh_2)(CH_2Z)_2$ (**3**). Mesylation of **2** leads to $MeSO_2OCH_2C(CH_2PPh_2)3{\cdot}Mo(CO)_3$ (**4**), which reacts with alkoxides to produce **3** in a sequence of reversed polarity. Ligands **5** [$ROCH_2C(CH_2PPh_2)_3$] are liberated from **3** by UV irridation of their solutions in the presence of pyridine *N*-oxide. Direct etherification of **1** is also possible in some cases after deprotonation of **1** by KO*t*Bu and subsequent reaction with an electrophile RX in the narrow temperature range between –10 and +20 °C. By this way, ω-methyl polyglycol ether functions are easily introduced resulting in $H_3C(OC_2H_4)_nOCH_2C(CH_2PPh_2)_3$ (**5g**, **h**).

Introduction

One of the properties of a ligand which has not been generally considered to be too important is its solubility in different solvents and the herewith introduced solubility of its coordination compounds. On the other hand it has been shown how solubility properties may considerably improve processes which rely on the catalytic activity of ligand-metal templates, one of the examples of even technical importance being the Rhone-Poulenc process.[1] In this case hydrophilic phosphane ligands are the reason for the advance.[2] Many other catalytic processes do in principle allow for this kind of modification[3], given that the ligand can be appropriately modified. Modifying ligands to enhance and specify solubility is thus of basic interest. Modifying ligands by attaching auxiliary groups, such as to allow the attachment of ligand-metal templates to a surface is another reason for putting more weight to the question of an appropriate functionalizability of a ligand.[3] Homogeneous processes may be transferred to heterogenous ones using this approach combining the advantages of both homogeneous and heterogeneous catalyses.[4] Modifying ligands such as to induce a self-assembly type of order in the phases derived from their coordination compounds is yet another point of interest in this topic.[5] The rapid development of chemical sensors[6] as well as of non-linear optical materials[7] will further increase the demand for ligands which do not only have the appropriate coordinative capabilities but do at the same time allow for easy-to-achieve modifications by additional functionalities in order to imprint the specific properties which are needed in each case to their coordination compounds.

As a consequence a well-thought-of strategy for designing a particular class of ligands will from the very beginning incorporate a functionality which may serve as a linker group such as to allow for all the modifications eventually needed. In a project concerned with the synthesis and application of tripod ligands $RCH_2C(CH_2X)(CH_2Y)(CH_2Z)$ much work has been devoted to the problem of designing a convergent strategy to introduce different donor groups[8a][8b][8c][8d][8e][8f][8g][8h], even enantioselective procedures have been worked out.[9a][9b][9c] The problem of introducing a linker group at the backbone has, however, not yet been solved in a convergent way. Wherever syntheses of ligands modified in this sense had been reported, the modified groups were incorporated from the very beginning of the syntheses.[8k][8m] Even though with the synthesis of $HOCH_2C(CH_2X)(CH_2Y)(CH_2Z)$[8k] the alcohol function appears to naturally lend itself to further functionalization, the steric bulk of the neopentane system hitherto precluded the scope of this reaction. Only silylation and esterification[8k] leading to R_3Si- and $RCOO-$ derivatives had been found to work. And even with these reactions the protection of donor functions X, Y, Z like PR_2 was found to be necessary. The functionalizations thus introduced strongly limit the potential application of these ligands due to their sensitivity to hydrolysis. An ether functionality would be far more superior. Despite continued efforts[8k][8l] to achieve etherification of the hydroxymethyl group of these neopentane-based ligands definitive solutions of this problem have only now been found. We report here on methods which allow for this type of modification of tripod ligands and which are at the same time tolerant to a broad

 © WILEY-VCH Verlag GmbH, D-69451 Weinheim, 1998 1434–1948/98/1010–1407 $ 17.50+.50/0

range of functionalities in the auxiliary group as well as in the donor set of the ligands.

Results and Discussion

Modification of Coordinated Ligands

There are two main reasons for the failure of the transformation of the CH_2OH group in $HOCH_2C(CH_2X)(CH_2Y)(CH_2Z)$ into an ether function: one of them being the sluggish reactivity of the neopentane system[10] and the other one being inherent in the sensitivity of the donor groups to electrophilic attack.[8k][8l] This second impediment may in part be overcome by appropriate protection of the donor groups e.g. adduct formation of PR_2 donors with borane to give protected PR_2-BH_3 entities which are less prone to electrophilic attack. A strategy which solves both problems at the same time may be envisaged in η^3-coordinating all three donor groups to one metal center. This should protect the donor groups and should at the same time reduce the steric crowding around the CH_2OH group at the neopentane framework with this steric crowding being the main reason for the reduced reactivity of neopentane derivatives.[10] It is observed that the tricarbonylmolybdenum fragment serves as an efficient template in this sense. Tripod tricarbonylmolybdenum complexes are easily accesible and remarkably stable.[8i][8k][8l] Thus, ligands **1** are transformed into their $Mo(CO)_3$ derivatives **2** (Scheme 1) with excellent yields (Experimental Section).

Scheme 1

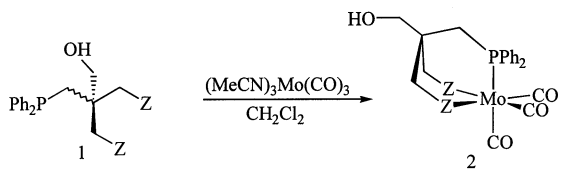

1a: Z = PPh_2
1b: Z = SBzl

2a: Z = PPh_2
2b: Z = SBzl

Their ν(CO) IR spectra (Experimental Section) are in accord with the C_3 symmetry of the $Mo(CO)_3$ chromophore which is somewhat disturbed by the two different donor functions in **2b** so that the E band is split into two discernable components. The NMR data (Tables 1 and 2, Experimental Section) are in full accord with the assigned constitution. Compound **2a** is deprotonated at the alcohol function by KO*t*Bu (Scheme 2). The potassium alkoxide thus obtained reacts with various electrophiles to produce the corresponding ethers **3**. The infrared and ^{31}P-NMR spectra (Experimental Section) as well as the ^{13}C- and ^{1}H-NMR data (Tables 1 and 2) are in full accord with the structures. Compounds **3** are obtained as analytically pure pale yellow microcrystalline solids, the structures of **3a** and **3b** have been determined by X-ray crystallography.[16]

While the above procedure relies upon transforming the CH_2OH function of **2a** into a nuleophilic group, a method

Table 1. ^{1}H-NMR data of **1b**, **2b**, **7**, **8a**, **8b**, **9a**, and **9b**

^{1}H NMR[a]	CH_2P	CH_2SBzl	CH_2OR	SCH_2Ph	R	H aromat.
1b, R = H	2.35, d, 2 H, 4.4[b]	2.66, s, 4 H	3.52, s, 2 H	3.62, s, 4 H	–	7.57–7.18, m, 20 H
2b, R = H	2.50, bs, 2 H	2.35, bs, 4 H	3.11, bs, 2 H	3.98 3.83, 2d, 4 H, 13.5[c]	–	7.57–7.18, m, 20 H
7, R = CH_2	–	2.93, s, 4 H	4.33, s, 2 H	3.73, s, 2 H	–	7.36–7.30, m, 10 H
8a, R = Me	2.41, d, 2 H, 4.0[b]	2.81 2.74, 2d, 4 H, 12.7[c]	3.25, s, 2 H	3.68, s, 4 H	3.03, s, 3 H	7.53–7.25, m, 20 H
8b, R = Et	2.44, d, 2 H, 3.8[b]	2.81, s, 4 H	3.35, s, 2 H	3.71, s, 4 H	3.22, q, 2 H, 6.9[d] 1.09, t, 3 H, 6.9[d]	7.58–7.27, m, 20 H
9a, R = Me	2.43, d, 2 H, 7.4[b]	2.39, s, 4 H	2.98, d, 2 H, 1.0[e]	3.68, s, 4 H	3.27, s, 3 H	7.53–7.25, m, 20 H
9b, R = Et	2.46–2.40, m, 2 H	2.40, s, 4 H	3.03, s, 2 H	4.00 3.93, 2d, 4 H, 15.0[c]	3.40, q, 2 H, 6.9[d] 1.17, t, 3 H, 6.9[d]	7.90–7.34, m, 20 H

[a] **1b, 7** and **8** in $CDCl_3$, **2b** in [D_8]THF, **9** in CD_2Cl_2. – [b] $^{2}J_{HP}$. – [c] $^{2}J_{HH}$. – [d] $^{3}J_{HH}$. – [e] $^{4}J_{HP}$ in Hz.

Table 2. ^{13}C-NMR data of **1b**, **2b**, **7**, **8a**, **8b**, **9a**, and **9b**

^{13}C NMR[a]	CH_2P	CH_2SBzl	CH_2OR	SCH_2Ph	C_qCH_2O	R	CO	C aromat.
1b, R = H	34.1, d, 15.5[c]	38.0, d, 10.1[d]	66.6, d, 8.3[d]	37.4, s	43.8, d, 10.9[e]	–	–	137.9–126.8, m
2b, R = H	31.5, d, 12.9[c]	36.5, d, 4.6[d]	73.5, d, 9.2[d]	48.8, d, 5.5[d]	43.5, d, 4.6[e]	–	223.4, d, 8.3[f], 220.3, d, 34.9[g]	139.6–128.4, m
7, R = CH_2	–	37.5–37.3, 2s[b]	79.8, s	37.5–37.3,2s[b]	43.6, s	–	–	137.9–126.9, 4s
8a, R = Me	35.0, d, 17.0[c]	38.7, d, 10.3[d]	76.0, d, 8.4[d]	38.3, s	44.0, d, 13.4[e]	58.7, s	–	139.8–127.4, m
8b, R = Et	35.0, d, 16.9[c]	38.7, d, 10.3[d]	73.6, d, 8.7[d]	38.3, s	44.0, d, 13.3[e]	66.6, s; 15.5, s	–	140.0–127.3, m
9a, R = Me	31.5, d, 11.7[c]	35.9, d, 4.4[d]	82.1, d, 8.8[d]	48.3, d, 5.8[d]	42.1, d, 5.5[e]	59.5, s	223.4, m	138.1–128.4, m
9b, R = Et	31.5, d, 12.0[c]	35.8, d, 4.2[d]	81.1, d, 9.2[d]	48.2, d, 5.8[d]	42.2, d, 5.2[e]	67.3, s; 15.1, s	223.3, d, 9.0[f], 220.1, d, 35.0[g]	138.1–128.4, m

[a] **1b, 7** and **8** in $CDCl_3$, **2b** in [D_8]THF, **9** in CD_2Cl_2. – [b] Assignment not unambigously possible. – [c] $^{1}J_{CP}$. – [d] $^{3}J_{CP}$. – [e] $^{2}J_{CP}$. – [f] $CO_{cis\text{-}P}$. – [g] $CO_{trans\text{-}P}$.

Scheme 2

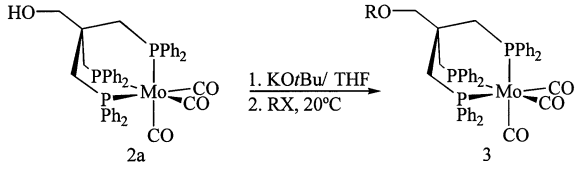

3a : R = Me
3b : R = Et
3c : R = Bzl
3d : R = 4-stilbenyle
3e : R = $Br(CH_2)_6$

Scheme 3

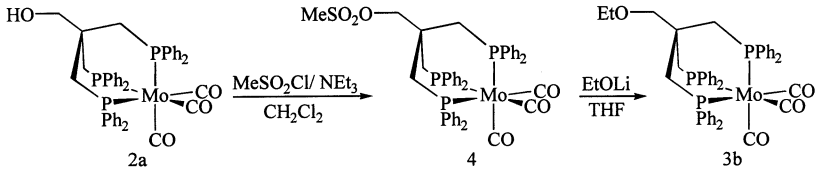

Scheme 4

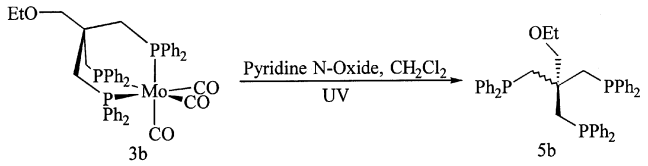

inverting the polarity by mesylation of the hydroxy group is also possible.

2a, when treated with an excess of mesyl chloride in the presence of NEt_3 (Scheme 3), gives the mesylate **4** which after chromatography is obtained analytically pure as a pale yellow microcrystalline solid (Experimental Section; Tables 4 and 5). The mesylate **4** reacts with LiOEt to give **3b** albeit in lower yields as compared to the yields obtained using the above procedure based on an inverted polarity. The procedure starting from **4** was therefore not further generalized. It should be noted that the free ligand $HOCH_2C(CH_2PPh_2)(CH_2Y)(CH_2Z)$ can not be mesylated[11] and even a change of the reaction conditions as described later did not work with mesyl chloride.

In order to make the above procedure useful for the synthesis of the corresponding free ligands decoordination of the $Mo(CO)_3$ template in **3** is necessary. An especially useful approach for this purpose has been developed by H. A. Mayer et al.[12], who found that tripod ligands containing P-donor functions may be decoordinated from their $Mo(CO)_3$ complexes by irridating their CH_2Cl_2 solutions in the presence of pyridine *N*-oxide. With **3b** as an example this procedure was shown to work equally well for the class of tripod ligands which are of concern in this paper. **3b** liberates the tripod ligand **5b** (Scheme 4).

The ligand has to be purified by chromatography since even under these specialized conditions oxidation at the phosphorus atoms is a minor side reaction. **5b** is obtained as an analytically pure colorless viscous material, the identity of which is evident from the ^{31}P-NMR and analytical data (Experimental Section) as well as from ^{1}H- and ^{13}C-NMR results (Tables 4 and 5).

Modification of Free Ligands

It had been shown that ether formation from **1a** is not possible under standard Williamson conditions.[8k] Neither change of the solvent nor change of the counter ion (Na^+, Li^+) was found to be a remedy in this situation[8k], nor did BH_3 protection of the phosphane donors cause a positive change. Lacking reactivity or quaternization at the phosphorus atoms were the seemingly unavoidable problems.[8k][11] We found now that **1a** after deprotonation with KO*t*Bu in THF does react with various electrophiles at temperatures below 20°C to give the corresponding ethers (Scheme 5).

Scheme 5

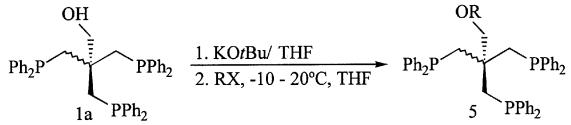

Table 3. Alkylation reagents RX and yields for the reaction of **1a** to **5a–h**

	R	X	Yield (%)
5a	Me	I	72
5b	Et	I	69
5c	$CH_3[CH_2]_9$	OTs	33
5d	$CH_3[CH_2]_{21}$	OTs	44
5e	$H_2C{=}CH[CH_2]_9$	OTs	38
5f	$Cl[CH_2]_6$	OTs	52
5g	$Me[OC_2H_4]_3$	OTs	53
5h	$Me[OC_2H_4]_n$, $n = 4-13$	OTs	[a]

[a] Yield cannot be determined due to separation problems of **5h** from the starting compounds.

The relative rates of ether formation or quaternization at the phosphorus atoms are different enough under these conditions to impede the extensive formation of quaternization products. As minor side products the phosphonium salts are separated by chromatography from the products **5** and the ligands **5** are obtained in fair yields by this procedure. They are colorless viscous oils in general; only **5a** could be obtained as a microcrystalline solid by recrystallization from CH_2Cl_2. The compounds **5a–5g** are obtained in an analytically pure state; the polyoxyethylene derivative **5h** is not completely separated from the starting materials.

Table 4. ^{1}H-NMR data of **2**, **3**, **4**, and **5**

^{1}H NMR [a]	CH_2P	CH_2OR	R	H aromat.
2a, R = H	2.30, br. s, 6H	3.56, br. s, 2 H	–	7.00–7.40, m, 30 H
3a, R = Me	2.31, br. s, 6H	3.28, br. s, 2 H	3.48, s, 3H	7.44–7.05, m, 30 H
3b, R = Et	2.35, br. s, 6H	3.36, br. s, 2 H	3.63, q, 2 H, 7.0[c]; 1.31, t, 3 H, 7.0[c]	7.43–7.06, m, 30 H
3c, R = Bzl	2.37, br. s, 6H	3.45, br. s, 2 H	4.66, s, 2H	7.37–7.05, m, 30 H
3d, R = 4-stilbenyl	2.36, br. s, 6H	3.44, br. s, 2 H	4.66, s, 2H	7.61–7.06, m, 41 H
3e, R = $Br[CH_2]_6$	2.32, br. s, 6H	3.32, br. s, 2 H	3.55, t, 6.3[c], CH_2O; 3.42, t, 6.7[c], CH_2Br; 1.89–1.50, m, 8 H, $CH_2CH_2CH_2$	7.37–7.04, m, 30 H
4, R = CH_3SO_2	2.32, br. s, 6H	4.11, br. s, 2 H	3.11, s, 3H	7.35–7.06, m, 30 H
5a, R = Me	2.61, d, 6 H, 2.6[b]	3.06, s, 2 H	2.51, s, 3H	7.27–7.43, m, 30 H
5b, R = Et	2.52, d, 6 H, 2.4[b]	3.11, s, 2 H	0.7, t, 3 H, 6.9[c]; 2.62, q, 2 H, 7.0[c]	7.26–7.40, m, 30 H
5c, R = $CH_3[CH_2]_9$	2.68, d, 6 H, 2.5[b]	3.11, s, 2 H	1.0, t, 3 H, 5.6[c]; 1.1–1.5, m, 16 H	7.90–7.34, m, 30 H
5d, R = $CH_3[CH_2]_{21}$	2.55, d, 6 H, 2.4[b]	3.16, s, 2 H	0.94–3.39, m, 45 H; 3.39, m, 2 H	7.27–7.60, m, 30 H
5e, R = $H_2C{=}CH[CH_2]_9$	2.63, d, 6 H, 2.3[b]	3.21, s, 2 H	1.1–1.6, m, 14 H; 2.11, m, 2H; 2.73, m, 2H; 5.04, m, 2 H; 5.92, m, 2 H	7.29–7.44, m, 30 H
5f, R = $Cl[CH_2]_6$	2.59, d, 6 H, 2.6[b]	3.21, s, 2 H	1–1.5, m, 6H; 1.7, q, 2 H, 6.8[c]; 2.73, t, 2 H, 6.0[c]; 3.50, t, 2 H, 6.8[c]	7.28–7.45, m, 30 H
5g, R = $Me[OC_2H_4]_3$	2.55, d, 6 H, 2.5[b]	2.86, s, 2 H	2.86, m,2H; 3.18, m, 4 H; 3.37, s, 3H; 3.51–3.56, m, 8 H	7.25–7.37, m, 30 H
5i, R = $NC[CH_2]_6$	2.56, d, 6 H, 2.6[b]	3.21, s, 2 H	1.1–1.6, m, 10 H; 2.22, t, 2 H, 7.0[c]; 2.71, m, 2 H	7.27–7.39, m, 30 H
5j, R = $HOOC[CH_2]_6$	2.57, d, 6 H, 2.4[b]	3.18, s, 2 H	1.1–1.5, m, 8 H; 2.32, m, 2H; 2.71, m, 2 H	7.27–7.40, m, 30 H
5k, R = $HOH_2C[CH_2]_6$	2.56, d, 6 H, 2.6[b]	3.21, s, 2 H	1.1–1.6, m, 10 H; 2.22, m, 2H; 2.70, m, 2 H	7.27–7.39, m, 30 H

[a] **3** and **4** in CD_2Cl_2, **2** and **5** in $CDCl_3$. – [b] $^2J_{HP}$. – [c] $^3J_{HH}$ in Hz.

Table 5. ^{13}C-NMR data of **3**, **4**, and **5**

^{13}C NMR[a]	CH_2P	CH_2OR	C_qCH_2OR	R	C aromat.	CO
3a, R = Me	32.9–32.4, m	87.5, q, 9.8[b]	42.8, q, 6.4[c]	60.8, s	139.9–129.6, m	[e]
3b, R = Et	31.6–31.1, m	84.1, q, 9.8[b]	41.6, q, 6.4[c]	67.4, s; 15.4, s	139.6–128.4, m	221.7–221.2, m
3c, R = Bzl	31.5–31.0, m	83.6, q, 9.5[b]	41.6, q, 6.4[c]	73.7, s	139.4–127.9, m	221.6–221.1, m
3d, R = 4-stilbenyl	31.5–31.0, m	83.5, q, 9.5[b]	41.6, q, 6.6[c]	73.4, s	139.4–126.8, m	221.6–221.0, m
3e, R = $Br[CH_2]_6$	31.5–31.0, m	84.3, q, 9.6[b]	41.6, q, 6.5[c]	71.7, 34.5, 33.3, 30.0, 28.4, 26.0, 6s	139.5–128.3, m	221.8–221.1, m
4, R = CH_3SO_2	32,2–31.7, m	80.8, q, 10.1[b]	42.4, q, 7.4[c]	39.5, s	139.8–129.8, m	[e]
5a, R = Me	37.8, d, 8.9[d]	78.36, s	42.4, m	57.3, s	139.7–128.0, m	–
5b, R = Et	37.5, m, 8.0[d]	85.4, s	42.5, m	14.4, s; 65.3, s	138.9–128.1, m	–
5c, R = $CH_3[CH_2]_9$	38.5, m, 9.0[d]	71.1, s	43.1, m	14.7, s; 23.2–32.4, m,	140.5–128.7, m	–
5e, R = $H_2C{=}CH[CH_2]_9$	38.5, d, 8.5[d]	71.0, s	43.2, m	26.5–34.3, m; 77.2, m; 114.6, s; 139.7, s	140.5–128.6, m	–
5f, R = $Cl[CH_2]_6$	35.3, m	66.1, s	40.1, m	21.0–28.3, m; 65.7, s	138.8–124.0, m	–
5g, R = $Me[OC_2H_4]_3$	37.7, d, 8.8[d]	71.7, s	42.6, m	58.8, s; 69.6–71.7, m	139.6–128.0, m	–
5i, R = $NC[CH_2]_6$	38.3, m			18.0–25.0, m	140.1–128.7, m	–
5j, R = $HOOC[CH_2]_6$	38.4, d, 9[d]	70.8, s	43.2, m	25.1–34.6, m, 179.8, s	140.6 – 128.7, m	–
5k, R = $HOH_2C[CH_2]_6$	38.3, m			18.0–25.0, m	140.1–128.7, m	

[a] **3** and **4** in CD_2Cl_2, **5** in $CDCl_3$. – [b] $^3J_{CP}$. – [c] $^2J_{CP}$. – [d] $^1J_{CP}$ in Hz. – [e] Due to worse solubility not observed.

The presence of different chain lengths in the product **5h** is evident from the mass spectra (Experimental Section) as well as from individual chromatographic bands for the major congeners of the mixture of oligomers acting as the auxiliary groups in **5h**. All compounds **5** show their ^{31}P resonances as a singlett at $\delta \approx -28$ (Experimental Section) as usual for the CH_2PPh_2 groups in tripod ligands.[8l] The ^{1}H-NMR spectra of **5a–5g** (Table 4) show the signals of all the chemically different groups of **5** in the correct integral ratio and with the expected J_{CP} couplings. The ^{13}C-NMR data (Table 5) are equally conclusive as to the constitution of the compounds.

It is observed that while iodide as a leaving group of the electrophile used to form the ether linkage works well in MeI and also in EtI as the electrophilic components, it is not apt for the introduction of components which contain longer chain alkyl constituents (**5e–5f**). In these cases, presumably by the elimination of HI, no products **5** are obtained. Using tosylate instead of iodide as the leaving group allows for the introduction of long-chain residues (**5c–5f**). These residues may well contain ω-olefinic functionalities (e.g. **5f**). The monomethylpolyoxyethylene function (**5g**, **5h**) may as well be introduced, with the corresponding tosylates which are themselves easily obtained from the commercial alcohols.[13] With the tris(oxyethylene) building block, which is commercially available as its analytically pure alcohol derivative **5g**, is formed correspondingly. The distribution characterizing the polymer mixture $Me(OC_2H_4)_nOH$

leads to a corresponding distribution of chain lengths in the product. The spread of compounds **5a**−**5h** shows that lipophilizing as well as hydrophilizing (**5g**, **h**) auxiliary groups may equally well be introduced by the above procedure. Examples **5e**, **5f** show that ω functionalization of alkyl chains is tolerated by the synthetic procedure, while further functionalization of the terminal double bond in **5e** has not yet been analyzed. Substitution of the chlorine function in **5f** has been investigated: **5f** in DMSO reacts with an excess of KCN to give the nitrile derivative **5i** which lends itself to a variety of further transformations (Scheme 6).

Scheme 6

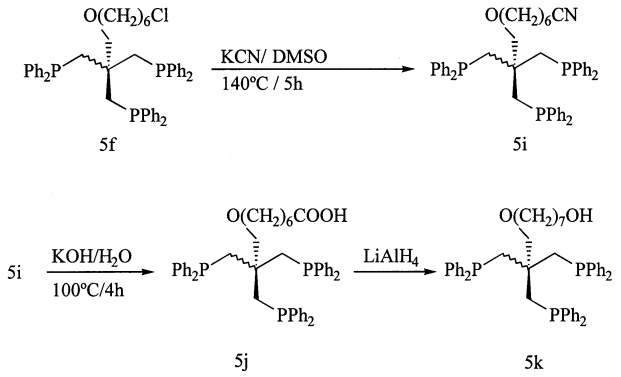

In order to test whether the reaction conditions just described would also work when other donor groups besides phosphanes are present in hydroxy-functionalized ligands of type **1** the mixed-donor set ligand **1b** was synthesized.

Scheme 7

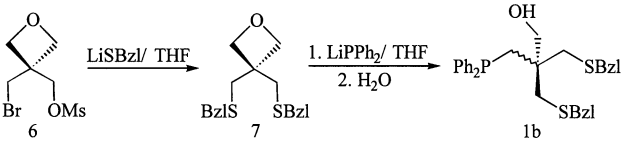

The functionalized oxetane **6** was transformed into **7** by reaction with LiSBzl. In a consequent step the oxetane ring in **6** was nucleophilically opened by $LiPPh_2$ (Scheme 7). After workup, **1b** was obtained as a colorless oil of moderate viscosity. The sequence of reactions used to form **1b** from the functionalized oxetane **6** had already been successfully applied in several principally analogous cases.[8a][8b][8c][8d][8l] It corresponds to an entry into the chemistry of hydroxy-functionalized tripod ligands which is of rather broad scope. While **6** has already been described[8g] compounds **7** and **1b** have been unknown and have therefore been fully characterized by elemental analysis, mass spectrometry and ^{31}P-NMR data where appropriate (Experimental Section) as well as by ^{1}H- and ^{13}C-NMR data (Tables 1 and 2).

The hydroxy function in **1b** is indeed transformed into an ether functionality under the conditions which have been found to be productive in the transformation of **1a**−**5** (Scheme 8). Compounds **8** are colorless oils which are unequivocally characterized by their analytical and spectroscopic data (Experimental Section; Tables 1 and 2).

Scheme 8

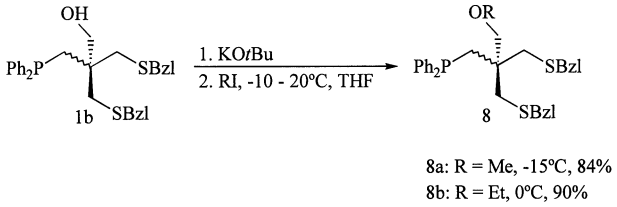

Compounds **8** contain three different ligand functionalities in principle (PPh_2, SBzl, OR). If they undergo η^3 coordination, different possibilities with respect to the formation of isomers exist in principle. It is observed that with the "soft" template $Mo(CO)_3$ only the P- and S-donor functions coordinate.

Scheme 9

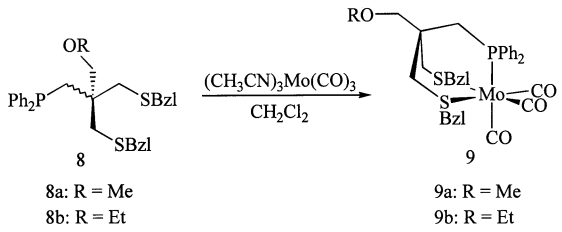

Upon reaction of **8** with $(CH_3CN)_3Mo(CO)_3$[14] the derivatives **9** are formed which contain the ligand in an η^3 coordination mediated by the two SBzl functions and the PPh_2 group (Scheme 9). Compounds **9** are microcrystalline yellow solids which are fully characterized with their analytic and spectroscopic data (Experimental Section; Tables 1 and 2). In compounds **9** as in compound **2b** two sets of carbonyl groups are expected. The ^{13}C-NMR resonances clearly distinguish between these two sets: the CO group *trans* to the phosphorus donor shows a large $^2J_{CP}$ coupling constant: (**2b**: 34.9 Hz; **9b**: 35.0 Hz) while the two carbonyl groups *cis* to the phosphorus atom are characterized by coupling constants of around 9 Hz (Table 2). The idealized symmetry of the $Mo(CO)_3$ entity is thus disturbed and as described for **2b** the ν(CO)-IR E bands of **9a** and **9b** are split into two distinct components (Experimental Section). The diastereotopicity of some of the CH_2 groups in **9** is only occasionally resolved in their ^{1}H-NMR (Table 1). The same statement applies for the diastereotopic differentation of some of the CH_2 groups in **8**, **1b**, and **2b** (Table 1). While with the selective coordination of P and S donors in **9** and the consequent exclusion of the OR donor from coordination, no problems arise with respect to the formation of a mixture of isomers it might well be that a template less soft than $Mo(CO)_3$ might change the situation. To test this hypothesis **5a** containing three phosphorus and one oxygen

donors was treated with $[Fe(CH_3CN)_6](BF_4)_2$[8l][8m][8n][8o] (Scheme 10).

Scheme 10

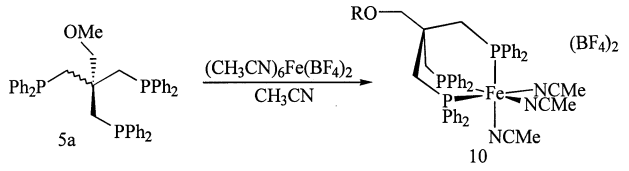

The propensity of the starting material to form tris(acetonitrile)iron cations had already been demonstrated.[8l][8m][8n][8o] With **5** as the ligand compound **10** is obtained as the only product. No signs of oxygen coordination are thus observed even when the less soft metal center Fe^{II} as compared to Mo^0 in **9** is coordinated. **10** is fully characterized by the usual analytical and spectroscopic techniques (Experimental Section).

Experimental Section

General: All manipulations were carried out under argon by means of standard Schlenk techniques. All solvents were dried by standard methods and destilled under argon. The $CDCl_3$, CD_2Cl_2, and $[D_8]$THF used for the NMR-spectroscopic measurements were degassed by three successive "freeze-pump-thaw" cycles and dried over 4-Å molecular sieves. The silica gel (Kieselgel z.A. 0.06−0.2 mm, J. T. Baker Chemicals B.V.) used for chromatography was degassed at 1 mbar for 24 h and saturated with argon. − NMR: Bruker Avance DPX 200 at 200.13 MHz (^1H), 50.323 MHz ($^{13}C\{^1H\}$), 81.015 MHz ($^{31}P\{^1H\}$)); chemical shifts (δ) in ppm with respect to $CDCl_3$ (^1H: δ = 7.27; ^{13}C: δ = 77.0), CD_2Cl_2 (^1H: δ = 5.32; ^{13}C: δ = 53.5) and $[D_8]$THF (^1H: δ = 3.58; ^{13}C: δ = 67.7) as internal standards, and chemical shifts (δ) in ppm with respect to 85% H_3PO_4 (^{31}P: δ = 0) as external standard. − IR: Bruker FT-IR IFS-66; CaF_2 cells. − MS: Finnigan MAT 8400; FAB: Nibeol (4-nitrobenzyl alcohol) or TEA (triethanol amine) matrices, respectively; EI: 70 eV. − Elemental analyses: Microanalytical laboratory of the Organisch-Chemisches Institut, Universität Heidelberg: With the equipment used, carbon values tend to be systematically too low in the presence of molybdenum or/and boron. Some of the analytical data given have to be interpreted with this in mind. − Melting points: Gallenkamp MFB-595 010; melting points are not corrected. − The oxetane **6** was prepared according to ref.[8g]. $[(CH_3CN)_3Mo(CO)_3]$ was obtained as described in ref.[14]. All other chemicals were commercially obtained and used without further purification.

Preparation of **1b**: A solution of lithium diphenylphosphide in THF (100 ml) was prepared by deprotonation of diphenylphosphane (8.2 g; 44 mmol) with *n*-butyllithium (17.6 ml; 44 mmol; 2.5 M in *n*-hexane) at 0°C. After stirring for 30 min, a solution of **7** (13.2 g; 40 mmol) in THF (100 ml) was added and the mixture refluxed for 2 h. The solvent was removed, water (100 ml) and diethyl ether (100 ml) were added, and the mixture was neutralized with 37% HCl. The aqueous phase was extracted with diethyl ether (2 × 100 ml) and the combined organic phases were dried and concentrated. The resulting residue was chromatographed on silica gel (20 cm, Ø = 10 cm). The fraction eluted with a mixture of petroleum ether (40/60)/diethyl ether (6:4; TLC control: R_f = 0.48) gave 15.5 g of **1b** as a colorless oil in 75% yield. − $C_{31}H_{33}OPS_2$ (516.7): calcd. C 72.07, H 6.44; found C 71.72, H 6.49. − MS(FAB); *m/z* (%): 517 (18) $[M^+ + 1]$, 425 (100) $[M^+ - C_7H_7]$. − $^{31}P\{^1H\}$ NMR ($CDCl_3$): δ = −26.0 (s). − For ^1H- and ^{13}C-NMR data see Tables 1 and 2.

General Procedure for the Preparation of the Molybdenum Complexes **2** *and* **9**: The given tripod ligands (vide infra) were dissolved in CH_2Cl_2 (30 ml), solid $(CH_3CN)_3Mo(CO)_3$ was added (302 mg; 1 mmol) and the mixtures were stirred for 1 h at room temperature. During the reactions the $(CH_3CN)_3Mo(CO)_3$ slowly dissolved and the colors of the solutions turned from light-yellow into yellow-brown. The reaction mixtures were concentrated to 5 ml and slow stepwise addition of 50 ml of petroleum ether (40/60) gave yellow to yellow-brownish, microcrystalline solids. The crude products were washed with petroleum ether (40/60) (2 × 50 ml) and diethyl ether (2 × 50 ml) and dried in vacuo.

Follwing the above procedure using **1b** (517 mg; 1 mmol) as the tripod ligand yielded 490 mg (70%) of **2b**, m.p. 220°C (dec.). With **1a** (640 mg; 1 mmol) as the tripod ligand 740 mg (90%) of **2a** were obtained, m.p. 225°C (dec.). Starting the procedure described above with **8a** (530 mg; 1 mmol) led to 600 mg (84%) of **9a**, m.p. 210°C (dec.). Crystals suitable for an X-ray analysis were obtained for **9a** by slow diffusion of diethyl ether into a solution of 100 mg of the microcystalline product in 5 ml of a mixture of CH_2Cl_2/toluene (1:1) at room temperature after 2 d. 650 mg (90%) **9b**, m.p. 205°C (dec.) was obtained if the starting compound for the above procedure was **8b** (545 mg; 1 mmol).

2a: $C_{44}H_{39}MoO_4P_3$ (820.7): − MS (EI); *m/z* (%): 822 (4) $[M^+]$, 738 (60) $[M^+ - 3\ CO]$, 523 (100) $[M^+ - 3\ CO - C_7H_7]$. − IR (CH_2Cl_2): $\tilde{\nu}$(CO) = 1937 cm^{-1} (s), 1845 (s, br.). − $^{31}P\{^1H\}$ NMR (CD_2Cl_2): δ = 14.5 (s).

2b: $C_{34}H_{33}MoO_4PS_2$ (696.7): calcd. C 58.45, H 4.76, P 4.44, S 9.16; found C 57.39, H 4.99, P 4.29, S 8.87. − MS (FAB); *m/z* (%): 698 (36) $[M^+]$, 614 (44) $[M^+ - 3\ CO]$, 523 (100) $[M^+ - 3\ CO - C_7H_7]$. − IR (CH_2Cl_2): $\tilde{\nu}$(CO) = 1932 cm^{-1} (s), 1829 (s, br.); 1817 (vs, br.). − $^{31}P\{^1H\}$ NMR ($[D_8]$THF): δ = 20.2 (s).

9a: $C_{35}H_{35}MoO_4PS_2$ (710.7): calcd. C 59.15, H 4.96, P 4.36, S 9.03; found C 57.66, H 5.06, P 4.16, S 8.80. − MS (FAB); *m/z* (%): 712 (14) $[M^+]$, 537 (4) $[M^+ - 3\ CO - C_7H_7]$. − IR (CH_2Cl_2): $\tilde{\nu}$(CO) = 1932 cm^{-1} (s), 1829 (v, br.), 1815 (s, br.). − $^{31}P\{^1H\}$ NMR ($[D_8]$THF): δ = 17.2 (s). − X-ray analysis see ref.[16].

9b: $C_{36}H_{37}MoO_4PS_2$ (724.7): calcd. C 59.66, H 5.15, P 4.27, S 8.85; found C 58.94, H 4.99, P 4.21, S 8.86. − MS (FAB); *m/z* (%): 726 (18) $[M^+]$, 642 (5) $[M^+ - 3\ CO]$, 551 (20) $[M^+ - 3\ CO - C_7H_7]$. − IR (CH_2Cl_2): $\tilde{\nu}$(CO) = 1932 cm^{-1} (s), 1829 (s, br.), 1815 (s, br.). − $^{31}P\{^1H\}$ NMR (CD_2Cl_2): δ = 16.1 (s).

For ^1H- and ^{13}C-NMR data see Tables 1 and 2.

General Procedure for the Preparation of the Molybdenum Complexes **3** *by Alkylation of* **2a**: Compound **2a** (815 mg; 1 mmol) was dissolved in THF (50 ml) and deprotonated with KO*t*Bu (112 mg; 1 mmol). While stirring the mixture for 1 h a light-yellow precipitate of the potassium salt of **2a** formed. The alkylation reagent as specified below was added. The mixture was stirred for 2 h during which the precipitate formed in the deprotonation step slowly dissolved again. The completion of the reaction was determined by TLC control: CH_2Cl_2/petroleum ether (40/60), 3:1; **2a**: R_f = 0.35 (tailing); **3**: R_f = 0.67−0.74 (no tailing). After removal of the solvent, the resulting residue was chromatographed on silica gel (10 cm, Ø = 4 cm). The fractions eluted with a mixture of CH_2Cl_2/petroleum ether (40/60), 3:1 (TLC control: R_f = 0.67−0.74) gave pale-yellow microcrystalline solids.

Following the above procedure compounds **3** were obtained by using as alkylation reagent CH_3I (284 mg, 2 mmol) to prepare **3a**

(790 mg, 95%), triethyloxonium tetrafluoroborate (380 mg, 2 mmol) to prepare **3b** (510 mg, 60%), benzyl bromide (340 mg, 2 mmol) to prepare **3c** (820 mg, 91%), 4-chloromethylstilbene (460 mg, 2 mmol) to prepare **3d** (960 mg, 95%), and 6-bromo-*n*-hexyl *p*-toluenesulfonate (670 mg, 2 mmol) to prepare **3e** (360 mg, 37%). Crystals suitable for X-ray analyses were obtained for **3a** and for **3b** by slow diffusion of diethyl ether into a solution of 100 mg of the microcystalline products in 5 ml of CH_2Cl_2 at room temperature after 1 d.

3a: $C_{45}H_{41}MoO_4P_3$ (834.7): calcd. C 64.58, H 4.92, P 11.12; found C 63.90, H 5.24, P 10.89. − MS (EI); *m/z* (%): 836 (30) [M^+], 808 (36) [M^+ − CO], 780 (60) [M^+ − 2 CO], 752 (100) [M^+ − 3 CO]. − IR (CH_2Cl_2): $\tilde{\nu}$(CO) = 1932 cm^{-1} (s), 1835 (s, br.). − $^{31}P\{^1H\}$ NMR (CD_2Cl_2): δ = 16.0 (s). − X-ray analysis see ref.[16].

3b: $C_{46}H_{43}MoO_4P_3$ (848.7): calcd. C 64.93, H 5.10, P 10.93; found C 64.87, H 5.26, P 10.76. − MS (EI); *m/z* (%): 850 (20) [M^+], 821 (30) [$M^+ - CH_2CH_3$], 793 (58) [M^+ − CO − CH_2CH_3], 766 (100) [M^+ − 3 CO]. − IR (CH_2Cl_2): $\tilde{\nu}$(CO) = 1929 cm^{-1} (s), 1833 (s, br.). − $^{31}P\{^1H\}$ NMR (CD_2Cl_2): δ = 15.9 (s). − X-ray analysis see ref.[16].

3c, $C_{51}H_{45}MoO_4P_3$ (910.7): calcd. C 67.26, H 4.98, P 10.20; found C 66.78, H 5.18, P 10.06. − MS (FAB); *m/z* (%): 912 (46) [M^+], 884 (30) [M^+ − CO], 856 (34) [M^+ − 2 CO], 828 (35) [M^+ − 3 CO]. − IR (CH_2Cl_2): $\tilde{\nu}$(CO) = 1929 cm^{-1} (s), 1829 (s, br.). − $^{31}P\{^1H\}$ NMR (CD_2Cl_2): δ = 15.8 (s).

3d: $C_{59}H_{51}MoO_4P_3$ (1012.9): calcd. C 69.96, H 5.54; found C 69.40, H 5.54. − MS (FAB); *m/z* (%): 1014 (80) [M^+], 986 (36) [M^+ − CO], 958 (64) [M^+ − 2 CO], 930 (54) [M^+ − 3 CO]. − IR (CH_2Cl_2): $\tilde{\nu}$(CO) = 1937 cm^{-1} (s), 1844 (s, br.). − $^{31}P\{^1H\}$ NMR (CD_2Cl_2): δ = 15.7 (s).

3e: $C_{50}H_{50}BrMoO_4P_3$ (983.7): calcd. C 61.05, H 5.12; found C 62.18, H 5.51. − MS (FAB); *m/z* (%): 984 (80) [M^+], 956 (50) [M^+ − CO], 928 (68) [M^+ − 2 CO], 900 (100) [M^+ − 3 CO]. − IR (CH_2Cl_2): $\tilde{\nu}$(CO) = 1937 cm^{-1} (s), 1844 (s, br.).

For ^1H- and ^{13}C-NMR data see Tables 3 and 4.

Preparation of **4**: NEt_3 (600 mg, 6 mmol) and methanesulfonyl chloride (570 mg, 5 mmol) were added to a solution of **2a** (819 mg, 1 mmol) in CH_2Cl_2 (50 ml). After stirring the light-yellow mixture for 30 min, water was added (50 ml). After separation of the phases, the aqueous phase was extracted with CH_2Cl_2 (2 × 50 ml) and the residue of the dried ($MgSO_4$) and concentrated organic phases was chromatographed on silica gel (10 cm, Ø = 4 cm). Concentrating the fractions eluted with a mixture of CH_2Cl_2/petroleum ether (40/60) (3:1; TLC control: R_f = 0.50) gave **4** as a pale-yellow microcrystalline product (810 mg, 90%). − $C_{45}H_{41}BrMoO_6P_3S$ (898.7): calcd. C 60.14, H 4.60; found C 58.71, H 4.73. − MS (EI); *m/z* (%): 899 (20) [M^+ − 1], 872 (26) [M^+ − CO], 844 (60) [M^+ − 2 CO], 816 (100) [M^+ − 3 CO]. − IR (CH_2Cl_2): $\tilde{\nu}$(CO) = 1927 cm^{-1} (s), 1844 (s), 1826 (s). − $^{31}P\{^1H\}$ NMR (CD_2Cl_2): δ = 14.0 (s). − For ^1H- and ^{13}C-NMR data see Tables 3 and 4.

Preparation of **3b** *Starting from* **4**: To a solution of lithium ethoxide in THF (50 ml), prepared by deprotonation of ethanol (138 mg, 3 mmol) with 1.2 ml of *n*-butyllithium (2.5 M in *n*-hexane) at 0°C, **4** (450 mg, 0.5 mmol) was added. After stirring the yellow mixture for 4 h at 50°C, the solvent was removed and the residue chromatographed on silica gel (10 cm, Ø = 4 cm). Concentrating the fractions eluted with a mixture of CH_2Cl_2/petroleum ether (40/60) (3:1; TLC control: R_f = 0.73) gave **3b** as a pale-yellow microcrystalline product (148 mg, 35%). − Analytical data: vide supra.

Liberating **5b** *from* **3b**: Compound **3b** (829 mg, 1 mmol) was dissolved in CH_2Cl_2 (200 ml), pyridine *N*-oxide was added (1.90 g, 20 mmol) and the reaction mixture was irradiated in a "Duran 50" ("Pyrex") apparatus with a mercury lamp (TQ 150 Hanau) at −5°C for 1 h. After removal of the solvent the brownish residue was chromatographed on silica gel. The fractions eluted with a mixture of petroleum ether (40/60)/diethyl ether (9:1; TCL control: R_f = 0.40) gave 401 mg (60%) of **5b** as a colorless, viscous oil. − Analytical data: vide supra.

Preparation of **7**: Compound **6** (13.0 g; 50 mmol) was dissolved in THF (100 ml) and the solution cooled to 0°C. A solution of lithium benzylthiolate (100 mmol in 300 ml of THF), obtained by deprotonation of 12.4 g (100 mmol) of benzylthiole with 40 ml of *n*-butyllithium (2.5 M in *n*-hexane) at 0°C, was slowly added and the mixture stirred for 4 h at room temperature to give a voluminous white precipitate of lithium mesylate and lithium bromide. The solvent was removed in vacuo, water (200 ml) and diethyl ether (200 ml) were added and the mixture was neutralized with 37% HCl. The aqueous phase was extracted with diethyl ether (2 × 150 ml) and the combined organic phases were dried and concentrated. Destillation of the residue (b.p. 205−210°C/1 mbar) yielded 14.9 g (90%) of **7** as a viscous, colorless oil. − $C_{19}H_{22}OS_2$ (330.5): calcd. C 69.07, H 6.72, S 19.37; found C 68.81, H 6.50, S 18.68. − MS (FAB); *m/z* (%): 331 (72) [M^+ + 1], 239 (100) [$M^+ - C_7H_7$]. − For ^1H- and ^{13}C-NMR data see Tables 1 and 2.

Preparation of **8a** *and* **8b**: For the synthesis of **8a** a solution of **1b** (5.17 g; 10 mmol) in THF (100 ml) was deprotonated with KO*t*Bu (1.12 g; 10 mmol). The mixture was cooled to −15°C, then CH_3I (1,42 g; 10 mmol) was slowly added (temperature was held below −10°C) and a white precipitate of potassium iodide instantaneously formed. The progress of the reaction was determined by TLC [petroleum ether (40/60)/diethyl ether, 6:4; **1b**: R_f = 0.48; **8a**: R_f = 0.80].

To synthesize **8b** a slightly modified procedure was applied: A solution of **1b** (2.58 g, 5 mmol) in 50 ml of THF was deprotonated with KO*t*Bu (560 mg, 5 mmol). The mixture was cooled to 0°C, iodethane (780 mg, 5 mmol) was slowly added and a white precipitate of potassium iodide slowly formed. After 10 min, the progress of the reaction was determined by TLC control [petroleum ether (40/60)/diethyl ether, 6:4; **1b**: R_f = 0.48; **8b**: R_f = 0.81]. After the first "deprotonation-alkylation" sequence, the reaction was incomplete. For obtaining higher yields it was necessary to repeat this sequence five times. The isolation procedures for **8a** and **8b** were similar:

After completion of the reaction, water was added (1 ml) and the mixture was allowed to warm to 20°C. The solvent was removed, water (100 ml) and diethyl ether (100 ml) were added und the mixture was neutralized with 37% HCl. The aqueous phase was extracted with diethyl ether (2 × 100 ml) and the combined organic phases were dried and concentrated. The resulting residue was chromatographed on silica gel (15 cm, Ø = 6 cm).

8a: The fraction eluted with a mixture of petroleum ether (40/60)/diethyl ether (6:4; TLC control: R_f = 0.8) gave 3.45 g of **8a** as a colorless oil in 65% yield. − $C_{32}H_{35}OPS_2$ (530.7): calcd. C 72.42, H 6.65, P 5.84; found C 71.95, H 7.03, P 5.46. − MS (FAB); *m/z* (%): 531 (34) [M^+ + 1], 439 (100) [$M^+ - C_7H_7$]. − $^{31}P\{^1H\}$ NMR ($CDCl_3$): δ = −26.4 (s).

8b: The fraction eluted with a mixture of petroleum ether (40/60)/diethyl ether (9:1; TLC control: R_f = 0.4) gave 1.91 g of **8b** as a colorless oil in a 70% yield. − $C_{33}H_{37}OPS_2$ (544.8): calcd. C 72.75, H 6.85, P 5.59, S 11.77; found C 72.77, H 7.13, P 5.58, S 11.75. − MS (FAB); *m/z* (%): 545 (18) [M^+ + 1], 453 (100) [$M^+ - C_7H_7$]. − $^{31}P\{^1H\}$ NMR ($CDCl_3$): δ = −26.8 (s). −For ^1H- and ^{13}C-NMR data see Tables 1 and 2.

General Procedure for the Preparation of Ethers **5** *by Direct Alkylation of* **1a**: Compound **1b** (640 mg; 1 mmol) was dissolved in THF (20 ml) and cooled to −5°C by means of an ice/salt bath. 1.5 equivalents of KO*t*Bu were added to the colorless solution, which immediately turned yellow. The mixture was stirred for 5 min and the given alkyl iodides or toluenesulfonic esters (vide infra) were added. In case of the alkyl iodides the mixture immediately became turbid white, in case of the toluenesulfonic esters the mixture was slowly brought to room temperature and the mixture became turbid yellow-brown. The completion of the reaction was determined by TLC control. Water (0.5 ml) was added and the solvent was removed in vacuo. The residue was dissolved in dichloromethane and filtered through silica gel. The solvent was removed and the residue was chromatographed on silica gel (15−25 cm, ∅ = 4 cm).

Following the above procedure compounds **5** were obtained by using as alkylation reagents iodomethane (982 mg, 6.91 mmol) to prepare **5a** (470 mg, 72%), iodoethane (200 mg, 1.33 mmol) to prepare **5b** (461 mg, 69%), *n*-decyl *p*-toluenesulfonate (667 mg, 2.14 mmol) to prepare **5c** (253 mg, 33%), *n*-docosanyl *p*-toluenesulfonate (510 mg, 1.06 mmol) to prepare **5d** (425 mg, 44%), undecenyl *p*-toluenesulfonate (475 mg, 1.46 mmol) to prepare **5e** (300 mg, 38%), 6-chloro-*n*-hexyl *p*-toluenesulfonate (347 mg, 1.2 mmol) to prepare **5f** (394 mg, 52%), triethyleneglycol monomethyl ether *p*-toluenesulfonic ester (400 mg, 1.25 mmol) to prepare **5g** (415 mg, 53%).

5a: $C_{42}H_{41}OP_3$ (654.1): calcd. C 77.04, H 6.32; found C 76.79, H 6.37. − MS (EI); *m/z* (%): 654 (11) [M^+], 577 (100) [M^+ − Ph], 469 (16) [M^+ − PPh_2]. − $^{31}P\{^1H\}$ NMR ($CDCl_3$): δ = −28.4 (s).

5b: $C_{43}H_{43}OP_3$ (668.7): calcd. C 77.22, H 6.49; found C 75.51, H 6.63. − MS (EI); *m/z* (%): 668 (10) [M^+], 591 (100) [M^+ − PPh_2], 485 (38) [M^+ − PPh_2]. − $^{31}P\{^1H\}$ NMR ($CDCl_3$): δ = −28.3 (s).

5c: $C_{51}H_{59}OP_3$ (780.5): calcd. C 78.48, H 7.56; found C 78.10, H 7.83. − MS (EI); *m/z* (%): 780 (9) [M^+], 703 (100) [M^+ − PPh_2], 595 (11) [M^+ − PPh_2]. − $^{31}P\{^1H\}$ NMR ($CDCl_3$): δ = −28.6 (s).

5d: $C_{63}H_{83}OP_3$ (949.3): calcd. C 79.71, H 8.81; found C 79.34, H 10.01. − MS (EI); *m/z* (%): 949 (17) [M^+], 872 (100) [M^+ − PPh_2], 764 (20) [M^+ − PPh_2]. − $^{31}P\{^1H\}$ NMR ($CDCl_3$): δ = −25.3 (s).

5e: $C_{52}H_{59}OP_3$ (792.5): calcd. C 78.75, H 7.50; found C 78.88, H 7.75. − MS (EI); *m/z* (%): 792 (20) [M^+], 715 (100) [M^+ − PPh_2]. − $^{31}P\{^1H\}$ NMR ($CDCl_3$): δ = −28.2 (s).

5f: $C_{47}H_{50}ClOP_3$ (759.3): calcd. C 74.35, H 6.58; found C 73.77, H 7.10. − MS (EI); *m/z* (%): 758 (10) [M^+], 681 (100) [M^+ − PPh_2], 573 (10) [M^+ − PPh_2]. − $^{31}P\{^1H\}$ NMR ($CDCl_3$): δ = −25.1 (s).

5g: $C_{48}H_{53}OP_3$ (786.9): calcd. C 73.27, H 6.79; found C 73.10, H 6.83. − MS(EI); *m/z* (%): 786 (9) [M^+], 709 (100) [M^+ − PPh_2], 601 (11) [M^+ − PPh_2]. − $^{31}P\{^1H\}$ NMR ($CDCl_3$): δ = −28.6 (s).

For ^{1}H- and ^{13}C-NMR data see Tables 3 and 4.

Preparation of **5i**: A solution of **5f** (759 mg, 1 mmol) in DMSO (3 ml) was slowly added to a stirred mixture of 1 g of KCN in 5 ml of DMSO at 90°C. After the addition, the mixture was heated to 140°C for 5 h. The solvent was removed and the residue was chromatographed on silica gel. The fractions eluted by a mixture of petroleum ether (40/60)/diethyl ether (3:1) at R_f = 0.30 were collected to give 300 mg (40%) of **5i** as a colorless oil after evaporation of the solvent. − $C_{48}H_{50}NOP_3$ (749.8): calcd. C 76.89, H 6.72, N 1.87; found C 76.40, H 6.75, N 1.61. − MS (FAB); *m/z* (%): 750 (33) [M^+], 672 (100) [M^+ − PPh_2], 564 (16) [M^+ − PPh_2]. − $^{31}P\{^1H\}$ NMR ($CDCl_3$): δ = −28.3 (s). − For ^{1}H- and ^{13}C-NMR data see Tables 3 and 4.

Preparation of **5j**: A solution of **5i** (430 mg , 0.6 mmol) in a 1:1 mixture of ethanol/water (25 ml) and KOH (580 mg, 10.4 mmol) was heated under reflux for 4 h. After cooling, the reaction mixture was acidified with 37% hydrochloric acid. The water phase was extracted with dichloromethane (3 ×), the organic phase was dried with $MgSO_4$, the solvent was removed in vacuo and the residue was chromatographed on silica gel. The fractions eluted with diethyl ether at R_f = 0.40 were collected to give 220 mg (48%) of **5j** as a colorless oil after evaporation of the solvent. − $C_{48}H_{51}O_3P_3$ (768.8): calcd. C 74.99, H 6.69; found C 74.42, H 6.82. − MS (FAB); *m/z* (%): 768 (35) [M^+], 691 (100) [M^+ − PPh_2], 582 (21) [M^+ − PPh_2]. − $^{31}P\{^1H\}$ NMR ($CDCl_3$): δ = −28.2 (s). − IR (Nujol): $\tilde{\nu}$(COO) = 1708 cm^{-1} (m). − For ^{1}H- and ^{13}C-NMR data see Tables 3 and 4.

Preparation of **5k**: A solution of **5j** (50 mg, 0.07 mmol) in THF (5 ml) was added to a stirred suspension of $LiAlH_4$ (30 mg, 0.8 mmol) in THF (5 ml). The mixture was heated under reflux for 2 h and after cooling to 20°C hydrolized with water. The products of hydrolysis were washed with dichloromethane, the combined organic phases were dried ($MgSO_4$) and the solvents were removed in vacuo. The residue, a colorless oil, was investigated by mass spectrometry and NMR spectroscopy. − $C_{48}H_{53}O_2P_3$ (755). − MS (FAB); *m/z* (%): 755 (27) [M^+], 678 (100) [M^+ − PPh_2], 571 (18) [M^+ − PPh_2]. − $^{31}P\{^1H\}$ NMR ($CDCl_3$): δ = −28.1 (s). − For ^{1}H-and ^{13}C-NMR data see Tables 3 and 4.

Preparation of **10**: Compound **5a** (654 mg, 1 mmol) was dissolved in acetonitrile (20 ml) and 476 mg (1 mmol) of $[Fe(CH_3CN)_6](BF_4)_2$, dissolved in 10 ml of acetonitrile, was added. The mixture immediately turned red and was stirred at room temperature for 1 h. The solvent was removed and the residue was washed with diethyl ether (3 ×). After drying in vacuo, 930 mg (92%) of **10** was obtained as a red powder. Crystals suitable for X-ray analysis were obtained by diffusion of diethyl ether into a solution of **10** in CH_2Cl_2 within 1 d at room temperature. − $C_{48}H_{50}B_2F_8FeN_3OP_3$ (1007.4): calcd. C 57.23, H 5.00, N 4.17; found C 54.04, H 6.83, N 4.18. − MS (FAB); *m/z* (%): 729 (100) [M^+ − 3 MeCN − B_2F_7], 655 (73) [free ligand], 576 (52) [free ligand-Ph]. − ^{1}H NMR ($CDCl_3$): δ = 2.03 (br. s, 2 H, OCH_2), 2.41 (br. s, 9 H, CH_3CN), 2.58 (br. s, 6 H, CH_2P), 3.61 (br. s, 3 H, CH_3O), 7.25-7.37 (br. m, 30 H, *H* arom.). − $^{13}C\{^1H\}$ NMR ($CDCl_3$): δ = 4.9 (s, CH_3CN); 129.3, 130.8, 132.4, 142 (m, *C* arom.). − $^{31}P\{^1H\}$ NMR ($CDCl_3$): δ = +31.7 (s). − IR (KBr): $\tilde{\nu}$(CN) = 2343 cm^{-1} (w), 2287 (m).

☆ Dedicated to Prof. Dr. *Achim Müller*, Universität Bielefeld, on the occasion of his 60th birthday.

[1] E. Kuntz (Rhone-Poulenc Ind.), FR-75-19407, **1975**; E. Kuntz (Rhone-Poulenc Ind.), FR-76-22824, **1976**; J. Junk (Rhone-Poulenc Ind.) FR-79-26994, **1979**.

[2] P. Behrens, G. Stucky, *Angew. Chem.* **1993**, *105*, 729−732; *Angew. Chem. Int. Ed. Engl.* **1993**, *32*, 696−699.

[3] W. A. Herrmann, C. W. Kohlpaintner, *Angew. Chem*. **1993**, *105*, 1588−1609; *Angew. Chem. Int. Ed. Engl.* **1993**, *32*, 1524−1545.

[4] B.Cornlis, *Angew. Chem.* **1997**, *109*, 1075−1095; *Angew. Chem. Int. Ed. Engl.* **1997**, *36*, 36−56.

[5] C. Tanford (Ed.), *The Hydrophobic Effect: Formation of Micelles and Biological Membranes*, 2nd ed., Wiley, New York, **1980**.

[6] A. Hulanicki, S. Glab, F. Ingman, Chemical Sensors: Definitions and Classification, *Pure Appl. Chem.* **1991**, *63*, 1247.

[7] Tobin J. Marks, Mark A. Ratner, *Angew. Chem*. **1995**, *107*, 167−187; *Angew. Chem. Int. Ed. Engl.* **1995**, *34*, 146−166.

[8] [8a] S. T. Liu, H. E. Wang, M. C. Cheng, S. M. Peng, *J. Or-*

ganomet. Chem. **1989**, *376*, 333−42. [8b] S. T. Liu, K. J. Liu, *Inorg. Chem.* **1990**, *29*, 4576−4579. [8c] S. T. Liu, G. J. Liu, C. H. Yieh, M. C. Cheng, S. M. Peng, *J. Organomet. Chem.* **1990**, *387*, 83−84. [8d] S. T. Liu, *J. Chinese Chem. Soc.* **1992**, *39*, 611−616. [8e] S. T. Liu, H. E. Wang, C. Y. Liu, M. C. Cheng, S. M. Peng, *Phosphorus Sulfur Silicon* **1992**, *69*, 201−211. [8f] S. Tsai, H. E. Wang, C. T. Huang, L. M. Yin, S. T. Liu, *Chem. Ber.* **1995**, *128*, 151−155. [8g] A. Muth, A. Asam, G. Huttner, A. Barth, L. Zsolnai, *Chem. Ber.* **1994**, *127*, 305−317. [8h] G. Reinhard, R. Soltek, A. Barth, O. Walter, L. Zsolnai, *Chem. Ber.* **1996**, *129*, 97−108. [8i] O. Walter, Th. Klein, G. Huttner, L. Zsolnai, *J. Organomet. Chem*. **1993**, *458*, 63−81. [8j] A. Jacobi, G. Huttner, U. Winterhalter, *Chem. Ber.* **1997**, *130*, 1279−1294. [8k] Th. Seitz, A. Muth, G. Huttner, Th. Klein, O. Walter, M. Fritz, L. Zsolnai, *J. Organomet. Chem*., **1994**, *469*, 155−162. [8l] Th. Seitz, A. Asam, G. Huttner, O. Walter, l. Zsolnai, *Z. Naturforsch*. **1995**, *50b*, 1287−1306. [8m] B. Janssen, V. Sernau, G. Huttner, A. Asam, O. Walter, M. Büchner, L. Zsolnai, *Chem. Ber.* **1995**, *128*, 63−70. [8n] A. Asam, B. Janssen, G. Huttner, L. Zsolnai, O. Walter, *Z. Naturforsch.* **1993**, *48b*, 1707−1714. [8o] A. Asam, B. Janssen, G. Huttner, L. Zsolnai, *Chem. Ber.* **1994**, *127*, 501−506. [8p]H. Heidel, J. Scherer, A. Asam, G. Huttner, O. Walter, L. Zsolnai, *Chem. Ber.* **1995**, *128*, 293−301.

[9] [9a] H. Heidel, G. Huttner, G. Helmchen, *Z. Naturforsch*. **1993**, *48b*, 1681. [9b]H. Heidel, G. Huttner, R.Vogel, G. Helmchen, *Chem. Ber.* **1994**, *127*, 271. [9c]H. Heidel, G. Huttner, L. Zsolnai, *Z. Naturforsch*. **1995**, *50b*, 729−734.

[10] C. K. Ingold, *Structure and Mechanism in Organic Chemistry*, 2nd ed., Cornell University Press, Ithaca, N. Y. **1969**.

[11] Th. Seitz, G. Huttner, M. Büchner, *Z. Naturforsch.* **1994**, *49b*, 1813−1817.

[12] P. Stössel, H. A. Mayer, C. Maichle-Mössmer, R. Fawzi, M. Steinmann, *Inorg. Chem.* **1996, 35**, 5860.

[13] F. Muth, *Methoden Org. Chem. (Houben-Weyl)* **1955**, vol. IX, p. 663−682.

[14] D. P. Tate, W. R. Knipple, J. M. Augl, *Inorg. Chem.* **1962**, *1*, 433.

[15] B. J. Hathaway, D. G. Holah, A. E. Underhill, *J. Chem. Soc.* **1962**, 244.

[16] Compounds **3a**, **3b**, **9a**, **10** were characterized by single-crystal X-ray analyses. The constitution as given above was corroborated in each case. Distances and angles are in the range characteristic of $(tripod)Mo(CO)_3$[8i][8k][8l] or $[(tripod)Fe(MeCN)_3]^{2+}$[8l][8m][8n][8o][8p] compounds throughout. Further details of the crystal-structure investigations may be obtained from the Fachinformationszentrum Karlsruhe, D-76344 Eggenstein-Leopoldshafen (Germany), on quoting the depository numbers CSD-407890 for **3a**, -407891 for **3b**, -407892 for **9a**, -407889 for **10**.

[98063]

Thiolate and Thioether Functions as Donor Groups X, Y in Tripod Ligands $RCH_2C(CH_2PPh_2)(CH_2X)(CH_2Y)$ – Synthesis and Coordination Chemistry☆

Rainer Soltek and Gottfried Huttner*

Anorganisch-Chemisches Institut der Universität Heidelberg,
Im Neuenheimer Feld 270, D-69120 Heidelberg, Germany
Fax: (internat.) + 49(0)6221/545707

Received March 16, 1998

Keywords: Tripod ligands / Molybdenum / Mixed donor set ligands / Thiole ligands / Thiolate ligands

Tripod ligands $RCH_2C(CH_2PPh_2)(CH_2X)(CH_2Y)$ (**1**) with X, Y = SAlkyl, SBzl selectively undergo reductive cleavage of the SBzl function with Li/NH_3/THF at –40 °C to produce $RCH_2C(CH_2PPh_2)(CH_2X)(CH_2Y)$ (**2**) (X, Y = SAlkyl, SH). In these mixed donor set ligands the SH functions are the least coordinative ones such that $[\eta^2$-$\{CH_3C(CH_2PPh_2)(CH_2SEt)$-$(CH_2SH)\}(CO)_4Mo]$ (**5**) is a stable compound with an uncoordinated SH function at the dangling arm of the ligand. If the SH functions of a potential tripod ligand are deprotonated the resulting thiolate functions are found to strongly coordinate in compounds such as $[\eta^3$-$\{CH_3C(CH_2PPh_2)_2(CH_2S)\}(CO)_3Mo]^-$ which are obtained as their lithium and sodium salts **6**. These highly reactive species may be stabilized by encapsulating their alkali counter ions in cryptands and the corresponding salts with [2,1,1]cryptand (**7a**) and [2,2,2]cryptand (**7b**) are far easier to handle than the cryptand-free progeners **6**. Alkylation of the coordinatively bound thiolate function in **6** leads to the corresponding thioether derivatives $[\eta^3$-$\{CH_3C(CH_2PPh_2)_2$-$(CH_2SR)\}(CO)_3Mo]$ (**8**).

Introduction

The coordination chemistry of tripod ligands $CH_3C(CH_2PPh_2)_3$ developed by L. Sacconi and his school has quite some unconventional features which show that the η^3 coordination of a neopentane-based tripod ligand is able to induce a reactive potential at the metal center which is otherwise not accessible[1][2]. The potential of this type of ligand should be greatly enhanced by an appropriate variation of the donor functions and in fact there is a promising chemistry with ligands of type $RC(CH_2X)_3$ containing donor functions X other than PPh_2[2][3][4]. A still broader scope of this chemistry could be envisaged if it were possible to synthesize ligands $CH_3C(CH_2X)(CH_2Y)(CH_2Z)$ with up to three different phosphorus donor groups. The difficulties characterizing the neopentane chemistry, which is at the basis of such syntheses, had only recently been overcome and neopentane-based tripod ligands with up to three different phosphorus donors have been described[5][6][7][8][9][10][11][12][13] with even enantioselective syntheses of such ligands having been reported[10]. The introduction of sulfur and nitrogen donors instead of phosphorus donor functions in this type of tripod ligand has by now not yet found a general solution. Even though different strategies for introducing these types of donor functions have been worked out for special cases[14][15][16][17][18]. It is shown in this paper how tripod ligands containing one or more thioether or thiolate donor functions may be obtained and how these molecules behave as ligands in their $[(CO)_3Mo]$ and $[(CO)_4Mo]$ derivatives.

Results and Discussion

Preparation of the Ligands

There are two main pathways to obtain tripod ligands containing thiole functions, one of them being the nucleophilic cleavage of thietanes by phosphides[15][16] and the other one relying upon the reductive cleavage of SBzl groups by lithium[15].

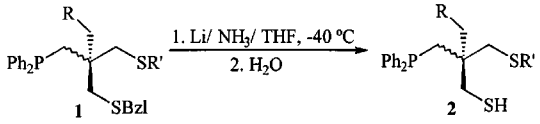

1	R	R′	**2**	R	R′
1a	H	Et	**2a**	H	Et
1b	H	*i*Pr	**2b**	H	*i*Pr
1c	H	Bzl	**2c**	H	H
1d	CH_3O	Bzl	**2d**	CH_3O	H

This second method was used to transform compounds **1**[18][19], containing at least one SBzl group into tripod ligands containing thiole functions (**2**).

Starting from compounds **1**[18][19] applying the "lithium reduction step"[15] to **1**, followed by hydrolytic workup gives the thiole tripod ligands **2**. **2a** and **2b**, containing one thiole function, are obtainted as colorless oils while **2c** and **2d**, bearing two thiole functions, are colorless microcrystalline solids. Their identity is proven by NMR and mass spectra

 © WILEY-VCH Verlag GmbH, D-69451 Weinheim, 1998 1434–1948/98/1010–1417 $ 17.50+.50/0

Table 1. ^{1}H-NMR data

^{1}H NMR[x] X,Y	CH_2P	CH_2X	CH_2Y	X	Y	CH_3C_q or CH_3OCH_2	aromat. H	cryptand
2a	2.36, d,	2.73,	2.72−2.67, m, 2 H	2.50, q, 2 H, 7.3[b]	1.29−1.24,	1.05, s,	7.55−7.32,	−
SEt, SH	2 H, 3.7[a]	s, 2 H		1.24, t, 3 H, 7.3[b]	m, 1 H	3 H	m, 10 H	
2b	2.35, d,	2.70,	2.67, d,	2.80, spt, 1 H, 6.6[b]	1.28−1.22,	1.03, s,	7.55−7.32,	−
S*i*Pr, SH	2 H, 3.3[a]	s, 2 H	2 H, 10.2[b]	1.28−1.22, m, 6H	m, 1 H	3 H	m, 10 H	
2c	2.34, d,	2.70, d,		1.16, t,		1.04, s,	7.51−7.28,	−
SH, SH	2 H, 3.7[a]	4 H, 8.8[b]		2 H, 9.0[b]		3H	m, 10 H	
2d	2.35, d,	2.75, d,		1.17, t,		3.27, s, 2H	7.56−7.35,	−
SH, SH,	2 H, 3.8[a]	4 H, 9.0[b]		2 H, 9.0[b]		3.10, s, 3H	m, 10 H	
3	2.35, d,	2.67, d,	−	1.25, t,	−	1.10, s,	7.57−7.39,	−
SH, −	2 H, 3.2[a]	2 H, 8.8[b]		1 H, 8.8[b]		6H	m, 10 H	
5	2.59, d,	2.93, 2.76,	2.48, 2.29, 2dd,	2.86, q, 2 H, 7.3[b]	1.17, t,	0.93, bs,	7.68−7.43,	−
SEt, SH	2 H, 7.6[a]	2d, 2 H, 7.3[b]	2 H, 13.9[c], 9.0[b]	1.45, t, 3 H, 7.3[b]	1 H, 9.0[b]	3H	m, 10 H	
6a	2.30, 2.05, 2dd,		2.14, s, 2 H	−	−	1.14, bs,	8.10−7.28,	−
PPh_2, S	4 H, 14.4[c], 7.4[a]					3H	m, 20 H	
6b	2.22, 1.94, 2dd,		2.05, s, 2 H	−	−	0.98, bs,	7.95−7.00,	−
PPh_2, S	4 H, 14.2[c], 6.6[a]					3H	m, 20 H	
6c	2.22, d,	2.35, 2.21, 2d,		−	−	2.78, s, 2H	8.10−7.28,	−
S, S	2 H, 9.0[a]	4 H, 12.8[c]	2.13, s, 2 H			3.13, s, 3H	m, 10 H	
7a		2.39, 2.05, 2dd,		−	−	1.14, bs,	8.09−7.21,	3.72−3.60, m, 20 H
PPh_2, S		4 H, 14.4[c], 7.2[a]	1.77, s, 2 H			3H	m, 20 H	2.95−2.60, m, 12 H
7b		2.05, 1.81, 2dd,		−	−	0.76, bs,	7.86−6.88,	3.44, 3.39, 2s, 24 H
PPh_2, S		4 H, 14.0[c], 7.0[a]	2.40, s, 2 H			3H	m, 20 H	2.46, bs, 12 H
8a		2.35, d,		−	2.18,	1.33, t,	7.77−7.12,	−
PPh_2, SMe		2 H, 6.2[a]	2.46, s, 2 H		s, 3H	3 H, 2.2[d]	m, 20 H	
8b		2.39−2.32,		−	2.40, q, 2 H, 7.3[b]	1.33, t,	7.76−7.05,	−
PPh_2, SEt		m, 4H	2.15, s, 2 H		1.18, t, 3 H, 7.3[b]	3 H, 2.5[d]	m, 20 H	
8c		2.37, 2.27, 2dd,		−	3.54,	1.23, t,	7.76−7.01,	−
PPh_2, SBzl		4 H, 15.3[c], 5.7[a]			s, 2 H	3 H, 2.5[d]	m, 25 H	

[x] **2** and **3** in $CDCl_3$, **5** and **8** in CD_2Cl_2, **6** in [D_8]THF, **7** in CD_3CN. − [a] $^2J_{HP}$. − [b] $^3J_{HH}$. − [c] $^2J_{HH}$. − [d] $^4J_{HP}$.

as well as by elemental analyses (Tables 1 and 2, Experimental Section). Judging from the variety of groups present in the starting compounds **1** the scope and selectivity of the applied method − i.e. generating thiole functions in tripod ligands by the reductive cleavage of SBzl functions − are quite broad. A limitation is, however, met when an SPh and an SBzl function are both present in **1**.

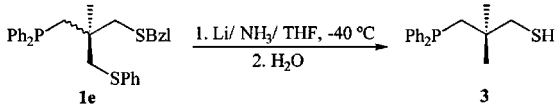

1e **3**

In this case the CH_2SPh group is cleaved at the CH_2S bond as is shown by the transformation of **1e** to **3** (Experimental Section, Tables 1 and 2).

Coordination Chemistry

The coordination chemistry of tripod ligands containing thiole functions has not been worked out in much detail. There are some compounds derived from such ligands with manganese[14] or nickel[15] as the coordinated metals; in each of these cases, however, the thiole function had been transformed into a thiolate functionality during the process of coordination. The coordination of RSH functions themselves is not too common even if they are not part of a tripod ligand[20]. Although even the coordination of H_2S as a two-electron donor has been observed[21] the reaction of RSH with coordinatively unsaturated ligand-metal entities appears to be hampered with difficulties. It has been found that the reaction of [$Cp(CO)_2MnTHF$], which in itself is a precursor of the 16-electron [$Cp(CO)_2Mn$] fragment, with RSH leads to the formation of the radical compunds [$Cp(CO)_2MnSR$] with a concommitant hydrogen abstraction of the thiole function[22]. It is not astonishing therefore that the reaction of $CH_3C(CH_2PPh_2)_2CH_2SH$ (**4**)[15] with [$(MeCN)_3(CO)_3Mo$] in CH_2Cl_2 does not result in isolabable and well-charcterizable tripod compounds of the hypothetical formula [η^3-{$CH_3C(CH_2PPh_2)_2CH_2S$}$(CO)_3Mo$]. Instead a yellow to brownish solution of what is obviously a mixture of compounds is obtained. Trying to isolate a definite compound from this mixture by transforming any SH functions into thiolate groups by NaH or *n*BuLi leads to a brownish product from which, however, no definite compounds could be isolated even after addition of crown ethers or cryptands as potential precipitating agents (see, however, the preparation of **7**, below).The yellow to brownish solutions which result from the deprotonation step (see above) are highly sensitive to air. They immediately change color at the first contact with a trace of oxygen to give deep blue solutions.

While the deep color reminds of the radical compounds [$Cp(CO)_2MnSR$][22] no definite product could be isolated either and the blue powders which remain after evaporation

Table 2. ^{13}C-NMR data

^{13}C NMR[x] X, Y	CH_2P	CH_2X	CH_2Y	X	Y	CH_3C_q CH_3OCH_2	orCH_3C_q	aromat. C	CO/ cryptand
2a SEt, SH	38.2, d, 16.5[a]	42.2, d, 9.6[b]	34.7, d, 10.1[b] 34.8, d,	27.5, s 14.8, s	–	24.8, d, 9.6[b]	39.0, d, 13.8[c]	139.2–128.1, m	–
2b S*i*Pr, SH	38.4, d, 16.5[a]	40.6, d, 9.6[b]	9.7[b] 33.9, d, 11.0[b]	36.2, s 23.4, s	–	24.9, d, 9.2[b]	38.8, d, 13.8[c]	139.1–128.0, m	–
2c SH, SH	37.1, d, 16.5[a]		30.0, d, 10.9[b] –	–	–	24.0, d, 9.2[b]	38.7, d, 12.9[c]	139.0–128.3, m	–
2b SH, SH	33.2, d, 16.8[a]		48.2, d, 6.0[b]	–	–	74.6, d, 8.7[b] 59.1, s	43.4, d, 12.3[c]	142.3–126.4, m	–
3 SH, –	40.9, d, 16.4[a]	38.4, d, 10.4[b] 37.7, d,	–	–	–	28.3, d, 9.1[b]	35.8, d, 13.3[c]	140.3–128.9, m	–
5 SEt, SH	38.7, d, 13.1[a]	6.7[b] 32.7, t,	–	38.6, d, 5.6[b] 13.7, s	–	27.4, d, 6.0[b]	39.1, d, 2.5[c]	138.2–128.8, m	[d]
6a PPh_2, S	36.5, pt, 8.5[a][b]	5.5[b] 34.9,	–	–	35.9, t, 9.0[b]	39.1, t, 4.4[c]	143.4–127.3, m	223.7, t, 8.7[c]; 223.0, dd, 41.0[e], 14.0[f]	
6b PPh_2, S	38.5, pt, 8.5[a][b]	bs	–	–	36.0, t, 8.4[b]	37.7, t, 4.4[c]	143.5–127.3, m	226.1–224.9, m	
7a PPh_2, S	37.9–34.8, m	43.9, t,	–	–	37.9–34.8, m		143.2–127.7, m	[d]; 68.96, 67.66, 65.92, 3s[g] 51.79, 50.51, 2s[h]	
7b PPh_2, S	37.9–34.9, m	4.6[b] 41.6, t,	–	–	37.9–34.9, m	37.7, t, 5.5[c]	143.2–127.8, m	[d]; 68.59, 67.71, 2s[g] 52.62, s[h]	
8a PPh_2, SMe	36.0, pt, 7.4[a][b]	4.6[b] 38.3, t,	–	27.7, t, 5.5[b]	37.7, t, 9.2[b]	38.2–38.0, m	139.9–128.6, m	220.8, m	
8b PPh_2, SEt	36.8, pt, 8.5[a][b]	4.4[b]		38.2–38.0, m 13.7, s	37.5, t, 8.7[b]	37.6–6.3, m	141.5–128.4, m	[d]	
8c PPh_2, SBzl	37.6–36.3, m			47.2, t, 5.1[b]	35.1, t, 8.3[b]		139.8–127.0, m	222.5–219.0, m	

[x] **2** and **3** in $CDCl_3$, **5** and **8** in CD_2Cl_2, **6** in [D_8]THF, **7** in CD_3CN – [a] $^1J_{CP}$ – [b] $^3J_{CP}$ – [c] $^2J_{CP}$ – [d] Due to worse solubility no ^{13}CO resonances observed. – [e] $^2J_{CPtrans}$. – [f] $^2J_{CPcis}$. – [g] CH_2O. – [h] CH_2N.

of the solvent give only very weak EPR signals and are not highly paramagnetic as would be expected for radical species when analyzed on a magnetic balance. Chromatography of the blue solutions on silica gel is of no help since the blue phase rather rapidly desintegrates during the process of elution. The nature of the compounds and intermediates obtained from **4** by the above procedure does remain unknown (see, however, the transformation of **4** to **7**, below).

In contrast to the reaction of **4** with $[(MeCN)_3(CO)_3Mo]$ the ligand **2a** reacts with the same reagent to produce the $(CO)_4Mo$ derivative **5** in fair yields.

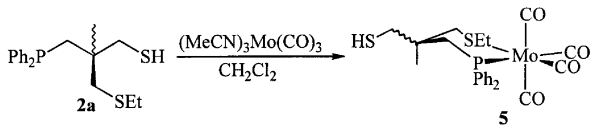

The formation of $(CO)_4Mo$ derivatives from $[(MeCN)_3(CO)_3Mo]$ is not an uncommon observation[17]. Even though no single crystals suitable for an X-ray analysis could be obtained from **5** its constitution as given is clear from spectroscopic data.

The $\tilde{\nu}_{CO}$ spectrum is characteristic for a $[(CO)_4Mo]$ entity[23]. The coordination of the phosphorus function is evident from its ^{31}P-NMR resonance which is found at δ = 20.0 in constrast to the chemical shift of the free ligand (δ = −26.9). The coordination of the SEt group is evidenced by a $^3J_{CP}$ coupling of 5.6 Hz to the α-carbon atom of the ethyl group (Table 2). There is no such coupling to the proton of the SH group of the dangling arm with the ^{1}H-NMR signal

Table 3. Infrared data of **5–8**

	Solvent	$\tilde{\nu}_{CO}$ [cm^{-1}]		
5	CH_2Cl_2	2020 (s)	1901 (s, br.)	1870 (s)
6a	THF	1911 (s)	1816 (s)	1787 (s)
6b	THF	1909 (s)	1815 (s)	1779 (s)
6c	THF	1885 (s)	1771 (s)	1718 (s)
7a	MeCN	1905 (s)	1809 (s)	1778 (s)
7b	MeCN	1909 (s)	1802 (s)	1763 (s)
8a	CH_2Cl_2	1927 (s)	1830 (s)	1795 (s)
8b	CH_2Cl_2	1929 (s)	1837 (s)	1811 (s)
8c	CH_2Cl_2	1934 (s)	1844 (s, br.)	

referring to this group being a clear-cut triplet as expected (Table 1). The CH_2 protons of the dangling arm are diastereotopic which, together with a coupling to the SH proton, results in a pattern of two doublets of doublets. ^{31}P decoupling substanciates the assignments. With correct mass spectra and elemental analyses the identity of **5** as shown is beyond doubt therefore.

The observation that in **5** the thiole function cannot compete with the donors present in the reaction solution suggests a different strategy: if the thiole function of the ligand is deprotonated the thiolate function thus formed should have better ligand capabilities such that tripodal coordination of the anionic ligands might ensue. If salts of these derivatives could be isolated protonation of the coordinated thiolate functions might well lead to coordinated SH functions in tripodal metal compounds.

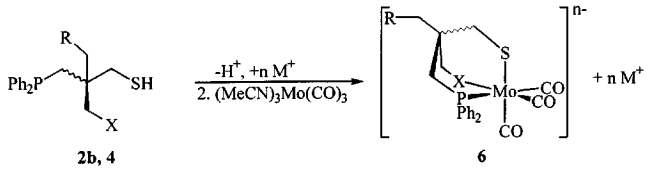

2b, 4 6

	R	X	6	R	X	M	*n*
4	H	PPh_2	**6a**	H	PPh_2	Li	1
2d	CH_3O	SH	**6b**	H	PPh_2	Na	1
			6c	CH_3O	S	Na	2

If the ligand **4** is deprotonated by *n*BuLi in THF and the resulting solution is treated with $[(MeCN)_3(CO)_3Mo]$ the lithium salt **6a** results, in which all three donor functions of the tripod ligand are engaged in coordination. **6a** is isolated from the reaction solution as its adduct with two molecules THF per unit by evaporating the solvent and washing the brown oily residue with petroleum ether in an ultrasonic bath. The product as isolated is very sensitive to oxygen and moisture so that its yellow solutions turn first green and finally blue under atmospheric conditions. Under unaerobic conditions the solutions are stable enough to warrant detailed analyses by NMR. The ^{1}H-, ^{13}C-, and ^{31}P-NMR spectra are in accord with the formula as given (Tables 1 and 2). The coordination of both phosphorus centers is apparent from the appearance of one single signal at $\delta = 21.6$. The coordination of the sulfide function is not definitely established by $^3J_{CP}$ coupling constants between the phosphorus nucleus and the methylene carbon atom to which the sulfur atom is bound, since $^3J_{CP}$ coupling through the ligand framework gives rise to values of similar magnitude[15]. From the three CH_2 groups of the chelate cage the one linked to the sulfur atom has two chemically equivalent hydrogen atoms and a singlet is observed for this group in the ^{1}H-NMR spectrum. The hydrogen atoms at the CH_2 groups linked to the phosphorus atoms are diastereotopic and give rise to two doublets of doublets (Table 1). The symmetry of **6a** is thus clearly reflected by its ^{1}H-NMR spectrum. The tridentate binding mode of the ligand on the other hand is not a necessary prerequisit to explain the spectra. Since **6a** contains two THF solvate molecules per formula unit (the ratio of THF/**6** is determined by integration of the $[H_8]$THF signals apparent for solutions of the compounds in isotopically pure $[D_8]$THF) it might be argued that the ligand is only acting in the bidentate fashion with one THF molecule occupying the vacant coordination site at the metal. Even the observation of a $\tilde{\nu}_{CO}$ IR pattern which corresponds to a $[(CO)_3Mo]$ entity (Table 3) does not differentiate between the two possibilities. An indication that the constitution of **6** as shown might be correct may be found in the values of the chemical shifts of the carbonyl carbon atoms of **6**. The two different classes of carbonyl groups (*trans* to P, *trans* to S) have their resonances in close vicinity which is well expected if the sulfur and phosphorus atoms act as the *trans* ligand but would not be easily explained if THF and P were in the corresponding positions. The pattern of the $^2J_{CP}$ coupling constants (Table 2) is in accord with an overall octahedral geometry of the compound. One argument in favor of the η^3 coordination of the ligand in **6a** comes from a comparison of the ^{13}C-NMR resonances observed for compounds which definitely contain the ligands in η^2 coordination (e.g. **5**) and a series of examples in ref.[18] where it was found that the relevant resonances of **6a** occur at different shift values which are much closer to the values characterictic for compounds with η^3 coordination (**8**) and a series of compounds in ref.[18]. Yet a stronger argument comes from the observation that the solvent-free salt obtained from **6a** by the addition of [2,1,1]cryptand (**7a**, see below) have their NMR resonances at approximately the same values as observed for **6a** (Tables 1 and 2).

Observations very similar to the results reported for **6a** are made for its sodium analogue **6b** which results when NaH is used as the deprotonating agent in the transformation of **4** to **6** (Tables 1−3). With **2d** as the starting material **6c** is formed under these conditions. **6b** as well as **6c**, when isolated as yellow powders following the workup procedure described for the synthesis of **6a**, are both found to contain two THF molecules per formula unit. The chemical shifts observed for the constitution of the compounds in the various NMR spectra are close to the ones reported for **6a** (Tables 1−3). In contrast to the situation in **6a**, instead of the protons at the CH_2S group now the protons at the CH_2P entity are chemically equivalent with the remaining two CH_2S groups showing the phenomenon of diastereotopicity in the case of **6c**. This symmetry property is clearly evident from the ^{1}H-NMR spectrum (Table 1).

Compounds **6** are rather difficult to handle due to their high sensitivity to oxygen and moisture as well as to the fact that the only solvent in which comparatively stable solutions are formed is THF while solvents with higher proton activity and/or oxidation power (e.g. CH_3CN, CH_3NO_2) lead to desintegration of the compounds.

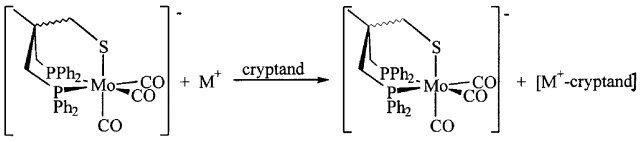

6 7

6	M	**7**	M	Cryptand
6a	Li	**7a**	Li	[2,1,1]cryptand
6b	Na	**7b**	Na	[2,2,2]cryptand

In the hope to increase the stability of the salt-like compounds cation scavengers were used to transform the lithium salt **6a** into its lithium [2,1,1]cryptand derivative **7a** and the sodium salt **6b** into its sodium [2,2,2]cryptand analogue **7b**. When the cryptand ligands are added to THF solutions of **6** the salts **7** form and precipitate from the solutions in the form of light-yellow microcrystalline powders. With respect to sensitivity and solubility compounds **7** differ

strongly from compounds **6**. Solutions of **7** in contrast to solutions of **6** do not undergo a rapid color change when exposed to the atmosphere even though a slow color change from light-yellow to light-green is observed on prolonged exposure to air. In constrast to compounds **6** which dissolves in THF, compounds **7** are only very sparingly soluble in this solvent. They are soluble, however, in CH_3CN or CH_3NO_2 without desintegration. The salt of type **7** formed from **6c** by the addition of [2,2,2]cryptand does not dissolve, neither in THF, nor in CH_3CN or CH_3NO_2, so that it could not be characterized. The identity of the anions present in **7** is clear from the negative-ion FAB mass spectra which show the peak for the molecule anion at $m/z = 653$ for both **7a** and **7b**. The close similarity of the anionic parts of **6** and **7** is evident from the close similarity of the relevant NMR data (Tables 1, 2). Shifts as well as coupling constants show only minor differences between the compounds **6** and **7**. Due to the low solubility of compounds **7** and due to an overlap of some of the signals arising from the cryptand ligands a detailed comparison is not possible for all of the signals (Tables 1, 2). The $\tilde{\nu}_{CO}$ IR spectra of compounds **6** and **7** are rather similar as well (Table 3). Taken together the similarity of all the spectral data obtained for **6** and **7** corroborates the structural assignments as elaborated for **6**. Comparing the spectral data obtained for **6a** and **6b** slight differences in chemical shifts as well as in the $\tilde{\nu}_{CO}$ IR data are apparent, the most propable explanation for this observation being that the counter ions are in some form associated with the complexes. It is astonishing to note that the ^{1}H-NMR data of **7a** and **7b** (Tables 1, 2) as well as the IR data (Table 3) of these compounds are slightly different as well. It must be assumed that the compounds are at least in part dissolved as ion pairs such that different properties of the cations are reflected by these data. The identity of the anionic part of **6** and **7** is as well documented by their cyclovoltammogrammes. Both the compounds **6a** and **7a** show a quasi-reversible oxidation at −410 mV vs. S.C.E. The slight difference between the values observed for **7a** and **7b**, if not due to experimental uncertainty, might again indicate that ion pairs are still solvated even with the alkali cation embedded in cryptands. The ratio of the anodic current to the cationic current is around 1.7 and the slope of the anodic current versus the scan rate (50−800 mV) is lower than the one predicted by the square root law[24] for a reversible process. When comparing **7a** and **7b** it is found that the quasi-reversible oxidation occurs at almost the same potential for both compounds (**7b**: −420 mV vs. S.C.E.).

To further corroborate the identity of **6** compound **6a** was treated with alkylating reagents which, based on the constitution assigned to **6**, should lead to the corresponding thioether-functionalized species. In fact **6a** reacts with a variety of electrophilic reagents to produce compounds **8**.

Mass spectra of **8** (FAB or EI) show the molecular ion peak in each case and elemental analyses correspond to the assigned constitution. The NMR data (Tables 1, 2) are as well in accord with their constitution; specifically, they show that the tripod ligand coordinates in a tridentate way.

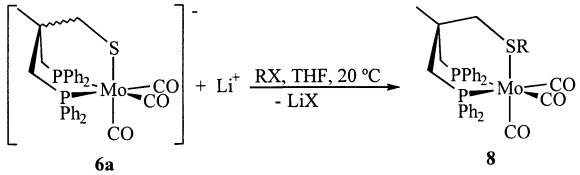

6a **8**

8	R	X
8a	Me	I
8b	Et	$Et_2O{\cdot}BF_4$
8c	Bzl	Br

This is evidenced by $^3J_{CP}$ coupling constants of around 6 Hz between the coordinated phosphorus atom and the α-carbon atom bonded to the coordinated sulfur center. The coupling constants should be zero if the SR entities would not be coordinated. In the case of **8c** the spectral data obtained for the free ligand[14] show that no P-$C_{\alpha S}$ coupling is observed if not both phosphorus and sulfur atom are coordinated to the same metal center. The presence or absence of diastereotopicity of the protons at the CH_2 groups of the chelate cage (Table 1) does again reflect the symmetry of the compounds as already discussed for **6**. The local symmetry of the $[(CO)_3Mo]$ chromophore reflects the constitutional C_s symmetry which is characteristic for all the compounds **6−8** so that instead of a two-band pattern (A_1, E) as expected for C_{3v} symmetry 3 $\tilde{\nu}_{CO}$ IR bands are observed in general. Only for **8c** the splitting of the E band is not large enough to make the two components derived from it decernible (Table 3).

A comparison of the IR data obtained for **6−8** is rewarding: the anionic compounds **6** and **7** show their absorptions at distinctly lower energy than the neutral compounds **8**. Within each class of compounds the differences are only minor as expected. The dianionic species **6c** has its absorptions at by far the lowest energies. The observed trends are in accord with the well-established rule that the higher the charge density at the metal center the lower the frequencies of the corresponding $\tilde{\nu}_{CO}$ absorptions. With respect to this rule trends observed for compounds **6−8** are in full agreement with their structural assignment derived by other methods as discussed before.

With the identity of **8** established beyond doubt it is clear that the SR group is coordinated in each case. For the type of ligand as present in **6a** and **6b** it had been shown for the neutral complex $[\eta^3\text{-}\{CH_3C(CH_2PPh_2)_2CH_2S\}(CO)_3Mn]$ that alkylation at the sulfur atom may well lead to decoordination with the vacant coordination site being occupied by the nucleofugic group of the alkylation reagent used (e.g. I^- with MeI as the reagent)[16]. This type of reaction is not observed when **6a** is treated with alkylation reagents independent of whether the nucleofugic group is I^- (MeI), Et_2O ($Et_3O{\cdot}BF_4$) or Br^- (BzlBr) even though the neutral manganese compound and the anionic molybdenum compound are isoelectronic ($[(CO)_3Mn]^+$ to $[(CO)_3Mo]$). The coordination of the nucleofugic group of the anionic part of the

electrophile to the metal center can well compete with the coordination of the neutral SR function in the presence of the cationic metal center in $[\eta^3\text{-}\{CH_3C(CH_2PPh_2)_2CH_2SR\}(CO)_3Mn]^+$ while with the neutral compounds $[\eta^3\text{-}\{CH_3C(CH_2PPh_2)_2CH_2SR\}(CO)_3Mo]$ (**8**) the anionic nucleophile is not competitive.

Conclusion

Taken together the observations described in this paper allow for the following statements:

– Neopentane-based tripod ligands $CH_3C(CH_2X)(CH_2Y)(CH_2Z)$ (X, Y, Z = PR_2, SR, S^-) are accessible by a convergent set of reactions. The reductive cleavage of SBzl functions in tripod ligands (some of the groups X, Y, Z = SBzl)[15][17][18][19] by lithium under spezialized conditions has a broad scope of application in this context.

– Tripod ligands containing thiolate functions (some of the groups X, Y, Z = S^-) form anionic $[(CO)_3Mo]$ derivatives which contain the ligands in a tridentate binding mode. The coordinatively bound thiolate functions are transformed into coordinated thioether functions upon reaction of the anions with alkylating reagents.

The financial support by the *Deutsche Forschungsgemeinschaft* (SFB 247) and the *Fonds der Chemischen Industrie* is gratefully acknowledged. We are grateful to *D. Günauer* (cyclovoltammetry), to *R. Rupp* (ESR) and to *P. Schober* (magnetic balance) for various help. One of us is indepted to the Graduierten Kolleg *Selektivität und Reaktivität in der organischen Synthese* for a fellowship.

Experimental Section

General: All manipulations are carried out under argon by means of standard Schlenk techniques. All solvents are dried by standard methods and destilled under argon. Water was degassed by five "pump-thaw" cycles and stored under argon. The $CDCl_3$, CD_2Cl_2 and $[D_8]$THF used for the NMR spectroscopic measurements were degassed by three successive "freeze-pump-thaw" cycles and dried over 4-Å molecular sieves. The silica gel (Kieselgel z.A. 0.06–0.2 mm, J. T. Baker Chemicals B.V.) used for chromatography was degassed at 1 mbar for 24 h and saturated with argon. – NMR: Bruker Avance DPX 200 at 200.13 MHz (^{1}H), 50.323 MHz ($^{13}C\{^1H\}$), 81.015 MHz ($^{31}P\{^1H\}$), 77.779 MHz (^{7}Li); chemical shifts (δ) in ppm with respect to $CDCl_3$ (^{1}H: δ = 7.27; ^{13}C: δ = 77.0), CD_2Cl_2 (^{1}H: δ = 5.32; ^{13}C: δ = 53.5) and $[D_8]$THF (^{1}H: δ = 3.58; ^{13}C: δ = 67.7) as internal standards, and chemical shifts (δ) in ppm with respect to 85% H_3PO_4 (^{31}P: δ = 0) and 1 M LiCl in D_2O (^{7}Li: δ = 0) as external standards. – IR: Bruker FT-IR IFS-66; CaF_2 cells. – MS: Finnigan MAT 8400; FAB: Nibeol (4-nitrobenzyl alcohol) or TEA (triethanol amine) matrices, respectively; EI: 70 eV. Mass spectra are referenced relative to the most abundant Mo isotop ($^{98}_{42}$Mo). Elemental analyses: Microanalytical laboratory of the Organisch-Chemisches Institut, Universität Heidelberg. With the procedures used carbon contents tend to be found too low in the presence of molybdenum. Some of the analytical data have to be interpreted with this in mind. – Melting points: Gallenkamp MFB-595 010; melting points are not corrected. – Cyclovoltammetry: EG&G Princeton Applied Research model 273; potentials in mV versus S.C.E at a glassy carbon electrode at 25°C; solutions of the compounds: 10^{-3} M in 0.1 M Bu_4NPF_6 in CH_2Cl_2. – **1a–c** and **e** were prepared accordingto ref.[18], **1d** was prepared according to ref.[19]. **4** can be obtained according to ref.[14]. $[(CH_3CN)_3(CO)_3Mo]$ was synthesized as described in ref.[25] and was always freshly prepared (using always fresh batches); [2,1,1]cryptand and [2,2,2]cryptand are abbreviations for 4,7,13,18-tetraoxa-1,10-diazabicyclo[8.5.5]eicosane and 4,7,13,16,21,24-hexaoxa-1,10-diazabicyclo[8.8.8]hexacosane, respectively. The latter ones and all other chemicals are commercially obtained and used without further purification.

Preparation of **2**: The given amount (vide infra) of **1** was dissolved in THF (50 ml), the solution was cooled to −50°C and liquid NH_3 was added (50 ml). After stirring for 10 min, the given amount (vide infra) of lithium was added. During the reaction the color of the mixture turned from deep blue to red. The reaction was finished when all lithium was consumed (4 h). Then water was added (5 ml) and the NH_3 was cautiously removed by letting the reaction mixture slowly warm up to 20°C. Finally, the THF was removed in vacuo. To the crude product water (50 ml) and diethyl ether (50 ml) were added and the mixture was neutralized with HCl. The phases were separated and the aqueous phase was extracted with diethyl ether (2 × 50 ml). The residue of the combined, dried and concentrated organic phases was purified by chromatography on silica gel in case of **2a**, **2b**, and **2e** (15 cm, Ø = 6 cm). Concentrating the fractions eluted by a mixture of petroleum ether (40/60)/diethyl ether (17:1; TLC control: R_f = 0.4 for **2a** and **2b**/29:1; TLC control: R_f = 0.45 for **2e**) gave the pure products **2a**, **2b** and **2e**. **2c** and **2d** were purified by recrystallization from petroleum ether (40/60) (20 ml). Completion of the crystallization was achieved by cooling the mixture down to −40°C for 1 h.

1a (1.6 g, 3.6 mmol) and Li (50 mg, 7.2 mmol) yielded 1.2 g (95%) of **2a** as a pasty, colorless oil. – $C_{19}H_{25}PS_2$ (348.5): calcd. C 65.48, H 7.23; P 8.89; S 18.40; found C 65.77, H 7.30, P 8.89, S 17.68. – MS (EI); *m/z* (%): 349 (50) [M^+ + 1], 319 (100) [$M^+ - C_2H_5$]. – $^{31}P\{^1H\}$ NMR ($CDCl_3$): δ = −26.9 (s).

1b (2.3 g, 5.0 mmol) and Li (69 mg, 10.0 mmol) yielded 1.7 g (93%) of **2b** as a pasty, colorless oil (even after prolonged drying, **2b** tenaciously withheld some solvent resulting in somewhat to high carbon values). – $C_{20}H_{27}PS_2$ (362.5): calcd. C 66.26, H 7.51; found C 67.11, H 7.48. – MS (FAB); *m/z* (%): 363 (70) [M^+ + 1], 319 (100) [$M^+ - C_3H_7$]. – $^{31}P\{^1H\}$ NMR ($CDCl_3$): δ = −26.8 (s).

1c (2.5 g, 5.0 mmol) and Li (138 mg, 10 mmol) yielded 1.4 g (85%) of **2c** as a colorless microcrsystalline solid. – MS (EI); *m/z* (%): 319 (100) [M^+ − 1]. – $^{31}P\{^1H\}$ NMR ($CDCl_3$): δ = −27.3 (s).

1d (2.6 g, 5.0 mmol) and Li (138 mg, 20.0 mmol) yielded 1.6 g (90%) of **2d** as a colorless microcrystalline solid. – $C_{18}H_{23}OPS_2$ (350.5): calcd. C 61.69, H 6.61, P 8.84, S 18.30; found C 61.63, H 6.77, P 8.84 S 18.58. – MS (FAB); *m/z* (%): 349 (100) [M^+]. – $^{31}P\{^1H\}$ NMR ($CDCl_3$): δ = −26.8 (s).

1e (1.9 g, 4.0 mmol) and Li (112 mg, 16.0 mmol) yielded 980 mg (85%) of **3** as a colorless, microcrystalline solid. – $C_{17}H_{21}PS$ (288.4): calcd. C 70.80, H 7.34; found C 71.26, H 7.64. – MS (FAB); *m/z* (%): 287 (100) [M^+ − 1]. – $^{31}P\{^1H\}$ NMR ($CDCl_3$): δ = −23.2 (s).

For ^{1}H- and ^{13}C-NMR data see Tables 1 and 2.

Preparation of **5**: Compound **2a** (349 mg, 1 mmol) was dissolved in CH_2Cl_2 (30 ml), solid $[(MeCN)_3(CO)_3Mo]$ was added (302 mg; 1 mmol) and the mixture was stirred for 1 h at room temperature. During the reaction the $[(MeCN)_3(CO)_3Mo]$ slowly dissolved and the color of the solution turned from light-yellow to yellow-brown.

The solvent was removed and the brown residue was chromagraphed on silica gel (15 cm, Ø = 6 cm). Concentrating the fractions eluted by a mixture of petroleum ether (40/60)/CH_2Cl_2 (1:3; TLC control: R_f = 0.75) gave 250 mg (45%) of **5** as a yellow microcrystalline solid, m.p. 150°C (dec.). – $C_{23}H_{35}MoO_4PS_2$ (556.5): calcd. C 49.64, H 4.53, P 5.57, found C 49.88, H 4.85, P 5.55. – MS (EI); *m/z* (%): 558 (8) [M^+], 530 (14) [M^+ – CO], 501 (10) [M^+ – CO – C_2H_5], 473 (6) [M^+ – 2 CO – C_2H_5], 444 (16) [M^+ – 3 CO – C_2H_5 – H]. – $^{31}P\{^1H\}$ NMR ($CDCl_3$): δ = 20.0 (s).

For IR -, ^1H- and ^{13}C-NMR data see Tables 1–3.

Preparation of **6**: 1 mmol of **2d** or **4** (vide infra) was dissolved in 30 ml of THF, the solution was cooled to 0°C and treated with NaH or *n*-butyllithium (vide infra). After stirring for 30 min, solid [$(MeCN)_3(CO)_3Mo$] (302 mg, 1 mmol) was added. During the reaction the color of the mixture turned light-brown. After stirring for another 30 min, the reaction mixture was concentrated to 3–5 ml and 30 ml of petroleum ether (40/60) was added. If oily products were obtained the mixtures were treated twice with 30 ml of petroleum ether (40/60) in an ultrasonic bath. The pure yellow microcrystalline products were obtained in quantitative yields by removing the solvent in vacuo. In all cases the products contained two molecules of THF per formula unit. When compounds **6** were prepared for a consecutive reaction the purification step did not need to be applied e.g. preparation of **7** or **8**.

4 (472 mg, 1 mmol) and *n*-butyllithium (2.5 M, 0.4 ml, 1 mmol) yielded 800 mg of **6a** · 2 THF. – $C_{32}H_{29}LiMoO_3P_2S \cdot 2\ C_4H_8O$ (800.5): calcd. C 59.85, H 5.65, P 7.72; found C 58.51, H 6.13, P 7.30. – $^{31}P\{^1H\}$ NMR ([D_8]THF): δ = 21.6 (s). – ^7Li NMR ([D_8]THF): δ = –0.33.

4 (472 mg, 1 mmol) and NaH (24 mg, 1 mmol) yielded 820 mg of **6b** · 2 THF. – $^{31}P\{^1H\}$ NMR ([D_8]THF): δ = 19.8 (s).

2d (350 mg, 1 mmol) and NaH (48 mg, 2 mmol) yielded 720 mg of **6c** · 2 THF. – $^{31}P\{^1H\}$ NMR ([D_8]THF): δ = 14.9 (s).

For IR, ^1H- and ^{13}C-NMR data see Tables 1–3.

Preparation of **7**: To a solution of 1 mmol of **6a** · 2 THF or **6b** · 2 THF (vide infra) in THF (30 ml) the given cryptand (vide infra) was added. While stirring the mixtures for 30 min, yellow precipitates formed. The precipitates were separated from the solvent and washed with petroleum ether (40/60). Drying in vacuo gave the pure yellow microcrystalline products in quantitative yields.

6a · 2 THF (800 mg, 1 mmol) and [2,1,1]cryptand (288 mg, 1 mmol) yielded 946 mg of **7a**. – $C_{46}H_{57}LiMoN_2O_7P_2S$ (946.9): calcd. C 58.35, H 6.07, N 2.96, P 6.54; found C 58.04, H 6.43, N 2.76, P 6.32. – MS (FAB negative); *m/z* (%): 653 (100) [M^-]. – $^{31}P\{^1H\}$ NMR (CD_3NO_2): δ = –20.4 (s). – ^7Li NMR ([D_8]THF): δ = –1.37.

6b · 2 THF (820 mg, 1 mmol) and [2,2,2]cryptand (376 mg, 1 mmol) yielded 1050 mg of **7b**. – $C_{50}H_{65}MoN_2NaO_9PS_2$ (1049.9): calcd. C 57.19, H 6.24, N 2.67; found C 58.51, H 6.31, N 2.48. – MS (FAB negative); *m/z* (%): 653 (60) [M^-]. – $^{31}P\{^1H\}$ NMR ([D_8]THF): δ = –19.8 (s).

For IR, ^1H- and ^{13}C-NMR data see Tables 1–3.

Preparation of **8**: To a solution of **6a** · 2 THF (800 mg, 1 mmol) in THF (30 ml) the given alkylation reagent (vide infra) was added and the mixture was stirred for 2 h. The solvent was removed and the brown residue was chromagraphed on silica gel (15 cm, Ø = 6 cm). Concentrating the fractions eluted by a mixture of petroleum ether (40/60)/CH_2Cl_2 (1:3; TLC control: R_f = 0.71–0.75) gave the pure compounds **8** as yellow microcrystalline solids. While **8a** and **8b** were obtained solvent-free, **8c** crystallized with 0.5 equivalents of CH_2Cl_2 per formula unit. The obtained yields were: **8a**: 488 mg (73%), m.p. 195°C (dec.); **8b**: 409 mg (60%), m.p. 188°C (dec.); **7c**: 493 mg (70%), m.p. 205°C (dec.).

8a: MeI (426 mg, 3 mmol). – $C_{33}H_{32}MoO_3P_2S$ (666.6): calcd. C 59.28, H 4.83, P 9.27; found C 58.31, H 4.87, P 9.09. – MS (EI); *m/z* (%): 668 (28) [M^+], 640 (40) [M^+ – CO], 612 (30) [M^+ – 2 CO], 584 (100) [M^+ – 3 CO]. – $^{31}P\{^1H\}$ NMR (CD_2Cl_2): δ = –18.1 (s).

8b: $Et_3O{\cdot}BF_4$ (513 mg, 3 mmol). – $C_{34}H_{34}MoO_3P_2S$ (680.6): calcd. C 59.82, H 5.02, P 9.08; found C 59.12, H 5.30, P 8.97. – MS (EI); *m/z* (%):682 (32) [M^+], 654 (46) [M^+ – CO], 626 (20) [M^+ – 2 CO], 596 (100) [M^+ – 3 CO]. – $^{31}P\{^1H\}$ NMR ([D_8]THF): δ = –22.5 (s).

8c: BzlBr (380 mg, 3 mmol). – $C_{39}H_{36}MoO_3P_2S \cdot 0.5\ CH_2Cl_2$ (785.2): calcd. C 60.42, H 4.75; found C 60.01, H 4.62. – MS (FAB); *m/z* (%): 744 (28) [M^+], 660 (46) [M^+ – 3 CO], 569 (14) [M^+ – 3 CO – Bzl], 471 (5) [M^+ – 3 CO – Bzl – Mo]. – $^{31}P\{^1H\}$ NMR (CH_2Cl_2): δ = –18.0 (s).

For IR, ^1H- and ^{13}C-NMR data see Tables 1–3.

☆ Dedicated to Prof. *H. P. Latscha* on the occasion of his 60th birthday.

[1] See, e.g.: [1a] L. Sacconi, S. Midollini, *J. Chem. Soc., Dalton Trans.* **1972**, 1213. – [1b] P. Dapporto, G. Fallani, S. Midollini, L. Sacconi, *J. Am. Chem. Soc.* **1973**, *95*, 2021. – [1c] M. Di Vaira, L. Sacconi, *Angew. Chem.* **1982**, *94*, 338; *Angew. Chem. Int. Ed. Engl.* **1982**, *21*, 330. – [1d] P. Dapporto, S. Midollini, A. Orlandini, L. Sacconi, *Inorg. Chem.* **1976**, *15*, 2678. – [1e] C. Mealli, S. Midollini, L. Sacconi, *Inorg. Chem.* **1978**, *17*, 632. – [1f] C. Mealli, L. Sacconi, *Inorg. Chem.* **1983**, *22*, 2786.

[2] [2a] C. Bianchini, C. Ghilardi, A. Meli, S. Midollini, A. Orlandini, *J. Organomet. Chem.* **1983**, *248*, C13. – [2b] C. Bianchini, A. Meli, A. Orlandini, L. Sacconi, *Angew. Chem.* **1980**, *92*, 1055; *Angew. Chem. Int. Ed. Engl.* **1980**, *19*, 1021. – [2c] C. Bianchini, A. Meli, A. Orlandini, L. Sacconi, *J. Organomet. Chem.* **1981**, *218*, 81. – [2d] J. Ott, M. Venanzi, C. A. Ghilardi, S. Midollini, A. Orlandini, *J. Organomet. Chem.* **1985**, *291*, 89.

[3] [3a] M. J. Burk, R. L. Harlow, *Angew. Chem.* **1990**, *102*, 1511; *Angew. Chem. Int. Ed. Engl.* **1990**, *29*, 1467. – [3b] M. J. Burk, J. E. Feaster, R. L. Harlow, *Tetrahedron: Asymmetry* **1991**, *2*, 569.

[4] [4a] T. G. Gardner, G. S. Girolami, *Organometallics* **1987**, *6*, 2551. – [4b] J.-P. Charland, E. J. Gabe, J. M. McCall, J. R. Morton, K. F. Preston, *Acta Crystallogr., C* **1987**, *43*, 48.

[5] O. Walter, T. Klein, G. Huttner, L. Zsolnai, *J. Organomet. Chem.* **1993**, *458*, 63.

[6] H. Heidel, G. Huttner, G. Helmchen, *Z. Naturforsch.* **1993**, *48b*, 1681.

[7] H. Heidel, G. Huttner, R. Vogel, G. Helmchen, *Chem. Ber.* **1994**, *127*, 271.

[8] A. Muth, G. Reinhard, G. Huttner, T. Seitz, T. Klein, L. Zsolnai, *Z. Naturforsch.* **1994**, *49b*, 889.

[9] T. Seitz, A. Muth, G. Huttner, *Chem. Ber.* **1994**, *127*, 1837.

[10] [10a] H. Heidel, G. Huttner, R. Vogel, G. Helmchen, *Chem. Ber.* **1994**, *127*, 271. – [10b] H. Heidel, G. Huttner, L. Zsolnai, *Z. Naturforsch.* **1995**, *50b*, 729.

[11] T. Seitz, A. Muth, G. Huttner, *Z. Naturforsch.* **1995**, *50b*, 1045.

[12] J. Scherer, G. Huttner, M. Büchner, J. Bakos, *J. Organomet. Chem.* **1996**, *520*, 45.

[13] J. Scherer, G. Huttner, M. Büchner, *Chem. Ber.* **1996**, *129*, 697.

[14] [14a] S.-T. Liu, H.-E. Eang, M.C. Cheng, S.-M. Peng, *J. Organomet. Chem.* **1989**, *376*, 333. – [14b] S.-T. Liu, K.-J. Liu, *Inorg. Chem.* **1990**, *29*, 4576. – [14c] S.-T. Liu, C.-L. Tsao, M.-C. Cheng, S.-M. Peng, *Polyhedron* **1990**, *9*, 2579. – [14d] S.-T. Liu, C.-H. Yieh, H.-P. Dai, *Proc. Natl. Sci. Counc.* **1995**, *19*, 1. – [14e] S.-T. Liu, D.-R. Hou, T.-C. Lin, M.-C. Cheng, S.-M. Peng, *Organometallics* **1995**, *14*, 1529. – [14f] S.-T. Liu, C.-H. Yieh, H.-J. Lu, *Phosphorus Sulfur Silicon* **1989**, *44*, 261. – [14g] S.-T. Liu, *J. Chin. Chem. Soc.* **1992**, *39*, 611. – [14h] H.-E. Wang, C.-Y. Liu, M.-C. Cheng, S.-M. Peng, S. -T. Liu, *Phosphorus Sulfur Silicon* **1992**, *69*, 201.

[15] G. Reinhard, R. Soltek, G. Huttner, A. Barth, O. Walter, *Chem. Ber.* **1996**, *129*, 97.
[16] S.-C. Tsai, H.-E- Wang, S.-T. Huang, L.-M- Yiin, S.-T. Liu, *Chem. Ber.* **1995**, *128*, 151.
[17] A. Jakobi, G. Huttner, U. Winterhalter, *Chem. Ber.* **1997**, *130*, 1279-1294.
[18] R. Soltek, G. Huttner, L. Zsolnai, A. Driess, *Inorg. Chim. Acta*, accepted for publication.
[19] P. Schober, R. Soltek, G. Huttner, L. Zsolnai, K. Heinze, A. Driess, *Eur. J. Inorg. Chem.*, accepted for publication.
[20] e.g.: [20a] H. Park, D. Minick, M. Draganjac, J. W. Crump, A. W. Cordes, E. M. Holt, *Proc. Arkansas Acad. Sci.* **1993**, *47*, 142. – [20b] H. Park, D. Minick, M. Draganjac, A. W. Cordes,R. L. Hallford, G. Eggleton, *Inorg. Chim. Acta* **1993**, *204,* 195. – [20c] M. Y. Darensbourg, E. M. Longridge, V. Payne, J. Reibenspies, C. G. Riordan, J. J. Springs, J. C. Calabrese, *Inorg. Chem.* **1990**, *29*, 2721. – [20d] D. Minick, M. Draganjac, J. W. Crump, A. W. Cordes, *J. Crystallogr. Spectrosc. Res.* **1993**, *23*, 629. – [20e] C. H. Winter, T. S. Lewkebandara, J. W. Proscia, A. L. Rheingold, *Inorg. Chem.* **1993**, *32*, 3807. – [20f] G. X. Jin, M. Herberhold, *Conf. Coord. Chem*. **1993**, *14*, 67.
[21] D. Sellmann, P. Lechner, F. Knoch, M. Moll, *J. Am. Chem. Soc.* **1992**, *114*, 922.
[22] P. Lau, H. Braunwarth, G. Huttner, D. Günauer, K. Evertz, W. Imhof, C. Emmerich, L. Zsolnai, *Organometallics* **1991**, *10*, 3861-3873.
[23] [23a] J. Weidlein, U. Müller, K. Dehnicke, *Schwingungsspektroskopie*, Georg Thieme Verlag, Stuttgart, **1989**. – [23b] F. A. Cotton, C. S. Kraihanzel, *J. Am. Chem. Soc.* **1962**, *84*, 4432. – [23c] C. S. Kreihanzel, F. A. Cotton, *Inorg. Chem*. **1963**, *2*, 533.
[24] [24a] B. Speiser, *Chem. Unserer Zeit* **1981**, *15*, 62. – [24b] J. Heinze, *Angew. Chem.* **1984**, *96*, 823; *Angew. Chem. Int. Ed. Engl.* **1984**, *23,* 831.
[25] D. P. Tate, W. R. Knipple, J. M. Augl, *Inorg. Chem.* **1962**, *1*, 433, [98064]

Complex Catalysis, LIV[◇]

Synthesis and Characterization of Organorhodium(I) Complexes with the Tridentate Ligand 2,6-Bis(diphenylphosphanylmethyl)pyridine [Rh(PNP)R] (R = CH_3, C_6H_5) and Their Reactivity toward Ethylene and Protic Acids

Christine Hahn[a], Michael Spiegler[b], Eberhardt Herdtweck[b], and Rudolf Taube*[b]

Institut für Anorganische Chemie, Universität Würzburg[a],
Am Hubland, D-97074 Würzburg, Germany
E-mail: christine.hahn@mail.uni-wuerzburg.de

Anorganisch-Chemisches Institut, Technische Universität München[b],
Lichtenbergstraße 4, D-85747 Garching, Germany
Fax: (internat.) + 49(0)89/289-13473

Received April 27, 1998

Keywords: Organorhodium(I) complexes / Tridentate ligand / Protolysis / Reductive elimination / C–H coupling

The organorhodium(I) complexes [Rh(PNP)R] [PNP = 2,6-bis(diphenylphosphanylmethyl)pyridine, R = CH_3 (**3a**), C_6H_5 (**3b**)] were synthesized from [Rh(PNP)(C_2H_4)]BF_4 (**1a**) and LiR and characterized by ^{31}P-, ^{1}H-, and ^{13}C-NMR spectroscopy and EI mass spectrometry. In a THF solution saturated with ethylene **3a** and **3b** form the five-coordinate ethylene organorhodium(I) complexes [Rh(PNP)R(C_2H_4)] (**5a**, **b**). The stable monohydridorhodium(III) complex [Rh(PNP)ClH(CH_3CN)]SO_3CF_3 (**7**) was obtained by the reaction of [Rh(PNP)Cl] with HSO_3CF_3 in a solution of THF/acetonitrile and characterized by X-ray crystallography. In a THF solution the organorhodium(I) complexes **3a**, **b** react upon the addition of either HSO_3CF_3 or $HNMe_3Cl$ with the immediate release of the respective hydrocarbon HR.

The hydroamination of ethylene was first achieved at room temp. and normal pressure by a cationic ethylenerhodium(I) complex [Rh(PPh_3)$_2$(Me_2CO)(C_2H_4)]PF_6[1]. However, the low productivity of this rhodium complex catalyst could not be improved by variation of the ligand sphere[2]. Therefore we started upon a series of model studies to investigate the reaction mechanism of the rhodium complex catalyzed hydroamination of olefins, trying to trace systematically those reaction steps considered crucial for the catalytic cycle by the use of the [2,6-bis(diphenylphosphanylmethyl)pyridine]rhodium(I) complex fragment [Rh(PNP)]$^+$ as a stable structural moiety for the respective model compounds. The hypothetical reaction mechanism of the catalyses is formulated in Scheme 1.

It was recently found that model complexes of the type **A** [Rh(PNP)(olefin)]X (olefin = ethylene, styrene; X = BF_4, PF_6, SO_3CF_3) are only in a thermodynamic equilibrium with the corresponding amine complex **E**. In this case no indication of a nucleophilic attack of the secondary amine at the C−C double bond could be detected[3]. On the other hand the nucleophilic attack of secondary amines (HNR_2) was succesful with related dicationic olefin palladium(II) complexes [Pd(PNP)(olefin)]BF_4 (olefin = ethylene, styrene), however the Pd−C σ-bond in the formed (β-aminoethyl)palladium(II) complexes [Pd(PNP)($CHR'CH_2NR_2$)]-

Scheme 1

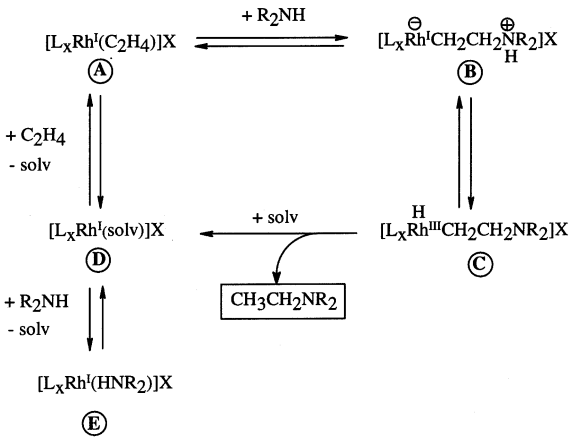

BF_4 (R′ = H, Ph) is so stable that it can not be cleaved protolytically under the reaction conditions[4].

It is known from other rhodium-catalyzed reactions, such as the hydrogenation of olefins[5][6], that the cleavage of the Rh−C σ-bond and the formation of the C−H bond can be realized by intramolecular reductive elimination, which is proposed as the product-forming step, cf. the formation of the ethylamine, shown as the step **C**→**D** in Scheme 1.

In this paper we report on the synthesis of related organorhodium(I) model complexes [Rh(PNP)R] (R = CH_3, C_6H_5) which were used to characterize the stability of the

[◇] Part LIII: R. Taube, H. Windisch, H. Hemling, H. Schumann, *J. Organomet. Chem.* **1998**, *555*, 201−210.

 © WILEY-VCH Verlag GmbH, D-69451 Weinheim, 1998 1434−1948/98/1010−1425 $ 17.50+.50/0

Rh−C σ-bond. For this purpose their reactivities toward ethylene and protic acids were investigated, and these results are presented here.

Results and Discussion

Synthesis and Characterization of [Rh(PNP)R]

The organorhodium(I) complexes [Rh(PNP)R] [R = CH_3 (**3a**), C_6H_5 (**3b**)] were synthesized from the cationic ethylenerhodium(I) complex [Rh(PNP)(C_2H_4)]BF_4 (**1a**)[3] with slightly more than three equiv. of the corresponding organyllithium compound, cf. Eq. 1.

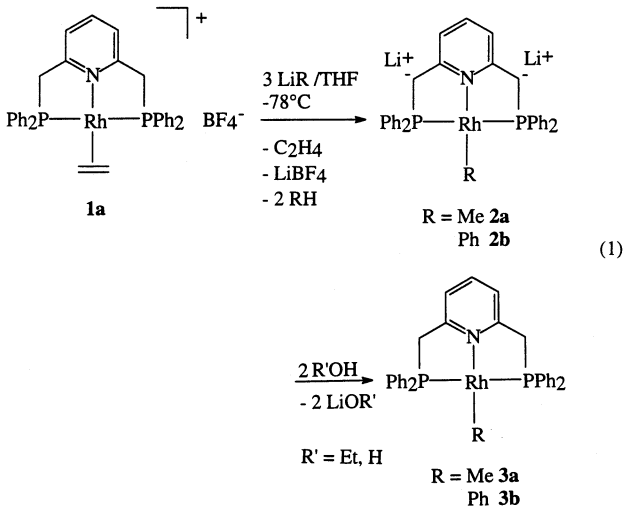

(1)

The intermediates **2a**, **b** formed were characterized in situ by NMR spectroscopy. The ^{31}P-NMR spectrum of the reaction solution of **1a** with 3.1 equiv. of $LiCH_3$ in [D_8]THF shows one doublet at δ = 17.2 (J_{P-Rh} = 148 Hz) which is shifted upfield by about 11 ppm compared to the starting complex **1a**. In the ^{1}H-NMR spectrum of this solution a signal is found at δ = 0.30 (td, J_{H-P} = 4.9 Hz, $J_{H-Rh} \approx 1$ Hz, CH_3) for the methyl group coordinated at the rhodium centre. The corresponding ^{13}C signal for the methyl group appears at δ = −15.4 (dt, J_{C-P} = 10.3 Hz, J_{C-Rh} = 27.5 Hz).

A virtual triplet in the ^{1}H-NMR spectrum at δ = 3.34 has an intensity of 2 H, consistent with deprotonated methylene groups of the PNP ligand in **2a**, while the corresponding ^{13}C signal is observed at δ = 58.0 (vt, N = 24.6 Hz), which is shifted downfield in comparison to that of **1a** (δ = 43.9, vt, N = 10.9 Hz). Thus, the NMR data suggests the formation of **2a**.

The formation of the analogous phenyl compound **2b** is suggested by the ^{31}P-NMR-spectroscopic investigation of a reaction solution of **1a** and 3.2 equiv. of LiC_6H_5 in THF, where again one doublet is observed, at δ = 16.7, showing the same phosphorus-rhodium coupling constant (J_{P-Rh} = 148 Hz) as that found for **2a**.

Upon reprotonation with ethanol or water these intermediates **2a**, **b** are converted into the neutral organorhodium(I) complexes **3a**, **b**. The methyl and the phenyl complexes which are obtained in good yields are reddish/brown air-sensitive solids which are soluble in THF and toluene, moderately soluble in ethanol, and insoluble in diethyl ether. In contrast to the structurally analogous organorhodium(I) complexes [Rh(PPh_3)$_3$R], which form spontaneously the *ortho*-metallated product [Rh(*o*-$C_6H_4PPh_2$)(PPh_3)$_2$] by release of the respective hydrocarbon HR[7], the complexes **3a**, **b** are quite stable as solid compounds under an inert gas, as well as in solution at room temp.

However, only a few stable square-planar alkyl- and arylrhodium(I) complexes of the type [Rh{R′P(CH_2CH_2-CH_2PPh_2)$_2$}R] (R′ = *t*Bu, Ph) are known[8]. The *ortho*-metallation of a PPh group in these complexes as well as in **3a**, **b** is obviously prevented by the chelating structure of the tridentate ligand.

The complexes **3a**, **b** were characterized by ^{31}P-, ^{1}H-, and ^{13}C-NMR spectroscopy and by EI mass spectrometry. In the ^{31}P-NMR spectra a doublet was found at δ = 28.9 (J_{P-Rh} = 177 Hz) for **3a**, and at δ = 20.6 (J_{P-Rh} = 180 Hz) for **3b**. These signals are shifted upfield and have a larger phosphorus-rhodium coupling constant compared to those of the related cationic (PNP)rhodium(I) complexes [Rh(PNP)L]X (L = HNR_2, py, CH_3CN, DMSO, olefin; X = BF_4, PF_6, SO_3CF_3) which are found in the region of δ = 31−41 with coupling constants of 126−157 Hz[3][9].

The ^{1}H-NMR signal for the methyl group of **3a** at δ = 0.19 (J_{H-P} = 6.2 Hz; J_{H-Rh} = 1.7 Hz), as well as the corresponding ^{13}C-NMR signal at δ = −20.8 (J_{C-P} = 11.7 Hz; J_{C-Rh} = 24.6 Hz), is shifted upfield in comparison to that found for the intermediate **2a**. The characteristic virtual triplet for the methylene group of the PNP ligand appears at δ = 3.88 in the ^{1}H-NMR spectrum, and at δ = 46.8 in the ^{13}C-NMR spectrum.

The ^{1}H-NMR signals for the phenyl moiety of **3b** are found at δ = 6.45, 6.57, and 7.36, and in the ^{13}C-NMR spectrum the corresponding signals are observed at δ = 119.0, 125.2, 140.9. While in the ^{1}H-NMR spectrum of **3b** the characteristic virtual triplet for the methylene group at δ = 4.02 is shifted slightly downfield compared to that of **3a**, the corresponding ^{13}C-NMR signal appears at the same chemical shift (δ = 46.8) as is found for **3a**.

In the EI mass spectra of **3a** and **3b** the respective peaks $[M]^+$ and $[M - R]^+$ could be observed.

A further piece of evidence for the formation of the twofold deprotonated intermediate **2a** is given by the reaction of **3a** with two equiv. of CH_3Li, cf. Eq. 2.

By the reaction of **2a** with D_2O the corresponding twofold deuterated methyl complex **4** is obtained and characterized by ^{1}H-NMR spectroscopy, where the signal for the methylene group is observed at δ = 3.87 with half the intensity found in the spectrum of **3a**. Accordingly, in the mass spectrum of **4**, the peaks for $[M]^+$ and $[M - CH_3]^+$ appear at the corresponding *m/z* values which are higher by two units than those found for **3a**.

This deprotonation reaction was also described for the structurally related [2,6-bis(diphenylphosphanylmethyl)-phenyl](methyl)platinum(II) complex, where an analogous

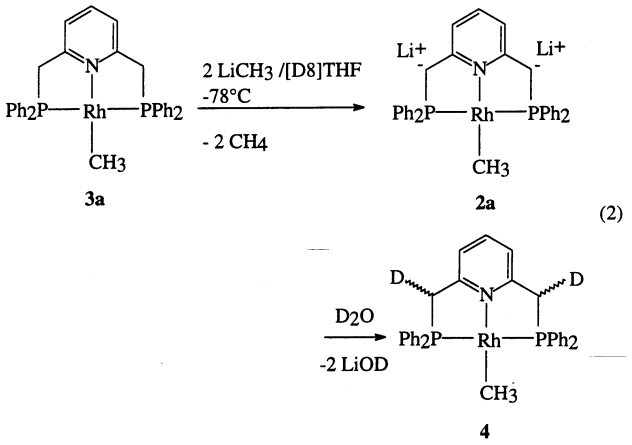

twofold deprotonated complex is obtained by the reaction with two equiv. of CH_3Li[10].

Reactivity of [Rh(PNP)R] toward Ethylene

Since the possibility of an insertion of an ethylene molecule into the Rh−C bond (cf. Scheme 1: e.g. in **B**) has to be taken into consideration as a side reaction during the hydroamination of ethylene, the investigation of the reactivity of the organorhodium(I) complexes **3a**, **b** toward ethylene was included in the model studies.

When a solution of **3a** or **3b** in THF saturated with ethylene was cooled down its colour changed reversibly from red (at room temp.) to orange-red (at −78°C). The formation of the corresponding five-coordinate ethylene organorhodium(I) complexes **5a**, **b** (cf. Eq. 3) is suggested by ^{1}H-NMR spectroscopy at room temp.: In addition to the slightly shifted signals for the coordinated PNP ligand and the organo moiety (see Experimental Section), relatively broad average signals at δ = 5.08 and δ = 4.36 are found for the methyl and phenyl complexes respectively, indicating an exchange between free and coordinated ethylene (the chemical shift of the average signal depends on the concentration of free ethylene).

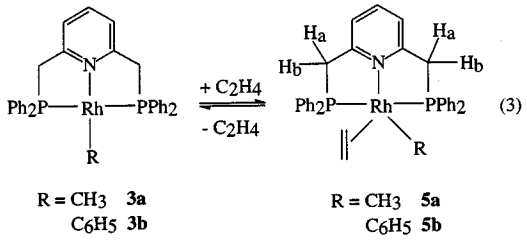

In the ^{31}P-NMR spectra of these solutions the doublets at δ = 39.0 (J_{P-Rh} = 152 Hz) and 27.5 (J_{P-Rh} = 171 Hz) are observed at room temp. for the methyl and phenyl complexes **5a**, **b** respectively; these are show a remarkable downfield shift compared to those found for **3a**, **b**. These features are in agreement with the coordination of an ethylene molecule. As a consequence of the increased coordination number the phosphorus−rhodium bond becomes weaker, as reflected by the decreased phosphorus-rhodium coupling constants.

The behaviour of the solution of **3b** (under ethylene in [D_8]THF and during the cooling) was monitored by a dynamic proton-NMR experiment. The chemical shifts of the spectra run in the temperature range room temp. to −80°C are summarized in Table 1.

By cooling the sample the average signal for the ethylene becomes very broad. The coalescence temp. lies between −20°C and −40°C. At −60°C a broad signal at δ = 5.36 for the free ethylene, and two broad signals at δ = 2.48 and 1.85 for the coordinated ethylene, are visible and the signal for the methylene protons of the PNP ligand at δ ≈ 4.1 begins to split into two signals. By cooling to −80°C the signals for free and coordinated ethylene become sharper, which indicates a slow exchange relative to the NMR time scale. At this temperature the five-coordinate complex **5b** has a relatively stable coordination geometry which is no longer of C_{2v} symmetry, consequently the signals for the methylene protons become inequivalent and there is a split into two doublets at δ = 4.16 and 4.06 (J_{H-H} = 14.8 Hz).

When the solvent was removed under vacuum from a solution of **5a** or **5b** a red solid remained, identified as **3a** or **3b**, respectively. This indicates a weak coordination of the ethylene at the organorhodium(I) complexes. No indication of an insertion of the ethylene into the Rh−C σ-bond could be observed, under these conditions, for either **3a** or **3b**.

Synthesis and Structure of [Rh(PNP)ClH(CH$_3$CN)]SO$_3$CF$_3$

In the proposed catalytic cycle of the hydroamination of ethylene (cf. Scheme 1) the liberation of the ethylamine from the (β-ammonioethyl)rhodium(I) complex **B** is assumed to be achieved by oxidative addition of the proton of the β-ammonio group at the rhodium centre, forming the (β-aminoethyl)(hydrido)rhodium(III) complex **C** from which the product is reductively eliminated in an irreversible reaction step.

As is known (monohydrido)rhodium(III) complexes can be obtained by the oxidative addition of protic acids to rhodium(I) complexes[11][12], which is demonstrated here by the reaction of [Rh(PNP)Cl] (**6**)[13] with HSO_3CF_3, cf. Eq. 4.

The (chloro)(hydrido)rhodium(III) complex [Rh(PNP)-ClH(CH$_3$CN)]SO$_3$CF$_3$ (**7**) obtained was isolated as an air-stable pale yellow solid and characterized by IR and ^{1}H-NMR spectroscopy. In the IR spectrum the band at 2138 cm^{-1} is assigned to the Rh−H vibration, the two bands at 2293 and 2366 cm^{-1} are observed for the end-on coordinated acetonitrile[14], and the corresponding bands for the triflate anion (see Experimental Section) suggest its non-coordination[15]. The ^{1}H-NMR signal of the hydrido ligand appears at δ = −15.99 as a broad triplet, while for the coordinated acetonitrile a singlet is observed at δ = 1.48. For the inequivalent methylene protons of the PNP ligand the corresponding two doublets of virtual triplets appear at δ = 4.22 and 4.83.

Table 1. Dynamic ^{1}H-NMR experiment of the solution of [Rh(PNP)(C_6H_5)] (**3a**) in [D_8]THF under ethylene (500 MHz)

T [°C]	py-4 (t)	PPh, Ph (m)	Ph (m)	CH_2	C_2H_4 free	coord.
23	7.52	7.08−7.34	6.48−6.57	4.05 vt	4.20 br.	
0	7.52	7.02−7.26	6.50−6.57	4.07 br.	3.96 br.	
−20	7.52	7.00−7.28	6.50−6.58	4.09 br.	3.9 br.	
−40	7.54	6.99−7.30	6.51−6.58	4.10 br.	5.3 br.	2.5 br.
−60	7.56	6.99−7.31	6.54−6.59	4.12 br. 4.09 br.	5.36 br.	2.50 br., 1.86 br.
−70	7.57	6.99−7.36	6.52−6.59	4.15 d 4.07 d J_{H-H} = 14.8 Hz	5.40 br.	2.48 br., 1.85 br.
−80	7.58	6.99−7.36	6.52−6.60	4.16 d 4.06 d J_{H-H} = 14.8 Hz	5.41 br.	2.48 d, 1.84 d J_{H-H} = 14.8 Hz

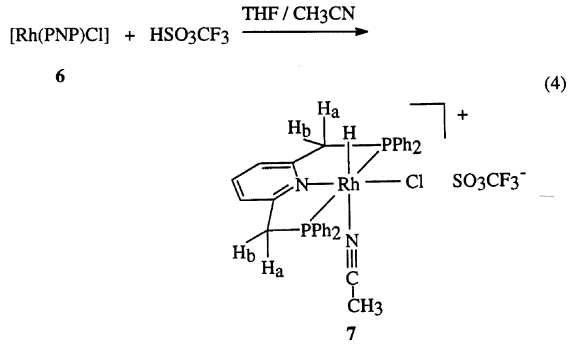

Single crystals of complex **7** were obtained from the mother liquor (THF/CH_3CN/diethyl ether) which stood three days at room temp. The molecular structure of the complex cation $[Rh(PNP)ClH(CH_3CN)]^+$ is shown in Figure 1. The Rh−Cl distance [2.3480(7) Å] is identical with that found for the chlororhodium(I) complex [Rh(PNP)Cl] [2.344(2) Å], while the Rh−N(1) distance [2.1451(19) Å] is significantly longer than the corresponding Rh−N bond length [1.984(3) Å] found in the (acetonitrile)rhodium(I) complex $[Rh(PNP)(CH_3CN)]BF_4$[9] due to the strong *trans* influence of the hydrido ligand. The Rh^{III}(PNP) fragment in **7** exhibits practically the same features of the bonding parameters as found in the Rh^{I}(PNP) fragment in **6** and in other Rh^{I}(PNP) complexes[3][9].

Figure 1. Platon[16] drawing of the complex cation $[Rh(PNP)ClH(CH_3CN)]^+$ of **7**

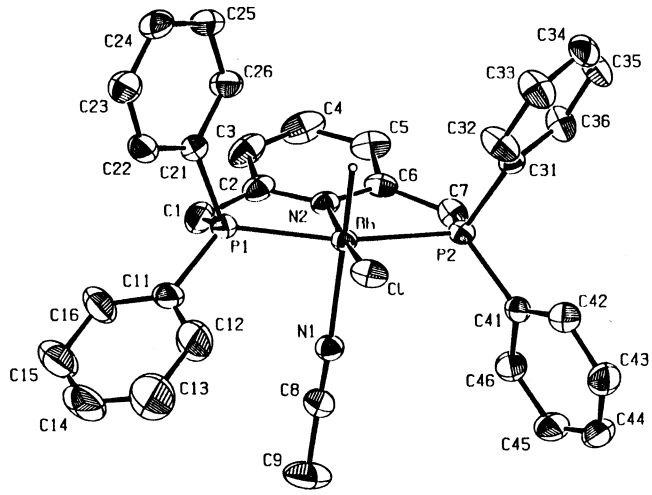

Reactivity of [Rh(PNP)R] toward Protic Acids

Analogous to the formation of the hydridorhodium(III) complex **7**, the reaction of the organorhodium(I) complexes **3a**, **b** with protic acids can be used as a simplified reaction model for the product-forming steps (**B** → **C** → **D** in Scheme 1). It is of interest to investigate the protolysis of [Rh(PNP)R], in one case in the presence of a weak coordinating anion X^- such as $CF_3SO_3^-$, and in another case with a stronger coordinating anion such as Cl^-. Thus, the proposed hydrido organorhodium(III) intermediates, either five-coordinate **I** or six-coordinate **II** (cf. Scheme 2), might show different reactivities concerning the reductive elimination of the hydrocarbon HR (discussed in detail by Milstein[6]).

First HSO_3CF_3 was added to a solution of **3a** or **3b** in THF. In the case of the methyl complex **3a** the release of the methane was observed immediately, visible as an evolution of gas, whereas from the phenyl complex **3b** the corresponding benzene was detected by gas chromatography of the reaction solution. However, no defined Rh^{I} complex could be isolated from the reaction solution. Obviously, the remaining $[Rh(PNP)]^+$ fragment (analogous to **D**, Scheme 1) cannot be stabilized either by the solvent (THF) or by the triflate anion. Decomposition of the reaction solution occurred and the formation of the dinuclear complex $[Rh_2(PNP)_3](SO_3CF_3)_2$ (**8**)[3] was detected by ^{31}P NMR.

However, when some acetonitrile was added to the reaction solution after the protolysis the corresponding cationic acetonitrile complex **9**[9] could be isolated, cf. Eq. 5.

According to the last step of the catalytic cycle (**D** → **A**, Scheme 1) the remaining $[Rh(PNP)]^+$ fragment can also be trapped with ethylene by formation of the cationic ethylene complex **1b**[3], cf. Eq. 6.

When cyclooctadiene was added after the protolyses of **3b** a dinuclear COD complex **10** was obtained, cf. Eq. 7, which was fully characterized by ^{31}P-, ^{1}H-, and ^{13}C-NMR

Table 2. Selected bond lengths [Å] and angles [°] for $[Rh(PNP)ClH(CH_3CN)]SO_3CF_3$ (**7**)

Rh−Cl(1)	2.3480(7)	Rh−P(1)	2.3013(7)	Rh−P(2)	2.2863(6)
Rh−N(1)	2.1451(19)	Rh−N(2)	2.0656(17)	P(1)−C(1)	1.841(3)
P(2)−C(7)	1.828(2)				
P(1)−Rh−P(2)	166.90(2)	Cl−Rh−P(1)	96.77(2)	Cl−Rh−P(2)	93.42(2)
Cl−Rh−N(1)	91.95(5)	Cl−Rh−N(2)	175.06(5)	P(1)−Rh−N(1)	91.02(5)
P(1)−Rh−N(2)	84.53(6)	P(2)−Rh−N(1)	96.85(5)	P(2)−Rh−N(2)	84.82(5)
N(1)−Rh−N(2)	92.83(7)				

Scheme 2

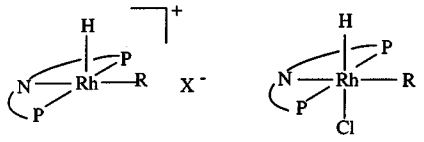

$$[Rh(PNP)R] + HSO_3CF_3 \xrightarrow{THF\,/\,CH_3CN} [Rh(PNP)(CH_3CN)]SO_3CF_3 + HR \quad (5)$$

R = Me **3a**, Ph **3b** — **9**

$$[Rh(PNP)R] + HSO_3CF_3 \xrightarrow{THF\,/\,C_2H_4} [Rh(PNP)(C_2H_4)]SO_3CF_3 + HR \quad (6)$$

R = Me **3a**, Ph **3b** — **1b**

spectroscopy (see Experimental Section). Thus, it is shown that the regeneration of the cationic olefin complex is possible after the elimination of the hydrocarbon, which is of great importance for the catalysis.

$$2\,[Rh(PNP)(C_6H_5)] + 2\,HSO_3CF_3 \xrightarrow{THF\,/\,COD} 2\,C_6H_6 +$$

3b

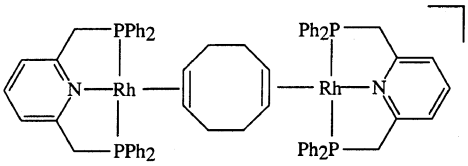

$$2\,SO_3CF_3^- \quad (7)$$

10

In another experiment trimethylammonium chloride was added to a solution of **3a** or **3b**. In both cases the respective hydrocarbon was also released immediately while the chlororhodium(I) complex **6** formed, which is poorly soluble in THF, began to precipitate and was filtered off after 4 h with a yield of 80−90%, cf. Eq. 8.

$$[Rh(PNP)R] + [HNMe3]Cl \xrightarrow{THF} [Rh(PNP)Cl] + HR + NMe3 \quad (8)$$

R = Me **3a**, Ph **3b** — **6**

Since a (hydrido)(phenyl)rhodium(III) complex $[Rh(PMe_3)_2(CO)(C_6H_5)HCl]$ could be detected upon the reaction of $[Rh(PMe_3)_2(CO)(C_6H_5)]$ with HCl, although only in solution at −40°C by NMR spectroscopy[17], the formation of a hydrido organo-PNP−rhodium(III) intermediate during the protolysis reaction described above might be postulated. Furthermore, the reductive elimination step from this complex seems to proceed without any kinetic inhibition, independent of the coordinating ability of the anion in the Brönsted acid used for protolysis.

Conclusions

The synthesis of the new organorhodium(I) complexes [Rh(PNP)R] (R = CH_3, C_6H_5) succeeded by the reaction of the cationic ethylene complex $[Rh(PNP)(C_2H_4)]BF_4$ with three equiv. of LiR. Organorhodium complexes containing deprotonated methylene groups of the PNP ligand occur as intermediates, which can be reprotonated with ethanol or water.

The square-planar coordination geometry of the organorhodium complexes is stabilized by the chelating structure of the tridentate PNP ligand, which avoids the release of the hydrocarbon HR by *ortho*-metallation of a PPh moiety.

The organorhodium(I) complexes [Rh(PNP)R] react with ethylene by the formation of five-coordinate complexes $[Rh(PNP)R(C_2H_4)]$ in which the ethylene is weakly coordinated and can be removed under vacuum. No indication of an insertion of the ethylene in the Rh−C σ-bond could be observed, which may be important to exclude the oligomerization of ethylene as a side reaction of the hydroamination.

As was shown a stable (monohydrido)rhodium(III) complex $[Rh(PNP)ClH(CH_3CN)]SO_3CF_3$ can be obtained by oxidative addition of HSO_3CF_3 to the chlororhodium(I) complex [Rh(PNP)Cl]. Upon protolysis with HSO_3CF_3 of the organorhodium(I) complexes [Rh(PNP)R] the hydrocarbons RH are liberated, and it is possible to trap the remaining Rh^I complex fragment with olefins, so the cationic olefin complex can be regenerated, which is as expected for the starting complex in the catalytic cycle of the hydroamination of olefins.

Independently, if a protic acid with a weakly coordinating (HSO_3CF_3) or a stronger coordinating anion ($HNMe_3Cl$) is used, the protolytic reaction of the organorhodium(I) complexes [RhPNP)R] [proceeding by intermediate formation of corresponding hydrido-organorhodium(III) complex] leads immediately in each case to the reductive elimination of the hydrocarbon HR. These results also suggest that the reductive elimination of the ethylamine (cf. Scheme 1) may proceed irreversibly and without kinetic inhibition, which is essential for a product-forming step closing the catalytic cycle. The proposed reaction mechanism for the hydroamination of olefins finds strong chemical support from these model reactions.

We thank Dr. *A. Porzel* of the *Institut für Pflanzenbiochemie* of the University of Halle for the measurement of the dynamic proton-resonance experiment and the *Deutsche Forschungsgemeinschaft* (*Sonderforschungsbereich 347* of the University of Würzburg) for financial support.

Experimental Section

General: All reactions were carried out under dry and oxygen-free argon or ethylene. Ethanol, acetone, $CDCl_3$ and [D_6]acetone were refluxed over 4-Å molecular sieves and made oxygen-free by bubbling argon through the liquid. THF and diethyl ether were refluxed in the presence of Na/benzophenone and [D_8]THF in the presence of K/Na alloy. Acetonitrile and DMSO were dried over 4-Å molecular sieves and distilled before use. HSO_3CF_3, $LiCH_3$ and LiC_6H_5 were obtained from Fluka. − IR: KBr pellets with a Perkin-Elmer FT-IR 16 spectrometer. − ^1H, $^{13}C\{^1H\}$, and $^{31}P\{^1H\}$ NMR: Varian Gemini 300 NMR spectrometer (300, 75, and 121 MHz respectively), ^1H- and ^{13}C-NMR shifts were referenced to the resonance of the residual protons of the solvents, the ^{31}P-NMR shifts were referenced to external 85% H_3PO_4. − Dynamic proton NMR: Varian Unity 500 NMR spectrometer (500 MHz). − EI MS: AMD 402 spectrometer (AMD Intectra) at 70 eV. − (C, H, and N): LECO CHN 932 analyzer. Rh elemental analysis was determined using a photometric method[18]. The Chrompack gas-chromatograph CP 9000 was used for the identification of liquid organic compounds.

Syntheses: [Rh(PNP)(C_2H_4)]BF_4 (**1a**) was prepared according to the procedure described in ref.[3].

[Rh(PNP)(CH_3)] (**3a**): 10.5 ml of a 1.6 M $LiCH_3$ solution in diethyl ether (3.2 equiv.) was added slowly at −78°C to a suspension of 3.6 g (5.2 mmol) of [Rh(PNP)(C_2H_4)]BF_4 (**1a**) in 20 ml of THF. The mixture was warmed up to room temp. and stirred for a further 10 min to give a red solution. The solvent was removed under reduced pressure. 20 ml of ethanol was added dropwise slowly at −78°C to the remaining red crystalline solid with rigorous stirring. After stirring for another 20 min at room temp., the reddish/brown solid was filtered off, washed with ethanol (2 ×), then with diethyl ether and dried under vacuum. After recrystallization of the crude product in hot THF, 2.2 g of **3a** (3.7 mmol, 71%), reddish/brown solid was isolated, temp. of decomposition 220−230°C. − ^{31}P NMR ([D_8]THF): δ = 28.89 (d, J_{P-Rh} = 177 Hz). − ^1H NMR([D_8]THF): δ = 0.19 (td, $^3J_{H-P}$ = 6.2 Hz, J_{H-Rh} = 1.7 Hz, 3 H, CH_3), 3.88 (vt, N_{H-P} = 3.9 Hz, 4 H, CH_2), 7.07 (d, J_{H-H} = 7.6 Hz, 2 H, *3,5*-py), 7.30 (m, 12 H, PPh), 7.49 (t, J_{H-H} = 7.6 Hz, 1 H, *4*-py), 7.78 (m, 8 H, PPh). − ^{13}C NMR([D_8]THF): δ = −20.8 (dt, $^2J_{C-P}$ = 11.7 Hz, J_{C-Rh} = 24.6 Hz, *C*H_3), 46.8 (vt, N_{C-P} = 9.7 Hz, *C*H_2), 120.8 (vt, N_{C-P} = 5.1 Hz, $C_{3,5\text{-py}}$), 128.6 (vt, N_{C-P} = 4.4 Hz, PC_{meta}), 129.3 (s, PC_{para}), 131.4 (s, $C_{4\text{-py}}$), 133.6 (vt, N_{C-P} = 7.5 Hz, PC_{ortho}), 138.3 (vt, N_{C-P} = 14.9 Hz, PC_{ipso}), 159.9 (vt, N_{C-P} < 3 Hz, $C_{2,6\text{-py}}$). − EI MS; *m/z* (%): 593 (100) $[M]^+$, 578 (62) $[M - CH_3]^+$. − $C_{32}H_{30}NP_2Rh$ (593.45): calcd. C 64.77, H 5.10, N 2.36, Rh 17.34; found C 64.26, H 5.04, N 2.63, Rh 17.88.

[Rh(PNP)(C_6H_5)] (**3b**): The complex **3b** was prepared in the same manner as described for **3a** from 3 g (4.3 mmol) of **1a** in 20 ml of THF and 7.5 ml of a ca. 1.8 M Et_2O/cyclohexane solution of LiC_6H_5 (13.4 mmol, 3.1 equiv.). When the solvent was removed from the red solution, a red oil remained which was treated with 20 ml of ethanol at −78°C by rigorously stirring, giving a reddish/brown suspension. After stirring for another 20 min, the solid was filtered off washed with ethanol (3 ×)and then with diethyl ether and dried under vacuum. The crude product was recrystallized in hot THF giving 2.1 g of **3b** (3.2 mmol, 75%), reddish/brown solid, temp. of decomposition 215−220°C. − ^{31}P NMR ([D_8]THF): δ = 20.6 (d, J_{P-Rh} = 180 Hz). − ^1H NMR ([D_8]THF): δ = 4.02 (vt, N_{H-P} = 3.8 Hz, 4 H, CH_2), 6.45 (t, J_{H-H} = 7.0 Hz, 1 H, H_{para}), 6.57 (t, J_{H-H} = 7.2 Hz, 2 H, H_{meta}), 7.21 (m, 14 H, PPh, *3,5*-py), 7.36 (d, J_{H-H} = 7.3 Hz, 2 H, H_{ortho}), 7.50 (m, 8 H, PPh), 7.60 (t, J_{H-H} = 7.6 Hz, 1 H, *4*-py). − ^{13}C NMR ([D_8]THF): δ = 46.8 (vt, N_{C-P} = 9.9 Hz, *C*H_2), 119.0 (s, C_{para}), 120.9 (vt, N_{C-P} = 5.2 Hz, $C_{3,5\text{-py}}$), 125.24 (s, C_{meta}), 128.5 (vt, N_{C-P} = 4.6 Hz, PC_{meta}), 129.3 (s, PC_{para}), 133.5 (s, $C_{4\text{-py}}$), 133.6 (vt, N_{C-P} = 6.9 Hz, PC_{ortho}), 137.9 (vt, N_{C-P} = 16.1 Hz, PC_{ipso}), 140.9 (vt, N_{C-P} = 3.8 Hz, C_{ortho}), 160.9 (vt, N_{C-P} < 3 Hz, $C_{2,6\text{-py}}$). − EI MS; *m/z* (100): 655 (6.7) $[M]^+$, 578 (0.1) $[M - C_6H_5]^+$. − $C_{37}H_{32}NP_2Rh$ (655.52): calcd. C 67.79, H 4.92, N 2.14, Rh 15.70; found C 63.92 (premature decomposition of the sample), H 5.03, N 1.91, Rh 15.58.

Alternatively the complexes could be obtained by reprotonation with 5 equiv. of H_2O which were added directly to the red reaction solution (**2a** or **2b**). The crude products **3a**, **b** precipitated after a few minutes from the THF solution and were isolated in yields of about 65%.

NMR-Spectroscopic Characterization of [Rh{2,6-($Ph_2PCHLi)_2$-(NC_5H_3)}(R)] [R = CH_3 (**2a**)*, C_6H_5* (**2b**)*]*

2a: (a) [Rh(PNP)(C_2H_4)]BF_4 (148 mg, 0.21 mmol, **1a**) was dissolved in 1 ml of [D_8]THF and 3.1 equiv. of solid $LiCH_3$ (0.66 mmol, obtained from 0.41 ml of a 1.6 M Et_2O solution by removing the solvent) were added at −78°C and warmed up to room temp. The NMR spectra, which were measured instantly from the red solution obtained are consistent with **2a**. − ^{31}P NMR ([D_8]THF): δ = 17.2 (d, J_{P-Rh} = 148 Hz). − ^1H NMR ([D_8]THF): δ = 0.30 (td, $^3J_{H-P}$ = 4.9 Hz, $J_{H-Rh} \approx$ 1 Hz, 3 H, CH_3), 3.34 (vt, N_{H-P} = 3.8 Hz, 2 H, C*H*), 5.10 (d, J_{H-H} = 7.6 Hz, 2 H, *3,5*-py), 6.06 (t, J_{H-H} = 7.6 Hz, 1 H, *4*-py), 6.92−7.05 (m, 12 H, PPh), 7.72 (m, 8 H, PPh). − ^{13}C NMR ([D_8]THF): δ = −15.4 (dt, $^2J_{C-P}$ = 10.3 Hz, J_{C-Rh} = 27.5 Hz, *C*H_3), 58.0 (vt, N_{C-P} = 24.6 Hz, *C*H), 92.3 (vt, N_{C-P} = 8.0 Hz, $C_{3,5\text{-py}}$), 126.1 (s, PC_{para}), 127.2 (vt, N_{C-P} = 4.2 Hz, PC_{meta}), 131.0 (s, $C_{4\text{-py}}$), 132.5 (vt, N_{C-P} = 6.6 Hz, PC_{ortho}), 148.6 (vt, N_{C-P} = 14.4 Hz, PC_{ipso}), 171.6 (vt, N_{C-P} < 3 Hz, $C_{2,6\text{-py}}$).

(b) [Rh(PNP)(CH_3)] (197 mg, 0.33 mmol, **3a**) was dissolved in 1 ml of [D_8]THF and 2.2 equiv. of solid CH_3Li (0.73 mmol, obtained from 0.46 ml of a 1.6 M Et_2O solution by removing the solvent) were added at −78°C and warmed up to room temp. The obtained red solution was instantly characterized by NMR spectroscopy. The ^{31}P-, ^1H-, and ^{13}C-NMR spectra are identical with those found for the reaction solution of **1a** and 3.1 equiv. of CH_3Li described in (a).

2b: The reaction solution of **1a** and 3.2 equiv. of C_6H_5Li (1.8 M solution in Et_2O/cyclohexane) in THF prepared in the same manner as described for **2a** was characterized by ^{31}P NMR (with external ref. C_6D_6): δ = 16.7 (d, J_{P-Rh} = 148 Hz).

Reaction of **2a** *with D_2O:* 5 equiv. of D_2O were added to a solution of **2a** in THF, which was prepared from **3a** and 2.2 equiv. of CH_3Li as described above. The reddish/brown crystalline solid which was precipitated was filtered off washed with ethanol and diethyl ether and dried under vacuum. The ^1H-NMR spectrum of the solid is consistent with [Rh{2,6-($Ph_2PCHD)_2$(NC_5H_3)}(CH_3)] (**4**). For the deuterated methylene group a multiplet at δ = 3.87 was found with an intensity of 2 H. All other signals of **4** agree with those of **3a**. − EI MS of **4**; *m/z* (%): 595 $[M]^+$ (81), 580 $[M - CH_3]^+$ (53).

Reaction of **3a**, **b** *with Ethylene:* The complexes **3a**, **b** were dissolved in [D_8]THF. The solutions were saturated with ethylene at −78°C. The five-coordinate complexes [Rh(PNP)R(C_2H_4)] [R = CH_3 (**5a**), C_6H_5 (**5b**)] were identified by ^{31}P- and ^{1}H-NMR spectroscopy.

5a: ^{31}P NMR ([D_8]THF): δ = 39.0 (d, J_{P-Rh} = 152 Hz). − ^{1}H NMR ([D_8]THF): δ = −0.54 (td, $^3J_{H-P}$ = 7.3 Hz, J_{H-Rh} = 1.5 Hz, 3 H, CH_3), 4.04 (vt, N_{H-P} = 3.0 Hz, 4 H, CH_2), 5.08 (br., average signal for free and coord. C_2H_4), 7.12−7.62 (m, 23 H, PPh, py).

5b: ^{31}P NMR ([D_8]THF): δ = 27.5 (d, J_{P-Rh} = 171 Hz). − ^{1}H NMR ([D_8]THF): δ = 4.05 (vt, N_{H-P} = 3.0 Hz, 4 H, CH_2), 4.36 (br., average signal for free and coord. C_2H_4), 6.45 (t, J_{H-H} = 7.3 Hz, 1 H, H_{para}), 6.55 (t, J_{H-H} = 7.3 Hz, 2 H, H_{meta}), 7.07−7.40 (m, 23 H, PPh, *3,5*-py, H_{ortho}), 7.54 (t, J_{H-H} = 7.9 Hz, 1 H, *4*-py).

[Rh(PNP)ClH(CH$_3$CN)]SO$_3$CF$_3$ (**7**): 0.2 ml of HSO_3CF_3 was added to a suspension of 345 mg (0.56 mmol) of [Rh(PNP)Cl][9][13] in 5 ml of THF and 1 ml of acetonitrile. The mixture changed its colour to pale yellow. After filtration of the solution, diethyl ether was added dropwise and a yellow/brown oil precipitated which crystallized to a pale yellow solid. The crude product was filtered off, washed with diethyl ether (2 ×), and recrystallized in acetone/diethyl ether to give 290 mg of **7** (0.38 mmol, 67%), temp. of decomposition 160−170°C. − IR (KBr): $\tilde{\nu}$ = 2366 cm^{-1}, 2293 (CH_3CN); 2138 (Rh−H); 1602, 1568 (py); 1261, 1223, 1159, 1030, 638, 572 (SO_3CF_3). − ^{1}H NMR ($CDCl_3$): δ = −15.9 (t, $^2J_{H-P}$ = 9.5 Hz, 1 H, Rh*H*), 1.49 (s, 3 H, NCH_3) 4.22 (dvt, J_{Ha-Hb} = 17.8 Hz, N_{H-P} = 4.6 Hz, 2 H, CH_a), 4.83 (dvt, J_{Ha-Hb} = 17.8 Hz, N_{H-P} = 4.6 Hz, 2 H, CH_b), 7.41−7.94 (m, 23 H, PPh, py).

Reactivity of **3a**, **b** *toward HSO$_3$CF$_3$:* (a) 1 equiv. of HSO_3CF_3 was added to a solution of 1 mmol of **3a** or **3b** in 8 ml of THF. In the case of the reaction with **3a** the evolution of methane was immediately visible. In the reaction solution of **3b** benzene was correspondingly detected by gas chromatography. By addition of diethyl ether to the respective reaction solutions dark red oil precipitated giving reddish/brown solids upon removal of the solvent in vacuum. The solids obtained from both reaction solutions contain the dinuclear complex [Rh_2(PNP)$_3$](SO_3CF_3)$_2$ (**8**) among decomposition products; detected by ^{31}P-NMR spectroscopy (δ = 43.9 dd, $J_{P(a)-Rh}$ = 139 Hz, $J_{P(a)-P(b)}$ = 39 Hz; δ = 26.4, dt $J_{P(b)-Rh}$ = 169 Hz)[3].

(b) In presence of CH_3CN: After the protolysis of **3a** or **3b** with HSO_3CF_3 (see above), 1 ml of acetonitrile was added to the reaction solution and stirred for 20 min at room temp. Upon dropwise addition of diethyl ether an orange/brown oil precipitated which crystallized after 1 d to give a brown/yellow solid which was filtered off washed with diethyl ether and dried under vacuum. In each case the solid was analyzed by ^{1}H-NMR spectroscopy as the pure acetonitrile complex [Rh(PNP)(CH_3CN)]SO_3CF_3 (**9**) when compared to the spectrum of an authentic sample prepared according to the procedure in the literature[9] (yield: 50−60%).

(c) In presence of ethylene: After the protolysis of **3a** or **3b** with HSO_3CF_3 (see above), the reaction solution was stirred for 20 min under ethylene at −78°C. The mixture was warmed up to room temp. Upon addition of diethyl ether to the solution an orange yellow crystalline solid precipitated which was filtered off, washed with diethyl ether and dried under vacuum. The solid was identified as the pure ethylene complex [Rh(PNP)(C_2H_4)]SO_3CF_3 (**1b**) by ^{1}H-NMR spectroscopy when compared to an authentic sample[3] (yield: 60−80%).

(d) In the presence of COD: 114 μl of HSO_3CF_3 was added to a solution of 830 mg (1.26 mmol) of [Rh(PNP)(C_6H_5)] (**3b**) in 8 ml of THF. After 5 min, 1.6 ml (12.6 mmol) of cyclooctadiene (COD) was added and stirred for 30 min while an orange yellow solid crystallized slowly from the solution. The solid was filtered off the next day. For recrystallization the solid was dissolved in acetone and precipitated after addition of diethyl ether to the solution. The crystalline solid was filtered off, washed with diethyl ether and dried under vacuum. The solid was characterized as [Rh_2(PNP)$_2$(COD)](SO_3CF_3)$_2$ (**10**) which was isolated in a yield of 520 mg (0.66 mmol, 53%), temp. of decomposition 232°C. − ^{31}P NMR ([D_6]acetone): δ = 41.2 (d, J_{P-Rh} = 142 Hz). − ^{1}H NMR ([D_6]acetone): δ = 1.18 (m, 4 H, COD), 2.25 (m, 4 H, COD), 4.09 (m, 4 H, COD), 4.36 (vt, N_{H-P} = 3.6 Hz, 4 H, CH_2), 7.37−7.81 (m, 23 H, PPh, py). − ^{13}C NMR ([D_6]acetone): δ = 44.7 (vt, N_{C-P} = 11.5 Hz, *C*H$_2$), 77.8 (d, J_{C-Rh} = 12 Hz), 122.7 (vt, N_{C-P} < 3 Hz, $C_{3,5\text{-py}}$), 129.9 (vt, N_{C-P} = 4.2 Hz, PC_{meta}), 131.0 (vt, N_{C-P} = 15.8 Hz, PC_{ipso}), 132.2 (s, PC_{para}), 134.5 (vt, N_{C-P} = 6.6 Hz, PC_{ortho}), 141.7 (s, $C_{4\text{-py}}$), 161.9 (vt, N_{C-P} < 3 Hz, $C_{2,6\text{-py}}$). − $C_{72}H_{66}F_6N_2O_6P_4Rh_2S_2$ (1563.15): calcd. C 55.31, H 4.26, N 1.79, Rh 13.17; found C 54.91, H 4.26, N 1.65, Rh 13.07.

Reactivity of **3a**, **b** *toward HNMe$_3$Cl:* 48 mg (0.5 mmol) of $HNMe_3Cl$, dissolved in 2 ml of THF, was added to a solution of 0.5 mmol of **3a** or **3b**, dissolved in 8 ml of THF. A red crystalline solid precipitated and, in the case of the methyl complex **3a**, an evolution of gas was observed immediately. In the reaction solution of **3b** benzene was detected by gas chromatography. After 4 h, the red solid was filtered off, washed with THF and diethyl ether and dried under vacuum. The solid was identified in each case as [Rh(PNP)Cl][9][13] (**6**) by ^{31}P-NMR and IR spectroscopy (yield: 80−90%).

Crystal-Structure Determination of **7**: A single crystal of approximate dimensions 0.64 × 0.28 × 0.08 mm was mounted inside a Lindemann glass capillary. Crystal data and structure refinement details are given in Table 3.

Table 3. Crystal data and structure refinement for **7**

Formula	$C_{34}H_{31}ClF_3N_2O_3P_2RhS$
Molecular mass	805.00
Crystal system	triclinic
Space group	*P*$\bar{1}$ (I. T. No. 2)
a [Å]	9.2052(5)
b [Å]	12.6582(8)
c [Å]	15.7936(10)
α [°]	79.231(7)
β [°]	74.202(6)
γ [°]	77.905(6)
V [Å^3]	1714.9(2)
Z	2
D(calcd.) [g cm^{-3}]	1.559
μ (Mo-K_α) [cm^{-1}]	7.8
F(000)	816
Θ range [°]	2.28−25.60
T [K]	193
Reflections, collected	10392
Independent reflections	5972
Data/restraints/parameters	5972/0/548
Goodness-of-fit on F^2	0.948
Final *R* indices [$I > 2\sigma(I)$]	$R1$ = 0.0249, $wR2$ = 0.0571
R indices (all data)	$R1$ = 0.0337, $wR2$ = 0.0588
Largest diff peak and hole [e Å^{-3}]	+0.53; −0.62

The data were measured with a STOE IPDS[18] using graphite-monochromated Mo-K_α radiation (λ = 0.71073 Å). A decay correction using the program DECAY[19] was applied. The structure was solved by direct methods[20], completed by subsequent difference Fourier syntheses, and refined by full-matrix least-squares procedures[21]. Final cycles of refinement converged at $R1 = \Sigma(\|F_o| -$

$||F_c||)/\Sigma|F_o| = 0.0249$ and $wR2 = [\Sigma w(F_o^2 - F_c^2)^2/\Sigma w(F_o^2)^2]^{1/2} = 0.0571$ for 4931 observed reflections [$I > 2\sigma(I)$]. All non-hydrogen atoms were refined with anisotropic displacement coefficients. All hydrogen atom positions were found in the difference map calculated from the model containing all non-hydrogen atoms. The hydrogen positions were refined with individual isotropic temperature parameters. Crystallographic data (excluding structure factors) for the structures reported in this paper have been deposited with the Cambridge Crystallographic Data Centre (CCDC-101416). Copies of the data can be obtained free of charge on application to CCDC, 12 Union Road, Cambridge CB2 1EZ, UK [Fax: (internat.) + 44-1223/336-033, E-mail: deposit@ccdc.cam.ac.uk].

[1] [1a] R. Taube in *Applied Homogeneous Catalysis with Organometallic Compounds* (Eds.: B. Cornils, W. A. Herrmann), Verlag Chemie, Weinheim, **1996**, vol. 1, pp. 507. – [1b] D. Steinborn, R. Taube, *Z. Chem.* **1986**, *26*, 349–359. – [1c] J.-J. Brunet, D. Neibecker, F. J. Niedercorn, *J. Mol. Catal.* **1989**, *49*, 235–259. – [1d] E. Krukowka, R. Taube, D. Steinborn, DD 296 909 A5 (10. 11. 88), **1988**; *Chem. Abstr.* **1992**, *116*, 213993b. – [1e] J.-J. Brunet, *Gazz. Chim. Ital.* **1997**, *127*, 111–118.

[2] [2a] E. Krukowka, Dissertation, TH Merseburg, **1985**. – [2b] R. Taube, Arbeits- und Ergebnisbericht **1992/1993/1994** des SFB 347 (Universität Würzburg): *Selektive Reaktionen Metall-aktivierter Moleküle*, p. 573.

[3] C. Hahn, J. Sieler, R. Taube, *Chem. Ber.* **1997**, *130*, 393–345.

[4] C. Hahn, A. Vitagliano, F. Giordano, R. Taube, *Organometallics* **1998**, *17*, 2060–2066.

[5] J. Halpern, *Pure Appl. Chem.* **1983**, *55,* 99–106.

[6] D. Milstein, *Acc. Chem. Res.* **1984**, *17*, 221–226.

[7] [7a] W. Keim, *J. Organomet. Chem.* **1968**, *14*, 179–184. – [7b] C. S. Cundy, M. F. Lappert, R. Pearce, *J. Organomet. Chem.* **1973**, *59*, 161–166.

[8] [8a] L. Dahlenburg, C. Prengel, *Organometallics* **1984**, *3*, 934–936. – [8b] L. Dahlenburg, C. Prengel, *J. Organomet. Chem.* **1983**, 241, 27–36.

[9] C. Hahn, J. Sieler, R. Taube, *Polyhedron* **1998**, *17*, 1183–1193.

[10] F. Gorla, L. M. Venanzi, A. Albinati, *Organometallics* **1994**, *13*, 43–54.

[11] T. E. Nappler, D. W. Meek, R. M. Kirchner, J. A. Ibers, *J. Am. Chem. Soc*. **1973**, *95*, 4194–4210.

[12] J. A. Tiethof, J. L. Peterson, D. W. Meek, *Inorg. Chem.* **1976**, *15*, 1365–1370.

[13] G. Vasapollo, P. Giannoccaro, C. F. Nobile, A. Sacco, *Inorg. Chim. Acta* **1981**, *48*, 125–128.

[14] B. N. Storhoff, H. C. Lewis, *Coord. Chem. Rev.* **1977**, *23*, 1–29.

[15] M. Aresta, E. Quaranta, *Organometallics* **1993**, *12*, 2032–2043.

[16] A. L. Spek, "PLATON-92", *Acta Crystallogr., Sect. A* **1990**, *46*, C34.

[17] S. E. Boyd, L. D. Field, T. W. Hambley, *Organometallics* **1992**, *12*, 1720–1724.

[18] B. Lange, Z. J. Vejdelek, *Kolorimetrische Analyse*, Verlag Chemie, **1982**, p. 232.

[19] *IPDS Operating System Version 2.8. STOE&CIE. GmbH*, Darmstadt, Gemany, **1997**.

[20] A. Altomare, G. Cascarano, C. Giacovazzo, A. Guargliardi, M. C. Burla, G. Polidori, M. Camalli *SIR-92*, University of Bari, Italy, **1992**.

[21] G. M. Sheldrick *SHELXL-93*, in *Crystallographic Computing 3* (Eds.: G. M. Sheldrick, C. Krüger, R. Goddard), Oxford University Press, England, **1993**, pp. 175–189.

[98113]

Generation of Gas-Phase Ge, Sn, and Pb Cluster Anions from Various Sources and Comparison to Solid-State Analogues

Thomas F. Fässler*, Hans-Joachim Muhr, and Markus Hunziker

Laboratorium für Anorganische Chemie der Eidgenössischen Technischen Hochschule Zürich,
Universitätstr. 6, CH-8092 Zürich, Switzerland
Fax: (internat.) + 41-1/632-1149
E-mail: faessler@inorg.chem.ethz.ch

Received February 19, 1998

Keywords: Mass spectrometry / Clusters / Germanium / Tin / Lead

Time-of-flight mass-spectrometric investigations show that laser desorption leads to anionic, large clusters of the elements (E) Ge, Sn, and Pb without special gas-phase clustering conditions and additional ionization processes. Ion formation strongly depends on the nature of the starting materials used during desorption experiments. Cluster anions from pure elements E were observed with a maximum of 6 atoms and their relative intensities decreased exponentially with increasing cluster size. Larger clusters are observed if alkali metals (K, Rb, and Cs) are present. Binary phases of nominal composition K_4E_9, ethylenediamine solutions of these phases, and crystalline compounds containing well-defined cluster anions as in $[K([2.2.2]\text{-crypt})]_3E_9$ are used as sources for desorption experiments. The latter results in the formation of clusters of 11 (Ge), 15 (Sn), and 13 (Pb) E atoms. Under similar conditions cations are observed at much lower intensities and the maximum cluster size is 6. For E = Ge anions containing two different kinds of atoms KGe_n^- are observed with relatively high abundance for n = 5, 9, and 10; KGe_{11}^- and KGe_{13}^- are also detected. The results are compared to the formation of clusters in binary alloys. Analogies to structurally characterized Zintl ions E_n^{x-} (x = 2, 3, 4) are given. The enhanced formation of cluster anions during the laser desorption process in the presence of electropositive metals indicates a more general application for anion formation in the gas phase.

Introduction

The relationship between the stability of gas-phase clusters and Zintl ions is of considerable interest[1][2]. The remarkable feature of anions of group-14 elements E (E = Ge, Sn, Pb) is their distinct tendency towards *cluster* formation in the solid state, in solution, and in the gas phase. The earliest studies on soluble E_n clusters were reported more than 100 years ago[3]. The systematic work of Kraus, Smyth, and Zintl[4][5] proved the existence of polyanions, such as Pb_9^{4-} and Pb_7^{4-}. Since then, several homoatomic cluster anions − so-called *Zintl ions* − have been structurally characterized, most of them as their $[K([2.2.2]\text{crypt})]^+$ and $[Na([2.2.2]\text{crypt})]^+$ salts[6]: E_5^{2-}, E_9^{x-} (x = 3, 4), and Ge_{10}^{2-}. Sn_9^{4-} and Pb_9^{4-} clusters stabilized by $Cr(CO)_3$ have also been isolated (Figure 1)[7]. Interestingly, there is only one structural report of an octahedral group-14 species $[SnCr(CO)_5]_6^{2-}$ characterized as $[K([2.2.2]\text{crypt})]^+$ salt[8].

The enhanced stability of these anions can be understood using Wade's electron counting rules for clusters[9]. Deltahedral n-vertex clusters are stable with $2n + 2$, $2n + 4$ and $2n + 6$ skeletal electrons and form *closo*-, *nido*-, and *arachno*-type clusters, respectively. As a result, E_n^{x-} clusters which are build up from group-14 elements should be especially favored independent of cluster size with the same relatively low charges of −2, −4, and −6. Deltahedral *closo* structures were predicted for $n \leq 24$[10] and are known for boranes and caboranes for $4 \leq n \leq 12$.

Figure 1. Structurally characterized homoatomic deltahedra E_n with n = 4, 5, 6, 9, 10 vertices; nine-atom clusters occur with different electron counts and structures between the *closo* and *nido* type; octahedral clusters are only known with stabilizing organometallic ligands (for further details see text)

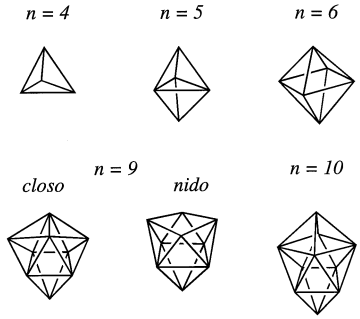

Several homoatomic clusters of the heavier group-14 elements were characterized by mass spectrometry. Under equilibrium conditions in Knudsen cell effusion, the abundance of tetrameric molecules is independent of the composition of the condensed starting material. Such precursors include binary to quaternary systems of group-14 to -16 elements, some of which also contain alkali metals[11]. The stability of these molecules correlates with their electron numbers (20 and 22 electrons) and hence with their possible structures (planar and tetrahedral)[12]. Cooling hot metal vapors using different techniques enables the production of larger cluster species and ultrasmall particles[1][13][14][15]. In

 © WILEY-VCH Verlag GmbH, D-69451 Weinheim, 1998 1434−1948/98/1010−1433 $ 17.50+.50/0

many cases electron bombardment or laser ionization generates positive cluster ions from neutral cluster beams. Positively and negatively charged cluster ions can be obtained by laser desorption[13] or injecting electrons from a biased filament[16]. Several mass-spectrometric investigations of larger group-13 to -16 clusters use the corresponding elements as ion sources. Gas-phase reaction and gas-aggregation techniques used for the binary systems Cs/Sn and Cs/Pb show intensity maxima for the molecules $Cs_3Sn_5^+$, $Cs_3Sn_9^+$, $Cs_5Sn_9^+$, and $Cs_3Pb_5^+$. Sn_{10}^+ is observed at low intensity. Larger clusters were not observed due to the limitation of the mass spectrometer[1].

The facile synthesis and isolation of molecular paramagnetic clusters E_9^{3-} in good yields[17] prompted us to investigate the gas-phase ion formation from samples that contain discrete cluster units. Here we report our time-of-flight (TOF) mass-spectrometric studies of $E_n^{+/-}$ ions (E = Ge, Sn, and Pb) generated by laser desorption in a commercially available TOF mass spectrometer. The generation of large, anionic clusters is achieved by laser desorption without gas-phase aggregation techniques.

In order to evaluate the dependency of the gas-phase cluster-ion formation on the ability of electron transfer and thus ion formation in the precursors, we investigated the following series of samples: pure elements (Ge, Pb); mixtures of the elements K and E = Ge, Pb; binary phases K_4E_9 (E = Ge, Sn, and Pb); ethylenediamine solutions of A_4E_9 (A = alkali metal, E = Ge, Sn, and Pb); $[K([2.2.2]crypt)]_3E_9$ salts containing isolated Zintl ions E_9^{3-} (E = Ge, Sn, and Pb).

Results

The resolution of the TOF spectrometer allows the identification of the isotopic distribution in the clusters up to a maximum cluster size of six atoms. As an example, the observed and simulated spectrum of Ge_4 is shown in Figure 2a, left where the five most abundant isotopes are used for the calculation (isotope mass, relative abundance: 69.9, 0.56; 71.9, 0.75; 72.9 ,0.21; 73.9, 1.00; 75.9, 0.21). Larger clusters appear as broader signals (Figure 2b, right). Typical mass spectra of the investigations are shown in Figures 3−5. The inserts show the mass spectra of delayed extraction. In Figures 3c and 4a higher mass regions are shown on enlarged intensity scales.

Figure 2. Comparison of the measured and simulated (lines) mass spectra of Ge_4 and Ge_{10}

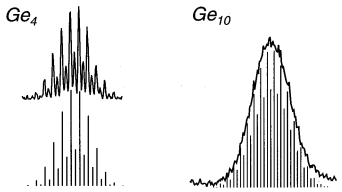

Pure Elements E = Ge, Pb

A typical spectrum of negatively charged Ge clusters generated by laser desorption from elemental germanium is shown in Figure 3a. All ion signals have the expected mass distribution due to the abundance of the different isotopes of Ge. The largest detected ion is a six-atom cluster. The relative intensities of the ion signals decrease exponentially with increasing cluster size. The relative intensities differ clearly from those recorded using vapor-phase condensation techniques. In these experiments cluster-size "magic numbers"[15][16][18] appear and a dependency of the cluster size distribution on the gas-aggregation technique is observed[14][19]. The size distribution for Ge and Pb cations are very similar, however, in the case of Pb also oxide formation Pb_3O_y with $y = 1-4$ is found.

Mixtures of K and E = Ge, Pb

If potassium is present during the laser evaporation process, the formation of larger anionic clusters occurs. The mass spectrum in Figure 3b reveals an exponential decay of the anion intensities from $n = 1$ to 6 for Ge. After a drop of relative intensity, larger clusters ($n = 7-10$) appear with similar intensities. An analogous spectrum is obtained with E = Pb (not shown). No mixed atom clusters KE_n^- are present. For E = Ge and Pb several oxide-containing anions are observed: Ge_2O^-, $Ge_2O_2^-$, $Ge_2O_3^-$, Ge_3O^-, $Ge_3O_2^-$, $Ge_3O_3^-$, $Ge_4O_2^-$ and the series $Pb_nO_{n+1}^-$ as well as $KPb_nO_{n+1}^-$ ($n = 2-6$) are predominant. The enhanced formation of oxides is probably caused by oxygen impurities in elemental potassium or partial oxidation of the surface of the samples during sample transfer to the mass spectrometer. Certainly, the alkali metal acts as an electron donor, and thus promotes the anion cluster formation in the plasma. Lead cation abundance using the mixture as source is similar to the mass distributions from pure metal sources.

Binary Phases of Nominal Composition "K_4E_9" (E = Ge, Sn, and Pb)

Recently, binary A/E = 4:9 phases have been structurally characterized for E = Ge and Sn and A = K, Rb, Cs[20]. They contain discrete E_9^{4-} cluster ions. In the case of E = Pb the existence of a 4:9 phase was discussed earlier[5]. The results of the desorption experiments are shown in Figure 3c for E = Ge. Clusters with maximum size $n = 13$ are observed. The ion signals of the homoatomic clusters Ge_n^- show a decay in intensity up to cluster size $n = 8$. The nine- and ten-atom clusters occur with similar intensities as the eight-atom cluster. Species containing 11 to 13 atoms are detected at lower relative intensities. The formation of mixed metal clusters KGe_n^- for $n = 5$, 9, and 10 is favored, accompained by ions with $n = 8$, 11, and 13 at lower intensities.

In the case of E = Sn and Pb, the anionic clusters occur with a stronger decay in relative intensity in the higher mass

Figure 3. Mass spectra of Ge_n^- clusters obtained from a) elemental Ge, b) mixture of K and Ge, c) K_4Ge_9, d) ethylenediamine extract of K_4Ge_9, and e) $[K([2.2.2]crypt)]_3Ge_9$, containing discrete Ge_9^{3-} clusters; inserts show spectra optimized for the higher mass regions (delayed extractions)

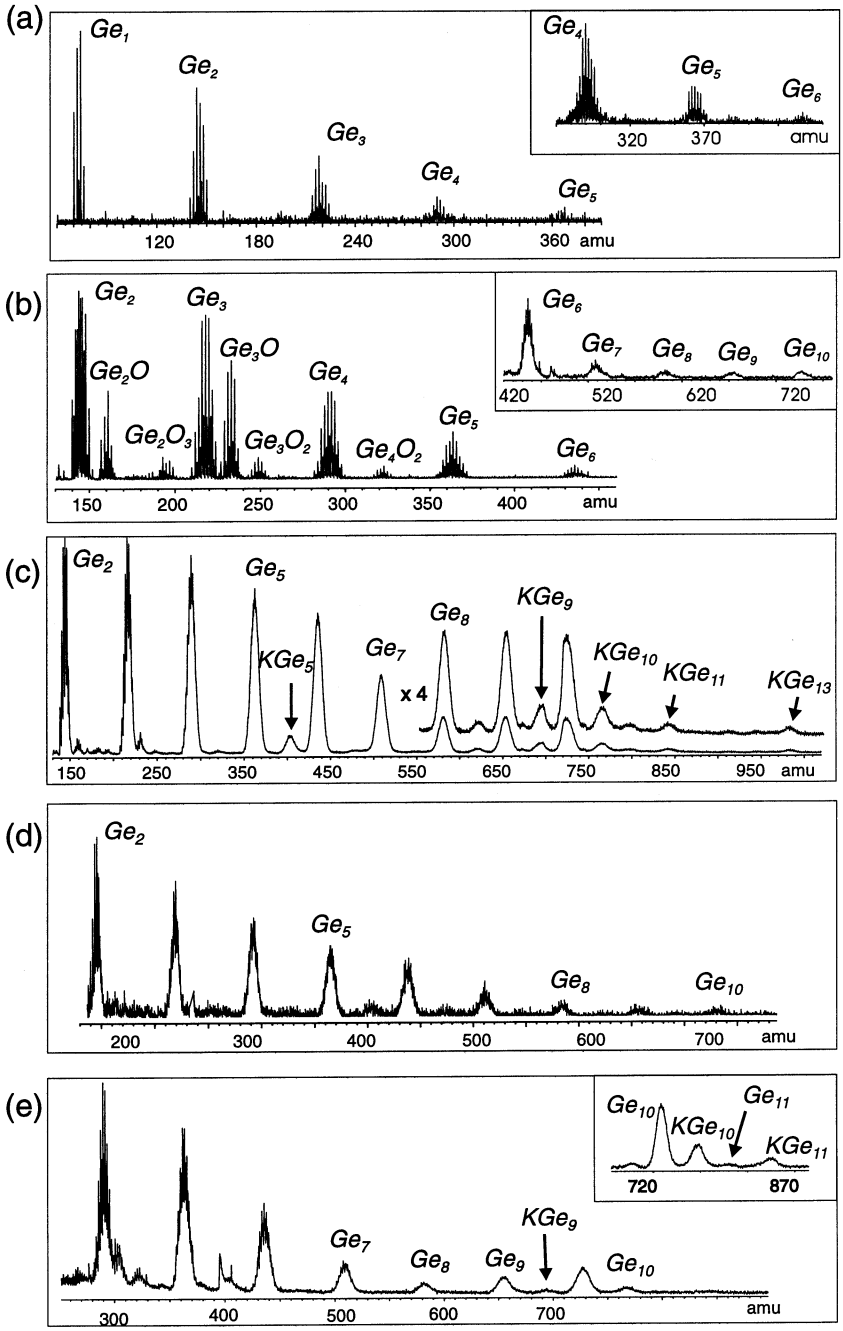

region and reach a maximum cluster size of 10 atoms. Mixed metal clusters KSn_n^- or KPb_n^- are absent but the anions $KSn_2O_3^-$, $KSn_3O_4^-$, KPb_9O^-, and $KPb_{10}O^-$ are present.

Ethylenediamine (en) Solutions of Phases of Nominal Composition "A_4E_9" (E = Ge, A = Na, K, Rb; E = Sn, Pb, A = K)

If phases of nominal composition Na_4E_9 (E = Ge, Sn) are dissolved in en, the crystalline product $[Na_4 \cdot x\ en]\ E_9$ ($x = 0-7$) can be isolated after slow evaporation of the solvent[21]. Using K instead of Na leads to products with similar compositions. The mass spectra of residues of en solutions of K_4Ge_9, K_4Sn_9, and K_4Pb_9 are shown in Figures 3d, 4a, and 5a, respectively. The spectra of the en solutions of Na_4Ge_9 (not shown), K_4Ge_9, Rb_4Ge_9 (not shown), and K_4Pb_9 reveal very similar mass distributions and relative intensities. E_n^- clusters are observed with an exponential decay of their intensities with increasing mass for $n \leq 10$. $NaGe_5^-$, KGe_5^-, KGe_6^-, $RbGe_5^-$, and $RbGe_{10}^-$ are also observed. In the lead system several oxides as dis-

cussed earlier are present. In K_4Sn_9 the occurrence of ion pairs Sn_n^- and Sn_n^- + 56 (±1) amu, corresponding to the mass of Sn_n and KSn_nO, respectively, is prominent. These peaks are present for $7 \leq n \leq 12$ (Figure 4a). Notice the high abundance of the $KSn_{11}O^-$ anion. For larger n the ternary ions show higher abundance than Sn_n^- anions.

Figure 4. Mass spectra of Sn_n^- clusters obtained from a) ethylenediamine extract of a solidified melt of nominal composition K_4Sn_9, and b) $[K([2.2.2]crypt)]_3Sn_9$, containing discrete Sn_9^{3-} clusters; for insert cf. caption of Figure 3

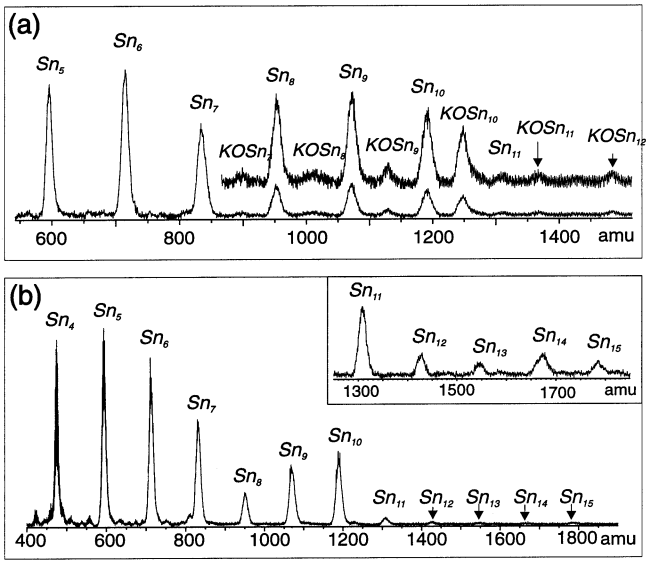

Figure 5. Mass spectra of Pb_n^- clusters obtained from a) ethylenediamine extract of a solidified melt of nominal composition K_4Pb_9, and b) $[K([2.2.2]crypt)]_3Pb_9$, containing discrete Pb_9^{3-} clusters; for inserts cf. caption of Figure 3

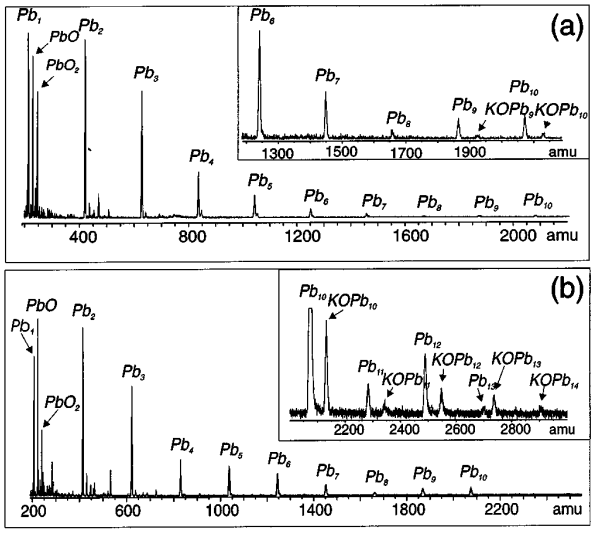

Compounds Containing E_9^{3-} Zintl Ions Separated by K-[2.2.2]crypt Units (E = Ge, Sn, Pb)

On use of the alkali-metal-sequestering reagent [2.2.2]crypt[6] crystalline compounds $[K-[2.2.2]crypt)]_3E_9$ containing discrete polyanions can be isolated from the en solutions of the A_4E_9 alloys[7][17]. Photodesorption and photoionization of these Ge, Sn, and Pb compounds leads to the formation of ions of size $1 \leq n \leq 11$ (Figure 3e), $1 \leq n \leq 15$ (Figure 4b), and $1 \leq n \leq 13$ (Figure 5b), respectively. An exceptional increase of abundance with respect to smaller clusters of cluster size $8 \leq n \leq 10$ is observed. The intriguing difference to the other experiments is the occurrence of larger clusters. For E = Ge the spectrum is very similar to that of "K_4Ge_9" (Figure 3c); however, mixed metal anions are less frequent. The same holds for E = Sn, where a very high abundance of E_{10} and the occurrence of a cluster series with $11 \leq n \leq 15$ at lower intensities is visible (Figure 4b). Desorption of the lead compound leads to a series of clusters $1 \leq n \leq 10$ with exponential decay of intensity (Figure 5b). The maximum size of Pb_n clusters is limited to $n = 13$. The higher mass region shows predominant peaks of ion pairs [Pb_n + 56 (±1) amu] as found in the case of Sn (Figure 4a), corresponding to the series KPb_nO^- with $n = 10-14$.

Discussion

We found that the relative abundance of ions depends strongly on the nature of the starting material used for the desorption process. The desorption conditions used in this investigation generate *cluster anions* from pure elements E with a maximum size of 6 atoms and display an exponential and monotone decrease of their relative intensities with increasing cluster size. In the case of E = Sn the results are consistent with a recent investigation using direct laser ablation of tin metal in an ICR cell[22]. We observe larger anionic clusters in the presence of alkali metals, e.g. from mixtures of the elements K/E, from phases of nominal composition K_4E_9, and from residues of ethylenediamine solutions of these phases. Clusters E_n with maximum size of 13, 12, and 10 atoms are found for E = Ge, Sn, and Pb, respectively. On use of compounds containing preformed E_9^{3-} clusters separated by large counterions $(K-[2.2.2]crypt)^+$, gas phase species with maximum sizes up to 15 E atoms are found (KGe_{11}^-, Sn_{15}^-, and $KOPb_{14}^-$). The general feature of the spectra is a decay of intensity as the number of constituent cluster atoms increases from one to seven and a minimum in intensity for clusters of eight atoms. Nine- and ten-atom clusters are found with similar or increased intensity relative to the abundance of eight-atom clusters. The increase of intensity of clusters with $n = 9$ and 10 are most pronounced in $[K-([2.2.2]crypt)]_3E_9$ as source. The maximum cluster size for *cations* is 6 atoms, however, much smaller intensities are measured.

The ion distributions do not correlate to photoelectron threshold energies and thus electron affinities of the E_n clusters, generated by other techniques. Higher values are ob-

served for $n = 5$ and 9 for Ge[23], 5 and 8 for Sn, and 5, 10, and 11 for Pb[18]. This is in contrast to the relative intensities observed in our experiments, where exponential decays with increasing size or intensity minima for $n = 8$ are found. Also, if electron affinity would dominate the occurrence of specific mass peaks in the spectra, a similar abundance of clusters should be found, independent of the sample used as starting material.

Conclusions and Comparison to Solid-State Analogues

Naked polyatomic ions of the type E_n^{x-} belong to the class of Zintl ions. Many of these ions cannot be described using classical electron counting rules such as the octet rule; thus, bonding models with electron delocalization (e.g. molecular orbital theory and related electron counting rules for clusters) are used for their electronic description. According to electron-counting rules for deltahedral clusters an *n*-vertex *closo*-deltahedron is stable if $n + 1$ skeletal orbitals are filled. As cluster size increases, a deviation from the expected number of electrons (or structures) is possible. Variable electron counts are especially observed for clusters of the heavier elements E, which have smaller HOMO-LUMO gaps[24]. Interestingly, ligand-free polyhedral clusters E_9 occur more frequently with additional electrons. E_9^{3-} and E_9^{4-} clusters with 21 and 22 skeletal electrons, respectively, possess deltahedral structures, albeit distorted and a compromise between tricapped trigonal prismatic (*closo*) and monocapped quadratic antiprismatic (*nido*)[7]. The E_n^- anions investigated here in the gas phase might correspond to $2n + 1$ skeletal electron clusters and might therefore also adopt to deltahedral structures. In other words the single-charged gas-phase anions might be regarded as *closo*-type clusters with a deficiency of one electron. Indeed, density functional studies on anionic Sn_n^- clusters confirm that the species adopt *closo* structures at the optimized minimum energies for $n = 5$, 6, and 7[22].

It has been pointed out earlier that clusters with one negative charge (e.g. E_n^-) are probably not stable in the solid state due to an inherent insufficient cation presence for anion separation[25]. Although no E_9^- species has been hitherto isolated from solution, the variability of electron numbers for these clusters makes the existence of singly charged ions with deltahedral structures more likely. Recent electrochemical investigations show that Ge_9^{3-} undergoes two pseudo reversible oxidative electron processes and therefore Ge_9^- might be a stable cluster. Oxidation of Sn_9^{3-} and Pb_9^{3-} in solution is possible, but is accompanied by an adsorption process making the interpretation more difficult[26]. Even more intriguing is the high abundance of KE_n^- ions. The formation of the mixed element clusters KGe_n^- for $n = 5$, 9, and 10 is predominant beside $n = 8$, 11, and 13 at lower intensities. Applying the *Zintl-Klemm-Busmann*[27] concept applicable to binary phases also to the KGe_n^- ions[1] – in other words transferring the valence electron from the more electropositive K atom to the element cluster – the doubly charged and according to Wades rules electron-precise Ge_n^{2-} Zintl ions result.

The exceptional occurrence of KGe_{13}^- and Sn_{15}^- anions attests to the possible existence of large Zintl ions. Remarkable is the fact that the counterion [K-[2.2.2]crypt]$^+$ is capable of good crystal packing also with very large anions such as C_{60}^{2-}[28]. However, large *n*-vertex polyhedra with $n > 10$ of the elements Ge and Sn are known only as structural units in three-dimensional anionic networks of Zintl phases. Pentagonal dodecahedra E_{20} which are centered by A atoms are found as linked building blocks in the Zintl phases A_4E_{22}[29] and $A_{6+x}E_{25}$[30].

In summary, we see a tendency for the formation of larger clusters, especially if preformed cluster units or electropositive elements are already present in the precursor. The latter point indicates a more general application for anion formation in plasmas. Owing to the possible variable electron counts of polyhedral clusters, the gas-phase monoanionic Zintl ions are in close relation to polyanions found in solution and in the solid state. Therefore these results suggest the possibility that large, discrete main-group clusters of Ge, Sn, and Pb may also exist in solution or in the solid state.

The authors like to thank Dr. *W. Amrein* for the use of the TOF mass spectrometer and the *Eidgenössische Technische Hochschule Zürich* for financial support.

Experimental Section

The elements Ge, Sn, Pb, and K, Na, Rb were purchased from Fluka and Aldrich and used without further purification. The syntheses of the binary phases, the ethylenediamine solutions of the latter, and the compounds [K-[2.2.2]crypt]$_3E_9$ are described elsewhere[17]. The mixtures of the elements K/E were prepared in an argon-filled dry-box by stirring the corresponding group-14 element with a slight excess (by weight) of molten alkali metal at 200°C. The solid samples were pressed in a recess of a stainless steel target of 3 mm in diameter. The ethylenediamine solutions of the binary A_4E_9 phases, as well as the acetonitrile solutions of [K-[2.2.2]crypt]E_9 salts were transferred to the target in an argon-filled dry-box and the solvent was subsequently removed under vacuum. During the transfer of the targets into the mass spectrometer, the samples were briefly exposed to air (approx. 5–10 s).

The mass analysis was carried out with a reflector time-of-flight (RETOF) mass spectrometer (Bruker Reflex™). Desorption and ionization of the clusters were achieved in a single step with a pulsed N_2 laser (337 nm, 3.7 eV, pulse duration: 3 ns; pulse frequency: 3–5 Hz) operating at a maximum pulse energy of 0.1 mJ. The spectra shown here are accumulations of 20–50 laser shots at acceleration voltages ranging from 7–15 kV in the negative ion mode. For each accumulation the laser power is adjusted slightly above the threshold level for detection of ion signals by the use of a variable attenuator. In order to enhance the intensity and resolution of ions with masses greater than 600 amu, ions of lower masses, i.e. shorter flight times, are ejected by applying an electric field between the two deflection plates by a rectangular signal triggered by the pulsed laser (delayed extraction). We like to emphasize that no special clustering conditions (e.g. gas expansion) are used for the generation of the clusters.

[1] T. P. Martin, *Angew. Chem.* **1986**, *98*, 197; *Angew. Chem., Int. Ed. Engl.* **1986**, *25*, 197.
[2] D. Schild, R. Pflaum, K. Sattler, E. Recknagel, *J. Phys. Chem.* **1987**, *91*, 2649; D. Schild, R. Pflaum, G. Riefer, E. Recknagel, *Z. Phys. D* **1989**, *12*, 235.
[3] A. Joannis, *C. R. Hebd. Seances Acad. Sci.* **1891**, *113*, 795.
[4] C. A. Kraus, *J. Am. Chem. Soc.* **1922**, *44*, 1216; F. H. Smyth, *J. Am. Chem. Soc.* **1917**, *39*, 1299; E. Zintl, J. Goubenau, W. Dullenkopf, *Z. Physikal. Chem.* **1931**, *A154*, 1.
[5] E. Zintl, A. Harder, *Z. Physikal. Chem.* **1931**, *154*, 47.
[6] crypt = [2.2.2]Cryptofix = 4,7,13,16,21,24-hexaoxa-1,10-diazobicyclo[8.8.8]hexacosane.
[7] For recent reviews see: J. D. Corbett, *Struct. Bonding* **1997**, *87*, 157; T. F. Fässler in *Metal Clusters in Chemistry* (Eds.: P. Braunstein, L. A. Oro, P. R. Raithby), Wiley-VCH Verlag, **1998**.
[8] B. Schiemenz, G. Huttner, *Angew. Chem.* **1993**, *105*, 295; *Angew. Chem. Int. Ed. Engl.* **1993**, *32*, 297.
[9] K. Wade, *Adv. Inorg. Chem. Radiochem.* **1976**, *18*, 1.
[10] L. D. Brown, W. N. Lipscomb, *Inorg. Chem.* **1977**, *16*, 2989.
[11] L. Poth, K. G. Weil, *Ber. Bunsenges. Phys. Chem.* **1992**, *96*, 1621; L. Poth, K. G. Weil, *J. Phys. Chem.* **1995**, *99*, 551; A. Hartmann, K. G. Weil, *Z. Phys. D* **1989**, *11*, 12; A. Hartmann, K. G. Weil, *Angew. Chem.* **1988**, *100*, 1111; *Angew. Chem. Int. Ed. Engl.* **1988**, *27*, 1091; A. Hartmann, K. G. Weil, *High Temp. Sci.* **1990**, *27*, 31.
[12] F. Hagelberg, S. Srinivas, N. Sahoo, T. P. Das, K. G. Weil, *Phys. Rev. A* **1996**, *53*, 353.
[13] K. LaiHing, R. G. Wheeler, W. L. Wilson, M. A. Duncan, *J. Chem. Phys.* **1987**, *87*, 3401; K. F. Willey, K. LaiHang, T. G. Taylor, M. A. Duncan, *J. Phys. Chem.* **1993**, *97*, 7435.
[14] T. P. Martin, H. Schaber, *J. Chem. Phys.* **1985**, *83*, 855.
[15] K. Sattler, J. Mühlebach, O. Echt, P. Pfau, E. Recknagel, *Phys. Rev. Lett.* **1981**, *47*, 160; J. Mühlebach, P. Pfau, K. Sattler, E. Recknagel, *Z. Phys. B − Condensed Matter* **1982**, *47*, 233; Y. Liu, Q.-L. Zhang, F. K. Tittel, R. F. Curl, R. E. Smalley, *J. Chem. Phys.* **1986**, *85*, 7434; J. R. Heath, Y. Liu, S. C. O′Brien, Q.-L. Zhang, R. F. Curl, F. K. Tittel, R. E. Smalley, *J. Chem. Phys.* **1986**, *83*, 5520.
[16] K. M. McHugh, H. W. Sarkas, J. G. Eaton, C. R. Westgate, K. H. Bowen, *Z. Phys. D* **1989**, *12*, 3.
[17] T. F. Fässler, M. Hunziker, *Inorg. Chem.* **1994**, *33*, 5380; T. F. Fässler, M. Hunziker, *Z. Anorg. Allg. Chem.* **1996**, *622*, 837.
[18] G. Ganteför, M. Gausa, K. H. Meiwes-Broer, H. O. Lutz, *Z. Phys. D* **1989**, *12*, 405.
[19] W. Schulze, B. Winter, I. Goldenfeld, *J. Chem. Phys.* **1987**, *87*, 2402.
[20] V. Queneau, S. C. Sevov, *Angew. Chem.* **1997**, *109*, 1818; *Angew. Chem. Int. Ed. Engl.* **1997**, *36*, 1754; H. G. von Schnering, M. Baitinger, U. Bolle, W. Carrillo-Cabrera, J. Curda, Y. Grin, F. Heinemann, J. Llanos, K. Peters, A. Schmeding, M. Somer, *Z. Anorg. Allg. Chem.* **1997**, *623*, 1037; V. Quéneau, S. C. Sevov, *Inorg. Chem.* **1998**, *37*, 1358.
[21] L. Diehl, K. Khodadadeh, D. Kummer, J. Strähle, *Chem. Ber.* **1976**, *109*, 3404; L. Diehl, K. Khodadedeh, D. Kummer, J. Strähle, *Z. Naturforsch.* **1976**, *31b*, 522; D. Kummer, L. Diehl, *Angew. Chem.* **1970**, *82*, 881; *Angew. Chem. Int. Ed. Engl.* **1970**, *9*, 895.
[22] P. Jackson, I. G. Dance, K. J. Fisher, G. D. Willett, G. E. Gadd, *Int. J. Mass Spec. Ion Processes* **1996**, *157/158*, 329.
[23] O. Chesnovsky, S. H. Yang, C. L. Pettiette, M. J. Craycraft, Y. Liu, R. E. Smalley, *Chem. Phys. Lett.* **1987**, *138*, 119.
[24] Variable electron counts are also possible for transition-metal carbonyl clusters containing bridging main-group elements. They show reversible oxidation and reduction processes: B. Eber, D. Buchholz, G. Huttner, T. F. Fässler, W. Imhof, M. Fritz, J. C. Jochims, J. C. Daran, Y. Jeannin, *J. Organomet. Chem.* **1991**, *401*, 49.
[25] J. D. Corbett, S. C. Sevov, *Z. Phys.* **1993**, *26*, 64.
[26] T. F. Fässler, Habilitation Thesis, ETH Zürich, **1997**.
[27] E. Busmann, *Z. Anorg. Allg. Chem.* **1961**, *313*, 90. W. Klemm, *Proc. Chem. Soc. London* **1959**, 329; E. Zintl, *Angew. Chem.* **1939**, *52*, 1.
[28] T. F. Fässler, A. Spiekermann, M. Spahr, R. Nesper, *Angew. Chem.* **1997**, *109*, 502; *Angew. Chem. Int. Ed. Engl.* **1997**, *36*, 486.
[29] The composition of the clathrate-I type was corrected from A_4E_{23} to $A_4E_{22}\square_1$ (E = Si, Ge; $\square$ = vacancy). Each vacancy creates four three-bonded atoms per 22 remaining E atoms; thus, these phases are also "electron-precise" *Zintl* phases ($[A^+]_4[E_{22}]^{4-}\square$): J. S. Kasper, P. Hagenmuller, M. Pouchard, C. Cros, *Science* **1965**, *150*, 1713; J. Gallmeier, H. Schäfer, A. Weiss, *Z. Naturforsch.* **1969**, *24b*, 655; H. G. von Schnering, *Nova Acta Leopoldina* **1985**, *59*, 168.
[30] R. Kröner, R. Nesper, H. G. von Schnering, *Z. Kristallogr.* **1988**, *182*, 164; J. Zhao, J. D. Corbett, *Inorg. Chem.* **1994**, *33*, 5721; T. F. Fässler, C. Kronseder, *Z. Anorg. Allg. Chem.* **1998**, *624*, 561; T. F. Fässler, *Z. Anorg. Allg. Chem.* **1998**, *624*, 569.
[98037]

New Synthetic Routes to Hydrotalcite-Like Compounds − Characterisation and Properties of the Obtained Materials

Umberto Costantino*, Fabio Marmottini, Morena Nocchetti, and Riccardo Vivani

Dipartimento di Chimica, Università di Perugia,
Via Elce di Sotto 8, I-06123 Perugia, Italy
Fax: (internat.) + 39(0)75/5855566
E-mail: ucost@unipg.it

Received March 18, 1998

Keywords: Layered double hydroxides / Hydrotalcite-like compounds / Magnesium / Aluminium / Intercalation

Hydrotalcite-like anionic clays of general formula $[M(II)_{1-x}M(III)_x(OH)_2]^{x+}[CO_3^{2-}{}_{x/2}]^{x-} \cdot m\ H_2O$ with M(III) = Al and M(II) = Mg, Ni, Zn have been prepared by precipitation of the hydroxycarbonates from the "homogeneous" solution after the thermally induced hydrolysis of urea. The effect of the temperature of precipitation, of the total metal cations concentration, of the molar fraction M(III)/M(III) + M(II) and of the molar fraction urea/M(II) + M(III) in solution on the composition and on the crystallinity degree of the samples has been investigated. The optimum conditions are reported to obtain micro-crystalline powders with a narrow distribution of particle size in a short time with a simple procedure. The compounds obtained have been characterised for chemical composition, thermal behaviour, particle-size distribution and BET-surface area. In addition, the crystal structure of $Mg_{0.67}Al_{0.33}(OH)_2\ (CO_3)_{0.165} \cdot 0.4\ H_2O$ has been refined by X-ray diffraction powder methods. The carbonate form has been converted into the chloride form by letting gaseous HCl flow over the hydrotalcite-like compounds, heated at 150 °C. The exchange of Cl^- anions with some alkoxide anions in the presence of the respective alkanols has been investigated. The exchange reaction was driven by the segregation of NaCl crystals poorly soluble in alkanols and led to the co-intercalation of the alkoxide ions together with the alkanol with the formation of a bi-layer of extended alkyl chain in the interlayer region of the Mg-Al hydrotalcite. The intercalation compound, washed with water, produces a hydrotalcite with Cl^- and OH^- as balancing anions.

Hydrotalcite-like compounds (HTlc) form, at present, a large class of inorganic materials, extensively studied as catalysts, precursors and supports of catalysts, anionic exchangers, sorbents, additives[1][2][3][4][5]. Furthermore, the HTlc are, practically, the only known family of layered solids with positively charged layers and interlayered charge balancing anions that may be replaced by ion-exchange processes. The structure of HTlc originates from the packing of layers built up in a manner similar to that found in brucite, the naturally occurring $Mg(OH)_2$. In this mineral, the Mg atoms are octahedrally co-ordinated by six oxygen atoms belonging to six OH groups; each OH group is, in turn, shared by three octahedral cations and points to the interlayer space[6]. When some of the Mg(II) cations are isomorphously replaced by Al(III) cations, carbonate anions are inserted between the metal hydroxide sheets to maintain the electroneutrality and the mineral hydrotalcite, with ideal formula $Mg_6Al_2(OH)_{16}CO_3 \cdot 4H_2O$, is obtained[7]. Hydrotalcite and hydrotalcite-like minerals are rare in nature but it is relatively simple and cheap to prepare these compounds on a laboratory scale.

The general formula of synthetic HTlc is often written as $[M(II)_{1-x}M(III)_x(OH)_2]^{x+}[A^{n-}{}_{x/n}]^{x-} \cdot m$ S, where M(II) may be Mg, Zn, Co, Ni, Mn, etc.; M(III) may be Al, Cr, Fe, V, Co, etc.; A^{n-} is the charged compensating anion (CO_3^{2-}, SO_4^{2-}, Cl^-, NO_3^-, organic anions, etc.); m the number of mols of co-intercalated solvent (S), generally water, per formula weight of compound. The number of mols x of M(III) cation per formula weight of compound, generally ranges between 0.2 and 0.33, and its value determines the charge density of the layer[3][4].

Most of the synthetic HTlc are prepared by co-precipitation of the chosen M(II) and M(III) hydroxides with diluted NaOH and/or $NaHCO_3$ or Na_2CO_3 solutions. Poorly crystalline samples are generally obtained, unless a low degree of supersaturation and a relatively high temperature are maintained during precipitation. However, to obtain well-crystallised samples a hydrothermal treatment, i.e. digestion of the gel at 180−200 °C under pressure, is often required[1][4]. In an attempt to prepare HTlc with a good degree of crystallinity using simpler methods, we turned our attention to methods known as precipitation from "homogeneous" solutions and found that the hydrolysis of urea in the presence of a mixture of M(II) and M(III) salts leads to the formation of HTlc with good crystallinity degree and a narrow distribution of particle size. This result is rather surprising since research papers and quantitative analysis textbooks[8][9] recommend the urea method for precipitating aluminium in the presence of magnesium.

This paper describes the preparative conditions of some HTlc anionic clays by the urea method, the physico-chemical characterisation of the products thereby obtained, and the preparation of some intercalation compounds with alkoxides. In addition, a novel method to convert the carbon-

 © WILEY-VCH Verlag GmbH, D-69451 Weinheim, 1998 1434−1948/98/1010−1439 $ 17.50+.50/0

ate form of HTlc into the chloride form, by gas-solid reaction is reported.

Results

Preparation of the Hydrotalcite-Like Compounds

Urea has a number of properties that makes its use as an agent for precipitation from "homogeneous" solution very attractive and it has long been used in gravimetric analysis to precipitate several metal ions as hydroxides or as insoluble salts when in the presence of a suitable anion[9]. Urea is a very weak Brønsted base (pK_b = 13.8), highly soluble in water, and its hydrolysis rate may be easily controlled by controlling the temperature of the reaction. According to Shaw and Bordeaux[10] the mechanism of hydrolysis consists of the formation of ammonium cyanate, as the rate-determining step, and the fast hydrolysis of the cyanate to ammoniun carbonate, i.e.:

$$CO(NH_2)_2 \rightarrow NH_4CNO$$
$$NH_4CNO + 2H_2O \rightarrow (NH_4)_2CO_3$$

The rate constant increases by about 200 times when the temperature is increased from 60 to 100°C. The hydrolysis of ammonium to ammonia and carbonate to hydrogen carbonate gives a pH of about 9, depending on the temperature. This pH is suitable for precipitating a large number of metal hydroxides.

After some preliminary positive tests, a wider investigation was undertaken to find the optimal conditions to produce, with a simple procedure, HTlc microcrystals of uniform size, well crystallised, and with the required stoichiometry. The following couples of cations, as chlorides, were considered: Mg(II)-Al(III); Zn(II)-Al(III); Ni(II)-Al(III). In the case of Zn(II), a weighed amount of ZnO was dissolved in a stoichiometric amount of 6 mol/dm^3 HCl solution.

Solid urea was added to 0.5 mol/dm^3 metal chloride solutions, having molar fraction M(III)/M(III) + M(II) equal to 0.33, until the molar ratio urea/M(II) + M(III) reached the value 3.3. The clear solutions were heated, under stirring, at temperatures between 60 and 100°C. As expected, longer precipitation times were observed for the lower temperatures. However, all the materials showed XRPD patterns typical of hydrotalcite-like compounds. A preliminary rough analysis of the variation of the crystallinity degree as a function of the precipitation temperature was made on the basis of the quality of the X-ray diffraction patterns of the samples, that is the number of reflections, their intensity and width at half-height. The results shown in Table 1 (see also Figure 1) indicate that hydrotalcite-like compounds with a good crystallinity degree were obtained in the 90−100°C temperature range after 24−36 h of precipitation.

Further characterisation was performed taking into account the preparation of the Mg-Al HTlc, maintaining the temperature at 100°C and the precipitation time at 36 h. Table 2 reports the composition, expressed as a molar fraction in the solid, X_{sol} = Al(III)/Al(III) + Mg(II), and the crystallinity degree of several samples, as a function of the total concentration of the cations, of their molar fraction in solution and of the urea/Al(III) + Mg(II) molar fraction. The data of Table 2 show that the variation of the indicated parameters does not markedly affect the crystallinity degree of the samples, even though the most crystalline samples were obtained at values of the urea/Al(III) + Mg(II) fraction close to 4 and at a value of the total metal ion concentration of 0.5 mol/dm^3. Temperature seems to be the most important parameter to control in order to produce well crystallised samples.

It is interesting to note that the molar fraction Al(III)/Al(III) + Mg(II) of the solids reaches values near to 0.32 even when the corresponding values in solution are as low as 0.2. As already discussed, the precipitation of the HTlc occurs at pH values of 8.5−9.0 (the hydrolysis pH of ammonium carbonate) and at these pH values the solubility of magnesium hydroxide is much higher than that of aluminium hydroxide. Therefore almost all the alluminium is co-precipitated with the magnesium ions to obtain a solid with the stoichiometry of two Mg(II) for each Al(III). This corresponds to an ideal disposition in the brucite-like sheet of each aluminium atom surrounded by six magnesium atoms. In general, the Al(III) molar fraction in the solid is higher than that in solution and it is possible to reach val-

Table 1. Effect of the temperature and time of precipitation on the crystallinity degree of the indicated HTlc's; conditions of precipitation: total metal ion concentration: 0.5 mol/dm^3; molar fraction M(III)/M(II) + M(III) = 0.33; molar fraction urea/M(II) + M(III) = 3.3

Precipitation		Crystallinity degree of the indicated HTlc[a]		
T [°C]	t [h]	Al-Mg	Al-Zn	Al-Ni
60	360	vl	vl	l
75	72	l	l	g
90	48	vg	vg	g
100	36	g	g	g

[a] g = good; l = low; v = very.

Figure 1. XRPD patterns of the Zn-Al-HTlc precipitated by urea hydrolysis at (a) 60°C, (b) 75°C, (c) 90°C, and (d) 100°C; the time of digestion is reported in Table 1

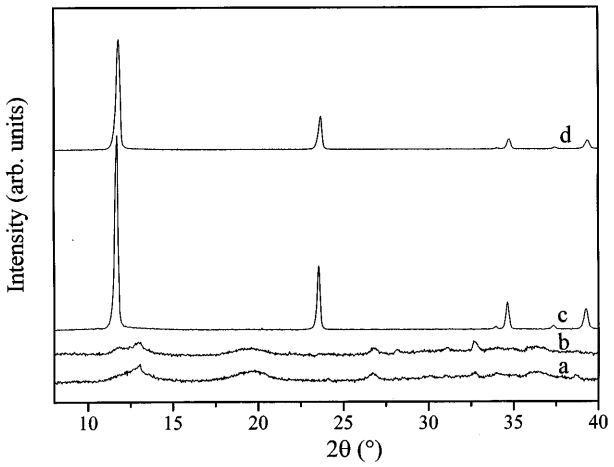

Table 2. Effect of the total metal ion concentration, of the molar fractions Al(III)/Al(III) + Mg(II) and urea/Al(III) + Mg(II) on the crystallinity degree and of the composition of Mg-Al-HTlc; temperature and precipitation time were 100°C and 36 h, respectively

	Solution		Solid		
Metal ion conc. [mol/dm^3]	Molar fraction Al(III)/Al(III)+Mg(II)	Molar fraction urea/Al(III)+Mg(II)	Molar fraction Al(III)/Al(III)+Mg(II)	Molar ratio CO_3^{2-}/Al(III)	Crystallinity degree[a]
0.1	0.33	3.3	0.36	–	l
0.5	0.20	4	0.32	–	fg
0.5	0.25	2	0.41	–	g
0.5	0.25	3.3	0.32	0.5	vg
0.5	0.25	4	0.34	0.49	m
0.5	0.33	2	0.38	–	g
0.5	0.33	3.3	0.34	0.5	vg
0.5	0.33	4	0.35	0.5	vg
0.5	0.33	6	0.36	0.5	m
0.5	0.40	4	0.40	0.48	vg
1	0.33	3.3	0.36	–	

[a] g = good; m = medium; l = low; f = fairly; v = very.

ues near to 0.44 value, indicated by Pausch et al.[11] as the maximum for a pure HTlc.

However, in order to prove the absence of co-precipitated $Al(OH)_3$ in the samples, the molar ratio CO_3^{2-}/Al^{3+} in the solid was determined. In all cases the molar ratio CO_3^{2-}/Al^{3+} in the solid was found to be near to 0.5 (see Table 2), as expected for pure HTlc and we may exclude the presence of co-precipitated aluminium hydroxide.

Therefore, the urea-method is not indicated for the preparation of Mg-Al HTlc with low charge density but allows the preparation of compounds with high charge density not easily obtainable with the other proposed procedures[4]. However, if the M(II) hydroxide is much more insoluble than the $Mg(OH)_2$, the HTlc obtained has a composition very near to that predicted from the composition of the solution. This is the case, for example, for the Zn-Al and Ni-Al systems. As may be seen from the data of Table 3 the Al molar ratio in the solid was found to be very near to that of the precipitating solutions.

Table 3. Effect of the metal ion concentration on the crystallinity degree and on the composition of Zn-Al-HTlc and Ni-Al-HTlc; conditions of precipitation: total metal ion concentration 0.5 mol/dm^3, molar fraction urea/M(II) + Al(III) = 3.3, temperature and time 100°C and 36 h

Molar fraction in solution Al(III)/Al(III) + M(II)	Molar fraction in the solid Al(III)/Al(III) + M(II)	Crystallinity degree[a]
M(II) = Zn		
0.20	0.23	g
0.25	0.28	g
0.33	0.35	vg
0.40	0.37	g
M(II) = Ni		
0.25	0.27	g
0.33	0.31	g

[a] g = good; v = very.

At the end of this investigation, we suggest the following simple procedure to obtain HTlc with a good crystallinity degree in a relatively short time. Solid urea is dissolved in a solution 0.5 mol/dm^3 in the chosen metal chlorides, [molar ratio M(III)/M(II) + M(III) equal to 0.33 M(III) = Al; M(II) = Mg or Ni or Zn], to reach urea/metal ions molar ratio of 3.3. The clear solution is maintained at 100°C, or even at the refluxing temperature, for 36 h. If the digestion time is prolonged, the crystallinity degree of the samples is slightly improved. The solids, separated from the solution, are washed with distilled water up to a negative test for chloride ions. Finally, they are air-dried and stored in a desiccator with P_4O_{10} at room temperature.

Physico-Chemical and Structural Characterisation

Empirical formula and water content were determined by thermoanalytical methods. Specific surface-area and particle-size distributions of selected samples were also measured. The crystallographic parameters of a well-crystallised Al-Mg HTlc were obtained from X-ray powder diffraction patterns.

Table 4 collects the data of composition, interlayer distance and B.E.T. specific surface area. The XRPD patterns of these samples are reported in Figure 2.

Table 4. Composition, interlayer distance and B.E.T. specific surface area for HTlc obtained by urea hydrolysis; conditions of precipitation: total metal ion concentration 0.5 mol/dm^3, molar ratio urea/M(II) + Al(III) = 3.3, temperature and time 100°C and 36 h

M(II)-M(III)-HTlc	Composition	d [Å]	Surface area [m^2/g]
Mg-Al	$[Mg_{0.67}Al_{0.33}(OH)_2](CO_3)_{0.165}\cdot 0.48\ H_2O$	7.57	24.1
Zn-Al	$[Zn_{0.65}Al_{0.35}(OH)_2](CO_3)_{0.175}\cdot 0.48\ H_2O$	7.55	24.9
Ni-Al	$[Ni_{0.69}Al_{0.31}(OH)_2](CO_3)_{0.155}\cdot 0.76\ H_2O$	7.98	47.4

Figure 3 shows the coupled TG-DTA curves of the Al-Mg and Al-Ni HTlc. The shape of the curves reflects the good crystallinity degree of the samples and, in both cases, the curves may be divided into two well-differentiated main regions. In the first one, ranging from 80 to 250°C there is a broad endothermic peak related to the dehydration of the

Figure 2. XRPD patterns of the HTlc obtained by urea hydrolysis: (a) $[Ni_{0.69}Al_{0.31}(OH)_2](CO_3)_{0.155}\cdot 0.76\ H_2O$; (b) $[Zn_{0.65}Al_{0.35}(OH)_2](CO_3)_{0.175}\cdot 0.48\ H_2O$; (c) $[Mg_{0.66}Al_{0.34}(OH)_2](CO_3)_{0.17}\cdot 0.48\ H_2O$; conditions of precipitation: total metal ion concentration 0.5 mol/dm^3, molar ratio urea/M(II) + Al(III) = 3.3, temperature and time 100°C and 36 h

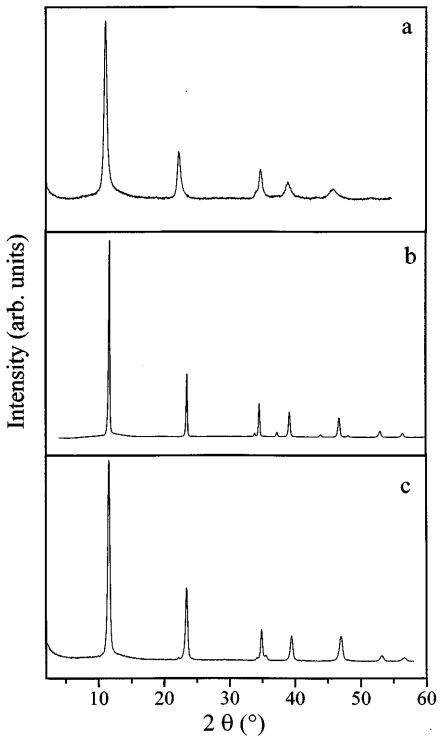

Figure 3. TG (solid line) and DTA (dashed line) curves of (a) Al-Mg-HTlc and (b) Al-Ni-HTlc previously equilibrated over P_4O_{10}; heating rate 5°C/min, air-flow 30 ml/min

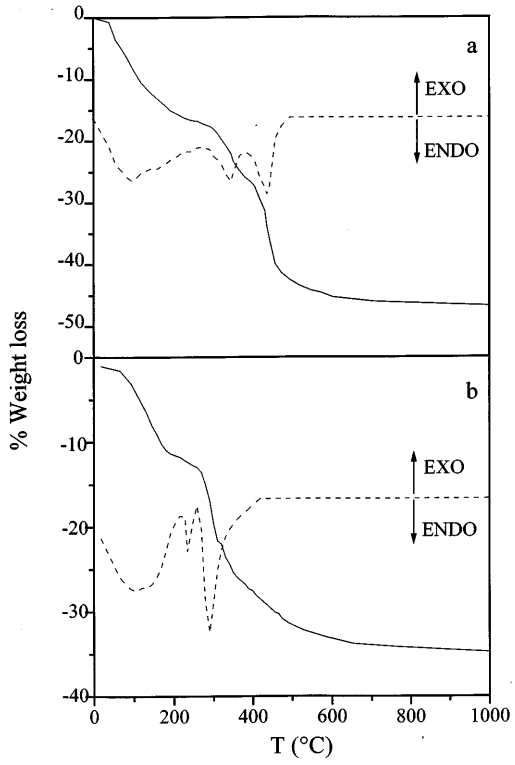

samples. The second region, corresponds to the weight loss due to the dehydroxylation and de-carbonation reactions, that, as discussed by Rey et al., overlap in this temperature range[12]. The XRD patterns of the samples heated at 1000°C show the typical reflections of MgO (or NiO) and of the $MgAlO_2$ (or $NiAlO_2$).

Figure 4 shows the cumulative particle-size distribution of the Mg-Al HTlc. It shows that more than 90% of particles have a diameter between 10 and 0.5 μm. The microcrystals are well formed and appear as hexagonal platelets, as shown in the SEM photograph (Figure 5).

Having at our disposition microcrystalline powders of good crystallinity degree, attempts were done to use the Rietveld method to refine the Al-Mg HTlc structure. Accurate positions of XRPD maxima were first determined by a peak-fitting procedure, using a pseudo Voigt function for the peak-profile description. The pattern was then indexed by the TREOR program[13] using the first 18 peaks. The parameters of the hexagonal cell found were a = 3.044 Å, c = 22.703 Å [$M(18)$ = 35] in good agreement with those already known[6]. All the reflection indexes followed the $-h + k + l = 3n$ rule, in agreement with the expected R-3m space group. The Rietveld refinement was then carried out by the GSAS program[14] using, as starting model, the structural parameters reported in ref.[7]. The refinement included a 5-terms Fourier cosine series function for the background and a modified pseudo Voigt peak-profile function. March-Dollase correction was employed to model

Figure 4. Population distribution as a function of equivalent spherical diameter for microcrystals of Al-Mg-HTlc

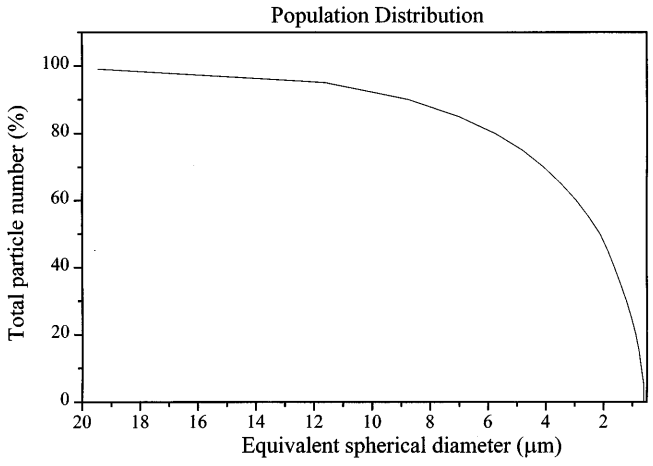

the preferred orientations. No corrections were made for absorption effects. The *003* reflection was not included in the refinement because of its strong asymmetry. When the refinement was stopped, the shifts in all the refined parameters were less than their estimated standard deviations, and the following residual values were reached: wRp = 8.7%; Rp = 6.6%; R_F = 4.4%. A difference Fourier map calculated at this stage, did not reveal any peak larger than 0.5 electron density units. The Rietveld plot is shown in Figure 6. The atomic parameters and main geometrical data ob-

Figure 5. SEM micrograph of Al-Mg-HTlc microcrystals

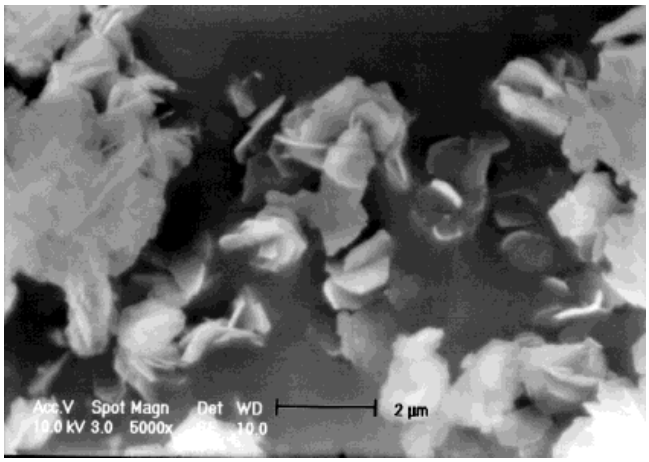

tained for $Mg_{0.67}Al_{0.33}(OH)_2$ $(CO_3)_{0.165}\cdot 0.4$ H_2O are reported in Tables 5, 6, and 7. They are in good agreement with those already published[7].

Figure 6. Experimental (+), calculated (−) and difference (lower) profiles for the $[Mg_{0.67}Al_{0.33}(OH)_2](CO_3)_{0.165}\cdot 0.4$ H_2O microcrystals

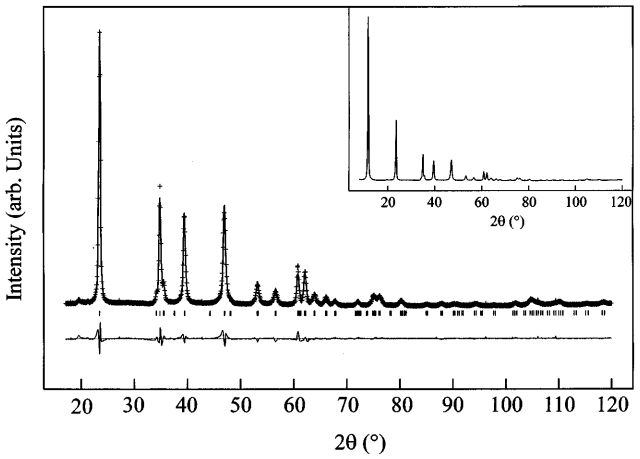

Table 5. Crystallographic data for $[Mg_{0.67}Al_{0.33}(OH)_2](CO_3)_{0.165}\cdot 0.48$ H_2O

Formula	$Mg_{0.67}Al_{0.33}O_{2.975}C_{0.165}H_{2.96}$
Formula weight	234.7
Crystal system	trigonal
Space group	*R*-3*m*
a [Å]	3.04535(9)
b [Å]	3.04535(9)
c [Å]	22.7010(13)
α [°]	90
β [°]	90
γ [°]	120
V [Å^3]	182.327(13)
Z	3
$d_{calcd.}$ [g/cm^3]	2.137
R_{wp}	0.1037
R_p	0.0798
R_F	0.0556
χ	3.51

Chemical Reactivity

A large research program, involving the ion-exchange properties, the interlayer reactivity, the storage in the interlayer region and subsequent release of species of pharmacological and biological interest has been undertaken to study the chemical reactivity of the HTlc, prepared by the urea method. Here we report new methods to convert the HTlc in the Cl^- and OH^- forms. These exchanged forms are commonly considered[4] the best precursors to intercalate other charged and neutral species even of large dimensions.

The carbonate anions fit well in the hexagonal arrangement of the hydroxy ions of the brucite-like sheets, and this accounts for their high affinity for HTlc[1]. The exchange of carbonate for others anions (Cl^-, NO_3^-, SO_4^{2-}) is then performed by treating the solid with diluted solutions of the corresponding mineral acid[15]. The exchange reaction is driven by the release of gaseous CO_2, but a concomitant slight dissolution of the solid can take place. To avoid these effects we used the gas-solid exchange reactions already employed to convert layered zirconium phosphate into some salt forms[16]. We passed a stream of water vapour and gaseous HCl through Mg-Al-CO_3 HTlc maintained at 140−160°C in a glass tube. At these temperatures Mg-Al-CO_3 HTlc has a very small CO_2 vapour pressure[17] and in the presence of hydrochloric acid the following reaction takes place:

$$Mg_{0.67}Al_{0.33}(OH)_2(CO_3)_{0.165} + 0.33\ HCl \rightarrow Mg_{0.67}Al_{0.33}(OH)_2Cl_{0.33} + 0.165\ CO_2 + 0.165\ H_2O$$

After preliminary positive tests, the procedure was optimised as follows: 1 g of Mg-Al CO_3 HTlc was heated at 150°C in a glass tube for one hour. A stream of N_2, passed through a 6 mol/dm^3 HCl solution at a flux of about 40 ml/min, was allowed to flow over the sample for 8 h. From time to time the presence of CO_2 was monitored by bubbling the escaping gas in barite solution. When the $Ba(OH)_2$ solution was clear, the heating was stopped and the sample recovered. Ion-chromatography analysis showed that the conversion was completed and the XRPD patterns (see Figure 7) showed that the material maintained a good crystallinity degree.

It is well known that Mg-Al HTlc may be obtained in the OH^- form taking advantage of the so-called "memory effect"[12]. According to this method, hydrotalcite in carbonate form is first heated to 400−450°C, the mixture of metal oxides thus obtained is then dispersed in water and reconstruction of the layered structure occurs, the positive charges being balanced by the OH^-. Alternatively, the chloride ions of Mg-Al-Cl HTlc may be replaced by hydroxide ions by equilibrating the solid with a diluted NaOH solution. A slight dissolution of the solid may also occur. However, in both cases a loss in crystallinity degree of the samples is observed.

Searching for methods that would lead to hydrotalcites in hydroxy form, in the cases in which they do not show the "memory effect" or when it is difficult to perform the ion exchange process in water, we considered the exchange of Cl^- for alkoxide ion in alkanol media. The alkoxide

Table 6. Positional and thermal parameters for $[Mg_{0.67}Al_{0.33}(OH)_2](CO_3)_{0.165}\cdot 0.48\ H_2O$

Name	*x/a*	*y/b*	*z/c*	100 U_{iso} [Å^2][a]	Occupancy
Mg	0.0	0.0	0.0	1.37(6)	2/3
Al	0.0	0.0	0.0	1.37(6)	1/3
O(1)	0.0	0.0	0.37631(10)	2.66(9)	1
O(2)	0.1075(10)	−0.1075(10)	0.50034(48)	1.98(22)	1/6
C	1/3	2/3	0.5003(5)	5.3(11)	1/12
H(1)	0.0	0.0	0.4220(17)	8.2(13)	1
H(2)	1/3	2/3	0.5006(5)	8.2(13)	1/2

[a] U_{iso} = mean square displacement, $B_{iso} = 8\pi^2\ U_{iso}$.

Table 7. Selected interatomic distances and angles for $[Mg_{0.67}Al_{0.33}(OH)_2](CO_3)_{0.165}\cdot 0.48\ H_2O$

Distances [Å]	
Mg,Al−O(1)	2.0107(11)
O(1)−O(1) across the layer	2.6264(34)
O(1)−O(2)	2.857(11)
C−O(2)	1.191(5)
Angles [°]	
O(1)−Mg,Al−O(1)	98.45(7)
O(1)−Mg,Al−O(1)	81.55(7)
O(2)−C−O(2)	119.980(27)

Figure 7. XRPD patterns of Mg-Al-Cl-HTlc obtained by streaming gaseous HCl through Mg-Al-CO_3-HTlc (a); the pattern of the parent compound is reported for comparison (b)

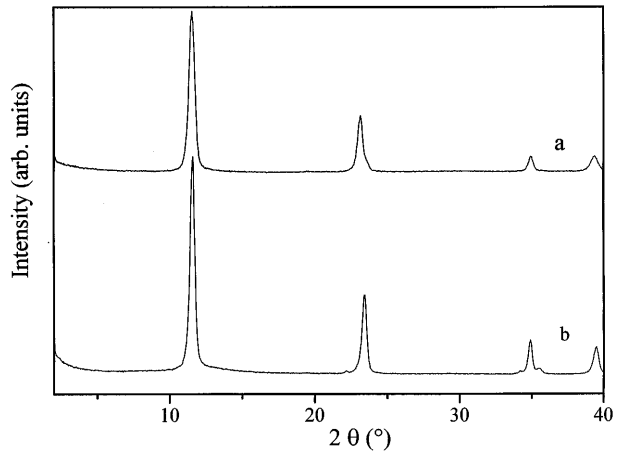

form, treated with water, would immediately give rise to the hydroxide form. Furthermore, it was of interest to see whether bases stronger than the OH^-, would be stabilised in the interlayer region of the hydrotalcites.

One gram of $Mg_{0.67}Al_{0.33}(OH)_2Cl_{0.33}$, prepared as above, and dehydrated at 150°C, was equilibrated in 100 cm^3 of ROH containing 0.1 mol/dm^3 of RONa (R = nC_3H_7, nC_4H_9, nC_5H_{11}, nC_6H_{13}) for two days at room temperature. The solid was separated from the solution by centrifuging under N_2. The equilibrating solution did not contain an appreciable amount of Cl^- ions as though the ion exchange process had not taken place. The XRPD patterns of the solid samples, still wet with the alkanol solution, showed indeed a large shift of the first diffraction maxima towards low angles, indicating that an intercalation process had occurred. Figure 8 shows the XRPD patterns of the sample treated with sodium butoxide in *n*-butanol. Two sharp reflections at 2Θ = 27.25° and 31.47°, typical of cubic NaCl, are present. The exchange Cl^-/RO^- has indeed occurred, driven by the segregation of NaCl crystals, insoluble in alkanols.

Figure 8. XRPD patterns of the Mg-Al-Cl-HTlc equilibrated with 0.1 mol/dm^3 sodium butoxide in *n*-butanol; the peaks of NaCl microcrystals are marked by an asterisk

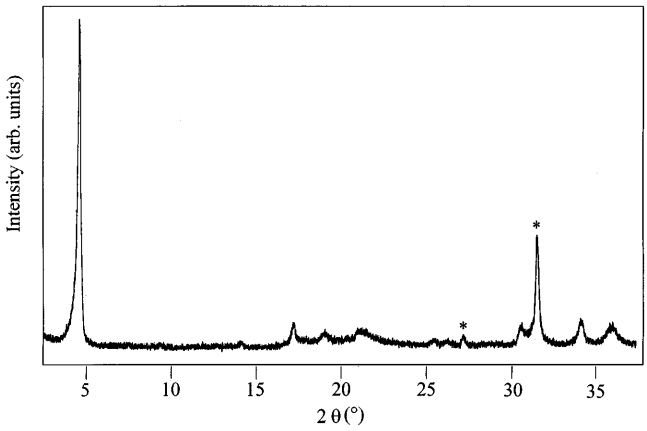

Figure 9 shows the interlayer distance of the alkoxide-exchanged HTlc as a function of the number of carbon atoms in the alkyl chain. Note that the intercept is close to the value of the interlayer distance of the compound in OH form, while the increment of the interlayer distance for each additional carbon atom, 2.3 Å/carbon atom, is consistent with the presence of a bi-layer of alkyl chain in the interlayer region. Since the cross-sectional area of a *trans-trans*-alkyl chains is estimated to be 18.6 Å[18] and the free area surrounding each positive charge on one side of the layer is 48 Å^2, the interpenetration of the alkyl chain of the alkoxide ions interacting with the two facing sides of the lamellae was expected to produce a monolayer similar to that depicted in Figure 10 and found in the intercalation of *n*-alkyl carboxylate anions[2]. The formation of the bi-layer may be explained by the fact that the Cl^-/RO^- exchange occurs in ROH media and that the alkanol molecules are co-intercalated to produce a bi-layer similar to the one shown in Figure 11. Treating the alkoxide-exchanged HTlc with water, we observed a partial washing of the NaCl crystals and a sudden increase of the pH of the washing solution. In the presence of water, the RO^- is readily transformed into the corresponding ROH and the OH^- assumes the role of bal-

ancing charge. No variation of the pH of the solution should occur. In the presence of Cl^- ions, however, some Cl^-/OH^- exchange takes place and the pH increases.

Figure 9. Interlayer distance of Mg-Al-HTlc exchanged with alkoxide ions in the presence of the corresponding *n*-alkanols as a function of the number of carbon atoms in the *n*-alkyl chain

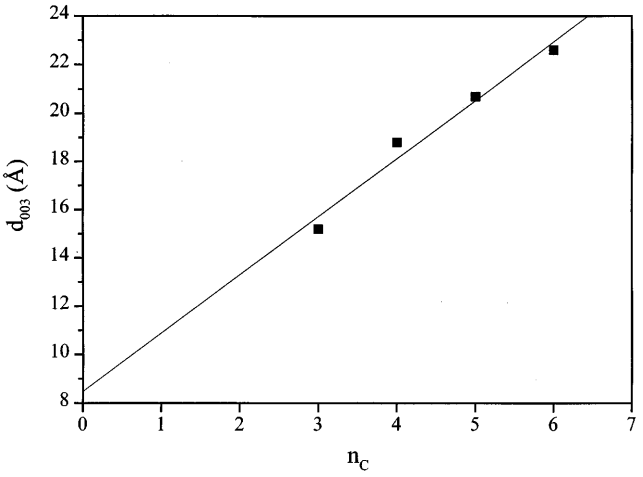

Figure 10. Schematic representation of a Mg-Al-HTlc intercalated with an interdigitate mono-layer of pentoxide anions

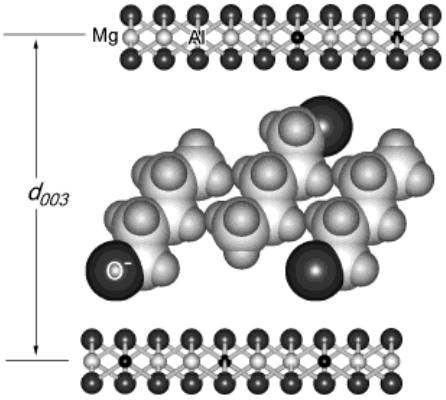

Figure 11. Schematic representation of a Mg-Al-HTlc intercalated with a bi-layer of pentoxide anions and pentanol molecules

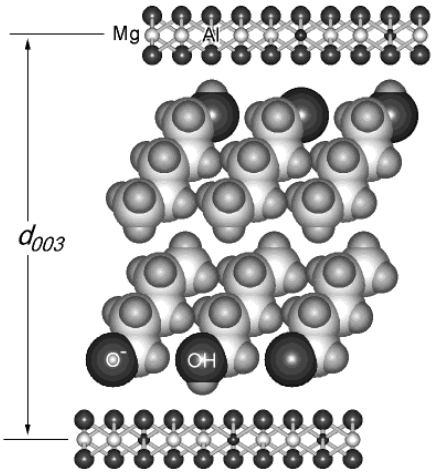

Conclusion

At present we do not know whether the urea method, proposed in this paper, to prepare HTlc has general applicability. Preliminary results indicate that the method also works well for the Mg-Fe-CO_3 and for the Al-Li-CO_3 HTlc. Some difficulties arise in the presence of cations such as Cr(III) or Cu(II). In such cases the method will require some modification and improvement. This is not surprising, if we agree with the concept already expressed by Riechle[1], that each layered double hydroxide requires its own procedure to be obtained in the best way. However, Mg-Al, Ni-Al and Zn-Al hydrotalcites have been obtained with the urea procedure and the materials have a high crystallinity degree and a narrow distribution of particle size. The high crystallinity degree has allowed the refinement of the structure with the Rietveld method.

A novel method to convert the carbonate into the chloride form, based on a gas-solid reaction has been proposed. Bases as strong as alkoxides were successfully intercalated. Further study is in progress to obtain the pure OH^- form, starting from alkoxide derivatives.

This work was supported by *M.U.R.S.T.* and *C.N.R.*

Experimental Section

Materials: All the reagents used were of analytical grade (C. Erba RPE-ACS). Alkoxides were prepared by a reaction of metallic sodium and the corresponding alkanol, previously dehydrated over CaO.

Analytical Procedures: To obtain the chemical composition of the HTlc, weighed amounts of the samples (ca. 100 mg) were dissolved in a few drops of concentrated HCl and diluted with water to 50 ml. The metal ion content of the latter solution was determined with standard EDTA titrations [Mg(II), Al(III), Ni(II), Zn(II)] and atomic absorption spectroscopy [Mg(II), Ni(II), Zn(II)]. The carbonate anion content of HTlc was obtained both with C elemental analysis and thermogravimetry. Anions, unlike carbonate, were determined by ion chromatography (DIONEX 2000 I/SP), after elution of the anion with 1 mol/dm^3 sodium carbonate solution. The water content was obtained by thermogravimetry.

Instrumentation: Coupled TG-DTG-DTA thermogravimetric curves were obtained with a Stanton-Redcroft STA 780 Analyzer at a heating rate of 5°C/min, under an air flow. − X-ray powder diffraction (XRPD) patterns were taken with a computer-controlled PW 1710 Philips diffractometer operating at 40 kV, 30 mA, using a PW 1820 goniometer, supplied with a bent graphite monochromator in the diffracted beam, and Cu-K_α radiation. XRPD patterns for indexing and structure refinement were taken with the step-scanning technique. The samples were prepared using the side-loading procedure in order to minimize preferred orientations. Diffractograms were collected from $2\Theta = 6$ to 120° using steps of 0.01° and a counting time of 20 s per step. − N_2 adsorption-desorption isotherms were taken by Sorptomatic 1800 supplied with an outgassing unit (C. Erba Strumentazione). − Particle-size distribution was obtained by means of an AccuSizer™ 770 Optical Particle Sizer, Santa Barbara, CA 93117, USA. − The scanning electron microscopy (SEM) photographs of the microcrystals were taken with a Philips XL30 apparatus.

[1] W. T. Reichle, *Solid State Ionics* **1986**, *22*, 135.
[2] M. Meyn, K. Beneke, G. Lagaly, *Inorg. Chem.* **1990**, *29,* 5201.
[3] A. de Roy, C. Forano, K. El Malki, J. P. Besse, in *Synthesis of Microporous Materials*; *Expanded Clays and Other Microporous Solids* (Ed.: M. L. Ocelli, H. E. Robson), vol. II, Van-Nostrand-Reinhold, New York **1992**, p. 108.
[4] F. Cavani, F. Trifirò, A. Vaccari, *Catal. Today* **1991**, *11*, 173.
[5] F. Trifirò, A. Vaccari, in *Comprehensive Supramolecular Chemistry* (Ed.: G. Alberti, T. Bein), vol. 7, Pergamon, Elsevier Science, Oxford, **1996**, chapter 8.
[6] H. R. Oswald, R. Asper, in *Physics and Chemistry of Materials with Layered Structures* (Ed.: R. M. A. Lieth), vol. 1, D. Reidel Publishing Company, Dordrecht, **1977**, p. 73.
[7] R. Allmann, *Chimia* **1970**, *24,* 99.
[8] H. H. Willard, N. Tang, *Ind. Eng. Chem.* **1937**, *9*, 357.
[9] A. I. Vogel, *Quantitative Inorganic Chemical Analysis*, 5th ed., Longman, Harlow, Essex, UK, **1989**, p. 424.
[10] W. H. R. Shaw, J. J. Bordeaux, *J. Am. Chem. Soc*. **1955**, *77*, 4729.
[11] I. Pausch, H. H. Lohse, K. Schürmann, R. Allmann, *Clay Clay Miner.* **1986**, *34*, 507.
[12] F. Rey, V. Fornès, *J. Chem. Soc., Faraday Trans.* **1992**, *88*, 2233.
[13] P. E. Werner, L. Eriksson, M. Westdhal, *J. Appl. Crystallogr.* **1985**, *18*, 367.
[14] A. C. Larson, R. B. Von Dreele, *Los Alamos National Laboratory Report*, No. LA-UR-86-748, **1987**.
[15] D. L. Bish, *Bull. Mineral*. **1980**, *103*, 170.
[16] A. Clearfield, J. M. Troup, *J. Phys. Chem*. **1970**, *74*, 314.
[17] J. Shen, J. M. Kobe, Yi Chen, J. A. Dumesic, *Langmuir* **1994**, *10*, 3902.
[18] A. I. Kitaigorodsky, *Molecular Crystals and Molecules*, Academic Press, New York, **1973**, chapter 1.

[98067]

Amino Acid Derivatives of Layered Zirconium Phosphates − α-Zirconium L-(+)-Serinephosphate and Zirconium L-(+)-Serinephosphate Phosphates

Umberto Costantino*, Morena Nocchetti, Fabio Marmottini, and Riccardo Vivani

Dipartimento di Chimica, Università di Perugia,
Via Elce di Sotto 8, I-06123 Perugia, Italy
Fax: (internat.) + 39-75/5855566
E-mail: ucost@unipg.it

Received April 20, 1998

Keywords: Layered compounds / Zirconium / Amino acids / Zirconium L-(+)-serinephosphates / Intercalation

A layered derivative of α-zirconium phosphate containing L-(+)-serine covalently attached to the inorganic layer has been prepared by allowing Zr fluoro complexes to decompose in the presence of L-(+)-phosphoserine. On the basis of thermogravimetric weight loss and C,H,N elemental analyses, the layered compound obtained has been formulated as $Zr[HOOCCH(NH_2)CH_2OPO_3]_2$. The X-ray powder diffraction pattern has been indexed with a monoclinic cell (a = 5.3737 Å, b = 9.3231 Å, c = 14.510 Å, β = 96.99°, Z = 2). FT-IR absorption spectra show that the serine groups attached to the inorganic layers are present as zwitterions. Thermal decomposition commences at ca. 250 °C and occurs in two steps: the first is due to a decarboxylation reaction, with the formation of the amino derivative $Zr(NH_2CH_2CH_2OPO_3)_2$, while the second is associated with pyrolysis of the organic moiety, leading to ZrP_2O_7. Despite the presence of the amino acid function in the interlayer region, the compound does not show intercalation ability towards cations or anions or polar species. However, compounds with a certain degree of microporosity and possessing ion-exchange and adsorption properties have been obtained by replacing some of the phosphoserine groups of the compound by HPO_4 groups, to produce the mixed layered derivatives $Zr[HOOCCH(NH_2)CH_2OPO_3]_{2-x}(HPO_4)_x$.

In 1978, Alberti and co-workers showed that it is possible to anchor organic functions to the layers of α-zirconium phosphate [α-$Zr(HOPO_3)_2$] by allowing fluorozirconium complexes to decompose in the presence of organophosphoric or -phosphonic acids[1]. As the complexing agent is slowly removed (i.e. as HF), layered zirconium organophosphates or -phosphonates of the general formulae $Zr(ROPO_3)_2$ or $Zr(RPO_3)_2$ (where R is the organic moiety) with structures similar to that of the inorganic analogue are obtained. This method has attracted the attention of many researchers since a large number of layered compounds with different properties and functionalities can be obtained simply by changing the nature of the R groups[2]. The sole limitation to synthesis is that only groups with a cross-section equal to or less than 24 $Å^2$ can be used, which corresponds to the free area around each POH group present on the surface of the layers of the parent α-$Zr(HOPO_3)_2$[3]. However, more voluminous groups may be attached to the α-layers if their dimensions are compensated for by introducing small groups R′ (e.g. H, OH, CH_3) so as to obtain compounds of the formula $Zr(RPO_3)_{2-x}(R'PO_3)_x$[4].

To date, many organic derivatives bearing different functional groups (alkyl, aryl, carboxylic acid, aldehydic, amino, etc.) and even macrocyclic ligands have been prepared and investigated[5][6][7][8][9]. However, only a few papers on layered derivatives bearing the amino acid function can be found in the literature[10][11], despite the fact this functional group is of interest with regard to its amphoteric character and in view of its ability to coordinatively bind transition metal ions.

We report herein on the results of an investigation of the layered compounds obtained by precipitating Zr^{IV} with L-(+)-phosphoserine or with a mixture of L-(+)-phosphoserine and phosphoric acid. The aim of the work was not only to prepare new derivatives incorporating the amino acid function but also to obtain new stationary phases for chiral recognition, by anchoring chiral groups to a stable and insoluble inorganic backbone.

Results

Preparation and Characterization of α-Zirconium L-(+)-Serinephosphate

Figure 1 shows a computer-generated model of the phosphoserine molecule. The cross-section, evaluated at the level of the amino acid group, is very near to 24 $Å^2$, the maximum permissible value for the preparation of stoichiometric zirconium organophosphates. However, before starting the synthetic procedures, experiments were carried out to assess the stability of the ester bond of phosphoserine in acidic media at 60°C, by recording ^{31}P-NMR spectra of such solutions at regular intervals. The hydrolysis of phosphoserine (0.2 M) in HCl (0.4 M) at this temperature was found to be a very slow process, the amount of phosphates in solution after 3 days accounting for less than 3% of the total phosphorus content (Figure 2). This result indicates that phosphoserine is sufficiently stable to be employed un-

 © WILEY-VCH Verlag GmbH, D-69451 Weinheim, 1998 1434−1948/98/1010−1447 $ 17.50+.50/0

der the synthesis conditions. Nevertheless, precipitates obtained following the procedure described in the experimental section, collected after 1−3 days, were found to contain increasing amounts of phosphates (from 5 to 10% of the total phosphorus content). In order to reduce the presence of phosphates in the precipitate, the rate of precipitation was increased by bubbling wet nitrogen into the reaction vessel. Under these conditions, the solid collected after 12 h did not contain appreciable amounts of phosphates. The X-ray powder diffraction (XRPD) pattern of the wet sample was almost identical to that of a sample dried over phosphorus pentoxide and further characterization was performed on the latter sample.

Figure 1. Ball-and-stick model of L-(+)-phosphoserine

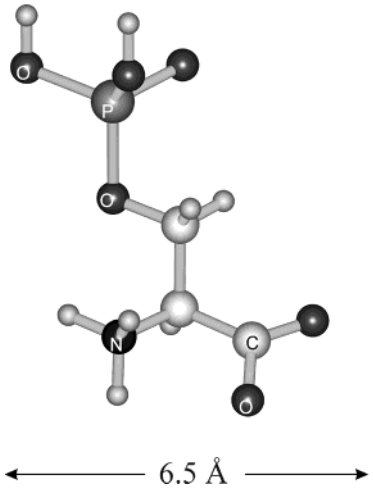

Figure 3 shows the thermogravimetric (TG) and differential thermal analysis (DTA) curves obtained at a heating rate of 5°C/min under oxygen. No appreciable loss is seen up to about 250°C, suggesting the absence of water of crystallization. Thermal decomposition starts at about 250°C and occurs in two steps. The first is very sharp and corresponds to the loss of 20% of the initial weight, while the second occurs over a much broader temperature range and leads to the formation of cubic ZrP_2O_7, as shown by the XRPD spectrum of a sample heated at 900°C. The total weight loss amounts to 42.1%, which is almost identical to that calculated (42.2%) for the following thermal decomposition:

$$Zr[HOOC-CH(NH_2)CH_2OPO_3]_2 + 5\ O_2 \rightarrow ZrP_2O_7 + 2\ NH_3 + 3\ H_2O + 6\ CO_2$$

Results of C,H,N elemental analyses were consistent to within 5% of the stoichiometry derived from TG data. Percentage weights calculated on the basis of the above formula and found values were: C 15.7, H 2.6, N 6.1, and C 15.2, H 2.8, N 5.8, respectively.

Figure 4 depicts the XRPD pattern obtained using the stepwise scanning procedure. The pattern was indexed, using the TREOR program[12], on the basis of a monoclinic cell with parameters a = 5.3737 Å, b = 9.3231 Å, c = 14.510 Å, β = 96.99°, $M(18)$ = 23, $F(18)$ = 30. Assuming

Figure 2. ^{31}P-NMR spectra of a sample of 0.2 M phosphoserine in 0.4 M HCl, using D_2O as solvent, maintained at 60°C for 30 min (spectrum a) and 3 d (spectrum b); peak labels are expressed in Hz

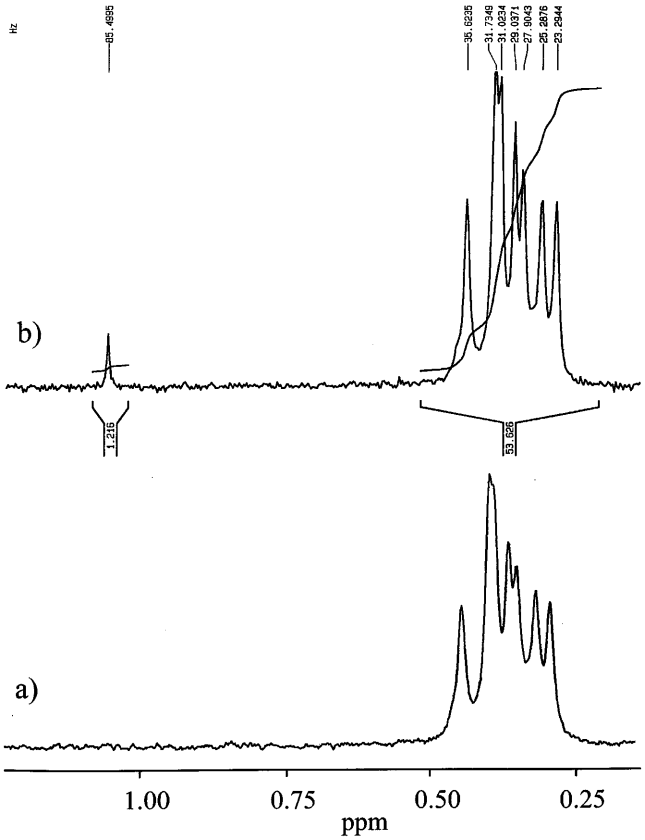

Figure 3. TG (solid line) and DTA (dotted line) curves of zirconium L-(+)-serinephosphate previously equilibrated over P_4O_{10}; heating rate 5°C/min, O_2 flow 30 ml/min

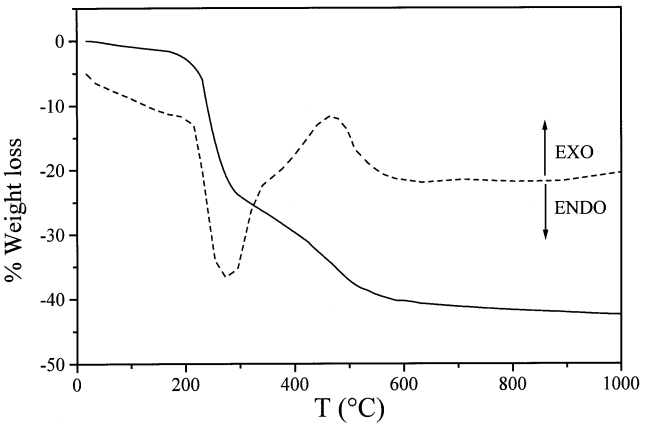

the presence of two formula weights in the unit cell volume (V = 721.5 Å^3), the calculated density (2.10 g cm^{-3}) is very near to the measured density (2.11 g cm^{-3}).

The XRPD pattern of the zirconium serinephosphate is typical of that of layered zirconium phosphate or phosphonates, with a strong first reflection (see Figure 4) corresponding to an interlayer distance (d) of 14.40 Å. Information about the type of layered structure can be obtained by determining the number (n) of moles of compound per

Figure 4. XRPD patterns of zirconium L-(+)-serinephosphate

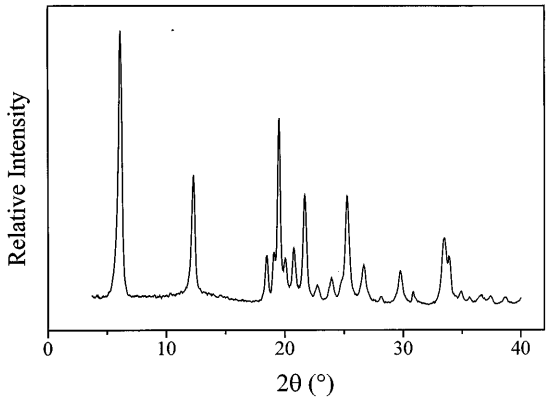

Figure 5. FT-IR absorption spectra of (a) L-(+)-phosphoserine, (b) zirconium L-(+)-serinephosphate

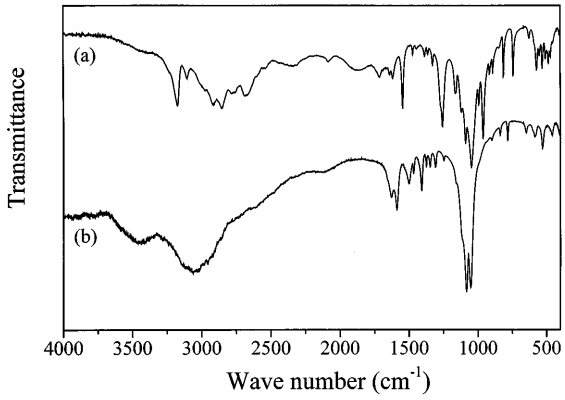

unit area of layer. This number is calculated from the ratio density × interlayer distance/formula weight, and is characteristic of the type of layer structure, being $6.8 \cdot 10^{-10}$ and $9.3 \cdot 10^{-10}$ mol cm^{-2} for the α- and γ-type compounds, respectively[13]. The *n* parameter of zirconium serinephosphate, calculated from the density of 2.11 g/cm^3, the interlayer distance of 14.40 Å, and the formula weight of 457.2 Da (from TG data), is $6.6 \cdot 10^{-10}$ mol cm^{-2}. This result is indicative of an α-type layer structure, where each layer consists of a planar arrangement of zirconium atoms bridged by the oxygen atoms of the phosphate groups, which are located alternatively above and below the zirconium plane. The *a* and *b* axes of the monoclinic cell lie in a plane parallel to the Zr atom plane and the area $a \times b/2$ corresponds to the free area around each phosphorus atom. This free area amounts to 25.1 Å^2, a value slightly higher than the 24 Å^2 typical for α-$Zr(HPO_4)_2$[3], probably because of the presence of the serine group bonded to the phosphate.

Further structural information was derived from a comparison of the IR absorption spectra of solid phosphoserine and zirconium serinephosphate (see Figure 5, spectra a and b, respectively). Both spectra show the typical bands of the protonated amino group and of the ionized carboxyl group. The region 1800−1300 cm^{-1} is particularly significant. The phosphoserine spectrum shows the typical amino acid I and II bands due to NH_3^+ deformations at 1640 and 1620 cm^{-1}, and the asymmetric stretching of the COO^- group at 1548 cm^{-1}. Furthermore, the absorption of the undissociated COOH group at 1717 cm^{-1} indicates that not all phosphoserine molecules are present as zwitterions. This absorption is absent in the zirconium serinephosphate spectrum (Figure 5, spectrum b). In addition, the I and II bands attributable to NH_3^+ deformation are split and shifted to lower wavenumbers (1628 and 1590 cm^{-1}), probably due to the hydrogen bonds being weaker in the layered compound. A similar shift is observed for the asymmetric stretching of the COO^- group (1501 cm^{-1})[14]. At higher wavenumbers (3700−3500 cm^{-1}), the zirconium serinephosphate spectrum shows a broad band, probably due to some water adsorbed on the surface microcrystals. Indeed, TG data do not show any bulk water loss. At lower wavenumbers, in the region 1300−800 cm^{-1}, the zirconium serinephosphate spectrum shows a complex system of bands attributable to the phosphate groups.

In conclusion, the data collected indicate that zirconium L-(+)-serinephosphate has a layered structure of the α-type, similar to that shown in Figure 6. This model representation was obtained by applying the Hyperchem MM+ force field (a modified version of the Allinger's original data set[15]) to a set of L-(+)-phosphoserine molecules to obtain a monolayer that fits the phosphate site distribution on each side of the inorganic matrix, which is assumed to be almost identical to that in α-$Zr(HOPO_3)_2$. It is interesting to note that when the layers are brought together, a hydrogen atom of the ammonium groups resides at such a distance from the oxygen atom of the carboxylic groups (2.6 Å) that allows the formation of hydrogen bonds. The layer −layer interactions are dominated by ionic and hydrogen bonds and the interlayer distance obtained from the model is similar to that measured from XRPD patterns.

Figure 6. Computer-generated model showing the packing of two layers of zirconium L-(+)-serinephosphate; the possible hydrogen bonds are indicated

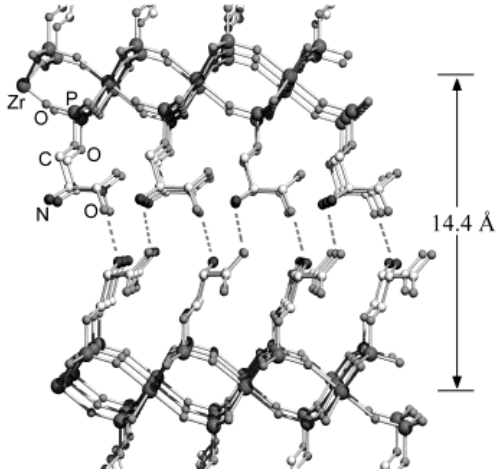

Once the empirical formula and the structural model had been established, it seemed of interest to reconsider the thermal decomposition process, since the TG data (see Figure 3) showed that, at about 250°C, the first sharp weight

loss (20% of the initial weight) was near to that (19.3%) calculated for the following process:

$$Zr[HOOCCH(NH_2)CH_2OPO_3]_2 \rightarrow Zr(NH_2CH_2CH_2OPO_3)_2 + 2\ CO_2$$

Further evidence for this reaction was gained by collecting XRPD spectra of zirconium serinephosphate maintained at different temperatures (see Figure 7), and by performing evolution gas analysis (EGA) on a sample heated to 900°C (see Figure 8). Both these experiments gave clear evidence that a clean decarboxylation reaction occurs. It can be seen from Figure 7 that the *d* value does not change up to about 200°C, but decreases from 14.4 Å to 12.1 Å at 250°C. At higher temperatures, the XRPD patterns become more and more disordered. It is interesting to note that the phase at 250°C has an interlayer distance similar to that of zirconium 2-aminoethylphosphonate (11.3 Å)[16]. Furthermore, the EGA profile (see Figure 8) shows a marked increase of the CO_2 partial pressure in the 250−300°C temperature range.

Figure 7. XRPD patterns of zirconium L-(+)-serinephosphate maintained at the indicated temperature

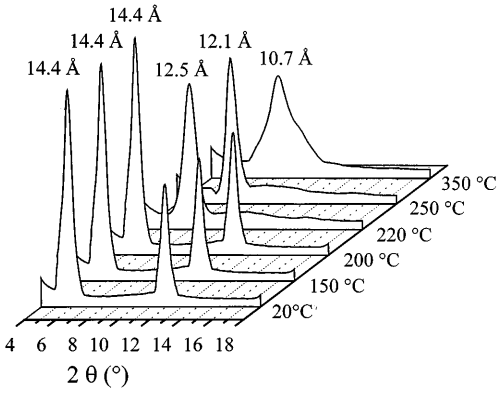

Figure 8. CO_2 partial pressure as a function of temperature in evolution gas analysis of zirconium L-(+)-serinephosphate

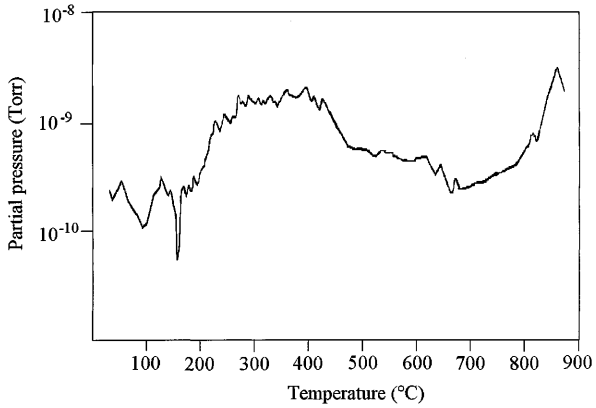

Considering the proposed structure, this new layered compound might be expected to behave as an amphoteric ion-exchange material, capable of taking up cations, anions and even neutral salts from solutions. Moreover, it could also be expected to act as an intercalating agent of polar molecules. Unfortunately, despite the numerous attempts made, the compound was found to be incapable of intercalating neutral species (alkanols, ethyleneglycol, propylamine, glycine), nor could it be titrated with NaOH or HCl solutions.

The lack of intercalation is probably due to the strong layer−layer interactions arising from the long-range ionic bonds between the zwitterions anchored to the surface of the layers, as well as from the network of interlamellar hydrogen bonds. The layer separation necessary for the insertion of the guest species seems to require a very high activation energy. However, it was observed that precipitates obtained after 3 days of precipitation time, which contained a small number of hydrogen phosphate groups, showed some exchange properties toward sodium ions. Therefore, zirconium serinephosphates in which some of the phosphoserine groups are replaced by phosphate groups were prepared, and their ion-exchange behaviour was investigated.

Preparation and Characterization of Zirconium L-(+)-Serinephosphate Phosphates

Several samples of zirconium serinephosphate phosphate, containing increasing amounts of phosphate groups, were prepared using the HF procedure[17] (see Experimental Section) starting from solutions with increasing mole fraction Xph = phosphoric acid/phosphoserine + phosphoric acid. The general trend shown by the system is summarized in Figure 9, where the approximate percentage composition of the phases obtained, identified by their interlayer distances, is plotted against the Xph in the precipitating solution. The percentage of a given phase was estimated from the intensity of the relevant first reflection in the XRPD powder pattern, which is assumed to be roughly proportional to the amount of that phase.

Figure 9. Percentage of the phases obtained in the system Zr(IV)/L-(+)-serinephosphate/phosphoric acid as a function of the molar fraction Xph (see text) in the precipitating solution

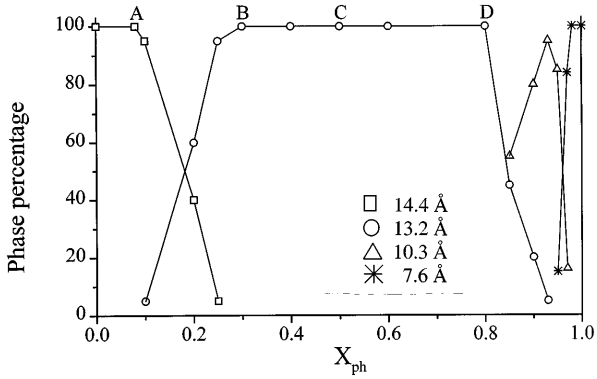

The system is discontinuous: initially, up to Xph ≈ 0.1, some phosphates replace an equivalent amount of serinephosphate groups in zirconium serinephosphate (14.4 Å) with slight modification of the XRPD patterns. When the maximum solubility of O_3POH groups in this latter phase is reached (the solid contains an average of one phosphate in every five groups), formation of a new phase with an

interlayer distance of 13.2 Å begins and the phase transition 14.4 → 13.2 Å is completed at Xph ≈ 0.3. The solids precipitated in the range 0.3 ≤ Xph ≤ 0.8 maintain about the same interlayer distance. Concomitantly, their phosphate content increases from one phosphate in every three groups to the idealized composition of two phosphates in every three groups.

A further increase in Xph produces another immiscible phase with a higher phosphate content and an interlayer distance of 10.3 Å, together with pure α-$Zr(HOPO_3)_2$ (interlayer distance 7.6 Å). It proved impossible to isolate the 10.3 Å phase in pure form. However, the spacing of 10.3 Å would be that expected for a mixed compound[18], in which a layer of serinephosphate containing phosphate groups regularly alternates with a layer containing only phosphates, i.e. (13.2 Å + 7.6 Å)/2 = 10.4 Å.

Some representative samples of the mixed compounds obtained by varying the Xph in solution (those marked with a capital letter in Figure 9) were characterized by thermal analysis, as well as by C, N elemental analysis in order to establish their empirical formulae. Figure 10 shows the weight-loss curves of the samples, previously conditioned at room temp. and 75% relative humidity, and the results of C, N elemental analyses. When heated at 1000°C, all samples show the typical XRPD pattern of cubic ZrP_2O_7. Assuming that all the zirconium and phosphorus present was transformed into zirconium pyrophosphate, and taking into account the experimental percentage weight loss, the formula weights were calculated at room temp. Furthermore, the results of C,N elemental analyses allow the determination of the number of moles of phosphoserine per formula weight, while the percentage weight losses at 150°C allow determination of the number of moles of water of hydration. The empirical formula of the mixed compounds can be written as $Zr[HOOCCH(NH_2)CH_2OPO_3]_{2-x}$-$[HOPO_3]_x \cdot n\ H_2O$. Table 1 shows the values of x and n for the samples examined, together with the interlayer distance taken from the XRPD patterns depicted in Figure 11. In addition, Table 1 includes the no. of mmol of exchangeable protons bound to the carboxylic and phosphate groups per gram of compound, calculated on the basis of the empirical formula. To assess their ion-exchange capacity, the samples were titrated with an NaOH solution in the presence of added NaCl. The potentiometric titration curves, shown in Figure 12, give experimental ion-exchange capacities very near to those that would be expected if only the protons of the P−OH groups were replaced by the sodium ions. Furthermore, the titration curves do not show any well-defined ion-exchange plateau, as though the Na^+ uptake process occurs without the phase transitions usually associated with ion-exchange processes in layered metal(IV) phosphates[19]. The XRPD patterns of the samples obtained after titration indicate that the uptake process occurs without appreciable alteration of the interlayer distance. It seems that the serinephosphate groups act as pillars, determining the interlayer distance, and that the ionogenic phosphate groups are randomly inserted between these pillars. Hence, the incoming sodium ions find sufficient space to be accommodated without an increase of the interlayer distance. In this context, it was of interest to examine the surface properties of the mixed compounds in comparison with those of the original zirconium serinephosphate.

Figure 10. Percent weight loss as a function of the temperature of the indicated samples previously equilibrated at 75% relative humidity at room temp. Heating rate 5°C/min, air flow; the C,N elemental analysis (percent by weight) of the same samples is reported in the inset

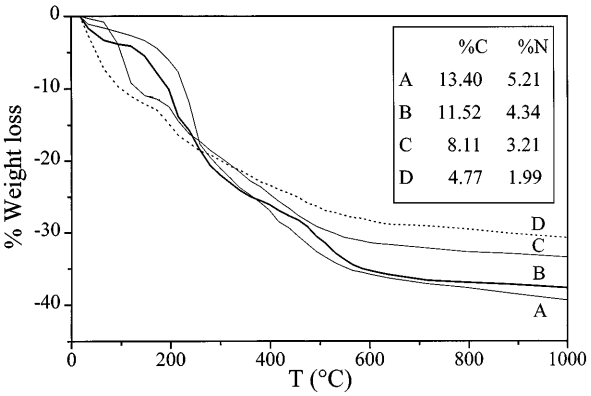

Figure 11. XRPD patterns of samples A and C (see text)

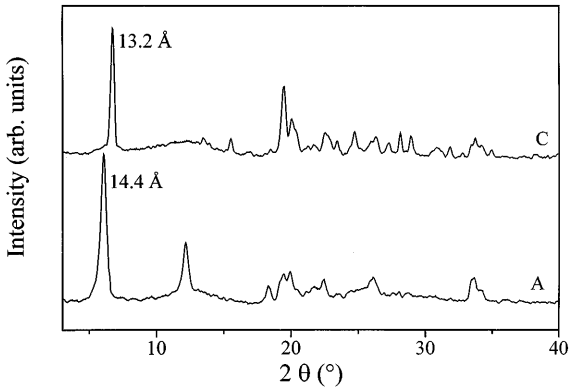

Table 1. Composition, interlayer distance, and calculated ion-exchange capacity of the two ionogenic groups of zirconium serinephosphate phosphates, obtained at the indicated values of mole fraction of phosphoric acid in solution (Xph)

Sample	Xph	$Zr[HOOCCH(NH_2)CH_2OPO_3]_{2-x}(HPO_4)_x \cdot n\ H_2O$ x	n	d [Å]	mmol H^+ [−COOH]/g	mmol H^+ [−POH]/g
A	0.1	0.36	0.65	14.4	3.75	0.823
B	0.25	0.60	1.14	13.2	3.29	1.41
C	0.5	1.1	2.05	13.2	2.26	2.76
D	0.8	1.4	2.62	13.2	1.57	3.66

N_2 adsorption isotherms of zirconium serinephosphate and of samples A and C were recorded. B.E.T. analysis of the isotherms gives specific surface areas of 5.5, 10.6, and 54.5 m^2/g, respectively. It seems that the replacement of serinephosphate groups by phosphates produces an increase in the specific surface area of the solids and the high surface area of sample C may be attributed to the presence of some microporosity in the interlayer region.

Figure 12. Potentiometric titration curves of the indicated samples with a 0.1 M NaOH solution in the presence of 0.1 M NaCl as added salt

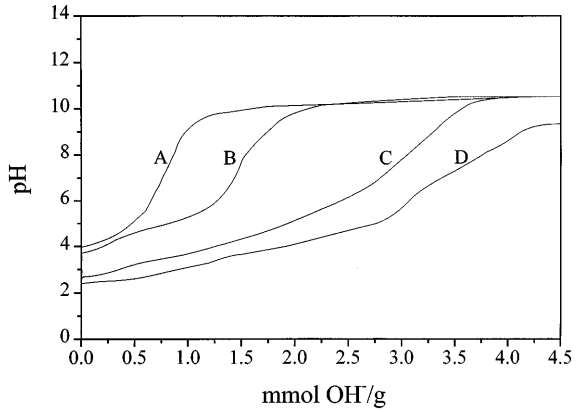

Conclusion

As noted by Clearfield in a recent monograph[7], one of the most exciting aspects of the chemistry of metal(IV) phosphates and phosphonates is the possibility of manipulating the inorganic layered backbone by "soft chemistry" procedures, so as to design materials with specific properties. The work reported herein shows that it is possible to anchor an amino acid function bearing a chiral centre to the α-layer. The α-zirconium serinephosphate obtained does not show the expected ion-exchange or intercalation properties. However, the interlayer region becomes accessible to sodium ions upon replacing some serinephosphate groups by phosphate groups. The zirconium serinephosphate phosphates obtained merit further study, e.g. with regard to investigation of their ion-exchange and intercalation properties with the aim of producing exfoliation of the layered microcrystals. Furthermore, new chiral stationary phases may be obtained by deposition of the exfoliated materials onto suitable supports. This may represent an alternative method to that suggested by Malluk and coworkers[20] based on the intercalation of a chiral receptor in the original α-zirconium phosphate.

Financial support of the *Consiglio Nazionale delle Ricerche* and of the *Ministero Università e Ricerca Scientifica e Tecnologica* is gratefully acknowledged.

Experimental Section

Materials: L-(+)-Phosphoserine (2-amino-3-phosphatylpropanoic acid) was purchased from Sigma and used as received. $ZrOCl_2 \cdot 8\ H_2O$ was a Merck product; all other chemicals were Carlo Erba RP-ACS reagents. − Zirconium serinephosphate and zirconium serinephosphate phosphates were prepared using the method of slow decomposition of zirconium fluoro complexes[3] in the presence of an aqueous solution of phosphoric acid and/or phosphoserine. The preparation conditions were as follows: molar ratio $Zr^{IV}/HF = 6$, molar ratio $P/Zr^{IV} = 3$, phosphoserine and/or phosphoric acid concentration 0.2 M, temperature of precipitation 60°C, time of precipitation 1−4 d. After precipitation, the microcrystals were separated from the solution, washed with distilled water up to pH ≈ 4, and finally dried at room temperature over a saturated NaCl solution (relative humidity ca. 75%) or over phosphorus pentoxide.

Instrumentation: The X-ray powder diffraction (XRPD) patterns of the samples were recorded by the stepwise scanning procedure (increment: $2\Theta = 0.02°$, time per step: 5 s) with a computer-controlled Philips PW 1710 diffractometer, using Ni-filtered Cu-K_α radiation. The XRPD patterns at different temperatures were obtained with an A. Paar HTK diffraction camera. − TG and DTA analyses were performed with a Stanton Redcroft thermal analyser (STA 781), with a heating rate of 5°C/min under an air or O_2 flow. This apparatus coupled with a Fisons mass spectrometer was used to obtain EGA curves. − N_2 adsorption and desorption isotherms were recorded with a Carlo Erba Sorptomatic 1800 apparatus. − C,H,N, elemental analyses were carried out with a Carlo Erba Model 1106 Analyser. Densities were determined pycnometrically at 20°C, using CCl_4 as the displacement liquid. − The molar ratios phosphate/serinephosphate in the products investigated were also estimated by liquid-state ^{31}P-NMR analysis with a Bruker AC 200 instrument, after dissolving 0.05 g of the sample in a small volume of conc. HF (ca. 0.5 ml) and D_2O as solvent. − The ion-exchange experiments were performed with a Mettler DK automatic titrator operating in equilibrium-point mode, by titrating 200 mg of the sample, suspended in 40 ml of 0.1 M NaCl solution, with 0.1 M NaOH solution under an N_2 stream.

[1] G. Alberti, U. Costantino, S. Allulli, N. Tomassini, *J. Inorg. Nucl. Chem.* **1978**, *40*, 1113.
[2] [2a] L. Maya, *Inorg. Nucl. Chem. Lett.* **1979**, *15*, 207. − [2b] M. B. Dines, P. M. Di Giacomo, *Inorg. Chem.* **1981**, *20*, 92. − [2c] M. B. Dines, P. C. Griffith, *Polyhedron* **1982**, *1*, 62. − [2d] Ortiz-Avila, A. Clearfield, *Inorg. Chem.* **1985**, *24*, 1773.
[3] J. M. Troup, A. Clearfield, *Inorg. Chem.* **1977**, *16*, 3311.
[4] [4a] M. B. Dines, P. M. Di Giacomo, K. P. Callahan, P. C. Griffith, R. H. Lane, R. E. Cooksey in *Chemically Modified Surfaces in Catalysis and Electrocatalysis*, vol. 192 (Ed.: J. S. Miller), ACS Symposium Series, Washington DC, **1982**, chapter 12. − [4b] G.Alberti, U. Costantino, J. Kornyei, M. L. Luciani Giovagnotti, *React. Polym.* **1985**, *4*, 1.
[5] G. Alberti, M. Casciola, U. Costantino, R. Vivani, *Adv. Mater.* **1996**, *8*, 291.
[6] G. Alberti in *Solid-State Supramolecular Chemistry: Two- and Three-Dimensional Inorganic Networks* (Eds.: G. Alberti, T. Bein), vol. 7 of the series *Comprehensive Supramolecular Chemistry* (Ed.: J. M. Lehn), Pergamon, Elsevier Science, Oxford, **1996**, chapter 5.
[7] A. Clearfield in *Progress in Inorganic Chemistry*, vol. 47 (Ed.: K. D. Karlin), John Wiley & Sons, New York, **1998**, 371−508.
[8] E. Brunet, M. Huelva, R. Vazquez, O. Juanes, J. C. Rodriguez-Ubis, *Chem. Eur. J.* **1996**, *2*, 1578.
[9] G. Alberti, L. Boccali, C. Dionigi, R. Vivani, V. I. Kalchenko, L. I. Atamas, *Supramol. Chem.* **1996**, *7*, 129.
[10] E. Jaimez, G. B. Hix, R. C. T. Slade, *J. Mater. Chem.* **1997**, *7*, 475.
[11] D. M. Poojary, B. Zhang, A. Clearfield, *Angew. Chem.* **1994**, *106*, 2420; *Angew. Chem. Int. Ed. Engl.* **1994**, *33*, 2324.
[12] P. E. Werner, L. Eriksson, M. Westdhal, *J. Appl. Crystallogr.* **1985**, *18*, 367.
[13] G. Alberti, U. Costantino, M. L. Luciani Giovagnotti, *J. Inorg. Nucl. Chem.* **1979**, *41*, 643.
[14] F. S. Parker, *Applications of Infrared Spectroscopy in Biochemistry, Biology, and Medicine*, Plenum Press, New York, **1971**, chapter 9.
[15] N. L. Allinger, *J. Am. Chem. Soc.* **1977**, *99*, 8127.
[16] M. Casciola, U. Costantino, A. Peraio, T. Rega, *Solid State Ionics* **1995**, *77*, 229.
[17] G. Alberti, E. Torracca, *J. Inorg. Nucl. Chem.* **1968**, *30*, 317.
[18] G. Alberti, U. Costantino, G. Perego, *J. Solid State Chem.* **1986**, *63*, 455.
[19] G. Alberti, *Acc. Chem. Res.* **1978**, *11*, 163.
[20] G. Cao, M. E. Garcia, M. Alcalà, L. F. Burgess, T. E. Mallouk, *J. Am. Chem. Soc.* **1992**, *114*, 7574.

[98114]

Adducts of Ferrocenylboranes and Pyridine Bases: Generation of Charge-Transfer Complexes and Reversible Coordination Polymers☆

Marco Fontani[b], Frank Peters[a], Wolfgang Scherer[a], Wolfgang Wachter[a], Matthias Wagner*[a], and Piero Zanello[b]

Anorganisch-chemisches Institut, Technische Universität München[a],
Lichtenbergstraße 4, D-85747 Garching b.München, Germany
Fax: (internat.) + 49(0)89/28913473
E-mail: wagner@arthur.anorg.chemie.tu-muenchen.de

Universitá di Siena, Dipartímento di Chimica[b],
Pian dei Mantellini 44, I-53100 Siena, Italy
Fax: (internat.) + 39-577/280405
E-mail: zanello@unisi.it

Received April 1, 1998

Keywords: Iron / Boron / Ferrocene / Charge-transfer complexes / Coordination polymers

Compared to parent ferrocene, the redox potential of the Fe^{II}/Fe^{III} transition is shifted to much more cathodic values in B–N adducts **1**·Do and **2**·$(Do)_2$ of borylated ferrocenes $FcBMe_2$ (**1**) and 1,1′-fc$(BMe_2)_2$ (**2**) with pyridine bases Do [Fc: $(C_5H_5)Fe(C_5H_4)$; fc: $(C_5H_4)Fe(C_5H_4)$; Do: γ-picoline, 4-(dimethylamino)pyridine, *N*-(*n*-propyl)-4-(4′-pyridyl)pyridinium hexafluorophosphate]. Electron donation by one single BMe_2·Do substituent at the cyclopentadienyl ligand is approximately equal to the positive inductive effect of the five methyl groups in a C_5Me_5 (cp^*) moiety. Using the bidentate nitrogen ligand 4,4′-bipyridine (bipy), the dark-purple dimetallic complex **1**·bipy·**1** is obtained upon reaction with 2 equiv. of **1**. **1**·bipy·**1** has been structurally characterized by X-ray crystallography. The compound tolerates loss of two electrons at the ferrocene groups, as well as two one-electron reductions at the bipy linker. Dark purple coloured coordination polymers [**2**·bipy]$_n$ are accessible from bipy and 1 equiv. of the diborylated derivative **2**. The intense colours of **1**·bipy·**1** and [**2**·bipy]$_n$ are indicative of charge-transfer interactions between the electron-rich ferrocene fragments and the viologen-like R_3B–bipy–BR_3 acceptor. Neat, solid [**2**·bipy]$_n$ is thermally stable up to 240 °C, but in the presence of toluene, polymerization is fully reversible at about 85 °C.

Introduction

Multimolecular arrays in which metal complexes are joined by rigid (electroactive) bridges represent a highly promising class of compounds, due to the potential properties of these materials such as electrical conductivity,[1] magnetism[2] and liquid-crystalline behaviour.[3] Two main lines of research that are particularly relevant in the context of this paper, concern: (a) Poly(ferrocenes) **A** derived from strained, ring-tilted *ansa*-ferrocenes by thermal[4][5] or catalytic[6] ring-opening polymerization (Figure 1). (b) Low-dimensional solids **B** comprised of coordinatively unsaturated metal complex fragments and bridging dihapto ligands. Among the latter, 4,4′-bipyridine (bipy) and 1,2-bis(4-pyridyl)ethane (pyetpy) are particularly prominent (**B**, Figure 1).[7]

Figure 1. Poly(ferrocenes) **A** and bipy-bridged coordination polymers **B**

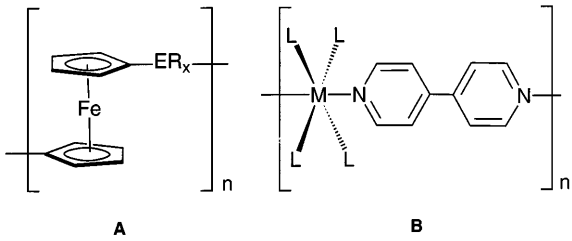

A **B**

E : e.g. Si, Ge, P, As

ML_4 : e.g. Fe(phthalocyaninato), Co(dimethylglyoximato)$_2$

Our group is currently developing a novel synthetic approach to oligonuclear complexes and organometallic polymers, which is based on the facile formation of boron−nitrogen bonds and thus provides a convenient means of connecting mononuclear metal-containing building blocks.[8][9][10][11] This concept appeared to us to be well-suited for the generation of molecular materials combining the advantages of poly(ferrocenes) (e.g. thermal and chemical inertness of the ferrocene backbone; reversible redox processes) and bipy coordination polymers (e.g. facile synthesis; electron-accepting properties of the bipy unit). It will be shown in this paper that, starting from readily available borylated ferrocenes,[12][13][14][15][16] the addition of 4,4′-bipyridine or 1,2-bis(4-pyridyl)ethane gives dimetallic complexes and polymeric materials by B−N adduct formation (Schemes 1 and 2).

A variety of intriguing properties can be expected to result from the combination of ferrocene and pyridine bases, and the following points will be addressed:

(1) The ligand 4,4′-bipyridine has two coordination sites, which may influence each other by the delocalized π-electron system. The question then arises as to what extent

 © WILEY-VCH Verlag GmbH, D-69451 Weinheim, 1998 1434−1948/98/1010−1453 $ 17.50+.50/0

N→B σ bonding at one nitrogen centre lowers the Lewis basicity of the remaining free N atom, i.e. whether the formation of $R_3B{\cdot}bipy{\cdot}BR_3$ involves stable and isolable $R_3B{\cdot}bipy$ intermediates.

(2) Closely related to the aforementioned question is the problem as to whether a bipy spacer allows electronic communication between two pendant ferrocenylborane units (**1**·bipy·**1**; Scheme 1).

Scheme 1

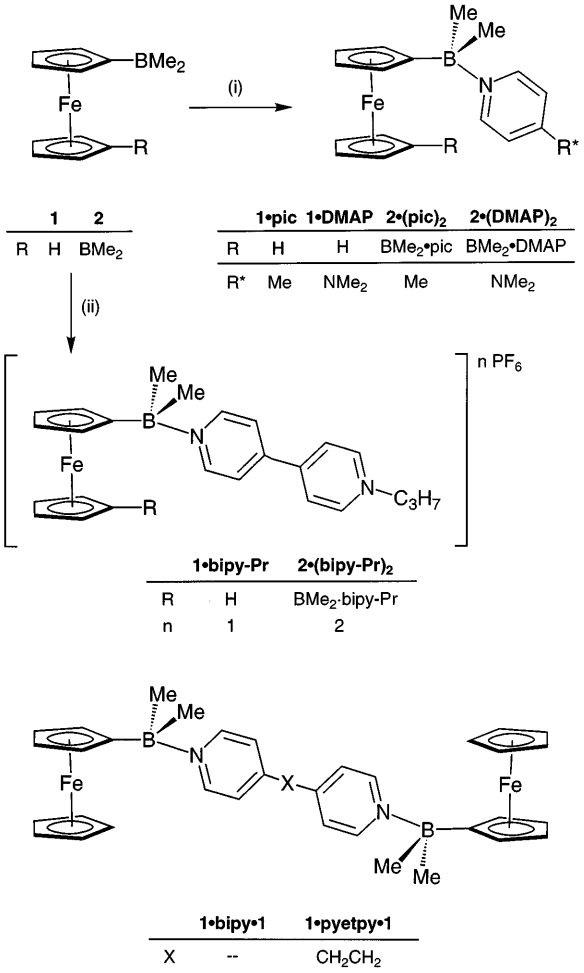

Reagents: (i) **1**·pic/**1**·DMAP: **1** + 1 pic/DMAP; toluene, ambient temp. **2**·$(pic)_2$/**2**·$(DMAP)_2$: **2** + 2 pic/DMAP; toluene, ambient temp. (ii) **1**·bipy-Pr: **1** + 1 bipy-Pr; acetonitrile, ambient temp. **2**·$(bipy\text{-}Pr)_2$: **2** + 2 bipy-Pr; acetonitrile, ambient temp.

Moreover, comparison of the electrochemical data of the Lewis acid/base complexes **1**·pic, **1**·DMAP, **2**·$(pic)_2$ and **2**·$(DMAP)_2$ (Scheme 1), featuring the moderately strong electron donor γ-picoline (pic; pK_a = 6.02; in water, 25°C)[17] on the one hand, and the more basic 4-(dimethylamino)pyridine (DMAP; pK_a = 9.71; in water, 20°C)[18] on the other, will yield information on the influence of tetracoordinate boron substituents on the redox potential of the ferrocene fragment.

(3) 4,4′-Bipyridine-1,1′-diyldiboranes **C** are analogues of the bis-quaternary salts of 4,4′-bipyridine ($\mathbf{D}^{2+}$, "viologens"), which behave as perfectly reversible two-step redox

Figure 2. B−N adducts **C** as structural and electrochemical analogues of the two-step redox system viologen $\mathbf{D}^{2+}$

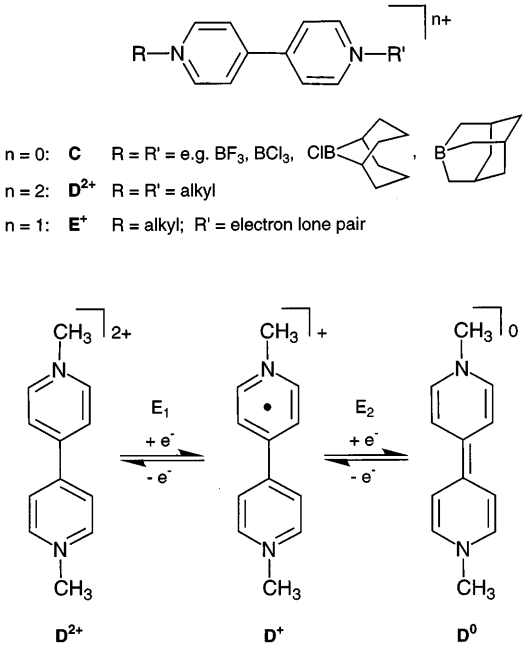

systems in polar aprotic solvents such as acetonitrile and dimethylformamide (Figure 2).[19]

Consequently, derivatives of $\mathbf{D}^{2+}$ have found widespread use as electron acceptors[20][21] and electron carriers,[22] and it is in the latter context that the incorporation of viologens into polymers has been thoroughly investigated.[23][24][25][26] To a large extent, these polymeric materials retain the chemical and electrochemical properties of the monomeric species $\mathbf{D}^{2+}$, although the first reduction (E_1) of polyviologens usually occurs at a more anodic, and the second (E_2) at a more cathodic potential, compared to the corresponding monomers. Thus, in polymeric viologens, the difference ΔE between the two potential values was found to be about twice as large as that in the monomers, and this effect is observable even in oligomers with only 2 or 3 repeating units.[25] This behaviour is indicative of a certain degree of electronic communication between the electroactive sites, which has been attributed to intramolecular interactions among neighbouring pendant viologen cation radicals. Given this background, it will be interesting to see how the electronic behaviour of polymeric viologens changes when the highly flexible backbones used to date are substituted for the more rigid 1,1′-ferrocenediyl spacer [cf. **2**·$(bipy\text{-}Pr)_2$; Scheme 1]. For a general discussion of $L_nM{\cdot}bipy{\cdot}ML_n$ adducts (ML_n: main-group Lewis acid) and the respective radicals formed upon one-electron reduction, the reader is referred to the work of Kaim et al.[27][28][29][30]

(4) The synthesis of aggregates composed of electron-donating ferrocene units and electron-accepting viologen bridges may lead to charge-transfer (CT) processes between the two components. This assumption is based on the observation of pronounced CT interactions between the ferrocene backbone and its pendant 2,2′-bipyridylboronium substituents in the case of related systems **F** (Figure 3).[31][32]

Figure 3. View of the charge-transfer complex **F**

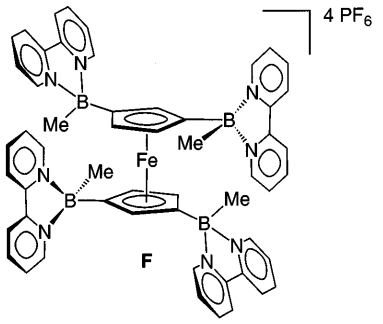

Results and Discussion

In the following, the numbers **1** and **2** are used to denote derivatives of mono- and diborylated ferrocenes, respectively. These numbers are followed by a specification of the coordinating pyridine, i.e. pic, DMAP, bipy, pyetpy and bipy-Pr [*N*-(*n*-propyl)-4-(4′-pyridyl)pyridinium hexafluorophosphate[26]]. The term "Do" stands for all these cited pyridine donors in general.

Synthesis

1·pic, **1**·DMAP and **2**·$(pic)_2$, **2**·$(DMAP)_2$ were prepared by mixing toluene solutions of the appropriate nitrogen base and **1** (molar ratio 1:1) or **2** (molar ratio 2:1) at ambient temperature (Scheme 1). Orange crystalline solids were obtained in almost quantitative yields. Even in solution, the compounds show only moderate sensitivity towards moisture, but **2**·$(pic)_2$ and **2**·$(DMAP)_2$ are rapidly oxidized on exposure to air (see below). The syntheses of the ionic adducts **1**·bipy-Pr and **2**·$(bipy\text{-}Pr)_2$ were performed in acetonitrile (Scheme 1). From the dark, purple-red reaction mixtures, the compounds were isolated as almost black crystals. The dinuclear complex **1**·bipy·**1**, which was obtained from toluene solutions of **1** and bipy (molar ratio 2:1), also forms dark-purple crystals and gives intensely red-coloured solutions in toluene as well as in chloroform. In contrast, the related compound **1**·pyetpy·**1** is orange, both in solution and in the solid state, and thus resembles the pic and DMAP adducts described above.

While alkyl bipyridinium systems $\mathbf{E}^+$ (R = alkyl; R′ = electron lone pair; n = 1) are readily accessible (Figure 2),[26] we have not been able to isolate a stable 1:1 adduct of bipy with **1**, even though this species is likely to be abundant in an equimolar solution of the two components. Communication of both nitrogen termini in bipy seems to be observable only when electrophiles of very high Lewis acidity are used for nitrogen coordination, and this condition is apparently not met with **1**.

When diborylated ferrocene **2** in $CHCl_3$ is layered with one equiv. of bipy in CH_2Cl_2, polymeric [**2**·bipy]$_n$ is obtained as a purple microcrystalline solid, which is insoluble in all common non-coordinating solvents. In an attempt to grow single crystals suitable for X-ray crystallography, we tried to slow down the reaction rate by replacing the highly Lewis acidic **2** with its corresponding picoline adduct **2**·$(pic)_2$ (Scheme 2). Using this method, black rhombic crystals of [**2**·bipy]$_n$ grew within 24 h, and it was shown that coordinated pic may be substituted for bipy, even though the former is a much stronger base [pic: pK_a = 6.02;[17] bipy: pK_a(1) = 4.82, pK_a(2) = 3.17;[33] in water, 25°C]. A driving force for this reaction clearly lies in the precipitation of [**2**·bipy]$_n$, which is thus continuously removed from the reaction mixture, thereby shifting the equilibrium towards polymer formation. Polymerization can be reversed by treating purple [**2**·bipy]$_n$ with excess picoline. From the resulting orange solutions, uncomplexed bipy and **2**·$(pic)_2$ can be recovered quantitatively. A polymeric product is also obtained from **2** or **2**·$(pic)_2$ upon reaction with one equiv. of 1,2-bis(4-pyridyl)ethane (pyetpy). Like the dinuclear species **1**·pyetpy·**1**, and unlike **1**·bipy·**1** and [**2**·bipy]$_n$, [**2**·pyetpy]$_n$ exhibits the orange colour usually observed for ferrocenes bearing tetracoordinate boron substituents.

Scheme 2. Preparation of the coordination polymers [**2**·bipy]$_n$ and [**2**·pyetpy]$_n$

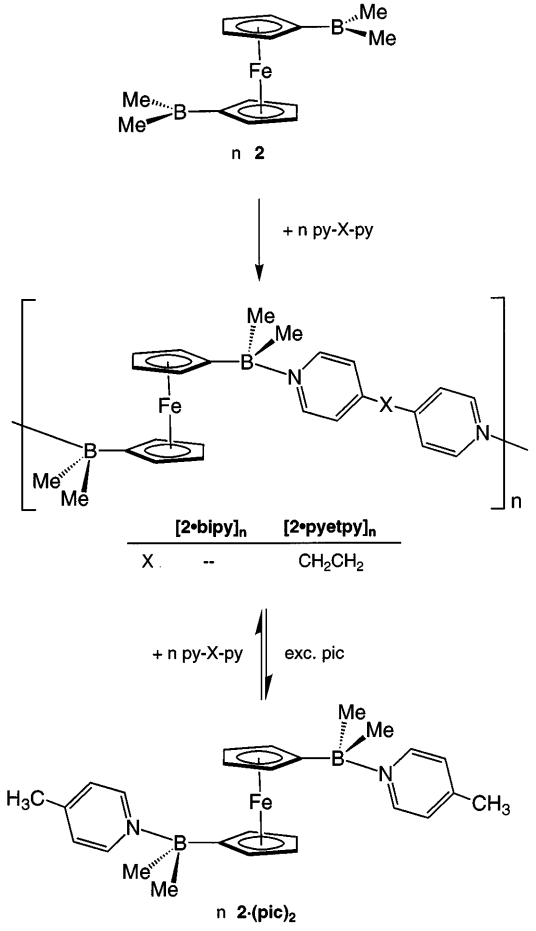

NMR Spectroscopy

It is a characteristic feature of B−N donor−acceptor compounds that a dynamic equilibrium exists in solution involving the four-coordinate species and the respective free acids and bases. The chemical shifts observed in the NMR spectra are thus a weighted average between those of the adducts and those of the uncomplexed components. Obviously, the relative amount of an adduct increases when the

solution becomes more concentrated. Therefore, we have used saturated solutions for all NMR spectroscopic measurements to ensure full reproducibility of the data and to obtain chemical shift values as close as possible to the resonances of **1**·Do and **2**·$(Do)_2$. Since the B−N adducts under investigation possess different solubilities in the chosen solvents ($CDCl_3$, CD_3CN), a quantitative comparison, particularly of their ^{11}B-NMR data, is problematic. We have therefore restricted the discussion of NMR spectra to a qualitative level.

Compared to the ^{11}B-NMR spectra of **1** [$\delta(^{11}B) = 70.5$] and **2** [$\delta(^{11}B) = 72.1$], the resonances of **1**·Do and **2**·$(Do)_2$ show large upfield shifts upon addition of the pyridine bases [$\delta(^{11}B) = -3.0$ to 15.0], giving good evidence for B−N adduct structures with four-coordinate boron centres.[34] The relative base strengths of the different pyridines are nicely reflected in the ^{11}B chemical shift values of the B−N complexes, with stronger donors leading to a better shielding of the boron centre: $\delta(^{11}B) = -3.0$ (**1**·DMAP), 0.4 (**1**·pic), 7.5 (**1**·bipy-Pr); 6.2 (**1**·pyetpy·**1**), 15.1 (**1**·bipy·**1**). A similar correlation holds for the adducts of diborylated **2**, but the ^{11}B-NMR signals of the diadducts generally appear at lower field compared to those of the corresponding monoadducts, e.g. $\delta(^{11}B) = 0.4$ (**1**·pic), 15.0 [**2**·$(pic)_2$]. When a large excess (0.5 ml) of pic is added to a solution of **2**·$(pic)_2$ in $CDCl_3$, the boron resonance closely approaches that of **1**·pic [**2**·$(pic)_2$ and excess of pic: $\delta(^{11}B) = 0.0$]. This finding is in good agreement with the assumption of a dissociation equilibrium, which is shifted towards adduct formation in the presence of free base. To gain a deeper insight into this phenomenon, we have investigated the dynamic behaviour of equimolar mixtures of **2** with pic and DMAP in [D_8]toluene at various temperatures by ^{11}B-NMR spectroscopy. In the case of pic, only one extremely broad resonance is detected at ambient temperature [$\delta(^{11}B) \approx 33$]. Upon warming, the signal sharpens considerably, but no significant change of its chemical shift is observed [+60°C: $\delta(^{11}B) = 35.0$; $h_{1/2} = 720$ Hz]. The signal vanishes upon cooling to +15°C. At −10°C, two very broad humps become visible at $\delta(^{11}B) = 70$ and 0, while at −50°C the resonances appear at $\delta(^{11}B) = 73.6$ ($h_{1/2} = 1780$ Hz) and −0.6 ($h_{1/2} = 720$ Hz). In the DMAP case, two ^{11}B-NMR signals are observed even at ambient temperature [$\delta(^{11}B) = 71.0$ ($h_{1/2} = 320$ Hz), −2.8 ($h_{1/2} = 640$ Hz)]. Coalescence of these signals occurs in the temperature range between +80 and +90°C, and at +110°C only one resonance is seen at $\delta(^{11}B) = 35$ ($h_{1/2} = 1360$ Hz). These data suggest that at ambient temperature, and when the N donor is of moderate basicity (pic), the base rapidly fluctuates between the two boron atoms of **2**. The observed ^{11}B-chemical shift is thus time-averaged. In contrast, the stronger donor DMAP comes to a rest at one of the BMe_2 centres under these conditions, and the ^{11}B-NMR spectrum is indicative of the presence of one tri- and one tetracoordinate boron atom. The free activation enthalpies $\Delta G^{\neq}$ of the dynamic processes can be estimated as 45 ± 2 kJ mol^{-1} (pic) and 58 ± 2 kJ mol^{-1} {DMAP; $\Delta G^{\neq} = 19.14\ T_c\ [10.32 + \log(T_c k_c^{-1}]$; $k_c = 2.22 \cdot \Delta\nu$}[35].

In the ^{1}H- and ^{13}C-NMR spectra, one observes only minor changes of the chemical shifts of the pyridine bases upon B−N adduct formation. This finding is in contrast to what was expected, since in the case of e.g. compounds **C**, a pronounced dependence of the bipy proton ^{1}H signals on the nature of the coordinated borane has been reported, e.g. R, R′ = BF_3: $\delta(^1H) = 8.63, 9.54$; R, R′ = 1-boraadamantane: $\delta(^1H) = 8.31, 8.84$ ([D_6]DMSO).[36] For most derivatives of **C**, these values are intermediate between those of free bipy [$\delta(^1H) = 7.79, 8.63$] and those of the bis-quaternary $\mathbf{D}^{2+}$ [R, R′ = CH_3: $\delta(^1H) = 8.68, 9.21$].[36] It has thus been argued that coordination of a highly Lewis acidic borane is mirrored by a pronounced deshielding of the bipy protons in the ^{1}H-NMR spectrum.[36] Even though this correlation may serve as a useful rule of thumb, a quantitative interpretation requires more detailed scrutiny, and other factors, such as magnetic anisotropy effects, also have to be taken into account. For example, the reasons why the bipy protons in the BF_3 adduct experience a large downfield shift, even though BF_3 is a rather weak electrophile,[37][38] still remain obscure.

The ^{1}H-NMR resonances of the $FcBMe_2$ moiety are more informative, showing characteristic upfield shifts upon treatment with pyridine bases: (a) The signal of the BMe_2 fragment, which appears at $\delta(^1H) = 0.82$ in uncomplexed **1**, is found in the corresponding B−N adducts at $\delta(^1H) = 0.30$ (**1**·bipy-Pr), 0.27 (**1**·pic), 0.16 (**1**·DMAP) and at $\delta(^1H) = 0.40$ (**1**·bipy·**1**), 0.29 (**1**·pyetpy·**1**). (b) The protons of the C_5H_4 ring bearing the boryl substituent resonate at $\delta(^1H) = 4.37, 4.59$ in the case of **1**, but are significantly more shielded in **1**·bipy-Pr [$\delta(^1H) = 4.08, 4.19$], **1**·pic [$\delta(^1H) = 4.03, 4.16$], **1**·DMAP [δ⊥ft parenthesis^{1}H) = 3.97, 4.09] and in **1**·bipy·**1** [$\delta(^1H) = 4.13, 4.27$] and **1**·pyetpy·**1** [$\delta(^1H) = 4.04, 4.18$]. These data clearly indicate that not only the ^{11}B-NMR spectra, but also the cited proton shifts can be taken as a measure of the pK_a values of the coordinating pyridines. Similar effects as described for **1** are operative in the case of diborylated derivatives, cf. **2**: $\delta(^1H) = 0.84$ (BCH_3), 4.31, 4.44 (C_5H_4); **2**·$(pic)_2$: $\delta(^1H) = 0.34$ (BCH_3), 3.99, 4.13 (C_5H_4).

The ^{13}C-NMR data of **1**, **2** on the one hand, and of **1**·Do, **2**·$(Do)_2$ on the other, show similar changes and therefore do not merit further discussion.

Infrared Spectroscopy

The infrared spectrum of a pyridine base is modified when the non-bonding pair of electrons on the nitrogen atom is donated into a vacant orbital of an electron acceptor. Consequently, a comparison of the IR data (KBr disc) of **1**, **2** and of the free donors Do with **1**·Do and **2**·$(Do)_2$ reveals a number of alterations characteristic of B−N adduct formation, which will be described here in detail for the oligometallic complexes **1**·bipy·**1** and [**2**·bipy]$_n$ only (Table 1).

B−N Vibration: The values of the B−N stretching modes are of particular importance in obtaining information about the stability of the Lewis acid/base pairs under investigation. The B−N frequencies of solid (KBr disc)

BCl_3·pyridine and BF_3·pyridine have been reported to occur at $\tilde{\nu}$ = 1113 cm^{-1}[39] and $\tilde{\nu}$ = 1112 cm^{-1}[40], respectively. For a series of complexes BX_3·pyridine (X: H, F, Cl, Br) in $CHCl_3$ solution, the corresponding bands are found in the 1102−1090 cm^{-1} interval. They are shifted to lower values when pyridines bearing electron-withdrawing substituents at the 4-position are used (e.g. BCl_3·4-chloropyridine: 1076 cm^{-1}).[41]

Table 1. Infrared bands [cm^{-1}] of selected compounds **1**·Do and **2**·$(Do)_2$ (KBr disc) in the characteristic regions 1650−1450 cm^{-1} (C=C and C=N stretch) and 1100−1050 cm^{-1} (B−N vibration)

1·pic	**1**·DMAP	**2**·$(pic)_2$	**2**·$(DMAP)_2$	**1**·bipy·**1**	[**2**·bipy]$_n$
1628	1636	1628	1638	1622	1622
–	1544	–	1552	1540	1540
1507	–	1508	–	1493	1493
1104	1104	–	–	1100	–
1068	1076	1066	1077	1075	1075
1058	1058	1047	1060	1058	1061

1·pic	**1**·DMAP	**2**·$(pic)_2$	**2**·$(DMAP)_2$	**1**·bipy·**1**	[**2**·bipy]$_n$
1606	1603			1590	1645
1563	1537			1531	1569
1497	1519			1487	1509

[a] *N*,*N*′-Bis(*n*-propyl)-4,4′-bipyridinium hexafluorophosphate.

1·bipy·**1** exhibits three bands in the region of interest ($\tilde{\nu}$ = 1100 cm^{-1}, 1075 cm^{-1}, 1058 cm^{-1}), while [**2**·bipy]$_n$ shows only two such absorptions at $\tilde{\nu}$ = 1075 cm^{-1} and 1061 cm^{-1} (Table 1). It can thus be concluded that the band at $\tilde{\nu}$ = 1100 cm^{-1} is probably not caused by a B−N vibration. The band at $\tilde{\nu}$ = 1075 cm^{-1} appears not only in **1**·bipy·**1** and [**2**·bipy]$_n$, but also in the IR spectra of the free Lewis acids **1** and **2**. Moreover, it does not show the isotope doublet structure ($^{10}B/^{11}B$) that would be expected for a vibration involving the motion of a boron atom. Given this background, the band at $\tilde{\nu}$ = 1058 cm^{-1} (1061 cm^{-1}) is tentatively assigned to the B−N stretching mode of **1**·bipy·**1** ([**2**·bipy]$_n$). It has to be concluded that the B−N bonds in **1**·Do and **2**·$(Do)_2$ are not very strong, which is in accord with the thermal behaviour of these compounds in solution, as well as with the NMR spectroscopic results outlined above.

C=C/C=N Vibration: The region between $\tilde{\nu}$ = 1650 cm^{-1} and $\tilde{\nu}$ = 1450 cm^{-1}, showing three bands at 1622 cm^{-1}, 1540 cm^{-1} and 1493 cm^{-1} both for **1**·bipy·**1**, and for [**2**·bipy]$_n$, also merits further discussion (Table 1). Neither **1** nor **2** exhibits significant absorptions in this region of the spectrum, and thus we may safely assume that these bands are due to C=N and C=C stretching modes of the bipy fragments. Compared to the free base, which shows bands at $\tilde{\nu}$ = 1590 cm^{-1}, 1531 cm^{-1} and 1487 cm^{-1} (KBr disc), the adduct absorptions are shifted by 32 cm^{-1}, 9 cm^{-1} and 6 cm^{-1} towards higher wavenumbers. Similar changes have previously been reported for other complexes of pyridines with main-group Lewis acids.[39][41] The pronounced shift of the highest energy band may therefore be used as a valuable diagnostic tool to investigate (a) the degree of **1**·bipy·**1** dissociation in solution on a very fast time scale, and (b) the molecular structure of solid [**2**·bipy]$_n$.

(a) All infrared frequencies exhibited by solid **1**·bipy·**1** (KBr disc) are also found in CH_2Cl_2 solution. The solution spectrum, however, reveals two additional weak bands ($\tilde{\nu}$ = 1597 cm^{-1}, 1517 cm^{-1}) in the characteristic region between $\tilde{\nu}$ = 1650 cm^{-1} and 1450 cm^{-1}, thereby indicating the presence of a second species that is not found in the solid state. Since the additional absorptions do not match those of free bipy in CH_2Cl_2 ($\tilde{\nu}$ = 1592 cm^{-1}, 1535 cm^{-1}, 1485 cm^{-1}), they are most likely caused by the monoadduct **1**·bipy. This molecule may be formed in a dynamic equilibrium by the dissociation of a small proportion of **1**·bipy·**1**, as has already been suggested from an inspection of the ^{11}B-NMR spectra.

(b) An intense band at $\tilde{\nu}$ = 1622 cm^{-1} and the absence of an absorption at $\tilde{\nu}$ = 1590 cm^{-1} in the infrared spectrum of [**2**·bipy]$_n$ provides strong evidence in favour of the proposed adduct structure. The amount of any free bipy that might have co-crystallized with [**2**·bipy]$_n$ is beyond the detection limit of the IR spectrometer. The question then remains as to whether [**2**·bipy]$_n$ consists mainly of short oligomeric fragments, or whether it is a well-organized coordination polymer. One way of distinguishing between these two structural motifs is to evaluate the amount of uncomplexed BMe_2 substituents or of terminal bipy units with one coordinating and one uncomplexed nitrogen atom. The two types of chain end should be equally abundant in [**2**·bipy]$_n$, but we will focus our attention on the latter, which is easier to detect by IR spectroscopy. Terminal bipy ligands have a less symmetrical environment than bridging bipy, which leads to the appearance of additional infrared lines. For example, monosubstituted [bipy-Pr]PF_6 exhibits (among others) four well-resolved C=C/C=N stretching frequencies at $\tilde{\nu}$ = 1597 cm^{-1}, 1548 cm^{-1}, 1526 cm^{-1} and 1496 cm^{-1}, whereas the bis-quaternary salt [Pr−bipy−Pr]$(PF_6)_2$ shows only two lines in this spectral range with intermediate values of $\tilde{\nu}$ = 1569 cm^{-1} and 1509 cm^{-1}. In the characteristic region, the frequency pattern of [**2**·bipy]$_n$ closely resembles that of [Pr−bipy−Pr]$(PF_6)_2$ and is absolutely identical with the IR spectrum of **1**·bipy·**1**. These findings suggest that there are far less terminal than internal bipy ligands present in [**2**·bipy]$_n$ and are thus consistent with the proposed polymeric structure. It should be noted, however, that on the basis of the infrared data discussed, the presence of cyclic structures *cyclo*-[**2**·bipy]$_n$ cannot be ruled out.

Solid-State Structure of 1·bipy·1

Dark-purple crystals of **1**·bipy·**1** (Figure 4, Table 2) were grown from toluene/hexane (1:1) in the triclinic space group $P\bar{1}$ with two crystallographically independent molecules in the asymmetric unit (**1**·bipy·$\mathbf{1}_A$, **1**·bipy·$\mathbf{1}_B$; 0.5 equiv. of disordered toluene in the crystal lattice). Selected bond lengths, angles and dihedral angles of both molecules are given in Table 3. The complete set of structural data of **1**·bipy·$\mathbf{1}_A$ and **1**·bipy·$\mathbf{1}_B$ is available on request.[42]

Since both molecules **1**·bipy·$\mathbf{1}_A$ and **1**·bipy·$\mathbf{1}_B$ possess rather similar structures within experimental error, only

Figure 4. Molecular structure of **1**·bipy·$\mathbf{1}_A$; the thermal ellipsoids are drawn at a 50% probability level

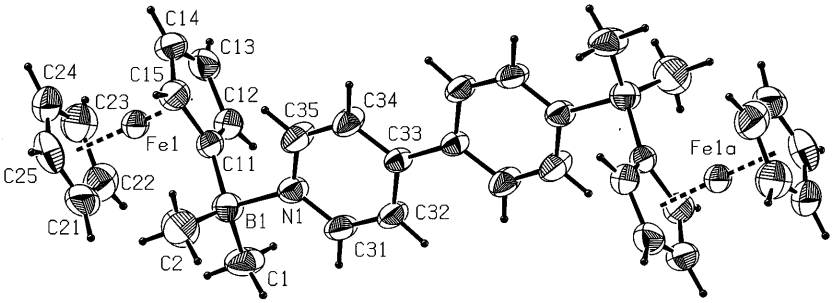

Table 2. Summary of crystallographic data of **1**·bipy·**1**

Formula	$C_{34}H_{38}B_2Fe_2N_2$
Form. wt.	608.00
Cryst. dimen. [mm]	0.20 × 0.13 × 0.13
Cryst. syst.	triclinic
Space group	$P\bar{1}$ (No. 2)
T [K]	293
a [Å]	8.7143(5)
b [Å]	13.8257(10)
c [Å]	15.8214(12)
α [°]	65.820(7)
β [°]	86.337(7)
γ [°]	75.376(7)
V [Å^3]	1680.9(2)
$D_{calcd.}$ [g·cm^{-3}]	1.201
Z	2
Radiation	Mo-K_α, 0.71073 Å
Total reflns.	19554
No. of uniq. reflns.	5965
No. of obsd. reflns.	4982 [all data]
No. of parameters	361
μ [cm^{-1}]	8.9
Final $R1$[a]	0.0319 [$I > 2\sigma(I)$]
Final $wR2$[b]	0.0558 [all data]
GooF[c]	0.72

[a] $R1 = \Sigma(||F_o| - |F_c||)/\Sigma|F_o|$. – [b] $wR2 = [\Sigma w (F_o^2 - F_c^2)^2/\Sigma w (F_o^2)^2]^{1/2}$. – [c] $GooF = [\Sigma w (F_o^2 - F_c^2)^2/(NO - NV)]^{1/2}$.

Table 3. Selected bond lengths [Å], angles and torsion angles [°] of **1**·bipy·$\mathbf{1}_A$ and **1**·bipy·$\mathbf{1}_B$

	1·bipy·$\mathbf{1}_A$	**1**·bipy·$\mathbf{1}_B$
B(1)−N(1)	1.682(5)	1.689(4)
B(1)−C(11)	1.617(4)	1.604(5)
N(1)−C(31)	1.334(3)	1.339(4)
N(1)−C(35)	1.339(4)	1.323(4)
C(31)−C(32)	1.359(4)	1.366(5)
C(32)−C(33)	1.389(4)	1.378(5)
C(33)−C(34)	1.380(3)	1.381(4)
C(34)−C(35)	1.355(4)	1.370(4)
C(33)−C(33a)	1.480(4)	1.479(4)
C(1)−B(1)−N(1)	107.5(3)	104.8(2)
C(2)−B(1)−N(1)	103.9(3)	104.5(2)
C(11)−B(1)−N(1)	103.7(3)	104.1(3)
C(1)−B(1)−C(2)	113.5(3)	114.6(3)
C(1)−B(1)−C(11)	112.9(3)	113.1(3)
C(2)−B(1)−C(11)	114.2(3)	114.2(3)
B(1)−N(1)−C(31)	122.9(2)	120.4(3)
B(1)−N(1)−C(35)	121.0(2)	123.6(2)
C(12)−C(11)−B(1)−N(1)	90.5(4)	88.6(3)
C(11)−B(1)−N(1)−C(35)	42.9(4)	4.3(3)
C(34)−C(33)−C(33a)−C(34a)	180.0(7)	180.0(2)

1·bipy·$\mathbf{1}_A$ is discussed here in detail. As has already been deduced from the NMR data, the compound consists of two ferrocenylborane moieties bridged by a doubly coordinating bipy ligand. An inversion centre is located between C(33) and C(33a), and the bipy unit adopts the planar conformation required for an effective viologen-like electron acceptor. This finding is somewhat peculiar, because 4,4′-bipyridines, as well as biphenyls, tend to be twisted about their central C−C bond so as to minimize non-bonding interactions between adjacent hydrogen atoms.[43]

Compared to pyridine (py) complexes of boron Lewis acids,[43] the boron−nitrogen bonds of **1**·bipy·$\mathbf{1}_A$ are rather long [B(1)−N(1) = 1.682(5) Å; cf. BF_3·py: B−N = 1.603(5) Å, BCl_3·py: B−N = 1.592(3) Å].[38][44] Nevertheless, the boron centres are fully pyramidalized with the relevant angles C(1)−B(1)−C(2) = 113.5(3)°, C(1)−B(1)−C(11) = 112.9(3)° and C(2)−B(1)−C(11) = 114.2(3)° being only slightly larger than the value expected for an sp^3-hybridized boron atom with ideal tetrahedral geometry (109.5°). The B−N vectors of **1**·bipy·$\mathbf{1}_A$ are almost orthogonal to the C_5H_4 rings of the pendant ferrocenyl substituents with a torsion angle C(12)−C(11)−B(1)−N(1) of 90.5(4)°. The plane of the bipy bridge in **1**·bipy·$\mathbf{1}_A$ shows a dihedral angle C(11)−B(1)−N(1)−C(35) of 42.9(4)° with respect to the B(1)−C(11) bond [**1**·bipy·$\mathbf{1}_B$ shows a significantly different value of 4.3(3)°]. In summary, crystalline **1**·bipy·**1** features the desired molecular architecture: Two electropositive ferrocenyl fragments are held in close proximity to a rigid electroactive linker by means of simple B−N adduct formation.

Electrochemistry

The potential values are referred to the Saturated Calomel Electrode (S.C.E.); where necessary, literature data used for comparison have been recalculated for S.C.E. as reference. All the ferrocene adducts studied here display the typical ferrocene-centred oxidation, showing features of chemical reversibility on the cyclic voltammetric time scale. However, the electrochemical behaviour of most of the present complexes was found to be dependent on the concentrations employed. This is illustrated in Figure 5, which shows the cyclic voltammetric responses of **1**·bipy-Pr in DMF at concentrations of 2.3 × 10^{-3} mol·dm^{-3} (Figure 5a) and 0.2 × 10^{-3} mol·dm^{-3} (Figure 5b).

Following the main oxidation step, a minor but significant reversible peak system appears in the more dilute

sample at about +0.5 V, which vanishes almost completely when the concentration of **1**·bipy-Pr is increased by one order of magnitude. This picture is qualitatively independent of the scan rate (0.02 Vs^{-1} to 2.00 Vs^{-1}). **1**·bipy-Pr, as well as most other bipy adducts under investigation here, also exhibits two sequential reversible reduction processes, which are most likely centred at the bipy ligand ($E^{\circ\prime}$ = −0.80 V, −1.33 V; Table 4). Again, a concentration-dependent chemical complication is readily detectable. The corresponding potential value ($E^{\circ\prime} \approx -0.9$ V) is intermediate between the formal electrode potentials of the first redox transition of bipy ($E^{\circ\prime}$ = −1.84 V; Table 4) and that of paraquat $\mathbf{D}^{2+}$ ($E^{\circ\prime}$ = −0.36 V; Table 4). Moreover, the feature occurs at a more negative electrode potential than is observed in the case of **1**·bipy-Pr and may thus be assigned to the reduction of uncomplexed $[bipy\text{-}Pr]^+$. This assumption was confirmed by investigating an authentic sample of $[bipy\text{-}Pr]PF_6$, which possesses redox potentials of $E^{\circ\prime}$ = −0.95 V and −1.66 V. Our attempts to obtain cyclic voltammograms of **1** suffered from poor reproducibility due to severe decomposition processes that accompanied the one-electron removal. The minor reversible oxidation wave at $E^{\circ\prime} \approx +0.5$ V is thus probably not attributable to a $\mathbf{1/1}^+$ transition, but may be tentatively assigned to the oxidation of parent ferrocene, formed by rapid decomposition of free **1** under the experimental conditions employed. It may be concluded, therefore, that the chemical complications observed at low concentrations of **1**·Do are indicative of a dynamic equilibrium between the B−N adducts and their constituent components, as has already been deduced from NMR and IR data.

Controlled potential coulometric tests performed on concentrated DMF solutions of **1**·bipy-Pr (E_w = +0.4 V) consume one electron per molecule. The colour of the solution turns to pale-green and the typical absorption (λ_{max} = 635 nm) of ferricinium derivatives is observed. Moreover, in confirmation of the chemical reversibility of the **1**·bipy-Pr/$[\mathbf{1}\cdot bipy\text{-}Pr]^+$ oxidation, cyclic voltammetry on the exhaustively oxidized solution gives a voltammetric profile quite complementary to that shown in Figure 5a.

Analysis[45] of the cyclic voltammetric anodic response with scan rates varying from 0.02 Vs^{-1} to 1.00 Vs^{-1} shows that (a) the current ratio i_{pc}/i_{pa} is equal to 1 throughout; (b) the current function $i_{pa}/v^{1/2}$ remains constant; (c) the peak-to-peak separation does not depart appreciably from the value of 59 mV theoretically expected for an electrochemically reversible one-electron process. The same diagnostic criteria essentially hold for both reduction steps. The electrochemical reversibility of these processes indicates that no significant structural reorganizations are involved. The relevant redox potentials are compiled in Table 4, together with the electrochemical characteristics of all other complexes under consideration.

In confirmation of the assumption that the oxidation process is centred on the ferrocene moiety and that the sequential reductions are centred on the bipy fragment, the relative peak heights of the cathodic vs. the anodic steps exactly reflect the ratio between the number of bipy and

Figure 5. Cyclic voltammetric responses recorded at a platinum electrode of DMF solutions containing $[NEt_4]PF_6$ (0.1 $mol\cdot dm^{-3}$) and **1**·bipy-Pr: (a) 2.3×10^{-3} $mol\cdot dm^{-3}$; (b) 0.2×10^{-3} $mol\cdot dm^{-3}$; scan rate 0.2 Vs^{-1}

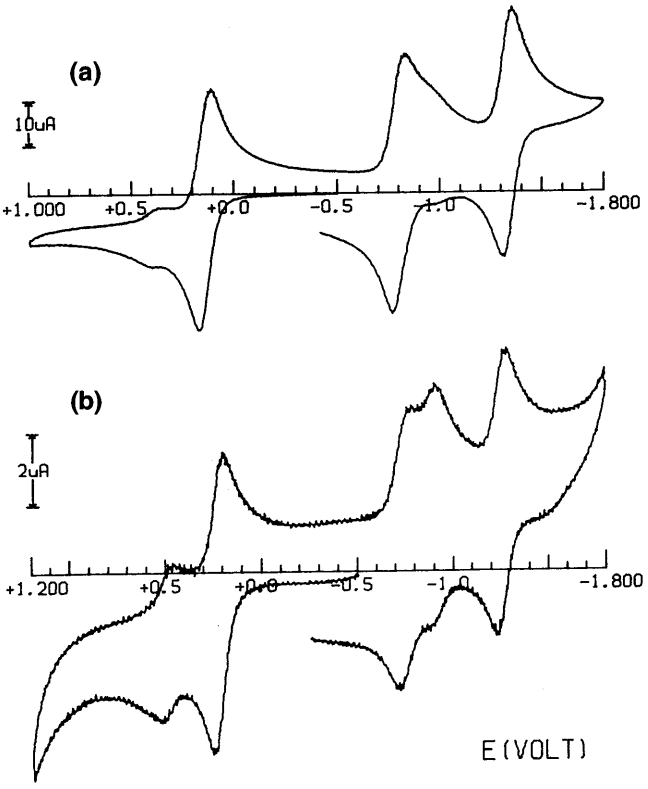

ferrocenyl units present in each molecule [i.e. **1**·bipy·**1**: 2:1; **2**·$(bipy\text{-}Pr)_2$: 1:2]. In passing, we note that the appearance of a single two-electron oxidation in the biferrocenyl complexes **1**·bipy·**1** and **1**·pyetpy·**1** suggests that no electronic communication between the outer ferrocenyl fragments takes place.

The presence of four-coordinate boron substituents in **1**·Do and **2**·$(Do)_2$ considerably lowers the oxidation potential of the central iron atoms. The effect is apparently additive, as can be seen from the $E^{\circ\prime}$ values of the parent ferrocene (+0.49 V), **1**·pic (+0.20 V) and **2**·$(pic)_2$ (−0.01 V) in DMF solution (Table 4). Oxidation generally occurs at somewhat more cathodic values in CH_2Cl_2. Most importantly, the oxidation potentials of **1**·pic ($E^{\circ\prime}$ = +0.20 V [DMF], +0.11 V [CH_2Cl_2]) and **2**·$(pic)_2$ ($E^{\circ\prime}$ = −0.01 V [DMF], −0.12 V [CH_2Cl_2]) are very close to those of Cp* FeCp ($E^{\circ\prime}$ = +0.12 [CH_3CN])[46] and Cp*FeCp* ($E^{\circ\prime}$ = −0.12 [CH_3CN]),[46] respectively. When pic is substituted by the more nucleophilic DMAP, a cathodic shift of the Fe^{II}/Fe^{III} transition is observed: $\Delta E^{\circ\prime}$(**1**·DMAP − **1**·pic) = −0.05 V [CH_2Cl_2], $\Delta E^{\circ\prime}$[**2**·$(DMAP)_2$ − **2**·$(pic)_2$] = −0.08 V [CH_2Cl_2]. We may therefore conclude that the electron-donating ability of a BMe_2·Do substituent attached to the Cp ligand is approximately equal to the positive inductive effect of the five methyl groups in (pentamethyl)cyclopentadienyl (Cp*). In addition, some fine-tuning of the Fe^{II}/Fe^{III} redox potential is possible by choosing pyridine bases of different pK_a values for boron coordination.

Table 4. Electrochemical and spectroscopic data characterizing the redox changes exhibited by the B−N adducts under study; formal electrode potentials $E^{\circ\prime}$ in V, vs. S.C.E.; peak-to-peak separations ΔE_p in mV, at 0.2 Vs^{-1}; wavelengths λ_{max} in nm for the oxidized ferricinium species

	$E^{\circ\prime}_{ox}$ (ΔE_p)	λ_{max}[a]	$E^{\circ\prime}_{red1}$ (ΔE_p)	$E^{\circ\prime}_{red2}$ (ΔE_p)	Solvent
1·pic	+0.20 (72)	[b]	–	–	DMF
	+0.11 (132)	[b]	–	–	CH_2Cl_2
1·DMAP	+0.18 (72)	[c]	–	–	DMF
	+0.06 (83)	648	–	–	CH_2Cl_2
1·bipy-Pr	+0.14 (76)	635	−0.80 (80)	−1.33 (62)	DMF
	+0.19 (96)	[b]	−0.78 (63)	−1.40 (71)	CH_2Cl_2
2·$(pic)_2$	−0.01 (73)	[c]	–	–	DMF
	−0.12 (121)	640	–	–	CH_2Cl_2
2·$(DMAP)_2$	−0.10 (73)	[c]	–	–	DMF
	−0.20 (86)	641	–	–	CH_2Cl_2
2·$(bipy\text{-}Pr)_2$	+0.02 (114)	[b]	−0.74 (89)	−1.30 (65)	DMF
	[d]	–	[d]	[d]	CH_2Cl_2
1·bipy·**1**	+0.17 (66)	[c]	−1.20 (72)	−1.75 (60)	DMF
	+0.15 (80)	627	−1.37 (128)	−1.91[e]	CH_2Cl_2
1·pyetpy·**1**	+0.21 (71)	[c]	–	–	DMF
	+0.11 (79)	630	–	–	CH_2Cl_2
bipy[f]	–	–	−1.84	−2.38	DMF
$\mathbf{D}^{2+}$[f]	–	–	−0.36	−0.80	DMF
FcH	+0.49 (72)	–	–	–	DMF
	+0.44 (90)	620	–	–	CH_2Cl_2

[a] Referred to the oxidized species. – [b] Not measured because of slow decomposition. – [c] Not measured. – [d] Not interpretable. – [e] Peak potential value. – [f] Ref.[6].

As expected, B−N adduct formation shifts the two reduction potentials of the bipy moiety by more than 0.6 V (DMF) towards more anodic values in the dimetallic complex **1**·bipy·**1** (bipy: $E^{\circ\prime}$ = −1.84 V, −2.38 V;[36] **1**·bipy·**1**: $E^{\circ\prime}$ = −1.20 V, −1.75 V). This effect is somewhat less pronounced than in the 9-boraadamantane adduct **C** [Figure 2; $E^{\circ\prime}$ = −1.10 V, −1.68 V (DMSO)],[36] which may be explained by the lower Lewis acidity of **1** bearing a strongly electron-donating ferrocenyl substituent. Like the Fc fragments in **1**·bipy·**1**, the two bipy-Pr substituents in **2**·$(bipy\text{-}Pr)_2$ do not show any significant degree of electronic communication.

UV/Vis Spectroscopy

In the solid state, all bipy complexes **1**·bipy·**1**, **1**·bipy-Pr, **2**·$(bipy\text{-}Pr)_2$ and [**2**·bipy]$_n$ exhibit an intense blue to purple colour, and single crystals of these compounds are almost black. We consider that these additional electronic absorptions, which cannot be attributed to internal transitions of bipy or the ferrocenylboranes **1** and **2**, are due to charge-transfer interactions between the electron-rich ferrocene donors and the electron-poor bipy diadducts. When the extended π-electron system of bipy is disrupted by inserting an ethylene spacer into its central C−C bond, the viologen-like electron acceptor is destroyed, and consequently the colour of the respective complexes changes to yellow (cf. **1**·pyetpy·**1**, [**2**·pyetpy]$_n$).

Somewhat surprisingly, the UV/Vis spectra of **1**·bipy·**1** and **1**·pyetpy·**1** are rather similar in solution (toluene, CH_2Cl_2) [λ_{max} = 447 nm (**1**·bipy·**1**); 447 nm (**1**·pyetpy·**1**)]. Several possible explanations for this phenomenon can be envisaged: (a) The Fc-to-bipy charge transfer may occur *inter*molecularly and thus require close contacts with specific spatial orientation of the individual complexes. These conditions are more likely to be met in the solid state rather than in dilute solution. (b) As has been shown by X-ray crystallography, the bipy bridge of **1**·bipy·**1** adopts a planar conformation in the crystal lattice. In solution, however, rotation about the central C(33)−C(33a) bond is to be expected, leading to a weakening of the electron acceptor due to the continuous perturbation of the π-electron system. (c) The Lambert-Beer law is only valid for highly dilute solutions. Since dilution favours dissociation of **1**·bipy·**1** and **1**·pyetpy·**1**, the UV spectra recorded under these conditions are not representative of the adduct complexes, but are most likely dominated by the bands of free **1**, bipy and pyetpy.

Thermal Analysis

To investigate the stability of solid **1**·bipy·**1** and [**2**·bipy]$_n$ more closely, differential thermal scans (DSC)[47] and thermogravimetric measurements (TG-MS)[48] were performed [heating rate: 10 $K \cdot min^{-1}$; inert gas flow (He): 16 sccm (DSC); 60 sccm (TGA)]. For comparison, the model compounds **1**·pic, **1**·DMAP and **2**·$(pic)_2$, **2**·$(DMAP)_2$ were included in this study.

All complexes show a sharp endothermic feature, followed by a broad, sometimes ill-defined, endothermic event at higher temperatures. With the exception of **2**·$(pic)_2$, the position of the first signal is independent of whether the thermal scans are run at constant pressure or at constant volume. In contrast, the second endothermic transition is markedly influenced by pressure and its onset temperature is generally shifted to higher values in a closed system (V = const.; Table 5).

These findings suggest that the first signal in each DSC plot is due to crystal melting, and this was confirmed by independent melting-point determinations, during which

Table 5. Results of DSC measurements

	1·pic	**1**·DMAP	**2**·$(pic)_2$	**2**·$(DMAP)_2$	**1**·bipy·**1**	$[\mathbf{2}\cdot bipy]_n$
$T(1)_{on}$[a]	127[c]/128[d]	156[c]/156[d]	165[c]/198[d]	244[c]/250[d]	180[c]/180[d]	240[c]/240[d]
$T(1)_p$[b]	130[c]/132[d]	160[c]/163[d]	182[c]/202[d]	254[c]/256[d]	182[c]/184[d]	245[c]/247[d]
$T(2)_{on}$[a]	–[c]/–[d]	–[c]/290[d]	–[c]/–[d]	–[c]/296[d]	–[c]/284[d]	–[c]/–[d]
$T(2)_p$[b]	195[c]/240[d]	290[c]/320[d]	–[c]/250[d]	280[c]/310[d]	240[c]/305[d]	260[c]/–[d]

[a] Onset temperature. – [b] Peak temperature of the first (1) and second (2) endothermic events. – [c] p = constant. – [d] V = constant.

the samples were viewed under a microscope. The much broader, less regular line shape recorded in most cases for the second endotherm, as well as its pressure dependence, indicates the occurrence of chemical transformations in the respective temperature range. At this stage, B–Cp and B–N bond rupture takes place, generating more volatile components such as the free pyridine bases, ferrocene, and the $(C_5H_5)Fe$ fragment (cf. $[\mathbf{2}\cdot bipy]_n$; Figure 6). The melting process of some adducts is thus accompanied by chemical decomposition. In these cases, it is not possible to accurately determine the onset temperatures $T(2)_{on}$ and therefore only the peak values $T(2)_p$ are given in Table 5. The melting points of **1**·pic to **2**·$(DMAP)_2$ show the expected influence of base strength, dipole moment, and molecular weight of the individual compounds. On going from pic to the more basic DMAP, the decomposition temperatures increase, which provides additional support for the assumption that the B–N bonds are the weakest parts in the molecular frameworks. No significant differences are found for the decomposition temperatures $T(2)_p$ of **1**·pic, **2**·$(pic)_2$ on the one hand, and of **1**·DMAP, **2**·$(DMAP)_2$ on the other. Hence, B–N adduct formation at one BMe_2 substituent seems to have little influence on the Lewis acidity of the second boron centre.

The dimetallic complex **1**·bipy·**1** and the coordination polymer $[\mathbf{2}\cdot bipy]_n$ possess high thermal stability in the solid state (Table 5). This finding is in contrast to the ready dissociation of $[\mathbf{2}\cdot bipy]_n$, even at moderate temperatures in toluene: As outlined above, $[\mathbf{2}\cdot bipy]_n$ is virtually insoluble in all common solvents at 20°C. At elevated temperature (T > 85°C), however, a slurry of $[\mathbf{2}\cdot bipy]_n$ in toluene is turned into a clear, orange-red solution, from which purple dendritic crystals are re-formed upon cooling (T < 70°C). This process may be repeated several times without significant decomposition of the material. The thermal behaviour of $[\mathbf{2}\cdot bipy]_n$ in the presence of a low-polarity solvent indicates that a reversible rupture of the oligomer backbone can be induced. Thermolysis of a slurry of $[\mathbf{2}\cdot bipy]_n$ in anhydrous and deaerated $[D_8]$toluene was also monitored by means of ^{1}H-NMR spectroscopy. Initially (20°C), the colourless supernatant shows no signals other than those of incompletely deuterated solvent. Upon heating to 80°C, however, resonances attributable to the mononuclear building blocks **2** [$\delta(^1H)$ = 0.84, 4.31, 4.44] and bipy [$(\delta(^1H)$ = 7.51, 8.72]

Figure 6. DSC, TG/DTG plots of $[\mathbf{2}\cdot bipy]_n$ and mass spectrometric analysis of thermolysis products

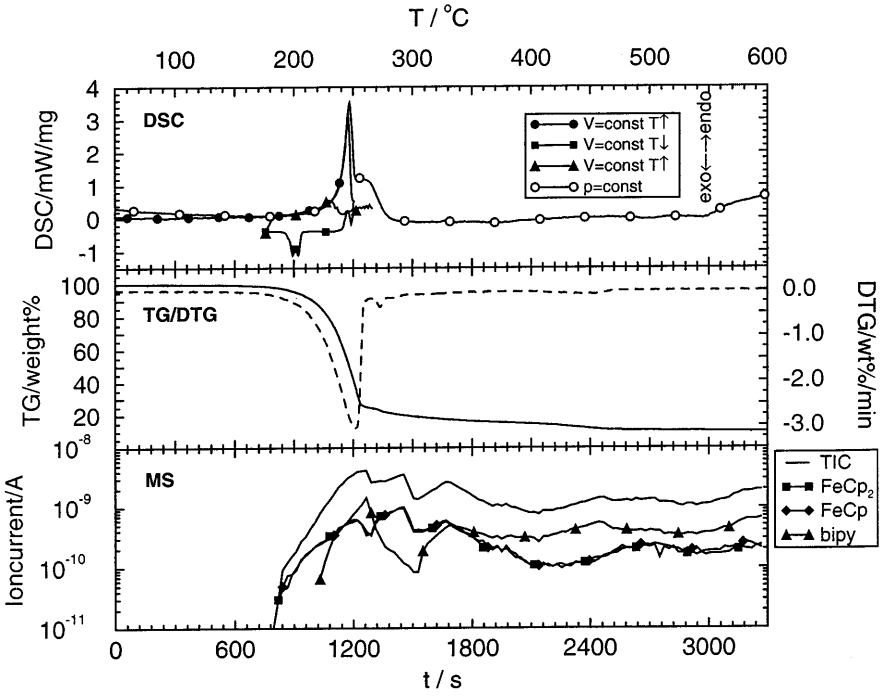

are detected in a molar ratio of 1:1. Some reversibility of the thermal transformation of [**2**·bipy]$_n$ is also maintained in the solid state (Figure 6).

When heating of the sample is stopped at 250°C under isochoric conditions and then the sample is cooled down again, an exothermic event is observed with an onset temperature $T(2)_{on}$ = 207°C and a peak temperature $T(2)_p$ = 200°C. A second heating scan again reveals an endothermic transition [$T(2)_p$ = 220°C] of lower intensity compared to the first scan.

Polymer Analysis

IR spectroscopy, DSC measurements and elemental analysis of neat [**2**·bipy]$_n$ suggest that this material consists of B−N coordination polymers. A solid-state ^{13}C-NMR spectrum of [**2**·bipy]$_n$ reveals that the compound crystallizes together with a small proportion of toluene. Otherwise, only the signals expected for well-defined polymeric [**2**·bipy]$_n$ are observed [$\delta(^{13}C)$ = 13.7 (BMe), 71.5 (Fc), 90.3 (Fc-*ipso*), 121.7, 143.9 (bipy), 147.2 (bipy-*ipso*)].

When a slurry of purple [**2**·bipy]$_n$ in CH_2Cl_2 is treated with excess pic, a clear orange solution is obtained (cf. Scheme 2), from which **2**·(pic)$_2$ and free bipy can be recovered in almost quantitative yield. This finding clearly demonstrates that the integrities of the molecular frameworks of **2** and bipy are maintained in [**2**·bipy]$_n$, and that its formation is not accompanied by unwanted side reactions. Moreover, it is evident that the copolymerization of **2** and bipy can not only be reversed by thermally induced B−N bond cleavage (see above), but also with the help of Lewis basic additives.

We have attempted to gather more detailed structural information on [**2**·bipy]$_n$ by X-ray crystallography. Unfortunately, we have not yet been able to obtain single crystals of sufficiently good quality to allow a full structure refinement (polysynthetic twins), although the polymeric nature of [**2**·bipy]$_n$ has been proven by a preliminary crystal structure solution.

Conclusion

A boron−nitrogen donor−acceptor bond is highly directional and is of a reversible nature. It can be very strong (H_3B-NH_3: 31 kcal·mol^{-1}), but the energy required for heterolytic dissociation may also be tuned over a wide range by judicious choice of appropriate substituents at the boron and nitrogen atoms. We therefore suggest consideration of B−N Lewis acid/base pairing as an alternative to hydrogen bonding for the generation of reversible polymer systems. Since an individual hydrogen bond is rather weak (3−7 kcal·mol^{-1}), only the cooperative action of many of them provides a linker that is sufficiently stable to build well-defined supramolecular aggregates.[49] The efficient control of cooperative phenomena requires very careful positioning of every single binding site, and this difficult task can be circumvented by employing B−N bonds instead.

On the basis of this B−N concept, organometallic polymers [**2**·bipy]$_n$ and [**2**·pyetpy]$_n$ have been synthesized from 1,1′-fc(BMe$_2$)$_2$, **2**, 4,4′-bipyridine, and 1,2-bis(4-pyridyl)-ethane, respectively. Neat [**2**·bipy]$_n$ is stable up to 240°C in the solid state. In the presence of toluene, however, the polymer is reversibly split into its constituent monomers upon warming to 85°C.

Apart from its role in establishing the polymer backbone, B−N adduct formation substantially changes the charge distribution of the ferrocene fragments and of the bipy bridges, as is evident from an investigation of the model complexes **1**·Do, **2**·(Do)$_2$ [Do: γ-picoline, 4-(dimethylamino)pyridine, *N*-(*n*-propyl)-4-(4′-pyridyl)pyridinium hexafluorophosphate], and **1**·Do·**1** [Do: 4,4′-bipyridine, 1,2-bis(4-pyridyl)ethane]: The donor strength of one BMe$_2$·Do substituent at ferrocene is equal to the electron-releasing effect of five methyl groups and consequently leads to a large cathodic shift of the Fe^{II}/Fe^{III} redox transition {e.g. $E°'$ = +0.44 V [CpFeCp, CH_2Cl_2]; +0.11 V [**1**·pic, CH_2Cl_2], +0.12 V [Cp*FeCp, CH_3CN]; −0.12 V [**2**·(pic)$_2$, CH_2Cl_2], −0.12 V [Cp*FeCp*, CH_3CN]}. For this reason, base adducts of ferrocenylboranes are an alternative to the widely used decamethylferrocene as electron donors in organometallic redox chemistry. In contrast to Cp*FeCp*, there are still four CH groups at each Cp ring of **1**·Do and **2**·(Do)$_2$ available for further functionalization, and the Fe^{II}/Fe^{III} redox potential is, moreover, tunable by selecting the appropriate pyridine base.

The electrochemical behaviour of the bipy linker is also sensitive to its coordination state, since each of the two one-electron reductions of parent 4,4′-bipyridine ($E°'$ = −1.84 V, −2.38 V; DMF) is shifted by about 0.6 V towards less negative values as a result of FcBMe$_2$ binding ($E°'$ = −1.20 V, −1.75 V [**1**·bipy·**1**; DMF]).

Destabilization of the ferrocene HOMO parallel to the stabilization of the bipy LUMO facilitates charge-transfer interactions between the two orbitals in **1**·bipy·**1**, **1**·bipy-Pr, **2**·(bipy-Pr)$_2$ and [**2**·bipy]$_n$, as indicated by the deep-purple colour of these compounds. In contrast, the ferrocene-free B−N adducts **C** (Figure 2), as well as the metal-containing complexes **1**·pyetpy·**1** and [**2**·pyetpy]$_n$ with two separated pyridine rings, exhibit the yellow colour usually observed for ferrocene derivatives bearing tetracoordinate boron substituents. The question as to whether charge-transfer in e.g. [**2**·bipy]$_n$ occurs within the polymeric rod or between two adjacent polymer chains will be subject of future investigations. Also attendant on the investigation of [**2**·bipy]$_n$ is the screening of a variety of bidentate Lewis bases other than bipy in order to increase the extent of charge delocalization in ferrocenylborane-containing coordination polymers. Promising results have already been obtained with pyrazine, which (a) brings adjacent ferrocene units into closer proximity, (b) is more rigid than bipy, and (c) forms bis-quaternary salts that are able to accept an electron at considerably more anodic potential values compared to *N*,*N*′-dialkylbipyridinium acceptors.[50][51]

We are grateful to Prof. Dr. *W. A. Herrmann* (Technische Universität München) for his generous support, to *H. Heise* for recording the solid-state ^{13}C-NMR spectra, and to *W. Hieringer* for helpful discussions. Financial funding by the *Deutsche Forschungsgemein-*

schaft (DFG) and the *Fonds der Chemischen Industrie* is acknowledged.

Experimental Section

All reactions and manipulations were carried out in dry, oxygen-free Ar using standard Schlenk glassware or in an Ar-filled dry-box. Solvents were freshly distilled under N_2 from Na/K alloy/benzophenone (hexane, toluene, THF) or from CaH_2 (CH_2Cl_2, CH_3Cl, CH_3CN) prior to use. − UV/Vis: Hewlett-Packard 8452 A. − IR: Perkin-Elmer 1650 FT-IR. − NMR: Jeol JMN-GX 400 and Bruker DPX 400 [abbreviations: s: singlet, d: doublet, t: triplet, vt: virtual triplet, br: broad, n.r.: multiplet expected but not resolved; pic: γ-picoline, DMAP: 4-(dimethylamino)pyridine, bipy: 4,4′-bipyridine, pyetpy: 1,2-bis(4-pyridyl)ethane, bipy-Pr: *N*-(*n*-propyl)-4-(4′-pyridyl)pyridinium hexafluorophosphate]. − ^{11}B-NMR spectra were referenced to external $BF_3{\cdot}Et_2O$. − MS (FAB/CI mode): Finnigan MAT 90. − Thermal analyses: Netzsch DSC 404 high-temperature furnace, thermocouple Pt/Rh, Perkin-Elmer TGA 7 thermobalance equipped with a Balzers QMG 420 mass spectrometer. − Elemental analyses: Microanalytical laboratory of the Technische Universität München. − The compounds **1**, **2**[15] and bipy-Pr[26] were synthesized according to literature procedures.

Preparation of **1**·pic: To a solution of **1** (0.25 g, 1.11 mmol) in toluene (10 ml) at ambient temperature, was added γ-picoline (0.10 g, 1.07 mmol) in toluene (5 ml) by means of a cannula. The resultant clear orange solution was stirred for 3 h and then concentrated to half of its original volume in vacuo, whereupon **1**·pic gradually precipitated as an orange crystalline solid. The precipitate was collected on a frit (G3), treated with cold hexane (−30°C) and dried in vacuo. The mother liquor was kept in a refrigerator (−30°C) for 12 h to yield a second crop. Yield 0.32 g (93%). − IR (KBr, cm^{-1}): $\tilde{\nu}$ = 1628 (vs), 1507 (m) (pic-C−C, C−N), 1104 (m), 1068 (m), 1058 (m) (B−N). − ^{11}B NMR (128.3 MHz, $CDCl_3$): δ = 0.4 ($h_{1/2}$ = 300 Hz). − ^{1}H NMR (400 MHz, $CDCl_3$): δ = 0.27 (s, 6 H, BCH_3), 2.35 (s, 3 H, pic-CH_3), 4.03 (vt, 2 H, *J* = 1.7 Hz, C_5H_4), 4.06 (s, 5 H, C_5H_5), 4.16 (vt, 2 H, *J* = 1.7 Hz, C_5H_4), 7.16 (d, 2 H, *J* = 6.6 Hz, pic-3-H, -5-H), 8.41 (d, 2 H, *J* = 6.6 Hz, pic-2-H, -6-H). − ^{13}C NMR (100.5 MHz, $CDCl_3$): δ = 11.1 (br, BCH_3), 21.0 (pic-CH_3), 67.9 (C_5H_5), 68.4, 71.7 (C_5H_4), n.o. (C_5H_4-*ipso*), 125.4 (pic-C-3, -C-5), 144.5 (pic-C-2, -C-6), 150.7 (pic-C-4). − $C_{18}H_{22}BFeN$ (319.04): calcd. C 67.77, H 6.95, N 4.39; found C 67.86, H 6.92, N 4.31.

Preparation of **1**·DMAP: **1** (0.34 g, 1.51 mmol) in toluene (10 ml) was treated with 4-(dimethylamino)pyridine (0.18 g, 1.47 mmol) in toluene (5 ml) at ambient temperature. The cloudy orange mixture was stirred for 1 h and then concentrated to half of its original volume in vacuo, whereupon an orange precipitate gradually formed. The precipitate was removed by filtration (G3 frit), triturated with hexane, and dried in vacuo. A second crop was obtained from the mother liquor upon storage at −30°C for 12 h. Yield 0.46 g (90%). − IR (KBr, cm^{-1}): $\tilde{\nu}$ = 1636 (vs), 1544 (m) (DMAP-C−C, C−N), 1104 (m), 1076 (m), 1058 (m) (B−N). − ^{11}B NMR (128.3 MHz, $CDCl_3$): δ = −3.0 ($h_{1/2}$ = 300 Hz). − ^{1}H NMR (400 MHz, $CDCl_3$): δ = 0.16 (s, 6 H, BCH_3), 3.02 (s, 6 H, NCH_3), 3.97 (vt, 2 H, *J* = 1.5 Hz, C_5H_4), 4.05 (s, 5 H, C_5H_5), 4.09 (vt, 2 H, *J* = 1.5 Hz, C_5H_4), 6.41 (d, 2 H, *J* = 6.6 Hz, DMAP-3-H, -5-H), 8.09 (d, 2 H, *J* = 6.6 Hz, DMAP-2-H, -6-H). − ^{13}C NMR (100.5 MHz, $CDCl_3$): δ = 10.9 (br, BCH_3), 39.2 (NCH_3), 67.8 (C_5H_5), 68.0, 71.5 (C_5H_4), n.o. (C_5H_4-*ipso*), 106.0 (DMAP-C-3, -C-5), 144.2 (DMAP-C-2, -C-6), 154.4 (DMAP-C-4). − $C_{19}H_{25}BFeN_2$ (348.08): calcd. C 65.56, H 7.24, N 8.05; found C 65.28, H 7.16, N 7.96.

Preparation of **1**·bipy-Pr: **1** (0.11 g, 0.49 mmol) in CH_3CN (3 ml) was treated with *N*-(*n*-propyl)-4-(4′-pyridyl)pyridinium hexafluorophosphate (0.17 g, 0.49 mmol) in CH_3CN (2 ml) at ambient temperature. The reaction mixture, which instantaneously took on a purple colour, was stirred for 1 h and then concentrated to a volume of 1 ml. Toluene (15 ml) was added, whereupon **1**·bipy-Pr precipitated quantitatively as a dark-purple microcrystalline solid, which was triturated with toluene (3 × 5 ml) and hexane (2 × 5 ml) and dried in vacuo overnight. Yield 0.25 g (90%). − IR (KBr, cm^{-1}): $\tilde{\nu}$ = 1646 (vs), 1627 (vs), 1552 (m), 1501 (m) (bipy-C−C, C−N), 1102 (m), 1079 (m), 1061 (m) (B−N). − ^{11}B NMR (128.3 MHz, CD_3CN): δ = 7.5 ($h_{1/2}$ = 350 Hz). − ^{1}H NMR (400 MHz, CD_3CN): δ = 0.30 (s, 6 H, BCH_3), 0.97 (t, 3 H, *J* = 7.5 Hz, CH_3), 2.01 (m, 2 H, CH_2CH_3), 4.06 (s, 5 H, C_5H_5), 4.08, 4.19 (n.r., 2 × 2 H, C_5H_4), 4.53 (t, 2 H, *J* = 7.6 Hz, NCH_2), 7.91, 8.29, 8.80, 8.87 (4 × d, 4 × 2 H, *J* = 6.5 Hz, bipy). − ^{13}C NMR (100.5 MHz, CD_3CN): δ = 10.5 (CH_3), 11.0 (br, BCH_3), 25.3 (CH_2CH_3), 64.0 (NCH_2), 69.2 (C_5H_5), 70.0, 72.5 (2 × br, C_5H_4), n.o. (C_5H_4-*ipso*), 124.4, 127.7, 144.6, 146.1, 148.5, 153.5 (bipy). − $C_{25}H_{30}BF_6FeN_2P$ (570.15): calcd. C 52.67, H 5.30, N 4.91; found C 52.33, H 5.25, N 4.92.

Preparation of **1**·bipy·**1**: At ambient temperature, a colourless solution of 4,4′-bipyridine (0.25 g, 1.60 mmol) in toluene (10 ml) was added dropwise to an orange-red solution of **1** (0.73 g, 3.23 mmol) in toluene (10 ml). The reaction mixture, which instantaneously took on a dark-brown colour, was stirred for 3 h, whereupon a purple microcrystalline solid gradually precipitated. All insolubles were collected on a frit (G3), triturated with toluene (5 ml) and hexane (5 ml), and dried in vacuo. The filtrate was kept at −30°C overnight to yield a second crop. Yield 0.91 g (94%). X-ray quality crystals were obtained from toluene/hexane (1:1) at −30°C. − IR (KBr, cm^{-1}): $\tilde{\nu}$ = 1622 (vs), 1540 (m), 1493 (m) (bipy-C−C, C−N), 1100 (s), 1075 (s), 1058 (s) (B−N); IR (CH_2Cl_2, cm^{-1}): $\tilde{\nu}$ = 1622 (vs), 1597 (w), 1538 (w), 1517 (vw), 1489 (m) (bipy-C−C, C−N), 1104 (s), 1076 (s), 1058 (s) (B−N). − UV (CH_2Cl_2): λ = 239, 447 nm. − ^{11}B NMR (128.3 MHz, $CDCl_3$): δ = 15.1 ($h_{1/2}$ = 700 Hz). − ^{1}H NMR (400 MHz, $CDCl_3$): δ = 0.40 (s, 12 H, BCH_3), 4.08 (s, 10 H, C_5H_5), 4.13, 4.27 (2 × n.r., 2 × 4 H, C_5H_4), 7.53 (d, 4 H, *J* = 5.5 Hz, bipy-3-H, -5-H), 8.72 (d, 4 H, *J* = 5.5 Hz, bipy-2-H, -6-H). − ^{13}C NMR (100.5 MHz, $CDCl_3$): δ = 10.8 (br, BCH_3), 68.5 (C_5H_5), 70.3, 72.8 (C_5H_4), n.o. (C_5H_4-*ipso*), 122.2 (bipy-C-3, -C-5), 145.9 (bipy-C-4), 147.4 (bipy-C-2, -C-6). − $C_{34}H_{38}B_2Fe_2N_2$ (608.00): calcd. C 67.17, H 6.30, N 4.61; found C 66.81, H 6.54, N 4.41.

Preparation of **1**·pyetpy·**1**: **1** (0.72 g, 3.19 mmol) in toluene (20 ml) was treated dropwise with 1,2-bis(4-pyridyl)ethane (0.29 g, 1.57 mmol) in toluene (10 ml) at ambient temperature. A yellow microcrystalline solid precipitated from the orange reaction mixture. The slurry was stirred for 3 h and the solid material was isolated by filtration. After trituration with toluene (5 ml) and hexane (5 ml), the product was dried in vacuo. Yield 0.96 g (84%). − IR (KBr, cm^{-1}): $\tilde{\nu}$ = 1623 (s), 1560 (w), 1506 (m), 1496 (m) (pyetpy-C−C, C−N), 1102 (m), 1069 (s), 1061 (m) (B−N). − UV (CH_2Cl_2): λ = 239, 447 nm. − ^{11}B NMR (128.3 MHz, $CDCl_3$): δ = 6.2 ($h_{1/2}$ = 900 Hz). − ^{1}H NMR (400 MHz, $CDCl_3$): δ = 0.29 (s, 12 H, BCH_3), 2.94 (s, 4 H, -CH_2-), 4.04 (vt, 4 H, *J* = 1.5 Hz, C_5H_4), 4.06 (s, 10 H, C_5H_5), 4.18 (vt, 4 H, *J* = 1.5 Hz, C_5H_4), 7.14 (d, 4 H, *J* = 6.0 Hz, pyetpy-3-H, -5-H), 8.48 (d, 4 H, *J* = 6.0 Hz, pyetpy-2-H, -6-H). − ^{13}C NMR (100.5 MHz, $CDCl_3$): δ = 10.9 (br, BCH_3), 34.8 (−CH_2−), 68.1 (C_5H_5), 69.2, 72.1 (C_5H_4), n.o. (C_5H_4-*ipso*), 124.4 (pyetpy-C-3, -C-5), 145.8 (pyetpy-C-2, -C-6), 151.8 (pyetpy-C-4). − $C_{36}H_{42}B_2Fe_2N_2$ (636.07)·C_7H_8 (92.14): calcd. C 70.92, H 6.92, N 3.85; found C 70.97, H 6.67, N 3.79.

Preparation of **2**·$(pic)_2$: **2** (0.43 g, 1.62 mmol) in toluene (10 ml) was treated with a solution of γ-picoline (0.33 g, 3.54 mmol) in

toluene (5 ml) at ambient temperature. The resultant orange slurry was stirred for 1 h. Insoluble material was collected on a frit (G3), triturated with hexane (5 ml), and dried in vacuo. Yield 0.59 g (81%). − IR (KBr, cm^{-1}): $\tilde{\nu}$ = 1628 (s), 1508 (m) (pic-C−C, C−N), 1066 (s), 1047 (s) (B−N). − ^{11}B NMR (128.3 MHz, $CDCl_3$): δ = 15.0 ($h_{1/2}$ = 300 Hz). − ^1H NMR (400 MHz, $CDCl_3$): δ = 0.34 (s, 12 H, BCH_3), 2.37 (s, 6 H, pic-CH_3), 3.99, 4.13 (2 × n.r., 2 × 4 H, C_5H_4), 7.15 (d, 4 H, J = 6.0 Hz, pic-3-H, -5-H), 8.44 (d, 4 H, J = 6.0 Hz, pic-2-H, -6-H). − ^{13}C NMR (100.5 MHz, $CDCl_3$): δ = 10.9 (br, BCH_3), 21.1 (pic-CH_3), 71.0, 72.6 (C_5H_4), n.o. (C_5H_4-*ipso*), 125.2 (pic-C-3, -C-5), 145.6 (pic-C-2, -C-6), 149.8 (pic-C-4). − $C_{26}H_{34}B_2FeN_2$ (452.04): calcd. C 69.08, H 7.58, N 6.20; found C 68.58, H 7.38, N 6.10.

Preparation of **2**·$(DMAP)_2$: The compound was synthesized similarly to **2**·$(pic)_2$ using **2** (0.18 g, 0.68 mmol) and 4-(dimethylamino)-pyridine (0.17 g, 1.39 mmol). Yield 0.28 g (81%). − IR (KBr, cm^{-1}): $\tilde{\nu}$ = 1638 (vs), 1552 (s) (DMAP-C−C, C−N), 1077 (m), 1060 (m) (B−N). − ^{11}B NMR (128.3 MHz, $CDCl_3$): δ = −2.3 ($h_{1/2}$ = 500 Hz). − ^1H NMR (400 MHz, $CDCl_3$, 55°C): δ = 0.39 (s, 12 H, BCH_3), 3.01 (s, 12 H, NCH_3), 4.01, 4.16 (2 × n.r., 2 × 4 H, C_5H_4), 6.42 (d, 4 H, J = 6.6 Hz, DMAP-3-H, -5-H), 8.12 (d, 4 H, J = 6.6 Hz, DMAP-2-H, -6-H). − ^{13}C NMR (100.5 MHz, $CDCl_3$, 55°C): δ = 10.6 (br, BCH_3), 39.2 (NCH_3), 71.8, 73.1 (C_5H_4), n.o. (C_5H_4-*ipso*), 106.1 (DMAP-C-3, -C-5), 144.4 (DMAP-C-2, -C-6), 154.7 (DMAP-C-4). − $C_{28}H_{40}B_2FeN_4$ (510.13): calcd. C 65.93, H 7.90, N 10.98; found C 65.44, H 7.77, N 10.74.

Preparation of **2**·$(bipy\text{-}Pr)_2$: The compound was synthesized similarly to **1**·bipy-Pr from **2** (0.19 g, 0.71 mmol) and *N*-(*n*-propyl)-4-(4′-pyridyl)pyridinium hexafluorophosphate (0.49 g, 1.42 mmol). Yield 0.42 g (60%). − IR (KBr, cm^{-1}): $\tilde{\nu}$ = 1645 (vs), 1624 (s), 1550 (m), 1496 (m), 1470 (m) (bipy-C−C, C−N), 1072 (w), 1062 (m) (B−N). − ^{11}B NMR (128.3 MHz, CD_3CN): δ = 15.1 ($h_{1/2}$ = 500 Hz). − ^1H NMR (400 MHz, CD_3CN): δ = 0.42 (br, 12 H, BCH_3), 0.97 (t, 6 H, J = 7.5 Hz, CH_3), 2.01 (m, 4 H, CH_2CH_3), 4.05, 4.18 (2 × n.r., 2 × 4 H, C_5H_4), 4.52 (t, 4 H, J = 7.6 Hz, NCH_2), 7.88, 8.30, 8.76, 8.88 (4 × d, 4 × 4 H, J = 6.5 Hz, bipy). − ^{13}C NMR (100.5 MHz, CD_3CN): δ = 10.5 (CH_3), 11.0 (br, BCH_3), 25.3 (CH_2CH_3), 64.0 (NCH_2), 73.0, 74.0 (2 × br, C_5H_4), n.o. (C_5H_4-*ipso*), 124.1, 127.4, 144.1, 146.0, 149.2, 153.9 (bipy). − $C_{40}H_{50}B_2F_{12}FeN_4P_2$ (954.27)·0.4 C_7H_8 (92.14): calcd. C 51.87, H 5.41, N 5.65, Fe 5.63; found C 51.92, H 5.45, N 5.68, Fe 5.23.

Preparation of [**2**·bipy]$_n$: A red solution of **2** (0.13 g, 0.49 mmol) in $CHCl_3$ (15 ml) was layered firstly with neat CH_2Cl_2 (15 ml) and secondly with a solution of 4,4′-bipyridine (0.08 g, 0.51 mmol) in THF (10 ml). After 12 h, mixing of all three phases was complete and a purple microcrystalline precipitate had formed, which was found to be insoluble in all common solvents at ambient temperature. Yield 0.20 g (96%). − IR (KBr, cm^{-1}): $\tilde{\nu}$ = 1622 (vs), 1540 (m), 1493 (m) (bipy-C−C, C−N), 1075 (s), 1061 (s) (B−N). − $[C_{24}H_{28}B_2FeN_2]_n$ (421.97)$_n$: calcd. C 68.31, H 6.69, N 6.64; found C 67.91, H 6.62, N 6.48.

Preparation of [**2**·pyetpy]$_n$: A solution of 1,2-bis(4-pyridyl)ethane (0.13 g, 0.71 mmol) in toluene (20 ml) was added dropwise with stirring to **2** (0.19 g, 0.71 mmol) in toluene (20 ml). The resultant orange slurry was stirred for 4 h, the insoluble material was collected on a frit (G3), triturated with hexane (5 ml), and dried in vacuo. The product was found to be insoluble in all common solvents at ambient temperature. Yield 0.25 g (78%). − IR (KBr, cm^{-1}): $\tilde{\nu}$ = 1626 (vs), 1567 (w), 1506 (m) (pyetpy-C−C, C−N), 1073 (m), 1059 (s) (B−N). − $[C_{26}H_{32}B_2FeN_2]_n$ (450.03)$_n$: calcd. C 69.39, H 7.17, N 6.22; found C 69.33, H 7.27, N 6.26.

X-ray Crystal Structure Analysis of **1**·bipy·**1**:[42] A selected purple crystal of **1**·bipy·**1** was placed in perfluorinated oil and mounted in a glass capillary on an Image Plate Diffraction System (IPDS, STOE). Final lattice parameters were obtained by least-squares refinement of 2988 reflections (graphite monochromator, λ = 0.71073 Å, Mo-K_α). Empirical formula $C_{34}H_{38}B_2Fe_2N_2$, formula weight = 608.00, triclinic system, space group $P\bar{1}$ (I.T. no.: 2); a = 8.7143(5) Å, b = 13.8257(10) Å, c = 15.8214(12) Å, α = 65.820(7), β = 86.337(7), γ = 75.376(7), V = 1680.9(2) Å^3, crystal size 0.20 × 0.13 × 0.13 mm, Z = 2, F(000) = 636. Data were collected at 293 K, distance from crystal to image plate 70 mm (10.2° < Θ < 24.7°), 300 images collected, 0° < φ < 300°, Δφ = 1°, exposure time 5 min. Data were corrected for Lorentz and polarization terms.[52] A decay and absorption correction (μ = 8.9 cm^{-1}) was performed using the program DECAY;[52] 19554 data measured, 4982 independent reflections used for refinement. The structure was solved by direct methods and refined with standard difference Fourier techniques.[53] All hydrogen atoms of **1**·bipy·**1** were calculated in ideal positions (riding model). **1**·bipy·**1** crystallizes together with 0.5 equiv. of toluene (NMR spectroscopy; elemental analysis). Severe disorder of the toluene molecules precluded their structural refinement to any satisfactory level. We have therefore applied the "squeeze" routine[54] to remedy this disordered solvent problem (potential solvent accessible area: 293 Å^3). Number of parameters refined: 361, 13.8 data per parameter, weighting scheme w = 1/[$\sigma^2(F_o^2)$ + (0.0176·P)^2] where P = (F_o^2 + 2·F_c^2)/3, shift/error < 0.001 in the last cycle of refinement, residual electron density +0.15 eÅ^{-3}, −0.18 eÅ^{-3}, *R1* = 0.0319 [I > 2σ(I)], *wR2* = 0.0558 (all data), the minimized function was Σw(F_o^2 − F_c^2)^2. Neutral atom scattering factors for all atoms and anomalous dispersion corrections for the non-hydrogen atoms were taken from the *International Tables for X-ray Crystallography.*[55] All calculations were performed with a DEC 3000 AXP workstation with the STRUX-V system,[56] incorporating the programs PLATON-92,[57] PLUTON-92,[57] SHELXS-86,[58] SIR-92,[53] and SHELXL-93.[59]

Electrochemical Measurements: Cyclic voltammetry and controlled potential coulometry were performed in deaerated dimethylformamide (DMF) and CH_2Cl_2 solutions containing [NEt_4][PF_6] (0.1 mol·dm^{-3}) and [NBu_4][ClO_4] (0.2 mol·dm^{-3}), respectively, as supporting electrolytes. All potential values are referred to the Saturated Calomel Electrode (S.C.E.). The apparatus for electrochemistry measurements is described in ref.[60].

☆ Dedicated to Professor *Heinrich Nöth* with gratitude on the occasion of his 70th birthday.

[1] I. Manners, *Angew. Chem.* **1996**, *108*, 1712−1731; *Angew. Chem. Int. Ed. Engl.* **1996**, *35*, 1602−1621.
[2] D. W. Bruce, D. O'Hare, *Inorganic Materials*, Wiley, New York, **1992**.
[3] L. Oriol, J. L. Serrano, *Adv. Mater.* **1995**, *7*, 348−369.
[4] D. A. Foucher, B.-Z. Tang, I. Manners, *J. Am. Chem. Soc.* **1992**, *114*, 6246−6248.
[5] I. Manners, *Adv. Organomet. Chem.* **1995**, *37*, 131−168.
[6] J. B. Sheridan, K. Temple, A. J. Lough, I. Manners, *J. Chem. Soc., Dalton Trans.* **1997**, 711−713.
[7] T. L. Hennigar, D. C. MacQuarrie, P. Losier, R. D. Rogers, M. J. Zaworotko, *Angew. Chem.* **1997**, *109*, 1044−1046; *Angew. Chem. Int. Ed. Engl.* **1997**, *36*, 972−973.
[8] F. Jäkle, T. Priermeier, M. Wagner, *Chem. Ber.* **1995**, *128*, 1163−1169.
[9] F. Jäkle, K. Polborn, M. Wagner, *Chem. Ber.* **1996**, *129*, 603−606.
[10] F. Fabrizi de Biani, F. Jäkle, M. Spiegler, M. Wagner, P. Zanello, *Inorg. Chem.* **1997**, *36*, 2103−2111.
[11] E. Herdtweck, F. Peters, W. Scherer, M. Wagner, *Polyhedron* **1998**, *17*, 1149−1157.
[12] J. C. Kotz, E. W. Post, *Inorg. Chem.* **1970**, *9*, 1661−1669.

[13] W. Ruf, M. Fueller, W. Siebert, *J. Organomet. Chem.* **1974**, *64*, C45−C47.
[14] T. Renk, W. Ruf, W. Siebert, *J. Organomet. Chem.* **1976**, *120*, 1−25.
[15] W. Ruf, T. Renk, W. Siebert, *Z. Naturforsch., B* **1976**, *31b*, 1028−1034.
[16] A. Appel, H. Nöth, M. Schmidt, *Chem. Ber.* **1995**, *128*, 621−626.
[17] H. C. Brown, X. R. Mihm, *J. Am. Chem. Soc.* **1955**, *77*, 1723−1726.
[18] J. M. Essery, K. Schofield, *J. Chem. Soc.* **1961**, 3939−3953.
[19] S. Hünig, H. Berneth, *Top. Curr. Chem.* **1980**, *92*, 1−44.
[20] A. J. Bard, A. Ledwith, H. J. Shine, *Adv. Phys. Org. Chem.* **1976**, *13*, 155−278.
[21] A. J. Bard, *Nature* **1995**, *374*, 13.
[22] P. Hanson, *Adv. Heterocycl. Chem.* **1979**, *25*, 205−301.
[23] A. Factor, G. E. Heinsohn, *J. Polym. Sci. B* **1971**, *9*, 289−295.
[24] M. S. Simon, P. T. Moore, *J. Polym. Sci., Polym. Chem. Ed.* **1975**, *13*, 1−16.
[25] H. Sato, T. Tamamura, *J. Appl. Polym. Sci.* **1979**, *24*, 2075−2085.
[26] H. Kamogawa, H. Mizuno, Y. Todo, M. Nanasawa, *J. Polym. Sci.* **1979**, *17*, 3149−3157.
[27] W. Kaim, *Chem. Ber.* **1981**, *114*, 3789−3800.
[28] W. Kaim, *J. Organomet. Chem.* **1983**, *241*, 157−169.
[29] A. Lichtblau, H.-D. Hausen, W. Schwarz, W. Kaim, *Inorg. Chem.* **1993**, *32*, 73−78.
[30] J. Fiedler, S. Zalis, A. Klein, F. M. Hornung, W. Kaim, *Inorg. Chem.* **1996**, *35*, 3039−3043.
[31] F. Fabrizi de Biani, T. Gmeinwieser, E. Herdtweck, F. Jäkle, F. Laschi, M. Wagner, P. Zanello, *Organometallics* **1997**, *16*, 4776−4787.
[32] F. Peters, M. Wagner, manuscript in preparation.
[33] P. Krumholz, *J. Am. Chem. Soc.* **1951**, *73*, 3487−3492.
[34] H. Nöth, B. Wrackmeyer, *Nuclear Magnetic Resonance Spectroscopy of Boron Compounds*, in *NMR Basic Principles and Progress* (Eds.: P. Diehl, E. Fluck, R. Kosfeld), Springer Verlag, Berlin, **1978**.
[35] H. Friebolin, *Basic One- and Two-Dimensional NMR Spectroscopy*, 2nd ed., Verlag Chemie, Weinheim, **1992**.
[36] S. Hünig, I. Wehner, *Liebigs Ann. Chem.* **1989**, 299−301.
[37] H. C. Brown, R. R. Holmes, *J. Am. Chem. Soc.* **1956**, *78*, 2173−2176.
[38] K.-H. Töpel, K. Hensen, J. W. Bats, *Acta Crystallogr., C* **1984**, *40*, 828−830.
[39] N. N. Greenwood, K. Wade, *J. Chem. Soc.* **1960**, 1130−1141.
[40] H. Luther, D. Mootz, F. Radwitz, *J. Prakt. Chemie* **1957**, *5*, 242−259.
[41] A. R. Katritzky, *J. Chem. Soc.* **1959**, 2049−2051.
[42] Further details of the crystal structure investigations are available on request from the Fachinformationszentrum Karlsruhe, Gesellschaft für wissenschaftlich-technische Information mbH, D-76344 Eggenstein-Leopoldshafen (Germany), on quoting the depository number CSD-408518.
[43] F. H. Allen, O. Kennard, R. Taylor, *Acc. Chem. Res.* **1983**, *16*, 146−153.
[44] K.-H. Töpel, K. Hensen, M. Trömel, *Acta Crystallogr., B* **1981**, *37*, 969−971.
[45] E. R. Brown, J. Sandifer, in *Physical Methods in Chemistry: Electrochemical Methods* (Eds.: B. W. Rossiter, J. F. Hamilton), Wiley, New York, **1986**.
[46] A. Togni, T. Hayashi (Eds.), *Ferrocenes*, VCH Verlagsgesellschaft, Weinheim, **1995**.
[47] P. J. Haines, *Thermal Methods of Analysis, Principles, Applications and Problems*, Blackie Academic Press, London, **1995**. Note: Only a qualitative interpretation of data obtained under isochoric conditions is possible due to the limited stability of the aluminum crucibles used. At temperatures exceeding 250°C, large pressure build-up may lead to some leakage such that the reaction volume is no longer strictly constant.
[48] H.-G. Wiedemann, G. Bayer, *Top. Curr. Chem.* **1978**, *77*, 67−140.
[49] R. P. Sijbesma, F. H. Beijer, L. Brunsveld, B. J. B. Folmer, J. H. K. K. Hirschberg, R. F. M. Lange, J. K. L. Lowe, E. W. Meijer, *Science* **1997**, *278*, 1601−1604.
[50] H.-D. Hausen, A. Schulz, W. Kaim, *Chem. Ber.* **1988**, *121*, 2059−2061.
[51] J. Baumgarten, C. Bessenbacher, W. Kaim, T. Stahl, *J. Am. Chem. Soc.* **1989**, *111*, 2126−2131.
[52] IPDS Operating System Version 2.6. STOE & CIE GmbH, Darmstadt, Germany, **1995**.
[53] A. Altomare, G. Cascarano, C. Giacovazzo, A. Guagliardi, M. C. Burla, G. Polidori, M. Camalli, *SIR-92*, University of Bari, Italy, **1992**.
[54] A. Spek, *SQUEEZE, An Effective Cure for the Disordered Solvent Syndrome in Crystal Structure Refinement*, ACA-94, Atlanta, USA, **1994**, Abstract M05 (p. 66).
[55] *International Tables for Crystallography*, vol. C, tables 6. 1. 1. 4 (pp. 500−502), 4.2.6.8 (pp. 219−222) and 4.2.4.2 (pp. 193−199) (Ed.: A. J. C. Wilson), Kluwer Academic Publishers, Dordrecht, **1992**.
[56] G. Artus, W. Scherer, T. Priermeier, E. Herdtweck, *STRUX-V, A Program System to Handle X-ray Data*, TU München, Germany, **1994**.
[57] A. L. Spek, *Acta Crystallogr., A* **1990**, *46*, C34.
[58] G. M. Sheldrick, *SHELXS-86: Program for Crystal Structure Solutions*, Universität Göttingen, Germany, **1986**.
[59] G. M. Sheldrick, "SHELXL-93" in *Crystallographic Computing 3* (Eds.: G. M. Sheldrick, C. Krüger, R. Goddard), Oxford University Press, **1993**.
[60] C. Bianchini, F. Laschi, D. Masi, F. M. Ottaviani, A. Pastor, M. Peruzzini, P. Zanello, F. Zanobini, *J. Am. Chem. Soc.* **1993**, *115*, 2723−2730.

[98092]

Gradient-Enhanced 2D Multinuclear NMR and X-ray Diffraction Studies of Reaction Products of Dimethyltin(IV) Salicylaldoximate with Chiral Alcohols

Abdelkrim Meddour[a][+], Abdeslam Bouhdid[b], Marcel Gielen[b], Monique Biesemans[a,b], Frédéric Mercier[a,b], Edward R. T. Tiekink[c], and Rudolph Willem*[a,b]

High Resolution NMR Centre (HNMR)[a] and Laboratory of General and Organic Chemistry (AOSC)[b],
Free University of Brussels (VUB),
Pleinlaan 2, B-1050 Brussels, Belgium
Fax: (internat.) + 32-2/629-3281
E-mail: rwillem@vub.ac.be

Department of Chemistry, The University of Adelaide[c],
Australia 5005

Received April 8, 1998

Keywords: Dimethyltin salicylaldoximates / Chiral ligands / Proton-tin HMQC NMR / X-ray structure / Trinuclear microclusters

The complex {[$(CH_3)_2Sn]_2$[$(CH_3)_2SnO$](OCH$_3$)(HONZO)(ONZO)} (**3**) [ONZOH is the oximate residue, *o*-(–ON=CH–C_6H_4–OH), HONZO the corresponding phenolate residue, *o*-(HON=CH–C_6H_4–O–), and ONZO the dibasic species *o*-(–ON=CH–C_6H_4–O–), all derived from salicylaldoxime, *o*-(HON=CH–C_6H_4–OH)] reacts with an excess of racemic (*d,l*)-2-methyl-1-butanol to afford the μ_2-substitution product **5a** {[$(CH_3)_2Sn]_2$[$(CH_3)_2SnO$][$OCH_2CH(CH_3)CH_2CH_3$](HONZO)(ONZO)]}. Crystallographic characterisation of the trinuclear microcluster **5a** shows the presence of the monobasic HONZO ligand in a tridentate μ_2-O,N mode and of the dibasic ONZO ligand in a tridentate O,N,O mode. This coordination mode leads to one seven-coordinate and two five-coordinate tin centers that are linked by a μ_3-oxo function. The coordination geometries are distorted pentagonal bipyramidal and trigonal bipyramidal, respectively. The two low-coordinate tin atoms are linked by the alkoxide ion. The corresponding chiral (*S*)-2-methyl-1-butanol reacts analogously to yield **5b**. By contrast, reaction of **3** with chiral secondary alcohols (2-butanol or 1-phenyl-1-ethanol), in various molar ratios, failed to provide the corresponding μ_2-alkoxy complex. Instead, pure crystals of {[$(CH_3)_2Sn]_2$[$(CH_3)_2SnO$](OH)(HONZO)(ONZO)} (**2a**) were isolated.

Introduction

Reaction of salicylaldoxime, *o*-(HON=CH−C_6H_4−OH), and diorganotin(IV) oxide, R_2SnO (R = Me, *n*-Bu), yields small clusters represented as [$(R_2Sn)_2(R_2SnO)$(ONZOH)(HONZO)(ONZO)] (**1b**: R = *n*-Bu; **2b**: R = Me), where ONZOH is the oximate residue *o*-(−ON=CH−C_6H_4−OH), HONZO is the phenolate *o*-(HON=CH−C_6H_4−O−), and ONZO is the dibasic species *o*-(−ON=CH−C_6H_4−O−), associated with salicylaldoxime[1]. Their general structure is displayed in Figure 1[1].

Attempts to crystallize crude **1b** or **2b** with hydroxylated solvents usually lead to substitution compounds like the μ_2-hydroxy-bridged compound **1a** (R = *n*-Bu)[1a], or a μ_2-alkoxy-bridged compound (R = Me)[1b], as e.g. **3**, the μ_2-bridged ONZOH unit being eliminated as salicylaldoxime (HONZOH).

Such compounds undergo facile reversible μ_2-nucleophilic substitutions with protonated nucleophiles, according to Scheme 1[2][3].

X-ray data on several such compounds reveal that ligand A is planar, with Sn(1), Sn(2) and Sn(3) being coplanar. By contrast, ligand B is dramatically twisted since the atom N18 is 0.3 Å away from the mean plane of the aromatic ring with which it is associated[1a][1b][2]. As a consequence, these derivatives have a chiral skeleton in the solid state.

In order to assess whether this skeleton chirality could be detected in solution, we prepared dimethyltin salicylaldoximate derivatives containing a ligand with a chiral center bridging the Sn(2) and Sn(3) tin atoms. Provided the chirality of the cluster skeleton would be maintained in solution, it should indeed be observable through the formation of the diastereoisomers necessarily obtained[4].

This paper presents solid-state and solution characterization by X-ray diffraction and 1D- and 2D-NMR spectroscopy, mainly gradient assisted[5] ^{1}H-^{13}C HMQC[6a] and HMBC[6b][6c] and ^{1}H-^{119}Sn HMQC[7], of compounds derived from the reaction of **3** with chiral alcohols. The first tris(dimethyltin) disalicylaldoximate with a chiral μ_2-bridged alkoxy ligand is reported.

Results and Discussion

Synthesis

Reaction of **3** with an excess of racemic (*d,l*)-2-methyl-1-butanol provides, after recrystallization from dichlorometh-

[+] Present address: Laboratoire de Chimie Structurale Organique, Université de Paris-Sud, Bât. 410, ICMO, CNRS URA no. 1384, F-91405 Orsay Cedex, France.

 © WILEY-VCH Verlag GmbH, D-69451 Weinheim, 1998 1434−1948/98/1010−1467 $ 17.50+.50/0

Figure 1. General structure, with atom labelling, of compounds from several condensation reactions between di-*n*-butyl or dimethyltin(IV) oxide and salicylaldoxime (HONZOH); HOZNO represents the salicylaldoximate residue bound to O40 by the oxygen atom of its oximate moiety[1][2][3]; Nu stands for a nucleophile μ_2-bridging the five-coordinate tin atoms Sn2 and Sn3

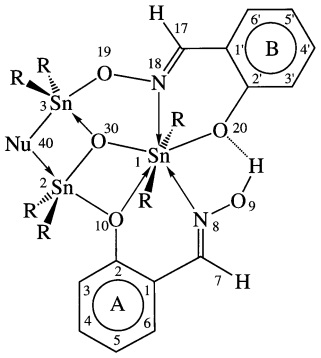

	Nu	R
1a	HO	n-Bu
1b	HOZNO	n-Bu
2a	HO	Me
2b	HOZNO	Me
3	MeO	Me
4	F	Me
5	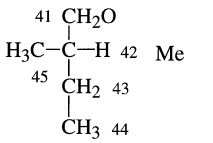	Me

Scheme 1

$$[(R_2Sn)_2(R_2SnO)(Nu)(HONZO)(ONZO)] + Nu'\text{-}H \rightleftharpoons [(R_2Sn)_2(R_2SnO)(Nu')(HONZO)(ONZO)] + Nu\text{-}H$$

ane/hexane (1:1), pure crystals of μ_2-(*d,l*)-2-methylbutoxydimethyltin salicylaldoximate (**5a**) (Figure 1). Similarly, crystals of μ_2-(*S*)-2-methylbutoxydimethyltin salicylaldoximate (**5b**) were obtained starting from (*S*)-(−)-2-methyl-1-butanol.

By contrast, reaction of **3** with chiral secondary alcohols (2-butanol or 1-phenyl-1-ethanol), in various molar ratios, failed to provide the corresponding crystalline μ_2-alkoxy complex. Instead, pure crystals of **2a** were isolated; the compound **2a** was observed so far only as a transient[1b][2][3], where the μ_2-methoxy moiety of **3** is substituted for a μ_2-hydroxy one.

NMR analysis of the crude product obtained by reaction of **3** with secondary alcohols revealed the presence of the desired μ_2-(*sec*)-alkoxy compound in small fractions, depending on the starting alcohol, in addition to **3** and **2b**. Monitoring the reaction of **3** with (*d,l*)-2-butanol by ^1H, ^{13}C and ^{119}Sn NMR reveals an equilibrium mixture with the μ_2-1-methylpropoxy compound as a minor species, even when the secondary alcohol is used in large excess. This result implies that a μ_2-alkoxy moiety bridging Sn(2) and Sn(3) is more stable when it originates from a primary alcohol than from a secondary one, probably due to steric hindrance of the latter.

X-ray Diffraction Analysis of Compound 5a

The molecular structure of **5a** resembles closely those found for related systems[1][2][3] and hence, only a brief description of **5a** is given (Figure 2).

Figure 2. Molecular structure and crystallographic numbering scheme employed for **5a**

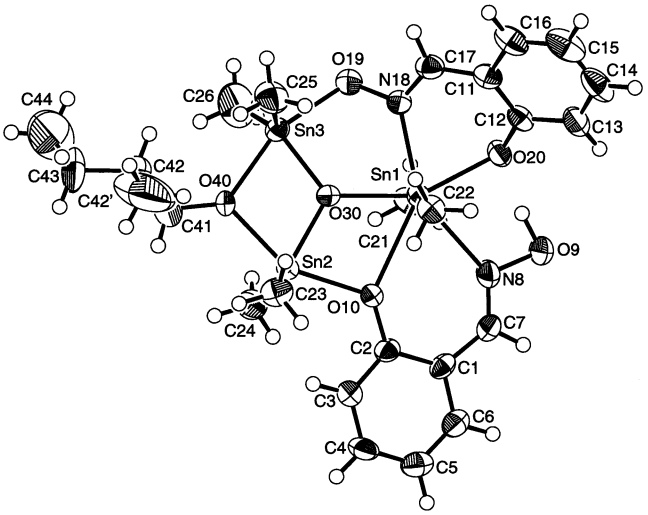

There are two distinct coordination geometries about the tin atoms in the trinuclear structure. The Sn(1) atom is seven-coordinate, existing in a distorted pentagonal bipyramidal geometry with the methyl substituents occupying axial positions, C−Sn−C is 167.4(3)°. The equatorial plane is defined by the phenoxide O(10) and O(20) atoms, the oxime N(8) and N(18) atoms and an oxo O(30) atom. In this description, the Sn(1) atom lies 0.0012(4) Å out of the plane in the direction of the C(21) atom. The remaining tin atom geometries are based on trigonal bipyramidal geometries defined by the oxo O(30) atom, the alkoxide O(40) atom, two methyl substituents and for Sn(2) the phenoxide O(10) atom and for Sn(3) the oxime O(19) atom. The Sn(2) atom lies 0.0932(4) Å above the $C_2O(30)$ trigonal plane in the direction of the O(10) atom and the deviation of the Sn(3) atom from the $C_2O(30)$ plane is 0.0324(4) Å, in the direction of the O(19) atom. The geometric parameters describing **5a** (Table 1) are in essential agreement with those found in the analogous T = Me, Et, *n*Pr and *i*Pr structures[1b]. Notable features in the structure include the presence of the tri-coordinate O(30) atom, the symmetric alkoxide bridge [Sn(2)−O(40) is 2.164(4) Å and Sn(3)−O(40) is 2.174(4) Å], and an intramolecular hydrogen bond formed between the O(9)*H* and O(20) atoms such that O(9)*H*···O(20) is 1.59 Å and O(9)−H···O(20) is 166°. The crystal structure of **5a** is comprised of equal amounts of the *R* and *S* forms of the chiral alcohol, i.e. is racemic.

An investigation of the structure of the chiral *S* form of the compound, i.e. **5b**, was also undertaken[8]. The crystal

Table 1. Selected bond lengths [Å] and angles [°] for **5a**

Sn(1)−O(10)	2.634(4)	Sn(1)−O(20)	2.193(4)
Sn(1)−O(30)	2.171(4)	Sn(1)−N(8)	2.543(6)
Sn(1)−N(18)	2.291(5)	Sn(1)−C(21)	2.091(7)
Sn(1)−C(22)	2.103(7)	Sn(2)−O(10)	2.149(4)
Sn(2)−O(30)	2.001(4)	Sn(2)−O(40)	2.164(4)
Sn(2)−C(23)	2.104(7)	Sn(2)−C(24)	2.102(7)
Sn(3)−O(19)	2.115(5)	Sn(3)−O(30)	1.999(4)
Sn(3)−O(40)	2.174(4)	Sn(3)−C(25)	2.097(8)
Sn(3)−C(26)	2.077(9)	O(9)−N(8)	1.425(7)
O(10)−C(2)	1.349(7)	O(19)−N(18)	1.368(7)
O(20)−C(12)	1.333(7)	N(8)−C(7)	1.284(8)
N(18)−C(17)	1.276(8)		
O(10)−Sn(1)−O(20)	142.5(1)	O(10)−Sn(1)−O(30)	65.2(1)
O(10)−Sn(1)−N(8)	67.6(2)	O(10)−Sn(1)−N(18)	142.2(2)
O(10)−Sn(1)−C(21)	88.4(2)	O(10)−Sn(1)−C(22)	81.8(2)
O(20)−Sn(1)−O(30)	152.3(1)	O(20)−Sn(1)−N(8)	75.1(2)
O(20)−Sn(1)−N(18)	75.1(2)	O(20)−Sn(1)−C(21)	89.9(2)
O(20)−Sn(1)−C(22)	93.2(2)	O(30)−Sn(1)−N(8)	132.4(2)
O(30)−Sn(1)−N(18)	77.4(2)	O(30)−Sn(1)−C(21)	90.7(2)
O(30)−Sn(1)−C(22)	92.2(2)	N(8)−Sn(1)−N(18)	150.2(2)
N(8)−Sn(1)−C(21)	82.0(2)	N(8)−Sn(1)−C(22)	87.0(2)
N(18)−Sn(1)−C(21)	97.7(2)	N(18)−Sn(1)−C(22)	94.8(2)
C(21)−Sn(1)−C(22)	167.4(3)	O(10)−Sn(2)−O(30)	78.2(2)
O(10)−Sn(2)−O(40)	151.7(2)	O(10)−Sn(2)−C(23)	100.1(2)
O(10)−Sn(2)−C(24)	97.4(2)	O(30)−Sn(2)−O(40)	73.6(2)
O(30)−Sn(2)−C(23)	115.0(2)	O(30)−Sn(2)−C(24)	116.5(3)
O(40)−Sn(2)−C(23)	93.1(2)	O(40)−Sn(2)−C(24)	93.8(2)
C(23)−Sn(2)−C(24)	127.9(3)	O(19)−Sn(3)−O(30)	85.3(2)
O(19)−Sn(3)−O(40)	158.2(2)	O(19)−Sn(3)−C(25)	95.3(3)
O(19)−Sn(3)−C(26)	91.4(3)	O(30)−Sn(3)−O(40)	73.4(2)
O(30)−Sn(3)−C(25)	111.1(3)	O(30)−Sn(3)−C(26)	119.0(4)
O(40)−Sn(3)−C(25)	96.6(3)	O(40)−Sn(3)−C(26)	94.9(3)
C(25)−Sn(3)−C(26)	129.8(4)	Sn(1)−O(10)−Sn(2)	97.1(1)
Sn(1)−O(10)−C(2)	138.7(4)	Sn(2)−O(10)−C(2)	124.2(4)
Sn(3)−O(19)−N(18)	116.1(4)	Sn(1)−O(20)−C(12)	122.2(4)
Sn(1)−O(30)−Sn(2)	119.3(2)	Sn(1)−O(30)−Sn(3)	128.0(2)
Sn(2)−O(30)−Sn(3)	112.7(2)	Sn(2)−O(40)−Sn(3)	100.3(2)
Sn(1)−N(8)−O(9)	109.8(4)	Sn(1)−N(8)−C(7)	139.1(5)
Sn(1)−N(18)−O(19)	119.6(4)	Sn(1)−N(18)−C(17)	125.0(5)

structure obtained for a crystal chosen from the recrystallisation of **5b** shows the presence of both the *S* form as well as a small amount of the *R* form. The asymmetric unit contains two pseudo-centrosymmetrically related molecules. One site contains 100% of the *S* form, while the other site contains 58.6% of the *R* form, giving a 1.414(22):0.586 ratio of the two forms in the crystal investigated. A number of crystals were examined and similar results were obtained each time, including under conditions of low temperature (200 K). Presumably, the centrosymmetric structure packing ($P2_1/c$) is thermodynamically favoured implying that the better grown crystals have a higher percentage of the minor component[8]. The geometric features determined for **5b** are as described for the racemic species.

Solution-State Structure

Dissolving dimethyltin salicylaldoximates usually gives rise to minor species involved in a complex equilibrium, among which **2b** and the dimethyl analogue of m_2[1a]. In benzene solution, **5** remains the major species. By contrast, when **2a** is dissolved in C_6D_6, it remains only as a minor species, the transient signals of m_2 dominating the ^{119}Sn NMR spectrum. This is accompanied by an important precipitation in the NMR tube. This observation is accounted for by the reaction of Scheme 2.

Scheme 2

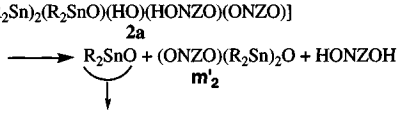

The structures of m'_2, and of its resulting dimer, m_2, proposed from comparable observations[1a] on the corresponding di-*n*-butyltin compound **1a**, are shown in Figure 3. Further evidence to the reaction of Scheme 2 is the observation of the oximic ^{1}H resonance of free salicylaldoxime.

In $CDCl_3$, the transient fractions remain low. Lowering the temperature increases the fraction of **2a** in the mixture, enabling its full NMR characterization at 270 K.

Table 2 presents an overview of the ^{1}H, ^{13}C, and ^{119}Sn chemical shifts and coupling constants associated with the dimethyltin moieties. The ^{1}H,^{13}C and ^{119}Sn resonances of **5** and **2a** were assigned with exactly the same strategy as reported previously for **2b**, **3** and **4**, using 2D gradient-enhanced ^{1}H-^{13}C HMQC and HMBC spectroscopy[5][6][7] and ^{1}H-^{119}Sn HMQC spectroscopy[1][2][3][6], evidencing the same basic tritin cluster structure for **5** and **2a** as for **2b** and

Figure 3. Transients generated from dissolving compound **2a** in C_6D_6 (see text)

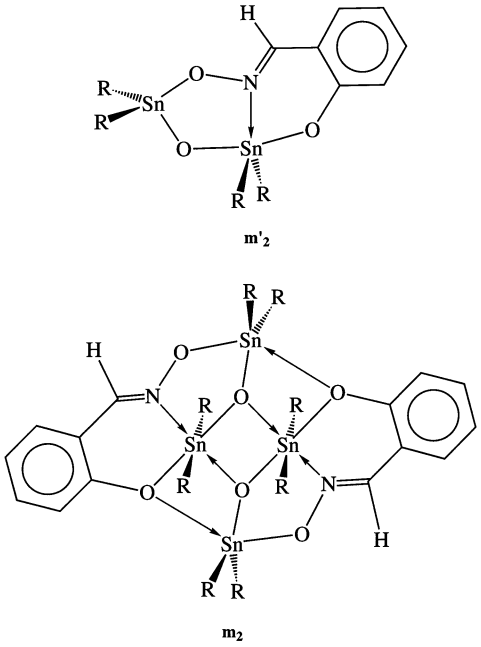

of Sn(1), probably because the latter are too remote from the chiral center.

NMR spectra of **5** do not show any evidence of skeletal chirality in dimethyltin salicylaldoximate in addition to that arising from the chiral alkoxide moiety. Indeed, additional skeletal chirality observable on the NMR time scale should have provided two racemic diastereoisomers resulting in further unequal duplication of the ^{119}Sn resonances of all three Sn(1), Sn(2) and Sn(3) atoms. This expectation remained unfulfilled in spite of the very high sensitivity to the electronic environment of the ^{119}Sn nucleus evidenced by its wide chemical shift range (3000 ppm)[4][9]. Hence, it can be concluded that the observed splitting of equal intensity in the ^{1}H and ^{13}C resonances for **5** is due to a pairwise anisochrony of the two methyl groups within each of the five-coordinate tin atoms generated by their vicinity to the stereogenic carbon centre of the chiral alkoxy ligand.

Conclusion

This paper has addressed several issues unsolved so far in the chemistry of tris(dimethyltin) disalicylaldoximates. First, a chiral group could be incorporated for the first time

Table 2. ^{119}Sn-, ^{13}C- and ^{1}H-NMR data for the dimethyltin moieties of compounds **5** and **2a**[a]

Compd.	Moiety	δ(^{119}Sn)	^{n}J(^{119}Sn-$^{119/117}$Sn)[b]	δ(^{13}C)	^1J(^{13}C-$^{119/117}$Sn)	δ(^{1}H)	^2J(^{1}H-^{119}Sn)
5[c]	$Me_2Sn(1)$	−458.0	356; /[d]	14.82	1107/1058	1.103	114
	$Me_2Sn(2)$	−141.8	102; 64	2.56/2.51	637/603	0.517/0.511	75
	$Me_2Sn(3)$	−130.6	351; 104	−0.16/−0.27	661/636	0.493/0.491	75
2a[e]	$Me_2Sn(1)$	−458.5	/;/[d]	14.04	1104/1062	0.813	111
	$Me_2Sn(2)$	−142.6	66; 66	4.44	677/648	0.793	76
	$Me_2Sn(3)$	−130.9	339; 72	1.89	669/640	0.623	76

[a] Chemical-shift data in ppm and coupling constants in Hz. − [b] Averaged values from unresolved ^{n}J(^{119}Sn-^{119}Sn) and ^{n}J(^{119}Sn-^{117}Sn) coupling satellites in ^{119}Sn spectrum. − [c] Spectrum recorded from a C_6D_6 solution of **5** at 303 K. − [d] Invisible satellites because of broad ^{119}Sn(1) resonance feet. − [e] Spectrum recorded from a $CDCl_3$ solution of **2a** at 270 K.

3 (Figure 1). The ^{1}H-^{119}Sn HMQC cross peaks of **5** and **2a** reviewed in Table 3, similar to those of **1a**, **1b**, **2b** and **3**, support this conclusion, as do all the ^1J(^{13}C-$^{119/117}$Sn), ^{n}J(^{119}SN−O-$^{119/117}$Sn), and ^2J(^{1}H-$^{119/117}$Sn) coupling data.

Characteristically, the ^{1}H-^{119}Sn HMQC spectrum of **5** shows a cross peak between the two diastereotopic protons, H(41A) and H(41B) of the 2-methylbutoxy group, and both Sn(2) and Sn(3) atoms. In the case of **2a**, a correlation is observed between the hydroxy proton, H(40), and both Sn(2) and Sn(3) tin atoms. These correlations are in agreement with the binding site of the entering nucleophile between Sn(2) and Sn(3).

The ^{1}H and ^{13}C methyl resonances of Sn(2) and Sn(3) in compound **5** are duplicated (Table 2). This is in agreement with the pairwise diastereotopism of the Sn(2) and Sn(3) methyl groups due to the presence of the chiral carbon atom C(42) (see below). These features are observed both in **5a**, obtained from racemic (*R,S*)-2-methyl-1-butanol, and **5b** from enantiomerically enriched (*S*)-2-methyl-1-butanol. Such an anisochrony is not observed for the methyl groups

into such a complex. Second, the limits of the reactivity of these complexes towards alcohols have clearly been defined. Thus, while primary alcohols smoothly react towards the corresponding μ_2-alkoxy-substituted complex, even when the substituent on the CH_2OH moiety is rather bulky, secondary alcohols, apart from 2-propanol[1b], fail to yield the corresponding μ_2-substitution products. A steric effect from a moderately bulky group is responsible for this. Third, the first clear evidence of chirality-related anisochrony of the two methyl groups on the dimethyltin moieties demonstrates that their diastereotopism can be induced on the NMR time scale only by the introduction of a μ_2-bridged chiral group into the complex. Accordingly, this rules out that the skeletal chirality displayed by these microclusters in the crystalline state remains observable in solution on the ^{119}Sn-NMR time scale, no anisochrony being visible without chiral substituent. This suggests a fast inversion of the skeletal chirality on this time scale. Last, albeit unexpected, the μ_2-hydroxy-bridged complex could be fully isolated, having been observed only as a transient so far[1][2]. Actu-

Table 3. ^{1}H-^{119}Sn correlation data as obtained from 2D ^{1}H-^{119}Sn HMQC spectra of **5** and **2a**[a][b]

Compd.	Tin atom	δ(^{119}Sn)	Oximic protons	Other protons
5[c]	Sn(1)	−460.0	H(17): 8.226, $^3J < 2$ H(7): 8.143, $^3J < 2$	H(9): 13.881, $^3J < 2$ CH_3[d]: 1.103, ^2J = 114
	Sn(2)	−141.8	H(17): 8.226, $^5J < 2$	H(3): 6.244, $^4J < 2$ H(41A): 3.074, ^3J = 12 H(41B): 2.955, ^3J = 11 CH_3−Sn(1): 1.103, $^4J < 2$ CH_3[d]: 0.517/0.511, ^2J = 75
	Sn(3)	−130.6	H(17): 8.226, $^4J < 2$	H(41A): 3.074, ^3J = 13 H(41B): 2.955, ^3J = 14 CH_3−Sn(1): 1.103, $^4J < 2$ CH_3[d]: 0.493/0.491, ^2J = 75
2a[e]	Sn(1)	−458.5	H(17): 8.133, $^3J < 2$ H(7): 8.006, $^3J < 2$	H(9): 13.536, $^3J < 2$ CH_3[d]: 0.813, ^2J = 111 CH_3−Sn(2): 0.793, $^4J < 2$
	Sn(2)	−142.6	H(17): 8.133, $^5J < 2$	H(3): 6.366, $^4J < 2$ H(40): 2.406, $^2J < 2$ CH_3[d]: 0.793, ^2J = 76 CH_3−Sn(3): 0.623, $^4J < 2$
	Sn(3)	−130.9	H(17): 8.133, ^4J <2	H(40): 2.406, $^2J < 2$ CH_3−Sn(1): 0.813, $^4J < 2$ CH_3[d]: 0.623, ^2J = 76

[a] ^{1}H chemical shift and ^nJ(^{1}H-^{119}Sn) are given for each proton that correlates with a ^{119}Sn resonance (see Figure 1 for labelling). − [b] Chemical shifts are given in ppm and coupling constants in Hz. − [c] Spectrum recorded from a C_6D_6 solution of **5** at 303 K. − [d] Methyl group bound to the considered tin atom. − [e] Spectrum recorded from a $CDCl_3$ solution of **2a** at 270 K.

ally, this complex appears to be the only one that can be generated from the reaction mixture when the synthesis of complexes involving chiral μ_2-bridged secondary alkoxy groups is attempted. Noteworthy is that the resulting complex reaction mixture smoothly evolves by crystallization to the single μ_2-hydroxy complex, just by taking up water present in the medium, either in the solvent and/or in the atmosphere.

The financial support of the *Fund for Scientific Research − Flanders (Belgium)* (*FKFO*, grant no. 2.0094.94) and of the Belgian *Nationale Loterij* (grant no. 9.0006.93) is gratefully acknowledged (R. W., M. B.). A post-doctoral grant of the *Fund for Scientific Research − Flanders (Belgium)* (grant V10/6-AB-D12073) is gratefully acknowledged (A. M.). We thank Mrs *I. Verbruggen* for recording routine NMR spectra. The authors also thank the *Australian Research Council* for support of this work (*E. R. T. T.*).

Experimental Section

General: The samples were prepared by dissolving ca. 40 mg of product in 0.5 ml of solvent. NMR spectra of compounds **5a** and **5b** were recorded at 303 K in C_6D_6 and those of compound **2a** were recorded at 270 K in $CDCl_3$. ^{1}H-, ^{13}C- and ^{119}Sn-NMR spectra were recorded with a Bruker AMX500 spectrometer equipped with a digital lock and operating at 500.13, 125.77 and 186.50 MHz, respectively. Chemical shifts are in ppm, coupling constants in Hz. The ^{119}Sn reference frequency was calculated from the absolute frequency of Me_4Sn, Ξ = 37.290 665 MHz[10]. ^{13}C and ^{1}H chemical shifts were respectively referenced to the ^{13}C resonance of the solvent at δ = 128.0 (C_6D_6) or 77.0 ($CDCl_3$) and to the residual ^{1}H solvent resonance at δ = 7.15 (C_6D_5H) or 7.24 ($CHCl_3$); multiplicity patterns in ^{1}H spectra are: d: doublet; dd: doublet of doublets; ddd: doublet of doublets of doublets; s: singlet; m: complex pattern; nr: non resolved. ^nJ(^{1}H-^{1}H) coupling constants are given between parentheses. ^nJ(^{1}H-^{119}Sn), ^1J(^{13}C-$^{119/117}$Sn), and ^2J(^{119}Sn-$^{119/117}$Sn) coupling constants are given in Table 2 and not repeated here. Broad-band ^{1}H-decoupled ^{13}C and ^{119}Sn spectra were recorded using Bruker standard pulse sequences. All heteronuclear correlation-spectroscopy experiments consisted of gradient-enhanced versions of the standard ^{1}H-^{119}Sn HMQC and ^{1}H-^{13}C HMQC or HMBC pulse sequences, implemented in exactly the same way as explained elsewhere and processed in the magnitude mode[1b].

X-ray Diffraction Studies: Intensity data for a colourless crystal of **5a** were collected at 200 K with a Rigaku AFC6R diffractometer employing Mo-K_α radiation (λ = 0.71073 Å) and the ω-2θ scan technique to $2\theta_{max}$ = 50.0°. The data set was corrected for Lorentz and polarisation effects[11] as well as for absorption employing an empirical procedure (range of transmisison factors: 0.756 to 1)[12]. Data that satisfied the $I \geq 3.0\sigma(I)$ criterion of observability were used in the subsequent analysis. Crystal data and refinement details are given in Table 4.

Table 4. Crystallographic data for **5a**

Formula	$C_{25}H_{40}N_2O_6Sn_3$
Formula weight	820.7
Crystal system	monoclinic
Space group	$P2_1/c$
a [Å]	8.865(5)
b [Å]	17.64(1)
c [Å]	19.52(1)
β [°]	92.49(6)
V [Å^3]	3048(3)
Z	4
Crystal dimensions [mm]	0.11 × 0.37 × 0.47
$\rho_{calcd.}$ [g cm^{-3}]	1.788
$F(000)$	1608
No. of data collected	5970
No. of unique data	5591
No. of reflections with $I \geq 3.0\sigma(I)$	4144
No. of refined parameters	325
R	0.035
R_w	0.041
Residual ρ_{max} [e Å^{-3}]	0.73

The structure was solved by direct methods[13] and refined by a full-matrix least-squares procedure based on F[11]. Non-hydrogen atoms were refined with anisotropic displacement parameters and hydrogen atoms were included in the model at their calculated positions (C−H 0.95 Å). The refinement was continued until convergence employing sigma weights, i.e. $1/\sigma^2(F)$. Selected interatomic parameters are collected in Table 1 and the crystallographic numbering scheme employed is shown in Figure 2 which was drawn with ORTEP[14] at 50% probability ellipsoids. Crystallographic data (excluding structure factors) for the structure reported in this paper have been deposited with the Cambridge Crystallographic Data Centre as supplementary publication no. CCDC-101351. Copies of the data can be obtained free of charge on application

to CCDC, 12 Union Road, Cambridge CB2 1EZ, UK [Fax: + 44-1223-336−033; E-mail: deposit@ccdc.cam.ac.uk].

Compound **3**: Compound **3** was synthesized as previously described[1b].

Compound **5a**: To a solution of 1.000 g (1.31 mmol) of **3** in 10 ml of dichloromethane was added a solution of 0.598 g (6.8 mmol, 5.2 equiv.) of (*d,l*)-2-methyl-1-butanol in 10 ml of dichloromethane. The mixture was stirred for 5 min and the solvent was evaporated under vacuum. Recrystallization in dichloromethane/hexane (1:1) of the precipitate obtained provided 0.942 g of pure **5a** crystals suitable for X-ray analysis (yield: 88%). The compound starts melting under decomposition at 116°C. − $C_{25}H_{40}N_2O_6Sn_3$ (820.67): calcd. C 36.6, H 4.9, N 3.4; found C 36.6, H 5.2, N 3.4. − ^{1}H NMR (C_6D_6, 500.13 MHz; for complex patterns, the centre of ^{1}H-^{13}C HMQC cross peaks is given): δ = 13.88 [s, OH(9)], 8.23 (s, 17-H), 8.14 (s, 7-H), 7.07 (mnr, 3′-H), 7.06 (mnr, 4′-H), 7.04 (mnr, 4-H), 6.847 (dd, *J* = 7.7, 1.9 Hz, 6-H), 6.823 (dd, *J* = 7.6, 1.1 Hz, 6′-H), 6.605 (ddd, *J* = 7.4, 7.4, 0.8 Hz, 5-H), 6.570 (ddd, *J* = 7.6, 6.5, 1.8 Hz, 5′-H), 6.244 (d, *J* = 8.2 Hz, 3-H), 3.074 (dd, *J* = 10.9, 6.5 Hz, 41A-H), 2.955 (dd, *J* = 10.9, 7.0 Hz, 41B-H), 1.30 (mnr, 43A-H), 1.103 [s, CH_3 (Sn-1)]; 1.06 (mnr, 42-H), 0.81 (mnr, 43B-H), 0.78 (mnr, 44-H), 0.684 (d, *J* = 6.6 Hz, 45-H), 0.517 [s, Sn(2)−CH_3], 0.511 [s, Sn(2)−CH_3], 0.493 [s, Sn(3)−CH_3], 0.491 [s, Sn(3)−CH_3]. − ^{13}C NMR (C_6D_6, 125.76 MHz): δ = 162.6 (C-2′), 161.0 (C-2), 154.6 (C-17), 149.9 (C-7), 135.6 (C-6), 132.4 (C-4′), 132.1 (C-6′), 131.0 (C-4), 120.9 (C-3′), 120.7 (C-1), 119.4 (C-1′), 117.9 (C-3), 117.2 (C-5′), 117.1 (C-5), 68.5 (C-41), 38.8 (C-42), 26.3 (C-43), 16.5 (C-45), 14.8 [C−Sn(1)], 11.4 (C-44), 2.56 [C−Sn(2)], 2.51 [C−Sn(2)], −0.16 [C−Sn(3)], −0.27 [C−Sn(3)]. − ^{119}Sn NMR (C_6D_6, 186.50 MHz): −130.6 Sn(3), −141.8 Sn(2), −458.0 Sn(1).

Compound **5b**: Synthesis is the same as for **5a**, using 0.592 g of (*S*)-(−)-2-methyl-1-butanol; yield 53%. The compound starts melting under decomposition at 109°C. − $C_{25}H_{40}O_6N_2Sn_3$ (820.67): calcd. C 36.6, H 4.9, N 3.4; found C 36.1, H 5.0, N 3.4. − NMR spectra of **5b** are identical to those of **5a**.

Compound **2a**: Same procedure as for **5a**, using 1.000 g of **3** and 0.492 g (6.6 mmol, 5.1 equiv.) of (*d,l*)-2-butanol; recrystallization from dichloromethane/hexane (1:4); yield 59%. The compound starts melting under decomposition at 99°C. − $C_{20}H_{30}O_6N_2Sn_3$ (750.54): calcd. C 32.0, H 4.0, N 3.7; found C 32.1, H 4.1, N 3.6. − ^{1}H NMR ($CDCl_3$, 500.13 MHz): δ = 13.536 [s, OH(9)], 8.133 (s, 17-H), 8.006 (s, 7-H), 7.227 (ddd, *J* = 8.6, 7.2, 1.8 Hz, 4′-H), 7.17 (mnr, 4-H), 7.15 (mnr, 6-H), 7.104 (dd, *J* = 7.7, 1.7 Hz, 6′-H), 6,824 (d, *J* = 8.0 Hz, 3′-H), 6.746 (t, *J* = 7.4 Hz, 5-H and 5′-H), 6.366 (d, *J* = 8.1 Hz, 3-H), 2.406 (s, 40-H), 0.813 [s, Sn(1)−CH_3], 0.793 [s, Sn(2)−CH_3], 0.623 [s, Sn(3)−CH_3]. − ^{13}C NMR ($CDCl_3$, 125.76 MHz): δ = 161.4 (C-2′), 160.4 (C-2), 154.1 (C-17), 149.6 (C-7), 134.9 (C-6), 131.9 (C-4′), 131.7 (C-6′), 131.1 (C-4), 120.3 (C-3′), 119.4 (C-1), 118.7 (C-1′), 117.5 (C-3), 116.9 (C-5′), 116.5 (C-5), 14.0 [Sn(1)−CH_3], 4.4 [Sn(2)−CH_3], 1.9 [Sn(3)−CH_3]. − ^{119}Sn NMR ($CDCl_3$, 186.50 MHz): δ = −130.9 [Sn(3)], −142.6 [Sn(2)], −458.5 [Sn(1)].

[1] [1a] F. Kayser, M. Biesemans, M. Bouâlam, E. R. T. Tiekink, A. El Khloufi, J. Meunier-Piret, A. Bouhdid, K. Jurkschat, M. Gielen, R. Willem, *Organometallics* **1994**, *13*, 1098−1113 and 4126. − [1b] R. Willem, A. Bouhdid, F. Kayser, A. Delmotte, M. Gielen, J. C. Martins, M. Biesemans, B. Mahieu, E. R. T. Tiekink, *Organometallics* **1996**, *15*, 1920−1929.

[2] R. Willem, A. Bouhdid, A. Meddour, C. Camacho-Camacho, F. Mercier, M. Gielen, M. Biesemans, F. Ribot, C. Sanchez, E. R. T. Tiekink, *Organometallics* **1997**, *16*, 4377−4385.

[3] A. Meddour, F. Mercier, J. C. Martins, M. Gielen, M. Biesemans, R. Willem, *Inorg. Chem.* **1997**, *36*, 5712−5715.

[4] E. L. Eliel, S. H. Wilen, L. N. Mander, *Stereochemistry of Organic Compounds*, Wiley-Interscience, **1994**.

[5] [5a] J. Keeler, R. T. Clowes, A. L. Davis, E. D. Laue, *Meth. Enzymol.* **1994**, *239*, 145−207. − [5b] J.-M. Tyburn, I. M. Bereton, D. M. Doddrell, *J. Magn. Reson.* **1992**, *97*, 305−312. − [5c] J. Ruiz-Cabello, G. W. Vuister, C. T. W. Moonen, P. Van Gelderen, J. S. Cohen, P. C. M. Van Zijl, *J. Magn. Reson.* **1992**, *100*, 282−302. − [5d] G. W. Vuister, R. Boelens, R. Kaptein, R. E. Hurd, B. K. John, P. C. M. Van Zijl, *J. Am. Chem. Soc.* **1991**, *113*, 9688−9690.

[6] [6a] A. Bax, R. H. Griffey, B. L. Hawkins, *J. Magn. Reson.* **1983**, *55*, 301−315. − [6b] A. Bax, M. F. Summers, *J. Am. Chem. Soc.* **1986**, *108*, 2093−2094. − [6c] A. Bax, M. F. Summers, *J. Magn. Reson.* **1986**, *67*, 565−569.

[7] [7a] F. Kayser, M. Biesemans, M. Gielen, R. Willem, *J. Magn. Reson.* **1993**, *A102*, 249−252. − [7b] J. C. Martins, P. Verheyden, F. Kayser, M. Gielen, R. Willem, M. Biesemans, *J. Magn. Reson.* **1997**, *124*, 218−222. − [7c] F. Kayser, M. Biesemans, M. Gielen, R. Willem, *Advanced Applications of NMR to Organometallic Chemistry* (Eds.: M. Gielen, R. Willem, B. Wrackmeyer), Wiley, Chichester, **1996**, chapter 3, p. 45−86.

[8] A. D. Rae, E. R. T. Tiekink, unpublished results.

[9] B. Wrackmeyer, *Annu. Rep. NMR Spectrosc.* **1985**, *16*, 73−184.

[10] [10a] A. G. Davies, P. G. Harrison, J. D. Kennedy, R. J. Puddephatt, T. N. Mitchell, W. McFarlane, *J. Chem. Soc. A* **1969**, 1136−1141. − [10b] J. Mason, *Multinuclear NMR*, Plenum Press, New York, **1987**, p. 625−629.

[11] *TEXSAN, Structure Analysis Package*, Molecular Structure Corporation, TX, **1992**.

[12] N. Walker, D. Stuart, *Acta Crystallogr., Sect. A* **1983**, *39*, 158−166.

[13] P. T. Beurskens, G. Admiraal, G. Beurskens, W. P. Bosman, S. García-Granda, J. M. M. Smits, C Smykalla, *The DIRDIF program system, Technical Report of the Crystallography Laboratory*, University of Nijmegen, The Netherlands, **1992**.

[14] C. K. Johnson, *ORTEP-II, Report ORNL-5138*, Oak Ridge National Laboratory, Oak Ridge, TN, **1976**.

[98100]

Electronic Communication in $[Co_2(CO)_6]_2$-Diyne and $[Co_2(CO)_4(dppm)]_2$-Diyne Complexes

Domenico Osella*, Luciano Milone, Carlo Nervi, and Mauro Ravera

Dipartimento di Chimica IFM, Università di Torino,
via P. Giuria 7, I-10125 Torino, Italy
Fax: (internat.) + 39-11/6707855
E-mail: osella@ch.unito.it

Received April 15, 1998

Keywords: Electrochemistry / Mixed-valent compounds / Alkynecobalt complexes / Through-bond interactions / Through-space interactions

The electrochemical behaviour of the $[Co_2(CO)_6]_2$(μ-R–C≡C–L–C≡C–R) and $[Co_2(CO)_4(dppm)]_2$(μ-R–C≡C–L–C≡C–R) series is reported. Qualitative evidence suggests that both through-space and through-bond interactions are operating with different relative weight depending on the spacer L.

Introduction

Organometallic polymers with unsaturated bridging units are currently the subject of much research because of their potential as non-linear optical (NLO) materials[1][2], liquid crystals[3][4], and quasi-one-dimensional conductors[5]. The properties of such materials can be tuned by varying the organic link or by adjusting the metal itself. Poly-yne segments are recognised to allow long-distance electronic interactions through π-delocalization[6][7][8][9][10][11][12]. Several studies have been performed on organometallic "rigid rod" polymers, Lapinte[13] and Gladysz[14] have demonstrated that conjugated C_2 to C_{20} σ-acetylide bridges constitute the most efficient link between organometallic redox-active termini. Recently, we have investigated the electronic communication between redox-active clusters joined with diynes in a σ/π fashion[15][16][17], although this kind of interaction is suspected to reduce the π-conjugation.

Electrochemistry represents a simple tool to evaluate the extent of the electronic interaction between two redox centres[18][19][20][21]. When there is no electronic interaction between two redox cores, the $E^{\circ\prime}$ values differ only by a small statistical factor[22] (ca. 36 mV at 298 K) and in polarography/CV a single wave/peak is observed. On the other hand, when there is charge delocalization over the two centres, the $E^{\circ\prime}$ values for the redox processes differ up to about 700 mV[23], giving two, more or less resolved, waves/peaks.

In this paper, we study a large series of complexes where the redox centres are either "$Co_2(CO)_6$" or "$Co_2(CO)_4$(dppm)" moieties and the bidentate ligand is a μ-R−C≡C−L−C≡C−R chain[15][16][24]. The "Co_2-alkyne" electrochemical reduction is reasonably well understood[24][25], although fast ECE processes complicate its behaviour. Phosphane ligand substitution in $Co_2(CO)_6$(μ-alkyne) has been extensively studied mainly by Robinson et al.[26][27][28][29][30][31] The $Co_2(CO)_{6-n}(PR_3)_n$(alkyne) series exhibits a further electrochemically and chemically reversible 1e oxidation[24] only when n = 3, 4 and R = OMe. Similar behaviour has recently been observed for $Co_2(CO)_4$(dppm)(μ-alkyne) derivatives[32].

Results and Discussion

Complexes $[Co_2(CO)_6]_2$(μ-diyne) have been synthesised by reaction of $Co_2(CO)_8$ with the appropriate ligand[33] (Figure 1).

The subsequent CO substitution was achieved by thermal reaction of the $[Co_2(CO)_6]_2$(μ-diyne) with dppm [bis(diphenylphosphanyl)methane, $Ph_2P-CH_2-PPh_2$][34] (Scheme 1).

Scheme 1

$$2\ Co_2(CO)_8 + R-C\equiv C-L-C\equiv C-R \rightarrow [Co_2(CO)_6]_2(R-C\equiv C-L-C\equiv C-R) + 4\ CO$$

$$[Co_2(CO)_6]_2(R-C\equiv C-L-C\equiv C-R) + 2\ Ph_2P-CH_2-PPh_2 \rightarrow [Co_2(CO)_4(Ph_2P-CH_2-PPh_2)]_2(R-C\equiv C-L-C\equiv C-R) + 4\ CO$$

In most cases, in order to increase the yields of the desired compounds, $Co_2(CO)_6$(dppm) was employed as starting reagent[35].

Scheme 2

$$Co_2(CO)_8 + Ph_2P-CH_2-PPh_2 \rightarrow Co_2(CO)_6(Ph_2P-CH_2-PPh_2) + 2\ CO$$

$$2\ Co_2(CO)_6(Ph_2P-CH_2-PPh_2) + (R-C\equiv C-L-C\equiv C-R) \rightarrow [Co_2(CO)_4(Ph_2P-CH_2-PPh_2)]_2(R-C\equiv C-L-C\equiv C-R) + 4\ CO$$

Some substituted complexes were not stable enough to be isolated from both the pathways, namely $[Co_2(CO)_4(dppm)]_2(H-C\equiv C-CH_2-CH_2-C\equiv C-H)$, $[Co_2(CO)_4(dppm)]_2(H_3C-C\equiv C-C\equiv C-CH_3)$, and $[Co_2(CO)_4(dppm)]_2[Me_3Si-C\equiv C-C\equiv C-SiMe_3]$.

At room temperature, all diyne complexes **1**−**10** undergo an *apparently* single two-electron reduction process in the relative CV responses. However, as the temperature is low-

 © WILEY-VCH Verlag GmbH, D-69451 Weinheim, 1998 1434−1948/98/1010−1473 $ 17.50+.50/0

Figure 1. Sketch of structures of complexes **1**−**19**; CO ligands are omitted for clarity

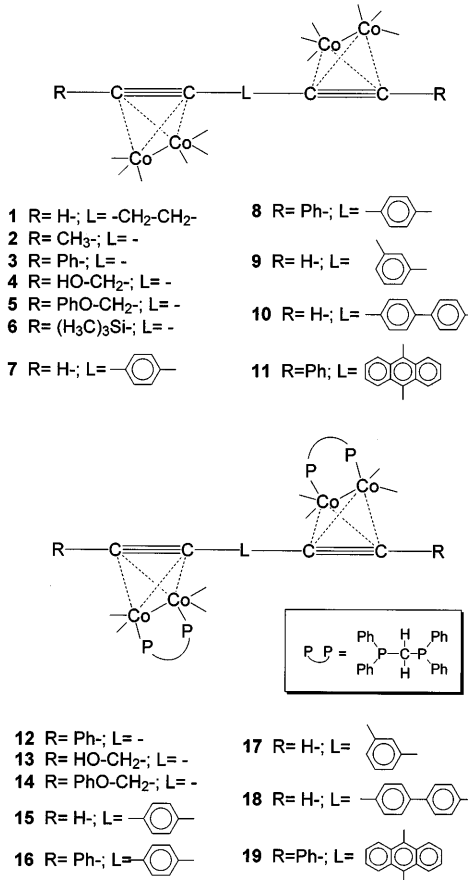

ered and/or the scan rate is increased, the chemical complications involving the primary radical anions are quenched so that two peak couples, corresponding to subsequent 1e reductions and showing full chemical reversibility, are observed[16][17].

For complexes **1**−**6**, two distinct peak couples are clearly observed in CV, at −30°C, allowing the calculation of the relevant formal electrode potentials $E^{\circ\prime}$ as $(E_p^c + E_p^a)/2$ (Table 1). Generally speaking, the external substituents R of the diyne affect the half-life of the electrogenerated monoanion; hydrogen substituents, in particular, give faster decomposition: in every case such complications can be eliminated by further raising the scan rate.

The complexes $[Co_2(CO)_4(dppm)]_2(R-C\equiv C-L-C\equiv C-R)$ (**12**−**19**) are interesting molecules as they have two identical redox centres which can undergo both reduction and oxidation processes. At ambient temperature, the cathodic scans mirror those of the parent compounds, albeit with a higher degree of chemical reversibility; the study of their $\Delta E^{\circ\prime}$ values requires low temperature. In contrast, two peak couples corresponding to Nernstian and chemically reversible 1e oxidation processes are always observed in the anodic region (Figure 2). It is worth mentioning that at low temperature (−30°C) such oxidation processes become electrochemically quasi-reversible, as testified by the increased ΔE_p values.

Figure 2. Electrochemical response of a THF solution of **12** ($1\cdot10^{-3}$ M) on a GC electrode at room temperature: SWV at 30 Hz (top) and CV at 0.2 V s^{-1}(bottom)

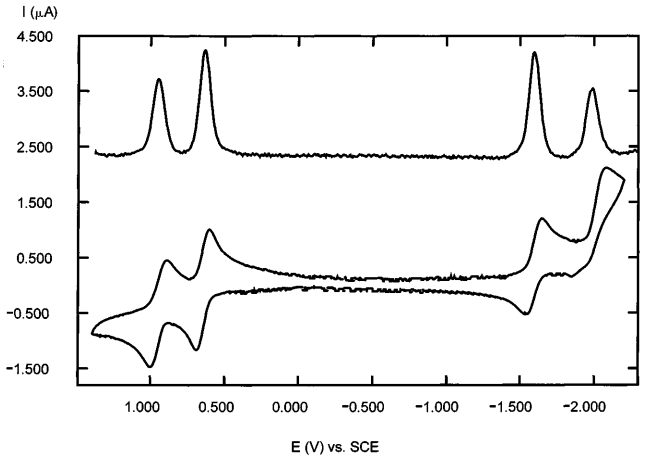

Certainly, the presence of dppm, which allows reversible oxidations to be observed at room temperature, facilitates the experimental work and, furthermore, permits the evaluation of the electronic communication for compounds such as **19**, where the aromatic 9,10-bis(phenylethynyl)anthracene gives reduction processes which overlap with those of the redox centres under study. In fact, no indication of electronic interaction could be obtained for **11**[17].

For complexes **7**−**10** and **15**−**19**, where the aromatic spacer is interpolated between the "Co_2C_2" moieties, the $E^{\circ\prime}$ values cannot be immediately evaluated from the CV responses at low temperature since the peaks are partially overlapped. We successfully employed a computer-assisted technique for peak resolution enhancement called *semi-derivative voltammetry*[36][37], where the CV data are first semi-integrated and then differentiated with respect to time (Figure 3). Alternatively, we used the Square Wave Voltammetry (SWV) technique[38] to resolve this overlapping. The relevant $E^{\circ\prime}$ values obtained from the above described techniques are in agreement (±10 mV) and are reported in Table 1.

For all compounds **1**−**19** the $\Delta E^{\circ\prime}$ values suggest a low to moderate electronic communication between the two bimetallic cores (formally corresponding to class-II mixed-valence systems in the Hush-Robin-Day formulation)[39][40].

Through-Bond and Through-Space Electronic Interaction

A large amount of data have been published on the metal−metal interactions in binuclear complexes M−L−M′ evaluated by electrochemistry. However, there are only rare attempts to rationalise this collection of potentials by using the distinction between through-space and through-bond interaction. Although both represent approximations, they can be distinguished via specially designed models. Through-space is the solvent-dependent coulombic interaction within the molecule and through-bond is both the so-called inductive (by successive polarisation of the bonds)

Figure 3. Cyclic voltammograms (top) and corresponding semiderivative voltammograms (bottom) of a THF solution of **16** on a GC electrode at 0.2 V s^{-1}; the cathodic scan is recorded at −30°C, the anodic scan at room temperature; Fc* = decamethylferrocene, added as an internal standard

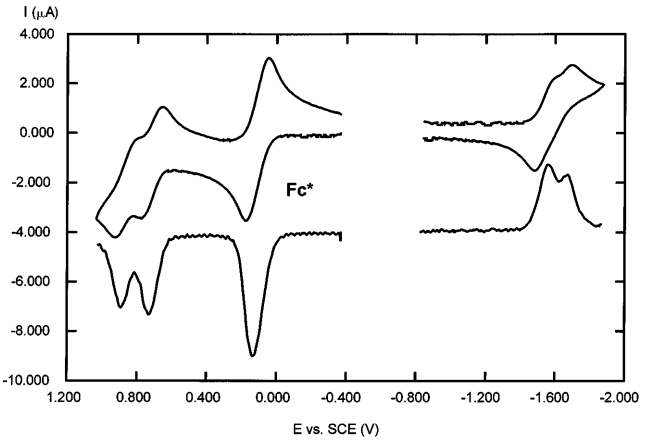

Table 1. Electrochemical data for complexes **1**−**11**, evaluated in THF containing $[Bu_4N][PF_6]$ (0.1 M) at −30°C, GC working electrode

Complex	$E^{\circ\prime}$(0,0/0,1−) [V vs. SCE]	$E^{\circ\prime}$(0,1−/1−,1−) [V vs. SCE]	$\Delta E^{\circ\prime}$ [mV]
1	−0.96	−1.11	150
2	−0.81	−1.27	460
3	−0.80	−1.20	400
4	−0.83	−1.16	330
5	−0.79	−1.20	410
6	−0.80	−1.28	480
7	−0.91	−1.02	110
8	−0.87	−1.01	140
9	−0.93	−1.07	140
10	−0.93	−1.01	80
11	[a]	[a]	[a]

[a] Not evaluated because of overlapping of the reduction of the 9,10-bis(phenylethynyl)anthracene.

and mesomeric (delocalised) effects[41]. It seems to be generally true that extensive intervening π-bond systems facilitate electron communication while σ-bond networks help less. However, a σ-bond system is strongly preferable to transmission across free space.

Complex **1**, having a $-CH_2-CH_2-$ spacer (a region of saturation), shows a $\Delta E^{\circ\prime}$ value about three times lower than those of complexes **2**−**6** but similar to those of complexes **7**−**9** where a phenylene spacer is present (Table 1). This comparison suggests that through-space interaction may be operative in complex **1**, especially if one considers that the $-CH_2-CH_2-$ chain is flexible enough to allow the two redox "Co_2C_2" centres to be in close contact.

In a simple electrostatic model the dependence of comproportionation constant K_c on the distance between the redox centres has been discussed by Reimers and Hush[42]; ln K_c, and hence $\Delta E^{\circ\prime}$[22][43][44][45], is found to be inversely related to both the distance between the redox centres and the dielectric constant (ε) of the solvent. On passing from THF (ε = 7.5) to acetone (ε = 21.0) to acetonitrile (ε = 36.6), $\Delta E^{\circ\prime}$ of compound **1** has decreasing values of 150, 90, and 50 mV, respectively. Although ion pairing effects play a role especially in the presence of supporting electrolyte in high concentration (0.1 M $[NBu_4][PF_6]$), the trend is consistent with this view[*]. The general tendency for the remaining **2**−**10** complexes is as follows: (i) compounds **2**−**6** (having a direct C−C bond between the two subunits) show a weaker dependence of $\Delta E^{\circ\prime}$ values on the solvent, suggesting that a residual through-space electronic interaction is still operative; (ii) compounds **7**−**10** (having large π-delocalised spacer) show negligible dependence of $\Delta E^{\circ\prime}$ values on the solvent indicating that the through-bond electronic coupling is dominant.

Complexes **7** and **9** (as well as **15** and **17**) are two substitutional isomers, *para* and *meta* respectively. Their $\Delta E^{\circ\prime}$ experimental values are very similar. In contrast, in a purely through-bond model, the *para* isomer is expected to show stronger electronic interaction than the *meta* isomer, due to a higher degree of mixing between aryl and acetylenic orbitals.

A closer inspection of the available solid-state structures indicates that the "Co−Co" centres (a *naive* attempt of localisation of the redox cores) are not so far apart; i.e. the distance is about 4.43 Å in $[Co_2(CO)_6]_2(PhC{\equiv}C-C{\equiv}CPh)$[46] and 4.36 Å in $[Co_2(CO)_4(dppm)]_2(PhC{\equiv}C-C{\equiv}CPh)$[32], so that the substitution of CO groups by dppm does not alter substantially the aforementioned distance. Only in $[Co_2(CO)_6]_2(HC{\equiv}C-C_6H_4-C{\equiv}CH)$[47] such a distance increases up to 8.60 Å and in $[Co_2(CO)_6]_2(Me_3SiC{\equiv}C-C_6H_4-C_6H_4-C{\equiv}CSiMe_3)$[47] is 12.8 Å.

For complexes **12**−**19** we obtained slightly different values for $\Delta E^{\circ\prime}{}_{red}$ (measured at −30°C, when complete chemical reversibility is achieved for both reductions) and $\Delta E^{\circ\prime}{}_{ox}$ (measured at the same temperature for comparison purpose) (Table 2), although the trend is clearly the same. If the electronic communication were purely through-space one should foresee identical $\Delta E^{\circ\prime}$ values for oxidation and reduction. On the contrary, for extensive π-delocalization the $\Delta E^{\circ\prime}$ values depend on the character of both HOMO (depopulated by oxidation) and LUMO (populated by reduction) and should be, in principle, different. These orbitals have been postulated to be essentially Co−Co in character (bonding and antibonding, respectively) by simple EHT calculations on the model derivative $Co_2(CO)_6(H-C{\equiv}C-C{\equiv}C-H)$[48]. EHT calculations (CACAO package)[49] on the model complex $Co_2(CO)_4(H_2P-CH_2-PH_2)(H-C{\equiv}C-C{\equiv}C-H)$[**] confirm that the HOMO's composition is mainly metal−metal bonding in character (ca. 57%) with small contributions of

[*] In the electrochemical context, $\Delta E^{\circ\prime}$ seems to be a good parameter to compare electronic interactions between redox centres in different solvents because it should be free of liquid junction potential errors, which effect each $E^{\circ\prime}$ equally.

[**] The geometry of the model complex $Co_2(CO)_4(H_2P-CH_2-PH_2)(H-C{\equiv}C-C{\equiv}C-H)$ was build up from the known structure of $Co_2(CO)_4(Ph_2P-CH_2-PPh_2)(Ph-C{\equiv}C-C{\equiv}C-Ph)$[32] by formal removal of the phenyl groups and substitution with hydrogen atoms (imposing a C−H distance of 1.10 A and a P−H distance of 1.34 A).

Table 2: Electrochemical data for complexes **12−19**, evaluated in THF containing $[Bu_4N][PF_6]$ (0.1 M), GC working electrode

Complex	$E°(0,0/0,1-)$[b]	$E°(0,1-/1-,1-)$[b]	$\Delta E°'_{red}$[b]	$E°(0,0/0,1+)$[b]	$E°(0,1+/1+,1+)$[b]	$\Delta E°'_{ox}$[b]	$\Delta E°'_{ox}$[c]
12	−1.67	−2.07	400	+0.61	+0.95	340	390
13	−1.66	−1.93	270	+0.57	+0.85	280	250
14	−1.56	−2.02	460	+0.61	+0.92	310	260
15	−1.62	−1.70	80	+0.66	+0.77	110	110
16	−1.57	−1.64	70	+0.74	+0.89	150	150
17	−1.66	−1.74	80	+0.68	+0.78	100	100
18	−1.60	−1.67	70	+0.73	+0.81	80	90
19	[a]	[a]	[a]	+0.75	+0.84	90	100

[a] Not evaluated because of overlapping of the reduction of the 9,10-bis(phenylethynyl)anthracene. − [b] At −30°C. − [c] At 20°C.

the butadiyne π-orbitals (ca. 5%) and of diphosphane (ca. 4%). Similarly, the LUMO′s composition is mainly metal−metal antibonding in character (ca. 49%) with partial contribution of the diyne (ca. 11%) and negligible contribution of diphosphane. This similar but not identical composition does not allow any firm conclusion on the nature of interactions.

The bulk of results suggests that for all the compounds under investigation through-space interaction is always operative with different weight depending on the nature of the spacer L. The $\Delta E°'$ values (80−90 mV) evaluated for complexes **10** and **18**, having the larger aromatic spacer employed for the series, represent the limit of "purely" through-bond interactions.

We thank the *Ministero dell' Università e della Ricerca Scientifica e Tecnologica* (MURST, Rome), the *Centro Nazionale delle Ricerche* (CNR, Rome), and the *European Union* (EU, Brussells) (COST Chemistry Action D5/0008/93) for financial support. We are indebted to Professors *C. Amatore* (Ecole Normale Superieure, Paris) and *C. Mealli* (CNR, Florence) for useful discussions.

Experimental Section

Electrochemical Methods and Instrumentation: Electrochemical measurements were performed using EG&G PAR 273 or EG&G PAR 263 electrochemical analysers interfaced to personal computers employing PAR M270 Electrochemical Software. A standard three-electrode cell was constructed so that it allowed the tip of the reference system to approach the working electrode closely. An aqueous saturated calomel electrode (SCE) (separated from the cell solution with a Luggin probe) was the operational reference electrode at room temperature and all potentials are referred to SCE. A silver wire was used as a pseudo-reference for the low temperature measurements. The stability of the pseudo-reference electrode was verified by adding decamethylferrocene as an internal standard; the $Fc^*(0/1+)$ potential was evaluated in the same experimental conditions to be +0.11 V vs. SCE in THF[50][51]. The working electrode was a glassy carbon (GC) disk (diameter = 0.1 cm) sealed in inert resin. The voltammetric responses were recorded in THF $1\cdot10^{-3}$ M in electroactive material and 0.1 M in supporting electrolyte, $[Bu_4N][PF_6]$.

Preparation of $[Co_2(CO)_6]_2$-Diyne Complexes **1−11**: In a typical preparation stoichiometric amounts of the appropriate alkyne and $Co_2(CO)_8$ were allowed to react at room temperature, for 1 h in CH_2Cl_2 (35 ml/mmol) in a Schlenk tube under nitrogen. The reaction mixture was filtered through silica gel to remove any insoluble impurities and the filtrate taken to dryness in vacuum. The complex was then purified by recrystallisation from hexane at −20°C. Yields 70−80%. Since the spectroscopic characteristics of similar complexes have been previously discussed[52], the IR, ^{1}H- and ^{31}P-NMR spectroscopic data and elemental analyses of each new compound are simply reported as follows:

1: $C_{18}H_6Co_4O_{12}$: calcd. C 33.26, H 0.93; found C 33.20, H 0.90. − IR (CH_2Cl_2); ν_{CO}: 2091m, 2056vs, 2026vs cm^{-1}. − ^{1}H NMR ($CDCl_3$): δ = 6.09 (s, 2 H, ≡C*H*), 3.16 (s, 4 H, −CH_2−).

2: $C_{18}H_6Co_4O_{12}$: calcd. C 33.26, H 0.93; found C 33.00, H 0.92. − IR (CH_2Cl_2); ν_{CO}: 2100m, 2080s, 2057vs, 2029s, 2021s cm^{-1}. − ^{1}H NMR ($CDCl_3$): δ = 2.74 (s, 6 H, −CH_3).

4: $C_{18}H_6Co_4O_{14}$: calcd. C 31.70, H 0.89; found C 31.50, H 0.90. − IR (CH_2Cl_2); ν_{CO}: 2103m, 2083s, 2061vs, 2034sh, 2028s cm^{-1}. − ^{1}H NMR ($CDCl_3$): δ = 6.09 (d, 4 H, $^3J_{HH}$ = 5.6 Hz, −CH_2−), 2.87 (t, 2 H, $^3J_{HH}$ = 5.6 Hz, −O*H*),

5: $C_{30}H_{14}Co_4O_{14}$: calcd. C 43.20, H 1.69; found: C 43.15, H 1.72. − IR (CH_2Cl_2); ν_{CO}: 2105m, 2085s, 2063vs, 2034s, 2029s cm^{-1}. − ^{1}H NMR ($CDCl_3$): δ = 7.36−6.99 (m, 10 H, Ph), 5.24 (s, 4 H, −CH_2−).

6: $C_{22}H_{18}Co_4O_{12}Si_2$: calcd. C 34.48, H 2.37; found C 34.40, H 2.30. − IR (CH_2Cl_2); ν_{CO}: 2099m, 2078s, 2059vs, 2032s, 2020s cm^{-1}. − ^{1}H NMR ($CDCl_3$): δ = 0.42 (s, 18 H, −CH_3).

9: $C_{22}H_6Co_4O_{12}$: C 37.86, H 0.87; found: C 37.70, H 0.85. − IR (CH_2Cl_2); ν_{CO}: 2092m, 2060vs, 2028vs cm^{-1}. − ^{1}H NMR ($CDCl_3$): δ = 7.70−7.30 (m, 4 H, C_6H_4), 6.39 (s, 2 H, ≡C*H*).

10: $C_{28}H_{10}Co_4O_{12}$: calcd. C 43.44, H 1.30; found C 43.39, H 1.32. − IR (CH_2Cl_2); ν_{CO}: 2093m, 2057vs, 2028vs cm^{-1}. − ^{1}H NMR ($CDCl_3$): δ = 7.60 (s, 8 H, Ph), 6.43 (s, 2 H, ≡C*H*).

Preparation of $[Co_2(CO)_4(dppm)]_2$-Diyne Complexes **12−19**: Stoichiometric amounts of the appropriate alkyne and $Co_2(CO)_6$(dppm), prepared according to a literature procedure[35], were heated at reflux in benzene for 2 h, under nitrogen. The hot reaction mixture was filtered through silica gel to remove any insoluble impurities and the filtrate taken to dryness in vacuum. The complex was then purified by recrystallisation from hexane/CH_2Cl_2 at −20°C. Yields 60−70%. Noteworthy, the co-ordination of two dppm ligands to the available Co−Co units is inferred by the presence of two complex multiplets in the region δ = 4.3−3.2, as expected for an ABX_2 pattern (X = ^{31}P) in the ^{1}H-NMR spectra[53] and by a single resonance in the region δ = 36−43 in the ^{31}P-NMR spectra.

13: $C_{64}H_{50}Co_4O_{10}P_4$: calcd. C 57.42, H 3.76; found C 57.382, H 3.7. − IR (CH_2Cl_2); ν_{CO}: 2033 (w), 2002vs, 1968m cm^{-1}. − ^{1}H NMR ($CDCl_3$): δ = 7.56−7.04 (m, 40 H, Ph), 5.31 (s, br., 4 H, −CH_2−), 4.17, 3.22 (m, 4 H, P−CH_2−P), 2.20 (s, br., 2 H, −O*H*). − ^{31}P NMR ($CDCl_3$): δ = 39.8 (s).

14: $C_{76}H_{58}Co_4O_{10}P_4$: calcd. C 61.23, H 3.92; found C 61.19, H 3.89. – IR (CH_2Cl_2); ν_{CO}: 2034 (w), 2005vs, 1971m cm^{-1}. – ^1H NMR ($CDCl_3$): δ = 7.50–6.40 (m, 50 H, Ph), 5.63 (s, 4 H, $-CH_2-$), 4.30, 3.26 (m, 4 H, $P-CH_2-P$). – ^{31}P NMR ($CDCl_3$): δ = 39.5 (s).

15: $C_{68}H_{50}Co_4O_8P_4$: calcd. C 60.29, H 3.72; found: C 60.25, H 3.70. – IR (CH_2Cl_2); ν_{CO}: 2021s, 1995vs, 1970s cm^{-1}. – ^1H NMR ($CDCl_3$): δ = 7.78–6.92 (m, 44 H, Ph and C_6H_4), 5.82 (t, $^3J_{HP}$ = 3.1 Hz, 2 H, $\equiv CH$), 4.31, 3.20 (m, 4 H, $P-CH_2-P$). – ^{31}P NMR ($CDCl_3$): δ = 43.2 (s).

16: $C_{80}H_{58}Co_4O_8P_4$: calcd. C 63.76, H 3.88; found C 63.70, H 3.80. – IR (CH_2Cl_2); ν_{CO}: 2021s, 1997vs, 1971s cm^{-1}. – ^1H NMR ($CDCl_3$): δ = 7.80–6.92 (m, 54 H, Ph and C_6H_4), 4.27, 3.25 (m, 4 H, $P-CH_2-P$). – ^{31}P NMR ($CDCl_3$): δ = 35.6 (s).

17: $C_{68}H_{50}Co_4O_8P_4$: calcd. C 60.29, H 3.72; found C 60.19, H 3.69. – IR (CH_2Cl_2); ν_{CO}: 2021s, 1997vs, 1969s cm^{-1}. – ^1H NMR ($CDCl_3$): δ = 7.88–6.80 (m, 44 H, Ph and C_6H_4), 5.82 (t, $^3J_{HP}$ = 3.2 Hz, 2 H, $\equiv CH$), 3.62, 3.11 (m, 4 H, $P-CH_2-P$). – ^{31}P NMR ($CDCl_3$): δ = 43.1 (s).

18: $C_{74}H_{54}Co_4O_8P_4$: calcd. C 62.12, H 3.80; found C 62.00, H 3.60. – IR (CH_2Cl_2); ν_{CO}: 2021s, 1995vs, 1970s cm^{-1}. – ^1H NMR ($CDCl_3$): δ = 8.00–6.80 (m, 48 H, Ph and C_6H_4), 5.81 (t, $^3J_{HP}$ = 3.1 Hz, 2 H, $\equiv CH$), 3.61, 3.18 (m, 4 H, $P-CH_2-P$). – ^{31}P NMR ($CDCl_3$): δ = 43.2 (s).

19: $C_{88}H_{62}Co_4O_8P_4$: calcd. C 65.77, H 3.89; found C 65.69, H 3.80. – IR (CH_2Cl_2); ν_{CO}: 2022s, 1997vs, 1973s cm^{-1}. – ^1H NMR ($CDCl_3$): δ = 8.88–6.82 (m, 58 H, Ph and $C_{14}H_8$), 3.45, 3.23 (m, 4 H, $P-CH_2-P$). – ^{31}P NMR ($CDCl_3$): δ = 36.5 (s).

[1] G. D. Stucky, S. R. Marder, J. Sohn. *Materials for Nonlinear Optics; Chemical Perspectives,* American Chemical Society, Washington, DC, **1991.**
[2] R. A. Hahn, D. Bloor, *Organic Materials for Non-Linear Optics,* The Royal Society of Chemistry, London, **1989.**
[3] A. Abe, N. Kimura, S. Tabata, *Macromolecules* **1991**, *24*, 6238–6243.
[4] T. Kaharu, H. Matsubara, S. Takahashi, *J. Mater. Chem.* **1991**, *1*, 145–146.
[5] G. Frapper, M. Kertesz, *Inorg. Chem.* **1993**, *32*, 732–740.
[6] W. Beck, B. Niemer, M. Wieser, *Angew. Chem. Int. Ed. Engl.* **1993**, *32*, 923–949.
[7] H. Lang, *Angew. Chem. Int. Ed. Engl.* **1994**, *33*, 547–550.
[8] J. S. Schumm, D. L. Pearson, J. M. Tour, *Angew. Chem. Int. Ed. Engl.* **1994**, *33*, 1360–1362.
[9] U. H. F. Bunz, *Angew. Chem. Int. Ed. Engl.* **1996**, *35*, 969–971.
[10] J. E. Sheats, C. E. Carraher, C. U. Pittman, M. Eldin, B. Currel, *Inorganic and Metal-Containing Polymeric Materials*, Plenum Press, New York, **1990.**
[11] D. W. Bruce and D. O′Hare, *Inorganic Materials,* Wiley, New York, **1992.**
[12] J. L. Bredas and R. R. Chance, *Optoelectronic and Molecular Electronics,* Kluwer, Dordrecht, **1990.**
[13] N. Le Narvor, L. Toupet, C. Lapinte, *J. Am. Chem. Soc.* **1995**, *117*, 7129–7138.
[14] M. Brady, W. Weng, Y. Zihou, J. W. Seyler, A. J. Amoroso, A. M. Arif, M. Böhme, G. Frenking, J. A. Gladysz, *J. Am. Chem. Soc.* **1997**, *119*, 775–788.
[15] D. Osella, O. Gambino, C. Nervi, M. Ravera, M. V. Russo, G. Infante, *Gazz.Chim.Ital.* **1993**, *123*, 579–582.
[16] D. Osella, L. Milone, C. Nervi, M. Ravera, *J. Organomet. Chem.* **1995**, *488*, 1–7.
[17] N. Duffy, J. McAdam, C. Nervi, D. Osella, M. Ravera, B. H. Robinson, J. Simpson, *Inorg. Chim. Acta* **1996**, *247*, 99–104.
[18] G. H. Worth, B. H. Robinson, J. Simpson, *Appl. Organomet. Chem.* **1990**, *4*, 481–491.
[19] G. H. Worth, B. H. Robinson, J. Simpson, *Organometallics* **1992**, *11*, 3863–3874.
[20] B. H. Robinson, J. Simpson, *Paramagnetic Organometallic Species in Activation, Selectivity and Catalysis*, Reidel, Dordrecht, The Netherlands, **1987**, pp 18.
[21] J. W. Merkert, W. E. Geiger, M. N. Paddon-Row, A. M. Oliver, A. L. Rheingold, *Organometallics* **1992**, *11*, 4109–4116.
[22] F. A. Ammar, J. M. Savéant, *J. Electroanal.Chem.* **1973**, *47*, 115–125.
[23] It is interesting to note that the electron-transfer sequence in which the second wave is negative of the first wave by ca. 0.7 V is very similar to that of aromatic hydrocarbons, having a singly degenerated LUMO. This ΔE° represents, to a first approximation, the energy necessary to overcome charge repulsion for setting two electrons in the same orbital: T. M. Mc Kinney, *J. Electroanal. Chem.* **1980**, *10*, 97.
[24] C. M. Arewgoda, P. H. Rieger, B. H. Robinson, J. Simpson, S. V. Visco, *J. Am. Chem. Soc.* **1982**, *104*, 5633–5640.
[25] D. Osella, J. Fiedler, *Organometallics* **1992**, *11*, 3875–3878.
[26] L. V. Casagrande, T. Chen, P. H. Rieger, B. H. Robinson, J. Simpson, S. V. Visco, *Inorg. Chem.* **1984**, *23*, 2019–2025.
[27] R. F. Heck, *J. Am. Chem. Soc.* **1963**, *85*, 657–661.
[28] R. P. Aggarwal, N. G. Connelly, M. C. Crespo, B. J. Dunne, P. M. Hopkins, A. G. Orpen, *J. Chem. Soc., Chem. Commun.* **1989**, 33–35.
[29] R. P. Aggarwal, N. G. Connelly, M. C. Crespo, B. J. Dunne, P. M. Hopkins, A. G. Orpen, *J. Chem. Soc., Dalton Trans.* **1992**, 655–662.
[30] C. M. Arewgoda, B. H. Robinson, J. Simpson, *J. Chem. Soc., Chem. Commun.* **1982**, 284–285.
[31] C. M. Arewgoda, B. H. Robinson, J. Simpson, *J. Am. Chem. Soc.* **1983**, *105*, 1893–1903.
[32] C. J. McAdam, N. W. Duffy, B. H. Robinson, J. Simpson, *Organometallics* **1996**, *15*, 3935–3943.
[33] R. S. Dickson, P. J. Fraser, *Adv. Organometal. Chem.* **1977**, *12*, 323–377.
[34] L. S. Chia, W. R. Cullen, M. Franklin, A. R. Manning, *Inorg. Chem.* **1975**, *14*, 2521–2526.
[35] T. Fukumoto, Y. Matsumura, R. Okawara, *J. Organomet. Chem.* **1974**, *69*, 437–444.
[36] J. J. Toman, S. D. Brown, *Anal. Chem.* **1981**, *53*, 1497–1504.
[37] J. C. Myland, K. B. Oldham, *Anal. Chem.* **1988**, *60*, 62–66.
[38] J. H. Christie, J. A. Turner, R. A. Osteryoung, *Anal. Chem.* **1977**, *49*, 1899–1903.
[39] G. C. Allen, N. S. Hush, *Prog. Inorg. Chem.* **1967**, *8*, 357–389.
[40] M. B. Robin, P. Day, *Adv. Inorg. Chem. Radiochem.* **1967**, *10*, 247–422.
[41] K. Bowden, E. J. Grubbs, *Chem. Soc. Rev.* **1996**, *25*, 171.
[42] J. R. Reimers, N. Hush, *Inorg. Chem.* **1990**, *29*, 3686–3697.
[43] D. S. Polcyn, I. Shain, *Anal. Chem.* **1966**, *38*, 370–375.
[44] R. L. Myers, I. Shain, *Anal. Chem.* **1969**, *41*, 980–980.
[45] F. A. Ammar, J. M. Savéant, *J. Electroanal.Chem.* **1973**, *47*, 215–221.
[46] B. F. G. Johnson, J. Lewis, P. R. Raithby, D. A. Wilkinson, *J. Organomet. Chem.* **1991**, *408*, C9–C12.
[47] C. E. Housecroft, B. F. G. Johnson, M. S. Khan, J. Lewis, P. R. Raithby, M. E. Robson, D. A. Wilkinson, *J. Chem. Soc., Dalton Trans.* **1992**, 3171–3178.
[48] D. Osella, R. Rossetti, C. Nervi, M. Ravera, M. Moretta, J. Fiedler, L. Pospísil, E. J. Samuel, *Organometallics* **1997**, *16*, 695–700.
[49] C. Mealli, D. M. Proserpio, *J. Chem. Educ.* **1990**, *67*, 399–402.
[50] U. Kölle, F. Khouzami, *Angew. Chem. Int. Ed. Engl.* **1980**, *19*, 640–641.
[51] W. E. Geiger, *Organometallic Radical Processes*, Elsevier, Amsterdam, **1990**, pp 144.
[52] B. Happ, T. Bartik, C. Zucchi, M. C. Rossi, F. Ghelfi, G. Pályi, G. Váradi, G. Szalontai, I. T. Horváth, A. Chiesi-Villa, C. Guastini, *Organometallics* **1995**, *14*, 809–819.
[53] B. E. Hanson, J. S. Mancini, *Organometallics* **1983**, *2*, 126–128.

[98106]

The Photochemistry of $M_3(CO)_{12}$ (M = Ru, Os) with Pyrazole and Its Substituted Derivatives

Nicholas E. Leadbeater*, Jack Lewis, Paul R. Raithby, and Gregory P. Ward

Centre for Inorganic Photochemistry, Department of Chemistry,
Lensfield Road, Cambridge, CB2 1EW, U.K
Fax: (internat.) + 44-1223/336362
E-mail: nel1000@cam.ac.uk

Received April 15, 1998

Keywords: Photochemistry / Ruthenium / Osmium / Clusters / Nitrogen heterocycles

The photochemistry of $M_3(CO)_{12}$ [M = Ru (**1a**), Os (**1b**)] with pyrazole, 3,5-dimethylpyrazole, and 3,5-diphenylpyrazole is documented. With **1a**, photolysis with pyrazole leads to the substitution product $HRu_3(CO)_{10}(C_3H_3N_2)$ (**2a**). In the case of **1b**, the initial product is the *ortho*-metallated species $HOs_3(CO)_{10}(C_3H_3N_2)$ (**3b**), heating of which yields $HOs_3(CO)_{10}(C_3H_3N_2)$ (**2b**). Photolysis of **1a** and **1b** with 3,5-dimethylpyrazole yields $HRu_3(CO)_{10}(C_3HMe_2N_2)$ (**4a**) and $HOs_3(CO)_{10}(C_3HMe_2N_2)$ (**4b**), respectively. The molecular structure of **4b** has been determined by X-ray crystallography. There is no reaction on photolysis of **1a** and **1b** with 3,5-diphenylpyrazole.

The reaction chemistry of cluster carbonyl complexes with nitrogen-heterocyclic ligands has received little attention as compared to that of other ligands such as phosphanes[1].This may be attributed in part to the harsh conditions frequently required to prepare N-heterocycle complexes, reactions often resulting in cluster degradation or the formation of complex products[2]. Our research has led us to investigate the photochemistry of ruthenium and osmium complexes with a number of ligand systems[3][4]. Photochemistry offers a simple, and often highly selective, route to organometallic compounds, overcoming large enthalpy barriers. As a consequence, it is often possible to prepare complexes that are otherwise inaccessible by conventional thermochemical routes[3][4][5].

The trinuclear cluster $Ru_3(CO)_{12}$ (**1a**) serves as a prototype for the photoreactivity of more complex examples. Our studies have shown that, by broad-band UV irradiation of a dichloromethane solution of **1a** in the presence of a two-electron donor ligand, high yields of photofragmentation products can be obtained[6]. This opens a route to substituted mononuclear ruthenium and osmium complexes. Although there has been much work on the synthetic potential of the reactive intermediates generated by photofragmentation of **1a**, the corresponding photosubstitution pathway is still relatively unexplored[7]. Our research has shown that, simply by changing the solvent from dichloromethane to ethyl acetate, ether, or acetonitrile, it is possible to prepare photosubstitution products from **1a** this enabling the synthesis of substituted cluster products[8].

A range of trinuclear complexes can be formed on photolysis of **1a** and its osmium analogue $Os_3(CO)_{12}$ (**1b**) with pyridine and bipyridine[9]. The work documented here focuses on the photochemistry of **1a** and **1b** with pyrazole and its substituted derivatives. The aim of the investigation was to prepare photochemically a number of trinuclear carbonyl complexes containing nitrogen heterocycles as ligands since these compounds may well have the ability to act as efficient catalysts for key industrial synthetic transformations[10].

Results and Discussion

The results from the investigations are summarised in Scheme 1 and all spectroscopic data are shown in Table 1.

Photoreactions with Pyrazole

Broad-band UV photolysis of an ethyl acetate solution of **1a** in the presence of an excess of pyrazole leads, within 30 min, to the formation of the substitution product $HRu_3(CO)_{10}(\mu_N{:}\mu_N\text{-}C_3H_3N_2)$ (**2a**). The ^{1}H-NMR spectrum of **2a** shows a symmetrical arrangement of the pyrazolide group and, in the IR spectrum, the complex does not show any bands assignable to μ-CO groups.

The formation of **2a** from **1a** is a relatively inefficient process, the photoreactions taking some considerable time. To explain this, the mechanism for photosubstitution needs to be considered. By using matrix-isolation and flash-photolysis techniques key intermediates involved in the photosubstitution pathway of **1a** have been generated[11]. The primary photoreaction is the dissociation of CO to form the coordinatively unsaturated fragment $[Ru_3(CO)_{11}]$. This fragment is highly selective in its chemistry, reaction with photoejected CO is eight times faster than with added PPh_3[11]. Therefore, in the case of an added ligand, L, photosubstitution of CO by L is in competition with recombination of the unsaturated triruthenium fragment with photoejected CO.

Due to the increased stability of trinuclear osmium complexes over their ruthenium analogues, different products are often formed. Broad-band UV photolysis of an ethyl acetate solution of **1b** in the presence of an excess of pyrazole leads, within 45 min, to the relatively insoluble *ortho*-

 © WILEY-VCH Verlag GmbH, D-69451 Weinheim, 1998 1434−1948/98/1010−1479 $ 17.50+.50/0

Table 1. Spectroscopic data for the complexes prepared in this study

Compound[a]	IR Spectrum[b]	^{1}H-NMR Spectrum[c]	Mass Spectrum[d]
$Ru_3(CO)_{12}$ (**1a**)	2059(vs), 2027(s), 2007(m)	–	–
$Os_3(CO)_{12}$ (**1b**)	2068(s), 2035(s), 2014(m), 2002(m)	–	–
$HRu_3(CO)_{10}(C_3H_3N_2)$ (**2a**)	2107(m), 2072(s), 2066(vs), 2030(s), 2016(vs), 1999(m), 1984(w)	7.5 (d, 2 H), 6.2 (t, 1 H), −13.45 (s)	653 (653 calcd.)
$HOs_3(CO)_{10}(C_3H_3N_2)$ (**2b**)	2109(m), 2070(s), 2061(vs), 2024(s), 2003(vs), 1994(s), 1979(w)	7.15 (d, 2 H), 5.89 (t, 1 H), −13.49 (s)	923 (924 calcd.)
$HOs_3(CO)_{10}(C_3H_3N_2)$ (**3b**)	2103(m), 2060(s), 2052(vs), 2024(s), 2013(vs), 1999(s), 1979(w), 1956(w)	8.9 (br., 1 H), 7.15 (d, 1 H), 6.22 (d, 1 H), −15.12 (s, 1 H)	924 (924 calcd.)
$HRu_3(CO)_{10}(C_3HMe_2N_2)$ (**4a**)	2108(w), 2074(s), 2064(vs), 2032(m), 2019(s), 1997(m), 1985(w), 1967(w)	5.72 (s, 1 H), 2.04 (s, 6 H), −13.24 (s, 1 H)	680 (681 calcd.)
$HOs_3(CO)_{10}(C_3HMe_2N_2)$ (**4b**)	2107(w), 2067(vs), 2060(vs), 2034(m), 2019(s), 1998(m), 1976(w)	5.29 (s, 1 H), 1.89 (s, 6 H), −13.22 (s, 1 H)	952 (952 calcd.)

[a] Compound numbers refer to text. – [b] In CH_2Cl_2unless stated otherwise. – [c] In $CDCl_3$ unless stated otherwise. – [d] Based on ^{192}Os, ^{101}Ru.

Scheme 1. A summary of the results reported

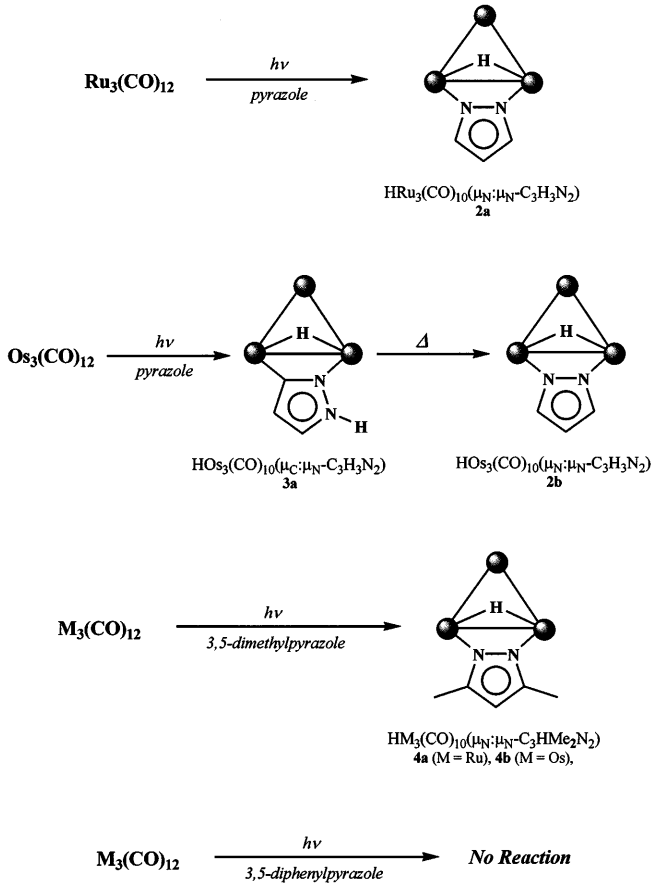

metallated complex $HOs_3(CO)_{10}(\mu_C{:}\mu_N\text{-}C_3H_3N_2)$ (**3b**). Retention of the N−H bond is evident from the spectral data and, because of this and the solubility problem, separation by chromatography is difficult since the acidic amine group interacts with the silica gel surface. Heating **3b** in boiling xylene in the absence of light yields the osmium analogue of **2a**, $HOs_3(CO)_{10}(\mu_N{:}\mu_N\text{-}C_3H_3N_2)$ (**2b**). The *ortho*-metallated complex **3b**, has been reported previously, as a minor product in the reaction of the lightly ligated complex $Os_3(CO)_{10}(MeCN)_2$ with pyrazole under reflux in benzene, the major product being **2b**[12]. This shows clearly one of the benefits of photochemistry over conventional thermolytic routes; the reaction conditions being mild and less stable complexes often being formed. This has also been shown in the reaction of **1a** and **1b** with pyridine, photolysis leading initially to the relatively unstable complex $Os_3(CO)_{11}(C_5H_5N)$ before orthometallating to form the more stable $HOs_3(CO)_{10}(C_5H_4N)$, the latter being the only thermolytic product[9].

Of note is that there is no evidence for the formation of the *ortho*-metallated analogue of **3b**, $HRu_3(CO)_{10}(\mu_C{:}\mu_N\text{-}C_3H_3N_2)$ (**3a**) in the photochemical reaction of **1a** with pyrazole or in the case of reaction of $Ru_3(CO)_{10}(MeCN)$ with the heterocycle, both routes leading to **2a**.

Photolysis of **2b** and **3b** over a longer time period 1−2 h results in the formation of a black precipitate, this being uncharacterised at present. It is, however, proposed that the black products are charged in nature, due to their insolubility in common organic solvents. This is not wholly unexpected since the photochemistry of $Ru(CO)_5$ with polydentate heterocycles has been show to result in Ru^{III} complexes as a result of a proposed photooxidation process[13]. This occurs regardless of the temperature at which the photolysis is undertaken.

Photoreactions with 3,5-Dimethylpyrazole

With 3,5-dimethylpyrazole, there is no scope for the formation of orthometallated products. Photolysis leads to the $\mu_N{:}\mu_N$ substitution products $HRu_3(CO)_{10}(\mu_N{:}\mu_N\text{-}C_3HMe_2N_2)$ (**4a**) and $HOs_3(CO)_{10}(\mu_N{:}\mu_N\text{-}C_3HMe_2N_2)$ (**4b**) in the cases of **1a** and **1b**, respectively. Again, prolonged photolysis of the reaction products leads to decomposition and photooxidation.

Photoreactions with 3,5-Diphenylpyrazole

When ethyl acetate solutions of **1a** and **1b** containing 3,5-diphenylpyrazole are irradiated, no net photoreaction is observed. This is attributed to the considerable steric shielding of the nitrogen atom of the pyrazole ring in 3,5-diphenylpyrazole and the concomitant steric hindrance to formation of complexes with the clusters.

The Molecular Structure of $HOs_3(CO)_{10}(\mu_N{:}\mu_N\text{-}C_3HMe_2N_2)$ (4b)

The molecular structure of $HOs_3(CO)_{10}(\mu_N{:}\mu_N\text{-}C_3HMe_2N_2)$ (**4b**) has been determined by single-crystal X-ray diffraction studies and is shown in Figure 1. Selected bond lengths and angles are reported in Table 2.

Figure 1. The molecular structure of $HOs_3(CO)_{10}(\mu_N{:}\mu_N\text{-}C_3HMe_2N_2)$ (**4b**)

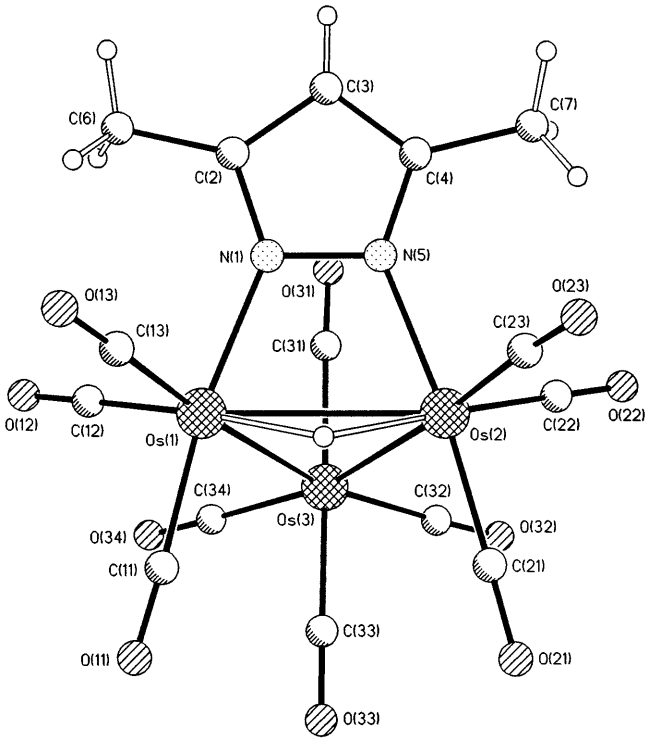

Table 2. Selected bond lengths [Å] and angles [°] for **4b**

Os(1)−Os(3)	2.8704(9)	N(1)−C(2)	1.35(2)
Os(1)−Os(2)	2.9243(13)	N(1)−N(5)	1.38(2)
Os(2)−Os(3)	2.8652(10)	C(2)−C(3)	1.41(2)
Os(1)−N(1)	2.116(11)	C(3)−C(4)	1.38(2)
Os(2)−N(5)	2.114(10)	C(4)−N(5)	1.34(2)
Os(3)−Os(1)−Os(2)	59.26(2)	C(22)−Os(2)−Os(3)	85.1(5)
Os(3)−Os(2)−Os(1)	59.43(3)	C(23)−Os(2)−Os(3)	175.3(4)
Os(2)−Os(3)−Os(1)	61.31(3)	C(22)−Os(2)−Os(1)	139.4(5)
N(1)−Os(1)−Os(3)	87.3(3)	C(23)−Os(2)−Os(1)	116.1(4)
N(1)−Os(1)−Os(2)	68.6(3)	C(32)−Os(3)−Os(2)	98.6(5)
N(5)−Os(2)−Os(3)	88.0(3)	C(34)−Os(3)−Os(1)	97.9(5)
N(5)−Os(2)−Os(1)	68.6(3)	N(5)−N(1)−Os(1)	111.3(8)
C(12)−Os(1)−Os(3)	85.9(4)	N(1)−N(5)−Os(2)	111.5(8)
C(13)−Os(1)−Os(3)	175.9(5)	C(2)−N(1)−N(5)	108.4(11)
C(12)−Os(1)−Os(2)	141.0(4)	C(4)−N(5)−N(1)	108.8(11)
C(13)−Os(1)−Os(2)	117.2(5)		

The solid-state structure of **4b** is consistent with that in solution, the heterocyclic unit bridging one of the Os−Os bonds. The two unbridged Os−Os bond lengths (mean 2.875 Å) in **4b** are very similar to those in $Os_3(CO)_{12}$ **1b** (mean 2.867 Å)[14]. The bridged Os−Os bond is significantly longer at 2.9243 Å. The hydride was not located directly in the Fourier difference map but its position was determined using the program HYDEX[15]. The pyrazolate unit, which is inclined at an angle of 102.4° to the Os_3 plane, coordinates with one nitrogen atom axially bonded to Os(1) and one nitrogen atom axially bonded to Os(2) [Os(1)−N(1) = 2.116(11) Å; Os(1)−N(5) = 2.114(10) Å]. The complex possesses a similar molecular architecture to that of the related complexes $HOs_3(CO)_{10}[\mu_2\text{-}2,3\text{-}\eta^2\text{-}NNN(O)C_6H_4]$[16] (**5b**) and $HOs_3(CO)_{10}(\mu\text{-}\eta^2\text{-}N{=}NPh)$[17] (**6b**) prepared from the reactions of $Os_3(CO)_{10}(MeCN)_2$ and 1-hydroxybenzotriazole and phenyldiazonium tetrafluoroborate, respectively. In both **5b** and **6b**, there is extension of the Os−Os bond bridged by the heterocycle and hydride ligand, as in **4b**. The heterocyclic unit is inclined at an angle of 102.5° in **5b** and at 103.25° in **6b**. In all three structures, a survey of the *cis*-diequatorial angles around the triosmium framework shows that the angles are larger than the remaining *cis*-diequatorial OC−Os−Os angles [for **4b**: C(23)−Os(2)−Os(1) = 116.1(4), C(13)−Os(1)−Os(2) = 117.2(5), C(34)−Os(3)−Os(1) = 97.9(5), C(32)−Os(3)−Os(2) = 98.6(5)]. Compared to the free pyrazole ligand, coordination to **4b** has remarkable little effect, the bond lengths being almost unchanged within the remit of statistical significance[18].

Conclusions

The photolysis of ethyl acetate solutions of $M_3(CO)_{12}$ [M = Ru (**1a**), Os (**1b**)] with pyrazole and 3,5-dimethylpyrazole leads to photosubstitution products. With pyrazole, **1a** forms the substitution product $HRu_3(CO)_{10}(\mu_N{:}\mu_N\text{-}C_3H_3N_2)$ (**2a**) but, in the case of osmium, the *ortho*-metallated complex $HOs_3(CO)_{10}(\mu_C{:}\mu_N\text{-}C_3H_3N_2)$ (**3b**) can be isolated. Heating **3b** yields the osmium analogue of **2a**, $HOs_3(CO)_{10}(\mu_N{:}\mu_N\text{-}C_3H_3N_2)$ (**2b**). Photolysis of **1a** and **1b** with 3,5-dimethylpyrazole yields the substitution products $HRu_3(CO)_{10}(\mu_N{:}\mu_N\text{-}C_3HMe_2N_2)$ (**4a**) and $HOs_3(CO)_{10}(\mu_N{:}\mu_N\text{-}C_3HMe_2N_2)$ (**4b**), respectively. With 2,6-diphenylpyrazole no net photoreaction is observed.

Girton College Cambridge is thanked for a Research Fellowship. This work was funded in part by the *UK Engineering and Physical Sciences Research Council* and *Johnson-Matthey plc* is acknowledged for the generous loan of ruthenium chloride. Advice and assistance from *G.P. Shields* is greatly appreciated.

Experimental Section

General Experimental: Unless stated otherwise, all syntheses were performed under dry nitrogen using standard Schlenk techniques. All photochemical reactions were performed in a specially designed glass reaction vessel fitted with a nitrogen bubbler, reflux condenser and dry-ice cooling finger. A 125-W mercury arc broad-band UV lamp was used as the irradiation source and reflectors placed around the reaction vessel to maximise efficiency. All reagents were purchased from commercial sources and used as received unless noted otherwise. Literature methods were used to prepare the starting material compounds $Ru_3(CO)_{12}$ (**1a**)[19] and $Os_3(CO)_{12}$ (**1b**)[20]. Purification of the reaction products was by thin layer chromatography (laboratory prepared glass plates coated to a thickness of 1.0 mm with Merck Kieselgel 60 F_{254}) using light petroleum ether as eluent.

Physical Measurements: Infrared (IR) spectra were recorded in NaCl solution cells (path length 0.5 mm) using a Perkin-Elmer PE 1710 Fourier transform infrared spectrometer. All values quoted are in wavenumbers (cm^{-1}). – The ^1H-NMR spectra were recorded using a Bruker AM400, WM250, or WP80SY Fourier transform NMR spectrometer and data reported using the chemical shift scale in units of ppm relative to the solvent resonance. – Fast atom bombardment (FAB) mass spectra were recorded using a KRATOS MS-50 spectrometer, with either 3-nitrobenzyl alcohol or thioglycerol as a matrix and CsI as calibrant. – IR, NMR, and mass spectral data are collected in Table 1.

Photolyses

An Ethyl Acetate Solution of $Ru_3(CO)_{12}$ (**1a**) *with Pyrazole:* An ethyl acetate solution of **1a** (30 mg in 150 ml) containing excess pyrazole (9.6 g) was irradiated using the broad-band UV source. The reaction was deemed complete when there was no further change in the IR spectrum (30 min). From comparison with literature data it was proposed that the yellow-orange cluster formed in 60% yield was $HRu_3(CO)_{10}(\mu_N{:}\mu_N\text{-}C_3H_3N_2)$ (**2a**)[21]. Prolonged photolysis of the reaction mixture (1 h) led to decomposition.

An Ethyl Acetate Solution of $Os_3(CO)_{12}$ (**1b**) *with Pyrazole:* The photolysis was performed as with **1a** but using **1b** (40 mg in 150 ml) and 16 mg of the heterocycle. The yellow-green *ortho*-metallated cluster $HOs_3(CO)_{10}(\mu_C{:}\mu_N\text{-}C_3H_3N_2)$ (**3b**) was formed in 60% yield after 45 min, as characterised by comparison with literature data[12]. The product is not particularly soluble and sticks to the silica gel surface of TLC plates. As a result, an eluent of 2:1 petroleum ether/dichloromethane was used for purification. Prolonged photolysis of the reaction mixture (1 h) led to decomposition. Heating a solution of **3b** in refluxing xylene for 1 h led to the formation of $HOs_3(CO)_{10}(\mu_N{:}\mu_N\text{-}C_3H_3N_2)$ (**2b**) in 70% yield.

An Ethyl Acetate Solution of $Ru_3(CO)_{12}$ (**1a**) *with 3,5-Dimethylpyrazole:* The photolysis was performed as with pyrazole but using 3,5-dimethylpyrazole (16 mg) as the heterocycle. The yellow cluster $HRu_3(CO)_{10}(\mu_N{:}\mu_N\text{-}C_3HMe_2N_2)$ (**4a**) was formed in 60% yield after 30 min. Prolonged photolysis of the reaction mixture (1 h) led to decomposition.

An Ethyl Acetate Solution of $Os_3(CO)_{12}$ (**1b**) *with 3,5-Dimethylpyrazole:* The photolysis was performed as with **1a** but using $Os_3(CO)_{12}$ (**1b**) (40 mg in 150 ml) and 24 mg of the heterocycle. The yellow cluster $HOs_3(CO)_{10}(\mu_N{:}\mu_N\text{-}C_3HMe_2N_2)$ (**4b**) was formed in 50% yield after 45 min. Prolonged photolysis of the reaction mixture (1 h) led to decomposition.

An Ethyl Acetate Solution of $Ru_3(CO)_{12}$ (**1a**) *and $Os_3(CO)_{12}$* (**1b**) *with 3,5-Diphenylpyrazole:* The photolyses were performed as with pyrazole but using 3,5-diphenylpyrazole (26 mg for **1a**, 35 mg for **1b**) as the heterocycle. No net photoreaction was observed in each case.

Determination of the Molecular Structure of $HOs_3(CO)_{10}(\mu_N{:}\mu_N\text{-}C_3HMe_2N_2)$ (**4b**) *by Single-Crystal X-ray Diffraction*

Crystal Data: $C_{15}H_8N_2O_{10}Os_3$, M = 946.83, monoclinic, space group $P2_1/c$ (no. 14), a = 16.392(3), b = 7.636(2), c = 18.536(4) Å, β = 115.53(3), U = 2093.6(8) Å^3 (from refinement of 2θ values of 25 independent reflections), Z = 4, D_c = 3.004 gcm^{-3}, T = 293 K, yellow-orange rectangular plate 0.50 × 0.40 × 0.40 mm, μ(Mo-K_α) = 18.216 mm^{-1}, F(000) = 1680.

Data Collection and Processing: All X-ray measurements were made with graphite monochromated Mo-K_α radiation (λ = 0.71073 Å) with a Stoe-Siemens diffractometer using the ω-θ scan mode, 4994 reflections collected, 3681 independent (R_{int} = 0.0454) ($-19 \le h \le 19$, $-8 \le k \le 9$, $-22 \le l \le 22$; $5.5° \le 2\theta \le 50°$). Semi-empirical absorption correction based on ψ-scan data was applied (minimum and maximum transmission factors 0.153 and 0.288, respectively)[22].

Structure Solution and Refinement: The osmium atom positions were determined by direct methods (SHELXTL-PLUS)[23] and all non-hydrogen atoms located by subsequent Fourier difference syntheses. Full-matrix least-squares refinement on F^2 (SHELXL-93)[24] was performed with anisotropic displacement parameters for all non-hydrogen atoms. Hydrogen atoms were placed in idealised positions and allowed to ride on the relevant carbon atom. The hydride ligand was located using the program HYDEX. In the final cycles of refinement, a weighting scheme of the form $w^{-1} = [\sigma(F_o^2) + 0.053P^2 + 10.46P]$ [where $P = (F_o^2 + 2F_c^2)/3$] was introduced which produced a flat analysis of variance. At final convergence (max Δ/σ = 0.001), $wR(F^2)$ = 0.1025 for all data, $R(F)$ = 0.0865 for 2801 observed reflections [$I > 2\sigma(I)$] and 188 parameters. The final difference synthesis showed no Δρ above 2.882 or below −1.390 eÅ^{-3}, the major features lying near the osmium atoms.

Crystallographic data (excluding structure factors) for the structure reported in this paper have been deposited with the Cambridge Crystallographic Data centre as supplementary publication no. CCDC-101356. Copies of the data can be obtained free of charge on application to the CCDC, 12 Union Road, Cambridge, CB2 1EZ [Fax: int. code + 44-1223/336-033; E-mail: deposit@ccdc.cam.ac.uk].

[1] See for example: [1a] M. I. Bruce in *Comprehensive Organometallic Chemistry* (Eds.: G. Wilkinson, F. G. A. Stone, E. W. Abel), Pergamon Press, Oxford, **1982**, vol. 4. – [1b] K. Burgess, *Polyhedron* **1984**, *3*, 1175. – [1c] E. C. Constable, *Polyhedron* **1984**, *3*, 1037.

[2] [2a] F. Calderazzo, C. Floriaini, R. Henzi, F. l'Eplattinier, *J. Chem. Soc. A* **1969**, 1378. – [2b] R. L. Bennett, M. I. Bruce, B. L. Goodall, M. Z. Iqbal, F. G. A. Stone, *J. Chem. Soc., Dalton Trans.* **1972**, 1787.

[3] A. J. Edwards, N. E. Leadbeater, J. Lewis, P. R. Raithby, *J. Organomet. Chem.* **1995**, *512*, 13.

[4] [4a] N.E. Leadbeater, *J. Chem. Soc., Dalton Trans.* **1995**, 2923. – [4b] N. E. Leadbeater, J. Lewis, P. R. Raithby, *J. Organomet. Chem.* **1997**, 251.

[5] P. C. Ford, *J. Organomet. Chem.* **1990**, *383*, 339.

[6] A. J. Edwards, N. E. Leadbeater, J. Lewis, P. R. Raithby, *J. Organomet. Chem.* **1995**, *503*, 15.

[7] N. E. Leadbeater, *J. Chem. Soc., Dalton Trans.* **1995**, 2923.

[8] N. E. Leadbeater, *J. Organomet. Chem.*, in press.

[9] N. E. Leadbeater, J. Lewis, P. R. Raithby, G. N. Ward, *J. Chem. Soc., Dalton Trans.* **1997**, 2511.

[10] [10a] H. Kuroda, *Pure. Appl. Chem.* **1992**, *64*, 1449. – [10b] M. Haukka, T. Venäläinen, P. Hirva, T. A. Pakkanen, *J. Organomet. Chem.* **1996**, *509*, 163. – [10c] *Catalysis in C_1 Chemistry* (Ed.: W. Keim), Reidel, Dodrecht, **1983**. – [10d] M. Haukka, L. Alvila, T. A. Pakkanen, *J. Mol. Catal.* **1995**, *102*, 79. – [10e] R. Usón, L. A. Oro, M. T. Pinillos, M. Royo, E. Pastor, *J. Mol. Catal.* **1982**, *14*, 375. – [10f] P. Kalck, A. Thorez, M. T. Pinillos, L. A. Oro, *J. Mol. Catal.* **1985**, *31*, 311. – [10g] E. Alessio, G. Clauti, G. Mestroni, *J. Mol. Catal.* **1985**, *29*, 77. – [10h] E. Alessio, G. Zassinovich, G. Mestroni, *J. Mol. Catal.* **1983**, *18*, 113.

[11] [11a] J. A. DiBenedetto, D. W. Ryba, P. C. Ford, *Inorg Chem.* **1989**, *28*, 3503. – [11b] J. G. Bentsen, M. S. Wrighton, *J. Am. Chem. Soc.* **1987**, *109*, 4530.

[12] J. R. Shapley, D. E. Samkoff, C. Bueno, M. R. Churchill, *Inorg Chem.* **1982**, *21*, 634.

[13] G. R. Haire, N. E. Leadbeater, J. Lewis, P. R. Raithby, A. J. Edwards, E. C. Constable, *J. Chem. Soc., Dalton Trans.* **1997**, 2997.

[14] M. R. Churchill, B. G. De Boer, *Inorg Chem.* **1977**, *16*, 878.

[15] A. G. Orpen, *J. Chem. Soc., Dalton. Trans.* **1980**, 2509.

[16] K.-L. Lu, S. Kumaresan, Y-S. Weng, J. R. Hwu, *Organometallics* **1994**, *13*, 3170.

[17] D. E. Samkoff, J. R. Shapley, M. R. Churchill, H. J. Wasserman, *Inorg. Chem.* **1984**, *23*, 397.
[18] F. Krebs Laesen, M. S. Lehmann, I. Søtofte, S. E. Rasmussen, *Acta Chem. Scand.* **1970**, *24*, 3248.
[19] C. R. Eady, P.F Jackson, B. F. G. Johnson, J. Lewis, M. C. Malatesta, M. McPartlin, W. J. H. Nelson, *J. Chem. Soc., Dalton. Trans.* **1980**, 383.
[20] B. F. G. Johnson, J. Lewis, *Inorg. Synth.* **1976**, *16*, 47.
[21] M. I. Bruce, M. G. Humphrey, M. R. Snow, E. R. T. Tiekink, R. C. Wallis, *J. Organomet. Chem.* **1986**, *314*, 311.
[22] A. C. T. North, D. C. Phillips, F. S. Mathews, *Acta Crystallogr., Sect A* **1968**, *24*, 351.
[23] G. M. Sheldrick, *SHELXL-PLUS program for solving, refining and displaying crystal structures from diffraction data*, University of Göttingen, Germany, **1990**.
[24] G. M. Sheldrick, *SHELXL-93 program for crystal structure refinement*, University of Göttingen, Germany, **1993**.

[98108]

β-Diiminato Complexes of V^{III} and Ti^{III} − Formation and Structure of Stable Paramagnetic Dialkylmetal Compounds

Peter H. M. Budzelaar*[a][+], A. Bart van Oort[a], and A. Guy Orpen[b]

Shell Research and Technology Centre Amsterdam[a],
P. O. Box 38000, NL-1030 BN Amsterdam, The Netherlands

School of Chemistry, University of Bristol[b],
Bristol BS8 1TS, United Kingdom

Received April 20, 1998

Keywords: Titanium / Vanadium / Polymerizations / Diimine / Dialkylmetal compounds

(Mono-β-diiminato)titanium(III) and -vanadium(III) dichlorides $LMCl_2$ [L = ArNC(R)CHC(R)NAr$^-$] are easily accessible from the metal trichlorides and LLi in THF. The crystal structures of $LVCl_2$ (Ar = 2,6-*i*$Pr_2C_6H_3$, R = Me) and $LTiCl_2$ (Ar = 2,4,6-$Me_3C_6H_2$, R = Me and Ar = 2,4,6-$Me_3C_6H_2$, R = *t*Bu) reveal tetrahedral metal environments. Treatment of $LVCl_2$ with alkyllithium reagents affords surprisingly stable dialkylvanadium(III) compounds; the structure of $LV(n\text{Bu})_2$ (Ar = 2,6-*i*$Pr_2C_6H_3$, R = Me) is similar to that of the dichloride. The corresponding dialkyltitanium(III) compounds are less stable; only the dimethyl derivatives could be obtained in pure form (from $LTiCl_2$ and MeMgI), and only for ligands bearing 2,6-disubstituted aryl groups. The structure of $LTiMe_2$ (Ar = 2,4,6-$Me_3C_6H_2$, R = Me) is also similar to that of the dichloride. Reaction of $LTiMe_2$ with $B(C_6F_5)_3$ produces a catalyst for α-olefin polymerization, but the corresponding V^{III} derivatives are inactive.

Introduction

The development of metallocene catalysis has led to intense interest in the generation and reactivity of early transition alkylmetal compounds. Neutral dialkylmetal compounds, in particular, are of great importance as precursors of catalytically active cationic monoalkyl species. Most of the work in this area has concentrated on diamagnetic d^0 complexes of group-III and -IV metals. It is still unclear whether d^1 or d^2 complexes can be as efficient in olefin polymerization as their d^0 analogues, and this lack of insight is at least partly due to the unavailability of suitable catalyst precursors. However, work by Theopold on d^3 chromium systems demonstrates that well-defined paramagnetic homogeneous polymerization catalysts are certainly possible.[1]

We report herein on the preparation of Ti^{III} (d^1) and V^{III} (d^2) complexes containing a β-diiminato ancillary ligand. The β-diimine ligand has not been widely used in organometallic chemistry. Some Pd^{II} and Ni^{II} complexes have been prepared recently; in comparison with related α-diimine complexes they showed a much lower activity in Brookhart-type olefin polymerization.[2] Collins has recently reported the synthesis of several Zr^{IV} complexes of β-diimines.[3]

One advantage of β-diimines is that ligand variation, in both the ligand backbone and the substituent at the nitrogen atom, is relatively easy. This has allowed us to probe the consequences of steric effects in the present study (Scheme 1 shows the ligands studied and the abbreviations used here). We have concentrated on the $\mathbf{L^1}$ and $\mathbf{L^2}$ ligands, because the Ti and V dichloride and dimethyl derivatives were found to crystallize well, and only examined the use of the other ligands in selected cases.[4]

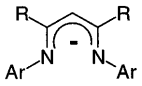

Ligand Syntheses

The two main routes for the synthesis of β-diimines are summarized in Scheme 1. The most convenient route (**A**) is condensation of a β-diketone with an (aromatic) amine.[5] The second route (**B**) is especially useful for very bulky diimines,[6] where the route **A** condensation is very sluggish. Route **B** is also applicable to the synthesis of asymmetrically substituted diimines (different Ar groups). The ligands used in the present work were all prepared by one of these two methods. Lappert has reported a more exotic synthesis of silyl-substituted diiminates from bis(trimethylsilyl)methyllithium and nitriles.[7]

Dichloride Complexes

Complexes $LMCl_2$ (M = Ti^{III}, V^{III}; L ≠ $\mathbf{L^4}$ or $\mathbf{L^6}$) are conveniently prepared by reaction in THF of $MCl_3(THF)_3$ with the lithium salt of the β-diimine (prepared in situ from the free diimine and *n*BuLi). After evaporation of the solvent, the complex is extracted with toluene and purified by

[+] Present address: Department of Inorganic Chemistry, University of Nijmegen, Toernooiveld 1, NL-6525 ED Nijmegen, The Netherlands; E-mail: budz@sci.kun.nl

 © WILEY-VCH Verlag GmbH, D-69451 Weinheim, 1998 1434−1948/98/1010−1485 $ 17.50+.50/0

Scheme 1. β-Diimine ligand syntheses

Route **A**.

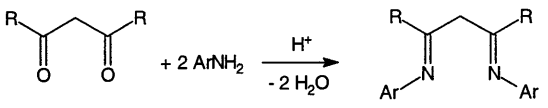

	R	Ar	ref
L^1	Me	2,4,6-$Me_3C_6H_2$	this work
L^2	Me	2,6-(*i*-Pr)$_2C_6H_3$	2
L^3	Me	2-MeC_6H_4	this work
L^4	Me	C_6H_5	5

Route **B**.

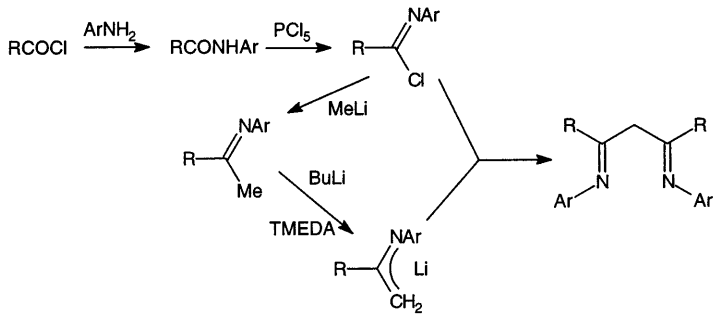

L^5	*t*-Bu	2,4,6-$Me_3C_6H_2$	this work
L^6	*t*-Bu	2,6-(*i*-Pr)$_2C_6H_3$	this work

crystallization from toluene or hexane. In several instances, we initially observed formation of a THF complex; repeated distillation of toluene (at 1 bar) from a solution of the complex was found to be a convenient method for removal of this THF.

The $\mathbf{L^4}$ complexes tenaciously retain 2 molecules of complexed THF. Treatment of $VCl_3(THF)_3$ with $\mathbf{L^4}$Li in THF results in precipitation of dark-green needles of poorly soluble $\mathbf{L^4}VCl_2(THF)_2$. Most of the coordinated THF can be removed by the above-mentioned toluene distillation, but the resulting product is an ill-defined black substance. $\mathbf{L^4}TiCl_2(THF)_2$ is poorly soluble even in hot THF or toluene/THF mixtures; small amounts can be crystallized from THF as dark-brown needles. Reaction of the THF complex with Me_3SiI[8] removes the coordinated THF but also exchanges the chlorides for iodides, giving dark-red $\mathbf{L^4}TiI_2$, which is fairly soluble in toluene and diethyl ether.

All the dichlorides are stable at room temperature, but are highly sensitive to air and moisture. They are paramagnetic and exhibit strongly broadened NMR spectra that could not be fully interpreted. Complexes $\mathbf{L^2}VCl_2$ (Figure 1), $\mathbf{L^1}TiCl_2$ (Figure 2), and $\mathbf{L^5}TiCl_2$ (Figure 3) were characterized by X-ray diffraction. They are monomeric and show the expected distorted tetrahedral surrounding of the metal center. In the case of the bulky $\mathbf{L^2}$ ligand, the metal atom has moved out of the NCCCN plane of the ligand. This allows the aryl groups at the nitrogen atoms to tilt, thus relieving steric repulsion between the chlorides and the isopropyl substituents. Movement of the metal atom out of the NCCCN plane has also been observed in the sterically hindered zirconium complex [$Me_3SiNC(t\text{Bu})CHC(t\text{Bu})NSiMe_3$]$ZrCl_3$[7] and in the tin derivative [$Me_3SiNC(t\text{Bu})CHC(t\text{Bu})NSiMe_3$]$SnMe_2Cl$,[7] whereas the unhindered tin complex [$HNC(t\text{Bu})CHC(t\text{Bu})NH$]$SnMe_2Cl$[7] and the lanthanide complex [$PhNC(Me)CHC(Me)NPh$]$GdBr_2(THF)_2$[9] have essentially planar skeletons. The *neutral* β-diimine complex ($H\mathbf{L^2}$)$NiBr_2$ and the *C*-metallated [$Pd(NCMe)_3$][μ-C:N,N′-$\mathbf{L^2}$][$Pd(NCMe)_2$]$^{3+}$ also have non-planar diimine skeletons.[2] The strongly non-planar structure recently reported for ($\mathbf{L^4}$)(indenyl)$ZrCl_2$ by Collins was described as partially η^5;[3] the nonplanarity of our $\mathbf{L^2}VCl_2$ complex is clearly not pronounced enough to warrant such a description.

Figure 1. X-ray structure of L^2VCl_2[a]

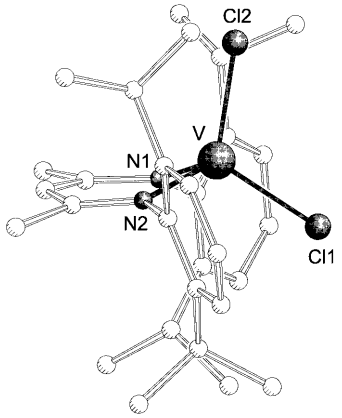

[a] Selected structure data: V−N1 1.940(2), V−N2 1.963(2), V−Cl1 2.242(1), V−Cl2 2.234(1) Å; N1−V−N2 94.0(1), Cl1−V−Cl2 114.3(1)°.

Surprisingly, we were unable to prepare transition metal complexes of the bulkiest ligand ($\mathbf{L^6}$). Neither the lithium salt nor the potassium salt reacted with $TiCl_3$ in refluxing THF, despite the fact that in the less hindered systems ligand transfer occurs even at room temperature. With VCl_3, some kind of reaction took place, but no vanadium diiminate was formed. It occurred to us that the steric repulsion between the backbone *t*Bu groups and the substituents at the nitrogen atoms might destabilize the geometry needed

Figure 2. X-ray structure of L^1TiCl_2[a]

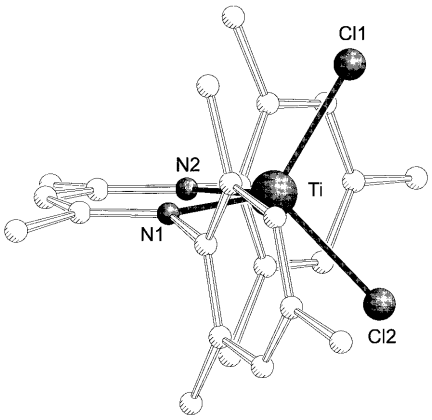

[a] Selected structure data: Ti−N1 1.983(3), Ti−N2 1.964(3), Ti−Cl1 2.294(1), Ti−Cl2 2.295(1) Å; N1−Ti−N2 84.2(1), Cl1−Ti−Cl2 106.34(5)°.

Figure 3. X-ray structure of L^5TiCl_2[a]

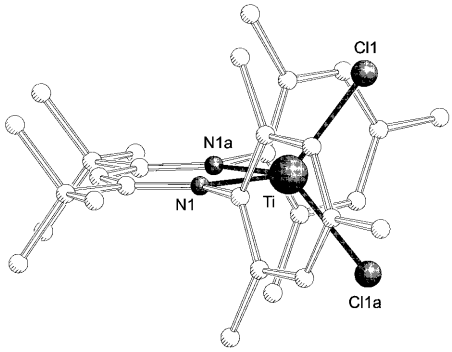

[a] Selected structure data: Ti−N1 1.986(1), Ti−Cl1 2.2966(6) Å; N1−Ti−N1a 83.88(8), Cl1−Ti−Cl1a 104.57(3)°.

for chelation, for example by enforcing a *trans* arrangement of the *t*Bu and diisopropylphenyl groups around the C=N bonds. However, the X-ray structure of the salt $\mathbf{L^6}$Li(THF) (Figure 4) shows a normal chelate structure. The most likely explanation for the failure to form Ti and V complexes is still a steric one. The *t*Bu groups enforce a larger C−N−C angle [compare the values of 119 and 120° in $\mathbf{L^2}VCl_2$ and 121 and 122° in $\mathbf{L^1}TiCl_2$ to 128° in $\mathbf{L^5}TiCl_2$ and 127 and 129° in $\mathbf{L^6}$Li(THF)], thus restricting the amount of space in the open "wedge" between the aryl groups. Also, the possibility of strain relief by aryl group tilting as found in $\mathbf{L^2}VCl_2$ is probably limited by the *t*Bu groups. Thus, there is still enough space in the center of the open wedge for the single THF molecule in $\mathbf{L^6}$Li(THF), but the isopropyl groups might cause severe repulsion at the two tetrahedral positions of the chlorides in a hypothetical $\mathbf{L^6}MCl_2$ molecule.

Dialkylvanadium(III) Compounds

Treatment of complexes $LVCl_2$ with alkyllithium compounds (MeLi, *n*BuLi) in diethyl ether affords easy access to dialkylmetal compounds LVR_2. These complexes were found to be unexpectedly stable. For example, $\mathbf{L^2}V(n\text{Bu})_2$,

Figure 4. X-ray structure of L^6Li(THF)[a]

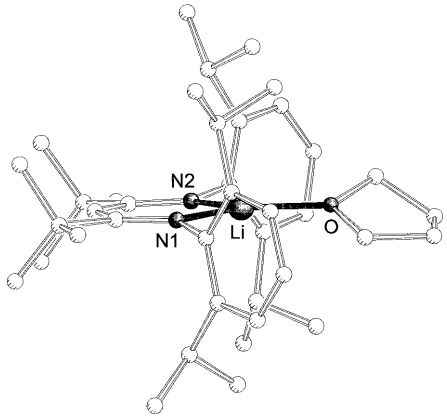

[a] Selected structure data: Li−N1 1.927(6), Li−N2 1.927(6), Li−O 1.910(6) Å; N1−Li−N2 100.2(3), N1−Li−O 130.9(3), N2−Li−O 128.8(3)°.

which is formally a 10-*e* complex (or at most a 14-*e* complex, if π-donation from both nitrogen atoms is included in the count) and contains 4 β-hydrogen atomss, could be crystallized from warm (50°C) hexane without significant decomposition. The X-ray structure of this complex (Figure 5) shows a tetrahedral environment of the metal centre, similar to that in the dichloride. There is some disorder in one of the *n*-butyl groups, but the structure is otherwise unremarkable. There is no evidence for significant agostic interactions or short intermolecular contacts.

Not many dialkylvanadium(III) compounds are known. Two examples bearing tridentate amido ligands have been reported: Edwards obtained a compound formulated as $[(Me_2PCH_2CH_2)_2N]VMe_2$ as an oil from the reaction of the dichloride with MeLi;[10] he also obtained the crystalline complex $[(Et_2NCH_2CH_2)_2N]VMe_2$ in a similar manner.[11] $CpVMe_2(PMe_3)_2$[12] and $CpVR_2(PMe_3)$ (R = CH_2CMe_3, CH_2CMe_2Ph, CH_2SiMe_3)[13] have been reported by the group of Teuben. None of these complexes have been characterized by X-ray diffraction, but the crystal structure of the metallated alkyl-aryl complex $CpV(CH_2CMe_2\text{-}o\text{-}C_6H_4)(PMe_3)_2$ has been determined and shows a rather long V−C(alkyl) distance of 2.194(3) Å.[13] The *tri*alkyl complex $[(Me_3CCH_2)_3V]_2(\mu\text{-}N_2)$ has much shorter V−C bonds [2.026(2) Å];[14] those in our complex $\mathbf{L^2}V(n\text{Bu})_2$ are intermediate [2.062(5) Å].

Dialkyltitanium(III) Compounds

The related dialkyltitanium(III) compounds were found to be less stable. For ligands bearing 2,6-disubstituted aryl groups, $LTiMe_2$ complexes are best prepared from $LTiCl_2$ and MeMgI in diethyl ether. Addition of 1 equiv. of dioxane, evaporation of the solvent, and extraction with hexane gave an impure product, which could be purified further by crystallization from hexane. The $LTiMe_2$ complexes all have an intense dark-blue colour. The structure of $\mathbf{L^1}TiMe_2$ (Figure 6) shows the expected tetrahedral environment of the metal centre and is very similar to that of

Figure 5. X-ray structure of $L^2V(n\text{Bu})_2$[a]

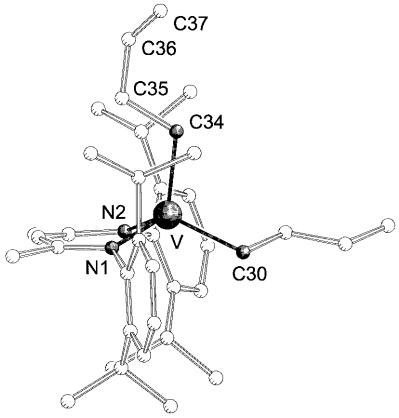

[a] Selected structure data: V–N1 1.997(4), V–N2 1.991(4), V–C30 2.062(5), V–C34 2.062(5) Å; N1–V–N2 94.5(2), C30–V–C34 109.6(2)°; the apparent near-eclipsed confirmation of the C34–C37 butyl chain is caused by a disorder in the positions of C35 and C36, probably between two possible *gauche* conformations.

Figure 6. X-ray structure of L^1TiMe_2[a]

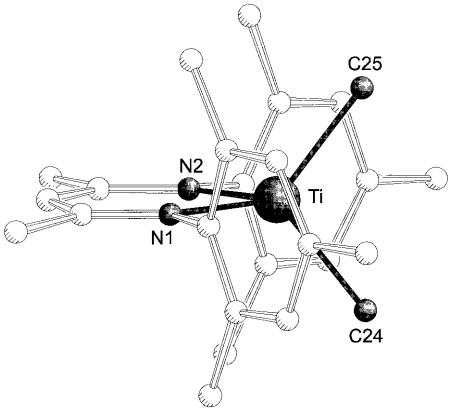

[a] Selected structure data: Ti–N1 1.989(2), Ti–N2 1.989(2), Ti–C24 2.131(3), Ti–C25 2.123(3) A; N1–Ti–N2 85.33(7), C24–Ti–C25 104.5(1)°.

the dichloride. Paramagnetic alkyltitanium compounds are relatively rare, and only a few examples not bearing cyclopentadienyl substituents have been described. Arnold has reported the synthesis of a *mono*methyltitanium(III) benzamidinate complex, $[PhC(NSiMe_3)_2]_2TiMe$,[15] and suggested that the unusually short Ti–C bond in this complex, 2.120(5) Å, was due to the low coordination number (5) of the Ti atom. The coordination number of Ti in $\mathbf{L^1}TiMe_2$ is even lower (4), but the Ti–C bond lengths [2.123(3) and 2.131(3) Å] are not shorter than those in the benzamidinate compound. However, the benzamidinato ligand should be "harder" than the diiminato ligand, and this is reflected in much longer Ti–N bonds [2.104(3), 2.164(3), 2.095(3), and 2.160(3) Å, vs. 1.989(2) Å in $\mathbf{L^1}TiMe_2$], which might compensate for the difference in coordination number. Cummins has reported the X-ray structure of $[\eta^1\text{-}(t\text{Bu})(\text{Ar})\text{N}][\eta^3\text{-}(t\text{Bu})(\text{Ar})\text{N}]\text{TiCH}(SiMe_3)_2$ (Ar = 3,5-$Me_2C_6H_3$), which has a Ti–C distance of 2.137(7) Å.[16] Edwards has reported the preparation of $[(Et_2NCH_2CH_2)_2N]TiMe_2$, which was characterized by elemental analysis and ESR; no further details of its stability and reactivity were given.[11] Gambarotta has prepared several anionic dialkyltitanium(III) compounds $(R_2N)_2Ti(\mu\text{-}R')_2Li(TMEDA)$ and $[(R_2N)_2Ti(R')_2]^-[Li(TMEDA)_2]^+$.[17]

The presence of sufficient steric shielding appears to be essential for the stability of the product. Whereas $LTiMe_2$ complexes bearing *2,6-disubstituted* aryl groupss were found to be reasonably stable at room temperature, the bis(*o-tolyl*) ($\mathbf{L^3}$) derivative decomposes within 1 h (an impure product could be obtained by carrying out the reaction and isolation at −10°C). The di*phenyl* ($\mathbf{L^4}$) derivative was initially formed upon addition of MeMgI to $LTiCl_2$ (as indicated by the deep-blue colour), but within ca. 10 seconds the colour had changed to green-brown, indicating rapid decomposition. We could not find any conditions under which the rate of formation was sufficiently high and the decomposition slow enough to allow isolation of $\mathbf{L^4}TiMe_2$.

Higher alkyl derivatives are less stable than the methyl complexes. A few large, dark-blue crystals of what appeared to be $\mathbf{L^1}TiEt_2$ were obtained by rapid work-up of the reaction product from $\mathbf{L^1}TiCl_2$ and EtMgBr in Et_2O, but even during crystallization at −20°C the initially blue hexane solution turned green, indicating partial decomposition. The crystals themselves were fully decomposed after 1 night at room temperature. No further attempts were made to prepare higher alkyl compounds.

Polymerization Experiments

Even though they are coordinatively unsaturated, the dialkylmetal compounds themselves were found to be unreactive towards olefins. Treatment with MAO or $EtAlCl_2$ resulted in transfer of the β-diimine ligand to Al, and no significant polymerization activity was observed. The reaction of $LVMe_2$ complexes with 1 equiv. of $B(C_6F_5)_3$ produced a brown solution, possibly containing the ionic species, but no polymerization activity was observed with propene, and only a very low activity with ethene.

The corresponding Ti complexes proved to be significantly more active. Reaction of $\mathbf{L^1}TiMe_2$ with $B(C_6F_5)_3$ in benzene produced a red-brown solution, possibly containing $\mathbf{L^1}TiMe^+MeB(C_6F_5)_3^-$. This solution was found to be active in the polymerization of propene and 1-hexene, producing atactic materials, although activities in propene polymerization (see Table 1) are not very high compared to those of metallocene catalysts. The molecular weight distribution is rather narrow ($M_w/M_n \approx 1.58-1.78$) indicating relatively slow chain transfer. The polymerization is not "living", since propene absorption almost stopped after 15 min. The stoichiometry of the reaction indicates the formation of ca. 1 chain per metal atom. NMR analysis of the product did not reveal any unsaturated end groups. These facts suggest that the polymerization does *not* terminate by β-elimination, but by a different mechanism which prevents initiation of a new chain. One possibility is reaction with impurities in the feed (since there is no scavenger present

Table 1. Propene polymerization experiments[a]

Entry	Cat.	Co-cat.	Solvent	Time [min]	Activity[b][c]	Remarks
1	$\mathbf{L^1}TiMe_2$	$B(C_6F_5)_3$	benzene	30	62000/96000	
2		$B(C_6F_5)_3$	benzene	120	25000	0.05 mmol cat, co-cat.
3		$B(C_6F_5)_3$	benzene	30	14000/33000	50°C; exotherm
4		$B(C_6F_5)_3$	toluene	10	–	
5		$B(C_6F_5)_3$	bromobenzene	10	–	
6		$Ph_3C^+B(C_6F_5)_4^-$	benzene	30	–	
7		$PhMe_2NH^+$ $B(C_6F_5)_4^-$	benzene	30	53000/101000	
8		$PhMe_2NH^+$ $B(C_6F_5)_4^-$	benzene	30	2000/8100	0.05 mmol cat, co-cat.
9	$\mathbf{L^5}TiMe_2$	$B(C_6F_5)_3$	benzene	30	0/2000/10000	
10	$\mathbf{L^2}TiMe_2$	$B(C_6F_5)_3$	benzene	30	2000	

[a] 0.1 mmol of cat. and co-cat., 25 ml of solvent, 5–6 bar propene, room temperature. – [b] (g olefin)/(mol Ti)·h. – [c] Multiple entries are results from separate experiments.

in this system), but alkyl transfer to the ligand cannot be excluded: Floriani observed transfer of alkyl groups from Zr^{IV} to the imine carbon atoms of the macrocyclic bis(diiminato) ligand tmtaa.[18] Reproducibility of the activities is poor (see the different activities given for entries 1, 3, 7, 8, 9 in the table). We found that the time taken to prepare the catalyst mixture and the laboratory temperature had a significant influence, indicating that the catalyst is not very stable.

Curiously, polymerization activity is virtually zero if toluene is used as the solvent instead of benzene (entries 1 and 3). Inhibition of polymerization by toluene has been noted for a closely related Ti^{IV} di*amide* catalyst by McConville,[19] but he did not report on the effect of benzene in the same system. McConville attributed the effect of toluene to the formation of a toluene complex. Our observed difference between benzene and toluene might have a similar cause, since toluene is a somewhat stronger donor than benzene. However, we do not consider this very likely since some activity was observed when the reaction was carried out at a lower temperature in toluene. Chemical reaction with toluene (e.g. benzylic C–H activation) could be an alternative explanation.

The catalyst system used here allows only a limited amount of "tuning". Increasing the steric hindrance at the metal centre was found to have a deleterious effect on activity (compare entries 1 and 10). *Reduction* of steric hindrance was not possible since the required $LTiMe_2$ precursors are unstable (see above). Use of the less coordinating anion $B(C_6F_5)_4^-$ also decreased activity (entries 1 and 6), possibly because of faster catalyst decomposition. Activity is also lower at higher temperature (entries 1 and 3), again indicating catalyst decomposition. Thus, the scope of this Ti^{III} catalyst appears to be rather limited.

Conclusions

β-Diimine complexes $LMCl_2$ of Ti^{III} and V^{III} are easily prepared. The corresponding dialkylmetal compounds are unexpectedly stable when M = V, but they do not seem to give rise to active polymerization catalysts. The corresponding dialkyltitanium(III) compounds are much less stable, but catalysts generated from $LTiMe_2$ and $B(C_6F_5)_3$ show activity in α-olefin polymerization. The reasons for these differences are unclear and point out the need for a more detailed understanding of the reactivity of paramagnetic non-d^0 systems

Experimental Section

General: All manipulations involving lithium, potassium, and transition metal compounds were performed in standard Schlenk glassware under an inert atmosphere. Reagents were used as received. Solvents were dried by distillation from sodium under argon prior to use. – ^{1}H- and ^{13}C-NMR spectra were recorded using Varian XL-200 and Varian VXR-300 instruments, respectively. – The metal chlorides $TiCl_3(THF)_3$ and $VCl_3(THF)_3$[20], the ligands $\mathbf{L^2}H$[2] and $\mathbf{L^4}H$[5] and the borane $B(C_6F_5)_3$[21] were prepared according to literature methods. For some syntheses of vanadium compounds, $VCl_3(THF)_3$ was prepared in situ by refluxing anhydrous VCl_3 in THF prior to reaction with a lithium β-diiminate.

L²Li: 76 g of $\mathbf{L^2}H$ was dissolved in 200 ml of THF. To a cooled solution of 10.2 g of *n*BuLi in 250 ml of hexane was added 25 ml of diisopropylamine, and this solution was slowly added to the cooled solution of $\mathbf{L^2}H$. The mixture was warmed to room temperature and the solvents were removed in vacuo. The crude product was crystallized from hexane (+65°C/–20°C) to give light-yellow crystals of the composition $\mathbf{L^2}Li(THF)$ (by NMR) (ca. 70 g, 80%). – ^{1}H NMR (C_6D_6): δ = 7.28 (*m*-H), 7.20 (*p*-H), 5.14 (C*H*C=N), 2.03 (CH_3C=N), 1.30, 1.40, 3.55 (*i*Pr), 1.02, 2.83 (THF). – ^{13}C NMR ([D_8]THF): δ = 150.3 (*i*-C), 141.4 (*o*-C), 123.4 (*m*-C), 123.1 (*p*-C), 163.4 (*C*=N), 92.7 (*C*HC=N), 28.4 (*C*H_3C=N), 24.8, 24.0 (*C*H_3CH), 23.3 (*C*HCH$_3$).

L¹H was prepared by a similar route to that used for $\mathbf{L^2}H$:[2] A mixture of 25.03 g of acetylacetone (0.25 mol), 67.6 g of 2,4,6-trimethylaniline (0.5 mol), and 20.8 ml of 12 N hydrochloric acid (0.25 mol) was heated to 120°C for 4 h. Water was allowed to distil from the reaction mixture and heating was continued at 140°C overnight. Thereafter, the solids produced were crystallized from refluxing ethanol. Two fractions were collected, the second fraction after treatment with diethyl ether. Yield of crude $\mathbf{L^1}H$·HCl: 87.6 g (94%). – ^{1}H NMR ($CDCl_3$): δ = 2.65 (1-H), 4.29 (3-H), 6.74 (*m*-H), 1.94 (α*o*-H), 2.23 (α*p*-H), 4.88 (NH). – ^{13}C NMR ($CDCl_3$): δ = 21.1 (C-1), 171.5 (C-2), 90.5 (C-3), 139.7 (*i*-C), 135.5 (*o*-C), 130.0 (*m*-C), 132.7 (*p*-C), 17.5 (α*o*-C), 21.2 (α*p*-C). A mixture of 60.2 g of crude $\mathbf{L^1}H$·HCl (162 mmol), 30 ml of triethylamine (218 mmol), 200 ml of dichloromethane, and 100 ml of water was stirred

for 1 h until all solids had dissolved and a clear separation of the two layers had occurred. The organic phase was removed, dried with magnesium sulfate, filtered, and the solvent was removed in vacuo. The resulting thick oil was dried in vacuo at 100°C for 4 h (to remove small amounts of 2,4,6-trimethylaniline). The crude product **L[1]H** was isolated as a brown solid, yield 46.2 g (85%), and was used as such, without further purification, for reaction with transition metal chlorides. – ^{1}H NMR ($CDCl_3$): δ = 1.68 (1-H), 4.85 (3-H), 6.85 (*m*-H), 2.25 (α*o*-H), 2.11 (α*p*-H). – ^{13}C NMR ($CDCl_3$): δ = 20.3 (C-1), 160.9 (C-2), 93.3 (C-3), 141.1 (*i*-C), 131.8 (*o*-C), 128.4 (*m*-C), 133.4 (*p*-C), 18.2 (α*o*-C), 20.8 (α*p*-C).

L[5]H was prepared by procedures similar to those used by Knorr and Weiss for bulky diimines.[6] – (a) To a mixture of 67.6 g of 2,4,6-trimethylaniline (0.5 mol) and 50.6 g of triethylamine (0.5 mol) in 800 ml of dichloromethane was slowly added a solution of 60.3 g of pivaloyl chloride (0.5 mol) in 200 ml of dichloromethane. After the addition was completed, the reaction mixture was refluxed for 1 h and then extracted with 2 × 250 ml water. The organic fraction was dried with magnesium sulfate, filtered, and the solvent was removed in vacuo. The resulting yellow oil was treated with diethyl ether, yielding a white, microcrystalline powder. This powder was filtered off and dried. Yield: 96 g (88%) of crude 2,2-dimethyl-*N*-(2,4,6-trimethylphenyl)propionamide. – ^{1}H NMR ($CDCl_3$): δ = 1.32 (3-H), 6.86 (*m*-H), 2.14 (α*o*-H), 2.25 (α*p*-H). – ^{13}C NMR ($CDCl_3$): δ = 176.5 (C-1), 39.2 (C-2), 27.8 (C-3), 136.6 (*i*-C), 135.1 (*o*-C), 128.8 (*m*-C), 131.3 (*p*-C), 18.1 (α*o*-C), 20.9 (α*p*-C).

(b) To a slurry of 96 g (438 mmol) of the crude amide in 1 l of toluene, 91.15 g of phosphorus pentachloride (438 mmol) was added in small portions. During the course of the addition, HCl gas was liberated and the reaction mixture became a clear yellow solution. After the addition was completed, the reaction mixture was stirred overnight. The solvent was distilled off, first toluene followed by the formed $POCl_3$. Finally, the product was distilled at 85°C (4 mbar oil pump). Yield: 88.8 g (85%) of 1-chloro-2,2-dimethyl-1-(2,4,6-trimethylphenylimino)propane. – ^{1}H NMR ($CDCl_3$): δ = 1.43 (3-H), 6.88 (*m*-H), 2.03 (α*o*-H), 2.29 (α*p*-H). – ^{13}C NMR ($CDCl_3$): δ = 155.3 (C-1), 43.8 (C-2), 28.5 (C-3), 143.1 (*i*-C), 125.9 (*o*-C), 128.4 (*m*-C), 133.1 (*p*-C), 17.5 (α*o*-C), 20.8 (α*p*-C).

(c) To 32.5 g of 1-chloro-2,2-dimethyl-1-(2,4,6-trimethylphenylimino)propane (137 mmol) in 200 ml of diethyl ether was added 170 ml of 1.6 M methyllithium in diethyl ether (274 mmol). The solution became warm and methane gas was evolved. The reaction mixture was stirred for 1 h at room temperature. After careful hydrolysis with water and subsequent extraction, the organic fraction was dried with magnesium sulfate, filtered, and distilled at 106–108°C (3 mbar oil pump). Yield: 27.6 g (93%) of 3,3-dimethyl-2-(2,4,6-trimethylphenylimino)butane. – ^{1}H NMR ($CDCl_3$): δ = 1.61 (1-H), 1.27 (4-H), 6.81 (m-H), 1.93 (α*o*-H), 2.25 (α*p*-H). – ^{13}C NMR ($CDCl_3$): δ = 15.2 (C-1), 177.0 (C-2), 40.3 (C-3), 28.0 (C-4), 146.3 (*i*-C), 125.1 (*o*-C), 128.4 (*m*-C), 131.2 (*p*-C), 17.5 (α*o*-C), 20.7 (α*p*-C).

(d) To a cooled (–78°C) mixture of 10.85 g of 3,3-dimethyl-2-(2,4,6-trimethylphenylimino)butane (50 mmol) and 5.8 g of *N,N,N′N′*-tetramethylethylenediamine (TMEDA) (50 mmol) in 100 ml of hexane was added 31.25 ml of 1.6 M *n*-butyllithium in hexane (50 mmol). The reaction mixture was allowed to warm to room temperature and was then stirred overnight, resulting in a cloudy, slightly yellow slurry. To this was added dropwise 11.875 g of 1-chloro-2,2-dimethyl-1-(2,4,6-trimethylphenylimino)propane (50 mmol) in 75 ml of hexane. The reaction temperature was maintained below reflux temperature with water-bath cooling. After the addition was completed, the mixture was refluxed for 1 h. Then, 100 ml of water and 100 ml of diethyl ether were added and the product was extracted. The aqueous layer was extracted once with 100 ml of diethyl ether. The combined organic fractions were dried with magnesium sulfate, filtered, and the solvent was evaporated in vacuo. The product was crystallized from refluxing ethanol. Yield: 15.88 g (76%). The NMR spectra show separate peaks due to the imine-enamine and bis(imine) (minor component) forms. – ^{1}H NMR ($CDCl_3$) of imine-enamine form: δ = 1.14 (1-H), 5.43 (4-H), 6.71 (*m*-H), 2.20 (α*o*-H), 2.14 (α*p*-H), 13 (NH); of bis(imine) form (all peaks broad): δ = 0.8–1.4 (1-H), 3.2 (4-H), 1.9 (α*o*-H), 2.23 (α*p*-H), 6.75 (*m*-H). – ^{13}C NMR ($CDCl_3$) of imine-enamine form: δ = 30.4 (C-1), 40.3 (C-2), 170 (C-3), 91 (C-4), 143 (*i*-C), 131.3 (*o*-C), 128.7 (*m*-C), 132.7 (*p*-C), 19.2 (α*o*-C), 20.9 (α*p*-C).

L[6]H was prepared by a route similar to that used for **L[5]H**. – (a) To a mixture of 44.3 g of 2,6-diisopropylaniline (0.25 mol) and 25.3 g of triethylamine (0.25 mol) in 400 ml of dichloromethane was slowly added a solution of 30.145 g of pivaloyl chloride (0.25 mol) in 100 ml of dichloromethane. After the addition was completed, the reaction mixture was refluxed for 1.5 h. It was then diluted with 500 ml of dichloromethane and extracted with water (3 × 100 ml). The organic fraction was dried with magnesium sulfate, filtered, and the solvent was removed in vacuo. The resulting yellow oil was treated with diethyl ether to yield a white microcrystalline powder. This powder was filtered off and dried. Yield: 65.5 g (100%) of crude *N*-(2,6-diisopropylphenyl)-2,2-dimethylpropionamide. – ^{1}H NMR ($CDCl_3$): δ = 1.36 (3-H), 7.15–7.25 (*m*-, *p*-H), 3.00 (α-H), 1.19 (β-H), 6.8 (NH). – ^{13}C NMR ($CDCl_3$): δ = 177.1 (C-1), 39.2 (C-2), 28.7 (C-3), 131.4 (*i*-C), 146.1 (*o*-C), 123.3 (*m*-C), 128.0 (*p*-C), 23.5 (α-C), 27.8 (β-C).

(b) To a slurry of 65.5 g of *N*-(2,6-diisopropylphenyl)-2,2-dimethylpropionamide (0.25 mol) in 500 ml of benzene, 52 g of phosphorus pentachloride (0.25 mol) was added in small portions. During the course of the addition, HCl gas was liberated and the reaction mixture became a clear yellow solution. After the addition was completed, the reaction mixture was stirred for 1 h. The solvent was then distilled off, first benzene followed by the formed $POCl_3$. Finally, the product was distilled at 85°C (4 mbar oil pump). Yield: 54.4 g (78%) of 1-chloro-1-(2,6-diisopropylphenylimino)-2,2-dimethylpropane.[22] – ^{1}H NMR ($CDCl_3$): δ = 1.44 (3-H), 7.14 (*m*-, *p*-H), 2.75 (α-H), 1.2 (β-H). – ^{13}C NMR ($CDCl_3$): δ = 154.6 (C-1), 43.9 (C-2), 28.4 (C-3), 143.1 (*i*-C), 136.4 (*o*-C), 122.9 (*m*-C), 124.4 (*p*-C), 23 (α-, β-C).

(c) To 32.76 g of 1-chloro-1-(2,6-diisopropylphenylimino)-2,2-dimethylpropane (117 mmol) in 100 ml of diethyl ether was added a large excess of 200 ml of 1.6 M methyllithium in diethyl ether (320 mmol). The solution became warm and methane gas was evolved. The reaction mixture was stirred for 3 h at room temperature and then carefully (!) hydrolysed with water. After extraction, the organic fraction was dried with magnesium sulfate, filtered, and distilled at 75°C (2 mbar oil pump). Yield: 27.9 g (92%) of 2-(2,6-diisopropylphenylimino)-3,3-dimethylbutane. – ^{1}H NMR ($CDCl_3$): δ = 1.7 (1-H), 1.3 (4-H), 7.0–7.3 (*m*-, *p*-H), 2.71 (α-H), 1.15, 1.18 (β-H). – ^{13}C NMR ($CDCl_3$): δ = 15.9 (C-1), 176.4 (C-2), 40.4 (C-3), 28.0 (C-4), 146.6 (*i*-C), 135.7 (*o*-C), 122.7 (*m*-C), 122.6 (*p*-C), 27.8 (α-C), 22.8, 23.0 (β-C).

(d) To a cooled (–78°C) mixture of 27.9 g 2-(2,6-diisopropylphenylimino)-3,3-dimethylbutane (107.5 mmol) and 12.5 g of *N,N,N′N′*-tetramethylethylenediamine TMEDA (107.5 mmol) in 100 ml of hexane was added 67.5 ml of 1.6 M *n*-butyllithium in hexane (107.5 mmol). The reaction mixture was allowed to warm

to room temperature and then stirred overnight. A sticky white slurry was obtained, which was treated dropwise with 30.1 g of 1-chloro-1-(2,6-diisopropylphenylimino)-2,2-dimethylpropane (107.5 mmol) in 75 ml of hexane. The reaction temperature was maintained below reflux temperature with water-bath cooling. After the addition was completed, the mixture was refluxed for 1 h. Then, 100 ml of water and 100 ml of diethyl ether were added and the product was extracted. The aqueous layer was extracted once with 100 ml of diethyl ether. The combined organic fractions were dried with magnesium sulfate, filtered, and the solvent was evaporated in vacuo. The product was crystallized from refluxing hexane. Two fractions of white crystals (35.86 and 7.47 g) were collected; combined yield 43.33 g (80%) of **L⁶**H. The NMR spectra show separate peaks due to the imine-enamine and bis(imine) (minor component) forms. – ^{1}H NMR ($CDCl_3$) of imine-enamine form: δ = 1.08 (1-H), 5.42 (4-H), 6.94 (*m*-, *p*-H), 3.26 (α-H), 1.02, 1.22 (β-H), 4.9 (NH); of bis(imine) (all peaks broad): δ = 0.8−1.4 (1-H, β-H), 2.4−2.8 (α-H), 6.9−7.2 (*m*-, *p*-H). – ^{13}C NMR ($CDCl_3$) of imine-enamine form: δ = 31.3 (C-1), 41.3 (C-2), 169.3 (C-3), 94.7 (C-4), 142.7 (*i*-C), 141.3 (*o*-C), 123.1 (*m*-C), 122.9 (*p*-C), 28.9 (α-C), 22.5, 25.8 (β-C).

L⁶Li: To a cooled (−78°C) mixture of 1.0 g of **L⁶**H (2 mmol) and 202 mg of diisopropylamine in 15 ml of THF was added 1.25 ml 1.6 of M *n*BuLi in hexane. The reaction mixture was allowed to warm to room temperature and then refluxed for a short time (10 min). The solvent was evaporated in vacuo and the product was crystallized from refluxing hexane, yielding beautiful yellow crystals of **L⁶**Li·THF. – ^{1}H NMR (C_7D_8): δ = 1.26 (1-H), 5.11 (4-H), 6.8−7.0 (*m*-, *p*-H), 3.36 (α-H), 1.03, 1.29 (β-H). – ^{13}C NMR (C_7D_8): δ = 33.3 (C-1), 44.1 (C-2), 170.1 (C-3), 92.2 (C-4), 150.9 (*i*-C), 139.5 (*o*-C), 122.9 (*m*-C), 121.6 (*p*-C), 27.9 (α-C), 23.1, 25.3 (β-C).

L⁶K: To a stirred suspension of 0.16 g (4 mmol) of KH (dispersion in mineral oil, washed with hexane to remove the oil) in 25 ml of THF, 1.0 g (2 mmol) of **L⁶**H was added in small portions. The yellowish solution was stirred at 65°C for 1 h and then filtered. The THF was removed in vacuo, and the product was washed with hexane to give off-white **L⁶**K (0.9 g, 90%). – ^{1}H NMR ([D_8]THF): δ = 1.16−1.19 (1-H, β-H), 3.85 (4-H), 6.84 (*m*-H), 6.51 (*p*-H), 3.35 (α-H). – ^{13}C NMR ([D_8]THF): δ = 31.4 (C-1), 42.2 (C-2), 168 (br., C-3), 88.4 (C-4), 153.7 (*i*-C), 137.8 (*o*-C), 122.3 (*m*-C), 117.0 (*p*-C), 28.1 (α-C), 23.8, 25.4 (β-C).

L³H: (a) A mixture of 46.9 g of *o*-toluidine (438 mmol) and 48.2 g of acetylacetone (481 mmol) in 500 ml of toluene, plus a few drops of H_2SO_4, was heated under reflux in a Dean-Stark apparatus for the azeotropic removal of water. After 16 h, the reaction mixture was cooled to room temperature and the solvent was removed in vacuo. The product was distilled at 118°C (5 mbar) to give 4-*o*-tolylamino-3-penten-2-one as a light-yellow oil (75.3 g, 91%). – ^{1}H NMR ($CDCl_3$): δ = 1.86 (CH_3C=N), 2.10 (CH_3C=O), 2.27 (*o*-CH_3), 5.19 (C*H*), 7.0−7.3 (Ar-H), 12.3 (NH). – ^{13}C NMR ($CDCl_3$): δ = 29.0 (CH_3C=O), 196.0 (CH_3C=O), 97.0 (*C*H), 161.1 (CH_3C=N), 19.5 (CH_3C=N), 137.4 (arom. C-1), 133.8 (arom. C-2), 130.7 (arom. C-3), 126.2 (arom. C-4), 126.3 (arom. C-5). 126.2 (arom. C-6), 18.0 (*o*-CH_3).

(b) A mixture of 47.3 g of 4-*o*-tolylamino-3-penten-2-one (250 mmol) and 35.9 g of *o*-toluidine hydrochloride (250 mmol) was refluxed in the minimum volume of ethanol for dissolution of both components. Cooling the reaction mixture to room temperature yielded yellow crystals of the monohydrochloride of 2,4-di-*o*-tolyliminopentane (63.1 g, 80%). – ^{1}H NMR (CD_3OD): δ = 2.68 (CH_3C=N), 2.06 (*o*-CH_3), 4.64 (CH), 4.89 (NH), 6.8−7.3 (Ar-H). – ^{13}C NMR (CD_3OD): δ = 22.0 (CH_3C=N), 171.5 (CH_3C=N), 92.4 (*C*H), 136.5 (arom. C-1), 135.6 (arom. C-2), 132.2 (arom. C-3), 127.7 (arom. C-4), 129.8 (arom. C-5), 128.2 (arom. C-6), 17.4 (*o*-CH_3).

(c) A mixture of 7.87 g of 2,4-di-*o*-tolyliminopentane·HCl (25 mmol), 7 ml of triethylamine (50 mmol), 100 ml of dichloromethane, and 100 ml of water was stirred for 1 h until all solids had dissolved and a clear separation of the two layers had occurred. The organic phase was removed, dried with magnesium sulfate, filtered, and the solvent was removed in vacuo. The resulting thick yellow oil was dried in vacuo for 16 h. The product was isolated as a yellow oil (6.36 g, 91%). – ^{1}H NMR ($CDCl_3$): δ = 1.97 (CH_3C=N), 2.27 (*o*-CH_3), 4.98 (CH), 12.6 (NH), 6.9−7.3 (Ar-H). – ^{13}C NMR ($CDCl_3$): δ = 20.7 (CH_3C=N), 159.8 (CH_3C=N), 96.5 (*C*H), 144.6 (arom. C-1), 130.7 (arom. C-2), 130.2 (arom. C-3), 123.6 (arom. C-4), 126.1 (arom. C-5), 123.0 (arom. C-6), 16.3 (*o*-CH_3).

L¹VCl₂: Vanadium trichloride (7.865 g, 50 mmol) was refluxed for 3 h in 100 ml of THF to form $VCl_3(THF)_3$. A solution of 16.725 g (50 mmol) of **L¹**H in 100 ml of THF was cooled to −78°C. To this was added 31.4 ml (50 mmol) of 1.6 M *n*-butyllithium in hexane, and the mixture was allowed to warm to room temperature. The orange/yellow solution thus obtained was added to the pink/red slurry of $VCl_3(THF)_3$ resulting in an immediate colour change to an intense dark brown-red. The reaction mixture was refluxed for an additional 1 h. The solvent was then removed in vacuo, and the residue was dried at 80°C in vacuo. It was then washed with 50 ml of hexane, dried, and extracted with 200 ml of toluene. The product was crystallized from toluene as red crystals. Two fractions were obtained (7.425 g and 5.4 g). Yield: 12.825 g (56%). – $C_{23}H_{29}Cl_2N_2V$ (455.34): calcd. C 60.67, H 6.42, Cl 15.57, N 6.15, V 11.19; found C 60.39, H 6.26, Cl 15.45, N 6.00, V 10.95.

L¹VMe₂: To a suspension of 9.3 g of **L¹**VCl_2 (20.4 mmol) in 150 ml of diethyl ether, cooled to −78°C, was slowly added 25.65 ml of a solution of methyllithium in diethyl ether (1.6 M, 40.8 mmol). The mixture was allowed to warm to room temperature and the solvent was removed in vacuo. Crystallization from hexane (+40°C/−20°C) gave dark-brown crystals. Yield: 5.42 g (64%). – $C_{25}H_{35}N_2V$ (414.51): calcd. C 72.44, H 8.51, N 6.76, V 12.29; found C 72.18, H 8.33, N 6.71, V 12.10, Cl < 0.1.

L¹TiCl₂: To a solution of 6.69 g of **L1**H (20 mmol) in 50 ml of THF, cooled to −78°C, was added 6.3 ml (20 mmol) 1.6 of M *n*BuLi in hexane, and the mixture was allowed to warm to room temperature. Then, 3.7 g of solid $TiCl_3(THF)_3$ (20 mmol) was added and the reaction mixture was refluxed overnight. A colour change from green to dark brown took place. The solvent was then removed in vacuo and 100 ml of toluene was added. The resulting solution was reduced in volume by 20 ml by distillation of toluene along with residual THF and/or hexane. The warm, deep-red solution was filtered and the filtrate was concentrated, at reflux temperature, until crystals appeared. After leaving the solution to stand overnight, deep-red crystals were collected. Yield: 7.32 g (81%). – $C_{23}H_{29}Cl_2N_2Ti$ (452.30): calcd. C 61.08, H 6.46, Cl 15.68, N 6.19, Ti 10.59; found C 60.90, H 6.62, Cl 15.76, N 6.03, Ti 10.45.

L¹TiMe₂: 1. *Using MeLi:* To a stirred suspension of 1.0 g (2.2 mmol) of **L¹**$TiCl_2$ in 20 ml of diethyl ether, cooled to −80°C, was slowly added 2.8 ml (4.4 mmol) of a 1.6 M solution of MeLi in diethyl ether. The mixture was allowed to warm to 0°C, whereupon a deep-blue colour appeared. The solvent was then removed in vacuo, and the residue was quickly extracted with two 15-ml portions of hexane. The combined hexane fractions were concentrated in vacuo to a volume of ca. 2.5 ml and after storage overnight at

−20°C, a dark-blue crystalline solid was isolated. The yield of this synthesis was rather variable, but was usually in the range 10−50%. The isolated product was found to be stable at room temperature, both in solution and in the solid state. Crystals for X-ray diffraction were obtained by recrystallization from pentane (+25°C/−20°C).

2. *Using MeMgI:* To a stirred suspension of 1.0 g (2.2 mmol) of $\mathbf{L^1}TiCl_2$ in 20 ml of diethyl ether was slowly added a solution of 1.06 g (4.4 mmol) of $MeMgI(Et_2O)$ in 15 ml of diethyl ether. The mixture immediately turned deep-blue. The solvent was removed in vacuo, and the residue was extracted with two 15-ml portions of hexane. Concentration of the solution and cooling to −20°C gave dark-blue crystals of the product (0.64 g, 70%).

Attempted Synthesis of $\boldsymbol{L^1TiEt_2}$*:* To a stirred suspension of 1.0 g (2.2 mmol) of $\mathbf{L^1}$TiCl2 in 20 ml of diethyl ether, cooled to −20°C, was slowly added a solution of 0.92 g (4.4 mmol) of $EtMgBr(Et_2O)$ in 15 ml of diethyl ether. The mixture immediately turned deep-blue. It was allowed to warm to 5°C and then cooled once more to −20°C. The solvent was then removed in vacuo, and the residue was quickly extracted with two 15-ml portions of hexane. Concentration of the combined extracts at −20°C and storage at this temperature overnight gave a few very large, dark-blue crystals of the product. These decomposed within a day at room temperature, both in solution and in the solid state, leading to unidentified brown products with liberation of ethane.

$\boldsymbol{L^2VCl_2}$*:* Vanadium trichloride (7.865 g, 50 mmol) was refluxed for 2 h in 150 ml of THF to form $VCl_3(THF)_3$. To this was added a solution of 24.84 g of $\mathbf{L^2}$Li(THF) (50 mmol) in 50 ml of THF and the reaction mixture was refluxed for 30 min resulting in a deep brown-red colouration. The solvent was then removed in vacuo and the residue was dried at 100°C, whereupon it slowly turned dark green. It was then washed with 25 ml hexane, dried, and crystallized from toluene as very dark-green crystals. Yield: 22.15 g (82%). − $C_{29}H_{41}Cl_2N_2V$ (539.50): calcd. C 64.56, H 7.66, Cl 13.14, N 5.19, V 9.44; found C 64.30, H 7.52, Cl 13.00, N 5.03, V 9.55.

$\boldsymbol{L^2VMe_2}$: To a solution of 2.7 g of $\mathbf{L^2}VCl_2$ (5 mmol) in 25 ml of diethyl ether, cooled to −80°C, was slowly added 6.28 ml of methyllithium in diethyl ether (1.6 M, 10 mmol). The stirred mixture was allowed to warm to room temperature and then refluxed for 1.5 h. The resulting solution was filtered through a fine frit and the solvent was removed in vacuo. Crystallization from hexane gave dark-brown crystals. Yield: 1.12 g, second crop 0.4 g, total yield: 1.52 g (61%).

$\boldsymbol{L^2V(nBu)_2}$*:* To a suspension of 1.0 g of $\mathbf{L^2}VCl_2$ (1.7 mmol) in 10 ml of toluene, cooled to −80°C, was slowly added 2.1 ml of a solution of *n*BuLi (1.6 M in hexane). The stirred mixture was allowed to warm to room temperature. The solvents were then removed in vacuo, and the product was extracted with a small amount of warm hexane. After leaving the resulting solution to stand for 1 week at −20°C, large, dark-brown crystals were deposited.

$\boldsymbol{L^2TiCl_2}$*:* A solution of 4.967 g of $\mathbf{L^2}$Li(THF) (20 mmol) and 3.7 g of $TiCl_3(THF)_3$ in 50 ml of THF was refluxed overnight. The colour of the reaction mixture changed from light green to dark green. The solvent was then removed in vacuo and 75 ml of toluene was added. The resulting solution was reduced in volume by 20 ml by distillation of toluene along with residual THF and/or hexane. A further 20 ml of fresh toluene was added and distilled off once more. The warm, deep-red/brown solution was filtered and the filtrate was concentrated, at reflux temperature, until crystals appeared. After storage overnight, deep-red/brown crystals were deposited. Yield: 2.85 g (53%).

$\boldsymbol{L^2TiMe_2}$*:* This was prepared in the same manner as $\mathbf{L^1}$TiMe2 (Grignard route). The residue after the reaction was sticky, and extraction with hexane was far from complete; from 1.0 g of $\mathbf{L^2}TiCl_2$, we obtained only 0.09 g (10%) of $\mathbf{L^2}TiMe_2$ as dark-blue needles from hexane.

$\boldsymbol{L^5VCl_2}$*:* Vanadium trichloride (1.57 g, 10 mmol) was refluxed for 2 h in 25 ml of THF to form $VCl_3(THF)_3$. A solution of 4.19 g (10 mmol) of $\mathbf{L^5}$H in 25 ml of hexane was cooled to −78°C. To this was added 6.25 ml (10 mmol) of 1.6 M *n*-butyllithium solution in hexane and the mixture was allowed to warm to room temperature. The reaction mixture slurry was stirred overnight and then a small amount of THF was added until a clear yellow solution was obtained. This yellow solution was added to the pink/red slurry of $VCl_3(THF)_3$ and the mixture was refluxed for 1 d. The solvent was then removed in vacuo and the residue was crystallized from toluene (30 ml) to afford dark-red crystals. Yield: 2.07 g (38%). − $C_{29}H_{41}Cl_2N_2V$ (539.50): calcd. C 64.56, H 7.66, Cl 13.14, N 5.19, V 9.44; found C 64.81, H 7.72, Cl 12.93, N 5.18, V 9.55.

$\boldsymbol{L^5TiCl_2}$*:* To a mixture of 5.66 g of $\mathbf{L^5}$H (13.5 mmol) in 30 ml of hexane was added 8.5 ml (13.5 mmol) of 1.6 M *n*BuLi in hexane. The reaction mixture was allowed to warm to room temperature and then stirred overnight. The initially clear yellow solution became a yellow slurry. To this, 5.0 g of $TiCl_3(THF)_3$ (13.5 mmol) and 30 ml of THF were added and the mixture was refluxed overnight. The solvent was then removed in vacuo and 75 ml of toluene was added. The resulting solution was reduced in volume by 10 ml by distillation of toluene along with residual THF and/or hexane. The warm, deep-red solution was filtered and the filtrate was concentrated, at reflux temperature, until crystals appeared. After storage overnight, deep-red crystals separated. Yield: 4.36 g (74%). − $C_{29}H_{41}Cl_2N_2Ti$ (536.46): calcd. C 64.93, H 7.70, Cl 13.22, N 5.22, Ti 8.93; found C 64.89, H 7.56, Cl 13.32, N 5.18, Ti 8.79.

$\boldsymbol{L^5TiMe_2}$*:* This was prepared in the same manner as $\mathbf{L^1}TiMe_2$ (MeLi route) but crystallized more easily and was typically obtained in 70% yield as dark-blue crystals.

Attempted Synthesis of $\boldsymbol{L^3TiMe_2}$*:* $\mathbf{L^3}TiCl_2$ was prepared in the same manner as $\mathbf{L^1}TiCl_2$. However, the compound did not crystallize well from toluene, and so an excess of hexane was added to the dark-brown toluene solution to precipitate the product as a brown-green powder. To a stirred suspension of 1.0 g (2.5 mmol) of crude $\mathbf{L^3}TiCl_2$ in 20 ml of diethyl ether, cooled to −10°C, was slowly added a cooled solution of 1.21 g (5.1 mmol) of $MeMgI(Et_2O)$ in 15 ml of diethyl ether. The solution turned deep-blue. After 1 min, 0.43 ml of 1,4-dioxane was added, the solvent was removed in vacuo, and the residue was extracted with two cold (−10°C) 15-ml portions of hexane. Evaporation of the solvent left a dark-blue solid, which upon hydrolysis produced variable amounts of methane (but always less than 2 equivalents based on $\mathbf{L^3}TiMe_2$). All attempts at purification or crystallization resulted in the disappearance of the blue color, indicating decomposition.

$\boldsymbol{L^4VCl_2(THF)_2}$*:* Vanadium trichloride (7.9 g, 50 mmol) was refluxed for 3 h in 100 ml of THF to form $VCl_3(THF)_3$. A slurry of 14.3 g (50 mmol) of $\mathbf{L^4}H \cdot HCl$ in 100 ml of THF was cooled to −78°C. To this was added 63 ml (100 mmol) of 1.6 M *n*-butyllithium in hexane, and the mixture was allowed to warm to room temperature. The resulting orange/yellow solution was added to the cooled, pink/red slurry of $VCl_3(THF)_3$. An immediate colour change to very dark green was observed and small crystals were formed. After leaving the mixture to stand overnight, the supernatant was decanted, the crystals were washed with 50 ml of THF, and dried in vacuo. Yield: 20.8 g (81%). − $C_{25}H_{33}N_2VO_2Cl_2$

(515.40): calcd. C 58.26, H 6.45, Cl 13.76, N 5.44, V 9.88; found C 57.93, H 6.23, Cl 14.01, N 5.60, V 10.10.

L^4VMe_2: To a slurry of 1.03 g (2 mmol) of **L^4**VCl2(THF)$_2$ in 30 ml of THF, cooled to −78°C, was added 2.5 ml (4 mmol) of 1.6 M methyllithium in diethyl ether. The reaction mixture was allowed to warm to room temperature, whereupon the colour changed from dark green/blue to dark red. The solvent was then removed in vacuo, and the product was redissolved in diethyl ether. Filtration of the resulting solution and evaporation of the solvent yielded the product as a solid foam. Because of its high solubility, we were unable to purify the product further; the number of methyl groups still present in the complex was determined by controlled hydrolysis. A 430-mg (1.3 mmol) portion of the solid foam was dissolved in the minimum volume of dichloromethane and the complex was deliberately decomposed with 1 ml of methanol. The volume of evolved gas was measured as 58 cm^3 (2.6 mmol).

$L^4TiCl_2(THF)_2$: To a solution of *n*BuLi (2.6 ml of a 1.6 M solution in hexane; 4.2 mmol) in 15 ml of THF, cooled to −40°C, was added 0.7 ml (4.8 mmol) of diisopropylamine. The resulting mixture was added to a solution of 1.0 g (4.0 mmol) of **L^4**H in 15 ml of THF and the solvent was removed in vacuo (50°C, 1 h). The residue was taken up in 10 ml of THF, and the resulting solution was slowly added to a suspension of 1.48 g (4.0 mmol) of $TiCl_3(THF)_3$ in 25 ml of THF. The mixture was heated to 50°C and after 10 min the solvent was removed in vacuo. The residue was quickly[23] extracted with two 25-ml portions of toluene. After the addition of 1 ml of THF to the combined extracts and leaving the solution to stand, brown crystals of **L^4**$TiCl_2(THF)_2$ were deposited (1.4 g, 70%). The product could be recrystallized from toluene/THF mixtures, but its solubility is low even in hot solvent mixtures.

L^4TiI_2: To a suspension of **L^4**$TiCl_2(THF)_2$ (0.5 g, 1 mmol) in 25 ml of benzene was added 0.78 g (0.56 mmol) of Me_3SiI. The mixture was stirred for 4 h at 70°C, during which it turned violet. The solvent was then removed in vacuo, the residue was washed with hexane, and crystallized from toluene/hexane to give red-purple crystals of **L^4**TiI_2 (0.43 g, 80%).

Polymerization Experiments: Under argon, a glass Büchi miniclave was charged with benzene (21 ml) followed by 41 mg of tris(pentafluorophenyl)borane (0.1 mmol) in 2 ml of benzene. The solvent was then saturated with propene and the dimethyltitanium compound (0.1 mmol) in 2 ml of benzene was introduced. The dark blue/green colour of the diminatodimethyltitanium compound immediately disappeared and a clear, red solution was formed. The propene pressure was maintained at 5−6 bar for 30 min. The propene pressure was then released and the solution was poured into 200 ml of methanol. The polymer produced was filtered off and dried in vacuo at 100°C.

X-ray Structure Determinations: All crystals were mounted in thin-walled glass capillaries under N_2 and held in place with silicone grease. Diffraction measurements were made with a Siemens P3m diffractometer fitted with an LT-1 crystal cooling device, using graphite-monochromated Mo-K_α radiation (λ = 0.71073 Å). Unit cell dimensions were determined from carefully centered reflections in the range 15.0° < 2θ < 40.0°. Diffracted intensities were measured in a unique volume of reciprocal space for 4.0° < 2θ < 50.0° by Wyckoff ω scans. Three check reflections were measured again after every 100 ordinary data over the period of data collection in order to monitor and correct for crystal decay and long term intensity fluctuations. Duplicate and equivalent measurements were averaged and systematic absences were deleted. Absorption corrections were applied based on azimuthal scan data and Lorentz and polarization corrections were applied. The structures were solved by Patterson and Fourier methods. All non-hydrogen atoms were assigned anisotropic displacement parameters and all hydrogen atoms were given fixed isotropic displacement parameters and constrained to idealized geometries (C−H 0.96 Å, methyl H−C−H 109.5°). Full-matrix least-squares refinements were against F_o or F_o^2. Weights, *w*, were adjusted to minimize the variation in *S* as a function of F_o. Final difference electron density maps showed no

Table 2. Details of X-ray structure determinations

Compound	**L^2**VCl_2	**L^1**$TiCl_2$	**L^5**$TiCl_2$	**L^6**Li(THF)	**L^2**V(*n*Bu)$_2$	**L^1**$TiMe_2$
Formula	$C_{29}H_{41}Cl_2N_2V$	$C_{23}H_{29}Cl_2N_2Ti$	$C_{29}H_{41}Cl_2Ti$	$C_{39}H_{61}LiN_2O$	$C_{37}H_{59}N_2V$	$C_{25}H_{35}N_2Ti$
Mass	539.5	452.3	536.4	580.8	582.8	411.5
T [K]	200	213	200	200	200	200
Crystal size [mm]	0.25 × 0.65 × 0.7	0.3 × 0.6 × 0.6	0.6 × 0.55 × 0.45	0.4 × 0.5 × 0.6	0.4 × 0.4 × 0.65	0.45 × 0.45 × 0.75
Crystal system	monoclinic	triclinic	monoclinic	monoclinic	monoclinic	monoclinic
Space group[25]	$P2_1/c$ (No. 14)	$P\bar{1}$ (No. 2)	$C2/c$	$P2_1/n$ (No. 14)	$P2_1/c$ (No. 14)	$P2_1/n$ (No. 14)
a [Å]	17.177(5)	8.198(3)	14.592(3)	9.541(3)	12.903(3)	8.233(3)
b [Å]	13.170(4)	8.719(3)	9.096(2)	17.911(6)	13.042(4)	23.097(7)
c [Å]	13.842(4)	17.859(6)	21.727(5)	21.711(7)	21.489(7)	12.598(3)
α [°]	90	90.68(3)	90	90	90	90
β [°]	109.11(2)	93.43(3)	95.43(2)	95.44(2)	92.85(2)	94.60(3)
γ [°]	90	113.91(3)	90	90	90	90
V [Å^3]	2958.8(15)	1163.9(7)	2870.9(11)	3694(2)	3612(2)	2387.9(13)
Z	4	2	4	4	4	4
$d_{calcd.}$ [g cm^{-3}]	1.21	1.29	1.24	1.05	1.07	1.14
Transmission (min./max.)	0.755/0.917	0.722/0.921	0.574/0.618	(no correction, μ = 0.61 cm^{-1})	0.737/0.808	0.733/0.821
F(000)	1144	474	1140	1280	1272	884
Measured	5703	4076	2614	7197	6913	4555
Unique	5225	4067	2520	6495	6310	4186
Used	4119, $I > 2\sigma(I)$	4056, $I > -3\sigma(I)$	2519, $I > -3\sigma(I)$	3607, $I > 2\sigma(I)$	3859, $I > 2\sigma(I)$	4184, $I > -3\sigma(I)$
Parameters	337	253	161	388	361	295
R	0.041	0.048 [3611 data with $I > 2\sigma(I)$]	0.033 [2266 data with $I > 2\sigma(I)$]	0.063	0.070	0.038 [3562 data with $I > 2\sigma(I)$]
wR	0.049	0.142 (all data)	0.038 (all data)	0.065	0.071	0.108 (all data)
S	1.42	1.16	1.52	1.45	1.59	1.13

chemically significant features (with one exception noted below). All calculations were carried out using programs of the SHELXTL-PLUS and SHELXL-93 packages.[24] Complex neutral-atom scattering factors were used. Table 2 gives further details of the individual structure determinations. The γ and δ carbon atoms of one of the butyl chains of $\mathbf{L^2}V(n\mathrm{Bu})_2$ showed large thermal parameters, and significant electron density features were found close to these atoms. This clearly implies some kind of disorder in the chain, but no satisfactory multisite model was derived.

Crystallographic data (excluding structure factors) have been deposited with the Cambridge Crystallographic Data Centre as supplementary publication no. CCDC-101413. Copies of the data can be obtained free of charge on application to CCCD, 12 Union Road, Cambridge CB2 1EZ, U.K. [Fax: (internat.) + 44-1223/336033; E-mail: deposit@ccdc.cam.ac.uk].

[1] P. A. White, J. Calabrese, K. H. Theopold, *Organometallics* **1996**, *15*, 5473; Y. Liang, G. A. P. Yap, A. L. Rheingold, K. H. Theopold, *Organometallics* **1996**, *15*, 5284; K. H. Theopold, *Eur. J. Inorg. Chem.* **1998**, *1*, 15.

[2] J. Feldman, S. J. McLain, A. Parthasarathy, W. J. Marshall, J. C. Calabrese, S. D. Arthur, *Organometallics* **1997**, *16*, 1514.

[3] M. Rahim, N. J. Taylor, S. Xin, S. Collins, *Organometallics* **1998**, *17*, 1315.

[4] Theopold has very recently reported on studies of Ti^{III}, V^{III}, and Cr^{III} complexes of the $\mathbf{L}^4$ ligand: W.-K. Kim, L. MacAdams, M. Fevola, L. Liable-Sands, A. L. Rheingold, K. Theopold, 215th ACS National Meeting, Division of Inorganic Chemistry, Dallas, **1998**, *Conference Abstract* 279.

[5] G. Scheibe, *Chem. Ber.* **1923**, *56*, 1923; J. E. Parks, R. H. Holm, *Inorg. Chem.* **1968**, *7*, 1408.

[6] R. Knorr, A. Weiss, *Chem. Ber.* **1982**, *115*, 139.

[7] P. B. Hitchcock, M. F. Lappert, D.-S. Liu, *J. Chem. Soc., Chem. Commun.* **1994**, 1699 and 2637.

[8] H. van der Heijden, C. J. Schaverien, A. G. Orpen, *Organometallics* **1989**, *8*, 255.

[9] D. Drees, J. Magull, *Z. Anorg. Allg. Chem.* **1994**, *620*, 814.

[10] A. A. Danopoulos, P. G. Edwards, *Polyhedron* **1989**, *8*, 1339.

[11] A. R. Wills, P. G. Edwards, M. Harman, M. B. Hursthouse, *Polyhedron* **1989**, *8*, 1457; A. R. Wills, P. G. Edwards, *J. Chem. Soc., Dalton Trans.* **1989**, 1253.

[12] B. Hessen, J. H. Teuben, T. H. Lemmen, J. C. Huffman, K. G. Caulton, *Organometallics* **1985**, *4*, 946; B. Hessen, T. M. Lemmen, H. J. G. Luttikhedde, J. H. Teuben. J. L. Petersen, J. C. Huffman, S. Jagner, K. G. Caulton, *Organometallics* **1987**, *6*, 2354.

[13] B. Hessen, A. Meetsma, J. H. Teuben, *J. Am. Chem. Soc.* **1989**, *111*, 5977; B. Hessen, J.-K. F. Buijink, A. Meetsma, J. H. Teuben, G. Helgesson, M. Håkansson, S. Jagner, A. L. Spek, *Organometallics* **1993**, *12*, 2286.

[14] J.-K. F. Buijink, A. Meetsma, J. H. Teuben, *Organometallics* **1993**, *12*, 2004.

[15] J. R. Hagadorn, J. Arnold, *J. Am. Chem. Soc.* **1996**, *118*, 893.

[16] A. R. Johnson, W. M. Davis, C. C. Cummins, *Organometallics* **1996**, *15*, 3825.

[17] R. K. Minhas, L. Scoles, S. Wong, S. Gambarotta, *Organometallics* **1996**, *15*, 1113.

[18] L. Giannini, E. Solari, S. de Angelis, T. R. Ward, C. Floriani, A. Chiesi-Villa, C. Rizzoli, *J. Am. Chem. Soc.* **1995**, *117*, 5801.

[19] J. D. Scollard, D. H. McConville, *J. Am. Chem. Soc.* **1996**, *118*, 10008; J. D. Scollard, D. H. McConville, N. C. Payne, J. J. Vittal, *Macromolecules* **1996**, *29*, 5241.

[20] L. E. Manzer, *Inorg. Synth.* **1982**, *21*, 135.

[21] A. G. Massey, A. J. Park, *J. Organomet. Chem.* **1964**, *2*, 245.

[22] F. Cramer, K. Baer, *Chem. Ber.* **1960**, *93*, 1231.

[23] The crystalline product is rather insoluble, but we usually found that the crude product first dissolves and only starts to crystallize after a period of a few hours or days. If, for some reason, crystallization starts *before* extraction is complete, the best way to proceed is to extract the residue with a fairly large volume of hot toluene containing a few drops of THF.

[24] G. M. Sheldrick, *SHELXTL-PLUS Rev 4.2*, Göttingen, Germany, **1990**; *SHELXL-93*, Göttingen, Germany, **1993**.

[25] T. Hahn (Ed.), *International Tables for Crystallography*, vol. A ("Space Group Symmetry"), 2nd ed., D. Reidel, Dordrecht, **1984**.

[98117]

Untypical Regioselectivity of Carbon Dioxide Coupling with Titanocene Complexes of Phenyl(trimethylsilyl)acetylene by Using the *meso*-1,2-Ethylene-1,1′-bis(η^5-tetrahydroindenyl) Ligand System

Dominique Thomas[a], Normen Peulecke[a], Vladimir V. Burlakov[b], Wolfgang Baumann[a], Anke Spannenberg[a], Rhett Kempe[a], and Uwe Rosenthal*[a]

Abteilung "Komplexkatalyse", Institut für Organische Katalyseforschung an der Universität Rostock e.V.[a],
Buchbinderstr. 5−6, D-18055 Rostock, Germany

Institute of Organo-Element Compounds, Russian Academy of Sciences[b],
Vavilov Str. 28, Moscow 117813, Russian Federation

Received April 27, 1998

Keywords: Alkyne complexes / Titanium / *ansa*-Metallocenes / Carbon dioxide fixation / C–C coupling / Metallacycles / Regioselectivity

The reaction of [*meso*-(ebthi)$TiCl_2$] [ebthi = 1,2-ethylene-1,1′-bis(η^5-tetrahydroindenyl)] with magnesium in the presence of the alkynes $Me_3SiC{\equiv}CSiMe_3$ and $PhC{\equiv}CSiMe_3$ resulted in the formation of the complexes [*meso*-(ebthi)Ti(η^2-$Me_3SiC_2SiMe_3$)] (**1**) and [*meso*-(ebthi)Ti(η^2-PhC_2SiMe_3)] (**2a** and **2b**), which were isolated and then characterized by their NMR spectra. Due to incomplete reduction the Ti^{III} complex [*meso*-(ebthi)Ti(THF)Cl] (**3**) was also obtained as a by-product of these reactions. By insertion into the Ti–CPh bond carbon dioxide reacted with the titanacyclopropene structure of the alkyne complex [*meso*-(ebthi)Ti(η^2-PhC_2SiMe_3)] (**2a**), with untypical regioselectivity to yield the α-silyl-substituted *meso*-(ebthi)titanafuranone **6a**. In the analogous reactions of the complexes [(thi)$_2$Ti(η^2-PhC_2SiMe_3)] (thi = η^5-tetrahydroindenyl), [*rac*-(ebthi)Ti(η^2-PhC_2SiMe_3)], and [$Cp^*{}_2$Ti(η^2-PhC_2SiMe_3)] with carbon dioxide typical regioselectivity (insertion into the M–CSi bond of the titanacyclopropene) was observed, yielding the β-silyl-substituted titanafuranones **7**, **8a**, and **9**. These results show that insertion of carbon dioxide into the M–C bond of the titanacyclopropene structure of the alkynemetallocene complexes is governed by the substitution pattern of the alkyne and the steric enviroment around the metal center. The complexes **3**, **6a**, and **7** were investigated by X-ray crystal structure analysis.

A large number of reviews concerning the cooordination chemistry, the stoichiometric reactions, and the catalytic activation of carbon dioxide have been published.[1] In this series of publications little has been reported concerning insertion reactions of carbon dioxide into the metallacyclopropene structure of alkynetitanocene and -zirconocene complexes, although the nature of the observed products shows a strong dependence on the different Cp substituents, the alkynes, and the metals used. To the best of our knowledge Scheme 1 summarizes all the different types of reaction products previously described.

The first results of this chemistry came from Vol′pin et al.[2] who trapped the benzyne complex [Cp_2Ti(η^2-*o*-C_6H_4)] during the thermal decomposition of Cp_2TiPh_2 by a reaction with CO_2 to give the titanabenzofuranone complex **I**. The titanafuranone **VI** as well as the dimeric carboxylate complex **XI** (not isolated or characterized) were said to be the result of the interaction of a solution of [CpCp*Ti(η^2-PhC_2CPh)] with CO_2.[3] Recently, we have shown that dimeric compounds such as **VIII** and **X** are the primary products in the reactions of alkynetitanocene complexes [Cp_2Ti(η^2-RC_2R)] (R = Ph, Me_3Si) with CO_2[4] and that only after subsequent interaction with oxygen the titanafuranone complexes **II** and **III**[4] are formed. In the first step a coupling of only half the amount of the alkynes with CO_2 occurs, and not the direct coupling of all the alkyne to metallafuranones. Other complexes of this type **IV** and **V** were also described.[5]

The chemoselectivity for coupling of the alkyne and CO_2, as well as the structures of the products obtained, depends strongly on the substituents of the Cp ligands and the alkynes. In the reaction of CO_2 with the permethyltitanocene complex [$Cp^*{}_2$Ti(η^2-$Me_3SiC_2SiMe_3$)] the alkyne is not coupled and the carbonate-bridged complex **XII**[6a][6b] was obtained. When [$Cp^*{}_2$Ti(Me)Ph] was thermolyzed in the presence of CO_2 the benzyne complex [$Cp^*{}_2$Ti(η^2-*o*-C_6H_4)] was trapped, and the complex **VII** formed.[6c] In the reaction of [Cp_2Ti(η^2-Me_3SiC_2tBu)] and CO_2[4d] the products obtained are another carbonate-bridged complex **XIII**, the carbon monoxide complex [$Cp_2Ti(CO)_2$], and the free alkyne.

In the reaction of the alkynezirconocene complex [Cp_2Zr(THF)(η^2-$Me_3SiC_2SiMe_3$)] with CO_2 only the zirconafuranone **XIV** was obtained, which has a dimeric structure.[7]

Whereas, e.g. for nickel(0) complexes with unsymmetrically substituted alkynes, the regioselectivity of the carbon dioxide coupling reaction was studied both theoretically[1r] and experimentally[1s][1t], fewer results have been reported on the regioselectivity of these reactions with titanocene

 © WILEY-VCH Verlag GmbH, D-69451 Weinheim, 1998 1434−1948/98/1010−1495 $ 17.50+.50/0

Scheme 1

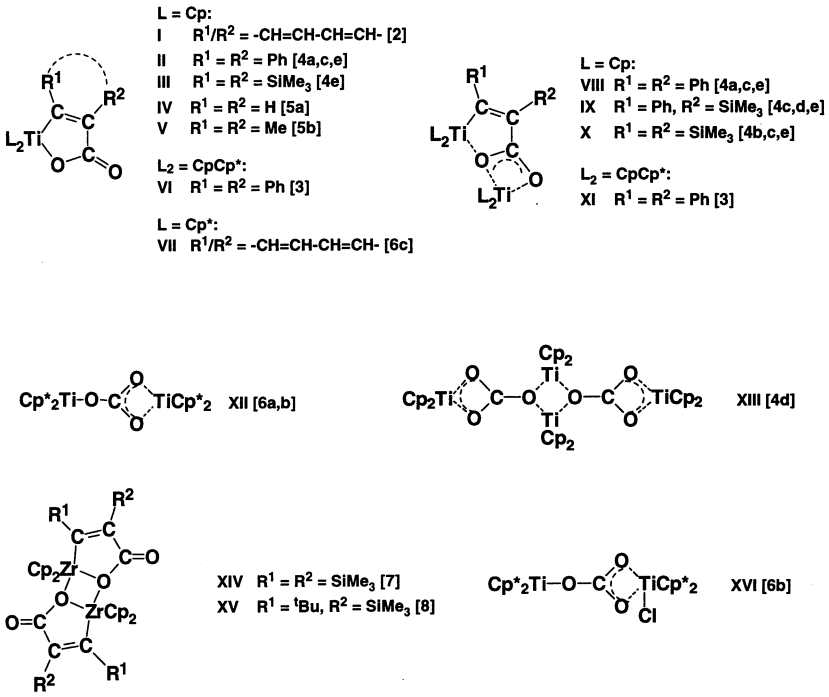

and zirconocene complexes. Using the unsymmetrically disubstituted alkynes $PhC{\equiv}CSiMe_3$ and $tBuC{\equiv}CSiMe_3$, an insertion of carbon dioxide at the silicon-substituted carbon atom is typical for titanocene as well as zirconocene, yielding the (vinylcarboxylato)titanium complex **IX**[4d] and the dimeric zirconocene compound **XV**,[8] respectively (see explanation below).

Here we report on a strategy to change the regioselectivity of the insertion of carbon dioxide into titanocene complexes, using $PhC{\equiv}CSiMe_3$, by the use of different ligand systems.

Results

Complex Syntheses

Starting Materials: The preparation of the complexes $[Cp_2Ti(\eta^2\text{-}PhC_2SiMe_3)]$,[4c][11] $[(thi)_2Ti(\eta^2\text{-}PhC_2SiMe_3)]$ (thi = tetrahydroindenyl),[12] and [*rac*-(ebthi)Ti(η^2-$Me_3SiC_2SiMe_3$)][13] has been described recently. In order to investigate the influence of the ligand system on the regiochemistry of insertion reactions we prepared the alkyne complexes [*meso*-(ebthi)Ti(η^2-$Me_3SiC_2SiMe_3$)] (**1**) and [*meso*-(ebthi)Ti(η^2-PhC_2SiMe_3)] (**2**) by the same procedure (Eq. 1).

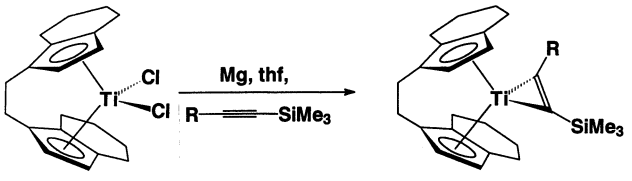

1 R= SiMe3
2a R= Ph

As a consequence of the *meso*-ebthi ligand we obtained the complex **2** as a mixture (3:1) of the two diastereomeric products **2a** (major isomer) and **2b** (minor isomer), which could not be seperated by crystallization. The ratio in which the two diastereomers are formed can be explained if one considers the different steric requirements of the alkyne substituents. In the major isomer the bulky trimethylsilyl group could be located at the less hindered side of the molecule, while the flat phenyl group could be situated between the two saturated rings. This assumption was proven by ^{1}H-NOESY NMR investigations (see below).

One by-product in the reaction of [*meso*-(ebthi)$TiCl_2$] with magnesium in THF in the presence of $Me_3SiC{\equiv}CSiMe_3$ is the Ti^{III} complex **3**, as the result of an incomplete reduction (Eq. 2).

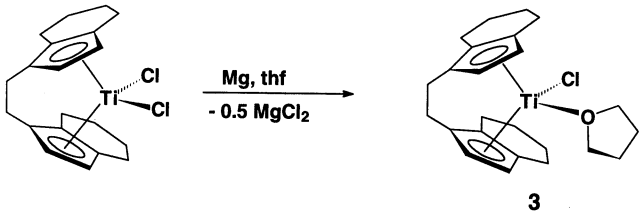

3

Regioselectivity: Three general questions must be kept in mind when determining the regioselectivity of the coupling of carbon dioxide with phenyl(trimethylsilyl)acetylene:

(i) What is the overall regioselectivity in the raw material (before the workup)?

(ii) Is the regioisomer identified by the X-ray crystal structure determination identical with the bulk product, as determined by NMR investigations?

(iii) Is there any cycloreversion of one regioisomer leading to the "opposite" product?

Complex **1** with the symmetrically substituted bis(trimethylsilyl)acetylene reacts with CO_2 to give the titanafuranone **5**, where the bulky Me_3Si groups are located at the sterically less hindered side of the complex, while the CO_2 is situated between the two saturated rings, as verified by NOE experiments. For **2a** an unusual insertion reaction was observed at the phenyl-substituted carbon atom and the complex **6a** was isolated in a high yield of 87% (Eq. 3). No other isomers were detected by NMR investigation of the raw material. The structure of the unexpected product **6a,** with the Me_3Si group in α-position, was proven by NMR investigations (NOE experiments) and confirmed by an X-ray crystal structure analysis (see below).

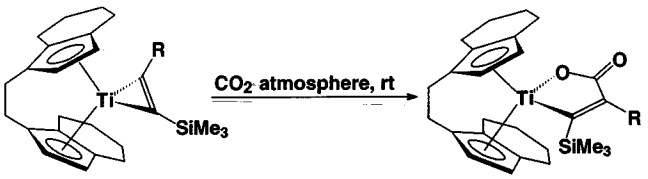

1 R = $SiMe_3$ **5 R = $SiMe_3$**
2a R = Ph **6a R = Ph**

The opposite regioselectivity was observed in the reaction of the corresponding alkyne complex [$(thi)_2Ti(\eta^2$-$PhC_2SiMe_3)$] with CO_2. The titanafuranone **7** was formed by insertion of CO_2 at the silicon-substituted carbon atom (Eq. 4). A by-product, detected by NMR and in a very low yield (5%), is presumed to be the titanafuranone resulting from CO_2 insertion at the Ti−CPh bond.

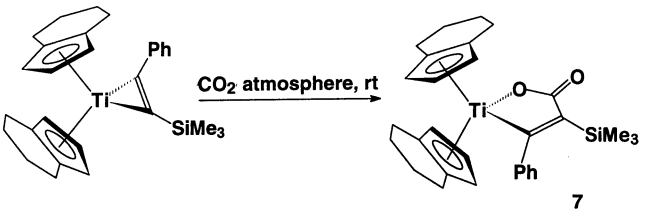

7

The opposite regioselectivity, compared to the reaction course from complex **2a** to **6a**, was also found in the reaction of the bridged alkyne complex [*rac*-(ebthi)Ti(η^2-Me_3SiC_2Ph)] **4** with carbon dioxide to yield the complex **8a** (Eq. 5).

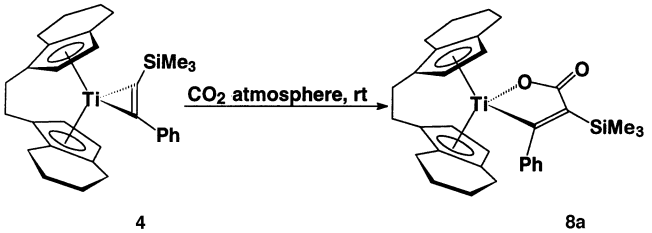

4 **8a**

This regioselectivity is identical to that obtained in the reaction of the (alkyne)permethyltitanocene complex [$Cp^*_2Ti(\eta^2$-$Me_3SiC_2Ph)$][4c] with carbon dioxide, which gives the complex **9** as the sole product (Eq. 6).

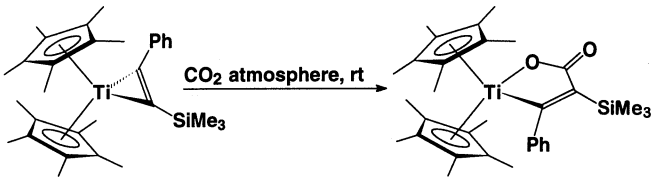

9

NMR and Structural Investigations: The regio- and stereochemistry of the reactions were investigated by ^{1}H- and ^{13}C-NMR methods. The ^{1}H-NOESY spectra of the isomer **2a** feature NOE cross peaks from the CH protons of ebthi (^{1}H: δ = 4.88, d, ^3J = 3.0 Hz, 2 H, CH ebthi; δ = 7.28, d, ^3J = 3.0 Hz, 2 H, CH ebthi) to the trimethylsilyl group. This clearly indicates that the Me_3Si group is located at the sterically less hindered side of the complex. For the minor isomer **2b** the analogous NOE signals could not be observed. Similarly, a strong NOE is found at the cyclopentadienyl doublets for titanafuranone **6a** upon irradiation of the $SiMe_3$ protons, proving a close proximity, and hence silyl substitution, at C_α relative to Ti.

The position of the silyl group at the metallafuranone (α or β) can also be determined from proton-coupled ^{13}C-NMR spectra, where characteristic and clearly distinguishable patterns occur for the trimethylsilyl- and phenyl-substituted carbon atoms. The C_α signal appears at very low field (δ > 230); the C_β and the carbonyl signals are found at δ ≈ 160 (see Experimental Section). Surprisingly, there is no clear influence of the substituents on the chemical shifts, and the C_α signal of the product with the "opposite" regiochemistry (**6a**) exhibits a very similar shift compared to that of the other titanafuranones (**6a**: C_α-$SiMe_3$: δ = 237.4; **7**: C_α-Ph: δ = 239.2; **8a**: C_α-Ph: δ = 236.2), and the same observation is made for the shifts of C_β. This is not understood because Me_3Si groups very often give a more extended low-field shift for signals of C atoms in the β position to the silicon atom (see also complex **5**: C_α: δ = 264.9).[8] Complex **3** was investigated by X-ray crystal-structure analysis (see Figure 1). To clarify the regioselectivity and to understand it from the perspective of the structures of the products obtained, the complexes **6a** and **7** were investigated by X-ray crystal-structure analysis (see Figures 2 and 3).

Discussion

Preparation of Starting Complexes

The complex [*rac*-(ebthi)Ti(η^2-$Me_3SiC_2SiMe_3$)] was recently prepared in high yield by the reduction of [*rac*-(ebthi)$TiCl_2$] with magnesium in THF at room temp. in the presence of bis(trimethylsilyl)acetylene.[13] Using the same procedure to prepare [*meso*-(ebthi)Ti(η^2-$Me_3SiC_2SiMe_3$)] (**1**), the titanium(III) complex **3** is obtained as a by-product. The incomplete reduction seems to be the consequence of

Figure 1. Molecular structure of **3**[a]

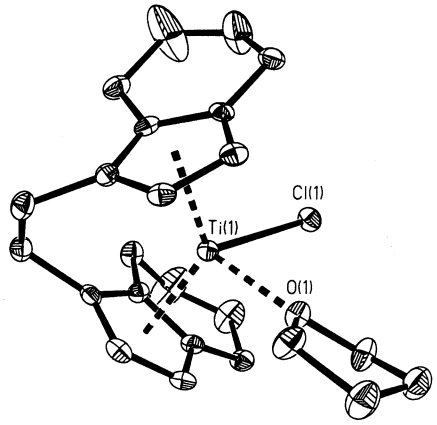

[a] Selected distances [Å] and angles [°]: Ti1−Cl1 2.447(1), Ti1−O1 2.257(3); Cl1−Ti1−O1 83.10(8), Cp′−Ti1−Cp′ 130.8(1).

Figure 2. Molecular structure of **6a**[a]

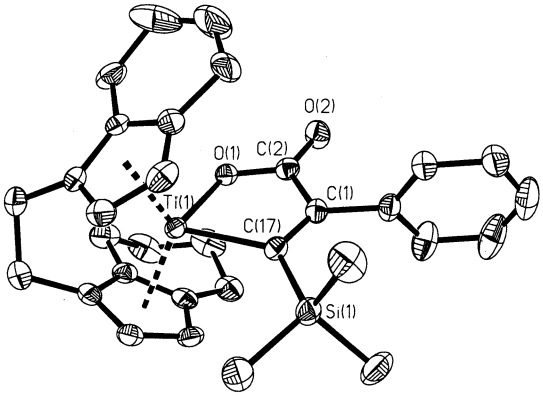

[a] Selected distances [Å] and angles [°]: Ti1−O1 1.950(2), Ti1−C17 2.184(3), C1−C17 1.348(4), C1−C2 1.499(4); O1−Ti1−C17 80.2(1), C1−C17−Si1 122.7(2), C17−C1−C21 127.0(3), Cp′−Ti1−Cp′ 130.9(1).

Figure 3. Molecular structure of **7**[a]

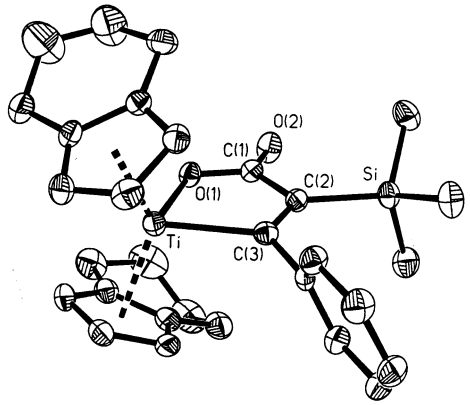

[a] Selected distances [Å] and angles [°]: Ti−C3 2.190(3), Ti−O1 1.938(2), C2−C3 1.362(4), C1−C2 1.490(4); O1−Ti−C3 77.96(9), C22−C3−C2 121.7(3), Si−C2−C3 128.6(2), Cp′−Ti−Cp′ 134.5(1).

the steric situation in the *meso*-ebthi isomer, where the ligand shields one face of the molecule. Detailed investigations concerning the reduction of $[Cp_2TiCl_2]$ by magnesium in THF without the alkyne had shown the chlorine-bridged $Ti-(\mu\text{-}Cl)_2-Mg$ species to be formed in one of the first steps of the reactions.[14] It seems reasonable to assume that steric reasons influence the reaction pathway and lead to the formation of Ti^{III} complexes such as **3**. A similar complex $[Cp^*_2Ti(THF)Cl]$ was also indicated as a by-product during the preparation of $[Cp^*_2Ti(\eta^2\text{-}Me_3SiC_2SiMe_3)]$. The reaction of the mother liquor with CO_2 gave not only **XII** but also **XVI** (see Scheme 1), apparently formed due to the presence of incompletely reduced Ti^{III} complex in the solution.[6b] Interestingly, **3** is a monomer and coordinates a THF ligand. In a series of well-known complexes $[(C_5H_{5-n}Me_n)TiX]$ (n = 0, 1, 3−5; X = Cl, Br, I) it was shown that an increase in n in the range n = 3−5 is connected with an increasing tendency to monomerize and to coordinate THF. This was explained primarily by considering the electron-donating properties of the Me groups.[15] Additionally, in **3** the threefold substituted Cp ligand is fixed in such a position that a dimerization seems to be unfavourable. The complexes with an unsymmetrically substituted alkyne, $[$*meso*-(ebthi)$Ti(\eta^2\text{-}PhSiC_2SiMe_3)]$ (**2**), and the corresponding racemic compound **4** were prepared by the same procedure.

Regioselectivity

All titanocene and zirconocene complexes with unsymmetrically disubstituted alkynes of the type $[Cp_2Ti(\eta^2\text{-}RC_2SiMe_3)]$ or $[Cp_2Zr(thf)(\eta^2\text{-}RC_2SiMe_3)]$ are characterized by longer M−CSi than M−CR distances.[4d][8] This is explained electronically by assuming a (d-p)-π interaction of silyl groups, which reduces the electron density from the alkyne resulting in a positive charge on the CR group and a shorter M−CR bond, or by steric reasons resulting from the bulky $SiMe_3$ groups. The result of these effects is a kinetically favored reaction at the M−CSi bond to give the β-silyl-substituted metallacycles. In some cases a subsequent cycloreversion in solution to the thermodynamically more stable α-silyl product[4d][8] was observed.

The regioselectivity of the CO_2 insertion, influenced by the alkyne substituents, is characterized by insertions into the M−CSi bond (e.g as found. in **IX** and **XV**). For these complexes no cycloreversion could be observed. In this respect, the regioselectivity found in **6a** is unexpected and opposite: insertion into the M−CPh bond.

Regarding the stereochemical possibilities for the CO_2 insertion into the metallacyclopropene structure of the diastereomers **2a** and **2b,** in total four reaction products were expected, as indicated in Scheme 2.

For the major complex **2a** the attack of CO_2 occurs at the M−C−Ph bond to give the complex **6a**, and the other regioisomer, **6b,** was not found. There are three different explanations for the observed regioselectivity shown by the product obtained:

Scheme 2

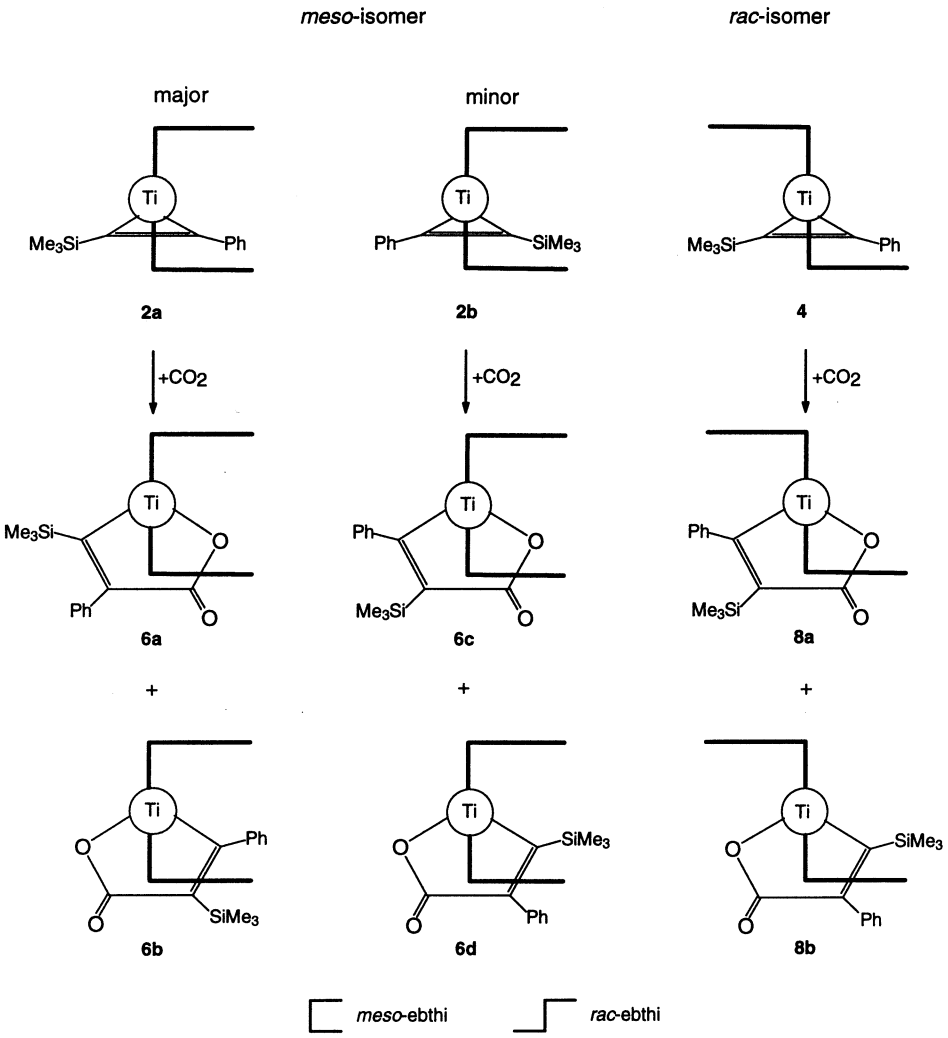

(i) In the starting complex [*meso*-(ebthi)Ti(η^2-PhC_2SiMe_3)] the larger $SiMe_3$ groups are preferentially located at the nonsubstituted sides of the Cp′s, whereas the flat phenyl groups are between the cyclohexanediyl substituents (a similar situation is verified in complex **3** with the smaller chlorine atom and larger THF molecule). The insertion of CO_2 occurs in the M−CPh bond in order to minimize the steric restrictions between the saturated ring units and the phenyl group.

(ii) The Me_3Si group comes into the α position to the metal center which is in many metallacycles thermodynamically favoured (after cycloreversion) as shown by a number of coupling reactions of silylalkynes.[4d][8]

(iii) It seems possible that in the starting complex **2a** the M−CPh distances become nearly identical or longer, compared to the M−CSi bonds, due to the steric interactions of the phenyl groups and the cyclohexanediyl substituents. This could be the reason for the other regioselectivity, since all Cp complexes show longer M−CSi than M−CPh bonds.

Complex **2b** seems to form two insertion products, **6c** and **6d**. This is surprising because the steric repulsion between the bulky Me_3Si group and the tetramethylene unit should lead to a uniform reaction and only one product (**6c**). So far the separation and unambiguous characterization of the insertion products formed has failed and a stereochemical statement is not possible.

Compared to this "unusual" regioselectivity, the "normal" insertion of carbon dioxide into the complexes [$(thi)_2$Ti(η^2-PhC_2SiMe_3)], [*rac*-(ebthi)Ti(η^2-Me_3SiC_2Ph)], and [Cp^*_2Ti(η^2-Me_3SiC_2Ph)] follows the rules discussed above, with insertions at the M−CSi bond to the β-silyl-substituted metallacycles.

The reaction product **9** of the (alkyne)permethyltitanocene complex [Cp^*_2Ti(η^2-Me_3SiC_2Ph)] with carbon dioxide, differs from the dinuclear complex **IX**[4c][4d][4e] (Scheme 1) which was observed in the reaction of the corresponding titanocene complex [Cp_2Ti(η^2-Me_3SiC_2Ph)] with carbon dioxide. Interestingly, in the reaction of the corresponding permethylzirconocene complex [Cp^*_2Zr(η^2-Me_3SiC_2Ph)][16] with carbon dioxide a 1:1 mixture of the two possible regioisomers was obtained.[17]

Conclusion

The regioselectivity of the carbon dioxide insertion into titanocene complexes with unsymmetrically disubstituted alkynes of the type [$L_2Ti(\eta^2$-PhC_2SiMe_3)] is influenced by the nature of the ligands L used. With L_2 = Cp_2, Cp^*_2, thi_2 or *rac*-ebthi the "normal" reaction at the M−CSi bond to give the β-silyl-substituted titanafuranones was observed. With L_2 = *meso*-ebthi the opposite regioselectivity gives, after insertion into the M−CPh bond, the α-silyl-substituted titanacycle.

In all reactions investigated, the regioselectivity identified by X-ray crystal structure determination is consistent with the results of NMR investigations. In most reactions only one regioisomer was obtained. There are no hints of any cycloreversion leading to the "opposite" regioisomeric titanafuranone, as e.g. found in corresponding metallacyclic compounds.[4d][8]

Steric interactions seem to be the reason for the different regioselectivity and, after these considerations, the fixation of the tetrahydroindenyl units in a certain position by the *ansa* bridge is the most important feature in understanding the unusual regioselectivity for carbon dioxide insertion.

Experimental Section

General Remarks: All operations were carried out under argon with standard Schlenk techniques. Prior to use, solvents were freshly distilled from sodium tetraethylaluminate under argon. Deuterated solvents were treated with sodium or sodium tetraethylaluminate, distilled and stored under argon. − NMR: Bruker ARX 400 at 9.4 T (chemical shifts given in ppm relative to TMS; the signals of the aliphatic ebthi protons have not been analyzed). − Melting points: Sealed capillaries with a Büchi 535 apparatus. − Elemental analyses: Leco CHNS-932 elemental analyzer.

Preparation of [meso-(ebthi)Ti(η^2-$Me_3SiC_2SiMe_3$)] (**1**): 0.03 g (1.5 mmol) of magnesium cuttings and 0.34 ml (1.5 mmol) of bis(trimethylsilyl)acetylene were added to a suspension of 0.53 g (1.4 mmol) of [*meso*-(ebthi)$TiCl_2$] in 15 ml of THF. The mixture was stirred at 45°C until the color changed from red to black/brown. After that, the solution was stirred at room temp. for 2 h, the solvent removed in vacuo and the brown solid residue dissolved in 15 ml of *n*-hexane. After filtration and repeated removal of the solvent, brown/yellow needles of **1** crystallized from the oil at −78°C. The crystals were collected by filtration after washing with *n*-hexane at −78°C. Yield: 0.42 g (62%); m.p. 142−145°C. − ^{1}H NMR ([D_6]benzene): δ = −0.20 (s, 9 H, $SiMe_3$), 0.09 (s, 9 H, $SiMe_3$), 4.32 (d, ^3J = 3.0 Hz, 2 H, CH ebthi), 7.83 (d, ^3J = 3.0 Hz, 2 H, CH ebthi). − ^{13}C NMR ([D_6]benzene): δ = 1.1, 4.4 ($SiMe_3$), 23.5, 23.6, 24.4, 26.3, 26.7 (CH_2 ebthi), 113.8, 114.3 (CH ebthi), 122.7, 126.0, 129.0 (C ebthi), 242.1, 254.3 (C alkyne). − $C_{28}H_{42}Si_2Ti$ (482.7): calcd. C 69.67, H 8.77; found C 68.69, H 8.56. − IR (Nujol): $\tilde{\nu}$ = 1589 cm^{-1}.

Preparation of the Complexes [meso-(ebthi)Ti(η^2-Me_3SiC_2Ph)] (**2a** and **2b**): As described above for **1**, 0.37 g (0.96 mmol) of [*meso*-(ebthi)$TiCl_2$], 24 mg (1.0 mmol) of magnesium cuttings, and 0.20 ml (1.0 mmol) of phenyl(trimethylsilyl)acetylene yielded the red/brown alkynemetallocene complexes **2a** and **2b**, as indicated by both NMR and IR. The product was isolated in the same manner as described for **1**, but only a red brown oil was obtained which was a mixture (3:1) of the diastereomeric products **2a** (major) and **2b** (minor). Yield: 0.21 g of **2a** and **2b** (45%). − ^{1}H NMR ([D_6]benzene) of major isomer **2a**: δ = −0.02 (s, 9 H, $SiMe_3$), 4.88 (d, ^3J = 3.0 Hz, 2 H, CH ebthi), 6.6−7.5 (m, 5 H, Ph), 7.29 (d, ^3J = 3.0 Hz, 2 H, CH ebthi). − ^{1}H NMR ([D_6]benzene) of minor isomer **2b**: δ = 0.19 (s, 9 H, $SiMe_3$), 4.38 (d, ^3J = 3.0 Hz, 2 H, CH ebthi), 6.6−7.5 (m, 5 H, Ph), 7.44 (d, ^3J = 3.0 Hz, 2 H, CH ebthi). − ^{13}C NMR ([D_6]benzene) of major isomer **2a**: δ = 0.6 ($SiMe_3$), 23.4, 23.4, 23.7, 25.5, 27.3 (CH_2 ebthi), 112.1, 114.5 (CH ebthi), 122.5, 123.5, 125.2 (C ebthi), 127.6, 131.2 (CH Ph, *para* not found), 139.7 (C Ph), 220.1, 224.9 C(alkyne). − ^{13}C NMR([D_6]benzene) of minor isomer **2b**: δ = 3.9 ($SiMe_3$), 23.4, 23.8, 24.3, 25.9, 27.2 (CH_2 ebthi), 112.5, 113.2 (CH ebthi), 145.7 (C Ph, further ebthi and Ph signals not unambiguously identified), 210.3, 227.9 C(alkyne). − $C_{31}H_{38}SiTi$ (486.6): calcd. C 76.52, H 7.87; found C 76.04; H 7.72.

Preparation of [meso-(ebthi)Ti(THF)Cl] (**3**): The method used was as described above for **1** {starting with 0.31 g of [*meso*-(ebthi)$TiCl_2$]} but after the reaction a second extraction of the brown solid with 20 ml of THF yielded a dark blue solution, which was reduced to ca. 5 ml and stored at −30°C. After 72 h at −30°C, blue crystals (57 mg, 17%) formed, which were washed with cold *n*-hexane and isolated by filtration. M.p. decomposition, loss of THF in vacuo. − $C_{24}H_{32}ClOTi$ (419.9): calcd.C 68.66, H 7.68; found: C 68.02; H 7.63.

Preparation of [rac-(ebthi)Ti(η^2-Me_3SiC_2Ph)] (**4**): The method used was as described above for **1**. 0.32 g (0.84 mmol) of [*rac*-(ebthi)$TiCl_2$], 21 mg (0.86 mmol) of magnesium cuttings, and 0.17 ml (0.86 mmol) of phenyl(trimethylsilyl)acetylene yielded the alkynemetallocene complex **4**, which was isolated as a black oil. After standing for one week, the oil solidified as black crystals (0.29 g, 90%), which were washed with cold *n*-hexane (−30°C) to obtain analytical pure material, m.p. 156°C. − ^{1}H NMR ([D_6]benzene): δ = 0.15 (s, 9 H, $SiMe_3$), 4.23 (d, ^3J = 3.0 Hz, 1 H, CH ebthi), 4.54 (d, ^3J = 3.2 Hz, 1 H, CH ebthi), 6.66 (2 H, Ph *ortho*), 6.92 (1 H, Ph *para*), 7.07 (2 H, Ph *meta*), 8.10 (d, ^3J = 3.2 Hz, 1 H, CH ebthi), 8.50 (d, J = 3.0 Hz, 1 H, CH ebthi). − ^{13}C NMR ([D_6]benzene): δ = 2.1 ($SiMe_3$), 22.9, 23.2, 23.4, 23.7, 23.7, 23.9, 25.3, 25.3, 26.5, 26.6 (CH_2 ebthi), 111.7, 112.8, 113.8, 114.0 (CH ebthi), 128.0, 130.2 (CH Ph, *para* not found), 124.6, 124.8, 124.8, 126.0, 126.1, 127.5 (C ebthi), 141.2 (C Ph), 213.8, 220.8 C(alkyne). − $C_{31}H_{38}SiTi$ (486.6): calcd. C 76.52, H 7.87; found C 75.97, H 7.81. − IR (Nujol): $\tilde{\nu}$ = 1638 cm^{-1}.

Preparation of **5**: 0.48 g (1.0 mmol) of [*meso*-(ebthi)Ti(η^2-$Me_3SiC_2SiMe_3$)] was dissolved in a mixture of THF/*n*-hexane (3:1) (ca. 10 ml) which was exposed to CO_2. The color of the solution changed from red/brown to orange. After standing 24 h at −78°C, 0.37g (0.70 mmol, 70%) of red needles of complex **5** precipitated from the solution; m.p. > 240°C. − ^{1}H NMR ([D_8]THF): δ = 0.05 (s, 9 H, α-$SiMe_3$), 0.17 (s, 9 H, β-$SiMe_3$), 5.83 (d, ^3J = 3.1 Hz, 2 H, CH ebthi), 6.54 (d, ^3J = 3.1 Hz, 2 H, CH ebthi). − ^{13}C NMR ([D_8]THF): δ = 3.0, 3.6 ($SiMe_3$), 22.1, 22.9, 23.6, 24.7, 29.3 (CH_2 ebthi), 113.0, 115.3 (CH ebthi), 129.9, 132.5, 133.8 (C ebthi), 161.5, 171.7 (C_β titanacycle), 264.9 (C_α titanacycle). − $C_{29}H_{42}O_2Si_2Ti$ (526.7): calcd. C 66.13, H 8.03. found C 66.32, H 7.98. − IR (Nujol): $\tilde{\nu}$ = 1610 cm^{-1}.

Preparation of **6a**: 200 mg (0.41 mmol) of [*meso*-(ebthi)Ti(η^2-Me_3SiC_2Ph)] was dissolved in 10 ml of a mixture of THF/*n*-hexane (3:1) which was exposed to CO_2. The color of the solution changed from red/brown to orange. After standing 36 h at −30°C, light red crystals of **6a** crystallized from the solution which were then isolated by filtration to yield 137 mg (63%); m.p. >240°C. − ^{1}H NMR ([D_8]THF): δ = −0.25 (s, 9 H, $SiMe_3$), 5.86 (d, ^3J = 3.0 Hz, 2 H,

CH ebthi), 6.66 (d, ^3J = 3.0 Hz, 2 H, CH ebthi), 7.08 (2 H, Ph *ortho*), 7.15 (3 H, Ph *meta*/*para*). − ^{13}C NMR ([D$_8$]THF): δ = 2.4 ($SiMe_3$), 22.1, 22.8, 23.8, 24.6, 29.4 (CH_2 ebthi), 112.8, 115.7 (CH ebthi), 130.0, 132.3, 133.4 (C ebthi), 126.5 (*p*-Ph), 127.3, 130.5 (CH Ph), 144.4 (*i*-Ph), 158.1 (*C*-Ph), 162.6 (CO), 237.4 (*C*-$SiMe_3$). − $C_{32}H_{38}O_2TiSi$ (530.62): calcd. C 72.43, H 7.22. found C 71.95, H 7.29. − IR (Nujol): $\tilde{\nu}$ = 1240 cm^{-1}.

Preparation of **7**: 200 mg (0.43 mmol) of [(thi)$_2$Ti(η^2-Me_3Si-C_2Ph)][12] was dissolved in 5 ml of a mixture of THF/*n*-hexane (3:1) which was exposed to CO_2. The color of the solution changed from dark red to orange. After standing 24 h at 0°C, light red crystals crystallized from the solution. Filtration yielded 188 mg of **7** (87%); m.p. 185°C. − ^{1}H NMR ([D$_8$]THF): δ = −0.16 (s, 9 H, $SiMe_3$), 1.58 (m, 4 H, thi), 1.74 (m, 2 H, thi), 1.88 (m, 2 H, thi), 1.98 (ddd, ^2J = 16 Hz, ^3J = 5 and 7 Hz, 2 H, α-CH_2 thi), 2.47 (dt, ^2J = 16 Hz, ^3J = 6 Hz, 2 H, α-CH_2 thi), 2.77 (dt, ^2J = 17 Hz, ^3J = 6 Hz, 2 H, α-CH_2 thi), 2.92 (dt, ^2J = 17 Hz, ^3J = 6 Hz, 2 H, α-CH_2 thi), 5.20 (t, J = 3 Hz, 2 H, β-CH thi), 6.44 (dd, J = 2 and 3 Hz, 2 H, α-CH thi), 6.57 (dd, J = 2 and 3 Hz, 2 H, α-CH thi), 6.92 (2 H, Ph *ortho*), 6.97 (1 H, Ph *para*), 7.16 (2 H; Ph *meta*). − ^{13}C NMR ([D$_8$]THF): δ = 1.0 ($SiMe_3$) 22.8, 22.8, 25.3, 25.4 (CH_2 thi), 110.2, 111.8, 119.9 (CH thi), 124.9 (*o*-Ph), 125.5 (*p*-Ph), 128.2 (*m*-Ph), 131.4, 134.7 (C thi), 150.5 (*i*-Ph) 155.5 (*C*-$SiMe_3$), 164.8 (CO), 239.2 (*C*-Ph). − MS (70eV); *m*/*z* (%): 504.6 [M$^+$], 286 [(thi)$_2$Ti$^+$]. $C_{30}H_{36}O_2SiTi$ (504.6): calcd. C 71.41, H 7.19; found C 71.45, H 7.04.

Preparation of **8a**: As described above for **6a**, 143 mg [*rac*-(ebthi)$_2$Ti(η^2-Me_3SiC_2Ph)] yielded, after exposure to CO_2 and recrystallization from THF/*n*-hexane (1:1) (ca. 3 ml), 112 mg (72%) of **8a** as orange needles, m.p. 268°C (decomposition). − ^{1}H NMR ([D$_8$]THF) δ = −0.10 (s, 9 H, $SiMe_3$), 5.35 (d, ^3J = 2.8 Hz, 1 H, CH ebthi), 5.57 (d, ^3J = 3.2 Hz, 1 H, CH ebthi), 6.40 (d, ^3J = 3.2 Hz, 1 H, CH ebthi), 6.89 (2 H, Ph *ortho*), 7.07 (1 H, Ph *para*), 7.18 (2 H, Ph *meta*), 7.55 (d, ^3J = 2.8 Hz, 1 H, CH ebthi). − ^{13}C NMR ([D$_8$]THF): δ = 1.8 ($SiMe_3$), 21.6, 22.2, 22.3, 22.7, 23.9, 24.3, 24.3, 24.6, 28.7, 28.9 (CH_2 ebthi), 111.4, 114.7, 117.0, 123.3 (CH ebthi), 126.1, 129.7, 133.0, 133.8, 134.6, 136.2 (C ebthi), 126.9 (*p*-Ph), 127.9, 128.2 (CH Ph), 147.7 (*i*-Ph), 156.4 (*C*−$SiMe_3$), 164.6 (CO), 236.2 (*C*−Ph). − $C_{32}H_{38}O_2TiSi$ (530.62): calcd. C: 72.43, H: 7.22; found C: 72.04, H: 7.04.

Preparation of **9**: 344 mg (0.70 mmol) of [Cp*$_2$Ti(η^2-Me_3Si-C_2Ph)][4c] was dissolved in 15 ml of *n*-hexane under argon and the resulting solution filtered. Argon was then carefully removed in vacuo, and the flask with the solution filled with CO_2 at 20°C. After standing 24 h at 20°C, dark red crystals had formed, which were filtered, washed with cold *n*-hexane and dried in vacuo. Yield 266 mg of **9** (71%); m.p. 173−174°C. − ^{1}H NMR ([D$_8$]THF): δ = 0.01 (s, 9 H, $SiMe_3$), 1.86 (s, 30 H, C_5Me_5), 6.58 (m, 2 H, *o*-Ph), 7.04 (m, 1 H, *p*-Ph), 7.15 (m, 2 H, *m*-Ph). − ^{13}C NMR ([D$_8$]THF): δ = 2.0 ($SiMe_3$), 12.3 ($C_5\mathit{Me}_5$), 126.9 (C_5Me_5), 126.6 (*p*-Ph), 127.8 (*m*-Ph), 129.8 (*o*-Ph), 146.5 (*i*-Ph), 154.7 (*C*−$SiMe_3$), 166.1 (CO), 244.1 (*C*−Ph). − IR (Nujol): $\tilde{\nu}$ = 1620 (CO), 1237 ($SiMe_3$) cm^{-1}. − MS (70eV); *m*/*z* (%): 537 [M$^+$]. − $C_{32}H_{44}O_2SiTi$ (536.7): calcd. C 71.62, H 8.62; found C 71.76, H 8.63.

X-ray Crystallographic Study of Complexes **3**, **6a**, *and* **7**: Data were collected with a STOE-IPDS diffractometer using graphite-monochromated Mo-K_α radiation. The structures were solved by direct methods (SHELXS-86)[9] and refined by full-matrix least-squares techniques against F^2 (SHELXL-93)[10]. The hydrogen atoms were included at calculated positions. All other nonhydrogen atoms were refined anisotropically. Cell constants and other experimental details were collected and are recorded in Table 1. XP (SIEMENS Analytical X-ray Instruments, Inc.) was used for structure representations. Further details of the crystal-structure investigations are available on request from the Cambridge Crystallographic Data Centre, on quoting the depository number CCDC-101470.

Table 1. Crystallographic data of **3**, **6a**, and **7**

	3	**6a**	**7**
cryst. color, habit	green, prism	red-orange, prism	red, prism
cryst. system	monoclinic	monoclinic	orthorhombic
space group	$P2_1/c$	$P2_1/n$	*Pbca*
lattice constants			
a [Å]	8.161(1)	11.482(2)	15.027(3)
b [Å]	16.512(2)	16.295(2)	17.111(3)
c [Å]	15.114(2)	14.874(2)	20.612(4)
β [°]	97.370(11)	92.700(11)	
Z	4	4	8
T [K]	200(2)	293(2)	293(2)
μ(Mo-K_α) [mm^{-1}]	0.568	0.378	0.393
θ range [°]	1.83−24.34	1.85−24.33	1.98−24.33
no. of rflns. (measd.)	5942	8187	12238
no. of rflns. (indep.)	3235	4388	3564
no. of rflns. (obsd.)	2139	3272	2809
no. of parameters	244	325	307
$R1$ [$I > 2\sigma(I)$]	0.056	0.047	0.041
$wR2$ (all data)	0.165	0.128	0.119

[1] Selected examples: [1a] R. Eisenberg, D. E. Hendriksen, *Adv. Catal.* **1979**, *28*, 119. − [1b] D. J. Darensbourg, R. A. Kudaroski, *Adv. Organomet. Chem.* **1983**, *22*, 129. − [1c] D. R. Palmer, R. van Eldik, *Chem. Rev.* **1983**, *83*, 651. − [1d] D. Walther, *Coord. Chem. Rev.* **1987**, *79*, 135. − [1e] A. Behr, *Angew. Chem.* **1988**, *100*, 681; *Angew. Int. Ed. Engl.* **1988**, *27*, 129. − [1f] A. Behr, *Aspects Hom. Catal.* **1988**, *6*, 59. − [1g] P. Braunstein, D. Matt, D. Nobel, *Chem. Rev.* **1988**, *88*, 747. − [1h] I. S. Kolomnikov, T. V. Lysak, *Russ. Chem. Rev. (Engl. Tranl.)* **1990**, *59*, 344. − [1i] D. Walther, *Nachr. Chem. Tech. Lab.* **1992**, *40*, 1214. − [1j] M. Aresta, E. Quaranta, I. Tommasi, *New J. Chem.* **1994**, *18*, 133. − [1k] W. Leitner, *Angew. Chem.* **1995**, *107*, 2391; *Angew. Chem. Int. Ed. Engl.* **1995**, *34*, 2207. − [1l] P. G. Jessop, T. Ikariya, R. Noyori, *Chem. Rev.* **1995**, *95*, 259. − [1m] A. R. Cutler, P. K. Hanna, J. C. Vites, *Chem. Rev.* **1988**, *88*, 1383. − [1n] M. Aresta, E. Quaranta, I. Tommasi, P. Giannoccaro, A. Ciccarese, *Gazz. Chim. Ital.* **1995**, *125*, 509. − [1o] K. Tanaka, *Adv. Inorg. Chem.* **1995**, *43*, 409. − [1p] K. K. Pandey, *Coord. Chem. Rev.* **1995**, *140*, 37. − [1q] W. Leitner, *Coord. Chem. Rev.* **1996**, *153*, 257. − [1r] S. Sakaki, K. Mine, T. Hamada, T. Arai, *Bull. Chem. Soc. Jpn.* **1995**, *68*, 1873. − [1s] E. Dunach, S. Derien, J. Perichon, *J. Organomet. Chem.* **1989**, *364*, C33. − [1t] S. Derien, E. Dunach, J. Perichon, *J. Am. Chem. Soc.* **1991**, *113*, 8447.

[2] I. S. Kolomnikov, T. S. Lobeeva, V. V. Gorbachevskaja, G. G. Alexandrov, Yu. T. Struchkov, M. E. Vol′pin, *J. Chem. Soc. Chem. Commun.* **1971**, 972.

[3] B. Demersemann, R. Mahé, P. H. Dixneuf, *J. Chem. Soc., Chem. Commun.* **1984**, 1394.

[4] [4a] V. B. Shur, V. V. Burlakov, A. I. Yanovsky, Yu. T. Struchkov, M. E. Vol'pin, *Metalloorg. Khim.* **1988**, *1*, 475. − [4b] V. V. Burlakov, U. Rosenthal, A. I. Yanovsky, Yu. T. Struchkov, O. G. Ellert, V. B. Shur, M. E. Vol'pin, *Metalloorg. Khim.* **1989**, *2*, 1193; *Organomet. Chem. USSR* **1989**, *2*, 633. − [4c] V. V. Burlakov, A. V. Polyakov, A. I. Yanovsky, Yu. T. Struchkov, V. B. Shur, M. E. Vol'1pin, U. Rosenthal, H. Görls, *J. Organomet. Chem.* **1994**, *476*, 197. − [4d] C. Lefeber, A. Ohff, A. Tillack, W. Baumann, R. Kempe, V. V. Burlakov, U. Rosenthal, H. Görls *J. Organomet. Chem.* **1995**, *501*, 179. − [4e] V. V. Burlakov, A. I. Yanovsky, Yu. T. Struchkov, U. Rosenthal, A. Spannenberg, R. Kempe, O. G. Ellert, V. B. Shur, *J. Organomet. Chem.* **1997**, *542*, 105.

[5] [5a] H. G. Alt, G. S. Herrmann, M. D. Rausch, D. T. Mallin, *J. Organomet. Chem.* **1988**, *356*, C53. − [5b] H. G. Alt, G. S. Herrmann, *J. Organomet. Chem.* **1990**, *390*, 159.

[6] [6a] V. V. Burlakov, U. Rosenthal, F. M. Dolgushin, A. I. Yanovsky, Yu. T. Struchkov, O. G. Ellert, V. B. Shur, M. E. Vol′pin,

Metalloorg. Khim. **1992**, *5*, 1231; *Organomet. Chem. USSR* **1992**, *5*, 593. – [6b] V. V. Burlakov, F. M. Dolgushin, A. I. Yanovsky, Yu. T. Struchkov, V. B. Shur, U. Rosenthal, U. Thewalt *J. Organomet. Chem.* **1996**, *522*, 241. – [6c] G. A. Luinstra, J. H. Teuben, *Organometallics* **1992**, *11*, 1793.
[7] U. Rosenthal, A. Ohff, M. Michalik, H. Görls, V. V. Burlakov, V. B. Shur, *Organometallics* **1993**, *12*, 5016.
[8] C. Lefeber, A. Ohff, A. Tillack, W. Baumann, R. Kempe, V. V. Burlakov, U. Rosenthal, *J. Organomet. Chem.* **1995**, *501*, 189.
[9] Sheldrick, G. M. *Acta Crystallogr.* **1990**, *A46*, 467.
[10] G. M. Sheldrick, *SHELXL-93*, University of Göttingen, Göttingen, Germany, **1993**.
[11] U. Rosenthal, H. Görls, V. V. Burlakov, V. B. Shur, M. E. Vol′pin, *J. Organomet. Chem.* **1992**, *426*, C53.
[12] N. Peulecke, W. Baumann, R. Kempe, V. V. Burlakov, U. Rosenthal, *Eur. J. Inorg. Chem.* **1998**, *3*, 419.
[13] C. Lefeber, W. Baumann, A. Tillack, R. Kempe, H. Görls, U. Rosenthal, *Organometallics* **1996**, *15*, 3486.
[14] D. W. Stephan, *Organometallics* **1992**, *11*, 996.
[15] K. Mach, J. B. Raynor, *J. Chem. Soc., Dalton Trans.* **1992**, 683.
[16] A.K. List, K. Koo, A. L. Rheingold, G. L. Hillhouse, *Inorg. Chim. Acta* **1998**, *270*, 339.
[17] V. V. Burlakov, U. Rosenthal, unpublished results.

[98129]

Pyrazolato Metal Complexes: Synthesis, Characterization and X-ray Crystal Structures of Rhenium(I) Derivatives

G. Attilio Ardizzoia*[a], Girolamo LaMonica[a], Angelo Maspero[a], Massimo Moret[b], and Norberto Masciocchi*[b]

Dipartimento di Chimica Inorganica, Metallorganica e Analitica, Università di Milano e Centro CNR[a], Via Venezian, 21, I-20133 Milano, Italy

Dipartimento di Chimica Strutturale e Stereochimica Inorganica, Università di Milano e Centro CNR[b], Via Venezian, 21, I-20133 Milano, Italy

Received May 5, 1998

Keywords: Pyrazolato ligands / Rhenium / Carbonylmetal complexes / Crystal structure / Hydrogen bonds

The mononuclear complexes $[Re(CO)_3(Hpz)_2Br]$ (**1**) and $[Re(CO)_3(Hdmpz)_2Br]$ (**2**) were obtained by treating $[Re(CO)_5Br]$ with pyrazole (Hpz) or 3,5-dimethylpyrazole (Hdmpz). Complex **1** reacted with triethylamine affording a mixture of the ionic dinuclear derivative $(Et_3NH)[Re_2(CO)_6(pz)_2Br]$ (**3**) and of the mononuclear species $[Re(CO)_3(Hpz)_2(pz)]$ (**4**). Complex **4** was obtained in a pure form by carrying out the reaction in the presence of excess free pyrazole. Treatment of **4** with pyridine afforded the $[Re(CO)_3(py)(Hpz)(pz)]$ species (**6**). The analogues of **4** and **6** with Hdmpz, i.e. $[Re(CO)_3(Hdmpz)_2(dmpz)]$ (**7**) and $[Re(CO)_3(py)(Hdmpz)(dmpz)]$ (**8**) were also synthesized. All species were characterized in solution by ^{1}H-NMR spectroscopy, while the crystal structures of complexes **1**, **3**, **4** and **6** were determined by single-crystal X-ray diffraction analysis. The $[(CO)_3Re(\mu\text{-}pz)_2(\mu\text{-}Br)Re(CO)_3]^-$ anion represents the first structurally characterized species containing rhenium(I) atoms bridged by μ-pyrazolate ligands.

Introduction

The rapid development of the coordination and organometallic chemistry of the pyrazolate anion and its derivatives has been witnessed in recent years[1]. Thanks to the possibility of modifying the steric and electronic properties of the pyrazole ligand by the action of the substituents of the heterocyclic ring, pyrazolates, which possess two adjacent nucleophilic sites, give rise to a versatile and varied chemistry. For example, it is well known that pyrazolates (i) can act as monodentate, *exo*- or even *endo*-bidentate anionic ligands[1], (ii) can afford, for the same stoichiometry, oligomers of different nuclearities (and polymers) depending on the synthetic methods used[2] and (iii) have been shown to possess a rather wide conformational variability,[2c][3] despite possessing a stiff heterocyclic ring.

In the recent past we have been active in the field of metal pyrazolates and have reported extensively on copper, silver and palladium species, demonstrating the structural versatility caused by the pyrazolate ligand and the catalytic activity of some of its complexes[2c][4]. Our continual interest in evaluating the coordination properties of this class of ligands led us to explore the synthesis and reactivity of rhenium(I) pyrazolate derivatives, a field so far scarcely investigated.

The easily accessible mononuclear carbonylrhenium(I) complex $[Re(CO)_5Br]$ was found to be an excellent starting material for the synthesis of pyrazole- and pyrazolatorhenium(I) derivatives. In this paper we report the synthesis, spectroscopic and structural characterization of a series of rhenium(I) species derived by direct reaction of $[Re(CO)_5Br]$ with pyrazole (Hpz) and 3,5-dimethylpyrazole (Hdmpz).

Results and Discussion

The reaction of $[Re(CO)_5Br]$ with pyrazole in toluene at 80°C afforded quantitatively a white product, revealed by analysis as $[Re(CO)_3(Hpz)_2Br]$ (**1**), produced by the substitution of two carbonyl groups with two pyrazole molecules (eq. 1).

$$[Re(CO)_5Br] + 2\ Hpz \rightarrow [Re(CO)_3(Hpz)_2Br]\ (\mathbf{1}) + 2\ CO \qquad (1)$$

The IR spectrum of **1**, recorded in toluene, shows three strong $\tilde{\nu}$(CO) bands at 2031, 1929 and 1897 cm^{-1} typical for a *fac* structure [the spectrum of the alternative *mer* geometry would show two strong and one weak $\tilde{\nu}$(CO) bands][5]. Evidence for a similar geometry, the most plausible taking in account the *trans* effect of the carbonyl groups, was also found in earlier substitution studies on $[Re(CO)_5Br]$ with nitrogen[6] or phosphorous[7] ligands. An X-ray crystal-structure determination provided an unambiguous confirmation of the assigned geometry (see later).

It is noteworthy that the monosubstituted product, i.e. $[Re(CO)_4(Hpz)Br]$, could not be isolated (even by carrying out the reaction with a Hpz/Re ratio < 2 and employing a decarbonylating agent such as Me_3NO), nor did the IR spectra of the reaction mixture show any indication of a spectroscopically detectable monosubstituted intermediate. On the contrary, in earlier studies on the substitution of CO with PPh_3 in $[Re(CO)_5Br]$, the intermediate formation of

 © WILEY-VCH Verlag GmbH, D-69451 Weinheim, 1998 1434−1948/98/1010−1503 $ 17.50+.50/0

monosubstitution derivatives was proved by means of IR spectroscopy[7a].

The ^{1}H-NMR spectrum of **1** recorded in CD_2Cl_2 at 20°C shows three sharp signals at δ = 6.29 [C(4)−*H*], 7.53 [C(3)−*H*] and 7.66 [C(5)−*H*][8], and a broader signal at δ = 11.7 assignable to N−*H* protons. The presence of only one set of signals for each pyrazole hydrogen atom reveals the equivalence of the two pyrazole molecules coordinated to the rhenium centre. The scrambling process which equalizes the 3 and 5 sites, frequently found in complexes containing anionic *mono*dentate pyrazolate ligands[9], is in this case absent. Indeed, in complexes containing neutral pyrazoles, the interchange of the nitrogen sites requires simultaneous proton transfer and metal hopping, and is, therefore, expected to be more difficult. Accordingly, the dynamic behaviour observed for [Ir(CO)(PPh$_3$)(dmpz)] disappears upon protonation to the corresponding Hdmpz derivative[9a]. The NMR characterization of various pyrazole complexes revealed both static[10] and dynamic[11] behaviour. On lowering the temperature to −80°C, all signals split as a result of the coupling C(3)−*H*/C(4)−*H*, C(5)−*H*/C(4)−*H* and of N−*H* with the three heterocyclic C−*H* protons, leading to a very complex spectrum because of partial overlapping of the signals. N−*H* irradiation allows a simplification of the ^{1}H-NMR spectrum of **1** to three resonances, a doublet [δ = 7.65, $J_{5,4}$ = 2.2 Hz, C(5)−*H*], a second doublet [δ = 7.53, $J_{3,4}$ = 1.8 Hz, C(3)−*H*] and a pseudotriplet centred at δ = 6.29 [C(4)−*H*]. Similar features were previously reported for the pyrazoleplatinum(II) derivative [(C$_6$Cl$_5$)$_2$Pt(Hpz)$_2$][10a].

Table 1. IR (toluene) and ^{1}H-NMR (CD_2Cl_2, 198 K) data for complexes **1**−**8**

	Complex	IR [cm^{-1}]	^{1}H NMR					
			δ				$J_{3,4}$ [Hz]	$J_{5,4}$ [Hz]
		ν̃(CO)	C(4)−*H*[a]	C(3)−*H*[b]	C(5)−*H*[b]	**N**−H		
1	[Re(CO)$_3$(Hpz)$_2$Br]	2031, 1929, 1897	6.29	7.53	7.65	11.2	1.80	2.20
2	[Re(CO)$_3$(Hdmpz)$_2$Br]	2028, 1925, 1893	5.96	2.20[c]	2.27[c]	10.7	–	–
3	[Re$_2$(CO)$_6$(pz)$_2$Br](Et$_3$NH)	2008, 1899 (br.)	6.11	7.77	7.77	1.73[d]	2.05	2.05
			6.17	7.80	7.80		1.99	1.99
4	[Re(CO)$_3$(Hpz)$_2$(pz)]	2024, 1916, 1902	6.35	7.67	7.80	14.6	1.75	2.37
6	[Re(CO)$_3$(Hpz)(pz)(py)]	2023, 1915, 1898	6.28	7.55	7.85	18.2	1.95	2.15
7	[Re(CO)$_3$(Hdmpz)$_2$(dmpz)]	2018, 1907, 1893	5.79	2.02[c]	2.13[c]	13.1	–	–
8	[Re(CO)$_3$(Hdmpz)(dmpz)(py)]	2017, 1906, 1893	5.76	2.04[c]	2.15[c]	17.8	–	–

[a] Triplets or pseudo-triplets − [b] Doublets − [c] C*H*$_3$ signals − [d] Et$_3$N*H*$^+$, other signals at 1.22 (t, C*H*$_2$) and 3.04 (d, C*H*$_3$).

Scheme 1

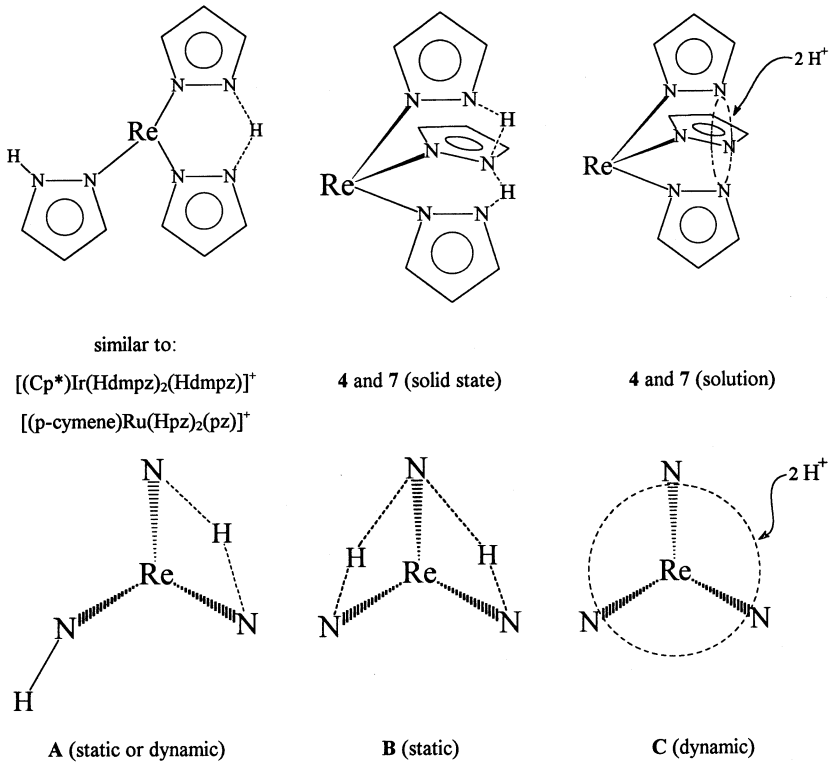

When $[Re(CO)_5Br]$ was treated with Hdmpz, the $[Re(CO)_3(Hdmpz)_2Br]$ species (**2**) was similarly obtained. Its IR spectrum (toluene solution) shows three strong $\tilde{\nu}$(CO) bands at 2028, 1925, and 1893 cm^{-1}. On the basis of a comparison between the IR and ^{1}H-NMR spectra of **1** and **2** (see Table 1) we assign to the latter species a structure identical to **1**. Note, however, the significant red-shift of all resonances, ca. 4 cm^{-1}, caused by the higher basicity of Hdmpz compared to Hpz.

A closely related rhenium(I) species, $[Re(CO)_3(Hdmpz)_2Cl]$, derived by the breakdown of the tridentate pyrazolylborate ligand into pyrazole fragments, was fortuitously obtained by reaction of $[Re(CO)_4Cl]_2$ with $K[HB(dmpz)_3]$[12].

Reaction of 1 with Triethylamine

When monitoring the treatment of $[Re(CO)_3(Hpz)_2Br]$ with Et_3N in toluene at 60°C using IR spectroscopy, the $\tilde{\nu}$(CO) absorptions of the starting complex were observed to disappear along with the simultaneous appearance of a complex pattern of CO bands. The changes in the IR spectrum were accompanied by the formation of a white precipitate. The work-up of the reaction mixture (see Experimental Section) led to the isolation of two rhenium(I) complexes, both exhibiting $\tilde{\nu}$(CO) bands in their IR spectra (eq. 2).

$$[Re(CO)_3(Hpz)_2Br] + Et_3N \rightarrow \mathbf{3} + \mathbf{4} + (Et_3NH)Br \quad (2)$$

Complex **3**, sparingly soluble in toluene, was isolated in an analytically pure form, whereas the second species, **4**, soluble in the reaction medium, was always recovered contaminated by variable amounts of **3**; only by employing an alternative synthetic route was it possible to isolate **4** in a pure form (see later).

Complex **3** shows two strong bands at 2008 and 1899 cm^{-1}, the latter, broader, is probably due to the superposition of two different bands. Additionally, a broad absorption attributable to the $\tilde{\nu}$(N−H) of the triethylammonium cation is also observed. On the basis of elemental analysis and spectroscopic data, the ionic dinuclear formulation $(Et_3NH)[Re_2(CO)_6(pz)_2Br]$ was assigned to complex **3**. As later shown by an X-ray crystal structure analysis, the two rhenium centres are held together by one bromide and two pyrazolate bridges.

Care must be paid in order to exclude moisture from the reaction medium because the presence of adventitious water in solvents or reactants caused the formation of the hydroxo-bridged $(Et_3NH)[Re_2(CO)_6(pz)_2(OH)]$ species (**5**), formally derived by hydrolysis of the bromide bridge in complex **3**, and characterized by an ancillary X-ray diffraction study[13].

Reaction of 1 with Triethylamine in the Presence of Pyrazole

When reaction 2 was carried out in the presence of excess pyrazole, complex **4** could be obtained in analytically pure form as the unique reaction product. On the basis of elemental analysis and spectroscopic data, it was formulated as monomeric $[Re(CO)_3(Hpz)_2(pz)]$ species (**4**) (eq. 3).

$$[Re(CO)_3(Hpz)_2Br] + Et_3N + Hpz \rightarrow [Re(CO)_3(Hpz)_2(pz)]\ (\mathbf{4}) + (Et_3NH)Br \quad (3)$$

The IR spectrum of **4**, recorded in toluene, shows three strong $\tilde{\nu}$(CO) bands at 2024, 1916, and 1902 cm^{-1}, suggesting a *fac* geometry in this case too. An additional broad band centred at about 2850 cm^{-1} (nujol mull) indicates the presence of hydrogen bonds between the pyrazole and pyrazolate groups. The proposed formulation was confirmed by an X-ray diffraction study (see later).

The simultaneous formation of complexes **3** and **4** in reaction 2 can therefore be rationalized by taking into account the stoichiometries of formation of **3** and **4** (eq. 4a and b).

$$2\,[Re(CO)_3(Hpz)_2Br] + 2\,Et_3N \rightarrow (Et_3NH)[Re_2(CO)_6(pz)_2Br]\ (\mathbf{3}) + 2\,Hpz + (Et_3NH)Br \quad (4a)$$

$$[Re(CO)_3(Hpz)_2Br] + Hpz + Et_3N \rightarrow [Re(CO)_3(Hpz)_2(pz)]\ (\mathbf{4}) + (Et_3NH)Br \quad (4b)$$

The pyrazole released in eq. 4a, as a result of the presence of Et_3N, is deprotonated to the pyrazolate anion, which is

Scheme 2

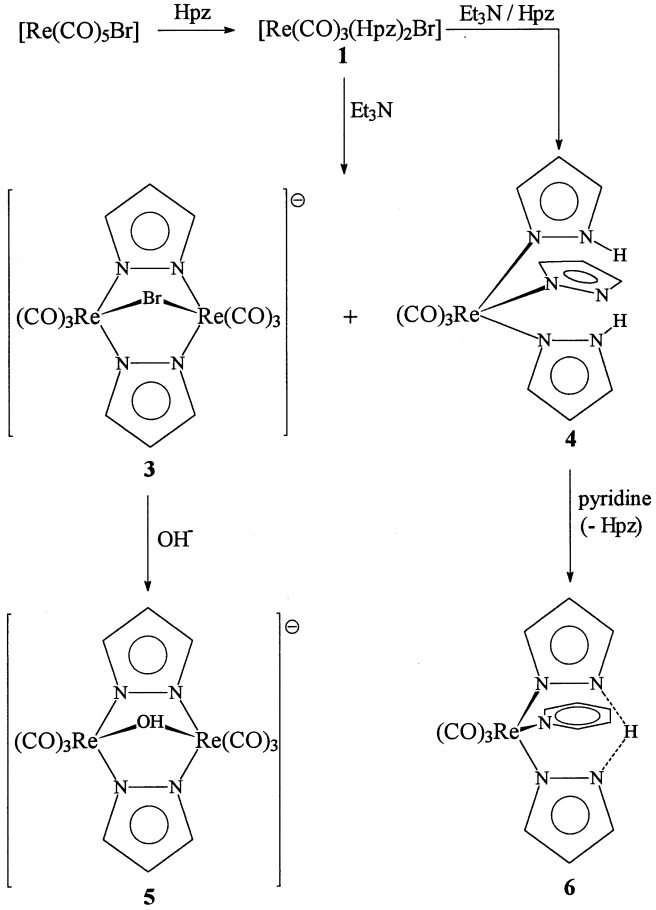

responsible for the nucleophilic substitution of the bromide anion on the starting $[Re(CO)_3(Hpz)_2Br]$ derivative. In the light of these observations, it is reasonable to exclude the intermediacy of **3** in the formation of complex **4** in eq. 3, the more probable reaction pathway being a direct substitution of the terminal bromide anion by the pyrazolate anion generated in situ in the reaction medium.

The ^{1}H-NMR spectrum of **4**, recorded in CD_2Cl_2 at 298 K, shows three resonances: a doublet centred at $\delta = 7.80$ ($J_{4,5} = 2.37$ Hz), a second doublet centred at $\delta = 7.67$ ($J_{3,4} = 1.75$ Hz) and a pseudotriplet (due to partial overlapping of two doublets) at $\delta = 6.35$. In addition, a broad peak at $\delta \approx 13$, due to N−*H*, is found. The spectral features do not change appreciably on lowering the temperature down to 198 K. The first two doublets can easily be assigned to the 3,5 protons of the heterocyclic ring, and, taking into account that $J_{4,5}$ is usually larger than $J_{3,4}$[14], the doublet downfield can likely be assigned to the C(5)−*H* protons. The pseudotriplet is due to the C(4)−*H* coupled to the 3 and 5 protons. As a matter of fact, the ^{1}H-NMR spectrum of **4** clearly shows that both (neutral) pyrazoles and the pyrazolate ligand appear identical on the NMR time scale. Although a static conformation with the two pyrazole *N*-hydrogen atoms sharing the same uncoordinated pyrazolate nitrogen atom cannot be completely ruled out, an (N)−H intramolecular exchange, producing a dynamic hydrogen bonding between the three pyrazole/pyrazolate ligands is probably more realistic. Indeed, of the three conformations which can be envisaged for a $(CO)_3Re(Hpz)_2(pz)$ molecule (see Scheme 1), only a dynamic proton exchange as depicted in C is in full agreement with our spectroscopic observations. It is useful to compare the chemical shift of the N−*H* protons for complex **4** [$\delta = 12.8$ (298 K); 14.6 (198 K)] to that found in the palladium(II) derivative $[Pd(dmpz)_2(Hdmpz)_2]_2$[15] ($\delta = 18.1$, 198 K). In the latter, the presence of very strong hydrogen bonds, shown also by IR bands at 2400 and 1900 cm^{-1}, caused the dramatic downfield shift of the N−*H* signals [free Hdmpz: $\delta = 13.1$ (CD_2Cl_2, 0.5 M)], and the total rigidity of the molecular framework. In contrast, the chemical shift of the N−*H* protons in **4** is close to that of free pyrazole [$\delta = 12.6$ (CD_2Cl_2, 0.5 M)], thus suggesting a rather flexible $(Hpz)_2(pz)$ system with dynamic exchange of the H atoms.

When complex **4** is treated with pyridine, the substitution of only one pyrazole molecule takes place, giving the mononuclear $[Re(CO)_3(py)(Hpz)(pz)]$ (**6**) derivative, (eq. 5).

$$[Re(CO)_3(Hpz)_2(pz)] + py \rightarrow [Re(CO)_3(Hpz)(pz)(py)]\ (\mathbf{6}) + Hpz \quad (5)$$

The IR spectrum of **6** shows, in the carbonyl region, three strong bands at 2023, 1915 and 1898 cm^{-1}. Furthermore, a broad band in the region 3300−3400 cm^{-1}, attributable to hydrogen bonds, is also observed. Significantly, the ^{1}H-NMR spectrum of **6** (toluene, 298 K) shows the N−*H* resonance as a very sharp peak at $\delta = 18.2$, indicating the presence of a strong hydrogen bond equalizing the pyrazole and pyrazolate ligands (as revealed by the signals of the carbon protons of the heterocyclic rings, see Table 1), stabilizing the complex and hampering, in our opinion, the substitution of the second pyrazole molecule, even when reaction 5 is performed with excess pyridine.

*Intra*molecular hydrogen bonds between pyrazole and pyrazolate ligands have been previously observed by ^{1}H-NMR spectroscopy in rhenium(V)[16], iridium(III)[17], palladium(II)[10] and platinum(II)[10] derivatives, and confirmed by means of X-ray crystallography[10][17], but in no case was the chemical shift of the N−*H* protons found so downfield shifted as in **6**.

Employing 3,5-dimethylpyrazole in place of pyrazole, the related $[Re(CO)_3(Hdmpz)_2(dmpz)]$ (**7**) and $[Re(CO)_3(py)(Hdmpz)(dmpz)]$ (**8**) derivatives have been obtained. As revealed by ^{1}H-NMR spectroscopy (see Table 1), the solution behaviour of complexes **7** and **8** is quite similar to that of the related derivatives **4** and **6**, indicating that the steric hindrance of the methyl substituents on the pyrazole ring plays a minor role. A different situation was found for the iridium(III) couple $[(Cp^*)Ir(Hpz)(pz)_2]$ and $[(Cp^*)Ir(Hdmpz)(dmpz)_2]$, where the presence of the more sterically demanding Hdmpz ligand prevented the formation of a (dynamic) *bifurcated* hydrogen bond, such as that observed in the Hpz analogue[17a]. The larger ionic radius is probably responsible for these differences.

A synopsis of the spectroscopic data for complexes **1**−**8** is collected in Table 1, and Scheme 2 summarizes the reactions discussed above.

Crystal Structures of 1, 4 and 6

All these compounds are mononuclear species, packed in space by normal van der Waals contacts. Their ORTEP drawings are shown in Figures 1−3, together with a partial labelling scheme.

Table 2 reports the significant bond lengths and angles for **1**, **4** and **6**. These three compounds belong to the class of octahedral rhenium(I) species, bearing three carbonyl ligands in a *fac* disposition. The remaining coordination sites are occupied by one negatively charged ligand (pyrazolate or bromide) and two neutral fragments, such as pyrazole and/or pyridine. Despite this formal distinction, when both Hpz and pz fragments are present in the same molecule, such as in **4** and **6**, one might suspect that assignment of the Hpz/pz nature could be dubious. This is indeed the case for the hydrogen-bonded ligands of **6**, which, sharing a common H atom [N2−H 1.36(5) and N4−H 1.28(4) Å], show a very short N···N distance of 2.561(8) Å {in agreement with the ^{1}H-NMR spectrum and with other pyrazole/pyrazolato complexes such as $[M(C_6F_5)(Hpz)(pz)]$, (M = Pd, Pt)[10a], $[Zn_2(Hdmpz)_2(dmpz)_4]$[18], $[Co(Hdmpz)_2(dmpz)_4]$[19], $[(\eta^5\text{-}C_5Me_5)Ir(dmpz)_2(Hdmpz)]$[17a] and $[(\eta^6\text{-p-cymene})Ru(Hpz)_2(pz)]^+$[20]}.

In contrast, the situation in **4** is much clearer: Two H atoms are bound to two (different) neutral ligands, with both N−H vectors pointing toward the bare nitrogen atom of the

Figure 1. ORTEP drawing of the $[Re(CO)_3(Hpz)_2Br]$ species with partial labelling scheme; thermal ellipsoids drawn at the 30% probability level; hydrogen atoms are omitted for clarity; primed atoms are generated by the $-x, y, -z - 1/2$ symmetry operation

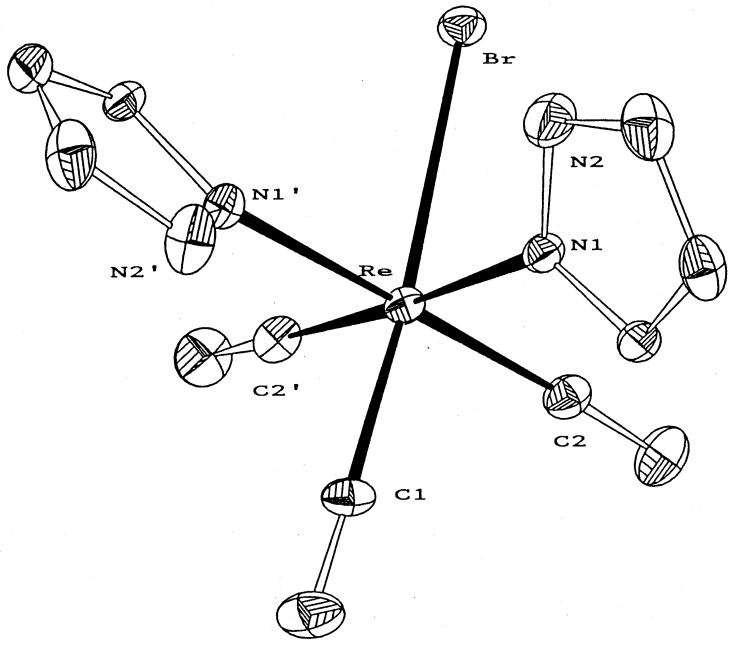

Figure 2. ORTEP drawing of the $[Re(CO)_3(Hpz)_2(pz)]$ species with partial labelling scheme; thermal ellipsoids drawn at the 30% probability level; hydrogen atoms connected to carbon vatoms are omitted for clarity; at the drawing resolution, the other independent molecule looks similar

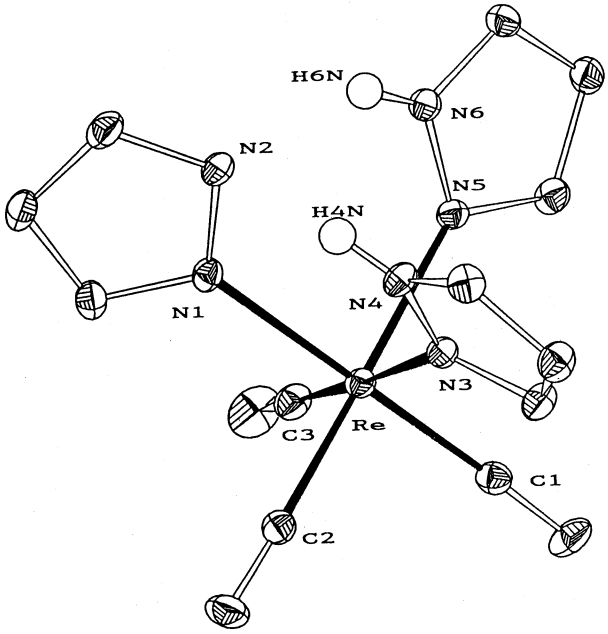

Figure 3. ORTEP drawing of the $[Re(CO)_3(Hpz)(pz)(py)]$ species with partial labelling scheme; thermal ellipsoids drawn at the 30% probability level; hydrogen atoms connected to carbon atoms are omitted for clarity

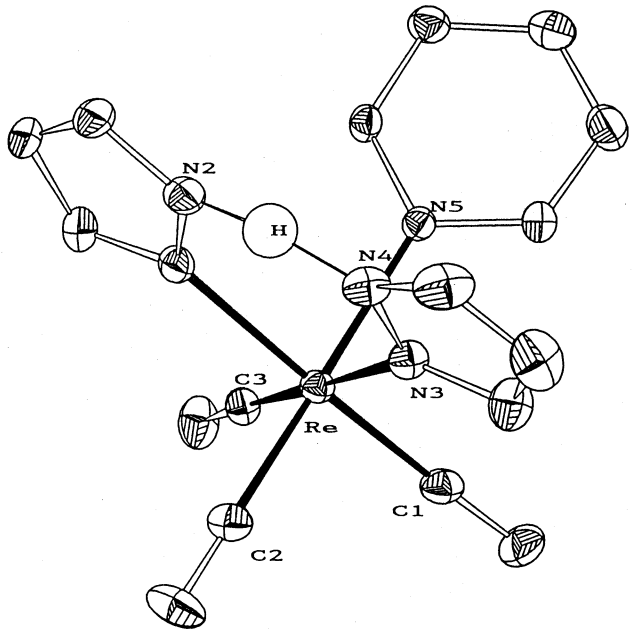

remaining pz fragment [four N−H···N interactions in the range 2.749(7)−2.883(6) Å]. This is indeed observed in both crystallographically independent molecules and confirmed by an ancillary successful crystal-structure determination of **7**[21], with a (crystallographically unique) N−H···N contact of 2.751 Å, clearly demonstrating the N−H···N···H−N nature of this interaction. Therefore, *in the solid state*, molecules of **4** and **7** are better represented by the static picture B (see Scheme 1). When no pyrazolates are present, such as in **1**, the nitrogen atoms of the neutral Hpz ligands in A are found to lie far apart from each other (ca. 5.27 Å). However, a short N−H···Br *inter*molecular hydrogen bond is present in

Table 2. Selected bond lengths [Å] and angles [°] for **1**, **4** and **6**; e.s.d.'s in parentheses

	1	**4**[a]	**6**
Re−C avg.	1.94	1.913	1.888
Re−C1	1.94(4)	1.924(5)	1.882(6)
Re−C2	1.921(9)	1.915(4)	1.881(6)
Re−C3	1.913(5)	1.902(6)	
Re2−C13		1.902(5)	
Re2−C14		1.913(5)	
Re2−C15		1.910(5)	
C−O avg.	1.13	1.152	1.171
C1−O1	1.12(4)	1.152(5)	1.184(6)
C2−O2	1.132(10)	1.156(5)	1.171(6)
C3−O3	1.139(5)	1.157(5)	
C13−O13		1.161(5)	
C14−O14		1.150(5)	
C15−O15		1.152(5)	
Re−C1−O1	178(2)	176.4(4)	177.9(5)
Re−C2−O2	178.5(8)	178.5(4)	179.0(5)
Re−C3−O3	178.7(5)	177.6(5)	
Re2−C13−O13		176.2(4)	
Re2−C14−O14		179.1(5)	
Re2−C15−O15		178.4(4)	
Re−N1	2.187(6)	2.187(3)	2.183(4)
Re−N3	2.211(3)	2.191(4)	
Re−N5	2.195(3)	2.227(4)	
Re2−N7		2.188(3)	
Re2−N9		2.199(3)	
Re2−N11		2.190(3)	
Re−Br	2.641(5)		
N···H···N		2.877(5)	2.561(8)
		2.755(4)	
		2.883(6)	
		2.749(7)	

[a] Two independent molecules in the asymmetric unit.

the solid state, with an estimated length of 2.645(8) Å for H2···Br.

In the absence of strained cyclic rings, such as that observed in $Re(CO)_3Cl(died)$ (died = *N*,*N*′-diisopropylethylenediimine), where the N−Re−N angle is as low as 72.72°[22], the *cis* octahedral angles about the rhenium atoms are fairly regular and range from 83.4(2) to 95.7(3)°. Analogously, the digonal geometry of the CO carbon atoms is also maintained [Re−C−O in the range 176.4(4)−179.0(5)°]. In all three compounds the Re−C distances are similar [1.881(6)−1.94(4) Å] and fall close to the mean value observed for the 28 ReC_3N_2X structures (X = F, Cl, Br) deposited in the CCDC file (1.907 Å). If a minor chemical effect is sought, one can envisage that the presence of a more basic[23] ligand (py) in **6** than in **4** (Hpz) slightly shortens the Re−C interactions [from 1.913 (**4**) to 1.888 Å (**6**), typical e.s.d.'s of 0.005 Å]; this effect, i.e. the presence of a stronger π back-donation in **6** than in **4**, can also be seen in the C−O values [1.152 (**4**) vs. 1.171 Å in **6**]. Re−N bond lengths lie in the range 2.183(4)−2.227(4) Å (CCDC avg. value, 2.208 Å).

Crystal Structure of 3

Crystals of **3** contain anionic, dinuclear $[(CO)_3Re(\mu\text{-}pz)_2(\mu\text{-}Br)Re(CO)_3]^-$ species and triethylammonium cations, packed in space by Coulombic forces and weak(er) van der Waals contacts. An ORTEP drawing of the anion is shown in Figure 4, together with a partial labelling scheme and a list of chemically relevant bond lengths and angles. The rhenium atoms in **3** exhibit an octahedral geometry, with *fac*-carbonyl ligands, and fulfil the 18-electron rule without the need for a

Figure 4. ORTEP drawing of the $[Re_2(CO)_6(pz)_2(Br)]^-$ anion with partial labelling scheme; thermal ellipsoids drawn at the 30% probability level[a]

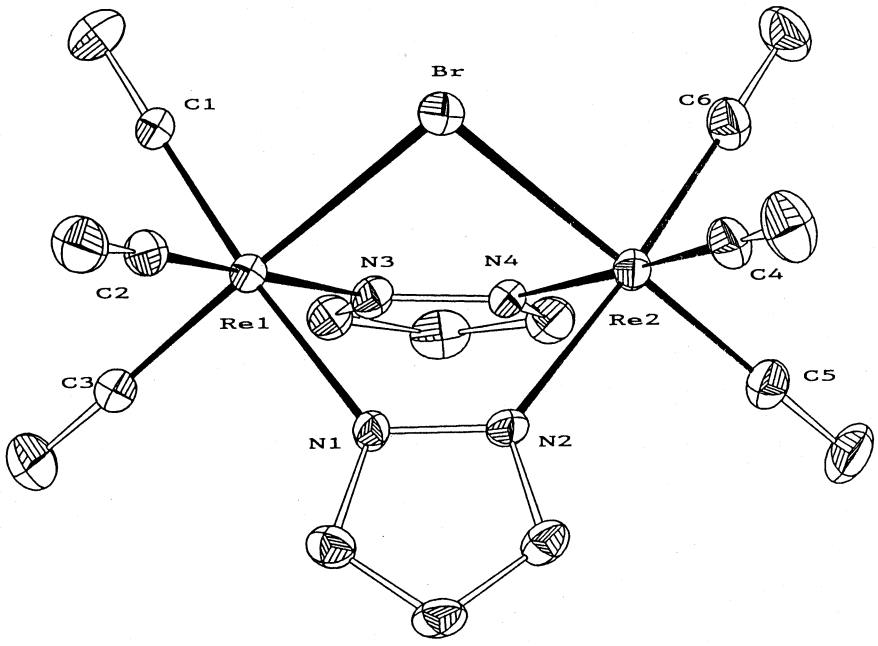

[a] Selected bond lengths [Å] and angles [°]: Re···Re 3.825(1), Re(1)−Br 2.654(1), Re(2)−Br 2.641(1), Re−C avg. 1.895, C−O avg. 1.16; Re(1)−Br−Re(2) 92.51(4), Re−C−O 177(1)−180(1); hydrogen atoms are omitted for clarity.

direct metal−metal bond. The $[(CO)_3Re(\mu\text{-}pz)_2(\mu\text{-}Br)Re(CO)_3]^-$ anion represents the first structurally characterized species containing rhenium(I) atoms bridged by μ-pyrazolate ligands.

A similar rhenium(V) species $[ReO\{\eta^2\text{-}B(pz)_4\}(\mu\text{-}pz)]_2(\mu\text{-}O)$, has been recently reported[16], and showed a nonbonding Re···Re interaction of 3.425 Å. In addition, the synthesis and spectroscopic properties of an oxorhenium(VII) species, possibly a dimer containing two pz bridges, $[ReO_3(\mu\text{-}pz)]_2$, have long been known[24], but, in the absence of single crystals of suitable quality, this species could not be characterized any further. Therefore, the observed nonbonding Re−Re separation, 3.825(1) Å, cannot usefully be compared to other cases. However, it appears, among pyrazolato-bridged complexes, to be rather long, even though rare examples with exceptionally distant metals (up to 4.56 Å) have been reported for polydentate complex pyrazolates[25]. In spite of the presence of a triple (pz, pz, Br) bridge which, avoiding overcrowding of ligands at the metal centres, should shorten the Re···Re distance, such a long Re···Re contact is certainly determined by the simultaneous presence of large metals (leading to Re−N distances of about 2.17 Å) and a rather bulky bridging anion, the bromide, with Re−Br interactions of about 2.65 Å. The above observations agree well with the coordination versatility of pz groups (which are known to form single- to quadruple-bridged[26] systems), capable of bridging metal atoms which are as close as 2.353 Å or even acting as *endo*bidentate η^2 ligands[9b][27]. Also in this case, *inter*molecular hydrogen bonds are found. Indeed, if the nitrogen-bonded proton is added to the triethylammonium cation in the ideal position, one can devise an N−H···Br contact with a Br···H distance of, say, 2.90 Å. During our studies of the crystal structure of **3**, a crystal which eventually was characterized as the product of bromine hydrolysis, containing hydroxo, rather than bromide, bridges[13] came fortuitously to our attention. In order to maintain the hydrogen-bond network, which properly stabilizes the crystal, an extra water molecule was found in its asymmetric unit, leading to a $\mu\text{-}OH\cdots(H_2O)\cdots H-N(Et)_3$ fragment replacing the $Br\cdots H-N(Et)_3$ contact of **3**. In **5**, as expected, replacement of Br by a smaller hydroxo group lowers the intermetallic distance to 3.659(1) Å.

Conclusion

The synthesis and structural properties of a series of mononuclear and dinuclear pyrazolate complexes of rhenium(I) have been described. In particular, we foresee that the mononuclear derivatives $[Re(CO)_3(Hpz)_2(pz)]$ (**4**) and $[Re(CO)_3(Hdmpz)_2(dmpz)]$ (**6**) may act as useful synthetic precursors in building heteropolynuclear metal complexes.

In fact, **4** and **6** belong to a limited class of complexes that, from a coordination point of view, are comparable to the protonated tris(pyrazolyl)borate molecules[28]. The other members of this class, $[(\eta^5\text{-}C_5Me_5)Ir(Hpz)(pz)_2]$[17a], $[(\eta^6\text{-}p\text{-cymene})Ru(Hpz)(pz)_2]$[20] and $[(\eta^6\text{-mesitylene})Ru(Hpz)(pz)_2]$[29] when deprotonated to the anionic fragments $[(\eta^5\text{-}C_5Me_5)Ir(pz)_3]^-$, $[(\eta^6\text{-}p\text{-cymene})Ru(pz)_3]^-$ and $[(\eta^6\text{-mesitylene})Ru(pz)_3]^-$, have been shown to behave in some respect as the tris(pyrazolyl)borate anion, acting as organometallic ligands toward a variety of metal ions[29][30].

Accordingly, preliminary results[31] with group-7 and -11 metals show that, in the presence of appropriate deprotonating agents, complex **4** results in the dianionic species $[Re(CO)_3(pz)_3]^{2-}$, capable of coordination through the lone pairs of the three monodentate pyrazolate groups on a single or on two different metal centres, leading to bi- and trimetallic species. In this way, an analogy with the Kläui tripod-like metallorganic ligands such as $[(\eta^5\text{-}C_5H_5)M\{P(O)R_2\}_3]^-$ (M = Co, Rh) can be drawn[32]. Finally, the use of complexes **4** and **6** in the synthesis of bimetallic derivatives with potential catalytic applications is currently under investigation and will be the subject of a forthcoming paper.

This work was supported by the *Ministero dell' Università e della Ricerca Scientifica e Tecnologica* (*MURST*) and by the *Italian Consiglio Nazionale delle Ricerche* (*CNR*). The technical support of Mr. *Gianni Mezza* is also acknowledged.

Experimental Section

General: Solvents were dried and purified by standard methods. Pyrazole and 3,5-dimethylpyrazole (Aldrich Chemical Co.) were used as supplied. $[Re(CO)_5Br]$ was prepared according to literature procedures[33]. − Infrared spectra were taken with a BIO RAD FTIR 7 instrument. − ^{1}H-NMR spectra were acquired with a Bruker AC-200 FT spectrometer operating at 200.13 MHz. − Elemental analyses (C, H, N) were performed at the Microanalytical Laboratory of this University. All reactions were carried out under dry nitrogen using standard Schlenk techniques.

[Re(CO)$_3$(Hpz)$_2$Br] (**1**): $[Re(CO)_5Br]$ (400 mg, 0.98 mmol) was dissolved in 10 ml of toluene and solid pyrazole (200 mg, 2.94 mmol) was added under stirring. The solution was kept at 80°C until no change in the IR spectrum was observed (about 4 h) and then concentrated to dryness. The white residue was treated with 3 ml of water, filtered off and dried under vacuum (414 mg, 87%). − $C_9H_8BrN_4O_3Re$ (486): calcd. C 22.23, H 1.66, N 11.53; found C 22.22, H 1.67, N 11.52. − Crystals suitable for X-ray structure analysis were obtained by slow diffusion of *n*-hexane into a dichloromethane solution of **1**.

[Re(CO)$_3$(Hdmpz)$_2$Br] (**2**): Prepared in a similar way, employing 3,5-dimethylpyrazole in place of pyrazole (yield 85%). − $C_{13}H_{16}BrN_4O_3Re$ (542): calcd. C 28.78, H 2.98, N 10.33; found C 28.85, H 2.84, N 10.34.

(Et$_3$NH)[Re$_2$(CO)$_6$(pz)$_2$(Br)] (**3**): To a toluene solution of **1** (400 mg, 0.823 mmol) maintained at 50°C, triethylamine (0.5 ml) was added under stirring. In a few minutes a white precipitate formed. After 6 h, the solid was separated by filtration, washed with water (2 ml), and dried under vacuum (yield about 30%). − $C_{18}H_{22}BrN_5O_6Re_2$ (857): calcd. C 25.20, H 2.59, N 8.17; found C 25.28, H 2.65, N 8.21. − The mother liquors were concentrated to dryness and the residue treated with water. A mixture of variable amounts of **3** and **4** (on the basis of the IR spectrum) was always obtained (see text).

[Re(CO)$_3$(Hpz)$_2$(pz)] (**4**): $[Re(CO)_5Br]$ (1.03 g, 2.54 mmol) was added to a solution of pyrazole (0.920 g, 13.5 mmol) in toluene (20 ml) containing 0.5 ml of triethylamine. The solution was maintained

Table 3. Summary of X-ray single-crystal data and structure-refinement parameters

Compound	**1**	**3**	**4**	**6**
Formula	$C_9H_8BrN_4O_3Re$	$C_{18}H_{22}BrN_5O_6Re_2$	$C_{12}H_{11}N_6O_3Re$	$C_{14}H_{12}N_5O_3Re$
Formula weight	486.30	856.72	473.47	484.49
Crystal system	Monoclinic	Monoclinic	Monoclinic	Monoclinic
Space group	*C*2/*c*	$P2_1/n$	$P2_1/n$	$P2_1/n$
a [Å]	7.247(3)	8.189(2)	15.699(3)	9.049(4)
b [Å]	14.258(4)	16.190(4)	13.173(4)	12.356(4)
c [Å]	13.029(3)	18.983(4)	16.376(4)	14.427(4)
β [°]	91.31(4)	99.53(2)	115.13(2)	93.17(2)
V [Å^3]	1345.9(7)	2482.1(10)	3066.0(13)	1610.6(10)
Z	4	4	8	4
F(000)	896	1592	1792	920
D(calcd.) [g cm^{-3}]	2.400	2.293	2.051	1.998
Temperature [K]	293(2)	293(2)	293(2)	293(2)
Diffractometer	CAD4	SMART	SMART	SMART
Radiation [Å]	0.71069	0.71069	0.71069	0.71069
Absorption coeff [mm^{-1}]	12.002	11.396	7.948	7.566
Crystal size [mm]	400 × 80 × 50	200 × 100 × 100	200 × 80 × 20	40 × 40 × 40
Scan method	ω	ω	ω	ω
Scan interval [°]	1.0 + 0.35 tan θ	0.30[a]	0.30[a]	0.30[a]
Max time per refl. [s]	50	30[a]	40[a]	60[a]
θ range [°]	3.13−24.97	1.66−26.90	1.51−26.84	2.17−26.97
Index ranges	$-8 \le h \le 8$, $0 \le k \le 16$, $0 \le l \le 15$	$-10 \le h \le 6$, $-16 \le k \le 19$, $-22 \le l \le 23$	$-19 \le h \le 19$, $-16 \le k \le 12$, $-11 \le l \le 23$	$-10 \le h \le 11$, $-15 \le k \le 12$, $-12 \le l \le 18$
Reflections collected	1185	12734	15039	8202
Independent reflections	1185 [*R*(int) = 0.0000]	4786 [*R*(int) = 0.0324]	5892 [*R*(int) = 0.0208]	3093 [*R*(int) = 0.0391]
Crystal decay	none	none	none	none
Min. transmission factor	0.294	0.637	0.621	0.804
Refinement method		*Full-matrix least-squares on F_o^2		
Obsd. reflection criterion	> 2σ(*I*)	> 2σ(*I*)	> 2σ(*I*)	> 2σ(*I*)
Data/restraints/parameters	1185/0/96	4786/6/254	5892/0/397	3093/2/212
Goodness-of-fit[b] on F_o^2	1.386	1.022	0.929	0.921
R indices[c] [$F_o > 4\sigma(F_o)$] *R*1, *wR*2	0.0230, 0.0924	0.0414, 0.0904	0.0199, 0.0434	0.0286, 0.0362
R indices (all data) *R*1, *wR*2	0.0252, 0.0939	0.0720, 0.1005	0.0291, 0.0444	0.0605, 0.0396
Largest diff. peak and hole [e Å^{-3}]	1.017 and −1.036	1.220 and −1.249	0.327 and −1.272	0.495 and −0.513
Weighting scheme[d] [a]	0.0587	0.0494	0.0188	0.0085

[a] Frame width and exposure time per frame. − [b] $GOF = [\Sigma w(F_o^2 - F_c^2)^2/(n-p)]^{1/2}$ (where *n* is the number of reflections and *p* is the number of refined parameters). − [c] $R1 = \Sigma\|F_o| - |F_c\| / \Sigma|F_o|$, $wR2 = [\Sigma w(F_o^2 - F_c^2)^2 / \Sigma wF_o^4]^{1/2}$. − [d] $w = 1/[\sigma(F_o^2) + (a\,P)^2]$ where $P = (F_o^2 + 2F_c^2)/3$.

under stirring at 80°C for 6 h, the formation of $(Et_3NH)Br$, insoluble in the reaction medium, being observed. The solvent was then evaporated to dryness and the residue dissolved in the minimum amount of ethanol (2 ml). The addition of water caused the precipitation of **4** as a white product. The product was filtered, washed with water and dried under vacuum (yield 1.08 g, 90%). − $C_{12}H_{11}N_6O_3Re$ (474): calcd. C 30.38, H 2.34, N 17.72; found C 30.50, H 2.24, N 17.34.

[Re(CO)$_3$(Hdmpz)$_2$(dmpz)] (**7**): Obtained in a similar way employing Hdmpz (yield 90%). − $C_{18}H_{23}N_6O_3Re$ (558): calcd. C 38.70, H 4.15, N 15.05; found C 38.52, H 4.01, N 14.91. − Crystals suitable for X-ray structure analysis were obtained by slow concentration of toluene solutions of **4** or **7**.

[Re(CO)$_3$(py)(Hpz)(pz)] (**6**): Pyridine (1 ml) was added to a solution of **4** (300 mg, 0.634 mmol) in toluene. The clear solution was maintained under stirring at 50°C for 3 h. The solvent was then evaporated to dryness and the residue was dissolved in ethanol (1 ml). Addition of water caused the precipitation of **6** as a white product. The complex was filtered, washed with water and dried under vacuum (yield 240 mg, 78%). − $C_{14}H_{12}N_5O_3Re$ (485): calcd. C 34.64, H 2.49, N 14.43; found C 34.64, H 2.52, N 14.37. −Crystals suitable for X-ray structure analysis were obtained from an *n*-hexane solution of complex **6** kept at −25°C.

[Re(CO)$_3$(Hdmpz)(dmpz)(py)] (**8**): Obtained similarly starting from complex **7** (yield 80%). − $C_{18}H_{20}N_6O_3Re$ (555): calcd. C 38.91, H 3.63, N 15.14; found C 39.40, H 3.57, N 15.53.

Crystallography[34]: Crystals of **1**, **3**, **4** and **6** were studied by conventional single-crystal X-ray methods; an overview of the methodology used can be found in ref.[35]. A list of crystal data, refinement parameters and final agreement factors is reported in Table 3.

[1] [1a] S. Trofimenko, *Chem. Rev.* **1972**, *72*, 497−509. − [1b] S. Trofimenko, *Prog. Inorg. Chem.* **1986**, *34*, 115−210. − [1c] G. La Monica, G.A. Ardizzoia, *Prog. Inorg. Chem.* **1997**, *46*, 151−238. − [1d] J. E. Cosgriff, G. B. Deacon, *Angew. Chem.* **1998**, *110*, 298−299; *Angew. Chem. Int. Ed.* **1998**, *37,* 286−287.

[2] [2a] N. Masciocchi, M. Moret, P. Cairati, A. Sironi, G.A. Ardizzoia, G. La Monica, *J. Am. Chem. Soc.* **1994**, *116*, 7668−7676. − [2b] M. K. Ehlert, S. J. Rettig, A. Storr, R. C. Thompson, J. Trotter, *Can. J. Chem.* **1990**, *68*, 1444−1449. − [2c] G. A. Ardizzoia, S. Cenini, G. La Monica, N. Masciocchi, M. Moret, *Inorg. Chem.* **1994**, *33,* 1458−1463. − [2d] H. H. Murray, R. G. Raptis, J. P. Fackler, Jr. *Inorg. Chem.* **1988**, *27*, 26−33. − [2e] R. G. Raptis, J. P. Fackler, Jr. *Inorg. Chem.* **1988**, *27*, 4179−4182.

[3] [3a] G. A. Ardizzoia, M. Angaroni, G. La Monica, N. Masciocchi, M. Moret, *J. Chem. Soc., Dalton Trans.* **1990**, 2277−2281. − [3b] G. A. Ardizzoia, E. M. Beccalli, G. La Monica, N. Masciocchi, M. Moret, *Inorg. Chem.* **1992**, *31*, 2706−2711. − [3c] M. Angaroni, G. A. Ardizzoia, G. La Monica, E. M. Beccalli, N. Masci-

occhi, M. Moret, *J. Chem. Soc., Dalton Trans.* **1992**, 2715−2721.
[4] G. A. Ardizzoia, M. Angaroni, G. La Monica, F. Cariati, S. Cenini, M. Moret, N. Masciocchi, *Inorg. Chem.* **1991**, *30*, 4347−4353.
[5] R. J. Angelici, F. Basolo, A. J. Poe, *J. Am. Chem. Soc.* **1963**, *85*, 2215−2219.
[6] [6a] A. M. Sladkov, N. A. Vasneva, A. A. Johansson, V. V. Derunov, *Inorg. Chim. Acta* **1977**, *25*, L97−L99. − [6b] J. R. Wagner, D. G. Hendricker, *J. Inorg. Nucl. Chem.* **1975**, *37*, 1375−1379.
[7] [7a] D. A. Brown, R. T. Sane, *J. Chem. Soc. A* **1971**, 2088−2090. − [7b] E. W. Abel, G. Wilkinson, *J. Chem. Soc.* **1959**, 1501−1505.
[8] The numbering scheme of pyrazole and derivatives usually consider the heterocyclic ring as a 1*H*-azole coordinated to the metal centre through the N-2 lone pair.
[9] [9a] A. L. Bandini, G. Banditelli, F. Bonati, G. Minghetti, F. De Martin, M. Manassero, M. *J. Organomet. Chem.* **1984**, *269*, 91−105. − [9b] D. Röttger, G. Erker, M. Grehl, R.Fröhlich, R. *Organometallics* **1994**, *13*, 3897−3902.
[10] [10a] G. Lopez, J. Ruiz, C. Vicente, J. M. Martì, G. Garcia, P. A. Chaloner, P. B. Hitchcock, R. M. Harrison, *Organometallics* **1992**, *11*, 4090−4096. − [10b] H. Daamen, A. Oskam, D. J. Stufkens, H. W. Waaijers, *Inorg. Chim. Acta* **1979**, *34*, 253−260.
[11] G. W. Bushnell, K. R. Dixon, D. T. Eadie, S. R. Stobart, *Inorg. Chem.* **1981**, *20*, 1545−1552.
[12] J. A. McCleverty, I. Wolochowicz, *J. Organomet. Chem.* **1979**, *169*, 289−291.
[13] Crystal data for $(Et_3NH)[(CO)_3Re(\mu\text{-}pz)_2(\mu\text{-}OH)Re(CO)_3]\cdot H_2O$: $C_{18}H_{25}N_5O_8Re_2$, formula weight 811.83 $gmol^{-1}$; monoclinic, *Cc*; a = 13.875(4), b = 13.573(2), c = 13.771(2) Å, β = 101.96(1)°; V = 2537.1(9) Å^3, μ = 95.8 cm^{-1}; Z = 4; $\rho_{calcd.}$ = 2.125 g cm^{-3}; $R1$ = 0.020 and $wR2$ = 0.039 for 4802 observed data [$I > 4\sigma(I)$] and 258 refined parameters.
[14] A. R. Katritzky, in *Comprehensive Heterocyclic Chemistry* (Eds.: A. R. Katritzky, C. W. Rees), Pergamon Press, Oxford, **1984**, vol. 5, p. 182.
[15] G. A. Ardizzoia, G. La Monica, S. Cenini, M. Moret, N. Masciocchi, *J. Chem. Soc., Dalton Trans.* **1996**, 1351−1357.
[16] A. Paulo, A. Domingos, I. Santos, *Inorg. Chem.* **1996**, *35*, 1798−1807.
[17] [17a] D. Carmona, L. A. Oro, M. P. Lamata, J. Elguero, M. C. Apreda, C. Foces-Foces, F. H. Cano, F.H. *Angew. Chem.* **1986**, *98*, 1091−1092; *Angew. Chem. Int. Ed. Engl.* **1986**, *25*, 1114−1115. − [17b] D. Carmona, L A. Oro, M. P. Lamata, M. L. Jimeno, J. Elguero, A. Belguesi, P. Lux, P. *Inorg. Chem.* **1994**, *33*, 2196−2203.
[18] M. K. Ehlert, S. J. Rettig, A. Storr, R. C. Thompson, J. Trotter, *Can. J. Chem.* **1990**, *68*, 1494−1498.
[19] M. K. Ehlert, S. J. Rettig, A. Storr, R. C. Thompson, J. Trotter, *Can. J. Chem.* **1993**, *71*, 1425−1436.
[20] D. Carmona, J. Ferrer, L. A. Oro, M. C. Apreda, C. Foces-Foces, F. H. Cano, J. Elguero, M. L. Jimeno, *J. Chem. Soc., Dalton Trans.* **1990**, 1463−1476.
[21] Crystal data for $[(CO)_3Re(Hdmpz)_2(dmpz)]$: $C_{18}H_{23}N_6O_3Re$, formula weight 557.62 $gmol^{-1}$; monoclinic, $P2_1/m$; a = 8.135(1), b = 14.119(3), c = 9.464(1) Å, β = 97.93(1)°; V = 1076.6(3) Å^3, μ = 56.7 cm^{-1}; Z = 2; $\rho_{calcd.}$ = 1.720 g cm^{-3}; $R1$ = 0.022 and $wR2$ = 0.061 for 1806 observed data [$I > 4\sigma(I)$] and 147 refined parameters.
[22] A. J. Graham, D. Arkigg, B. Sheldrick, B. *Cryst. Struct. Commun.* **1977**, *6*, 577−586.
[23] J. Reedijk in *Comprehensive Coordination Chemistry* (Eds.: G. Wilkinson, R. D. Gillard, J. A. McCleverty), Pergamon Press, Oxford, **1987**, vol. 2, p. 73.
[24] I. A. Degnan, W. A. Hermann, E. Herdtwek, *Chem. Ber.* **1990**, *123*, 1347−1349.
[25] N. Sakagami, M. Nakahanada, K. Ino, A. Hioki, S. Kaizaki, *Inorg. Chem.* **1996**, *35*, 683−688.
[26] A. R. Barron, G. Wilkinson, M. Motevalli, H. B. Hursthouse, *Polyhedron* **1985**, *4*, 1131−1134.
[27] [27a] C. W. Eigenbrot, Jr., K. N. Raymond, *Inorg. Chem.* **1981**, *20,* 1553−1556. − [27b] C. W. Eigenbrot, Jr., K. N. Raymond, *Inorg. Chem.* **1982**, *21,* 2653−2660. − [27c] I. A. Guzei, G. A. Baboul, G. P. A. Yap, A. L. Rheingold, H. B. Schegel, C. H. Winter, *J. Am. Chem. Soc.* **1997**, *119*, 3387−3388. − [27d] I. A. Guzei, G. P. A. Yap , C. H. Winter, *Inorg. Chem.* **1997**, *36*, 1738−1739.
[28] S. Trofimenko, *Chem. Rev.* **1993**, *93*, 943−980.
[29] D. Carmona, F. J. Lahoz, R. Atencio, A. J. Edwards, L. A. Oro, M. P. Lamata, M. Esteban, S. Trofimenko, *Inorg. Chem.* **1996**, *35*, 2549−2557.
[30] [30a] D. Carmona, F. J. Lahoz, L. A. Oro, M. P. Lamata, S. Buzarra, S. *Organometallics* **1991**, *10*, 3123−3131. − [30b] D. Carmona, L. A. Oro, M. P. Lamata, M. L. Jimeno, J. Elguero, A. Belguise, P. Lux, *Inorg. Chem.* **1994**, *33*, 2196−2203. − [30c] D. Carmona, J. Ferrer, R. Atencio, F. Lahoz, L. A. Oro, M. P. Lamata, *Organometallics* **1995**, *14*, 2057−2065.
[31] G. A. Ardizzoia, G. La Monica, A. Maspero, N. Masciocchi, M. Moret, *25th Italian Chemical Society Meeting − Inorganic Division*, Alessandria (Italy), **1997**, September 1−5, Abstract P10.
[32] W. Kläui, *Angew. Chem.* **1990**, *102*, 661−671; *Angew. Chem. Int. Ed. Engl.* **1990**, *29*, 627−637.
[33] M. O. Albers, E. Singleton, N. J. Coville, *Inorg. Synth.* **1990**, *28*, 160−165.
[34] Crystallographic data for the structure reported in this paper have been deposited with the Cambridge Crystallographic Data Centre as supplementary publication no. CCDC-101428. Copies of the data can be obtained free of charge on application to CCDC, 12 Union Road, Cambridge CB2 1EZ, UK.
[35] G. A. Ardizzoia, A. Maspero, G. La Monica, M.Moret, N. Masciocchi, *Inorg. Chem.* **1997**, *36*, 2321−2328

[98137]

A Preliminary Study of Host-Guest Interactions in Polymeric Clathrates – An Ab Initio Study of the Model Complexes Benzene/X_2 (X = F, Cl, Br, I)

Giuseppe Milano[a], Gaetano Guerra[a], and Luigi Cavallo*[b]

Dipartimento di Chimica, Università di Salerno[a],
Baronissi, I-84081 Salerno, Italy

Dipartimento di Chimica, Università degli Studi di Napoli "Federico II"[b],
Via Mezzocannone 4, I-80134 Napoli, Italy
E-mail: cavallo@chemna.dichi.unina.it

Received May 7, 1998

Keywords: Arene complexes / Ab initio calculations / Polymeric clathrates / Host-guest chemistry

A systematic ab initio investigation of the complexes benzene/halogen molecules is presented. For the whole halogen series, the T-shaped geometry is clearly favored relative to the sandwich geometry. This preference is rationalized in terms of the electrostatic fields generated by the interacting molcules. Higher binding energies have been calculated on going from /F_2 to /I_2 molecular complexes.

Introduction

Van der Waals interactions of aromatic systems are of considerable interest because they often play an important structure-determining role. These interactions control such diverse phenomena as porphyrin aggregation, the packing of aromatic molecules, and the base-base interactions in DNA. For this reason, a large number of experimental as well as theoretical papers have been devoted to the study of the weak interactions in prototype systems of the type benzene/benzene, benzene/H_2O, benzene/NH_3, benzene/N_2, benzene/alkane, and benzene/hydrogen halide.[1][2]

Another phenomenon of considerable interest that is often controlled by these interactions is the sorption of small molecules in polymers,[3][4] the economic importance of which, e.g. in the packaging industry and in the field of membrane separation processes, is well known. For instance, systematic studies of the sorption of various molecules in amorphous polymeric materials based on atactic polystyrene have allowed correlations to be made between the structures of the small molecules and the relevant sorption parameters.[3] Moreover, studies of the sorption of halogenated aliphatic molecules have led to molecular models of absorption that involve interactions of the halogen atoms with the phenyl groups of the polymeric absorbents.[5] However, experimental and theoretical studies of the molecular interactions responsible for the sorption phenomena are made difficult by the dynamic intramolecular and intermolecular disorder that is characteristic of the swollen polymeric phases.

Recently, semicrystalline polymeric materials based on syndiotactic polystyrene that are able to absorb small molecules, not only in the amorphous phase but also in the cavities of suitable crystalline phases, have been described.[6][7][8][9] It has also been found that the same classes of molecules that are suitable for sorption into atactic polystyrene based samples,[3] are absorbed both into amorphous and crystalline phases of syndiotactic polystyrene samples.[6][7][8][9] Furthermore, it is remarkable that at low activities these small molecules are preferentially (or exclusively) absorbed as guests in the crystalline phase to form clathrates.[9] This suggests that the host-guest interactions in clathrate structures are similar to the interactions between the polymer and small molecules in the amorphous phase.

X-ray diffraction[10][11] and FT-IR-spectroscopic[9] studies on these clathrate samples can give detailed experimental information regarding the molecular interactions that occur between the guest molecules and the host polymer in the crystalline cavities. In particular, the number and distances of the intermolecular interactions, the preferred relative orientations of the guest and host, as well as possible preferential guest conformations can be established. Finally, it is worth noting that the study of host-guest interactions in these polymeric clathrates is also relevant due to the potential applications of nanoporous materials based on syndiotactic polystyrene for water and air purification and, more generally, for chemical separations.[6]

The clathrate structure of syndiotactic polystyrene incorporating two I_2 molecules per cavity has been well characterized by X-ray diffraction study.[7] The I_2 molecule interacts significantly with only two phenyl rings, and the I_2 molecular axis is almost perpendicular to the planes of the phenyl rings. Moreover, X-ray studies of the benzene/Cl_2[12] and benzene/Br_2[13] systems have shown that a T-shaped geometry (see Figure 1), with the halogen molecule almost aligned along the C_{6v} symmetry axis of the benzene, is preferred. Furthermore, IR-spectroscopic studies indicate that an axial or slightly bent structure is also adopted in nitrogen matrices.[14][15] However, despite the great interest in these complexes, a systematic theoretical description of

 © WILEY-VCH Verlag GmbH, D-69451 Weinheim, 1998 1434–1948/98/1010–1513 $ 17.50+.50/0

the benzene/X_2 (X = F, Cl, Br, I) series is still lacking. To the best of our knowledge, of this series only the benzene/I_2 complex has been studied in detail from a theoretical point of view.[16][17][18] For this reason, we have carried out a systematic study of the interactions occurring in the ground state of the model systems benzene/X_2 (X = F, Cl, Br, I) using the second-order Møller-Plesset (MP2) theory.

Methods

The interaction energy, ΔE, of the complexes was evaluated as the sum of the self-consistent field interaction energy, ΔE_{SCF},[19] and the correlation interaction energy, ΔE_{COR},[19] where ΔE_{COR} was calculated using MP2 theory.[19] We applied the supermolecule approach.[1] Thus, the interaction energy was obtained as the difference between the energy of the complex and the energies of the free benzene and halogen molecules. All the calculated interaction energies were basis set superposition error (BSSE) free.[19] For the BSSE evaluation, the counterpoise method of Boys and Bernardi was used.[20] All the calculations were performed using the GAMESS package.[21]

The geometries of the benzene (R_{C-C} = 1.406 and R_{C-H} = 1.08 Å) and halogen molecules (R_{F-F} = 1.34, R_{Cl-Cl} = 1.99, R_{Br-Br} = 2.28, R_{I-I} = 2.68 Å) were kept rigid, and only the distance between the centres of mass of the benzene and halogen molecules, R, was varied. To locate the BSSE-free minimum energy geometries, the potential energy surface was scanned simply by varying the distance R. To save computer time, we used the 6-31G basis set for the C and H atoms,[22] augmented with single d and p polarization functions,[22] respectively, and the SBK effective core potential (ECP) and valence basis set, augmented with a d polarization function, for the halogens.[23] To assess the dependence of the interaction energy on the particular basis set used, single-point energy calculations were performed on the minimum energy geometries obtained from the potential energy surface scan. In these cases, a double-ζ basis set, DZ, augmented with two d polarization functions on the C atoms, was adopted for the benzene.[24] Finally, test calculations were performed using the SBK ECP basis set on the C atoms of the benzene as well. Due to the fact that envisaged extensions of this work will focus on systems of considerably larger size (polymer cavities containing guest molecules), we decided to use basis sets of moderate size only.

Results

As already suggested by other authors,[1] for benzene-containing molecular complexes the total interaction energy is mainly determined by the electrostatic (quadrupole-quadrupole) interaction, essentially included in the ΔE_{SCF} contribution, and by the dispersion energy, essentially included in the ΔE_{COR} contribution. For this reason, the selection of suitable basis sets requires that one-electron properties, in particular the quadrupole moment, Q_{zz}, be reproduced with good accuracy.

Table 1 shows the Hartree-Fock quadrupole moments of the molecules considered in the present study. As reported previously,[1] for the benzene molecule the 6-31G basis set, even augmented by two polarization functions on the carbon atoms, underestimates the quadrupole moment. On the other hand, with the DZ basis set reasonable values for the quadrupole moment are obtained, even in the absence of polarization functions.

Table 1. Quadrupole moments of the benzene and halogen molecules at the Hartree-Fock level

Molecule	Basis set	Polarization exponents	Q_{zz} [a.u.]
C_6H_6	6-31G		−6.59
	6-31G d, p	C: 0.80, H: 1.10	−6.52
	6-31G 2d	C: 1.60, 0.40	−6.36
	DZ		−7.19
	DZ 2d	C:1.5, 0.375	−7.38
	DZ 2d, 2p	C:1.5, 0.375; H: 2.0, 0.5	−7.20
	SBK d	C: 0.80	−6.30
	Experimental[a]		−7.4
F_2	SBK		−0.09
	SBK d	0.80	+0.40
	SBK 2d	1.60, 0.40	+0.48
	Extended basis set[b]		+0.41
	Extended basis set[c]		+0.56
	Experimental[d]		+0.65
Cl_2	SBK		+0.78
	SBK d	0.750	+1.97
	SBK 2d	1.500, 0.375	+2.73
	DZ		+0.95
	DZ 2d	1.500, 0.375	+2.74
	Extended basis set[b]		+2.51
	Extended basis set[e]		+2.26
	Experimental[f]		+2.40
Br_2	SBK		+1.88
	SBK d	0.389	+3.85
	SBK 2d	0.778, 0.195	+4.24
	Extended basis set[b]		+3.55
I_2	SBK		+3.08
	SBK d	0.266	+6.06
	SBK 2d	0.532, 0.133	+6.21
	Extended basis set[b]		+4.17
	Extended basis set[g]		+4.49

[a] J. Vrbancich, G. L. D. Ritchie, *J. Chem. Soc., Faraday Trans. 2* **1980**, *76*, 648. – [b] P. A. Straub, A. D. McLean, *Theo. Chim. Acta* **1974**, *32*, 227. – [c] G. Maroulis, A. J. Thakkar, *J. Chem. Phys.* **1989**, *90*, 366. – [d] G. H. Cheeseman, A. J. T. Finney, *Theo. Chim. Acta* **1970**, *15*, 33. – [e] G. Maroulis, *Chem. Phys. Lett.* **1992**, *199*, 244. – [f] A. D. Buckingham, L. Graham, J. H. Williams, *Mol. Phys.* **1983**, *49*, 703. – [g] G. Maroulis, A. J. Thakkar, *Mol. Phys.* **1991**, *73*, 1235.

On the contrary, for the halogen molecules, both with DZ (for F_2 and Cl_2) and ECP (for the whole series) basis sets, the quadrupole moments are clearly underestimated in the absence of polarization functions. For F_2 and Cl_2, the DZ and ECP basis sets augmented with two polarization functions provide reasonable values of Q_{zz}, whereas for the heavier Br_2 and I_2 halogen molecules Q_{zz} is overestimated.

Table 2 shows the calculated minimum energy distances, BSSE-free, and the interaction energy contributions for the benzene/X_2 molecular complexes. Clearly, the T-shaped geometry is preferred for each of the halogens. This result is in

Table 2. Energy contributions to the total interaction energy, BSSE-free, for the benzene/X_2 molecular complexes in the T-shaped and sandwich geometries

/X_2	Geometry	C_6H_6 Basis Set	Halogen Basis Set	R_e[a] [Å]	ΔE_{SCF} [kcal/mol]	ΔE_{COR} [kcal/mol]	ΔE_{TOT} [kcal/mol]
/F_2	T-shaped	6-31G d,p	SBK d	3.9	+0.33	−1.00	−0.67
	T-shaped	DZ 2d	SBK 2d		+0.36	−1.38	−1.02
	T-shaped	SBK d	SBK d		+0.55	−0.98	−0.43
	Sandwich	6-31G d,p	SBK d	3.8	+0.27	−0.48	−0.21
	Sandwich	DZ 2d	SBK 2d		+0.30	−0.77	−0.47
	Sandwich	SBK d	SBK d		+0.30	−0.52	−0.22
/Cl_2	T-shaped	6-31G d,p	SBK d	4.6	−0.01	−1.10	−1.11
	T-shaped	DZ 2d	SBK 2d		−0.27	−1.99	−2.26
	T-shaped	DZ 2d	DZ 2d		−0.20	−2.00	−2.20
	T-shaped	SBK d	SBK d		+0.21	−1.12	−0.91
	Sandwich	6-31G d,p	SBK d	4.4	+0.38	−0.58	−0.20
	Sandwich	DZ 2d	SBK 2d		+0.46	−1.10	−0.64
	Sandwich	DZ 2d	DZ 2d		+0.48	−1.16	−0.68
	Sandwich	SBK d	SBK d		+0.35	−0.62	−0.27
/Br_2	T-shaped	6-31G d,p	SBK d	4.7	−0.20	−1.88	−2.08
	T-shaped	DZ 2d	SBK 2d		−0.36	−3.06	−3.42
	T-shaped	SBK d	SBK d		+0.18	−1.95	−1.77
	Sandwich	6-31G d,p	SBK d	4.4	+0.71	−1.03	−0.32
	Sandwich	DZ 2d	SBK 2d		+0.64	−1.79	−1.15
	Sandwich	SBK d	SBK d		+0.62	−1.19	−0.57
/I_2	T-shaped	6-31G d,p	SBK d	4.9	+0.17	−2.71	−2.54
	T-shaped	DZ 2d	SBK 2d		+0.05	−4.28	−4.23
	T-shaped	SBK d	SBK d		+0.84	−2.81	−1.97
	Sandwich	6-31G d,p	SBK d	4.6	+0.86	−1.29	−0.43
	Sandwich	DZ 2d	SBK 2d		+0.73	−2.06	−1.33
	Sandwich	SBK d	SBK d		+0.71	−1.40	−0.69

[a] Optimized intermolecular distance, BSSE-free.

agreement with X-ray structural investigations of benzene/Cl_2[12] and benzene/Br_2[13] complexes, which have shown that the T-shaped geometry is the most probable. The minimum energy distances R, between the centres of mass of the benzene and halogen molecules for the T-shaped structures are 3.9, 4.6, 4.7, and 4.9 Å for F_2, Cl_2, Br_2, and I_2, respectively. The calculated values of R are overestimated by roughly 0.3 Å (4.27 and 4.34 Å in the crystalline structures of the benzene/Cl_2 and benzene/Br_2 complexes, respectively). The T-shaped geometry for the benzene/X_2 complexes is also in agreement with the structures indicated by infrared absorption spectra of the Cl_2, Br_2 and I_2 complexes with benzene in nitrogen matrices,[14][15] and with previous ab initio studies on the benzene/I_2 complex.[16][17][18]

As already outlined,[1] the rationalization of the preferred geometry in molecular complexes with benzene is essentially related to the electrostatic interaction (quadrupole-quadrupole) between the two molecules. In order to rationalize the preferred geometry in terms of electrostatic interactions, the electrostatic fields generated by the two interacting molecules are depicted in Figure 1. In the T-shaped geometry, negative and positive regions of the electrostatic potential of the benzene and halogen molecules face each other, whereas in the sandwich geometry regions of electrostatic potential of the same sign face each other. As a consequence, the electrostatic interactions clearly favour the T-shaped geometry relative to the sandwich geometry.

Our analysis is in agreement with the previously reported rationalization based on the quadrupole-quadrupole electrostatic interaction. In order to optimize this interaction, and depending on the sign of the quadrupole moment of

Figure 1. Schematic representation of the T-shaped and sandwich geometries for the benzene/I_2 complex; the distance R between the centres of mass of the two molecules, which was varied during the potential energy surface scan, is indicated; the electrostatic fields generated by the two molecules are also indicated; starting from the 0.0 contours (dotted lines), positive and negative contours of the electrostatic field (continuous and dashed lines, respectively) are shown; the isopotential curves are spaced by 1 kcal/mol

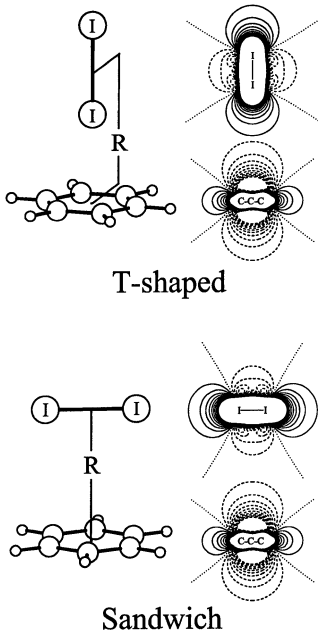

the two molecules that form the molecular complex, either T-shaped (benzene/benzene and benzene/I_2) or sandwich (benzene/N_2) geometries are adopted. Considering that all

the halogen molecules have quadrupole moments of the same sign, it is reasonable to assume that the T-shaped structure is the preferred geometry throughout the benzene/X_2 series.

This rationalization is also supported by the fact that the ΔE_{SCF} contribution always favours the T-shaped geometry. Moreover, the repulsive electrostatic interaction in the sandwich geometry pushes the two molecules far apart, and this reduces the strength of the attractive dispersion interactions. As a consequence, the ΔE_{COR} energy contribution also favours the T-shaped geometry.

As regards the total binding energy, more stable complexes are observed on going from the very weakly bound F_2 to I_2, both for T-shaped and sandwich geometries. The calculated value for the T-shaped benzene/I_2 complex, 2.54 kcal/mol, is in fair agreement with the heat of formation of this complex in the gas phase, as determined by spectrometric methods (2.0−2.6 kcal/mol).[25] Previous ab initio calculations led to binding energies of 1.91[16] and 2.07[18] kcal/mol. By using the DZ basis set for benzene and the SBK ECP set for the halogens, and augmenting these basis sets with two standard polarization functions on the C and halogen atoms, the same trend is observed, i.e. higher binding energies on going from F_2 to I_2. With this basis set, which should be of better quality, the binding energies are probably overestimated. In fact, for the T-shaped benzene/I_2 complex this basis set gives a binding energy of 4.23 kcal/mol. Finally, by using the SBK ECP basis set for the C atoms of benzene as well, results fairly similar to those obtained using the 6-31G basis set are obtained. However, there is a decrease in the energy difference between the sandwich and the more stable T-shaped geometry [ΔE(sandwich − T-shaped) = 0.46, 0.89, 1.76, and 2.11 kcal/mol using the 6-31G basis set for the benzene, and 0.21, 0.52, 1.20, and 1.28 kcal/mol using the SBK ECP basis set for the benzene, for F_2, Cl_2, Br_2, and I_2, respectively].

The results shown in Table 2 clearly indicate that the ΔE_{SCF} contribution is virtually independent of the basis set used, and that the increase in the binding energy is essentially due to the dispersion term, ΔE_{COR}. It is also apparent that the ΔE_{COR} contribution is not yet converged. Due to the fact that we have mixed a DZ basis set with a split-valence ECP basis set, we checked the reasonability of this mixing by using, for the Cl_2 complex only, a DZ all-electron basis set. The results obtained with the ECP were in very good agreement with the all-electron results. Thus, we believe that the basis set mixing that we have used represents a reasonable approximation.

In the last part of our study, we investigated the feasibility of oblique structures. In Figure 2, the BSSE-free interaction energies of the oblique geometries of the benzene/Cl_2 and benzene/I_2 complexes are plotted as a function of the angle α between the halogen−halogen bond and the C_{6v} symmetry axis of the benzene. Since in the bent structures the distance R is not re-optimized, we confined our analysis to structures close to the T-shaped geometry, that is, to values of $\alpha \leq 40°$. The geometries at $\alpha = 0°$ correspond to the minimum energy T-shaped geometries of the Cl_2 and I_2 complexes. It is clear that the T-shaped geometries of the two complexes represent only shallow minima, and that large oscillations might easily be achieved. In fact, α deformations of 20−30° require less than 0.5 kcal/mol. Our results support the hypothesis that in photoexcitation experiments the excitation process occurs in bent conformations, i.e. the conformations with the largest transition moment.[18]

Figure 2. MP2 BSSE-free interaction energy as a function of α for the benzene/Cl_2 and benzene/I_2 complexes; the 6-31G d,p and ECP SBK 2d basis sets were used for the benzene and halogen molecules, respectively

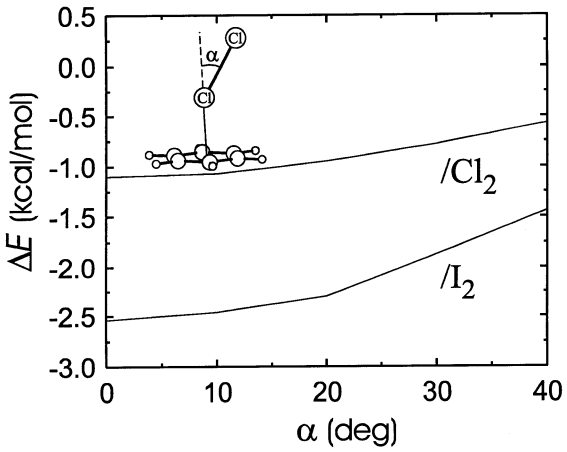

Conclusions

A systematic investigation of benzene/halogen molecule complexes in the ground state has indicated that the T-shaped geometry is preferred relative to the sandwich geometry for each of the halogens. The calculated minimum energy distances for the benzene/Cl_2 and benzene/Br_2 complexes (for which X-ray structures are available) overestimate the experimental values by roughly 0.3 Å. Moreover, irrespective of the particular basis set used, higher binding energies have been calculated on going from benzene/F_2 to benzene/I_2 molecular complexes. The relative stability of the T-shaped and sandwich geometries is essentially determined by the electrostatic quadrupole-quadrupole interaction. This can clearly be visualized in terms of the electrostatic potential generated by the interacting molecules. Finally, we note that the T-shaped geometry represents only a shallow minimum, and that environmental effects (i.e. crystal packing or inert matrices) can reasonably force the adoption of oblique geometries.

We thank Prof. *V. Barone* of the University of Naples and Dr. *A. Peluso* of the University of Salerno for useful discussions. The financial support of the *Ministero dell' Università e della Ricerca Scientifica e Tecnologica* and of the *Consiglio Nazionale delle Ricerche* of Italy is gratefully acknowledged.

[1] P. Hobza, H. L. Selzle, E. W. Schlag, *Chem. Rev.* **1994**, *94*, 1767.
[2] H. J. Neusser, H. Krause, *Chem. Rev.* **1994**, *94*, 1829.
[3] L. A. Errede, *Adv. Polym. Sci.* **1991**, *99*, 1.
[4] L. A. Errede, *J. Phys. Chem.* **1996**, *100*, 9918.

[5] L. A. Errede, *J. Phys. Chem.* **1991**, *95*, 1836.
[6] G. Guerra, C. Manfredi, M. Rapacciuolo, P. Corradini, G. Mensitieri, M. A. Del Nobile. *Ital. CNR RM94A00030 (21/1/94)*.
[7] C. De Rosa, G. Guerra, V. Petraccone, B. Pirozzi, *Macromolecules* **1997**, *30*, 4147.
[8] C. Manfredi, M. A. Del Nobile, G. Mensitieri, G. Guerra, M. Rapacciuolo, *J. Polym. Sci., Polym. Phys. Ed.* **1997**, *35*, 133.
[9] G. Guerra, C. Manfredi, P. Musto, S. Tavone, *Macromolecules* **1998**, *31*, 1329.
[10] Y. Chatani, T. Inagaki, Y. Shimane, H. Shikuma, *Polymer* **1993**, *34*, 4841.
[11] C. De Rosa, P. Rizzo, O. Ruiz de Ballesteros, V. Petraccone, G. Guerra, *Polymer*, in press.
[12] O. Hassel, K. O. Strømme, *Acta Chem. Scand.* **1959**, *13*, 1781.
[13] O. Hassel, K. O. Strømme, *Acta Chem. Scand.* **1958**, *12*, 1146.
[14] L. Fredin, B. Nelander, *Mol. Phys.* **1974**, *27*, 885.
[15] L. Fredin, B. Nelander, *J. Am. Chem. Soc.* **1974**, *96*, 1672. A. Engdahl, B. Nelander, *J. Chem. Phys.* **1983**, *78*, 6563.
[16] E. Kochanski, J. Prissette, *Nouv. J. Chim.* **1980**, *4*, 509.
[17] I. Jano, *Theor. Chim. Acta.* **1985**, *66*, 341.
[18] E. Lenderink, K. Duppen, F. P. X. Everdij, J. Mavri, R. Torre, D. A. Wiersma, *J. Phys. Chem.* **1996**, *100*, 7822.
[19] W. J. Hehre, L. Radom, P. von R. Schleyer, J. A. Pople, *Ab Initio Molecular Orbital Theory*, John Wiley & Sons, New York, **1986**.
[20] S. F. Boys, F. Bernardi, *Mol. Phys.* **1970**, *19*, 553.
[21] M. W. Schmidt, K. K. Baldridge, J. A. Boatz, S. T. Elbert, M. S. Gordon, J. H. Jensen, S. Koseki, N. Matsunaga, K. A. Nguyen, S. Su, T. L. Windus, M. Dupuis, J. A. Montgomery, *J. Comput. Chem.* **1993**, *14*, 1347.
[22] P. C. Hariharan, J. A. Pople, *Theor. Chim. Acta* **1973**, *28*, 213. M. M. Francl, W. J. Hehre, J. S. Binkley, M. S. Gordon, D. J. DeFrees, J. A. Pople, *J. Chem. Phys.* **1982**, *77*, 3654.
[23] W. J. Stevens, H. Basch, M. Krauss, *J. Chem. Phys.* **1984**, *81*, 6026. W. J. Stevens, H. Basch, M. Krauss, *Can. J. Chem.* **1992**, *70*, 612.
[24] T. H. Dunning, *J. Chem. Phys.* **1970**, *53*, 2823.
[25] D. Atack, O. K. Rice, *J. Phys. Chem.* **1954**, *58*, 1017. F. T. Lang, R. L. Strong, *J. Am. Chem. Soc.* **1965**, *87*, 2345. W. K. Duerksen, M. Tamres, *J. Am. Chem. Soc.* **1968**, *90*, 1379. T. D. McLean, B. B. Ratcliff, J. Z. Pastalan, K. K. Innes, *J. Quant. Spectrosc. Radiat. Transfer* **1989**, *42*, 445.

[98140]

Contribution to the Chemistry of Boron, 243[◇]

Synthesis and Structures of Dimesityldiboranes(4)☆

Herbert Hommer, Heinrich Nöth*, Jörg Knizek[+], Werner Ponikwar[+], and Holger Schwenk-Kircher[+]

Institut für Anorganische Chemie der Universität München,
Meiserstraße 1, D-80333 München, Germany
Fax: (internat.) +49(0)89/5902451

Received May 8, 1998

Keywords: *B*,*B*′-Dimesityldiborane(4) dihalides / *B*,*B*′-Diamino-*B*,*B*′-dimesityldiboranes(4) / *B*,*B*′-Di-*tert*-butyloxy-*B*,*B*′-dimesityldiborane(4) / *B*,*B*′-Dimesityl-*B*,*B*′-di(organylthio)diborane(4) / NMR spectroscopy / X-ray structures

An efficient route to *B*,*B*′-dihalo-*B*,*B*′-dimesityldiboranes(4) is reported, as well as the conversion of these and of *B*,*B*′-dimesityl-*B*,*B*′-dimethoxydiborane(4) into other *B*,*B*′-dimesityldiboranes $B_2mes_2X_2$ (X = OR, SR, NR_2, NHR). The substituents X influence the shielding of the ^{11}B nucleus in the expected manner. Hindered rotation about the B–N bond is observed for X = pyrrolyl, while in solution there is free rotation about the B–C bond. However, X-ray structural results reveal that the mesityl group is almost orthogonal to the B(B)CY plane in the solid state. The shortest B–B bond is observed in $mes_2B_2I_2$, indicating that the iodide is the strongest Lewis acid in the reported series of $mes_2B_2Y_2$ compounds. This is also reflected in short B–C bonds. Moreover, the two mes(Y)B units also approach orthogonality in these diborane(4) compounds, and thus enforce this as a typical structural feature of diborane(4) derivatives. For this reason, the planar C(N)B–B(N)C unit of *B*,*B*′-di(benzylamino)-*B*,*B*′-dimesityldiborane(4) is regarded as exceptional for aminodiboranes(4).

Introduction

Although B_2Cl_4, the first diborane(4) compound, was synthesized as long ago as 1925[2], the intensive study of diborane(4) derivatives only began in the early 1960s, when an easy access to $B_2(NMe_2)_4$ was found[3][4]. Because $B_2(NMe_2)_4$ can be converted into $B_2(NMe_2)_3X$ or *sym*-$B_2(NMe_2)_2X_2$ (X = Cl, Br) by reaction with BX_3, a very useful synthon for the synthesis of amino-substituted diborane(4) derivatives was available on a preparative scale[4]. It was soon recognized that the stability of diborane(4) compounds B_2X_4 could be enhanced by increasing the electronic and steric shielding at the boron centers, so as to suppress decomposition into BX_3 and $(BX)_n$[5]. Thus, $B_2(NMe_2)_4$ is the most stable derivative due to N−B π-bonding in addition to the steric effect of the Me_2N groups, while B_2Me_4 remains unknown. Nevertheless, the first stable tetraorganyldiborane(4) derivatives, such as $(t\mathrm{Bu})_2\mathrm{B}-\mathrm{B}(t\mathrm{Bu})\mathrm{Me}$[6] and $(t\mathrm{Bu})_2\mathrm{B}-\mathrm{B}(t\mathrm{Bu})(\mathrm{CH}_2t\mathrm{Bu})$[7], were reported in 1980, demonstrating that only steric hindrance is required for the stabilization of diborane(4) species of this type. Although the *tert*-butyl groups are able to prevent redox disproportionation of these tetraalkyldiborane(4) derivatives, the halogenated species $t\mathrm{Bu}_2\mathrm{B}_2\mathrm{X}_2$ (X = Cl, Br) decompose readily[8].

While in alkyl-substituted diborane(4) derivatives the boron−carbon bonds can be described purely as σ-bonds, a B−C π-interaction can be expected in cases where aryl substituents are attached at the boron atoms, as the π-electrons of the aryl ligand can interact with the empty p-orbital of the boron atom. This has been documented in several examples[9][10]. Therefore, aryl-substituted diborane(4) derivatives might be expected to show an enhanced stability in comparison with their alkyl counterparts due to B−C π-bonding in B_2R_4. Indeed, some aryl-substituted diborane(4) derivatives such as $mes_2B-B(mes)Ph$ and $mes_2B-B(mes)CH_2SiMe_3$ are thermally stable, although little evidence for π-bonding or hyperconjugation was found[11].

We now report on the synthesis and crystallographic characterization of a variety of mesityl-substituted diborane(4) derivatives. These studies were undertaken in order to gain further insight into the stabilities, electronic properties, and conformations of such species.

Synthesis

As mentioned above, $B_2(NMe_2)_4$ and $B_2(NMe_2)_2X_2$ (X = Cl, Br) are key species in diborane(4) chemistry. The reaction of bis(dimethylamino)diborane(4) dichloride with mesityllithium, mesLi, for example, leads to $mes_2B_2(NMe_2)_2$[12][13] (Eq. 1a), which can be converted into $mes_2B_2(OMe)_2$ in very good yield according to Eq. 1b[11][13].

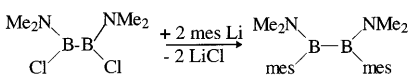

(1a)

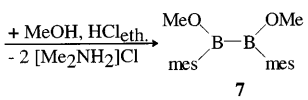

(1b)

7

[◇] For Part 242, see ref.[1].
[+] Crystal structure determination.

 © WILEY-VCH Verlag GmbH, D-69451 Weinheim, 1998 1434−1948/98/1010−1519 $ 17.50+.50/0

As shown in Eqs. 2 and 3, $mes_2B_2(OMe)_2$ itself can be further used as a starting material for the synthesis of various mesityl-substituted diboranes(4), e.g. the dihalides $mes_2B_2X_2$. In particular, the iodide **1c** is readily available under mild conditions and is obtained in good yield. Additionally, several diaminodimesityldiboranes(4) **2**–**6** were synthesized by allowing $mes_2B_2(OMe)_2$ to react with LiNH*t*Bu or $mes_2B_2Cl_2$ to react with amines or lithium amides (Eqs. 3, 4a, and 4b).

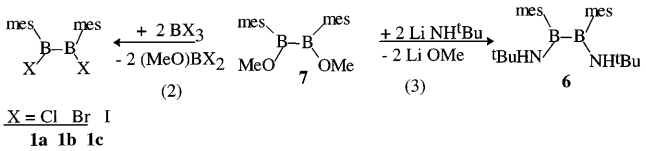

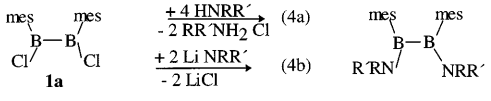

amine		Li NRR´		
$MeNH_2$	**2**	Li NH*i*Pr	**4**	bzl = benzyl
$bzlNH_2$	**3**	Li pyr	**5**	pyr = pyrrolyl

Although all these reactions provided the diaminodimesityldiboranes(4) in yields > 70%, better results were obtained when lithium amides were allowed to react with $mes_2B_2Cl_2$ rather than $mes_2B_2(OMe)_2$. This is due to the enhanced reactivity of the halogenated species. Moreover, the reactions can be carried out at lower temperatures and in less time. Furthermore, compared to the preparation of di(benzylamino)dimesityldiborane(4) (**3**) by the amine route, where a voluminous precipitate of benzylammonium chloride is formed, the by-product LiCl precipitates as a fine powder, and the reaction mixture can be stirred more readily. On the other hand, the method using amines as auxiliary bases can be advantageous when gaseous amines such as $MeNH_2$ are employed. $mes_2B_2(NHtBu)_2$ is also obtained in good yield by ligand exchange from $mes_2B_2(OMe)_2$ according to Eq. 3, but not by dehalogenation of haloboranes to diboranes(4), as shown in Eq. 5. The latter method fails when bulky substituents are attached to the boron atom.

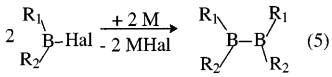

Earlier attempts to synthesize dialkyldialkoxydiboranes(4) as well as dialkyldialkylthiodiboranes(4) were unsuccessful, and compounds of the type $R_2B_2X_2$ (X = OR, SR) were regarded as unstable as only borane(III) derivatives could be isolated[5]. Thus, only a few dialkyldiborane(4) derivatives with elements of the sixth main group are known[8]. In order to avoid redox disproportionation of these derivatives into R_2BX and "BX", one *t*Bu group was attached at each boron atom in order to stabilize the diborane(4) compounds. However, most of these dialkyldiborane(4) compounds are liquids and structural characterization by X-ray diffraction has as yet been impossible[8]. In order to gain further structural insight into the conformation of dialkoxydimesityldiborane(4) derivatives and to compare them with the structure of $mes_2B_2(OMe)_2$ (**7**)[11] (see Eq. 1b), we synthesized $mes_2B_2(OtBu)_2$ (**8**) (Eq. 6), as well as several mercapto derivatives $mes_2B_2(SR)_2$. The latter were prepared from $mes_2B_2Cl_2$ with either a mixture of the respective thiol and Et_3N as auxiliary base, or with lithium mercaptides, as shown in Eqs. 7a, 7b, and 7c. The best results were obtained using the latter method.

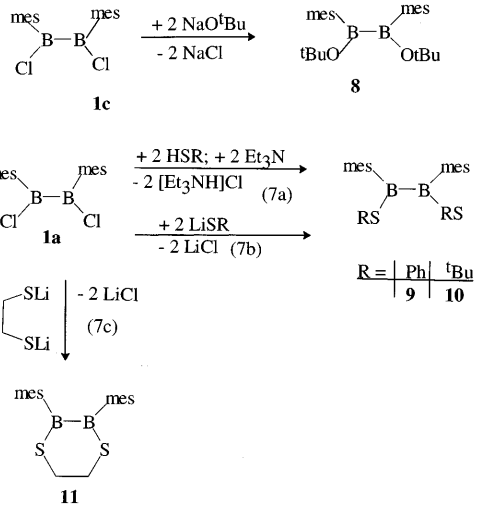

Efforts were also made to synthesize phosphanyl-substituted dimesityldiborane(4) derivatives. However, the reactions of $mes_2B_2Cl_2$ and LiPH*t*Bu in a 1:1 and in a 1:2 stoichiometry, as well as the reaction with one equivalent of Li_2PtBu, led only to ill-defined, multicomponent mixtures, as was evident from the many signals in the ^{11}B-NMR spectra, which ranged from $\delta = 90$ to -25. On the other hand, when $mes_2B_2Cl_2$ was allowed to react with lithiated 1,2-bis(isopropylphosphanyl)benzene, a planar heteroaromatic B–P–C cyclic product was formed in quantitative yield[14].

NMR Spectra

The ^{11}B-NMR shifts of the amino derivatives **2**–**6** are found in the range $\delta = 45-60$, which is typical for diaminodiorganyldiboranes(4)[15]. The signals for $B_2mes_2(NHR)_2$ compounds (R = Me, *i*Pr, *t*Bu) are shifted to higher field compared to those of $(Me_2N)mesB-Bmes(NMe_2)$ [$\delta^{11}B$ ($CDCl_3$) = 55]. The magnitude of the shift difference increases in the order NHMe < NHBz < NH*i*Pr < NH*t*Bu ($\delta^{11}B$ = 48.3, 47.9, 46.3, and 45.3, respectively) as the branching of R at the nitrogen atom increases. On the contrary, the ^{11}B resonance shows a deshielding ($\delta = 60.5$ for **5**) when an aromatic amine ligand is attached to the boron atoms, because the electrons of the p_z orbital at the nitrogen atom contribute to the aromaticity of the pyrrole heterocycle. Consequently, the B–N bonds possess less π-bond character. Nevertheless, the ^1H- and ^{13}C-NMR spectra show a discrete signal for each H and C atom of the pyrrole ligand, indicating hindered rotation of this subunit at ambient temperature, and therefore N–B back bonding (vide infra).

In analogy to borane(3) derivatives, the replacement of an amino group by an alkoxy group leads to a deshielding of the ^{11}B nucleus due to the higher electronegativity of the substituent. The resonance signals of the two alkoxy compounds **7** and **8** are found at $\delta^{11}B \approx 60$ (±5) depending on the solvent. In the ^{13}C-NMR spectra, the signals of the oxygen-bonded carbon atoms of the alkoxy ligands are shifted to lower field by about 5−7 ppm compared to those of the free alcohol[16]. This effect can be explained in terms of an O−B π-back donation, reducing the electron deficiency at the boron atom, leading to a deshielding of the respective C atom.

Within the dimercaptodimesityldiborane(4) series, the ^{11}B-NMR signals span a range from $\delta = 69-81$. The thiophenolate derivative **9** shows the least shielded boron atom ($\delta^{11}B = 80.6$), while those of the cyclic dithiadiborinane **11** ($\delta^{11}B = 69.4$) are the best shielded among these compounds. Furthermore, the signal of the latter compound shows a relatively narrow half-width of ca. 210 Hz, while the signals of the acyclic derivatives exhibit half-widths of 1000−1550 Hz. In analogy to the alkoxydiboranes(4) **7** and **8**, the signals of the sulfur-bonded carbon atoms of the mercapto ligands are shifted to lower field compared with those of the free thiol[16], indicating partial π-character of the S−B bond (vide infra). The magnitude of shift difference is about 4−8 ppm, as is observed for the alkoxy analogues.

Molecular Structures

In order to obtain information on the preferred conformations, and to gain further insight into steric and/or electronic effects of the ligands in the solid state of dimesityldiboranes(4), X-ray structure determinations of some representative derivatives were carried out.

Table 1 shows that the B−B bond lengths span a range from 1.709(5) Å in **5** to 1.735(7) Å in **8**. These can be compared with the B−B bond lengths in tetraaminodiboranes(4) **12**[17] and **13**[18] [1.693(9) Å and 1.750(8) Å, respectively]. Within the amino-substituted dimesityldiborane(4) series, compounds **6** and **3** show B−N bond lengths between 1.388(5) Å and 1.394(2) Å. These are slightly shorter than those in **12** and **13** (average of 1.415 and 1.426 Å)[17][18] and correspond, within the limits of significance, to the values determined for mes(Me$_2$N)B−B(NMe$_2$)mes (1.40 Å)[12]. It is interesting to note that the B−N bond lengths to the aromatic pyrrole ligands in compound **5** are significantly longer [1.434(4) and 1.438(4) Å] compared to those in the non-aromatic analogues mes$_2$B$_2$(NMe$_2$)$_2$[12] and mes$_2$B$_2$(NH*t*Bu)$_2$ **6**.

As expected, the boron atoms reside in planar environments (sum of bond angles = 360°). Nevertheless, although the NBC$_{mes}$ bond angles of the bis(dimethylamino)- as well as the dimesityldipyrrolyldiborane(4) are all 120 ± 2.5°, in compound **6** this angle is widened to 126.7° due to the steric repulsion between the mesityl and *tert*-butylamino groups. Consequently, the B−B−N bond angle in **6** is reduced to 114.9°. It is quite interesting that compounds **3** and **6** exhibit point group symmetry C_i in the solid state and thus possess planar $C_2B_2N_2$ skeletons. Normally, diborane(4) derivatives show a dihedral angle between the two planes at the boron atoms in the range 60−80°. It seems that only packing effects are responsible for the conformation in the solid state, because no intermolecular interactions between the molecules other than van der Waals contacts are detectable.

A comparison of the crystal structures of mes$_2$B$_2$(OMe)$_2$ (**7**)[11] and mes$_2$B$_2$(O*t*Bu)$_2$ (**8**) reveals no significant differences in the B−B, B−O, and B−C bond lengths. The B−B bonds are only marginally longer than in the tetraalkoxy-substituted diborane(4) **14** [1.711(6) Å][19], but are significantly longer compared to those in compounds **15a** and **15b**, where the B−B bond lengths are 1.687(3) and 1.684(3), respectively[20]. The B−O bonds of **8** [1.348(6) and 1.366(7) Å] are intermediate between single and double bond lengths (1.46 and 1.26 Å)[21], indicating partial B−O π-bonding[22][23]. In comparison, the B−O bonds in mes$_2$B(OMe) (1.352 Å)[23] and compound **16** (average 1.367 Å)[24] are equally long, while in the triborane(5) derivative **17** a value of 1.396(5) Å is observed[25]. Due to enhanced steric repulsion between the *tert*-butyloxy group and the mesityl ligand, the OBC$_{mes}$ angles in **8** are widened to 128° compared with the corresponding bond angles in the methoxy derivative **7** [121.9(5)° and 123.2(5)°][11]. B−B−O and B−B−C$_{mes}$ bond angles are smaller (114.8−116.9°) as the sum of the bond angles around each boron atom is 360°. Most probably as a result of the aforementioned steric repulsion, the B−O−C$_{t\mathrm{Bu}}$ angles in **8** are even wider (131°) than the B−O−C$_{Me}$ angles in **7** (121° and 123.4°) and mes(OMe)B−Bmes$_2$ [125.0(9)°][11], but are very similar to that in compound **17** [130.7(4)°][25].

Table 1. Selected bond lengths [Å] and angles [°] for compounds **3**, **5**, **6**, **8**, and **10**

Compound	**5**	**3**	**6**	**8**	**10**
Formula	$C_{26}H_{30}B_2N_2$	$C_{32}H_{38}B_2N_2$	$C_{26}H_{42}B_2N_2$	$C_{26}H_{40}B_2O_2$	$C_{26}H_{40}B_2S_2$
d_{BB}	1.709(5)	1.717(4)	1.732(8)	1.735(7)	1.712(6)
$d_{B(1)X(1)}$[a]	1.434(4)	1.394(2)	1.388(5)	1.348(6)	1.771(4)
$d_{B(2)X(2)}$[a]	1.438(4)	1.394(2)	1.388(5)	1.366(7)	1.771(4)
$d_{B(1)C(1)}$[a]	1.576(5)	1.590(2)	1.578(5)	1.595(7)	1.576(5)
$d_{B(1)C(10)}$[a]	1.578(4)	1.590(2)	1.578(5)	1.578(8)	1.572(5)
angle betw. planes at B(1) and B(2)	1.0	58.8	180 (“*trans*”)	110.9	115.2
angle betw. planes at B(1) and C(1)	86.4		79.5	83.6	88.5
angle betw. planes at B(2) and C(10)	86.4		79.5	94.0	92.1

[a] X is either N, O or S.

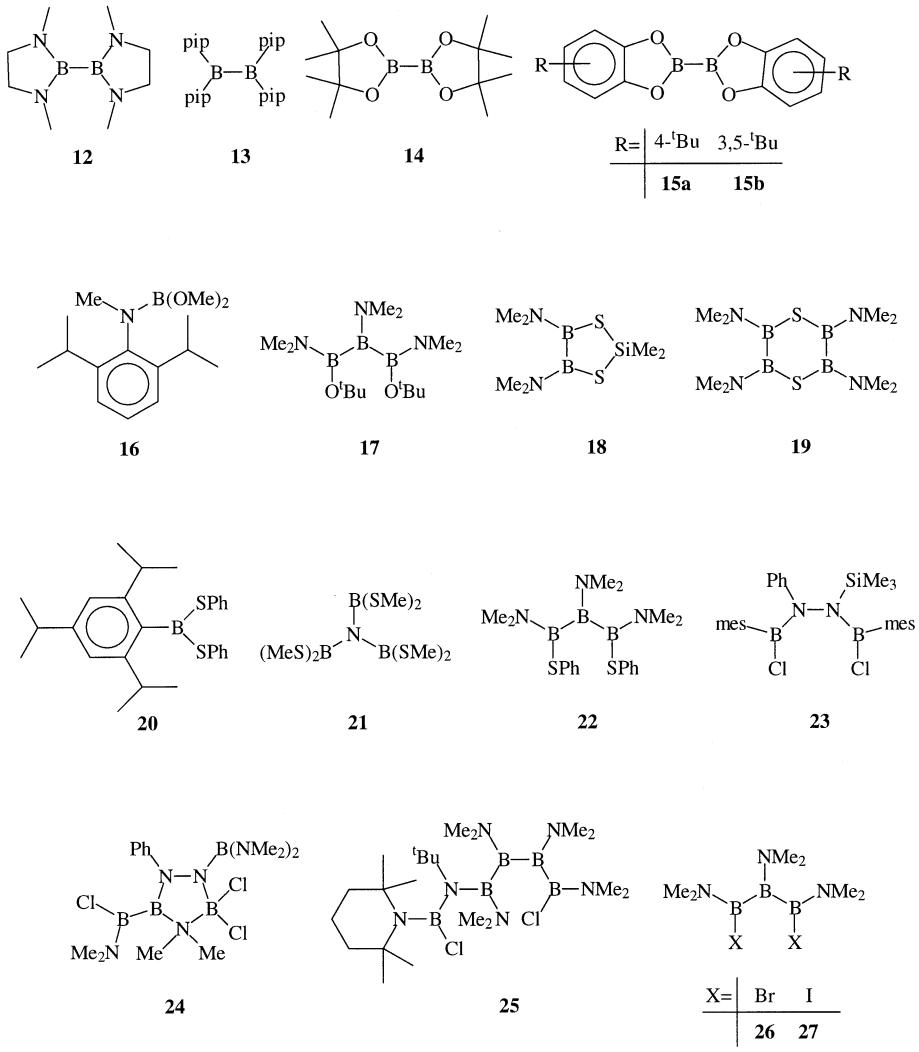

Figure 1. ORTEP representation of the molecular structure of **3**; esd's in parentheses; thermal ellipsoids are represented at a 25% probability level

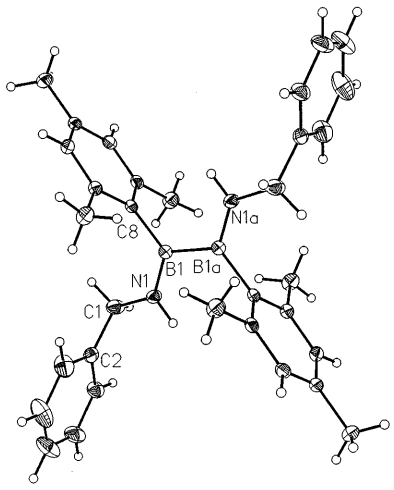

Figure 2. ORTEP representation of the molecular structure of **6**; esd's in parentheses; thermal ellipsoids are represented at a 25% probability level

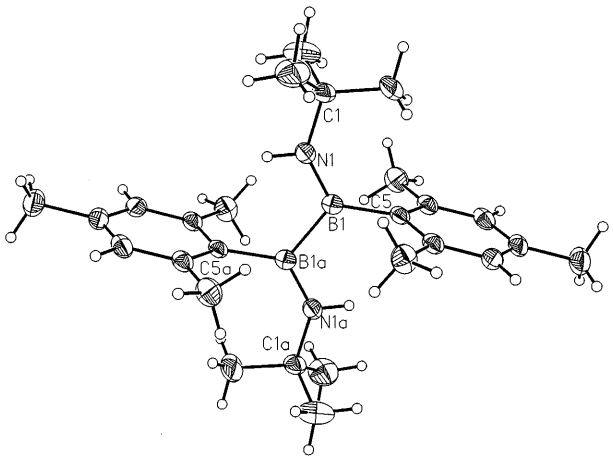

The mercaptodiborane(4) mes(*t*BuS)B−B(S*t*Bu)mes (**10**) exhibits a B−B bond length of 1.712(6) Å, which is intermediate between the corresponding bond lengths of the amino-substituted B−S heterocycles **18** [1.72(1) Å] and **19** [1.66(1) and 1.69(1) Å][26]. The B−S distance in **10** was found to be 1.771(4) Å, which is intermediate between a

Figure 3. ORTEP representation of the molecular structure of **5**; esd′s in parentheses; thermal ellipsoids are represented at a 25% probability level

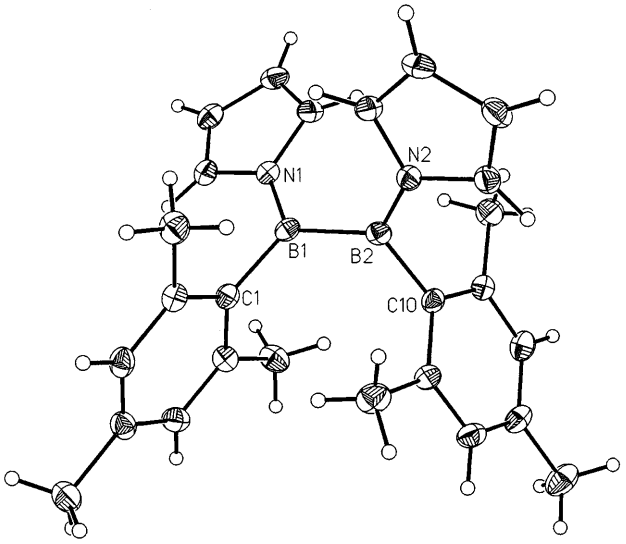

Figure 4. ORTEP representation of the molecular structure of **8**; esd′s in parentheses; thermal ellipsoids are represented at a 25% probability level[a]

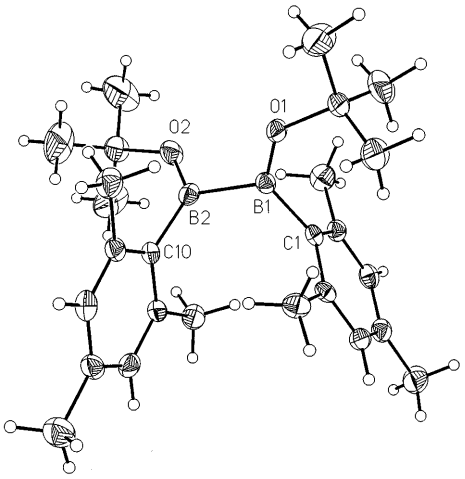

[a] Selected bond angles [°]: O1−B1−C1 128.1(4), O1−B1−B2 116.9(4), C1−B1−B2 114.9(4), O2−B2−C10 128.2(4), O2−B2−B1 114.8(5), C10−B2−B1 116.9(4), B1−O1−C19 130.7(3), B2−O2−C23 131.0(4).

B−S single bond (1.89 Å) and a B−S double bond (1.69 Å)[21]. Similar B−S bond lengths were observed in the trithiadiborolanes $(MeB)_2S_3$ (1.803 Å)[27a] and $(ClB)_2S_3$ (1.794 Å)[27b], as well as in the tris(methylthio)borane $B(SMe)_3$ (1.805 Å)[28], where partial S−B π-bonding is discussed. Furthermore, the B−S bond length in **10** matches very well those found in the acyclic derivatives mes_2BSMe [1.787(6) Å][23] and mes_2BSPh [1.790(6) Å][29], as well as in compounds **20** [1.799(6) and 1.802(6) Å][30] and **21** (average 1.80 Å)[30]. In molecules with less B−S π-bond character, such as the triborane(5) **22**, the B−S bonds are noticeably longer [1.864(2) and 1.849(2) Å][25].

The $S-B-C_{mes}$ angles are on average 128.5° and are thus of the same order as those in the *tert*-butyloxy analogue **8**,

Figure 5. ORTEP representation of the molecular structure of **10**; esd′s in parentheses; thermal ellipsoids are represented at a 25% probability level[a]

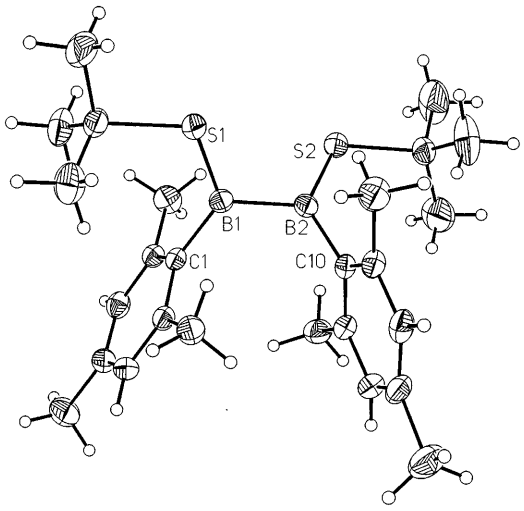

[a] Selected bond angles [°]: C1−B1−B2 118.0(3), C1−B1−S1 127.6(3), B2−B1−S1 114.4(3), C10−B2−B1 115.5(3), C10−B2−S2 129.4(3), B1−B2−S2 115.1(3), B1−S1−C19 114.0(2), B2−S2−C23 114.1(2).

but the B−B−S and $B-B-C_{mes}$ angles are smaller (114.4° and 118.0°, respectively). Owing to the steric repulsion between the mesityl ligand and the *tert*-butyl group, the $B-S-C_{tBu}$ angles in **10** are larger (114°) than those in $mes_2B(SMe)$ (109.8°)[23] or in the derivatives **20**−**23**, where B−S−R angles in the range 104.8−107.3° were measured[25][29][30].

The mesityl rings adopt an orientation almost perpendicular to the plane around the boron centers. This is a common feature of all the newly studied compounds.

Table 2. Selected bond lengths [Å] and interplanar angles [°] for compounds **1a**, **1b**, and **1c**

	1a	**1b**	**1c**
Formula	$C_{18}H_{22}B_2Cl_2$	$C_{18}H_{22}B_2Br_2$	$C_{18}H_{22}B_2I_2$
d_{BB}	1.680(6)	1.673(6)	1.664(9)
$d_{B(1)Hal(1)}$	1.770(5)	1.928(4)	2.165(6)
$d_{B(2)Hal(2)}$	1.774(4)	1.932(4)	2.158(7)
$d_{B(1)C(1)}$	1.551(5)	1.557(5)	1.558(8)
$d_{B(1)C(10)}$	1.558(6)	1.560(5)	1.548(8)
dihedr. angle HalB−BHal	73.4	71.6	71.5
angle betw. planes at B(1) and C(1)	88.5	87.5	88.5
angle betw. planes at B(2) and C(10)	85.8	88.6	85.9

The crystal structures of the dihalogenodimesityldiborane(4) compounds reveal some interesting characteristics. Among all studied diborane(4) compounds, they exhibit the shortest B−B bonds. With an average of 1.67 Å, they are at the lower end of the range for B−B single bonds and, within the series, an interesting trend is observed (Table 2). Surprisingly, the bond lengths vary in a manner opposite to what might have been expected. As the covalent radius of the halogen atom increases on going from chlorine to iodine, the

Figure 6. ORTEP representation of the molecular structure of **1a**; esd's in parentheses; thermal ellipsoids are represented at a 25% probability level

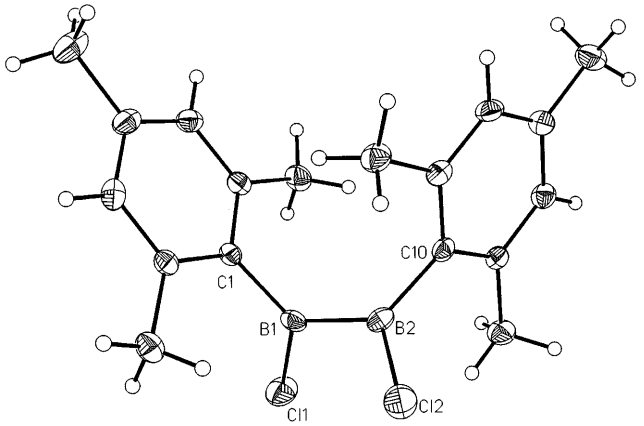

Figure 7. ORTEP representation of the molecular structure of **1b**; esd's in parentheses; thermal ellipsoids are represented at a 25% probability level

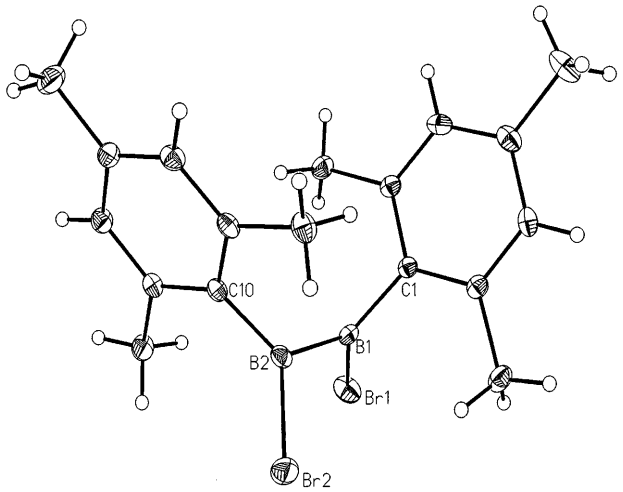

Figure 8. ORTEP representation of the molecular structure of **1c**; esd's in parentheses; thermal ellipsoids are represented at a 25% probability level

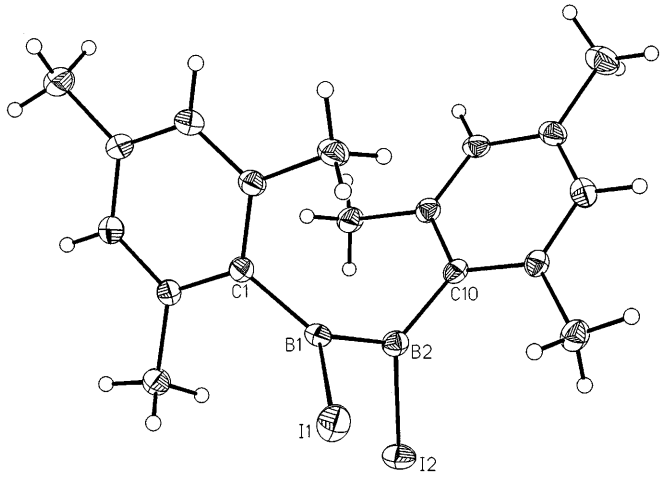

B−B distances *decrease*. This shrinkage is contrary to expectation in terms of the *−I* effect of the halogen atoms, but fits the Lewis acidity scale of the boron halides. We regard this as further experimental evidence that π-bonding at boron halides decreases on ascending the series F > Cl > Br > I, with the consequence that in most cases the iodides are the most Lewis acidic compounds among such species. Moreover, electron diffraction experiments on the tetrahalodiboranes(4) B_2Cl_4[31] and B_2Br_4[32] show the same trend and lengths 1.70(7) Å and 1.69(2) Å], although these distances have large standard errors associated with them and do not differ significantly. At 1.68(2) Å[12], the B−B bond length in $(Me_2N)_2B_2Br_2$ fits very well into this series. The B−Cl bond lengths in **1a** (see Table 2) are significantly shorter than those observed for compounds **23**[33] [1.790(4) Å, 1.805(4) Å] and **24**[33] [1.814(5) Å]. This implies partial π-bond character. In comparison, the B−Cl bond lengths in the tetraborane(6) derivative **25**[25] are 1.809(5) Å for the terminal boron atom of the tetraborane chain and 1.870(4) Å for the di(aminoboryl) subunit. The same trend, i.e. a short B−Hal bond length, is also observed in B_2Br_4. The B−Br bond lengths in **1b** [1.928(4) Å, 1.932(4) Å] are obviously short, since a single bond would be expected to have a length of 1.99 Å [atomic radii of boron (0.85 Å) and bromine (1.14 Å)[21]], as observed in $(Me_2N)_2B_2Br_2$[12] [1.97(1) Å and 1.99(1) Å] and in compound **26**[25] [1.99(1) Å and 2.00(1) Å]. Even $mes_2B_2I_2$ exhibits a B−I bond length (average 2.16 Å) that is slightly smaller than the sum of the atomic radii[21] (0.85 Å and 1.33 Å, giving 2.18 Å). In this respect, it is interesting to note that the diiodotriborane(5) derivative **27** has longer B−I bonds [2.224(6) and 2.237(6) Å][25], which seems to be due to the presence of the amino groups.

However, all the halogen derivatives **1a**−**1c** show the common feature of shorter $B-C_{mes}$ bonds compared to the compounds listed in Table 1. In all cases, the mesityl rings are almost orthogonally orientated with respect to the plane at the boron atom. Furthermore, irrespective of the nature of the halogen atom, compounds **1a**−**1c** exhibit an X−B−B−X dihedral angle of 71°.

Conclusions

A comparison of the chemistry of *B*,*B'*-di-*tert*-butyldiboranes(4) with that of *B*,*B'*-dimesityldiboranes(4) reveals the higher stability of the latter compounds. This is particularly evident for the dihalides $mes_2B_2X_2$ (X = Cl, Br, I) and $tBu_2B_2X_2$. Because there is *no* significant electronic contribution to stabilize the B−B bond by decreasing the electron deficiency at the boron atoms by X by B−C π-bonding, it is evident that the stability of $R_2B_2Y_2$ compounds with respect to dismutation into B^I and B^{III} species is kinetically but not thermodynamically controlled. This is also supported by the geometry of the structure of *B*,*B'*-dimesityldiborane(4) in the solid state, because possible π-overlap as in 1,4-butadienes is prevented by an almost orthogonal arrangement of the CB(B)Y planes and the C_3B plane to the B(C)B(Y) plane. All the structural and chemical evidence collected for diborane(4) derivatives indicates that the B−B bond lengths are primarily determined by the character of the group Y. Thus, it appears that kinetically stable tetraorganyldiboranes B_2R_4 can be prepared with bulky groups R,

as verified for $B_2(tBu)_3SiMe_3$[6] and similar compounds. The former may be used to generate $B_2H_2(tBu)SiMe_3$, an unstable molecule that may be used to determine whether hydroboration or diboration prevails in kinetic experiments.

We are grateful to the *Fonds der Chemischen Industrie* and the *Chemetall GmbH* for support of our research, and to the technical staff at the *Institute of Inorganic Chemistry* for recording NMR, IR and mass spectra, as well as for performing elemental analyses.

Experimental Section

Schlenk techniques were used in all experiments with nitrogen gas as a blanket. Solvents were dried by standard procedures. Commercial chemicals were purified before use as necessary. Literature procedures were employed for the preparation of $B_2(NMe_2)_4$[3][4], $(Me_2N)_2B_2Cl_2$[4], $mes_2B_2(NMe_2)_2$[13], $mes_2B_2(OMe)_2$[13], and $mes_2B_2Cl_2$[13]. − NMR: Bruker AC-P 200 (^{11}B), Jeol GSX 270 (^1H, ^{13}C); standards: int. TMS, ext. $BF_3{\cdot}OEt_2$. − IR: Perkin-Elmer 325. − MS: Varian CH7 (70 eV). − X-ray analyses: Siemens P4 and Nicolet R3m diffractometer, Mo-K_α radiation, graphite monochromator.

B,B′-Dibromo-B,B′-dimesityldiborane(4) (**1b**): To a stirred suspension of $mes_2B_2(OMe)_2$ (510 mg, 1.6 mmol) in 60 ml of hexane at −30°C was added BBr_3 (1.00 g, 3.99 mmol, 0.38 ml). The reaction mixture was allowed to warm to 0°C and was kept at this temperature for at least 1 h. A clear, light-yellow solution resulted. The solution was stored at −20°C overnight, and then concentrated to a volume of about 20 ml. At −20°C, yellow crystals of $mes_2B_2Br_2$ (**1b**) separated (450 mg, 1.1 mmol). A second crop of **1b** was isolated by reducing the volume of the solution still further. Total yield: 0.53 g (80%); m.p. 98−101°C. **1b** can be stored under an inert atmosphere at low temperatures (< −20°C) for several months without decomposition. Even in solution at −20°C, **1b** is stable for weeks, while at ambient temperature it decomposes readily into $mesBBr_2$ ($\delta^{11}B$ = 62.8) and other boron-containing compounds [$\delta^{11}B$ = 42.5, 30 (br.), −6]. − NMR (C_6D_6): δ^1H = 2.05 (s, 6 H, *p*-CH_3), 2.18 (s, 12 H, *o*-CH_3), 6.58 (s, 4 H, *m*-H). − $\delta^{11}B$ = 86 ($h_{1/2} \approx$ 1000 Hz). − $\delta^{13}C$ = 21.1 (*p*-CH_3), 22.3 (*o*-CH_3), 127.8 (*m*-C), 135.7 (*o*-C), 139.3 (*p*-C), *ipso*-C signal not obsd. − $C_{18}H_{22}B_2Br_2$ (419.80): calcd. C 51.50, H 5.28; found C 51.20, H 5.13.

B,B′-Diiodo-B,B′-dimesityldiborane(4) (**1c**): To a stirred solution of $mes_2B_2(OMe)_2$ (1.21 g, 3.76 mmol) in 40 ml of hexane, a solution of BI_3 (3.51 g, 8.94 mmol, 19% excess) in hexane (60 ml) was added at 0°C with the exclusion of light. After stirring for 2 h at this temperature, an ^{11}B-NMR spectrum showed the signals of excess BI_3 ($\delta^{11}B$ = −7.5), of $(MeO)BI_2$ ($\delta^{11}B$ = 6.5), and of $mes_2B_2I_2$ ($\delta^{11}B$ = 89). Insoluble material was then removed by filtration and the filtrate was stored at −20°C overnight. A small amount of $mes_2B_2I_2$ (**1c**) was obtained in the form of yellow crystals, suitable for X-ray diffraction. Fractional crystallization by reducing the volume of the solution in a stepwise manner to about 30 ml, provided additional **1c**. Yield: 1.32 g (2.57 mmol, 68%); m.p. ca. 89°C (decomp.). − NMR (C_6D_6): δ^1H = 2.08 (s, 6 H, *p*-CH_3), 2.21 (s, 12 H, *o*-CH_3), 6.59 (s, 4 H, *m*-H). − $\delta^{11}B$ = 89. − $\delta^{13}C$ = 21.1 (*p*-CH_3), 23.0 (*o*-CH_3), 128.5 (*m*-C), 134.1 (*o*-C), 139.3 (*p*-C), *ipso*-C signal not obsd. − $C_{18}H_{22}B_2I_2$ (513.78): calcd. C 42.08, H 4.32; found C 40.20, H 4.36.

B,B′-Dimesityl-B,B′-bis(methylamino)diborane(4) (**2**): At −30°C, methylamine (3.0 ml, 68 mmol) was condensed into a stirred solution of $mes_2B_2Cl_2$ (1.80 g, 5.44 mmol) in 50 ml of hexane, resulting in the immediate precipitation of methylammonium chloride. The reaction mixture was allowed to warm to ambient temp. while stirring overnight. After separation of the solid (0.88 g, 119% "$[MeNH_3]Cl$"), the solvent and all volatile materials were removed in vacuo. The residue was treated with 50 ml of hexane, and insoluble material was removed by centrifugation for 10 min (1200 rpm). The clear solution was then stored at −78°C, whereupon **2** precipitated as a white solid. Yield: 1.55 g (4.84 mmol, 89%). Within 2 d, **2** crystallized in the form of colorless cubes in an NMR tube, m.p. 190°C. − NMR ($CDCl_3$): δ^1H = 2.17 (s, 12 H, *o*-CH_3), 2.30 (s, 6 H, *p*-CH_3), 2.49 (d, 6 H, NMe, $^3J_{HH}$ = 8 Hz), 4.7 (br., 2 H, NH), 6.81 (s, 4 H, *m*-H). − $\delta^{11}B$ = 48.3. − $\delta^{13}C$ = 21.2 (*p*-CH_3), 21.7 (*o*-CH_3), 31.4 (NMe), 127.0 (*m*-C), 135.7 (*p*-C), 138.4 (*o*-C), *ipso*-C signal not obsd. − $C_{20}H_{30}B_2N_2$ (320.10): calcd. C 75.05, H 9.45, N 8.75; found C 74.66, H 9.31, N 8.22.

B,B′-Di(benzylamino)-B,B′-dimesityldiborane(4) (**3**): $mes_2B_2Cl_2$ (1.77 g, 5.35 mmol) was dissolved in 60 ml of pentane and the flask was placed in an ice bath. Under stirring, benzylamine (2.50 ml, 2.46 g, 22.9 mmol) was added, resulting in the immediate precipitation of benzylammonium chloride. The suspension was allowed to warm to ambient temp., and then stirring was continued for a further 4 h. The insoluble material was then removed by filtration (1.98 g), and the filtrate was concentrated to dryness in vacuo. Since the residue was found to be moderately soluble in pentane and hexane, it was treated with a few mls of pentane and the solid was recovered by filtration. After drying in vacuo, **3** was obtained as a white powder (1.20 g, 2.54 mmol, 47%), essentially pure on the basis of its NMR spectra. Recrystallization from 5 ml of diethyl ether gave colorless crystals, suitable for X-ray diffraction; m.p. 115−117°C. − NMR ($CDCl_3$): δ^1H = 2.26 (s, 12 H, *o*-CH_3), 2.30 (s, 6 H, *p*-CH_3), 4.08 (d, 4 H, CH_2, $^3J_{HH}$ = 7.3 Hz), 5.16 (t, 2 H, NH), 6.82 (s, 4 H, *m*-H), 7.14−7.27 (m, 10 H, Ph). − $\delta^{11}B$ = 47.9 ($h1/2 \approx$ 980 Hz). − $\delta^{13}C$ = 21.1 (*p*-CH_3), 22.0 (*o*-CH_3), 49.0 (CH_2), 126.5 (*m*-mes), 126.8 (*p*-Ph), 127.0 (*o*-Ph), 128.2 (*m*-Ph), 135.7 (*p*-mes), 138.2 (*o*-mes), 141.2 (*ipso*-Ph), *ipso*-mes signal not obsd. − $C_{32}H_{38}B_2N_2$ (472.29): calcd. C 81.38, H 8.11, N 5.93; found C 80.98, H 8.00, N 5.84.

B,B′-Di(isopropylamino)-B,B′-dimesityldiborane(4) (**4**): $mes_2B_2Cl_2$ (1.37 g, 4.14 mmol) was dissolved in 30 ml of hexane and the solution was cooled to −35°C. To the stirred solution, a suspension of iPr_2NLi (0.54 g, 8.27 mmol) in 20 ml of hexane was added. After allowing the mixture to warm to ambient temp. overnight, the insoluble material (LiCl) was removed by filtration. The filtrate was then concentrated in vacuo to a volume of about 20 ml. Compound **4** separated as a white solid at −50°C. Yield: 1.34 g (3.56 mmol, 86%); m.p. 185°C. − NMR ($CDCl_3$): δ^1H = 0.91 (d, 12 H, CH*Me*, $^3J_{HH}$ = 8 Hz), 2.18 (s, 12 H, *o*-CH_3), 2.31 (s, 6 H, *p*-CH_3), 3.12 (sept, 2 H, C*H*Me), 4.55 (d, 2 H, NH), 6.80 (s, 4 H, *m*-H). − $\delta^{11}B$ = 46.3. − $\delta^{13}C$ = 21.2 (*p*-CH_3), 22.0 (*o*-CH_3), 25.5 (CH*Me*), 46.1 (*C*HMe), 126.8 (*m*-C), 135.2 (*p*-C), 138.4 (*o*-C), 141.0 (*ipso*-C, low intensity). − $C_{24}H_{38}B_2N_2$ (376.20): calcd. C 76.63, H 10.18, N 7.45; found C 76.77, H 10.50, N 7.23.

B,B′-Dimesityl-B,B′-dipyrrolyldiborane(4) (**5**): To a solution of $mes_2B_2(OMe)_2$ (2.04 g, 6.17 mmol) in 50 ml of toluene at 0°C, was added a suspension of pyrLi (0.90 g, 12.3 mmol) in 20 ml of hexane. The reaction mixture was stirred overnight at ambient temp. All solid material was then removed by filtration (0.58 g), the filtrate was concentrated to a volume of 15 ml in vacuo, and cooled to −20°C. Colorless crystals, suitable for X-ray diffraction were obtained after recrystallization from *n*-hexane. Yield: 5.1 g, (2.0 mmol, (82%); m.p. 148−150°C. − NMR ($CDCl_3$): δ^1H = 1.90 (s, 12 H, *o*-CH_3), 2.30 (s, 6 H, *p*-CH_3), 6.41, 6.53 (each m, 4 H, $H_{2,3}$-

Table 3. Crystal data and parameters related to data collection and structure solution of the mesityl-substituted diboranes(4); all crystals were monoclinic

Compound	**5**	**3**	**6**	**8**	**10**	**1a**	**1b**	**1c**
Formula	$C_{26}H_{30}B_2N_2$	$C_{32}H_{38}B_2N_2$	$C_{26}H_{42}B_2N_2$	$C_{26}H_{40}B_2O_2$	$C_{26}H_{40}B_2S_2$	$C_{18}H_{22}B_2Cl_2$	$C_{18}H_{22}B_2Br_2$	$C_{18}H_{22}B_2I_2$
Formula weight	392.14	472.26	404.24	406.20	438.32	330.88	419.80	513.78
Cryst. size [mm]	0.3 × 0.2 × 0.2	0.5 × 0.4 × 0.4	0.35 × 0.25 × 0.2	0.65 × 0.6 × 0.4	0.6 × 0.5 × 0.4	0.4 × 0.2 × 0.2	0.25 × 0.2 × 0.2	0.2 × 0.2 × 0.1
Space group	$P2_1/c$	$P2_1/n$	$P2_1/c$	$P2_1/c$	$P2_1/n$	$P2_1/c$	$P2_1/c$	$P2_1/c$
a [Å]	17.931(7)	10.8233(2)	10.051(4)	18.656(4)	8.941(4)	8.169(3)	8.2064(2)	8.2702(2)
b [Å]	8.610(3)	10.5265(1)	16.029(8)	12.180(2)	24.264(10)	29.805(11)	29.7746(4)	29.8558(9)
c [Å]	15.077(4)	13.4730(1)	8.722(3)	11.936(2)	12.589(7)	7.592(2)	7.6856(2)	7.9733(2)
β [°]	99.10(1)	112.483(1)	106.98(2)	107.28(3)	93.54(4)	98.321(2)	98.070(1)	97.335(1)
V [Å3]	2298(1)	1418.33(3)	1344(1)	2589.8(8)	2725.9(22)	1829(1)	1859.32(7)	1952.60(9)
Z	4	2	2	4	4	4	4	4
$d_{calcd.}$ [Mg/m^3]	1.133	1.106	0.999	1.042	1.068	1.202	1.500	1.748
μ [mm^{-1}]	0.064	0.063	0.056	0.062	0.206	0.348	4.353	3.215
F(000)	840	508	444	888	952	696	840	984
T [K]	183(3)	193(2)	183(3)	298	298	193(3)	193(2)	193(2)
2θ [°]	4−49.4	4−49.4	4.2−57.8	2.28−44.00	3.36−44.10	13.62−49.42	2.74−59.06	2.72−58.62
Index range	$-21 < h < 21$ $-10 < k < 10$ $-17 < l < 13$	$-11 < h < 12$ $-12 < k < 12$ $-15 < l < 15$	$-12 < h < 12$ $-20 < k < 20$ $-11 < l < 8$	$-19 < h < 19$ $-12 < k < 0$ $-1 < l < 8$	$0 < h < 9$ $0 < k < 25$ $-13 < l < 13$	$-9 < h < 9$ $-35 < k < 34$ $-8 < l < 8$	$-10 < h < 10$ $-38 < k < 38$ $-9 < l < 9$	$-10 < h < 9$ $-39 < k < 38$ $-10 < l < 10$
Refl. coll.	10651	6617	7546	3109	3614	8504	10780	11501
Refl. indep.	3453	2021	2512	2569	3361	2480	3686	3853
Refl. obsd. [> 4σ(F)]	2780	1758	1239			2147	2945	2937
Absorp. corr.	none	none	none	none	none	none	Sadabs	Sadabs
R	7.95	4.6	8.31	7.24	5.11	6.79	4.14	4.69
$wR2$	5.19	11.5	16.88			13.41	10.05	12.66
GooF	0.220	1.063	1.208	1.544	1.011	1.222	1.069	1.168
diff. peak [e/Å^3]		0.212	0.196	0.374	0.244	0.263	0.781	1.524

$_{pyr}$), 6.74 (s, 4 H, *m*-H), 6.81, 7.25 (each m, 4 H, $H_{1,4\text{-pyr}}$). − $\delta^{11}B$ = 60 ($h_{1/2} \approx 1500$ Hz). − $\delta^{13}C$ = 21.1 (*o*-CH_3), 21.7 (*p*-CH_3), 114.8, 115.6 (pyr-C-3, -C-4), 126.9, 127.1 (pyr-C-2, -C-5), 129.6 (*m*-C_{mes}), 137.2 (*o*-C_{mes}), 137.6 (*p*-C_{mes}), 138.2 (*ipso*-C_{mes}, br. low intensity). − $C_{26}H_{30}B_2N_2$ (392.16): calcd. C 79.63, H 7.71, N 7.14; found C 79.39, H 7.68, N 7.00.

B,B′-Di(tert-butylamino)-B,B′-dimesityldiborane(4) (**6**): $mes_2B_2(OMe)_2$ (0.86 g, 2.7 mmol) was dissolved in 25 ml of hexane and 15 ml of diethyl ether. A suspension of *t*BuNHLi (0.42 g, 5.3 mmol) was added at 0°C, and the resulting mixture was stirred at ambient temp. for 2 d. The reaction was completed by heating the suspension for 4 h. The insoluble material (0.25 g) was removed by filtration and the filtrate was concentrated to a volume of 25−30 ml. After 5 d, colorless crystals separated. A second crop of **6** was isolated after storage of the mother liquor at −20°C for 2 weeks. Total yield: 0.75 g (1.9 mmol, 70%); m.p. 194−195°C. − NMR (C_6D_6): δ^1H = 0.91 (s, 18 H, CMe_3), 2.25 (s, 6 H, *p*-CH_3), 2.40 (s, 12 H, *o*-CH_3), 4.99 (s, 2 H, NH), 6.88 (s, 4 H, *m*-H). − $\delta^{11}B$ ($CDCl_3$) = 45.3. − $\delta^{13}C$ (C_6D_6) = 21.3 (*o*-CH_3), 22.9 (*p*-CH_3), 31.6 (CMe_3), 52.9 (CMe_3), 127.7 (*m*-C), 135.4 (*p*-C), 137.3 (*o*-C), *ipso*-C signal not obsd. − $C_{26}H_{42}B_2N_2$ (404.26): calcd. C 77.25, H 10.47, N 6.93; found C 77.08, H 10.40, N 6.92.

B,B′-Di(tert-butyloxy)-B,B′-dimesityldiborane(4) (**8**): Dichlorodimesityldiborane(4) (0.90 g, 2.7 mmol) was dissolved in 40 ml of hexane. At −35°C, a suspension of NaO*t*Bu (0.52 g, 5.4 mmol) in 30 ml hexane was added to the stirred solution. Stirring was continued overnight, while the mixture was allowed to reach ambient temp. The insoluble material (0.34 g) was removed by filtration and the filtrate was kept at −20°C, resulting in the deposition of 0.83 g of **8** (2.05 mmol, 75%) in the form of cubic crystals within 1 d; m.p. 158−162°C. − NMR (C_6D_6): δ^1H = 1.27 (s, 18 H, $OCMe_3$), 2.00 (s, 12 H, *o*-CH_3), 2.23 (s, 6 H, *p*-CH_3), 6.63 (s, 4 H, *m*-H). − $\delta^{11}B$ = 57.0. − $\delta^{13}C$ = 21.1 (*p*-CH_3), 22.1 (*o*-CH_3), 30.8 ($OCMe_3$), 77.4 ($OCMe_3$), 126.8 (*m*-C), 135.6 (*p*-C), 136.8 (*o*-C), *ipso*-C signal not obsd. − MS (70 eV); *m/z* (%): 406 (2) [$M^{\bullet+}$], 349 (100) [$M^{\bullet+}$ − *t*Bu], 333 (27) [$M^{\bullet+}$ − O*t*Bu], 173 (90) [$M^{\bullet+}$ − *t*Bu − C_4H_8 − mesH], 147 (85) [$M^{\bullet+}$ − *t*Bu − C_4H_8 − OBmes]. − $C_{26}H_{40}B_2O_2$ (406.23): calcd. C 76.88, H 9.93; found C 75.06, H 9.52.

B,B′-Dimesityl-B,B′-di(phenylthio)diborane(4) (**9**): (a) To a stirred solution of $mes_2B_2Cl_2$ (1.20 g, 3.66 mmol) in 35 ml of hexane at −30°C, was added a mixture of thiophenol (0.81 g, 7.3 mmol) and triethylamine (0.74 g, 7.3 mmol, 1.01 ml), dissolved in 10 ml of hexane. A voluminous white precipitate of [Et_3N·HCl] formed immediately. To allow better stirring, the reaction mixture was quickly warmed to 0°C and 20 ml of benzene was added. After stirring overnight, the solid was removed by filtration (0.96 g, 95% [Et_3NH]Cl), and the filtrate was concentrated to dryness in vacuo. After adding 20 ml of hexane to the residue, insoluble material was removed by filtration. Cooling the clear filtrate to −20°C yielded 0.70 g of **9** (1.46 mmol, 40%).

(b) To a stirred solution of $mes_2B_2Cl_2$ (0.89g, 2.96 mmol) in 30 ml of hexane at −35°C was added a suspension of LiSPh (0.69 g, 5.9 mmol) in 20 ml of hexane. The reaction mixture was allowed to warm to ambient temp. and then stirred overnight. The white precipitate (0.30 g, 120% "LiCl") was removed by filtration and the filtrate was concentrated to a volume of approximately 30 ml. Storing this solution at −50°C yielded a colorless crystalline mass within 3 d, which was collected and dried in vacuo. The crystals turned slightly yellowish, but no decomposition was detectable. Yield 0.96 g (2.01 mmol, 68%); m.p. 58−62°C. − NMR ($CDCl_3$): δ^1H = 1.95 (s, 12 H, *o*-CH_3), 2.13 (s, 6 H, *p*-CH_3), 6.54 (s, 4 H, *m*-H), 7.0−7.12 (m, 10 H, Ph). − $\delta^{11}B$ = 80.6. − $\delta^{13}C$ = 21.0 (*p*-CH_3), 22.0 (*o*-CH_3), 126.9 (*m*-C_{mes}), 127.3 (*p*-C_{Ph}), 128.3 (*o*-C_{Ph}), 131.2 (*m*-C_{Ph}), 134.0 (*i*-C_{Ph}), 135.6 (*o*-C_{mes}), 136.6 (*p*-C_{mes}), 137.8

(*i*-C_{mes}). – $C_{30}H_{32}B_2S_2$ (478.34): calcd. C 75.33, H 6.74, S 13.41; found C 75.04, H 6.74, S 13.45.

B,B′-Di(tert-butylthio)-B,B′-dimesityldiborane(4) (**10**): To a solution of $mes_2B_2Cl_2$ (1.62 g, 4.89 mmol) in 70 ml of hexane at −40°C was added a suspension of Li*S*t*B*u (0.94 g, 9.8 mmol) in 30 ml of hexane. The reaction mixture was stirred overnight while it warmed to ambient temp. The insoluble material (0.49 g, 118% "LiCl") was filtered off, and the light-yellow filtrate was stored at −20°C. Colorless, rectangular crystals of **10** separated. On concentrating the solution still further to less than half of its original volume, a second crop of **10** was obtained. Total yield: 1.80 g (84%); m.p. 183−185°C. – NMR ($CDCl_3$): δ^1H = 1.24 (s, 18 H, CMe_3), 1.91 (s, 12 H, *o*-CH_3), 2.23 (s, 6 H, *p*-CH_3), 6.65 (s, 4 H, *m*-H). – $\delta^{11}B$ = 77.0. – $\delta^{13}C$ = 21.0 (*p*-CH_3), 22.3 (*o*-CH_3), 32.0 (CMe_3), 49.2 (CMe_3), 127.1 (*m*-C), 135.7 (*o*-C), 136.3 (*p*-C), *ipso*-C signal not obsd. – MS (70 eV); *m/z* (%): 438 (11) [$M^{\bullet+}$], 381 (26) [$M^{\bullet+}$ − *t*Bu], 324 (100) [$M^{\bullet+}$ − 2 *t*Bu], 219 (10) [mesBS*t*Bu$^+$], 162 (100) [mesBS$^{\bullet+}$]. – $C_{26}H_{40}B_2S_2$ (438.36): calcd. C 71.24, H 9.42, S 14.63; found C 71.08, H 8.92, S 13.70.

2,3-Dimesityl-1,4,2,3-dithiadiborinane (**11**): To a solution of $mes_2B_2Cl_2$ (1.00 g, 3.02 mmol) in 40 ml of hexane at −35°C was added a suspension of dilithium ethanedithiolate (0.32 g, 3.0 mmol) in 30 ml of hexane. The reaction mixture was allowed to warm to ambient temp. and stirring was continued overnight. The white precipitate (0.28 g, 109% "LiCl") was separated, and the filtrate was concentrated to dryness in vacuo. The yellow residue was treated with 30 ml of hexane, centrifuged for 10 min (1200 rpm), and the clear solution was stored at −20°C. Within 3 d, a yellow crystalline mass had formed, which was separated and dried in vacuo. Yield: 0.43 g of **11** (1.2 mmol, 40%), m.p. 115−118 °C. – NMR ($CDCl_3$): δ^1H = 2.17 (s, 6 H, *p*-CH_3), 2.20 (s, 12 H, *o*-CH_3), 2.55 (s, 4 H, CH_2), 6.71 (s, 4 H, *m*-H). – $\delta^{11}B$ = 69.4. – $\delta^{13}C$ = 21.1 (*p*-CH_3), 22.5 (*o*-CH_3), 30.5 (CH_2), 127.8 (*m*-C), 136.6 (*p*-C), 137.0 (*o*-C), *ipso*-C signal not obsd. – $C_{20}H_{26}B_2S_2$ (352.18): calcd. C 68.21, H 7.44, S 18.21; found C 68.33, H 7.78, S 17.26.

X-ray Structure Determinations: Single crystals were either sealed in glass capillaries under argon or were covered and mounted with perfluoroether oil on glass fibres. The setting angles of 15−20 well-centered reflections were used for the determination of the dimensions of the unit cells (Siemens P4) or the data on 60 frames collected with a Siemens P4 instrument equipped with a CCD detector. Data collection was performed by using a graphite monochromator and Mo-K_α radiation, either in the ω/2θ scan mode with variable scan speed, or in the hemisphere mode with 10 s exposures per frame and Δω = 0.3. Data reduction was performed by applying Lorentz and polarization corrections or with the SAINT routine. The structures were solved by direct methods; non-hydrogen atoms were refined anisotropically and, unless stated otherwise, H atoms were refined in calculated positions using a riding model. Programs used: SHELXTL-PC plus[34] and SHELXL-93/97[35]. A summary of the data is given in Table 3. Crystallographic data have been deposited with the Cambridge Crystallographic Data Centre as supplementary publication no. CCDC-102212 (**5**), -102213 (**6**), -102214 (**3**), -102211 (**8**), -102210 (**10**), -102209 (**1a**), -102208 (**1b**), -102207 (**1c**). Copies of the data can be obtained free of charge on application to CCCD, 12 Union Road, Cambridge CB2 1EZ, U.K. [Fax: (internat.) +44-1223/336033; E-mail: deposit@ccdc.cam.ac.uk].

☆ Dedicated to Prof. Dr. Dr. h. c. *Hans Bock* on the occasion of his 70th birthday.

[1] J. Knizek, I. Krossing, H. Nöth, W. Ponikwar, *Eur. J. Inorg. Chem.* **1998**, 505−509.
[2] A. Stock, A. Brandt, H. Fischer, *Ber. Dtsch. Chem. Ges.* **1925**, *58*, 653−655.
[3] R. J. Brotherton, A. L. McClosky, L. L. Petterson, H. J. Steinberg, *J. Am. Chem. Soc.* **1960**, *82*, 6242−6245.
[4] H. Nöth, W. Meister, *Chem. Ber.* **1961**, *94*, 509−514.
[5] H. Nöth, P. Fritz, *Z. Anorg. Allg. Chem.* **1963**, *324*, 129−145.
[6] W. Biffar, H. Nöth, H. Pommerening, *Angew. Chem.* **1980**, *92*, 63; *Angew. Chem. Int. Ed. Engl.* **1980**, *19*, 56.
[7] K. Schlüter, A. Berndt, *Angew. Chem.* **1980**, *92*, 64; *Angew. Chem. Int. Ed. Engl.* **1980**, *19*, 57.
[8] H. Pommerening, Ph. D. Thesis, University of Munich, **1979**.
[9] J. D. Odom, in *Comprehensive Organometallic Chemistry* (Eds.: G. Wilkinson, F. G. A. Stone, E. W. Abel), Pergamon Press, Oxford, **1984**, vol. 1, chapter 5.
[10] [10a] R. Hunold, J. Allwohn, G. Baum, W. Massa, A. Berndt, *Angew. Chem.* **1988**, *100*, 961−963; *Angew. Chem. Int. Ed. Engl.* **1988**, *27*, 961−963. – [10b] R. A. Bartlett, P. P. Power, *Organometallics* **1986**, *5*, 1916−1917.
[11] A. Moezzi, M. M. Olmstead, R. A. Bartlett, P. P. Power, *Organometallics* **1992**, *11*, 2383−2388.
[12] A. Moezzi, M. M. Olmstead, P. P. Power, *J. Chem. Soc., Dalton Trans.* **1992**, 2429−2434.
[13] R. Hunold, Ph. D. Thesis, University of Marburg, **1988**.
[14] B. Kaufmann, R. Jetzfellner, E. Leissring, K. Issleib, H. Nöth, *Chem. Ber.* **1997**, *130*, 1677−1692.
[15] H. Nöth, B. Wrackmeyer, *NMR Spectroscopy of Boron Compounds*, vol. 14, *NMR Basic Principles and Applications* (Eds.: P. Diehl, E. Fluck, R. Kosfeld), Springer Publ., Heidelberg, Berlin, New York, **1978**.
[16] H. O. Kalinowsky, S. Berger, S. Braun, *13*C-NMR-Spektroskopie, G. Thieme Publ., Stuttgart, New York, **1984**.
[17] H. Fußstetter, J. C. Huffman, H. Nöth, H. Schaefer, *Z. Naturforsch., B* **1976**, *31*, 1441−1445.
[18] D. Loderer, H. Nöth, H. Pommerening, W. Rattay, H. Schick, *Chem. Ber.* **1994**, *127*, 1605−1611.
[19] H. Nöth, *Z. Naturforsch., B* **1984**, *39*, 1463−1466.
[20] P. Nguyen, G. Lesley, N. J. Taylor, T. B. Marder, N. L. Pickett, W. Clegg, M. R. J. Elsegood, N. C. Norman, *Inorg. Chem.* **1994**, *33*, 4623−4624.
[21] A. F. Holleman, E. Wiberg, *Lehrbuch der Anorganischen Chemie*, 91−100th ed., Walter de Gruyter Publ., Berlin, New York, **1985**.
[22] P. Finocchiaro, D. Gust, K. Mislow, *J. Am. Chem. Soc.* **1973**, *95*, 7029−7036.
[23] M. T. Ashby, N. A. Sheshtawy, *Organometallics* **1994**, *13*, 236−243.
[24] W. Maringgele, H. Knop, D. Bromm, A. Meller, S. Dielkus, R. Herbst-Irmer, G. M. Sheldrick, *Chem. Ber.* **1992**, *125*, 1807−1813.
[25] G. Linti, D. Loderer, H. Nöth, K. Polborn, W. Rattay, *Chem. Ber.* **1994**, *127*, 1909−1922.
[26] H. Nöth, H. Fußstetter, H. Pommerening, T. Taeger, *Chem. Ber.* **1980**, *113*, 342−357. [27a] H. M. Seip, R. Seip, W. Siebert, *Acta Chem. Scand.* **1973**, *27*, 15−20. – [27b] A. Almenningen, H. M. Seip, P. Vassbotn, *Acta Chem. Scand.* **1973**, *27*, 21−25.
[28] R. Johansen, E. Wisloff-Nilssen, H. M. Seip, W. Siebert, *Acta Chem. Scand.* **1973**, *27*, 3015−3020.
[29] R. Wehmschulte, K. Ruhlandt-Senge, M. M. Olmstead, M. A. Petrie, P. P. Power, *J. Chem. Soc., Dalton Trans.* **1994**, 2113−2117.
[30] H. Nöth, R. Staudigl, W. Storch, *Chem. Ber.* **1981**, *114*, 3024−3043.
[31] R. R. Ryan, K. Hedberg, *J. Chem. Phys.* **1969**, *50*, 4986.
[32] D. D. Danielson, K. Hedberg, *J. Am. Chem. Soc.* **1979**, *101*, 3199−3203.
[33] H. Hommer, H. Nöth, H. Sachdev, H. Schmidt, H. Schwenk, *Chem. Ber.* **1995**, *128*, 1187−1194.
[34] *SHELXTL-PC plus*, Siemens Analytical Instruments.
[35] G. M. Sheldrick, *SHELXL-97*, University of Göttingen, **1997**.

[98143]

Mass-Spectrometric Experiments together with Electronic Structure Calculations Support the Existence of the Elusive Ammonia Oxide Molecule and Its Radical Cation☆

Mark Brönstrup, Detlef Schröder, Ilona Kretzschmar, Christoph A. Schalley[+], and Helmut Schwarz*

Institut für Organische Chemie der Technischen Universität Berlin,
Straße des 17. Juni 135, D-10623 Berlin
Fax: (internat.) + 49(0)30/314-21102
E-mail: schw0531@www.chm.tu-berlin.de

Received May 12, 1998

Keywords: Ab initio calculations / Mass spectrometry / Gas-phase chemistry / Ammonia oxide / Hydroxylamine

Mass-spectrometric experiments were combined with ab initio calculations to explore the cationic and neutral $[H_3,N,O]^{\bullet+/0}$ potential energy surfaces and relevant anionic species. The calculations predict the existence of three stable cationic and neutral $[H_3,N,O]^{\bullet+/0}$ isomers, i.e. ammonia oxide $H_3NO^{\bullet+/0}$ ($\mathbf{1}^{\bullet+/0}$), hydroxylamine $H_2NOH^{\bullet+/0}$ ($\mathbf{2}^{\bullet+/0}$) and the imine-water complex $HNOH_2^{\bullet+/0}$ ($\mathbf{3}^{\bullet+/0}$). Hydroxylamine **2** represents the most stable isomer on the neutral surface (E_{rel} = 0), and the metastable isomers **1** (E_{rel} = 24.8 kcal mol^{-1}) and **3** (E_{rel} = 61.4 kcal mol^{-1}) are separated by barriers of 49.5 kcal mol^{-1} and 64.2 kcal mol^{-1}, respectively. Adiabatic ionization of **2** (IE_a = 9.15 eV) yields $\mathbf{2}^{\bullet+}$, which is 21.4 kcal mol^{-1} more stable than $\mathbf{1}^{\bullet+}$ and 36.4 kcal mol^{-1} more stable than $\mathbf{3}^{\bullet+}$. The barriers associated with the isomerizations of the cations are 58.6 kcal mol^{-1} for $\mathbf{2}^{\bullet+} \rightarrow \mathbf{1}^{\bullet+}$ and 71.4 kcal mol^{-1} for $\mathbf{2}^{\bullet+} \rightarrow \mathbf{3}^{\bullet+}$. Collisional activation (CA) and unimolecular decomposition (MI) experiments allow for a clear distinction of $\mathbf{1}^{\bullet+}$ from $\mathbf{2}^{\bullet+}$. Besides, neutralization/reionization (NR) experiments strongly support the gas-phase existence of the long-sought neutral ammonia oxide.

Introduction

The generation of ammonia oxide (**1**) represents a major challenge to experimentalists working in the field of elusive molecules, as there is a striking discrepancy between the numerous quantum chemical studies,[1] which predict a distinct stability of the molecule, and the still scarce experimental evidence.[2] Moreover, it has recently been stated that "the *possible* characterization of two metastable isomers of hydroxylamine ... would be a significant step forward towards the understanding of important aspects of N/O/H chemistry."[2a]

The fact that homologs of **1** like trialkylamine oxides are well-known, storable compounds indicates that the atom connectivity R_3N-O is not inherently unstable. Therefore, for R = H the main problem is to prevent the isomerization of **1** to the more stable hydroxylamine (**2**). This can occur in two ways, i.e. either a unimolecular [1,2]-H shift or a bi- or termolecular acid/base-catalyzed path, of which we presume the latter to be energetically favorable. Such an acid/base-catalyzed isomerization can be circumvented by generating the species of interest in the diluted gas phase of a mass spectrometer. The generation and characterization of several elusive ionic and neutral molecules has been achieved during the last decade by combining advanced mass-spectrometric techniques, like collisional activation (CA) and neutralization/reionization (NR), with appropriate theoretical means.[3][4]

Nowadays, theoretical calculations of small systems, like $[H_3,N,O]$, can achieve an accuracy such that they do complement the experimental results. Therefore, we have performed a series of mass-spectrometric experiments and calculated all relevant structures of the cationic and neutral $[H_3,N,O]$ surfaces with a G2-like ab initio method; also the anionic species are briefly discussed (see below). The neutral surface was reexamined using the same level of theory, as previous theoretical studies did not include the relevant exit channels. For the sake of simplicity and readability, the potential energy surfaces (PES) of the different charge states are calibrated to the respective global minima, which are set to zero (E_{rel} = 0). As all the experiments start from cationic states, the cationic PES will be discussed first.

Theoretical Results

The relative energies of all relevant species of the $[H_3,N,O]^{\bullet+}$ surface are displayed in Table 1. Ionized hydroxylamine ($\mathbf{2}^{\bullet+}$) represents the global minimum (E_{rel} = 0) and possesses a planar structure. Mulliken analysis reveals that the spin density is distributed between the nitrogen (0.80) and the oxygen atom (0.20). This indicates that the unpaired electron is mainly located on the nitrogen atom, but that there is also exchange with the adjacent oxygen lone pairs. As a consequence, the N−O bond length is significantly shortened compared to neutral hydroxylamine (128 pm vs. 144 pm, see below). A [1,2]-H shift from the nitrogen to the oxygen atom requires an energy of 58.6 kcal mol^{-1} and leads to the ammonia oxide cation ($\mathbf{1}^{\bullet+}$), which

[+] Present address: The Skaggs Institute for Chemical Biology, The Scripps Research Institute, 10550 North Torrey Pines Road, La Jolla, CA, 92037, USA.

 © WILEY-VCH Verlag GmbH, D-69451 Weinheim, 1998 1434−1948/98/1010−1529 $ 17.50+.50/0

is a minimum with E_{rel} = 21.4 kcal mol^{-1}. Thus, the calculations suggest that the ammonia oxide cation (**1**$^{\bullet+}$) is trapped in a potential well which may be deep enough to capture **1**$^{\bullet+}$ without facile isomerization to **2**$^{\bullet+}$ or dissociation. With respect to the lowest lying direct exit channel for the dissociation of $[H_3,N,O]^{\bullet+}$, i.e. loss of H$^{\bullet}$ (E_{rel} = 69.7 kcal mol^{-1}), unimolecular isomerization **1**$^{\bullet+}$ ⇌ **2**$^{\bullet+}$ is, however, conceivable. The ammonia oxide cation (**1**$^{\bullet+}$) has C_s symmetry due to a small Jahn-Teller distortion of the C_{3v}-symmetric molecule. The unpaired electron is located on the oxygen atom (spin density = 1.05). In contrast to hydroxylamine, the N−O bond is not shortened, but slightly elongated upon ionization of the neutral **1** (138 pm vs. 135 pm, see below); this can be explained in terms of a diminished electrostatic interaction compared to the neutral $H_3N^+-O^-$ zwitterion. Another minimum structure of $[H_3,N,O]^{\bullet+}$ is obtained by a [1,2]-H shift from the nitrogen to the oxygen atom starting from hydroxylamine. The resulting distonic ion **3**$^{\bullet+}$ (E_{rel} = 36.4 kcal mol^{-1}) can be regarded as an ion-dipole complex between the imine fragment (*IE* = 13.49 eV) and the water cation (*IE* = 12.612 eV).[5] The barrier associated with this [1,2]-H shift (E_{rel} = 71.4 kcal mol^{-1}) implies that the $NH_2OH^{\bullet+}$/$NHOH_2^{\bullet+}$ isomerization is disfavored compared to the $NH_2OH^{\bullet+}$/$NH_3O^{\bullet+}$ equilibrium. Moreover, the exit channel for loss of H$^{\bullet}$ to yield H_2NO^+ **4**$^+$ is lower in energy (E_{rel} = 69.7 kcal mol^{-1}) and has much smaller entropical restrictions than the rearrangement **2**$^{\bullet+}$ → **3**$^{\bullet+}$. Therefore, we expect that $NHOH_2^{\bullet+}$ (**3**$^{\bullet+}$), can hardly be generated by isomerization starting from **1**$^{\bullet+}$ and **2**$^{\bullet+}$ when the $[H_3,N,O]^{\bullet+}$ surface is accessed experimentally. A further proton shift from the nitrogen to the oxygen atom and consecutive fragmentation yields H_3O^+ and N (^4S) as the lowest lying exit channel of the cationic PES (E_{rel} = 49.3 kcal mol^{-1}). However, as H_3O^+ and N (^4S) can only be produced after spin crossing and extensive isomerization, severe kinetic restrictions are imposed on this otherwise thermochemically favorable exit channel.

Cleavage of one of the N−H bonds in ionized hydroxylamine (**2**$^{\bullet+}$) gives H$^{\bullet}$ and *cis*- or *trans*-$HNOH^+$ (**5**$^+$) with E_{rel} = 87.0 kcal mol^{-1} (*trans*) and 93.6 kcal mol^{-1} (*cis*), respectively (Table 2).[6] Further exit channels of $[H_3,N,O]^{\bullet+}$ yield $HNO^{\bullet+}$ (**6**$^{\bullet+}$) and H_2 (E_{rel} = 58.4 kcal mol^{-1}), $NOH^{\bullet+}$ (**7**$^{\bullet+}$) and H_2 (E_{rel} = 73.2 kcal mol^{-1}), or NO^+, **8**$^+$, H_2, and H$^{\bullet}$ (E_{rel} = 77 kcal mol^{-1}). Although these exit channels are low in energy, they are associated with significant activation barriers. Thus, the transition state **TS 1**$^{\bullet+}$**/6**$^{\bullet+}$ for 1,1-elimination of H_2 from **1**$^{\bullet+}$ has a relative energy of 89.5 kcal mol^{-1}, and the transition state **TS 2**$^{\bullet+}$**/7**$^{\bullet+}$ for the analogous 1,1-elimination of H_2 from **2**$^{\bullet+}$ has a relative energy of 92.3 kcal mol^{-1}. Despite an intensive search from several starting geometries, a transition state for a formal 1,2-elimination from **2**$^{\bullet+}$ could not be located. Instead, optimization leads to two transition structures **TS 5**$^+$**/6**$^{\bullet+}$ and **TS 4**$^+$**/6**$^{\bullet+}$, which are featured by linear O−H−H (**TS 5**$^+$**/6**$^{\bullet+}$) and N−H−H (**TS 4**$^+$**/6**$^{\bullet+}$) arrangements. An analysis of the internal reaction coordinate (IRC) reveals that the respective reaction pathways correspond to an attack of a hydrogen atom at H_2NO^+ (**4**$^+$) and at $HNOH^+$ (**5**$^+$), respectively, to yield $HNO^{\bullet+}$ (**6**$^{\bullet+}$) and H_2. Although the barriers associated with these transition structures are comparable to those for **TS 1**$^{\bullet+}$**/6**$^{\bullet+}$ and **TS 2**$^{\bullet+}$**/7**$^{\bullet+}$, it is hard to imagine that **TS 4**$^+$**/6**$^{\bullet+}$ or **TS 5**$^+$**/6**$^{\bullet+}$ can be reached, because instead of a long-range H migration starting from **1**$^{\bullet+}$ or **2**$^{\bullet+}$, an irreversible loss of the migrating hydrogen atom appears to be favored. Therefore, it is suggested that the only ways to produce $HNO^{\bullet+}$/H_2 from $[H_3,N,O]^{\bullet+}$ proceed by 1,1-eliminations (**TS 1**$^{\bullet+}$**/6**$^{\bullet+}$ and **TS 2**$^{\bullet+}$**/7**$^{\bullet+}$). Two different pathways of NO^+ generation from $[H_3,N,O]^{\bullet+}$ are conceivable: Either H_2 elimination to yield $[H,N,O]^{\bullet+}$ precedes H$^{\bullet}$ abstraction, or H$^{\bullet}$ is lost first to yield **4**$^+$ and/or **5**$^+$, which can subsequently be dehydrogenated to NO^+. The calculations predict that the initial H_2 eliminations either from **1**$^{\bullet+}$ or from **2**$^{\bullet+}$ are strongly favored by at least 66.1 kcal mol^{-1} compared to the dehydrogenations of **4**$^+$ and **5**$^+$ (Figure 1). Therefore, it can be concluded that only the pathway involving loss of H_2 followed by loss of H$^{\bullet}$ is relevant for NO^+ production in the present context.

Losses of one or several hydrogen atoms do not reveal information about the connectivity of the $[H_3,N,O]^{\bullet+}$ precursors. For a structural elucidation, fragments arising from cleavage of the N−O bond are decisive: Cleavage of N−O in **2**$^{\bullet+}$ into NH_2^+ ($^3B_1$) and OH$^{\bullet}$ has an energy demand of E_{rel} = 104.0 kcal mol^{-1}, whereas the N−O cleavage of **1**$^{\bullet+}$ to yield O (^3P) and $NH_3^{\bullet+}$ requires E_{rel} = 79.4 kcal mol^{-1}. For **2**$^{\bullet+}$, the calculations predict a competition of two processes: The direct bond cleavage into NH_2^+ ($^3B_1$) and OH$^{\bullet}$ is energetically disfavored, but has probably no kinetic restriction. In contrast, while the production of $NH_3^{\bullet+}$ + O

Table 1. Total energies *E* in Hartree for $[H_3, N, O]^{\bullet+/0}$ species; *E* = *E*[CCSD(T)/6-311G(d,p)] + *E*[MP2/6-311+G(3df,2p)] − *E*[MP2/6-311G(d,p)] + ZPVE

Species	Total energy in Hartree
NH_3O (**1**)	−131.453218
$^3NH_3O$ (^{3}**1**)	−131.403453
NH_3O, with geometry of **1**$^{\bullet+}$	−131.451865
NH_2OH (**2**)	−131.492710
$^3NH_2OH$ (^{3}**2**)	−131.399248
NH_2OH, gauche,gauche conf.	−131.486162
NH_2OH, with geometry of **2**$^{\bullet+}$	−131.444508
$NHOH_2$ (**3**)	−131.394834
MECP $^1NH_3O$/$^3NH_3O$	−131.387307
TS 1/2	−131.413806
TS 2/3	−131.390428
TS 2/6	−131.314067
TS 2/7	−131.351575
TS 1/6	−131.375234
$NH_3O^{\bullet+}$ (**1**$^{\bullet+}$)	−131.119145
$NH_3O^{\bullet+}$, with geometry of **1**	−131.118677
$NH_2OH^{\bullet+}$ (**2**$^{\bullet+}$)	−131.156460
$NH_2OH^{\bullet+}$, with geometry of **2**	−131.098877
$NHH_2O^{\bullet+}$ (**3**$^{\bullet+}$)	−131.098450
TS 1$^{\bullet+}$**/2**$^{\bullet+}$	−131.063322
TS 2$^{\bullet+}$**/6**$^{\bullet+}$	−131.001773
TS 1$^{\bullet+}$**/6**$^{\bullet+}$	−131.013807
TS 2$^{\bullet+}$**/6**$^{\bullet+}$	−131.042749
TS 2$^{\bullet+}$**/7**$^{\bullet+}$	−131.009346
TS 5$^+$**/6**$^{\bullet+}$	−131.001773
TS 4$^+$**/6**$^{\bullet+}$	−131.015157

Table 2. Total energies E in Hartree for $[H_3,N,O]^{\bullet+/0}$ fragmentation products; $E = E$[CCSD(T)/6-311G(d,p)) + E(MP2/6-311+G-(3df,2p)] − E[MP2/6-311G(d,p)] + ZPVE

Species	Total energy in Hartree
$H_2NO^{\bullet}$ (**4**$^{\bullet}$)	−130.871158
trans-$HNOH^{\bullet}$ (**5**$^{\bullet}$)	−130.860474
cis-$HNOH^{\bullet}$ (**5**$^{\bullet}$)	−130.852498
HNO (**6**)	−130.282162
^{3}NOH (**7**)	−130.237766
$NO^{\bullet}$ (**8**$^{\bullet}$)	−129.701610
NH_3	−56.435131
^3O	−74.966971
$OH^{\bullet}$	−75.625497
$H_2N^{\bullet}$	−55.770735
H_2	−1.160442
H	−0.499810
^4N	−54.510044
^3NH	−55.126862
^1NH	−55.060045
H_2O	−76.308577
NH_2O^+ (**4**$^+$)	−130.545642
trans-$NHOH^+$ (**5**$^+$)	−130.517986
cis-$NHOH^+$ (**5**$^+$)	−130.507510
$NHO^{\bullet+}$ (**6**$^{\bullet+}$)	−129.902885
$NOH^{\bullet+}$ (**7**$^{\bullet+}$)	−129.879370
NO^+ (**8**$^+$)	−129.373546
TS 4$^+$/8$^+$	−130.404296
TS 5$^+$/8$^+$	−130.383696
$NH_3^{\bullet+}$	−56.062959
$^1NH_2^+$	−55.316852
$^3NH_2^+$	−55.365182
$H_2O^{\bullet+}$	−75.847343
$NH^{\bullet+}$	−54.636206
H_3O^+	−76.56788

and $NH_3^{\bullet+}$ is favored due to thermochemical *and* kinetic reasons.

The profile of the neutral $[H_3,N,O]$ surface resembles its cationic counterpart as far as the hydroxylamine/ammonia oxide region is concerned. Hydroxylamine (**2**) again represents the global minimum and has two C_s-symmetrical conformers which differ in energy by 4.1 kcal mol^{-1} (E_{rel} = 0 for θ_{HNOH} = 125.1°, E_{rel} = 4.1 kcal mol^{-1} for θ_{HNOH} = 57.4°). Hydroxylamine (**2**) can isomerize to ammonia oxide (**1**) by a [1,2]-H shift with an energy barrier of 49.5 kcal mol^{-1}. **1** lies 24.8 kcal mol^{-1} higher in energy than **2**, but may be captured as a metastable molecule due to the reverse barrier of 24.7 kcal mol^{-1} towards isomerization to **2** and a barrier of 48.9 kcal mol^{-1} associated with fragmentation into HNO and H_2. The N−O bond in **1** is significantly shorter than in **2** (135 pm vs. 144 pm), which can be rationalized with an electrostatic attraction of the zwitterionic **1** and the repulsion of lone pairs in **2**. The two molecules are predicted to differ also in other physical properties such as dipole moments[7] (μ = 5.63 D for **1** and 0.788 D for **2**) or vertical ionization energies[8][9] (IE_v = 9.1 eV for **1** and 10.72 eV for **2**). Two factors are mainly responsible for the fact that vertically ionized hydroxylamine is 36.1 kcal mol^{-1} above the minimum geometry of the cation. First, the minimum-energy conformation of **2**$^{\bullet+}$ is planar, while C_s-symmetrical, neutral **2** has a dihedral HNOH angle of 125°. Secondly, the N−O bond lengths in **2** and **2**$^{\bullet+}$ differ significantly (Figures 3 and 4). In contrast, the geometry changes upon adiabatic ionization of **1** are negligible, and IE_a and

Figure 1. Potential energy surface of cationic $[H_3,N,O]^{\bullet+}$; zero-point corrected energies given in kcal mol^{-1} relative to $H_2NOH^{\bullet+}$ (**2**$^{\bullet+}$)

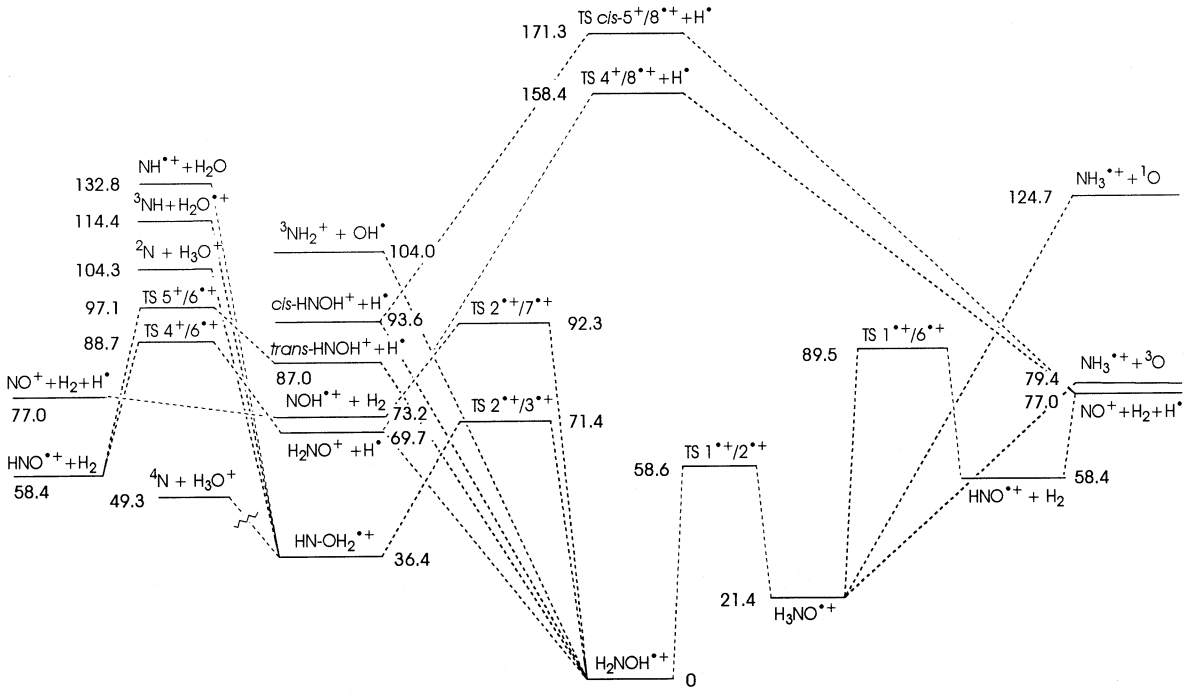

is lower in energy, it is kinetically hampered due to the entropic restrictions associated with **TS 1**$^{\bullet+}$**/2**$^{\bullet+}$. For ionized ammonia oxide, however, the direct fragmentation into O

IE_v differ by no more than 0.29 kcal mol^{-1}. As a result, the vertical ionization energies of hydroxylamine (IE_v = 10.72 eV) and ammonia oxide (IE_v = 9.1 eV) differ by as much

Figure 2. Potential energy surface of neutral $[H_3,N,O]$; zero-point corrected energies given in kcal mol^{-1} relative to H_2NOH (**2**)

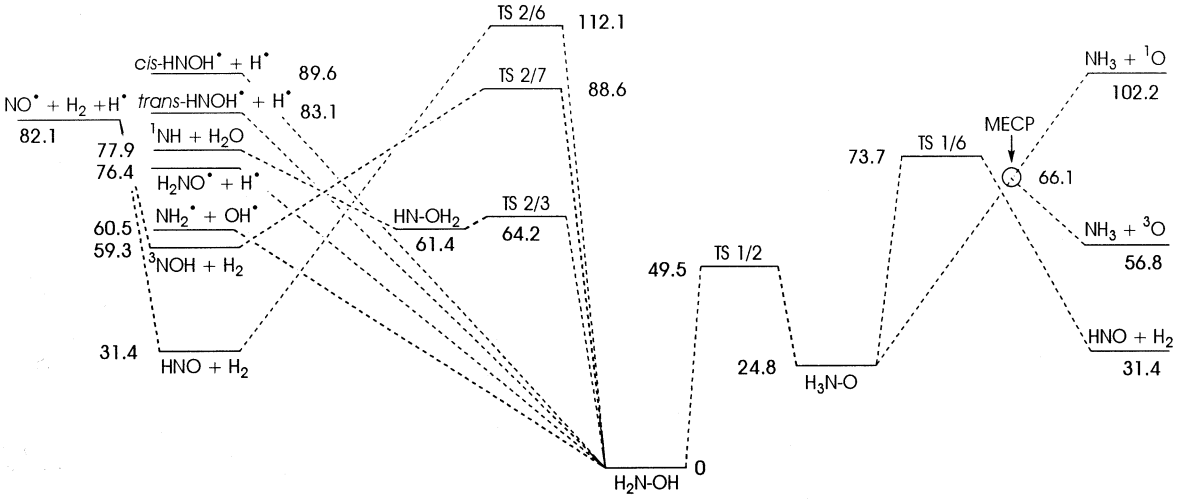

as 1.6 eV, although IE_a is comparable for both isomers.[8][9] A similar difference can be discerned for the recombination processes of an electron with the cations to the neutral molecules. In fact, these pronounced differences in physical properties may enable an experimental distinction of these two isomers.

The stability of the third neutral isomer, the imine-water complex **3**, has very much decreased compared to the cationic surface. The minimum structure is hardly more stable than the transition state of the [1,2]-H shift **TS 2/3**, and a further internal energy of 16.5 kcal mol^{-1} is sufficient to dissociate the molecule into ^{1}NH and H_2O. Dissociation into ^{3}NH and H_2O is exothermic by 25.5 kcal mol^{-1}, but a spin-forbidden process for **^{1}3**.

The relative heights of the exit channels are also different from the cationic surface, especially as far as the structure-indicative channels involving N−O bond cleavage are concerned. In this respect, dissociation of $[H_3,N,O]$ into $H_2N^•$ and $OH^•$ represents the lowest lying, barrier-free exit channel with a relative energy of 60.5 kcal mol^{-1}, whereas the spin-allowed dissociation into O (^1D) and NH_3 becomes quite unfavorable with a relative energy of 102.2 kcal mol^{-1}. Therefore, the dissociation behaviour of the neutral isomers is expected to be quite different from that of the cations, in that for $[H_3,N,O]$ formation of $H_2N^•$ and $OH^•$ should be more pronounced than $NH_2^+ + OH^•$ for $[H_3,N,O]^{•+}$. The relative stability of the closed-shell pair HNO + H_2 (31.4 kcal mol^{-1}) is much higher than $H^•$ losses to yield the open-shell pairs $H_2NO^• + H^•$ (76.4 kcal mol^{-1}), *trans*-$HNOH^• + H^•$ (83.1 kcal mol^{-1}) and *cis*-$HNOH^• + H^•$ (89.6 kcal mol^{-1}). However, HNO + H_2 formation is again hampered by significant activation barriers of 73.7 kcal mol^{-1} for 1,1-elimination from H_3NO and of 112.1 kcal mol^{-1} for 1,2-elimination from H_2NOH. Besides, NOH (^{3}A″) and H_2 (E_{rel} = 59.3 kcal mol^{-1}) are obtained by 1,1-elimination of H_2 from H_2NOH, which is associated with a barrier of 88.6 kcal mol^{-1}.

Figure 3. Calculated bond lengths in pm and angles in degrees of relevant cationic $[H_3,N,O]^{•+}$ species; for geometries of $[H_2,N,O]^+$ species pertinent to the present work, see ref.[6]

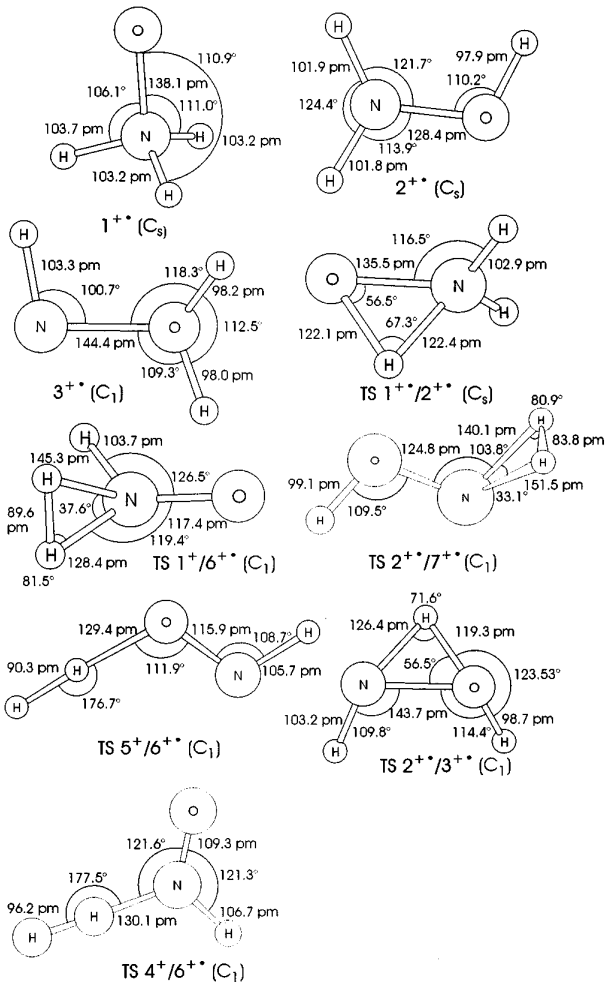

Figure 4. Calculated bond lengths in pm and angles in degrees of relevant neutral $[H_3,N,O]$ species

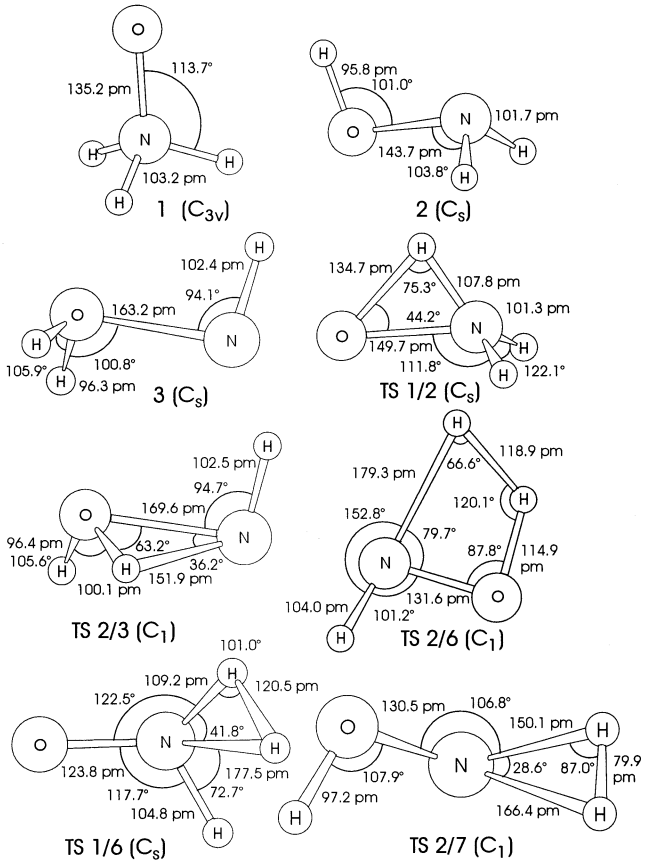

The $NH_3 + O$ (^3P) exit channel has a comparatively low relative energy of 56.8 kcal mol^{-1}, but cannot be entered from the singlet surface in a spin-allowed manner. However, two processes that eventually yield $^3O + NH_3$ should be mentioned briefly: (i) The dissociation of ^3H_3NO (^{3}**1**), which has an energy of 56 kcal mol^{-1} relative to **2** and 31.2 kcal mol^{-1} relative to $^1NH_3O$ (^{1}**1**), is spin-allowed. However, the N−O distance in geometry-optimized ^{3}**1** is 296 pm, revealing that the structure actually corresponds to a $^3O\cdots NH_3$ van der Waals complex with a binding energy of only 0.8 kcal mol^{-1}. A triplet structure for H_2NOH could not be located, but a second minimum on the triplet surface corresponding to $H_2N^{\bullet}\cdots H-O^{\bullet}$ with r_{N-H} = 200 pm was found with an energy of 58.7 kcal mol^{-1} relative to ^{1}**2**, only 1.9 kcal mol^{-1} below the separated species $H_2N^{\bullet}$ and $HO^{\bullet}$. (ii) In addition, the $NH_3 + O$ (^3P) exit channel might be accessed by spin crossing of ^{1}**1** en route to oxygen dissociation. The highest spin crossing probability is achieved at geometries where both spin states possess the same energy. Therefore, the minimum energy crossing point (MECP) for the H_3N-O dissociation was located with a recently developed method.[10] Most efficient crossing is expected at N−O distances of 192 pm, where the molecule has an energy of 66.1 kcal mol^{-1} relative to **1**.

As far as $[H_3,N,O]^{\bullet-}$ anions are concerned, three minimum structures could be located that all correspond to weakly bound ion-dipole complexes.[4][11] The respective relative energies are E_{rel} = 0 for $HNH^{\bullet}\cdots OH^-$, E_{rel} = 3.1 kcal mol^{-1} for $HOH\cdots NH^{\bullet-}$ and E_{rel} = 7.7 kcal mol^{-1} for $H_2NH\cdots O^{\bullet-}$. None of the complexes possesses an intact N−O bond, and dissociations into $H_2N^{\bullet}$ and OH^- (E_{rel} = 15.3 kcal mol^{-1}), NH_3 and $O^{\bullet-}$ (E_{rel} = 23.3 kcal mol^{-1}) or into $HN^{\bullet-}$ and H_2O (E_{rel} = 27.3 kcal mol^{-1}) can occur easily. We would like to point out that both neutral isomers **1** and **2** possess negative vertical electron affinities, i.e. EA_v = −22.8 kcal mol^{-1} for **1** and EA_v = −47.4 kcal mol^{-1} for **2**. Thus, theory strongly suggests that a distinction of neutral **1** and **2** by electron attachment experiments, which have been applied successfully to the generation and identification of the neutral singlet water oxide molecule,[4][11] is not feasible for the $[H_3,N,O]$ system.

In conclusion, the quantum chemical calculations predict the existence of three $[H_3,N,O]^{\bullet+/0}$ isomers. Whereas the shapes of the neutral and cationic PES are similar concerning the hydroxylamine/ammonia oxide tautomerism, distinct differences exist with respect to the energetics of the fragmentation channels.

Experimental Results

The analysis of the hydroxylamine/ammonia oxide system based on dissociation products is hampered by an analytical problem, because the structure-indicative cleavages of the N−O bonds lead to fragments of equal masses, i.e. $NH_2^{\bullet}$ and O (both 16 amu) as well as NH_3 and $OH^{\bullet}$ (both 17 amu). Therefore, we decided to carry out additional experiments with the fully deuterated analogs $[D_3,N,O]$, such that the combination of the two sets of data allows for a deconvolution of the overlapping fragments, i.e. ND_2 and OD (both 18 amu) as well as ND_3 and D_2O (both 20 amu). In order to produce the three different isomers $\mathbf{1}^{\bullet+}$, $\mathbf{2}^{\bullet+}$, and $\mathbf{3}^{\bullet+}$, the following precursors were chosen. (i) A mixture of NH_3 and N_2O was subjected to chemical ionization in which one may envision N_2O as a donor for atomic oxygen to afford ammonia oxide cation $\mathbf{1}^{\bullet+}$. (ii) Pure hydroxylamine was ionized to (predominantly) yield $\mathbf{2}^{\bullet+}$. (iii) Surprisingly, electron ionization of an aqueous N_3H solution also yields reasonable amounts of $[H_3,N,O]^{\bullet+}$, and high mass-resolution and labeling experiments assured that the selected beam actually had the desired elemental composition. The mechanism of $[H_3,N,O]^{\bullet+}$ formation could not be established and seems particularly obscure for N_3H/H_2O. Although we cannot exclude rigorously ion-molecule reactions, the fact that the highest yields of $[H_3,N,O]^{\bullet+}$ are obtained under electron ionization conditions suggests that a volatile, hitherto uncharacterized N,H,O compound is liberated from an aqueous mixture of NaN_3 and H_2SO_4. Methods (i) and (iii) gave similar spectra (Table 3), but the $[H_3,N,O]^{\bullet+}$ intensities obtained from N_3H/H_2O were much higher than those from NH_3/N_2O. Thus, in the following discussion, the fragmentation patterns obtained for ionized

NH_2OH are compared with those for N_3H/H_2O and their deuterated analogues.

Table 3. Relative intensities of fragments generated from different $[H_3,N,O]$ and $[D_3,N,O]$ precursors

$[H_3,N,O]$ Experiment	Precursors	Fragment mass in amu 33	32	31	30	19	18	17	16	15	14
	NH_2OH		100	20	2			0.4	0.5		
MI	NH_3/N_2O		100	5				2			
	HN_3/H_2O		100	6	1			4			
	NH_2OH		100	18	27	0.4	1	3	4	0.6	0.2
CA	NH_3/N_2O		100	12	16	0.4	1	5	3	1	0.2
	HN_3/H_2O		100	14	19	1	2	11	4	1	0.2
	NH_2OH	100	71	12	20		1	11	16	3	1
NR	NH_3/N_2O	100	48	14	17			15	19	1	
	HN_3/H_2O	100	62	16	21	1	2	17	22	7	2
NR-CA	NH_2OH		100	24	38		2	9	13	2	2
	HN_3/H_2O		100	30	40			30	20		

$[D_3,N,O]$ Experiment	Precursors	Fragment mass in amu 36	34	32	30	22	20	18	16	14
	ND_2OD		100	2	1		0.5	0.6		
MI	ND_3/N_2O		100				4			
	DN_3/D_2O		100	1			12			
	ND_2OD		100	15	18	1	7	10	1	0.5
CA	ND_3/N_2O		100	10	13	1	14	9	2	1
	DN_3/D_2O		100	15	14	1	15	8	1	0.2
	ND_2OD	100	56	9	10		7	27	5	1
NR	ND_3/N_2O	100	31	5	10		6	15	2	
	DN_3/D_2O	100	56	17	18		15	51	17	2
NR-CA	ND_2OD		100	26	34		18	25	4	

The intensities of the metastable ion (MI) spectra are low, consistent with the fact that $[H_3,N,O]$ has only few degrees of freedom for the storage of internal energy. In all spectra, the by far dominant process corresponds to $H^\bullet$ loss to yield $[H_2,N,O]^+$, which is the lowest lying barrier-free exit channel of the system. However, as already mentioned neither this nor the other hydrogen loss channels are indicative as far as structural aspects are concerned. Thus, the following discussion is primarily based on the structurally indicative signals due to N−O bond cleavage. Unimolecular dissociation of ionized hydroxylamine yields fragments of masses 16 and 17 in a 1.3:1 ratio, while only mass 17 is observed in the MI experiment using the HN_3/H_2O mixture as precursor. Accordingly, the MI spectrum of $[D_3,N,O]^{\bullet+}$ obtained from DN_3/D_2O gives rise to a single signal at mass 20, which demonstrates that exclusively $ND_3^{\bullet+}$ is formed. In comparison, the MI spectrum of $ND_2OD^{\bullet+}$ is featured by two peaks at $m = 18$ and $m = 20$ in a 1.2:1 ratio, indicating that ND_2^+ as well as $ND_3^{\bullet+}$ are produced with ND_2^+ slightly dominating. Further, the combined analysis of the results obtained for the unlabeled and the labeled ions suggests that contributions of oxygen-containing fragments are minor in the MI mass spectra. This is consistent with the order of the *IE*s of the complementary fragments arising from $[H_3,N,O]$, i.e. $IE(NH_2) = 11.4$ eV vs. $IE(OH) = 13.0$ eV and $IE(NH_3) = 10.2$ eV vs. $IE(O) = 13.6$ eV.[5]

An increase of the internal energy of the molecules by collisional activation leads to much more abundant fragmentations. In addition, a fraction of "hot" molecules possesses lifetimes long enough to allow for extensive rearrangements preceding decomposition, which is indicated by fragments like $H_2O^{\bullet+}$ and H_3O^+ (or $D_2O^{\bullet+}$ and D_3O^+, respectively). Nonetheless, collisional activation with ions having keV energies promotes characteristic direct bond cleavages which are valuable for a structural characterization.

Due to collision-induced isomerization, the differences in the CA spectra of the two precursors are less pronounced compared to the metastable ion decay patterns. However, whereas ionized hydroxylamine shows an *m*/*z* 16/17 ratio of 1.3:1, this ratio amounts to 1:2.7 for the ion observed from the HN_3/H_2O mixture (Figures 5a and 5b). Analogous results are obtained with the deuterated compounds, in that the 18/20 ratio for ND_2OD is 1.4:1, as compared to 1:1.9 for the DN_3/D_2O mixture. In order to probe whether an alteration of the ion internal energy has any effect, CA spectra of $\mathbf{2}^{\bullet+}$ were also recorded at various ionization energies ranging from 10 to 100 V under EI conditions; in addition, **2** was ionized under CI conditions at higher source pressures. Except for the $HNO^{\bullet+}/NO^+$ ratio (see below), both variations, however, did not lead to significant changes of fragmentation patterns, suggesting that internal energy effects can be neglected to a first approximation.

The differences in the MI and CA spectra of the two precursors prove that the ion beam produced via HN_3/H_2O cannot consist of $\mathbf{2}^{\bullet+}$ alone. In fact, the absence of the signal at 16 amu in the MI spectra suggests that rather a pure beam of ammonia oxide ($\mathbf{1}^{\bullet+}$) is produced. The dominant

Figure 5. Mass spectra of $[H_3,N,O]^{\bullet+}$ ions generated from HN_3/H_2O and NH_2OH, respectively, as neutral precursors; CA spectra for HN_3/H_2O (a) and NH_2OH (b), $^{+}NR^{+}$ spectra for HN_3/H_2O (c) and NH_2OH (d), and $^{+}NR^{+}$/CA spectra for HN_3/H_2O (e) and NH_2OH (f)

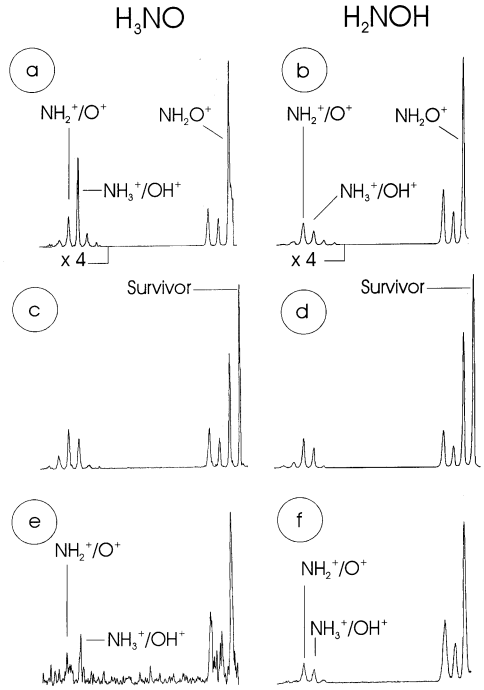

signal corresponds to $NH_3^{\bullet+}$, which is in line with an NH_3-O connectivity, whereas the dominant fragment of the NH_2OH precursor is NH_2^+, as expected for the NH_2-OH connectivity. In both MI and CA experiments, the HN_3/H_2O couple gives rise to a much more distinct and characteristic 16/17 ratio compared to NH_2OH. An explanation can be derived from the cationic potential energy surface. The $NH_3^{\bullet+}$ + O (^3P) exit channel is much lower in energy compared to NH_2^+ + $OH^{\bullet}$ (58 kcal mol^{-1} vs. 104 kcal mol^{-1}). Starting from $\mathbf{2}^{\bullet+}$, two decomposition paths compete. Compared to the direct bond cleavage to yield NH_2^+ + OH, the $NH_3^{\bullet+}$ + O exit channel is energetically favored, but entropically severely disfavored due to the necessity of a hydrogen migration. Especially in the MI experiment, the ions can store only a relatively low amount of internal energy; therefore, a fraction of molecules does not possess enough energy to access direct bond cleavage, but undergoes isomerization instead. Another indication for the formation of $\mathbf{1}^{\bullet+}$ from HN_3/H_2O is the fact that the intensity of the N–O cleavage relative to the base peak is much smaller for NH_2OH compared to HN_3/N_2O. A common feature of the CA spectra of both precursors is that NO^+ formation is more pronounced than $[H,N,O]^{\bullet+}$ formation, although the $NO^+/H_2/H^{\bullet}$ exit channel is 18.6 kcal mol^{-1} higher in energy than $HNO^{\bullet+}/H_2$ and 3.8 kcal mol^{-1} higher than $NOH^{\bullet+}/H_2$. The theoretical results show that for $[H,N,O]^{\bullet+}$ production, barriers of 89.5 kcal mol^{-1} for 1,1-elimination from $\mathbf{1}^{\bullet+}$ and of 92.3 kcal mol^{-1} for 1,1-elimination from $\mathbf{2}^{\bullet+}$ have to be overcome. Therefore, *every* generated $[H,N,O]^{\bullet+}$ + H_2 unit has an internal excess energy of at least 19.1 kcal mol^{-1}. This excess energy is sufficient to convert a considerable fraction of $[H,N,O]^{\bullet+}$ immediately to NO^+ and $H^{\bullet}$. It was found that the $NO^+/[H,N,O]^{\bullet+}$ ratio varies easily with experimental conditions, pointing to a high sensitivity of this particular ratio towards the internal energy. Unimolecular decomposition of both precursors yields, next to dominant $H^{\bullet}$ loss, small amounts of $[H,N,O]^{\bullet+}$ and NO^+, the $[H,N,O]^{\bullet+}$ signal being higher in each case. In contrast to that, unimolecular decomposition of $\mathbf{4}^+$ and $\mathbf{5}^+$ produces mainly NO^+ and only minor amounts of $HNO^{\bullet+}$ cation.[6] Therefore, it can be concluded that at least in the low-energy regime, $[H,N,O]^{\bullet+}$ and NO^+ fragments in $[H_3,N,O]^{\bullet+}$ are not generated via $[H_2,N,O]^+$ as an intermediate, but produced on a different way, probably by H_2 elimination; this conjecture is completely in line with the theoretical predictions. Finally, it should be noted that signals due to H_3O^+ ions are minor in CA spectra and not observed at all in MI spectra of both precursors, although fragmentation into H_3O^+ and N (^4S) is predicted to be the thermodynamically most favorable exit channel of $[H_3,N,O]^{\bullet+}$. Obviously, access to this fragmentation is severely hampered by the kinetic restrictions associated with extensive isomerization and spin crossing.

After having shown that two different cationic $[H_3,N,O]^{\bullet+}$ precursors can be distinguished, an experimental differentiation of the corresponding neutral counterparts **1** and **2** is attempted. One approach to neutral ammonia oxide is based on the strategy shown in Scheme 1. Thus, a precursor molecule H_2N-OR is protonated with a suitable CI gas. If the preferred protonation site is nitrogen, and if the group R can form a stable cation, metastable ion decay of H_3N^+-O-R may lead to R^+ and neutral ammonia oxide (H_3NO). This route can be followed by performing CIDI (collision induced dissociative ionization) experiments in which after deflection of all charged species from the beam, the neutrals are subsequently reionized and detected.[12] CIDI experiments were performed with $H_2NOSiMe_3$ (**9**), $H_2NOSiMe_2Ph$, and $H_2NOSi\mathit{t}BuPh_2$ as precursors.[13] Although the stabilities of the cationic leaving groups should increase in the order $SiMe_3^+ < SiMe_2Ph^+ < Si\mathit{t}BuPh_2^+$, meaningful CIDI spectra could only be obtained for **9**. This is probably a consequence of the fact that the effective kinetic energies of the neutral $[H_3,N,O]$ fragments decrease with increasing size of the precursor, which lowers the reionization yields of $[H_3,N,O]$. The MI spectrum of $H_3NOSiMe_3^+$, which was generated by protonation of **9** with methane as CI gas,[14] is featured by losses of 15 amu (30%), 16 amu (100%), and 33 amu (50%), demonstrating that the heaviest neutral fragment lost is actually $[H_3,N,O]$. The most important feature of the CIDI spectrum is that reionized neutral $[H_3,N,O]$ constitutes the base peak in the spectrum. According to the MI spectrum, no peaks with masses higher than 33 should be present in a pure CIDI spectrum. Small signals between 40 and 47 amu indicate, however, that few NR processes occur due to diffusion of the reionization gas through the deflector region of the mass spectrometer.[12] The key issue is, however,

whether the peak at *m*/*z* 33 can be assigned unambiguously to reionized ammonia oxide. Mainly two concerns discard the CIDI experiment as a proof. Although theory predicts that *N*-protonation of **9** is favored over *O*-protonation by 16 kcal mol^{-1}, it cannot be excluded that a fraction of molecules is protonated at the oxygen atom, because the protonation with methane as CI gas is strongly exothermic at either side, i. e. 86.4 kcal mol^{-1} and 70.4 kcal mol^{-1}, respectively.[15] Thus, one might argue that the observed reionized [H_3,N,O] stems from the *O*-protonated species, which produces hydroxylamine concomitantly with the generation of $SiMe_3^+$. Moreover, even if exclusive initial *N*-protonation is assumed, one cannot rule out a possible [1,2]-H shift from the nitrogen to the oxygen atom prior to or concerted with $SiMe_3^+$ loss. Both objectives would be disprovable if it was possible to examine *N*-protonated $Me_3SiNHOH$, but this compound has not been synthesized yet. Due to the concerns mentioned, for the time being the CIDI experiments should be regarded as an experimental hint for neutral ammonia oxide rather than a proof.

Scheme 1

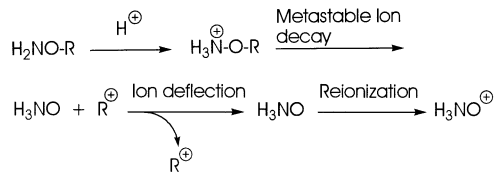

In a different approach to generate the neutral [H_3,N,O] molecule, the cationic beam was neutralized with xenon, and after removal of all ionic species from the beam, the neutrals were reionized with oxygen, subsequently mass-analyzed and detected.[3] The base peak of all neutralization-reionization spectra belongs to intact [H_3,N,O], which demonstrates the distinct stability of neutral [H_3,N,O] (Figures 5c and 5d). As low-mass fragments represent a superposition of decompositions of the projectile ion, the neutral transient, and the reionized species, structural information of the neutrals is difficult to achieve from fragment ion analysis. However, we note that the most intense peak in the lower mass region corresponds to $NH_2^\bullet$ ($ND_2^\bullet$) for both precursors, in line with the theoretical predictions for this exit channel.

The mere observation of an NR survivor ion arising from cationic ammonia oxide does, however, not prove the existence of neutral ammonia oxide, as the structural integrity might have been lost by isomerization at the neutral stage. Therefore, the structure of reionized [H_3,N,O] survivor ions was examined by a collisional activation experiment (Figures 5e and 5f). For H_2NOH and its deuterated analog, CA and NR/CA spectra are practically indistinguishable, which proves that no significant isomerization occurs at the neutral stage. The corresponding NR/CA experiment with the ammonia oxide precursor was conducted close to the detection limit of the instrument. Although the signal-to-noise ratio is poor, it can be seen that the fragmentation pattern in the structurally indicative region again resembles the observed CA pattern for the ammonia oxide cation rather than that of ionized NH_2OH (Fig. 5e and 5f). Thus, at least a complete isomerization **1** → **2** at the neutral stage seems improbable. Further, the intense survivor ion in NR spectra indicates favorable Franck-Condon factors for single-electron reduction to neutral **1**, being in line with the fact that the geometries of neutral and cationic ammonia oxide are very similar. The $NH_2^+/NH_3^{\bullet+}$ ratio in the NR/CA spectrum of $\mathbf{2}^{\bullet+}$ (Figure 5f) also implies that hydroxylamine does not isomerize during the NR experiment, in spite of the much less favorable Franck-Condon overlap of cation and neutral.

In conclusion, relevant points of the cationic and neutral $[H_3,N,O]^{\bullet+/0}$ surface have been calculated on a high theoretical level, predicting the existence of three different [H_3,N,O] isomers. Information obtained from the experiments, combined with the theoretical results, show that two cationic $[H_3,N,O]^{\bullet+}$ species can be distinguished in the gas phase. Furthermore, the experiments strongly suggest the existence of neutral ammonia oxide, although a definitive proof cannot be provided yet. This ambiguity is probably due to (i) the fact that the differences of the NR spectra of $\mathbf{1}^{\bullet+}$ and $\mathbf{2}^{\bullet+}$ are minor suggesting a compensation of Franck-Condon effects in conjunction with the different fragmentation channels accessible and (ii) the failure to perform $^-CR^+$ and/or $^-NR^+$ experiments as far as meaningful information about connectivity is concerned. Nonetheless, the NR/CA experiments presented here are very much in favor of the generation of $\mathbf{1}^{\bullet+}$ upon ionization of HN_3/H_2O as well as the generation of neutral ammonia oxide **1**.

We are grateful to the *Deutsche Forschungsgemeinschaft*, the *Fonds der Chemischen Industrie*, and the *Volkswagen-Stiftung* for financial support. M. B. and I. K. acknowledge the *Stiftung Stipendien-Fonds des Verbandes der Chemischen Industrie* for Ph. D. scholarships. We thank Dr. *J. N. Harvey* for helpful discussions concerning the quantum chemical calculations.

Experimental Section

The experiments were performed with a modified VG/ZAB/HF/AMD four-sector mass spectrometer of *BEBE* configuration (*B* stands for magnetic and *E* for electric sector), which has been described in detail elsewhere.[16] NH_2OH and N_3H/H_2O were ionized by a beam of electrons (100 eV) in an electron ionization source (repeller voltage ca. 30 V). NH_3/N_2O mixtures were ionized under chemical ionization conditions. The ions of interest were accelerated to 8 keV and mass-selected by means of *B*(1)/*E*(1) at a resolution of $m/\Delta m \geq 3000$; isobaric impurities, i.e. O_2H^+ and $N_2H_5^+$ for [H_3,N,O] or $N_2D_4^{\bullet+}$ and $D_2O_2^{\bullet+}$ for [D_3,N,O] were either absent or baseline-resolved. Unimolecular fragmentations occurring in the field-free region preceding the second magnet are referred to as metastable ion spectra. For collisional activation experiments, helium (80% transmission, T) was admitted to a collision cell located between *E*(1) and *B*(2). In these MI and CA experiments, the ionic fragments were recorded by scanning *B*(2). For comparison with the NR/CA spectra (see below), MI and CA experiments were also performed with *B*(1)/*E*(1)/*B*(2)-mass-selected ions, scanning products with *E*(2). For NR experiments, cations were neutralized

by collisions with xenon (80% T); unreacted ions were removed from the beam. Subsequent reionization of the neutrals was achieved by collision with oxygen (80% T), and the resulting cationic fragments were recorded by scanning *B*(2). For NR/CA experiments, the survivor ions of the NR experiment were mass-selected with *B*(2), collided with helium (80% T), and the produced fragments were recorded by scanning *E*(2). In order to improve the signal-to-noise ratio, 5−100 spectra were accumulated and online-processed with the AMD-Intectra data system.

ND_2OD was obtained by repeated recrystallization of pure NH_2OH in CH_3CH_2OD. Pure NH_2OH was deliberated from $NH_2OH \cdot HCl$ with NaOEt.[17] ND_3 was produced by deuterolysis of Mg_3N_2 with D_2O. Aqueous HN_3 was produced by dropping concentrated sulfuric acid into a solution of NaN_3 in water. The concentration of HN_3 solutions was about 1−5%. $H_2NOSiMe_3$, $H_2NOSiMe_2Ph$, and $H_2NOSitBuPh_2$ were synthesized by treating hydroxylamine with the corresponding chlorosilanes $ClSiR_3$ in dichloromethane.[18] All chemicals were introduced in the ion source via the metal-free teflon/glass inlet system.[19]

Ab initio quantum-mechanical calculations were performed with IBM RS/6000 workstations and Pentium PCs using Gaussian 94.[20] For trimethylsilyl-substituted species, geometries were fully optimized at the HF/6-31G* level, and single-point energies were calculated at the MP2/6-31G* level. For all other species, full geometry optimizations and frequency calculations were carried out at the MP2/6-311G(d,p) level. The effect of using larger basis sets and a better correlation treatment was examined by performing single-point MP2/6-311+G(3df,2p) and CCSD(T)/6-311G(d,p) calculations at the previously optimized geometries. These results were further used to determine extrapolated[21] CCSD(T)/6-311+G(3df,2p) energies in an approach similar to the well-known G2 method.[23] All data in Tables 1 and 2 include the unscaled MP2/6-311G** zero-point energy corrections. The relative energy of ^1O was determined by adding the experimental value for the $^3P \rightarrow {}^1D$ excitation (1.967 eV)[24] to the calculated total energy of ^3O. Analogously, the relative energy of ^2N was determined by adding the experimental value for the $^4S \rightarrow {}^2D$ excitation (2.383 eV)[24] to the calculated total energy of ^4N. The minimum energy crossing point (MECP) of H_3NO was located by employing a recently developed hybrid method[10] which calculates energy gradients at the MP2/6-311G(d,p) level and energies of stationary points at the CCSD(T)/6-311G(d,p) level. The geometries of both spin states were adjusted until the energy difference between them was smaller than 0.06 kcal mol^{-1}.

☆ Dedicated to Professor Dr. *Ernst Schmitz*, Berlin, on the occasion of his 70th birthday.

[1] [1a] B. Kallies, R. Mitzner, *J. Phys. Chem. B* **1997**, *101*, 2959. − [1b] T. P. Cunningham, D. L. Cooper, J. Gerrat, P. B. Karadakov, M. Raimondi, *Int. J. Quantum Chem.* **1996**, *60*, 393. − [1c] R. Ponec, M. Krack, K. Jug, *Theor. Chim. Acta* **1996**, *93*, 165. − [1d] N. N. Kharabaev, V. V. Rachkovskii, A. D. Garnovkii, *Zh. Obshch. Khim.* **1995**, *65*, 1650 (*Chem. Abstr.* **1996**, *125*, 151522x). − [1e] R. D. Bach, A. L. Owensby, C. Gonzales, H. B. Schlegel, J. J. W. McDouall, *J. Am. Chem. Soc.* **1991**, *113*, 6001. − [1f] S. M. Bachrach, *J. Org. Chem.* **1990**, *55*, 1016. − [1g] Y.-Z. Han, D.-Z. Zhu, C.-D. Zhao, *Chin. J. Chem.* **1990**, *5*, 405. − [1h] J. A. Pople, K. Raghavachari, M. J. Frisch, J. S. Binkley, P. v. R. Schleyer, *J. Am. Chem. Soc.* **1983**, *105*, 6389. − [1i] F. Grein, J. L. Lawlor, *Theor. Chim. Acta* **1983**, *63*, 161. − [1j] H. Wallmeier, W. Kutzelnigg, *J. Am. Chem. Soc.* **1979**, *101*, 2804. − [1k] C. Trindle, D. D. Shillady, *J. Am. Chem. Soc.* **1973**, *95*, 703.

[2] [2a] D. Luckhaus, *Ber. Bunsenges. Phys. Chem.* **1997**, *101*, 346. − [2b] B. Kuhn, O. V. Boyarkin, T. R. Rizzo, *Ber. Bunsenges. Phys.* **1997**, *101*, 339. − [2c] D. Luckhaus, *J. Chem. Phys.* **1997**, *106*, 8409. − [2d] M. N. Hughes, K. Shrimanker, *Inorg. Chim. Acta* **1976**, *18*, 69.

[3] [3a] C. A. Schalley, G. Hornung, D. Schröder, H. Schwarz, *J. Chem. Soc. Rev.* **1998**, *27*, 91. − [3b] N. Goldberg, H. Schwarz, *Acc. Chem. Res.* **1994**, *27*, 347. − [3c] F. Turecek, *Org. Mass Spectrom.* **1992**, *27*, 1087.

[4] Two problems closely related to $[H_3,N,O]$ concerning the $HOOH/H_2OO$ and the $HNNH/H_2NN$ tautomerism have been investigated by mass spectrometry: For $[H_2,O_2]$, see: D. Schröder, C. A. Schalley, N. Goldberg, J. Hrušák, H. Schwarz, *Chem. Eur. J.* **1996**, *2*, 1235; for $[H_2,N_2]$, see: N. Goldberg, M. C. Holthausen, J. Hrušák, W. Koch, H. Schwarz, *Chem. Ber.* **1993**, *126*, 2753.

[5] S. G. Lias, J. F. Liebmann, J. L. Holmes, R. D. Levin, W. G. Mallard, *J. Phys. Chem. Ref. Data* **1988**, *17*, 695.

[6] For a combined MS and theoretical study of $[H_2,N,O]^+$ ions, see: [6a] D. Schröder, F. Grandinetti, J. Hrušák, H. Schwarz, *J. Phys. Chem* **1992**, *96*, 4841. − [6b] F. Grandinetti, J. Hrušák, D. Schröder, H. Schwarz, *J. Phys. Chem.* **1992**, *96*, 2100. − [6c] C. Lifshitz, P. J. A. Ruttink, G. Schaftenaar, J. K. Terlouw, *Mass Spectrom. Rapid Commun.* **1987**, *1*, 61.

[7] Our calculated dipole moments agree fairly well with the experimentally determined values of 0.59 D for hydroxylamine (taken from *Selected Values of Electric Moments for Molecules in the Gas Phase*, U.S. Department of Commerce, National Bureau of Standards, **1967**) and of 5.0 D for Me_3NO (taken from: N. Hacket, R. J. W. Fevre, *J. Chem. Soc.* **1961**, 1612).

[8] The discrepancy between our calculated value for $IE_a(\mathbf{2}) = 9.15$ eV and the literature values (9.6 eV[9a] and 10.0 eV[9b]) derived from photoelectron spectra is quite high. We ascribe it to the absence of the 0-0 transition in the experiment, yielding an overestimation of IE_a. The calculated value for $IE_v(\mathbf{2}) = 10.72$ eV and the experimental values (10.6 eV[9a] and 10.56 eV[9b]) agree much better.

[9] [9a] I. A. Koppel, U. M. Mölder, R. J. Pikver, *Org. React.* **1983**, *20*, 45. − [9b] R. E. Kutina, G. L. Goodman, J. Berkowitz, *J. Chem. Phys.* **1982**, *77*, 1664.

[10] [10a] J. N. Harvey, M. Aschi, H. Schwarz, W. Koch, *Theor. Chem. Acc.* **1998**, *99*, 95. − [10b] D. Schröder, C. Heinemann, H. Schwarz, J. N. Harvey, S. Dua, S. J. Blanskby, J. H. Bowie, *Chem. Eur. J.*, in press.

[11] [11a] J. Hrušák, H. Friedrichs, H. Schwarz, H. Razafinjanahary, H. Chermette, *J. Phys. Chem.* **1996**, *100*, 100. − [11b] S. Humbel, I. Demachy, P. C. Hilberty, *Chem. Phys. Lett.* **1995**, *247*, 126.

[12] [12a] M. J. Polce, S. Beranova, M. J. Nold, C. Wesdemiotis, *J. Mass Spectrom.* **1996**, *31*, 1073. − [12b] J. L. Holmes, A. A. Mommers, *Org. Mass Spectrom.* **1984**, *19*, 460. − [12c] P. C. Burgers, J. L. Holmes, A. A. Mommers, J. E. Szulejko, J. K. Terlouw, *Org. Mass Spectrom.* **1984**, *19*, 442.

[13] Attempts to protonate $F_3CCONHOH$ and $H_2NOCOCF_3$ lead to loss of HF instead of the desired loss of neutral H_3NO.

[14] Whereas protonation with H_2 was not feasible, use of isobutane as CI gas gave the same results as with methane.

[15] The heats of reaction were determined by substracting the proton affinity of methane (132 kcal mol^{-1}) from the calculated proton affinity for *N*- and *O*-protonation of **9**. The calculated total energies including zero point corrections are −538.8831 hartree for $H_2NOSiMe_3$, −539.4069 hartree for $H_3NOSiMe_3^+$ and −539.2033 hartree for $H_2NOHSiMe_3^+$.

[16] [16a] C. A. Schalley, D. Schröder, H. Schwarz, *Int. J. Mass Spectrom. Ion Processes* **1996**, *153*, 173. − [16b] R. Srinivas, D. Sülzle, W. Koch, C. H. DePuy, H. Schwarz, *J. Am. Chem. Soc.* **1991**, *113*, 5970. − [16c] R. Srinivas, D. Sülzle, T. Weiske, H. Schwarz, *Int J. Mass Spectrom. Ion Processes* **1991**, *107*, 368.

[17] R. Steudel, P. W. Schenk in *Handbuch der präparativen anorganischen Chemie* (Ed.: G. Brauer), F. Enke Verlag, Stuttgart, **1975**, p. 464.

[18] J. C. Bottaro, C. D. Clifford, A. Dodge, *Synth. Commun.* **1985**, *15*, 1333.

[19] C. A. Schalley, R. Wesendrup, D. Schröder, T. Weiske, H, Schwarz, *J. Am. Chem. Soc.* **1995**, *117*, 7711.

[20] M. J. Frisch, G. W. Trucks, H. B. Schlegel, P. M. W. Gill, B. G. Johnson, M. A. Robb, J. R. Cheeseman, T. Keith, G. A. Petersson, J. A. Montgomery, K. Raghavachari, M. A. Al-Laham, V. G. Zakrzewski, J. V. Ortiz, J. B. Foresman, J. Cioslowski, B. B. Stefanov, A. Nanayakkara, M. Challacombe, C. Y. Peng, P. Y. Ayala, W. Chen, M. W. Wong, J. L. Andres, E. S. Replogle, R. Gomperts, R. L. Martin, D. J. Fox, J. S. Binkley, D. J. Defrees,

J. Baker, J. P. Stewart, M. Head-Gordon, C. Gonzalez, J. A. Pople, *Gaussian 94, Revision E.1*, Gaussian, Inc., Pittsburgh PA, **1995**.
[21] E[CCSD(T)/6-311+G(3df,2p)] ≈ E[CCSD(T)/6-311G(d,p)] + E[MP2/6-311+G(3df,2p)] − E[MP2/6-311G(d,p)] + ZPVE; for details, see ref.[22].
[22] [22a] C. W. Bauschlicher, H. Partridge, *J. Chem. Phys.* **1995**, *103*, 1788. − [22b] L. A. Curtiss, K. Raghavachari, P. C. Redfern, J. A. Pople, *J. Chem. Phys.* **1997**, *106*, 1063.
[23] L. A. Curtiss, K. Raghavachari, G. W. Trucks, J. A. Pople, *J. Chem. Phys.* **1991**, *94*, 7221.
[24] G. Herzberg, *Molecular Spectra and Molecular Structure*, vol. 1, 2nd ed., Krieger Publishing Company, Malabar, **1993**, p. 447.
[98147]

The Inferior p-Donor Ability of Phosphanyl versus Amino Substituents: Consequences on the Stability and Reactivity of Phosphanyl- and Aminocarbenes

Stéphanie Goumri, Yann Leriche, Heinz Gornitzka, Antoine Baceiredo, and Guy Bertrand*

Laboratoire de Chimie de Coordination du CNRS,
205 route de Narbonne, F-31077 Toulouse Cédex, France
Fax: (internat.) + 33-5/61553003
E-mail: gbertran@lcctoul.lcc-toulouse.fr

Received May 14, 1998

Keywords: Carbenes / Insertions / Donor systems / Phosphorus heterocycles

Bis(diisopropylamino)(trimethylstannyl)phosphane (**2**) reacts with the (chloromethylene)diisopropylammonium salt **1** affording the *C*-phosphanyl-substituted iminium salt **3** (67 % yield), which features a short C–N (1.284 Å) and a long P–C bond (1.850 Å), a planar iminium nitrogen atom and a pyramidalized phosphorus atom. Deprotonation of **3** leads to the enamine **8** (92 % yield), while addition of sodium methoxide followed by thermolysis of the resulting hemiaminal **9** (90 % yield) gives rise to the azaphosphetane **10** (85 % yield), by intramolecular CH insertion of the transiently formed (amino)(phosphanyl)carbene **6**.

Introduction

The genuine carbene nature of stable phosphanylcarbenes **A**[1] and diaminocarbenes **B**[2] is still a debatable topic.[3] Part of the debate relates to the role of the heteroatom substituents. Indeed, in the ground state, both **A** and **B** feature a heteroatom−carbon multiple-bond character.[4] In a recent paper, Schleyer et al[5] mentioned that "the *inherent* p donor capabilities of the heavier elements are as large as or larger than their second row counterparts" but add that "the superior ability of nitrogen compared to phosphorus to act as a p donor is due to the ease in achieving the optimum planar configurations with sp^2 hybridization". Here we report our preliminary results concerning the synthesis of an "(amino)(phosphanyl)carbenium salt",[6][7] and the generation of an (amino)(phosphanyl)carbene.

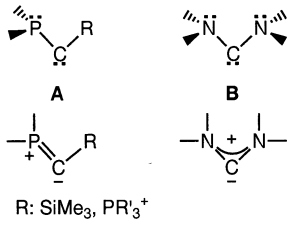

Results and Discussion

The "[bis(diisopropylamino)phosphanyl](diisopropylamino)carbenium salt" **3** was obtained in 67% yield, along with chlorotrimethylstannane, on reaction of the (chloromethylene)ammonium salt **1**[8a] with the stannylphosphane **2**[9] (Scheme 1). Only one signal is observed in the ^{1}H- and ^{13}C-NMR spectra for the four CH groups of the amino substituents bonded to the phosphorus atom, while two signals are detected for the two CH groups of the amino group directly bonded to the carbon atom. Thus, in solution, derivative **3** has to be regarded as *C*-phosphanyl-substituted iminium salt **3a**. Single crystals of **3** suitable for an X-ray diffraction study were grown from a dichloromethane/ether solution at −20°C. The molecular structure of **3** along with pertinent geometric parameters are shown on Figure 1. The C(1) and N(1) atoms are planar (sum of the angles: 359.9 and 359.8°, respectively) while the phosphorus atom is strongly pyramidalized (sum of the angles: 308.48°). The C(1)−P (1.850 Å) and the C(1)−N(1) (1.284 Å) bond lengths are in the range expected for C−P single and C=N double bonds, respectively. Therefore, in solution and in the solid state, derivative **3** has to be regarded as *C*-phosphanyl-substituted iminium salt **3a**, and not as (*C*-aminomethylene)phosphonium salt **3b**,[10] clearly demonstrating the superior p donor ability of the nitrogen compared to the phosphorus atom toward carbenium centers.

Scheme 1

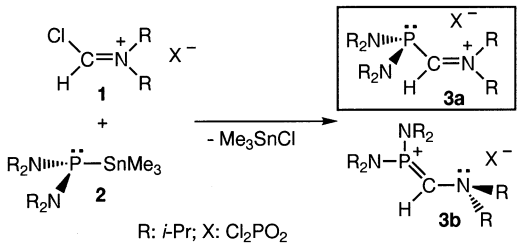

Recently, the bis(diisopropylamino)carbene **5** has been obtained by a reaction of the corresponding formamidinium chloride **4** with LDA.[8a] However, this synthetic method appeared inappropriate to generate the (amino)-

 © WILEY-VCH Verlag GmbH, D-69451 Weinheim, 1998 1434−1948/98/1010−1539 $ 17.50+.50/0

Figure 1. Molecular structure of **3**[a]

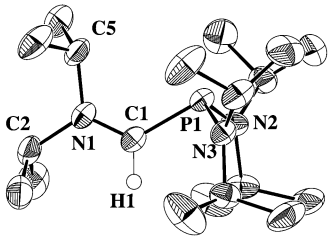

[a] Selected bond lengths [Å] and angles [°]: C(1)−N(1) 1.284(4), C(1)−P(1) 1.850(3), C(1)−H(1) 0.99(4); N(2)−P(1)−N(3) 113.90(12), N(3)−P(1)−C(1) 97.93(13), N(2)−P(1)−C(1) 96.65(13), N(1)−C(1)−P(1) 124.6(2), N(1)−C(1)−H(1) 115.6(2.2), P(1)−C(1)−H(1) 119.7(2.2), C(1)−N(1)−C(2) 121.3(3), C(1)−N(1)−C(5) 120.2(7), C(2)−N(1)−C(5) 118.3(7), N(1)−C(2)−C(3) 110.3(3), N(1)−C(2)−C(4) 110.3(3).

(phosphanyl)carbene **6**. Indeed, LDA reacts with **3**, but leads to the enamine **8** (92% yield), probably through the transient formation of the azomethine ylide **7**, followed by a prototropic rearrangement (Scheme 2).

In order to generate the (amino)(phosphanyl)carbene **6**, the synthetic method developed by Enders et al. was used.[11] Compound **3** was first treated with sodium methoxide affording the hemiaminal **9** in 90% yield, which was subsequently thermolyzed at 160°C under vacuum. Instead of the desired carbene **6**, the azaphosphetane **10** was obtained in 85% yield. The formation of heterocycle **10** clearly results from a regio- and stereoselective intramolecular insertion of the transient carbene **6** into a methine C−H bond of an isopropylamino group bonded to P. The same regio- and stereoselectivity have already been observed with the diphosphanylcarbene **11**.[12] Note that CH insertions are typical reactions for transient singlet carbenes, but have never been observed with diaminocarbenes[13] (Scheme 3).

Conclusion

For cationic species, the experimental results reported here clearly corroborate the theory:[5] an amino substituent has a better p-donor ability than a phosphanyl substituent. For carbenes with comparable steric hindrance, it was already known that the diaminocarbenes are stable,[8b] while the diphosphanylcarbenes are only transient intermediates;[12] the (amino)(phosphanyl)carbenes seem also to be unstable. Therefore, from these results and those previously

Scheme 2

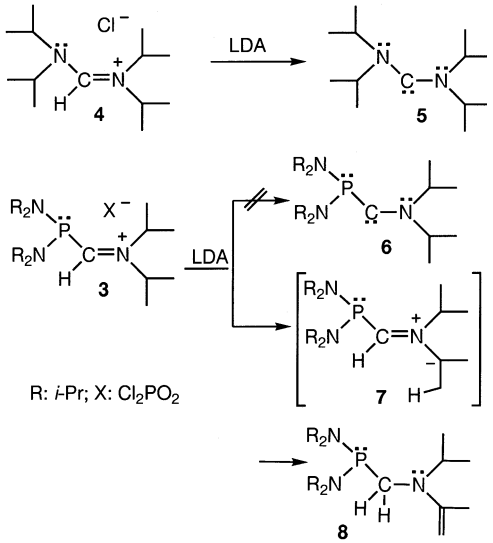

reported in the literature, it seems clear that the stabilization of singlet[14] carbenes can at least be achieved by two strong p-donor substituents *which can easily adopt a planar configuration*, and by the combination of a weak p donor with a p-acceptor substituent,[15] such as in **A**.

We thank the *CNRS* for financial support of this work, and the *Alexander von Humboldt Foundation* for a grant to H. G.

Experimental Section

General: All experiments were performed under dry argon. Melting points are uncorrected. ^{1}H-, ^{13}C-, and ^{31}P-NMR spectra were recorded with Brucker AC80, AC200, WM250, or AMX400 spectrometers. ^{1}H- and ^{13}C-chemical shifts are reported in ppm relative to Me_4Si as external standard. ^{31}P-NMR downfield chemical shifts are expressed with a positive sign, in ppm, relative to external 85% H_3PO_4. Mass spectra were obtained with a Ribermag R10 10E instrument. Conventional glassware was used.

3: To a CH_2Cl_2 solution (5 ml) of (chloromethylene)ammonium salt **1** (0.28 g, 1 mmol) was added at −78°C one equivalent of [bis(diisopropylamino)]trimethylstannylphosphane (**2**) (0.39 g, 1 mmol). The solution was allowed to warm to room temperature (r.t.) and stirred for a further 30 min. After evaporation of the solvent under vacuum, the residue was dissolved in a minimum of CH_2Cl_2. Compound **3** was precipitated as a yellow solid (0.32 g, 67%) by adding Et_2O. M.p. 153°C. − ^{31}P NMR (32 MHz, $CDCl_3$):

Scheme 3

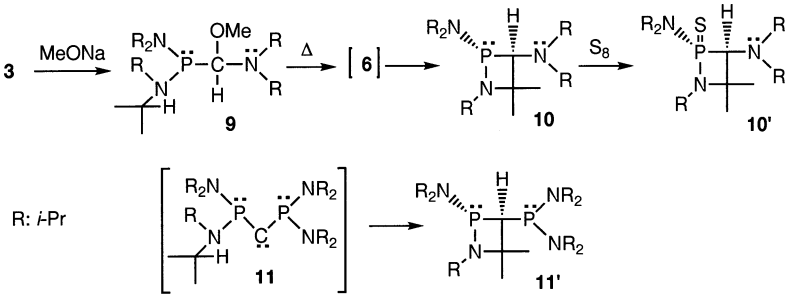

δ = 32.3 (N_2P), −10.3 (PO_2). − ^{1}H NMR (200 MHz, $CDCl_3$): δ = 9.78 (s, 1 H; CH), 5.22 [sept, ^3J(H,H) = 6.6 Hz, 1 H, CNCH], 4.21 [sept d, ^3J(H,H) = 6.7 Hz, ^4J(P,H) = 2.3 Hz, 1 H, CNCH], 3.80 [sept d, ^3J(H,H) = 6.6 Hz, ^3J(P,H) = 5.9 Hz, 4 H, PNCH], 1.61 [d, ^3J(H,H) = 6.6 Hz, 6 H, CNCHCH_3], 1.46 [d, ^3J(H,H) = 6.7 Hz, 6 H, CNCHCH_3], 1.28 [d, ^3J(H,H) = 6.6 Hz, 12 H, PNCHCH_3], 1.16 [d, ^3J(H,H) = 6.6 Hz, 12 H, PNCHCH_3]. − ^{13}C NMR (50 MHz, $CDCl_3$): δ = 183.6 [d, ^1J(P,C) = 21.7 Hz, P-C], 59.6 [d, ^3J(P,C) = 32.9 Hz, CN*C*H], 54.9 (s, CN*C*H), 49.0 [d, ^2J(P,C) = 12.3 Hz, PNCH], 25.0 [d, ^3J(P,C) = 6.2 Hz, PNC*C*H_3], 23.6 [d, ^3J(P,C) = 6.6 Hz, PNC*C*H_3], 23.0 (s, CNC*C*H_3), 19.1 (s, CNC*C*H_3). − $C_{19}H_{43}Cl_2N_3O_2P_2$ (477.2): calcd. C 47.70, H 9.06, N 8.78; found C 47.41, H 9.50, N 8.57.

Crystal-Structure Determination of **3**: $C_{19}H_{43}Cl_2N_3O_2P_2$, M = 478.40, monoclinic, $P2_1/c$, a = 15.205(2) Å, b = 10.3700(10) Å, c = 17.201(3) Å, β = 90.91(2)°, V = 2711.8(6) Å^3, Z = 4, ρ_c = 1.172 Mg m^{-3}, F(000) = 1032, λ = 0.71073 Å, T = 173(2) K, μ(Mo-K_α) = 0.375 mm^{-1}, crystal size 0.6 × 0.4 × 0.3 mm, 2.29° < θ < 23.26°, 17995 reflections (3686 independent, R_{int} = 0.0425, completness 88.7%) were collected with a STOE-IPDS diffractometer. The structure was solved by direct methods (SHELXS-97)[16] and 381 parameters were refined with 191 restraints using the least-squares method on F^2.[17] Largest electron density residue: 0.635 e Å^{-3}, R_1 [for $F > 2\sigma(F)$] = 0.0432 and wR_2 = 0.1174 (all data) with $R_1 = \Sigma\ F_o - F_c\ /\Sigma\ F_o$ and $wR_2 = [\Sigma w(F_o^2 - F_c^2)^2/\Sigma w(F_o^2)^2]^{0.5}$. A disorder of the anion was refined anisotropically on two positions with the occupancy 0.85/0.15, and a disorder of the two isopropyl groups was also refined anisotropically on two positions with the occupancies 0.61/0.39 and 0.59/0.41 using ADP and distance restraints. Crystallographic data (excluding structure factors) have been deposited with the Cambridge Crystallographic Data Center as supplementary publication No. CCDC-101971. Copies of the data can be obtained free of charge on application to CCDC, 12 Union Road, Cambridge CB2 1EZ, UK (Fax: int. code + 44-1223/336-033; E-mail: deposit@ccdc.cam.ac.uk).

8: To a THF solution (5 ml) of the *C*-phosphanyl-substituted iminium salt **3** (0.48 g, 1 mmol) was added one equivalent of LDA (0.11 g, 1 mmol) in THF solution (4 ml) at −78°C. The reaction mixture was allowed to warm to r.t. and stirred for a further 30 min. After evaporation of the solvent in vacuo, the residue was extracted with pentane (10 ml). After filtration and evaporation of pentane, compound **8** was obtained as a yellow oil (0.31 g, 92%). − ^{31}P NMR (32 MHz, $CDCl_3$): δ = 45.8. − ^{1}H NMR (400 MHz, $CDCl_3$): δ = 4.57 [d, ^5J(P,H) = 2.4 Hz, 1 H, =CH_2], 4.55 [dd, ^2J(P,H) = 0.8 Hz, ^5J(P,H) = 0.8 Hz, 1 H, =CH_2], 3.71 [sept, ^3J(H,H) = 6.7 Hz, 1 H, CNCH], 3.40 [sept d, ^3J(H,H) = 6.6 Hz, ^3J(P,H) = 10.2 Hz, 4 H, PNCH], 3.26 [d, ^2J(P,H) = 10.3 Hz, 2 H, PCH_2], 1.94 [m, ^4J(H,H) = 0.7 Hz, ^5J(P,H) = 1.0 Hz, 3 H, CH_3C=], 1.34 [d, ^3J(H,H) = 6.6 Hz, 12 H, PNCHCH_3], 1.31 [d, ^3J(H,H) = 6.6 Hz, 12 H, PNCHCH_3], 1.17 [d, ^3J(H,H) = 6.7 Hz, 6 H, NCHCH_3]. − ^{13}C NMR (100 MHz, $CDCl_3$): δ = 149.2 [d, ^3J(P,C) = 2.6 Hz, >C=], 94.8 [d, ^4J(P,C) = 13.5 Hz, =CH_2], 49.9 [d, ^3J(P,C) = 5.1 Hz, CNCH], 47.6 [d, ^2J(P,C) = 10.9 Hz, PNCH], 44.5 (s, P-CH_2), 25.4 [d, ^3J(P,C) = 6.8 Hz, PNC*C*H_3], 24.7 [d, ^3J(P,C) = 6.8 Hz, PNC*C*H_3], 23.0 (s, *C*H_3C=), 19.5 (s, NC*C*H_3). − MS (NH_3, CI); *m*/*z*: 344 [M + 1].

9: To a THF solution (15 ml) of the *C*-phosphanyl-substituted iminium salt **3** (0.48 g, 1 mmol) was added at r.t. one equivalent of MeONa (0.05 g, 1 mmol). The reaction mixture was stirred for 30 min. After evaporation of the solvent in vacuo, the residue was extracted with pentane (20 ml). After filtration and evaporation of the solvent, compound **9** was obtained as a yellow powder (0.34 g, 90%). M.p. 189−190°C. − ^{31}P NMR (32 MHz, $CDCl_3$): δ = 60.6. − ^{1}H NMR (250 MHz, C_6D_6): δ = 4.38 [d, ^2J(P,H) = 3.5 Hz, 1 H, P-CH],3.56 (m, 6 H, NCH), 3.23 (s, 3 H, OCH_3), 1.24-1.11 (m, 36 H, CH_3). − ^{13}C NMR (100 MHz, $CDCl_3$): δ = 94.8 [d, ^1J(P,C) = 7.5 Hz, P-CH], 54.7 (s, OCH_3), 48.5 [d, ^2J(P,C) = 11.9 Hz, PNCH], 48.0 [d, ^2J(P,C) = 8.8 Hz, PNCH], 45.3 [d, ^3J(P,C) = 3.6 Hz, NCH], 24.6, 24.5, 24.4, 23.4 (s, CH_3). − $C_{20}H_{46}N_3OP$ (375.3): calcd C 63.96, H 12.34, N 11.19; found C 62.98, H 12.95, N 10.68.

10: 0.1 g (0.27 mmol) of neat hemiaminal **9** was heated at 160°C in vacuo. During this process, methanol was evolved and compound **10**, a yellow oil, was obtained as the distillate (0.09 g, 85%) and characterized by ^{31}P-NMR spectroscopy (32 MHz, C_6D_6): δ = 111.3.

10′: A THF solution of **10** (0.08 g) was stirred for 3 h at r.t. with an excess of elemental sulfur. After filtration and evaporation of the solvent, **10′** (0.09 g, 95%) was isolated by column chromatography on silica gel (hexane/ether, 98:2, R_F = 0.4). M.p. 79−80°C. − ^{31}P NMR (162 MHz, $CDCl_3$): δ = 86.1. − ^{1}H NMR (400 MHz, $CDCl_3$): δ = 3.87 (m, 3 H, CHNP), 3.49 [sept, ^3J(H,H) = 6.7 Hz, 2 H, CHNCP], 3.48 [d, J(P,H) = 20.3 Hz, 1 H, CH_{ring}], 1.43 (s, 3 H, CH_{3ring}), 1.40 [d, ^3J(H,H) = 7.3 Hz, 6 H, CH_3CHNP], 1.38 [d, ^3J(H,H) = 8.6 Hz, 6 H, CH_3CHNP], 1.36 [d, ^3J(H,H) = 6.8 Hz, 3 H, CH_3CHNC], 1.25 [d, J(P,H) = 1.1 Hz, 3 H, CH_{3ring}], 1.21 [d, ^3J(H,H) = 6.4 Hz, 3 H, CH_3CHN], 1.10 [d, ^3J(H,H) = 6.4 Hz, 6 H, CH_3CHNC], 1.01 [d, ^3J(H,H) = 6.4 Hz, 6 H, CH_3CHNC]. − ^{13}C NMR (100 MHz, $CDCl_3$): δ = 70.7 [d, J(P,C) = 62.9 Hz, CH_{ring}], 62.7 [d, J(P,C) = 19.3 Hz, C_{ring}], 46.9 [d, ^2J(P,C) = 1.0 Hz, PNCH], 45.8 (s broad, PNCH), 45.1 (s, NCH), 31.1 [d, J(P,C) = 27.6 Hz, CH_3], 24.3 [d, J(P,C) = 6.5 Hz, *C*H_3CHNP], 23.9 (s, *C*H_3CHN), 23.7 [d, J(P,C) = 2.9 Hz, *C*H_3CHNP], 23.4 (s, *C*H_3CHN), 23.2 [d, J(P,C) = 5.5 Hz, *C*H_3CHN], 21.6 (s, *C*H_3CHN). − $C_{19}H_{42}N_3PS$ (375.3): calcd. C 60.76, H 11.27, N 11.19; found C 60.32, H 10.94, N 10.62. − The relative configuration of the chiral phosphorus and carbon atoms has been established by comparison of the NMR data of **10′** with those of the thioxo derivative **11′**.[12]

[1] G. Bertrand, R. Reed, *Coord. Chem. Rev.* **1994**, *137*, 323.

[2] [2a] A. J. Arduengo III, R. Krafczyk, *Chemie Unserer Zeit* **1998**, *32*, 6. − [2b] W. A. Herrmann, C. Köcher, *Angew. Chem.* **1997**, *109*, 2256; *Angew. Chem. Int. Ed. Engl.* **1997**, *36*, 2162.

[3] [3a] R. Dagani, *Chem. Eng. News* **1991**, *69*, 19. − [3b] M. Regitz, *Angew. Chem.* **1991**, *103*, 691; *Angew. Chem. Int. Ed. Engl.* **1991**, *30*, 674. − [3c] R. Dagani, *Chem. Eng. News* **1994**, *72*, 20. − [3d] M. Regitz, *Angew. Chem.* **1996**, *108*, 791; *Angew. Chem. Int. Ed. Engl.* **1996**, *35*, 725.

[4] For theoretical studies see: [4a] M. T. Nguyen, M. A. McGinn, A. F. Hegarty, *Inorg. Chem.* **1986**, *25*, 2185. − [4b] D. A. Dixon, K. D. Dobbs, A. J. Arduengo III, G. Bertrand, *J. Am. Chem. Soc.* **1991**, *113*, 8782. − [4c] M. Soleilhavoup, A. Baceiredo, O. Treutler, R. Ahlrichs, M. Nieger, G. Bertrand, *J. Am. Chem. Soc.* **1992**, *114*, 10959. − [4d] Boehme, C., Frenking, G. *J. Am. Chem. Soc.* **1996**, *118*, 2039. − [4e] C. Heinemann, T. Müller, Y. Apeloig, H. Schwarz, *J. Am. Chem. Soc.* **1996**, *118*, 2023. − [4f] G. Raabe, K. Breuer, D. Enders, J. H. Teles, *Z. Naturforsch.* **1996**, *51A*, 95.

[5] J. Kapp, C. Schade, A. M. El-Nahasa, P. von R. Schleyer, *Angew. Chem.* **1996**, *108*, 2373; *Angew. Chem. Int. Ed. Engl.* **1996**, *35*, 2236 and references therein.

[6] A cyclic compound of this type, not allowing the synthesis of the corresponding carbene has been reported: N. Burford, J. A. C. Clyburn, S. V. Sereda, T. S. Cameron, J. A. Pincock, M. Lumsden, *Organometallics* **1995**, *14*, 3762.

[7] For a review on heteroatom stabilized carbenium ions see: H. Grützmacher, C. M. Marchand, *Coord. Chem. Rev.* **1997**, *163*, 287.

[8] [8a] R. W. Alder, P. R. Allen, M. Murray, A. G. Orpen, *Angew. Chem.* **1996**, *108*, 1211; *Angew. Chem. Int. Ed. Engl.* **1996**, *35*, 1121. – [8b] R. W. Alder, M. E. Blake, *J. Chem. Soc., Chem. Commun.* **1997**, 1513.
[9] H. R. G. Bender, E. Niecke, M. Nieger, H. Westermann, *Z. Anorg. Allg. Chem.* **1994**, *620*, 1194.
[10] [10a] O. Guerret, G. Bertrand, *Acc. Chem. Res.* **1997**, *30*, 486. – [10b] M. Driess, H. Grützmacher, *Angew. Chem.* **1996**, *108*, 900; *Angew. Chem. Int. Ed. Engl.* **1996**, *35*, 829.
[11] D. Enders, K. Breuer, G. Raabe, J. Runsink, J. H. Teles, J. P. Melder, K. Ebel, S. Brode, *Angew. Chem.* **1995**, *107*, 1119; *Angew. Chem. Int. Ed. Engl.* **1995**, *34*, 1021.
[12] M. J. Menu, Y. Dartiguenave, M. Dartiguenave, A. Baceiredo, G. Bertrand, *Phosphorus Sulfur Silicon* **1990**, *47*, 327.
[13] Carbene CH insertion reactions reported by Wanzlick in the 1960s involve the corresponding olefin, as demonstrated later. See ref.[8b] and references therein.
[14] For persistent triplet carbenes, see: H. Tomioka, *Acc. Chem. Res.* **1997**, *30*, 315.
[15] To date, there are no examples of stable carbenes featuring the combination of p-donor and σ-attracting substituents, although CF_3CSF_3 and F_5SCSF_3 might be considered as representatives of this category: K. Seppelt, *Angew. Chem.* **1991**, *103*, 399; *Angew. Chem. Int. Ed. Engl.* **1991**, *30*, 361.
[16] G. M. Sheldrick, *Acta Crystallogr.* **1990**, *A46*, 467.
[17] G. M. Sheldrick, *SHELXL-97, Program for Crystal Structure Refinement*, University of Göttingen, **1997**.

[98152]

A Very-High-Spin Molecule: Preparation, Characterization and Magnetic Properties of an Fe^{III}–Gd^{III} Complex with an $S = 12/2$ Ground State

Jean-Pierre Costes*, Arnaud Dupuis, and Jean-Pierre Laurent

Laboratoire de Chimie de Coordination du CNRS, UPR 8241 liée par convention à l'Université Paul Sabatier,
205, route de Narbonne, F-31077 Toulouse Cedex, France
Fax: (internat.) + 33-5/61553003
E-mail: costes@lcc-toulouse.fr

Received May 27, 1998

Keywords: High-spin molecule / 3d-4f complex / Heterodinuclear complex / Fe–Gd complex / Ferromagnetism

The tripodal ligand tris[4-(2-hydroxy-3-methoxyphenyl)-3-aza-3-buten]amine (H_3vantren) offers two coordination sites, an inner N_4O_3 one and an outer O_6 one. Therefore, it can successively encapsulate two different metal ions, a 3d(III) ion in the N_4O_3 site, and a 4f(III) ion in the O_6 site. This general route to homo- and heterodinuclear complexes has been exploited for the preparation of the vantrenFeGd$(NO_3)_3 \cdot 2\ H_2O$ complex (**2**), featuring a high-spin iron centre. This compound has been characterized by chemical analysis and mass spectrometry (FAB^+). Its magnetic properties have been investigated and show that the (Fe,Gd) pair (**2**) exhibits a ferromagnetic interaction of low intensity [$J = 0.50(5)$ cm^{-1}]. The resulting $S = 12/2$ ground state is, most probably, the highest spin ground state that can be expected for a dinuclear complex.

Introduction

In recent years, there has been increasing interest in the magnetic properties of dinuclear complexes composed of either 4f and 3d ions or of identical 4f ions.[1][2][3][4][5][6][7] This interest has been largely focused on the Cu−Gd couple, but one of our aims is to extend this work to other M−Gd couples (M being a 3d cation such as Ni^{2+},[8] Co^{2+},[9] or VO^{2+}[10]). As for the strategies used to prepare these polynuclear complexes, tripodal ligands derived from tris(2-aminoethyl)amine have so far been employed as hosts for 3d or 4f ions, leading to mononuclear (3d or 4f) and homodinuclear (4f, 4f) complexes.[11][12][13][14][15][16][17][18][19][20][21][22][23][24][25][26][27] Very recently, it has been shown that a mononuclear (4f) complex prepared from a novel tripodal ligand can be deprotonated to incorporate an Ni^{2+} ion.[28] Also relevant to the present paper is the use of 3d-block tripods in obtaining self-assembled triple-stranded heterodinuclear (3d, 4f) complexes.[29][30] The structural determination of an $Fe^{II}-La^{III}$ complex has been carried out.[30]

We have also demonstrated the effectiveness of the potentially decadentate tripodal Schiff base H_3vantren[31] {tris[4-(2-hydroxy-3-methoxyphenyl)-3-aza-3-buten]amine} in generating hetero- (4f, 4f′) as well as homo-dimetallic (4f, 4f) species. A schematic representation of the ligand H_3vantren is given in Figure 1. The aim of the present contribution is to demonstrate the ability of this tripodal ligand to successively incorporate 3d and 4f ions, thereby affording vantrenFe (**1**) and vantrenFeGd$(NO_3)_3 \cdot 2\ H_2O$ (**2**), and to report the magnetic properties of these complexes. At this point we should mention an $Fe^{III}-La$ complex prepared with a compartmental Schiff base ligand, for which neither a structural determination nor magnetic properties were reported.[24]

Figure 1. Schematic representation of the H_3vantren ligand

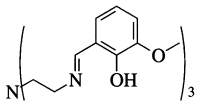

Results and Discussion

The tripodal H_3saltren ligand, obtained by reaction of salicylaldehyde with tris(2-aminoethyl)amine (tren), and its 5-chloro- ($H_3$5-Clsaltren) and 3-methoxy-substituted (H_3vantren) analogues, react with 3d(III) ions and particularly with Fe^{III} to yield neutral complexes formulated as saltrenFe.[18][19][20][24] The iron centre in 5-ClsaltrenFe[19] resides in an N_3O_3 environment, with the bridgehead nitrogen atom not being involved in coordination. A similar situation is found in vantrenMn.[20][24]

H_3vantren is a potentially decadentate tripodal ligand with two different complexation sites: an inner N_4O_3 site and an outer O_6 site. These differ in their size and nature, thus making easier the stepwise complexation of different metal ions. The marked preference of iron(III) for the inner site has been clearly demonstrated,[18][19] but we have recently shown that 4f metal ions can also be complexed in this deprotonated coordination site.[31] The bridgehead nitrogen atom that caps the structure is "tucked in", with its lone pair of electrons directed towards the Yb^{3+} ion.[31] The same disposition has been observed in mononuclear (Gd, Dy, or Yb) complexes of tripodal ligands.[12][32][33] However, in our case, the bonding interaction is expected to be

 © WILEY-VCH Verlag GmbH, D-69451 Weinheim, 1998 1434−1948/98/1010−1543 $ 17.50+.50/0

weak, as indicated by the N(2)−Yb separation of 2.626(4) Å, which is significantly larger than the related distances involving the imino nitrogen atoms [2.448(5) to 2.494(4) Å].[31] Furthermore, the difference in ionic radii between 3d(III) and 4f(III) centres induces a large difference in bond lengths between the Fe−N(imine), Fe−O(phenolato) and the Ln−N(imine), Ln−O(phenolato) bonds, respectively, [Fe−N: 2.185(7) Å; Yb−N: 2.448(5)−2.494(4) Å and Fe−O: 1.953(6) Å; Yb−O: 2.259(3)−2.329(3) Å]. This large difference is not expected to be a stabilizing factor for the desired 3d(III)−4f(III) pairs.

Infrared spectra of vantrenFe (**1**) and vantrenFeGd$(NO_3)_3\cdot 2\ H_2O$ (**2**) mainly serve to reveal the presence of water and nitrate ions in **2**. Bands attributable to bidentate nitrates are observed at 1462 and 1335 cm^{-1}. A splitting of the 1620 cm^{-1} band for **1** into two bands at 1615 and 1641 cm^{-1} for **2** is also observed.

In addition to the analytical results, important information is provided by positive-ion FAB mass spectrometry. The main peak appears at m/z = 602 (100%) for the vantrenFe compound. This value together with the isotopic feature is attributable to the $[vantrenFe + 1]^+$ ion. In the case of vantrenFeGd$(NO_3)_3\cdot 2\ H_2O$, the signal corresponding to $[vantrenFeGd(NO_3)_2]^+$ is not observed. However, a signal appears at m/z = 821. This corresponds to the $[vantrenFeGd(NO_3)]^+$ ion, suggesting a change in the oxidation state of a metal centre (Fe or Gd). A similar observation has been made in previous reports.[1][3][8][9][10] The existence of a species such as [vantrenFeGd$(NO_3)_2]_2\cdot Gd(NO_3)_5$ is ruled out by the analytical results and the absence of a signal attributable to the $[Gd(NO_3)_5]^-$ anion in the FAB^- spectrum.[31]

The temperature dependence of the magnetic susceptibility over the range 5−300 K for vantrenFeGd$(NO_3)_3\cdot 2\ H_2O$ is shown in Figure 2 in the $\chi_M T$ vs. T form, the applied magnetic field being equal to 0.05 T. At 300 K, $\chi_M T$ is equal to 12.17 cm^3 K mol^{-1}, which roughly corresponds to the value expected for two uncoupled metal ions (12.25 cm^3 K mol^{-1}). On lowering the temperature, $\chi_M T$ remains practically constant until 80 K and then increases, reaching a maximum of 16.55 cm^3 K mol^{-1} at 5 K. The behaviour observed in the 300−5 K range is indicative of a ferromagnetic interaction between the Gd^{III} and Fe^{III} ions. The maximum value of 16.55 is lower than the value of 21 cm^3 K mol^{-1} that would be expected for the spin state S = 6 resulting from ferromagnetic coupling between Gd^{III} (S = 7/2) and Fe^{III} (S = 5/2), both ions having g values of 2.0. The decrease of $\chi_M T$ observed below 5 K is most likely attributable to saturation effects or to zero-field splitting. In this instance, the experimental results obtained between 5 and 300 K can be analysed on the basis of a spin-only Hamiltonian for isotropic exchange $H = -JS_{Fe}\cdot S_{Gd}$. The six low-lying spin levels, $E(6) = 0$, $E(5) = 6J$, $E(4) = 11J$, $E(3) = 15J$, $E(2) = 18J$ and $E(1) = 20J$ are characterized by different g values[34], $g_6 = (7g_{Gd} + 5g_{Fe})/12$, $g_5 = (37g_{Gd} + 23g_{Fe})/60$, $g_4 = (27g_{Gd} + 13g_{Fe})/40$, $g_3 = (19g_{Gd} + 5g_{Fe})/24$, $g_2 = (13g_{Gd} - g_{Fe})/12$, $g_1 = (9g_{Gd} - 5g_{Fe})/4$. Finally, the experimental data may be fitted to the following expression:

$$\chi_M T = \frac{N\beta^2}{k}\,\frac{91g_6^2 + 55g_5^2 e(\frac{-6J}{kT}) + 30g_4^2 e(\frac{-11J}{kT}) + 14g_3^2 e(\frac{-15J}{kT}) + 5g_2^2 e(\frac{-18J}{kT}) + g_1^2 e(\frac{-20J}{kT})}{13 + 11e(\frac{-6J}{kT}) + 9e(\frac{-11J}{kT}) + 7e(\frac{-15J}{kT}) + 5e(\frac{-18J}{kT}) + 3e(\frac{-20J}{kT})}$$

In the 5−300 K temperature range, a satisfactory fit [$R = \Sigma(\chi_{obs.}T - \chi_{calcd.}T)^2/\Sigma(\chi_{obs.}T)^2 = 2.4\cdot 10^{-4}$] is obtained for the following set of parameters: g_{Fe} = 1.96, g_{Gd} = 2.00, J = 0.50(5) cm^{-1}. In order to account for the decrease of the product below 5 K, a θ parameter has been introduced to gauge second-order effects. Then, the best fit over the 2−300 K temperature range yields g_{Fe} = 1.96, g_{Gd} = 2.00, J = 0.66(5) cm^{-1} and θ = −0.46 K, with $R = 1.0\cdot 10^{-4}$.

Figure 2. Thermal dependence of $\chi_M T$ for LFeGd$(NO_3)_3\cdot 2\ H_2O$ **2** at 0.05 T; the solid line corresponds to the best data fit

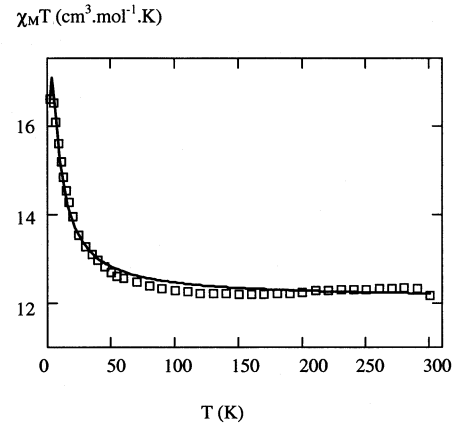

The sign of the magnetic interaction between the Fe^{3+} and Gd^{3+} ions is definitively supported by the field dependence of the magnetization M at 5 K. In Figure 3, the experimental values of M have been fitted to the Brillouin function, yielding g = 1.94 and S = 5.6 with $R = \Sigma[M_{calcd.} - M_{obsd.}]^2/\Sigma[M_{obsd.}]^2 = 2.5\cdot 10^{-3}$. The S value differs little from the value (S = 12/2) expected for a ferromagnetic ground state. Although the agreement cannot be considered as perfect, we can state that the experimental magnetization is larger than that for isolated Gd^{III} and Fe^{III} metal ions. In spite of the lack of a structural determination, the ferromagnetic behaviour confirms the existence of a genuine strictly dinuclear Fe−Gd complex.

Based on the structural determination of $[vantrenYbLa(NO_3)_2]^+$,[31] a possible structure for **2** has been obtained using CAChe molecular modelling software. It is shown in Figure 4. This view indicates that the bridgehead nitrogen atom is not involved in coordination to the iron centre, in full agreement with structural determinations of complexes of $3d^{III}$ elements with H_3vantren[24] or similar ligands.[19][20][22]

Finally, the main purpose of this paper is to report the first example of a discrete heterodinuclear $Fe^{III}-Gd^{III}$ complex that displays ferromagnetic behaviour. In this respect, the $Fe^{3+}-Gd^{3+}$ pair resembles the $Cu^{2+}-Gd^{3+}$,[1][3] $Ni^{2+}-Gd^{3+}$,[8] $Co^{2+}-Gd^{3+}$,[9] and $VO^{2+}-Gd^{3+}$[10] pairs

Figure 3. Field dependence of the magnetization; the solid line corresponds to the best data fit (cf. text)

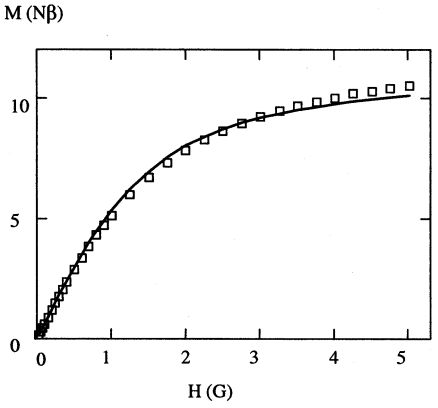

Figure 4. Possible structure of **2** based on CAChe molecular modelling software; the H atoms are not shown

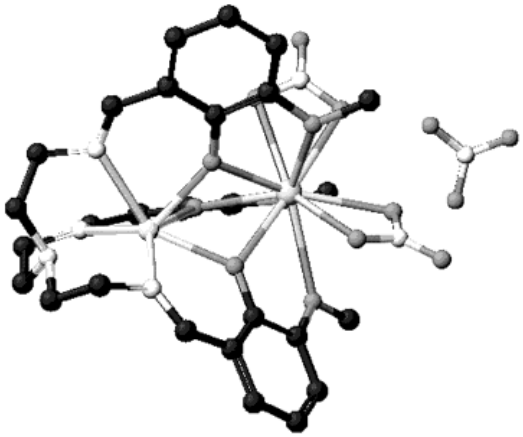

described previously. In the case of the $Cu^{2+}-Gd^{3+}$ couple, it has been proposed[35][36] that the stabilization of the parallel spin state arises from coupling between the $Cu^{II}-Gd^{III}$ ground configuration and the $Cu^{III}-Gd^{II}$ charge-transfer excited configuration, in which an electron is transferred from the singly occupied 3d-type copper orbital to an empty 5d-type gadolinium orbital. There is no obvious reason why this mechanism could not be operative in the case of the $Fe^{3+}-Gd^{3+}$ couple as well. Indeed, although the ligands involved in these different complexes are not identical, they all give rise to phenolato bridges, two with 3d(II) and three with 3d(III) metal ions. We emphasize that the value $S = 12/2$ is most probably the highest spin ground state that can be expected for a dinuclear complex. Theoretically, a higher value ($S = 14/2$) could result from a ferromagnetic coupling between two Gd^{3+} ions, but the available data[5][7] show that such a magnetic state is unlikely.

We thank Dr. *A. Mari* for his contribution to the magnetic measurements and Mrs. *S. Richelme* (Service Commun de Spectrométrie de Masse) for her contribution to the mass-spectral data.

Experimental Section

Materials and Methods: All starting materials were purchased from Aldrich and were used without further purification. Elemental analyses were carried out by the Service de Microanalyse du Laboratoire de Chimie de Coordination, Toulouse (C, H, N). Magnetic susceptibility data were collected from a powdered sample of the compound using a SQUID-based sample magnetometer with a QUANTUM Design Model MPMS instrument. All data were corrected for diamagnetism of the ligand, as estimated from Pascal's constants[38] ($-381\cdot10^{-6}$ emu mol^{-1} for **2**). Positive-ion FAB mass spectra were recorded in DMF as solvent with 3-nitrobenzyl alcohol as the matrix with a Nermag R10-10 spectrometer.

Tris[4-(2-hydroxy-3-methoxyphenyl)-3-aza-3-buten]amine: This ligand was obtained as described previously.[37]

Tris[4-(2-hydroxy-3-methoxyphenyl)-3-aza-3-buten]aminato-(3−)iron(III) (**1**): To a mixture of H_3vantren (0.55 g, 1 mmol) and anhydrous $FeCl_3$ (0.16 g, 1 mmol) in methanol (25 ml) was added triethylamine (0.3 g, 3 mmol). The mixture was heated under stirring for 20 min and, after cooling, the black precipitate produced was filtered off and washed with methanol and diethyl ether. Yield: 0.5 g (85%). − $C_{30}H_{33}FeN_4O_6$ (601.4): calcd. C 59.9, H 5.5, N 9.3; found C 59.6, H 5.3, N 9.1. − MS (FAB^+, 3-nitrobenzyl alcohol matrix): $m/z = 602$ $[LFe + 1]^+$.

Tris[4-(2-hydroxy-3-methoxyphenyl)-3-aza-3-buten]aminato-(3−)iron(III)gadolinium(III)·2 H_2O (**2**): A mixture of vantrenFe (0.5 g, $8.3\cdot10^{-4}$ mol) and $Gd(NO_3)_3\cdot6\,H_2O$ (0.37 g, $8.3\cdot10^{-4}$ mol) in acetone (20 ml) was heated under stirring for 15 min. After cooling, the resulting precipitate was filtered off and washed with acetone and diethyl ether. Yield: 0.8 g (97%). − $C_{30}H_{37}FeGdN_7O_{17}$ (980.7): calcd. C 36.7, H 3.8, Fe 5.7, Gd 16.0, N 10.0; found C 36.4, H 3.6, Fe 5.6, Gd 15.2, N 9.7. − MS (FAB^+, 3-nitrobenzyl alcohol matrix): $m/z = 821$ $[LFeGd(NO_3)]^+$.

[1] J. P. Costes, F. Dahan, A. Dupuis, J. P. Laurent, *Inorg. Chem.* **1996**, *35*, 2400−2402 and refs. therein.
[2] I. Ramade, O. Kahn, Y. Jeannin, F. Robert, *Inorg. Chem.* **1997**, *36*, 930−936 and refs. therein.
[3] J. P. Costes, F. Dahan, A. Dupuis, J. P. Laurent, *Inorg. Chem.* **1997**, *36*, 3429−3433 and refs. therein.
[4] S. Wang, Z. Pang, K. D. L. Smith, Y. Hua, C. Delippe, M. J. Wagner, *Inorg. Chem.* **1995**, *34*, 908−917 and refs. therein.
[5] A. Panagiotopoulos, T. F. Zafiropoulos, S. P. Perlepes, E. Bakalbassis, I. Masson-Ramade, O. Kahn, A. Terzis, C. P. Raptopoulou, *Inorg. Chem.* **1995**, *34*, 4918−4920 and refs. therein.
[6] I. A. Kahwa, S. Folkes, D. J. Williams, S. V. Ley, C. A. O'Mahoney, G. L. McPherson, *J. Chem. Soc., Chem. Comm.* **1989**, 1531−1533 and refs. therein.
[7] J. P. Costes, A. Dupuis, J. P. Laurent, *Inorg. Chim. Acta* **1998**, *268*, 125−130 and refs. therein.
[8] J. P. Costes, F. Dahan, A. Dupuis, J. P. Laurent, *Inorg. Chem.* **1997**, *36*, 4284−4286.
[9] J. P. Costes, F. Dahan, A. Dupuis, J. P. Laurent, *C. R. Acad. Sci.*, in press.
[10] J. P. Costes, A. Dupuis, J. P. Laurent, *J. Chem. Soc., Dalton Trans.* **1998**, 735−736.
[11] A. Smith, S. J. Rettig, C. Orvig, *Inorg. Chem.* **1988**, *27*, 3929−3934.
[12] D. J. Berg, S. J. Rettig, C. Orvig,. *J. Am. Chem. Soc.* **1991**, *113*, 2528−2532.
[13] L. Yang, S. Liu, E. Wong, S. J. Rettig, C. Orvig, *Inorg. Chem.* **1995**, *34*, 2164−2178.
[14] U. Casellato, S. Tamburini, P. Tomasin, P. A. Vigato, M. Botta, *Inorg. Chim. Acta* **1996**, 247, 143−145.
[15] P. Blech, C. Floriani, A. Chiesti-Villa, C. Guastini, *J. Chem. Soc., Dalton Trans.* **1990**, 3557−3561.
[16] P. L. Jones, A. J. Amoroso, J. C. Jeffery, J. A. McCleverty, E. Psillakis, L. H. Rees, M. D. Ward, *Inorg. Chem.* **1997**, *36*, 10−18.
[17] O. Kocian, K. W. Chiu, R. Demeure, B. Gallez, C. J. Jones, J. R. Thornback, *J. Chem. Soc., Perkin Trans. 1* **1994**, 527−535.
[18] J. A. Broomhead, D. J. Robinson, *Aust. J. Chem.* **1968**, *21*, 1365−1367.

[19] D. F. Cook, D. Cummins, E. D. McKenzie, *J. Chem. Soc., Dalton Trans.* **1976**, 1369−1375.
[20] N. W. Alcock, D. F. Cook, E. D. McKenzie, J. M. Worthington, *Inorg. Chim. Acta* **1980**, *38*, 107−112.
[21] P. G. Sim, E. Sinn, *J. Am. Chem. Soc.* **1981**, *103*, 241−243.
[22] Y. Elerman, M. Kabak, I. Svoboda, M. Geselle, *Acta Crystallogr.* **1994**, *C50*, 1694−1696.
[23] G. A. McLachlan, G. D. Fallon, L. Spiccia, *Acta Crystallogr.* **1996**, *C52*, 309−312.
[24] A. Aguiari, E. Bullita, U. Casselato, P. Guerriero, S. Tamburini, P. A. Vigato, *Inorg. Chim. Acta* **1997**, *219*, 135−146.
[25] S. Liu, L. Gelmini, S. J. Rettig, R. C. Thompson, C. Orvig, *J. Am. Chem. Soc.* **1992**, *114*, 6081−6087.
[26] L. Yang, S. Liu, S. J. Rettig, C. Orvig, *Inorg. Chem.* **1995**, *34*, 4921−4925.
[27] H. C. Aspinall, M. R. Tillotson, *Inorg. Chem.* **1996**, *34,* 2163−2164.
[28] S. J. Archibald, A. J. Blake, S. Parsons, M. Schröder, R. E. P. Winpenny, *J. Chem. Soc., Dalton Trans.* **1997**, 173−179.
[29] C. Piguet, G. Bernardinelli, J. C. G. Bünzli, S. Petoud, G. Hopfgartner, *J. Chem. Soc., Chem. Comm.* **1995**, 2575−2577.
[30] C. Piguet, E. Rivara-Minten, G. Bernardinelli, J. C. G. Bunzli, G. Hopfgartner, *J. Chem. Soc., Dalton Trans.* **1997**, 421−433.
[31] J. P. Costes, F. Dahan, A. Dupuis, S. Lagrave, J. P. Laurent, *Inorg. Chem.* **1998**, *37*, 153−155.
[32] M. G. B. Drew, O. W. Howarth, C. J. Harding, N. Martin, J. Nelson, *J. Chem. Soc., Chem. Comm.* **1995**, 903−905.
[33] F. Avecilla, R. Bastida, A. de Blas, D. E. Fenton, A. Macias, A. Rodriguez, T. Rodriguez-Blas, S. Garcia-Granda, R. Corzo-Suarez, *J. Chem. Soc., Dalton Trans.* **1997**, 409−413.
[34] A. Bencini, D. Gatteschi, *EPR of Exchange Couples Systems*, Springer-Verlag, Berlin, **1990**.
[35] M. Andruh, I. Ramade, E. Codjovi, O. Guillou, O. Kahn, J. C. Trombe, *J. Am. Chem. Soc.* **1993**, *115*, 1822−1829.
[36] O. Guillou, R. L. Oushoorn, O. Kahn, E. Bakalbassis, K. Boubekeur, P. Batail, *Angew. Chem. Int. Ed. Engl.* **1992**, *31*, 626−628.
[37] S. Liu, L. W. Yang, S. J. Rettig, R. C. Thompson, C. Orvig, *Inorg. Chem.* **1993**, *32*, 2773−2778.
[38] P. Pascal, *Ann. Chim. Phys.* **1910**, *19*, 5−70.

[98164]

New Imidazabole Derivatives: Dimers of Carbene–Borane Adducts

Itzia I. Padilla-Martínez*[a], Francisco J. Martínez-Martínez[a], Armando López-Sandoval[a], Katia I. Girón-Castillo[a], Marco A. Brito[a], and Rosalinda Contreras*[b]

Departamento de Química, Unidad Profesional Interdisciplinaria de Biotecnología del Instituto Politécnico Nacional[a],
Av. Acueducto s/n Barrio La Laguna Ticomán, México, D. F. 07340 México
Fax: (internat.) + 52-5/729-6000 ext. 56325
E-mail: ipadilla@vmredipn.ipn.mx

Departamento de Química, Centro de Investigación y de Estudios Avanzados del Instituto Politécnico Nacional[b],
A. P. 14-740, México, D. F. 07000 México
Fax: (internat.) +52-5/747-7113
E-mail: rcontrer@mail.cinvestav.mx

Received May 20, 1998

Keywords: Imidazaboles / Carbene–borane adducts / Azole–borane adducts

The preparation and characterization of five new imidazabole derivatives is reported: 1,5-dibenzyl-4,4,8,8-tetrahydroimidazabole (**2**), 4,4,8,8-tetrafluoro-1,5-dimethylimidazabole (**3**), 4,4-difluoro-8,8-dihydro-1,5-dimethylimidazabole (**4**), 4,4,8,8-tetrachloro-1,5-dimethylimidazabole (**5**), and 4,4,8,8-tetraethyl-1,5-dimethylimidazabole (**6**). The structures of compounds **2**–**6** as dimeric carbene–borane adducts rather than dimeric *N*-borane adducts are discussed on the basis of NMR (**2**–**6**) and X-ray diffraction data (**2**, **3**, **5** and **6**).

Introduction

Heterocyclic boron hydrides have found broad application in catalysis[1]. Examples of an important class of these compounds named pyrazaboles were first synthesized in 1966 and since then they have been exhaustively studied[2]. This class of compounds features two $-BR_2-$ moieties bridging two pyrazole rings through their nitrogen atoms. Recently, two series of related compounds have been synthesized, one incorporating pyridine derivatives[3] and the other five-membered azole rings with an N−C−X moiety (X = N, S)[4]. The common, distinguishing feature of both series is that the $-BR_2-$ moiety links the two heterocyclic rings via nitrogen and carbon atoms that are both highly nucleophilic, and hence the question arises as to whether they should be considered as aza- or carbene−borane adducts. The former compounds may be compared with pyridine derivatives[5], which are very stable, but there have been virtually no studies on the azole derivatives. In this paper, the synthesis of five new imidazabole derivatives **2**−**6** is reported with a view to delineating factors that might allow a distinction to be made between C−B and N−B donation. The molecular structures of these compounds based on NMR and X-ray diffraction data are strongly indicative that compounds **1**−**6** are dimers of carbene−borane adducts rather than dimers of *N*-borane adducts (Scheme 1)[*].

Scheme 1

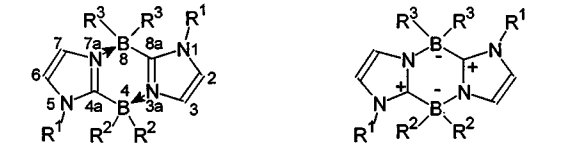

1 $R^1 = CH_3$, $R^2 = R^3 = H$; **2** $R^1 = CH_2C_6H_5$, $R^2 = R^3 = H$
3 $R^1 = CH_3$, $R^2 = R^3 = F$; **4** $R^1 = CH_3$, $R^2 = F$, $R^3 = H$
5 $R^1 = CH_3$, $R^2 = R^3 = Cl$; **6** $R^1 = CH_3$, $R^2 = R^3 = CH_2CH_3$

Results and Discussion

Synthesis

We have previously reported the synthesis of 4,4,8,8-tetrahydroimidazabole (**1**) from its *N*-methylimidazole−*N*-borane adduct[4]. The imidazabole **2** has been prepared from the 1-benzylimidazole−*N*-borane adduct in an analogous manner (Scheme 2). In order to examine the chemical stability and the molecular structures of imidazaboles (N−B−C fragment) and to compare them with pyrazaboles (N−B−N fragment), some derivatives of the parent imidazabole **1** have been synthesized (Scheme 3).

The chemical stabilities and reactivities of imidazaboles have been found to be very similar to those of pyrazaboles[2b][6]. Compounds **1**−**6** are very stable, even under the strongly acidic and oxidizing conditions of the reaction medium. Fluorination of **1** was performed with $BF_3 \cdot OEt_2$; formation of 4,4,8,8-tetrafluoro-1,5-dimethylimidazabole (**3**)

[*] Note added in proof (July 30, 1998): Other examples of carbene−boranes derived from imidazole have been recently reported: A. Wacker, H. Pritzkow, W. Siebert, *Eur. J. Inorg. Chem.* **1998**, 843−849.

 © WILEY-VCH Verlag GmbH, D-69451 Weinheim, 1998 1434−1948/98/1010−1547 $ 17.50+.50/0

Scheme 2

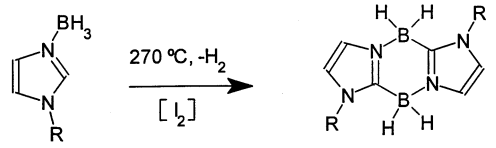

1 R = CH_3
2 R = $CH_2C_6H_5$

Scheme 3

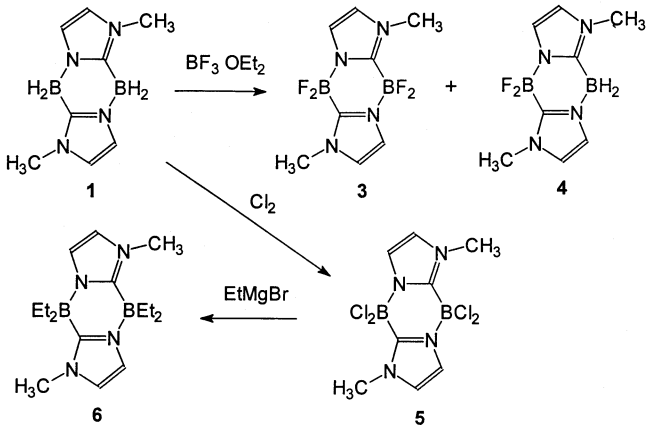

and of the mixed compound 4,4-difluoro-8,8-dihydro-1,5-dimethylimidazabole (**4**) reveals that the reaction proceeds with opening of the central $C_2B_2N_2$ ring in a similar manner as in pyrazaboles[7]. Chlorination of **1** with molecular chlorine gave compound **5**, whereas bromination with Br_2 (Scheme 4) proceeded with central ring rupture via the 4,4,8,8-tetrabromo-1,5-dimethylimidazabole (observed by NMR) to give the 1-methylimidazole−tribromoborane adduct ($\delta^{11}B = -2.2$) by HBr addition. Reaction of compound **5** with MgEtBr in diethyl ether afforded **6** in good yield. The aforementioned reactions demonstrate the similar reactivity and stability of imidazabole compounds compared to pyrazabole compounds.

Scheme 4

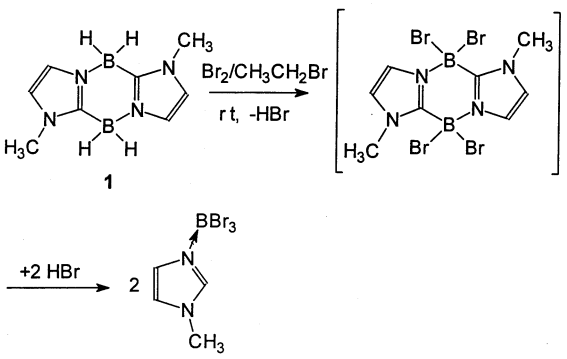

Molecular Structures

The molecular structures of compounds **1**−**6** can be viewed as dimers of imidazole *N*-borane adducts with a simple N→B dative bond (structure **A**) or as dimers of a 2-ylidene−borane adduct (carbene adduct) with a C−B dative bond (structure **B**) (Scheme 1), similar to that described by Arduengo[8]. In order to establish the structures of the imidazaboles **2**−**6**, comparisons were made with the reported stable monomeric carbene−borane adducts 2-borane−1,2,3,4-tetramethylimidazoline (**7**) and 2-trifluoroborane−1,2,3,4-tetramethylimidazoline (**8**)[9], as well as with the N→B adducts *N*-borane−1-methylimidazole (**9**)[10] and indolylborane−*N*-methylimidazole (**10**)[11] (Scheme 5).

Scheme 5

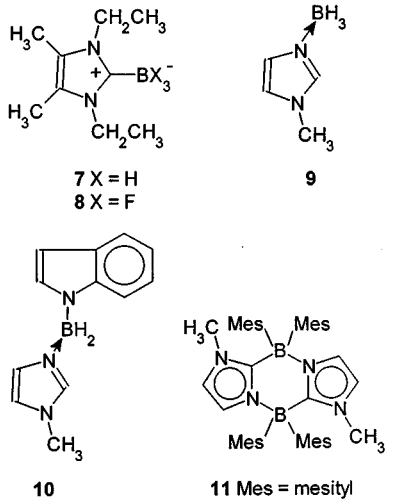

7 X = H
8 X = F

9

10

11 Mes = mesityl

NMR Studies

Compounds **2**−**6** have been characterized by their ^1H-, ^{11}B- and ^{13}C-NMR data (Table 1). The ^{11}B chemical-shift values are at lower frequencies relative to those of the pyrazabole analogues [$\delta^{11}B(H_2B$-μpz-$BH_2) = -8.8$, $\delta^{11}B(F_2B$-μpz-$BF_2) = 0.2$, $\delta^{11}B(Cl_2B$-μpz-$BCl_2) = 2.1$, $\delta^{11}B(Et_2B$-μpz-$BEt_2) = 2.2$, pz = pyrazabole][7a][12], in accordance with the change from the NBN to the NBC fragment. However, ^{11}B chemical shifts do not allow a distinction to be made between N→B coordination **A** and N−B covalent bonding **B** in tetracoordinated compounds (Scheme 1). If $\delta^{11}B$ values of similar N→B coordinated adducts and of N−B covalently-bonded borates are compared {$\delta^{11}B(Me_2HN{\rightarrow}BH_3) = -13.5$ vs. $\delta^{11}B(Me_2N{-}BH_3^-) = -14.7$; $\delta^{11}B(H_3N{\rightarrow}BMe_3) = -8.7$ vs. $\delta^{11}B(H_2N{-}BEt_3^-) = -9.8$; and $\delta^{11}B$[(*N*-methylimidazole)→BH_2−pyrrole] = −7.8 vs. $\delta^{11}B(pz_2{-}BH_2^-) = -7.4$}[11][12], no significant differences are apparent. On the other hand, coupling constants ^1J(B−X, X = F, C) appear to be more characteristic and do allow a distinction between N→B adducts and N−B covalently-bonded compounds. Coupling constants ^1J(B−F) for **3** and **4** are larger (43 and 54 Hz, respectively)

Table 1. $\delta^{11}B$, $\delta^{13}C$ and $\delta^{1}H$ in ppm, [^{1}J(B−X)], [^{1}J(C−H)] and [^{3}J(H−H)]] in Hz of imidazabole derivatives **2**−**6**[a], 2-borane−1,2,3,4-tetramethylimidazoline (**7**), 2-trifluoroborane−1,2,3,4-tetramethylimidazoline (**8**) and *N*-borane−1-methylimidazole (**9**)

Compd.	$\delta^{11}B$, [^{1}J(B−X)] X = H, F, C	$\delta^{13}C$(8a)	$\delta^{13}C$(2)	$\delta^{13}C$(3)	$\delta^{13}C$(R)	$\delta^{1}H$(2)	$\delta^{1}H$(3)	$\delta^{1}H$(R)
2[b]	−18.6, $h_{1/2}$ = 265	164.0 (br.)	124.3	119.1	50.7	6.96 [1.9]	6.78 [1.9]	5.11
3	0.5 [43]	[c]	123.7 [197]	119.7 [197]	34.2	7.47 [1.7]	7.34 [1.7]	3.96
4[d]	0.9 [54] (BF_2)	[c]	123.1 (C2)	118.7 (C3)	34.4 (N1)	7.43 [1.8]	7.41 [1.8]	3.83 (N1)
	−18.3 [101] (BH_2)		123.6 (C6)	122.5 (C7)	33.5 (N3a)	7.44 [1.5]	7.17 [1.5]	3.60 (N3a)
5	−1.6	[c]	121.4 [199]	126.5 [203]	35.4	7.78 [1.8]	7.67 [1.8]	4.02
6[e]	−6.3 [54]	164.0 (br.)	121.1 [190]	120.4 [192]	34.3	6.88 [1.7]	6.08 [1.7]	3.12
7[f]	−34.9 [86]	167.3 (C2) [51.5]	122.9 (C5)	122.9 (C4)	32.1			3.50
8[g]	1.48 [38]	[c]	125.7 (C5)	125.7 (C4)	32.8			3.71
9[h]	−18.4 [98]	136.9 (C2)	121.5 (C5)	127.1 (C4)	34.9	6.95	6.97	3.75

[a] **2**−**4** and **5** in $CDCl_3$ and **6** in C_6D_6. − [b] Phenyl protons as a multiplet at δ = 7.28; $\delta^{13}C$ = 128.8 (*o*-C), 127.9 (*m*-C), 128.0 (*p*-C) and 136.4 (*i*-C). − [c] Not observed. − [d] Mixed with signal of **3**. − [e] Ethyl: CH_2: $\delta^{13}C$ = 17.9 (br.), $\delta^{1}H$ = 0.95 (m); CH_3: $\delta^{13}C$ = 11.4, $\delta^{1}H$ = 0.80 [7.3]. − [f] CD_2Cl_2[9]. − [g] CD_2Cl_2[9]. − [h] $CDCl_3$[11].

than in the pyrazabole analogues (23 and 22 Hz)[7a] and are intermediate between that in the adduct $Me_3N{\rightarrow}BEtF_2$ (65 Hz)[7a] and the reported value (37.6 Hz) for the carbene adduct 2-trifluoroborane−1,2,3,4-tetramethylimidazoline (**8**)[9]. Moreover, the value of the coupling constant ^{1}J(B−C) found for **6** (54 Hz) is close to that of the 2-ylidene adduct 2-borane−1,2,3,4-tetramethylimidazoline (**7**) (51.5 Hz)[9].

^{13}C chemical-shift values have proved to be a useful tool in establishing the nature of the N→B coordinative bond and to distinguish it from N−B covalent bonding[10]. The ^{13}C signal of C4 of 1-methyl imidazole (δ = 129.2) is shifted upon coordination to δ = 127.1 in the $N{\rightarrow}BH_3$ adduct **9** and to δ = 122.4 in the 1,3-dimethylimidazolium cation[10]. The ^{13}C signal of C3 (C4 in imidazoles) in compounds **2**−**6** is shifted to lower frequencies (Δδ ≈ 7−10 ppm), which is clearly indicative of N−B covalent bond formation. $\delta^{13}C$ values for C3 of **2**−**6** are in agreement with $\delta^{13}C$ values reported for C4 and C5 of the carbene adducts **7** and **8**. $\delta^{13}C$ signals for C8a of **2**−**6** are either extremely broad or are not observed at all as a result of the partially relaxed scalar $^{13}C-^{11}B$ spin-spin coupling[12]. When present, these are found in the range reported for **7**. On the other hand, $^{1}J(^{13}C,1H)$ values of C2 and C3 lie in the typical range for a neutral imidazole ring[10], in spite of the development of a positive charge delocalized over the whole ring. The C−H coupling pattern helped to unequivocally assign the ^{13}C signals for C2 and C3 in **3**, **5** and **6**. The signal for C2 appears as a double multiplet due to coupling with the 2-H, 3-H and CH_3 hydrogen atoms. These findings confirm that the canonical form with N−B covalent bonding makes the principal contribution to the structures of compounds **2**−**6**.

X-ray Structure Analysis

The molecular structure of the imidazabole **1** found by X-ray diffraction analysis was previously reported to have the space group $P2_1$ (monoclinic)[4]. However, the structure has since been resolved in space group $P2_1/n$ and this resulted in better parameters. The corrected molecular structure of imidazabole **1** is shown in Figure 1. Molecular structures of the imidazaboles **2**, **3**, **5** and **6** are shown in Figures 2−5 and selected bond lengths and angles are summarized in Table 2 (those pertaining to the central ring $C_2B_2N_2$) and Table 3 (those of the imidazole ring). Compounds **1**−**3**, **5** and **6** have a crystallographic centre of inversion. Thus, only one half of the "dimeric" molecule occupies the asymmetric unit.

Figure 1. Molecular structure of imidazabole **1**[a]

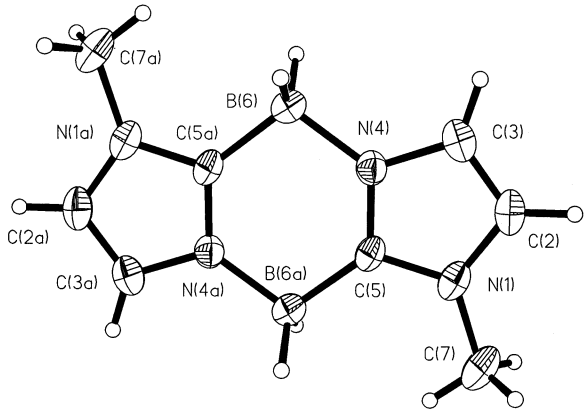

[a] Selected bond lengths [pm] and angles [°]: B(6)−N(4) 155.4(4), B(6A)−C(5) 159.0(4), N(1)−C(2) 136.7(4), C(2)−C(3) 133.3(4), C(3)−N(4) 138.5(3), N(4)−C(5) 134.6(3), C(5)−N(1) 135.5(3), N(1)−C(7) 145.2(3); B(6A)−C(5)−N(4) 127.7(2), N(4)−B(6)−C(5A) 106.8(2), B(6)−N(4)−C(5) 125.5(2), N(1)−C(5)−B(6A) 125.8(2), C(3)−N(4)−B(6) 125.6(2), N(1)−C(2)−C(3) 107.5(3), C(2)−C(3)−N(4) 107.5(3), C(3)−N(4)−C(5) 108.9(2), N(1)−C(5)−N(4) 106.4(2), C(2)−N(1)−C(5) 109.6(2), C(2)−N(1)−C(7) 126.1(2), C(5)−N(1)−C(7) 124.4(3).

The geometry around the boron atoms in **1**−**3** and **5** is of a slightly distorted tetrahedron (92% tetrahedron character, THC)[13], whereas in compound **6** it is a highly distorted tetrahedron (41% THC), probably due to steric effects. The central $C_2B_2N_2$ ring is almost planar, in contrast with the pyrazabole analogues, which are observed in chair, boat or planar conformations. The mean B−N(4) length in compounds **1**−**3** and **5** is intermediate between that of a coordinate bond $N(sp^2)-B(sp^3)$ [157.8(8) pm][11] and a covalent bond $N(sp^2)-B(sp^3)$ [151.3(2) pm][11]. This bond is significantly elongated [158.6(5) pm] in **6**, probably due to steric

Figure 2. Molecular structure of imidazabole **2**[a]

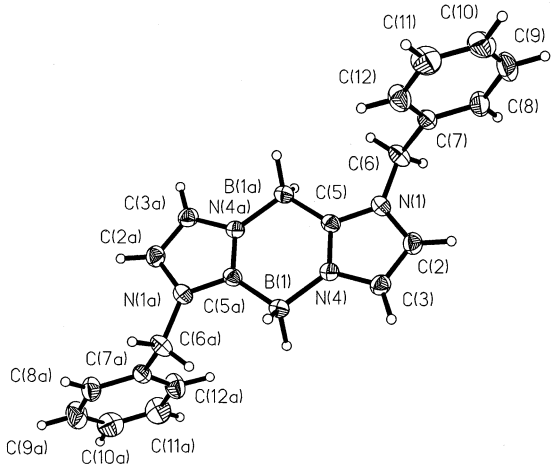

[a] Selected bond lengths [pm] and angles [°]: B(1)−N(4) 155.5(2), B(1A)−C(5) 158.6(2), N(1)−C(2) 137.3(2), C(2)−C(3) 133.7(2), C(3)−N(4) 137.8(2), N(4)−C(5) 133.7(2), C(5)−N(1) 134.9(2), N(1)−C(6) 146.0(2); B(1A)−C(5)−N(4) 126.7(1), N(4)−B(1)−C(5A) 107.4(1), B(1)−N(4)−C(5) 125.9(1), N(1)−C(5)−B(1A) 126.4(1), C(3)−N(4)−B(1) 125.3(1), N(1)−C(2)−C(3) 106.6(2), C(2)−C(3)−N(4) 108.1(2), C(3)−N(4)−C(5) 108.8(1), N(1)−C(5)−N(4) 106.9(1), C(2)−N(1)−C(5) 109.7(1), C(2)−N(1)−C(6) 124.9(1), C(5)−N(1)−C(6) 125.4(1).

Figure 3. Molecular structure of imidazabole **3**[a]

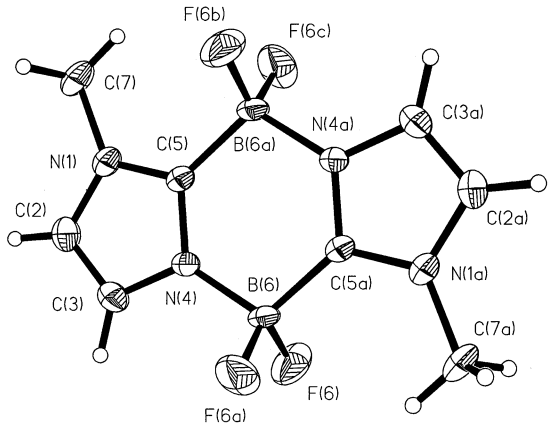

[a] Selected bond lengths [pm] and angles [°]: (B6)−N(4) 155.2(4), B(6A)−C(5) 161.1(5), N(1)−C(2) 137.1(5), C(2)−C(3) 133.0(5), C(3)−N(4) 137.9(4), N(4)−C(5) 134.3(4), C(5)−N(1) 133.8(4), N(1)−C(7) 146.7(4), B(6)−F(6) 137.9(3), B(6)−F(6B) 137.9(3); B(6A)−C(5)−N(4) 126.1(3), N(4)−B(6)−C(5A) 108.2(2), B(6)−N(4)−C(5) 125.7(3), N(1)−C(5)−B(6A) 126.6(3), C(3)−N(4)−B(6) 126.0(3), N(1)−C(2)−C(3) 107.3(3), C(2)−C(3)−N(4) 107.8(3), C(3)−N(4)−C(5) 108.3(3), N(1)−C(5)−N(4) 107.3(3), C(2)−N(1)−C(5) 109.2(3), C(2)−N(1)−C(7) 125.8(3), C(5)−N(1)−C(7) 125.0(3), F(6B)−B(6)−F(6) 109.4(3), F(6)−B(6)−N(4) 108.7(2), F(6)−B(6)−C(5A) 110.9(2).

Figure 4. Molecular structure of imidazabole **5**[a]

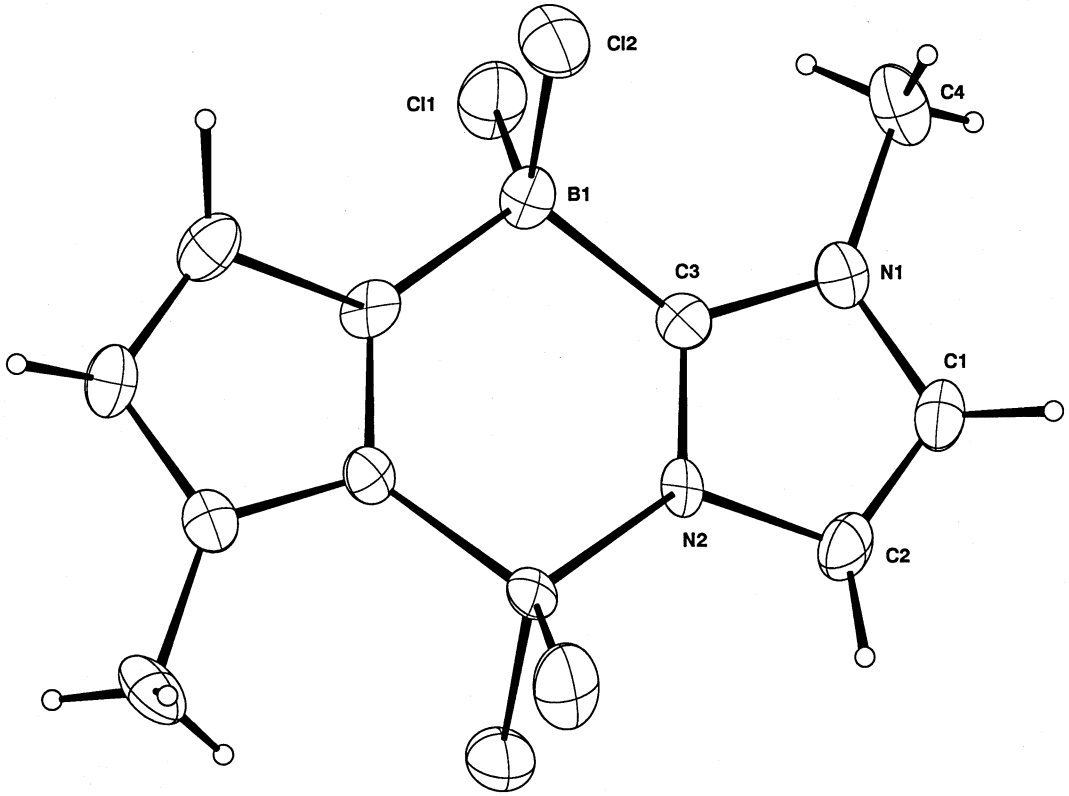

[a] Selected bond lengths [pm] and angles [°]: (B1)−N(2) 153.4(8), B(1)−C(3) 159.3(9), N(1)−C(1) 137.0(8), C(1)−C(2) 133.3(9), C(2)−N(2) 139.8(8), N(2)−C(3) 134.0(7), C(3)−N(1) 134.6(7), N(1)−C(4) 147.3(8), B(1)−Cl(1) 184.6(4); B(1)−C(3)−N(2) 125.3(5), N(2)−B(1)−C(3) 108.4(5), B(1)−N(2)−C(3) 126.3(5), N(1)−C(3)−B(1) 126.7(5), C(2)−N(2)−B(1) 125.4(5), N(1)−C(1)−C(2) 108.6(5), C(1)−C(2)−N(2) 106.7(6), C(2)−N(2)−C(3) 108.3(5), N(1)−C(3)−N(2) 107.9(5), C(1)−N(1)−C(3) 108.4(5), C(1)−N(1)−C(4) 126.3(5), C(3)−N(1)−C(4) 125.3(5), Cl(1)−B(1)−Cl(2) 111.1(4), Cl(1)−B(1)−N(2) 108.6(3), Cl(1)−B(1)−C(3) 110.0(3).

effects, but it is shorter than that in the analogous pyrazabole [167(6)−172(6) pm][14]. The B−C(5) bonds lie in the typical range for a B(sp^3)−C(Ar) linkage of 160.3(8) pm[15]. The B−C(5) bond length in **3** [161.1(5) pm] is slightly longer than in 2-trifluoroborane−1,2,3,4-tetramethylimidazoline (**8**) [160.3(3) pm]. These figures suggest that the molecular structures of imidazaboles **1**−**6** should be considered as carbene−borane dimers.

Figure 5. Molecular structure of imidazabole **6**[a]

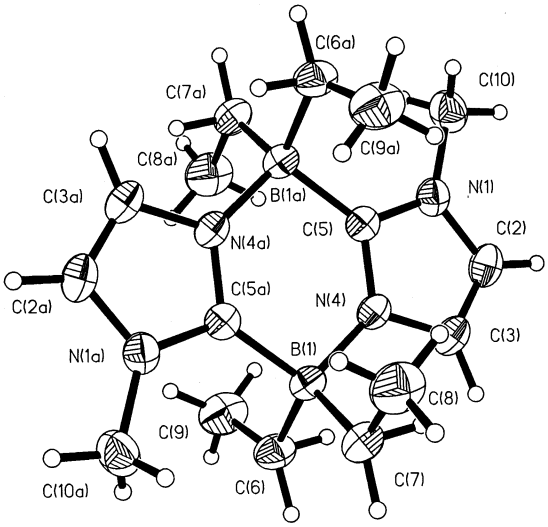

[a] Selected bond lengths [pm] and angles [°]: B(1)−N(4) 158.6(5), B(1A)−C(5) 161.4(5), N(1)−C(2) 136.0(5), C(2)−C(3) 131.9(5), C(3)−N(4) 138.3(4), N(4)−C(5) 133.7(4), C(5)−N(1) 135.9(4), N(1)−C(10) 145.7(5), B(1)−C(6) 162.8(5), B(1)−C(7) 162.6(5); B(1A)−C(5)−N(4) 127.2(3), N(4)−B(1)−C(5A) 104.2(2), B(1)−N(4)−C(5) 128.5(3), N(1)−C(5)−B(1A) 126.5(3), C(3)−N(4)−B(1) 122.9(3), N(1)−C(2)−C(3) 107.4(3), C(2)−C(3)−N(4) 108.2(3), C(3)−N(4)−C(5) 108.6(3), N(1)−C(5)−N(4) 106.3(3), C(2)−N(1)−C(5) 109.5(3), C(2)−N(1)−C(10) 123.8(3), C(5)−N(1)−C(10) 126.6(3), C(6)−B(1)−C(7) 109.3(3), C(6)−B(1)−N(4) 109.3(3), C(6)−B(1)−C(5A) 111.3(3), C(6)−B(1)−N(4) 109.3(3), C(6)−B(1)−C(5A) 111.3(3).

Table 2. Selected bond lengths [pm] and angles [°] of the central $C_2B_2N_2$ ring of imidazaboles **1**−**3**, **5** and **6**

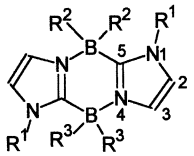

1 $R^1 = CH_3$, $R^2 = R^3 = H$; **2** $R^1 = CH_2C_6H_5$, $R^2 = R^3 = H$
3 $R^1 = CH_3$, $R^2 = R^3 = F$; **5** $R^1 = CH_3$, $R^2 = R^3 = Cl$;
6 $R^1 = CH_3$, $R^2 = R^3 = CH_2CH_3$

	1	**2**	**3**	**5**[a]	**6**
B−R			137.9(3)	184.6(4)	162.8(5), 162.6(5)
B−N(4)	155.4(4)	155.5(2)	155.2(4)	153.4(8)	158.6(5)
B−C(5)	159.0(4)	158.6(2)	161.1(5)	159.3(9)	161.4(5)
R−B−R			109.4(3)	111.1(4)	109.3(3)
N(4)−B−C(5)	106.8(2)	107.4(1)	108.2(2)	108.4(5)	104.2(2)
B−N(4)−C(5)	125.5(2)	125.9(1)	125.7(3)	126.3(5)	128.5(3)
B−C(5)−N(4)	127.7(2)	126.7(1)	126.1(3)	125.3(5)	127.2(3)

[a] The numbering scheme is as that used for imidazaboles **1**−**3** and **6**.

The most categorical evidence for this conclusion comes from a comparison of the molecular structures of **1**−**3** and **5** with that of 4,4,8,8-tetramesityl-1,5-dimethylimidazabole **11**[16], the latter being characteristic of an imidazole *N*-borane adduct dimer. This compound exhibits a boat conformation of the central $C_2B_2N_2$ ring, with an angle between the two imidazole rings of 128°, in contrast with the fully planar structure found in imidazaboles **1**−**6**. The B−N bond length [163.8(4) pm] is larger than the corresponding bond lengths in imidazaboles **1**−**3**, **5** and **6**, which lie in the typical range for weak N→B adducts[17]. The marked contrast between these structures confirms that compounds **1**−**6** have to be considered as 2-ylidene−borane adducts (carbene−boranes).

The geometry of the imidazole ring is strongly modified when 2-ylidene adducts are formed. Table 3 shows bond lengths and angles related to the imidazole ring for compounds **1**−**3**, **5** and **6**, 2-trifluoroborane−1,3,4,5-tetramethylimidazoline (C−B coordination) (**8**)[9], and indolylborane−*N*-methylimidazole adduct (N→B coordination) (**10**)[11]. The main difference between the latter two lies in the N−C−N fragment. The bond length N(4)−C(5) [130.1(5) pm] is shorter than C(5)−N(1) [132.0(6) pm] in the N→B adduct **10**, whereas both have the same large value [135.2 (2) pm] in the C−B adduct **8**. These bonds in **1**−**3**, **5** and **6** are practically equivalent and have the same value as that in the C−B adduct **8**. The angle N(1)−C(5)−N(4) is wider in the C−B adduct **8** [104.7(1)°] than in the N−B adduct **10** [111.2(4)°]. In the opposite sense, the angles C(3)−N(4)−C(5) and C(2)−N(1)−C(5) become equal and are wider in the C−B adduct **8** [111.2(1)°] than in the N−B adduct **10** [106.2(4)° and 106.3(4)°, respectively]. Both these angles in **1**−**3**, **5** and **6** have a value intermediate between those found in the N−B and C−B adducts. These findings and the planarity found for all the structures reported here strongly support a significant contribution from the C−B adduct to the resonance structure and indicate that the positive charge is delocalized over the fragment N−C−N according to structure **C**, instead of over the fully delocalized resonance structure **D** (Scheme 6).

It follows from the aforementioned changes that as the groups attached to boron become bulkier, the resulting structure resembles more the N→B adduct. On the other hand, the B−C(5) length becomes longer (Table 2) as the electronegativity of the boron substituent increases (Pauling values: H 2.20, C 2.55, Cl 3.16, F 3.98)[18]. These observations demonstrate that both steric and electronic effects on the boron atom determine the degree of carbene−borane or *N*-borane dimer character of the structure.

Conclusion

NMR and X-ray diffraction experiments confirm that compounds **1**−**6** are dimers of carbene−borane adducts rather than *N*-borane adducts. The main differences between these structures are most clearly apparent in the imidazole

Table 3. Selected bond lengths [pm] and bond angles [°] of the imidazole ring in imidazaboles **1**−**3**, **5** and **6**, 2-trifluoroborane−1,2,3,4-tetramethylimidazoline (**8**) (C−B adduct)[9], and pyrrolylborane−*N*-methylimidazole adduct (**10**) (N−B adduct)[11]; the numbering scheme is as that used in Table 2

	8[a]	**1**	**2**	**3**	**5**	**6**	**10**[a]
N(1)−C(2)	139.2(2)	136.7(4)	137.3(2)	137.1(5)	137.4(4)	136.0(5)	135.4(7)
C(2)−C(3)	135.0(2)	133.3(4)	133.7(2)	133.0(5)	133.7(4)	131.9(5)	132.0(8)
C(3)−N(4)	139.3(2)	138.5(3)	137.8(2)	137.9(4)	136.9(4)	138.3(4)	135.7(6)
N(4)−C(5)	135.2(2)	134.6(3)	133.7(2)	134.3(4)	134.0(3)	133.7(4)	130.1(5)
C(5)−N(1)	135.2(2)	135.5(3)	134.9(2)	133.8(4)	133.8(4)	135.9(4)	132.0(6)
N(1)−C(5)−N(4)	104.7(1)	106.4(2)	106.8(1)	107.3(3)	107.3(2)	106.3(3)	111.2(4)
C(3)−N(4)−C(5)	111.2(1)	108.9(2)	108.8(1)	108.3(3)	108.7(2)	108.6(3)	106.2(4)
C(2)−N(1)−C(5)	111.1(1)	109.6(2)	109.7(1)	109.2(3)	108.4(5)	109.5(3)	106.3(4)

[a] For comparison purposes, the numbering scheme has been changed to the ring numbering followed in imidazaboles.

Scheme 6

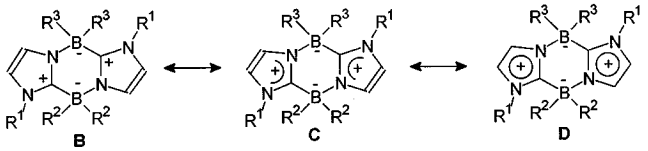

N−C−N fragment bond lengths and angles and in the N−B bond lengths. The $C_2B_2N_2$ ring in compounds **1**−**6** is quite stable, even under the strongly acidic and oxidizing conditions used for the synthesis of such species. Imidazabole compounds **1**−**6** are the first examples of cyclic dimers of carbene−borane adducts to be reported.

We thank Professor *M. J. Rosalez-Hoz*, Mr. *F. Roberts* and Mr. *M. A. Leyva-Ramírez* for performing the X-ray diffraction studies

Experimental Section

General Remarks: All solvents were freshly distilled and dried before use according to established procedures. *N*-Methylimidazole, $BF_3 \cdot OEt_2$, Cl_2, Br_2 and Mg (granules) were commercial products. $BH_3 \cdot THF$ solution was prepared according to reported methods[19]. − Melting points (uncorrected): Gallenkamp apparatus. − IR (KBr): Perkin-Elmer 16F, PC spectrometer. − $^1H/^{13}C$ NMR: Jeol GXS 270 (270.67/67.94 MHz), TMS as external standard. − ^{11}B NMR: Jeol GXS 270 (86.84 MHz), $Et_2O \cdot BF_3$ as external standard ($\Xi^{11}B$ = 32.083971 MHz). − Elemental analyses were performed by Oneida Research Services, Whitesboro, N.Y. − The X-ray diffraction studies were performed with an Enraf-Nonius CAD4 diffractometer [λ(Mo-K_α) = 71.069 pm, monochromator: graphite, T = 293 K, ω-2θ scan]. Cell parameters were determined by least-squares refinement on diffractometer angles for 24 automatically centered reflections. Absorption corrections were not necessary; corrections were made for Lorentz and polarization effects. Solution and refinement: direct methods (SHELXS-86) for

Table 4. Crystallographic data for imidazaboles **1**−**3**, **5** and **6**

	1[a]	**2**[a]	**3**[a]	**5**[b]	**6**[a]
formula	$C_8H_{14}B_2N_4$	$C_{20}H_{22}B_2N_4$	$C_4H_7BF_2N_2$	$C_8H_{10}B_2Cl_4N_4$	$C_{16}H_{30}B_2N_4$
molecular mass [g/mol]	187.85	340.04	131.93	325.62	300.06
crystal system	monoclinic	triclinic	monoclinic	monoclinic	monoclinic
space group	$P2_1/n$	$P\bar{1}$	$I2/m$	$C2/m$	$P2_1/n$
a [pm]	867.2(2)	644.90(10)	752.0(2)	1230.5(9)	788.2(2)
b [pm]	632.50(10)	791.6(2)	693.60(10)	711.5(4)	1031.0(2)
c [pm]	978.0(2)	698.8(2)	1125.6(2)	817.4(4)	1127.7(2)
α [°]	90.00	108.85(3)	90.00	90.00	90.00
β [°]	100.70(3)	101.33(3)	109.37 (3)	108.38(6)	93.47(3)
γ [°]	90.00	93.47(3)	90.00	90.00	90.00
V 10^3 [nm^3]	527.1(2)	464.2(2)	553.9(2)	679.1(7)	914.7(3)
Z	2	1	4	2	2
$d_{calcd.}$ [g cm^{-3}]	1.184	1.216	1.582	1.59	1.089
2θ range [°]	6.96−49.92	4.48−51.92	5.76−52.58		5.36−51.94
reflections measured	984	1916	1237	702	1884
unique reflections	927	1806	618	655	1795
reflns. used with $(F_o)^2 > 4\sigma(F_o)^2$	709	1356	548	548 $(F_o)^2 > 3\sigma(F_o)^2$	1047
R (int)	0.0338	0.0176	0.0674	0.024	0.0191
no. of variables	64	127	52	52	100
final R indices [$F > 4\sigma(F)$]	0.0618	0.0417	0.0685	0.045 [$F > 3\sigma(F)$]	0.0722
Rw	0.1808	0.1210	0.2217	0.047 $w = 1/\sigma^2$	0.2368
goodness of fit	1.114	0.992	1.156	5.4	1.093
min. res. density [10^{-6} e/pm^{-3}]	−0.317	−0.175	−0.645	−0.38	−0.386
max. res. density [10^{-6} e/pm^{-3}]	0.340	0.200	0.351	0.47	0.406

[a] Program for structure solution and refinement: SHELXL-93[20]. − [b] Program for structure solution and refinement: CRYSTALS[21].

structure solution. The SHELXL[20] and CRYSTALS (version 9, **1994**)[21] software packages were used for refinement and data output. All hydrogen atoms in structures **1**, **3**, **5** and **6** were refined as riding atoms. Experimental parameters are listed in Table 4. Crystallographic data (excluding structure factors) for the structures reported in this paper have been deposited with the Cambridge Crystallographic Data Centre as supplementary publication no. CCDC-101913 (**1**), -101909 (**2**), -101910 (**3**), -101912 (**5**), -101911 (**6**). Copies of the data can be obtained free of charge on application to CCDC, 12 Union Road, Cambridge CB2 1EZ, UK [Fax: int. code +44(1223)336-033; E-mail: deposit@ccdc.cam.ac.uk].

1,5-Dibenzyl-4,4,8,8-tetrahydroimidazabole (**2**): 2.00 g (11.6 mmol) of 2-borane−1-benzylimidazole, prepared as described previously[11], was left to stand overnight at 0 °C in the presence of a solution of one small I_2 crystal in 1 ml of dry benzene. The mixture was then heated in a sand bath at 290 °C until hydrogen evolution had ceased. Crystallization from a saturated solution in toluene at −20 °C gave 0.637 g of **2** (32%) as a white, crystalline powder, m.p. 204−205 °C. Crystals suitable for X-ray structure analysis were obtained from a CH_2Cl_2 solution at −17 °C. − IR (KBr): $\tilde{\nu}_{max}$ = 2354 cm^{-1} (B−H), 1636 (C=N), 1206 (B−N). − $C_{20}H_{22}N_4B_2$ (340.04): calcd. C 70.64, H 6.52, N 16.49; found C 70.92, H 6.88, N 16.67.

4,4,8,8-Tetrafluoro-1,5-dimethylimidazabole (**3**) *and 4,4-Difluoro-8,8-dihydro-1,5-dimethylimidazabole* (**4**): To 10 ml of $BF_3 \cdot OEt_2$ was added 1.0 g of **1** and the mixture was stirred for a week. Excess $BF_3 \cdot OEt_2$ was then distilled off in vacuo, and the residual solid was washed with CH_2Cl_2 and then with THF to give 262 mg of a white solid composed of 95 parts of **3** (36% overall yield) and 5 parts of **4** (2.2% overall yield). Suitable crystals of **3** for X-ray structure analysis were obtained from acetone solution; m.p. 277 °C. − IR (KBr): $\tilde{\nu}_{max}$ = 1684 cm^{-1} (C=N), 1162 (B−N), 842 (B−F). − $C_8H_{10}N_4B_2F_4$ (259.81): calcd. C 36.98, H 3.88, N 21.56; found C 37.69, H 4.13, N 21.39. − The THF solution was found to contain a 1:1 mixture of **3** and **4**, from which the NMR spectra of **4** were obtained.

4,4,8,8-Tetrachloro-1,5-dimethylimidazabole (**5**): 2.00 g (10.6 mmol) of imidazabole **1** was dissolved in 30 ml of CH_2Cl_2. Molecular chlorine was bubbled through this solution until a yellow-green color persisted. After stirring for 1 h, the product formed was filtered off to afford 2.8 g (81%) of **5** as a white, crystalline solid, m.p. > 310 °C. − IR (KBr): $\tilde{\nu}_{max}$ = 1628 cm^{-1} (C=N), 1096 (B−N), 770 (B−Cl). − $C_8H_{10}N_4B_2Cl_4$ (325.63): calcd. C 29.51, H 3.10, N 17.21; found C 29.41, H 3.15, N 17.32.

4,4,8,8-Tetraethyl-1,5-dimethylimidazabole (**6**): A suspension of 124 mg of magnesium and a small amount of iodine in 10 ml of diethyl ether was stirred for 2 h. Then, 0.40 ml (5.1 mmol) of ethyl bromide was added and, after 1 h, a solution of 331 mg (1.02 mmol) of **5** in 100 ml of diethyl ether. The resulting mixture was refluxed under nitrogen for 4 h. After cooling overnight, 295 mg (96%) of crystals suitable for X-ray structure analysis were obtained; m.p. 200 °C. − IR (KBr): υ_{max} = 1684 cm^{-1} (C=N), 1074 (B−N). − $C_{16}H_{30}N_4B_2$ (300.06): calcd. C 64.05, H 10.08, N 18.67; found C 64.64, H 9.72, N 18.83.

[1] K. Burgess, M. Ohlmeyer, *Chem. Rev.* **1991**, *91*, 1179−1191.
[2] [2a] S. Trofimenko, *J. Am. Chem Soc*. **1966**, *88*, 1842−1844. − [2b] S. Trofimenko, *J. Am. Chem. Soc*. **1967**, *89*, 4948−4952. − [2c] S. Trofimenko, *J. Am. Chem. Soc.* **1967**, *89*, 3170−3177. − [2d] S. Trofimenko, *Inorg. Chem*. **1969**, 1714−1716. − [2e] S. Trofimenko, *Acc. Chem. Res.* **1971**, *4*, 17−22. − [2f] S. Trofimenko, *Chem. Rev.* **1972**, *72*, 497−509. − [2g] K. Niedenzu, K. R. Woodrum, *Inorg. Chem*. **1989**, 28, 4022−4026.
[3] T. G. Hodgkins, *Inorg. Chem.* **1993**, *32*, 6115−6116.
[4] I. I. Padilla-Martínez, M. J. Rosalez-Hoz, R. Contreras, S. Kerschl, B. Wrackmeyer, *Chem. Ber.* **1994**, *127*, 343−346.
[5] T. G. Hodgkins, D. R. Powell, *Inorg. Chem.* **1996**, *35*, 2140−2148.
[6] [6a] K. Niedenzu, H. Nöth, *Chem. Ber*. **1983**, *116*, 1132−1153. − [6b] E. Hanecker, T. G. Hodgkins, K. Niedenzu, H. Nöth, *Inorg. Chem.* **1985**, *24*, 459−462. − [6c] W. J. Layton, K. Niedenzu, P. M. Niedenzu, S. Trofimenko, *Inorg. Chem*. **1985**, *24*, 1454−1460.
[7] [7a] C. M. Clarke, M. K. Das, E. Hanecker, K. Niedenzu, P. M. Niedenzu, H. Nöth, R. Warner, *Inorg. Chem*. **1987**. *26*, 2310−2317. − [7b] M. K. Das, A. L. DeGraffenreid, K. D. Edwards, L. Komorowski. J. F. Mariategui, B. W. Miller, M. T. Mojesky, K. Niedenzu, *Inorg. Chem*. **1988**, *27*, 3085−3089.
[8] [8a] A. J. Arduengo, III, H. V. R. Dias, R. L. Harlow, M. Kline, *J. Am. Chem. Soc.* **1992**, *114*, 5530−5534. − [8b] A. J. Arduengo, III, H. V. R. Dias, J. C. Calabrese, F. Davidson, *J. Am. Chem. Soc.* **1992**, *114*, 9724−9725.
[9] N. Kuhn, G. Henkel, T. Kratz, J. Kreutzberg, R. Boese, A. H. Maulitz, *Chem. Ber.* **1993**, *126*, 2041−2045.
[10] I. I. Padilla-Martínez, A. Ariza-Castolo, R. Contreras, *Magn. Reson. Chem.* **1993**, *31*, 189−193.
[11] I. I. Padilla-Martínez, M. J. Rosalez-Hoz, H. Tlahuext, C. Camacho-Camacho, A. Ariza-Castolo, R. Contreras, *Chem. Ber.* **1996**, *129*, 441−449.
[12] B. Wrackmeyer, *Ann. Rep. NMR Spectrosc*. **1988**, *20*, 61−203.
[13] S. Toyota, M. Oki, *Bull. Chem. Soc. Jpn*. **1992**, *65*, 1832−1840.
[14] E. M. Holt, S. L. Tebben, S. L. Holt, K. J. Watson, *Acta Crystallogr.* **1977**, *B33*, 1986−1988.
[15] F. H. Allen, O. Kennard, D. G. Watson, L. Brammer, G. Orpen, R. Taylor, *J. Chem. Soc., Perkin Trans 2* **1987**, S1.
[16] K. Okada, R.Suzuki, M. Oda, *J. Chem. Soc., Chem. Commun*. **1995**, 2069−2070.
[17] M. A. Dvorak, R. S. Ford, R. D. Suenram, F. J. Lovas, K. R. Leopold, *J. Am. Chem. Soc.* **1992**, *114*, 108−115.
[18] A. L. Allred, *J. Inorg. Nucl. Chem*. **1961**, *17*, 215−221.
[19] H. C. Brown, *Organic Synthesis via Boranes*, Wiley Interscience, New York, **1975**.
[20] G. W. Sheldrick, *SHELXTL-93*, University of Göttingen, **1993**.
[21] D. J. Watkin, J. R. Carruthers, P. W. Betteridge, *CRYSTALS, An Advanced Crystallographic Program System,* Chemical Crystallography Laboratory, University of Oxford, Oxford, **1988**.

[98187]

Schiff-Base Podates − X-ray, NMR and Ab Initio Molecular-Orbital Studies of the Cadmium(II) Complexes of Linear and Three-Armed Podands in Solution and Solid State

Anu Jäntti[a], Michael Wagner[a,b], Reijo Suontamo[a], Erkki Kolehmainen[a], and Kari Rissanen*[a]

Department of Chemistry, University of Jyväskylä[a],
P. O. Box 35 (Survontie 9), FIN-40351, Jyväskylä, Finland
Fax: (internat.) + 358-14/602501
E-mail: Kari.Rissanen@jyu.fi

Organisch-Chemisches Institut, Westfälische Wilhelms-Universität Münster[b],
Corrensstraße 40, D-48149 Münster, Germany
Fax: (internat.) + 49(0)251/83-39772

Received April 2, 1998

Keywords: Schiff-bases / Helical structures / Structure elucidation / NMR spectroscopy / Ab initio calculations

Cadmium(II) complexes of two Schiff bases, 1,3-di(pyridine-2-carboxaldimino)propane ($C_{15}H_{16}N_4$, **L1**)[1] and tris[4-(2′-pyridyl)-3-aza-3-butenyl]amine ($C_{24}H_{27}N_7$, **L2**)[2] are described. An efficient route utilising molecular sieves for the synthesis of Schiff bases is presented. The ligands **L1** and **L2** can be described as linear and three-armed podands, respectively, **L1** being conformationally flexible and **L2** preorganised. Cadmium perchlorate in methanol with **L1** yields a crystalline complex $[Cd(\mathbf{L1})_2](ClO_4)_2$ (**1**), the structure of which was determined by X-ray structure analysis. The complex **1** has an unusual nonsymmetrical 8-coordinated helical structure and crystallizes in an acentric space group (*Cc*, no. 9) as a pure enantiomer due to spontaneous resolution. Solution studies of **1** in $CHCl_3$/DMSO (10:1) and pure DMSO were performed using ^{1}H-, ^{13}C-, ^{113}Cd-NMR and ^{1}H,^{15}N z-GS HMBC spectroscopy and they suggest a reorientation of **1** into the more symmetrical 4-coordinate complex due to the flexible nature of **L1**. The preorganised, potentially tetra-, hexa- or heptadentate, three-armed podand **L2** and its in situ complexation with the Cd^{2+} cation were investigated by ^{1}H-, ^{13}C-, ^{113}Cd-NMR and ^{1}H,^{15}N z-GS HMBC spectroscopy. The results support the formation of a highly symmetrical helical 6-coordinate podate $[Cd\mathbf{L2}](NO_3)_2$ (**2**). The structure of **2** has also been verified by ab initio HF-MO calculations using a standard 3-21G* basis set (Lan2DZ for Cd).

There is a growing interest in finding alternative approaches for the design of new inexpensive and easy-to-prepare ligand/podand systems. Hannon and coworkers have described a simple and inexpensive way to prepare imine-based rigid ligands that can form a triple-helicate structure with proper metal ions.[3a] Schiff-base complexes are considered to be among the most important stereochemical models in main-group and transition-metal coordination chemistry due to their preparative accessibility and structural variety.[4] The Schiff-base ligands and podands are not so well studied as their macrocyclic and macrobicyclic counterparts. In particular, the macrocyclic Schiff bases have been synthesized, as their metal complexes, through the [1+1] or [2+2] condensation of proper bis-amines and bis-aldehydes, using metal ions as templates.[5] In the absence of templating metal ions the reactions give poor yields and oligomeric/polymeric products. On the other hand, by using metal ions, it is often very difficult or impossible to remove the template from the macrocycle. Schiff-base helical structures are still rare[3a] and only a few examples exist for similar Schiff-base cryptates[3b]. Earlier we reported the synthesis and some metal complexes of the podand **L1**[1]. **L1** has a short flexible spacer between the two metal-binding sites, thus giving a tweezer-like bite to a single transition-metal ion. As an alternative approach to prepare Schiff-base compounds we used activated molecular sieves to increase yields in the nontemplated synthesis for a known podand **L2**[2]. **L2** offers a chemically similar complexation site, but now preorganised for *endohedral* 4-, 6- or 7-coordination. We selected the Cd^{2+} ion as a probe for a study of the solution complexation, since it has very versatile coordination behaviour and ^{113}Cd NMR has proved to be an excellent tool to monitor complex formation.[6] In this work we report the preparation of Cd^{II} complex from **L1** (Scheme 1) and the definitive characterization of the complex in the solid state by X-ray diffraction together with the synthesis of three-armed podand **L2** derived from tris(2-aminoethyl)-amine (TREN) and 2-pyridylcarbaldehyde and its in situ complexation with Cd^{2+} (Scheme 2). The Cd^{II} complexes **1** and **2** were investigated by ^{1}H-, ^{13}C-, ^{113}Cd-NMR and 2-D (two-dimensional) ^{1}H,^{15}N z-GS HMBC (z-gradient selected heteronuclear multiple-bond coherence) spectroscopy and the complex **2** also by an ab initio HF-MO calculation.

Results and Discussion

Although **L1** itself is a liquid its complexation with Cd^{II} perchlorate in methanol produced crystals suitable for X-ray diffraction study (Table 1 in Experimental Section). The

 © WILEY-VCH Verlag GmbH, D-69451 Weinheim, 1998 1434−1948/98/1010−1555 $ 17.50+.50/0

Scheme 1

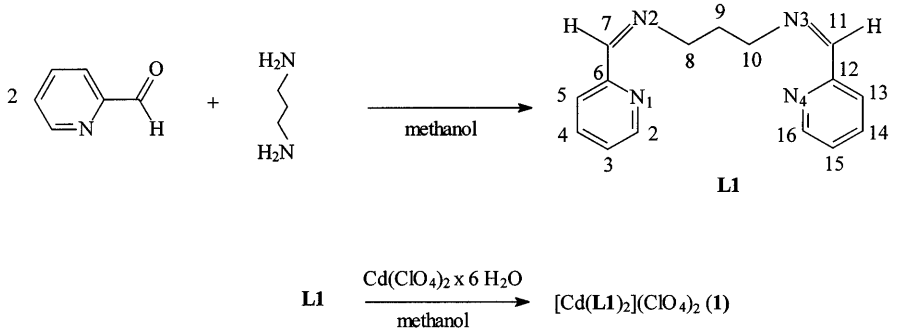

Scheme 2

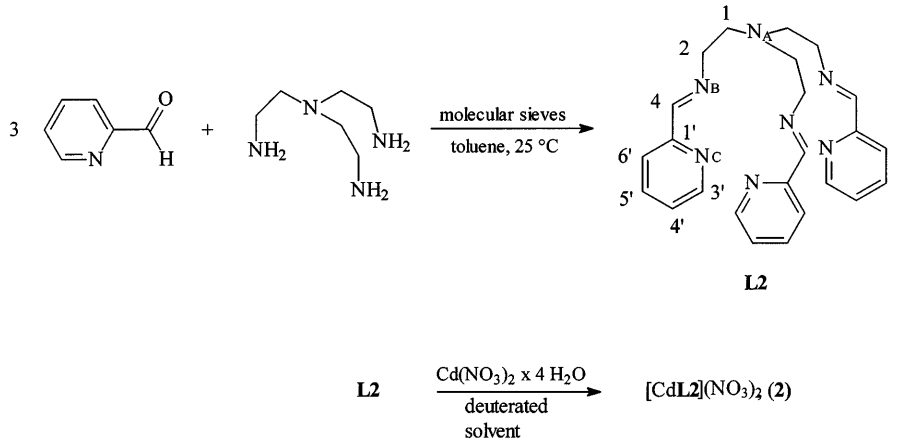

molecular structure of Cd^{II} complex **1** is displayed in Figure 1. The complex **1** is formed by coordination of two **L1** podands into a single cadmium ion. Due to its flexible nature **L1** acts as a pseudo-macrocyclic tetradentate ligand, thus resulting in a sandwich-type of 8-coordinated 1:2 complex.

Similar 8-coordination for Cd^{II} has been observed in some macrocyclic complexes.[7] The observed bond lengths and angles are consistent with the literature.[8][9] Selected bond lengths and angles for complex **1** of the Cd^{2+} ion are presented in Figure 1. To our great surprise complex **1** crystallized in an acentric space group and a detailed inspection of the structure revealed a helical arrangement of **L1** [in pseudo-macrocyclic conformation, the nonbonded intramolecular contact distances between the *ortho*-H atoms (H2, H16) are 223 pm (**L1**A) and 246 pm (**L1**B)] around the Cd^{II} ion. In some cases crystallization from a racemic solution of helical molecules can induce spontaneous resolution of the enantiomers and a mixture of enantiomerically pure crystals can be obtained[10]. The helical arrangement of the ligands results from the sterical factors around the Cd^{II} ion. The covalent radius of Cd^{II} ion is too small to bind all eight spatially neighbouring N atoms in a symmetrical cubic coordination, thus creating a twist of approximately 64° between the lower and upper ligand (Figure 2).

The four N atoms in a single **L1** ligand form a nearly symmetrical square plane (torsion angles for N1a−N2a−N3a−N4a and N1b−N2b−N3b−N4b are −4.63 and −3.69°, respectively) with almost equal nonbonded contact distances between the N atoms (N1a···N2a = 270.9 pm, N2a···N3a = 287.2 pm, N3a···N4a = 272.4 pm and N1a···N4a = 324.2 pm; N1b···N2b = 277.4 pm, N2b···N3b = 280.3 pm, N3b···N4b = 273.6 and N1b···N4b = 328.2 pm). The conformation of **L1** in the complex **1** is very close to an aza-crown conformation with all N atom lone pairs pointing in the same direction. The least-squares planes for the pyridine−imine (N1, C2−C7, N2 and N3, C11−C16, N4) parts show that they are nearly planar and the angles between the planes within the coordinated **L1** are quite similar: (N1a → N2a) and (N3a → N4a) 86.02°; (N1b → N2b) and (N3b → N4b) 75.80° The packing of the molecules in the unit cell along the *b* axis is shown in Figure 3. The weak π-stacking interactions between the two adjacent and co-planar pyridine rings along the *c* axis stabilise the packing. The distance between the co-planar pyridine rings is 416 pm.

Figure 1. The molecular structure of compound **1** [DIAMOND drawing with 20% (size reduced to improve clarity) probability ellipsoids (all non-hydrogen atoms), the uncoordinated perchlorate anions have been omitted for clarity][a]

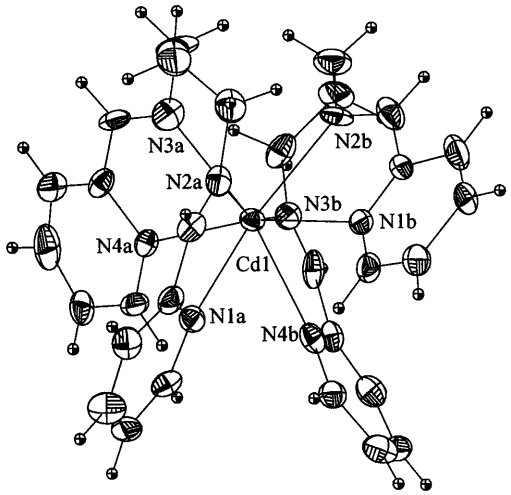

[a] Selected bond lengths [pm] and angles [°]: Cd1−N1a (−N1b) 256.3(14) [251.8(18)], Cd1−N2a (−N2b) 247.7(17) [251.8(14)], Cd1−N3a (−N3b) 250.9(20) [250.9(20)], Cd1−N4a (−N4b) 246.9(15) [259.5(19)]; N4a−Cd1−N3b 71.6(6), N4a−Cd1−N1b 169.0(2), N3b−Cd1−N2a 161.6(3), N4a−Cd1−N3a 65.9(6), N3b−Cd1−N3a 95.7(6), N2a−Cd1−N3a 70.3(6), N3b−Cd1−N1b 109.8(5), N3a−Cd1−N1b 124.0(6), N4a−Cd1−N2b 122.5(5), N1b−Cd1−N2b 66.9(5), N1b−Cd1−N1a 91.5(5), N3b−Cd1−N1a 32.0(6), N1a−Cd1−N4b 77.6(2), N2b−Cd1−N1a 156.0(5), N2a−Cd1−N4b 131.4(6), N4a−Cd1−N1a 80.2(5), N4a−Cd1−N4b 91.2(5).

In order to obtain some information about the structure of the metal complex **1** in solution we also carried out ^{113}Cd-NMR and 2-D ^{1}H,^{15}N z-GS HMBC measurements in [D$_6$]DMSO. The metal complex shows only one strong ^{113}Cd signal at δ = 84.4 measured from external 0.1 M aqueous Cd(ClO$_4$)$_2$ (δ = 0.0). This result can be regarded as good evidence for the reorientation of the unsymmetrical complex **1** into a more symmetrical tetracoordinate complex. This result is also in good agreement with the value for the tetracoordinate Cd^{2+} complex (δ = 95) reported by Munataka et al.[6b]

The ^{15}N chemical shift of the imine nitrogen atoms changes from δ = −35.8 for the free ligand to δ = −62.2 for the cadmium complex **1**. The signal of the pyridine nitrogen atoms at δ = −62.6 of the free ligand, is not visible in the ^{1}H,^{15}N z-GS HMBC correlation map of the cadmium complex of **L1** in solution, although the delay for evolution of long-range couplings was increased to 200 ms. The ^{15}N-NMR chemical shifts of the ligand itself are in agreement with those reported for (*Z*)-*N*-benzylidenecyclohexylamine (δ = −36.4[11]) and 2-methylpyridine (δ = −62.6[12]). The absence of the ^{1}H,^{15}N z-GS HMBC correlation can be due to (i) too small a scalar coupling constant $J(^{1}H,^{15}N)$ to allow magnetization transfer between proton and ^{15}N or (ii) a dynamic process taking place inside the complex at room temperature.

We have also investigated the complexation properties of tris[4-(2′-pyridyl)-3-aza-3-butenyl]amine (**L2**) in solution

Table 1. Crystal data, data collection and structure refinement for compound **1**

Crystal data	
Formula	$C_{30}H_{32}CdCl_2N_8O_8$
M_r	815.94
Crystal system	Monoclinic
Space group	*Cc* (No. 9)
Wavelength, Mo-K_α [Å]	0.71073
Crystal size [mm]	0.4 × 0.4 × 0.3
a [pm]	1809.3(4)
b [pm]	1065.7(3)
c [pm]	1753.1(5)
β [°]	95.85(2)
V [nm^3]	3.3627(2)
D_c [g cm^{-1}]	1.612
Z	4
F(000)	1656
μ (Mo-K_α) [mm^{-1}]	0.870
Data collection	
T [K]	293(2)
Scan mode	ω/2θ
hkl range	*h* 0 → 21 *k* 0 → 12 *l* −20 → 20
$\theta_{min/max}$ [°]	2.22/24.97
Measured reflections	3068
Unique reflections	3068
Refls. used for refinement	2570
Absorption correction	ψ scans
T_{min}/T_{max}	0.84/0.99
Refinement	
Refinement method on F^2	Full-matrix least-squares on F^2
Data/restraints/parameters	3068/44/392
H atoms (found/calcd.)	0/32
Final *R* values [$I > 2\sigma(I)$]	
*R*1[a]	0.0475
*wR*2[b]	0.1285
(shift/error)$_{max}$	< 0.001
Goodness-of-fit on F^2 (*S*)	1.079
ρ_{fin}(max/min) [e Å^{-3}]	0.673/−1.224

[a] $R1 = \Sigma||F_o| - |F_c||/\Sigma|F_o|$. − [b] $wR_2 = \{\Sigma[w(F_o^2 - F_c^2)^2]/[\Sigma[w(F_o^2)]\}^{1/2}$; $w = 1/[\delta^2(F_o^2) + (ap)^2 + bp]$; $p = (F_o^2 + 2F_c^2)/3$; $a = 0.0946$; $b = 8.58$. − $S = [\Sigma[w(F_o^2 - F_c^2)^2]/(n - p)]^{1/2}$.

Figure 2. A view of the coordination sphere showing the twist between the lower and upper ligand (the coordinating bonds are presented as dotted bars and the non-bonded intramolecular distances as thick solid bars)

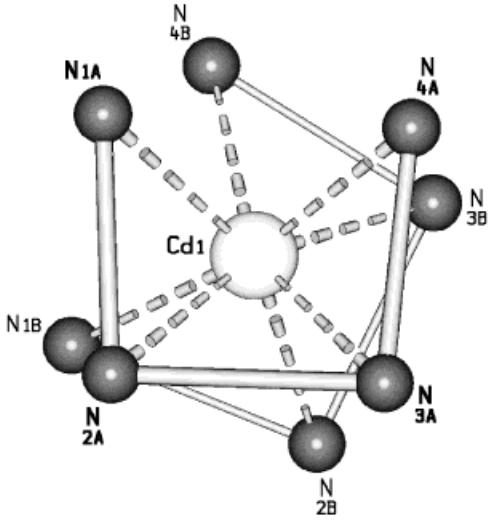

Figure 3. The packing of the molecules in the unit cell along the *b* axis

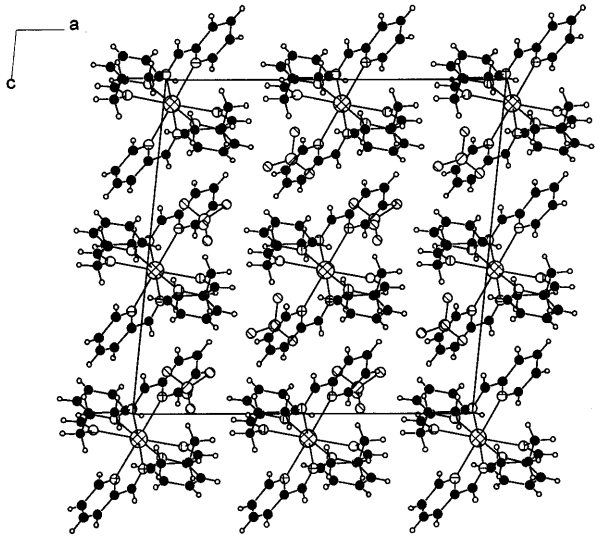

with Cd^{2+} using ^{1}H-, ^{13}C-, ^{113}Cd-NMR and 2-D $^{1}H,^{15}N$ z-GS HMBC spectroscopy. The measurements show that Cd^{2+} [added as $Cd(NO_3)_2 \cdot 4\ H_2O$] is efficiently complexed with the ligand **L2** forming tris[4-(2′-pyridyl)-3-aza-3-butenyl]aminecadmium(II) (**2**).

The metal complex **2** exhibits a strong ^{113}Cd signal at $\delta = 188.1$ in $CDCl_3$/[D_6]DMSO (10:1). From the fact that only one ^{113}Cd signal is observed it can be concluded that the potentially heptadentate Schiff-base ligand **L2** provides a highly symmetrical time-averaged complexation site for the Cd^{2+} cation. Furthermore, the more deshielded chemical shift value of **2** in comparison with **1** suggests that the coordination number must be larger in **2** than in **1**, as shown by Munataka et al.[6b]

A comparison of the $^{1}H,^{15}N$ z-GS HMBC correlation map of the free ligand **L2** with that of the cadmium complex **2** reveals that both pyridyl- and Schiff-base nitrogen atoms coordinate towards the cadmium cation. Due to the interaction with the metal centre the ^{15}N-NMR chemical shifts are moved upfield by approximately 50 ppm for each N atom compared with the free ligand **L2**. In [D_6]DMSO the ^{15}N-NMR chemical shift of the Schiff-base nitrogen atoms changes from $\delta = -38.9$ of **L2** to $\delta = -90.0$ in **2**. The pyridine nitrogen atoms show a shift from $\delta = -62.2$ to $\delta = -113.0$, respectively. The $^{1}H,^{15}N$ z-GS HMBC correlation map does not show any cross peak at room temperature due to the tertiary nitrogen atom N_A.

From the X-ray studies of related tris[4-(2′-pyridyl)-3-aza-3-butenyl]aminemetal complexes[2] it is already known that the bridging tertiary nitrogen atom N_A should also be coordinating. This assumption is further supported by the present ab initio calculation carried out on tris[4-(2′-pyridyl)-3-aza-3-butenyl]aminecadmium(II) (**2**) with a full geometry optimization at the HF/3-21G* (using Lan2DZ

Table 2. Calculated Cartesian atomic coordinates of the optimized standard orientation for the cation $[Cd\mathbf{L2}]^{2+}$ in $[Cd\mathbf{L2}](NO_3)_2$ (**2**)

Atom	*x*	*y*	*z*	Atom	*x*	*y*	*z*
Cd(1)	0.327679	0.115479	−0.116882	H(1AA)	4.242137	−0.409747	0.616059
N(A)	2.989909	0.359778	−0.871631	H(1BA)	4.594015	1.252063	0.215507
N(BA)	1.767749	0.124783	1.705724	H(1AB)	4.422504	−1.106293	−1.487278
N(BB)	1.114459	−1.706196	−1.320791	H(1BB)	3.172969	−0.741547	−2.652850
N(BC)	0.907513	2.353453	−0.654099	H(1AC)	2.433796	1.235742	−2.673551
N(CA)	−0.456477	−1.470165	1.649774	H(1BC)	3.965292	1.838415	−2.064705
N(CB)	−1.380929	−0.683573	−1.744201	H(2AA)	3.578743	0.914095	2.483553
N(CC)	−1.419530	1.666177	0.660750	H(2BA)	2.612870	1.997155	1.495694
C(1A)	3.788146	0.540514	0.370504	H(2AB)	2.676744	−2.254262	−0.064183
C(1B)	3.367161	−0.884064	−1.599658	H(2BB)	2.789114	−2.967091	−1.674338
C(1C)	2.961904	1.532508	−1.778203	H(2AC)	2.147590	3.507315	−1.936604
C(2A)	2.959017	0.981227	1.595700	H(2BC)	2.816624	3.153870	−0.359261
C(2B)	2.526131	−2.074039	−1.118607	H(4A)	2.151676	−0.617145	3.580905
C(2C)	2.244584	2.739249	−1.178054	H(4B)	0.685271	−3.135606	−2.729425
C(4A)	1.518982	−0.590757	2.707267	H(4C)	0.223119	4.287073	−0.616247
C(4B)	0.369533	−2.281908	−2.150254	H(3′A)	−2.103666	−2.257197	0.720052
C(4C)	0.054743	3.243325	−0.399196	H(3′B)	−2.852297	0.710329	−1.444561
C(1′A)	0.331912	−1.472820	2.731171	H(3′C)	−2.626556	0.344378	1.657186
C(1′B)	−0.996225	−1.782350	−2.408261	H(4′A)	−2.684997	−3.765472	2.593520
C(1′C)	−1.218263	2.932485	0.278310	H(4′B)	−4.420500	−0.296887	−3.062499
C(3′A)	−1.509052	−2.281728	1.608649	H(4′C)	−4.339934	2.030504	2.229239
C(3′B)	−2.584515	−0.170967	−1.983798	H(5′A)	−1.246286	−3.759834	4.613101
C(3′C)	−2.515077	1.360925	1.350639	H(5′B)	−3.725300	−2.343116	−4.278651
C(4′A)	−1.830568	−3.125481	2.660123	H(5′C)	−3.997017	4.372728	1.489814
C(4′B)	−3.462284	−0.740765	−2.892955	H(6′A)	0.724458	−2.261354	4.669779
C(4′C)	−3.472215	2.310958	1.670299	H(6′B)	−1.475936	−3.284162	−3.837361
C(5′A)	−1.026964	−3.121522	3.782083	H(6′C)	−1.936577	4.936403	0.235822
C(5′B)	−3.072291	−1.877534	−3.569435				
C(5′C)	−3.277275	3.614069	1.260539				
C(6′A)	0.077533	−2.280765	3.817006				
C(6′B)	−1.812595	−2.407909	−3.322603				
C(6′C)	−2.124876	3.931822	0.554219				

Table 3. Selected bond lengths [Å] and bond angles [°] and some TAP structural parameters for the cation $[Cd\mathbf{L2}]^{2+}$ in $[Cd\mathbf{L2}](NO_3)_2$ (**2**)

Cd(1)−N(A)	2.778	C(2B)−N(BB)	1.473	C(3′A)−C(4′A)	1.386
Cd(1)−N(BA)	2.323	C(2C)−N(BC)	1.487	C(3′B)−C(4′B)	1.386
Cd(1)−N(BB)	2.321	N(BA)−C(4A)	1.256	C(3′C)−C(4′C)	1.386
Cd(1)−N(BC)	2.373	N(BB)−C(4B)	1.255	C(4′A)−C(5′A)	1.380
Cd(1)−N(CA)	2.500	N(BC)−C(4C)	1.259	C(4′B)−C(5′B)	1.379
Cd(1)−N(CB)	2.491	C(4A)−C(1′A)	1.479	C(4′C)−C(5′C)	1.380
Cd(1)−N(CC)	2.462	C(4B)−C(1′B)	1.477	C(5′A)−C(6′A)	1.389
N(A)−C(1A)	1.488	C(4C)−C(1′C)	1.475	C(5′B)−C(6′B)	1.389
N(A)−C(1B)	1.490	C(1′A)−N(CA)	1.338	C(5′C)−C(6′C)	1.388
N(A)−C(1C)	1.483	C(1′B)−N(CB)	1.340	C(5′C)−C(6′C)	1.388
C(1A)−C(2A)	1.544	C(1′C)−N(CC)	1.338	C(6′A)−C(1′A)	1.377
C(1B)−C(2B)	1.535	N(CA)−C(3′A)	1.330	C(6′B)−C(1′B)	1.376
C(1C)−C(2C)	1.527	N(CB)−C(3′B)	1.330	C(6′C)−C(1′C)	1.377
C(2A)−N(BA)	1.471	N(CC)−C(3′C)	1.330		

N(BA)−Cd(1)−N(BB)	101.5	C(4A)−N(BA)−Cd(1)	120.0
N(BA)−Cd(1)−N(BC)	91.28	C(4B)−N(BB)−Cd(1)	120.1
N(BA)−Cd(1)−N(CA)	69.05	C(4C)−N(BC)−Cd(1)	117.1
N(BA)−Cd(1)−N(CB)	159.9	C(1′A)−N(CA)−Cd(1)	112.8
N(BA)−Cd(1)−N(CC)	100.9	C(1′B)−N(CB)−Cd(1)	112.9
N(BB)−Cd(1)−N(BC)	122.7	C(1′C)−N(CC)−Cd(1)	113.5
N(BB)−Cd(1)−N(CA)	88.57	C(3′A)−N(CA)−Cd(1)	127.8
N(BB)−Cd(1)−N(CB)	69.02	C(3′B)−N(CB)−Cd(1)	127.9
N(BB)−Cd(1)−N(CC)	154.0	C(3′C)−N(CC)−Cd(1)	127.1
N(BC)−Cd(1)−N(CA)	146.6	C(1A)−C(2A)−N(BA)	109.2
N(BC)−Cd(1)−N(CB)	108.8	C(1B)−C(2B)−N(BB)	106.8
N(BB)−Cd(1)−N(CC)	69.57	C(1C)−C(2C)−N(BC)	110.8
N(CA)−Cd(1)−N(CB)	92.47	C(1A)−N(A)−C(1B)	111.9
N(CA)−Cd(1)−N(CC)	87.35	C(1A)−N(A)−C(1C)	115.1
N(CB)−Cd(1)−N(CC)	85.50	C(1B)−N(A)−C(1C)	111.5
C(2A)−N(BA)−Cd(1)	116.5	N(A)−C(1A)−C(2A)	114.2
C(2B)−N(BB)−Cd(1)	116.8	N(A)−C(1B)−C(2B)	110.8
N(2C)−N(BC)−Cd(1)	123.0	N(A)−C(1C)−C(2C)	113.2

Coordination polyhedron model values[a]	$[Cd\mathbf{L2}]^{2+}$ (this work)	$[Zn\mathbf{L2}]^{2+}$ in $[Zn\mathbf{L2}](BF_4)_2$[b]
twist angle ϕ [°]	47	45.9
$M-N_A$ [pm]	277.8	301.3
$M-N_6$ [pm]	2.344	2.180
a	3.36	3.29
c	3.29	3.14
a/*c*	1.02	1.05
"bite" *b*	2.79	2.64

[a] For the definition of the model, see ref.[2a]. − [b] See ref.[2a].

basis set for Cd) level of theory. Calculated Cartesian atomic coordinates of **2** are collected in Table 2.

The calculated Cd^{2+} ($4d^{10}$) complex **2** and the analogous Zn^{2+} ($3d^{10}$) complex[2a] have a similar distorted trigonal antiprism (TAP) 6-coordinated structure, as might be expected. Selected bond lengths and bond angles of **2**, together with some TAP structural model parameters,[2a] are given in Table 3.

The six Cd−N distances are calculated to be between 232 pm and 250 pm as shown in Table 3 and are in agreement with the experimental range from 246.9 pm to 259.5 pm found for complex **1** (see Figure 1). The size of the coordination polyhedron in **2**, given by $M-N_6$ (the weighted mean of all M−N bond length, $M-N_A$ not included)[2a] is calculated to be 241.2 pm (weighted by δ = 2.0 pm for each bond length). The model parameters are in fair agreement when the larger size of Cd^{II} ion compared to Zn^{II} ion is taken into account. The distance between the bridgehead nitrogen atom N_A and the metal centre is calculated as 278 pm. This distance is long for an actual bond but is clearly less than 295 pm which is the sum of the covalent radius of Cd (141 pm) and the van der Waals radius of N (154 pm),[13] indicating a moderate non-bonding interaction. It is also clearly shorter than found in the Zn analogue, see Table 3. Consequently, the calculated structure of **2** allows more flexibility in that part of complex where N_A is located than for the other nitrogen atoms coordinated to Cd^{2+}. These results also can explain the fact that in $^1H,^{15}N$ z-GS HMBC experiments, nitrogen atom N_A did not give any cross peak. An ab initio optimized structure of the cation $[Cd\mathbf{L2}]^{2+}$ is shown in Figure 4.

Such an indicated dynamic process, involving the protons at C2 close to the bridgehead nitrogen atom N_A is indeed observed and can easily be studied by ^1H NMR.

At 303 K the ^1H-NMR spectrum of **2** in $CDCl_3$/$[D_6]$DMSO (10:1) shows one broad singlet for the methylene protons of C2 at δ = 3.51. This signal broadens even further when the sample is cooled down to 287 K. Further cooling leads to a splitting of this singlet into two separate signals with a multiplet splitting. At 253 K the dynamics of the diastereotopic protons 2-H and 2′-H are frozen out completely and then their separation is 86.6 Hz. Using now

Figure 4. An ab initio optimized structure and a van der Waals representation of the cation $[Cd\mathbf{L2}]^{2+}$

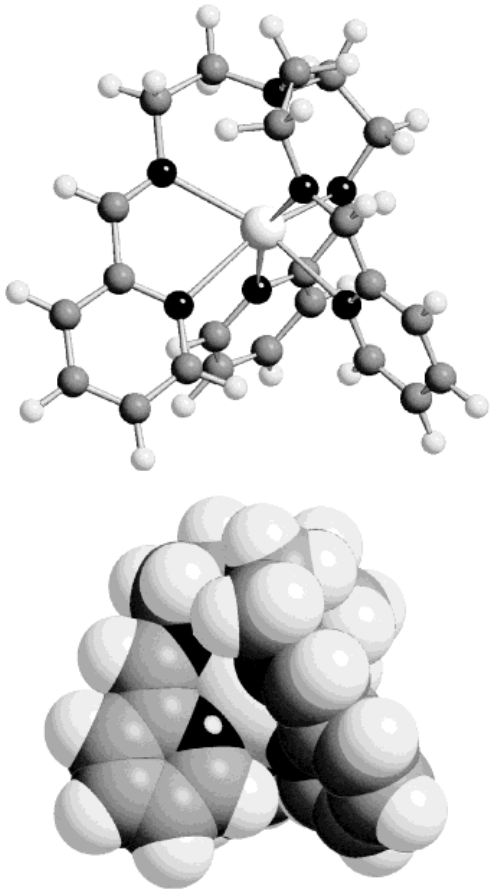

the Guttowsky−Holm equation[14] modified by Green[15] the activation barrier of the proton topomerization can be calculated as $\Delta G^{\neq}(287\ K) = 56.1 \pm 2.1$ kJ/mol. In contrast to above, the ^{1}H-NMR signals of the aromatic protons do not show significant temperature dependency. This finding also points to a well-defined geometry of the complexation site with strong binding interactions between the Cd^{2+}cation and the pyridine and Schiff-base nitrogen atoms.

This work was carried out with the financial support of *The Finnish Academy* (E. K.), The *Ministry of the Education of Finland* (A. J.) and *Deutsche Akademische Austauschdienst* (M. W.). Part of this work was done in the Organisch-Chemisches Institut, Westfälische Wilhelms-Universität Münster, Germany, for which the financial support of *The Finnish Academy* (A. J.) is gratefully acknowledged. Mr. *Reijo Kauppinen* is thanked for his help with NMR measurements.

Experimental Section

General: Metal salts, 2-pyridylcarbaldehyde and 1,3-diaminopropane were purchased from Merck, tris(2-aminoethyl)amine from Aldrich, powdered molecular sieves (3 Å) from Acros and used as received without further purification. Condensation reactions with molecular sieves were carried out under N_2, using a modified Schlenk technique. NMR spectra were recorded with either a Bruker Avance DRX 500 or a Bruker Avance DPX 250 FT NMR spectrometer. The ^{113}Cd-NMR chemical shift scale was fixed to the signal of a 1-mm diameter capillary tube containing 0.1 M aqueous or ethanolic (in low temperature runs) solutions of $Cd(ClO_4)_2$ inserted coaxially inside the 5-mm NMR tube as an external standard ($\delta = 0.0$). External neat nitromethane was used for the calibration in the case of ^{15}N-NMR experiments. The mass spectrum of **L1** was run with a VG AutoSpec HRMS spectrometer and the HRMS measurement of **L2** was recorded at 70 eV with a MAT 312 Finnigan mass spectrometer. IR spectra of **L2** were recorded with a Nicolet 5DXC FT-IR spectrometer, using KBr pellets.

Crystal-Structure Determinations: A specimen of suitable quality and size of compound **1** was mounted on top of a glass fibre and used for measurements of precise cell constants and intensity data collection with an Enraf Nonius CAD4 diffractometer [Mo-K_α radiation, λ(Mo-K_α) = 0.71073 Å]. During data collection three standard reflections were measured periodically as a general check of crystal and instrument stability. No significant changes were observed for compound **1**, where the data was corrected for decay (−1.4%). Lp correction was applied and intensity data were corrected for absorption effects (max $T = 0.99$, min $T = 0.84$). The atomic scattering factors and anomalous dispersion factors were taken from the International Tables for X-ray Crystallography.[16] The structure was solved by direct methods (SHELXS-86[17]) and completed by full-matrix least-squares techniques against F^2 (SHELXL-93[18]). All non-hydrogen atoms were refined anisotropically. Geometrical restraints were used to prevent anomalous bond lengths for the perchlorate anions. Calculations were performed with the hydrogen atoms in their idealized calculated positions (C−H distance 0.93 Å for aromatic CH and 0.97 Å for CH_2) and allowed to ride on their corresponding carbon atoms with fixed isotropic temperature factors ($U_{iso(fix)} = 1.2 \times U_{eq}$ of the attached C atom). Further information on crystal data, data collection and structure refinement are summarized in Table 1. Selected interatomic distances and angles are shown in the caption to Figure 1. The plots were generated with the program DIAMOND[19] and SCHAKAL92[20]. Crystallographic data (excluding structure factors) for the structure reported in this paper have been deposited with the Cambridge Crystallographic Data Centre as supplementary publication no. CCDC-101258. Copies of the data can be obtained free of charge on application to CCDC, 12 Union Road, Cambridge CB2 1EZ, UK [Fax: int. code +44(1223)336033; E-mail: deposit@ccdc.cam.ac.uk].

Ab Initio Molecular-Orbital Calculations: A full optimization of the structure of tris[4-(2′-pyridyl)-3-aza-3-butenyl]aminecadmium-(II) (**2**) was performed at the ab initio HF level of theory using gradient techniques with the Gaussian 94 set of programs.[21] The effective core potential (ECP) standard basis set Lan2DZ[22] was utilized for cadmium. The full-electron standard basis set 3-21G*[23] was used for all other atoms. A starting MM^+ structure for the ab initio calculations was optimized using the HyperChem 4.5 program.[24]

1,3-Bis(pyridine-2-carboxaldimino)propane (**L1**): We have earlier reported the synthesis of **L1**.[1] The structure of **L1** was further characterized by elemental analysis, ^{1}H/^{13}C NMR, ^{1}H,^{13}C HMQC and ^{1}H,X (X = ^{13}C,^{15}N) HMBC as well as mass spectrometry. All attempts to crystallize **L1** failed. − ^{1}H NMR (CD_3OD, 250.13 MHz, 303 K): δ = 2.15 (m, 9-H), 3.80 (m, 8-H, 10-H), 7.46 (t, 3-H), 7.88 (d, 4-H), 8.00 (m, 5-H), 8.41 (s, 7-H, 11-H), 8.59 (m, 2-H). − ^{13}C NMR (CD_3OD, 62.90 MHz, 303 K): δ = 32.5 (C-9), 59.8 (C-8, C-10), 122.8 (C-5), 126.6 (C-3), 138.6 (C-4), 150.2 (C-2), 155.1 (C-6), 163.5 (C-7, C-11). − ^{1}H,^{15}N z-GS HMBC

([D$_6$]DMSO, 250.13 MHz/25.35 MHz, 303 K): δ = −35.8/7.46 (N-4/3-H), −62.6/8.41 (N-3/7-H and 11-H). − MS (75 eV); *m/z* (%): 252 [M$^+$]. − $C_{15}H_{16}N_4$ (252.32): calcd. C 71.40, H 6.39, N 22.20; found C 68.82, H 6.32, N 21.49. Owing to the difficulties in purifying **L1**, satisfactory elemental analysis could not be obtained.

Bis{1,3-bis(pyridine-2-carboxaldimino)propane}cadmium(II) Perchlorate {[Cd(**L1**$_2$)](ClO$_4$)$_2$ (**1**)}: To 2.00 mmol of **L1** in 10 ml of methanol was added dropwise methanolic Cd(ClO$_4$)$_2$·6 H$_2$O (1.00 mmol in 10 ml of MeOH) until precipitation was observed. The solution was allowed to stand overnight during which time yellowish crystals of the complex formed. Yield 54%. The crystals were separated by filtration and washed with acetone and a suitable crystal was selected for the X-ray diffraction study.− ^{1}H NMR ([D$_6$]DMSO, 250.13 MHz, 303 K): δ = 1.86 (m, 9-H), 3.73 (m, 8-H, 10-H), 7.68 (m, 3-H), 7.91 (m, 5-H), 8.11 (m, 4-H), 8.57 (s, 7-H, 11-H), 8.75 (m, 2-H). − ^{13}C NMR ([D$_6$]DMSO, 125.75 MHz, 303 K): δ = 31.8 (C-9), 57.8 (C-8, C-10), 125.6 (C-5), 127.4 (C-3), 139.4 (C-4), 149.5 (C-6), 149.9 (C-2), 161.2 (C-7, C-11). − $^{1\,H,13}$C z-GS HMQC ([D$_6$]DMSO, 250.13 MHz/62.90 MHz, 303 K): δ = 125.6/7.91 (C-5, 5-H), 127.4/7.68 (C-3, 3-H), 139.4/7.91 (C-4, 5-H), 139.4/8.11 (C-4, 4-H), 149.9/8.75 (C-2, 2-H), 161.2/8.57 (C-7, C-11, 7-H, 11-H). − ^{1}H,^{15}N z-GS HMBC ([D$_6$]DMSO, 250.13 MHz/25.35 MHz, 303 K): δ = −62.2/8.57 (N-3/7-H and 11-H). − ^{113}Cd NMR {[D$_6$]DMSO, 110.94 MHz, 348 K, calibration with 0.1 M aqueous Cd(ClO$_4$)$_2$}: δ = 84.4.

Tris[4-(2′-pyridyl)-3-aza-3-butenyl]amine (**L2**): 10.0 g of molecular sieves (3 Å, powdered) was thoroughly activated at 500°C in vacuo (oil pump). After addition of 90 ml of toluene, 0.51 ml (500 mg, 3.42 mmol) of tris(2-aminoethyl)amine and 0.98 ml (1.10 g, 10.3 mmol) of 2-pyridylcarbaldehyde, the resulting suspension was stirred under nitrogen at room temperature (23°C) for 12 h. The molecular sieves were then removed by filtration. After evaporation of the solvent, the slightly yellowish oil was dried under vacuum (oil pump). The yield of **L2** was 1.23 g (87%). − IR (NaCl): $\tilde{\nu}$ = 3053 (m) cm^{-1}, 3007 (m), 2940 (vs), 2906 (vs), 2886 (vs), 2850 (vs), 1648 (vs), 1587 (vs), 1567 (vs), 1468 (vs), 1436 (vs), 1352 (m), 1292 (m), 1146 (m), 1066 (s), 1045 (s), 992 (s), 773 (vs), 754 (s), 617 (m). − ^{1}H NMR (CDCl$_3$, 500.13 MHz, 303 K): δ = 2.97 (t, ^3J = 6.8 Hz, 6 H, 1-H), 3.75 (t, ^3J = 6.8 Hz, 6 H, 2-H), 7.22 (m, 3 H, 4′-H), 7.64 (m, 3 H, 5′-H), 7.87 (m, 3 H, 6′-H), 8.30 (s, 3 H, 4-H), 8.56 (m, 3 H, 3′-H). − ^{1}H NMR(CD$_3$CN, 500.13 MHz, 303 K): δ = 2.93 (t, ^3J = 6.5 Hz, 6 H, 1-H), 3.72 (dt, ^3J = 6.5 Hz, ^4J = 1.3 Hz, 6 H, 2-H), 7.32 (m, 3 H, 4′-H), 7.72 (m, 3 H, 5′-H), 7.89 (m, 3 H, 6′-H), 8.28 (s, 3 H, 4-H), 8.56 (m, 3 H, 3′-H). − ^{1}H NMR ([D$_6$]DMSO, 250.13 MHz, 303 K): δ = 2.88 (t, ^3J = 6.3 Hz, 6 H, 1-H), 3.69 (t, ^3J = 6.3 Hz, 6 H, 2-H), 7.36 (m, 3 H, 4′-H), 7.73 (m, 3 H, 5′-H), 7.86 (m, 3 H, 6′-H), 8.30 (s, 3 H, 4-H), 8.56 (m, 3 H, 3′-H) . − ^{13}C NMR (CDCl$_3$, 125.75 MHz, 303 K): δ = 55.3 (C-1), 59.8 (C-2), 121.2 (C-6′), 124.5 (C-4′), 136.4 (C-5′), 149.3 (C-3′), 154.5 (C-1′), 162.2 (C-4). − ^{13}C NMR (CD$_3$CN, 125.75 MHz, 303 K): δ = 56.1 (C-1), 60.5 (C-2), 121.4 (C-6′), 125.6 (C-4′), 137.5 (C-5′), 150.3 (C-3′), 155.8 (C-1′), 163.5 (C-4) . − ^{1}H,^{13}C HMQC (CD$_3$CN, 500.13/125.75 MHz, 303 K): δ = 56.1/2.93 (C-1, 1-H), 60.5/3.72 (C-2, 2-H), 121.4/7.89 (C-6′, 6′-H), 125.6/7.32 (C-4′, 4′-H), 137.5/7.72 (C-5′, 5′-H), 150.3/8.56 (C-3′, 3′-H), 163.5/8.28 (C-4, 4-H). − ^{1}H,^{13}C HMBC (CDCl$_3$, 500.13 MHz/125.75MHz, 303 K): δ = 55.3/3.75 (C-1/2-H), 59.8/2.97 (C-2/1-H), 59.8/8.30 (C-2/4-H), 121.2/7.22 (C-6′/4′-H), 121.2/8.30 (C-6′/4-H), 124.5/7.87 (C-4′/6′-H), 136.4/8.56 (C-5′/3′-H), 149.3/7.22 (C-3′/4′-H), 149.3/7.64 (C-3′/5′-H), 154.5/7.64 (C-1′/5′-H), 154.5/8.30 (C-1′/4-H), 154.5/8.56 (C-1′/3′-H), 162.2/3.75 (C-4/2-H). − ^{1}H,^{15}N z-GS HMBC (CDCl$_3$, 25.35 MHz/250.13 MHz, 303 K): δ = −42.0/2.97 (N$_B$/1-H), −42.0/8.30 (N$_B$/4-H), −66.8/7.22 (N$_C$/4′-H), −347.0/3.75 (N$_A$/2-H). − ^{1}H,^{15}N z-GS HMBC ([D$_6$]DMSO, 25.35 MHz/250.13 MHz, 303 K): δ = −38.9/2.88 (N$_B$/1-H), −38.9/8.30 (N$_B$/4-H), −62.2/7.36 (N$_C$/4′-H), −62.2/7.73 (N$_C$/5′-H), −62.2/8.56 (N$_C$/3′-H), −347.1/3.69 (N$_A$/2-H). − HR MS (75 eV) (C$_{24}$H$_{27}$N$_7$): calcd. 413.23279, found 413.23191.

In Situ Preparation of Tris[4-(2′-pyridyl)-3-aza-3-butenyl]aminecadmium(II) Nitrate {[Cd**L2**](NO$_3$)$_2$ (**2**)}: 31 mg (74.5 μmol) of tris[4-(2′-pyridyl)-3-aza-3-butenyl]amine (**L2**) was dissolved in 0.5 ml of CDCl$_3$. The solution was mixed with a portion of 8.0 mg (25.9 μmol) of Cd(NO$_3$)$_2$·4H$_2$O. To this mixture [D$_6$]DMSO was added dropwise until the precipitate was dissolved. The ^{1}H-NMR chemical-shift changes unambiguously revealing the complex formation between Cd^{2+}cation and **L2**, the molar ratio **2**/**L2** being 1:3 at this stage. After another addition of 15.0 mg (48.6 μmol) of the Cd salt the Schiff base **2** was completely complexed with Cd^{2+} cation. The same procedure was also carried out in pure [D$_6$]DMSO. − ^{1}H NMR (CDCl$_3$/[D$_6$]DMSO = 10:1, 500.13 MHz, 303 K): δ = 2.70 (m, 6 H, 1-H), 2.79 (br. s, 8 H, H$_2$O), 3.51 (br. s, 6 H, 2-H and 2-H′), 7.29 (m, 6 H, 3′-H and 4′-H), 7.68 (m, 3 H, 6′-H), 7.80 (m, 3 H, 5′-H), 8.58 (s, 3 H, 4-H). − ^{1}H NMR (CDCl$_3$/[D$_6$]DMSO = 10:1, 500.13 MHz, 253 K): δ = 2.65 (m, 6 H, 1-H), 3.27 (br. s, 8 H, H$_2$O), 3.38 (m, 3 H, 2-H or 2-H′), 3.55 (m, 3 H, 2-H′ or 2-H), 7.25 (m, 6 H, 3′-H and 4′-H), 7.67 (m, 3 H, 6′-H), 7.79 (m, 3 H, 5′-H), 8.56 (s, 3 H, 4-H). − ^{1}H NMR([D$_6$]DMSO, 250.13 MHz, 303 K): δ = 3.01 (br. s, 6 H, 1-H), 3.77 (br. s, 8 H, H$_2$O), 3.83 (br. s, 6 H, 2-H), 7.72 (m, 6 H, 3′-H and 4′-H), 8.08 (m, 3 H, 6′-H), 8.28 (m, 3 H, 5′-H), 8.94 (s, 3 H, 4-H) . − Variable-temperature ^{1}H NMR: $\Delta G^{\neq}(T_C)$ = R·T_C ln [(R·T_C·21/2)/(2π·N$_A$·h·Δν)], $\Delta G^{\neq}$(287 K) = 56.1 kJ mol^{-1} ± 2.1 kJ mol^{-1}, T_C = 287 K (coalescense temperature), Δν (253 K) = 86.6 Hz [difference of the baseline-separated signals of the observed protons (dynamics frozen out)], R = 8.3144 J K^{-1} mol^{-1} (gas constant), N$_A$ = 6.0220 × 10^{23} mol^{-1} (Avogadro's number), h = 6.6262 × 10^{-34} J s (Planck constant). − ^{13}C NMR (CDCl$_3$/[D$_6$]DMSO = 10:1, 125.75 MHz, 303 K): δ = 53.9 (C-1), 54.2 (C-2), 128.5 (C-3′ or C-4′), 129.0 (C-6′), 140.4 (C-5′), 146.3 (C-1′), 148.3 (C-4′ or C-3′), 162.2 (C-4). − ^{13}C NMR (CDCl$_3$/[D$_6$]DMSO = 10:1, 125.75 MHz, 253 K): δ = 53.3 (C-1), 53.9 (C-2), 128.0 (C-3′ or C-4′), 128.4 (C-6′), 140.3 (C-5′), 145.8 (C-1′), 148.0 (C-4′ or C-3′), 161.8 (C-4). − ^{1}H,13C HMQC (CDCl$_3$/[D$_6$]DMSO = 10:1, 500.13 MHz/125.75MHz, 303 K): δ = 53.9/2.70 (C-1/1-H), 54.2/3.51 (C-2/2-H), 128.5/7.29 (C-4′andC-3′/4′-H and 3′-H), 129.0/7.68 (C-6′/6′-H), 140.4/7.80 (C-5′/5′-H), 148.3/7.29 (C-3′ and C-4′/3′-H and 4′-H), 162.2/8.58 (C-4/4-H). − ^{1}H,^{13}C z-GS HMBC (CDCl$_3$/[D$_6$]DMSO = 10:1, 250.13 MHz/62.90MHz, 303 K): δ = 54.2/8.58 (C-2/4-H), 128.5/7.29 (C-3′ and C-4′/4′-H and 3′-H), 128.5/7.68 (C-3′ and C-4′/6′-H), 128.5/7.80 (C-3′ and C-4′/5′-H), 129.0/8.58 (C-6′/4-H), 140.4/7.29 (C-5′/3′-H and 4′-H), 146.3/7.29 (C-1′/3′-H and 4′-H), 146.3/7.68 (C-1′/6′-H), 146.3/7.80 (C-1′/5′-H), 146.3/8.58 (C-1′/4-H), 148.3/7.80 (C-3′/5′-H), 162.2/7.68 (C-4/6′-H). − ^{1}H,^{15}N z-GS HMBC (CDCl$_3$/[D$_6$]DMSO = 10:1, 250.13 MHz/25.35 MHz, 303 K): δ = −91.6/2.70 (N$_B$/1-H), −91.6/8.58 (N$_B$/4-H), −113.7/7.29 (N$_C$/3′-H and 4′-H),-113.7/7.68 (N$_C$/6′-H), −113.7/7.80 (N$_C$/5′-H), −113.7/8.58 (N$_C$/4-H). Cross peaks for the nitrogen atom N$_A$ could not be detected at 303 K. − ^{1}H,^{15}N z-GS HMBC ([D$_6$]DMSO, 25.35 MHz/250.13 MHz, 303 K): δ = −90.0/8.94 (N$_B$/4-H), −113.0/7.72 (N$_C$/3′-H and 4′-H), −113.0/8.94 (N$_C$/4-H). Cross peaks for the nitrogen atom N$_A$ could not be detected at 303 K. − ^{113}Cd NMR {CDCl$_3$/[D$_6$]DMSO = 10:1, 110.94 MHz, 303 K, calibration with ethanolic 0.1 M Cd(ClO$_4$)$_2$}: δ = 227.0. − ^{113}Cd NMR {CDCl$_3$/[D$_6$]DMSO = 10:1, 110.94 MHz, 303 K, calibration with aqueous 0.1 M Cd(ClO$_4$)$_2$}: δ = 188.1.

[1] A. Jäntti, K. Rissanen and J. Valkonen, *Acta Chem. Scand.*, in press.
[2] [2a] R. M. Kirchner, C. Mealli, M. Bailey, N. Howe, L. P. Torre, L. J. Wilson, L. C. Andrews, N. J. Rose, E. C. Lingafelter, *Coord. Chem. Rev.* **1987**, *77*, 89−163. [2b] J. A. Thomas, A. Davison, A. G. Jones, *Inorg. Chim. Acta* **1991**, *184*, 99−105. [2c] L. J. Wilson, N. J. Rose, *J. Am. Chem. Soc.* **1968**, *90*, 6041−6045.
[3] [3a] M. J. Hannon,C. J. Painting, A. Jackson, J. Hamblin and W. Errington, *J. Chem. Soc., Chem. Commun.* **1997**, 1807−1808. [3b] J. de Mendoza, E. Mesa, J.-C. Rodriquez-Ubis, P. Vazguez, F. Vögtle, P.-M. Windscheif, K. Rissanen, J.-M. Lehn, D. Lilienbaum and R. Ziessel, *Angew. Chem. Int. Ed. Eng.* **1991**, 1331−1333.
[4] A. D. Garnovskii, A. L. Nivorozhkin and V. I. Minkin, *Coord. Chem. Rev.* **1993**, *126*, 1−69.
[5] S. M. Nelson, *Pure Appl. Chem.* **1980**, *52*, 2461−2476.
[6] [6a] J. Ratilainen, K. Airola, E. Kolehmainen and K. Rissanen, *Chem. Ber.* **1997**, 1353−1359. [6b] M. Munataka, S. Kitagawa and F. Yagi, *Inorg. Chem*. **1986**, *25*, 964−970.
[7] M. G. B. Drew, J. de O. Cabral, M. F. Cabral, F. S. Esho and S. M. Nelson, *J. Chem. Soc., Chem. Commun.* **1979**, 1033−1035.
[8] J. M. Epstein, J. C. Dewan, D. L. Kepert and A. H. White, *J. Chem. Soc., Dalton Trans.* **1974**, 1949−1954.
[9] K. R. Adam, S. Donnelly, A. J. Leong, L. F. Lindoy, B. J. McCool, A. Bashall, M. R. Dent, M. McPartlin, D. E. Fenton and P. A. Tasker, *J. Chem. Soc., Dalton Trans.* **1990**, 1635−1643.
[10] H. Sleiman, P. Baxter, J.-M. Lehn, K. Airola and K. Rissanen, *Inorg. Chem.* **1997**, 4734−4742.
[11] P. W. Westerman, R. E. Botto and J. D. Roberts, *J. Org. Chem*. **1978**, *43*, 2590−2596.
[12] R. E. Botto and J. D. Roberts, *J. Org. Chem*. **1977**, *42*, 2247−2249.
[13] J. Emsley, *The Elements*, Clarendon Press, Oxford, Great Britain, **1989**.
[14] H. Friebolin, *Ein-und zweidimensionale NMR-Spektroskopie*, Verlag Chemie, Weinheim, **1988**.
[15] M. L. H. Green, L.-L. Wong, A. Sella, *Organometallics* **1992**, *11*, 2660−2668.
[16] *International Tables for X-Ray Crystallography*, vol IV, The Kynoch Press, Birmingham, England, **1974**.
[17] G. M. Sheldrick, *Acta Cryst.* **1990,** *A46*, 467−473.
[18] G. M. Sheldrick, *SHELXL-93, A Program for the Refinement of Crystal Structures*, University of Göttingen, Germany, **1993**.
[19] G. Bergerhoff, *DIAMOND, Visual Crystal Structure Information System*, version 1.0.4, Bonn, Germany, **1995**.
[20] E. Keller, *SCHAKAL92, A FORTRAN Program for the Graphic Representation of Molecular and Crystallographic Models*, University of Freiburg, Freiburg, Germany, **1992**.
[21] M. J. Frisch, G. W. Trucks, H. B. Schlegel, P. M. W. Gill, B. G. Johnson, M. A. Robb, J. R. Cheeseman, T. Keith, G. A. Petersson, J. A. Montgomery, K. Raghavachari, M. A. Al-Laham, V. G. Zakrzewski, J. V. Ortiz, J. B. Foresman, C. Y. Peng, P. Y. Ayala, W. Chen, M. W. Wong, J. L. Andres, E. S. Replogle, R. Gomperts, R. L. Martin, D. J. Fox, J. S. Binkley, D. J. Defrees, J. Baker, J. P. Stewart, M. Head-Gordon, C. Gonzales and J. A. Pople, *Gaussian 94, Revision B3*, Gaussian Inc., Pittsburgh, PA, **1995**.
[22] P. J. Hay and W. R. Wadt, *J. Chem. Phys.* **1985**, *82*, 299−310.
[23] K. D. Dobbs and W. J. Hehre, *J. Comp. Chem*. **1987**, *8*, 880−893.
[24] *HyperChem, Release 4.5*, Hypercube, Inc., Gainesville, **1995**.
[98093]

Palladium-Induced Intramolecular Pyridine-Allyl Coupling Reactions: Formation of N-Bridgehead Heterocycles with a Stable C–N Bond

Jaganaiden Chengebroyen, Mary Grellier, and Michel Pfeffer*

Laboratoire de Synthèses Métallo-induites, Université Louis Pasteur,
4 rue Blaise Pascal, F-67070 Strasbourg, France
Fax: (internat.) + 33-3/88454667
E-mail: pfeffer@chimie.u-strasbg.fr

Received April 24, 1998

Keywords: *ortho*-Alkenylpyridines / C–H Activation / Palladium / Pyridine-allyl coupling / Indolizinium derivatives

In the presence of stoichiometric amounts of bis(acetonitrile)dichloropalladium(II) the *ortho*-alkenylpyridines 2-but-3′-en-1′-ylpyridine (**1**), 2-pent-5′-en-1′-ylpyridine (**2**), 2-hex-5′-en-1′-ylpyridine (**3**), 2-hept-6′-en-1′-ylpyridine (**4**) and 2-methyl-6-pent-4′-en-1′-ylpyridine (**5**) led to a mixture of coordination compounds such as 2-alken-1′-ylpyridine-κN:$\kappa^2 C$-dichloropalladium(II) and bis(2-alken-1′-ylpyridine-κN)-dichloropalladium(II) together with 2-pent-4-ene-1′,3′-diylpyridine-κN:$\kappa^3 C$-chloropalladium(II) and 2-hex-4-en-1′,3′-diylpyridine-κN:$\kappa^3 C$-chloropalladium(II) in the case of **2** and **3** respectively. The latter were quantitatively demetallated in the presence of an excess of triphenylphosphane to yield tris(triphenylphosphane)palladium(0), 2-vinyl-2,3-dihydroindolizinium chloride and 2-prop-1′-en-1′-yl-2,3-dihydroindolizinium chloride, respectively, by a regioselective addition of the pyridine unit onto the more congested terminal carbon atom of the allyl fragment.

Introduction

The formation of an intramolecular C−N bond between an amine and an olefin activated in the presence of palladium complexes, has been extensively studied. Indeed, Hegedus and co-workers[1] have shown that for primary and secondary amines this amine-olefin coupling reaction, yielding a new C−N bond, results mainly from the addition of the amine to the alkene which has been activated towards nucleophilic addition through coordination to the palladium center. Moreover, recent studies from our group revealed that tertiary amines could also be used as nucleophiles in a different type of C−N coupling reaction to afford cationic and neutral heterocyclic compounds[2]. Here the key step is the formation of an (η^3-allyl)Pd^{II} intermediate by a palladium-assisted C−H activation process. We deemed it of great importance to check whether this coupling reaction could be extended to other nitrogen-containing systems such as those containing an sp^2-hybridised nitrogen atom. We were especially interested in nitrogen nucleophiles in pyridinic systems in these heterocyclisation reactions. It is noteworthy that prior to the work described herein the intramolecular C−N coupling of a nitrogen atom at an allylic position was limited mainly to primary or secondary amines as nitrogen-containing nucleophiles[3]. We can note that heterocycles obtained in this novel way [i.e. by intramolecular addition of a pyridine unit onto a (allyl)Pd derivative] would furnish N-bridgehead heterocycles, many of which display interesting biological properties[4].

The substrates we have chosen for this study are *ortho*-alkenylpyridine derivatives bearing a terminal olefin separated by a chain of carbon atoms of variable length, in the *ortho* position of the pyridine (Scheme 1).

Scheme 1. *ortho*-Alkenyl pyridines (*o*-AlkPy)

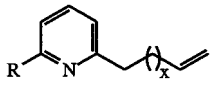

1: x = 1; R = H
2: x = 2; R = H
3: x = 3; R = H
4: x = 4; R = H
5: x = 2; R = Me

We report herein the reactivity of the pyridine derivatives **1**−**5** (they are called *o*-AlkPy from now on) in the presence of a palladium(II) complex and base, and we compare this to the reactions observed previously for tertiary amines. We will also describe the interactions between the nitrogen atom and/or the alkene unit and the Pd^{II} center, define under which structural conditions an allylic C−H activation can take place, and, finally study the depalladation of the thus formed organopalladium species affording the anticipated heterocyclic compounds.

Results

Synthesis of the *ortho*-Alkenylpyridines

The *o*-AlkPy ligands **1**−**5** are synthesised according to a known procedure[5]. It is based principally on a C−C coupling reaction between a 2-methylpyridyllithium derivative (prepared in situ) and an alkenyl bromide (Scheme 2).

 © WILEY-VCH Verlag GmbH, D-69451 Weinheim, 1998 1434−1948/98/1010−1563 $ 17.50+.50/0

Scheme 2. Synthesis of *ortho*-alkenylpyridines

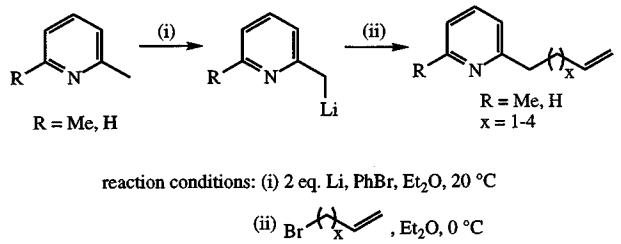

Ligand-Pd^{II} Interaction

The reaction of the *ortho*-alkenylpyridines **1**−**5** with stoichiometric amounts of $PdCl_2(MeCN)_2$ (1:1) leads to the formation of new coordination chelate complexes (Scheme 3). The stability of these compounds (**1a**, **2a** and **5a**) enabled their characterisation both in the solid state and in solution. This is in marked contrast to the corresponding derivatives obtained previously with *ortho*-alkenylaniline or -benzylamine which were only characterised in solution as they were too unstable to be isolated in the solid state.[2a] The structure of compound **2a** was determined by ^{1}H-NMR and IR spectroscopy, microanalysis and mass spectrometry while compounds **1a** and **5a** were identified by comparison of their ^{1}H-NMR spectra with that of **2a** and confirmed by their combustion analyses.

The downfield shift of the *ortho* proton of the pyridine ring in the proton-NMR spectrum of **2a** indicates that the nitrogen atom is coordinated to the Pd atom. The coordination of the olefinic double bond is evidenced by the shielding of all the protons in the lateral chain. Moreover, this is confirmed by the fact that when the chelate complexes are treated with one equivalent of PPh_3 or NEt_3, used to displace the alkene-Pd interaction, the chemical shifts of the latter protons are indeed almost identical to the values observed for the free ligand. In addition, the elemental analysis of **2a** gave a ratio of 1:2:1 with respect to palladium, chlorine and the *o*-AlkPy ligand **2**; the mass spectrum is in agreement with a monomeric species which was expected due to its solubility. Finally, two absorptions with mean intensities corresponding to the frequencies of two Pd−Cl vibrations are seen in the far-IR spectrum: the higher value is assigned to the vibration frequency of the Pd−Cl bond *trans* to N, and the lower one, to the Pd−Cl bond *trans* to the olefin[6][7].

Scheme 3. Chelate-type interaction between the *o*-AlkPy ligands and Pd^{II}

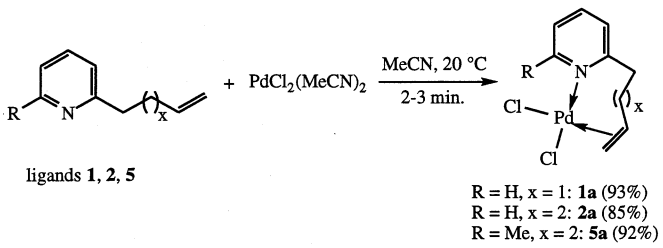

In order to check whether it would be possible to generate an (η^3-allyl)Pd^{II} complex by deprotonation at the allylic position, as it was observed in the case of tertiary amines[2a][2b], the chelate adduct **2a** was treated with a base. Indeed, the corresponding (η^3-allyl)Pd^{II} analogue was formed. Nevertheless, its poor yield (less than 10%) due to the formation of a secondary product of the type $PdCl_2(\mathbf{2})_2$ (see below), incited us to investigate optimum conditions to generate the (allyl)Pd complex.

Ligand-Pd^{II}-Base Interaction: Formation of (η^3-Allyl)Pd^{II} Complexes

The products of the one-pot reaction of the *o*-AlkPy ligands **1**−**5** with one equivalent of $PdCl_2(MeCN)_2$ and a base were studied. The reaction conditions and the products formed are indicated in Table 1 below. Several important remarks can be made concerning these results. Firstly, the nature of the final products seems to depend not only on the number of carbon atoms (*n*) between the nitrogen atom and the terminal olefin but also on the nature of R (R = Me, H). In fact, the formation of an (η^3-allyl)palladium(II) complex, analogous to that obtained in the case of tertiary amines, is limited to the cases where R = H and *n* = 4, 5. In other terms, no allylpalladium complex is observed for *n* larger than 5: the same observation was made in the case of tertiary amines where a different reactivity was noticed for the same length of the carbon chain separating the terminal olefin and the sp^3-hybridised nitrogen atom[2a][2b]. Given that the number of carbon atoms between the nitrogen atom and the allylic fragment in these two (η^3-allyl)Pd^{II} complexes (**2d** and **3d** in Table 1) is the same, we are inclined to believe that in the case of pyridinoolefins, the formation of the allyl complex is under thermodynamic control. However, the formation, in all cases and whatever the reaction conditions, of an important quantity of a secondary product (existing as two isomers except for **5c**) consisting of two *o*-AlkPy ligands and two chlorine atoms coordinated to the same palladium center, limits the yield of the allyl complex for *n* = 4, 5 and R = H. The latter organopalladium compounds **2d** and **3d** are indeed the minor products obtained during this reaction. All attempts (use of different reaction conditions, solvents or bases) to optimise its yield were unsuccessful: 18% was the maximum yield obtained for **2d** [the $PdCl_2(\mathbf{2})_2$ adduct remained the major product of the reaction] when heating a mixture of **2**, 1 equivalent of $PdCl_2(MeCN)_2$ and 2.5 equivalents of NaOAc in MeCN at 65°C for 3 h.

It is worth noting that the stability of these $PdCl_2$(ligand)$_2$ adducts depends on the value of *n*. For *n* < 4 (i.e for **1**), this adduct was not stable and was not isolated although a proton-NMR spectrum of the reaction mixture revealed unambiguously its presence in solution. When *n* increases, a higher yield of the adducts reflects an increase in their stability. A plausible explanation, based on observations from L. D. Pettit's group[5], is the increase in the basicity of the nitrogen atom as it moves further away from the olefinic

double bond with a negative inductive effect. Consequently, the donor ability of the nitrogen atom, via its lone pair of electrons, increases. This is confirmed by the chemioselective formation of this adduct in the case $n = 6$ (compounds **4b** and **4c**). In addition, for longer aliphatic chains ($n = 5$ and 6) this adduct is obtained with an isomerisation of the double bond in the lateral carbon chain of the pyridino-olefin ligand. The latter reaction is rationalised by a classical 1,3-hydrogen shift as described by Sen[8] and others[9]. Finally, the simplicity of the ^{1}H- and ^{13}C-NMR spectra (compared to those obtained for a mixture of the two isomers) suggests the formation of only one isomer of the $PdCl_2$(*o*-AlkPy)$_2$ adduct for ligand **5**. An increase in the steric bulk around the nitrogen atom resulting from the presence of a methyl group in the second *ortho* position of the pyridine ring would most probably favour the formation of the *anti* isomer **5c** rather than the *syn* isomer.

As shown in Scheme 4, ligand **2** is metallated by the palladium salt $PdCl_2(MeCN)_2$ in the presence of 2 equivalents of K_2CO_3 in MeCN to afford the (η^3-allyl)Pd^{II} complex **2d** and the two isomers **2b** and **2c** of the adduct $PdCl_2$(**2**)$_2$ as the main products, along with some palladium black and traces of unidentified products. After Celite filtration, **2d** (15%) and a mixture of isomers **2b** and **2c** (30%) were isolated by column chromatography on silica gel using ethyl acetate as eluant.

The (η^3-allyl)Pd^{II} complex **2d** was structurally characterised by microanalysis and ^{1}H- and ^{13}C-NMR spectroscopy. The ^{1}H-NMR spectrum shows the presence of the expected signals for an η^3-allyl fragment: a multiplet at $\delta \approx 5.5$ corresponding to H_b, coupled to H_a, H_c and H_d (Scheme 4); the terminal CH_2 group with the characteristic *syn* ($^3J_{HbHc}$ = 6.68 Hz), *anti* ($^3J_{HbHd}$ = 11.87 Hz) and *gem* ($^2J_{HcHd}$ = 1.1 Hz) couplings. The intramolecular coordination of the ni-

Table 1. Ligand-Pd^{II}-base interaction

Entry	Ligands (o-AlkPy)	Products formed	Conditions / yield [a]
1	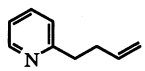 **1** (n = 3)	$PdCl_2$(**1**)$_2$ (**1b**, **1c**)	1,5 eq.K_2CO_3, MeCN, 65°C, 2h / [b]
2	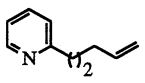 **2** (n = 4)	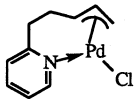 **2d** + $PdCl_2$(**2**)$_2$ (**2b**, **2c**)	2 eq. K_2CO_3, MeCN, 20 °C, 4 days / (**2b** + **2c**): 30% **2d** : 15%
3	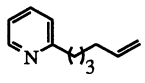 **3** (n = 5)	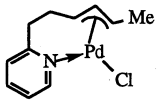 **3d** + $PdCl_2$(**3**)$_2$ (**3b**, **3c**)	2 eq. NaOAc, MeCN, 20 °C, 1 night / (**3b** + **3c**): 34% **3d** : 10%
4	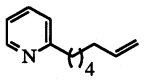 **4** (n = 6)	$PdCl_2$(**4**)$_2$ (**4b**, **4c**)	1,5 eq. NaOAc, MeCN, 65 °C, 1 night / (**4b** + **4c**): 40%
5	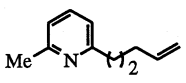 **5** (n = 4)	$PdCl_2$(**5**)$_2$ (**5c**)	1,5 eq. NaOAc, MeCN, 65 °C, 3h / 41%

[a] Yield of the pure products after a column chromatography on silica gel. – [b] Unstable product, not isolated but characterised in solution by ^{1}H NMR.

Scheme 4

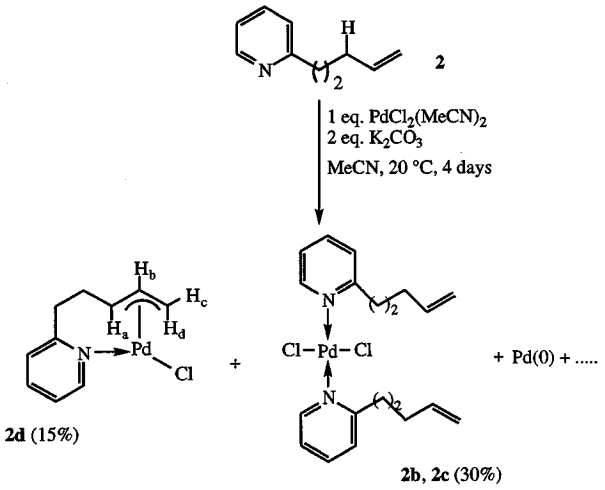

trogen atom is evidenced by the deshielding of the *ortho* proton (δ = 9.4 compared to 8.4 for the free ligand). The ^{1}H-NMR spectrum of **2d** indicates the presence of only one isomer in which the coupling constant between H_b and H_a is characteristic for two protons in an *anti* position ($^3J_{HaHb}$ = 11.5 Hz) suggesting that the carbon chain is in a *syn* position to H_b.

The $PdCl_2(\mathbf{2})_2$ adduct results from the higher affinity of a palladium(II) center for an sp^2-nitrogen atom. This compound was characterised by ^{1}H and ^{13}C NMR, elemental analysis and IR. The ^{1}H-NMR spectrum shows two distinct doublets of doublets in a 1:1 ratio at $\delta \approx 9$. In the presence of a drop of deuterated pyridine this spectrum remained unchanged but with a larger excess, the free *o*-AlkPy ligand **2** and the yellow adduct $PdCl_2(pyr\text{-}D_5)_2$ were formed. All these observations seem to indicate that the terminal olefin of the lateral chain is not coordinated and that a simple adduct is formed by the coordination of *o*-AlkPy ligand **2** on the palladium(II) center. The combustion analysis is in agreement with the presence of two chlorine atoms and two ligands around one atom of palladium. The far-IR spectrum of this compound shows only one large and intense band at 347 cm^{-1}: this vibration frequency is characteristic of a Pd−Cl bond *trans* to a chlorine atom[6][7]. Thus these data indicate that the $PdCl_2(\mathbf{2})_2$ adduct is a mixture of two isomers, in a 1:1 ratio. For one of these isomers, the two lateral carbon chains are on the same side of the coordination plane of the palladium center (*syn* isomer) and in the other isomer, they are opposite each other with respect to this plane (*anti* isomer). The (η^3-allyl)Pd^{II} complex **3d** and the mixture of isomers **3b** and **3c** (Scheme 5) were isolated in an analogous way to that described for **2d**, **2b** and **2c**. Their structures were determined mainly by ^{1}H and ^{13}C NMR. The proton NMR of **3d** shows the presence of only one compound where the multiplet at δ = 5.5 characteristic of H_b, the central proton of the allylic unit is no longer observed. Instead a triplet at δ = 5.3 was found, indicating that H_b is coupled with H_a and H_c, two magnetically equivalent protons. This suggests that the (η^3-allyl)Pd^{II} complex has the *syn* configuration. The presence of the methyl group is confirmed by a doublet integrating for three protons at δ = 1.55 and with a coupling constant $^3J_{HHc}$ of 6.3 Hz. Finally, evidence for the intramolecular coordination of the nitrogen atom comes from the shielding of the *ortho* proton (δ = 9.41 compared to 8.47 for the free ligand). The structure of the *syn*-(η^3-allyl)Pd^{II} complex **3d** was confimed by ^{13}C-DEPT NMR.

Scheme 5

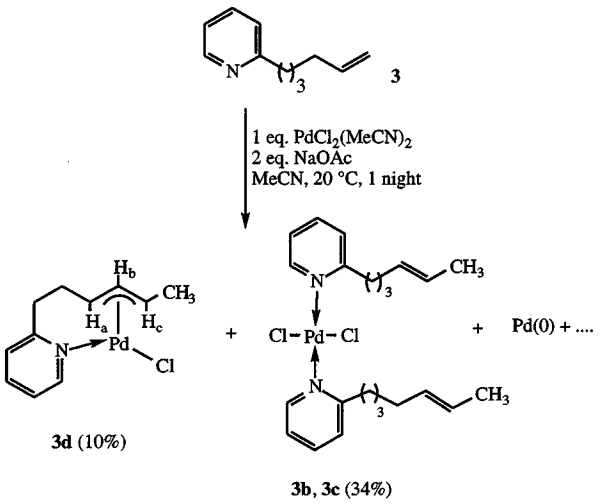

The aspect of the ^{1}H-NMR spectrum of the mixture **3b** and **3c** is also markedly different from that observed for the mixture of isomers **2b** and **2c**: the integration of the multiplets in the olefinic region indicates the presence of fewer olefinic protons (8 instead of 12). On the other hand, we noticed the appearence of a new multiplet integrating for 12 protons at δ = 1.7 and corresponding to the methyl groups. In addition, the ^{13}C-DEPT NMR spectrum shows a signal for methyl groups, thereby confirming the isomerisation of the olefinic double bond in ligand **3** during the course of the reaction and prior to the allylic deprotonation leading to the allyl complex. The same isomerisation process was observed in the case of ligand **4** and the analogous mixture of isomers **4b** and **4c** was isolated and characterised (see Table 1).

Formation of Cationic N-Bridgehead Heterocycles

The (η^3-allyl)Pd^{II} complexes **2d** and **3d** are stable in air and in solution. However, in the presence of an excess (3.5−4 equivalents) of triphenylphosphane in MeOH or MeCN at room temperature, they can be easily demetallated[10]. An orange-yellow solution was obtained together with the precipitation of a pale yellow solid. A proton NMR of the reaction mixture indicated the presence of only one organic compound and the characteristic signals of the phosphane ligands in a Pd^0 complex, $Pd(PPh_3)_n$. After filtration through Celite and anion exchange using KPF_6 in MeOH, the cationic N-heterocycles **2f** and **3f** (Scheme 6) were obtained as pure beige solids. These heterocyclic com-

pounds are indolizinium derivatives incorporating an sp^2-hybridised nitrogen atom shared between a pyridine ring and a 5-membered ring.

Scheme 6

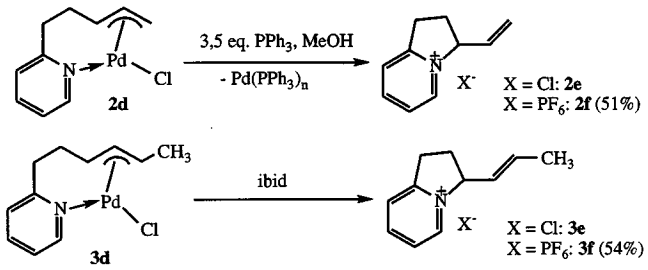

The structures of compounds **2f** and **3f** were deduced from ^1H and ^{13}C NMR, mass spectrometry and combustion analysis. The proton-NMR spectrum of **2f** is rather simple and shows not only that all the protons are different but also that the protons of the lateral carbon chain resonate at lower frequencies compared to those observed for compound **2d**: this general shielding is best explained by the presence of a positive charge on the nitrogen atom. The diastereotopicity of the protons of both CH_2 groups in **2f** is due to the presence of a stereogenic center α to the nitrogen atom. The structure of compound **3f** was deduced by comparaison of its ^1H- and ^{13}C-NMR spectra with those of **2f**.

Discussion

This study was aimed at defining the reactivity of *ortho*-alkenylpyridine ligands with a Pd^{II} center in the presence of a base. We intended to extend the scope of the unusual reactions that were observed for the related *ortho*-alkenylanilines or -benzylamines under similar conditions, i.e. the palladium-mediated heterocyclisation of these ligands which occured via the formation of C−N bonds at the allylic position[2].

We have noticed one major similarity between tertiary amines and pyridine derivatives concerning the above-mentioned heterocyclisation process: the addition of the nucleophile (amine or pyridine) always takes place at an allylic terminal (i.e. after an allylic deprotonation in the presence of a base) instead of a direct nucleophilic addition on the activated olefin due to its coordination to a Pd^{II} center, as observed in the case of primary and secondary amines[1]. Indeed, the results we have obtained clearly demonstrate that there is very little similarity between these types of nitrogen ligands and the corresponding pyridine derivatives, since in the present work we have mainly observed the formation of stable pyridine−palladium adducts. This result is not surprising as it is well known that Pd^{II} has a much larger affinity to a pyridine nitrogen atom as compared to an sp^3-hybridised tertiary amine nitrogen atom[11].

However, in two cases we could observe the formation of some (η^3-allyl)Pd-containing complexes by a C−H activation reaction. It is interesting to note that (i) this moiety has only been observed for two ligands and (ii) that both compounds do have the same geometry around the (Py-allyl)Pd unit: in both cases a CH_2-CH_2 chain is found between the pyridine ring and one extremity of the allylic unit. This is due to the stabilisation of the π-allyl fragment by an intramolecular coordination of the pyridine, thereby confering an ideal coordination geometry for the palladium atom in an analogous manner to that observed for a Pd(benzylamine-allyl) derivative[2a].

Moreover, for ligand **3** a prior C−H migration is essential in order to obtain the same type of stabilised (Py-allyl)Pd compound observed for ligand **2** (see Table 1). However, this C−H migration occurs only once since for ligand **4**, we observed only the formation of the bis(*ortho*-alkenylpyridine)palladium adduct. This behaviour is in marked contrast to that of the corresponding ligands bearing an sp^3-hybridised tertiary amine unit[2a][2b], for which the formation of the (η^3-allyl)Pd moiety was always possible (although it could not be isolated in each case studied) regardless of the number of carbon atoms between the olefin and the N atom. We interpret this as a consequence of the strong coordination of the sp^2-hybridised nitrogen atom of the pyridine moiety to the Pd center prior to the C−H activation at the allylic position by this metal, whereas for the tertiary amine alkene derivatives the interaction of the alkene to the palladium center seems to be the key step of the metallation process, yielding the (π-allyl)Pd derivatives in a quantitative way.

Although the corresponding (η^3-allyl)Pd^{II} complexes have been observed for pyridine derivatives, their yields are low (less than 20%) compared to those for tertiary amine analogues. These compounds are most likely formed by the intermediacy of the monomeric chelate adduct where both the nitrogen atom and the olefin are coordinated to the palladium atom (its presence in solution was unambiguously identified by ^1H NMR of the reaction mixture at the beginning of the reaction). However, the C−H activation process takes place only partially since the compounds with two ligands per palladium, $PdCl_2$(*o*-AlkPy)$_2$, are the major products of the reaction. Nevertheless, once they are formed no reverse reaction could be envisaged to transfer one species into the other; this result seems to indicate clearly the absence of any type of equilibrium between these two Pd^{II} compounds. One may anticipate, from our failed attempts to increase the yields of the allylic compounds starting from **2a** for instance, that the formations of these two classes of compounds are in competition with each other; however, in the absence of any reliable kinetic data we cannot conclude about this important mechanistic point.

It is, however, interesting to note the ease with which the allylic compounds can be demetallated to yield quantitatively heterocyclic compounds with a stable C−N bond even in the presence of Pd^0 formed. Indeed, even if some rare examples of (allyl)Pd^{II} complexes analogous to that observed for the pyridino-olefins are known for quinoline derivatives[12], the cyclisation reaction by the addition of an sp^2-nitrogen atom on an allylic fragment has never been

studied until now. One of the reasons is, most probably, a reversible reaction implying a C−N bond rupture, between the pyridinium ion formed and the simultaneous obtention of Pd^0 during the demetallation reaction. Indeed, allylpyridinium moities synthesised by other methods are used to generate in the presence of Pd^0 an (η^3-allyl)Pd^{II} complex and a trisubstituted pyridine (playing the role of a neutral leaving group) by an oxidative addition of the C−N bond on the Pd^{II} center[13]. Moreover, another reason which may justify that hitherto only few studies have been carried out concerning pyridine-allyl coupling reactions yielding new C−N bonds, is the result of the recent study carried out on the reversible intermolecular addition of a pyridine on an allylic unit[14]. Thus, this reversibility reflects the instability of the C−N^+ bond formed during this study.

The demetallation of the (η^3-allyl)Pd^{II} compounds is induced by an intramolecular attack of the sp^2-hybridised nitrogen atom on the allylic fragment and this can occur either as an endo- or exocyclisation yielding different cyclic products. In the case of substrate **2d** or **3d**, only one heterocycle is obtained by the formation of a new C−N bond between the sp^2-nitrogen and the more substituted carbon atom C_α to give a 5-membered heterocycle (Scheme 7). We have, therefore, a remarkably high regioselectivity when taking into account the two possible electrophilic centers on the allylic fragment.

Scheme 7

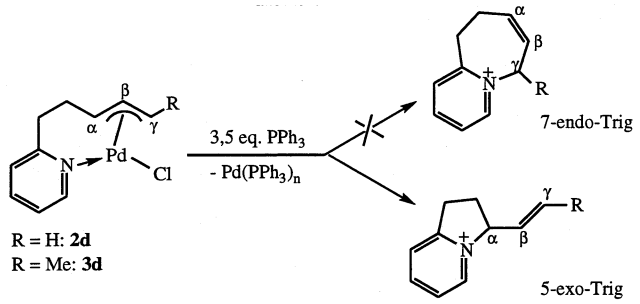

According to Baldwin rules governing the formation of cyclic products[15], both the formation of the 5-membered heterocycle and that of the 7-membered one are favoured processes. It is, however, accepted that the formation of 5-membered rings is more frequent than that of 7-membered derivatives[16]. An important observation is the fact that in the case of tertiary amines, for the closely related (π-allyl)Pd compounds (i.e. those having 3 carbon atoms between the N atom and the allylic fragment) the endocyclisation process was exclusively observed[2a]. This highlights the difference of the strength of the N−Pd bond in the latter case as compared to the pyridine compounds: the endocyclisation could only take place via an intermediate in which the NR_2 unit was not coordinated to the palladium atom. On the other hand, for the pyridine-containing compounds the exocyclisation could be achieved without dissociation of the Py−Pd bond by a *cis* migration of the N atom to the more substituted allylic carbon atom; however, this assumption merits a more substantial mechanistic study.

Moreover, in the case of substrate **3d**, the exocyclisation should be even more favorable owing to the steric effect of the methyl group at the external (C_γ) allylic carbon atom. Consequently, the nucleophilic attack at this position becomes more difficult[17].

Conclusion

The present study shows that even if there is a remarkable difference in affinity to a palladium(II) center between a pyridinic sp^2-nitrogen and a tertiary amino sp^3-nitrogen atom, it is possible to generate the (η^3-allyl)Pd^{II} analogue of the pyridino-olefin derivative. The demetallation of the latter complex yields, regioselectively and in mild conditions, a stable cationic N-heterocycle by the intramolecular formation of a C−N bond between the pyridinic nitrogen atom and the allylic C_3 unit. Nevertheless, the low yield of the allylpalladium complex associated with the fact that it is observed in only a few cases, considerably limits the scope of this elegant cyclisation reaction for the formation of cationic N-bridgehead heterocycles. Consequently, new methods to generate selectively and quantitatively the key (η^3-allyl)Pd^{II} intermediate are under investigation.

J. C. thanks the *Ministère de la Recherche et de l'Enseignement Supérieur* for partial financial support of this work.

Experimental Section

General: All the reactions described herein were carried out without any particular precaution unless otherwise stated. All the solvents used were dried beforehand and distilled under nitrogen. The other commercial starting materials were utilised without further purification. Filtrations to remove the black deposit of metallic palladium formed during the depalladation reactions, were performed using Celite pads. Column chromatography was carried out either on silica gel (Geduran SI 60; 0.063−0.200 mm) or on alumina 90 (Activity II−III mesh; 0.063−0.200 mm) from Merck. ^{1}H- (300.13 or 200.13 MHz), ^{13}C- (75.47 or 50.32 MHz) and ^{31}P-NMR spectra (81 MHz) were recorded with AC 300 and AC 200 Bruker instruments and externally referenced to TMS. Coupling constants (J) are given in Hertz. All deuterated solvants were dried with molecular sieves (4 Å) and stored under nitrogen. Combustion analyses were performed by the Service Central de Microanalyses du CNRS, Université Louis Pasteur, Strasbourg, France or by that of Vernaison, France. All Mass spectra were performed by the Laboratoire de Spectroscopie de Masse de l'Université Louis Pasteur, Strasbourg. IR spectra were recorded with an IRFT Bruker instrument and the absorption bands are given in cm^{-1}.

Ligands Synthesis: Ligands **1** and **2** were prepared according to published procedures[5]. Ligands **3**, **4** and **5** were synthesised in an analogous manner. The analytical data for these ligands are listed below.

Ligand **1**: Yellow oil (83%). − ^{1}H NMR ($CDCl_3$): δ = 8.45−8.43 (m, 1 H, H_o), 7.48 (td, 1 H, H_m, ^3J = 8.4 Hz, ^4J = 1.9 Hz), 7.09 (d, 1 H, H_m, ^3J = 19.2 Hz), 7.04−6.97 (m, 1 H, Ar, H_p), 5.86−5.73 (m, 1 H, HC=C), 5.01−4.87 (m, 2 H, C=CH_2, $^3J_{trans}$ = 17.1 Hz, $^3J_{cis}$ = 10.2 Hz), 2.83−2.78 (m, 2 H, Ar-CH_2), 2.47−2.39 (m, 2 H, CH_2). − ^{13}C NMR ($CDCl_3$): δ = 161.4, 149.2, 137.7, 136.2, 123.0, 121.0, 115.1 (aromatic and olefinic), 37.7, 33.7 (CH_2).

Ligand **2**: Pale yellow oil (78%). − The indices allocated to certain protons are given in Figure 1. − ^{1}H-NMR ($CDCl_3$): δ = 8.45 (d, 1 H, H_a, $^3J_{HaHb}$ = 3.4 Hz), 7.52 (m, 1 H, H_c), 7.03 (m, 2 H, H_b + H_d), 5.80 (m, 1 H, H_k, $^3J_{HkHm}$ = 18.8 Hz, $^3J_{HkHl}$ = 9.3 Hz), 4.92 (m, 2 H, H_l + H_m, $^2J_{HlHm}$ = 1.8 Hz), 2.74 (t, 2 H, Ar-CH_2), 2.06 (m, 2 H, CH_2−CH=), 1.80 (m, 2 H, CH_2-CH_2-CH=).

Figure 1. Numbering scheme for the protons of ligand **2**

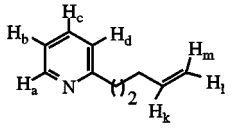

Ligand **3**: Orange yellow oil (94%). − ^{1}H NMR ($CDCl_3$): δ = 8.47 (d, 1 H, H_o, ^3J = 4.8 Hz); 7.54 (td, 1 H, H_m, ^3J = 7.7, Hz, ^4J = 1.8 Hz), 7.10 (d, 1 H, H_m, ^3J = 7.8 Hz); 7.07−7.02 (m, 1 H, H_p), 5.82−5.71 (m, 1 H, HC=C), 5.01−4.88 (m, 2 H, H_2C=C), 2.76 (t, 2 H, Ar-CH_2, ^3J = 7.7 Hz), 2.11−2.03, 1.78−1.67, 1.49−1.38 (3 m, 6 H, CH_2). − ^{13}C NMR ($CDCl_3$): δ = 162.3, 149.2, 138.8, 136.3, 122.7, 120.9 (aromatic and olefinic), 38.3, 33.6, 29.4, 28.7 (CH_2). − MS; *m/z*: 162 (M^+ + H), 120 (M^+ − C_3H_5), 106 (M^+ − C_4H_7), 93 (M^+ − C_5H_8).

Ligand **4**: Yellow oil (93%). − ^{1}H NMR ($CDCl_3$): δ = 8.52−8.50 (m, 1 H, Ar, H_o), 7.56 (td, 1 H, Ar, ^3J = 7.7 Hz, ^4J = 1.9 Hz), 7.12 (d, 1 H, Ar, ^3J = 7.8 Hz), 7.09−7.05 (m, 1 H, Ar), 5.86−5.72 (m, 1 H, HC=C), 5.01−4.89 (m, 2 H, C=CH_2), 2.77 (t, 2 H, Ar−CH_2, ^3J = 7.6 Hz), 2.09−2.01, 1.78−1.68, 1.48−1.32 (3 m, 8 H, CH_2). − ^{13}C NMR ($CDCl_3$): δ = 162.3, 149.1, 138.9, 136.1, 122.6, 120.8 (aromatic and olefinic CH), 114.2 (olefinic CH_2), 38.3, 33.6, 29.7, 28.8, 28.7 (CH_2).

Ligand **5**: Pale yellow oil (80%). − ^{1}H NMR ($CDCl_3$): δ = 7.45 (t, 1 H, Ar, ^3J = 7.7 Hz), 6.94−6.90 (m, 2 H, Ar), 5.87−5.75 (m, 1 H, HC=C), 5.04−4.92 (m, 2 H, C=CH_2), 2.74 (t, 2 H, Ar-CH_2, ^3J = 7.7), 2.51 (s, 3 H, CH_3), 2.14−2.07, 1.84−1.74 (2 m, 4 H, CH_2). − ^{13}C NMR ($CDCl_3$): δ = 161.5, 157.7, 138.5, 136.4, 120.4, 119.5, 114.8 (aromatic and olefinic), 37.9, 33.5, 29.3 (CH_2), 24.6 (CH_3). − MS; *m/z*: 161 (M^+), 160 (M^+ − H), 120 (M^+ − C_3H_5), 107 (M^+ − C_4H_6).

Synthesis of the Chelate Adducts

Compound **2a**: To a suspension of $PdCl_2(MeCN)_2$ (0.93 g; 3.6 mmol) in acetonitrile (40 ml) was added dropwise a solution of ligand **2** (0.525 g; 3.6 mmol). The yellow suspension became gradually homogeneous with increasing amounts of the ligand. The reaction mixture was stirred for 10 min at room temperature. After removal of the solvent by evaporation, drying, washing with ether (2 × 40 ml), compound **2a** was obtained as a fine, orange-coloured powder (0.985 g; yield 85%). − ^{1}H NMR ($CDCl_3$): δ = 8.63 (d, 1 H, H_{ortho}, ^3J = 5.5 Hz), 7.83 (t, 1 H, H_{para}, ^3J = 7.7 Hz), 7.38−7.34 (m, 2 H, H_{meta}), 6.43−6.31 (m, 1 H, CH_2=C*H*), 5.78 (dd , 1 H, CH_2=CH, ^3J = 7.7 Hz, ^2J = 2.1 Hz), 4.95−4.83 (m, 1 H, Ar−CH_2), 4.68 (d, 1 H, CH_2=CH, ^3J = 14.7 Hz), 3.39−3.32 (m, 1 H, Ar−CH_2), 2.61−2.48, 2.34−2.16, 2.07−1.89, 0.95−0.88 (4 m, 4 H, CH_2). − IR (polyethylene pellet): 341 (br, m, νPd−Cl *trans* to N); 308 (br, m, νPd−Cl *trans* to the olefin). − MS (FAB); *m/z*: 328 (M^+ + 3H), 254 [M^+ − 2 Cl)]. − $C_{10}H_{13}Cl_2NPd$ (324.5): calcd. C 37.01, H 4.04, N 4.32; found C 37.10, H 4.12, N 4.38.

Compounds **1a** and **5a** were synthesised in the same way as described for compound **2a** above.

Compound **1a**: Dark yellow solid (93%). − ^{1}H NMR ($CDCl_3$): δ = 8.93 (d, 1 H, H_o, ^3J = 5.6 Hz), 7.85 (t, 1 H, H_m, ^3J = 7.5 Hz), 7.40−7.26 (m, 2 H, H_p + H_m), 6.91−6.78 (m, 1 H, C=CH), 5.85 (d, 1 H, C=CH_2, $^3J_{cis}$ = 8.2 Hz), 4.41 (d, 1 H, C=CH_2, $^3J_{trans}$ = 14.1 Hz), 3.92 (td, 1 H, CH_2, ^3J = 12.6 Hz), 3.34−3.27, 2.80−2.77, 1.70−1.54 (3 m, 3 H, CH_2). − $C_9H_{11}Cl_2NPd$ (310.5): calcd. C 34.79, H 3.54, N 4.51; found C 34.65, H 3.36, N 4.71.

Compound **5a**: Orange yellow solid (92%). − ^{1}H NMR ($CDCl_3$): δ = 7.71 (t, 1 H, Ar, ^3J = 7.5 Hz), 7.24 (d, 1 H, Ar, ^3J = 8.3 Hz), 7.17 (d, 1 H, Ar, ^3J = 7.7 Hz), 6.55−6.35 (m, 1 H, C=CH), 5.65 (d, 1 H, C=CH_2, ^3J = 7.1 Hz), 5.18−5.07 (m, 1 H, CH_2), 4.57 (d, 1 H, C=CH_2, ^3J = 14.5 Hz), 3.40−3.32 (m, 1 H, CH_2), 3.28 (s, 3 H, CH_3), 2.63−2.43, 2.25−2.10, 2.05−1.85, 1.05−0.82 (4 m, 4 H, CH_2). − $C_{11.6}H_{16.4}Cl_2NPd$ (**5a** + 0.1 C_6H_{14}) (the solvent was detected in the ^{1}H-NMR spectrum) (347.2): calcd. C 40.11, H 4.70, N 4.03; found C 40.14, H 4.45, N 4.11.

Synthesis of the (η^3-Allyl)palladium Complex **2d** *and of the Mixture* **2b** + **2c**: A suspension containing ligand **2** (1.3 g, 8.8 mmol), $PdCl_2(MeCN)_2$ (2.3 g, 8.8 mmol) and 2 equiv. of NaOAc (1.45 g, 17.6 mmol) in acetonitrile (50 ml) was heated at 65°C for 3 h. A red solution with a considerable deposit of metallic palladium was thus obtained. After filtration of the Pd^0 so formed through Celite, the clear solution was concentrated to dryness. The brown oily residue was then extracted with CH_2Cl_2 (ca. 5 ml). A column chromatography using silica gel and ethyl acetate as eluant allowed the migration of a first yellow band corresponding to the mixture **2b** + **2c**. After solvent evaporation, a yellow solid was obtained (1.25 g; yield 30%). Then a second yellow fraction containing compound **2d** was collected (0.412 g; yield 16%).

Compound **2d**: Figure 2 indicates the indices attributed to certain protons.

Figure 2. Numbering scheme for the protons of ligand **2d**

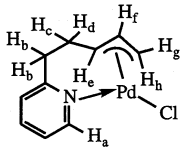

^{1}H NMR ($CDCl_3$): δ = 9.36 (d, 1 H, H_a, $^3J_{HaH}$ = 5.2 Hz), 7.73, 7.30 (2 m, 3 H, *meta* and *para* protons), 5.45 (m, 1 H, H_f, $^3J_{HfHh}$ = 11.87 Hz, $^3J_{HfHg}$ = 6.68 Hz, $^3J_{HfHe}$ = 11.5 Hz), 3.94 (d, 1 H, H_g), 3.72 (m, 1 H, H_e, $^3J_{HeHc}$ = 5.6 Hz), 3.12 (m, 2 H, H_b, $^3J_{HbHc}$ = 6.74 Hz, $^3J_{HbHd}$ = 3.15 Hz), 2.88 (d, 1 H, H_h), 2.05 (m, 1 H, H_c), 1.85 (m, 1 H, H_d). − ^{13}C NMR ($CDCl_3$): δ = 158.2, 152.2, 138.7, 124.9, 122.9 (aromatic), 111.7, 81.4, 55.9 (allylic), 41.6, 26.4 (CH_2). − $C_{12}H_{16}ClNOPd$ (**2d** + 0.5 $C_4H_8O_2$) (the solvent was detected in the ^{1}H-NMR spectrum) (332.1): calcd. C 43.37, H 4.82, N 4.22; found C 43.74, H 4.81, N 4.42.

Compounds **2b** + **2c**: ^{1}H NMR ($CDCl_3$): δ = 9.02 (d, 2 H, H_o, ^3J = 5.0 Hz), 8.90 (d, 2 H, H_o, ^3J = 4.9 Hz), 7.68 (td, 4 H, H_m, ^3J = 7.5 Hz, ^4J = 1.6 Hz), 7.30−7.18 (m, 8 H, H_m + H_p), 6.05−5.93 (m, 4 H, C=CH), 5.29−5.05 (m, 8 H, C=CH_2), 3.96−3.92 (m, 8 H, CH_2), 2.42−2.18 (m, 16 H, CH_2). − ^{13}C NMR ($CDCl_3$): δ = 164.0, 152.7, 152.2, 138.2, 138.0, 125.4, 124.5, 122.6 (aromatic carbon atoms and olefinic CH), 115.7 (olefinic CH_2), 39.5, 38.9, 33.8, 33.4, 28.2 (CH_2). − IR (polyethylene pellet): 347 (br, s, νPd−Cl *trans* to Cl). − $C_{20}H_{26}Cl_2N_2Pd$ (471.7): calcd. C 50.91, H 5.52, N 5.94; found C 51.62, H 5.52, N 5.63.

Synthesis of Indolizinium Derivatives **2e** *and* **2f**: The reaction of the allylpalladium complex **2d** (220 mg, 0.76 mmol) with 3.5 equivalents of triphenylphosphane (700 mg, 2.66 mmol) in methanol (20 ml), at room temperature and under nitrogen, gave an orange solu-

tion together with a yellow solid that precipitated after only a few minutes of reaction. The reaction mixture was allowed to stir for 1 h. Then after filtration of the fine yellow solid, the filtrate was concentrated to dryness to give an orange oily residue. Column chromatography on alumina using a mixture of ether and methanol (80:20) as eluant, enabled the migration of a yellow band corresponding to the cationic heterocycle **2e** (100 mg, crude yield 72%). Compound **2f** (PF_6^- as conter anion) was obtained pure as a beige solid by treating **2e** with KPF_6 in methanol (112 mg, yield 51%). The indices attributed to the different protons in compounds **2e** and **2f** are indicated in Figure 3.

Figure 3. Numbering scheme for the protons of ligand **2e**

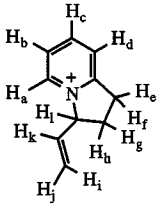

Compound **2e**: ^{1}H NMR ($CDCl_3$): δ = 8.97 (d, 1 H, H_a, ^3J = 5.9 Hz), 8.42 (t, 1 H, H_c, ^3J = 7.7 Hz), 8.09 (d, 1 H, H_d, ^3J = 7.9 Hz), 7.93 (t, 1 H, H_b, ^3J = 6.7 Hz), 6.13 (dd, 1 H, H_l, ^3J = 15.2, 7.6 Hz), 6.00−5.88 (m, 1 H, H_k), 5.68 (d, 1 H, H_i, $^3J_{trans}$ = 16.8 Hz), 5.54 (d, 1 H, H_j, $^3J_{cis}$ = 10.0 Hz), 3.70−3.59, 2.83−2.77, 2.31−2.24 (4 m, 4 H, H_e + H_f + H_g + H_h). − ^{13}C NMR ($CDCl_3$): δ = 158.1, 145.7, 140.7, 132.8, 126.3, 125.3 (aromatic and olefinic CH), 124.6 (olefinic CH_2), 73.4 (N−CH), 31.6, 28.6 (CH_2). − MS (without Cl^-); *m/z*: 146 (M^+), 117 [M^+ − (vinyl + 2H)].

Compound **2f**: ^{1}H NMR ([D_6]acetone): δ = 8.89 (d, 1 H, H_a, ^3J = 6.4 Hz), 8.64 (t, 1 H, H_c, ^3J = 8.6 Hz), 8.24 (d, 1 H, H_d, ^3J = 7.8 Hz), 8.11 (t, 1 H, H_b, ^3J = 6.8 Hz), 6.28−6.17 (m, 1 H, H_k), 5.81−5.68 (m, 1 H, H_l), 5.75 (d, 1 H, H_i, $^3J_{trans}$ = 17.0 Hz), 5.69 (d, 1 H, H_j, $^3J_{cis}$ = 10.2 Hz), 3.83−3.58, 3.05−2.85, 2.62−2.42 (3 m, 4 H, H_e + H_f + H_g + H_h). − $C_{10}H_{12}F_6NP$ (291.2): calcd. C 41.24, H 4.12, N 4.81; found C 40.76, H 4.01, N 4.58.

Synthesis of the (η^3-Allyl)palladium Complex **3d** *and of the Mixture* **3b** + **3c**: To a mixture containing ligand **3** (0.76 g, 4.7 mmol) and $PdCl_2(MeCN)_2$ (1.22 g, 4.7 mmol) in acetonitrile (50 ml) were added 2 equiv. of NaOAc (0.77 g, 9.4 mmol). The reaction mixture was stirred overnight at room temperature. A red solution along with a deposit of black metallic palladium was obtained. After filtration through Celite and concentration of the filtrate to dryness, the brown oily residue was extracted with a minimum amount of CH_2Cl_2. Column chromatography on silica gel using a mixture of ether and acetone (85:15) as eluant, allowed the migration of a first yellow band containing a mixture of isomers **3b** + **3c** (0.473 g, yield 34%), followed by the migration of a second yellow fraction corresponding to the allylpalladium complex **3d** (0.142 g, yield 10%).

Compound **3d**: ^{1}H NMR ($CDCl_3$): δ = 9.41 (d, 1 H, Ar, H_o, ^3J = 5.3 Hz), 7.73 (td, 1 H, Ar, ^3J = 7.7 Hz, ^4J = 1.8 Hz), 7.34−7.27 (m, 2 H, Ar), 5.30 (t, 1 H, $H_{central\ allylic}$, ^3J = 10.8 Hz), 3.83−3.65 (m, 1 H, $H_{allylic}$), 3.53−3.43 (m, 1 H, $H_{allylic}$), 3.19−3.01 (m, 2 H, CH_2), 2.13−1.98 (m, 1 H, CH_2), 1.91−1.71 (m, 1 H, CH_2), 1,55 (d, 3 H, CH_3, ^3J = 6.3 Hz). − ^{13}C NMR ($CDCl_3$): δ = 158.4, 152.7, 138.5, 124.9, 122.8 (aromatic), 112.6, 76.9, 73.7 (allylic), 41.3, 26.4 (CH_2), 17.9 (CH_3).

Compounds **3b** + **3c**: ^{1}H NMR ($CDCl_3$): δ = 9.13−8.80 (m, 4 H, Ar, H_o), 7.67 (t, 4 H, Ar, H_m, ^3J = 6.4 Hz), 7.40−7.08 (m, 8 H, Ar, H_p),, 5.75−5.40 (m, 8 H, C=CH), 3.90 (br s, 8 H, H_2C−C=), 2.60−2.03 (m, 16 H, CH_2), 1.85−1.58 (m, 12 H, CH_3). − ^{13}C NMR ($CDCl_3$): δ = 164.3, 160.6, 152.5, 152.1, 138.2, 130.4, 126.3, 126.1, 125.3, 122.4, 121.4 (aromatic and olefinic), 39.6, 39.1, 32.6, 28.9, 26.6, 23.0, 22.5 (CH_2), 18.1,14.1 (CH_3). − $C_{22.6}H_{31.2}Cl_{3.2}N_2Pd$ (**3b**, **3c** + 0.6 CH_2Cl_2) (the solvent was detected in the ^{1}H-NMR spectrum) (550.8): calcd. C 49.27, H 5.67, N 5.09; found C 49.18, H 5.35, N 5.28.

Synthesis of the Indolizinium Derivatives **3e** *and* **3f** : Compound **3e** was prepared by a similar procedure to that described for **2e**, starting from **3d** (70 mg; 0.23 mmol) and yielding **3e** (36 mg). Compound **3f**, with PF_6^- as counterion instead of Cl^-, was obtained pure as a pale yellow solid (38 mg; yield 54%), by treating a methanol solution of **3e** with KPF_6, followed by a column chromatography on alumina using the same system of eluant as for **2e**.

Compound **3e**: ^{1}H NMR ($CDCl_3$): δ = 8.95 (d, 1 H, H_o, ^3J = 6.1 Hz), 8.37 (td, 1 H, H_m, ^3J = 6.5 Hz, ^4J = 2.0 Hz), 7.99 (d, 1 H, H_m, ^3J = 7.9 Hz), 7.93 (t, 1 H, H_p, ^3J = 6.8 Hz), 6.49−6.37 (m, 1 H, C=C*H*Me, ^3J = 6.5 Hz), 6.23 (dd, 1 H, N−C*H*, ^3J = 8.4, 16.6 Hz), 5.59−5.50 (m, 1 H, *H*C=C), 3.87−3.73, 3.61−3.51, 2.92−2.82, 2.33−2.20 (4 m, 4 H, CH_2), 1.85 (dd, 3 H, CH_3, ^3J = 6.6 Hz, ^4J = 1.6 Hz). − MS (without Cl^-); *m/z*: 160 (M^+), 132 (M^+ − C_2H_4), 106 (M^+ − C_4H_6), 95 (M^+ − C_5H_7).

Compound **3f**: ^{1}H NMR ([D_6]acetone): δ = 8.86 (d, 1 H, H_o, ^3J = 6.2 Hz), 8.60 (t, 1 H, H_m, ^3J = 7.7 Hz), 8.19 (d, 1 H, H_m, ^3J = 7.7 Hz), 8.06 (t, 1 H, H_p, ^3J = 6.6 Hz), 6.37−6.26 (m, 1 H, C=C*H*Me), 5.86−5.77 (m, 1 H, *H*C=C), 5.69 (dd, 1 H, N−C*H*, ^3J = 8.1, 16.3 Hz), 3.78−3.61, 2.95−2.70, 2.51−2.38 (3 m, 4 H, CH_2),1.87 (dd, 3 H, CH_3, ^3J = 6.6 Hz, ^4J = 1.6 Hz). − ^{13}C NMR (CD_3OD): δ = 160.5, 146.5, 141.0, 138.9, 127.4, 127.0 (aromatic and olefinic CH), 126.0 (CH_2 olefinic), 75.2 (N−CH), 32.1, 30.0 (CH_2), 18.1 (CH_3). − $C_{11}H_{14}F_6NP$ (305.2): calcd. C 43.28, H 4.59, N 4.59; found: C 43.02, H 4.41, N 4.37.

Synthesis of the Mixture of Isomers **4b** *and* **4c**: To a solution containing $PdCl_2(MeCN)_2$ (0.78 g, 3.0 mmol) and ligand **4** (0.528 g, 3.0 mmol) in acetonitrile (40 ml) were added 1.5 equiv. of NaOAC (0.37 g, 4.5 mmol). The reaction mixture was heated at 65°C overnight. The black deposit of palladium(0) thereby formed was filtered off using a Celite pad. Then, after evaporation of the solvent, the brown oily residue obtained was extracted using a minimum of CH_2Cl_2. Column chromatography on silica gel with ethyl acetate as eluant allowed the migration of a yellow band containing the mixture **4b** + **4c** (0.335 g, yield 42%). − ^{1}H NMR ($CDCl_3$): δ = 9.00 (d, 2 H, H_o, ^3J = 4.5 Hz), 8.89 (d, 2 H, H_o, ^3J = 5.0 Hz), 7.67 (t, 4 H, Ar, ^3J = 3.7 Hz), 7.26 (br t, 4 H, Ar), 7.19 (t, 4 H, Ar, ^3J = 6.5 Hz), 5.40−5.60 (m, 8 H, HC=CH), 3.92 (t, 8 H, H_2C−C=, ^3J = 7.6 Hz), 2.43−1.95 (m, 24 H, CH_2), 1.80−1.55 (m, 12 H, CH_3). − ^{13}C NMR ($CDCl_3$): δ = 159.5, 147.7, 147.3, 133.2, 126.2, 126.1, 120.5, 120.1, 117.6 (aromatic and olefinic), 35.2, 34.6, 27.6, 24.9,24.7, 24.0, 23.4 (CH_2), 13.1 (CH_3). − $C_{24}H_{34}Cl_2N_2Pd$ (527.9): calcd. C 54.61, H 6.45, N 5.31; found C 53.58, H 5.97, N 4.76.

Synthesis of Compound **5c**: A mixture containing ligand **5** (0.72 g, 4.5 mmol), $PdCl_2(MeCN)_2$ (1.17 g, 4.5 mmol) and 1.5 equiv. of NaOAc (0.55 g, 6.8 mmol) in 50 ml of acetonitrile was heated at 65°C for 3 h. An orange solution containing some black palladium was observed. After filtration through a Celite pad, the solvent was evaporated and the brown oily residue formed was extracted using a minimum of CH_2Cl_2. Column chromatography on silica gel with a mixture of CH_2Cl_2 and hexane (90:10) as eluant allowed the migration of a yellow band. After evaporation of the solvents, compound **5c** was obtained as a beige solid (0.93 g, yield 41%). − ^{1}H

NMR ($CDCl_3$): δ = 7.56 (td, 2 H, Ar, ^3J = 7.7 Hz, ^4J = 3.4 Hz), 7.10 (d, 4 H, Ar, ^3J = 7.6 Hz), 6.03−5.90 (m, 2 H, HC=C), 5.21−5.06 (m, 4 H, C=CH_2), 4.30−4.23 (m, 4 H, CH_2), 3.63 (s, 6 H, CH_3), 2.37−2.44, 2.21−2.11 (2 m, 8 H, CH_2). − ^{13}C NMR ([D_6]acetone): δ = 165.0, 161.2, 139.8, 139.1, 124.3, 123.1, 115.7 (aromatic and olefinic), 40.1, 34.3, 29.1 (CH_2), 27.9 (CH_3). − $C_{25}H_{37}Cl_2N_2Pd$ (**5c** + 0.5 C_6H_{14}) (the solvent was detected in the ^{1}H-NMR spectrum) (542.9): calcd. C 55.31, H 6.82, N 5.16; found C 55.32, H 6.39, N 5.22.

[1] [1a] L. S. Hegedus, *Angew. Chem.* **1988**, *100*, 1147; *Angew. Chem. Int. Ed. Engl.* **1988**, *27*, 1113 and references cited.

[2] [2a] P. A. van der Schaaf, J. P. Sutter, M. Grellier, G. P. M. van Mier, A. L. Spek, G. van Koten, M. Pfeffer, *J. Am. Chem. Soc.* **1994**, *116*, 5134. − [2b] M. Grellier, PhD thesis, Louis Pasteur University, Strasbourg, France, **1996**. − [2c] M. Grellier, M. Pfeffer, G. van Koten, *Tetrahedron Lett.* **1994**, *35*, 2877. − [2d] M. Pfeffer. J. P Sutter, A. DeCian, J. Fischer, *Inorg. Chim. Acta* **1994**, *220*, 115.

[3] See for example: P. J. Harrington "Transition Metal Allyl Complexes: Pd, W, Mo-assisted Nucleophilic Attack" in *Comprehensive Organometallic Chemistry II* (Eds.: E. W. Abel, F. G. A. Stone, G. Wilkinson), Pergamon Press, Oxford, **1995**, vol. 12, p. 803−807 and references cited therein.

[4] H. Fukuda, K. Watanabe, Y. Kudo, *Chem. Pharm. Bull.* **1970**, *18*, 1299−1304. − S. M. Shanbhag, H. J. Fulkarni, B. B. Gaitonde, *Jpn. J. Pharmacol.* **1970**, *20*, 482−487. − R. J. Alaimo, *J. Med. Chem.* **1975**, *18*, 1145. − B. M. Trost, S. A. Godleski, J. P. Genêt, *J. Am. Chem. Soc.* **1978**, *100*, 3930. − P. Dätwyler, R. Ott-Longoni, E. Schöpp, M. Hesse, *Helv. Chim. Acta* **1981**, *64*, 1959−1963. − C. Subramanyam, J. P. Mallano, J. A. Dority, Jr., W. G. Earley, V. Kumar, L. D. Aimone, B. Ault, M. S. Miller, D. A Luttinger, D. L. DeHaven-Hudkins, *J. Med. Chem.* **1995**, *38*, 21−27. − R. Sutherland *"beta lactam antibiotic review"*, *Antibiot. Chemother.*, 7th ed. (engl.) (Eds.: O'Grady, Francis, Churchill, Livingstone), Edinburgh, UK, **1997**, p. 256−305. − E. R. de Oliveira, F. Dumas, J. d′Angelo, *Tetrahedron Lett.* **1997**, *38*, 3723.

[5] [5a] M. Israeli, D. K. Laing, L. D. Pettit *J. Chem. Soc., Dalton Trans.* **1974**, 2194−2197. − [5b] B. T. Heaton, D. J. A. Mc Caffrey *J. Chem. Soc., Dalton Trans.* **1979**, 1078.

[6] M. Pfeffer, P. Braunstein, J. Dehand, *Spectrochim. Acta* **1974**, *30A*, 341.

[7] [7a] D. M. Adams, *Metal-Ligand and Related Vibrations*, Arnold, London, **1967**, pp. 74−75. − [7b] P. L. Goggin *J. Chem. Soc., Dalton Trans.* **1974**, 1483 and references cited.

[8] A. Sen, T. W. Lai, *Inorg. Chem.* **1984**, *23*, 3257 and references cited.

[9] [9a] R. F. Heck *Organotransition Metal Chemistry: A mechanistic approach* (Eds.: P. M. Maitlis, F. G. A. Stone, R. West), Academic Press, New York and London, **1974**, p. 81. − [9b] M. Tsutsui, A. Courtney, *Adv. Organomet. Chem.* **1978**, *16*, 241.

[10] [10a] M. Pfeffer, J. P. Sutter, M. A. Rotteveel, A. De Cian, J. Fischer, *Tetrahedron* **1992**, *48*, 2427. − [10b] M. Pfeffer, J. P. Sutter, A. De Cian, J. Fischer, *Organometallics* **1993**, *12*, 1167.

[11] See for example: C. F. J. Barnard, M. J. H. Russel, "Palladium" in *Comprehensive Coordination Chemistry: The Synthesis, Reactions, Properties of Coordination compounds* (Eds.: G. Wilkinson, R. D. Gillard, J. A. McCleverty), Pergamon Press, Oxford, **1987**, vol. 5, p. 1115−1117 and references cited therein.

[12] R. Hüttel, B. Rau, *J. Organomet. Chem.* **1977**, *139*, 103−105.

[13] R. Malet, M. Morena-Mañas, R. Pleixats, *Organometallics* **1994**, *13*, 397.

[14] L. Canovese, F. Visentin, P. Uguagliati, F. Di Bianca, S. Antonaroli, B. Crociani, *J. Chem. Soc., Dalton Trans.* **1994**, 3113.

[15] Baldwin rules: J. E. Baldwin *J. Chem. Soc., Chem. Commun.* **1976**, 734.

[16] A. Heuman, M. Réglier, *Tetrahedron* **1995**, *51*, 975 and references cited.

[17] H. W. Bersch, R. Ribman, D. Schon, *Arch. Pharm.* **1982**, *315*, 749.

[98124]

Synthesis of the First Neutral Spiro Selenium(II) Complex Containing a True Square Planar Se(Se_4) Core – Preparation and Crystal Structure of Bis[*N*-(diphenylphosphanylselenoyl)-*P*,*P*-diphenylphosphanylselenoic amidato-*Se*, *Se'*]selenium(II)☆

Raymundo Cea-Olivares*[a], Graciela Canseco-Melchor[a], Verónica García-Montalvo[a], Simón Hernández-Ortega[a], and Josef Novosad[b]

Instituto de Química, Universidad Nacional Autónoma de México[a],
Circuito Exterior, Ciudad Universitaria, México 04510 D.F., México
Fax: (internat.) + 52-5/6162203
E-mail: cea@servidor.unam.mx

Inorganic Chemistry Department, Masaryk University[b],
61137 Brno, Czech Republik

Received March 23, 1998

Keywords: Selenium / Spiro compounds / Phosphazene heterocycles / Chelates

The Bis[*N*-(diphenylphosphanylselenoyl)-*P*,*P*-diphenylphosphanylselenoic amidato-*Se*,*Se'*]selenium(II) (**1**) was prepared by treating [K{N($SePPh_2$)$_2$}] with [Se{S_2P(O-*i*Pr)$_2$}$_2$] in THF. The title compound was characterized by means of IR and ^{31}P-NMR spectroscopy and positive-ion FAB mass spectrometry and elemental analysis. The molecular structure was determined using single-crystal X-ray diffraction. The Se(Se_4) core exhibited a quasi perfect square planar geometry. Two selenide ligands are coordinated symmetrically to the central atom forming a spiro complex.

Introduction

The extraordinary ability of the anions $[R_2P(X)NP(X)R_2]^-$ (R = Me, Ph; X = O, S, Se) to form very unusual carbon-free chelate complexes is well known. Some examples are the tetrahedral [M{N($SPMe_2$)$_2$-*S*,*S'*}$_2$] (M = Ni, Fe)[1], the six-coordinated lanthanide complexes [Ln{N($OPPh_2$)$_2$-*O*,*O'*}$_2$][2], the true square planar tellurium(II) complex [Te{N($SPPh_2$)$_2$-*S*,*S'*}$_2$][3] and recently the square planar tin(II) complex [Sn{N($SePPh_2$)$_2$-*Se*,*Se'*}$_2$][4] with the first example of such a geometry for Sn^{II}. The great flexibility of these chelate rings with wide variations in the ring angles (P−N−P, M−X−P, X−P−N) and large bites X···X enables the central atom to "reveal" its preference for a particular geometry, since there is no restrictions imposed by the presence of rigid organic rings, e. g. the β-diketonates, or small rings, with great stereochemical restrictions, like the dithiophosphates or dithiophosphinates.

Twenty years ago, Husebye et al. classified five types of geometries for divalent sulphur, selenium and tellurium complexes with bidentate dithio and related ligands[5]. Complexes of class I are trapezoid planar tetracoordinated with all intramolecular ligand bonds. Class-II compounds are also trapezoid planar, however two of the ligand bonds are intramolecular and the other two intermolecular. Class-III compounds are mainly represented by the bis(4-morpholinethiocarbonyl) trisulfide with a "zigzag" framework; *trans* square planar complexes with monodentate ligands correspond to class IV and bidentate square planar molecules to class V. In 1982, Husebye et al. used the imidotetraphenyldithiodiphosphinate anion as a chelating ligand with a very large bite, in order to synthesis true square planar complexes (class V) with Te^{II} and Se^{II}. They obtained [Te{N($SPPh_2$)$_2$-*S*,*S'*}$_2$][3] which was a true square planar Te^{II} compound (a class-V complex), while the structure of the selenium analogous compound, [Se{N($SPPh_2$)$_2$-*S*,*S'*}$_2$], was intermediate between class I and class II, yet much closer to a class-II complex[6].

The number of compounds where the selenium atom is surrounded by four selenium atoms [Se(Se_4) core] are quite scarce. The bis(*N*,*N*-diethyldiselenocarbamate)Se^{II} is a class-I trapezoid planar complex[7]. The bis(diethyldiselenophosphinate)Se^{II} is a class-II complex[8]. The low-temperature ^{77}Se-NMR solution data of the analogous bis(diisobutildiselenocarbamate) of Se^{II} suggests a four-coordinated structure[9]. Another example with bidentate ligands corresponds to the dianionic complex [(Bu_4N)$_2${Se[Se_2C=$C(CN)_2$]$_2$}], with intrachelating Se−Se−Se angles of 75° and an $SeSe_4E_2$ (E = lone pair) distorted octahedral geometry[10]. Several examples of polyselenide derivatives containing the anion $[Se\{Se_5\}_2]^{-2}$ are known. This anion exhibits a geometry close to the square planar one[11]. The square planar Se_5 moiety with monodentate ligands was observed in tetrakis[*N*-methylbenzothiazole)-3*H*-selenone]selenium(II) tetrafluoroborate (class-IV complex)[12]. However, there are no examples of neutral true square planar neutral complexes containing the Se(Se_4) core and bidentate ligands (a class-V complexes) in the literature.

We decided to synthesise the compound [Se{N($SePPh_2$)$_2$-*Se*,*Se'*}$_2$] to determine whether it is a class-V complex, or

 © WILEY-VCH Verlag GmbH, D-69451 Weinheim, 1998 1434−1948/98/1010−1573 $ 17.50+.50/0

isotructural with [Se{N(SPPh$_2$)$_2$-*S,S′*}$_2$] (a class-II compound).

Results and Discussion

Treatment of [K{N(SePPh$_2$)$_2$}] with [Se{S$_2$P(O-*i*Pr)$_2$}$_2$] in THF at room temperature, yielded [Se{N(SePPh$_2$)$_2$-*Se,Se′*}$_2$] (**1**). The compound was purified by thin layer chromatography. Attempts of purification by normal recrystallization methods were unsuccessful because the compound tends to decompose giving red selenium, free ligand, and other compounds. Derivative **1** was characterized on the basis of its elemental analysis and its ^{31}P-NMR, IR and positive-ion FAB MS data and by X-ray crystallography. It is a yellow-orange, air-stable solid, that tends to decompose in solution, soluble in polar organic solvents such as $CHCl_3$, yet insoluble in ethanol or hexane.

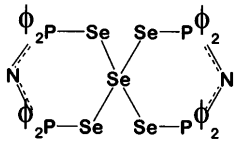

1

^{31}P-NMR spectra show that all phosphorus atoms are equivalent. As with other main-group complexes with this ligand, in the IR spectrum the assignments of the phosphazene bands were relatively easy, after identification of the usual phenyl group bands common to the [(PPh$_2$X)$_2$N]$^-$ ligands[13] . Individual assignments of the ν(PSe) bands is not fully possible because of the overlap with the corresponding PNP vibrations.

To date, few P−Se vibrations have been clearly assigned[14]. The FAB mass spectrum of the compound exhibits a low-intensity signal for the corresponding molecular ion, but rather intense peaks resulting from the expected first fragmentations. The most intense peak containing selenium corresponds to [Se(PPh$_2$)$_2$N$^+$]. Since the FAB mass spectrum was obtained in solution, it also shows some fragments due to a decomposition product, e.g. [{Ph$_2$P(Se)NP(Ph$_2$)}$_2$O; *m/z*: 944 and 864]. All the observed signals exhibit the expected isotopic pattern.

Description of the Structure

The structure is built of discrete neutral [Se{N(SePPh$_2$)$_2$-*Se,Se′*}$_2$] molecules, the central selenium atom is coordinated to four other selenium atoms, forming two six-membered carbon-free chelate rings, in a typical spiro arrangement. There are two crystallographically independent molecules in the cell (**1a** and **1b**). According to the cell parameters, **1** is isomorphic with the yellow [Sn{N(SePPh$_2$)$_2$-*Se,Se′*}$_2$] [*a* = 10.124(5), *b* = 13.085(4), *c* = 18.260 Å, α = 89.42(2), β = 82.75(2) , γ = 77.62(2)°] [4] and [Te{N(SPPh$_2$)$_2$-*S,S′*}$_2$] [*a* = 10.187(1), *b* = 12.929(5), *c* = 18.282(3) Å, α = 89.04(2) , β = 82.98(1) , γ = 77.40(2)°][3]. Figure 1 presents the inner coordination sphere, with angles and distances for molecules **1a** and **1b**, whereas Figure 2

Figure 1. The inner coordination sphere in **1a** and **1b**

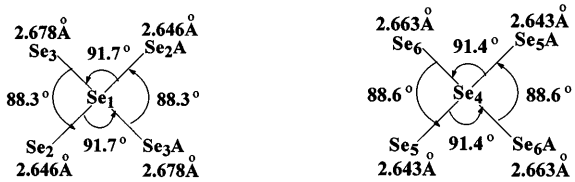

1a **1b**

Figure 2. ORTEP plot of **1a** and **1b**, independent molecules of [Se{N(SePPh$_2$)$_2$-*Se,Se′*}$_2$]

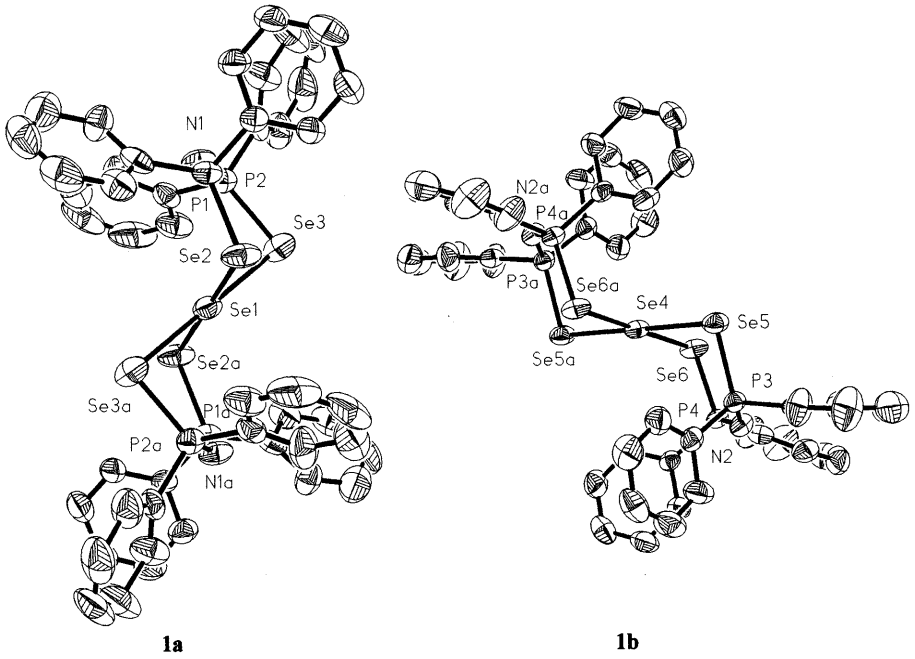

1a **1b**

shows the molecular structures and atomic labelling scheme of compound **1**.

The most remarkable feature of the structure is the square planar character of the selenium coordination sphere. The $SeSe_4$ core is coplanar [$\Sigma\{Se-Se-Se\} = 360°$] with *trans*-Se−Se−Se angles of 180.0(1)°. There is a slight asymmetry in the Se−Se bond lengths in both molecules [long ones of 2.678(1) and 2.663(1) Å and short ones of 2.646(1) and 2.643(1) for **1a** and **1b**, respectively]. These values are similar with those found in polyselenide anions[14]. The Se···Se bite of 3.708(2) Å is intermediate between the values of 3.667(4) and 3.771(3) Å found in [Te{N(SPPh$_2$)$_2$-*S,S′*}$_2$]. As in [Sn{N(SePPh$_2$)$_2$-*Se,Se′*}$_2$], the main difference between molecules **1a** and **1b** lies in the Se−Se−P angle [96.3(1) and 88.7(1)° for **1a**, and 97.1(1) and 96.9(1)° for **1b**]. The values of the P−N−P angles for **1a** and **1b**, [139.5(5) and 136.4(5)°] are also extraordinary large − larger than that found in the free ligand [132.3(2)°][14]. Since it is expected that the coordination of the donor atoms should contract the angle, the opening is indicative of the high flexibility of the P−N−P system and explains the ability of this ligand to form unusual structures. The endocyclic Se−Se−Se angles [88.31(4) and 88.67(3)°] are smaller than the corresponding exocyciclic ones [91.69(4) and 90.46(3)°].

The existence of this new neutral square planar structure for a Se^{II} compounds, demonstrates the ability of the $[Ph_2P(Se)NP(Se)Ph_2]^-$ anion to fulfill the preferences imposed by the central atom, in function of the great flexibility of the phosphazenic system and the soft character of the donor atoms.

We thank the *Mexican National Council of Science and Technology*, CONACYT (Grant 109P-E) for financial support and Prof. Dr. *Husebye* for his comments and suggestions.

Experimental Section

The experiments were carried out with the exclusion of air and moisture, under argon.The solvents were purified and dried by the usual methods. Se{S$_2$P(O*i*Pr)$_2$}$_2$][17] and bis[*N*-diphenylphosphanylselenoyl)-*P,P*-diphenylphosphanylselenoyl)amide[15] were prepared by literature methods. The latter was converted to its potassium salt by the reaction with KO*t*Bu according to a previously described procedure[16]. − ^{31}P NMR: Varian VXS 300S (121 MHz, external standard 85% H_3PO_4). − FAB MS (3-nitrobenzyl alcohol support): Jeol JMS-SX102A, positive-ion mode. − IR (KBr): Perkin-Elmer 283B. − Elemental analysis : Galbraith Laboratories.

Bis(imidotetraphenyldiselenodiphosphanyl-Se,Se′)selenium(II) (**1**): A solution of 3.0 g (5.1 mmol) of [K{N(SePPh$_2$)$_2$}], in 50 ml of THF was added to a stirred solution of bis(diisopropyldithiophosphato)selenium(II) (1.30 g, 2.5 mmol) in 50 ml of THF. An orange solution was formed, the solvent was evaporated at low pressure and the obtained solid was washed with ethanol and filtered. 10% of the solid was subjected to a thin layer chromatographic separation using hexane/ethyl acetate as eluent (90:10). The less polar layer was separated and extracted with CH_2Cl_2 to obtain the desired compound (m. p. 210°C). Yield 62% (based on of the chromatographic separated portion). Crystals suitable for X-ray crystallography were obtained by solvent diffusion in a chloroform/*n*-hexane mixture at room temperature. − ^{31}P NMR ($CDCl_3$): δ = 34.35 (s). − IR (KBr): $\tilde{\nu}$ = 3053 cm^{-1} w [νCH)], 1211 s [νP−N)], 1177 s [ν(P−N)/δ(CH)], 744 m [ν(P−N)], 689 vs [ϕ(CC), Ph], 532 vs [γ(PNP)/ν(P−Se)]. − MS (FAB$^+$, $CHCl_3$, for ^{80}Se); *m/z*: 1164 [M$^+$], 1087 [M − Ph$^+$], 622 [Se{N(SePPh$_2$)$_2$}$^+$], 544 [(SePPh$_2$)$_2$-N$^+$], 464 [Se(PPh$_2$)$_2$N$^+$], 384 [(PPh$_2$)$_2$N$^+$], 307 [(Ph$_2$PNPPh$^+$]. − $C_{48}H_{40}N_2P_4Se_5$ (1163.5): calcd. C 49.55, H 3.46; found C 49.11, H 3.36. − Mol. mass 1164 (FAB MS; CH_3Cl for ^{80}Se).

Crystal-Structure Analysis: Data collection was performed at room temperature with a Siemens P4 four-circle diffractometer by using graphite-monochromated Mo-K_α radiation ((= 0.71073 Å). Crystal Data: $C_{48}H_{40}N_2P_4Se_5$, M = 1163.5, orange prisms, 0.24 × 0.20 × 0.12 mm; triclinic, space group $P\bar{1}$ (No. 2), a = 10.158(2), b = 13.090(2), c = 18.239(5) Å, α = 89.42(2), β = 82.56(2), γ = 77.72(2)°, V = 2349.4(1) Å^3, Z = 2, D_x = 1.645 Mg m^{-3}, μ(Mo-K_α) = 4.070 mm^{-1}, T = 293 K, F(000) = 1144, number of reflections: 8742 (8231 independent, R_{int} = 0.048), $R(F)$ = 0.041, $wR(F)$ = 0.034 (536 parameters). Structure Solution and Refinement: The structure was solved by direct methods and refined by full-matrix least-squares calculations using the program system SHELXTL-Plus (PC-version)[18]. Absorption effects were corrected by face-index numerical methods. H atoms were refined using a riding model (U = 0.06), while non-hydrogen atoms were refined anisotropically. The crystal structure data (excluding structure factors) have been deposited with the Cambridge Crystallographic Data Centre as supplementary publication no. CCDC-101279. Copies of the data can be obtained free of charge on application to CCDC, 12 Union Road, Cambridge CB2 1EZ, UK [Fax: int code + 44(1223)336-033; E-mail: deposit@ccdc.cam.ac.uk].

☆ Dedicated to Professor *Heinrich Nöth* on the ocassion of his 70th birthday.

[1] M. R. Churchill, J. Wormald, *Inorg. Chem.* **1971**, *10*, 1778. − M.R. Churchill, J. Cooke, J.P. Fennessey, J. Wormald, *Inorg. Chem.* **1971**, *10*, 1031.
[2] I. Rodríguez, C. Alvarez, J. Gómez-Lara, R. Cea-Olivares, *Lanthanide Actinide Res.* **1985-6**, *1*, 253. − N. Platzer, H. Rudler, C. Alvarez, L. Barkaoui, B. Denise, N. Goasdoué, M. N. Rager, J. Vaissermann, J. C. Daran, *Bull. Soc. Chim. Fr.* **1995**, *132*, 95.
[3] S. Bjørnevåg, S. Husebye, K. Maartmann-Moe, *Acta Chem. Scand. A* **1982**, *36*, 195.
[4] R. Cea-Olivares, J. Novosad, J. D Woollins, A. M. Z. Slawin, V. García-Montalvo, G. Espinosa Pérez , P. García y García. *J. Chem. Soc., Chem. Comm.* **1996**, 519. − V. García-Montalvo, J. Novosad, P. Kilian, J. D. Woollins, A. M. Z. Slawin, P. García y García, M. López-Cardoso, G. Espinosa-Pérez, R. Cea-Olivares, *J. Chem. Soc., Dalton Trans.* **1997**, 1025.
[5] N. J. Brøndmo, J. Esperås, S. Husebye, *Acta Chem. Scand. A* **1975**, *29*, 93. − H. Graver, S. Husebye, *Acta Chem. Scand. A* **1975**, *29*, 14.
[6] S. Husebye, K. Maartmann-Moe, *Acta Chem. Scand. A* **1983**, *37*, 219.
[7] R. O. Gould, C. L. Jones, E. J. Savage, T. A. Stephenson, *J. Chem. Soc., Dalton Trans.* **1976**, 908.
[8] S. Husebye, G. Helland-Madsen, *Acta Chem. Scand. A* **1969**, *23*, 1398.
[9] Y. Masaki, K. Kobayashi, *Tetrahedron Lett.* **1989**, *30*, 2813.
[10] H. U. Hummel, E. Fischer, T. Fischer, D. Gruss, A. Franke, W. Dietzsch, *Chem. Ber.* **1992**, *125*, 1565.
[11] M. G. Kanatzidis, S. P. Huang, *Coord. Chem. Rev.* **1994**, *130*, 509.
[12] C. Adamo, F. Demartin, P. Deplano, F. A. Devillanova, F. Isaia, F. Lelj, V. Lippolis, P. Lukes, M. L. Mercuri, *J. Chem. Soc., Chem. Comm.* **1996**, 873.
[13] R. Cea-Olivares, V. García-Montyalvo, J. Novosad, J. D. Woolllins, R. A. Toscano, G. Espinosa-Pérez,. *Chem. Ber.* **1996**, *129*, 919, and references cited therein.

[14] V. Krishnan, R. A. Zingaro, *Inorg. Chem.* **1969**, *8*, 2337. − J. Ellermann, A. A. M. Demuth, W. Bauer, *Z. Naturforsch., B* **1986**, *41*, 863. − J. Ellermann, J. Sutler, F. A. Knoch, M. Moll, *Chem. Ber*. **1994**, *127*, 1015.
[15] P. Bhattacharyya, J. Novosad, J. Phillip, A. M. Z. Slawin, D. J. Williams, J. D. Woollins, *J. Chem. Soc., Dalton Trans.* **1995**, 1607.
[16] A. Schmidpeter, H. Groeger, *Z. Anorg. Allg. Chem*. **1966**, *345*, 106.
[17] S. Husebye, *Acta Chem. Scand. A* **1965**, *19*, 1045.
[18] Siemens, *SHELXTL PLUS, Release 4.0*, for Siemens R3 Crystallographic, Madiso, WI, **1998**.

[98074]

An Unprecedented, Copper-Mediated, In-Situ Multi-Step Ligand Formation – Synthesis, Structure, and Magnetism of Bis(μ-methoxo)bis[nitrato(2-methoxymethylamino-3-methylpyridine)copper(II)]☆

Saeid Amani Komaei[a][+], Gerard A. van Albada[a], Ilpo Mutikainen[b], Urho Turpeinen[b], and Jan Reedijk*[a]

Leiden Institute of Chemistry, Gorlaeus Laboratories, Leiden University[a],
P. O. Box 9502, NL-2300 RA Leiden, Netherlands
E-mail: reedijk@chem.leidenuniv.nl

Laboratory of Inorganic Chemistry, Department of Chemistry, University of Helsinki[b],
P. O. Box 55 (A. I.Virtasen aukio 1), SF-00014 Helsinki, Finland

Received August 13, 1998

Keywords: Copper / Methoxo-bridged complexes / Crystal structure

A novel chelating ligand, synthesized in situ within the coordination sphere of Cu^{II} from 2-amino-3-methylpyridine, MeOH, and dioxygen from the air, is found to form a strongly coupled, dinuclear methoxo-bridged Cu^{II} compound with the formula $[Cu(L)(CH_3O)(NO_3)]_2$ (L = 2-methoxymethylamino-3-methylpyridine). The geometry around the copper atom is square pyramidal and the Cu–Cu distance within the dinuclear unit is 3.011(2) Å with an Cu–O–Cu angle of 103.13(8)°. Synthesis, X-ray crystal structure, and magnetism are reported.

In situ ligand formations in the presence of metal ions are not uncommon[1][2][3], and several cases are known of such reactions, like Schiff-base couplings and the formation of phthalocyanins[1][2][3]. The metal ion in these cases acts as a template, to facilitate the ring closure or the addition. Cases where a multi-step ligand reaction occurs are relatively rare. Our recent studies towards the formation of formamidines[4] have prompted us to further investigations of such reactions with aminopyridine ligands. We now wish to report a most unusual case of a three-step reaction (see Scheme 1) in which 2-amino-3-methylpyridine first forms a Schiff base with formaldehyde − in situ formed gradually by MeOH oxidation − which subsequently reacts with Cu-coordinated methanol to a 2-methoxymethylamino-3-methylpyridine chelating ligand. Copper(II) is known to be a catalyst for the air oxidation of methanol to formaldehyde[5]. The Schiff-base reaction is followed by the third step in which a methanol molecule inserts into the imine double bond[6a], resulting in the dinuclear compound: $[Cu(L)(CH_3O)(NO_3)]_2$ (in which L = 2-methoxymethylamino-3-methylpyridine). The first oxidation must originate from dioxygen from the air, as the reaction does not occur under argon. In fact deliberate addition of CH_2O accelerates the reaction. Under argon only a methoxo-bridged dinuclear Cu^{II} compound with the starting ligand, 2-amino-3-methyl-pyridine, is formed (see Experimental Section).

Scheme 1. Proposed reaction scheme (R = 3-methylpyridin-2-yl)

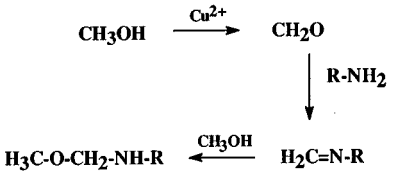

Structural analysis of the title compound reveals a dinuclear methoxo-bridged dinuclear unit with a centre of symmetry located between two copper ions (see Figure 1). The Cu atom has a square-pyramidal geometry with a basal plane formed by a nitrogen atom of the ligand, two oxygen atoms of the bridging methoxo molecules and an oxygen atom of the coordinating nitrate anion. The Cu−N distance and the Cu−O distances are in the normal range of ca. 2.00 Å[7]. The angles of the basal plane are almost linear [O1a−Cu1−O11 168.71(6), O1−Cu1−N11 170.61(7)°]. The apical site is occupied by the ether oxygen atom (O20) of the ligand with a distance of 2.318(2) Å and with the angle O20−Cu1−N11 of 93.09(9)°. The most striking feature of the structure is the presence of the newly synthesized ligand 2-methoxymethylamino-3-methylpyridine. Synthesis of methoxomethylamino compounds is known[6], however, in some cases they are unstable[6c]. In fact the present ligand might quite well be stabilized by the Cu chelation.

The Cu−Cu distance within the dinuclear unit is 3.011(2) Å with an Cu−O−Cu angle of 103.13(8)°. These distances and angles can be compared with some methoxo-bridged Cu^{II} dinuclear compounds which have also distances of ca. 3.0 Å and an angle of about 103°[8]. The lattice structure is stabilized by stacking between the pyridine rings of different units (ring−ring distance of 3.613 Å) and by a relatively strong hydrogen-bonding of an amino-nitrogen atom and an oxygen atom of the nitrate anion [N17···O13 = 2.939(9) Å].

[+] On leave from Chemistry Department, Arak University, Arak, Iran.

 © WILEY-VCH Verlag GmbH, D-69451 Weinheim, 1998 1434−1948/98/1111−1577 $ 17.50+.50/0

Figure 1. Plot of the structure with atom-labelling scheme; H atoms are omitted for clarity[a]

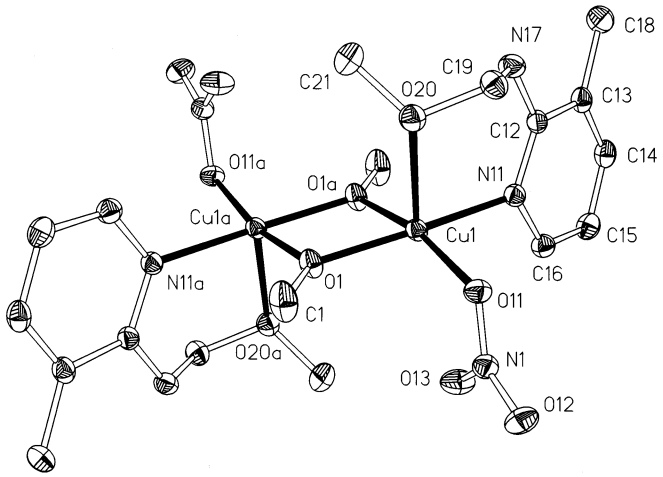

[a] Selected bond lengths [Å] and angles [°]: Cu1−O1 1.917(2), Cu1−O1a 1.9270(17), Cu1−N11 1.998(2), Cu1−O11 2.0267(18), Cu1−O20 2.318(2), Cu1−Cu1a 3.011(2); O1−Cu1−O1a 76.87(8), O1−Cu1−N11 170.61(7), O1a−Cu1−N11 94.22(8), O1−Cu1−O11 96.50(8), O1a−Cu1−O11 168.71(6), N11−Cu1−O11 91.81(8), O1−Cu1−O20 91.85(9), O1a−Cu1−O20 103.27(9), N11−Cu1−O20 93.09(9), O11−Cu1−O20 85.91(8), Cu1−O1−Cu1a 103.13(8) ($a = -x, -y, -z$).

The ligand-field spectrum reveals a broad band with a centre around $14.6 \cdot 10^3$ cm^{-1}, which is common for a square pyramidal geometry[9]. A typical infrared vibration is found at 3349 cm^{-1} as a strong sharp peak, attributed to the N−H vibration. The anion vibrations of the nitrate are found at 1453 and 1299 cm^{-1} (a splitting of 154 cm^{-1}) which is in the range for didentate coordinating nitrate[10]. In the present case one of the oxygen atoms of the nitrate anion has a strong bonding to the Cu^{II} ion and the second oxygen atom (O13) is involved in a strong intermolecular hydrogen bonding (see above).

The powder EPR spectrum at 77 K only shows a very weak signal with a $g_{\perp}$ of 2.06, a resolved $g_{||}$ of 2.32, with $A_{||}$ of 14.2 mT, typical for a $CuNO_3(O)$ chromophore[9]. Given the dinuclear nature, this weak signal must originate from a mononuclear impurity. Even a nitrogen superhyperfine structure is observed with 3 lines, which also agrees with one nitrogen donor atom per Cu. In frozen solution (DMF) at 77 K a similar spectrum is obtained, indicative of monomerisation in solution. Low-temperature solid-state powder magnetic susceptibility recorded in the region 250−5 K, shows an almost diamagnetic species below 200 K. A preliminary fit with $g = 2.10$ results in a $-2J$ value over 500 cm^{-1}.

Summarizing, it is concluded that an MeOH oxidation reaction occurs initiated by the Cu^{II} ion. However, other factors, like the strength of the anion, must contribute as well, since weaker coordinating anions like perchlorate and triflate under identical conditions, do not yield such a reaction product.

Further work will deal with related ligands yielding this structure and with oxidation reaction studies to obtain more information about the reaction process.

The work described in the present paper has been supported by the *Leiden University Study group WFMO* (Werkgroep Fundamenteel Materialen Onderzoek). Use of the services and facilities of the *Dutch National NWO/SURF Expertise Center CAOS/CAMM,* under grant numbers SON 326-052 and STW NCH99.1751, is gratefully acknowledged. Dr. *J. G. Haasnoot* and Dr. *W. L. Driessen* are thanked for their helpful suggestions.

Experimental Section

General: Ligand-field spectra were recorded with a Perkin-Elmer Lambda 900 spectrophotometer using the diffuse-reflectance technique, with MgO as a reference. X-band powder EPR spectra were obtained with a Jeol RE2x electron spin resonance spectrometer using DPPH ($g = 2.0036$) as a standard. Magnetic susceptibilities were measured in the temperature range 5−300 K with a Manics DSM-8 susceptometer. Data were corrected for magnetization of the sample holder and for diamagnetic contributions, which were estimated from the Pascal constants[11].

Synthesis: 2-Amino-3-methylpyridine was obtained from Acros Organics; 0.6 mmol of $Cu(NO_3)_2 \cdot 3\,H_2O$ and 1.2 mmol of 2-amino-3-methylpyridine were each dissolved in ca. 10 ml of methanol. The copper solution was added carefully to the ligand solution and filtered to remove any undissolved material. The blue solution was kept at room temp., and after a few days blue crystalline material was obtained from the solution which turned green. The product was filtered and air-dried. Adding a little sodium hydroxide or heating the solution yields the same blue compound. Yield ca. 80%. − $C_{18}H_{30}Cu_2N_6O_{10}$ (617.56): calcd. C 35.01, H 4.90, Cu 20.50, N 13.61; found 35.07 C, 5.12 H, 20.12 Cu, 13.85 N.

Using a higher L/M ratio (L/M = 4:1 or 6:1) a violet methoxo-bridged dinuclear Cu^{II} compound with the formula $[Cu_2(2\text{-amino-3-methylpyridine})_4(CH_3O)_2](NO_3)_2$ was obtained. This structure is confirmed by elemental and X-ray crystal structure analysis[13]. The same compound is derived when the present reaction (L/M ratio 2:1) is carried out under argon.

X-ray Crystal Structure Analysis: Crystal data for $[Cu(C_8H_{12}N_2O)(CH_3O)(NO_3)]_2$: $C_{18}H_{30}Cu_2N_6O_{10}$, $M = 617.56$, triclinic, space group $P\bar{1}$ (no.2), $a = 8.336(5)$, $b = 8.734(5)$, $c = 10.357(5)$ Å, $\alpha = 109.24(5)$, $\beta = 91.99(5)$, $\gamma = 113.13(4)°$, $V = 642.9(6)$ $Å^3$, $Z = 1$, $D_c = 1.595$ g cm^{-3}, $T = 193$ K, $\mu(\text{Mo-}K_\alpha) = 1.715$ mm^{-1}, $F(000) = 318$, $R1 = 0.0299$, $wR2 = 0.0804$ with $I > 2\sigma(I)$, $S = 1.084$, 3982 data collected, 2627 data used, 163 parameters. A blue crystal with dimensions of $0.48 \times 0.45 \times 0.27$ mm was selected, mounted to the glass fiber using the oil-drop method[12a]. Rigaku AFC-7S diffractometer, graphite-monochromated Mo-K_α radiation ($\lambda = 0.71073$ Å), ω-2θ scans. Data reduction using the TEXSAN[12b] package. The intensity data were corrected for Lorentz and polarization effects and for absorption and extinction. All non-H atoms were refined anisotropically. H atoms were situated from difference Fourier map and refined isotropically. The structure was solved using direct methods (SHELXS-86)[12c]. The weighting scheme $w = 1/[\sigma^2(F_o^2) + (0.0457 \cdot P)^2 + 0.3867 \cdot P]$, where $P = (F_o^2 + 2 \cdot F_c^2)/3$ was adopted. Full-matrix least-squares refinement method on F^2 was applied, using the SHELXL-93[12d] package.

Crystallographic data (excluding structure factors) for the structure in this paper have been deposited with the Cambridge Crystallographic Data Centre as supplementary publication no. CCDC-102597. Copies of the data can be obtained free of charge on appli-

cation to CCDC, 12 Union Road, Cambridge CB2 1EZ, UK [Fax: (internat.) + 44(1223)336-033, E-mail: deposit@ccdc.cam.ac.uk].

☆ Dedicated to Professor *Bernt Krebs* on the occasion of his 60th birthday.

[1] See e.g: [1a] U. Casellato, P. A. Vigato, M. Vidali, *Coord. Chem. Rev.* **1977**, *23*, 31−117. − [1b] J. C. Brown, J. G. Wardeska, *Inorg. Chem.* **1982**, *21*, 1530−1534. − [1c] S. A. Warda, P. Dahlke, S. Wocadlo, W. Massa, C. Friebel, *Inorg. Chim. Acta* **1998**, *268*, 117−124.

[2] See e.g.: [2a] C. C. Leznoff, A. B. P. Lever (Eds.), *Phthalocyanines. Properties and Applications*, vol. I−III, VCH Publ., New York, **1989−1993**. − [2b] C. Wang, M. R. Bryce, A. S. Batsanov, J. A. K. Howard, *Chem. Eur. J.* **1997**, *3*, 1679−1690 (and references citied therein). − [2c] M. Hanack, M. Lang, *Adv. Mater.* **1994**, *6*, 819−833.

[3] A. M. García, J. Manzur, M. T. Garland, R. Baggio, O. González, O. Peña, E. Spodine, *Inorg. Chim. Acta* **1996**, *248*, 247−255.

[4] G. A. v. Albada, I. Mutikainen, U. Turpeinen, J. Reedijk, *Eur. J. Inorg. Chem.* **1998**, 547−549.

[5] [5a] H. Werner, D. Herein, G. Schulz, U. Wild, R. Schlögl, *Catal. Lett.* **1997**, *49*, 109−119. − [5b] P. R. Davies, G. G. Mariotti, *Catal. Lett.* **1997**, *43*, 261−266.

[6] [6a] J. Barluenga, A. M. Bayón, P. Campos, G. Asensio, E. Gonzalez-Nuñez, Y. Molina, *J. Chem. Soc., Perkin Trans. 1* **1988**, 1631−1636. − [6b] P. J. Campos, I. Lamaza, M. A. Rodríguez, *Tetrahedron Lett.* **1997**, *38*, 6741−6744. − [6c] H.-J. Ha, Y.-G. Ahn, *Synth. Commun.* **1995**, *25*, 969−975.

[7] [7a] G. A. v. Albada, M. T. Lakin, N. Veldman, A. L. Spek, J. Reedijk *Inorg. Chem*, **1995**, *34*, 4910−4917. − [7b] G. A. v. Albada, W. J. J. Smeets, A. L. Spek, J. Reedijk, *Inorg. Chim. Acta* **1997**, *260*, 151−161.

[8] [8a] R. D. Willett, G. L. Breneman, *Inorg. Chem.* **1983**, *22*, 326−329. − [8b] C. Fukuhara, K. Tsuneyoshi, K. Katsura, N. Matsumoto, S. Kida, M. Mori, *Bull. Chem. Soc. Jpn.* **1989**, *62*, 3939−3943. − [8c] S.-M. Peng, Y.-N. Lin, *Acta. Crystallogr.* **1986**, *C42*, 1725−1731. − [8d] M. Sterns, *J. Cryst. Mol. Struct.* **1971**, *1*, 383−387.

[9] B. J. Hathaway, in *Comprehensive Coordination Chemistry* (Eds.: G. Wilkinson, R. D. Gill, J. A. McCleverty), Pergamon Press, Oxford, **1987**, vol. 5.

[10] K. Nakamoto, *Infrared and Raman Spectra of Inorganic and Coordination Compounds*, John Wiley & Sons, 4th ed., New York, **1986**.

[11] I. M. Kolthoff, P. J. Elving, *Treatise on Analytical Chemistry*, Interscience Publ., New York, **1963**, vol. 4, part 1.

[12] [12a] T. Kottke, D. Stalke, *J. Appl. Crystallogr.* **1993**, *26*, 615−619. − [12b] *TEXSAN, Single Crystal Structure Analysis Software*, version 1.6, Molecular Structure Corporation, The Woodlands, TX 77381, USA, **1993**. − [12c] G. M. Sheldrick, *SHELXS86, Program for crystal structure determination*, University of Göttingen, Germany, **1986**. − [12d] G. M. Sheldrick, *SHELXL93, Program for crystal structure refinement,*. University of Göttingen, Germany, **1993**.

[13] S. Amani Komaei, G. A. van Albada, I. Mutikainen, U. Turpeinen, J. Reedijk, in preparation.

[98275]

Solution Study, Crystal Structure and Relaxivity Properties of a Gd^{3+} Complex with an Uncharged Macrocyclic Ligand Bearing Four Amidic Side Arms

Lucia Alderighi[a], Antonio Bianchi*[a], Luisella Calabi[b], Paolo Dapporto[c], Claudia Giorgi[a], Pietro Losi[b], Lino Paleari[b], Paola Paoli[c], Patrizia Rossi[a], Barbara Valtancoli[a], and Mario Virtuani[b]

Department of Chemistry, University of Florence[a],
Via Maragliano 75/77, I-50144 Florence, Italy
Fax: (internat.) + 39-55/354845
E-mail: bianchi@chim1.unifi.it

Research and Development Division, Braeeo SpA[b],
Via E. Folli 50, I-20134 Milan, Italy
Fax: (internat.) + 39-2/26410678

Department of Energetics, University of Florence[c],
I-50144 Florence, Italy

Received April 6, 1998

Keywords: Gadolinium complexes / Gadolinium / Magnetic Resonance Imaging (MRI) / Contrast agents / Polyaminopolycarboxylic ligands

Equilibrium data on the interaction of DTMA [(DTMA = DOTA tetrakis(methylammide)] with Gd^{3+} in aqueous solution, properties of the complexes formed in the pH range 0.6–11.8, water proton relaxation rate enhancement, and the crystal structure analysis of the $[Gd(DTMA)H_2O]^{3+}$ complex are reported. In the crystal structure the metal ion is bound to the nitrogen atoms of the tetraazamacrocyclic moiety, to the amidic oxygen atoms, and to an oxygen atom of a water molecule. The nine donors are located at the vertices of a distorted square antiprism, which is capped by the coordinated water oxygen atom in the axial position. In solution $[Gd(DTMA)]^{3+}$ is not very stable [$\log K_{ML}$ = 12.8(1)] and gives rise to the formation of $[Gd(DTMA)OH]^{2+}$ [pK_a = 7.9(1)] and $[Gd(HDTMA)]^{4+}$ [$\log K_{(ML+H)}$ = 3.4(1)]. The proton solvent relaxivity of aqueous complex solutions assumes a constant value in the pH range 3–8, increasing at higher and lower pH. For pH > 3 the data are in good agreement with a previous study on the same compound. For pH < 3 a new interpretation is presented, based on the formation of $[Gd(HDTMA)]^{4+}$ and the release of Gd^{3+}.

A recent communication by Aime et al.[1] reported the interesting observations of the enhancement of the nuclear relaxation rate of water protons brought about by the $[Gd(DTMA)]^{3+}$ complex [(DTMA = DOTA tetrakis-(methylammide)] in aqueous solution. This presented for the first time a distinct evaluation of the water and prototropic exchange rates for a Gd^{3+}-coordinated solvent molecule. The uncharged DTMA ligand was selected in order to assess the contribution of prototropic exchange to the overall water exchange between the complex and the bulk solvent, as it had been observed that the exchange lifetime of Gd^{3+}-coordinated water molecules increases with decreasing negative charge of the Gd^{3+} complex. Actually, the nuclear transverse relaxation rate of ^{17}O nuclei of the solvent observed for the $[Gd(DTMA)]^{3+}$ complex is the slowest water exchange rate so far reported for a lanthanide(III) complex[1].

Aqueous solutions containing the triflate salt of $[Gd(DTMA)]^{3+}$ revealed a peculiar pH dependence of the longitudinal solvent relaxivity[2] (R_{1p}): R_{1p} assumes a constant value (ca. 2.6 $mM^{-1}s^{-1}$) in the pH range 2−8, increasing at higher and lower pH ($R_{1p} \approx 5.8$ $mM^{-1}s^{-1}$ at pH = 11−12 and $R_{1p} \approx 5.4$ $mM^{-1}s^{-1}$ at pH = 0.5). In the pH range 2−8 the low relaxivity values are consistent with a purely outer-sphere contribution[3]. ^{19}F-NMR measurements performed in this pH range were indicative of strong ion pairing between the complex $[Gd(DTMA)]^{3+}$ and the counterions $CF_3SO_3^-$[1]. The increase in relaxivity for pH > 8 was attributed to the additional contribution to ^1H-R_{1p} deriving from a prototropic exchange caused by the presence of the hydroxo species $[Gd(DTMA)OH]^{2+}$, while the increase in relaxivity in very acidic solutions was attributed to the acid-catalyzed dissociation of the ion pairs formed by $[Gd(DTMA)]^{3+}$ with the counterions[1]. The interpretation of the relaxivity behavior in acidic solutions was

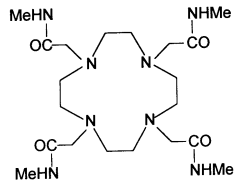

DTMA

 © WILEY-VCH Verlag GmbH, D-69451 Weinheim, 1998 1434−1948/98/1111−1581 $ 17.50+.50/0

based on the assumption that the complex $[Gd(DTMA)]^{3+}$ is the only species present in such media, as suggested by the ^1H- and ^{13}C-NMR spectra of the analogous $[Eu(DTMA)]^{3+}$ complex.

Results and Discussion

A parallel but independent study performed in our laboratories on the same compound led to the determination of the crystal structure[4][5][6][7][8] of the $[Gd(DTMA)H_2O]^{3+}$ cation, to the identification of the Gd^{3+} complexes formed in solution by DTMA in the pH range 2.5−10, and to the determination of equilibrium constants of these complexes[9]. This elucidated some aspects of the system and completed the picture outlined by the previous work[1].

DTMA actually acts as an octadentate ligand toward Gd^{3+}, forming a tight structure where a water molecule is accommodated in the ninth position. Crystals of $[Gd(DTMA)H_2O](ClO_4)_3 \cdot NaClO_4 \cdot 3\ H_2O$[10] are composed of $[Gd(DTMA)H_2O]^{3+}$ cations, sodium ions, perchlorate counterions and water of crystallization. The metal ion is bound to the nitrogen atoms of the tetraazamacrocyclic moiety and to the amidic oxygen atoms provided by the four side arms, and finally to an oxygen atom of a water molecule (Figure 1).

Figure 1. Molecular structure (ORTEP[11] draw) of the $[Gd(DTMA)H_2O]^{3+}$ cation[a]

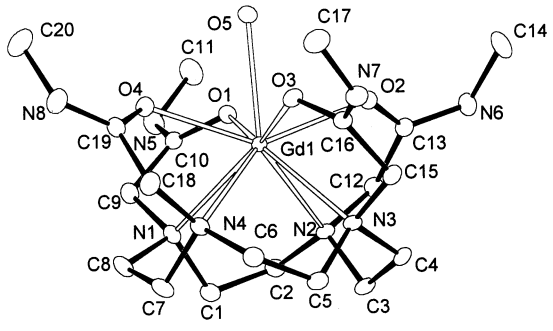

[a] Selected interatomic distances [Å] and angles [°]: Gd(1)−O(2) 2.351(5), Gd(1)−O(3) 2.351(4), Gd(1)−O(4) 2.393(5), Gd(1)−O(1) 2.455(5), Gd(1)−O(5) 2.461(5), Gd(1)−N(4) 2.621(6), Gd(1)−N(1) 2.626(5), Gd(1)−N(3) 2.648(5), Gd(1)−N(2) 2.649(5); O(2)−Gd(1)−O(3) 84.1(2), O(5)−Gd(1)−N(1) 123.1(2), O(2)−Gd(1)−O(4) 142.3(2), N(4)−Gd(1)−N(1) 69.2(2), O(3)−Gd(1)−O(4) 83.7(2), O(2)−Gd(1)−N(3) 74.9(2), O(2)−Gd(1)−O(1) 81.8(2), O(3)−Gd(1)−N(3) 66.1(2), O(3)−Gd(1)−O(1) 145.1(2), O(4)−Gd(1)−N(3) 130.4(2), O(4)−Gd(1)−O(1) 88.3(2), O(1)−Gd(1)−N(3) 138.3(2), O(2)−Gd(1)−O(5) 73.4(2), O(5)−Gd(1)−N(3) 130.9(2), O(3)−Gd(1)−O(5) 74.1(2), N(4)−Gd(1)−N(3) 68.5(2), O(4)−Gd(1)−O(5) 69.0(2), N(1)−Gd(1)−N(3) 106.0(2), O(1)−Gd(1)−O(5) 71.3(2), O(2)−Gd(1)−N(2) 66.7(2), O(2)−Gd(1)−N(4) 142.5(2), O(3)−Gd(1)−N(2) 130.7(2), O(3)−Gd(1)−N(4) 74.0(2), O(4)−Gd(1)−N(2) 142.6(2), O(4)−Gd(1)−N(4) 65.7(2), O(1)−Gd(1)−N(2) 70.9(2), O(1)−Gd(1)−N(4) 132.3(2), O(5)−Gd(1)−N(2) 127.8(2), O(5)−Gd(1)−N(4) 126.5(2), N(4)−Gd(1)−N(2) 105.6(2), O(2)−Gd(1)−N(1) 131.1(2), N(1)−Gd(1)−N(2) 68.6(2), O(3)−Gd(1)−N(1) 142.4(2), N(3)−Gd(1)−N(2) 68.3(2), O(4)−Gd(1)−N(1) 74.5(2), O(1)−Gd(1)−N(1) 65.4(2).

The nine donors are located at the vertices of a distorted square antiprism, capped by the coordinated water oxygen atom in the axial position. Similar coordination spheres were found for other Gd^{3+} complexes with analogous ligands derived from the 1,4,7,10-tetraazacyclododecane macrocycle[12]. The four nitrogen atoms supplied by the macrocyclic ligand are in a well-defined plane, while the maximum deviation from the mean plane formed by the four amidic oxygen atoms is 0.025(5) Å. The oxygen atom of the water molecule is ca. 1.7 Å away from the mean O1−O2−O3−O4 plane, with the Gd−O5 bond direction almost perpendicular to this plane (87°). The metal ion is significantly shifted towards the mean plane of the oxygen donors with respect to the plane described by the four nitrogen atoms (0.74 vs. 1.59 Å, respectively). The Gd−N bond lengths [2.621(5)−2.649(6) Å], the Gd−O amidic bond lengths [2.351(5)−2.455(5) Å], as well as the Gd−O water distance [2.461(5) Å, see Figure 1] compare well with those previously reported for analogous gadolinium(III) complexes[12]. Concerning the ligand, the tetraaza ring adopts the [3333] C corners conformation[13], with the four side arms, which are folded towards the macrocyclic cavity, in a head-to-tail arrangement. The four amidic nitrogen atoms have a significant sp^2 character, thus the usual π conjugation takes place in each amidic functional group enhancing the donor capability of the carbonylic oxygen atoms.

The molecular packing reveals a large number of H-bond contacts (< 3.0 Å) involving the water of crystallization, the oxygen atoms of the perchlorate anions and various hydrogen and nitrogen atoms of the ligand, while the sodium ion is six-coordinated [Na−O bond lengths range from 2.413(9) to 2.80(1) Å] by four perchlorate oxygen atoms and two water molecules of crystallization. It is worth noting that the oxygen atom O5 of the Gd^{3+}-coordinated water molecule is very close [2.92(1) Å] to an oxygen atom of a perchlorate ion. This suggests the presence of a strong hydrogen bond between $[Gd(DTMA)H_2O]^{3+}$ and a counterion, offering a model for the ion pairing occurring in solution[1] between the complex and $CF_3SO_3^-$.

Gd^{3+} complexation by DTMA is very slow; solutions containing the metal ion and the ligand in the pH range 2.5−8 require several days to equilibrate at 298.1 K. For this reason the speciation of the system was performed by using an out-of-cell batch technique in which 40 solutions corresponding to different points in a conventional potentiometric titration were allowed to equilibrate at 298.1 K[9]. The same procedure was adopted to study the Eu^{3+}/DTMA system. The formation constants[9] determined for the complexes formed at equilibrium (0.1 mol dm^{-3} Me_4NNO_3, 298.1 ± 0.1 K) are listed in Table 1, which also contains the ligand protonation constants determined under the same experimental conditions.

The $[Gd(DTMA)]^{3+}$ complex is not very stable [$\log K$ = 12.8(1)] if compared with the analogous complex with DOTA ($\log K = 24.67$)[14], demonstrating the lower coordinating ability toward Gd^{3+} of amidic groups with respect to carboxylate groups[15]. Starting from neutral pH the metal-bound water molecules in $[Gd(DTMA)H_2O]^{3+}$ dissociate

Table 1. Logarithms of the equilibrium constants of the Gd^{3+} and Eu^{3+} complexation reactions with DTMA, determined in 0.1 mol dm^{-3} Me_4NNO_3 at 298.1 ± 0.1 K[a]

reaction	log *K*
$DTMA + H^+ \rightleftharpoons HDTMA^+$	9.27(1)
$HDTMA^+ + H^+ \rightleftharpoons H_2DTMA^{2+}$	5.55(2)
$H_2DTMA^{2+} + H^+ \rightleftharpoons H_3DTMA^{3+}$	1.56(7)
$Gd^{3+} + DTMA \rightleftharpoons [Gd(DTMA)]^{3+}$	12.8(1)
$[Gd(DTMA)]^{3+} + H^+ \rightleftharpoons [Gd(HDTMA)]^{4+}$	3.4(1)
$[Gd(DTMA)]^{3+} + OH^- \rightleftharpoons [Gd(DTMA)OH]^{2+}$	5.8(1)
$Eu^{3+} + DTMA \rightleftharpoons [Eu(DTMA)]^{3+}$	13.17(4)
$[Eu(DTMA)]^{3+} + OH^- \rightleftharpoons [Eu(DTMA)OH]^{2+}$	6.83(5)

[a] Values in parentheses are standard deviations on the last significant figure

[pK_a = 7.9(1)] giving rise to the hydroxo complex $[Gd(DTMA)OH]^{2+}$, while for pH < 5 $[Gd(DTMA)]^{3+}$ undergoes protonation to produce the species $[Gd(HDTMA)]^{4+}$. Due to the reduced coordinating ability of DTMA toward Gd^{3+}, the uncoordinated metal ion is present in acidic media at pH < 4 (Figure 2).

Figure 2. Distribution diagram of the complexed species formed by DTMA with Gd^{3+} as a function of pH in 0.1 mol dm^{-3} Me_4NNO_3 solution at 298.1 K; [DTMA] = $[Gd^{3+}] = 1 \times 10^{-3}$ mol dm^{-3}

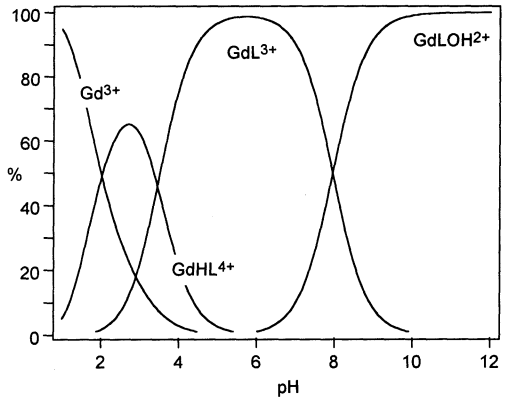

As can be seen in Table 1, DTMA displays almost the same tendency to bind Gd^{3+} and Eu^{3+}, but $[Eu(DTMA)H_2O]^{3+}$ demonstrates a higher propensity than $[Gd(DTMA)H_2O]^{3+}$ to form the hydroxylated complex [pK_a = 7.0(1)], and does not form protonated species.

Hence, the use of the Eu^{3+} complex with DTMA as a model for the Gd^{3+}/DTMA system led Aime et al. to ignore the formation of $[Gd(HDTMA)]^{4+}$ in their interpretation of the relaxivity properties in acidic media.

Measurement of water relaxation times in the presence of the gadolinium complex, performed with 0.1 mol dm^{-3} Me_4NNO_3 solutions after equilibration in the pH range 0.6−11.8, confirmed the pH dependence of relaxivity found by Aime et al.[1] in the presence of $CF_3SO_3^-$ at pH > 3. This accounts for similar properties of NO_3^- and $CF_3SO_3^-$ in the formation of ion pairs with the complex. However for pH values < 3 the relaxivity increases with decreasing pH more rapidly than previously reported[1] for measurements performed shortly after solution acidification. The equilibrium data obtained for the Gd^{3+}/DTMA system (Table 1) confirm the role played by $[Gd(DTMA)]^{3+}$ and $[Gd(DTMA)OH]^{2+}$ in determining the relaxivity properties of solutions at pH > 3 containing the complex, offering a new interpretation of the relaxivity behavior observed at pH < 3. Actually, in acidic solutions at equilibrium the relaxivity increases with increasing concentration of free Gd^{3+} (released by the complex upon acid-catalyzed dissociation), and at pH ≈ 0.5, where complete complex dissociation occurs (Figure 2), approaches the value expected (ca. 11 $mM^{-1}s^{-1}$) at such pH for a solution of Gd^{3+} in the ionic medium employed.

On the other hand, potentiometric measurements performed on $[Gd(DTMA)]^{3+}$ in acidic solutions indicate that the monoprotonated complex is formed after rather short equilibration times (2−3 h), while complex dissociation is expected[1] to produce significant concentrations of uncoordinated Gd^{3+} only after many hours.

Complex protonation produces a more open structure around Gd^{3+}, which means either an increase in the metal-ion hydration number or a wider diffusion of water molecules in proximity of the paramagnetic centre; both phenomena are expected[3] to imply an enhancement of the relaxation rate of water protons.

Therefore, the Gd^{3+}/DTMA system gives different relaxivity responses in acidic media, depending on the equilibration times of the complex; relaxivity increases with decreasing pH due to: i) the formation of the monoprotonated $[Gd(HDTMA)]^{4+}$ complex, after short equilibration times, ii) the presence of uncoordinated Gd^{3+} ion after long equilibration times. Both effects can be present simultaneously.

We believe that the relaxation properties of $[Gd(DTMA)]^{3+}$ observed by Aime et al. in acidic solutions are principally connected with the first factor.

Indeed, the results on the Gd^{3+}/DTMA system have a direct impact in the research about paramagnetic contrast agents for magnetic resonance imaging, suggesting that modulation of water proton relaxivity can be achieved by tuning the solution pH under kinetic control of the Gd^{3+}/ligand complexation reaction. Furthermore, the results described here demonstrate the necessity to be very prudent in the use of Eu^{3+} complexes as models for the corresponding Gd^{3+} systems.

We are grateful to Mr. *Massimo Foresti*, Dr. *Palma Mariani*, Mrs. *Lucia Monti*, and Dr. *Stefano Seniori Costantini* for technical assistance

[1] S. Aime, A. Barge, M. Botta, D. Parker, A. S. De Sousa, *J. Am. Chem. Soc.* **1997**, *119*, 4767−4768.
[2] Relaxivity is defined as the nuclear magnetic relaxation rate increase of water nuclei per unit concentration of the paramagnetic complex.
[3] R. B. Lauffer, *Chem. Rev.* **1987**, *87*, 901−927.
[4] Crystal data: $[Gd(DTMA)H_2O](ClO_4)_3 \cdot NaClO_4 \cdot 3\ H_2O$, triclinic, *P*1, *a* = 11.558(6), *b* = 13.251(9), *c* = 14.713(9) Å, α = 94.29(9), β = 109.65(8), γ = 102.97(6)°, *V* = 2040(4) $Å^3$, *Z* =

2, $D_{calcd.}$ = 1.80 g cm^{-3}, T = 298 K, graphite-monochromated Mo-K_α radiation, λ = 0.71069 Å, μ = 19.9 cm^{-1}; data collection with an Enraf Nonius CAD4 automatic diffractometer, $\theta-2\theta$ scan, $2\theta \leq 50°$, 7622 reflections, 6377 observed [$I > 2\sigma(I)$] data, absorption correction by DIFABS[5]. The structure, solved by direct methods of SIR92[6] and refined[7] by full-matrix least squares against F^2 (non-H atoms anisotropic, the hydrogen atoms of the macrocyclic ligand were placed in calculated positions and treated with an overall temperature factor refined to 0.053 Å^2, 528 variables/7111 data) to $wR2$ = 0.139, goodness-of-fit 1.06, $R(F$, obs. data) = 0.050. The Fourier difference map did not allow us to localize the hydrogen atoms of the Gd-coordinated water molecule. Geometrical parameters were obtained by using PARST93[8]. Further information on the crystal-structure determination has been deposited with the Cambridge Crystallographic Data Centre as supplementary publication no. CCDC-101378 and may be obtained from CCDB, 12 Union Road, Cambridge CB2 1EZ, UK [Fax: (internat.) + 44-1223/336033; e-mail: deposit@ccdc.cam.ac.uk]

[5] N. Walker, D. D. Stuart, *Acta Crystallogr., Sect. A* **1983**, *39*, 158−166.

[6] A. Altomare, G. Cascarano, C. Giacovazzo, A. Guagliardi, M. C. Burla, G. Polidori M. Camalli, *J. Appl. Crystallogr.* **1994**, *27*, 435.

[7] G. M. Sheldrick, *SHELXL93 − Program for the Refinement of Crystal Structures*, University of Göttingen, Germany, **1993**.

[8] M. Nardelli, *Comput. Chem.* **1983**, *7*, 95−98.

[9] Equilibrium constants were obtained by means of potentiometric titrations in 0.1 mol dm^{-3} Me_4NNO_3 at 298.1 ± 0.1 K. Under such conditions pK_w = 13.83(1). Out-of-cell experiments were performed by employing individual solutions equilibrated at 298.1 ± 0.1 K. The pH of these solution was recorded at intervals until no further pH drift was observed. E.m.f. data were processed by using the HYPERQUAD program (P. Gans, A. Sabatini, A. Vacca, *Talanta* **1996**, *43*, 1739−1753).

[10] Crystals of $[Gd(DTMA)H_2O](ClO_4)_3 \cdot NaClO_4 \cdot 3\,H_2O$ were obtained by slow concentration at room temp. of aqueous solutions containing equimolar quantities of DTMA and $GdCl_3$ in the presence of a tenfold excess of $NaClO_4$. Satisfactory elemental analyses were obtained for the various samples prepared.

[11] C. K Johnson, *ORTEPII*, Report-5138, Oak Ridge National Laboratory, Tennessee, USA, **1973**.

[12] S. Aime, P. L. Anelli, M. Botta, F. Fedeli, M. Grandi, P. Paoli, F. Uggeri, *Inorg. Chem*. **1992**, *31*, 2422; K. Kumar, C. A. Chang, L. C. Francesconi, D. D. Dischino, M. F. Malley, J. Z. Gougoutas, M. F. Tweedle, *Inorg. Chem*. **1994**, *33*, 3567−3575; S. I. Kang, R. S. Ranganathan, J. E.Emswiler, K. Kumar, J. Z. Gougoutas, M. F. Malley, M. F. Tweedle, *Inorg. Chem*. **1993**, *32*, 2912−2918.

[13] *Stereochemical and Stereophysical Behaviour of Macrocycles* (Ed.: I. Bernal), Elsevier, Amsterdam, **1987**, p 34−45.

[14] A. Bianchi, L. Calabi, L. Ferrini, P. Losi, F. Uggeri, B Valtancoli, *Inorg. Chim. Acta* **1996**, *249*, 13−15.

[15] H. Maumela, R. D. Hancock, L. Carlton, J. H. Reibenspies, K. P. Wainwright, *J. Am. Chem. Soc.* **1995**, *117*, 6698−6707.

[98101]

Synthesis and Reactivity of Silicon Transition Metal Complexes, 44[◇]
Metallosilanols and Metallosiloxanes, 17[◇◇]

Regiospecific Hydroxylation of Metallodisilanes of the Iron Group – An Impressive Example of the Transition Metal Effect

Wolfgang Malisch*[a], Heinrich Jehle[a], Stephan Möller[a], Chantu Saha-Möller[b], and Waldemar Adam[b]

Institut für Anorganische Chemie der Universität Würzburg[a],
Institut für Organische Chemie der Universität Würzburg[b],
Am Hubland, D-97074 Würzburg, Germany
Fax: (internat.) + 49(0)931/888-4618
E-mail: Wolfgang.Malisch@mail.uni-wuerzburg.de

Received April 23, 1998

Keywords: Metallodisilanes / Oxofunctionalization / Metallodisilandiols / Silanetriols / Metallosiloxanes

Reaction of the ferriodisilanes $C_5R_5(OC)_2Fe–Si_2H_5$ [R = H (**1a**), Me (**1b**)] with dimethyldioxirane leads to selective insertion of oxygen into the α-Si–H bonds to yield the ferriodihydroxydisilanes $C_5R_5(OC)_2Fe–Si(OH)_2–SiH_3$ [R = H (**2a**), Me (**2b**)]. Another access to yield **2a** is opened by hydrolysis of the dichloro(ferrio)disilane $Cp(OC)_2Fe–SiCl_2–SiH_3$ (**3a**). Treatment of the pentachloro(metallo)disilanes $C_5H_5(OC)_2Fe–Si_2Cl_5$ (**4a**) and $C_5Me_5(OC)_2Ru–Si_2Cl_5$ (**4b**) with water results in regiospecific hydroxylation of the β-silicon atom to generate metallodisilanetriols $C_5R_5(OC)_2M–SiCl_2–Si(OH)_3$ [M = Fe, R = H (**5a**); M = Ru, R = Me (**5b**)]. Controlled condensation of **5b** with $Me_2Si(H)Cl$ leads to the novel rutheniosiloxane $C_5Me_5(OC)_2Ru–SiCl_2–Si(OSiMe_2H)_3$ (**6**).

Introduction

Due to their important role as intermediates in the technical synthesis of silicones[1] organosilanoles have been the subject of extensive studies over several decades[2]. Recently, in context with our studies on the reactivity of functionalized silicon transition metal complexes we have established a new type of silanol containing an Si-bonded transition metal fragment. Access to these metallosilanols is opened by the hydrolysis of halo(metallo)silanes[3] and by the oxygenation of metallosilanes with dimethyldioxirane[4]. Especially the second approach which even allows transformation of metal-bound SiH_3 groups to $Si(OH)_3$ moieties is favored by the strong electron donor capacity of the transition metal fragment which in addition guarantees high stability with respect to condensation. We now focused our interest on metallodisilanes and pentachloro(metallo)disilanes $L_nM–SiX_2–SiX_3$ (X = H, Cl) where two extremely different types of Si–X units are present and which can be regarded as attractive model compounds for the demonstration of the directing effect of transition metal fragments. We have examined this possibility using the metallodisilanes of the iron group [$L_nM = C_5R_5(OC)_2Fe/Ru$ (R = H, Me)] accessible by simple routes[5]. We now report that the transition metal effect can create novel types of disilanyl ligands in which either the α- or the β-silicon atom is fully substituted by hydroxy groups.

[◇] Part 43: Ref.[5a].
[◇◇] Part 16: S. Möller, H. Jehle, W. Malisch, W. Seelbach in: *Organosilicon Chemistry III: From Molecules to Materials* (Eds.: N. Auner, J. Weis), VCH, Weinheim **1998**, p. 267–270.

Results and Discussion

Treatment of the ferriodisilanes **1a–b** with a solution of dimethyldioxirane in acetone at −78°C results in the formation of the ferriodihydroxydisilanes **2a**, **b**, the first complexes with an $H_3Si–Si(OH)_2$ ligand (Eq. 1).

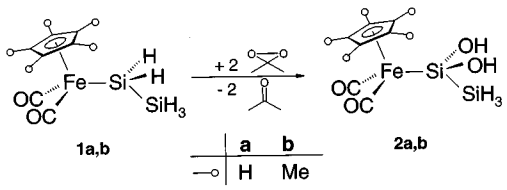

(1)

The dihydroxydisilanes **2a**, **b** are isolated as pale yellow solids in excellent yields [89% (**2a**), 83% (**2b**)] within hours and are barely soluble in aliphatic or aromatic solvents. The solubility in THF or acetone is reasonable but light-induced decomposition occurs in these solutions within 12–16 h. However, unlimited storage under nitrogen at −20°C is possible. Further hydroxylation of **2a**, **b** with a large excess of dimethyldioxirane does not lead to the expected metallopentahydroxydisilane due to extensive decomposition.

Another approach to **2a**, **b** starting from the ferriodisilanes applies in the first step the regiospecific transformation of **1a**, **b** into the corresponding dichloro(ferrio)disilanes **3a**, **b** by H/Cl exchange with CCl_4 as described recently[6], followed by treatment with water. Hydrolysis of **3a**, **b** in the presence of Et_3N as an auxiliary base takes place only in

 © WILEY-VCH Verlag GmbH, D-69451 Weinheim, 1998 1434–1948/98/1111–1585 $ 17.50+.50/0

the case of **3a** (Eq. 2). Generated **2a** is isolated after 14 hours in 81% yield.

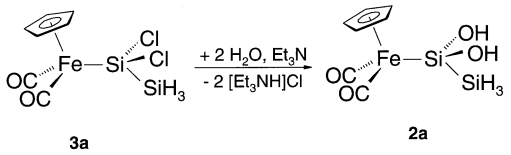

3a 2a (2)

The dichloro(ferrio)disilane **3b** does not show an analogous tendency for Cl/OH exchange according to Eq. (2), indicating that the electron-releasing capability of the Cp* $(OC)_2Fe$ fragment, which exceeds that of the $Cp(OC)_2Fe$ fragment, too strongly reduces the electrophilicity of the α-silicon atom.

In contrast to the reactions of Eq. (1) in which the metal fragment activates the α-silicon atom with respect to electrophilic attack, nucleophilic exchange activity of this silicon atom is extremely reduced. This fact allows regiospecific hydroxylation in the β-position of the pentachloro(metallo)disilanes **4a**, **b** by base-assisted hydrolysis. Cl/OH exchange is complete within 12 hours at room temperature yielding the dichloro(metallo)trihydroxydisilanes **5a**, **b** as beige, rather air-stable solids (Eq. 3).

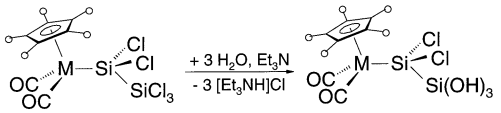

4a,b 5a,b (3)

	a	b
—	H	Me
M	Fe	Ru

Remarkable is the stability of the metallodisilanetrioles **5a**, **b** with respect to self-condensation. Apparently, the Si−OH group stabilization by the "transition metal effect" is working even at the β-silicon atom. This property renders **5a**, **b** useful as precursors for selective formation of unusual siloxane arrangements at the β-silicon atom. A first example is realized by base-assisted condensation of **5b** with chlorodimethylsilane to give the novel (ruthenio-silyl)(siloxy)trisiloxane **6** as a deep yellow solid after recrystallization from *n*-pentane at −78°C (yield: 74%) (Eq. 4).

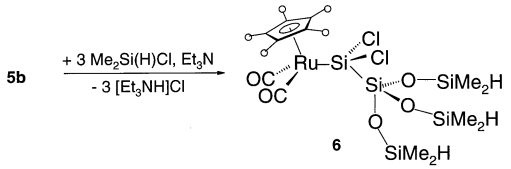

(4)

The ruthenio complex **6** is characterized by a high number of Si functionalities which can be used for further hydroxylation or introduction of transition metal fragments by oxidative addition.

In forthcoming publications we will report on these transformations and further regiospecific reactions of metallodisilanes using the "transition metal effect".

We gratefully acknowledge financial support from the *Deutsche Forschungsgemeinschaft* (SFB 347: *"Selective Reaktionen Metall-aktivierter Moleküle"*; Schwerpunktprogramm *"Spezifische Phänomene in der Siliciumchemie"*) as well as from the the *Fonds der Chemische Industrie.*

Experimental Section

All operations were performed under purified and dried nitrogen with the Schlenk-type technique. Solvents were dried according to conventional procedures, distilled, and saturated with N_2 prior to use. − NMR: Bruker AMX 400 (400.1 MHz, 100.6 MHz, and 79.5 MHz for ^1H, ^{13}C, and ^{29}Si, respectively). [D_6]Benzene as a solvent (unless otherwise stated): $\delta_H = 7.15$, $\delta_C = 128.0$; [D_6]acetone: $\delta_H = 2.04$, $\delta_C = 206, 29.8$; for ^{29}Si ^2H-lock internal, rel. to TMS external. − IR: Perkin-Elmer 283. − Melting points: Du Pont 9000 Thermal Analysis System. − Starting materials: $C_5R_5(OC)_2Fe-SiH_2-SiH_3$ (R = H, Me)[5], $C_5Me_5(OC)_2Ru-SiH_2-SiH_3$[5].

1. *1-[Dicarbonyl(η⁵-cyclopentadienyl)ferrio]-1,1-dihydroxydisilane* (**2a**)

A) *Dimethyldioxirane Route:* A solution of 150 mg (0.62 mmol) of $Cp(OC)_2Fe-Si_2H_5$ (**1a**) in 5 ml of toluene was combined with 16.5 ml (1.24 mmol) of a 1.4 M solution of dimethyldioxirane in acetone at −78°C leading to a rapid change of colour from yellow to orange. The reaction mixture was warmed up to room temperature within 50 min, unsoluble material separated, and volatiles were removed in vacuo. Remaining **2a** was washed with pentane and dried in vacuo. − Yield 146 mg (89%).

B) *Hydrolysis Route:* A solution of 537 mg (1.70 mmol) of $Cp(OC)_2Fe-SiCl_2-SiH_3$ (**3a**) in 15 ml of Et_2O was combined with 63 mg (3.5 mmol) of H_2O and 353 mg (3.4 mmol) of Et_3N at 0°C and the reaction mixture stirred for 10 h in the dark. Following the work-up procedure of A) **2a** was obtained in 81% yield. − Yellow microcrystalline powder. − M.p. 66°C (decomp.). − $C_7H_{10}FeO_4Si_2$ (264.92): calcd. C 27.32, H 2.49; found C 27.38, H 2.63. − ^1H NMR: δ = 3.95 (s, H_5C_5), 3.88 (s, br., 2 H, HO), 3.76 [s, ^1J(SiH) = 196.0 Hz, 3 H, H_3Si]. − ^{13}C NMR: δ = 214.6 (s, CO), 85.07 (s, C_5H_5). − ^{29}Si NMR: δ = 99.88 (s, α-Si), −100.1 (s, β-Si). − IR (toluene): $\tilde{\nu}$ = 3372 cm^{-1} [m, br., ν(OH)]; 2135 [m, ν(SiH)]; 2000 (vs), 1953 (vs) [ν(CO)].

2. *1-[Dicarbonyl(η⁵-pentamethylcyclopentadienyl)ferrio]-1,1-dihydroxydisilane* (**2b**): According to 1. A) from 130 mg (0.42 mmol) of **1b** and 11 ml (0.84 mmol) of a 1.3 M solution of dimethyldioxirane in acetone after 80 min. − Yield: 98 mg (89%). − Yellow, microcrystalline powder. − M.p. 65°C (decomp.). − $C_{12}H_{20}FeO_4Si_2$ (340.31): calcd. C 42.35, H 5.92; found C 42.26, H 6.01. − ^1H NMR: δ = 3.57 [s, ^1J(SiH) = 182.0 Hz, 3 H, H_3Si], 2.28 (s, br., 2 H, HO), 1.58 [s, 15 H, $(H_3C)_5C_5$]. − ^{13}C NMR: δ = 215.9 (s, CO), 95.70 [s, $C_5(CH_3)_5$], 9.69 [s, $(CH_3)_5C_5$]. − ^{29}Si NMR: δ = 96.70 [s, $Si(OH)_2$], −95.26 (s, SiH_3). − IR (toluene): $\tilde{\nu}$ = 3479 cm^{-1} [m, br., ν(OH)]; 2107 [m, ν(SiH)], 1986 (vs), 1931 (vs) [ν(CO)].

3. *1,1-Dichloro-1-dicarbonyl(η⁵-cyclopentadienyl)ferrio]-2,2,2-trihydroxydisilane* (**5a**): A solution of 1.01 g (2.46 mmol) of $Cp(OC)_2Fe-Si_2Cl_5$ (**4a**) in 50 ml of Et_2O was combined with 132 mg (7.38 mmol) of H_2O and 747 mg (7.38 mmol) of Et_3N. The reaction mixture was stirred for 12 h at room temperature, followed by separation of insoluble material. After removal of volatiles, the remaining residue was washed with 15 ml of *n*-pentane, filtered, and dried in vacuo. − Yield: 740 mg (84%). − Pale yellow, microcrystalline powder. − M.p. 64°C (decomp.). − $C_7H_8Cl_2FeO_5Si_2$ (355.06): calcd. C 23.68, H 2.27; found C 23.81, H 2.39. − ^1H

NMR: δ = 4.48 (s, 5 H, H_5C_5), 3.96 (s, br, 3 H, HO). − ^{13}C NMR: δ = 212.9 (s, CO), 84.51 (s, C_5H_5). − IR (THF): $\tilde{\nu}$ = 3481 cm^{-1} [s, br., ν(OH)]; 2000 (vs), 1946 (vs) [ν(CO)].

4. *1,1-Dichloro-1-dicarbonyl(η^5-pentamethylcyclopentadienyl)ruthenio]-2,2,2-trihydroxydisilane* (**5b**): According to 3. from 260 mg (0.49 mmol) of **4b**, 26.5 mg (1.47 mmol) of H_2O and 150 mg (1.47 mmol) of Et_3N in 50 ml of Et_2O after stirring for 12 h. − Yield: 110 mg (47%). − Pale yellow, microcrystalline powder. − M.p. 57°C (decomp.). − $C_{12}H_{18}Cl_2O_5RuSi_2$ (470.42): calcd. C 30.69, H 3.87; found C 30.64, H 3.86. − ^{1}H NMR ([D$_6$]acetone): δ = 2.20 (s, 3 H, HO), 1.92 [s, 15 H, $(H_3C)_5C_5$]. − ^{13}C NMR ([D$_6$]acetone): δ = 204.47 (s, CO), 100.58 [s, $C_5(CH_3)_5$], 10.64 [s, $(CH_3)_5C_5$]. − IR (Et_2O): $\tilde{\nu}$ = 3473 cm^{-1} [s, br., ν(OH)]; 2001 (vs), 1944 (vs) [ν(CO)].

5. *3-{[Dicarbonyl(η^5-pentamethylcyclopentadienyl)ruthenio]-dichlorosilyl}-3-(dimethylsiloxy)-1,1,5,5-tetramethyltrisiloxane* (**6**): 321 mg (3.40 mmol) of $Me_2Si(H)Cl$ and 343 mg (3.39 mmol) of Et_3N in 20 ml of Et_2O were added dropwise to a solution of 402 mg (1.13 mmol) of $C_5Me_5(OC)_2Ru-SiCl_2-Si(OH)_3$ (**5b**) in 10 ml of Et_2O. After stirring for 8 h, volatiles were removed in vacuo. The residue was extracted with 15 ml of *n*-pentane and **6** crystallized at −78°C. − Yield: 113 mg (74%). − Yellow waxy solid. − M.p.: 77°C (decomp.). − $C_{18}H_{36}Cl_2O_5Si_5Ru$ (644.85): calcd. C 33.52, H 5.63; found C 33.21, H 5.50. − ^{1}H NMR: δ = 5.19 [sept, ^3J(HSiCH) = 2.8 Hz, ^1J(HSi) = 202.5 Hz, 3 H, HSi], 1.86 [s, 15 H, $(H_3C)_5C_5$], 0.51 [d, ^3J(HSiCH) = 2.8 Hz, 18 H, $(H_3C)Si$]. − ^{13}C NMR: δ = 203.3 (s, CO), 99.7 [s, $C_5(CH_3)_5$] 10.2 [s, $(CH_3)_5C_5$], 1.4 (s, CH_3). − ^{29}Si NMR: δ = −10.14 (s, β-Si), −27.00 (s, δ-Si) [α-silicon signal was not observed]. − IR (toluene): $\tilde{\nu}$ = 2117 cm^{-1} [s, ν(SiH)]; 1995 (vs), 1936 (vs) [ν(CO)].

[1] W. Noll, *Chemistry and Technology of Silicones*, VCH, Weinheim, **1968**.

[2] H. J. Holdt, G. Schott, E. Popowski, H. Kelling, *Z. Chem.* **1983**, *23*, 252. − L. Fabry, *Rev. Silicon, Germanium, Tin, Lead Compd.* **1985**, *4*, 349. − J. Ackermann, V. Demrath, *Chem. Unserer Zeit* **1989**, *23*, 86−99. − R. Murugawel, A. Voigt, M. G. Walawalkar, H. W. Roesky, *Chem. Rev.* **1996**, *96*, 2205−2236. − R. Murugawel, V. Chandraheskar, H. W. Roesky, *Acc. Chem. Res.* **1996**, *29*, 183−189. − P. D. Lickiss, *Adv. Inorg. Chem.* **1995**, *42*, 147−262.

[3] W. Ries, T. Albright, J. Silvestre, I. Bernal, W. Malisch, *Inorg. Chim. Acta* **1986**, *111*, 119−128.

[4] W. Adam, U. Azzena, F. Prechtl, K. Hindahl, W. Malisch, *Chem. Ber.* **1992**, *125*, 1409−1411. − S. Möller, O. Fey, W. Malisch, W. Seelbach, *J. Organomet. Chem.* **1996**, *507*, 239−244. − W. Malisch, R. Lankat, S. Schmitzer, J. Reising; *Inorg. Chem.* **1995**, *34*, 5701−5702. − W. Adam, R. Mello, R. Curci, *Angew. Chem.* **1990**, *102*, 916−917; *Angew. Chem. Int. Ed. Engl.* **1990**, *29*, 890−891. − W. Adam, A. K. Smerz, *Bull. Soc. Chim. Belg.* **1996**, *105*, 581−599.

[5] [5a] W. Malisch, H. Jehle, S. Möller, G. Thum, J. Reising, A. Gbureck, V. Nagel, C. Fickert, W. Kiefer, *Eur. J. Inorg. Chem.*, submitted ((I98123)). − [5b] B. Stadelmann, P. Lassacher, H. Stüger, E. Hengge, *J. Organomet. Chem.* **1994**, *482*, 201−206.

[6] R. B. King, K. H. Pannell, C. R. Bennett, M. Ishaq, *J. Organomet. Chem.* **1969**, *19*, 327. − W. Malisch, M. Kuhn, *Chem. Ber.* **1974**, *107*, 2835−2851. − W. Malisch, W. Ries, *Chem. Ber.* **1979**, *112*, 1304−1315.

[98125]

Transition Metal Substituted Phosphanes, Arsanes, and Stibanes, LXII[◇]

Insertion of Diazoacetic Ester into the P–H Bond of the Cationic Primary and Secondary Phosphane-Substituted Iron Complexes $[Cp(OC)_2Fe–P(Ph)(R)H]^+$ (R = Ph, Me) and $[(R'C_5H_4)(OC)_2Fe–P(R)H_2]^+$ [R = *t*Bu, Ph, Mes; R′ = H, Neomenthyl (NM)]

Wolfgang Malisch*, Katharina Thirase, Franz-Josef Rehmann, Joachim Reising, and Norbert Gunzelmann

Institut für Anorganische Chemie der Universität Würzburg,
Am Hubland, D-97074 Würzburg, Germany
Fax: (internat.) + 49(0)931/888-4618
E-mail: Wolfgang.Malisch@mail.uni-wuerzburg.de

Received May 12, 1998

Keywords: (Phosphane)iron complexes / P–H function / Insertion / Diazoacetic ester / Iron / P ligands

Treatment of the cationic secondary (phosphane)iron complexes $[Cp(OC)_2Fe–P(Ph)(R)H]BF_4$ (R = Ph, Me) (**1a**, **b**) with diazoacetic ester (**2**) yields the novel complex salts $\{Cp(OC)_2Fe–P(Ph)(R)[N(H)–N=C(H)CO_2Et]\}BF_4$ (R = Ph, Me) (**3a**, **b**) by insertion of the terminal nitrogen atom of **2** into the P–H bond of **1a**, **b**. Reaction of the primary (phosphane)iron complexes $[(R'C_5H_4)(OC)_2Fe–P(R)H_2]BF_4$ [R = *t*Bu, Ph, Mes; R′ = H, neomenthyl (NM)] (**4a–e**) with **2** affords the complex salts $\{(R'C_5H_4)(OC)_2Fe–P(R)(H)[N(H)–N=C(H)CO_2Et]\}BF_4$ (**5a–d**) or $\{(R'C_5H_4)(OC)_2Fe–P(R)[N(H)–N=C(H)CO_2Et]_2\}BF_4$ (**6a–d**), depending on the molar ratio. The structures of **5c** and **6b** are proved by X-ray analysis.

Introduction

Our investigations into the reactivity of primary phosphane-substituted iron complexes of the type $[Cp(OC)_2Fe–P(R)H_2]BF_4$ (R = alkyl, aryl) towards organoisothiocyanates have revealed that in the presence of Et_3N the corresponding ferriophosphanes $Cp(CO)_2Fe–P(H)R$ are formed as intermediates. This will subsequently lead to the product of a P–H insertion[2] or a combination of P–H insertion and [2+3] cycloaddition[1]. This result clearly contrasts with the reactivity of ferriodiorganophosphanes $Cp(OC)_2Fe–PR_2$ which in all cases were found to form the [2+3] cycloadducts $Cp(OC)Fe–PR_2–C(S)–N(R')–C^a(=O)(Fe–C^a)$[3a] with the heterocumulenes. A comparable reaction was observed with electron-deficient alkynes[3b][3c][3d][3e].

Now we have utilized this synthetic strategy for functionalization of phosphane ligands by transformation of metal-coordinated primary and secondary phosphanes with diazoacetic ester.

Results

Preferentially, the complex salts $\{Cp(OC)_2[H(R)(R')P]Fe\}BF_4$ (R = H, Me, Ph; R′ = *t*Bu, Ph, Mes) were used, which feature a simple structure and are easily accessible by thermal carbon monoxide/phosphane exchange from the cation $[Cp(OC)_3Fe]^+$.

Reaction of **1a**, **b** with diazoacetic ester (**2**) in dichloromethane at room temperature yields the insertion products **3a**, **b** after 24 h which are obtained as yellow, microcrystalline powders in high yields (87%) after precipitation with ether [Eq. (1)].

The cation of **3a**, **b** bears a functional phosphane ligand characterized by a hydrazone unit formed by insertion of the terminal nitrogen atom of **2** into the P–H bond of **1a**, **b**. The constitution of **3a**, **b** is deduced from the NMR spectroscopic data that show a doublet resonance for the N–H proton [δ = 8.61 (**3a**)/8.43 (**3b**); ^2J(PNH) = 16.7 (**3a**)/22.0 Hz (**3b**)] and a singlet resonance for the CH(=N) proton [δ = 7.35 (**3a**)/7.31 (**3b**)] in the ^{1}H-NMR spectra. The insertion of **2** causes a significant low-field shift of the ^{31}P-NMR resonance from δ = 31.8/10.8 for the secondary phosphane in the starting material **1a**, **b** to δ = 114.1/108.0 for the phosphanylhydrazone in the product **3a**, **b**. The IR spectra show the expected $\nu(CO)_{sym}$ and $\nu(CO)_{asym}$ absorptions at approximately 2050 and 2020 cm^{-1}.

In contrast to the insertion reaction of the metal-coordinated secondary phosphanes $\{Cp(OC)_2Fe–PR_2H\}^+$ (R = alkyl, aryl) with isothiocyanates which requires a base (e.g. Et_3N)[3a] the insertion of diazoacetic ester according to Eq. (1) proceeds without an auxiliary base. Since metallodiorganophosphanes, formed by deprotonation of secondary cationic phosphane complexes, have been shown to be essential intermediates for the insertion process, diazoacetic ester itself must act as the base. In accordance with this experience a reaction sequence for the formation of **3a**, **b** appears reasonable in which primarily the cation of **1a**, **b** is

[◇] Part LXI: Ref.[1].

 © WILEY-VCH Verlag GmbH, D-69451 Weinheim, 1998 1434–1948/98/1111–1589 $ 17.50+.50/0

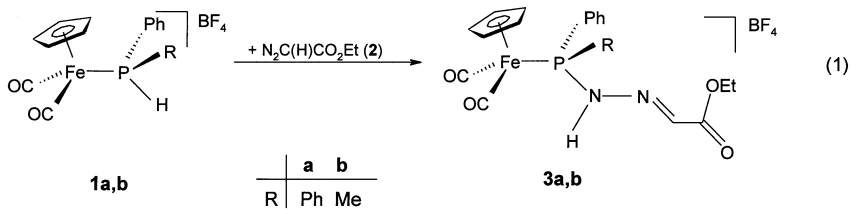

deprotonated by diazoacetic ester to generate the phosphido species **A** followed by coupling between the terminal nitrogen atom and the phosphido phosphorus atom leading to intermediate **B** (Scheme 1). Protonation at the *P*-bound nitrogen atom gives **3a**, **b** under release of diazoacetic ester.

An insertion into one or both of the P−H bonds can be expected in the reaction of **2** with coordinated primary phosphanes. Especially the monoinsertion is of interest as it generates a stereogenic functionalized phosphorus atom. From this point of view it appears attractive to study the possibility of its asymmetrically induced formation using a chirally modified Cp ligand. In a first approach we introduced the easily accessible neomenthyl cyclopentadienyl unit[4][5].

Reaction of the primary (phosphane)iron complexes **4a−d** with **2** in acetonitrile at room temperature in a molar ratio of 1:1 yields the phosphanylhydrazone complexes **5a−d** within 2 d [Eq. (2a)]. The analogous reaction of **4a−c**, **e** with two equivalents of **2** leads to the formation of the metallophosphanyldihydrazone species **6a−d** by insertion of **2** into both the P−H bonds [Eq. (2b)]. Complexes **5a−d** and **6a−d** are obtained in good yields as yellow, microcrystalline powders after precipitation with ether from the concentrated reaction mixture.

The monoinsertion products **5a−d** are of particular interest, since they do not only contain a chiral phosphorus atom but also offer the possibility of further derivatization of the R_2P-H moiety. The NMC_5H_4 substituted compound **5d** is obtained as a 1:1 mixture of two epimers, which means that the chiral ring ligand has no effect on the stereochemical course of the coupling process[6]. Compound **5d**, however, should offer the possibility of separating the stereoisomers with (*R*) and (*S*) configuration at the phosphorus atom by chromatography[6][7].

In accordance with the postulated constitution the ^{1}H-NMR spectra of **5a−d/6a−d** show the resonances of the NH and CH protons in the typical ranges of δ = 8.20−8.98 (N−H) and 7.02−8.47 (C−H). The resonance of the *P*-bonded hydrogen atom in **5a−d** at δ = 7.68−8.59 shows a doublet splitting with a P−H coupling constant of about 400 Hz. The ^{31}P-NMR resonances of the secondary phosphane ligands in **5a−d** at δ = 64.9−113.8 exhibit a significant shift of about 120 ppm to lower field in relation to the starting materials **4a−d**. Relative to the secondary phosphane in **5a−c**, the tertiary phosphane in **6a−c** displays an additional shift of about 50 ppm (**5/6a**) or 80 ppm (**5/6b**, **c**).

The structures of the insertion products **5a−d/6a−d** deduced from the spectroscopic data are confirmed by X-ray analysis of **5c** und **6b**, demonstrating an exclusive formation of the (*E*) isomer at to the C=N double bond.

Molecular Structures of 5c and 6b

The complex salts **5c** (Figure 1) and **6b** (Figure 2) have an octahedral arrangement of the ligands CO, Cp, and P(H)(Mes)[N(H)−N=C(H)−C(O)OEt] or P(Ph)[N(H)−N=C(H)−C(O)OEt]$_2$, respectively, indicated by the bond angles of C1−Fe−C2 92.0(5)° (**5c**)/93.4(3)° (**6b**), C1−Fe−P 93.9(5)° (**5c**)/91.4(2)° (**6b**), and C2−Fe−P 95.0(8)° (**5c**)/95.0(2)° (**6b**). The Fe−C(O) distances of 1.757(12) Å (Fe−C1)/1.769(11) Å (Fe−C2) (**5c**), 1.753(7) Å (Fe−C1)/1.785(6) Å (Fe−C2) (**6b**) as well as the Fe−P distances [*d*(Fe−P) = 2.208(17) Å (**5c**)/2.1909(15) Å (**6b**)] are in good agreement with known values[1][2]. The substituents at the phosphorus atom show a nearly perfectly staggered conformation of ligands at the iron atom. In **5c** the bulky mesityl unit adopts the *anti* position to the Cp ligand [Cp(Z)−Fe−P−C10 173.47°], while in compound **6b** this position is occupied by a hydrazone unit [Cp(Z)−Fe−P−N1 167.64°]. As a consequence the other two substituents in both molecules are oriented *trans* to the CO ligands [**5c**: H−P−Fe−C2 165.0(8)°, N1−P−Fe−C1−173.1(5)°; **6b**: C10−P−Fe−C2 175.7(3)°, N3−P−Fe−C1 −159.4(3)°].

The phosphorus atoms exhibit a distorted tetrahedral conformation with the largest bond angles including the metal center [**5c**: N1−P−Fe 112.2(3)°, H−P−Fe 116.3(35)°, C10−P−Fe 118.7(2)°; **6b** N3−P−Fe 112.9(2)°, N1−P−Fe 113.8(2)°, C10−P−Fe 115.5(2)°]. The P−H distance of 1.39(8) Å is in good agreement with the expected values {[Cp(OC)(Me$_3$P)Fe−P(H)(*t*Bu)Me]I: 1.40(5) Å[8]; PH_3: 1.439 Å[9]}. The hydrazone units are characterized by N−N single bonds for N1−N2[10] [1.374(9) Å (**5c**)/1.368(6)

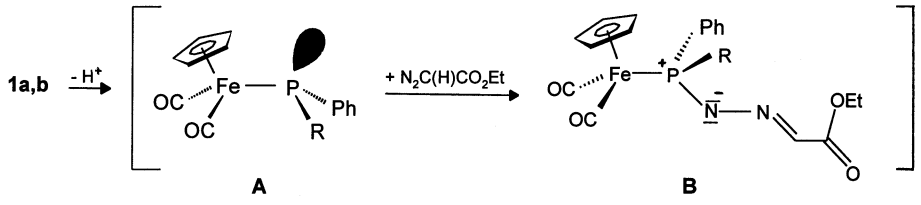

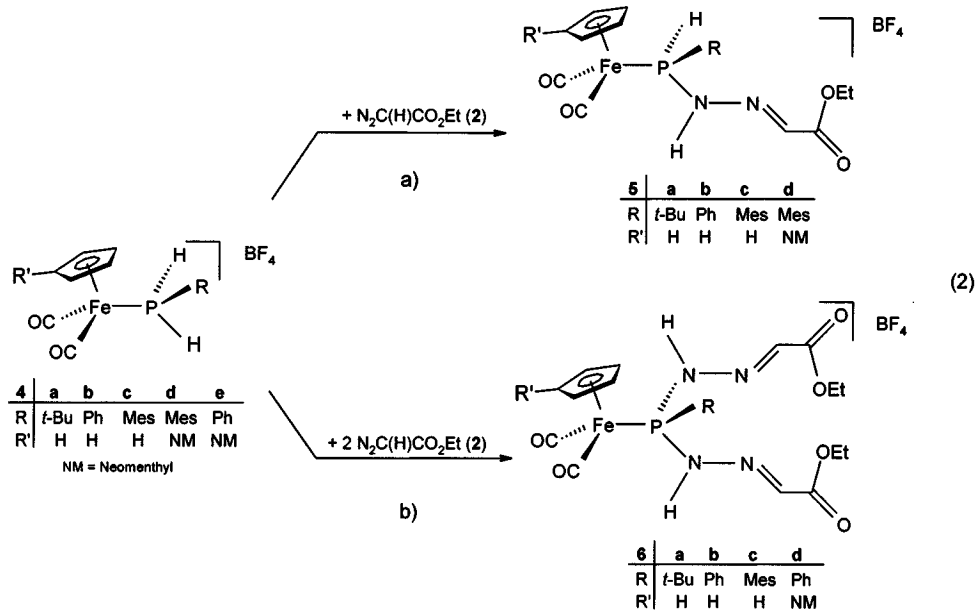

4	a	b	c	d	e
R	*t*-Bu	Ph	Mes	Mes	Ph
R'	H	H	H	NM	NM

5	a	b	c	d
R	*t*-Bu	Ph	Mes	Mes
R'	H	H	H	NM

6	a	b	c	d
R	*t*-Bu	Ph	Mes	Ph
R'	H	H	H	NM

Figure 1. ORTEP plot of $Cp(OC)_2Fe-P(H)(Mes)[N(H)-N=C(H)-CO_2Et]BF_4$ (**5c**)[a]

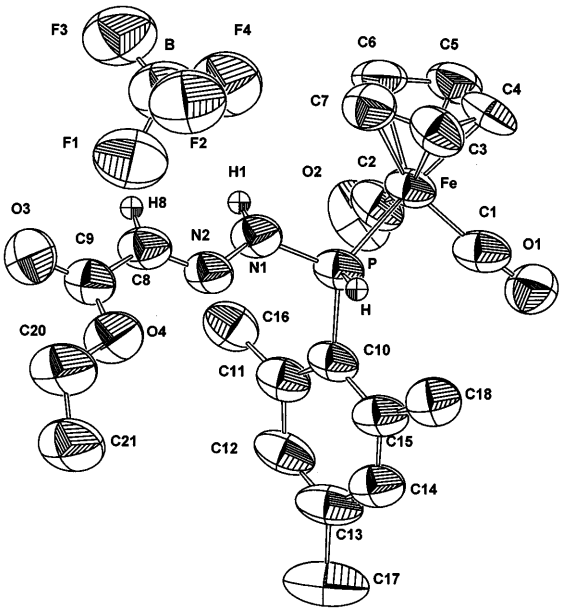

[a] Selected bond lengths [Å], bond and torsion angles [°]: Fe−P 2.208(17), Fe−C1 1.757(12), Fe−C2 1.769(11), P−N1 1.647(8), P−C10 1.807(8), N1−N2 1.374(9), N2−C8 1.254(11), P−H 1.39(8), N1−H1 0.85(8); C1−Fe−C2 92.0(5), C1−Fe−P 93.9(5), C2−Fe−P 95.0(8), N1−P−C10 109.8(4), N1−P−Fe 112.2(3), N2−N1−P 120.4(6), C8−N2−N1 117.2(7), N2−C8−C9 121.6(9), N2−C8−H8 119.2(5), C9−C8−H8 119.2(6), N1−P−H 99.9(34), Fe−P−H 116.3(35), N2−N1−H1 117.6(59), P−N1−H1 120.8(58); C1−Fe−P−N1 −173.1(5), C2−Fe−P−N1 −80.8(5), N2−C8−C9−O3 177.8(9), N1−P−C10−C15 −137.5, Fe−P−C10−C15 91.3(6).

Figure 2. ORTEP plot of $\{Cp(OC)_2Fe-P(Ph)[N(H)-N=C(H)-CO_2Et]_2\}BF_4$ (**6b**)[a]

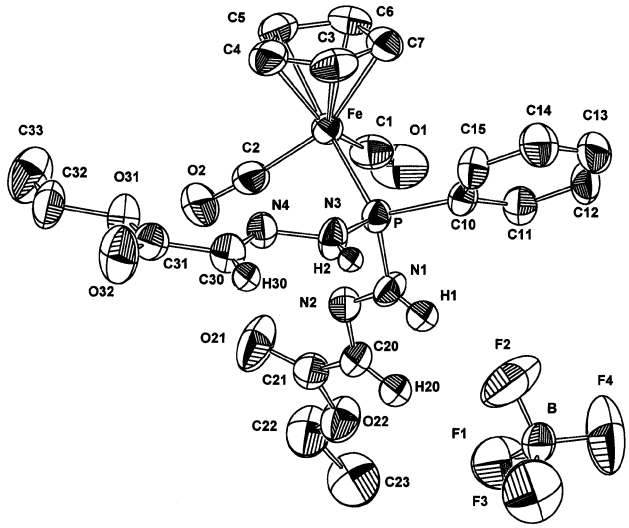

[a] Selected bond lengths [Å], bond and torsion angles [°]: Fe−C1 1.753(7), Fe−C2 1.785(6), Fe−P 2.1909(15), P−N3 1.667(4), P−N1 1.670(5), P−C10 1.796(5), N1−N2 1.368(6), N2−C20 1.263(6), N3−N4 1.367(5), N4−C30 1.256(6); C1−Fe−C2 93.4(3), C1−Fe−P 91.4(2), C2−Fe−P 95.0(2), N3−P−N1 108.9(2), N3−P−Fe 112.9(2), N1−P−Fe 113.8(2), C10−P−Fe 115.5(2), C20−N2−N1 117.8(4), N4−N3−P 118.0(4), C30−N4−N3 118.5(4); N3−P−N1−N2 96.1(4), C10−P−N1−N2 −155.4(4), P−N1−N2−C20 180.0(4), N1−P−N3−N4 −96.5(4), C10−P−N3−N4 156.2(4), P−N3−N4−C30 173.9(4), N2−C20−C21−O22 163.5(5), N4−C30−C31−O32 −170.2(6).

Å (**6b**)] and N3−N4 (**6b**) [1.367(5) Å], and values typical of a C=N double bond[11] for N2−C8 (**5c**) [1.254(11) Å], N2−C20 (**6b**) [1.263(6) Å] and N4−C30 (**6b**) [1.256(6) Å]. The structural units N(H)−N=C(H)C−(O)OEt are nearly planar [N−N−C−C: −178.5(8)° (**5c**), −174.5(4)° and 176.7(5)° (**6b**)] and exhibit (*E*) configuration; the *P*-bound nitrogen atoms N1 (**5c**, **6b**) and N3 (**6b**) as well as the sp^2-hybridized C=N carbon atoms C8 (**5c**) and C20, C30 (**6c**) show nearly ideal planarity (sum of angles: 358.8°−360.0°).

We have demonstrated that diazoacetic ester is a reagent which easily inserts into P−H bonds of metal-coordinated primary and secondary phosphanes. This procedure can be used to build up novel phosphane ligands at the metal center. Controlled monoinsertion in the case of primary

phosphanes leads to chiral secondary phosphane ligands which possess a high synthetic potential because of the P−H moiety which is useful for further derivatization.

Support of this research by the *Deutsche Forschungsgemeinschaft* (Sonderforschungsbereich 347, "*Selektive Reaktionen Metall-aktivierter Moleküle*") and the *Fonds der Chemischen Industrie* is gratefully acknowledged.

Experimental Section

General: All manipulations were performed under purified nitrogen with standard Schlenk techniques. Solvents were rigorously dried with an appropiate drying agent and distilled under nitrogen prior to use. − ^{1}H-, ^{13}C-, and ^{31}P-NMR spectra were obtained with a Bruker AMX 400 spectrometer. − Infrared spectra were recorded in solution with a Perkin-Elmer 283 grating spectrometer in NaCl cells with 0.1 mm path lengths. − Melting points were determined by Differential Thermo Analysis (DTA) with a Du Pont Thermal Analysis System 9000. − Elemental analyses were performed in the laboratories of the *Institut für Anorganische Chemie*. − $[Cp(OC)_3Fe]BF_4$[12] and $[(NMC_5H_4)(OC)_3Fe]BF_4$[6] were prepared according to literature procedures. $N_2C(H)CO_2Et$ was obtained commercially and used without further purification.

1) *General Procedure for the Preparation of {Cp(OC)$_2$[H(R)(Ph)P]Fe}BF$_4$ [R = Ph, Me (**1a**, **b**)], {Cp(OC)$_2$[H$_2$(R)P]Fe}BF$_4$ [R = tBu, Ph, Mes (**4a**−**c**)] and {(NMC$_5$H$_4$)(OC)$_2$[H$_2$(R)P]Fe}BF$_4$ [R = Mes, Ph (**4d**, **e**)]:* A cooled (0°C) solution of 3.50 mmol of $[Cp(OC)_3Fe]BF_4$ or $[(NMC_5H_4)(OC)_3Fe]BF_4$ in 20 ml of acetonitrile was combined with an equimolar amount of the appropriate phosphanes R(Ph)PH (R = Me, Ph) or RPH_2 (R = *t*Bu, Ph, Mes). The mixture was stirred for 10 h at 60°C and then reduced in vacuo to a volume of 8 ml. Precipitation of the product was achieved by addition of 10 ml of ether. The product was separated by filtration, washed with 10 ml of ether and dried in vacuo. − Yield > 85%. − Yellow to orange microcrystalline powders. − M.p.: **1a**: 123°C; **1b**: 143°C; **4a**: 177−179°C (dec.); **4b**: 178°C (dec.); **4c**: 137°C (dec.); **4d**: 76°C; **4e**: 78°C.

1a: ^{1}H NMR ([D$_3$]acetonitrile, 400.1 MHz): δ = 8.02−7.62 (m, 10 H, H_5C_6); 7.45 [d, ^1J(PH) = 418 Hz, 1 H, H−P]; 5.50 [d, ^3J(PFeCH) = 2.0 Hz, 5 H, H_5C_5]. − ^{13}C NMR ([D$_3$]acetonitrile, 100.6 MHz): δ = 209.8 [d, ^2J(PFeC) = 24.4 Hz, C=O]; 133.3 (s, C-4); 133.2 [d, ^2J(PCC) = 10.7 Hz, C-2/6]; 130.8 [d, ^3J(PCCC) = 11.3 Hz, C-3/5]; 129.9 [d, ^1J(PC) = 54.1 Hz, C-1]; 89.1 (s, C_5H_5). − ^{31}P NMR ([D$_3$]acetonitrile, 162.0 MHz): δ = 31.8. − IR (acetonitrile): ν(PH) = 2302 (w); ν(CO) = 2054 (s); 2016 (s) cm^{-1}. − $C_{19}H_{16}BF_4FeO_2P$ (449.96): calcd. C 50.72, H 3.58; found C 50.56, H 3.38.

1b: ^{1}H NMR ([D$_3$]acetonitrile, 400.1 MHz): δ = 7.80−7.55 (m, 5 H, H_5C_6); 6.50 [dq, ^1J(PH) = 372 Hz, ^3J(HPCH) = 6.18 Hz, 1 H, H−P]; 5.45 [d, ^3J(PFeCH) = 2.1 Hz, 5 H, H_5C_5]; 2.11 [dd, ^2J(HCP) = 12.1 Hz, ^3J(HCPH) = 6.2 Hz, 3 H, H_3CP]. − ^{31}P NMR ([D$_3$]acetonitrile, 162.0 MHz): δ = 10.8. − IR (acetonitrile): ν(CO) = 2054 (s); 2010 (s) cm^{-1}. − $C_{14}H_{14}BF_4FeO_2P$ (387.89): calcd. C 43.35, H 3.64; found C 43.90, H 3.71.

4a: ^{1}H NMR ([D$_3$]acetonitrile, 400.1 MHz): δ = 5.78 (s, 5 H, H_5C_5); 5.12 [d, ^1J(PH) = 384.0 Hz, 2 H, H−P]; 1.27 [d, ^3J(PCCH) = 21.3 Hz, 9 H, $(H_3C)_3C$]. − ^{13}C NMR ([D$_3$]acetonitrile, 100.6 MHz): δ = 209.5 [d, ^2J(PFeC) = 24.1 Hz, C=O]; 88.1 (s, C_5H_5); 31.7 [d, ^1J(PC) = 31.5 Hz, $C(CH_3)_3$]; 29.4 [d, ^2J(PCC) = 3.7 Hz, $C(CH_3)_3$]. − ^{31}P NMR ([D$_3$]acetonitrile, 162.0 MHz): δ = 3.4. − IR (acetonitrile): ν(PH) = 2390 (w); ν(CO) = 2057 (vs); 2009 (vs) cm^{-1}. − $C_{11}H_{16}BF_4FeO_2P$ (353.87): calcd. C 37.33, H 4.56; found C 37.41, H 4.57.

4b: ^{1}H NMR ([D$_3$]acetonitrile, 400.1 MHz): δ = 7.71−7.52 (m, 5 H, H_5C_6); 6.16 [d, ^1J(PH) = 407.8 Hz, 2 H, H−P]; 5.42 [d, ^3J(PFeCH) = 2.1 Hz, 5 H, H_5C_5]. − ^{13}C NMR ([D$_3$]acetonitrile, 100.6 MHz): δ = 209.0 [d, ^2J(PFeC) = 24.9 Hz, C=O]; 133.5 [d, ^2J(PCC) = 10.1 Hz, C-2/6]; 132.1 [d, ^4J(PCCCC) = 2.9 Hz, C-4]; 130.3 [d, ^3J(PCCC) = 11.5 Hz, C-3/5]; 124.0 [d, ^1J(PC) = 57.2 Hz, C-1]; 88.5 (s, C_5H_5). − ^{31}P NMR ([D$_3$]acetonitrile, 162.0 MHz): δ = −29.5. − IR (acetonitrile): ν(PH) = 2398 (w); ν(CO) = 2060 (vs); 2015 (vs) cm^{-1}. − $C_{13}H_{12}BF_4FeO_2P$ (373.86): calcd. C 41.76, H 3.24; found C 41.53, H 2.93.

4c: ^{1}H NMR ([D$_3$]acetonitrile, 400.1 MHz): δ = 7.04 (s, 2 H, H−C); 6.09 [d, ^1J(PH) = 400.4 Hz, 2 H, H−P]; 5.49 [d, ^3J(PFeCH) = 2.3 Hz, 5 H, H_5C_5]; 2.43 (s, 6 H, 2-H_3C); 2.27 (s, 3 H, 4-H_3C). − ^{13}C NMR ([D$_3$]acetonitrile, 100.6 MHz): δ = 209.3 [d, ^2J(PFeC) = 24.1 Hz, C=O]; 143.3 [d, ^4J(PCCCC) = 1.5 Hz, C-4]; 141.6 [d, ^2J(PCC) = 8.0 Hz, C-2/6]; 141.6 [d, ^3J(PCCC) = 9.0 Hz, C-3/5]; 126.4 [d, ^1J(PC) = 58.4 Hz, C-1]; 88.4 (s, C_5H_5); 21.6 [d, ^3J(PCCC) = 9.7 Hz, 2/6-CH_3]; 20.9 (s, 4-CH_3).−^{31}P NMR ([D$_3$]acetonitrile, 162.0 MHz): δ = −61.2. − ^{19}F NMR ([D$_3$]acetonitrile, 376.5 MHz): δ = −150.2. − IR (acetonitrile): ν(PH) = 2397 (w); ν(CO) = 2058 (vs), 2015 (vs) cm^{-1}. − $C_{16}H_{18}BF_4FeO_2P$ (415.94): calcd. C 46.20, H 4.36; found C 46.28, H 4.18.

4d: ^{1}H NMR (400.1 MHz, $CDCl_3$): δ = 6.90 [s, 2 H, H−C]; 6.22 [s, ^1J(HP) = 407.5 Hz, 1 H, H_2P]; 6.20 [s, ^1J(HP) = 405.8 Hz, 1 H, H_2P]; 5.63/5.54/5.48/5.44 (s, 4 H, H_4C_5); 2.87 (s, 1 H, 6-H, $H_{19}C_{10}$); 2.40 (s, 6 H, *o*-H_3C); 2.24 (s, 3 H, *p*-H_3C); 0.90 (d, ^3J(HCCH) = 5.8 Hz, 3 H, H_3C); 0.85 [d, ^3J(HCCH) = 5.9 Hz, 3 H, H_3C]: 0.74 [d, ^3J(HCCH) = 5.9 Hz, 3 H, H_3C]; 1.86−0.73 (m, 9 H, $H_{11}C_{10}$). − ^{13}C NMR (100.6 MHz, $CDCl_3$): δ = 209.13 [d, ^2J(CFeP) = 23.7 Hz, CO]; 142.23 [d, ^3J(CCCP) = 2.1 Hz, C-4, $C_6H_2(CH_3)_3$]; 140.69 [d, ^3J(CCCP) = 8.6 Hz, C-3, C-5, $C_6H_2(CH_3)_3$]; 130.12 [d, ^2J(CCP) = 9.00 Hz, C-2, C-6, $C_6H_2(CH_3)_3$]; 117.39 [d, ^1J(CP) = 58.2 Hz, C-1, $C_6H_2(CH_3)_3$]; 111.89 (s, C-1, C_5H_4); 90.44/90.17/88.10/84.56 (s, C-2, C-3, C-4, C-5, C_5H_4); 47.88 (s, C-6, $C_{10}H_{19}$); 43.72 (s, C-11, $C_{10}H_{19}$); 35.41 (s, C-7, $C_{10}H_{19}$); 34.78 (s, C-9, $C_{10}H_{19}$); 29.46 (s, C-10, $C_{10}H_{19}$); 27.91 (s, C-12, $C_{10}H_{19}$); 24.15 (s, C-8, $C_{10}H_{19}$); 22.27/21.80/21.70/21.60/21.13/20.51 (s, C-13, C-14, C-15, $C_{10}H_{19}$, *o*-CH_3, *p*-CH_3). − ^{31}P NMR (162.0 MHz, $CDCl_3$): δ = −60.24. − IR (acetonitrile): ν(CO) = 2049 (s), 2005 (s) cm^{-1}. − $C_{26}H_{36}BF_4FeO_2P$ (554.20): calcd. C 56.35, H 6.55; found C 56.51, H 6.74.

4e: ^{1}H NMR (400.1 MHz, CD_3CN): δ = 7.80−7.62 (m, 5 H, H_5C_6); 6.25 [d, ^1J(HP) = 404.00 Hz, 2 H, H_2P]; 5.79/5.49/5.33/5.22 (s, 4 H, H_4C_5NM); 2.98 (s, 1 H, 6-H, $H_{19}C_{10}$); 0.95 [d, ^3J(HCCH) = 6.4 Hz, 3 H, H_3C]; 0.91 [d, ^3J(HCCH) = 6.2 Hz, 3 H, H_3C]; 0.81 [d, ^3J(HCCH) = 6.5 Hz, 3 H, H_3C]; 1.94−0.84 (m, 9 H, H_9C_7). − ^{13}C NMR (100.6 MHz, CD_3CN): δ = 208.93 [d, ^2J(CFeP) = 24.7 Hz, CO]; 208.90 [d, ^2J(CFeP) = 24.7 Hz, CO]; 123.27 [d, ^2J(CP) = 57.2 Hz, C-1, CP]; 132.78 [d, ^2J(CCP) = 10.5 Hz, C-2, C_6H_5P]; 132.39 [d, ^3J(CCCP) = 3.3 Hz, C-3, C-6, C_6H_5P]; 129.97 [d, ^2J(CCP) = 12.1 Hz, C-6, C_6H_5P]; 112.97 (s, C-1, C_5H_4); 90.85/90.76/96.67/84.11 (s, C-2, C-3, C-4, C-5, C_6H_4); 47.83 (s, C-6, $C_{10}H_{19}$); 43.34 (s, C-11, $C_{10}H_{19}$); 35.27 (s, C-7, $C_{10}H_{19}$); 34.89 (s, C-9, $C_{10}H_{19}$); 29.54 (s, C-10, $C_{10}H_{19}$); 27.76 (s, C-12, $C_{10}H_{19}$); 24.13 (s, C-8, $C_{10}H_{19}$); 21.82/21.40/20.10 (s, C-13, C-14, C-15, CH_3). − ^{31}P NMR (162.0 MHz, CD_3CN): δ = −28.87. − IR (acetonitrile): ν(CO) = 2052 (s), 2007 (s) cm^{-1}. − $C_{23}H_{30}BF_4FeO_2P$ (512.11): calcd. C 53.94, H 5.90; found C 54.06, H 6.03.

2) *Dicarbonyl(η⁵-cyclopentadienyl)[(ethoxycarbonylmethylenehydrazino)diphenylphosphane]iron(II) Tetrafluoroborate* (**3a**): 99 mg (0.87 mmol) of $N_2C(H)CO_2Et$ (**2**) was added to a solution of 300 mg (0.67 mmol) of $\{Cp(OC)_2[H(Ph)_2P]Fe\}BF_4$ (**1a**) in 11 ml of dichloromethane. After stirring for 24 h at room temperature, the reaction mixture was reduced in vacuo to a volume of 2 ml. Addition of 20 ml of ether afforded precipitation of **3a** which was separated by filtration, washed with three portions of 5 ml of ether, and dried in vacuo. − Yield 327 mg (87%). − Yellow microcrystalline powder. − M.p. 170°C (dec.). − ^{1}H NMR ([D$_3$]acetonitrile, 400.1 MHz): δ = 8.61 [d, ^2J(PNH) = 16.7 Hz, 1 H, HN], 7.62−7.46 (m, 10 H, H_5C_6), 7.35 (s, 1 H, HC), 5.25 [d, ^3J(PFeCH) = 1.4 Hz, 5 H, H_5C_5], 4.14 [q, ^3J(HCCH) = 7.1 Hz, 2 H, H_2C], 1.19 [t, ^3J(HCCH) = 7.1 Hz, 3 H, H_3C]. − ^{13}C{^{1}H} NMR ([D$_3$]acetonitrile, 100.6 MHz): δ = 208.4 [d, ^2J(PFeC) = 26.6 Hz, CO], 162.2 (s, CO_2), 136.0−129.2 (m, C_6H_5, C=N), 88.3 (s, C_5H_5), 60.8 (s, CH_2), 13.1 (s, CH_3). − ^{31}P{^{1}H} NMR ([D$_3$]acetonitrile, 162.0 MHz): δ = 114.1 (s). − IR (acetonitrile): ν(CO) = 2055 (s), 2009 (s); ν(C=O) = 1740 (s) cm^{-1}. − $C_{23}H_{22}BF_4FeN_2O_4P$ (564.06): calcd. C 48.98, H 3.93, N 4.97; found C 48.60, H 3.70, N 4.61.

3) *Dicarbonyl(η⁵-cyclopentadienyl)[(ethoxycarbonylmethylenehydrazino)(methyl)(phenyl)phosphane]iron(II) Tetrafluoroborate* (**3b**): Prepared as described for **3a** from 250 mg (0.65 mmol) of $\{Cp(OC)_2[H(Me)(Ph)P]Fe\}BF_4$ (**1b**) and 109 mg (0.96 mmol) of $N_2C(H)CO_2Et$ (**2**) in 10 ml of dichloromethane. − Yield 282 mg (87%). − Yellow microcrystalline powder. − M.p. 98°C (dec.). − ^{1}H NMR ([D$_3$]acetonitrile, 400.1 MHz): δ = 8.43 [d, ^2J(PNH) = 22.0 Hz, 1 H, HN], 7.52−7.39 (m, 5 H, H_5C_6), 7.31 (s, 1 H, HC), 5.28 [d, ^3J(PFeCH) = 1.3 Hz, 5 H, H_5C_5], 4.14 [q, ^3J(HCCH) = 7.2 Hz, 2 H, H_2C], 2.20 [d, ^2J(PCH) = 10.1 Hz, 3 H, H_3CP], 1.19 [t, ^3J(HCCH) = 7.2 Hz, 3 H, H_3C]. − ^{13}C{^{1}H} NMR ([D$_3$]acetonitrile, 100.6 MHz): δ = 208.1 (d, ^2J(PFeC) = 27.6 Hz, CO), 162.2 (s, CO_2), 136.2−128.7 (m, C_6H_5, C=N), 87.7 (s, C_5H_5), 60.7 (s, CH_2), 19.2 [d, ^1J(PC) = 39.2 Hz, CH_3P], 13.1 (s, CH_3). − ^{31}P{^{1}H} NMR ([D$_3$]acetonitrile, 162.0 MHz): δ = 108.0 (s). − IR (acetonitrile): ν(CO) = 2045 (s), 2000 (vs); ν(C=O) = 1713 (s) cm^{-1}. − $C_{18}H_{20}BF_4FeN_2O_4P$ (501.99): calcd. C 43.06, H 4.02, N 5.58; found C 42.83, H 3.88, N 4.22.

4) *{tert-Butyl[(E)-ethoxycarbonylmethylenehydrazino]phosphane}dicarbonyl(η⁵-cyclopentadienyl)iron(II) Tetrafluoroborate* (**5a**): 60 mg (0.53 mmol) of $N_2C(H)CO_2Et$ (**2**) was added to a solution of 200 mg (0.57 mmol) of $\{Cp(OC)_2[H_2(tBu)P]Fe\}BF_4$ (**4a**) in 10 ml of acetonitrile. After stirring for 48 h at room temperature, the solution was reduced in vacuo to a volume of 1 ml. Addition of 3 ml of ether afforded precipitation of **5a**, which was separated by filtration, washed with three portions of 5 ml of ether and dried in vacuo. − Yield 198 mg (74%). − Beige microcrystalline powder. − M.p. 113°C (dec.). − ^{1}H NMR ([D$_3$]acetonitrile, 400.1 MHz): δ = 7.68 [d, ^2J(PNH) = 19.8 Hz, 1 H, HN], 7.15 (s, 1 H, CH), 6.76 [d, ^1J(PH) = 411.0 Hz, 1 H, HP], 5.51 [d, ^3J(PFeCH) = 1.9 Hz, 5 H, H_5C_5], 4.26−4.17 (m, 2 H, H_2C), 1.39 [d, ^3J(PCCH) = 18.4 Hz, 9 H, $(H_3C)_3C$], 1.31 (m, 3 H, H_3C). − ^{13}C{^{1}H} NMR ([D$_3$]acetonitrile, 100.6 MHz): δ = 208.4 [d, ^2J(PFeC) = 24.1 Hz, CO], 207.9 [d, ^2J(PFeC) = 23.1 Hz, CO], 162.3 (s, CO_2), 134.4 [d, ^3J(PNNC) = 14.1 Hz, C=N], 86.1 (s, C_5H_5), 60.3 (s, CH_2), 38.2 [d, ^1J(PC) = 27.2 Hz, CP], 28.7 [d, ^2J(PCC) = 3.0 Hz, $(CH_3)_3C$], 12.9 (s, CH_3). − ^{31}P{^{1}H} NMR ([D$_3$]acetonitrile, 162.0 MHz): δ = 113.8 (s). − ^{19}F NMR ([D$_3$]acetonitrile, 376.5 MHz): δ = −149.9. − IR (acetonitrile): ν(CO) = 2055 (s), 2013 (s); ν(C=O) = 1713 (m) cm^{-1}. − $C_{15}H_{22}BF_4FeN_2O_4P$ (467.97): calcd. C 38.50, H 4.74, N 5.99; found C 39.01, H 4.92, N 6.21.

5) *Dicarbonyl(η⁵-cyclopentadienyl){[(E)-ethoxycarbonylmethylenehydrazino](phenyl)phosphane}iron(II) Tetrafluoroborate* (**5b**): Prepared as described for **5a** from 200 mg (0.53 mmol) of $\{Cp(OC)_2[H_2(Ph)P]Fe\}BF_4$ (**4b**) and 57 mg (0.50 mmol) of $N_2C(H)CO_2Et$ (**2**) in 10 ml of acetonitrile. − Yield 191 mg (74%). − Yellow microcrystalline powder. − M.p. 106°C (dec.). − ^{1}H NMR ([D$_3$]acetonitrile, 400.1 MHz): δ = 8.59 [d, ^1J(PH) = 404.0 Hz, 1 H, HP], 8.47 [d, ^2J(PNH) = 24.4 Hz, 1 H, HN], 7.75−7.22 (m, 5 H, H_5C_6), 7.19 (s, 1 H, CH), 5.27 [d, ^3J(PFeCH) = 1.3 Hz, 5 H, H_5C_5], 4.20 [q, ^3J(HCCH) = 7.2 Hz, 2 H, H_2C], 1.27 [t, ^3J(HCCH) = 7.2 Hz, 3 H, H_3C]. − ^{13}C{^{1}H} NMR ([D$_3$]acetonitrile, 100.6 MHz): δ = 209.3 [d, ^2J(PFeC) = 29.6 Hz, CO], 208.7 [d, ^2J(PFeC) = 29.7 Hz, CO], 163.5 (s, CO_2), 137.5 [d, ^3J(PNNC) = 17.1 Hz, C=N], 133.5 [d, ^2J(PCC) = 10.1 Hz, C-2/6], 133.1 [d, ^4J(PCCCC) = 2.1 Hz, C-4], 131.6 [d, ^3J(PCCC) = 11.1 Hz, C-3/5], 129.4 [d, ^1J(PC) = 52.3 Hz, C-1], 88.6 (s, C_5H_5), 62.1 (s, CH_2), 14.4 (s, CH_3). − ^{31}P{^{1}H} NMR ([D$_3$]acetonitrile, 162.0 MHz): δ = 86.6 (s). − ^{19}F NMR ([D$_3$]acetonitrile, 376.5 MHz): δ = −150.7. − IR (acetonitrile): ν(CO) = 2058 (s), 2016 (s); ν(C=O) = 1716 (m) cm^{-1}. − $C_{17}H_{18}BF_4FeN_2O_4P$ (487.97): calcd. C 41.84, H 3.72, N 5.74; found C 41.92, H 3.79, N 5.81.

6) *Dicarbonyl(η⁵-cyclopentadienyl){[(E)-ethoxycarbonylmethylenehydrazino](2,4,6-trimethylphenyl)phosphane}iron(II) Tetrafluoroborate* (**5c**): Prepared as described for **5a** from 200 mg (0.48 mmol) of $\{Cp(OC)_2[H_2(Mes)P]Fe\}BF_4$ (**4c**) and 55 mg (0.47 mmol) of $N_2C(H)CO_2Et$ (**2**) in 10 ml of acetonitrile. − Yield 201 mg (79%). − Yellow microcrystalline powder. − M.p. 135°C (dec.). − ^{1}H NMR ([D$_3$]acetonitrile, 400.1 MHz): δ = 8.20 [d, ^2J(PNH) = 24.0 Hz, 1 H, HN], 8.19 [d, ^1J(PH) = 407.2 Hz, 1 H, HP], 7.26 (s, 1 H, HC), 7.03 [d, ^4J(PCCCH) = 4.4 Hz, 2 H, *meta*-H], 5.45 [d, ^3J(PFeCH) = 2.0 Hz, 5 H, H_5C_5], 4.20 [q, ^3J(HCCH) = 7.2 Hz, 2 H, H_2C], 2.41 (s, 6 H, 2/6-H_3C), 2.29 (s, 3 H, 4-H_3C), 1.25 [t, ^3J(HCCH) = 7.2 Hz, 3 H, H_3C]. − ^{13}C{^{1}H] NMR ([D$_3$]acetonitrile, 100.6 MHz): δ = 209.3 [d, ^2J(PFeC) = 25.2 Hz, CO], 208.4 [d, ^2J(PFeC) = 23.1 Hz, CO], 163.0 (s, CO_2), 144.1 [d, ^4J(PCCCC) = 1.1 Hz, C-4], 135.6 [d, ^3J(PNNC) = 16.1 Hz, C=N], 134.8 (s, C-3/5), 130.6 (s, C-2/6), 123.7 [d, ^1J(PC) = 59.4 Hz, C-1], 90.6 (s, C_5H_5), 61.6 (s, CH_2), 21.4 [d, ^3J(PCCC) = 8.8 Hz, 2/6-CH_3], 20.7 (s, 4-CH_3), 13.9 (s, CH_3).−^{31}P{^{1}H} NMR ([D$_3$]acetonitrile, 162.0 MHz): δ = 64.9 (s). − ^{19}F NMR ([D$_3$]acetonitrile, 376.5 MHz): δ = −151.1. − IR (acetonitrile): ν(CO) = 2059 (s), 2017 (s); ν(C=O) = 1736 (m) cm^{-1}. − $C_{20}H_{24}BF_4FeN_2O_4P$ (530.05): calcd. C 45.32, H 4.56, N 5.29; found C 45.57, H 4.71, N 5.45.

7) *Dicarbonyl{[(E)-ethoxycarbonylmethylenehydrazino](2,4,6-trimethylphenyl)phosphane}[η⁵-(c-2-isopropyl-t-5-methylcyclohexan-r-1-yl)cyclopentadienyl]iron(II)} Tetrafluoroborate* (**5d**): Prepared as described for **5a** from 150 mg (0.27 mmol) of $\{(NMC_5H_4)(OC)_2[H_2(Mes)P]Fe\}BF_4$ (**4d**) and 30 mg (0.27 mmol) of $N_2C(H)CO_2Et$ (**2**) in 10 ml of acetonitrile. − Yield 150 mg (83%). − Yellow microcrystalline powder. − M.p. 93°C (dec.). − ^{1}H NMR (400.1 MHz, [D$_3$]acetonitrile): δ = 8.35 [dd, ^1J(PH) = 434.2 Hz, ^3J(HPNH) = 4.4 Hz, 1 H, HP], 8.34 [dd, ^1J(PH) = 434.0 Hz, ^3J(HPNH) = 4.4 Hz, 1 H, HP], 8.21 [d, ^2J(PNH) = 24.8 Hz, 2 H, HN], 7.30 (s, 2 H, HC), 7.08 [d, ^4J(PCCCH) = 4.00 Hz, 4 H, *meta*-H], 5.80 (m, 1 H, H_4C_5), 5.75 (m, 1 H, H_4C_5), 5.55 (m, 1 H, H_4C_5), 5.49 (m, 1 H, H_4C_5), 5.28 (m, 2 H, H_4C_5), 5.24 (m, 1 H, H_4C_5), 5.20 (m, 1 H, H_4C_5), 4.25 [q, ^2J(HCCH) = 7.2 Hz, 2 H, H_2C-O], 4.24 [q, ^2J(HCCH) = 7.2 Hz, 2 H, H_2C-O], 3.04 (m, 1 H, 6-H, NMH_4C_5), 3.01 (m, 1 H, 6-H, NMH_4C_5), 2.47 [s, 12 H, 2-CH_3, 6-CH_3, $(H_3C)_3C_6H_2$], 2.34 [s, 6 H, 4-CH_3, $(H_3C)_3C_6H_2$], 1.86−1.84 (m, 2 H, 9/9′-H, NMH_4C_5), 1.84−1.82 (m, 2 H, 11/11′-H, NMH_4C_5), 1.73−1.71 (m, 2 H, 8/8′-H, NMH_4C_5), 1.69−1.66 (m, 2 H, 12-H, NMH_4C_5), 1.57−1.50 (m, 2 H, 11/11′-H, NMH_4C_5), 1.39−1.32 (m, 2 H, 7-H, NMH_4C_5), 1.32−1.29 (m, 2 H, 10-H,

NMH_4C_5), 1.30 [t, ^2J(HCCH) = 7.2 Hz, 6 H, OCH_2CH_3], 1.15−1.10 (m, 2 H, 8/8′-H, NMH_4C_5), 1.10−0.94 (m, 2 H, 9/9′-H, NMH_4C_5), 0.97 [d, ^3J(HCCH) = 6.0 Hz, 3 H, 13-H, NMH_4C_5], 0.96 [d, ^3J(HCCH) = 6.4 Hz, 3 H, 13-H, NMH_4C_5), 0.93 [d, ^3J(HCCH) = 6.4 Hz, 3 H, 15-H, NMH_4C_5], 0.92 [d, ^3J(HCCH) = 6.4 Hz, 3 H, 15-H, NMH_4C_5], 0.82 [d, ^3J(HCCH) = 6.8 Hz, 3 H, 14-H, NMH_4C_5], 0.81 [d, ^3J(HCCH) = 6.4 Hz, 3 H, 14-H, NMH_4C_5]. − $^{13}C\{^1H\}$ NMR (100.6 MHz, [D$_3$]acetonitrile): δ = 210.32 [d, ^2J(CFeP) = 26.16 Hz, CO], 209.44 [d, ^2J(CFeP) = 22.14 Hz, CO], 209.38 [d, ^2J(CFeP) = 23.14 Hz, CO], 163.28 (s, CO_2), 144.24 [s, C-4, $C_6H_2(CH_3)_3$], 135.96 [s, *C*HC(O)OEt], 135.81 [s, *C*HC(O)OEt], 135.88 [m, C-2, C-6, $C_6H_2(CH_3)_3$], 131.77 [m, C-3, C-5, $C_6H_2(CH_3)_3$], 124.22 [d, ^1J(CP) = 58.36 Hz, C-1, $C_6H_2(CH_3)_3$], 124.13 [d, ^1J(CP) = 59.36 Hz, C-1, $C_6H_2(CH_3)_3$], 114.00 (s, C-1, C_5H_4), 113.78 (s, C-1, C_5H_4), 91.84 (s, C-2, C-3, C-4, C-5, C_5H_4), 91.30 (s, C-2, C-3, C-4, C-5, C_5H_4), 91.06 (s, C-2, C-3, C-4, C-5, C_5H_4), 90.99 (s, C-2, C-3, C-4, C-5, C_5H_4), 88.77 (s, C-2, C-3, C-4, C-5, C_5H_4), 88.72 (s, C-2, C-3, C-4, C-5, C_5H_4), 85.47 (s, C-2, C-3, C-4, C-5, C_5H_4), 84.55 (s, C-2, C-3, C-4, C-5, C_5H_4), 61.79 (s, OCH_2CH_3), 48.55 (s, C-7, NMC_5H_4), 48.43 (s, C-7, NMC_5H_4), 43.73 (s, C-11, NMC_5H_4), 43.43 (s, C-11, NMC_5H_4), 35.94 (s, C-6, NMC_5H_4), 35.84 (s, C-6, NMC_5H_4), 35.39 (s, C-9, NMC_5H_4), 30.07 (s, C-10, NMC_5H_4), 29.96 (s, C-10, NMC_5H_4), 28.35 (s, C-12, NMC_5H_4), 24.64 (s, C-8, NMC_5H_4), 22.35 (s, C-15, NMC_5H_4), 22.29 (s, C-15, NMC_5H_4), 21.93 (s, C-13, NMC_5H_4), 21.91 (s, C-13, NMC_5H_4), 21.76 (s, 2-CH_3, 6-CH_3, $(CH_3)_3C_6H_2$), 21.71 [s, 2-CH_3, 6-CH_3, $(CH_3)_3C_6H_2$], 21.67 [s, 2-CH_3, 6-CH_3, $(CH_3)_3C_6H_2$], 21.62 [s, 2-CH_3, 6-CH_3, $(CH_3)_3C_6H_2$], 20.94 [s, 4-CH_3, $(CH_3)_3C_6H_2$], 20.62 (s, C-14, NMC_5H_4), 20.59 (s, C-14, NMC_5H_4), 14.24 (s, OCH_2CH_3), 14.23 (s, OCH_2CH_3). − $^{31}P\{^1H\}$ NMR (162.0 MHz, [D$_3$]acetonitrile): δ = 65.48 (s), 65.03 (s). − ^{19}F NMR (376.5 MHz, [D$_3$]acetonitrile): δ = −151.4. − IR (acetonitrile): ν(CO) = 2049 (s), 2008 (s) cm^{-1}. − $C_{30}H_{42}BF_4FeN_2O_4P$ (668.30): calcd. C 53.92, H 6.33, N 4.19; found C 54.34, H 6.17, N 4.09.

Figure 3. Atom labeling in the neomenthylcyclopentadienyl ligand

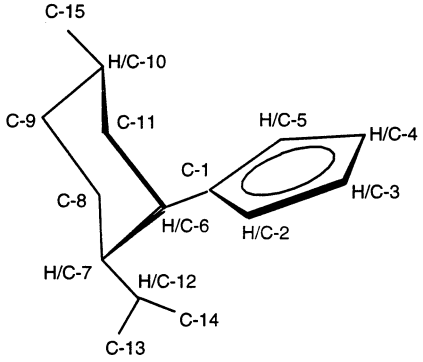

8) *{(tert-Butyl)bis[(E)-ethoxycarbonylmethylenehydrazino]-phosphane}dicarbonyl(η^5-cyclopentadienyl)iron(II)} Tetrafluoroborate* (**6a**): Prepared as described for **5a** from 200 mg (0.57 mmol) of $\{Cp(OC)_2[H_2(tBu)P]Fe\}BF_4$ (**4a**) and 112 mg (0.98 mmol) of $N_2C(H)CO_2Et$ (**2**) in 10 ml of acetonitrile. − Yield 212 mg (77%). − Beige microcrystalline powder. − M.p. 145°C (dec.). − ^1H NMR ([D$_3$]acetonitrile, 400.1 MHz): δ = 8.51 [d, ^2J(PNH) = 13.2 Hz, 2 H, HN], 7.32 (s, 2 H, HC), 5.44 (s, 5 H, H_5C_5), 4.21−4.09 (m, 4 H, H_2C), 1.31 [d, ^3J(PCCH) = 16.8 Hz, 9 H, $(H_3C)_3C$], 1.27 [t, ^3J(HCCH) = 6.8 Hz, 6 H, H_3C]. − $^{13}C\{^1H\}$ NMR ([D$_3$]acetonitrile, 100.6 MHz): δ = 208.9 [d, ^2J(PFeC) = 27.1 Hz, CO], 166.0 (s, CO_2), 135.3 [d, ^3J(PNNC) = 16.1 Hz, C=N], 85.6 (s, C_5H_5), 62.5 (s, CH_2), 40.9 [d, ^1J(PC) = 39.9 Hz, CP], 25.7 [d, ^2J(PCC) = 3.7 Hz, $(CH_3)_3C$], 13.6 (s, CH_3). − $^{31}P\{^1H\}$ NMR ([D$_3$]acetonitrile, 162.0 MHz): δ = 166.8 (s). − ^{19}F NMR ([D$_3$]acetonitrile, 376.5 MHz): δ = −148.5. − IR (acetonitrile): ν(CO) = 2058 (s), 2019 (s); ν(C=O) = 1732 (m) cm^{-1}. − $C_{19}H_{28}BF_4FeN_4O_6P$ (582.08): calcd. C 39.21, H 4.85, N 9.63; found C 39.41, H 4.93, N 9.78.

9) *Dicarbonyl(η^5-cyclopentadienyl){bis[(E)-ethoxycarbonylmethylenehydrazino](phenyl)phosphane}iron(II) Tetrafluoroborate* (**6b**): Prepared as described for **5a** from 200 mg (0.53 mmol) of $\{Cp(OC)_2[H_2(Ph)P]Fe\}BF_4$ (**4b**) and 114 mg (1.00 mmol) of $N_2C(H)CO_2Et$ (**2**) in 10 ml of acetonitrile. − Yield 220 mg (75%). − Light yellow microcrystalline powder. − M.p. 176°C (dec.). − ^1H NMR ([D$_3$]acetonitrile, 400.1 MHz): δ = 8.86 (s, 2 H, HN), 7.73−7.37 (m, 5 H, H_5C_6), 7.02 [d, ^4J(PNNCH) = 1.2 Hz, 2 H, HC], 5.27 [d, ^3J(PFeCH) = 1.5 Hz, 5 H, H_5C_5], 4.21 [q, ^3J(HCCH) = 7.2 Hz, 4 H, H_2C], 1.27 [t, ^3J(HCCH) = 7.2 Hz, 6 H, H_3C]. − $^{13}C\{^1H\}$ NMR ([D$_3$]acetonitrile, 100.6 MHz): δ = 208.7 [d, ^2J(PFeC) = 29.2 Hz, CO], 163.4 (s, CO_2), 137.3 [d, ^3J(PNNC) = 17.1 Hz, C=N], 134.1 [d, ^4J(PCCCC) = 1.7 Hz, C-4], 133.1 [d, ^1J(PC) = 82.5 Hz, C-1], 131.6 [d, ^2J(PCC) = 11.1 Hz, C-2/6], 130.5 [d, ^3J(PCCC) = 12.1 Hz, C-3/5], 89.1 (s, C_5H_5), 62.0 (s, CH_2), 14.3 (s, CH_3). − $^{31}P\{^1H\}$ NMR ([D$_3$]acetonitrile, 162.0 MHz): δ = 132.3 (s). − ^{19}F NMR ([D$_3$]acetonitrile, 376.5 MHz): δ = −151.1. − IR (acetonitrile): ν(CO) = 2059 (s), 2018 (s); ν(C=O) = 1738 (m) cm^{-1}. − $C_{21}H_{24}BF_4FeN_4O_6P$ (602.05): calcd. C 42.03, H 3.70, N 9.34; found C 41.85, H 3.90, N 9.11.

10) *Dicarbonyl(η^5-cyclopentadienyl){bis[(E)-ethoxycarbonylmethylenehydrazino](2,4,6-trimethylphenyl)phosphane}iron(II) Tetrafluoroborate* (**6c**): Prepared as described for **5a** from 200 mg (0.48 mmol) of $\{Cp(OC)_2[H_2(Mes)P]Fe\}BF_4$ (**4c**) and 112 mg (0.98 mmol) of $N_2C(H)CO_2Et$ (**2**) in 10 ml of acetonitrile. − Yield 218 mg (69%). − Yellow microcrystalline powder. − M.p. 184°C (dec.). − ^1H NMR ([D$_3$]acetonitrile, 400.1 MHz): δ = 8.72 (s, 2 H, HN), 7.16 (s, 2 H, HC), 6.88 [d, ^4J(PNNCH) = 4.0 Hz, 2 H, *meta*-H], 5.17 (s, 5 H, H_5C_5), 4.03 [q, ^3J(HCCH) = 6.8 Hz, 4 H, H_2C], 2.26 [d, ^4J(PCCCH) = 1.0 Hz, 6 H, 2-H_3C], 2.13 (s, 3 H, 4-H_3C), 1.09 [t, ^3J(HCCH) = 6.8 Hz, 6 H, H_3C]. − $^{13}C\{^1H\}$ NMR ([D$_3$]acetonitrile, 100.6 MHz): δ = 202.3 [d, ^2J(PFeC) = 36.2 Hz, CO], 156.2 (s, CO_2), 137.3 [d, ^4J(PCCCC) = 3.0 Hz, C-4], 135.1 [d, ^3J(PNNC) = 20.0 Hz, C=N], 128.8 [d, ^2J(PCC) = 17.1 Hz, C-2/6], 126.3 [d, ^3J(PCCC) = 10.1 Hz, C-3/5], 120.5 [d, ^1J(PC) = 66.4 Hz, C-1], 82.2 (s, C_5H_5), 54.9 (s, CH_2), 17.4 [d, ^3J(PCCC) = 3.9 Hz, 2-CH_3], 13.9 (s, 4-CH_3), 7.4 (s, CH_3). − $^{31}P\{^1H\}$ NMR ([D$_3$]-acetonitrile, 162.0 MHz): δ = 139.14 (s). − ^{19}F NMR ([D$_3$]acetonitrile, 376.5 MHz): δ = −149.0. − IR (acetonitrile): ν(CO) = 2056 (s), 2013 (s); ν(C=O) = 1730 (m) cm^{-1}. − $C_{24}H_{30}BF_4FeN_4O_6P$ (644.15): calcd. C 44.75, H 4.69, N 8.70; found C 44.57, H 4.71, N 8.53.

11) *Dicarbonyl{bis[(E)-ethoxycarbonylmethylenehydrazino]-(phenyl)phosphane}[η^5-(c-2-isopropyl-t-5-methylcyclohexan-r-1-yl)-cyclopentadienyl]iron(II)} Tetrafluoroborate* (**6d**): Prepared as described for **5a** from 200 mg (0.36 mmol) of $\{NMC_5H_4(OC)_2[H_2(Ph)P]Fe\}BF_4$ (**4e**) and 117 mg (1.03 mmol) of $N_2C(H)CO_2Et$ (**2**) in 10 ml of acetonitrile. − Yield 246 mg (81%). − Yellow microcrystalline powder. − M.p. 179°C (dec.). − ^1H NMR ([D$_3$]acetonitrile, 400.1 MHz): δ = 8.98 (s, 2 H, HN), 7.78−7.61 (m, 5 H, H_5C_6), 7.40 (s, 2 H, HC), 5.58 (s, 1 H, H_4C_5), 5.30 (s, 1 H, H_4C_5), 5.07 (s, 1 H, H_4C_5), 4.93 (s, 1 H, H_4C_5), 4.22 [q, ^3J(HCCH) = 7.2 Hz, 2 H, H_2C-O], 4.14 [q, ^3J(HCCH) = 7.2 Hz, 2 H, H_2C-O], 2.63 (s, 1 H, 6-H, *NM*H_4C_5], 1.87 (s, 1 H , 12-H, *NM*H_4C_5), 1.81 (m, 2 H, 9/9′-H, *NM*H_4C_5), 1.73 (m, 2 H, 11/11′-H, *NM*H_4C_5), 1.63 (m, 2 H, 8/8′-H, *NM*H_4C_5), 1.32 (s, 1 H, 7-H, *NM*H_4C_5), 1.27 [t, ^3J(HCCH) = 7.2 Hz, 6 H, H_3C], 0.86 [d, ^3J(HCCH) = 6.0 Hz,

6 H, 13/14-H, *NM*H_4C_5], 0.72 [d, ^3J(HCCH) = 6.4 Hz, 3 H, 15-H, *NM*H_4C_5]. – $^{13}C\{^1H\}$ NMR ([D_3]acetonitrile, 100.6 MHz): δ = 205.8 [d, ^2J(PFeC) = 26.7 Hz, CO], 167.5 (s, CO_2), 133.4 [d, ^3J(PNNC) = 16.1 Hz, C=N], 130.1 [d, ^4J(PCCCC) = 2.0 Hz, C-4], 129.2 [d, ^1J(PC) = 82.0 Hz, C-1], 127.8 [d, ^3J(PCCC) = 11.0 Hz, C-3/5], 126.6 [d, ^2J(PCC) = 12.0 Hz, C-2/6], 112.1 (s, C-1, C_5H_4), 87.9 (s, C-2, C_5H_4), 87.2 (s, C-3, C_5H_4), 84.5 (s, C-4, C_5H_4), 82.5 (s, C-5, C_5H_4), 58.1 (s, CH_2-O), 57.8 (s, CH_2-O), 44.7 (s, C-7, *NM*C_5H_4), 39.8 (s, C-11, *NM*C_5H_4), 38.1 (s, C-6, *NM*C_5H_4), 31.8 (s, C-9, *NM*C_5H_4), 26.1 (s, C-10, *NM*C_5H_4), 24.6 (s, C-12, *NM*C_5H_4), 20.8 (s, C-8, *NM*C_5H_4), 18.7 (s, C-15, *NM*C_5H_4), 18.2 (s, C-14, *NM*C_5H_4), 16.8 (s, C-13, *NM*C_5H_4), 10.5 (s, CH_3). – $^{31}P\{^1H\}$ NMR ([D_3]acetonitrile, 162.0 MHz): δ = 132.5 (s). – ^{19}F NMR ([D_3]acetonitrile, 376.5 MHz): δ = −150.8. – IR (acetonitrile): ν(CO) = 2062 (s), 2021 (s); ν(C=O) = 1740 (m) cm^{-1}. – $C_{31}H_{42}BF_4FeN_4O_6P$ (740.32): calcd. C 50.29, H 5.72, N 7.57; found C 50.27, H 5.45, N 7.19.

12) *X-ray Analysis of* **5c** *and* **6b**: Yellow crystals suitable for X-ray analysis were obtained by slow diffusion of diethyl ether into a saturated solution of {$Cp(OC)_2Fe-P(H)(Mes)[N(H)-N=C(H)-CO_2Et]$}$BF_4$ (**5c**) or {$Cp(OC)_2Fe-P(Ph)[N(H)-N=C(H)-CO_2Et]_2$}$BF_4$ (**6b**), in acetonitrile at room temperature.

5c: $C_{20}H_{24}BF_4FeN_2O_4P$, M_r = 530.05, monoclinic, space group $P2_1/n$ (No. 14), a = 9.490(3), b = 22.433(5), c = 11.483(7) Å, β = 103.71(1)°, V = 2375(2) Å^3, Z = 4, $D_{calcd.}$ = 1.482 g·cm^{-3}, CAD4 diffractometer (Enraf-Nonius), radiation type: Mo-K_α, wavelength: λ = 0.71073 Å, graphite monochromator, crystal size: 0.20 × 0.20 × 0.15 mm, temperature: 293(2) K, scale range: 1.81° < Θ < 24.96°, F(000): 1088, total reflections: 5723, observed reflections: 2542 with [I > 2.0 σ(I)], absorption coefficient: μ = 0.764 mm^{-1}, semi-empirical absorption correction[13] (T_{min}/T_{max}: 0.5586/0.9988), structure solution: SHELXS-86[14] with Patterson methods, structure refinement: SHELXL-93[15] (392 parameters), R_1 = 0.1001, wR_2 = 0.3413[16].

6b: $C_{21}H_{24}BF_4FeN_4O_6P$, M_r = 602.05, triclinic, space group $P\bar{1}$ (No. 2), a = 7.643(2), b = 12.590(2), c = 14.694(1) Å, α = 75.77(1), β = 82.61(2), γ = 82.88(2)°, V = 1352.9(4) Å^3, Z = 2, $D_{calcd.}$ = 1.478 g·cm^{-3}, CAD4 diffractometer (Enraf-Nonius), radiation type: Mo-K_α, wavelength: λ = 0.71073 Å, graphite monochromator, crystal size 0.25 × 0.20 × 0.15 mm, temperature: 293(2) K, scale range: 1.67° < Θ < 23.92°, F(000): 616, total reflections: 4048, observed reflections: 2623 with [I > 2.0 σ(I)], absorption coefficient: μ = 0.688 mm^{-1}, semi-empirical absorption correction[13] (T_{min}/T_{max}: 0.9564/0.9995), structure solution: SHELXS-86[14] with Patterson methods, structure refinement: SHELXL-93[15] (439 parameters), R_1 = 0.0489, wR_2 = 0.1099[16].

[1] W. Malisch, K. Thirase, J. Reising, *J. Organomet. Chem.*, submitted.
[2] W. Malisch, K. Thirase, J. Reising, *Z. Naturforsch.*, submitted.
[3] [3a] W. Malisch, A. Spörl, K. Thirase, O. Fey, *J. Organomet. Chem.*, submitted. – [3b] W. F. McNamara, E. N. Duesler, R. T. Paine, *Organometallics* **1986**, *5*, 1747–1749. – [3c] M. T. Ashby, J. H. Enemark, *Organometallics* **1987**, *6*, 1318–1323. – [3d] M. T. Ashby, J. H. Enemark, *Organometallics* **1987**, *6*, 1323–1327. – [3e] M. T. Ashby, J. H. Enemark, D. L. Lichtenberger, *Inorg. Chem.* **1988**, *27*, 191–197.
[4] [4a] S. G. Davies, *Tetrahedron Lett.* **1986**, *27*, 3787–3790. – [4b] S. G. Davies, *Aldrichim. Acta* **1990**, *23*, 31–37. – [4c] H. Brunner, *Angew. Chem.* **1991**, *103*, A-310–A-313. – [4d] H. Brunner, *Adv. Organomet. Chem.* **1980**, *18*, 151–201.
[5] G. Consiglio, F. Morandini, *Chem. Rev.* **1987**, *87*, 761–778.
[6] W. Malisch, N. Gunzelmann, K. Thirase, M. Neumayer, unpublished.
[7] E. Cesarotti, H. B. Kagan, R. Goddard, C. Krüger, *J. Organomet. Chem.* **1978**, *162*, 297–309.
[8] [Cp(OC)(Me_3P)Fe–P(H)(*t*Bu)Me]I: Yellow powder. – M.p. 181°C (decomp.). – ^{31}P NMR ([D_3]acetonitrile, 162.0 MHz): δ = 51.2/49.6 [d, ^2J(PFeP) = 55.7/56.7 Hz, PH]; 31.2/30.8 [d, ^2J(PFeP) = 55.7/56.7 Hz, $P(CH_3)_3$]. – Monoclinic, space group: $P2_1/c$ (No. 14), a = 12.960(2), b = 11.5569(15), c = 13.077(7) Å, β = 104.52(2)°. – Manuscript in preparation.
[9] T. Ohishi, Y. Shiotani, M. Yamashita, *Organometallics* **1994**, *13*, 4641–4642.
[10] *CRC, Handbook of Chemistry and Physics*, 59th ed. (Ed.: R. C. Weast), CRC, Boca Raton **1978**, F-215.
[11] G. Häfelinger, *Chem. Ber.* **1970**, *103*, 2902–2921.
[12] [12a] B. D. Dombek, R. J. Angelici, *Inorg. Chim. Acta* **1973**, *7*, 345–347. – [12b] W. E. Williams, F. J. Lalor, *J. Chem. Soc., Dalton Trans.* **1973**, 1329–1332.
[13] Enraf-Nonius, *Structure Determination Package*, Enraf-Nonius, Delft, The Netherlands **1984**.
[14] G. M. Sheldrick, *SHELXS-86* in: G. M. Sheldrick, C. Krüger, R. Goddard (Eds.), *Crystallographic Computing 3*, Oxford University Press, **1985**, p. 175.
[15] G. M. Sheldrick, *SHELXL-93, Program for structure refinement*, Göttingen, **1993**.
[16] Crystallographic data (excluding structure factors) for the structures reported in this paper have been deposited at the Cambridge Crystallographic Data Centre as supplementary publication no. CCDC-101577 (**5c**) and -101578 (**6b**). Copies of the data can be obtained free of charge on application to CCDC, 12 Union Road, Cambridge CB2 1EZ (Fax: + 44-1223/336-033; E-mail: deposit@ccdc.cam.ac.uk).

[I98141]

Organophosphorus Compounds, 131[◇]

Tricyclic Phosphorus-Carbon Compounds – Synthesis by Oligomerization of Kinetically Stabilized Phosphaalkynes☆

Andreas Hoffmann[a], Andreas Mack[a], Richard Goddard[b], Paul Binger[b][+], and Manfred Regitz*[a]

Fachbereich Chemie der Universität Kaiserslautern[a],
Erwin-Schrödinger-Straße, D-67663 Kaiserslautern, Germany
Fax: (internat.) + 49(0)631/205-3921
E-mail: regitz@rhrk.uni-kl.de

Max-Planck-Institut für Kohlenforschung[b],
Kaiser-Wilhelm-Platz 1, D-45470 Mühlheim a. d. Ruhr, Germany
Fax: (internat.) + 49(0)208/306-2890

Received May 27, 1998

Keywords: Phosphaalkynes / Cooligomerization / Phosphaalkyne cyclooligomers / Cage compounds, phosphorus-carbon-aluminum / Cage compounds, phosphorus-carbon-gallium

When trialkylaluminum reagents **2** bearing sterically demanding substituents are allowed to react with phosphaalkynes **1** a highly selective phosphaalkyne cyclotrimerization with incorporation of one organometal unit occurs (→ **5a–d**). The resulting triphosphaalatricycloheptenes **5** are able to function as ligands in transition metal complexes (→ **6a**,**b**), as illustrated by the reactions of **5a** with nonacarbonyldiiron or the pentacarbonyltungsten tetrahydrofuran complex. When triethylgallium (**7**) is allowed to react with phosphaalkynes **1**, tricyclic phosphorus-carbon-gallium compounds are generated (→ **8a**,**b**).

Introduction

Phosphorus-carbon cage compounds have attained increasing importance in the chemistry of low-coordinated phosphorus over the past few years. Even complicated polycyclic systems can be obtained specifically by means of various synthetic strategies[2]. One versatile concept involves the initiation of a phosphaalkyne cyclooligomerization with the help of a Lewis acid[3]. Thus, for example, the tetracyclic product **3** is obtained in high selectivity from the reaction of *tert*-butylphosphaalkyne (**1a**) with triethylaluminum (**2a**)[4][5]. A phosphaalkyne cyclooligomerization with incorporation of the Lewis acid **2a** is also observed when diethyl ether is used in place of pentane as solvent; however, in this case the cyclooligomerization process of **1a** with **2a** ends at the stage of the polycyclic betaine **4**[4][6].

The results described here represent an extension of the investigations on the preparation of the cage compounds **3** and **4** and concern the use of triorganoaluminum reagents bearing sterically demanding substituents as well as triorganogallium reagents as reaction partners for the phosphaalkynes **1**. Furthermore, the reaction behavior of a selected phosphorus-carbon-aluminum cage compound towards transition metal carbonyl complexes is discussed.

[+] Present address: Fachbereich Chemie der Universität Kaiserslautern, Erwin-Schrödinger-Straße, D-67663 Kaiserslautern, Germany; Fax: (internat.) + 49(0)631/205-3921.

Scheme 1

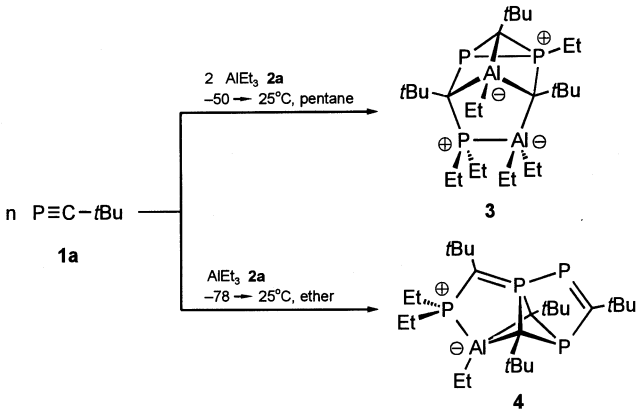

Results and Discussion

Generation of the Triphosphaalatricycloheptenes (1 → 5)

Neither the cage compound **3** nor the polycyclic system **4** are formed in the reactions of the phosphaalkynes **1a–c** with the triorganoaluminum reagents **2b**,**c** bearing voluminous substituents. Instead a cyclotrimerization of the organophosphorus compounds **1** with incorporation of one trialkylaluminum unit occurs[7]. The triphosphaalatricycloheptenes **5a–d** formed in this way can be isolated by bulb-to-bulb distillation or recrystallization from non-polar

 © WILEY-VCH Verlag GmbH, D-69451 Weinheim, 1998 1434–1948/98/1111–1597 $ 17.50+.50/0

solvents and are obtained in moderate to good yields (36−82%) as yellow oils (**5a**−**c**) or a yellow solid (**5d**).

Scheme 2

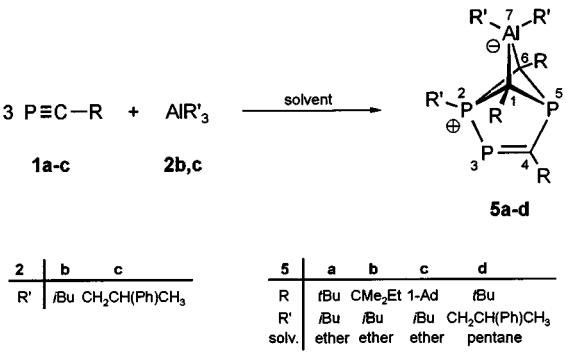

Elemental analyses and mass-spectrometric data clearly show that the polycyclic compounds **5** have the constitutions of 3:1 adducts of the respective phosphaalkyne **1** with the triorganoaluminum reagent **2**. The NMR spectra of products **5** also provide valuable diagnostic information which is discussed in detail below for the example of product **5a** (R = *t*Bu; R′ = *i*Bu).

Relevant information about the degree of oligomerization is provided by the ^{31}P-NMR spectrum which contains three signals which must result from a single molecule on account of the observed ABX spin system. The signal at low field (δ = 223.3) may unequivocally be assigned to the $\lambda^3\sigma^2$ phosphorus atom P-3[8] and its large $^1J_{P,P}$ coupling constant of 299.2 Hz confirms the adjacency to the onium phosphorus atom P-2 (δ = 53.9). The remaining signal at δ = 36.5 (P-5) is split into a double doublet by two $^2J_{P,P}$ couplings (32.2 and 19.0 Hz).

The ^{1}H-NMR spectrum of compound **5a** shows two signals for the *tert*-butyl groups (integration ratio 2:1) and a total of nine signals for the three, chemically non-equivalent isobutyl groups. A two-dimensional NMR spectrum was needed to clarify the spatial relationships between the protons (^{1}H,^{1}H-COSY-45 experiment). The signal at lowest field (δ = 2.36) is assigned to the protons of the α-methylene group at the onium phosphorus atom P-2. It is split by one H,H and two H,P couplings (7.3 and 2.0 Hz). The methyl hydrogen atoms of the isobutyl group at P-2 furnish the signal at δ = 0.96; the methine hydrogen signal occurs at δ = 2.08−2.22. The signal group at δ = 0.46, 2.08−2.22 and 1.24 as well as that at δ = 0.64, 2.22−2.32 and 1.25 can each be assigned to one of the two isobutyl groups at the aluminum atom. However, a distinction between these two alkyl groups is not possible.

The ^{13}C-NMR-spectral data are also in harmony with the proposed structure for the polycyclic product **5a**. The signal of the phosphaalkene carbon atom C-4 is especially characteristic: it appears at relatively high field (δ = 104.4) and is split into a double doublet (50.2 and 13.4 Hz)[9]. A signal with a chemical shift of δ = 44.7 is observed for the two skeletal sp^3-carbon atoms C-1 and C-6. The signal for the methylene carbon atom at the $\lambda^4\sigma^4$-phosphorus atom (P-2) appears at relatively low field (δ = 47.2) and is split into a double doublet by two C,P couplings (24.6 and 10.5 Hz)[10].

A conclusive mechanism for the formation of the polycyclic system **5** cannot be given at present since it has not been possible to isolate or even to detect any of the occurring intermediates by NMR spectroscopy. Even so it is plausible to assume that the first step in the sequence is an attack of the Lewis acid **2** at the carbon atom of the phosphaalkyne **1**.

Metalation Reaction of the Triphosphaalatricycloheptene (5 → 6)

It has been shown elsewhere that phosphorus-carbon-aluminum cage compounds are able to act as ligands in transition metal complexes[5][6]. Complexation of the triphosphaalatricycloheptene **5a** with a carbonylmetal fragment can be realized in an analogous manner. Thus, reactions of compound **5a** with nonacarbonyldiiron[11] or the in situ generated pentacarbonyltungsten tetrahydrofuran complex[12] proceed at room temperature to furnish the transition metal complexes **6a**,**b** in practically quantitative yields (^{31}P-NMR monitoring). After recrystallization from appropriate solvents, compound **6a** is obtained as a dark-red solid (84% yield) and compound **6b** as an orange solid (76% yield).

Scheme 3

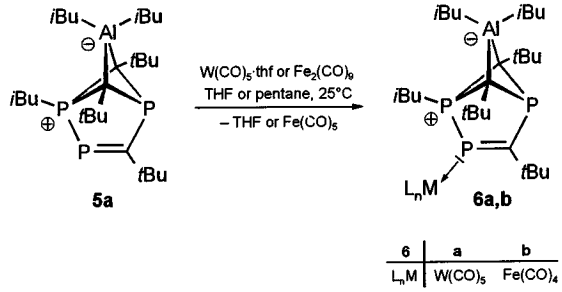

The success of the metalation reaction is immediately apparent from the IR spectra of the reaction products **6a**,**b**. Three carbonyl bands appear in each spectrum in the expected wavenumber ranges (**6a**: $\tilde{\nu}$ = 2064, 1992, 1970 cm^{-1}; **6b**: $\tilde{\nu}$ = 2076, 1960, 1948 cm^{-1}). The mass spectra of the compounds **6a**,**b** show that in both cases only one 16-valence-electron fragment has been coordinated to the polycyclic system of **5a**. The $\lambda^3\sigma^2$-phosphorus atom of the P−C double bond functions as two-electron donor to the metal center as is confirmed by the ^{31}P-NMR spectra. Accordingly, the chemical shift of the phosphorus atom P-3 is only marginally influenced by addition of the metal fragment (**5a**: δ = 223.3; **6a**: δ = 232.2; **6b**: δ = 191.0); however, the P-2/P-3 coupling constant is markedly reduced by almost 100 Hz. Furthermore, in the case of the polycyclic compound **6b** the signal at lowest field exhibits a characteristic $^1J_{P,W}$ coupling constant of 234.1 Hz[13].

Both the ^{1}H- and the ^{13}C-NMR spectra are in accord with the proposed structures: they confirm retention of the tricyclic skeleton in the course of the transformations **5a**

→ **6a**,**b**. In addition, the ^{13}C-NMR spectra proved relevant information about the hapticity of the polycyclic ligands. In the cases of **6a**,**b** the signals of the double-bond carbon atom C-4 experience only slight shifts to higher field in comparison to that of C-4 in the uncomplexed tricyclic compound **5a**. This finding supports the formulation of the transition metal complexes **6a**,**b** as end-on complexes and eliminates the possibility of the existence of a metallophosphacyclopropane structural unit[14].

Although the simple complexation of the tricyclic compound **5a** can easily be achieved under mild reaction conditions, it was not possible to effect complexation of a second 16-valence-electron species. Even in the presence of a large excess of the complexing reagent, the phosphorus atom P-5 remained unchanged. It is probable that the $\lambda^3\sigma^3$-phosphorus atom is sterically so strongly shielded by the three neighboring *tert*-butyl groups and by one of the isobutyl groups on the aluminum atom that an attack of the electrophilic carbonylmetal is not possible.

Generation of the Triphosphagallatricycloheptenes (1 → 8)

In many cases the chemistry of triorganogallium reagents **7** resembles that of the corresponding aluminum compounds **2**[15]. The Lewis acid **7** should thus also be able to initiate a phosphaalkyne cyclooligomerization. Indeed, when a mixture of a phosphaalkyne **1** and triethylgallium (**7**) in diethyl ether is stirred at room temperature for several days its color changes from colorless to orange-brown. Monitoring of the course of reaction by ^{31}P-NMR spectroscopy is indicative of a cyclotrimerization of the organophosphorus compound **1**. After removal of volatile materials under vacuum, recrystallization of the residue from a non-polar solvent furnishes the compounds **8a**,**b** in the

Scheme 4

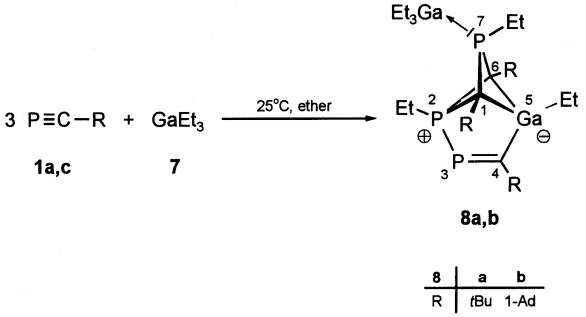

form of yellow crystals in yields of 49 and 43%, respectively.

The structural relationships between the polycyclic compounds **8** and **5** are clear: both cage compounds have a tricyclo[3.2.0.0^{2,6}]hept-3-ene skeleton. In the case of **8** however, an additional, exocyclic triethylgallium unit is coordinated at a phosphorus atom of the polycyclic system. In addition, the positions of a phosphorus atom and a gallium atom are exchanged in comparison to the polycyclic skeleton of **5**.

Elemental analytical data confirm that compound **8** is composed of three molecules of phosphaalkyne **1** and two molecules of triethylgallium (**7**). The molecular ion peak is not present in the mass spectra of **8** although the fragment ions ($M^+ - Et_3Ga$) are observed in each case.

The NMR spectra provide diagnostic information about the constitutions of compounds **8**. In the case of **8a** the degree of oligomerization is apparent from the three signals appearing in the ^{31}P-NMR spectrum as an ABX spin system. The signal with the chemical shift δ = 253.6 is assigned to the $\lambda^3\sigma^2$-phosphorus atom[8]; the onium phosphorus atom P-2 produces the signal at δ = 41.6. The direct connection between these two phosphorus atoms is reflected in the coupling constant of 336.8 Hz. The signal at δ = 38.2 (P-7) is less characteristic and is split into a double doublet by two $J_{P,P}$ couplings (40.2 Hz and 25.0 Hz).

Information on the constitution of **8a** is also provided by the ^{1}H-NMR spectrum. The signals were assigned with the help of a two-dimensional NMR spectrum (^{1}H,^{1}H-COSY-45 experiment). In addition to two signals for the *tert*-butyl groups (integration ratio 2:1) there is a total of eight signals resulting from the six ethyl substituents. The two multiplets at low field (δ = 2.30−2.37 and δ = 2.05−2.10) are assigned to the α-methylene groups at the phosphorus atoms P-2 and P-7. Furthermore, the ethyl groups of the exocyclic triethylgallium unit give rise to a triplet at δ = 1.52 and a quadruplet at δ = 0.80 in the ^{1}H-NMR spectrum.

The ^{13}C-NMR spectrum is also in accord with the proposed structure for the polycyclic compound **8a**. The signal for the phosphaalkene carbon atom C-4 appears at relatively high field (δ = 79.0) while the two sp^3-skeletal carbon atoms C-1 and C-6 give rise to a double doublet (J = 23.2 and 16.7 Hz) at δ = 46.5.

The constitutions of the cyclooligomerization products were finally confirmed by an X-ray crystallographic analysis of **8a**. Crystals of the tricyclic compound **8a** are monoclinic, space group $P2_1/n$ (no. 14). A plot of the crystal structure is shown in Figure 1.

The central structural element of compound **8a** is a tricyclo[3.2.0.0^{2,6}]hept-3-ene system bearing an exocyclic triethylgallium unit. The double-bond carbon atom, all phosphorus atoms as well as the gallium atoms lie in the same plane. The sp^3-carbon atoms C-1 and C-2 are arranged in mirror symmetry around this plane.

The bond lengths and angles for compound **8a** are all of the expected magnitude; this holds especially for the P-2−P-3 linkage [2.203(2) Å; ref.[16]: 2.249 Å] and the P−C double bond [1.682(5) Å; ref.[17]: 1.670 Å]. A further characteristic feature, already observed in the structures of the polycyclic compounds **3** and **4**, is the shortening of the P−C single bonds to a $\lambda^4\sigma^4$-phosphorus atom [P-2−C-1: 1.818(4) Å; P-2−C-2: 1.811(5) Å; ref.[16]: 1.80 Å]. In contrast, the distances between the neighboring carbon atoms and the phosphorus atom P-1 are in the typical range for $\lambda^3\sigma^3$-P−C bonds [P-1−C-1: 1.869(4) Å; P-1−C-2: 1.879(4) Å; ref.[16]: 1.86 Å]. These observations, together with the P-1−Ga-2-separation of 2.581(1) Å [ref.[18]: 2.553(2)], support

Figure 1. Molecular structure of **8a**[a]

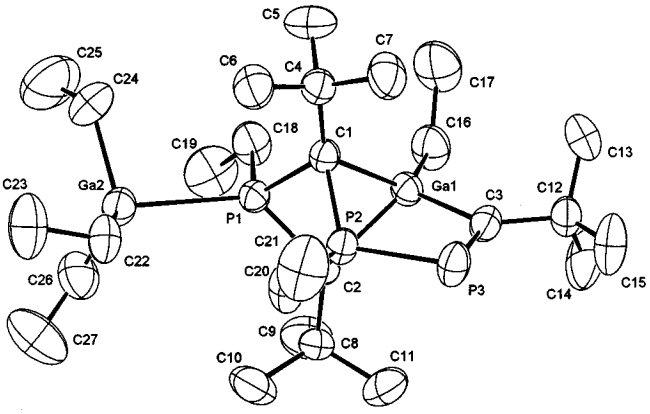

[a] Selected bond lengths [Å] and angles [°]: P1−C1 1.869(4), P1−C2 1.879(4), P2−C1 1.818(4), P2−C2 1.811(5), C2−Ga1 2.145(4), C1−Ga1 2.180(4), P2−P3 2.203(2), P3−C3 1.682(5), C3−Ga1 2.037(5), P1−P2 2.544(2), P1−Ga1 2.872(1), P2−Ga1 2.584(1), P1−Ga2 2.581(1); C3−Ga1−C1 101.6(2), C2−P1−C1 78.6(2), C3−Ga1−C2 102.6(2), C2−Ga1−C1 66.6(2), C2−P2−C1 81.7(2), C2−P2−P3 113.7(2), C1−P2−P3 113.9(2), C3−P3−P2 92.1(2), P2−C1−P1 87.3(2), P3−C3−Ga1 113.1(3), P1−C2−Ga1 90.8(2), P2−C2−Ga1 81.1(2), P2−C2−P1 87.2(2).

the existence of a donor-acceptor bond between the exocyclic triethylgallium unit and the polycyclic skeleton.

Again in this case of a cyclooligomerization of a kinetically stabilized phosphaalkyne **1** with triethylgallium (**7**), the question of the mechanism of formation of the polycyclic system **8** cannot be answered unambiguously. However, it is still reasonable to assume that the first step also involves an attack of the Lewis acid **7** at the carbon atom of the phosphaalkyne **1**.

We thank the *Fonds der Chemischen Industrie* for generous financial support and for post-graduate grants (to A. H. and A. M.).

Experimental Section

General Remarks: The reactions were carried out under argon (purity > 99.998%) in a previously oven-dried and evacuated apparatus (Schlenk techniques). The solvents were dried by standard procedures (*n*-pentane, diethyl ether and THF: Na/K alloy), distilled and stored under argon. Melting points: Mettler FP 61 (heating rate: 3°C/min). − FT-IR spectra: Perkin-Elmer infrared spectrometer 16PC. − Mass spectra: Finnigan MAT 90 spectrometer. − NMR spectra: Bruker AMX 400 (^{1}H: 400 MHz, ^{13}C: 101 MHz, ^{31}P: 162 MHz) and Bruker AC 200 (^{31}P: 81 MHz) spectrometers, solvent as internal standard (^{1}H and ^{13}C); the chemical shifts for ^{31}P are relative to external 85% orthophosphoric acid. Compounds **1a**[19], **1b**[20], **1c**[19], **2c**[15] were prepared by published methods. Compounds **2b**, **7** were purchased from Aldrich and used without further purification.

1,4,6-Tri-tert-butyl-2,7,7-triisobutyl-3,5-diphospha-2-phosphonia-7-aluminatotricyclo[3.2.0.0^{2,6}]hept-3-ene (**5a**): To a magnetically stirred solution of 0.94 g (4.75 mmol) of triisobutylaluminum (**2b**) in diethyl ether (10 ml) was added 1.67 g (16.68 mmol) of phosphaalkyne **1a**. After the reaction mixture had been heated to 100°C for 10 h in a Schlenk pressure tube, all volatile components were removed at 25°C/10^{-3} mbar. The remaining crude product was purified by bulb-to-bulb distillation (150°C/10^{-3} mbar): 1.56 g, 66% yield, yellow oil. − IR (pentane, cm^{-1}): $\tilde{\nu}$ = 1210 (s), 1200 (s), 1090 (s), 810 (s), 790 (s), 680 (s). − ^{31}P NMR (C_6D_6): δ = 36.5 (dd, $^2J_{P,P}$ = 32.2 Hz, $^2J_{P,P}$ = 19.0 Hz, P-5), 53.9 (dd, $^1J_{P,P}$ = 299.2 Hz, $^2J_{P,P}$ = 32.2 Hz, P-2), 223.3 (dd, $^1J_{P,P}$ = 299.2 Hz, $^2J_{P,P}$ = 19.0 Hz, P-3). − ^{1}H NMR (C_6D_6): δ = 0.46 [d, $^3J_{H,H}$ = 7.2 Hz, 2 H, AlCH_2CH(CH$_3$)$_2$], 0.64 [dd, $^4J_{H,P}$ = 2.3 Hz, $^3J_{H,H}$ = 7.1 Hz, 2 H, AlCH_2CH(CH$_3$)$_2$], 0.96 [d, $^3J_{H,H}$ = 6.7 Hz, 6 H, P-2-CH$_2$CH(CH_3)$_2$], 1.05 [s, 18 H, 2 C(CH_3)$_3$], 1.24 [d, $^3J_{H,H}$ = 6.5 Hz, 6 H, AlCH$_2$CH(CH_3)$_2$], 1.25 [d, $^3J_{H,H}$ = 6.5 Hz, 6 H, AlCH$_2$CH(CH_3)$_2$], 1.37 [s, 9 H, C(CH_3)$_3$], 2.08−2.22 [m, 2 H, AlCH$_2$CH(CH$_3$)$_2$ and P-2-CH$_2$CH(CH$_3$)$_2$], 2.22−2.32 [m, 1 H, AlCH$_2$CH(CH$_3$)$_2$], 2.36 [d-pseudo-t, $^2J_{H,P}$ = 7.3 Hz, $J_{H,P}$ = 2.0 Hz, $^3J_{H,H}$ = 7.3 Hz, 2 H, P-2-CH_2CH(CH$_3$)$_2$]. − ^{13}C NMR (C_6D_6): δ = 24.7 [pseudo-t, $J_{C,P}$ = 4.9 Hz, $J_{C,P}$ = 4.9 Hz, P-2-CH$_2$CH(*C*H$_3$)$_2$], 26.3 [s, broad, 2 Al*C*H$_2$CH(CH$_3$)$_2$], 26.8 [s, broad, CH$_2$*C*H(CH$_3$)$_2$], 27.8 [d, $J_{C,P}$ = 3.1 Hz, CH$_2$*C*H(CH$_3$)$_2$], 27.9 [s, CH$_2$*C*H(CH$_3$)$_2$], 29.1 [s, AlCH$_2$CH(*C*H$_3$)$_2$], 29.3 [s, AlCH$_2$CH(*C*H$_3$)$_2$], 32.1 [pseudo-t, $J_{C,P}$ = 9.0 Hz, $J_{C,P}$ = 9.0 Hz, C-4-C(*C*H$_3$)$_3$], 34.6 [dd, $J_{C,P}$ = 7.5 Hz, $J_{C,P}$ = 5.5 Hz, C-1/6-C(*C*H$_3$)$_3$], 35.8 [s, broad, 3*C*(CH$_3$)$_3$], 44.7 (d-pseudo-t, $^1J_{C,P}$ = 20.8 Hz, $J_{C,P}$ = 10.4 Hz, $J_{C,P}$ = 10.4 Hz, C-1/6), 47.2 [dd, $^1J_{C,P}$ = 24.6 Hz, $J_{C,P}$ = 10.5 Hz, P-2-*C*H$_2$CH(CH$_3$)$_2$], 104.4 (dd, $^1J_{C,P}$ = 50.2 Hz, $^1J_{C,P}$ = 13.4 Hz, C-4). − MS (CI, 120 eV); *m/z* (%): 500 (5) [M$^+$ + 2 H], 499 (17) [M$^+$ + H], 442 (24) [M$^+$ − C$_4$H$_8$], 441 (100) [M$^+$ − C$_4$H$_9$], 341 (4) [M$^+$ − C$_4$H$_9$ − PC$_5$H$_9$]. − $C_{27}H_{54}AlP_3$ (498.63): calcd. C 65.04, H 10.92; found C 63.5, H 11.2.

1,4,6-Tris(1,1-dimethylpropyl)-2,7,7-triisobutyl-3,5-diphospha-2-phosphonia-7-aluminatotricyclo[3.2.0.0^{2,6}]hept-3-ene (**5b**): To a magnetically stirred solution of 0.20 g (1.00 mmol) of triisobutylaluminum (**2b**) in diethyl ether (10 ml) was added 0.40 g (3.50 mmol) of phosphaalkyne **1b** (32 mol-% solution in hexamethyldisiloxane). After the reaction mixture had been heated to 100°C for 6 h in a Schlenk pressure tube, all volatile components were removed at 25°C/10^{-3} mbar. The remaining crude product was purified by bulb-to-bulb distillation (200°C/10^{-3} mbar): 0.25 g, 46% yield, yellow oil. − IR (pentane, cm^{-1}): $\tilde{\nu}$ = 1380 (s), 1362 (m), 1166 (m), 1100 (m), 1060 (m), 1014 (m), 796 (m), 670 (s). − ^{31}P NMR (C_6D_6): δ = 36.7 (dd, $^2J_{P,P}$ = 32.8 Hz, $^2J_{P,P}$ = 18.7 Hz, P-5), 52.7 (dd, $^1J_{P,P}$ = 299.1 Hz, $^2J_{P,P}$ = 32.8 Hz, P-2), 228.7 (dd, $^1J_{P,P}$ = 299.1 Hz, $^2J_{P,P}$ = 18.7 Hz, P-3). − ^{1}H NMR (C_6D_6): δ = 0.56 [d, $^3J_{H,H}$ = 7.2 Hz, 2 H, AlCH_2CH(CH$_3$)$_2$], 0.76 [dd, $J_{H,P}$ = 2.3 Hz, $^3J_{H,H}$ = 7.1 Hz, 2 H, AlCH_2CH(CH$_3$)$_2$], 0.82 [t, $^3J_{H,H}$ = 7.5 Hz, 6 H, 2 C(CH$_3$)$_2$CH$_2$CH_3], 0.87 [t, $^3J_{H,H}$ = 7.5 Hz, 3 H, C(CH$_3$)$_2$CH$_2$CH_3], 0.96 [d, $^3J_{H,H}$ = 6.6 Hz, 6 H, CH$_2$CH(CH_3)$_2$], 1.01 [s, broad, 6 H, C(CH_3)$_2$CH$_2$CH$_3$], 1.04 [s, broad, 6 H, C(CH_3)$_2$CH$_2$CH$_3$], 1.31 [d, $^3J_{H,H}$ = 6.5 Hz, 6 H, CH$_2$CH(CH_3)$_2$], 1.33 [d, $^3J_{H,H}$ = 6.5 Hz, 6 H, CH$_2$CH(CH_3)$_2$], 1.33 [s, broad, 6 H, C(CH_3)$_2$CH$_2$CH$_3$], 1.45−1.55 [m, 4 H, 2 C(CH$_3$)$_2$CH_2CH$_3$], 1.79 [q, 2 H, $^3J_{H,H}$ = 7.5 Hz, C(CH$_3$)$_2$CH_2CH$_3$], 2.12−2.23 [m, 1 H, CH$_2$CH(CH$_3$)$_2$], 2.22−2.31 [m, 1 H, CH$_2$CH(CH$_3$)$_2$], 2.30−2.41 [m, 1 H, CH$_2$CH(CH$_3$)$_2$], 2.45 [pseudo-t, broad, $^2J_{H,P}$ = 6.2 Hz, $^3J_{H,H}$ = 6.2 Hz, 2 H, P-2-CH_2CH(CH$_3$)$_2$]. − ^{13}C NMR (C_6D_6): δ = 9.2 [s, C(CH$_3$)$_2$CH$_2$*C*H$_3$], 9.3 [s, 2 C(CH$_3$)$_2$CH$_2$*C*H$_3$], 24.7 [pseudo-t, $J_{C,P}$ = 5.0 Hz, $J_{C,P}$ = 5.0 Hz, P-2-CH$_2$CH(*C*H$_3$)$_2$], 27.0 [s, broad, CH$_2$*C*H(CH$_3$)$_2$], 27.8 [d, $J_{C,P}$ = 3.0 Hz, CH$_2$*C*H(CH$_3$)$_2$], 27.9 [s, CH$_2$*C*H(CH$_3$)$_2$], 29.1 [s, AlCH$_2$CH(*C*H$_3$)$_2$], 29.3 [s, AlCH$_2$CH(*C*H$_3$)$_2$], 30.1 [pseudo-t, broad, $J_{C,P}$ = 6.3 Hz, $J_{C,P}$ = 6.3 Hz, 2 C(*C*H$_3$)$_2$CH$_2$CH$_3$], 30.9 [pseudo-t, $J_{C,P}$ = 6.1 Hz, $J_{C,P}$ = 6.1 Hz, C(*C*H$_3$)$_2$CH$_2$CH$_3$], 38.5 [pseudo-t, $J_{C,P}$ = 2.2 Hz, $J_{C,P}$ = 2.2 Hz, 2 C(CH$_3$)$_2$*C*H$_2$CH$_3$], 39.1 [dd, $J_{C,P}$ = 8.5 Hz, $J_{C,P}$ = 5.8 Hz, C-4-C(CH$_3$)$_2$CH$_2$CH$_3$], 40.1 [m, *C*(CH$_3$)$_2$CH$_2$CH$_3$], 47.3 [m, C1/6 and P-2-*C*H$_2$CH(CH$_3$)$_2$], 105.3 (dd, $^1J_{C,P}$ = 51.5 Hz, $^1J_{C,P}$ = 14.0 Hz, C-4)[21]. − MS (EI, 70 eV); *m/z* (%): 540 (1) [M$^+$], 484 (14)

[$M^+ - C_4H_8$], 483 (48) [$M^+ - C_4H_9$], 427 (41) [$M^+ - C_4H_9 - C_4H_8$], 369 (100) [$M^+ - 3\ C_4H_9$]. – MS (CI, 120 eV); *m/z* (%): 541 (17) [$M^+ + H$], 483 (37) [$M^+ - C_4H_9$], 345 (100) [$M^+ - 3\ C_4H_8 - Al$]. – HR MS (EI): calcd. 540.3723; found 540.3755. – $C_{30}H_{60}AlP_3$ (540.70).

1,4,6-Triadamant-1-yl-2,7,7-triisobutyl-3,5-diphospha-2-phosphonia-7-aluminatotricyclo[3.2.0.0^{2,6}]hept-3-ene (**5c**): To a magnetically stirred solution of 0.15 g (0.76 mmol) of triisobutylaluminum (**2b**) in diethyl ether (10 ml) was added 0.47 g (2.66 mmol) of phosphaalkyne **1c**. After the reaction mixture had been stirred at room temperature for 3 weeks, all volatile components were removed at 120°C/10^{-3} mbar. The remaining crude product was taken up in pentane and purified by recrystallization at low temperatures: 0.20 g, 36% yield, yellow oil. – ^{31}P NMR (C_6D_6): δ = 26.5 (dd, $^2J_{P,P}$ = 33.2 Hz, $^2J_{P,P}$ = 16.3 Hz, P-5), 51.7 (dd, $^1J_{P,P}$ = 299.4 Hz, $^2J_{P,P}$ = 33.2 Hz, P-2), 227.3 (dd, $^1J_{P,P}$ = 299.4 Hz, $^2J_{P,P}$ = 16.3 Hz, P-3). – ^{1}H NMR (C_6D_6): δ = 0.54 [d, $^3J_{H,H}$ = 7.3 Hz, 2 H, AlCH_2CH(CH$_3$)$_2$], 0.72 [d, broad, $^3J_{H,H}$ = 7.3, 2 H, AlCH_2CH(CH$_3$)$_2$], 1.05 [d, $^3J_{H,H}$ = 6.6 Hz, 6 H, CH$_2$CH(CH_3)$_2$], 1.30 [d, $^3J_{H,H}$ = 6.4 Hz, 6 H, CH$_2$CH(CH_3)$_2$], 1.30 [d, $^3J_{H,H}$ = 6.5 Hz, 6 H, CH$_2$CH(CH_3)$_2$], 1.58–2.16 (m, 45 H, Ad-H), 2.19–2.33 [m, 3 H, 3 CH$_2$CH(CH$_3$)$_2$], 2.50 [pseudo-t, broad, $^2J_{H,P}$ = 6.8 Hz, $^3J_{H,H}$ = 6.8 Hz, 2 H, P-2-CH_2CH(CH$_3$)$_2$]. – ^{13}C NMR (C_6D_6): δ = 24.8 [s, broad, P-2-CH$_2$CH(*C*H$_3$)$_2$], 26.7 [s, broad, 2 Al*C*H$_2$CH(CH$_3$)$_2$], 27.3 [s, broad, CH$_2$*C*H(CH$_3$)$_2$], 28.0 [s, CH$_2$*C*H(CH$_3$)$_2$], 28.1 [s, CH$_2$*C*H(CH$_3$)$_2$], 29.1 (s), 29.3 (s), 29.4 (s), 29.5 (s, 6 Ad-C), 36.8 (s, 3 Ad-C), 37.1 (s, 6 Ad-C), 38.3 (s, 2 Ad-C), 44.1 (s, Ad-C), 45.1 (s, broad, 3 Ad-C), 47.3 [m, C-1/6 and P-2-*C*H$_2$CH(CH$_3$)$_2$], 48.1 [pseudo-t, $J_{C,P}$ = 6.0 Hz, $J_{C,P}$ = 6.0 Hz, 6 Ad-C], 105.7 (dd, $^1J_{C,P}$ = 50.8 Hz, $^1J_{C,P}$ = 13.4 Hz, C-4). – MS (EI, 70 eV); *m/z* (%): 732 (1) [M^+], 675 (2) [$M^+ - C_4H_9$], 591 (5) [M^+ – Al(C_4H_9)$_2$], 325 (34) [$M^+ - 2\ H - 3\ C_{10}H_{15}$], 135 (100) [$C_{10}H_{15}^+$]. – $C_{45}H_{72}AlP_3$ (732.97).

1,4,6-Tri-tert-butyl-2,7,7-tris(2-phenylpropyl)-3,5-diphospha-2-phosphonia-7-aluminatotricyclo[3.2.0.0^{2,6}]hept-3-ene (**5d**): To a magnetically stirred solution of 0.31 g (0.80 mmol) of triorganoaluminum **2c** in pentane (8 ml) was added 0.28 g (2.80 mmol) of phosphaalkyne **1a** at −78°C. After the reaction mixture had been allowed to warm to room temperature and stirred for 3 d, all volatile components were removed at 25°C/10^{-3} mbar. Recrystallization from pentane at +4°C gave pure **5d** as a mixture of four diastereomers (**A**–**D**): 0.45 g, 82% yield, yellow crystals, m.p. 128–130°C. – IR (KBr, cm^{-1}): $\tilde{\nu}$ = 3024 (w, C=CH), 2956 (s, CH), 2862 (s, CH), 1600 (w), 1492 (m), 1452 (m), 1386 (w), 1360 (m), 1028 (m), 806 (m), 760 (s), 700 (s). – ^{31}P NMR (C_7D_8, 105°C): **5dA**: δ = 43.8 (dd, $^2J_{P,P}$ = 34.9 Hz, $^2J_{P,P}$ = 17.6 Hz, P-5), 60.0 (dd, $^1J_{P,P}$ = 299.9 Hz, $^2J_{P,P}$ = 34.9 Hz, P-2), 230.0 (dd, $^1J_{P,P}$ = 299.9 Hz, $^2J_{P,P}$ = 17.6 Hz, P-3). – **5dB**: δ = 43.8 (dd, $^2J_{P,P}$ = 34.9 Hz, $^2J_{P,P}$ = 15.6 Hz, P-5), 60.0 (dd, $^1J_{P,P}$ = 299.9 Hz, $^2J_{P,P}$ = 34.9 Hz, P-2), 229.9 (dd, $^1J_{P,P}$ = 299.9 Hz, $^2J_{P,P}$ = 15.6 Hz, P-3). – **5dC**: δ = 42.0 (dd, $^2J_{P,P}$ = 35.2 Hz, $^2J_{P,P}$ = 18.8 Hz, P-5), 57.7 (dd, $^1J_{P,P}$ = 306.7 Hz, $^2J_{P,P}$ = 35.2 Hz, P-2), 229.0 (dd, $^1J_{P,P}$ = 306.7 Hz, $^2J_{P,P}$ = 18.8 Hz, P-3). – **5dD**: δ = 42.0 (dd, $^2J_{P,P}$ = 35.2 Hz, $^2J_{P,P}$ = 18.8 Hz, P-5), 57.6 (dd, $^1J_{P,P}$ = 306.4 Hz, $^2J_{P,P}$ = 35.2 Hz, P-2), 228.8 (dd, $^1J_{P,P}$ = 306.4 Hz, $^2J_{P,P}$ = 18.8 Hz, P-3). – ^{1}H NMR (C_6D_6): δ = 0.86 (s, broad, 24 H), 0.91 (s, broad, 12 H), 0.96 (s, broad, 24 H), 1.01 (s, broad, 12 H), 1.19-1.24 (m, 16 H), 1.30 (s, broad, 36 H), 1.59–1.69 (m, 36 H), 2.67–2.87 (m, 4 H), 2.89–3.00 (m, 4 H), 3.22–3.38 (m, 8 H), 3.43–3.50 (m, 4 H), 6.99–7.19 (m, 28 H), 7.22–7.28 (m, 16 H), 7.33–7.42 (m, 8 H), 7.48–7.52 (m, 8 H). – ^{13}C NMR (C_6D_6): δ = 24.1 (s), 25.6 (m), 26.8 (s, broad), 27.9 (s), 28.0 (s), 28.1 (s), 28.3 (s), 28.8 (s), 29.1 (s), 32.0 (m), 34.5 (m), 35.4 (m), 35.6 (m), 38.2 (s, broad), 39.2 (s, broad), 39.3 (s, broad), 44.3–44.8 (m, 4 C-1/6), 46.2–46.9 [m, 4 P-2-*C*H$_2$CH(Ph)CH$_3$], 104.4 (d, broad, $^1J_{C,P}$ = 50.3 Hz, 4 C-4), 125.5 (s, broad), 125.6 (s, broad), 126.8 (m), 127.2 (s, broad), 127.3 (s, broad), 127.4 (s, broad), 128.6 (s, broad), 128.7 (m), 129.3 (m), 145.1 (s, broad), 153.4 (d, $J_{C,P}$ = 14.4 Hz), 153.5 (s). – MS (EI, 70 eV); *m/z* (%): 684 (1) [M^+], 683 (2) [$M^+ - H$], 564 (100) [$M^+ - H - C_9H_{11}$], 465 (60) [$M^+ - C_9H_{11} - PC_5H_9$], 365 (59) [$M^+ - C_9H_{11} - 2\ PC_5H_9$], 265 (74) [$M^+ - C_9H_{11} - 3\ PC_5H_9$], 119 (31) [$C_9H_{11}^+$]. – $C_{42}H_{60}AlP_3$ (684.85).

Tetracarbonyl{(3-η)-1,4,6-tri-tert-butyl-2,7,7-triisobutyl-3,5-diphospha-2-phosphonia-7-aluminatotricyclo[3.2.0.0^{2,6}]hept-3-ene}iron (**6a**): Nonacarbonyldiiron (0.54 g, 1.50 mmol) was added to a solution of triphosphaalatricycloheptene **5a** (0.25 g, 0.50 mmol) in pentane (15 ml) at 25°C. The reaction mixture was allowed to stir for 2 d, followed by a filtration to remove all insoluble components. Recrystallization of the crude product from the remaining solution at −78°C provided 0.28 g of **6a** (84%), red crystals, m.p. 108 – 110°C. – IR (pentane, cm^{-1}): $\tilde{\nu}$ = 2064 (s, CO), 1992 (s, CO), 1970 (s, CO), 1260 (w), 1100 (w), 1020 (w), 812 (w), 670 (m), 634 (m). – ^{31}P NMR (C_6D_6): δ = 39.4 (dd, $^2J_{P,P}$ = 50.1 Hz, $^2J_{P,P}$ = 19.0 Hz, P-5), 48.2 (dd, $^1J_{P,P}$ = 206.0 Hz, $^2J_{P,P}$ = 50.1 Hz, P-2), 232.2 (dd, $^1J_{P,P}$ = 206.0 Hz, $^2J_{P,P}$ = 19.0 Hz, P-3). – ^{1}H NMR (C_6D_6): δ = 0.43 [d, $^3J_{H,H}$ = 7.2 Hz, 2 H, AlCH_2CH(CH$_3$)$_2$], 0.69 [d, broad, $^3J_{H,H}$ = 5.7 Hz, 2 H, AlCH_2CH(CH$_3$)$_2$], 1.02 [s, broad, 6 H, CH$_2$CH(CH_3)$_2$], 1.10 [s, 18 H, 2 C(CH_3)$_3$], 1.25 [d, $^3J_{H,H}$ = 6.3 Hz, 6 H, CH$_2$CH(CH_3)$_2$], 1.28 [d, $^3J_{H,H}$ = 6.6 Hz, 6 H, CH$_2$CH(CH_3)$_2$], 1.35 [s, 9 H, C(CH_3)$_3$], 2.14–2.25 [m, 1 H, CH$_2$CH(CH$_3$)$_2$], 2.26–2.32 [m, 1 H, CH$_2$CH(CH$_3$)$_2$], 2.35–2.46 [m, 3 H, CH$_2$CH(CH$_3$)$_2$ and P-2-CH_2CH(CH$_3$)$_2$]. – ^{13}C NMR (C_6D_6): δ = 24.8 [d, $^3J_{C,P}$ = 7.0 Hz, P-2-CH$_2$CH(*C*H$_3$)$_2$], 25.3 [d, $J_{C,P}$ = 4.8 Hz, CH$_2$*C*H(CH$_3$)$_2$], 25.7 [s, broad, 2 Al*C*H$_2$CH(CH$_3$)$_2$], 27.8 [s, broad, 2 CH$_2$*C*H(CH$_3$)$_2$], 29.0 [s, AlCH$_2$CH(*C*H$_3$)$_2$], 29.1 [s, AlCH$_2$CH(*C*H$_3$)$_2$], 31.7 [pseudo-t, $J_{C,P}$ = 10.1 Hz, $J_{C,P}$ = 10.1 Hz, C-4-C(*C*H$_3$)$_3$], 34.2 [pseudo-t, $J_{C,P}$ = 6.5 Hz, $J_{C,P}$ = 6.5 Hz, C-1/6-C(*C*H$_3$)$_3$], 35.4 [s, broad, C-1/6-*C*(CH$_3$)$_3$ and C-4-*C*(CH$_3$)$_3$], 44.3 [m, P-2-*C*H$_2$CH(CH$_3$)$_2$ and C-1/6], 101.3 (dd, $^1J_{C,P}$ = 51.0 Hz, $^1J_{C,P}$ = 15.9 Hz, C-4), 215.1 (d, $^2J_{C,P}$ = 12.0 Hz, 4 CO). – MS (CI, 120 eV); *m/z* (%): 667 (14) [$M^+ + H$], 609 (19) [$M^+ - 2\ CO - H$], 499 (49) [$M^+ + H - Fe(CO)_4$], 442 (24) [$M^+ - Fe(CO)_4 - C_4H_8$], 441 (100) [$M^+ - Fe(CO)_4 - C_4H_9$]. – $C_{31}H_{54}AlFeO_4P_3$ (666.51).

Pentacarbonyl{(3-η)-1,4,6-tri-tert-butyl-2,7,7-triisobutyl-3,5-diphospha-2-phosphonia-7-aluminatotricyclo[3.2.0.0^{2,6}]hept-3-ene}tungsten (**6b**): A solution of hexacarbonyltungsten (0.35 g, 1.00 mmol) in THF (50 ml) was irradiated at 0°C. After 0.5 h triphosphaalatricycloheptene **5a** (0.20 g, 0.40 mmol) in THF (5 ml) was added at 25°C and the reaction mixture was allowed to stir for 14 h, followed by evaporation of all volatile components (25°C/10^{-3} mbar). The residue was extracted with pentane (10 ml) and filtered. Recrystallization at −78°C from the same solvent provided 0.25 g of **6b** (76%), orange crystals. – IR (pentane, cm^{-1}): $\tilde{\nu}$ = 2076 (m, CO), 1960 (s, CO), 1948 (s, CO), 1260 (m), 1100 (m), 1018 (m), 806 (m). – ^{31}P NMR (C_6D_6): δ = 40.0 (dd, $^2J_{P,P}$ = 52.7 Hz, $^2J_{P,P}$ = 15.6 Hz, P-5), 59.6 (dd, $^2J_{P,W}$ = 24.4 Hz, $^1J_{P,P}$ = 199.0 Hz, $^2J_{P,P}$ = 52.7 Hz, P-2), 191.0 (dd, $^1J_{P,W}$ = 234.1 Hz, $^1J_{P,P}$ = 199.0 Hz, $^2J_{P,P}$ = 15.6 Hz, P-3). – ^{1}H NMR (C_6D_6): δ = 0.47 [d, $^3J_{H,H}$ = 7.3 Hz, 2 H, AlCH_2CH(CH$_3$)$_2$], 0.72 [dd, $J_{P,H}$ = 2.6 Hz, $^3J_{H,H}$ = 7.3 Hz, 2 H, AlCH_2CH(CH$_3$)$_2$], 1.05 [d, $^3J_{H,H}$ = 6.4 Hz, 6 H, CH$_2$CH(CH_3)$_2$], 1.10 [s, 18 H, 2 C(CH_3)$_3$], 1.26 [d, $^3J_{H,H}$ = 6.5 Hz, 6 H, CH$_2$CH(CH_3)$_2$], 1.29 [d, $^3J_{H,H}$ = 6.5 Hz, 6 H, CH$_2$CH(CH_3)$_2$], 1.41 [s, 9 H, C(CH_3)$_3$], 2.14–2.25 [m, 1 H, CH$_2$CH(CH$_3$)$_2$], 2.25–2.33 [m, 1 H, CH$_2$CH(CH$_3$)$_2$], 2.46–2.59 [m, 3 H, CH$_2$CH(CH$_3$)$_2$ and P-2-CH_2CH(CH$_3$)$_2$]. – ^{13}C NMR (C_6D_6): δ =

25.2 [d, $J_{C,P}$ = 7.0 Hz, P-2-$CH_2CH(CH_3)_2$], 25.4 [d, $J_{C,P}$ = 4.9 Hz, $CH_2CH(CH_3)_2$], 26.5 [s, broad, 2 $AlCH_2CH(CH_3)_2$], 27.7 [s, $CH_2CH(CH_3)_2$], 27.8 [s, $CH_2CH(CH_3)_2$], 29.0 [s, $AlCH_2CH(CH_3)_2$], 29.1 [s, $AlCH_2CH(CH_3)_2$], 32.4 [pseudo-t, $J_{C,P}$ = 10.3 Hz, $J_{C,P}$ = 10.3 Hz, C-4-$C(CH_3)_3$], 34.2 [pseudo-t, $J_{C,P}$ = 6.8 Hz, $J_{C,P}$ = 6.8 Hz, C-1/6-$C(CH_3)_3$], 35.5 [s, broad, C-1/6-$C(CH_3)_3$ and C-4-$C(CH_3)_3$], 44.4 [dd, $^1J_{C,P}$ = 23.2 Hz, $J_{C,P}$ = 8.6 Hz, P-2-$CH_2CH(CH_3)_2$], 45.9 (m, C-1/6), 101.3 (dd, $^1J_{C,P}$ = 50.5 Hz, $^1J_{C,P}$ = 15.0 Hz, C-4), 195.9 (d, $^2J_{C,P}$ = 8.1 Hz, $^1J_{C,W}$ = 130.4 Hz, 4 *cis*-CO), 198.4 (d, $^2J_{C,P}$ = 31.8 Hz, *trans*-CO). – MS (CI, 120 eV); *m/z* (%): 823 (1) [M^+ + H], 767 (3) [M^+ + H – 2 CO], 683 (2) [M^+ + H – 5 CO], 499 (21) [M^+ + H – $W(CO)_5$], 441 (100) [M^+ + H – $W(CO)_5$ – C_4H_{10}]. – $C_{32}H_{54}AlO_5P_3W$ (822.53).

Triethyl{(7-η)-1,4,6-tri-tert-butyl-2,5,7-triethyl-3,7-diphospha-2-phosphonia-5-gallatotricyclo-[3.2.0.0^{2,6}]hept-3-ene}gallium (**8a**): To a magnetically stirred solution of 0.25 g (1.60 mmol) of triethylgallium (**7**) in diethyl ether (10 ml) was added 0.48 g (4.80 mmol) of phosphaalkyne **1a**. After the reaction mixture had been stirred at room temperature for 48 h, all volatile components were removed at 25°C/10^{-3} mbar. The remaining crude product was taken up in pentane and purified by recrystallization at +4°C: 0.48 g, 49% yield, yellow crystals, m.p. 45–48°C. – IR (pentane, cm^{-1}): $\tilde{\nu}$ = 1360 (s), 1260 (s), 1238 (m), 1100 (s), 1020 (s), 806 (s), 692 (m), 656 (m). – ^{31}P NMR (C_6D_6): δ = 38.2 (dd, $^2J_{P,P}$ = 40.2 Hz, $^2J_{P,P}$ = 25.0 Hz, P-7), 41.6 (dd, $^1J_{P,P}$ = 336.8 Hz, $^2J_{P,P}$ = 40.2 Hz, P-2), 253.6 (dd, $^1J_{P,P}$ = 336.8 Hz, $^2J_{P,P}$ = 25.0 Hz, P-3). – ^{1}H NMR (C_6D_6): δ = 0.80 [q, $^3J_{H,H}$ = 8.1 Hz, 6 H, $Ga(CH_2CH_3)_3$], 0.94 (q, $^3J_{H,H}$ = 8.0 Hz, 2 H, $GaCH_2CH_3$), 1.03 [s, 18 H, 2 C-1/6-$C(CH_3)_3$], 1.30–1.35 (m, 6 H, 2 PCH_2CH_3), 1.31 [d, $J_{P,H}$ = 1.5 Hz, 9 H, C-4-$C(CH_3)_3$], 1.36 (t, $^3J_{H,H}$ = 8.0 Hz, 3 H, $GaCH_2CH_3$), 1.52 (t, $^3J_{H,H}$ = 8.1 Hz, 9 H, 3 $GaCH_2CH_3$), 2.05–2.10 (m, 2 H, PCH_2CH_3), 2.30–2.37 (m, 2 H, PCH_2CH_3). – ^{13}C NMR (C_6D_6): δ = 7.1 (s, broad, CH_2CH_3), 10.8 (s, CH_2CH_3), 10.9 (d, $J_{C,P}$ = 4.9 Hz, CH_2CH_3), 11.0 (d, $J_{C,P}$ = 4.8 Hz, CH_2CH_3), 11.8 (d, $J_{C,P}$ = 13.2 Hz, CH_2CH_3), 12.0 (s, CH_2CH_3), 14.1 (d, $J_{C,P}$ = 14.6 Hz, CH_2CH_3), 18.8 (s, broad, CH_2CH_3), 29.2 [pseudo-t, $J_{C,P}$ = 26.8 Hz, $J_{C,P}$ = 26.8 Hz, C-4-$C(CH_3)_3$], 31.6 [d, $J_{C,P}$ = 13.6 Hz, C-4-$C(CH_3)_3$], 34.4 [dd, $J_{C,P}$ = 7.5 Hz, $J_{C,P}$ = 4.9 Hz, C-1/6-$C(CH_3)_3$], 35.1 [dd, $J_{C,P}$ = 4.9 Hz, $J_{C,P}$ = 1.6 Hz, C-1/6-$C(CH_3)_3$], 46.5 (dd, $^1J_{C,P}$ = 23.2 Hz, $^1J_{C,P}$ = 16.7 Hz, C-1/6), 79.0 (d, broad, $^1J_{C,P}$ = 15.0 Hz, C-4). – MS (EI, 70 eV); *m/z* (%): 457 (34) [M^+ + H – $Ga(C_2H_5)_3$], 428 (100) [M^+ – $Ga(C_2H_5)_3$ – C_2H_4], 328 (76) [M^+ – $Ga(C_2H_5)_3$ – C_2H_4 – PC_5H_9], 227 (93) [M^+ – $Ga(C_2H_5)_3$ – C_2H_5 – 2 PC_5H_9]. – HR MS (EI, 70 eV); [M^+ – $Ga(C_2H_5)_3$]: calcd. 456.1755; found 456.1761. – $C_{27}H_{57}Ga_2P_3$ (614.10): calcd. C 52.81, H 9.36; found C 50.28, H 9.00.

Triethyl{(7-η)-1,4,6-triadamant-1-yl-2,5,7-triethyl-3,7-diphospha-2-phosphonia-5-gallatotricyclo[3.2.0.0^{2,6}]hept-3-ene}gallium (**8b**): To a magnetically stirred solution of 0.13 g (0.83 mmol) of triethylgallium (**7**) in diethyl ether (10 ml) was added 0.44 g (2.50 mmol) of phosphaalkyne **1c**. After the reaction mixture had been stirred at room temperature for 72 h, all volatile components were removed at 25°C/10^{-3} mbar. The remaining crude product was taken up in pentane and purified by recrystallization at +4°C: 0.30 g, 43% yield, yellow crystals. – IR (pentane, cm^{-1}): $\tilde{\nu}$ = 1260 (s), 1100 (s), 1020 (s), 806 (s). – ^{31}P NMR (C_6D_6): δ = 36.1 (dd, $^1J_{P,P}$ = 333.8 Hz, $^2J_{P,P}$ = 58.6 Hz, P-2), 40.3 (dd, $^2J_{P,P}$ = 58.6 Hz, $^2J_{P,P}$ = 27.2 Hz, P-7), 257.0 (dd, $^1J_{P,P}$ = 333.8 Hz, $^2J_{P,P}$ = 27.2 Hz, P-3). – ^{1}H NMR (C_6D_6): δ = 1.22 (q, $^3J_{H,H}$ = 7.9 Hz, 2 H, CH_2CH_3), 1.35–2.20 (m, 71 H, CH_2CH_3 and Ad-H), 2.35–2.45 (m, 2 H, PCH_2CH_3). – MS (CI, 120 eV); *m/z* (%): 661 (1) [M^+ – $Ga(C_2H_5)_3$ – C_2H_5], 495 (25) [M^+ – $Ga(C_2H_5)_3$ – 2 C_2H_6 – $C_{10}H_{15}$], 255 (100) [M^+ – $Ga(C_2H_5)_3$ – C_2H_6 – 3 $C_{10}H_{15}$]. – $C_{45}H_{75}Ga_2P_3$ (848.44).

Crystal Structure Analysis of **8a**[22]: Enraf-Nonius CAD4 diffractometer, graphite monochromator, Mo-K_α radiation, structure solution by heavy-atom method (SHELXS-97[23]) and structure refinement by SHELXL-97[24]; monoclinic, space group $P2_1/n$; lattice constants a = 11.191(2), b = 20.303(3); c = 15.156(2) Å, β = 107.95(1)°, V = 3276.0(7) Å^3, Z = 4, μ(Mo-K_α) = 1.804 mm^{-1}, crystal size 0.25 × 0.35 × 0.39 mm; θ_{max} = 27.4°; 7470 independent reflections (R_{int} = 0.0453) measured of which 3670 were considered observed with $I > 2\sigma(I)$; analytical absorption correction: max./min. transmission 0.5061/0.6588; max./min. residual electronic density 0.351 and −0.475 e/Å^3. 289 parameters [C, Ga and P anisotropic, the positions of the H atoms were calculated for idealized positions ($d_{C\text{-}H}$ = 0.980 Å)]; R_1 = 0.0462; wR^2 = 0.1009.

[1] M. Schmitz, S. Leininger, U. Bergsträßer, M. Regitz, *Heteroatom Chem.*, in press.

[2] See for example: [2a] M. Regitz, T. Wettling, B. Breit, M. Birkel, B. Geißler, U. Bergsträßer, S. Barth, P. Binger, *Phosphorus Sulfur* **1993**, *76*, 1–4. – [2b] R. Streubel, *Angew. Chem.* **1995**, *107*, 478–480; *Angew. Chem. Int. Ed. Engl.* **1995**, *34*, 436–438. – [2c] M. Regitz, A. Hoffmann, U. Bergsträßer, in *Modern Acetylene Chemistry* (Eds.: F. Diederich, P. Stang), VCH, New York **1995**, p. 173. – [2d] M. Regitz, T. Wettling, R. Fäßler, B. Breit, B. Geißler, M. Julino, A. Hoffmann, U. Bergsträßer, *Phosphorus Sulfur* **1996**, *109/110*, 425–428. – [2e] A. Mack, M. Regitz, *Chem. Ber.* **1997**, *130*, 823–834.

[3] [3a] G. Becker, W. Becker, R. Knebl, H. Schmidt, U. Hildenbrand, M. Westerhausen, *Phosphorus Sulfur* **1987**, *30*, 349–352. – [3b] B. Breit, U. Bergsträßer, G. Maas, M. Regitz, *Angew. Chem.* **1992**, *104*, 1043–1046; *Angew. Chem. Int. Ed. Engl.* **1992**, *31*, 1055–1058. – [3c] B. Breit, M. Regitz, *Chem. Ber.* **1996**, *129*, 489–494.

[4] B. Breit, A. Hoffmann, U. Bergsträßer, L. Ricard, F. Mathey, M. Regitz, *Angew. Chem.* **1994**, *106*, 1541–1543; *Angew. Chem. Int. Ed. Engl.* **1994**, *33*, 1491–1493.

[5] A. Hoffmann, B. Breit, M. Regitz, *Chem. Ber.* **1997**, *130*, 255–259.

[6] A. Hoffmann, S. Leininger, M. Regitz, *J. Organomet. Chem.* **1997**, *539*, 61–66.

[7] A similar Lewis acid induced cyclotrimerization takes place, when tantalum pentachloride is allowed to react with phosphaalkyne **1a**[3a].

[8] For the ^{31}P-NMR absorptions see, for example: J. C. Tebby, *Handbook of Phosphorus-31 Nuclear Magnetic Resonance Data*, CRC Press, Boca Raton, **1991**, p. 29.

[9] See, for example: J. G. Verkade, L. D. Quin, *Phosphorus-31-NMR-Spectroscopy in Stereochemical Analysis*, VCH, Deerfield Beach, **1987**, p. 446.

[10] The structure of the cyclotrimerization product **5d** is confirmed by an X-ray structure analysis. Due to the unsatisfactory quality of the data, the bond lengths and bond angles are not discussed.

[11] P. S. Braterman, W. J. Wallace, *J. Organomet. Chem.* **1971**, *30*, C17–C18.

[12] W. Strohmeier, F.-J. Müller, *Chem. Ber.* **1969**, *102*, 3608–3612.

[13] Ref.[9], p. 430.

[14] [14a] R. H. Neilson, R. J. Thoma, I. Vickovic, W. H. Watson, *Organometallics* **1984**, *3*, 1132–1133. – [14b] R. Appel, C. Casser, *Tetrahedron Lett.* **1984**, *25*, 4109–4112.

[15] G. Bähr, P. Burba, H. Lehmkuhl, K. Ziegler, in *Houben-Weyl: Methoden der Organischen Chemie* (Ed.: E. Müller), vol. 13/4 ("Metallorganische Verbindungen Al, Ga, In, Tl"), 4th ed., **1970**, p. 315.

[16] D. R. Lide, *CRC Handbook of Chemistry and Physics*, 73rd ed., CRC Press, Boca Raton, **1992**, chapter 9–1.

[17] R. Appel, in *Multiple Bonds and Low Coordination in Phosphorus Chemistry* (Eds.: M. Regitz, O. J. Scherer), Thieme, Stuttgart, **1990**, p. 160.

[18] G. Müller, J. Lachmann, *Z. Naturforsch., B: Chem. Sci.* **1993**, *48*, 1544–1554.

[19] W. Rösch, T. Allspach, U. Bergsträßer, M. Regitz in *Synthetic Methods of Organometallic and Inorganic Chemistry*, vol. 3 (Ed.: H. H. Karsch), Thieme, Weinheim, **1996**, pp. 11.

[20] W. Rösch, U. Vogelbacher, T. Allspach, M. Regitz, *J. Organomet. Chem.* **1986**, *306*, 39−53.
[21] Note: the signals of $AlCH_2CH(CH_3)_2$ and $C(CH_3)_2CH_2CH_3$ cannot be reported since they are obscured by other signals.
[22] Crystallographic data (excluding structure factors) for the structure reported in this paper have been deposited with the Cambridge Crystallographic Data Centre as supplementary publication no. CCDC-101440. Copies of the data can be obtained free of charge on application to CCDC, 12 Union Road, Cambridge CB2 1EZ, UK [fax: int. code + 44(1223)336-033; e-mail: deposit@ccdc.cam.ac.uk].
[23] G. M. Sheldrick, *SHELXS-97*, *Program for Crystal Structure Solution*, Universität Göttingen, **1997**.
[24] G. M. Sheldrick, *SHELXL-97*, *Program for Crystal Structure Refinement*, Universität Göttingen, **1997**.

[98161]

A Novel Route to Formaldehyde and Thioformaldehyde Rhodium Complexes☆

Helmut Werner*[a], Margarete Steinmetz[a], Karl Peters[b], and Hans Georg von Schnering[b]

Institut für Anorganische Chemie der Universität Würzburg[a],
Am Hubland, D-97074 Würzburg, Germany

Max-Planck-Institut für Festkörperforschung[b],
Heisenbergstraße 1, D-70506 Stuttgart, Germany

Received June 9, 1998

Keywords: Rhodium / Carbenoide metal complexes / Formaldehyde complexes / Thioformaldehyde complexes / Cyclopentadienyl complexes

The acetoxymethyl rhodium compounds $[(\eta^5\text{-}C_5R_5)Rh(CH_2OAc)(L)I]$ (**4**, **13**–**16**) which were prepared from the chloromethyl derivatives $[(\eta^5\text{-}C_5R_5)Rh(CH_2Cl)(L)I]$ and sodium acetate in benzene/acetic acid as solvent, reacted with $AgPF_6$ to give the chelate complexes $[(\eta^5\text{-}C_5R_5)Rh\{\kappa^2\text{-}C,O\text{-}CH_2OC(Me)O\}(L)]PF_6$ (**19**–**23**) in excellent yields. Treatment of these complexes with KOH in methanol led to the elimination of the acetyl group and to the formation of the formaldehyde compounds $[(\eta^5\text{-}C_5R_5)Rh(\eta^2\text{-}CH_2O)(L)]$ (**24**–**27**). The related thioformaldehyde complexes $[(\eta^5\text{-}C_5Me_5)Rh(\eta^2\text{-}CH_2S)(L)]$ (**46**, **47**) and $[(\eta^5\text{-}C_5H_5)Rh(\eta^2\text{-}CH_2S)(PMe_3)]$ (**50**) were obtained on a similar route. Studies on the reactivity of the formaldehyde derivatives revealed that the Rh–CH_2O bond is rather labile and the CH_2O ligand easily converted to a CO group.

In a series of papers we have recently shown[1] that cobalt and rhodium half-sandwich type complexes, which contain $MI(CH_2I)$ as a molecular unit, can be transformed to the corresponding thio-, seleno-, and telluroformaldehyde metal derivatives upon treatment with SH^-, SeH^-, and TeH^-, respectively (see Scheme 1). Due to the lone electron pairs at the chalcogen atom of the CH_2E ligand, these compounds behave as Lewis bases and react with in situ generated 16-electron fragments such as $[W(CO)_5]$ or $[(\eta^5\text{-}C_5H_5)Mn(CO)_2]$ to give dinuclear hetero-metallic complexes with the aldehyde CH_2E in a bridging position.[1d][2] First attempts to complete the series of compounds $[(\eta^5\text{-}C_5R_5)M(\eta^2\text{-}CH_2E)(L)]$ by those with E = O failed. The reaction of the respective precursor $[(\eta^5\text{-}C_5R_5)M(L)(L')]$ with monomeric formaldehyde was rather slow and in most cases led to a mixture of products among which the carbonyl complexes $[(\eta^5\text{-}C_5R_5)M(CO)(L)]$ were the dominating species. Therefore, we had to develop a different synthetic route. The present paper describes that for M = Rh the key to success was the preparation of metalated acetic acid derivatives $[Rh]CH_2OC(O)CH_3$ as intermediates which could be converted in two steps to the coordinated formaldehyde ligand. Some related results to this work were already reported.[3]

Scheme 1

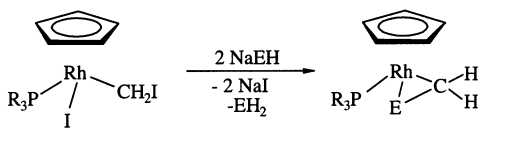

Results

Preparation of $RhCH_2OAc$ Precursors

The carbenoide rhodium complex **1**, which can easily be prepared from $[C_5Me_5Rh(CO)_2]$ and CH_2I_2,[4] reacts quite smoothly in polar solvents with sodium acetate. While in acetone a mixture of products is formed, the reaction of **1** with excess NaOAc in methanol leads to the methoxymethyl compound **2** in good yield. In contrast, the starting material **1** and NaOAc react in ethanol to give two products **3** and **4** (see Scheme 2), which could be separated by chromatographic techniques. Although the desired acetoxy derivative **4** is the dominating species provided that an excess of sodium acetate is used, the separation of the two compounds on Al_2O_3 results in the partial conversion of **4**

Scheme 2. [Ac = CH_3CO]

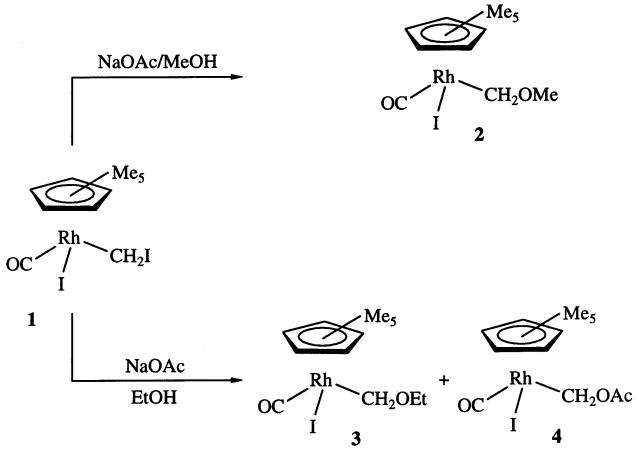

 © WILEY-VCH Verlag GmbH, D-69451 Weinheim, 1998 1434–1948/98/1111–1605 $ 17.50+.50/0

Scheme 3. [Ac = CH_3CO]

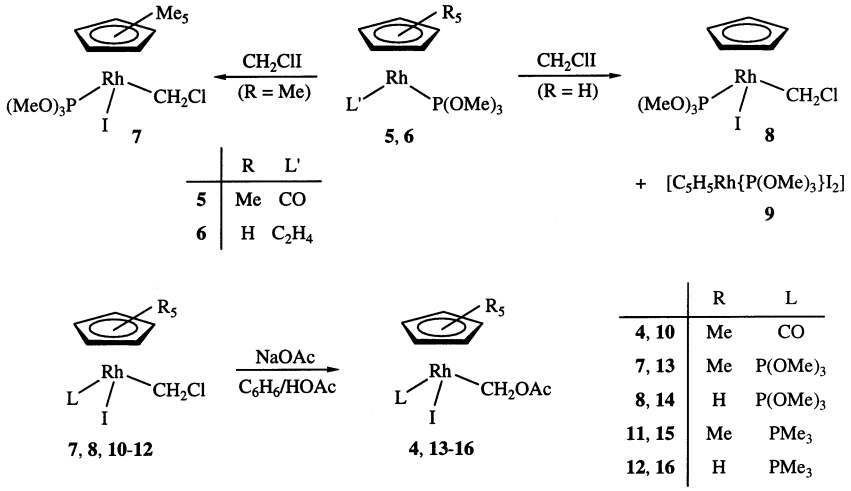

to the dinuclear complex [{(η^5-C_5Me_5)Rh(μ-CO)}$_2$]. Therefore, the isolated yield is rather low.

The method of choice for the preparation of **4** is the reaction of **7** with excess NaOAc in a mixture of benzene and glacial acetic acid as the solvent. Under these conditions, not only **4** but also the half-sandwich type Rh−CH_2OAc complexes **13**−**16** (Scheme 3) have been obtained in 80−85% yield. The synthesis of the formerly unknown chloromethyl rhodium(III) precursors **7** and **8** was achieved by oxidative addition (followed by elimination of CO or C_2H_4) of CH_2ClI to [(η^5-C_5Me_5)Rh(CO){$P(OMe)_3$}] and [(η^5-C_5H_5)Rh(C_2H_4){$P(OMe)_3$}], respectively. We note that the rate of formation of **15** from **11** is significantly higher than from [(η^5-C_5Me_5)Rh(CH_2I)(PMe_3)I][4] which can be understood by the HSAB concept: Substitution of the hard chloride by the hard nucleophile OAc^- is favoured compared to the displacement of the soft iodide by acetate.[5]

The acetoxymethyl derivatives **4** and **13**−**16** are yellow to red-brown microcrystalline solids, which are air-stable and soluble in common organic solvents. The most typical feature of the ^{1}H-NMR spectra of **4** and **13**−**16** is the appearance of two distinct signals for the methylene protons of the CH_2OAc group which due to Rh-H, H-H, and in some cases P-H coupling are split into doublets of doublets or appear as doublets of doublets of doublets. Since the size of ^3J(PH), which depends on the mutual orientation of the phosphorus and the hydrogen atoms of the $PRhCH_2$ unit,[6] differs considerably (e.g. between 0 Hz and 8.8 Hz for **15**), we assume that the rotation around the Rh−CH_2O axis is partially hindered and the conformations **A** or **B** (Figure 1) are preferred. A similar observation has already been made for compounds such as **12** and [(η^5-C_5H_5)Rh(CH_2X)-(PMe_3)X] (X = Br, I)[7] as well as for related cyclopentadienyliron derivatives [(η^5-C_5H_5)Fe(CH_2R)(CO)(PR'_3)] (R = Ph, $SiMe_3$).[8]

Figure 1. Conformations of compounds [(η^5-C_5R_5)Rh(CH_2X)(L)I] (X = Cl, OAc) viewed along the Rh−C axis. Due to the formally octahedral geometry the bond angle P−Rh−I is assumed to be 90° (see also ref.[8])

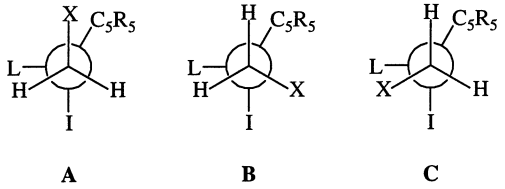

Conversion of $RhCH_2OAc$ to Rh(η^2-CH_2O) Complexes

Attempts to convert the acetoxymethyl compounds **4** and **13**−**16** to the corresponding formaldehyde complexes by using different nucleophiles failed.[9] Whereas treatment of **4** with NaOMe in methanol/benzene or with *n*BuLi in benzene led mainly to decomposition (and to the formation of small amounts of [{(η^5-C_5Me_5)Rh(μ-CO)}$_2$]), the reaction of **15** with NaOMe in methanol or with NaOH in water/benzene in the presence of [$PhCH_2NEt_3$]Cl (TEBA) as phase-transfer catalyst gave mainly the mononuclear compound [(η^5-C_5Me_5)Rh(CO)(PMe_3)].[10] Although the ^{1}H-NMR spectrum of the reaction mixture formed from **15** and NaOMe in CD_3OD showed that besides the carbonyl complex [(η^5-C_5Me_5)Rh(CO)(PMe_3)] the corresponding formaldehyde compound **26** (see Scheme 5) is probably formed, the attempts to separate the two C_5Me_5Rh species by chromatographic techniques failed. One noteworthy result is that from the mixture of products obtained upon treatment of the trimethylphosphite complex **14** with two equiv of *n*BuLi in benzene/hexane the half-sandwich type rhodium(III) derivatives **17** and **18** (Scheme 4) could be isolated in low yield. The ^{1}H NMR data as well as the mass spectra and (in the case of **17**) the elemental analysis revealed that both in **17** and **18** a Rh−C_6H_5 bond is present, the phenyl group originating either from benzene or from in situ generated LiPh, respectively.

The methodology for the successful preparation of the formaldehyde rhodium complexes **24**−**27** is outlined in Scheme 5. Instead of an attack of a nucleophile to the carbon atom of the acetoxy unit of **4** and **13**−**16** the first step involves the cleavage of the Rh−I linkage by $AgPF_6$. This is followed by the formation of a five-membered chelate

Scheme 4. [Ac = CH_3CO]

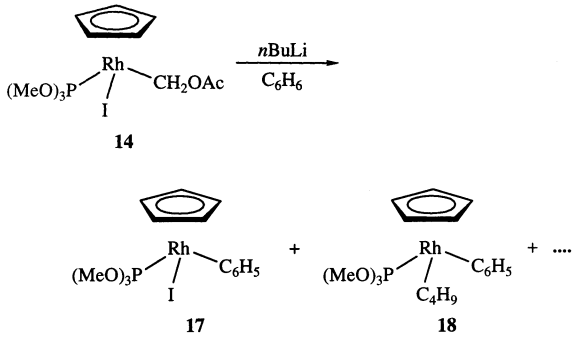

ring. Since the coordination of the carbonyl oxygen atom to the metal increases the δ+ charge at the C=O carbon atom, a subsequent nucleophilic attack at this carbon is preferred. Finally, the products **24**–**27** are obtained in moderate yield. It should be emphasized that even treatment of the highly reactive bis(trimethylphosphane) compounds $[(\eta^5\text{-}C_5H_5)Rh(PMe_3)_2]$ and $[(\eta^5\text{-}C_5Me_5)Rh(PMe_3)_2]$[11] with formaldehyde does not lead to **26** and **27** but instead gives the carbonyl derivatives $[(\eta^5\text{-}C_5H_5)Rh(CO)(PMe_3)]$ and $[(\eta^5\text{-}C_5Me_5)Rh(CO)(PMe_3)]$.

Scheme 5

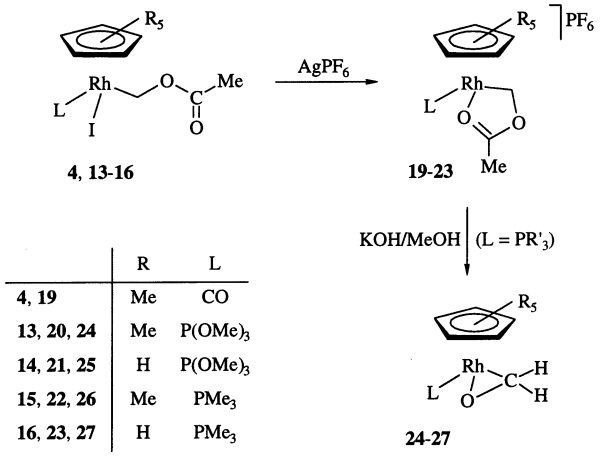

	R	L
4, 19	Me	CO
13, 20, 24	Me	$P(OMe)_3$
14, 21, 25	H	$P(OMe)_3$
15, 22, 26	Me	PMe_3
16, 23, 27	H	PMe_3

The chelate complexes **19**–**23** are yellow to orange-yellow air-stable solids which in nitromethane display the conductivity expected for 1:1 electrolytes. The spectroscopic data of **19**–**23** and of the non-ionic precursors **4** and **13**–**16** differ insofar, as in the ^{13}C NMR spectra of **19**–**23** the signal of the C=O carbon atom is shifted significantly (16–20 ppm) to lower field due to the interaction of the acetyl moiety with the metal. In the IR spectra of the chelate compounds the C=O stretching frequency is also reduced and appears at 1600–1610 cm^{-1} compared with 1700–1720 cm^{-1} for **4** and **13**–**16**, respectively. For the dicyclopentadienylvanadium complexes $[(\eta^5\text{-}C_5H_5)_2V\{\eta^1\text{-}CH_2OC(O)R\}Cl]$ and $[(\eta^5\text{-}C_5H_5)_2V\{\kappa^2\text{-}C,O\text{-}CH_2OC(R)O\}]BPh_4$ an almost identical trend has been observed.[12]

The result of the X-ray crystal structure analysis of **22** is shown in Figure 2. The acetoxymethyl unit acts as a bidentate ligand and forms a nearly planar five-membered ring with the rhodium center. The distance C2–O1 [1.240(8) Å] indicates significant double bond character which is in agreement with the bonding pattern shown for **19**–**23** in Scheme 5. The corresponding C=O bond length in the vanadium complex $[(\eta^5\text{-}C_5H_5)_2V\{\kappa^2\text{-}C,O\text{-}CH_2OC(Me)O\}]^+$ is 1.236(4) Å[12] and thus almost identical to that in **22**. Compared with C2–O1, the distance C2–O3 [1.307(8) Å] is considerably longer and quite similar to the C–O(W) distance found in $[(\eta^5\text{-}C_5H_5)W(CO)_3(OAc)]$.[13] The Rh–C4 bond length [2.067(6) Å] is somewhat shorter than in related cationic cyclopentadienylrhodium compounds such as $[(\eta^5\text{-}C_5H_5)Rh(CH_2NC_5H_5)(PMe_3)I]^+$ [14] and $[(\eta^5\text{-}C_5H_5)\text{-}RhCH_3(CO)(PPh_2R)]^+$ [R = NHCH(Me)Ph][15] which could be due to the electronic effect caused by the OAc group. The Rh–C4–O3 bond angle is 109.7(4)° which is consistent with the sp^3 hybridization of the CH_2 carbon atom. The distances between rhodium and the carbon atoms of the C_5Me_5 ring are in the usual range for complexes containing the $C_5Me_5Rh(PMe_3)$ unit.[16] However, as has previously been observed for those half-sandwich type compounds with π-donating ligand,[7][17] the metal–carbon bond lengths [Rh–C5 and Rh–C6] *trans* to this ligand are shorter than the other Rh–C(ring) distances.

Figure 2. Molecular structure of **22**[a] (thermal elipsoids with 50% probability)

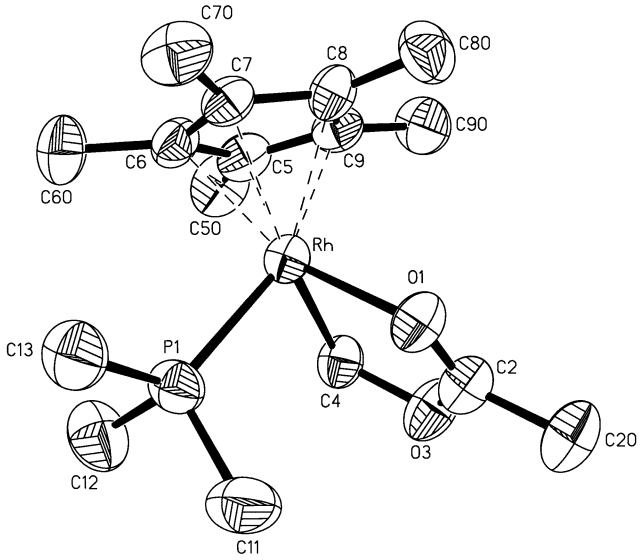

[a] Selected bond lengths [Å] and angles [°]: Rh–P1 2.300(2), Rh–O1 2.112(4), Rh–C4 2.067(6), Rh–C5 2.170(6), Rh–C6 2.179(6), Rh–C7 2.254(6), Rh–C8 2.230(7), Rh–C9 2.198(6), O1–C2 1.240(8), C2–O3 1.307(8), C2–C20 1.501(9), O3–C4 1.471(7); P1–Rh–O1 91.3(1), P1–Rh–C4 87.7(2), O1–Rh–C4 77.9(2), Rh–O1–C2 113.9(4), O1–C2–O3 122.2(6), O1–C2–C20 122.6(6), O3–C2–C20 115.2(6), C2–O3–C4 116.0(5), Rh–C4–O3 109.7(4).

The second step of the synthesis of compounds **24**–**27** (see Scheme 5) proved to be difficult. Treatment of the acetoxymethyl complexes **20**–**23** with NaOMe or KOH in methanol at room temperature gave in each case a mixture of products with the carbonyl and the formaldehyde compounds $[(\eta^5\text{-}C_5R_5)Rh(CO)(L)]$ and $[(\eta^5\text{-}C_5R_5)Rh(\eta^2\text{-}CH_2O)(L)]$ as the dominating species. Attempts to separate

these mixtures by chromatographic techniques led mainly to the isolation of the Rh−CO complexes. However, the rate of the decomposition of the formaldehyde derivatives to $[(\eta^5\text{-}C_5R_5)Rh(CO)(L)]$ could be considerably reduced if the reaction of **20**−**23** with base was carried out at low temperature. After the reaction mixture was worked up at 0°C, oily products were obtained which could partly be converted to yellow-brown microcrystalline solids. Since the formaldehyde compounds **24**−**27** are not only labile (and air-sensitive) but also readily soluble in pentane, the yield of the isolated solids did not exceed 30%.

Even more labile than the trimethylphosphite and trimethylphosphane complexes **24**−**27** is the corresponding carbonyl derivative $[(\eta^5\text{-}C_5Me_5)Rh(\eta^2\text{-}CH_2O)(CO)]$. Addition of excess NaOMe to a solution of **19** in methanol at −78°C led initially to the formation of a clear yellow solution which rapidly turned blue if the same work-up procedure was used as applied for **24**−**27**. The isolated product consisted of both $[(\eta^5\text{-}C_5Me_5)Rh(CO)_2]$ and the dinuclear compound $[\{(\eta^5\text{-}C_5Me_5)Rh(\mu\text{-}CO)\}_2]$. However, the ^{1}H-NMR spectrum of the reaction mixture in CD_3OD at −40°C displayed two doublets of doublets at δ 5.67 [J(RhH) = 4.4, J(HH) = 6.1 Hz] and 5.46 [J(RhH) = 0.6, J(HH) = 6.1 Hz] and one doublet at δ 1.66 [J(RhH) = 0.4 Hz] which can be assigned to the CH_2 and C_5Me_5 protons of $[(\eta^5\text{-}C_5Me_5)Rh(\eta^2\text{-}CH_2O)(CO)]$, respectively.

With regard to the spectroscopic data of the isolated formaldehyde complexes, we note that at least in the case of **25**, **26**, and **27** for the methylene protons of the coordinated CH_2O ligand two distinct signals (both doublets of doublets of doublets) have been observed. The ^2J(HH) coupling of 18.2−21.5 Hz lies between that of free formaldehyde (42.2 Hz) and ethylenoxide (5.5 Hz)[18] and indicates some double bond character for the C−O bond. The H-H coupling constant of **25**−**27** is quite similar to that of the cationic rhenium compound $[(\eta^5\text{-}C_5H_5)Re(\eta^2\text{-}CH_2O)(NO)(PPh_3)]^+$ (16.6 Hz)[19] for which according to the structural data also a partial C−O double bond character has been postulated. We note that a three-membered MCO ring as shown in Scheme 6 dominates the structural chemistry of formaldehyde complexes containing the $Zr(C_5H_5)_2$ unit which is probably due to the higher oxophilicity of electron-poor transition-metal centres.[12][20]

To find out whether complexes that are structurally related to **19**−**23** are also suitable starting materials for the generation of formaldehyde rhodium derivatives, compounds **28** and **29** (Scheme 6) have been prepared. Both were obtained via the same route as **16** and **23** and characterized by elemental analysis and spectroscopic means. However, treatment of **29** with various bases led to a mixture of products among which **27** could not be exactly identified.

Scheme 6

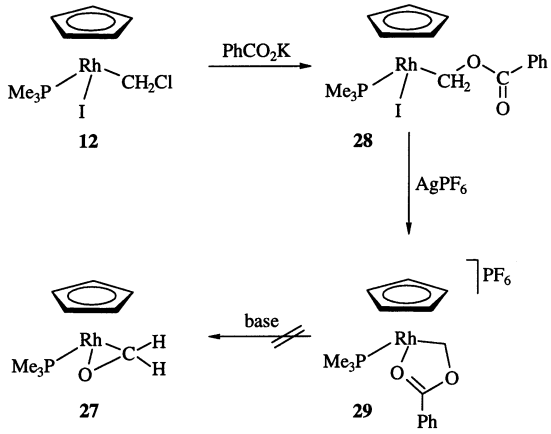

Reactions of Rh(η^2-CH_2O) Complexes

The striking lability of the formaldehyde rhodium complexes $[(\eta^5\text{-}C_5R_5)Rh(\eta^2\text{-}CH_2O)(L)]$ initiated a series of experiments aimed to find out whether during the decomposition besides the carbonyl derivatives other compounds are formed too. If the course of the thermal decomposition of **24**, **26**, and **27** in C_6D_6 is studied in an NMR tube at room temperature, the complexes $[(\eta^5\text{-}C_5R_5)Rh(CO)(L)]$ indeed are the most dominating species among the observed products. After completion of the reaction the spectroscopically determined yield of the carbonyl compounds is 80−90%. Hydrido complexes such as $[(\eta^5\text{-}C_5Me_5)RhH_2(PMe_3)]$[21] could not be detected. The most surprising discovery was that in contrast to the thermolysis of **24** which gave almost quantitatively $[(\eta^5\text{-}C_5Me_5)Rh(CO)\{P(OMe)_3\}]$,[22] the corresponding reaction of **25** led to a mixture of **31** and **32** (Scheme 7) in the ratio of ca. 70:30 under the same conditions (benzene, 25°C). If a somewhat higher concentration of **25** is used, the relative amount of the dinuclear complex increases and, after fractional crystallization, the isolated yield of **31** (which is a green moderately air-sensitive solid) is about 40%.

Scheme 7

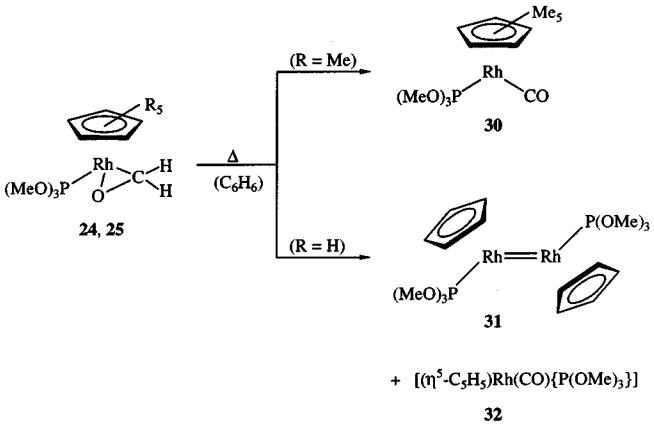

The structural proposal for **31** is mainly supported by the mass spectrum and the NMR spectroscopic data. In the mass spectrum peaks for M^+, $M^+ - P(OMe)_3$, and $M/2^+$ are observed, which is in agreement with the presence of a dinuclear framework. The ^{1}H-NMR spectrum displays two signals for the protons of the C_5H_5 and $P(OMe)_3$ ligands,

while the ^{31}P-NMR spectrum displays only a single resonance, its splitting being consistent with a spectrum of an AA′XX′ type (A,A′ = ^{31}P; X, X′ = ^{103}Rh). Since compound **31** is formally an analogue of the well-known carbonyl complex [{(η^5-C_5Me_5)Rh(μ-CO)}$_2$] (the structural data of which indicate the presence of a metal−metal double bond),[23] we tentatively assign a similar bonding pattern also to **31**. The spectroscopic data are of course not conclusive as to the *cis* or *trans* disposition of the two cyclopentadienyl (and equally the two phosphite) ligands.

The question of why compound **25** but not the related complexes **24**, **26**, and **27** decomposes by loss of formaldehyde and formation of a dinuclear product can not be answered definitively. It should be noted, however, that only in the mass spectra of **24**, **26**, and **27** the peak of the molecular ion M^+ appears, while the corresponding peak (m/z = 322) is missing in the mass spectrum of **25**. On the other hand, only in the latter the ion CH_2O^+ is observed with relatively high intensity. A plausible explanation of these results is that due to the less pronounced donor character of C_5H_5 compared to C_5Me_5 and of $P(OMe)_3$ compared to PMe_3, the metal-to-formaldehyde bond of compound **25** is the weaker and can be cleaved more easily than in the C_5Me_5Rh and $Rh(PMe_3)$ counterparts. The loss of formaldehyde from **25** would generate the 16-electron species [(η^5-C_5H_5)Rh{$P(OMe)_3$}] which dimerizes preferentially and does not react with CH_2O or benzene. The carbonyl complexes [(η^5-C_5R_5)Rh(CO)(L)] as the preferred products of the thermal decomposition of **24**, **26**, and **27** (and in part also of **25**) are probably formed via the formyl(hydrido)metal intermediates [(η^5-C_5R_5)RhH(CHO)(L)] which eliminate H_2 to give the final products. There is ample evidence for this pathway, particular due to the work by Thorn[24] and Roper et al.[25]

The reactions of **24**, **26**, and **27** with methyltriflate follow an unexpected course. In contrast to several other formaldehyde metal complexes which react with HX or RX by attack of the electrophile to the CH_2O oxygen atom,[12][25b][26] on treatment of **24**, **26**, or **27** with $CF_3SO_3CH_3$ no $RhCH_2OCH_3$ species could be detected. Instead the triflates of the cationic complexes **33**−**35** were formed. While the isolated yield of **33** and **34** was high, that of **35** was rather low which could be due to the lability of the Rh−CO bond in the rhodium(III) species. The PF_6 salts of the cations [(η^5-C_5R_5)Rh(CH_3)(CO)(PMe_3)]$^+$ (R = H, Me) were previously prepared in our laboratory either from the acyl derivative [(η^5-C_5Me_5)Rh{$C(O)CH_3$}(PMe_3)I] and $AgPF_6$[10] or by salt metathesis from [(η^5-C_5H_5)Rh(CH_3)(CO)(PMe_3)]I and NH_4PF_6[27]. We assume that compounds **33**−**35** are formed via the carbonyl complexes [(η^5-C_5R_5)Rh(CO)(L)] and that the electrophile $CF_3SO_3CH_3$ strongly facilitates the conversion of **24**, **26**, and **27** to [(η^5-C_5R_5)RhH(CHO)(L)] and subsequently to [(η^5-C_5R_5)Rh(CO)(L)]. This mechanistic proposal is supported by the observation that upon addition of methyltriflate to solutions of the starting material a rapid evolution of gas (H_2) is observed.

Scheme 8

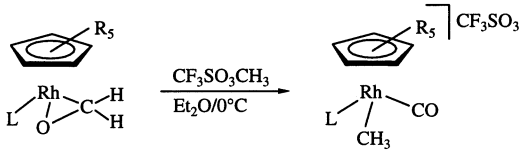

24, 26, 27 **33-35**

	R	L
33	Me	$P(OMe)_3$
34	Me	PMe_3
35	H	PMe_3

The formaldehyde complexes **26** and **27** react with CF_3SO_3H in a less straightforward manner and afford a mixture of products. Among those the cations [(η^5-C_5R_5)RhH(CO)(PMe_3)]$^+$ could be identified by ^{1}H-NMR spectroscopy.[10][27] Treatment of **26** and **27** with CH_2I_2 leads to the fast displacement of CH_2O (detected by ^{1}H NMR) and to the formation of [(η^5-C_5Me_5)Rh(CH_2I)(PMe_3)I][4] and [(η^5-C_5H_5)Rh(CH_2I)(PMe_3)I],[7] respectively. Compounds **26** and **27** behave thus analogously to the carbonyl and ethene derivatives [(η^5-C_5Me_5)Rh(CO)(PMe_3)] and [(η^5-C_5H_5)Rh(C_2H_4)(PMe_3)]. The noteworthy difference is, however, that the reactions of **26** and **27** with CH_2I_2 proceed much faster than those of the corresponding carbonyl and ethene complexes which is probably due to the weaker Rh−CH_2O compared to the Rh−CO and Rh−C_2H_4 bond.

Thioacetate− and Thioformaldehyde−Rhodium Complexes

The methodology used for the preparation of [(η^5-C_5R_5)Rh(η^2-CH_2O)(L)] (**24**−**27**) could also be applied for the synthesis of the corresponding thioformaldehyde complexes [(η^5-C_5R_5)Rh(η^2-CH_2S)(L)]. The investigations, which were carried out to obtain the respective precursors, are summarized in Schemes 9 and 10. Reaction of the starting material **36** with excess CH_3COSK in benzene/thioacetic acid led not only to cleavage of the CH_2−I but also to that of the Rh−I and Rh−C bonds and gave the bis(thioacetato)rhodium(III) compound **37** in nearly 80% yield. In contrast, treatment of **36** with one equiv of CH_3COSK in benzene/ethanol afforded a mixture of **38** and the known ethoxymethyl complex **39**,[3] which could be separated by fractional crystallization from pentane. The isolated yield of **38** was about 60%. If the separation of **38** and **39** was attempted by column chromatography using deactivated Al_2O_3, loss of the CH_2 fragment of the CH_2SAc ligand of **38** occurred and the half-sandwich rhodium(III) compound **40** was obtained. Both **37** and **38** as well as **40** were characterized by elemental analyses, mass spectra and IR and NMR spectroscopic techniques.

The preparation of the pentamethylcyclopentadienyl complexes **43** and **44** from the $RhCH_2I$ precursors **41** and **42** and CH_3COSK in benzene/ethanol proceeded in a clear manner and gave the expected products almost quantita-

Scheme 9. [Ac = CH_3CO]

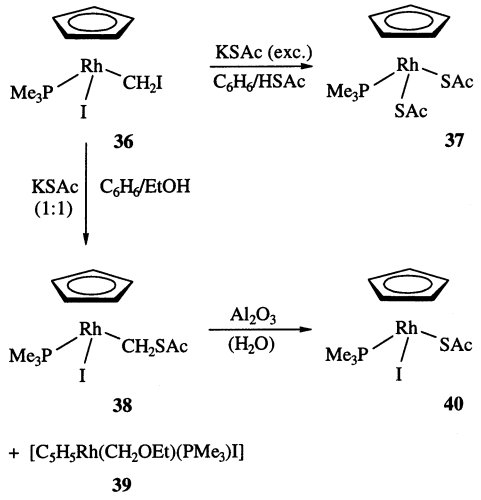

tively. In this case, no byproducts such as [(η^5-C_5Me_5)Rh(CH_2OEt)(L)I] [L = $P(OMe)_3$, PMe_3] were observed. The reaction of **42** with an excess of potassium thioacetate led both to the cleavage of the CH_2-I and the Rh−I bond and produced the thioacetatorhodium(III) derivative **45**. The same compound was obtained from **44** and an equimolar amount of CH_3COSK. The ^{1}H-NMR spectra of complexes **38**, **43**, and **44**, each containing a $RhCH_2SAc$ unit, display two distinct signals for the diastereotopic CH_2 protons which are well separated (by 0.2 to 0.7 ppm) and due to Rh-H, P-H, and H-H coupling appear as doublets of doublets of doublets.

Scheme 10. [Ac = CH_3CO]

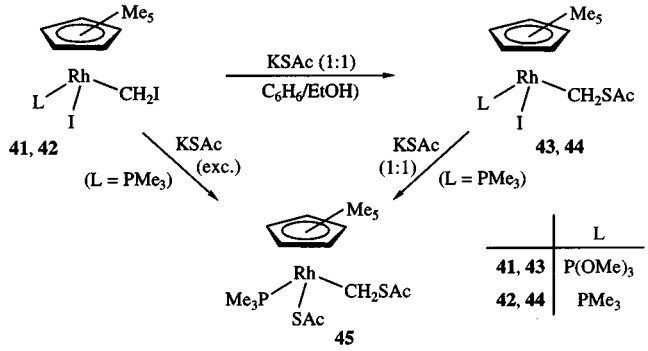

The thioformaldehyde complexes **46** and **47** can be prepared in two different ways (see Scheme 11) using either the neutral derivatives **43** and **44** or the cationic compounds **48** and **49** as starting materials. The latter were prepared similar to the above mentioned chelate complexes **19**−**23** from **43** or **44** and $AgPF_6$ in acetone. The conversion of **48** and **49** to the thioformaldehyde compounds **46** and **47** proceeded then analogously as described for the Rh(η^2-CH_2O) counterparts.

Scheme 11. [Ac = CH_3CO]

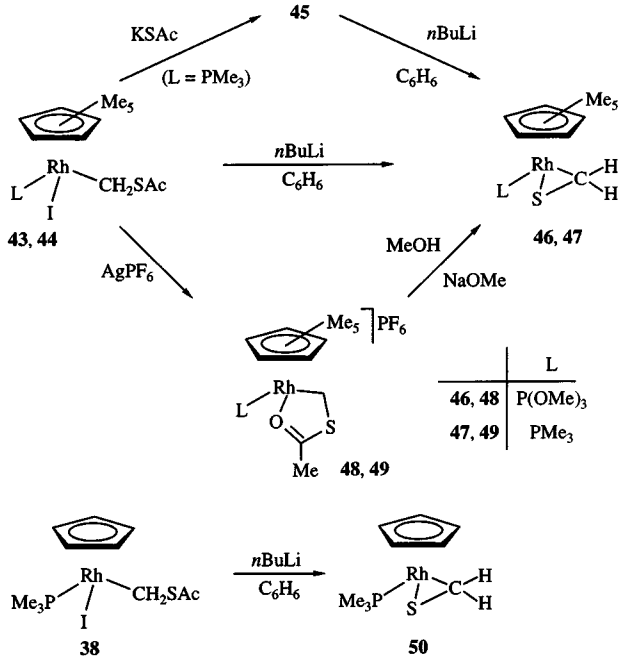

However, in contrast to **24**−**27** the Rh(η^2-CH_2S) complexes **46** and **47** can also be prepared directly from **43** and **44** upon treatment with *n*BuLi in benzene/hexane. After the reaction mixture was worked up by column chromatography using Al_2O_3, the isolated yield of **46** and **47** was 75%. The (η^5-C_5H_5)Rh derivative **50**, which had previously been prepared from **36** and two molar equivalents of NaSH,[1a][1d] was obtained on the same route. In this context it should be reminded that treatment of **14** (a related species to **38** with a $RhCH_2OAc$ linkage) did not yield the corresponding formaldehyde complex **25**, probably due to the lability of the Rh−CH_2O bond toward the organolithium reagent. We note that the ^{1}H-, ^{13}C-, and ^{31}P-NMR spectra of **46** and **47** are quite similar to those of the cyclopentadienyl complexes [(η^5-C_5H_5)Rh(η^2-CH_2E)(L)] (E = S, Se, Te; L = PMe_3, PMe_2Ph, P*i*Pr_3)[1d] and thus deserve no further comment.

Discussion

The present investigation has shown that carbenoide rhodium compounds containing $Rh(CH_2X)I$ as a molecular fragment are not only useful starting materials for the synthesis of thio-, seleno-, and telluroformaldehyde complexes[1] but also open up a preparative route to corresponding formaldehyde metal derivatives. Although several examples are known which prove that compounds of the general composition [M(η^2-CH_2O)L_n] can be obtained from an appropriate precursor and free formaldehyde,[12][25][28] this method of synthesis failed for complexes such as [(η^5-C_5R_5)Rh(η^2-CH_2O)(L)]. The main reason for this is the lability of the Rh−CH_2O bond which is

illustrated by our studies concerned to the reactivity of the isolated compounds **24**−**27**. The preferred pathway of decomposition seems to be the conversion of [Rh](CH_2O) to [Rh](CO) and H_2 ([Rh] = [(η^5-C_5R_5)Rh(L)]) which is noteworthy insofar as the reverse reaction, i.e. the formation of [M](CH_2O) from [M](CO) and hydrogen, is described as an important step in the metal-assisted hydrogenation of carbon monoxide.[29] Presently the state of the art is that electron-poor transition metal centers are more suitable to stabilize the M−CH_2O bond than electron-rich counterparts which is probably due to the well-known oxophilicity of d^o-d^4 systems.[30] Electron-rich transition metal centers prefer to coordinate thio- and selenoformaldehyde instead of CH_2O, which has first been shown by Roper et al.[31] and has also been confirmed by this work as well as by previous studies from our laboratory.[1]

We acknowledge the support for this work by the *Deutsche Forschungsgemeinschaft* and the *Fonds der Chemischen Industrie*. Moreover, we are also grateful to Mrs. *R. Schedl* and Mr. *C. P. Kneis* for elemental analyses and DTA measurements as well as to Mrs. *M. L. Schäfer* and Dr. *W. Buchner* for recording the NMR spectra.

Experimental Section

All operations were carried out in an inert gas atmosphere with the Schlenk technique. The starting materials **1**,[4] **5**,[22] **6**,[32] **10**−**12**,[4][7] **36**,[32] and **41**, **42**[4] were prepared as described in the literature. CH_3COSK (KSAc) was prepared as a white microcrystalline solid from equimolar amounts of KOH and thioacetic acid in ethanol and used without further purification. − MS: Varian MAT CH7. − IR: Perkin-Elmer 397. − NMR: Varian EM 360 L, Bruker WH 90, AC 200, and WM 400. − Melting points: DTA. − Conductivity measurements (in CH_3NO_2) with conductometer Schott CG 851; Λ in $cm^2\Omega^{-1}mol^{-1}$.

1. Preparation of [(η^5-C_5Me_5)Rh(CH_2OMe)(CO)I] (**2**): A suspension of 85.1 mg (0.16 mmol) of **1** in 5 ml of methanol was treated with 13.5 mg (0.25 mmol) of CH_3CO_2Na and stirred for 3 h at room temp. The solvent was removed and the residue was extracted with 10 ml of ether. The extract was brought to dryness in vacuo and the residue was dissolved in 1 ml of pentane. After the solution was stored for 12 h at −78°C, a red-brown microcrystalline solid precipitated which was filtered, washed with small portions of pentane (−20°C) and dried; yield 45 mg (64%); m. p. 77°C (dec.). − IR (C_6H_6): $\tilde{\nu}$ = 2007 cm^{-1} [ν(CO)]. − ^{1}H NMR (200 MHz, C_6D_6): δ = 5.30 [dd, *J*(RhH) = 2.0, *J*(HH) = 3.8 Hz, 1 H, one H of C*H*$_2$OMe], 5.15 [dd, *J*(RhH) = 5.1, *J*(HH) = 3.8 Hz, 1 H, one H of C*H*$_2$OMe], 3.03 (s, 3 H, OCH_3), 1.68 [d, *J*(RhH) = 0.5 Hz, 15 H, C_5Me_5]. MS (70 eV); *m/z* (%) = 438 (10) [M^+], 393 (10) [M^+ − CH_2OMe], 365 (100) [$C_5Me_5RhI^+$], 266 (2) [$C_5Me_5Rh(CO)^+$], 238 (10) [$C_5Me_5Rh^+$]. − $C_{13}H_{20}IO_2Rh$ (438.1): calcd. C 35.64, H 4.60; found C 34.97, H 4.88.

2. Reaction of **1** *with CH_3CO_2Na in Ethanol:* A solution of 135.3 mg (0.25 mmol) of **1** in 5 ml of ethanol was treated with 20.9 mg (0.26 mmol) of CH_3CO_2Na and stirred for 15 h at room temp. The solvent was removed, the residue was extracted with 10 ml of benzene and after the extract was concentrated to ca. 2 ml in vacuo, it was chromatographed on Al_2O_3 (neutral, activity grade IV, height of column 5 cm). With benzene/pentane (1:1), a brown-yellow fraction was eluted which after removal of the solvent and recrystallization of the residue from ether/pentane gave red-brown crystals of **3**; yield 68 mg (60%). Subsequently with benzene, first a deep blue fraction containing [(η^5-$C_5Me_5Rh)_2$(μ-CO)$_2$] and then a yellow fraction was eluted. The latter was brought to dryness in vacuo, the residue was washed with pentane (0°C) and dried. A yellow solid of **4** was obtained; yield 19 mg (16%). − **3**: m. p. 96°C (dec.). − IR (C_6H_6): $\tilde{\nu}$ = 2010 cm^{-1} [ν(CO)]. − ^{1}H NMR (200 MHz, $CDCl_3$): δ = 5.26 [dd, *J*(RhH) = 2.0, *J*(HH) = 3.7 Hz, 1 H, one H of C*H*$_2$OEt], 5.06 [dd, *J*(RhH) = 5.0, *J*(HH) = 3.7 Hz, 1 H, one H of C*H*$_2$OEt], 3.44, 3.22, 1.20 [ABX_3 spin system, $J(H_AH_X)$ = 7.2, $J(H_BH_X)$ = −7.2, $J(H_AH_B)$ = 9.5 Hz, 5 H, $OCH_AH_BC(H_X)_3$], 1.96 [d, *J*(RhH) = 0.5 Hz, 15 H, C_5Me_5]. − MS (70 eV); *m/z* (%) = 452 (10) [M^+], 393 (9) [M^+ − CH_2OEt], 365 (100) [$C_5Me_5RhI^+$], 266 (3) [$C_5Me_5Rh(CO)^+$], 238 (14) [$C_5Me_5Rh^+$]. − $C_{14}H_{22}IO_2Rh$ (452.1): calcd. C 37.19, H 4.90; found C 37.45, H 5.03.

3. Preparation of [(η^5-C_5Me_5)Rh(CH_2OAc)(CO)I] (**4**): A solution of 152.3 mg (0.34 mmol) of **10** in 2 ml of benzene was treated with a solution of 258 mg (3.16 mmol) of CH_3CO_2Na in 2 ml of acetic acid (100%) and stirred for 3 h at 50°C. After cooling to room temp., the solvent was removed, the oily residue was extracted with 15 ml of benzene and the extract was brought to dryness in vacuo. A yellow solid was obtained which was washed with small portions of pentane (0°C) and dried; yield 103 mg (65%); m. p. 116°C (dec.). − IR (KBr): $\tilde{\nu}$ = 2020 cm^{-1} [ν(CO)], 1715 cm^{-1} [ν(C=O)]. − ^{1}H NMR (200 MHz, C_6D_6): δ = 6.20 [dd, *J*(RhH) = *J*(HH) = 2.2 Hz, 1 H, one H of C*H*$_2$OAc], 4.93 [dd, *J*(RhH) = 4.4, *J*(HH) = 2.2 Hz, 1 H, one H of C*H*$_2$OAc], 1.70 (s, 3 H, OCH_3), 1.53 [d, *J*(RhH) = 0.5 Hz, 15 H, C_5Me_5]. − ^{13}C NMR (22.5 MHz, $CDCl_3$): δ = 188.7 [d, *J*(RhC) = 78.0 Hz, Rh(CO)], 170.3 [s, *C*(O)CH_3], 104.5 [d, *J*(RhC) = 4.4 Hz, *C*$_5$Me$_5$], 55.6 [d, *J*(RhC) = 22.8 Hz, $RhCH_2$], 21.3 [s, C(O)*C*H_3], 10.1 [br. s, C_5(*C*H_3)$_5$]. − $C_{14}H_{20}IO_3Rh$ (465.1): calcd. C 36.06, H 4.32, Rh 22.09; found C 36.01, H 4.24, Rh 21.80.

4. Preparation of [(η^5-C_5Me_5)Rh(CH_2Cl){P($OMe)_3$}I] (**7**): A solution of 236.1 mg (0.61 mmol) of **5** in 8 ml of ether was treated under continuous stirring dropwise with 80 μl (1.10 mmol) of CH_2ClI. Evolution of gas (CO) was observed. The solution was stirred for 2 h at room temp. and then concentrated to ca. 2 ml in vacuo. After pentane (ca. 5 ml) was added, the solution was stored for 12 h at −78°C. Orange-red crystals precipitated which were filtered, washed with small quantities of pentane (−20°C) and dried; yield 203 mg (62%); m. p. 106°C (dec.). − ^{1}H NMR (200 MHz, C_6D_6): δ = 5.17 [ddd, *J*(RhH) = 8.0, *J*(PH) = 1.9, *J*(HH) = 6.0 Hz, 1 H, one H of C*H*$_2$OAc], 4.49 [ddd, *J*(RhH) = 1.6, *J*(PH) = 4.4, *J*(HH) = 6.0 Hz, 1 H, one H of C*H*$_2$OAc], 3.64 [d, *J*(PH) = 11.5 Hz, 9 H, P$(OMe)_3$], 1.79 [dd, *J*(RhH) = 0.3, *J*(PH) = 4.3 Hz, 15 H, C_5Me_5]. − ^{13}C NMR (22.5 MHz, C_6D_6): δ = 101.5 [dd, *J*(RhC) = *J*(PC) = 4.4 Hz, *C*$_5$Me$_5$], 54.2 [d, *J*(PC) = 6.6 Hz, P$(OMe)_3$], 35.5 [dd, *J*(RhC) = 30.2, *J*(PC) = 19.1 Hz, $RhCH_2$], 9.6 [d, *J*(RhC) = 2.2 Hz, C_5(*C*H_3)$_5$]. − ^{31}P NMR (36.2 MHz, C_6D_6): δ = 133.1 [d, *J*(RhP) = 253.1 Hz]. − MS (70 eV); *m/z* (%) = 538 (2) [M^+], 489 (66) [M^+ − CH_2Cl], 365 (100) [$C_5Me_5RhI^+$], 362 (2) [$C_5Me_5RhP(OMe)_3^+$], 238 (8) [$C_5Me_5Rh^+$]. − $C_{14}H_{26}ClIO_3PRh$ (538.6): calcd. C 31.22, H 4.87; found C 31.21, H 4.92.

5. Preparation of [(η^5-C_5H_5)Rh(CH_2Cl){P($OMe)_3$}I] (**8**) *and [(η^5-C_5H_5)Rh{P($OMe)_3$}I_2]* (**9**): A solution of 219.5 mg (0.69 mmol) of **6** in 3 ml of benzene was treated dropwise with 85 μl (1.17 mmol) of CH_2ClI and stirred for 28 h at room temp. A red-violet solid **9** precipitated. After addition of 10 ml of benzene to the reaction mixture, the solid was separated from the mother liquor, washed with acetone and ether, and dried; yield 38 mg (10%). The mother liquor was concentrated to 2−3 ml in vacuo and treated dropwise with 15 ml of pentane. A red-brown solid **8**

was formed which was filtered, repeatedly washed with small portions of ether (0°C), and dried; yield 188 mg (58%).

8: m. p. 89°C (dec.). – ^{1}H NMR (200 MHz, C_6D_6): δ = 5.47 [ddd, *J*(RhH) = 4.0, *J*(PH) = 1.4, *J*(HH) = 5.6 Hz, 1 H, one H of CH_2Cl], 5.27 [dd, *J*(RhH) = 0.3, *J*(PH) = 3.2 Hz, 5 H, C_5H_5], 4.73 [ddd, *J*(RhH) = 1.8, *J*(PH) = 9.8, *J*(HH) = 5.6 Hz, 1 H, one H of CH_2Cl], 3.53 [d, *J*(PH) = 11.8 Hz, 9 H, $P(OMe)_3$]. – ^{13}C NMR (22.5 MHz, C_6D_6): δ = 92.4 [dd, *J*(RhC) = *J*(PC) = 3.7 Hz, C_5H_5], 54.0 [d, *J*(PC) = 5.9 Hz, $P(OMe)_3$], 27.3 [dd, *J*(RhC) = 26.5, *J*(PC) = 17.2 Hz, $RhCH_2$]. – ^{31}P NMR (36.2 MHz, C_6D_6): δ = 133.4 [d, *J*(RhP) = 245.6 Hz]. – MS (70 eV); *m/z* (%) = 468 (2) [M^+], 419 (31) [$M^+ - CH_2Cl$], 341 (8) [$M^+ - I$], 295 (26) [$C_5H_5RhI^+$], 292 (9) [$C_5H_5RhP(OMe)_3^+$], 168 (28) [$C_5H_5Rh^+$]. – $C_9H_{16}ClIO_3PRh$ (468.5): calcd. C 23.08, H 3.44, Rh 21.97; found C 23.33, H 3.57, Rh 22.15.

9: m. p. 96°C (dec.). – ^{1}H NMR (60 MHz, CD_3NO_2): δ = 5.97 [dd, *J*(RhH) = 0.4, *J*(PH) = 1.3 Hz, 5 H, C_5H_5], 4.34 [d, *J*(PH) = 10.8 Hz, 9 H, $P(OMe)_3$]. – ^{31}P NMR (36.2 MHz, $CDCl_3$): δ = 116.0 [d, *J*(RhP) = 211.4 Hz]. – MS (70 eV); *m/z* (%) = 546 (21) [M^+], 419 (100) [$M^+ - I$], 295 (83) [$C_5H_5RhI^+$], 168 (60) [$C_5H_5Rh^+$]. – $C_8H_{14}I_2O_3PRh$ (545.9): calcd. C 17.60, H 2.58; found C 17.82, H 2.62.

6. Preparation of [(η^5-C_5Me_5)Rh(CH_2OAc){$P(OMe)_3$}I] (**13**): A solution of 165.5 mg (0.31 mmol) of **7** in 6 ml of benzene was treated with a solution of 194.9 mg (1.60 mmol) of CH_3CO_2Na in 4 ml of acetic acid (100%) and stirred for 6 h at room temp. The solvent was removed, the residue was extracted with 20 ml of ether, and after the extract was filtered, the filtrate was concentrated to ca. 5 ml in vacuo. Pentane (ca. 5 ml) was added and the solution was stored for 12 h at −78°C. Orange-red crystals precipitated which were separated from the mother liquor, washed twice with 2 ml portions of pentane (−20°C) and dried; yield 134 mg (77%); m. p. 70°C (dec.). – IR (KBr): $\tilde{\nu}$ = 1712 cm^{-1} [ν(C=O)]. – ^{1}H NMR (200 MHz, C_6D_6): δ = 5.92 [ddd, *J*(RhH) = 8.2, *J*(PH) = 2.2, *J*(HH) = 6.0 Hz, 1 H, one H of CH_2OAc], 5.10 [ddd, *J*(RhH) = 0.7, *J*(PH) = 4.4, *J*(HH) = 6.0 Hz, 1 H, one H of CH_2OAc], 3.53 [d, *J*(PH) = 10.5 Hz, 9 H, $P(OMe)_3$], 1.78 (s, 3 H, OCH_3), 1.70 [dd, *J*(RhH) = 0.4, *J*(PH) = 4.2 Hz, 15 H, C_5Me_5]. – ^{13}C NMR (22.5 MHz, C_6D_6): δ = 170.4 [s, *C*(O)CH_3], 101.4 [dd, *J*(RhC) = *J*(PC) = 4.4 Hz, *C*$_5$Me$_5$], 57.2 [dd, *J*(RhC) = 27.2, *J*(PC) = 17.7 Hz, $RhCH_2$], 54.0 [d, *J*(PC) = 5.9 Hz, $P(OMe)_3$], 21.2 [s, C(O)*C*H$_3$], 9.7 [d, *J*(RhC) = 1.5 Hz, C$_5$(*C*H$_3$)$_5$]. – ^{31}P NMR (36.2 MHz, C_6D_6): δ = 136.4 [d, *J*(RhP) = 256.1 Hz]. – MS (70 eV); *m/z* (%) = 562 (1) [M^+], 489 (58) [$M^+ - CH_2OAc$], 365 (100) [$C_5Me_5RhI^+$], 362 (1) [$C_5Me_5RhP(OMe)_3^+$], 238 (9) [$C_5Me_5Rh^+$]. – $C_{16}H_{29}IO_5PRh$ (562.2): calcd. C 34.18, H 5.20, Rh 18.31; found C 34.48, H 5.39, Rh 18.13.

7. Preparation of [(η^5-C_5H_5)Rh(CH_2OAc){$P(OMe)_3$}I] (**14**): Compound **14** was prepared analogously to **13** by using 210.2 mg (0.45 mmol) of **8** (in 6 ml of benzene) and 250 mg (3.05 mmol) of CH_3CO_2Na (in 2 ml of 100% acetic acid) as starting materials; time of reaction 90 min at 25°C. Red-brown microcrystalline solid; yield 173 mg (78%); m. p. 76°C (dec.). – IR (KBr): $\tilde{\nu}$ = 1700 cm^{-1} [ν(C=O)]. – ^{1}H NMR (200 MHz, C_6D_6): δ = 6.70 [ddd, *J*(RhH) = *J*(HH) = 4.8, *J*(PH) = 1.4 Hz, 1 H, one H of CH_2OAc], 5.83 [ddd, *J*(RhH) = 2.4, *J*(PH) = 8.5, *J*(HH) = 4.8 Hz, 1 H, one H of CH_2OAc], 5.23 [dd, *J*(RhH) = 0.5, *J*(PH) = 3.1 Hz, 5 H, C_5H_5], 3.47 [d, *J*(PH) = 10.5 Hz, 9 H, $P(OMe)_3$], 1.72 (s, 3 H, OCH_3). – ^{13}C NMR (22.5 MHz, C_6D_6): δ = 169.9 [s, *C*(O)CH_3], 91.0 [dd, *J*(RhC) = *J*(PC) = 4.2 Hz, C_5H_5], 53.9 [d, *J*(PC) = 5.9 Hz, $P(OMe)_3$], 49.3 [dd, *J*(RhC) = 25.0, *J*(PC) = 15.4 Hz, $RhCH_2$], 21.6 [s, C(O)*C*H$_3$]. – ^{31}P NMR (36.2 MHz, C_6D_6): δ = 135.8 [d, *J*(RhP) = 248.6 Hz]. – MS (70 eV); *m/z* (%) = 492 (1) [M^+], 419 (100) [$M^+ - CH_2OAc$], 365 (50) [$M^+ - I$], 295 (70) [$C_5H_5RhI^+$], 292 (18) [$C_5H_5RhP(OMe)_3^+$], 168 (58) [$C_5H_5Rh^+$]. – $C_{11}H_{19}IO_5PRh$ (492.1): calcd. C 26.85, H 3.89, Rh 20.92; found C 27.06, H 3.98, Rh 21.35.

8. Preparation of [(η^5-C_5Me_5)Rh(CH_2OAc)(PMe_3)I] (**15**): Compound **15** was prepared analogously to **4** by using 321.3 mg (0.47 mmol) of **11** (in 5 ml of benzene) and 308.3 mg (3.76 mmol) of CH_3CO_2Na (in 5 ml of 100% acetic acid) as starting materials; time of reaction 5 h at 25°C. An orange-yellow oil was obtained which upon addition of 0.5 ml of pentane gave an orange-yellow microcrystalline solid; yield 190 mg (78%); m. p. 83°C (dec.). – IR (KBr): $\tilde{\nu}$ = 1708 cm^{-1} [ν(C=O)]. – ^{1}H NMR (200 MHz, C_6D_6): δ = 5.57 [ddd, *J*(RhH) = 2.1, *J*(PH) = 8.8, *J*(HH) = 6.5 Hz, 1 H, one H of CH_2OAc], 5.23 [dd, *J*(RhH) = 5.1, *J*(HH) = 6.5 Hz, 1 H, one H of CH_2OAc], 1.70 (s, 3 H, OCH_3), 1.59 [dd, *J*(RhH) = 0.3, *J*(PH) = 2.7 Hz, 15 H, C_5Me_5], 1.35 [dd, *J*(RhH) = 0.7, *J*(PH) = 10.3 Hz, 9 H, PMe_3]. – ^{13}C NMR (22.5 MHz, C_6D_6): δ = 170.3 [s, *C*(O)CH_3], 99.3 [dd, *J*(RhC) = 4.4, *J*(PC) = 2.9 Hz, *C*$_5$Me$_5$], 60.1 [dd, *J*(RhC) = 30.2, Hz, *J*(PC) = 15.4, $RhCH_2$], 21.1 [s, C(O)*C*H$_3$], 17.4 [d, *J*(PC) = 32.4 Hz, PMe_3], 10.0 [br. s, C$_5$(*C*H$_3$)$_5$]. – ^{31}P NMR (36.2 MHz, C_6D_6): δ = 4.8 [d, *J*(RhP) = 157.8 Hz]. – MS (70 eV); *m/z* (%) = 514 (6) [M^+], 441 (100) [$M^+ - CH_2OAc$], 365 (83) [$C_5Me_5RhI^+$], 314 (2) [$C_5Me_5Rh(PMe_3)^+$], 238 (5) [$C_5Me_5Rh^+$]. – $C_{16}H_{29}IO_2PRh$ (514.2): calcd. C 37.37, H 5.70; found C 37.28, H 6.07.

9. Preparation of [(η^5-C_5H_5)Rh(CH_2OAc)(PMe_3)I] (**16**): Compound **16** was prepared analogously to **4** by using 140.1 mg (0.33 mmol) of **12** (in 2 ml of benzene) and 270 mg (3.30 mmol) of CH_3CO_2Na (in 1 ml of 100% acetic acid) as starting materials; time of reaction 6 h at 25°C. After recrystallization from ether (25°C to −78°C) orange-red crystals were obtained; yield 125 mg (85%); m. p. 106°C (dec.). – IR (KBr): $\tilde{\nu}$ = 1720 cm^{-1} [ν(C=O)]. – ^{1}H NMR (200 MHz, $CDCl_3$): δ = 6.60 [dd, *J*(RhH) = 4.9, *J*(HH) = 5.7 Hz, 1 H, one H of CH_2OAc], 5.42 [dd, *J*(RhH) = 0.4, *J*(PH) = 1.4 Hz, 5 H, C_5H_5], 4.97 [ddd, *J*(RhH) = 2.6, *J*(PH) = 8.3, *J*(HH) = 5.7 Hz, 1 H, one H of CH_2OAc], 1.78 [dd, *J*(RhH) = 0.8, *J*(PH) = 11.1 Hz, 9 H, PMe_3], 1.70 (s, 3 H, OCH_3). – ^{13}C NMR (22.5 MHz, C_6D_6): δ = 169.5 [s, *C*(O)CH_3], 89.9 [dd, *J*(RhC) = *J*(PC) = 3.7 Hz, C_5H_5], 51.5 [dd, *J*(RhC) = 27.2, *J*(PC) = 13.4, $RhCH_2$], 19.6 [d, *J*(PC) = 33.8 Hz, PMe_3], 18.9 [s, C(O)*C*H$_3$]. – ^{31}P NMR (36.2 MHz, C_6D_6): δ = 10.3 [d, *J*(RhP) = 160.0 Hz]. – MS (70 eV); *m/z* (%) = 444 (3) [M^+], 371 (100) [$M^+ - CH_2OAc$], 295 (23) [$C_5H_5RhI^+$], 244 (73) [$C_5H_5Rh(PMe_3)^+$], 168 (35) [$C_5H_5Rh^+$]. – $C_{11}H_{19}IO_2PRh$ (444.0): calcd. C 29.75, H 4.31, Rh 23.18; found C 30.01, H 4.40, Rh 23.53.

10. Reaction of Compound **14** *nBuLi:* A solution of 276.5 mg (0.56 mmol) of **14** in 20 ml of benzene was treated under continuous stirring with 0.8 ml of a 1.41 M solution (1.12 mmol) of *n*BuLi in hexane at room temp. After the reaction mixture was stirred for 1 h, the solvent was removed and the residue was extracted with 20 ml of ether. The extract was brought to dryness in vacuo, the oily residue was dissolved in 2 ml of benzene and the solution was chromatographed on Al_2O_3 (neutral, activity grade IV, height of column 5 cm). With hexane, a yellow fraction was eluted from which upon evaporation of the solvent a light yellow oil **18** was obtained; yield 8 mg (3%). Further elution with benzene gave a red fraction which was brought to dryness in vacuo. The residue was dissolved in 10 ml of ether, the extract was concentrated to ca. 1 ml and then stored for 12 h at −20°C. A red-brown microcrystalline solid **17** precipitated which was washed with small portions of pentane and dried; yield 21 mg (8%).

17: ^{1}H NMR (60 MHz, $CDCl_3$): δ = 8.20, 7.07 (both m, 5 H, C_6H_5), 5.03 [dd, *J*(RhH) = 0.5, *J*(PH) = 3.2, 5 H, C_5H_5], 3.32 [d, *J*(PH) = 11.7 Hz, 9 H, $P(OMe)_3$]. − MS (70 eV); *m/z* (%) = 496 (7) [M^+], 419 (11) [$M^+ - C_6H_5$], 292 (100) [$C_5H_5RhP(OMe)_3^+$], 168 (69) [$C_5H_5Rh^+$]. − $C_{14}H_{19}IO_3PRh$ (496.1): calcd. C 33.90, H 3.86; found C 33.56, H 3.98.

18: ^{1}H NMR (60 MHz, C_6D_6): δ = 7.64, 7.37 (both m, 5 H, C_6H_5), 5.17 [dd, *J*(RhH) = 0.4, *J*(PH) = 2.2 Hz, 5 H, C_5H_5], 3.28 [d, *J*(PH) = 11.4 Hz, 9 H, $P(OMe)_3$] 1.1 (br. m, 9 H, C_4H_9). − MS (70 eV); *m/z* (%) = 462 (2) [M^+], 292 (100) [$C_5H_5RhP(OMe)_3^+$], 168 (56) [$C_5H_5Rh^+$].

11. Preparation of [(η^5-C$_5$Me$_5$)Rh{κ^2-C,O-CH$_2$OC(Me)O}(CO)]PF$_6$ (**19**): A solution of 81.2 mg (0.17 mmol) of **4** in 5 ml of acetone was treated under continuous stirring with a solution of 42.9 mg (0.17 mmol) of $AgPF_6$ in 2 ml of acetone at room temp. A pale yellow precipitate of AgI was rapidly formed. After the reaction mixture was stirred for 20 min, it was filtered and the filtrate was concentrated to ca. 2 ml in vacuo. Upon addition of 20 ml of ether, the solution was rigorously stirred until a yellow microcrystalline solid precipitated. This was filtered, washed twice with 5 ml portions of ether and dried; yield 69 mg (83%); dec. temp. 109°C. − Λ = 66 $cm^2\Omega^{-1}mol^{-1}$. − IR (nujol): $\tilde{\nu}$ = 2030 cm^{-1} [ν(CO)], 1605 [ν(C=O)]. − ^{1}H NMR (200 MHz, CD_3NO_2): δ = 6.23 [dd, *J*(RhH) = 0.5, *J*(HH) = 6.0 Hz, 1 H, one H of $RhCH_2$], 5.63 [dd, *J*(RhH) = 4.0, *J*(HH) = 6.0 Hz, 1 H, one H of $RhCH_2$], 2.23 (s, 3 H, CH_3), 1.92 [d, *J*(RhH) = 0.4 Hz, 15 H, C_5Me_5]. − ^{13}C NMR (22.5 MHz, CD_3NO_2): δ = 190.7 [d, *J*(RhC) = 70.5 Hz, Rh(CO)], 187.9 (s, C=O), 107.6 [d, *J*(RhC) = 5.2 Hz, C_5Me_5], 81.0 [d, *J*(RhC) = 23.5 Hz, $RhCH_2$], 18.6 [s, C(O)CH_3], 9.3 [br. s, $C_5(CH_3)_5$]. − $C_{14}H_{20}F_6O_3PRh$ (484.2): calcd. C 37.74, H 4.17; found C 37.44, H 4.31.

12. Preparation of [(η^5-C$_5$Me$_5$)Rh{κ^2-C,O-CH$_2$OC(Me)O}{P(OMe)$_3$}]PF$_6$ (**20**): Compound **20** was prepared analogously to **19** by using 131.7 mg (0.24 mmol) of **13** and 59.9 mg (0.24 mmol) of $AgPF_6$ as starting materials. Yellow microcrystalline solid; yield 131 mg (94%); dec. temp. 66°C. − Λ = 80 $cm^2\Omega^{-1}mol^{-1}$. − IR (nujol): $\tilde{\nu}$ = 1600 cm^{-1} [ν(C=O)]. − ^{1}H NMR (200 MHz, CD_3NO_2): δ = 5.91, 5.77 [both part of an ABPX spin system; from $^1H\{^{31}P\}$: *J*(RhH) = 0.3 and 4.2, *J*(HH) = 6.4 Hz, 1H each, $RhCH_2$], 3.77 [d, *J*(PH) = 11.8 Hz, 9 H, $P(OMe)_3$], 2.14 (s, 3 H, CH_3), 1.76 [dd, *J*(RhH) = 0.4, *J*(PH) = 4.4 Hz, 15 H, C_5Me_5]. − ^{13}C NMR (50.3 MHz, CD_3NO_2): δ = 186.3 (s, C=O), 103.2 [dd, *J*(RhC) = 5.3, *J*(PC) = 3.4 Hz, C_5Me_5], 82.1 [dd, *J*(RhC) = 25.9, *J*(PC) = 23.1 Hz, $RhCH_2$], 53.8 [d, *J*(PC) = 4.7 Hz, $P(OMe)_3$], 18.5 [s, C(O)CH_3], 9.2 [br. s, $C_5(CH_3)_5$]. − ^{31}P NMR (36.2 MHz, CD_3NO_2): δ = 129.4 [d, *J*(RhP) = 256.1 Hz]. − $C_{16}H_{29}F_6O_5P_2Rh$ (580.3): calcd. C 33.12, H 5.04; found C 33.38, H 5.26.

13. Preparation of [(η^5-C$_5$H$_5$)Rh{κ^2-C,O-CH$_2$OC(Me)O}{P(OMe)$_3$}]PF$_6$ (**21**): Compound **21** was prepared analogously to **19** by using 90.2 mg (0.18 mmol) of **14** and 45.4 mg (0.18 mmol) of $AgPF_6$ as starting materials. Yellow microcrystalline solid; yield 87 mg (94%); dec. temp. 112° C. − Λ = 65 $cm^2\Omega^{-1}mol^{-1}$. − IR (nujol): $\tilde{\nu}$ = 1600 cm^{-1} [ν(C=O)]. − ^{1}H NMR (200 MHz, CD_3NO_2): δ = 7.37 [ddd, *J*(RhH) = 4.5, *J*(PH) = 1.4, *J*(HH) = 6.2 Hz, 1 H, one H of $RhCH_2$], 5.88 [ddd, *J*(RhH) = 0.3, *J*(PH) = 28.3, *J*(HH) = 6.2 Hz, 1 H, one H of $RhCH_2$], 5.85 [dd, *J*(RhH) = 0.6, *J*(PH) = 2.8 Hz, 5 H, C_5H_5], 3.80 [d, *J*(PH) = 12.0 Hz, 9 H, $P(OMe)_3$], 2.17 (s, 3 H, CH_3). − ^{13}C NMR (22.5 MHz, CD_3NO_2): δ = 188.1 (s, C=O), 91.4 [dd, *J*(RhC) = *J*(PC) = 4.4 Hz, C_5H_5], 73.0 [dd, *J*(RhC) = 23.5, *J*(PC) = 20.6 Hz, $RhCH_2$], 54.3[d, *J*(PC) = 4.4 Hz, $P(OMe)_3$], 17.9 [s, C(O)CH_3]. − ^{31}P NMR (36.2 MHz, CD_3NO_2): δ = 128.2 [d, *J*(RhP) = 242.7 Hz]. − $C_{11}H_{19}F_6O_5P_2Rh$ (510.1): calcd. C 25.90, H 3.75, Rh 20.17; found C 25.81, H 3.91, Rh 19.78.

14. Preparation of [(η^5-C$_5$Me$_5$)Rh{κ^2-C,O-CH$_2$OC(Me)O}(PMe$_3$)]PF$_6$ (**22**): Compound **22** was prepared analogously to **19** by using 67.0 mg (0.13 mmol) of **15** and 36.1 mg (0.14 mmol) of $AgPF_6$ as starting materials. Orange-yellow microcrystalline solid; yield 59 mg (85%); dec. temp. 60°C. − Λ = 84 $cm^2\Omega^{-1}mol^{-1}$. − IR (nujol): $\tilde{\nu}$ = 1608 cm^{-1} [ν(C=O)]. − ^{1}H NMR (200 MHz, CD_3NO_2): δ = 5.86 [ddd, *J*(RhH) = 4.0, *J*(PH) = 0.3, *J*(HH) = 7.4 Hz, 1 H, one H of $RhCH_2$], 5.55 [ddd, *J*(RhH) = *J*(HH) = 7.4, *J*(PH) = 27.7 Hz, 1 H, one H of $RhCH_2$], 2.16 (s, 3 H, CH_3), 1.73 [dd, *J*(RhH) = 0.3, *J*(PH) = 2.6 Hz, 15 H, C_5Me_5], 1.48 [dd, *J*(RhH) = 0.8, *J*(PH) = 10.4 Hz, 9 H, PMe_3]. − ^{13}C NMR (50.3 MHz, CD_3NO_2): δ = 186.1 (s, C=O), 101.4 [dd, *J*(RhC) = *J*(PC) = 3.0 Hz, C_5Me_5], 84.6 [dd, *J*(RhC) = 28.5 Hz, $RhCH_2$], 18.8 [s, C(O)CH_3], 13.8 [d, *J*(PC) = 31.0 Hz, PMe_3], 9.5 [br. s, $C_5(CH_3)_5$]. − ^{31}P NMR (36.2 MHz, CD_3NO_2): δ = 2.3 [d, *J*(RhP) = 159.3 Hz]. − $C_{16}H_{29}F_6O_2P_2Rh$ (532.3): calcd. C 36.11, H 5.49, Rh 19.34; found C 36.05, H 5.31, Rh 19.70.

15. Preparation of [(η^5-C$_5$H$_5$)Rh{κ^2-C,O-CH$_2$OC(Me)O}(PMe$_3$)]PF$_6$ (**23**): Compound **23** was prepared analogously to **19** by using 96.2 mg (0.22 mmol) of **16** and 58.0 mg (0.23 mmol) of $AgPF_6$ as starting materials. Orange-yellow microcrystalline solid; yield 83 mg (81%); dec. temp. 68°C. − Λ = 78 $cm^2\Omega^{-1}mol^{-1}$. − IR (nujol): $\tilde{\nu}$ = 1605 cm^{-1} [ν(C=O)]. − ^{1}H NMR (200 MHz, CD_3NO_2): δ = 7.37 [ddd, *J*(RhH) = 4.2, *J*(PH) = 0.8, *J*(HH) = 6.8 Hz, 1 H, one H of $RhCH_2$], 5.60 [ddd, *J*(RhH) = 0.3, *J*(PH) = 19.7, *J*(HH) = 6.8 Hz, 1 H, one H of $RhCH_2$], 5.57 [dd, *J*(RhH) = 0.6, *J*(PH) = 1.3 Hz, 5 H, C_5H_5], 2.18 (s, 3 H, CH_3), 1.63 [dd, *J*(RhH) = 0.8, *J*(PH) = 11.5 Hz, 9 H, PMe_3]. − ^{13}C NMR (22.5 MHz, CD_3NO_2): δ = 187.5 (s, C=O), 90.6 [dd, *J*(RhC) = 5.2, *J*(PC) = 2.9 Hz, C_5H_5], 75.4 [dd, *J*(RhC) = 25.7, *J*(PC) = 14.7 Hz, $RhCH_2$], 17.0 [s, C(O)CH_3], 16.2 [d, *J*(PC) = 33.1 Hz, PMe_3]. − ^{31}P NMR (36.2 MHz, CD_3NO_2): δ = 12.5 [d, *J*(RhP) = 150.3 Hz]. − $C_{11}H_{19}F_6O_2P_2Rh$ (462.1): calcd. C 28.59, H 4.15, Rh 22.27; found C 28.42, H 4.11, Rh 22.00.

16. Preparation of [(η^5-C$_5$Me$_5$)Rh(η^2-CH$_2$O){P(OMe)$_3$}] (**24**): A suspension of 89.7 mg (0.15 mmol) of **20** in 5 ml of methanol was treated at 0°C under continuous stirring with 98.1 mg (1.40 mmol) of KOH. A yellow-brown solution was formed of which after it was stirred for 10 min at 0°C, the solvent was removed in vacuo. The residue was extracted twice with 5 ml of cold ether (0°C) and the combined extracts were brought by cooling with an ice bath to dryness in vacuo. The remaining yellow-brown oil was dissolved in 2 ml of pentane (0°C) and the solution was stored for 10 h at −78°C. A yellow-brown microcrystalline solid precipitated which was filtered, washed twice with small quantities of pentane (−20°C) and dried; yield of oily product 38 mg (62%), yield of solid material 15 mg (26%); m. p. 36°C (dec.). − IR (C_6H_6): $\tilde{\nu}$ = 2805 cm^{-1} [ν(CH_2)], 1220 [ν(C−O)]. − ^{1}H NMR (200 MHz, C_6D_6): δ = 4.62 (m, 2 H, CH_2O), 3.52 [d, *J*(PH) = 12.2 Hz, 9 H, $P(OMe)_3$], 1.89 [dd, *J*(RhH) = 0.5, *J*(PH) = 3.4 Hz, 15 H, C_5Me_5]. − ^{13}C NMR (50.3 MHz, C_6D_6): δ = 97.6 [dd, *J*(RhC) = *J*(PC) = 4.4 Hz, C_5Me_5], 78.1 [dd, *J*(RhC) = 12.0, *J*(PC) = 5.9 Hz, CH_2O], 51.1 [br. s, $P(OMe)_3$], 10.0 [s, $C_5(CH_3)_5$]. − ^{31}P NMR (36.2 MHz, C_6D_6): δ = 149.2 [d, *J*(RhP) = 311.1 Hz]. − MS (70 eV); *m/z* (%) = 392 (2) [M^+], 390 (32) [$M^+ - 2$ H], 362 (100) [$M^+ - CH_2O$], 238 (49) [$C_5Me_5Rh^+$], 30 (2) [CH_2O^+]. − $C_{14}H_{26}O_4PRh$ (392.2): calcd. C 42.87, H 6.68; found C 42.59, H 6.70.

17. Preparation of [(η^5-C$_5$H$_5$)Rh(η^2-CH$_2$O){P(OMe)$_3$}] (**25**): Compound **25** was prepared analogously to **24** by using 95.3 mg (0.19 mmol) of **21** and 88.7 mg (1.26 mmol) of KOH as starting

materials. Yellow-brown solid; yield of oily product 43 mg (71%), yield of solid material 13 mg (22%); m. p. 43°C (dec.). – IR (C_6H_6): $\tilde{\nu}$ = 2825 cm^{-1} [$\nu(CH_2)$], 1232 [$\nu(C-O)$]. – ^1H NMR (200 MHz, C_6D_6): δ = 5.56 [ddd, J(RhH) = 2.5, J(PH) = 0.5, J(HH) = 21.5 Hz, 1 H, one H of CH_2O], 5.29 [dd, J(RhH) = 0.8, J(PH) = 2.6 Hz, 5 H, C_5H_5], 4.60 [ddd, J(RhH) = 2.0, J(PH) = 5.1, J(HH) = 21.5 Hz, 1 H, one H of CH_2O], 3.80 [d, J(PH) = 12.4 Hz, 9 H, $P(OMe)_3$]. – ^{13}C NMR (100.6 MHz, C_6D_6): δ = 86.1 [dd, J(RhC) = J(PC) = 3.1 Hz, C_5H_5], 72.6 [dd, J(RhC) = 13.6, J(PC) = 4.9 Hz, CH_2O], 51.6 [br. s, $P(OMe)_3$]. – ^{31}P NMR (36.2 MHz, C_6D_6): δ = 150.1 [d, J(RhP) = 299.2 Hz]. – $C_9H_{16}O_4PRh$ (322.1): calcd. C 33.56, H 5.01; found C 33.54, H 4.81.

18. Preparation of [(η^5-C_5Me_5)Rh(η^2-CH_2O)(PMe_3)] (**26**): Compound **26** was prepared analogously to **24** by using 105.6 mg (0.20 mmol) of **22** and 85.9 mg (1.22 mmol) of KOH as starting materials. Brownish microcrystalline solid; yield of oily product 39 mg (56%), yield of solid material 20 mg (29%); m. p. 25°C (dec.). – IR (C_6H_6): $\tilde{\nu}$ = 2800 cm^{-1} [$\nu(CH_2)$], 1210 [$\nu(C-O)$]. – ^1H NMR (200 MHz, C_6D_6): δ = 4.48 [ddd, J(RhH) = 3.0, J(PH) = 0.6, J(HH) = 18.2 Hz, 1 H, one H of CH_2O], 4.15 [ddd, J(RhH) = 2.4, J(PH) = 6.1, J(HH) = 18.2 Hz, 1 H, one H of CH_2O], 1.87 [dd, J(RhH) = 0.4, J(PH) = 2.2 Hz, 15 H, C_5Me_5], 0.99 [dd, J(RhH) = 0.9, J(PH) = 8.9 Hz, 9 H, PMe_3]. – ^{13}C NMR (50.3 MHz, C_6D_6): δ = 96.5 [dd, J(RhC) = J(PC) = 3.3 Hz, C_5Me_5], 74.4 [dd, J(RhC) = 14.0, J(PC) = 6.6 Hz, CH_2O], 15.8 [d, J(PC) = 25.7 Hz, PMe_3], 10.7 [s, $C_5(CH_3)_5$]. – ^{31}P NMR (36.2 MHz, C_6D_6): δ = 2.8 [d, J(RhP) = 190.3 Hz]. – MS (70 eV); *m/z* (%) = 344 (2) [M^+], 342 (23) [M^+ – 2 H], 314 (100) [M^+ – CH_2O], 238 (25) [$C_5Me_5Rh^+$], 30 (2) [CH_2O^+]. – $C_{14}H_{26}OPRh$ (344.3): calcd. C 48.85, H 7.61 Rh 29.83; found C 48.34, H 7.55, Rh 29.50.

19. Preparation of [(η^5-C_5H_5)Rh(η^2-CH_2O)(PMe_3)] (**27**): Compound **27** was prepared analogously to **24** by using 98.7 mg (0.21 mmol) of **23** and 103.6 mg (1.48 mmol) of KOH as starting materials. Brownish microcrystalline solid; yield of oily product 39 mg (56%), yield of solid material 20 mg (29%); m. p. 39°C (dec.). – IR (C_6H_6): $\tilde{\nu}$ = 2790 cm^{-1} [$\nu(CH_2)$], 1215 [$\nu(C-O)$]. – ^1H NMR (60 MHz, C_6D_6): δ = 5.70 [ddd, J(RhH) = 2.8, J(PH) = 0.5, J(HH) = 19.8 Hz, 1 H, one H of CH_2O], 5.07 [dd, J(RhH) = 0.3, J(PH) = 1.2 Hz, 5 H, C_5H_5], 4.03 [ddd, J(RhH) = 2.1, J(PH) = 5.0, J(HH) = 19.8 Hz, 1 H, one H of CH_2O], 0.90 [dd, J(RhH) = 0.8, J(PH) = 10.4 Hz, 9 H, PMe_3]. – ^{13}C NMR (100.6 MHz, C_6D_6): δ = 85.0 [br. s, C_5H_5], 67.9 [m, CH_2O], 17.7 [d, J(PC) = 28.4 Hz, PMe_3]. – ^{31}P NMR (36.2 MHz, C_6D_6): δ = 8.0 [d, J(RhP) = 193.5 Hz]. – MS (70 eV); *m/z* (%) = 274 (4) [M^+], 272 (30) [M^+ – 2 H], 244 (100) [M^+ – CH_2O], 168 (50) [$C_5H_5Rh^+$], 30 (4) [CH_2O^+]. – $C_9H_{16}OPRh$ (274.1): calcd. C 39.44, H 5.88, Rh 37.54; found C 39.73, H 6.16, Rh 38.09.

20. Preparation of [(η^5-C_5H_5)Rh{$CH_2OC(O)Ph$}(PMe_3)I] (**28**): A solution of 87.1 mg (0.21 mmol) of **12** in 4 ml acetone/benzene (1:1) was treated with 79.3 mg (0.49 mmol) of $PhCO_2K$ and stirred for 20 h at 50–60°C. After the reaction mixture was cooled to room temp., the solvent was removed and the residue was extracted with 15 ml of ether. The extract was concentrated to ca. 3 ml in vacuo and upon storing for 6 h at –78°C gave orange-red crystals. The crystals were separated from the mother liquor, washed twice with pentane (0°C) and dried; yield 59 mg (56%); m. p. 142°C (dec.). – IR (KBr): $\tilde{\nu}$ = 1712 cm^{-1} [$\nu(C=O)$]. – ^1H NMR (200 MHz, C_6D_6): δ = 8.1, 7.2 (both m, 5 H, C_6H_5), 7.00 [ddd, J(RhH) = 4.8, J(PH) = 0.3, J(HH) = 5.6 Hz, 1 H, one H of $RhCH_2$], 5.33 [ddd, J(RhH) = 1.4, J(PH) = 8.4, J(HH) = 5.6 Hz, 1 H, one H $RhCH_2$], 5.05 [dd, J(RhH) = 0.6, J(PH) = 1.4 Hz, 5 H, C_5H_5], 1.37 [dd, J(RhH) = 0.8, J(PH) = 11.2 Hz, 9 H, PMe_3]. – ^{31}P NMR (36.2 MHz, C_6D_6): δ = 10.0 [d, J(RhP) = 153.3 Hz]. – $C_{16}H_{21}IO_2PRh$ (506.1): calcd. C 37.97, H 4.18; found C 37.67, H 4.61.

21. Preparation of [(η^5-C_5H_5)Rh{κ^2-C,O-$CH_2OC(Ph)O$}(PMe_3)]PF_6 (**29**): A solution of 60.7 mg (0.12 mmol) of **28** in 3 ml of acetone was treated dropwise with a solution of 30.4 mg (0.12 mmol) of $AgPF_6$ in 2 ml of acetone. The reaction mixture was stirred for 10 min at room temp. and then filtered. The filtrate was concentrated to ca. 2 ml in vacuo and under vigorous stirring 15 ml of ether was added. An orange-yellow precipitate was formed which was separated from the mother liquor, washed twice with ether and dried; yield 52 mg (83%); dec. temp. 75°C. – IR (nujol): $\tilde{\nu}$ = 1602 cm^{-1} [$\nu(C=O)$]. – ^1H NMR (60 MHz, $(CD_3)_2CO$): δ = 8.1, 7.7 (both m, 5 H, C_6H_5), 6.17 (m, 1 H, one H of $RhCH_2$), 5.80 [dd, J(RhH) = 0.6, J(PH) = 1.2 Hz, 5 H, C_5H_5], 1.73 [dd, J(RhH) = 0.8, J(PH) = 11.8 Hz, 9 H, PMe_3], signal of one H of $RhCH_2$ partly covered by signal of C_5H_5. – ^{31}P NMR (36.2 MHz, CD_3NO_2): δ = 12.8 [d, J(RhP) = 150.4 Hz]. – $C_{16}H_{21}F_6O_2P_2Rh$ (524.2): calcd. C 36.66, H 4.04; found C 36.73, H 4.29.

22. Thermal Decomposition of **24**: A solution of 36.4 mg (0.09 mmol) of **24** in 0.5 ml of benzene was stored for 5 h at room temp. The reaction was controlled by measuring the ^1H-NMR spectrum in time intervals of ca. 20 min. After 5 h, the signals of **24** disappeared and new signals corresponding to **30**[22] were observed; yield ca 85%.

23. Thermal Decomposition of **25**: A solution of 50.6 mg (0.16 mmol) of **25** in 0.5 ml of benzene was stored for 6 d at room temp. The reaction was controlled by measuring the ^1H-NMR spectrum in time intervals of ca. 2–3 h. After 6 d, the signals of **25** disappeared and new signals corresponding to **31** and **32**[33] were observed; yield almost quantitative; ratio **31**/**32** = 70:30.

24. Preparation of [{(η^5-C_5H_5)RhP($OMe)_3$}$_2$] (**31**): A solution of 88.2 mg (0.27 mmol) of **25** in 0.6 ml of benzene was stored for 7 d at room temp. A characteristic change of color from yellow-brown to deep green occurred. The solvent was removed, the residue was washed twice with 2 ml portions of pentane and then extracted with 10 ml of ether . The extract was concentrated to ca. 1 ml in vacuo and stored for 12 h at –78°C. A green microcrystalline solid precipitated which was repeatedly washed with small quantities of pentane and dried; yield 30.5 mg (39%). – ^1H NMR (60 MHz, C_6D_6): δ = 5.57 [dd, J(RhH) = 0.6, J(PH) = 2.2 Hz, 5 H, C_5H_5], 3.57 [d, J(PH) = 13.1 Hz, 9 H, $P(OMe)_3$]. – ^{31}P NMR (36.2 MHz, C_6D_6): δ = 161.8 [pseudo-quartet, spectrum of AA′XX′ type, N = J(AX) + J(AX′) = 277.6 Hz]. – MS (70 eV); *m/z* (%) = 584 (8) [M^+], 460 (6) [M^+ – $P(OMe)_3$], 292 (88) [$M/2^+$], 233 (100) [$(C_5H_5)_2Rh^+$], 168 (67) [$C_5H_5Rh^+$]. – $C_{16}H_{28}O_6P_2Rh_2$ (584.2): calcd. C 32.90, H 4.83; found C 32.96, H 4.82.

25. Preparation of [(η^5-C_5Me_5)Rh(CH_3)(CO){$P(OMe)_3$}]CF_3SO_3 (**33**): A solution of 47.1 mg (0.12 mmol) of **24** in 3 ml of ether was treated dropwise with 14 µl (0.12 mmol) of $CF_3SO_3CH_3$ at 0°C. Evolution of gas was observed and a pale yellow solid precipitated. After the cooling vessel was removed, the solid was separated from the mother liquor, repeatedly washed with ether and dried; yield 37 mg (55%). – IR (CH_2Cl_2): $\tilde{\nu}$ = 2060 cm^{-1} [$\nu(CO)$]. – ^1H NMR (60 MHz, CD_2Cl_2): δ = 3.78 [d, J(PH) = 11.8 Hz, 9 H, $P(OMe)_3$], 1.86 [dd, J(RhH) = 0.4, J(PH) = 5.0 Hz, 15 H, C_5Me_5], 0.75 [dd, J(RhH) = 2.2, J(PH) = 6.1 Hz, 3 H, $RhCH_3$]. – ^{31}P NMR (36.2 MHz, $CDCl_3$): δ = 120.2 [d, J(RhP) = 218.8 Hz]. – $C_{16}H_{27}F_3O_7PRhS$ (554.3): calcd. C 34.67, H 4.91; found C 34.31, H 5.00.

26. Preparation of [(η^5-C_5Me_5)Rh(CH_3)(CO)(PMe_3)]CF_3SO_3 (**34**): Compound **34** was prepared analogously to **33** by using 44.6

mg (0.13 mmol) of **26** and 15 µl (0.13 mmol) of $CF_3SO_3CH_3$ as starting materials. Pale yellow solid; yield 45 mg (69%). − IR (CH_2Cl_2): $\tilde{\nu}$ = 2045 cm^{-1} [ν(CO)]. − ^1H NMR (200 MHz, CD_2Cl_2): δ = 1.85 [dd, *J*(RhH) = 0.3, *J*(PH) = 3.1 Hz, 15 H, C_5Me_5], 1.55 [dd, *J*(RhH) = 0.8, *J*(PH) = 11.0 Hz, 9 H, PMe_3], 0.51 [dd, *J*(RhH) = 2.2, *J*(PH) = 5.7 Hz, 3 H, $RhCH_3$]. − ^{31}P NMR (36.2 MHz, $CDCl_3$): δ = 4.8 [d, *J*(RhP) = 126.5 Hz]. − $C_{16}H_{27}F_3O_4PRhS$ (506.3): calcd. C 37.95 H 5.38; found C 37.56, H 5.23.

27. Preparation of [(η⁵-C_5H_5)Rh(CH_3)(CO)(PMe_3)]CF_3SO_3 (**35**): Compound **35** was prepared analogously to **33** by using 60.3 mg (0.22 mmol) of **27** and 25 µl (0.22 mmol) of $CF_3SO_3CH_3$ as starting materials. The crude product (dark oil) was dissolved in 8 ml of CH_2Cl_2, the solution was filtered and the filtrate was brought to dryness in vacuo. The residue was dissolved in 1 ml of methanol and the solution was layered with 10 ml of ether. Light brown crystals precipitated which were separated from the mother liquor, washed with ether and dried; yield 16 mg (16%). − IR (CH_2Cl_2): $\tilde{\nu}$ = 2055 cm^{-1} [ν(CO)]. − ^1H NMR (200 MHz, CD_3NO_2): δ = 5.73 [dd, *J*(RhH) = 0.3, *J*(PH) = 1.4 Hz, 5 H, C_5H_5], 1.85 [dd, *J*(RhH) = 0.9, *J*(PH) = 10.8 Hz, 9 H, PMe_3], 1.03 [dd, *J*(RhH) = 2.3, *J*(PH) = 5.2 Hz, 3 H, $RhCH_3$]. − ^{31}P NMR (36.2 MHz, $(CD_3)_2CO$): δ = 12.8 [d, *J*(RhP) = 125.1 Hz]. − $C_{11}H_{17}F_3O_4PRhS$ (436.2): calcd. C 30.29 H 3.91; found C 29.80, H 4.08.

28. Preparation of [(η⁵-C_5H_5)Rh(PMe_3)($SAc)_2$] (**37**): A solution of 146 mg (0.35 mmol) of **36** in 1 ml of benzene and 2 ml of thioacetic acid was treated with 302.9 mg (2.65 mmol) of KSAc at room temp. After the reaction mixture was stirred for 1 h, the solvent was removed and the residue was extracted with 10 ml of benzene. The extract was brought to drynesss in vacuo and upon addition of 1 ml of ether and 1 ml of pentane the oily residue was crystallized to give an orange solid; yield 105 mg (76%); m. p. 150°C (dec.). − IR (C_6H_6): $\tilde{\nu}$ = 1625 cm^{-1} [ν(C=O)]. − ^1H NMR (60 MHz, C_6D_6): δ = 5.40 [dd, *J*(RhH) = 0.4, *J*(PH) = 2.0 Hz, 5 H, C_5H_5], 2.57 (s, 6 H, $SCCH_3$), 1.32 [dd, *J*(RhH) = 0.9, *J*(PH) = 11.7 Hz, 9 H, PMe_3]. − ^{31}P NMR (36.2 MHz, C_6D_6): δ = 12.2 [d, *J*(RhP) = 120.0 Hz]. − MS (70 eV); *m/z* (%) = 394 (7) [M^+], 319 (100) [M^+ − SAc], 244 (65) [$C_5H_5Rh(PMe_3)^+$], 168 (16) [$C_5H_5Rh^+$]. − $C_{12}H_{20}O_2PRhS_2$ (394.3): calcd. C 36.58, H 5.11; found C 36.18, H 5.09.

29. Preparation of [(η⁵-C_5H_5)Rh(CH_2SAc)(PMe_3)I] (**38**): A solution of 104.2 mg (0.25 mmol) of **36** in 4 ml C_6H_6/EtOH (1:1) was treated with 28.3 mg (0.25 mmol) of KSAc and stirred for 1 h at room temp. The solvent was removed, the residue was extracted with 10 ml of benzene and the extract was brought to dryness in vacuo. The residue was now extracted with 5 ml of pentane and the dark red extract was worked up as described below. The remaining solid was dissolved in 2 ml of ether and then 2 ml of pentane was added. After the solution was stored for 12 h at −78°C orange-red crystals of **38** were formed which were separated from the mother liquor, washed twice with pentane and dried; yield 67 mg. The pentane extract was also brought to dryness in vacuo, the residue was dissolved in 1 ml of benzene and the solution was chromatographed on Al_2O_3 (neutral, activity grade IV, height of column 4 cm). With benzene, a red fraction was eluted which upon work up gave red-brown needles of **39**[3]; yield 23 mg (21%). − **38**: m. p. 142°C (dec.). − IR (C_6H_6): $\tilde{\nu}$ = 1670 cm^{-1} [ν(C=O)]. − ^1H NMR (200 MHz, C_6D_6): δ = 4.87 [dd, *J*(RhH) = 0.5, *J*(PH) = 1.6 Hz, 5 H, C_5H_5], 4.10 [ddd, *J*(RhH) = 4.8, *J*(PH) = 3.8, *J*(HH) = 9.2 Hz, 1 H, one H of $RhCH_2$], 3.44 [ddd, *J*(RhH) = 2.2, *J*(PH) = 6.9, *J*(HH) = 9.2 Hz, 1 H, one H of $RhCH_2$], 2.14 (s, 3 H, $SCCH_3$), 1.34 [dd, *J*(RhH) = 0.7, *J*(PH) = 11.1 Hz, 9 H, PMe_3]. − ^{31}P NMR (36.2 MHz, C_6D_6): δ = 7.3 [d, *J*(RhP) = 150.0 Hz]. − MS (70 eV); *m/z* (%) = 371 (95) [M^+ − CH_2SAc], 333 (88) [M^+ − I], 295 (27) [$C_5H_5RhI^+$], 244 (100) [$C_5H_5Rh(PMe_3)^+$], 168 (57) [$C_5H_5Rh^+$]. − $C_{11}H_{19}IOPRhS$ (460.1): calcd. C 28.71, H 4.16; found C 28.48, H 3.84.

30. Preparation of [(η⁵-C_5H_5)Rh(PMe_3)(SAc)I] (**40**): a) A solution of 50.3 mg (0.11 mmol) of **38** in 1.5 ml of benzene was chromatographed on Al_2O_3 (neutral, activity grade IV, height of column 4 cm). With benzene, an orange-yellow fraction was eluted from which the solvent was removed in vacuo. To the oily residue 1 ml of pentane was added and after the mixture was stirred for 1 h an orange solid was obtained; yield 45 mg (91%). − b) A solution of 131.8 mg (0.25 mmol) of **36** in 1.5 ml of benzene and 3 ml of thioacetic acid was treated with 30.1 mg (0.26 mmol) of KSAc and stirred for 2 h at room temp. The solvent was removed, the residue was extracted with 10 ml of benzene and the extract was concentrated to ca. 2 ml in vacuo. The ^1H-NMR spectrum of the solution revealed that the major component of the crude product was **38**. The solution was chromatographed on Al_2O_3 (neutral, activity grade IV, height of column 4 cm) and with benzene two fractions were eluted. The first fraction contained a mixture of products among which **37** could be detected. The second fraction was worked up analogously as described for a) to give an orange microcrystalline solid; yield 80 mg (72%); m. p. 118°C (dec.). − IR (C_6H_6): $\tilde{\nu}$ = 1620 cm^{-1} [ν(C=O)]. − ^1H NMR (200 MHz, C_6D_6): δ = 5.20 [dd, *J*(RhH) = 0.3, *J*(PH) = 1.9 Hz, 5 H, C_5H_5], 2.57 (s, 3 H, $SCCH_3$), 1.50 [dd, *J*(RhH) = 0.7, *J*(PH) = 11.9, 9 H, PMe_3]. − MS (70 eV); *m/z* (%) = 446 (1) [M^+], 371 (50) [M^+ − SAc], 319 (17) [M^+ − I], 295 (16) [$C_5H_5RhI^+$], 244 (60) [$C_5H_5Rh(PMe_3)^+$], 168 (36) [$C_5H_5Rh^+$]. − $C_{10}H_{17}IOPRhS$ (446.1): calcd. C 26.93, H 3.84; found C 27.24, H 3.81.

31. Preparation of [(η⁵-C_5Me_5)Rh(CH_2SAc){$P(OMe)_3$}I] (**43**): A solution of 87.9 mg (0.14 mmol) of **41** in 3 ml of benzene was treated under stirring with a solution of 16.0 mg (0.14 mmol) of KSAc in 1.5 ml of ethanol. After the reaction mixture was continuously stirred for 1 h at room temp., the solvent was removed and the residue was extracted with 10 ml of ether. The extract was brought to dryness in vacuo, the oily residue was washed with 0.5 ml of ethanol and 3 ml of pentane was added. Upon storing for 12 h at −78°C an orange-red solid precipitated which was washed twice with pentane and dried; yield 61 mg (75%). − IR (C_6H_6): $\tilde{\nu}$ = 1670 cm^{-1} [ν(C=O)]. − ^1H NMR (200 MHz, $CDCl_3$): δ = 3.77 [d, *J*(PH) = 11.2 Hz, 9 H, $P(OMe)_3$], 3.20 [ddd, *J*(RhH) = 5.2, *J*(PH) = 2.6, *J*(HH) = 8.4 Hz, 1 H, one H of $RhCH_2$], 2.99 [ddd, *J*(RhH) = 3.2, *J*(PH) = 5.0, *J*(HH) = 8.4 Hz, 1 H, one H of $RhCH_2$], 2.23 (s, 3 H, $SCCH_3$), 1.87 [dd, *J*(RhH) = 0.3, *J*(PH) = 4.5 Hz, 15 H, C_5Me_5]. − ^{13}C NMR (22.5 MHz, C_6D_6): δ = 198.9 (s, C=O), 101.0 [dd, *J*(RhC) = *J*(PC) = 4.4 Hz, C_5Me_5], 54.2 [d, *J*(PC) = 6.6 Hz, $P(OMe)_3$], 29.7 (s, $SCCH_3$), 9.6 [d, *J*(RhC) = 1.5 Hz, $C_5(CH_3)_5$], 5.3 [dd, *J*(RhC) = 27.2, *J*(PC) = 19.1 Hz, $RhCH_2$]. − ^{31}P NMR (36.2 MHz, C_6D_6): δ = 133.6 [d, *J*(RhP) = 248.6 Hz]. − MS (70 eV); *m/z* (%) = 489 (24) [M^+ − CH_2SAc], 365 (41) [$C_5Me_5RhI^+$], 362 (100) [M^+ − CH_2SAc − I], 238 (46) [$C_5Me_5Rh^+$]. − $C_{16}H_{29}IO_4PRhS$ (578.3): calcd. C 33.23, H 5.06; found C 33.47, H 5.18.

32. Preparation of [(η⁵-C_5Me_5)Rh(CH_2SAc)($PMe)_3$I] (**44**): Compound **44** was prepared analogously to **43** by using 87.1 mg (0.15 mmol) of **42** and 17.1 mg (0.15 mmol) of KSAc as starting materials. The ether extract was concentrated to ca. 1 ml in vacuo and then stored for 12 h at −78°C. Orange microcrystalline solid; yield 58 mg (73%); m. p. 137°C (dec.) − IR (C_6H_6): $\tilde{\nu}$ = 1665 cm^{-1} [ν(C=O)]. − ^1H NMR (200 MHz, C_6D_6): δ = 3.60 [ddd, *J*(RhH) =

2.4, J(PH) = 5.0, J(HH) = 8.2 Hz, 1 H, one H of $RhCH_2$], 3.17 [ddd, J(RhH) = J(PH) = 4.1 Hz, J(HH) = 8.2 Hz, 1 H, one H of $RhCH_2$], 2.19 (s, 3 H, $SCCH_3$), 1.72 [dd, J(RhH) = 0.3, J(PH) = 2.8 Hz, 15 H, C_5Me_5], 1.30 [dd, J(RhH) = 0.9, J(PH) = 10.1 Hz, 9 H, PMe_3]. – ^{13}C NMR (22.5 MHz, C_6D_6): δ = 198.7 (s, C=O), 98.8 [dd, J(RhC) = 5.2, J(PC) = 3.7 Hz, C_5Me_5], 29.6 (s, $SCCH_3$), 17.4 [d, J(PC) = 32.4 Hz, PMe_3], 10.0 [br. s, $C_5(CH_3)_5$], 5.9 [dd, J(RhC) = 28.7, J(PC) = 15.4, $RhCH_2$]. – ^{31}P NMR (36.2 MHz, C_6D_6): δ = 2.1 [d, J(RhP) = 140.1 Hz]. – MS (70 eV); m/z (%) = 441 (93) [$M^+ - CH_2SAc$], 365 (100) [$C_5Me_5RhI^+$], 314 (7) [$M^+ - CH_2SAc - I$], 238 (8) [$C_5Me_5Rh^+$]. – $C_{16}H_{29}IOPRhS$ (530.3): calcd. C 36.24, H 5.51; found C 35.83, H 5.53.

33. Preparation of [(η^5-C_5Me_5)Rh(CH_2SAc)(PMe_3)SAc] (**45**): a) A solution of 131.2 mg (0.25 mmol) of **42** in 2 ml of benzene was treated with a solution of 98.5 mg (0.86 mmol) of KSAc in 1 ml of ethanol and stirred for 30 min at room temp. The solvent was removed, the residue was extracted with 10 ml of ether and the extract was concentrated to ca. 1 ml in vacuo. Upon addition of 2 ml of pentane, the solution was stored for 12 h at −78°C. Yellow crystals precipitated which were separated from the mother liquor and dried; yield 80 mg (67%). – b) A solution of 56.6 mg (0.10 mmol) of **44** in 1 ml of benzene was treated with a solution of 12.2 mg (0.11 mmol) of KSAc in 0.5 ml of ethanol. After the reaction mixture was worked up as described for a), a yellow solid was obtained; yield 28 mg (58%); m. p. 163°C (dec.). – IR (C_6H_6): $\tilde{\nu}$ = 1660, 1609 cm^{-1} [ν(C=O)]. – ^{1}H NMR (200 MHz, C_6D_6): δ = 2.70 [ddd, J(RhH) = 2.5, J(PH) = 7.2, J(HH) = 8.5 Hz, 1 H, one H of $RhCH_2$], 2.55, 2.15 (both s, 3 H each, $SCCH_3$), 1.63 [dd, J(RhH) = 0.3, J(PH) = 2.9 Hz, 15 H, C_5Me_5], 1.24 [dd, J(RhH) = 0.9, J(PH) = 10.2 Hz, 9 H, PMe_3], signal of one H of $RhCH_2$ not exactly located. – ^{31}P NMR (36.2 MHz, C_6D_6): δ = 2.2 [d, J(RhP) = 140.0 Hz]. – MS (70 eV); m/z (%) = 478 (0.1) [M^+], 389 (44) [$M^+ - CH_2SAc$], 313 (88) [$C_5Me_5Rh(SAc)^+$], 314 (22) [$C_5Me_5Rh(PMe_3)^+$], 238 (13) [$C_5Me_5Rh^+$]. – $C_{18}H_{32}O_2PRhS_2$ (478.5): calcd. C 45.19, H 6.74; found C 45.35, H 6.46.

34. Preparation of [(η^5-C_5Me_5)Rh(η^2-CH_2S){$P(OMe)_3$}] (**46**): a) A solution of 81.7 mg (0.14 mmol) of **43** in 8 ml of benzene was treated with 85 μl of a 1.6 M solution (0.14 mmol) of nBuLi in hexane and stirred for 10 min at room temp. The solvent was removed and the residue was extracted with 10 ml of pentane. The extract was brought to dryness in vacuo, the oily residue was dissolved in 2 ml of benzene and the solution was chromatographed on Al_2O_3 (neutral, activity grade IV, height of column 5 cm). With benzene, an orange fraction was eluted from which the solvent was removed. The oily residue was dissolved in 8 ml of pentane, the solution was filtered, the filtrate was concentrated to ca. 2 ml and then stored for 12 h at −78°C. Orange-yellow crystals precipitated which were separated from the mother liquor and dried; yield 42 mg (75%). – b) A solution of 85.7 mg (0.14 mmol) of **48** in 5 ml of methanol was treated at room temp. with an excess (ca. 50 mg) of $NaOCH_3$. After the reaction mixture was stirred for 10 min, the solvent was removed and the residue was extracted with 15 ml of pentane. The extract was concentrated to ca. 2 ml in vacuo and then stored for 12 h at −78°C. Orange-yellow crystals; yield 42 mg (73%); m. p. 76°C (dec.). – ^{1}H NMR (90 MHz, C_6D_6): δ = 3.91 [ddd, J(RhH) = 2.7, J(PH) = 0.9, J(HH) = 8.6 Hz, 1 H, one H of CH_2S], 3.34 [d, J(PH) = 12.0 Hz, 9 H, $P(OMe)_3$], 1.77 [dd, J(RhH) = 0.7, J(PH) = 3.9 Hz, 15 H, C_5Me_5], signal of one H of CH_2S partly covered by signal of $P(OMe)_3$. – ^{13}C NMR (50.3 MHz, C_6D_6): δ = 98.5 [dd, J(RhC) = J(PC) = 4.5 Hz, C_5Me_5], 51.5 [d, J(PC) = 6.3 Hz, $P(OMe)_3$], 49.5 [dd, J(RhC) = 18.9, J(PC) = 7.4 Hz, CH_2S], 9.7 [s, $C_5(CH_3)_5$]. – ^{31}P NMR (36.2 MHz, C_6D_6): δ = 143.4 [d, J(RhP) = 290.3 Hz]. – MS (70 eV); m/z (%) = 408 (52) [M^+], 362 (100) [$M^+ - CH_2S$], 238 (40) [$C_5Me_5Rh^+$]. – $C_{14}H_{26}O_3PRhS$ (408.3): calcd. C 41.18, H 6.42; found C 41.50, H 6.55.

35. Preparation of [(η^5-C_5Me_5)Rh(η^2-CH_2S)(PMe_3)] (**47**): Compound **47** was prepared analogously to **46** either by using 68.1 mg (0.15 mmol) of **44** and 90 μl of a 1.6 M solution (0.15 mmol) of nBuLi in hexane or 78.4 mg (0.14 mmol) of **49** and ca. 50 mg of $NaOCH_3$ as starting materials. Orange-brown microcrystalline solid; yield 41 mg (76%) from **44** and 34 mg (68%) from **49** as starting material; m. p. 81°C (dec.). – ^{1}H NMR (200 MHz, C_6D_6): δ = 3.87 (m, 2 H, CH_2S), 1.87 [dd, J(RhH) = 0.5, J(PH) = 2.4 Hz, 15 H, C_5Me_5], 1.07 [dd, J(RhH) = 0.9, J(PH) = 9.0 Hz, 9 H, PMe_3]. – ^{13}C NMR (50.3 MHz, C_6D_6): δ = 96.6 [dd, J(RhC) = J(PC) = 4.4 Hz, C_5Me_5], 46.6 [dd, J(RhC) = 19.9, J(PC) = 5.5 Hz, CH_2S], 15.9 [d, J(PC) = 28.5 Hz, PMe_3], 10.1 [s, $C_5(CH_3)_5$]. – ^{31}P NMR (36.2 MHz, C_6D_6): δ = 4.9 [d, J(RhP) = 184.6 Hz]. – MS (70 eV); m/z (%) = 360 (55) [M^+], 314 (100) [$M^+ - CH_2S$], 238 (21) [$C_5Me_5Rh^+$]. – $C_{14}H_{26}PRhS$ (360.3): calcd. C 46.67, H 7.27; found C 46.48, H 7.52.

36. Preparation of [(η^5-C_5Me_5)Rh{κ^2-C,O-$CH_2SC(Me)O$}-{$P(OMe)_3$}]PF_6 (**48**): Compound **48** was prepared analogously to **19** by using 130.0 mg (0.22 mmol) of **43** and 56.5 mg (0.22 mmol) of $AgPF_6$ as starting materials. Orange-yellow solid; yield 117 mg (89%); dec. temp. 69°C. – Λ = 82 $cm^2\Omega^{-1}mol^{-1}$. – IR (nujol): $\tilde{\nu}$ = 1565 cm^{-1} [ν(C=O)]. – ^{1}H NMR (60 MHz, $(CD_3)_2CO$): δ = 3.83 [d, J(PH) = 11.6 Hz, 9 H, $P(OMe)_3$], 3.37 (m, 2 H, $RhCH_2$), 2.40 (s, 3 H, $SCCH_3$), 1.77 [dd, J(RhH) = 0.3, J(PH) = 4.5 Hz, 15 H, C_5Me_5]. – ^{13}C NMR (22.5 MHz, CD_3NO_2): δ = 226.4 (s, C=O), 103.0 [dd, J(RhC) = 5.9, J(PC) = 4.2 Hz, C_5Me_5], 54.0 [d, J(PC) = 5.9 Hz, $P(OMe)_3$], 27.1 [s, $C(O)CH_3$], 21.5 [dd, J(RhC) = 27.9, J(PC) = 22.8 Hz, $RhCH_2$], 9.2 [d, J(RhC) = 2.2 Hz, $C_5(CH_3)_5$]. – ^{31}P NMR (36.2 MHz, CD_3NO_2): δ = 126.7 [d, J(RhP) = 251.6 Hz]. – $C_{16}H_{29}F_6O_4P_2RhS$ (596.3): calcd. C 32.23, H 4.90; found C 32.10, H 5.11.

37. Preparation of [(η^5-C_5Me_5)Rh{κ^2-C,O-$CH_2SC(Me)O$}-(PMe_3)]PF_6 (**49**): Compound **49** was prepared analogously to **19** by using 159.4 mg (0.30 mmol) of **44** and 78.2 mg (0.31 mmol) of $AgPF_6$ as starting materials. Orange-yellow solid; yield 54 mg (96%); dec. temp. 96°C. – Λ = 73 $cm^2\Omega^{-1}mol^{-1}$. – IR (nujol): $\tilde{\nu}$ = 1552 cm^{-1} [ν(C=O)]. – ^{1}H NMR (200 MHz, $(CD_3)_2CO$): δ = 3.29 [ddd, J(RhH) = 2.9, J(PH) = 0.3, J(HH) = 9.5 Hz, 1 H, one H of $RhCH_2$], 3.07 [ddd, J(RhH) = 9.5, J(PH) = 18.9 J(HH) = 9.5 Hz, 1 H, on H of $RhCH_2$], 2.36 (s, 3 H, $SCCH_3$), 1.71 [dd, J(RhH) = 0.3, J(PH) = 2.7 Hz, 15 H, C_5Me_5], 1.52 [dd, J(RhH) = 0.7, J(PH) = 10.5 Hz, 9 H, PMe_3]. – ^{13}C NMR (22.5 MHz, CD_3NO_2): δ = 226.1 (s, C=O), 100.8 [dd, J(RhC) = 5.9, J(PC) = 2.9 Hz, C_5Me_5], 27.3 [s, $C(O)CH_3$], 21.7 [dd, J(RhC) = 30.2, J(PC) = 15.4 Hz, $RhCH_2$], 13.6 [d, J(RhC) = 30.9 Hz, PMe_3], 9.3 [br. s, $C_5(CH_3)_5$]. – ^{31}P NMR (36.2 MHz, CD_3NO_2): δ = 4.0 [d, J(RhP) = 156.3 Hz]. – $C_{16}H_{29}F_6OP_2RhS$ (548.3): calcd. C 35.05, H 5.33; found C 34.66, H 5.45.

38. Preparation of [(η^5-C_5H_5)Rh(η^2-CH_2S)(PMe_3)] (**50**): Compound **50** was prepared analogously to **46** by using 68.1 mg (0.15 mmol) of **38** and 90 μl of a 1.6 M solution (0.15 mmol) of nBuLi in hexane as starting materials. The yellow microcrystalline solid **50** was identified by comparison of the NMR spectroscopic data with those of an authentic sample;[1d] yield 34 mg (79%).

39. X-ray Structure Determination of Compound **27**[34]: Single crystals of **27** were grown by slow diffusion of ether to a solution of **27** in nitromethane at room temp. Crystal data: orthorhombic, space group $Pbca$, a = 16.857(5), b = 23.538(6), c = 11.048(3) Å, Z = 8, $d_{calcd.}$ = 1.613 g cm^{-3}, μ(Mo-K_α) = 0.98 mm^{-1}; crystal size

0.9 × 1.35 × 0.2 mm; Nicolet P3 diffractometer, Mo-K_α radiation, graphite monochromator; ω scan, $2\Theta_{max} = 55°$; 4276 reflections scanned, 4053 unique reflections, 3919 reflections with $F > 3\sigma(F)$. Intensity data were corrected for Lorentz and polarization effects and a geometrical absorption correction was applied. The structure was solved by the Patterson method. Atomic coordinates and the anisotropic thermal parameters of the non-hydrogen atoms were refined by full-matrix least- squares. The positions of all hydrogen atoms were calculated according to ideal geometry (distance C−H = 0.95 Å). $R = 0.065$, $R_w = 0.070$ [weighting scheme $1/\sigma^2(F)$]; reflections-to-parameter ratio 16.00; residual electron density 2.31 eÅ^{-3}.

☆ Dedicated to Professor *Warren R. Roper* on the occasion of his 60th birthday.

[1] [1a] W. Paul, H. Werner, *Angew. Chem.* **1983**, *95*, 333−334; *Angew. Chem. Int. Ed. Engl.* **1983**, *22*, 316−317. − [1b] L. Hofmann, H. Werner, *J. Organomet. Chem.* **1983**, *255*, C41−C45. − [1c] L. Hofmann, H. Werner, *Chem. Ber.* **1985**, *118*, 4229−4238. − [1d] H. Werner, W. Paul, W. Knaup, J. Wolf, G. Müller, J. Riede, *J. Organomet. Chem.* **1988**, *358*, 95−121.

[2] H. Werner, W. Paul, *Angew. Chem.* **1984**, *96*, 68−69; *Angew. Chem. Int. Ed. Engl*. **1984**, *23*, 58−59.

[3] M. Steinmetz, H. Werner, *J. Organomet. Chem.* **1989**, *369*, 309−319.

[4] W. Paul, H. Werner, *Chem. Ber.* **1985**, *118*, 3032−3040.

[5] [5a] R. G. Pearson, *J. Am. Chem. Soc.* **1963**, *85*, 3533−3539. − [5b] H. Werner, *Chem. unserer Zeit* **1967**, *1*, 135−139.

[6] C. Benezra, *J. Am. Chem. Soc.* **1973**, *95*, 6890−6894.

[7] H. Werner, W. Paul, R. Feser, R. Zolk, P. Thometzek, *Chem. Ber.* **1985**, *118*, 261−274.

[8] [8a] K. Stanley, M. C. Baird, *J. Am. Chem. Soc.* **1975**, *97*, 4292−4298. − [8b] B. K. Hunter, M. C. Baird, *Organometallics* **1985**, *4*, 1481−1483. − [8c] S. G. Davies, I. M. Dordor-Hedgecock, K. H. Sutton, M. Whittaker, *J. Am. Chem. Soc.* **1987**, *109*, 5711−5719.

[9] M. Steinmetz, Dissertation Universität Würzburg **1987**.

[10] H. Werner, B. Klingert, *J. Organomet. Chem.* **1981**, *218*, 395−407.

[11] [11a] H. Werner, W. Hofmann, *Chem. Ber.* **1977**, *110*, 3481−3493. − [11b] H. Werner, B. Heiser, B. Klinglert, R. Dölfel, *J. Organomet. Chem.* **1982**, *240*, 179−190.

[12] S. Gambarotta, C. Floriani, A. Chiesi-Villa, C. Guastini, *Organometallics* **1986**, *5*, 2425−2433.

[13] H. Werner, J. Roll, R. Zolk, P. Thometzek, K. Linse, M. L. Ziegler, *Chem. Ber.* **1987**, *120*, 1553−1564.

[14] H. Werner, O. Schippel, J. Wolf, M. Schulz, *J. Organomet. Chem.* **1991**, *417*, 149−162.

[15] S. Quinn, A. Shaver, V. W. Day, *J. Am. Chem. Soc.* **1982**, *104*, 1096−1099.

[16] Inter alia: [16a] R. A. Periana, R. G. Bergman, *J. Am. Chem. Soc.* **1986**, *108*, 7332−7346 and 7346−7355. − [16b] W. D. Jones, V. L. Chandler, F. J. Feher, *Organometallics* **1990**, *9*, 164−174. − [16c] S. T. Belt, M. Helliwell, W. D. Jones, M. G. Partridge, R. N. Perutz, *J. Am. Chem. Soc.* **1993**, *115*, 1429−1440. − [16d] A. D. Selmeczy, W. D. Jones, M. G. Partridge, R. N. Perutz, *Organometallics* **1994**, *13*, 522−532.

[17] [17a] H. Werner, J. Wolf, U. Schubert, *Chem. Ber.* **1983**, *116*, 2848−2854. − [17b] H. Werner, L. Hofmann, W. Paul, U. Schubert, *Organometallics* **1988**, *7*, 1106−1111.

[18] M. Hesse, H. Meier, B. Zeeh, *Spektroskopische Methoden der organischen Chemie*, 2. Ed., Thieme, Stuttgart **1984**, p. 144 and 183.

[19] W. E. Buhro, S. Georgiou, J. M. Fernandez, A. T. Patton, C. E. Strouse, J. A. Gladysz, *Organometallics* **1986**, *5*, 956−965.

[20] [20a] G. Erker, U. Hoffmann, R. Zwettler, P. Betz, C. Krüger, *Angew. Chem.* **1989**, *101*, 644−645; *Angew. Chem. Int. Ed. Engl.* **1989**, *28*, 630−631. − [20b] G. Erker, F. Sosna, U. Hoffmann, *J. Organomet. Chem.* **1989**, *372*, 41−52. − [20c] G. Erker, M. Mena, S. Werner, C. Krüger, *J. Organomet. Chem.* **1990**, *390*, 323−331. − [20d] G. Erker, M. Bendix, R. Petrenz, *Organometallics* **1994**, *13*, 456−461.

[21] [21a] K. Isobe, P. M. Bailey, P. M. Maitlis, *J. Chem. Soc.*, *Dalton Trans.* **1981**, 2003−2008. − [21b] W. D. Jones, F. J. Feher, *J. Am. Chem. Soc.* **1984**, *106*, 1650−1663.

[22] H. Werner, B. Klingert, *J. Organomet. Chem.* **1982**, *233*, 365−371.

[23] M. Green, D. R. Hankey, J. A. K. Howard, P. Louca, F. G. A. Stone, *J. Chem. Soc., Chem. Commun.* **1983**, 757−758.

[24] D. L. Thorn, *Organometallics* **1982**, *1*, 197−204.

[25] [25a] K. L. Brown, G. R. Clark, C. E. L. Headford, K. Marsden, W. R. Roper, *J. Am. Chem. Soc.* **1979**, *101*, 503−505. − [25b] G. R. Clark, C. E. L. Headford, K. Marsden, W. R. Roper, *J. Organomet. Chem.* **1982**, *231*, 335−360.

[26] Y.-H. Huang, J. A. Gladysz, *J. Chem. Educ.* **1988**, *65*, 298−303.

[27] R. Feser, H. Werner, *J. Organomet. Chem.* **1982**, *233*, 193−204.

[28] Representative examples: [28a] H. Berke, W. Bankhardt, G. Huttner, J. von Seyerl, L. Zsolnai, *Chem. Ber.* **1981**, *114*, 2754−2768. − [28b] H. Berke, G. Huttner, G. Weiler, L. Zsolnai, *J. Organomet. Chem.* **1981**, *219*, 353−362. − [28c] J. Okuda, G. E. Herberich, *Angew. Chem.* **1985**, *97*, 400−401; *Angew. Chem. Int. Ed. Engl.* **1985**, *24*, 402−403. − [28d] R. A. Head, *J. Chem. Soc.*, *Dalton Trans.* **1982**, 1637−1639.

[29] [29a] E. L. Muetterties, J. Stein, *Chem. Rev.* **1979**, *79*, 479−490. − [29b] W. A. Herrmann, *Angew. Chem.* **1982**, *94*, 118−131; *Angew. Chem. Int. Ed. Engl.* **1982**, *21*, 117−130. − [29c] U. Pidun, G. Frenking, *Chem. Eur. J.* **1998**, *4*, 522−540; and refs. therein.

[30] [30a] R. E. LaPointe, P. T. Wolczanski, *J. Am. Chem. Soc.* **1986**, *108*, 3535−3537. − [30b] A. van Asselt, B. J. Burger, V. C. Gibson, J. E. Bercaw, *J. Am. Chem. Soc.* **1986**, *108*, 5347−5349.

[31] [31a] T. J. Collins, W. R. Roper, *J. Organomet. Chem.* **1978**, *159*, 73−89. − [31b] A. F. Hill, W. R. Roper, J. M. Waters, A. H. Wright, *J. Am. Chem. Soc.* **1983**, *105*, 5939−5940.

[32] H. Werner, L. Hofmann, R. Feser, W. Paul, *J. Organomet. Chem.* **1985**, *281*, 317−347.

[33] H. G. Schuster-Woldan, F. Basolo, *J. Am. Chem. Soc.* **1966**, *88*, 1657−1663.

[34] Crystallographic data (excluding structure factors) for the structure reported in this paper have been deposited with the Cambridge Crystallographic Data Centre as supplementary publication no. CCDC-101821. Copies of the data can be obtained free of charge on application to the Director, CCDC, 12 Union Road, Cambridge CB2 1EZ, UK [fax: (internat.) +44(1223)336−033; e-mail: deposit@chemcrys.cam.ac.uk].

[98183]

Structure of 2,4,6-Tri-*tert*-butyl-1,3,5-triphosphabenzene and of 2,4-Di-*tert*-butyl-1,3-diphosphabenzene: X-ray Analysis, Photoelectron Spectra and Molecular Orbital Calculations☆

Rolf Gleiter*[a], Holger Lange[a], Paul Binger*[b], Jörg Stannek[b], Carl Krüger[b], Joachim Bruckmann[b], Ulrich Zenneck*[c], and Susanne Kummer[c]

Organisch-Chemisches Institut der Universität Heidelberg[a],
Im Neuenheimer Feld 270, D-69120 Heidelberg, Germany,

Max-Planck-Institut für Kohlenforschung[b],
Kaiser-Wilhelm-Platz 1, D-45470 Mülheim a. d. Ruhr, Germany,

Institut für Anorganische Chemie der Universität Erlangen-Nürnberg[c],
Egerlandstraße 1, D-91058 Erlangen, Germany

Received June 16, 1998

Keywords: 1,3,5-Triphosphabenzene / 1,3-Diphosphabenzene / Photoelectron spectroscopy / Molecular orbital calculations

The structure of 2,4,6-tri-*tert*-butyl-1,3,5-triphosphabenzene (**1**) as well as the He(I) photoelectron spectra of **1** and 2,4-di-*tert*-butyl-1,3-diphosphabenzene (**2**) have been investigated. It was found that **1** is planar with average C–P–C angles of 109.3° (±0.3°) and P–C–P angles of 130.7° (± 0.4°). All P–C bond lengths amount to 1.727 (± 0.008) Å. The PE spectra were interpreted by comparison with the results of ab initio calculations (RHF/ 6-31G*). They reveal a splitting of the lone pairs on P in **2** of 0.7 eV.

With the synthesis of 2,4,6-tri-*tert*-butyl-1,3,5-triphosphabenzene (2,4,6-tri-*tert*-butyl-1λ^3,3λ^3,5λ^3-triphosphinine) (**1**)[1] and of 2,4-di-*tert*-butyl-1,3-diphosphabenzene (2,4-di-*tert*-butyl-1λ^3,3λ^3-diphosphinine) (**2**)[2] the family of phosphorus-containing heterobenzenes is now nearly complete. Earlier investigations led to the synthesis of λ^3-phosphinine **4**[3], numerous substituted λ^3-phosphinines[4] and also of one example of a 1λ^3,4λ^3-diphosphinine **3**.[5] The latter compound, 2,3,5,6-tetrakis(trifluormethyl)-1λ^3,4λ^3-diphosphinine, is stable only in solution. According to their NMR-spectroscopic data (^{31}P, ^{1}H, ^{13}C) mono-, di- and triphosphinines can be conceived as 6π heteroarenes and therefore their trivial names as phosphabenzenes are justified.

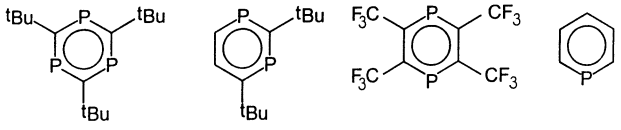

1 2 3 4

In order to gain more information about the electronic structure of the two recently prepared diphospha- and triphosphabenzenes **2** and **1**[1][2], we investigated their PE spectra and interpreted the results on the basis of Hartree-Fock ab initio calculations adopting a 6-31G* basis. Furthermore, we present the results of a single-crystal structure analysis of the triphosphabenzene **1** in this paper.

Suitable crystals of compound **1** for an X-ray analysis were obtained as little yellow plates from a pentane solution of **1** at −30°C. As shown in Figure 1 the triphosphabenzene derivative **1** is completely planar. However, in contrast to benzene or pyridine, but in accordance with phosphinines[4] 1,3,5-triphosphinine **1** is far from being regular hexagonal. The average C−P−C angles are 109.3° (±0.3°) (C−C−C angle in benzene 120°, C−N−C angle in pyridine 117°, C−P−C angle in phosphine 101−103°C). In order to accommodate this angular change the P−C−P angles have to exceed 120°. In triphosphabenzene **1** the average P−C−P angles are 130.7° (±0.4°) (P−C−C and C−C−C angles in phosphinines 122−120°[4]). All P−C bond lengths of the P_3C_3 ring are equal with average bond lengths of 1.727 (±0.008) Å, and are in the range of those found for phosphinines (1.73−1.75 Å),[4] considerably longer than P=C bond lengths in phosphaalkenes (1.66−1.68 Å).[6] All these results point towards a delocalization of the six π-electrons of the triphosphabenzene **1**. Our calculations (C_3 symmetry, RHF/6-31G*) reveal geometrical parameters for **1** which are close to the experiment (C=P: calcd. 1.730 Å, found 1.727 Å; C−P−C: calcd. 110.6°, found 109.6°; P−C−P: calcd. 129.4°, found 130.3°).[7]

The He(I) photoelectron (PE) spectra of **1** and **2** are shown in Figure 2. The vertical ionization energies, $I_{v,j}$, are collected in Table 1. The PE spectrum of **1** shows one broad band centered at 8.2 eV separated by 1.8 eV from the next one at 10.0 eV. The PE spectrum of **2** shows also a broad peak at 8.6 eV and a smaller one at 9.5 eV. The ratio between the areas below both peaks in **2** is approximately 3:1.

To assign the PE spectra of **1** and **2** to various ionization processes we assume the validity of Koopmans' theorem[8] which allows us to correlate the recorded vertical ionization

 © WILEY-VCH Verlag GmbH, D-69451 Weinheim, 1998 1434−1948/98/1111−1619 $ 17.50+.50/0

Figure 1. Molecular structure of **1**[a]

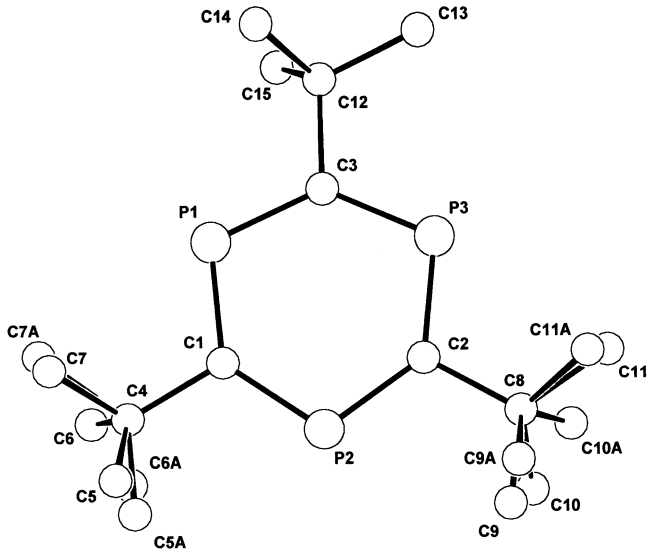

[a] Selected bond lengths [Å] and angles [°]: P1−C1 1.725(5), P1−C3 1.729(5), P2−C1 1.724(5), P2−C2 1.719(4), P3−C2 1.727(4), P3−C3 1.718(4), C3−C12 1.558(6), C1−C4 1.551(7); P1−C1−P2 130.3(3), P2−C2−P3 130.8(3), P1−C3−P3 130.9(3), C1−P1−C3 109.3(2), C1−P2−C2 109.6(2), C2−P3−C3 109.0(2).

energies, $I_{v,j}$, with the calculated orbital energies, $-\varepsilon_j$. To derive the orbital energies we use the Hartree-Fock ab initio method adopting a 6-31G* basis.[9] The results of our calculations are based on the optimized geometries of **1** and **2** and are listed in Table 1.

The calculations predict for **2** three relatively close-lying occupied molecular orbitals (MOs) at 8.38, 8.93 and 9.29 eV, well separated from a fourth one at 10.76 eV.

We assume that the ionizations from these four MOs give rise to two peaks; the first one is due to the overlap of three close-lying bands. The calculations predict that the two highest occupied MOs are of π type followed by linear combinations of the phosphorus lone pairs. All four are shown schematically in Figure 3.

The plausibility of this assignment can be checked by comparing the PE spectrum of **2** with that of phosphabenzene (**4**)[10] and 1,3,5-tri-*tert*-butylphosphabenzene (**5**).[11] The ionization energy of the phosphorous lone pair of **4** was found at 10.0 eV and of **5** at 8.6 eV. These values allow us to estimate the inductive effect of one *tert*-butyl group to 0.47 eV. This leads to the center of gravity of the two lone pairs in **2** at 9.1 eV. This value agrees very well with that found for bands 3 and 4 in the PE spectrum of **2**. A comparison between the energy difference of band 3 and 4 in the PE spectrum of **2** and the values for the corresponding orbital energies show that the calculated energy splitting of the lone pairs is twice as large as the measured one. The splitting of the bands assigned to the lone pairs in **2** (0.7 eV) is half the value found in the PE spectrum of pyrimidine.[12] We ascribe this to the higher p character of the lone pairs in pyrimidine (73%) as compared to 2,4-di-*tert*-butyl-1,3-diphosphabenzene **2** (41%).

Our assignment of the first bands of the PE spectrum of **1** is also based on the comparison between the results of a HF-SCF calculation and the PE experiment. This comparison suggests to assign the first peak in the PE spectrum of **1** to four strongly overlapping bands corresponding to the transition from 27e(π) and 26e(n). The shoulder at 10 eV is assigned to 27a(π). All four MOs are shown in Figure 3.

Figure 2. He(I) photoelectron spectra of **1** and **2**

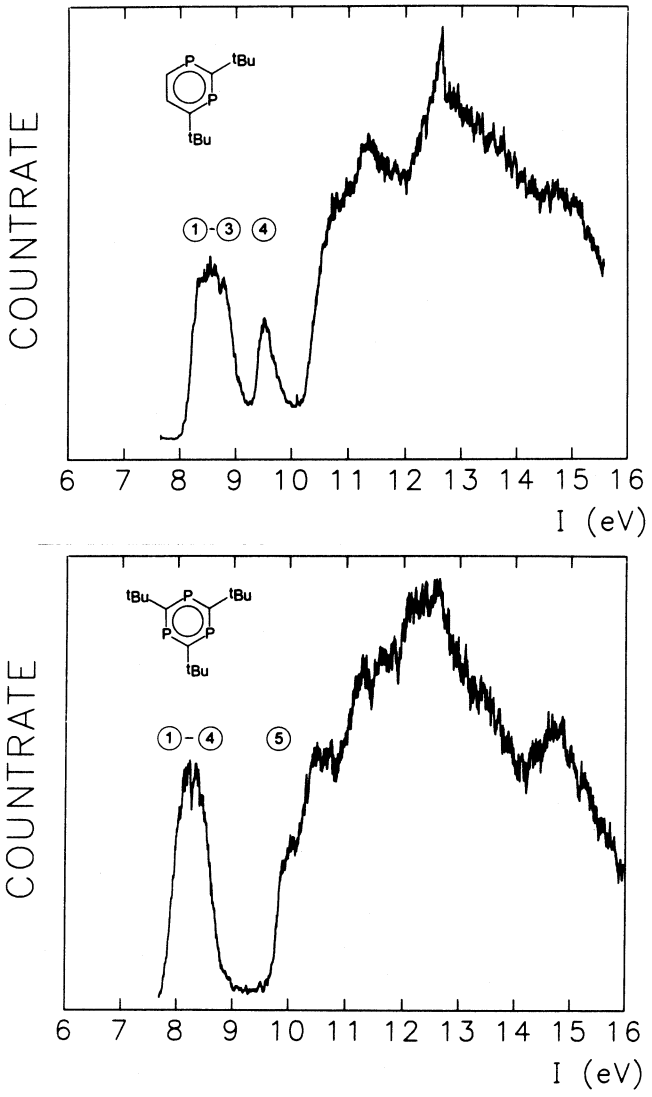

Table 1. Vertical ionization energies, $I_{v,j}$, and calculated orbital energies, $-\varepsilon_j$, of **1** and **2**

	band	$I_{v,j}$ [eV]	assignment	$-\varepsilon_j$ [eV]
1	1	8.2	27 e (π)	8.51
	2			
	3	8.3	26e (n)	9.16
	4			
	5	10.0	27a (π)	11.46
2	1	8.5	61a (π)	8.38
	2	8.6	60a (π)	8.93
	3	8.8	59a (n-)	9.29
	4	9.5	58a (n+)	10.76

Figure 3. Schematic representation of the highest occupied molecular orbitals of **1**and **2**

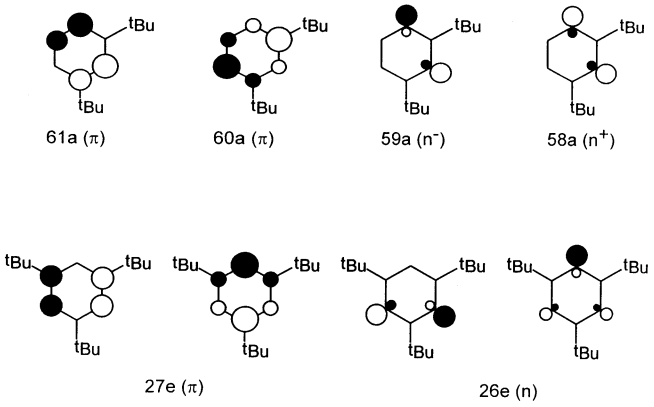

The assignment of the π bands of **1** yields a center of gravity of 8.8 eV. This value is close to that found for **5** (8.9 eV).

We are grateful to *A. Flatow* for recording the PE spectra of **1** and **2**. We thank the *Deutsche Forschungsgemeinschaft (Graduiertenkolleg "Phosphor als Bindeglied verschiedener chemischer Disziplinen")*, the *Fonds der Chemischen Industrie* and the *BASF Aktiengesellschaft*, Ludwigshafen, for financial support.

Experimental Section

The He(I) PE spectra of **1** and **2** were recorded with a PS18 spectrometer (Perkin Elmer). The recording temperatures were 80°C for **1** and 25°C for **2**. The calibration was performed with Ar and Xe. A resolution of 20 meV on the $P_{3/2}$ Ar line was obtained. The MO calculations on **1** and **2** were carried out with the Gaussian 94 program.[9] The orbital energies are based on the optimized geometries of **1** and **2**.

Crystal Structure Analysis of **1**[13]: Enraf-Nonius CAD4 diffractometer (Cu-K_α radiation), T = 293 K; structure solution by heavy atom method (SHELXS-86[14]) and structure refinement by SHELXL-93[15]; monoclinic, space group $C2/c$, lattice constants a = 31.281(3), b = 6.047(1), c = 19.458(1) Å, β = 93.96(3)°, V = 3672.0(6) Å^3, Z = 8, μ(Mo-K_α) = 2.876 mm^{-1}, crystal size 0.25 × 0.24 × 0.11 mm, Θ_{max} = 33.16°, 4206 measured reflections (R_{int} = 0.04), 3756 independent of which 2262 were considered observed with $I > 2\sigma(I)$, ψscan absorption correction; min./max, transmission 0.860/0.999, max. residual electronic density 0.54 e/Å^3. 157 parameters C and P anisotropic (except the disordered atoms at C4 and C8), the positions of the H atoms were calculated for idealized positions (d_{C-H} = 0.980 Å), R_1 = 0.0909, wR^2 = 0.2438.

☆ Dedicated to Professor *Hans Bock* on the occasion of his 70th birthday.

[1] P. Binger, S. Leininger, J. Stannek, B. Gabor, R. Mynott, J. Bruckmann, C. Krüger, *Angew. Chem.* **1995**, *107*, 2411; *Angew. Chem. Int. Ed. Engl.* **1995**, *34*, 2227.
[2] D. Böhm, F. Knoch, S. Kummer, U. Schmidt, U. Zenneck, *Angew. Chem.* **1995**, *107*, 251; *Angew. Chem. Int. Ed. Engl.* **1995**, *34*, 198.
[3] A. J. Ashe III, *J. Am. Chem. Soc.* **1971**, *93*, 3293.
[4] G. Märkl in *Multiple Bonds and Low Coordination in Phosphorus Chemistry* (Ed. M. Regitz, O. J. Scherer), Thieme, Stuttgart **1990**, p. 220.
[5] Y. Kobayashi, J. Kumadaki, A. Ohsawa, H. Hamana, *Tetrahedron Lett.* **1977**, 867; C. G. Krespan, B. C. McKusick, T. L. Cairns, *J. Am. Chem. Soc.* **1960**, *82*, 1515; C. G. Krespan, *J. Am. Chem. Soc.* **1961**, *83*, 3432.
[6] F. H. Allen, O. Kennard, D. G. Watson, L. Brammer, A. G. Orpen, R. Tayler, *J. Chem. Soc. Perkin Trans. 2* **1987**, S1.
[7] The calculated values for **1** would also be in line with the MP2/6-31G* results of S. R. Bachrach. P. Magdalinos, *J. Molec. Struct. (Theochem.)* **1996**, *368*, 1, reported for the parent system if one assumes that the authors have mixed up the C−P−C and P−C−P angles for 1,3,5-triphosphabenzene.
[8] T. Koopmans, *Physica* **1934**, *1*, 104.
[9] We used the *Gaussian 94* program by M. J. Frisch, G. W. Trucks, H. B. Schlegel, P. M. W. Gill, B. G. Johnson, M. A. Robb, J. R. Cheeseman, T. Keith, G. A. Petersson, J. A Montgomery, K. Raghavachari, M. A. Al-Laham, V. G. Zakrzewski, J. V. Ortiz, J. B. Foresman, J. Cioslowski, B. B. Stefanov. A. Nanayakkara, M. Challacombe, C. Y. Peng, P. Y. Ayala, W. Chen, M. W. Wong, J. L. Andres, E. S. Replogle, R. Gomperts, R. L. Martin, D. J. Fox, J. S. Binkley, D. J. Defrees, J. Baker, J. P. Stewart, M. Head-Gordon, C. Gonzalez, J. A. Pople, Gaussian, Inc., Pittsburgh, PA, **1995**.
[10] C. Batich, E. Heilbronner, V. Hornung, A. J. Ashe III, D. T. Clark, K. T. Bobley, D. Kilcast, I. Scanlan, *J. Am. Chem. Soc.* **1973**, *95*, 928.
[11] H. Oehling, W. Schäfer, A. Schweig, *Angew. Chem.* **1971**, *83*, 723; *Angew. Chem. Int. Ed. Engl.* **1971**, *10*, 656.
[12] R. Gleiter, E. Heilbronner, V. Hornung, *Helv. Chim. Acta* **1972**, *55*, 255.
[13] Crystallographic data (excluding structure factors) for the structure reported in this paper have been deposited with the Cambridge Crystallographic Data Centre as supplementary publication no. CCDC-101646. Copies of the data can be obtained free of charge on application to CCDC, 12 Union Road, Cambridge CB2 1EZ, UK [fax: int. code +44(1223)336-033, e-mail: deposit@ccdc.cam.ac.uk].
[14] G. M. Sheldrick, *SHELXS-86, Program for Crystal Structure Solution*, Universität Göttingen, **1986**.
[15] G. M. Sheldrick, *SHELXL-93, Program for Crystal Structure Refinement*, Universität Göttingen, **1993**.

[98188]

Organic Syntheses via Transition Metal Complexes, XCVII[◇]

Mesoionic Pyrrolium Complexes and Dihydropyrroles by Cycloaddition of (Non-enolizable) Imines to an [(1-Alkynyl)carbene]tungsten Complex☆

Rudolf Aumann*, Zhengkun Yu[+], Roland Fröhlich[++], and Frank Zippel[++]

Organisch-Chemisches Institut der Universität Münster,
Orléans-Ring 23, D-48149 Münster, Germany

Received June 2, 1998

Keywords: (1-Alkynyl)carbene complexes / Pyrroles / Imines / Mesoionic compounds / Tungsten complexes

Reaction of the [(1-alkynyl)carbene]tungsten complex $(CO)_5W{=}C(OEt)C{\equiv}CPh$ (**1a**) with non-enolizable imines, e.g. 9-fluorenone imines **2** [NR = N(*i*Pr), N(*c*-C_6H_{11})], affords novel mesoionic pyrrolium carbonyltungstates **3** (by [3+2] cycloaddition) together with dihydropyrroles **4** (by dichotomy of the C=N bond and subsequent insertion of the carbene carbon atom into an NC–H bond). Cross-conjugated azametallatrienes **6** and pentacarbonyltungsten complexes **7** of the dihydropyrroles **4** have been identified to be precursors to compound **4**. Compounds **3b**, **4a**, and **6a** have been characterized by X-ray crystal structure analyses.

Reactions of imines with group-VI heteroatom-stabilized carbene complexes of the Fischer-type are varied and have provided some useful synthetic applications. Depending on the type of carbene complex and the imine, nucleophilic substitution at the carbene carbon atom,[2] condensation at the α-carbon atom (under thermal conditions) or formation of β-lactams[3] (under the influence of sun light) is achieved. The latter type of reaction has been extensively studied by Hegedus et al., and many *N*-substituted imines have been converted into β-lactams. Reactions of imines with α,β-unsaturated carbene complexes are channeled by competing 4-addition of the nitrogen atom to a C=C (or C≡C) bond, and by 2-addition to the M=C, respectively. For example, reactions of *NH*-ketimines $R_2C{=}NH$ (R = alkyl, aryl) with the [(1-alkynyl)carbene]chromium complex $(CO)_5Cr{=}C(OEt)C{\equiv}CPh$ (**1b**) were shown to afford mainly 5-aza-1-chroma-1,3,5-hexatrienes $(CO)_5Cr{=}C(OEt)CH{=}C(Ph)N{=}CR_2$ by 4-addition.[4] Alkenyl *NH*-imidates $R^2CH{=}CR^1{-}C(OEt){=}NH$ (R^1, R^2 = Ph, Me, H) and (1-alkynyl)-carbene complexes **1a**, **b** (M = W, Cr) were found to produce 5-aza-1-metalla-1,3,5,7-octatetraenes $(CO)_5M{=}C(OEt){-}CR{=}CR{-}N{=}C(OEt){-}CR^1{=}CHR^2$ (R = alkyl, aryl) by 4-addition, but also 2,5-diethoxy-2*H*-pyrrole and 2,4-diethoxy-2*H*-dihydroazete complexes, both of which by 2-addition (in an overall [3+2] and [2+2] cycloaddition, respectively).[5] Furthermore, reactions of both alkenyl *N(alkyl)*-imines, and -imidates, respectively, involve participation of the alkenyl unit, but lead to different types of products with (1-alkynyl)carbene complexes **1a**, **b**. Whilst the alkenyl *N(alkyl)*-imines, e.g. PhCH=CH−CH=N(*i*Pr) yield (dihydropyridinyl)carbene complexes (in an overall [4+2] cycloaddition initiated by 4-addition) and mesoionic 1-azonia-5*H*-cycloheptatrien-3-yl carbonylmetalates (in an overall [4+3] cycloaddition initiated by 2-addition),[6][7] alkenyl *N(alkyl)*-imidates, e.g. $RCH{=}CH{-}C(OEt)NR^1$ (R, R^1 = aryl, alkyl) were found to afford binuclear compounds as the only products, resulting from a domino [4+2] and [2+2] cycloaddition of two equivalents of compound **1**.[8] Thus, with respect to the addition of α,β-unsaturated imines to (1-alkynyl)carbene complexes **1**, it should be noted that open-chain adducts as well as four- and five-membered *N*-heterocyclic rings are obtained from *N*-unsubstituted alkenyl imidates, whilst bicyclic systems are generated from *N*-substituted alkenyl imidates, and six- and seven-membered rings are generated from *N*-substituted alkenylimines (but supposedly not from *N*-unsubstituted alkenylimines).

Reaction of (1-Alkynyl)carbene Complex 1a with Non-enolizable Imines 2

The investigation of fundamental reaction paths of imines and imidates with (1-alkynyl)carbene complexes **1** was extended to aliphatic compounds. It was found that enolizable imidates, e.g., *O*-alkyl lactims $\sim(CH_2)_n{-}N{=}C(OR){\sim}$ (n = 3−6) and (1-alkynyl)carbene complexes **1a**, **b** gave 1-azacycloalkene derivatives as the main products, involving the transfer of an α-hydrogen atom.[1] Focusing more strongly on the reactivity of the C=N bonds in aliphatic systems, it was envisaged that non-enolizable imines might yield pyrrolium (= azoniacyclopentadiene) complexes by [3+2] cycloaddition of a C_3 unit of compounds **1** to the C=N bond (Scheme 1). This reaction mode was anticipated as an extension of the recently described access to cyclopen-

[◇] Part XCVI: Ref.[1].
[+] On leave of absence from Dalian Institute of Chemical Physics, Chinese Academy of Sciences, P. O. Box 110, 116023 Dalian, China.
[++] X-ray structure analyses.

 © WILEY-VCH Verlag GmbH, D-69451 Weinheim, 1998 1434−1948/98/1111−1623 $ 17.50+.50/0

tadienes by [3+2] cycloaddition of (1-alkynyl)carbene complexes to HC=C(N) bonds.[9]

Scheme 1. [3+2] Cycloaddition of [(1-alkynyl)carbene]tungsten complex **1a** to olefines and imines, respectively

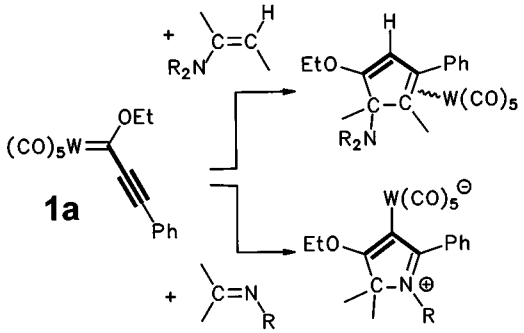

Reaction of the (1-alkynyl)carbene complex **1a** with non-enolizable imines, like fluorenone imines **2a**, **b** at 90°C, 2 h, molar ratio 1:1, affords two types of compounds in a clean reaction: (a) novel pyrrolium complexes **3a**, **b** as minor and (b) dihydropyrroles **4a**, **b** as major products (Scheme 2). Compounds **3** and **4** were isolated by chromatography on silica gel and characterized spectroscopically as well as by X-ray crystal structure analyses. Whilst it is quite obvious that compounds **3** are generated in an overall [3+2] cycloaddition as outlined above (Scheme 1), formation of compounds **4** seems to involve a more complicated reaction sequence (v.s.).

Scheme 2. Two different routes to pyrrole derivatives from non-enolizable imines 2 and (1-alkynyl)carbene complex **1a**

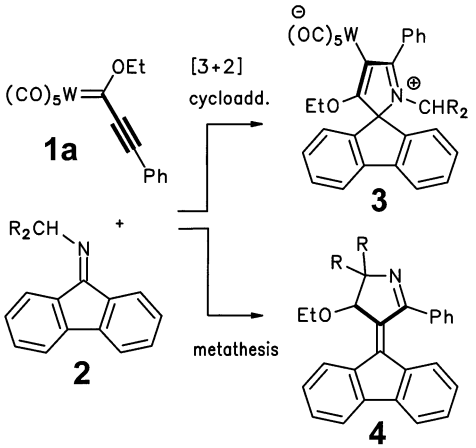

2–4	R,R	[3] + [4]	[3]/[4]
a	Me,Me	93%	1:8
b	$-[CH_2]_4-$	89%	2:7

Spectroscopy and Structure Determinations

The mesoionic character of the novel pyrrolium compounds **3** is indicated in its ^{13}C-NMR spectrum by a characteristic upfield shift of the signal W–*C*(ring) (**3a**: δ = 187.9; **3b**: δ = 187.3), which now is observed in a range similar to that found for iminium carbonylmetalates[10] derived from vinylogous seven-membered *N*-heterocyclic ligands[7] (W–*C*: δ = 181.9).[6c] Furthermore, the signal of *C*=N$^+$ is appreciably shifted downfield (**3a**: δ = 198.2; **3b**: δ = 197.3) if compared to a normal C=N bond. Compounds **3** are first representatives of a (supposedly) large group of mesoionic pyrrolium complexes, which, like sydnones and related species,[11] can not be satisfactorily described by Lewis formulas excluding charge separation. In line with expectation, compounds **3** were found to undergo hydrolysis of the enol ether unit with formation of a spiro compound **5** as the only detectable product, in addition to $W(CO)_6$ (Scheme 3).

Scheme 3. Hydrolysis of zwitterionic pyrrolium complexes **3**

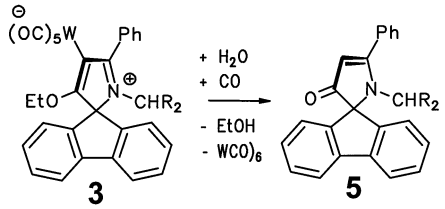

Structural details of spiro compounds **3** are based on a crystal structure analysis of compound **3b** (Figure 1, Table 1). The distance W–C4 [2.276(4)] Å is longer than in non-heteroatom (carbene)tungsten complexes, such as $(CO)_5W{=}CPh_2$ [2.15(1)][12] and even longer than in pyrylium pentacarbonyltungstates, e.g. 2.193(5).[13] In line with the mesoionic character of compound **3b** is the pattern of alternating bond lengths found in the *N*-heterocyclic ring [N–C2 1.474(5), C2–C3 1.517(5), C3–C4 1.357(5), C4–C5 1.434(6), C5–N 1.324(5) Å] and an essentially planar arrangement of the bonds to the nitrogen atom (sum of valence angles is 360.0°). The plane defined by the five-membered heterocycle bisects the angle between two neighboring carbonyltungsten groups, C3–C4–W–C41 –37.5 (4)°, and is arranged almost perpendicular to the phenyl group, C4–C5–C50–C51 97.6 (5)°.

Figure 1. Molecular structure of the mesoionic pyrrolium complex **3b**

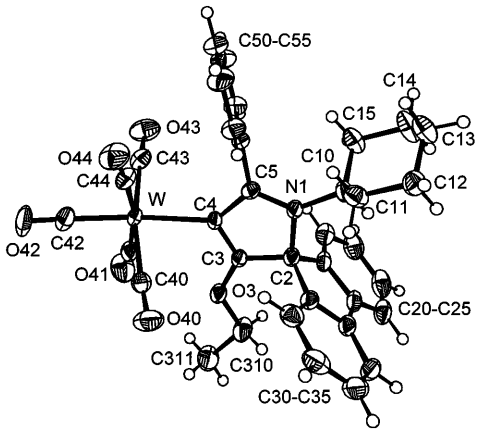

The structure of the dihydropyrroles **4a**, **b** is based on the ^1J-, ^2J-, and $^3J(^{13}C,^1H)$ coupling constants in the NMR

Table 1. Selected bond lengths [Å] and angles [°] for pyrrolium compound **3b**

N(1)−C(5)	1.324(5)	N(1)−C(2)−C(3)	100.5(3)
N(1)−C(2)	1.474(5)	N(1)−C(2)−C(20)	112.8(3)
N(1)−C(10)	1.485(5)	C(3)−C(2)−C(20)	117.0(3)
C(2)−C(3)	1.517(5)	N(1)−C(2)−C(30)	112.7(3)
C(2)−C(20)	1.521(6)	C(3)−C(2)−C(30)	112.4(3)
C(2)−C(30)	1.535(6)	C(20)−C(2)−C(30)	102.0(3)
C(3)−O(3)	1.331(5)	O(3)−C(3)−C(4)	121.9(4)
C(3)−C(4)	1.357(5)	O(3)−C(3)−C(2)	125.1(3)
C(4)−C(5)	1.434(6)	C(4)−C(3)−C(2)	112.8(3)
C(4)−W	2.276(4)	C(3)−C(4)−C(5)	103.3(3)
C(5)−C(50)	1.488(5)	C(3)−C(4)−W	123.7(3)
O(3)−C(310)	1.434(5)	C(5)−C(4)−W	132.1(3)
C(310)−C(311)	1.496(7)	N(1)−C(5)−C(4)	114.6(3)
		N(1)−C(5)−C(50)	122.6(4)
C(5)−N(1)−C(2)	108.7(3)	C(4)−C(5)−C(50)	122.7(4)
C(5)−N(1)−C(10)	132.5(3)	C(3)−O(3)−C(310)	123.7(4)
C(2)−N(1)−C(10)	118.8(3)	O(3)−C(310)−C(311)	107.0(4)
N(1)−C(2)−C(3)	100.5(3)		

spectra, as well as on a crystal structure analysis of compound **4a** (Figure 2, Table 2). The *N*-heterocyclic ring exhibits the expected pattern of bond lengths [C1−C2 1.514(3), C2−C3 1.554(4), C3−N4 1.489(3), N4−C5 1.291(3), C1−C5 1.481(3) Å] and is slightly twisted against the fluorenylidene unit, C5−C1−C6−C7 18.0 (4)°.

Figure 2. Molecular structure of the dihydropyrrol **4a**

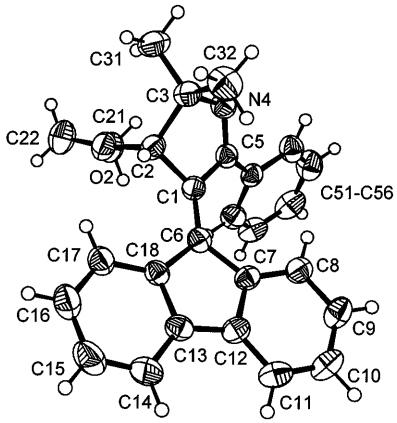

Table 2. Selected bond lengths [Å] and angles [°] for dihydropyrrole **4a**

C(1)−C(6)	1.352(3)	O(2)−C(2)−C(1)	115.5(2)
C(1)−C(5)	1.481(3)	O(2)−C(2)−C(3)	114.6(2)
C(1)−C(2)	1.514(3)	C(1)−C(2)−C(3)	100.4(2)
C(2)−O(2)	1.428(3)	C(21)−O(2)−C(2)	115.5(2)
C(2)−C(3)	1.554(4)	O(2)−C(21)−C(22)	109.4(2)
O(2)−C(21)	1.428(3)	N(4)−C(3)−C(31)	110.7(2)
C(21)−C(22)	1.503(4)	N(4)−C(3)−C(32)	108.3(2)
C(3)−N(4)	1.489(3)	C(31)−C(3)−C(32)	110.0(2)
C(3)−C(31)	1.522(4)	N(4)−C(3)−C(2)	104.0(2)
C(3)−C(32)	1.528(4)	C(31)−C(3)−C(2)	113.9(2)
N(4)−C(5)	1.291(3)	C(32)−C(3)−C(2)	109.8(2)
C(5)−C(51)	1.477(3)	C(5)−N(4)−C(3)	108.9(2)
		N(4)−C(5)−C(51)	119.9(2)
C(6)−C(1)−C(5)	131.0(2)	N(4)−C(5)−C(1)	113.2(2)
C(6)−C(1)−C(2)	124.8(2)	C(51)−C(5)−C(1)	126.0(2)
C(5)−C(1)−C(2)	103.5(2)		

Reaction Course

Since there is ample precedence for reactions of (1-alkynyl)carbene complex $(CO)_5W{=}C(OEt)C{\equiv}CPh$ (**1a**) with nitrogen bases N (and also phosphanes) to form zwitterionic adducts $^{-}(OC)_5W{-}C(OEt){=}C{=}C(Ph)N^{+}$ as initial products,[14] it is suggested for the present case that an intermediate **A** might be generated from addition of an imine **2** to the (1-alkynyl)carbene complex **1a**. A zwitterionic species **A** might act as precursor to both a five-membered cycloadduct **3** and a four-membered dihydroazete derivative **B** (Scheme 4).

Scheme 4. Competing [3+2] and [2+2] cycloadditions of (1-alkynyl)carbene complex **1a** to the C=N bond of non-enolizable imines **2**

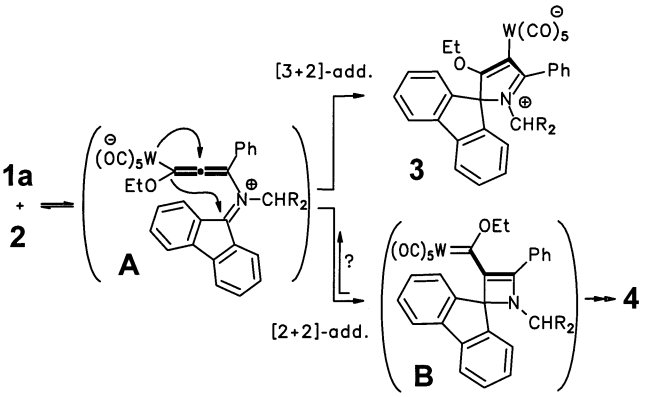

It is suggested that dihydroazetes **B** would be key intermediates en route to dihydropyrroles **4**. This assumption is supported by the fact that organometallic intermediates **6** and **7** could be isolated and characterized.

Organometallic Reaction Intermediates

Reaction of (1-alkynyl)carbene complex **1a** with fluorenone imines **2** at 20°C (instead of 90°C, as it has been applied for the reaction given in Scheme 2), affords two colored compounds **6** and **7**, which were isolated by column chromatography on silica gel (Scheme 5). It could be easily demonstrated that the azametallatriene unit of compounds **6** in solution undergoes a thermally induced ring closure to give dihydropyrroles **7**, from which finally pyrroles **4** and $W(CO)_6$ are obtained as the only products.

Scheme 5. Organometallic intermediates en route to dihydropyrroles **4**

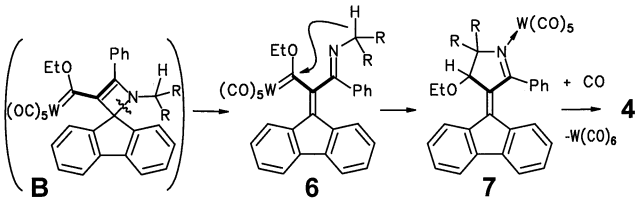

	yield [%]		yield [%]
3a	11	**3b**	20
4a	48	**4b**	35
6a	30	**6b**	13
7a	–	**7b**	4

Cross-Conjugated Azametallatrienes 6

Since the signal of the W=C group in the ^{13}C-NMR spectra of compounds **6** (**6a**: δ = 321.8; **6b**: δ = 321.2) is observed in a range typical of non-conjugated (carbene)-tungsten complexes, e.g. $(CO)_5W{=}C(OEt)Me$ (δ = 319.6), little or no π-conjugation is expected within the W=C−C=C moiety. Furthermore, π-conjugation is not expected to be effective within the C=C−C=N group, since the *C*=N signal (**6a**: δ = 157.9; **6b**: δ = 157.8) appears in the normal range. Strong distortion from planarity of the W=C−C=C as well as of the C=C−C=N unit [W−C1−C2−C3 −109.0(3), N28−C21−C2−C3 −94.0(4)°] is confirmed by an X-ray structure analysis of compound **6a** (Figure 3, Table 3). It should be noted that the structural features of the M=C−C(=C)−C=N backbone in compound **6a** are unique and different from that of other cross-conjugated azametallatrienes, e.g. $(CO)_5W{=}C(OEt){-}C(=CHNC_4H_8){-}C(Ph){=}NPh$,[15] in which partial planarisation of the $(CO)_5W{=}C{-}C{=}C(N)$ portion of the ligand is achieved by π-electron delocalization. Rapid equilibration of diastereomers by rotation about the C1−C2 bond of **6a** is indicated by dynamic line-broadening of the ^{1}H-NMR signals of the diastereotopic OCH_2 group at 20°C.

Figure 3. Molecular structure of the cross-conjugated azametallatriene **6a**

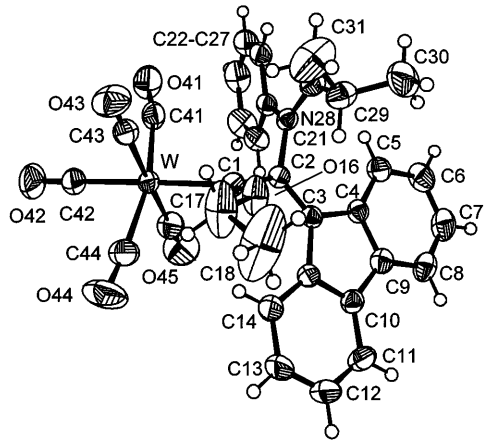

Table 3. Selected bond lengths [Å] and angles [°] for cross-conjugated azametallatriene **6a**

W−C(1)	2.180(3)	O(16)−C(1)−W	130.0(2)
C(1)−O(16)	1.309(4)	C(2)−C(1)−W	125.3(2)
C(1)−C(2)	1.504(4)	C(3)−C(2)−C(1)	123.2(2)
C(2)−C(3)	1.351(4)	C(3)−C(2)−C(21)	123.0(2)
C(2)−C(21)	1.520(4)	C(1)−C(2)−C(21)	113.7(2)
C(21)−N(28)	1.270(4)	N(28)−C(21)−C(22)	117.7(2)
C(21)−C(22)	1.493(4)	N(28)−C(21)−C(2)	124.0(2)
N(28)−C(29)	1.474(4)	C(22)−C(21)−C(2)	118.3(2)
C(29)−C(31)	1.519(6)	C(21)−N(28)−C(29)	122.5(3)
C(29)−C(30)	1.521(5)	N(28)−C(29)−C(31)	108.3(3)
O(16)−C(17)	1.459(4)	N(28)−C(29)−C(30)	107.1(3)
C(17)−C(18B)	1.43(2)	C(31)−C(29)−C(30)	112.6(4)
C(17)−C(18A)	1.45(2)	C(1)−O(16)−C(17)	123.3(3)
		C(18B)−C(17)−O(16)	111.4(12)
O(16)−C(1)−C(2)	104.7(2)	C(18A)−C(17)−O(16)	106.5(11)

Structural characterization of compound **7b** is based on NMR spectra. The sets of ^{13}C- and ^{1}H-NMR signals of dihydropyrrole **4b** and its pentacarbonyltungsten derivative **7b** are quite similar. Characteristic downfield shifts are observed for the signals *C*=N (**4b**: δ = 170.2; **7b**: δ = 179.2) and *C*−N (**4b**: δ = 77.1; **7b**: δ = 83.3).

This work was supported by the *Volkswagen-Stiftung* and the *Fonds der Chemischen Industrie*. Experimental assistance by *Barbara Hildmann* is gratefully acknowledged.

Experimental Section

All operations were performed under argon. Dried solvents were used in all experiments. − Melting points are not corrected. − Instrumentation: ^{1}H- and ^{13}C-NMR spectra were obtained with Bruker WM 300, WP 360 and Varian U 600 spectrometers (multiplicities were determined by DEPT. Chemical shifts refer to δ_{TMS} = 0.00. ^{13}C shifts were assigned on the basis of ^1J(CH) and $^{2,3}J$(CH) correlation experiments). Low-temperature NMR measurements were carried out with Bruker AM 360 instrument. − Other analyses: IR Diglab FTS 45; MS Finnigan MAT 312; elemental analysis, Perkin-Elmer 240 elemental analyzer; TLC, Merck DC-Alufolien Kieselgel 60 F_{254}. R_f values refer to TLC tests. − Column-chromatographic purifications were made on Merck Kieselgel 100.

(Fluoren-9-ylidene)alkylamine (**2**) was obtained in high yields by condensation of 9-fluorenone (1.80 g, 10 mmol) with the corresponding amine (10 mmol) in 30 ml of pentane and 15 g of molecular sieves (Acros, 4 Å) at 20°C, 24 h, and were purified by distillation prior to use.

Pentacarbonyl[5-(2,2'-biphenylene)-4-ethoxy-1-isopropyl-2-phenyl-1-azoniacyclopenta-1,3-dien-3-yl]tungstate (**3a**), *3-Ethoxy-4-(fluoren-9-ylidene)-2,2-dimethyl-5-phenyl-3,4-dihydro-2H-pyrrole* (**4a**), *Pentacarbonyl[1-ethoxy-2-(fluoren-9-ylidene)-3-(isopropylimino)-3-phenylprop-1-ylidene]tungsten* (**6a**): To pentacarbonyl(1-ethoxy-3-phenyl-2-propyn-1-ylidene)tungsten (**1a**) (482 mg 1.00 mmol) in a 3-ml screw-top vessel is added (fluoren-9-ylidene)isopropylamine (**2a**) (221 mg, 1.00 mmol) in 3 ml of toluene. The mixture is shaken until homogeneity (ca. 3 min). After ca. 5 min at 20°C, a dark oil begins to precipitate which consists of compound **3a** and $W(CO)_6$. After compound **1a** is consumed completely (ca. 2 d at 20°C according to TLC), the supernatant is decanted and the solid washed with *n*-pentane (3 × 1 ml). The solution is separated by chromatography on silica gel. Elution with pentane/dichloromethane (2:1) affords a brown fraction with compound **6a** (R_f = 0.4 in pentane/dichloromethane, 2:1, 215 mg, 30%, brown crystals from pentane at −40°C, mp 102°C). Elution with diethyl ether affords a yellow fraction of compound **4a** (180 mg, 48%, R_f = 0.8 in diethyl ether, yellow crystals from cyclohexane/dichloromethane (4:1) at −78°C, mp 106°C). The solid residue of the reaction mixture (ca. 240 mg) is dissolved in dichloromethane (ca. 3 ml). $W(CO)_6$ is removed by crystalization at −15°C and compound **3a** is obtained from the mother liquor at 20°C after addition of pentane (2 ml) (ca. 78 mg, 11%, amber-colored crystals). If **1a** (52 mg, 0.11 mmol) and **2a** (22 mg, 0.10 mmol) in 1 ml of C_6D_6 are heated to 90°C for 2 h the ^{1}H-NMR spectrum of the solution shows signals of compounds **4a** and **3a** in a molar ratio of 8:1 as the only products. Removal of the solvent gives a residue of 39 mg, which corresponds to 82% of compound **4a** and 11% of compound **3a**.

3a: ^{1}H NMR (C_6D_6, 600 MHz): δ = 7.33, 7.26 and 7.18 (2:2:1 H; "d", "t", "t"; Ph), 7.30 (2 H, d, 4′-H and 5′-H), 7.10 (2 H, t, 3′-H and 6′-H), 7.05 (2 H, d, 1′-H and 8′-H), 6.95 (2 H, t, 2′-H

and 7′-H), 3.29 and 0.70 (2:3 H; q and t, OCH_2CH_3), 2.73 (1 H, quint, NCH), 0.18 [6 H, d, $CH(CH_3)_2$]. − ^{13}C NMR (C_6D_6): δ = 204.8 and 201.8 [1:4, C_q each, *cis*- and *trans*-CO $W(CO)_5$], 198.2 (C_q, C2), 187.9 (C_q, C3), 142.8 (2 C_q, C8a′ and C9a′), 137.3 (2 C_q, C4a′ and C4aa′), 136.0 (C_q, *i*-C Ph), 135.8 (C_q, C4), 130.9 (2 CH, C2′ and C7′), 130.3 (*p*-CH Ph), 129.8 (2 CH, C3′ and C6′), 128.1 (2 *m*-CH Ph), 127.8 (2 *o*-CH Ph), 124.5 (2 CH, C1′ and C8′), 121.6 (2 CH, C4′ and C5′), 84.2 (C_q, C5 ≡ C9′), 65.9 (OCH_2), 50.8 (NCH), 22.4 [$C(CH_3)_2$], 14.8 (OCH_2CH_3). − IR (diffuse reflection): $\tilde{\nu}$ [cm^{-1} (%)] = 2048.5 (30), 1975.0 (10), 1950.4 (20), 1895.2 (100), 1858.5 (80) [ν(C≡O)]. − $C_{32}H_{25}NO_6W$ (703.4): calcd. C 54.64, H 3.58, N 1.99; found C 54.61, H 3.69, N 2.05.

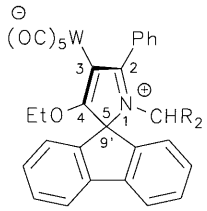

3

4a: ^1H NMR (C_6D_6, 600 MHz): δ = 8.49 (1 H, d, ^3J = 7.7 Hz, 8′-H), 7.85 and 7.04 (2:3 H, broad each, Ph), 7.45 (1 H, d, ^3J = 7.4 Hz, 1′-H), 7.35 (1 H, d, ^3J = 7.5 Hz, 5′-H), 6.87 (1 H, d, ^3J = 7.9 Hz, 4′-H); 7.24, 7.18, 7.08, and 6.90 (1 H each, t each, 2′-H, 3′-H, 6′-H and 7′-H), 5.07 (1 H, s, 3-H), 3.52 and 3.34 (1:1 H, m each, OCH_2), 1.68 and 1.12 [3:3 H, s each, $C(CH_3)_2$], 1.02 (3 H, t, OCH_2CH_3). − ^{13}C NMR (C_6D_6): δ = 170.2 (C_q, C=N, C5), 141.9 and 141.8 (C_q each, C4 and C9′), 140.4 (C_q, C8a′), 140.1 (C_q, C9a′), 138.4 (C_q, C4aa′), 136.6 (C_q, C4a′), 136.3 (C_q, *i*-C Ph); 130.1 (2 C), 129.7, 129.2, 128.9, 128.8 (2 C, broad), 128.1 (2 C), 126.64, 126.63, 119.9 and 119.6 (CH each, fluorene and Ph), 90.6 (CH, C3), 74.4 (C_q, C2), 62.3 (OCH_2), 27.8 and 22.9 [$C(CH_3)_2$], 15.8 (OCH_2CH_3). − MS (70 eV); *m/z* (%): 379 (100) [M^+], 350 (30) [M^+ − Et], 332 (5), 322 (5), 265 (70) [M^+ − $NCMe_2$ − HCOEt], 215 (5), 165 (10) [fluorenyl], 146 (10), 104 (50), 58 (15). − $C_{27}H_{25}NO$ (379.5): calcd. C 85.45, H 6.64, N 3.69; found C 85.53, H 6.55, N 3.85.

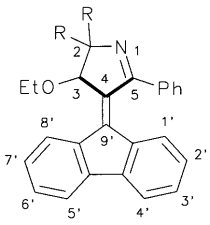

4

X-ray Crystal Structure Analysis of **4a**:[16] Formula $C_{27}H_{25}NO$, M = 379.48, 0.30 × 0.20 × 0.20 mm, a = 14.371(4), b = 8.989(1), c = 16.259(4) Å, β = 92.12(2)°, V = 2098.9(8) Å^3, $\rho_{calcd.}$ = 1.201 g cm^{-3}, μ = 0.72 cm^{-1}, empirical absorption correction with φ-scan data (0.975 ≤ C ≤ 0.999), Z = 4, monoclinic, space group $P2_1/c$ (No. 14), λ = 0.71073 Å, T = 293 K, ω/2θ scans, 4422 reflections collected (+h, −k, ±l), [(sinθ)/λ] = 0.62 Å^{-1}, 4248 independent and 1858 observed reflections [$I \geq 2\,\sigma(I)$], 265 refined parameters, R = 0.048, wR^2 = 0.093, max. residual electron density 0.19 (−0.23) e Å^{-3}, hydrogen atoms calculated and refined as riding atoms.[17]

6a: ^1H NMR (C_6D_6): δ = 8.40 (2 H, s broad, *o*-H Ph); 7.71, 7.56, 7.39 and 7.29 (1 H each, "d" each; 1′-H, 4′-H, 5′-H and 8′-H); 7.16, 7.10, 6.89 and 6.59 (1 H each, "t" each; 2′-H, 3′-H, 6′-H and 7′-H), 7.00 (3 H, m broad, *m*- and *p*-H Ph), 4.81 (1 H, sept, NCH), 4.78 and 4.26 (1 H each, m broad each, OCH_2), 1.19 and 1.17 [6 H, d, $C(CH_3)_2$], 1.03 (3 H, t, OCH_2CH_3). − ^{13}C NMR (C_6D_6): δ = 321.8 (C_q, W=C), 203.4 and 196.8 [1:4, C_q each, *trans*- and *cis*-CO, $W(CO)_5$], 157.9 (C_q, C=N, C3), 152.2 (C_q, C9′); 144.6, 142.3, 141.8, 137.7, 137.0, and 134.7 (C_q each, C2, C4a′, C4aa′, C8a′, C9a′, and *i*-C Ph); 130.8, 129.9 (2 C), 129.7, 129.5, 128.7 (2 C), 127.8, 127.3, 127.0, 126.9, 120.5, and 120.1 (CH each, fluorene and Ph), 81.2 (OCH_2), 53.8 (NCH), 25.5 and 24.1 [$C(CH_3)_2$], 13.6 (OCH_2CH_3). − IR (hexane): $\tilde{\nu}$ [cm^{-1} (%)] = 2072.0 (35), 1994.7 (10), 1964.8 (60), 1945.0 (100) [ν(C≡O)]. − MS (70 eV); *m/z* ^{184}W (%): 703 (1) [M^+], 647 (1) [M^+ − 2 CO], 619 (3) [M^+ − 3 CO], 563 (2) [M^+ − 5 CO], 504 (2), 463 (2), 379 (100) [M^+ − $W(CO)_5$], 350 (35), 322 (6), 265 (65), 180 (10), 165 (25), 111 (15), 104 (75), 83 (35), 71 (55), 57 (80). − $C_{32}H_{25}NO_6W$ (703.4): calcd. C 54.64, H 3.58, N 1.99; found C 54.63, H 3.70, N 2.00.

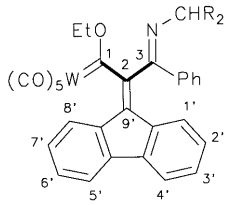

6

X-ray Crystal Structure Analysis of **6a**:[16] Formula $C_{32}H_{25}NO_6W$, M = 703.38, 0.30 × 0.30 × 0.10 mm, a = 9.962(2), b = 12.281(2), c = 12.929(2) Å, α = 88.20(1), β = 85.64(2), γ = 66.31(1)°, V = 1444.3(4) Å^3, $\rho_{calcd.}$ = 1.617 g cm^{-3}, μ = 40.43 cm^{-1}, empirical absorption correction with φ-scan data (0.788 ≤ C ≤ 0.999), Z = 2, triclinic, space group $P\bar{1}$ (No. 2), λ = 0.71073 Å, T = 293 K, ω/2θ scans, 6134 reflections collected (±h, ±k, +l), [(sinθ)/λ] = 0.62 Å^{-1}, 5861 independent and 5338 observed reflections [$I \geq 2\,\sigma(I)$], 375 refined parameters, R = 0.020, wR^2 = 0.052, max. residual electron density 1.02 (−0.90) e Å^{-3}, C18 refined as splitted atom, hydrogen atoms calculated and refined as riding atoms.[17]

Pentacarbonyl[5-(2,2′-biphenylene)-1-cyclohexyl-4-ethoxy-2-phenyl-1-azoniacyclopenta-1,3-dien-3-yl]tungstate (**3b**), *3-Ethoxy-4-(fluoren-9-ylidene)-2-pentamethylene-5-phenyl-3,4-dihydro-2H-pyrrole* (**4b**), *Pentacarbonyl[1-ethoxy-3-cyclohexylimino-2-(fluoren-9-ylidene)-3-phenylprop-1-ylidene]tungsten* (**6b**), *Pentacarbonyl[3-ethoxy-4-(fluoren-9-ylidene)-2-pentamethylene-5-phenyl-3,4-dihydro-2H-pyrrole]tungsten* (**7b**): To pentacarbonyl(1-ethoxy-3-phenyl-2-propyn-1-ylidene)tungsten (**1a**) (482 mg, 1.00 mmol) in a 3-ml screw-top vessel is added fluoren-9-ylidenecyclohexylamine (**2b**) (260 mg, 1.00 mmol) in 2.5 ml of pentane. The mixture is shaken until it becomes homogeneous. After ca. 1−2 h at 20°C, a dark precipitate begins to form consisting of compound **3b** and $W(CO)_6$. After ca. 2−3 d at 20°C (TLC), the reaction is almost complete. The supernatant is decanted and the solid residue washed with toluene (3 × 1 ml). Pentane and toluene extracts are combined, brought to dryness (20°C, 10 Torr) and separated by chromatography on silica gel with pentane/dichloromethane (2:1) to give successively a small amount of red compound **7b** (R_f = 0.6 in pentane/dichloromethane, 2:1, 30 mg, 4%), the brown compound **6b** (R_f = 0.4 in pentane/dichloromethane 2:1, 100 mg, 13%, brown crystals from pentane at −40°C). Elution with diethyl ether affords yellow product **4b** (131 mg, 35%, R_f = 0.3 in pentane/diethyl ether (10:1),

yellow crystals from toluene/pentane 1:1 at −15°C, mp 172°C). The solid residue of the reaction mixture (ca. 260 mg) is dissolved in dichloromethane (ca. 3 ml). $W(CO)_6$ is removed by crystalization at −15°C and compound **3b** is obtained from the mother liquor at 20°C after addition of pentane (2 ml) (ca. 150 mg, 20%, amber-colored crystals). If **1a** (52 mg, 0.11 mmol) and **2b** (26 mg, 0.10 mmol) in 1 ml of C_6D_6 are heated to 90°C for 2 h the ^{1}H-NMR spectrum of the solution shows signals of compounds **4b** and **3b** in a molar ratio of ca. 3.5:1 as the only detectable products. Removal of the solvent and of $W(CO)_6$ leaves a residue of 44 mg, which corresponds to 69% of the pyrrol derivative **4b** and 20% of compound **3b**.

3b: ^{1}H NMR (C_6D_6, 600 MHz): δ = 7.38, 7.30, and 7.22 (2:2:1 H; d, t, t; Ph), 7.36 (2 H, d, 4′-H and 5′-H), 6.99 (2 H, t, 3′-H and 6′-H), 7.15 (2 H, t, 2′-H and 7′-H), 7.10 (2 H, d, 1′-H and 8′-H), 3.30 and 0.70 (2:3 H; q and t, OCH_2CH_3), 2.50 (1 H, m, NCH); 0.98, 0.90, 0.80, 0.75, and 0.11 (2 H each, CH_2 cyclohexyl). − ^{13}C NMR (C_6D_6): δ = 204.8 and 201.0 [1:4, C_q each, *cis*- and *trans*-CO $W(CO)_5$], 197.3 (C_q, C2), 187.1 (C_q, C3), 142.1 (2 C_q, C8a′ and C9a′), 136.5 (2 C_q, C4a′ and C4aa′), 135.6 (C_q, *i*-C Ph), 134.3 (C_q, C4), 130.5 (2 CH, C2′ and C7′), 129.7 (*p*-CH Ph), 129.0 (2 CH, C3′ and C6′), 127.9 (2 *m*-CH Ph), 127.2 (2 *o*-CH Ph), 124.0 (2 CH, C1′ and C8′), 121.1 (2 CH, C4′ and C5′), 83.6 (C_q, C5 ≡ C9′), 65.2 (OCH_2), 59.6 (NCH); 32.9, 25.7, 24.2 (2:2:1, CH_2 each, cyclohexyl), 14.3 (OCH_2CH_3). − IR (diffuse reflection): $\tilde{\nu}$ [cm^{-1} (%)] = 2048.3 (30), 1975.1 (10), 1950.7 (20), 1895.3 (100), 1858.9 (80) [ν(C≡O)]. − MS (70 eV); *m/z* ^{184}W (%): 743 (1) [M^+], 687 (1) [M^+ − 2 CO], 659 (3) [M^+ − 3 CO], 603 (2) [M^+ − 5 CO], 391 (60), 308 (100). − $C_{35}H_{29}NO_6W$ (743.5): calcd. C 56.54, H 3.93, N 1.88; found C 56.33, H 3.71, N 1.97.

4b: ^{1}H NMR (C_6D_6, 600 MHz): δ = 8.56 (1 H, d, ^3J = 7.4 Hz, 8′-H), 7.90 and 7.10 (2:3 H, broad each, Ph), 7.45 (1 H, d, 1′-H), 7.35 (1 H, d, 5′-H); 7.25, 7.16, 7.04, and 6.90 (1 H each, t each, 2′-H, 3′-H, 6′-H, and 7′-H), 6.63 (1 H, d, ^3J = 7.9 Hz, 4′-H), 5.29 (1 H, s, 3-H), 3.52 and 3.38 (1:1 H, m each, OCH_2); 2.15, 1.72, 1.50, 1.31 (2:2:2:2, CH_2 each, cyclohexyl), 1.03 (3 H, t, OCH_2CH_3). − ^{13}C NMR (C_6D_6): δ = 170.2 (C_q, C=N, C5), 141.9 and 141.8 (C_q each, C4 and C9′), 140.7 (C_q, C8a′), 140.3 (C_q, C9a′), 138.3 (C_q, C4aa′), 136.8 (C_q, C4a′), 136.2 (C_q, *i*-C Ph); 130.0, 129.7, 129.2, 128.9 (2 C), 128.8 (2 C, broad), 128.1 (2 C), 126.6, 126.5, 119.9, and 119.6 (CH each, fluorene and Ph), 88.9 (CH, C3), 77.1 (C_q, C2), 62.1 (OCH_2); 37.4, 32.2, 26.3, 24.4, 23.4 (CH_2 each, cyclohexyl), 15.9 (OCH_2CH_3). − MS (70 eV); *m/z* (%): 419 (100) [M^+], 390 (30) [M^+ − Et], 265 (70), 165 (10) [fluorenyl], 146 (10), 104 (30). − $C_{30}H_{29}NO$ (419.6): calcd. C 85.88, H 6.97, N 3.34; found C 85.59, H 6.85, N 3.45.

6b: ^{1}H NMR (C_6D_6): δ = 8.40 (2 H, s broad, *o*-H Ph); 7.70, 7.52, 7.40, and 7.26 (1 H each, "d" each; 1′-H, 4′-H, 5′-H, and 8′-H); 7.13, 7.10, 6.80, and 6.54 (1 H each, "t" each; 2′-H, 3′-H, 6′-H, and 7′-H), 7.05 (3 H, m broad, *m*- and *p*-H Ph), 4.82 (1 H, "t", NCH), 4.78 and 3.95 (1 H each, m broad each, OCH_2), 1.80 and 1.20 (5 H each, m each broad, cyclohexyl), 0.87 (3 H, t, OCH_2CH_3). − ^{13}C NMR (C_6D_6): δ = 321.2 (C_q, W=C), 202.2 and 196.9 [1:4, C_q each, *trans*- and *cis*-CO, $W(CO)_5$], 157.8 (C_q, C=N, C3), 152.5 (C_q, C9′); 141.9, 141.5, 137.7, 137.1, 136.3, and 132.4 (C_q each, C2, C4a′, C4aa′, C8a′, C9a′, and *i*-C Ph); 130.8, 129.9 (2 C), 129.7, 129.5, 128.7 (2 C), 127.8, 127.3, 127.0, 126.9, 120.5, and 120.1 (CH each, fluorene and Ph), 80.6 (OCH_2), 61.9 (NCH); 33.9, 26.1, 24.5, 24.3, and 22.7 (CH_2 each, cyclohexyl), 13.9 (OCH_2CH_3). − IR (hexane): $\tilde{\nu}$ [cm^{-1} (%)] = 2071.9 (30), 1994.4 (10), 1964.7 (60), 1945.3 (100) [ν(C≡O)]. − MS (70 eV); *m/z* ^{184}W (%): 743 (1) [M^+], 715 (1) [M^+ − CO], 659 (1) [M^+ − 3 CO], 603 (1) [M^+ − 5 CO], 419 (100) [M^+ − $W(CO)_5$], 390 (60), 265 (60).

7b: ^{1}H NMR (C_6D_6, 600 MHz): δ = 8.70 (1 H, d, ^3J = 7.4 Hz, 8′-H), 7.98 and 7.15 (2:3 H, broad each, Ph), 7.22 (1 H, d, 5′-H), 7.12 (1 H, d, 1′-H), 7.08 (1 H, dd, 6′-H), 7.05 (1 H, dd, 7′-H), 6.84 (1 H, dd, 2′-H), 6.46 (1 H, dd, 3′-H), 6.16 (1 H, d, 4′-H), 5.46 (1 H, s, 3-H), 3.46 and 3.37 (1:1 H, m each, OCH_2); 2.78, 2.47, 1.84, 1.80, 1.56, 1.44, 1.42, 1.24, 1.15, 1.10, and 1.02 (1 H each, m each, cyclohexyl), 1.03 (3 H, t, OCH_2CH_3). − ^{13}C NMR (C_6D_6): δ = 201.8 and 198.8 [C_q each, *cis*- and *trans*-CO $W(CO)_5$], 179.2 (C_q, C=N, C5), 147.3 and 142.3 (C_q each, C4 and C9′), 142,2 (C_q, C9a′), 140.0 (C_q, C8a′), 108.7 (C_q, C4aa′), 137.6 (C_q, C4a′), 136.0 (C_q, *i*-C Ph); 131.5, 131.0, 130.1, 128.2, 128.5, 128.3, 127.7, 126.8, 120.0 (CH each, fluorene); 129.8, 129.0 and 128.3 (CH each broad, Ph), 83.2 (C_q, C2), 82.7 (CH, C3), 61.1 (OCH_2); 36.6, 35.4, 25.3, 24.4, 24.2 (CH_2 each, cyclohexyl), 15.5 (OCH_2CH_3). − IR (hexane): $\tilde{\nu}$ [cm^{-1} (%)] = 2063.7 (30), 1982.6 (10), 1928.2 (100), 1914.2 (60) [ν(C≡O)]. − MS (70 eV); *m/z* ^{184}W (%): 743 (10) [M^+], 715 (40) [M^+ − CO], 659 (50) [M^+ − 3 CO], 603 (40) [M^+ − 5 CO], 543 (100), 419 (80) [M^+ − $W(CO)_5$], 390 (60), 265 (60).

X-ray Crystal Structure Analysis of **3b**:[16] Formula $C_{35}H_{29}NO_6W$, M = 743.47, 0.50 × 0.30 × 0.10 mm, a = 9.626(2), b = 16.259(3), c = 19.291(3) Å, β = 91.51(1)°, V = 3018.2(10) Å^3, $\rho_{calcd.}$ = 1.636 g cm^{-3}, μ = 38.75 cm^{-1}, empirical absorption correction via φ-scan data (0.684 ≤ C ≤ 0.999), Z = 4, monoclinic, space group $P2_1/c$ (No. 14), λ = 0.71073 Å, T = 223 K, ω/2θ scans, 6296 reflections collected (±h, −k, −l), [(sinθ)/λ] = 0.62 Å^{-1}, 6110 independent and 5305 observed reflections [$I \geq 2\,\sigma(I)$], 389 refined parameters, R = 0.031, wR^2 = 0.083, max. residual electron density 1.54 (−2.24) e Å^{-3} close to tungsten, hydrogen atoms calculated and refined as riding atoms.[17]

3-(2,2′-Biphenylene)-1-isopropyl-5-phenyl-1,2-dihydropyrrol-3-one (**5a**): Pentacarbonyl[1-isopropyl-4-ethoxy-2-phenyl-1-azoniacyclopenta-1,3-dien-3-yl]tungstate (**3a**) (70 mg, 0.10 mmol) in $CHCl_3$ (1 ml) is treated with water (1.8 mg, 0.01 mmol) for 6 h at 20°C. Evaporation of the solvent leaves compound **5a** together with $W(CO)_6$. − ^{1}H NMR (C_6D_6): δ = 7.46 (2 H, d, 4′-H and 5′-H), 7.35 (2 H, d, 1′-H and 8′-H), 7.26 (2 H, "t", *m*-H Ph), 7.17 and 7.08 (2 H each, dd each; 2′-H, 3′-H, 6′-H, and 7′-H), 7.09 (3 H, *o*- and *p*-H Ph), 5.40 (1 H, s, 4-H), 3.41 (1 H, m, NCH), 0.50 [6 H, d, $CH(CH_3)_2$]. − ^{13}C NMR (C_6D_6): δ = 195.5 (C_q, C=O), 179.3 (C_q, C5), 143.9 (2 C_q, C8a′ and C9a′), 142.5 (2 C_q, C4a′ and C4aa′), 133.6 (C_q, *i*-C Ph); 129.6, 128.9, and 128.6 (CH each, 1:2:2, Ph), 124.2 (2 CH, C2′ and C7′), 120.8 (2 CH, C3′ and C6′), 101.1 (CH, C4), 82.3 (C_q, C2 ≡ C9′), 49.7 (NCH), 23.1 [$C(CH_3)_2$]. − IR (diffuse reflection): $\tilde{\nu}$ [cm^{-1} (%)] = 1675.5 (100) [ν(C=O)].

3-(2,2′-Biphenylene)-1-cyclohexyl-5-phenyl-1,2-dihydropyrrol-3-one (**5b**): Pentacarbonyl[1-cyclohexyl-4-ethoxy-2-phenyl-1-azoniacyclopenta-1,3-dien-3-yl]tungstate (**3b**) (74 mg, 0.10 mmol) in $CHCl_3$ (1 ml) is treated with water (1.8 mg, 0.10 mmol) for 6 h at 20°C. Evaporation of the solvent leaves compound **5b** together with $W(CO)_6$. − ^{1}H NMR (C_6D_6): δ = 7.52 (2 H, d, 4′-H and 5′-H), 7.40 (2 H, d, 1′-H and 8′-H), 7.31 (2 H, "d", *o*-H Ph), 7.19 and 7.09 (2 H each, dd each; 2′-H, 3′-H, 6′-H and 7′-H), 7.15 and 7.12 (2:1 H, *m*- and *p*-H Ph), 5.41 (1 H, s, 4-H), 3.29 (1 H, m, NCH); 1.40, 1.00, 0.85, 0.42, and 0.21 (3:3:2:1:1, CH_2 cyclohexyl). − ^{13}C NMR (C_6D_6): δ = 195.5 (C_q, C=O), 179.4 (C_q, C5), 144.1 (2 C_q, C8a′ and C9a′), 142.4 (2 C_q, C4a′ and C4aa′), 133.6 (C_q, *i*-C Ph); 129.6, 128.9, and 128.6 (CH each, 1:2:2, Ph), 124.4 (2 CH, C2′ and C7′), 120.9 (2 CH, C3′ and C6′), 100.6 (CH, C4), 82.2 (C_q, C2 ≡ C9′), 58.9 (NCH); 34.2, 26.2, and 25.0 (CH_2 each, 2:2:1, cyclohexyl). − IR (diffuse reflection): $\tilde{\nu}$ [cm^{-1} (%)] = 1676.1 (100) [ν(C=O)].

[☆] Dedicated to Professor *E. O. Fischer* on the occasion of his 80th birthday

[1] Part XCVI: R. Aumann, Z. Yu, R. Fröhlich, *Organometallics* **1998**, *117*, 2897.

[2] E. O. Fischer, H. Hollfelder, F.R. Kreissl, W. Uedelhoven, *J. Organomet. Chem.* **1976**, *113*, C31.

[3] L. S. Hegedus, M. A.. McGuire, L. M. Schultze, Y. Chen, O. P. Anderson, *J. Am. Chem. Soc.* **1984**, *106*, 2680.

[4] F. Funke, M. Duetsch, F. Stein, M. Noltemeyer, A. de Meijere, *Chem. Ber.* **1994**, *127*, 911.

[5] R. Aumann, R. Fröhlich, F. Zippel, *Organometallics* **1997**, *16*, 2571.

[6] [6a] J. Barluenga, M. Tomás, J. A. López-Pelegrín, E. Rubio, *Tetrahedron Lett.* **1997**, *38*, 3981. – [6b] R. Aumann, Z. Yu, see ref. [142] in ref.[14]. – [6c] R. Aumann, Z. Yu, R. Fröhlich, *J. Organomet. Chem.* **1997**, *549*, 311.

[7] J. Barluenga, M. Tomás, E. Rubio, J.A. López-Pelegrín, S. García-Granda, P. Pertierra, *J. Am. Chem. Soc.* **1996**, *118*, 695.

[8] R. Aumann, B. Hildmann, R. Fröhlich, *Organometallics* **1998**, *17*, 1197.

[9] [9a] R. Aumann, K. Roths, M. Grehl, *Synlett* **1993**, 669. – [9b] R. Aumann, M. Kößmeier, K. Roths, R. Fröhlich, *Synlett* **1994**, 1041. – [9c] R. Aumann, K. Roths, M. Läge, B. Krebs, *Synlett* **1993**, 667. – [9d] A. G. Meyer, R. Aumann, *Synlett* **1995**, 1011. – [9e] R. Aumann, A. G. Meyer, R. Fröhlich, *Organometallics* **1996**, *15*, 5018. – [9f] R. Aumann, M. Kößmeier, F. Zippel, *Synlett* **1997**, 621.

[10] R. Aumann, K. Roths, R. Fröhlich, *Organometallics* **1997**, *16*, 5893.

[11] For a review see, e.g.: [11a] Y. Noël, *Bull. Soc. Chim. Fr.* **1964**, *5*, 173. – [11b] F. H. Stewart, *Chem. Rev.* **1964**, *64*, 129.

[12] C. P. Casey, T. J. Burkhardt, C. A. Bunnell, J. C. Calabrese, *J. Am. Chem. Soc.* **1977**, *99*, 2127.

[13] R. Aumann, K. Roths, B. Jasper, R. Fröhlich, *Organometallics* **1996**, *15*, 1257.

[14] See, e.g., review: R. Aumann, H. Nienaber, *Adv. Organomet. Chem.* **1997**, *41*, 163.

[15] R. Aumann, B. Jasper, R. Fröhlich, *Organometallics* **1995**, *14*, 3167.

[16] Data sets were collected with an Enraf Nonius CAD4 diffractometer using an FR591 rotating anode generator. Programs used: data reduction MolEN, structure solution SHELXS-86, structure refinement SHELXL-93, graphics DIAMOND.

[17] Crystallographic data (excluding structure factors) for the structures reported have been deposited with the Cambridge Crystallographic Data Centre. Copies of the data can be obtained free of charge by quoting the depository numbers CCDC-102622, -102623 and -102624, the names of the authors, and the journal citation on application to CCDC, 12 Union Road, Cambridge CB2 1EZ, UK [fax: int code + 44-12238 336-033, e-mail: deposit@ccdc.cam.ac.uk].

[I98171]

Synthesis, Structure, and Physical Properties of Tetraalkylammonium Bis(5,6-dihydro-1,4-dithiin-2,3-diselenolato)nickelate, $(R_4N)[Ni(ddds)_2]$ (R = Me, Et, and *n*Bu), and Neutral Complex $[Ni(ddds)_2]_2$

Hideki Fujiwara*[a], Emiko Ojima[a], Hayao Kobayashi[a], Thierry Courcet[b], Isabelle Malfant*[b], and Patrick Cassoux[b]

Institute for Molecular Science[a],
Myodaiji, Okazaki 444–8585, Japan,
Fax: (internat.) +81-564/54-2254
E-mail: fuji@ims.ac.jp

Equipe Prècurseurs Molèculaires et Matèriaux LCC-CNRS[b],
205 route de Narbonne, F-31077 Toulouse Cedex, France

Received June 2, 1998

Keywords: Metal complexes / Organic conductors / Selenium / Magnetic properties

Novel metal complexes $(R_4N)[Ni(ddds)_2]$ (R = Me, Et and *n*Bu, ddds = 5,6-dihydro-1,4-dithiin-2,3-diselenolate) have been prepared and their crystal structures determined. The intraligand Se–Se distance is longer than that between the inner sulfur atoms of the five-member ring of the $M(dddt)_2^-$ sulfur analogue and is almost equal to the S–S distance in the six-member ring. Consequently, two-dimensional intermolecular close contacts are expected, and observed in $Ni(ddds)_2$ complexes. The neutral $Ni(ddds)_2$ species was obtained by electrochemical oxidation from the monoanionic $(nBu_4N)[Ni(ddds)_2]$ complex. X-Ray crystal structure analyses of this neutral species show that two $Ni(ddds)_2$ are connected by the two Ni–Se bonds. Thus, the $Ni(ddds)_2$ entities form $[Ni(ddds)_2]_2$ dimers which are arranged face-to-face and rotated by about 90° with respect to each other. The electrochemical behavior of $(nBu_4N)[Ni(ddds)_2]$ indicates the possible formation of cation-radical species. The room temperature magnetic susceptibility measurements showed that the $(R_4N)[Ni(ddds)_2]$ complexes are paramagnetic with μ_{eff} = 1.77–1.83 μ_B, corresponding to one unpaired electron per molecular formula. The temperature dependence of the magnetic susceptibility of $(Et_4N)[Ni(ddds)_2]$ is indicative of weak long-range antiferromagnetic ordering below 9 K. The dimerization in $[Ni(ddds)_2]_2$ results in a strong antiferromagnetic spin coupling within the dimer, and explain the non magnetic state observed for this compound.

Introduction

The development of new organic conductors has made great strides over the last two decades since the discovery in 1973 of the first synthetic metal, i.e., tetrathiafulvalene−tetracyano-*p*-quinodimethane(TTF·TCNQ).[1][2][3][4] Along this line, bis(ethylenedithio)tetrathiafulvalene (BEDT-TTF) has taken a leading role, and a large number of new organic superconductors have been derived from this molecule.[5] On the other hand, the study of transition-metal bis(dithiolene) complexes has an even longer history[6][7] than that of the TTF-based systems and has been an area of great interest because the salts of these complexes show various crystal structures and conducting properties depending on the nature of the central metal atom and counter ion, and the oxidation state.[8] These salts show a tendency to form one-dimensional structure and, consequently, most of those that exhibit high metal-like conductivity at ambient pressure become insulator at low temperature. However, no less than eight superconductors have been discovered within the series of $M(dmit)_2$-based complexes (dmit = 2-thioxo-1,3-dithiole-4,5-dithiolate), namely, $(TTF)[Ni(dmit)_2]_2$, α- and α′-$(TTF)[Pd(dmit)_2]_2$, $(Me_4N)[Ni(dmit)_2]_2$, β-$(Me_4N)[Pd(dmit)_2]_2$, $(Et_2Me_2N)[Pd(dmit)_2]_2$, α-(EDT-TTF)$[Ni(dmit)_2]_2$,[9] and, most recently, β′-$(Et_2Me_2P)[Pd(dmit)_2]_2$.[10]

Among the many chemical modifications of $M(dmit)_2$ systems subsequently studied, metal complexes of 5,6-dihydro-1,4-dithiin-2,3-dithiolate $[M(dddt)_2]$ were synthesized for the first time about ten years ago.[11][12] They have a planar structure remarkably similar to that of BEDT-TTF in which the central C=C bond of BEDT-TTF is substituted by a metal ion. The neutral $M(dddt)_2$ complexes (M = Ni, Pd, Pt, and Au) may be used as donor components in the preparation of partially-oxidized conducting cation-radical salts (as for BEDT-TTF), some of them exhibiting metallic temperature dependence down to low temperature.[13] In this context, the development of selenium analogue compounds of $M(dddt)_2$ has attracted our interest because the expected increase of the dimensionality resulting from enhanced transverse chalcogen−chalcogen interaction obtained through selenium substitution. This increase of the dimensionality is known to stabilize the metallic state by suppressing low-dimensional instabilities (such as the Peierls transition[14]) at low temperature. For example, such a strong stabilization of metallic state has been observed in salts derived from BETS (BETS = bis(ethylenedithio)tetraselenafulvalene),[15] the selenium ana-

 © WILEY-VCH Verlag GmbH, D-69451 Weinheim, 1998 1434−1948/98/1111−1631 $ 17.50+.50/0

logue of BEDT-TTF, and new BETS-based organic superconductors have been recently discovered.[16] Thus, selenium substitution has been applied to $Ni(dddt)_2$ compounds and we report herein on the synthesis, structure and physical properties of new selenium containing metal complexes $(R_4N)[Ni(ddds)_2]$ (ddds = 5,6-dihydro-1,4-dithiin-2,3-diselenolate; R = Me, Et, *n*Bu[17]) and of the neutral $[Ni(ddds)_2]_2$ complex.

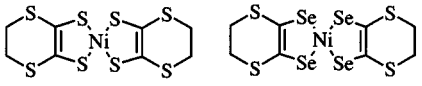

$Ni(dddt)_2^-$ $Ni(ddds)_2^-$**(1)**

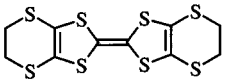

BEDT-TTF

Results and Discussion

The synthesis of tetraalkylammonium salts of $[Ni(ddds)_2]^-$ **1** was performed as follows: the disodium diselenolate ligand, $Na_2(ddds)$ **3**, was generated as a reddish orange solution by the hydrolytic cleavage of 4,5-ethylenedithio-1,3-diselenol-2-one **2** with 20% sodium ethoxide in dry THF at 0°C.[15b] Nickel complexes were obtained as the tetramethylammomium, tetraethylammonium and tetra-*n*-butylammonium salts, respectively, by successive treatment with an ethanol solution of nickel dichloride hexahydrate and the corresponding tetraalkylammonium bromide. The resulting precipitates were collected and washed with methanol and recrystallized in acetone or acetone/isopropanol (1:1) to afford dark green and air stable crystals. All the complexes were found by X-ray crystal analysis and elemental analysis to have a 1:1 cation/anion stoichiometry, indicating that the expected dianionic nickel complexes are easily air-oxidized to their monoanionic species in the course of preparation.

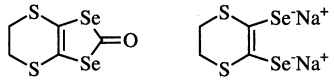

2 **3**

The neutral $Ni(ddds)_2$ species can be prepared by electrochemical oxidation of the monoanionic $(nBu_4N)[Ni(ddds)_2]$ complex in the presence of tetra-*n*-butylammonium perchlorate in acetonitrile. Needle-shaped black single crystals grew on the anode within about 2−3 weeks. In the course of research aiming at coupling $[Ni(ddds)_2]^-$ with nonlinear optical or magnetic cations,[18] the neutral $Ni(ddds)_2$ compound has been also unexpectedly obtained by electrochemical oxidation of $(nBu_4N)[Ni(ddds)_2]$ in the presence of (DAMP)I (4-dimethylamino-1-methylpyridinium iodide), $(HPMS)(PF_6)$ {4′-[2(hydroxymethyl)pyrrolidinyl]-1-methylstilbazolium hexafluorophosphate} and $[Cu(bpy)_2](PF_6)_2$ (bpy = 2,2′-bipyridine). In the last case, two apparently different phases (needles and blocks) of the neutral complex were obtained. Finally, the $Ni(ddds)_2$ neutral complex can be also obtained as black powder by chemical oxidation by iodine of $(nBu_4N)[Ni(ddds)_2]$. However, these powder material being extremely insoluble, the compound could not be recrystallized to obtain pure single crystal samples.

As previously reported,[17] the cyclic voltammogram of $(nBu_4N)[Ni(ddds)_2]$ shows two pairs of reversible redox waves corresponding to the $[Ni(ddds)_2]^{2-}/[Ni(ddds)_2]^-$ and $[Ni(ddds)_2]^-/[Ni(ddds)_2]$ couples. The potentials of the first and second waves (−0.60 V and +0.16 V vs Ag/AgCl, respectively) are about 0.1 V higher than those of the $(nBu_4N)[Ni(dddt)_2]$ sulfur analogue (−0.71 and +0.03 V[11][12]), suggesting that selenium substitution results in a decrease of the electron-donating ability. The redox potential of the $[Ni(ddds)_2]^{2-}/[Ni(ddds)_2]^-$ couple (−0.60 V) is very low, especially when compared to that of the corresponding $[Ni(dmit)_2]^{2-}/[Ni(dmit)_2]^-$ couple (−0.18 V[9a]) and this accounts for the spontaneous air-oxidation of the expected dianionic $(R_4N)_2[Ni(ddds)_2]$ salts observed during the synthesis. Moreover, the cyclic voltammogram of $(nBu_4N)[Ni(ddds)_2]$ also shows an irreversible oxidation wave at +0.71 V, reminiscent to that observed for (nBu_4N)-$[Ni(dddt)_2]$ (+0.99 V[11][12]), indicating the possible formation of cation-radical salts. Up to date, however, because of the low solubility of neutral $Ni(ddds)_2$, or the low stability of derived positively charged species, all attempts to grow crystals of such cation-radical salts failed.

Crystal structure analyses were performed for the monoanionic $(R_4N)[Ni(ddds)_2]$ and neutral $[Ni(ddds)_2]$ complexes. The crystal and experimental data are summarized in Table 4.

The molecular structure of the $[Ni(ddds)_2]^-$ anions and the atomic numbering schemes of the three studied $(R_4N)[Ni(ddds)_2]$ complexes are shown in Figure 1. Selected bond lengths and angles are gathered in Tables 1 and 2. Very similar bond lengths are observed in the three cases. The average C=C double bond length in the $[Ni(ddds)_2]^-$ anions, 1.357 Å, is almost the same as in $[Ni(dddt)_2]^-$ anions, 1.363 Å,[11a][11d][11c] indicating a similar electronic state. The mean Ni−Se distance in the $[Ni(ddds)_2]^-$ anion, 2.27 Å, is longer than that of the corresponding Ni−S distance in the $[Ni(dddt)_2]^-$ anion, 2.132(9) Å,[11c] but the difference of both values (0.14 Å) is in fact almost equal to that between the atomic covalent radius of sulfur and selenium. The intramolecular Se−Se distances, Se(1)−Se(2) = 3.268(3) and Se(3)−Se(4) = 3.267(3) Å, are longer than that between the corresponding sulfur atoms of the inner five-member ring of $[Ni(dddt)_2]^-$, 3.068(3) Å,[11a] and are closer to the S−S distances in the outer six-member ring, S(1)−S(2) = 3.451(8) and S(3)−S(4) = 3.461(7) Å. This suggests that the expansion of the electron clouds of the chalcogen atoms is nearly uniform towards the transverse direction over the whole $[Ni(ddds)_2]^-$ anion, which is in contrast with the case of $[Ni(dddt)_2]^-$ (see below).

The overall structural arrangements of the three monoanionic $(R_4N)[Ni(ddds)_2]$ complexes are also different

Figure 1. ORTEP drawings and atomic numbering schemes of the anion moieties (a) $(Me_4N)[Ni(ddds)_2]$, (b) $(Et_4N)[Ni(ddds)_2]$, and (c) $(nBu_4N)[Ni(ddds)_2]$

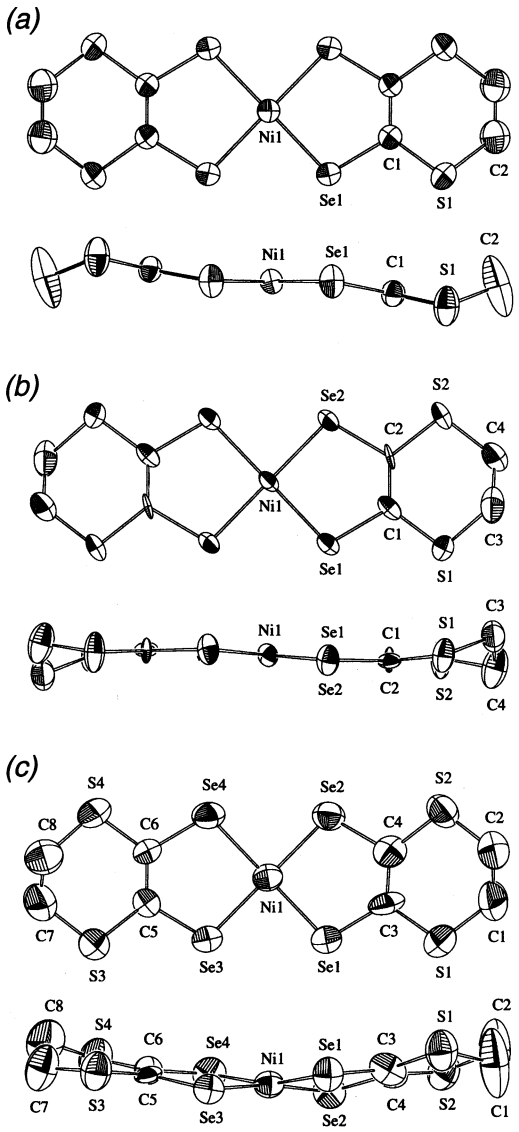

from those of the corresponding $R_4N[Ni(dddt)_2]$ (R = Me, Et, *n*Bu) sulfur analogues:[11a][11d][11c]

– $(Me_4N)[Ni(ddds)_2]$: One tetramethylammonium cation and one $[Ni(ddds)_2]^-$ anion are crystallographically independent. The Ni atom of $[Ni(ddds)_2]^-$ and the N(1) atom of the tetramethylammonium cation are located in the mirror plane (*ab* plane) and on the center of inversion. The C(4) atom of the tetramethylammonium cation is in the mirror *ab* plane. Therefore, the tetramethylammonium cation is octahedrally disordered. As shown in Figure 2a, the cations and anions are stacked alternately along the *b* axis and form a layered structure in the *ab* plane. Only the terminal ethylenedithio bridges are slightly overlapping each other. On the other hand, the $[Ni(ddds)_2]^-$ anions are arranged in a zigzag manner along the *c* axis and there is one short intermolecular Se(1)···S(1) contact [3.781(2) Å] between adjacent layers (Figure 2b). The $[Ni(ddds)_2]^-$ anion has a slightly chair-like structural arrangement with a dihedral angle of 11.01° and exhibits a completely planar coordination around the central nickel atom. The terminal C(2)–C(2)* bond length has a very short value, 1.34(2) Å, compared to the C–C single bond lengths (about 1.51 Å) usually observed in analog compounds.[11][12] The C(2) carbon atom has a large temperature factor [B_{eq} = 10.7(4)], indicating a conformational flexibility of the ethylene bridge.

Table 1. Selected bond lengths [Å] for $Ni(ddds)_2$ complexes

	(Me_4N)-$[Ni(ddds)_2]$	(Et_4N)-$[Ni(ddds)_2]$	(nBu_4N)-$[Ni(ddds)_2]$	$[Ni(ddds)_2]_2$
Ni(1)–Se(1)	2.2672(8)	2.284(3)	2.263(3)	2.332(1)
Ni(1)–Se(2)		2.259(2)	2.270(3)	2.311(1)
Ni(1)–Se(3)			2.267(3)	2.280(1)
Ni(1)–Se(4)			2.268(3)	2.284(1)
Se(1)–C(1)	1.885(6)	1.88(2)		
Se(2)–C(2)		1.88(2)		
Se(1)–C(3)			1.84(2)	1.881(8)
Se(2)–C(4)			1.91(2)	1.895(7)
Se(3)–C(5)			1.89(2)	1.871(7)
Se(4)–C(6)			1.86(2)	1.858(8)
C(1)–C(1)*	1.35(1)			
C(1)–C(2)		1.35(2)		
C(3)–C(4)			1.37(2)	1.368(10)
C(5)–C(6)			1.36(2)	1.384(10)
C(1)–S(1)	1.746(6)			
C(3)–S(1)		1.80(2)	1.79(2)	1.718(8)
C(4)–S(2)		1.78(3)	1.74(2)	1.734(8)
C(5)–S(3)			1.75(2)	1.748(7)
C(6)–S(4)			1.75(2)	1.740(8)
S(1)–C(2)	1.753(8)			
S(1)–C(1)		1.77(2)	1.78(3)	1.75(1)
S(2)–C(2)		1.75(2)	1.76(2)	1.77(1)
S(3)–C(7)			1.80(2)	1.79(1)
S(4)–C(8)			1.81(2)	1.76(1)
C(2)–C(2)*	1.34(2)			
C(3)–C(4)		1.52(3)		
C(1)–C(2)			1.35(3)	1.34(1)
C(7)–C(8)			1.37(2)	1.23(1)

– $(Et_4N)[Ni(ddds)_2]$: The Ni atom of $[Ni(ddds)_2]^-$ is located on the center of inversion and the $[Ni(ddds)_2]^-$ anion moiety is almost planar except for the slightly staggered ethylene bridge. The N(1) atom of the tetraethylammonium cation is also located on the center of inversion and two carbon atoms connected to the nitrogen atom are disordered on two positions [C(5) and C(9), C(8) and C(10)] with occupancy factor of 0.5. The anions form a one-dimensional array along the *a*-axis and there are several intermolecular Se···Se or Se···S contacts between the adjacent anions, indicating strong side-by-side interaction along the *a* axis (Figure 3a). On the other hand, each donor array is completely separated by a layer containing the tetraethylammonium cations and there is no interaction between the anion layers (Figure 3b).

– $(nBu_4N)[Ni(ddds)_2]$: The unit cell contains one crystallographically independent tetrabutylammonium cation and one $[Ni(ddds)_2]^-$ anion. Figure 4 shows the projection onto the *bc* plane. Neither a stacking, nor a columnar structural arrangement of the anions is observed. Only one S···S contact [3.542(10) Å] between anions is found (dotted lines in Figure 4). Each anion is surrounded by a counter tetrabu-

Table 2. Bond angles [°] involving the nickel atom in $Ni(ddds)_2$ complexes

	$(Me_4N)[Ni(ddds)_2]$	$(Et_4N)[Ni(ddds)_2]$	$(nBu_4N)[Ni(ddds)_2]$	$[Ni(ddds)_2]_2$
Se(1)−Ni(1)−Se(1)	92.23(4)			
Se(1)−Ni(1)−Se(2)		88.28(8)	92.2(1)	90.80(5)
Se(2)−Ni(1)−Se(4)			89.2(1)	85.29(5)
Se(3)−Ni(1)−Se(4)			92.2(1)	91.39(5)
Se(1)−Ni(1)−Se(3)			88.3(1)	90.13(5)
Se(1)−Ni(1)−Se(2)*				90.43(5)
Se(2)−Ni(1)−Se(2)*				97.33(4)
Se(3)−Ni(1)−Se(2)*				89.83(4)
Se(4)−Ni(1)−Se(2)*				109.69(5)
Ni(1)−Se(1)−C(1)	102.7(2)	103.3(7)		
Ni(1)−Se(2)−C(2)		103.7(5)		
Ni(1)−Se(1)−C(3)			102.6(5)	102.0(2)
Ni(1)−Se(2)−C(4)			103.2(6)	102.7(2)
Ni(1)−Se(3)−C(5)			102.6(5)	103.4(2)
Ni(1)−Se(4)−C(6)			103.6(5)	103.1(2)

Figure 2. Crystal structures of $(Me_4N)[Ni(ddds)_2]$ projected onto the (a) *ab*-plane and (b) *ac*-plane. − The intermolecular contact Se(1)−S(1) (−1/2 + *x*, 3/2 − *y*, 1/2 − *z*) is 3.781(2) Å

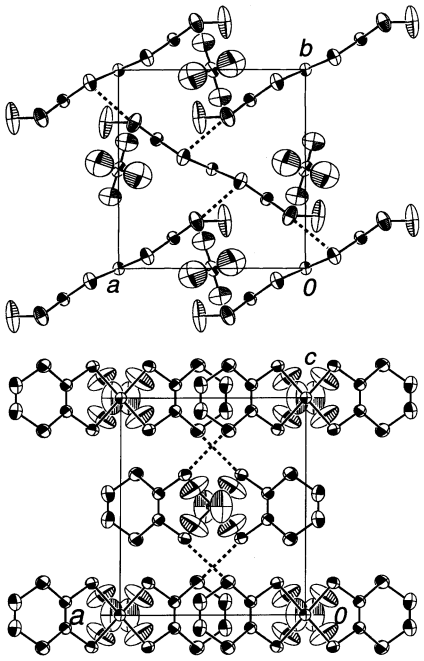

Figure 3. Crystal structures of $(Et_4N)[Ni(ddds)_2]$ projected onto the (a) *ab*-plane and (b) *bc*-plane. − The intermolecular contacts are Se(1)−S(2) (1 + *x*, *y*, *z*) = 3.750(7), Se(2)−S(2) (−*x*, 1 − *y*, −*z*) = 3.766(8), and Se(2)−Se(2) (−*x*, 1 − *y*, −*z*) = 3.975(5) Å. Two disordered carbons of cation moiety are omitted for clarity

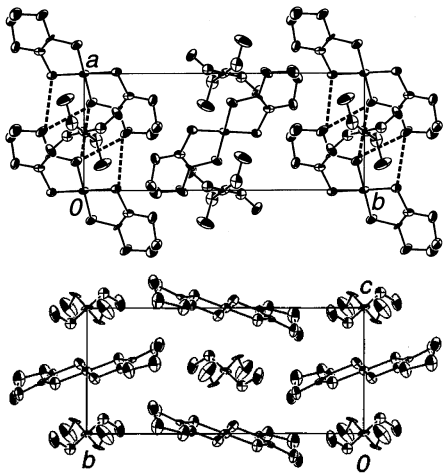

Figure 4. Crystal structure of $(nBu_4N)[Ni(ddds)_2]$ projected onto the *bc*-plane. − The intermolecular contact S(4)−S(4) (1 − *x*, −*y*, −*z*) is 3.542(10) Å

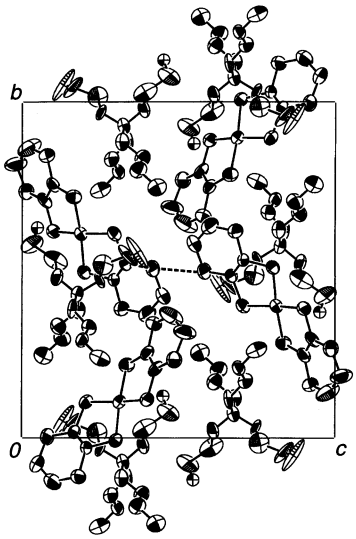

tylammonium cations. The nickel atom is coordinated to the four selenium atoms in a slightly distorted square planar geometry with a dihedral angle of 15.7° between the two five-member rings. This situation is different from that observed in the case of the other complexes with R = Me, Et, in which the coordination geometry around the nickel atom is strictly planar for symmetry reason. This is probably due to the steric hindrance of the bulky tetrabutylammonium cation. Each of the two chelating ligands is almost planar except for the ethylene bridge.

A stated above (see also Experimental Section), two, apparently different phases of the neutral $Ni(ddds)_2$ complex have been obtained, a needle-shaped one and a block-shaped one. The structures of these two phases have been independently determined and are in fact identical.[19] Two $Ni(ddds)_2$ units related by a center of inversion (symmetry

operation $1 - x$, $1 - y$, $2 - z$) are strongly dimerized and connected by the two Ni−Se(2) [2.496(1) Å] bonds to each other [the Ni(1)−Ni(1) distance is 3.178(2) Å]. Consequently, the neutral $Ni(ddds)_2$ complex should be more appropriately described as a dimer, $[Ni(ddds)_2]_2$ (Figure 5). The square coordination around nickel is distorted with a dihedral angle of 21.3°. Within each $Ni(ddds)_2$ entity of the dimer, the nickel atom is displaced by about 0.27 Å from the optimal plane of the four selenium atoms towards the axial selenium atom of the other $Ni(ddds)_2$ entity of the dimer. The large thermal ellipsoids of C(1), C(7) and C(8) and the small C(1)−C(2) and C(7)−C(8) distance indicate a conformational disorder of ethylene bridges. This disorder has been treated in the case of the block phase,[19] but no essential change in the description of the structure results from this treatment. The two ligand parts are heavily crooked and adopt a butterfly-wing shape conformation, probably caused by the steric hindrance introduced by the very short interplanar distance (2.84 Å for the $NiSe_4$ core of $Ni(ddds)_2$ entity). This structure is quite different from that reported for the neutral $Ni(dddt)_2$ analogue complex in which the $Ni(dddt)_2$ entities form uniform stacks and do not connect to each other[12], and rather resembles the dianion structure of $(Bu_4N)_2[Co(dddt)_2]_2$.[20] In $[Ni(ddds)_2]_2$, the $Ni(ddds)_2$ entities form real face-to-face dimers rotated by about 90° with respect to each other (Figure 6). This crystal structure is reminiscent of those reported for neutral BEDT-TTF,[21] or BETS,[15c], though in these compounds there are no actual chemical bonds between the two entities forming the so called "dimer". The $[Ni(ddds)_2]_2$ complexes are arranged side-by-side along the *a*-axis and produce a one-dimensional array. There are several Se(S)···Se(S) contacts between adjacent dimers as indicated by the dotted lines in Figure 7a. This is consistent with the value of the shape ratio *C* {0.98 for the $Ni(ddds)_2$ entity in $[Ni(ddds)_2]_2$} which had been proposed to evaluate the possible extent of the transversal intermolecular interaction in such chalcogen-based compounds.[15c] This $C = 0.98$ value is very close to that calculated for a rectangular shape ($C = 1$), which is predicted as the most favorable one for high intermolecular interaction.

The bond lengths of the ddds ligands in $[Ni(ddds)_2]_2$ are nearly identical, within standard deviations, to those observed for the monoanionic $(R_4N)[Ni(ddds)_2]$ complexes. Especially the C=C double bond length does not change upon oxidation to the neutral species. These results indicate that the decrease of electron density does not occur within the ddds ligands, but it is the central nickel atom which is oxidized. This oxidation of nickel may explain the formation of a pentahedral intradimer coordination bond and the $[Ni(ddds)_2]_2$ dimer structure. Such a situation is quite different from that observed for the $Ni(dddt)_2$ sulfur analogue system. It was inferred from Raman spectra of $Ni(dddt)_2$ that nickel could be unambiguously described as a d^8 ion and that the dddt ligands were involved in oxidation and reduction.[22] Thus, substitution of selenium for sulfur atoms in the dddt ligand seems to affect coordination of the ligand to nickel and change the electron configuration of the resulting neutral complex.

Figure 5. (a) ORTEP drawing and atomic numbering scheme of the neutral $[Ni(ddds)_2]_2$ complex and (b) the side view. The second molecule is generated by symmetry operation $1 - x$, $1 - y$, $2 - z$

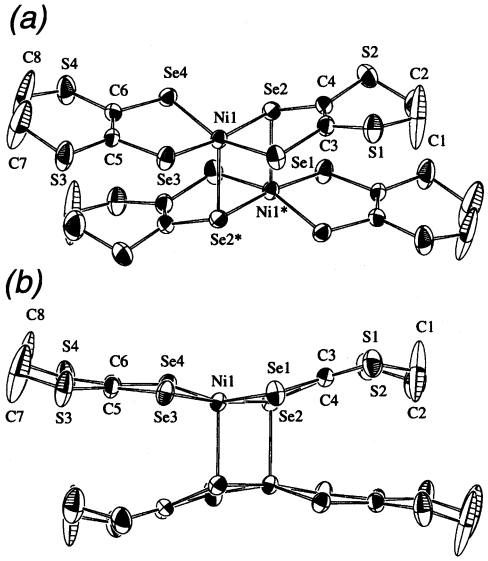

Figure 6. Crystal structure of neutral $[Ni(ddds)_2]_2$ projected onto the *bc*-plane

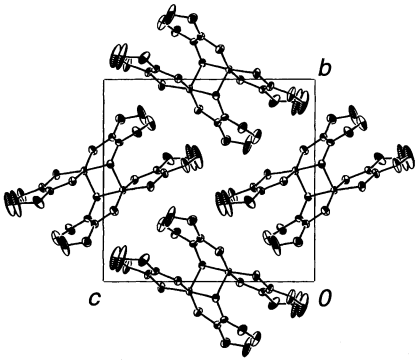

The room temperature magnetic susceptibilities of monoanionic $(R_4N)[Ni(ddds)_2]$ and neutral $[Ni(ddds)_2]_2$ complexes were measured by SQUID magnetometer at 1 Tesla. As shown in Table 3, all the monoanionic complexes show paramagnetism with $\mu_{eff} = 1.77 - 1.83\ \mu_B$ corresponding to one unpaired electron per molecular formula {1.73 μ_B for $s = 1/2$, $g = 2$ spins from the equation of $\mu_{eff}/\mu_B = g[s(s + 1)]^{1/2}$}. On the other hand, no magnetic moment was detected for the neutral $[Ni(ddds)_2]_2$ complex. This non-magnetic state can be explained by the stabilization of a singlet ground state in the $Ni(ddds)_2$ moiety, but more probably, as the X-ray results show that the $Ni(ddds)_2$ entities are structurally strongly dimerized in the neutral species, by a strong antiferromagnetic spin coupling within the dimer.

The temperature dependence of static magnetic susceptibility was measured for the monoanionic complexes. The tetramethylammonium salt showed a Curie-Weiss temperature dependence with a small positive Weiss temperature

Figure 7. Dimer array of neutral $[Ni(ddds)_2]_2$ (a) viewed along the molecular long axis and (b) projected onto the molecular plane. – The interdimer contacts are Se(1)–Se(4) (1 + *x*, *y*, *z*) = 3.993(1), Se(3)–S(4) (1 + *x*, *y*, *z*) = 3.663(3), Se(3)–Se(4) (1 + *x*, *y*, *z*) = 3.807(2), S(3)–S(4) (1 + *x*, *y*, *z*) = 3.639(4), and Se(2)–Se(4) (–*x*, 1 – *y*, 2 – *z*) = 3.897(2) A

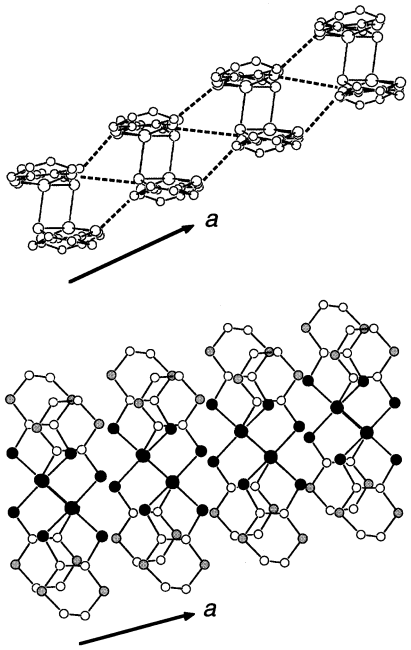

Table 3. Magnetic Properties of $(R_4N)[Ni(ddds)_2]$ at 1 Tesla.

	Magnetic susceptibility/ μ_B at room temperature	Weiss temperature/ K[a]
$(Me_4N)[Ni(ddds)_2]$	1.81	+1.0
$(Et_4N)[Ni(ddds)_2]$	1.77	–18.0
$(nBu_4N)[Ni(ddds)_2]$	1.83	–4.0

[a] Weiss temperature was obtained from the Curie-Weiss law.

(θ = +1.0 K), indicating a slight short-range ferromagnetic interaction between anions. The tetrabutylammonium salt also obeyed a Curie-Weiss law, but the Weiss temperature is –4.0 K indicative of a weak antiferromagnetic interaction. However, both these salts did not show any phase transitions down to 2 K.

By contrast, the magnetic moment of the tetraethylammonium complex decreases as temperature decreases and a strong antiferromagnetic interaction is observed, as indicated by a large Weiss temperature of θ = –18 K in the high temperature region (Figure 8). Furthermore, the temperature dependence suddenly changes around 10 K, and below 9 K the magnetic susceptibility indicates a slight field dependence under magnetic fields below 100 Gauss, suggesting the occurrence of a weak long-range antiferromagnetic ordering. This phenomenon seems to be derived from the side-by-side strong interaction along the one-dimensional array of anions of $(Et_4N)[Ni(ddds)_2]$ (vide supra). A similar situation has been reported for the tetraethylammonium salt of $Ni(dddt)_2$.[11a]

Figure 8. Temperature dependence of magnetic susceptibility and magnetic moment of $(Et_4N)[Ni(ddds)_2]$ measured at 1 Tesla

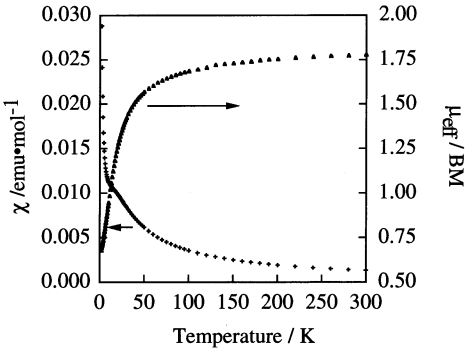

Conclusions

The selenium substitution of inner sulfur atoms in $Ni(dddt)_2$ complexes was expected to increase the transverse intermolecular interaction and therefore to stabilize metallic state. Indeed, in the resulting $Ni(ddds)_2$ complexes studied in this work, the intraligand Se–Se distance is longer than that of the corresponding inner sulfur atoms in the $M(dddt)_2$ complexes and is almost equal to the S–S distance in the outer six-member ring. Thus, two-dimensional intermolecular close contacts were expected and observed in the $Ni(ddds)_2$ complexes. This intermolecular interaction accounts for the strong antiferromagnetic interaction and weak long-range antiferromagnetic ordering observed for $(Et_4N)[Ni(ddds)_2]$. The neutral $Ni(ddds)_2$ species was obtained by electrochemical oxidation from the monoanionic $(nBu_4N)[Ni(ddds)_2]$ complex. X-Ray crystal structure analyses revealed that in this neutral species intermolecular Ni–Se bonds are formed, resulting in a $[Ni(ddds)_2]_2$ dimer compound. Given the promising CV data indicating the possible formation of cation–radical salts, several attempts, using various electrochemical procedures, were made to prepare such cation–radical salts starting from the neutral $[Ni(ddds)_2]_2$ molecule, but they all failed. This is probably due to the low solubility of $[Ni(ddds)_2]_2$ in common solvents. However, changing the nature of the metal may alleviate this difficulty and we are now engaged in the preparation of other $M(ddds)_2$ complexes such as those with M = Au.

Experimental Section

General: Microanalyses were performed by the Organic Elemental Analysis Center, Department of Chemistry, School of Science, the University of Tokyo, and by the Microanalyses Service at the LCC-CNRS, Toulouse. – ^1H NMR: JEOL FT-NMR EX-270N (270 MHz for ^1H), [D_6]acetone as solvent, TMS as internal standard. – IR: PERKIN-ELMER FTIR-1600.

4,5-Ethylenedithio-1,3-diselenol-2-one was synthesized by literature methods.[15b] THF was distilled over sodium and benzophenone and acetonitrile was distilled over calcium hydride under

Table 4. Crystallographic data for $Ni(ddds)_2$ complexes

	$(Me_4N)[Ni(ddds)_2]$	$(Et_4N)[Ni(ddds)_2]$	$(Bu_4N)[Ni(ddds)_2]$	$[Ni(ddds)_2]_2$ [19]
formula	$C_3H_5N_{0.25}Ni_{0.25}SSe$	$C_8H_{14}N_{0.5}Ni_{0.5}S_2Se_2$	$C_{24}H_{44}NNiS_4Se_4$	$C_8H_8NiS_4Se_4$
crystal color, habit	black, needle	black, plate	black, plate	black, needle
crystal system	orthorhombic	monoclinic	monoclinic	monoclinic
formula weight	170.27	368.59	849.40	606.93
a/Å	9.464(3)	8.022(1)	9.668(5)	6.589(3)
b/Å	10.052(4)	18.350(2)	19.260(3)	14.722(2)
c/Å	11.166(2)	8.733(2)	18.099(2)	15.366(1)
β/°		107.90(2)	97.87(2)	90.86(2)
V/Å^3	1062.2(9)	1223.3(4)	3338(1)	1490.5(6)
space group	*P*nnm	$P2_1$/n	$P2_1$/c	$P2_1$/n
Z, formula units	8	4	4	4
D_{calc}/g·cm^{-3}	2.129	2.001	1.690	2.705
dimensions, mm	0.40 × 0.10 × 0.10	0.40 × 0.15 × 0.03	0.60 × 0.20 × 0.05	0.40 × 0.10 × 0.10
μ/cm^{-1}	81.56	70.90	52.08	116.05
$2\theta_{max}$/°	59.9	50.0	55.0	60.0
total reflections	1797	2235	7698	4520
reflections used	635 (I>3.0σ(I))	815 (I>3.0σ(I))	2359 (I>3.0σ(I))	2318 (I>3.0σ(I))
parameters/*Fo*	10.58	5.86	7.66	15.05
scan width	1.15+0.50 tanθ	1.26+0.50 tanθ	0.94+0.50 tanθ	1.37+0.50 tanθ
ω scan speed	8.0° min^{-1}	8.0° min^{-1}	8.0° min^{-1}	8.0° min^{-1}
R [a], R_w [b]	0.039, 0.029	0.059, 0.057	0.065, 0.054	0.040, 0.033
GOF	1.57	1.63	2.65	1.54
Max/min transmission	1.00/0.90	1.00/0.52	1.00/0.47	1.00/0.79
T/K	296	296	296	296

[a] $R=\Sigma\|\|Fo\| - |Fc\|\|/\Sigma|Fo|$. – [b] $R_w = [\Sigma w(|Fo| - |Fc|)^2/\Sigma w|Fo|^2]^{1/2}$.

nitrogen and stored in the refrigerator until use. Tetra-*n*-butylammonium perchlorate was recrystallized from ethyl acetate, and dried in vacuo. All other reagents were used without purification.

Synthesis of (Me$_4$N)[Ni(ddds)$_2$]: 4,5-Ethylenedithio-1,3-diselenol-2-one (0.302 g; 1.00 mmol) was hydrolyzed with a 20% ethanol solution of sodium ethoxide (1.50 g; 4.40 mmol) in dry THF (10.0 ml), at 0°C and under nitrogen. The color of the solution changed from yellow to reddish-orange as the reaction proceeded. The solution was stirred for 2 hours and a reddish-pink precipitate formed. A solution of nickel(II) chloride hexahydrate (0.128 g; 0.538 mmol) in ethanol (30.0 ml) was added dropwise to the reaction mixture and the resulting solution was stirred for 2 hours at 0°C. The obtained dark brown solution was treated with a solution of tetramethylammonium bromide (0.172 g; 1.12 mmol) in ethanol (10.0 ml), for 1 hour at 0°C, and warmed to room temperature. The resulting dark green precipitate was collected by filtering, washed with methanol and recrystallized from acetone to afford 0.240 g (0.352 mmol) of air-stable needle-shaped dark green crystals in 71% yield. – $C_{12}H_{20}NNiS_4Se_4$ (681.08): calcd. C 21.16, H 2.96, N 2.06, S 18.83, Se 46.37; found C 21.30, H 2.85, N 2.17, S 18.56, Se 46.79. – $\tilde{\nu}$ (KBr) = 2904 cm^{-1}, 1472, 1397, 1278, 1164, 943, 678.

The other $(R_4N)[Ni(ddds)_2]$ complexes with R = Et and *n*Bu were obtained by a procedure similar to that described above for $(Me_4N)[Ni(ddds)_2]$:

Synthesis of (Et$_4$N)[Ni(ddds)$_2$]: Obtained from 4,5-ethylenedithio-1,3-diselenol-2-one (0.303 g; 1.00 mmol), a 20% ethanol solution of sodium ethoxide (1.47 g; 4.31 mmol), a solution of nickel (II) chloride hexahydrate (0.126 g; 0.531 mmol) in ethanol (20.0 ml) and a solution of tetraethylammonium bromide (0.219 g; 1.04 mmol) in ethanol (20.0 ml), as air-stable plate-shaped dark green crystals in 82% yield (0.301 g, 0.408 mmol) – $C_{16}H_{28}NNiS_4Se_4$ (737.18): calcd. C 26.07, H 3.83, N 1.90, S 17.40; found C 26.12, H 3.74, N 2.18, S 17.35. – $\tilde{\nu}$ (KBr) = 2968 cm^{-1}, 2912, 1474, 1398, 1280, 1172, 999, 870, 780.

*Synthesis of (n*Bu$_4$N)[Ni(ddds)$_2$]:* Obtained from 4,5-ethylenedithio-1,3-diselenol-2-one (0.308 g; 1.02 mmol), a 20% ethanol solution of sodium ethoxide (1.41 g; 4.13 mmol), a solution of nickel (II) chloride hexahydrate (0.120 g; 0.505 mmol) in ethanol (30.0 ml) and a solution of tetrabutylammonium bromide (0.172 g; 0.534 mmol) in ethanol (10.0 ml), as air-stable plate-shaped dark green crystals in 84% yield (0.362 g, 0.426 mmol). – $C_{24}H_{44}NNiS_4Se_4$ (849.40): calcd. C 33.94, H 5.22, N 1.65, S 15.10; found C 33.67, H 5.20, N 1.61, S 15.08. – $\tilde{\nu}$ (KBr) = 2954 cm^{-1}, 2923, 2866, 1408, 1377, 1282, 687, 682. – ^{1}H NMR δ = 3.39 (m, 8 H, SCH_2CH_2S), 1.87 (m, 8 H, NCH_2), 1.82 (m, 8 H, NCH$_2$CH_2), 1.50 (m, 8 H, NCH$_2$CH$_2$CH_2), 1.03 (m, 12 H, CH_3).

Electrochemical Synthesis of [Ni(ddds)$_2$]$_2$

Method A: (*n*Bu$_4$N)[Ni(ddds)$_2$] (10 mg) and tetra-*n*-butylammonium perchlorate (51 mg) were dissolved in 15 ml of acetonitrile under nitrogen. Electrochemical oxidation of this solution was carried out with a constant current of 1.0 μA at room temperature. Needle-shaped black single crystals grew on the anode within about 2–3 weeks.

Method B: A solution of (*n*Bu$_4$N)[Ni(ddds)$_2$] (15 mg) in acetonitrile (11 ml) was prepared under nitrogen and placed in the anodic compartment of a U-shaped electrochemical cell. A solution of $Cu(bpy)_2(PF_6)_2$ (14 mg) in acetonitrile was prepared under nitrogen and placed in the cathodic compartment of the cell. Electrochemical oxidation was carried out with a constant current of 0.25 μA at room temperature. Needle-shaped black and block-shaped black single crystals grew on the anode and on the low porosity glass frit between the anodic and cathodic compartments within about ten days.

In both cases, the obtained crystals were filtered, washed with ethanol, and air-dried at room temperature. – $C_{16}H_{16}Ni_2S_8Se_8$ (1213.86): calcd. C 15.83, H 1.35; found C 16.30, H 1.35. – $\tilde{\nu}$ (KBr) = 2945 cm^{-1}, 2906, 2866, 1365, 1324, 1272, 679, 668.

Electrochemical Measurements: Cyclic voltammetry data were obtained using a BAS 100B/W electrochemical workstation. The

measurements were performed at 20°C in benzonitrile containing 0.1 M tetra-*n*-butylammonium hexafluorophosphate as supporting electrolyte with platinum working- and counter-electrode, and a BAS RE-1B Ag/AgCl reference electrode (scan rate: 200 mV s^{-1}).

Magnetic Susceptibility Measurements: Magnetic susceptibility measurements of $(R_4N)[Ni(ddds)_2]$ (R = Me, Et, *n*Bu) and $[Ni(ddds)_2]_2$ were performed on Quantum Design MPMS2 and MPMS7 magnetometers in the temperature range from 2 K to 300 K. The samples were wrapped with a clean aluminum foil whose magnetic susceptibility was separately measured and subtracted. The diamagnetic contribution was calculated from the Pascal's constants.

X-Ray Crystallographic Studies: Data collection for the $(R_4N)[Ni(ddds)_2]$ and needle-shaped crystals of $[Ni(ddds)_2]_2$ was performed on a Rigaku AFC-5R diffractometer with graphite monochromated Mo-*Kα* radiation (λ = 0.71069 Å) and a rotating anode generator. Intensities were collected by the ω-2θ scan technique. Lorentz-polarization (Lp) correction and empirical absorption correction based on azimuthal scans of several reflections were applied. The experimental details and crystal data are listed in Table 4. The structure was solved by direct method (MULTAN88[23] for neutral $[Ni(ddds)_2]_2$ and SHELXS86[24] for other complexes). The atomic scattering factors were taken from the International Tables for X-ray Crystallography.[25] The non-hydrogen atoms were anisotropically refined by full-matrix least-squares method. Hydrogen atoms were included but not refined. All calculations were performed using the teXsan crystallographic software package of Molecular Structure Cooperation[26]. Data collection for the block-shaped crystals of $[Ni(ddds)_2]_2$ was performed on a STOE IPDS (imaging plate diffraction system) using monochromatic Mo-*Kα* radiation (λ = 0.71013 Å), The structure was solved by direct methods (SHELXS-86[24]). Crystal data are given in ref.[19]. Experimental details, atomic coordinates, bond lengths and angles can be found in the Supporting Information section. Crystallographic data (excluding structure factors) for the structures reported in this manuscript have been deposited with the Cambridge Crystallographic Data Centre. The deposition numbers are CCDC-101694, -101695, and -101696 for the $(R_4N)[Ni(ddds)_2]$ (R = Me, Et, *n*Bu) compounds, respectively, 101697 for the needle-shaped $[Ni(ddds)_2]_2$, and 101556 for the block-shaped $[Ni(ddds)_2]_2$. Copies of the data can be obtained free of charge on application to The Director, CCDC, 12 Union Road, GB-Cambridge CB12 1EZ [Fax: (internat.) + 44(0)1223/336−033, E-mail: deposit@ccdc.cam.ac.uk].

[1] J. Ferraris, D. O. Cowan, V. Walatka, Jr., J. H. Perlstein, *J. Am. Chem. Soc.* **1973**, *95*, 948−949.

[2] Reviews: [2a] K. Bechgaard, D. Jérome, *Sci. Am.* **1982**, *247*, 50−59. − [2b] J. M. Williams, A. J. Schultz, U. Geiser, K. D. Carlson, A. M. Kini, H. H. Wang, W. K. Kwok, M.-H. Whangbo, J. E. Schirber, *Science* **1991**, *252*, 1501−1508. − [2c] G. Saito, *Phosphorus, Sulfur, and Silicon* **1992**, *67*, 345−360.

[3] [3a] *Organic Superconductors* (Eds.: T. Ishiguro, K. Yamaji), Springer-Verlag Berlin, Heidelberg, **1990**. − [3b] *The Physics and Chemistry of Organic Superconductors* (Eds.: G. Saito, S. Kagoshima), Springer-Verlag Berlin, Heidelberg, **1990**. − [3c] J. M. Williams, J. R. Ferraro, R. J. Thorn, K. D. Carlson, U. Geiser, H. H. Wang, A. M. Kini, M.-H. Whangbo, *Organic Superconductors*, Prentice Hall, New Jersey, **1992**.

[4] Recent Proceedings of International Conferences: [4a] *Synth. Met.* **1995**, *69−71* (Eds.: Y. W. Park, H. Lee). − [4b] *Synth. Met.* **1997**, *84−86* (Eds.: Z. V. Vardeny, A. J. Epstein).

[5] [5a] A. Kobayashi, R. Kato, H. Kobayashi, S. Moriyama, Y. Nishio, K. Kajita, W. Sasaki, *Chem. Lett*. **1987**, 459−462. − [5b] H. Urayama, H. Yamochi, G. Saito, K. Nozawa, T. Sugano, M. Kinoshita, S. Sato, K. Oshima, A. Kawamoto, J. Tanaka, *Chem. Lett*. **1988**, 55−58. − [5c] A. M. Kini, U. Geiser, H. H. Wang, K. D. Carlson, J. M. Williams, W. K. Kwok, K. G. Vandervoort, J. E. Thompson, D. L. Stupuka, D. Jung, M.-H. Whangbo, *Inorg. Chem.* **1990**, *29*, 2555−2557. − [5d] J. M. Williams, A. M. Kini, H. H. Wang, K. D. Carlson, U. Geiser, L. K. Montgomery, G. J. Pyrka, D. M. Watkins, J. M. Kommers, S. J. Boryschuk, A. V. Strieby-Crouch, W. K. Kwok, J. E. Schirber, D. L. Overmyer, D. Jung, M. -H. Whangbo, *Inorg. Chem*. **1990**, *29*, 3272−3274.

[6] [6a] G. N. Schrauzer, V. P. Mayweg, *J. Am. Chem. Soc*. **1962**, *84*, 3221. − [6b] H. B. Gray, R. Williams, I. Bernal, E. Billing, *J. Am. Chem. Soc*. **1962**, *84*, 3596−3597.

[7] [7a] J. A. McCleverty, *Prog. Inorg. Chem*. **1968**, *10*, 49. − [7b] H. B. Gray, *Transition Met. Chem*. **1965**, *1*, 239−287. − [7c] G. N. Schrauzer, *Transition Met. Chem.* **1968**, *4*, 299−335. − [7d] R. Eisenberg, *Prog. Inorg. Chem*. **1970**, *12*, 295−369. − [7e] R. P. Burns, C. A. McAuliffe, *Adv. Inorg. Chem. Radiochem.* **1986**, *22*, 303−348.

[8] P. Cassoux, L. Valade, H. Kobayashi, A. Kobayashi, R. A. Clark, A. E. Underhill, *Coord. Chem. Rev.* **1991**, *110*, 115−160.

[9] [9a] P. Cassoux, L. Valade, in *Inorganic materials*, 2nd edn (Eds.: D. W. Bruce, D. O′Hare) J. Wiley & Sons, Chichester, **1996**, 1−64. − [9b] P. Cassoux, J. S. Miller, in *Chemistry of Advanced Materials*, (Eds.: L. V. Interrante, M. J. Hampden-Smith) Wiley−VCH, New York, **1998**, 19−72.

[10] R. Kato, Y. Kashimura, S. Aonuma, N. Hanasaki, H. Tajima, *Solid State Commun.* **1998**, in the press.

[11] [11a] C. T. Vance, R. D. Bereman, J. Bordner, W. E. Hatfield, J. H. Helms, *Inorg. Chem*. **1985**, *24*, 2905−2910. − [11b] R. Kato, H. Kobayashi, A. Kobayashi, Y. Sasaki, *Bull. Chem. Soc. Jpn.* **1986**, *59*, 627−630. − [11c] A. J. Schultz, H. H. Wang, L. C. Soderholm, T. L. Sifter, J. M. Williams, K. Bechgaard, M.-H. Whangbo, *Inorg. Chem*. **1987**, *26*, 3757−3761. − [11d] J. H. Welch, R. D. Bereman, P. Singh, D. Haase, W. Hatfield, M. L. Kirk, *Inorganica Chimica Acta* **1989**, *162*, 89−96.

[12] H. Kim, A. Kobayashi, Y. Sasaki, R. Kato, H. Kobayashi, *Bull. Chem. Soc. Jpn.* **1988**, *61*, 579−581.

[13] [13a] E. B. Yagubskii, A. I. Kotov, A. G. Khomenko, L. I. Buravov, A. I. Schegolev, R. P. Shibaeva, *Synth. Met*. **1992**, *46*, 255−259. − [13b] E. B. Yagubskii, L. A. Kushch, V. V. Gritsenko, O. A. Dyachenko, L. I. Buravov, A. G. Khomenko, *Synth. Met*. **1995**, *70*, 1039−1041. − [13c] L. A. Kushch, V. V. Gritsenko, L. I. Buravov, A. G. Khomenko, G. V. Shilov, O. A. Dyachenko, V. A. Merzhanov, E. B. Yagubskii, R. Rousseau, E. Canadell, *J. Mater. Chem*. **1995**, *5*, 1633−1638. − [13d] L. A. Kushch, S. V. Konovalikhin, L. I. Buravov, A. G. Khomenko, G. V. Shilov, K. Van, O. A. Dyachenko, E. B. Yagubskii, C. Rovira, E. Canadell, *J. Phys. I France* **1996**, *6*, 1555−1565.

[14] R. E. Peierls, in *Quantum Theory of Solids,* Oxford University Press, **1955**, p. 108.

[15] [15a] R. R. Schumaker, V. Y. Lee, E. M. Engler, *IBM Research Report* **1983**. − [15b] R. Kato, H. Kobayashi, A. Kobayashi, *Synth. Met.* **1991**, *41−43*, 2093−2096. − [15c] T. Courcet, I. Malfant, K. Pokhodnia, P. Cassoux, *New J. Chem.* **1998**, 585−589.

[16] [16a] H. Kobayashi, T. Udagawa, H. Tomita, K. Bun, T. Naito, A. Kobayashi, *Chem. Lett*. **1993**, 1559−1562. − [16b] H. Kobayashi, H. Tomita, T. Naito, H. Tanaka, A. Kobayashi, T. Saito, *J. Chem. Soc., Chem. Commun*. **1995**, 1225−1226. − [16c] L. K. Montgomery, T. Burgin, T. Miebach, D. Dunham, J. C. Huffman, J. E. Schirber, *Mol. Cryst. Liq. Cryst*. **1996**, *284*, 73−84. − [16d] H. Tanaka, A. Kobayashi, T. Saito, K. Kawano, T. Naito, H. Kobayashi, *Adv. Mater*. **1996**, *8*, 812−815. − [16e] H. Kobayashi, H. Tomita, T. Naito, A. Kobayashi, F. Sakai, T. Watanabe, P. Cassoux, *J. Am. Chem. Soc.* **1996**, *118*, 368−377.

[17] Part of these results has been reported in a preliminary communication, H. Fujiwara, E. Arai, H. Kobayashi, *J. Chem. Soc., Chem. Commun*. **1997**, 837−838.

[18] I. Malfant, unpublished results. Such a coupling of DAMP cations has been achieved with [Ni(dmit)2], I. Malfant, R. Andreu, P. G. Lacroix, C. Faulmann, P. Cassoux, *Inorg. Chem.* **1998**, *37*, 3361−3370.

[19] *Crystal Data*: black block, $C_8H_8Se_4S_4Ni$, M = 607.0, monoclinic, space group $P2_1/n$, unit cell at 160K: a = 6.539(1), b = 14.639(2), c = 15.324(2) Å, β = 90.62(2)°, V = 1466.8 $Å^3$, D_c = 2.75 g/cm^3 for Z = 4. μ_c = 116.8 cm^{-1} corrections from absorption effects. 2218 independent reflections with $I > 0$ $\sigma(I)$. The non-hydrogen atoms were refined anisotropically. Disorder has been treated on two carbons C(7), C(8) of one terminal ethylene group. Hydrogens atoms were included but not refined. The

structure was refined by full-matrix least squares to $R = 0.035$, $R_w = 0.029$. Atomic coordinates, bond lengths and angles, and thermal parameters are available in the Supporting Information.

[20] J. H. Welch, R. D. Bereman, P. Singh, C. Moreland, *Inorg. Chim. Acta* **1989**, *158*, 17−25.

[21] H. Kobayashi, A. Kobayashi, Y. Sasaki, G. Saito, H. Inokuchi, *Bull. Chem. Soc. Jpn.* **1986**, *59*, 301−302.

[22] H. H. Wang, S. B. Fox, E. B. Yagubskii, L. A. Kushch, A. I. Kotov, M.-H. Whangbo, *J. Am. Chem. Soc.* **1997**, *119*, 7601−7602.

[23] *MULTAN88:* T. Debaerdemaeker, G. Germain, P. Main, L. S. Refaat, C. Tate, M. M. Woolfson, computer programs for the automatic solution of crystal structures from X-ray diffraction data, University of York, U. K., **1988**.

[24] *SHELXS86:* G. M. Sheldrick, in *Crystallographic Computing 3* (Eds.: G. M. Sheldrick, C. Kruger, R. Goddard) Oxford University Press, **1985**, 175−189, .

[25] D. T. Cromer, J. T. Waber, in *International Tables for X-ray Crystallography*, vol. 4, Kynoch Press, Birmingham, England, Table 2.2 A, **1974**.

[26] *teXsan:* Crystal Structure Analysis Package, Molecular Structure Cooperation, **1985** & **1992**.

[98172]

How to Predict Conformations Accessible to a Molecule in Solution: Validation of a Force Field-Based Prediction of NOE Distances by Comparison with the Experimental Data for the Series of Compounds $CH_3C[CH_2P(Bzl)R]_3Mo(CO)_3$ (R = Ph, *m*-Xyl)☆

Stefan Beyreuther, Johannes Hunger, Sven Cunskis, Tammo Diercks, Axel Frick, Eckart Planker, and Gottfried Huttner*

Anorganisch-Chemisches Institut der Universität Heidelberg,
INF 270, D-69120 Heidelberg, Germany
Fax: (internat.) +49 (0)6221/54-5707
E-mail: NOE@indi.aci.uni-heidelberg.de

Received June 4, 1998

Keywords: *tripod* Molybdenum(CO)$_3$ compounds / Conformational ensembles in solution / Modelling NOE contacts / MM2* Force field calculations / Packing forces

NMR-NOE analysis of the three compounds (*RRS*/*SSR*)-$CH_3C(CH_2PPhBz)_3Mo(CO)_3$ (**1**), (*RRR*/*SSS*)-$CH_3C(CH_2PPhBz)_3Mo(CO)_3$ (**2**), and (*RRR*/*SSS*)-$CH_3C[CH_2P(m\text{-Xyl})Bz]_3Mo(CO)_3$ (**3**), leads to experimental values for a number of intramolecular H···H contacts in each case. By the very nature of the NOE method, and with the type of molecules studied here, these values have to be understood as a Boltzmann weighted average over all the conformations accessible to the molecules in solution. – A Boltzmann weighted force field approach is used to predict these values on the basis of sets of force field parameters derived earlier for this class of compounds. The agreement between observed and calculated NOE distances is highly satisfactory in each case (rms = 0.2 Å to 0.3 Å). By a statistical analysis it is shown that the predictions made by applying this Boltzmann weighted force field approach are highly significant. There is only a chance of 3 in 100 000 that this quality of prediction might be obtained by chance. This is taken as a validation, albeit indirect, of the energy scale reproduced by the force field parameters as developed. The methods described give a detailed insight into the conformational flexibility of molecules of the type studied. Solid state structures of the molecules are also correctly modelled by the force field used.

Introduction

When force field methods are used to predict possible structural arrangements of coordination compounds, the parameters describing the interactions involving the metal atom are generally deduced from solid-state structures of a series of similar compounds. An optimisation method based on Genetic Algorithms has been proposed as an unbiased method to derive such parameters from a set of solid-state molecular structures.[1] The success of this novel methodology has been demonstrated by correctly predicting general trends as well as specific conformations in the chemistry of *tripod*Mo(CO)$_3$ compounds [*tripod* = $CH_3C(CH_2X)(CH_2Y)(CH_2Z)$, X, Y, Z = PRR′]. It remains an open question as to whether force field approaches developed on the basis of solid-state molecular structures might have some bearing on the behaviour of molecules in solution. Since most reactions in coordination chemistry, including those mediating homogeneous catalysis, in fact take place in solution, this is a serious question. Only if it can be shown that the conformational properties of coordination compounds in solution are appropriately modelled by these methods, can these methods be of help to the preparative chemist in the design and optimisation of ligand-metal-templates with predefined properties. In order to address this problem, information about the conformational behaviour of coordination compounds in solution is clearly necessary.

It has long been known that the Nuclear Overhauser Effect (NOE) allows the determination of H···H distances of molecules in solution.[2] The application of this type of distance measurement in solution has for decades been the preserve of the specialist. Only in recent years have NMR techniques, both methods and equipment, been developed to a state where this kind of measurement might even become a routine tool. Indeed, NMR analysis of protein structures[3] has made enormous progress in the last few years.[4]

In the chemistry of small molecules including the subclass of coordination compounds considered here, NOE measurements are routine only in their qualitative form, i.e. to find out whether two protons in a given molecule are close together or far away from each other. In a quantitative way the method is not used too often in this context. One reason for this is evident: it is rather easy to obtain a crystal structure determination once a compound has been crystallised. A second reason is more intricate: the number of H···H distances accessible to NOE measurements in small molecules is generally too low to uniquely define a structure. There is kind of a paradox: if a molecule increases in size, the number of NOE distances increases and, even

 © WILEY-VCH Verlag GmbH, D-69451 Weinheim, 1998 1434–1948/98/1111–1641 $ 17.50+.50/0

though a larger molecule will have more degrees of freedom in conformational space, the increased number of measurable distances may well counterbalance this increase so that proteins with (depending on the kind and degree of labelling) 200 or more amino acids may be fully structurally characterised by this method, while simple structures such as the ones considered in this paper still pose severe problems. Nevertheless NOE data represent the most valuable and easy way to access information about an ensemble of conformations of molecules in solution.

It is the purpose of this paper to analyse the appropriateness of the force field description[1] of *tripod*$Mo(CO)_3$ compounds[5][6] by comparing the NOE distances measured for a specific molecule with those predicted by the straightforward application of the force field model. This type of analysis is performed for the three coordination compounds **1**−**3** (Figure 1).

Figure 1. Schematic representation of compounds **1** to **3**. The configuration at the phosphorus centers of the racemates to which the paper refers is indicated by the (*R*/*S*) nomenclature

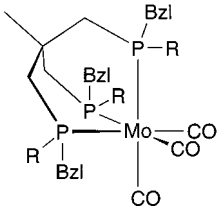

1 R=C_6H_5 (RRS/SSR)
2 R=C_6H_5 (RRR/SSS)
3 R=3,5-xylyl (RRR/SSS)

Results

Compound 1

Three compounds of the type *tripod*$Mo(CO)_3$[5][6] (**1**−**3**, Figure 1) have been selected for this analysis in the hope that the number of short and hence detectable H···H contacts might be sufficient to warrant a detailed comparison of measured and calculated H···H distances. All three compounds are chiral and the NMR analysis has been performed on the racemate in each case. In addition, compounds **1** and **2** are diastereomers. It was expected that the reduced symmetry of **1** relative to **2**, together with the bulkiness of the substituents, would strongly differentiate the conformational behaviour of these two isomers so that a maximum of information would result from their analysis.

Compound **1** was a member of the data base used to derive the force field approach and its solid state structure[5] is neatly reproduced[1] by the force field as developed.[1] A projection of the structure of **1** as determined by X-ray analysis is given in Figure 2 (the plane of projection is defined by the three P atoms). The designators of the hydrogen atoms that are involved in NOE contacts, as shown in Figure 2, refer to the contacts given in Table 1.

The NOE distances elaborated for **1** in solution in CD_2Cl_2 at 275 K (see Experimental Section) do not fully agree with the distances observed in the crystal structure. This is not an unexpected result since **1**, especially given its benzylic constituents, is expected to have a high degree of flexibility (Figure 2).

Figure 2. Projection of the structure of **1** onto the plane defined by the phosphorus atoms of $CH_3C(CH_2PPhBzl)_3Mo(CO)_3$. The numbering scheme used throughout is indicated as is the configuration at the phosphorus centers for the (*RRS*) enantiomer of the racemic pair of **1** studied

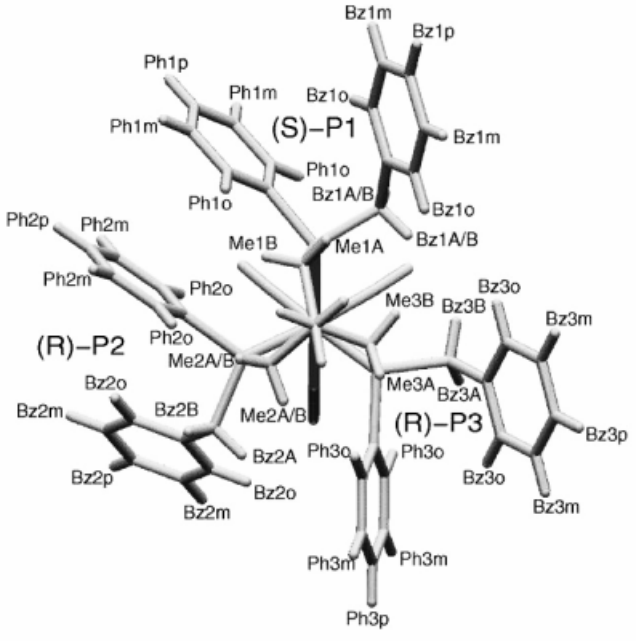

Table 1. Proton-proton distances in **1** as determined by NOE analysis (solution) and X-ray analysis (single crystal) in comparison with these distances as calculated from the force field approach

proton 1	proton 2	d_{NOE} [Å]	$d_{X\text{-}ray}$ [Å]	$d_{Boltzmann}$ [Å][a] *mm2f*	*mm2t*
Bz1A/B	Bz1o	2.30(10)	2.37(1)	2.42	2.43
Bz2A	Bz2o	2.60(15)	2.35(1)	2.45	2.44
Bz2B	Bz2o	2.50(15)	2.56(1)	2.46	2.47
Bz3A	Bz3o	2.60(10)	2.57(1)	2.46	2.46
Bz3B	Bz3o	2.40(15)	2.37(2)	2.47	2.45
Me1/3A	Bz1o	2.50(10)	2.57(2)	2.45	2.41
Me1/3B	Bz1o	2.80(10)	2.49(1)	2.91	2.76
Me2A/B	Bz2o	2.70(15)	4.57(0)	2.44	2.42
Me3A	Bz3o	2.60(15)	3.44(2)	3.17	3.16
Me1/3B	Bz3o	2.80(10)	2.46(1)	2.35	2.34
Me1A	Ph1o	2.20(10)	2.90(3)	2.75	2.74
Me3A	Ph3o	2.00(15)	2.04(2)	2.06	2.08
Me2A/B	Ph2o	2.10(15)	1.84(1)	2.05	2.09
Me3A	Bz2o	2.60(15)	6.29(2)	3.09	2.78
Bz2A	Ph2o	2.60(10)	4.40(1)	2.91	2.84
Bz3A	Ph3o	2.60(15)	2.47(1)	2.61	2.72
Bz3o	Ph3o	2.80(15)	3.19(0)	2.99	3.08
Bz2o	Ph3o	2.20(15)	3.66(0)	3.06	3.34
Bz3o	Bz1o	2.90(20)	2.78(0)	3.06	3.24
rms	[Å]	−	1.16	0.34	0.38

[a] *mm2f* and *mm2t* refer to different sets of force field parameters.[1] Column header $d_{Boltzmann}$ refers to the Boltzmann weighted average of the relevant distances in each case. − [b] rms deviation between the experimental NOE distances and the distances derived by the methods given in the respective column headers.

A flexible molecule like **1** might adopt a number of different conformations in solution and a distance extracted from NOE measurements is some kind of weighted average of all these individual distances between a specific pair of H atoms. Due to the fact that the NOE decreases with the inverse sixth power of the distance, there is an experimental limit to H···H contacts leading to NOE signals, which in the present analysis is around 3 Å. Even if only a narrow range of H···H contacts somewhere between 2 and 3 Å has been accessible by NMR for **1**, these distances are quite restrictive as far as the range of possible conformations is concerned. A number of different approaches have been used in the literature to transform the limited information available from a few NOE distances into structural models that are not excluded by the measurements.[7][8] All of these approaches use the constraints set by the measured NOE distances in one way or another to find acceptable conformations.[9]

A different approach is taken in the work described here. Be it assumed for the moment that a force field approach exists that correctly describes the energy hypersurface pertaining to a molecule, and that all the energy minima at this hypersurface are hence correctly placed in both position and in energy (relative to the energy of the global minimum). In this case the Boltzmann weighted average of the NOE-relevant geometric functions should reproduce the average of this function as observed. The function itself is, according to the physics of NOE, proportional to the inverse of the sixth power of the distance between a pair of hydrogen atoms. The NOE distances, as determined by measurement, thus present a criterion to evaluate and possibly validate a specific force field description.[10] Since molecules like **1**−**3** are still small enough for a complete and systematic search to be performed on the energy hypersurface defined by the force field they allow these lines of investigation to be followed.

To effectively scan all of the relevant conformational space[11] defined by the three rotations of phenyl groups (φ, Figure 3), the six rotational parameters describing the orientations of the benzyl groups (ψ, ω, Figure 3), and the three parameters describing the skew of the chelate cage (τ, Figure 3), the following simplifications were introduced to generate an appropriate set of starting conformations. The skew of the scaffolding was represented by just one torsion τ, thus effectively imposing C_3 symmetry on the torsional arrangement of this cage to start with. This simplification is well warranted given the observations made on 82 *tripod* metal compounds whose conformation had been statistically analysed[11] as well as by the observations made on a sample of *tripod*$Mo(CO)_3$ compounds.[1] Of course this constraint imposed on the starting conformations does not exclude the fact that during the conformational search any type of deviation from this C_3 symmetry will occur. The conformational space that has to be analysed is 10-dimensional, i.e. 3 × PPh- (φ) plus 6 × PBzl-rotations (ψ, ω) plus 1 cage twist (τ). A complete grid search was performed. The resolution for producing the starting conformations was defined by any combination of the values of the torsion angles τ, φ, ψ and ω (Figure 3) as given in Table 2. This leads to 11 664 (= $2{\cdot}3^3{\cdot}3^3{\cdot}2^3$) starting geometries.

Figure 3. Schematic drawing corresponding to Figure 2 with the definition of the conformational variables φ, ψ, ω, and τ shown. The definition illustrated here is also adopted for **2** and **3**

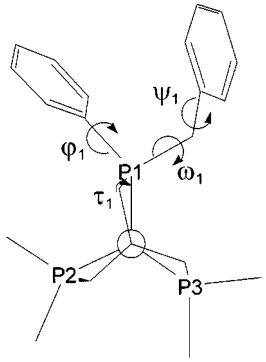

Table 2. Grid values for generating the starting geometries of **1**−**3**[a]

	τ [°]	φ [°]	ψ [°]	ω [°]	combinations	C_3 symmetric starting geometries
1	20 −20	60 0 −60	120 0 −120	90 0	11664	− 11664
2,**3**	20 −20	60 0 −60	120 0 −120	90 0	11664	2·3·3·2 = 36 3912

[a] There are 11 664 combinations in each case. Due to the constitutional C_3 symmetry of **2** and **3** the number of geometrically independent starting geometries is reduced to 3912 in these cases.

In a sterically crowded molecule like **1** this a priori setting of conformations may lead to unforeseeable entangling of the individual constituents of the molecule and so the *rubberband* protocol[12] was applied during refinement: the bonds radiating from the phosphorus atoms to the phenyl and benzyl groups were elongated to a distance of 4 Å initially, moving these groups away from the core of the molecule to begin with. During refinement these distances were then allowed to relax in a stepwise manner back to the normal. Entangling of the groups is elegantly[12] avoided by this procedure.

The starting conformations as defined were then allowed to adapt to the force field by an energy minimisation procedure. Depending on the force field implementation used, 191 (*mm2f*[1]) or 165 (*mm2t*[1]) conformations corresponding to local energy minima on the hypersurface were finally found. To illustrate the part of conformational space occupied by these conformations they were clustered according to the distance separating them in the 10-dimensional conformational space as defined by φ, ψ, ω, and τ. The lowest energy conformation in each cluster was used to represent its conformational characteristics. An overlay of these conformations is shown in Figure 4 arranged according to the sense of the torsion of the chelate cage.

It is evident that there is a smaller spread in the orientation of the phenyl groups as compared to that of the

Figure 4. Graphical representation of the section of conformational space occupied by the local minima on the *mm2f* hypersurface of **1**

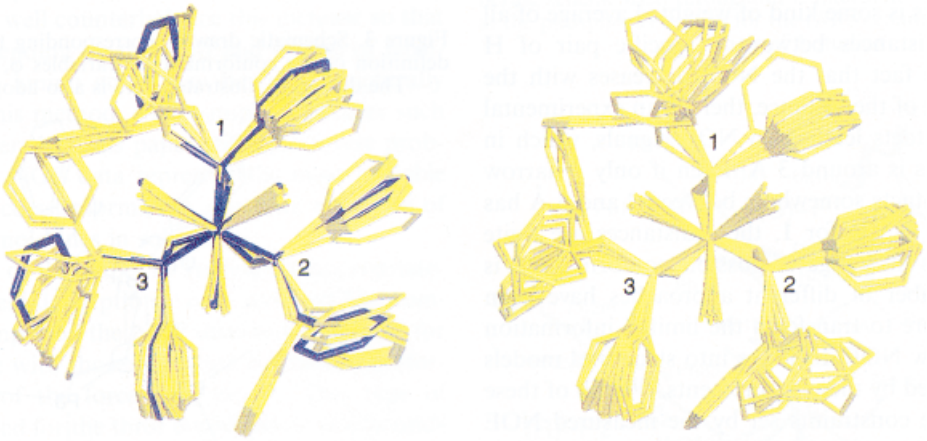

[a] The conformation adopted by **1** in the solid state is shown in blue. On the left hand side conformations with $\tau >= 0°$ are shown; the right hand side represents conformations with $\tau < 0°$. In order to make the diagram clearer the conformations were clustered with respect to their distance in conformational space so that each conformation shown represents the properties within each cluster. Note that the sense of numbering is opposite to the one given in Figure 2 due to the opposing directions of view taken in Figures 2 and 4.

benzyl residues. The conformation as determined by X-ray analysis is also indicated in Figure 4.

An alternative view of the diversity of possible orientations of the individual groups is presented by the histographic analyses of the φ-, ω-, ψ-, and τ-values adopted by the minimum energy conformations (Figure 5).

It is seen that the torsion around the P−C-bonds of the benzylic substituents ω basically conforms to the threefold rotational potential as expected. The different type of neighbourhood of benzyl group 2 in comparison to benzyl groups 1 and 3, i.e. benzyl group 2 having two phenyl neighbours (Figure 2) and benzyl groups 1 and 3 having one phenyl and one benzyl neighbour (Figure 2), is mirrored by a difference in the appearance of the corresponding histograms (compare the percentage values given in Figure 5). The histogram referring to the phenyl rotations φ (Figure

Figure 5. Histographic representation of the variance of the conformational parameters characterising the geometry of **1**

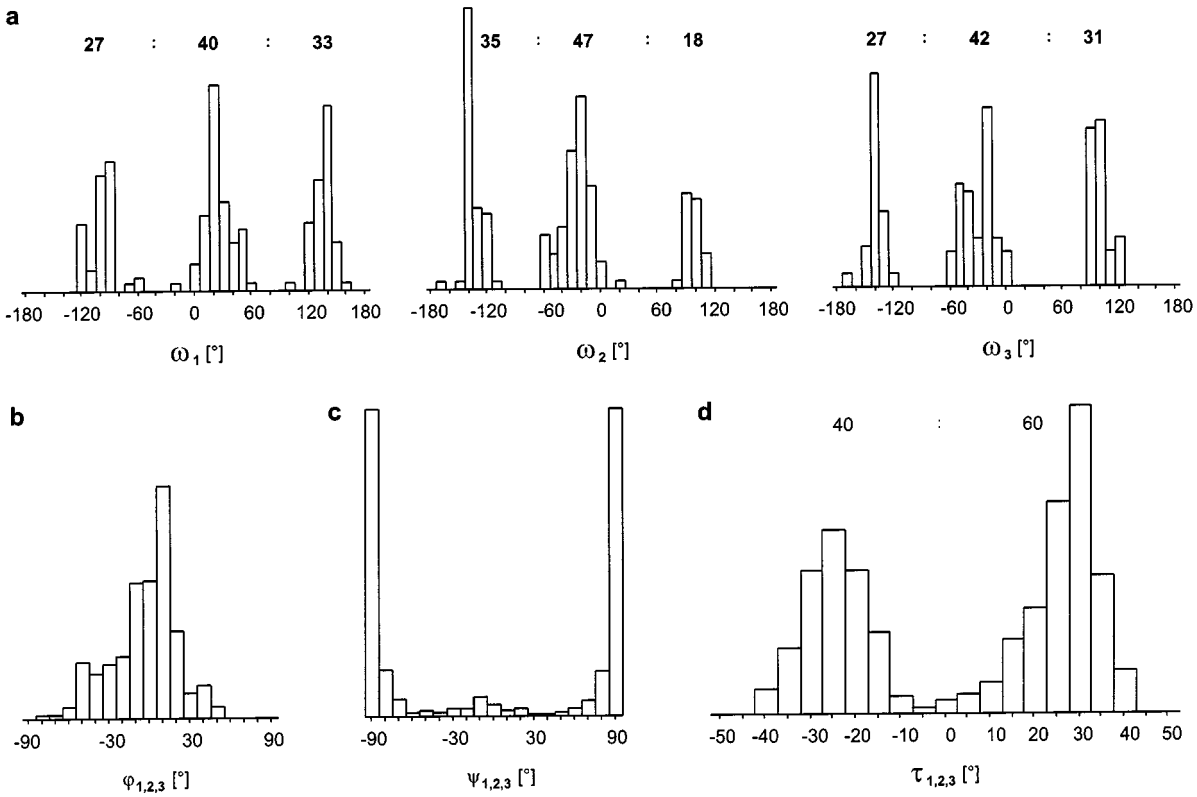

5) shows considerable spread while the histogram referring to the rotation ψ of the phenyl groups at the benzylic positions shows a marked preference at ±90°. The reason for this is that these phenyl groups are by and large outside the sterically crowded part of the molecule and can thus adopt the optimal orientation with respect to the neighbouring CH_2 groups, while the phosphorus-bound phenyl groups have to respond to the steric strain within the core of the molecule. As shown by the histogram, the space accessible to the torsion of the chelate cage (τ) is densely populated not only at the values of ±20° as set for the starting conformations but also at larger and smaller values. Since the analysis was done for the *RRS* enantiomer of the racemic pair **1**, the asymmetry in the distribution of τ values (Figure 5) is not at all unexpected (two (*R*)-configured PRR′ groups opposing only one (*S*)-configured group of this type).

The spread of the conformations, which correspond to local minima on the hypersurface as depicted in Figure 4 and Figure 5, makes no reference to their relative energy. The conformation as found in the crystal structure is at a computed energy of 5 kJ·mol^{-1} (*mm2f*) or 9 kJ·mol^{-1} (*mm2t*) above the global minimum, which differs from it by a 120° rotation around ω_2. As this amount of energy may easily be compensated for by the energy of the crystal lattice this result is not disturbing. With respect to the observation that the NOE distances are not consistent with the crystal structure, it is even a favourable observation. Indeed, none of the conformations, independent of their energy, is able to reproduce the observed NOE distances with an rms of less then 0.57 Å. If it is assumed that just two conformations would be sufficient to reproduce these distances, then all possible pairwise combinations of conformations should be analysed with their relative percentage of contribution being evaluated by a least squares procedure. By testing this hypothesis it was found that the best solution still has an rms deviation of 0.47 Å from the NOE distances. Analysing all possible combinations of three and even four conformations (combinatorial explosion does practically impede the analysis for higher multiples!) does not improve the agreement dramatically (3 conformations: rms = 0.43 Å; 4 conformations: rms = 0.43 Å). A favourable agreement between observed and calculated distances is, however, obtained when a Boltzmann weighted average (referring to d^{-6}) is taken over the complete set of minimum energy conformations. The rms deviation between observed and calculated average distances over all observable H···H pairs amounts to 0.34 Å for the *mm2f* force field and 0.38 Å for the *mm2t* approach (Table 1).

In order to develop a feeling for the relevance of this type of agreement and hence for the relevance of the Boltzmann weighting scheme employed, the following computer experiment was performed: for each conformation the relative energy was set at random in the range between 0.0 and 100 kJ/mol. This randomly generated energy was used to weight each conformation according to the Boltzmann scheme. The weighted average of the relevant distances was calculated and the calculated distances were compared with the measured ones so as to characterise each of these experiments by the corresponding rms value. This experiment was repeated with 10 000 sets of random weights generated in this way. The result of this computer experiment is shown in Figure 6 (**1**) in histographic form.

Figure 6. Computer experiments relevant to the significance of the approach used to predict NOE distances

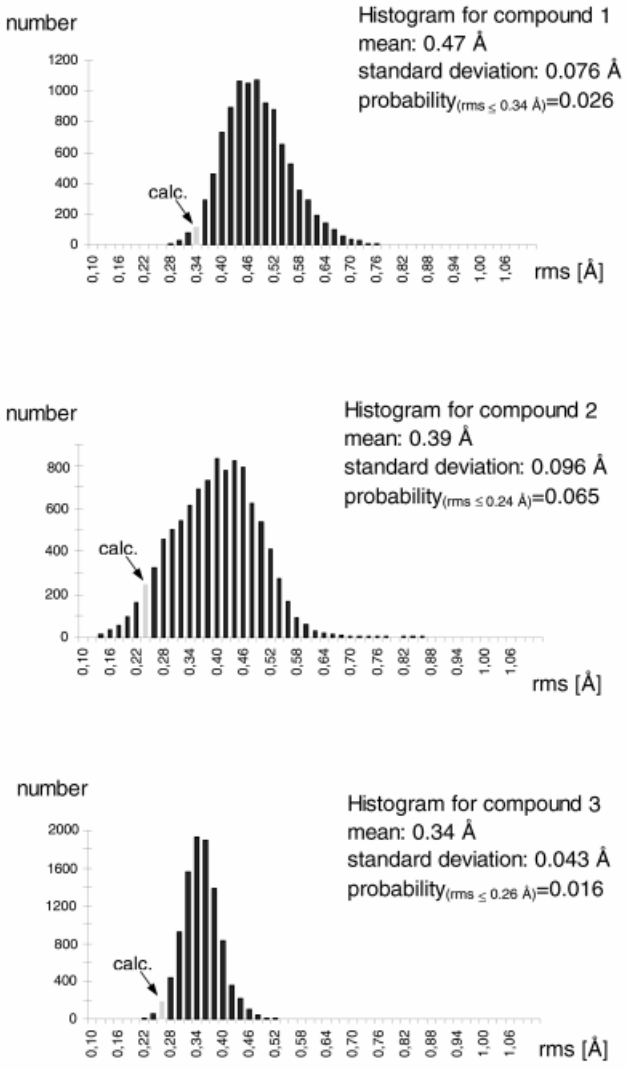

[a] 10 000 computer experiments were performed in each case. All conformations corresponding to local minima on the *mm2f* hypersurfaces were taken into account. NOE distances were calculated as a Boltzmann type average over all these conformations with the Boltzmann weights set at random in each experiment. For each experiment the rms deviation between the observed and the calculated NOE distances was derived. The spread of these rms values is shown in the diagrams and it is seen that the agreement obtained when the weights are derived by the force field (calc) is rather good. It is highly improbable that this quality of agreement could be fortuitous. The probability of the hypothesis that the results represented by the bars designated with "calc" might be fortuitous is below 7% for each individual compound. The probability that the quality of fit obtained by the approach taken might be fortuitous for all three compounds is in fact less than 3 in 100 000.

It is clear that the 10 000 rms numbers thus generated are not at all exhaustive with respect to the number of possible combinations of conformations and the weights attributed to them. In principle, an exhaustive solution would only be obtained after an infinite number of experiments of this

type; even if a discrete approximation were taken in order to allow as many different weights as there are conformations, the total number of combinations between conformations and weights would be $n!$ for a given number n of conformations! The histograms obtained will nevertheless approximate the distribution of possible solutions. It is observed that an rms value as good as that obtained by the Boltzmann weighting scheme as applied is highly unlikely to occur by chance. The probability of obtaining a solution with an rms value of 0.34 Å or lower by chance is only around 3% (Figure 6). The hypothesis that the quality of fit as obtained by using the energies derived from the force field in the Boltzmann weighting approach might be fortuitous may therefore be denied ata high level of significance.

The approach taken here to reproduce the observed NOE contacts by a force field approach was equally applied to compounds **2** and **3** (see below). The histograms reproducing the distribution of rms values as obtained from 10 000 computer experiments are also given in Figure 6. It is seen that the probability of obtaining the quality of fit (Figure 6, calc) derived from using the energies calculated by the force field approach fortitiously is less than 10 (**2**) and 5 (**3**) percent for these compounds. The probability of achieving the degree of approximation as obtained by applying the Boltzmann weighting scheme on the basis of the force field energies for all three compounds fortitiously is less than 3 in 100 000 as judged from the product of the probabilities given for each compound in Figure 6.

Compound 2

As indicated above the type of analysis as described for **1** was repeated with two additional compounds.The conformational space of **2** was defined by the same set of torsional parameters as already described for **1** (Figure 3). The grid spacing used to populate this space with starting conformations was numerically equal to the one used in the analysis of **1**. From the 11 664 starting conformations thus generated only a subset is symmetrically independent: those conformations that correspond to a C_3 symmetric arrangement occur only once each. The number of such conformations amounts to $2\cdot3\cdot3\cdot2 = 36$ in accordance with the number of values allowed for τ, φ, ω, and ψ. All the others will be represented at three symmetry related points in conformational space as three isoenergetic conformations. Each of these triplets corresponds to just one symmetrically independent conformation. The total number of independent conformations is thus $36 + (11664 - 36)/3 = 3912$ (Table 2). Force field refinement starting from these 3912 points in conformational space leads to 68 (*mm2f*) or 50 (*mm2t*) minimum energy conformations of which nine (*mm2f*) or eight (*mm2t*) have C_3-symmetry. Independent of the parameter set used (*mm2t, mm2f*), the conformation observed for **2** in the crystal closely corresponds to the global minimum in each case. This is a satisfactory result in that compound **2** had not been incorporated in the data base used to derive the force field approach.[1] There is some slight discrepancy between the calculated and the observed conformations as far as the precise orientation of two of the benzyl groups is concerned (Figure 7a).

Figure 7. Comparison of calculated (blue) and observed conformations of **2**; (a) free molecule; (b) molecule embedded in the crystal

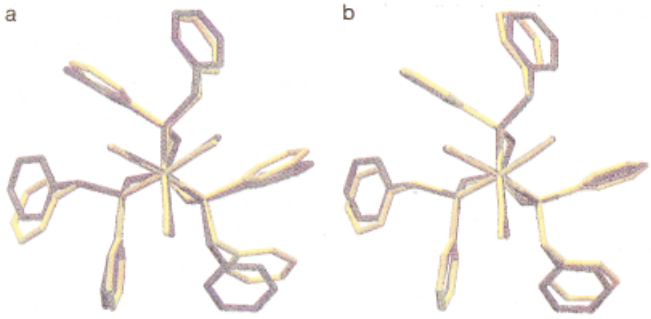

Assuming that this discrepancy might be caused by the environment of **2** in the crystal, a force field refinement of the structure in its solid state environment was performed. Contributions from all the atoms that are at a maximum distance of 8 Å from any atom of the molecule to be refined were taken into account. The atoms in this crystal environment were held at fixed positions during refinement. A view of the crystal environment as generated by the nineteen neighbouring molecules that meet the above criterion is given in Figure 8.

Figure 8. Crystal environment of **2** (blue: specified molecule, yellow: crystal surrounding)

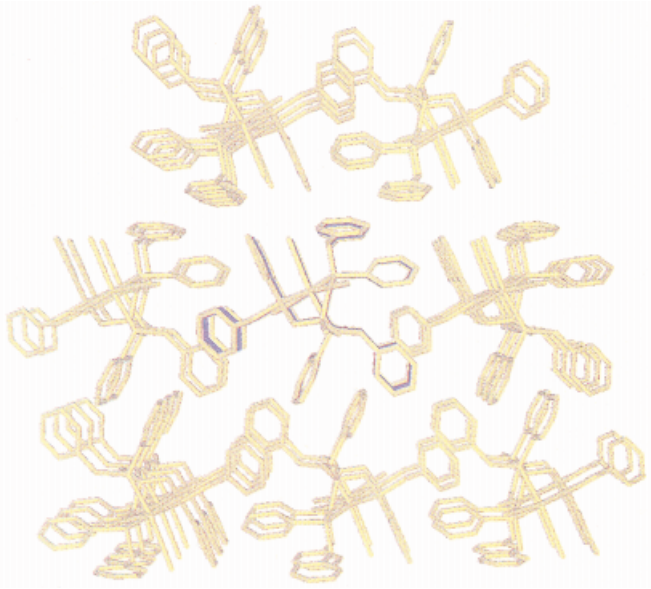

The result of this refinement is shown in Figure 7b (*mm2f*). The agreement between the calculated and the observed structures is significantly increased and the rms difference between the observed and the calculated structures decreases from 0.53 Å to 0.26 Å when the crystal environment is taken into account.

If the ensemble of conformations obtained by the minimisation process is systematically analysed, it is observed that the main difference between the individual confor-

mations may be traced back to the relative orientations that the benzyl groups occupy as characterised by ω. Three individually favourable conformations are possible for each such group, corresponding to the threefold potential governing this rotation (Figure 5). With reference to the coordination polyhedron, these three positions may be described in the following way: the benzyl group may point backward away from the carbonyl groups with its phenyl residue oriented such that it is close to the phenyl group that is directly bound to the phosphorus atom that supports both groups. Referring to Figure 9 this type of orientation is designated as **x**.

Figure 9. Relative orientation of the benzyl groups in **2** and letter codes used to specify them

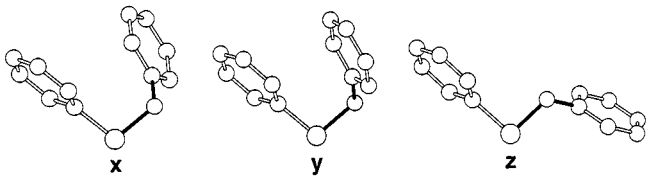

[a] The plots refer to a plane of projection and direction of view as used in Figure 7.

On the other hand, the benzyl group still pointing backward may be oriented such that its phenyl residue is close to the phenyl residue sustended by the neighbouring phosphorus atom (**z**, Figure 9). A third type of orientation (designated as **y**, Figure 9) results when the benzyl group is oriented towards the side of the carbonyl ligands with its phenyl part close to the phenyl residue supported by the same phosphorus atom. It is observed that there is an energetic preference for the orientations termed **x**. The sequence of orientations **xxx** < **xxy**, **xxz** < **xyy** < **xyz**, **xzy** < **yyy**, **xzz** < **yyz** < **zzy** < **zzz** (e.g. **xxy**: ω_1 = **x**, ω_2 = **x**, ω_3 = **y**; **x**, **y**, **z**: Figure 9) is found by ranking the orientations according to the energy at which they are observed for the first time amongst the manifold obtained from the conformational search procedure. This energetic ordering is also apparent by the selection of conformations shown in Figure 10 where the relative energies of some prototypic conformations are indicated.

An NOE analysis of **2** resulted in a number of NOE distances (Table 3). The protons involved in these NOE contacts and the designators used for them are shown in Figure 11.

It is seen from Table 3 that the conformation as found in the crystal already reproduces the NOE distances with an rms of only 0.28 Å. It might therefore appear that the conformation adopted by **2** in solution is close to that observed in the crystal, which itself is very close to the conformation calculated as the global minimum (see above).

On the other hand, based on the assumption that the force field approach correctly reproduces the energy hypersurfaces, a Boltzmann weighted average of the relevant geometric parameters should give an unbiased estimate of the NOE distances. Application of this procedure to the 68 conformations corresponding to the 68 energy minima obtained (*mm2f*, see above) leads to an rms discrepancy between the observed and the calculated NOE distances of 0.24 Å. In summing up the individual terms, appropriate care was taken to correctly handle symmetry: while C_1 symmetric conformations will appear at three different points in conformational space, reflecting the constitutional symmetry of the problem, C_3 symmetric conformations will occur just once. For instance, if φ2, φ3, and φ5 [or ω1, ω2, and ω3 etc. (Figure 3)] each have different values, their cyclic permutation will project itself into conformational space onto three different points; if on the other hand the values for φ1, φ3, φ5 etc. are equal, any cyclic permutation will project itself onto one and the same point in this space. The weight accounting for C_3 symmetric conformations is therefore only one third of those showing C_1 symmetry. Application of the same procedure to the conformations obtained by the *mm2t* parameter set likewise gave an rms of 0.33 Å. The result obtained by considering just the minimal energy conformation (rms = 0.25 Å) and that obtained by a Boltzmann weighted average over all conformations are not significantly different (Figure 6, **2**). It is observed that other single conformations, as well as pairwise combinations of conformations, numerically give an even better agreement of 0.19 Å (*mm2f*, single conformation: E_{rel} above global minimum: 5.9 kJ·mol) and 0.13 Å [*mm2f*, 2 conformations: E_{rel} = 5.9 (64%) and 21.1 kJ·mol^{-1} (36%)] respectively. With respect to the computer experimental distribution of rms values (Figure 6) these results are not totally unexpected. There are obviously weighted combinations of conformations in each case analysed (Figure 6) that lead to an rms value lower than that obtained by using the relative energies as the weighting criterion (bars designated with "calc" in Figure 6). This Boltzmann weighted average, however, is an a priori prediction of what the NOE distances should be. These predictions are not left to chance but a definitive formula is used to make these predictions and it is seen from Figure 6 that, by using this predictor, reliable predictions are made for completely independent sets of experiments (**1**−**3**). With the predictor being based on sound physical grounds this result is especially satisfying and, by its very methodology, is far superior to any method involving a posteriori fitting of the weights of individual conformations to achieve optimal agreement.

A caveat is in place here: as shown in the histograms (Figure 6) and in the paragraph above, there are always weighted linear combinations of conformations that neatly reproduce the NOE values with rms values that are even below the ones obtained with the Boltzmann predictor (Figure 6), and there are even single conformations (see above) that meet this criterion. These conformations would, of course, be found as the appropriate solutions by applying a distance geometry approach[8] and would naturally be considered to be very important because of the excellent agreement. In the light of the Boltzmann predictor it appears that these solutions, even though numerically excellent, might well be far from reality. Only if the energy of the relevant conformations is appropriately taken into account, as in the case of the Boltzmann predicting scheme, will a somewhat more realistic view be gained. We feel that

Figure 10. Conformations of **2** ranked according to increasing energy

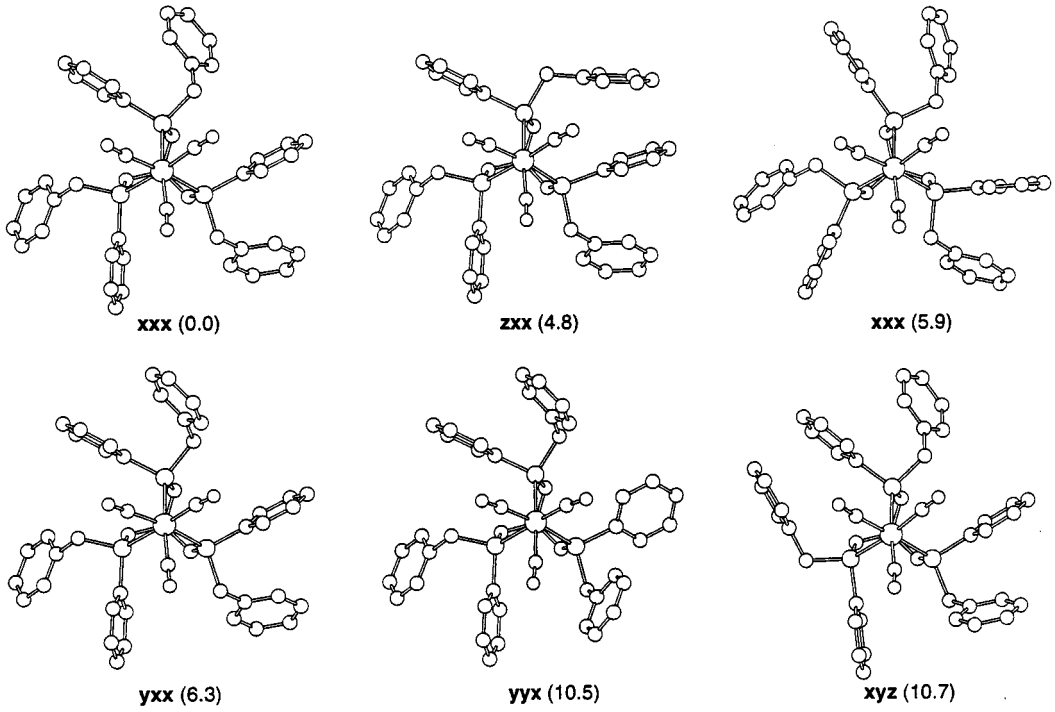

[a] From the complete set of minimum energy conformations as obtained by an exhaustive conformational search applying the parameter set *mm2f* those members are selected for which a specific arrangement (**x**, **y**, **z**, see Figure 8) of a benzyl group is first observed when scanning through these conformations in the direction of increasing energy.

Table 3. Proton-proton distances in **2** as determined by NOE analysis (solution) and X-ray analysis (single crystal) in comparison with these distances as calculated from the force field approach. Meaning of abbreviations see Figure 11 and legend to Table 1

proton 1	**proton 2**	d_{NOE} [Å]	$d_{X\text{-}ray}$ [Å]	$d_{Boltzmann}$ [Å] *mm2f*	*mm2t*
Pho	Bzo	3.16(7)	2.91(0)	3.21	3.48
Pho	BzB	2.73(5)	2.60(1)	2.89	3.11
Pho	MeB	2.18(6)	1.95(1)	2.23	2.38
Pho	MeA	2.41(5)	2.23(1)	2.44	2.58
Bzo	BzB	2.63(5)	2.53(1)	2.73	2.84
Bzo	BzA	2.53(5)	2.23(2)	2.73	2.83
Bzo	MeB	2.60(8)	3.16(1)	3.20	3.19
Bzo	MeA	2.62(3)	2.55(1)	2.50	2.63
BzA	MeA	2.89(4)	2.67(1)	3.01	3.12
rms	[Å]	–	0.28	0.24	0.33

Figure 11. Projection of the structure of **2** onto the plane defined by the three phosphorus atoms. The numbering scheme used throughout is indicated, as is the configuration at the phosphorus centers for the (*RRR*) enantiomer of the racemic pair of **2** studied

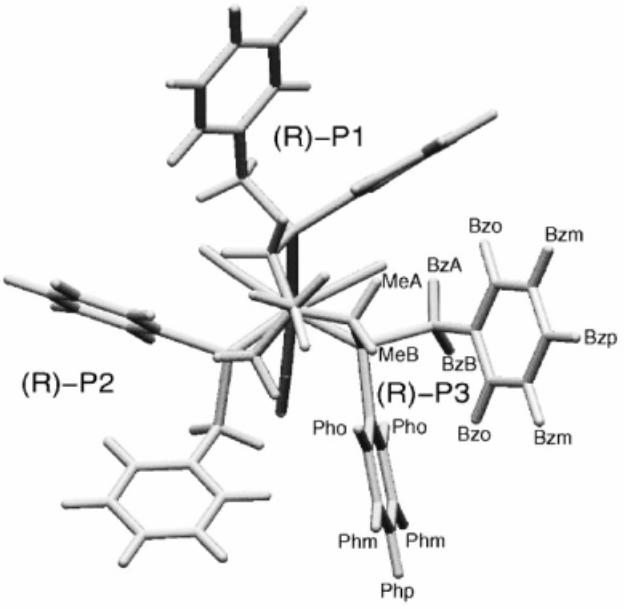

the approach taken here, while taking away the simple and aesthetically appealing picture of just one dominating conformation, is perhaps more relevant in a physical sense.

Force field based approaches to evaluate NOE distances of conformationally flexible coordination compounds had of course already been used. In this context C. R. Landis has described a very thorough attempt to derive the conformational flexibility of a series of catalytically relevant rhodium complexes containing chiral biphosphines[12] as well as of other coordination compounds.[13] His use of the force field approach is, however, restricted to an a posteriori fit of observed NOE distances to weighted averages of force field derived conformations. These conformations are in turn obtained by clustering individual conformations to a tractable number of average conformations. It was observed, as it is in this paper, that linear combinations of the conformations may be found that neatly reproduce the observed NOE′s. In such an approach any information about the relative energies of the conformations is com-

pletely neglected. No attempt to incorporate these force field derived energies is made. In contrast, in the present paper an a priori prediction of the expected NOE distances is made using all the conformations as well as their energies as given by the force field. With the above caveat in mind the physical relevance of these two approaches might be quite different.

Compound 3

Having been made curious by the results obtained so far, a third molecule (**3**) was analysed by the same type of procedure. Compound **3** is an analogue of **2**: it is a chiral compound, the racemate of which has been analysed. The configuration at each of the three chiral phosphorus centers in **3** is the same (the situation is analogous to the one in **2**). The phenyl substituents at the phosphorus centers in **2** are replaced by 3,5-$Me_2C_6H_3$ residues in **3**. A complete conformational search applying the procedures as already described (see Table 2) reduced the set of 3912 starting conformations to 158 (*mm2f*) or 104 (*mm2t*) conformations corresponding to minimum energy positions on the hypersurface. The conformation of **3** as observed in the solid state is reproduced by these calculations as the global minimum with an rms difference of only 0.46 Å (*mm2f*). The parameter set mm2t gives an equally good agreement (rms = 0.46 Å). The difference between the two estimates (*mm2f* / *mm2t*) is only 0.09 Å.

If the NOE data are compared with the appropriate H···H distances characterising the global minimum conformation, an rms agreement of 0.27 Å is observed (Figure 12, Table 4).

Figure 12. Projection of the structure of **3** onto the plane defined by the three phosphorus atoms. The numbering scheme used throughout is indicated, as is the configuration at the phosphorus centers for the (*RRR*) enantiomer of the racemic pair of **3** studied

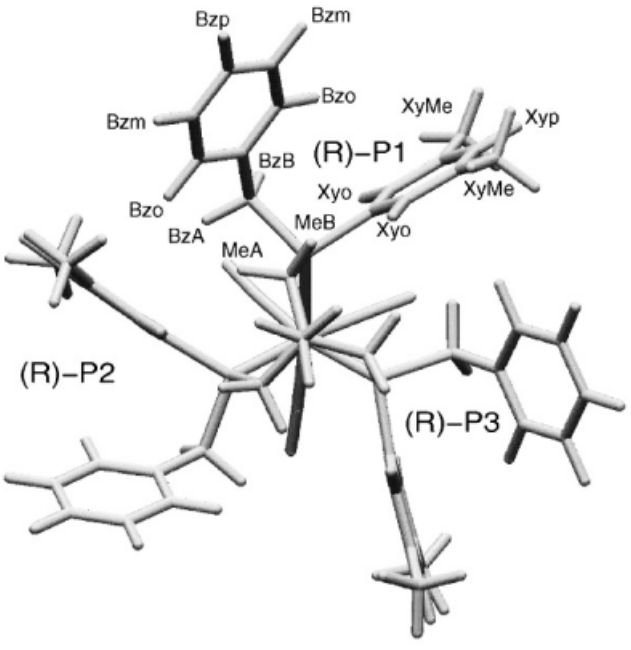

Table 4. Proton-proton distances in **3** as determined by NOE analysis (solution) and X-ray analysis (single crystal) in comparison with these distances as calculated from the force field approach. Meaning of abbreviations see Figure 12 and legend to Table 1

proton 1	**proton 2**	d_{NOE} [Å]	$d_{X\text{-}ray}$ [Å]	$d_{Boltzmann}$ [Å] *mm2f*	*mm2t*
Xyo	MeA	2.36(9)	2.51(1)	2.25	2.26
Xyo	MeB	2.00(7)	2.06(1)	2.07	2.16
Xyo	BzA	2.94(11)	3.24(1)	2.83	3.45
Xyo	BzB	2.54(9)	2.68(1)	2.68	2.74
Xyo	Bzo	2.82(12)	3.12(0)	2.95	3.12
Bzo	BzB	2.42(9)	2.43(1)	2.58	2.64
Bzo	MeA	2.63(10)	2.54(1)	2.35	2.39
Bzo	MeB	2.64(10)	2.87(2)	2.98	3.18
Bzo	BzA	2.43(9)	2.32(2)	2.56	2.58
Bzo	XyMe	2.96(11)	2.52(0)	2.60	2.72
MeA	XyMe	3.29(14)	3.83(1)	3.73	3.93
BzA	MeA	2.83(13)	2.63(4)	2.83	2.85
rms	[Å]	–	0.27	0.24	0.34

A Boltzmann-weighted average taken over the whole conformational ensemble leads to rms values of 0.24 Å (*mm2f*) and 0.34 Å (*mm2t*). The hypothesis that it is the ensemble of conformations and not just the one global minimum conformation that gives rise to the observed NOE distances is therefore acceptable. The distribution of rms values given in Figure 6 (**3**) shows that the solution obtained by applying the Boltzmann weighting scheme (calc) has a high level of significance. It is interesting to note that in the case of **3**, in a similar way to the findings made for **2**, there are pairs of conformations that, irrespective of their relative energy, are able to reproduce the experimental findings when used in appropriately weighted combinations. The best pair of such combinations leads to an rms value of only 0.14 Å (*mm2f*) even though the relative energies of the two contributing conformations are computed well above the global minimum (conformation 1: 42%, E_{rel} = 0.0 kJ/mol; conformation 2: 58%, E_{rel} = 24.8 kJ/mol). The best single conformation still gives an rms of 0.24 Å (E_{rel} = 7.5 kJ/mol). This may again be taken as a warning against the application of a merely distance based search procedure that does not appropriately account for the energetic distribution. This warning of course applies to the analysis of highly flexible molecules that are neither thermodynamically nor kinetically trapped in just one single conformation. When this happens, as is usually observed for proteins, the dimensionality of the problem is reduced and a distance based approach will generally lead to one statically correct solution as soon as there are enough NOE data points available to uniquely define the topology.[4]

For flexible small molecules the approach taken here appears to be a more reliable one as compared to mere distance geometry calculations. However, a prerequisite for this approach to work is a force field approximation that reproduces the molecular conformations on an energy hypersurface that is not distorted too far from reality.

Assessment of the Force Fields

Two sets of parameters describing the interactions involving the molybdenum heavy atom were applied in the work described in this paper. Both of these sets had been derived by an optimisation procedure involving Genetic Algorithms[1] on the basis of a large number of solid state conformations. It had already been argued[1] that the parameter set *mm2t* which, as an extension of the *mm2f* set, includes a number of torsional parameters might not be too reliable in view of the insufficient variance of the data basis with respect to these variables.[1] It is now found that in the analysis of **1**−**3** there is a tendency (Tables 1, 3, 4) for the *mm2f* set to better reproduce the experiments. While the static structures, i.e. individual conformations, are closely equivalent when calculated with the two sets of parameters, the dynamic situation analysed in this paper is better reproduced by the *mm2f* parameter set. This means that the energy scales produced by the two sets are different and the one implied by *mm2f* is the more realistic one.

The quality of fit obtained in modelling NOE distances suggests that the relative energies according to which the conformations are sorted by the force field are somehow on scale to reality. Otherwise an agreement such as that observed would not be expected. A more rigorous validation of the statement that the force field correctly assigns relative energies would of course consist in directly comparing energy differences accessible to measurement with their force field derived counterparts. The result of such a test will be described in a forthcoming paper.

Conclusion

With the force field approach used minimum energy conformations are correctly reproduced. It is found that the solid state structures of **2** and **3** correspond to conformations at globally minimal energy. The rms deviation of observed (X-ray) and calculated structures is less than 0.5 Å in each case.

It is observed that the average distances as determined for molecules **1**−**3** by NOE techniques are well reproduced by the force field model. While it is always possible to find weighted linear combinations of conformations that will reproduce the NOE distances, and while even one single conformation irrespective of its energy might give a good fit to the NOE data by an a posteriori analysis, the method reported here makes use of an a priori predictor: a Boltzmann weighted average taken over all conformations that correspond to minima on the relevant hypersurfaces will predict NOE distances with a highly satisfactory agreement. By a statistical analysis of the results obtained it is shown that the agreement achieved is far better than might be expected if it were a chance result. In fact the quality of the results obtained by applying the Boltzmann weighting scheme is estimated to have a statistical probability of below 3 in 100 000, lending considerable significance to the predictor as applied. The fact that this is so is in favour of the statement that the force field approach as applied does correctly place the conformations in space as well as in energy on the molecular hypersurface. It is also evident, however, that more stringent analyses with a more direct experimental access to energy differences have to be performed in order to independently justify the use of the approach reported.

We gratefully acknowledge financial support from the *Deutsche Forschungsgemeinschaft*, the *Fonds der Chemischen Industrie*, and the *Hermann-Schlosser-Foundation.*

Experimental Section

NMR Analysis: Compounds **1**−**3** were obtained as previously described.[5][6] All measurements were carried out with a Bruker DPX200 (200.130 MHz, 50.323 MHz, and 81.014 MHz for ^{1}H, ^{13}C, and ^{31}P, respectively). For ^{1}H- and ^{13}C-NMR spectra CD_2Cl_2 was used as solvent ($\delta_H = 5.31$, $\delta_C = 53.8$), TMS as external standard, for ^{31}P NMR 85% H_3PO_4 ($\delta = 0$) as external standard. For NMR analysis almost completely saturated solutions of the compounds in CD_2Cl_2 sealed in nmr tubes under argon were used. Unequivocal assignment of all the ^{1}H, ^{13}C, and ^{31}P resonances was performed by a combination of 1D and 2D experiments[14] ({^{1}H-^{13}C}-HMQC,[15] {^{1}H-^{13}C}-HMBC,[16] DQF-COSY,[17] TOCSY[18]). Experimental conditions are listed in Table 5. Assignment and shifts of the ^{1}H-NMR signals of compounds **1**−**3** are given in Table 6.

Two dimensional NOE measurements[19] were performed for each compound at a number of different mixing times. As an example the spectrum obtained for **3** with a mixing time of 200 ms is shown in Figure 13.

Figure 13. NOESY spectrum of **3** with 200 ms mixing time. The section referring to the arene protons is shown in the inlay in a magnified form. The numbers given in the diagram also refer to Table 7. Black: negative signals; grey: positive signals

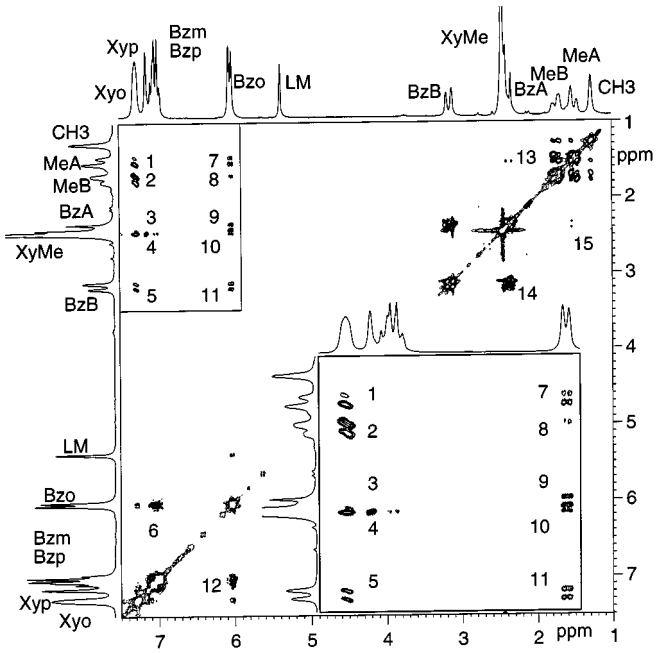

In general, the two integral values[20] thus obtained for each correlation were found to be in good agreement. In some cases the value of the integral taken from below the main diagonal was found to be definitely smaller than the one taken from above it. This discrepancy is a systematic one and indicates that, in those cases

where it appeared, the relaxation time was insufficient to allow for a complete relaxation. This will always lead to integrals that are smaller than the maximum obtainable by one NOE effect and it is therefore good practice to take the above diagonal value as the more appropriate data. The initial slope of integral value versus mixing time was evaluated in each case. Correlation coefficients were generally better than 95% (Figure 14) but occasionally coefficients as low as 70% were obtained.

Figure 14. Evolution of NOE cross polarisation with mixing time. The Figure refers to **3** with the pairs Xyo-MeB (upper trace) and Xyo-MeA (lower trace) as two examples

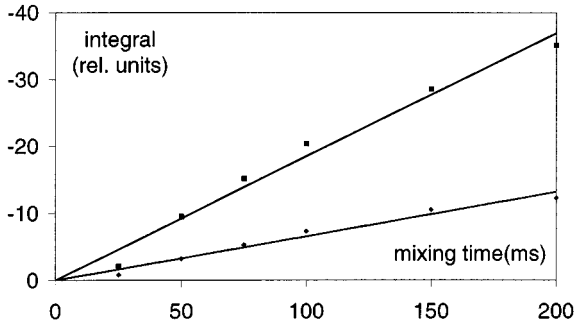

were analysed by three different approaches and the results of these are given in Table 7.

In one approach all the slopes were transformed into distances using the Bzm-Bzo reference (Table 7, aromatic reference). Transformation of the same data using the BzA-BzB distance for all data led to a slightly different set of distances (Table 7, aliphatic reference). In yet another approach the reference distance taken from the arene protons was applied to contacts between aromatic protons. The CH_2 reference distance was applied to contacts between aliphatic protons. Distances between aliphatic and aromatic protons were evaluated by applying the mean between the constants derived from the arene and from the methylene references (Table 7, individual reference). The spread of distances thus calculated (Table 7) from three different systematic approaches is a kind of a measure of the systematic error introduced by the systematically different procedures of evaluation. It is seen that for individual distances the maximum deviation between the three estimates amounts to around 0.3 Å. The average deviation between the three estimates is only $\sigma = 0.1$ Å in the mean. This is in agreement with the estimate of the reliability of the NOE distances determined for **1**−**3** as inferred from the calculus of error propagation. By whatever means an estimate for the reliability of the NOE derived dis-

Table 5. Setup of NMR experiments

2D-Experiment	**{^{13}C-^{1}H}-HMQC** [15]	**{^{13}C-^{1}H}-HMBC** [16]	**DQF-COSY** [17]	**TOCSY**[18]	**NOESY**[19]
Pulse Program[a]	invbtp	inv4lplrnd	cosydftp	mlevtp	noesytp
Spectral Width F_2 [Hz]	1302	1302	1302	1302	1302
Time Domain F_2 [Word]	2 K	2 K	2 K	2 K	2 K
Size F_2 [Word]	1 K	1 K	2 K	1 K	1 K
Spectral Width F_1 [Hz]	6039	6039	1302	1302	1302
Time Domain F_1 [Word]	512	512	512	256	256
Size F_1 [Word]	1 K	1 K	1 K	512	512
Scans	44	44	32	32	32
Mixing Time [ms]	250	60	−	125	10−1400
Relaxation Delay [s]	2	2	1.5	1.0	2

[a] The acronyms in this row refer to pulse sequences supplied under these names for the BRUKER series of instruments.

As far as the distances pertinent to the slopes in each case are concerned, this uncertainty is not dramatic because the physics of the NOE process are such that the distances are proportional to the sixth root of the slopes. Application of the laws of error propagation to the data sets obtained shows that the maximum error inferred from the uncertainty in the slopes is less than 0.1 Å in every case. Reference distances are needed in order to transform the values obtained for the slopes into estimates of proton-proton distances. There are up to three possible choices for such distances for the compounds **1**−**3**: as a standard tool of the absolute assessment of distances, the distance between two vicinal methylene protons at a CH_2 group is often used. This type of reference distance is available for all three compounds (CH_2 in the chelate cage, CH_2 of the benzyl groups, standard value: 1.75 Å). Another standard tool which is often used as an absolute reference is the distance between the protons at *o*- and *m*-positions of a six membered arene ring (accepted standard value: 2.45 Å). The data for compound **1** were evaluated using: Bz2A-Bz2B, Bz3A-Bz3B, Bz1o-Bz1m, Bz2o-Bz2m, Bz3o-Bz3m. The NOE distances of compound **2** were evaluated on the basis of the methylene distance BzA-BzB (Figure 11) as well as on the basis of the Bzo-Bzm distance.

For compound **3** the same type of two different reference distances was used. In order to develop a feel for the reliability of the distances obtained by the different ways of evaluation, the data tances is made, this estimate is around 0.1 Å on average. Since there is no a priori argument as to which of the three approaches applied to evaluate the data should be preferred, the mean of the three estimates[21] was considered throughout (Table 7, average) when experimental and modelled distances had to be compared. The data are thus good enough to allow for the assessment of the force field approach as described.

Force Field Calculations: The commercial program set MacroModel[22] was used for the calculations throughout. Starting conformations were generated using a program, written in C, for this purpose.[1] The torsion angles used to define these conformations have the following meanings (see Figure 3):

φ: torsion angle Du−P−C_{ipso}−C_{ortho} with the position of the Dummy atom Du generated and defined as given[1]

τ: torsion angle Mo−P−$C_{methylene(cage)}$−C

ω: torsion angle Du−P−$C_{methylene(benzyl)}$−C_{ipso}

ψ: torsion angle P−$C_{methylene(benzyl)}$−C_{ipso}−C_{ortho}.

To avoid entangling of individual groups in the starting conformations as well as during refinement, a rubberband protocol was used.[12] The P−C bonds radiating to the phenyl and benzyl substituents respectively were stretched to an initial value of 4 Å with the direction of these bonds unchanged. For the purpose of refine-

Table 6. ^{1}H-NMR data for compounds **1**–**3**

Nucleus	Molecule 1 Group 1[a]	Molecule 1 Group 2[a]	Molecule 1 Group 3[a]	Molecule 2	Molecule 3
Me	———	1.32 (bs, 3 H, [2.1])[f]	———	1.24 (bs, 3 H)	1.23 (bs, 3 H)
MeA	1.83–2.10 (m, 4 H, $^2J_{HH}$ 16.0)[b], [e]	1.42–1.58 (m, 2 H, $^2J_{HH}$ 16.0)[b]	1.83–2.10 (m, 4 H, $^2J_{HH}$ 16.0)[b], [e]	1.57 (d, 3 H, $^2J_{HH}$ 13.0)	1.46 (d, 3 H, $^2J_{HH}$ 15.0)
MeB				1.76 (d, 3 H, $^2J_{HH}$ 13.0)	1.64 (d, 3 H, $^2J_{HH}$ 15.0)
BzA	3.46 (dd, 1 H, $^2J_{HH}$ 14.0, [3.9])[c]	2.88 (dd, 1 H, $^2J_{HH}$ 14.6, [2.9])[c]	3.58 (dd, 1 H, $^2J_{HH}$ 14.4, [3.8])[c]	2.38 (d, 3 H, $^2J_{HH}$ 14.0)	2.32 (d,3 H, $^2J_{HH}$ 14.0)
BzB	3.31 (dd, 1 H, $^2J_{HH}$ 14.0, [2.4])[c]	2.38 (d, 1 H, $^2J_{HH}$ 14.6)	3.19 (d, 1 H, $^2J_{HH}$ 14.4)	3.13 (d, 3 H, $^2J_{HH}$ 14.0)	3.11 (d, 3 H, $^2J_{HH}$ 14.0)
Pho/Xyo	7.18–7.22 (m, 2 H)[g]	6.95–7.03 (m, 8 H)[e], [g]	7.63–7.78 (m, 2 H)[g]	7.61 (bs, 6 H)[g]	7.28 (bs, 6 H) [Xyo][g]
Phm/XyMe	6.95–7.03 (m, 8 H)[d], [e], [g]	6.95–7.03 (m, 8 H)[d], [e], [g]	7.45–7.55 (m, 3 H)[d], [g]	7.41–7.58 (m, 9 H)[d], [g]	2.39 (s, 18 H) [XyMe][g]
Php/Xyp					7.27 (s, 3 H) [Xyp][g]
Bzo	6.65 (d, 2 H, $^3J_{HH}$ 4.0)	5.97 (d, 2 H, $^3J_{HH}$ 7.0)	6.46 (d, 2 H, $^3J_{HH}$ 5.4)	5.95 (d, 6 H, $^3J_{HH}$ 7.2)	5.97 (d, 6 H, $^3J_{HH}$ 7)
Bzm, Bzp	7.05–7.12 (m, 9 H)[d]	6.83–6.93 (m, 9 H)[d]	7.12–7.18 (m, 9 H)[d]	6.89–7.12 (m, 9 H)[d]	6.91–7.15 (m, 9 H)[d]

[a] The three $CH_2P(Ph)(Bzl)$ groups of **1** are chemically different. Refering to the designators given in Figure 2, data given in row "nucleus xyz" and column "group i" refer to proton xyiz, e.g. the data in the line MeA and the column "group 1" refer to the Me1A. For **2** and **3** these groups are chemically equivalent. – [b] Higher order multiplets, $^2J_{HH}$ coupling constants were determined by DQF-COSY experiments. – [c] The $^2J_{PH}$ coupling-value is given in square brackets. – [d] Higher order multiplets, see for example Bzm, Bzp, Figure 13. The NOE′s observed in this spectral range are by virtue of the geometry of the compounds (Figures 1, 11, 12) due to the dipolar interactions with the *meta*-protons in each case. – [e] Signals of individual groups overlap. – [f] The $^4J_{PH}$ coupling-value is given in square brackets. – [g] The value is given for the phenyl-protons Pho, Phm, or Php respectively; the xylyl-protons are marked by "xyz" in square brackets

Table 7. Dependence of the NOE distances of **3** on relevant reference distances[a]

crosspeak No.	interaction	slope	distance estimates [Å] aromatic reference	aliphatic reference	individual reference	average
1	Xyo/MeA	0.073(2)	2.46(3)	2.25(5)	2.37(3)	2.36(9)
2	Xyo/Meb	0.193(3)	2.09(3)	1.91(5)	2.01(3)	2.00(7)
3	Xyo/BzA	0.020(1)	3.06(3)	2.80(5)	2.95(3)	2.94(11)
4	Xyo/XyMe	0.048(2)	2.64(3)	2.41(5)	2.54(3)	2.53(9)
5	Xyo/BzB	0.047(5)	2.65(3)	2.42(5)	2.55(3)	2.54(9)
6	Xyo/Bzo	0.027(2)	2.90(3)	2.65(5)	2.90(3)	2.82(12)
–	Xyp/XyMe	0.049(1)	2.63(3)	2.40(5)	2.53(3)	2.52(9)
7	Bzo/MeA	0.038(7)	2.75(4)	2.51(6)	2.64(4)	2.63(10)
8	Bzo/MeB	0.037(11)	2.76(6)	2.52(7)	2.65(5)	2.64(10)
9	Bzo/BzA	0.061(5)	2.53(3)	2.31(5)	2.44(3)	2.43(9)
10	Bzo/XyMe	0.019(3)	3.09(4)	2.83(5)	2.97(4)	2.96(11)
11	Bzo/BzB	0.063(9)	2.52(3)	2.31(5)	2.43(3)	2.42(9)
12	Bzo/Bzm	0.075(11)	2.45(4)	2.24(5)	2.45(4)	2.38(10)
13	BzA/MeA	0.022(3)	3.00(4)	2.74(5)	2.74(3)	2.83(13)
14	BzA/BzB	0.328(74)	1.91(5)	1.75(6)	1.75(5)	1.80(8)
15	MeA/XyMe	0.009(3)	3.49(6)	3.19(7)	3.19(6)	3.29(14)

[a] Crosspeak refers to the numbering scheme shown in Figure 12; the numbers refer to the numbers assigned to individual crosspeaks (Figure 13). Slope derived from measurements at different mixing times; the numbers in brackets refer to the standard deviation in terms of the least significant digit given in each case. Aromatic reference: The Bzm-Bzo distance (Figure 12) is used throughout. Aliphatic reference: The BzA-BzB distance (Figure 12) is used throughout. Individual reference: The reference distances BzA-BzB (aliphatic) and Bzm-Bzo (aromatic) are used where appropriate. For contacts between aromatic and aliphatic protons the mean between the two estimates is taken. The integrals of the crosspeaks were interpreted with reference to the mean of the two estimates. The numbers given in brackets for these three columns refer to the standard deviations inferred from the standard deviations of the slopes. Average designates the mean derived from the three values in the three columns at left; the numbers in brackets are the root mean square deviations from the mean.

ment these artificial restraints were reduced in a stepwise manner: reducing the distance after every hundred iterations to values of 3 Å, 2.5 Å, and 2.1 Å. The force constants referring to the artificially elongated bonds were set at 100.0, 175.18, 583.4, 1166.7 kJ/Å^2 mol in the sequence given. In the last step, now applying the original P–C equilibrium bond length and the original force constants using the *mm2f* / *mm2** force field (1166.7 kJ/mol = 2.91 mdyn/Å), refinement was performed without constraints (convergence criteria: maximum number of iterations = 99 999, convergence gradient: 0.01 Å/iteration).

The Polak Ribiere Conjugate Gradient algorithm was used for energy minimisation.[23]

In each case the refinement resulted in a largely reduced number of different conformations, each of which corresponding to at least a local minimum (for exact numbers: see text). Once all the conformations were known, the following procedure was applied: for each of the conformations the NOE relevant distances were extracted in the following way: whenever a pair of protons to which the NOE measurement refers could be uniquely assigned, the distances rel-

evant to such pairs were calculated. In those cases where the nmr experiments could not differentiate between constitutionally equivalent sets of protons, as for instance in the case of the conformationally diastereotopic pair of *ortho*-protons at a phenyl residue or, in some cases, for the configurationally diastereotopic protons at a methylene position, the shortest contact amongst the set of experimentally indiscernible contacts of this type was used. Whenever configurationally equivalent, but conformationally different groups were analysed, e.g. PBzPh in **2**, all the contacts relevant to these groups were calculated and again the shortest one was taken as the representative. This means that contacts involving the methyl groups of the 3,5-xylyl groups in **3** were extracted by calculating up to 72 individual distances. This number results from the fact that three methyl protons have to be considered for each individual methyl group; there are six such groups representing a total of 18 different methyl proton positions. If these protons are involved in contacts to *ortho*-hydrogens of the benzyl groups, two positions of these protons at the left hand side as well as on the right hand side are potential candidates thus multiplying the number of possible origins of the protons which may be at three different fixed positions, to a total of $18 \times 4 = 72$.

The diastereotopic protons at the CH_2 constituents of the chelate cages, as well as of the CH_2 phenyl substituents, had been uniquely assigned in the nmr experiments with the exception of the protons Bz1A/B (Figure 2) and Me2A/B (Figure 2) for compound **1**. Independent of this assignment, which had been possible in most cases, the analysis of contacts involving these groups was done without incorporating this specification. All possible combinations corresponding to a specific assignment referring to these groups were evaluated in each case. The quality of the assignment was judged by calculating a Boltzmann weighted average over all conformations with this specific assignment and comparing the predicted distances with the observed ones. For compounds **2** and **3** the assignment as originally deduced from nmr analysis was reproduced by this procedure. With compound **1** the situation is more difficult due to its low symmetry. The best fit was obtained with the assignment shown in Figure 2. To evaluate the sums of states a temperature of $T = 300$ K was used throughout in accordance with the measuring temperature of the NOE experiments.

In order to answer the question of how well the NOE distances might be reproduced on the basis of a combination of just a few conformations, a program was written to find the best linear combination of the weights with which these conformations will contribute. The constraint that the sum of the weights has to add up to one has been incorporated in terms of a Lagrangean multiplier.[24][25]

In order to optimise the structure of compound **2** in its crystal environment, the complete set of those 19 molecules in its neighbourhood was selected for which at least one contact to the given molecule is shorter than 8 Å (Figure 8). This environment was fixed to the coordinate values found in the crystal structure and the selected molecule that is embedded by this crystal surrounding was refined. The crystal environment was generated by using the appropriate feature in the MSI program package, refinement was performed by using MacroModel. The calculations were carried out on two Silicon Graphics Indigo^2 MIPS R4400 workstations, 200 MHz, 128 MB RAM, operating under IRIX 5.3.

☆ Dedicated to Professor *Hans Bock* on the occation of his 70th birthday.

[1] J. Hunger, S. Beyreuther, G. Huttner, U. Radelof, K. Allinger, *Europ. J. Inorg. Chem.* **1998**, 693−702.
[2] F. Anet, A. Bourn, *J. Am. Chem. Soc.* **1965**, *87*, 5250−5251.
[3] K. Wüthrich, *Acta Cryst. D* **1995**, *51*, 249−270.
[4] The volumes of *nature structural biology* demonstrate the continously increasing number of protein structures which have been solved by NMR techniques.
[5] O. Walter, T. Klein, G. Huttner, L. Zsolnai, *J. Organomet. Chem.* **1993**, 63−81.
[6] M. Büchner, G. Huttner, U. Winterhalter, A. Frick, *Chem. Ber.* **1997**, *130*, 1379−1392.
[7] A. E. Torda, W. F. v. Gunsteren, in K. B. Lipkowitz, D. B. Boyd (Eds.): *Reviews in Computational Chemistry*, *Vol. 3,* VCH Publishers, Inc., New York **1992**, p. 143−172.
[8] J. M. Blaney, J. S. Dixon, in K. B. Lipkowitz, D. B. Boyd (Eds.): *Reviews in Computational Chemistry*, *Vol. 5,* VCH Publishers, Inc., New York **1994**, p. 299−335.
[9] For a recent application of distance geometry methods see H. Steinhagen, M. Reggelin, G. Helmchen, *Angew. Chem.* **1997**, *109*, 2199−2202. For molecular dynamics simulations which make use of distance constraints as well as of constraints derived from a Boltzmann weighting scheme see: J. Fennen, A. E. Torda and W. F. van Gunsteren, *Journal of Biomol. NMR*, **1995**, 6, 163−170.
[10] The underlying assumption is of course that the system is in its thermodynamic equilibrium. For the compounds studied this means that none of the rotations of either phenyl or benzyl groups is slowed down to such an extent that this assumption would not be valid. For the present case complete dynamic equilibration of the conformers is observed on the NMR time scale.
[11] S. Beyreuther, J. Hunger, G. Huttner, S. Mann, L. Zsolnai, *Chem. Ber.* **1996**, *129*, 745−757.
[12] J. S. Giovannetti, C. M. Kelly, C. R. Landis, *J. Am. Chem. Soc.* **1993**, *115*, 4040−4057.
[13] [13a] C. P. Casey, S. L. Hallenbeck, J. Monty Wright and C. R. Landis, *J. Am. Chem. Soc.* **1997**, 119, 9680−9690. – [13b] C. Landis, V. Allured, *J. Am. Chem. Soc.* **1991**, 113, 9493−9499.
[14] [14a] T. Dierks, Diplomarbeit, Heidelberg **1995**. – [14b] S. Cunskis, Diplomarbeit, Heidelberg **1996**.
[15] A. Bax, R. H. Griffey, B. L. Hawkins, *J. Magn. Reson.* **1983**, *55*, 301−315.
[16] A. Bax, M. F. Summers, *J. Am. Chem. Soc.* **1986**, *108*, 2093−2094.
[17] M. Rance, O. W. Sørensen, G. Bodenhausen, G. Wagner, R. R. Ernst, K. Wüthrich, *Biochem. Biophys. Res. Commun.* **1983**, *117*, 479−485.
[18] L. Braunschweiler, R. R. Ernst, *J. Magn. Reson.* **1983**, *53*, 521−528.
[19] [19a] J. Jeener, B. H. Meier, P. Bachmann, R. R. Ernst, *J. Chem. Phys.* **1979**, *69*, 4546−4553. – [19b] D. Neuhaus, M. Williamson, *The Nuclear Overhauser Effect in Structural and Conformational Analysis*, VCH, New York, **1989**.
[20] XWIN-NMR 1.3, Bruker, **1995**.
[21] "*Medio tutissimus ibis"*, Ovid, *Metamorphoses*, II, 137.
[22] The *mm2* force field as implemented in Macromodel 5.0 (*mm2**) has been used throughout (see F. Mohamadi, N. G. J. Richards, W. C. Guida, R. Liskamp, M. Lipton, C. Caufield, G. Chang, T. Hendrickson, W. C. Still, *J. Comp. Chem.* **1990**, *11*, 440−467).
[23] E. Polak, G. Ribiere, *Revue Francaise Informat. Recherche Operationelle* **1969**, *16*, 35.
[24] P. S. Shenkin, D. L. Yarmush, R. M. Fine, H. Wang, C. Levinthal, *Biopolymers* **1987**, *26*, 2053.
[25] R. Courant, *Vorlesungen über Differential- und Integralrechnung. Zweiter Band. Funktionen mehrerer Veränderlicher*, *3rd* ed., Springer Heidelberg, **1955**.

[I98175]

Anionic Tetranuclear Platina-β-diketonates of Platina-β-diketones – Organometallic Analogues of Platinum Blue Complexes

Michael Gerisch[a], Clemens Bruhn[a], Andrea Porzel[b], and Dirk Steinborn*[a]

Institut für Anorganische Chemie der Martin-Luther-Universität Halle-Wittenberg[a],
Kurt-Mothes-Straße 2, D-06120 Halle (Saale), Germany
Fax: (internat.) +49 (0)345/5527028
E-mail: steinborn@chemie.uni-halle.de

Institut für Pflanzenbiochemie[b],
Weinberg 3, D-06120 Halle (Saale), Germany

Received June 24, 1998

Keywords: Metalla-β-diketones / Platinum / Bis(acyl)-bridged complexes / Platinum blues / Metal–metal interactions

The platina-β-diketone $[Pt_2\{(COMe)_2H\}_2(\mu\text{-}Cl)_2]$ (**1**) reacts with aliphatic amines [nBuNH$_2$, (iPr)$_2$NH, NEt$_3$], N-methylaniline, and N,N-dimethylaniline, as well as with strong bases, such as a proton sponge or [NMe$_4$]OH, in an equimolar ratio to give the anionic platina-β-diketonato complexes of platina-β-diketones $[BH]_2[\{Cl_2Pt(\mu\text{-}COMe)_2Pt[(COMe)_2H]\}_2]$ (**3**) {B = nBuNH$_2$ (**3a**), (iPr)$_2$NH (**3b**), NEt$_3$ (**3c**), PhNHMe (**3d**), PhNMe$_2$ (**3e**), $C_{10}H_6(NMe_2)_2$ [1,8-bis(dimethylamino)naphthalene] (**3f**) and $[NMe_4]_2[\{Cl_2Pt(\mu\text{-}COMe)_2Pt[(COMe)_2H]\}_2]$ (**3g**)}. All complexes were characterized by microanalysis, and by ^{1}H-NMR and IR spectroscopy. X-ray structure analyses reveal that in the solid state the complexes **3a** · 0.5 CH_2Cl_2 and **3g** · 2 CH_2Cl_2 consist of tetranuclear dianions with zigzag Pt_4 chains [Pt–Pt–Pt angle: 122.92(3)° (**3a**), 119.30(6)° (**3g**)]. The central Pt···Pt distances [**3a**: 3.171(1) Å, **3g**: 3.176(1) Å] give evidence for closed shell d^8-d^8 interactions. Thus, these bis(acyl)-bridged complexes can be regarded as organometallic analogues of platinum blue complexes.

The dinuclear platina-β-diketone $[Pt_2\{(COMe)_2H\}_2(\mu\text{-}Cl)_2]$ (**1**), prepared by the reaction of hexachloroplatinic(IV) acid with silyl-substituted acetylenes in n-butanol, proved to be an electronically unsaturated complex with a kinetically labile ligand sphere[1]. When compared to Lukehart's mononuclear metalla-β-diketones $[L_xM\{(COR)_2H\}]$ (**A**)[2] (L = CO, Cp; M = Mo, W, Mn, Re, Fe, Os), which are electronically saturated and kinetically stable complexes, the complex **1** exhibits a fundamentally different reactivity. These complexes **A** were shown to react with primary amines to give the corresponding metalla-β-ketoimines **B**[3] [Scheme 1(i)] and, after deprotonation (**A′**), with metal salts to give the metalla-β-diketonato metal complexes **C** [Scheme 1(ii) and (iii)][4]. Recently, we reported that the platina-β-diketone **1** reacts with aniline or p-toluidine to yield platina-β-diketonato complexes of platina-β-diketones $[\{(RNH_2)ClPt(\mu\text{-}COMe)_2Pt[(COMe)_2H]\}_2]$ (R = Ph **2a**, pMeC$_6$H$_4$ **2b**) [Scheme 1(iv)][5]. These complexes are neutral complexes containing tetranuclear zigzag Pt_4 chains in the solid state.

Here we report on the reaction of the platina-β-diketone **1** with primary, secondary, and tertiary aliphatic amines, and with N-methyl- and N,N-dimethylaniline as well as with strong bases such as a proton sponge and [NMe$_4$]OH, to give anionic platina-β-diketonato complexes of platina-β-diketones.

Scheme 1. (i) RNH_2; (ii) – H^+; (iii) $[L'_xM']^+$; (iv) 2 RNH_2 (– $[RNH_3]Cl$)

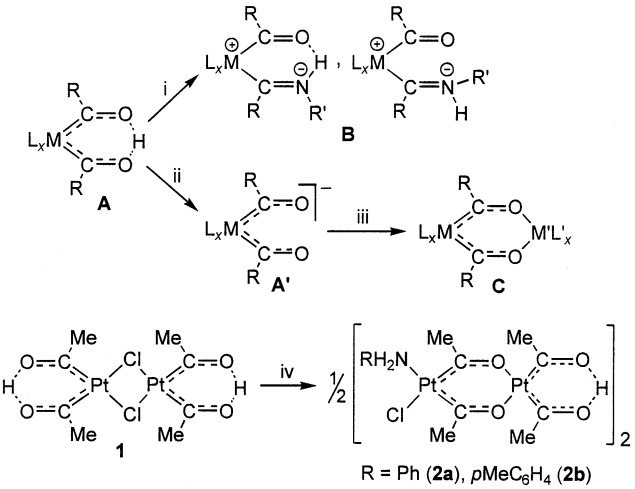

Results and Discussion

Treatment of $[Pt_2\{(COMe)_2H\}_2(\mu\text{-}Cl)_2]$ (**1**) with one equiv. of n-butylamine (nBuNH$_2$), diisopropylamine [(iPr)$_2$NH], triethylamine (NEt$_3$), N-methylaniline (PhNHMe), N,N-dimethylaniline (PhNMe$_2$), or the proton sponge 1,8-bis(dimethylamino)naphthalene [$C_{10}H_6$-(NMe$_2$)$_2$] in dichloromethane at ambient temperature af-

 © WILEY-VCH Verlag GmbH, D-69451 Weinheim, 1998 1434–1948/98/1111–1655 $ 17.50+.50/0

fords, in moderate to good yield (56−82%), the anionic platina-β-diketonato complexes of platina-β-diketones $[BH]_2[\{Cl_2Pt(\mu\text{-}COMe)_2Pt[(COMe)_2H]\}_2]$ [B = nBuNH$_2$ (**3a**), (iPr)$_2$NH (**3b**), NEt$_3$ (**3c**), PhNHMe (**3d**), PhNMe$_2$ (**3e**), $C_{10}H_6(NMe_2)_2$ (**3f**)] [Scheme 2(i)]. An analogous reaction carried out with tetramethylammonium hydroxide forms the complex $[NMe_4]_2[\{Cl_2Pt(\mu\text{-}COMe)_2Pt\text{-}[(COMe)_2H]\}_2]$ (**3g**) in a yield of 60% [Scheme 2(ii)]. No well defined products could be obtained with an excess of amines or [NMe$_4$]OH.

Scheme 2. (i) nBuNH$_2$, (iPr)$_2$NH, NEt$_3$, PhNHMe, PhNMe$_2$ or $C_{10}H_6(NMe_2)_2$ (1:1); (ii) [NMe$_4$]OH (1:1; − H$_2$O)

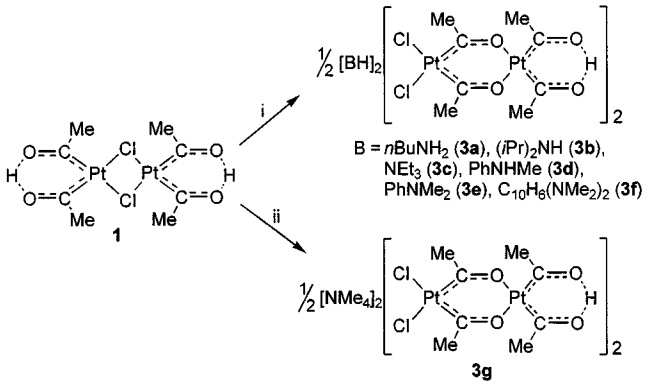

Complex **3a** was obtained as orange crystals and the complexes **3b**, **3c**, and **3f** were obtained as yellow, microcrystalline solids. The complexes **3d** and **3e** were isolated as orange rubberlike solids. After drying briefly, the complex **3g**·CH_2Cl_2 was obtained as orange crystals. All anionic platina-β-diketonato complexes of platina-β-diketones **3** are air-sensitive and decompose between 79 and 110°C. Thus, their thermal stability is similar to that of the neutral platina-β-diketonates of platina-β-diketones **2** [m.p. (dec) = 90−93°C][5], but smaller than that of the starting complex **1** [m.p. (dec) = 183 C][1]. In solution (CH_2Cl_2) complexes of **3** decompose at room temp. within less than 1 h, whereas at low temperatures (< −50°C) the solutions are stable over a period of one week.

Spectroscopic Investigations

At room temp. the ^{1}H-NMR spectra of the anionic complexes **3** show only one broad signal for the methyl protons ($\delta \approx 2.4$). With the exception of the complex **3d**, four methyl resonances are found at low temperatures (< −20°C). These methyl resonances form two pairs, the signals within each pair having the same intensity; and the ratio of intensities between the two pairs of signals being ca. 70:30 in all cases. Because all of the complexes are only slightly soluble in CD_2Cl_2 at −25°C, and due to the restricted thermal stability of these solutions, the carbonyl carbon atoms could not be detected by conventional ^{13}C-NMR spectroscopy. However, from the ^{1}H,^{13}C shift-correlation 2D-NMR spectra of **3g** via one (HMQC) and three bonds (HMBC), recorded at −25°C, the ^{13}C-chemical shifts of the four methyl groups and the corresponding four chemically inequivalent carbonyl carbon atoms (Figure 1) can be extracted and are found to be in in the range δ = 233.2−248.8.

Figure 1. HMBC spectrum of **3g** showing the range of the carbonyl carbon resonances

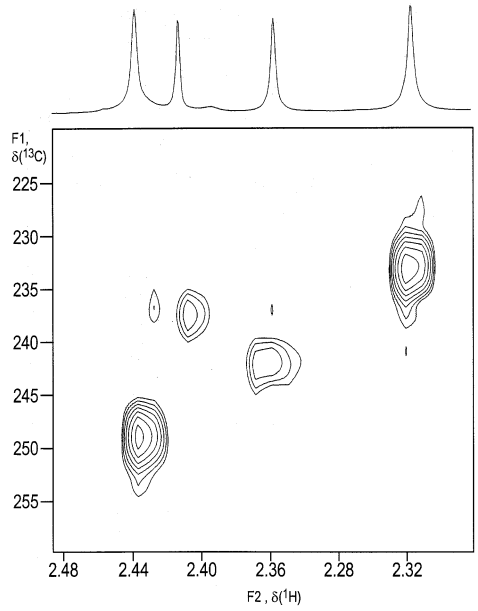

The temperature dependence of the ^{1}H-NMR spectra points to a dynamic process at room temp. and to the existence of two isomers at temperatures below −20°C. Taking into account the fact that the neutral complex **2b** is dinuclear in chloroform solution at room temp.[5], one isomer should be the dinuclear species **3′** (Scheme 3). **3′** could be in equilibrium with either the tetranuclear complex **3′′** (as was found in the solid state) or with the deprotonated starting complex **1′** (Scheme 3).

The proton resonances of the hydrogen-bonded hydrogen atoms in all anionic platina-β-diketonato complexes of platina-β-diketones **3** appear as a broad signal at $\delta \approx 20$, indicating a downfield shift of about 4 ppm with respect to the platina-β-diketone **1** ($\delta \approx 16$).

Two strong bands in the carbonyl region are found in the IR spectra of the complexes **3**: $\tilde{\nu}$ = 1524−1534 cm^{-1} for the bridging μ-acyl groups in the platina-β-diketonato unit and $\tilde{\nu}$ = 1552−1556 cm^{-1} for the platina-β-diketone unit. In the neutral complexes **2**, there were two bands observed at 1514 cm^{-1} and 1535 cm^{-1} for the bridging μ-acyl unit (the splitting is due to the unsymmetric coordination of the platinum centre) and one band at 1545 cm^{-1} (**2a**) and 1553 cm^{-1} (**2b**), for the platina-β-diketone unit. The C−O stretching vibration in the platina-β-diketone **1** also appears in this region ($\tilde{\nu}$ = 1548 cm^{-1}).

Crystal Structures

The crystal structures of **3a**·0.5 CH_2Cl_2 and **3g**·2 CH_2Cl_2 were obtained by X-ray diffraction analyses. The ORTEP diagram of the anion in **3g**·2 CH_2Cl_2 is shown in

Scheme 3. Possible isomers of the anion $[Cl_2Pt(\mu\text{-}COMe)_2Pt\{(COMe)_2H\}]^-$ (**3**) in solution

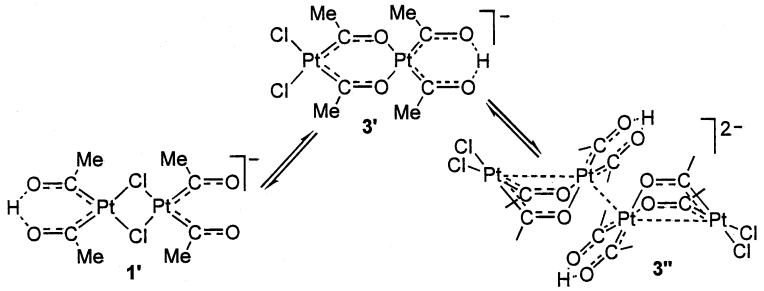

Figure 2. ORTEP-III plot[14] of the anion in **3g**·2 CH_2Cl_2[a], showing atom numbering (displacement ellipsoids at 30% probability); only the H atom in the hydrogen bridge is shown

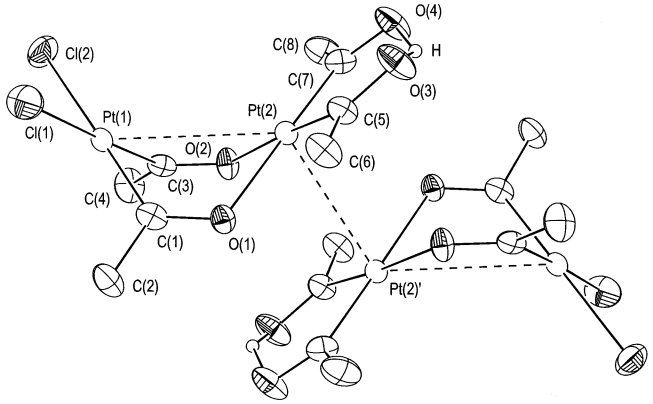

[a] Selected interatomic distances [Å] and angles [°]; values concerning **3a**·0.5 CH_2Cl_2 are given in square brackets: Pt(1)−Cl(1) 2.412(2) [2.417(4)], Pt(1)−Cl(2) 2.408(2) [2.424(4)], Pt(1)−C(1) 1.940(8) [1.91(1)], Pt(1)−C(3) 1.941(8) [1.96(1)], Pt(2)−C(5) 1.94(1) [1.90(2)], Pt(2)−C(7) 1.939(8) [1.93(1)], Pt(2)−O(1) 2.148(5) [2.139(7)], Pt(2)−O(2) 2.138(5) [2.129(8)], C(1)−O(1) 1.25(1) [1.26(1)], C(3)−O(2) 1.27(1) [1.26(2)], C(5)−O(3) 1.25(1) [1.27(2)], C(7)−O(4) 1.26(1) [1.25(2)], O(3)···O(4) 2.397(8) [2.40(2)], Pt(1)···Pt(2) 3.358(1) [3.336(1)], Pt(2)···Pt(2′) 3.176(1) [3.171(1)]; Pt(1)−Pt(2)−Pt(2′) 119.30(6) [122.92(3)], [Pt(1)Cl(1)Cl(2) C(1)C(3)]/[Pt(2)O(1)O(2)C(5)C(7)] 89.1(2) [89.6(3)].

Figure 2. The representation of the anion in **3a**·0.5 CH_2Cl_2 is not shown due to the close similarities to **3g**·2 CH_2Cl_2. Both complexes exhibit crystallographically imposed inversion symmetry. Bond lengths and bond angles of complexes **3a**·0.5 CH_2Cl_2 and **3g**·2 CH_2Cl_2 do not differ significantly. Minor differences were found in the Pt(1)···Pt(2) distance [**3a**: 3.336(1) Å, **3b**: 3.358(1) Å] and in the Pt(1)−Pt(2)−Pt(2′) angle [**3a**: 122.92(3)°, **3b**: 119.30(6)°].

Platinum is square-planar coordinated by two Cl and two C atoms, and by two O and two C atoms, respectively. The Pt−C bond lengths [1.90(1)−1.96(1) Å] and the C−O bond lengths [1.25(1)−1.27(2) Å] are in each case equivalent to within 3σ, and do not differ significantly from those in the platina-β-diketone **1** and in the neutral platina-β-diketonato complexes of platina-β-diketones **2** [d(Pt−C) = 1.95(1)−2.00(2) Å; d(C−O) = 1.21(3)−1.26(1) Å][1][5]. The Pt−O distances [2.129(8)−2.148(5) Å] and the Pt−Cl distances [2.408(2)−2.424(4) Å] are in the range of those observed in **2** [d(Pt−O) = 2.15(1)−2.18(1) Å; d(Pt−Cl) = 2.409(6)/2.390(4) Å]. The O···O distances in the intramolecular O···H···O bonds [**3a**: 2.40(2) Å, **3g**: 2.397(8) Å] are essentially the same as those in the complexes **1** and **2** [2.28(4)−2.37(2) Å].

As for the complexes **2**[5], complexes **3a**·0.5 CH_2Cl_2 and **3g**·2 CH_2Cl_2 are "head-to-head" dimers forming Pt_4 "zigzag" chains. Analogous Pt_4 units are found in platinum blue complexes that were first prepared (1908) by treating an aqueous solution of $[PtCl_2(MeCN)_2]$ with silver nitrate[6] and were structurally characterized (1977) as amidato bridged complexes especially by Lippard[7].

The conformations of the zigzag Pt_4 chains are very similar in all four complexes **2** and **3**. The Pt···Pt distances between the two central platinum atoms [**3a**: 3.171(1)/**3g**: 3.176(1) Å] indicate relatively strong closed shell d^8-d^8 interactions[8]. Similar values are observed in the "classical" platinum blue complexes with platinum in the average oxidation state of 2.0 [d(Pt···Pt) = 2.87−3.24 Å][9], and in platinum(II) complexes with columnar structures [d(Pt···Pt) = 3.09−3.60 Å][10].

In complexes **2** and **3** the coordination planes of Pt(1) and Pt(2) are inclined at angles of 76.4(4)°−89.6(4)°[11]. In the classical platinum blue complexes these angles are markedly smaller (18−40°)[7][9][12]. This may be due to the different numbers of bridging atoms (two in complexes **2** and **3** vs. three in the platinum blue complexes). In accordance with this, the Pt(1)−Pt(2)−Pt(2′) angles in complexes **2** and **3** are distinctly smaller than in the platinum blues [119.30(6)−127.52(3)° vs. 158−170°][7][9][12]. Furthermore, in all complexes **2** and **3,** the central Pt···Pt distances {mean value d[Pt(2)···Pt(2′)] = 3.171 Å} are shorter than the distances between the ligand-bridged platinum atoms {mean value d[Pt(1)···Pt(2)] = 3.284 Å}. The reverse order is observed in the classical platinum blue complexes[7][9][12].

The comparison made between the platina-β-diketonato complexes of platina-β-diketones **2** and **3** and the classical platinum blue complexes reveals many structural similarities. Thus, the bis(acyl)-bridged complexes **2** and **3** can be regarded as organometallic analogues of platinum blue complexes. The investigations show that stable organometallics with Pt_4 chains can appear as neutral complexes **2**[5] or as anionic complexes **3**. Investigations are in progress to synthesize analogous cationic complexes.

Financial support by the *Deutsche Forschungsgemeinschaft* and by the *Fonds der Chemischen Industrie*, as well as gifts of chemicals by the companies *Degussa* (Hanau) and *Merck* (Darmstadt), are gratefully acknowledged.

Experimental Section

All reactions were performed under an Ar atmosphere using standard Schlenk techniques. The solvents were dried and distilled prior to use. − IR: Galaxy Mattson 5000 FT-IR spectrometer using CsBr pellets. − NMR: Varian Gemini 200, VXR 400, and Unity 500 spectrometers. Chemical shifts are relative to C*H*DCl$_2$ (δ_H = 5.32), C*D*$_2$Cl$_2$ (δ_C = 53.8), C*H*Cl$_3$ (δ_H = 7.24), and C*D*Cl$_3$ (δ_C = 77.0) as internal references. − Microanalyses (C, H, N, Cl): University of Halle microanalytical laboratory using CHNS-932 (LECO) and Vario EL (elementar Analysensysteme) elemental analyzers. − The complex [Pt$_2${(COMe)$_2$H}$_2$(μ-Cl)$_2$] (**1**) was prepared according to the literature method[1]. Other chemicals were commercial materials used after distillation or without further purification.

General Procedure for the Synthesis of [BH]$_2$[{Cl$_2$Pt(μ-COMe)$_2$Pt[(COMe)$_2$H]}$_2$] (**3**): The amine [*n*BuNH$_2$; (*i*Pr)$_2$NH; NEt$_3$; PhNHMe; PhNMe$_2$; C$_{10}$H$_6$(NMe$_2$)$_2$] (0.32 mmol) was added to a stirred suspension of [Pt$_2${(COMe)$_2$H}$_2$(μ-Cl)$_2$] (**1**) (200 mg, 0.32 mmol) in dichloro methane (3 ml) at ambient temp., producing a yellow/orange solution within 1 min. Diethyl ether (5 ml) was added and a precipitate was formed within 2 d at −40°C which was filtered off, washed with diethyl ether, and dried briefly in vacuo.

(*B* = *nBuNH$_2$*) (**3a**): Orange crystals. − M.p. (dec) 84−86°C. − Yield: 169 mg (76%). − IR: $\tilde{\nu}$ = 1556 cm^{-1} (sh, CO), 1531 (s, CO), 274 (w, PtCl), 249 (w, PtCl). − ^{1}H NMR (293 K, CDCl$_3$): δ = 0.92 [t, 3 H, N(CH$_2$)$_3$C*H*$_3$], 1.42 [sext, 2 H, N(CH$_2$)$_2$C*H*$_2$], 1.77 (quin, 2 H, NCH$_2$C*H*$_2$), 2.36 [s(br), 6 H, COC*H*$_3$], 2.38 [s(br), 6 H, COC*H*$_3$], 3.10 (t, 2 H, NC*H*$_2$), 7.53 [s(br), 3 H, N*H*$_3$], ca 19.5 [s(br), 1 H, O*H*O]. − ^{1}H NMR (248 K, CDCl$_3$): δ = 0.92 [t, 3 H, N(CH$_2$)$_3$C*H*$_3$], 1.39 [sext, 2 H, N(CH$_2$)$_2$C*H*$_2$], 1.77 (quin, 2 H, NCH$_2$C*H*$_2$), 2.31 (s, 1.8 H, COC*H*$_3$), 2.33 (s, 4.2 H, COC*H*$_3$), 2.36 (s, 1.8 H, COC*H*$_3$), 2.46 (s, 4.2 H, COC*H*$_3$), 3.09 (sext, 2 H, NC*H*$_2$), 7.54 (s, 3 H, N*H*$_3$), 20.10 (s, 1 H, O*H*O). − C$_{12}$H$_{25}$Cl$_2$NO$_4$Pt$_2$ (708.40): calcd. C 20.35, H 3.56, Cl 10.01, N 1.98; found C 20.13, H 3.49, Cl 10.20, N 1.85.

[*B* = *(iPr)$_2$NH*] (**3b**): Yellow crystals. − M.p. (dec) 95−97°C. − Yield: 190 mg (82%). − IR: $\tilde{\nu}$ = 1556 cm^{-1} (sh, CO), 1534 (s, CO), 275 (w, PtCl), 250 (w, PtCl). − ^{1}H NMR (293 K, CDCl$_3$): δ = 1.45 (d, 12 H, NCHC*H*$_3$), 2.3−2.5 (m, 12 H, COC*H*$_3$), 3.38 (sept, 2 H, NC*H*CH$_3$), 8.33 [s(br), 2 H, N*H*$_2$], resonance for O*H*O not observed. − ^{1}H NMR (248 K, CDCl$_3$): δ = 1.44 (d, 12 H, NCHC*H*$_3$), 2.31 (s, 4.2 H, COC*H*$_3$), 2.36 (s, 1.8 H, COC*H*$_3$), 2.48 (s, 1.8 H, COC*H*$_3$), 2.51 (s, 4.2 H, COC*H*$_3$), 3.38 (sept, 2 H, NC*H*CH$_3$), 8.24 (s, 2 H, N*H*$_2$), 20.02 [s(br), 1 H, O*H*O]. − C$_{14}$H$_{29}$Cl$_2$NO$_4$Pt$_2$ (736.45): calcd. C 22.83, H 3.97, Cl 9.63, N 1.90; found C 22.47, H 3.83, Cl 10.36, N 1.99.

(*B* = *NEt$_3$*) (**3c**): Yellow microcrystals. − M.p. (dec) 90−92°C. − Yield: 139 mg (60%). − IR: $\tilde{\nu}$ = 1553 cm^{-1} (sh, CO), 1530 (s, CO), 280 (w, PtCl), 257 (w, PtCl). − ^{1}H NMR (293 K, CDCl$_3$): δ = 1.37 (t, 9 H, NCH$_2$C*H*$_3$), 2.3−2.5 (m, 12 H, COC*H*$_3$), 3.21 (dq, 6 H, NC*H*$_2$CH$_3$, $^3J_{NH,H}$ = 5.1 Hz), 9.08 [s(br), 1 H, N*H*], resonance for O*H*O not observed. − ^{1}H NMR (248 K, CDCl$_3$): δ = 1.34 (t, 9 H, NCH$_2$C*H*$_3$), 2.31 (s, 4.4 H, COC*H*$_3$), 2.35 (s, 1.6 H, COC*H*$_3$), 2.42 (s, 1.6 H, COC*H*$_3$), 2.51 (s, 4.4 H, COC*H*$_3$), 3.19 (dq, 6 H, NC*H*$_2$CH$_3$, $^3J_{NH,H}$ = 5.3 Hz), 8.71 (s, 1 H, N*H*), 20.06 (s, 1 H, O*H*O). − C$_{14}$H$_{29}$Cl$_2$NO$_4$Pt$_2$ (736.45): calcd. C 22.83, H 3.97, Cl 9.63, N 1.90; found C 22.56, H 3.86, Cl 10.04, N 1.94.

(*B* = *PhNHMe*) (**3d**): Orange rubberlike solid. − Yield: 131 mg (56%). − IR: $\tilde{\nu}$ = 1556 cm^{-1} (sh, CO), 1531 (s, CO), 274 (w, PtCl), 249 (w, PtCl). − ^{1}H NMR (293 K, CDCl$_3$): δ = 2.2−2.6 (m, 12 H, COC*H*$_3$), 3.01 (s, 3 H, NC*H*$_3$), 7.1−7.4 (m, 5 H, C*H*), 11.61 [s(br), 2 H, N*H*$_2$], resonance for O*H*O not observed. − ^{1}H NMR (248 K, CDCl$_3$): δ = 2.2−2.5 (m, 12 H, COC*H*$_3$), 3.09 (s, 3 H, NC*H*$_3$), 7.42 (m, 3 H, *m*,*p*-C*H*), 7.60 (m, 2 H, *o*-C*H*), 10.55 (s, 2 H, N*H*$_2$), 20.03 [s(br), 1 H, O*H*O]. − C$_{15}$H$_{23}$Cl$_2$NO$_4$Pt$_2$ (742.41): calcd. C 24.27, H 3.12, Cl 9.55, N 1.89; found C 24.88, H 3.43, Cl 10.36, N 2.05.

(*B* = *PhNMe$_2$*) (**3e**): Orange rubberlike solid. Yield: 148 mg (62%). − IR: $\tilde{\nu}$ = 1554 cm^{-1} (sh, CO), 1530 (s, CO), 274 (w, PtCl), 251 (w, PtCl). − ^{1}H NMR (293 K, CDCl$_3$): δ = 2.3−2.6 (m, 12 H, COC*H*$_3$), 3.12 (d, 6 H, NC*H*$_3$, $^3J_{NH,H}$ = 1.2 Hz), 7.37 (m, 5 H, C*H*), ca 10.8 [s(br), 1 H, N*H*], resonance for O*H*O not observed. − ^{1}H NMR (248 K, CDCl$_3$): δ = 2.21 (s, 4.6 H, COC*H*$_3$), 2.39 (s, 1.4 H, COC*H*$_3$), 2.44 (s, 1.4 H, COC*H*$_3$), 2.52 (s, 4.6 H, COC*H*$_3$), 3.25 (s, 6 H, NC*H*$_3$), 7.36 (t, 1 H, *p*-C*H*), 7.47 (m, 2 H, *m*-C*H*), 7.57 (d, 2 H, *o*-C*H*), 11.8 (s, 1 H, N*H*), 20.03 [s(br), 1 H, O*H*O]. − C$_{16}$H$_{25}$Cl$_2$NO$_4$Pt$_2$ (756.44): calcd. C 25.41, H 3.33, Cl 9.37, N 1.85; found C 25.13, H 3.67, Cl 10.25, N 1.94.

[*B* = *C$_{10}$H$_6$(NMe$_2$)$_2$*] (**3f**): Yellow microcrystals. − M.p. (dec) 108−110°C. − Yield: 182 mg (68%). − IR: $\tilde{\nu}$ = 1552 cm^{-1} (sh, CO), 1529 (s, CO), 271 (w, PtCl), 248 (w, PtCl). − ^{1}H NMR (293 K, CDCl$_3$): δ = 2.3−2.5 [s(br), 12 H, COC*H*$_3$], 3.27 (d, 12 H, NC*H*$_3$, $^3J_{H,H}$ = 2.8 Hz), [7.69 (t, 2 H, $^3J_{H,H}$ = 7.7 Hz), 7.80 (dd, 2 H, $^3J_{H,H}$ = 7.7 Hz, $^4J_{H,H}$ = 1.1 Hz), 7.99 (dd, 2 H, $^3J_{H,H}$ = 8.4 Hz, $^4J_{H,H}$ = 0.7 Hz)], 18.85 (s, 1 H, N*H*N), resonance for O*H*O not observed. − ^{1}H NMR (233 K, CD$_2$Cl$_2$): δ = 2.27 (s, 4.4 H, COC*H*$_3$), 2.35 (s, 1.6 H, COC*H*$_3$), 2.45 (s, 1.6 H, COC*H*$_3$), 2.48 (s, 4.4 H, COC*H*$_3$), 3.21 (d, 12 H, NC*H*$_3$, $^3J_{H,H}$ = 2.8 Hz), [7.69 (t, 2 H, $^3J_{H,H}$ = 7.8 Hz), 7.80 (dd, 2 H, $^3J_{H,H}$ = 7.5 Hz, $^4J_{H,H}$ = 0.8 Hz), 7.97 (dd, 2 H, $^3J_{H,H}$ = 8.4 Hz, $^4J_{H,H}$ = 0.7 Hz)], 19.15 (s, 1 H, N*H*N), 20.1 [s(br), 1 H, O*H*O], Resonances of the aromatic H atoms are given in brackets. − C$_{22}$H$_{32}$Cl$_2$N$_2$O$_4$Pt$_2$ (849.56): calcd. C 31.10, H 3.80, Cl 8.35, N 3.30; found C 30.47, H 3.97, Cl 9.16, N 3.10.

Synthesis of [NMe$_4$]$_2$[{Cl$_2$Pt(μ-COMe)$_2$Pt[(COMe)$_2$H]}$_2$] (**3g**·CH$_2$Cl$_2$): A 2.2 M solution of [NMe$_4$]OH in methanol (142 μl, 0.32 mmol) was added to a stirred suspension of [Pt$_2${(COMe)$_2$H}$_2$(μ-Cl)$_2$] (**1**) (200 mg, 0.32 mmol) in dichloromethane (3 ml) at ambient temp., immediately producing an orange solution. On standing overnight (−40°C), orange crystals precipitated from solution, which were filtered off at −78°C, washed with diethyl ether, and dried briefly in vacuo. − M.p. (dec) 79−81°C. − Yield: 142 mg (60%). − IR: $\tilde{\nu}$ = 1553 cm^{-1} (sh, CO), 1524 (s, CO), 271 (w, PtCl), 256 (w, PtCl). − ^{1}H NMR (293 K, CD$_2$Cl$_2$): δ = 2.2−2.5 [s(br), 12 H, COC*H*$_3$], 3.39 (s, 12 H, NC*H*$_3$), resonance for O*H*O not observed. − ^{1}H NMR (248 K, CD$_2$Cl$_2$): δ = 2.28 (s, 4.0 H, COC*H*$_3$), 2.36 (s, 2.0 H, COC*H*$_3$), 2.41 (s, 2.0 H, COC*H*$_3$), 2.44 (s, 4.0 H, COC*H*$_3$), 3.33 (s, 12 H, NC*H*$_3$), ca 20.0 [s(br), 1 H, O*H*O]. − C$_{24}$H$_{50}$Cl$_4$N$_2$O$_8$Pt$_4$·CH$_2$Cl$_2$ (1501.72): calcd. C 19.99, H 3.49, Cl 14.16, N 1.86; found C 20.00, H 3.63, Cl 14.51, N 1.96. HMQC (248 K, CD$_2$Cl$_2$): δ(^{1}H/^{13}C) = 2.28/37.6 (*C*H$_3$), 2.36/41.4 (*C*H$_3$), 2.41/40.6 (*C*H$_3$), 2.44/42.6 (*C*H$_3$), 3.33/53.8 (N*C*H$_3$). − HMBC (248 K, CD$_2$Cl$_2$): δ(^{1}H/^{13}C) = 2.28/233.2 (C*H*$_3$, *C*O), 2.36/242.1 (C*H*$_3$, *C*O), 2.41/237.6 (C*H*$_3$, *C*O), 2.44/248.8 (C*H*$_3$, *C*O).

Crystal Structure Determination of Complexes **3a**·0.5 CH$_2$Cl$_2$ *and* **3g**·2 CH$_2$Cl$_2$: Crystals were taken directly from the solution and selected under perfluoro ether. A suitable crystal was quickly mounted on a glass fiber. Intensity data were collected on a Stoe IPDS diffractometer with Mo-K_α radiation (0.71073 Å, graphite monochromator). A summary of the crystallographic data, the data collection parameters and the refinement parameters is given in Table 1. Absorption corrections were carried out numerically. The structures were solved by direct methods using *SHELXS*-86[13] and refined with full matrix least squares routines against F^2 using

Table 1. Crystal data and details on the structure determination of complexes **3a**·0.5 CH_2Cl_2 and **3g**·2 CH_2Cl_2

compound	**3a**·0.5 CH_2Cl_2	**3g**·2 CH_2Cl_2
Empirical formula	$C_{24.5}H_{51}Cl_5N_2O_8Pt_4$	$C_{26}H_{54}Cl_8N_2O_8Pt_4$
Formula weight	1459.28	1586.67
Crystal system	monoclinic	monoclinic
Space group	*C*2/c (no. 15)	$P2_1/a$ (no. 14)
a [Å]	34.648(7)	14.932(2)
b [Å]	10.540(2)	9.372(1)
c [Å]	13.557(3)	18.023(5)
β [°]	57.42(2)	112.34(2)
Z	4	2
V [Å^3]	4172(2)	2332.8(7)
$D_{calcd.}$ [g cm^{-3}]	2.323	2.259
F(000)	2692	1472
μ(MoK_α) [cm^{-1}]	13.730	12.453
Crystal size	0.2 × 0.2 × 0.1	0.24 × 0.13 × 0.04
Temperature [K]	298(2)	223(2)
θ (min., max.) [°]	2.05, 24.00	2.44, 24.07
Recip. latt. segment *h*	−42 → 41	−16 → 17
k	−13 → 12	−10 → 10
l	−16 → 16	−20 → 20
Measured reflections	11890	15148
Independent refl. [$R_{int.}$]	3274 [0.1354]	3631 [0.1029]
$T_{min}/T_{max.}$	0.09/0.22	0.04/0.49
Observed reflections	2209	3187
Parameters	186	248
*R*1, *wR*2 [$I>2\sigma(I)$]	0.0430/0.0857	0.0328/0.0815
*R*1, *wR*2 (all data)	0.0737/0.0944	0.0389/0.0842
S	0.917	1.053
Min. and max. resd. electron dens. [e/A^3]	−2.427 and 1.256	−1.443 and 2.615

SHELXL-93[13]. All non-H atoms were refined with anisotropic displacement parameters. As a result of disorder in **3a**·0.5 CH_2Cl_2 the two outer C atoms of the butyl group in the cation $[n\text{BuNH}_3]^+$ were refined isotropically. The H atoms were added to the model in their calculated positions and refined isotropically, except for the bridging H-atom in **3g**·2 CH_2Cl_2, which was found in the difference Fourier map.

Crystallographic data (excluding structure factors) for the structures reported in this paper have been deposited at the Cambridge Crystallographic Data Center as supplementary publication no. CCDC-101858 (**3a**·0.5 CH_2Cl_2) and no. CCDC-101859 (**3g**·2 CH_2Cl_2), respectively. Copies of the data can be obtained free of charge on application to CCDC, 12 Union Road, Cambridge, CB2, 1EZ, UK [Fax: (internat.) + 44(0)1223/336-033; E-mail: deposit@ccdc.cam.ac.uk].

[1] D. Steinborn, M. Gerisch, K. Merzweiler, K. Schenzel, K. Pelz, H. Bögel, J. Magull, *Organometallics* **1996**, *15*, 2454−2457.

[2] Reviews: [2a] C. M. Lukehart, *Acc. Chem. Res.* **1981**, *14*, 109−116. − [2b] C. M. Lukehart, *Adv. Organomet. Chem.* **1986**, *25*, 45−71.

[3] [3a] C. M. Lukehart, J. V. Zeile, *J. Am. Chem. Soc.* **1978**, *100*, 2774−2778. − [3b] C. M. Lukehart, J. V. Zeile, *Inorg. Chem.* **1978**, *17*, 2369−2374. − [3c] K. P. Darst, C. M. Lukehart, *Inorg. Chim. Acta* **1980**, *41*, 239−243. − [3d] C. M. Lukehart, M. Raja, *Inorg. Chem.* **1982**, *21*, 1278−1280. − [3e] D. Afzal, C. M. Lukehart, *Inorg. Chem.* **1983**, *22*, 3954−3956.

[4] [4a] C. M. Lukehart, G. P. Torrence, *Inorg. Chem.* **1979**, *18*, 3150−3155. − [4b] C. M. Jensen, Y. J. Chen, H. D. Kaesz, *J. Am. Chem. Soc.* **1984**, *106*, 4046−4047. − [4c] P. G. Lenhert, C. M. Lukehart, P. O. Sotiropoulos, K. Srinivasan, *Inorg. Chem.* **1984**, *23*, 1807−1810. − [4d] D. Xu, H. D. Kaesz, S. I. Khan, *Inorg. Chem.* **1991**, *30*, 1341−1344. − [4e] E. Lippmann, C. Robl, H. Berke, H. D. Kaesz, W. Beck, *Chem. Ber.* **1993**, *126*, 933−940.

[5] D. Steinborn, M. Gerisch, F. W. Heinemann, C. Bruhn, *J. Chem. Soc., Chem. Commun.* **1997**, 843−844.

[6] K. A. Hoffmann, G. Bugge, *Ber. Dtsch. Chem. Ges.* **1908**, *41*, 312−314.

[7] Reviews: [7a] J. K. Barton, S. J. Lippard, *Ann. N. Y. Acad. Sci.* **1978**, *313*, 686−700. − [7b] S. J. Lippard, *Science* **1982**, *218*, 1075−1082.

[8] P. Pyykkö, *Chem. Rev.* **1997**, *97*, 597−636.

[9] [9a] L. S. Hollis, S. J. Lippard, *J. Am. Chem. Soc.* **1981**, *103*, 1230−1232. − [9b] L. S. Hollis, S. J. Lippard, *Inorg. Chem.* **1983**, *22*, 2600−2604. − [9c] J. P. Laurent, P. Lepage, F. Dahan, *J. Am. Chem. Soc.* **1982**, *104*, 7335−7336. − [9d] G. Bernadinelli, P. Castan, R. Soules, *Inorg. Chim. Acta* **1986**, *120*, 205−207. − [9e] L. S. Hollis, S. J. Lippard, *J. Am. Chem. Soc.* **1983**, *105*, 3494−3503. − [9f] K. Matsumoto, H. Miyamae, H. Moriyama, *Inorg. Chem.* **1989**, *28*, 2959−2964.

[10] [10a] W. B. Connick, R. E. Marsh, W. P. Schaefer, H. B. Gray, *Inorg. Chem.* **1997**, *36*, 913−922. − [10b] J. M. Williams, *Adv. Inorg. Chem. Radiochem.* **1983**, *26*, 235−268.

[11] In ref.[5] the angles between the normals to the planes are given [**2a**: 95.7(6)°, **2b**: 103.6(4)°], which are the supplemental angles to α.

[12] [12a] J. K. Barton, H. N. Rabinowitz, D. J. Szalda, S. J. Lippard, *J. Am. Chem. Soc.* **1977**, *99*, 2827−2829. − [12b] J. K. Barton, S. A. Best, S. J. Lippard, R. A. Walton, *J. Am. Chem. Soc.* **1978**, *100*, 3785−3788. − [12c] J. K. Barton, D. J. Szalda, H. N. Rabinowitz, J. V. Waszczak, S. J. Lippard, *J. Am. Chem. Soc.* **1979**, *101*, 1434−1441. − [12d] J. K. Barton, C. Caravana, S. J. Lippard, *J. Am. Chem. Soc.* **1979**, *101*, 7269−7277. − [12e] T. V. O'Halloran, P. K. Mascharak, I. D. Williams, M. M. Roberts, S. J. Lippard, *Inorg. Chem.* **1987**, *26*, 1261−1270. − [12f] K. Matsumoto, K. Sakai, K. Nishio, Y. Tokisue, R. Ito, T. Nishide, Y. Shichi, *J. Am. Chem. Soc.* **1992**, *114*, 8110−8118.

[13] G. M. Sheldrick, *SHELXS-86*, *SHELXL-93*, *Programs for Crystal Structure Determination*; University of Göttingen, Göttingen, **1986**, **1993**.

[14] M. N. Burnett, C. K. Johnson, *ORTEP-III: Oak Ridge Thermal Ellipsoid Plot Program for Crystal Structure Illustrations*, Oak Ridge National Laboratory Report ORNL-6895, **1996**.

[98199]

The Formation of Macrocyclic Compounds Containing Two Ga–Ga Bonds by the Reaction of Tetraalkyldigallane(4) $R_2Ga–GaR_2$ [R = $CH(SiMe_3)_2$] with Dicarboxylic Acids

Werner Uhl*, Thomas Spies, and Wolfgang Saak

Fachbereich Chemie der Universität,
Postfach 2503, D-26111 Oldenburg, Germany
Fax (internat.): +49 (0)441/ 798-3352

Received June 29, 1998

Keywords: Gallium / Low-valent compounds / Macrocycles

Tetrakis[bis(trimethylsilyl)methyl]digallane(4) **1** reacts with dicarboxylic acids like 1,4-benzenedi(methylcarboxylic) acid, 1,4-cyclohexanedicarboxylic acid, 1,6-hexanedicarboxylic acid, and 1,4-butanedicarboxylic acid (adipinic acid) by the release of two equivalents of bis(trimethylsilyl)methane and the retention of the Ga–Ga bond. Products are formed, in which the very short Ga–Ga bonds (237.7 pm on average) are bridged by two carboxylato groups. Two of these moieties are connected in each compound by two spacers (dimethylbenzene, cyclohexane, hexane, or butane) to form macrocyclic compounds with up to 22 atoms in the resultant heteroatomic rings. The dimeric form is also observed in solution. For comparison, the synthesis and structure of the product of the reaction of **1** with 1-adamantanecarboxylic acid is included, which also has the Ga–Ga bond (239.1 pm) bridged by two carboxylato groups.

Recently we published the reactions of tetrakis[bis(trimethylsilyl)methyl]digallane(4) **1**[1] with aromatic carboxylic acids. Remarkably, these reactions did not lead to the expected cleavage of the Ga−Ga bond of **1** as observed for the corresponding dialuminium or diindium derivatives[2], but two alkyl substituents were replaced by two carboxylato groups, and two equivalents of bis(trimethylsilyl)methane were released in an almost quantitative yield[3]. As shown in Scheme 1, the bidentate carboxylato ligands of the products occupy bridging positions across the Ga−Ga bond, which is significantly shortened to 238.5(2) pm compared with that of the starting compound **1** [254.1(1) pm][1]. In contrast, a terminal coordination of chelating diphenyltriazenido ligands was observed in a digallium compound obtained by the reaction of **1** with diphenyltriazene[4]. Also, the product of the reaction with dibenzoylmethane showed a terminal arrangement of the chelating groups[5], which have, however, two atoms more in the resulting heterocycle. The reason for the different coordination is not well understood; it may depend on the distance between the coordinating atoms (bite), and we hope to clarify this problem by the synthesis of some derivatives by systematically changing the size of the chelating groups. In this context, we report here on the structural characterization of the first example of a digallium compound with aliphatic carboxylato ligands in order to exclude an electronic influence of the aromatic groups on the coordination mode.

The reactions of **1** with carboxylic acids yielded the products almost quantitatively without any NMR spectroscopically detectable by-products[3]. Therefore, we were interested in the behavior of bifunctional dicarboxylic acids, which could give two different products: (i) The dicarboxylato ligand might be bound to only one digallium fragment in a chelating manner. But from molecular models it can be deduced that such an intramolecular coordination is not easy to achieve and requires long carbon chains to avoid considerable steric stress in the molecule. (ii) The dicarboxylato ligands could bridge two digallium units by an intermolecular coordination to form dimeric or oligomeric species. The oligomerization of the products would open an easy route to the synthesis of interesting new macrocyclic compounds. The reactions of some dicarboxylic acids with **1** and the complete characterization of the products is described in this article.

Scheme 1

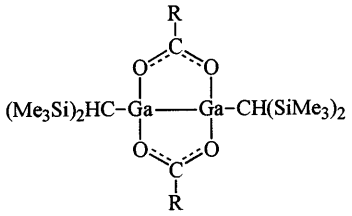

R = -4-Br-C_6H_4

Reaction of Digallane(4) 1 with 1-Adamantanecarboxylic Acid

Two equivalents of 1-adamantanecarboxylic acid reacted rapidly with **1** in *n*-pentane at low temperature, and the yellow color of the digallium(4) compound disappeared already at −15°C. As shown by a NMR spectrum of the reac-

 © WILEY-VCH Verlag GmbH, D-69451 Weinheim, 1998 1434−1948/98/1111−1661 $ 17.50+.50/0

tion mixture, exactly two equivalents of bis(trimethylsilyl)-methane were released per formula unit of **1** (Eq. 1). The colorless, crystalline product (**2**) was isolated after evaporation and recrystallization from pentane in a yield of 79%. Product **2** is readily soluble in hydrocarbons. It is a monomer in benzene solution, as shown by the cryoscopical molar mass determination. The NMR resonances of the methine hydrogen and carbon atoms of the $CH(SiMe_3)_2$ substituents bound to gallium (^1H: $\delta = -0.30$; ^{13}C: $\delta = 4.0$) show a significant high-field shift relative to those of the starting compound **1** (^1H: $\delta = 1.11$; ^{13}C: $\delta = 25.9$[1]), which is very characteristic of an enhancement of the coordination number of the Ga atoms from 3 to 4[3][4][5][6]. The stretching vibration of the CO_2 group with a delocalized electronic π bond is observed in the IR spectrum at 1530 cm^{-1}.

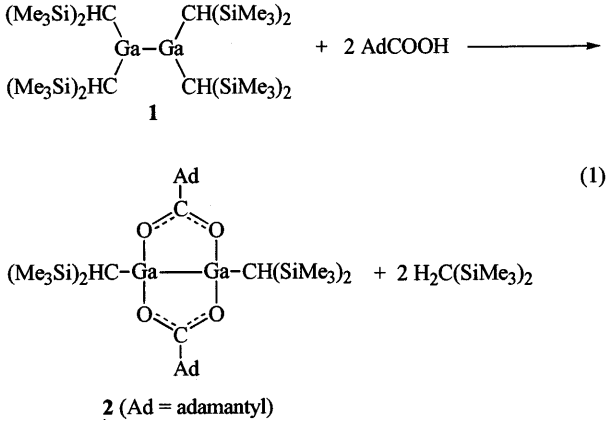

(1)

Reactions of 1 with Dicarboxylic Acids

The reactions of dicarboxylic acids with **1** were much slower than those with the monocarboxylic acids and required reaction times of several days in *n*-pentane at room temperature or some hours in boiling solvents. While, as expected, two equivalents of bis(trimethylsilyl)methane with respect to **1** were released in all reactions, only four acids reacted successfully to gave isolable products in high purity (Eq. 2): 1,4-benzenedi(methylcarboxylic) acid (product **3**), 1,4-cyclohexanedicarboxylic acid (product **4**), 1,6-hexanedicarboxylic acid (product **5**), and 1,4-butanedicarboxylic acid (adipinic acid) (product **6**). In contrast, other acids like maleic acid, 1,2- and 1,4-benzenedicarboxylic acid, 4,4′-oxydibenzoic acid and 2,2-dimethylpropane-1,3-dicarboxylic acid (glutaric acid) yielded only oily residues with mixtures of many unknown products, from which no compound could be isolated in a pure form. The products **3** to **6** were isolated after recrystallization in excellent yields of more than 80%.

The spectroscopic properties of the compounds **3** to **6** are very similar to those described above for **2** with the monocarboxylato ligand. The NMR resonances of the methine groups bound to gallium are shifted to high field (^1H: $\delta = -0.31$ to -0.47; ^{13}C: $\delta = 4.2$ to 4.5) relative to those of digallane(4) **1**, as expected for the enhancement of the coordination number at the Ga atoms to 4. The integration of

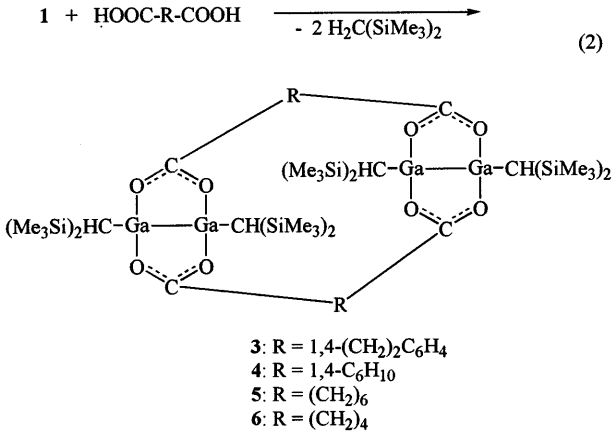

the ^1H-NMR spectra clearly reveals one dicarboxylato ligand each Ga_2R_2 formula unit. In the IR spectra of **3** to **6**, the most characteristic absorptions are those of the CO_2 stretching vibrations in a quite narrow range between 1539 and 1549 cm^{-1}. All products are dimeric in benzene solution as shown by the cryoscopical molar mass determination, so that compounds were formed, which contain two Ga_2R_2 moieties bridged by two dicarboxylato bridges.

Crystal Structures of 2, 3, and 4

The molecular structure of compound **2** is depicted in Figure 1. It is quite similar to the structure of the recently published *p*-bromobenzoate derivative[3] and has the Ga−Ga bond bridged by two adamantyl carboxylato groups. The Ga−Ga bond [239.1(1) pm] is shorter than that of the tetraalkyl compound **1** [254.1(1) pm][1], which may be caused by the carboxylato bridges with a short distance between the coordinating atoms of 223.2 pm on average. Both Ga−Ga distances lie within the broad range of known bond lengths between Ga atoms[7]. Two five-membered heterocycles are formed by the chelating coordination of the Ga−Ga bond, which are almost ideally planar and show a maximum deviation of an atom from the plane of 1.8 and 2.5 pm. Remarkably, these heterocycles arrange perpendicular to one another, and the angle between both chelating groups is 89.3°. The C−Ga−Ga−C center of the molecule is almost linear with large mean C−Ga−Ga angles of 158.7°. Thus, the coordination of the carboxylato groups seems to be based mainly on an interaction with two p orbitals of each Ga atom.

Compounds **3** and **4** contain macrocycles (Figures 2 and 3), and two digallium dicarboxylato units are bridged by hydrocarbon groups. The structure around the Ga−Ga bond of both molecules **3** and **4** is quite similar to that observed in compound **2**. Each Ga−Ga bond is bridged by two carboxylato groups, which results in short Ga−Ga bond lengths of 237.85 pm on average (**3**) and 237.46(4) pm (**4**). The C−Ga−Ga−C moieties are almost linear with C−Ga−Ga angles of 156.6° (**3**) and 155.8° (**4**). As in **2**, the Ga_2O_2C heterocycles are perpendicular to each other, and

Figure 1. Molecular structure and numbering scheme of compound **2**; the thermal ellipsoids are drawn at the 40% probability level; the carbon atoms of one of the disordered adamantyl groups are drawn with an arbitrary radius[a]

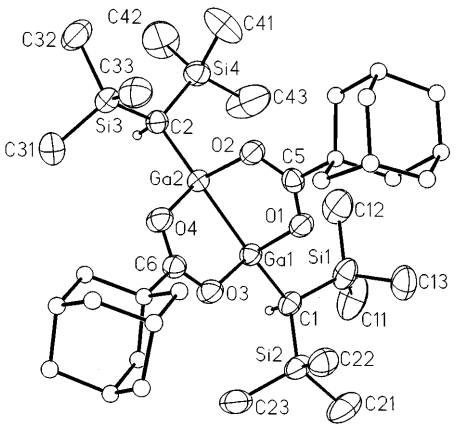

[a] Selected bond lengths [pm] and angles [°]: Ga1−Ga2 239.1(1), Ga1−O1 200.2(2), Ga1−O3 200.4(2), Ga1−C1 195.4(3), Ga2−O2 200.6(2), Ga2−O4 201.6(2), Ga2−C2 195.8(3), O1−Ga1−O3 91.1(1), O2−Ga2−O4 91.5(1), Ga2−Ga1−O1 87.67(8), Ga2−Ga1−O3 88.16(8), Ga1−Ga2−O2 87.80(8), Ga1−Ga2−O4 87.25(8), Ga2−Ga1−C1 158.4(1), Ga1−Ga2−C2 159.0(1).

the angles between the chelating ligands show values of 88.5° and 87.3° in **3** and 88.2° in **4**.

These digallium dicarboxylato groups are bridged by a dimethylbenzene group in compound **3** to form a macrocycle containing 22 atoms. The aromatic rings do not, however, adopt the parallel arrangement, which is often observed in phenyl compounds and is caused by weak interactions between the delocalized π electrons, but the rings are perpendicular to one another with an angle between the normals of the planes of 93.1°. The reason is the very long distance between the aromatic rings (C701−C711 583 pm) forced by the geometry of the coordination of the Ga atoms. This distance is much longer than detected or calculated for compounds with a bonding interaction between phenyl groups, in which the separation between the carbon atoms of the phenyl rings is below 400 pm[8]. As can be seen from Figure 2 a quite unsymmetric molecular structure results in the solid state with the Ga−Ga bonds not arranged parallel, but their vectors subtend an angle of 94.4°.

In contrast, **4**, which has bridging cyclohexane groups, is a highly symmetric compound (Figure 3). **4** is located on a crystallographic center of symmetry, and the Ga−Ga bonds adopt a parallel arrangement. The cyclohexane rings have a chair conformation, and one bond to a carbonyl group occupies an axial position (C5−C51), while the other one (C54−C6′) is in an equatorial position. From this conformation, an almost rectangular cage results in the center of the molecule.

The results described here clearly confirm that the reaction of digallane(4) **1** with dicarboxylic acids is a powerful method for the synthesis of large macrocycles. It is of particular interest now to synthesize corresponding macrocyclic compounds that contain heteroatoms like N or S and could possibly act as ligands for the complexation of cations.

Figure 2. Molecular structure and numbering scheme of compound **3**; the thermal ellipsoids are drawn at the 40% probability level; methyl groups are omitted for clarity[a]

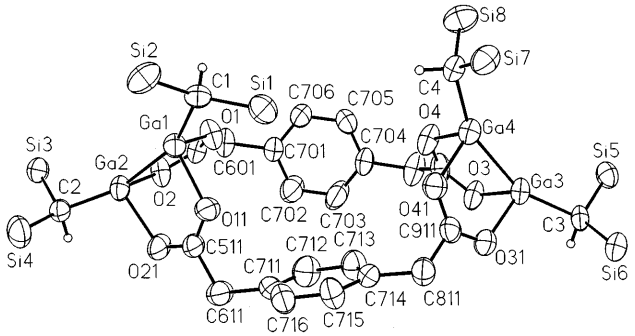

[a] Selected bond lengths [pm] and angles [°]: Ga1−Ga2 238.29(8), Ga3−Ga4 237.41(9), Ga1−O1 199.6(3), Ga1−O11 200.2(3), Ga1−C1 194.9(5), Ga2−O2 201.1(3), Ga2−O21 201.5(3), Ga2−C2 194.6(4), Ga3−O3 200.7(3), Ga3−O31 200.3(3), Ga3−C3 195.4(4), Ga4−O4 201.0(3), Ga4−O41 201.0(4), Ga4−C4 195.0(5), mean values: Ga−Ga−O 88.0, O−Ga−O 91.8, Ga−Ga−C 156.6.

Figure 3. Molecular structure and numbering scheme of compound **4**; the thermal ellipsoids are drawn at the 40% probability level; methyl groups are omitted for clarity[a]

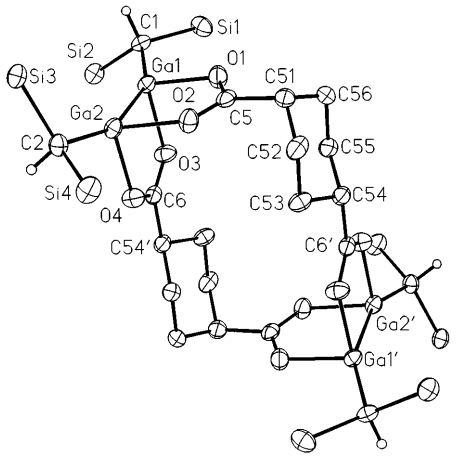

[a] Selected bond lengths [pm] and angles [°]: Ga1−Ga2 237.46(4), Ga1−O1 202.9(2), Ga1−O3 199.7(2), Ga1−C1 195.2(2), Ga2−O2 199.8(2), Ga2−O4 201.1(2), Ga2−C2 195.8(2), O1−Ga1−O3 91.30(8), O2−Ga2−O4 92.19(7), Ga2−Ga1−O1 87.83(5), Ga2−Ga1−O3 87.40(5), Ga1−Ga2−O2 88.16(5), Ga1−Ga2−O4 88.48(5), Ga2−Ga1−C1 155.22(7), Ga1−Ga2−C2 156.37(7).

We are grateful to the *Deutsche Forschungsgemeinschaft* and the *Fonds der Chemischen Industrie* for generous financial support.

Experimental Section

General: All procedures were carried out under purified argon in dried solvents (diisopropyl ether and toluene with Na/benzophenone, *n*-pentane with $LiAlH_4$). Compound **1** was synthesized as described in ref.[1], commercially available 1-adamantanecarboxylic acid, 1,4-benzenedi(methylcarboxylic) acid, and 1,4-butanedicarboxylic acid were sublimed in vacuo before use, and 1,6-hexanedicarboxylic acid and 1,4-cyclohexanedicarboxylic acid were used without further purification.

Reaction of **1** *with 1-Adamantanecarboxylic Acid, Synthesis of* **2**: Solid 1-adamantanecarboxylic acid (0.207 g, 1.15 mmol) was added

Table 1. Crystal data and data-collection parameters for **2**, **3**, and **4**

	2	**3**	**4**
Formula	$C_{36}H_{68}O_4Ga_2Si_4$	$C_{48}H_{92}Ga_4O_8Si_8$	$C_{44}H_{96}Ga_4O_8Si_8$
Crystal system	triclinic	triclinic	triclinic
Space group	P−1; No. 2 [9]	P−1; No. 2 [9]	P−1; No. 2 [9]
Z	2	2	1
T [K]	293(2)	293(2)	213(2)
$d_{calcd.}$ [g/cm^3]	1.231	1.241	1.283
a [pm]	1270.3(3)	1361.0(1)	1099.7(1)
b [pm]	1306.2(3)	1403.2(1)	1203.6(1)
c [pm]	1499.9(3)	1926.8(2)	1368.1(1)
α [°]	102.06(3)	72.940(9)	64.19(1)
β [°]	112.35(3)	84.33(1)	86.78(1)
γ [°]	96.08(3)	82.49(1)	89.69(1)
V [10^{-30} m^3]	2203.2(8)	3480.5(5)	1627.2(2)
μ [mm^{-1}]	1.364	1.709[a]	1.826[a]
Crystal size [mm]	0.30 × 0.30 × 0.76	0.23 × 0.30 × 0.38	0.45 × 0.50 × 0.80
Diffractometer	AED 2	AED 2	IPDS
Radiation	Mo-K_α; graphite monochromator		
Range	$3 \le 2\Theta \le 48°$	$3° \le 2\Theta \le 46°$	$4.8° \le 2\Theta \le 52°$
Reciprocal space	$-14 \le h \le 13$	$-14 \le h \le 14$	$-13 \le h \le 13$
	$-14 \le k \le 14$	$-14 \le k \le 15$	$-14 \le k \le 14$
	$0 \le l \le 17$	$0 \le l \le 21$	$-16 \le l \le 16$
Scan mode	ω−2Θ	ω−2Θ	157 exposures; Δφ 1.4°
Independent reflections	6892	9624	5892
Number of reflections with $F > 4\ \sigma(F)$	5603	6907	4949
Parameters	546	637	301
$R = \Sigma\|\|F_o\| - \|F_c\|\|/\Sigma\|F_o\|$ $[F > 4\ \sigma\ (F)]$	0.0438	0.0534	0.0301
$wR^2 = \{\Sigma w(F_o^2 - F_c^2)^2/\Sigma w\ (F_o^2)^2\}^{1/2}$ (all data)	0.0782	0.0792	0.0588
Max./min. residual [10^{30} e/m^3]	0.724/−0.283	0.472/−0.279	0.590/−0.482

[a] Empirical absorption correction. − [b] Program: SHELXTL, SHELXL-93[10]; solutions by direct methods; full matrix refinement with all independent structure factors.

to a cooled (−50°C) solution of yellow digallane(4) **1** (0.445 g, 0.574 mmol) in 25 ml of *n*-pentane. The mixture was stirred and slowly warmed to room temperature. The color changed from yellow to colorless at a temperature of −15°C. The solvent was distilled off in vacuo, the residue was thoroughly dried in vacuo and recrystallized from *n*-pentane (20/−30°C). Yield: 0.370 g (79%), colorless crystals. − M. p. (argon, sealed capillary): 174°C. − ^{1}H NMR (C_6D_6, 300 MHz): δ = 2.02 (12 H, CH_2 of adamantyl), 1.85 (6 H, CH of adamantyl), 1.54 (12 H, CH_2 of adamantyl), 0.35 (36 H, $SiMe_3$), −0.30 (2 H, $GaCHSi_2$). − ^{13}C NMR (C_6D_6, 75.5 MHz): δ = 190.1 (CO_2), 41.9 (*ipso*-C of adamantyl, 39.7, 36.7, and 28.4 (adamantyl), 4.0 ($GaCSi_2$), 3.5 ($SiMe_3$). − IR (CsBr, paraffin): $\tilde{\nu}$ = 1580 vw, 1530 s cm^{-1} νCO_2; 1462 vs, 1377 vs paraffin; 1310 s, 1256 s, 1242 s δCH_3; 1186 vw, 1181 vw, 1169 vw, 1113 w, 1105 w, 1090 w νCC; 1015 vs δCH; 976 m, 949 s, 907 w, 843 vs, 797 s, 775 s, 758 s, 723 m ρCH_3(Si); 679 s, 671 s ν_{as}SiC; 627 w, 613 w ν_sSiC; 515 s, 500 s, 465 w, 422 m νGaC, νGaO; 370 vw, 355 vw, 339 vw δSiC. − MS (CI, three most intensive peaks): 815.1, 817.1, 818.1 (all M^+ + H) corresponding with a calculated isotope pattern. − $C_{36}H_{68}O_4Si_4Ga_2$ (816.7): calcd. Ga 17.1, found Ga 16.9. − Mol. mass: 769 (cryoscopically in benzene).

Reaction of **1** *with Ddicarboxylic Acids, General Procedure for the Syntheses of the Compounds* **3** *to* **6**: The solid dicarboxylic acids were added to a cooled (−50°C) solution of an equimolar quantity of yellow digallane(4) **1** (about 0.5 g) in 25 ml of *n*-pentane. The mixtures were warmed to room temperature and stirred for 2 d (**4**) or heated under reflux for 1.5 h (**5** and **6**) or 14 h (**3**). The color changed in each reaction from yellow to colorless. A small quantity of an unknown solid precipitated during the synthesis of **3**, which was filtered off. The filtrate was concentrated and cooled to −50°C to obtain colorless crystals of **3**. The other reaction mixtures were evaporated to dryness and thoroughly dried in vacuo to completely remove $CH_2(SiMe_3)_2$. The residues were recrystallized from different solvents (20/−30°C): **4** from toluene, **5** from diisopropyl ether and **6** from *n*-pentane.

Characterization of **3**: Yield: 83%, colorless crystals. − M. p. (argon, sealed capillary): 140°C (dec.). − ^{1}H NMR (C_6D_6, 300 MHz): δ = 6.88 (8 H, phenyl), 3.37 (8 H, CH_2), 0.27 (72 H, $SiMe_3$), −0.31 (4 H, $GaCHSi_2$). − ^{13}C NMR (C_6D_6, 75.5 MHz): δ = 184.3 (CO_2), 133.2 (*ipso*-C of phenyl), 129.2 (2,3,5,6-C of phenyl), 42.9 (CH_2), 4.5 ($GaCSi_2$), 3.3 ($SiMe_3$). − IR (CsBr, paraffin): $\tilde{\nu}$ = 1549 s cm^{-1} νCO_2; 1462 vs, 1377 vs paraffin; 1292 m, 1262 sh, 1246 s δCH_3; 1204 w, 1181 vw, 1165 vw, 1117 vw, 1078 vw νCC; 1013 s δCH; 930 m, 868 s, 843 vs, 787 m, 775 m, 758 s, 727 s ρCH_3(Si); 687 m, 669 s ν_{as}SiC; 638 w, 625 m, 611 w ν_sSiC; 563 vw, 523 m, 463 w, 422 w νGaC, νGaO; 378 vw, 353 vw, 334 vw δSiC. − MS (CI, three most intensive peaks): 1299.0, 1301.0, 1302.6 (all M^+ + H) corresponding with a calculated isotope pattern. − $C_{48}H_{92}O_8Si_8Ga_4$ (1300.8): calcd. Ga 21.4, found Ga 21.0. − Mol. mass: 1262 (cryoscopically in benzene).

Characterization of **4**: Yield: 85%, colorless crystals. − M. p. (argon, sealed capillary): 192°C (dec.). − ^{1}H NMR (C_6D_6, 300 MHz): δ = 2.2 to 1.2 (very broad, 20 H, cyclohexyl), 0.30 (72 H, $SiMe_3$), −0.47 (4 H, $GaCHSi_2$). − ^{13}C NMR (C_6D_6, 75.5 MHz): δ = 186.7 (CO_2), 41.7 (*ipso*-C of cyclohexyl), 26.8 (2,3,5,6-C of cyclohexyl), 4.2 ($GaCSi_2$), 3.4 ($SiMe_3$). − IR (CsBr, paraffin): $\tilde{\nu}$ = 1603 vw, 1539 w cm^{-1} νCO_2; 1462 vs, 1377 vs paraffin; 1304 w, 1258 sh, 1248 w δCH_3; 1204 vw, 1145 w, 1113 m, 1082 s, 1040 s νCC; 1013 s δCH; 918 w, 845 m, 791 w, 777 w, 758 w, 721 m ρCH_3(Si); 687 vw, 673 w, 669 w ν_{as}SiC; 627 w ν_sSiC; 517 s, 461 s νGaC, νGaO; 382 vw, 345 vw δSiC. − $C_{44}H_{96}O_8Si_8Ga_4$ (1256.8): calcd. Ga 22.2, found Ga 22.1. − Mol. mass: 1205 (cryoscopically in benzene).

Characterization of **5**: Yield: 86%, colorless crystals. − M. p. (argon, sealed capillary): 130°C (dec.). − ^{1}H NMR (C_6D_6, 300 MHz): δ = 2.18 (t, 8 H, CH_2CO$_2$), 1.48 and 1.06 (each m, 8 H, CH_2CH_2), 0.32 (72 H, $SiMe_3$), −0.32 (4 H, $GaCHSi_2$). − ^{13}C NMR (C_6D_6, 75.5 MHz): δ = 186.2 (CO_2), 36.5, 28.9 and 25.7 (CH_2), 4.3 ($GaCSi_2$), 3.4 ($SiMe_3$). − IR (CsBr, paraffin): $\tilde{\nu}$ = 1611 w, 1543 s cm^{-1} νCO$_2$; 1464 vs, 1377 vs paraffin; 1307 m, 1302 w, 1258 sh, 1248 s δCH$_3$; 1167 w, 1140 w, 1098 w, 1080 w νCC; 1015 s δCH; 939 m, 934 m, 843 vs, 785 m, 777 m, 758 m, 721 m ρCH$_3$(Si); 673 m ν_{as}SiC; 625 w, 613 w ν_sSiC; 525 vw, 515 w, 463 vw, 422 vw νGaC, νGaO; 388 vw, 338 vw δSiC. − $C_{44}H_{100}O_8Si_8Ga_4$ (1260.1): calcd. Ga 22.1, found Ga 22.3. − Mol. mass: 1135 (cryoscopically in benzene).

Characterization of **6**: Yield: 85%, colorless crystals. − M. p. (argon, sealed capillary): 125°C (dec.). − ^{1}H NMR (C_6D_6, 300 MHz): δ = 2.10 (m, 8 H, CH_2CO$_2$), 1.41 (m, 8 H, CH_2CH_2), 0.30 (72 H, $SiMe_3$), −0.33 (4 H, $GaCHSi_2$). − ^{13}C NMR (C_6D_6, 75.5 MHz): δ = 185.7 (CO_2), 36.2 and 25.1 (CH_2), 4.3 ($GaCSi_2$), 3.3 ($SiMe_3$). − IR (CsBr, paraffin): $\tilde{\nu}$ = 1545 m cm^{-1} νCO$_2$; 1458 vs, 1377 vs paraffin; 1331 w, 1312 m, 1248 s δCH$_3$; 1196 vw, 1150 w, 1113 w, 1082 w νCC; 1013 s δCH; 947 m, 932 m, 843 vs, 775 w, 758 m, 721 m ρCH$_3$(Si); 673 m ν_{as}SiC; 625 m, 613 w ν_sSiC; 523 w, 515 w, 463 w, 428 w, 401 vw νGaC, νGaO; 353 vw, 345 vw δSiC. − $C_{40}H_{92}O_8Si_8Ga_4$ (1204.7): calcd. Ga 23.1, found Ga 22.9. − Mol. mass: 1143 (cryoscopically in benzene).

Crystal Structure Determinations: Single crystals of the compounds **2**, **3**, and **4** were obtained by recrystallization from cyclopentane, diisopropyl ether, and toluene, respectively. Crystal data and structure refinement parameters are given in Table 1[11]. The adamantyl groups in **2** are rotationally disordered, and the carbon atoms with the exception of those attached to the carbonyl groups (C51 and C61) were refined in two positions with occupancy factors of 0.5. **4** is located on a crystallographic inversion center.

[1] W. Uhl, M. Layh, T. Hildenbrand, *J. Organomet. Chem.* **1989**, *364*, 289−300.
[2] W. Uhl, R. Graupner, S. Pohl, W. Saak, W. Hiller, M. Neumayer, *Z. Anorg. Allg. Chem.* **1997**, *623*, 883−891.
[3] W. Uhl, I. Hahn, H. Reuter, *Chem. Ber.* **1996**, *129*, 1425−1428.
[4] W. Uhl, I. Hahn, R. Wartchow, *Chem. Ber./Recueil* **1997**, *130*, 417−420.
[5] W. Uhl, R. Graupner, I. Hahn, T. Spies, W. Frank, *Eur. J. Inorg. Chem.* **1998**, 355−360.
[6] W. Uhl, I. Hahn, M. Koch, M. Layh, *Inorg. Chim. Acta* **1996**, *249*, 33−39; W. Uhl, R. Graupner, I. Hahn, *Z. Anorg. Allg. Chem.* **1997**, *623*, 565−572; W. Uhl, R. Gerding, F. Hannemann, *ibid.* **1998**, *624*, 937−944.
[7] X. He, R. A. Bartlett, M. M. Olmstead, K. Ruhlandt-Senge, B. E. Sturgeon, P. P. Power, *Angew. Chem.* **1993**, *105*, 761−762; *Angew. Chem. Int. Ed. Engl.* **1993**, *32*, 717−718; D. Loos, H. Schnöckel, D. Fenske, *Angew. Chem.* **1993**, *105*, 1124−1125; *Angew. Chem. Int. Ed. Engl.* **1993**, *32*, 1059−1060; W. Hönle, G. Gerlach, W. Weppner, A. Simon, *J. Solid State Chem.* **1986**, *61*, 171−180; G. Linti, W. Köstler, *Angew. Chem.* **1996**, *108*, 593−595; *Angew. Chem. Int. Ed. Engl.* **1996**, *35*, 550−552; G. Linti, R. Frey, M. Schmidt, *Z. Naturforsch., B. Chem. Sci.* **1994**, *49*, 958−962; M. Julien-Pouzol, S. Jaulmes, M. Guittard, F. Alapini, *Acta Crystallogr. B* **1979**, *35*, 2848−2851; A. Kuhn, A. Chevy, R. Chevalier, *Acta Crystallogr. B* **1976**, *32*, 983−984; S. Paashaus, R. Kniep, *Z. Naturforsch., B. Chem. Sci.* **1990**, *45*, 667−678; D. S. Brown, A. Decken, A. H. Cowley, *J. Am. Chem. Soc.* **1995**, *117*, 5421−5422; A. K. Saxena, H. Zhang, J. A. Maguire, N. S. Hosmane, A. H. Cowley, *Angew. Chem.* **1995**, *107*, 378−380; *Angew. Chem. Int. Ed. Engl.* **1995**, *34*, 332−334; X.-W. Li, W. T. Pennington, G. H. Robinson, *J. Am. Chem. Soc.* **1995**, *117*, 7578−7579; X.-W. Li, Y. Xie, P. R. Schreiner, K. D. Gripper, R. C. Crittendon, C. F. Campana, H. F. Schaefer, G. H. Robinson, *Organometallics* **1996**, *15*, 3798−3803; B. Beagley, S. M. Godfrey, K. J. Kelly, S. Kungwankunakorn, C. M. McAuliffe, R. G. Pritchard, *J. Chem. Soc., Chem. Commun.* **1996**, 2179−2180; M. C. Kuchta, J. B. Bonanno, G. Parkin, *J. Am. Chem. Soc.* **1996**, *118*, 10914−10915; A. H. Cowley, A. Decken, C. A. Olazabal, *J. Organomet. Chem.* **1996**, *524*, 271−273.
[8] G. D. Smith, R. L. Jaffe, *J. Phys. Chem.* **1996**, *100*, 9624−9630. W. Uhl, F. Hannemann, R. Wartchow. *Organometallics* **1998**, in press.
[9] T. Hahn (Ed.), *International Tables for Crystallography, Space Group Symmetry*, Kluwer Academic Publishers, Dordrecht-Boston-London, **1989**, vol. A.
[10] *SHELXTL-Plus REL. 4.1*, Siemens Analytical X-RAY Instruments Inc., Madison, USA, **1990**; G. M. Sheldrick *SHELXL-93, Program for the Refinement of Structures*, Universität Göttingen, **1993**.
[11] The crystallographic data of **2**, **3** and **4** (excluding structure factors) were deposited with the Cambridge Crystallographic Data Centre as supplementary publication no. CCDC-102026 (**2**), -102027 (**3**), and -102028 (**4**). Copies of the data can be obtained free of charge on application to The Director, CCDC, 12 Union Road, GB-Cambridge CB2 1EZ, UK [Fax: Int. Code+(1223) 336−033; E-mail: deposit@chemcrys.cam.ac.uk].

[98203]

Head-to-Head versus Head-to-Tail Dimerizations of Transient Silenes – The Solvent-Dependent Regiospecifity of the Dimerization of 2-(2-Methoxyphenyl)-1,1-bis(trimethylsilyl)silene

Kathleen Schmohl[a], Matthias Blach[a], Helmut Reinke[a], Rhett Kempe[b], and Hartmut Oehme*[a]

Fachbereich Chemie der Universität Rostock[a],
D-18051 Rostock, Germany
Fax: (internat.) +49(0)381/498-1763

Institut für Organische Katalyseforschung an der Universität Rostock e.V.[b],
D-18055 Rostock, Germany

Received July 22, 1998

Keywords: Silicon / Silenes / 1,2-Disilacyclobutanes / 1,3-Disilacyclobutanes / Eliminations

The regiospecifity of the dimerization of the transient 2-(2-methoxyphenyl)-1,1-bis(trimethylsilyl)silene (**6**), synthesized by base-initiated trimethylsilanolate elimination from (2-methoxyphenyl)[tris(trimethylsilyl)silyl]methanol (**5**) according to a modified Peterson mechanism, decisively depends on the donating ability of the solvent in which the silene is generated. In ether, **6** undergoes a formal [2 + 2] dimerization to afford 3,4-bis(2-methoxyphenyl)-1,1,2,2-tetrakis(trimethylsilyl)-1,2-disilacyclobutane (**12**), whereas in toluene the head-to-tail [2 + 2] cyclodimer, 2,4-bis-(2-methoxyphenyl)-1,1,3,3-tetrakis(trimethylsilyl)-1,3-disilacyclobutane (**13**) was obtained. 1,1-Bis(trimethylsilyl)-2-(2,4,6-trimethoxyphenyl)silene (**18**), similarly made by a modified Peterson reaction, under the same conditions reacted with the eliminated trimethylsilanolate with readdition at the polar Si=C bond to give, after hydrolysis,2-(2,4,6-trimethoxybenzyl)-1,1,1,3,3,3-hexamethyl-2-(trimethylsiloxy)trisilane (**19**). A possible mechanism explaining the solvent-dependent regiospecificity of the dimerization of **6** is discussed. The structures of **12** and **13** were determined on the basis of NMR and MS data as well as X-ray structural analyses.

In the absence of trapping agents, sterically congested transient silenes undergo rapid dimerizations, in which head-to-head as well as head-to-tail reactions are observed[1]. The factors influencing the mode of dimerization are not clear, but, obviously, increasing polarity of the Si=C bond favors a head-to-tail coupling. Transient 1,1-bis(trimethylsilyl)silenes, made by the photolysis of acyl-tris(trimethylsilyl)silanes[2] or by a modified Peterson reaction[2][3][4], generally dimerize in a head-to-head mode. The reaction is supposed to proceed through radical intermediates[5]. After Si−Si bond formation the resulting diradicals stabilize with the formation of products, the structures of which depend on the nature of the substituents at the silene carbon atom (Eq. 1). 1,2-disilacyclobutanes **1** are usually obtained as the formal head-to-head [2 + 2] cyclodimers of the transient 1,1-bis(trimethylsilyl)silenes. When at least one of the silene C substituents is an aryl group, moderately stable tetrahydro-2,3-disilanaphthalenes **2**[6] are in some cases isolated as the kinetically preferred formal [2 + 4] silene dimers, which on thermal treatment gradually isomerize to give **1**. Silenes containing α hydrogen in the substituent at the silene C atom ("allylic" hydrogen) stabilize preferentially under hydrogen transfer to give linear dimers **3**[2][3a][5][7].

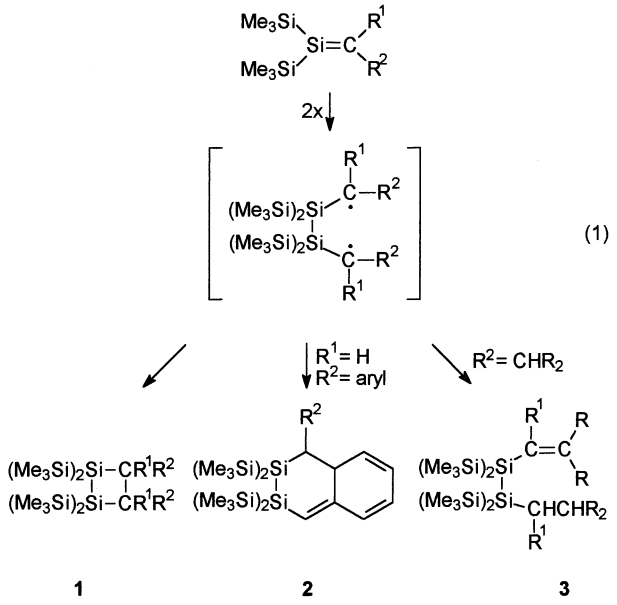

(1)

Recently we found that 2-(2-dimethylaminophenyl)-1,1-bis(trimethylsilyl)silene (**4**) dimerizes exclusively in a head-to-tail reaction affording the respective 1,3-disilacyclobutane[4]. This unusual regiospecificity was discussed as being effected by the 2-dimethylamino group of the aromatic substituent, causing an intermolecular interaction with the electrophilic silene silicon atom of a neighboring silaethene molecule. This donor−acceptor interaction finally leads to a head-to-tail dimerization following a mechanism, which is discussed later in this text. In this paper we describe the synthesis and dimerization behavior of 2-(2-methoxyphenyl)-1,1-bis(trimethylsilyl)silene, i.e. the dimethylamino do-

 © WILEY-VCH Verlag GmbH, D-69451 Weinheim, 1998 1434−1948/98/1111−1667 $ 17.50+.50/0

nor group in the above-mentioned silaethene is replaced by a methoxy group, to examine the proposed cyclodimerization mechanism.

The Generation and Cyclodimerization Behavior of the Transient 2-(2-Methoxyphenyl)-1,1-bis(trimethylsilyl)silene (6)

2-(2-Methoxyphenyl)-1,1-bis(trimethylsilyl)silene (**6**) was generated by the base-induced elimination of trimethylsilanol from (2-methoxyphenyl)-[tris(trimethylsilyl)silyl]-methanol (**5**) according to a modified Peterson mechanism. The alcohol **5** was obtained by the standard method[7] from tris(trimethylsilyl)silylmagnesium bromide and 2-methoxybenzaldehyde (Eq. 2).

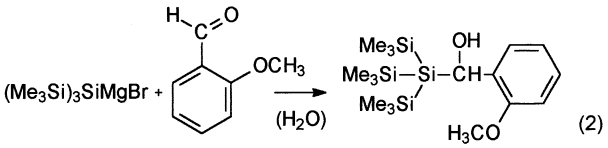

(2)

5

Interestingly, the outcome of the deprotonation reaction of **5** with organolithium reagents markedly depended on the solvent in which the reaction was carried out, and on the reaction conditions applied. Thus, the reaction of **5** with excess phenyllithium in ether led to the trisilane **8** (Eq. 3). This experiment is generally our standard method to check the clean trimethylsilanolate elimination from the starting 1-hydroxyalkyl-tris(trimethylsilyl)silane and the formation of the respective silene[7]. **8** was formed by immediate addition of excess phenyllithium to the Si=C bond of generated **6**, affording after hydrolysis the trisilane **8** . The high yield, in which **8** was obtained (84%), indicates a straightforward silene formation according to the modified Peterson mechanism.

The deprotonation of **5** with stoichiometric quantities of phenyllithium in ether at low temperature (starting at −78 °C and allowing the solution to warm up to room temperature) led to a complex mixture of components, from which only small quantities of a resultant silene product **11** could be separated in a pure form. On the basis of IR, NMR, and MS data, and particularly by means of an X-ray structural analysis it was identified as the silane **11** (Eq. 3). Its formation is interpreted as the result of the addition of phenyllithium at the polar Si=C bond of **6** giving an organolithium derivative **7** which attacks a further silene molecule. The resulting organolithium intermediate **9** undergoes a rapid rearrangement, a 1,4-Si,C-trimethylsilyl migration, with formation of the lithium silanide **10**, which is hydrolyzed during the aqueous workup affording **11**. Such trimethylsilyl migrations are not unusual; some years ago we observed a similar 1,3-Si,C shift[9], and the isomerization **9**→**10** is easily understood in terms of the particular stabilization of the silaanion by the phenyl and trimethylsilyl substituents. As we noticed, the deprotonation step of **5** proceeds comparatively slowly. Assuming that the elimination of lithium trimethylsilanolate is a fast process, the

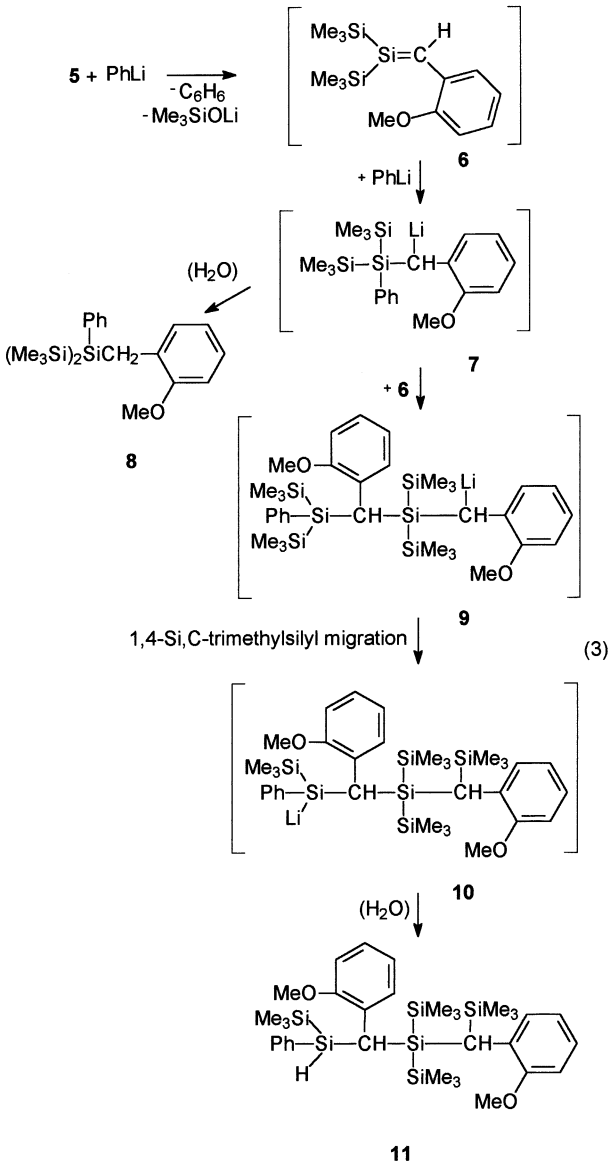

generated silene will always meet an effective excess of phenyllithium, which initiates this side reaction. The molecular structure of **11** is illustrated in Figure 1. The significant deviations from standard values of the bond distances and angles given characterize **11** as a considerably congested compound.

The clean generation of **6** by deprotonation of **5** with PhLi, indicated by the formation of **8** in high yield, led to the assumption that the mixture of unidentified compounds obtained by the reaction of **5** with stoichiometric quantities of PhLi in ether may probably consist of the various isomers of the formal [2 + 4] head-to-head cycloadducts **2** of the silene **6** (see Eq. 1). These products are known to undergo an isomerization on thermal treatment to give the thermodynamically stable 1,2-disilacyclobutane. This was the reason for changing the procedure of the reaction of **5** with equimolar quantities of PhLi in ether in such a way that after warming-up of the mixture to room temperature and subsequent removal of the solvent the residue was dis-

Figure 1. Molecular structure of **11** in the crystal [H atoms (except Si4-H and C1-H) omitted, ORTEP, 30% probability level][a]

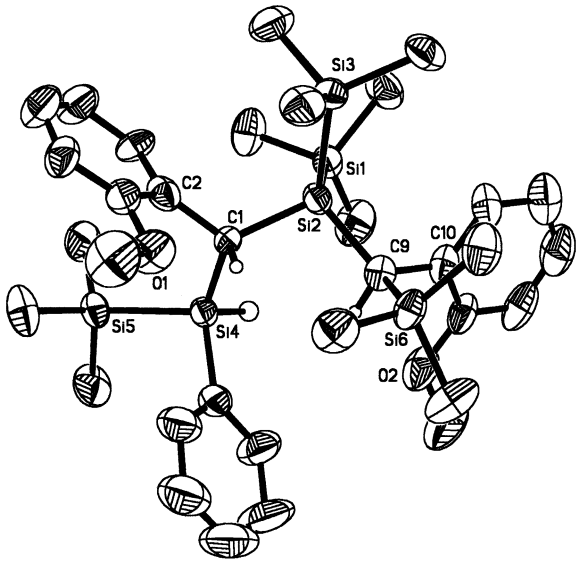

[a] Selected bond lengths [Å] and angles [°]: C1−Si2 1.912(5), C1−Si4 1.891(5), Si1−Si2 2.491(3), Si2−Si3 2.379(2), Si4−Si5 2.351(2), Si2−C9 1.873(6), C9−Si6 1.885(6); C1−Si2−C9 103.6(7), C9−Si2−Si3 118.7(2), C1−Si2−Si3 107.7(2), C1−Si2−Si1 113.3(2), Si1−Si2−Si3 107.02(9), C1−Si4−Si5 117.1(2).

Figure 2. Molecular structure of *E*-**12** in the crystal [H atoms (except the ring-CH) omitted, ORTEP, 30% probability level][a]

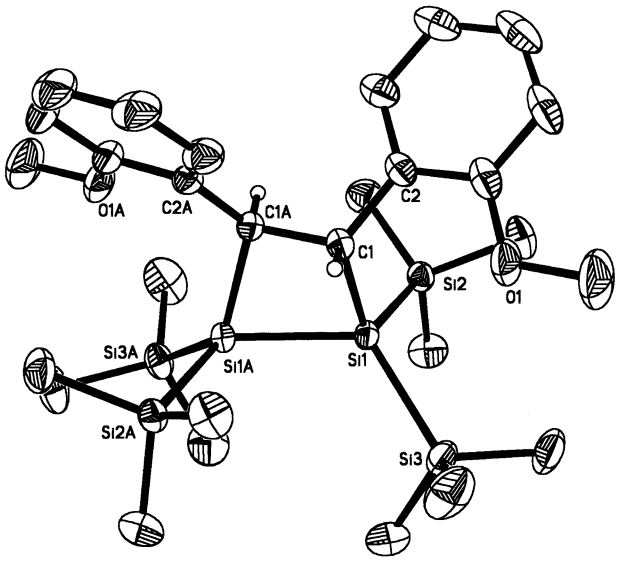

[a] Selected bond lengths [Å] and angles [°]: C1−C1A 1.549(5), C1−Si1 1.953(2), Si1−Si1A 1.3477(13), C1−C2 1.507(3), Si1−Si2 2.3589(10), Si1−Si3 2.3585(10); C1−Si1−Si1A 76.05(7), C1−C1A−Si1A 98.57(9), C1−Si1−Si2 107.52(8), C1−Si1−Si3 124.79(8), Si2−Si1−Si3 109.51(4).

solved in toluene and heated under reflux for 4 h. Aqueous workup actually afforded 42% of (*E*/*Z*)-3,4-di(2-methoxyphenyl)-1,1,2,2-tetrakis(trimethylsilyl)-1,2-disilacyclobutane (**12**). Repeated recrystallization from acetone gave pure (*E*)-**12**.

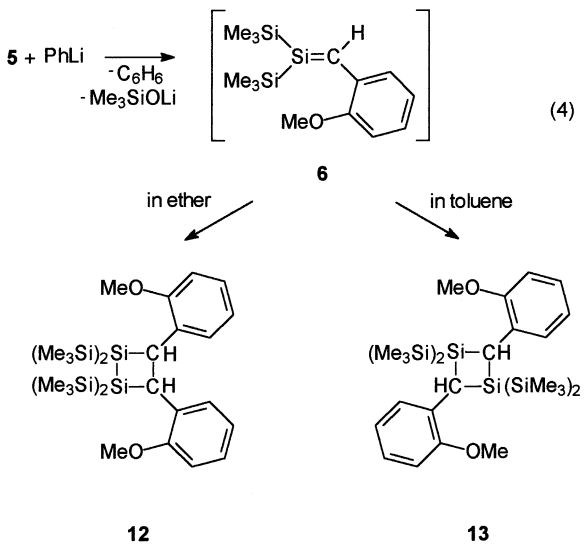

Compound **12** is the expected formal head-to-head [2 + 2] cyclodimer of the silene **6**. Its structure was elucidated by a full spectral analysis and an X-ray structural analysis characterizing the compound investigated as the C_2 symmetrical (*E*)-isomer (Figure 2). The four-membered ring is folded, the torsional angle Si1−Si1−C1−C1 being 24.7°. The C1−Si1 distances are slightly elongated, but most structural parameters are within the expected range.

As mentioned above, the outcome of the reaction of **5** with organolithium reagents decisively depends on the solvent used. A number of products were identified when **5** was deprotonated with equimolar quantities of methyllithium or *n*-butyllithium in toluene at low temperature and the mixture stirred after warming up to room temperature for 4 days. Besides unreacted **5**, traces of **16** and large quantities of a polymeric material a solid compound was isolated, which was unambiguously identified as the 1,3-disilacyclobutane **13**, the formal head-to-tail cyclodimer of the silene **6**. The structure elucidation of **13** was performed by NMR and MS investigations as well as by an X-ray structural analysis. As seen in Figure 3, the compound isolated in a yield of 27% is the (*E*)-isomer of the 1,3-disilacyclobutane **13**. The ring is planar. Apart from slightly elongated ring Si−C distances, which are considered as being due to steric congestion, the bond parameters are in the expected range. The reaction of **5** with organolithium reagents in pentane under the same conditions afforded (*E*)-**13** in 16% yield.

The byproduct **16** is the result of a 1,3-migration of one trimethylsilyl group from the central silicon atom to the alkoxid oxygen atom of deprotonated **5**, followed by hydrolysis of the silanide formed (Eq. 5). The same H-silane **16** is obtained in high yield by treatment of **5** with sodium hydride in ether. Such Si,O migrations were observed for the first time by Brook et al.[8] and appear to be typical of the behavior of 1-hydroxyalkylpolysilanes towards base[7].

Whereas the silene **6**, generated in ether, dimerizes to give the "normal" head-to-head product, a change of the solvent causes a complete reversal of the dimerization regiospecificity. Actually, the yield of **13** was not very high, but it should be emphasized that in the product mixture of the reaction

Figure 3. Molecular structure of *E*-**13** in the crystal [H atoms (except the ring-CH) omitted, ORTEP, 30% probability level][a]

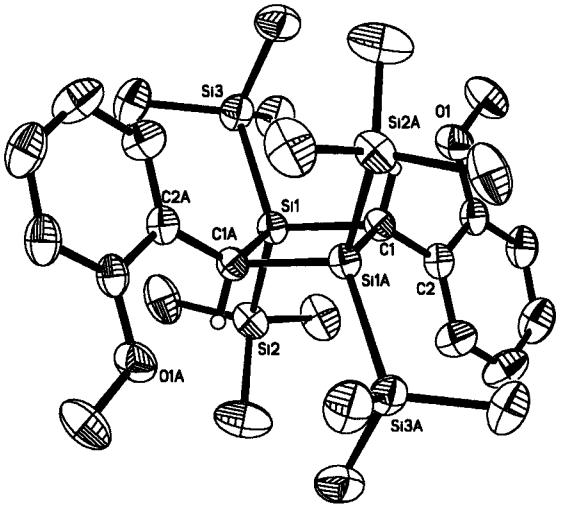

[a] Selected bond lengths [Å] and angles [°]: C1−Si1 1.923(2), Si1−Si2 2.3682(11), Si1−Si3 2.3668(11); C1−Si1−C1A 91.14(10), Si1−C1−Si1A 88.86(10).

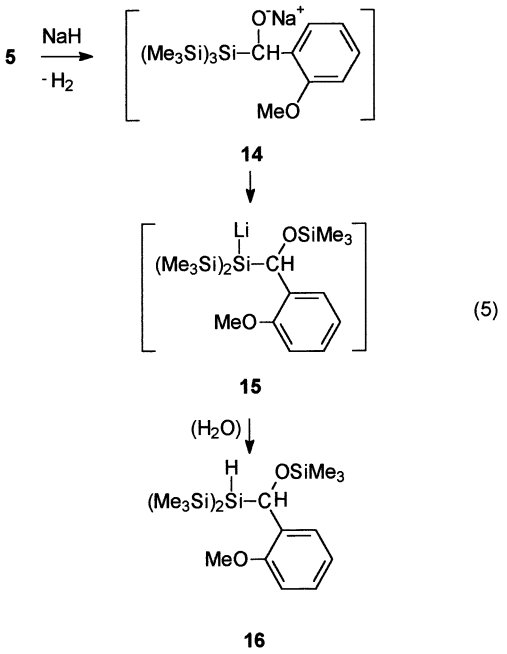

(5)

of **5** with methyllithium in toluene no silene head-to-head dimer **12** could be detected. Similarly, no trace of the head-to-tail dimer **13** was observed after the reaction of **5** with MeLi in ether.

This solvent-dependent behavior of the silene **6** is fully consistent with the model proposed for the dimerization of 2-(2-dimethylaminophenyl)-1,1-bis(trimethylsilyl)silene (**4**), affording (in this case also in ether) exclusively the head-to-tail dimer. The deviation of **4** from the usual dimerization pattern of 1,1-bis(trimethylsilyl)silenes was discussed as a consequence of a strong donor−acceptor interaction of the dialkylamino group with the electrophilic silene silicon atom[4]. An effective intramolecular donor−acceptor interaction, which actually is expected to lead to an increase in the polarity of the silene double bond, thus facilitating a head-to-tail dimerization, is rather unlikely for steric reasons. We assume that the head-to-tail dimerization of **4** is achieved by an intermolecular donor−acceptor interaction, the *ortho*-dimethylamino group acting as some kind of anchor. Its interaction with the electrophilic silene silicon atom of a neighboring molecule and the attack of the activated nucleophilic silene carbon atom at the Si=C group of the first silene molecule possibly initiate a head-to-tail dimerization through a cyclic seven-membered transition state. This picture, outlined in eq. 6, can directly be transferred to the dimerization of **6** in toluene.

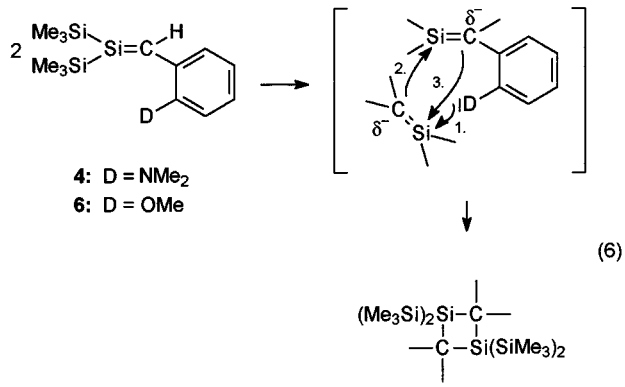

(6)

Of course, the donating ability of the dialkylamino group of **4** is much stronger than that of the methoxy group in **6**. Therefore the dimerization mode of **4** is solvent independent. On the other hand, in case of the generation of the silene **6** in ether, the donor solvent competes successfully with the weakly donating *o*-methoxy group, interrupting the intermolecular interaction. Thus, when ether is used as the solvent, the dimerization of **6** follows the usual reaction pattern providing the head-to-head product **12**.

The Reaction of (2,4,6-Trimethoxyphenyl)[tris(trimethylsilyl)-silyl]methanol (17) with Potassium *tert*-Butoxide

1,1-Bis(trimethylsilyl)-2-(2,4,6-trimethoxyphenyl)silene (**18**), generated through the modified Peterson mechanism from (2,4,6-trimethoxyphenyl)[tris(trimethylsilyl)silyl]methanol (**17**) offers the same structural requirements for following a dimerization pattern comparable to that of **6** and was therefore included in our studies. Unexpectedly, the reaction of **17** with MeLi or PhLi in ether as well as in toluene proceeded very slowly. Better results were obtained when potassium *tert*-butoxide was used as the deprotonating base. However, the reaction of **17** with *t*BuOK in both solvents gave no silene dimer, and we obtained a colorless oil, which was identified as 2-(2,4,6-trimethoxyphenyl)-1,1,1,3,3,3-hexamethyl-2-(trimethylsiloxy)trisilane (**19**) (Eq. 7).

The siloxane **19** is formed by readdition of the silanolate, just eliminated from **17**, at the Si=C bond of the silene **18**. This behavior is typical for highly congested silenes generated by the Peterson process[3b][10]. Obviously, the increase

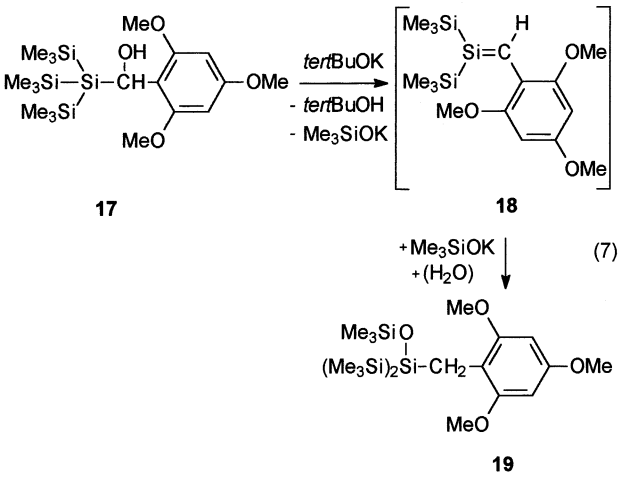

of the bulkiness of the substituent at the silene carbon atom diminishes the dimerization tendency making the silanolate addition the dominating process.

We gratefully acknowledge the support of our research by the *Deutsche Forschungsgemeinschaft* and the *Fonds der Chemischen Industrie.* We thank Dr. *M. Michalik,* Dr. *W. Baumann* and Prof. *N. Stoll* for recording the NMR and MS spectra.

Experimental Section

General: All reactions involving organometallic reagents were carried out under purified argon. − NMR: Bruker AC 250 or Bruker ARX 300, tetramethylsilane as internal standard. − IR: Nicolet 205 FT-IR. − MS: Intectra AMD 402, chemical ionization with isobutane as the reactant gas. − $(Me_3Si)_3SiLi \cdot 3$ THF[11] and **17**[12] were prepared as reported in the literature.

(2-Methoxyphenyl)[tris(trimethylsilyl)silyl]methanol (**5**): As described previously[7], 14.7 g (0.03 mol) of $(Me_3Si)_3SiLi \cdot 3$ THF were converted in ether with an equimolar quantity of $MgBr_2$ into $(Me_3Si)_3SiMgBr$ and to this suspension 4.1 g (0.03 mol) of 2-methoxybenzaldehyde were added at −78°C. After stirring for 2 h the mixture was allowed to warm up to room temperature, diluted HCl was added, the organic layer was separated, dried with $MgSO_4$, and evaporated. The residue was purified by Kugelrohr distillation (150°C / 0.03 Torr). Yield 8.7 g (75%) pale yellow crystals, m.p. 48°C. **5** is rather unstable and should be kept in the cold. At room temperature the solid gradually decomposes to an oily product of unidentified structure. Attempts to recrystallize **5** were therefore also unsuccessful. − IR (cap.): $\tilde{\nu}$ = 3523 cm^{-1} (OH free), 3439 (OH ass.). − ^{1}H NMR ([D$_6$]benzene): δ = 0.28 (s, $SiCH_3$, 27 H), 1.30 (d, ^3J = 4.0 Hz, OH, 1 H), 3.27 (s, OCH_3, 3 H), 5.38 (d, ^3J = 4.0 Hz, CH, 1 H), 6.42−7.49 (m, ArH, 4 H). − ^{13}C NMR ([D$_6$]benzene): δ = 1.8 ($SiCH_3$), 54.2 (OCH_3), 62.6 (COH), 109.8, 121.0, 126.8, 127.2 (arom. CH), 136.3, 154.5 (arom. quart. C). − ^{29}Si NMR ([D$_6$]benzene): δ = −12.8 ($SiMe_3$)$_3$, − 68.8 (*Si*$SiMe_3$). − MS: *m/z* (%): 383 (6) [M^+ − H], 367 (100) [M^+ − OH]. − $C_{17}H_{36}O_2Si_4$ (384.82): calcd. C 53.06, H 9.43; found C 52.58, H 8.85).

(2-Methoxybenzyl)-1,1,1,3,3,3-hexamethyl-2-phenyltrisilane (**8**)*:* To a solution of 0.5 g (1.3 mmol) of **5** in 20 ml of ether a fivefold molar excess of PhLi was added at room temperature. After stirring for 2 h diluted HCl was added, the ethereal phase separated and dried with $MgSO_4$. The oily product obtained after evaporation was purified by chromatography (silica gel, heptane/ethyl acetate, 20:1) to give 0.4 g (84%) **8**. − ^{1}H NMR ([D$_6$]benzene): δ = 0.16 (s, $SiCH_3$, 18 H), 2.75 (s, CH_2, 2 H), 3.27 (s, OCH_3, 3 H), 6.49−7.61 (m, ArH, 9 H). − ^{13}C NMR ([D$_6$]benzene): δ = −0.2 ($SiCH_3$), 13.9 (CH_2), 54.3 (OCH_3), 110.2, 120.7, 125.9, 128.0, 128.2, 130.3, 135.6 (aromat. CH), 130.0, 137.9, 156.7 (aromat. quart. C). − MS: *m/z* (%) = 357 (8.5) [M^+ − CH_3], 299 (100) [M^+ − $CSiMe_3$]. − $C_{20}H_{32}OSi_3$ (372.73): calcd. C 64.45, H 8.65; found C 64.56, H 8.74.

2,4-Bis(2-methoxyphenyl)-1-phenyl-1,3,3,4-tetrakis(trimethylsilyl)-1,3-disilabutane (**11**): An equimolar quantity of phenyllithium was added to a solution of 0.5 g (1.3 mmol) of **5** in ether at −78°C and stirred for 2 h. After warming of the mixture to room temperature, diluted HCl was added, the organic layer separated, dried with $MgSO_4$, and evaporated. Chromatographic separation of the residue (silica gel, heptane) and recrystallization of the product from acetone gave 0.04 g (9.2%) of **11**. Colorless crystals, m.p. 255°C. − IR (KBr): $\tilde{\nu}$ = 2094 cm^{-1} (SiH). − ^{1}H NMR ([D$_6$]benzene): δ = − 0.18, 0.13, 0.20, 0.28 (4s, $SiCH_3$, 4 × 9 H), 2.87 (s, CH, 1H), 3.28 and 3.58 (2s, OCH_3, 2 × 3 H), 3.44 and 5.06 (2d, ^3J = 5.4 Hz for both, SiH and PhSiCH, 3 × 1 H), 6.48−7.92 (m, ArH, 13 H). − ^{13}C NMR ([D$_6$]benzene): δ = −1.5, 0.5, 2.8, 3.4 ($SiCH_3$), 9.4, 15.6 (CH), 54.2, 54.4 (OCH_3), 110.0, 110.3, 119.8, 120.9, 121.9, 125.4, 125.6, 125.7, 128.8, 132.3, 132.4, 133.3, 135.9, 138.3, 138.4, 155.7 (aromat.C). − ^{29}Si NMR ([D$_6$]benzene): δ = − 22.3 *Si*($SiMe_3$)$_2$, −16.7, −16.3, −15.2 (Si*Si*Me_3, SiH), 1.6 ($CSiMe_3$). − MS: *m/z* (%) 622 (2) [M^+], 651 (7) [M^+ − CCH_3], 593 (100) [M^+ − $CSiMe_3$]. − $C_{34}H_{58}O_2Si_6$ (667.34): calcd. C 61.19, H 8.76; found C 61.33, H 8.72.

(E)-3,4-Bis(2-methoxyphenyl)-1,1,2,2-tetrakis(trimethylsilyl)-1,2-disilacyclobutane (**12**): An equimolar quantity of PhLi was given to a stirred solution of 0.5 g (1.3 mmol) of **5** in 25 ml of ether. After warming up to room temperature, the solvent was removed in vacuo, 20 ml of toluene were added and the solution was refluxed for 4 h. After addition of diluted HCl the organic phase was separated, dried with $MgSO_4$, and evaporated. The oily residue crystallized after addition of a few ml of *n*-heptane to give 0.16 g (42%) of (*E*/*Z*)-**12**, repeated recrystallization from acetone afforded pure (*E*)-**12**, m.p. 175°C. − ^{1}H NMR ([D$_6$]benzene): δ = 0.17, 0.44 (2s, $SiCH_3$, 2 × 18 H), 3.45 (s, OCH_3, 6 H), 4.18 (s, ring CH, 2 H), 6.51−7.12 (m, ArH, 8 H). − ^{13}C NMR ([D$_6$]benzene): δ = 1.9, 2.0 ($SiCH_3$), 29.8 (ring C), 54.7 (OCH_3), 109.4, 120.8, 125.0, 126.5 (arom. CH), 133.4, 156.2 (arom. quart. C). − ^{29}Si NMR ([D$_6$]benzene): δ = −49.9 (ring Si), −14.0, −11.3 ($SiMe_3$). − MS: *m/z* (%): 589 (22) [M^+ + H], 573 (12) [M^+ − CCH_3], 515 (19) [M^+ − $CSiMe_3$], 348 (100) [M^+ − $C(Me_3Si)_2SiSi(SiMe_3)_2$]. − $C_{28}H_{52}O_2Si_6$ (589.24): calcd. C 57.08, H 8.90; found C 57.30, H 8.79.

(E)-2,4-Bis(2-methoxyphenyl)-1,1,3,3-tetrakis(trimethylsilyl)-1,3-disilacyclobutane (**13**): To 0.6 g (1.6 mmol) of **5**, dissolved in 25 ml of toluene, an equimolar quantity of *n*BuLi was added under stirring at −78°C. The solution was allowed to warm up to room temperature within 2 h and afterwards it was refluxed for 4 h. After hydrolysis the organic layer was separated, dried with $MgSO_4$ and evaporated to give an oily residue which crystallized on addition of some heptane. Repeated recrystallization from heptane afforded 0.06 g (13%) of colorless crystals of (*E*)-**13**, m.p. 235°C. − ^{1}H NMR ([D$_6$]benzene): δ = 0.28 (s, $SiCH_3$, 36 H), 3.37 (s, OCH_3, 6 H), 3.87 (s, ring CH, 2 H), 6.47−7.67 (m, ArH, 8 H). − ^{13}C NMR ([D$_6$]benzene): δ = 0.6 ($SiCH_3$), 7.6 (ring C), 54.9 (OCH_3), 110.2, 120.3, 124.4, 130.5 (arom. CH), 133.5, 156.6 (arom. quart. C). − ^{29}Si NMR ([D$_6$]benzene): δ = −13.4 (ring Si), −13.9 ($SiMe_3$). − MS: *m/z* (%): 589 (3) [M^+ + H], 573 (6) [M^+ − CCH_3], 515 (100)

Table 1. Crystal and structure solution data of **11**, **12**, and **13**

	11	**12**	**13**
Formula	$C_{34}H_{58}O_2Si_6$	$C_{28}H_{52}O_2Si_6$	$C_{28}H_{52}O_2Si_6$
M [g·mol^{-1}]	667.34	589.24	589.24
a [Å]	17.429(2)	17.138(3)	21.324(4)
b [Å]	12.104(2)	10.323(2)	10.130(2)
c [A]	19.984(2)	21.022(3)	17.056(3)
β [°]	94.630(10)	105.59(4)	99.06(3)
V [Å^3]	4202.1(9)	3582.2(11)	3638.3(12)
$\rho_{calcd.}$ [g·cm^{-3}]	1.055	1.093	1.076
Z	4	4	4
Crystal system	Monoclinic	Monoclinic	Monoclinic
Space group	$P2_1/c$	C2/c	C2/c
F(000) [e]	1448	1280	1280
μ (Mo-K_α) [mm^{-1}]	0.224	0.255	0.251
Radiation λ [A]	0.71073	0.71073	0.71073
Diffractometer	Siemens P4	Siemens P4	Stoe-IPDS
Crystal size	0.94 × 0.62 × 0.56	0.88 × 0.60 × 0.38	0.6 × 0.5 × 0.4
Temperature [°C]	293	293	293
Data collection Mode	omega scan	omega scan	laser-scanned imaging plate
Scan range (2θ) [°]	3.94−42.00	4.02−44.00	3.86−48.62
hkl range	−1/18 −1/13 −1/18	−1/18 −11/1 −1/18	−24/24 −11/11 −24/24
Measured refl.	5703	2806	9445
Unique refl.	4519	2198	2914
Observed refl.	3573	1984	2139
$I \geq 2\sigma(I)$	2σ (I)	2σ (I)	2σ (I)
Refined param.	380	163	189
$R1$	0.0768	0.0444	0.038
$wR2$ for all	0.2158	0.1238	0.109
GoF for all	1.027	1.088	1.047

[M^+ − $CSiMe_3$]. − $C_{28}H_{52}O_2Si_6$ (589.24): calc. C 57.08, H 8.90; found C 57.14, H 8.91.

(2-Methoxyphenyl)bis(trimethylsilyl)silyltrimethylsiloxymethane (**16**): To a stirred solution of 0.6 g (1.6 mmol) of **5** in 35 ml of ether a catalytic amount of sodium hydride was added at −78°C. After warming up to room temperature water was added, the organic layer separated and dried with $MgSO_4$. Evaporation gave a colorless oil, which was purified by chromatography (silica gel, heptane/ethyl acetate, 30:1). − IR (cap.): $\tilde{\nu}$ = 2074 cm^{-1} (SiH). − ^{1}H NMR ([D$_6$]benzene): δ = 0.09 (s, $OSiCH_3$, 9 H), 0.25 (s, $SiSiCH_3$, 18 H), 3.37 (s, OCH_3, 3 H), 3.68 (d, ^3J = 2.45 Hz, SiH, 1 H), 5.67 (d, ^3J = 2.52 Hz, CH, 1 H), 6.50−7.67 (m, ArH, 4 H). − ^{13}C NMR ([D$_6$]benzene): δ = 0.3, 0.6, 0.8 ($SiCH_3$), 54.6 (OCH_3), 61.2 (CH), 109.9, 120.9, 126.7, 127.2 (arom. CH), 135.6, 154.2 (arom. quart. C). − ^{29}Si NMR ([D$_6$]benzene): δ = −52.9 (SiSiMe$_3$), −15.0, −15.3 (SiSiMe$_3$), 17.7 (OSiMe$_3$). − MS: *m/z* (%): 384 (3) [M^+], 311 (90) [M^+ − $CSiMe_3$], 209 (100) [M^+ − $CHSi(SiMe_3)_2$]. − $C_{17}H_{36}O_2Si_4$ (384.82): calcd. C 53.06, H 9.43; found C 52.88, H 9.39.

2-(2,4,6-Trimethoxbenzyl)-1,1,1,3,3,3-hexamethyl-2-(trimethylsiloxy)trisilane (**19**): To a solution of 0.55 g (1.2 mmol) of **17** in 30 ml of toluene the equimolar quantity of *t*BuOK was added at −78°C. The mixture was allowed to warm up gradually to room temperature and was then heated under reflux for 4 h. Hydrolysis, separation and drying of the organic phase and evaporation gave a colorless oil, which was purified by chromatography (silica gel, heptane/ethyl acetate, 20:1), yield 0.23 g (59%). − IR (cap.): $\tilde{\nu}$ = 1062 cm^{-1} (SiOSi). − ^{1}H NMR ([D$_6$]benzene): δ = 0.18 (s, OS-iCH_3, 9 H), 0.21 (s, $SiSiCH_3$, 18 H), 2.72 (s, CH_2, 2 H), 3.39 (s, OCH_3, 6 H), 3.42 (s, OCH_3, 3 H), 6.12 (s, ArH, 2 H). − ^{13}C NMR ([D$_6$]benzene): δ = −1.3 ($SiSiCH_3$), 2.3 ($OSiCH_3$), 12.9 (CH_2), 54.8 (*o*-OCH_3), 54.9 (*p*-OCH_3), 90.6 (arom. CH), 109.1, 157.9, 158.7 (arom. quart. C). − ^{29}Si NMR ([D$_6$]benzene): δ = −19.6 (SiSi-*t*Me$_3$), 0.9 (*Si*SiMe$_3$), 6.3 (OSiMe$_3$). − MS: *m/z* (%): 445 (1) [M^++H], 429 (10) [M^+ − CCH_3], 371 (100) [M^+ − $CSiMe_3$], 355 (12) [M^+ − $COSiMe_3$]. − $C_{19}H_{40}O_4Si_4$ (444.87): calcd. C 51.30, H 9.06; found C 51.23, H 9.03.

Crystal-Structure Determination of **11**, **12**, *and* **13**: The crystal-structure determinations were performed on a SIEMENS P4 four-circle diffractometer with graphite monochromator in the case of compounds **11** and **12** and on a STOE IPDS system with graphite monochromator for **13**. The structures were solved by direct methods (Siemens SHELXTL, 1990, Siemens Analytical X-ray Inst. Inc. for **11** and **12** and SHELXS-86[13] for **13**) and refined by the full-matrix least-squares method of Siemens SHELXTL, Ver. 5.03 (**11**, **12**) and SHELXL-93[14] (**13**). All non-hydrogen atoms were refined anisotropically. The hydrogen atoms were put into theoretical positions and refined using the riding model.

Crystallographic data (excluding structure factors) for the structures reported in this paper have been deposited with the Cambridge Crystallographic Data Centre as supplementary publication no. CCDC-102330 (**11**), CCDC-102331 (**12**), and CCDC-102332 (**13**). Copies of the data can be obtained free of charge on application to The Director, CCDC, 12 Union Road, Cambridge CB2 1EZ, UK [Fax: (internat.) +44(1223) 336-033; e-mail: deposit@ccdc.cam.ac.uk].

[1] G. Raabe, J. Michl in *The Chemistry of Organic Silicon Compounds* (Eds. S. Patai, Z. Rappoport), Wiley, New York, **1989**, p. 1100.
[2] D. Bravo-Zhivotovskii, V. Braude, A. Stanger, M. Kapon, Y. Apeloig, *Organometallics* **1992**, *11*, 2326−2328.
[3] [3a] J. Ohshita, Y. Masaoka, M. Ishikawa, *Organometallics* **1992**, *10*, 3775−3776. − [3b] J. Ohshita, Y. Masaoka, M. Ishikawa, T. Takeuchi, *Organometallics* **1993**, *12*, 876−879.
[4] C. Krempner, D. Hoffmann, R. Kempe, H. Oehme, *Organometallics* **1997**, *16*, 1828−1832 and literature cited therein.
[5] A. G. Brook, J. W. Harris, J. Lennon, M. ElSheikh, *J. Am. Chem. Soc.* **1979**, *101*, 83−95; A. G. Brook, K. M. Baines, *Adv. Organomet. Chem.* **1986**, *25*, 1−38; K. M. Baines, A. G. Brook, *Organometallics* **1987**, *6*, 692−696.
[6] C. Krempner, H. Reinke, H. Oehme, *Chem. Ber.* **1995**, *128*, 1083−1088; D. Hoffmann, H. Reinke, H. Oehme, *Z. Naturforsch.* **1996**, *51b*, 370−376.
[7] C. Krempner, H. Reinke, H. Oehme, *Chem. Ber.* **1995**, *128*, 143−149.
[8] A. G. Brook, J. J. Crusciel, *Organometallics* **1984**, *3*, 1317−1318.
[9] H. Oehme, R. Wustrack, A. Heine, G. M. Sheldrick, D. Stalke, *J. Organomet. Chem.* **1993**, *452*, 33−39.
[10] A. G. Brook, P. Chiu, J. McClenaghnan, A. J. Lough, *Organometallics* **1991**, *10*, 3292−3301; F. Luderer, H. Reinke, H. Oehme, *J. Organomet. Chem.* **1996**, 510, 181−188.
[11] G. Gutekunst, A. G. Brook, *J. Organomet. Chem.* **1982**, *225*, 1−3.
[12] K. Sternberg, H. Oehme, *Eur. J. Inorg. Chem.* **1998**, 177−181.
[13] G. M. Sheldrick, *SHELXS-86*, Universität Göttingen, **1986**.
[14] G. M. Sheldrick, *SHELXL-93*, Universität Göttingen, **1993**.

[98244]

Selective Catalytic Oxidation of Alcohols by a Ruthenium-Copper Bifunctional System Using Molecular Oxygen

Karl S. Coleman, Christian Y. Lorber, and John A. Osborn*

Laboratoire de chimie des métaux de transition et de catalyse, URA au CNRS 424, Université Louis Pasteur, Institut Le Bel, 4, rue Blaise Pascal, F-67070 Strasbourg, France
E-mail: osborn@chimie.u-strasbg.fr

Received February 2, 1998

Keywords: Ruthenium / Copper / Oxidations / Catalysis / Alcohols

The oxidation of allylic and benzylic alcohols to aldehydes can be carried out at room temperature with molecular oxygen, in the presence of the bifunctional ruthenium-copper system (nPr$_4$N)(RuO$_4$)–CuCl acting as the catalyst.

The oxidation of alcohols to aldehydes and ketones is a fundamental reaction in organic synthesis, and numerous oxidizing reagents are available to effect this key transformation.[1] In most instances, these reagents are used in stoichiometric amounts and are very often toxic such as the chromium oxidants used in vast amounts in both the laboratory and industry.[1] However, with the ever-growing environmental and economic concerns the development of catalytic processes for alcohol oxidation is becoming increasingly important.

A particularly noteworthy process has been described by Griffith et al.[2] who reported the use of the high oxidation state oxoruthenium compound tetra-*n*-propylammonium perruthenate (nPr$_4$N)(RuO$_4$), TPAP, as a mild catalyst for the oxidation of alcohols with *N*-methylmorpholine *N*-oxide, NMO, as the secondary oxidizing source. More recently, we reported the catalytic oxidation of primary alcohols to aldehydes with *cis*-dioxymolybdenum(VI) complexes and sulfoxides as the co-oxidant.[3] Although both of the above function well as catalytic systems, unpleasant and harmful by-products, amine and sulfide respectively, are produced. This limits the use of these catalysts on an industrial scale. The quest for catalytic systems that use inexpensive, nontoxic, molecular oxygen in the air as the secondary oxidant remains a particularly important goal for the development of a "green method" for converting alcohols to carbonyl products on an industrial scale.[4]

Relatively few ruthenium-based catalytic systems using air or molecular oxygen have been reported for the dehydrogenation of alcohols. These include the trinuclear ruthenium carboxylates [Ru$_3$O(O$_2$CR)$_6$L$_3$]^n (R = CH$_3$ or C$_2$H$_5$; L = H$_2$O or PPh$_3$; n = 0, +1)[5], the ruthenium(II) species [RuCl$_2$(PPh$_3$)$_3$][6], RuO$_2\cdot x$H$_2$O[7], the binuclear [Ru$_2$O$_6$(C$_5$H$_5$N)$_4$]$\cdot$3.5H$_2$O[8], the bimetallic system RuCl$_3$–Co(OAc)$_2$[9] and the triple catalytic system [RuCl(OAc)(PPh$_3$)$_3$]–hydroquinone–[Co(salophen)(PPh$_3$)][10] where H$_2$salophen = *N*,*N*′-bis(salicylidene)-*O*-phenylenediamine. However, these catalysts are rarely selective and are often limited as rather high reaction temperatures and high pressures of molecular oxygen are required and low turnover numbers are observed.

Recently, during the preparation of our manuscript Ley[11] and Markó[12] have communicated the use of tetra-*n*-propylammonium perruthenate, (nPr$_4$N)(RuO$_4$), in the presence of molecular oxygen, as a catalytic oxidant of both primary and secondary alcohols. Markó[12] has also observed that the presence of CuCl$\cdot$phenanthroline (5 mol-%) and K$_2$CO$_3$ (200 mol-%) produced a retarding effect in the oxidation of 4-chlorobenzyl alcohol. We wish to communicate some of our recent results on a similar (nPr$_4$N)(RuO$_4$)–CuCl bimetallic system which is a selective and efficient catalytic system for the oxidation of alcohols with molecular oxygen under mild conditions (25°C), producing water as the only stoichiometric by-product, Scheme 1.

The catalytic oxidation of various alcohols takes place smoothly at 25°C with (nPr$_4$N)(RuO$_4$) (1 mol-%), CuCl (1 mol-%), and 2-aminopyridine (5 mol-%) in the presence of 1 atm of molecular oxygen in toluene, dichloromethane, or acetonitrile. The results are presented in Table 1. The addition of powdered 4-Å molecular sieves results in slightly increased rates, as previously observed in oxidations with (nPr$_4$N)(RuO$_4$) and NMO.[2] This may be because the water formed as a by-product in the reaction degrades the catalyst. Allylic and benzylic alcohols are oxidized with nearly

Scheme 1

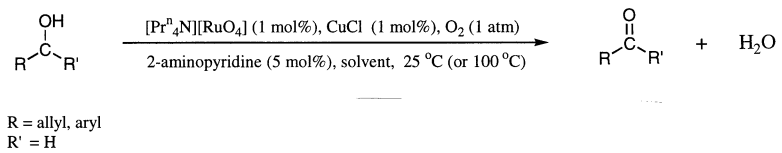

R = allyl, aryl
R′ = H

 © WILEY-VCH Verlag GmbH, D-69451 Weinheim, 1998 1434–1948/98/1111–1673 $ 17.50+.50/0

Table 1. Oxidation of alcohols to carbonyl compounds catalysed by a ruthenium−copper bifunctional system[a]

Entry	Substrate	t [h]	Product	Yield[b] (%)	Selectivity (%)
1	4-$MeOC_6H_4CH_2OH$[c][d]	24	4-$MeOC_6H_4CHO$	5[e]	56
2	4-$MeOC_6H_4CH_2OH$[c]	17	4-$MeOC_6H_4CHO$	100	100
3	4-$MeOC_6H_4CH_2OH$[c][f]	27	4-$MeOC_6H_4CHO$	50	100
4	4-$MeOC_6H_4CH_2OH$[g]	25	4-$MeOC_6H_4CHO$	71	100
5	4-$MeOC_6H_4CH_2OH$[h]	24	4-$MeOC_6H_4CHO$	61	100
6	4-$MeOC_6H_4CH_2OH$	23	4-$MeOC_6H_4CHO$	52	100
7	4-$ClC_6H_4CH_2OH$	26	4-ClC_6H_4CHO	40	100
8	4-$CF_3C_6H_4CH_2OH$	26	4-$CF_3C_6H_4CHO$	41	100
9	2,4-$Cl_2C_6H_3CH_2OH$	25	2,4-$Cl_2C_6H_3CHO$	51	100
10	2,6-$Cl_2C_6H_3CH_2OH$	25	2,6-$Cl_2C_6H_3CHO$	12	100
11	cinnamyl alcohol[c]	26	cinnamaldehyde	94	100
12	cinnamyl alcohol	29	cinnamaldehyde	47	100
13	$C_6H_5CH_2OH$	21	C_6H_5CHO	61	100
14	$C_6H_5CH_2OH$[i]	2	C_6H_5CHO	90	100
15	$C_6H_5CD_2OH$[i]	2	C_6H_5CDO	41	100
16	2-buten-1-ol	17	2-buten-1-al	53	100
17	2-methyl-2-propen-1-ol	24	2-methyl-2-propen-1-al	32	100
18	1-butanol	43	1-butanal	9	100
19	1-hexanol[c]	24	1-hexanal	1	100
20	1-decanol	50	1-decanal	6	100
21	1-decanol[c]	24	1-decanal	1	100
22	2-butanol	72	2-butanone	1	100
23	L-menthol	72	L-menthone	1	100
24	cyclobutanol[i]	43	cyclobutanone[j]	44	100
25	cyclohexanol	39	cyclohexanone	6	100
26	cyclohexanol[c]	27	cyclohexanone	1	100

[a] General reaction conditions: ($n$$Pr_4N$)($RuO_4$) (1 mol-%), CuCl (1 mol-%), 2-aminopyridine (5 mol-%), 0.5 g of powdered 4-Å molecular sieves, 6 ml of dichloromethane, 1 atm of molecular oxygen, and temperature 25°C. − [b] GC determination. − [c] Toluene (6 ml), 100°C. − [d] In the absence of ($n$$Pr_4N$)($RuO_4$). − [e] 4% conversion to the corresponding acid. − [f] In the absence of a nitrogen donor ligand. − [g] Acetonitrile (6 ml), 50°C. − [h] Acetonitrile (6 ml), 25°C. − [i] 20 equivalents of substrate. − [j] Determined by ^{1}H-NMR spectroscopy.

total selectivity to aldehydes with no further oxidation to the corresponding acids observed. Slightly improved rates can be observed in toluene at 100°C (***WARNING:*** Attempted oxidation of 1-butanol in toluene at 100°C resulted in an explosion) and acetonitrile at 50°C. The bifunctional ($n$$Pr_4N$)($RuO_4$)−CuCl catalyst was found to be very selective, with only benzylic and allylic alcohols undergoing any significant oxidation. Aliphatic primary alcohols such as 1-butanol (entry 18) and 1-decanol (entry 20) remain effectively unchanged under the same conditions at 25°C in dichloromethane or acetonitrile, and increasing the temperature to 100°C with toluene as the solvent has little effect (entry 21). Similarly, secondary alcohols were found to undergo very little oxidation (cyclohexanol, entry 25 and 26) or not at all (2-butanol, entry 22 and L-menthol, entry 23), a notable exception being cyclobutanol (entry 24) which was slowly oxidised in dichloromethane. We believe that the dehydrogenation of cyclobutanol results from it being less sterically encumbered than other more common secondary alcohols. The oxidation reactions, therefore, appear to be sensitive to steric factors near the alcohol functional group. This is further supported by the increase in rate of oxidation of 2,4-dichlorobenzyl alcohol (entry 9) compared with 2,6-dichlorobenzyl alcohol (entry 10). This has been observed in the ($n$$Pr_4N$)($RuO_4$)/NMO system[2] but it would seem to a lesser degree, as a range of secondary alcohols readily undergo oxidation with this system. This suggests that as with the ($n$$Pr_4N$)($RuO_4$)/NMO system, the bifunctional ($n$$Pr_4N$)($RuO_4$)−CuCl reagent is sterically demanding, with oxidation presumably occurring through the intermediacy of ruthenate esters. The selectivity of the ruthenium-copper catalyst is significantly different to that of the Griffith ($n$$Pr_4N$)($RuO_4$)/NMO system[2] and the ($n$$Pr_4N$)($RuO_4$)/$O_2$ system of Ley[11] and Markó[12], where benzylic, allylic and aliphatic primary alcohols and secondary alcohols are all readily oxidized. As with the Griffith, Ley, and Markó systems, functional groups such as double bonds remain intact during the oxidations.

The role of the copper compound is unclear. Varying the copper complex used in the system from CuCl to Cu($OCOCH_3$)$_2$, CuO, or [Cu($MeCN$)$_4$][PF_6] has little effect on the rate of oxidation; CuCl shows marginally improved initial rates. The concentration of the copper complex seems to be significant as the addition of 10 equivalents results only in stoichiometric oxidation. The addition of the nitrogen donor ligand (2-aminopyridine) causes a marked improvement on the rate of oxidation (compare entry 2 and 3). This may be as a result of complexation to the copper complex resulting in a more soluble species which is more efficient in activating or binding the molecular oxygen.[13] UV/Vis spectroscopy and electrospray mass spectrometry preclude any involvement of the nitrogen donor ligand with ($n$$Pr_4N$)($RuO_4$). Similar conlusions have been reached for RuO_4 which, unlike OsO_4, is unable to form simple adducts with nitrogen donor ligands.[8][14]Varying the nitrogen donor ligand from 2-aminopyridine to pyridine, 4-dimethylaminopyridine, or 2,6-lutidine has little effect on the rate of oxidation. However, addition of a bidentate nitrogen donor ligand, e.g. 2,2′-bipyridyl results in a decrease in catalytic activity as also noted by Markó.[12]

The observation that cyclobutanol is oxidized to cyclobutanone with total selectivity (entry 24) by this bifunctional catalyst would suggest one-electron processes are not involved in the oxidation process.[15] Similarly, studies on the oxidation of a series of *para*-substituted benzyl alcohols $RC_6H_4CH_2OH$ [R = OMe (entry 6), Cl (entry 7), CF_3 (entry 8), and H (entry 13)] show no correlation with Hammett σ parameters. Hence, benzyl radicals would appear not to be involved in the catalytic process, a conclusion which is further supported by the observation that radical traps, such as 2,4,6-tri-*tert*-butylphenol, have no effect on the rate of oxidation. In kinetic isotope effect experiments, the overall rate of the catalytic oxidation of $C_6H_5CH_2OH$ (entry 14) and $C_6H_5CD_2OH$ (entry 15) in parallel experiments yields the value of $k_H/k_D = 2.2$, indicating that C−H cleavage is involved in the rate-determining step. The nature of the action of the bifunctional ruthenium−copper catalyst is unclear and is currently under further investigation.

Finally, we have found that both the simple $(n\mathrm{Pr}_4\mathrm{N})(\mathrm{RuO}_4)/\mathrm{O}_2$ and $(n\mathrm{Pr}_4\mathrm{N})(\mathrm{RuO}_4)/\mathrm{Cu}/\mathrm{O}_2$ systems give very dark heterogeneous solutions during catalysis. Preliminary experiments seem to indicate the formation of colloidal material in these reactions. We have used different separation methods (e.g. centrifuging and membrane filtration) to remove the major part of the solid material formed. However, the residual solution contains particulate matter (ca. 200 nm, determined by photo correlation spectroscopy) and, interestingly, is still catalytically active. Therefore, whether the catalysis occurs heterogeneously or homogeneously remains unknown. Studies on more stable bifunctional systems are underway to clarify this point.

We gratefully acknowledge the support of this work by the *Centre National de la Recherche Scientifique*. K. S. C. also wishes to thank the *European Commission* for a *Marie Curie Research Fellowship* (ERBFMBICT971873).

Experimental Section

General: Most of the reagents were used without further purification except for the solvents, dichloromethane, acetonitrile, and toluene, which were dried and distilled prior to use. The catalyst $(n\mathrm{Pr}_4\mathrm{N})(\mathrm{RuO}_4)$ and all the substrates described in Table 1 were purchased from Aldrich Chemicals or Lancaster Synthesis. The analyses of the catalytic reactions were carried out with a Hewlett Packard 5890 Series II Gas Chromatograph equipped with a flame ionisation detector (FID) and a methyl silicone gum column of length 10 m, diameter 0.53 mm and 2.65 μm film thickness. ^{1}H-NMR spectra were recorded with a Bruker AC300 spectrometer and referenced internally to TMS.

General Procedure for the Oxidation of Alcohols: In a typical oxidation experiment the alcohol (100 mol-%) and 2-aminopyridine (5 mol-%) were dissolved in dichloromethane (6 ml), and powdered 4-Å molecular sieves added. After stirring the mixture for 10 min at 25°C under an atmosphere of molecular oxygen the copper complex (1 mol-%) was added followed by $(n\mathrm{Pr}_4\mathrm{N})(\mathrm{RuO}_4)$ (1 mol-%). The reaction was monitored by GC, with each sample taken from the reaction first filtered through a small plug of silica gel and washed with diethyl ether to remove any metal compounds.

[1] B. M. Trost, I. Fleming (Eds.), *Comprehensive Organic Synthesis*, **1991**, vol. 7 ("Oxidation"), Pergamon Press, UK; W. J. Mijs, C. R. H. I. De Jonge (Eds.), *Organic Synthesis by Oxidation with Metal Compounds*, Plenum Press, New York, **1986**.
[2] W. P. Griffith, S. V. Ley, G. P. Whitcombe, A. D. White, *J. Chem. Soc., Chem. Commun*. **1987**, 1625−1627; W. P. Griffith, S. V. Ley, S. P. Marsden, J. Norman, *Synthesis* **1994**, 639−666.
[3] C. Y. Lorber, J. A. Osborn, I. Pauls, *Bull. Soc. Chim. Fr*. **1996**, *133*, 755−758.
[4] S. M. Brown, P. R. Giles, I. E. Markó, M. Tsukazaki, C. J. Urch, *Science* **1996**, *274*, 2044−2046.
[5] C. Bilgrien, S. Davies, R. S. Drago, *J. Am. Chem. Soc.* **1987**, *109*, 3786−3787.
[6] S. Ito, M. Matsumoto, *J. Chem. Soc., Chem. Commun*. **1981**, 907−908.
[7] M. Matsumoto, N. Watanabe, *J. Org. Chem*. **1984**, *49*, 3435−3436.
[8] A. C. Dengel, A. M. El-Hendawy, W. P. Griffith, C. A. O'Mahoney, D. J. Williams, *J. Chem. Soc., Dalton Trans.* **1990**, 737−742.
[9] N. Hirai, S.-I. Murahashi, T. Naota, *J. Org. Chem*. **1993**, *58*, 7318−7319.
[10] J.-E. Backvall, R. L. Chowdhury, U. Karlsson, *J. Chem. Soc., Chem. Commun.* **1991**, 473−475.
[11] R. Lenz, S. V. Ley, *J. Chem. Soc. Perkin Trans 1* **1997**, 3291−3292.
[12] S. M. Brown, I. Chellé-Regnaut, P. R. Giles, I. E. Markó, M. Tsukazaki, C. J. Urch, *J. Am. Chem. Soc*. **1997**, *119*, 12661−12662.
[13] G. Davies, M. A. El Sayed, R. E. Fasano, *Inorg. Chim. Acta* **1983**, *71*, 95−99.
[14] M. El-Hendawy, W. P. Griffith, M. N. Moussa, F. I. Taha, *J. Chem. Soc., Dalton Trans.* **1989**, 901−906.
[15] W. P. Griffith, *Chem. Soc. Rev.* **1992**, *21*, 179−185.

[I98019]

Isolation of Enantiomers of a Range of Tris(bidentate)ruthenium(II) Species Using Chromatographic Resolution and Stereoretentive Synthetic Methods

Todd J. Rutherford[a], Paul A. Pellegrini[b], Janice Aldrich-Wright[b], Peter C. Junk[a], and F. Richard Keene*[a]

School of Biomedical and Molecular Sciences, James Cook University,[a]
Townsville, Queensland 4811, Australia
Fax: (internat.) + 61-7/47814600
E-mail: Richard.Keene@jcu.edu.au

Faculty of Business & Technology, University of Western Sydney[b]
Macarthur, N. S. W. 2560, Australia

Received March 19, 1998

Keywords: Chirality / Ruthenium / Chiral resolution / Nitrogen heterocycles / Carbonyl complexes

A range of chiral building blocks of the type Δ- or Λ-$[Ru(pp)_2(CO)_2]^{2+}$ {pp = bidentate ligands bpy (2,2′-bipyridine), phen (1,10-phenanthroline) and Me_2bpy (4,4′-dimethyl-2,2′-bipyridine)} have been synthesized, and their enantiomeric purity and absolute configurations determined by CD and NMR studies. Decarbonylation using trimethylamine oxide in the presence of the respective pp ligand at room temperature produced the corresponding tris(bidentate) species $[Ru(pp)_3]^{2+}$ with retention of configuration at the ruthenium(II) centre. A general chromatographic technique for resolution of tris-homoleptic complexes of the type $[Ru(pp)_3]^{2+}$ was investigated, with the absolute configurations of the resolved complexes confirmed by CD studies, and the X-ray structural analyses of Δ-(–)-$[Ru(Me_2bpy)_3]$[(–)-*O*,*O*′-dibenzoyl-L-tartrate] and Λ-(+)-$[Ru(phen)_3]$[(+)-*O*,*O*′-di-4-toluoyl-D-tartrate]. Resolution is also reported for the analogous species containing three potential bridging ligands, $[Ru(bpm)_3]^{2+}$ and $[Ru(HAT)_3]^{2+}$ (bpm = 2,2′-bipyrimidine; HAT = 1,4,5,8,9,12-hexaazatriphenylene). The versatility of the chromatographic procedure was demonstrated by the resolution of a series of bis-heteroleptic complexes $[Ru(pp)_2(pp')]^{2+}$ {pp′ = dpq (dipyrido[3,2-*d*:2,3′-*f*]quinoxaline), dpqc (dipyrido[3,2-*a*:2,3-*d*]-6,7,8,9-tetrahydrophenazine), and dppz {dipyrido[3,2-*a*:2,3′-*d*]phenazine)}.

Introduction

Ruthenium(II) complexes of polypyridyl ligands have received considerable attention as potential chromophoric components in photochemical molecular devices,[1] largely as a consequence of their synthetic versatility, and favourable photophysical and redox properties.[2][3][4]

For polynuclear assemblies based on such octahedral metal centres, stereoisomerism may occur by virtue of chirality or geometrical isomerism in the individual components, particularly when bidentate ligands are involved.[5][6][7] Since the initial chiral resolution of $[Ru(bpy)_3]^{2+}$ (bpy = 2,2′-bipyridine),[8][9][10] increasing attention has been drawn to the stereochemistry of this species and its analogues as a result of the differential interactions of the enantiomeric forms {e.g. of Δ- and Λ-$[Ru(phen)_3]^{2+}$ (phen = 1,10-phenanthroline)} with certain biological molecules such as DNA or oligonucleotides.[11][12][13][14] Additionally, the chiral resolution of $[Ru(pp)_2(BL)]^{2+}$,[15] $[Ru(pp)(pp')(BL)]^{2+}$,[16] {pp = bidentate polypyridyl ligand and BL = bridging ligand}, $[Ru(pp)_2(X)_2]^{n+}$ {X = py, CO, Cl^-, and CN^-},[15][17][18][19][20] and $[Ru(pp)(pp')(py)_2]^{n+}$[16] species have also been investigated in terms of their potential use as chiral building blocks for oligonuclear assemblies with predetermined stereochemistry.[6][7]

In the utilization of these species as chiral building blocks in stereoselective syntheses, or in the investigation of chiral interactions, it is required that they be available in optically pure form and have known absolute configurations. Generally, the chiral resolutions of bis(bidentate)- and tris(bidentate)ruthenium(II) complexes of polypyridyl ligands have been achieved by diastereoisomeric salt formation,[8][10][15][19][20][21][22][23][24] or chromatographic techniques.[15][16][25][26][27][28][29][30][31] The absolute configuration of a number of these enantiomeric forms have been assigned by exciton analysis of their circular dichroism (CD) spectra,[19][32][31][32][33][34][35][36] although more recently X-ray analyses have unambiguously confirmed the absolute configurations of Λ-$[Ru(bpy)_2(py)_2]^{2+}$[37] and Λ-$[Ru(phen)_3]^{2+}$.[38]

We recently communicated details of the chiral resolution of a series of dicarbonyl complexes of the type $[Ru(pp)_2(CO)_2]^{2+}$ {where pp = bpy, phen, and Me_2bpy (= 4,4′-dimethyl-2,2′-bipyridine)} and demonstrated their potential as chiral building blocks in the stereoselective synthesis of oligonuclear assemblies with predetermined stereochemistry.[15] We now report in detail the chiral resolution procedures and assignment of their absolute configurations, an NMR method of determining their optical purity, and the stereochemical consequences of their decarbonylation reactions. Also discussed is the development of a general chromatographic resolution technique for a variety of tris(bidentate)ruthenium(II) species and the factors which in-

 © WILEY-VCH Verlag GmbH, D-69451 Weinheim, 1998 1434–1948/98/1111–1677v $ 17.50+.50/0

fluence this resolution procedure. X-ray structural analyses of Δ-(−)-[Ru(Me_2bpy)$_3$]{(−)-*O,O′*-dibenzoyl-L-tartrate} and Λ-(+)-[Ru(phen)$_3$]{(+)-*O,O′*-di-4-toluoyl-D-tartrate} were used in combination with CD studies to confirm the absolute configurations of the tris(bidentate) species.

Results and Discussion

Dicarbonyl Species

Stereochemistry

Chiral resolutions of the cations $[Ru(bpy)_2(CO)_2]^{2+}$, $[Ru(phen)_2(CO)_2]^{2+}$, and $[Ru(Me_2bpy)_2(CO)_2]^{2+}$ were achieved by conventional diastereoisomeric salt formation as the antimonyl-(+)- or -(−)-tartrate salts. The CD spectra of the Λ-(+)- and Δ-(−)-$[Ru(phen)_2(CO)_2](PF_6)_2$ and Λ-(+)- and Δ-(−)-$[Ru(bpy)_2(CO)_2](PF_6)_2$ are shown in Figure 1; assignments of the absolute configurations of the three cations are discussed below.

Figure 1. CD spectra of the enantiomeric forms of $[Ru(bpy)_2(CO)_2]^{2+}$; Δ (——) and Λ (·····), and $[Ru(phen)_2(CO)_2]^{2+}$; Δ (------) and Λ (-·-·-·-)

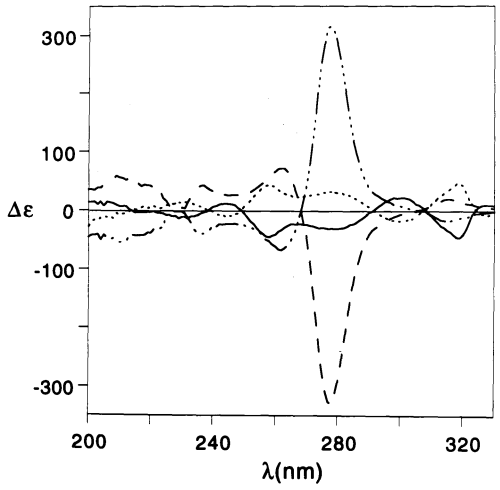

Cation-exchange chromatography utilizing a chiral eluent {e.g. sodium (−)-*O,O′*-dibenzoyl-L-tartrate}[15] was attempted as a resolution procedure but was found to be experimentally difficult due to the colourless character of these dicarbonyl complexes.

Chiral Lanthanide-Shift Reagent Studies

^{1}H-NMR techniques have provided an accurate and definitive method for the determination of enantiomeric purity of a variety of ruthenium(II) complexes of polypyridyl ligands. Such studies involve the addition to the complex of a chiral lanthanide-induced shift reagent[15][20][39][40][41][42] or tartrate derivative,[28] which causes a discrimination in the chemical shifts between the two enantiomeric forms. In the present work, the lanthanide-shift reagent studies of $[Ru(pp)_2(CO)_2]Cl_2$ (pp = bpy, phen, and Me_2bpy) were performed in [D_3]acetonitrile or [D_2]dichloromethane solutions: a non-polar solvent such as [D_2]dichloromethane is preferable in such studies,[40] but for solubility reasons [D_3]acetonitrile was required for the former two complexes. For all three dicarbonyl complexes, chemical shift discriminations between the enantiomeric forms were observed upon the addition of tris[3-(trifluoromethylhydroxymethylene)-*d*-camphorato]europium(III), Eu(tfc)$_3$, with the largest and most pronounced effects occurring for $[Ru(Me_2bpy)_2(CO)_2]Cl_2$ measured in [D_2]dichloromethane solution.

The effect of the sequential addition of Eu(tfc)$_3$ on the ^{1}H-NMR spectrum of $[Ru(bpy)_2(CO)_2]Cl_2$ is shown in Figure 2, where all the protons exhibited an induced downfield chemical shift of a magnitude influenced by their environment. The distinction between the enantiomers can be seen most clearly by comparison of the H3′ and H5′ proton resonances in Figures 2d and 2e (the racemate and a sample enriched in the Λ-(+) form, respectively, under similar conditions).

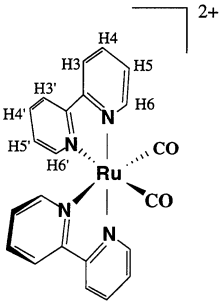

The complexes $[Ru(phen)_2(CO)_2]Cl_2$ and $[Ru(Me_2bpy)_2(CO)_2]Cl_2$ also showed an induced downfield chemical shift and chiral descrimination. Intersection of initial and final slopes in plots of the induced perturbation in chemical shift as a function of added Eu(tfc)$_3$ for $[Ru(phen)_2(CO)_2]Cl_2$ and $[Ru(bpy)_2(CO)_2]Cl_2$ indicated a ca. 1:1 adduct with the shift reagent. For the complex $[Ru(Me_2bpy)_2(CO)_2]Cl_2$, the ratio of shift reagent to complex exceeded unity.

Figure 2. The effect of [Eu(tfc)$_3$] on the ^{1}H-NMR (300 MHz; CD_3CN) spectrum of $[Ru(bpy)_2(CO)_2]Cl_2$; {a = no Eu(tfc)$_3$; b = 0.25 equiv.; c = 0.6 equiv.; d = 1 equiv.; e ≈ 1 equiv.; sample enriched in Λ isomer}; ^{1}H labelling scheme shown in text}

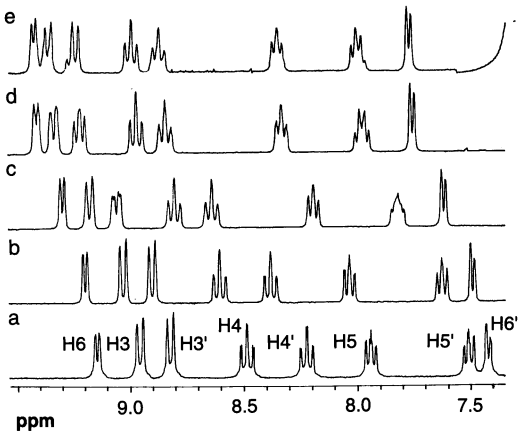

Stereochemical Consequences of the Decarbonylation Reaction

The stereochemical consequences of the decarbonylation reaction with trimethylamine *N*-oxide (TMNO) were investigated by treating the enantiomerically pure Λ-(+)-$[Ru(phen)_2(CO)_2]^{2+}$, Δ-(−)-$[Ru(bpy)_2(CO)_2]^{2+}$ and Λ-(+)-$[Ru(Me_2bpy)_2(CO)_2]^{2+}$ species (see below for absolute configuration assignments) with the ligands phen, bpy, and Me_2bpy under a variety of conditions, as given in Table 1. The $[Ru(pp)_3]^{2+}$ products from the reactions were isolated and the corresponding $[\alpha]_D$ values compared with those of the independently fully resolved products, allowing an assessment of the enantiomeric excess (*ee*) of the products formed under the various decarbonylation conditions. ^{1}H-NMR techniques utilizing the chiral shift reagent $[Eu(tfc)_3]$ were also used to confirm these *ee* determinations.

Previous studies[15][43] of the decarbonylation reactions of enantiomerically-enriched $[Ru(bpy)_2(CO)_2]^{2+}$ indicated that the three parameters which most significantly influenced the degree of stereoretention were temperature, solvent and ligand concentration. In order to maintain chiral integrity during the decarbonylation process, reaction conditions involved use of the solvent 2-methoxyethanol, ligand concentrations of ca. 10-fold or higher excess and low reaction temperatures. Photoracemization was not observed, but light was excluded in this study as a precaution.[15][43]

All reactions were observed to proceed with complete or near-complete retention of configuration at room temperature, whereas racemization occurred to varying degrees for all complexes at elevated temperatures. The most likely stage at which racemization might occur is subsequent to the removal of one carbonyl group, when competition for the "free" (or solvated) coordination site may occur between the uncoordinated nitrogen of an incoming monodentate pp ligand and a rearrangement involving one of the coordinated bidentate pp ligands. The extent of *racemization* during the decarbonylation reaction agrees with work previously completed by the authors, which demonstrated that retention of *geometric* integrity of an analogous dicarbonyl complex incorporating two non-symmetrical polypyridyl ligands occurred at 25°C, but isomerization took place at elevated temperatures.[44]

Absolute Configuration Determinations

Assignment of the absolute configurations of (+)- and (−)-$[Ru(phen)_2(CO)_2]^{2+}$ and (+)- and (−)-$[Ru(bpy)_2(CO)_2]^{2+}$ was achieved by their reaction with a third bidentate ligand to yield a tris(bidentate) product of known chirality. To ensure the decarbonylation reactions occurred with complete retention of configuration, the reactions were performed at room temperature and in subdued light (see above). The decarbonylation of (−)-$[Ru(bpy)_2(CO)_2]^{2+}$ with TMNO in 2-methoxyethanol in the presence of a 10-fold excess of bpy yielded the product Δ-(−)-$[Ru(bpy)_3]^{2+}$[36] with $[\alpha]_D = -816$ (compared with the literature value of −819[9]). This observation established a Δ configuration for (−)-$[Ru(bpy)_2(CO)_2]^{2+}$ and confirmed complete retention of configuration under those decarbonylation reaction conditions.

The absolute configuration of Λ-(+)-$[Ru(phen)_3]^{2+}$ has been assigned by CD[36] and X-ray crystallographic studies[38] and confirmed in the present work. It was formed by decarbonylation of (+)-$[Ru(phen)_2(CO)_2]^{2+}$ in the presence of phen, but otherwise under identical conditions to those described above for the formation of Δ-(−)-$[Ru(bpy)_3]^{2+}$, thus indicating the Λ configuration for (+)-$[Ru(phen)_2(CO)_2]^{2+}$ (see above). The product showed $[\alpha]_D = +1395$ compared with the literature value of +1340.[10]

The decarbonylation of (+)-$[Ru(Me_2bpy)_2(CO)_2]^{2+}$ under the same conditions described above but in the presence of Me_2bpy yielded the Λ-(+)-$[Ru(Me_2bpy)_3]^{2+}$ product (configuration determined by X-ray structural determination, Figure 4). The synthesized Λ-(+)-$[Ru(Me_2bpy)_3]^{2+}$ showed $[\alpha]_{546} = +1000$ compared to the independently resolved (+)-$[Ru(Me_2bpy)_3]^{2+}$ complex (see below) where $[\alpha]_{546} = +1045$, which may suggest that minor racemization (< 4%) occurs under the above reaction conditions.

The electronic spectrum of $[Ru(phen)_2(CO)_2]^{2+}$ exhibited a strong absorption band at ca. 275 nm which is assigned to an intraligand $\pi \rightarrow \pi^*$ transition, while the weak bands at

Table 1. Stereochemical consequences of the decarbonylation reactions of Δ- or Λ-$[Ru(pp)_2(CO)_2]^{2+}$ {where pp = phen, bpy, or Me_2bpy}

$[Ru(pp)_2(CO)_2]^{2+}$ precursor	Reaction conditions[a]	$[Ru(pp)_3]^{2+}$ product $[\alpha]_D$	Column resolution $[\alpha]_D$	Literature[b] $[\alpha]_D$	Enantiomeric excess (*ee*)
Λ-(+)-[pp = phen]	25°C	+1395	+1400	+1340	> 0.99
	45°C	+1330			0.95
	60°C	+1134			0.82
	120°C	+980			0.74
	200°C[c]	+938			0.70
Δ-(−)-[pp = bpy]	25°C	−816	−823	−819	> 0.99
	120°C	−254			0.50
	120°C[d]	−300			0.53
Λ-(+)-[pp = Me_2bpy]	25°C	+1000[e]	+1045[e]		0.96
	120°C	+920[e]			0.88

[a] All reactions were performed in subdued light using 2-methoxyethanol as solvent, with 10-fold excess of pp and 3-fold excess of TMNO unless otherwise specified. – [b] Optical rotations measured in water as Cl^- or I^- salt for phen and bpy, respectively. – [c] Reaction conditions of ethylene glycol as solvent and heating under microwave conditions. – [d] Reaction conditions of 30-fold excess of bpy, 20-fold excess of TMNO and 2-methoxyethanol as solvent. – [e] Optical rotations measured as PF_6^- salts in CH_3CN as solvent at λ = 546 nm.

340 and 350 nm are most likely to be $d\pi \rightarrow \pi^*$ transitions.[45][46] The intense circular dichroism band at ca. 280 nm (phen long-axis polarization transition) for (+)-$[Ru(phen)_2(CO)_2]^{2+}$ is strongly positive and the circular dichroism band at higher energy (ca. 260 nm) negative (Figure 1), confirming the (+) isomer as having the Λ absolute configuration.[33]

The electronic spectrum of $[Ru(bpy)_2(CO)_2]^{2+}$ was dominated by $\pi \rightarrow \pi^*$ transitions in the region of ca. 200−300 nm.[45][46] The long-axis polarized transitions of bpy occur at ca. 300 nm:[33] the CD band at 315 nm for the (+)-enantiomer is strongly positive and the high energy band at 300 nm is negative (Figure 1), confirming the assignment as Λ-(+)-$[Ru(bpy)_2(CO)_2]^{2+}$. For the complexes $[Ru(bpy)_2(CO)_2]^{2+}$ and $[Ru(phen)_2(CO)_2]^{2+}$, the lower energy long-axis polarized transitions were red-shifted relative to those reported for the $[Ru(pp)_2(py)_2]^{2+}$ analogues,[19][33] presumably due to the electron-withdrawing carbonyl ligands. Accordingly, the two methods used to determine the absolute configurations of the chirally resolved dicarbonyl complexes (i.e. stereoselective syntheses and CD studies) were in agreement.

Tris(bidentate) Complexes

Stereochemistry

During the course of this study, a chromatographic technique was developed for the resolution of tris(bidentate)ruthenium(II) complexes. The technique is based on a cation-exchange mechanism (SP Sephadex C-25 support) with the mode of resolution significantly influenced by the differential association of the chiral anions of the eluent with the enantiomeric forms of the complex.[30][31] As Sephadex has a dextran base and is itself chiral, it believed to significantly influence the resolution procedure, as demonstrated by the chiral resolution of $[\{Ru(Me_2bpy)_2\}_2(\mu\text{-bpm})]^{4+}$[30] and $[Ru(bpq)_3]^{2+}$ {bpq = 2,3-bis(2-pyridyl)quinoxaline} with the achiral eluent sodium toluene-4-sulfonate.[47]

The resolutions of a number of ruthenium(II) complexes involving α,α′-diimine ligands have recently been reported using CM and SP Sephadex C-25 and (+ or −)-SbOtart salts as eluents.[25][27][28] Generally, these resolution procedures have required the collection of a series of fractions to obtain the resolved complex. The procedure reported below resulted in the clear separation into two bands (i.e. the two enantiomeric forms) of every mononuclear complex examined.

The study was based primarily on the resolution of the four tris-homoleptic tris(bidentate) complexes $[Ru(pp)_3]^{2+}$ (pp = bpy, phen, Me_2bpy, and Me_4bpy), although a number bis-heteroleptic complexes $[Ru(pp)_2(pp')]^{2+}$ were examined to demonstrate the generality of the resolution procedure. The CD spectra of Δ- and Λ-$[Ru(bpy)_3]^{2+}$ and Δ- and Λ-$[Ru(phen)_3]^{2+}$ resolved by the technique were in excellent agreement with the spectra reported previously.[35] The CD spectra of Δ-(−)- and Λ-(+)-$[Ru(Me_2bpy)_3]^{2+}$ and Δ- and Λ-$[Ru(Me_4bpy)_3]^{2+}$ are shown in Figure 3 (the determination of the absolute configuration of Δ-(−)-$[Ru(Me_2bpy)_3]^{2+}$ is discussed below). The Cotton effects of the three complexes $[Ru(pp)_3]^{2+}$ (pp = bpy, Me_2bpy, and Me_4bpy) were near identical, as expected because of their electronic and structural similarity.

Figure 3. CD spectra of the enantiomeric forms of $[Ru(Me_2bpy)_3]^{2+}$; Δ (·····) and Λ (——), and $[Ru(Me_4bpy)_3]^{2+}$; Δ (-···-···-) and Λ (------)

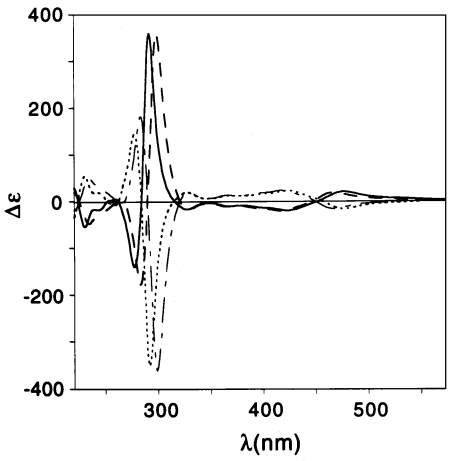

Chromatographic Resolutions of Tris-homoleptic Tris(bidentate) Species

In the chromatographic resolutions, large variations in efficiencies were observed between the different eluents for the same complex and between different complexes for the same eluent {where a decreased distance for column resolution ("effective column length", ECL) indicates a more efficient resolution}, as shown in Table 2. ^{1}H-NMR studies have suggested that there is a differential association between the above complexes and the anions in the eluent solutions which involves π-stacking and hydrophobic interactions.[30][31] This is further supported by the X-ray structure of Λ-$[Ru(bpy)_2(py)_2]$\{(+)-*O,O′*-dibenzoyl-L-tartrate\}[37] Δ-$[Ru(Me_2bpy)_3]$\{(−)-*O,O′*-dibenzoyl-L-tartrate\} and Λ-(+)-$[Ru(phen)_3]$\{(+)-*O,O′*-di-4-toluoyl-D-tartrate\}; the latter two are reported herein. The associations leading to the chromatographic resolution are believed to involve three-way interaction between the complex, the chiral eluent and the Sephadex support.[31]

Chromatographic resolution using aqueous sodium (−)-*O,O′*-dibenzoyl-L-tartrate as the eluent is significantly more efficient in complexes containing methyl-substituted ligands {$[Ru(bpy)_3]^{2+}$ (ECL = 55 cm) > $[Ru(Me_2bpy)_3]^{2+}$ (ECL = 30 cm) > $[Ru(Me_4bpy)_3]^{2+}$ (ECL = 20 cm) or $[Ru(Me_4bpy)_2(bpm)]^{2+}$ (ECL = 25 cm) > $[Ru(Me_4bpy)_3]^{2+}$ (ECL = 20 cm)}. For these complexes in which there is an increase in resolution efficiency, it is also noted that there is an enhanced rate-of-travel down the column.

While sodium (−)-*O,O′*-di-4-toluoyl-L-tartrate is more efficient than sodium (+)-*O,O′*-di-4-toluoyl-D-tartrate solution as an eluent in the resolution of $[Ru(bpy)_3]^{2+}$ (ECL = 30 cm and 55 cm, respectively), the opposite is true for $[Ru(Me_2bpy)_3]^{2+}$ (ECL = 80 cm and 30 cm, respectively)

Table 2. Chromatographic resolution efficiency for a range of polypyridyl complexes of ruthenium(II)

Complex	Effective column length (ECL)[a]			
	sodium (−)-*O,O′*-dibenzoyl-L-tartrate[b]	sodium (+)-*O,O′*-dibenzoyl-D-tartrate[b]	sodium (−)-*O,O′*-di-*p*-toluoyl-L-tartrate[b]	sodium (+)-*O,O′*-di-*p*-toluoyl-D-tartrate[b]
$[Ru(bpy)_3]^{2+}$	55		30	120
$[Ru(bpy)_2(Me_2bpy)]^{2+}$				65
$[Ru(Me_2bpy)_2(bpy)]^{2+}$				70
$[Ru(Me_2bpy)_3]^{2+}$	30	> 120	80	22
$[Ru(phen)_3]^{2+}$	70	24	80	25
$[Ru(Me_4bpy)_3]^{2+}$	20		40	> 120
$[Ru(Me_4bpy)_2(bpm)]^{2+}$ [15]	25			
$[Ru(bpm)_3]^{2+}$	60			
$[Ru(Me_4bpy)(phen)(bpm)]^{2+}$ [16]	45			
$[Ru(HAT)_3]^{2+}$	50			
$[Ru(bpy)_2(HAT)]^{2+}$ [48]			> 400	ca. 300
$[Ru(phen)_2(HAT)]^{2+}$ [48]	200			

[a] ECL given in cm; error ± 2.5 cm. − [b] Eluent concentrations at 0.075 M.

and $[Ru(Me_4bpy)_3]^{2+}$ (ECL = 40 cm and 20 cm, respectively). The apparent anomaly may arise from increased steric interactions between the toluoyl substituent in the anion and the methyl substituents on the ligands, which diminish the association between the eluent anion and the substrate cation and thus reduce the degree of chiral discrimination.

Chromatographic resolution using sodium (+)-*O,O′*-di-4-toluoyl-D-tartrate solution as the eluent is also more efficient for resolution of complexes with increased numbers of methyl-substituted ligands, although not with the same predicability as in the case above {e.g. $[Ru(bpy)_3]^{2+}$ (ECL = 120 cm) > $[Ru(bpy)_2(Me_2bpy)]^{2+}$ (ECL = 65 cm) ≈ $[Ru(bpy)(Me_2bpy)_2]^{2+}$ (ECL = 70 cm) compared with $[Ru(Me_4bpy)_3]^{2+}$ (ECL > 120 cm)}. The apparent anomaly in the resolution efficiency of $[Ru(Me_4bpy)_3]^{2+}$ may also have its origins in competing steric interactions, as described above.

The degree of aromaticity of the polypyridyl ligand also has a significant influence in the resolution efficiency. For example, the resolution of $[Ru(phen)_3]^{2+}$ was significantly more efficient than $[Ru(bpy)_3]^{2+}$ using both the (+)-tartrate salts as eluents.

The order of elution of the two enantiomeric forms was also observed to be significantly influenced by the chirality of the eluent. For example, elution of the complex $[Ru(bpy)_3]^{2+}$ with sodium (−)-*O,O′*-di-4-toluoyl-L-tartrate solution or sodium (−)-*O,O′*-dibenzoyl-L-tartrate solutions resulted in resolution with the first eluted band (Band 1) as the Δ-(−) enantiomer and the second eluted band (Band 2) as Λ-(+) enantiomer. This elution order is reversed when eluting with aqueous sodium (+)-*O,O′*-di-4-toluoyl-D-tartrate and sodium (+)-*O,O′*-dibenzoyl-D-tartrate (Table 3). This observation suggests the Δ enantiomer of the complex has a higher degree of association with the (−) forms of the two anions, reducing its effective charge (relative to the Λ enantiomer), and thus leading to the resolution.

However, this "band switching" was not observed in the complexes containing ligands with one or more methyl-substituents (e.g. $[Ru(bpy)_2(Me_2bpy)]^{2+}$ and $[Ru(Me_2bpy)_3]^{2+}$); in those cases the (−)-enantiomer was eluted first independent of the eluent or its chirality. This is presumably a result of the increased hydrophobic interactions between the Sephadex support and the methyl-substituted ligands, leading to the chirality of the Sephadex dominating the elution order of the enantiomeric forms. For the elution order of the enantiomers of $[Ru(bpy)_3]^{2+}$ and $[Ru(phen)_3]^{2+}$ to be dependent on the chirality of the eluent, the interaction between the complex and the eluent must be significantly greater than the interaction of the enantiomeric forms with the Sephadex support. The involvement of the support in the chromatographic resolution of dinuclear complexes has also been reported previously.[30] These simultaneous interactions of the target cation with the support itself and the chiral anion of the eluent may be cooperative or in opposition, with the consequence that the two enantiomeric forms of the eluent have unequal efficiencies in achieving the resolution of a particular substrate.

The study demonstrates the effectiveness of the technique for the chiral resolution of tris(bidentate) polypyridyl complexes of ruthenium, and provides an appreciation of the factors involved for efficient chiral resolution in terms of the nature of the interactions between the complex, Sephadex support and the chiral eluent.

X-ray Structural Studies

The X-ray crystal structures of (−)-$[Ru(Me_2bpy)_3]$\{(−)-*O,O′*-dibenzoyl-L-tartrate\}·6 H_2O (**1**; Figure 4) and (+)-$[Ru(phen)_3]$\{(+)-*O,O′*-di-4-toluoyl-D-tartrate\}·8 H_2O (**2**; Figure 5) are reported. The incorporation of an anion of known chirality allowed ready and unambiguous assignment of the absolute configuration of the respective cations as Δ and Λ. Such assignments are significant: while there have been a number of structural determinations of tris(bidentate)ruthenium(II) complexes containing polypyridyl ligands, a vast majority have involved racemic samples. There are in fact very few structural confirmations of chirality within complexes of this genre, and in view of recent interest in the control of the stereochemistry of polymetallic assemblies incorporating such centres as components,[6][7][49] such confirmations are timely. In this case, the determination of the chirality of the (+)-$[Ru(phen)_3]^{2+}$ cation as Λ

Table 3. Chromatographic elution order for the enantiomeric forms of $[Ru(pp)_2(pp')]^{2+}$ and $[Ru(pp)_3]^{2+}$ with various resolving agents as eluents

Complex	Elution band (Band 1 eluted first)	Elution order of the enatiomeric forms: sodium (−)-*O,O′*-dibenzoyl-L-tartrate[a]	sodium (+)-*O,O′*-dibenzoyl-D-tartrate[a]	sodium (−)-*O,O*-di-*p*-toluoyl-L-tartrate[a]	sodium (+)-*O,O*-di-*p*-toluoyl-D-tartrate[a]
$[Ru(bpy)_3]^{2+}$	Band 1	Δ-(−)		Δ-(−)	Λ-(+)
	Band 2	Λ-(+)		Λ-(+)	Δ-(−)
$[Ru(bpy)_2(Me_2bpy)]^{2+}$	Band 1				Δ-(−)
	Band 2				Λ-(+)
$[Ru(Me_2bpy)_2(bpy)]^{2+}$	Band 1				Δ-(−)
	Band 2				Λ-(+)
$[Ru(Me_2bpy)_3]^{2+}$	Band 1	Δ-(−)	Δ-(−)	Δ-(−)	Δ-(−)
	Band 2	Λ-(+)	Λ-(+)	Λ-(+)	Λ-(+)
$[Ru(phen)_3]^{2+}$	Band 1	Δ-(−)	Λ-(+)	Δ-(−)	Λ-(+)
	Band 2	Λ-(+)	Δ-(−)	Λ-(+)	Δ-(−)
$[Ru(Me_4bpy)_3]^{2+}$	Band 1	Δ-(−)		Δ-(−)	Δ-(−)
	Band 2	Λ-(+)		Λ-(+)	Λ-(+)

[a] Eluent concentration 0.075 M.

confirms earlier CD analyses based on exciton theory,[32][33][34][35][36] and the recent structural determination by Maloney and MacDonnell,[38] which utilised the technique of fractal analysis in the assignment. Bond lengths and angles are typical for such complexes.[38][50][51][52][53]

Figure 4. X-ray structure of one of the unique Δ-(−)-$[Ru(Me_2bpy)_3]^{2+}$ cations in compound (−)-$[Ru(Me_2bpy)_3]${(−)-*O,O′*-dibenzoyl-L-tartrate} (**1**) which resides on a two-fold rotation axis; hydrogen atoms have been omitted for clarity

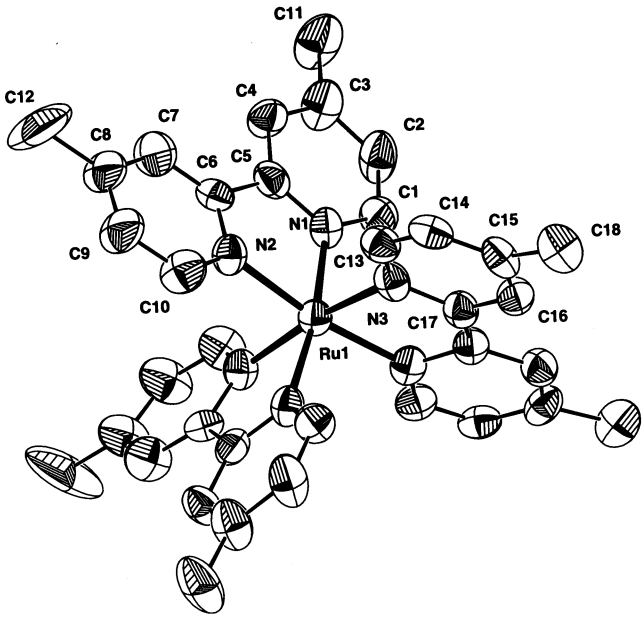

The packing diagram for the structure of **2** is shown in Figure 6, and attention is draw to a particular feature. The $[Ru(phen)_3]^{2+}$ cations form layers which alternate with layers containing water molecules. The (+)-*O,O′*-di-4-toluoyl-D-tartrate anions are positioned such that the tartrate backbone (containing the two carboxylate functionalities) reside in the water layer (hydrophilic), while the toluoyl rings penetrate into a virtually hydrophobic region in the complex cations where they essentially π-stack with the phenanthroline rings. The distance between the toluoyl and phenanthroline rings varies in the range 3.4−3.9 Å, which is consistent with π-stacking, for which a spacing of ca. 3.5 Å is considered normal.[54] While this present observation is made in the solid state, the interaction supports our proposal for the mode of association of anions with such complexes in solution (based on ^{1}H-NMR evidence),[30][31] which we assert is a major contributing factor to the mechanism of separation of complexes (and their stereoisomers) in cation-exchange chromatographic techniques involving the organic counter-anions in the eluents.

Figure 5. X-ray structure of the Λ-(+)-$[Ru(phen)_3]^{2+}$ cation in complex Λ-(+)-$[Ru(phen)_3]${(+)-*O,O′*-di-4-toluoyl-D-tartrate}·8 H_2O (**2**); hydrogen atoms have been omitted for clarity

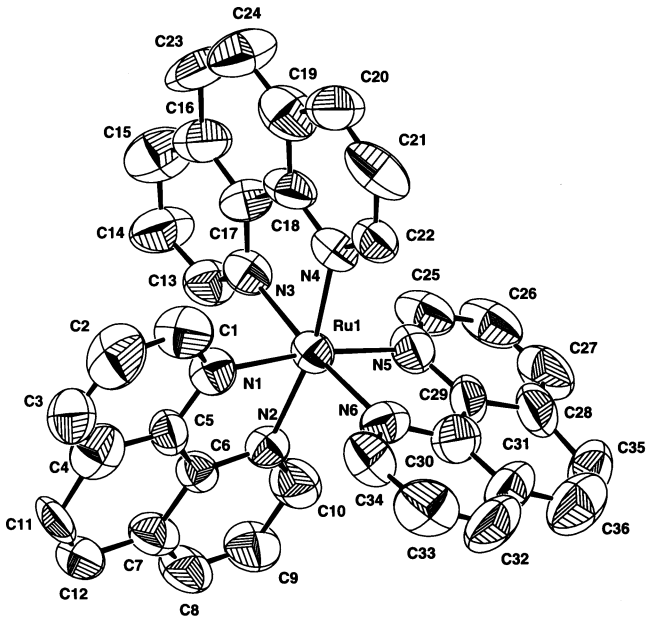

Chiral Resolutions of Heteroleptic Tris(bidentate) Species

To demonstrate the versatility of the chromatographic techniques and stereoretentive synthetic procedures, a range of bis-heteroleptic complexes $[Ru(pp)_2(pp')]^{2+}$ were also re-

Figure 6. Packing diagram for Λ-(+)-[Ru(phen)$_3$]{(+)-*O,O′*-di-4-toluoyl-D-tartrate}·8 H_2O (**2**) showing penetration of the toluoyl residues of the anion into the hydrophobic cationic layer; the carboxylate groups reside in the hydrophilic layer; water molecules have been omitted for clarity

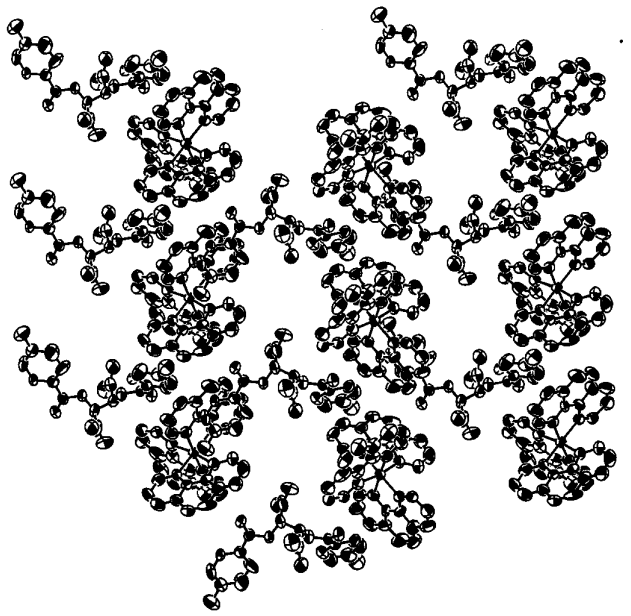

solved. Each of the complexes [Ru(bpy)$_2$(pp′)]$^{2+}$ and [Ru(Me$_2$bpy)$_2$(pp′)]$^{2+}$ {pp′ = phen (1,10-phenanthroline), dpq (dipyrido[3,2-*d*:2,3′-*f*]quinoxaline), dpqc (dipyrido[3,2-*a*:2,3-*d*]-6,7,8,9-tetrahydrophenazine), and dppz {dipyrido[3,2-*a*:2,3′-*d*]phenazine)}, and [Ru(phen)$_2$(pp′′)]$^{2+}$ (pp′′ = dpq, dpqc, and dppz) were resolved by the cation-exchange chromatographic procedure on SP Sephadex C-25 support using sodium (−)-*O,O′*-dibenzoyl-L-tartrate solution as eluent. Aqueous K (+)-SbOtart solution was also used as eluent for the resolution of [Ru(phen)$_2$(dpqc)]$^{2+}$ and [Ru(phen)$_2$(dppz)]$^{2+}$. Additionally, [Ru(bpy)$_2$(dpqc)]$^{2+}$ and [Ru(bpy)$_2$(dppz)]$^{2+}$ were also obtained in specific enantiomeric forms by the reaction of the respective ligands with resolved [Ru(bpy)$_2$(py)$_2$]$^{2+}$.[19]

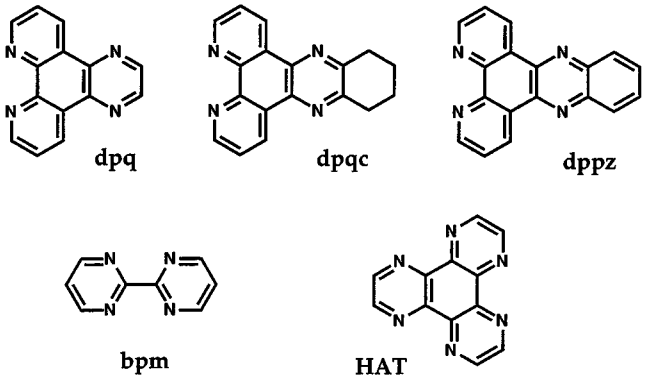

This general method for chiral resolution is significant as there have been a number of studies of the nature of the interaction of such complexes with polynucleotides, aimed at the assessment of their potential as photoprobes in sequencing and in cleavage reactions of DNA.[12][13][14]

Analogous bis-heteroleptic complexes [Ru(Me$_2$bpy)$_2$(bpy)]$^{2+}$, [Ru(Me$_2$bpy)(bpy)$_2$]$^{2+}$, [Ru(Me$_2$bpy)$_2$(phen)]$^{2+}$, and [Ru(bpy)(phen)$_2$]$^{2+}$ were also resolved chromatographically {aqueous sodium (+)-*O,O′*-dibenzoyl-D-tartrate solution eluent}. It is also noted that we have previously reported the chromatographic resolution of a tris-heteroleptic species, [Ru(phen)(Me$_4$bpy)(bpm)]$^{2+}$, using aqueous sodium (−)-*O,O′*-dibenzoyl-L-tartrate solution as eluent.[16]

The incorporation of potential bridging ligands such as 2,2′-bipyrimidine (bpm) or 1,4,5,8,9,12-hexaazatriphenylene (HAT) in such chiral tris(bidentate) metal centres provides the potential basis of stereochemical control in the construction of polymetallic ligand-bridged assemblies.[6][7] In such a context, we also chromatographically resolved the tris-homoleptic complexes [Ru(bpm)$_3$]$^{2+}$ and [Ru(HAT)$_3$]$^{2+}$ by these techniques using 0.1 M sodium (−)-*O,O′*-dibenzoyl-L-tartrate solution as eluent.

Summary

The chiral building blocks Δ- and Λ-[Ru(pp)$_2$(CO)$_2$]$^{2+}$ (where pp = bpy, phen, and Me$_2$bpy) were obtained by diastereoisomeric salt formation, and their enantiomeric purity established by ^{1}H-NMR spectroscopy using the chiral lanthanide-shift reagent [Eu(tfc)$_3$]. These species were demonstrated to undergo decarbonylation to form tris(bidentate) complexes with retention of stereochemical integrity under certain reaction conditions. Their absolute configurations were established by comparison of the configuration of the products with the the X-ray crystal structure determinations of the diastereoisomeric salts Δ-(−)-[Ru(Me$_2$bpy)$_3$]{(−)-*O,O′*-dibenzoyl-L-tartrate} and Λ-(+)-[Ru(phen)$_3$]{(+)-*O,O′*-di-4-toluoyl-D-tartrate}, and comparison of CD spectra with compounds whose configuration has previously assigned by exciton analysis.

The development of a cation-exchange chromatographic resolution procedure provided an efficient means of obtaining a wide range of enantiomerically-pure tris(bidentate)ruthenium(II) complexes containing polypyridyl ligands, which have application as chiral building blocks for oligomeric assemblies, or as chiral probes for biological molecules (e.g. polynucleotides, DNA).

This work was supported by the *Australian Research Council,* and Research Grants Schemes with both *James Cook University* and the *University of Western Sydney.* We thank Professor *R. S. Vagg* for access to the CD facilities at Macquarie University, and Ms. *Sue Butler* for measurement of the CD spectra at the University of Wollongong. We are grateful to Dr. *Nick Fletcher* and Dr. *Brett Yeomans* for useful comments on the manuscript.

Experimental Section

Materials, Instrumentation, and Techniques: The following chemicals were used without further purification: 2,2′-bipyridine (bpy, 99+%; Aldrich), 1,10-phenanthroline (phen, 99+% anhydrous; Aldrich), 4,4′-dimethyl-2,2′-bipyridine (Me$_2$bpy, 99%; Aldrich),

tris[3-(trifluoromethylhydroxymethylene)-*d*-camphorato]europium-(III) {Eu(tfc)$_3$, 97%; Fluka}, ruthenium(III) chloride hydrate ($RuCl_3$, 99.9%; Strem), potassium hexafluorophoshate (KPF_6, 98%; Aldrich), 2,3-bis(2-pyridyl)pyrazine (dpp, 98%; Aldrich), 2,2′-bipyrimidine (bpm, 98+%; Lancaster), sodium hydroxide (BDH), sodium chloride (BDH), sodium toluene-4-sulfonate (95%; Aldrich), potassium antimonyl (+)-tartrate hydrate {K(+)-SbOtart, 99+%, $[\alpha]_D$ = +141; Aldrich}, (−)-*O,O′*-di-4-toluoyl-L-tartaric acid (98+%, $[\alpha]_D$ = −139; Fluka), (+)-*O,O′*-di-4-toluoyl-D-tartaric acid (97%, $[\alpha]_D$ = +139; Aldrich), (+)-*O,O′*-dibenzoyl-D-tartaric acid (99%, $[\alpha]_D$ = +117; Fluka), (−)-*O,O′*-dibenzoyl-L-tartaric acid (99+%, $[\alpha]_D$ = −117; Fluka), tetra-*n*-butylammonium bromide (TBABr, 99%; Aldrich), tetra-*n*-butylammonium iodide (TBAI, 98+%; BDH) and tetraethylammonium chloride (TEACl, > 98%; Fluka).

The ligands dpq,[55] dpqc,[56] and dppz[57] were prepared as reported previously.

$[Ru(pp)_2Cl_2]$,[58] $[Ru(CO)_2Cl_2]_n$, $[Ru(pp)(CO)_2Cl_2]$, and $[Ru(pp)_2(CO)_2](PF_6)_2$ pp = Me_2bpy, phen, and bpy),[59] $[Ru(OH_2)_6]$(toluene-4-sulfonate)$_2$,[60] and $[Ru(DMSO)_4Cl_2]$ (DMSO = dimethyl sulfoxide)[61] were prepared as reported previously. $[Ru(bpy)_3](PF_6)_2$, $[Ru(Me_2bpy)_3](PF_6)_2$, $[Ru(bpy)_2(Me_2bpy)](PF_6)_2$ $[Ru(Me_2bpy)_2(bpy)](PF_6)_2$, $[Ru(Me_4bpy)_3](PF_6)_2$ and $[Ru(phen)_3](PF_6)_2$ were synthesized in a manner similar to the literature methods,[62] except that they were isolated as the PF_6^- salts by addition of KPF_6. Their ^{1}H-NMR and electronic spectra were in agreement with those reported previously.[4][63][64] Δ- and Λ-$[Ru(bpy)_2(py)_2]^{2+}$ were obtained by diastereoisomeric salt fomation with the chiral anion *O,O′*-dibenzoyltartrate, as described previously.[18][19]

Trifluoromethanesulfonic acid (3 M) was distilled under vacuum prior to use. Trimethylamine *N*-oxide hydrate (TMNO, Aldrich) was sublimed under vacuum at 120°C and stored under argon. 4,4′,5,5′-Tetramethyl-2,2′-bipyridine (Me_4bpy) was kindly supplied by Michael Quagliotto and was prepared according to a literature method.[16][65] Silver antimonyl (−)-tartrate {Ag (−)-SbOtart} and silver antimonyl (+)-tartrate {Ag (+)-SbOtart} were prepared according to a literature method.[66]

Electronic spectra, elemental analyses, and optical rotations were recorded as described previously.[48] CD (circular dichroism) spectra were measured using either a Jobin Yvon Dichrograph 6 or a JASCO-500C spectropolarimeter. Mass spectra were recorded with a Fisons/VG Biotech Quattra (Altrinchem, U.K.) instrument which is a tandem mass spectrometer with quadrupoles for MS1 and MS2, each with a mass range of 4000 amu for single-charged ions, a hexapole collision cell and photomultiplier detectors. The samples were dissolved in acetonitrile (50−100 pmol/μl).

Chromatographic procedures were carried out using SP Sephadex C-25 cation exchanger as the support and aqueous sodium chloride, sodium toluene-4-sulfonate, sodium (−)-*O,O′*-dibenzoyl-L-tartrate, sodium (+)-*O,O′*-dibenzoyl-D-tartrate, sodium (−)-*O,O′*-di-4-toluoyl-L-tartrate or sodium (+)-*O,O′*-di-4-toluoyl-D-tartrate solutions as eluents. The tartrate salts were prepared by the neutralization of the respective acids with sodium hydroxide. The support was contained in a column approximately 100 cm long × 2 cm diameter and the flow rate was controlled at ca. 1.5 ml/min. When necessary, the column was sealed enabling the complex to be recycled several times down its length with the aid of a peristaltic pump: in these cases, an "effective column length" (ECL) for the separation represents the length of support travelled by the sample for visual band separation. All chromatography was carried out in subdued light.

X-Ray Crystal Structure Determinations: Crystals of (−)-$[Ru(Me_2bpy)_3]$\{(−)-*O,O′*-dibenzoyl-L-tartrate\} (**1**) and (+)-$[Ru(phen)_3]$\{(+)-*O,O′*-di-4-toluoyl-D-tartrate\} (**2**) were grown by slow concentration of aqueous solutions of the respective salts. Unique room-temperature diffractometer data sets ($T \approx 295$ K; monochromatic Mo-K_α radiation, $\lambda = 0.7107_3$ Å; 2θ/θ scan mode; 2−50°) were measured on an Enraf-Nonius CAD4 diffractometer, yielding N_o independent reflections, N_o with $I > 3\sigma(I)$ being considered "observed" and used in the large-block least-squares refinements.

For both compounds, anisotropic thermal parameters were refined for all non-hydrogen atoms, except the oxygen atoms of the hydration water molecules (due to high thermal motion and disorder, see below). Hydrogen atoms were placed in calculated positions and were not refined. Two oxygen atoms in compound **1** were disordered and were successfully modelled with half occupancies {O(5w), O(6w), O(7w) and O(8w)}. Likewise in compound **2** two water molecules were also disordered and were modelled with half occupancies {O(1w), O(4w), O(5w) and O(7w)}. Conventional residuals R, R_w on F are quoted, statistical weights derivatives of $\sigma^2(I) = \sigma^2(I_{diff}) + 0.0004\sigma^4(I_{diff})$ being used. Neutral atom complex scattering factors were employed, and computation was by the XTAL 3.4 program system, implemented by S. R. Hall.[67] A summary of crystal data and data collection is compiled in Table 4 and structures are shown in Figures 4 and 5; material deposited comprises all atomic coordinates and thermal parameters, complete bond lengths and angles and full non-hydrogen atom geometries.

Synthetic and Stereochemical Studies

Homoleptic Dicarbonyl Ruthenium(II) Complexes: The $[Ru(phen)_2(CO)_2](PF_6)_2$ species was converted to the bromide salt by metathesis with TBABr in acetone. For ^{1}H-NMR, UV/Vis, and ORD measurements, the bromide salt was converted to the chloride by anion-exchange chromatography. $[Ru(Me_2bpy)_2(CO)_2](PF_6)_2$ and $[Ru(bpy)_2(CO)_2](PF_6)_2$ were converted to the respective bromide salts by metathesis with TBABr in 2-butanone. The chloride salts were obtained as described above.

^{1}H NMR ([D$_3$]acetonitrile): *[Ru(phen)$_2$(CO)$_2$]Cl$_2$:* δ = 7.63 [m, 4 H], 8.25 [d, 2 H, J = 9 Hz], 8.29 [dd, 2 H, J = 5.5, 8 Hz], 8.36 [d, 2 H, J = 9 Hz], 8.71 [dd, 2 H, J = 5.5, 1.5 Hz], 9.10 [d, 2 H, J = 8 Hz], 9.60 [d, 2 H, J = 5 Hz]. *[Ru(bpy)$_2$(CO)$_2$]Cl$_2$:* δ = 7.42 [d, 2 H, J = 5 Hz], 7.51 [ddd, 2 H, J = 8, 6, 1 Hz], 7.94 [ddd, 2 H, J = 8, 6, 1 Hz], 8.22 [td, 2 H, J = 8, 1 Hz], 8.48 [td, 2 H, J = 8, 1 Hz], 8.82 [d, 2 H, J = 8 Hz], 8.96 [d, 2 H, J = 8 Hz], 9.14 [d, 2 H, J = 5 Hz]. − ^{1}H NMR ([D$_2$]dichloromethane): *[Ru(Me$_2$-bpy)$_2$(CO)$_2$]Cl$_2$:* δ = 2.57 [s, 6 H], 2.61 [s, 6 H], 7.37 [m, 4 H], 7.78 [d, 2 H, J = 5.5 Hz], 9.04 [d, 2 H, J = 5.5 Hz], 9.11 [s, 2 H], 9.28 [s, 2 H]. UV/Vis [λ (ε), H_2O]: *[Ru(phen)$_2$(CO)$_2$]Cl$_2$:* 226 nm (57900), 274 (52100), 305 (15000). *[Ru(bpy)$_2$(CO)$_2$]Cl$_2$:* 210 nm (35600), 250 (26200), 306 (24800). *[Ru(Me$_2$bpy)$_2$(CO)$_2$]Cl$_2$:* 214 nm (43800), 252 (26900), 302 (23300), 312 (22900).

Λ-[Ru(phen)$_2$(CO)$_2$]\{(+)-SbOtart\}$_2$·3 H$_2$O: $[Ru(phen)_2(CO)_2]Br_2$ (1.369 g, 2.019 mmol) was stirred in the minimum of distilled water for dissolution, and Ag(+)-SbOtart (1.589 g, 4.038 mmol) added. The mixture was stirred over glass balls for ca. 30 min in subdued light, then filtered through Celite to remove AgBr, and the filtrate concentrated to dryness. Yield 2.00 g, 90%. − $C_{33}H_{26}N_4O_{17}RuSb_2$: calcd. C 36.2, H 2.39, N 5.1%; found: C 36.2, H 2.25, N 5.0%.

(+)-$[Ru(phen)_2(CO)_2]$\{(+)-SbOtart\}$_2$ was dissolved in a minimum volume of hot water and methanol added dropwise until the appearance of a faint cloudiness. The mixture was stored at 4°C

Table 4. Crystal data and summary of data collection for complexes **1** and **2**

Compound	(−)-[Ru(Me_2bpy)$_3$]{(−)-*O,O′*-dibenzoyl-L-tartrate}·6 H_2O (**1**)	(+)-[Ru(phen)$_3$]{(+)-*O,O′*-di-4-toluoyl-D-tartrate}·8 H_2O (**2**)
Molecular formula	$C_{54}H_{60}N_6O_{14}Ru$	$C_{56}H_{56}N_6O_{16}Ru$
Molecular weight	1118.2	1170.2
Crystal system	Monoclinic	Monoclinic
Space group	*C*2 (no. 5)	$P2_1$ (no. 4)
F(000)	2328	1212
Cell constants		
a [Å]	16.520(5)	10.597(2)
b [Å]	26.279(2)	24.921(2)
c [Å]	15.073(3)	11.634(2)
α [deg]	90	90
β [deg]	115.47(2)	99.78(1)
γ [deg]	90	90
V [Å^3]	5908(4)	3028.2(8)
Molecules/unit cell (*Z*)	4	2
D_c [g cm^{-3}]	1.257	1.265
μ [cm^{-1}]	3.3	3.3
A* min., max.	1.107, 1.138	1.125, 1.144
Crystal dimensions [mm]	0.62 × 0.40 × 0.36	0.42 × 0.42 × 0.38
σ cutoff	3σ	2σ
No. reflcections collected *(N)*	5326	5456
No. observed reflections (N_o)	4128	3512
No. parameters varied	655	680
R	0.058	0.064
R_w	0.067	0.071

overnight, the product collected and the precipitation procedure repeated a further two times. The precipitate was collected and either converted to the Cl^- salt by anion exchange or precipitated by the addition of KPF_6 to yield [Ru(phen)$_2$(CO)$_2$]Cl_2 or [Ru(phen)$_2$(CO)$_2$](PF_6)$_2$, respectively. Λ-(+)-[Ru(phen)$_2$(CO)$_2$]Cl_2: $[\alpha]_{365}$ (water) = +2320, $[M]_{365}$ (water) = +13640. Λ-(+)-[Ru(phen)$_2$(CO)$_2$](PF_6)$_2$: CD [λ (Δε), CH_3CN] = 211 nm (−55), 236 (−40), 262(−67), 278 (+315), 316 (−17).

The enantiomeric form was obtained in an analogous manner, using Ag(−)-SbOtart.

Δ-(−)-[Ru(phen)$_2$(CO)$_2$]Cl_2: $[\alpha]_{365}$ (water) = −2330 and $[M]_{365}$ (water) = −13710. Δ-(−)-[Ru(phen)$_2$(CO)$_2$](PF_6)$_2$: CD [λ (Δε), CH_3CN] = 211 nm (+54), 236(+41), 262 (+70), 278 (−322), 316 (+19).

Δ-[Ru(bpy)$_2$(CO)$_2$]{(+)-SbOtart}$_2$·2 H_2O: [Ru(bpy)$_2$(CO)$_2$]{(+)-SbOtart}$_2$·2 H_2O was prepared in an identical manner to that described above, using [Ru(bpy)$_2$(CO)$_2$]Br_2 in place of [Ru(phen)$_2$(CO)$_2$]Br_2. − $C_{29}H_{24}N_4O_{16}RuSb_2$: calcd. C 33.8, H 2.35, N 5.3; found C 33.8, H 2.31, N 5.3. − The diastereoisomer was recrystallized four times from methanol, the collected product being washed with cold methanol, ether, and air-dried. The product was then converted to the chloride and hexafluorophosphate salts as described above. Δ-(−)-[Ru(bpy)$_2$(CO)$_2$]Cl_2: $[\alpha]_{365}$ (water) = −1020 and $[M]_{365}$ (water) = −5570. Δ-(−)-[Ru(bpy)$_2$(CO)$_2$](PF_6)$_2$: CD [λ (Δε), CH_3CN] = 231 nm (−13), 244 (+11), 258 (−46), 278 (−31), 301 (+22), 319 (−47), 327 (+9).

The enantiomeric form was obtained in an analogous manner, using Ag(−)-SbOtart. Λ-(+)-[Ru(bpy)$_2$(CO)$_2$]Cl_2: $[\alpha]_{365}$ (water) = +1025 and $[M]_{365}$ (water) = +5545. Λ-(+)-[Ru(bpy)$_2$(CO)$_2$](PF_6)$_2$: CD [λ (Δε), CH_3CN] = 231 nm (+13), 244 (−10), 258 (+43), 278 (+31), 301 (−18), 319 (+45), 327 (−8).

(+)-[Ru(Me$_2$bpy)$_2$(CO)$_2$]{(+)-SbOtart}$_2$·H_2O: [Ru(Me$_2$bpy)$_2$(CO)$_2$]{(+)-SbOtart}$_2$·H_2O was prepared in an identical manner to that described above using [Ru(Me$_2$bpy)$_2$(CO)$_2$]Br_2 in place of [Ru(phen)$_2$(CO)$_2$]Br_2. − $C_{33}H_{30}N_4O_{15}RuSb_2$: calcd. C 37.1, H 2.83, N 5.3; found C 37.4, H 2.72, N 5.3. − The diastereoisomer was recrystallized twice from methanol. The product was stirred with boiling methanol (ca. 20 ml) and collected by filtration while hot. The precipitate was washed with methanol, ether, and air-dried. The product was then converted to the chloride and hexafluorophosphate salts as described above. (+)-[Ru(Me$_2$bpy)$_2$(CO)$_2$]Cl_2: $[\alpha]_{365}$ (water) = +840 and $[M]_{365}$ (water) = +5006.

Decarbonylation Reactions of Δ- or Λ-[Ru(pp)$_2$(CO)$_2$]$^{2+}$

Λ-(+)-[Ru(phen)$_3$]Cl_2: (+)-[Ru(phen)$_2$(CO)$_2$](PF_6)$_2$ (20 mg, 0.0247 mmol) was dissolved in 2-methoxyethanol (10 ml) and the solution purged with N_2 for 20 min prior to the addition of phen (44 mg, 0.247 mmol). TMNO (12 mg, 0.116 mmol) was then added and the reaction mixture stirred at room temperature in subdued light for 72 h. The reaction mixture was diluted with water and the product purified by cation exchange chromatography (SP Sephadex C25, eluent 0.2 M NaCl). The orange band was collected and precipitated as the PF_6^- salt by the addition of a saturated solution of KPF_6, which was collected by filtration and washed with water, ether, and air dried. Yield: 8 mg, 40%. NMR spectra were in agreement with those published previously for $[Ru(phen)_3]^{2+}$.[63][68] Λ-(+)-[Ru(phen)$_3$](PF_6)$_2$: $[\alpha]_{546}$ (CH_3CN) = +2000. The complex was converted to the chloride salt by metathesis from acetone solution using TEACl. $[\alpha]_D$ (water) = +1385; ref.[10][35] +1340.

The above reaction was repeated at a series of temperatures and reaction times, with all other conditions remaining identical, and $[\alpha]_D$ values measured as the chloride salts in water: 45°C for 24 h; yield 48%, $[\alpha]_D$ = +1330; 60°C for 6 h; yield 62%, $[\alpha]_D$ = +1134; 120°C for 3 h; yield 75%, $[\alpha]_D$ = +980. Microwave (low power) using ethylene glycol/10% water for 40 s; yield 78%, $[\alpha]_D$ = +938.

Δ-(-)-[Ru(bpy)$_3$]I_2: Bpy (30 mg, 0.197 mmol) was dissolved in 2-methoxyethanol (5 ml) and the solution purged with N_2 for 20 min. (−)-[Ru(bpy)$_2$(CO)$_2$](PF_6)$_2$ (15 mg, 0.0197 mmol) and TMNO (10 mg, 0.133 mmol) were added and the mixture stirred at room temperature for 72 h in subdued light, and after addition of water purification was achieved as described for Λ-(+)-[Ru(phen)$_3$]Cl_2.

Yield: 9 mg, 58%. The NMR spectrum was in agreement with the literature.[63][68] The complex was converted to the iodide salt by metathesis with TBAI in 2-butanone solution. $[\alpha]_D$ and $[M]_D$ (water) = −816 and −6740 respectively; ref.[9][35] $[\alpha]_D$ and $[M]_D$ = −819and −6750, respectively.

The above reaction was repeated at 120°C for 3 h with all other conditions identical; yield 81%, $[\alpha]_D$ = −254.

The above reaction was repeated at 120°C for 3 h with a 30-fold excess of bpy and 20-fold excess of TMNO with all other conditions identical; yield 85%, $[\alpha]_D$ = −300.

Λ-(+)-[Ru(Me$_2$bpy)$_3$]Cl$_2$: (+)-[Ru(Me$_2$bpy)$_3$]Cl$_2$ was formed by the decarbonylation of (+)-[Ru(Me$_2$bpy)$_2$(CO)$_2$](PF$_6$)$_2$ in the presence of an excess of Me$_2$bpy, but otherwise under identical conditions to those described for Λ-(+)-[Ru(phen)$_3$]Cl$_2$; yield 40%. The NMR spectrum was in agreement with that described previously.[63] Λ-(+)-[Ru(Me$_2$bpy)$_3$](PF$_6$)$_2$ $[\alpha]_{546}$ (CH_3CN) = +972 and $[M]_{546}$ = +9164. Chromatographically resolved Λ-(+)-[Ru(Me$_2$bpy)$_3$](PF$_6$)$_2$ (see below): $[\alpha]_{546}$ = +1045 and $[M]_{546}$ = +9845. (See above for X-ray structural determination of absolute configuration.)

The above reaction was repeated at 120°C for 3 h with all other conditions identical; yield 84%, $[\alpha]_D$ = +920.

Chromatographic Resolutions: The chromatographic resolutions of the mononuclear complexes were all achieved by cation-exchange chromatography (SP Sephadex C-25) using 0.075 M solutions of the eluent specified in the text. The impact of the enantiomeric identity of the eluent anion on the efficiency of the chromatographic resolution procedure {quoted as ECL for the chiral resolution (cm)}, and on the order of elution of the chiral forms of the cation (sign of optical rotation quoted at 589 nm, or the sign of Δε from the CD spectra at the MLCT absorption maximum at ca. 450 nm), was investigated by separately examining the resolution of complex {30 mg} with the eluents sodium (+)- and (−)-*O,O′*-dibenzoyltartrate and sodium (+)- and (−)-*O,O′*-di-4-toluoyltartrate.

Δ.Λ-[Ru(phen)$_3$]$^{2+}$: Chromatographic resolution was achieved using aqueous sodium (−)-*O-O′*-dibenzoyl-L-tartrate solution as the eluent (ECL ≈ 60 cm). The two bands were collected and the products isolated as the PF_6^- salts by addition of a saturated aqueous solution of KPF_6. The two products were converted to the chloride salts by anion exchange. By comparisons with the literature,[35][38] Band 1 (eluted first) was assigned as Δ-(−)-[Ru(phen)$_3$]$^{2+}$ and Band 2 (eluted second) as Λ-(+)-[Ru(phen)$_3$]$^{2+}$ with $[\alpha]_D$ (water) = −1310 and +1400 respectively (literature values of −1330 and +1340).[10] − CD [λ (Δε), CH_3CN]: Δ-(−): 227 nm (−19), 234 (33), 259 (437), 268 (−602), 296 (−72), 385 (+7), 419 (15), 464 (−22); Λ-(+): 227 (10), 234 (−33), 259 (−430), 268 (582), 296 (87), 385 (−7), 419 (−15), 464 (23).

Elution with sodium (−)-*O,O′*-dibenzoyl-L-tartrate, sodium (+)-*O,O′*-dibenzoyl-D-tartrate, sodium (−)-*O,O′*-di-4-toluoyl-L-tartrate and sodium (+)-*O,O′*-di-4-toluoyl-D-tartrate solutions demonstrated resolution at ECL ≈ 70 cm (Band 1 having a negative and Band 2 a positive rotation), ECL ≈ 30 cm (Band 1 positive), ECL ≈ 80 cm (Band 1 negative) and ECL ≈ 25 cm (Band 1 positive) respectively.

Δ.Λ-[Ru(bpy)$_3$]$^{2+}$: Chromatographic resolution was achieved for [Ru(bpy)$_3$]$^{2+}$ using aqueous sodium (−)-*O,O′*-dibenzoyl-L-tartrate solution at ECL ≈ 55 cm {$[\alpha]_{546}$ (water; I^- salt) − Band 1 = −824 and Band 2 = +817} (literature values of −819[9][35]), sodium (−)-*O,O′*-di-4-toluoyl-L-tartrate at ECL ≈ 30 cm (Band 1 negative rotation) and sodium (+)-*O,O′*-di-4-toluoyl-D-tartrate at ECL ≈ 120 (Band 1 positive rotation). − CD [λ (Δε), CH_3CN]: Δ-(−): 240 nm (24), 257 (−12), 278 (149), 292 (−331), 323 (21), 358 (12), 418 (23), 469 (−18); Λ-(+): 240 (−23), 257 (12), 278 (−147), 292 (347), 323 (−20), 358 (−12), 418 (−22), 469 (18).

Λ-(+)/Δ-(−)-[Ru(Me$_2$bpy)$_3$]$^{2+}$: Chromatographic resolution was achieved for [Ru(Me$_2$bpy)$_3$]$^{2+}$ using aqueous sodium (−)-*O,O′*-dibenzoyl-L-tartrate solution at ECL ≈ 30 cm, $[\alpha]_{546}$ and $[M]_{546}$ (CH_3CN; PF_6^-): Band 1 = −1060 and −10027 respectively and Band 2 = +1045 and +9845, respectively; sodium (−)-*O,O′*-di-4-toluoyl-L-tartrate at ECL ≈ 80 cm (Band 1 negative rotation); and sodium (+)-*O,O′*-di-4-toluoyl-D-tartrate at ECL ≈ 22 cm (Band 1 negative). − CD [λ (Δε), CH_3CN]: Δ-(−): 231 (54), 260 (−7), 277 (142), 292 (−351), 328 (18), 367 (11), 424 (21), 477 (−17); Λ-(+): 231 (−55), 260 (4), 277 (−141), 292 (357), 328 (−18), 367 (−11), 424 (−21), 477 (19).

Λ-(+)/Δ-(−)-[Ru(Me$_4$bpy)$_3$]$^{2+}$: Chromatographic resolution was achieved for [Ru(Me$_4$bpy)$_3$]$^{2+}$ using aqueous sodium (−)-*O,O′*-dibenzoyl-L-tartrate solution at ECL ≈ 20 cm, $[\alpha]_{546}$ and $[M]_{546}$ (CH_3CN; PF_6^-): Band 1 = −831 and −8530 respectively and Band 2 = 839 and +8631 respectively, and for sodium (−)-*O,O′*-di-4-toluoyl-L-tartrate eluent at ECL ≈ 40 cm (Band 1 negative rotation), sodium(+)-*O,O′*-di-4-toluoyl-D-tartrate eluent at ECL > 120 cm (Band 1 negative). − CD [λ (Δε), CH_3CN]: Δ-(−): 234 nm (49), 283 (180), 299 (−361), 329 (19), 366 (12), 418 (22), 468 (−17); Λ-(+): 234 (−48), 283 (−178), 299 (357), 329 (−19), 366 (−12), 418 (−22), 468 (17).

(+)/(−)-[Ru(Me$_2$bpy)$_2$(bpy)]$^{2+}$ and [Ru(Me$_2$bpy)(bpy)$_2$]$^{2+}$: Chromatographic resolution was observed for [Ru(Me$_2$bpy)$_2$(bpy)]$^{2+}$ and [Ru(Me$_2$bpy)(bpy)$_2$]$^{2+}$ using aqueous sodium (+)-*O,O′*-di-4-toluoyl-D-tartrate solution as eluent, where ECL ≈ 65 and 70 cm, respectively (Band 1 negative rotation).

[Ru(pp)$_2$(pp′)](PF$_6$)$_2$ {pp = bpy or Me$_2$bpy; pp′ = phen, dpq, dpqc, or dppz} and [Ru(phen)$_2$(pp′′)](PF$_6$)$_2$ {pp′′ = dpq, dpqc, or dppz} were synthesized by a literature procedure.[69] The respective [Ru(pp)$_2$Cl$_2$] precursor in 50% aqueous ethanol was refluxed in the presence of a slight excess of the third bidentate ligand for 2 h. Ethanol was evaporated from the solution, which was filtered before the dropwise addition of a saturated solution of KPF_6 to give an orange precipitate which was collected by filtration, washed with ice/water, and dried at 100°C. The complexes were purified by chromatography on alumina (acetonitrile eluent). the major band collected and concentrated to dryness. Yields were typically in the range 60−80%. Mass spectra *m/z* observed for all species were within 0.5 amu of the values calculated for [Ru(pp)$_2$(pp′)](PF$_6$)$^+$. ^{1}H-NMR spectra were consistent with the complex formulations. Visible spectra [λ_{max} (MLCT) (ε), CH_3CN]: [Ru(bpy)$_2$(phen)]$^{2+}$ 452 (14900); [Ru(bpy)$_2$(dpq)]$^{2+}$ 449 (14500); [Ru(bpy)$_2$(dpqc)]$^{2+}$ 451 (16200); [Ru(bpy)$_2$(dppz)]$^{2+}$ 448 (16400); [Ru(Me$_2$bpy)$_2$(phen)]$^{2+}$ 456 (14100); [Ru(Me$_2$bpy)$_2$(dpq)]$^{2+}$ 439 (13900); [Ru(Me$_2$bpy)$_2$(dpqc)]$^{2+}$ 452 (15200); [Ru(Me$_2$bpy)$_2$(dppz)]$^{2+}$ 443 (16100); [Ru(phen)$_2$(dpq)]$^{2+}$ 446 (17300); [Ru(phen)$_2$(dpqc)]$^{2+}$ 448 (14300); [Ru(phen)$_2$(dppz)]$^{2+}$ 439 (16100).

Chiral Resolution of [Ru(pp)$_2$(pp′)]$^{2+}$ Cations: All cations were chromatographically resolved on SP Sephadex C-25 support using as eluent aqueous 0.1 M sodium (−)-*O,O′*-dibenzoyl-L-tartrate solution containing 5% acetone to maintain complex solubility. In all cases, two distinct enantiomer bands were observable within ECL ≈ 1.5−2 m, and the separated bands were collected after 3 m of passage down the column. The enantiomer with a negative Δε in the CD spectrum at the absorption maximum (ca. 450 nm) was invariably eluted first; by comparison with the CD characteristics of similar complexes (see above), these were assigned the Δ

absolute configuration. CD [λ (Δε), CH_3CN]: $[Ru(bpy)_2(phen)]^{2+}$ Δ 380 nm (58), 457 (−56) and Λ 380 (−59), 457 (55); $[Ru(bpy)_2(dpq)]^{2+}$ Δ 400 (79), 461 (−67) and Λ 400 (−81), 461 (66); $[Ru(bpy)_2(dpqc)]^{2+}$ Δ 412 (62), 468 (−54) and Λ 412 (−64), 468 (54); $[Ru(bpy)_2(dppz)]^{2+}$ Δ 395 (64), 461 (−58) and Λ 395 (−70), 461 (58); $[Ru(Me_2bpy)_2(phen)]^{2+}$ Δ 400 (53), 465 (−54) and Λ 400 (−59), 457 (56.5); $[Ru(Me_2bpy)_2(dpq)]^{2+}$ Δ 415 (53.6), 476 (−38.8) and Λ 415 (−54), 476 (40); $[Ru(Me_2bpy)_2(dpqc)]^{2+}$ Δ 386 (51), 464 (−46) and Λ 386 (−60), 464 (46); $[Ru(Me_2bpy)_2(dppz)]^{2+}$ Δ 390 (63), 467 (−51) and Λ 390 (−70), 467 (51);$[Ru(phen)_2(dpq)]^{2+}$ Δ 396 (30), 456 (−52) and Λ 396 (−33), 456 (51); $[Ru(phen)_2(dpqc)]^{2+}$ Δ 407 (40), 467 (−54) and Λ 407 (−43), 467 (58); $[Ru(phen)_2(dppz)]^{2+}$ Δ 405 (41), 458 (−49) and Λ 405 (−55), 458 (61) {incomplete separation}.

The complexes $[Ru(phen)_2(dpqc)]^{2+}$ and $[Ru(phen)_2(dppz)]^{2+}$ could also be separated using aqueous 0.1 M potassium antimonyl (+)-tartrate solution (containing 10% acetone) as eluent (ECL ≈ 3 m).

The enantiomers of the complexes $[Ru(bpy)_2(dpqc)]^{2+}$ and $[Ru(bpy)_2(dppz)]^{2+}$ were also obtained by the stereoretentive reactions of Δ- or Λ-$[Ru(bpy)_2(py)_2]^{2+}$ with dpqc or dppz, in an analogous manner to that described previously.[18][19]

Synthesis of $[Ru(bpm)_3](PF_6)_2$: $[Ru(H_2O)_6]$(toluene-4-sulfonate)$_2$[60] (100 mg, 0.079 mmol) and bpm (62 mg, 0.394 mmol) were added to ethylene glycol (30 ml) and heated in a microwave oven (medium high) for 45 s. The reaction mixture was diluted with distilled water and purified by cation-exchange chromatography (SP Sephadex C-25, 0.2 M NaCl). The product was precipitated from the orange band by addition of KPF_6, collected and washed with water and diethylether. Yield = 140 mg, 62%. − $C_{24}H_{18}F_{12}N_{12}P_2Ru$: calcd. C 33.3, H 2.09, N 19.4; found: C 33.2, H 2.08, N 19.4. − UV/Vis data was in agreement with the literature.[70] − ^{1}H NMR ([D$_3$]acetonitrile): δ = 9.12 (dd, 6 H, *J* = 5, 2 Hz], 8.15 (dd, 6 H, *J* = 5, 2 Hz], 7.59 (t, 6 H, *J* = 5.5 Hz].

Resolution of $[Ru(bpm)_3]^{2+}$: Resolution was achieved by cation-exchange chromatography using 0.1 M sodium (−)-*O,O′*-dibenzoyl-L-tartrate as the eluent (ECL ≈ 150 cm). The two bands were collected and the enantiomers precipitated by the addition of a saturated solution of KPF_6, reprecipitated twice from acetone/water solution by the addition of KPF_6, collected, washed with cold water and diethyl ether. Comparisons with similar compounds,[15][19][35] enabled the assignment of Δ-(−)-$[Ru(bpm)_3]^{2+}$ (Band 1) $[\alpha]_{546}$ = −909 and $[\alpha]_D$ = −454, CD [λ (Δε), CH_3CN]: 235 nm (+51), 254 (+45), 268 (−210), 320 (−19), 411 (+22), 468 (−14) and Λ-(+)-$[Ru(bpm)_3]^{2+}$ (Band 2) $[\alpha]_{546}$ = +890 and $[\alpha]_D$ = +451, CD [λ (Δε), CH_3CN]: 235 nm (−48), 254 (−40), 268 (+200), 320 (+19), 411 (−21), 468 (+14).

Synthesis of $[Ru(HAT)_3](PF_6)_2$: $[Ru(HAT)_3]^{2+}$ was synthesiszd in a similar manner to that described by Kirsch-De Mesmaeker et al.[71] $[Ru(DMSO)_4Cl_2]$ (65 mg, 0.2 mmol) was dissolved in distilled water (60 ml) and degassed with N_2 for 20 min. HAT (233 mg, 0.99 mmol) was added and the mixture refluxed for 48 h. The reaction mixture was allowed to cool, then filtered to remove unreacted HAT. The orange product was purified by cation-exchange chromatography (SP Sephadex C-25, 0.2 M NaCl) and collected as described above. Yield 140 mg, 64%. − UV/Vis [λ (ε), CH_3CN]: 212 (63800), 274 (64300), 414 (sh), 436 (14180).[71][72] − ^{1}H NMR ([D$_3$]acetonitrile): δ = 9.40 (s, 6 H), 9.14 (d, 6 H, *J* = 2.5 Hz), 8.43 (d, 6 H, *J* = 2.5 Hz).

Resolution of $[Ru(HAT)_3]^{2+}$: Resolution was achieved by cation-exchange chromatography using 0.1 M sodium (−)-*O,O′*-dibenzoyl-L-tartrate solution as the eluent (ECL ≈ 80 cm). The two bands were collected and precipitated by the addition of a saturated solution of KPF_6, reprecipitated twice from acetone/water solution by the addition of KPF_6, collected, washed with cold water, and diethyl ether. Comparisons with similar compounds,[15][19][35] Λ-(+)-$[Ru(HAT)_3]^{2+}$ (Band 1) $[\alpha]_{546}$ = +974 and $[\alpha]_{589}$ = +623, CD [λ (Δε), CH_3CN]: 232 (+8), 250 (−15), 262 (+4), 282 (−6), 314 (+48), 406 (−13), 462 (+12) and Δ-(−)-$[Ru(HAT)_3]^{2+}$ (Band 2) $[\alpha]_{546}$ = −940 and $[\alpha]_{589}$ = −618, CD (λ nm (Δε), CH_3CN): 232 (−8), 250 (+15), 262 (−2), 282 (+7), 314 (−45), 406 (+14), 462 (−11).

Chiral Lanthanide Shift Reagent Studies: All complexes were converted to the Cl^- salts for the chiral-lanthanide shift reagent (CLSR) studies, which were performed on *rac*- and Δ- or Λ-$[Ru(bpy)_2(CO)_2]Cl_2$, $[Ru(phen)_2(CO)_2]Cl_2$, $[Ru(Me_2bpy)_2(CO)_2]Cl_2$ and $[Ru(Me_4bpy)_2(CO)_2]Cl_2$ in [D$_3$]acetonitrile for the former two and [D$_2$]dichloromethane for the latter two complexes. Mol ratios of [Complex]/[CLSR] varied from 0 to 2, depending on solvent and complex. Shift reagent studies were also performed on $[Ru(Me_2bpy)_3]Cl_2$ in [D$_2$]dichloromethane and $[Ru(Me_4bpy)_3]Cl_2$ in [D$_2$]dichloromethane and [D$_3$]acetonitrile. Complexes were dissolved in the solvent at concentrations between $3\cdot10^{-2}$ M and $3\cdot10^{-3}$ M.

[1] V. Balzani, F. Scandola, *Supramolecular Photochemistry*, Ellis Horwood, Chichester, **1991**.
[2] K. Kalyanasundaram, *Coord. Chem. Rev.* **1982**, *46*, 159−244.
[3] V. Balzani, A. Juris, M. Venturi, S. Campagna, S. Serroni, *Chem. Rev.* **1996**, *96*, 759−833.
[4] A. Juris, S. Barigelletti, S. Campagna, V. Balzani, P. Belser, A. von Zelewsky, *Coord. Chem. Rev.* **1988**, *84*, 85−277.
[5] A. von Zelewsky, *Stereochemistry of Coordination Compounds*, Wiley, Chichester, **1995**.
[6] F. R. Keene, *Coord. Chem. Rev.* **1997**, *166*, 122−159.
[7] F. R. Keene, *Chem. Soc. Rev.* **1998**, 27, 185−193.
[8] F. H. Burstall, *J. Chem. Soc.* **1936**, 173−175.
[9] F. P. Dwyer, E. C. Gyarfas, *J. Proc. Roy. Chem. Soc. N.S.W.* **1949**, *83*, 174−176.
[10] F. P. Dwyer, E. C. Gyarfas, *J. Proc. Roy. Chem. Soc. N.S.W.* **1949**, *83*, 170−173.
[11] A. Shulman, F. P. Dwyer, *Chelating Agents and Metal Chelates* (Eds.: F. P. Dwyer, D. P. Mellor), Academic Press, New York, **1964**, pp. 383−439.
[12] A. M. Pyle, J. K. Barton, *Prog. Inorg. Chem.* **1990**, *38*, 413−475.
[13] A. Kirsch-De Mesmaeker, J.-P. Lecomte, J. M. Kelly, *Top. Curr. Chem.* **1996**, *177,* 25−76.
[14] R. E. Holmlin, P. J. Dandliker, J. K. Barton, *Angew. Chem.* **1997**, *109,* 2830−2848; *Angew. Chem. Int. Ed. Engl.* **1997**, *36*, 2715−2730.
[15] T. J. Rutherford, M. G. Quagliotto, F. R. Keene, *Inorg. Chem.* **1995**, *34*, 3857−3858.
[16] B. T. Patterson, F. R. Keene, *Inorg. Chem.* **1998**, *37*, 645−650.
[17] A. Yamagishi, K. Naing, Y. Goto, M. Taniguchi, M. Takahashi, *J. Chem. Soc., Dalton Trans.* **1994**, 2085−2089.
[18] X. Hua, A. von Zelewsky, *Inorg. Chem.* **1991**, *30*, 3796−3798.
[19] X. Hua, A. von Zelewsky, *Inorg. Chem.* **1995**, *34*, 5791−5797.
[20] R. T. Watson, J. L. Jackson, J. D. Harper, K. A. Kane-Maguire, L. A. P. Kane-Maguire, N. A. P. Kane-Maguire, *Inorg. Chim. Acta* **1996**, *249*, 5−7.
[21] F. P. Dwyer, E. C. Gyarfas, *Proc. Roy. Soc. N.S.W.* **1949**, *83*, 263−265.
[22] B. Bosnich, F. P. Dwyer, *Aust. J. Chem.* **1966**, *19*, 2229−2233.
[23] J. A. A. Sagues, R. D. Gillard, D. H. Smalley, P. A. Williams, *Inorg. Chim. Acta* **1980**, *43*, 211−216.
[24] C. Hiort, P. Lincoln, B. Norden, *J. Am. Chem. Soc.* **1993**, *115*, 3448−3454.
[25] K. Naing, M. Takahashi, M. Taniguchi, A. Yamagishi, *Bull. Chem. Soc. Jpn.* **1994**, *67*, 2424−2429.
[26] J. R. Aldrich-Wright, I. Greguric, R. S. Vagg, K. Vickery, P. A. Williams, *J. Chromatogr. A* **1995**, *718*, 436−443.
[27] C. M. Dupureur, J. K. Barton, *Inorg. Chem.* **1997**, *36*, 33−43.
[28] I. Greguric, J. R. Aldrich-Wright, J. G. Collins, *J. Am. Chem. Soc.* **1997**, *119*, 3621−3622.

[29] C. M. Shelton, K. E. Seaver, J. F. Wheeler, N. A. P. Kane-Maguire, *Inorg. Chem.* **1997**, *36*, 1532−1533.
[30] N. C. Fletcher, P. C. Junk, D. A. Reitsma, F. R. Keene, *J. Chem. Soc., Dalton Trans.* **1998**, 133−138.
[31] N. C. Fletcher, F. R. Keene, *Chem. Eur. J*, submitted.
[32] B. Bosnich, *Inorg. Chem.* **1968**, *7*, 2379−2386.
[33] B. Bosnich, *Inorg. Chem.* **1968**, *7*, 178−180.
[34] A. J. McCaffery, S. F. Mason, *Proc. Chem. Soc.* **1963**, 211−212.
[35] A. J. McCaffery, S. F. Mason, B. J. Norman, *J. Chem. Soc. A* **1969**, 1428−1441.
[36] S. F. Mason, B. J. Norman, *J. Chem. Soc. A* **1969**, 1442−1447.
[37] B. Kolp, H. Viebrock, A. von Zelewsky, D. Abeln, unpublished work.
[38] D. J. Maloney, F. M. MacDonell, *Acta Crystallogr., C: Cryst. Str.* **1997**, *53*, 705−707.
[39] G. R. Sullivan, *Top. Stereochem.* **1978**, *10*, 287−329.
[40] J. K. Barton, J. S. Nowick, *J. Chem. Soc., Chem. Commun.* **1984**, 1650−1652.
[41] H.-Y. Mei, J. K. Barton, *J. Am. Chem. Soc.* **1986**, *108*, 7414−7416.
[42] S. S. David, J. K. Barton, *J. Am. Chem. Soc.* **1993**, *115*, 2984−2985.
[43] M. G. Quagliotto, Honours Dissertation, James Cook University, **1993**.
[44] T. J. Rutherford, D. A. Reitsma, F. R. Keene, *J. Chem. Soc., Dalton Trans.* **1994**, 3659−3666.
[45] J. M. Kelly, C. M. O′Connell, J. G. Vos, *J. Chem. Soc., Dalton Trans.* **1986**, 253−258.
[46] N. C. Thomas, J. Fischer, *J. Coord. Chem.* **1990**, *21*, 119−128.
[47] B. T. Patterson, Honours Dissertation, James Cook University, **1997**.
[48] T. J. Rutherford, O. Van Gijte, A. Kirsch-De Mesmaeker, F. R. Keene, *Inorg. Chem.* **1997**, *36*, 4465−4474.
[49] A. von Zelewsky, *Chimia* **1994**, *48*, 331−335.
[50] D. P. Rillema, D. S. Jones, H. A. Levy, *J. Chem. Soc., Chem. Commun.* **1979**, 849−851.
[51] R. Schachter, C. G. Michel, M. A. Kuck, J. A. Baumann, D. J. Olego, L. G. Polgar, P. M. Raccah, W. E. Spicer, *Appl. Phys. Lett.* **1984**, *45*, 277−279.
[52] D. P. Rillema, D. S. Jones, C. Woods, H. A. Levy, *Inorg. Chem.* **1992**, *31*, 2935−2938.
[53] J. M. Harrowfield, A. N. Sobolev, *Aust. J. Chem.* **1994**, *47*, 763−767.
[54] J. M. Harrowfield, *J. Chem. Soc., Dalton Trans.* **1996**, 3165−3171.
[55] J. Aldrich-Wright, PhD Thesis, Macquarie University, **1993**.
[56] I. Greguric, Honours Dissertation, University of Western Sydney (Macarthur), **1994**.
[57] E. Amouyal, A. Homsi, J.-C. Chambron, J.-P. Sauvage, *J. Chem. Soc., Dalton Trans.* **1990**, 1841−1845.
[58] B. P. Sullivan, D. J. Salmon, T. J. Meyer, *Inorg. Chem.* **1978**, *17*, 3334−3341.
[59] P. A. Anderson, G. B. Deacon, K. H. Haarmann, F. R. Keene, T. J. Meyer, D. A. Reitsma, B. W. Skelton, G. F. Strouse, N. C. Thomas, J. A. Treadway, A. H. White, *Inorg. Chem.* **1995**, *34*, 6145−6157.
[60] P. Bernhard, M. Biner, A. Ludi, *Polyhedron* **1990**, *9*, 1095−1097.
[61] I. P. Evans, A. Spencer, G. Wilkinson, *J. Chem. Soc., Dalton Trans.* **1973**, 204−209.
[62] T. Togano, N. Nagao, M. Tsuchida, H. Kumakura, K. Hisamatsu, F. S. Howell, M. Mukaida, *Inorg. Chim. Acta* **1992**,*195*, 221−225.
[63] E. C. Constable, J. Lewis, *Inorg. Chim. Acta* **1983**,*70*, 251−253.
[64] S. F. McClanahan, R. F. Dallinger, F. J. Holler, J. R. Kincaid, *J. Am. Chem. Soc.* **1985**, *107*, 4853−4860.
[65] L. Della Ciana, W. J. Dressick, D. Sandrini, M. Maestri, M. Ciano, *Inorg. Chem.* **1990**, *29*, 2792−2798.
[66] H. A. Goodwin, E. C. Gyarfas, D. P. Mellor, Aust. J. Chem. **1958**, *11,* 428−431.
[67] S. R. Hall, G. S. D. King, J. M. Stewart, *Xstal3.4 User's Manual,* University of Western Australia, **1995**.
[68] M. J. Cook, A. P. Lewis, G. S. G. McAuliffe, *Org. Magn. Reson.* **1984**, *22*, 388−394.
[69] G. M. Brown, T. R. Weaver, F. R. Keene, T. J. Meyer, *Inorg. Chem.* **1976**, *15*, 190−196.
[70] D. P. Rillema, G. Allen, T. J. Meyer, D. Conrad, *Inorg. Chem.* **1983**, *22*, 1617−1622.
[71] A. Kirsch-De Mesmaeker, L. Jacquet, A. Masschelein, F. Vanhecke, K. Heremans, *Inorg. Chem.* **1989**, *28*, 2465−2470.
[72] L. Jacquet, A. Kirsch-De Mesmaeker, *J. Chem. Soc., Faraday Trans.* **1992**, *88*, 2471−2480.

[98068]

Phosphanyl-Amino Complexes of Nickel(II): Synthesis and Structure

Laura Crociani[a], Francesco Tisato[a], Fiorenzo Refosco[a], Giuliano Bandoli*[b], and Benedetto Corain[c][+]

Istituto di Chimica e Tecnologia dei Materiali Avanzati, C. N. R.[a],
C. so Stati Uniti, 4, I-35020 Padova, Italy

Dipartimento di Scienze Farmaceutiche, Università di Padova[b],
Via Marzolo 5, I-35131 Padova, Italy
Fax: (internat.) + 39-49/8275345

Institut für Organische Chemie und Biochemie, TU München[c],
Lichtenbergstraße 4, D-85747 Garching, Germany

Received April 3, 1998

Keywords: Phosphanyl-amine / Nickel / Coordination chemistry / Pentacoordinate Ni complexes / Tetracoordinate Ni complexes

New neutral pentacoordinate nickel(II) complexes of the type $[NiCl_2(PR_3)(P^{\frown}N)]$ [PR_3 = PMe_3, PMe_2Ph, $PMePh_2$; $P^{\frown}N$ = 2-(diphenylphosphanyl)aniline ($P^{\frown}NH_2$), *N*-methyl-2-(diphenylphosphanyl)aniline ($P^{\frown}NHMe$), *N,N*-dimethyl-2-(diphenylphosphanyl)aniline ($P^{\frown}NMe_2$)], as well as cationic tetracoordinate nickel(II) complexes of the type $[NiCl(PR_3)(P^{\frown}N)]^+$ have been synthesized and characterized both in the solid state and in solution. Interesting X-ray structural data have been collected for each class of compounds, which show, inter alia, that the pentacoordinate neutral complexes can be isolated in two different molecular forms, namely square-pyramidal or bipyramidal-trigonal.

Introduction

The synthesis of metal complexes stabilized by $P^{\frown}N$ ligands and particularly phosphanyl-amines has attracted considerable attention in recent years[1]. The ligands 2-(diphenylphosphanyl)pyridine and 2-(diphenylphosphanyl)aniline give rise to interesting examples. The first is known to exhibit a very versatile coordination behavior towards numerous transition metal centers[2], both in mono- and polynuclear complexes. Remarkably, in these complexes it acts as either a monodentate, a bidentate chelating, or a bidentate bridging ligand. In its monodentate mode, the phosphane ligating site normally exhibits the strongest bonding ability towards metal centers such as nickel(II)[3], cobalt(I)[3], ruthenium(II)[4][5], rhodium(I)[4][6], and palladium(II)[4][7][8]. Conversely, the coordination chemistry of 2-(diphenylphosphanyl)aniline[9] has been widely investigated because of its ability to behave as a bidentate chelating amino[10], amido[11], or imido[12] ligand. This behavior has been further developed in the synthesis of new macrocyclic chelate compounds such as P_2N_2 ligands, which have previously been tested in these laboratories[13]. In particular, the reactivity of the tetradentate ligand *N,N′*-bis[2-(diphenylphosphanyl)phenyl]propane-1,3-diamine, H_2dppd, toward technetium and rhenium has been investigated. This tetradentate phosphanyl-amine behaves both as a ligand and as a reducing agent towards $[MO_4]^-$ (M = Tc, Re) to give hexacoordinate neutral oxo-M^V phosphanyl-amido complexes of the general formula [MO(dppd)X], X = Cl, OH, OMe, OEt, O_2CCF_3.

Similarly, P_2N_2 ligands such as *N,N′*-bis[2-(diphenylphosphanyl)phenyl]ethane-1,2-diamine and *N,N′*-bis[2-(diphenylphosphanyl)phenyl]propane-1,3-diamine have been employed as efficient ligands for preparing unprecedented and previously elusive copper(II) phosphane complexes[14]. These were subjected to X-ray structural analyses and were found to be characterized by authentic thermodynamic stability that was not attributable to kinetic inertness[15]. The finely balanced *soft-hard* character of the $\{P_2N_2\}$ ligating set has been proposed to play a major role in underlying this important result.

The various properties of phosphanyl-amino ligands prompted us to undertake a systematic study aimed at preparing both neutral and cationic nickel(II) complexes of the type shown in Scheme 1 and to evaluate the potential of the cationic species as "SHOP"-type catalysts[16].

Scheme 1

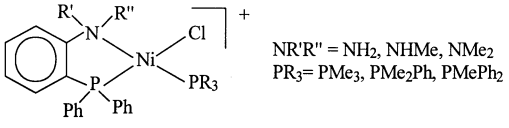

In this paper, we report on the detailed development of this project. Some of the results reported herein were anticipated in a preliminary report[17].

[+] Humboldt Stipendiat − on leave of absence from Dipartimento di Chimica Ingegneria Chimica e Materiali, Via Vetoio Coppito Due, I-67010 L′Aquila, Italy and from Centro di Studio sulla Stabilità e Reattività dei Composti di Coordinazione, CNR, c/o Dipartimento di Chimica Inorganica Metallorganica e Analitica, Università di Padova, via Marzolo 1, I-35131 Padova, Italy.

Supporting information for this article is available on the WWW under http://www.wiley-vch.de/home/eurjic or from the author.

 © WILEY-VCH Verlag GmbH, D-69451 Weinheim, 1998 1434−1948/98/1111−1689 $ 17.50+.50/0

Results and Discussion

A general overview of the scope of the synthetic results is given in Scheme 2. The compounds are obtained upon substitution of one monodentate phosphane by the bidentate one, which chelates the metal through both the P and N atoms.

Scheme 2

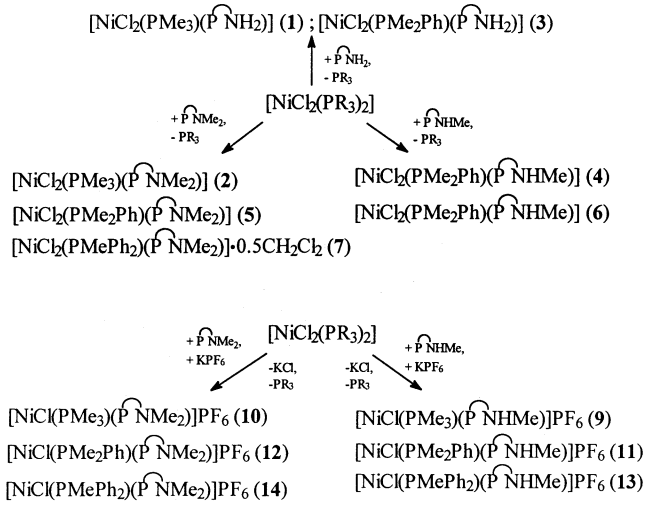

$[NiCl_2(PR_3)_2]$ complexes react readily with 2-(diphenylphosphanyl)aniline, $P^{\frown}NH_2$, *N*-methyl-2-(diphenylphosphanyl)aniline, $P^{\frown}NHMe$, and *N*,*N*-dimethyl-2-(diphenylphosphanyl)aniline, $P^{\frown}NMe_2$ (hereafter referred to as $P^{\frown}N$), usually in MeCN solution, to give pentacoordinate species of the type $[NiCl_2(PR_3)(P^{\frown}N)]$ (Table 1).

The same reaction, carried out in CH_2Cl_2 in the presence of KPF_6 as a scavenger of one Cl^- ligand per Ni atom, successfully leads to tetracoordinated species of the type $[NiCl(PR_3)(P^{\frown}N)]^+$ (Table 1), except in the case of $P^{\frown}NH_2$. The action of this tertiary phosphanyl-primary amine on $[NiCl_2(PR_3)_2]$ (PR_3 = PMe_2Ph and $PMePh_2$) leads to the bis-bidentate species $[Ni(P^{\frown}NH_2)_2]^{2+}$[18], and/or to the mononuclear phosphorane-imino complex $[NiCl(PMe_3)(P^{\frown}NP)]^+$[19], [$P^{\frown}NP$ = *N*-(trimethylphosphoranyl)-2-(diphenylphosphanyl)aniline], when PMe_3 is incorporated into the starting material as a mono-tertiary phosphane.

The formation of the pentacoordinate $[NiCl_2(PR_3)(P^{\frown}N)]$ complexes is achieved under stoichiometric conditions in a homogeneous phase after a few hours of reaction time at room temperature. The products can be isolated as analytically pure species either upon spontaneous precipitation or after the addition of Et_2O. All these compounds are rather unstable in solution when exposed to air. Nevertheless, they can be recrystallized from e.g. CH_2Cl_2 (see Experimental Section) and their MeCN solutions provide conductivity measurements consistent with non-conducting species (Table 1).

Table 1. Selected synthetic and physicochemical data of $[NiCl_2(PR_3)(P^{\frown}N)]$ and $[NiCl(PR_3)(P^{\frown}N)]^+$[a] complexes

Complex	Color	Crystal structure[b]	μ_{eff} [BM]	Λ_M[c] [Ω^{-1} cm^2mol^{-1}]	ν_{N-H} δ_{N-H} [cm^{-1}][d]	^1H NMR δ[e]	P{^1H} NMR δ[e]	λ_{max}[f] [nm] in solution	λ_{max}[d] [nm] in the solid state
2	Blue	n.d.	1.3	n.c.[g]		Paramagnetic solutions, signals from +18.0 to −2.0		485, 570, 725	380, 600, 800
3	Blue	spy	Diam. [h]	n.c.[g]	ν_{as}[i] 3236 m, ν_s[l] 3134 m, δ 1602 m	1.78 (s, 6 H), 2.67 (m, 2 H), 6.33−8.38 (m, 19 H)	−5.2 (br s, 1P), 38.6 (br s, 1P)	475, 610 sh	490 sh, 620
4·0.5 MeCN	Blue	n.d.	0.7	n.c.[g]	3241 s	Paramagnetic solutions, signals from +18.0 to −2.0		475, 630 sh	550, 690 sh
6·C_6H_6	Green	tb	3.4	n.c.[g]	3262 s	Paramagnetic solutions, signals from +18.0 to −1.0		430, 610 sh, 1055	400 sh, 620, 1050
9	Yellow	sp	Diam.[h]	180	3191 m	1.23 (s, 9 H), 2.87 (d, 3 H), 4.85 (m, 1 H), 7.20−7.95 (m, 14 H)	−144 (sept,1 P), −9.8 (dd, 1 P), 42.5 (d, 1 P)	265 (4.49), 290 sh, 430 (2.89)	430
10	Yellow	n.d.	Diam.[h]	190		1.26 (d, 9 H), 3.19 (s, 6 H), 7.12−8.15 (m, 14 H)	−144 (sept, 1 P), −9.51 (d, 1 P), 38.1 (d, 1 P)	240 (4.16), 270 sh, 435 (2.76)	445
11	Red-orange	n.d	Diam.[h]	158	3229 m	1.64 (s, 6 H), 2.04 (d, 3 H), 4.94 (m, 1 H), 7.12−8.15 (m, 19 H)	−144 (sept, 1 P), 1.30 (m, 1 P), 48.0 (m, 1 P)	295 (4.06), 322 (4.05), 430 (2.76)	450
13·C_6H_6	Yellow	sp	Diam.[h]	171	3251 m	2.01 (d, 3 H), 2.33 (s, 3 H), 7.10−7.84 (m, 24 H)	−146 (sept, 1 P), 6.91 (d, 1 P), 37.6 (d, 1 P)	275 (4.08), 310 (4.02), 435 (2.81)	445

[a] PF_6^- salts. − [b] X-ray authenticated: n.d. = not determined; spy = square-pyramidal; tb = trigonal-bipyramidal; sp = square-planar. − [c] In MeCN. − [d] KBr plates. − [e] $CDCl_3$ for **2**, **3**, **4**·0.5 MeCN, and **6**·C_6H_6; CD_2Cl_2 for **9**, **10**, **11**, and **13**·C_6H_6. − [f] The data refer to solutions in CH_2Cl_2, ca. 10^{-2} M for **2**, **3**, **4**·0.5 MeCN, and **6**·C_6H_6 and 10^{-3}−10^{-5} M for **9**, **10**, **11**, and **13**·C_6H_6; lg ε values in parentheses. − [g] n.c. = non-conducting. − [h] Diam. = diamagnetic. − [i] ν_{as} = ν asymmetric. − [l] ν_s = ν symmetric.

The formation of the tetracoordinate $[NiCl(PR_3)(P^{\frown}N)]^+$ complexes can also be readily achieved under essentially stoichiometric conditions, by removal of KCl, concentration of the reaction solution, and addition of Et_2O. Cationic complexes $[NiCl(PR_3)(P^{\frown}N)]^+$ can be readily recrystallized from suitable solvent mixtures, such as CH_2Cl_2/EtOH/Et_2O or CH_2Cl_2/EtOH/C_6H_6.

The ability of nickel(II) to give charged and neutral pentacoordinate complexes is well-documented in the literature[20]. Thus, numerous high-spin distorted trigonal-bipyramidal and square-pyramidal complexes are known, which usually contain *hard* donor sites. Quite a few low-spin distorted trigonal-bipyramidal complexes have also been described and, conversely, they typically exhibit an overall *soft* coordination sphere. To the best of our knowledge, only four examples of pentacoordinate complexes with an $\{NP_2Cl_2\}$ donor set have been reported in the literature[17][21][22]; the data presented herein allow the possibility of analyzing this coordination sphere, which is otherwise only poorly documented. The geometry of complex **3** (vide infra) is intermediate between square-pyramidal and trigonal-bipyramidal and this complex is diamagnetic. On the other hand, complexes **5**, **6**·CH_2Cl_2, and **7** are trigonal-bipyramidal and paramagnetic. Ligand sets high in the spectrochemical series are predicted[20] to give diamagnetic trigonal-bipyramidal complexes, but in our case the situation is reversed. Apparently, the ligand field exerted by our ligand set is not large enough to produce a singlet fundamental electronic state. Moreover, complexes **2** and **4** are characterized by magnetic moment values formally corresponding to less than two unpaired electrons (Table 1), which have previously been observed and discussed[23] in terms of a thermally controlled equilibrium between singlet and triplet states. However, the data collected prevent us from invoking such an equilibrium as the sole factor responsible for the magnetic behavior of complexes **2** and **3**.

The $\{NP_2Cl\}$ chromophore invariably produces square-planar nickel(II) complexes for all the PR_3 and $P^{\frown}N$ ligands employed, the structures of which have been validated by single-crystal X-ray analyses. The spectra in the visible range and the diamagnetism of all the complexes **9**, **10**, **11**, and **13**·C_6H_6 are in accordance with this structure[20]. The position of the *d-d* band at 430−450 nm (Table 1) indicates that the $\{NP_2Cl\}$ chromophore is appreciably lower in the spectrochemical series than e.g. $\{P_2(CN)_2\}$[24], for which this band appears at ca. 350 nm. These bands are also observed in solution (lg ε values are also reasonable) and the conductivity figures are consistent with classical behavior of these square-planar nickel complexes.

Proton NMR spectra of the paramagnetic pentacoordinate complexes in $CDCl_3$ show signals spread over the range from δ = +20 to −14. Conversely, complexes **1** and **3**, which retain the unsubstituted phosphanyl-amine $P^{\frown}NH_2$, are diamagnetic; their spectra allow the assignment of the coordinated phosphanyl-amine protons at δ = 2.60 and of the methyl groups of the mono-tertiary phosphanes at δ = 1.26 and 1.78 for **1** and **3**, respectively. These diamagnetic species are subject to fluxional behavior at room temperature in $CDCl_3$ solution, since the $^{31}P\{^1H\}$ spectra exhibit broad signals that lack the multiplicity that would be expected given the presence of two magnetically non-equivalent phosphorus donors in the coordination sphere.

On the other hand, the $^{31}P\{^1H\}$ spectra of square-planar cationic complexes indicate the existence of two types of phosphorus donors; in fact, a double doublet pattern is usually observed, the position of which is primarily determined by the nature of the mono-tertiary phosphane. In addition, a septuplet centred at δ = −144 establishes the presence of the hexafluorophosphate counterion. The methyl groups incorporated at the phosphorus and/or nitrogen donors are distinguishable on the basis of their chemical shifts and relative integrals in the proton spectra, which, where appropriate, also show the coordinated amine protons at δ = 4.90.

X-ray Structure Analysis

In the neutral complexes **3** (Figure 1) and **6**·CH_2Cl_2 (Figure 2), the coordination around the Ni^{II} center is distorted trigonal-bipyramidal with the two axial positions occupied by the phosphorus atom of the monodentate phosphane and by the nitrogen atom of the bidentate ligand ($P^{\frown}NH_2$ in **3** and $P^{\frown}NHMe$ in **6**·CH_2Cl_2). The equatorial sites accommodate the remaining phosphorus of the phosphanylamine and the two Cl donors. The Ni atom is displaced from the equatorial plane in the direction of P(2), by 0.13 Å in **3** and by 0.18 Å in **6**·CH_2Cl_2. The $P^{\frown}N$ ligand mean plane of **3** makes a dihedral angle of 94.6° with the equatorial plane, while the corresponding angle in **6**·CH_2Cl_2 is 67.5°. The five-membered chelate ring, roughly planar in **3** (maximum deviation of 0.05 Å by the nitrogen atom; torsion angles between −6.8° and +9.3°), assumes an envelope (C_s) conformation in **6**·CH_2Cl_2, as shown by the deviation (0.29 Å) of the nitrogen atom and the torsion angle values (from −30.5° to +35.0°). Moreover, superposition of the two structures (Figure 3) gives a high r.m.s. value (0.56 Å) when the fitting is performed on the 12 atoms labelled in the pertinent figure. Based on these differences, the geometry of **3** could alternatively be described as distorted square-pyramidal (Figure 4). In this description, the base could be regarded as comprising the P,N donors of the ligand, the P(2) atom of the monodentate phosphane, and Cl(1). The Ni atom is displaced from the base by +0.27 Å in the direction of Cl(2), but the deviations of the other donors are also dramatic [P(1) −0.31 Å, N(1) +0.35 Å, Cl(1) −0.32 Å and P(2) +0.28 Å]. Moreover, the *trans* angle P(1)−Ni−Cl(1) is only 148.29(6)°, while the *cis* angle P(1)−Ni−Cl(2) is widened to 110.82(6)°. In conclusion, the coordination geometry of **3** is intermediate between trigonal-bipyramidal and square-pyramidal and, accordingly, application of the τ index[25] gives a value of 0.46 (1.0 for trigonal-bipyramidal; 0.0 for square-pyramidal).

In the cationic complexes **9** (Figure 5) and **13**·MeOH (Figure 6), the coordination geometry around Ni^{II} can be

Figure 1. ORTEP view of complex **3**; hydrogen atoms are omitted for clarity; the thermal ellipsoids are drawn at 40% probability

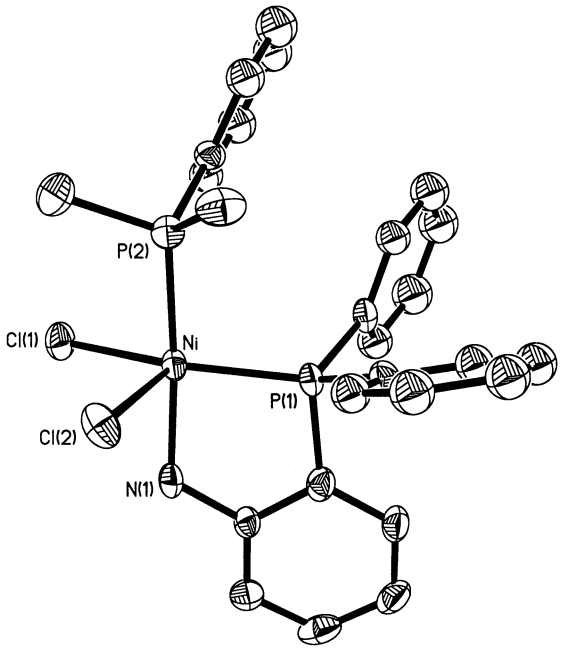

Figure 2. ORTEP view of complex **6**·CH_2Cl_2; hydrogen atoms and the CH_2Cl_2 molecule are omitted for clarity; the thermal ellipsoids are drawn at 40% probability

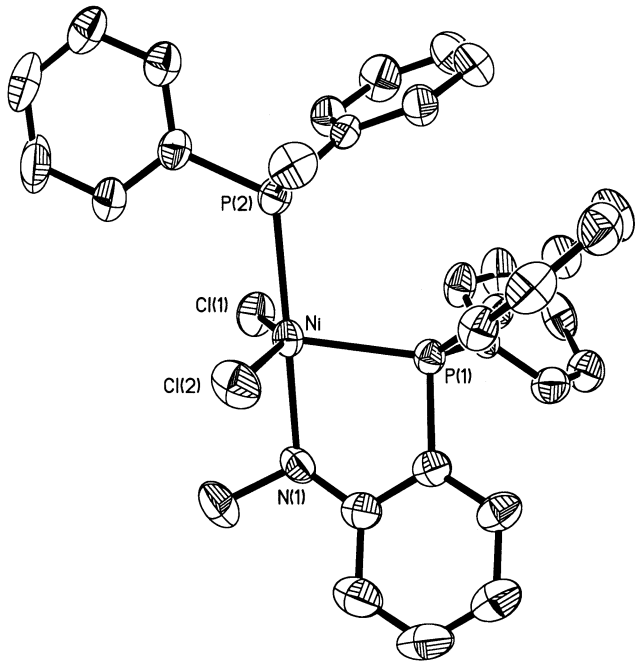

Figure 3. Superposition of geometries of **3** (—) and **6**·CH_2Cl_2 (---)

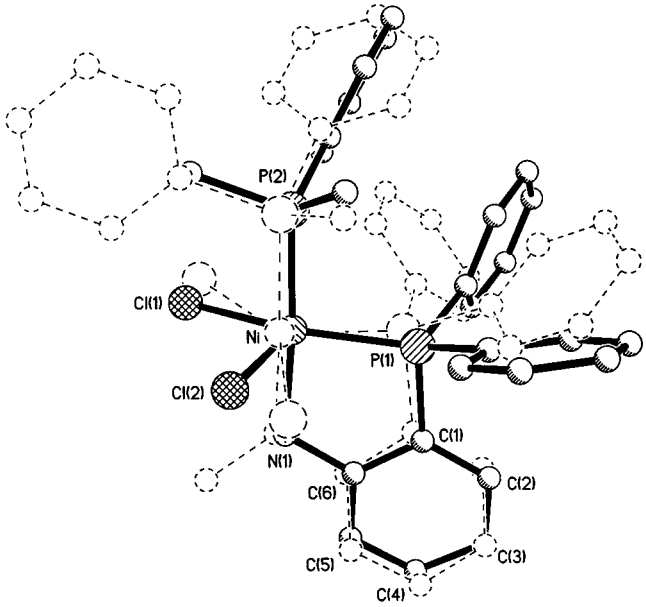

Figure 4. ORTEP view of complex **3** showing the square-pyramidal geometry; hydrogen atoms are omitted for clarity; the thermal ellipsoids are drawn at 40% probability

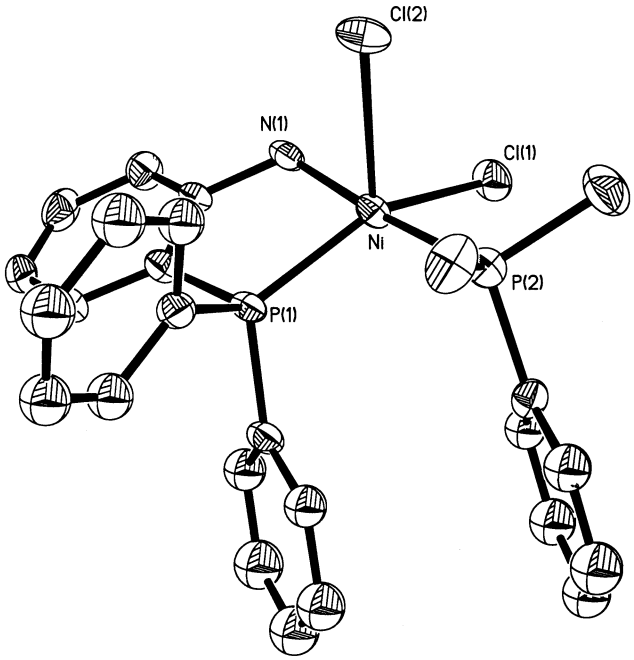

described as square-planar, with the two phosphorus donors located in a mutual *cis* arrangement and the remaining two positions occupied by the secondary amine nitrogen of the bidentate P⌒NHMe ligand and by the Cl donor. The nickel coordination spheres are distorted (Table 2) and the four donor atoms deviate from the mean coordination plane by ±0.17 Å in **9** and by ±0.10 Å in **13**·MeOH. The P⌒N ligand mean plane makes a dihedral angle with the mean coordination plane of 18.8° in **9** and of 23.9° in **13**·MeOH. The conformation of the five-membered NiPCCN chelate ring results in a twist-envelope (C_2) form (torsion angles between −14.2° and 13.2° in **9** and between −24.2° and 19.4° in **13**·MeOH) and superposition of the two structures (Figure 7) reveals only minor differences in the relative orientations of the phenyl rings, the r.m.s. value being 0.13 Å when the fitting is performed on the 11 atoms labelled in the pertinent figure.

For each of the four complexes, the packing does not give rise to intermolecular contacts shorter than the sum of the

Figure 5. ORTEP view of complex **9**; hydrogen atoms and the PF_6^- anion are omitted for clarity; the thermal ellipsoids are drawn at 40% probability

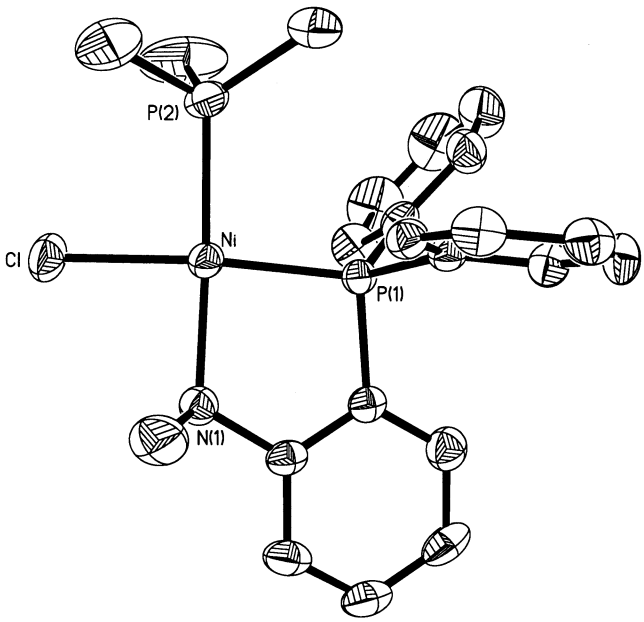

Figure 6. ORTEP view of complex **13**·MeOH; hydrogen atoms, the PF_6^- anion and the MeOH molecule are omitted for clarity; the thermal ellipsoids are drawn at 40% probability

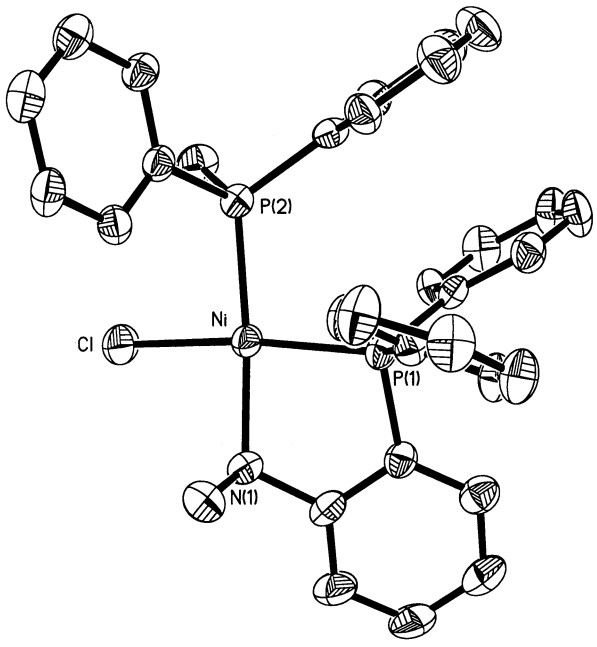

Figure 7. Superposition of geometries of **9** (—) and **13**·MeOH (- - -)

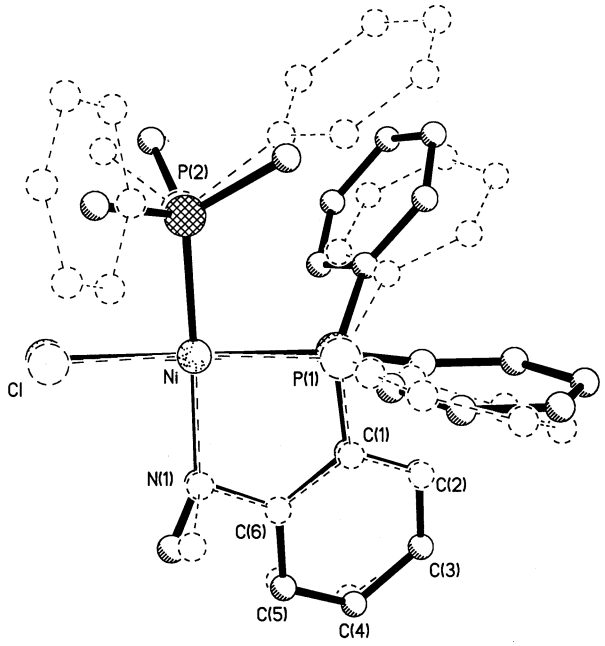

Table 2. Selected bond lengths [Å] and angles [°] for **3**, **6** · CH_2Cl_2, **9**, and **13** · MeOH

	3	**6** · CH_2Cl_2
Ni−Cl(1)	2.249(2)	2.307(2)
Ni−Cl(2)	2.565(2)	2.298(2)
Ni−P(1)	2.170(2)	2.330(2)
Ni−P(2)	2.189(2)	2.380(2)
Ni−N(1)	1.963(4)	2.212(4)
Cl(1)−Ni−Cl(2)	99.78(6)	144.59(6)
Cl(1)−Ni−P(1)	148.29(6)	109.17(6)
Cl(1)−Ni−N(1)	87.5(1)	84.8(1)
Cl(2)−Ni−P(2)	90.65(6)	92.24(6)
Cl(2)−Ni−P(1)	110.82(6)	104.09(6)
P(2)−Ni−N(1)	175.6(1)	177.6(1)
	9	**13**·MeOH
Ni−Cl	2.200(2)	2.177(2)
Ni−P(1)	2.137(1)	2.156(2)
Ni−P(2)	2.195(2)	2.204(2)
Ni−N(1)	1.987(4)	1.998(6)
Cl−Ni−P(1)	165.91(6)	171.36(9)
Cl−Ni−P(2)	89.53(6)	88.68(9)
Cl(1)−Ni−N(1)	88.7(1)	87.9(1)
P(1)−Ni−P(2)	95.87(6)	98.05(8)
P(1)−Ni−P(2)	87.0(1)	85.8(2)
P(2)−Ni−N(1)	174.8(1)	174.0(2)

van der Waals radii and there are no possibilities for hydrogen bonding. The Ni(II)−donor atom bond lengths in the $[NiCl_2(PR_3)(P^{\frown}N)]$ and $[NiCl(PR_3)(P^{\frown}N)]^+$ complexes merit some comment. Thus, the spread of their values (Table 3) might seem unexpectedly large (Ni−Cl in the range 2.177−2.567 Å; Ni−P 2.139−2.400 Å and Ni−N 1.963−2.353 Å), but this can be rationalized on the basis of coordination number, c.n., and/or geometry arguments. In fact, comparison of the distances with the pertinent "reference" values retrieved from the Cambridge Structural Database (CSD)[26] reveals the following features. (i) The Ni^{II}−Cl distances (mean value of 2.196 Å when c.n. = 4, and of 2.288 Å with c.n. = 5) are slightly shorter than the corresponding CSD values [2.22 (219 obs.) and 2.34 Å (88 obs.), respectively], but they confirm the finding that on going from c.n. 4 to 5 the distance increases. This trend also holds for the Ni−P and Ni−N distances. The Ni−Cl(2) distance in **3** [2.567(2) Å] represents an exception, being the

Table 3. Selected structural data for $[NiCl_2(PR_3)(P^{\frown}N)]$ and $[NiCl(PR_3)(P^{\frown}N)]PF_6$ complexes

	Geometry[a]	Ni−Cl [Å]	Ni−PR_3 [Å]	Ni−P [Å]	Ni−N [Å]	$P^{\frown}N_{bite}$ [°]	Ni−N−$C_{chelate}$ [°]	Ref.[b]
$[NiCl_2(PMe_2Ph)(P^{\frown}NMe_2)]$	tb	2.276(2) 2.284(2)	2.372(2)	2.290(2)	2.353(4)	77.9(1)	109.2(5)	**5**
$[NiCl_2(PMePh_2)(P^{\frown}NHMe)]\cdot CH_2Cl_2$	tb	2.298(2) 2.307(2)	2.380(2)	2.330(2)	2.212(4)	79.9(1)	112.3(3)	**6**·CH_2Cl_2
$[NiCl_2(PMePh_2)(P^{\frown}NMe_2)]\cdot 0.5CH_2Cl_2$	tb	2.288(3) 2.272(3)	2.400(5)	2.310(3)	2.325(8)	78.7(2)	108.5(5)	**7**
$[NiCl_2(PMe_2Ph)(P^{\frown}NH_2)]$	tb/spy	2.249(2) 2.567(2)	2.189(2)	2.170(2)	1.963(4)	86.3(2)	119.8(3)	**3**
$[NiCl(PMe_3)(P^{\frown}NP)]PF_6$ [c]	sp	2.217(2)	2.192(2)	2.159(3)	2.011(7)	83.1(2)	113.8(5)	**8**
$[NiCl(PMe_3)(P^{\frown}NHMe)]PF_6$	sp	2.200(2)	2.195(2)	2.137(1)	1.987(4)	87.0(1)	116.7(3)	**9**
$[NiCl(PMePh_2)(P^{\frown}NHMe)]PF_6\cdot MeOH$	sp	2.177(2)	2.177(2)	2.156(2)	1.998(6)	85.8(2)	115.2(5)	**13**·MeOH
$[NiCl(PMePh_2)(P^{\frown}NMe_2)]PF_6$	sp	2.189(5)	2.207(5)	2.139(5)	2.056(8)	86.8(2)	114.9(6)	**14**

[a] tb = trigonal-bipyramidal; spy = square-pyramidal; sp = square-planar. − [b] **3**, **6**·CH_2Cl_2, **9**, **13**·MeOH in present work; **5** in ref.[21]; **7** and **14** in ref.[17]; **8** in ref.[19]. − [c] $P^{\frown}NP$ = *N*-(trimethylphosphoranyl)-2-(diphenylphosphanyl)aniline.

second longest distance ever reported in the literature[27]. In the square-pyramidal description (Figure 4), this axial elongation can be correlated with the electron density in the d_{z^2} orbital for the d^8 ion, leading to a pronounced metal−halide electron-electron repulsion. (ii) The geometry seems to govern the Ni−P bond lengths. The corresponding mean values in the trigonal-bipyramidal complexes average 2.310 Å and 2.384 Å for the chelating phosphane ligand and the unidentate ligand axially bonded to Ni^{II}, respectively. The magnitude of this "axial effect" (ca. 0.07 Å) is consistent with similar values encountered in the CSD file. In square-planar complexes, the corresponding mean values are 2.148 Å and 2.193 Å and a parallel situation is presented by **3**, since values of 2.189 Å and 2.170 Å are observed. (iii) The Ni^{II}−N distances in cationic complexes with c.n. = 4 (mean value 2.01 Å) are dramatically shorter than those in the neutral complexes with c.n. = 5 (mean value 2.30 Å), but the paucity of literature data prevents us from making a reliable comparison. In any case, the Ni−N(C_{sp^2})H_2 value of **3** (1.963 Å) conforms to those of the square-planar complexes. Similarly, the P−Ni−N bite angle (86.3°) of **3** closely approaches the mean value (85.6°) found in the four analogous complexes with c.n. 4, while it is compressed to 78.8° in those with c.n. = 5. Finally, the Ni−N−C angle of the five-membered chelate ring averages 115.2° in complexes with c.n. = 4, while it is compressed to 110.0° when the c.n. becomes 5.

Conclusions

Phosphanyl-amines $P^{\frown}NH_2$, $P^{\frown}NHMe$, $P^{\frown}NMe_2$ exhibit good coordination properties towards the nickel(II) center, affording stable neutral pentacoordinate $[NiCl_2(PR_3)(P^{\frown}N)]$ and cationic tetracoordinate $[NiCl(PR_3)(P^{\frown}N)]^+$ complexes starting from the corresponding $[NiCl_2(PR_3)_2]$ precursor.

The neutral pentacoordinate species $[NiCl_2(PR_3)(P^{\frown}N)]$ feature a rather unusual $\{NP_2Cl_2\}$ donor set. Their behavior can be satisfactorily accounted for considering the data collected in the course of this study. The range of magnetic moments they exhibit is unexpected in view of the donor set $\{NP_2Cl_2\}$ and of their crystal structures. While it is possible to assign a trigonal-bipyramidal structure to complex **6**, in analogy to related compounds such as $[NiCl_2(PMe_2Ph)(P^{\frown}NMe_2)]$[21] and $[NiCl_2(PMePh_2)(P^{\frown}NMe_2)]\cdot 0.5\ CH_2Cl_2$[17], complex **3** has a structure intermediate between trigonal-bipyramidal and square-pyramidal, which accounts for the very long Ni−Cl distance.

The cationic tetracoordinate species $[NiCl(PR_3)(P^{\frown}N)]^+$ can be derived from the corresponding $[NiCl_2(PR_3)_2]$ precursor only by the addition of KPF_6 in order to remove one Cl^- ligand per Ni atom. NMR spectra and crystal structures indicate that these complexes consist of the *cis*-P,P isomer. Comparison of some structural features such as the Ni−N, Ni−Cl, and Ni−P bond lengths confirms the finding that on going from c.n. = 4 to 5 the distances increase. In particular, Ni−N is dramatically shorter than the CSD reference value, but the paucity of literature data prevents us from making firm conclusions from this observation.

Benedetto Corain is grateful to the *Alexander von Humboldt Foundation* for supporting his activities at TU München.

Experimental Section

General: All chemicals and solvents were of analytical grade and were used as received unless otherwise stated. The starting $[NiCl_2(PR_3)_2]$ (PR_3 = PMe_3, PMe_2Ph, $PMePh_2$) complexes were prepared according to the literature[28][29], as were the ligands $P^{\frown}NH_2$[9], $P^{\frown}NHMe$[9], and $P^{\frown}NMe_2$[30]. − IR: Mattson 3030 Fourier-transform spectrometer. − UV/Vis in the solid state: Cary 5-E spectrophotometer (1200−220 nm), diffuse reflectance method. − UV/Vis in solution: Cary 17D spectrophotometer (1200−220 nm), ca. 10^{-2} M solutions in CH_2Cl_2 for the pentacoordinate complexes in 0.1-cm cells and 10^{-3}−10^{-5} M solutions in CH_2Cl_2 for square-planar and cationic complexes in 1-cm cells. − NMR: Bruker AC-200 (200 MHz for ^1H and ^{31}P). For ^1H NMR, $CDCl_3$ or CD_2Cl_2 as solvent, TMS as internal standard; for $^{31}P\{^1H\}$ NMR, $CDCl_3$ or CD_2Cl_2 as solvent, 85% aqueous H_3PO_4 as external standard. − Conductivity measurements: Amel conductimeter Mod. 131, ca. 10^{-3} M solutions in MeCN at 25°C. − Magnetic susceptibility measurements: Cahn 2000 microbalance. − Elemental analyses (C, H, N): Fisons EA 1108 elemental analyzer.

[NiCl$_2$(PMe$_3$)(P⌒NMe$_2$)] (**2**): To a solution of 0.196 g of [NiCl$_2$(PMe$_3$)$_2$] (0.68 mmol) in 10 ml of MeCN was added 0.209 g of P⌒NH$_2$ (0.68 mmol). The blood-red solution immediately darkened and was stirred under dinitrogen at room temperature for 3 h. The solution was then concentrated to a volume of 3 ml under a flow of dinitrogen. A dark-blue powder precipitated, which was collected by filtration, washed with 5 ml of Et$_2$O, 5 ml of *n*-hexane and 0.5 ml of EtOH, and dried in vacuo. Yield: 0.140 g (40%). − IR (KBr): $\tilde{\nu}$ = 3047 cm^{-1} s, 1580 m, 1481 m, 1437 s, 1094 s, 959 vs, 753 m, 514 m. − ^{1}H NMR (CDCl$_3$): Several signals in the region δ = +18.0 to −2.0. − $C_{23}H_{29}Cl_2NNiP_2$ (483.01): calcd. C 54.05, H 5.73, N 2.74; found C 54.64, H 5.67, N 2.43.

[NiCl$_2$(PMe$_2$Ph)(P⌒NH$_2$)] (**3**): To a solution of 0.108 g of [NiCl$_2$(PMe$_2$Ph)$_2$] (0.27 mmol) in 10 ml of MeCN was added 0.075 g of P⌒NH$_2$ (0.27 mmol) and the mixture was stirred under dinitrogen at room temperature. The blood-red solution immediately turned dark. After 5 min, a blue compound precipitated and after 15 min the solid was collected by filtration, washed several times with MeCN, and dried in vacuo. Yield: 0.111 g (85%). Crystals were grown by slow evaporation of the solvent from CH$_2$Cl$_2$ solutions. − IR (KBr): $\tilde{\nu}$ = 3236 cm^{-1} m, 3179 m, 3093 s, 1555 m, 1478 m, 1433 s, 1095 m, 914 vs, 698 m, 512 m. − ^{1}H NMR (CDCl$_3$): δ = 1.78 [s, 6 H, P(C*H*$_3$)$_2$], 2.67 (m, 2 H, N*H*$_2$), 6.33−8.38 (m, 19 H, aromatic). − ^{31}P{^{1}H} NMR (CDCl$_3$): δ = −5.2 (br. s, 1 P, *P*Me$_2$), 38.6 (br., 1 P, *P*⌒NH$_2$). − $C_{26}H_{27}Cl_2NNiP_2$ (545.08): calcd. C 57.29, H 5.00, N 2.57; found C 57.17, H 5.37, N 2.57.

[NiCl$_2$(PMe$_2$Ph)(P⌒NHMe)] (**4**): To a solution of 0.100 g of [NiCl$_2$(PMe$_2$Ph)$_2$] (0.25 mmol) in 5 ml of MeCN was added 0.073 g of P⌒NHMe (0.25 mmol) and the mixture was stirred under dinitrogen at room temperature. After 30 min, a blue compound precipitated and after 3 h the solid was collected by filtration, washed twice with 6 ml of *n*-hexane, and dried in vacuo. Yield: 0.065 g (44%). − IR (KBr): $\tilde{\nu}$ = 3246 cm^{-1} w, 3051 s, 2247 w, 1580 m, 1481 m, 1435 s, 1098 s, 913 s, 742 m, 487 s. − ^{1}H NMR (CDCl$_3$): Several signals in the region δ = +18.0 to −2.0. − $C_{27}H_{29}Cl_2NNiP_2 \cdot 0.5\ CH_3CN$ (579.64): calcd. C 58.02, H 5.31, N 3.62; found C 57.75, H 5.06, N 3.64.

[NiCl$_2$(PMePh$_2$)(P⌒NHMe)] (**6**): To a blood-red solution of 0.101 g of [NiCl$_2$(PMePh$_2$)$_2$] (0.19 mmol) in 10 ml of MeCN and 0.5 ml of CH$_2$Cl$_2$ was added 0.055 g of P⌒NHMe (0.19 mmol). The red solution immediately turned brown. After stirring under dinitrogen at room temperature for 3 h, the solution was concentrated to dryness under reduced pressure. The residue was washed with 0.4 ml of MeCN and 0.4 ml of CH$_2$Cl$_2$, and then redissolved in 10 ml of CH$_2$Cl$_2$ and 1.5 ml of C$_6$H$_6$. Addition of 23 ml of Et$_2$O caused the precipitation of a green solid, which was collected by filtration, washed with 5 ml of Et$_2$O, and dried in vacuo. Yield: 0.080 g (60%). Crystals were grown by slow evaporation of the solvent from CH$_2$Cl$_2$ solutions. − IR (KBr): $\tilde{\nu}$ = 3262 cm^{-1} w, 1580 m, 1471 s, 1434 s, 1099 m, 885 s, 685 vs, 502 s. − ^{1}H NMR (CDCl$_3$): Several signals in the region δ = +18.0 to −1.0. − $C_{32}H_{31}Cl_2NNiP_2 \cdot C_6H_6$ (699.3): calcd. C 65.26, H 5.34, N 2.00; found C 65.38, H 5.44, N 1.74.

[NiCl(PMe$_3$)(P⌒NHMe)]PF$_6$ (**9**): To a mixture of 0.131 g of [NiCl$_2$(PMe$_3$)$_2$] (0.46 mmol) and 0.117 g of KPF$_6$ (0.64 mmol) in 10 ml of CH$_2$Cl$_2$ was added 0.134 g of P⌒NHMe (0.46 mmol) under stirring. The blood-red mixture immediately turned dark-red. After 3 h, a yellow solid had been deposited, which was filtered off, washed with 2 ml of H$_2$O, recrystallized from a 1:2 MeCN/Et$_2$O solution (30 ml), and dried in vacuo. The filtrate was concentrated to dryness under reduced pressure and the residue was recrystallized as above, giving a second crop of the yellow solid. Yield: 0.195 g (70%). Crystals suitable for X-ray analysis were grown by slow evaporation of the solvent from CH$_2$Cl$_2$ solutions. − IR (KBr): $\tilde{\nu}$ = 3191 cm^{-1} m, 1583 m, 1462 m, 1104 w, 838 vs (P−F), 557 s. − ^{1}H NMR (CD$_2$Cl$_2$): δ = 1.23 [s, 9 H, P(C*H*$_3$)$_3$], 2.87 (d, $^3J_{HH}$ = 6 Hz, 3 H, NC*H*$_3$), 4.85 (m, 1 H, N*H*), 7.20−7.95 (m, 14 arom. H). − ^{31}P{^{1}H} NMR (CD$_2$Cl$_2$): δ = −144 (sept., J_{PF} = 711 Hz, 1 P, *P*F$_6^-$), −7.80 (m, 1 P, *P*Me$_3$), 42.5 (m, 1 P, *P*⌒NHMe). − $C_{22}H_{27}ClF_6NNiP_3$ (606.56): C 43.56, H 4.50, N 2.31; found C 43.42, H 4.16, N 2.16.

[NiCl(PMe$_3$)(P⌒NMe$_2$)]PF$_6$ (**10**): To a mixture of 0.082 g of [NiCl$_2$(PMe$_3$)$_2$] (0.29 mmol) and 0.074 g of KPF$_6$ (0.40 mmol) in 10 ml of CH$_2$Cl$_2$ was added 0.089 g of P⌒NH$_2$ (0.25 mmol) and the mixture was stirred at room temperature. The blood-red solution immediately turned orange-red. After 3 h, the mixture was filtered and concentrated to a volume of 4 ml under a flow of dinitrogen. Addition of 12 ml of Et$_2$O caused the precipitation of a yellow-orange solid, which was collected by filtration, washed with H$_2$O, and dried in vacuo. The solid was recrystallized from CH$_2$Cl$_2$/EtOH/C$_6$H$_6$ (10:1:19) (20 ml). Yield: 0.121 g (67%). − IR (KBr): $\tilde{\nu}$ = 3070 cm^{-1} w, 1580 m, 1483 m, 1436 s, 1097 m, 836 vs (P−F), 558 s. − ^{1}H NMR (CD$_2$Cl$_2$): δ = 1.26 [d, 9 H, $^2J_{HP}$ = 12.5 Hz, P(C*H*$_3$)$_3$], 3.19 [s, 6 H, N(C*H*$_3$)$_2$], 7.12−8.15 (m, 14 H, aromatic). − ^{31}P{^{1}H} NMR (CD$_2$Cl$_2$): δ = −144 (sept, 1 P, J_{PF} = 713 Hz, *P*F$_6^-$), −9.51 (d, 1 P, $^2J_{PP}$ = 107 Hz, *P*Me$_3$), 38.1 (d, 1 P, $^2J_{PP}$ = 107 Hz, *P*⌒NMe$_2$). − $C_{23}H_{29}ClF_6NNiP_3$ (620.59): calcd. C 44.51, H 4.71, N 2.26; found C 44.41, H 4.56, N 2.26.

[NiCl(PMe$_2$Ph)(P⌒NHMe)]PF$_6$ (**11**): To a mixture of 0.155 g of [NiCl$_2$(PMe$_2$Ph)$_2$] (0.38 mmol) and 0.138 g of KPF$_6$ (0.75 mmol) in 1 ml of CH$_2$Cl$_2$ was added 0.111 g of P⌒NHMe (0.38 mmol) and the mixture was stirred at room temperature. The blood-red mixture slowly turned red-orange. After 3 h, the solution was filtered and concentrated to a volume of 5 ml under a flow of dinitrogen. Addition of 15 ml of Et$_2$O caused the precipitation of an orange solid, which was collected by filtration, washed with H$_2$O, and dried in vacuo. The solid was recrystallized from CH$_2$Cl$_2$/EtOH/C$_6$H$_6$ (7:1.5:19) (27.5 ml). Yield: 0.153 g (60%). − IR (KBr): $\tilde{\nu}$ = 3229 cm^{-1} m, 1584 m, 1506 m, 1437 s, 1102 m, 837 vs (P−F), 557. − ^{1}H NMR (CD$_2$Cl$_2$): δ = 1.64 [s, 6 H, P(C*H*$_3$)$_2$], 2.96 (d, 3 H, $^3J_{HH}$ = 6 Hz, NC*H*$_3$), 4.94 (m, 1 H, N*H*), 6.90−8.04 (m, 19 H, aromatic). − ^{31}P{^{1}H} NMR (CD$_2$Cl$_2$): δ = −144 (sept, 1 P, J_{PF} = 713 Hz, *P*F$_6^-$), 1.30 (m, 1 P, *P*Me$_2$Ph), 48.0 (m, 1 P, *P*⌒NHMe). − $C_{27}H_{29}ClF_6NNiP_3$ (668.63): calcd. C 48.55, H 4.38, N 2.10; found C 48.71, H 4.38, N 2.03.

[NiCl(PMePh$_2$)(P⌒NHMe)]PF$_6$ (**13**): To a mixture of 0.132 g of [NiCl$_2$(PMePh$_2$)$_2$] (0.25 mmol) and 0.092 g of KPF$_6$ (0.50 mmol) in 10 ml of CH$_2$Cl$_2$ was added 0.073 g of P⌒NHMe (0.25 mmol) and the mixture was stirred at room temperature. The blood-red mixture immediately turned red-orange. After 3 h, the solution was filtered and concentrated to a volume of 4 ml under a flow of dinitrogen. Addition of 16 ml of Et$_2$O caused the formation of a red-orange oil, which was separated by decantation. After dissolution of the oil in 7 ml of CH$_2$Cl$_2$, 18 ml of C$_6$H$_6$ was added and upon stirring an orange-yellow solid precipitated. This solid was collected by filtration, washed with H$_2$O, dried in vacuo, and recrystallized from CH$_2$Cl$_2$/EtOH/C$_6$H$_6$ (6:1.5:17) (24.5 ml). Yield: 0.112 g (60%). Crystals were grown from CH$_2$Cl$_2$/MeOH/C$_6$H$_6$/Et$_2$O solutions. − IR (KBr): $\tilde{\nu}$ = 3251 cm^{-1} m, 1581 m, 1436 s, 1099 w, 840 vs (P−F), 557 s. − ^{1}H NMR (CDCl$_3$): δ = 2.01 (d, 3 H, $^3J_{HP}$ = 13 Hz, PC*H*$_3$), 2.33 (s, 3 H, NC*H*$_3$), 7.10−7.84 (m, 26 H, aromatic). − ^{31}P{^{1}H} NMR (CDCl$_3$): δ = −146 (sept., 1 P, J_{PF} = 713 Hz, *P*F$_6^-$), 6.91 (d, 1 P, $^2J_{PP}$ = 83 Hz, *P*Me$_2$Ph), 37.6 (d, 1 P, $^2J_{PP}$ = 83 Hz, *P*⌒NHMe). − $C_{32}H_{31}ClF_6NNiP_3 \cdot C_6H_6$ (808.82): calcd. C 56.08, H 4.59, N 1.72; found C 56.99, H 4.55, N 1.65.

X-ray Crystal Structure Determinations: Many of the details of the structure analyses carried out on complexes **3**, **6**·CH_2Cl_2, **9**, and **13**·MeOH are listed in Table 4.

Table 4. Crystallographic details for complexes **3**, **6** · CH_2Cl_2, **9**, and **13**·MeOH

	3	**6**·CH_2Cl_2	**9**	**13**·MeOH
formula	$C_{26}H_{27}Cl_2NNiP_2$	$C_{33}H_{33}Cl_4NNiP_2$	$C_{22}H_{27}ClF_6NNiP_3$	$C_{33}H_{35}ClF_6NNiOP_3$
cryst. system	monoclinic	triclinic	monoclinic	triclinic
space group	$P2_1/n$, (No.14)	$P\bar{1}$ (No.2)	$P2_1/n$, (No.14)	$P\bar{1}$ (No.2)
a [Å]	11.937(5)	9.763(4)	11.856(3)	10.008(1)
b [Å]	13.348(4)	10.002(3)	13.669(4)	13.395(2)
c [Å]	15.575(4)	18.115(9)	16.575(5)	14.598(2)
α [°]	90	77.89(3)	90	101.50(1)
β [°]	92.37(3)	77.85(3)	96.54(2)	105.02(1)
γ [°]	90	87.36(3)	90	104.56(1)
V [Å^3]	2479(1)	1691(1)	2669(1)	1745.5(3)
Z	4	2	4	2
D_{calcd} [Mg/m^3]	1.460	1.251	1.510	1.444
μ [mm^{-1}]	1.142	1.008	1.061	0.825
F(000)	1128	728	1240	784
cryst. size [mm]	0.20 × 0.30 × 0.20	0.15 × 0.10 × 0.20	0.25 × 0.25 × 0.25	0.15 × 0.15 × 0.15
Θ range [°]	2.3−25.0	2.6−22.5	2.5−22.5	2.2−21.5
indep. refl.	4387	4429	3500	4013
refl. with $I > 2\sigma(I)$	2633	3295	2956	2798
no. of parameters	215	385	289	414
$R1$[a], $wR2$ [b] [$I > 2\sigma(I)$]	0.043, 0.106	0.041, 0.112	0.045, 0.158	0.055, 0.139
$R1$, $wR2$ (all data)	0.082, 0.121	0.062, 0.123	0.054, 0.163	0.094, 0.165
GooF on F^2	0.745	0.987	1.509	1.182
max/min. resid. dens. [eÅ^{-3}]	0.90, −0.48	0.53, −0.49	0.87, −0.84	0.69, −0.46
extinction coeff. F_c*[c]	0.0000(6)	−	0.0039(11)	0.0000(11)

[a] $R = \Sigma\|F_o| - |F_c\|/\Sigma|F_o|$. − [b] $wR2 = [\Sigma w(F_o^2 - F_c^2)^2/\Sigma(w|F_o|^2)]^{1/2}$. − [c] $F_c^* = kF_c[1 + (0.001 \times F_c^2\lambda^3/\sin 2\Theta)]^{-1/4}$.

Crystallographic measurements were made at 293 K with a Siemens Nicolet R3m/V four-circle diffractometer using graphite-monochromated Mo-K_α radiation (λ = 0.71073 Å) (ω−2Θ scan technique). The unit cell was determined by the automatic indexing of 50 centered reflections at 2Θ > 21°. The rather poor quality of crystals of **13**·MeOH was manifested in broad scan-widths during initial search routines with the diffractometer and the diffracting ability of the sample dropped with increasing Bragg angle; much of the higher angle data collected were deemed to be weak. As a consequence, the data collection for **13**·MeOH was restricted to 2Θ = 43°. Corrections for Lorentz polarization effects and extinction were applied in all cases, while an empirical absorption correction, based on ψ scans for six reflections at χ ≈ 90°, was applied only for compounds **3** and **13**·MeOH (minimum and maximum transmission factors 0.63−0.87 and 0.49−0.68 for **3** and **13**·MeOH, respectively). In fact, for **6**·CH_2Cl_2 and **9**, azimuthal scan data proved such correction to be unnecessary. The structures were solved by Patterson methods and refined by full-matrix least-squares methods on F^2 using the SHELXTL/PC[31] and SHELXL-93[32] suites of programs. Atomic scattering factors and anomalous dispersion parameters were taken from ref.[33]. Non-hydrogen atoms were assigned anisotropic thermal parameters, with the exception of the disordered atoms of **6**·CH_2Cl_2, **9**, and **13**·MeOH. The hydrogen atoms were constrained to ride on the atom to which they were attached. The isotropic thermal parameters for the methyl H atoms were refined with 1.5 times, and for all phenyl H atoms with 1.2 times the U_{eq} value of the corresponding atom. On the contrary, the hydrogen atoms attached to nitrogen atoms were located in the final difference maps, but were not included in the refinement. During the refinement procedure it became apparent that the CH_2Cl_2 molecule in **6**·CH_2Cl_2, the PF_6^- anion in **9**, and the MeOH molecule in **13**·MeOH were disordered. The CH_2Cl_2 molecule of **6**·CH_2Cl_2 was found to be severely disordered into a number of partially occupied sites with occupancies of ca. 0.7, 0.2, and 0.1, but efforts to refine these values were not successful and hence this matter was not pursued further. The PF_6^- anion of **9** was modelled using partial F atom occupancies, such that the central P atom had two 100%, four 66% and four 33% occupied F atoms around it. This model still gave rather high thermal parameters (ca. 0.10 Å^2 for all atoms), but resulted in an overall improvement in the structure. Finally, the MeOH molecule of **13**·MeOH was located in a disordered position and was included at half occupancy.

Selected bond lengths and angles are listed in Table 2.

Further details of the crystal structure determination can be ordered from the Fachinformationszentrum Karlsruhe, D-76344 Eggenstein-Leopoldshafen, Germany, on quoting the depository numbers CSD-408520 (**3**), -408521 (**6**·CH_2Cl_2), -408522 (**9**), -408523 (**13**·MeOH).

[1] [1a] C. A. McAuliffe, W. Levason, *Studies in Inorganic Chemistry 1: Phosphine, Arsine and Stibine Complexes of the Transition Elements*, Elsevier, Amsterdam, **1979**, pp. 27−28. − [1b] S. Park, M. P. Johnson, D. M. Roundhill, *Organometallics* **1989**, *8*, 1700−1707. − [1c] E. Farnetti, G. Nardin, M. Graziani, *J. Chem. Soc., Chem. Commun.* **1988**, 1264−1265. − [1d] D. Hedden, D. M. Roundhill, *Inorg. Chem.* **1986**, *25*, 9−15.
[2] Z.-Z. Zhang, H. Cheng, *Coord. Chem. Rev.* **1996**, *147*, 1−39.
[3] X. Guan, W. Zhao, S. Zhang, Y. Fang, X. Yun, D. Kon, Y. Li, *Fenzi Cuihua* **1992**, *6*, 303−307.
[4] G. Bruno, C. G. Arena, D. Drommi, F. Faraone, F. Nicolò, *J. Organomet. Chem.* **1995**, *485*, 115−121.
[5] N. Lugan, G. Lavigne, J. J. Bonnet, *Inorg. Chem.* **1987**, *26*, 585−590.
[6] J. P. Farr, M. M. Olmstead, A. L. Balch, *Inorg. Chem.* **1983**, *22*, 1229−1235.
[7] W. Zhao, X. Guan, S. Zhang, Y. Fang, H. Wang, R. Wang, *Huaxue Xuebao* **1992**, *50*, 300−305.
[8] G. De Munno, G. Bruno, C. G. Arena, D. Drommi, F. Faraone, *J. Organomet. Chem.* **1993**, *450*, 263−267.
[9] M. K. Cooper, J. M. Downes, P. A. Duckworth, E. R. T. Tiekink, *Aust. J. Chem.* **1992**, *45*, 595−609 and refs. therein.
[10] [10a] M. K. Cooper, J. M. Downes, *J. Chem. Soc., Chem. Com-*

mun. **1981**, 381−382. − [10b] M. K. Cooper, J. M. Downes, *Inorg. Chem.* **1978**, *17*, 880−884.
[11] [11a] C. W. G. Ansell, M. McPartlin, P. A. Tasker, M. K. Cooper, P. A. Duckworth, *Inorg. Chim. Acta* **1983**, *76*, L135. − [11b] M. K. Cooper, H. J. Goodwin, M. McPartlin, J. M. Rosalky, *Inorg. Chim. Acta* **1983**, *76*, L155−L156.
[12] F. Refosco, F. Tisato, G. Bandoli, C. Bolzati, A. Dolmella, A. Moresco, M. Nicolini, *J. Chem. Soc., Dalton Trans.* **1993**, 605−618.
[13] F. Refosco, F. Tisato, A. Moresco, G. Bandoli, A. Dolmella, C. Bolzati, *Inorg. Chem.* **1995**, *34*, 1779−1787 and refs. therein.
[14] [14a] F. Tisato, F. Refosco, F. Vallotto, G. Pilloni, C. Corvaja, B. Corain, *J. Chem. Soc., Chem. Commun.* **1994**, 2397−2398. − [14b] F. Tisato, F. Refosco, G. Bandoli, G. Pilloni, B. Corain, *J. Chem. Soc., Dalton Trans.* **1994**, 2471−2472.
[15] G. Pilloni, G. Bandoli, F. Tisato, B. Corain, *J. Chem. Soc., Chem. Commun.* **1996**, 433−434.
[16] [16a] S. Y. Desjardins, K. J. Cavell, H. Jin, B. W. Skelton, A. H. White, *J. Organomet. Chem.* **1996**, *515*, 233−243. − [16b] M. C. Bonnet, F. Dahan, A. Ecke, W. Keim, R. P. Schulz, I. Tkachenko, *J. Chem. Soc., Chem. Commun.* **1994**, 615−616. − [16c] G. J. Britovsek, W. Keim, S. Mecking, D. Sainz, T. Wagner, *J. Chem. Soc., Chem. Commun.* **1993**, 1632−1634. − [16d] W. Keim, *Angew. Chem. Int. Ed. Engl.* **1990**, *29*, 235−244; *Angew. Chem.* **1990**, *102*, 251−260. − [16e] E. F. Lutz, *J. Chem. Educ.* **1986**, *63*, 202−203.
[17] L. Crociani, B. Corain, F. Refosco, F. Tisato, A. Dolmella, S. Gatto, G. Bandoli, *Z. Kristallogr.* **1997**, *212*, 745−751.
[18] M. K. Cooper, P. A. Duckworth, T. W. Hambley, K. Henrick, M. McPartlin, G. J. Organ, A. Parekh, *J. Chem. Soc., Dalton Trans.* **1989**, 1067−1073.
[19] L. Crociani, F. Refosco, F. Tisato, G. Bandoli, B. Corain, *J. Am. Chem. Soc.* **1998**, 2973−2974.
[20] L. Sacconi, F. Mani, A. Bencini, in *Comprehensive Coordination Chemistry* (Eds.: G. Wilkinson, R. D. Gillard, J. A. McCleverty), Pergamon Press, New York, **1987**, vol. 5, pp. 45−68.
[21] L. Crociani, F. Refosco, F. Tisato, S. Gatto, B. Corain, *Inorg. Chim. Acta* **1996**, *249*, 131−133.
[22] P. E. Kyba, R. E. Davis, S.-T. Liu, K. A. Hassett, S. B. Larson, *Inorg. Chem.* **1985**, *24*, 4629−4634.
[23] W. S. Kelly, G. H. Ford, S. M. Nelson, *J. Chem. Soc. A* **1971**, 388−396.
[24] P. Rigo, A. Turco, *Coord. Chem. Rev.* **1974**, *13*, 133−172.
[25] A. W. Addison, T. N. Rao, J. Reedijk, J. Van Rijn, G. C. Verschoor, *J. Chem. Soc., Dalton Trans.* **1984**, 1349−1356.
[26] F. H. Allen, S. Bellard, M. D. Bruce, B. A. Cartwright, A. Doubleday, H. Higgs, T. Hummelink, B. G. Hummelink-Peters, O. Kennard, W. D. Motherwell, J. R. Rodgers, D. G. Watson, The Cambridge Crystallographic Data Centre: Computer-based Search, Retrieval, Analysis and Display of Information. *Acta Crystallogr., B* **1979**, *35*, 2331−2339; CSD Database, Release 5.14, October **1997**.
[27] L. G. Scanlon, Y.-Y. Tsao, K. Toman, S. C. Cummings, D. W. Meek, *Inorg. Chem.* **1982**, *21*, 2707−2712.
[28] O. Dahl, *Acta Chem. Scand.* **1969**, *23*, 2342−2353.
[29] E. A. Allen, W. Wilkinson, *Spectrochim. Acta* **1974**, *30A*, 1219−1224.
[30] H. P. Fritz, I. R. Gordon, K. E. Schwarzahans, L. M. Venanzi, *J. Chem. Soc.* **1965**, 5210−5216.
[31] G. M. Sheldrick, *SHELXTL/PC. Version 5.03,* Siemens Analytical X-ray Instruments Inc., Madison, Wisconsin, USA, **1994**.
[32] G. M. Sheldrick, *SHELXL-93*, University of Göttingen, Germany, **1990**.
[33] *International Tables for X-ray Crystallography*, vol. IV, Kynoch Press, Birmingham, **1974**.

[I98102]

Magnesium Anthracene Systems, 10[◇]

Nanocrystalline Zintl Phases from Main-Group Metal Chlorides and Magnesium Anthracene or Activated Magnesium

Ingo Abraham, Lorraine E. Aleandri, Borislav Bogdanović*, Uwe Kolb, Martin Lagarden, and Klaus Schlichte

Max-Planck-Institut für Kohlenforschung,
Kaiser-Wilhelm-Platz 1, D-45470 Mülheim an der Ruhr, Germany
Fax: (internat.) + 49(0)208/306-2980
E-mail: bogdanovic@mpi-muelheim.mpg.de

Received April 14, 1998

Keywords: Magnesium anthracene / Active magnesium / Zintl phases / Magnesium intermetallics / EXAFS spectroscopy

Ga, Tl, Sn, Pb, As, Sb, Bi, Cd, and Hg chlorides react with magnesium anthracene · 3 THF (MgA), anthracene-activated magnesium, or "active magnesium" (Mg*) in THF, generating the respective Mg intermetallics in a nanocrystalline or amorphous state (Eqs. 1–3). Mg intermetallics accessible through the wet-chemical route can be exploited by metathetical exchange reactions for the preparation of other, highly active intermetallics and alloys; EXAFS investigation of X-ray amorphous Cu–Sn and Pd–Pb solids thus prepared (Eqs. 13 and 14) shows that they are true bimetallic alloys (solid solutions).

Introduction

In recent publications[1] we have reported the preparation of a series of so-called inorganic Grignard reagents from transition-metal chlorides and organomagnesium compounds or "active magnesium" (Mg*). These soluble systems can be used as reagents for the synthesis of intermetallics and alloys in a finely divided, usually nanoparticulate, state[1]. In contrast to transition-metal chlorides, it was found[1b] that chlorides of heavier group 12−15 metals (MCl_n) in THF react with magnesium anthracene · 3 THF[2] (MgA), Mg*, or ordinary magnesium powder in the presence of catalytic amounts of MgA[3], with formation of magnesium intermetallics (Mg_qM), also in a finely divided, highly active state[4]; the reactions can be described by eqs. 1−3. When MgA is used as the reducing agent (Eq. 1), the reaction progress can be monitored by measuring the increase in anthracene (A) concentration in the reaction solution with time. In some cases, it is advantageous to run the reaction shown in Eq. 1 in two steps. In the first step, MCl_n is reduced to the metallic state in a highly active form (M*, Eq. 1a); subsequently, M* with additional MgA is transformed into Mg_qM (Eq. 1b). In the following, we give an account of the preparation, characterization, and possible application of magnesium intermetallics obtained via these routes[1b][4][5].

$$MCl_n + \left(\frac{n}{2}+q\right)MgA \longrightarrow Mg_qM\downarrow + \frac{n}{2}MgCl_2 + \left(\frac{n}{2}+q\right)A \quad (1)$$

$$MCl_n + \frac{n}{2}MgA \longrightarrow M^*\downarrow + \frac{n}{2}MgCl_n + \frac{n}{2}A \quad (1a)$$

$$M^* + qMgA \longrightarrow Mg_qM\downarrow + qA \quad (1b)$$

$$MCl_n + \left(\frac{n}{2}+q\right)Mg^* \longrightarrow Mg_qM\downarrow + \frac{n}{2}MgCl_2 \quad (2)$$

$$MCl_n + \left(\frac{n}{2}+q\right)Mg \xrightarrow{MgA(A)} Mg_qM\downarrow + \frac{n}{2}MgCl_2 \quad (3)$$

Results

Mg−Ga and Mg−Tl Intermetallics

The Ga-rich Zintl phase Mg_2Ga_5[6] has previously been prepared in bulk form by melting stoichiometric mixtures of high-purity Mg and Ga metal sealed in Ta[6a] or pyrex crucibles[6c]. The preparation of Mg_2Ga_5 in a finely divided, highly reactive crystalline form can now be achieved via a two-step reaction. In the first step (Eq. 4) $GaCl_3$ is reduced with MgA at low temperature to give a highly active gallium (Ga*) suspension in THF. After separating the active metal from $MgCl_2$ and anthracene, Ga* can be converted, with additional MgA, into Mg_2Ga_5 (Eq. 5). Mg_2Ga_5 is obtained as a black pyrophoric powder contaminated with $MgCl_2$, A, and THF (Table 3; Expt. 1).

$$2\,GaCl_3 + 3\,MgA \xrightarrow{-78°C \rightarrow RT} 2\,Ga^*\downarrow + 3\,MgCl_2 + 3\,A \quad (4)$$

$$5\,Ga^* + 2\,MgA \xrightarrow{RT} Mg_2Ga_5\downarrow + 2\,A \quad (5)$$

[◇] Part 9: R. Benn, B. Bogdanović, M. Brüning, H. Grondey, W. Herrmann, H.-G. Kinzelmann, K. Seevogel, *Chem. Ber.* **1993**, *126*, 225

 © WILEY-VCH Verlag GmbH, D-69451 Weinheim, 1998 1434−1948/98/1111−1699 $ 17.50+.50/0

The XRD pattern of the Mg_2Ga_5 thus prepared (Figure 1) is in accordance with that reported in the literature[7].

Figure 1. X-ray powder diffraction patterns of Mg_2Ga_5, prepared from $GaCl_3$ and MgA; o, diffraction line of Ga

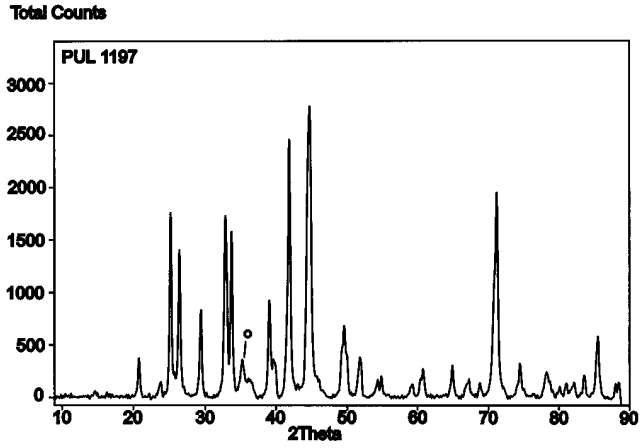

The Mg−Tl Zintl phase MgTl[8][9] can now be prepared in a microcrystalline (nanocrystalline?) form by treating TlCl with an excess of MgA in THF (Eq. 6; Expt. 3.2). MgTl was obtained as a silvery shining powder with the composition $Mg_{0.88}TlCl_{0.01}(CH_2)_{0.2}$. A DSC analysis of the powder showed a weak endothermic peak at 202.7°C (onset temperature; MgTl + Tl eutectic; ref.[10], 202°C) and an intense endothermic peak at 351.3°C (onset temperature) corresponding to the melting point of MgTl (ref.[10], 358°C).

$$TlCl + 1.5\,MgA \longrightarrow MgTl\downarrow + 0.5\,MgCl_2 + 1.5\,A \qquad (6)$$

This result, together with the Mg/Tl ratio of 0.88:1 found through elemental analysis, reveals the presence of Tl in the MgTl thus prepared. However, the XRD powder pattern of this material (Figure 2) exhibited only the diffraction lines of MgTl[11]. The Tl particles if present are, therefore, most likely X-ray amorphous.

Figure 2. X-ray powder diffraction pattern of MgTl, prepared from TlCl and MgA

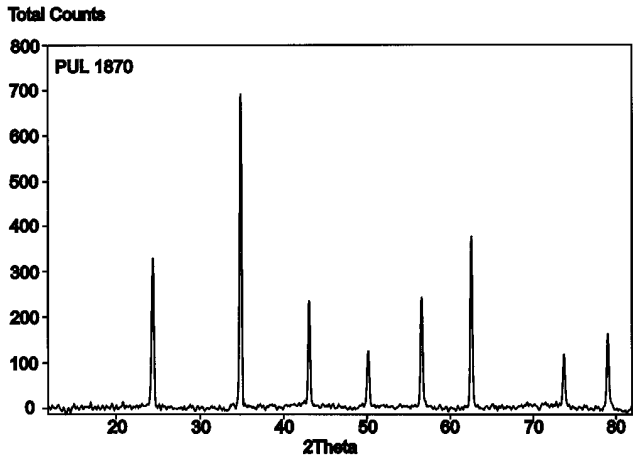

Mg−Sn and Mg−Pb Intermetallics

Mg forms Zintl phases of the type Mg_2E, E = Ge, Sn, Pb[8] with group 14 metals which crystallize in CaF_2 antiisomorphous structures. Their high melting points reflect the heteropolar character of the bonds between the respective elements. The preparation of Mg_2E in bulk form has been carried out by melting the components in an inert atmosphere in sealed iron or corundum crucibles[8][12].

The reaction of $SnCl_2$ with MgA in THF, as a method for the preparation of Sn or Mg_2Sn, both in a finely divided state, has been investigated in some detail (Table 4). If the reaction is conducted in the 1:1 molar ratio at room or low temperature (Expts. 4.1 and 4.2), a highly reactive, pyrophoric, black form of metallic Sn of 97−98% purity (Sn*, Eq. 7) is obtained. Sn* prepared at low temperature (Expt. 4.2) shows only diffuse Sn and no Mg_2Sn diffraction lines in the XRD spectrum. The high reactivity of Sn* prepared according to Eq. 7 is demonstrated by, amongst other things, its reaction with MgA in THF leading to Mg_2Sn (see below Eq. 10; Expt. 4.6); commercial Sn powder does not react with MgA under such conditions.

$$SnCl_2 + MgA \longrightarrow Sn^*\downarrow + MgCl_2 + A \qquad (7)$$

Reaction of $SnCl_2$ with MgA in the molar ratio of 1:2 gives a mixture of Sn* and Mg_2Sn (Expt. 4.3), which, with additional $SnCl_2$ can again be converted into Sn* (Eq. 8).

$$SnCl_2 + 2\,MgA \longrightarrow \underbrace{(0.5\,Sn^* + 0.5\,Mg_2Sn)}\downarrow + MgCl_2 + 2\,A \qquad (8)$$

$$SnCl_2 \longrightarrow 2\,Sn^* + MgCl_2$$

In order to produce Mg_2Sn free of Sn*, it is necessary to react $SnCl_2$ with MgA in an excess amount with respect to Eq. 9 (e.g. in the molar ratio 1:4, Expt. 4.4). The Mg_2Sn obtained is free of Sn or of the Sn−Mg_2Sn eutectic, according to DSC analysis. The TEM photograph of the Mg_2Sn thus prepared (Figure 3) reveals aggregates of nonuniform nanocrystals of 10−50-nm size.

$$SnX_2 + 3\,MgA \longrightarrow Mg_2Sn\downarrow + MgX_2 + 3\,A \qquad (9)$$

X = Cl, Br

On the basis of the widening of the strongest diffraction line in the XRD of this material, an average particle size of 40 ± 4 nm has been estimated, in agreement with the TEM result.

The progress of the reaction of Sn halides with MgA in the molar ration of 1:4.1 at 0°C is represented in Figure 4. Under these conditions (Expt. 4.5) $SnCl_2$ and $SnBr_2$ yielded Mg_2Sn with specific surface areas of 70 and 130 m^2g^{-1}, respectively. X-ray powder diffraction showed sharp Mg_2Sn diffraction lines only. SnI_2 (Figure 4) under the same conditions did not react completely, while hardly any reaction

Figure 3. High-resolution TEM photograph of Mg_2Sn prepared from $SnCl_2$ and MgA

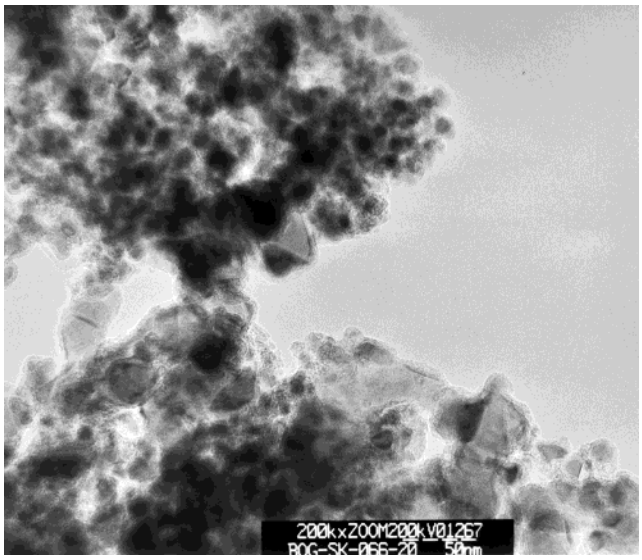

at all was observed with SnF_2, probably due to the insolubility of SnF_2 and MgF_2 in THF.

3A/Mg_2Sn is, in both cases, only reached after ca. 50 h. The reaction is further slowed down when Sn* is separated from $MgCl_2$ and A prior to the reaction with additional MgA (−◆−). Since the reduction of $SnCl_2$ by MgA to Sn* (Eq. 7) is apparently much more rapid than the conversion of Sn* with MgA in Mg_2Sn, it is reasonable to assume that Sn* also acts as an intermediate in the direct formation of Mg_2Sn from $SnCl_2$ and MgA (Eq. 10). The X-ray diffraction pattern of Mg_2Sn prepared according to the two-step reaction (Expt. 4.6) is shown in Figure 5.

$$SnCl_2 + MgA \xrightarrow{\text{rapid}} Sn^{*}\downarrow + MgCl_2 + A \xrightarrow[\text{slow}]{2\ MgA} Mg_2Sn + MgCl_2 + 3\ A \qquad (10)$$

The preparation of Mg_2Pb by the wet-chemical method can be carried out by using either stoichiometric amounts of MgA (Eq. 11) or commercial Mg powder with MgA acting as a "phase transfer catalyst"[1f][13] (Eq. 12). Reaction of $PbCl_2$ with MgA in the molar ratio of 1:3.7 in THF (Expt. 5.1) yielded microcrystalline pyrophoric intermetallic Mg_2Pb which, according to its elemental composition ($Mg_{1.84}Pb$) and X-ray diffractogram, contained minute amounts of Pb. On the other hand, Mg_2Pb which was shown using XRD to contain only traces of Pb (Figure 6)

Figure 4. Progress of the formation reaction of Mg_2Sn from Sn halides (SnX_2) and MgA (1:4.1; [SnX_2] = 0.06 mol/l) in THF at 0°C; −■−, $SnCl_2$, one-step reaction; −▬−, $SnCl_2$, two-step-reaction; −◆−, $SnCl_2$, two-step reaction, Sn* separated from $MgCl_2$ and A; −▲−, $SnBr_2$; −✳−, SnI_2; −×−, SnF_2

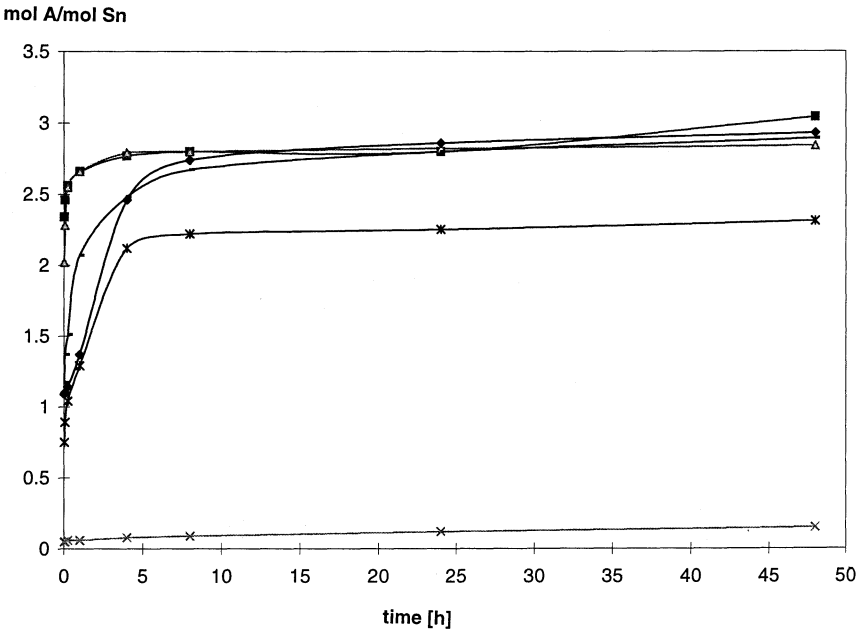

The preparation of Mg_2Sn with a high specific surface area (85 m^2g^{-1}) and free of Sn* is also possible via the two-step reaction. Accordingly, $SnCl_2$ is first reacted with MgA in the molar ratio of 1:1 at room temperature, thus generating Sn*, and then at 0°C with 3 additional equivalents of MgA, giving Mg_2Sn (Expt. 4.6).

As can further be seen in Figure 4, the rate of the two-step reaction (Expt. 4.6; −▬−) is somewhat slower than that of the direct reaction (−■−); but the final ratio of ca. was obtained by reacting $PbCl_2$ with Mg powder and 10 mol-% of MgA at 0°C (Expt. 5.2).

Cu(Mg)−Sn and Pd−Pb Alloys from Mg_2Sn and Mg_2Pb and the Respective Metal Halides

According to preliminary investigations, the highly reactive Mg intermetallics accessible by the wet-chemical route

Figure 5. X-ray powder diffraction pattern of Mg_2Sn prepared from $SnCl_2$ and MgA in the two-step reaction

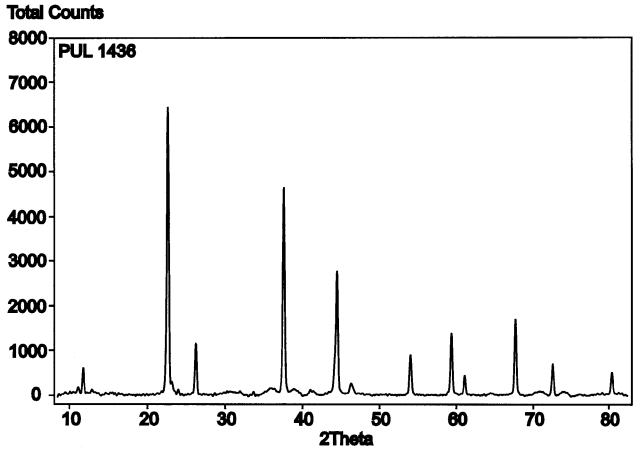

$$PbCl_2 + 3\,MgA \xrightarrow[-78°C \rightarrow RT]{THF} Mg_2Pb(+Pb)\downarrow + MgCl_2 + 3\,A \quad (11)$$

$$PbCl_2 + 3\,Mg \xrightarrow[0\,°C]{THF/MgA} Mg_2Pb(+Pb)\downarrow + MgCl_2 \quad (12)$$

Figure 6. X-ray powder diffraction pattern of Pb_2Sn prepared from $PbCl_2$ and Mg powder in the presence of 10 mol-% of MgA; o, diffraction lines of Pb

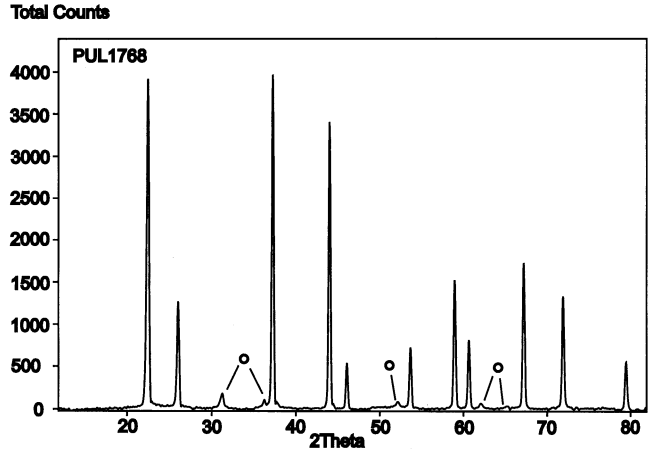

(Eqs. 1−3) can be exploited for the preparation of other intermetallics and alloys in a highly active state. As demonstrated in the following, wet-chemically prepared Mg_2Sn and Mg_2Pb react with Cu and Pd chlorides, respectively in THF with exchange of Mg by the metal in question. The reactions can thus be envisaged as a route for the preparation of intermetallics and alloys complementary to that of applying "inorganic Grignard reagents"[1] (see Introduction).

Cu−Sn[14] and Pd−Pb alloys[15] are accessible via metallurgical methods. A colloidal Pd−Pb alloy has recently been prepared by Bönnemann et al.[16] by means of co-reduction of the corresponding metal salts. Pd−Pb metal combinations can be used as catalysts for the *cis*-selective hydrogenation of alkynes to alkenes (Lindlar catalyst)[16][17] and for the hydrodechlorination of chlorofluorocarbons (CFCs)[18].

In order to provide starting materials with a high dispersion and reactivity, Mg_2Sn and Mg_2Pb utilized for the reactions with metal halides were prepared at low temperatures (Expts. 4.8 and 5.1). Mg_2Sn prepared at low temperatures (Expt. 4.7) is, indeed, highly dispersed, as demonstrated by its broad but weak diffraction lines in XRD.

Reactions of Mg_2Sn with $CuCl_2$ and of Mg_2Pb with $PdCl_2$ in the molar ratio of 1:2 (THF, room temperature) gave in quantitative yields solids of the compositions ca. $Cu_{1.6}Mg_{0.2}Sn(MgCl_2)_{0.1}(CH_2)_{0.4}$ (Expt. 6.1) and ca. $Pd_{1.9}Pb(MgCl_2)_{0.1}Cl_{0.1}(CH_2)_{0.9}$ (Expt. 6.2), respectively. From the compositions of the solids and the amount of Mg^{2+} analyzed in THF solutions, it can be concluded that exchange reactions have taken place in the sense of Eqs. 13 and 14. In the first case (Eq. 13), however, these reactions amount only to roughly 80%.

$$Mg_2Sn + 2CuCl_2 \longrightarrow "Cu_2Sn"\downarrow + 2\,MgCl_2 \quad (13)$$

$$Mg_2Pb + 2\,PdCl_2 \longrightarrow "Pd_2Pb"\downarrow + 2\,MgCl_2 \quad (14)$$

According to the Cu−Sn[14] and Pd−Pb[15] phase diagrams, intermetallic compounds of the compositions Cu_2Sn and Pd_2Pb are not known. The X-ray diffractogram for wet-chemically prepared Cu(Mg)−Sn alloy showed weak diffuse reflections (Cu?, Sn) only. After heating a sample to 145 or 400°C, weak diffraction lines for Cu_6Sn_5[19] appeared in the X-ray powder pattern. XRD of the wet-chemically prepared Pd−Pb alloy showed the presence of Pb, but upon programmed heating to 300 or 400°C (in steps of 50°C), the spectrum showed weak diffraction lines for Pd_3Pb[20].

In order to gain more information about their structure, both nonannealed X-ray amorphous alloys were investigated using extended X-ray absorption fine structure (EXAFS) spectroscopy.

Structural Characterization of the Wet-Chemically Prepared Cu(Mg)−Sn and Pd−Pb Alloys Using EXAFS

The Fourier transforms of the $k^3\chi(k)$ functions at the Cu- and Sn-*K* absorption edges of the Cu(Mg)−Sn alloy are dominated by a single peak which at the Cu-*K* edge (Figure 7) is markedly split. An adaption of the Fourier-filtered $k^3\chi(k)$ functions requires, for the Sn central atom, a single coordination shell of Cu atoms. For the Cu central atom, a fit with only a single coordination shell is not possible. Two coordination shells consisting of Cu and Sn backscatterers are needed to reproduce the Cu-*K* EXAFS spectrum. Although only a limited *k* range (3−10 $Å^{-1}$) is available, a clear distinction between Cu and Sn backscatterers is possible. Using only Cu backscatterers, no fit is possible. The structural parameters of the Cu(Mg)−Sn alloy as determined by EXAFS spectroscopy are summarized in Table 1.

The agreement between the values for the Cu−Sn distance (2.68 Å) and for the EXAFS Debye-Waller factor σ

Figure 7. Unfiltered experimental (solid line) and fitted (broken line) $k^3\chi(k)$ functions and their Fourier transforms of the Cu(Mg)−Sn alloy at the Cu- (A) and Sn-K (B) absorption edges

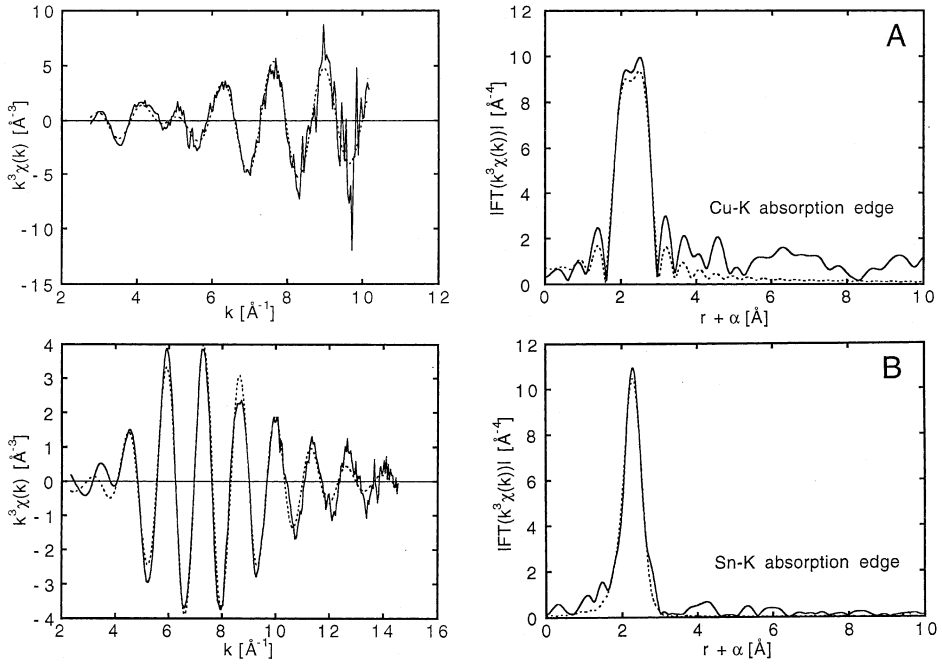

Table 1. Structural parameters of the Cu(Mg)−Sn alloy before annealing determined by EXAFS spectroscopy

absorber	backscatterer	r [Å]	N	σ [Å]
Sn	Cu	2.68	6.5	0.113
Cu	Sn	2.68	2.6	0.114
	Cu	2.56[a]	2.9	0.098

[a] The Cu−Cu distance corresponds to that of the bulk metal.

(0.113 and 0.114) obtained by analysis of the Cu and Sn data shows the structural parameters to be reliable. Although no further-reaching model can be proposed, the structural data (Table 1) allow the following conclusions to be made: (1) for the Sn central atom only Cu backscatterer atoms are observed; the neat Sn phase can therefore only be present to a very low extent, the greatest part of Sn being alloyed with Cu; (2) structural models which postulate the majority of Sn atoms to be on the surface of Cu particles can be excluded because for the Sn central atom ca. 6.5 Cu backscatter atoms are found; (3) the low number of atoms in the coordination shells is characteristic of extremely small metal particles having a large proportion of surface atoms and consisting of no more than a few dozen metal atoms. Coordination numbers determined by EXAFS spectroscopy are influenced by the quality of samples, thus for more accurate determination of coordination numbers further experiments are necessary. This is also especially true for EXAFS investigations of the annealed sample, which exhibit diffractometrically detectable phases and which point to higher coordination numbers; (4) Cu backscatterers at a distance of 2.56 Å are shown to be present using Cu-K EXAFS spectroscopy, demonstrating that a pure Cu phase is present.

The Fourier transforms of the experimental $k^3\chi(k)$ functions at the Pd-K and Pb-L_{III} absorption edges of the Pb(Mg)Pd alloy also show one single peak with a small shoulder at low r values. The nonfiltered, experimental and fitted $k^3\chi(k)$ functions and their Fourier transforms are shown in Figure 8. The curve-fitting procedure shows that the experimental $k^3\chi(k)$ functions at both the Pd-K and at the Pb-L_{III} absorption edge are dominated by the contribution of Pd backscatterers. Therefore, from the analysis of the Pb-L_{III} absorption spectrum, it can be concluded that the Pb atoms are mostly alloyed to Pd. Variations of the structural parameters of the Pd backscatterers influence the agreement between nonfiltered, experimental and fitted $k^3\chi(k)$ functions much more than variations of the structural parameters of the Pb backscatterers.

Both $k^3\chi(k)$ functions can be reproduced by inclusion of only two coordination shells of Pb and Pd atoms. For the final fits, the EXAFS Debye-Waller factors σ_{Pb-Pd} and

Table 2. Structural parameters of the Pd−Pb alloy before annealing determined by EXAFS spectroscopy

absorber	backscatterer	r [Å]	N	σ [Å]
Pb	Pd	2.8	4.2	0.103[a]
	Pb	3.6	1.9	0.144
Pd	Pb	2.8	2.6	0.103[a]
	Pd	2.8	4.6	0.091

[a] For the final fits, the EXAFS Debye−Waller factors σ_{Pb-Pd} and σ_{Pd-Pb} were constrained to the same value.

σ_{Pd-Pb} were constrained to the same value. The results of the curve fitting procedures are listed in Table 2.

The agreement between the values for the Pb−Pd distance (2.80 Å) derived from both $k^3\chi(k)$ functions confirms the reliability of these structural parameters too.

Figure 8. Unfiltered experimental (solid line) and fitted (broken line) $k^3\chi(k)$ functions and their Fourier transforms for the Pb−Pd alloy at the Pt-L_{III} (A) and the Pd-K (B) absorption edges

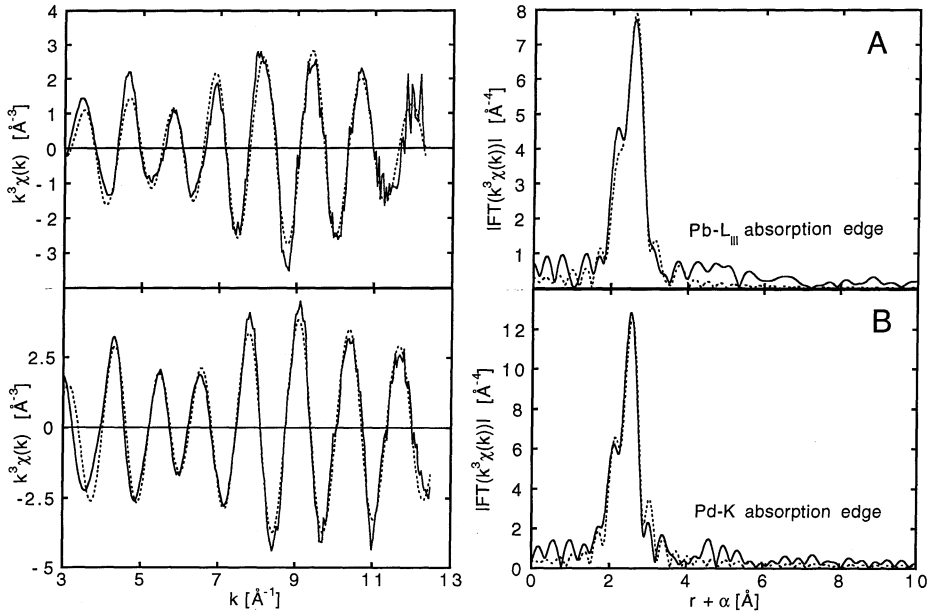

The data allow the following conclusions to be made: (1) only Pd backscatterers can be seen in the first coordination shell of the Pb atoms, suggesting that Pb is predominantly alloyed with Pd and at most a small fraction of Pb atoms exist as a pure Pb phase; (2) Pb atoms contribute significantly to the Pd-K EXAFS spectrum; a considerable part of the Pd atoms are therefore alloyed to Pb atoms; (3) because Pd atoms can also be seen in the first coordination shell of Pd atoms, and the determined Pd−Pd distance of 2.8 Pd Å is close to the Pd−Pd distance in bulk Pd (2.75 Å), a considerable fraction of Pd atoms seem additionally to be present in the form of bulk Pd.

Mg−As, Mg−Sb and Mg−Bi Intermetallics

As, Sb and Bi (M) together with Mg form Zintl phases of the formula Mg_3M_2[8]. Mg_3As_2 has been prepared by Zintl and Huseman[21] from As vapour and Mg at elevated temperatures under hydrogen. Mg_3Sb_2 and Mg_3Bi_2 have been obtained in bulk form by melting stoichiometric mixtures of pure metals in sealed steel crucibles.[8][21][22]

A highly reactive, pyrophoric form of magnesium (Mg*) with specific surface areas of 13−36 m^2g^{-1} can be generated by decomposing MgA in an organic solvent, such as toluene (Eq. 15).[23] By reacting $AsCl_3$, or $BiCl_3$ in THF with the Mg* thus obtained, it is possible to prepare the corresponding Zintl phases Mg_3M_2* in a finely divided, highly active, pyrophoric state (Eq. 16).

Mg_3As_2 (Expt. 7.1) is obtained by this method as a deep-brown, X-ray amorphous powder, with a specific surface area of 167.7 m^2g^{-1}. After annealing (400°C), the presence

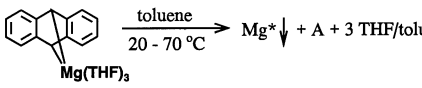

(15)

$$2\,MCl_3 + 6\,Mg^* \xrightarrow[RT]{THF} Mg_3M_2 \downarrow + 3\,MgCl_2 \qquad (16)$$

M = As, Bi

of Mg_3As_2 was proved by X-ray diffraction[24] (Figure 9). $BiCl_3$ reacted with Mg* in THF (Expt. 7.2) to give a black pyrophoric powder with the composition $Mg_{1.45}Bi(MgCl_2)_{0.06}(CH_2)_{0.8}$, whose X-ray diffractogram (without annealing; Figure 10) exhibited strong diffraction lines for Mg_3Bi_2[25] and weak ones for Bi.

Reaction of $SbCl_3$ with MgA in THF (Eq. 17; Expt. 7.3) yielded a highly pyrophoric powder with the composition $Mg_{1.49}Sb(MgCl_2)_{0.03}(CH_2)_{1.4}$. The carbon in the solid was shown to be present in the form of THF and anthracene. An X-ray powder pattern of the sample (Figure 11) after annealing (400°C) demonstrated, however, the presence of a mixture of Mg_3Sb_2[26] and Sb.

$$2\,SbCl_3 + 6\,MgA \longrightarrow Mg_3Sb_2(+Sb)\downarrow + 3\,MgCl_2 + 6\,A \qquad (17)$$

Mg−Cd and Mg−Hg Intermetallics

$CdCl_2$ reacted with commercial Mg powder (molar ratio 1:2.2) in THF in the presence of catalytic amounts MgA

Figure 9. X-ray powder diffraction pattern of Mg_3As_2, prepared from $AsCl_3$ and Mg* (after annealing, 400°C)

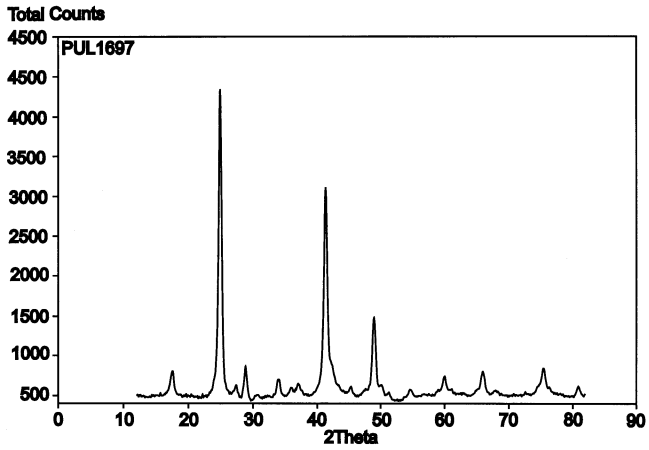

Figure 10. X-ray powder diffraction pattern of Mg_3Bi_2, prepared from $BiCl_3$ and Mg*; o, diffraction lines of Bi

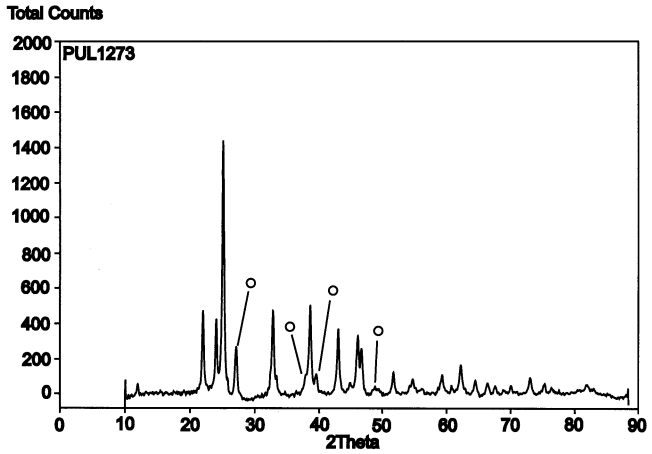

Figure 11. X-ray powder diffraction pattern of Mg_3Sb_2 (+ Sb), prepared from $SbCl_3$ and MgA; o, diffraction lines of Sb (after annealing, 400°C)

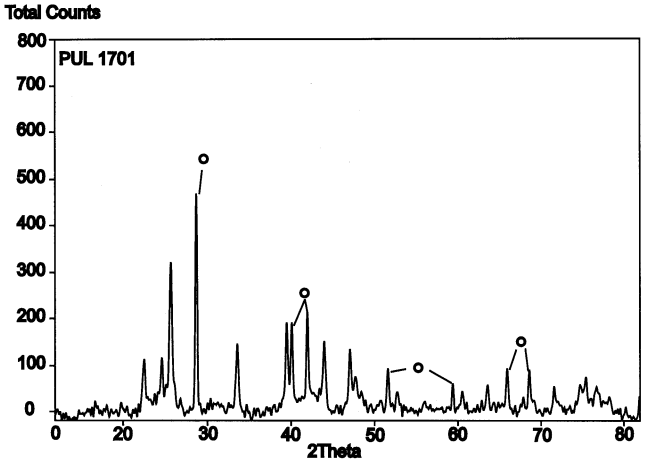

to give a solid of composition $Mg_{1.28}Cd(MgCl_2)_{0.02}(CH_2)_{1.9}$ (Expt. 8.1) which exhibited strong X-ray powder diffraction lines for MgCd and a weak reflection for $MgCd_3$[27] (Figure 12). The formation of a mixture of Mg−Cd intermetallics and the presence of ca. 30% of Cd in the reaction solution, probably indicate a more complex reaction course than that given by Eq. 18.

$$CdCl_2 + 2\,Mg \xrightarrow{MgA/THF} MgCd\downarrow + MgCl_2 \qquad (18)$$

The reaction of $HgCl_2$ with MgA (molar ratio 1:3.8) in THF takes place with a rapid liberation of 2.0 mol anthracene/mol $HgCl_2$ and formation of a finely divided solid having the composition $Mg_{1.32}Hg$ (Expt. 8.2); the X-ray powder pattern of the solid exhibited only sharp diffraction lines for MgHg[28] (Figure 13; Eq. 19).

$$HgCl_2 + 2\,MgA \xrightarrow{THF} MgHg\downarrow + MgCl_2 + 2\,A \qquad (19)$$

Figure 12. X-ray powder diffraction pattern of MgCd (o, $MgCd_3$), prepared from $CdCl_2$ and Mg in the presence of 10 mol-% of MgA

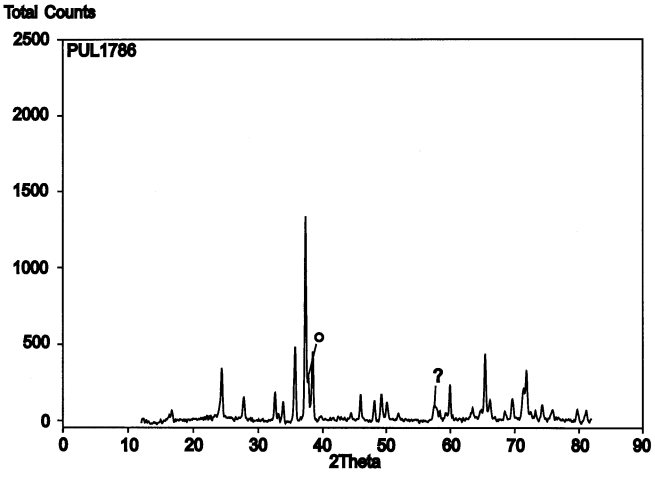

Figure 13. X-ray powder diffraction pattern of MgHg, prepared from $HgCl_2$ and MgA

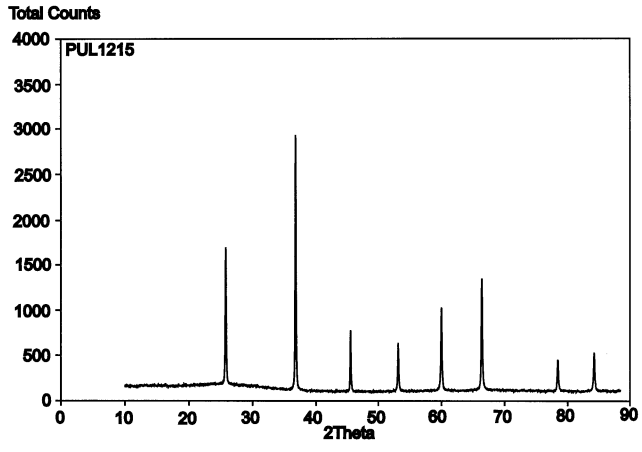

Conclusion

Magnesium intermetallics with heavier group 12−15 metals, which were previously known only in bulk form[8], can now be prepared in a highly active, nanocrystalline or amorphous state using a wet-chemical method (Eqs. 1−3).

They have, through metathetical exchange reactions (Eqs. 13 and 14), a synthetic potential as reagents for inorganic and organometallic chemistry, especially for the preparation of bimetallic noble metal−main-group metal heterogeneous catalysts[16][17][18][29][30]. In this sense, they represent main-group metal counterparts of inorganic Grignard reagents[1] (see Introduction). In addition, the low-temperature, kinetically controlled processes, such as for example in Eqs. 13 and 14, may be suitable for the preparation of as yet unknown metastable systems.

The authors thank Prof. Dr. *C. Krüger*, Dr. *C. Lehmann*, Dr. *B. Tesche*, and their coworkers (Max-Planck-Institut für Kohlenforschung) for conducting and discussing the XRD, DSC, TEM, and EDX analyses, and Dr. *J. S. Bradley* for useful comments. Financial support by the *Fonds der Chemischen Industrie* is gratefully acknowledged.

Experimental Section

Instruments: X-ray diffraction patterns: STOE, STAD/2/PL powder diffractometer, Cu-$K_{\alpha 1}$ radiation; the samples were filled into glass capillaries. HREM images: field emission TEM, Hitachi HF 2000, 200 keV. DSC: DuPont 9900; four points temperature and heat calibration method; heating rate, 10°C/min; Al crucible. EXAFS[31] spectra were recorded at station 9.2 at the SRS, Daresbury using a Si(220) double-crystal monochromator (storage-ring conditions: ca. 2.0 GeV, 150−200 mA). In all cases, data were collected in transmission mode. For the measurements, the material was mixed with PE and pressed to form self-supporting wafers. During the experiments the samples were kept under argon. To eliminate higher harmonics the second monochromator crystal was detuned, reducing the intensity of the X-ray beam to 65% (Pd-*K* and Sn-*K* absorption edges) or 50% (Pb-L_{III}, Cu-*K* absorption edges) of its maximum value. During the experiments, the energy calibration of the monochromator was checked with metal foils. Photoelectron threshold energies of 24350 eV, 29202 eV, 13055eV, and 8981 eV were chosen for the Pd-*K*, Sn-*K*, Pb-L_{III} and Cu-*K* absorption edges, respectively. Data evaluation was performed in *k* space using the program package[32] and amplitude and phase data calculated with the program FEFF6[33]. The usable *k* ranges were 2.9−10.2 $Å^{-1}$ at the Cu-*K* edge, 2.4−14.3 $Å^{-1}$ at the Sn-*K* edge, 2.8−12.2 $Å^{-1}$ at the Pb-L_{III} edge and 2.4−12.3 $Å^{-1}$ at the Pd-*K* edge.

Analyses: Elemental analyses and AAS measurements: Dornis and Kolbe, Mülheim an der Ruhr, Germany.

Materials: Magnesium anthracene·3 THF (MgA).[2] Mg powder (270 mesh, PK-31), purchased from the Eckart-Werke, Fürth, Germany, was used in all experiments unless otherwise stated. THF was boiled for several hours over MgA[2] and subsequently distilled under argon. All experiments and manipulations with air-sensitive materials were performed under dry argon. Vacuum = 0.1−0.2 mbar; high vacuum = 10^{-3} mbar.

Two-Step Preparation of Mg_2Ga_5. − Active Gallium (Ga) from $GaCl_3$ and MgA (Expt. 3.1):* 13.0 g (31 mmol) of MgA was suspended in 50 ml of THF. 50 ml of a 0.45 M solution of $GaCl_3$ in THF (22.5 mmol; $GaCl_3$ solutions in THF must be stored at ≤ −20°C, because at room temperature the solution eventually solidifies due to cationic polymerisation of THF) was added over a period of 0.5 h into the stirred MgA suspension previously cooled to −78°C. The colour of the suspension changed from orange to a dark brownish black. The stirred suspension was allowed to warm up to room temperature over a period of 18 h to give a black suspension. The Ga* was allowed to settle on the bottom of the flask and the green- or yellow-coloured supernatant liquid was removed. The solid was washed with several portions of fresh THF until the supernatant liquid was colourless. The metal could also be isolated by separating the reaction slurry using a centrifuge and, after washing, transferring the solid suspended in fresh THF, into a Schlenk flask.

Mg_2Ga_5 from Ga and MgA:* 3.67 g (8.7 mmol) of MgA was transferred at room temperature to the Ga* suspension (see above) in 100 ml of THF. The reaction mixture immediately turned green (reaction of MgA with residual $MgCl_2$ to form the radical anion complex $Mg_2Cl_3(THF)_6^+ A^{-\bullet}$[34]). After stirring at room temperature for 24 h, the product was allowed to settle from the suspension (now dark grey- or black-coloured), washed with several portions of THF, and dried under high vacuum. 1.53 g (83%) of Mg_2Ga_5 was obtained as a crystalline, black pyrophoric powder. Only diffraction lines corresponding to Mg_2Ga_5[7] were noted in the X-ray powder diffraction pattern (Figure 1).

MgTl from TlCl and MgA (Expt. 3.2): Solid TlCl (1.18 g, 4.92 mmol) was added in small portions to a stirred suspension of MgA (15.0 mmol) in THF (100 ml) at room temperature. From time to time 1.0-ml samples were taken from the stirred suspension, quenched with 3.0 ml of a toluene/CH_3OH mixture (25:1 vol./vol.) containing a known amount of *n*-$C_{16}H_{34}$ as an internal standard and the content of A in quenched samples determined by GC. Dependence of the concentration of A in solution (mol A/mol Tl) from the reaction time (h): 0.21(0.17), 0.43(1.0), 1.29(8), 1.37(24), 1.52(120).

After 170 h, the black suspension was filtered, the precipitate washed several times with THF (until the washing liquids become colourless) and dried in vacuum. MgTl (0.95 g, 81%) was obtained as a silvery shining powder. For the discussion of the DSC analysis of MgTl, see the general section. The X-ray diffractogram of MgTl is shown in Figure 2.

Sn from $SnCl_2$ and MgA at Room Temperature (Expt. 4.1):* To a cooled and stirred suspension of 6.45 g (15.4 mmol) of MgA in 50 ml of THF was added, in one portion, a solution of 3.21 g (16.9 mmol) of anh. $SnCl_2$ in 50 ml of THF; the temperature of the reaction mixture rose from 13 to 25°C and a black solid precipitated. During the subsequent stirring of the reaction mixture at room temperature, samples (2 ml) of the solution were taken, and by complexometric titration it was determined that the deposition of tin had already been completed after about 3 min. After this time, upon the hydrolysis of an aliquot of the solution, a molar ratio of A/9,10-dihydroanthracene (DHA) of 30:1 was determined by GC. The suspension was filtered, the precipitate was washed with THF and dried under vacuum. 1.34 g of a black powder was obtained which had the composition and the specific surface area as given in Table 4.

Sn from $SnCl_2$ and MgA at Low Temperatures (Expt. 4.2):* A cooled (ca. −30°C) solution of $SnCl_2$ in THF was added to a stirred suspension of MgA in THF which had been cooled to −70°C. The suspension was allowed to warm up to room temperature (24 h) and thereafter stirred at room temperature for another 24 h. A small part of Sn* was isolated by filtration, washing with THF and drying under vacuum. The Sn* thus obtained exhibited in XRD only broad, diffuse diffraction lines for Sn.

Preparation of the Sn/Mg_2Sn = 1:1 Mixture from $SnCl_2$ and MgA and the Subsequent Reaction of the Mixture with $SnCl_2$ to give Sn* (Expt. 4.3):* To a stirred solution/suspension of 6.94 g (16.6

Table 3. Mg_2Ga_5 and MgTl from MCl_n (M = Ga, Tl) and MgA

expt.	MCl_n [g] (mmol)	MgA [mmol]	MCl_n/MgA molar ratio	THF	react. temp. [°C]/ react. time [h]	solid [g]	*elem. composition [%] Mg M Cl C H* empirical formula	yield[a] [%]	DSC	XRD
1	$GaCl_3$ 3.96 (22.5)	31.0	1:1.38	100	−78/0.5 −78 → r. t./18	not isolated				
		8.7	0:0.39		r. t./24	1.53	*13.7 85.1 0.17 0.61 0.30* $Mg_{2.31}Ga_5Cl_{0.02}C_{0.2}H_{1.2}$	83	n.d.	Mg_2Ga_5 (Figure 1)
2	TlCl 1.18 (4.92)	15.0	1:3	100	r. t./170	0.95	*9.0 85.8 0.15 0.91 0.19* $Mg_{0.88}TlCl_{0.01}C_{0.2}H_{0.5}$	81	see text	MgTl (Figure 2)

[a] Based on M.

mmol) of MgA in 50 ml of THF was added dropwise a solution of 1.56 g (8.2 mmol) of anhydrous $SnCl_2$ dissolved in 50 ml of THF at room temperature over a period of 1 h, whereupon a black suspension formed. After stirring at room temperature for 1 h, a 2-ml sample of the suspension was protolyzed with 2 ml of a mixture of toluene/CH_3OH, 25:1, (using *n*-$C_{16}H_{34}$ as an internal standard) and analyzed by GC, whereafter the batch contained 15.4 mmol of anthracene and 0.3 mmol of 9,10-dihydroanthracene. Analysis of the deep-blue THF solution by complexometry showed 9.4 mmol of Mg^{2+} and 0.01 mmol of Sn. The suspension was filtered, and the solid was washed with THF until the washing liquid was colourless. After drying under vacuum, 1.17 g of black pyrophoric solid was obtained which had the composition Mg 12.4, Sn 60.5, C 1.9, H 0.3% (Mg/Sn = 1:1). After hydrolysis (H_2O + 5 N H_2SO_4, 1:1) of a sample of the solid and GC analysis of the organic portion, the solid contained 0.03% of anthracene. According to the X-ray powder analysis the solid was a mixture of Mg_2Sn with elemental Sn.

The preparation of the 1:1 mixture of Mg_2Sn + Sn* was repeated in the same manner as described above and was confirmed by X-ray powder analysis of an isolated small sample of the solid. The moist solid left after filtration was suspended in 50 ml of THF, the stirred suspension was mixed with a solution of 8.2 mmol of $SnCl_2$ in 47 ml of THF, and the mixture was stirred at room temperature for 7 h. The suspension was filtered and the solid was washed with THF and dried under vacuum. According to the X-ray diffractogram, only Sn, with no Mg_2Sn, was present in the solid.

Mg_2Sn from $SnCl_2$ and MgA (Expt. 4.4): 35 ml of a 0.217 M solution of $SnCl_2$ in THF (7.6 mmol) was added dropwise within 15 min to a stirred suspension of 12.82 g (30.6 mmol) of MgA in 100 ml of THF. (Solutions of $SnCl_2$ in THF are stable at room temperature for only ca. 15 min, but can be stored for long periods of time at −20°C.) The colour of the suspension changed from orange to olive green-black during the slightly exothermic reaction. After stirring for 3 h, the suspension was filtered (D4 sinter) and the solid washed with ca. 100-ml aliquots of THF. The filtrate was yellow-green (unreacted MgA) and at the final washing colourless. GC analysis of the combined filtrate showed 25.5 mmol of A and 3.4 mmol of DHA to be present. The black solid was dried under vacuum. Mg_2Sn (1.39 g, 87%) was obtained as a crystalline, black pyrophoric powder with the composition and the specific surface area as given in Table 4. A DSC analysis of a sample of Mg_2Sn thus prepared showed no endothermic peak up to 300°C (confirming the absence of Sn, m.p. 231.97°C, or of a Sn−Mg_2Sn eutectic, m.p. 203.5°C), but a weakly exothermic peak at 219°C. An X-ray diffractogram of a sample of Mg_2Sn was in accordance with the line diagram of Mg_2Sn from ref.[35].

The TEM photograph of Mg_2Sn taken from the experiment is reproduced in Figure 3; point-by-point EDX analyses of the nanocrystals gave Mg/Sn ratios ranging between 1.7 and 2.7, the majority of analyses giving a value of 2.0. Traces of Cl but no free Mg or Sn could be identified by EDX. The results confirm the formation of the intermetallic Mg_2Sn.

Monitoring of the Reaction $SnCl_2$ and MgA to form Mg_2Sn at 0°C (Expt. 4.5): 32.1 mmol of MgA was suspended in 125 ml of THF, the suspension was cooled to 0°C and kept at that temperature throughout the experiment by means of a cryostat. To the stirred suspension were added 1.48 g (7.8 mmol) of solid $SnCl_2$. 2.0 ml samples were taken periodically (see Figure 4) from the stirred suspension, quenched with a standard solution (see Expt. 3.2) and the content of A and DHA in the hydrolyzed samples with respect to the standard were determined by GC analysis. Analogous experiments were also carried out with equimolar amounts of SnF_2, $SnBr_2$, and SnI_2, and the same amounts of MgA and solvent. The results are graphically represented in Figure 4.

The Two-step Preparation of Mg_2Sn from $SnCl_2$ and MgA (Expt. 4.6): A solution of 7.7 mmol of $SnCl_2$ in 30 ml of THF was added dropwise to a stirred suspension of 7.7 mmol of MgA in 100 ml of THF. The black suspension of Sn* was stirred at room temperature for 1 h. The suspension was then cooled down to 0°C and an additional 24.5 mmol of MgA added. The progress of the stirred-batch reaction at 0°C was monitored as described in Expt. 4.5 and is represented graphically in Figure 4. The Mg_2Sn thus prepared was isolated and analyzed as described for Expt. 4.4; X-ray diffractogram, see Figure 5.

Mg_2Sn from $SnCl_2$ and MgA at Low Temperature (Expts. 4.7 and 4.8): The experiments were conducted in an analogous manner to Expt. 4.4, except that $SnCl_2$ was added to MgA each time at −70°C and, thereafter, the temperature of the reaction mixtures slowly raised from −70°C to room temperature (see Table 4). The Mg_2Sn thus prepared (Expt. 4.7) exhibited in the X-ray diffractogram only broad diffuse reflections characteristic of the intermetallic and Sn. The Mg_2Sn prepared in Expt. 4.8 was used for the reaction with $CuCl_2$ to form a Cu−Sn alloy (see Expt. 6.1).

Mg_2Pb from $PbCl_2$ and MgA at Low Temperatures (Expt. 5.1): The experiment was conducted in the same manner as Expts. 4.7 and 4.8. The XRD powder pattern of the reaction product was consistent with Mg_2Pb, except for very weak reflections for Pb; Mg_2Pb thus prepared was used for the reaction with $PdCl_2$ to form a Pd−Pb alloy (Expt. 6.2).

Mg_2Pb from $PbCl_2$, Mg Powder and 10 mol-% of MgA (Expt. 5.2): A suspension of 1.69 g (6.1 mmol) of $PbCl_2$, 19.1 mmol of

Table 4. Sn* and Mg_2Sn from $SnCl_2$ and MgA

expt.	$SnCl_2$ [g] (mmol)	MgA [mmol]	$SnCl_2$/MgA molar ratio	THF	react. temp. [°C]/ react. time [h]	solid [g]	*elem. composition [%] Mg Sn Cl C H* empirical formula	yield[a] [%]	sp. surf. area [m^2g^{-1}]	XRD
1	3.21 (16.9)	15.4	1:0.9	100	r. t./2	1.34	*1.2 96.8 0.35 nd* $Mg_{0.06}SnCl_{0.01}$	65	16.2	nd
2	8.20 (43.3)	40.0	1:0.92	280	−70 → r. t./24 r. t. / 24	0.94[b]	*0.57 97.9 0.74 0.44 0.1* $Mg_{0.03}SnCl_{0.02}C_{0.04}H_{0.1}$	nd	nd	Sn
3	1.56 (8.2)	16.6	1:2	100	r. t./1	1.17	*12.4 60.5 nd 1.9 0.3* $MgSnCl_{0.3}H_{0.6}$	73	nd	Mg_2Sn[c] + Sn
4	1.44 (7.6)	30.6	1:4	135	r. t./3	1.39	*26.8 61.8 1.3 8.8 1.1* $Mg_{2.1}SnCl_{0.07}C_{1.4}H_{2.0}$	87	72.8	Mg_2Sn[d]
5	1.48 (7.8)	32.1	1:4.1	125	0/48	1.21	*25.4 62.0 1.5 9.4 1.4* $Mg_2SnCl_{0.08}C_{1.5}H_{2.7}$	81	70.3	Mg_2Sn[e] (+ Sn)
6	1.44 (7.6)	7.7	1:1	130	r. t./1					
		24.5	0:3.2		0/122	1.21	*27.8 63.6 0.75 2.3 0.6* $Mg_{2.13}SnCl_{0.04}C_{0\cdot4}H_{1.0}$	81	85.5	Mg_2Sn[e][f]
7	5.31 (28.0)	97.3	1:3.5	300	−70 → −40/2 −40 → r. t./22	5.32	*22.4 59.1 2.1 9.3 1.4* $Mg_{1.85}SnCl_{0.1}C_{1.6}H_{2.8}$	95	54.8	
8	2.49 (13.1)	45.4	1:3.5	220	−70 → r. t./6 r. t./96	[g]				

[a] Based on Sn. − [b] Only a small fraction of the solid was isolated. − [c] Reaction with $SnCl_2$ to give Sn, see text. − [d] TEM photograph, see Figure 3. − [e] Progression of the reaction with time, see Figure 4. − [f] XRD in Figure 5. − [g] Not isolated; used for the reaction with $CuCl_2$ (Expt. 6.1).

Mg powder and 1.9 mmol of MgA in 200 ml of THF was stirred for 10 days at 0°C. During the first 24 h of reaction the total amount of Mg^{2+} analyzed in the THF solution increased to 7.3 mmol and, thereafter, remained constant. Hydrolysis of an aliquot of the THF solution gave 1.5 mmol of *n*-butanol, expressed in terms of the whole solution (GC analysis) − the product of THF cleavage by Mg[23a]. Mg_2Pb was isolated from the THF solution in the same way as described in Expt. 4.4. XRD powder pattern in Figure 6.

A Cu(Mg)Sn Alloy from Mg_2Sn and $CuCl_2$ (Expt. 6.1): The Mg_2Sn suspension in THF (Expt. 4.8) was allowed to settle, the green supernatant solution was syphoned off, 50 ml of THF was added to the Mg_2Sn, the resulting suspension was stirred for 30 min, and the solution was again syphoned off. This operation was repeated two more times. Then, Mg_2Sn was suspended in 100 ml of fresh THF, the suspension was mixed with 3.48 g (25.9 mmol) of anhydrous $CuCl_2$ and was stirred at room temperature for 65 h. The black suspension was filtered, the solid was washed 4 or 5

Table 5. Mg_2Pb from $PbCl_2$ and MgA or Mg powder and 10 mol-% of MgA

expt.	$PbCl_2$ [g] (mmol)	MgA or Mg + MgA [mmol]	Pb/Mg ratio	THF	react. temp. [°C]/ react. time [h]	solid [g]	*elem. composition [%] Mg Pb Cl C H* empirical formula	yield[a] [%]	sp. surf. area [m^2g^{-1}]	XRD
1	4.84 (17.4)	MgA 64.7	1:3.7	300	−78 → r. t./24 r. t./72	4.70	*15.3 70.7 1.0 4.5 0.6* $Mg_{1.84}PbCl_{0.08}C_{1.1}H_{1.8}$	92	10.7	Mg_2Pb[b] (+ Pb)
2	1.69 (6.1)	Mg 19.1 + MgA 1.9	1:3.5	200	0/260[c]	1.56	*15.6 71.6 0.98 3.3 0.5* $Mg_{1.86}PbCl_{0.08}C_{0.8}H_{1.4}$	90	nd	Mg_2Pb[d] (+ Pb)

[a] Based on Pb. − [b] Used for the reaction with $PdCl_2$ (Expt. 6.2). − [c] According to the amount of Mg^{2+} in the THF solution, the reaction was complete after ca. 20 h. − [d] XRD powder pattern in Figure 6.

Table 6. Cu−Sn and Pd−Pb alloys from Mg_2Sn, Mg_2Pb and the respective metal chlorides ($M'Cl_2$)

expt.	Mg_2M [g] (mmol)	$M'Cl_2$ (mmol)	Mg_2M: $M'Cl_2$ molar ratio	THF [ml]	react. time[a] [h]	solid [g]	*elem. composition [%] M' Mg M Cl C H* empirical formula	yield[b] [%]	sp. surf. area [m^2g^{-1}]	XRD
1	Mg_2Sn (13.1)	$CuCl_2$ (25.9)	1:2	150	65	3.23	*41.5 2.4 47.6 1.9 3.6 0.5* $Cu_{1.64}Mg_{0.25}SnCl_{0.13}C_{0.4}H_{1.2}$	99	31.2	Cu_6Sn_5 + Cu_3Sn[c]
2	Mg_2Pb (2.14)	$PdCl_2$ (4.8)	1:2.2	30	170	0.99	*44.4 0.6 45.4 2.4 1.4 0.3* $Pd_{1.90}Mg_{0.12}PbCl_{0\cdot31}C_{0.9}H_{1.4}$	100	18.9	Pd_3Pb +Pd_3Pb_2[c]

[a] Room temperature. − [b] Based on M. − [c] After heating the sample to 400°C.

times with THF and was dried under high vacuum, yielding 3.23 g of an Mg-containing Cu−Sn alloy which had the composition shown in Table 6. The EXAFS spectra of the Cu(Mg)Sn alloy are shown in Figure 7 and discussed in the text. In the filtrate of the batch were found 20.6 mmol of Mg^{2+} by way of an analysis (79%).

A Pd(Mg)Pb Alloy from Mg_2Pb and $PdCl_2$ (Expt. 6.2): 0.85 g (4.8 mmol) of anhydrous $PdCl_2$ was added to a stirred suspension of 0.63 g of Mg_2Pb from Expt. 5.1 (2.14 mmoles Pb) in 30 ml of THF. The suspension was stirred for 7 d at room temperature, filtered and the resulting solid washed with THF and dried under high vacuum. Yield: 0.99 g of a black powder of the composition as given in Table 6. The EXAFS spectra of the Pd(Mg)Pb alloy are shown in Figure 8 and discussed in the text. Mg^{2+} content of the filtrate: 4.1 mmol.

Mg_3As_2 from $AsCl_3$ and Mg (Expt. 7.1):* 9.21 g (22.2 mmoles) of MgA was suspended in 400 ml of toluene and stirred at room temperature for 24 h yielding a fine grey suspension of Mg*. Most of the solvent toluene was removed by decanting leaving ca. 40 ml of toluene with Mg*. After adding 100 ml of THF and 1.30 g (7.15 mmol) of $AsCl_3$ to Mg*/THF suspension, the reaction mixture was stirred for 5 d at room temperature. After filtration, washing with THF and pentane, and drying under vacuum, 0.95 g of Mg_3As_2 was obtained as a deep brown pyrophoric powder. XRD powder pattern in Figure 9.

Mg_3Bi_2 from $BiCl_3$ and Mg (Expt. 7.2):* The experiment was conducted in the same manner as in Expt. 7.1. XRD powder pattern in Figure 10.

(Mg_3Sb_2 + Sb) from $SbCl_3$ and MgA (Expt. 7.3): $SbCl_3$ was added to the stirred suspension of MgA in THF. The reaction mixture was stirred for several days at room temperature. The solid was isolated in the same manner as described in Expt. 7.1. After a hydrolytic work-up of the solid, THF and anthracene were identified in the organic phase by mass spectrometry.

MgCd(+ $MgCd_3$) from $CdCl_2$, Mg Powder and a Catalytic Amount of MgA (Expt. 8.1): A mixture of 1.33 g (7.24 mmol) of anhydrous $CdCl_2$ and 0.38 g (15.8 mmol) of Mg powder in 100 ml of THF was stirred at room temperature for 72 h; during this time, no reaction took place between $CdCl_2$ and Mg, as shown by the absence of any $MgCl_2$ in the THF solution. After addition of 1.0 mmol of MgA, the mixture was stirred for an additional 48 h, after which 11.0 mmol of Mg in the form of $MgCl_2$ (65.4% of the total amount of Mg used) was determined by complexometry in the solution (Cd^{+2} ions were masked by addition of KCN). After further stirring for several days, the concentration of $MgCl_2$ in the THF solution remained almost unchanged. Filtration, washing with THF and drying under high vacuum yielded 0.91 g of a grey powder with the composition given in Table 8. The X-ray pattern of the powder (Figure 12) exhibited, in addition to one weak signal

Table 7. Mg_3M_2 (M = As, Sb, Bi) Zintl phases from MCl_3 and Mg*, Mg powder or MgA

expt.	MCl_3 [g] (mmol)	M*(Mg) or MgA [mmol]	MCl_3/Mg molar ratio	THF [ml]	reaction[a] time [h]	solid [g]	*elem. composition [%] Mg M Cl C H* empirical formula	yield[b] [%]	sp. surf. area [m^2g^{-1}]	XRD
1	$AsCl_3$ 1.30 (7.15)	Mg* 22.2	1:3.1	100	120	0.95	*27.2 55.3 3.3 6.7 1.3* $Mg_{1.51}AsCl_{0.12}C_{0.8}H_{1.8}$	98	167.7	Mg_3As_2[c][d] (+ MgO)
1a	$AsCl_3$	Mg 19.8	1:3.2	50	72	0.66	*29.7 60.8 2.3 1.6 0.4* $Mg_{1.50}AsCl_{0.08}C_{0.2}H_{0.5}$		55.3	Mg_3As_2 (+ Mg + As)[e]
2	$BiCl_3$ 2.25 (7.14)	Mg* 22.3	1:3.1	100	48	1.80	*14.1 80.2 1.5 3.5 0.6* $Mg_{1.51}BiCl_{0.11}C_{0.8}H_{1.5}$	97	67.9	Mg_3Bi_2 (+ Bi)[f]
3	$SbCl_3$ 1.55 (6.78)	MgA 21.7	1:3.2	160	290	1.29	*19.4 64.3 1.2 8.9 1.5* $Mg_{1.51}SbCl_{0.06}C_{1.4}H_{2.8}$	100	153.9	Mg_3Sb_2 + Sb[g]

[a] Room temperature. − [b] With respect to M. − [c] After 24 h at 400°C. − [d] XRD in Figure 9. − [e] After heating the sample to 400°C for 24 h, X-ray diffractogram shows only Mg_3As_2. − [f] Untempered sample; XRD in Figure 10. − [g] After the sample had been heated to 400°C for 24 h; XRD in Figure 11.

Table 8. Mg−Cd and Mg−Hg intermetallics from the corresponding metal chlorides and Mg powder in the presence of MgA, or MgA

Expt.	MCl_2 [g] (mmol)	Mg + MgA or MgA (mmol)	MCl_2/Mg molar ratio	THF [ml]	react. time[a] [h]	solid [g]	*elem. composition [%] Mg M Cl C H* empirical formula	yield[b] [%]	sp. surf. area [m^2g^{-1}]	XRD
1	$CdCl_2$ (1.33) (7.24)	Mg (15.8) +MgA (1.0)	1:2.2	100	72	0.91	*17.4 62.4 0.5 12.9 2.3* $Mg_{1.29}CdCl_{0.03}C_{1.94}H_{1.19}$	70	nd	MgCd[c] (+ $MgCd_3$) (Figure 12)
2	$HgCl_2$ 1.06 (3.9)	MgA (14.9)	1:3.8	40	120	0.82	*12.1 75.8 0.1 6.0 0.6* $Mg_{1.32}HgCl_{0.01}C_{1.32}H_{1.65}$	79	12.1	MgHg[c] (Figure 13)

[a] At room temperature. − [b] With respect to M. − [c] Untempered sample.

for $MgCd_3$, strong reflections for MgCd. 30 ml of the total 171 ml of the THF solution was evaporated to dryness under vacuum, giving 0.675 g of a solid (5.1 wt.-% Cd; 1.73 mmol of Cd).

MgHg from $HgCl_2$ and MgA (Expt. 8.2): 1.06 g (3.9 mmol) of $HgCl_2$ was added to a stirred suspension of 6.24 g (14.9 mmol) of MgA in 40 ml of THF. After 10 min of stirring, a 1.0 ml sample was taken from the stirred suspension, quenched with 5.0 ml of the standard solution (Expt. 3.2) and analyzed by gas chromatography. Found: 2 A/Hg. (After stirring for a further 120 h, the amount of A increased to 2.5 A/Hg.) Isolation of MgHg was carried out as described above for MgCd. XRD powder pattern (nontempered) in Figure 13.

[1] [1a] L. E. Aleandri, B. Bogdanović, P. Bons, Ch. Dürr, A. Gaidies, Th. Hartwig, S. C. Huckett, M. Lagarden, U. Wilczok, R. A. Brand, *Chem. Mater.* **1995**, *7*, 1153. – [1b] B. Bogdanović, U. Wilczok (Studiengesellschaft Kohle mbH), Europ. Pat. Appl. 0469463, **1992**; *Chem. Abstr.* **1993,** *118*, 24647x. – [1c] L. E. Aleandri, B. Bogdanović, A. Gaidies, D. J. Jones, S. Liao, A. Michalowicz, J. Rozière, A. Schott, *J. Organomet. Chem.* **1993**, *459*, 87. – [1d] L. E. Aleandri, B. Bogdanović, Ch. Dürr, S. C. Huckett, D. J. Jones, U. Kolb, M. Lagarden, J. Rozière, U. Wilczok, *Chem. Eur. J.* **1997**, *3*, 1710. Reviews: – [1e] L. E. Aleandri, B. Bogdanović, Ch. Dürr, D. J. Jones, J. Rozière, U. Wilczok, *Adv. Mater.* **1996**, *8*, 600. – [1f] L. E. Aleandri, B. Bogdanović in *Active Metals* (Ed: A. Fürstner), VCH, Weinheim, **1996**, chapter 8.

[2] [2a] B. Bogdanović, S. Liao, K. Schlichte, U. Westeppe in *Synthetic Methods of Organometallic and Inorganic Chemistry* (Ed: W.A. Herrmann), vol. 1, p. 47, Thieme Verlag, Stuttgart, **1996**. – [2b] B. Bogdanović, S. Liao, K. Schlichte, U. Westeppe in *Organometallic Syntheses* (Eds: R. B. King, J. J. Eisch), Elsevier, Amsterdam, **1988**, vol. 4, p. 410. – [2c] B. Bogdanović, S. Liao, R. Mynott, K. Schlichte, U. Westeppe, *Chem. Ber.* **1984**, *117*, 1378.

[3] Ordinary Mg powder in the presence of catalytic amounts of MgA (or anthracene) has been applied as a reducing agent in the preparation of finely divided homometallic powders and transition metal complexes: [3a] H. Bönnemann, B. Bogdanović, R. Brinkmann, D.-W. He, B. Spliethoff, *Angew. Chem.* **1983**, *95*, 749; *Angew. Chem., Int. Ed. Engl.* **1983**, *22*, 728. – [3b] H. Bönnemann, B. Bogdanović, R. Brinkmann, B. Spliethoff, D.-W. He, *J. Organomet. Chem.* **1993**, *451*, 23; see also ref.[1f].

[4] Preliminary communication: L. E. Aleandri, B. Bogdanović, M. Lagarden, K. Schlichte, Abstracts of Papers, 24. GDCh-Hauptversammlung, Hamburg, 5–11 September **1993**, Abstract AC, 173, VCH, Hamburg, **1993**; see also ref.[1f] and B. Bogdanović, K. Schlichte in *Synthetic Methods of Organometallic and Inorganic Chemistry* (Ed.: W.A. Herrmann), Thieme Verlag, Stuttgart, **1996**, vol.1, p. 49.

[5] In recent years, there has been an increasing activity with regard to the synthesis and investigation of intermetallic compounds, especially of Zintl phases and ions: [5a] S. M. Kauzlarich (Ed.), *Chemistry, Structure and Bonding of Zintl Phases and Ions*, VCH Publishers, Inc., New York, **1996**. – [5b] B. Eisenmann, *Angew. Chem.* **1993**, *105*, 1764; *Angew. Chem., Int. Ed. Engl.* **1993**, *32*, 1693. – [5c] R. Nesper, *Angew. Chem.* **1991**, *103*, 805; *Angew. Chem., Int. Ed. Engl.* **1991**, *30*, 789. – [5d] C. J. Warren, D. M. Ho, R. C. Haushalter, A. B. Bocarsly, *Angew. Chem.* **1993**, *105*, 1684; *Angew. Chem., Int. Ed. Engl.* **1993**, *32*, 1646. – [5e] G. Sauthoff, *Intermetallics*, VCH, Weinheim, **1995**.

[6] [6a] G. S. Smith, Q. Johnson, D. H. Wood, *Acta Crystallogr.* **1969**, *B25*, 554. – [6b] A. A. Nayeb-Hashemi, J. B. Clark, *Bull. Alloy Phase Diagr.* **1985**, *6*, 434. – [6c] P. Feschotte, K. Yvon, *J. Less-Common Met.* **1990**, *158*, 89. – [6d] M. Notin, E. Belbacha, J. Charles, J. Hertz, *J. Alloys Comp.* **1991**, *176*, 25. – [6e] T. B. Massalski, J. G. Murray, L. H. Bennett, H. Baker, *Binary Alloy Phase Diagrams*, American Society for Metals, Metals Park, Ohio, 1st printing, **1986**, vol. 1 and 2, p. 1142–1143.

[7] PDF-2, ICCD, International Center for Diffraction Data, Newton Square, PE, USA, **1993**, [25–227].

[8] H. Schäfer, B. Eisenmann, W. Müller, *Angew. Chem.* **1973**, *85*, 742; *Angew. Chem., Int. Ed. Engl.* **1973**, *12*, 694.

[9] W. Hume-Rothery, G. V. Raynor, *J. Inst. Met.* **1938**, *63*, 201.

[10] Ref.[6e], p. 1556.

[11] Ref.[7], [3–846].

[12] [12a] G. Bauer, J. Tiesler, *Z. Anorg. Allg. Chem.* **1950**, *262*, 319. – [12b] G. H. Grosch, K.-J. Range, *J. Alloys Comp.* **1996**, *235*, 250.

[13] B. Bogdanović, *Acc. Chem. Res.* **1988**, *21*, 261.

[14] Ref.[6e], p. 964–5.

[15] Ref.[6e], p. 1831–34.

[16] [16a] H. Bönnemann, W. Brijoux, K. Siepen, J. Hormes, R. Franke, J. Pollman, J. Rothe, *Appl. Organomet. Chem.*, in press. – [16b] K. Siepen, Dissertation, RWTH Aachen, **1996**.

[17] J. G. Ulan, E. Kuo, W. F. Maier, *J. Org. Chem.* **1987**, *52*, 3126.

[18] R. Ohnishi, I. Suzuki, M. Ichikawa, *Chem. Lett.* **1991**, 841.

[19] Ref.[7], [2–717].

[20] Ref.[7], [20–827].

[21] E. Zintl, E. Husemann, *Z. Phys. Chem.* **1933**, *B 21*, 138.

[22] E. Zintl, *Z. Elektrochem.* **1934**, *40*, 142.

[23] [23a] E. Bartmann, B. Bogdanović, N. Janke, S. Liao, K. Schlichte, B. Spliethoff, J. Treber, U. Westeppe, U. Wilczok, *Chem. Ber.* **1990**, *123*, 1517. – [23b] E. Bartmann, B. Bogdanović, N. Janke, S. Liao, K. Schlichte, B. Spliethoff, J. Treber, U. Westeppe, U. Wilczok in *Synthetic Methods of Organometallic and Inorganic Chemistry* (Ed.: W.A. Herrmann), Thieme Verlag, Stuttgart, **1996**, vol. 1, p. 39.

[24] Ref.[7], [4–458].

[25] Ref.[7], [4–464].

[26] Ref.[7], [29–131].

[27] Ref.[7], MgCd [8–389], $MgCd_3$ [29-264].

[28] Ref.[7], [20–319].

[29] R. Ohnishi, W.-G. Wang, M. Ichikawa, *Appl. Catal. A* **1994**, *113*, 29.

[30] [30a] O. A. Feretti, C. Lucas, J. P. Candy, J. -M. Basset, B. Didillon, F. LePeltier, *J. Mol. Catal. A* **1995**, *103*, 125 and references therein. – [30b] J. Toyir, M. Leconte, G. P. Niccolai, J. -P. Candy, J. -M. Basset, *J. Mol. Catal. A* **1995**, *100*, 61. – [30c] K. Yoshikawa, Y. Iwasawa, *J. Mol. Catal. A* **1995**, *100*, 115.

[31] H. Bertagnolli, T. S. Ertel, *Angew. Chem.* **1994**, *106*, 15; *Angew. Chem., Int. Ed. Engl.* **1994**, *33*, 45.

[32] T. S. Ertel, H. Bertagnolli, S. Hückmann, U. Kolb, D. Peter, *Appl. Spectrosc.* **1992**, *46*, 690.

[33] [33a] J. J. Rehr, R. C. Albers, *Phys. Rev.* **1990**, *B 41*, 8139. – [33b] J. J. Rehr, J. Mustre de Leon, S. I. Zabinsky, R. C. Albers, *J. Am. Chem. Soc.* **1991**, *113*, 5135. – [33c] J. Mustre de Leon, J. J. Rehr, S. I. Zabinsky, R. C. Albers, *Phys. Rev.* **1991**, *B 44*, 4146. – [33d] J. J. Rehr, S. I. Zabinsky, R. C. Albers, *Phys. Rev. Lett.* **1992**, *69*, 3397.

[34] B. Bogdanović, N. Janke, C. Krüger, R. Mynott, K. Schlichte, U. Westeppe, *Angew. Chem.* **1985**, *97*, 972; *Angew. Chem., Int. Ed. Engl.* **1985**, *24*, 960.

[35] Ref.[7], [7-274].

[98104]

Electrografting of Acrylic and Methacrylic Monomers onto Metals: Influence of the Relative Polarity and Donor–Acceptor Properties of the Monomer and the Solvent

Noëlle Baute[a], Philippe Teyssié[a], Lucien Martinot[b][+], Marc Mertens[a][++], Philippe Dubois[a][+++], and Robert Jérôme*[a]

University of Liège, Center for Education and Research on Macromolecules (CERM)[a],
Sart Tilman, B6, B-4000 Liège, Belgium

University of Liège, Laboratory of Analytical Chemistry and Radiochemistry[b],
Sart Tilman, B16, B-4000 Liège, Belgium

Received April 14, 1998

Keywords: Materials science / Surface chemistry / Electrochemistry / Organic-inorganic hybrid composites / Donor-acceptor systems

The possibility of grafting a series of alkyl polyacrylates and polymethacrylates onto a nickel cathode by electropolymerization of the parent monomers has been investigated and has emphasized the critical importance of the solvent used. Indeed, the intensity of the inhibition peak, which is the electrochemical mark of the cathode passivation as result of the polymer grafting, clearly depends on both the polarity and the donor-acceptor properties of the solvent. The Gutmann concept is used to account for these experimental results. An increase in the donicity of the solvent used for the electrochemical medium has allowed, for the very first time, several polyacrylates and polymethacrylates [such as poly(ethyl acrylate), poly(methyl methacrylate), and poly(2-trimethylsilyloxyethyl methacrylate)] to be electrografted onto Ni. This observation is consistent with a competition process between the monomer and the solvent for being adsorbed on the cathode and amassing in its very close vicinity. The outcome of this competition is controlled by the relative polarity (in case of low donicity) and the relative donor-acceptor properties (when the difference is high enough) of the monomer/solvent pair, and by the monomer concentration (in case of weak competition). A semi-quantitative relationship has also been observed between the monomer ability to be electrografted and the electron-accepting character of the vinyl β-carbon atom as measured by ^{13}C NMR.

Introduction

Although electrochemistry is a well-known technique for coating various conducting substrates by an organic polymer, the achievement of a stable polymer-metal association is usually a challenge, since a poor and short-lived interfacial adhesion is the rule[1][2].

According to the pioneering work by Lécayon et al.[3][4], we have confirmed in a previous paper[5] that polyacrylonitrile (PAN) could be cathodically electrografted onto several transition metals (Ni, Cu, Fe), and made clear that peak I, observed by voltammetry (Figure 1) is the mark of the grafting reaction. The term grafting, which implies a chemical bonding of the polymer to the metal, has been used by these authors on the basis of X-ray emission spectroscopy (EXES) analysis[6]. This quite unusual and promising reaction, originally reported in acetonitrile (ACN), which is a nonsolvent for the polymer (PAN), has been confirmed in a good solvent such as dimethylformamide (DMF)[5]. This observation is a convincing evidence for a highly stable interaction between PAN and the metal in the potential range of peak I. When this potential is increased further (Figure 1, peak II), the originally "grafted" PAN is debonded and dissolved in DMF and the polymerization occurs in solution[7][8].

Figure 1. Voltammetry of AN on nickel in a 0.05 M TEAP solution in DMF; [AN] 0.5 M; $v = 20$ mVs^{-1}

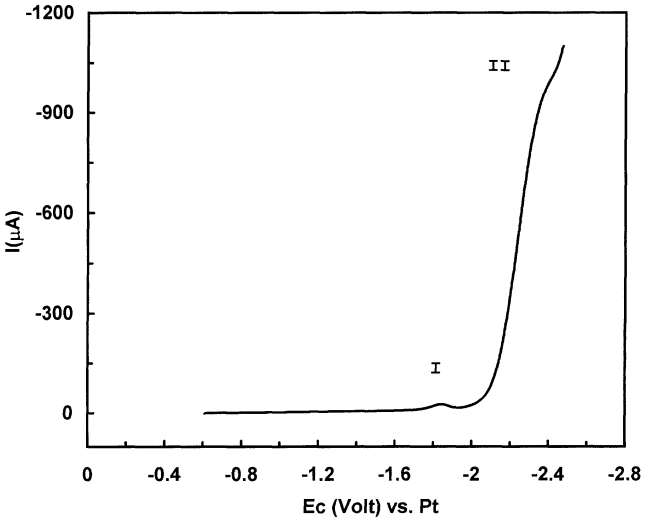

[+] Research associate of the Inter-University Institute for Nuclear Sciences (Brussels).
[++] Current address: Norton Performance Plastics, avenue du Parc 18, B-4650 Chaîneux, Belgium.
[+++] Current address: Laboratory of Polymeric Materials and Composites, University of Mons-Hainaut, Place du Parc 20, B-7000 Mons, Belgium.

 © WILEY-VCH Verlag GmbH, D-69451 Weinheim, 1998 1434–1948/98/1111–1711 $ 17.50+.50/0

Until now, only very few monomers are known for their capability of being grafted onto a metallic cathode. In addition to polyacrylonitrile that has been most extensively studied, grafting of poly(*p*-chlorostyrene) has been reported some years ago by Deniau et al.[9]. This conclusion might, however, be distorted by the parasitic loss of the chlorine atom simultaneously observed. A cross-linking reaction[10] gives a better account for the intrinsic insolubility of that polymer in the solvent used (ACN) and thus for the presence of the deposited film. The case of polymethacrylonitrile, recently reported by Tanguy et al.[11][12], is less ambiguous, since this polymer is known to be soluble in the reaction medium (ACN). Furthermore, according to these authors, infrared spectra did not show any structural modification indicating cross-linking[11]. Nevertheless, they noted that the electrografting of polymethacrylonitrile in acetonitrile strongly depended on the monomer concentration, without giving a satisfactory explanation for this experimental observation.

It is clear from the "state of the art" that the actual weakness of the electrografting reaction is the severe restriction on the choice of the polymer to be grafted. Discovery of new monomers prone to electrografting and able to make a stable organic coating reactive is highly desirable for specific technological applications (adhesion in composite materials, ...). The purpose of this paper is to search for experimental conditions under which the electrografting reaction known for acrylonitrile and methacrylonitrile could be extended to a large set of vinyl monomers. There is indeed a complete lack of information that could serve as a guideline for increasing the range of electrografted organic coating. It is interesting to note that the problem of polymer adhesion on various surfaces in different solvents has been discussed in terms of acid-base interactions between polymer and solid, polymer and solvent, and solvent and solid, in order to explain polymer deposition in a particular medium[13][14]. The problem is, however, more complex when the polymer is formed in situ by electropolymerization, since an additional partner has to be considered, i.e. the monomer. Furthermore, at the very first step of the process, only monomer and solvent may compete for adsorption on the metal, which is actually the electrode where electropolymerization is initiated. Once a polymer is formed, sites originally available to polymerization initiation would be progressively occupied until the complete passivation of the electrode. Nevertheless, during the whole process, a competitive monomer/solvent adsorption on sites left unoccupied has to be operative and to control the electrochemical reaction. It is therefore of prime importance to focus on the monomer adsorption on the cathode, a prerequisite step for the polymer grafting according to the early works by Lécayon et al.[15]. In line with these considerations, the adsorption of acrylonitrile ($CH_2=CH_3-CN$, the most widely studied monomer) from gas phase and liquid phase has been experimentally studied in case of metal substrates, i.e. copper[16], gold[17], platinum[18], silver[19], and nickel[20]. According to theoretical models, acrylonitrile interacts with the surface of copper, nickel, and iron[8][21] through both nitrile group and vinyl end, whereas it does not interact strongly with zinc[22]. These authors have also shown that formation of a σ complex between the β-carbon atom of the acrylonitrile C−C double bond and the metal atom is favorable in a moderate electric field, the nitrile substituent of the monomer being aligned along the field[8]. All these results emphasize the importance of the monomer adsorption. The voltammetric curves also suggest that an adsorbed species is involved in the charge-transfer step[23]. The important role played by the solvent in interfacial adsorption processes has been known for a long time in electrochemical experiments[24]. Displacement of solvent molecules by an electroactive molecule is the rule[25] and competitive adsorption of different species is a phenomenon commonly observed in these experiments[26]. Consistently, we have recently reported on the influence of the solvent polarity on the acrylonitrile electrografting, in particular on the monomer concentration in the electrical double layer of the electrode[7]. In this paper, we will discuss the problem of the competitive monomer/solvent adsorption for a series of solvent/monomer pairs, in reference to the well-known Gutmann donor−acceptor concept[27][28], which is a widely accepted criterion in electrochemical processes[29][30]. It will be shown, that the adequate choice of the solvent donor−acceptor properties with respect to the monomer, is a very powerful tool for qualitatively predicting the electrografting of a series of polymers widely used for technological applications [such as poly(ethyl acrylate), poly(methyl methacrylate) and poly(2-trimethylsilyloxyethyl methacrylate)] (Scheme 1), and known as "ungraftable" until now. A semiquantitative criterion will be proposed to evaluate the grafting capacity of new monomers and which solvent would be most appropriate to this purpose.

Results and Discussion

It has been observed for the first time that an acrylate other than acrylonitrile, i.e. ethyl acrylate, could be grafted onto nickel, just by substituting DMF for the commonly used ACN solvent. This observation has led to the detailed analysis reported in this paper.

For the sake of completeness, it must be noted that the widely described behavior of acrylonitrile will serve as a reference to establish whether the grafting of the monomers considered in this work, occurs or not. Numerous criteria have thus to be considered and have been systematically checked for each monomer considered in this study. Since the aim of this paper is to report on the critical effect of the solvent on the electrografting course, this systematic part of the work is not detailed here, but summarized as follows[5].(i) Both passivation (peak I) and diffusion (peak II) peaks can be observed in the recorded voltammograms (see Figure 1 as an example). (ii) When electrolysis is carried out in the potential range of peak I (Ep1), a thin polymer film is formed on the cathode, even in a good solvent for the polymer. No cross-linking reaction may account for this insolubility. When a second forward scan is carried out in this

potential range, the current intensity cannot be recovered as a consequence of the cathode passivation. Except when mentioned in the discussion, no unbound polymer is formed in the potential range of peak I, as attested by a lack of polymer precipitation when the electrochemical bath is poured into a nonsolvent for this polymer. The intensity of peak I (ip1) decreases when the monomer concentration is increased as result of a more rapid formation of an insulating film. No linear relationship between ip1 and $v^{1/2}$ can be found (v is the potential scanning rate). (iii) ip2 increases with the monomer concentration and a linear relationship between ip2 and $v^{1/2}$ confirms the diffusion-controlled origin of peak II. Chain propagation then occurs independently of the cathode (as confirmed by precipitation of the polymer from the electrochemical bath).

Ethyl Acrylate (EA) Reduction in Acetonitrile (ACN) and in Dimethylformamide (DMF)

Cathodic scans have been carried out in an extended range of EA concentration ($5{\cdot}10^{-2}$ to 2 M) in ACN, and only one reduction peak of high intensity is observed (Figure 2a). This unique peak has been previously identified as a diffusion peak, since the peak intensity (ip2) linearly increases with the square root of the potential scanning rate[5]. ip2 is also observed to increase upon increasing EA concentration, while its potential (Ep2) becomes more cathodic. Polymerization then occurs in the electrochemical solution.

The experiments have been repeated in DMF. Starting from the lowest concentration (10^{-2} M), as in ACN, the diffusion peak alone was noticed. Above 0.5 M EA concentration, this unique peak splits in two resolved components of highly different intensity, as shown by voltammetry on nickel in Figure 2b. Actually, the resolution of the two peaks (thus the distance they are apart from each other) increases and the intensity of peak I (ip1) decreases, when the monomer concentration is increased (Table 1). As previously concluded from the AN electrografting[5], the voltammogram strongly depends on the monomer concentration and on the polymerization kinetics. When the EA concentration is increased, the time required for the formation of an insulating film onto the cathode decreases, and so does ip1 since the inhibition occurs faster. When electrolysis is carried out in the potential range of peak I, the current drops down to zero and only a residual current is observed when the potential scan is repeated. Even though the experiment was conducted in DMF, a good solvent for poly(ethyl acrylate) (PEA), a film is clearly bound on the nickel electrode and is responsible for the cathodic passivation. Infrared spectroscopy carried out ex situ confirms the deposition of a PEA film (Figure 3a), since the IR spectrum is identical to the one recorded for a reference PEA film prepared by free-radical polymerization (Figure 3b). The four main bands at 2983, 1740, 1456 and 1183 cm^{-1} have been assigned to $\nu_{as}(CH_2)$, $\nu(C{=}O)$, $\delta(CH_2)$, and $\nu(C{-}O)$.

As discussed in a previous paper[7], the solvent polarity has a critical effect on the electrografting and this has been

Figure 2. Voltammetry of EA on nickel in a 0.05 M TEAP solution in: a) ACN, [EA] = $5{\cdot}10^{-2}$ M; b) DMF, [EA] = 2 M; v = 20 mVs^{-1}

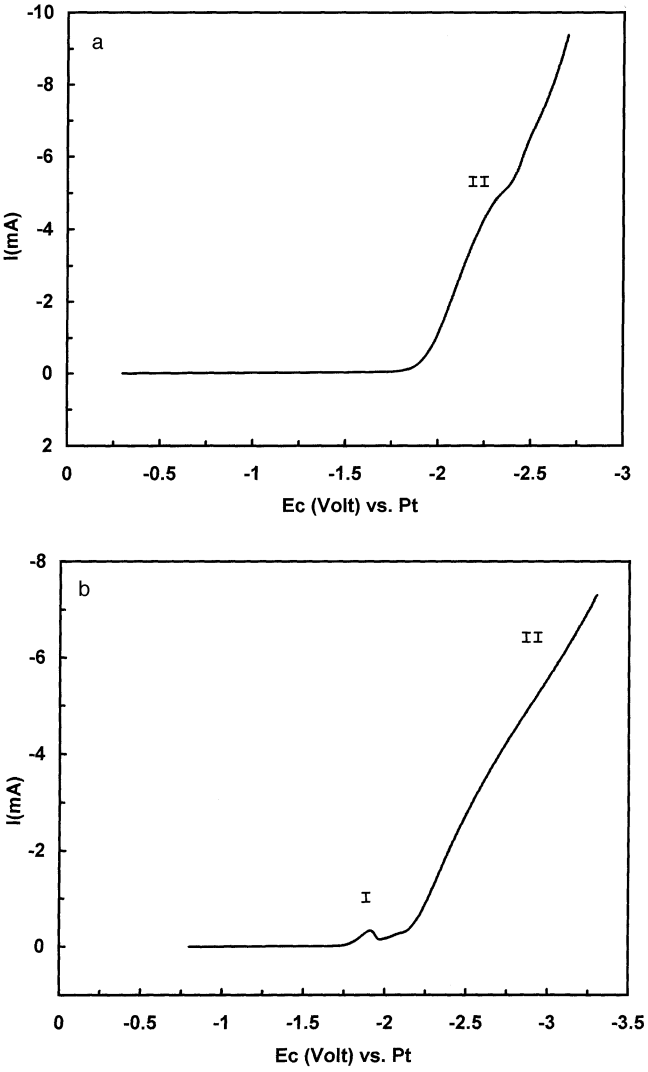

Table 1. Intensities of peak I (ip1) for various EA concentrations in DMF; v = 20mVs^{-1}

Solvent	[EA] = 0.1 M	[EA] = 0.5 M	[EA] = 1 M	[EA] = 2 M
DMF	[a]	500 μA	400 μA	300 μA

[a] Peak I superimposed to peak II.

explained by a competition between the solvent and the monomer. Depending on this competition, the actual monomer concentration at the cathode will be or will not be high enough for observing the cathode passivation. Since ACN and DMF have a very comparable polarity [ε(ACN) = 38.0; ε(DMF) = 36.1], this parameter cannot explain why EA is not electrografted to the cathode in ACN, although it is in DMF above a defined concentration, all the other conditions being the same. The Gutmann donor-acceptor approach[27][28] could however be a better basis for the qualitative comparison of the solvent and the

Figure 3. Infrared spectrum of a) a PEA film deposited on Ni from a solution of [EA] = 2 M in DMF at potential of peak I; b) a free-radically prepared PEA casted onto a Ni plate

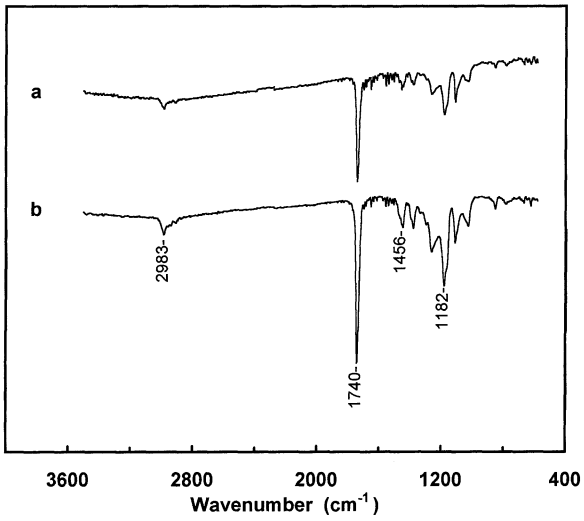

monomer and their possible competition for the occupancy of the cathode surface. The donor number is characteristic of the solvation, coordination, and adsorption properties of the solvent. It is defined for each solvent as the numerical value of the enthalpic variation that occurs when the donor is added to the reference acceptor. Quantitative measurements have been carried out by Gutmann et al.[33], in case of a number of O- and certain N-containing solvent molecules added to antimony(V) chloride as the reference acceptor in 1,2-dichloroethane (the donor number of which has been assigned to 0). The acceptor number[28] is defined as a dimensionless number related to the relative chemical shift of ^{31}P in Et_3PO dissolved in the particular solvent. Hexane and $Et_3PO-SbCl_5$ in 1,2-dichloroethane are the references, to which the acceptor numbers 0 and 100, respectively, have been assigned. Antimony(V) chloride has been used as a standard for both acceptor number and donor number, in order to emphasize the relationship between acceptor properties and their conjugate donicity. Table 2 lists the donor number, the acceptor number and dielectric constant for the solvents which are used in this study. It is interesting to note that the acceptor number decreases from ACN to HMPA, thus in the reverse order to that of the donor number, although this observation is not the rule within the Gutmann scale. Under these specific conditions, the tendency of the solvents (used in this study) to be adsorbed may be discussed in terms of either donor numbers or acceptor numbers. Since the donor number of these solvents (Table 2) extend over ca. half the donor number scale (0−38.8) whereas the acceptor number (Table 2) cover a very short range of the acceptor number scale (0−129), the main discussion will refer to the donor number of the solvent without losing sense. DMF is clearly a stronger donor and a poorer acceptor than ACN. When AN and EA are compared (Scheme 1), the ester substituent of the polymerizable C−C double bond in EA is less efficient than the nitrile substituent in AN in triggering an electron delocalization. In the chemisorption model proposed by Lécayon et al.[15], AN would be properly oriented in the electric field at the cathode, as a result of the strong electron-withdrawing nitrile substituent. The acidic extremity (i.e. the β-carbon atom) of AN would accordingly be in an ideal position with respect to the reactive sites on the cathode (considered as a Lewis base). The β-carbon atom of EA has a lower acceptor capability than AN, which may be a key issue, since adsorption in electrochemistry (here on the cathode) is always a competitive process[24] between the adsorbate (the monomer in this case) and the solvent. Indeed, for an adsorbate molecule to occupy a surface site, a number of solvent molecules have to be displaced. It is therefore quite reasonable to assume that the electrografting of a monomer can only occur in a solvent which has a lower tendency to be adsorbed onto the cathode site, i.e. a solvent which is a poorer acceptor and/or a better donor.

Scheme 1

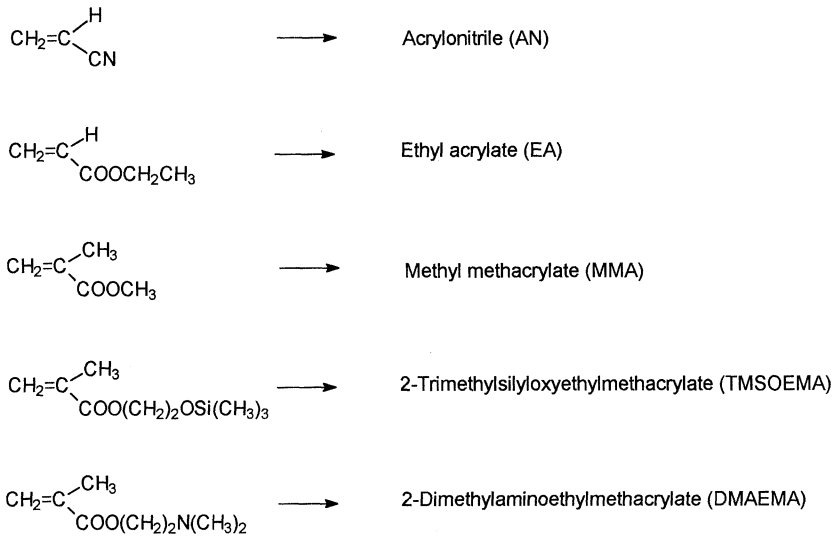

Table 2. Donor number, acceptor number, and dielectric constant of different solvents

Solvents	Donor number[28]	Acceptor number[28]	Dielectric constant[28]
ACN	14.1	19.3	38.0
PC	15.1	18.3	65.0
DMF	26.6	16.0	36.1
PY	33.1	14.2	12.3
HMPA	38.8	10.6	30.0

Several series of experiments are proposed in this paper to support this hypothesis. In a first step, the EA/DMF solution has been added with ACN in order to check the extent to which the electrochemical mark of the electrografting is perturbed.

In a second step, the electropolymerization of AN will be compared in four solvents: ACN, PC, PY, and HMPA, that are all nonsolvents for PAN. ACN and PC have a low and similar donicity, but highly different polarity. The donicity of PY and HMPA is high and quite comparable, whereas the polarity is very different (Table 2). The same cathode (Ni) and the same conducting salt (Et_4NClO_4, $5\cdot10^{-2}$ M) will be used in all the experiments.

Finally, three methacrylic monomers: methyl methacrylate (MMA), 2-dimethylaminoethyl methacrylate (DMAEMA), and 2-trimethylsilyloxyethyl methacrylate (TMSOEMA) will be studied for investigating the possible effect of the monomer structure on their ability to be grafted onto the cathode.

Ethyl Acrylate (EA) Reduction in a Mixture of DMF and ACN

Figure 4 compares the voltammetric cathodic scans of a 1M EA solution in DMF modified by an increasing percentage of ACN. The monomer concentration is kept unchanged in all the experiments. When EA is electrografted in DMF, the intensity of the inhibition peak is ca. −400μA (Figure 4a). When the relative amount of ACN in the EA/DMF solution is increased, the intensity of peak I increases, whereas the resolution between peak I and peak II decreases (Figure 4 b, c). The dependence of ip1 on the ACN percentage in the EA/DMF solution is such that the cathode is more slowly inhibited, in agreement with a lower EA concentration at the cathode. This observation suggests that the co-solvent (ACN in this case) competes with the monomer for adsorption on the cathode. Since ACN and DMF have the same polarity and are both good solvents for PEA, only a significant difference in the donor-acceptor properties can explain the experimental observations in Figure 4.

Scheme 2 illustrates this extreme situation where the monomer (e.g. EA) is a poorer acceptor than the solvent (e.g. ACN) and is so far unable to displace the solvent molecules in order to be adsorbed on the cathode sites. No inhibition peak is observed on the voltammogram but only a diffusion peak: this indicates that the monomer reduction

Figure 4. Voltammetry of EA on nickel (v = 20 mVs^{-1}) in a DMF solution, [EA] = 1 M, Ip1 dependence on the addition of ACN: a) without ACN; b) + 3% of the volume; c) + 12% of the volume

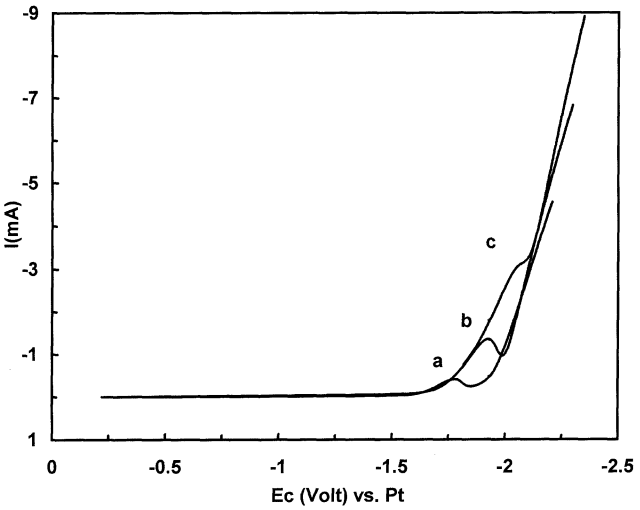

can occur at a more cathodic potential, as confirmed by the polymer formation in solution.

Scheme 2

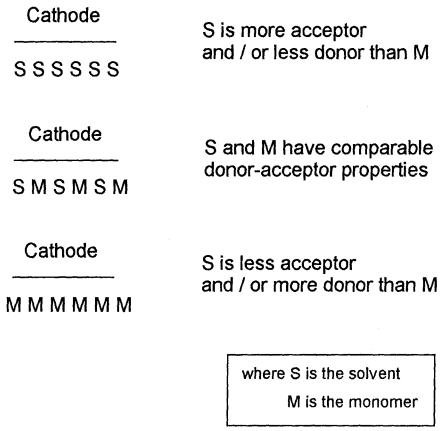

Comparative Reduction of Acrylonitrile (AN) in ACN and PC, in PY and HMPA

Table 3 shows that the intensity of peak I (ip1) increases when PC is substituted for ACN at constant monomer (AN) concentration, thus when polarity is increased in case of solvents of low donicity. Figure 5 shows voltammograms of AN in PY. The intensity of peak I is much lower than in ACN and PC for the same monomer concentration (Table 3). As a rule, the cathode inhibition is controlled by the monomer concentration and ip1 systematically decreases as the AN concentration is increased[5]. So, the small ip1 value in PY might be explained by a high local AN concentration in the electrical double layer and a more rapid formation of an insulating film. As previously discussed the low polarity may account for the experimental observations[6], but the

effect of the solvent donicity may not be ignored. In order to appreciate the relative importance of solvent polarity and solvent donicity, hexamethylphosphoramide (HMPA) which has a high and comparable donicity as PY, but which is 2.5 times more polar has been used. Table 3 shows that there is no significant difference in the voltammograms in PY and HMPA since ip1 remains almost unchanged when HMPA is substituted for PY, all the other conditions being the same. From Table 3, we can draw the conclusion that the solvent polarity has a decisive effect on the AN electrografting only when the solvent is a good enough acceptor and a poor donor (see ACN/PC pair). When the solvent is a poor acceptor and a good enough donor (PY/HMPA pair), the polarity has no longer a significant influence, since that solvent has a small tendency to be adsorbed onto the cathode. Although neglected until now, the relative donor-acceptor properties of the monomer/solvent pair must be considered when the monomer electrografting is concerned.

Table 3. Intensity of peak I (ip1) for various AN concentrations in ACN, PC, PY, HMPA; $v = 20$ mVs^{-1}

Solvents	[AN] = $5\cdot10^{-2}$ M	[AN] = 0.1 M	[AN] = 0.5 M	[AN] = 2 M
ACN	[a]	370 μA	30 μA	25 μA
PC	[a]	650 μA	90 μA	60 μA
PY	25−30 μA	15−20 μA	[b]	[b]
HMPA	30−35 μA	15−17 μA	[b]	[b]

[a] Peak I superimposed to peak II. − [b] Peak I intensity to weak to be detected.

Figure 5. Voltammetry of AN on nickel in a 0.05 M TEAP solution in PY: a) [AN] = $2\cdot10^{-2}$ M; b) [AN] = $5\cdot10^{-2}$ M; c) [AN] = 0.1 M; $v = 20$ mVs^{-1}

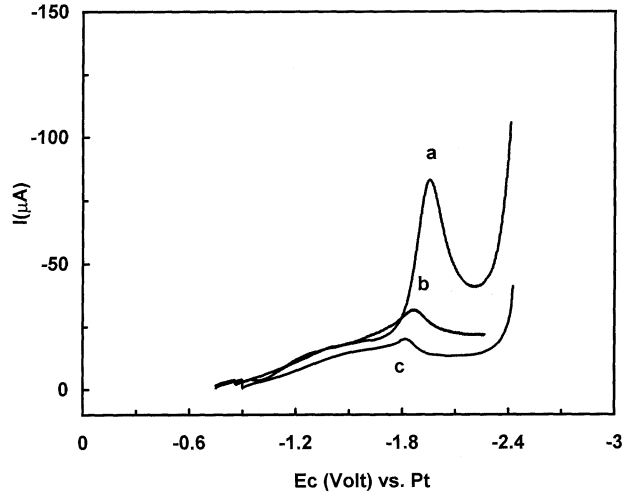

Scheme 2 summarizes the main experimental observations, that lead to the following conclusions: (i) As previously pointed out, no electrografting occurs when the solvent is a better acceptor than the monomer, to the point where the solvent is preferably adsorbed on the cathode to the exclusion of the monomer. (ii) When the monomer and the solvent have quite comparable donor-acceptor properties, the adsorption on the cathode is controlled by their relative polarity, the more polar compound being preferably adsorbed. (iii) If the solvent is a better donor and a poor acceptor (compared to the monomer), its tendency to adsorption is low, and any difference in polarity has no remarkable effect on the inhibition peak. The propensity of the monomer to be electrografted will be enhanced by increasing its electron acceptor capability compared to the solvent. Then the inhibition could be so fast that peak I is no longer observed because of an extremely low intensity. The only way to observe it, would be to decrease the monomer concentration.

Methyl Methacrylate (MMA) Reduction in ACN and in DMF

Although donor and acceptor numbers are available for a series of traditional solvents, no pertinent information has been reported in case of monomers, at least to our best knowledge. This situation has prompted us to compare three methacrylate monomers, different by the substituent in the ester group and accordingly by the acceptor properties of the β-carbon of the polymerizable double bond (Scheme 1). The monomers have also been selected on the basis of the "reactivity" of the ester group in order to provide the final organic coating with adhesive properties towards a polymeric matrix, e.g. for producing composite materials. Methyl methacrylate (MMA), the most widely used methacrylate, 2-hydroxyethyl methacrylate (HEMA), and 2-dimethylaminoethyl acrylate (DMAEMA) have been considered in this study (Scheme 1).

Electroreduction of MMA has been first studied in ACN, and only one diffusion peak has been observed, indicating that the solvent is preferably adsorbed onto the cathode within a monomer concentration range of 0.1 M to 3 M.

In reference to Scheme 2, DMF, i.e. a solvent of a higher donicity than ACN (Table 2) was substituted for ACN, in order to increase the probability for the monomer to be preferably adsorbed on the cathode. At MMA concentrations smaller than 2 M, only one reduction peak (diffusion peak) is observed. Beyond 2 M, this unique peak splits into two steadily resolved components. Figure 6 shows the voltammogram when the MMA concentration is 3 M. Undoubtedly when MMA concentration is increased, the intensity of the less cathodic peak rapidly decreases (Table 4) and the resolution between the two peaks increases. This behavior is typical of the inhibition peak observed in experiments conducted with AN and EA. The main difference with respect to these monomers, has to be found in the high concentration required to evidence the MMA electrografting. This observation indicates that MMA can only successfully compete for adsorption onto the cathode when its relative abundance with respect to DMF is high enough. The same experimental observations have been reported for methacrylonitrile[11], which is a poorer acceptor than acrylonitrile due to the electron donating effect of the α-methyl substituent.

Figure 7 shows the cathodic response of a 2 M MMA solution in DMF when the cathodic scan of the potential

Figure 6. Voltammetry of MMA on nickel in a 0.05 M TEAP solution in DMF, [MMA] = 3 M; v = 20 mVs^{-1}

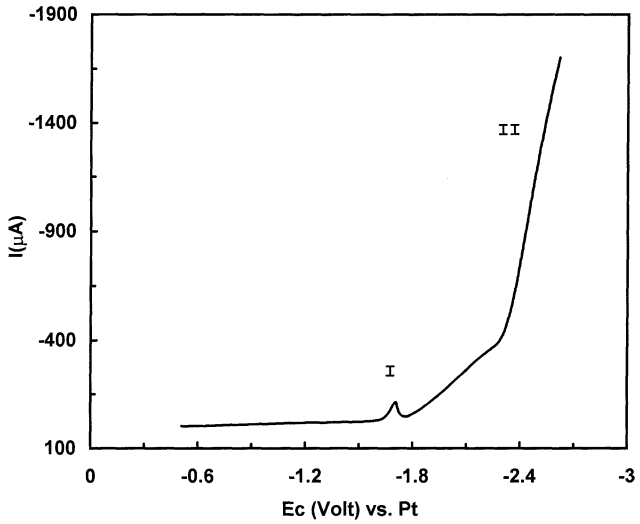

Table 4. Intensity of peak I (ip1) for various MMA concentrations in DMF; v = 20 mVs^{-1}

[MMA] = 0.5 M	[MMA] = 1 M	[MMA] = 2 M	[MMA] = 3 M
[a]	[a]	160 μA	90 μA

[a] Peak I superimposed to peak II.

range of peak I followed by a 20-s voltage hold is repeated. In contrast to what happens when this experiment is conducted with acrylic monomers such as AN or EA, the cathode is not fully passivated after one scan. Indeed, ip1 decreases slowly upon repeated cathodic scans. A film is clearly seen by the naked eye on the cathode when it is withdrawn from the electrochemical cell after one scan. When the number of scans is increased, the PMMA coating is seen as a thick gel-like layer poorly adhering to the metal. This result is quite surprising and in contrast with previously published data for PAN. Indeed the PAN film thickness measured ex situ by ellipsometry does not change when the cathodic scans are repeated in the potential range of peak I[34]. The IR spectrum of the polymer coating (dried in vacuo but not rinsed with solvent) (Figure 8a) confirms the PMMA deposition, the main absorption bands at 3006, 1739, and 1151 cm^{-1} being assigned to $\nu_{as}(CH_2)$, $\nu C{=}O$), and $\nu C{-}O$), respectively. However, the intensity of the absorption bands decreases if the electrode is previously washed with THF, i.e. a good solvent for PMMA, (comparison of Figures 8a and 8b). Since only the polymer chains strongly bound to the electrode remain on it after the washing step, one may suppose that unbound polymer chains are produced simultaneously to grafted ones, which may lead to unreliable film thickness. Consistently, PMMA is formed in solution as demonstrated by PMMA precipitation from the electrochemical bath in methanol (nonsolvent for PMMA, solvent for Et_4NClO_4). This observation is very similar to that one reported by Tanguy et al. for the electrografting of methacrylonitrile (MAN)[11]. Measurements performed with a quartz crystal microbalance[12] have shown that unbound polymethacrylonitrile chains are embedded in a thin layer of grafted ones. On the basis of that observation valid for one monomer (MAN), the authors have proposed a mechanism of "oligomer grafting" instead of the "monomer grafting" they claimed until now[15]. This revision of the grafting mechanism, which is not essential for the purpose of this paper, might, however, be hasty, since unbound polymers in the potential range of peak I (at which the grafting occurs) have never been observed in case of acrylic monomers (such as AN or EA). This observation is actually confined to the electrografting of methacrylates, i.e. methacrylonitrile and MMA, and is certainly not a general behavior. Although the high concentration of methacrylonitrile and MMA which is required for electrografting is in a qualitative agreement with the competitive solvent/monomer adsorption concept, it is not clear yet why unbound methacrylate chains are observed in

Figure 7. Voltammetry of MMA on nickel in a 0.05 M TEAP solution in DMF carried out in the potential range of peak I, [MMA] = 2 M; v = 20 mVs^{-1}: a) first scan; b) second scan

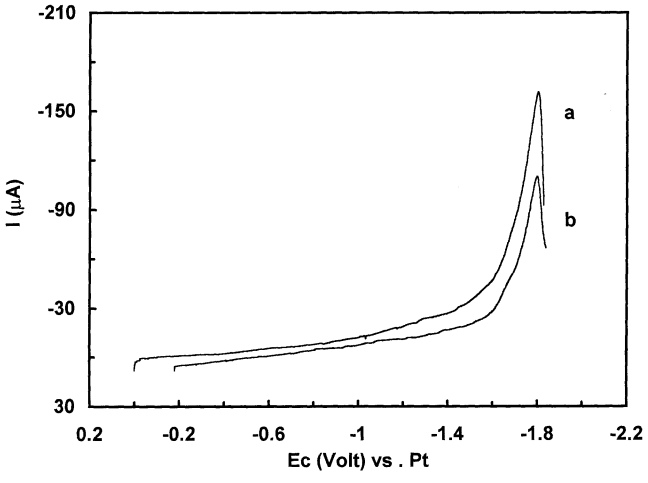

Figure 8. Infrared spectrum of a PMMA film deposited on Ni from a solution of [MMA] = 3 M in DMF at potential of peak I: a) before rinsing with THF; b) after rinsing with THF

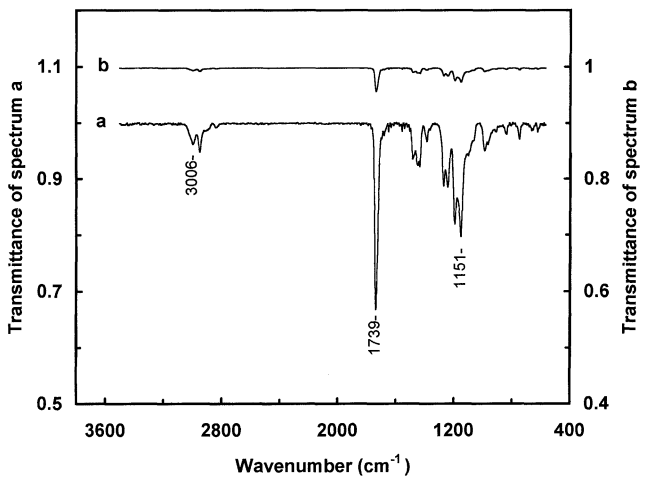

the potential range of peak I. This problem will be discussed in a forthcoming paper.

TMSOEMA and DMAEMA Reduction in ACN and DMF

Nowadays an increasing interest is paid to 2-hydroxyethyl methacrylate (HEMA)[35] and the parent poly(HEMA), which are suitable biomaterials for implants because of their lack of toxicity and their high resistance to degradation[36]. Furthermore, hydroxy groups are reactive towards various topcoats (paint, varnish) that could be used for imparting specific properties to the metal substrate. HEMA may, however, not be used as such, because of the interference of the hydroxy proton reduction. It is the reason why HEMA has to be protected by a trimethylsilyl group, which is easily removed after polymerization. Electrochemical experiments have been conducted with the protected monomer (TMSOEMA) in ACN. Within the 0.1 M to 2 M concentration range, only a diffusion peak is observed. Nevertheless, the classical grafting "signature" has been observed in DMF (poorer acceptor and better donor than ACN) beyond a 0.1 M concentration (Figure 9). It must be noted that in agreement with what happens for MMA and MAN, unbound PTMSOEMA is also embedded in the thin layer of grafted chains when the electropolymerization is conducted in the potential range of peak I.

Finally, the grafting of the third methacrylate, DMAEMA, remained impossible in ACN and in DMF, suggesting so that this monomer cannot compete with these solvents for adsorption onto the cathode.

Figure 9. Voltammetry of TMSOEMA on nickel in a 0.05 M TEAP solution in DMF: a) [TMSOEMA] = 0.1 M; b) [TMSOEMA] = 0.2 M; c) [TMSOEMA] = 0.5 M; v = 20 mVs^{-1}

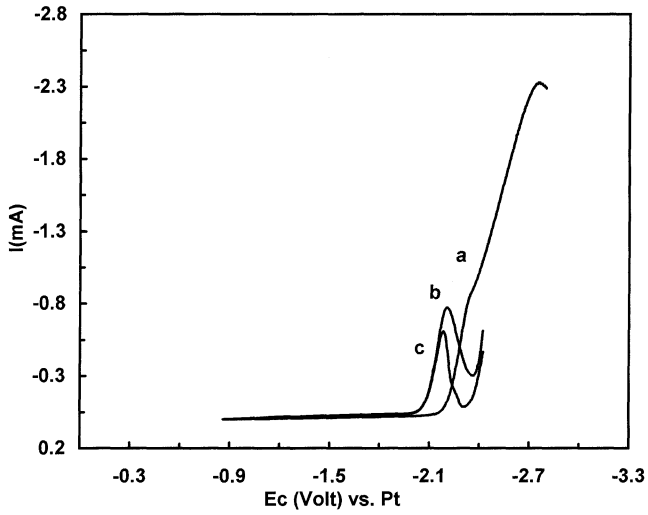

Tentative Prediction of the Cathodic Monomer Grafting

From the experimental results reported in this paper, it appears that the ability of vinyl monomers to be electrografted onto a metal, strongly depends on the electron deficiency of the β-carbon atom double bond. In case of radical copolymerization, the monomer reactivity can be predicted by the Alfrey-Price Q−e scheme[37]. According to these authors, the electrostatic factor e is representative of the monomer polarity and thus of the electron-donor (or -acceptor) character of the vinyl substituent. A linear relationship[38] has been found between the ^{13}C-NMR chemical shifts of the β-carbon atom of the double bond [δ(C-β)] and the corresponding e values[39][40]. By analogy the ^{13}C-NMR spectra of the monomers considered in this paper have been recorded in mixed DMF/$CDCl_3$ solutions. The experimental δ(C-β) values agree with the previously reported data when plotted against e (Figure 10) and they are consistent with an electrografting propensity that decreases when the vinyl β-carbon atom is more shielded, thus less inclined to accept electrons. AN has clearly the less shielded β-carbon atom and is thus the best competitor towards the solvents, since vinyl chloride and vinyl acetate have the more shielded β-carbon atom and have no chance to be adsorbed onto the cathode and to be electrografted as confirmed experimentally. According to the electrochemical experiments reported in this paper, EA is more competitive than MMA towards DMF in agreement with the inductive effect of the α-methyl group in MMA that counterbalances the electron-withdrawing effect of the ester group so that the electron delocalization of the MMA double bond is less pronounced than in EA. This conclusion agrees with the relation of δ(C-β) shown in Figure 10 for EA and MMA. This qualitative consistency is, however, no longer observed when TMSOEMA and DMAEMA are concerned. In a similar way, Figure 10 cannot explain why DMAEMA is not electrografted in DMF. This behavior also remains unexplained when inductive or mesomeric effects are considered. It could, however, be explained by the presence of the silicon group in TMSOEMA and of amino group in DMAEMA. The silicon atom (electron acceptor) can contribute to the monomer adsorption and thus to the electro-

Figure 10. ^{13}C-NMR chemical shifts [δ(C-β)] of monomers vs the corresponding e values: a) AN; b) EA; c) TMSOEMA; d) MMA; e) DMAEMA; f) vinyl chloride; g) vinyl acetate

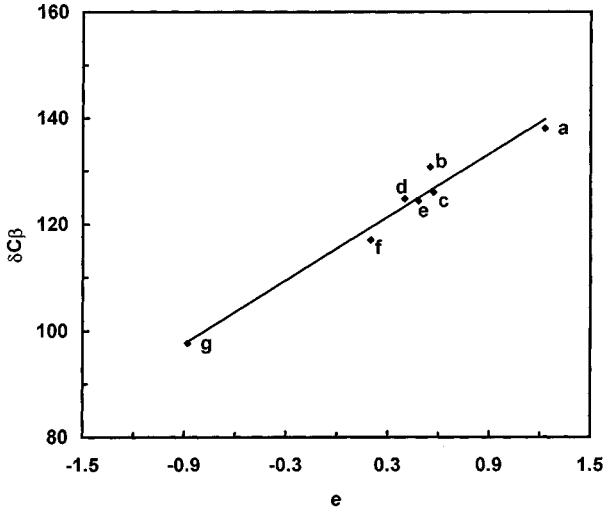

grafting, whereas the amino group (electron donor) can prevent this adsorption from occurring. These assumptions will be supported by theoretical calculations in a forthcoming paper.

Concluding Remarks

The important potentiality of grafting monomers other than AN has been demonstrated in this paper. We have indeed observed that under suitable conditions, ethyl acrylate (EA), and some methacrylates can be electrografted on e.g. nickel, thus with creation of a stable polymer−metal interface, although the reaction is carried out in a good solvent for the polymer. It is now clear that the choice of the solvent for the cathodic grafting of vinyl monomers has a decisive effect on the issue of the electrochemical reaction by deciding whether a strong chemisorption of the electropolymerized material occurs or not.

The explanation for this solvent effect has to be found in a competition between the solvent and the monomer for the localization at the electrode. The issue of this competition strongly depends on the relative donor-acceptor properties and polarity of the solvent with respect to the monomer as confirmed by a great effect on the potential and intensity of the inhibition peak. The polarity of the solvent is more important as this solvent is a better electron-acceptor (and a poorer donor) than the monomer and has thus higher probability to be adsorbed onto the cathode. Conversely, the effect of the solvent polarity decreases when the solvent is a poor acceptor (and a good donor), thus when this solvent has less chance to be in the electrical double layer. If solvent and monomer have a comparable liability to be adsorbed at the cathode, then the monomer concentration has a decisive effect on the grafting issue.

One important criterion for the cathodic electrografting of a monomer is the choice of a solvent with a weaker acceptor character and higher donicity than the monomer, provided that this solvent is not electroactive in the potential range of interest. As a consequence of this rule, the more the substituent of the polymerizable double bond decreases the acceptor capacity of the monomer, the smaller the ability of this monomer to be electrografted. The measurement of the ^{13}C-NMR chemical shifts for the β-carbon atom of the vinyl double bond could accordingly serve as a preliminary semiquantitative tool for predicting the grafting ability of new monomers. However, some problems can arise when the monomer substituent contains atoms or groups of atoms that do not influence too much the β-carbon atom although they can contribute to the cathode adsorption by their electron acceptor or donor capacity.

A theoretical model accounting for the competitive adsorption of monomer/solvent pairs is currently studied and will be the topic of a forthcoming paper.

The authors are grateful to the *Services Fédéraux des Affaires Scientifiques, Techniques et Culturelles* in the frame of the *"Pôles d'Attraction Interuniversitaires: Chimie and Catalyse Supramoléculaire"*. They thank the *R & D groupe Cockerill Sambre* for continuous interest and *M. Micheels* for her technical assistance.

Experimental Section

Acrylonitrile (AN: Aldrich, > 99%), ethyl acrylate (EA: Acros, 99.5%), methyl methacrylate (MMA: Acros, 99%), 2-(dimethylamino)ethyl methacrylate (DMAEMA: Acros, 98%), and acetonitrile (ACN: Acros, p.a.) were dried over calcium hydride (Acros: 93%) and distilled under reduced pressure. Dimethylformamide (DMF: Acros, p.a.) was dried over phosphorus pentoxide (Acros 98%) and distilled at 70°C under reduced pressure. Propylene carbonate (PC: Acros, 99%) and 2-hydroxyethyl methacrylate (HEMA: Acros, 96%) were dried over molecular sieves 4 Å for 24 h and distilled at 85°C and 50°C, respectively, under reduced pressure. Pyridine (PY: Acros, 99.5%) was dried over potassium hydroxide (Acros: 98%) for 2 h at 120°C and distilled at 40°C under reduced pressure. Hexamethylphosphoramide (HMPA: Aldrich 99%) was dried over calcium hydride for 24 h and distilled at 80°C under reduced pressure. Tetraethylammonium perchlorate (TEAP: Fluka, > 99%) was heated in vacuum at 80°C for 12 h prior to use.

2-Trimethylsilyloxyethyl methacrylate (TMSOEMA) was synthesized by adding dropwise chlorotrimethylsilane (ClTMS: Acros, 98%) to a mixture of previously dried HEMA and triethylamine (Acros, 99%) in tetrahydrofuran (THF: Acros, p.a.)[31]. The reaction was carried out in THF at 0°C, under an inert and dry atmosphere and stirring for 12 h. Triethylamine hydrochloride was filtered off, and THF distilled off under reduced pressure. The residue was purified just before use by distillation under reduced pressure at 50°C. The product was then identified as TMSOEMA by ^{1}H-NMR spectroscopy [i. e. presence of the trimethylsilyl $-Si(CH_3)_3$ resonance at $\delta = 0.1$ and absence of the hydroxy −OH resonance at $\delta = 3.3$]. The purity was ascertained to be higher than 99.5% by gas chromatography.

Voltammetry (CV) experiments were carried out with each monomer (10^{-2} to 2 M), dissolved in an appropriate solvent containing tetraethylammonium perchlorate (TEAP) as a conducting salt ($5 \cdot 10^{-2}$ M).

The water content was measured by the Karl-Fischer method (Tacussel aqua processor) and ascertained to be lower than 5 ppm. All the experiments were carried out in a glove-box at room temperature under an inert (lower than 10 ppm in oxygen) and dry atmosphere.

The potentiostat used for the voltammetry experiments was a PAR-E. G&G model 273A. The electrochemical cells are described elsewhere[5]. Potentials were measured against a Pt pseudo-reference electrode. The nickel working electrodes of 2 cm^2 area, were mechanically polished with an alumina suspension in water, washed with heptane and acetone, and finally treated overnight in vacuum at 150°C. The residual nickel oxide on the electrode surface was then electrochemically reduced in an ACN/TEAP solution in the glove-box just prior to electropolymerization. The oxide layer was completely removed as assessed by a reduction current dropping down to zero after several potential scans. The rapid transfer of the cathode from one solution to the other within the glove box ensures the absence of oxide at the metal substrate, which is a prerequisite for polymer grafting[32].

A reference poly(ethyl acrylate) sample (PEA) was prepared by free radical polymerization of EA in DMF (0.5 M solution) initiated by 2,2′-azobis(2-methylpropionitrile) (AIBN: Acros, 98%) at 60°C for 6 h. The polymer was precipitated in methanol, washed several times with methanol in order to remove the unreacted monomer and AIBN, and dried in vacuo at 40°C for 24 h. A PEA film was solvent-casted (DMF) onto nickel plates, such that infrared spectra could be recorded by the same technique as for the electrografted films.

Except for specific treatment mentioned in the discussion all the electrografted films were carefully rinsed with a good solvent for the polymer in order to remove any ungrafted chains and conducting salt, and dried in vacuo for 2 h before characterization.

IR spectra were recorded ex situ with a BRUKER (Equinox IFS 66) FTIR spectrometer equipped with a grazing angle accessory (83°) and a polarizer (Specac KRS-5). – ^{13}C-NMR data were recorded in a mixed DMF/$CDCl_3$ medium with a BRUKER AM 400 apparatus operating at 100 MHz.

[1] B. Yurttas, L. Toppare, V. Akbulut, *J. Macromol. Sci.* **1988**, *A25*, 219.
[2] S. N. Bhadani, Q. Ansari, S. K. S. Gupta, *J. Appl. Polym. Sci.* **1992**, *44*, 121.
[3] G. Lécayon, C Le Gressus, A. Le Moel, Eur. Patent no. 0038244, **1981**; *Chem. Abstr.* **1982**, *96*, 21350m.
[4] C. Boiziau, G. Lécayon, *Recherche* **1988**, *19*, 888.
[5] M. Mertens, C. Calberg, L. Martinot, R. Jérôme, *Macromolecules* **1996**, *29*, 4910–4918.
[6] P. Jonnard, F. Vergand, P. F. Staub, C. Bonnelle, G. Deniau, C. Bureau, G. Lécayon, *Surf. Interface Anal*. **1996**, *24*, 339.
[8] M. Mertens, C. Calberg, N. Baute, R. Jérôme, L. Martinot, *J. Electroanal. Chem.* **1998**, *441*, 237–244.
[8] V. Geskin, R. Lazzaroni, M. Mertens, R. Jérôme, J. L. Brédas, *J .Chem. Phys.* **1996**, *105*, 3278.
[9] G. Deniau, G. Lécayon, P. Viel, G. Zalczer, C. Boiziau, G. Hennico, J. Delhalle, *J. Chem. Soc., Perkin Trans. 2* **1990**, 1433.
[10] J. Levisalles, B. Castro, M. Jozefowicz, *Chimie Organique, Flammarion Sciences* **1973**, *2*, 92.
[11] J. Tanguy , G. Deniau, C. Auge, G. Zalczer, G. Lécayon, *J. Electroanal. Chem*. **1994**, *337*, 114.
[12] J. Tanguy, G. Deniau, G. Zalczer, G. Lécayon, *J. Electroanal. Chem.* **1996**, *417*, 175–184.
[13] F. M. Fowkes, in *Physicochem. Aspects Polym. Surf.* (K. L. Mittal, Ed.), Plenum Press, New York, **1983**, vol 2, 583–603.
[14] D. L. Allara, F. M. Fowkes, J. Noolandi, G. W. Rubloff, M. V. Tirrel, *Mater. Sci. and Eng*. **1986**, *83*, 213–226.
[15] G. Lécayon, Y. Bouizem, C. Le Gressus, C. Reynaud, C. Boiziau, C. Juret, *Chem. Phys. Lett*. **1982**, *91*, 506.
[16] B. H. Loo, T. Kato, *Surf. Sci*. **1993**, *284*, 167.
[17] A. Bewick, C. Gibilaro, M. Razaq, J. W. Russel, *J. Electron Spectrosc. Relat. Phenom*. **1983**, *30*, 191.
[18] P. Parent, G. Laffon, G. Tourillon, A. Cassuto, *J. Phys. Chem*. **1995**, *99*, 5058.
[19] G. Xue, J. Dong, J. Zhang, Y. Sun, *Polymer* **1994**, *35*, 723.
[20] J. Perreau, C. Reynaud, C. Boiziau, *Surf. Sci.* **1985**, *162*, 776.
[21] X. Crispin, V. Geskin, R. Jérôme, R. Lazzaroni, J. L. Brédas, *Proceeding of the international Conference on Polymer-Solid Interfaces*, Namur, Belgium, **1996**, in press.
[22] C. Fredrikson, R. Lazzaroni, J. L. Brédas, M. Mertens, R. Jérôme, *Chem. Phys. Lett*. **1996**, *258*, 356.
[23] M. O. Bernard, C. Bureau, J. M. Soudan, G. Lécayon, *J. Electroanal. Chem*. **1997**, *431,* 153–162
[24] J. Lawrence, R. Parsons, *J. Phys. Chem*. **1969**, *73*, 3577.
[25] J. O′M. Bockris, M. A. V. Devanathan, K. Müller, *Proc. R. Soc.* **1963**, *274A*, 55.
[26] B. Roelfs, C. Schroeter, T. Solomun, *Ber. Bunsenges. Phys.* **1997**, *101*, 1105.
[27] V. Gutmann, *Coordination Chemistry in Non-Aqueous Solutions*, Springer-Verlag, New-York, **1968**.
[28] V. Gutmann, *The Donor-Acceptor Approach to Molecular Interactions*, Plenum Press, New York, **1978**.
[29] V. V. Kuznetsov, V. P. Grigor′ev, L. G. Bozhenko, *Elektrokhimiya* **1980**, *16*, 495.
[30] M. Munakata, S. Kitagawa, M. Miyazima, *Inorg. Chem*. **1985**, *24*, 1638–1643.
[31] B. Ivan, J. P. Kennedy, P. W. Mackey, *Polymeric Drugs and Drugs Delivery System* (Eds.: L. Dunn, R. M. Ottenbrite), *ACS Symp. Book Ser*., vol. 469, Am. Chem. Soc., Washington, D. C., **1991**, p. 203–212.
[32] Y. Bouizem, F. Chao, M. Costa, A. Tadjeddine, G. Lécayon, *J. Electroanal. Chem.* **1984**, *172*, 101–121.
[33] V. Gutmann, A. Steininger, E. Wychera, *Monatsh. Chem.* **1966**, *97*, 460.
[34] C. Calberg, M. Mertens, R. Jérôme, X. Arys, A. M. Jonas, R. Legras, *Thin Solid Films* **1997**, *310*, 148–155.
[35] J. P. Montheard, M. Chatzopoulos, D. Chappard, *J. Macromol. Sci. – Rev. Macromol. Chem. Phys.* **1992**, *C32*, 1–34.
[36] J. Kalal, *Makromol. Chem., Suppl*. **1984**, *7*, 31.
[37] T. Alfrey, C. Price, *J. Polym. Sci.* **1947**, *2*, 101.
[38] J. J. Herman, P. Teyssié, *Macromolecules* **1978**, *11*, 839.
[39] R. E. Greenley, *J. Macromol. Sci. Chem*. **1980**, *14*, 427.
[40] E. C. Leonard, *High Polymers,* vol. 24(1), Wiley Interscience, New York, (*Vinyl and Diene Monomers*), part 1, Wiley Interscience, **1970**.

[I98105]

Anionic Monosubstituted Cyclopentadienylsamarium Derivatives: Catalysts for a Stereospecific Isoprene Polymerization

Denise Baudry-Barbier*, Nicolas Andre, Alain Dormond, Christine Pardes, Philippe Richard, Marc Visseaux, and Cheng Jian Zhu

Université de Bourgogne, Faculté des Sciences Gabriel, Laboratoire de Synthèse et d'Electrosynthèse Organométalliques (L.S.E.O.-U.M.R. 5632),
6 bd Gabriel, F-21000 Dijon, France

Received April 15, 1998

Keywords: Samarium / Allyl complexes / Carbene adducts / Organolanthanides / *trans*-Polyisoprene

New alkyl and allyl complexes **1**–**3** {**1**: $[Cp'_2Sm(C_3H_5)]_n$, Cp′ = $Me_3CC_5H_4$; **2**: $[Me_4C_2(C_5H_4)_2]Sm(C_3H_5)_2Li(dme)$, dme = $(CH_3OCH_2CH_2OCH_3)$; **3**: $Cp'_2SmMe_2Li(dioxane)$} were synthesized from $(Cp'_2SmCl)_2$ and from the magnesium derivative $[Me_4C_2(C_5H_4)_2]SmCl \cdot MgCl_2(THF)_4$ (**4**). The ansa anionic complex **2** exhibited good activity for the stereospecific 1,4-*trans* polymerization of isoprene, whereas the neutral derivative **1** was inactive. In the same way, the anionic complex $[Cp'_2SmMe_2]Li(dioxane)$ (**3**) was found to be an ethylene polymerization catalyst of very short lifetime. The lack of reactivity of **1** is related to the associated structure of this coordinatively unsaturated complex: this fact was established by the formation of the carbene adduct $Cp'_2Sm(C_3H_5)[C(NiPr)_2(CMe)_2]$ (**1′**). Crystals of **1′** were isolated but this new compound undergoes a partial rearrangement into a tris-Cp′ species in solution. Similar behaviour is observed for the analogous complex $Cp'_2SmCl[C(NiPr)_2(CMe)_2]$ (**1′′**). The X-ray crystal structure revealed the formation of the adduct, as a toluene solvate, which exists in benzene solution in equilibrium with Cp'_3Sm and $Cp'SmCl_2[C(NiPr)_2(CMe)_2]_2$. The catalytic behaviour of **2** is compared with that of other early lanthanide derivatives.

Introduction

Isoprene polymerization, in relation to the chemistry of elastomers and adhesives, is of current interest[1]. Hydrido- or alkylmetallocenes of lanthanides are efficient catalysts for ethylene polymerization in the absence of the methyl aluminoxane reagent MAO[2][3]. However, the compounds Cp_2*LnH or Cp^*_2LnR, Cp* = C_5Me_5 or related bridged systems, are almost completely unreactive for the polymerization of α-olefins or dienes[4]. We were interested in the determination of the limits of stability of less hindered metallocene hydrides[5] of the early lanthanides and established that the hydride $[Cp'_2SmH]_2$, Cp′ = $Me_3CC_5H_4$, can be observed in solution, whereas the analogous neodymium hydride is only a transient species[6][7]. In this Cp′ series, or preferably in an analogous ansa cyclopentadienyl series [to avoid the easy redistribution leading to tris(cyclopentadienyl) derivatives], it was therefore necessary to synthesize alkyl or allyl derivatives that would be stable compounds capable of catalyzing the diene (and especially isoprene) polymerization without addition of a co-catalyst. The microstructure of a polymer is, to a large extent, controlled by the mode of coordination of the monomer to the catalyst: in a Cp'_2SmR moiety, even when R is a non-bulky alkyl or allyl ligand, only one vacant site will be readily accessible and, consequently, a stereospecific 1,4-*trans* polymerization is expected[8].

Results and Discussion

Synthesis of *tert*-Butylcyclopentadienyl Complexes

The methyl derivative $(Cp'_2SmMe)_2$[5] had been synthesized from $(Cp'_2SmCl)_2$[9] by addition of MeLi. The neutral allylic derivative $[Cp'_2Sm(C_3H_5)]_n$ (**1**) was obtained in a similar way using the dioxane adduct of allyl lithium[10] (Scheme 1).

Scheme 1

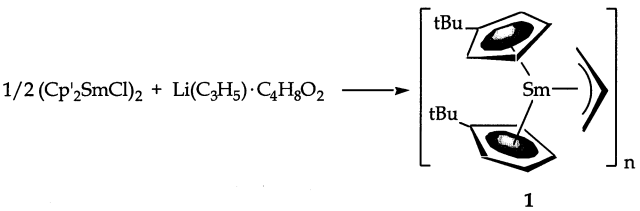

1

Compound **1** was isolated in an analytically pure state as a red oil. Due to the fact that no ether ligand remained coordinated, it was inferred that this compound was dimeric or polymeric. Attempts to obtain a monomeric solvated form by crystallization in the presence of oxygenated solvents were unsuccessful. However, crystals could be obtained in the presence of another Lewis base, i.e. the stable carbene 1,3-diisopropylimidazoline-2-ylidene $C(NiPr)_2$-

 © WILEY-VCH Verlag GmbH, D-69451 Weinheim, 1998 1434–1948/98/1111–1721 $ 17.50+.50/0

$(CMe)_2$[11], which has recently been used as a ligand in lanthanide compounds[12]. The nitrogen analysis of these thin red plates was consistent with the formula of a mono adduct $Cp'_2Sm(C_3H_5)[C(NiPr)_2(CMe)_2]$ (**1′**). The crystals were not suitable for X-ray structural analysis because the melting point was just above ambient temperature and, consequently, crystals melted in the sealed capillary. Surprisingly, the ^{1}H-NMR spectrum (C_6D_6 solution) of these monocrystals showed the known signals of Cp'_3Sm (ca. 10%) in addition to the set of signals due to the adduct (90%). A partial redistribution of the ligands could be involved, although no signals corresponding to the concomitant formation of a mono Cp′ derivative were detected.

Although we could not establish unambiguously the behaviour of $Cp'_2Sm(C_3H_5)[C(NiPr)_2(CMe)_2]$ (**1′**) in solution, this was possible in the case of another carbene adduct. Addition of one equivalent of the carbene $C(NiPr)_2(CMe)_2$ to a toluene solution of $(Cp'_2SmCl)_2$ allowed the isolation of yellow crystals [see ORTEP view (Figure 1) and Experimental Section] of an analytically pure toluene solvate of the adduct $Cp'_2SmCl[C(NiPr)_2(CMe)_2]$ (**1″**).

1:3 ratio. The percentage of the carbene adduct **1″** was a function of the concentration and it was found to be higher (nearly 80%) in dilute solution. This equilibrium (Scheme 2) is slow in the NMR timescale and Spin Saturation Transfer (SST) experiments could not be performed.

Scheme 2

$$2\,Cp'_2SmCl[C(N^iPr)_2(CMe)_2] \rightleftharpoons Cp'SmCl_2[C(N^iPr)_2(CMe)_2]_2 + Cp'_3Sm$$

1"

Synthesis of Ansacyclopentadienyl Complexes

An ansa compound was synthesized from $SmCl_3(THF)_3$ and the Grignard reagent $[Me_4C_2(C_5H_4MgCl)_2](THF)_4$[13]. The X-ray crystal structure of two related samarium complexes $[\{Me_4C_2(C_5H_4)_2\}SmCl(THF)MgCl_2(THF)_3]$ and $[\{Me_4C_2(C_5H_4)_2\}SmCl(THF)]_2$ have been described elsewhere[14][15]. The reasons for the formation of one or other of these complexes were not clear given that the starting

Figure 1. ORTEP view of the solid-state structure of $(Cp'_2SmCl[C(NiPr)_2(CMe)_2]$ (**1″**); for reasons of clarity, ellipsoids are set to the 30% probabity level and the toluene solvate molecule is not represented[a]

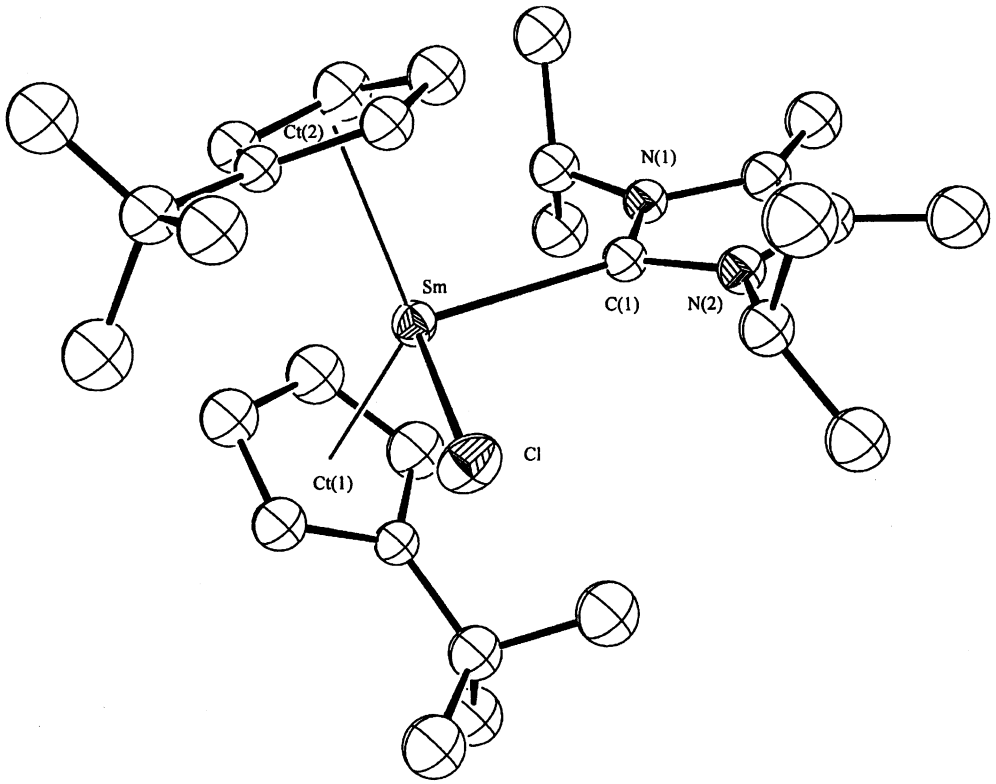

[a] Selected bond lengths [Å] and angles [°]: Sm−C(1) 2.62(2), Sm−Cl 2.648(4), Sm−Ct(1) 2.45(1), Sm−Ct(2) 2.44(1); Ct(1)−Sm−Ct(2) 128.6(14), Ct(1)−Sm−C(1) 106.3(9), Ct(1)−Sm−Cl 107.9(7), Ct(2)−Sm−C(1) 101.8(9), Ct(2)−Sm−Cl 105.6(6), C(1)−Sm−Cl 104.2(3).

After dissolution of these crystals in C_6D_6, the NMR spectrum showed the presence of three compounds: **1″**, a second adduct identified as $Cp'SmCl_2[C(NiPr)_2(CMe)_2]_2$ on the basis of the NMR data, and the unavoidable Cp'_3Sm. The integral values for the Cp signals of $Cp'SmCl_2[C(NiPr)_2(CMe)_2]_2$ and Cp'_3Sm were, as expected, in a

materials and the experimental procedures were quite similar. NMR data were not mentioned and, consequently, it was not established wether the two complexes could be distinguished in solution. The formation of a related monomeric complex, $[Me_4C_2(C_5H_4)_2]SmCl(THF)$, had also been reported, and this involved the oxidative addition of *tert*-

Table 1. ^{1}H-NMR data of complexes **1**−**4** [C_6D_6, δ vs. TMS, 298 K]

Complex	C_5H_4	CMe_3 or $(CMe_2)_2$	allyl or alkyl	carbene $C(NiPr)_2(CMe)_2$
$[Cp'_2Sm(C_3H_5)]_n$	13.21 (4 H)	−2.81 (18 H)	16.79 (1 H)	−
1	9.21 (4 H)		9.56 (2 H)	
			6.43 (2 H)	
$Cp'_2Sm(C_3H_5),C(NiPr)_2(CMe)_2$	12.72 (4 H)	−2.51 (18 H)	15.97 (1 H)	3.91 (m, 2 H);
1′	9.21 (4 H)		8.10 (4 H)	1.72 (6 H);
				1.47 (d, 12 H)
$Cp'_2SmCl,C(N^iPr)_2(CMe)_2$	11.38; 10.45	1.18 (18 H)	−	3.95 (m, 2 H);
1″	8.15; 7.94			0.91 (6 H);
	(2 H each)			0.57 (12 H)
$Cp'SmCl_2,[C(NiPr)_2(CMe)_2]_2$	10.72 (2 H)	−0.5 (br 9 H)	−	1.51 (d, 24 H);
1‴	11.57 (2 H)			0.01 (s, 12 H);
				H signal not located
$[Me_4C_2(C_5H_4)_2]Sm(C_3H_5)_2$	7.94 (4 H)	1.70 (12 H)	9.53 (m, 2 H)	3.35 (dme, 4 H)
Li(dme), **2**[a]	5.77 (4 H)		8.61 (br., 4 H)	3.19 (dme, 6 H)
			7.07 (br., 4 H)	
Cp'_2SmMe_2Li(dioxane)	9.77 (4 H)	−0.05 (18 H)	−5.12 (s, 6 H)	4.15 (dioxane, 8 H)
3	9.07 (4 H)			
$[Me_4C_2(C_5H_4)_2]SmCl(THF)$	15.31 (4 H)	1.25 (12 H)	−	3.73 (THF, 16 H)
$MgCl_2(THF)_3$, **4**	8.05 (4 H)			1.34 (THF, 16 H)

[a] In C_4D_8O.

butyl chloride to the Sm^{II} compound $[Me_4C_2(C_5H_4)_2]Sm$. In this case NMR data were obtained[16].

Initially we tried to investigate the reaction on an NMR-scale preparation. By mixing stoichiometric amounts of $SmCl_3(THF)_3$ and $[Me_4C_2(C_5H_4MgCl)_2](THF)_4$ in C_6D_6, a yellow solution and a white precipitate of salts were obtained. The solution was transferred into another tube and the solvent removed under reduced pressure to remove the excess THF originating from the Grignard reagent. After redissolution in C_6D_6, the NMR spectrum showed the presence of four remaining THF molecules per $[Me_4C_2(C_5H_4)_2]Sm$ moiety and no further loss of THF was observed when the same process was repeated. This was interpreted in terms of the formation of the mixed samarium-magnesium compound, $[\{Me_4C_2(C_5H_4)_2\}SmCl(THF)\text{-}MgCl_2(THF)_3]$ (**4**).

The synthesis was then performed on a larger scale, in THF, as described in the literature[15]. After the usual work-up, the NMR spectrum of the crude orange-yellow solid was very different from the one recorded in the previous synthesis (directly in the NMR tube) and could not be interpreted in terms of the formation of a well-defined pure compound. Further attempts were made using toluene as the solvent, but similar results were obtained. It was concluded that if evidence for the quantitative formation of a unique complex was provided by NMR experiments, then the handling of the mixture, leading to undefined materials, was not recommended.

The one-pot synthesis of an allylic derivative was therefore undertaken, initially on an NMR scale, by adding a stoichiometric amount of C_3H_5Li(dioxane) to the crude deuterated benzene solution obtained, as described previously, by mixing $SmCl_3(THF)_3$ and the Grignard reagent $[Me_4C_2(C_5H_4MgCl)_2](THF)_4$. A reaction occurred immediately and a pink-red precipitate deposited, which was partially soluble in the presence of the oxygenated solvents (7 THF + 2 dioxane). At 70°C the NMR spectrum showed a two-allyl signal pattern {2 H and 8 H per $[Me_4C_2(C_5H_4)_2]Sm$ moiety}, revealing a dynamic exchange process. The poor solubility, along with these integral values, indicated that the new complex was an anionic bis(allylic) complex. At ambient temperature the allylic signals coalesced and only the signals due to the ansa ligand could be detected. This could be interpreted as evidence for the partial dissociation of allyl ligands.

The synthesis was then performed on a bulk scale, in toluene, with two equivalents of $C_3H_5Li\cdot$dioxane. The crude compound contained THF and dioxane, which were exchanged by dissolution in DME. The red expanded oil obtained after removal of the solvents was washed with ether and finally gave a red powder of analytically pure **2**, $[Me_4C_2(C_5H_4)_2]Sm(C_3H_5)_2Li(DME)$. This new compound was not soluble in either toluene or benzene: its NMR spectrum was recorded in $[D_8]$THF and the allyl ligands exhibited a typical η^3 three-signal (1 H, 2 H, and 2 H) pattern.

The dianionic ansa cyclopentadienyl ligand $[Me_4C_2(C_5H_4)_2]^{2-}$ was chosen in order to avoid the disproportionation of the bis(cyclopentadienyl) derivatives of the lighter lanthanides[17][18]. Moreover, the stereoelectronic properties of a $[Me_4C_2(C_5H_4)_2]Sm$ moiety should be similar to those of a $(Me_3CC_5H_4)_2Sm$ unit, except that the angle between the metal center and the centroids of the rings would be slightly smaller in the case of an ethylene bridge[19] (the ring-centroid−Yb−ring-centroid angle is 121° and 121.3° in $[Me_4C_2(C_5H_4)_2]YbCl_2,Mg_2Cl_3\cdot 7$ THF[17] and $(Me_3CC_5H_4)_2YbCl\cdot THF$[20], respectively). In addition, in the ansa ligand the rotation of the Cp rings[21][22] is not possible and the effective size of the ligand is therefore smaller. The saturation of the coordination sphere of the metal atom therefore occurs in a different manner: in the Cp′ series, $Cp'_2YbCl\cdot THF$[20] is neutral

whereas the homologous ansa complex $[Me_4C_2(C_5H_4)_2]YbCl_2 \cdot Mg_2Cl_3 \cdot 7\ THF$[17] is anionic.

In a similar manner, the reaction of an equimolar amount of C_3H_5Li with $(Cp'_2SmCl)_2$ leads to a dimer (or a polymer, although the high solubility of **1** in pentane suggests an oligomeric structure), showing that a neutral species is preferred. In the case of the ansa compound, a monomeric anionic complex **2** is formed.

In the presence of an excess of allyl ligand, no anionic compound was formed in the Cp′ series: a redistribution leading to a mixture of Cp'_3Sm[9] and $Sm(C_3H_5)_4Li(dioxane)$[23] was observed (Scheme 3).

Scheme 3

$$3\ Cp'_2Sm(C_3H_5) + Li(C_3H_5)\cdot C_4H_8O_2 \longrightarrow 2\ Cp'_3Sm + Sm(C_3H_5)_4Li\cdot C_4H_8O_2$$

Nevertheless, on using the small monohapto methyl ligand, a bis(alkyl)-anionic complex was obtained in the Cp′ series: treatment of $(Cp'_2SmMe)_2$ or $(Cp'_2SmCl)_2$ with one or two equivalents of MeLi, respectively, led to the same compound Cp'_2SmMe_2Li. After addition of one molar equivalent of $(Cp'_2SmCl)_2$ the neutral dimer could be recovered.

Scheme 4

$$Cp'_2SmMe_2Li + 1/2\ (Cp'_2SmCl)_2 \longrightarrow (Cp'_2SmMe)_2$$

The anionic bis(methyl) compound was isolated in an analytically pure form (pale yellow microcrystals) as a dioxane adduct: $Cp'_2SmMe_2Li \cdot dioxane$.

Catalysis

Allylic lanthanide derivatives are known to catalyse the polymerization of dienes[24] and the new complexes **1** and **2** were tested in the polymerization of isoprene.

The anionic complex **2** was found to be efficient (the turn-over number amounts to ca. 260 mol of isoprene per mol of lanthanide catalyst per hour) and very stereospecific (95%) for 1,4-*trans* polymerization (see Table 2). Molecular weights are in the expected range for this type of polymerization test[1].

The neutral complex **1** was found to be inactive and its carbene adduct **1′** was found to be almost inactive. This implies that the $[Cp'_2Sm(C_3H_5)]_n$ compound remains strongly associated and isoprene does not possess a sufficiently strong ligand ability [unlike, for example, the nucleophilic carbene $C(NiPr)_2(CMe)_2$] to dissociate the starting material. Attempts to create a more accessible metallic center by addition of 1 equivalent of yttrium chloride as a Lewis acid led to a system of very low activity (yield of polyisoprene 2%).

In contrast, the dissociation of an allylic ligand in the anionic compound **2** is easy and allows the coordination of the diene. The precedent for this ligand dissociation was postulated for other anionic allyllanthanide compounds[8] tested in the polymerization of butadiene.

The tetraallylneodymium complex $Nd(C_3H_5)_4Li(dioxane)_{1.5}$ had been previously found to be a specific (86% of *trans*-1,4-polybutadiene) catalyst for butadiene polymerization[10]. We found that for the polymerization of isoprene, tetraallyllanthanide complexes are less specific (31% and 28% of *trans*-1,4-polyisoprene for neodymium and samarium, respectively). This reaction was thus very dependent on the steric hindrance of the monomer.

In the same way, $C_3H_5Li(dioxane)$ leads to a high (ca. 53%) percentage of *cis* 1-4 polyisoprene; the participation of this species could be invoked for the polymerization obtained from the tetraallylic compounds and this has been discussed previously[8]. However, for the anionic bisallylic complexes (or systems) its role appears negligible because those systems led to an almost pure 1,4-*trans* polymer.

Scheme 5

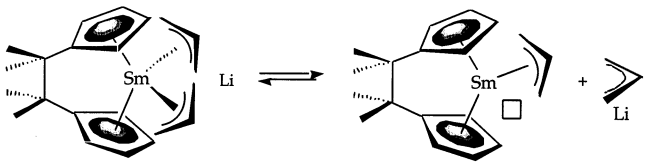

The performances of other allylic systems towards isoprene polymerization are presented in Table 2 (**A**, the neodymium analogue of **2**, and **B**, an alkoxide derivative, tris-*tert*-butyloxy − "tritox" −). The catalysts are prepared in situ and may contain salts and an excess of oxygenated sol-

Table 2. Polymerization of isoprene (50°C, ratio isoprene/catalyst = 1500)

Catalyst	Yield (%)	$\bar{M}_w$	*trans*-1,4 (%)	*cis*-1,4 (%)	3,4 (%)	Reaction time [h]	T.O.[a] [h^{-1}]
$[Cp'_2Sm(C_3H_5)]_n$ **1**	0						
$[Me_4C_2(C_5H_4)_2]Sm(C_3H_5)_2Li(dme)$, **2**	62	8000	95	1	4	12	260
$(C_3H_5)Li(dioxane)$	100	−	27	53	20	2.5	110
$Sm(C_3H_5)_4Li(dioxane)$	55	24000	28	45	27	3	200
$Nd(C_3H_5)_4Li(dioxane)_{1.5}$[b]	75	1500	31	39	30	4	150
system A	30	37000	97	0	3	6	50
system B	30	46000	91	0	9	21	50

[a] T.O. = mol of monomer transformed/mol of catalyst/h. − [b] Was found to be inactive in the presence of 4 THF per Nd atom.

vents as ligands, which could modify the process of dissociation of the allylic ligand. Indeed, we found this to be the case for the tetraallylneodymium complex Nd-$(C_3H_5)_4Li(dioxane)_{1.5}$, in which the activity decreases in the presence of 1 THF per molecule, and it becomes inactive with 4 THF per molecule. The turn-over values (Table 2) are lower than for **2**, nevertheless, the catalytic activity is well in evidence: in each case the same stereocontrol is observed, with predominant formation of 1,4-*trans*-polyisoprene.

The ansa and the tritox complexes possess more bulky ligands than the tetraallyl complexes. The isolated complexes are tetracoordinated, and in solution it also seems that no more than four coordination sites are accessible. After the decoordination of the allyl ligand, only one site will be vacant for the coordination of the monomer. As a consequence, a very high stereoselectivity (89 to 95% of 1,4-*trans* polymer) is observed.

The anionic complex **3**, $Cp'_2SmMe_2Li(dioxane)$, was found to be very active (T.O. = 25000 mol of ethylene transformed/mol of catalyst/h) towards the polymerization of ethylene in the absence of MAO, but only within five minutes[25]. The rapid loss of activity was attributed to the ease of rearrangement leading to the inactive tris derivative.

The neutral dimer $(Cp'_2SmMe)_2$ had already been found to be very poorly active towards hydrogenolysis. This lack of reactivity was related to its dimeric structure[5].

Conclusion

New organometallic complexes of samarium have been synthesized, $[Cp'_2Sm(C_3H_5)]_n$ and its carbene adduct $Cp'_2Sm(C_3H_5)[C(NiPr)_2(CMe)_2]$, $[Me_4C_2(C_5H_4)_2]Sm(C_3H_5)_2Li(dme)$, and $Cp'_2SmMe_2Li(dioxane)$. The structures of these complexes are strongly dependent on steric factors: neutral monoallylic and anionic bis(allylic) complexes were characterized. Related complexes were prepared in situ. An X-ray structure analysis could be obtained for $Cp'_2SmCl[C(NiPr)_2(CMe)_2]$, which undergoes rearrangement in solution. The catalytic behaviour of all these new complexes towards polymerization was investigated. Anionic complexes are active: $Cp'_2SmMe_2Li(dioxane)$ is an ethylene polymerization catalyst with a short lifetime and the ansa bis(allylic) complex is a stereospecific 1,4-*trans*-polymerization catalyst.

The authors wish to thank *G. De Demo*, *BTS Chimie Chalon/Saône* (France), for S.E.C. analysis of the polymers.

Experimental Section

All manipulations were carried out under purified nitrogen in a Jacomex glove box or under argon using standard vacuum techniques. Solvents were distilled from the appropriate drying agent, stored over Na/benzophenone and vacuum-transferred to reaction vessels. ^1H- and ^{13}C-NMR spectra were recorded with AC 200 and DRX 500 Bruker spectrometers (297 K). − Polymer Analysis: Molecular weights and polydispersities were obtained by Steric Exclusion Chromatography (S.E.C.) on a Spectra-Physics chromatograph equipped with two detectors (a UV and a refractive index detector) connected in series. The calibration was carried out with PL-Lab polystyrene standards (EasiCal® PS-1, range $\bar{M}_w$ = 580−8.5 × 10^6). Each measurement was performed at 25°C in toluene as eluent, with a 1 ml/min flow rate. Two connected PL-Lab 5μ mixed-C 300 × 7.5 mm columns were used. The calculations for I_p and $\bar{M}_n$ were performed using GPC-Plus® software. Structural analysis of polyisoprene was conducted by ^{13}C- and ^1H-NMR spectroscopy and compared to commercially available samples. The isomeric purity was first evaluated by $^{13}C\{^1H\}$ sequences and then confirmed on the basis of ^1H-NMR data. − $SmCl_3(THF)_3$ and $NdCl_3(THF)_3$[26], $(Cp'_2SmCl)_2$ and $(Cp'_2SmMe)_2$[5] $C_3H_5Li(dioxane)$[10], 1,3-diisopropylimidazoline-2-ylidene $C(NiPr)_2(CMe)_2$[11], tritoxLi[27], $(C_3H_5)_4NdLi(dioxane)_{1.5}$[10], and $[Me_4C_2(C_5H_4MgCl)_2](THF)_4$[13] were prepared as described. $(C_3H_5)_4SmLi(dioxane)$ was synthesized following the procedure described for its neodymium homologue and its NMR data were in accordance with the original synthesis[23]. Ethereal solutions of MeLi were purchased from Aldrich. The diene (isoprene 99%) was dried over molecular sieves and distilled twice to remove the stabiliser. Elemental analyses were performed with a Fisons EA 1108 CHONS apparatus.

$[Cp'_2Sm(C_3H_5)]_n$ (**1**): A solution of $(Cp'_2SmCl)_2$ (0.39 g, 0.91 mmol) was added at −78°C to a slurry of $C_3H_5Li(dioxane)$ (0.13 g, 0.91 mmol) in toluene (20 ml). The mixture was stirred at −78°C for 30 min, and then warmed to room temperature for another 30 min. The solution turned red and LiCl was deposited. After filtration, the solvent was removed under reduced pressure and the residue extracted with pentane (3 × 30 ml). After evaporation of the pentane, a deep red oil was obtained (0.27 g, yield 68%). − $C_{21}H_{31}Sm$ (433.88): calcd. C 58.14, H 7.20; found C 58.27, H 7.33. − ^1H NMR (C_6D_6): δ = 16.79 (s, 1 H), 13.21 (s, 4 H), 9.56 (s, 2 H), 9.21 (s, 4 H), 6.43 (s, 2 H), −2.81 (s, 18 H).

A mixture of 10 mg (23 μmol) of **1** and 3 mg (22 μmol) of $C_3H_5Li(dioxane)$ in C_6D_6 was stirred by sonification, and Cp'_3Sm and $(C_3H_5)_4SmLi$ slowly precipitated from the mixtute and these compounds were detected by NMR.

$Cp'_2Sm(C_3H_5)$, $C(NiPr)_2(CMe)_2$ (**1′**): A mixture of **1** (0.247 g, 0.57 mmol) and 1 equiv. (0.103 g) of $C(NiPr)_2(CMe)_2$ in 20 ml of toluene was stirred at room temperature for 12 h. The solvent was evaporated and the residue extracted with pentane (3 × 20 ml). After filtration and concentration, a dark red solid was obtained (0.273 g, yield 78%). The NMR analysis revealed the presence of the adduct **1′**: ^1H NMR (C_6D_6): δ = 15.97 (s, 1 H), 12.72 (s, 4 H), 9.21 (s, 4 H), 8.10 (s, 4 H), 3.91 (m, 2 H), 1.72 (s, 6 H), 1.47 (d, 12 H), −2.51 (s, 18 H). This compound was accompanied by 10% of Cp'_3Sm. To remove the yellow contaminant Cp'_3Sm, the solid was washed with cold pentane. Red/black crystals were obtained by a further dissolution in pentane (15 ml), followed by filtration and slow concentration to a volume of ca. 3 ml. These crystals seemed suitable for X-ray analysis and one was mounted in a capillary tube. However, the crystal had melted after only a few minutes of exposure. After dissolution in deuterated benzene, NMR showed the invariable presence of 10% of Cp'_3Sm. − $C_{32}H_{51}N_2Sm$ (614.18): calcd. N 4.56; found N 4.58.

Cp'_2SmCl, $C(NiPr)_2(CMe)_2$ (**1″**): To a mixture of $(Cp'_2SmCl)_2$ (0.36 g, 0.84 mmol) and $C(NiPr)_2(CMe)_2$ (0.255 g, 1.41 mmol) was added 30 ml of toluene. The mixture was stirred at room temperature overnight and then filtered. The yellow solution was concentrated slowly to ca. 5 ml. Yellow crystals were collected 12 h later. The crystals were washed with pentane (10 ml) and dried under vacuum. Total yield: 0.235 g, 40%. A crystal was found that was

suitable for X-ray structure analysis (see below for further details), which revealed the presence of one toluene molecule per samarium atom. – Toluene adduct $C_{36}H_{54}ClN_2Sm$ (700.70): calcd. C 61.71, H 7.71, N 4.00; found C 61.24, H 7.93, N 4.37.

^{1}H-NMR analysis of the dissolved crystals revealed the presence of three compounds in solution (C_6D_6): **1″**: δ = 11.38 (s, 2 H), 10.45 (s, 2 H), 8.15 (s, 2 H), 7.94 (s, 2 H), 3.95 (m, 2 H), 1.18 (s, 18 H), 0.91 (s, 6 H), 0.57 (d, 12 H); Cp_3Sm and $Cp'SmCl_2[C(NiPr)_2(CMe)_2]_2$; **1‴**: δ = 10.72 (s, 2 H), 11.57 (s, 2 H), 1.51 (d, 24 H), 0.01 (s, 12 H), −0.5 (br., 9 H).

[Me$_4$C$_2$(C$_5$H$_4$)$_2$]Sm(C$_3$H$_5$)$_2$Li(dme) (**2**): (a) In an NMR tube a mixture of 9.17 mg (19.3 μmol) of $SmCl_3(THF)_3$ and 12 mg (19.3 μmol) of $[Me_4C_2(C_5H_4MgCl)_2](THF)_4$ was stirred by sonification in 0.4 ml of C_6D_6 and then the mixture was warmed at 60°C. First a pale yellow, and then an orange yellow colour developed, and after 20 min the reaction was complete; the ^{1}H-NMR spectrum recorded was consistent with $[Me_4C_2(C_5H_4)_2]SmClMgCl_2(THF)_n$. – NMR ($C_6D_6$) δ = 15.51 (s, 4 H), 8.16 (s, 4 H), 1.51 (s, 18 H). – After evaporation of the solvents, C_6D_6 (0.4 ml) was added. NMR analysis revealed the presence of $[Me_4C_2(C_5H_4)_2]SmCl(THF)MgCl_2(THF)_3$ (**4**) as the unique product. – NMR (C_6D_6): δ = 15.31 (s, 4 H), 8.05 (s, 4 H), 3.73 (s, 16 H), 1.34 (s, 16 H), 1.25 (s, 12 H). – 2 equivalents (5.28 mg) of $C_5H_3Li(C_4H_8O_2)$ were added, the solution became pink/red and a reddish precipitate was deposited that was partially soluble in the presence of the oxygenated solvents (7 THF + 2 dioxane molecules per Sm atom). – **2**: ^{1}H NMR (C_6D_6; 298 K): δ = 8.09 (s, 4 H), 5.97 (s, 4 H), 3.34 (dioxane + THF), 1.89 (s, 12 H), 1.25 (THF), the allylic signals could not be detected; (343 K): δ = 8.54 (s, 4 H), 7.99 (br., 2 H), 6.62 (s, 4 H), 5.76 (br., 8 H), 3.36 (dioxane + THF), 1.81 (s, 12 H), 1.32 (THF).

(b) A toluene solution of $[Me_4C_2(C_5H_4)_2]SmCl(THF)\cdot MgCl_2(THF)_2$ (**4**) was prepared following the published procedure[14] from 0.5 g (1.06 mol) of $SmCl_3(THF)_3$ and 0.66 g (1.06 mol) of $[Me_4C_2(C_5H_4MgCl)_2](THF)_4$ in 20 ml of toluene (instead of THF). Salts were removed by filtration and, at −30°C and with vigourous stirring, 0.29 g (2.12 mmol) of $C_3H_5Li(C_4H_8O_2)$ was added to the bright orange solution. The mixture turned pink within a few minutes and the temperature was allowed to rise to 20°C. Salts were removed by filtration and the solvent was evaporated under reduced pressure to give a red paste. This paste was dissolved in dimethoxyethane (20 ml) and the solvent was evaporated. The crude product was an expanded oil which was washed with ether (3 × 15 ml) to finally give a brick-red powder (yield 60%). – ^{1}H NMR (C_4D_8O): δ = 9.53 (m, 2 H), 8.61 (br., 4 H), 7.94 (s, 4 H), 7.07 (br., 4 H), 5.77 (s, 4 H), 3.35 (dme, 4 H), 3.19 (dme, 6 H), 1.70 (s, 12 H). – Crystals could be obtained as thin plates in a 75−25% mixture of dimethoxyethane and diethyl ether. – $C_{26}H_{40}LiO_2Sm$ (541.95): calcd. C 57.62, H 7.44; found C 57.20, H 7.29.

Cp′$_2$SmMe$_2$Li(dioxane) (**3**): To a stirred solution of $(Cp'_2SmCl)_2$ (0.39 g, 0.91 mmol) in toluene (30 ml) was slowly added, at −78°C, a 1 M ethereal solution of MeLi (2.0 μl, 2.0 mmol). The mixture was stirred for 2 h and then warmed to room temperature and stirred for a further 30 min. The mixture turned pale yellow and LiCl was deposited. The solution was filtered and the solvent evaporated. The residue was extracted with toluene (2 × 10 ml). The clear solution was concentrated and microcrystals were formed. After evaporation of the toluene, the powder was washed with pentane (2 × 10 ml) and dried in vacuo; a pale yellow solid was obtained (0.25 g, yield 64%) that was sparingly soluble in aromatic solvents. – ^{1}H NMR (C_6D_6): δ = 9.16 (s, 4 H), 8.86 (s, 4 H), −0.01 (s, 18 H), −4.08 (s, 6 H). – The solid was dissolved in 30 ml of toluene, a slight excess of dioxane (50 μl) was added and the solution was stirred for 1 h at ambient temperature. Slow evaporation of the solvent under reduced pressure gave pale yellow crystals. – ^{1}H NMR (C_6D_6): δ = 9.77 (s, 4 H), 9.07 (s, 4 H), 4.15 (s, 8 H), −0.05 (s, 18 H), −5.12 (s, 6 H). – $C_{24}H_{40}SmLiO_2$ (517.92): calcd. C 55.66, H 7.79; found C 55.29, H 7.85.

Crystal Data for Cp′$_2$ClSm·C(NiPr)$_2$(CMe)$_2$: $C_{29}H_{46}ClN_2Sm\cdot C_7H_8$, M = 700.6, monoclinic, space group $P2_1/c$, a = 13.351(2), b = 17.005(3), c = 16.443(2) Å, β = 101.011(12)°, V = 3664(1) Å^3, Z = 4, D_c = 1.27 gcm^{-3}, μ(Mo-K_α) = 1.7 mm^{-1}. A yellow crystal was mounted on a capillary on an Enraf-Nonius CAD4 diffractometer at 20°C. Unfortunately, the crystal underwent rapid decomposition under X-ray exposure and only the first shell of data with 17.90° < θ < 20.58° was used to solve and refine the structure (decay = 82%). The solution was obtained by interpretation of the Patterson map[28] and refined on F^2 using all the 1228 independent reflections collected[29]. Due to the lack of data, only the samarium and chlorine atoms were anisotropically refined. Hydrogen atoms were included, when possible, at their calculated positions. The Cp rings were constrained to a regular pentagon and the toluene ring to a regular hexagon. The methyl group of the toluene solvate was not located. The final agreement indices are $R_w(F^2)$ = 0.124 and $R(F)$ = 0.102 for all data (1228 independent reflections) and 135 parameters; $R(F)$ = 0.047 for 822 data with $I > 2\sigma(I)$; goodness of fit = 0.94 and Δρ = 0.344 and −0.260 e Å^{-3}. Crystallographic data (excluding structure factors) for the structure reported in this paper have been deposited with the Cambridge Crystallographic Data Centre as supplementary publication No. CCDC-101393. Copies of the data can be obtained free of charge on application to CCDC, 12 Union Road, Cambridge CB21EZ, UK [Fax: internat. +44-1223/336-033; E-mail: deposit@ccdc.cam.ac.uk].

In situ Preparation of Catalytic Systems. – System A: In an NMR tube was placed 12 mg of $[Me_4C_2(C_5H_4MgCl)_2](THF)_4$, 9 mg of $NdCl_3(THF)_3$, and 5.3 mg of C_3H_5Li(dioxane). 0.5 ml of C_6D_6 was added and the mixture was stirred by sonification until the signals of the starting materials totally disappeared: a bright green colour developed and white salts precipitated. The benzene (and the excess THF and dioxane) was evaporated and the residue dissolved in toluene. The toluene solution was transferred into a flask and the solvents were evaporated. The green solid was used for polymerization.

System B: To a C_6D_6 solution of 8 mg of tris-*tert*-butylmethanol – "tritoxH" – (dried over molecular sieves), was added 10.3 mg of $(C_3H_5)_4NdLi(dioxane)_{1.5}$. The tube was heated (60°C) and the mixture stirred by sonification, which led to a green, sparingly soluble material; very large allylic signals with paramagnetic shifts in the range δ = −10 to −50 and a paramagnetic *tert*-butyl signal at δ = 10 were observed in the ^{1}H-NMR spectrum. The solvent was partially evaporated, THF was added and the solvents partially evaporated once again. The green solid was then soluble in benzene and the solution was transferred into the polymerization flask. The solvents were evaporated before isoprene was added.

Polymerization Experiments: (1) Diene polymerization: The catalyst (10 mg) was introduced into a flask connected to a vacuum line. The diene (3 ml) was then condensed on to it and the stirred solution was heated at 50°C during 5 h. Depending on the activity of the catalyst, the mixture can become highly viscous; the flask was opened to the air and the contents dissolved in the required volume (5−15 ml) of toluene. The toluene solution was poured into 200 ml of ethanol and the polymer precipitated. The liquors were

decanted and the solid dried (12 Torr, 1−2 d) and weighed before sampling for analysis (^{1}H and ^{13}C NMR, molecular weight, polydispersity).

(2) Ethene polymerization: the reaction was conducted at 60°C and *p*(ethene) = 4 bar[25].

[1] D. J. Wilson, *Makromol. Chem. Macromol. Symp.* **1993**, *66*, 273−288.
[2] B. J. Burger, M. E. Thomson, W. D. Cotter, J. E. Bercaw, *J. Am. Chem. Soc.* **1990**, *112*, 1566.
[3] G. Jeske, H. Lauke, H. Mauermann, P. N. Swepston, H. Schumann, T. J. Marks, *J. Am. Chem. Soc.* **1985**, *107*, 8091−8103.
[4] W. J. Evans, D. M. Decoster, J. Greaves, *Organometallics* **1996**, *15*, 3210−3221.
[5] D. Baudry, A. Dormond, B. Lachot, M. Visseaux, G. Zucchi, *J. Organomet. Chem.* **1997**, *547*, 157−165.
[6] M. Visseaux, D. Baudry, A. Dormond, C. T. Qian, *C. R. Acad. Sci. Paris* **1996**, *323*, 415−419.
[7] M. Visseaux, D. Baudry, A. Dormond, C. T. Qian, *J. Organomet. Chem.*, in press.
[8] R. Taube, H. Windisch, S. Maiwald, *Macromol. Symp.* **1995**, *89*, 393−409.
[9] A. L. Wayda, *J. Organomet. Chem.* **1989**, *361*, 73−78.
[10] R. Taube, S. Maiwald, J. Sieler, *J. Organomet. Chem.* **1996**, *513*, 37−47.
[11] N. Kuhn, T. Kratz, *Synthesis* **1993**, *6*, 561−562.
[12] W. A. Herrmann, F. C. Munck, G. R. J. Artus, O. Runte, R. Anwander, *Organometallics* **1997**, *16*, 682−688.
[13] H. Schwemlein, H. H. Brintzinger, *J. Organomet. Chem.* **1983**, *254*, 69−73.
[14] C. Sun, G. Wei, Z. Jin, W. Chen, *J. Organomet. Chem.* **1993**, *453*, 67−64.
[15] C. Sun, G. Wei, Z. Jin, W. Chen, *Polyhedron* **1994**, *13*, 1483−1487.
[16] A. Recknagel, F. T. Edelmann, *Angew. Chem. Int. Ed. Engl.* **1991**, *30* , 693; *Angew. Chem.* **1991**, *103*, 720.
[17] P. Yan, N. Hu, Z. Jin, W. Chen, *J. Organomet. Chem.* **1990**, *391*, 313−320.
[18] C. T. Qian, C. Ye, H. Lu, Y. Li, Y. Huang, *J. Organomet. Chem.* **1984**, *263*, 333−343.
[19] J. A. Smith, J. Von Seyerl, G. Huttner, H. H. Brintzinger, *J. Organomet. Chem.* **1979**, *173*, 175−185.
[20] Q. Shen, M. Qi, J. Guan, Y. Lin, *J. Organomet. Chem.* **1991**, *406*, 353−361.
[21] A. Cano, T. Cuenca, P. Gomez-Sal, A. Manzanero, P. Royo, *J. Organomet. Chem.* **1996**, *526*, 227−235.
[22] W. D. Luke, A. Streitwieser, *J. Am. Chem. Soc.* **1981**, *103*, 3241−3243.
[23] M. Brunelli, S. Poggio, U. Pedretti, G. Lugli, *Inorg. Chim. Acta* **1987**, *131*, 281−85.
[24] R. Taube, H. Windisch, H. Weissenborn, H. Hemling, H. Schumann, *J. Organomet. Chem.* **1997**, *548*, 229−236.
[25] Polymerization tests were performed by Dr. C. Boisson at the Laboratoire de Chimie des Procédés de Polymérisation, Director Dr. R. Spitz, Lyon, France.
[26] M. D. Taylor, C. P. Carter, *J. Inorg. Nucl. Chem.* **1962**, *24*, 387.
[27] T. V. Lubben, P. T. Wolczanski, G. D. Van Duyne, *Organometallics* **1984**, *3*, 977−983.
[28] G. M. Sheldrick, *SHELXS: Program for Crystal Structure Determination*, University of Göttingen, **1997**.
[29] G. M. Sheldrick, *SHELXL: Program for Crystal Structure Refinement*, University of Göttingen, **1997**.

[I98107]

Advances in the Reactivity of Amido-Bridged Binuclear Carbonylruthenium Complexes – Derivative Chemistry of the Cationic Complex $[Ru_2(\mu\text{-dan})(\mu\text{-H})(CO)_6][BF_4]$ (H_2dan = 1,8-Diaminonaphthalene)

Javier A. Cabeza*, Jorge García-Díez, and Víctor Riera

Departamento de Química Orgánica e Inorgánica, Instituto de Química Organometálica "Enrique Moles", Universidad de Oviedo-CSIC, E-33071 Oviedo, Spain
Fax: (internat.) +34-985103446
E-mail: jac@sauron.quimica.uniovi.es

Received April 20, 1998

Keywords: Ruthenium / Cationic complexes / Hydrido complexes / N ligands / P ligands

The reactivity of the cationic amido-bridged binuclear ruthenium carbonyl complex $[Ru_2(\mu\text{-dan})(\mu\text{-H})(CO)_6]^+$ (H_2dan = 1,8-diaminonaphthalene) (**2**) with some anionic and neutral nucleophilic reagents has been investigated. The reaction of **2** with halide anions gives neutral products, $[Ru_2X(\mu\text{-dan})(\mu\text{-H})(CO)_5]$ [X = Cl (**3**), Br (**4**), I (**5**)], which result from the regiospecific substitution of the halide anion for one of the CO ligands *trans* to the bridging hydride. Compound **3** is more conveniently prepared by treatment of the neutral complex $[Ru_2(\mu\text{-dan})(CO)_6]$ with gaseous hydrogen chloride. The reaction of **2** with triphenylphosphane affords the disubstituted product of C_{2v} symmetry $[Ru_2(\mu\text{-dan})(\mu\text{-H})(PPh_3)_2(CO)_4]^+$ (**7a**), which can be transformed into the asymmetric isomer **7b** under thermal conditions (70 °C, 10 h) or under acid catalysis ($[HOEt_2][BF_4]$, 18 °C, 1 min). Such isomerization reactions can be prevented by adding an excess of triphenylphoshane to the solutions. The complexes **7a** and **7b** can also be prepared by treating the neutral complex $[Ru_2(\mu\text{-dan})(PPh_3)_2(CO)_4]$ with $[HOEt_2][BF_4]$ in the presence (for **7a**) or in the absence (for **7b**) of triphenylphoshane. In addition, compound **3** reacts with triphenylphoshane at room temperature to give the symmetric cationic complex **7a** , whereas the reaction of complex **5** with triphenylphoshane requires higher temperature and gives the asymmetric isomer **7b**.

Introduction

The interest in the synthesis and reactivity of late-transition-metal amido complexes has grown considerably[1]. This research activity has been carried out in parallel to investigations on binuclear carbonylruthenium(I) complexes[2]. In connection with these two research fields, we have previously reported the synthesis of the binuclear amido-bridged carbonylruthenium(I) complex $[Ru_2(\mu\text{-dan})(CO)_6]$ (H_2dan = 1,8-diaminonaphthalene) (**1**)[3][4]. Reactivity studies on compound **1** have shown that it can be protonated at the metal atoms to give the cationic derivative $[Ru_2(\mu\text{-dan})(\mu\text{-H})(CO)_6]^+$ (**2**) and that it readily undergoes carbonyl substitution reactions with phosphane ligands to give disubstituted derivatives such as $[Ru_2(\mu\text{-dan})(PPh_3)_2(CO)_4]$[4]. The basicity and the *cis*-labilizing character of the bridging amido ligand have been suggested as the factors responsible for the observed reactivity. However, compound **1** does not react with hard ligands, such as the halide anions[5].

As cationic complexes should be more prone than their neutral precursors to undergo reactions with basic reagents[6][7], and as the protonation of neutral complexes should increase the hard character of the metal atoms, we thought it would be interesting to study the substitution chemistry of the cationic compound **2** and to compare it with that of its neutral precursor **1**. No such a comparative study is known for binuclear complexes, although related studies with trinuclear carbonylruthenium clusters have been reported[7].

Results and Discussion

Reactions with Halide Anions

Treatment of the ionic compound $[Ru_2(\mu\text{-dan})(\mu\text{-H})(CO)_6][BF_4]$ (**2**$[BF_4]$) with dichloromethane solutions of [PPN]X (X = Cl, Br, I) or $[Et_4N]$Br led to the instantaneous formation of the neutral derivatives $[Ru_2X(\mu\text{-dan})(\mu\text{-H})(CO)_5]$ [X = Cl (**3**), Br (**4**), I (**5**)] in quantitative spectroscopic (IR) yields. However, this synthetic method did not lead to analytically pure products because the complexes could not be efficiently separated from the ionic tetrafluoroborate byproducts Q$[BF_4]$ (Q = PPN, Et_4N) by either fractional crystallization (similar solubility in organic solvents) or chromatographic methods (the complexes did not elute on silica and alumina). In addition, treatment of **2**$[BF_4]$ with an excess of solid KX (X = Cl, Br, I) in dichloromethane also gave compounds **3**–**5**, but the reactions were slow. The bromo and iodo complexes **4** and **5** were efficiently prepared in pure form by this method, requiring reaction times of 40 and 20 h, respectively. The reaction of **2**$[BF_4]$ with KCl was very slow, being incomplete (ca. 70% conversion) after one week. It should be noted that KCl is nearly insoluble in chlorinated solvents, and that **2**$[BF_4]$ undergoes

 © WILEY-VCH Verlag GmbH, D-69451 Weinheim, 1998 1434–1948/98/1111–1729 $ 17.50+.50/0

deprotonation in basic solvents such as acetone, THF, or water, thus preventing the use of such solvents in the reactions. The most convenient method to prepare the chloro complex **2** in pure form turned out to be the treatment of the neutral hexacarbonyl complex **1** with a dichloromethane solution of HCl.

Scheme 1

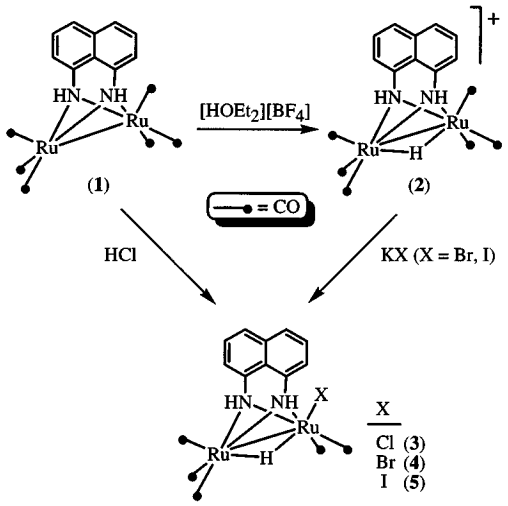

The structure proposed for compounds **3**−**5** in Scheme 1 is based on their analytical and spectroscopic data. Their IR spectra are nearly identical, suggesting a common structure for the three compounds, showing the ν(CO) absorptions at lower wavenumbers (2115−1985 cm^{-1}) than those of the cationic starting complex **2** (2136−1991 cm^{-1})[4]. Their ^{1}H-NMR spectra (Table 1) show one hydride resonance and four resonances for the dan ligand (three aromatic and one N*H*), indicating the presence of a mirror plane that divides the dan ligand into two identical halves. The $^{13}C\{^1H\}$-NMR sprectrum of compound **5** (taken as a representative example) shows three carbonyl resonances in a 2:2:1 ratio (relaxation delay 2 s), confirming the presence of five CO ligands. Interestingly, only the smallest carbonyl signal is split into a doublet in the proton-coupled ^{13}C-NMR spectrum, indicating that only one CO ligand is in a *trans* position to the hydride. Thus, these data confirm the structure shown in Scheme 1 and rule out an alternative structure which would have the hydride and halide ligands in terminal and bridging positions, respectively.

It seems that the *acidic* (and not merely the *cationic*) character of complex **2** might be responsible for the observed reactivity. In fact, complex **2** could reversibly protonate the halide anions to give the corresponding hydrogen halides which would then react in a *concerted* way with the conjugated base **1** to give the substituted products **1**−**3**.

As halide anions are worse π-acceptor ligands than carbon monoxide, the substitution of halide anions for carbonyl ligands in ruthenium complexes has been previously observed only on a few occasions on neutral[8][9] and cationic[6b][6c][10] carbonyl cluster compounds. As mentioned in the Introduction, the neutral compound **1** does not react with halide anions[5]. Curiously, it has been reported that the anionic binuclear osmium(I) complexes $[PPN][Os_2X(\mu\text{-}O_2CMe)_2(CO)_5]$ (X = Cl, I) can be prepared by treatment of the solvated complex $[Os_2(\mu\text{-}O_2CMe)_2(CO)_5(thf)]$ with [PPN]X[11]. Unfortunately, all attempts to prepare any solvated derivative of complex **1** were unsuccessful.

Table 1. Comparative ^{1}H- and $^{31}P\{^1H\}$-NMR data for compounds **2**−**7**[a]

Comp.	δ_H(μ-H)	δ_H(dan)	δ_P(PPh_3)
2[b][c]	−10.95 (s)	7.82 (d) [7.7], 7.60 (d) [7.7], 7.43 (t) [7.7], 7.56 (s, br.)	
3	−15.30 (s)	7.62 (dd) [7.6, 1.1], 7.25 (t) [7.6], 7.16 (dd) [7.6, 1.1], 5.14 (s, br.)	
4	−14.37 (s)	7.65 (dd) [7.6, 1.1], 7.29 (t) [7.6], 7.35 (dd) [7.6, 1.1], 5.05 (s, br.)	
5	−12.56 (s)	7.60 (dd) [7.6, 1.0], 7.28 (t) [7.6], 7.14 (dd) [7.6, 1.1], 4.85 (s, br.)	
6[b]		6.83 (d) [7.8], 6.39 (t) [7.8], 5.98 (d) [7.8], 4.23 (s, br.)	27.7 (s)
7a	−9.63 (t) {41.4}	6.73 (d) [7.9], 6.54 (d) [7.9], 6.29 (t) [7.9], 5.24 (s, br.)	37.6 (s)
7b	−10.10 (dd) {43.5, 7.4}	7.45 (d) [7.7], 6.85 (t) [7.5], 6.67 (t) [7.7], 5.87 (d) [7.5], 2.26 (s, br.)[d]	49.4 (s), 38.9 (s)

[a] Spectra recorded in $CDCl_3$; multiplicities are given in parentheses; coupling constants (Hz) are given in square brackets [$J_{H\text{-}H}$] or braces {$J_{H\text{-}P}$}. − [b] Data taken from ref.[4]. − [c] Spectrum recorded in $(CD_3)_2CO$ containing 10% $[HOEt_2][BF_4]$. − [d] Other resonances of the dan ligand are obscured by those of the PPh_3 ligand.

Reactions with Triphenylphosphane

Complex **2** reacted instantaneously with triphenylphosphane at room temperature to give the disubstituted derivative $[Ru_2(\mu\text{-dan})(\mu\text{-H})(PPh_3)_2(CO)_4]^+$ (**7a**), regardless of the ratio of the reactants. The use of a phosphane/complex ratio smaller than two resulted in a mixture of **7a** and unreacted **2**. The symmetric (C_{2v}) structure shown for the cation **7a** in Scheme 2 is based on spectroscopic data. The $^{31}P\{^1H\}$- and ^{1}H-NMR spectra (Table 1) are consistent with the existence of two mirror planes, since they only show one singlet in the $^{31}P\{^1H\}$ spectrum and five resonances in the ^{1}H spectrum (four for the dan ligand and one for the hydride). In particular, the hydride resonance is a triplet with a large J(H-P) coupling constant (41.4 Hz). It is generally accepted that large (> 20 Hz) ^2J(H-P) coupling constants are indicantive of a trans arrangement of hydride and phosphane ligands on a metal carbonyl complex[7], although some exceptions to this rule have been reported for pentacoordinated iron complexes[12].

In an attempt to make **7a**$[BF_4]$ by an alternative route, we treated a dichloromethane solution of the symmetric (C_{2v}) neutral disubstituted compound $[Ru_2(\mu\text{-dan})(PPh_3)_2(CO)_4]$ (**6**) with an excess of $[HOEt_2][BF_4]$ in diethyl ether. The reaction was instantaneous but, to our surpise, the product was not **7a** but the asymmetric isomer **7b** (Scheme 2), as inferred from its $^{31}P\{^1H\}$ spectrum, which consists of two singlet resonances, and from its ^{1}H spectrum, which shows

Scheme 2

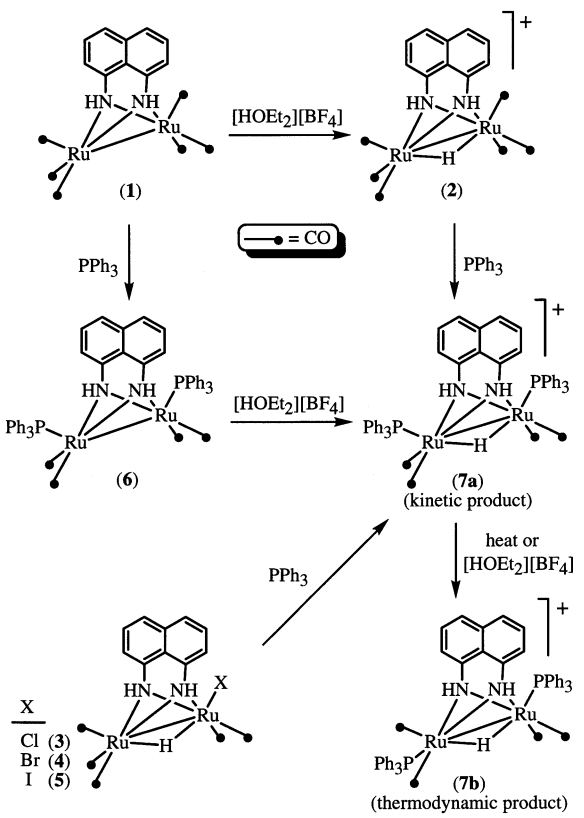

the hydride resonance as a doublet of doublets with J(H-P) coupling constants (43.5 and 7.4 Hz) in agreement with a structural assignment in which the hydride is *trans* to a phosphorus atom and *cis* to the other[7].

The reactions of the halide derivatives **3** and **5** with triphenylphosphane were also studied. The chloro complex **3** reacted slowly (6 h) with two equivalents triphenylphosphane in 1,2-dichloroethane at room temperature to give the symmetric cationic derivative **7a**. No monosubstituted derivatives were detected when the reaction was monitored by IR or $^{31}P\{^1H\}$ NMR. Curiously, no reaction was observed with the iodo derivative **5** under the same conditions, but it gave the asymmetric cationic derivative **7b** within 30 min when the reaction was carried out at reflux.

The above results prompted us to try to establish whether the transformations of **7a** into **7b** or of **7b** into **7a** were possible. We found that (a) complex **7a** can be quantitatively transformed into **7b** under thermal conditions (1,2-dichloroethane, reflux temperature) and that the rate of the cation isomerization depends on the accompanying anion, being faster for chloride (30 min) than for tetrafluoroborate (10 h), (b) the isomerization reaction is catalysed by acids, since the addition of $[HOEt_2][BF_4]$ to a dichloromethane solution of **7a** at room temperature resulted in its instantaneous transformation into **7b**, (c) this isomerization process is inhibited by the presence of free triphenylphosphane, regardless of the presence of acid in the solution, and (d) by no means could the transformation of **7b** into **7a** be achieved. Therefore, it is clear that **7a** is the kinetic isomer and that **7b** is the thermodynamic isomer, and that the isomerization takes place through a dissociative mechanism which requires the decoordination of triphenylphosphane in the activation step.

To our knowledge, no previous isomerization reactions of phosphane-substituted ligand-bridged binuclear ruthenium complexes have been described, but a few examples of such reactions have been reported for trinuclear clusters[7].

Further work on the reactivity of binuclear cationic carbonylruthenium complexes, extending the reactions to other P-donor ligands, such as phosphites, diphosphanes, etc., is in progress.

Financial support from the *Dirección General de Enseñanza Superior* (Project PB95−1042) is gratefully acknowledged.

Experimental Section

General: IR: Perkin-Elmer FT 1720-X. − NMR: Bruker AC-200 and AC−300, 20°C, internal TMS (for ^1H and ^{13}C) or external 85% H_3PO_4 (for ^{31}P) as standards. − Microanalyses: Perkin Elmer 2400. − Solvents were dried with sodium diphenyl ketyl (diethyl ether, hydrocarbons) or CaH_2 (dichloromethane, 1,2-dichloroethane) and distilled under nitrogen prior to use. The reactions were carried out under nitrogen with Schlenk vacuum-line techniques, and were routinely monitored by solution IR spectroscopy (carbonyl stretching region). Compounds **1**, **2**, and **6** were prepared as described previously[4]. A saturated solution of HCl in dichloromethane was prepared by bubbling gaseous HCl (formed by addition of 98% sulfuric acid to solid NaCl) through the solvent. All the other reagents were purchased from Aldrich and were used as received.

[$Ru_2Cl(\mu$-dan$)(\mu$-H$)(CO)_5$] (**3**): A saturated solution of HCl in dichloromethane (2 ml) was added to a solution of compound **1** (100 mg, 0.190 mmol) in the same solvent (10 ml). The original pale yellow colour slightly darkened and the IR spectrum of the resulting solution revealed the complete transformation of **1** into a new compound. The solvent was removed under reduced pressure and the residue was washed with hexane (2 × 10 ml) and dried to give complex **3** as a yellow solid (83 mg, 82%). − $C_{15}H_9ClN_2O_5Ru_2$ (534.86): calcd. C 33.68, H 1.70, N 5.24; found C 33.21, H 1.46, N, 4.91. − IR (CH_2Cl_2): $\tilde{\nu}$ = 2115 cm^{-1} (m), 2053 (s), 1985 (m).

[$Ru_2Br(\mu$-dan$)(\mu$-H$)(CO)_5$] (**4**): Solid KBr (96 mg, 0.807 mmol) was added to a solution of **2**[BF_4] (50 mg, 0.081 mmol) in dichloromethane (10 ml). The resulting suspension was stirred for 40 h, when the IR spectrum of the solution revealed the absence of the starting material. The suspension was filtered through a Celite filter and the resulting yellow solution was concentrated to dryness. The solid residue was washed with hexane (2 × 5 ml) and dried to give complex **4** as a yellow solid (35 mg, 75%). − $C_{15}H_9BrN_2O_5Ru_2$ (579.31): calcd. C 31.10, H 1.57, N 4.84; found C 30.91, H 1.66, N 4.65. − IR (CH_2Cl_2): $\tilde{\nu}$ = 2115 cm^{-1} (m), 2052 (s), 1987 (m).

[$Ru_2I(\mu$-dan$)(\mu$-H$)(CO)_5$] (**5**): Solid KI (132 mg, 0.795 mmol) was added to a solution of **2**[BF_4] (50 mg, 0.081 mmol) in dichloromethane (10 ml). The resulting suspension was stirred for 20 h, when the IR spectrum of the solution revealed the absence of the starting material. The suspension was filtered through a Celite filter and the resulting solution was concentrated to dryness. The solid residue was washed with hexane (2 × 5 ml) and dried to give complex **5** as a yellow-orange solid (34 mg, 67%). − $C_{15}H_9IN_2O_5Ru_2$

(626.31): calcd. C 28.77, H 1.45, N 4.47; found C 28.51, H 1.58, N 4.09. – IR (CH_2Cl_2): $\tilde{\nu}$ = 2114 cm^{-1} (m), 2051 (s), 1986 (m). – $^{13}C\{^1H\}$ NMR (CD_2Cl_2): δ = 196.9 (2 CO), 190.2 (2 CO), 181.9 (1 CO), 148.7 (2 C), 135.4 (1 C), 126.1 (2 C), 125.3 (1 C), 124.5 (2 C), 114.7 (2 C) (all singlets); the resonances at δ = 181.9, 126.1, 124.5, and 114.7 are split into doublets in the proton-coupled spectrum.

[$Ru_2(\mu$-dan)(μ-H)(PPh_3)$_2$(CO)$_4$][BF_4] (**7a**[BF_4], symmetric isomer): Solid **2**[BF_4] (25 mg, 0.041 mmol) was added to a stirred solution of PPh_3 (22 mg, 0.084 mmol) in dichloromethane (10 ml). The reaction was instantaneous (IR). No changes were observed in the IR spectrum of this solution after 20 h. The solvent was removed under reduced pressure and the residue was washed with hexane (2 × 5 ml) and dried to give **7a**[BF_4] as a yellow solid (36 mg, 80%). – $C_{50}H_{39}BF_4N_2O_4P_2Ru_2$ (1082.79): calcd. C 55.46, H 3.63, N 2.59; found C 54.92, H 3.94, N 2.30. – IR (CH_2Cl_2): $\tilde{\nu}$ = 2063 cm^{-1} (s), 2047 (m), 1998 (s).

[$Ru_2(\mu$-dan)(μ-H)(PPh_3)$_2$(CO)$_4$][BF_4] (**7b**[BF_4], asymmetric isomer): An excess of [$HOEt_2$][BF_4] (0.2 ml, 60% solution in diethyl ether) was added to a solution of complex **6** (100 mg, 0.100 mmol) in dichloromethane (10 ml). The reaction was instantaneous (IR).- The solvent was removed under reduced pressure and the oily residue was washed with diethyl ether (3 × 5 ml) and dried to give **7b**[BF_4] as a yellow solid (87 mg, 80%). – $C_{50}H_{39}BF_4N_2O_4P_2Ru_2$ (1082.79): calcd. C 55.46, H 3.63, N 2.59; found C 55.42, H 3.83, N 2.39. – IR (CH_2Cl_2): $\tilde{\nu}$ = 2063 cm^{-1} (m), 2051 (s), 2000 (s). – $^{13}C\{^1H\}$ NMR ($CDCl_3$): δ = 196.5 (d, *J* = 11.1 Hz, 1 CO), 196.4 (d, *J* = 12.6 Hz, 1 CO), 194.7 (d, *J* = 12.9 Hz, 1 CO), 190.4 (t, *J* = 10.9 Hz, 1 CO), 150.3 (1 C), 147.4 (1 C), 135–112 (complex mixture of signals).

Protonation of Complex **6** *in the Presence of Triphenylphosphane:* An excess of [$HOEt_2$][BF_4] (0.2 ml, 60% solution in diethyl ether) was added to a solution of PPh_3 (105 mg, 0.400 mmol) and complex **6** (100 mg, 0.100 mmol) in dichloromethane (10 ml). After 3 min, the IR spectrum of the resulting solution showed only the presence of the symmetric complex **7a**, remaining unchanged after 12 h. The solvent was removed under reduced pressure and the residue was washed with diethyl ether (3 × 5 ml) and dried to give pure **7a**[BF_4] (IR, ^{31}P NMR) (75 mg, 69%).

Reaction of Complex **3** *with Triphenylphosphane:* A solution of complex **3** (100 mg, 0.187 mmol) and triphenylphosphane (98 mg, 0.375 mmol) in 1,2-dichloroethane (10 ml) was stirred at room temperature for 6 h, when the IR spectrum of the solution showed the complete transformation of **3** into the symmetric cationic derivative **7a**.

Reaction of Complex **5** *with Triphenylphosphane:* A solution of complex **5** (35 mg, 0.056 mmol) and triphenylphosphane (30 mg, 0.113 mmol) in 1,2-dichloroethane (10 ml) was stirred at room temperature for 1 h, but no reaction was observed (IR). The solution was then heated to reflux temperature. After 30 min, the IR spectrum showed the complete transformation of **5** into the asymmetric cationic derivative **7b**.

Thermal Isomerization of **7a** *to* **7b**: A solution of **7a**[BF_4] (50 mg, 0.046 mmol) in 1,2-dichloroethane (20 ml) was stirred at reflux temperarure. The reaction was monitored by IR spectroscopy, which showed the complete transformation of **7a** into **7b** after 10 h. When the chloride salt **7a**[Cl] was used as starting material, under analogous conditions, the transformation of **7a** into **7b** took only 30 min.

Acid-Catalysed Isomerization of **7a** *to* **7b**: [$HOEt_2$][BF_4] (0.2 ml, 60% solution in diethyl ether) was added to a solution of **7a**[BF_4] (50 mg, 0.046 mmol) in dichloromethane (20 ml). The IR spectrum of the resulting solution showed the complete transformation of **7a** into **7b**.

[1] For reviews on late-transition-metal amido complexes, see: [1a] M. D. Fryzuk, C. D. Montgomery, *Coord. Chem. Rev.* **1989**, *95*, 1–40. – [1b] H. E. Bryndza, *Chem. Rev.* **1988**, *88*, 1163–1188.

[2] For a review on binuclear ruthenium(I) complexes containing N-donor ligands, see: J. A. Cabeza, J. M. Fernández-Colinas, *Coord. Chem. Rev.* **1993**, *126*, 319–336.

[3] J. A. Cabeza, V. Riera, M. A. Pellinghelli, A. Tiripicchio, *J. Organomet. Chem.* **1989**, *376*, C23-C25.

[4] J. A. Cabeza, J. M. Fernández-Colinas, V. Riera, M. A. Pellinghelli, A. Tiripicchio, *J. Chem. Soc., Dalton Trans.* **1991**, 371–377.

[5] J. A. Cabeza, J. M. Fernández-Colinas, unpublished results.

[6] [6a] J. A. Cabeza, I. del Río, V. Riera, F. Grepioni, *Organometallics* **1995**, *14*, 3124–3126. – [6b] J. A. Cabeza, I. del Río, V. Riera, F. Grepioni, *Organometallics* **1997**, *16*, 812–815. – [6c] J. A. Cabeza, I. del Río, V. Riera, S. García-Granda, S. B. Sanni, *Organometallics* **1997**, *16*, 1743–1748.

[7] [7a] P. L. Andreu, J. A. Cabeza, V. Riera, C. Bois, Y. Jeannin, *J. Chem. Soc., Dalton Trans.* **1990**, 3347–3353. – [7b] P. L. Andreu, J. A. Cabeza, M. A. Pellinghelli, V. Riera, A. Tiripicchio, *Inorg. Chem.* **1991**, *30*, 4611–4616. – [7c] P. L. Andreu, J. A. Cabeza, J. L. Cuyás, V. Riera, *J. Organomet. Chem.* **1992**, *427*, 363–368. – [7d] P. L. Andreu, J. A. Cabeza, V. Riera, *Inorg. Chim. Acta* **1991**, *186*, 225–230.

[8] See, for example: [8a] G. Lavigne, H. D. Kaesz, *J. Am. Chem. Soc.* **1984**, *106*, 4647–4648. – [8b] N. Lugan, G. Lavigne, J. M. Soulie, S. Fabre, P. Kalck, J. Y. Saillard, J. F. Halet, *Organometallics* **1995**, *14*, 1712–1731 and references therein.

[9] See, for example: [9a] S. H. Han, G. L. Geoffroy, B. D. Dombek, A. L. Rheingold, *Inorg. Chem.* **1988**, *27*, 4355–4361. – [9b] T. Chin-Choy, W. T. Harrison, G. D. Stucky, N. Keder, P. C. Ford, *Inorg. Chem.* **1989**, *28*, 2028–2029 and references therein.

[10] J. A. Cabeza, F. J. Lahoz, A. Martín, *Organometallics* **1992**, *11*, 2754–2756.

[11] A. J. Deeming, N. P. Randle, M. B. Hursthouse, R. L. Short, *J. Chem. Soc., Dalton Trans.* **1987**, 2473–2477.

[12] C. E. Ash, M. Y. Darensbourg, M. B. Dahl, *J. Am. Chem. Soc.* **1987**, *109*, 4173–4180.

[98118]

New Monomers for Organometallic Poly-*p*-xylylenes: Synthesis of Silyl-, Germyl- and Stannyl[2.2]paracyclophane Derivatives☆

Elena Popova[a], Dmitrii Antonov[b], Elena Sergeeva[b], Evgenii Vorontsov[b], Adam Stash[a], Valeria Rozenberg*[b], and Henning Hopf*[c]

Karpov Institute of Physical Chemistry[a],
Vorontsovo Pole 10, 103064 Moscow, Russia
E-mail: gerasim@cc.nifhi.ac.ru

A. N. Nesmeyanov Institute of Organoelement Compounds, Russian Academy of Science[b],
Vavilova 28, 117813 Moscow, Russia
E-mail: lera@ineos.ac.ru

Institute of Organic Chemistry, Techical University of Braunschweig[c],
Hagenring 30, D-38106 Braunschweig, Braunschweig
E-mail: h.hopf@tu-bs.de

Received May 4, 1998

Keywords: Cyclophanes / σ-Bonded silyl-, germyl-, stannyl derivatives / Grignard reactions

Symmetrically 4,16-disubstituted (**3a–c**) and bridged (**6a**, **b**) organometallic paracyclophane derivatives have been synthesized for use as monomeric precursors of organometallic poly-*p*-xylylenes. Both types of compounds were obtained by lithiation of the appropriately substituted paracyclophane bromides (**1** or **4**) and subsequent quenching of the resulting lithioparacyclophane derivatives with organometallic electrophiles. For the synthesis of 4,16-bis(trimethylsilyl)[2.2]paracyclophane (**3a**) we also examined the Grignard reaction, and as a result the first successful use of a 4,16-bis Grignard reagent is described. According to the spectral data, the bridged compounds **6a, c** are formed as diastereomeric mixtures of a *meso*- and a *d,l* form. The diastereomers were separated by fractional recrystallization and characterized.

Although numerous functional groups have been introduced into the [2.2]paracyclophane nucleus[1], relatively little is known about these bridged aromatic compounds when they bear metal-containing substituents. To date, only mono(trimethylstannyl)-[2], 4,16-bis(triphenylphosphanegold)-[3], and several trimethylsilyl-substituted paracyclophane derivatives[4] have been synthesized, among them the *meso* and *d,l* diastereomers of dimethylbis([2.2]paracyclophan-4-yl)silane[5].

In principle, these derivatives could find wide application. They are not only of interest because of their stereochemical properties − any monosubstituted [2.2]paracyclophane is chiral, regardless of the position of the substituent in the system − but they could serve as ligands for new metal complexes and be used as monomeric precursors of novel, metal-containing polymers. The parent hydrocarbon is an important monomer in polymer chemistry − the poly-*p*-xylylene (PPX) polymer derived from it is called parylene®. Recently, we succeeded in preparing PPX films containing nanosize metal particles[6][7], which could be used as sensor devices for the detection of gaseous compounds in air[8]. In our methodology, developed for the preparation of polymer−metal nanocomposites, an organometallic PPX film (A or B in Scheme 1) is first produced by pyrolytic polymerization of the corresponding disubstituted or bridged paracyclophane monomers.

Scheme 1. PPX films containing silyl, germyl and stannyl functions

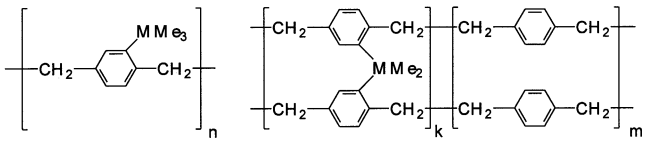

Further annealing of the polymers A and B leads to cleavage of the M−C bonds and the formation of metal nanocrystals in a polymer matrix. In contrast to the previously reported methods[9], we were able to obtain polymer coatings of uniform thickness that contained evenly distributed metal particles. Preliminary investigations on Ge-containing nanocomposites have shown these systems to be very promising sensor materials for air humidity[8].

In this paper we report on the synthesis of new disubstituted (**3a−c**, M = Si, Ge, Sn) and bridged (**6a**, **b**, M = Ge,

 © WILEY-VCH Verlag GmbH, D-69451 Weinheim, 1998 1434−1948/98/1111−1733 $ 17.50+.50/0

Sn; for Si compound see ref.[5]) paracyclophane monomers, which we plan to employ as monomers for the aforementioned polymer synthesis.

Results and Discussion

Dibromide **1** was obtained according to ref.[10] and lithiated with excess *n*-butyllithium in diethyl ether[11]. The resulting intermediate dilithio derivative **2** was then treated with trimethylsilyl chloride, trimethylgermanium bromide or trimethyltin chloride to yield the derivatives **3a–c** (Scheme 2).

Scheme 2. The preparation of dimetallated [2.2]paracyclophanes

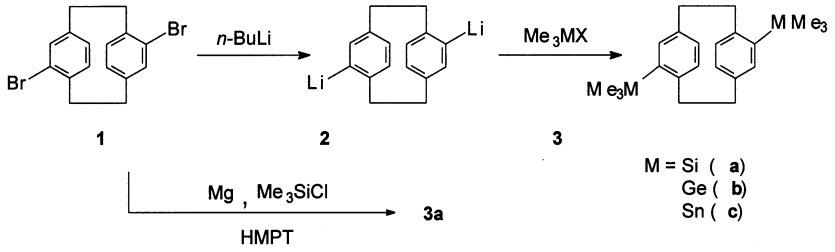

It is known that aromatic silylation can also be performed via organomagnesium reagents[12]. In the paracyclophane series, the mono Grignard reagent has been prepared and used for the synthesis of [2.2]paracyclophane-4-carboxylic acid[13]. Also, the coupling reaction of 4-bromo-[2.2]paracyclophane has been carried out via an organomagnesium intermediate[14]. To study the applicability of the organomagnesium route for the preparation of **3a**, we used the Barbier procedure[15], which has been applied previously for the synthesis of polysilylated benzenes[16]. In this approach, the aryl halide, magnesium and trimethylsilyl chloride are refluxed together in hexamethyl phosphoric triamide (HMPT) in a one-pot reaction. Compared with the lithation of **1**, this required more severe conditions (HMPT, heating, longer reaction time) and produced **3a** in substantially lower yield. Nevertheless, this metallation/quenching is the first example of the successful application of a disubstituted organomagnesium paracyclophane derivative in synthesis.

The bridged paracyclophane derivatives **6a**, **b** were synthesized from the monobromide **4**[17] via the monolithiated cyclophane **5**[18] (Scheme 3).

Scheme 3. The preparation of metal-bridged [2.2]paracyclophanes

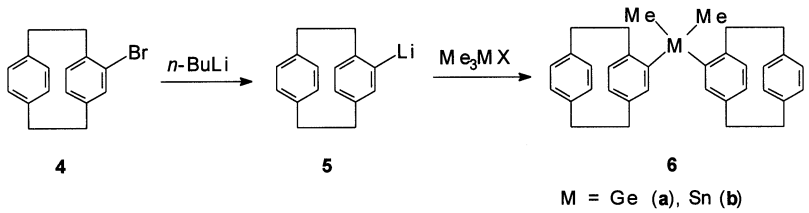

One of the most striking properties of [2.2]paracyclophanes is their planar chirality, which appears as soon as one hydrogen atom of the parent molecule is replaced by another substituent, with the substituents being introduced into the aromatic nuclei in most cases. Since compounds **6a**, **b** are constructed from two chiral elements, they could in principle be obtained as a mixture of diastereomers, a chiral *d,l* enantiomeric pair and an achiral *meso* form (Scheme 4).

In both cases, the reaction mixtures were analyzed by HPLC (RP-18, methanol or methanol/water) and ^{1}H-NMR spectroscopy. The title compounds were indeed shown to have been formed as a diastereomeric mixture. According

Scheme 4. The *d,l* and *meso* form of a metal-bridged [2.2]paracyclophane

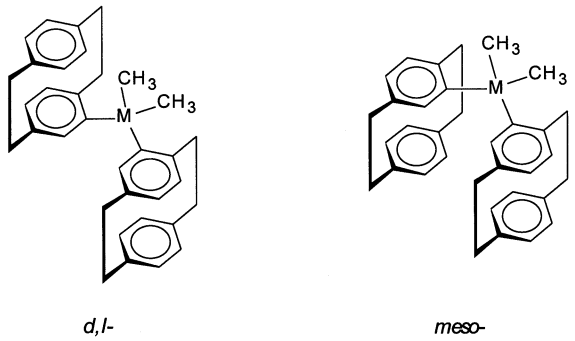

to their ^{1}H-NMR data, the diastereomers **6a**, **b** are formed in a *d,l*/*meso* ratio of about 2:1. The diastereomers could be separated by fractional recrystallization, with the *meso* form usually precipitating from the mixture. The separation of **6b** from the reaction mixture is difficult, since this compound is not stable on silica gel. Fractional recrystallization of the reaction mixture in this case only leads to the *meso* dia-

stereomer in pure form. Full spectral characterization of the diastereomers obtained was performed (see Experimental Section).

The chiral enantiomeric and the *meso* stereoisomers of both compounds **6a**, **b** could also be distinguished directly. Thus, the protons of CH_3 groups in the chiral isomer are related by a C_2 axis, so that they are homotopic and give rise to a single singlet. The corresponding protons in the *meso* form are surrounded by different chiral paracyclophane moieties and are therefore diastereotopic. The signals of these groups are detected as two singlets with a shift difference of 0.2 ppm. It is noteworthy that although the *meso* forms of **6a**, **b** can be unambiguously characterized by ^{1}H-NMR spectroscopy, in the ^{13}C-NMR spectra of these compounds the signals of the methyl C atoms are not resolved.

Furthermore, crystals suitable for an X-ray structural determination could be obtained in the case of *d,l*-**6a**′′. According to X-ray data, the [2.2]paracyclophanyl units of this derivative are very similar to one another and display the typical [2.2]paracyclophane geometry (Figure 1).

Figure 1. The structure of *d,l*-**6a**′′ in the crystal; radii are arbitrary

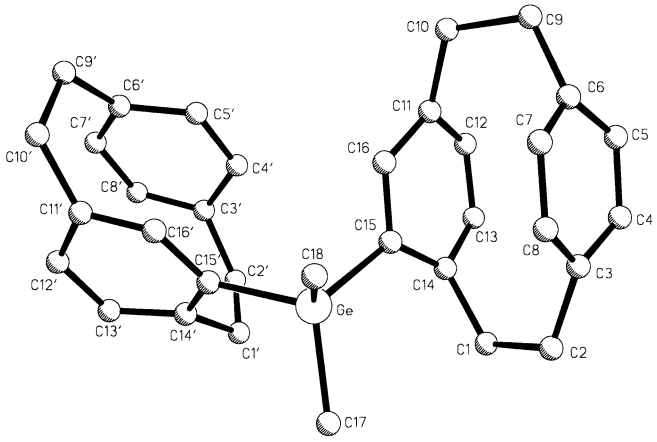

The aromatic rings are puckered into a boat form, with the bridgehead carbon atoms displaced out of the plane formed by the remaining four carbon atoms of the rings by 0.153−0.163 Å for the unsubstituted, and by 0.168−0.175 Å for the substituted rings. The C(sp^3)−C(sp^3) bond lengths of the ethano bridges range from 1.554 to 1.568 Å, i.e. they are slightly shorter than that in the parent [2.2]-paracyclophane molecule[5]. The lengths of the germanium−carbon bonds (such as Ge−C15) to the paracyclophanyl groups range from 1.955 to 1.962 Å, consistent with what is normally observed for Ge−Ar bonds[19].

The use of these new [2.2]paracyclophanes as monomers for novel metal-containing polymers is under active investigation, and we hope to report on these studies shortly.

This work was supported by the *Fonds der Chemischen Industrie* and the *Russian Funds for Fundamental Investigations* (project 96-03-33620).

Experimental Section

General: ^{1}H and ^{13}C NMR: Bruker AM-400 (400.13 and 100.6 MHz, for ^{1}H and ^{13}C, respectively), $CDCl_3$ as solvent, TMS as internal standard. − MS: Varian CH5, EI (70 eV). − IR: Nicolet 320 FT-IR spectrometer. − UV/Vis: Hewlett-Packard 8452A. − Column chromatography: Kieselgel 60, 70−230 mesh (Merck, Darmstadt). − Diastereomer compositions were determined by analytical HPLC (Milton-Roy HPLC system, methanol/water, 19:1, reversed-phase (S_5 octadecylsilane, SiC_{18} Spherisorb). − Et_2O was distilled from benzophenone ketyl under argon immediately prior to use. Dichloromethane was distilled from P_2O_5. Hexamethylphosphortriamide (HMPT) was distilled from CaH_2 in vacuo and stored under nitrogen. $(CH_3)_3SiCl$, $(CH_3)_3GeBr$, $(CH_3)_2GeCl_2$ were distilled from CaH_2. Other reagents were purchased from Aldrich and were used without purification.

4,16-Bis(trimethylsilyl)[2.2]paracyclophane (**3a**) *via Organolithium Compound* **2**: To a stirred suspension of 1.0 g (2.73 mmol) of **1** in 60 ml of dry diethyl ether under nitrogen, was added 9.76 ml of a 1.64 M *n*BuLi solution in hexane (16 mmol). The reaction mixture was stirred for 3 h, and then 2.03 ml (16 mmol) of $(CH_3)_3SiCl$ was added by means of a syringe over a period of 15 min. The reaction mixture was stirred overnight, heated for an additional 1 h, and then quenched with saturated NH_4Cl solution. The organic layer was washed several times with water, and dried with Na_2SO_4. The solvent was evaporated under reduced pressure. Column chromatography of the residue (pentane/dichloromethane, 8:1) gave 0.64 g (67%) of **3a**, m.p. 156°C. − IR (KBr): $\tilde{\nu}$ = 2930 cm^{-1} (m), 2880 (w), 1240 (s), 1105 (m), 905 (m), 860 (s), 842 (s), 832 (s), 755 (m), 720 (m). − UV/Vis (CH_3CN): λ_{max} (lg ε) = 230 nm (3.95), 255 (3.27), 266 (3.06). − ^{1}H NMR ($CDCl_3$): δ = 0.4 (s, 18 H, CH_3), 2.96−3.35 (m, 8 H, CH_2CH_2), 6.29 (d, *J* = 7.8 Hz, 2 H, 8-, 12-H), 6.37 (dd, *J* = 7.8, *J* = 1.9 Hz, 2 H, 7-, 13-H), 6.82 (d, *J* = 1.9 Hz, 2 H, 5-, 15-H). − ^{13}C NMR ($CDCl_3$): δ = 1.00 (s, CH_3), 35.67, 35.82 (s, C-1, -2, -9, -10), 133.47, 134.37, 137.15, 137.9, 138.76, 146.2 (s, all C-Ar). − MS (70 eV); *m/z* (%): 352 (10) [M$^+$], 337 (13), 176 (100), 160 (85), 145 (15). − $C_{22}H_{32}Si_2$ (352.67): calcd. C 74.93, H 9.15; found C 74.80, H 8.74.

4,16-Bis(trimethylsilyl)[2.2]paracyclophane (**3a**) *via an Organomagnesium Derivative:* Under nitrogen, 0.36 g (14.9 mmol) of magnesium and 2.0 g (5.46 mmol) of **1** in dry HMPT (8 ml) were placed in a two-necked round-bottomed flask equipped with a dropping funnel and a condenser, and the mixture was stirred for 10 min. Then, 2.52 ml (19.86 mmol) of $(CH_3)_3SiCl$ was added, the mixture was heated to 50°C, and reaction was initiated by adding a few drops of 1,2-dibromomethane (frothing and temperature increase). The reaction mixture was refluxed at 60°C for 40 h and, after cooling to room temp., was hydrolyzed by pouring it into a 0.5% sodium hydrogen carbonate solution, while the neutrality of the solution was tested at regular intervals. The resulting mixture was extracted with hexane, and the organic phase was washed several times with water and dried with Na_2SO_4. The solvent was evaporated under reduced pressure, and column chromatography of the residue on silica gel (pentane/dichloromethane, 8:1) gave 0.8 g (42%) of **3a**.

4,16-Bis(trimethylgermanyl)[2.2]paracyclophane (**3b**): 4,16-Dilithio[2.2]paracyclophane (**2**) was obtained as described above from 1.0 g (2.73 mmol) of **1** and 9.76 ml (16 mmol) of *n*BuLi (1.64 M solution in hexane). Subsequent reaction of **2** with 2.05 ml (16 mmol) of $(CH_3)_3GeBr$ and work-up of the reaction mixture were performed as in the case of **3a**. Column chromatography on silica gel of the resulting solid (heptane/benzene, 6:1) afforded 0.39 g (32%) of **3b**, m.p. 158−159°C. − IR (KBr): $\tilde{\nu}$ = 2925 cm^{-1} (m),

2900 (w), 1225 (m), 1105 (w), 905 (m), 855 (s), 840 (s), 822 (s), 750 (w), 720 (m). − UV/Vis (CH_3CN): λ_{max} (lg ε) = 230 nm (4.03), 255 (3.30), 266 (3.10). − ^1H NMR ($CDCl_3$): δ = 0.48 (s, 18 H, CH_3), 2.94−3.33 (m, 8 H, CH_2CH_2), 6.30 (br. s, 4 H, 7-, 8-, 12-, 13-H), 6.72 (br. s, 2 H, 5-, 15-H). − ^{13}C NMR ($CDCl_3$): δ = 1.14 (s, CH_3), 34.22, 34.38 (s, C-1, -2, -9, -10), 131.92, 132.38, 134.85, 136.70, 140.32, 143.70 (s, all C-Ar). − MS (70 eV); *m/z* (%): 444 (29) [M^+], 429 (25), 310 (24), 222 (100), 207 (78), 177 (30), 118 (46). − $C_{22}H_{32}Ge_2$ (441.72): calcd. C 59.83, H 7.30, Ge 32.87; found C 59.73, H 7.24.

4,16-Bis(trimethylstannyl)[2.2]paracyclophane (**3c**): 10 ml of a 3.0 N *n*BuLi solution in hexane (30 mmol) was added to a stirred suspension of 0.50 g (1.37 mmol) of **1** in 50 ml of dry diethyl ether under argon. The reaction mixture was stirred for 5 h, and then a solution of 5.98 g (30 mmol) of $(CH_3)_3SnCl$ in dry diethyl ether was added dropwise over a period of 30 min. The reaction mixture was left overnight, and was then quenched with saturated NH_4Cl solution. The organic layer was washed several times with water and dried with Na_2SO_4. The solvent was evaporated under reduced pressure to give 0.45 g (62%) of **3c**, m.p. 162−164°C. − IR (KBr): $\tilde{\nu}$ = 2922 cm^{-1} (m), 2886 (w), 1170 (s), 1100 (s), 1050 (s), 920 (w), 868 (s), 860 (s), 845 (s), 762 (s), 722 (w). − UV/Vis (CH_3CN): λ_{max} (lg ε) = 230 nm (4.20), 2.55 (3.39), 266 (3.18). − ^1H NMR ($CDCl_3$): δ = 0.35 [dt, 18 H, $J(^{117}Sn\text{-}H)$ = 51.6 Hz, $J(^{119}Sn\text{-}H)$ = 53.6 Hz, CH_3], 2.94−3.16 (m, 4 H, CH_2CH_2), 3.24−3.34 (m, 4 H, CH_2CH_2), 6.26 (dd, J_1 = 7.8, J_2 = 1.9 Hz, 2 H, 7-, 13-H), 6.37 (d, J = 7.8 Hz, 2 H, 8-, 12-H), 6.71 (d, J = 1.9 Hz, 2 H, 5-, 15-H). − ^{13}C NMR ($CDCl_3$): δ = −9.36 (s, CH_3), 34.36, 36.48 (s, C-1, -2, -9, -10), 131.13, 132.67, 136.61, 137.31, 142.85, 145.34 (s, all C-Ar). − MS (70 eV); *m/z* (%): 534 (2.5) [M^+], 519 (10) [$M^+ - CH_3$], 253 (100), 223 (34), 185 (64), 165 (62), 104 (84). − $C_{22}H_{32}Sn_2$ (533.88): calcd. C 49.50, H 6.04, Sn 44.46; found C 49.87, H 5.91, Sn 44.20.

Dimethylbis([2.2]paracyclophane-4-yl)germane (**6a**): To a stirred solution of 1.0 g (3.49 mmol) of **4** in dry diethyl ether (80 ml) under dry nitrogen, was added 2.5 ml of a 1.64 M *n*BuLi solution in hexane (4.1 mmol). After 3 h, 0.2 ml (1.75 mmol) of $Ge(CH_3)_2Cl_2$ was slowly added by means of a syringe, the reaction mixture was stirred for 2 h, and left to stand overnight. Saturated aqueous NH_4Cl solution was then added, the organic layer was washed twice with water, and dried with Na_2SO_4. The solvent was removed in vacuo, and the residue was separated by column chromatography on silica gel using CCl_4 as eluent, to afford a diastereomeric mixture of **6a** (1.28 g, 71%). − MS (70 eV); *m/z* (%): 518 (68) [M^+], 503 (95), 414 (36), 399 (56), 309 (42), 205 (100), 191 (78), 104 (36). − $C_{34}H_{36}Ge$ (517.25): calcd. C 78.95, H 7.02, Ge 14.03; found C 78.98, H 7.08. − The diastereomeric mixture was recrystallized from 2-propanol/dichloromethane (5:1, v/v). The precipitated solid was removed by filtration: 0.71 g (40%) of dimethyl-*meso*-bis([2.2]paracyclophane-4-yl)germane (**6a′**): M.p. 244°C. − IR (KBr): $\tilde{\nu}$ = 2923 cm^{-1} (s), 2891 (m), 2850 (m), 1410 (w), 1237 (w), 902 (m), 833 (m), 798 (s), 720 (s), 576 (m). − UV/Vis (CH_3CN): λ_{max} (lg ε) = 228 nm (4.54), 256 (3.86), 266 (3.64). − ^1H NMR ($CDCl_3$): δ = 0.72 (s, 3 H, CH_3), 0.92 (s, 3 H, CH_3), 2.67−3.27 (m, 16 H, CH_2CH_2), 6.20 (dd, J_1 = 7.8, J_2 = 1.3 Hz, 2 H), 6.30 (dd, J_1 = 7.8, J_2 = 1.3 Hz, 2 H), 6.38 (d, J = 7.8 Hz, 2 H, 8-, 8′-H), 6.44 (dd, J_1 = 7.8, J_2 = 1.6 Hz, 2 H, 7-, 7′-H), 6.55 (m, 4 H), 6.73 (d, J = 1.6 Hz, 2 H, 5-, 5′-H). − ^{13}C NMR ($CDCl_3$): δ = 35.65 (s, 6 C), 36.35 (s, 2 C) (C-1, -1′, -2, -2′, -9, -9′, -10, -10′), 132.51, 132.56, 132.94, 133.40, 134.16, 134.29, 137.00, 138.77, 139.41, 139.78, 140.40, 145.65 (s, all C-Ar). − The filtrate, after concentration and recrystallization of the residue from hexane, yielded 0.18 g (10%) of dimethyl-*d,l*-bis([2.2]paracyclophane-4-yl)germane (**6a′′**): M.p. 163°C. − IR (KBr): $\tilde{\nu}$ = 2923 cm^{-1} (s), 2891 (m), 2850 (m), 1410 (m), 1237 (m), 902 (m), 833 (m), 805 (s), 718 (s), 580 (w). − UV/Vis (CH_3CN): λ_{max} (lg ε) = 228 nm (4.28), 256 (3.76), 266 (3.60). − ^1H NMR ($CDCl_3$): δ = 0.89 (s, 3 H, CH_3), 2.80−3.27 (m, 16 H, CH_2CH_2), 6.07 (dd, J_1 = 7.9, J_2 = 1.7 Hz, 2 H), 6.33 (dd, J_1 = 7.9, J_2 = 1.7 Hz, 2 H), 6.37−6.49 (m, 4 H), 6.51−6.62 (m, 4 H), 6.76 (d, J = 1.9 Hz, 2 H). − ^{13}C NMR ($CDCl_3$): δ = −0.67 (s, CH_3), 34.15, 34.21, 34.36, 34.68 (C-1, -1′,-2, -2′, -9, -9′, -10, -10′), 131.10 (2 C), 131.41, 131.78, 131.71 (2 C), 135.49, 136.96, 137.98, 138.24, 139.34, 143.85 (s, all C-Ar).

Dimethylbis([2.2]paracyclophane-4-yl)stannane (**6b**): Monolithio[2.2]paracyclophane **5** was obtained as described above from 1.0 g (3.49 mmol) of **4** and 2.5 ml (4.1 mmol) of *n*BuLi (1.64 M solution in hexane). Subsequent reaction of **4** with 0.387 g (1.75 mmol) of $(CH_3)_2SnCl_2$ and work-up of the reaction mixture were performed as in the case of **6a**. Since this compound is not stable on silica gel, the mixture of diastereomers could not be separated by column chromatography. Recrystallization (three times) from 2-propanol/dichloromethane (4:1, v/v) yielded 0.85 g (43%) of dimethyl-*meso*-bis([2.2]paracyclophane-4-yl)stannane (**6b′**): M.p. 208°C. − IR (KBr): $\tilde{\nu}$ = 2926 cm^{-1} (s), 2890 (m), 2851 (s), 1410 (w), 1181 (w), 1092 (m), 898 (w), 742 (m), 720 (s), 520 (m), 510 (m). − UV/Vis (CH_3CN): λ_{max} (lg ε) = 228 nm (4.51), 256 (3.85), 266 (3.62). − ^1H NMR ($CDCl_3$): δ = 0.61 [dt, 3 H, $J(^{117}Sn\text{-}H)$ = 51.6 Hz, $J(^{119}Sn\text{-}H)$ = 53.6 Hz, CH_3], 0.77 [dt, 3 H, $J(^{117}Sn\text{-}H)$ = 51.6 Hz, $J(^{119}Sn\text{-}H)$ = 53.6 Hz, CH_3], 2.71−3.29 (m, 16 H, CH_2CH_2), 6.21 (br d, 2 H), 6.36 (br d, 2 H), 6.40−6.59 (m, 8 H), 6.76 (br s, 2 H). − ^{13}C NMR ($CDCl_3$): δ = 35.73, 35.75, 35.80, 38.16 (s, C-1, -2, -9, -10), 132.72, 132.87, 133.05, 133.20, 133.61, 134.21, 138.84, 139.25, 139.34, 139.90, 143.81, 146.90 (s, all C-Ar). − MS (70 eV); *m/z* (%): 564 (100) [M^+], 549 (98), 445 (74), 413 (16), 309 (32), 205 (84), 191 (58), 135 (18), 104 (36). − $C_{34}H_{36}Sn$ (563.35): calcd. C 72.49, H 6.44; found C 71.95, H 6.07.

X-ray Crystallographic Study of Dimethyl-d,l-bis([2.2]paracyclophan-4-yl)germane (*d,l*-**6a′′**): Crystal data: $C_{34}H_{36}Ge$, 517.25 g mol^{-1}, a = 14.001(3), b = 17.814(4), c = 10.554(2) Å, β = 93.09 (3)°, V = 2628.5 (10) $Å^3$, Z = 4, d = 1.307 mg/m^3, monoclinic crystals, space group $P2(1)/c$. Data collection: A colorless prism of dimensions 0.45 × 0.30 × 0.28 mm was mounted in inert oil. Data were collected to $2\theta_{max}$ = 50° [$I > 2\sigma(I)$] with an Enraf-Nonius CAD-4 diffractometer, Mo-K_α radiation (λ = 0.71073 Å), β-filter monochromator. Of 1965 measured data, 1844 were unique (R_{int} = 0.0155). μ = 1.186 mm^{-1}, T = 20°C. The structure was solved by direct methods and refined anisotropically on F^2 (program SHELXL-93, G. M. Sheldrick, Univ. Göttingen). Hydrogen atoms were refined in isotropic approximation. The final $wR^2(F^2)$ was 0.0553 for 461 parameters. Conventional $R(F)$ = 0.022, S = 1.086; max Δ/σ < 0.001; max Δρ 0.332 e$Å^{-3}$. Crystallographic data (excluding structure factors) for the structure *d,l*-**6a′′** reported in this paper have been deposited with the Cambridge Crystallographic Data Centre as supplementary publication no. CCDC-101369. Copies of the data can be obtained free of charge on application to CCDC, 12 Union Road, Cambridge CB2 1EZ, UK [Fax: (int. code) + 44(1223)336-033; E-mail: deposit@ccdc.cam.ac.uk; World Wide Web: http://www.ccdc.cam.ac.uk].

☆ Dedicated to Professor *Heinrich Nöth* on the occasion of his 70th birthday.

[1] F. Vögtle, *Cyclophane Chemistry*, John Wiley & Sons, Chichester, **1993**.

[2] V. A. Nikanorov, V. I. Rozenberg, V. G. Kharitonov, E. V. Yatsenko, V. V. Mikulshina, N. A. Bumagin, I. P. Belezkaya, V. N. Guryshev, V. I. Yur′ev, O. A. Reutov, *Organomet. Chem. USSR* **1991**, *4*, 338−341.

[3] V. I. Rozenberg, V. G. Kharitonov, E. V. Yatsenko, E. V. Smyslova, K. I. Grandberg, M. V. Galakhov, V. V. Mikulshina, V. A. Nikanorov, V. N. Guryshev, V. I. Yur′ev, O. A. Reutov, *Organomet. Chem. USSR* **1991**, *4*, 336−338.
[4] M. Stobbe, O. Reiser, T. Thiemann, R. G. Daniels, A. de Meijere, *Tetrahedron Lett.* **1986**, *27*, 2353−2356.
[5] P. G. Jones, L. Ernst, I. Dix, L. Wittkowski, *Acta Crystallogr.* **1997**, C53, 612−615.
[6] V. V. Zagorski, M. A. Petrukhina, G. B. Sergeev, V. I. Rozenberg, V. G. Kharitonov Pat. 2, 017, 547 (Cl. B05D1/38), 15 Aug **1994**, Appl. 5, 060, 992, 2 Jul **1992** (Russ).
[7] G. N. Gerasimov, E. L. Popova, E. V. Nikolaeva, S. N. Chvalun, E. I. Grigoriev, L. I. Trakhtenberg, V. I. Rozenberg, H. Hopf. *Macromol. Chem. Phys.*, in press.
[8] H. Hopf, G. N. Gerasimov, E. I. Grigoriev, S. N. Chvalun, V. I. Rozenberg, E. L. Popova, E. V. Nikolaeva, S. V. Zavialov, L. I. Trakhtenberg, *Adv. Mater., Chem. Vapor Deposition* **1997**, *3*, 197−200.
[9] M. P. Andrews, G. A. Ozin, *Chem. Mater.* **1989**, *1*, 174 −187.
[10] V. A. Nikanorov, V. G. Kharitonov, E. V. Yatsenko, D. P. Krut′ko, M. V. Galakhov, S. O. Yakushin, V. V. Milulshina, V. I. Rozenberg, V. N. Guryshev, V. P. Yur′ev, O. A. Reutov, *Bull. Acad. Sci. USSR, Div. Chem. Sci.* **1991**, *41*, 1430−1434.
[11] A. Izuoka, S. Murata, T. Sugawara, H. Iwamura, *J. Am. Chem. Soc.* **1987**, *109*, 2631−2639.
[12] D. Habich, F. Effenberger, *Synthesis* **1979**, 841−876.
[13] J. L. Marshall, L. Hall, *Tetrahedron* **1981**, *37*, 1271−1275.
[14] P. Kuz, *Pol. J. Chem.* **1994**, *68*, 1983−1988.
[15] C. Blomberg, F. A. Hartog, *Synthesis* **1977**, 18−30.
[16] P. Bourgeois, R. Calas, E. Jausseaume, J. Gerval, *J. Organomet. Chem.* **1975**, *84*, 165−175.
[17] H. J. Reich, D. J. Cram, *J. Am. Chem. Soc.* **1969**, *91*, 3534−3543.
[18] K. Krohn, H. Rieger, H. Hopf, D. Barett, P. G. Jones, *Chem. Ber.* **1990**, *B123*, 1729−1732.
[19] A. Karipides, D. A. Haller, *Acta Crystallogr.* **1972**, *B28*, 2889−2894.

[98134]

Homogeneous and Biphasic Nickel-Catalyzed Isomerization of Allylic Alcohols

Hervé Bricout[a], Eric Monflier*[a], Jean-François Carpentier[b], and André Mortreux[b]

Université d'Artois, Laboratoire de Physicochimie des Interfaces et Applications, Faculté des Sciences J. Perrin[a],
Rue Jean Souvraz, S.P.18, F-62307 Lens, France
Fax: (internat.) +33-3/21791717
E-mail: monflier@univ-artois.fr

Laboratoire de Catalyse Hétéroge̊ne et Homogène associé au CNRS, URA CNRS 402[b],
B. P. 108, F-59652 Villeneuve d'Ascq, France

Received May 4, 1998

Keywords: Isomerization / Allylic alcohol / Nickel / Homogeneous catalysis / Two-phase catalysis

The nickel-catalyzed isomerization of geraniol and prenol in homogeneous and two-phase systems has been investigated. The best results in terms of activity and selectivity have been obtained in homogeneous systems with a bis(cycloocta-1,5-diene)nickel(0)/1,4-bis(diphenylphosphanyl)butane/trifluoroacetic acid combination. Catalyst deactivation occurs in the course of the reaction owing to coordination of the formed aldehyde group to the nickel species or as a result of protonolysis of hydrido- or (π-allyl)nickel complexes.

Introduction

The ability of homogeneous nickel complexes to promote double-bond positional isomerization of simple alkenes and polyenes as well as skeletal isomerization of some dienes is well documented[1]. While the reactions of unfunctionalized alkenes have been quite extensively studied, the case of alkenes bearing polar functional groups has received less attention. Thus, there have been only two reports on the nickel-catalyzed isomerization of allylic alcohols[2][3][4]. The first describes the selective transformation of allyl alcohol into propanal in the presence of a catalytic amount of the Ni^{I} complex $Ni_2(CN)_2(dppb)_3$ [dppb = 1,4-bis(diphenylphosphanyl)butane], which is either preformed or generated in situ from $Ni(dppb)_2$ and HCN[2]. The second describes a sluggish catalytic system consisting of ethylene(tri-*o*-tolyl phosphite)nickel(0) and hydrogen chloride for the isomerization of various allylic alcohols[3]. Surprisingly, although the catalytic isomerization of terpenic alcohols and related compounds could be of great industrial interest[4h], no attention has been directed towards these substrates in the previous studies.

Our continuing interest in the reactivity of zerovalent nickel−phosphane catalysts towards allylic substrates[5] has led us to explore the catalytic activity of various homogeneous Ni^0/diphosphane/acid systems in the isomerization of geraniol and prenol. We report herein that nickel efficiently catalyzes this process and point out how the catalyst is deactivated in the course of the reaction. An alternative water-soluble catalytic system has also been developed and evaluated.

Results and Discussion

In the light of literature reports and of our own work[5], we decided to use as catalyst precursor the complex $Ni(dppb)_2$, which is easily generated in situ from $Ni(COD)_2$ and two equiv. of dppb[6]. Preliminary experiments aimed at evaluating the efficiencies of the added Brønsted acids were first conducted using geraniol (**1**) as the substrate. Besides the expected isomerization product, citronellal (**2**), several compounds were formed in variable amounts depending on the reaction conditions (Scheme 1). Thus, some of the **2** present was converted into the diastereomeric alcohols isopulegol (**3**) and neoisopulegol (**4**) as a result of a proton-catalyzed cyclization process[7]. Two further side-products **5** and **6** were generated due to esterification of the starting substrate by the carboxylic acid added as a co-catalyst, and acetalization of **2** by **1**, respectively. The results are summarized in Table 1.

The isomerization of **1** did not proceed when 1.5 mol-% of $Ni(dppb)_2$ was used at 80°C in the absence of a co-catalyst (entry 1) or in the presence of methanol (entry 2). In these cases, only small amounts of the dehydration products of **1**, i.e. myrcene (**8**) and ocimene (**9**) were formed, most probably by oxidative addition of **1** followed by a β-H elimination process as these products were not observed in the absence of the nickel catalyst (Schemes 2 and 6).

The addition of 4 equiv. of acetic acid (with respect to Ni) allowed the selective, but sluggish formation of **2** (entry 3). An increase in the amount of acetic acid up to 50 equiv. improved the catalytic activity, but the selectivity significantly decreased with time because of the formation of the ester **5** as a side-product (entry 4). Use of TFA as the co-catalyst proved much more advantageous. With 1 equiv., an almost total selectivity for **2** could be observed, although the reaction stopped after 2 h, reaching a maximum of 30% conversion of **1**. Increasing the amount of TFA up to 2 or 4 equiv. led to a slight improvement of the catalytic activity in the initial stages of the reaction, but the limitation of termination of the reaction after ca. 50% conversion was

 © WILEY-VCH Verlag GmbH, D-69451 Weinheim, 1998 1434−1948/98/1111−1739 $ 17.50+.50/0

Scheme 1. Isomerization of geraniol (**1**) into citronellal (**2**) and reaction side-products

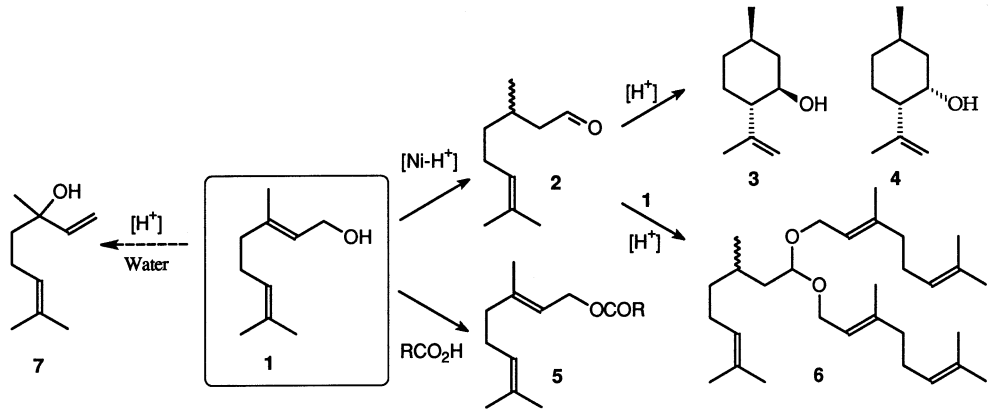

Table 1. Nickel-catalyzed isomerization of geraniol[a]

Entry	Acid (equiv.)[b]	Time [h]	Conv. **1**[c] [mol-%]	Yield **2** [mol-%]	Sel. **2**[c] [mol-%]	Sel. **3** + **4**[c][d] [mol-%]	Sel. **5**[c] [mol-%]	Sel. **6**[c] [mol-%]	Sel. **7**[c] [mol-%]
1	–	16	2[e]	0	0	0	0	0	< 1
2	MeOH (50)	18	3[e]	0	0	0	0	0	< 1
3	AcOH (4)	2	2	2	> 99	< 1	< 1	< 1	< 1
4	AcOH (50)	0.5	19	18	98	< 1	2	< 1	< 1
		2	25	23	92	< 1	6	2	< 1
		16	41	29	71	4	20	5	< 1
5	TFA (1)	0.5	25	25	> 99	< 1	< 1	< 1	< 1
		2	30	30	> 99	< 1	< 1	< 1	< 1
		16	30	30	> 99	< 1	< 1	< 1	< 1
6	TFA (2)	0.5	31	31	> 99	< 1	< 1	< 1	< 1
		2	46	45	97	< 1	< 1	3	< 1
		16	54	49	90	5	< 1	5	< 1
7	TFA (4)	0.5	33	30	91	5	4	< 1	< 1
		2	46	38	82	10	3	5	< 1
		16	58	47	80	10	1	9	< 1
8[f]	TFA (4)	0.5	10	1	10	0	0	0	90
		2	34	1	3	0	0	0	97
		16	65	3	5	0	0	0	95
9[g]	TFA (4)	0.5	10	8	80	4	0	0	16
		2	15	13	86	4	0	0	10
		16	19	14	74	11	0	0	15
10[g]	HCl (4)	0.5	9	8	88	1	0	0	11
		2	15	13	86	4	0	0	10
		16	19	14	74	12	0	14	
11[h]	TFA (4)[h]	0.5	20	8(19)[i]	40(96)[j]	4	< 1	< 1	< 1
		2	31	5(30)[i]	17(96)[j]	4	< 1	< 1	< 1
		16	72	8(69)[i]	11(95)[j]	5	< 1	< 1	< 1

[a] Reaction conditions: $Ni(COD)_2$ 0.13 mmol, dppb 0.26 mmol, geraniol (**1**) 9.1 mmol, toluene 5 ml, $T = 80°C$. – [b] mol equivalent of protic co-reagent with respect to Ni. – [c] Selectivity = (mmol of product)/(mmol of converted geraniol) × 100; conversion of **1** and selectivities of the formed products were determined by quantitative GLC analysis. – [d] The **3**/**4** ratio was always 60:40. – [e] Myrcene and ocimene account for the conversion. – [f] Two-phase system: $Ni(COD)_2$ 0.13 mmol, dppbts 0.26 mmol, geraniol (**1**) 9.1 mmol, toluene 5 ml, water 10 g, $T = 110°C$. – [g] Same conditions as in footnote [f] except water 5 g and dimethylformamide 5 g. – [h] Reaction conducted in the presence of butane-1,2-diol (13.7 mmol, 1.5 equiv. with respect to **1**). – [i] The first value indicates the yield of free citronellal (**2**) and the value in brackets the total yield including free and acetalized citronellal (**2** + **15**). – [j] The first value indicates the selectivity for free citronellal (**2**) and the value in brackets the total selectivity including free and acetalized citronellal (**2** + **15**).

still observed (entries 6, 7). Moreover, the presence of an excess of acid with respect to nickel catalyst promoted the cyclization and acetalization, and to a lesser extent the esterification (entry 7).

Similar results were also obtained for the isomerization of prenol (**10**) into isovaleraldehyde (**11**) using the $Ni(dppb)_2$/TFA (1:2) catalyst system (Scheme 3). Besides **11**, the isomeric 3-methyl-3-buten-1-ol (**12**), resulting from isomerization of the double bond in the carbon backbone, was also formed in small amounts. The results are summarized in Table 2.

With 1 equiv. of TFA with respect to $Ni(dppb)_2$, isomerization rapidly ceased, thus allowing the attainment of modest yields only (Table 2, entry 13). On the other hand, excess TFA proved to be detrimental to the selectivity due to acetalization of **11** to give **13** (Table 2, entry 15). A TFA/

Scheme 2. Suggested formation of myrcene (**8**) and ocimene (**9**) from geraniol (**1**)

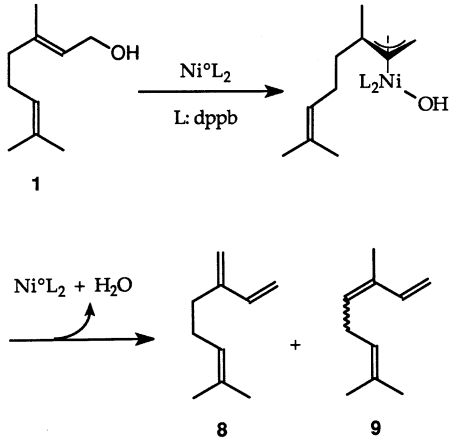

In order to gain further insight into the aforementioned limitation to the extent of conversion, an experiment was conducted with the $Ni(dppb)_2$/TFA (1:2) catalytic system, in which the temperature was varied during the course of the reaction. The experiment was started at room temperature and the temperature was increased when the progress of the reaction was seen to falter (Figure 1).

It was found that the limit to the degree of conversion of **1** into **2** increased with temperature, i.e. 5% at 20°C, 13% at 50°C, and ca. 50% at 80°C. As the isomerization of allylic alcohols is a non-reversible process[8], the above data cannot stem from a thermodynamic control of the reaction and are much more likely to be attributable to catalyst deactivation. In fact, we assume that the aldehydes **2** or **11** reversibly coordinate to Ni[9] to form an inactive species, the stability of which would decrease with temperature (Scheme 4).

Scheme 3. Isomerization of prenol (**10**) into isovaleraldehyde (**11**) and reaction side-products

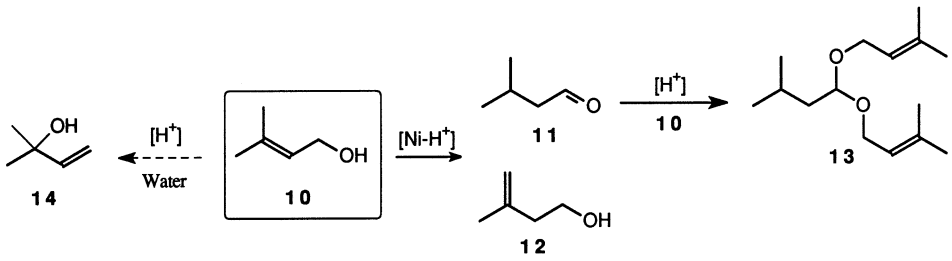

Table 2. Nickel-catalyzed isomerization of prenol[a]

Entry	TFA (equiv.)[b]	Time [h]	Conv. **10**[c] [mol-%]	Yield **11** [mol-%]	Sel. **11**[c] [mol-%]	Sel. **12**[c] [mol-%]	Sel. **13**[c] [mol-%]	Sel. **11**[d] [mol-%]	Sel. **14**[d] [mol-%]
12	0	18	25[e]	0	0	0	0	0	0
13	1	0.5	28	26	92	7	1	93	0
		2	34	31	91	7	2	93	0
		16	35	31	89	8	3	93	0
14	2	0.5	40	34	85	6	9	94	0
		2	55	45	82	5	13	95	0
		16	65	47	72	5	23	95	0
15	4	0.5	46	30	66	3	31	97	0
		2	67	37	55	2	43	98	0
		16	82	43	52	3	45	97	0
16[f]	4[f]	0.5	23	11	47	0	0	47	53
		2	32	12	38	0	0	38	62
		16	55	12	22	0	0	22	78
17[g]	4[g]	0.5	36	10(32)[h]	26(89)[i]	2	9	98	0
		2	47	5(44)[h]	10(94)[i]	2	4	98	0
		4	59	5(57)[h]	8(96)[i]	2	2	98	0
		16	92	5(90)[h]	5(98)[i]	2	0	98	0

[a][b] See Table 1. – [c] Selectivity = (mmol of product)/(mmol of converted prenol) × 100; conversion of **10** and selectivities of the formed products were determined by quantitative GLC analysis. – [d] Calculated selectivity for attainable isovaleraldehyde after hydrolysis. – [e] Isoprene accounts for the conversion. – [f] Two-phase system: $Ni(COD)_2$ 0.13 mmol, dppbts 0.26 mmol, prenol (**10**) 9.1 mmol, toluene 5 ml, water 5 g, dimethylformamide 5 g, $T = 110$°C. – [g] Reaction conducted in the presence of butane-1,2-diol (13.7 mmol, 1.5 equiv. with respect to **11**). – [h] The first value indicates the yield of free isovaleraldehyde (**11**) and the value in brackets the total yield including free and acetalized isovaleraldehyde (**11** + **16**). – [i] The first value indicates the selectivity for free isovaleraldehyde (**11**) and the value in brackets the total selectivity including free and acetalized isovaleraldehyde (**11** + **16**).

Ni ratio of 2 appeared to be a good compromise (Table 2, entry 14) but, as in the case of geraniol, a rapid decrease in the catalytic activity after 2 h of reaction and a limit to the degree of conversion was observed.

To check this hypothesis, two approaches were considered:

(i) The first of these involved the use of an aqueous/organic two-phase system where the organic compounds, i.e.

Figure 1. Influence of the temperature on the isomerization of geraniol (**1**) into citronellal (**2**); experimental conditions: $Ni(COD)_2$: 0.13 mmol, dppb: 0.26 mmol, **1**: 9.1 mmol, toluene: 5 ml, TFA: 0.52 mmol

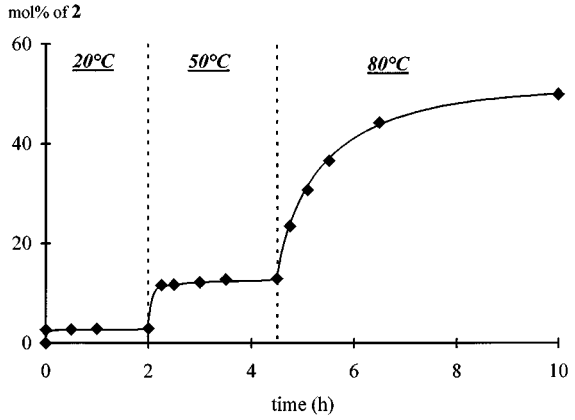

Scheme 4. Reversible coordination of the aldehyde to the nickel center

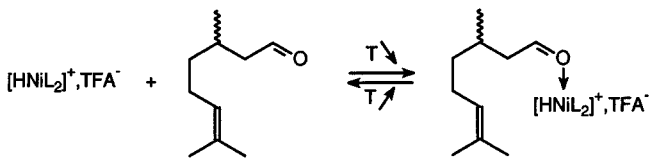

the allylic alcohol and the aldehyde, were in a different phase from that containing the catalytic system. In such a system, the coordination of the aldehyde group should be less favorable. Unfortunately, the performance of the corresponding water-soluble catalytic system, i.e. a nickel complex of tetrasulfonated 1,4-bis(diphenylphosphanyl)butane in an acidic aqueous solution[10], turned out to be rather disappointing (entries 8–10). Indeed, in a genuine two-phase system, i.e. without a co-solvent, the isomerization of **1** into linalool (**7**) was the major reaction (Scheme 1) and **2** was obtained only in very poor yield (3%, entry 8). Experiments conducted in the absence of a nickel catalyst proved unequivocally that **7** is formed by a proton-assisted process[11]. Such a process did not occur in homogeneous media, probably because of the lower stability of the intermediate allylic carbocation in non-polar organic media. Interestingly, the use of a co-solvent such as dimethylformamide (DMF) reduces the polarity of the aqueous layer and consequently suppresses this undesirable reaction. Indeed, although this catalytic system gave **2** in poor yields irrespective of the acid used, the selectivity for the desired aldehyde reached 86%, compared to 3% without DMF (entries 9, 10). Owing to the high solubility of prenol in water, it is noteworthy that DMF does not suppress the proton-catalyzed side reaction (Table 2, entry 16). Furthermore, in all biphasic reactions, a rapid colour change of the aqueous layer from orange to pale-green was observed, thus indicating an irreversible catalyst decay.

(ii) The second approach involved trapping of the aldehyde by acetalization, by including an excess of butane-1,2-diol in the reaction mixture (Scheme 5). Butane-1,2-diol was preferred to ethane-1,2-diol for trapping of the aldehydes because of its total solubility in the reaction mixture.

Scheme 5. Acetalization of citronellal (**2**) and isovaleraldehyde (**11**) by butane-1,2-diol

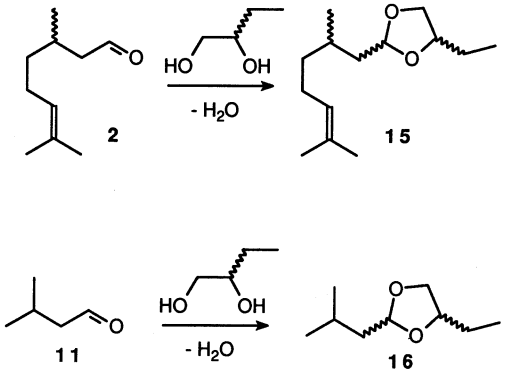

Under these conditions, higher final yields of aldehyde derivatives and higher conversions of **1** and **10** compared to the runs conducted without butane-1,2-diol were obtained. For instance, for the isomerization of **1**, the amounts of by-products **3**–**6** were significantly decreased in favour of **2** and the corresponding dioxolane **15** (entry 11). In the case of **10**, aldehyde **11** was produced in essentially 90% yield in 16 h (compared with 47% yield in the absence of butane-1,2-diol; Table 2, entry 17). These results are clearly fully supportive of the aforementioned hypothesis of a competitive coordination between the double bond of the alcohol and the aldehyde function to the Ni.

However, even in the presence of butane-1,2-diol, substrates **1** and **10** could not be completely converted and a limit to the degree of conversion was still observed. As the coordination of the aldehyde group leads to unreactive but stable species (Figure 1, vide supra), the progressive loss of activity in the course of the reaction cannot be attributed

Figure 2. Isomerization of geraniol (**1**) into citronellal (**2**) as a function of time and initial mixture composition; test ◇: $Ni(COD)_2$: 0.13 mmol, dppb: 0.26 mmol, **1**: 9.1 mmol, toluene: 5 ml, TFA: 0.26 mmol, test +: $Ni(COD)_2$: 0.13 mmol, dppb: 0.26 mmol, **1**: 4.5 mmol, **2**: 4.5 mmol, toluene: 5 ml, TFA: 0.26 mmol

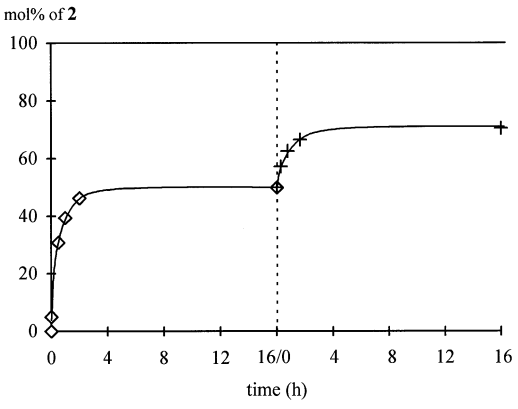

Scheme 6. Suggested catalytic cycle for isomerization of allylic alcohols and irreversible deactivation pathways of the catalyst

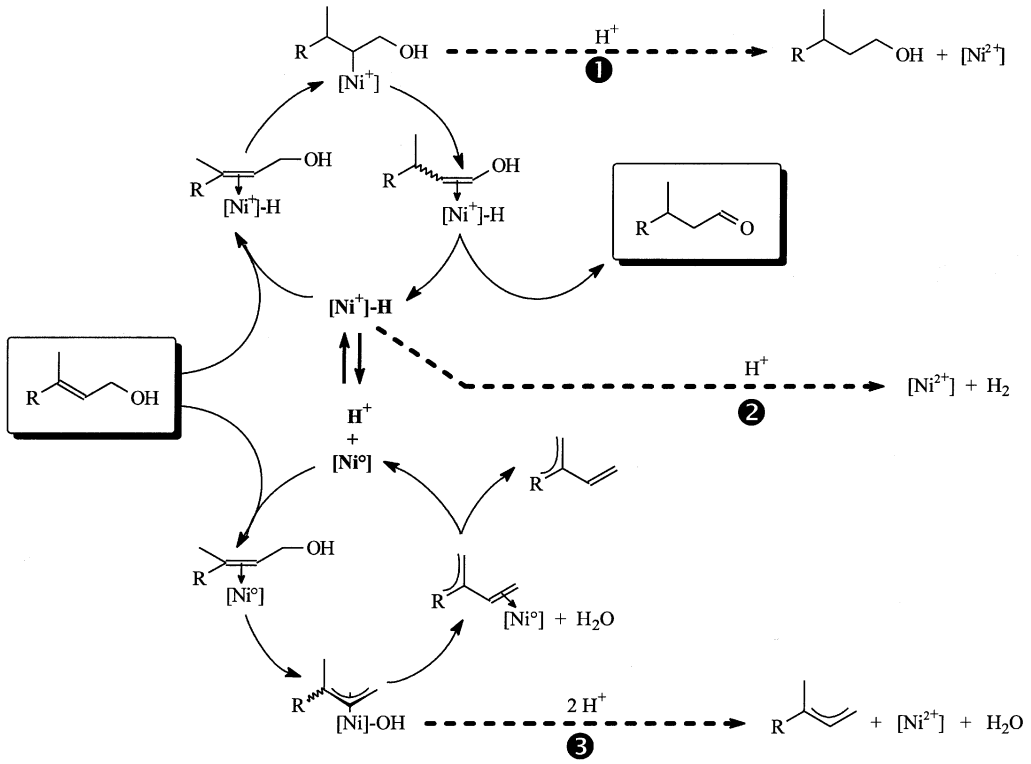

to this phenomenon, but rather to a slow and irreversible catalyst decay. The latter was confirmed by carrying out two further separate experiments under the same reaction conditions, i.e. the isomerization of pure **1** and of a 50:50 mixture of **1** and **2** (Figure 2).

In the first case, the conversion reached 50%, i.e. the same composition as the starting mixture of the second experiment, while in the second case 40% of the **1** initially present was isomerized. This clearly indicates that the **2**/Ni ratio is not the sole parameter affecting the catalytic activity. A further experimental indication of the catalyst decay came from the aforementioned progressive colour change of the homogeneous and biphasic solutions in the course of the reactions. Possible mechanistic pathways for this catalyst deactivation are the well-known protonolysis of the active hydride−nickel species[12] or of a π-allyl− or alkyl−nickel species resulting from allylic alcohol insertion into the hydride−nickel bond during the isomerization catalytic cycle (pathways 1, 2, and 3 in Scheme 6).

Conclusion

Although catalyst deactivation appears to be a non-negligible reaction, this study proves that the Ni^0/1,4-bis(diphenylphosphanyl)butane/trifluoroacetic acid combination is efficient for the isomerization of the trisubstituted carbon−carbon double bond in terpenic alcohols and related compounds. Thus, provided that the reaction is conducted in the presence of butane-1,2-diol, a turnover number of 60 and a selectivity of 98% for the free and acetalized isovaleraldehydes can be attained using a homogeneous system. Further experiments aimed at increasing the stability of the catalytic system and with a view to performing asymmetric isomerization are currently under way in our laboratories.

Experimental Section

General: Bis(cycloocta-1,5-diene)nickel, 1,4-bis(diphenylphosphanyl)butane (dppb), trifluoroacetic acid (TFA), geraniol (**1**), and prenol (**8**) were purchased from Strem Chemicals or Aldrich Chemical Co. in the highest available purity and used without further purification. The sodium salt of tetrasulfonated 1,4-bis(diphenylphosphanyl)butane (dppbts) was synthesized according to a literature procedure[13]. All catalytic reactions were performed under nitrogen using standard Schlenk techniques. All solvents and liquid reagents were degassed by two freeze-thaw cycles prior to use.

General Procedure for Isomerization Reactions of Allylic Alcohols: In a typical experiment (Table 1, entry 6), to $Ni(COD)_2$ (36 mg, 0.13 mmol) in a 50-ml glass reactor fitted with a Teflon cap was added a degassed solution of dppb (111 mg, 0.26 mmol) in toluene (5 ml). The solution rapidly turned orange. After 15 min of magnetic stirring, geraniol (**1**) (1.4 g, 9.1 mmol), decane (0.5 g, GLC internal standard) and finally a toluene solution of TFA (0.6 M, 0.85 ml, 0.51 mmol) were added. The solution immediately became deep-red-orange. Quantitative GLC analysis of this solution (Chrompack, CP Sil 5-CB column, 25 m × 0.32 mm) indicated that 5 mol-% of **1** had been converted into citronellal (**2**). The solution was stirred at 80°C and the reaction was monitored by removing aliquots and subjecting them to GLC analysis. A progressive colour change deep-red-orange to yellow was observed. Reactions in the presence of butane-1,2-diol were conducted in a similar manner.

All products were identified by comparison of retention times and spectral properties with those of authentic samples.

General Procedure for Isomerization Reactions of Allylic Alcohols in Biphasic Media: In a typical experiment, $Ni(COD)_2$ (35 mg, 0.13 mmol), dppbts (217 mg, 0.26 mmol), and either water (10 g) or a mixture of water (5 g) and dimethylformamide (5 g) were introduced under nitrogen into a glass tube reactor. After stirring with a magnetic bar for 2 h at 80°C, the solution took on an orange color and the insoluble $Ni(COD)_2$ had disappeared. This solution was then added to a mixture of **1** (1.4 g, 9.1 mmol), toluene (5 ml), and the chosen acid (0.52 mmol). The resulting mixture was stirred at 1000 rpm at 110°C and the reaction was monitored by GLC analysis of aliquots withdrawn from the organic phase.

[1] P. W. Jolly, G. Wilke, *The Organic Chemistry of Nickel*, Academic Press, New York, **1975**, vol. 2.

[2] [2a] B. Corain, G. Puosi, *J. Catal.* **1973**, *30*, 403−408. − [2b] B. Corain, *Gazz. Chim. Ital.* **1972**, *102*, 687−695.

[3] C. F. Lochow, R. G. Miller, *J. Org. Chem.* **1976**, *41*, 3020−3022.

[4] Isomerization of allylic alcohols proceeds with many other transition metal catalysts; *Molybdenum*: [4a] Y. Lin, X. Lu, *J. Organomet. Chem.* **1983**, *251*, 321−325. − *Iron*: [4b] G. F. Emerson, R. Pettit, *J. Am. Chem. Soc.* **1962**, *84*, 4591−4592. − [4c] R. Damico, T. J. Logan, *J. Org. Chem.* **1967**, *32*, 2356−2358. − [4d] F. G. Cowherd, J. L. von Rosenberg, *J. Am. Chem. Soc.* **1969**, *91*, 2157−2158. − *Rhodium*: [4e] W. Strohmeier, L. Weigelt, *J. Organomet. Chem.* **1975**, *86*, C17−C19. − [4f] C. Botteghi, G. Giacomelli, *Gazz. Chim. Ital.* **1976**, *106*, 1131−1134. − [4g] H. Alper, K. Hachem, *J. Org. Chem.* **1980**, *45*, 2269−2270. − [4h] M. Kitamura, K. Manabe, R. Noyori, H. Takaya, *Tetrahedron Lett.* **1987**, *28*, 4719−4720. − [4i] J. Park , C. S. Chin, *J. Chem. Soc., Chem. Commun.* **1987**, 1213−1214. − [4j] S. H. Bergens, B. Bosnich, *J. Am. Chem. Soc.* **1991**, *113*, 958−967. − [4k] A. M. Trzeciak, J. J. Ziolkowski, *Gazz. Chim. Ital.* **1994**, *124*, 403−409. − *Iridium*: [4l] D. Baudry, M. Ephritikhine, H. Felkin, *New J. Chem.* **1978**, *2*, 355−356. − [4m] C. S. Chin, J. Park, C. Kim, S. Y. Lee, J. H. Shin, J. B. Kim, *Catal. Lett.* **1988**, *1*, 203−206.

[5] [5a] H. Bricout, J. F. Carpentier, A. Mortreux, *J. Chem. Soc., Chem. Commun.* **1995**, 1863−1864. − [5b] H. Bricout, J. F. Carpentier, A. Mortreux, *Tetrahedron Lett.* **1996**, *37*, 6105−6108. − [5c] H. Bricout, J. F. Carpentier, A. Mortreux, *J. Chem. Soc., Chem. Commun.* **1997**, 1393−1394. − [5d] H. Bricout, J. F. Carpentier, A. Mortreux, *Tetrahedron* **1998**, *54*, 1073−1084.

[6] As an isolated $Ni(dppb)_2$ complex and a mixture of $Ni(COD)_2$ and two equiv. of dppb gave comparable results, all experiments in the course of this work were conducted by generating the catalyst precursor in situ from $Ni(COD)_2$ and two equiv. of dppb.

[7] This process has been reported to occur in the presence of Lewis[7a] and Brønsted[7b] acid catalysts: [7a] Y. Nakatani, K. Kawashima, *Synthesis* **1978**, *2*, 147−148. − [7b] C. Dean, D. Whittaker, *J. Chem. Soc., Perkin Trans. 2* **1990**, 1275−1277 and references cited therein.

[8] No geraniol could be detected in a control experiment using citronellal as the substrate.

[9] A variety of Ni coordination complexes of aldehydes and ketones have been reported:

[9a] Y.-H. Huang, J. A. Gladysz, *J. Chem. Educ.* **1988**, *65*, 298−300 and references cited therein. − [9b] Y.-J. Kim, K. Osakada, A. Yamamoto, *Bull. Chem. Soc. Jpn.* **1989**, *62*, 964−966.

[10] H. Bricout, A. Mortreux, E. Monflier, *J. Organomet. Chem.* **1998**, *553*, 469−471.

[11] J. M. Grosselin, C. Mercier, G. Allmang, F. Grass, *Organometallics* **1991**, *10*, 2126−2133.

[12] C. A. Tolman, *J. Am. Chem. Soc.* **1970**, *92*, 4217−4222.

[13] A. Andriollo, A. Bolivar, F. A. Lopez, D. E. Paez, *Inorg. Chim. Acta* **1995**, *238*, 187−197.

[98135]

The 3,5-Dichlorotrifluorophenyl Ligand, a Useful Tool for the Study of Coordination Modes and Dynamic Behavior of Complexes of Palladium and Platinum

M. Aránzazu Alonso, Juan A. Casares, Pablo Espinet*, Jesús M. Martínez-Ilarduya, and Celeste Pérez-Briso

Departamento de Química Inorgánica, Facultad de Ciencias, Universidad de Valladolid,
E-47005 Valladolid, Spain
Fax: (internat.) +34/983423013
E-mail: espinet@cpd.uva.es

Received May 6, 1998

Keywords: Palladium / Platinum / Aryl rotation / Through-space coupling interactions / Turnstile mechanism

The square-planar complexes $[MR_2L_2]$ (M = Pd, Pt; R = 3,5-$C_6Cl_2F_3$) [L_2 = $OPPyPh_2$ (Py = 2-pyridyl); $SPPyPh_2$; $OPPy_2Ph$; DMBI (3,3′-dimethyl-2,2′-biindazole); OPPyPh(NHTol-*p*); *p*-TolNPPy_2Ph] have been prepared by treating *cis*-$[MR_2(THF)_2]$ (THF = tetrahydrofuran) with the appropriate chelate ligands. The ^{19}F-NMR spectra of these complexes show the presence of intramolecular through-space F-F couplings between *ortho*-fluorine atoms of nonequivalent R groups, which provide information for the assignment of the different *ortho*-fluorine signals and can be used to study the dynamic behavior of the mentioned complexes such as: a) Rotation of the R group in either Pd or Pt complexes, at the same or at different rates for each R groups depending on the neutral ligand; and b) exchange of the coordination sites of the chelating ligand, either by Berry or by turnstile mechanisms. The activation parameters for some of the processes are given.

Introduction

Fluoroaryl ligands have been profusely used in organometallic chemistry because of the stability of their complexes, which enables the isolation of compounds not easily obtained with nonfluorinated analogs[1]. The thermal stability of the complexes obtained is such that it allows not only their use as models in mechanistic studies, but also the synthesis of some thermotropic metal-containing liquid crystals[2]. Another advantage of fluoroaryl ligands is the simplicity of their ^{19}F-NMR spectra relative to the usually blurred ^{1}H-NMR aromatic region. Although higher field NMR instruments have decreased the importance of this second advantage, for detailed mechanistic and dynamic studies fluoroaryl ligands, particularly the pentafluorophenyl group, are still preferred[3].

However, the simplicity of the ^{19}F-NMR spectra of C_6F_5 derivatives is often deceptive. In the course of our work on asymmetric *cis*-bis(pentafluorophenyl) derivatives of palladium and platinum we have used systematically ^{19}F-^{19}F COSY-NMR experiments to help with the assignment of the two sets of ^{19}F signals of the two nonequivalent C_6F_5 rings. This methodology permits to observe the presence of scalar coupling cross-peaks between the *ortho*-fluorine signals of different C_6F_5 groups, although clear observation of the splitting pattern due to these couplings is possible only for few complexes, by selective-decoupling experiments on the F_{meta} nuclei when these have almost coincident chemical shifts. The observation of through-space coupling is not uncommon in ^{19}F-NMR spectroscopy, and it has been reported that the magnitude of the coupling depends on the distance between the interacting nuclei[4]. A detailed study of these *J*(F-F) has been carried out for the different atropisomers of $[Pd(2\text{-}C_6BrF_4)_2L_2]$ and $[Pd(3\text{-}C_6BrF_4)_2L_2]$ (L_2 = $OPPy_2Ph$, 2 tht, etc.), establishing that through-space interactions contribute importantly to them[5]. This study revealed that the magnitude of the coupling between *ortho*-fluorine atoms at the same side of the coordination plane (*syn*) in *cis*-bis(polyfluorophenyl) complexes is larger than that for *ortho*-fluorine atoms at different sides (*anti*) (Figure 1). Hence, even if the ^{19}F-NMR spectra show well-separated chemical shifts and well-resolved signals for each inequivalent nucleus (which is a quite common case), in complexes with two or more fluoroaryl rings coordinated to the same metallic center the presence of through-space F-F couplings prevents easy simulation of the spin system, measurement of *J*(F-F) values, and the use of line-shape analysis (LSA) for quantitative measurement of dynamic processes when pentafluorophenyl or tetrafluorophenyl groups are used.

Figure 1. F-F coupling constants measured in $[Pd(2\text{-}C_6BrF_4)_2L_2]$ complexes

In order to minimize this undesired complication we have started to use 3,5-dichlorotrifluorophenyl instead of the pentafluorophenyl[6]. In this group the spin system is very simple: The coupling between the fluorine atoms in position

 © WILEY-VCH Verlag GmbH, D-69451 Weinheim, 1998 1434−1948/98/1111−1745 $ 17.50+.50/0

2 and 4, and between those in 4 and 6, is usually less than the half-height band width; then any multiplicity observed in the signals in the ^{19}F-NMR spectra is due only to intra-ring or inter-ring coupling of nuclei in the *ortho* position to the metal center (F_{ortho}). We will show here that this allows more stereochemical and dynamic information to be obtained than with the pentafluorophenyl rings, since the changes in the spin system due to the maintenance or not of the through-space coupling is an additional source of information. Another important advantage is that the longitudinal relaxation times T_1 for the F nuclei of 3,5-$C_6Cl_2F_3$ (1.5 to more than 3 s) are much longer than for C_6F_5, thus increasing the range of validity of the magnetization-transfer (MT) experiments for low exchange rates[7].

Results

The complexes [MR_2L_2] (M = Pd, **a** or Pt, **b**; R = 3,5-$C_6Cl_2F_3$) [L_2 = $OPPyPh_2$ (Py = 2-pyridyl), **1**; $SPPyPh_2$, **2**; $OPPy_2Ph$, **3**; DMBI (3,3′-dimethyl-2,2′-biindazole), **4**; OPPyPh(NHTol-*p*), **5**; *p*-TolNPPy_2Ph, **6**] were obtained by substitution of tetrahydrofuran in *cis*-[$MR_2(THF)_2$] under gentle conditions (Figure 2).

Figure 2. Ligands used to prepare complexes **1**−**6**

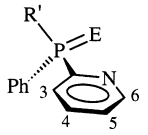

1 (E = O, R′ = Ph), **2** (E = S, R′ = Ph),
5 (E = O, R′ = NHTol-*p*),
6 (E = NTol-*p*, R′ = Py)

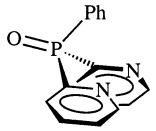

3

4

The solid-state IR spectra for all the isolated complexes show the characteristic infrared absorptions of the R group, and the presence of a split band in the region 710−670 cm^{-1} is in accordance with the presence of a *cis*-MR_2 arrangement[6a]. The shift to lower wavenumbers observed for ν(P=E) [E = O, S, N(C_6H_4Me-*p*)] for complexes **1**, **2**, **5**, and **6** relative to those of the free ligands[8][9] (see Experimental Section) suggests that, at least in the solid state, they are acting as E,N(Py) chelates. This is confirmed for their solutions by molecular-mass determinations with a vapor-pressure osmometer, which indicate monomeric species, and by the $^{31}P\{^1H\}$-NMR spectra which show the presence of only one isomer. However, the $OPPy_2Ph$ ligand behaves as N,N chelate in complexes **3**, as found for the C_6F_5 analogues[9b].

In the 300-MHz ^{1}H-NMR spectra of complexes **1**, **2**, **3**, **5**, and **6** the resonances due to the Py groups can be detected, although in some cases they overlap with Ph peaks. The analysis of the Py first-order subspectra is trivial[10]. The H^6 (the atom on C^6 in the Py groups) signal corresponds to a multiplet slightly broadened by the quadrupolar effect of the ^{14}N nucleus. Its chemical shift is very sensitive to coordination of the group and, when coordinated, to the *cis* ligand[9][11]. For a coordinated Py group in these complexes H^6 has a negative coordination-induced shift value, indicating its close proximity to the shielding zone of the adjacent R ring. The same effect is observed in the ^{1}H-NMR spectrum of **4**, where the H^7 (and $H^{7'}$) signal of the coordinated DMBI shows a clear upfield shift relative to the free ligand[12].

The complexes studied here have different symmetry elements giving rise to different chemical or magnetic equivalence situations in the ^{19}F-NMR spectra in a static situation. Moreover, they undergo some dynamic processes. Altogether they constitute good models of the possible static and dynamic circumstances that can occur in square-planar coordination, and illustrate how the 3,5-$C_6Cl_2F_3$ groups behave, or how they reflect these circumstances. Each situation is discussed in turn in the following. A schematic representation of the group, as shown in Figure 3, is used in the figures.

Figure 3. Schematic representation of the 3,5-$C_6Cl_2F_3$ group

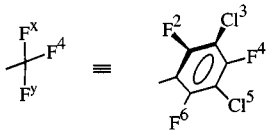

Complexes of Type I: [$MR_2(OPPyPh_2)$] (1) and [$MR_2(SPPyPh_2)$] (2)

These complexes have been studied both in $CDCl_3$ and [D_6]acetone solutions. The ligands $OPPyPh_2$ and $SPPyPh_2$ are coordinated through the pyridine nitrogen and the oxygen (in **1**) or the sulfur atom (in **2**) in an almost planar chelate ring. We have shown previously that there is a fast envelope-shift movement of the chelating ring, with a very low activation energy, which allows us to consider the five-membered metallacycle as planar for the rest of the discussion[9]. Thus, in a static situation the complexes have a C_s symmetry and the four F_{ortho} should give rise to an AA′BB′ spin system (Figure 4). The rotation of the R groups around the Pd−C bond in these complexes would produce exchange of chemically equivalent but magnetically inequivalent F_{ortho} nuclei.

Variable-temperature studies of **1a** and **1b** in $CDCl_3$ reveal that at room temperature the rotation of at least one of the R groups (most probably that *cis* to the oxygen atom, R^a, according to the results obtained for the related complexes **5**; see later) is fast, but on cooling the rotation is arrested. Thus, the appearance of the F_{ortho} signals changes from multiplets at low temperature, corresponding to an AA′BB′ spin system with J(AA′) and J(BB′) ≈ 0, to triplets (A_2B_2 system) as a result of the rotation of R^a which

Figure 4. Static structure of complexes of type I, and interconversion of the F_{ortho} as a result of the rotation of R[a]

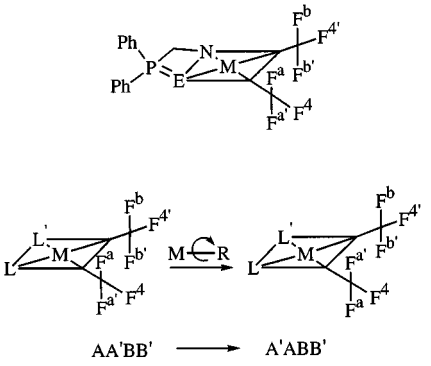

interconverts the *ortho*-fluorine atoms as shown in Figure 4.

It is possible to obtain kinetic data for the rotation of R by LSA provided that the different J values can be estimated by simulation of the static spectrum (Table 1). However, the variation of the coupling constants with temperature observed, and the short range of temperatures in which the line-shape changes are detectable [which is related to $J(AB) - J(AB')$] prevent accurate calculation of activation parameters other than $\Delta G^{\neq}$. With these limitations, only the spectra of **1a** in $CDCl_3$ and [D_6]acetone at 235.2 K have been simulated, yielding similar values of $\Delta G^{\neq}$ (Table 2). For **1b** we could not obtain numerical values of $\Delta G^{\neq}$, but the change in the appearance of the F_{ortho} signals shows that it is probably in the same order of magnitude.

The room temperature ^{19}F-NMR spectra of **2a** and **2b** in $CDCl_3$ and [D_6]acetone show that their F_{ortho} signals give rise to an AA′BB′ spin system indicating a rigid structure for these complex in which the R groups are not rotating around the Pd−C bond. However, on raising the temperature from 293 K to 332 K the appearance of the *ortho*-fluorine signals undergoes changes characteristic of the rotation of at least one of the R groups (Figure 5). These changes are more evident for **2b** in a shorter temperature interval, showing the smaller difference between $J(AB)$ and $J(AB')$ (Table 1) which average their values in the fast exchange limit. The values of $\Delta G^{\neq}$ calculated for **2a** ([D_6]acetone) and **2b** ($CDCl_3$) at 324.7 K are in accordance with the higher steric hindrance imposed by the bulkier S atom (or the Py group) compared to the O atom[9b].

Another possible process in compounds of type I is that N and O (in **1**) or S (in **2**) exchange their sites. In the fast-exchange limit all the F_{ortho} signals of both R groups should average, and also their F_{para} signals. In practice, this limit is not reached for any of the complexes, but above 282 K this exchange is easily detected for **1a** in [D_6]acetone by the broadening of all the signals. The temperature dependence of the exchange rate, measured by MT experiments and

Table 1. ^{19}F-NMR data for the *ortho*-fluorine region of selected complexes

Complex Solvent, T [K]	δ^{19}F (J_{FPt} [Hz]) F^a, F^b F^c, F^d	J_{FF} [Hz] J_{ab}, J_{ac}, J_{ad} J_{bc}, J_{bd}, J_{cd}
[PdR_2(OPPyPh$_2$)] (**1a**) $CDCl_3$, 208.4	−91.21, −91.21 −89.71, −89.71	0.0, 8.3, 3.8 3.8, 8.3, 0.0
[PtR_2(OPPyPh$_2$)] (**1b**) $CDCl_3$, 208.4	−94.16 (423), −94.16 (423) −93.19 (504), −93.19 (504)	$J_{ac} + J_{ad} = 8.3$ $J_{bc} + J_{bd} = 8.3$[a]
[PdR_2(SPPyPh$_2$)] (**2a**) [D_6]acetone, 293	−86.95, −86.95 −87.88, −87.88	0.0[b], 9.1, 3.2 3.2, 9.1, 1.7[b]
[PtR_2(SPPyPh$_2$)] (**2b**) $CDCl_3$, 293	−91.70 (420), −91.70 (420) −92.55 (427), −92.55 (427)	0.0[b], 5.3, 3.2 3.2, 5.3, 0.5[b]
[PdR_2(OPPy$_2$Ph)] (**3a**) $CDCl_3$, 208.4	−88.36, −91.48 −88.36, −91.48	0.7, J_{ac}[c], 1.6 1.6, J_{bd}[c], 0.7
[PtR_2(OPPy$_2$Ph)] (**3b**) $CDCl_3$, 208.4	−90.56 (390), −93.81 (399) −90.56 (390), −93.81 (399)	0.7, J_{ac}[c], 1.6 1.6, J_{bd}[c], 0.7
[PdR_2(DMBI)] (**4a**) $CDCl_3$, 293	−86.79, −91.05 −91.05, −86.79	−1.8, 8.2, 0.6[d] 4.8[d], 8.2, −1.8
[PdR_2{OPPyPh(NHTol-*p*)}] (**5a**) [D_6]acetone, 208.4	−89.42, −88.48 −87.80, −88.04	0.0, 6.4, 3.8 3.8, 7.0, 0.0
[PtR_2{OPPyPh(NHTol-*p*)}] (**5b**) [D_6]acetone, 208.4	−92.11, −90.92 −90.96, −91.13[e]	[a]
[PdR_2(*p*-TolNPPy$_2$Ph)] (**6a**) [D_6]acetone, 293	−88.44, −87.33 −86.72, −87.27	0.0, 11.1, 2.8 2.8, 14.8, 0.0
[PtR_2(*p*-TolNPPy$_2$Ph)] (**6b**) [D_6]acetone, 293	−90.50 (431), −89.10 (421) −89.32 (465), −89.88 (428)	2.4, 8.3, 2.4 2.4, 14.2, 2.4

[a] It is not possible to estimate all the coupling constants. − [b] The spectrum is unaffected if these coupling constants are interchanged. − [c] The magnitude of these coupling constants does not affect significatively the appearance of the spectrum. − [d] The spectrum is unaffected by the interchange of these coupling constants and their values reflect probably some distortions. − [e] Two broad satellites.

Table 2. Activation parameters for the different processes observed for complexes **1**−**6** (standard deviations in parentheses)

Complex	Process	Method	$\Delta G_{298}^{\neq}$ [kJ mol^{-1}][a]	$\Delta H^{\neq}$ [kJ mol^{-1}]	$\Delta S^{\neq}$ [J K^{-1} mol^{-1}]
1a[b]	rotation R^a	LSA	53.6 (0.3)[d]		
1a[b]	exchange $R^a \rightleftharpoons R^b$	MT + LSA	65.5 (0.5)	53.1 (0.4)	−41.5 (1.3)
1a[c]	rotation R^a	LSA	54.4 (0.5)[d]		
1a[c]	exchange $R^a \rightleftharpoons R^b$	MT	77.9 (0.8)[e]		
2a[b]	rotation R^a	LSA	75.1 (0.5)[f]		
2a[b]	exchange $R^a \rightleftharpoons R^b$	MT	79.42 (0.12)[e]		
2b[c]	rotation R^a	LSA	74.9 (0.5)[f]		
3a[c]	rotation R	MT and LSA	60.8 (0.7)	57.6 (0.5)	−10.7 (1.6)
3b[c]	rotation R	MT and LSA	60.2 (0.2)	56.3 (0.1)	−13.4 (0.5)
4[c]	rotation R	MT	85.92 (0.07)[g]		
5a[b]	rotation R^a	MT and LSA	55.1 (0.7)	45.4 (0.4)	−32.6 (1.8)
5a[b]	exchange $R^a \rightleftharpoons R^b$	MT and LSA	68.3 (0.6)	54.0 (0.4)	−48.1 (1.4)
5b[b]	rotation R^a	LSA	52.4 (1.3)	42.9 (0.8)	−32 (3)
6a[b]	exchange $R^a \rightleftharpoons R^b$	MT	75.95 (0.04)[e]		
6b[b]	rotation R^a	LSA	69 (2)	59.4 (1.7)	−32 (6)

[a] Unless otherwise stated. − [b] In [D_6]acetone. − [c] In $CDCl_3$. − [d] Measured only at 235.2 K. − [e] Measured only at 298 K. − [f] Measured only at 324.7 K. − [g] Measured only at 329.1 K.

Figure 5. Temperature dependence of the AA′ part in the range 290−332 K for **2a** ([D_6]acetone) and **2b** ($CDCl_3$)

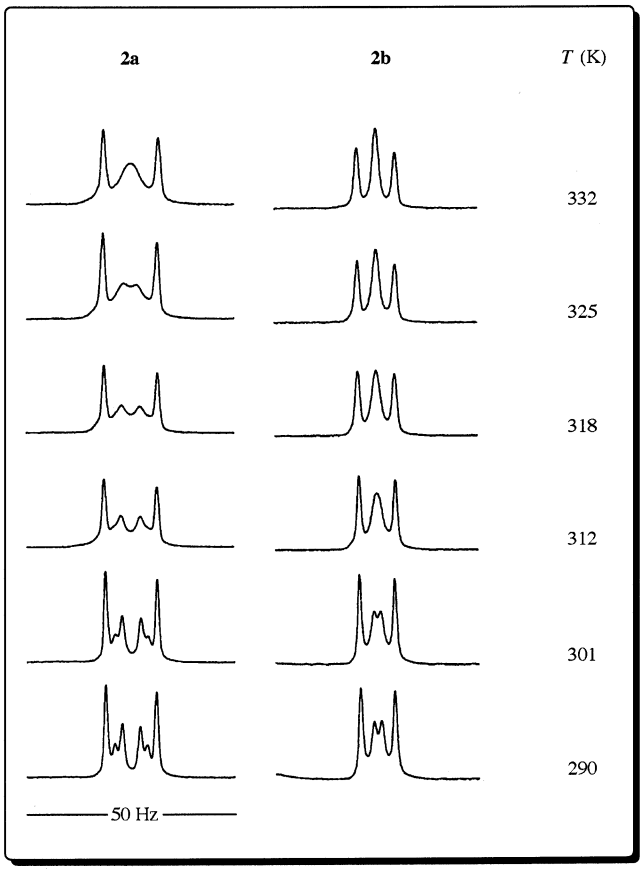

LSA on the F_{para} signals, allows us to calculate the activation parameters collected in Table 2. The exchange is solvent-dependent, and in $CDCl_3$ it is clearly much slower. The behavior of **2a** in [D_6]acetone is similar but with a lower rate; although the signals do not become broad it has been possible to measure k_{exch} at 298 K by MT experiments. In the platinum complexes, **1b** and **2b**, the exchange is not observed by MT.

The most plausible interpretation of this dependence on both the solvent and the metal center is a double substitution mechanism in which the solvent substitutes the weaker end of the chelating ligand (the oxygen atom in **1** or the sulfur or the Py nitrogen atom in **2**) at a rate measurable only in the kinetically labile Pd^{II} complexes, followed by the intramolecular substitution of the Py by the O or S atom, or by a reorganization in a pentacoordinate intermediate and the extrusion of the solvent molecule. However, the data available do not unequivocally support this hypothesis.

Complexes of Type II: [$MR_2(OPPy_2Ph)$] (3)

A detailed study of the related complexes [$M(C_6F_5)_2(OPPy_2Ph)$] has been recently published[9b]. The complexes [$MR_2(OPPy_2Ph)$] (**3**) have a C_s symmetry. In the slow-exchange limit the spin system of the F_{ortho} nuclei is AA′BB′ although the signals appear as broad singlets (approximately 4 Hz band width at half-height). The exchange, produced indistinctly by R rotation or by N,N exchange, renders equivalent the two sides above and below the coordination plane. Thus, in the fast-exchange limit the spin system becomes A_4 (Figure 6). In the case of **3**, the exchange is due to R rotation in the square-planar species without dissociation, which was measured and quantified by MT experiments or by LSA (Table 2).

Complexes of Type III: [$PdR_2(DMBI)$] (4a)

These complexes have a C_2 symmetry, common in enantiomerically pure ligands. With the ligand DMBI only the palladium compound has been studied, since with platinum an insoluble product was formed. The spin system of the F_{ortho} nuclei is again AA′BB′, but now the stereochemically

Figure 6. Interconversion of the F_{ortho} as a result of the rotation of R or by N,N exchange, and variable temperature ^{19}F-NMR spectra of [$PdR_2(OPPy_2Ph)$] (**3a**) in the F_{ortho} region

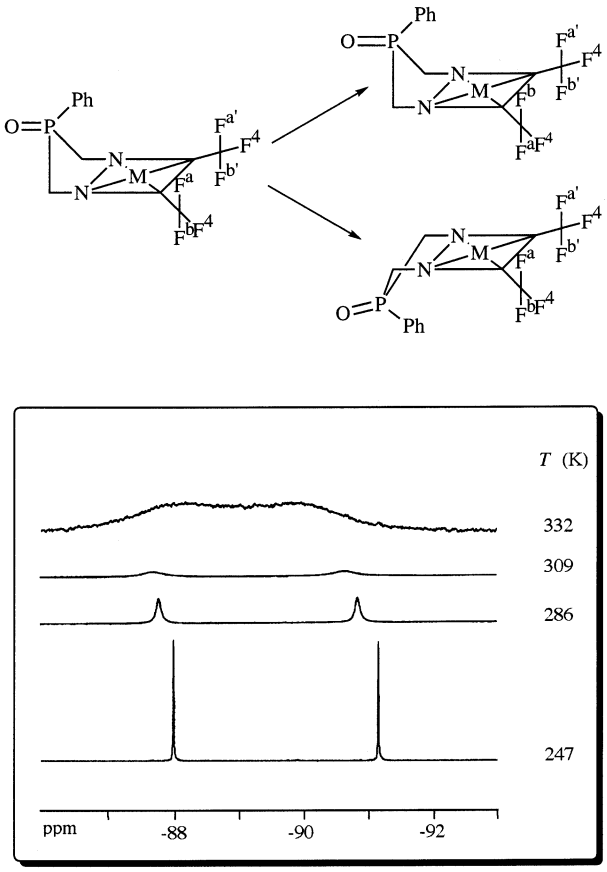

inequivalent nuclei are at the same side of the coordination plane (Figure 7). The origin of the nonplanarity of the coordinated DMBI is the methyl-methyl interaction. The twist of both indazole moieties about the N−N bond brings the protons H^7 and $H^{7'}$ close to the upfield F_{ortho} nuclei, which show some unresolved coupling (it can be removed by ^{1}H irradiation).

In this type of complexes the rotation of the aryl group should produce the equivalence of the *ortho*-fluorine nuclei (A_4). On the other hand, the two R groups (or their F_{para}) are equivalent by symmetry, so any exchange between the N coordination sites will not produce any observable effect, unless it occurs with concurrent R rotation. The latter should be the case if the exchange of coordination sites involved ligand dissociation, since R rotation becomes faster in a three-coordinate intermediate. The very slow exchange of the *ortho*-fluorine nuclei detected by MT at 329.1 K (Table 2) indicates a quite hindered rotation of the R groups in the tetracoordinate species.

Complexes of Type IV: [MR_2{OPPyPh(NHTol-*p*)}] (5) and [MR_2(*p*-TolNPPy_2Ph)] (6)

Complexes of type IV have the lowest symmetry, and in all the fluorine atoms are chemically inequivalent, giving

Figure 7. Static structure of complexes type III, and the AA′ part of the AA′BB′ spin system of the F_{ortho} for **4a** ($CDCl_3$, 293 K)

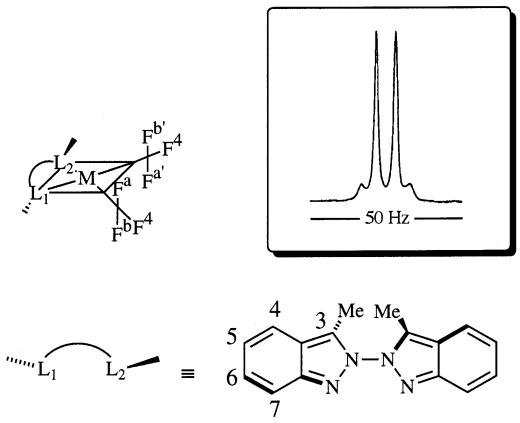

rise to an ABCD spin system in the low-exchange limit. The rotation of each group can be studied separately and also the stereochemistry of the exchange of the coordination sites of the chelated ligand.

As we have already mentioned, IR and ^{1}H- and ^{31}P{^{1}H}-NMR data indicate that the ligand OPPyPh(NHTol-*p*) is acting as O,N(Py) chelate in complexes **5**, like $OPPyPh_2$ in complexes **1**. In addition, only one stereoisomer is detected in solution for both complexes **5**, due to a rapid amine inversion process. Accordingly, four signals are expected in their ^{19}F-NMR spectra for the nonequivalent F_{ortho} nuclei. However, their ^{19}F-NMR spectra in [D_6]acetone at 293 K show only three signals in the F_{ortho} region, two of them with some splitting and the other very broad, in an intensity ratio of 1:1:2. This indicates that the two complexes behave similarly with one of the R groups (R^a) rotating fast at room temperature around the M−C bond, and the other apparently static. This is illustrated in Figure 8. The exchange interconverts the *ortho*-fluorine atoms according to the scheme ABCD ⇌ BACD, and F^4 and $F^{4'}$ remain unaffected.

Irradiation at room temperature of the broad signals assigned to R^a in **5a** and **5b** (F^a and F^b in Figure 8) led to the following results: For **5a** a simplification of the signals corresponding to R^b (the nonrotating group) from triplets to singlets is observed, which shows that for R^b $J(F^c\text{-}F^{4'})$ and $J(F^d\text{-}F^{4'})$ are smaller than the half-height band width. If the irradiation is used to presaturate the signal, a remarkable loss of intensity is observed in the others, confirming that a slow exchange is occurring between R^a and R^b. This last process will be further analyzed below considering the *para*-fluorine signals. For **5b** a simplification in R^b signals also occurs. Irradiation gives rise to two doublets from which it is possible to measure $J(F^c\text{-}F^d) = 2.8$ Hz.

At low temperature the rotation of the R^a group is arrested leading to inequivalence of its two F_{ortho} nuclei. The coalescence temperatures for **5a** and **5b** are 281 and 269 K, respectively.

For **5a** at temperatures below 258 K there is a change in the appearance of the signals; the *ortho*-fluorine atoms of R^b change from triplets in system A_2CD, with $J(CD) = 0$

Hz] to doublets of doublets [ABCD with $J(AB) = J(CD) = 0$ Hz]. Thus, in the slow-exchange limit the spectrum of the palladium complex **5a** consists of four doublets of doublets (Table 1, Figure 8). The signal assignment of the fluorine atoms on the same side of the coordination plane is straightforward considering the relative magnitudes of their coupling constants. Unfortunately, ^{1}H-^{19}F NOE experiments do not give clear results and it is not possible to tell F^a and F^c from F^b and F^d.

The activation parameters for the rotation of R^a in **5a** (Table 2) were determined by MT experiments and LSA in the range 200−282 K. The exchange between the N and O coordination sites in **5a** is also observable (Figure 8), and it has been possible to perform kinetic studies by MT experiments and LSA in the range 275−330 K in the F_{para} region, to determine the corresponding activation parameters.

Figure 8. Illustration of the rotation of R^a and the exchange between the N and O coordination sites for complexes **5**, and variable-temperature ^{19}F-NMR spectra of [PdR_2{OPPyPh(NHTol-*p*)}] (**5a**) in the F_{ortho} region

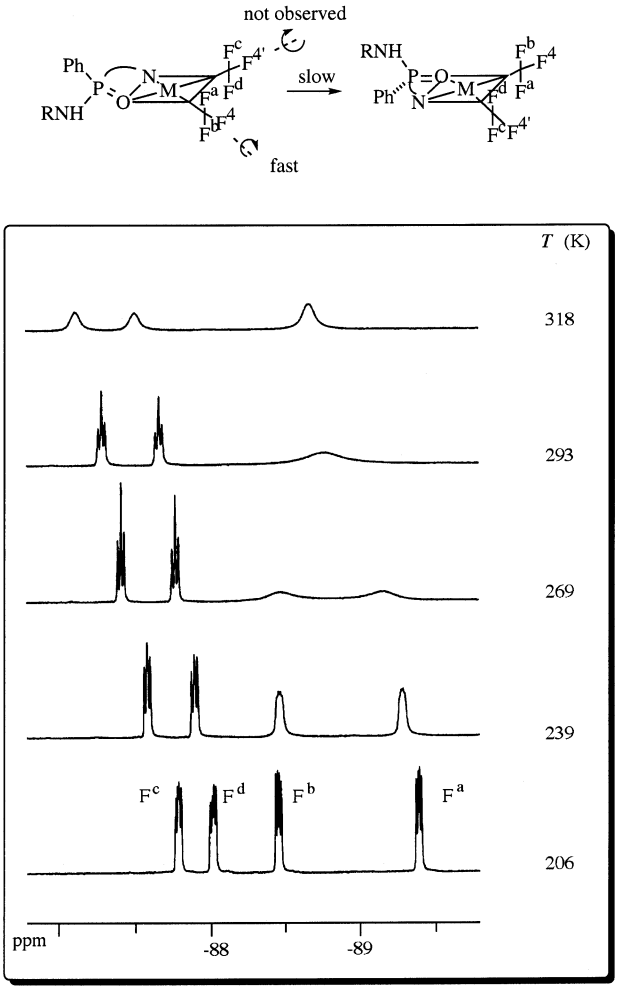

For the platinum complex **5b** LSA was performed in the temperature range in which the F_{ortho} signals are broad. There is no detectable exchange between R^a and R^b in this complex. The values of $^3J(^{195}Pt$-$^{19}F)$ measured in this complex confirm the assignment of R^a and R^b made in **5a**[6a][9b][13].

The room-temperature ^{1}H-NMR spectra of **6a** and **6b** in [D_6]acetone display the signals expected for two nonequivalent Py groups, one of them coordinated, and the ^{19}F-NMR spectra reveal four distinct fluorine environments associated with the F_{ortho} of the two nonequivalent R groups, which corresponds to a static structure for both complexes. Thus, their room-temperature spectra resemble the low-temperature spectra of **5a** and **5b** but with larger through-space coupling constants. When the temperature was increased **6a** and **6b** behaved differently. For **6b** a noticeable broadening of two F_{ortho} signals was observed and although the fast-exchange limit was not reached, this feature corresponds to the rotation of one of the R groups (R^a). Accordingly, the fine structure of the F_{ortho} signals of the nonrotating group (R^b) modified its appearance due to averaging of the couplings with the F_{ortho} of the rotating ring, in agreement with the simulated spectra. A good set of simulated band shapes was obtained for the spectra recorded, and the activation parameters derived are given in Table 2. Neither exchange between R^a and R^b, nor between the nonequivalent Py groups was detected for **6b** up to 325 K.

For **6a** only a slight broadening of the F_{ortho} signals was observed at 325 K, being the aryl rotation slow in the *J* time scale. MT experiments on ^{1}H Py signals and on ^{19}F F^4 signals of **6a** at 298 K confirm the slow exchanges between R^a and R^b [$k_{exch}(R^a \rightarrow R^b) = 0.30 \pm 0.01$] and between the nonequivalent Py groups [$k_{exch}(Py_{free} \rightarrow Py_{coord}) = 0.38 \pm 0.06$]. The similarity of both k_{exch} values (identical within the error limit) suggests that the two exchanges are produced by the same mechanism. The MT experiments on the *ortho*-fluorine nuclei at 298 K show a multi-step transfer (Figure 9). After the selective inversion of F^a, the intensity of the F^b signal decreased 30% after 0.6 s due to the rotation of the R group. There is also MT to F^c, which decreased 10% after 0.8 s, and to a smaller extent to F^d, which decreased 5% after 0.8 s (using the same numbering scheme as for complexes **5** in Figure 8). This experiment shows that the rotation of R^a is faster than the exchange between the N and N′ sites, and that the N,N′ exchange is stereoselective, since the magnetization is transferred from F^a preferentially to F^c. When the same experiment was performed by inversion of F^c there was simultaneous transfer to F^d and F^a, which decreased 10% after 1 s, while the transfer to F^b was slower and the signal decreased 7% after 1.4 s. Then the rotation of R^b has a rate comparable to the N,N′ exchange. The very low transfer of magnetization from F^a to F^d in the first experiment, or from F^c to F^b in the second, seems to be due to the fact that there is no transfer form the selectively inverted signal, but from the others when the MT has affected them. This selectivity supports a faster rotation for one of the aryl groups than for the other, as observed for **6b** and also for complexes **5**. It also suggests that the exchange between aryl groups takes place by a turnstile mechanism, with coordination of the free Py group to produce a square-pyramidal intermediate, supporting our previous observation that

Figure 9. Top: evolution of the signals of F^d (△), F^c (○) and F^b (+) after the selective inversion of F^a (▼) in complex **6a** ([D_6]acetone, 298 K); bottom: the same experiment by selective inversion of F^c

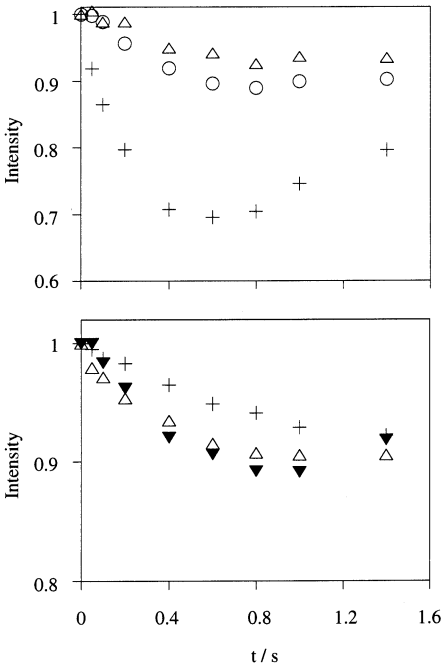

turnstile mechanisms are preferred to Berry mechanism for ligands favoring square-pyramidal geometry[14].

Conclusions

The compounds described in this paper allow the study of the inter-ring F-F coupling constants in *cis*-bis(3,5-dichlorotrifluorophenyl)palladium and -platinum units. In addition, they show that the use of this partially fluorinated ligand greatly facilitates their characterization and the study of their behavior in solution, which reveals the occurrence of the following processes: (a) fluoroaryl rotation, and (b) exchange between the coordination sites of the chelating ligand. The $\Delta G^{\neq}$ values associated with the aryl rotation processes (Table 2) reinforce our previous ideas suggesting that the rate of aryl rotation in square-planar complexes depends mainly on the steric hindrance by the atoms (or groups of atoms) coordinated to the metal center *cis* to the aryl ligand[9b].

Conversely, the patterns observed for the fluorine signals can be used to assign the coordination mode of the neutral ligands, or to detect some dynamic processes they might be undergoing. Thus, exchange between the coordination sites of the chelating ligand has been observed for the palladium complexes **1a**, **2a**, **5a**, and **6a**, and the low values of $\Delta S^{\neq}$ for **1a** and **5a** suggest an associative mechanism by a pentacoordinate mechanism. An incoming solvent does not impose any geometric restriction in the pentacoordinate intermediate, so a Berry mechanism seems most probable[15], but when the pentacoordination is achieved with the aid of one arm of the chelating ligand with a small bite angle (as for **6a**), the turnstile mechanism seems to be preferred[14].

We are very grateful to Dr. *A. L. Casado* for helpful discussions. Financial support was granted by the *Dirección General de Enseñanza Superior* (Project No. PB96-0363) and the *Junta de Castilla y León* (Project No. VA18/97). The *Ministerio de Educación y Cultura* is gratefully acknowledged for a fellowship to M. A. A.

Experimental Section

General Considerations: All reactions were performed under nitrogen in deoxygenated solvents, although subsequent manipulations were carried out in air, except where otherwise stated. Solvents were dried by standard methods and freshly distilled under nitrogen prior to use[16]. − C,H,N analyses were obtained with a Perkin-Elmer 2400B microanalyzer. − Molecular-mass determinations were carried out with a Knauer vapour-pressure osmometer, in $CHCl_2CHCl_2$ at 303 K (the solubility of **3b**, **4a**, and **5b** was too low to carry out this determination). − IR spectra were recorded (in the range 4000−200 cm^{-1}) with a Perkin-Elmer 883 spectrophotometer using samples mulled in Nujol between polyethylene films. − ^1H-, ^{19}F-, and $^{31}P\{^1H\}$-NMR spectra were recorded with a Bruker ARX 300 spectrometer (300.13, 282.35, and 121.44 MHz, respectively) equipped with a VT-100 variable-temperature unit. Temperature calibration was performed before measurements using the temperature-dependent chemical shift differences of the ^1H resonances of methanol (175−313 K) or ethylene glycol (310−410 K)[17]. Chemical shifts are relative to TMS (^1H), $CFCl_3$ at 293 K (^{19}F), or external 85% H_3PO_4 (^{31}P), with downfield values reported as positive. In some of the kinetic studies the magnetization transfer from a selective inverted peak was observed as a function of time. The selective excitation was executed using the known 1-1 sequence or with a Gaussian-shaped soft pulse, and the data analysis was carried out as described in the literature[18]. The computer simulation of the variable-temperature NMR spectra was carried out by line-shape analysis using the standard DNMR 6 program[19]. − The following starting materials were prepared according to published procedures: $OPPyPh_2$[20], $SPPyPh_2$[21], $OPPy_2Ph$[20], DMBI[22], *cis*-$[MR_2(THF)_2]$[6a]. The monophosphazene (*p*-MeC_6H_4)$NPPy_2Ph$ was synthesized by reaction of equimolar amounts of PPy_2Ph (made as reported for PPy_3[23], but starting from $PPhCl_2$) and the organic azide[24] in toluene. Hydrolysis in chloroform of this monophosphazene produced the ligand $OPPyPh\{NH(C_6H_4Me\text{-}p)\}$.

Preparation of the Complexes [MR_2L_2]: To a solution of *cis*-$[MR_2(THF)_2]$ (0.2 mmol) in 20 ml of $CHCl_3$ was added 0.2 mmol of the ligand ($OPPyPh_2$: 56 mg; $SPPyPh_2$: 60 mg; $OPPy_2Ph$: 56 mg; DMBI: 53 mg; OPPyPh(NHTol-*p*): 62 mg; *p*-$TolNPPy_2Ph$: 74 mg). The solution was stirred for 1 h and then concentrated to ca. 5 ml and stored at 243 K. Yellow or white crystals precipitated which were filtered off, washed with diethyl ether, and vacuum-dried.

[$PdR_2(OPPyPh_2)$] (**1a**): Yield: 132 mg (84%). − IR (cm^{-1}): $\tilde{\nu}$ = 1134 (P=O) (free ligand 1203), 706, 692 (R). − ^1H NMR ($CDCl_3$, 293 K): δ = 7.99 (m, 1 H, H^6 Py), 7.95 (m, 1 H, H^4 Py), 7.90−7.45 (12 H). − ^{19}F NMR ($CDCl_3$, 293 K): δ = −88.91 (t, *J* = 7 Hz, 2 F, F_{ortho}), −90.68 (t, *J* = 7 Hz, 2 F, F_{ortho}), −118.68 (s, 1 F, F_{para}), −119.68 (s, 1 F, F_{para}). − $^{31}P\{^1H\}$ NMR ($CDCl_3$, 293 K): δ = 49.8 (free ligand 21.5). − $C_{29}H_{14}Cl_4F_6NOPPd$ (785.61): calcd. C 44.34, H 1.80, N 1.78; found C 44.49, H 1.90, N 1.76. − Molecular mass: calcd. 786; found 808.

[$PtR_2(OPPyPh_2)$] (**1b**): Yield: 149 mg (85%). − IR (cm^{-1}): $\tilde{\nu}$ = 1134 (P=O) (free ligand 1203), 708, 695 (R). − ^1H NMR ($CDCl_3$,

293 K): δ = 8.30 (m, J_{HPt} = 23 Hz, 1 H, H^6 Py), 8.06 (m, 1 H, H^4 Py), 7.77 (m, 1 H, H^5 Py), 7.71−7.59 (10 H, Ph), 7.53 (m, 1 H, H^3 Py). − ^{19}F NMR ($CDCl_3$, 293 K): δ = −92.33 (t, J = 4.4 Hz, J_{FPt} = 505 Hz, 2 F, F_{ortho}), −93.44 (t, J = 4.4 Hz, J_{FPt} = 427 Hz, 2 F, F_{ortho}), −120.16 (s, 1 F, F_{para}), −120.67 (s, 1 F, F_{para}). − $^{31}P\{^1H\}$ NMR ($CDCl_3$, 293 K): δ = 55.2 (J_{PPt} = 37 Hz) (free ligand 21.5). − $C_{29}H_{14}Cl_4F_6NOPPt$ (874.30): calcd. C 39.84, H 1.61, N 1.60; found C 40.06, H 2.13, N 1.53. − Molecular mass: calcd. 874; found 887.

[PdR$_2$(SPPyPh$_2$)] (**2a**): Yield: 135 mg (84%). − IR (cm^{-1}): ν̃ = 701, 686 (R), 631 (P=S) (free ligand 645). − ^{1}H NMR ($CDCl_3$, 293 K): δ = 8.20 (m, 1 H, H^6 Py), 7.90 (m, 1 H, H^4 Py), 7.85−7.60 (10 H, Ph), 7.46 (m, 1 H, H^5 Py), 7.36 (m, 1 H, H^3 Py). − ^{19}F NMR ($CDCl_3$, 293 K): δ = −89.31 (m, 2 F, F_{ortho}), −89.44 (m, 2 F, F_{ortho}), −118.75 (s, 1 F, F_{para}), −120.30 (s, 1 F, F_{para}). − $^{31}P\{^1H\}$ NMR ($CDCl_3$, 293 K): δ = 47.9 (free ligand 38.1). − $C_{29}H_{14}Cl_4F_6NPPdS$ (801.67): calcd. C 43.45, H 1.76, N 1.75; found C 43.79, H 1.93, N 1.84. − Molecular mass: calcd. 802; found 818.

[PtR$_2$(SPPyPh$_2$)] (**2b**): Yield: 103 mg (58%). − IR (cm^{-1}): ν̃ = 698, 687 (R), 629 (P=S) (free ligand 645). − ^{1}H NMR ($CDCl_3$, 293 K): δ = 8.48 (m, J_{HPt} = 28 Hz, 1 H, H^6 Py), 8.00 (m, 1 H, H^4 Py), 7.85−7.55 (10 H, Ph), 7.45 (m, 1 H, H^5 Py), 7.34 (m, 1 H, H^3 Py). − ^{19}F NMR ($CDCl_3$, 293 K): δ = −91.70 (m, J_{FPt} = 419 Hz, 2 F, F_{ortho}), −92.55 (m, J_{FPt} = 427 Hz, 2 F, F_{ortho}), −119.85 (s, 1 F, F_{para}), −121.37 (s, 1 F, F_{para}). − $^{31}P\{^1H\}$ NMR ($CDCl_3$, 293 K): δ = 47.2 (J_{PPt} = 82 Hz) (free ligand 38.1). − $C_{29}H_{14}Cl_4F_6NPPtS$ (890.36): calcd. C 39.12, H 1.59, N 1.57; found C 38.94, H 1.83, N 1.33. − Molecular mass: calcd. 890; found 865.

[PdR$_2$(OPPy$_2$Ph)] (**3a**): Yield: 134 mg (85%). − IR (cm^{-1}): ν̃ = 1216 (P=O) (free ligand 1207), 703, 688 (R). − ^{1}H NMR ($CDCl_3$, 293 K): δ = 8.76−8.62 (4 H, H^6 + H^3 Py), 8.13 (m, 2 H, H^4 Py), 7.84−7.59 (m, 5 H, Ph), 7.55 (m, 2 H, H^5 Py). − ^{19}F NMR ($CDCl_3$, 293 K): δ = −87.75 (br., 2 F, F_{ortho}), −90.79 (br., 2 F, F_{ortho}), −118.49 (s, 2 F, F_{para}). − $^{31}P\{^1H\}$ NMR ($CDCl_3$, 293 K): δ = 20.7 (free ligand 17.7). − $C_{28}H_{13}Cl_4F_6N_2OPPd$ (786.60): calcd. C 42.76, H 1.67, N 3.56; found C 42.72, H 1.99, N 3.40. − Molecular mass: calcd. 787; found 773.

[PtR$_2$(OPPy$_2$Ph)] (**3b**): Yield: 145 mg (83%). − IR (cm^{-1}): ν̃ = 1217 (P=O) (free ligand 1207), 708, 689 (R). − ^{1}H NMR ($CDCl_3$, 293 K): δ = 8.87 (m, J_{HPt} = 33 Hz, 2 H, H^6 Py), 8.71 (m, 2 H, H^3 Py), 8.17 (m, 2 H, H^4 Py), 7.80−8.50 (7 H). − ^{19}F NMR ($CDCl_3$, 293 K): δ = −90.06 (br., J_{FPt} = 386 Hz, 2 F, F_{ortho}), −93.07 (br., J_{FPt} = 394 Hz, 2 F, F_{ortho}), −119.32 (s, 2 F, F_{para}). − $^{31}P\{^1H\}$ NMR ($CDCl_3$, 293 K): δ = 22.3 (J_{PPt} = 166 Hz) (free ligand 17.7). − $C_{28}H_{13}Cl_4F_6N_2OPPt$ (875.29): calcd. C 38.42, H 1.50, N 3.20; found C 38.51, H 1.70, N 3.26.

[PdR$_2$(DMBI)] (**4a**): Yield: 138 mg (90%). − IR (cm^{-1}): ν̃ = 700, 693 (R). − ^{1}H NMR ($CDCl_3$, 293 K): δ = 7.56 (d, J = 8.6 Hz, 2 H, $H^{4,4'}$ DMBI), 6.84 (dd, J = 8.6 and 6.6 Hz, 2 H, $H^{5,5'}$ DMBI), 6.50 (dd, J = 8.8 and 6.6 Hz, 2 H, $H^{6,6'}$ DMBI), 5.53 (d, J = 8.8 Hz, 2 H, $H^{7,7'}$ DMBI), 3.12 (s, 6 H, Me DMBI). − ^{19}F NMR ($CDCl_3$, 293 K): δ = −86.79 (m, 2 F, F_{ortho}), −91.05 (m, 2 F, F_{ortho}), −118.31 (s, 2 F, F_{para}). − $C_{28}H_{14}Cl_4F_6N_4Pd$ (768.65): calcd. C 43.75, H 1.84, N 7.29; found C 43.81, H 1.91, N 7.15.

[PdR$_2${OPPyPh(NHTol-p)}] (**5a**): Yield: 114 mg (70%). − IR (cm^{-1}): ν̃ = 3341 (N−H), 1143 (P=O) (free ligand 1202), 704, 693 (R). − ^{1}H NMR ([D$_6$]acetone, 293 K): δ = 8.53 (d, J_{HP} = 12.4 Hz, 1 H, NH), 8.38−8.27 (3 H), 8.18 (m, 1 H, H^4 Py), 8.08 (m, 1 H, H^6 Py), 7.87−7.65 (4 H), 7.40−7.08 (m, 4 H, C_6H_4), 2.24 (s, 3 H, Me). − ^{19}F NMR ([D$_6$]acetone, 293 K): δ = −87.27 (t, J = 6.2 Hz, 1 F, F_{ortho}), −87.64 (t, J = 6.4 Hz, 1 F, F_{ortho}), −88.72 (vbr., 2 F, F_{ortho}), −119.49 (s, 1 F, F_{para}), −120.03 (s, 1 F, F_{para}). − $^{31}P\{^1H\}$ NMR ([D$_6$]acetone, 293 K): δ = 37.7 (free ligand 11.6). − $C_{30}H_{17}Cl_4F_6N_2OPPd$ (814.65): calcd. C 44.23, H 2.10, N 3.44; found C 43.88, H 2.24, N 3.25. − Molecular mass: calcd. 815; found 779.

[PtR$_2${OPPyPh(NHTol-p)}] (**5b**): Yield: 128 mg (71%). − IR (cm^{-1}): ν̃ = 3342 (N−H), 1139 (P=O) (free ligand 1202), 705, 689 (R). − ^{1}H NMR ([D$_6$]acetone, 293 K): δ = 8.76 (d, J_{HP} = 13 Hz, 1 H, NH), 8.40−8.20 (5 H), 7.88−7.65 (4 H), 7.40−7.06 (m, 4 H, C_6H_4), 2.23 (s, 3 H, Me). − ^{19}F NMR ([D$_6$]acetone, 293 K): δ = −90.40 (m, J_{FPt} = 508 Hz, 1 F, F_{ortho}), −90.71 (m, J_{FPt} = 512 Hz, 1 F, F_{ortho}), −91.26 (br., J_{FPt} = 424 Hz, 2 F, F_{ortho}), −121.32 (s, 1 F, F_{para}), −121.37 (s, 1 F, F_{para}). − $^{31}P\{^1H\}$ NMR ([D$_6$]acetone, 293 K): δ = 44.6 (broad satellites) (free ligand 11.6). − $C_{30}H_{17}Cl_4F_6N_2OPPt$ (903.34): calcd. C 39.89, H 1.90, N 3.10; found C 39.91, H 1.96, N 3.21.

[PdR$_2$(p-TolNPPy$_2$Ph)] · CHCl$_3$ (**6a**·$CHCl_3$): Yield: 119 mg (60%). − IR (cm^{-1}): ν̃ = 1270 (P=N) (free ligand 1316), 699, 689 (R). − ^{1}H NMR ([D$_6$]acetone, 293 K): δ = 8.95 (m, 1 H, H^6 Py_{free}), 8.67 (m, 1 H, H^3 Py_{free}), 8.30−8.15 (3 H), 8.10−8.00 (m, 2 H, Ph), 8.02 (s, 1 H, $CHCl_3$), 7.97 (m, 1 H, H^3 Py_{coord}), 7.83−7.70 (3 H), 7.67−7.58 (m, 2 H, Ph), 6.73−6.52 (m, 4 H, C_6H_4), 1.97 (s, 3 H, Me). − ^{19}F NMR ([D$_6$]acetone, 293 K): δ = −86.72 (dd, J = 11.1 and 2.8 Hz, 1 F, F_{ortho}), −87.27 (m, J = 14.8 and 2.8 Hz, 1 F, F_{ortho}), −87.33 (m, J = 14.8 and 2.8 Hz, 1 F, F_{ortho}), −88.44 (dd, J = 11.1 and 2.8 Hz, 1 F, F_{ortho}), −119.95 (s, 1 F, F_{para}), −121.93 (s, 1 F, F_{para}). − $^{31}P\{^1H\}$ NMR ([D$_6$]acetone, 293 K): δ = 27.7 (free ligand −6.1). − $C_{35}H_{20}Cl_4F_6N_3PPd \cdot CHCl_3$ (995.12): calcd. C 43.45, H 2.13, N 4.22; found C 43.79, H 2.22, N 4.04. − Molecular mass: calcd. 876; found 850.

[PtR$_2$(p-TolNPPy$_2$Ph)]·0.5 CHCl$_3$ (**6b**·0.5 $CHCl_3$): Yield: 124 mg (61%). − IR (cm^{-1}): ν̃ = 1273 (P=N) (free ligand 1316), 711, 701 (R). − ^{1}H NMR ([D$_6$]acetone, 293 K): δ = 8.96 (m, 1 H, H^6 Py_{free}), 8.73 (m, 1 H, H^3 Py_{free}), 8.55 (m, J_{HPt} = 29 Hz, 1 H, H^6 Py_{coord}), 8.30 (m, 1 H, H^4 Py_{coord}), 8.25 (m, 1 H, H^4 Py_{free}), 8.10−7.98 (m, 2 H, Ph), 8.02 (s, 0.5 H, $CHCl_3$), 7.93 (m, 1 H, H^3 Py_{coord}), 7.81 (m, 1 H, H^5 Py_{free}), 7.78−7.68 (2 H), 7.65−7.57 (m, 2 H, Ph), 6.84−6.54 (m, 4 H, C_6H_4), 1.98 (s, 3 H, Me). − ^{19}F NMR ([D$_6$]acetone, 293 K): δ = −89.10 (dt, J = 14.2 and 2.4 Hz, J_{FPt} = 428 Hz, 1 F, F_{ortho}), −89.32 (dt, J = 8.3 and 2.4 Hz, J_{FPt} = 458 Hz, 1 F, F_{ortho}), −89.88 (dt, J = 14.2 and 2.4 Hz, J_{FPt} = 430 Hz, 1 F, F_{ortho}), −90.50 (dt, J = 8.3 and 2.4 Hz, J_{FPt} = 434 Hz, 1 F, F_{ortho}), −121.53 (s, 1 F, F_{para}), −123.11 (s, 1 F, F_{para}). − $^{31}P\{^1H\}$ NMR ([D$_6$]acetone, 293 K): δ = 31.2 (J_{PPt} = 67 Hz) (free ligand −6.1). − $C_{35}H_{20}Cl_4F_6N_3PPt \cdot 0.5\ CHCl_3$ (1024.12): calcd. C 41.64, H 2.02, N 4.10; found C 41.48, H 2.06, N 4.10. − Molecular mass: calcd. 964; found 949.

[1] [1a] A. J. Canty in *Comprehensive Organometallic Chemistry* (Eds.: E. W. Abel, F. G. A. Stone, G. Wilkinson), Pergamon Press, Oxford, **1995**, vol. 9, chapter 5. − [1b] P. M. Maitlis, P. Espinet, M. J. H. Russell. in *Comprehensive Organometallic Chemistry* (Eds.: E. W. Abel, F. G. A. Stone, G. Wilkinson), Pergamon Press, Oxford, **1982**, vol. 6, chapter 38.4. − [1c] R. Usón, J. Forniés, *Adv. Organomet. Chem.* **1988**, *28*, 219−297.

[2] R. Bayón, S. Coco, P. Espinet, C. Fernández-Mayordomo, J. M. Martín-Alvarez, *Inorg. Chem.* **1997**, *36*, 2329−2334.

[3] For recent examples see: [3a] A. L. Casado, J. A. Casares, P. Espinet, *Organometallics* **1997**, *16*, 5730−5736. − [3b] K. G. Orrell, A. G. Osborne, V. Sik, M. V. da Silva, *J. Organomet. Chem.* **1997**, *530*, 235−246. − [3c] A. Gelling, M. D. Olsen, K. G. Orrell, A. G. Osborne, V. Sik, *Chem. Commun.* **1997**, 587−588. − [3d] E. W. Abel, A. Gelling, K. G. Orrell, A. G. Osborne, V. Sik, *Chem. Commun.* **1996**, 2329−2330. − [3e] A. C. Albéniz, P. Espinet, Y.-S. Lin, *J. Am. Chem. Soc.* **1996**, *118*, 7145−7152 and references therein.

[4] L. Ernst, K. Ibrom, *Angew. Chem.* **1995**, *107*, 2010−2012; *Angew. Chem. Int. Ed. Engl.* **1995**, *34*, 1881−1882.
[5] A. C. Albéniz, A. L. Casado, P. Espinet, *Organometallics* **1997**, *16*, 5416−5423.
[6] [6a] P. Espinet, J. M. Martínez-Ilarduya, C. Pérez-Briso, A. L. Casado, M. A. Alonso, *J. Organomet. Chem.* **1998**, *551*, 9−20. − [6b] A. L. Casado, P. Espinet, *Organometallics* **1998**, *17*, 954−959.
[7] [7a] J. Sandström, *Dynamic NMR Spectroscopy*, Academic Press, London, **1982**, chapter 4. − [7b] J.-J. Delpuech in *Dynamics of Solutions and Fluid Mixtures by NMR* (Ed.: J.-J. Delpuech), John Wiley & Sons, Chichester, **1995**, chapter 3.
[8] [8a] F. A. Cotton, R. D. Barnes, E. Bannister, *J. Chem. Soc.* **1960**, 2199−2203. − [8b] M. G. King, G. P. McQuillan, *J. Chem. Soc. A* **1967**, 898−901.
[9] [9a] J. A. Casares, S. Coco, P. Espinet, Y.-S. Lin, *Organometallics* **1995**, *14*, 3058−3067. − [9b] J. A. Casares, P. Espinet, J. M. Martínez-Ilarduya, Y.-S. Lin, *Organometallics* **1997**, *16*, 770−779.
[10] G. E. Griffin, W. A. Thomas, *J. Chem. Soc. B* **1970**, 477−479.
[11] [11a] P. K. Byers, A. J. Canty, *Organometallics* **1990**, *9*, 210−220. − [11b] R. E. Rülke, J. M. Ernsting, A. L. Spek, C. J. Elsevier, P. W. N. M. van Leeuwen, K Vrieze, *Inorg. Chem.* **1993**, *32*, 5769−5778. − [11c] E. W. Abel, K. G. Orrell, A. G. Osborne, H. M. Pain, V. Sick, M. B. Hursthouse, K. M. A. Malik, *J. Chem. Soc.*, *Dalton Trans.* **1994**, 3441−3449.
[12] A. C. Albéniz, J. C. Cuevas, P. Espinet, J. de Mendoza, P. Prados, *J. Organomet. Chem.* **1991**, *410*, 257−263.
[13] [13a] R. Usón, J. Forniés, M. Tomás, B. Menjón, C. Fortuño, A. J. Welch, D. E. Smith, *J. Chem. Soc., Dalton Trans.* **1993**, 275−280. − [13b] R. Usón, J. Forniés, M. A. Usón, S. Herrero, *J. Organomet. Chem.* **1993**, *447*, 137−144. − [13c] J. M. Casas, L. R. Falvello, J. Forniés, A. Martín, *Inorg. Chem.* **1996**, *35*, 56−62.
[14] J. A. Casares, P. Espinet, *Inorg. Chem.* **1997**, *36*, 5428−5431.
[15] M. L. Tobe in *Comprehensive Coordination Chemistry* (Eds.: G. Wilkinson, R. D. Gillard, J. A. McCleverty), Pergamon Press, Oxford, **1987**, vol. 1, chapter 7, p. 318−320.
[16] D. D. Perrin, W. L. F. Armarego, *Purification of Laboratory Chemicals*, 3rd ed., Pergamon Press, Oxford, **1988**.
[17] A. L. Van Geet, *Anal. Chem.* **1970**, *42*, 679−680.
[18] M. L. H. Green, A. Sella, L.-L. Wong, *Organometallics* **1992**, *11*, 2650−2659.
[19] DNMR6, *Quantum Chemical Program Exchange (QCPE 633)*, Indiana University, Bloomington, IN, **1995**.
[20] G. R. Newkome, D. C. Hager, *J. Org. Chem*. **1978**, *43*, 947−949.
[21] F. G. Mann, J. Watson, *J. Org. Chem*. **1948**, *13*, 502−531.
[22] J. C. Cuevas, J. de Mendoza, P. Prados, *J. Org. Chem*. **1988**, *53*, 2055−2066.
[23] K. Kurtev, D. Ribola, R. A. Jones, D. J. Cole-Hamilton, G. Wilkinson, *J. Chem. Soc., Dalton Trans.* **1980**, 55−58.
[24] R. O. Lindsay, C. F. H. Allen, *Org. Synth., Coll. Vol.* **1955**, *3*, 710−711.

[98136]

Silicon Compounds with Strong Intramolecular Steric Interactions, 68[◇]

Silylene Reactions with Nitrogen Multiple Bonds: Additions and Rearrangements☆

Manfred Weidenbruch*[a], Susanne Olthoff[a], Wolfgang Saak[a], and Heinrich Marsmann[b]

Fachbereich Chemie der Universität Oldenburg[a],
Carl-von-Ossietzky-Straße 9–11, D-26111 Oldenburg, Germany

Fachbereich Chemie der Universität-GH Paderborn[b],
Warburger Straße 100, D-33095 Paderborn, Germany

Received May 20, 1998

Keywords: Silicon / Silylene / Azobenzene / 1-Adamantyl azide / Addition reactions

Reactions of the sterically encumbered silylenes R_2Si**:** (R = 2,4,6-$Me_3C_6H_2$, 2,4,6-$iPr_3C_6H_2$) with azobenzene are thought to proceed via the [2+1] cycloaddition products, followed by insertion of the N–N single bond into the *ortho*-C–H bond of one of the phenyl rings or into the C–*H*Me_2 bond of one of the *ortho*-isopropyl groups to furnish the 1,3-diaza-2-silaindan (**4**) or 1-aza-2-silaindan (**5**) derivatives, respectively. The reactions of these silylenes with 1-adamantyl azide seem to proceed through the silanimines and 4-azahomoadamantene intermediates which, by [2+2] cycloadditions, afford the 1,3-diaza-2-silacyclobutane derivatives **11** and **12**. The structures of **4**, **5**, **11**, and **12** were determined by X-ray crystallography.

Introduction

The addition of silylenes, R_2Si**:**, to homo- and heteronuclear multiple bonds is now an established method for the preparation of three-membered ring systems containing silicon atoms. The reactions are particularly facilitated by the presence of bulky alkyl or aryl groups which hinder subsequent rearrangements of the primarily formed three-membered rings.[2][3] However, the course of silylene addition to nitrogen−nitrogen double bonds is still somewhat ambiguous. Even though the first − and as yet only − diazasilirane of the type **3** was prepared in 1982 by a different route,[4] a structural characterization of this three-membered ring system has not yet been achieved. Recently, Ando et al.[5] reported on the photolysis of hexamesitylcyclotrisilane, which is known to decompose into dimesitylsilylene and tetramesityldisilene on exposure to light,[6] in the presence of azobenzene. Although the [2+2] cycloaddition product of the disilene to the N=N double bond was completely characterized, the putative [2+1] cycloaddition product of the silylene was only obtained in the form of a hydrolysis product of the diazasilirane ring system.

We now describe the reactions of two diarylsilylenes bearing sterically demanding substituents with azobenzene and with 1-adamantyl azide (**6**) and the unusual addition and rearrangement products isolated thereby.

[◇] Part 67: See ref.[1].

Results and Discussion

Irradiation of a solution of the trisilane **1**, which results in the silylene R_2Si**:** (R = 2,4,6-$Me_3C_6H_2$) together with hexamethyldisilane, in the presence of azobenzene furnished, after separation of a brown oil, colorless crystals for which the analytical and mass-spectral data were in agreement with reported values[2][5] suggestive of a 1:1 adduct of type **3**. However, the NMR- and IR-spectral data were not concordant with this proposal because they demonstrated, for example, the presence of an N−H bond in the molecule. The structure of this addition product was elucidated by X-ray crystallography which revealed that the bicyclic system **4** with a 1,3-diaza-2-silaindan skeleton (Figure 1) had been formed instead of the expected three-membered ring compound **3**.

The reaction of dimesitylsilylene with azobenzene presumably proceeds through an addition of the electron-sextet species to the N=N double bond to furnish **3** as an intermediate. The well-known weakness of the N−N single bond[7] which in this case will experience a further lowering of the bond dissociation energy by its incorporation into a strained three-membered ring probably provides the driving force for the cleavage of this bond with the simultaneous formation of one N−H and one N−C bond. The result is the more or less strain-free five-membered ring part of the bicyclic compound **4**. Surprisingly, this simple bicyclic compound apparently represents the first example of a novel ring system. A search of the Cambridge Crystallographic

 © WILEY-VCH Verlag GmbH, D-69451 Weinheim, 1998 1434−1948/98/1111−1755 $ 17.50+.50/0

Scheme 1

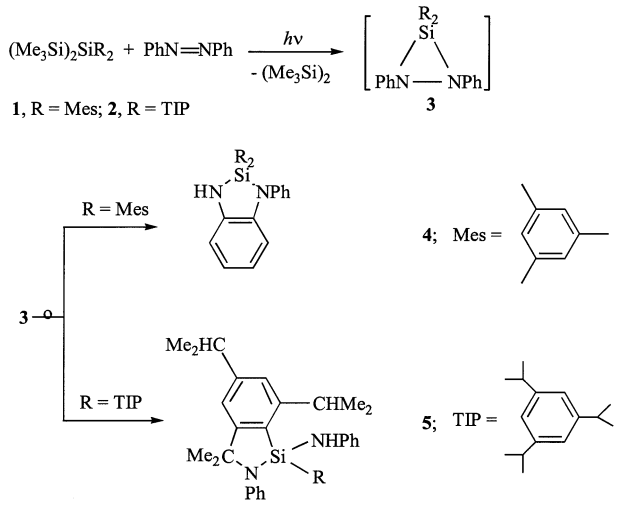

Figure 1. Molecular structure of **4** in the crystal (hydrogen atoms omitted)[a]

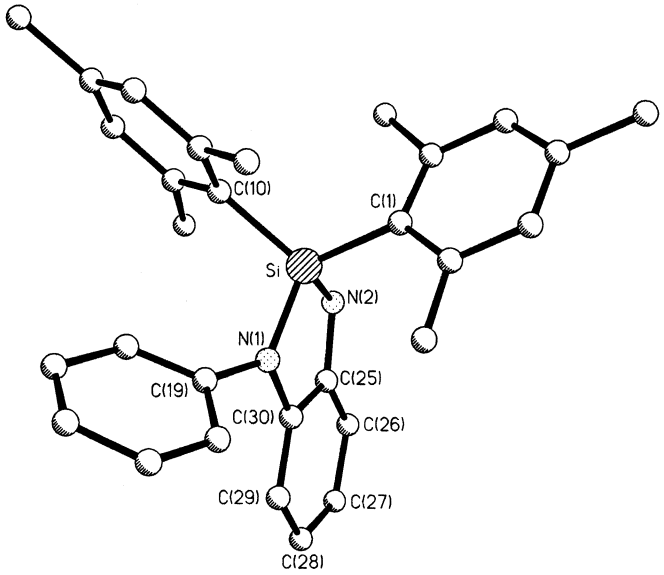

[a] Selected bond lengths [pm] and angles [°]: Si−C(1) 191.7(5), Si−C(10) 192.5(5), Si−N(1) 174.9(8), Si−N(2) 173.1(7); N(1)−Si−N(2) 90.8(4).

Data File revealed only one novel silylene with a similar atomic arrangement.[8]

In order to determine whether this reaction behavior is applicable to other silylenes, we allowed the trisilane **2**, photolysis of which furnishes hexamethyldisilane and the sterically highly overcrowded bis(2,4,6-triisopropylphenyl)silylene, to react with azobenzene under otherwise identical conditions. We isolated a light yellow crystalline product whose elemental analysis and mass-spectral data were again indicative of a 1:1 adduct of the starting materials. However, similarly to compound **4**, the spectroscopic data did not support the formation of an azadisilirane **3** as reaction product. The first assumption of a product analogous to **4** was not confirmed by the X-ray-crystallographic analysis (Figure 2). Although product **5** also contains a five-membered ring as a part of a bicyclic system, the product is not formed by insertion of the nitrogen atom into the *ortho*-C−H bond of the phenyl ring but rather by insertion into a methine C−H bond of one of the *ortho*-isopropyl groups. Assuming the siladiazirane **3** as an intermediate, the subsequent preferred reaction course apparently depends on the bulk of the substituents at the silicon atom and leads to the product with the least ring strain.

With regard to the relatively low yields of **4** (33%) and **5** (17%) it is obvious that several competitive reactions occur which, however, could not be elucidated.

Figure. 2. Molecular structure of **5** in the crystal (hydrogen atoms omitted)[a]

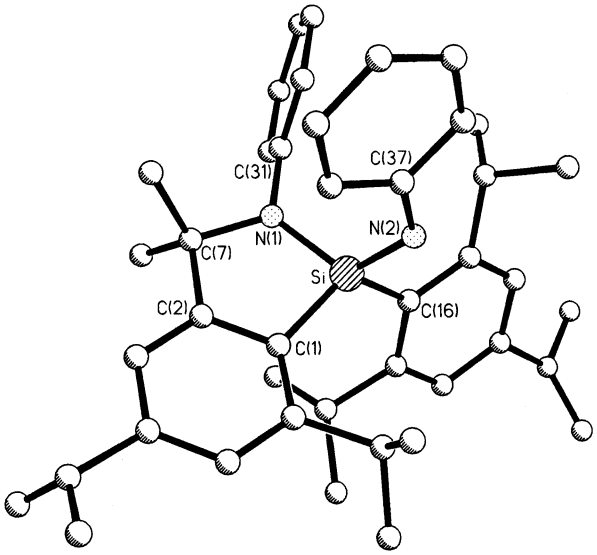

[a] Selected bond lengths [pm] and angles [°]: Si−C(1) 186.1(4), Si−C(16) 194.6(4), Si−N(1) 172.0(6), Si−N(2) 173.4(6); N(1)−Si−N(2) 116.8(3), C(1)−Si−C(16) 124.1(2).

A different form of nitrogen−nitrogen multiple bond is present in the covalent azides and can be described by the two mesomeric forms $R-N=N^+=N^- \leftrightarrow R-N^-=N^+\equiv N$. Which of the two forms dominates depends strongly on the nature of the substituent R.[9] A few years ago we investigated the reactions of the sterically overcrowded tri-*tert*-butylsilyl azide with silylenes bearing voluminous substituents. These reaction were assumed to proceed through cleavage of molecular nitrogen to the nitrene $t\mathrm{Bu_3Si-N}$ and reaction of this species with the silylenes to furnish the silanimines $t\mathrm{Bu_3Si-N=SiR_2}$. Most of these products, however, proved to be unstable and underwent various subsequent reactions. Thus, for example, the product obtained from dimesitylsilylene undergoes [1,5]-hydrogen shift followed by a conrotatory electrocyclic ring closure to afford a silacyclobutene derivative.[10] The reactions of 1-adamantyl azide (**6**) with the trisilanes **1** and **2** described in the present paper follow a completely different and previously unobserved course.

Cophotolysis of **6** and the trisilane **1** affords, through cleavage of nitrogen and hexamethyldisilane, colorless crystals of a compound shown by elemental analytical and spectroscopic data to be a 2:1 adduct of the nitrene **7** and dimes-

Scheme 2

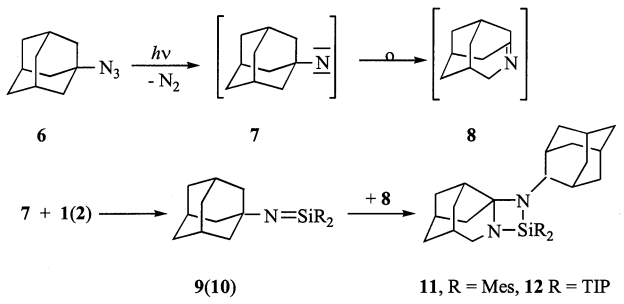

itylsilylene. The constitution of the isolated, crystalline product was elucidated by X-ray crystallography (Figure 3) and unexpectedly found to be that of the 1,3-diaza-2-silacyclobutane derivative **11** in which one of the nitrogen atoms is incorporated into a 4-homoazaadamantane unit.

Figure. 3. Molecular structure of **11** in the crystal (hydrogen atoms omitted)[a]

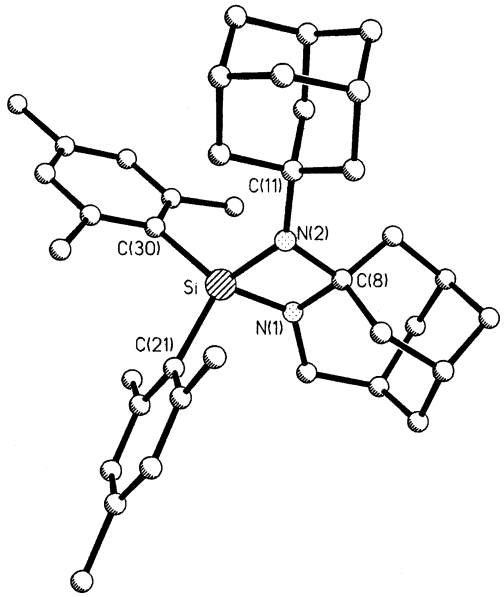

[a] Selected bond lengths [pm] and angles [°] for **11** and **12**: For **11**: Si−N(1) 173.6(5), Si−N(2) 173.3(4), N(1)−C(8) 147.7(7), N(2)−C(8) 150.0(7); N(1)−Si−N(2) 77.6(2), Si−N(1)−C(8) 94.4(3), N(1)−C(8)−N(2) 93.8(4), Si−N(2)−C(8) 93.7(3). For **12**: Si−N(1) 172.7(4), Si−N(2) 172.5(4), N(1)−C(8) 148.7(5), N(2)−C(8) 151.1(5); N(1)−Si−N(2) 78.8(2), Si−N(1)−C(8) 93.5(2), N(1)−C(8)−N(2) 93.9(3), Si−N(2)−C(8) 92.7(2).

In order to explain the formation of **11** it must be assumed that two parallel reactions with similar reaction rates occur. Firstly, the azide **6** is transformed via the nitrene **7** to the 4-azahomoadamantan-3-ene (**8**). The occurence of the latter intermediate upon photolysis of **6** has been confirmed by numerous trapping reactions.[11] Concomitantly, the silylene generated from the trisilane reacts with another molecule of nitrene **7** to furnish the silanimine **9**. A [2+2] cycloaddition of the two intermediates **8** and **9** would then provide a plausible rationale for construction of the novel polycyclic ring system **11**.

The differing reaction behaviors of **1** and **2** in cophotolysis with azobenzene prompted us to allow the silylene bearing sterically more demanding substituents generated from **2** to react with the azide **6**. Irradiation of a mixture of the two components furnished colorless crystals consisting, similarly to the case of **11**, of a 2:1 adduct of the nitrene **7** and the silylene. Once again, the complicated NMR spectra did not furnish diagnostic information about the structure of the isolated compound. However, X-ray crystallography did indeed reveal that the structure of the product **12** was analogous to that of **11** so that a separate view of the structure is not necessary.[12] Compound **12** is also presumed to be the result of an analogous reaction sequence while the somewhat higher yield (**12**: 38%; **11**: 25%) is attributed to the higher stability of the silanimine **10**.

Financial support of our work by the *Deutsche Forschungsgemeinschaft* and the *Fonds der Chemischen Industrie* is gratefully acknowledged.

Experimental Section

All manipulations were performed under dry nitrogen or argon by using Schlenk techniques. Solvents were purified, dried, and distilled under argon. − ^{1}H, ^{13}C, and ^{29}Si NMR: Bruker AM 300 or Bruker AMX 300. − MS: Varian MAT 212. − IR: Bio-Rad FTS-7. − Elemental analyses: Analytische Laboratorien, D-51779 Lindlar, Germany. − Photolyses were carried out by using a high-pressure mercury immersion lamp (Heraeus TQ 150).

3-Phenyl-2,2-bis(2,4,6-trimethylphenyl)-1,3-diaza-2-silaindan (**4**): At room temp., a solution of **1** (0.41 g, 1.0 mmol) and azobenzene (0.19 g, 1.0 mmol) in 80 ml of *n*-pentane was irradiated for 6 h. After this time, the volatile compounds were distilled off and the residue redissolved in a minimum amount of *n*-pentane. Cooling to −50°C provided a brown oil which was separated by decantation. Cooling of the remaining solution at −30°C furnished 0.150 g (33% yield) of colorless, air-sensitive crystals of **4**, m.p. 171°C. − ^{1}H NMR (C_6D_6): δ = 2.03 (s, 6 H), 2.25 (s, 12 H), 3.6 (s, 1 H, NH), 6.45−7.39 (m, 9 H), 6.63 (s, 4 H). − ^{13}C NMR (C_6D_6): δ = 21.01, 24.11, 111.21, 112.08, 118.17, 119.77, 124.67, 127.34, 129.23, 129.76, 134.07, 138.96, 139.61, 140.19, 143.12, 143.27. − MS (CI, isobutane); *m/z* (%): 449 (100) [MH^+]. − IR (nujol): $\tilde{\nu}$ [cm^{-1}] = 3418 (w, NH). − $C_{30}H_{32}N_2Si$ (448.67): calcd. C 80.30, H 7.18; found C 80.16, H 7.13.

[5,7-Diisopropyl-3,3-dimethyl-2-phenyl-1-(2,4,6-triisopropylphenyl)-2-aza-1-sila-1-indanyl]phenylamine (**5**): A solution of **2** (0.58 g, 1.0 mmol) and azobenzene (0.19 g, 1.0 mmol) in 80 ml of *n*-pentane was irradiated for 7 h at room temp. All volatile compounds were distilled off and the residue was redissolved in a minimum amount of *n*-hexane. Cooling at −30°C afforded 0.110 g (17% yield) of pale yellow crystals of **5**, m.p. 158°C. − ^{1}H NMR (C_6D_6): δ = 1.00 (d, 6 H, $^3J_{H,H}$ = 6.35 Hz), 1.17 (d, 6 H, $^3J_{H,H}$ = 7.0 Hz), 1.22 (d, 6 H, $^3J_{H,H}$ = 7.0 Hz), 1.24 (d, 6 H, $^3J_{H,H}$ = 7.0 Hz), 1.33 (d, 6 H, $^3J_{H,H}$ = 6.35 Hz), 1.55 (s, 3 H), 1.60 (s, 3 H), 2.72 (sept, 1 H), 2.84 (sept, 1 H), 3.21 (sept, 1 H), 3.60 (br., 2 H), 4.45 (s, 1 H, NH), 6.63−7.10 (m, 10 H), 7.15 (s, 2 H), 7.22 (s, 1 H), 7.24 (s, 1 H). − ^{13}C NMR (C_6D_6): δ = 23.30, 23.87, 23.96, 26.02, 29.09, 31.60, 34.18, 34.48, 34.83, 35.89, 65.26 (C_q, ring), 117.69, 118.89, 119.89, 122.14, 125.94, 129.03, 129.41, 129.56, 131.88, 133.86, 143.51, 146.91, 150.60, 151.86, 154.04, 156.99. − ^{29}Si NMR (C_6D_6): δ = −26.82. − MS (CI, isobutane); *m/z* (%): 618

Table 1. Crystallographic data of **4**, **5**, **11**, and **12**

	4	**5**	**11**	**12**
formula	$C_{30}H_{32}N_2Si$	$C_{42}H_{56}N_2Si$	$C_{98}H_{52}N_2Si \cdot C_5H_{12}$	$C_{50}H_{76}N_2Si \cdot 1/2\ C_5H_{12}$
mol. mass	448.67	616.98	637.05	769.92
cryst. dimension [mm]	0.38 × 0.34 × 0.27	0.63 × 0.29 × 0.11	0.68 × 0.49 × 0.38	0.61 × 0.49 × 0.30
cryst. system	orthorhombic	monoclinic	triclinic	orthorhombic
space group	$P2_12_12_1$	$P2_1/c$	$P\bar{1}$	$Pccn$
a [pm]	925.1(2)	2093.8(4)	1149.0(1)	1647.6(1)
b [pm]	971.0(2)	912.8(2)	1172.1(1)	3762.3(3)
c [pm]	2837(1)	1990.2(4)	1543.6(2)	1521.5(1)
α [°]	90	90	74.74(1)	90
β [°]	90	98.48(3)	83.50(1)	90
γ [°]	90	90	70.73(1)	90
V [× 10^6 pm^3]	2549(1)	3762(1)	1892.6(3)	9431.4(1)
Z	4	4	2	8
$d_{calcd.}$ [g cm^{-3}]	1.169	1.089	1.118	1.084
μ [mm^{-1}]	0.112	0.092	0.093	0.085
scan method	ω	ω-2θ	ω-2θ	ω
2θ(max) [°]	48	42	48	46
no. of unique reflections	2306	4593	5940	6538
no. of observed reflections	1604	2648	4664	3971
parameters	250	349	378	471
R [$I > 2\ \sigma(I)$]	0.081	0.095	0.097	0.085
$wR2$	0.185	0.210	0.263	0.175

(60) [MH$^+$]. − IR (KBr): $\tilde{\nu}$ [cm^{-1}] = 3422 (m, NH). − $C_{42}H_{56}N_2Si$ (616.98): calcd. C 81.70, H 9.14, N 4.54; found C 79.86, H 9.16, N 4.25.

Formation of Compound **11**: A solution of **1** (0.41 g, 1.0 mmol) and **6** (0.36 g, 2.0 mmol) in 80 ml of *n*-pentane was irradiated for 7 h at room temp. All volatile compounds were removed by vacuum distillation and the residue was redissolved in a minimum amount of DME. Cooling at 4°C yielded 0.150 g (25% yield) of colorless crystals of **11**, m.p. 211°C. − ^{1}H NMR (C_6D_6): δ = 1.33−1.81 (accumulation of signals, 15 H), 1.85 (s, 6 H), 1.95−3.13 (accumulation of signals, 27 H), 6.65 (s, 2 H), 6.83 (s, 1 H), 6.88 (s, 1 H). − ^{13}C NMR (C_6D_6): δ = 21.09, 29.57, 30.07, 30.46, 32.92, 34.29, 34.40, 35.50, 36.94, 40.60, 44.93, 47.14, 49.46, 51.25, 53.24, 88.45, 128.30, 128.92, 129.88, 130.14, 136.55, 136.75, 137.55, 139.01, 140.88, 141.32, 143.21, 144.35. − ^{29}Si NMR: δ = −10.52. − MS (CI, isobutane); *m/z* (%): 565 (100) [MH$^+$]. − $C_{38}H_{52}N_2Si$ (564.86): calcd. C 80.80, H 9.28, N 4.96; found C 78.20, H 9.81, N 4.56.

Formation of Compound **12**: At room temp., a solution of **2** (0.52 g, 1.0 mmol) and **6** (0.36 g, 2.0 mmol) in 80 ml of *n*-pentane was irradiated for 8 h, after which the reaction was shown to be complete by the dissappearance of **2** (TLC monitoring). All volatile compounds were distilled off and the residue redissolved in a minimum amount of *n*-pentane. Cooling at 4°C afforded 0.280 g (38% yield) of colorless crystals of **12**, m.p. 242°C. − ^{1}H NMR (C_6D_6): δ = 0.30 (d, br., 6 H), 1.21−1.31 (accumulation of signals, 21 H), 1.31−1.72 (accumulation of signals, 24 H), 1.90−2.90 (accumulation of signals, 15 H), 2.75 (sept, 2 H), 3.09 (sept, 1 H), 3.23 (sept, 1 H), 5.13 (sept, 1 H), 5.68 (sept, 1 H), 6.95 (s, 1 H), 6.96 (s, 1 H), 7.21 (s, 2 H). − ^{13}C NMR (C_6D_6): δ = 23.02, 23.07, 23.10, 24.11, 24.63, 24.92, 25.14, 25.15, 25.52, 26.18, 26.69, 29.18, 29.57, 30.26, 30.50, 30.65, 33.05, 34.47, 34.50, 34.59, 35.10, 35.48, 36.59, 36.83, 40.84, 45.87, 47.38, 50.27, 52.97, 53.29, 87.76, 121.63, 122.47, 122.73, 122.85, 136.34, 136.71, 149.51, 150.50, 152.86, 153.19, 154.10, 155.43. − ^{29}Si NMR (C_6D_6): δ = −10.87. − MS (CI, isobutane); *m/z* (%): 733 (100) [MH$^+$]. − $C_{50}H_{76}N_2Si$ (733.24): calcd. for **12** · 1/2 pentane C 79.96, H 10.11, N 3.72; found C 79.84, H 10.81, N 3.57.

X-ray Structural Analyses of Compounds **4**, **5**, **11**, *and* **12**: Crystal and numerical data of the structure determinations are given in Table 1.[12] In each case, the crystal was mounted in a thin-walled glass capillary. Data collection was performed at room temp. with a Siemens Stoe AED 2 diffractometer using graphite-monochromated Mo-K_α radiation. The structures were solved by direct-phase determination using the Siemens SHELXTL PLUS and SHELX 93[13] program systems and refined by full-matrix least-squares techniques. Hydrogen atoms were placed in the calculated positions, and all other atoms were refined anisotropically.

☆ Dedicated to Professor *Walter Jansen* on the occasion of his 60th birthday.

[1] M. Weidenbruch, A. Grybat, W. Saak, E.-M. Peters, K. Peters, *Monatsh. Chem.,* in press.
[2] Review: Y. Kabe, W. Ando, *Adv. Strain Org. Chem.* **1993**, *3*, 59−136.
[3] Review: M. Weidenbruch, *Coord. Chem. Rev.* **1994**, *130*, 275−300.
[4] J. Hluchy, U. Klingebiel, *Angew. Chem.* **1982**, *94*, 292; *Angew. Chem. Int. Ed. Engl.* **1982**, *21*, 301.
[5] A. Sakakibara, Y. Kabe, T. Shimizu, W. Ando, *J. Chem. Soc., Chem. Commun.* **1991**, 43−44.
[6] Review: M. Weidenbruch, *Chem. Rev.* **1995**, *95*, 1479−1493.
[7] J. Emsley, *Die Elemente*, Walter de Gruyter, Berlin, **1994**, p. 178.
[8] B. Gehrhus, M. F. Lappert, J. Heinicke, R. Boese, D. Blaser, *J. Chem. Soc., Chem. Commun.* **1995**, 1931−1932.
[9] S. S. Zigler, K. J. Haller, R. West, M. S. Gordon, *Organometallics* **1989**, *8*, 1656−1660 and references cited therein.
[10] M. Weidenbruch, B. Brand-Roth, S. Pohl, W. Saak, *J. Organomet. Chem.* **1989**, *379*, 217−222.
[11] T. Sasaki, S. Eguchi, T. Okano, *J. Org. Chem.* **1981**, *41*, 4474−4477.
[12] Crystallographic data (excluding structure factors) for the structures reported in this paper have been deposited with the Cambridge Crystallographic Data Center as supplementary publication no. CCDC-101486. Copies of the data can be obtained free of charge on application to the Director, CCDC, 12 Union Road, Cambridge CB21EZ, U.K. [fax: int. code + (1223)336-023. e-mail: deposit@ccdc.cam.ac.uk].
[13] G. M. Sheldrick, *SHELXL 93*, Universität Göttingen, Germany, **1993**.

[I98158]

New Tripodal N_3S Ligands and Some Zinc Complexes Thereof☆

Rainer Burth, Andreas Stange, Markus Schäfer, and Heinrich Vahrenkamp*

Institut für Anorganische und Analytische Chemie der Universität Freiburg,
Albertstraße 21, D-79104 Freiburg, Germany

Received May 22, 1998

Keywords: Tripodal ligands / Nitrogen–sulfur ligands / Zinc complexes / Structure determination

Attachment of 2-pyridylmethyl units to cysteine amide and 2-mercaptobenzylamine leads to the new tripodal N_3S ligands N^{α}-(4-methylbenzoyl)-L-cysteine-bis(2-pyridylmethyl)amide (**CBPA-H**) and 2-mercaptobenzyl-bis(2-pyridylmethyl)amine (**MBPA-H**). Their treatment with zinc halides yields the neutral complexes **L** · ZnHal (Hal = Cl, Br, I). With zinc perchlorate **MBPA** forms the ionic compound [**L** · Zn] ClO_4, presumed to be a thiolate bridged dimer. Structure determinations of **MBPA** · ZnHal (Hal = Cl, Br) have confirmed the tripodal nature of the ligand in the trigonal-bipyramidal complexes.

Metal ions in biological systems are coordinated by the aminoacids′ side chain donor functions (O of aspartate and glutamate, N of histidine, S of cysteine). In terms of modelling their structural and functional properties this asks for the design of ligands with an arrangement of the donor atoms similar to that in the protein. As a result modern model ligands are polydentate and chelating.

For complexes modelling zinc enzymes the requirements on the suitability of the polydentate ligands are especially pronounced, because the zinc ion profits neither from preferred coordination numbers or geometries nor from ligand field effects. Typically, all attempts to model the tetrahedral $ZnNS_2O$ coordination in the enzyme alcohol dehydrogenase[1] using amine-bisthiols as tridentate NS_2 ligands have resulted in thiolate-bridgted oligonuclear zinc complexes so far[2][3][4][5]. The high tendency for thiolate bridging has prevented the formation of the desired complexes, and similarly the highly preferred tetrahedral ZnN_2S_2 coordination has rendered futile many efforts invested in the synthesis of N_2S or N_3S ligands[6][7][8].

The ligands of choice for zinc complex model chemistry seem to be the tripodal ones, especially when they serve the further need of encapsulating the zinc ion by suitably attached substituents. The best results so far have been achieved here with the pyrazolylborates[9][10][11]. The pyrazolylborates, however, are confined for synthetic reasons to be N_3 ligands, and only recently have ways been found to modify them in the form of N_2S[12] or NS_2[13] ligands. It is this limitation of the pyrazolylborates that has directed the attention of other researchers and ourselves to the class of tetradentate tripodal ligands derived from ammonia, for which tripicolylamine (**A**) is the prototype. Ligands of this class can be synthesized step by step from ammonia or amines, and in the mono- and difunctionalized variants **B** and **C** all kinds of donor functions can be incorporated[14]. Thereby the disadvantage of these ligands in zinc model chemistry (their tetradentate nature) may be overcome by their versatility.

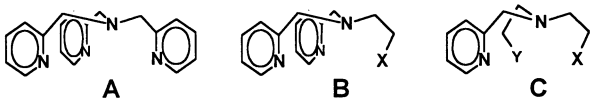

In the field of zinc model complexes N_4 ligands like **A** have been used mostly so far[15], followed by N_3O ligands like **B**[16]. We have contributed variations of **A**[17][18][19] and complexes of N_3O ligands with caboxylate and phenolate functions including a chiral variant[20][21][22]. In this paper we wish to present two thiolate-containing ligands of type **B**. **CBPA-H** is a derivative of cysteine, **MBPA-H** one of 2-mercaptobenzylamine. To our knowledge no such thiolate ligands with a N_3S donor set have been reported so far[23][24]. Some simple zinc complexes of the two ligands have been prepared to establish an entry to the modelling of zinc enzymes in which the metal is anchored, among others, by one thiolate function to the protein.

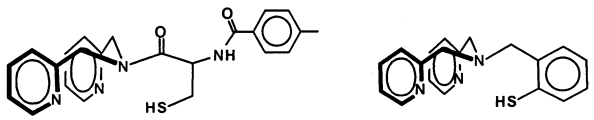

Ligand Synthesis

Both new ligands are derived from amine thiols, derivatized to contain two additional pyridyl donor functions. For the syntheses this meant that the thiol functions had to be protected until the last synthetic step. We found the use of the corresponding disulfides to be the only approach to do that. Schemes 1 and 2 show the reaction sequences.

 © WILEY-VCH Verlag GmbH, D-69451 Weinheim, 1998 1434–1948/98/1111–1759 $ 17.50+.50/0

Scheme 1. Synthesis of **CBPA-H**. Abbreviations: CAIBE = isobutylchloroformate, NMM = *N*-methylmorpholine, TFA = trifluoroacetic acid, MBC = 4-methylbenzoylchloride, DTE = dithioerythritol

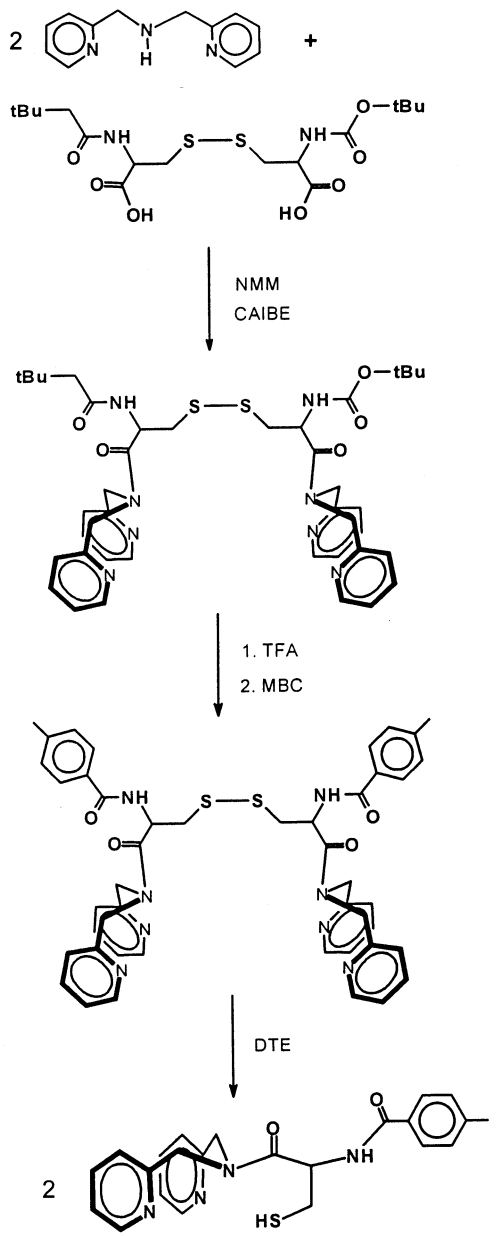

Scheme 2. Synthesis of **MBPA-H**

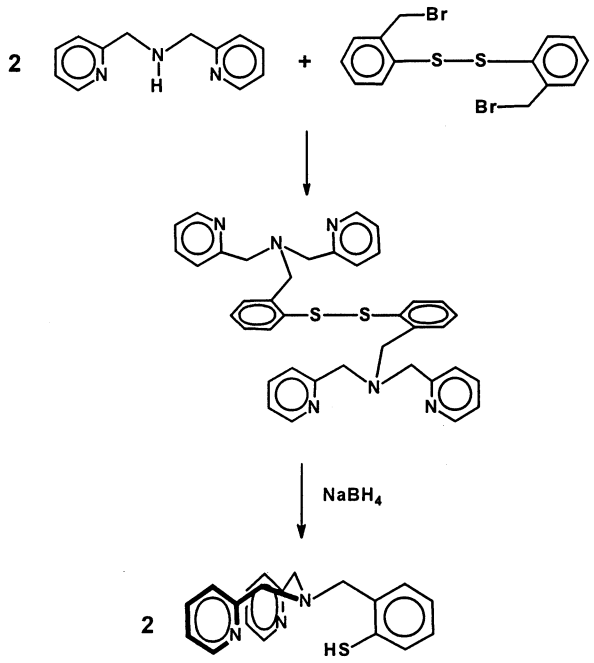

Ligand **CBPA-H** was obtained from cystine (in the *t*Boc protected form) by the standard procedures of activation, coupling, and deprotection. Ligand **MBPA-H** resulted from bis[(2-bromomethyl)phenyl] disulfide[25] in two reaction steps. The two pyridyl donor functions were introduced in the form of dipicolylamine in both cases. The sluggish reactions of the voluminous molecules allowed only mediocre overall yields. After the reductive cleavage of the disulfide precursors the thiol ligands had to be purified by HPLC. Thereby **CBPA-H** and **MBPA-H** were obtained pure, as evidenced by ^{1}H-NMR spectroscopy, but containing variable amounts of trifluoroacetic acid. Their identification rests on the spectra, their EI mass spectra showing the parent peak, and the full characterization of their zinc complexes.

Zinc Complexes

Reactions of **CBPA-H** with the zinc halides in acetonitrile in the presence of triethylamine produced complexes **1a**−**c** in good yields. **1a**−**c** precipitate from the reaction solutions and are soluble only in very polar solvents like water, DMSO or DMF. In addition to the spectra (see below) a EI mass spectrum of **1c** has verified the identity and monomeric nature of the complexes.

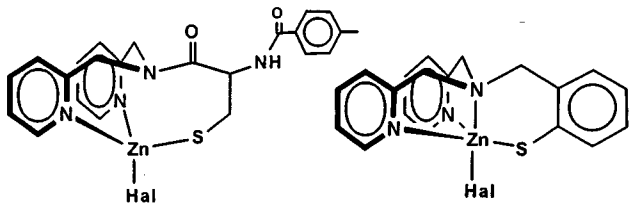

1a: Hal = Cl
1b: Hal = Br
1c: Hal = I

2a: Hal = Cl
2b: Hal = Br
2c: Hal = I

It was possible to prepare the zinc halide complexes of ligand **MBPA-H** the same way. **2a**−**c** could, however, be obtained in a more convenient way when after the last synthetic step in the formation of **MBPA-H**, i.e. the disulfide cleavage with $NaBH_4$, the corresponding hydrohalic acid was used for acidification and the corresponding zinc halide was added in excess. After neutralization **2a**−**c** were precipitated in a crystalline form. **2a**−**c** are of equally low solubility as **1a**−**c** in nonpolar solvents. This time in addition

to the spectra the structure determinations (see below) ascertained the constitution of the complexes.

When $HClO_4$ was used as before for acidifying and zinc perchlorate was added, complex **3** was precipitated. **3** could not be obtained in the form of X-ray quality crystals, nor were informative MS data obtained from it. Its ^{1}H-NMR spectrum is, however quite similar to that of the zinc perchlorate derivative of the analogous phenolate containing ligand which was characterized by a structure determination[22]. We therefore feel safe in assigning the given constitution to **3**. In contrast to the molecular complexes **1** and **2** the ionic complex **3** has a reasonable solubility not only in water, but also in methanol. It is therefore conceivable that a derivative chemistry of $[MBBA \cdot Zn]^+$ species may start with **3**.

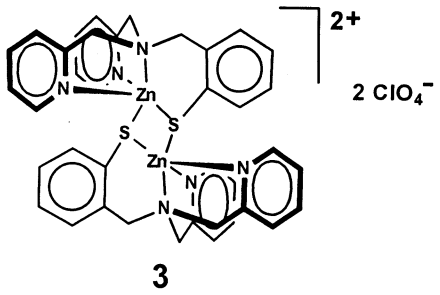

3

Product Identification

The free ligands are characterized by their ^{1}H-NMR spectra (see Experimental). In their IR spectra they show the SH band and their typical double bond bands. The pertinent ^{1}H-NMR data of the zinc halide complexes are listed in Tables 1 and 2 in comparison to those of the free ligands. Typical coordination shifts are observed for the pyridyl H_A and for the NCH_2 signals. In the IR spectra of the zinc halide complexes (see Experimental Section) the SH band is missing as expected, and the intense pyridine band around 1600 cm^{-1} is shifted to lower wavenumbers. As a rule, the IR and ^{1}H-NMR spectra of complexes **2** are very similar to those of the zinc complexes of the ligand which is the phenolate analogue of **MBPA**[22]. This holds also for complex **3** whose IR and NMR data (see Table 2) are noticeably different from those of complexes **2**.

Table 1. Characteristic ^{1}H-NMR data (DMSO, 50°C, δ [ppm]/*J* [Hz]) of the free ligand **L** = **CBPA-H** and its zinc complexes

	L	**1a**	**1b**	**1c**
CH_3	2.31	2.35	2.35	2.36
SCH_2	2.70/m	2.77/m	2.78/m	2.81/m
NCH_2[a]	4.38−4.61	4.67−5.11	4.71−5.22	4.67−5.28
Py-H_A^1	8.25/5.7	8.66/5.7	8.69/5.7	8.71/5.7
Py-H_A^2	8.63/5.7	8.99/br	8.96/br	8.91/5.7

[a] Multiplets due to the inequivalence of the CH protons and due to superposition by the Cys-CH_α signal.

Table 2. Characteristic ^{1}H-NMR data (DMSO, 50°C, δ [ppm]/*J* [Hz]) of the free ligand **L** = **MBPA-H** and its zinc complexes

	L	**2a**	**2b**	**2c**	**3**
N-CH_2-Ph	3.68	3.78	3.81	3.93	3.82
N-CH_2-Py^1	3.82/s	3.94/15.9	3.97/16.1	3.98/16.1	4.21/br
N-CH_2-Py^2	−	4.05/15.9	4.08/16.1	4.09/16.1	−
Py-H_A	8.69/6.2	9.15/4.4	9.13/5.2	8.79/4.7	7.48

Confirmation of the tetradentate nature of the tripodal ligands and the molecular nature of the halide complexes was obtained by the structure determinations of **2a** and **b**. The two compounds are isostructural and share the property that the asymmetric unit contains two independent molecules. Hence only **2a** is discussed here. Figure 1 shows one of the two molecules. The geometrical differences between the two molecules are significant, becoming most visible for the axial and equatorial intraligand angles.

Figure 1. Molecular structure of complex **2a**. Pertinent bond lengths and angles: molecule 1: Zn−Cl 2.371(1), Zn−S 2.289(1), Zn−N1 2.091(2), Zn−N2 2.096(2), Zn−N3 2.304(2) Å; N3−Zn−Cl 170.52(4), N1−Zn−N2 107.00(7), N1−Zn−S 121.58(6), N2−Zn−S 126.75(6)°. Molecule 2: Zn−Cl 2.335(1), Zn−S 2.302(1), Zn−N1 2.092(2), Zn−N2 2.100(2), Zn−N3 2.325(2); N3−Zn−Cl 163.79(5), N1−Zn−N2 124.23(7), N1−Zn−S 108.49(5), N2−Zn−S 120.27(6)°

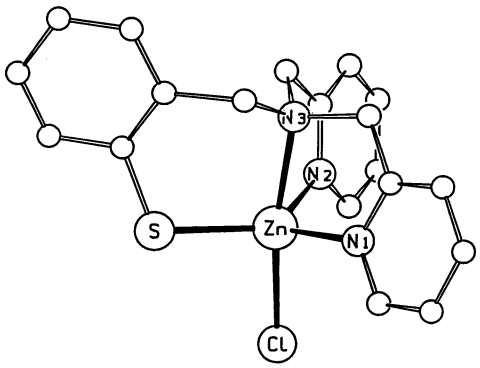

The coordination geometry of the complexes is severely distorted trigonal bipyramidal. The distortion cannot be related to the binding preferences of the tripodal ligand, as the two independent molecules are distorted in quite different ways. Furthermore the complex whose molecular shape is most similar to that of **2a**, i.e. the one with oxygen in place of sulfur[22], shows yet another kind of distortion and does not crystallize with two independent molecules. This is a good demonstration of the fact that the transitions between trigonal bipyramidal and square pyramidal geometries are "soft" in the coordination chemistry of zinc. The bond lengths at zinc are in the normal range. For the axial ligands the Zn−Cl bond length is at the upper end of the range observed for axial Zn−Cl bonds[22][26][27][28][29], and correspondingly the Zn−N3 bond length is at the lower end of its range[15][16][17][18][20][21][22][26][27][28][29]. To our knowledge no other zinc complexes with a ZnN_3SHal ligand set have been described yet.

Conclusions

This paper has shown that tripodal ligands offering a N_3S donor set for trigonal bipyramidal metal complexes with equatorial N_2S coordination are accessible, though with some synthetic effort. As a first step in exploiting their zinc complex chemistry the compounds L·ZnHal have been prepared which may serve as a starting point for obtaining functional species L·Zn−X. In the complexes L·Zn−Hal the tendency of the thiolate sulfur to bridge two zinc ions is suppressed. It seems to be operative, however, in the cationic species $[(MBPA)Zn]^+$ resulting in its existence as a sulfur-bridged dimer.

This work was supported by the *Deutsche Forschungsgemeinschaft*. We thank *A. Trösch* and *M. Tesmer* for help with the spectra and the structure determinations.

Experimental Section

General experimental methods and measuring techniques: see ref.[30]. All reactions were carried out in a nitrogen atmosphere. Starting materials were obtained commercially or prepared according to the given references. The complete ^{1}H-NMR data are given here for the two ligands only. Those of the complexes are very similar except for the resonances given in Tables 1 and 2.

Ligand Syntheses

CBPA-H: Step 1: 5.00 g (11.35 mmol) of bis(*tert*-butyloxycarbonyl)-L,L-cystine in 100 ml of THF at −15°C were stirred and treated with 2.49 ml (2.29 g, 22.70 mmol) of NMM and 2.94 ml (3.09 g, 22.70 mmol) of CAIBE. After 15 min 4.51 g (22.70 mmol) of bis(2-pyridylmethyl)amine were added. Within 24 h of stirring the temperature was raised to ambient. After filtration and evaporation to dryness the residue was picked up in 200 ml of ethylacetate. The solution was extracted three times with 70 ml of water, three times with 70 ml of a 4% $NaHCO_3$ solution, and five times with 100 ml of water. After drying with Na_2SO_4, filtration, and evaporation to dryness 8.25 g (91%) of bis(*tert*-butoxycarbonyl)-L,L-cystinebis[bis(2-pyridylmethyl)amide] remained as a colourless solid.

Step 2: The material obtained in the preceding step (8.25 g, 10.28 mmol) was treated with 50 ml of TFA and stirred for 2 h. Then the mixture was evaporated to dryness and the remaining brownish oil washed three times with 20 ml of ether. 13.22 g of a colourless powder remained which corresponds to a quantitative formation of L,L-cystinebis[bis(2-pyridylmethyl)amide] as the TFA adduct.

Step 3: The product obtained (13.22 g, 10.27 mmol) was dissolved in 100 ml of THF and treated at 0°C with 12.43 ml (11.43 g, 112.8 mmol) of NMM and then 3.42 ml (3.96 g, 25.67 mmol) 4-methylbenzoylchloride. After stirring for 24 h at room temp. the mixture was filtered and evaporated to dryness. After dissolving the residue in 300 ml of ethylacetate the yellow solution was washed three times with 60 ml of a 4% $NaHCO_3$ solution and then five times with 100 ml of water. After drying with Na_2SO_4 the solution was evaporated to dryness leaving behind 6.73 g (78%) of bis(4-methylbenzoyl)-L,L-cystinebis[bis(2-pyridylmethyl)amide] as a brownish oil.

Step 4: The brownish oil (6.73 g, 8.02 mmol) was dissolved in 70 ml of methanol and treated with 1.61 g (10.43 mmol) of DTE in 10 ml of methanol and then 12 ml of 0.2 M NaOH. After stirring for 4 h, 5 ml of TFA were added and then the mixture evaporated to dryness. The remaining brownish oil was dissolved in 80 ml of water and the solution washed four times with 30 ml of ether. After freeze-drying 6.83 g of the raw product remained as a yellowish oil. This was purified by HPLC using a reversed phase column (Merck LiChrosorb RP 18, 7 μm) eluting first for 45 min with acetonitrile/water/TFA (20:80:0.1) and then 20 min with acetonitrile/water/TFA (60:40:0.1). After freeze-drying 2.23 g (20%) of N^{α}-4-methylbenzoyl-L-cysteinebis(2-pyridylmethyl)amide (**CBPA-H**) were obtained as a pale yellow, very hygroscopic powder. The product contains approx. 2.5 mole equivalents of TFA as determined by potentiometric titration.

$C_{23}H_{24}N_4O_2S \cdot 2.5\ CF_3COOH$ (420.5 + 285.1), calcd.: C 47.66, H 3.79, N 7.94; found: C 47.47, H 3.91, N 8.07. − IR (KBr): $\tilde{\nu}$ = 3306 s (NH), 2516 w (SH), 1675 s (carboxylate), 1537 m (amide). −^{1}H NMR (D_2O): 2.18 [s, 3 H, CH_3], 2.84 [dd, J = 6.7, 14.1 Hz, 2 H, Cys-C_bH], 4.98 − 5.51 [m, 5 H, NCH_2 and Cys-C_aH], 7.09 [d, J = 8.0 Hz, 2 H, Ph (3,5)], 7.27 [d, J = 8.0 Hz, 2 H, Ph (2,6)], 7.55 [t, J = 6.7 Hz, 1 H, Py-H_B], 7.78 [d, J = 7.3 Hz, 1 H, Py-H_D], 7.87 [t, J = 6.7 Hz, 1 H, Py-$H_{B'}$], 8.19 [d, J = 7.3 Hz, 1 H, Py-$H_{D'}$], 8.28 [dt, J = 7.3, 1.3 Hz, 1 H, Py-H_C], 8.39 [dt, J = 7.3, 1.3 Hz, 1 H, Py-$H_{C'}$], 8.45 [d, J = 6.7 Hz, 1 H, Py-H_A], 8.59 [d, J = 6.7 Hz, 1 H, Py-$H_{A'}$].

MBPA-H: Step 1: 3.20 g (7.92 mmol) of bis[(2-bromomethyl)phenyl]disulfide were dissolved in 50 ml of dioxane. A mixture of 3.15 g (15.84 mmol) of bis(2-pyridylmethyl)amine and 2.21 ml (1.60 g, 15.84 mmol) of triethylamine in 50 ml of dioxane was added dropwise with stirring. The resulting red mixture was stirred overnight, filtered, and the filtrate evaporated to dryness. The remaining red oil was picked up in 200 ml of dichloromethane, washed three times with 20 ml of a 4% $NaHCO_3$ solution and then five times with 50 ml of water. After drying with Na_2SO_4 the solution was evaporated to dryness, the remaining red oil was dissolved in cyclohexane/ethylacetate (1/1) and chromatographed with neutral Al_2O_3, activity V, to yield 2.98 g (63%) of bis[{2-bis(2-pyridylmethyl)aminomethyl}phenyl] disulfide as an orange oil.

Step 2: 212 mg (0.331 mmol) of the product obtained before were dissolved in 30 ml of methanol. 50 mg (1.32 mmol) of $NaBH_4$ were added with stirring, resulting in a colour change of the solution from orange to yellow. After stirring overnight the mixture was evaporated to dryness. The residue was picked up in 10 ml of doubly distilled water and acidified to pH 6 with TFA. The solution was extracted three times with 20 ml of dichloromethane. The combined extracts were evaporated to dryness. Purification by HPLC as above using water/acetonitrile/TFA (80:20:0.1) as eluent yielded 191 mg (47%) of [*N*,*N*-bis(2-pyridylmethyl)-*N*-(2-mercaptobenzyl)]-amine (**MBPA-H**) as a yellow oil. The product contains approx. 2.5 mole equivalents of TFA as determined by potentiometric titration.

$C_{19}H_{19}N_3S \cdot 2.5\ CF_3COOH$ (321.4 + 285.1), calcd.: C 47.53, H 3.57, N 6.93; found: C 47.88, H 3.55, N 7.17. − IR (KBr): = $\tilde{\nu}$ = 2498w (SH), 1684s (carboxylate), 1620s, 1588m (pyridine). ^{1}H NMR ($CDCl_3$): 3.79 [s, 2 H, NCH_2Ph], 4.25 [s, 1 H, SH], 4.32 [s, 4 H, NCH_2Py], 6.95−7.35 [m, 4 H, Ph], 7.62−7.73 [m, 2 H, Py-H_B], 7.90 [d, J = 7.8 Hz, 2 H, Py-H_D], 8.13−8.24 [m, 2 H, Py-H_C], 8.83 [d, J = 5.6 Hz, 2 H, Py-H_A], 13.27 [s, 3 H, Py-NH^+].

Complex **1a**: To 134 mg (0.19 mmol) of **CBPA-H**·2.5 TFA in 30 ml of acetonitrile were added with stirring 0.09 ml (67 mg, 0.67 mmol) of triethylamine and 26 mg (0.19 mmol) of $ZnCl_2$ in 5 ml of acetonitrile. After reducing the volume to 10 ml in vacuo the solution was allowed to stand, slowly precipitating the product. Filtration, washing with a few ml of cold acetonitrile and drying in vacuo yielded 55 mg (56%) of colourless **1a** of m.p. 252°C. − $C_{23}H_{23}ClN_4O_2SZn$ (520.4), calcd.: C 53.09, H 4.45, N 10.77, Zn

Table 3. Crystallographic details

	2a	**2b**
formula	$C_{19}H_{18}ClN_3SZn$	$C_{19}H_{18}BrN_3SZn$
mol. mass	421.3	465.7
cryst. from	methanol	methanol/water
crystal size [mm]	1.0 × 0.9 × 0.9	0.4 × 0.5 × 0.4
space group	*P*-1	*P*-1
Z	4	4
a [Å]	10.378(2)	10.361(1)
b [Å]	13.191(3)	13.244(1)
c [Å]	14.361(3)	14.423(1)
α [°]	107.84(3)	107.92(1)
β [°]	105.92(3)	105.75(1)
γ [°]	94.52(3)	93.95(1)
V [Å^3]	1771.0(6)	1787.1(2)
d (calc.) [g·cm^{-3}]	1.58	1.73
temp. [K]	200	183
μ (Mo-*Kα*) [mm^{-1}]	1.66	3.73
Θ range [°]	2.9−26.0	2.6−26.0
hkl range	*h*: −12 to 0 *k*: −16 to 16 *l*: −17 to 17	h: −12 to 0 k: −16 to 16 l: −17 to 17
refl. measd.	7342	7424
indep. refl.	6936	7011
obs. refl. [$I>2\sigma(I)$]	6520	6017
parameters	451	451
refl. refined	6936	7008
R_1 (obs. refl.)	0.029	0.041
wR_2 (all refl.)	0.087	0.130
residual el. density e/A^3	+0.8 −0.6	+1.0 −2.1

12.57; found: C 51.95, H 4.41, N 10.70, Zn 12.97. − IR (KBr): $\tilde{\nu}$ = 3373s (NH), 1669vs, 1651s (amide bands).

1b: Like **1a** from 219 mg (0.31 mmol) of **CBPA-H**·2.5 TFA, 0.15 ml (110 mg, 1.09 mmol) of triethylamine and 70 mg (0.31 mmol) of $ZnBr_2$. Yield 95 mg (54%) of colourless **1b**, m.p. 255°C. − $C_{23}H_{23}BrN_4O_2SZn$ (564.8), calcd.: C 48.91, H 4.10, N 9.92, Zn 11.58; found: C 49.31, H 4.21, N 10.25, Zn 11.94. − IR (KBr): $\tilde{\nu}$ = 3366m (NH), 1670s, 1652s (amide bands).

1c: Like **1a** from 183 mg (0.26 mmol) of **CBPA-H**·2.5 TFA, 0.12 ml (92 mg, 0.91 mmol) of triethylamine and 85 mg (0.26 mmol) of ZnI_2. Yield 98 mg (62%) of colourless **1c**, m.p. 257°C. − $C_{23}H_{23}IN_4O_2SZn$ (611.8), calcd.: C 45.15, H 3.79, N 9.16; found: C 45.28, H 3.70, N 9.13. − IR (KBr): $\tilde{\nu}$ = 3363m (NH), 1672s, 1650s (amide bands).

2a: 150 mg (0.23 mmol) of bis[{2-bis(2-pyridylmethyl)aminomethyl}phenyl] disulfide (**BAPD**) in 15 ml of methanol were treated with 35 mg (0.92 mmol) of $NaBH_4$ in 15 ml of methanol. After stirring for 4 h 15 ml of water, 1 ml of conc. HCl and 125 mg (0.92 mmol) of $ZnCl_2$ in 5 ml of methanol were added. A saturated aqueous solution of $NaHCO_3$ was slowly added until $Zn(OH)_2$ began to precipitate. Then the mixture was filtered twice and the resulting clear solution slowly reduced to two thirds its volume under reduced pressure. The resulting precipitate was filtered off, washed with a few ml of cold methanol and dried in vacuo, yielding 52 mg (27%) of colourless **2a**, m.p. 248°C (dec.). − $C_{19}H_{18}ClN_3SZn$ (421.3), calcd.: C 54.17, H 4.31, N 9.97, Zn 15.52; found: C 54.05, H 4.38, N 9.95, Zn 15.83. − IR (KBr): $\tilde{\nu}$ = 1604s, 1569m (pyridine bands).

2b: Like **2a** from 150 mg (0.23 mmol) of **BAPD**; 35 mg(0.92 mmol) of $NaBH_4$, 207 mg (0.92 mmol) of $ZnBr_2$ and 1 ml of conc. HBr. Yield 79 mg (37%) of colourless **2b**, m.p. 262°C (dec.). − $C_{19}H_{18}BrN_3SZn$ (465.7), calcd.: C 49.00, H 3.90, N 9.02; found: C 48.25, H 3.81, N 8.77. − IR (KBr): $\tilde{\nu}$ = 1606 s, 1572 m (pyridine bands).

2c: Like **2a** from 150 mg (0.23 mmol) of **BAPD**, 35 mg (0.92 mmol) of $NaBH_4$, 294 mg (0.92 mmol) of ZnI_2, and 1 ml of conc. HI. Yield 92 mg (39%) of pale-yellow **2c**, m.p. 274°C (dec.). − $C_{19}H_{18}IN_3SZn$ (512.7), calcd.: C 44.51, H 3.54, N 8.20; found: C 43.90, H 3.40, N 7.89. − IR (KBr): $\tilde{\nu}$ = 16.05 s, 1570 m (pyridine bands).

3: Like **2a** from 150 mg (0.23 mmol) of **BAPD**, 35 mg (0.92 mmol) of $NaBH_4$, 343 mg (0.92 mmol) of $Zn(ClO_4)_2 \cdot 6\ H_2O$, and 1 ml of conc. $HClO_4$. Yield 156 mg (35%) of colourless **3**, m.p. 181°C. − $C_{19}H_{18}ClN_3O_4SZn$ (485.3), calcd.: C 47.03, H 3.74, N 8.66, Zn 13.47; found: C 48.11, H 3.75, N 8.59, Zn 13.10. − IR (KBr): $\tilde{\nu}$ = 1606s, 1574 m (pyridine bands), 1092 vs (ClO_4).

Structure Determinations[31]: Crystals were obtained from the reaction solutions. Diffraction data were recorded with the ω/2θ technique on a Nonius CAD4 diffractometer fitted with a molybdenum tube (K_α, λ = 0.7107 Å) and a graphite monochromator. No absorption corrections were applied. The structures were solved with direct methods and refined anisotropically with the SHELX program suite[32]. Hydrogen atoms were included with fixed distances and isotropic temperature factors 1.2 times those of their attached atoms. Parameters were refined against F^2. The *R* values are defined as $R_1 = \Sigma F_o - F_c / \Sigma F_o$ and $wR_2 = [\Sigma[w(F_o^2 - F_c^2)^2 / \Sigma[w(F_o^2)^2]]^{1/2}$. Drawings were produced with SCHAKAL[33]. Table 3 lists the crystallographic data.

☆ Dedicated to Prof. *Bernt Krebs* on the occasion of his 60th birthday.

[1] C. I. Bränden, H. Eklund, B. Nordström, T. Boiwe, G. Söderlund, E. Zeppezauer, I. Ohlsson, A. Akeson, *Proc. Natl. Acad. Sci. U. S.* **1973**, *70*, 2439−2442. H. Cho, S. Ramaswamy, B. V. Plapp, *Biochemistry* **1997**, *36*, 382−389.
[2] N. J. Curtis, R. S. Brown, *Can. J. Chem.* **1981**, *59*, 65−75.
[3] B. Kaptein, L. Wang-Griffin, G. Barf, R. M. Kellogg, *J. Chem. Soc. Chem. Commun.* **1987**, 1457−1459; B. Kaptein, G. Barf, R. M. Kellogg, F. van Bolhuis, *J. Org. Chem.* **1990**, *55*, 1890−1901.
[4] M. Bochman, K. J. Webb, M. B. Hursthouse, M. Mazid, *J. Chem. Soc. Chem. Commun.* **1991**, 1735−1737.
[5] U. Brand, H. Vahrenkamp, *Z. Anorg. Allg. Chem.* **1996**, *622*, 213−218.
[6] Quite often ZnN_2S_2 coordination occurs even at the expense of other donor functions being unused when a ligand contains one SH and one heterocyclic nitrogen donor. For examples see refs.[7] and[8].
[7] U. Brand, H. Vahrenkamp, *Inorg. Chem.* **1995**, *34*, 3285−3293.
[8] U. Brand, H. Vahrenkamp, *Chem. Ber.* **1996**, *129*, 435−440.
[9] N. Kitajima, W. B. Tolman, *Prog. Inorg. Chem.* **1995**, *43*, 419−531.
[10] G. Parkin, *Adv. Inorg. Chem.* **1995**, *42*, 291−393.
[11] S. Trofimenko, *Chem. Rev.* **1993**, *93*, 943−980.
[12] P. Ghosh, G. Parkin, *J. Chem. Soc. Chem. Commun.* **1998**, 413−414.
[13] C. Kimblin, T. Hascall, G. Parkin, *Inorg. Chem.* **1997**, *36*, 5680−5681.
[14] cf. *Comprehensive Coordination Chemistry* (Eds.: G. Wilkinson, R. D. Gillard, J. A. McCleverty) Pergamon Press, Oxford, **1982**, vol. 2.
[15] For a recent example, cf. H. Adams, N. A. Bailey, D. E. Fenton, Q.-Y. He, *J. Chem. Soc. Dalton Trans.* **1997**, 1533−1539.
[16] For a recent example, cf. H. Adams, N. A. Bailey, D. E. Fenton, Q.-Y. He, *J. Chem. Soc. Dalton Trans.* **1996**, 2857−2865.
[17] R. Gregorzik, U. Hartmann, H. Vahrenkamp, *Chem. Ber.* **1994**, *127*, 2117−2122.
[18] U. Hartmann, R. Gregorzik, H. Vahrenkamp, *Chem. Ber.* **1994**, *127*, 2123−2127.
[19] R. Burth, H. Vahrenkamp, *Z. anorg. allg. Chem.* **1998**, *624*, 381−385.
[20] A. Abufarag, H. Vahrenkamp, *Inorg. Chem.* **1995**, *34*, 2207−2216.

[21] A. Abufarag, H. Vahrenkamp, *Inorg. Chem.* **1995**, *34*, 3279−3284.
[22] A. Trösch, H. Vahrenkamp, *Eur. J. Inorg. Chem.* **1998**, 827−832.
[23] For a triazacyclononane-derived N_3S ligand cf. R. P. Houser, J. A. Halfen, V. G. Young, N. J. Blackburn, W. B. Tolman, *J. Am. Chem. Soc.* **1995**, *117*, 10745−10746.
[24] For related thioether ligands cf. K. Takahashi, E. Ogawa, N. Oishi, Y. Nishida, S. Kida, *Inorg. Chim. Acta* **1982**, *66*, 97-103.
[25] D. Pearson, *J. Polymer. Sci.* **1955**, *17*, 221−233.
[26] J. W. Canary, C. S. Allen, J. M. Castagnetto, Y. Wang, *J. Am. Chem. Soc.* **1995**, *117*, 8484−8485.
[27] A. Marzotto, D. A. Clemente, G. Valle, *Acta Crystallogr., Sect. C.* **1994**, *C 50*, 1451−1456.
[28] N. Matsumoto, T. Akui, A. Okyoshi, H. Okawa, *Bull. Soc. Chim. Jpn.* **1988**, *61*, 2250−2252.
[29] R. J. Sime, R. F. Dodge, A. Zalkin, D. H. Templeton, *Inorg. Chem.* **1971**, *10*, 537−541.
[30] M. Förster, R. Burth, A. K. Powell, T. Eiche, H. Vahrenkamp, *Chem. Ber.* **1993**, *126*, 2643−2648.
[31] The crystallographic data of the structures described in this paper were deposited with the Cambridge Crystallographic Data Centre as "supplementary publication no. CCDC-101628 (for **2a**) and -101629 (for **2b**)". Copies of these data are available free of charge from the following address: The Director, CCDC, 12 Union Road, GB-Cambridge CB2 1EZ (Telefax: Int. +44-1223/ 336 033; E-mail: deposit@chemcrys.cam.ac.uk).
[32] G. M. Sheldrick, *SHELX-86* and *SHELXL-93*, Programs for Crystal Structure Determination, Universität Göttingen, **1986** and **1993**.
[33] E. Keller, Program *SCHAKAL*, Universität Freiburg, **1993**.
[I98159]

Thermodynamic Stability of Zirconium(IV) Complexes with Hydroxy Ions

Anne Veyland, Laurent Dupont, Jean-Claude Pierrard, Jean Rimbault, and Michel Aplincourt*

GRECI, Université de Reims Champagne-Ardenne,
B. P. 1039, F-51687 Reims Cédex 2, France

Received May 27, 1998

Keywords: Zirconium(IV) / Hydroxy ion / Complexes / Protometry / Equilibrium constant / Solubility product

A protometric study on the speciation of zirconium(IV) was performed in an aqueous solution at 25 °C in KNO_3 and four ionic strengths (0.2, 0.5, 1, and 2 mol·dm^{-3}). This study indicates the formation of the soluble species $Zr(OH)_3^+$, $Zr_2(OH)_7^+$, and $Zr(OH)_4$ in the pH range 1.5–3.5. The use of an appropriate titration technique allows the precipitation of the zirconium hydroxide to be limited. The overall stability constants β_{mlh} of these three hydroxo complexes were computed and refined, by the program PROTAF, for each ionic strength. The solubility product *K*s of $Zr(OH)_4$ was calculated by taking these β_{mlh} constants into account. The thermodynamic values were determined by extrapolation at zero ionic strength (Specific ion Interaction Theory method): log $\beta°_{10-3}$ = –0.52 (0.01); log$\beta°_{20-7}$ = −2.22(0.07); log$\beta°_{10-4}$ = −4.52 (0.07); log*K*s° = −55.26(0.08).

For about fifty years zirconium has been a strategic metal. Its importance in the military and industrial nuclear fields is due to its mechanical and thermal properties and its outstanding resistance to corrosion, as well as to a low neutron capture cross-section. It is an essential constituent of the core of the nuclear power station and for confining fissile materials.

The running of nuclear installations relies on the processing of nuclear fuels and fission by-products, but also on the long-term storage, in protected sites, of confined materials which have acquired an appreciable radioactivity.

In the long-term one may expect the possibility of corrosion and fissuring of the confining containers leading to a contamination of soils and waters.

Modelling programs which take into account the whole local physical parameters as well as the physicochemical data allow the quantification of these contamination risks. The values used for these simulations, especially those relating to zirconium, have to be as reliable as possible in order to yield realistic estimations.

The chemistry of zirconium(IV) in aqueous media is dominated by the complexation of Zr^{4+} with OH^-. The data currently available on zirconium hydroxide complexes comes from studies carried out (essentially) before 1975[1][2][3][4][5][6][7][8][9]. The advanced species formulae and, above all, the values of the corresponding complexation constants, seem questionable.

Baes and Mesmer[10] have reviewed bibliographical results concerning zirconium hydrolysis in aqueous solution. When the zirconium concentration is low (< 10^{-4} mol·dm^{-3}), they conclude that there is formation of mononuclear complexes $Zr(OH)_h^{(4-h)+}$ where $h = 1-5$.

According to these two authors, only the stability of the $ZrOH^{3+}$ species has been determined with a reasonable accuracy: log $\beta_{10-1} = 0.3 \pm 0.05$ at zero ionic strength[9]. The hydrolysis constants of the more hydrolysed complexes [$Zr(OH)_2^{2+}$ through to $Zr(OH)_5^-$] are only rough estimates [for instance log $K \leq -1.8$ for the equilibrium $ZrOH^{3+} + H_2O \rightleftharpoons Zr(OH)_2^{2+} + H^+$]. Increasing zirconium concentration induces the formation of polynuclear species $Zr_m(OH)_h^{(4m-h)+}$. In accordance with studies from Zielen and Connick[2], Johnson and Kraus[11], and Angstadt and Tyree[12], Baes and Mesmer conclude that the existence of a trimer, $Zr_3(OH)_4^{8+}$ or $Zr_3(OH)_5^{7+}$, and of the tetramer $Zr_4(OH)_8^{8+}$ is probable.

Aja et al.[13] also published a review concerning the aqueous chemistry of zirconium(IV). They principally take into account the results obtained by Russian scientists[5][6][8][14]. They consider that the values of the formation constants of the mononuclear hydroxide complexes depend little on the ionic strength and the nature of the supporting electrolyte. For these constants, they have retained average values which are very different from those given by Baes and Mesmer.

More recently, Adair et al.[15] published an article entitled "A review of the aqueous chemistry of the zirconium-water system" in which they simply give the same values of constants that Baes and Mesmer indicated for the mono- and polynuclear zirconium hydroxide complexes at 25°C.

In short, numerous studies deal with the formation of zirconium-hydrolysed complexes in aqueous solution but many discrepancies exist from one author to another concerning the major species formed and the values of the corresponding constants of formation. It must be pointed that in these studies the stoichiometry of the soluble species have not been experimentally determined.

The purposes of the present work are:

– The study of the complexation reactions between zirconium(IV) and hydroxy ions in aqueous solution. The stoichiometry of soluble species are determined from the position of the equivalent points on the titration curves and from the initial pH of the zirconium oxychloride solutions.

 © WILEY-VCH Verlag GmbH, D-69451 Weinheim, 1998 1434−1948/98/1111−1765 $ 17.50+.50/0

– The determination of the thermodynamical constants corresponding to the formation of the complex species by using the Specific ion Interaction Theory (SIT method).

Results

Stoichiometry of Complexes Formed

At the beginning of the titrations (pH < 2), the initial concentration of protons in $ZrOCl_2$ solutions corresponds to the liberation of one equivalent of proton per zirconium atom and to the formation of $Zr(OH)_3^+$ according to:

$$Zr(OH)_2^{2+} + 2\ H_2O \rightarrow Zr(OH)_3^+ + H_3O^+$$

Figure 1 shows that the potentiometric titration curve of the system $ZrOCl_2/HNO_3$ (curve b) is displaced to the right relative to the curve of nitric acid alone (curve a). In order to facilitate the interpretation of the results, the pH value is given versus the number (m) of OH^- equivalents per zirconium mol, calculated after the neutralisation of nitric acid. The derivative curve c shows two equivalent points at pH = 4 and pH = 8 which correspond to 1.5 and 2 equiv. of OH^- added, respectively. Both equivalent points correspond to the formation of species which contain 3.5 and 4 OH^- per zirconium atom according to:

$$Zr(OH)_3^+ + H_3O^+ + 1.5\ OH^- \rightarrow Zr(OH)_{3.5}^{0.5+} + 2\ H_2O$$
$$\text{and } Zr(OH)_3^+ + H_3O^+ + 2\ OH^- \rightarrow Zr(OH)_4 + 2\ H_2O$$

For the species "$Zr(OH)_{3.5}^{0.5+}$", computation led us to envisage the formation of the dimer $Zr_2(OH)_7^+$. As for the species "$Zr(OH)_4$", they are very likely to be polymeric species in which the ratio $[OH^-]/[Zr]$ is equal to four. For simplicity, these polymeric species are denoted as $[Zr(OH)_4]_n$.

Figure 1. Titration curves for (a) nitric acid ($4\cdot10^{-2}$ mol·dm^{-3}), (b) zirconium oxychloride ($8\cdot10^{-3}$ mol·dm^{-3}) in the presence of nitric acid ($4\cdot10^{-2}$ mol·dm^{-3}), (c) derivative curve of (b); the pH is given versus the number (m) of OH^- equivalents per zirconium, calculated after neutralisation of nitric acid

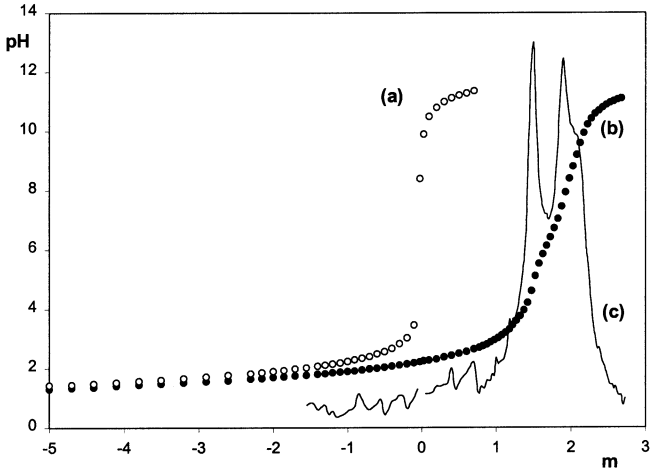

Precipitation occured after pH = 3.5 when the complex $Zr_2(OH)_7^+$ was still predominant. This means that the solid phase has a composition close to the composition of a ionic salt in which $Zr_2(OH)_7^+$ is associated with a counter anion, either nitrate or chloride.

To refine the composition of the solid phase several analyses were made. The precipitate was separated from the solution by centrifugation and filtration and washed with KNO_3. The solid was then dispersed in a KNO_3 solution which was titrated with KOH (0.1 mol dm^{-3}). The titration curve obtained shows that hydrolysis still occcurs at pH > 3.5, because we obtain one equivalent point at pH = 8.5 for 0.5 equiv. of OH^- added. This point corresponds to the formation of the polymeric species $[Zr(OH)_4]_n$ which confirms the previous formation of an insoluble salt at pH = 3.5. Chloride ions were titrated in the supernatant by potentiometry. The result indicates that all the chloride ions are present in solution and, consequently, that the solid phase does not contain any chloride. Infrared spectra of the solid phase were recorded and shows a band at 1380 nm which confirms the presence of nitrate anion.

A similar trend is observed in perchlorate medium; precipitation occurs at pH = 3.5, the titration curves show two inflexion points at pH = 4.4 for 1.75 equiv. of OH^- and pH = 8.5 for 2 equiv. of OH^-. These points correspond to the formation of species having the stoichiometry $Zr_3(OH)_{11}^+$ and $[Zr(OH)_4]_n$, respectively.

Determination of Stability Constants

The overall stability constants are related to the general equilibrium:

$$m\ Zr^{4+} + 2h\ H_2O \rightleftharpoons Zr_m(OH)_h^{(4m-h)+} + h\ H_3O^+$$

$$\beta^c_{m0-h} = \frac{[Zr_m(OH)_h^{(4m-h)+}][H_3O^+]^h}{[Zr^{4+}]^m}$$

The neutralisation curves were computed taking into account the species $Zr(OH)_3^+$, and $Zr_2(OH)_7^+$ and also the soluble monomeric species $Zr(OH)_4$. The concentration range of zirconium used in the calculation varies from 10^{-3} to 8×10^{-3} mol·dm^{-3}. The validity of the hypothesis was checked for lower concentrations up to 8×10^{-5} mol·dm^{-3} of Zr^{IV}. For the calculation of stability constants, data obtained in the heterogeneous phase was removed. However, further simulations were made over the whole pH range to confirm the stoichiometry of the insoluble species. Calculated curves were in good agreement with experiment over the whole pH range studied. We have included in our hypothesis the formation of polynuclear species cited in the literature[1][2][7][11][12]. After calculation, polynuclear species were not selected, and improved least square refinements were found considering only the three species previously proposed.

The precision on some log β_{10-4} values is weak because in the homogeneous phase $Zr(OH)_4$ can be considered as a very minor species. The species distribution curve shows

Table 1. Overall stability constants of $Zr(OH)_3^+$, $Zr(OH)_4$, and $Zr_2(OH)_7^+$[a] (KNO_3 medium, 25 ± 0.1°C)

I [mol·dm^{-3}]	log β^c_{10-3}	logβ^c_{20-7}	logβ^c_{10-4}
0.2	−2.02 (0.01)	−5.26 (0.04)	−6.09 (0.03)
0.5	−2.18 (0.01)	−5.39 (0.04)	−6.7 (0.2)
1	−2.27 (0.01)	−5.48 (0.04)	−6.71 (0.04)
1[b]	−2.29 (0.05)	−5.56 (0.11)	−6.51 (0.08)
2	−1.77 (0.03)	−4.35 (0.05)	−6.9 (0.3)

[a] Values in parentheses represent 1 σ standard deviation. – [b] $NaClO_4$ medium, 25 ± 0.1°C.

that its proportion in solution is lower than 10% at pH = 4.0. It is also interesting to note that for I = 1 mol·dm^{-3}, the values of the stability constants were similar in nitrate and perchlorate media, which seems to indicate that there is no complexation between zirconium and nitrate ions.

Determination of Solubility Products

The values of the solubility product of zirconium hydroxide $Zr(OH)_4$ proposed in the literature[3][4] vary between 10^{-52} and 10^{-54}, but it is worth pointing out that most of the authors do not take into account the stability constants of soluble species in their calculations.

In our experiments, the solubility product is determined from the pH value and the free concentration of Zr^{4+} calculated for each solution from the stability constants of the soluble species $Zr(OH)_3^+$ and $Zr_2(OH)_7^+$, using the following expression where [Zr(t)] is the total concentration of zirconium:

$$\frac{2\beta_{20-7}}{[H_3O^+]^7}[Zr^{4+}]^2 + \left(1 + \frac{\beta_{10-3}}{[H_3O^+]^3}\right)[Zr^{4+}] - [Zr(t)] = 0$$

The solubility product is then calculated using the usual expression $Ks = [Zr^{4+}][OH^-]^4$.

The mean values of the logarithms of the solubility products are reported in Table 2 for the four different ionic strengths.

Table 2. Solubility products of $Zr(OH)_4$; (KNO_3 medium, 25 ± 0.1°C)

I [mol·dm$^-$]^3	log Ks [a]
0.2	−52.71 (0.05)
0.5	−52.49 (0.06)
1	−52.72 (0.06)
2	−53.49 (0.03)

[a] Values in parentheses represent 1 σ standard deviation.

Determination of the Thermodynamical Formation Constants

The constants of formation have been determined in solution containing KNO_3 as supporting electrolyte (0.2−2 mol·dm^{-3}). The specific interaction theory[20][21][22][23] is used for the comparison of data at different ionic strengths and also for the calculation of the thermodynamic formation constants corresponding to the standard state.

The activity coefficient of a cation i of charge z is calculated from the following expression:

$$\log \gamma_i = -z_i^2 \, D + \Sigma_j \, \varepsilon(i, j) \times m_j$$

where $D = \dfrac{0.5091\sqrt{I_m}}{1+1.5\sqrt{I_m}}$ is the Debye-Hückel term (for long-range electrostatic interactions); $\varepsilon(i, j)$ is the specific interaction coefficient between the cation i of charge z and the others ions j of opposite charge in the solution and m_j is the molality of the ions j.

In our study, the concentration of the nitrate ions of the supporting electrolyte KNO_3 is much larger than these of the other ionic species. Consequently, it is the main contributor to the value of log γ_i:

$$\log \gamma_i = -z_i^2 \, D + \varepsilon(i, NO_3^-) \times I_m$$

with I_m ionic strength equal to the molal concentration of the supporting electrolyte.

For the general formation reaction,

$$m \, Zr^{4+} + 2 \, h \, H_2O \rightleftharpoons Zr_m(OH)_h^{(4m-h)+} + h \, H_3O^+$$

$$\beta^c_{m0-h} = \frac{[Zr_m(OH)_h^{(4m-h)+}][H_3O^+]^h}{[Zr^{4+}]^m}$$

The apparent stability constant β^c_{m0-h} is calculated from the molar concentrations of the reacting species. This value is then converted to molality units (β^m_{m0-h} value) according to the conversion factors determined by Baes and Mesmer[10]. Finally, the thermodynamical stability constant β°_{m0-h} is determined from the experimental constants β^m_{m0-h}, by using a weighted linear extrapolation to zero ionic strength.

$$\beta^\circ_{m0-h} = \frac{a_{Zr_m(OH)_h^{(4m-h)+}} \, a_{H_3O^+}^h}{a_{Zr^{4+}}^m \, a_{H_2O}^{2h}}$$

The expression of the logarithm of the thermodynamical stability constant may be written as:

$$\log \beta^\circ_{m0-h} = \log \beta^m_{m0-h} + \log \gamma_{Zr_m(OH)_h^{(4m-h)+}} + h \cdot \log \gamma_{H_3O^+} - m \cdot \log \gamma_{Zr^{4+}} - 2h \cdot \log a_{H_2O}$$

with the logarithms activity coefficients:

$$\log \gamma_{Zr_m(OH)_h^{(4m-h)+}} = -(4m-h)^2 \cdot D + \varepsilon(Zr_m(OH)_h^{4m-h)+}, NO_3^-) \cdot I_m$$
$$\log \gamma_{H_3O^+} = -D + \varepsilon(H_3O^+, NO_3^-) \cdot I_m$$
$$\log \gamma_{Zr^{4+}} = -16 \, D + \varepsilon(Zr^{4+}, NO_3^-) \cdot I_m$$

Consequently:

$$\log \beta^m_{m0-h} + D\,[16m - h - (4m - h)^2] - 2h \log a_{H_2O} = \log \beta^o_{m0-h} - \Delta\varepsilon \cdot I_m$$

where $\Delta\varepsilon$ is the summation of the specific interaction terms:

$$\Delta\varepsilon = \varepsilon[Zr_m(OH)_h^{(4m-h)+}, NO_3^-] + h\varepsilon[H_3O^+, NO_3^-] - m\varepsilon[Zr^{4+}, NO_3^-]$$

Since the solvent is a chemically reacting species, its activity must be calculated and incorporated into the expression for the thermodynamic constant.

$$\log a_{H_2O} \approx \frac{-2 \cdot \Phi \cdot I_m}{55.51 \cdot \ln(10)} \quad (I_m = m_{K+} = m_{NO_3^-})$$

Φ is the osmotic coefficient which can be calculated from Stockes[24] equation.

Figure 2. Extrapolation of the logarithm of the thermodynamical formation constant of $Zr(OH)_3^+$ by weighted linear regression

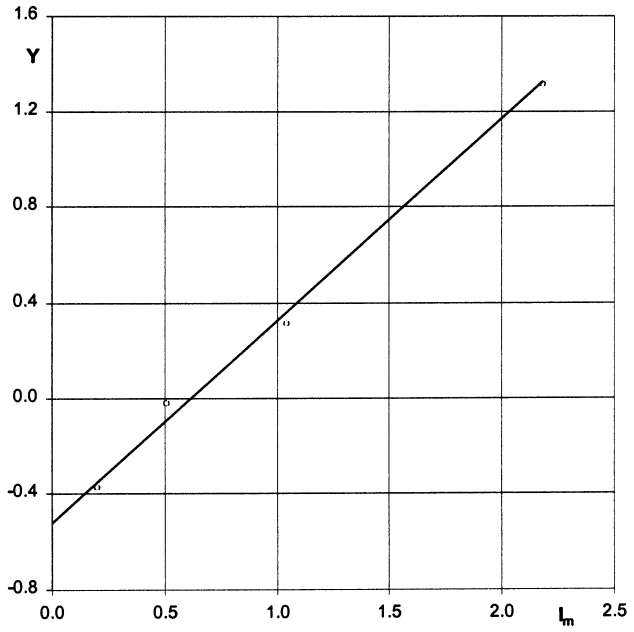

The value of $\log \beta^\circ_{m0-h}$ is obtained using a weighted linear regression of the quantity Y as a function of the ionic strength[25].

$$Y = \log \beta^m_{m0-h} + D[16m - h - (4m - h)^2] - 2h \log a_{H_2O} = \log \beta^\circ_{m0-h} - \Delta\varepsilon \cdot I_m$$

This procedure has been applied for the determination of $\log \beta^\circ_{10-3}$, $\log \beta^\circ_{20-7}$, $\log \beta^\circ_{10-4}$, and $\log K^\circ_s$ solubility product of $Zr(OH)_4$. For the determination of $\log \beta^\circ_{10-3}$ see, for example, Figures 2 and 3. All the results are reported in Table 3.

Discussion

The hydrolysis reactions of zirconium(IV) have been monitored by protometry, using a specific titration procedure which consist of adding the titrant very slowly (0.5 µl per 5 s) with vigorous stirring. This procedure avoids the precipitation of insoluble hydroxide at the tip of the burette and errors on the measurement of pH values.

Figure 3. Variation of the logarithm of the experimental formation constant of complex $Zr(OH)_3^+$ as a function of ionic strength (molality)

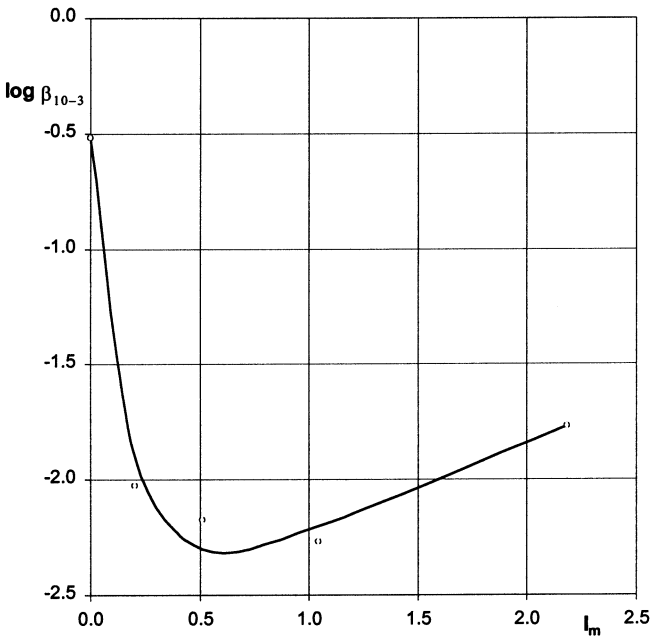

Table 3. Thermodynamic values of the logarithms of the formation constants of soluble complexes and of the solubility product of $Zr(OH)_4$; values in parentheses represent 1 σ standard deviation

$Zr(OH)_3^+$	$\log \beta^\circ_{10-3}$	−0.52 (0.01)
$Zr_2(OH)_7^+$	$\log \beta^\circ_{20-7}$	−2.22 (0.07)
$Zr(OH)_4$	$\log \beta^\circ_{10-4}$	−4.52 (0.07)
$Zr(OH)_4$	$\log Ks^\circ$	−55.26 (0.08)

In order to verify that pH measurements realised with KOH of 0.1 mol·dm^{-3} were not influenced by kinetic phenomena, we have also used KOH of $2.5 \cdot 10^{-2}$ mol·dm^{-3}. With the same rate of KOH addition (0.5 µl per 5 s) a protometric titration lasted for about one week. The pH measurements lead to stability constants values identical with those obtained with KOH of 0.1 mol·dm^{-3}.

The stability constants values of Zr hydrolysed complexes, reported by Baes and Mesmer[10] and Aja et al.[13], have been estimated from results contained in several publications. Different methods have been used in these works for studying Zr hydrolysis (e.g.: solvent extraction, spectroscopy, complexometry, solubility measurements). It must be noted that the values of Aja et al. take no account of the ionic strength variation. For calculating the thermodynamic constants values, Baes and Mesmer admit that the ionic strength dependence of β_{mlh} is similar to that found in the case of other cations, e.g. U^{4+}.

In this work, the protometric titrations of zirconium oxychloride solutions by KOH allow verification of the consistency between our obtained values and those reported by Baes and Mesmer and Aja et al. In the pH range where the solutions are homogeneous (pH $\leq$ 3.5), the experimental pH values were compared to those calculated from the sta-

bility constants. For example, in the Figure 4 the experimental titration curve of zirconium oxychloride solution ($4\cdot10^{-3}$ mol·dm^{-3}) in the presence of nitric acid ($2\cdot10^{-2}$ mol·dm^{-3}) is represented. The calculated curves obtained by using Baes and Mesmer or Aja et al. constants are represented by dashed lines. The stability constants given at zero ionic strength by Baes and Mesmer were calculated for $I = 1$ by using the relation between β_{mlh} and I they indicate in their paper[10] ($\log \beta_{10-1} = -0.6$; $\log \beta_{10-2} = -2.3$; $\log \beta_{10-3} = -6.3$; $\log \beta_{10-4} = -11.0$; $\log \beta_{10-5} = -17.1$; $\log \beta_{30-4} = 4.5$ or $\log \beta_{30-5} = 5.2$; $\log \beta_{40-8} = 8.0$).

Figure 4. Titration curves of zirconium oxychloride solution ($4\cdot10^{-3}$ mol·dm^{-3}) in the presence of nitric acid ($2\cdot10^{-2}$ mol·dm^{-3}); ionic strength = 1; KOH = 1 mol·dm^{-3}; ▲ experimental curve, (—) calculated curve with our results, (-----) calculated curves with results of Baes and Mesmer[10] or Aja et al.[13]

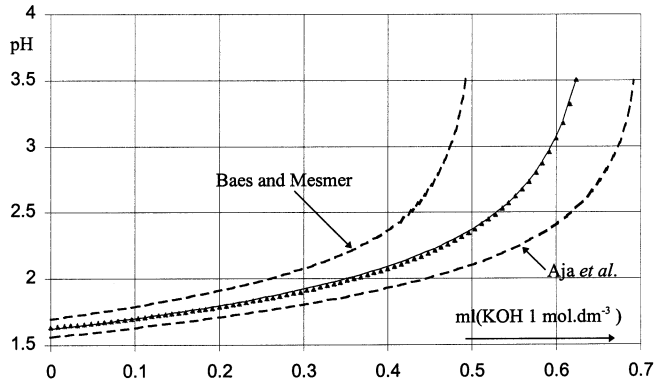

There is a large discrepancy between the experimental curve and the two calculated curves. By using the results of Baes and Mesmer, the plot of the distribution curves of the different mono- and polynuclear hydroxo complexes shows that $Zr_4(OH)_8^{8+}$ is practically the only species formed. This tetrameric ion is that encountered in the solid zirconium oxychloride, so the dissolution of this solid compound should not modify the pH solution, which disagrees with our observations and with those of Larsen and Gammill[1]. On the other hand, the constants values reported by Aja et al. lead to the predominance of $Zr(OH)_4$ at pH = 1.5−3.5. Under these conditions, the studied solutions would not be homogeneous because of the precipitation of $[Zr(OH)_4]_n$.

For all these reasons, we have envisaged the existence of other soluble species under our experimental conditions ($1.5 \leq$ pH ≤ 3.5, and $8\cdot10^{-5}$ mol·dm$^{-3} \leq [Zr] \leq 8\cdot10^{-3}$ mol·dm^{-3}). Our hypotheses are based on the following experimental results:

− The pH value at the beginning of the titrations corresponds to the liberation of one equivalent of proton per zirconium and therefore to the formation of the $Zr(OH)_3^+$ species.

− The positions of the equivalent points of the titration curves at 1.5 (in nitrate medium), 1.75 (in perchlorate medium) and 2 equiv. of OH^- per zirconium. These positions are independent of the zirconium concentration which indicates that the stoichiometry of the formed species is well defined: $Zr_2(OH)_7^+$ in nitrate medium and $Zr_3(OH)_{11}^+$ in perchlorate medium.

− The existence of $Zr_2(OH)_7^+$ is confirmed by the precipitation of the ionic salt $[Zr_2(OH)_7]NO_3$ at pH ≈ 3.5.

In short, at the beginning of the titrations, one may expect the formation of the $Zr(OH)_3^+$ species. The hydrolysis of this species leads to the formation of soluble $Zr(OH)_4$ which is always a very minor species in solution because, when its concentration increases, $Zr(OH)_4$ bonds to $Zr(OH)_3^+$ by hydroxo bridges leading to $Zr_2(OH)_7^+$. Then, in KNO_3 medium, at pH > 3.5, there is a precipitation and the probable formation of polymeric species such as $Zr_3(OH)_{11}^+$ $[Zr_2(OH)_7^+ + Zr(OH)_4]$ or $Zr_4(OH)_{15}^+$ $[Zr_3(OH)_{11}^+ + Zr(OH)_4]$. When the acidity of the solution decreases the existence of the $Zr_4(OH)_{15}^+$ species has also been suggested by Gimblett and Massey[26]. Then, according to these authors, the complex ion $Zr_4(OH)_{15}^+$ hydrolyses to a neutral tetrameric hydroxide which polymerises slowly to form colloidal particles and ultimately a solid hydroxide precipitate. Finally, at the second equivalence point of the titration curves (pH ≈ 6), the precipitated species is very likely to be a polymer of the formula $[Zr(OH)_4]_n$ because this precipitate does not dissolve in solution, even in very acidic medium.

Conclusion

The aqueous chemistry of zirconium(IV) can be explained by the formation of the soluble species $Zr(OH)_3^+$, $Zr_2(OH)_7^+$, and $Zr(OH)_4$ in KNO_3 media, in the pH range of 1.5−3.5 and for zirconium concentrations varying from $8\cdot10^{-5}$ to $8\cdot10^{-3}$ mol·dm^{-3}.

The formation constants of the species $Zr(OH)_3^+$, $Zr_2(OH)_7^+$, and $Zr(OH)_4$ as well as the solubility product of zirconium hydroxide have been determined in KNO_3 media at four ionic strengths. The values of these β_{mlh} constants were extrapolated to the standard state in order to determine the thermodynamic constants $\beta°_{mlh}$. The $\beta°_{mlh}$ constants were determined at zero ionic strength by putting the Specific ion Interaction Theory (SIT method) into practice.

We have also obtained some results in heterogeneous medium, at pH > 10, which lead us to consider the formation of the $Zr(OH)_5^-$ species. Unfortunately, these results cannot be used in this case to determine the formation constant of $Zr(OH)_5^-$. A useful evaluation of the solubility of zirconium(IV) in aqueous medium is obtained by plotting the total zirconium concentration (on a logarithmic scale) as a function of pH (Figure 5).

Such a plot shows that the insoluble species $Zr(OH)_4$ is predominant between pH = 5 and pH = 12. This species distribution diagram was established at pH > 8 by using the result of Sheka et al.[3] for the formation constant of $Zr(OH)_5^-$ ($\log \beta°_{10-5} \approx -19.3$).

We thank the *Agence Nationale pour la gestion des Déchets Radioactifs (ANDRA)* for financial support.

Figure 5. Speciation of hydroxy zirconium complexes in equilibrium with solid $Zr(OH)_4$ (25°C, $I = 0$); the thick line represents the total zirconium concentration in solution; Zr^{4+} (–·–·–); $Zr(OH)_4$ (+ +); $Zr_2(OH)_7^+$ (– – –); $Zr(OH)_3^+$ (a); $Zr(OH)_5^-$ (b)

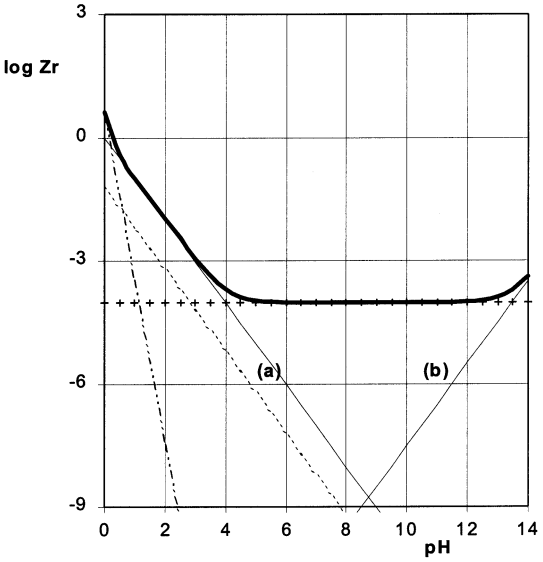

Experimental Section

Reagents: All chemicals used were of analytical grade. Zirconium oxychloride and potassium nitrate were purchased from Fluka. Nitric acid and potassium hydroxide were purchased from Merck. Solutions of zirconium oxychloride were prepared with an excess of nitric acid ($[H_3O^+]/[Zr] = 5$) to prevent the formation of less reactive polymers[16]. These solutions were standardised by edta titration using an excess of Fe^{III} ions, and salicylic acid as an indicator following the procedure described by Kragten et al.[16] and Milner et al.[17]. Potassium nitrate stock solutions were filtered on Millipore filters (pore size 1.2 μm) before use and storage.

Protometric Measurements: All measurements were performed at 25 ± 0.1°C. Experiments were made at different ionic strengths (I = 0.2, 0.5, 1, and 2 mol·dm^{-3}) and adjusted with potassium nitrate. A few experiments were carried out in sodium perchlorate medium to ensure that there is no complexation reaction with nitrate ions.

The protometric measurements were carried out in a thermoregularized cell with a nitrogen stream over the solution to avoid dissolution of carbon dioxide. The glass electrode Metrohm type "U" has a very low alkaline error. The reference element Hg/Hg_2Cl_2 was in contact with a solution containing KCl of a concentration of 0.1 mol·dm^{-3} and a variable concentration of KNO_3 to adjust ionic strength to the required value. The procedures and apparatus used for protometric measurements have been previously described[18]. For pH values below 2, a polynomial correction was used.

Because of the slow kinetics of the hydrolysis reactions, and also because of the formation of local precipitate as a consequence of the addition of the alkaline reagent, experimental procedures have been refined in order to obtain accurate and reproducible pH measurements. Titrations were made under the conditions of vigorous stirring and very slow addition of the titrant (0.5 μl per 5 s), so for high concentrations of zirconium, a titration can last several days.

Solutions of zirconium oxychloride in the concentration range of $8\cdot10^{-5}$ to $8\cdot10^{-3}$ mol·dm^{-3} were titrated by KOH (0.1 mol·dm^{-3}) up to pH = 12. Further titrations with a less concentrated reagent (KOH of 0.04 mol·dm^{-3}) were performed to ensure that the equilibrium is effectively reached throughout the experiments. The results were similar in both cases and so validate the titration procedure.

Solubility Measurements: The solubility of zirconium hydroxide $Zr(OH)_4$ was measured as a function of pH at four ionic strengths in order to evaluate its solubility product. Zirconium hydroxide was prepared by the precipitation of zirconyl chloride with ammonia. An amount of solid was introduced in zirconyl chloride solutions of variable concentration and ionic strength. After the equilibrium was reached (up to 15 d), the solutions were centrifuged and filtered using a Sartorius filter (pore size 0.45 μm). The pH value and the total concentration of zirconium for the supernatant were determined. The pH ranged from 1 to 3.5 and the zirconium concentration varied from 0.1 to 0.001 mol dm^{-3}. For each ionic strength a series of ten solutions was prepared.

Computations: The protometric data were processed by the computer program Protaf[19] in order to obtain the best-fit chemical model and refined stability constants β_{mlh} (β_{mlh} refers to the species $M_mL_lH_h$; a negative h value refers to the hydroxy ion). The program Protaf, which is based on the weighted least squares of the residues of the experimental variables (volume of titrant, pH), allows a simultaneous processing of ten titrations, each including 150 pairs of data (volume, pH).

[1] E. M. Larsen, A. M. Gammill, *J. Am. Chem. Soc.* **1950**, *72*, 3615.
[2] A. J. Zielen, R. E. Connick, *J. Am. Chem. Soc.* **1956**, *78*, 5785.
[3] I. A. Sheka, T. V. Pevzner, *Russ. J. Inorg. Chem.* **1960**, *5*, 1119.
[4] P. N. Kovalenko, K. N. Bagdasarov, *Russ. J. Inorg. Chem.* **1961**, 6, 272.
[5] V. M. Peshkova, N. V. Mel′chakova, S. G. Zhemchuzhin, *Russ. J. Inorg. Chem.* **1961**, *6*, 630.
[6] A. S. Solovkin, A. I. Ivantsov, *Russ. J. Inorg. Chem.* **1966**, *11*, 1013.
[7] H. Bilinski, M. Branica, L. G. Sillen, *Acta Chem. Scand.* **1966**, *20*, 853.
[8] V. A. Nazarenko, O. V. Mandzhgaladze, *Russ. J. Inorg. Chem.* **1969**, *14*, 639.
[9] N. Noren, *Acta Chem. Scand.* **1973**, *27*, 1369.
[10] C. F. J. Baes, R. E. Mesmer, in *The Hydrolysis of Cations*, Wiley & Sons, New York, **1976**.
[11] J. S. Johnson, K. A. Kraus, *J. Am. Chem. Soc.* **1956**, *78*, 3937.
[12] R. L. Angstadt, S. Y. Tyree, *J. Inorg. Nuclear Chem.* **1962**, *24*, 913.
[13] S. U. Aja, S. A. Wood, A. E. William-Jones, *Applied Geochem.* **1995**, *10*, 603.
[14] A. S. Solovkin, S. V. Tsvetkova, *Russ. Chem. Rev.* **1962**, *31*, 655.
[15] J. H. Adair, H. G. Krarup, S. Venigalla, T. Tsukada, *Mat. Res. Soc. Symp. Proc*. **1997**, *432*, 101.
[16] J. Kragten, A. Parczewski, *Talanta* **1981**, *28*, 149.
[17] G. W. C. Milner, P. J. Phennah, *Analyst* **1981**, *79*, 475.
[18] M. Aplincourt, C. Gerard, R. P. Hugel, J. C. Pierrard, J. Rimbault, A. Bertrandie, B. Magny, P. J. Siret, *Polyhedron* **1992**, *11*, 1161.
[19] R. Fournaise, C. Petitfaux, *Talanta* **1987**, *34*, 385.
[20] J. M. Brønsted, *J. Am. Chem. Soc.* **1922**, *44*, 938.
[21] J. M. Brønsted, *J. Am. Chem. Soc.* **1922**, *44*, 877.
[22] G. Scatchard, *Chem. Rev.* **1936**, *19*, 309.
[23] H. E. A. Guggenheim, in *Applications of Statistical Mechanics*, Clarenden, Oxford, **1966**.
[24] R. H. Stockes, "Thermodynamics of Solution" in *Activity Coefficients in Electrolyte Solutions*, vol. I, CRC Press, Boca Raton, Florida, **1979**.
[25] H. Wanner, I. Grenthe, in *Guidelines for the Extrapolation to Zero Ionic Strength, TDB-2 (revision 2)*, OECD Nuclear Energy Agency, France, **1992**.
[26] F. G. R. Gimblett, B. H. Massey, *Inorg. Chem.* **1979**, *9*, 2038.
[98162]

NMR Investigation on the Solution Structure and Dynamic Behaviour of 1,2-Diphenyl-1,2-bis(trimethylsilyl)ethanediyldilithium

Alois Fürstner*, Günter Seidel, Hans-Egbert Mons, and Richard Mynott

Max-Planck-Institut für Kohlenforschung,
Kaiser-Wilhelm-Platz 1, D-45470 Mülheim/Ruhr, Germany
Fax: (internat.) + 49(0)208/306-2980
E-mail: fuerstner@mpi-muelheim.mpg.de; mynott@mpi-muelheim.mpg.de

Received June 6, 1998

Keywords: Dianions / Organolithium compounds / Reductive metallation / HOESY / Lithium NMR

1,2-Diphenyl-1,2-bis(trimethylsilyl)ethene (**5**) undergoes a smooth reductive metallation with metallic lithium to yield the corresponding dilithioethane derivative (Li_2·**5**). The structure of this new compound in [D_8]THF solution was determined by NMR spectroscopy (^{1}H, ^{13}C, ^{6}Li, ^{7}Li NMR and ^{6}Li,^{1}H-HOESY). It is shown that the phenyl rings have a high quinoid character and that the lithium cations are relatively mobile.

Introduction

It has been known since 1928 that stilbene (**1**, R = H) and related aryl-substituted ethene derivatives (**1**, R = alkyl, aryl) react readily with alkali metals to afford π-delocalized benzylic carbanions[1][2]. Similar reductive metallations can be achieved with ethenylsilanes **2a–c**[3], in which the negative charges are stabilized by the adjacent silyl substituents. In compounds such as **3a–c**, both stabilizing effects are present[4].

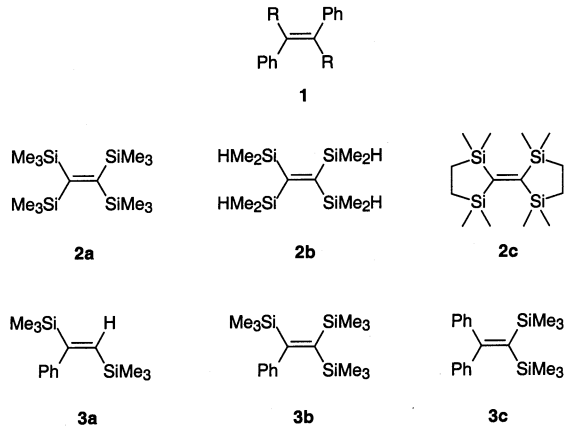

These metallations proceed in a stepwise fashion: a first single electron transfer (s.e.t.) leads to short-lived radical anions which rapidly undergo a second s.e.t. to afford the corresponding dianions[5]. The latter have attracted considerable attention in recent years as stabilized analogues of the still elusive 1,2-dilithioethane[6]. Several in-depth studies employing X-ray crystallography or NMR have provided a detailed – but rather static – picture of the bonding situation in such dimetallic compounds[1][2][3][4]. In the following we describe not only the solution structure of a further missing congener of this series, i. e. the dilithio derivative of 1,2-diphenyl-1,2-bis(trimethylsilyl)ethene (Li_2·**5**), but also show that within this molecule the metal cations are highly mobile.

Results and Discussion

Recently, McMurry-type coupling reactions have been extended to substrates other than aldehydes and ketones[7]. We found that aromatic acylsilanes react reasonably well with low-valent titanium [Ti] to afford the corresponding 1,2-disilylethene derivatives as the major products.

Scheme 1

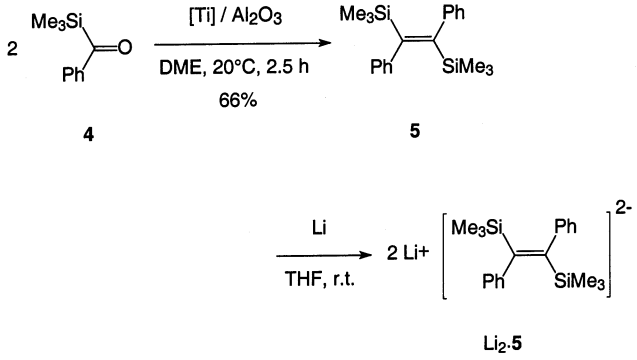

Specifically, treatment of benzoyltrimethylsilane **4** with [Ti] formed from $TiCl_3$ and "high surface sodium" (Na/Al_2O_3)[8] as the preferred coupling agent provides compound **5** in 66% yield as colorless crystals[9]. This product undergoes a smooth reductive metallation on exposure to an excess of lithium metal in thoroughly dried and degassed THF, leading to a dark-red solution of the corresponding dianion Li_2·**5**. This derivative is thermally stable for prolonged periods of time and can be isolated as a dark-red solid upon removal of the THF. However, Li_2·**5** is extremely sensitive in solution as well as in the solid state towards

 © WILEY-VCH Verlag GmbH, D-69451 Weinheim, 1998 1434–1948/98/1771–1774 $ 17.50+.50/0

traces of air which immediately re-convert it into the starting disilylethene **5**.

Although various conditions have been used to crystallize the compound, no crystals of $Li_2 \cdot$ **5** suitable for an X-ray analysis have been obtained. Therefore the structure of this compound was studied by NMR spectroscopy. A complete and unambiguous assignment of the ^1H and ^{13}C spectra (Table 1) was achieved using 2D-NMR techniques.

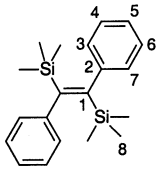

5

Table 1. ^1H- and ^{13}C-NMR data for **5** and Li_2·**5** in [D_8]THF at 303 K; arbitrary numbering as shown

Position	^{13}C NMR				^1H NMR		
	5	Li_2·**5**	$\Delta\delta$[a]	$^1J_{(C,H)}$	**5**	Li_2·**5**	$\Delta\delta$[a]
1	159.1	69.4	−89.7				
2	145.8	153.1	7.3				
3	128.0	107.4	−20.6	159.3	7.04	5.89	−1.15
4	127.6	127.0	−0.6	159.9	7.27	6.05	−1.22
5	125.6	97.9	−27.7	160.0	7.18	4.93	−2.25
6	127.6	130.5	2.9	159.9	7.27	6.27	−1.00
7	128.0	117.6	−10.4	159.3	7.04	6.18	−0.86
8	0.2	2.3	2.1	120.0	−0.36	0.00	0.36

[a] $\Delta\delta_n = [\delta_n(Li_2 \cdot \mathbf{5}) - \delta_n(\mathbf{5})]$.

As can be seen from Table 1, five proton and six ^{13}C signals are observed at 303 K for the phenyl groups. Detailed analysis of these spectra and further experiments including COSY revealed that the two arene groups are equivalent but that within each group all the carbon atoms and protons are different. The number of signals in the ^1H- and ^{13}C-NMR spectra is unchanged when the sample is cooled to 193 K and no broadening of any of these signals is observed (cf. Experimental Section). Thus, the phenyl groups remain equivalent on the NMR time scale over the range 300 K to 193 K.

The inequivalence of the *ortho* positions (3 and 7) and of the *meta* positions (4 and 6) within each phenyl group indicates that the barrier to rotation about the C-1,C-2 bond in Li_2·**5** must be high. No exchange cross peaks could be detected in a ^{13}C 2D-EXSY spectrum recorded at 303 K. Taking into account the relatively high signal-to-noise ratio of this 2D spectrum and that the cross peaks due to exchange were not larger than the peak-to-peak noise, the barrier to rotation of the arene ring is estimated to be at least 90 kJ/mol.

The resonance of C-1 is observed at $\delta = 69.4$, i. e. an upfield shift of 89.7 ppm relative to the olefin **5** ($\delta = 159.1$). Moreover, the ^{13}C data indicate that the negative charges are also delocalized to a large extent over the arene rings. Specifically, the *para*-^{13}C signal of C-5 resonates at $\delta = 97.9$, corresponding to a low-frequency shift of ca. 27.7 ppm by comparison with the signal of **5**. Similarly, the *ortho* signals ($\delta = 107.4$ and 117.6) are shifted to lower frequency by 20.6 and by 10.4 ppm. These observations and the high barrier to rotation indicate that the phenyl substituents have a strong quinoid character, a conclusion which is in accordance with previous studies on related ethylene anions[3][4].

Further structural information was gained from the lithium-NMR spectra. Both the ^7Li-NMR spectra of the natural abundance compound and ^6Li spectra of a ^6Li-enriched sample were measured. Surprisingly, the temperature dependence of the ^6Li- and ^7Li-NMR spectra contrasts strongly with that observed for the ^1H- and ^{13}C-NMR spectra. At 293 K a single, broadened signal is observed in the ^6Li spectrum (88.3 MHz) at $\delta_{Li} = -2.4$ (linewidth 500 Hz), which on lowering the temperature splits into two well-resolved lines at $\delta_{Li} = -0.8$ and -3.8 (Figure 1). The separation of these signals (3.0 ppm) is large as compared to the usual range of lithium chemical shifts[10], suggesting that the environments of the lithium cations are rather different. This result is in contrast to previous investigations on dilithioethane derivatives, in which the Li signals either coincide or resonate within a narrow shift range[3][4].

Figure 1. ^7Li-NMR (233.3 MHz) spectrum (top) and ^6Li-NMR (88.3 MHz) spectrum (bottom) of Li_2·**5** recorded at 193 K

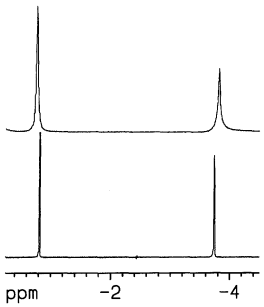

The ^6Li-enriched samples were prepared to obtain additional information on the *location* of the cations using ^6Li,^1H heteronuclear Overhauser effects, which were measured using the 2D HOESY (HOESY = heteronuclear Over-

hauser effect spectroscopy) technique[10][11]. The HOESY spectrum reveals strong cross peaks between the lithium signal at $\delta_{Li} = -3.8$ and the TMS group, the *ortho* proton at $\delta_H = 5.89$ (3-H) and the adjacent *meta* proton (4-H). Additional, but weaker, cross peaks are found to the *para* proton (5-H) and the other *ortho* proton (7-H). The HOESY cross peaks of the second lithium signal at $\delta_{Li} = -0.8$ are weaker and correlate with the TMS group and both *ortho* protons (Figure 2). Since ^{6}Li,^{1}H heteronuclear Overhauser effects can only be detected over short distances[10], these results show that *both* lithium cations must be close to the organic anion and that in Li_2·**5** tight ion contacts are present. ^{6}Li- and ^{7}Li-NMR spectra recorded in the presence of excess TMEDA support this conclusion: although TMEDA usually dissects oligomeric organolithium compounds in solution, the lithium chemical shifts of Li_2·**5** are hardly affected even when 2.5 equivalents of TMEDA are added.

Figure 2. ^{6}Li,^{1}H-HOESY-NMR spectrum (contour plot) of Li_2·**5** recorded in [D$_8$]THF at 193 K

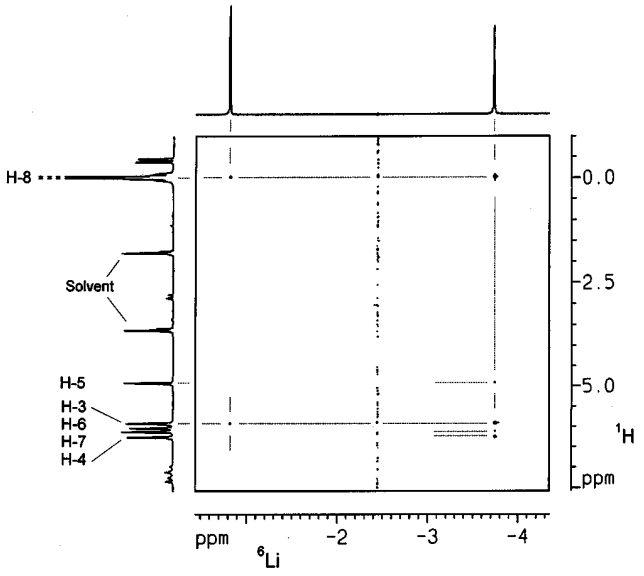

Table 1 also documents the large differences between the chemical shifts of the *ortho* carbon atoms C-3 and C-7 in Li_2·**5** (10.2 ppm). The signal shifted more strongly to high field arises from the *ortho* carbon atom on side of the ring having the stronger interaction with Li. Similarly, significant shift differences are found between the *meta* carbon atoms C-4/C-6 (3.5 ppm), as well as the *ortho* protons H-3/H-7 (0.29 ppm) and the *meta* protons H-4/H-6 (0.22 ppm). We interpret these data and the HOESY spectra described above as showing that the lithium cation giving rise to the resonance at $\delta = -3.8$ interacts with the phenyl groups, particularly with the sides of these groups towards the inside of the molecule (Figure 3). If the lithium atom interacts with both phenyl rings simultaneously, then the dianion cannot be planar: the torsional angle about the C-1, C-1′ bond must be reduced to ca. 90°. This is also consistent with ^{1}H-NOE data, since strong cross peaks are observed between the trimethylsilyl protons and both *ortho* protons of the arenes. Note also that the non-planar scaffold of Li_2·**5** implies an axially chiral environment. A schematic representation of the structure and bonding situation in Li_2·**5** is given in Figure 3.

Figure 3. Schematic representation of the structure and bonding situation in Li_2·**5**

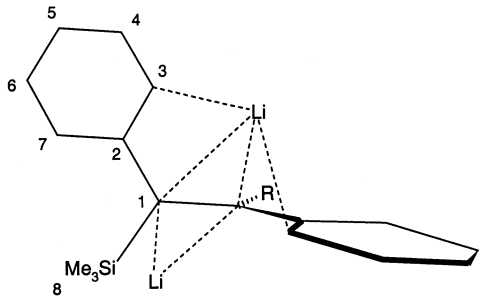

There is evidence that additional fast exchange processes are occurring. In both, the ^{6}Li and ^{7}Li spectra, the Li signal at $\delta = -0.8$ becomes narrower when the temperature is reduced to below 250 K but the Li signal at $\delta = -3.8$ remains somewhat broadened. This is apparently caused by additional exchange phenomena involving this lithium atom alone which remain fast on the NMR time scale. It is possible that the lithium cation jumps between different sites on the phenyl groups and the observed broadening may be due to a slowing of this rate of exchange. However, we have no corroborating evidence for this from the ^{1}H- or ^{13}C-NMR spectra and this interpretation remains speculative. When TMEDA is added to the sample, this phenomenon becomes much more marked. Not only does the high-field ^{6}Li signal below 200 K split into two signals of intensities ca. 2:1 but in this case the phenyl *ortho* proton signal also shows similar behaviour.

In summary, the NMR data are consistent with the presence of contact ionic interactions in Li_2·**5** with the anion having a C_2-symmetrical twisted, axially chiral conformation with a torsional angle of about 90°. As a result of their high quinoid character, the phenyl rings cannot rotate. On time average the two lithium cations are found on the plane orthogonal to the central C−C bond and passing through its midpoint. At room temperature the lithium cations exchange locations with one another rapidly but at 193 K this exchange is slow on the NMR time scale. One of the lithium cations lies between the phenyl rings and interacts strongly with the *ortho* positions.

We thank the *Fonds der Chemischen Industrie*, Frankfurt, for generous financial support.

Experimental Section

General: All reactions as well as the sample preparations for NMR were carried out under Ar using Schlenk techniques. All glassware was thoroughly flame-dried in vacuo. Natural abundant Li and ^{6}Li powder (Aldrich, 95% ^{6}Li, dispersion in mineral oil) were repeatedly washed with pentane and dried in vacuo prior to

use. [D_8]THF was dried by distillation from Na/K alloy and transferred under Ar. Substrate **5** was prepared by a McMurry-type coupling reaction as previously described[9a].

NMR Spectroscopy: All the NMR spectra were measured with a Bruker DMX-600 NMR spectrometer: ^{1}H (600.2 MHz), ^{6}Li (88.3 MHz), ^{7}Li (233.3 MHz), and ^{13}C (150.9 MHz). The chemical shifts were determined relative to the β-methylene signals of the solvent and converted to the TMS scale (^{1}H, β-CH_2, δ_H = 1.78; ^{13}C, β-CH_2, δ_C = 25.2). The sequence of proton signals 3-H to 6-H was determined in the COSY spectrum and confirmed by NOESY. These assignments were transferred to ^{13}C using data from the ^{1}H,^{13}C correlation. The strongest ^{6}Li,^{1}H cross-peaks in the HOESY spectrum were to the protons at 5.89 (*ortho*) and 6.27 (adjacent *meta*), allowing the "outer" and "inner" sides of the phenyl ring to be identified. The lithium chemical shifts are given relative to external 0.1 M LiBr in THF solution (0 ppm). The HOESY experiments were recorded using the experiment hoesytp from the standard Bruker pulse library using a mixing time of 1.8 s (256 experiments each of 64 scans, 1 K in f_2, magnitude calculation in f_1, exponential multiplication in both dimensions using lb = 2).

Preparation of Diphenyl-1,2-bis(trimethylsilyl)ethanediyldilithium (Li_2·**5**). To a stirred suspension of lithium powder (35 mg, 5.04 mmol) in 5 ml of [D_8]THF was added a solution of alkene **5** (144 mg, 0.44 mmol)[9a] in 5 ml of [D_8]THF. The reaction mixture turned dark-red within a few minutes and stirring was continued overnight. An aliquot of the supernatant dark-red liquid was transferred via cannula into a thoroughly dried NMR tube, the rest was filtered off and concentrated to afford a dark-red amorphous solid. – ^{7}Li NMR ([D_8]THF, 303 K) δ = −2.2, $\Delta\nu_{1/2}$ = 265 Hz. – ^{7}Li NMR ([D_8]THF, 193 K) δ = −0.78, −3.82. – ^{1}H NMR ([D_8]THF, 193 K): δ = 6.25, 6.10, 6.02, 5.92, 4.91, −0.03. – ^{13}C NMR ([D_8]THF, 193 K) δ = 153.0, 130.6, 127.0, 117.0, 107.4, 97.9, 68.2. – After addition of TMEDA: ^{1}H NMR ([D_8]THF, 303 K): δ = 6.27, 6.19, 6.03, 5.90, 4.95, 0.02. – ^{1}H NMR ([D_8]THF, 193 K): δ = 6.25, 6.17, 5.98, 5.87, 4.90, −0.02. – ^{7}Li NMR ([D_8]THF, 193 K): δ = −2.2, $\Delta\nu_{1/2}$ = 350 Hz. – ^{7}Li NMR ([D_8]THF, 193 K): δ = −0.75, −3.68 (br.). – For the assignment and additional data see Table 1.

[1] [1a] W. Schlenk, E. Bergmann, *Justus Liebigs Ann. Chem*. **1928**, *463*, 106–125. – See the following for leading references: [1b] H. Bock, T. Hauck, C. Näther, *Organometallics* **1996**, *15*, 1527–1529. – [1c] H. Bock, K. Ruppert, D. Fenske, *Angew. Chem*. **1989**, *101*, 1717–1719; *Angew. Chem. Int. Ed. Engl*. **1989**, *28*, 1685–1688. – [1d] Y. Yokoyama, T. Koizumi, O. Kikuchi, *Chem. Lett*. **1991**, 2205–2208. – [1e] M. Walczak, G. D. Stucky, *J. Am. Chem. Soc*. **1976**, *98*, 5531–5539. – [1f] M. Walczak, G. D. Stucky, *J. Organomet. Chem*. **1975**, *97*, 313–323. – [1g] J. G. Smith, E. Oliver, T. J. Boettger, *Organometallics* **1983**, *2*, 1577–1582. – [1h] J. E. Gano, E. J. Jacob, P. Sekher, G. Subramaniam, L. A. Ericksson, D. Lenoir, *J. Org. Chem*. **1996**, *61*, 6739–6743. – [1i] J. F. Garst, *J. Am. Chem. Soc*. **1971**, *93*, 6312–6313. – [1j] P. Schade, T. Schäfer, K. Müllen, D. Bender, K. Knoll, K. Bronstert, *Chem. Ber*. **1991**, *124*, 2833–2841.

[2] [2a] For a timely review see: A. Maercker in *Lithium Chemistry. A Theoretical and Experimental Overview* (Eds.: A.-M. Sapse, P. v. R. Schleyer), Wiley, New York, **1995**, p. 477–577. – [2b] W. N. Setzer, P. v. R. Schleyer, *Adv. Organomet. Chem*. **1985**, *24*, 353–451.

[3] [3a] A. Sekiguchi, T. Nakanishi, C. Kabuto, H. Sakurai, *J. Am. Chem. Soc*. **1989**, *111*, 3748–3750. – [3b] A. Sekiguchi, M. Ichinohe, C. Kabuto, H. Sakurai, *Bull. Chem. Soc. Jpn*. **1995**, *68*, 2981–2988. – [3c] A. Sekiguchi, M. Ishinohe, M. Takahashi, C. Kabuto, H. Sakurai, *Angew. Chem*. **1997**, *109*, 1577–1579; *Angew. Chem. Int. Ed. Engl*. **1997**, *36*, 1533–1534.

[4] [4a] B. Böhler, D. Hüls, H. Günther, *Tetrahedron Lett*. **1996**, *37*, 8719–8722. – [4b] A. Sekiguchi, M. Ichinohe, T. Nakanishi, C. Kabuto, H. Sakurai, *Bull. Chem. Soc. Jpn*. **1995**, *68*, 3215–3220.

[5] For electrochemical studies on the reduction of aryl-substituted ethene derivatives see: [5a] J. L. Muzyka, M. A. Fox, *J. Org. Chem*. **1991**, *56*, 4549–4552. – [5b] M. O. Wolf, H. H. Fox, M. A. Fox, *J. Org. Chem*. **1996**, *61*, 287–294 and references cited therein.

[6] See the following for leading references: [6a] A. J. Kos, E. D. Jemmis, P. v. R. Schleyer, R. Gleiter, U. Fischbach, J. A. Pople, *J. Am. Chem. Soc*. **1981**, *103*, 4996–5002. – [6b] L. Manceron, L. Andrews, *J. Phys. Chem*. **1986**, *90*, 4515–4528. – [6c] V. Rautenstrauch, *Angew. Chem*. **1975**, *87*, 254–255; *Angew. Chem. Int. Ed. Engl*. **1975**, *14*, 259–260. – [6d] B. Bogdanovic, B. Wermeckes, *Angew. Chem*. **1981**, *93*, 691–693; *Angew. Chem. Int. Ed. Engl*. **1981**, *20*, 684–686. – [6e] A. Maercker, B. Grebe, *J. Organomet. Chem*. **1987**, *334*, C21–C23. – [6f] N. J. R. van E. Hommes, F. Bickelhaupt, G. W. Klumpp, *Angew. Chem*. **1988**, *100*, 1100–1107; *Angew. Chem. Int. Ed. Engl*. **1988**, *27*, 1083–1084.

[7] Review: A. Fürstner, B. Bogdanovic, *Angew. Chem*. **1996**, *108*, 2583–2609; *Angew. Chem. Int. Ed. Engl*. **1996**, *35*, 2442–2469.

[8] Reviews: [8a] A. Fürstner (Ed.), *Active Metals. Preparation, Characterization, Applications*, VCH, Weinheim, **1996**, p. 381–426. – [8b] A. Fürstner, in *Encyclopedia of Reagents for Organic Synthesis* (Ed.: L. A. Paquette), Wiley, New York, **1995**, p. 4180–4181.

[9] [9a] A. Fürstner, G. Seidel, B. Gabor, C. Kopiske, C. Krüger, R. Mynott, *Tetrahedron* **1995**, *51*, 8875–8888. – [9b] For the development of low-valent titanium on alumina and related reagents see: A. Fürstner, G. Seidel, *Synthesis* **1995**, 63–68.

[10] For a review see: W. Bauer, in *Lithium Chemistry, A Theoretical and Experimental Overview* (Eds.: A.-M. Sapse, P. v. R. Schleyer), Wiley, New York, **1995**, p. 125–172.

[11] See the following for leading references on ^{1}H$^{6(7)}$Li HOESY spectroscopy: [11a] W. Bauer, P. v. R. Schleyer, *Magn. Res. Chem*. **1988**, *26*, 827–833. – [11b] W. Bauer, G. Müller, R. Pi, P. v. R. Schleyer, *Angew. Chem*. **1986**, *98*, 1130–1132. – [11c] W. Bauer, L. Lochmann, *J. Am. Chem. Soc*. **1992**, *114*, 7482–7489. – [11d] W. Bauer, T. Clark, P. v. R. Schleyer, *J. Am. Chem. Soc*. **1987**, *109*, 970–977. – [11e] W. Bauer, P. v. R. Schleyer, *J. Am. Chem. Soc*. **1989**, *111*, 7191–7198. – [11f] D. Hoffmann, W. Bauer, P. v. R. Schleyer, *Chem. Commun*. **1990**, 208–211. – [11g] W. Bauer, F. Hampel, *Chem. Commun*. **1992**, 903–905. – [11h] L. D. Field, M. G. Gardiner, B. A. Messerle, C. L. Raston, *Organometallics* **1992**, *11*, 3566–3570. – [11i] L. A. Paquette, M. R. Sivik, W. Bauer, P. v. R. Schleyer, *Organometallics* **1994**, *13*, 4919–4927. – [11j] G. Hilmersson, O. Davidsson, *Organometallics* **1995**, *14*, 912–918. – [11k] S. Berger, F. Müller, *Chem. Ber*. **1995**, *128*, 799–802. – [11l] T. Roelle, R. W. Hoffmann, *J. Chem. Soc., Perkin Trans. 2* **1995**, 1953–1954. – [11m] M. Wenzel, D. Lindauer, R. Beckert, R. Boese, E. Anders, *Chem. Ber*. **1996**, *129*, 39–44. – [11n] J. M. Saa, G. Martorell, A. Frontera, *J. Org. Chem*. **1996**, *61*, 5194–5195. – [11o] L. Glendenning, N. Bampos, L. D. Field, *Bull. Chem. Soc. Jpn*. **1996**, *69*, 2025–2029. – [11p] G. Hilmersson, P. I. Arvidsson, O. Davidsson, M. Haakansson, *Organometallics* **1997**, *16*, 3352–3362. – [11q] M. R. Sivik, W. Bauer, P. v. R. Schleyer, L. A. Paquette, *Organometallics* **1996**, *15*, 5202–5208.

[I98174]

Transformation of 3,4-Bis(isopropylidene)-2,5-dichloro-1,2,5-thiadiborolane into *nido*-2,4,5-Thiadicarbahexaborane(5) Derivatives − Formation and Computational Elucidation of a Thiadicarbanonaborane(8) with a *ni*-9<IV+IV> Configuration☆

Volker Beez[a], Peter Greiwe[a], Hans Pritzkow[a], Matthias Hofmann[b], Paul v. R. Schleyer*[b,c], and Walter Siebert*[a]

Anorganisch-Chemisches Institut der Universität Heidelberg[a],
Im Neuenheimer Feld 270, D-69120 Heidelberg, Germany

Computer-Chemie-Centrum, Institut für Organische Chemie[b],
der Universität Erlangen-Nürnberg,
Nägelsbachstraße 25, D-91054 Erlangen, Germany

Center for Computational Quantum Chemistry, University of Georgia[c],
Cedar Street 1004, Athens, GA 306052−2525, USA

Received June 4, 1998

Keywords: 3,4-Bis(isopropylidene)-1,2,5-thiadiborolane / *nido*-2,4,5-Thiadicarbahexaboranes(5) / Isomeres / Thiadicarbanonaborane(8) / IGLO

The 3,4-bis(isopropylidene)-2,5-dichloro-1,2,5-thiadiborolane (**5b**), obtained from 3,4-bis(dichloroboryl)-2,5-dimethyl-2,4-hexadiene (**4**) and $(Me_3Si)_2S$, reacts with $Li[RBH_3]$ (R = H, C_6H_5, C_6Me_4H) to yield the corresponding derivatives of the *nido*-4,5-diisopropyl-2,4,5-thiadicarbahexaboranes **2**. Replacements of the chlorine atoms in **5b** with two hydrido, or with one hydrido and one aryl (phenyl or duryl) group, followed by the hydroboration of the isopropylidene substituents with RBH_2 (R = H, C_6H_5, C_6Me_4H) lead to four *nido*-2,4,5-thiadicarbahexaboranes (**2a–d**) in low yields. Their composition follows from MS and NMR data; not refined X-ray structural data of **2d** support the proposed skeletal structure. In addition to **2a**, larger thiacarboranes were detected by GC/MS and ^{11}B NMR. The structure of the nine-vertex cluster **6a** could be identified by applying the ab initio/IGLO/NMR method. Geometry optimizations at the MP2(fc)/6–31G* level rule out the C_s *nido*-$SC_2B_6H_8$ isomer **7**. The C_{2v} structure of **6** consists of a nine-vertex cluster with two elongated B–B distances. As this 22e cluster **6** represents an exception to the Wade rules, the nature of the bonding of nine-vertex clusters with different electron counts is discussed.

The thiacarboranes and thiadicarboranes with nine to eleven skeletal atoms, *arachno*-SCB_7H_{11}[1][2], *arachno*-SCB_8H_{12}[2], *nido*-SCB_9H_{11}[2], *arachno*-$SC_2B_6H_{10}$[3], *nido*-$SC_2B_8H_{10}$,[4][5][6] have been obtained from the reactions of neutral carboranes or their anions with sulfur or sulfur compounds. Among the smaller but still unknown thiacarboranes, the *nido*-$SC_2B_3H_5$ cluster (**2**) is of particular interest to us, since it could be isoelectronic with 2,3,5-tricarbahexaborane(7) (**1**)[7]. Formal replacement of the CH_2 group in **1** by sulfur leads to **2**. The axial hydrogen in **1** bends and is involved to some extent in a 3c,2e CHB bonding.[7][8] The reaction of the $C_2B_{10}H_{13}^-$ anion with $KHSO_3$ in acid degrades the carborane and incorporates a sulfur atom to yield *arachno*-8,6-$SCH_2B_7H_9$[5]. The analogous reaction of **1** or its anion $C_3B_3H_6^-$ with $KHSO_3$ does not seem feasible, because no BH groups should be eliminated. Such BH units are needed to abstract the oxygen atoms of $KHSO_3$ (as is the case with $C_2B_{10}H_{13}^-$). The structurally and electronically related *nido*-$SC_2B_8H_{10}$ (**3**) is obtained in aqueous solution from the reaction of $K_2S_2O_5$ with K[7,8-$C_2B_9H_{12}$]. One BH group and a hydrogen atom are replaced by a sulfur atom to give **3**. The cluster **3** differs from **2** by the $(BH)_5$ belt.

We now present our results on the designed synthesis of derivatives of **2**, obtained from the hydroboration substitution reactions of the unsaturated 1,2,5-thiadiborolane derivative **5b**. Other products are formed as well. Of these, the thiadicarbanonaborane **6a** could be identified by GC-MS, ^{11}B-NMR spectra, and by applying the ab initio/IGLO/NMR method.

Scheme 1

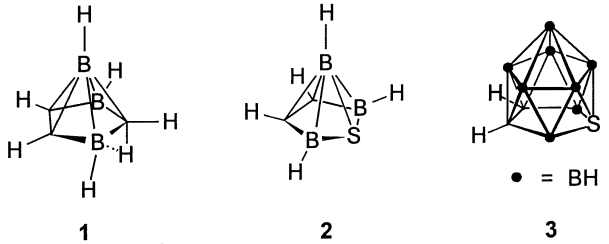

1 **2** **3**

 © WILEY-VCH Verlag GmbH, D-69451 Weinheim, 1998 1434−1948/98/1111−1775 $ 17.50+.50/0

Results and Discussion

The reaction of 3,4-bis(dichloroboryl)-2,5-dimethyl-2,4-hexadiene (**4**)[9] with hexamethyldisilathiane leads to elimination of chlorotrimethylsilane to give 3,4-bis(isopropylidene)-2,5-dichloro-1,2,5-thiadiborolane (**5b**) in 86% yield (Scheme 1). Compound **5b** is isolated as a slightly yellow liquid[10] by distillation in vacuum. It is extremely air- and moisture-sensitive due to the high reactivity conferred by the B−Cl and B−S bonds. The composition of **5b** follows from NMR and MS data, whereas the assignment of the ^{1}H- and ^{13}C-NMR signals for the *exo*- and *endo*-methyl

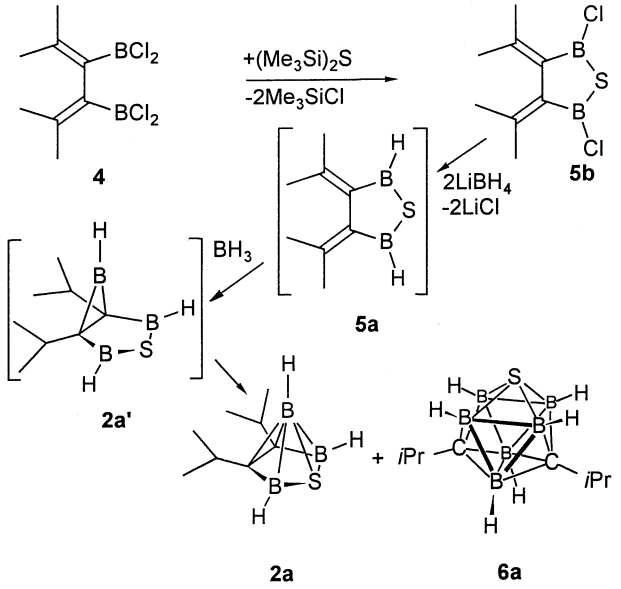

substituents of the isopropylidene groups was not possible.

The reactions of **5b** with lithium borates, Li[RBH$_3$] (R = H, C_6H_5, C_6Me_4H), yield several products. We presume that the first step involves substitution of the chlorine atoms in **5b** by hydrogen from $LiBH_4$ to give **5a**, but it was not isolated. In the next step, BH_3, formed in situ, hydroborates the double bonds of **5b**. The bicyclic organothiaborane **2a′** is an isomer of the product **2** whose existence as an intermediate may be supposed, but was not proven.With the formation of the *nido*-thiacarborane **2a** the coordination numbers increase from three to six for the apex boron atom and from three to four for the basal boron atoms. In addition to **2a**, other products are formed which could not be separated completely by distillation. The ^{11}B-NMR spectrum shows low-field signals for organoboranes and organothiaboranes as well as high-field signals. Unexpectedly, the GC-MS spectrum of the reaction mixture exhibits the molar peak for the thiadicarbanonaborane(8) derivative **6a** at m/z = 213 with the correct isotopic pattern for six boron atoms. In the {^{1}H}^{11}B-NMR spectrum three sets of signals at δ = 1.3/2.2 (intensity ratio ca. 2:1), −20.1/−20.7 (ca. 1:2) and at −28.2/−33.8 (ca. 1:2) are observed, the latter signals are assigned to **6a**.

If S were to contribute four bonding electrons, the product S(CR)$_2$(BH)$_6$ would have a 22 skeletal electron count[11]; this suggests a nine-vertex *nido* cluster. Structure **7** is a *ni*-9<V> cluster with a pentagonal open face. The MP2(fc)/6−31G* optimized structure of **7** is shown in Figure 1 together with the computed IGLO ^{11}B-NMR chemical shifts for **2** and **6**. The experimental 2:1 ^{11}B intensity pattern would be in line with structure **7** only if the S atom fluctuated from one BBB capping position to the other. However, the averaged theoretical shifts (4.3, −6.4) which might result from such fluctuation are in gross disagreement with the experimental values (−28.2, −33.8). Hence, structure **7** can be discarded from consideration. While the sulfur atom is at the vertex of lowest connectivity (k = 3), the carbon atoms in **7** are placed at k = 5 and not at the more favorable $k = 4x$ positions. For alternatives with carbons in the open face (at k = 4 positions), more than the observed two signals in the ^{11}B NMR spectrum are expected.

Figure 1. Computed geometries and ^{11}B chemical shifts of $SC_2B_3H_5$(**2**), C_s isomer $SC_2B_6H_8$ (**7**), and C_{2v} isomer $SC_2B_6H_8$ (**6**)

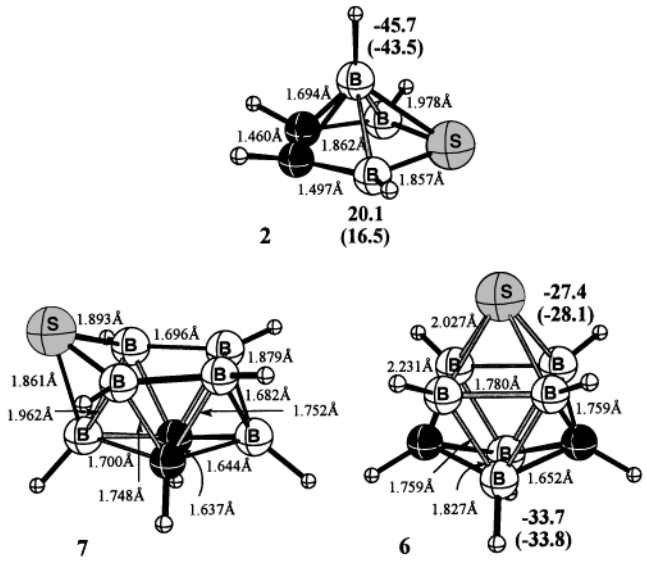

A C_{2v} starting geometry, where the S resides above a BBBB rectangular face, would be optimized to structure **6**; it is 66.3 kcal mol^{-1} lower in energy than **7**. Since the chemical shifts computed for **6** are very close to the values measured for **6a**, both have the same basic structure. The framework of **6** can be regarded as a triply capped trigonal prism and all hetero atoms are at the capping k = 4 positions. There are two large BB separations (2.23 Å) which suggest that the cluster should be considered as a *ni*-9<IV+IV> cluster with two tetragonal faces[12]. Such a cluster would be consistent with the *nido* electron count provided the S atom contributes four to a total of 22 skeletal electrons. For clarification we applied the NBO localization scheme.[13] Only one lone pair orbital on sulfur with an occupancy close to 2 (1.966) was found. This implies that the remaining four valence electrons are involved in cluster bonding which results in a *nido* electron count for $SC_2B_6H_8$, **6** (22 skeletal electrons).

The parent nine-vertex cluster anion *closo*-[B_9H_9]$^{2-}$is unusual in having non-degenerate frontier orbitals: HOMO-1, HOMO, and LUMO (A_1', A_2', and A_2'', respectively). This

implies that addition of two or removal of two or even four skeletal electrons need not cause symmetry reduction and disruption of the basic D_{3h} cluster structure. However, reduction or oxidation of $[B_9H_9]^{2-}$ changes the cluster B−B separations depending on the bonding and antibonding character of the occupied MOs. Both addition and removal of two electrons from $[B_9H_9]^{2-}$ elongate the B1-B1′ and shorten the B1−B1 distance (for numbering the atoms compare Table 2). The same effects are observed if all three capping HB vertices in $[B_9H_9]^{2-}$ are replaced by isolobal HC^+ groups to give the isoelectronic $[C_3B_6H_9]$ species: "hypo-*closo*", "*closo*", or "*nido*" (Table 2). With capping sulfur atoms (S^{2+} is isolobal to HC^+), adding two electrons to *closo*-$[S_3B_6H_6]^{4+}$ also results in shortening of B1−B1 and elongation of B1−B1′. However, the B1−B1′ bonds are larger in $[S_3B_6H_6]^{4+}$ and $[S_3B_6H_6]^{2+}$ than in the other cases. Hence, the large B1−B1′ separation (2.231 Å) involving the S cap in **6** turns out to be normal for a *nido* electron count in the nine-vertex cluster. This is in agreement with structural data of the unusual silicid compound $Rb_{12}Si_{17}$, which contains four crystallographically different Si_9^{4-} clusters besides Si_4^{4-} tetrahedra. Three of them (**B**, **C**, and **D**) are described as tricapped trigonal prisms elongated along the threefold axes. The cluster **B** has two long edges (3.09) and one short edge (2.63 Å).[14] In the Zintl phase K_4Pb_9 two different clusters, a monocapped square antiprism and an elongated tricapped trigonal prism with two long edges (3.90) and one short edge (3.45 Å) are present.[15]

Scheme 2

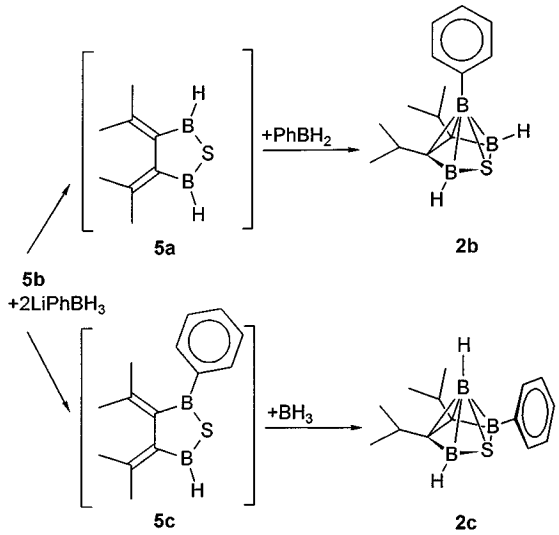

The analogous reaction of **5b** with lithium phenylborate yields the isomers **2b** and **2c** which could not be separated. According to the NMR data, the isomers are formed in a 5:1 molar ratio, the isomer with the phenyl group in the apex position being favored. This finding indicates that the chlorine atoms in **5b** are predominantly substituted by hydrogen atoms (leading to **2b**) rather than by the phenyl group (**2c**).

In order to study the steric influence of the aryl group on the formation of isomers, **5b** was reacted with lithium durylborate. Surprisingly this reaction leads to derivative **2d** with the duryl group in a basal position (Figure 2). This result may be interpreted in terms of the different reactivities of the lithium borates.

Spectra and Structural Characterization

The ^{11}B-NMR data support the assigned structures of the compounds **2a−d**. Their substitution patterns follow from the ^{1}H- coupled ^{11}B-NMR spectra, which clearly show doublets for **2a**, **c**, **d** at high field (δ = −39 to −41). The absence of this signal for **2b** indicates that the phenyl group is in the apex position. Both **2a** and **2b** have C_s symmetry, whereas **2c** and **2d** have C_1 symmetry and show three different ^{11}B-NMR signals in a 1:1:1 ratio. The ^{1}H-NMR spectra of **2c** and **2d** exhibit two sets of signals for the isopropyl group, in agreement with C_1 symmetry. The ^{13}C-NMR data also support the proposed constitutions. Since a mixture of compounds was present, it was not possible to assign the ^{1}H- and ^{13}C-NMR signals to **6a**.

Despite numerous crystallisation attempts, only **2d** yielded single crystals. A structure analysis was carried out on a crystal belonging to the orthorhombic space group $Pn2_1a$ with a = 7.518 (5), b = 20.12 (2), c = 12.86 (1) Å, V = 1946 Å^3, Z = 4. The bad quality of the crystals yielded only a very limited data set, which allowed the solution of the structure but not a reliable refinement. However, the analysis supports the proposed connectivity of the atoms in a *nido* arrangement. Due to the large uncertainty in bond distances and angles these details are not discussed here. The computed geometry parameters of **2** (see Figure 1) should be reliable and closely resemble the geometric features of **2a** as suggested by the close agreement between experimental ^{11}B-NMR chemical shifts for **2a** and values computed for **2**. The open five-membered face is essentially planar (the angle between the BCCB and the BSB plane is 176.1°) and the bond lengths S−B = 1.857, B−C = 1.497, C−C = 1.460 Å are shorter than in the analogous *nido*-thiadicarbaundecaborane(10) **3** (S−B = 1.915, B−C = 1.597, C−C = 1.542 Å).[16]

Computational Details

Geometries of **2**, **6**, and **7** have been optimized at HF/6−31G* and MP2(fc)/6−31G* levels of theory using the Gaussian 94 program.[17] The structures correspond to local minima on the SCF potential energy surface as shown by analytical frequency calculations (absence of imaginary frequencies). Chemical shifts have been computed with the IGLO program[18] applying Huzinaga's basis set[19] of DZ or II′ quality in the recommended contraction scheme[18c]. A gas phase chemical shift of 16.6 ppm[20] for B_2H_6 and shielding constants of 115.6 (DZ) and 103.0 (II′) have been used as reference to the experimental standard, $BF_3 \cdot OEt_2$.

Figure 2. Molecular structure of compound **2d**

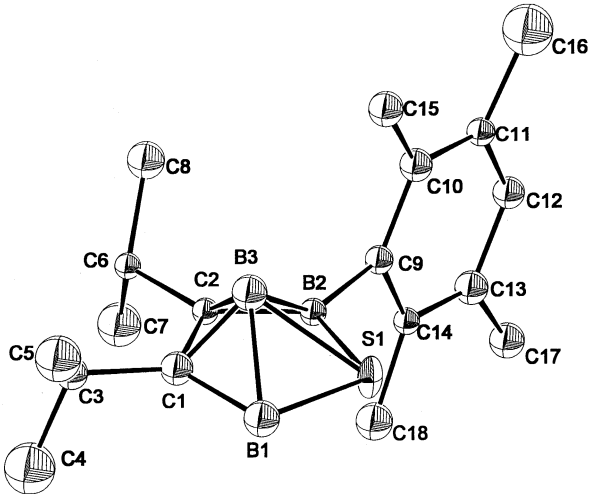

Model compounds listed in Table 2 have been optimized by the B3LYP DFT (density functional theory) method using the three parameter exchange parameter by Becke (B3)[21] and the correlation functional by Lee, Yang, and Parr (LYP),[22] including both local and non-local terms, as implemented in Gaussian 94.[17]

Table 1. Computed chemical shifts[a] for **2**, **6**, and **7** in comparison to experimental values

2, C_s	DZ	−45.7 (B1)	+20.1 (B2,5)
Exp. **2a**		*−43.5 (1 B)*	*+16.5 (2 B)*
7, C_s	DZ	31.0 (B1), −22.5 (B8)	−6.0 (B2,5), −6.8 (B6,8)
7, C_s av.	DZ	+4.3 (B1,8)	−6.4 (B2,5,6,8)
6, C_{2v}	DZ	−32.5 (B1,3)	−25.6 (B5,6,7,8)
6, C_{2v}	II′	−33.7 (B1,3)	−27.4 (B5,6,7,8)
Exp. **6a**		*−33.8 (2 B)*	*−28.1 (4 B)*

[a] δ^{11}B.

Table 2. Computed distances[a] in nine-vertex clusters having tricapped trigonal prism structures (D_{3h}- or D_{3h}-like) and different numbers of skeletal electrons

$[B_9H_9]^q$	B1−B1[b]	B1−B1′[c]	B1−B2[d]
$q = 2+$	1.947	2.133	1.772
$q = 0$	1.795	2.022	1.751 "hypo-closo"
$q = 2-$	1.987	1.792	1.712 "closo"
$q = 4-$	1.803	2.157	1.791 "nido"
$[B_6H_6(CH)_3]^q$	B1−B1	B1−B1′	B1−C
$q = 3+$	1.904	2.148	1.704 "hypo-closo"
$q = 1+$	2.021	1.796	1.611 "closo"
$q = 1-$	1.761	2.036	1.651 "nido"
$[B_6H_6(S)_3]^q$	B1−B1	B1−B1′	B1−S
$q = 4+$	2.122	2.091	1.978 "closo "
$q = 2+$	1.782	2.345	1.999 "nido "
$[B_6H_6(CH)_2S]$	B1−B1	B1−B1′	B1−X
at CH cap:	1.759	1.827	1.652 "nido"[c]
at S cap:	1.780	2.231	2.027

[a] //B3LYP/6−31G* geometries. − [b] Distance in the $(B1)_3$ deltahedral base. − [c] Distance between the deltahedral bases $(B1)_3$ and $(B1')_3$. − [d] Distance between B1 and the capping atom B2, CH, or S. − [e] //RMP2(fc)/6−31G*.

Support of this work by the *Deutsche Forschungsgemeinschaft* (SFB 247), the *Fonds der Chemischen Industrie*, and the *BASF AG* is gratefully acknowledged.

Experimental Section

All reactions and manipulations were performed in dry glassware under argon by using standard Schlenk techniques. Solvents were distilled from appropriate drying agents under argon before use. − $Et_2O \cdot BF_3$ was used as the external standard for ^{11}B NMR. As internal standards for ^{1}H-and ^{13}C-NMR spectra the signals of the deutero solvents were used and calculated for TMS. NMR: $CDCl_3$ solutions, Bruker AC 200. − MS: Varian MAT CH7 and GCMS HP 5971. − The following starting materials were prepared by methods described in literature: 3,4-bis(dichloroboryl)-2,5-dimethyl-2,4-hexadiene (**4**)[9], lithium phenylborate[9], lithium durylborate[23]. Hexamethyldisilathiane and lithium borate were commercially obtained.

2,5-Dichloro-3,4-bis(isopropylidene)-1,2,5-thiadiborolane (**5b**): 6.84 g (38.4 mmol) of hexamethyldisilathiane were added dropwise to a solution of 10.44 g (38.4 mmol) of **4** in 150 ml of n-hexane at 0° C. After 4 h heating to reflux, the solvent was removed under vacuum. Distillation yielded 7.68 g (33.0 mmol, 86%) of slightly yellow **5b**, b.p. 61° C/ $8 \cdot 10^{-3}$ Torr. − ^{1}H NMR ($CDCl_3$, 200 MHz): δ = 1.74, 2.21 (2 s, 2×6 H, $CCH_{3\ exo}$ or *endo*). − ^{11}B NMR ($CDCl_3$, 64 MHz): δ = 62. − ^{13}C NMR ($CDCl_3$, 50 MHz): δ = 23.1, 26.6 (2 s, $CCH_{3\ endo}$ or *exo*), 142 [s, br, $BCC(CH_3)_2$], 149.7 [s, $C(CH_3)_2$]. − MS(EI), *m/z* (%) = 232 [M^+] (42.0), 217 [$M^+ - CH_3$] (39.4), 190 [$M^+ - C_3H_6$] (17.8), 41 ($C_3H_5^+$, 78.7).

nido-4,5-Diisopropyl-2,4,5-thiadicarbahexaborane(5) (**2a**): 215 mg (9.87 mmol) of lithium borate were suspended in 20 ml of hexane and 880 mg (3.78 mmol) of **5b** in 5 ml of hexane were added at −78° C. After 1 h at this temp. the mixture was stirred 12 h at room temp.. The suspension was filtered and the solvent was removed under vacuum. Distillation yielded 70 mg (0.39 mmol, 10%) of colorless impure **2a**, b.p. 70° C/1.5 Torr, which could not be separated from **6a** and other by-products. − ^{1}H-NMR data of **2a** ($CDCl_3$, 200 MHz): δ = 1.17, 1.27 [2 d, 2×6 H, $HC(CH_3)_2$, $^3J_{H,H}$ = 6,8 Hz *endo* or *exo*], 2.45 [sept, 2 H, $HC(CH_3)_2$, $^3J_{H,H}$ = 6.8 Hz], (HB not detected). − ^{11}B-NMR data of **2a** ($CDCl_3$, 64 MHz): δ = −43.5 (d, 1 B, $^1J_{B,H}$ = 208 Hz), 16.5 (d, 2 B, $^1J_{B,H}$ = 167 Hz). MS(EI) data of **2a** : *m/z* (%) = 178 [M^+] (40.9), 163 [$M^+ - CH_3$] (17.5), 135 [$M^+ - C_3H_7$] (19.1), 41 [$C_3H_5^+$] (100). − ^{11}B-NMR data of **6a** ($CDCl_3$, 64 MHz): δ = −28.1 (d, 2 B, $^1J_{B,H}$ = 179 Hz), −33.8 (d, 1 B, $^1J_{B,H}$ = 173 Hz). − MS(EI) data of **6a**: *m/z* (%) = 213 [M^+] (100), 198 [$M^+ - CH_3$] (33.0), 170 [$M^+ - C_3H_7$] (29.6), 41 [$C_3H_5^+$] (15.5).

Mixture of nido-4,5-Diisopropyl-1-phenyl-2,4,5-thiadicarbahexaborane(5) (**2b**) *and nido-4,5-Diisopropyl-3-phenyl-2,4,5-thiadicarbahexaborane(5)* (**2c**): 780 mg (8.0 mmol) of lithium phenylborate were suspended in 50 ml of hexane and 930 mg (4.0 mmol) of **5b** solved in 20 ml of hexane were added under reflux conditions. After 2 h at this temp. the mixture was stirred 12 h at room temp.. The suspension was filtered and the solvent was removed under vacuum. Distillation yielded 180 mg (0.7 mmol, 18%) of colorless **2b**, **c**, b.p. 60−75° C/ $5 \cdot 10^{-2}$ Torr. − NMR data of **2b**: ^{1}H NMR ($CDCl_3$, 200 MHz): δ = 1.27, 1.32 [2d, 2x6 H, $HC(CH_3)_{2\ endo}$ or *exo*, $^3J_{H,H=6}$,8 Hz], 2.75 [sept, 2 H, $HC(CH_3)_2$, $^3J_{H,H}$ = 6,8 Hz], 7.12−7.67 (m, 5 H, C_6H_5). − ^{11}B NMR ($CDCl_3$, 64 MHz): δ = −31.8 (s, 1 B), 20.0 (d, 2 B, $^1J_{B,H}$ = 155 Hz). − ^{13}C NMR ($CDCl_3$, 50 MHz): δ = 24.4, 25.6 (2 s, $CCH_{3\ endo}$ or *exo*), 27.8 [s, $HC(CH_3)_2$], 127.4, 127.6 (2 s, *ortho*- or *meta*-C), 138.6 (s, *para*-C),

(CB not detected). NMR data of **2c**: ^{1}H NMR ($CDCl_3$, 200 MHz): δ = 1.00, 1.13, 1.25, 1.34 [4d, 4×3 H, HC(CH_3)$_2$, $^3J_{H,H}$ = 6.8 Hz], 2.53 [sept, 2 H, $HC(CH_3)_2$, $^3J_{H,H}$ = 6,8 Hz], 7.12−7.67 (m, 5 H, C_6H_5). − ^{11}B NMR ($CDCl_3$, 64 MHz): δ = −41.4 (d, 1 B, $^1J_{B,H}$ = 206 Hz), 15.3 (d, 1 B, $^1J_{B,H}$ = 172 Hz), 27.5 (s, 1B). − ^{13}C NMR ($CDCl_3$, 50 MHz): δ = 23.6, 23.9, 24.0, 24.9 [4 s, HC(CH_3)$_2$], 27.1, 28.8 [2 s, H*C* (CH_3)$_2$], 131.2, 133.9 (2 s, *ortho*- or *meta*-C), 138.6 (s, *para*-C), (CB not detected). − MS(EI): *m*/*z* (%) = 254 [M^+] (100), 239 [$M^+ - CH_3$] (13.1), 211 [$M^+ - C_3H_7$] (24.2), 41 [$C_3H_5^+$] (93.8).

nido-4,5-Diisopropyl-3-duryl-2,4,5-thiadicarbahexaborane(5) (**2d**): 1.6 g (10.0 mmol) of lithium durylborate were suspended in 100 ml of hexane and 1.16 mg (5.0 mmol) of **5b** solved in 100 ml of hexane were added under reflux conditions. After 2 h at this temp. the mixture was stirred 12h at room temp., then filtered, and the solvent was removed under vacuum. Sublimation yielded 480 mg (1.5 mmol, 31%) of colorless **2d**, s.p. 105° C/ $5\cdot10^{-2}$ Torr. − ^{1}H NMR ($CDCl_3$, 200 MHz): δ = 1.01, 1.12, 1.26, 1.34 [4d, 4×3 H, HC(CH_3)$_2$, $^3J_{H,H}$ = 6,8 Hz], 2.15, 2.24, 2.26, 2.32 (4 s, 4×3 H, *ortho*- or *meta*-CH_3), 2.50, 2.56 [2 sept, 2×1 H, $HC(CH_3)_2$, $^3J_{H,H}$ = 6,8 Hz], 7.00 (s, 1 H, *para*-CH). − ^{11}B NMR ($CDCl_3$, 64 MHz): δ = −39.5 (d, 1 B, $^1J_{B,H}$ = 203 Hz), 16.0 (d, 1 B, $^1J_{B,H}$ = 145 Hz), 28.4 (s, 1 B). − ^{13}C NMR ($CDCl_3$, 50 MHz): δ = 19.9, 20.4, 20.5, 20.6 (4 s, *ortho*- or *meta*- C*C*H_3), 22.9, 23.0, 24.9, 25.7 [4 s, HC(CH_3)$_2$], 27.7, 27.8 [2 s, H*C*(CH_3)$_2$], 109, 121 (2 s, br, CB), 131.7, 133.2, 133.3, 135.0 (4 s, *ortho*- or *meta*-*C*CH_3), 138.0 (s, *para*-CH). − MS(EI): *m*/*z* (%) = 310 [M^+] (100), 295 [$M^+ - CH_3$] (5.0), 267 [$M^+ - C_3H_7$] (62.2), 41 [$C_3H_5^+$] (49.8).

☆ Dedicated to Professor *Peter Jutzi* on the occasion of his 60th birthday.

[1] J. Plesek, T. Jelinek, B. Stibr, S. Hermanek, *J. Chem. Soc., Chem Commun.* **1988**, *5*, 348−349.

[2] J. Holub, J. D. Kennedy, T. Jelinek, B. Stibr, *J. Chem. Soc., Dalton Trans.* **1994**, *8*, 1317−1323.

[3] K. Base, S. Hermanek, F. Hanousek, *J. Chem. Soc., Chem. Commun.* **1984**, *5*, 299−300.

[4] V. A. Brattsev, S. P. Knyazev, G. N. Danilova, V. I. Stanko, *Zh. Obshch. Khim.* **1975**, *45*, 1393−1394.

[5] J. Plesek, S. Hermanek, Z. Janousek, *Coll. Czech. Chem. Commun.* **1977** , *42*, 785−792

[6] Z. Janousek, J. Plesek, Z. Plzak, *Coll. Czech. Chem. Commun.* **1979**, *44*, 2904−2907.

[7] A. Feßenbecker, A. Hergel, R. Hettrich, V. Schäfer, W. Siebert, *Chem. Ber.* **1993**, *126*, 2205−2210.

[8] M. Hofmann, M. A. Fox, R. Greatrex, R. E. Williams, P. v. R. Schleyer, *J. Organomet. Chem.* **1998**, *550*, 331−340.

[9] J. Hauß, A. Krämer, H. Pritzkow, W. Siebert, *Z. Naturforsch.* **1994**, *49b*, 1677−1683.

[10] V. Beez, Dissertation, Universität Heidelberg (**1997**).

[11] K. Wade, *Adv. Inorg. Chem. Radiochem.* **1976**, *18*, 1; D. M. P. Mingos, *Adv. Organomet. Chem.* **1977**, *15*, 1.

[12] R. E. Williams in *Adv. in Boron Chemistry* **1997**, 15−29, The Royal Society of Chemistry, Cambridge, Ed.: W. Siebert.

[13] A. E. Reed, L. A. Curtiss, F. Weinhold, *Chem. Rev.* **1988**, *88*, 899.

[14] V. Quéneau, E. Todorov, S. C. Sevov, *J. Am. Chem. Soc.* **1998**, *120*, 3263.

[15] V. Quéneau, S. C. Sevov, *Inorg. Chem.* **1998**, *37*, 1358.

[16] D. Hnyk, M. Hofmann, P. v. R. Schleyer, M. Bühl, D. W. H. Rankin, *J. Phys. Chem.* **1996**, *100*, 3435−3440.

[17] M. J. Frisch, G. W. Trucks, H. B. Schlegel, P. M. W. Gill, B. G. Johnson, M. A. Robb, J. R. Cheeseman, T. Keith, G. A. Petersson, J. A. Montgomery, K. Raghavachari, M. A. Al-Laham, V. G. Zakrzewski, J. V. Ortiz, J. B. Foresman, J. Cioslowski, B. B. Stefanov, A. Nanayakkara, M. Challacombe, C. Y. Peng, P. Y. Ayala, W. Chen, M. W. Wong, J. L. Andres, E. S. Replogle, R. Gomperts, R. L. Martin, D. J. Fox, J. S. Binkley, D. J. Defrees, J. Baker, J. P. Stewart, M. Head-Gordon, C. Gonzalez, J. A. Pople, *Gaussian 94*, Revision E.2, *Gaussian, Inc.*, Pittsburgh PA, **1995**.

[18] [18a] W. Kutzelnigg, *Israel. J. Chem.*, **1980**, *19*, 193. − [18b] M. Schindler, W. Kutzelnigg, *J. Chem. Phys.* **1982**, *76*, 1919. − [18c] W. Kutzelnigg, U. Fleischer, M. Schindler, *NMR: Basic Princ. Prog.* **1990**, *23*, 165.

[19] S. Huzinaga, *Approximate Atomic Wave Functions*, University of Alberta, Edmonton, **1971**.

[20] T. P. Onak, H. L. Landesman, R. E. Williams, *J. Phys. Chem.* **1959**, *63*, 1533.

[21] A. D. Becke, *J. Chem. Phys. 98*, **1993**, 5648.

[22] C. Lee, W. Yang, R. G. Parr, *Physical Review* **1988**, *B 37*, 785.

[23] A. Berndt, *Angew. Chem.* **1993**, *105*, 1034; *Angew. Chem. Int. Ed. Engl.* **1993**, *32*, 985.

[I98176]

First Synthesis and Structural Characterization of Neutral Chelated *syn*-Facial Bimetallic (η^5-Cyclohexadienyl)benzylidene Complexes from Tetracarbonyl[2-{(η^6-phenyl)tricarbonylchromium(0)-$\kappa C^{2'}$}pyridine-κN]manganese(I) Derivatives

Jean-Pierre Djukic[a], Aline Maisse[a], Michel Pfeffer*[a], Karl Heinz Dötz*[b], and Martin Nieger[c]

Laboratoire de Synthèses Métallo-Induites de l'Université L. Pasteur, UMR 7513[a],
4, rue Blaise Pascal, F-67070 Strasbourg, France
Fax: (internat.) +33 (0)3/ 88 45 46 67
E-mail: pfeffer@chimie.u-strasbg.fr

Kekulé-Institut für Organische Chemie und Biochemie der Universität Bonn[b],
Gerhard-Domagk Straße 1, D-53121 Bonn, Germany
Fax: (internat.) +49 (0)228/ 73 58 13
E-mail: doetz@uni-bonn.de

Institut für Anorganische Chemie der Universität Bonn[c],
Gerhard-Domagk Straße 1, D-53121 Bonn, Germany

Received June 6, 1998

Keywords: Chromium / Manganese / Nucleophilic additions / Metal–metal interactions / Helical structure

Reaction of tetracarbonyl[2-{(η^6-phenyl)tricarbonylchromium-$\kappa C^{2'}$}pyridine-κN]manganese(I), **2a**, with phenyllithium quantitatively affords an acylmanganese anion **3a** that can be isolated and spectroscopically characterized. In-situ *O*-alkylation of the latter anion by means of $MeOSO_2CF_3$ at low temperature, yields a new neutral *syn*-facial heterobimetallic analog **4a** of (η^5-cyclohexadienyl)-benzylidene complexes. The treatment of bimetallic carbonyl complexes of 3-methyl, 2-phenyl-pyridine and 2-phenyl-quinoline, **2b** and **2c**, with PhLi and subsequently with $MeOSO_2CF_3$ affords deep purple crystalline products **4b** and **4c** that have been structurally characterized by X-ray diffraction analyses. The molecular structures of **4b** and **4c** display, among other features, an overall helical shape with a pronounced π-stacking of the aromatic groups and a weak interaction between the chromium and the manganese centered units.

Introduction

We recently reported that cyclomanganated 2-phenylpyridine derivatives undergo a nucleophilic attack at a coordinated carbonyl ligand upon treatment with aryllithium reagents[1]. ^{13}C-NMR and IR spectroscopic measurements have revealed the formation of anionic acylmetalate intermediates which were shown to be prone either to decomposition by a reductive elimination process when kept in a solution at ambient temperature or to conversion into new chelated η^3-benzylic manganese complexes upon alkylation with $MeOSO_2CF_3$. These results demonstrated that chelated octahedral (tetracarbonyl)manganese(I) complexes display a reactivity toward organolithium reagents similar to that of the widely studied hexacarbonylmetal complexes of the chromium triade[2]. To our knowledge, this constituted the first report for a non-oxidative chemical transformation producing a new class of organomanganese compounds from cyclomanganated substrates[3]. In our continuing efforts to find new reactivity patterns for cyclomanganated aromatics we were naturally lead to study the behaviour of the peculiar class of chelated complexes derived from (η^6-arene)tricarbonylchromium complexes[4]. We[4a][4b] and other authors[4c] did previously report that such bimetallic complexes can be readily synthesized in preparative scale. Some examples have been used in the stereoselective insertion reactions of alkynes leading to π-coordinated indenol complexes[4c]. Herein, we report that the addition of phenyllithium to cyclomanganated 2-[(η^6-phenyl)-tricarbonylchromium]pyridine yields an air- and temperature-sensitive acylmanganate intermediate. Further alkylations of this and other analogous anionic intermediates afford novel neutral chelated *syn*-facial heterobimetallic (η^5-cyclohexadienyl)benzylidene complexes in which the two metallic centers, e.g. chromium and manganese, are involved in a weak metal−metal interaction that resembles a metal−metal dative bond[5].

Results and Discussion

1. Synthesis of Chelated Bimetallic (η^5-Cyclohexadienyl)benzylidene Complexes 4a−c

The reaction of an orange solution of complex **2a** with 1 equiv. of phenyllithium in DME[6] at −50°C yielded within

 © WILEY-VCH Verlag GmbH, D-69451 Weinheim, 1998 1434−1948/98/1111−1781 $ 17.50+.50/0

seconds a dark brown solution containing the acylmanganate **3a**-Li (Scheme 1). In order to properly characterize this reaction product we isolated the latter and exchanged the lithium cation for the more bulky PPN^+ counter cation. The $^{13}C\{^1H\}$-NMR analysis of the resulting compound, e.g. **3a**-PPN, confirmed the presence of only one product. In the carbonyl ligand resonance region we detected singlets at δ = 219.7, 222.9, and 231.1 that we assigned to the ^{13}C resonances of the $Mn(CO)_3$ group, an intense signal at δ = 237.5 produced by the carbonyl ligands of the $Cr(CO)_3$ moiety and a downfield singlet at δ = 289.5 attributed to the acyl carbon of the benzoyl group located on the manganese center. From this spectrum it was clear that the nucleophilic attack did not take place at a carbonyl ligand of the $Cr(CO)_3$ moiety but rather selectively at a CO ligand located on the manganese center. Similar chemical shifts for the carbonyl ligands of the $Mn(CO)_3$ group were previously obtained for lithium (benzoyl)(tricarbonyl)[2-(phenyl-$\kappa C^{2'}$), pyridine-κN]manganate(I)[1].

The infrared spectrum of **3a**-PPN in CH_2Cl_2 displays three intense absorption bands at 1972, 1930, and 1847 cm^{-1}, a shoulder at 1878 cm^{-1} and a weak band at 1560 cm^{-1} that may be assigned to as the C−O streching vibration of the benzoyl group. The former set of three intense signals can be considered reasonably as the result of the overlap of the two sets of A_1+E vibration modes related to the *fac*-$L_3Cr(CO)_3$ group and to a *fac*-$L_3Mn(CO)_3$ moiety. A *mer*-$L_3Mn(CO)_3$ moiety resulting from a nucleophilic attack at an equatorial CO ligand would have given three distinct absorption bands, e.g. $2A_1+B_2$, with the two A_1 vibration modes showing up at the higher frequencies[7].

Analogous anionic intermediates can be prepared starting from **2b** and **2c** by reaction with PhLi under experimental conditions similar to those used for the formation of **3a**-Li. In situ alkylation of the anionic adducts originating from **2a−c** at −20°C with $MeOSO_2CF_3$ gave rise to a dramatic change in colour of the reaction mixture from dark brown to dark red. Isolation of the corresponding reaction products afforded after chromatographic purification, the complexes **4a**, **4b**, and **4c** in 67, 70 and 45% yield respectively (based on the starting bimetallic substrates).

2. Molecular Structures of Complexes 4b and 4c

Crystallization of compounds **4b** (Figure 1) and **4c** (Figure 2) from mixtures of dichloromethane and hexane at −18°C afforded crystals suitable for X-ray crystal structure analysis. Details of data collection and refinement are summarized in Table 3. Selected interatomic distances, bond angles and torsion angles are given in Table 1 for compound **4b** and in Table 2 for compound **4c**.

The two molecules represented in Figures 1 and 2 reveal a quite compact intramolecular arrangement. Both metal-carbonyl fragments are coordinated to the same face of the organic ligand and the carbonyl ligands occupy positions that minimize steric interactions. The average Cr−Mn distance of 3.03 Å indicates interaction between what may be considered a formally closed shell 18 electron chromium(0) center and an electron-deficient 16 electron manganese(I) center. Obviously, the electron bookkeeping for each metal and the transcription of the relevant formulae rise several questions. At first glance, resonance forms depicted for **4a−c** in Scheme 1 have different chemical meanings[8]. The formula denoted as **A** includes a dative bond between the two metals whereas **B**, includes a single covalent bond. A choice between these two formulations must rely at least on thorough theoretical investigations that are not available so far for the type of bridging ligand described here. To our knowledge, only a few theoretical studies are available on donor-acceptor or dative transition metal-metal interactions involving[9] or not[10] bridging ligands. This ambiguity was already addressed for other bimetallic compounds that fit neither of the two aforementioned metal to metal interaction types[11]. At this stage of our study, we chose an intermediate "dashed bond" formulation for the molecular structures of **4a−c** which emcompasses the main structural informations extracted from the two available molecular structures (vide infra). In this formulation, the dashed lines indicate interactions of uncertain nature.

A close analysis of the metal-centered bond angles for the chelated $Mn(CO)_3$ fragment indicates that in both **4b** and **4c** the manganese atom is located in a slightly distorted octahedral coordination geometry (Tables 1 and 2). In this

Scheme 1

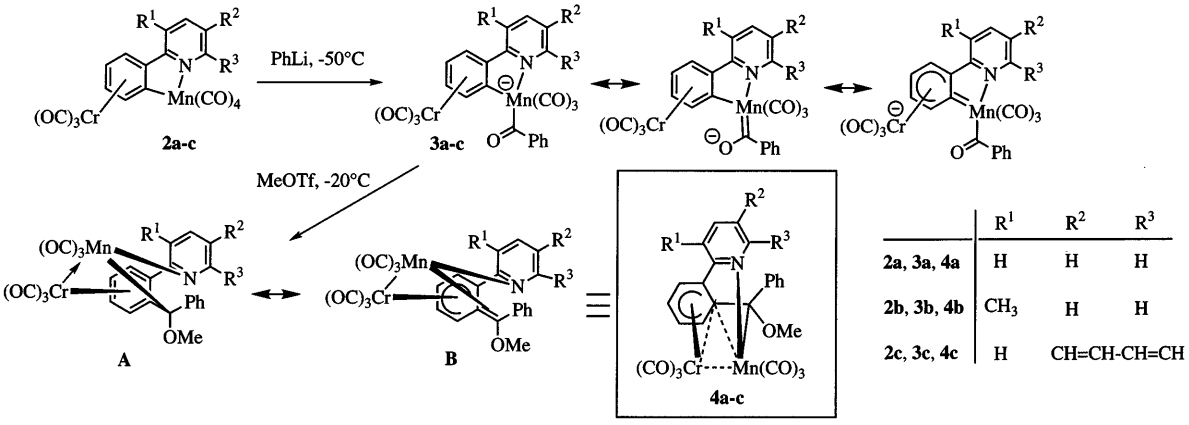

	R^1	R^2	R^3
2a, 3a, 4a	H	H	H
2b, 3b, 4b	CH_3	H	H
2c, 3c, 4c	H	CH=CH-CH=CH	

Figure 1. ORTEP diagram and atom numbering scheme of the molecular structure of **4b**. Ellipsoids are scaled to enclose 30% of the electronic density

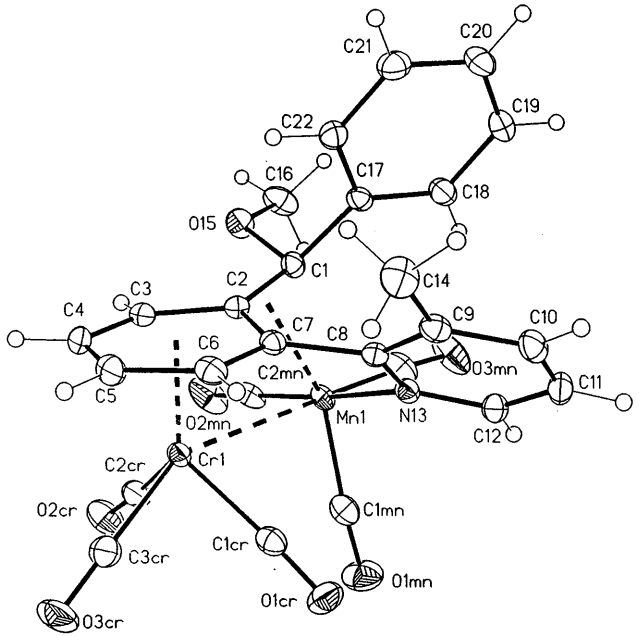

Table 1. Selected bond lengths, angles, and torsion angles for **4b**

Bond lengths [Å]		Bond angles [deg]	
Mn(1)−C(3Mn)	1.769(2)	C(1)−Mn(1)−Cr(1)	86.20(5)
Mn(1)−C(2Mn)	1.8129(19)	C(2)−Mn(1)−Cr(1)	49.76(4)
Mn(1)−C(1Mn)	1.8249(19)	C(7)−Mn(1)−Cr(1)	44.00(3)
Mn(1)−C(1)	2.1493(17)	N(13)−Mn(1)−Cr(1)	85.03(4)
Mn(1)−C(2)	2.4034(18)	C(1Mn)−Mn(1)−Cr(1)	90.86(6)
Mn(1)−C(7)	2.9401(18)	C(2Mn)−Mn(1)−Cr(1)	92.65(6)
Mn(1)−Cr(1)	3.0336(4)	C(3Mn)−Mn(1)−Cr(1)	178.06(6)
Cr(1)−C(3Cr)	1.8394(19)	C(1)−Mn(1)−C(2)	36.67(6)
Cr(1)−C(1Cr)	1.8595(19)	O(15)−C(1)−C(17)	109.64(13)
Cr(1)−C(2Cr)	1.870(2)	C(1Cr)−Cr(1)−C(3Cr)	82.59(8)
Cr(1)−C(5)	2.1891(18)	C(3Cr)−Cr(1)−C(2Cr)	82.76(9)
Cr(1)−C(4)	2.2112(18)	C(1Cr)−Cr(1)−C(2Cr)	97.52(8)
Cr(1)−C(6)	2.2125(17)		
Cr(1)−C(3)	2.2308(17)	Torsion angles [deg]	
Cr(1)−C(7)	2.2396(16)	C(1)−C(2)−C(7)−C(8)	−16.4(2)
Cr(1)−C(2)	2.3576(17)	C(6)−C(7)−C(8)−C(9)	−47.1(2)
C(1)−O(15)	1.429(2)	C(2)−C(7)−C(8)−N(13)	−42.9(2)
C(1)−C(2)	1.452(2)		
C(1)−C(17)	1.522(2)		
C(2)−C(3)	1.437(2)		
C(2)−C(7)	1.454(2)		
C(3)−C(4)	1.392(2)		
C(4)−C(5)	1.410(3)		
C(5)−C(6)	1.414(3)		
C(6)−C(7)	1.405(2)		
C(7)−C(8)	1.490(2)		
C(1Cr)−O(1Cr)	1.153(2)		
C(2Cr)−O(2Cr)	1.146(2)		
C(3Cr)−O(3Cr)	1.154(2)		
C(16)−O(15)	1.424(2)		

configuration the chromium atom, the pyridyl or quinolinyl group, and two carbonyl ligands occupy four equatorial positions, the two axial positions being held by the pseudo-benzylic carbon C(1) and by the third carbonyl ligand. The pseudo-benzylic and heterocyclic rings connected through C(7)−C(8) are twisted around this axis by about 45° [torsion angle C(2)−C(7)−C(8)−N(13) for **4b**: −42.9(2)°, for **4c**: 137.38(19)°] which is about 5° more than that observed for the mononuclear analog **5**[1].

The geometry of the $Cr(CO)_3$ moiety does not change dramatically from that commonly observed in (η^6-arene)-tricarbonylchromium complexes. The two chromium-bound CO ligands that are oriented towards the manganese center form a OC−Cr−CO bond angle of approximately 96° which may be considered intermediate between the average value of 89° generally observed in common (η^6-arene)tricarbonylchromium complexes[12] and the value of 105° for neutral tricarbonyl(η^5-cyclohexadienyl)(triphenyltin)chromium(*Cr-Sn*) complexes[13]. This relatively wide angle reflects not only a steric hindrance but also some peculiar bonding interactions between the chromium center and its surrounding ligands[14].

We reported previously[1] that in complex **5** the manganese center was more likely bound to the benzylic ligand through a η^1:η^2 bonding mode rather than via an ideal symmetric η^3 allylic-like mode. This conclusion was based on the analysis of the metal-to-carbon atom distances. The shortest distance of 2.104(4) Å was obtained for the pseudo-benzylic carbon-to-Mn bond, C1−Mn (Scheme 2), and the longest distance of 2.438(4) Å for the *ipso*-aromatic carbon-to-Mn bond C7−Mn (Scheme 2).

Figure 2. ORTEP diagram and atom numbering scheme of the molecular structure of **4c**. Ellipsoids are scaled to enclose 30% of the electronic density

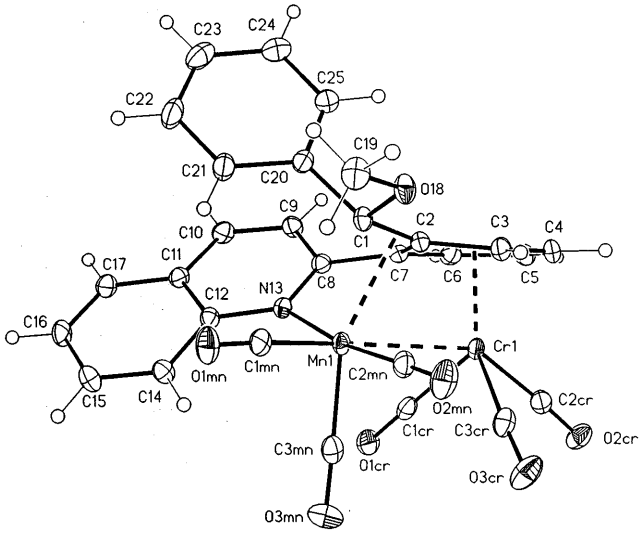

In **4b** and **4c** the corresponding average Mn(1)−C(7) bond distance of 2.91 Å is beyond the range of generally accepted C−Mn bond lengths of either σ- or π-coordinated carbon atoms[15]. The Mn(1)−C(2) (2.40 Å and 2.36 Å) and Mn(1)−C(1) (2.15 Å) are consistent with an altered π-type coordination between Mn(1), C(1), and C(2) even though the C(1)−C(2) bond distance of 1.45 Å in **4b** and **4c** is longer than that of a typical metal-coordinated C=C bond. This is supported by the fact that amongst all the aromatic

Table 2. Selected bond lengths, angles, and torsion angles for **4c**

Bond lengths [Å]		Bond angles [deg]	
Mn(1)−C(3Mn)	1.8339(16)	C(1)−Mn(1)−Cr(1)	87.81(4)
Mn(1)−C(2Mn)	1.8000(16)	C(2)−Mn(1)−Cr(1)	50.71(3)
Mn(1)−C(1Mn)	1.7759(16)	C(7)−Mn(1)−Cr(1)	44.09(3)
Mn(1)−C(1)	2.1494(15)	N(13)−Mn(1)−Cr(1)	85.78(3)
Mn(1)−C(2)	2.3619(14)	C(1Mn)−Mn(1)−N(13)	98.52(6)
Mn(1)−C(7)	2.8908(15)	C(2Mn)−Mn(1)−Cr(1)	91.07(6)
Mn(1)−Cr(1)	3.0444(3)	C(3Mn)−Mn(1)−Cr(1)	85.89(5)
Cr(1)−C(3Cr)	1.8713(17)	C(1)−Mn(1)−C(2)	37.29(6)
Cr(1)−C(1Cr)	1.8637(16)	C(20)−C(1)−O(18)	111.68(11)
Cr(1)−C(2Cr)	1.8479(16)	C(2Cr)−Cr(1)−C(1Cr)	84.26(7)
Cr(1)−C(5)	2.1972(15)	C(2Cr)−Cr(1)−C(3Cr)	81.90(6)
Cr(1)−C(4)	2.2203(15)	C(1Cr)−Cr(1)−C(3Cr)	94.96(7)
Cr(1)−C(6)	2.2180(15)		
Cr(1)−C(3)	2.2460(15)	Torsion angles [deg]	
Cr(1)−C(7)	2.2323(14)	C(1)−C(2)−C(7)−C(8)	−16.3(2)
Cr(1)−C(2)	2.3957(14)	C(9)−C(8)−C(7)−C(2)	−45.5(2)
C(1)−O(18)	1.4263(18)	C(6)−C(7)−C(8)−C(9)	−45.5(2)
C(1)−C(2)	1.456(2)	C(3)−C(2)−C(7)−C(6)	−13.7(2)
C(1)−C(20)	1.517(2)	C(2Mn)−Mn(1)−Cr(1)−C(3Cr)	33.40(7)
C(2)−C(3)	1.437(2)	C(3Mn)−Mn(1)−Cr(1)−C(3Cr)	−56.83(7)
C(2)−C(7)	1.446(2)	C(3Mn)−Mn(1)−Cr(1)−C(1Cr)	41.57(7)
C(3)−C(4)	1.394(2)	C(2)−C(7)−C(8)−N(13)	137.38(19)
C(4)−C(5)	1.415(3)		
C(5)−C(6)	1.411(3)		
C(6)−C(7)	1.409(2)		
C(7)−C(8)	1.481(2)		
C(1Cr)−O(1Cr)	1.1472(19)		
C(2Cr)−O(2Cr)	1.1527(19)		
C(3Cr)−O(3Cr)	1.151(2)		
C(19)−O(18)	1.4202(19)		

carbon atoms bound to the chromium, C(2) is the farthest with an average Cr(1)−C(2) bond distance for **4b** and **4c** of 2.38 Å as compared to the remainder average Cr(1)−C_{Ar} bond distance of 2.22 Å. A reasonable compromise to describe the coordination mode of atom C(2) is to present it as a part of a multicenter bonding system (Scheme 1).

The asymmetric bonding mode of the arene can be well characterized by the angle θ defined as the angle formed between the mean planes C(3)−C(2)−C(7) and C(3)−C(4)−C(5)−C(6)−C(7) in complexes **4b−c**. The calculation of the least square planes indicated no major deviation from the plane for C(5). The calculated values of θ were 8.3° for **4b** and 11.0° for **4c**. In other terms the structural features of the coordinated arene rather confirm a quasi η^5-coordination to the $Cr(CO)_3$ group[16].

As previously underlined for complex **5** (Scheme 2), compounds **4b** and **4c** possess a marked helicity characterized by the overlying of the aromatic rings originating from the N-heterocycles and the phenyl group attached to C(1). In the compounds described herein, the spacial arrangement of the aromatic rings implies relevant geometric distortions of the coordinated arene. Indeed, atoms C(1) and C(8) are forced in opposite directions with respect to the mean plane of the chromium-coordinated arene ring [C(1) towards the uncomplexed arene ring and C(8) towards manganese]. This distortion is evident in both complexes as the torsion angle C(1)−C(2)−C(7)−C(8) amounts 16°.

Scheme 2

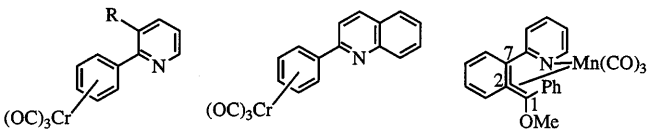

1a, R= H
1b, R= Me

1c

5

3. Spectroscopic Properties of Complexes 4a−c

The infrared spectra of compounds **4a−c** present four different signals at approximate frequencies of 2010 (sharp and strong), 1960 (strong), 1924 (medium and broad), and 1890 (medium and broad) cm^{-1} in CH_2Cl_2. This pattern is consistent with the overlap of two A_1+E vibration modes patterns of the *fac*-$Cr(CO)_3$ (1960 and 1890 cm^{-1}) and *fac*-$Mn(CO)_3$ (2010 and 1924 cm^{-1}) fragments, respectively.

A rough comparison of the frequency of the E mode absorption band produced by the chromium tripod in **4a−c** with that of the simple monometallic complexes **1a−c** (Scheme 2) informs about the magnitude of the electron density exchange between the manganese and the chromium atoms. For instance, if we consider both complexes **1a** (Scheme 2) and **4a**, the absorption band arising from the E vibration mode of the $Cr(CO)_3$ fragment undergoes a relative bathochromic shift $\Delta\nu_E$ ($\Delta\nu_E = \nu_{E1a} - \nu_{E4a}$) upon

intimate interaction with the $L_2Mn(CO)_3$ moiety of about 10 cm^{-1} suggesting an electron density transfer from the manganese to the chromium center. Similar values can be calculated for the couples **1b/4b** and **1c/4c**. It must be pointed out that the value of Dn_E is only a rough estimation since the coordinated arenes in **1a/4a** are slightly different in nature.

A more reliable comparative study can be based on the carbonyl ligand absorptions of complexes **4a** and **5** that differ by the absence of the $Cr(CO)_3$ moiety in the latter compound[1]. One may consider the A_1 absorption bands of the $Mn(CO)_3$ fragment that are detected at 2000 cm^{-1} in CH_2Cl_2 for **5** and at 2010 cm^{-1} in CH_2Cl_2 for **4a**. A new bathochromic shift value can be defined as

$$\Delta\nu_{Cr} = \nu_{Mn-Cr} - \nu_{Mn},$$

with ν_{Mn} defining the frequency of the A_1 mode band in the η^3-benzyl manganese complex **5** and ν_{Mn-Cr} designing the corresponding A_1 mode band in the *syn*-facial heterobimetallic compound **4a**. The difference of 10 cm^{-1} obtained for **5** and **4a** confirms a loss of electron density on the Mn-centered fragment as a consequence of the concomittant interaction with the $Cr(CO)_3$ moiety and structural rearrangements of the molecule. A similar effect of 8 cm^{-1} for $\Delta\nu_{Cr}$ is obtained for compound **4c** and its monometallic η^3-benzylic analog[1].

The ^{1}H-NMR spectra of compounds **4a**−**c** recorded at room temperature display very similar features. In all three cases the protons of the arene coordinated to the $Cr(CO)_3$ tripod resonate at ca. δ = 4.3−5.3 as two doublets and one triplet each integrating one proton and at ca. δ = 6.3 as a triplet integrating also one proton. A combination of two dimensional NMR experiments − e.g. COSY, NOESY and ^{1}H-^{13}C heteronuclear correlation − and the careful analysis of the multiplicities allowed the exact assignment of the proton resonances of the coordinated arene of compound **4a**. For instance, we assigned the signals at δ = 4.28 (d, 1 H), 4.39 (d, 1 H), 5.23 (t, 1 H), and 6.32 (m, 2 H) to respectively H^6, H^3, H^4, and H^5; the latter overlaps with a signal of the pyridyl group. This wide outspreading of the ^{1}H resonances of the coordinated arene over a range of 2 ppm is reminiscent of that observed in tricarbonyl(η^5-cyclohexadienyl)chromium complexes[17]. It suggests that the arene coordinated to the chromium center in **4a** as well as in **4b** and **4c** has a much more pronounced η^5-cyclohexadienyl character than that suspected in reported cases of anionic (η^5-cyclohexadienyl)benzylidenetricarbonylchromium complexes[18]. Indeed, in known structurally characterized examples of tricarbonyl(η^5-cyclohexadienyl)chromium complexes the protons at the 2-, 3-, and 4-positions with respect to the sp^3 carbon atom resonate at δ = 2.4, 3.7, and 6.0, respectively. The analogy made here lies on the assumption that at least H^3, H^4, and H^5 in complex **4a** are not submitted to some peculiar intramolecular magnetic anisotropy. Proton H^6 that resonates at a much lower frequency than H^4 may have underwent a slight shielding produced by the vicinal twisted pyridyl group. The significant geometrical distortions observed in the molecular structures of **4b** and **4c** support a "partial" η^5-bonding mode for the coordinated arene group.

Similarly to the observations made for complex **5**[1], the proton resonances of the phenyl group attached to the

Figure 3. Temperature dependence of the ^{1}H NMR spectrum of **4a** in $CDCl_3$ in the so-called aromatic region. Asterisks designate the signals originating from the "slowly" rotating phenyl group

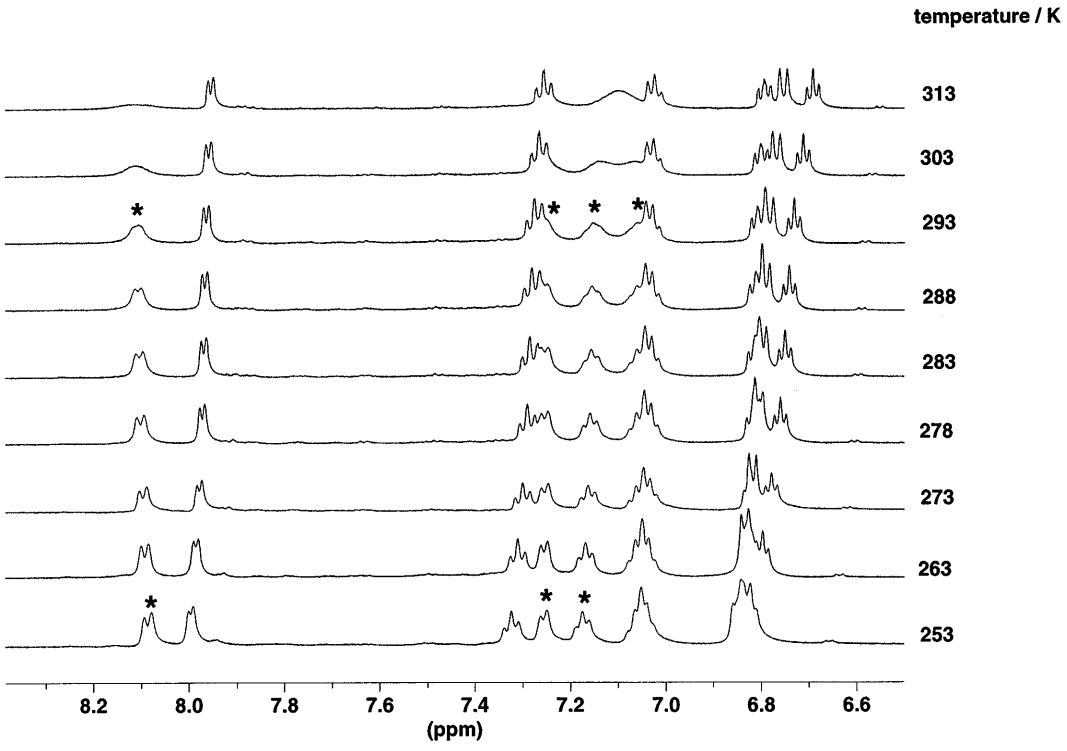

Figure 4. Temperature dependence of the ^{13}C-NMR resonances of the $Cr(CO)_3$ carbonyl ligands of **4a** in [D_8]THF. The asteriks indicate the signals that are involved in a dynamic process

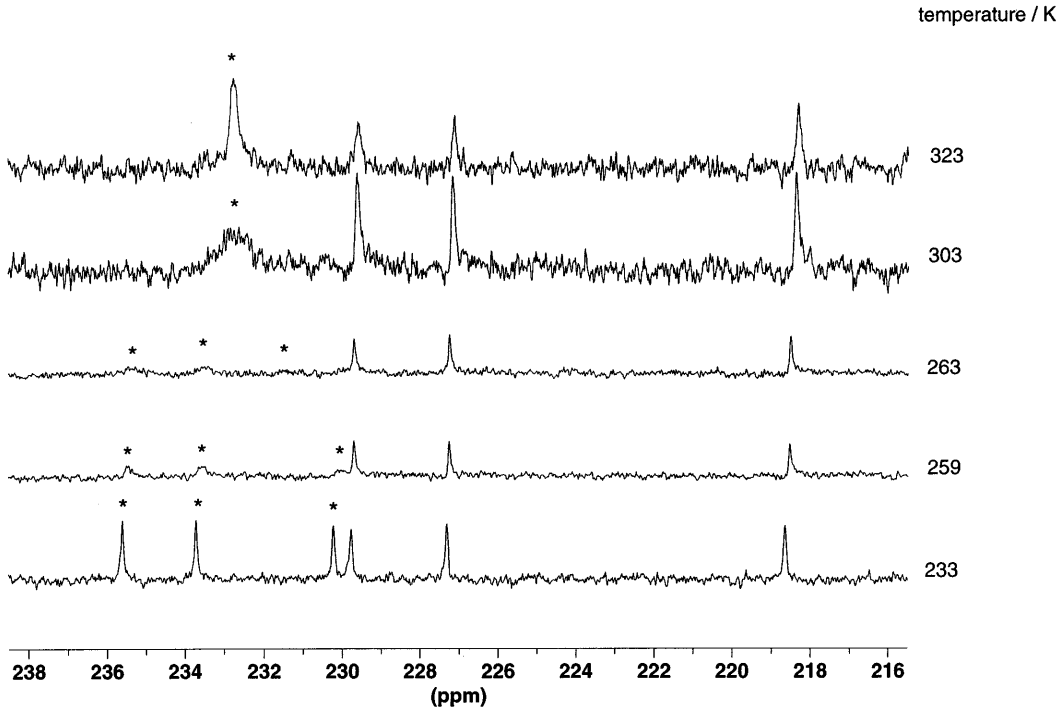

pseudo-benzylic carbon of complexes **4a** and **4c** display a clear temperature dependence. At 293 K in [D_6]acetone, the signals of the phenyl group of **4a** appear as broad signals at δ = 7.10, 7.30, and 8.10 (Figure 3).

Cooling the sample to 253 K induces the decoalescence of these broad peaks, and leads to a consecutive sharpening of the signals and an increased resolution (Figure 3). Hence at that temperature, one may detect three distinct signals, a doublet at δ = 8.08 (*ortho* proton), a doublet at δ = 7.26 (*ortho* proton) and a triplet at δ = 7.18. The other signals produced by the phenyl fragment, two triplets for instance, remain mostly hidden behind several intense multiplets attributed to the protons of the pyridyl group approximately at δ = 7.05 and 6.85. Due to the large separation in frequency between two exchanging protons the coalescence temperature of the two-site-exchange systems composed of two related doublets and two related triplets is not readily detectable. Heating the sample even up to 313 K did not provide a clear localization of the fast exchange signals (Figure 3).

Complex **4b** behaves in a slightly different way since at room temperature the signals of the phenyl group reflect, in the NMR time scale, a pattern consistent with a slow two site exchange[19]. Among the seven signals that can be readily observed at 298 K in deuterated acetone in the range from 6.7 to 8.5 ppm two resolved signals produced by the phenyl group are clearly separated from the rest of the spectrum and are detected at δ = 7.88 (d, 1 H) and 7.21 (t, 1 H). The integration of the overall area of the spectrum in the δ = 6.7−8.5 range confirms the presence of eight aromatic protons.

The steric bulk encountered in both molecular structures of **4b** and **4c** implies an underlying fluxional behavior of the $Cr(CO)_3$ rotor. Consequently, the ^{13}C-NMR spectra of **4a**−**c** performed at 298 K show a broad signal at about δ = 233 accounting for the rotating $Cr(CO)_3$ moiety and three sharp signals at δ = 229, 228, and 218 that can be assigned undoubtedly to the carbonyl resonances of the chelated static $Mn(CO)_3$ fragment. Variable-temperature NMR experiments were carried out with [D_8]THF solutions of compound **4a** (Figure 4).

At 233 K, complete decoalescence already took place and the resulting spectrum reveals, apart from the resonances of the manganese-coordinated carbonyl ligands at δ = 229.7, 227.3, and 218.6, three other low field sharp singlets at δ = 235.6, 233.7, and 230.2 consistent with a $Cr(CO)_3$ moiety which rotates relatively slowly in an asymmetric environment[20] (Figure 4). Further experiments are underway with ^{13}CO enriched samples that should yield the main thermodynamical factors related to the hindered rotation of $Cr(CO)_3$.

4. Discussion

The facile cyclomanganation of (η^6-arene)tricarbonylchromium complexes bearing nitrogen based chelating ligands has offered us an interesting starting point for the further exploration of possible applications of chelated $Mn(CO)_4$ complexes. In a recent paper we addressed the reactivity of 2-phenylpyridine−$Mn(CO)_4$ complexes toward organolithium reagents. This study indicated that the reac-

tivity of these metallacycles, that may also be formulated as *cis*-$L_2Mn(CO)_4$, toward organolithium reagents, RLi, corresponds to that of the intensively studied $M(CO)_6$ complexes (M = Cr, Mo, W). The main difference between these two systems is the fact that addition of RLi in the reaction involving $Mn(CO)_4$ chelates takes place exclusively at an axial carbonyl ligand. The trapping of the anionic acyl intermediates and subsequent NMR analyses never provided evidence for the formation of more than one anionic isomer. A study carried out with an analogous $Re(CO)_4$ complex allowed us to isolate and characterize an acetylrhenate complex that bears the CH_3CO- fragment at an axial position, *trans* to a CO ligand[21]. The addition of PhLi to the bimetallic starting materials selectively takes place at one carbonyl ligand of the $Mn(CO)_4$ moiety. Given the steric bulk of the $Cr(CO)_3$ tripod the *exo* axial CO ligand of the $Mn(CO)_4$ fragment is preferred to undergo a facile nucleophilic addition leading to a benzoylmanganate intermediate. The resulting anionic intermediate is greatly stabilized by a large delocalisation of the negative charge throughout the molecule. Three limit formulae may account reasonably for the charge redistribution as it is shown in Scheme 1 for **3a–c**.

We proposed in our early studies[1] that the treatment of the anionic acyl manganates by a hard alkylating agent such as MeOTf may yield a transient electrophilic alkoxyalkylidene complex[22]. A similar proposal can be made here (Scheme 3).

Scheme 3

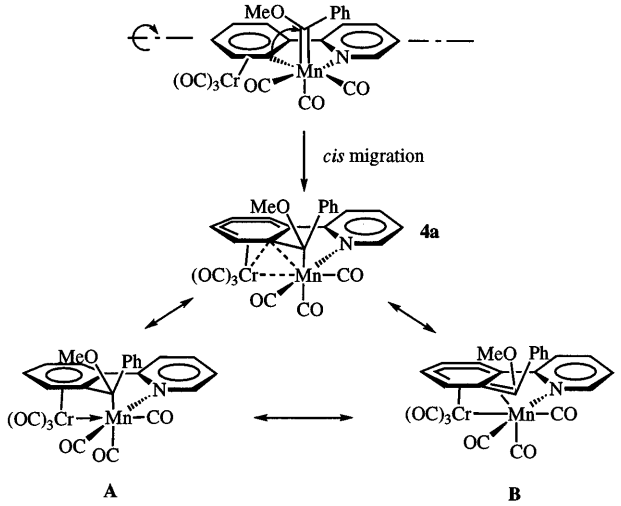

We speculate that such a species may undergo a *cis*-migration of the $Cr(CO)_3$-coordinated phenyl group to the manganese bound alkylidene carbon atom resulting in a *syn*-arrangement of the two tricarbonylmetal fragments (Scheme 3). We already reported that in the process leading to **5** the manganese atom must coordinate in part to the vicinal aromatic ligand to meet the 18 valence electrons requirement. In the new compounds presented here, this electronic requirement seems to be met through a dative or a donor-acceptor interaction with the saturated chromium atom. The results of the low temperature ^{13}C-NMR experiments done with **4a** indicate that $Cr(CO)_3$ still behaves as a rotor and that the Mn–Cr interaction must be quite weak. Indeed, each complete rotation of the $Cr(CO)_3$ tripod must correspond to at least three single metal-metal bond disruptions.

In a very recent study Ceccon and co-workers have reported the preparation and the structural chacterization of *syn*-facial heterobimetallic complexes *syn*-[$Cr(CO)_3$-μ,η:η-indenyl–ML] (M = Rh[23], L = COD, $(CO)_2$, NBD; M = Ir[24], L = COD). In most of these cases a weak non-covalent chromium-metal interaction, Cr–M, is invoked to explain the stability of the complexes. Similar to our two examples the $Cr(CO)_3$ tripod is shifted away from its common η^6 bonding mode to rather pronounced η^5 and η^4 hapticities. In general, a relevant distortion of the indenyl ligand accompanies these peculiar metal–metal interactions. Although a hindered rotation of the $Cr(CO)_3$ tripod is very likely it is not mentioned. The latter Cr–M interactions are even suspected by the authors to thermodynamically stabilize the *syn*-facial isomers whereas the analogous *trans* bimetallic complexes offer a much different reactivity. Depending on the steric bulk and the electronic nature of the ligand coordinating either Rh or Ir in these cases the Cr–M (M = Rh, Ir) distances vary from typically 3.07 Å (M = Ir, L = COD) to 3.3 Å (M = Rh, L = NBD). Similar significant differences for the Cr–Mn interatomic distance are not observed for **4b** and **4c**. However, we definitively may assess that metal-metal electronic interactions play a role. Ceccon′s *syn*-facial heterobimetallic complexes are synthesized by a ligand exchange reaction between $(CH_3CN)_3Cr(CO)_3$ and a η^3 coordinated indenyl iridium or rhodium complex in THF. A similar synthetic pathway applied to complex **5** did not yield compound **4a** even when the ligand-exchange reaction was done at 80°C in DME.

The main common trend that exists between the three crystallographically characterized complexes **5**, **4b**, and **4c** is the overlaying of the phenyl, pyridyl, and quinolinyl groups. This is well illustrated by the overlap diagrams grouped in the upper part of Figure 5 which outlines that in the more sterically hindered complexes **4b-c** the overlay of the phenyl and the N-heterocyclic ring is larger. In the lower part of Figure 5 the dashed lines indicate those interatomic distances between the two stacked rings that are inferior or equal to 3.5 ±0.1 Å, a value generally ascertained for optimal stabilizing π-stacking interactions in polyaromatic molecules or in crystal lattices of aromatic compounds[25]. The values of the interplanar angles between the phenyl group and the vicinal N-heterocycle in **4b–c** are 34.9° and 25.0°.

It is well established that the nature of the inter- or intramolecular π-stacking interactions is determined by five different categories of effects: the Van der Waals and electrostatic interactions, the induction energy, the charge-transfer and the desolvation of each molecule/fragment before interaction. Each of these effects depends directly on the nature of the aromatics that are involved and contributes in various orders of magnitude in a given interaction[25b].

It is noteworthy that the process which leads to the *syn*-facial bimetallic complexes afford solely the eclipsed stereo-

Figure 5. π-Stacking of phenyl and N-heterocyclic groups in compounds **5**, **4b**, **4c**. The adjacent aromatic ring has been omitted for clarity. a) top views and overlap diagrams. b) side views of the stakking interactions: the dashed bonds indicate interatomic distances that are shorter than 3.5 ± 0.1 Å

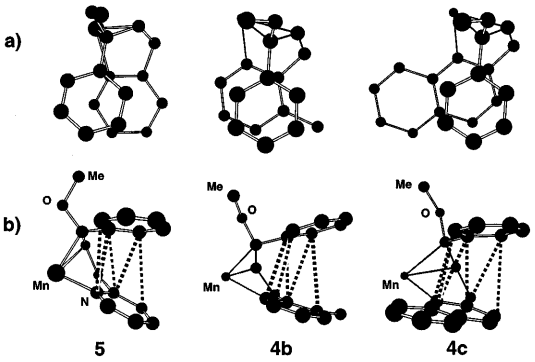

isomers in which the phenyl group eclipses the N-heterocycle as in **5** and **4b−c**. The other possible staggered product, which was not detected, would place the methoxy group above the heterocycle. At this point one might propose that the apparent selectivity of the reaction leading to **5** and **4a−c** from the alkylation of the corresponding acylmanganate species stems from a thermodynamic control that favors the eclipsed isomer through an intramolecular π-π interaction. Further experiments are underway to verify this hypothesis.

In conclusion, the reaction of cyclomanganated (η^6-arene)tricarbonylchromium complexes with PhLi and subsequent treatment with MeOTf yields new *syn*-facial heterobimetallic cyclohexadienylbenzylidene complexes in which the manganese atom interacts directly with the metal centre of the $Cr(CO)_3$ tripod. Although the exact nature of this interaction is not yet established it ressembles a donor-acceptor metal-metal bond. In this paper we have described a new methodology for the synthesis of *syn*-facial organobimetallic complexes and we have found a novel application of cyclometallated (η^6-arene)tricarbonylchromium complexes. We intend to further investigate the mechanistic aspects of their formation as well as the theoretical underlying issues.

We gratefully acknowledge the financial support provided by the *Centre National de la Recherche Scientifique*, the *Deutsche Forschungsgemeinschaft* and the *Fonds der Chemischen Industrie*. We thank Ms. *Ulrike Weynand* (Kékulé Institute of Organic Chemistry and Biochemistry − University of Bonn) for performing the low temperature NMR experiments and Dr. *Kamel Harrata* for HR-MS measurements.

Experimental Section

General: All reactions were carried out under a dry nitrogen atmosphere. (η^6-Arene)tricarbonylchromium complexes were prepared using the procedure of Pauson and co-workers[26]. Benzylpentacarbonylmanganese[27] and complexes **1a**, **2a**, **1b**, and **2b** were prepared by following literature procedures[4b]. The reaction products were separated by flash chromatography on silica gel (Merck, 60 μm) under a dry nitrogen atmosphere. High-resolution mass spectra were recorded at the Mass Spectrometry Service of the Iowa State University, U.S.A. Elemental analyses were done in presence of a combustion aid (V_2O_5) at the "Service de Microanalyse de l'Institut de Chimie", Strasbourg, France. Subambient temperature NMR experiments were done at the Analytical Center of the Chemical Institutes, University of Bonn, Germany. − IR: Perkin-Elmer FT. − NMR: Bruker AC 300, DRX 500 (300 MHz and 500 MHz for ^{1}H, 75 MHz and 125 MHz for ^{13}C). ^{13}C NMR spectra reported herein were all done with proton decoupling. The atom numbering used in the systematic nomenclature of the undermentioned compounds does not follow necessarily the one used for convenience throughout the results and discussion parts.

2-[(η^6-Phenyl)tricarbonylchromium]quinoline (**1c**): In a mixture of 8 ml of THF and 80 ml of di-*n*-butyl ether were dissolved 2-phenylquinoline (0.94 g, 4.58 mmol) and hexacarbonylchromium (1.51 g, 6.87 mmol). The resulting mixture was brought to refluxed for 51 hours under an atmosphere of nitrogen until signs of decomposition appeared in the reaction medium. The solution was cooled to room temperature and filtred over Celite, and both the solvents and the unreacted $Cr(CO)_6$ were removed under reduced pressure. The crude oily residue was then redissolved in dry diethyl ether and the solution mixed with silica gel. The solvent was removed under reduced pressure, and the resulting coated silica gel was loaded on the top of a silica gel column packed in dry and degassed hexane. The unreacted arene ligand was eluted first with CH_2Cl_2/hexane (4:6). The 2-[(η^6-phenyl)tricarbonylchromium]-quinoline complex, **1c**, was then eluted with CH_2Cl_2/hexane (8:2). The solvents were evaporated under reduced pressure. Recrystallization from dry hexane gave 1.17 g of **1c** (75%) as orange crystals, m.p. 130°C. − IR (CH_2Cl_2): $\tilde{\nu}$ = 1971 (CO), 1897 cm^{-1} (CO). − ^{1}H NMR ($CDCl_3$): δ = 5.52 (m, 3 H, H_{ArCr}), 6.37 (d, *J* = 5.4 Hz, 2 H, H_{ArCr}), 7.56 (t, *J* = 7.1 Hz, 1 H, H_{Ar}), 7.65 (d, *J* = 8.8 Hz, 1 H, H_{Ar}), 7.74 (t, *J* = 7.6 Hz, 1 H, H_{Ar}), 7.83 (d, *J* = 8.3 Hz, 1 H, H_{Ar}), 8.10 (d, *J* = 8.5 Hz, 1 H, H_{Ar}), 8.22 (d, *J* = 8.3 Hz, 1 H, H_{Ar}). − ^{13}C NMR ($CDCl_3$): δ = 91.8 (C_{ArCr}), 92.6 (C_{ArCr}), 92.7 (C_{ArCr}), 105.2 (C_{ArCr}), 117.6, 127.0, 127.5, 127.7, 129.6, 130.1, 137.0, 147.7, 153.4, 232.4 (Cr-*CO*). − $C_{18}H_{11}CrNO_3$ (341.3): calcd. C 63.29, H 3.22, N 4.10; found C 63.51, H 3.16, N 4.10.

*[2-[(η^6-Phenyl-κ$C^{1'}$)tricarbonylchromium](quinoline-κ*N*)]tetracarbonylmanganese* (**2c**): A solid mixture of complex **1c** (275 mg, 0.806 mmol) and $PhCH_2-Mn(CO)_5$ (253 mg, 0.887 mmol) was dissolved in a minimum volume (10 ml) of dry heptane and gently stirred at the boiling temperature of the solvent. After 4 hours, the reaction mixture was cooled to room temperature, and evaporated under reduced pressure. The residue was redissolved in CH_2Cl_2 and mixed with silica gel. The solvent was removed under reduced pressure, and the resulting coated silica gel loaded on the top of a silica gel column packed with dry and degassed hexane. [2-{(η^6-Phenyl-κ$C^{1'}$)tricarbonylchromium}(quinoline-κ*N*)]-tetracarbonylmanganese, **2c**, was eluted with CH_2Cl_2/hexane (4:6). The solvents were then evaporated under reduced pressure and recrystallization of the resulting solid from dry hexane gave 267 mg of **2c** (65%), red crystals, m.p. 190°C (decomposition). − IR (CH_2Cl_2): $\tilde{\nu}$ = 2086, 2007, 1985, 1955, 1944, 1884 cm^{-1}. − ^{1}H NMR ($CDCl_3$): δ = 5.47 (t, *J* = 6.2 Hz, 1 H, H_{ArCr}), 5.58 (t, *J* = 6.4 Hz, 1 H, H_{ArCr}), 5.92 (d, *J* = 6.1 Hz, 1 H, H_{ArCr}), 6.24 (d, *J* = 6.3 Hz, 1 H, H_{ArCr}), 7.63−7.71 (m, 2 H, H_{Ar}), 7.85 (m, 2 H, H_{Ar}), 8.32 (d, J = 8.5 Hz, 1 H, H_{Ar}), 8.62 (d, J = 9.3 Hz, 1 H, H_{Ar}). − ^{13}C NMR ($CDCl_3$): δ = 90.05 (C_{ArCr}), 92.72 (C_{ArCr}), 92.86 (C_{ArCr}), 104.69 (C_{ArCr}), 112.83 (C_{ArCr}), 116.93 (C_{ArCr}), 127.5, 127.9, 128.4, 129.1, 131.7 139.7 140.1, 149.8, 167.3 210.2 (Mn-*CO*), 211.1 (Mn-*CO*), 212.5 (Mn-*CO*), 220.1 (s, Mn-*CO*), 234.5 (s, Cr-*CO*). − $C_{22}H_{10}CrMnNO_7$ (507.3): calcd. C 52.09, H 1.99, N 2.76; found C 52.23, H 1.99, N 2.72.

General Procedure for the Synthesis of Complexes **4a**−**c**: Bimetallic complexes **2a-c** were separately dissolved in DME and the solution was cooled to −50°C. A solution of phenyllithium (1.8 M in cyclohexane/ether, Aldrich Chemicals) was then added and the temperature of the reaction mixture was allowed to reach −20°C. After 10 min at −20°C, the reaction mixture was cooled to −40°C. Methyltrifluoromethanesulfonate was added and the reaction mixture slowly warmed to room temperature. The solvent was removed in vaccuo and the residue dissolved in CH_2Cl_2 and mixed with silica gel, the solvent removed under reduced pressure. The resulting coated silica gel was loaded on the top of a silica gel column that was packed in dry and degassed hexane and eluted with mixtures of CH_2Cl_2 and hexane.

2-{2',3',4',5',6'-η⁵-[1'(α-methoxybenzylidene-κC^α)cyclohexadienyl-κC^1']tricarbonylchromium}(pyridine-κN)tricarbonylmanganese(Cr-Mn) (**4a**): Complex **2a** (413 mg, 0.90 mmol), PhLi (0.55 ml, 0.99 mmol), MeOTf (0.14 ml, 1.26 mmol). Chromatography on SiO_2 with CH_2Cl_2/hexane (7:3). Evaporation of the solvents gave 331 mg of **4a** (67%), as a red amorphous powder, m.p. 200−210°C (decomposition). − IR (CH_2Cl_2): $\tilde{\nu}$ = 2010.0, 1962.1, 1929.1, 1885.8 cm^{-1}. − ^1H NMR (C_3D_6O): δ = 3.29 (s, 3 H, OMe), 4.47 (d, *J* = 7.5 Hz, 1 H, H_{ArCr}), 4.82 (d, *J* = 6.3 Hz, 1 H, H_{ArCr}), 5.56−5.61 (m, 1 H, H_{ArCr}), 6.68−6.80 (m, 3 H), 7.01 (d, *J* = 7.0 Hz, 1 H), 7.09 (broad, 2 H, H_{Ar}), 7.25 (t, *J* = 7.9 Hz, 2 H), 7.93 (d, *J* = 5.5 Hz, 1 H), 8.08 (broad, 1 H). − ^1H NMR (CD_2Cl_2): δ = 3.33 (s, 3 H, OMe), 4.28 (d, 1 H, H_{ArCr}), 4.39 (d, 1 H, H_{ArCr}), 5.23 (t, 1 H, H_{ArCr}), 6.32 (m, 2 H), 6.57 (m, 1 H), 6.97−7.04 (m, 2 H, H_{Ar}), 7.10 (broad), 7.20 (broad), 7.84 (d, 1 H, H_{Ar}), 8.10 (broad). − ^{13}C NMR (CD_2Cl_2): δ = 55.2 (Me), 80.3 (C_{ArCr}), 82.9 (C_{ArCr}), 85.9 (C_{ArCr}), 88.7 (1 C, C_{ArCr}), 91.5 (C_{ArCr}), 91.6 (C_{ArCr}), 96.6, 118.8, 123.4, 127.0, 128.1, 131.3 (broad, 1 C), 134.5 (broad, 1 C), 138.0, 142.5, 152.9 , 159.0 , 220.3 (1 C, Mn-*CO*), 229.3 (1 C, Mn-*CO*), 231.0 (1 C, Mn-*CO*), 234.1 (broad, 3 C, Cr-*CO*). − $C_{25}H_{16}CrMnNO_7$ (549.34): calcd. C 54.66, H 2.94, N 2.55; found C 54.82, H 2.92, N 2.51.

[2-{2',3',4',5',6'-η⁵-[1'(α-methoxy-benzylidene-κC^α)cyclohexadienyl-κC1']tricarbonylchromium},3-methylpyridine-κN]tricarbonylmanganese(Cr−Mn) (**4b**): Complex **2b** (387 mg, 0.82 mmol) in 10 ml of DME at −50°C. Addition of PhLi (0.50 ml, 0.90 mmol), MeOTf (0.12 ml, 1.08 mmol). Chromatography on SiO_2 with CH_2Cl_2/hexane (7:3). Evaporation of the solvents gave 323 mg of **4b** (70%) as red crystals, m.p. 210°C (decomposition). − IR (CH_2Cl_2): $\tilde{\nu}$ = 2009, 1960, 1927, 1884 cm^{-1}. − MS (EI): *m/z* = 562.9 $[M]^+$, 507.0 $[M - 2\ CO]^+$, 479.1 $[M - 3\ CO]^+$, 395.1 $[M - 4\ CO - Mn]^+$, 340.1, 310.1, 257.2. − ^1H NMR (C_3D_6O): δ = 1.86 (s, 3 H, Me), 3.33 (s, 3 H, OMe), 4.43 (dd, ^3J = 7.4 Hz ^4J = 1.1 Hz, 1 H, H_{ArCr}), 4.74 (dd, ^3J = 6.2 Hz ^4J = 1.2 Hz, 1 H, H_{ArCr}), 5.49−5.54 (m, 1 H, H_{ArCr}), 6.60−6.70 (m, 2 H), 6.98−7.05 (m, 3 H), 7.21 (broad, 1 H, H_{Ar}), 7.37 (broad, 1 H), 7.85 (broad, 1 H), 7.88 (d, *J* = 5.5 Hz, 1 H). − ^{13}C NMR (CD_2Cl_2): δ = 21.2 (Me), 56.7 (OMe), 82.0 (C_{ArCr}), 85.5 (C_{ArCr}), 87.0 (C_{ArCr}), 90.9 (C_{ArCr}), 91.2 (C_{ArCr}), 93.0 (C_{ArCr}), 100.4 124.3, 128.8, 129.6, 130.0 132.5, 133.8, 135.0, 141.9, 144.3, 152.2, 157.7, 222.0 (1 C, Mn-*CO*), 231.4 (1 C, Mn-*CO*), 232.6 (1 C, Mn-*CO*), 236.5 (broad, 3 C, Cr-*CO*). − $C_{26}H_{18}CrMnNO_7$ (563.36): calcd. C 55.43, H 3.22, N 2.49; found C 56.71, H 2.83, N 2.45.

[2-{2',3',4',5',6'-η⁵-[1'(α-methoxybenzylidene-κC^α)cyclohexadienyl-κC^1']tricarbonylchromium}quinoline-κN]tricarbonylmanganese(Cr-Mn) (**4c**): Complex **2c** (226 mg, 0.44 mmol), PhLi (0.27 ml, 0.49 mmol), MeOTf (0.10 ml, 0.90 mmol). Chromatography on SiO_2 with CH_2Cl_2/hexane (5:5). Evaporation of the solvents gave 119 mg of **4c** (45%) as red crystals, m.p. 190°C (decomposition). − MS (EI): *m/z* 599.0 $[M]^+$, 542.9 $[M - 2\ CO]^+$, 433.1 $[M - 3\ CO - Cr]^+$, 372.9, 344.9, 293.2. − IR (CH_2Cl_2): $\tilde{\nu}$ = 2009, 1960, 1927, 1885 cm^{-1}. − ^1H NMR (CD_2Cl_2): δ = 3.34 (s, 3 H, OMe), 4.25 (dd, ^3J = 6.1 Hz ^4J = 1.4 Hz, 1 H, H_{ArCr}), 4.37 (dd, ^3J = 7.5 Hz ^4J = 0.9 Hz, 1 H, H_{ArCr}), 5.23−5.26 (m, 1 H, H_{ArCr}), 6.36 (d, *J* = 8.5 Hz, 1 H, H_{Ar}), 6.40 (td, ^3J = 6.1 Hz ^4J = 0.9 Hz, 1 H, H_{ArCr}), 6.57 (broad, 1 H, H_{Ar}), 6.85−6.87 (m, 1 H, H_{Ar}), 7.06 (broad, 1 H, H_{Ar}), 7.32 (broad, 1 H, H_{Ar}), 7.43 (broad, 1 H, H_{Ar}), 7.48−7.51 (m, 3 H), 7.87−7.91 (m, 1 H), 8.46−8.48 (m, 1 H). − ^{13}C NMR (CD_2Cl_2): δ = 55.4 (OMe), 81.2, 81.9, 85.1, 88.3, 90.9, 91.7, 96.9, 116.7, 127.4−129.0 (m, 8 C), 132.6, 134.2, 139.6, 142.1, 147.8, 160.6, 221.0 (1 C, Mn-*CO*), 231.8 (2 C, Mn-*CO*), 234.9 (broad, 3 C, Cr-*CO*). − $C_{29}H_{18}CrMnNO_7$ (599.40): calcd. C 58.11, H 3.03, N 2.34; found C 58.31, H 2.92, N 2.28. − High-resolution MS (EI) for $C_{29}H_{18}CrMnNO_7$: calcd. 598.986921; found (deviation) 598.98786 (1.4 ppm).

Isolation and Spectroscopic Characterization of Complex **3a**-PPN: A THF solution of complex **2a** was combined with a solution of phenyllithium in hexane at −50°C. The resulting dark orange solution was warmed to −20°C after 40 min and evaporated. The resulting oily residue was triturated with hexane. The supernatant was removed and the air and temperature sensitive solid residue dried under vacuum and added with PPN^+Cl^-. The solid mixture was dissolved in a minimum amount of dichloromethane. A few drops of diethyl ether were added to the solution in order to induce the precipitation of LiCl and the mixture filtered through celite. The filtrate was then evaporated under vacuum and the oily redish

Table 3. Details of data collection and refinement for compounds **4b** and **4c**

Compound	**4b**	**4c**
Formula	$C_{26}H_{18}NO_7CrMn \cdot CH_2Cl_2$	$C_{29}H_{18}NO_7CrMn$
M_r	648.3	599.4
Crystal system	monoclinic	triclinic
Space group	$P2_1/n$ (No.14)	$P\bar{1}$ (No.2)
a [Å]	9.5000(2)	8.8643(2)
b [Å]	13.6195(2)	9.8096(2)
c [Å]	20.9739(2)	15.6363(3)
α [deg]	90	76.387(1)
β [deg]	101.175(1)	74.656(1)
γ [deg]	90	72.519(1)
V [Å^3]	2662.26(7)	1232.55(4)
Z	4	2
crystal size [mm^3]	0.40 × 0.20 × 0.15	0.35 × 0.30 × 0.10
ρ_{calc} [g·cm^{-3}]	1.62	1.62
μ [mm^{-1}]	1.131	1.005
F(000)	1312	608
Diffractometer	Nonius Kappa-CCD	Nonius Kappa-CCD
Radiation	Mo-*K*	Mo-*K*α
λ [Å]	0.71013	0.71013
T [K]	123(2)	123(2)
max 2θ, [deg]	56.6	56.6
index range	$-12 < h < 12$ $-17 < k < 17$ $-23 < l < 23$	$-11 < h < 11$ $-13 < k < 12$ $-20 < l < 20$
No. of data	32570	19147
No. of unique data	5498	4557
R_{int}	0.024	0.019
No. of data with $I>2\sigma(I)$	4805	4193
Parameters/Restraints	353/16	353/0
$R(F)$ for $I>2\sigma(I)$	0.032	0.026
$wR2(F^2)$ for all data	0.090	0.074
goodness of fit on F^2	1.09	1.06
largest diff. peak and hole [e·Å^{-3}]	0.816/−0.840	0.271/−0.456

residue washed twice with diethyl ether to induce crystallization of **3a**-PPN. Elemental analysis of the latter did not provide satisfactory values due to fast decomposition during the sample preparation process. – IR (CH_2Cl_2): $\tilde{\nu}$ = 1972 (m), 1930 (m), 1844 (vs), 1558 (w) cm^{-1}. – ^1H NMR (CD_2Cl_2): 5.23 (t,1 H), 5.36 (t, 1 H), 5.95 (d, 1 H), 6.27 (d, 1 H), 6.95–7.19 (m, 6 H), 7.16–7.71 (m, 32 H), 8.90 (d, 1 H). – ^{13}C NMR (CD_2Cl_2): 90.8 (C_{ArCr}), 91.2 (C_{ArCr}), 93.3 (C_{ArCr}), 105.8, 118.6, 121.2, 123.7 , 126.3 , 126.9, 127.1, 127.7, 129.8 (m, PPN^+), 132.4 (m, PPN^+), 134.0 (s, PPN^+), 135.3, 153.0, 154.8, 164.3, 164.8, 168.8, 219.7 (Mn-*CO*), 222.9 (Mn-*CO*), 231.1 (Mn-*CO*), 237.5 (Cr-*CO*), 289.5 (Ph*CO*-Mn).

Procedure for the Structure Determination of **4b** *and* **4c**: The molecular structures of **4b** and **4c** were solved by direct methods (SHELXTL-Plus)[28]. The non hydrogen atoms were refined anisotropically on F^2 (SHELXL-93)[29]. Hydrogen atoms were refined isotropically using a riding model. An empirical absorption correction was applied (**4b**: $T_{max./min.}$ = 0.4956/0.4442, **4c**: $T_{max./min.}$ = 0.7996/0.6693). In **4b** the solvent is disordered. Further details are given in Table I. Crystallographic data (excluding structure factors) for the structures reported in this paper have been deposited with the Cambridge Crystallographic Data Centre as supplementary publication no. CCDC-101430. Copies of the data can be obtained free of charge on application to The Director, CCDC, 12 Union Road, Cambridge CB2 1EZ, UK [Fax: int. code +44 (1223) 336–033; e-mail: deposit@ccdc.cam.ac.uk].

[1] J.-P. Djukic, K. H. Dötz, M. Pfeffer, A. De Cian, J. Fischer, *Organometallics* **1997**, *16*, 5171.

[2] [2a] E. O. Fischer, A. Maasböl, *Angew. Chem.,* **1964**, *76*, 645; E. O. Fischer, A. Maasböl, *Angew. Chem., Int. Ed. Engl.* **1964**, *3*, 580. – [2b]K. H. Dötz, P. Hofmann, F. R. Kreissl, U. Schubert, K. Weiss, E. O. Fischer, Eds.,*Transition Metal Carbene Complexes*; VCH: Weinheim, Germany, **1983**. – [2c]W. D. Wulff, *in Comprehensive Organometallic Chemistry II* (Eds.: E. W. Abel, F. G. A. Stone, G. Wilkinson), Pergamon, Oxford, U.K., **1995**; Vol. 12, pp 470. – [2d]M. J. Winter, *in Comprehensive Organometallic Chemistry II* (Eds.: E. W. Abel, F. G. A. Stone, G. Wilkinson), Pergamon, Oxford, U. K., **1995**, Vol. 5, pp 155.

[3] T. C. Flood, *in Comprehensive Organometallic Chemistry II* (Eds.: E. W. Abel, F. G. A. Stone, G. Wilkinson), Pergamon, Oxford, U.K., **1995**, Vol. 6, pp 21–78.

[4] [4a] J. P. Djukic, A. Maisse, M. Pfeffer, A. De Cian, J. Fischer, *Organometallics* **1997**, *16*, 657. – [4b]J.-P. Djukic, A. Maisse, M. Pfeffer, *J. Organomet. Chem.* **1998**, accepted for publication. – [4c]G. R. Clark, M. R. Metzler, G. Whitaker, P. D. Woodgate, *J. Organomet. Chem.* **1996**, *513*, 109.

[5] [5a] F. W. B. Einstein, R. K. Pomeroy, P. Rushman, A. C. Willis, *Organometallics* **1985**, *4*, 250. – [5b]R. D. Barr, M. Green, K. Marsden, F. G. A. Stone, P. Woodward, *J. Chem. Soc., Dalton Trans.* **1983**, 507. – [5c]L. W. Arndt, M. Y. Darensbourg, T. Delord, B. Terscinska-Bancroft, *J. Am. Chem. Soc.* **1986**, *108*, 2617. – [5d]H. B. Davis, F. W. B. Einstein, P. G. Glavina, T. Jones, R. K. Pomeroy, P. Rushman, *Organometallics* **1989**, *8*, 1030.

[6] List of the abbreviations used throughout this article: DME, 1,2-dimethoxyethane; THF, tetrahydrofuran; MeOTf, methyltriflate or methyltrifluoromethanesulfonate; PPN, bis(triphenylphosphoranylidene)ammonium; PhLi, phenyllithium; MeLi, methyllithium; COD, cyclooctadiene; NBD, norbornadiene.

[7] F. A. Cotton, C. S. Kraihanzel, *J. Am. Chem. Soc.* **1962**, *84*, 4432.

[8] F. W. B. Einstein, M. C. Jennings, R. Krentz, R. K. Pomeroy, P. Rushman, A. C. Willis, *Inorg. Chem.* **1987**, *26*, 1341.

[9] R. D. Barr, T. B. Marder, A. G. Orpen, I. D. Williams, *J. Chem. Soc., Chem. Commun.* **1984**, 112.

[10] H. Nakatsuji, M. Hada, A. Kawashima, *Inorg. Chem.* **1992**, *31*, 1740.

[11] A. A. Hock, O. S. Mills, *Acta Cryst.* **1961**, *14*, 139.

[12] A. D. Hunter, L. Shilliday, W. S. Furey, M. J. Zaworotko, *Organometallics* **1992**, *11*, 1550 and references quoted therein.

[13] [13a] E. P. Kündig, A. F. Cunningham, P. Paglia, D. P. Simmons, G. Bernardinelli, *Helv. Chim. Acta* **1990**, *73*, 386. – [13b]J.-P. Djukic, F. Rose-Munch, E. Rose, Y. Dromzee, *J. Am. Chem. Soc.* **1993**, *115*, 6434. – [13c]J.-P. Djukic, F. Rose-Munch, E. Rose, F. Simon, Y. Dromzee, *Organometallics* **1995**, *14*, 2027.

[14] T. A. Albright, P. Hofmann, R. Hoffmann, *J. Am. Chem. Soc.* **1977**, *99*, 7546.

[15] [15a] C. B. Knobler, S. Schreiber-Crawford, H. D. Kaesz, *Inorg. Chem.* **1975**, *14*, 2062. – [15b]J. B. Sheridan, R. S. Padda, K. Chaffee, C. Wang, Y. Huang, R. Lalancette, *J. Chem. Soc., Dalton Trans.* **1992**, 1539. – [15c]M. Brookhart, W. Lamanna, M. B. Humphrey, *J. Am. Chem. Soc.* **1982**, *104*, 2117. – [15d]E. Jeong, Y. K. Chung, *J. Organomet. Chem.* **1992**, *434*, 225. [15e] L. H. P. Gommans, L. Main, B. K. Nicholson, *J. Organomet. Chem.* **1985**, *284*, 345.

[16] R. Hoffmann, P. Hofmann, *J. Am. Chem. Soc.* **1976**, *98*, 598.

[17] M. F. Semmelhack, H. T. Hall, R. Farina, M. Yoshifuji, G. Clark, T. Bargar, K. Hirotsu, J. Clardy, *J. Am. Chem. Soc.* **1979**, *101*, 3535.

[18] A. Ceccon, A. Gambaro, A. M. Romanin, A. Venzo, *J. Organomet. Chem.* **1983**, *254*, 199.

[19] J. Sandström, in *Dynamic NMR Spectroscopy*, Academic Press, London, U. K., **1984**.

[20] [20a] P. A. Downton, B. G. Sayer, M. J. McGlinchley, *Organometallics* **1992**, *11*, 3281. – [20b]G. Hunter, R. L. MacKay, P. Kremminger, W. Weissensteiner, *J. Chem. Soc., Dalton Trans.* **1991**, 3349. – [20c]K. V. Kilway, J. S. Siegel, *Organometallics* **1992**, *11*, 1426.

[21] J.-P. Djukic, K. H. Dötz, M. Pfeffer, J. Fischer, A. De Cian, *Inorg. Chem.* **1998**, *37*, 3649.

[22] [22a] E. O. Fischer, E. Offhaus, *Chem. Ber.* **1969**, *102*, 2549. – [22b]J. R. Moss, M. Green, F. G. A. Stone, *J. Chem. Soc, Dalton Trans.* **1973**, 975. – [22c]M. J. Webb, R. P. Stewart, W. A. G. Grahams, *J. Organomet. Chem.* **1973**, *59*, C21. – [22d]W. K. Dean, W. A. G. Grahams, *J. Organomet. Chem.* **1976**, *120*, 73. – [22e]M. J. McGeary, J. L. Templeton, *J. Organomet. Chem.* **1987**, *323*, 199. – [22f]J. B. Sheridan, R. S. Padda, K. Chaffee, C. Wang, Y. Huang, R. Lalancette, *J. Chem. Soc., Dalton Trans.* **1992**, 1539. – [22g]Y.-J. Lee, S.-J. Kim, C.-H. Kang, J. Ko, S. O. Kang, P. J. Carroll, *Organometallics* **1998**, *17*, 1109.

[23] [23a] C. Bonifaci, A. Ceccon, A. Gambaro, P. Ganis, S. Santi, G. Valle, A. Venzo, *Organometallics* **1993**, *12*, 4211. – [23b]C. Bonifaci, A. Ceccon, A. Gambaro, P. Ganis, S. Santi, G. Valle, A. Venzo, *J. Organomet. Chem.* **1995**, *492*, 35.

[24] P. Ceccheto, A. Ceccon, A. Gambaro, S. Santi, P. Ganis, R. Gobetto, G. Valle, A. Venzo, *Organometallics* **1998**, *17*, 752.

[25] for leading references please see: [25a] T. Dahl, *Acta Chem. Scand.* **1994**, *48*, 95. – [25b]C. A. Hunter, *Chem.Soc. Rev.* **1994**, 101.

[26] C. A. L. Mahaffy, P. L. Pauson, *Inorg. Synth.* **1978**, *19*, 154.

[27] M. I. Bruce, M. I. Liddell, G. N. Pain *Inorg. Synth.* **1989**, *26*, 172.

[28] G. M. Sheldrick, *SHELXTL-Plus*, Siemens Analytical X-ray Instruments Inc., Madison, Wi., USA, **1989**.

[29] G. M. Sheldrick, *SHELXL-93*, Universität Göttingen, Federal Republic of Germany, **1993**.

[98179]

Metal Complexes of Biologically Important Ligands, CVIII [◇]

Metal Complexes of Alkyne-Bridged α-Amino Acids☆

Bernd Kayser, Janina Altman, Heinrich Nöth[2], Jörg Knizek[2], and Wolfgang Beck*

Institut für Anorganische Chemie der Ludwig-Maximilians-Universität,
Meiserstraße 1, D-80333 München, Germany

Received June 8, 1998

Keywords: *p*-Ethynylphenylalanine / Alkyne-bridged α-amino acids / N,O-Chelate complexes / Ferrocenes / Schiff bases / Platinum / Gold

The palladium-mediated coupling of *p*-ethynylphenylalanine (*p*-epa) with different halogenated benzenes yielded alkyne-bridged α-amino acids. A series of cationic mono- to hexanuclear $(Ph_3P)_2Pt$ complexes with the anions of *p*-ethynylphenylalanine and alkynyl- or benzene-bridged di-, tri-, tetra- and hexa-ethynyl phenylalanines as N,O-chelate ligands was prepared. *N*-*t*-Boc-*p*-ethynylphenylalanine methyl ester was metal-substituted to give complexes of the types $Ph_3PAu\text{-}C{\equiv}C\text{–}R$ and $(Et_3P)_2Pt(C{\equiv}CR)_2$. The benzene-bridged di-, tri-, tetra- and hexa-*p*-ethynylphenylalanine methyl esters form Schiff bases with ferrocene aldehyde and a tripodal ligand was obtained from $Ph_2PCH_2CH_2CH_2NH_2$ and the benzene-bridged triethynylphenyl-alanine. The structure of $(Ph_3P)_2Pt[NH_2C(H)(CH_2C_6H_4C{\equiv}CH)CO_2]^+\ BF_4^-$ was determined by X-ray diffraction.

Non-proteinogenic amino acids influence the biological properties of peptides and are useful for the synthesis of peptidomimetics[3]. The synthesis of unnatural amino acids is based either on electrophilic[4] or nucleophilic[5] equivalents. A valuable building block for the derivatization of phenylalanines has been developed by Schwabacher et al.[6]. *p*-Iodophenylalanine was used as starting material to build, under palladium catalysis, amino acids which are bridged by a heteroatom[6] or the iodo substituent was replaced by sulfur-containing fragments or trimethyltin[7]. The palladium-mediated coupling of terminal acetylides with *p*-iodophenylalanine afforded fluorescent marker molecules[8a], which find growing attention in organometallic chemistry[8b-e]. Undheim et al. and Savi et al. reported the Pd-catalyzed synthesis of a series of α,α′-hydrocarbon bis(α-amino acids), including α,α′-alkynyl-bridged bis(glycines) and of alkyne−bridged oxazolidines[9].

By means of the Heck[10], especially the Sonogashira reaction[11], we were able to synthesize various acetylide-bridged phenylalanines[12a]. *p*-Ethynylphenylalanine was proven to be a potent inhibitor of the enzyme tryptophan-hydroxylase[13]; therefore structural details of this compound appear of interest. The bis-, tris-, tetra- and hexapodal[12b] amino acids should be useful starting compounds in peptide chemistry, for the synthesis of organic as well as metallo-dendrimers[14], and for linearly-bridged metal complexes with unusual optical or electrical properties[15]. The scope of organometallic complexes of α-amino acids and peptides has been recently reviewed[16].

In this paper we wish to present the coordination chemistry of the new amino acid derivatives.

[◇] For part CVII see ref.[1].

Results and Discussion

Chloro-bridged metal complexes have proven to be ideal starting materials for the synthesis of N,O-α-aminocarboxylate metal compounds[16]. We have chosen the chloro-bridged complexes $[(Ph_3P)_2Pt(\mu\text{-}Cl)_2Pt(PPh_3)_2]^{2+}$, $(Et_3P)(Cl)Pd(\mu\text{-}Cl)Pd(Cl)(PEt_3)$ and $Cp^*(Cl)Rh(\mu\text{-}Cl)_2Rh(Cl)Cp^*$ from which N,O-chelates with natural α-amino acids have been obtained in our group.[16][17][18][19]

The reaction of the chloro-bridged cationic complex $\{[(Ph_3P)_2Pt(\mu\text{-}Cl)]_2\}\{BF_4\}_2$ with the anion of *p*-ethynylphenylalanine yielded the cationic N,O-chelate **1**.

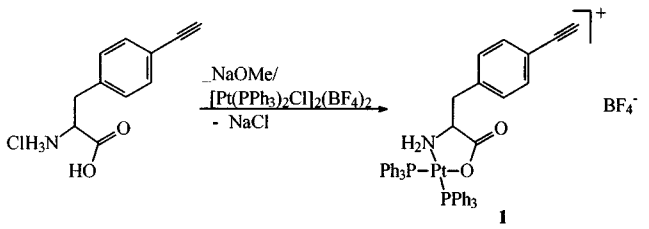

1

Suitable crystals for structure determination by X-ray diffraction of **1** were obtained by liquid-liquid diffusion of diethyl ether into an methanolic solution of **1** at room temperature. By this means the structure of the new non-proteinogenic amino acid *p*-ethynylphenylalanine (*p*-epa)[12a] has been established. The Pt−ligand atom distances are close to those of similar complexes, e.g. $(nBu_3P)(Cl)Pt(O_2CCH_2N{=}C(H)NMe_2)$[20a], (dppe)Pt[N(COMe)$CH_2$-$CO_2$][20b] and $(Ph_3P(Cl)Pt(NH_2CMe_2CO_2)$[20c].
The bond angle C11−C10−C7 is not exactly linear.

The analogous reactions of bis-, tris-, tetra- and hexa-ethynylphenylalanine derivatives gave the cationic complexes **2**−**7**.

 © WILEY-VCH Verlag GmbH, D-69451 Weinheim, 1998 1434−1948/98/1111−1791 $ 17.50+.50/0

Figure 1. Structure of complex **1**[a]

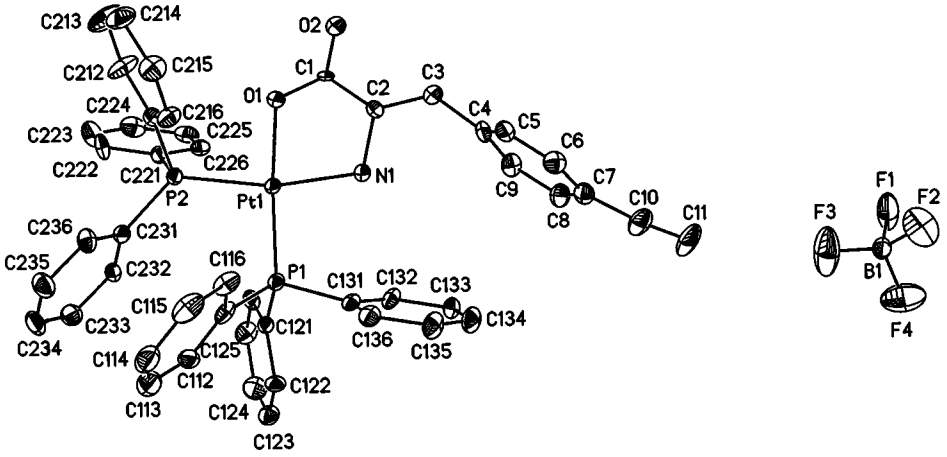

[a] Selected bond lengths [pm] and angles [°]: Pt−P1 225.3 (2), Pt−P2 225.8 (2), Pt−N1 209.5 (8), Pt−O1 207.1 (7), C10−C11 117.2 (17); N1−Pt−P2 165.9 (2), N1−Pt−P1 95.0 (2), O1−Pt−N1 81.0 (3), O1−Pt−P2 85.18 (19), C7−C10−C11 173.1 (16).

The IR spectra of the compounds **2**−**7** exhibit characteristic absorptions for η^2-coordinated α-amino carboxylates at $\nu \approx 1675\ cm^{-1}$ next to the ν(C≡C) vibrations at $\nu \approx 2205\ cm^{-1}$. The high symmetry of **2**−**7** is manifested in the ^{1}H- and ^{13}C-NMR spectra. Only one set of signals is observed. The ^{31}P-NMR spectra show a set of double doublets due to the different ligands *trans* to the P atoms with corresponding platinum satellites (^{195}Pt- ^{31}P coupling).

Terminal acetylide functions in organic molecules have successfully been used to build metal acetylide complexes which are also of interest for nonlinear optics. On the other hand the metal atom of bis(acetylide) complexes can func-

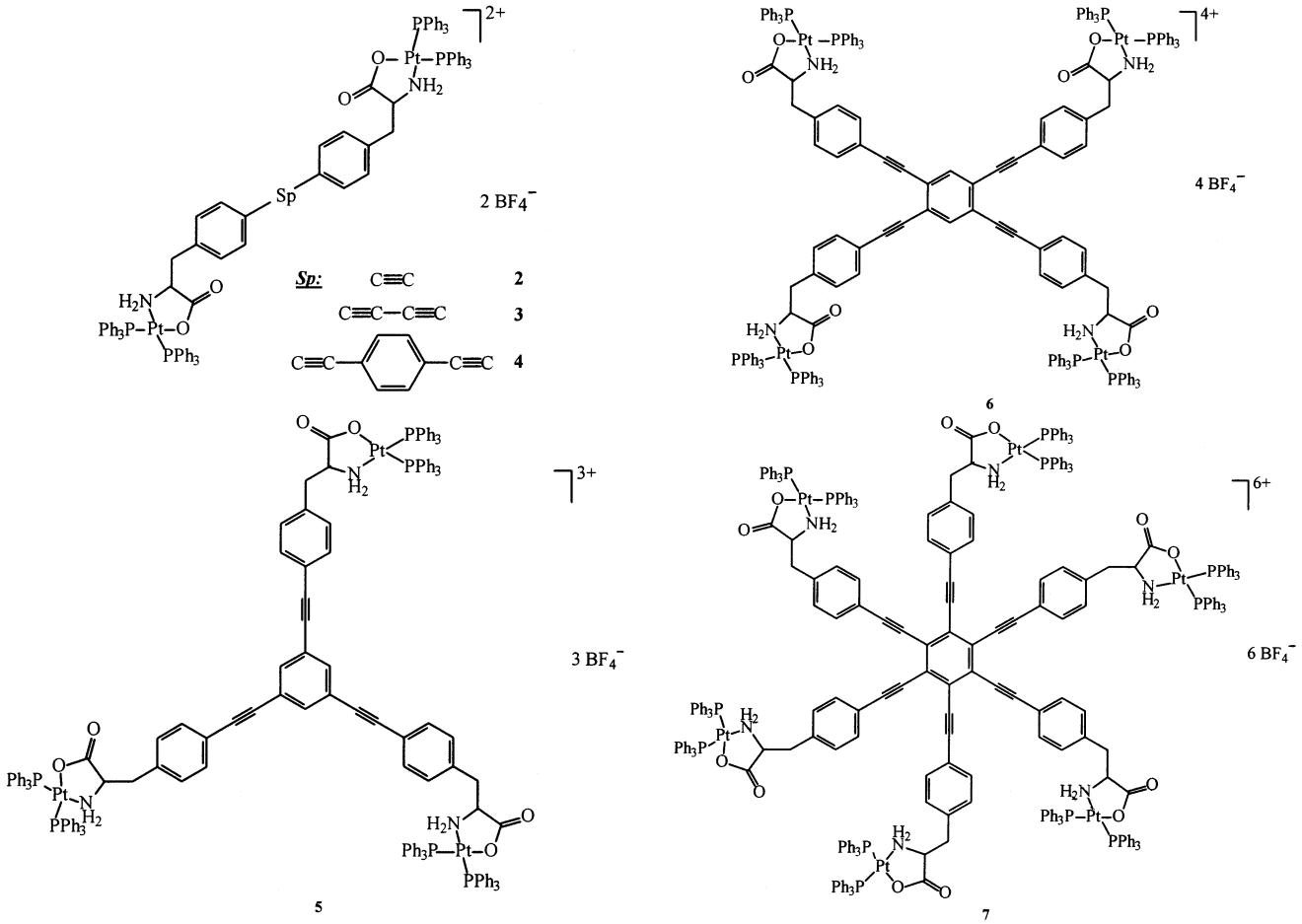

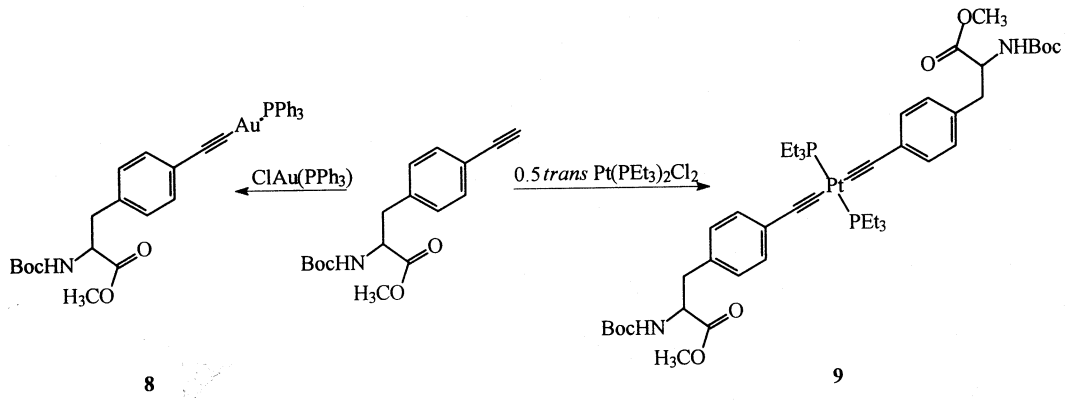

8 **9**

tion as a linker and support the conjugation of biological molecules[21]. Following known procedures[22] *p*-epa was treated with Ph_3PAuCl and *trans*-$(Ph_3P)_2PtCl_2$ to yield the compounds **8** and **9**.

Complexes **8** and **9** were characterized by IR-, ^1H-, ^{13}C- and ^{31}P-NMR spectroscopy. For **9** the characteristic $\nu(C{\equiv}C)$ absorption is found at 2103 cm^{-1}. The other spectroscopic data could be compared to similar known compounds[22].

Ferrocenyl Schiff base complexes of amino acids find application as lipophilic and chromophoric groups for masking of peptide bonds[23a]. Also interactions of the redoxac-

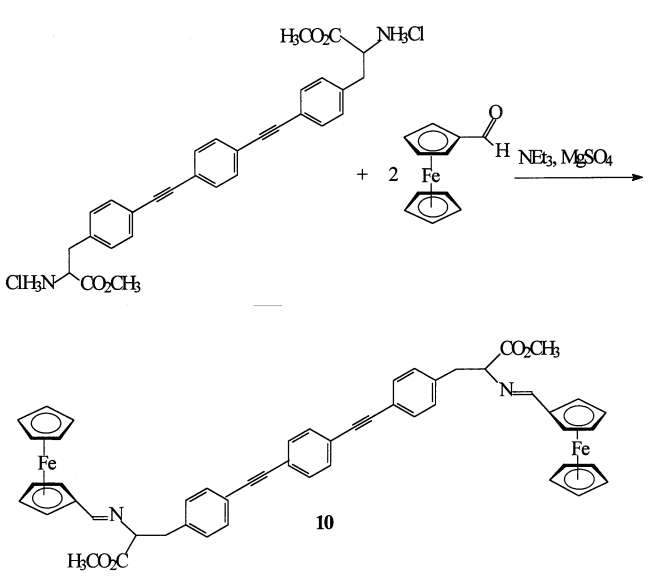

10

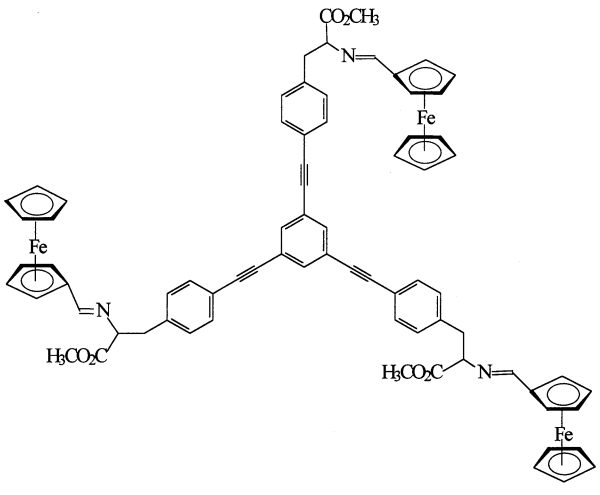

11

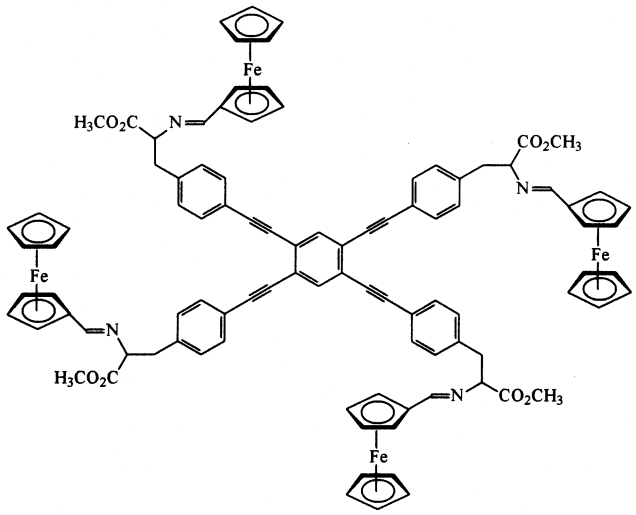

12

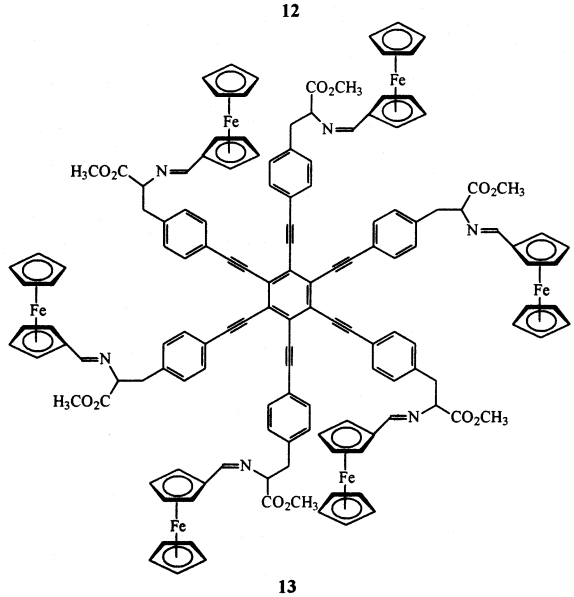

13

tive ferrocenyl unit and redoxactive enzymes are objects of investigations[23b]. The condensation between ferrocenecarbaldehyde and the corresponding phenylalanine esters afforded the orange Schiff base complexes **10**−**13**. For recent examples of star-shaped metal complexes derived from 1,3,5-triethynylbenzene as in **5** and **11** see ref.[24].

The successful formation of the Schiff base is proven by the intense ν(C=N) IR absorption band at 1636 cm^{-1} and by the imine proton signal (δ ≈ 7.90) in the ^{1}H-NMR spectrum. The ^{1}H-NMR signal of the H atom at α-C was not observed. A correlated ^{1}H/^{1}H-NMR experiment showed that the α-proton has the same chemical shift as the OCH_3 group of the methyl ester.

Using common methods of peptide chemistry the tripodal tris amino acid was derivatized and treated with 3-diphenylphosphanyl-*n*-propylamine to give the tripodal phosphane ligand **14** which may function as a tridentate chelate ligand. The reaction of **14** with 0.5 equivalents of $[Rh(COD)Cl]_2$ (COD = 1,5-cyclooctadiene) gave no defined compound, probably because the phosphane groups are not pre-organized. On the other hand the reactions of **14** with 1,5 equivalents of $[(Et_3P)PdCl(\mu\text{-}Cl)]_2$ or [Cp* $RhCl(\mu\text{-}Cl)]_2$ (Cp* = pentamethylcyclopentadienyl) yielded the three core complexes **15** and **16**.

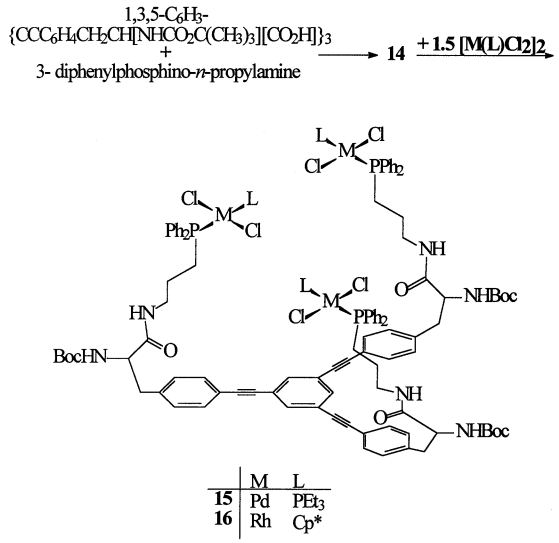

The ^{31}P-NMR spectrum of **15** shows several signal sets due to *cis* and *trans* isomers with the most intensive one having a coupling constant of 538 Hz. This coupling constant is typical for *trans*-situated phosphanes[25]. In contrast, compound **16** is formed as one isomer with a doublet in the ^{31}P-NMR spectrum due to the $^1J_{Rh\text{-}P}$ coupling of 143 Hz.

Generous support by *Deutsche Forschungsgemeinschaft*, *Fonds der Chemischen Industrie* and *Wacker Chemie*, München, is gratefully acknowledged. We thank *Degussa AG*, Hanau, for gifts of chemicals.

Experimental Section

General: All reactions were carried out in dry solvents under argon. − NMR: Jeol GSX 270 (^{1}H 270.0; ^{13}C 67.9; ^{31}P 109.3 MHz). Tetramethylsilane as internal standard; H_3PO_4 (85%) as external standard. − IR: 5ZDX FT-IR. − $ClAu(PPh_3)$[26], *trans*-$Pt(PEt_3)_2Cl_2$ [27a], $\{[(Ph_3P)_2Pt(\mu\text{-}Cl)]_2\}\{BF_4\}_2$ [28], $[(Et_3P)PdCl(\mu\text{-}Cl)]_2$ [27b], [Cp* $RhCl(\mu\text{-}Cl)]_2$ [29], 3-diphenylphosphanyl-*n*-propylamine[30] and the acetylide-substituted phenylalanines were prepared according to literature procedures[12]. Formylferrocene was purchased from Fluka and stored in the dark under argon.

$\{(Ph_3P)_2Pt[(NH_2)(O_2C)CHCH_2C_6H_4C{\equiv}CH]\}BF_4$ (**1**): To a solution of 34 mg (0.15 mmol) of *p*-ethynylphenylalanine hydrochloride in 10 ml of methanol was added 0.30 mmol of NaOMe and the mixture was stirred for 5 min. at room temperature. After addition of a solution of 120 mg (0.075mmol) of $\{[(Ph_3P)_2Pt(\mu\text{-}Cl)]_2\}\{BF_4\}_2$ in 10 ml of dichloromethane, the mixture was stirred for additional 3 h. The volatiles were evaporated, the residue was washed two times with 5 ml of water and dried at 50°C in vacuo. The resulting powder was finally recrystallized several times from dichloromethane/diethyl ether. Yield 121 mg (81%), colorless powder, m.p. 250°C (decomp.). − IR (KBr): $\tilde{\nu}$ = 3295 cm^{-1} m (NH_2), 1654 s (CO_2), 1084 s (BF_4). − ^{1}H NMR ($CDCl_3$): δ = 2.85 (dd, ^2J = 14.6 Hz, ^3J = 3.4 Hz, 1 H, CH′H), 3.13 (dd, ^2J = 14.6 Hz, ^3J = 7.5 Hz, 1 H, CHH′), 3.16 (s, 1 H, CH), 3.19−3.30 (m, 1 H, CH), 3.98−4.12 (m, 2 H, NH_2), 6.95 (d, ^3J = 8.1 Hz, 2 H, C_6H_4), 7.15−7.50 (m, 32 H, C_6H_4, PPh_3). − ^{13}C NMR ($CDCl_3$): δ = 38.90 (CH_2), 56.58 (CH), 77.76 (C≡*C*H), 83.41 (*C*≡CH), 120.85, 125.33 (d, ^1J = 84.1 Hz, *i*-PPh_3), 126.38 (d, ^1J = 83.5 Hz, *i*-PPh_3), 128.61 (d, ^3J = 11.4 Hz, *m*-PPh_3), 129.17 (d, ^3J = 11.5 Hz, *m*-PPh_3), 129.60, 131.66 (d, ^4J = 2.3 Hz, *p*-PPh_3), 132.21 (d, ^4J = 2.2 Hz, *p*-PPh_3), 132.66, 133.91 (d, ^2J = 10.8 Hz, *o*-PPh_3), 134.59 (d, ^2J = 10.6 Hz, *o*-PPh_3), 136.91, 182.94 (CO_2). − ^{31}P NMR ($CDCl_3$): δ = 7.70 (d, ^2J = 24.3 Hz, ^1J = 3586 Hz), 8.54 (d, ^2J = 24.3 Hz, ^1J = 3484 Hz). − $C_{47}H_{40}BF_4NO_2P_2Pt$ (994.7): calcd. C 56.75, H 4.05, N 1.41; found C 56.80, H 4.05, N 1.15.

$\{(Ph_3P)_2Pt[(NH_2)(CO_2)CHCH_2C_6H_4C{\equiv}CC_6H_4CH_2CH(CO_2)(NH_2)]Pt(PPh_3)_2\}\{BF_4\}_2$ (**2**): The reaction was carried out as described for **1** with 43 mg (0.10 mmol) of the ligand of **2** as dihydrochloride, 0.40 mmol of NaOMe, 160 mg (0.10 mmol) of $\{[(Ph_3P)_2Pt(\mu\text{-}Cl)]_2\}\{BF_4\}_2$ for 16 h. Yield 178 mg (91%), colorless powder, m.p. 220°C (decomp.). − IR (KBr): $\tilde{\nu}$ = 3303 cm^{-1} m (NH_2), 1676 s (CO_2), 1084 s (BF_4). − ^{1}H NMR ($CDCl_3$+CD_3OD): δ = 2.99 (dd, ^2J = 14.9 Hz, ^3J = 4.9 Hz, 2 H, CH′H), 3.11 (dd, ^2J = 14.9 Hz, ^3J = 7.6 Hz, 2 H, CHH′), 3.97−4.08 (m, 2 H, CH), 6.99 (d, ^3J = 8.3 Hz, 4 H, C_6H_4), 7.10−7.47 (m, 64 H, C_6H_4, PPh_3). − ^{13}C NMR ($CDCl_3$+CD_3OD): δ = 38.69 (CH_2), 56.48 (CH), 89.33 (C≡C), 121.75, 124.94 (d, ^1J = 77.0 Hz, *i*-PPh_3), 125.85 (d, ^1J = 74.9 Hz, *i*-PPh_3), 128.40 (d, ^3J = 11.4 Hz, *m*-PPh_3), 128.97 (d, ^3J = 11.3 Hz, *m*-PPh_3), 129.26, 131.64, 132.01 (*p*-PPh_3), 132.17 (*p*-PPh_3), 133.53 (d, ^2J = 10.3 Hz, *o*-PPh_3), 134.21 (d, ^2J = 10.5 Hz, *o*-PPh_3), 135.94, 183.71 (CO_2). − ^{31}P NMR ($CDCl_3$+CD_3OD): δ = 7.54 (d, ^2J = 24.1 Hz, ^1J = 3610 Hz), 8.29 (d, ^2J = 24.1 Hz, ^1J = 3466 Hz). − $C_{92}H_{78}B_2F_8N_2O_4P_4Pt_2$ (1963.3): calcd. C 56.28, H 4.01, N 1.43; found C 55.72, H 4.08, N 1.34.

$\{(Ph_3P)_2Pt[(NH_2)(CO_2)CHCH_2C_6H_4C{\equiv}CC{\equiv}CC_6H_4CH_2CH(CO_2)(NH_2)]Pt(PPh_3)_2\}\{BF_4\}_2$ (**3**): The reaction was carried out as described for **1** with 45 mg (0.10 mmol) of the ligand of **3** as dihydrochloride, 0.40 mmol of NaOMe, 160 mg (0.10 mmol) of $\{[(Ph_3P)_2Pt(\mu\text{-}Cl)]_2\}\{BF_4\}_2$ for 16 h. Yield 184 mg (93%), colorless powder, m.p. 235°C (decomp.). − IR (KBr): $\tilde{\nu}$ = 3303, 3223 cm^{-1} m (NH_2), 1679 s (CO_2), 1084 s (BF_4). − ^{1}H NMR

($CDCl_3$+CD_3OD): δ = 2.90−3.04 (m, 4 H, CH_2), 3.95−4.03 (m, 2 H, CH), 6.97 (d, ^3J = 7.8 Hz, 4 H, C_6H_4), 7.16−7.46 (m, 64 H, C_6H_4, PPh_3). − ^{13}C NMR ($CDCl_3$+CD_3OD): δ = 38.86 (CH_2), 56.66 (CH), 74.22, 81.34 (C≡C), 120.28, 125.05 (d, ^1J = 79.8 Hz, *i*-PPh_3), 126.03 (d, ^1J = 78.1 Hz, *i*-PPh_3), 128.53 (d, ^3J = 11.4 Hz, *m*-PPh_3), 129.09 (d, ^3J = 11.2 Hz, *m*-PPh_3), 129.44, 131.74 (*p*-PPh_3), 132.25 (*p*-PPh_3), 132.96, 133.65 (d, ^2J = 11.1 Hz, *o*-PPh_3), 134.38 (d, ^2J = 10.3 Hz, *o*-PPh_3), 137.34, 183.43 (d, ^3J = 5.2 Hz, CO_2). − ^{31}P NMR ($CDCl_3$+CD_3OD): δ = 7.43 (d, ^2J = 24.4 Hz, ^1J = 3506 Hz), 8.47 (d, ^2J = 24.4 Hz, ^1J = 3445 Hz). − $C_{94}H_{78}B_2F_8N_2O_4P_4Pt_2 \times CH_2Cl_2$ (2072.3): calcd. C 55.06, H 3.89, N 1.35; found C 54.60, H 3.92, N 1.30.

{1,4-C_6H_4[C≡$CC_6H_4CH_2CH(CO_2)(NH_2)$ $Pt(PPh_3)_2$]$_2$}-{BF_4}$_2$ (**4**): The reaction was carried out as described for **1** with 53 mg (0.10 mmol) of the ligand of **4** as dihydrochloride, 0.40 mmol of NaOMe, 160 mg (0.10 mmol) of {[$(Ph_3P)_2Pt(\mu\text{-}Cl)$]$_2$}{$BF_4$}$_2$ for 16 h. Yield 184 mg (89%), colorless powder, m.p. 260°C (decomp.). − IR (KBr): $\tilde{\nu}$ = 3299, 3223 cm^{-1} m (NH_2), 2213 (C≡C), 1666 s (CO_2), 1084 s (BF_4). − ^{1}H NMR ($CDCl_3$): δ = 2.89 (dd, ^2J = 13.6 Hz, ^3J = 4.3 Hz, 2 H, CH′H), 3.13 (dd, ^2J = 13.6 Hz, ^3J = 7.2 Hz, 2 H, CHH′), 3.32−3.47 (m, 2 H, CH), 3.98−4.19 (m, 4 H, NH_2), 7.01 (d, ^3J = 8.3 Hz, 4 H, C_6H_4), 7.12−7.49 (m, 64 H, C_6H_4, PPh_3), 7.59 (s, 4 H, C_6H_4). − ^{13}C NMR ($CDCl_3$): δ = 38.70 (CH_2), 56.50 (CH), 89.50, 90.75 (C≡C), 121.81, 122.88, 125.01 (d, ^1J = 78.9 Hz, *i*-PPh_3), 125.90 (d, ^1J = 76.4 Hz, *i*-PPh_3), 128.49 (d, ^3J = 11.2 Hz, *m*-PPh_3), 129.05 (d, ^3J = 11.1 Hz, *m*-PPh_3), 129.28, 131.44, 131.71, 132.08 (*p*-PPh_3), 132.26 (*p*-PPh_3), 133.57 (d, ^2J = 10.6 Hz, *o*-PPh_3), 134.27 (d, ^2J = 10.8 Hz, *o*-PPh_3), 135.97, 183.75 (d, ^3J = 4.0 Hz, CO_2). − ^{31}P NMR ($CDCl_3$): δ = 7.71 (d, ^2J = 24.2 Hz, ^1J = 3595 Hz), 8.55 (d, ^2J = 24.2 Hz, ^1J = 3446 Hz). − $C_{100}H_{82}B_2F_8N_2O_4P_4Pt_2 \times 1/2\ CH_2Cl_2$ (2105.9): calcd. C 57.48, H 3.98, N 1.33; found C 57.29, H 4.23, N 1.25.

{1,3,5-C_6H_3[C≡$CC_6H_4CH_2CH(CO_2)(NH_2)$ $Pt(PPh_3)_2$]$_3$}-{BF_4}$_3$ (**5**): The reaction was carried out as described for **1** with 75 mg (0.10 mmol) of the ligand of **5** as trihydrochloride, 0.60 mmol of NaOMe, 240 mg (0.15 mmol) of {[$(Ph_3P)_2Pt(\mu\text{-}Cl)$]$_2$}{$BF_4$}$_2$ for 16 h. Yield 256 mg (84%), colorless powder, m.p. 270°C (decomp.). − IR (KBr): $\tilde{\nu}$ = 3300, 3225 cm^{-1} m (NH_2), 2208 (C≡C), 1674 s (CO_2), 1085 s (BF_4). − ^{1}H NMR ($CDCl_3$+CD_3OD): δ = 2.89−3.15 (m, 6 H, CH_2), 4.03 (pt, ^3J = 6.4 Hz, 3 H, CH), 6.98 (d, ^3J = 8.0 Hz, 6 H, C_6H_4), 7.10−7.46 (m, 96 H, C_6H_4, PPh_3), 7.69 (s, 3 H, C_6H_3). − ^{13}C NMR ($CDCl_3$+CD_3OD): δ = 38.73 (CH_2), 56.58 (CH), 87.95, 90.17 (C≡C), 121.27, 123.87, 124.99 (d, ^1J = 79.0 Hz, *i*-PPh_3), 125.95 (d, ^1J = 77.4 Hz, *i*-PPh_3), 128.45 (d, ^3J = 11.3 Hz, *m*-PPh_3), 129.02 (d, ^3J = 11.4 Hz, *m*-PPh_3), 131.67 (*p*-PPh_3), 132.11 (*p*-PPh_3), 132.18, 133.89 (d, ^2J = 10.6 Hz, *o*-PPh_3), 133.89, 134.25 (d, ^2J = 10.6 Hz, *o*-PPh_3), 136.41, 183.56 (CO_2). − ^{31}P NMR ($CDCl_3$+CD_3OD): δ = 7.56 (d, ^2J = 24.0 Hz, ^1J = 3623 Hz), 8.53 (d, ^2J = 24.0 Hz, ^1J = 3440 Hz). − $C_{147}H_{120}B_3F_{12}N_3O_6P_6Pt_3 \times CH_2Cl_2$ (3141.1): calcd. C 56.59, H 3.91, N 1.34; found C 56.49, H 4.00, N 1.17.

{1,2,4,5-C_6H_2[C≡$CC_6H_4CH_2CH(CO_2)(NH_2)$ $Pt(PPh_3)_2$]$_4$}-{BF_4}$_4$ (**6**): The reaction was carried out as described for **1** with 73 mg (0.075 mmol) of the ligand of **6** as tetrahydrochloride, 0.60 mmol of NaOMe, 240 mg (0.15 mmol) of {[$(Ph_3P)_2Pt(\mu\text{-}Cl)$]$_2$}{$BF_4$}$_2$ for 16 h. Yield 261 mg (86%), brown powder, m.p. 276°C (decomp.). − IR (KBr): $\tilde{\nu}$ = 3299, 3225 cm^{-1} m (NH_2), 2198 (C≡C), 1674 s (CO_2), 1084 s (BF_4). − ^{1}H NMR ($CDCl_3$+CD_3OD): δ = 2.82 (dd, ^2J = 14.1 Hz, ^3J = 11.2 Hz, 4 H, CH′H), 3.08−3.20 (m, 4 H, CHH′), 4.03−4.17 (m, 4 H, CH), 6.99 (d, ^3J = 7.7 Hz, 8 H, C_6H_4), 7.09−7.45 (m, 128 H, C_6H_4, PPh_3), 7.76 (s, 2 H, C_6H_2). − ^{13}C NMR ($CDCl_3$+CD_3OD): δ = 39.04 (CH_2), 56.68 (CH), 87.74, 95.49 (C≡C), 121.05, 125.05 (d, ^1J = 89.7 Hz, *i*-PPh_3), 125.25, 126.03 (d, ^1J = 88.9 Hz, *i*-PPh_3), 128.38 (d, ^3J = 11.6 Hz, *m*-PPh_3), 128.89 (d, ^3J = 10.9 Hz, *m*-PPh_3), 129.23, 131.57 (*p*-PPh_3), 131.95, 132.04 (*p*-PPh_3), 133.56 (d, ^2J = 10.6 Hz, *o*-PPh_3), 134.02, 134.33 (d, ^2J = 10.5 Hz, *o*-PPh_3), 136.89, 183.46 (CO_2). − ^{31}P NMR ($CDCl_3$+CD_3OD): δ = 7.40 (d, ^2J = 23.9 Hz, ^1J = 3622 Hz), 8.47 (d, ^2J = 23.9 Hz, ^1J = 3440 Hz). − $C_{194}H_{158}B_4F_{16}N_4O_8P_8Pt_4 \times CH_2Cl_2$ (4133.7): calcd. C 56.65, H 3.90, N 1.35; found C 56.10, H 3.99, N 1.15.

{1,2,3,4,5,6-C_6[C≡$CC_6H_4CH_2CH(CO_2)(NH_2)$ $Pt(PPh_3)_2$]$_6$}-{BF_4}$_6$ (**7**): The reaction was carried out as described for **1** with 71 mg (0.05 mmol) of the ligand of **7** as hexahydrochloride, 0.60 mmol of NaOMe, 240 mg (0.15 mmol) of {[$(Ph_3P)_2Pt(\mu\text{-}Cl)$]$_2$}{$BF_4$}$_2$ for 16 h. Yield 244 mg (81%), brown powder, m.p. 300°C (decomp.). − IR (KBr): $\tilde{\nu}$ = 3304, 3231 cm^{-1} m (NH_2), 2198 (C≡C), 1675 s (CO_2), 1084 s (BF_4). − ^{1}H NMR ($CDCl_3$+CD_3OD): δ = 2.82 (pt, *J* = 11.9 Hz, 6 H, CH′H), 3.19 (pt, *J* = 10.7 Hz, 6 H, CHH′), 4.29 (pt, ^3J = 14.7 Hz, 6 H, CH), 7.09−7.51 (m, 204 H, C_6H_4, PPh_3). − ^{13}C NMR ($CDCl_3$+CD_3OD): δ = 39.18 (CH_2), 56.47 (CH), 87.23, 99.70 (C≡C), 120.92, 125.32 (d, ^1J = 110.8 Hz, *i*-PPh_3), 126.29 (d, ^1J = 108.1 Hz, *i*-PPh_3), 127.82, 128.56 (d, ^3J = 10.7 Hz, *m*-PPh_3), 129.02 (d, ^3J = 12.8 Hz, *m*-PPh_3), 129.72, 131.59 (*p*-PPh_3), 132.12 (*p*-PPh_3), 132.18, 133.74 (d, ^2J = 10.0 Hz, *o*-PPh_3), 134.61 (d, ^2J = 8.9 Hz, *o*-PPh_3), 137.63, 183.14 (CO_2). − ^{31}P NMR ($CDCl_3$+CD_3OD): δ = 7.32 (d, ^2J = 23.6 Hz, ^1J = 3623 Hz), 8.79 (d, ^2J = 23.6 Hz, ^1J = 3477 Hz). − $C_{288}H_{234}B_6F_{24}N_6O_{12}P_{12}Pt_6 \times 2\ CH_2Cl_2$ (6203.9): calcd. C 56.14, H 3.86, N 1.35; found C 55.53, H 4.09, N 1.18.

General Procedure for the Preparation of the σ*-Acetylide Metal Complexes* **8** *and* **9**: To a solution of 99 mg (0.20 mmol) of $ClAu(PPh_3)$ or 100 mg (0.20 mmol) of *trans*-$Pt(PEt_3)_2Cl_2$ in 10 ml of diethylamine were added 67 mg (0.22 mmol) or 133 mg (0.44 mmol) of *N*-*t*-Boc-4-ethynyl-L-phenylalanine methyl ester and a catalytic amount of CuI. The solutions were stirred at room temp. for 3 h in the dark and the volatiles were evaporated. The residues were each extracted with a mixture of dichloromethane/diethyl ether (1/3; 5 ml) and the solvent was evaporated. The resulting precipitates were washed with pentane (2 × 10 ml) and dried in vacuo.

$(PPh_3)Au${C≡$CC_6H_4CH_2CH[NHCO_2C(CH_3)_3](CO_2Me)$} (**8**): Yield 131 mg (86%), colorless powder, m.p. 99°C (decomp.). − IR (KBr): $\tilde{\nu}$ = 3439 cm^{-1} (NH), 1743 m, 1713 s (CO_2, CON). − ^{1}H NMR ($CDCl_3$): δ = 1.39 (s, 9 H, CH_3), 2.93−3.09 (m, 2 H, CH_2), 3.65 (s, 3 H, CH_3), 4.53 (pq, ^3J = 6.1 Hz, 1 H, CH), 4.92 (d, ^3J = 8.4 Hz, 1 H, NH), 6.99 (d, ^3J = 8.1 Hz, 2 H, C_6H_4), 7.39−7.56 (m, 17 H, PPh_3, C_6H_4). − ^{13}C NMR ($CDCl_3$): δ = 28.36 [$C(CH_3)_3$], 38.32 (CH_2), 52.55 (CH_3), 54.39 (CH), 79.94 [$C(CH_3)_3$], 83.35, 105.09 (C≡C), 123.62, 128.99, 129.21 (d, ^3J = 11.4 Hz, *m*-PPh_3), 131.67, 131.80 (d, ^1J = 8.9 Hz, *i*-PPh_3), 132.57, 134.35 (d, ^2J = 13.7 Hz, *o*-PPh_3), 134.70 (24 C, C_6H_4, PPh_3), 155.14 (CON), 172.40 (CO_2). − ^{31}P NMR ($CDCl_3$): δ = 42.84. − $C_{35}H_{35}NO_4PAu \times 1/2\ CH_2Cl_2$ (804.1): calcd. C 53.02, H 4.51, N 1.74; found C 52.54, H 4.13, N 1.46.

trans-$(PEt_3)_2Pt${C≡$CC_6H_4CH_2CH[NHCO_2C(CH_3)_3](CO_2Me)$}$_2$ (**9**): Yield 182 mg (88%), yellow powder, m.p. 135°C (decomp.). − IR (KBr): $\tilde{\nu}$ = 3443 cm^{-1} (NH), 2102 s (C≡C), 1745 m, 1715 s (CO_2, CON). − ^{1}H NMR ($CDCl_3$): δ = 1.46 (dt, ^3J = 8.3 Hz, ^3J = 7.8 Hz, 18 H, CH_3), 1.35 (s, 18 H, CH_3), 2.10 (tq, ^2J = 7.4 Hz, ^3J = 7.8 Hz, 12 H, CH_2), 2.88−3.02 (m, 4 H, CH_2), 3.65 (s, 6 H, CH_3), 4.48 (pq, ^3J = 7.2 Hz, 2 H, CH), 4.87 (d, ^3J = 8.3 Hz, 2 H, NH), 6.89 (d, ^3J = 8.0 Hz, 4 H, C_6H_4), 7.13 (d, ^3J = 8.0 Hz, 4 H, C_6H_4). − ^{13}C NMR ($CDCl_3$): δ = 8.22 (t, ^2J = 12.2

Hz, CH_3), 16.16 (t, ^1J = 17.9 Hz, CH_2), 28.18 [C(CH_3)$_3$], 37.95 (CH_2), 52.15 (CH_3), 54.23 (CH), 79.87 [C(CH_3)$_3$], 109.00, 128.99, 131.09, 132.62 (12 C, C_6H_4), 155.23 (CON), 172.55 (CO_2). − ^{31}P NMR ($CDCl_3$): δ = 11.50 (^1J = 2371 Hz). − $C_{46}H_{70}N_2O_8P_2Pt$ (1036.1): calcd. C 53.33, H 6.81, N 2.70; found C 52.71, H 6.67, N 2.69.

1,4-C_6H_4[-C≡C$C_6H_4CH_2CH(CO_2CH_3)(N=C$-Fc)] (**10**): To a solution of 112 mg (0.20 mmol) of the ligand of **4** as dihydrochloride dimethyl ester in 20 ml of dichloromethane were added 61.8 µl (0.44 mmol) of triethylamine. The solution was stirred at room temperature for 15 min, 96 mg (0.44 mmol) of ferrocenealdehyde and 150 mg of $MgSO_4$ were added and stirring was continued for 24 h in the dark. The precipitate was separated by centrifugation, the volatiles were evaporated from the supernatant solution, and the residue was extracted with a mixture of diethyl ether/tetrahydrofuran (3/1; 2 × 15 ml). The solvent was evaporated, the resulting precipitate was washed with pentane (3 × 10 ml) and dried in vacuo. Yield 138 mg (79%), orange powder, m.p. 108°C (decomp.). − IR (KBr): $\tilde{\nu}$ = 2216 cm^{-1} w (C≡C), 1737 s (CO_2), 1635 s (C=N). − ^{1}H NMR ($CDCl_3$): δ = 3.16 (dd, ^2J = 14.1 Hz, ^3J = 8.8 Hz, 2 H, CH′H), 3.34 (dd, ^2J = 14.1 Hz, ^3J = 5.1 Hz, 2 H, CHH′), 3.73 (s, 6 H, CH_3), 4.02 (s, 12 H, CH, C_5H_5), 4.36 (s, 4 H, C_5H_5), 4.60 (s, 2 H, C_5H_5), 4.65 (s, 2 H, C_5H_5), 7.19 (d, ^3J = 8.1 Hz, 4 H, C_6H_4), 7.42 (d, ^3J = 8.1 Hz, 4 H, C_6H_4), 7.47 (s, 4 H, C_6H_4), 7.93 (s, 2 H, CH). − ^{13}C NMR ($CDCl_3$): δ = 39.30 (CH_2), 52.08 (CH_3), 68.70, 68.92, 69.09, 70.79 (C_5H_5), 74.72 (CH), 79.34 (C_5H_5), 88.99, 91.04 (C≡C), 121.21, 123.06, 129.66, 131.45, 137.87, 138.55 (18 C, C_6H_4), 164.71 (C=N), 171.81 (CO_2). − $C_{52}H_{44}N_2O_4Fe_2$ (872.6): calcd. C 71.57, H 5.08, N 3.21; found C 71.57, H 5.22, N 3.84.

1,3,5-C_6H_3[-C≡C-C_6H_4-CH_2-$CH(CO_2CH_3)(N=C$-Fc)] (**11**): The reaction was carried out as described for **10** with 70 mg (0.10 mmol) of the ligand of **5** as trihydrochloride trimethyl ester, 45.7 µl (0.33 mmol) of triethylamine and 70 mg (0.33 mmol) of ferrocenealdehyde. Yield 107 mg (84%), orange powder, m.p. 123°C (decomp.). − IR (KBr): $\tilde{\nu}$ = 2211 cm^{-1} w (C≡C), 1740 s (CO_2), 1636 s (C=N). − ^{1}H NMR ($CDCl_3$): δ = 3.15 (dd, ^2J = 14.0 Hz, ^3J = 9.0 Hz, 3 H, CH′H), 3.34 (dd, ^2J = 14.0 Hz, ^3J = 4.6 Hz, 3 H, CHH′), 3.73 (s, 9 H, CH_3), 4.05 (s, 18 H, CH, C_5H_5), 4.36 (s, 6 H, C_5H_5), 4.58 (s, 3 H, C_5H_5), 4.63 (s, 3 H, C_5H_5), 7.20 (d, ^3J = 8.1 Hz, 6 H, C_6H_4), 7.41 (d, ^3J = 8.1 Hz, 6 H, C_6H_4), 7.52 (s, 3 H, C_6H_3), 7.93 (s, 3 H, CH). − ^{13}C NMR ($CDCl_3$): δ = 39.30 (CH_2), 52.30 (CH_3), 68.68, 68.92, 69.10, 70.74, 70.79 (C_5H_5), 74.76 (CH), 79.39 (C_5H_5), 87.70, 90.32 (C≡C), 120.96, 123.93, 129.65, 131.66, 133.83, 138.69 (24 C, C_6H_4, C_6H_3), 164.69 (C=N), 171.82 (CO_2). − $C_{75}H_{63}N_3O_6Fe_3$ × 1/2 CH_2Cl_2 (1312.3): calcd. C 69.09, H 4.92, N 3.20; found C 68.98, H 4.60, N 3.23.

1,2,4,5-C_6H_2[-C≡C-C_6H_4-CH_2-$CH(CO_2CH_3)(N=C$-Fc)] (**12**): The reaction was carried out as described for **10** with 51 mg (0.05 mmol) of the ligand of **6** as tetrahydrochloride tetramethyl ester, 30.5 µl (0.22 mmol) of triethylamine and 47 mg (0.22 mmol) of ferrocenealdehyde. Yield 67 mg (80%), orange powder, m.p. 132°C (decomp.). − IR (KBr): $\tilde{\nu}$ = 2204 cm^{-1} w (C≡C), 1739 s (CO_2), 1636 s (C=N). − ^{1}H NMR ($CDCl_3$): δ = 3.06−3.22 (m, 4 H, CH′H), 3.27−3.38 (m, 4 H, CHH′), 3.72 (s, 12 H, CH_3), 4.04 (s, 24 H, CH, C_5H_5), 4.34 (s, 8 H, C_5H_5), 4.57 (s, 4 H, C_5H_5), 4.64 (s, 4 H, C_5H_5), 7.11−7.23 (m, 8 H, C_6H_4), 7.39−7.48 (m, 8 H, C_6H_4), 7.62 (s, 2 H, C_6H_2), 7.92 (s, 4 H, CH). − ^{13}C NMR ($CDCl_3$): δ = 39.41 (CH_2), 52.42 (CH_3), 68.81, 68.91, 69.15, 70.85, 70.88 (C_5H_5), 74.65 (CH), 79.32 (C_5H_5), 87.54, 95.32 (C≡C), 121.20, 125.13, 129.80, 131.77, 134.90, 138.91 (30 C, C_6H_4, C_6H_2), 164.83 (C=N), 171.87 (CO_2). − $C_{98}H_{82}N_4O_8Fe_4$ × CH_2Cl_2 (1752.1): calcd. C 67.86, H 4.83, N 3.20; found C 67.00, H 4.73, N 3.30.

1,2,3,4,5,6-C_6[-C≡C-C_6H_4-CH_2-$CH(CO_2CH_3)(N=C$-Fc)] (**13**): The reaction was carried out as described for **10** with 75 mg (0.05 mmol) of the ligand of **7** as hexahydrochloride hexamethyl ester, 45.7 µl (0.33 mmol) of triethylamine and 70 mg (0.33 mmol) of ferrocenealdehyde. Yield 96 mg (78%), orange powder, m.p. 131°C (decomp.). − IR (KBr): $\tilde{\nu}$ = 2206 cm^{-1} w (C≡C), 1739 s (CO_2), 1636 s (C=N). − ^{1}H NMR ($CDCl_3$): δ = 3.15 (dd, ^2J = 13.6 Hz, ^3J = 9.2 Hz, 6 H, CH′H), 3.36 (dd, ^2J = 13.6 Hz, ^3J = 5.2 Hz, 6 H, CHH′), 3.75 (s, 18 H, CH_3), 4.06 (s, 36 H, CH, C_5H_5), 4.37 (s, 12 H, C_5H_5), 4.58 (s, 6 H, C_5H_5), 4.68 (s, 6 H, C_5H_5), 7.16 (d, ^3J = 8.2 Hz, 12 H, C_6H_4), 7.44 (d, ^3J = 8.2 Hz, 12 H, C_6H_4), 7.95 (s, 6 H, CH). − ^{13}C NMR ($CDCl_3$): δ = 39.34 (CH_2), 52.33 (CH_3), 68.75, 68.96, 69.15, 70.84 (C_5H_5), 74.65 (CH), 79.30 (C_5H_5), 87.23, 99.13 (C≡C), 121.25, 127.22, 129.74, 131.73, 139.05 (42 C, C_6H_4, C_6), 164.73 (C=N), 171.78 (CO_2). − $C_{144}H_{120}N_6O_{12}Fe_6$ × 2 CH_2Cl_2 (2631.3): calcd. C 66.63, H 4.75, N 3.19; found C 66.23, H 4.89, N 3.14.

1,3,5-C_6H_3{C≡C$C_6H_4CH_2CH[NHCO_2C(CH_3)_3][CO_2$-$(CH_2)_3PPh_2]\}_3$ (**14**): To a solution of 94 mg (0.10 mmol) of the ligand of **5** as *N*-Boc-protected triacid in 5 ml of tetrahydrofuran was added a solution of 98 mg (0.40 mmol) of 3-diphenylphosphanyl-*n*-propylamine in 5 ml of tetrahydrofuran and 38.0 µl (0.30 mmol) of *N*-ethylmorpholine. The solution was cooled to 0°C and 81 mg (0.60 mmol) of 1-hydroxybenzotriazole and 96 mg (0.50 mmol) of 1-[3-(dimethylamino)propyl]-3-ethylcarbodiimide hydrochloride were added. After stirring for 24 h, evaporation of the solvent gave a colorless residue from which the product was isolated by flash chromatography (silica gel, 30 cm, CH_2Cl_2/methanol 30:1). Yield 123 mg (76%), colorless powder, m.p. 185°C. − IR (KBr): $\tilde{\nu}$ = 3322 cm^{-1} m (NH), 2211 w (C≡C), 1706 s, 1684 s, 1651 s (CO_2, CON). − ^{1}H NMR ($CDCl_3$): δ = 1.37 (s, 27 H, CH_3), 1.46−1.60 (m, 6 H, CH_2), 1.93 (pt, ^3J = 7.9 Hz, 6 H, CH_2), 3.03 (pd, ^3J = 5.3 Hz, 6 H, CH′H, CH_2), 3.24 (dd, ^2J = 13.1 Hz , ^3J = 7.0 Hz, 6 H, CHH′, CH_2), 4.23 (pq, ^3J = 7.2 Hz, 3 H, CH), 5.00 (m, 3 H, NH), 5.79 (t, ^3J = 6.2 Hz, 3 H, NH), 7.16 (d, ^3J = 8.1 Hz, 6 H, C_6H_4), 7.26−7.42 (m, 36 H, C_6H_4, PPh_2), 7.58 (s, 3 H, C_6H_3). − ^{13}C NMR ($CDCl_3$): δ = 24.97 (d, ^2J = 10.4 Hz, CH_2), 25.74 (d, ^1J = 18.4 Hz, CH_2), 28.16 [C(CH_3)$_3$], 38.53 (CH_2), 40.33 (d, ^3J = 14.9 Hz, CH_2), 55.73 (CH), 80.28 [C(CH_3)$_3$], 87.99, 90.27 (C≡C), 121.42, 124.02, 128.50, 128.69 (d, ^3J = 10.3 Hz, *m*-PPh_2), 129.52, 131.99, 132.79 (d, ^2J = 18.5 Hz, *o*-PPh_2), 134.00, 137.65, 138.30 (d, ^1J = 13.9 Hz, *i*-PPh_2, 60 C, C_6H_4, C_6H_3, PPh_2), 155.42, 171.01 (CON). − ^{31}P NMR ($CDCl_3$): δ = −16.14. − $C_{99}H_{105}N_6O_9P_3$ × 2 H_2O(1654.9): calcd. C 71.98, H 6.65, N 5.08; found C 71.77, H 6.26, N 4.77.

General Procedure for the Preparation of the Complexes **15** *and* **16**: To a solution of 81 mg (0.05 mmol) of ligand **14** in 10 ml of dichloromethane were added 45 mg of [(Et_3P)PdCl(µ-Cl)]$_2$ or 46 mg of [Cp*RhCl(µ-Cl)]$_2$ (0.075 mmol each). The solutions were stirred at room temp. for 16 h, concentrated in vacuo and the residues were washed with 10 ml of diethyl ether and 30 ml of pentane.

1,3,5-C_6H_3{C≡C$C_6H_4CH_2CH[NHCO_2C(CH_3)_3][CO_2$-$(CH_2)_3PPh_2]Pd(PEt_3)(Cl)_2\}_3$ (**15**): Yield 123 mg (98%), yellow powder, m.p. 183°C (decomp.). − IR (KBr): $\tilde{\nu}$ = 3428 cm^{-1} m (NH), 2213 (C≡C), 1713, 1677 s (CON), 354, 329 w (Pd−Cl). − ^{1}H NMR ($CDCl_3$): δ = 0.93 (dt, $^3J_{PH}$ = 17.8 Hz, $^3J_{HH}$ = 7.7 Hz, 27 H, CH_3, B), 1.16 (dt, $^3J_{PH}$ = 16.5 Hz, $^3J_{HH}$ = 7.5 Hz, 27 H, CH_3, A), 1.37 (s, 18 H, CH_3, A+B), 1.51−1.65 (m, 6 H, CH_2, A+B), 1.81−1.95 (m, 18 H, CH_2, A+B), 2.14−2.32 (m, 6 H, CH_2, A+B), 2.89−3.41 (m, 12 H, CH_2, A+B), 4.25−4.40 (m, 3 H, CH, A+B), 5.09 (d, ^3J = 6.8 Hz, 3 H, NH, A+B), 6.52 (t, ^3J = 5.0 Hz, 3 H, NH, A+B), 7.19 (d, ^3J = 8.2 Hz, 4 H, C_6H_4), 7.29−7.84 (m,

39 H, C_6H_4, C_6H_3, PPh_2). – ^{13}C NMR ($CDCl_3$): δ = 8.23, 8.60 (d, ^2J = 1.5 Hz; 3.2 Hz, CH_3, A+B), 14.33 (dd, ^1J = 25.7 Hz, ^3J = 3.1 Hz, CH_2, A), 16.70 (d, ^1J = 30.4 Hz, CH_2, B), 21.99 (d, ^1J = 27.8 Hz, CH_2, A+B), 24.00 (CH_2, A+B), 28.26 [$C(CH_3)_3$, A+B], 39.20 (CH_2, A+B), 39.74 (d, ^2J = 14.4 Hz, CH_2, A+B), 55.64 (CH, A+B), 79.83 [$C(CH_3)_3$, A+B], 87.77, 90.55 (C≡C, A+B), 121.07, 124.02, 128.39–133.69 (m, 6 C, C_6H_4, C_6H_3, PPh_2, A+B), 133.95, 137.93, 155.12 (CON, A+B), 170.93 (CON, A+B). – ^{31}P NMR ($CDCl_3$): δ = 11.37 (d, $^2J_{trans}$ = 538 Hz), 14.85 (d, $^2J_{cis}$ = 234 Hz), 25.09 (d, $^2J_{trans}$ = 538 Hz), 30.15 (d, $^2J_{cis}$ = 234 Hz). – $C_{117}H_{150}Cl_6N_6O_9P_6Pd_3$ (2502.3): calcd. C 56.16, H 6.04, N 3.36; found C 56.51, H 5.95, N 3.34.

1,3,5-C_6H_3{C≡$CC_6H_4CH_2CH[NHCO_2C(CH_3)_3][CO_2(CH_2)_3PPh_2]Rh(Cp^*)(Cl)_2$}$_3$ (**16**): Yield 123 mg (97%), orange powder, m.p. 209°C (decomp.). – IR (KBr): $\tilde{\nu}$ = 3341 cm^{-1} m (NH), 2213 (C≡C), 1713, 1674 s (CON). – ^1H NMR ($CDCl_3$): δ = 1.29 (s, 18 H, CH_3), 1.31 (s, 15 H, CH_3), 1.42–1.58 (m, 6 H, CH_2), 2.47–3.19 (m, 18 H, CH_2), 4.29 (pq, ^3J = 6.7 Hz, CH), 5.13–5.37 (m, 3 H, NH), 6.24–6.46 (m, 3 H, NH), 7.18 (d, ^3J = 7.6 Hz, 6 H, C_6H_4), 7.32 (d, ^3J = 7.6 Hz, 6 H, C_6H_4), 7.38–7.52 (m, 18 H, PPh_2), 7.58 (s, 3 H, C_6H_3), 7.69–7.86 (m, 12 H, PPh_2). – ^{13}C NMR ($CDCl_3$): δ = 8.62 (Cp^*), 23.48 (CH_2), 26.74 (d, ^1J = 28.7 Hz, CH_2), 28.20 [$C(CH_3)_3$], 38.68 (CH_2), 39.86 (d, ^2J = 13.4 Hz, CH_2), 55.34 (CH), 79.57 [$C(CH_3)_3$], 87.51, 90.69 (C≡C), 98.69 (dd, J_{PC} = 6.7 Hz, J_{RhC} = 2.4 Hz, cp^*), 120.72, 124.11, 128.35 (dd, J_{PC} = 9.8 Hz, J_{RhC} = 3.9 Hz, PPh_2), 129.62, 130.89 (d, J_{PC} = 12.3 Hz, PPh_2), 131.53, 133.28 (d, J_{PC} = 9.6 Hz, PPh_2), 133.67, 133.92 (d, J_{PC} = 9.0 Hz, PPh_2), 138.38, 155.19 (CON,), 170.01 (CON). – ^{31}P NMR ($CDCl_3$): δ = 27.34 (d, J_{RhP} = 143 Hz). – $C_{129}H_{150}Cl_6N_6O_9P_3Rh_3 \times CH_2Cl_2$ (2627.9): calcd. C 59.42, H 5.83, N 3.19; found C 59.59, H 6.08, N 3.10.

X-ray-Structural Determination of **1**: $C_{47}H_{40}BF_4NO_2P_2Pt$, MW = 994.64, crystal size 0.15 × 0.15 × 0.1mm^3. The slightly yellow prism was covered with perfluoropolyether oil, mounted on a glass fiber and centered at 183(2) K. All reflections in the range 2 θ = 13.7–49.4° (index ranges $-33 < h < 33$, $-33 < k < 33$, $-10 < l < 17$) were measured by using a Siemens P4 diffractometer equipped with a CCD area detector. Hexagonal, space group $R3$, a = 28.708(5), b = 28.708(5), c = 14.458(3) Å, V = 10320(4) Å^3, Z = 9, d(calcd.) = 1.440 Mg/m^3, = 3.182 mm^{-1}, F(000) = 4446, independent reflections 6091 [R(int) = 0.0534], 5890 observed with $I > 4\,\sigma(I)$; at semiempirical absorption correction, max./min. transmission 0.972/0.698. The structure was solved by the heavy-atom method, and the non-hydrogen atoms were refined anisotropically. H atoms in calculated positions were included – the final refinement against F^2 using a riding model (SHELX93 programs). 523 variables, $R1$ = 0.0408, $wR2$ = 0.1015, largest residual peak: 2.624 e/Å^3 close to Pt.

Crystallographic data (excluding structure factors) for the structures reported in this paper have been deposited with the Cambridge Crystallographic Data Center as supplementary publication no. CCDC-102301. Copies of the data can be obtained free of charge on application to CCDC, 12 Union Road, Cambridge CB2 1EZ, UK [fax: (+44)1223-336-033; e-mail: deposit@ccdc.cam.ac.uk].

☆ Dedicated to Professor *Meinhart Zenk* on the occasion of his 65th birthday.

[1] Part 107: K. Sünkel, W. Hoffmüller, W. Beck, *Z. Naturforsch.*, in press.

[2] X-ray structure analysis of **1**.

[3] [3a] M. J. Burk, J. R. Lee, J. P. Martinez, *J. Am. Chem. Soc.* **1994**, *116*, 10847–10848 and literature cited therein. – [3b] A. Giannis, T. Kolter, *Angew. Chem.* **1993**, *105*, 1303–1326; *Angew. Chem. Int. Ed. Engl.* **1993**, *32*, 1244.

[4] [4a] R. M. Williams, J. A. Hendrix, *J. Org. Chem.* **1990**, *55*, 3723–3828. – [4b] D. Ben-Ishai, J. Altman, Z. Bernstein, N. Peled, *Tetrahedron* **1978**, *34*, 467–473. – [4c] S. Jaroch, T. Schwarz, W. Steglich, P. Zistler, *Angew. Chem.* **1993**, *105*, 1803–1805; *Angew. Chem. Int. Ed. Engl.* **1993**, *32*, 1771. – [4d] V. A. Burgess, C. J. Easton, M. P. Hay, P. J. Steel, *Aust. J. Chem.* **1988**, *41*, 701–710. – [4e] G. Apitz, M. Jäger, S. Jaroch, M. Kratzel, L. Schäffeler, W. Steglich, *Tetrahedron* **1993**, *49*, 8223–8232. – [4f] Th. Bretschneider, W. Miltz, P. Münster, W. Steglich, *Tetrahedron* **1988**, *44*, 5403–5414. – [4g] P. Münster, W. Steglich, *Synthesis* **1987**, 223–225.

[5] [5a] M. J. O'Donnell, R. L. Polt, *J. Org. Chem.* **1982**, *47*, 2663–2666. – [5b] U. Schöllkopf, U. Groth, C. Deng, *Angew. Chem.* **1981**, *93*, 793–795; *Angew. Chem. Int. Ed. Engl.* **1981**, *20*, 798. – [5c] S. Blank, D. Seebach, *Angew. Chem.* **1993**, *105*, 1780–1781; *Angew. Chem. Int. Ed. Engl.* **1993**, *32*, 1765.

[6] H. Lei, M. S. Stoakes, K. P. B. Herath, J. Lee, A. W. Schwabacher, *J. Org. Chem.* **1994**, *59*, 4206–4210.

[7] [7a] S. Rajagopalan, G. Radke, M. Evans, J. M. Tomich *Synth. Commun.* **1996**, *26*, 1431–1440. – [7b] S. A. Metwally, H. H. Coenen, G. Stöcklin, *Bull. Chem. Soc. Jpn.* **1987**, *60*, 4437–4440. – [7c] E. Morera, G. Ortar, *Synlett* **1997**, 1403–1405.

[8] [8a] G. T. Crisp, J. Gore, *Tetrahedron* **1997**, *53*, 1523–1544. – [8b] G. Jaouen, A. Vessières, I. S. Butler, *Acc. Chem. Res.* **1993**, *26*, 361–369. – [8c] A. Gorfti, M. Salmain, G. Jaouen, M. J. McGlinchey, A. Bennouna, A. Mousser, *Organometallics* **1996**, *15*, 142–151. – [8d] A. Varenne, A. Vessières, M. Salmain, S. Durand, P. Brossier, G. Jaouen, *Anal. Biochem.* **1996**, *242*, 172–179. – [8e] B. Kayser, K. Polborn, W. Steglich, W. Beck, *Chem. Ber.* **1997**, *130*, 171–177.

[9] [9a] M. Lange, K. Undheim, *Tetrahedron* **1998**, *54*, 5337–5344. – [9b] S. Rødbotten, T. Benneche, K. Undheim, *Acta Chem. Scand.* **1997**, *51*, 873–880 and references therein. – [9c] G. T. Crisp, Y.-L. Jiang, P. J. Pullman, Ch. De Savi, *Tetrahedron* **1997**, *53*, 17489–17500.

[10] [10a] A. de Meijere, F. E. Meyer, *Angew. Chem.* **1994**, *106*, 2473–2506; *Angew. Chem. Int. Ed. Engl.* **1994**, *33*, 2379. – [10b] R. F. Heck, *Org. React.* **1982**, *27*, 345–390.

[11] [11a] C. E. Castro, E. J. Gaughan, D. C. Owsley, *J. Org. Chem.* **1966**, *31*, 4071–4078. – [11b] K. Sonogashira, Y. Tohda, N. Hagihara, *Tetrahedron Lett.* **1975**, 4467–4470.

[12] [12a] B. Kayser, J. Altman, W. Beck, *Tetrahedron* **1997**, *53*, 2475–2484. – [12b] The synthesis of hexakis(*p*-ethynylphenylalanine)benzene will be reported elsewhere.

[13] A. H. Stokes, Y. Xu, H. Tamir, M. D. Gershon, PO. Butkerait, B. Kayser, J. Altman, W. Beck, K. Vrana, *Molecular Pharmacology*, submitted.

[14] [14a] G. R. Newhome, C. N. Moorefield, F. Vögtle, *Dendritic Molecules*, VCH Verlagsgesellschaft, Weinheim, **1996**. – [14b] M. T. Reetz, G. Lohmer, R. Schwickardi, *Angew. Chem.* **1997**, *109*, 1559–1562; *Angew. Chem. Int. Ed. Engl.* **1997**, *36*, 1526–1529. – [14c] W. T. S. Huck, B. Snellink-Ruël, F. C. J. M. van Veggel, D. N. Reinhoudt, *Organometallics* **1997**, *16*, 4287–4291.

[15] [15a] N. J. Long, *Angew. Chem.* **1995**, *107*, 37–56; *Angew. Chem. Int. Ed. Engl.* **1995**, *34*, 21. – [15b] S. R. Marder, *Inorganic Materials*, p. 136, Wiley Chichester, **1992**. – [15c] M. Sinclair, D. Moses, K. Akagi, A. J. Heeger, *Mater. Research Society Proceedings* **1988**, *109*, 205. – [15d] I. R. Whitall, M. G. Humphrey, S. Houbrechts, J. Maes, A. Persoons, S. Schmid, D. C. R. Hookless, *J. Organomet. Chem.* **1997**, *544*, 277–283. – [15e] R. J. Puddephatt, *Chem. Commun.* **1998**, 1055–1062. – [15f] J. R. Whittall, A. M. McDonagh, M. G. Humphrey, M. Samoc, *Adv. Organomet. Chem.* **1997**, *42*, 291–362.

[16] K. Severin, R. Bergs, W. Beck, *Angew. Chem.* **1998**, *110*, 1722–1743; *Angew. Chem. Int. Ed. Engl.* **1998**, *37*, 1634–1654.

[17] B. Olgemöller, L. Olgemöller, W. Beck, *Chem. Ber.* **1981**, *114*, 2971–2978; L. Olgemöller, Ph. D. Thesis, University of Munich, **1985**.

[18] W. Beck, M. Girnth, *Chem. Ber.* **1976**, *109*, 965–969.

[19] R. Krämer, K. Polborn, H. Wanjek, I. Zahn, W. Beck, *Chem. Ber.* **1990**, *123*, 767–778; D. Carmona, A. Mendozza, F. J. Lahoz, L. A. Oro, M. P. Lanata, E. San José, *J. Organomet. Chem.* **1990**, *396*, C17–C21.

[20] [20a] E. Ambach, U. Nagel W. Beck, *Chem. Ber.* **1982**, *116*, 659–668. – [20b] R. D. W. Kemmitt, S. Mason, J. Fawcett, D. R. Russell, *J. Chem. Soc., Dalton Trans.* **1992**, 1165–1176 –

[20c] A. Lombardi, O. Maglio, V. Pavone, B. Di Blasio, M. Saviano, F. Nastri, C. Pedoni, E. Benedetti, *Inorg. Chim. Acta* **1993**, *204*, 87−92.

[21] [21a] H. Dibowski, F. P. Schmidtchen, *Angew. Chem.* **1998**, *110*, 487−489; *Angew. Chem. Int. Ed. Engl.* **1998**, *37*, 476−478. − [21b] D. Osella, G. Dutto, C. Nervi, M. J. McGlinchey, A. Vessiéres, G. Jaouen, *J. Organomet. Chem.* **1997**, *533*, 97−102.

[22] [22a] M. I. Bruce, E. Horn, J. G. Matisons, M. R. Snow, *Aust. J. Chem.* **1984**, *37*, 1163−1170. − [22b] K. Sanogaslira, Y. Fujihusa, T. Yatake, N. Toyoshina, S. Takahaski, N. Hagihery, *J. Organomet. Chem.* **1978**, *145*, 101−108. − [22c] G. K. Anderson, *Comprehensive Organometallic Chemistry II* (E. W. Abel, F. G. A. Stone, Ed.) Pergamon **1995**, *9*, 490−494. − [22d] A. Grohmann, H. Schmidbaur, *ibid.* **1995**, *3*, 3−9.

[23] [23a] H. Eckert, C. Seidel, *Angew. Chem.* **1986**, *98*, 168−170; *Angew. Chem. Int. Ed. Engl.* **1986**, *25*, 159. − [23b] K. Takada, D. J. Diaz, H. D. Abruna, I. Cuadrado, C. Casado, B. Alonso, M. Moran, J. Losada, *J. Am. Chem. Soc.* **1997**, *119*, 10763−10773; A. D. Ryabov, *Angew. Chem.* **1991**, *103*, 945−955; *Angew. Chem. Int. Ed. Engl.* **1991**, *30*, 931.

[24] N. J. Long, A. J. Martin, F. F. de Biani, P. Zanello, *J. Chem. Soc., Dalton Trans.* **1998**, 2017−2021 and references therein; R. J. Puddephatt, *Chem. Commun.* **1998**, 1055−1062; M. Uno, P. H. Dixneuf, *Angew. Chem.* **1998**, *110*, 1822−1824; *Angew. Chem. Int. Ed. Engl.***1998**, *37*, 1714−1717; H. Fink, N. J. Long, A. J. Martin, G. Opromolla, A. J. P. White, D. J. Willliams, P. Zanello, *Organometallics* **1997**, *16*, 2646−2650; T. Weyland, C. Lapinte, G. Frapper, M. J. Calhorda, J.-F. Halet, L. Toupet, *ibid.* **1997**, *16*, 2024−2031; R. R. Tykwinski, P. J. Stang, *ibid.* **1994**, *13*, 3203−3208; M. S. Khan, D. J. Schwartz, N. A. Pasha, A. K. Kakkar, B. Lin, P. R. Raithby, J. Lewis, *Z. Anorg. Allg. Chem.* **1992**, *616*, 121−124; N. Ohshiro, F. Takei, K. Onitsuka, S. Takahashi, *Chem. Lett.* **1996**, 871−872; Th. J. J. Miller, H. J. Lindner, *Chem. Ber.* **1996**, *129*, 607−613.

[25] R. G. Ball, B. R. James, J. Trotter, D. W. Wang, *J. Chem. Soc., Chem. Commun.* **1979**, 460−461.

[26] M. I. Bruce, B. K. Nicholson, O. Bin Shawkataly, *Inorg. Synth.* **1989**, *26*, 324−328.

[27] [27a] G. W. Parshall, *Inorg. Synth.* **1970**, *12*, 27−28. − [27b] F. R. Hartley, *Organomet. Chem. Rev. Sect. A* **1970**, *6*, 119−137.

[28] [28a] W. P. Fehlhammer, W. A. Herrmann, K. Öfele (Ed. W. Brauer) *Handbuch d. Präp. Anorg. Chemie*, Enke Stuttgart, 3. Aufl. **1981**, *3*, 2015−2016. − [28b] W. Beck, K. v. Werner, *Chem. Ber.* **1971**, *104*, 2903. − [28c] P. M. Treichel, K. P. Wagner, W. J. Knebel, *Inorg. Chim. Acta* **1972**, *6*, 674−676.

[29] C. White, A. Yates, P. M. Maitlis, *Inorg. Synth.* **1992**, *29*, 228−234.

[30] [30a] D. A. Blinn, R. S. Button, V. Farazi, M. K. Neeb, C. L. Taplex, T. E. Trehearne, S. C. West, T. L. Kruger, B. N. Storhoff, *J. Organomet. Chem.* **1990**, *393*, 143−152. − [30b] M. Habib, H. Trujillo, C. A. Alexander, B. N. Storhoff, *Inorg. Chem.* **1985**, *24*, 2344−2349.

[I98182]

[*N*-Alkyl-(2-pyridyl)methanimine]copper(I) Complexes: Characterisation and Application as Catalysts for Atom-Transfer Polymerisation

David M. Haddleton*, David J. Duncalf, Dax Kukulj, Martin C. Crossman, Stuart G. Jackson, Stefan A. F. Bon, Andrew J. Clark, and Andrew J. Shooter

Department of Chemistry, University of Warwick,
Coventry, CV4 7AL, United Kingdom
Fax: (internat.) + 44-1203/524112
E-mail: msrgs@csv.warwick.ac.uk

Received July 3, 1998

Keywords: Atom-transfer polymerisation / Methyl methacrylate / Copper(I) / Schiff base

The synthesis and characterisation of a series of novel bis(imine)copper(I) complexes and their use in atom-transfer polymerisation of methyl methacrylate is described. Several *N*-alkyl-(2-pyridyl)methanimines (alkyl = *n*-butyl, isobutyl, *sec*-butyl, *n*-propyl) and *N*-(*n*-propyl)-1-(2-pyridyl)ethanimine as ligands have been fully characterised. Three bis[*N*-alkyl-(2-pyridyl)methanimine]copper(I) complexes, $[Cu\{(C_5H_4N)CH=N(iBu)\}_2][BF_4]$, $[Cu\{(C_5H_4N)C(CH_3)=N(nPr)\}_2][PF_6]$, and $[Cu\{(C_5H_4N)CH=N(sBu)\}_2][BF_4]$ have been structurally characterised; all having a distorted tetrahedral arrangement of co-ordinating nitrogen atoms surrounding the metal centre. All of the catalysts were found to be effective atom-transfer polymerisation catalysts for the polymerisation of MMA in hydrocarbon solution. However, it was discovered that the performance of the catalysts containing *n*-alkyl substituents was superior to those containing branched alkyl substituents. The presence of branching in the alkyl substituent results in a reduction of reaction rate and a corresponding broadening of the polydispersity index.

Introduction

Copper complexes containing chelating bis(imine) ligands are used increasingly as catalysts for a wide range of synthetic organic reactions.[1] Chiral ligands, in particular, are finding use in asymmetric organic catalysis,[2] such ligands being simply prepared from commercially available, and enantiomerically pure, primary amines. Atom-transfer addition, ATA, a technique used to effect organic transformation reactions, utilises transition-metal complexes[3] to promote carbon−carbon bond formation.[4] Transition-metal complexes able to function as halogen carriers with an available $n+1$ oxidation state, e.g. Cu^{I}/Cu^{II} are typical catalysts for ATA.

Recently, this chemistry has been extended and modified for use in polymerisation reactions. The groups of Matyjaszewski[5a][5b][5c][5d] and Sawamoto,[5e][5f][5g][5h] working independently from each other have reported the use of transition-metal-mediated polymerisation derived from the ATA reaction. It is believed that the mechanism of atom-transfer polymerisation depends upon the formation of a favourable equilibrium, shown in Scheme 1, where: R_n-X represents both the initiator and dormant polymer chain, X and X′ halogen atoms, L_m an unspecified, *m*, number of donor ligands and $R^{\bullet}$ represents both the initiating species and the propagating polymeric radical. The position of the equilibrium is pivotal to the control of the polymerisation reaction; easily oxidised complexes, i.e. catalysts having a too stable $n+1$ oxidation state, cause a movement to the right of the equilibria, ultimately resulting in a relatively high concentration of free radicals. At high free-radical concentration termination occurs by radical−radical combination and/or disproportionation, which results in a lack of control over the polymerisation and results in polymer having an increased polydispersity index, PDI, and ultimately loss of the linear relationship between the number-average molecular mass, M_n, and the ratio of monomer to initiator which is observed for *living polymerisation*. Conversely, if the metal complex is unable to increase its oxidation number then the equilibria will lie far to the left and the rate of polymerisation reaction will be too slow to lead to useful products on a sensible time-scale. Propagation of the polymerisation takes place from, an as yet, undetermined active centre. The active centre is either a carbon-centred free radical or a metal-complexed radical, or insertion at the metal centre takes place. At present a free-radical process is preferred by most authors but the exact mechanism is proving very difficult to determine unequivocally.

Scheme 1

$$R_n-X + [L_mCu(I)X'] \rightleftharpoons [R_n\ldots X\ldots CuL_mX'] \rightleftharpoons R_n^{\bullet} + [XCuL_mX']$$

The ligand choice is considered crucial in controlling the position of the equilibrium either by acting as electron donors, or acceptors, to the metal centre. In systems where copper(I) halides are used the ligand also serves to solubilise the particularly insoluble copper salt, and perhaps more importantly, the low-lying LUMO π* orbital, present in the conjugated π system (N=C-C=N) of the ligand, is able to accept electron density from the metal centre, which is

 © WILEY-VCH Verlag GmbH, D-69451 Weinheim, 1998 1434−1948/98/1111−1799 $ 17.50+.50/0

thought to be central to the action of these particular atom-transfer polymerisation catalysts.

Recently, we have reported on the use of a series of *N*-alkyl-(2-pyridyl)methanimine ligands which, when complexed with copper halides, give rise to highly effective atom-transfer polymerisation catalysts.[6] We have been interested in examining the structure of atom-transfer catalysts with a view to further understanding the mechanism of the reaction. Ultimately, we believe this to help in the optimisation of the ligands/catalysts for each monomer system thus giving greater control over this rapidly emerging polymerisation chemistry. The mode of co-ordination of this type of Schiff base ligand to metal centres in both the solution and solid state has been reported to vary depending upon many variables. Indeed in the case of copper(I) complexes, a simple change in the counter-ion can dramatically alter the nature of the predominant species[7]. Thus, structural determinations may play an important role in elucidating the mechanism of atom-transfer polymerisation. The results presented in this paper show how increasing the steric hindrance in the alkyl group of the imine ligand affects the kinetics of the polymerisation and the dramatic effects these apparently small changes in ligand have on the molecular mass control and molar mass distribution of the resulting poly(methyl methacrylate). Three of the catalysts used in this work have been fully characterised by single-crystal X-ray diffraction. Similar "*living*" polymerisation systems mediated by transition-metal complexes have been reported by a range of other research groups[8].

Results and Discussion

The *N*-alkyl-(2-pyridyl)methanimine ligands, **L1**−**L5** (see Scheme 2), were prepared from the condensation of 2-pyridinecarboxaldehyde (or 2-acetylpyridine in the case of **L5**) with the respective primary amine. Figure 1(a) shows the ^{1}H-NMR spectrum of **L1**, and Figure 1(b) shows the spectrum of the complex between **L1** and CuBr, **C1** (see Scheme 3)[9]. The assignments were made using NOE difference experiments by irradiating at H^6 so as to determine H^4 long−range COSY and ^{1}H-^{13}C heteronuclear correlation. The remaining ring protons were assigned by further decoupling experiments. In solution the ligand can exist in the *trans* conformation; however, on complexation to copper(I) we observe changes in the spectrum associated with the ligand adopting a *cis* conformation. The signal of the imine proton H^6 shifts approximately 0.6 ppm downfield on complexation. Figures 2(a) and 2(b) show the ^{13}C{^{1}H}-NMR spectrum of **L1** and **C1**, respectively. The assignments were made using heteronuclear shift-correlated 2D-NMR experiments. The pair C^5/C^1 changes its relative position whilst C^6 remains at highest field. These proton and carbon ring assignments are applicable to all ligands used in this study.

Scheme 2

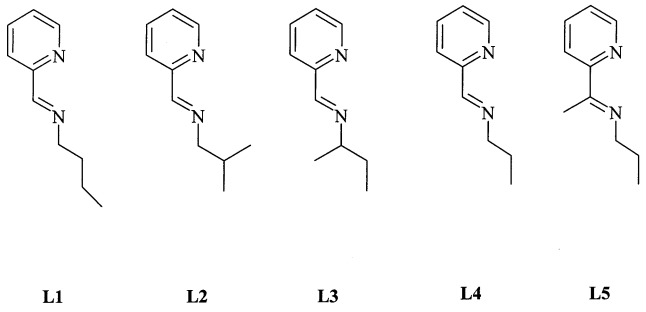

Figure 1. ^{1}H-NMR spectrum of (a) the free ligand **L1** and (b) the complex **C1** in [D_6]DMSO; (c) peak assignments

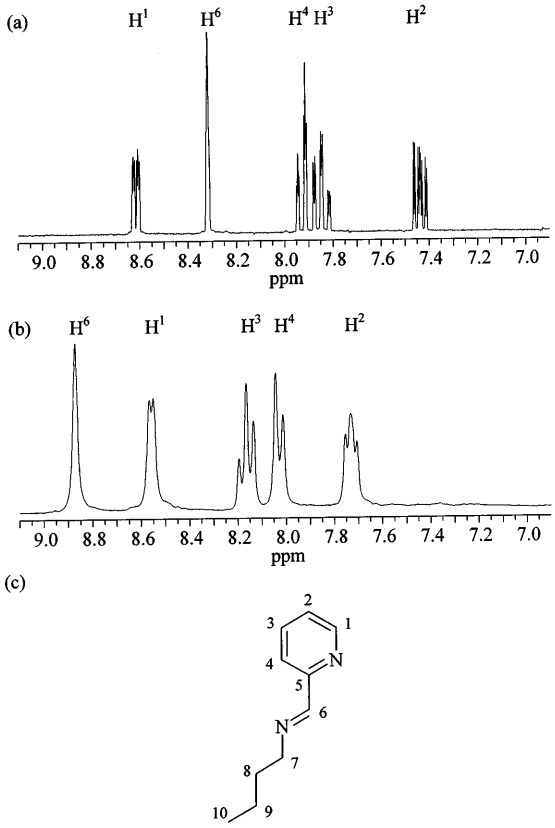

Scheme 3

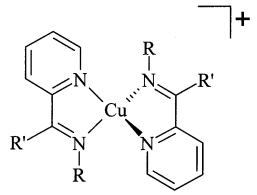

C1: R = *n*Bu, R′ = H; **C2**: *i*Bu, R′ = H; **C3**: R = *s*Bu, R′ = H; **C4**: R = *i*Pr, R′ = H; **C5**: R = *n*Pr; R′ = Me.

Polymerisation of Methyl Methacrylate Using C1 to C5 as Atom-Transfer Polymerisation Catalysts

Methyl methacrylate was polymerised in xylene solution at 90°C using ethyl 2-bromoisobutyrate as initiator in the

Figure 2. $^{13}C\{^1H\}$-NMR spectrum of (a) the free ligand **L1** and (b) the complex **C1** in [D_6]DMSO; the assignments were made using heteronuclear shift-correlated 2D-NMR experiments; for peak assignments see Figure 1(c)

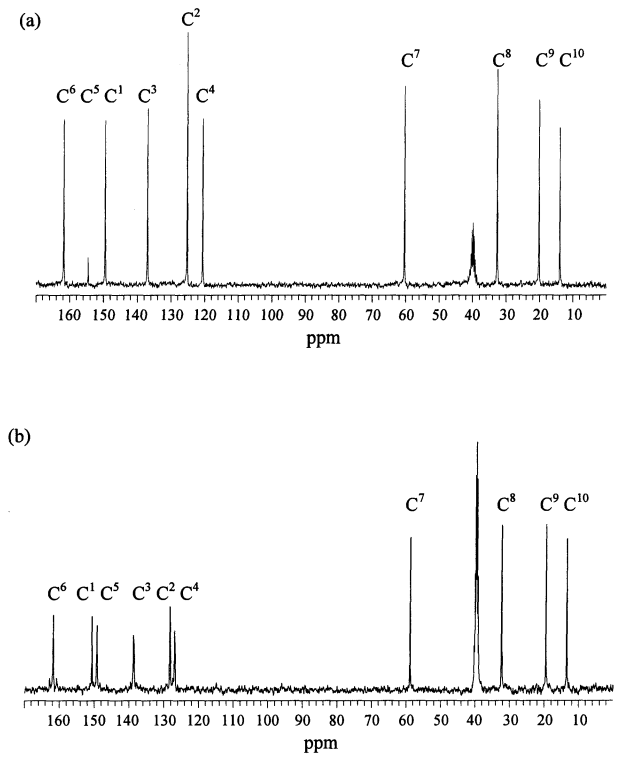

The effectiveness of the catalysts **C1**−**C5** for promoting controlled atom-transfer polymerisation was determined in three ways: (1) the relationship between the number-average molecular weight (M_n) and conversion to polymer. Living polymerisation processes lead to a linear increase in M_n with conversion.[6b] (2) The polydispersity index, PDI, of the polymer, free-radical polymerisation of methyl methacrylate has a PDI larger than 1.5. (3) The appearance of a first-order rate plot. For a living polymerisation a plot of ln $[M]_0/[M]$ against time gives a linear plot with the gradient equal to the pseudo first-order rate coefficient, k^{app}, which gives an indication of the rate of reaction. k^{app} is defined by Equation 1, where [M] is the monomer concentration, $[M]_0$ is the initial monomer concentration, k_p is the propagation rate coefficient, $[R^\bullet]$ is the concentration of active species, and t is time.

$$\ln [M]_0/[M] = k_p[R^\bullet]t = k^{app}t \quad (1)$$

Figure 3 shows the dependence of the number-average molecular weight (M_n) on polymer conversion for the catalysts **C1**−**C5**. In all cases, M_n increases approximately linearly with conversion, as is expected for a *living* polymerisation. The actual values of M_n are slightly higher than the theoretical line, which suggests that the initiator efficiency is less than unity i.e. the initiator is involved in secondary, as yet undetermined reactions such as coupling of carbon-centred radicals in the initial stages of the reaction. The presence of **C1**−**C5** catalysts (see Scheme 3). The catalysts were prepared in situ by the addition of ligands **L1**−**L5**, respectively, to CuBr in the xylene reaction solution. Polymer conversion and molecular weight data are listed in Table 1.

Table 1. Conversion and molecular-weight data for polymerisations using **C1**−**C5**

Catalyst	Time [min]	Conversion	M_n[a]	M_w[b]	PDI[c]	$M_{n,theo}$[d]	Initiator[e] efficiency	k^{app} [s^{-1}][f]
C1	60	0.195	2250	5000	2.22	1950	0.87	$1.00 \cdot 10^{-4}$
	120	0.536	6740	10000	1.49	5370	0.80	
	180	0.629	8200	12300	1.5	6300	0.77	
	240	0.782	10400	13800	1.33	7830	0.75	
C2	60	0.055	1250	1950	1.56	550	0.44	$1.15 \cdot 10^{-5}$
	120	0.061	1520	2450	1.61	610	0.40	
	180	0.118	1950	2930	1.5	1180	0.60	
	240	0.157	2100	3300	1.57	1570	0.75	
C3	60	0.007	530	689	1.3	70	0.13	$3.67 \cdot 10^{-6}$
	120	0.024	590	714	1.21	240	0.41	
	180	0.043	690	876	1.27	430	0.62	
	240	0.051	890	1230	1.38	510	0.57	
C4	60	0.19	3390	4510	1.33	1900	0.56	$7.15 \cdot 10^{-5}$
	120	0.35	4900	6320	1.29	3500	0.71	
	180	0.54	7100	8870	1.25	5400	0.76	
	240	0.66	9200	10900	1.19	6610	0.72	
C5	60	0.18	3290	4570	1.39	1800	0.55	$7.85 \cdot 10^{-5}$
	120	0.43	5340	7580	1.42	4300	0.81	
	180	0.58	6030	9280	1.54	5810	0.96	
	240	0.68	6850	10900	1.59	6810	0.99	

[a] Number-average molecular weight. − [b] Weight-average molecular weight. − [c] Polydispersity index = M_w/M_n. − [d] $M_{n,theo}$ = Conversion · [Monomer]/[Initiator]. − [e] Initiator efficiency = $M_{n,theo}/M_n$. − [f] Pseudo first-order rate coefficient determined from the slope of the line of best fit in Figure 4.

PDIs (Table 1) are narrower for polymer produced using catalysts **C1**, **C3**, and **C4**, than catalysts **C2** and **C5**, which are quite broad for a *living* polymerisation (> 1.5). In general the PDI becomes narrower during the course of the reaction.

Figure 3. Dependence of the number-average molecular weight, M_n, on conversion for polymerisations using catalysts **C1**−**C5**

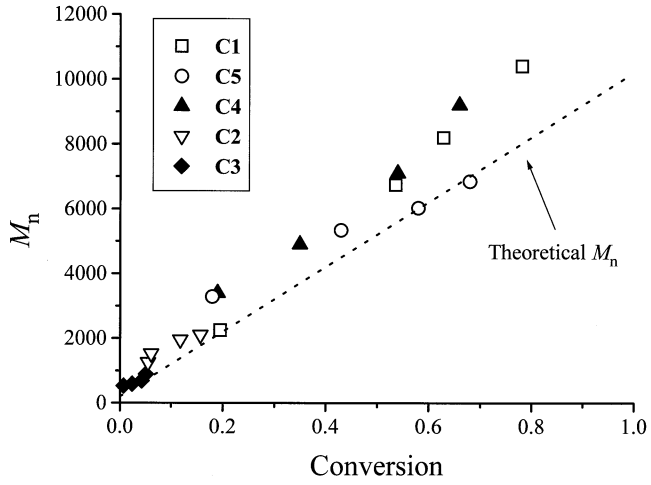

The first-order rate plots are shown in Figure 4. The lines through the data represent the best fit and correspond to the pseudo first-order rate coefficient, k^{app}. These plots are characteristic of *living* polymerisation;[6b] in all cases the plots are linear, indicating that the number of active species is constant and effects from termination of growing polymer chains by combination/disproportionation or chain transfer are not significant. It is immediately obvious, from Figure 4 and Table 1, that the catalysts **C2** and **C3** give a significantly lower rate of polymerisation (approximately one order of magnitude) than when **C1**, **C4**, and **C5** are used as catalysts . Thus, the catalysts using branched substituents at either the α or β positions in the ligand give significantly lower rates of polymerisation.

Figure 4. First-order log plots for polymerisations using catalysts **C1**−**C5**

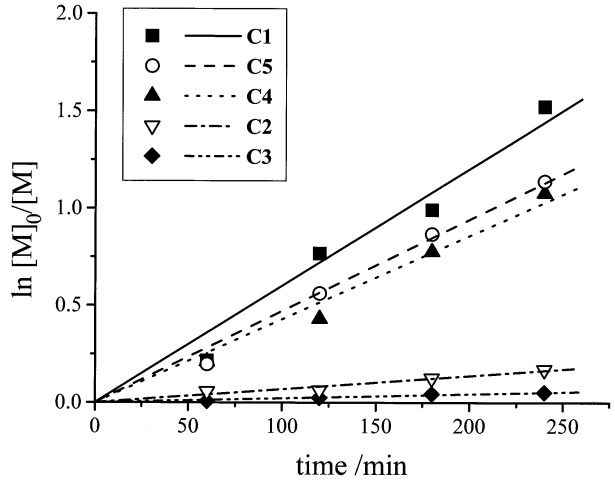

Overall, **C1** and **C4** show the best performance as atom-transfer polymerisation catalysts, giving both narrow PDI polymer and acceptable rates of reaction. Catalyst **C3** gives reasonable PDI but has a very low rate of reaction, **C5** gives good rate but broad PDI and **C2** is the least effective catalyst in this series, yielding both a low rate of reaction and broad PDI.

Single-Crystal X-ray Structural Study of Copper Complexes with L2, L3, and L5

X-ray structural studies were carried out for the compounds $Cu[BF_4]\cdot(\mathbf{L2})_2$, $Cu[BF_4]\cdot(\mathbf{L3})_2$, and $Cu[PF_6]\cdot(\mathbf{L5})_2$ which were isolated as crystalline salts from slowly cooled (5°C) solutions in methanol. Compounds formed from the reaction of $Cu(CH_3CN)_4[BF_4]$ with the ligands **L1** and **L4**, however, could not be isolated as crystals of suitable quality for X-ray analysis.

The compounds $Cu[BF_4]\cdot(\mathbf{L2})_2$, $Cu[BF_4]\cdot(\mathbf{L3})_2$, and $Cu[PF_6]\cdot(\mathbf{L5})_2$ all have the same basic distorted tetrahedral arrangement of co-ordinating nitrogen atoms which sur-

Figure 5. The crystal structure of $Cu[BF_4]\cdot(\mathbf{L2})_2$ (BF_4 counter ion not shown for clarity)

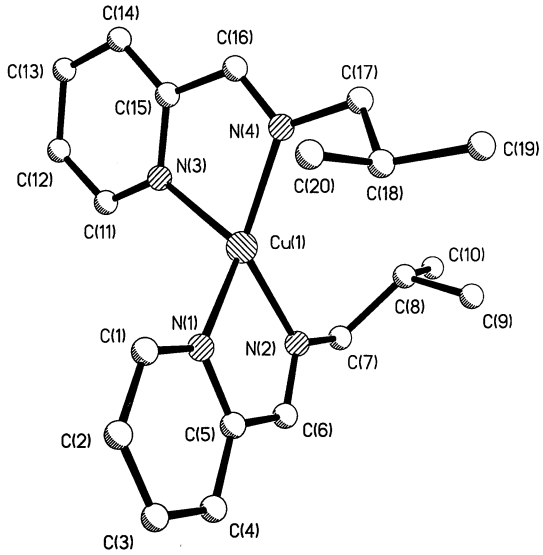

Figure 6. The crystal structure of $Cu[BF_4]\cdot(\mathbf{L3})_2$ (BF_4 counter ion not shown for clarity)

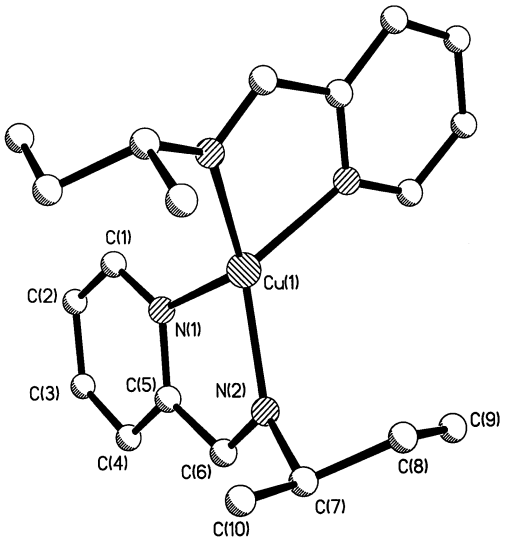

Figure 7. The crystal structure of $Cu[PF_6]\cdot(\mathbf{L5})_2$ (PF_6 counter ion not shown for clarity)

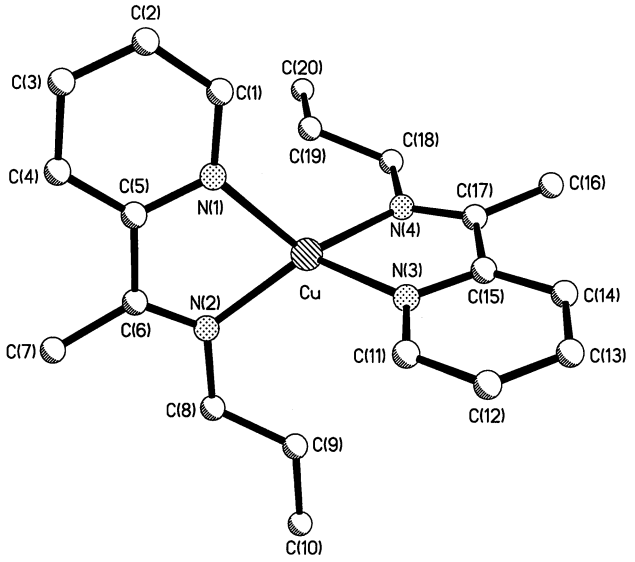

round the metal centre. Table 2 compares angles and average bond lengths to other similar published structures. The interligand dihedral angle between the mean planes defined by the central copper ion and each pair of chelating nitrogen atoms is 86.8° for $Cu[BF_4]\cdot(\mathbf{L2})_2$, 86.5° for $Cu[BF_4]\cdot(\mathbf{L3})_2$, and 85.3° for $Cu[PF_6]\cdot(\mathbf{L5})_2$ these values fall between 68° for the tetramethylbipyridine complex (entry 8) and 89.7° for the *N*-(α-methylbenzyl)-(2-pyridyl)methanimine complex (entry 4). The Cu−N bond lengths for $Cu[BF_4]\cdot(\mathbf{L2})_2$ are in the range of Cu(1)−N(1) = 2.080(3) Å, Cu(1)−N(2) = 2.005(2) Å, Cu(1)−N(3) = 2.047(3) Å, and Cu(1)−N(4) = 2.013(3) Å, for $Cu[BF_4]\cdot(\mathbf{L3})_2$ the Cu−N bond lengths are similar, with Cu(1)−N(1) = 2.092(2) Å and Cu(1)−N(2) = 2.008(2) Å. The Cu−N distances for $Cu[PF_6]\cdot(\mathbf{L5})_2$, tend to be, in most cases, somewhat shorter than those seen for $Cu[BF_4]\cdot(\mathbf{L2})_2$ and $Cu[BF_4]\cdot(\mathbf{L3})_2$, with Cu−N(1) = 2.028(2) Å, Cu−N(2) = 2.011(3) Å, Cu−N(3) = 2.034(3) Å, and Cu−N(4) = 2.001(2) Å. From Table 2 it can be seen that the average Cu−N bond lengths for $Cu[BF_4]\cdot(\mathbf{L2})_2$ and $Cu[BF_4]\cdot(\mathbf{L3})_2$ lie within the values measured for other $[CuL_2]^+$-type complexes, the average Cu−N distance for $Cu[PF_6]\cdot(\mathbf{L5})_2$ falling slightly below the other measured values. The N−Cu−N angles for $Cu[BF_4]\cdot(\mathbf{L2})_2$, $Cu[BF_4]\cdot(\mathbf{L3})_2$, and $Cu[PF_6]\cdot(\mathbf{L5})_2$ are similar and differ by only 0.37° at most, these values being comfortably within the estimated standard deviations.

Conclusion

A series of *N*-alkyl-(2-pyridyl)methanimines have been fully characterised. The bis[*N*-alkyl-(2-pyridyl)methanimine]copper(I) complexes characterised exhibit a distorted tetrahedral arrangement of co-ordinating nitrogen atoms surrounding the metal centre in the solid state. All of the catalysts tested were found to polymerise MMA effectively in hydrocarbon solution by an atom-transfer polymerisation process. Catalysts which contain *n*-alkyl substituents are more efficacious than those containing branched alkyl substituents in the imine group. The presence of branching in the alkyl substituent results in a loss of control over the polymerisation manifested by a slowing of the reaction rate and a broadening of the polydispersity index. The cause of these efffects of branching at the α-carbon atom of the imine on the final polymer properties is currently not known and is under further investigation in our laboratory.

We wish to thank the *EPSRC* (GR/K90364, MCC, DK; GR/L10314, DJD, SAFB; AMH, AJS studentships) for funding and *Courtaulds and Zeneca Specialties* for support of this work. We also thank Dr. *Adam Clarke* for help with the NMR analysis.

Table 2. Comparison of average bond-length and -angle data for $[Cu^I(L)_2]^+$ complexes

Ligand	Counter ion	C−$N_{acyclic}$	C−N_{cyclic}	C−C bond length [Å]	Cu−N	N−Cu−N angle [°]	Dihedral angle [°]	Ref.
L2	BF_4^-	1.277(4)	1.357(4)	1.457(5)	2.009	81.20(10)	86.8	This
		1.278(4)	1.344(4)	1.460(5)	2.064	80.97(10)		work
L3	BF_4^-	1.273(3)	1.654(3)	1.463(3)	2.08(2)	81.12(8)	86.2	This
					2.092(2)			work
L5	PF_6^-	1.279(4)	1.351(4)	1.479(5)	2.006	80.86(10)	85.3	This
		1.280(4)	1.353(4)	1.489(4)	2.031	80.64(11)		work
N-(α-methylbenzyl)-(2-pyridyl)methanimine[a][b]	BF_4^-	1.282	1.341	1.457	2.040	81.8	89.7	[10]
		1.273	1.370	1.456	2.030	82.3	85.1	
N-(*tert*-Butyl)-(2-pyridyl)methanimine	BF_4^-	1.270(4)	1.349(4)	1.467(5)	2.035	81.89(10)	81.9	[11]
1,4-Di-(*tert*-butyl)-1,4-diaza-1,3-butadiene	Br^-	1.263(4)	1.352(4)	1.470(4)	2.035	81.84(10)		
2,2′-Bipyridine	ClO_4^-	1.268(7)	1.290(7) [c]	1.453(8)	2.025(4)	82.2(2)	89.5	[11]
4,4′,6,6′-Tetramethyl-2,2′-bipyridine[b]	Cl^-	1.325(14)	1.385(15)	1.440(15)	2.021(11)	81.5(4)	75.2	[12]
1,10-Phenanthroline[b]	$CuBr_2^-$	1.347	1.360	1.488	2.040	81.35	68	[13]
2,9-Dimethyl-1,10-phenanthroline[b]	NO_3^-	1.366	1.352	1.428	2.039	82.2	76.8	[14]
		1.360	1.361	1.450	2.063	83.4	85.7	[15]

[a] There are two molecules in the asymmetric unit. − [b] Lengths are averaged for cyclic C−N (no estimated standard deviations for averaged data). − [c] Second acyclic bond.

Experimental Section

General Remarks: The reagents 2-pyridinecarboxaldehyde (Avocado, 99%), 2-acetylpyridine (Avocado, 98%), *n*-butylamine (Acros, 99.5%), isobutylamine (Avocado, 99%), *sec*-butylamine (Avocado, 99%), *n*-propylamine (Avocado, 99%), ethyl 2-bromoisobutyrate (Aldrich, 98%), xylene (Fisons, 99.8%), diethyl ether (BDH, 98%), and magnesium sulfate (Philip Harris) were used as received. Copper(I) bromide (Aldrich, 98%) was purified according to the method of Keller and Wycoff[10]. Methyl methacrylate (Aldrich, 99%) was purified by passing through a column of activated basic alumina to remove the inhibitor 4-methoxy phenol. All manipulations were performed using standard Schlenk line and syringe techniques under nitrogen.

NMR spectra were recorded using a Bruker WH 400 spectrometer. X-ray crystallographic data was collected with a Siemens R3m diffractometer.

Polymer conversions were determined by gravimetry and molecular-weight distributions were measured using size-exclusion chromatography (SEC), with a system equipped with a guard column, one 30-cm mixed E column (Polymer Laboratories) and a differential refractive-index detector, using tetrahydrofuran at 1 ml min^{-1} as the eluent. Poly(methyl methacrylate) standards in the range ($6 \cdot 10^4$ to 200 g mol^{-1}, Polymer laboratories) were used to calibrate the SEC.

N-Alkyl-(2-pyridyl)methanimine Ligands **L1**−**L4**: A solution of 2-pyridinecarboxaldehyde (15 g, 0.140 mol) in 100 ml of diethyl ether was placed into a 250-ml flask under dry nitrogen together with 2−3 g of anhydrous $MgSO_4$. The appropriate amount of amine was added dropwise to this solution. (**L1** nBuNH$_2$, **L2** iBuNH$_2$, **L3** sBuNH$_2$: 10.22 g, 0.140 mol; **L4** nPrNH$_2$: 8.26 g, 0.140 mol), with gentle cooling of the flask with iced water. After the addition of amine was complete, the reaction was stirred for ca. 3 h, after which time the solvent was removed by rotary evaporation and the residual oil further purified by vacuum distillation (**L1**, **L2**, **L3**, **L4**). The products were isolated as pale yellow liquids, yields were typically 94%.

L1: B.p. 105−106°C at 1.2 Torr. − IR: $\tilde{\nu}$ = 1649 cm^{-1} (C=N). − ^{1}H NMR (250 MHz, 298 K, $CDCl_3$): δ = 8.50 (d, J = 4.92 Hz, 1 H), 8.26 (s, 1 H), 7.86 (d, J = 7.72 Hz, 1H), 7.57 (t, J = 8.08 Hz, 1 H), 7.14 (m, J = 6.32 Hz, 1 H), 3.17 (t, J = 7.00 Hz, 2 H), 1.50 (quint, J = 7.00 Hz, 2 H), 1.13 (sext, J = 7.36 Hz, 2 H), 0.72 (t, J = 7.36 Hz, 3 H). −^{13}C{^{1}H} NMR (250 MHz, 298 K, [D$_6$]DMSO): δ = 161.57, 154.62, 149.29, 136.39, 124.47, 121.07, 61.15, 32.70, 20.34, 13.79. − MS (+EI); m/z: 163 [M$^+$].

L2: B.p. 179°C at 5.0 Torr. − IR: $\tilde{\nu}$ = 1636 cm^{-1} (C=N). − ^{1}H NMR (250 MHz, 298 K $CDCl_3$): δ = 8.53 (d, J = 4.53 Hz, 1 H), 8.25 (s, 1 H), 7.90 (d, J = 7.72 Hz, 1 H), 7.61 (t, J = 7.68 Hz, 1 H), 7.18 (m, J = 4.92 Hz, 1 H), 3.39 (d, J = 6.32 Hz, 2 H), 1.95 (sept, J = 6.68 Hz, 1 H), 0.87 (d, J = 6.68 Hz, 6 H). − ^{13}C{^{1}H} NMR (250 MHz, 298 K, $CDCl_3$): δ = 159.51, 154.56, 149.13, 136.22, 124.28, 121.13, 67.84, 30.30, 21.95. − MS (+EI): m/z: 163 [M$^+$].

L3: B.p. 74°C at 5.0 Torr. − IR: $\tilde{\nu}$ = 1630 cm^{-1} (C=N). − ^{1}H NMR (250 MHz, 298 K, $CDCl_3$), δ = 8.50 (d, J = 4.56 Hz, 1 H), 8.24 (s, 1 H), 7.86 (d, J = 7.68 Hz, 1 H), 7.57 (t, J = 7.36 Hz, 1H), 7.14 (dd, J = 4.92, 6.32 Hz, 1 H), 3.17 (sext, J = 6.32 Hz, 1 H), 1.50 (m, J = 7.72 Hz, 2H), 1.13 (d, J = 6.28 Hz, 3 H), 0.72 (t, J = 7.36 Hz, 3 H). −^{13}C{^{1}H} NMR (250 MHz, 298 K, $CDCl_3$): δ = 161.60, 154.49, 149.16, 136.29, 124.38, 120.96, 69.36, 29.27, 22.50.10.90. − MS (+EI); m/z: 163 [M$^+$].

L4: B.p. 50° at 0.2 Torr. − IR: $\tilde{\nu}$ = 1650 cm^{-1} (C=N). − ^{1}H NMR (250 MHz, 298 K, $CDCl_3$): δ = 8.44 (d, J = 4.24 Hz, 1 H), 8.20 (s, 1 H), 7.80 (d, J = 7.72 Hz, 1 H), 7.57 (t, J = 7.72 Hz, 1 H), 7.10 (t, J = 4.92 Hz, 1 H), 3.45 (t, J = 7.00 Hz, 2 H), 1.56 (sext, J = 7.00 Hz, 2 H), 0.77 (t, J = 7.36 Hz, 3 H). − ^{13}C{^{1}H} NMR (250 MHz, 298 K, $CDCl_3$): δ = 161.53, 154.50, 149.21, 136.29, 124.37, 120.97, 63.11, 23.58,11.65. − MS (+EI); m/z: 149 [M$^+$ + 1], 133 [M$^+$ − Me].

N-(n-Propyl)-1-(2-pyridyl)ethanimine (**L5**): A solution of 2-acetylpyridine (10 g, 0.0825 mol) in 60 ml of diethyl ether was placed in a 250-ml flask under dry nitrogen, together with 2−3 g of $MgSO_4$. The flask was cooled gently in iced water whilst *n*-propylamine (8 ml, 0.0973 mol) was added dropwise with stirring. After addition of the amine, the reaction was allowed to warm up to room temperature and the solution stirred overnight. After this time, the solvent was removed by rotary evaporation and the residual oil purified further by vacuum distillation. − B.p. 60°C at 0.4 Torr. − IR: $\tilde{\nu}$ = 1639 cm^{-1} (C=N). − ^{1}H NMR (250 MHz, 298 K, [D$_6$]DMSO): δ = 8.64 (d, J = 4.88 Hz, 1 H), 8.00 (d, J = 4.88 Hz, 1 H), 7.59 (m, J = 8.28, 7.33 Hz, 1 H), 7.16 (m, J = 7.33, 8.23 Hz, 1 H), 3.40 (t, J = 7.03 Hz, 2 H), 2.27 (s, 2 H), 1.70 (m, J = 7.33, 7.03 Hz, 2 H), 0.94 (t, J = 7.33 Hz, 2 H). − ^{13}C{^{1}H} NMR (250 MHz, 298°C, $CDCl_3$): δ = 166.51, 158.32, 148.48, 136.68, 124.28, 121.10, 54.58, 24.39,12.52, 14.21. − MS (+EI); m/z: 163 [M$^+$ + 1], 106 [M$^+$ − Et].

Bis[N-(isobutyl)-(2-pyridyl)methanimine]copper(I) Tetrafluoroborate (Cu[BF$_4$]·(**L2**)$_2$; [Cu{(C$_5$H$_4$N)CH=N(iBu)}$_2$][BF$_4$]): To a slurry of [Cu(CH$_3$CN)$_4$][BF$_4$][9b] (1.0 g, 3.22 mmol) in degassed methanol (30 ml) was added **L2** (1.008 g, 6.22 mmol) under nitrogen. The solution was stirred at room temperature overnight, filtered, and concentrated to ca. 10 ml. Slow cooling to 5°C resulted in the formation of red crystalline Cu[BF$_4$]·(**L2**)$_2$ (75%). − IR: $\tilde{\nu}$ = 1622 cm^{-1} [ν(C=N)]. − ^{1}H NMR (250 MHz, 298 K $CDCl_3$): δ = 8.63 (s, 1 H), 8.39 (d, 1 H), 8.05 (t, 1 H), 7.92 (d, 1 H), 7.61 (m, 1 H), 3.63 (d, 2 H), 2.00 (m, 1 H), 0.87 (d, 6 H). − ^{13}C{^{1}H} NMR (250 MHz, 298 K, $CDCl_3$) δ = 161.32, 150.66, 149.28, 138.93, 128.71, 127.42, 67.62, 30.20, 20.28. − MS (+EI) m/z : 387 [M$^+$], 225 [M$^+$ − **L2**].

Bis[N-sec-butyl)-(2-pyridyl)methanimine]copper(I) Tetrafluoroborate (Cu[BF$_4$]·(**L3**)$_2$; [Cu{(C$_5$H$_4$N)CH=N(sBu)}$_2$][BF$_4$]): An identical procedure to that used for Cu[BF$_4$]·(**L2**)$_2$, using **L3**, was followed yielding red crystals of Cu[BF$_4$]·(**L3**)$_2$ (70%). − IR: $\tilde{\nu}$ = 1620 cm^{-1} [ν(C=N)]. − ^{1}H NMR (250 MHz, 298 K, $CDCl_3$): δ = 8.72 (s, 1 H), 8.30 (d, 1 H), 7.96 (m, 2 H), 7.54 (m, 1 H), 3.71 (m, 1 H), 1.44 (br., 2 H), 1.13 (br., 3 H), 0.77 (t, 3 H). −^{13}C{^{1}H} NMR (250 MHz, 298 K, $CDCl_3$): δ = 159.68, 150.67, 148.39, 138.41, 127.79, 126.91, 66.65, 30.81, 22.50, 10.83. − MS (+EI); m/z: 387 [M$^+$], 225 [M$^+$ − **L3**].

Bis[N-(n-propyl)-1-(2-pyridyl)ethanimine}]copper(I) Hexafluorophosphate (Cu[PF$_6$]·(**L5**)$_2$; [Cu{(C$_5$H$_4$N)C(CH$_3$)=N(nPr)}$_2$]-[PF$_6$]): To a slurry of [Cu(CH$_3$CN)$_4$][PF$_6$][9b] (1.5 g, 4.839 mmol) in degassed methanol (40 ml) was added **L5** (1.568 g, 9.678 mmol) under nitrogen. The resulting red solution was stirred at room temperature overnight, filtered and concentrated to ca. 15 ml. Slow cooling to 5°C resulted in the formation of red crystalline Cu[PF$_6$]·(**L5**)$_2$ (65%). − IR: $\tilde{\nu}$ = 1591 cm^{-1} [ν(C=N)]. − ^{1}H NMR (250 MHz, 298 K, $CDCl_3$): δ = 8.37 (s, 1 H), 8.00 (br., 2 H), 7.55 (m, 1 H), 3.55 (br., 2 H), 2.42 (s, 3 H), 1.50 (m, 2 H), 0.74 (m, 3 H). − ^{13}C{^{1}H} NMR (250 MHz, 298 K, $CDCl_3$): δ = 164.5, 151.63, 147.60,137.41, 126.69, 123.59, 54.34, 23.34, 23.66, 14.26, 10.94. − MS (+EI); m/z: 387 [M$^+$], 225 [M$^+$ − **L5**].

Table 3. Summarized crystallographic data

(a) Crystal parameters	$Cu[BF_4]\cdot(\mathbf{L2})_2$	$Cu[BF_4]\cdot(\mathbf{L3})_2$	$Cu[PF_6]\cdot(\mathbf{L5})_2$
Formula	$C_{20}H_{28}BCuF_4N_4$	$C_{20}H_{28}BCuF_4N_4$	$C_{20}H_{28}PCuF_6N_4$
M	474.81	474.81	532.97
Crystal system	Monoclinic	Monoclinic	Monoclinic
spyace group	$P2_1/c$	$P2/n$	$P2_1/c$
a [Å]	8.850(2)	11.8712(6)	16.600(3)
b [Å]	23.609(5)	7.5742(4)	8.3920(2)
c [Å]	11.889(2)	12.4059(6)	17.300(4)
β [°]	107.02(3)	90.1050(10)	111.20(3)
V [Å^3]	2375.3(8)	1115.47(10)	2388.3(8)
Z	4	2	4
Crystal dimensions [mm]	0.4 × 0.30 × 0.20	0.50 × 0.40 × 0.30	0.30 × 0.20 × 0.20
Colour	Red	Red	Red
D_c [g·cm^{-3}]	1.328	1.414	1.482
μ(Mo-K_α) [mm^{-1}]	0.963	1.025	1.043
T [K]	200(2)	200(2)	200(2)
(b) Data collection[a]			
Data collected h	−9 to 11	−15 to 13	−21 to 21
(index ranges) k	−18 to 30	−9 to 10	−11 to 11
l	−10 to 11	−15 to 16	−9 to 22
Reflections collected	6291	6654	14624
Independent reflections	3484	2614	5612
Independent observed reflections [$F_o \leq 4\sigma(F_o)$]	2547	2182	4067
θ range [°]	1.73 to 26.49	2.37 to 28.59	1.32 to 28.59
F(000)	984	492	1096
Decay	< 1%	< 1%	< 1%
(c) Refinement			
R[b]	0.0387	0.0440	0.0543
$wR2$[c]	0.1007	0.1144	0.1491
Absorption correction	SADABS	SADABS	SADABS
S	0.994	1.079	1.090
Δ [e·Å^{-3}] (max, min)[d]	0.524, −0.420	0.475, −0.489	0.450, −0.417
Transmission max, min	1.000, 0.862	1.000, 0.1575	0.8552, 0.8464
Weighting scheme a, b[e]	0.0544, 0.000	0.0431, 0.7160	0.0588, 2.1880

[a] X-ray data collected with a Siemens 3-circle diffractometer equipped with a SMART CCD area detector; graphite-monochromated radiation Mo-K_α radiation (λ = 0.71073 Å). Anisotropic thermal parameters were used for all non-H atoms. Hydrogen atoms were inserted at calculated positions and fixed, with isotropic thermal parameters U = 0.08 Å^3. − [b] $R = \Sigma|F_o - F_c|/\Sigma F_o$ [for $F_o \geq 4\sigma(F_o)$]. − [c] $wR2 = \{\Sigma[w(F_o^2 - F_c^2)^2]/\Sigma[w(F_o^2)^2]\}^{1/2}$ for all data. − [d] Peaks of unsassigned residual electron density. − [e] $w^{-1} = \sigma^2(F_o^2) + aP + bP$, where $P = [\max(F_o^2,0) + 2F_c^2]/3$, where $\max(F_o^2,0)$ indicates that the larger of F_o^2 or 0 is taken, a and b are values set by the program.

Polymerisation Reactions: 0.134 g of CuBr ($9.35\cdot10^{-4}$ mol) was placed in a Schlenk tube, containing a magnetic stirring bead, and pumped/filled three times with nitrogen to remove air from the apparatus. Deoxygenated MMA (10 ml, 0.0935 mol) and deoxygenated xylene (20 ml) were added via syringe to the Schlenk tube at room temperature, followed by the appropriate ligand (2 molar equivalents on CuBr, $1.87\cdot10^{-3}$ mol). The Schlenk tube was then placed into an oil bath at 90°C with stirring, followed by the addition of the initiator, ethyl 2-bromoisobutyrate (0.137 ml, $9.35\cdot10^{-4}$ mol). Periodically, 1−2-ml samples were removed for conversion and molecular-weight analysis.

Crystal-Structure Determinations: Crystallographic data for complexes $Cu[BF_4]\cdot(\mathbf{2})_2$, $Cu[BF_4]\cdot(\mathbf{3})_2$, and $Cu[PF_6]\cdot(\mathbf{5})_2$ are summarised in Table 3. The corresponding molecular structures are shown in Figures 5−7. Suitable crystals were quickly glued to quartz fibres, coated with dry nujol, and cooled in the cold nitrogen gas stream of the diffractometer. The structures were solved by direct methods. Anisotropic thermal parameters were used for all non-H atoms, whilst hydrogen atoms were inserted at calculated positions and fixed, with isotropic thermal parameters (U = 0.08 Å^3), riding on the supporting atom. The structure solutions were carried out using SHELXTL[16a] version 5 software with a Silicon Graphics Indy workstation, refinements were carried out using SHELX 96[16b] software, minimising on the weighted R factor $wR2$. − Crystallographic data (excluding structure factors) for the structures reported in this paper have been deposited with the Cambridge Crystallographic Data Centre as supplementary publication no. CCDC-101884, -101885, -101886. Copies of the data can be obtained free of charge on application to CCDC, 12 Union Road, Cambridge CB2 1EZ, UK [Fax: int. code + 44(1223)336-033; E-mail: deposit@ccdc.cam.ac.uk].

[1] [1a] A. Togni, L. M. Venanzi, *Angew. Chem. Int. Ed. Engl.* **1994**, *33*, 497; *Angew. Chem.* **1994**, *106*, 517. − [1b] D. A. Evans, K. A. Woerpel, M. J. Scott, *Angew. Chem. Int. Ed. Engl.* **1992**, *31*, 430; *Angew. Chem.* **1992**, *104*, 439. − [1c] F. O. H. Pirrung, H. Hiemstra, W. N. Speckamp, B. Kaptein, H. Schoemaker, *Tetrahedron Lett.* **1994**, *50*, 12415.

[2] [2a] I. W. Davies, C. H. Senanayake, R. D. Carsen, T. R. Verhoeven, P. J. Reider, *Tetrahedron Lett.* **1996**, *37*, 1725. − [2b] R. Lowenthal, S. Masamune, *Tetrahedron Lett.* **1991**, *32*, 7373. − [2c] Y. Nishibayashi, K. Ohe, S. Uemura, *J. Chem. Soc., Chem.*

Commun. **1995**, 1245. – [2d] F. O. H. Pirrung, H. Hiermstra, W. N. Speckamp, B. Raptein, H. E. Schoemaker, *Synthesis* **1995**, 465.

[3] [3a] G. M. Lee, S.M. Weinreb, *J. Org. Chem.* **1990**, *55*, 1281. – [3b] H. Nagashima, H. Wakamatsu, K. Itoh, *J. Chem. Soc., Chem. Commun.* **1984**, 652. – [3c] H. Nagashima, N. Ozaki, M. Ishii, K. Seki, M. Washiyama, K. Itoh, *J. Org. Chem.* **1993**, *58*, 464.

[4] [4a] B. Giese, *Radicals in Organic Synthesis: Formation of Carbon-Carbon Bonds*, Pergamon, New York, **1988**. – [4b] J. Iqbal, B. Bhatia, N. K. Nayyar, *Chem. Rev.* **1994**, *94*, 519.

[5] [5a] J-S. Wang, K. Matyjaszewski, *J. Am. Chem. Soc.* **1995**, *117*, 5614. – [5b] T. Grimaud, K. Matyjaszewski, *Macromolecules* **1997**, *30*, 2216. – [5c] K. Matyjaszewski, T. E. Patten, J. Xia, *J. Am. Chem. Soc.* **1997**, *119*, 674. – [5d] K. Matyjaszewski, J-L. Wang, T. Grimaud, D. A. Shipp, *Macromolecules* **1998**, *31*, 1527. – [5e] M. Kato, M. Kamigaito, M. Sawamoto, T. Higashimura, *Macromolecules* **1995**, *28*, 1721. – [5f] M. Sawamoto, M. Kamigaito, *Trends Polym. Sci.* **1996**, *4*, 371. – [5g] J. Ueda, M. Matsuyama, M. Kamigaito, M. Sawamoto, *Macromolecules* **1998**, *31*, 557. – [5h] T. Nishikawa, T. Ando, M. Kamigaito, M. Sawamoto, *Macromolecules* **1997**, *30*, 2244

[6] [6a] D. M. Haddleton, C. B. Jasieczek, M. J. Hannon, A. J. Shooter, *Macromolecules* **1997**, *30*, 2190. – [6b] D. M. Haddleton, A. J. Clark, M. C. Crossman, D. J. Duncalf, A. M. Heming, S. R. Morsley, A. J. Shooter, *J. Chem. Soc., Chem. Commun.* **1997**, 1173. – [6c] D. M. Haddleton, C. Waterson, P. J. Derrick, C. Jasieczek, A. J. Shooter, *J. Chem. Soc., Chem. Commun.* **1997**, 683. – [6d] D.M. Haddleton, D. Kukulj, D. J. Duncalf, A. M. Heming, A. J.Shooter, *Macromolecules*, in press.

[7] [7a] H. T. Dieck, L. Stamp, *Z. Naturforsch., B* **1990**, *45*,1369. – [7b] V. G. Bahr, H. Thamlitz, *Z. Anorg. Allg. Chem*. **1951**, *267*, 161. – [7c] G. Van Koten, K. Vrieze, *Adv. Organomet. Chem*. **1982**, *21*, 151. – [7d] G Van Koten, K. Vroeze, *Recl. Trav. Chim. Pays-Bas* **1981**, *100*, 129.

[8] [8a] V. Percec, B. Barboiu, H.-J. Kim, *J. Am. Chem. Soc*. **1998**, *120*, 305. – [8b]] V. Percec, , H.-J. Kim, B. Barboiu *Macromolecules* **1997**, *30*, 6702. – [8c] V. Percec, B. Barboiu, M van der Sluis *Macromolecules* **1998**, *31,* 4053. – [8d] C. Granel, Ph. Dubois, R. Jerome, Ph. Teyssie, *Macromolecules* **1996**, *29*, 8576. – [8e] Ph. Lecomte, I. Drapier, Ph. Dubois, Ph. Teyssie, R. Jerome, *Macromolecules* **1997**, *30*, 7631, – [8f] B. B. Wayland, L. Basickes, S. Mukerjee, M. Wei, M. Fryd, *Macromolecules* **1997**, *30*, 8109.

[9] S. K. Sheppard, G. R. Eaton, S. S. Eaton, *Inorg. Chem.* **1989**, *28*, 4496.

[10] [10a] R. N. Keller, H. D. Wycoff, *Inorg. Synth.* **1947**, *2*, 1. – [10b] $[Cu(CH_3CN)_4][PF_6]$ was synthesised according to the method of Kubas and $[Cu(CH_3CN)_4][BF_4]$ was synthesised by a suitable modification to this method using HBF_4 in place of HPF_6. – [10c] G. J. Kubas, *Inorg. Synth.* **1990**, *28*, 68.

[11] D. M. Haddleton, A. J. Clark, D. J. Duncalf, A. M. Heming, D. Kukulj, A. J. Shooter, *J. Mat*. *Chem*. **1998**, 1525.

[12] M. Munikata, S. Kitagawa, A. Asahara, H. Masuda, *Bull. Chem. Soc. Jpn.* **1987**, *60*, 1927.

[13] J. F. Dobson, B. E. Green, P. C. Healy, C. H. L. Kennard, C. Pakawatchai, A. H. White, *Aust. J. Chem.* **1984**, *37*, 649.

[14] P. C. Healy, L. M. Englehardt, V. A. Patrick, A. White, *J. Chem. Soc., Dalton Trans.* **1985**, 2541.

[15] M. Munikata, M. Maekawa, S. K. Kitagawa, S. Matsuyama, H. Masuda, *Inorg. Chem.* **1989**, *28*, 4300.

[16] [16a] G. M. Sheldrick, *SHELXL 5.0*, Siemens Analytical Instruments, Madison, WI, **1994**. – [16b] G. M. Sheldrick, *SHELXL 96*, University of Göttengen, **1996**.

[I98213]

The Formation of $HAlX_2$ (X = Cl, Br) in the Thermolysis of Intramolecularly Coordinated Alanes $Me_2N(CH_2)_3AlX_2$: A Matrix Isolation Study

Jens Müller* and Bob Wittig

Institut für Anorganische Chemie der RWTH Aachen,
Professor-Pirlet-Straße 1, D-52056 Aachen, Germany
Fax: (internat.) +49 (0)241/ 888 8288
E-mail: jens.mueller@ac.rwth-aachen.de

Received July 10, 1998

Keywords: Aluminum hydrides / Matrix isolation / IR spectroscopy / Ab initio calculation / Thermolyses

High-vacuum thermolyses of the intramolecularly coordinated alanes $Me_2N(CH_2)_3AlX_2$ with X = Cl, Br (**1**, **2**) were investigated with matrix isolation techniques. Among the products, which were identified with IR spectroscopy, ab initio calculations, and known literature data, are monomeric $HAlCl_2$ and $HAlBr_2$. The experimental vibrational frequencies of these hydrides matches well the calculated harmonic frequencies at the MP2(fc)/6–311G+(2d, p) and B3LYP/6–311G+(2d, p) level of theory. Beside the monomeric $HAlX_2$, the argon matrices of the thermolysis experiments contained CH_4, HCN, $H_2C{=}CH_2$, $H_2C{=}NMe$, $[H_2CCHCH_2]^{\bullet}$, $H_2C{=}CHCH_3$, and AlX_n (n = 1–3; X = Cl or Br).

Introduction

The group-13 nitrides are promising materials for advanced microelectronic and optoelectronic devices.[1][2] Suitable single-source precursors for the chemical vapor deposition of AlN[3], GaN[4], and InN[5] are intramolecularly coordinated group-13 metal azides containing the 3-(dimethylamino)propyl ligand. Recently, we started to investigate these deposition reactions with the matrix isolation technique. We intend to trap reactive intermediates produced by the fragmentation of a single-source precursor on its pathway to the resulting nitride film. By the characterization of these molecules we expect to get insights into the reaction mechanisms of these CVD processes (e.g., Eq. 1), which so far are unknown.

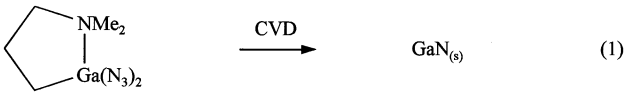

(1)

In order to get first results on the fragmentation pattern of intramolecularly coordinated molecules, we chose model compounds to begin with. In this article we report on gas-phase thermolysis experiments with the chloro- and the bromoalane, **1** and **2**, respectively.

Scheme 1

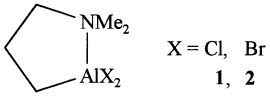

Results and Discussion

The two alanes **1** and **2** are volatile and moisture-sensitive compounds, which can be purified by sublimation in high vacuum. While the dichloro compound was published in 1991[6], no data on the bromide **2** has appeared in the literature.[7] As expected, compound **2** could readily be synthesized from aluminum bromide and $Li(CH_2)_3NMe_2$[8]. The crystal structures of **1** and **2** are unknown, but the ^{27}Al-NMR shift of δ = 139 for **1** and **2** clearly reveals the expected tetra-coordination of aluminum in solution.[3b][9]

We carried out a series of high-vacuum thermolyses of **1** and **2**, respectively (see Experimental Section). Between ambient temperature and oven temperatures of ca. 750°C the IR spectra of the matrix isolated alanes **1** and **2**, respectively, were unchanged. Around ca. 850°C new IR bands appeared, indicating the beginning of fragmentation; above ca. 950°C the typical IR absorptions of the precursors **1** or **2** could no longer be detected in the argon matrices.

Figure 1 shows a typical IR spectrum recorded after a thermolysis of the alane **2** at ca. 1000°C. The strongest absorption appears at 634.5 cm^{-1} followed by intensive bands at 476.0 and 1952.5 cm^{-1}. The latter lies in the characteristic region of aluminum−hydrogen stretching vibrations, which suggests the formation of a molecule with an AlH bond. Beside the experimental spectrum Figure 1 exhibits a theoretical IR spectrum of $HAlBr_2$ calculated at the B3LYP/6-311G+(2d, p) level of theory. Evidently, there is a good agreement between the major IR absorptions of the experimental spectrum and the theoretical one. In the case of the dichloro compound **1**, the AlH-stretching mode absorbs at 1966.0 cm^{-1}. Even without any calculation, there is no doubt that monomeric $HAlCl_2$ was formed in the pyrolysis of the alane **1**. This species has been synthesized photochemically in argon matrices before (Eq. 2) and was

 © WILEY-VCH Verlag GmbH, D-69451 Weinheim, 1998 1434−1948/98/1111−1807 $ 17.50+.50/0

Figure 1. Experimental and calculated IR spectra: X-axis, 250−2100 cm^{-1}; Y-axis, Absorbance (dimensionless). Spectrum A: products of the thermolysis of compound **2** at ca. 1000°C trapped in argon at 15 K (assignment $\nu_1-\nu_6$ see Table 1); a: $H_2C{=}NMe$[17] (2900.5[a], 2854.5[a], 1469.5, 1221.0, 1026.5 cm^{-1}), b: $H_2C{=}CH_2$[14a][16] (1440.0, 947.0 cm^{-1}), c: CH_4[14] (1305.0 cm^{-1}), d: $[H_2CCHCH_2]^{\bullet}$ [18] (801.0 cm^{-1}), e: $H_2C{=}CHCH_3$[19] (909.0 cm^{-1}), f: HCN[15] (3305.0[a], 721.0 cm^{-1}), g: $AlBr_3$[20] (508.5 cm^{-1}), h: AlBr[20] (357.5 cm^{-1}). The signal of $AlBr_2$[20] at 458.0 cm^{-1} is too weak to be seen in this spectrum. The strongest among the unassigned bands was found at 763.5 cm^{-1}[b] (see also text). Spectrum B: $HAlBr_2$ calculated at the B3LYP/6−311+G(2d, p) level (half band width of 2 cm^{-1})

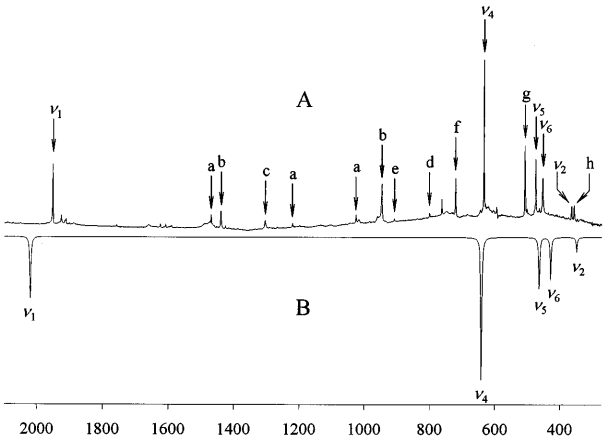

[a] Out of the depicted range; [b] For $HAlCl_2$ an unassigned signal was found at 770.0 cm^{-1}

unequivocally characterized by IR spectroscopy and normal coordinate analysis.[10] Within experimental error, the IR frequencies match with the published IR data of $HAlCl_2$ (Table 1, figures in braces).

In Table 1 the experimental and calculated vibrational data of $HAlCl_2$ and $HAlBr_2$ are compiled. The ab initio calculations predict C_{2v}-symmetrical equilibrium geometries for these aluminum hydrides (Table 2); thus, one expects six normal modes belonging to the irreducible representations A_1 (3), B_1 (2), and B_2 (1). In accordance with the calculations (Table 1) only five of the six modes were measured; the calculated frequencies of the XAlX-deformation vibration ν_3 are out of our detectable range of 240−4000 cm^{-1}.

Table 2. Calculated bond length (Å) and angles (deg) of $HAlCl_2$ and $HAlBr_2$[a]

	X = Cl	X = Br
AlH	1.552 (1.557)	1.554 (1.559)
AlX	2.093 (2.096)	2.259 (2.260)
XAlX	118.16 (118.47)	118.65 (119.37)

[a] MP2(fc)/6−311G+(2d, p) and B3LYP/6−311G+(2d, p); results of the B3LYP calculations in parentheses.

For reliable assignments of the IR bands we chose the MP2 and B3LYP methods with the 6-311G+(2d, p) basis set to calculate the harmonic frequencies. As known from the literature[11] MP2 results in higher wavenumbers compared with B3LYP, which is also valid for all of the calculated frequencies in Table 1. Usually, calculated wavenumbers are too large in comparison with the real values, but B3LYP often results in frequencies which are too small for the low energy modes.[12] From that point of view, the two alanes are illustrative examples: the AlH stretch ν_1, the only mode at high energy, is described slightly better by the B3LYP than by the MP2 calculations, while all other detected modes are below 655.0 cm^{-1} (ν_2, ν_4, ν_5, and ν_6) with mean observed/calculated frequency ratios of 0.995 ($HAlCl_2$) and 1.002 ($HAlBr_2$) for the MP2 calculations, whereas the respective ratios are 1.020 and 1.029 for the B3LYP method.

All experimental IR bands of $HAlCl_2$ are found at higher wavenumbers than those of $HAlBr_2$. This is mainly due to the higher molecular mass of bromine compared with chlorine; thus, the effect is strongly pronounced for the two AlX-stretching modes with differences between the chloro and the bromo derivative of 115.5 for ν_2 and 103.5 cm^{-1} for ν_5.

The dihaloalanes are most likely formed by β-hydrogen eliminations (Eq. 3).

There is evidence in the literature that the intramolecularly coordinated 3-(dimethylamino)propyl ligand can be split off by a β-hydrogen elimination pathway;[6a] and, indeed, allyldimethylamine was detected by NMR spec-

Table 1. Experimental and calculated vibrational data for $HAlCl_2$ and $HAlBr_2$. Experimental IR frequencies (cm^{-1}) and observed/calculated frequency ratios (in parentheses for MP2; in square brackets for B3LYP); harmonic frequencies (cm^{-1}) and intensities (in parentheses, km mol^{-1}) calculated at the MP2(fc)/6−311G+(2d, p) and the B3LYP/6−311G+(2d, p) level

			$HAlCl_2$			$HAlBr_2$		
			experimental [a]	MP2	B3LYP	experimental	MP2	B3LYP
A_1:	ν_1	ν(AlH)	1966.0 (0.9415) [0.9677] {1967.6}	2088.1 (110.2)	2031.6 (100.9)	1952.5 (0.9391) [0.9662]	2079.1 (116.2)	2020.9 (108.4)
	ν_2	$\nu_s(AlX_2)$	481.5 (0.9955) [1.0238] {481.3}[b]	483.7 (45.6)	470.3 (44.0)	366.0 (1.0186) [1.0472]	359.3 (29.7)	349.5 (27.6)
	ν_3	$\delta(AlX_2)$		161.9 (10.6)	159.1 (9.4)		107.7 (2.9)	107.2 (2.4)
B_1:	ν_4	δ(XAlH)	654.5 (0.9801) [0.9947] {654.5}	667.8 (334.0)	658.0 (288.7)	634.5 (0.9768) [0.9883]	649.6 (286.0)	642.0 (250.9)
	ν_5	$\nu_{as}(AlX_2)$	579.5 (0.9872) [1.0101] {578.9}[b]	587.0 (43.5)	573.7 (58.7)	476.0 (0.9996) [1.0241]	476.2 (90.6)	464.8 (91.6)
B_2:	ν_6	γ(H)	472.5 (1.0166) [1.0512] {471.8}	464.8 (122.2)	449.5 (102.7)	453.5 (1.0125) [1.0564]	447.9 (92.0)	429.3 (76.3)

[a] Wavenumbers in parentheses were taken from reference[10]. − [b] Listed are the wavenumbers concerning the main isotopomers.

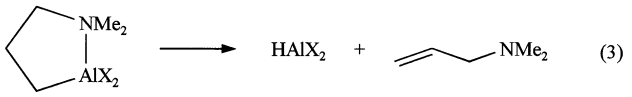

1, **2** X = Cl, Br

troscopy in the exhaust gases of the CVD process as shown by Eq. 1.[4b] The reverse reaction, the hydroalumination, is well known in organic and organometallic syntheses; the synthesis of 3-(dimethylamino)propylalane is given as an example (Eq. 4).[6b]

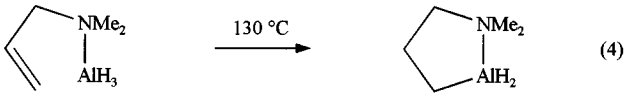

However, in none of the thermolysis experiments of compound **1** or **2** did we detect allyldimethylamine in argon matrices.[13] Beside the two dihaloalanes, we identified CH_4,[14] HCN,[15] $H_2C{=}CH_2$,[14a][16] $H_2C{=}NMe$,[17] $[H_2CCHCH_2]^{\bullet}$,[18] and $H_2C{=}CHCH_3$[19] (see Figure 1). One might believe that allyldimethylamine is produced by the thermolyses according to Eq. 3, and because the temperatures are so high that it is further pyrolyzed. In order to prove this speculation, we conducted thermolysis experiments with amine/argon mixtures (1:500). The fragmentation of the amine begins around 800°C, and at ca. 1150°C we could not detect any allyldimethylamine in argon matrices. All the mentioned above molecules were found, but they were produced in different ratios than for the thermolysis experiments of compound **1** and **2**, respectively. Furthermore, there were new, unidentified IR bands, which we have not identified so far. As mentioned before, allyldimethylamine was detected in the exhaust gases of the deposition reaction Eq. 1, and with increasing deposition temperatures increasing amounts of $H_2C{=}CH_2$ and NMe_3 were found; however, we did not find NMe_3 amoung the thermolyses products of compound **1** and **2**.

Among the pyrolysis products, the aluminum halide species AlX [X = Cl: 455.0 ($Al^{35}Cl$) and 450.0 ($Al^{37}Cl$) cm^{-1}; X = Br: 357.5 cm^{-1}], AlX_2 [X = Cl: 564.0 ($Al^{35}Cl_2$) and 561.5 ($Al^{35}Cl^{37}Cl$) cm^{-1}; X = Br: 458.0 cm^{-1}], and AlX_3 [X = Cl: 619.0 ($Al^{35}Cl_3$) and 615.0 ($Al^{35}Cl_2{}^{37}Cl$) cm^{-1}; X = Br: 508.5 cm^{-1}] could be unequivocally identified by comparison with known literature data.[20] At this point we will not suggest various reaction pathways which explain the AlX_n species, because they would be purely speculative; obviously, further experiments are necessary.

Conclusion

Up to date, only two monomeric aluminum hydrides of the type H_nAlX_{3-n} (n = 1−3) have been characterized, i.e., AlH_3[21] and $HAlCl_2$[10]; with $HAlBr_2$ we examined a third example. However, it is surprising that the hydrides $HAlX_2$ withstand the rather harsh thermolyses conditions. We hope to expand the method described in this paper to get access to new, reactive group-13 molecules. As mentioned in the introduction, **1** and **2** were chosen as model compounds for intramolecularly coordinated group-13 metal azides in order to get first insights into the fragmentation mechanism of these types of substances. The results reported here demonstrate that the fragmentation of the compounds **1** and **2** are not as simple as it seems at first glance. Further investigations are in progress and we will report on this outcome shortly.

We are grateful to the *Deutsche Forschungsgemeinschaft* for generous financial support and to the *Rechenzentrum der RWTH Aachen* for providing generous computer time. Especially, we would like to thank *T. Eifert* and *J. Risch* for their support, *P. Pilgram* for the synthesis of **2**, and *P. Geisler* for the construction of the thermolysis oven.

Experimental Section

General Remarks: All procedures for syntheses were carried out under a dry nitrogen atmosphere with standard Schlenk techniques. Solvents were dried by standard procedures, distilled, and stored under nitrogen and molecular sieves (4 Å). The reagents Me_2N-$(CH_2)_3AlCl_2$ (**1**)[6b] and $Li(CH_2)_3NMe_2$[8] were prepared according to the literature procedures. − NMR: Varian Unity 500 (ambient temp.; 499.843, 130.195, and 125.639 MHz for ^1H, ^{27}Al, and ^{13}C, respectively); calibrated against residual protons of the deuterated solvents. ^1H- and ^{13}C-chemical shift are reported relative to TMS and ^{27}Al-NMR values relative to the external standard [Al(acac)$_3$] in C_6D_6. As a result of the electric quadrupole moment of the ^{27}Al nucleus the carbon atoms bound to aluminum could not be detected in the ^{13}C-NMR measurement. − Elemental analyses (C, H, N): Carlo-Erba elemental analyzer, Model 1106. − MS: Finnigan MAT 95.

Dibromo[3-(dimethylamino)propyl]aluminum (**2**): 2.60 g (27.95 mmol) of $Li(CH_2)_3NMe_2$ were added to a solution of 7.45 g of $AlBr_3$ (27.95 mmol) in 50 ml of toluene, and the reaction mixture was stirred overnight. The suspension was filtered, and the solid was washed with two 10-ml portions of toluene. After removal of the solvent in high vacuum, sublimation (50−75°C, 10^{-3} mbar) gave 5.51 g of **2** (72%) as a colorless solid, m.p. 98−101°C. − ^1H NMR (C_6D_6): δ = 0.35 (t, ^3J = 7.78 Hz, 2 H, $AlCH_2$), 1.16 (pseudo quintet, ^3J = 6.71 Hz, 2 H, $AlCH_2CH_2$), 1.68 (t, ^3J = 6.41 Hz, 2 H, NCH_2), 1.70 (s, 6 H, CH_3). − $^{13}C\{^1H\}$ NMR (C_6D_6): δ = 20.02 ($AlCH_2CH_2$), 45.51 (CH_3), 62.12 (NCH_2). − ^{27}Al NMR (C_6D_6): δ = 139 ($h_{1/2}$ = 750 Hz). − MS (70 eV), *m/z* (%): 273 (100) [M^+], 245 (45) [$M^+ - C_2H_4$], 230 (76) [$M^+ - C_2H_5N$], 192 [M^+ − Br], 187 (41) [$M^+ - (CH_2)_3N(CH_3)_2$]. − $C_5H_{12}AlBr_2N$ (272.95): calcd. C 22.00, H 4.43, N 5.13; found C 21.66, H 4.50, N 5.11.

Matrix Isolation: The matrix apparatus consists of a vacuum line (Leybold Turbovac 151; Leybold Trivac D4B) and a Displex CSW 202 cryogenic closed-cycle system (APD Cryogenics Inc.) fitted with CsI windows. In a typical experiment the starting compound was kept in a small metal container in high vacuum at constant temperature (10^{-6} to 10^{-7} mbar; compound **1**: 35−50°C; compound **2**: 50−60°C), while a flow of argon was conducted over the sample (Linde 6.0; flow = 1.0 sccm; MKS mass flow controller type 1179). Subsequently, this gaseous mixture was passed through an Al_2O_3 tube (inner diameter of 1 mm; heated by tungsten wire coiled around the last 10 mm). The hot end of the pyrolysis tube was just 25 mm away from the cooled CsI window to assure that a maximum amount of volatile fragments emerging from the oven were trapped in the matrix. For the temperature determination of

the pyrolysis oven a current-to-temperature relation was measured with a thermocouple (Thermocoax: NiCr/NiAl) inside of the Al_2O_3 tube.

The concentrations of the samples in the matrices are unknown. Therefore, several experiments under various conditions were carried out to insure that the molecules were indeed matrix-isolated. The concentration of the samples decreases significantly at lower sublimation temperatures (20°C for **1** and 35°C for **2**), but no differences in the IR spectra were observed. At higher concentrations the half band widths of IR bands increased and new broad IR bands appeared indicating that notable parts of the molecule are no longer matrix-isolated under these conditions.

The IR spectra of the matrices (15 K) were recorded on a Perkin-Elmer FTIR 1720x from 240 to 4000 cm^{-1} with a resolution of 1 cm^{-1}.

Ab initio Calculations: The GAUSSIAN 94 package[22], run on a cluster of workstations (*Rechenzentrum der RWTH Aachen*), was applied for all ab initio calculations. The total energies E_h (in Hartrees) and the ZPVE (in kJ mol^{-1}; in parentheses) are as follows: – $HAlCl_2$: −1162.046298 (26.64) for MP2(fc)/6−311+G(2d, p); −1163.649857 (25.97) for B3LYP/6−311+G(2d, p). – $HAlBr_2$: −5387.697127 (24.64) for MP2(fc)/6−311+G(2d, p); −5391.474382 (24.01) for B3LYP/6−311+G(2d, p).

[1] D. A. Neumayer, J. G. Ekerdt, *Chem. Mater.* **1996**, *8*, 9−25, and references therein.

[2] A. C. Jones, P. O′Brien, *CVD of Compound Semiconductors*; VCH: Weinheim, **1997**.

[3] [3a] R. A. Fischer, A. Miehr, H. Sussek, H. Pritzkow, E. Herdtweck, J. Müller, O. Ambacher, T. Metzger, *J. Chem. Soc., Chem. Commun.* **1996**, 2685−2686. – [3b] J. Müller, R. A. Fischer, H. Sussek, P. Pilgram, R. Wang, H. Pritzkow, E. Herdtweck, *Organometallics* **1998**, *17*, 161−166.

[4] [4a] A. Miehr, M. R. Mattner, R. A. Fischer, *Organometallics*, **1996**, *15*, 2053−2059. – [4b] A. Miehr, O. Ambacher, W. Rieger, T. Metzger, E. Born, R. A. Fischer, *Chem. Vap. Deposition* **1996**, *2*, 51−55. – [4c] R. A. Fischer, A. Miehr, E. Herdtweck, M. R. Mattner, O. Ambacher, T. Metzger, E. Born, S. Weinkauf, C. R. Pulham, S. Parsons, *Chem. Eur. J.* **1996**, *2*, 1353−1358.

[5] R. A. Fischer, A. Miehr, T. Metzger, E. Born, O. Ambacher, H. Angerer, R. Dimitrov, *Chem. Mater.* **1996**, *8*, 1356−1359.

[6] [6a] H. Schumann, U. Hartmann, W. Wassermann, O. Just, A. Dietrich, L. Pohl, M. Hostalek, M. Lokai, *Chem. Ber.* **1991**, *124*, c 1113−1119. – [6b] U. Dümichen, K.-H. Thiele, T. Gelbrich, J. Sieler, *J. Organomet. Chem.* **1995**, *495*, 71−75.

[7] Compound **2** is mentioned in: R. A. Fischer, T. Priermeier, *Organometallics*, **1994**, *13*, 4306−4314.

[8] K.-H. Thiele, E. Langguth, G. E. Müller, *Z. Anorg. Allg. Chem.* **1980**, *462*, 152−158.

[9] J. Müller, U. Englert, *Chem. Ber.* **1995**, *128*, 493−497, and references therein.

[10] H. Schnöckel, *J. Mol. Struct.* **1978**, *50*, 275−280.

[11] [11a] A. P. Scott, L. Radom, *J. Phys. Chem.* **1996**, *100*, 16502−16513. – [11b] G. Rauhut, P. Pulay, *J. Phys. Chem.* **1995**, *99*, 3093−3100.

[12] A. Y. Timoshkin, H. F. Bettinger, H. F. Schaefer III, *J. Am. Chem. Soc.* **1997**, *119*, 5668−5678.

[13] For comparison with IR spectra of thermolysis experiments, we measured the IR spectrum of matrix isolated allyldimethylamine in argon (amine:argon ratio 1:500).

[14] [14a] G. Herzberg, *Molecular Spectra and Structure*, 1st ed., D. Van Nostrand Reinhold Company, Inc., Princeton, NJ, **1945**, Vol. II. – [14b] J. Müller, *J. Am. Chem. Soc.* **1996**, *118*, 6370−6376.

[15] [15a] D. E. Milligan, E. M. Jacox, *J. Chem. Phys.* **1963**, *39*, 712−715. – [15b] D. V. Lanzisera, L. Andrews, *J. Phys. Chem. A* **1997**, *101*, 824−830.

[16] L. Andrews, G. L. Johnson, B. J. Kelsall, *J Chem. Phys.* **1982**, *76*, 5767−5773.

[17] [17a] J. Hinze, R. F. Curl, Jr., *J. Am. Chem. Soc.* **1964**, *86*, 5068−5070. – [17b] I. Stolkin, T.-K. Ha, Hs. H. Günthard, *Chem. Phys.* **1977**, *21*, 327−347.

[18] [18a] G. Maier, H. P. Reisenauer, B. Rohde, K. Dehnicke, *Chem. Ber.* **1983**, *116*, 732−740. – [18b] J. W. Huang, W. R. M. Graham, *J. Phys, Chem.* **1990**, *93*, 1583−1596.

[19] L. Andrews, G. L. Johnson, B. J. Kelsall, *J. Am. Chem. Soc.* **1982**, *104*, 6180−6186.

[20] P. Hassanzadeh, A. Citra, L. Andrews, M. Neurock, *J. Phys. Chem.* **1996**, *100*, 7317−7325, and references therein.

[21] [21a] F. A. Kurth, R. A. Eberlein, H. Schnöckel, A. J. Downs, C. R. Pulham, *J. Chem. Soc., Chem. Commun.* **1993**, 1302−1304. – [21b] P. Pullumbi, Y. Bouteiller, L. Manceron, C. Mijoule, *Chem. Phys.* **1994**, *185*, 25−37.

[22] *Gaussian 94*, M. J. Frisch, G. W. Trucks, H. B. Schlegel, P. M. W. Gill, B. G. Johnson, M. A. Robb, J. R. Cheeseman, T. Keith, G. A. Petersson, J. A. Montgomery, K. Raghavachari, M. A. Al-Laham, V. G. Zakrzewski, J. V. Ortiz, J. B. Foresman, J. Cioslowski, B. B. Stefanov, A. Nanayakkara, M. Challacombe, C. Y. Peng, P. Y. Ayala, W. Chen, M. W. Wong, J. L. Andres, E. S. Replogle, R. Gomperts, R. L. Martin, D. J. Fox, J. S. Binkley, D. J. Defrees, J. Baker, J. P. Stewart, M. Head-Gordon, C. Gonzalez, and J. A. Pople, Gaussian, Inc., Pittsburgh PA, **1995**.

[98228]

New Organometallic Palladium(II) Complexes Containing P∩N Ligands – Synthesis, Characterization and X-ray Structure

Laura Crociani[a], Giuliano Bandoli[b][+], Alessandro Dolmella[b], Marino Basato*[c], and Benedetto Corain[d][++]

Istituto di Chimica e Tecnologia dei Materiali Avanzati, C. N. R.[a],
C. so Stati Uniti, 4, I-35020 Padova, Italy

Dipartimento di Scienze Farmaceutiche, Università di Padova[b],
Via Marzolo 5, I-35131 Padova, Italy
Fax: (internat.) +39 (0)49/8275345
E-mail: bandoli@pdfar3.dsfarm.unipd.it

Dipartimento di Chimica Inorganica, Metallorganica e Analitica, Università di Padova[c],
Via Marzolo 1, I-35131 Padova, Italy
Fax: (internat.)+39 (0)49/8275223
E-mail: basato@chim02.unipd.it

Institut für Organische Chemie und Biochemie[d],
TU München, Lichtenbergstraße 4, D-85747 Garching, Germany

Received April 6, 1998

Keywords: Phosphanyl-amine / Phosphanyl-imine / Palladium / Organometallic complexes / Crystal structure

New neutral organometallic palladium(II) complexes, [PdPhI($PNMe_2$)] (**1**), [PdPhI(PC=NMe)] (**2**), [PdPhI(PC=NEt)] (**3**), and [PdMeCl($PNMe_2$)] (**4**), {$PNMe_2$ means *N*,*N*-dimethyl-2-(diphenylphosphanyl)aniline; PC=NMe means *N*-[2-(diphenylphosphanyl)benzylidene]-*N*-methylamine; PC=NEt means *N*-[2-(diphenylphosphanyl)benzylidene]-*N*-ethylamine} have been synthesized by oxidative addition of PhI to [$Pd(dba)_2$] in the presence of the P∩N ligand (**1**–**3**), or by substitution reaction on [PdMeCl(COD)] with $PNMe_2$ (**4**). Cationic σ-organometallic species [PdR(PPh_3)(P∩N)]$^+$ are obtained upon treating complexes of the type [PdRX(P∩N)] with PPh_3 and $AgCF_3SO_3$ and consist predominantly of the *trans*-P,P isomer in $CDCl_3$ solution, as shown by NMR spectroscopic studies. The cationic η^3-allyl complex [Pd(η^3-all)($PNMe_2$)]PF_6 has also been prepared and characterized, both in solution and in the solid state. Compounds [PdPhI($PNMe_2$)] ($P2_1/n$), [PdPhI(PC=NMe)] ($P\bar{1}$), [PdPhI(PC=NEt)] ($P\bar{1}$), and [Pd(η^3-all)($PNMe_2$)]PF_6 ($P\bar{1}$) have been authenticated by X-ray analysis

Introduction

We have recently synthesized a number of nickel(II) complexes featuring mixed *soft-hard* coordination spheres[1][2][3] of the types {P_2NCl_2} and {P_2NCl}. The ultimate aim of this work was the evaluation of these species as potential catalysts in the oligomerization of olefins (Shell Higher Olefin Process, SHOP[4]). Although the catalytic results turned out to be unsatisfactory, P∩N ligands of the type depicted in Scheme 1 are expected to exhibit hemilabile behavior when coordinated to a *soft* metal center such like palladium(II)[5]. This feature, coupled with the known ability of palladium(II) complexes to promote catalytically a series of important C−C bond-forming reactions (such as the oligomerization of olefins[6], copolymerization of CO/ethylene[7], and the telomerization of butadiene[8]), prompted us to extend our investigations to this metal center[*].

Scheme 1

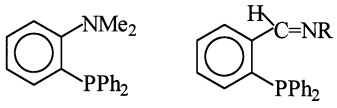

$PNMe_2$ **PC=NR**

The P∩N ligands employed in this work can be expected to exhibit rather different coordinating behavior. While the $PNMe_2$ ligand clearly contains *hard* (N) and *soft* (P) donor atoms and forms five-membered metal chelates[9], the imino nitrogen in PC=NR can be expected to possess appreciable *soft* character (π-acceptor properties) and the ligands clearly afford six-membered rings upon metal coordination. In this context, it is remarkable that the coordinating ability

[+] Corresponding author for crystallographic section.
[++] Humboldt Stipendiat − On leave of absence from Dipartimento di Chimica, Ingegneria Chimica e Materiali, Via Vetoio Coppito Due, I-67010 L′Aquila, Italy, and from Centro di Studio sulla Stabilità e Reattività dei Composti di Coordinazione, CNR, c/o Dipartimento di Chimica Inorganica Metallorganica e Analitica, Università di Padova, Via Marzolo 1, I-35131 Padova, Italy.

[*] Preliminary catalytic results indicate that the new complexes reported in this paper, [PdMe(PPh_3)($PNMe_2$)]$CF_3SO_3 \cdot C_6H_6$, and [Pd(η^3-all)($PNMe_2$)]PF_6, are efficient catalysts in the telomerization of butadiene with MeOH.

 © WILEY-VCH Verlag GmbH, D-69451 Weinheim, 1998 1434−1948/98/1111−1811 $ 17.50+.50/0

of these imino ligands remains largely unexplored, with the exception of their behavior towards rhodium(I)[10].

The importance of ligands based on a P,N set of donor atoms is well illustrated by other results obtained, e.g. by Vrieze with 1-(dimethylamino)-8-(diphenylphosphanyl)-naphthalene and 1-(dimethylamino)-3-(diphenylphosphanyl)propane[11], and by Venanzi with 2-(2-pyridyl)-4,5-dimethylphosphinine[12].

Results and Discussion

The investigated P$^{\frown}$N ligands form neutral and cationic η^3-allyl and σ organometallic complexes, characterized as (i) neutral complexes: [PdPhI($PNMe_2$)] (**1**), [PdPhI(PC=NMe)] (**2**), [PdPhI(PC=NEt)] (**3**), [PdMeCl($PNMe_2$)]·0.5 C_6H_6 (**4**), and (ii) cationic complexes: [PdMe(PPh_3)($PNMe_2$)]$CF_3SO_3\cdot C_6H_6$ (**5**), [PdPh(PPh_3)($PNMe_2$)]$CF_3SO_3\cdot 0.5\ C_6H_6$ (**6**), [PdPh(PPh_3)(PC=NMe)]$CF_3SO_3\cdot 0.5\ C_6H_6$ (**7**), [PdPh(PPh_3)(PC=NEt)]$CF_3SO_3\cdot 0.5\ C_6H_6$ (**8**), [Pd(η^3-all)($PNMe_2$)]PF_6 (**9**), where $PNMe_2$ means *N*,*N*-dimethyl-2-(diphenylphosphanyl)aniline, PC=NMe stands for *N*-[2-(diphenylphosphanyl)benzylidene]-*N*-methylamine, and PC=NEt for *N*-[2-(diphenylphosphanyl)benzylidene]-*N*-ethylamine.

While the phosphanylamine $PNMe_2$ is well-known as a ligand from the literature[9] and its reactivity with many metal centers[1][2][3][13], including palladium(II)[9], has been widely investigated, only a few rhodium(I)[10], molybdenum(0)[14], and iridium(I)[15] complexes with PC=NR (R = Me, Et) have been produced, and generally speaking, the coordination chemistry of ligands of this type has yet to be fully explored.

Synthesis and Characterization of the Neutral σ Organometallic Complexes [PdRX(P$^{\frown}$N)]

Two routes have been followed for the synthesis of complexes [PdPhI($PNMe_2$)] (**1**), [PdPhI(PC=NMe)] (**2**), [PdPhI(PC=NEt)] (**3**), and [PdMeCl($PNMe_2$)]·0.5 C_6H_6 (**4**), depending on the type of organic group. The phenyl complexes [PdPhI(P$^{\frown}$N)] were prepared by oxidative addition of iodobenzene to the palladium(0) complex [Pd($dba)_2$][16] (dba = dibenzylideneacetone) in the presence of the P$^{\frown}$N ligand (see Eq. 1)[17].

$$[Pd(dba)_2] + PhI + P^{\frown}N \xrightarrow[N_2,\ THF]{50\,^{\circ}C,\ 45\ min} [PdPhI(P^{\frown}N)] + 2\ dba \quad (1)$$

The complexes [PdPhI(P$^{\frown}$N)] were obtained as colored powders (yellow or pink-yellow) after filtration of the reaction mixture through Celite to eliminate metallic Pd, concentration of the filtrate to dryness, and repeated washing with Et_2O. No further recrystallization was necessary and crystals suitable for X-ray analysis could be grown by slow evaporation of the solvent from Me_2CO/MeOH solutions.

The methyl complex [PdMeCl($PNMe_2$)]·0.5C_6H_6 (**4**) was prepared by a substitution reaction on the complex [PdMeCl(COD)][18] (see Eq. 2) (COD = 1,5 cyclooctadiene), similar to that employed with related P$^{\frown}$N ligands[11].

$$[PdMeCl(COD)] + PNMe_2 \xrightarrow[N_2,\ C_6H_6,\ 24\ h]{r.t.} [PdMeCl(PNMe_2)]\cdot 0.5\ C_6H_4 + COD \quad (2)$$

Some IR and NMR spectroscopic data of the complexes [PdRX(P$^{\frown}$N)] and of the corresponding free ligands are reported in Table 1.

Direct evidence for the coordination modes of the ligands $PNMe_2$, PC=NMe, PC=NEt has been obtained from X-ray analyses of complexes **1**, **2**, and **3** (see below). The coordination of the P$^{\frown}$N ligands through both the P and N atoms has also been deduced in solution on the basis of NMR data, where the resonances of the ^{31}P nucleus and of the protons of the amino or imino alkyl groups are shifted towards lower fields than the corresponding resonances of the free ligand. NMR data also give useful information about the composition of the reaction product mixtures in $CDCl_3$ solutions. In fact, both reactions 1 and 2 produce only one isomer of complexes **2**–**4**, while [PdPhI($PNMe_2$)] (**1**) is obtained as a mixture of *trans* P,I and *cis* P,I isomers in a 3:1 ratio (Table 1). IR data are less helpful in distinguishing the type of coordination; in fact, the typical C=N stretching bands (at 1637 cm^{-1}) of the phosphanyl-imines PC=NMe and PC=NEt in the spectra of **2** and **3** are practically unchanged relative to those of the free ligands. However, at the same time, coordination of the ligand slightly affects the aromatic C=C stretching values.

The available data are not helpful in unambiguously establishing the geometries of [PdPhI(PC=NMe)] and [PdPhI(PC=NEt)], which are present as single isomers in solution. As a matter of fact, upon crystallization, the *trans*-P,I isomer is obtained. In contrast to these cases, the assignment of the molecular structure as *trans*-P,Cl in solution is possible for [PdMeCl($PNMe_2$)]·0.5 C_6H_6 by virtue of the $^3J_{PH}$ coupling constant value[11].

Synthesis and Characterization of the Cationic Palladium(II) Complexes

The cationic complexes of the type [PdR(PPh_3)(P$^{\frown}$N)]$^+$ (with $CF_3SO_3^-$ as the counterion), [PdMe(PPh_3)($PNMe_2$)]$^+\cdot C_6H_6$ (**5**), [PdPh(PPh_3)($PNMe_2$)]$^+\cdot 0.5\ C_6H_6$ (**6**), [PdPh(PPh_3)(PC=NMe)]$^+\cdot 0.5\ C_6H_6$ (**7**), [PdPh(PPh_3)(PC=NEt)]$^+\cdot 0.5\ C_6H_6$ (**8**), were synthesized by adding an $AgCF_3SO_3/PPh_3$ solution in Me_2CO to a CH_2Cl_2 solution of the corresponding neutral precursor [PdRX(P$^{\frown}$N)] at 0°C (see Eq. 3). Removal of the silver salt by filtration and recrystallization of the product from CH_2Cl_2, C_6H_6, and Et_2O afforded the pure products as white or off-white powders. Complexes **5**–**8** are stable in the solid state, but they tend to decompose slowly in solution (over a period of days).

Table 1. Selected IR and NMR absorptions of complexes [PdRX(P∩N)] and of the corresponding free ligands

	ν[a] (cm^{-1})		δ[b] (ppm), *J* (Hz)				
	C=C	C=N	CH_2	CH_3	H_{arom}	*H*C=N	$^{31}P\{^1H\}$
Complex **1**	1574			3.40 (s)[c], 3.66 (s)	6.63−6.72 (m), 6.88−6.99 (m), 7.22−7.89 (m)		24.3(s)[c], 37.3 (s)
$PNMe_2$	1570			2.58 (s)	6.50−7.50 (m)		−16.2 (s)
Complex **2**	1562	1637		4.00 (s)	6.38−6.68 (m), 7.04−7.68 (m)	8.00 (bs)	23.6 (s)
PC=NMe	1582	1640		3.38 (d) $^3J_{HH}$ = 1.8	6.80−6.97 (m), 7.13−7.48 (m), 7.89−8.05 (m)	8.85−8.95 (m) $^4J_{PH}$ = 4.8	−14.0 (s)
Complex **3**	1561	1637	4.42 (q) $^3J_{HH}$ = 7.3	1.22 (t) $^3J_{HH}$ = 7.3	6.40−6.68 (m), 6.99−7.70 (m)	8.00 (bs)	21.6 (s)
PC=NEt	1583	1637	3.49 (qd) $^4J_{HH}$ = 1.5, $^3J_{HH}$ = 4.4	1.10 (t) $^3J_{HH}$ = 4.4	6.75−6.95 (m), 7.13−7.56 (m), 7.91−8.03 (m)	8.84−8.93 (m) $^4J_{PH}$ = 4.8	−13.3 (s)
Complex **4**	1583			0.78 (d, Pd−CH_3) $^3J_{HP}$ = 2.9; 3.15 [s, N(CH_3)$_2$]	7.13−7.81 (m)		35.6 (s)

[a] In KBr: C=C refers to the aromatic C=C stretching, while C=N refers to the C=N stretching. − [b] In $CDCl_3$. − [c] More abundant isomer.

$$[PdRX(P^{\cap}N)] + AgCF_3SO_3 + PPh_3 \xrightarrow[CH_2Cl_2,\ Me_2CO]{0\,^{\circ}C,\ 45\ min} [PdR(PPh_3)(P^{\cap}N)]CF_3SO_3 + AgX \quad (3)$$

The more stable allyl complex $[Pd(\eta^3\text{-all})(PNMe_2)]PF_6$ (**9**) was obtained as a cream-coloured powder following a different synthetic procedure, employing $[Pd(\eta^3\text{-all})Cl]_2$[19], two equivalents of the ligand $PNMe_2$, and a large excess of KPF_6 (see Eq. 4).

$$[Pd(\eta^3\text{-all})Cl]_2 + PNMe_2 + 2\ KPF_6 \xrightarrow[CH_2Cl_2,\ 3\ h]{r.t.} 2\ [Pd(\eta^3\text{-all})(PNMe_3)]PF_6 + 2\ KCl \quad (4)$$

All the cationic complexes have been characterized by means of the usual physicochemical techniques. Molar conductivity values of 152 $ohm^{-1}cm^2mol^{-1}$ (see Experimental Section) confirm that they are uni-univalent electrolytes[20] and the presence of the anions $CF_3SO_3^-$ and PF_6^- is confirmed by very sharp, intense bands in their solid-state IR spectra at 1265 cm^{-1} [ν(S−O)] and 834 cm^{-1} [ν(P−F)], respectively[21].

In the case of complexes $[PdR(PPh_3)(P^{\cap}N)]^+$, the presence of two nonequivalent ^{31}P nuclei and the value of their coupling constants[22] (Table 2) permits the assignment of their molecular structures in $CDCl_3$ solution. This is fortunate, since no crystal structure could be determined. Thus, the $^{31}P\{^1H\}$ spectrum of $[PdPh(PPh_3)(PNMe_2)]^+$ is very informative and the complex is found to consist of a mixture of isomers (Figure 1), the *trans* isomer being prevalent (82%) (the terms *cis* and *trans* refer here to the mutual P positions).

Figure 1. The *trans* and *cis* isomers of complex **6**

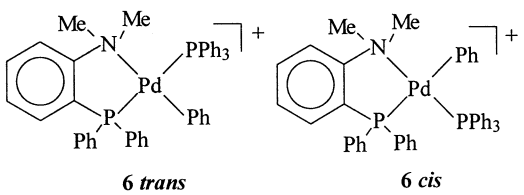

6 ***trans*** **6** ***cis***

In the $^{31}P\{^1H\}$ spectrum of complex **6** (Figure 2), the AB system ($^2J_{PP}$ = 372 Hz) is associated with the *trans* species, while the AX system ($^2J_{PP}$ = 24 Hz) is associated with the *cis* species.

Figure 2. $^{31}P\{^1H\}$-NMR spectrum of the mixture of isomers of complex **6**

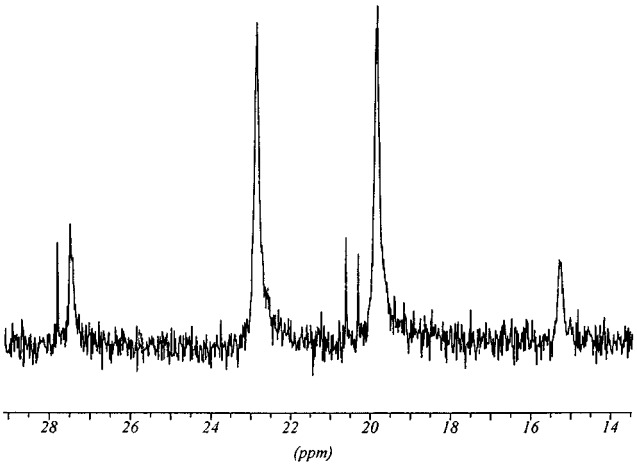

On the basis of these findings, and the values reported in Table 2, it can be stated that the phosphanyl-imino complexes **7** and **8** exhibit only the *trans* configuration.

The methyl σ organometallic cationic complex $[PdMe(PPh_3)(PNMe_2)]^+$ (**5**) gives rise to an interesting ^1H-NMR spectrum, which indicates the presence of the two expected isomers; while the *cis* species is stereochemically rigid at room temperature [the signal of the methyl group bound to palladium(II) of this isomer appears as a doublet of doublets at δ = 0.67 with $^3J_{HP}$ = 2.2 and 6.6 Hz] (Figure 3a), the *trans* species is stereochemically nonrigid. Broad signals at δ = 0.53 (Figure 3a) and δ = 2.87 can be attributed to the protons of the methyl group bound to palladium(II) and of the methyl groups of the dimethylamino ligand, respectively. This isomer is the prevalent species, as deduced from integration of the signals. In the $^{31}P\{^1H\}$ spectrum,

Table 2. NMR absorptions of the palladium(II) cationic complexes

Complex	CH_2	CH_3	δ (ppm)[a], J (Hz) H_{arom}	CH	$^{31}P\{^1H\}$
5		0.53 (bs, Pd−CH_3 *trans*), 0.67 (dd, Pd−CH_3 *cis*) $^3J_{HP}$ = 2.2, 6.6; 2.87 [bs, $N(CH_3)_2$ *trans*]; 3.25 [s, $N(CH_3)_2$ *cis*]	6.90−7.97 (m)		23.8 (d, *cis*) $^2J_{PP}$ = 26, 40.1 (d, *cis*) $^2J_{PP}$ = 26
6		2.76 (bs), 2.94 (s)	6.16−6.67 (m), 6.91−7.97 (m)		18.4 (d, *trans*) $^2J_{PP}$ = 372, 24.4 (d, *trans*) $^2J_{PP}$ = 372; 20.5 (d, *cis*) $^2J_{PP}$ = 24, 27.7 (d, *cis*) $^2J_{PP}$ = 24
7		2.87 (s)	6.30−6.49 (m), 6.65−6.79 (m), 6.88−8.05 (m)	8.21 (bs)	20.1 (d, *trans*) $^2J_{PP}$ = 376, 21.6 (d, *trans*) $^2J_{PP}$ = 376
8	3.03 (q) $^3J_{HH}$ = 7.3	0.54 (t) $^3J_{HH}$ = 7.3	6.32−6.53 (m), 6.69−6.80 (m), 7.00−7.92 (m)	8.33 (bs)	17.8 (d, *trans*) $^2J_{PP}$ = 389, 22.2 (d, *trans*) $^2J_{PP}$ = 389
9		3.45 (s)	6.40−6.68 (m), 6.99−7.70 (m)	2.90−3.80 (m, $H^{3\cdot}$,$H^{3'}$)[b], 4.17 (dd, H^1) $^3J_{HP}$ = 9.5, $^3J_{HH}$ = 13.9, 4.95 (dd, $H^{1'}$) $^3J_{HP}$ = 5.3, $^3J_{HH}$ = 7.7, 5.80−6.15 (m, H^2)	−141[c] (sept, J_{PF} = 708) 33.6 (s)

[a] In $CDCl_3$. − [b] $H^{1'}H^1C^1C^2H^2C^3H^{3'}H^3$, where C^1 is *trans* to P. − [c] In CD_3CN.

Figure 3. (a) ^{1}H-NMR signals of the methyl groups bound to palladium(II) of the mixture of isomers of complex **5** at 25°C; (b) ^{1}H-NMR signals of the methyl groups bound to palladium(II) of the mixture of isomers of complex **5** at −20°C

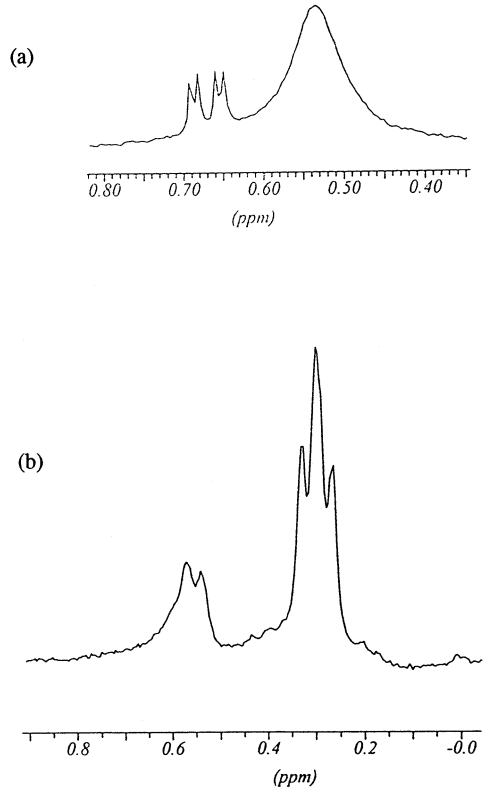

only the *cis* isomer gives rise to well-defined, sharp signals ($^2J_{PP}$ = 26 Hz).

Lowering of the temperature blocks the stereochemical nonrigidity of the *trans* species and at −20°C the AB system of the stereoisomer eventually appears (δ = 27.0 and δ = 31.7 with $^2J_{PP}$ = 375 Hz). The signal of the methyl group bound to palladium(II) (Figure 3b) becomes a triplet at δ = 0.30 with $^3J_{HP}$ = 6.5 Hz, this value being of the same order as the corresponding value of 5 Hz observed in the ^{1}H-NMR spectrum of *trans*-[PdMeI(PPh_3)$_2$][23].

We speculate that at low temperature (−20°C) the *trans* species is undissociated. When the temperature is increased, a fast dissociation process takes place so that the triplet, arising from the coupling of the protons of the methyl bound to palladium(II) with the two ^{31}P nuclei, merges into one very broad singlet. Considering the high *trans* effect of the phosphane group and the stabilization of the P∩N ligand due to the chelate effect, we postulate that this dissociation process involves the PPh_3 ligand, leading to a T-shaped intermediate (Figure 4).

Figure 4. Dissociation of the PPh_3 group and formation of a T-shaped intermediate in the case of *trans*-[PdMe(PPh_3)($PNMe_2$)]$^+$

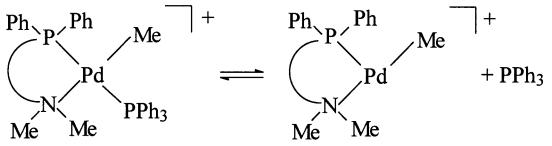

The complex [Pd(η^3-all)($PNMe_2$)]PF_6 is also stereochemically nonrigid in $CDCl_3$ as a consequence of a selective *syn-anti* interchange of the allyl protons *trans* to the NMe_2 group through the usual η^3−η^1−η^3 interconversion process (Scheme 2).

This fluxional phenomenon has been observed previously[24]. The PPh_2 group weakens the *trans* Pd−CH_2 bond, thus promoting the opening of the allyl ring and, by rotation about the σ bonds, the interchange of the *syn-anti* H^3 and $H^{3'}$ protons.

The relevant signal is not discernible in the ^{1}H-NMR spectrum owing to its partial overlap with that of the $N(CH_3)_2$ group (Figure 5) and only a broad absorption can be observed. On the contrary, the signals of the other three

Scheme 2

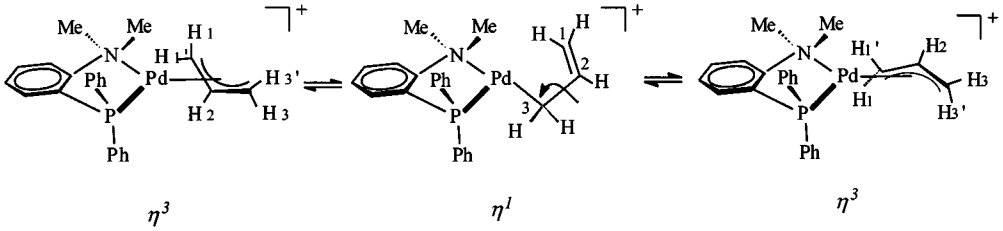

protons (Figure 6) are well defined: the multiplet between $\delta = 5.80$ and $\delta = 6.15$ is due to the central allyl proton H^2, while the two doublets of doublets at $\delta = 4.95$ ($^3J_{HH} = 7.7$ Hz and $^3J_{HP} = 5.3$ Hz) and at $\delta = 4.17$ ($^3J_{HH} = 13.9$ Hz and $^3J_{HP} = 9.5$ Hz) can be assigned to H^1 (*anti* in relation to H^2) and $H^{1'}$ (*syn* in relation to H^2), respectively, on the basis of the magnitudes of the coupling constants[25].

Figure 5. Overlapping of the signals of the protons of the $N(CH_3)_2$ group and of the protons H^3 and $H^{3'}$ in the ^{1}H-NMR spectrum of complex **9** in $CDCl_3$

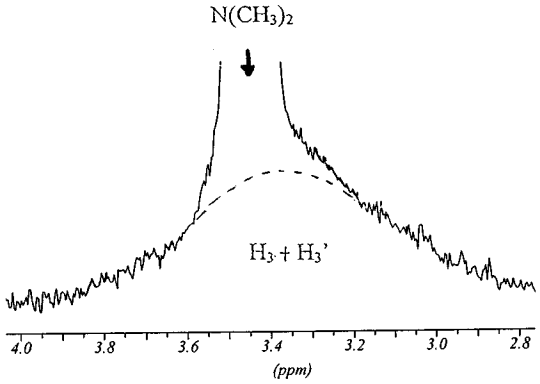

Figure 6. Signals of protons H^1, $H^{1'}$, and H^2 in the ^{1}H-NMR spectrum of complex **9** in $CDCl_3$

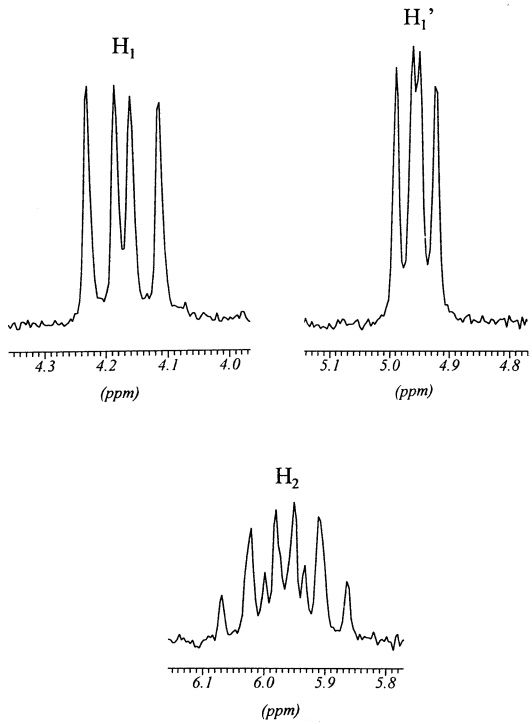

X-ray Structure

The unique portion of the unit cells is different in compounds **1**, **2**, **3**·3/2 H_2O, and **9**. In **1**, the asymmetric unit consists of a single molecule of the neutral complex [PdPhI($PNMe_2$)] (Figure 7), while two molecules of [PdPhI(PC=NMe)] are present in **2** (Figure 8). In **3**·3/2 H_2O, the unique portion comprises two molecules of [PdPhI(PC=NEt)], along with three molecules of water (Figure 9), and in **9** two molecules of the salt [Pd(η^3-C_3H_5)($PNMe_2$)]PF_6 are likewise present (Figure 10). In **2**, **3**·3/2 H_2O, and **9**, the geometries shown by the two such independent and chemically well-separated molecules are practically superimposable (Figure 11), the differences being restricted to minor features only. This is also confirmed by the fact that no bond distance differs by more than two standard deviations in any of these molecule pairs. Hence, in the present discussion, all geometrical parameters refer to the mean values.

In **1** and **9**, the bidentate P∩N ligand coordinates to palladium(II) forming a five-membered chelate ring, which adopts a somewhat envelope-like (C_s) conformation (pertinent torsion angles in the range from −16.1° to +16.1°). The

Figure 7. Molecular structure of **1**. H atoms have been omitted for clarity. Thermal ellipsoids are shown at the 40% probability level

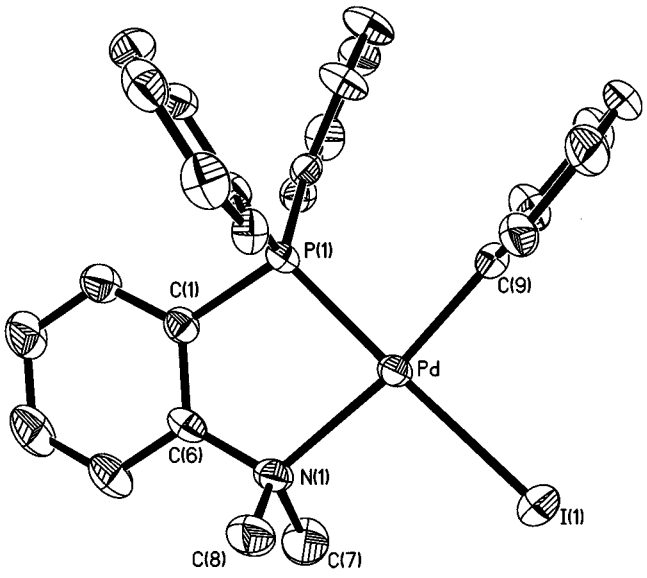

Figure 8. The asymmetric unit of **2**. H atoms have been omitted for clarity. Thermal ellipsoids are shown at the 40% probability level

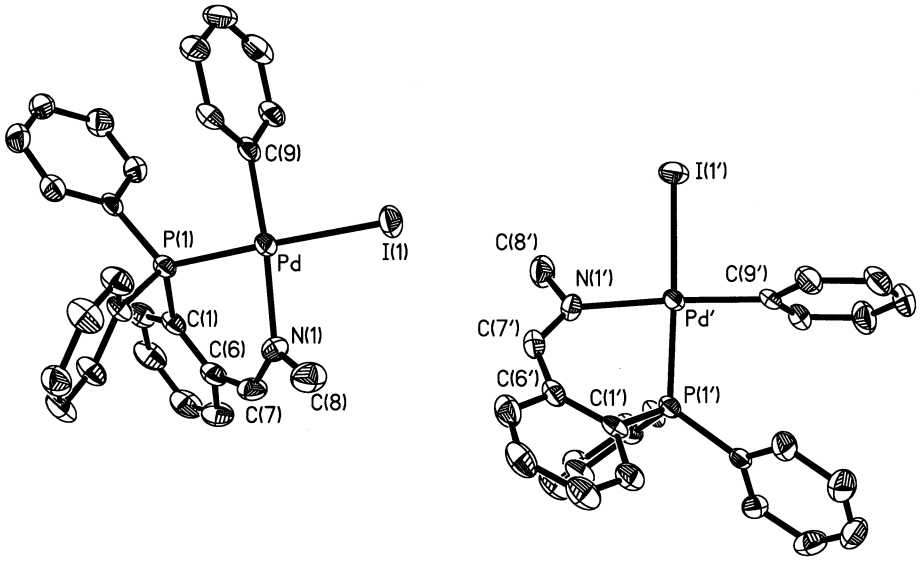

Figure 9. The asymmetric unit of **3**·3/2 H_2O. H atoms have been omitted for clarity. The C(9′) atom obscures N(1′).

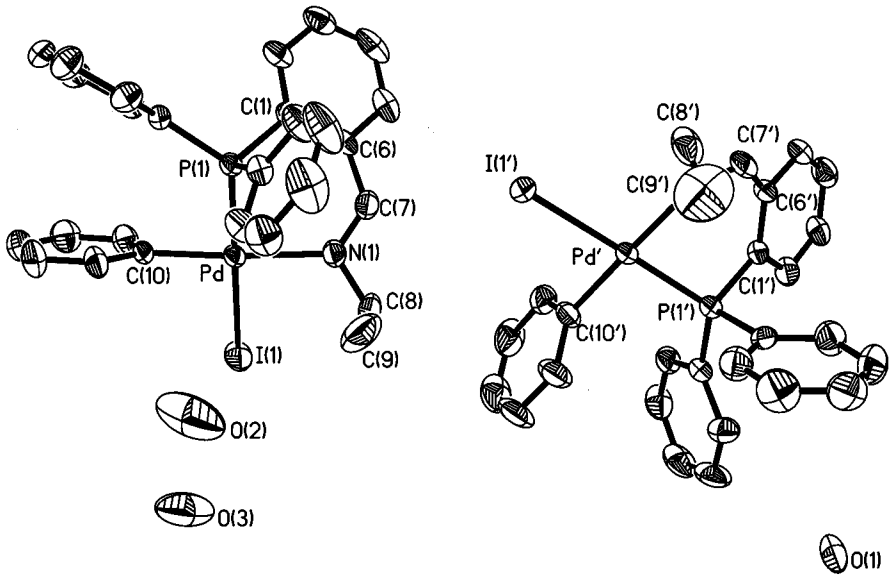

Figure 10. The asymmetric unit of **9**. H atoms have been omitted for clarity

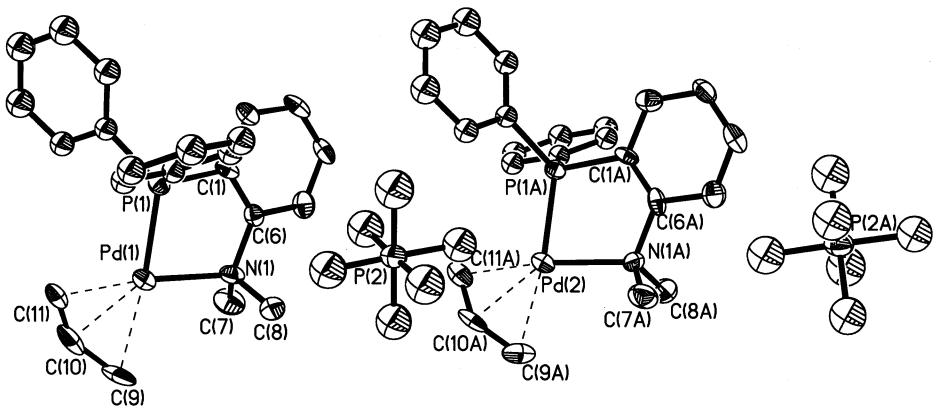

Figure 11. Superimposition of the two independent moieties of **2**, **3**·3/2 H_2O, and **9**. Weighted root mean square deviation of 0.02, 0.05, and 0.03 Å, respectively, when fitting is performed on the labelled atoms

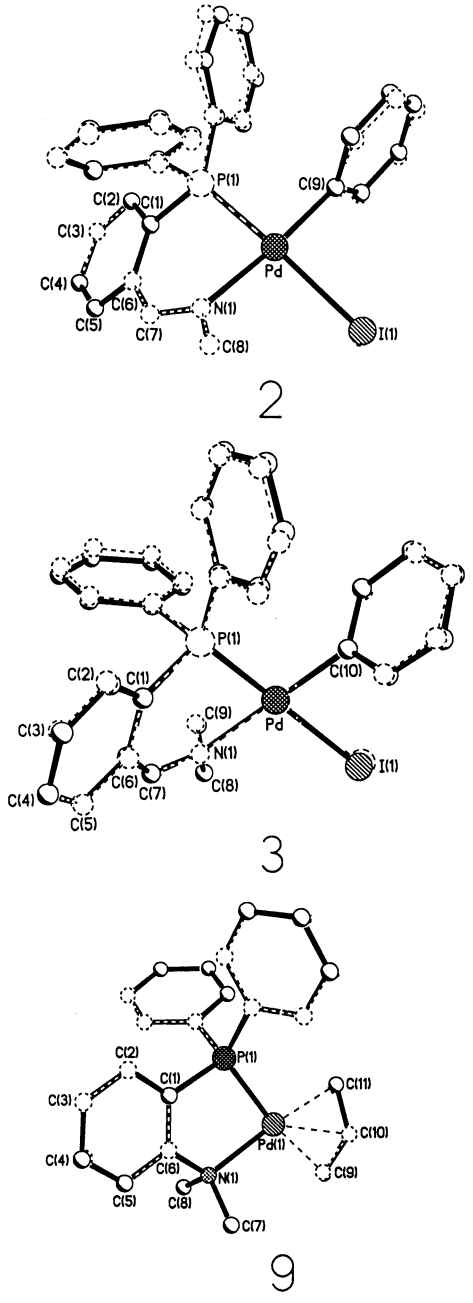

coordination sphere of **1** is completed by an iodide and a phenyl ligand, whereas the remaining coordination positions in **9** are occupied by the η^3-allyl ligand. In the latter compound, the coordination plane can be defined by the P,N donor atoms and by the terminal carbon atoms of the allyl group, the central carbon atom residing 0.50 Å above this plane. The mean plane defined by the eight atoms P(1), C(1)−(6), N(1) forms dihedral angles of 5.4° and 5.1° with the mean coordination plane in **1** and **9**, respectively. The P−N "bite" distance and the P−Pd−N angle are 3.00(1) Å and 85.1(3)° in both complexes. The Ph ligand in **1** is roughly orthogonal to the mean coordination plane (dihedral angle of 82.1°).

In **2** and **3**·3/2 H_2O, the P∩N ligand forms a six-membered chelate ring with the palladium(II) center. In this arrangement, the Pd and N(1) atoms in **2** deviate by +1.56 Å and +0.49 Å from the mean plane defined by the eight atoms P(1), C(1)−(7). The corresponding values in **3**·3/2 H_2O are +1.41 and +0.32 Å. The latter plane forms dihedral angles ("elbow angles") of 55.8° and 53.9° with the coordination plane in **2** and **3**·3/2 H_2O, respectively. In turn, the Ph ligand forms a dihedral angle with the coordination plane of 72.0° (in **2**) and of 75.3° (in **3**·3/2 H_2O). The "bite" distances and angles match those found in **1** and **9** [2.95(1) Å, 84.0(2)° in **2** and 3.00(1) Å, 85.8(2)° in **3**·3/2 H_2O].

The donor atoms deviate from the mean coordination plane by ±0.04 Å in **1**, ±0.07 Å in **2**, ±0.04 Å in **3**·3/2 H_2O, and ±0.06 Å in **9**, with the palladium(II) correspondingly out by 0.02, 0.02, 0.04, and 0.09 Å. In all the complexes, the major departure from the ideal square-planar geometry is manifested in the "bite" angle. From comparison of the distances with reference values obtained from the Cambridge Structural Database[26], the following comments can be made: (i) The Pd^{II}−I distance (mean 2.654 Å) is consistent with both the reference value (2.639 Å) derived from 164 observations and the sum of the covalent radii (1.33 + 1.31 Å)[27]; (ii) the Pd^{II}−P distance in the three neutral complexes (mean 2.228 Å), which is slightly shorter than that in the allyl cationic complex (2.260 Å), is remarkably shorter than the $Pd^{II}-PPh_3$ bond reference value (2.302 Å) encountered in 248 entries, and falls at the short end of a wide range (2.21−2.46 Å); (iii) the $Pd^{II}-C_{Ph}$ distance (mean 2.015 Å) matches the reference value (2.013 Å) derived from 34 observations, and (iv) the Pd^{II}−N distance in **1** (2.252 Å) is considerably longer than the corresponding distances in **2** and **3**·3/2 H_2O (mean 2.17 Å), which may be ascribed to the different environment of the nitrogen. Accordingly, on going from a five- to a six-membered chelate ring, the Pd−N(sp^3)−C angle (113.6°) widens to the mean value of 125.5° observed for Pd−N(sp^2)=C.

The packing observed for the four complexes does not show intermolecular contacts shorter than the sum of the van der Waals' radii, the shortest I−H approach being 3.1 Å. The opportunity for hydrogen bonding seems to be restricted to that between the water molecules of **3**·3/2 H_2O, which show O−O separations of 2.8 Å.

Conclusions

The phosphanyl-amine $PNMe_2$ and the phosphanyl-imines PC=NMe and PC=NEt are able to stabilize organometallic neutral and cationic palladium(II) complexes, acting as chelating bidentate ligands via their P and N donor atoms, forming five- or six-membered rings with the metal center in the expected manner.

The neutral complexes [PdRX(P∩N)] are stable species, both in solution and in the solid state. The phenyl com-

plexes [PdPhI(P⌒N)] and [PdMeCl(PNMe$_2$)] exist as the *trans*-P,I isomer in the solid state, as indicated by X-ray analysis, as well as *trans*-P,Cl isomer in solution, as deduced from the ^{1}H-NMR spectrum in $CDCl_3$.

The σ organometallic cationic complexes [PdR(PPh_3)(P⌒N)]$^+$ can be obtained by the reaction of the neutral precursor with PPh_3 and $AgCF_3SO_3$ and exist in solution mainly as *trans*-P,P species. In particular, a fluxional behavior is observed for *trans*-[PdMe(PPh_3)(PNMe$_2$)]$^+$, probably due to the dissociation of a PPh_3 molecule. The η^3-allyl complex [Pd(η^3-all)(PNMe$_2$)]PF_6, obtained from the dimer [Pd(η^3-all)Cl]$_2$ and a stoichiometric amount of $PNMe_2$ in the presence of excess KPF_6, also exhibits fluxional behavior in $CDCl_3$ solution, owing to the selective interchange of the protons of the CH_2 group *trans* to the phosphorus of the diphenylphosphanyl group.

Comparison of the crystal structure of [Pd(η^3-all)(PNMe$_2$)]PF_6 with those of the neutral complexes containing the phosphanyl-imines PC=NMe and PC=NEt reveals moderate differences relating to the size of the chelate ring in terms of bond lengths and the "bite" angle P−Pd−N.

This work was partially supported by *Progetto Strategico "Tecnologie Chimiche Innovative", Consiglio Nazionale delle Ricerche.* Benedetto Corain is grateful to the *Alexander von Humboldt Foundation* for supporting his activities at the TU München.

Experimental Section

General: All chemicals and solvents were of analytical grade and were used as received unless otherwise stated. Anhydrous Et_2O and C_6H_6 were distilled from potassium/benzophenone under N_2; anhydrous THF was freshly distilled from potassium/benzophenone under N_2. The complexes [Pd(dba)$_2$][16], [PdMeCl(COD)][18], [Pd(η^3-all)Cl]$_2$[19] and the ligands PNMe$_2$[9], PC=NR (R = Me, Et)[10] were synthesized according to literature procedures. − IR: Mattson 3030 Fourier transform spectrometer. − ^{1}H and ^{31}P{^{1}H} NMR: Bruker AC-200 (200 MHz for ^{1}H and 80.9 MHz for ^{31}P). Typical NMR samples were prepared by dissolving the complexes (20 mg) in 0.4 ml of the deuterated solvent. For ^{1}H NMR, $CDCl_3$ as solvent, TMS as internal standard; for ^{31}P{^{1}H} NMR, $CDCl_3$ as solvent, 85% aqueous H_3PO_4 as external standard. − Conductivity measurements: Amel conductimeter Model 131, ca. 10^{-3} M solutions in MeCN at 25°C. − Elemental analyses (C, H, N): Fisons EA 1108 elemental analyzer.

Synthesis of **1**−**3** − *General Procedure:* To a blood-red solution of 0.633 g of [Pd(dba)$_2$] (1.1 mmol) in 90 ml of dry THF at 50°C under N_2, a stoichiometric amount of the P⌒N ligand and 520 μl of PhI (4.4 mmol, d = 1.73 g/ml) were added, and the mixture was stirred under N_2 at the same temperature. After 45 min, the yellow-green mixture was concentrated under a flow of N_2 and filtered through Celite. The solvent was removed from the filtrate under reduced pressure and the residue was washed several times with Et_2O until the washings were colorless. The residual solid was then dried in vacuo. Crystals suitable for X-ray analysis were grown by slow evaporation of the solvent from Me_2CO/MeOH solutions (Crystals of complex **3** from Me_2CO/MeOH/H_2O solutions).

Synthesis of **4**: To a solution of 0.508 g of [PdMeCl(COD)] (0.19 mmol) in 60 ml of dry C_6H_6 under N_2, was added 0.058 g of the phosphanyl-amine $PNMe_2$ (0.19 mmol) and the mixture was stirred under N_2. After 15 min, a white solid began to precipitate. After 24 h, the pale-yellow mixture was filtered and the white solid was collected, washed with C_6H_6 and Et_2O, and dried in vacuo. The filtrate was concentrated under a flow of N_2 and upon addition of Et_2O a precipitate was formed. This was filtered off, washed with Et_2O and a small volume of THF, and dried in vacuo.

Synthesis of **5**−**8** − *General Procedure:* To a solution of the neutral complex [PdRX(P⌒N)] (0.41 mmol) in 5 ml of CH_2Cl_2 at 0°C under N_2, a solution containing 0.108 g of PPh_3 (0.41 mmol) and 0.106 g of $AgCF_3SO_3$ (0.41 mmol) in 3 ml of Me_2CO was added dropwise, resulting in immediate silver halide precipitation. After 45 min., the mixture was concentrated under a flow of N_2 and filtered, and the solvent was removed from the filtrate in vacuo. The residue was redissolved in CH_2Cl_2 and upon addition of Et_2O a precipitate was deposited, which was separated from the solution by decantation of the supernatant and redissolved in a small amount of CH_2Cl_2. Addition of C_6H_6 and Et_2O under vigorous stirring caused the formation of a solid, which was filtered off, washed with C_6H_6 and Et_2O, and dried in vacuo.

Synthesis of **9**: To a solution of 0.130 g of [Pd(η^3-all)Cl]$_2$ (0.36 mmol) in 10 ml of CH_2Cl_2 was added 0.265 g of KPF_6 (1.44 mmol) followed by 0.282 g of the ligand $PNMe_2$ (0.40 mmol), and the yellow mixture was stirred at room temperature. After 3 h, the colorless mixture was filtered and the filtrate was concentrated under reduced pressure. Addition of Et_2O caused the formation of a white precipitate, which was filtered off, washed with Et_2O, and dried in vacuo. The solid was recrystallized from MeCN and Et_2O and dried in vacuo. Crystals suitable for X-ray analysis were grown by slow evaporation of the solvent from CH_2Cl_2/EtOH/Et_2O solutions.

[PdPhI(PNMe$_2$)] (**1**): Yield 0.574 g (85%). − IR (KBr): ṽ = 3055 m cm^{-1}, 1574 m, 1469 s, 1433 s, 743 vs, 691 s, 500 vs. − $C_{26}H_{25}INPPd$ (615.79): calcd. C 50.71, H 4.10, N 2.28; found C 49.03, H 4.03, N 2.02.

[PdPhI(PC=NMe)] (**2**): Yield: 0.637 g (94%). − IR (KBr): ṽ = 3050 m cm^{-1}, 1637 m (C=N), 1562 m, 1478 m, 1434 s, 739 s, 688 s. − $C_{26}H_{23}INPPd$ (613.79): calcd. C 50.88, H 3.78, N 2.28; found C 50.73, H 4.01, N 2.13.

[PdPhI(PC=NEt)] (**3**): Yield: 0.421 g (61%). − IR (KBr): ṽ = 3043 m cm^{-1}, 1637 m (C=N), 1561 m, 1467 m, 1434 s, 727 vs, 691 vs. − $C_{27}H_{25}INPPd$ (627.82): calcd. C 51.65, H 4.02, N 2.23; found C 51.00, H 3.99, N 2.03.

[PdMeCl(PNMe$_2$)]·0.5 C_6H_6 (**4**): Yield: 0.074 g (78%). − IR (KBr): ṽ = 3049 w cm^{-1}, 1583 w, 1480 s, 1436 s, 748 s, 694 s, 502 s. − $C_{21}H_{23}ClNPPd \cdot 0.5\ C_6H_6$ (501.33): calcd. C 57.50, H 5.24, N 2.79; found C 55.32, H 5.15, N 2.69.

[PdMe(PPh$_3$)(PNMe$_2$)]$CF_3SO_3 \cdot C_6H_6$ (**5**): Yield: 0.252 g (67%). − IR (KBr): ṽ = 3053 w cm^{-1}, 1593 w, 1502 m, 1435 m, 1273 vs (S−O), 693 s, 636 s. − Λ_M (MeCN): 150 ohm^{-1}cm^{2}mol^{-1}. − $C_{40}H_{38}F_3NO_3P_2PdS \cdot C_6H_6$ (916.31): calcd. C 60.29, H 4.85, N 1.53, S 3.50; found C 60.93, H 5.56, N 1.63, S, 3.36.

[PdPh(PPh$_3$)(PNMe$_2$)]$CF_3SO_3 \cdot 0.5\ C_6H_6$ (**6**): Yield: 0.362 g (94%). − IR (KBr): ṽ = 3056 m cm^{-1}, 1564 m, 1473 m, 1437 s, 1263 vs (S−O), 691 s, 637 s. − Λ_M (MeCN): 152 ohm^{-1}cm^{2}mol^{-1}. − $C_{45}H_{40}F_3NO_3P_2PdS \cdot 0.5\ C_6H_6$ (939.32): calcd. C 61.37, H 4.62, N 1.48, S 3.41; found C 61.70, H 5.25, N 1.60, S 3.38.

[PdPh(PPh$_3$)(PC=NMe)]$CF_3SO_3 \cdot 0.5\ C_6H_6$ (**7**): Yield: 0.361 g (94%). − IR (KBr): ṽ = 3052 m cm^{-1}, 1641 m (C=N), 1564 m, 1482 m, 1435 s, 1261 vs (S−O), 693 s. − Λ_M (MeCN): 152 ohm^{-1}cm^{2}mol^{-1}. − $C_{45}H_{38}F_3NO_3P_2PdS \cdot 0.5\ C_6H_6$ (937.3): calcd.

Table 3. Crystal data and summary of data collection and refinement for [PdPhI($PNMe_2$)] (**1**), [PdPhI(PC=NMe)] (**2**), [PdPhI(PC=NEt)]·3/2 H_2O (**3**·3/2 H_2O), and [Pd(η^3-C_3H_5)($PNMe_2$)]PF_6 (**9**)

	1	**2**	**3**·3/2 H_2O	**9**
Empirical formula	$C_{26}H_{25}INPPd$	$C_{26}H_{23}INPPd$	$C_{27}H_{28}INO_{1.5}PPd$	$C_{23}H_{25}F_6NP_2Pd$
Form. weight	615.74	613.72	654.77	597.78
Crystal system	monoclinic	triclinic	triclinic	triclinic
Space group	$P2_1/n$	$P\bar{1}$	$P\bar{1}$	$P1$
a [Å]	9.283(2)	9.200(6)	11.972(4)	9.042(2)
b [Å]	16.645(4)	16.067(10)	15.356(5)	10.980(3)
c [Å]	15.542(4)	16.147(9)	15.874(6)	14.408(3)
α [°]	90	92.86(5)	105.03(3)	72.11(2)
β [°]	94.06(2)	90.95(5)	90.03(3)	71.86(2)
γ [°]	90	96.27(5)	96.63(3)	65.75(2)
V [Å^3]	2395.5(10)	2369(3)	2798(2)	1212.6(5)
Z	4	4	4	2
D_{calcd} [Mg/m^3]	1.707	1.721	1.554	1.637
μ [mm^{-1}]	2.143	2.167	1.843	0.955
λ [Å]	0.71073	0.71073	0.71073	0.71073
obsd. refl.	2512	5059	6798	2672
$R1$, $Rw2$[a]	0.0404, 0.1016	0.0469, 0.1211	0.0727, 0.2012	0.0398, 0.0997
GooF[b]	1.063	1.059	1.105	1.058

[a] $R1 = \Sigma\|F_o| - |F_c\|/\Sigma|F_o|$; $Rw2 = [\Sigma[w(F_o^2 - F_c^2)^2]/\Sigma[w(F_o^2)^2]]^{1/2}$. – [b] GooF = $[\Sigma[w(F_o^2 - F_c^2)^2]/(N_{obs} - N_{par})]^{1/2}$.

Table 4. Selected bond lengths [Å] and angles [°] for **1**, **2**[a], **3**·3/2 H_2O[a], and **9**[a]

	1	**2**		**3**·3/2H_2O		**9**	
Pd–I(1)	2.655(1)	2.664(2)	2.671(2)	2.628(1)	2.651(1)		
Pd–P(1)	2.208(2)	2.232(2)	2.239(2)	2.228(2)	2.235(3)	2.257(4)	2.263(5)
Pd–N(1)	2.252(5)	2.169(6)	2.172(6)	2.176(8)	2.166(8)	2.17(1)	2.17(1)
Pd–C(9)	2.029(6)	2.007(8)	2.026(7)			2.26(2)	2.19(2)
Pd–C(10)				2.007(8)	2.026(7)	2.15(2)	2.14(2)
P(1)–C(1)	1.819(6)	1.835(7)	1.828(7)	1.826(9)	1.830(9)	1.84(2)	1.85(2)
N(1)–C(6)	1.464(9)	1.26(1)	1.28(1)			1.47(2)	1.50(2)
N(1)–C(7)		175.6(1)	175.4(1)	1.29(1)	1.25(1)		
I(1)–Pd–P(1)	177.7(1)	175.6(1)	175.4(1)	178.3(1)	178.9(1)		
I(1)–Pd–N(1)	97.3(1)	94.6(2)	94.1(2)	94.0(2)	95.6(2)		
I(1)–Pd–C(9)	90.2(2)	89.8(2)	89.6(2)	88.0(2)	87.3(3)		
P(1)–Pd–N(1)	84.9(1)	84.2(2)	83.8(2)	86.2(2)	85.5(2)	85.2(3)	85.1(3)
P(1)–Pd–C(9)	87.7(2)	91.6(2)	92.7(2)			167.4(6)	167.4(6)
P(1)–Pd–C(10)				91.8(3)	91.6(3)	137.1(9)	137.0(8)
P(1)–Pd–C(11)						101.6(6)	102.0(6)
N(1)–Pd–C(9)	171.7(2)	174.9(3)	175.2(3)				
N(1)–Pd–C(10)				175.9(3)	174.7(4)	136.5(9)	136.7(9)
N(1)–Pd–C(11)						173.0(7)	172.4(7)
Pd–P(1)–C(1)	103.4(2)	105.7(3)	105.7(2)	106.4(3)	107.3(3)	100.8(5)	100.8(5)
Pd–N(1)–C(6)	112.6(4)					113.0(9)	112.6(9)
Pd–N(1)–C(7)		127.7(6)	126.7(5)	123.3(7)	124.7(7)		

[a] Since the asymmetric unit contains two independent molecules, two values are reported for each entry.

C 61.50, H 4.42, N 1.50, S 3.42; found C 60.74, H 4.59, N 1.32, S 3.31.

[PdPh(PPh$_3$)(PC=NEt)]CF$_3$SO$_3$ · 0.5 C$_6$H$_6$ (**8**): Yield: 0.316 g (81%). – IR (KBr): $\tilde{\nu}$ = 3056 m cm^{-1}, 1640 m (C=N), 1563 m, 1501 m, 1436 s, 1263 vs (S–O), 694 s, 636 s. – Λ_M (MeCN): 156 ohm^{-1}cm^{2}mol^{-1}. – $C_{46}H_{40}F_3NO_3P_2PdS \cdot 0.5\ C_6H_6$ (951.33): calcd. C 61.86, H 4.57, N 1.47, S 3.37; found C 61.25, H 4.86, N 1.37, S 3.19.

[Pd(η^3-all)(PNMe$_2$)]PF$_6$ (**9**): Yield: 0.200 g {93% based on [Pd(η^3-all)Cl]$_2$}. – IR (KBr): $\tilde{\nu}$ = 3061 w cm^{-1}, 1583 w, 1474 m, 1439 m, 834 vs (P–F), 556 s. – Λ_M (MeCN): 183 ohm^{-1}cm^{2}mol^{-1}. – $C_{23}H_{25}F_6NP_2Pd$ (597.83): calcd. C 46.20, H 4.22, N 2.34; found C 46.35, H 4.30, N 2.38.

X-ray Crystal Structure Determinations: The crystals were mounted on glass fibres, coated with epoxy resin, and were transferred to a Siemens Nicolet R3m/V four-circle automated diffractometer. Using graphite-monochromated Mo-K_α radiation, accurate cell parameters were determined and diffraction intensities (up to Θ 23°) were measured. Two standard reflections were measured after every 150 data points to check for crystal deterioration and/or misalignment. No significant deterioration in intensity was observed. Data were corrected for Lorentz, polarization and absorption (using ψ scans) effects.

The crystals of **3**·3/2 H_2O were found to be slightly sensitive to X-rays (decay of up to 19% during data collection) and decomposed after prolonged irradiation. Consequently, the empirical absorption correction was not applied. No unusually high correlation values were noted between any of the variables in the last cycle of full-matrix least-squares refinements on F^2 and the final difference maps were essentially featureless. Programs used and the sources of scattering factors are contained in the SHELXTL (PC version

4.20 or 5.03) software package provided by Siemens Analytical X-ray Instruments[28][29]. Some details of the data collection and refinements are given in Table 3. Selected bond distances and angles are presented in Table 4.

Further details of the crystal structure determination can be obtained from the Fachinformationszentrum Karlsruhe, D-76344 Eggenstein-Leopoldshafen, Germany, on quoting the depository numbers CSD 408513 (**1**), 408514 (**2**), 408515 (**3**·3/2 H_2O), and 408516 (**9**).

[1] L Crociani, F. Refosco, F. Tisato, S. Gatto, B. Corain, *Inorg. Chim. Acta* **1996**, *249*, 131−133.

[2] L. Crociani, B. Corain, F. Refosco, F. Tisato, A. Dolmella, S. Gatto, G. Bandoli, *Z. Kristallogr.* **1997**, *212*, 745−751.

[3] L. Crociani, F. Refosco, F. Tisato, G. Bandoli, B. Corain, *J. Am. Chem. Soc.* **1998**, *120*, 2973−2974.

[4] [4a] W. Keim, *Makromol. Chem. Macromol. Symp.* **1993**, *66*, 225−230. − [4b] W. Keim, *Angew. Chem. Int. Ed. Engl.* **1990**, *29*, 235−244. − [4c] E. F. Lutz, *J. Chem. Ed.* **1986**, *63*, 202−203.

[5] [5a] A. Bader, E. Lindner, *Coord. Chem. Rev.* **1991**, *108*, 27−110. − [5b] G. J. P. Britovsek, K. J. Cavell, W. Keim, *J. Mol. Catal. A: Chem.* **1996**, *110*, 77−87.

[6] [6a] G. M. DiRenzo, P. S. White, M. Brookhart, *J. Am. Chem. Soc.* **1996**, *118*, 6225−6234. − [6b] V. De Felice, M. E. Cucciolito, A. De Renzi, F. Ruffo, D. Tesauro, *J. Organomet. Chem.* **1995**, *493*, 1−11.− [6c] G. J. P. Britovsek, W. Keim, S. Mecking, D. Sainz, T. Wagner, *J. Chem. Soc., Chem. Commun.* **1993**, 1632−1634.

[7] [7a] L. K. Johnson, S. Mecking, M. Brookhart, *J. Am. Chem. Soc.* **1996**, *118*, 267−268. − [7b] B. Milani, L. Vicentini, A. Sommazzi, F. Garbassi, E. Chiarparin, E. Zangrando, G. Mestroni, *J. Chem. Soc., Dalton Trans.* **1996**, 3139−3144. − [7c] Z. Jiang, A. Sen, *J. Am. Chem. Soc.* **1995**, *117*, 4455−4467. − [7d] E. Drent, J. A. M. van Broekhoven, M. J. Doyle, *J. Organomet. Chem.* **1991**, *417*, 235−251.

[8] [8a] R. Patrini, M. Lami, M. Marchionna, F. Benvenuti, A. M. Raspolli Galletti, G. Sbrana, *J. Mol. Cat. A: Chem.* **1998**, *129*, 179−189. − [8b] J. Tsuji in *Palladium Reagents and Catalysts*, John Wiley & Sons, Chichester, U.K., **1996**, p. 427−429. − [8c] D. Commereuc, Y. Chauvin, *Bull. Soc. Chim. Fr.* **1974**, 652−656.

[9] H. P. Fritz, I. R. Gordon, K. E. Schwarzahans, L. M. Venanzi, *J. Chem. Soc.* **1965**, 5210−5216.

[10] [10a] C. A. Ghilardi, S. Midollini, S. Moneti, A. Orlandini, G. Scapacci, *J. Chem. Soc., Dalton Trans.* **1992**, 3371−3376. − [10b] H. Brunner, A. F. M. Mokhlesur Rahman, *Chem. Ber.* **1984**, *117*, 710−724.

[11] G. P. C. M. Dekker, A. Buijs, C. J. Elsevier, K. Vrieze, P. W. N. M. van Leeuwen, W. J. J. Smeets, A. L. Spek, Y. F. Wang, C. H. Stam, *Organometallics* **1992**, *11*, 1937−1948.

[12] B. Schmid, L. M. Venanzi, A. Albinati, F. Mathey, *Inorg. Chem.* **1991**, *30*, 4693−4699.

[13] [13a] E. Farnetti, G. Nardin, M. Graziani, *J. Chem. Soc., Chem. Commun.* **1988**, 1264−1265. − [13b] D. C. Mudalige, S. J. Rettig, B. R. James, W. R. Cullen, *J. Chem. Soc., Chem. Commun.* **1988**, 830−832. − [13c] D. M. Roundhill, R. A. Bechtold, S. G. N. Roundhill, *Inorg. Chem.* **1980**, *19*, 284−289. − [13d] T. B. Rauchfuss, F. T. Patino, D. M. Roundhill, *Inorg. Chem.* **1975**, *14*, 652−656. − [13e] T. B. Rauchfuss, D. M. Roundhill, *J. Am. Chem. Soc.* **1974**, 3098−3105. − [13f] T. B. Rauchfuss, D. M. Roundhill, *J. Organomet. Chem.* **1973**, *59*, C30−C32. − [13g] H. P. Fritz, I. R. Gordon, *J. Organomet. Chem.* **1966**, *5*, 103−105.

[14] T. B. Rauchfuss, *J. Organomet. Chem.* **1978**, *162*, C19−C22.

[15] P. Barbaro, C. Bianchini, F. Laschi, S. Midollini, S. Moneti, G. Scapacci, *Inorg. Chem.* **1994**, *33*, 1622−1630.

[16] M. F. Rettig, P. M. Maitlis, *Inorg. Synth.* **1977**, *17*, 134−137.

[17] [17a] W. De Graaf, J. Van Wegen, J. Boersma, A. L. Spek, G. van Koten, *Rec. Trav. Chim. Pays-Bas* **1989**, *108*, 275−277. − [17b] J. Andrieu, P. Braunstein, F. Naud, *J. Chem. Soc., Dalton Trans.* **1996**, 2903−2909.

[18] R. E. Rülke, A. L. Spek, C. J. Elsevier, P. W. N. M. van Leeuwen, K. Vrieze, *Inorg. Chem.* **1993**, *32*, 5769−5778.

[19] F. Hartley, S. R. Jones, *J. Organomet. Chem.* **1974**, *66*, 465−473.

[20] R. A. Walton, *Quart. Rev.* **1965**, *119*, 126−143.

[21] K. Nakamoto, *Infrared Spectra of Inorganic and Coordination Compounds*, J. Wiley & Sons, Inc., New York, **1963**, pp. 150, 169.

[22] C. A. McAuliffe, W. Levason, *Studies in Inorganic Chemistry 1: Phosphine, Arsine and Stibine Complexes of the Transition Elements*, Elsevier, Amsterdam, **1979**, p. 51.

[23] P. Fitton, M. P. Johnson, J. E. McKeon, *J. Chem. Soc., Chem. Commun.* **1968**, 6−7.

[24] R. Fernández-Galán, F. A. Jalón, B. R. Manzano, J. Rodríguez-de la Fuente, M. Vrahami, B. Jedlicka, W. Weissensteiner, G. Jogl, *Organometallics* **1997**, *16*, 3758−3768.

[25] S. Mecking, W. Keim, *Organometallics* **1996,** *15*, 2650−2656.

[26] F. H. Allen, S. Bellard, M. D. Brice, B.A. Cartwright, A. Doubleday, H. Higgs, T. Hummelink, B. G. Hummelink-Peters, O. Kennard, W. D. S. Motherwell, J. R. Rodgers, D. G. Watson, *Acta Crystallogr. B* **1979**, *35*, 2231; CSD Database, Release 5.14, October **1997**.

[27] G. Wulfsberg in *Principles of Descriptive Inorganic Chemistry* (Brooks/Cole Publ. Co.), Monterey, California, **1987**, p. 193.

[28] *Siemens SHELXTL (PC Version 4.20),* Siemens Industrial Automation, Inc., Madison, WI, **1990**.

[29] *Siemens SHELXTL (PC Version 5.03),* Siemens Industrial Automation, Inc., Madison, WI, **1994**.

[98097]

Theoretical Comparison of the Electronic Structures of $[PhN_2]^+$ and $[PhP_2]^+$ – Can the Benzenediphosphonium Cation Exist in the Gas Phase?

Geneviève Pfister-Guillouzo*[a], Anna Chrostowska[a], Jean-Marc Sotiropoulos[a], and Vadim D. Romanenko[b]

Laboratoire de Physico-Chimie Moléculaire, CNRS UMR 5624[a],
Avenue de l'Université, F-64000 Pau, France
Fax: (internat.) + 33(0)5599230-29
E-mail: genevieve.pfister@univ-pau.fr

Institute of Bioorganic Chemistry and Petrochemistry, National Academy of Sciences[b],
253660 Kiew 94, Murmanskaya St. 1, Ukraine

Received March 12, 1998

Keywords: Diazonium cations / Diphosphonium cations / Calculations / Ab initio methods

Ab initio quantum-chemical investigations are used to outline the main differences between the phenyldiazonium cation $[PhN_2]^+$ (**1a**,**b**) and its P analogue $[PhP_2]^+$ (**2a**,**b**). Our results show that in contrast to **1**, **2b** exists preferentially as a bridged structure. The phenyl ion affinity toward P_2 has been determined and suggests that the phenyldiphosphonium cation should be stable in the gas phase and that it is probably accessible by reaction between P_2 and Ph^+.

Introduction

The theoretical, structural and synthetic aspects of diazonium ions, $[RN_2]^+$, have been comprehensively studied and discussed in numerous monographs and reviews.[1] In contrast, data on the chemistry of their phosphorus analogues is much more limited. Thus, the sterically crowded salts $[Ar^*NP]^+ X^-$ ($Ar^* = 2,4,6\text{-}tBu_3C_6H_2$) are the only compounds isolated to date containing the phosphoazonium (phosphanetriylammonium) cation.[2] The area of the respective diphosphonium (phosphanetriylphosphonium) cations, $[RP_2]^+$, is even less well explored. Mass-spectrometric evidence has been presented for the formation of the $[iPr_2NP_2]^+$ cation,[3] but the characterization of this species by other physicochemical methods has yet to be accomplished. The closest approach to $[RP_2]^+$ cations has been our work on protonated *P*-aminodiphosphenes, $Ar^*-P=P-NR_2$.[4] We succeeded in the synthesis of the donor-stabilized arenediphosphonium cation, $[Ar^*PP(PPh_3)]^+$, but the free cation was found to be unstable and could not be directly observed in solution. It is evident that further synthetic design of diphosphonium ions requires a detailed theoretical examination of the electronic structure of these species and of the electronic influence of the substituent R on the stability and structure of the molecule. Earlier theoretical investigations on phosphorus analogues of diazonium ions based on ab initio calculations focused on the protonated $[HP_2]^+$[5a] and methyl-substituted $[MeNP]^+$, $[MePN]^+$ and $[MeP_2]^+$ species.[5b][5c][5d][5e] For the latter, the end-on structure appeared to be favoured. This fact could be rationalized in terms of a preference for a carbon coordination number of four. However, this hypothesis does not explain the end-on geometry adopted in the case of $[PhN_2]^+$. The purpose of this article is to compare the structures deduced from theory for $[PhN_2]^+$ and $[PhP_2]^+$ cations, so as to permit more considered interpretation of these geometrical preferences.

Computational Methods

Ab initio calculations were performed using Gaussian 94/DFT.[6][7] The optimization and the vibrational analysis were carried out at the RHF/6-31 G (d,p) level of theory with the inclusion of dynamic electron correlation at the MP2 (full)/6-31 G (d,p) level, as well as with density functional theory[8] using the hybrid Becke 3LYP[9] method in conjunction with the 6-31 G (d,p) basis set. The vibrational zero-point energies determined at the MP2 level and with the DFT method[10] are known to be accurate and were used unscaled. Graphical representations of the nature of the molecular orbitals were obtained using the Molden program.[11]

Results and Discussion

Phosphorus analogues of alkyldiazonium ions have recently been investigated theoretically by Glaser.[5c][5d][5e] In these reports, different geometric structures are advanced for RP_2^+, based on energetic considerations of a protonation process on the one hand, and a clear polarization of the P_2 fragment upon electrophilic attack on the other. However, no information is provided concerning the phenyldiphosphonium ion. In this work, we present the first theoretical investigation concerning the phenyl-substituted ion and its electronic characteristics.

Our theoretical approximation is more than adequate considering the large size of the molecule. Glaser[12] noted that regarding isomer stability of the phenyldiazonium ions, the MP2 results agree qualitatively with the CISD predic-

 © WILEY-VCH Verlag GmbH, D-69451 Weinheim, 1998 1434–1948/98/1111–1821 $ 17.50+.50/0

tions, but tend to underestimate the stability of the bridged structure. Furthermore, many studies have shown the quality of the results obtained using B3LYP to describe geometries, as well as in estimating heats of formation.[13]

Considering the phenyldiazonium ion, we found at both the MP2 and DFT levels, two local minima **1a** and **1b**, which are associated with the linear and the out-of-plane edge-on approaches of N−N to the singlet phenyl cation, respectively. These results are consistent with earlier theoretical research[12], and suggest that the dative bond description with an overall neutral N_2 moiety is clearly preferable. However, the latter less stable structure **1b** is isoenergetic with the dissociated phenyl cation and N_2, and is not accessible by reaction between these components.

For the benzenediphosphonium ion, two local minima are found at the same level of calculation, but linear end-on coordinated **2a** is less favoured than the symmetrically bridged local minimum **2b** by 16.29 kcal/mol [6-31 G (d,p)/MP2], 16.84 kcal/mol [6-31 G (d,p)/B3LYP]. Furthermore, regarding the affinity of P_2 towards the phenyl cation, our results suggest that **2b** should be stable in the gas phase. Affinities are calculated to be 52.83 kcal/mol by HF/MP2 (45.50 kcal/mol by B3LYP) for the end-on coordination, and 69.67 kcal/mol by HF/MP2 (61.79 kcal/mol by B3LYP) for the bridged local minimum. It should be pointed out that, in contrast to **1b**, the generation of the phenyldiphosphonium ion **2b** by reaction between P_2 and the phenyl cation is not excluded in the gas phase.

Energies and geometries of **1a**,**b** and **2a**,**b** are summarized in Figure 1. For **2a**, differences are apparent between the optimal geometries computed with MP2 and DFT. A linear structure is found at the DFT/6-31 G (d,p) and RHF/6-31 G (d,p) levels, but a bent geometry appears as a minimum at the MP2 (full)/6-31 G (d,p) level. The potential energy surface characteristics for the edge-on coordinated structure are greatly affected by electron correlation. Structure **2b** is calculated to be the only minimum (MP2 and DFT levels) corresponding to the out-of-plane edge-on approach. The distance C−P is proportionally shorter than the C−N distance in **1b**. This fact explains the widening of the P−C−P angle (60°) compared to the N−C−N angle (41°). It is noteworthy that theoretical models do not affect the P−C−P and C−P−P angles, which are quasi-similar. In addition, the bond length alternation suggests that the π electrons are not fully delocalized into the phenyl ring. A significant lengthening is observed for the C−C bond in the α position of C_{spiro} compared to that in the phenyldiazonium ion.

Figure 1. Energies and geometrical parameters of **1**(**a**,**b**) and **2**(**a**,**b**) calculated at the MP2/6-31 G** and B3LYP/6-31G** levels of theory. Total energies, E_{tot}, in atomic units; zero-point vibrational energies, ZPVE, in kcal/mol; angles in°, and bond lengths in Å

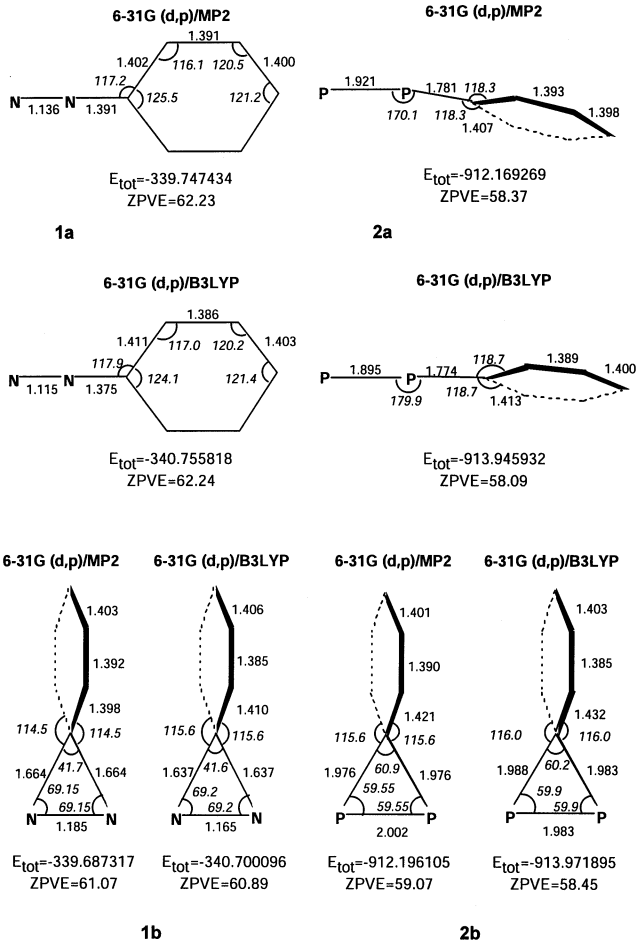

Figure 2. Charges of **1**(**a**,**b**) and **2**(**a**,**b**) calculated at the MP2/6-31 G** and B3LYP/6-31G** levels of theory

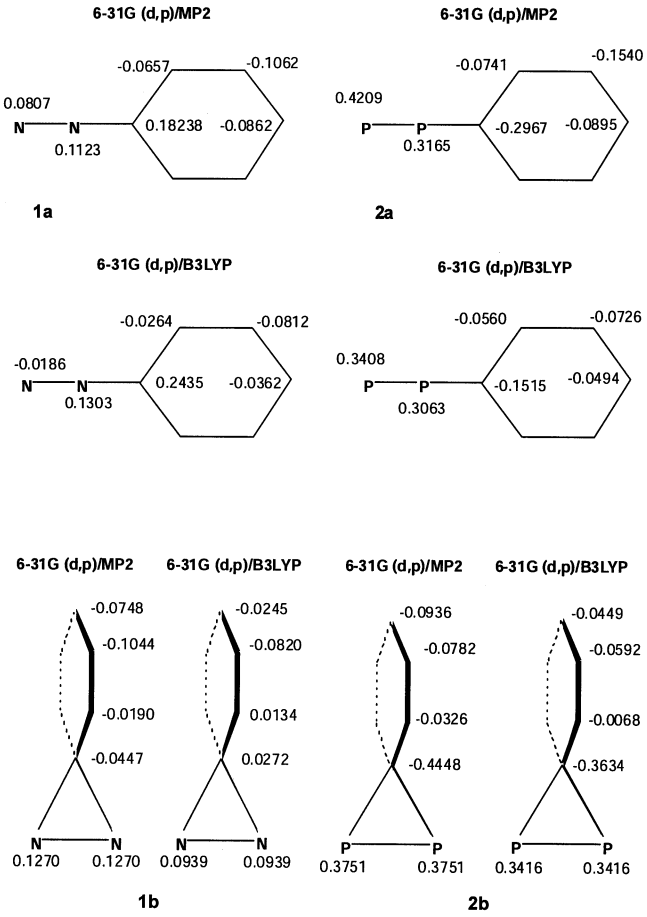

A key difference to the diazonium cation is seen in the polarization of these systems. Considering the charges displayed in Figure 2, it is clear that the positive charge (for **2a** and **2b**) is distinctly localized on the P−P moiety, while the stable structure of diazonium analogous **1a** can be viewed as a phenyl cation with a closely associated nitrogen molecule.

An examination of the molecular orbital interactions that occur in these two systems is clearly relevant, since these directly affect the nature of the preferentially adopted structure and thus will be a source of information with regard to the synthesis and detection of such species.

Localization and energetic positions of MOs allow us to visualize these interactions as in Figures 3 and 4[14]. If we analyse them for the end-on coordination structures **1a** and **2a**, they are very well described as an interaction between the σ_{XX} orbital and the LUMO of the phenyl cation [$\sigma_{XX} \rightarrow \sigma^*_{Ph}$ −17.29 eV (X = N), −13.32 eV (X = P)] and a back-donation from π_2 (phenyl cation) to the π^*_{XX} orbital of the same symmetry [$\pi_{2Ph} \rightarrow \pi^*_{XX}$ −12.78 eV (X = N), −11.75 eV (X = P)]. Furthermore, the formation of σ_{PC} becomes easier than that of σ_{NC} as a consequence of the σ_{PP} energetic position in comparison with that of σ_{NN}. In fact, experimentally determined ionic state energies for N_2 and P_2 [$^2\Sigma^+_g$ and $^2\Pi^+_u$ associated with the ejection of an electron from $^1\pi_u$ (π bond) and $^3\sigma_g$ (σ_{XX}) orbitals] are observed at 15.60, 16.98 and 10.81, 10.62 eV, respectively. The electron transfer should be more important in the case of P_2 than in the case of N_2, and the π back-donation is not expected to compensate this transfer. In agreement with this hypothesis, the charges are found to be negative at C_{ipso} and positive on the two phosphorus atoms. It is noteworthy that a slightly less pronounced polarization is obtained by using B3LYP than at the MP2 level.

Figure 3. Selected molecular orbitals (MO) of the linear compound **1a** calculated at the B3LYP/6-31 G** level

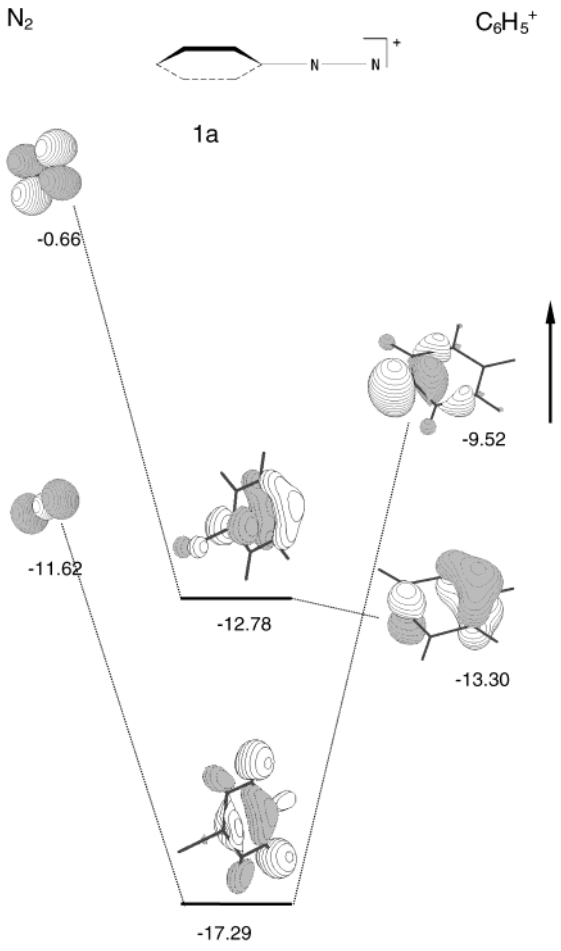

Figure 4. Selected molecular orbitals (MO) of the linear compound **2a** calculated at the B3LYP/6-31 G** level

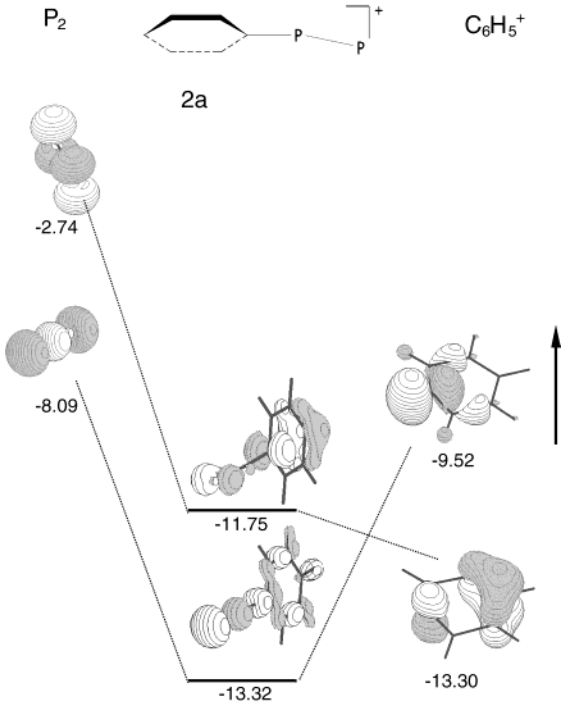

If we consider the bridged structures **1b** and **2b**, the LUMO σ^* of the phenyl cation is seen to interact with the π_{XX} orbital. Regarding the energetic gap between the LUMO Ph^+ and π_{XX}, this interaction will be easier in the case of P_2 (ΔE = 1.70 eV cf. 3.06 eV for N_2/Ph^+). This is well represented for the phosphonium ion by the MO at −14.38 eV.

We note that, in contrast to the aforementioned behaviour, in the case of N_2, a destabilizing interaction occurs between π_{NN} and the lower $\sigma_{Ph}{}^+$ orbitals. If we consider the charges, notable differences are evident in their distribution between the phenyldiphosphonium cation and the phenyldiazonium cation. The large positive charge localized on each phosphorus atom and the negative one on C_{ipso}, could be explained first of all by the high σ transfer, which is not sufficiently compensated by the π back-donation (vide infra).

Finally, π back-donation appears as for the linear molecule, involving the $\pi_{2Ph}{}^+$ and the π^*_{XX} orbitals, which can be visualized by the MO at −12.69 eV for the phosphorus compound, and at −13.29 eV for the nitrogen analogue.

Figure 5. Selected molecular orbitals (MO) of the bridged compound **1b** calculated at the B3LYP/6-31 G** level

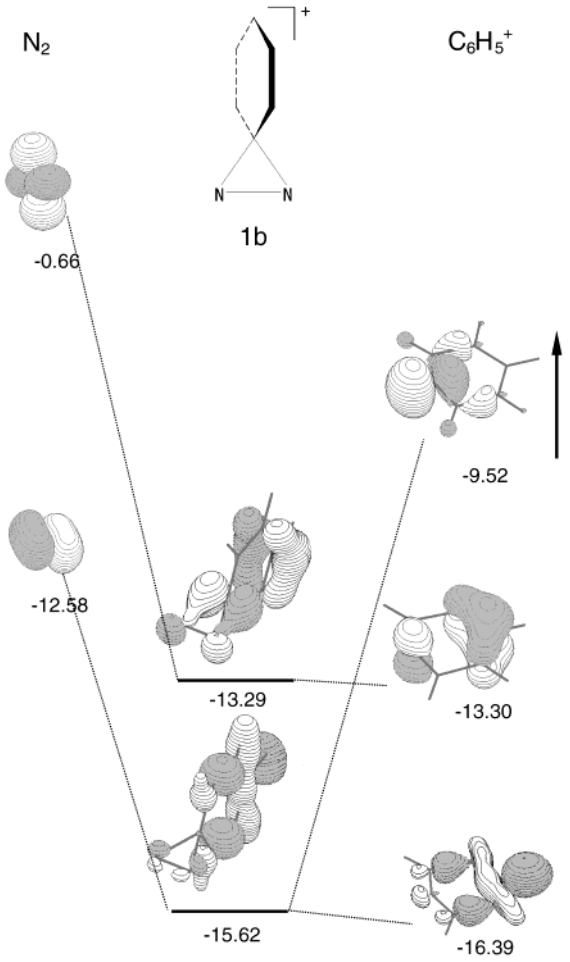

Figure 6. Selected molecular orbitals (MO) of the bridged compound **2b** calculated at the B3LYP/6-31 G** level

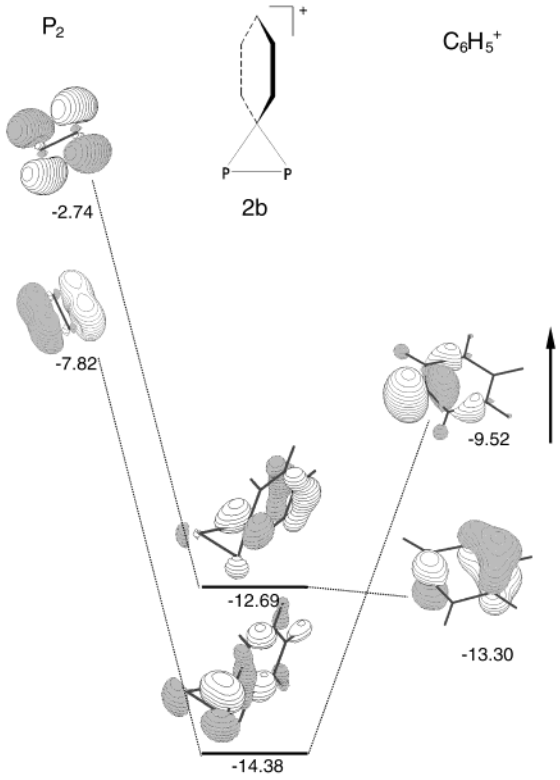

Why is the bridged form **2b** stabilized in comparison with the linear one? An explanation is found mainly in the stabilizing interactions and notably in the interaction $\pi^{+}_{PP} \rightarrow \sigma^{*}_{Ph}{}^{+}$, which is observed only in the bridged form. Naturally, other interactions play an important role in determining the stability of these systems, such as the interaction $\pi 2Ph^{+} \rightarrow \pi^{*}_{PP}$, but these are in fact found in both isomers. Nevertheless, the interaction $\pi^{+}_{PP} \rightarrow \sigma^{*}_{Ph}{}^{+}$ leads to a more effective overlap, compared with the $\sigma_{PP} \rightarrow \sigma^{*}_{Ph}{}^{+}$ interaction that exists in the linear form. In other words, the overlap is more effective with two phosphorus atoms (bridged form) than with only one (linear form). Finally, taking into account the energetic positions, the molecular orbitals π_{PP} and σ_{PP} remain localized on this moiety, while π_{NN} and σ_{NN} are mixed with the σ-MO from the phenyl ring (destabilizing interactions).

Conclusion

The new insight given by the present study shows that aromatic diphosphonium ions might be stable species. To date, all attempts to isolate these molecules have failed, mainly due to difficult kinetic control rather than because of thermodynamic factors. However, considering the σ^{*}_{PP}-MO energetic position (−7.69 eV) for the bridged structure, the availability of the diazonium ion complex, and the position of the corresponding σ* MO (−7.66 eV), we can reasonably expect that it should be possible to stabilize the system by means of nucleophilic assistance.

Financial support of this work by the *CNRS* (France) is gratefully acknowledged. We also thank the *Institut du Développement de Ressources en Informatique Scientifique* (*IDRIS*, Orsay, France), administered by the *CNRS*, for the calculation facilities, and Dr. *Gijs Schaftenaar* for allowing us to use his graphics program Molden. We also thank Mrs. *F. Gracian* for her invaluable help in the realization of the figures.

[1] [1a] K. H. Saunders, *The Aromatic Diazo Compounds*, 3rd ed., E. Arnold, London, **1985**. – [1b] S. Patai (Ed.), *The Chemistry of Diazonium and Diazo Groups,* Wiley Interscience, New York, **1978**, p. 511−591, 645−657. – [1c] W. Gerhartz (Ed.), *Ullmann's Encyclopedia of Industrial Chemistry*, VCH, Weinheim, New York, **1987**, vol. A8, p. 505. – [1d] L. G. Laing, *Arenediazonium Salts and Diazo Compounds*, in *Rodd's Chemistry of Carbon Compounds,* Elsevier, Amsterdam, London, New York, **1973**, vol. 3, section C, p. 11−88.

[2] [2a] E. Niecke, M. Nieger, F. Reichert, W. W. Schoeller, *Angew. Chem. Int. Ed. Engl.* **1988**, *27,* 1713. – [2b] E. Niecke, M. Nieger, F. Reichert, *Angew. Chem. Int. Ed. Engl.* **1988**, *27*, 1715. – [2c] N. Burford, T. S. Cameron, J. A. C. Clyburne, K. Eichele, K. N. Robertson, S. Sereda, R. E. Wasylishen, W. A. Whitla, *Inorg. Chem.* **1996**, *35*, 5460−5467, and references cited therein.

[3] E. Niecke, R. Streubel, M. Nieger, D. Stalke, *Angew. Chem. Int. Ed. Engl.* **1989**, *28*, 1673.

[4] [4a] V. D. Romanenko, V. L. Rudzevich, E. B. Rusanov, A. N. Chernega, A. Senio, J.-M. Sotiropoulos, G. Pfister-Guillouzo, M. Sanchez, *J. Chem. Soc., Chem. Commun.* **1995**, 1383−1385. – [4b] V. D. Romanenko, V. L. Rudzevich, E. B. Rusanov, A. N.

Chernega, A. Senio, J.-M. Sotiropoulos, G. Pfister-Guillouzo, M. Sanchez, *Phosphorus, Sulfur Silicon* **1996**, *111*, 200.

[5] [5a] M. T. Nguyen, N. J. Fitzpatrick, *Chem. Phys. Lett*. **1988**, *146*, 524−530. − [5b] T. Busch, W. W. Schoeller, E. Niecke, M. Nieger, H. Westermann, *Inorg. Chem*. **1989**, *28*, 4334−4340. − [5c] R. Glaser, C. J. Horan, G. S.-C. Choy, B. Harris, *J. Phys. Chem.* **1992**, *96*, 3689−3697, and references cited therein. − [5d] R. Glaser, C. J. Horan, P. E. Haney, *J. Phys. Chem.* **1993**, *97,* 1835. − [5e] R. Glaser, C. J. Horan, G. S.-C. Choy, B. L. Harris, *Phosphorus Sulfur* **1993**, *77*, 73−76.

[6] M. J. Frisch, G. W. Trucks, H. B. Schlegel, P. M. W. Gill, B. G. Johnson, M. A. Robb, J. R. Cheeseman, T. Keith, G. A. Petersson, J. A. Montgomery, K. Raghavachari, M. A. Al-Laham, V. G. Zahrzewski, J. V. Ortiz, J. B. Foresman, J. Cioslowski, B. B. Stefanov, A. Nanayakkara, M. Challacombe, C. Y. Peng, P. Y. Ayala, W. Chen, M. W. Wong, J. L. Andres, E. S. Replogle, R. Gomperts, R. L. Martin, D. J. Fox, J. S. Binkley, D. J. Defrees, J. Baker, J. P. Stewart, M. Head-Gordon, C. Gonzales, J. A. Pople, *Gaussian 94, Revision C.3*, Gaussian, Inc., Pittsburgh, PA, USA, **1995**.

[7] W. J. Hehre, L. Radom, P. v. R. Schleyer, J. A. Pople, *Ab Initio Molecular Orbital Theory*, John Wiley and Sons, New York, **1986**.

[8] [8a] N. H. March, *Electron Density Theory of Atoms and Molecules*, Academic Press, Inc., San Diego, CA, **1992**. − [8b] J. K. Labanowski, J. W. Andzelm (Eds.), *Density Functional Methods in Chemistry*, Springer-Verlag, New York, **1991**. − [8c] R. G. Parr, W. Yang, *Functional Theory of Atoms and Molecules*, Oxford University Press, New York, **1989**.

[9] Becke 3LYP: [9a] A. D. Becke, *Phys. Rev.* **1986**, *A33*, 2786. − [9b] A. D. Becke, *J. Chem. Phys.* **1988**, *88*, 2547. − [9c] C. Lee, W. Yang, R. G. Parr, *Phys. Rev.* **1988**, *B37*, 785.

[10] P. J. Stephens, F. J. Devlin, C. F. Chabalowski, M. J. Frisch, *J. Phys. Chem*. **1994**, *98*, 11623.

[11] See: http://www-srs.caos.kun.nl/schaft/molden

[12] R. Glaser, C. J. Horan, *J. Org. Chem.* **1995**, *60*, 7518−7528.

[13] M. J. Frisch, G. W. Trucks, J. R. Cheeseman, *Systematic Model Chemistries Based on Density Functional Theory: Comparison with Traditional Models and with Experiment* in: *Recent Developments and Applications of Modern Density Functional Theory, Theoretical and Computational Chemistry* (Ed.: J. M. Seminario), **1996**, vol. 4, pp. 679−707, Elsevier Science B.V.

[14] It is well known that ab initio orbitals do not derive from a purely one-electron Hamiltonian and therefore do not possess the property of associativity necessary to justify a construction from fragment orbitals. Thus, we preferred to present Kohn-Sham orbitals, which are more appropriate from this point of view.

[I98056]

Vinylidene Transition-Metal Complexes, 47[◇]

Synthesis and Molecular Structure of Six-Coordinate Dichlorodihydridoruthenium(IV) and Five-Coordinate Vinylideneruthenium(II) Complexes☆

Justin Wolf, Wolfram Stüer, Claus Grünwald, Olaf Gevert, Matthias Laubender, and Helmut Werner*

Institut für Anorganische Chemie der Universität Würzburg,
Am Hubland, D-97074 Würzburg, Germany

Received August 6, 1998

Keywords: Ruthenium / Terminal alkynes / Carbene complexes / Hydrido complexes / Vinylidene complexes

The dichlorodihydridoruthenium(IV) compound $[RuH_2Cl_2(PiPr_3)_2]$ (**4**) was prepared from $[RuCl_2(C_8H_{12})]_n$ (**3**), $PiPr_3$, and H_2 in 2-butanol via the chlorohydridoruthenium(II) derivative $[RuHCl(H_2)(PiPr_3)_2]$ (**5**) as an intermediate. The synthesis of **5** was achieved under similar conditions from **3**, $PiPr_3$, H_2, and 2-butanol in the presence of NEt_3. Compound **4**, which was characterized by X-ray crystal structure analysis, reacts with excess phenylacetylene to give the phenylvinylidene complex $[RuCl_2(=C=CHPh)(PiPr_3)_2]$ (**7**) and with propargylic alcohols or derivatives thereof to afford the vinylcarbene complexes $[RuCl_2(=CHCH=CR_2)(PiPr_3)_2]$ (**9**, **10**), respectively. From **5** and terminal alkynes RC≡CH the chlorohydridovinylidene compounds $[RuHCl(=C=CHR)(PiPr_3)_2]$ (**11**, **12**) were obtained. The phenylvinylidene complex $[RuCl_2(=C=CHPh)(PCy_3)_2]$ (**15**) was prepared from phenylacetylene and either $[RuH_2Cl_2(PCy_3)_2]$ (**14**) or one of the carbene derivatives $[RuCl_2(=CHR)(PCy_3)_2]$ (**16**, **17**) as starting materials. The X-ray crystal structure analysis of **15** confirms a distorted square-pyramidal geometry with the vinylidene ligand in the apical position. The interconversion of **4** to **5** and of the tricyclohexylphosphane counterparts **14** to **13** was achieved by hydrogen transfer from 2-propanol in the presence of PR_3. The reverse reaction occurs upon treatment of **5** or **13** with the corresponding phosphonium salt $[HPR_3]Cl$ or HCl, respectively.

In the course of our investigations aimed to prepare bis(trialkylphosphane) transition-metal complexes containing *coordinatively unsaturated* metal centers, we recently described the synthesis of the dichlorodihydridoosmium(IV) compounds $[OsH_2Cl_2(PiPr_3)_2]$ (**1**) and $[OsH_2Cl_2(PtBu_2Me)_2]$ (**2**), in which osmium, although six-coordinate, has 16 electrons in its valence shell.[1] These compounds, in particular **1**, have a rich chemistry which has opened the gate not only to carbyne- but also to vinylideneosmium complexes.[2][3]

Since it was known from our work on the reactivity of compounds such as $[MCl_2\{\kappa^2(P,O)\text{-}iPr_2PCH_2CH_2OMe\}_2]$ and $[MCl_2\{\kappa^2(P,O)\text{-}iPr_2PCH_2CO_2R\}_2]$ (M = Ru, Os) that the ruthenium derivatives react more readily with terminal alkynes and propargylic alcohols to give the corresponding vinylidene and allenylidene complexes,[4] we set out to prepare the hitherto unknown ruthenium(IV) compound $[RuH_2Cl_2(PiPr_3)_2]$ (**4**). After initial attempts with $RuCl_3 \cdot aq$ as starting material failed, we found that the reaction of $[RuCl_2(C_8H_{12})]_n$ (**3**) with triisopropylphosphane in 2-butanol under H_2 gave the dichlorodihydrido complex **4**.[5] Most recently, Caulton and coworkers reported the synthesis of the analogous compound $[RuH_2Cl_2(PtBu_2Me)_2]$ using our methodology with the cycloocta-1,5-diene derivative **3** as the starting material.[6]

In this article we describe the preparation and characterization of **4** and its PCy_3 counterpart **13**, and the use of these dichlorodihydridoruthenium(IV) compounds as well as of the related chlorohydrido(dihydrogen)ruthenium(II) derivatives to obtain five-coordinate vinylideneruthenium(II) complexes. Part of these studies has been communicated.[5]

Results and Discussion

As was mentioned above, instead of $RuCl_3 \cdot aq$, which reacts with $PiPr_3$ in boiling methanol to give $[RuHCl(CO)(PiPr_3)_2]$,[7] compound **3** has to be used as starting material for the preparation of **4** (Scheme 1). On treatment of a suspension of **3** in 2-butanol with 3 equiv. of $PiPr_3$ in the presence of H_2 a red solution is formed which, due to the ^1H- and ^{31}P-NMR spectra, contains the dihydrogen complex **5**. This compound was originally prepared by Chaudret et al. from $[Ru(\eta^4\text{-}C_8H_{12})(\eta^6\text{-}C_8H_{10})]$, $PiPr_3$, and $CHCl_3$ under 4 atm of dihydrogen.[8] If the red solution obtained from **3** was brought to dryness in vacuo and the oily residue recrystallized from ether, orange crystals of **4** (but not **5**) were

[◇] Part 46: H. Werner, P. Bachmann, M. Laubender, O. Gevert, *Eur. J. Inorg. Chem.* **1998**, 1217–1224.

 © WILEY-VCH Verlag GmbH, D-69451 Weinheim, 1998 1434–1948/98/1111–1827 $ 17.50+.50/0

Scheme 1

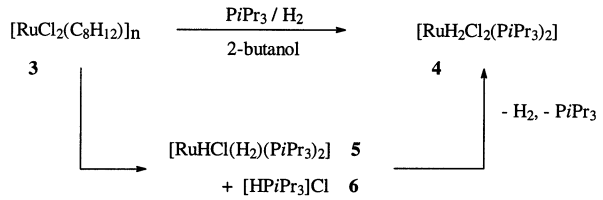

isolated in 92% yield. The conversion of **5** to **4** is promoted by the phosphonium salt **6** which is generated as a byproduct in the reaction of **3**, P*i*Pr$_3$, 2-butanol, and H_2.

In order to confirm the proposal that the initial product in the reaction of **3** with triisopropylphosphane under the conditions used is indeed the dihydrogen complex **5**, a suspension of the oligo- or polymeric cycloocta-1,5-diene compound **3** was treated with P*i*Pr$_3$/H_2 in 2-butanol in the presence of NEt_3 as a base. After removal of the solvent and extraction of the residue with pentane, a red oil was obtained which by comparison of the NMR data with those published by Chaudret is the dihydrogenruthenium(II) derivative **5**.[8] This compound reacts with the phosphonium salt [HP*i*Pr$_3$]Cl (**6**) in CH_2Cl_2 to afford, by evolution of gas (H_2), quantitatively P*i*Pr$_3$ and the dichlorodihydrido complex **4**. The latter is an orange solid which is readily soluble in CH_2Cl_2 and $CHCl_3$, but almost insoluble in hydrocarbons. The characteristic feature in the ^{1}H-NMR spectrum of **4** is the triplet resonance for the two hydrido ligands in the high-field region at $\delta = -12.30$.

The result of the X-ray crystal structure analysis of **4** is shown in Figure 1. The coordination geometry around the six-coordinate metal center is very similar to that of the osmium analogue **1**.[1a] It is best described as a somewhat distorted variant of a D_{4d} square antiprism with the two vacant coordination sites in alternate positions at one square base of this polyhedron. The other square base is made up by the two phosphorus atoms and the two hydrido ligands, the positions of which could be located in a difference Fourier synthesis. The Ru−P and Ru−Cl distances of **4** are almost identical to the corresponding bond lengths in **1**, and this is also true for the P−M−P, P−M−Cl, and Cl−M−Cl bond angles (M = Ru, Os). The distances Ru−H1 and Ru−H2 of 1.46(5) and 1.56(5) Å are in the range found for other hydridoruthenium(II) and -ruthenium(IV) complexes.[9] We note that recently Gusev, Berke, Eisenstein, Caulton et al. observed that the molecules [OsH_2X_2(P*i*Pr$_3$)$_2$] (X = Cl, Br, I) exist *in solution* as two rapidly interconverting isomers, one having C_2 symmetry (as seen in the crystal) and the other having no symmetry.[10] In contrast, the tricyclohexylphosphane derivative **13** which was prepared independently by Chaudret and coworkers[11] and by us (see below), shows a fluxional process attributed to the interconversion of two *symmetrical* isomers.

The dichlorodihydridoruthenium(IV) compound **4** does not only react with phenylacetylene[5] but also with propargylic alcohols and derivatives thereof. The results are summarized in Scheme 2. The reaction of **4** with PhC≡CH in CH_2Cl_2 yields a mixture of two products **7** and **8** of which the first is by far the most dominating species. Compound **7** is exclusively formed if the initially generated mixture, after removal of the solvent, is treated again with phenylacetylene and heated to 80°C for a short period of time. The isolated yield of **7** is then ca. 70%. The minor component

Figure 1. Molecular structure (ORTEP plot) of **4**;[a] the hydrogen atoms besides H1 and H2 are omitted for clarity

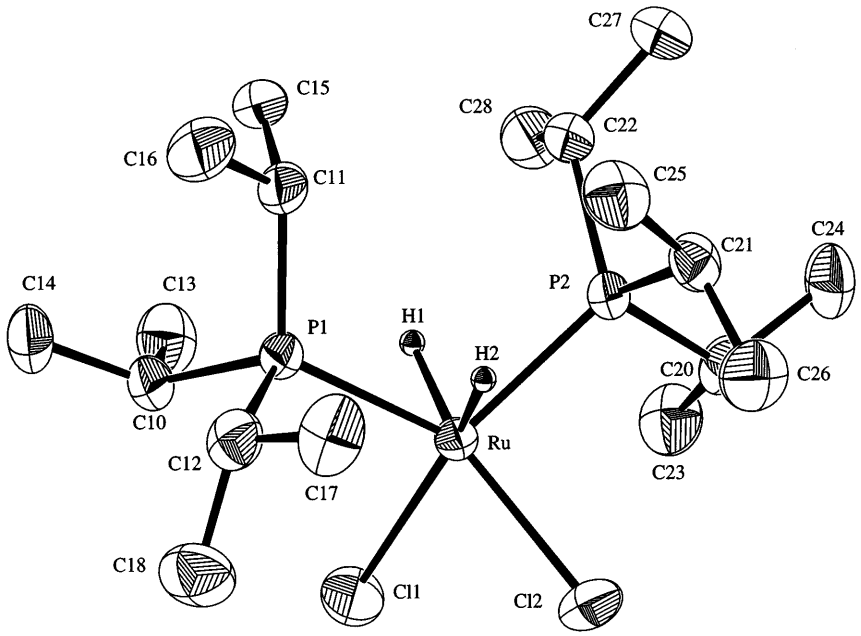

[a] Selected bond lengths [Å] and angles [°]: Ru−P1 2.270(1), Ru−P2 2.297(1), Ru−Cl1 2.400(1), Ru−Cl2 2.401(1), Ru−H1 1.46(5), Ru−H2 1.56(5); P1−Ru−P2 111.69(3), Cl1−Ru−Cl2 84.29(3), P1−Ru−Cl1 92.18(3), P1−Ru−Cl2 139.14(3), P2−Ru−Cl1 145.07(3), P2−Ru−Cl2 92.60(3).

of the reaction mixture is the benzylcarbene complex **8** which has already been characterized by X-ray crystal structure analysis.[5] Compound **8** belongs to the class of Grubbs-type carbene complexes $[RuCl_2(=CHR)(PR'_3)_2]$ that were originally prepared from $[RuCl_2(PPh_3)_3]$ and cyclopropene or diazoalkane derivatives[12] and are now widely used as highly active catalysts for olefin metathesis including ROMP and RCM.[13]

Scheme 2

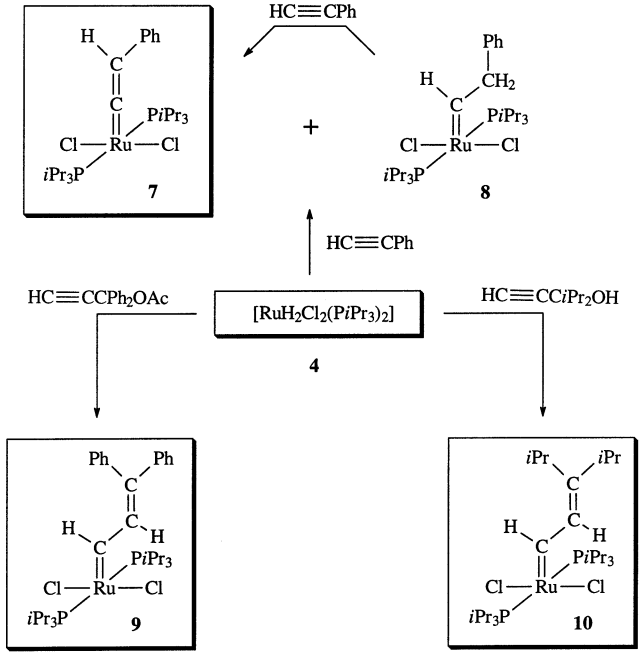

The vinylideneruthenium(II) compound **7** is a brown, only moderately air-sensitive solid that has been characterized by elemental analysis and spectroscopic techniques. The ^{13}C-NMR spectrum displays two triplets at δ = 341.1 and 109.3, which by comparison[4][14] are assigned to the α- and β-carbon atoms of the vinylidene ligand. In the ^{31}P-NMR spectrum a singlet resonance appears at δ = 29.0, the chemical shift of which is similar to that observed at δ = 27.2 for the PPh_3 ligands in $[RuCl_2(=C=CHtBu)(PPh_3)_2]$.[15] With regard to the mechanism of formation of **7**, we assume that the starting material **4**, containing a metal center with a 16-electron configuration, affords in the initial step of the reaction a 1:1 adduct with the alkyne. This seven-coordinate species could react by insertion of the alkyne into one of the Ru−H bonds to generate a hydrido(vinyl) intermediate (also with a 16-electron configuration at the metal center). This compound could then give upon addition of a second molecule of PhC≡CH, followed by reductive elimination of styrene, the alkyne complex $[RuCl_2(PhC{\equiv}CH)(PiPr_3)_2]$. The conversion of this species to the isomer **7** possibly occurs by a slippage of the π-bonded alkyne to an η^2-CH-coordinated complex which undergoes a 1,2-hydrogen migration to yield the final product. Quite recently, Wakatsuki et al. showed by ab initio MO calculations that the reaction of $[RuX_2(PPh_3)_3]$ with tBuC≡CH, which gives the compounds $[RuX_2(=C=CHtBu)(PPh_3)_2]$ (X = Cl, Br), follows a similar route.[16] It should be mentioned that the formation of styrene from **4** and phenylacetylene was confirmed by GC/MS analysis.

The synthesis of the vinylcarbene complexes **9** and **10** (Scheme 2) from **4** is a somewhat surprising result. Taking earlier work by Selegue,[17] Dixneuf,[18] and by some of us[4b][4c][19] into consideration, we anticipated that on treatment of **4** with propargylic alcohols $HC{\equiv}CCR_2OH$, in particular for R = Ph, allenylidenemetal derivatives $[RuCl_2(=C=C=CR_2)(PiPr_3)_2]$ would be formed. However, instead of these species the related vinylcarbene complexes **9** and **10** were obtained. We found that the reaction of **4** with $HC{\equiv}CCPh_2OH$ in CH_2Cl_2 leads to a mixture of products among which **9** could be detected as a major component by ^{1}H-NMR spectroscopy. In contrast, by using the corresponding acetate $HC{\equiv}CCPh_2OAc$ as a carbene source, compound **9** has been isolated in excellent yield. This (vinylcarbene)ruthenium(II) derivative was originally prepared by Grubbs and coworkers from $[RuCl_2(PPh_3)_3]$ and 1,1-diphenylcyclopropene followed by ligand exchange of PPh_3 for $PiPr_3$.[12c]

The formerly unknown complex **10**, which was isolated as a violet solid in 70% yield, resembles in its properties the diphenyl analogue **9**. The ^{1}H-NMR spectrum of **10** displays in the low-field region two doublets at δ = 19.56 and 8.06 with an H−H coupling of 11.2 Hz which is typical for an $M{=}CH{-}CH{=}CR_2$ unit.[12][14] In the ^{13}C-NMR spectrum of **10** the signal for the carbene-C atom appears at δ = 288.3 and is split into a triplet due to P−C coupling. Mechanistically, the formation of **9** and **10** from **4** is best understood if we assume that in analogy to the course of the reaction of **4** with phenylacetylene a functionalized hydrido(vinyl) species $[RuH(CH{=}CHCR_2OR')Cl_2(PiPr_3)_2]$ (R′ = H, Ac) is generated as an intermediate which yields the product by elimination of HOR′.

In a similar way to the dihydridoruthenium(IV) compound **4,** the hydridoruthenium(II) derivative **5** reacts with phenylacetylene to give the hydrido(phenylvinylidene) complex **11** (Scheme 3). Moreover, the parent hydrido(vinylidene) compound **12** was obtained from **5** and acetylene. Although a clean reaction between **5** and the terminal alkynes occurs, the isolated yields of **11** and **12** is only moderate (ca. 40%) mainly due to the good solubility of the products in pentane. Quite recently, Olivan, Eisenstein, and Caulton reported that on treatment of $[RuHCl(H_2)(PtBu_2Me)_2]$ with terminal alkynes RC≡CH the analogous hydrido(vinylidene) compounds $[RuHCl(=C=CHR)(PtBu_2Me)_2]$ (R = Ph, $SiMe_3$) are formed which, according to ab initio DFT calculations, possess a distorted trigonal-bipyramidal geometry with the phosphanes in the apical positions.[20] The osmium analogue of **11** was recently prepared by Esteruelas et al. by a different route, namely from the six-coordinate carbyne(hydrido) complex $[OsHCl_2(\equiv CCH_2Ph)(PiPr_3)_2]$ by elimination of HCl with NaOMe.[21]

The ^{13}C-NMR spectra of both **11** and **12** display in the low-field region the typical signals for the vinylidene α- and β-carbon atoms at δ = 329.3 and 109.7 (for **11**) and at δ =

Scheme 3

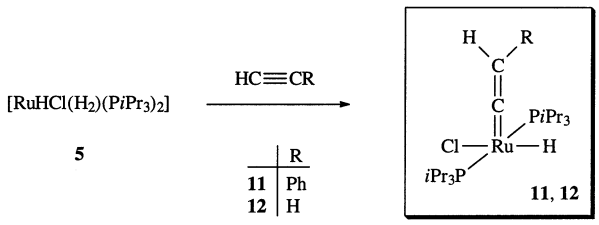

Scheme 4

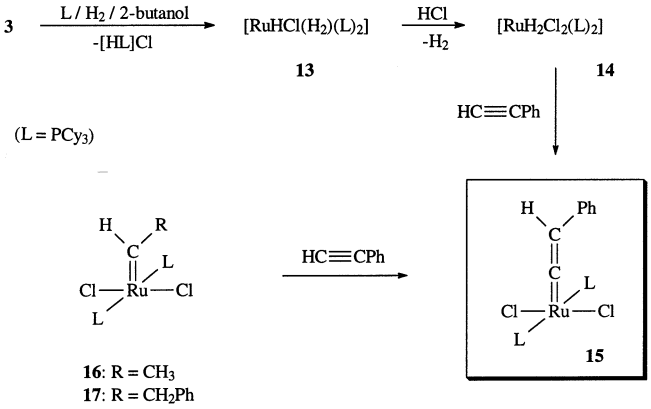

326.3 and 87.1 (for **12**) which are all split into triplets due to P−C coupling. In the ^{1}H-NMR spectrum the hydride resonance also appears as a triplet at $\delta = -12.48$ (for **11**) and −15.03 (for **12**). In contrast to **7**, the methyl groups of the triisopropylphosphane ligands in **11** and **12** are diastereotopic and thus two sets of signals are observed for the CH_3 protons and carbon nuclei in the NMR spectra. It should be mentioned that in agreement with recent work from our laboratory[22][23] compounds **11** and **12** react with the phosphonium chloride [HP*i*Pr$_3$]Cl to give the carbene complexes [RuCl$_2$(=CHCH$_2$R)(P*i*Pr$_3$)$_2$] (R = Ph, H) in excellent yield.

The analogues of the chlorohydrido and dichlorodihydrido compounds **5** and **4** with two PCy$_3$ instead of two P*i*Pr$_3$ ligands, **13** and **14**, are also accessible from the cycloocta-1,5-diene derivative **3** as the starting material. Like **5**, the corresponding ruthenium(II) complex **13** was first prepared by Chaudret and coworkers from the ruthenium(0) compound [Ru(η^4-C$_8$H$_{12}$)(η^6-C$_8$H$_{10}$)].[8] While this work was in progress,[24] Grubbs et al. published an experimental procedure for **13** that followed our methodology using the (cycloocta-1,5-diene)ruthenium(II) derivative **3** as the precursor.[25] Regarding the dichlorodihydridoruthenium(IV) complex **14**, very recently Chaudret and coworkers reported a synthesis which is different to that one described in this work and based on the reaction of the "polyhydride" [RuH$_2$(H$_2$)$_2$(PCy$_3$)$_2$] with aqueous HCl in ether.[11] The same authors also confirmed by VT NMR measurements that **14** shows a fluxional process in solution which is attributed to the interconversion between two stereoisomers having C_{2v} symmetry.[11] Our observations are in agreement with these results.[23]

Compound **14** does not only react with CO to give [RuHCl(CO)$_2$(PCy$_3$)$_2$][11] but also with phenylacetylene in the molar ratio of 1:10 to yield the vinylidene complex **15** (Scheme 4). Alternatively, **15** can be prepared upon treatment of the carbene derivatives **16** and **17** with PhC≡CH. In both cases the isolated yield is 60−70%. To the best of our knowledge, there has been only one other compound of the general composition [RuCl$_2$(=C=CHR)(PCy$_3$)$_2$] (with R = H) reported in the literature which was obtained from [RuCl$_2$(=CHPh)(PCy$_3$)$_2$] and a tenfold excess of allene.[12d][12e] The phenylvinylidene complex **15** (which is an almost air-stable solid) is only sparingly soluble in common organic solvents at room temperature and thus the ^{1}H-, ^{13}C-, and ^{31}P-NMR spectra were measured in $CDCl_3$ at 40°C. The NMR data for **15** and the related bis(triisopropylphosphane) complex are quite similar and therefore deserve no further comment.

The molecular structure of **15** is shown in Figure 2. The ORTEP plot reveals that the configuration around the metal center is distorted square-pyramidal with the vinylidene unit in the apical position. In the basal plane the two chloro and the two phosphane ligands are *trans* disposed. Although according to ab initio calculations this geometry represents the energy minimum on the potential surface,[16] it was found that in contrast to **15** the analogous compound [RuBr$_2$(=C=CH*t*Bu)(PPh$_3$)$_2$] possesses a trigonal-bipyramidal structure with the PPh$_3$ groups in the apical positions.[16] Therefore it seems that for the preferred configuration of the five-coordinate complexes steric requirements play a dominant role. The Ru−C1−C2 axis is nearly linear with an Ru−C1 distance that is slightly shorter than in [RuBr$_2$(=C=CH*t*Bu)(PPh$_3$)$_2$] [1.77(2) Å][16] and in the six-coordinate compound [RuCl$_2$(=C=CHPh){κ^1(*P*)-Me$_2$PCH$_2$CH$_2$OMe}{κ^2(*P,O*)-Me$_2$PCH$_2$CH$_2$OMe}] [1.815(2) Å][26] but almost identical to that in [RuCl$_2$(=C=CHPh)-{κ^1(*P*)-*i*Pr$_2$PCH$_2$CH$_2$OMe}{κ^2(*P,O*)-*i*Pr$_2$PCH$_2$CH$_2$OMe}] [1.749(7) Å].[4a] The P1−Ru−P2 axis is somewhat bent [169.82(7)°] and this is even more so for the Cl1−Ru−Cl2 unit [158.31(7)°]. The C1−C2 distance is in the expected range and this is true also for the Ru−Cl and Ru−P bond lengths.

Finally, a special comment is appropriate concerning the interconversion of the ruthenium(II) and ruthenium(IV) complexes **5** and **4** (see Scheme 5). In the context of the preparation of **4** from **3** it has already been mentioned that in this process compound **5** is generated as an intermediate which reacts with the byproduct **6**, after removal of 2-butanol, to give **4**. However, the surprising observation is that the red solution, which is initially formed from **3**, P*i*Pr$_3$, and H$_2$ in 2-butanol, is quite stable and can be stored for days without the conversion of the two components **5** and **6** to the ruthenium(IV) complex **4**.

In order to explain this seeming inconsistency it should be emphasized that although **5** and **6** react by elimination of H$_2$ to give **4** and P*i*Pr$_3$, in the presence of a secondary alcohol such as 2-butanol, or even better 2-propanol, the

Figure 2. Molecular structure (ORTEP plot) of **15**;[a] the hydrogen atoms are omitted for clarity

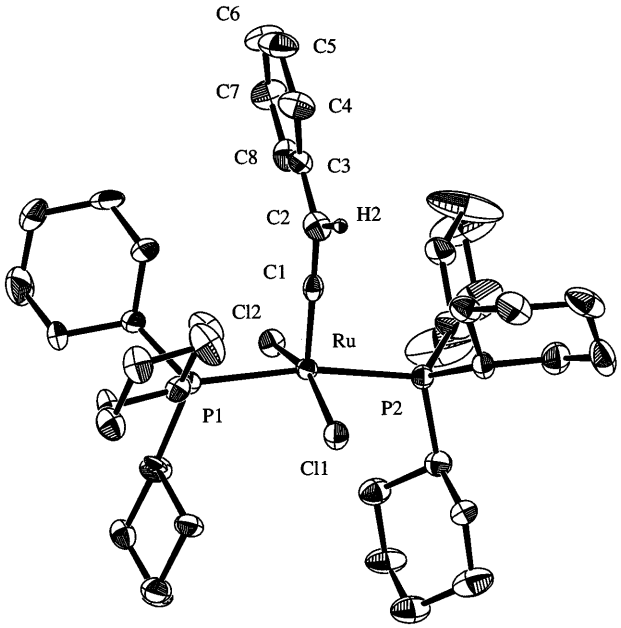

[a] Selected bond lengths [Å] and angles [°]: Ru−C1 1.747(7), Ru−P1 2.429(2), Ru−P2 2.410(2), Ru−Cl1 2.342(2), Ru−Cl2 2.355(2), C1−C2 1.33(1), C2−C3 1.45(1); C1−Ru−Cl1 102.8(2), C1−Ru−Cl2 98.9(2), C1−Ru−P1 94.6(2), C1−Ru−P2 94.9(2), P1−Ru−P2 169.82(7), P1−Ru−Cl1 88.97(7), P1−Ru−Cl2 88.42(6), P2−Ru−Cl1 85.47(7), P2−Ru−Cl2 93.59(7), Cl1−Ru−Cl2 158.31(7), Ru−C1−C2 178.2(6), C1−C2−C3 129.4(7).

Scheme 5

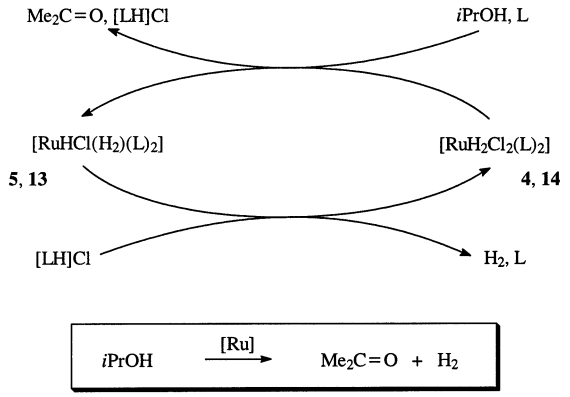

mixture of **4** and triisopropylphosphane is reconverted to **5** and **6**. The formation of acetone as a byproduct has been confirmed by GC/MS analysis which indicates that 2-propanol serves as the hydrogen source. An analogous but significantly slower reaction takes place between compound **14** and PCy_3 in 2-propanol. In this case the chlorohydrido complex **13** precipitates due to its lower solubility (compared with **5**) in the alcohol. The ^{31}P-NMR spectrum of the mother liquor indicates that besides **13** a small quantity of a sideproduct is formed which has not been identified as yet. For the conversion of **13** to **14** it is preferable to use instead of the phosphonium salt $[HPCy_3]Cl$ aqueous HCl as a proton source which yields the ruthenium(IV) compound almost quantitatively.

This work was supported by the *Deutsche Forschungsgemeinschaft* (SFB 347) and the Fonds der *Chemischen Industrie*. We are grateful to the latter in particular for a Kekulé stipend (to W. S.). Moreover, we thank Dr. *W. Buchner* and Mrs. *M.-L. Schäfer* for NMR measurements, Mrs. *R. Schedl* and Mr. *C. P. Kneis* for performing the elemental analyses and DTA measurements, and Mrs. *I. Geiter* for technical assistance. Generous support by the BASF AG and the Degussa AG (gifts of chemicals) is also gratefully acknowledged.

Experimental Section

All operations were carried out under argon using Schlenk techniques. The starting materials **3**,[27] and **16**, **17**[22] were prepared as described in the literature. The alkynes were commercial products from Aldrich, Strem, and ABCR. − NMR: Bruker AC 200 and AMX 400 [dvt = doublet of virtual triplets; $N = {}^3J(PH) + {}^5J(PH)$ or $^2J(PC) + {}^4J(PC)$, respectively]. − Melting points determined by DTA.

1. *Preparation of [$RuH_2Cl_2(PiPr_3)_2$]* (**4**): A suspension of 220 mg (0.79 mmol for $n = 1$) of **3** in 20 ml of 2-butanol was treated with 463 µl (2.37 mmol) of $PiPr_3$ and heated under hydrogen (1.5 bar) for 6 h at 80°C. Upon cooling the resulting red solution to room temperature, the solvent was removed in vacuo and 5 ml of diethyl ether was added to the oily residue. After 2 h, an orange solid crystallized, which was washed with 5 ml of diethyl ether and dried in vacuo; yield 359 mg (92%); m. p. 60°C (dec.). − ^1H NMR (200 MHz, CD_2Cl_2): δ = 2.30 (m, 6 H, PC*H*CH_3), 1.22 [dd, $J(PH) = 14.9$, $J(HH) = 7.1$ Hz, 36 H, PCHC*H*$_3$], −12.30 [t, $J(PH) = 19.0$ Hz, 2 H, RuH_2]. − ^{13}C NMR (100.6 MHz, CD_2Cl_2): δ = 29.7 (m, P*C*HCH$_3$), 19.6 (s, PCH*C*H$_3$). − ^{31}P NMR (162.0 MHz, CD_2Cl_2): δ = 103.2 (s). − $C_{18}H_{44}Cl_2P_2Ru$ (494.5): calcd. C 43.72, H 8.97, Ru 20.44; found C 43.41, H 8.83, Ru 19.85.

2. *Preparation of [$RuHCl(H_2)(PiPr_3)_2$]* (**5**) *from* **3**: A suspension of 119 mg (0.42 mmol für $n = 1$) of **3** in 15 ml of 2-butanol was treated with 200 µl (1.02 mmol) of $PiPr_3$ and 117 µl (0.84 mmol) of NEt_3 and then heated for 6 h under hydrogen (1.5 bar) at 80°C. Upon cooling to room temperature, the solvent was removed in vacuo and the orange residue was extracted with 15 ml of pentane. After the extract was brought to dryness in vacuo, a red oil was obtained which by comparison of the NMR data was identified as **5**.[8] Yield almost quantitative.

3. *Reaction of Compound* **5** *with [HPiPr$_3$]Cl* (**6**): A solution of compound **5**, prepared from 25 mg (0.09 mmol) of **3**, 45 µl (0.23 mmol) of $PiPr_3$ and 25 µl (0.18 mmol) of NEt_3 in 5 ml of 2-butanol, was brought to dryness in vacuo. The oily residue was extracted with 10 ml of pentane and, after removal of the solvent, was dissolved in 3 ml of CH_2Cl_2. The red solution was treated with 37 mg (0.19 mmol) of **6**, which led to a rapid evolution of gas (H_2). After the solution was stirred for 5 min, the solvent was removed and the remaining orange solid identified as **4** by comparison of the NMR data with those of an authentic sample. Yield almost quantitative.

4. *Preparation of [$RuCl_2(=C=CHPh)(PiPr_3)_2$]* (**7**): A solution of 142 mg (0.29 mmol) of **4** in 10 ml of CH_2Cl_2 was treated with 63 µl (0.57 mmol) of phenylacetylene and stirred for 5 min at room temperature. The solvent was removed in vacuo to give a red oil which according to the ^1H- and ^{31}P-NMR spectra consisted of a mixture of **7** (90%) and **8** (10%). The oily material was dissolved in 5 ml of benzene, the solution was treated with 30 µl (0.27 mmol)

of phenylacetylene and heated for 10 min at 80°C. After cooling to room temperature, the solvent was removed in vacuo and 3 ml of methanol were added to the brownish residue. Upon storing the mixture for 2 h, a brown microcrystalline solid was obtained which was separated from the mother liquor and dried in vacuo; yield 113 mg (66%); m. p. 97°C (dec.). – ^{1}H NMR (400 MHz, C_6D_6): δ = 7.23–7.02 (m, 5 H, C_6H_5), 4.71 [t, *J*(PH) = 3.6 Hz, 1 H, =C=C*H*Ph], 2.79 (m, 6 H, PC*H*CH_3), 1.29 [dvt, *N* = 13.2, *J*(HH) = 6.6 Hz, 36 H, PCHC*H*$_3$]. – ^{13}C NMR (100.6 MHz, C_6D_6): δ = 341.1 [t, *J*(PC) = 15.1 Hz, =*C*=CHPh], 133.8 [t, *J*(PC) = 2.5 Hz, *ipso*-C of C_6H_5], 128.5, 125.6, 124.4 (each s, C_6H_5), 109.3 [t, *J*(PC) = 4.3 Hz, =C=*C*HPh], 23.7 [vt, *N* = 19.0 Hz, P*C*HCH_3], 20.1 (s, PCH*C*H$_3$). – ^{31}P NMR (162.0 MHz, C_6D_6): δ = 29.0 (s). – $C_{26}H_{48}Cl_2P_2Ru$ (594.6): calcd. C 52.52, H 8.14; found C 52.85, H 7.86.

5. *Preparation of [RuCl$_2$(=CHCH=CPh$_2$)(PiPr$_3$)$_2$]* (**9**) *from* **4**: A solution of 116 mg (0.23 mmol) of **4** in 10 ml of CH_2Cl_2 was treated with 121 mg (0.48 mmol) of HC≡CCPh$_2$OAc and stirred for 1 h at room temperature. The solvent was removed in vacuo and 5 ml of pentane was added to the oily residue. After the mixture was stored for 2 h, a red solid precipitated which was filtered and dried in vacuo. It was identified by comparison of the ^{1}H- and ^{13}C-NMR data with those reported by Grubbs et al. for compound **9**.[12b]

6. *Preparation of [RuCl$_2$(=CHCH=CiPr$_2$)(PiPr$_3$)$_2$]* (**10**): A solution of 120 mg (0.24 mmol) of **4** in 10 ml of CH_2Cl_2 was treated with 85 µl (0.55 mmol) of HC≡CC*i*Pr$_2$OH and stirred for 10 min at 60°C. After cooling to room temperature, the solvent was removed in vacuo. Upon addition of 5 ml of pentane, a purple solid precipitated which was filtered and dried in vacuo; yield 103 mg (70%); m. p. 124°C (dec.). – ^{1}H NMR (400 MHz, C_6D_6): δ = 19.56 [d, *J*(HH) = 11.2 Hz, 1 H, =C*H*CH=C*i*Pr$_2$], 8.06 [d, *J*(HH) = 11.2 Hz, 1 H, =CHC*H*=C*i*Pr$_2$], 3.87 [sept, *J*(HH) = 6.8 Hz, 1 H, C*H*CH_3], 2.82 (m, 6 H, PC*H*CH_3), 2.38 [sept, *J*(HH) = 6.8 Hz, 1 H, C*H*CH_3], 1.24 [dvt, *N* = 13.2, *J*(HH) = 6.6 Hz, 36 H, PCHC*H*$_3$], 1.04, 0.98 both d, *J*(HH) = 6.8 Hz, 12 H, CHC*H*$_3$]. – ^{13}C NMR (100.6 MHz, C_6D_6): δ = 288.3 [t, *J*(PC) = 7.0 Hz, =*C*HCH=C*i*Pr$_2$], 152.4 [s, =CH*C*H=C*i*Pr$_2$], 143.3 [s, =*Ci*Pr$_2$], 30.8, 29.0 (both s, *C*HCH$_3$), 22.3 [vt, *N* = 19.8 Hz, P*C*HCH_3], 21.8, 19.4 (both s, PCH*C*H$_3$), 18.3 (s, CH*C*H$_3$). – ^{31}P NMR (162.0 MHz, C_6D_6): δ = 45.5 (s). – $C_{27}H_{58}Cl_2P_2Ru$ (616.7): calcd. C 52.59, H 9.48; found C 52.13, H 9.13.

7. *Preparation of [RuHCl(=C=CHPh)(PiPr$_3$)$_2$]* (**11**): A solution of compound **5**, prepared from 113 mg (0.40 mmol for *n* = 1) of **3**, 193 µl (0.99 mmol) of P*i*Pr$_3$, and 115 µl (0.83 mmol) of NEt_3 in 20 ml of 2-propanol under hydrogen, was brought to dryness in vacuo and the oily residue was extracted with 20 ml of hexane. The extract was treated with 96 µl (0.88 mmol) of phenylacetylene and the solution was stirred for 10 min at room temperature. The solvent was then removed at 0°C in vacuo, the residue was dissolved in 10 ml of pentane, and the solution was filtered through Celite. The filtrate was concentrated to ca. 4 ml and then stored at –78°C. Olive-green crystals precipitated which were separated from the mother liquor, washed with 2 ml of pentane (–20°C) and dried; yield 83 mg (37%); m. p. 78°C (dec.). – ^{1}H NMR (400 MHz, C_6D_6): δ = 7.16–6.87 (m, 5 H, C_6H_5), 4.36 [t, *J*(PH) = 3.4 Hz, 1 H, =C=C*H*Ph], 2.51 (m, 6 H, PC*H*CH_3), 1.24, 1.22 both m, in ^{1}H{^{31}P} d, *J*(HH) = 7.7 Hz, 36 H, PCHC*H*$_3$], –12.48 [t, *J*(PH) = 17.2 Hz, 1 H, RuH]. – ^{13}C NMR (100.6 MHz, C_6D_6): δ = 329.3 [t, *J*(PC) = 15.1 Hz, =*C*=CHPh], 133.8 [t, *J*(PC) = 2.5 Hz, *ipso*-C of C_6H_5], 128.5, 123.6, 123.5 (each s, C_6H_5), 109.7 [t, *J*(PC) = 3.5 Hz, =C=*C*HPh], 24.7 [vt, *N* = 19.4 Hz, P*C*HCH_3], 20.4, 20.2 (both s, PCH*C*H$_3$). – ^{31}P NMR (162.0 MHz, C_6D_6): δ = 50.4 (s). – $C_{26}H_{49}ClP_2Ru$ (560.2): calcd. C 55.75, H 8.82; found C 55.47, H 8.49.

8. *Preparation of [RuHCl(=C=CH$_2$)(PiPr$_3$)$_2$]* (**12**): A solution of compound **5**, prepared from 122 mg (0.43 mmol for *n* = 1) of **3**, 215 µl (1.10 mmol) of P*i*Pr$_3$, and 120 µl (0.87 mmol) of NEt_3 in 20 ml of 2-propanol under hydrogen, was brought to dryness in vacuo and the oily residue was extracted with 20 ml of hexane. A slow stream of acetylene was passed at –78°C through the hexane solution, which led to a rapid change of color from red to brown. The solvent was removed at 0°C in vacuo and the residue was worked up as described for **11**. A brown solid was obtained; yield 85 mg (41%); m. p. 83°C (dec.). – ^{1}H NMR (400 MHz, C_6D_6): δ = 2.64 (m, 8 H, PC*H*CH_3 and =C=CH_2), 1.28, 1.24 both m, in ^{1}H{^{31}P} d, *J*(HH) = 7.2 Hz, 36 H, PCHC*H*$_3$], –15.03 [t, *J*(PH) = 18.3 Hz, 1 H, RuH], signal of =C=C*H*$_2$ obscured by signal of PC*H*CH_3. – ^{13}C NMR (100.6 MHz, C_6D_6): δ = 326.3 [t, *J*(PC) = 14.6 Hz, =*C*=CH_2], 87.1 [t, *J*(PC) = 3.7 Hz, =C=*C*H$_2$], 24.4 [vt, *N* = 19.5 Hz, P*C*HCH_3], 20.4, 20.3 (each s, PCH*C*H$_3$). – ^{31}P NMR (162.0 MHz, C_6D_6): δ = 51.0 (s). – $C_{20}H_{45}ClP_2Ru$ (484.1): calcd. C 49.63, H 9.37; found C 49.36, H 9.11.

9. *Preparation of [RuHCl(H$_2$)(PCy$_3$)$_2$]* (**13**) *from* **3**: A suspension of 220 mg (0.79 mmol for *n* = 1) of **3** in 20 ml of 2-butanol was treated with 886 mg (3.16 mmol) of PCy_3 and heated for 6 h under hydrogen (1.5 bar) at 80°C. After the reaction mixture was cooled to room temperature, the solution was decanted from the precipitate. The orange solid was washed twice with 10 ml of 2-butanol and dried in vacuo. It was characterized by comparison of the ^{1}H- and ^{31}P-NMR data with those found in the literature.[8] Yield 470 mg (85%).

10. *Preparation of [RuH$_2$Cl$_2$(PCy$_3$)$_2$]* (**14**) *from* **13**: A solution of 130 mg (0.19 mmol) of **13** in 10 ml of CH_2Cl_2 was treated with 0.5 ml of a 2 M aequous solution of HCl and stirred for 3 h at room temperature. The resulting dark red mixture was cooled to –40°C to remove excess HCl and then filtered. The filtrate was brought to dryness in vacuo and the dark red microcrystalline solid was dried; yield 119 mg (87%); m. p. 74°C (dec.). –The ^{1}H- and ^{31}P-NMR data were identical to those reported by Chaudret et al.[11] – ^{13}C NMR (100.6 MHz, CD_2Cl_2): δ = 38.9 [d, *J*(PC) = 28.6 Hz, *ipso*-C of C_6H_{11}], 29.4 (s, C_6H_{11}), 27.4 [d, *J*(PC) = 11.0 Hz, C_6H_{11}], 26.1 (s, C_6H_{11}).

11. *Preparation of [RuCl$_2$(=C=CHPh)(PCy$_3$)$_2$]* (**15**): a) A solution of 119 mg (0.162 mmol) of **14** in 5 ml of CH_2Cl_2 was treated with 178 µl (1.62 mmol) of PhC≡CH at –78°C. After the solution was warmed to room temperature, it was stirred for 30 min and then concentrated to ca. 2 ml in vacuo. Addition of 10 ml of acetone led to the precipitation of a purple solid, which was filtered, washed twice with 10 ml of acetone, and dried; yield 91 mg (67%). – b) A solution of 172 mg (0.21 mmol) of **16** in 10 ml of benzene was treated with 226 µl (2.10 mmol) of PhC≡CH and the resulting brown solution heated for 15 h at 45°C. After the solution was cooled to room temperature, it was worked up as described for a); yield 103 mg (60%); m. p. 88°C (dec.). If instead of **16** the analogous compound **17** was used as starting material, the yield of the product was about the same. – ^{1}H NMR (200 MHz, $CDCl_3$, 40°C): δ = 7.14–7.07, 6.90–6.80 both m, 5 H, C_6H_5), 4.34 [t, *J*(PH) = 3.1 Hz, 1 H, =C=C*H*Ph], 2.70–2.54, 2.14–2.02, 1.68–1.50 (each m, C_6H_{11}). – ^{13}C NMR (50.3 MHz, $CDCl_3$, 40°C): δ = 342.8 [t, *J*(PC) = 15 Hz, =*C*=CHPh], 133.2, 127.9, 125.1, 123.3, (each s, C_6H_5) 108.6 (br s, =C=*C*HPh), 33.3 (vt, *N* = 22.0 Hz, *ipso*-C of C_6H_{11}), 30.1 (s, C_6H_{11}), 27.9 (vt, *N* = 8.0 Hz, C_6H_{11}). – ^{31}P NMR (81.0 MHz, $CDCl_3$, 40°C): δ = 22.0 (s). –

$C_{44}H_{72}Cl_2P_2Ru$ (834.98): calcd. C 63.29, H 8.69; found C 63.48, H 8.73.

12. *Conversion of Compound* **4** *to* **5** *with PiPr$_3$ and 2-Propanol:* In an NMR tube a suspension of 25 mg (0.05 mmol) of **4** in 0.5 ml of 2-propanol was treated with 20 µl (0.10 mmol) of P*i*Pr$_3$. After 2−3 min, a clear red solution was formed which due to the ^{1}H- and ^{31}P-NMR spectra contained the two compounds **5** and **6** in equimolar amounts. Moreover, the presence of acetone was confirmed by GC/MS analysis.

13. *Conversion of Compound* **14** *to* **13** *with PCy$_3$ and 2-Propanol:* A solution of 50 mg (0.068 mmol) of **14** in 5 ml of 2-propanol was treated with 76 mg (0.272 mmol) of PCy_3 at room temperature. Upon stirring for 12 h an orange precipitate was formed, which was filtered, washed with 2 ml of 2-propanol and dried in vacuo; yield 29 mg (61%).

14. *Determination of the X-ray Crystal Structure of* **15**[28] (for data of compound **4** see ref.[5]): Single crystals of **15** were grown upon cooling of a saturated solution of **15** in $CHCl_3$ from 50°C to room temperature. Crystal data (from 25 reflections, $4° < \Theta < 11°$): monoclinic; space group $P2_1/n$ (No. 14); a = 14.505(2), b = 16.816(1), c = 20.057(3) Å, β = 108.438(6)°; V = 4641(1) Å^3, Z = 4; $d_{calcd.}$ = 1.366 gcm^{-3}; µ(Mo-K_α) = 0.720 mm^{-1}; crystal size 0.15 × 0.10 × 0.10 mm; Enraf-Nonius CAD4 diffractometer, Mo-K_α radiation (0.71073 Å), graphite monochromator, zirconium filter (factor 16.4); T = 173(2) K; ω/θ scan, max. 2θ = 48°; 9081 reflections measured, 6500 independent ($R_{int.}$ = 0.0533), 4196 with $I > 2\sigma(I)$. Intensity data were corrected for Lorentz and polarization effects and an empirical absorption correction (Ψ scan method) was applied (min. transmission 98.29%). The structure was solved by the Patterson method (SHELXS-86)[29]. Atomic coordinates and the anisotropic thermal parameters of non-hydrogen atoms were refined by full-matrix least squares on F^2 (SHELXL-93)[30]. The positions of all hydrogen atoms except of H2 were calculated according to ideal geometry and refined by using the riding method. The position of H2 could be located in a final difference Fourier synthesis and refined with fixed U_{eq}. The asymmetric unit includes one molecule of $CHCl_3$ which was refined anisotropically without any restrictions. Conventional R = 0.0588 [for 4196 reflections with $I > 2\sigma(I)$], and weighted wR_2 = 0.1337 for all 6500 located reflections; reflection/parameter ratio 13.51; residual electron density +0.819/−0.685 eÅ^{-3}.

☆ Dedicated to Professor *Bernt Krebs* on the occasion of his 60th birthday.

[1] [1a] M. Aracama, M. A. Esteruelas, F. J. Lahoz, J. A. Lopez, U. Meyer, L. A. Oro, H. Werner, *Inorg. Chem.* **1991**, *30*, 288−293. − [1b] U. Meyer, Dissertation, Universtität Würzburg, **1988**.

[2] Carbyne complexes: [2a] J. Espuelas, M. A. Esteruelas, F. J. Lahoz, L. A. Oro, N. Ruiz, *J. Am. Chem. Soc.* **1993**, *115*, 4683−4689. − [2b] B. Weber, P. Steinert, B. Windmüller, J. Wolf, H. Werner, *J. Chem. Soc., Chem. Commun.* **1994**, 2595−2596.

[3] Vinylidene complexes: [3a] H. Werner, B. Weber, O. Nürnberg, J. Wolf, *Angew. Chem.* **1992**, *104*, 1105−1107; *Angew. Chem. Int. Ed. Engl.* **1992**, *31*, 1025−1027. − [3b] M. A. Esteruelas, L. A. Oro, N. Ruiz, *Organometallics* **1994**, *13*, 1507−1509. − [3c] B. Weber, Dissertation, Universität Würzburg, **1995**.

[4] [4a] H. Werner, A. Stark, M. Schulz, J. Wolf, *Organometallics* **1992**, *11*, 1126−1130. − [4b] H. Werner, A. Stark, P. Steinert, C. Grünwald, J. Wolf, *Chem. Ber.* **1995**, *128*, 49−62. − [4c] M. Martin, O. Gevert, H. Werner, *J. Chem. Soc., Dalton Trans.* **1996**, 2275−2283.

[5] C. Grünwald, O. Gevert, J. Wolf, P. González-Herreo, H. Werner, *Organometallics* **1996**, *15*, 1960−1962.

[6] M. Oliván, E. Clot, O. Eisenstein, K. G. Caulton, *Organometallics* **1998**, *17*, 3091−3100.

[7] M. A. Esteruelas, H. Werner, *J. Organomet. Chem.* **1986**, *303*, 221−231.

[8] [8a] T. Burrow, S. Sabo-Etienne, B. Chaudret, *Inorg. Chem.* **1995**, *34*, 2470−2472. − [8b] M. Christ, S. Sabo-Etienne, B. Chaudret, *Organometallics* **1994**, *13*, 3800−3804.

[9] [9a] P. Pertici, G. Vitulli, W. Porzio, M. Zocchi, *Inorg. Chim. Acta* **1979**, *37*, L521-L522. − [9b] J. W. Bruno, J. C. Huffman, K. G. Caulton, *Inorg. Chim. Acta* **1984**, *89*, 167−173. − [9c] H. Suzuki, D. H. Lee, N. Oshima, Y. Moro-oka, *Organometallics* **1987**, *6*, 1569−1575. − [9d] G. Jia, D. W. Meek, J. C. Galluci, *Inorg. Chem.* **1991**, *30*, 403−410. − [9e] J. F. Hartwig, R. A. Andersen, R. G. Bergman, *Organometallics* **1991**, *10*, 1875−1887.

[10] D. G. Gusev, R. Kuhlman, J. R. Rambo, H. Berke, O. Eisenstein, K. G. Caulton, *J. Am. Chem. Soc.* **1995**, *117*, 281−292.

[11] V. Rodriguez, S. Sabo-Etienne, B. Chaudret, J. Thoburn, S. Ulrich, H. −H. Limbach, J. Eckert, J. −C. Barthelat, K. Hussein, C. J. Marsden, *Inorg. Chem.* **1998**, *37*, 3475−3485.

[12] [12a] S. Nguyen, L. K. Johnson, R. H. Grubbs, *J. Am. Chem. Soc.* **1992**, *114*, 3974−3975. − [12b] G. C. Fu, S. Nguyen, R. H. Grubbs, *J. Am. Chem. Soc.* **1993**, *115*, 9856−9857. − [12c] S. Nguyen, R. H. Grubbs, J. W. Ziller, *J. Am. Chem. Soc.* **1993**, *115*, 9858−9859. − [12d] P. Schwab, M. B. France, J. W. Ziller, R. H. Grubbs, *Angew. Chem.* **1995**, *107*, 2179−2181; *Angew. Chem. Int. Ed. Engl.* **1995**, *34*, 2039−2041. − [12e] P. Schwab, R. H. Grubbs, J. W. Ziller, *J. Am. Chem. Soc.* **1996**, *118*, 100−110. − [12f] D. M. Lynn, S. Kanaoka, R. H. Grubbs, *J. Am. Chem. Soc.* **1996**, *118*, 784−790.

[13] [13a] R. H. Grubbs, S. J. Miller, G. C. Fu, *Acc. Chem. Res.* **1995**, *28*, 446−452. − [13b] A. S. K. Hashmi, *J. Prakt. Chem.* **1997**, 195−199. − [13c] A. Fürstner, *Top. Catal.* **1997**, *4*, 285−299. − [13d] M. Schuster, S. Blechert, *Angew. Chem.* **1997**, *109*, 2124−2144, *Angew. Chem. Int. Ed. Engl.* **1997**, *36*, 2036−2055.

[14] [14a] M. I. Bruce, A. G. Swincer, *Adv. Organomet. Chem.* **1983**, *22*, 59−128. − [14b] M. I. Bruce, *Chem. Rev.* **1991**, *91*, 197−257.

[15] Y. Wakatsuki, H. Yamazaki, N. Kumegawa, T. Satoh, J. Y. Satoh, *J. Am. Chem. Soc.* **1991**, *113*, 9604−9610.

[16] Y. Wakatsuki, N. Koga, H. Yamazaki, K. Morokuma, *J. Am. Chem. Soc.* **1994**, *116*, 8105−8111.

[17] J. P. Selegue, *Organometallics* **1982**, *1*, 217−218.

[18] [18a] H. Le Bozec, K. Ouzzine, P. H. Dixneuf, *J. Chem. Soc., Chem. Commun.* **1989**, 219−221. − [18b] A. Wolinska, D. Touchard, P. H. Dixneuf, *J. Organomet. Chem.* **1991**, *420*, 217−226. − [18c] N. Pirio, D. Touchard, L. Toupet, P. H. Dixneuf, *J. Chem. Soc., Chem. Commun.* **1991**, 980−982. − [18d] D. Pilette, K. Ouzzine, H. Le Bozec, P. H. Dixneuf, C. E. F. Rickard, W. R. Roper, *Organometallics* **1992**, *11*, 809−817. − [18e] D. Touchard, C. Morice, V. Cadierno, P. Haquette, L. Toupet, P. H. Dixneuf, *J. Chem. Soc., Chem. Commun.* **1994**, 859−860. − [18f] D. Touchard, N. Pirio, P. H. Dixneuf, *Organometallics* **1995**, *14*, 4920−4928. − [18g] D. Touchard, S. Guesmi, M. Bouchaib, P. Haquette, A. Daridor, P. H. Dixneuf, *Organometallics* **1996**, *15*, 2579−2581.

[19] [19a] H. Werner, T. Rappert, *Chem. Ber.* **1993**, *126*, 669−678. − [19b] H. Werner, T. Rappert, R. Wiedemann, J. Wolf, N. Mahr, *Organometallics* **1994**, *13*, 2721−2727. − [19c] T. Braun, P. Steinert, H. Werner, *J. Organomet. Chem.* **1995**, *488*, 169−176. − [19d] B. Windmüller, J. Wolf, H. Werner, *J. Organomet. Chem.* **1995**, *502*, 147−161. − [19e] H. Werner, *J. Chem. Soc., Chem. Commun.* **1997**, 903−910. − [19f] C. Grünwald, M. Laubender, J. Wolf, H. Werner, *J. Chem. Soc., Dalton Trans.* **1998**, 833−839. − [19g] H. Werner, C. Grünwald, P. Steinert, O. Gevert, J. Wolf, *J. Organomet. Chem.*, in press.

[20] M. Oliván, O. Eisenstein, K. G. Caulton, *Organometallics* **1997**, *16*, 2227−2229.

[21] M. Bourgault, A. Castillo, M. A. Esteruelas, E. Onate, N. Ruiz, *Organometallics* **1997**, *16*, 636−645.

[22] J. Wolf, W. Stüer, C. Grünwald, H. Werner, P. Schwab, M. Schulz, *Angew. Chem.* **1998**, *110*, 1165−1167; *Angew. Chem. Int. Ed. Engl.* **1998**, *37*, 1124−1126.

[23] W. Stüer, Dissertation, Universität Würzburg, in preparation.

[24] C. Grünwald, Dissertation, Universität Würzburg, **1998**.

[25] T. E. Wilhelm, T. R. Belderrain, S. N. Brown, R. H. Grubbs, *Organometallics* **1997**, *16*, 3867−3869.

[26] E. Lindner, M. Geprägs, K. Gierling, R. Fawzi, M. Steinmann, *Inorg. Chem.* **1995**, *34*, 6106−6117.

[27] M. O. Albers, E. Singleton, J. E. Yates, *Inorg. Synth.* **1989**, *26*, 251−254.

[28] Crystallographic data (excluding structure factors) for the structure reported in this paper have been deposited with the Cam-

bridge Crystallographic Data Centre as supplementary publication no. CCDC-102563 . Copies of the data can be obtained free of charge on application to CCDC, 12 Union Road, Cambridge CB2 1EZ, UK (Fax: internat. + 44-1223/336-033; E-mail: deposit@ccdc.cam.ac.uk).

[29] G. M. Sheldrick, *Acta Crystallogr., Sect. A* **1990**, *46*, 467.
[30] G. M. Sheldrick, *A Program for Crystal Structure Refinement*, University of Göttingen, **1993**.

[I98271]

Clusters as Ligands – Large Assemblies of Transition Metal Clusters

Xinjian Lei[a], Eduardo E. Wolf[b], and Thomas P. Fehlner*[a]

Department of Chemistry & Biochemistry[a]
and Department of Chemical Engineering[b]
University of Notre Dame
Notre Dame, IN 46556-5670, USA
Fax: (internat.) + 1-219/631-6652
E-mail: fehlner.1@nd.edu

Received July 30, 1998

Keywords: Clusters / Catalysis / Carboxylato complexes / Hydrogenations

A strategy of using functionalized clusters as ligands for cationic metal centers facilitates the construction of designed transition metal cluster assemblies. Examples of cluster metal carboxylates with conventional as well as novel structures are given and an application of these large molecular species to the generation of heterogeneous hydrogenation catalysts with unusual activities and selectivities is described.

The synthesis of complex species for defined chemical roles is one common goal of both organic and inorganic chemistry. In the latter area, the synthesis of complex extended solid-state structures from the elements under thermodynamic control, e.g., zeolites, provides an impressive example of the power of synthesis. Many of these subdisciplines are covered in the interdisciplinary area known supramolecular chemistry.[1]

Interest in the construction of large, complex inorganic species is driven by an eclectic set of applications which include molecular electronics[2], photochemically driven electron transfer[3], liquid crystalline materials[4], host-guest chemistry[5], cryptate chemistry[6], nanocluster borderline solids[7], chemical sensors[8], ferrimagnetic solids[9], and others. The structures involved range from one dimensional chains of clusters[10], to cluster aggregates[11], to rigid-rod polymers[12], to metal spheres[13], to supramolecular chiral networks[14], to supported clusters[15], to dendritic systems[16][17], and more. The synthetic approaches are equally varied and include step-wise formation of oligomers[18],

Xinjian Lei: After graduating with his M.S. from the Fujian Institute of Research on the Structure of Matter, Chinese Academy of Sciences, P. R. China in 1988, Xinjian Lei was a research associate in the following four years. He obtained his Ph.D. in inorganic chemistry in 1997 at the University of Notre Dame and continues as a research associate. His research has been focused on the synthesis, characterization, and reactivity of new cluster compounds, as well as their catalytic evaluation.

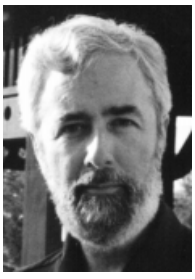

Eduardo E. Wolf: After receiving a B.S. degree from the University of Chile, Santiago, a M.S. degree from the University of California, Davis, and a Ph.D. degree from the University of California, Berkeley, Eduardo E. Wolf joined the faculty of the Chemical Engineering Department of the University of Notre Dame where he is presently hold the rank of Professor. He works in the area of catalysis and reaction engineering where he specializes in the design of novel catalytic materials and novel catalytic reactors.

Thomas P. Fehlner: After receiving a B.S. degree from Siena College and M.A and Ph.D. degrees from The Johns Hopkins University, Thomas P. Fehlner joined the faculty of the Chemistry Department of the University of Notre Dame where he is presently Grace-Rupley Professor of Chemistry. He has previously studied small inorganic species in the gas phase (reactivity of free BH_3, photoelectron spectra of unstable species) but more recently has worked on the syntheses of metallaboranes and organometallic cluster chemistry.

MICROREVIEWS: This feature introduces the readers to the authors' research through a concise overview of the selected topic. Reference to important work from others in the field is included.

 © WILEY-VCH Verlag GmbH, D-69451 Weinheim, 1998 1434–1948/98/1212–1835 $ 17.50+.50/0

modular assembly of rings[19][20], polymerization[21], development of molecular tinkertoys[22] and carborods.[23] Another synthetic approach, the use of functionalized main group[24][25][26], transition metal complexes[27][28] or clusters,[29][30][31][32] is of particular relevance to this contribution.

Our interest in large assemblies of clusters was piqued when we found that $(CO)_9Co_3(\mu_3\text{-}C(CH_2)_nOH$, a major product of the decomposition of $(CO)_4CoBH_2\cdot THF$ above 0 °C, crystallized in hexagonal columns with the hydrophilic hydrogen-bonded OH groups at the columnar axes and the hydrophobic metal carbonyl clusters on the surfaces (Scheme 1).[33] Even in solution this cluster derivative forms small aggregates reflecting its ambiphilic behavior. At the time, and still, the organization of metal clusters on various supports, principally for the generation of new catalysts, commanded considerable attention[34] and we wondered if suitably functionalized clusters would self-organize. This would eliminate the need for a complex substrate and, in doing so, introduce more uniformity into the cluster arrays.

As the weak forces holding $(CO)_9Co_3[\mu_3\text{-}C(CH_2)_nOH]$ molecules together seemed inadequate for our purposes, we sought functionalization that would permit a cluster to serve as a ligand in a classical Werner coordination compound, i.e., the metal cluster would simply replace the usual organic foliage of the typical ligand. These coordination compounds would constitute cluster assemblies in which the central metal cationic moiety would determine both the number of clusters (coordination number) and the spatial array of clusters (coordination geometry). In a sense, the relatively small, well-defined cationic metal center would replace the large substrate of the typical supported cluster.

The idea of cluster coordination compounds presented a number of attractive aspects. First, by using the established principles of coordination chemistry, we could construct a predetermined cluster array from monofunctional clusters. In principle, these cluster building blocks could be made di- and trifunctional in order to construct chains and nets as well. Indeed the Schauer group has made considerable progress in this direction by using bidentate cluster ligands in which main group atoms in the cluster itself act as ligating sites.[18][35][36][37] Curiously, monodentate clusters of the same type form trimeric rings by an intermolecular ligand displacement reaction on the cluster itself.[38] Second, metal clusters are very different from a typical organic substituent, e.g., CH_3R vs $(CO)_9Co_3(\mu_3\text{-}CR)$.[39][40][41][42][43][44][45][46][47] In terms of electronic effects, the metals within the clusters plus their ancillary ligands constitute electron reservoirs capable of donating or accepting electron density. The fact that even the smallest clusters have a substantial steric bulk must affect the products formed in cluster coordination reactions. Consequently, we expected to find significant differences between the coordination chemistry of a cluster ligand and that of a typical main group ligand.

Perhaps the most attractive aspect of an externally functionalized metal cluster is that cluster size, composition as well as ligand type and extension are quantities that can, in principle, be varied.[48] Unfortunately, cluster synthetic chemistry, although continuously developing, is in a rudimentary state relative to, e.g., organic ligand synthesis. Many cluster types are derived from reactions that are unselective thereby requiring tedious separations resulting in modest yields.[48] Much of the interesting structural chemistry[49] is based on metals such as Os and Rh which put an economic damper on thoughts of gram scale syntheses from low yield reactions. Thus, little of the cluster derivative chemistry in the literature was suitable for our purposes.

For these reasons we decided to focus on the well studied tricobalt akylidyne cluster system and began our exploration of cluster coordination chemistry using $(CO)_9Co_3(\mu_3\text{-}CCOOH)$ as a precursor to the corresponding cluster carboxylate ligand, $[(CO)_9Co_3(\mu_3\text{-}CCOO)]^-$.[40][41] This is a fortunate choice as metal carboxylate chemistry is a mature area of coordination chemistry of considerable interest.[50] Importantly, this cluster ligand precursor can be prepared in good yield from commercially available $Co_2(CO)_8$ and $Cl_3CC(O)OR$ on a multigram scale by undergraduates. Its main drawback, and one that figures in its chemistry, is cluster degradation which is facile under basic conditions. For this reason, simple salts of the free ligand $[(CO)_9Co_3(\mu_3\text{-}CCOO)]^-$ are unavailable and only efficient coordination reactions lead to simple chemistry. However, this cluster ligand is selective and metal carboxylate formation reactions are usually clean giving good to excellent yields even for obviously complex reaction pathways. In the following we highlight the varied coordination chemistry of

Scheme 1

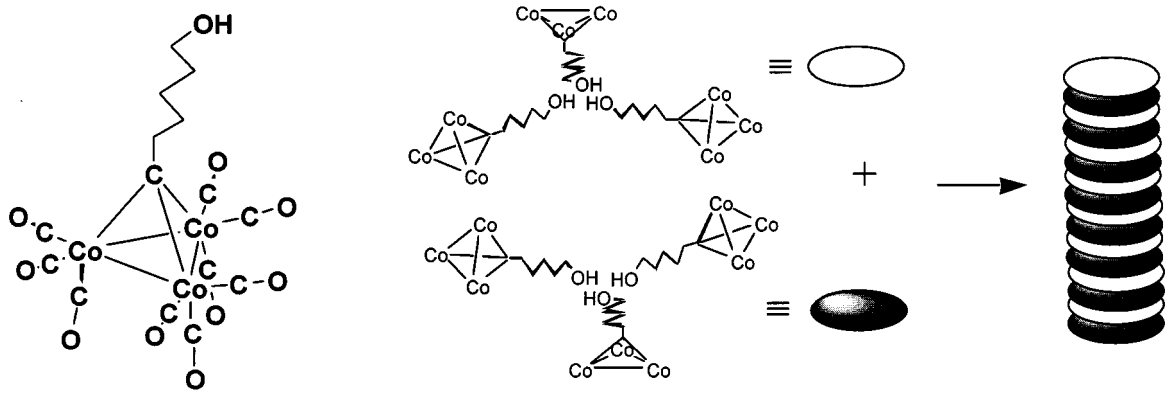

the $[(CO)_9Co_3(\mu_3\text{-}CCOO)]^-$ ligand established in our laboratory over the last few years.

Cluster Metal Carboxylate Chemistry

Organic carboxylate anions (RCO_2^-) have been known for over a hundred years as versatile ligands capable of forming metal carboxylates with almost all the metal elements in the periodic table. The resulting metal carboxylates exhibit a variety of core structures, coordination modes, and coordination numbers depending on the properties of the elements used.[50] Recently the chemistry of transition metal carboxylates has drawn renewed attention as such compounds can serve as precursors for the synthesis nanometer-sized polynuclear aggregates with unusual structural and magnetic properties. These compounds may also help to further improve our understanding of the transition from the molecular to the solid state in the biomineralization process or in the development of molecular magnets.[51][52][53]

Likewise, the chemistry of alkylidynetricobalt nonacarbonyl cluster compounds, $(CO)_9Co(\mu_3\text{-}CR)$, has been extensively investigated since the appearance of the first member of this class of compounds, $(CO)_9Co_3(\mu_3\text{-}CCH_3)$ in 1958.[41][54] These complexes are all deeply colored and most are air-stable in solution and in the solid state. In general the alkylidynetricobalt nonacarbonyls undergo degradation by oxidizing agents, bases, and nucleophiles. For example, reactions of potassium permanganate or water with $(CO)_9Co(\mu_3\text{-}CR)$ complexes lead to evolution of carbon monoxide, the formation of inorganic cobalt salts and carboxylic acids derived from the apical organic substituents. Fortunately from the point of view of the work described here, most alkylidynetricobalt nonacarbonyl complexes are soluble in organic solvents, stable toward protonic and Lewis acids, and possess an extensive chemistry.[34][41][42][48][55][56] Our interest in cluster assemblies joins these two fields, i.e. the carboxylic acid derivative of the alkylidynetricobalt nonacarbonyl complex, $(CO)_9Co(\mu_3\text{-}COOH)$, is used as a cluster carboxylate ligand precursor to synthesize cluster metal carboxylates.

Structures of the Cluster Metal Carboxylates

The principal means of characterization of the cluster metal carboxylates was single crystal X-ray diffraction. In all cases, the bond distances and angles of the tricobalt cluster substituents are unchanged within experimental error from those of free tricobalt clusters. In some cases, the cluster acid functions just like an organic carboxylic acid and analogs of known metal carboxylates are obtained. In other cases the combination of steric and electronic properties associated with the cluster substituent on the acid made novel structural types accessible. The compounds featured below illustrate analogs of organic carboxylates, unusual metal carboxylate structural types, and varied spatial arrangements of the tricobalt cluster assemblies. As will be seen, the cluster carboxylate ligand exhibits the same variety of coordination modes as organic metal carboxylates but also generates some novel structures.

Cluster Carboxylate Mimics of Known Metal Carboxylates

$[M_2\{(CO)_9Co_3(\mu_3\text{-}CCO_2)\}_4L_2]$ ($M = Co$, $L = THF$; $M = Mo$, $L = (CO)_9Co_3(\mu_3\text{-}CCO_2H)$:[57][58] As an example, the structure of $[Co_2\{(CO)_9Co_3(\mu_3\text{-}CCO_2)\}_4(THF)_2]$ is shown in Scheme 2. In this first scheme the complete structure from the crystallographic results is shown, and below, for clarity, a simplified structure. As some of the succeeding structures are considerably more cluttered, the representations have been simplified principally by removing the carbonyl ligands of the cobalt clusters. As with similar organic carboxylate analogs,[59] the cluster carboxylate ligands symmetrically bridge two cobalt centers. Consequently, the four tricobalt clusters are arranged in a square

Scheme 2

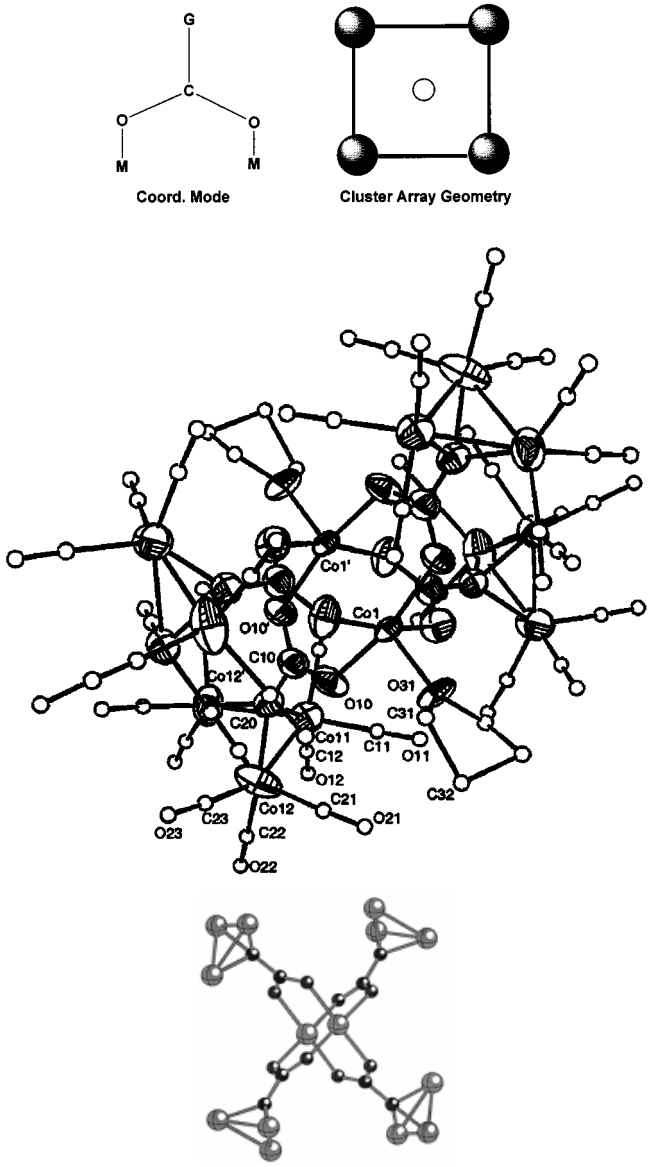

planar array perpendicular to Co−Co bond axis. Each metal atom is coordinated in the equatorial positions by four oxygen atoms from the four carboxylate ligands and in an axial position by one from the THF solvent.

[$M_4O\{(CO)_9Co_3(\mu_3\text{-}CCO_2)\}_6$] (M = Zn, Co): [60][61][62] As shown in Scheme 3, the core structure of the cluster zinc carboxylate consists of an M_4 tetrahedron with a centered oxygen atom. The six carboxylate moieties bridge the six metal-metal edges, resulting an octahedral spatial distribution of the tricobalt clusters. These cluster metal carboxylates are direct analogs of classical $M_4O(RCO_2)_6$ "basic" metal carboxylates which are known for M = Be, Zn, Co.[50]

Scheme 3

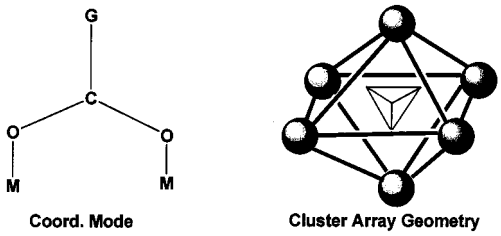

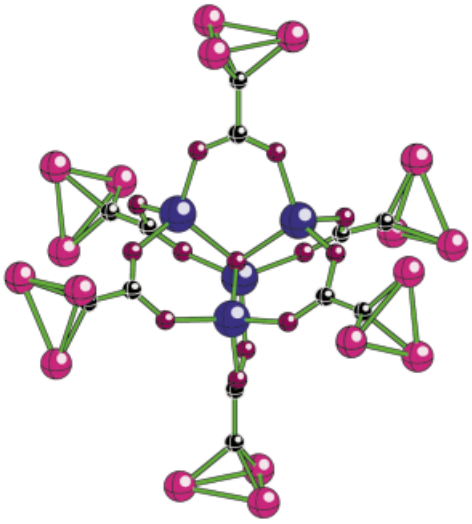

[$Ti_4O_4(OR)_4\{(CO)_9Co_3(\mu_3\text{-}CCO_2)\}_4$] (R = CH(Me)$_2$, $(CH_2)_3CH_3$, C_6H_5, 2,6-$(CH_3)_2$-C_6H_3):[63] The structure of the phenoxide derivative is shown in Scheme 4. The core is a distorted Ti_4O_4 cube with titanium and oxo oxygen atoms occupying alternate vertices. As expected, the coordination sphere of each Ti atom contains six oxygen atoms in a distorted octahedral arrangement. The cluster carboxylates bridge four of the six edges of the Ti_4 tetrahedron and the four tricobalt clusters lie roughly in a plane with one transoid pair being above and the other below the plane which results in a slightly distorted square-shape as indicated in Scheme 4. There is considerable open space in the structures, but this decreases with increasing size of the R group. One organic analog has been reported.[64]

Scheme 4

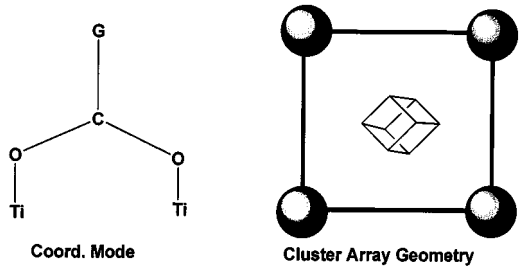

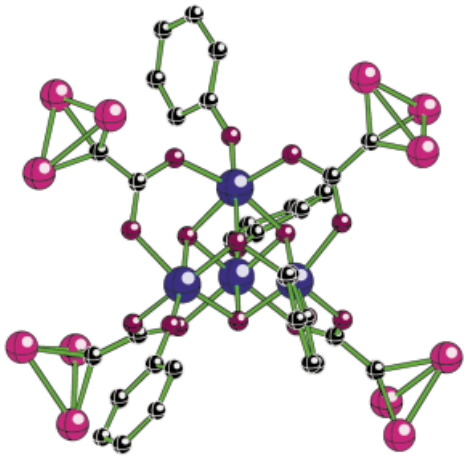

[$Ti_6O_4(OCH_2CH_3)_{12}\{(CO)_9Co_3(\mu_3\text{-}CCO_2)\}_4$] and [$Ti_6O_4(OCH(CH_3)_2)_4(1,2\text{-}O_2C_6H_4)_4\{(CO)_9Co_3(\mu_3\text{-}CCO_2)\}_4$]:[63] The structure of the first cluster metal carboxylate (Scheme 5) shows that it is a dimer of two Ti_3O_4 units linked together by TiO edges oriented so that the

Scheme 5

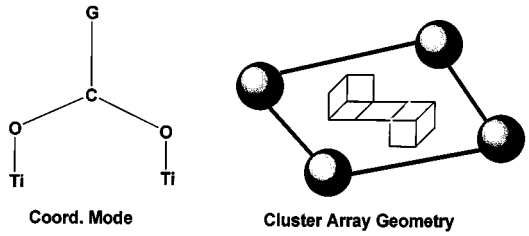

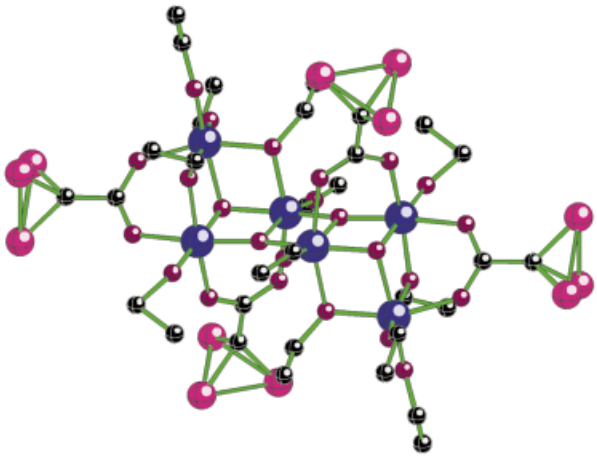

Scheme 6

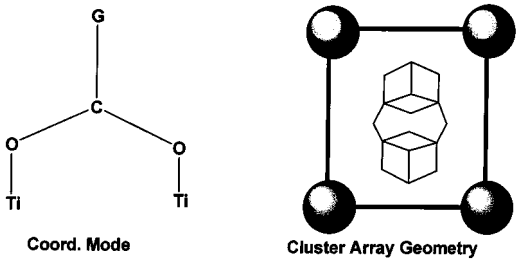

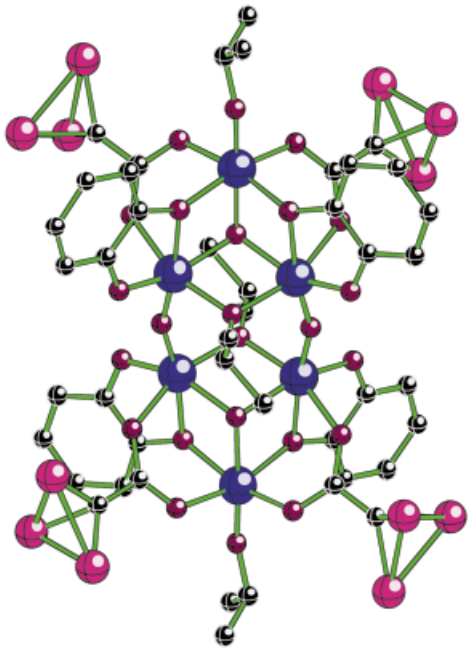

Ti_3O_4 units are related to each other by a crystallographic inversion center. Each Ti_3O_4 unit is bridged by two cluster ligands and the remaining coordination positions are occupied by six ethoxy ligands, two of which are bridging. The cluster carboxylates symmetrically bridge Ti centers, resulting a rhombic arrangement of the four tricobalt clusters elongated in the direction of the ladder-like Ti_6 core.

The structure of the second compound (Scheme 6) reveals that it is an isomeric form of the first resulting from different interconnects between the two Ti_3O_4 units. The catechol ligand uses one oxygen to bridge two Ti atoms and the other to coordinate to one of the two Ti centers in a terminal fashion. Each cluster carboxylate symmetrically bridges two Ti centers resulting a rectangular arrangement of the tricobalt clusters in the direction of the ladder-like Ti_6 core. Both cluster metal carboxylates have structurally characterized organic analogs[65][66][67][68]

Unique Cluster Metal Carboxylates

$[C_{10}H_6(NMe_2)_2][Co_2\{(CO)_9Co_3(\mu_3\text{-}CCO_2)\}_5]$:[69] As shown in Scheme 7, this anionic cluster metal carboxylate consists of two tetrahedral Co centers with very long Co−Co separation [3.47(4)Å]. The two Co atoms are held together by three bridging cluster ligands while the two remaining cluster ligands are terminally coordinated to each Co center in a unidentate fashion thereby generating a tetrahedral ligand environment for each Co atom and a triangular bipyramidal geometry for the spatial distribution of the five tricobalt clusters.

Scheme 7

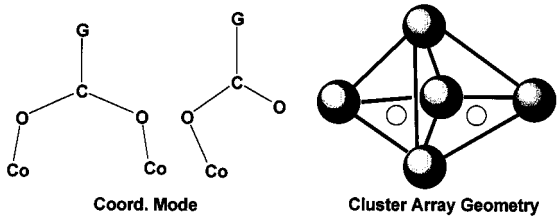

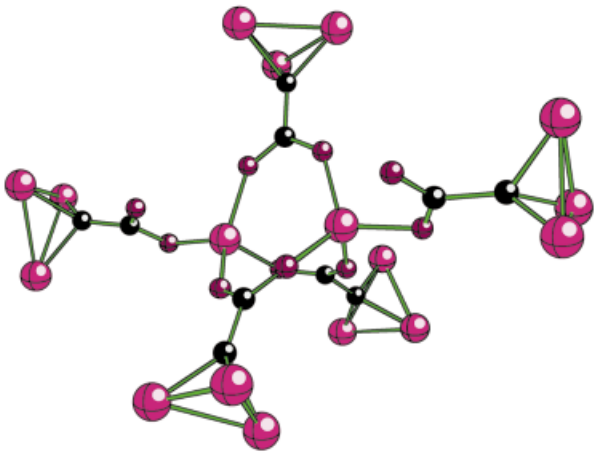

$[Zr_2(OCHMe_2)_4\{(CO)_9Co_3(\mu_3\text{-}CCO_2)\}_4]$:[63] This compound represents the first example of a structurally

Scheme 8

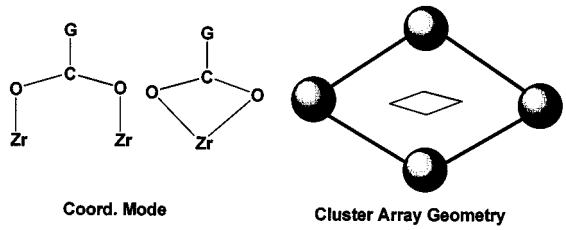

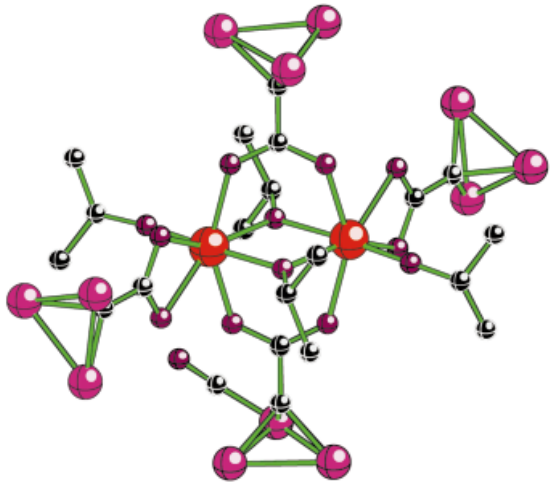

characterized zirconium alkoxy carboxylate. The structure (Scheme 8) reveals that there are two kinds of coordination modes for the cluster ligands, bridging and chelating. The coordination sphere of each zirconium atom is a slightly distorted pentagonal bipyramid in which the five equatorial positions are occupied with two oxygen atoms from a chelating cluster ligand, two from bridging cluster ligands, and one from a bridging isopropoxy group. The apical positions are occupied with oxygen atoms from one terminal and one bridging isopropoxy group. The spatial distribution of the four tricobalt clusters is a rhombic shape within which the rhombic Zr_2O_2 core is located.

[{Co(CO)$_3$}Cd$_3${(CO)$_9$Co$_3$(μ_3-CCO$_2$)}$_3$(THF)$_3$]:[70] This unusual hybrid compound consists of an equilateral triangle of Cd atoms capped with a $Co(CO)_3$ fragment with each Cd−Cd edge bridged by a cluster ligand (Scheme 9). In addition, each Cd atom is coordinated to a THF molecule. Although the bonding of the Cd_3Co core is very interesting, in terms of the spatial distribution of the clusters, the compound can be described as an equilateral triangle of tricobalt clusters in which an equilateral triangle of Cd atoms capped by a $Co(CO)_3$ fragment is inscribed.

Scheme 9

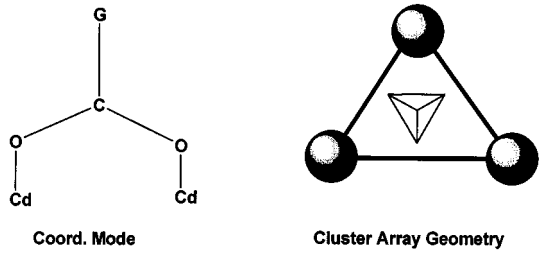

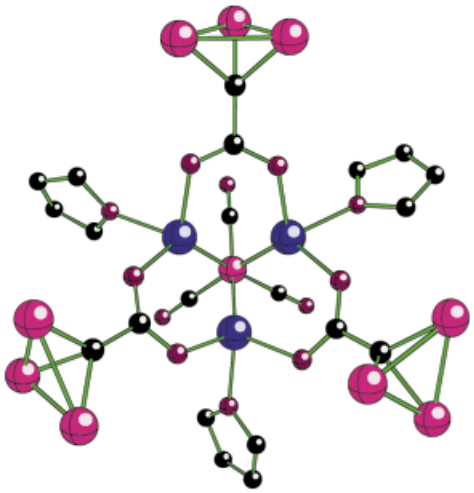

[{Co$_3$Ti(OMe)$_6$(HOMe)(THF){(CO)$_9$Co$_3$(μ_3-CCO$_2$)}$_3$}$_2$-(O$_2$CCO$_2$)]:[63] The structure (Scheme 10) consists of two complete $Co_3Ti(OMe)_4$ cubes, related by a inversion center, and joined by a bridging tetradentate oxalate ligand. The coordination environments of both the Ti and core Co atoms are both nearly octahedral. For a single cube, the three tricobalt clusters lie in an approximate plane, but the cluster planes of each cube are displaced with respect to each other, resulting a chair-like arrangement of

Scheme 10

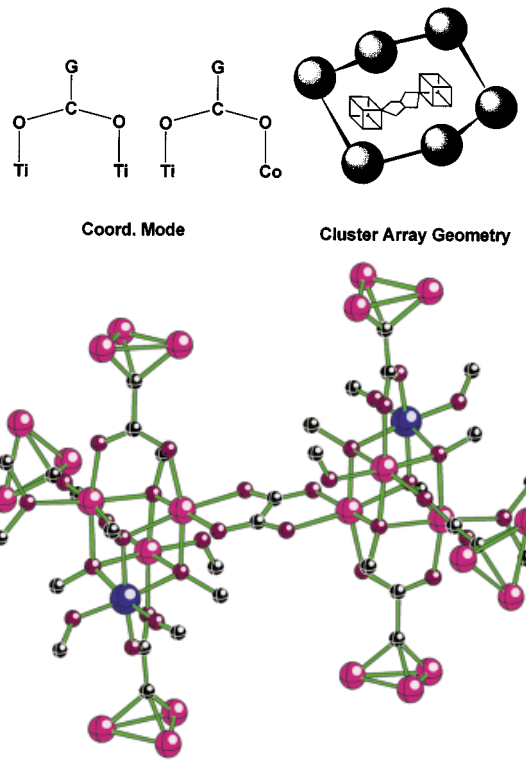

the six tricobalt clusters. The coordination modes of the cluster ligands fall into two groups: homonuclear bridging and heteronuclear bridging.

Scheme 11

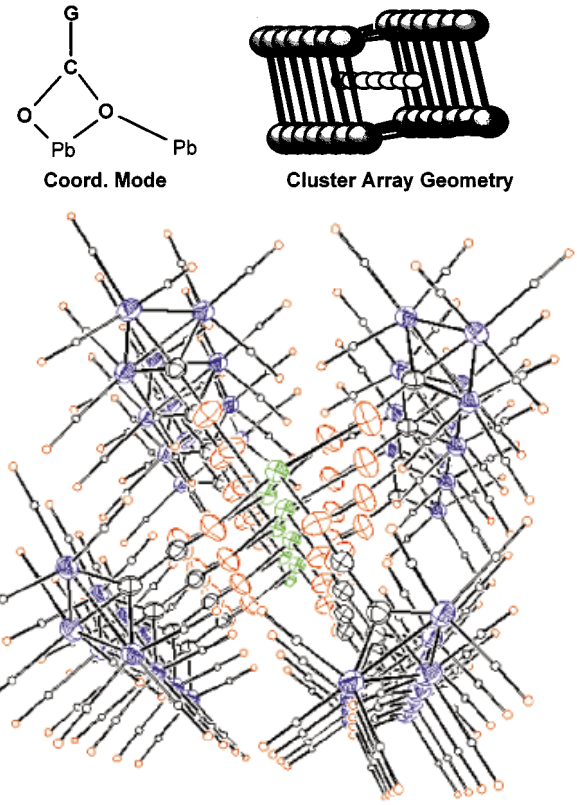

$[Pb\{(CO)_9Co_3(\mu_3\text{-}CCO_2)\}_2]_n$:[71] Each Pb atom is primarily coordinated by two cluster carboxylates but secondary Pb−O interactions occur between an oxygen atom of each chelating carboxylate and its adjacent Pb^{II} thereby generating a chainlike structure (Scheme 11) and unusual, solvent free six-coordinate Pb centers.[72] The three distinct Pb−O distances differ considerably. Viewed along the Pb−Pb direction, the tricobalt clusters generate an infinite square columnar array.

Synthetic Routes

The differences between the cluster acid and an organic acid originate in the instability of the metal framework, the capability of the cluster acting as either an electron donor or acceptor, and the steric bulk of the cluster. Consequently, some methods used to prepare organic metal carboxylates are not applicable to these cluster metal carboxylates, e.g., reactions involving carboxylate salts. Some of the successful approaches used for the metal cluster substituted acids are set out below.

Spontaneous Reaction: The cluster acid, $(CO)_9Co_3(\mu_3\text{-}CCO_2H)$, is soluble in polar solvents such as ether, THF, CH_2Cl_2, acetone, and methanol. However, when exposed to air, the solutions spontaneously precipitate the cluster oxo tetrametal carboxylate, $Co_4O\{(CO)_9Co_3(\mu_3\text{-}CCO_2)\}_6$ (Scheme 3) in high yield (Eq. 1).[61]

$$22\ (CO)_9Co_3(\mu_3\text{-}CCO_2H) + 7\ O_2 \rightarrow Co_4O\{(CO)_9Co_3(\mu_3\text{-}CCO_2)\}_6 + 44\ CO + 11\ H_2O \quad (1)$$

The origin of the Co^{II} ions is the tricobalt cluster which illustrates how the intrinsic lability of the metal cluster can control the coordination chemistry observed. Unless suitable precautions are taken, this reaction competes with all the other reactions described and generates unusable mixtures of products.

Reactions with Metal Alkyls: The preparation of anhydrous metal carboxylates using the elimination of an alkane from a metal alkyl as the driving force has been effectively used for the formation or organic metal carboxylates. Unlike the organic acids, $(CO)_9Co_3(\mu_3\text{-}CCO_2H)$ reacts with $ZnEt_2$ in ether giving a cluster oxo tetrametal carboxylate, $Zn_4O\{(CO)_9Co_3(\mu_3\text{-}CCO_2)\}_6$ (Scheme 3). A pathway involving formation of a cluster ester is postulated as shown in Eq. 2.[61]

$$8\ (CO)_9Co_3(\mu_3\text{-}CCO_2H) + 4\ ZnEt_2 \rightarrow Zn_4O\{(CO)_9Co_3(\mu_3\text{-}CCO_2)\}_6 + \{(CO)_9Co_3(\mu_3\text{-}CCO)\}_2O \quad (2)$$

Although the reaction of $(CO)_9Co_3(\mu_3\text{-}CCO_2H)$ and $CdMe_2$ under similar conditions may yield a simple cluster metal carboxylate, heating the reaction mixture in toluene at 70°C resulted in the formation of an unexpected product, $[\{(\mu_3\text{-}Co(CO)_3)\}Cd_3\{(CO)_9Co_3(\mu_3\text{-}CCO_2)\}_3(THF)_3]$ (Scheme 9) in good yield. Note that $(CO)_9Co_3(\mu_3\text{-}CCO_2H)$ also serves as a source of the $Co(CO)_3$ fragment that caps the Cd_3 triangle thereby demonstrating another way in which the metal cluster can participate in the reaction.

Exchange Reactions with Metal Carboxylates The exchange reactions between lower metal carboxylates and carboxylic acids have been used in the preparation of higher carboxylates. The lower carboxylic acid generated can be removed azeotropically from the reaction mixture when suitable solvents are employed. The reaction of binuclear carboxylates, $M(CH_3CO_2)_2$, (M = Cr, Mo,W, Cu) with $(CO)_9Co_3(\mu_3\text{-}CCO_2H)$ afforded a series of cluster carboxylates with the formula $[M_2(CH_3CO_2)_{4-n}\{(CO)_9Co_3(\mu_3\text{-}CCO_2)\}_nL_2]$ (L = the axial coordination ligand) via Eq. 3 with structures based on that illustrated in Scheme 2.[57][73][74]

$$n\ (CO)_9Co_3(\mu_3\text{-}CCO_2H) + [M(CH_3CO_2)_2]_2 \rightarrow [M\{(CO)_9Co_3(\mu_3\text{-}CCO_2)\}_n(CH_3CO_2)_{2-n}]_2 + n\ CH_3COOH \quad (3)$$

Although solvents often play an important role and are found coordinated in the product cluster metal carboxylates, this is not always the case. Organic lead carboxylates have a notable tendency to pick up water, but no coordinated or uncoordinated water is found in the crystal lattice of chain-like $[Pb\{(CO)_9Co_3(\mu_3\text{-}CCO_2)\}]_n$ (Scheme 11) even though present in the reaction system.[71]

Reactions with Metal Alkoxides and Aryloxides: The advantage of the reactions of metal alkoxides with carboxylic acids is that a variety of mixed alkoxide-carboxylate complexes can be produced by simply changing the stoichiometric ratios of the reactants.[67][68][75][76][77] The reaction of the cluster acids and group 4 alkoxides afforded cluster alkoxycarboxylates (Eqs. 4 and 5):

$$4\ (CO)_9Co_3(\mu_3\text{-}CCO_2H) + [Zr(OCHMe_2)4{\cdot}HOCHMe2]_2 \rightarrow [Zr_2\{(CO)_9Co_3(\mu_3\text{-}CCO_2)\}_4(OCHMe_2)_4] + 6\ HOCHMe_2 \quad (4)$$

$$4\ (CO)_9Co_3(\mu_3\text{-}CCO_2H) + Ti(OR)_4 \rightarrow [Ti_4O_4\{(CO)_9Co_3(\mu_3\text{-}CCO_2)\}_4(OR)_4] + 4\ ROH + 4\ ROR \quad (5)$$

Complex, Competitive Degradation: Some of the cluster carboxylates are unstable in the solution and undergo complicated redox reactions assisted by either the center metal or solvents to yield new cluster metal carboxylates. The exchange reaction of $Hg(CH_3CO_2)_2$ and $(CO)_9Co_3(\mu_3\text{-}CCO_2H)$ in CH_2Cl_2 led to $Hg\{(CO)_9Co_3(\mu_3\text{-}CCO_2)\}_2$ which is soluble in THF. Crystallization attempts in acetone led to the oxotetracobalt cluster, $[Co_4O\{(CO)_9Co_3(\mu_3\text{-}CCO_2\}_6]$ and mercury metal whereas crystallization in THF afforded $[Co_2\{(CO)_9Co_3(\mu_3\text{-}CCO_2\}_4(THF)_2]$ (Scheme 2) as well as mercury metal. It is believed that in solution a slow redox reaction takes place resulting in precipitation of either $[Co_4O\{(CO)_9Co_3(\mu_3\text{-}CCO_2\}_6]$ or $[Co_2\{(CO)_9Co_3(\mu_3\text{-}CCO_2\}_4(THF)_2]$. It is important to note that the direct reaction of cobalt acetate with $(CO)_9Co_3(\mu_3\text{-}CCO_2H)$ only generates the cluster oxo tetracobalt carboxylate.

With similar complexity, the reactions of $[M^{II}\{(CO)_9Co_3(\mu_3\text{-}CCO_2)\}_2]$ (M = Mn, Fe) with MeOH gave rise to $[M^{III}_2Co_2(MeO)_6(MeOH)_2\{(CO)_9Co_3(\mu_3\text{-}CCO_2)\}_4]$ with cubane-like cores.[78] Further, when $(CO)_9Co_3(\mu_3\text{-}CCO_2H)$ was treated with $Ti(OMe)_4$ in THF, a heteronuclear octameric species, $[\{Co_3Ti(OMe)_6(HOMe)(THF)\{(CO)_9Co_3(\mu_3\text{-}$

$CCO_2)\}_3\}_2(O_2CCO_2)]$ was isolated in good yield (Scheme 10). Both the Co^{II} ions and oxalate ligand arise from the degradation of the tricobalt cluster in situ.

Modified Cluster Acids and Their Reactivities

The $CpM(CO)_2$ (M=Mo, W) fragment can be substituted for one of the $Co(CO)_3$ fragments in $(CO)_9Co_3(\mu_3$-CR) to yield $CpM(CO)_2Co_2(CO)_6(\mu_3$-CR).[79] This method works well on a gram scale provided the acid group is protected as an ester from which the acid can be regenerated after metal fragment exchange.[80] The reaction of the heterometal cluster acids with Ti and Zr alkoxides was examined in order to directly compare their chemistry with that of $(CO)_9Co_3(\mu_3$-$CCO_2H)$. The compounds structurally characterized are $Zr_2(OH)_2\{CpMo(CO)_2Co(CO)_6(\mu_3$-$CCO_2)\}_6$ and $Ti_4O_4(OR)_4\{CpMo(CO)_2Co(CO)_6(\mu_3$-$CCO_2)\}_4$.[80] The former exhibits two bridging cluster ligands, four chelating cluster ligands, and two hydroxyl groups, generating a Zr_2O_{14} core and a coordination number of eight for each Zr center with an octahedral spatial distribution of the six modified clusters (Scheme 12). The Ti clusters show the same structural motif as those of tricobalt cluster ligands, i.e., that shown in Scheme 4.

Interestingly, the Cp rings of the $CpM(CO)_2$ moieties in all the compounds are proximal (Cp ring adjacent to the capping carbon) rather distal (Cp ring positioned away from the capping carbon) and the $CpM(CO)_2$ carbonyls are semibridging to the Co atoms. The exclusive presence of the proximal isomer of the coordinated cluster ligand relative to the more stable distal isomer for the uncoordinated cluster[81][82][83] reflects the existence of a cluster electronic effect in the coordination properties of the carboxylic group.

Scheme 12

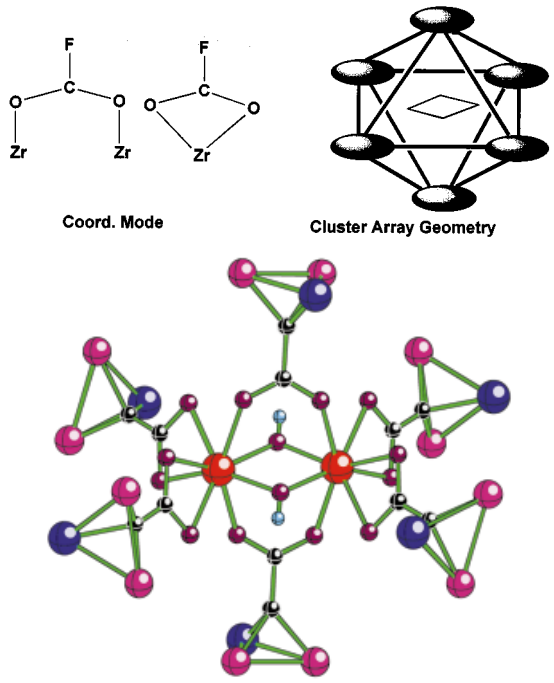

Reactivity and Physical Properties Imparted by the Cluster Substituent

Cluster substituted carboxylic acids are weaker acids than acetic acid and are expected to form more basic carboxylates.[61][80] It is not surprising, then, that the cluster substituent can alter the chemical selectivity of the carboxylate moiety. Thus, the reactions of the cluster acids with group 4 metal alkoxides exhibit significantly different chemistry than that of organic acids. For example, in contrast to acetic acid[68], the cluster carboxylate observed does not depend on the reaction stoichiometry. That this is a cluster effect is established by the reactivity of the modified cluster ligands, $CpM(CO)_2Co_2(CO)_6(\mu_3$-$CCO_2H)$. These are of similar size to the tricobalt cluster but under same reaction conditions the products from the reaction of the cluster acids with zirconium isopropoxide are different.

The physical properties of the cluster metal carboxylates show some interesting differences from those of their organic analogs. The presence of the carbonyl clusters has a large effect on the intermolecular interactions. For example, $[Ti_4O_4(OR)_4\{(CO)_9Co_3(\mu_3$-$CCO_2)\}_4]$ with molecular weights of ca. 2500 are soluble in hexane. All compounds are deeply colored, and their absorption spectra are similar to that of $(CO)_9Co_3(\mu_3$-$CCO_2H)$ with extinction coefficients roughly proportional to the number of the tricobalt units in the cluster arrays. Exceptions are $[M_2\{(CO)_9Co_3(\mu_3$-$CCO_2)\}_4]$ (M = Cr, Mo, W) which show intense absorption in the visible range, presumably due to the charge transfer from M center to the tricobalt units.[73]

As with organic metal carboxylates the IR bands associated with the $-CCO_2$ moiety provide useful fingerprints to distinguish and identify new compounds.[50] In the cluster metal carboxylates the carbonyl ligand stretching bands 1900 to 2200 cm^{-1} are also useful, albeit less sensitive, probes of coordination. These two regions provide useful fingerprints to distinguish and identify new compounds. In general, the deprotonation and coordination of a cluster acid results in a reduction of the number of carbonyl bands and the frequencies of the antisymmetrical and symmetrical stretching modes of the COO^- group are significantly decreased.

Cluster Arrays as Catalyst Precursors

Metal clusters are attractive catalysts or catalyst precursors[34][84] and the use of supported metal clusters potentially provides a catalyst with homogeneous set of multimetal active sites. Such a heterogeneous catalyst would preempt one of the most attractive aspects of homogenous catalysts while retaining those of heterogeneous catalysts. Indeed, recent work has been very promising.[15][85]

As already indicated in the introductory paragraphs, our approach is to limit the "support" to a minimal metal core thereby producing identical nanosized cluster assemblies with different shapes but related compositions. Indeed these cluster metal carboxylates may be considered as layered particles as shown in Scheme 13 with shapes ranging from

Scheme 13

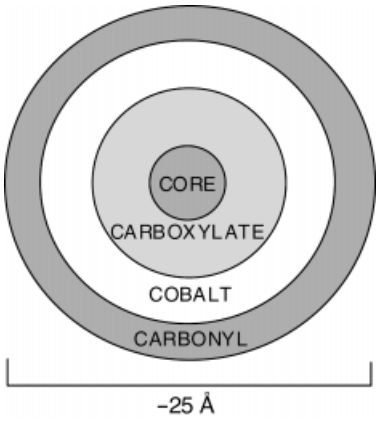

spheres to less symmetric solids. For the spherical particle, a cationic core is covered with a set of carboxylate moieties attached to a set of carbyne carbons, then a set of cobalt atoms, and, on the outside, a layer of carbonyl groups. In several of the compounds, one finds the 20 to 30 Å diameter molecular assemblies in a close-packed array in the solid state.

Ideally it was our intention to activate these species for catalysis by removing some or all of the external carbonyl ligands thereby forming reactive cobalt-covered nanoparticle spheres. Several issues had to be resolved experimentally. These included the relative lability of the outer Co−CO links vs the inner CCO_2−M links, the ease of metal diffusion resulting in Co crystallite formation (sintering), the surface areas of the active materials, and, most importantly, the catalytic activities and selectivities for selected reactions. In the following we describe the nature of the solid produced from the cluster assemblies by thermolysis, the catalytic properties of the solids in a standard hydrogenation reaction, and the unique properties of these catalysts for the selective hydrogenation of an α,β-unsaturated aldehyde to an unsaturated alcohol.

Properties of Solids Formed from Cluster Metal Carboxylates

The behavior of single crystals of cluster metal carboxylates on heating gave us the first indication of the special properties of these molecular cluster carboxylate solids.[86] For example, a single, well formed, shiny, dark colored crystal that diffracted X-rays was converted into a single smaller, but similarly shaped, apparent crystal with a metallic luster. The product did not, however, diffract X-rays and a close examination of the faces of the product showed extensive pitting. Indeed, density measurements revealed a substantial void volume in the product solid. Additional preliminary experiments also showed considerable hydrogenation activity and, thus, we set out to characterize the nature of these solids as well as their catalytic properties.

As long-range order in the molecular solids was lost on pyrolyzing the cluster carboxylates, unambiguous structure determination was out of the question. Further it appeared clear that there was some dependence of material properties on the activation procedure. Hence, the first efforts were directed towards establishing the nature of the chemical conversion of precisely characterized, but inactive, molecular precursors to amorphous, but active, solids.[87]

Thermal gravimetric analyses usually showed two stable regimes, i.e., a constant mass over a certain temperature range, depending on carboxylate structure type. Scheme 14 (labeled low temperature, LT, ca. 100−200°C: high temperature, HT, > ca. 200°C). Mass spectrometry showed that in the LT regime mainly CO loss occurred and CO_2 loss was predominant in the HT regime. Actual mass loss and gas composition suggested loss of the outer CO layer to reach to first regime and loss of the carboxylate links to reach the second regime. In situ IR measurements (DRIFTS) corroborated this interpretation in that the terminal carbonyl bands of the tricobalt disappeared followed by loss of the carboxylate bands as the temperature was raised.

Scheme 14

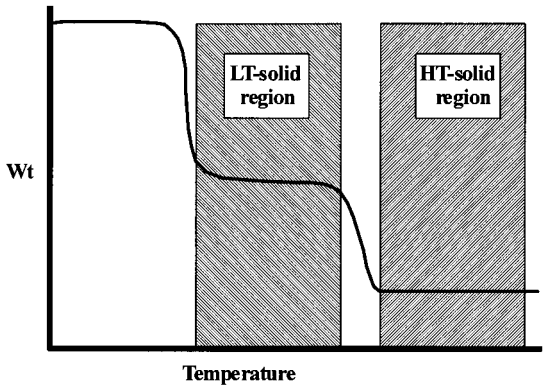

To say that only and all CO links are broken to reach the LT solids would be an oversimplification but it does appear that in the HT solids only the carbyne carbon remains in the amorphous product. This remaining carbon content is viewed as important in the same sense that main group elements are important in stabilizing amorphous metal alloys relative to crystallization.[88] This stability sustains the Co metal dispersion as well as the porous nature of the solid. However, there are limits and heating to 300°C and higher led to diffusion of the Co metal and the formation of α-Co crystallites detectable by X-ray diffraction.

The surface areas of the LT- and HT-solids ranged from 50 to 250 m^2/g which is well within usable range for catalytic purposes.[89] Heating to 300°C and higher led to loss of surface area which is consistent with the formation of the metal crystallites observed by X-ray diffraction. Transmission electron microscopy of cast thin films of the precursor, annealed to various temperatures, confirmed the porous nature of the solid implied by the density and surface area measurements. Electron diffraction of films heated to 300°C and higher showed cobalt crystallites of average size 100 Å. In the X-ray photoelectron spectroscopic experiments, the shift to lower binding energy on formation of the LT-, HT-solids is consistent with conversion of cobalt

carbonyl fragments to cobalt metal and reveals that both the LT- and HT-solids have cobalt metal on exposed surfaces.

A model for the chemical conversion of the molecular cluster metal carboxylates into the two solids based on these data is shown in Scheme 15. Loss of the external CO ligands reduces the size of the cluster assemblies which are still supported by internal core−cluster carboxylate bonds. Formation of inter-assembly metal−metal bonds follows thereby opening channels and generating an amorphous, high surface area, porous solid. Further heating leads to the destruction of the internal metal carboxylate bonding and the formation of larger metal aggregates of indeterminate structure, albeit with retention of significant surface area for the solid as a whole. These are the two meta-stable, amorphous, high surface area solids that were tested as catalysts.

Scheme 15

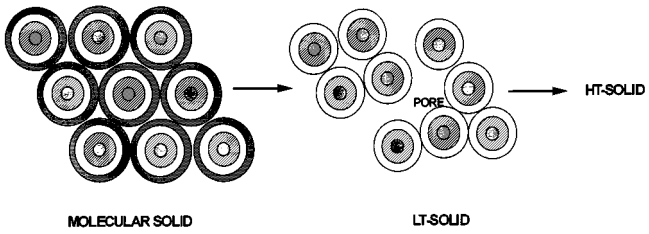

In order to establish the level of catalytic activity as well as to compare catalysts prepared from the different types of cluster metal carboxylates under a variety of conditions, the hydrogenation of 1,3-butadiene was used as a benchmark reaction.[90][74][89] This reaction was selected because the molecule is easily hydrogenated and high conversions can be achieved with small amounts of catalysts and relatively low temperatures. In addition, the reaction has been thoroughly studied with other transition and noble metal catalysts and a substantial literature exists for comparative purposes. In the event, the LT- and HT-solids tested were sufficiently active catalysts so that a gas phase, steady state flow system could be used for evaluation. This permitted a wide range of conditions to be expeditiously explored.

The activities and selectivities of the LT-solids produced from a variety cluster metal carboxylates showed similar, if not identical, behaviors. 1-Butene is the main product at low conversions whereas butane becomes the main product at high conversions.. On the other hand, the activities and selectivities of the HT-solids are markedly different from those of the LT-solids as well different among themselves. Core dependence appears to be important only for the HT-solids consistent with the model of solid formation summarized above. Importantly, these catalysts were stable (4−7 days on stream) and reproducible.

The catalytic behavior of solids produced from the tricobalt cluster alone and of conventional supported cobalt metal under identical conditions is very different from that of catalysts derived from the cluster arrays. This confirms that the catalytic behavior observed for the activated cluster assemblies is due in large part to properties derived from the cluster metal carboxylate precursors. Some carry over of structure from precursor to catalyst must take place in that octahedral and square planar cluster assemblies, both possessing cobalt cores, yield significantly different catalytic behaviors. The latter demonstrates structural as opposed to compositional control of activity and selectivity.

These studies suggest that carbonyl loss (outer cluster decomposition) before carboxylate ligand disruption is important and that core properties can modulate catalytic behavior but only for the HT-solids in which the cores are exposed. Chemical tests of these deductions were carried out. First, cluster metal carboxylates were synthesized using the very thermally stable 1,2-$C_2B_{10}H_{12}$ carborane as the external cluster. Thermolysis of these carboxylates resulted initially in the loss of CO_2 plus some free, intact carborane. This was followed by complex chemistry. The solids produced were of little use and clearly in this case the loss of the core-cluster bonding resulted in total collapse of the cluster assembly.[91] Second, a cluster lead carboxylate with an infinite chain-like structure was used as a catalyst precursor.[71] The LT-solid was an active catalyst with properties similar to any of the catalysts derived from tricobalt cluster metal carboxylates. However, the HT-solid was totally inactive and X-ray photoelectron spectroscopy showed the surface to be severely poisoned by lead metal. These observations are consistent with the model in which the LT-solid possesses an intact assembly core and the HT-solid a disrupted core.

Selective Hydrogenation of Crotonaldehyde

The selective hydrogenation of α,β-unsaturated aldehydes to unsaturated alcohols (path a, Scheme 16) is a challenging reaction for heterogeneous catalysis as C=C double bond reduction is thermodynamically favored at high temperatures and typical metal hydrogenation catalysts also favor C=C double bond reduction over the C=O double bond, i.e., path b in Scheme 16. For this reason a useful catalyst must have high activity at low temperatures as well as high selectivity for path a. As the catalytic solids derived from the cluster metal carboxylates expressed unusual activities and selectivity for the hydrogenation of butadiene, we were drawn to an investigation of the catalytic reduction of crotonaldehyde (2-butenal).[92][93][94]

Scheme 16

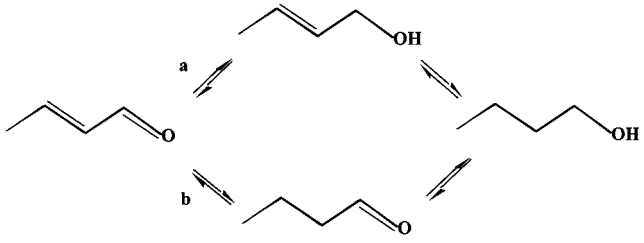

The catalyst activities and 2-butenol selectivities observed were good and depended on the type of metals in the core as well as the precursor structure. For cobalt core metals

the highest yield (28%) of 2-butenol resulted from the HT-solid produced from an octahedral cobalt cluster assembly with a cobalt core whereas the highest selectivity (100%) resulted from the HT-solid produced from a square planar cluster assembly also with a cobalt core. The activity and regioselectivity of the former material give the highest yield for a heterogeneously catalyzed reaction reported in the open literature. Results of kinetic studies show that this high regioselectivity resides in increased barrier heights for the various reaction steps. The simultaneous high activity requires the active participation of a large fraction of sites on the catalyst. That is, these solids show the behavior expected for catalysts that possess sites having a narrow activity distribution. This, in turn, is in accord with the model of these solids drawn from the spectroscopic as well as chemical studies.

The activities and selectivities of these catalysts are constant for periods of times that are several fold higher than those reported with supported catalysts and the materials do not show deactivation up to 50 hours of time on stream. Catalysts derived from tricobalt cluster assemblies with heterometal cores give uniformly poorer results relative to the homometallic systems of the same structure type. Solids produced from the tricobalt cluster alone were less active with poor selectivity.

Summary

We have demonstrated the coordination of cluster-substituted carboxylates to cationic metals as a successful strategy for the assembly of large transition metal cluster arrays. In terms of the coordination modes of the cluster carboxylate ligand, most exhibited by organic metal carboxylates have been observed. In terms of core structure, rhombic, tetrahedral, cubane-like, ladder-like, double cubane-like, as well as chain-like geometries have been generated. In terms of the spatial arrangement of the clusters, triangular, square, triangular bipyramidal, octahedral, chair-like, and column-like types have been observed. The observed compounds reveal the unique properties of the functionlized clusters as ligands over convertional organic carboxylates. These studies also show that the catalytic properties of solids produced from molecular cluster metal carboxylates depend on the molecular composition and structure of the cluster assembly. Further, the detailed catalytic behavior suggests that the high activities and unusual selectivities observed are derived from a high number of uniform active sites. Both conclusions are consistent with catalytic solids that "remember" their molecular origins. Although no practical catalyst has been uncovered for the selective crotonaldehyde reduction, only small changes in relative reaction barrier heights are needed to do so. In turn this suggests that relatively minor changes in precursor structure and composition are required. It remains to experimentally define these changes. This requires the continued development synthetic cluster chemistry in order to produce additional useful cluster ligands.

We thank our talented co-workers listed in the references for their contributions to the synthetic and catalytic chemistry and we appreciate the support of the *National Science Foundation*.

[1] J. L. Atwood, J. E. D. Davies, D. D. MacNicol, R. Vögtl, J.-M. Lehn, *Comprehensive Supramolecular Chemistry*; Pergamon Press: Oxford, **1996**.
[2] R. Gross-Lannert, W. Kain, B. Olbrich-Deussner, *Inorg. Chem.* **1990**, *29*, 5046.
[3] A. Harriman, F. Odobel, J.-P. Sauvage, *J. Am. Chem. Soc.* **1995**, *117*, 9461.
[4] M. H. Chisholm, M. R. Mackley, R. T. J. Marshall, E. F. Putilina, *Chem. Mater.* **1995**, *7*, 1938.
[5] X. Yang, C. B. Knobler, Z. Zheng, M. F. Hawthorne, *J. Am. Chem. Soc.* **1994**, *116*, 7142.
[6] L. Hao, J. J. Vittal, R. J. Puddephatt, *Inorg. Chem.* **1996**, *35*, 269.
[7] Y. Lin, R. G. Finke, *Inorg. Chem.* **1994**, *33*, 4891.
[8] G. O. Noonan, J. S. Ledford, *Chem. Mater.* **1995**, *7*, 1117.
[9] W. R. Entley, G. S. Girolami, *Inorg. Chem.* **1994**, *33*, 5165.
[10] N. Prokopuk, D. F. Shriver, *Inorg. Chem.* **1997**, *36*, 5609.
[11] X. Yang, C. B. Knobler, M. F. Hawthorne, *J. Am. Chem. Soc.* **1993**, *115*, 4904.
[12] M. J. Irwin, G. Jia, N. C. Payne, R. J. Puddephatt, *Organometallics* **1996**, *15*, 51.
[13] W. T. S. Huck, F. C. J. M. vanVeggel, B. L. Kropman, D. H. A. Blank, E. G. Keim, M. M. A. Smithers, D. N. Reinhoudt, *J. Am. Chem. Soc.* **1995**, *117*, 8293.
[14] S. Decurtins, H. W. Schmalle, R. Pellaux, P. Schneuwly, A. Hauser, *Inorg. Chem.* **1996**, *35*, 1451.
[15] M. S. Nashner, A. I. Frenkel, D. L. Adler, J. R. Shapley, R. G. Nuzzo, *J. Am. Chem. Soc.* **1997**, *119*, 7760.
[16] S. Campagna, A. Giannetto, S. Serroni, G. Denti, S. Trusso, F. Mallamace, N. Micali, *J. Am. Chem. Soc.* **1995**, *117*, 1754.
[17] I. Cuadrado, M. Morán, C. Casado, B. Alonso, F. Lobete, B. Garcia, M. Ibisate, J. Losada, *Organometallics* **1996**, *15*, 5278.
[18] M. R. Jordan, P. S. White, C. K. Schauer, M. A. Mosley III, *J. Am. Chem. Soc.* **1995**, *117*, 5403.
[19] P. J. Stang, K. Chen, A. M. Arif, *J. Am. Chem. Soc.* **1995**, *117*, 8793.
[20] K. L. Taft, C. D. Delfs, G. C. Papaefthymiou, S. Foner, D. Gatteschi, S. J. Lippard, *J. Am. Chem. Soc.* **1994**, *116*, 823.
[21] J. L. Wesemann, M. H. Chisholm, *Inorg. Chem.* **1997**, *36*, 3258.
[22] P. Kaszynski, A. C. Friedli, J. Michl, *J. Am. Chem. Soc.* **1992**, *114*, 601.
[23] X. Yang, W. Jiang, C. B. Knobler, M. F. Hawthorne, *J. Am. Chem. Soc.* **1992**, *114*, 9719.
[24] O. J. Scherer, H. Sitzmann, G. Wolmershäuser, *Angew. Chem., Int. Ed. Engl.* **1984**, *23*, 968; *Angew. Chem.* **1984**, *96*, 979.
[25] T. Schaper, W. Preetz, *Chem. Ber.* **1997**, *130*, 405.
[26] C. v. Hänisch, D. Fenske, F. Weigend, R. Ahlrichs, *Chem. Eur. J.* **1997**, *3*, 1494.
[27] D. H. Gibson, T.-S. Ong, M. Ye, *Organometallics* **1991**, *10*, 1811.
[28] F. A. Cotton, L. R. Falvello, A. H. Reid Jr., J. H. Tocher, *J. Organomet. Chem.* **1987**, *319*, 87.
[29] M. D. Westmeyer, M. A. Massa, T. B. Rauchfuss, S. R. Wilson, *J. Am. Chem. Soc.* **1998**, *120*, 114.
[30] M. W. Willer, J. R. Long, C. C. McLauchlan, R. H. Holm, *Inorg. Chem.* **1998**, *37*, 328.
[31] S. Onaka, M. Otsuka, A. Mizuno, S. Takagi, K. Sako, M. Otomo, *Chem. Lett.* **1994**, 45.
[32] U. Ritter, N. Winkhofer, R. Murugavel, A. Voigt, D. Stalke, H. W. Roesky, *J. Am. Chem. Soc.* **1996**, *118*, 8580.
[33] J. D. Basil, A. A. Aradi, N. K. Bhattacharyya, N. P. Rath, C. Eigenbrot, T. P. Fehlner, *Inorg. Chem.* **1990**, *29*, 1260.
[34] *Metal Clusters in Catalysis*; B. Gates, L. Guczi, H. Knözinger, Ed.; Elsevier: New York, 1986; Vol. 29.
[35] M. T. Bautista, P. S. White, C. K. Schauer, *J. Am. Chem. Soc.* **1991**, *113*, 8963.
[36] D. L. Sunick, P. S. White, C. K. Schauer, *Organometallics* **1993**, *12*, 245.
[37] B. E. Collins, Y. Koide, C. K. Schauer, P. S. White, *Inorg. Chem.* **1997**, *36*, 6172.
[38] R. D. Adams, D. Männing, B. E. Segmüller, *Organometallics* **1983**, *2*, 149.
[39] D. Seyferth, J. E. Hallgren, P. L. K. Hung, *J. Organomet. Chem.* **1973**, *50*, 265.

[40] D. Seyferth, J. E. Hallgren, C. S. Eschbach, *J. Am. Chem. Soc.* **1974**, *96*, 1730.
[41] D. Seyferth, *Adv. Organomet. Chem.* **1976**, *14*, 97.
[42] B. R. Penfold, B. H. Robinson, *Accts of Chem. Research* **1973**, *6*, 73.
[43] B. M. Peake, B. H. Robinson, J. Simpson, D. J. Watson, *Inorg. Chem.* **1977**, *16*, 405.
[44] S. B. Colbran, B. H. Robinson, J. Simpson, *Organometallics* **1983**, *2*, 943.
[45] P. N. Lindsay, B. M. Peake, B. H. Robinson, J. Simpson, *Organometallics* **1984**, *3*, 413.
[46] G. H. Worth, B. H. Robinson, J. Simpson, *J. Organomet. Chem.* **1990**, *387*, 337.
[47] G. H. Worth, B. H. Robinson, J. Simpson, *Organometallics* **1992**, *11*, 501.
[48] *The Chemistry of Metal Cluster Complexes*; D. F. Shriver, H. D. Kaesz, R. D. Adams, Ed.; VCH: New York, 1990.
[49] D. M. P. Mingos, D. J. Wales, *Introduction to Cluster Chemistry*; Prentice Hall: New York, **1990**.
[50] R. C. Mehrotra, R. Bohra, *Metal Carboxylates*; Academic Press: New York, **1983**, pp 396.
[51] K. L. Taft, G. C. Papaefthymiou, S. J. Lippard, *Science* **1993**, *259*, 1302.
[52] W. Micklitz, V. McKee, R. L. Rardin, L. E. Pence, G. C. Papaefthymiou, S. G. Bott, S. J. Lippard, *J. Am. Chem. Soc.* **1994**, *116*, 8061.
[53] S. M. J. Aubin, S. Spagna, H. J. Eppley, R. E. Sager, G. Christou, D. N. Hendrickson, *Chem. Commun.* **1998**, 803.
[54] R. Markby, I. Wender, R. A. Friedel, F. A. Cotton, H. W. Sternberg, *J. Am. Chem. Soc.* **1958**, *89*, 261.
[55] B. F. G. Johnson, J. Lewis, *Adv. Inorg. Chem. Radiochem.* **1981**, *24*, 225.
[56] C. Elschenbroich, A. Salzer, *Organometallics*; VCH: New York, **1989**.
[57] W. Cen, P. Lindenfeld, T. P. Fehlner, *J. Am. Chem. Soc.* **1992**, *114*, 5451.
[58] X. Lei, Ph.D. Thesis, Univ. Notre Dame, **1997**.
[59] F. A. Cotton, R. A. Walton, *Multiple Bonds Between Metal Atoms*; Wiley: New York, **1982**.
[60] W. Cen, K. J. Haller, T. P. Fehlner, *Inorg. Chem.* **1991**, *30*, 3120.
[61] W. Cen, K. J. Haller, T. P. Fehlner, *Inorg. Chem.* **1993**, *32*, 995.
[62] R. L. Sturgeon, M. M. Olmstead, N. E. Schore, *Organometallics* **1991**, *10*, 1649.
[63] X. Lei, M. Shang, T. P. Fehlner, *Organometallics* **1997**, *16*, 5289.
[64] S. G. Charnick, V. W. Day, W. J. Klemperer, *Personal Communication* **1996**,
[65] T. J. Boyle, C. J. Tafoya, B. Scott In *National ACS Meeting*; New Orleans, LA, **1996**; pp O62.
[66] T. J. Boyle, T. M. Alam, E. R. Mechenbier, B. L. Scott, J. W. Ziller, *Inorg. Chem.* **1997**, *36*, 3293.
[67] S. Doeuff, Y. Dromzee, F. Taulelle, C. Sanchez, *Inorg. Chem.* **1989**, *28*, 4439.
[68] T. J. Boyle, R. W. Schwartz, *Comments Inorg. Chem.* **1994**, *16*, 243.
[69] V. Calvo-Perez, M. Shang, G. P. A. Yap, A. L. Rheingold, T. P. Fehlner, *Polyhedron*, in press.
[70] W. Cen, K. J. Haller, T. P. Fehlner, *Organometallics* **1992**, *11*, 3499.
[71] X. Lei, M. Shang, A. Patil, E. E. Wolf, T. P. Fehlner, *Inorg. Chem.* **1996**, *35*, 3217.
[72] P. G. Harrison, A. T. Steel, *J. Organometal. Chem.* **1982**, *239*, 105.
[73] T. P. Fehlner, V. Calvo-Perez, W. Cen, *J. of Electron Spectr.* **1993**, *66*, 29.
[74] M. A. Bañares, L. Dauphin, X. Lei, W. Cen, M. Shang, E. E. Wolf, T. P. Fehlner, *Chem. Mater.* **1995**, *7*, 553.
[75] S. Doeuff, Y. Dromzee, C. Sanchez, *C. R. Acad. Sci. Paris, Ser. II* **1989**, *308*, 1409.
[76] I. Gautier-Luneau, A. Mosset, J. Galy, *Zeit. fur Kristallographie* **1987**, *180*, 83.
[77] P. Toledano, M. In, C. Sanchez, *C. C. R. Acad. Sci. Paris, Ser. II* **1991**, *313*, 1247.
[78] X. Lei, M. Shang, T. P. Fehlner, R. Werner, W. Haase, D. Hautot, G. J. Long, *J. Organomet. Chem.* **1997**, *541*, 57.
[79] M. Mlekuz, P. Bougeard, B. G. Sayer, R. Faggiani, C. J. L. Lock, M. J. McGlinchey, G. Jaouen, *Organometallics* **1985**, *4*, 2046.
[80] H. Shimomura, X. Lei, M. Shang, T. P. Fehlner, *Organometallics* **1997**, *16*, 5302.
[81] M. J. Chetcuti, P. A. M. Chetcuti, J. C. Jeffery, R. M. Mills, P. Mitrprachachon, S. J. Pickering, F. G. A. Stone, P. Woodward, *J. Chem. Soc., Dalton Trans.* **1982**, 699.
[82] H. Beurich, H. Vahrenkamp, *Angew. Chem., Int. Ed. Engl.* **1978**, *17*, 863.
[83] K. A. Sutin, L. Li, C. S. Frampton, B. G. Sayer, M. J. McGlinchey, *Organometallics* **1991**, *10*, 2362.
[84] W. L. Gladfelter, K. J. Roesselet In *The Chemistry of Metal Cluster Complexes* (Eds: D. F. Shriver, H. D. Kaesz and R. D. Adams), VCH: New York, **1990**; pp 329.
[85] M. S. Nashner, D. M. Somerville, P. D. Lane, D. L. Adler, J. R. Shapley, R. G. Nuzzo, *J. Am. Chem. Soc.* **1996**, *118*, 12964.
[86] W. Cen, Ph.D. Thesis, Univ. Notre Dame, **1992**.
[87] W. Cen, B. Ladna, T. P. Fehlner, A. E. Miller, D. Yue, *J. Organomet. Chem.* **1993**, *449*, 19.
[88] R. Hasegawa, *Glassy Metals: Magnetic, Chemical, and Structural Properties*; CRC Press: Boca Raton, FL, **1983**.
[89] M. A. Bañares, L. Dauphin, V. Calvo-Perez, T. P. Fehlner, E. E. Wolf, *J. Catal.* **1995**, *152*, 396.
[90] Z. Kalenik, B. Ladna, E. E. Wolf, T. P. Fehlner, *Chem. Mater.* **1993**, *5*, 1247.
[91] O. Kriz, A. L. Rehingold, M. Shang, T. P. Fehlner, *Inorg. Chem.* **1994**, *33*, 3777.
[92] M. Bañares, A. N. Patil, T. P. Fehlner, E. E. Wolf, *Catal. Lett.* **1995**, *34*, 251.
[93] A. N. Patil, M. A. Bañares, X. Lei, T. P. Fehlner, E. E. Wolf, *J. Catalysis* **1996**, *159*, 458.
[94] M. C. LaNeve, X. Lei, T. P. Fehlner, E. E. Wolf, *J. Catalysis* **1998**, *171*, 11.

[I98253]

Hypercoordinate P^{II}, P^{III}, and P^{IV} Phosphorus Derivatives with Intramolecular Coordination by Donor Groups

Claude Chuit and Catherine Reyé*

Laboratoire de Chimie Moléculaire et Organisation du Solide, UMR 5837 CNRS, Université Montpellier II,
Place E. Bataillon, F-34095 Montpellier Cedex 5, France
E-mail: reye@crit.univ-montp2.fr

Received July 20, 1998

Keywords: Intramolecular coordination / Donor groups / Phosphorus compounds / X-ray structures / Ligands exchange

This review describes phosphanes and phosphane derivatives as well as phosphenium salts in which increase in coordination number was achieved by intramolecular coordination of donor groups. This effect was established by X-ray crystal structure analysis and was also inferred from ^{1}H-NMR studies in solution. Where possible, comparison with the corresponding silicon compounds was made.

Contents

1. Introduction
2. Hypercoordinate P^{III} and P^{IV} Phosphorus Derivatives
2.1. Pentacoordinate Phosphonite, Phosphonate, and Thiophosphonate Compounds
2.2. Pseudo-Pentacoordinate Phosphanes and Pentacoordinate Phosphane Derivatives
2.3. Pseudo-Hexacoordinate Phosphanes and Hexacoordinate Phosphane Derivatives
2.4. Pseudo-Heptacoordinate Phosphanes
2.5. Reactivity of Pseudo-Hypercoordinate Phosphanes
2.6. Reactivity of Hypercoordinate Phosphonium Salts
3. Pseudo-Pentacoordinate Stabilized Phosphenium Salts
4. Conclusion

1. Introduction

It is well established that the silicon atom can extend its coordination number beyond four and that, in many cases, such an increase in coordination number can be achieved by intramolecular coordination of donor groups[1]. The phosphorus atom can also increase its coordination number through intramolecular coordination by donor groups[2]. However, this aspect has been mainly studied with regard to phosphoranes and this matter has recently been reviewed[3]. For our part, we have studied intramolecular coordination of NMe_2 donor groups in P^{III} and P^{IV} phosphorus compounds. The purpose of this review is to survey these compounds, with emphasis on the physical techniques used to establish their structures in the solid state and in

Claude Chuit was born in Paris in 1935. He obtained his Doctorat d'Etat from the University of Orsay under the supervision of Dr. H. Felkin. After one year of postdoctoral studies at the University of Stirling (Scotland) with the late Professor W. Parker, he spent 10 years in Professor J. F. Normant's laboratory at the University P. and M. Curie in Paris. Since 1980 he has worked on hypercoordinate silicon and phosphorus compounds in Professor R. Corriu's laboratory at the University of Montpellier. He was appointed Directeur de Recherche at the CNRS in 1990. His current interests concern the elaboration of materials by the sol-gel process.

Catherine Reyé was born in France (Deux Sèvres). She received her Ph.D. from the University of Montpellier II under the supervision of Professor R. J. P. Corriu. Her principal research interests were then focussed on the chemistry of hypercoordinate silicon and phosphorus compounds. Initially, she worked in the area of reactions catalyzed by nucleophiles involving hypercoordinate silicon intermediates. Subsequently, she studied the structure and the reactivity of hypercoordinate silicon and phosphorus compounds. Her current interests concern the study of hybrid organic-inorganic materials obtained by hydrolytic polycondensation.

MICROREVIEWS: This feature introduces the readers to the authors' research through a concise overview of the selected topic. Reference to important work from others in the field is included.

 © WILEY-VCH Verlag GmbH, D-69451 Weinheim, 1998 1434–1948/98/1212–1847 $ 17.50+.50/0

solution. Phosphanes with intramolecular N→P interactions are referred to as pseudo-hypercoordinate phosphanes, taking into account the phosphorus lone electron pair. Comparisons with the corresponding silicon compounds are made where analogies exist between hypercoordinate silicon and phosphorus chemistry[4][5]. Phosphenium salts stabilized by intramolecular coordination of two NMe_2 donor groups at the phosphorus atom are also surveyed. Analogies with the corresponding stabilized silylenium salts are noted.

Intramolecular chelation at the phosphorus atom can principally be achieved by using ligands **1**, **2**, and **3**, introduced by van Koten and co-workers[6] in tin chemistry, and used extensively in silicon chemistry[1]. Each of these has its own particularly interesting features. The rigid geometry of ligand **1**, in which the donor group is fixed in close proximity to the phosphorus centre, facilitate intramolecular coordination. In contrast, the geometry of ligand **2** does not enforce coordination to the phosphorus centre. However, a favourable conformation allowing interaction between the donor atom and the phosphorus atom exists, which is adopted when suitable substituents are also attached at the phosphorus. Finally, ligand **3** permits the study of mono- or bis-coordination at the phosphorus atom, also as a function of the other ligands. Furthermore, it allows the study of fluxional coordination-decoordination processes.

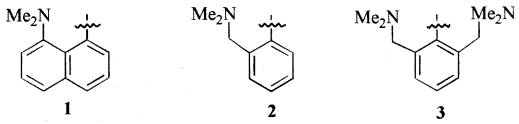

1 **2** **3**

2. Hypercoordinate P^{III} and P^{IV} Phosphorus Derivatives

2.1 Pentacoordinate Phosphonite, Phosphonate, and Thiophosphonate Compounds

An intramolecular N→P interaction was suggested for compound **4**[7] in view of its temperature-dependent ^{31}P-NMR spectrum, the chemical shift decreasing from δ = +125 at 25°C to δ = +121.4 at −80°C. This observation was attributed to an equilibrium between **4** and **4′** (Eq. 1).

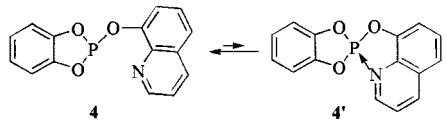

4 **4'** (1)

Following this result, we prepared compounds **5**, **6**, **7**, **8**, and **9**[8], which all include the potentially chelating ligand **2**. In Table 1, we report the ^{31}P-NMR resonances of **5**−**9**, alongside those of the corresponding phosphorus derivatives lacking the NMe_2 group.

Significant upfield shifts are observed for **5**, **6**, and **7**, suggesting N→P interactions in these derivatives. Such shifts were not evident for **8** and **9** and the lack of N→P interactions in **8** and **9** was confirmed by their ^{1}H-NMR spectra, in which the signal of the NMe_2 group appears as

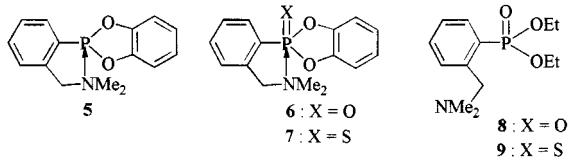

5 **6** : X = O, **7** : X = S **8** : X = O, **9** : X = S

Table 1. ^{31}P-NMR chemical shifts (at 293 K) of **5**−**9** compared to those of the corresponding phosphorus derivatives lacking NMe_2 groups

Compound	δ (ppm)	Compound	δ (ppm)	Δδ
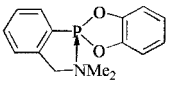 **5**	+130.7	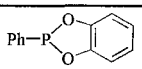	+177.0[9]	-46.0
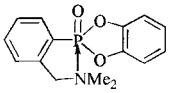 **6**	+13.3	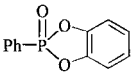	+35.7[10]	-22.4
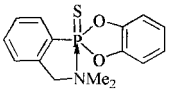 **7**	+72.9	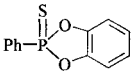	+107.1[11]	-34.2
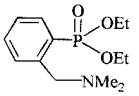 **8**	+19.6	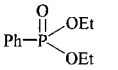	+16.9[12]	-2.7
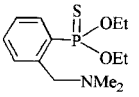 **9**	+83.3	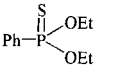	+86.7[8]	+0.4

a singlet over the temperature range studied (183−293 K) in both cases. In contrast, it was found that **7** is pentacoordinated at room temperature: Its ^{1}H-NMR spectrum displays two doublets attributable to the NMe_2 protons. These signals appear as doublets because of P,H coupling [^3J(PH) = 4.8 Hz]. The situation for **5** and **6** is intermediate. At 183 K, the ^{1}H-NMR spectra of **5** and **6** display two singlets for the NMe_2 protons. On raising the temperature, coalescence of these signals is observed ($\Delta G^{\neq}_{233K}$ = 48 kJ mol^{-1} for **5** and $\Delta G^{\neq}_{218K}$ = 46 kJ mol^{-1} for **6**). Two processes could explain the equivalence of the methyl groups, namely pseudorotation around the phosphorus atom or cleavage of the N→P bond with subsequent rotation about the CH_2−N bond and inversion at nitrogen prior to recoordination. In order to clarify this point, we prepared compound **10** bearing a ligand with an asymmetric benzylic carbon atom. From the ^{1}H-NMR spectrum at room temperature, it was inferred that **10** exists as two isomers in solution in an 80:20 ratio, the NMe_2 protons of each isomer appearing as sharp singlets. The major isomer was isolated and was found to slowly epimerize (CH_2Cl_2, 3 h, 20°C) to give the 80:20 equilibrium mixture. On lowering the temperature, the singlet attributable to the NMe_2 protons of the minor diastereoisomer splits into two signals ($\Delta G^{\neq}_{223K}$ = 47 kJ mol^{-1}), while the singlet of the major diastereoisomer gives only a broad signal ($\Delta G^{\neq}_{158K}$ = 32 kJ mol^{-1}). The equilibration of the diastereoisomers of **10** can be explained

by slow rotation about the P−C_{ipso} bond during the coordination-decoordination process. It is noteworthy that similar results have been observed for the tin derivative **11**[13], and the same explanation has been proposed.

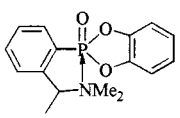

10

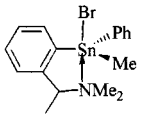

11

We have also prepared compounds **12**−**14**[8] incorporating ligand **1**, which imposes intramolecular coordination at the phosphorus atom. As a result, it is possible to study the permutational isomerization processes in these derivatives by dynamic ^{1}H-NMR spectroscopy. The ^{1}H-NMR spectra of **12**−**14** exhibit only one singlet for the NMe_2 protons at room temperature. However, on lowering the temperature, the singlet splits into two signals in each case. From the coalescence temperature of the methyl group signals (273 K for **12** and **13**; 255 K for **14**), $\Delta G^{\neq}$ values of 57−58 kJ mol^{-1} can be estimated for the pseudorotation processes in these three compounds. For **15**, only one singlet is observed for the *N*-methyl protons, even at low temperature, indicating either a facile permutational isomerization process about the phosphorus atom or a symmetrical arrangement of the molecule. Therefore, the X-ray crystal structure of this compound was determined (Figure 1). It reveals a dissymmetric geometry, the lone pair of the nitrogen atom being directed towards the phosphorus atom *trans* to a P−OEt bond, with an N−P distance of 2.87 Å. Furthermore, the basic pyramidal configuration around the phosphorus atom is only slightly deformed, so that the molecule can be described as a mono-capped tetrahedron in which the phosphorus atom is [4+1] coordinated[8]. Thus, the non-diastereotopy of the NMe_2 protons is probably due to a fast permutational isomerization process occurring at the phosphorus centre.

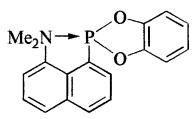

12

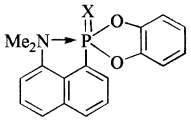

13 : X = O
14 : X = S

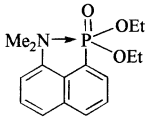

15

Figure 1. X-ray crystal structure of **15**

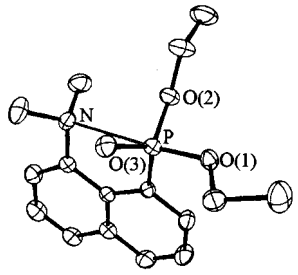

Similarly, Holmes et al.[14] have recently prepared the chloro and amino phosphites **16a** and **16b**, as well as the phosphate **17**. In these compounds, intramolecular S→P interactions are observed. Indeed, X-ray crystal structure determinations for these compounds have revealed S−P distances notably shorter than the sum of the van der Waals radii for phosphorus and sulfur (2.816, 2.952, and 3.114 Å for **16a**, **16b**, **17**, respectively), the geometry around the phosphorus atom being a pseudo-trigonal bipyramid for **16a** and **16b** and a trigonal bipyramid for **17**, with the eight-membered ring in the boat-boat conformation.

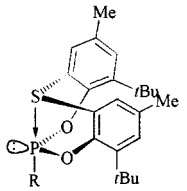

16 a : R = Cl
b : R = NMe_2

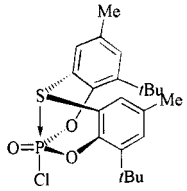

17

2.2 Pseudo-Pentacoordinate Phosphanes and Pentacoordinate Phosphane Derivatives

Phosphanes **18**[15−18], **19**[19,20], **20**[21], and **21**[22−24] have previously been prepared in order to study their abilities to act as mono- or bis-chelating ligands. However, to the best of our knowledge, the potential occurrence of N→P interactions has not been considered for these phosphanes, apart from in the case of **21**[22]. We have prepared phosphanes **21**[25], **22**[26], **23**[26], and **24**[27], as well as phosphane oxide **25**, phosphane sulphide **26**, and phosphonium salts **27**−**29**, all of which incorporate the rigid ligand **1**. X-ray crystal structure analyses of phosphanes **21**[25] and **23**[26] (Figure 2) and of the phosphonium salt **29**[26] reveal that the phosphorus atom resides in a nonsymmetric environment in each case, the lone pair of the nitrogen atom being directed towards the phosphorus atom *trans* to one P−C bond in **21** and **23**, and *trans* to the benzyl group in **29**[26]. The N−P distances in **21**, **23**, and **29** are 2.71, 2.62, and 2.83 Å, respectively, and these distances increase as a result of steric hindrance around the phosphorus atom. Furthermore, in these three compounds, the pyramidal configuration around the phosphorus atom is retained with only a slight deformation. Thus, the geometry of these compounds can be described as mono-capped tetrahedral, where the phosphorus atom is pseudo-[4+1]-coordinated in **21** and **23**, and [4+1]-coordinated in **29**. It is noteworthy that the silicon compound **30** also has a dissymmetrical structure, with the lone pair of the nitrogen atom directed towards the silicon atom, *trans* to an Si−C_{sp} bond[26], with an N−Si bond length of 2.72 Å.

Dynamic ^{1}H-NMR studies of compounds **21**−**28** have been carried out in solution. At 273 K, the spectrum of phosphane **21** (CD_2Cl_2/$CFCl_3$) exhibits a singlet due to the NMe_2 protons, which splits into two signals[25] on lowering the temperature. The same behaviour is observed for phosphane **23**[26] and the phosphane derivatives **25**−**28**[25,27].

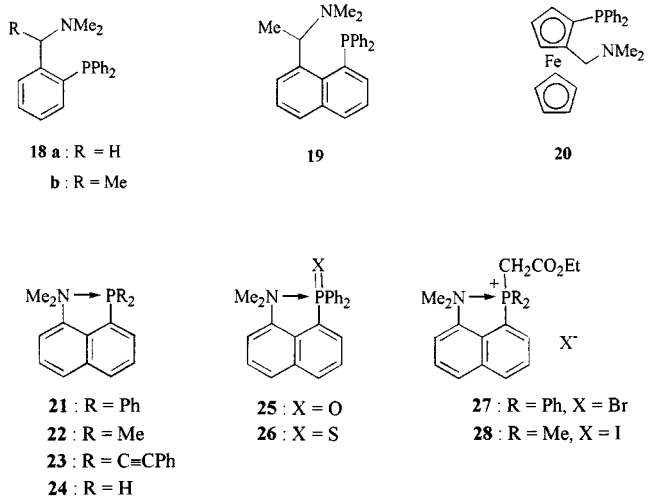

Figure 2. X-ray crystal structures of **21** (left) and **23** (right)

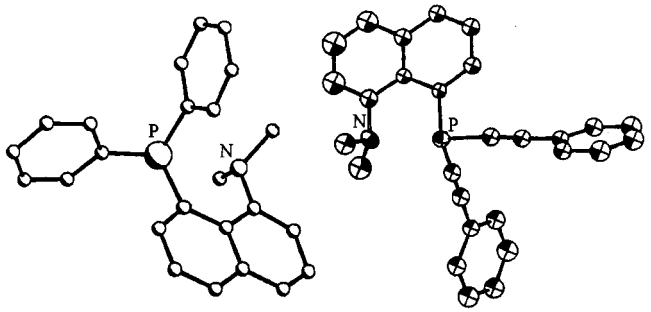

For phosphanes **22**[26] and **24**[27], only broadening of the singlet attributable to the NMe_2 protons is observed at 173 K. This shows that all these compounds (**21**−**29**) are pseudo-pentacoordinated or pentacoordinated in solution, with dissymmetrical geometries, in agreement with the solid-state structures of **21**, **23**, and **29**. In solution at room temperature they undergo a fast permutational isomerization process, the calculated $\Delta G^{\neq}$ values of which are reported in Table 2. These values indicate that isomerization is easier for phosphanes than for phosphane derivatives. This process should also be easier for compounds with Me substituents at the phosphorus atom than for compounds with Ph substituents, since the decoalescence of the NMe_2 signals could not be observed for phosphanes **22** or **24**. It is noteworthy that the behaviour in solution of the silicon compound **30**[26] has also been studied by ^{1}H-NMR spectroscopy. It is similar to that of **23**, with a $\Delta G^{\neq}$ value of 55.2 kJ mol^{-1} for the equivalence of the NMe_2 groups.

The diphosphane **31** has also been prepared[26]. It was found by ^{1}H-NMR studies that **31** and **21** show similar behaviour in solution. Thus, at room temperature, all the NMe_2 protons are equivalent and appear as a singlet, which splits into two signals at 178 K. This indicates that **31** is pentacoordinated in solution and undergoes a permutational isomerization process at room temperature. The calculated $\Delta G^{\neq}$ for this process is 36.8 kJ mol^{-1}, this value being very similar to that found for phosphane **21**.

Table 2. ^{1}H-NMR data (CD_2Cl_2) for NMe_2 groups and calculated $\Delta G^{\neq}$ values for the permutational isomerization process in compounds **21**, **23** and **25**−**28**

Compound	T (K)	δ (NMe_2)	T_c (K)	$\Delta G^{\neq}$
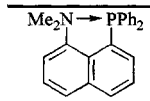 **21**	273	2.32	183	37.5[25]
	163	1.87-2.50		
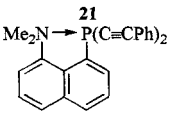 **23**	273	2.63	183	37.2[26]
	183	2.60 (broad)		
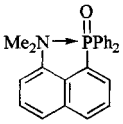 **25**	293	2.15	253	53.0[25]
	253	1.60-2.47		
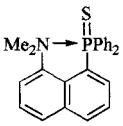 **26**	273	2.05	243	48.1[25]
	203	1.42-2.50		
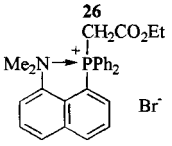 **27**	293	1.89	273	55.2[25]
	233	1.32-2.61		
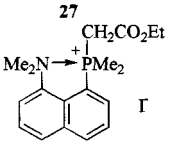 **28**	293	2.68	233	42.8[27]
	183	2.25-2.75		

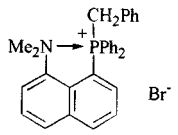
29

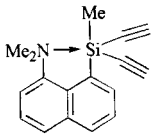
30

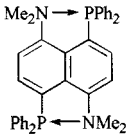
31

2.3 Pseudo-Hexacoordinate Phosphanes and Hexacoordinate Phosphane Derivatives

We have prepared phosphanes **32** and **33**, as well as their derivatives **34**−**37**. X-ray structure analyses of the phosphane **32**[28] and of phosphorus derivatives **35**[29] and **37**[28] have been performed (Figure 3). In each case, they reveal that the nitrogen lone pairs are directed towards the phosphorus atom, one NMe_2 group being *trans* to the P−Ph bond, while the other is opposite to a P−naphthyl bond with N−P−N angles of 102.4°, 94.9°, and 106.9°. The N−P distances are 2.70−2.73 Å in **35**, 2.78−2.79 Å in **32**, and 3.01 Å in **37**. The longer distance in **37** is probably due to the steric hindrance at the phosphorus atom, while the short distance in **35** is most probably attributable to the positive charge on the phosphorus atom. In each case, the pyramidal configuration around the phosphorus atom is retained and the geometries of these compounds correspond

to a bi-capped distorted tetrahedron (taking into account the nitrogen lone pair in **32**) rather than to a distorted octahedron. It is noteworthy that X-ray structure analysis of the analogous silicon compound **38**[30] showed the same geometry.

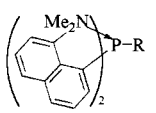

32 : R = Ph
33 : R = Me

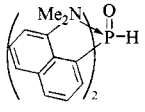

34

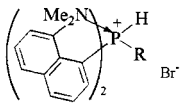

35 : R = Ph
36 R = H

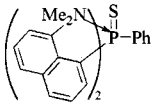

37

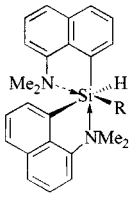

38 (R = H, F)

The solution ^{1}H-NMR spectra of phosphanes **32** and **33**, that of phosphane oxide **34**, and those of phosphonium salts **35** and **36**, at limiting temperatures for slow exchange, display four sharp signals attributable to the NMe_2 protons[31]. Selective irradiation of each methyl signal shows a transfer of saturation occurring between pairs of equivalent sites, one methyl of an NMe_2 group being equivalent to one methyl of the other NMe_2 group. At the same temperature, the ^{1}H-NMR spectra of these derivatives also show two discrete sets of naphthyl group signals. These data indicate that compounds **32**–**36** are hexacoordinated in solution, with dissymmetrical geometries, in agreement with the X-ray structures of **32**, **35**, and **37**. Furthermore, the ^{1}H-NMR spectra of these compounds are temperature-dependent. On raising the temperature there is coalescence of the four methyl signals into two essentially well-resolved signals (Table 3). Dynamic ^{1}H-NMR study of phosphonium salt **36**, which is the first known phosphonium salt with two P–H bonds, was not possible since it decomposes in solution at room temperature[27]. The ^{1}H-NMR spectrum of

Table 3. ^{1}H-NMR data for NMe_2 groups and calculated $\Delta G^{\neq}$ values for the permutational isomerization process in compounds **32**–**35**

Compound	Solvent	T (K)	δ (NMe_2)	$\Delta G^{\neq}$ (300 K)
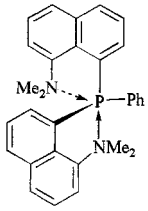	($CDBr_3$)	258	3.18, 1.94, 2.06, 2.93	62.3
		398	2.56[a]	
32				
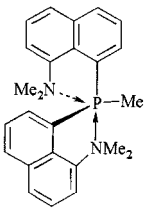	(toluene-d_8)	233	2.84, 1.63, 2.43, 2.69	57.5
		373	2.22, 2.54	
33				
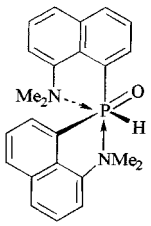	(toluene-d_8)	233	3.06, 1.92, 0.82, 2.71	56.2
		373	2.52, 1.92	
34				
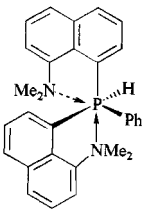	($CDBr_3$)	283	3.20, 1.67, 1.88, 3.02	59.9
		395	2.44, 2.49	
35				

[a] Unresolved doublet.

phosphane oxide **34** at 233 K shows a strongly deshielded signal at δ = 9.78. This downfield signal was assigned to the proton of the naphthyl group located in the deshielding zone of the P=O bond. This suggests that **34** adopts a conformation in which the N→P bond interaction is *trans* to the P=O bond (Figure 4). The coalescence of the four methyl group signals to give two signals can be explained

Figure 3. X-ray crystal structures of **32** (left), **35** (centre), and **37** (right)

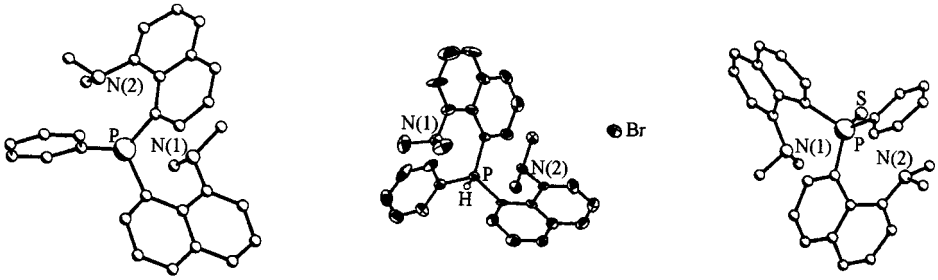

by a permutational isomerization process around the phosphorus atom, which occurs without cleavage of the N→P bond. The $\Delta G^{\neq}$ value for this process lies in the range 58−62 kJ mol^{-1} (Table 3). We note that similar solution behaviour was observed for the silicon compound **38** (R = F) by ^{1}H-NMR spectroscopy, the permutational isomerization process[32] taking place with a $\Delta G^{\neq}$ value of 62.4 kJ mol^{-1}.

Figure 4. Schematic representation of **34** and of the minor isomer of **37**

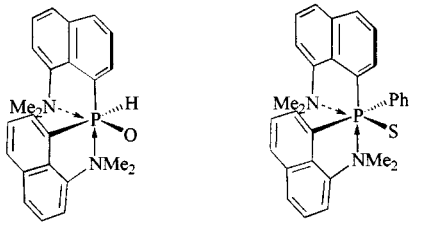

34 **37** (minor isomer)

Further raising of the temperature leads to the decomposition of **34** and **35** above 400 K. Coalescence of the two slightly separated signals into one was observed only for phosphane **32** (at 418 K in [D_4]-*o*-dichlorobenzene), thus indicating the cleavage of the N→P bond with an estimated $\Delta G^{\neq}$ value of 90 kJ mol^{-1}.

The solid-state ^{31}P-NMR spectrum of **37** shows one signal at δ = 50.9. In contrast, the ^{31}P-NMR spectrum of **37** in C_6D_6 displays two resonances at room temperature (at δ = 63.9 and δ = 53.5), which indicates that **37** exists as two isomers in solution. This was confirmed by a dynamic ^{1}H-NMR study. At the limiting temperature for slow exchange, the ^{1}H-NMR spectrum of **37** exhibits eight signals for the *N*-methyl protons, indicating the existence of two isomers in solution, the ratio of which depends on the solvent (50:50 in bromoform and 80:20 in toluene). Furthermore, comparison of the ^{31}P-NMR chemical shifts of **37** in solution and in the solid state shows that one of the isomers observed in solution (δ = 53.5) is presumably that present in the solid state (δ = 50.9). The structure of the other isomer (δ = 63.9 in C_6D_6) was inferred from a low-temperature ^{1}H-NMR study of the naphthyl protons. At 233 K (in [D_8]toluene), the ^{1}H-NMR spectrum of this isomer displays one signal at δ = 9.8, suggesting a structure similar to that of **34**, with the N→P bond lying *trans* to the P=S bond (Figure 4). COSY experiments on the mixture of isomers of **37** show that each methyl group of the NMe_2 groups exchanges with the other three, indicating an interconversion of the two isomers in solution. On raising the temperature, each methyl signal broadens, and they finally coalesce into a very broad signal at 373 K. Further raising of the temperature leads to the decomposition of the isomers at 405 K. Thus, two phenomena take place: (a) a permutational isomerization process occurring independently on each isomer, and (b) the interconversion of these isomers. This latter phenomenon was detected by means of COSY and NOESY experiments.

The ^{1}H-NMR spectra of **39** and **40** at room temperature show that these compounds are also hexacoordinated in solution, with dissymmetrical geometries[29]. Indeed, the ^{1}H-NMR spectrum of **39** exhibits four sharp singlets for the methyl groups and two sets of naphthyl proton signals. The PCH_2 protons are diastereotopic and appear as doublets of doublets. The ^{1}H-NMR spectrum of **40** displays eight singlets for the methyl groups and a multiplet for the diastereotopic PCH_2 protons, thus indicating that this compound exists as two isomers in solution, as in the case of **37**. Further evidence for the existence of two isomers is provided by the ^{31}P-NMR spectrum of **40**, which also exhibits two resonances.

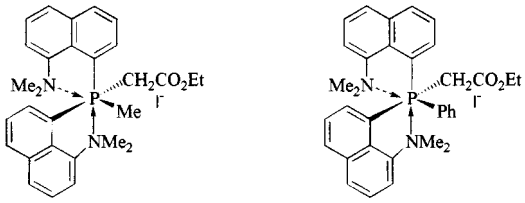

39 **40**

2.4 Pseudo-Heptacoordinate Phosphanes

The first pseudo-heptacoordinate P^{III} phosphorus derivative **41** was described by Paine and co-workers[33]. This complex was obtained by insertion of CS_2 into the P−N bond of the aminophosphane $P(NMe_2)_3$. Single-crystal X-ray structure analysis of **41** showed that the phosphorus centre is formally seven-coordinated, with six sulfur atoms (three short P−S bonds of mean length 2.178 Å and three long P−S bonds of mean length 2.966 Å) and the phosphorus lone pair forming a distorted capped trigonal antiprism.

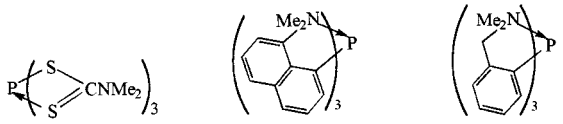

41 **42** **43**

We have prepared the phosphanes **42** and **43**[34], the X-ray crystal structures (Figure 5) of which reveal in both cases three weak N→P interactions with N−P distances of 2.80, 2.84, and 2.85 Å in **42** and 3.00, 3.01, and 3.07 Å in **43**. The pyramidal configuration around the phosphorus atom is retained and nitrogen coordination is observed *trans* to a P−C bond. Thus, the geometry of these phosphanes corresponds to a tri-capped tetrahedron[34] (taking into account the nitrogen lone pair). It is important to emphasize that phosphanes **42** and **43** adopt the same geometry, even though there is no steric constraint in phosphane **43** to force the NMe_2 groups to interact with the phosphorus centre. However, their ^{1}H-NMR spectra are notably different. Thus, while the ^{1}H-NMR spectrum of **43** exhibits only one sharp singlet for the methyl protons, even at low temperature, that of **42** displays two singlets for the

methyl protons, even up to 90°C (250 MHz). This notable difference indicates that N→P interactions are maintained in solution in the case of **42**, while an equilibrium between the opened and closed forms should be operative in solution for **43**. The same tri-capped tetrahedral geometry was also found in the silanes **44**[35] and **45**[36].

Figure 5. X-ray crystal structures of **42** (left) and **43** (right)

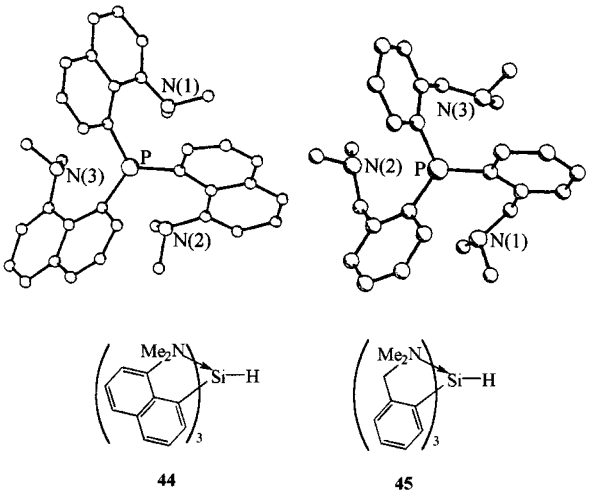

44 **45**

2.5 Reactivity of Pseudo-Hypercoordinate Phosphanes

The reactivity of phosphanes **21**, **32**, and **42**, incorporating one, two, or three 8-(dimethylamino)naphthyl ligands **1** decreases with the increasing number of ligands **1**, undoubtedly because of the increasing steric hindrance at the phosphorus atom and of the increasing number of N lone pairs in the P coordination sphere.

The reactivity of the pseudo-pentacoordinate phosphane **21** is very similar to that of triphenylphosphane. Thus, treatment of **21** with H_2O_2, S_8, CH_3I, or $BrCH_2CO_2Et$ affords the expected products in satisfactory yields[37] (58−65%). The pseudo-hexacoordinate phosphane **32** is less reactive than **21**. While its oxide and sulfide can be prepared under the classical reaction conditions in 60 and 67% yield, respectively, the formation of the phosphonium salt **40** required reaction with ICH_2CO_2Et for 24 h in refluxing toluene[27]. Finally, the reactivity of the pseudo-heptacoordinate phosphane **42**[34] is very different from that of **21** and **32**, as well as that of triphenylphosphane. It was not possible to obtain the corresponding oxide, nor the phosphane sulfide. However, reaction of **42** with CH_3I furnished the corresponding phosphonium salt in low yield (32%) after 10 days heating in a sealed tube at 100°C. In contrast, the pseudo-heptacoordinate phosphane **43**, incorporating three flexible ligands **2**, shows a reactivity similar to that of triphenylphosphane towards H_2O_2 or sulfur, but reacts with MeI to afford only the product of methylation at one amino group in 62% yield after 3 h at 100°C. This difference of reactivity between **42** and **43** towards MeI is consistent with their ^{1}H-NMR data in solution, which indicate a stronger N→P interaction in **42** than in **43**.

Phosphane **46**, incorporating the potentially bis-chelating ligand **3**, reacts with MeI to give the phosphonium salt **47** (Eq. 2), which undergoes a coordination-decoordination process in solution[38]. An X-ray structure determination of **47** (Figure 6) shows that the lone pairs of the two nitrogen atoms are directed symmetrically towards the phosphorus atom, with N−P distances of 3.14 and 3.16 Å. Furthermore, the tetrahedral geometry of the phosphorus atom is maintained so that the geometry around the phosphorus centre is that of a slightly distorted bi-capped tetrahedron. This conformation of the NCN ligand is similar to those found in transition-metal compounds incorporating this ligand[39]. During crystallization of **47**, a very small number of atypical crystals were found, the structure of which (Figure 6) revealed that they were composed of the ammonium salt **48**. The striking feature of this structure is that one methyl of the NMe_3^+ group is positioned close to the phosphorus atom, at a distance of 3.44 Å. This suggests that MeI could react with **46** to afford first the ammonium salt **48**, which should then undergo a fast rearrangement to **47** due to the favorable geometry of the NMe_3^+ group in relation to the P atom.

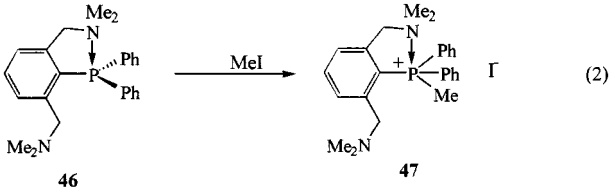

46 **47**

Figure 6. X-ray crystal structures of **47** (left) and **48** (right)

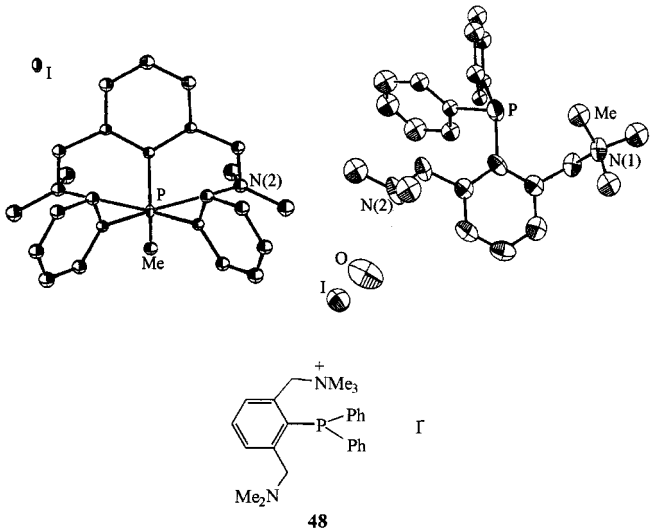

48

The reactivity of phosphanes **21**, **32**, and **42** towards transition-metal compounds was also investigated. The pseudo-pentacoordinate phosphane **21** may act as a monodentate ligand via the phosphorus atom or as a bidentate ligand via both the phosphorus and nitrogen atoms, depending on the experimental conditions. Thus, when $[(COD)PdCl_2]$ was allowed to react with 2 equiv. of **21**, complex **50** was formed, in which **21** coordinates to the Pd centre only via the phosphorus atom. On the other hand, **21** reacts with

Scheme 1

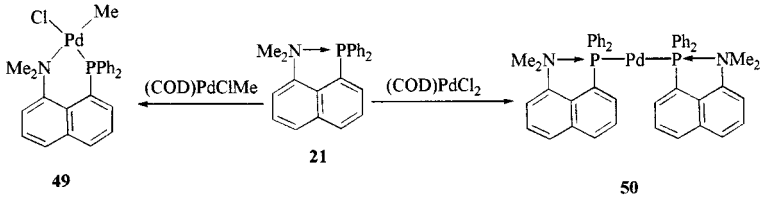

Scheme 2

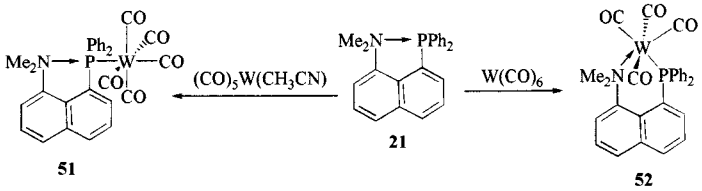

[(COD)PdClMe] as a bidentate ligand[24] to afford **49** (Scheme 1). Similarly, **21** reacts with $[(CO)_5W(CH_3CN)]$ as a monodentate ligand to afford complex **51** (Scheme 2), but with $W(CO)_6$ as a bidentate ligand to form complex **52**, the X-ray structure analysis[24] of which was performed. Phosphane **32** does not react appreciably with $W(CO)_6$ and no complex was isolated under these conditions. As regards phosphane **42**, it is completely unreactive towards $W(CO)_6$, as well as towards $[THF{\cdot}W(CO)_5]$. Phosphane **43**, incorporating three flexible ligands **2**, reacts with $W(CO)_6$ to give complex **53**, an X-ray structure determination[37] of which showed that the tungsten atom is complexed by one nitrogen atom and by the phosphorus centre, leaving two free NMe_2 groups. A similar bidentate carbonyltungsten complex **54** had previously been proposed[21] on the basis of IR and ^{1}H-NMR spectra. The pattern of CO stretching bands in the IR spectrum of complex **52** (2012, 1885, 1856 cm^{-1}) is similar to that seen for **54** (2018, 1889, 1832 cm^{-1}), but different from that in the case of complex **51** (2070, 1978, 1834 cm^{-1}). This latter spectrum closely resembles that of $Ph_3PW(CO)_5$ (2075, 1980, 1938 cm^{-1})[40].

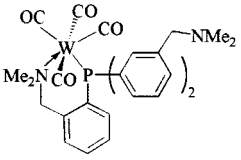

53

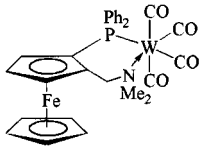

54

2.6 Reactivity of Hypercoordinate Phosphonium Salts

We have investigated the reactivity of some hypercoordinate phosphonium salts under Wittig conditions in order to study the effect of the N→P interaction on the rate and stereoselectivity of this reaction[29]. Some selected results are reported in Table 4. The pentacoordinate phosphonium salts **27** and **28** were found to react readily with benzaldehyde under Wittig conditions to give ethyl cinnamate, with **28** being more reactive than **27**. Furthermore, both substrates proved to be much more reactive than $Ph_3P^+CH_2CO_2Et$ under the same conditions, furnishing ethyl (*E*)-cinnamate with very good stereoselectivity. However, they were unreactive towards ketones under Wittig

Table 4. Results of Wittig reactions of phosphonium salts **27**, **28**, **39** and **40** with benzaldehyde under different experimental conditions; yields (*E*/*Z* ratio) of ethyl cinnamate

Phosphonium Salt	Reaction conditions: $NaNH_2$ / Et_2O [reaction times]	Reaction conditions: NaOH / C_6H_6 / H_2O [reaction times]
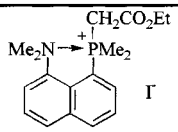 **28**	75% (95/5) [1 h]	40% (86/14) [5 min]
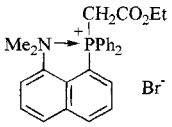 **27**	51% (99/1) [22 h]	77% (86/14) [2 h]
$Ph_3P^+CH_2CO_2Et$ Br^-	8% (97/3)	-
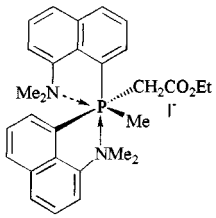 **39**	0% [44 h]	60% (92/8) [44 h]
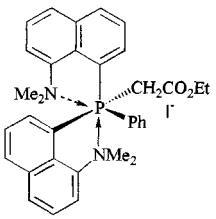 **40**	0% [96 h]	20% (97/3) [96 h]

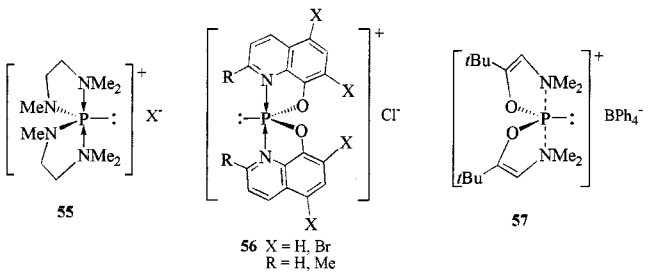

55 **56** X = H, Br; R = H, Me **57**

conditions. Due to the steric hindrance at the phosphorus atom, hexacoordinate phosphonium salts **39** and **40** are much less reactive than **27** and **28**. They react with PhCHO only under particular experimental conditions (Table 4), nevertheless showing good stereoselectivity. Thus, it can be concluded that electronic factors dominate over steric ones for compounds **27** and **28**, whereas for hexacoordinate phosphonium salts **39** and **40** incorporating two rigid ligands **1**, steric factors dominate the outcome of the Wittig reaction, resulting in poor reactivity.

3. Pseudo-Pentacoordinate Stabilized Phosphenium Salts

Phosphenium ions are reactive species[41] which can be stabilized by inter-[42–44] or intramolecular[45,46] coordination of donor groups on the phosphorus atom. The stabilization of phosphenium ions by twofold intramolecular coordination by nitrogen atoms was proposed by Schmutzler and Becker[47], who prepared the salt **55**. Subsequently, Lamandé and Munoz obtained salts **56**[48], the structures of which were inferred from ^{13}C- and ^{31}P-NMR studies. Finally, an X-ray crystal structure analysis of the salt **57**[49] revealed the pseudo-pentacoordination of the phosphorus atom in the cation, in a geometry close to a trigonal bipyramid, with N→P bond distances of 2.05 and 2.06 Å.

Ligand **3**, which has been found to stabilize silylenium ions[50–52], also permits the stabilization of phosphenium ions. Thus, reaction of the lithium derivative **58** with $PhPCl_2$ did not afford the phosphane $(Ar)_2PPh$, but rather an extremely air- and moisture-sensitive white powder **59** (Scheme 3), the ^1H-NMR spectrum of which featured two singlets for the NMe_2 protons and one AB pattern for the benzylic protons. The same ^1H-NMR pattern was found for the silylenium ion **62**[50–52]. Treatment of **59** with $NaPF_6$ furnished the corresponding hexafluorophosphate salt **60**, the ^{31}P-NMR spectrum of which exhibits two signals of equal intensity, one at $\delta = +95.5$, very close to that observed for **59**, and the other at $\delta = -143.6$ (PF_6^-). All these data are clearly consistent with an ionic structure for **59**. Reaction of this salt with $LiAlH_4$ afforded the phosphane **61** (Scheme 3), the ^{31}P-NMR chemical shift of which is upfield [$\delta = -77.5$, $^1J(PH) = 225$ Hz] with respect to that of Ph_2PH[53] ($\delta = -41.0$), thus suggesting an intramolecular N→P interaction. From the ^1H-NMR spectrum, it was inferred that phosphane **61** is pseudo-pentacoordinated at the phosphorus atom due to a rapid coordination-decoordination process of the NMe_2 groups. The increase in coordination number of the phosphorus atom in **61** gives rise to an unusual reactivity of the P−H bond. Indeed, **61** undergoes hydride abstraction upon reaction with Ph_3C^+-

Scheme 3

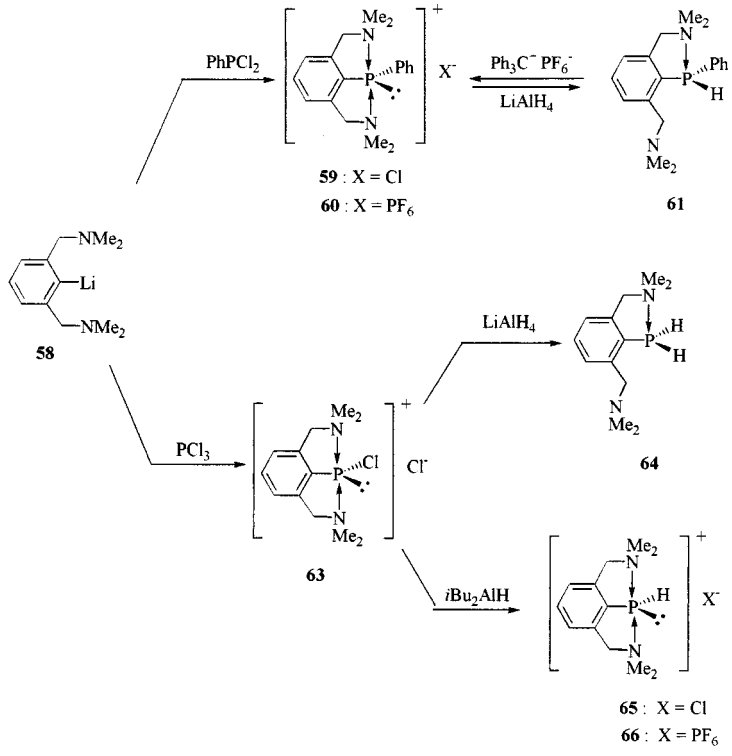

PF_6^- (Scheme 3), reforming the stabilized phosphenium salt **60**. It is noteworthy that hydride abstraction does not occur in the case of "classical" secondary phosphanes, but rather quaternization of the phosphane takes place[54]. The modification of the reactivity of a bond because of extra coordination is a well-known phenomenon in silicon chemistry[1], but has not previously been observed in phosphorus chemistry. Reaction of the lithium derivative **58** with PCl_3 gives rise to the phosphorus salt **63**, which was found to be extremely air- and moisture-sensitive. $LiAlH_4$ reduction of **63** gave phosphane **64**, while iBu$_2$AlH reduction unexpectedly afforded **65**, which represents the first stabilized phosphenium ion with a P−H σ bond (Scheme 3). The ^{1}H-NMR spectrum of this compound exhibits the same pattern for the NMe_2 and benzylic protons as **59**, indicating the coordination of both NMe_2 groups to the phosphorus atom[55]. The ^{1}H-NMR signals of the CH_2NMe_2 "arms" in the analogous P−Me salt **67**[27] are different from those in the case of salts **59** and **65**. At room temperature, the NMe_2 groups in **67** give rise to a single broad signal, while the benzylic protons appear as an AB pattern. On lowering the temperature, the NMe_2 signal splits into two signals and at 253 K the pattern due to the CH_2NMe_2 arms is the same as that seen for **59** and **65**. These observations can be explained in terms of a fast fluxional coordination-decoordination process of the NMe_2 groups at the phosphorus centre, which renders these groups equivalent at room temperature. However, the chirality at the phosphorus atom[27] is maintained, probably because of a slow rotation about the P−C_{ipso} bond, thus explaining the diastereotopy of the benzylic protons. An X-ray crystal structure determination of the hexafluorophosphate **66**[55] has confirmed the pseudo-pentacoordination at the phosphorus atom, the geometry of the cation being that of a distorted trigonal bipyramid with N−P distances of 2.08 and 2.07 Å, distances very close to those observed in the salt **57**.

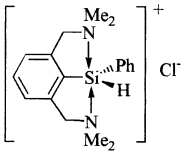

62

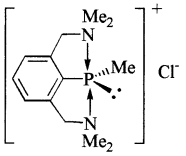

67

4. Conclusion

In this review, we have described hypercoordinate phosphorus compounds in which extra coordination at the phosphorus centre is provided by intramolecular interaction of strategically positioned NMe_2 groups. Pseudo-hypercoordinate phosphanes have structures very similar to those of the corresponding silicon derivatives with an Si−H bond, and both series of compounds show similar fluxional behaviour in solution. The N−P distances are generally rather long (2.7−3.0 Å), but amount to less than the sum of the van der Waals radii of phosphorus and nitrogen atoms (3.4 Å[56]). The geometry at the phosphorus atom invariably corresponds to a capped tetrahedron, which is generally somewhat distorted. It is noteworthy that the structural characteristics of the pseudo-hexacoordinate phosphanes and the hexacoordinate phosphane derivatives are quite different from those of the hexacoordinate phosphoranes in that the P−N distances are less than 2 Å[3] in the latter, which have octahedral geometries. This can be explained in terms of the generally high electronegativities of the ligands surrounding the phosphorus atoms in phosphoranes. Intramolecular N→P donor-acceptor interactions induce an increase in the reactivity of the phosphorus derivatives. Thus, the pentacoordinate phosphonium salts are much more reactive than the corresponding phosphorus derivatives lacking the NMe_2 groups. Indeed, an unusual reactivity of a P−H bond due to extra coordination at the phosphorus atom has been observed for the first time in the case of a hypercoordinate phosphane.

[1] C. Chuit, R. J. P. Corriu, C. Reyé, J. C. Young, *Chem. Rev.* **1993**, *93*, 1371−1448.
[2] R. R. Holmes, *Acc. Chem. Res.* **1979**, *12*, 257−265.
[3] C. V. Wong, D. K. Kennepohl, R. G. Cavell, *Chem. Rev.* **1996**, *96*, 1917−1951.
[4] [4a] R. J. P. Corriu, G. F. Lanneau, D. Leclerq, *Tetrahedron* **1980**, *36*, 1617−1626. − [4b] R. J. P. Corriu, G. F. Lanneau, D. Leclerq, *Tetrahedron* **1989**, *45*, 1959−1974.
[5] R. R. Holmes, *Chem. Rev.* **1996**, *96*, 927−950.
[6] [6a] G. van Koten, *Pure Appl. Chem*. **1989**, *61*, 1681−1694. − [6b] G. van Koten, *Pure Appl. Chem.* **1990**, *62*, 1155−1159. − [6c] J. T. B. H. Jastrzebski, G. van Koten, *Adv. Organomet. Chem*. **1993**, *35*, 241−294.
[7] C. B. Cong, G. Gence, B. Garrigues, M. Koenig, A. Munoz, *Tetrahedron* **1979**, *35*, 1825−1839.
[8] F. Carré, C. Chuit, R. J. P. Corriu, P. Montforte, N. K. Nayyar, C. Reyé, *J. Organomet. Chem*. **1995**, *499*, 147−154.
[9] V. V Vasil′ev, V. B. Lebedev, N. A. Razumova, *Zh. Obshch. Khim.* **1976**, *46*, 1739−1742; *Engl. Transl*. **1977**, 1690−1692.
[10] J. Gloede, H. Gross, *Z. Chem.* **1984**, *24*, 391−392.
[11] L. Z. Liu, B. Z. Cai, R. Y. Chen, *Acta Chim. Sin*. **1986**, *44*, 1249−1252.
[12] G. M. Kosolapoff, L. Maier, *Organic Phosphorus Compounds*, vol. 7, Wiley, Chichester, **1976**, p. 163.
[13] [13a] G. van Koten, J. G. Noltes, *J. Am. Chem. Soc.* **1976**, *98*, 5693−5395. − [13b] J. T. B. H. Jastrzebski, J. Boersma, G. van Koten, *J. Organomet. Chem*. **1991**, *413*, 43−53.
[14] D. J. Sherlock, A. Chandrasekaran, R. O. Day, R. R. Holmes, *Inorg. Chem.* **1997**, *36*, 5082−5089.
[15] T. B. Rauchfuss, F. T. Patino, D. M. Roundhill, *Inorg. Chem*. **1975**, *14*, 652−656.
[16] N. C. Payne, D. W. Stephan, *Inorg. Chem*. **1982**, *21*, 182−188.
[17] H. J. Kreuzfeld, C. Döbler, H. P. Abicht, *J. Organomet. Chem*. **1987**, *336*, 287−292.
[18] A. Kinting, H. J. Kreuzfeld, H. P. Abicht, *J. Organomet. Chem*. **1989**, *370*, 343−349.
[19] K. Yamamoto, A. Tomita, J. Tsuji, *Chem. Lett*. **1978**, 3−6.
[20] L. Horner, G. Simons, *Z. Naturforsch*. **1984**, *39b*, 504−511.
[21] J. C. Kotz, C. L. Nivert, J. M. Lieber, R. C. Reed, *J. Organomet. Chem*. **1975**, *84*, 255−267.
[22] G. P. Schiemenz, E. Papageorgiou, *Phosphorus Sulfur* **1982**, *13*, 41−59.
[23] L. Horner, G. Simons, *Phosphorus Sulfur* **1983**, *15*, 165−175.
[24] G. P. C. M. Dekker, A. Buijs, C. J. Elsevier, K. Vrieze, P. W. N. M. van Leeuwen, W. J. J. Smeets, A. L. Spek, Y. F. Wang, C. H. Stam, *Organometallics* **1992**, *11*, 1937−1948.
[25] C. Chuit, R. J. P. Corriu, P. Montforte, C. Reyé, J. P. Declercq, A. Dubourg, *J. Organomet. Chem*. **1996**, *511*, 171−175.
[26] D. Guy, Doctorat of the University of Montpellier II, **1997**.
[27] M. Chauhan, Doctorat of the University of Montpellier II, **1996**.
[28] M. Chauhan, C. Chuit, R. J. P. Corriu, C. Reyé, J. P. Declercq, A. Dubourg, *J. Organomet. Chem*. **1996**, *510*, 173−179.

[29] F. Carré, M. Chauhan, C. Chuit, R. J. P. Corriu, C. Reyé, *Phosphorus Sulfur Silicon* **1997**, *123*, 181−195.
[30] C. Brelière, R. J. P. Corriu, M. Poirier, G. Royo, J. Zwecker, *Organometallics* **1989**, *8*, 1831−1833.
[31] M. Chauhan, C. Chuit, A. Fruchier, C. Reyé, to be published.
[32] C. Brelière, R. J. P. Corriu, G. Royo, J. Zwecker, *Organometallics* **1989**, *8*, 1834−1836.
[33] R. W. Light, L. D. Hutchins, R. T. Paine, C. F. Campana, *Inorg. Chem*. **1980**, *19*, 3597−3604.
[34] C. Chuit, R. J. P. Corriu, P. Montforte, C. Reyé, J. P. Declercq, A. Dubourg, *Angew. Chem.* **1993**, *105*, 1529−1531; *Angew. Chem. Int. Ed. Engl.* **1993**, *32*, 1430−1432.
[35] C. Brelière, F. Carré, R. J. P. Corriu, G. Royo, *Organometallics* **1988**, *7*, 1006−1008.
[36] N. Auner, R. Probst, F. Hahn, E. Herdtweck, *J. Organomet. Chem*. **1993**, *459*, 25−41.
[37] P. Montforte, Doctorat of the University of Montpellier II, **1994**.
[38] F. Carré, C. Chuit, R. J. P. Corriu, A. Mehdi, C. Reyé, *J. Organomet. Chem*. **1997**, *529*, 59−68.
[39] M.H.P. Rietveld, D.M. Grove, G. van Koten, *New J. Chem.* **1997**, *21*, 751−771.
[40] S. Grimm, D. Wheatland, W. McFarlane, *J. Am. Chem. Soc.* **1967**, *89*, 5573−5577.
[41] [41a] A. H. Cowley, R. A. Kemp, *Chem. Rev.* **1995**, *85*, 367−382. − [41b] M. Sanchez, M. R. Mazières, L. Lamandé, R. Wolf, in *Multiple Bonds and Low Coordination in Phosphorus Chemistry* (Eds.: M. Regitz, O. J. Scherer), Georg Thieme, Stuttgart, **1990**, p. 129−148.
[42] R. W. Kopp, A. C. Bond, R. W. Parry, *Inorg. Chem*. **1976**, *15*, 3042−3046.
[43] C. Payrastre, Y. Madaule, J. G. Wolf, T. C. Kim, M. R. Mazières, R. Wolf, M. Sanchez, *Heteroatom Chem*. **1992**, *3*, 157−162.
[44] R. Reed, R. Réau, F. Dahan, G. Bertrand, *Angew. Chem.* **1993**, *105*, 464−465; *Angew. Chem. Int. Ed. Engl.* **1993**, *32*, 399−401.
[45] T. Kaukorat, I. Neda, R. Schmutzler, *Coord. Chem. Rev.* **1994**, *137*, 53−107.
[46] R. Bartsch, M. Sanchez, R. Wolf, *Phosphorus Sulfur* **1988**, *35*, 89−92.
[47] W. Becker, R. Schmutzler, *Phosphorus Sulfur* **1988**, *36*, 231−239.
[48] L. Lamandé, A. Munoz, *Tetrahedron Lett.* **1991**, *32*, 75−78.
[49] Y. V. Balitzky, S. E. Pipko, A. D. Sinitsa, A. N. Chernega, Y. G. Gololobov, *Phosphorus Sulfur Silicon* **1993**, *75*, 167−170; S. E. Pipko, Y. V. Balitzky, A. D. Sinitsa, Y. G. Gololobov, *Tetrahedron Lett*. **1994**, *35*, 165−168.
[50] C. Chuit, R. J. P. Corriu, A. Mehdi, C. Reyé, *Angew. Chem.* **1993**, *105*, 1372−1375; *Angew. Chem. Int. Ed. Engl*. **1993**, *32*, 1311−1313.
[51] M. Chauhan, C. Chuit, R. J. P. Corriu, C. Reyé, *Tetrahedron Lett*. **1996**, *37*, 845−848.
[52] M. Chauhan, C. Chuit, R. J. P. Corriu, A. Mehdi, C. Reyé, *Organometallics* **1996**, *15*, 4326−4333.
[53] D. G. Gorenstein, D. O. Shah, in *Phosphorus* ^{31}P NMR − Principles and Applications, Academic Press, New York, **1984**, p. 553.
[54] J. B. Lambert, J. H. So, *J. Org. Chem*. **1991**, *58*, 5960−5962.
[55] J. P. Bezombes, F. Carré, C. Chuit, R. J. P. Corriu, A. Mehdi, C. Reyé, *J. Organomet. Chem*. **1997**, *535*, 81−90.
[56] A. Bondi, *J. Phys. Chem*. **1964**, *68*, 441−451.

[I98234]

Caesium Control of the Coordination Chemistry of *t*Bu-calix[6]arene towards Uranyl

Pascal C. Leverd*, Patrick Berthault, Monique Lance and Martine Nierlich

CEA-Saclay, Service de Chimie Moléculaire, bat 125,
F-1191 Gif sur Yvette, France
Fax: (internat.) + 33(0)1/69086640
E-mail: leverd@drecam.cea.fr

Received June 3, 1998

Keywords: Calixarenes / Uranyl / Caesium / Supramolecular chemistry

The reaction of $[UO_2Cl_4]^{2-}$ with *t*Bu-calix[6]arene (H_6L) is made possible by the presence of Cs^+ leading to the formation of a trimetallic inclusion complex. An alkali metal can definitely influence the coordination chemistry of *t*Bu-calix[6]arene.

Calixarenes as ligands is a fast developing field of supramolecular chemistry. However, it almost exclusively concerns calix[4]arene derivatives.[1] Amongst all metal complexes currently studied, those of the lanthanides[2] and actinides[3] are receiving particular attention due to environmental needs.[4] Although calix[6]arene derivatives were soon recognised as matching the coordination geometry required by the uranyl ion,[5] it has not been possible to isolate the simple inclusion complex with UO_2^{2+}. Structural information on how this family of ligands binds to metals are still scarce[6][3d]. Recently, Gibson suggested that "alkali-metal ions could influence the coordination and reactivity of calix[4]arene at transition metal centres".[7] In order to test this idea for larger calixarenes, we decided to study the possible effect of an alkali metal on the reactivity of *t*Bu-calix[6]arene (H_6L) towards uranyl. We report here the dramatic influence of Cs^+ on the reaction of H_6L with $[UO_2Cl_4]^{2-}$ and the synthesis, X-ray determination, and NMR study of the new caesium inclusion complex $[Cs][HNC_5H_5]_3[UO_2Cl_2]_2[H_2L]\cdot 7\ NC_5H_5$ (**1**).

When $[HNC_5H_5]_2[UO_2Cl_4]$[8] was treated with H_6L in pyridine, no reaction was observed. Even after refluxing the two components for 12 hours, the ^1H NMR of the calixarene and the visible spectrum of the uranyl cation were identical to the ones of the starting materials.

Scheme 1

$$2\ [HNC_5H_5]_2[UO_2Cl_4] + H_6L \xrightarrow[\text{pyridine}]{} \text{no reaction}$$

However, when one equivalent of caesium triflate was added to the mixture, the pale yellow colour immediately turned to a deep red.

Scheme 2

$$2\ [HNC_5H_5]_2[UO_2Cl_4] + H_6L \xrightarrow[\text{pyridine}]{Cs^+} [Cs][HNC_5H_5]_3[UO_2Cl_2]_2[H_2L] + 4\ [HNC_5H_5]Cl$$

The solution was allowed to stand and after two days red crystals of **1** suitable for X-ray crystallography (59% yield) were isolated as the sole reaction product. The structure was solved and revealed an heterotrimetallic complex of *t*Bu-calix[6]arene where two uranyl cations and a caesium atom were coordinated to the macrocycle (Figure 1).

Of the ten pyridine molecules found in the lattice, six were found to form three pyridinium dimers (N−H···N bond distance of 2.66 Å), implying that the macrocycle was deprotonated four times to result in the observed stoichiometry for **1**: $[Cs][HNC_5H_5]_3[UO_2Cl_2]_2[H_2L]\cdot 7\ NC_5H_5$.

The two uranyl cations are bound in an external fashion to the macrocycle through the deprotonated oxygen of the phenolate groups. Mean U=O, U−O, and U−Cl bond distances are 1.789(7), 2.214(8), and 2.711(4) Å, respectively, and are comparable with those of the literature.[3b][3c][3d][3e][3f][5c][9] The geometry around uranyl is four-coordinate equatorial with the two phenolate oxygen atoms and the two chloride atoms in *cis* arrangements. This arrangement is unprecedented for an anionic moiety of uranyl ($[UO_2X_2Y_2]^{2-}$) and the only related example found in the literature is the *cis* arrangement of two phosphane oxides and two chlorides in $[UO_2Cl_2(OPPh_3)_2]$.[9]

The caesium cation is bound to the two protonated oxygens of the calixarene that do not form bonds with uranium [O(6) and O(3)]. The mean Cs−O distance is 3.045(8) Å, in agreement with the one found for coordinate bonds in crown ether (3.0−3.3 Å)[10] or in complexes where coordination of an alcohol group to caesium was observed [3.006(6)−3.323(7) Å][11]. More unusual are the short contacts of 3.390(9) and 3.454(8) Å found between the caesium and the two uranyl oxygen atoms [O(1B) and O(2B)]. Although they can not formally be considered as bonds, those interactions probably help to stabilise the caesium inside its host. The alkali cation is also bound in nearly a η^6-fashion to the faces of the two phenolic rings. Cs−C distances range between 3.41(1) and 3.87(1) Å, and the three shortest distances correspond to the phenol- and methylene-substituted

 © WILEY-VCH Verlag GmbH, D-69451 Weinheim, 1998 1434−1948/98/1212−1859 $ 17.50+.50/0

Figure 1. X-ray structure of compound **1** [a] A: side view, B: bottom view. *t*Bu groups have been omitted for clarity

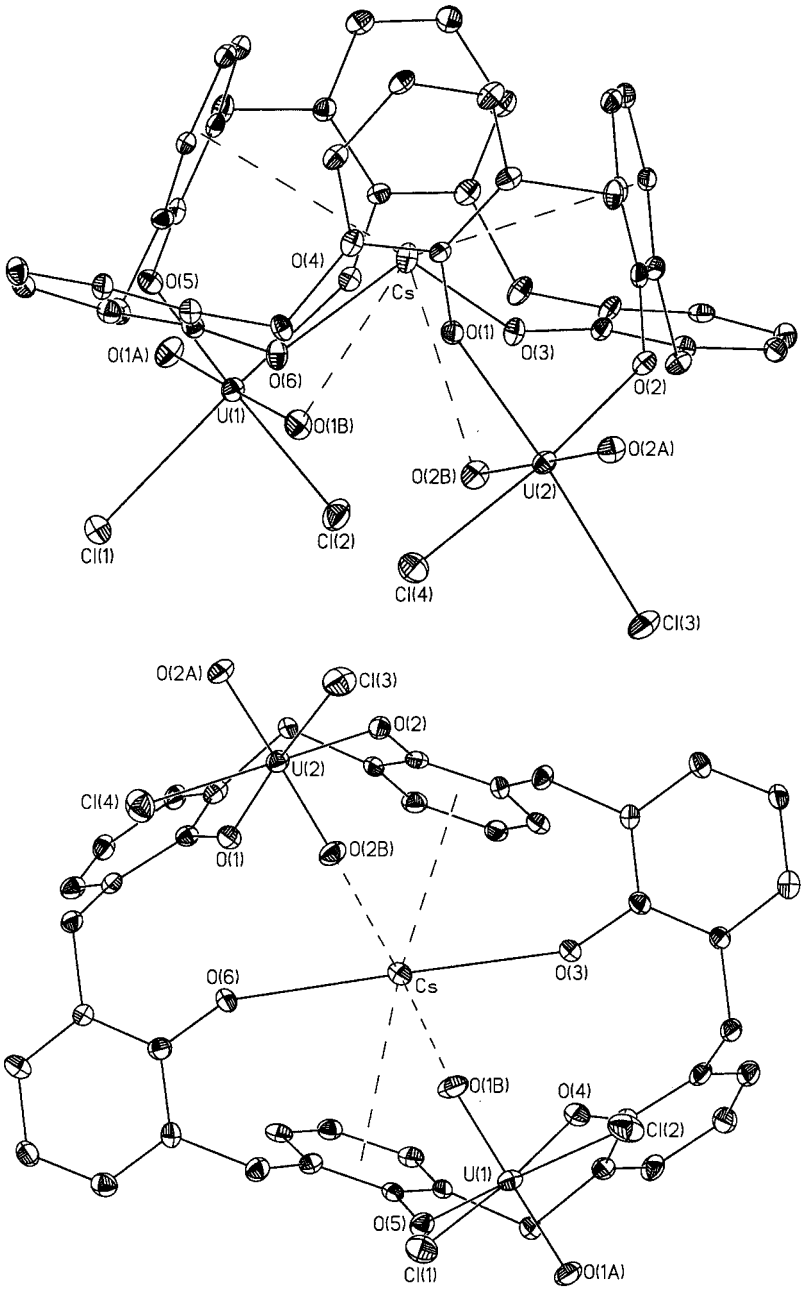

[a] Selected bond lengths [Å] and angles [°] with estimated standard deviations in parentheses: U(1)−O(1A) 1.788(7), U(1)−O(1B) 1.788(7), U(1)−O(4) 2.235(8), U(1)−O(5) 2.196(8), U(1)−Cl(1) 2.723(4), U(1)−Cl(2) 2.708(4), U(2)−O(2A) 1.791(7), U(2)−O(2B) 1.792(7), U(2)−O(1) 2.228(7), U(2)−O(2) 2.197(7), U(2)−Cl(3) 2.694(3), U(2)−Cl(4) 2.718(4), Cs−O(1B) 3.389(8), Cs−O(2B) 3.454(8), Cs−O(3) 3.021(7), Cs−O(6) 3.067(8), O(4)−U(1)−O(5) 87.7(3), O(4)−U(1)−Cl(2) 90.0(2), O(5)−U(1)−Cl(1) 92.5(2), Cl(1)−U(1)−Cl(2) 89.9(1), O(1)−U(2)−O(2) 86.2(3), O(1)−U(2)−Cl(4) 87.9(2), O(2)−U(2)−Cl(3) 95.2(2), Cl(3)−U(2)−Cl(4) 90.9(1), O(3)−Cs−O(6) 133.5(2).

positions. The mean Cs−centroid distance is 3.35(1) Å. The shortest Cs−C separations are shorter than those found for caesium−methyl (3.53 Å),[12] and for caesium complexes of *t*Bu-calix[4]arene and bis(homooxa)-*t*Bu-calix[4]arene [3.53(1) to 4.17(1) Å, with a Cs−centroid distance of 3.57(1) Å].[13] They are more in the range of those found for selective caesium extractants like 1,3-calix[4]arene crowns [3.273(5)−3.770(5) Å] although in the latter, the alkali cation is only bound in η^2 or η^3 fashion to the phenolic faces.[14] The short Cs−O and Cs−C distances in **1** imply that caesium is strongly bound within the macrocycle, which, in the case of a ligand as flexible as *t*Bu-calix[6]arene,[15] seems to indicate that the alkali cation guest is not held within the cavity by the suitable size of the host as noticed for the calix[4]arene analogues,[13a][16] but participates in holding together the ligand conformation. The crystal structure of **1** is not only a rare example of a metal complex of an underivatized calix[6]arene,[6a][6c][6e][3d] but is also the first crystallographic example of cationic π-bonding to the inner faces of the phenolic rings of anything other

than a calix[4]arene derivative.

The organic macrocycle adopts a pinched-cone conformation reminiscent of that found in the other complex of H_6L and uranyl present in the literature,[3d] but is more distorted. In compound **1**, the angle formed by the two planes of the phenolic rings bound to caesium by their oxygen atoms [O(3) and O(6)] is 18(1)°, and the one formed by the two phenolic rings bound in a polyhapto fashion to caesium, and therefore brought towards each other, is 32(2)°, inverted with respect to the cone conformation (relative to 62° and 11° for equivalent positions in reference 3d).

Synthesis of the analytically pure compound on a preparative scale was achieved by treating $[Cs]_2[UO_2Cl_4]$[8] with H_6L in pyridine.

^{1}H- and ^{133}Cs-NMR spectroscopy was employed to obtain information about the role of caesium in the formation of the complex. One equivalent of caesium triflate was added to a solution of H_6L in pyridine and a significant shift (−23 ppm) for the caesium signal was observed, as well as the enlargement and shift of the signals of the acidic protons [+0.57 ppm, Full Width at Half Maximum (FWHM) +53 Hz] and methylenic protons (−0.02 ppm, FWHM +7 Hz), demonstrating the modification of the geometry of the calixarene and the formation of a complex with the alkali metal. Although from these NMR data, it is not possible to draw conclusions about the resulting shape of the macrocycle, or the kind of bonding involved, it is possible to imagine that the formation of such Cs−*t*Bu-calix[6]arene species could then enable the reaction with uranyl.

Scheme 3

$$2\,[UO_2Cl_4]^{2-} + [H_6L] + Cs^+ \rightarrow '[Cs{-}H_6L]' \rightarrow [Cs][UO_2Cl_2]_2[H_2L]^{3-}$$

Unlike the reaction with calix[4]arene complexes of Nb and Ta where metallation of the ligand has been used to bind alkali metal cations in the cavity,[17] the reaction with the alkali metal occurs prior to reaction with uranium in the formation of **1**.

Contrary to observations for the free ligand, the ^{1}H-NMR spectrum of **1** is characteristic of the restricted motion of the macrocycle, with methylene, *tert*-butyl, and phenyl protons split into several resonances. ^{133}Cs-NMR spectrum of **1** exhibits three peaks, none of them corresponding to the signal of free Cs^+ as obtained for caesium triflate, thus demonstrating that encapsulation of the alkali metal is retained in solution. The three peaks proved to be in slow exchange, but no coalescence could be obtained by temperature change (276 to 346 K) or by addition of excess caesium triflate (up to one equivalent). We assume that this set of peaks could be due to different positions of the caesium atom inside its host, as observed for the calix[4]arene derivatives.[13b]

In conclusion, we have found that the reaction of *t*Bu-calix[6]arene with $UO_2Cl_4^{2-}$ could be activated by the presence of caesium. We have characterised a heterotrimetallic complex displaying external coordination of uranyl and inclusion of caesium. The evidence of an initial interaction between the calixarene and Cs^+ demonstrates the influence of the alkali metal on the coordination chemistry reaction. Studies are currently in progress to determine the exact nature of the interaction of caesium and *t*Bu-calix[6]arene in pyridine, and to extend this research to other calixarenes and to other alkali metals.

Experimental Section

General: All experiments were carried out with exclusion of air and moisture in a glove box. ^{1}H- and ^{133}Cs-NMR spectra were recorded in [D$_5$]pyridine on a Bruker DRX-500 spectrometer at T = 297 K. All NMR tubes were charged to obtain a Cs^+ concentration of approximately 2 mmol/l. The 65.6 MHz ^{133}Cs-NMR spectra were calibrated externally relatively to a 0.5 mol/l D_2O solution of CsBr. − Elemental analyses were performed at Service de Microanalyse, CNRS, 91191 Gif-sur-Yvette.

[Cs][HNC$_5$H$_5$]$_3$[UO$_2$Cl$_2$]$_2$[H$_2$L] (**1**): $[Cs]_2[UO_2Cl_4]$ (CAS no. 17631-98-0) (0.28 g, $4{\cdot}10^{-4}$ mol) was treated with H_6L (0.20 g, $2{\cdot}10^{-4}$ mol) in pyridine (30 ml) at 323 K for 12 hours. After filtration of a white powder of CsCl, the solution was concentrated and compound **1** was obtained as a red powder. After recrystallisation in pyridine, the powder was dried under vacuum and gave satisfactory elemental analysis for $[Cs][HNC_5H_5]_3[UO_2Cl_2]_2[H_2L]$ (0.27 g, $1.3{\cdot}10^{-4}$ mol, 65%). − ^{1}H NMR δ = 1.34 (m, 18 H, *t*Bu), 1.21 (m, 36 H, *t*Bu), 3.39, 3.82, 4.00, 4.11, 5.31, 6.16, 6.54 (br s, 12 H, ArCH$_2$Ar), 6.86, 7.24, 7.30, 7.41, 7.78 (12 H, ArH), 9.86, 12.75 (5 H, H$^+$): − ^{133}Cs NMR δ = 23 (br s, 20 Cs), −78(br s, 10 Cs), −128 (br s, 24 Cs). − $C_{81}H_{98}Cl_4CsN_3O_{10}U_2$ (2023): calcd. C 48.05, H 4.84, N 2.08; found C 47.98, H 5.09, 2.41.

Reaction of H_6L with Caesium Triflate: An NMR tube was charged with H_6L (10 mg, $1{\cdot}10^{-2}$ mmol) in [D$_5$]pyridine (0.4 ml) and caesium triflate (3 mg, $1{\cdot}10^{-2}$ mmol) was added. − ^{1}H NMR δ = 1.21 (s, 54 H, *t*Bu), 4.10 (s, 12 H, ArCH$_2$Ar, FWHM = 15 Hz), 7.31 (s, 12 H, ArH), 11.37 (br s, 6 H, H$^+$, FWHM = 97 Hz), − ^{133}Cs NMR δ = −5(br).

Reference ^{1}H NMR Spectrum of H_6L: δ = 1.21 (s, 54 H, *t*Bu), 4.12 (s, 12 H, ArCH$_2$Ar, FWHM = 8 Hz), 7.29 (s, 12 H, ArH), 10.80 (br s, 6 H, H$^+$, FWHM = 44 Hz).

Reference ^{133}Cs NMR spectrum of Caesium Triflate: δ = 18(s).

X-ray Crystallographic Study: Crystal data of **1**; $C_{116}H_{133}Cl_4CsN_{10}O_{10}U_2$ (2578.09), 0.75 × 0.55 × 0.40 mm^3, triclinic, $P\bar{1}$, Z = 2, a = 15.391(4), b = 17.059(7), c = 24.356(4) Å, α = 83.86(3), β = 88.60(2), γ = 67.60(4)°, V = 5877(3) Å^3, ρ_{calcd} = 1.457g.cm^{-3}, F(000) = 2572, $2\theta_{max}$ = 24°, μ_{Mo} = 3.206 cm^{-1}, Enraf-Nonius Mach 3 diffractometer (ω/2θ scans, T = 293 K, Mo-*Kα* radiation λ = 0.71069 Å). The structure was solved by the heavy-atom method and refined on F^2 using SHELXTL with all atoms considered as anisotropic except solvated pyridine molecules which were constrained to regular hexagons. One of them was found to be disordered over two positions which could be refined to final occupations 0.89(2) and 0.13(2). Absorption was corrected using ψ-scans (min. transmission = 57.7%, max. transmission = 99.9%). 15765 measured reflections, 11403 of which were considered as observed ($I > 2\sigma I$), 823 refined parameters, $R1$ = 0.0608 , $wR2$ = 0.1558 (all data), residual electron density 0.82 eÅ^{-3}. Crystallographic data (excluding structure factors) have been deposited with the Cambridge Crystallographic Data Centre as supplementary publication no. CCDC-101252. Copies of the data can be obtained free of charge on application to CCDC, 12 Union

Road, Cambridge CB2 1EZ, UK [Fax: (internat.) + 44-1223/336-033; E-mail: deposit@ccdc.cam.as.uk].

[1] C. Wieser, C. B. Dieleman, D. Matt, *Coord. Chem. Rev.* **1997**, *165*, 93−161.
[2] J.-C. Bünzli, J. M. Harrowfield, in *Calixarenes, A Versatile Class of Macrocyclic Compounds*, (Eds.: J. Vicens, V. Böhmer), Kluwer Academic Publishers, Dordrecht, **1990**, pp. 211−231.
[3] [3a] J. M. Harrowfield, M. I. Ogden, A. H. White, *J. Chem. Soc., Dalton Trans.* **1991**, 2625−2632. − [3b] J. M. Harrowfield, M. I. Ogden, A. H. White, *J. Chem. Soc., Dalton Trans.* **1991**, 979−985. − [3c] P. Thuéry, M. Nierlich, *J. Incl. Phenom*. **1997**, *27*, 13−20. − [3d] P. Thuéry, M. Lance, M. Nierlich, *Supramol. Chem*. **1996**, *7*, 183−185. − [3e] *t*Bu-Calix[7]arene complex of uranyl, P. Thuéry, M. Nierlich, M. I. Ogden, J. M. Harrowfield, *Supramol. Chem.*, in press. − [3f] P. Thuéry, N. Keller, M. Lance, J.-D. Vigner, M. Nierlich, *Acta Cryst*. **1995**, C51, 1570−1574.
[4] [4a] L. Cecille, *Radioactive Waste Management and disposal*, Elsevier, London, New York, **1991**. − [4b] L. Cecille, M. Casarci, L. Pietrelli, *New Separation Chemistry Techniques for Radioactive Waste and other Specific Applications*, Elsevier, London, New York, **1991**.
[5] [5a] S. Shinkai, H. Koreishi, K. Ueda, T. Arimura, O. Manabe, *J. Am. Chem. Soc.* **1987**, *109*, 6371. − [5b] S. Shinkai, Y. Shiramama, H. Satoh, O. Manabe, T. Arimura, K. Fujimoto, Tsutomu Matsuda, *J. Chem. Soc., Perkin Trans.* **1989**, 1167−1171. − [5c] P. Thuéry, N. Keller, M. Lance, J.-D. Vigner, M. Nierlich, *New J. Chem*. **1995**, *19*, 619−625.
[6] [6a] J. M. Smith, S. G. Bott, *Chem. Commun*. **1996**, 377−378. − [6b] F. J. Parlevliet, A. Olivier, W. G. J. de Lange, P. C. J. Kamer, H. Kooijman, A. L. Speck, P. W. N. M. van Leeuwen, *Chem. Commun.* **1996**, 583−584. − [6c] S. G. Bott, A. W. Coleman, J. L. Atwood, *J. Chem. Soc., Chem. Commun*. **1986**, 610−611. − [6d] G. D. Andreetti, G. Calestani, F. Ugozzoli, A. Arduini, E. Ghidini, A. Pochini, R. Ungaro, *J. Incl. Phenom*. **1987, 5**, 123−126. − [6e] L. M. Engelhardt, B. M. Furphy, J. M. Harrowfield, D. L. Kepert, A. H. White, F. R. Wilner, *Aust. J. Chem*. **1988**, *41*, 1465−1476.
[7] V. G. Gibson, C. Redshaw, W. Clegg, M. R. J. Elsegood, *Chem. Commun*. **1997**, 1605−1606.
[8] G. V. Ellert, V. V. Tsakin, Yu. N. Mikhailov, V. G. Kuznetsov, *Russ. J. Inorg. Chem*. **1965**, *10*, 7, 858−862.
[9] S. B. Akona, J. Fawcett, J. H. Holloway, D. R. Russel, I. Leban, *Acta Cryst*. **1991**, C47, 45−48.
[10] D. E. Fenton, in *Comprehensive Coordination Chemistry, Vol. 3*, (Eds.: J. A. McCleverty, R. D. Gillard, G. Wilkinson), Pergamon Press, Oxford, **1987**, 1−80.
[11] [11a] D. C. Luehrs, K. Bowman-James, *J. Mol. Struc*. **1994**, *321*, 251−254. − [11b] Y. Habata, S. Akatori, *J. Chem. Soc., Dalton Trans.* **1996**, 3871−3882. − [11c] N. Kasuga, S. Nakahama, K. Yamaguchi, Y. Ohashi, K. Hori, *Bull. Chem. Soc. Jpn*. **1991**, *64*, 3548−3556.
[12] E. Weiss, H. Koster, *Chem. Ber*. **1977**, *110*, 717−720
[13] [13a] J. M. Harrowfield, M. I. Ogden, W. R. Richmond, A. H. White, *J. Chem. Soc., Chem. Commun*. **1991**, 1159−1161. − [13b] R. Assmus, V. Böhmer, J. M. Harrowfield, M. I. Ogden, W. R. Richmond, B. W. Skelton, A. H. White, *J. Chem. Soc., Dalton Trans.* **1993**, 2427−2433.
[14] [14a] R. Ungaro, A. Casnati, F. Ugozzoli, A. Pochini, J.-F. Dozol, C. Hill, H. Rouquette, *Angew. Chem.* **1994**, *106*, 1551; *Angew. Chem. Int. Ed. Engl*. **1994**, *33*, 1506−1509. − [14b] P. Thuéry, M. Nierlich, J. C. Bryan, V. Lamare, J.-F. Dozol, Z. Asfari, J. Vicens, *J. Chem. Soc., Dalton Trans.* **1997**, 4191−4202.
[15] C. D. Gutsche, *Calixarenes*, Monographs in Supramolecular Chemistry, The Royal Society of Chemistry, Cambridge, **1989**, 97−98.
[16] F. Inokuchi, Y. Miyahara, T. Inazu, S. Shinkai, *Angew. Chem.* **1995**, *107*, 1459−1462; *Angew. Chem. Int. Ed. Engl*. **1995**, *34*, 1364−1366.
[17] A. Zanotti-Gerosa, E. Solari, C. Floriani, A. Chiesi-Villa, C. Rizzoli, *Chem. Commun*. **1997**, 183−184.

[I98173]

Ligand-to-Ligand Charge Transfer in (2,2′-Biquinoline)bis(cyclopentadienyl)-zirconium(IV) – Absorption and Emission in the Visible Range

Horst Kunkely and Arnd Vogler*

Institut für Anorganische Chemie, Universität Regensburg,
D-93040 Regensburg, Germany

Received August 11, 1998

Keywords: Charge transfer / Absorption spectra / Luminescence / Metallocenes / Zirconium complexes

The lowest energy electronic transition of [(cyclopentadienyl)$_2$Zr^{IV}(2,2′-biquinoline)]$^{2+}$, which appears in absorption at λ_{max} = 360 nm and in emission at λ_{max} = 518 nm, is of the Cp$^-$ → biq ligand-to-ligand charge-transfer-type.

Coordination compounds which contain reducing and oxidizing ligands are frequently characterized by long-wavelength ligand-to-ligand charge-transfer (LLCT) absorptions in their electronic spectra[1][2]. Such optical electron transfer between two ligands is a special type of light-induced charge separation which plays an important role in areas such as artificial photosynthesis[3] and nonlinear optics[4]. In the case of LLCT a metal mediates the electronic interaction between donor and acceptor. Appropriate acceptor ligands include 1,2-diimines (e.g. 2,2′-bipyridyl), while anions such as thiolates can be donor ligands. As yet little attention has been paid to organometallic compounds, although recently photoreactive LLCT states have been identified in complexes with alkyl anions as donor ligands[5][6][7][8]. However, in general, the large potential of organometallic compounds for optical LLCT has not yet been utilized. The present report includes an investigation of novel features such as $C_5H_5^-$ ligands as donors and an early transition metal as a template and mediator. Moreover, we report on emission from a LLCT state of an organometallic compound, which we believe to be a new observation. Finally, some intriguing analogies between our target compound and the photosynthetic reaction center will be mentioned.

The desired complex [Cp$_2$Zr(biq)]$^{2+}$ (Cp$^-$ = $C_5H_5^-$ and biq = 2,2′-biquinoline) was designed taking into account the following considerations. Cp$^-$ is a suitable donor ligand as indicated by the appearance of long-wavelength LMCT absorptions in the spectra of complexes such as Cp_2Fe^+[2][9][10][11] or $CpReO_3$[2][12]. The metallocene moiety Cp_2M^{IV} (M = Ti, Zr, Hf) provides an obliquely oriented pair of Cp$^-$ ligands and a d^0 metal center, which can provide no interference from low-energy LF and MLCT states. Moreover Zr^{IV}, in contrast to Ti^{IV}, is barely oxidizing[2][13]. Accordingly, low-energy Cp$^-$ → Zr^{IV} LMCT transitions do not occur. 1,2-Diimines such as 2,2′-bipyridyl (bipy) or 9,10-phenanthroline (*o*-phen) are well-known electron acceptors in CT transitions[9][10][14][15]. Complexes of the type [Cp$_2$Ti^{IV}(diimine)]$^{2+}$, with bipy and *o*-phen, have been prepared previously[16]. Unfortunately, the corresponding Zr^{IV} complexes are not stable, and undergo a dissociation owing to the tendency of Cp_2ZrL_2 complexes to expand their coordination sphere to Cp_2ZrL_3[17][18][19]. However, if bulkier ligands are introduced Cp_2ZrL_2 complexes become stable because access to a further ligand is blocked[18]. As a bidentate diimine the ligand biq meets this requirement, and the complex [Cp$_2$Zr(biq)]$^{2+}$ is prepared by the reaction of $Cp_2Zr(THF)(CF_3SO_3)_2$[19] with biq. Mixing of the colourless solutions leads to the precipitation of a bright yellow crystalline material.

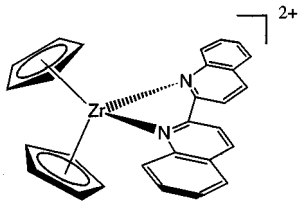

The electronic spectrum of [Cp$_2$Zr(biq)]$^{2+}$ (Figure 1) shows absorptions at λ_{max} = 360 (ε/dm^3 mol^{-1} cm^{-1} = 7700), 341 (8800), 329 (7400), 315 (5300), 304 (sh, 4300), 262 nm (20400). The bands at 341, 329, 315, 304, and 262 nm appear at almost the same wavelength as those of free biq and are thus attributed to intraligand (IL) transitions. However, while Cp_2Zr^{IV} compounds such as Cp_2ZrCl_2 and related complexes are colourless, [Cp$_2$Zr(biq)]$^{2+}$ is bright yellow owing to a new absorption at λ_{max} = 360 nm which extends into the visible spectral region. The complex is solvatochromic, and the longest wavelength absorption undergoes a blue shift with increasing solvent polarity (Figure 2[20]). This band is assigned to an LLCT transition[1][2] from the $(Cp^-)_2$ donor ligands to the biq acceptor, and the intensity of the band is consistent with this assignment. Complexes of the type $Cp_2M^{IV}L_2$ with M = Ti, Zr, and Hf including [Cp$_2$Ti(diimine)]$^{2+}$ are pseudotetrahedral[16] (C_{2v}). The highest occupied orbitals of such Cp_2ML_2 compounds

 © WILEY-VCH Verlag GmbH, D-69451 Weinheim, 1998 1434–1948/98/1212–1863 $ 17.50+.50/0

Figure 1. Electronic absorption (a, – – – – –) and emission (e, ·····) spectra of $2.18 \cdot 10^{-5}$ M $[Cp_2Zr(biq)]^{2+}$ at room temp. under argon in THF in a 1-cm cell; emission: $\lambda_{exc} = 380$ nm, intensity in arbitrary units

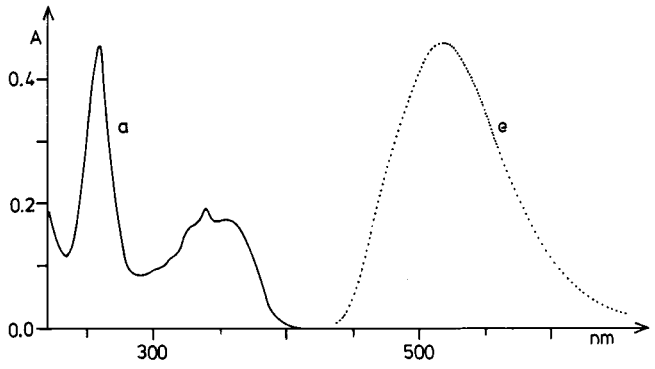

Figure 2. Energies of the LLCT absorption ($\tilde{\nu}_{max}$) of $[Cp_2Zr(biq)]^{2+}$ plotted against solvent parameters E^*_{MLCT}[20]

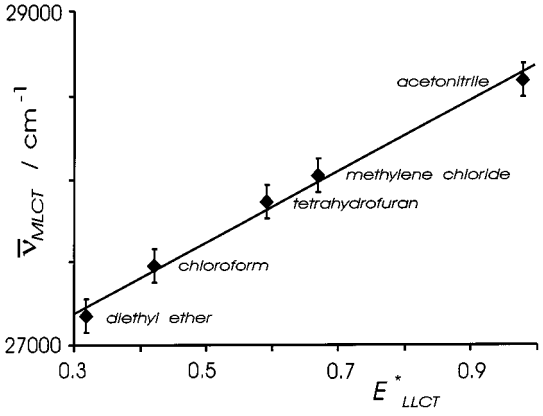

are derived from the Cp^- ligands and are of the b_2, b_1, a_2, and a_1 symmetry in close energetic proximity[21]. The LUMO is a π^* orbital (b_1) at the diimine ligand. While the $b_2 \rightarrow b_1$ transition is forbidden the other $Cp^- \rightarrow$ biq LLCT transitions ($b_1 \rightarrow b_1$, $a_2 \rightarrow b_1$ and $a_1 \rightarrow b_1$) are allowed[22].

The cation $[Cp_2Zr(biq)]^{2+}$ shows a bright yellow/green luminescence at $\lambda_{max} = 518$ nm in solution (Figure 1) and 524 nm in the solid state at room temp. The quantum yield of the emission is $\phi = 0.01$ (calibrated by comparison with rhodamine B)[23]. This luminescence is not of the intraligand (biq) type, and this is indicated by the absence of any vibrational structure at 77 K, since at low temperatures structured bands are typical for intraligand emissions[24][25]. The excitation spectrum matches the absorption spectrum and it is concluded that the luminescence originates from the lowest energy LLCT excited state, which is most likely to be a triplet state, in agreement with the general behavior of diamagnetic complexes with metals of the second transition row.

In summary, the lowest energy transition of $[Cp_2Zr(biq)]^{2+}$ is of the LLCT type and involves an electron transfer from the $(Cp^-)_2$ moiety to biq (absorption) and back (emission). The complex shares some remarkable features with the photosynthetic reaction center, which is characterized by a pair of two bacteriochlorophyll molecules in close proximity but in an oblique orientation. In the primary photochemical step this "special pair" undergoes a light-induced electron transfer to an electron acceptor. A variety of models have been developed to mimic the initial charge separation in the reaction center. In $[Cp_2Zr(biq)]^{2+}$ the special pair corresponds to both $C_5H_5^-$ ligands, which are also planar π-electron systems in an oblique orientation. However, in both the natural system and artificial models[3] charge separation takes place by excited-state electron transfer, whilst in our organometallic model it occurs as an optical transition since the metal facilitates an electronic coupling of donor and acceptor.

Other aspects of our observations may be also of interest as metallocene dihalides are well known to exhibit antitumor activity[26][27]. Since extended planar ligands can intercalate in DNA[28] the luminescence of $[Cp_2Zr(biq)]^{2+}$ and related compounds may be utilized to monitor such interactions. In this context it should be also mentioned that a few reports on the luminescence of some other d^0 complexes[29][30][31][32][33] including metallocene derivatives[34][35][36] have appeared recently. In these cases the emission apparently originates from LMCT excited states.

This work was supported by the *Deutsche Forschungsgemeinschaft*.

Experimental Section

General: Absorption spectra: Hewlett Packard 8452A diode array spectrophotometer, spectrograde solvents. – Emission and excitation spectra: Hitachi 850 spectrofluorometer equipped with a Hamamatsu 928 photomultiplier for measurements up to 900 nm. – Luminescence spectra: Corrected for monochromator and photo-multiplier efficiency variations. Absolute emission quantum yields were determined by comparison of the integrated emission intensity with that of Rhodamine B under identical conditions such as exciting wavelength, optical density, and apparatus parameters.

Preparation of [$Cp_2Zr(biq)(CF_3SO_3)_2$]: All solvents were dried and saturated with argon. The starting chemicals were used as purchased without further purification. A solution of 1.28 g ($5 \cdot 10^{-3}$ mol) of $AgCF_3SO_3$ in 10 ml of THF was added to a solution of 0.73 g ($2.5 \cdot 10^{-3}$ mol) of Cp_2ZrCl_2 in 10 ml of THF. The combined solutions were stirred for 30 min. AgCl precipitated and was removed by filtration. A solution of 1.02 g ($4 \cdot 10^{-3}$ mol) of biq in 40 ml of THF was added to the filtrate under strirring. The solution immediately turned intensely yellow and yellow crystals started to deposit. After 1 h, the crude product was collected by filtration and washed with a little THF/ether, and dried under vacuum. The product was purified by repeated recrystallization from THF/ether, yield: 0.6 g (31%). – $C_{30}F_6H_{22}N_2O_6S_2Zr$ (775.86): calcd. C 46.44, H 2.86, N 3.61; found C 46.52, H 2.98, N 3.69.

[1] A. Vogler, H. Kunkely, *Comments Inorg. Chem.* **1990**, *9*, 201.
[2] A. Vogler, H. Kunkely, *Comments Inorg. Chem.* **1997**, *19*, 283.
[3] For a recent review, see: A. Harriman, J. P. Sauvage, *Chem. Soc. Rev.* **1996**, *25*, 41.
[4] For a recent review, see: K. Clays, E. Hendrickx, T. Verbiest, A. Persoons, *Adv. Mater.* **1998**, *10*, 463.
[5] D. J. Stufkens, A. Vlcek, Jr., *Spectrum* **1996**, *9*, 2.
[6] H. Kunkely, A. Vogler, *J. Organomet. Chem.* **1993**, *453*, 269.

[7] H. Kunkely, A. Vogler, *J. Photochem. Photobiol. A: Chem.* **1996**, *94*, 135.
[8] H. Kunkely, A. Vogler, *J. Organomet. Chem.* **1998**, *553*, 517.
[9] A. B. P. Lever, *Inorganic Electronic Spectroscopy*, Elsevier Science B.V., Amsterdam, **1984.**
[10] G. L. Geoffrey, M.S. Wrighton, *Organometallic Photochemistry*, Academic Press, New York, **1979.**
[11] Y. S. Sohn, D. N. Hendrickson, H. B. Gray, *J. Am. Chem. Soc.* **1971**, *93*, 3603.
[12] W. A. Herrmann, F. E. Kühn, D. A. Fiedler, M. R. Mattner, M. R. Geisberger, H. Kunkely, A. Vogler, S. Steenken, *Organometallics* **1995**, *14*, 5377.
[13] H. Kunkely, A. Vogler, *Inorg. Chim. Acta* **1997**, *254*, 195.
[14] M. A. Fox, M. Chanon, *Photoinduced Electron Transfer*, Elsevier, Amsterdam, **1988**.
[15] K. Kalyanasundaram, *Photochemistry of Polypyridine and Porphyrin Complexes*, Academic Press, London, **1992**.
[16] U. Thewalt, Berhalter, *J. Organomet. Chem.* **1986**, *302*, 193.
[17] U. Thewalt, W. Lasser, *J. Organomet. Chem.* **1984**, *276*, 341.
[18] W. Lasser, U. Thewalt, *J. Organomet. Chem.* **1986**, *302*, 201.
[19] U. Thewalt, W. Lasser, *Z. Naturforsch., B* **1983**, *38b*, 1501.
[20] D. M. Manuta, A. J. Lees, *Inorg. Chem.* **1983**, *22*, 3825.
[21] M. R. M. Bruce, A. Kenter, D. R. Tyler, *J. Am. Chem. Soc.* **1984**, *106*, 639.
[22] C. Herzberg, *Molecular Spectra and Molecular Structure*, Van Nostrand Reinhold Company, New York, **1966**.
[23] C. A. Parker, W. T. Rees, *Analyst (London)* **1960**, *85*, 587.
[24] A. Juris, S. Campagna, I. Bidd, J.-M. Lehn, R. Ziessel, *Inorg. Chem.* **1988**, *27*, 4007.
[25] L. Wallace, C. Woods, D. P. Rillema, *Inorg. Chem.* **1995**, *34*, 2875 and references cited therein.
[26] For reviews, see: [26a] P. Köpf-Maier, H. Köpf, *Drugs Future* **1986**, *11*, 297. – [26b] P. Köpf-Maier, H. Köpf, *Struct. Bonding* **1988**, *70*, 105. – [26c] P. Köpf-Maier, H. Köpf, in *Metal Compounds in Cancer Chemotherapy* (Ed.: S. P. Fricker), Chapman & Hall, London, **1994**, p.109.
[27] M. M. Harding, G. Mokdsi, J. P. Mackay, M. Prodigalidad, S. Wright Lucas, *Inorg. Chem.* **1998**, *37*, 2431.
[28] R. E. Holmlin, E. D. A. Stemp, J. K. Barton, *J. Am. Chem. Soc.* **1996**, *118*, 5236.
[29] H. Kunkely, T. Türk, C. Teixeira, C. de Meric de Bellefon, W. A. Herrmann, A. Vogler, *Organometallics* **1991**, *10*, 2090.
[30] T. P. Pollagi, T. C. Stoner, R. F. Dallinger, T. M. Gilbert, M. D. Hopkins, *J. Am. Chem. Soc.* **1991**, *113*, 703.
[31] K. S. Heinselman, M. D. Hopkins, *J. Am. Chem. Soc.* **1995**, *117*, 12340.
[32] D. S. Williams, D. W. Thompson, A. V. Korolev, *J. Am. Chem. Soc.* **1996**, *118*, 6526.
[33] D. S. Williams, A. V. Korolev, *Inorg. Chem.* **1998**, *37*, 3809.
[34] B. R. Pfennig, M. E. Thompson, A. B. Bocarsly, *J. Am. Chem. Soc.* **1989**, *111*, 8947.
[35] S. Paulson, B. P. Sullivan, J. V. Caspar, *J. Am. Chem. Soc.* **1992**, *114*, 6906. V. W.-W. Yam, G.-Z. Qi, K.-K. Cheung, *J. Organomet. Chem.* **1997**, *548*, 289.

[I98273]

An Amidinate Ligand with a Pendant Amine Functionality; Synthesis of a Vanadium(III) Complex and Ethene Polymerization Catalysis[+]

Menno J. R. Brandsma, Edward A. C. Brussee, Auke Meetsma, Bart Hessen*, and Jan H. Teuben

Center for Catalytic Olefin Polymerization, Department of Chemistry, University of Groningen, Nijenborgh 4, NL-9747 AG Groningen, The Netherlands
E-mail: hessen@chem.rug.nl

Received September 3, 1998

Keywords: Vanadium / Amidinate / Ethene Polymerization / Catalysis

A new type of amidinate ancillary ligand has been prepared, which incorporates a pendant tertiary amine functionality. The crystal structure of a vanadium(III) derivative, $[SiMe_3NC(Ph)NCH_2CH_2NMe_2]VCl_2(THF)$ (**1**), shows that the ligand can adopt a facial geometry, with an unusual distortion of the amidinate nitrogen bearing the pendant functionality. With $AlEt_2Cl$ cocatalyst the compound **1** produces a single-site catalytic system for the polymerization of ethene.

Amidinates $[RC(NR')_2]^-$ are extensively being used as ligands for transition metals, lanthanides as well as main group elements, in which they act most frequently as bidentate 4-electron monoanionic ligands.[1] Various routes are available to prepare amidinates with a range of substitution patterns, and steric and electronic features of these ligands are readily varied.[2] For Group 4 transition metals, amidinates have been used as ancillary ligands in olefin polymerization catalysts.[3] The applicability of these ligands could be enhanced considerably with the ability to introduce additional functionalities as pendant groups on the amidinate ligand framework. In this contribution we describe the synthesis of such a functionalized amidinate, $[SiMe_3NC(Ph)NCH_2CH_2NMe_2]^-$, which has a pendant (dimethylamino)ethyl group attached to one of the amidinate nitrogens. A *facial* coordination mode of this ligand is illustrated by the structure of a vanadium(III) derivative, $[SiMe_3NC(Ph)NCH_2CH_2NMe_2]VCl_2(THF)$ (**1**), indicating that the new ligand may be compared with other, well-known face-capping monoanionic ligands like tris(pyrazoyl)borate and cyclopentadienyl. Compound **1** is active in the polymerization of ethene when activated by $AlEt_2Cl$ cocatalyst.

The synthesis of the (dimethylamino)ethyl-functionalized benzamidinate $[SiMe_3NC(Ph)NCH_2CH_2NMe_2]^-$ is based on the well-known reaction of lithium trimethylsilylamides with benzonitrile to give lithium *N*-(trimethylsilyl)benzamidinates.[2a] A suitable silylamide, $Me_2NCH_2CH_2NHSiMe_3$ was prepared by reaction of $Me_2NCH_2CH_2NH_2$ with Me_3SiCl and NEt_3 as base (in a preparation similar to that of $Me_2NCH_2CH_2N(Me)SiMe_3$[4a]), and isolated by vacuum distillation. Lithiation with *n*BuLi yields the lithium amide $Me_2NCH_2CH_2N(Li)SiMe_3$ which was obtained as a crystalline solid.[4b] This lithium amide readily reacts with benzonitrile in THF solvent to give the functionalized lithium benzamidinate $[SiMe_3NC(Ph)NCH_2CH_2NMe_2]Li$ (Scheme 1). The route appears to be quite versatile, and this methodology should be applicable to a range of *N*-monofunctionalized, *N'*-trimethylsilyl benzamidinates.

Scheme 1

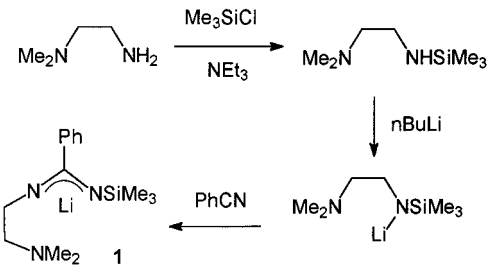

Reaction of one equivalent of $[SiMe_3NC(Ph)NCH_2CH_2NMe_2]Li$ with $VCl_3(THF)_3$ in THF produces the highly air sensitive, paramagnetic (by ^1H NMR), green V(III) mono(amidinate) dichloride complex[5] $[SiMe_3NC(Ph)NCH_2CH_2NMe_2]VCl_2(THF)$ (**1**), which was obtained as crystals suitable for X-ray diffraction by diffusion of pentane vapor into a THF solution of the compound. The structure of **1** (Figure 1) shows a distorted octahedral coordination of the metal, with the functionalized amidinate ligand adopting a facial geometry. The amidinate nitrogen bearing the (dimethylamino)ethyl functionality, N(2), is distinctly non-planar, the sum of the angles around N(2) being 336.4° as compared to 359.9° for N(1). This is unusual for metal amidinates, and may suggest that the ligand has partial amido-imine character. Indeed, the V−N(2) distance is 0.1 Å shorter than V−N(1), but the C(1)−N distances in the amidinate backbone differ only slightly (if significantly), with C(1)−N(1) being 0.017 Å

[+] Netherlands Institute for Catalysis Research (NIOK) publication no. RUG-98-4-03

 © WILEY-VCH Verlag GmbH, D-69451 Weinheim, 1998 1434−1948/98/1212−1867 $ 17.50+.50/0

Figure 1. ORTEP diagram of the molecular structure of **1**. Hydrogen atoms are omitted for clarity. The unlabeled atoms are carbon[a]

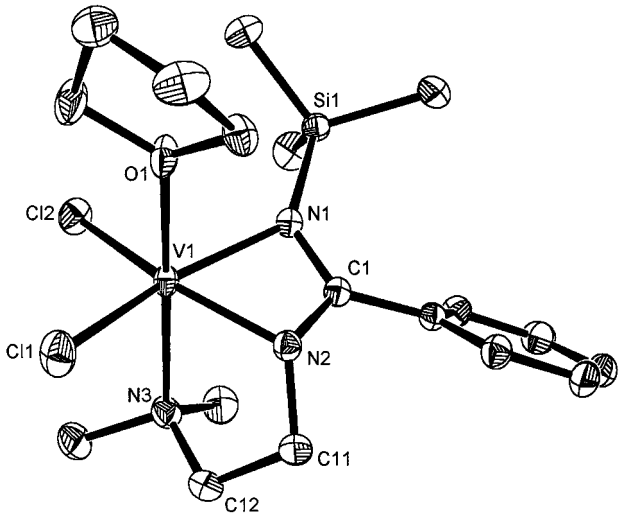

[a] Selected interatomic distances [Å] and angles [°]: V−Cl(1) = 2.3477(5), V−Cl(2) = 2.3153(4), V−O = 2.103(1), V−N(1) = 2.124(1), V−N(2) = 2.016(1), V−N(3) = 2.230(1), C(1)−N(1) = 1.322(2), C(1)−N(2) = 1.339(2), Cl(1)−V−Cl(2) = 106.47(2), O−V−N(3) = 172.50(5), N(1)−V−N(2) = 64.10(4), N(1)−V−N(3) = 100.62(5), N(2)−V−N(3) = 74.91(5), N(1)−V−Cl(1) = 156.44(3), N(2)−V−Cl(2) = 151.99(4), V−N(2)−C(1) = 93.77(8), V−N(2)−C(11) = 121.41(9), C(11)−N(2)−C(1) = 121.21(9), N(1)−C(1)−N(2) = 111.4(1).

(8σ) shorter than C(1)−N(2). A highly asymmetrically bound amidinate was also observed in $[MeC(N\mathit{i}Pr)_2]_2Ge$ (with a relatively small nonplanarity of one of the amidinate nitrogen atoms), but this only showed similarly small differences in the C−N distances of the amidinate backbone.[6]

The geometry around the metal center in **1** is significantly more distorted than in other octahedral vanadium(III) complexes with monoanionic tridentate ligands such as Tp* VCl_2L (Tp* = (3,5-dimethyl-1-pyrazoyl)borate; L = DMF,[7] 4-methylpyridine[8]). In the latter complexes, the N−V−N angles and V−N distances involving the tridentate ligand are all rather similar (around 86° and 2.12 Å respectively), whereas in **1** both features vary over a considerable range [from 64.10(4)° to 100.62(5)° and from 2.016(1) Å to 2.230(1) Å respectively].

When activated with $AlEt_2Cl$ (20 mol per mol V), **1** catalyzes the polymerization of ethene in toluene. Table 1 shows activity and GPC data for 30 minutes ethene polymerization runs at three different temperatures (30, 50, and 80°C). The catalyst is most active at 30°C, with a productivity of 447 kg mol^{-1} h^{-1} bar^{-1}, and the product molecular weight distribution is characteristic for the presence of a single active site. At 50°C the overall productivity drops substantially, indicating a limited thermal stability of the catalyst. At 80°C catalyst decomposition is rapid, and the molecular weight distribution of the polyethene formed is bimodal. For comparison, polymerization runs with a vanadium catalyst with an unfunctionalized amidinate ligand, $\{[PhC(NSiMe_3)_2]VCl_2(THF)\}_2$ (**2**), are given in Table 1 as well. At 30°C this system has a substantially lower activity than **1**/$AlEt_2Cl$, and forms polyethene with a significantly higher molecular weight. The catalyst activity is higher at 50°C but this is accompanied by a broadening of the polymer molecular weight distribution. Again, this system suffers from catalyst degradation at 80°C accompanied by formation of a bimodal distribution of the PE product. Thus the introduction of a pendant Lewis-base functionality on the benzamidinate ligand significantly increases the polymerization activity of the homogeneous V^{III} amidinate catalyst system at temperatures close to ambient, but does not improve the thermal stability of the catalytic species.

In conclusion, we have developed a convenient route to a new amidinate ligand with a tethered dialkylamine functionality. A vanadium(III) complex with this ligand was prepared and structurally characterized, revealing the possibility of this ligand to adopt a facial coordination mode. As such, this ligand is complementary to the familiar, more symmetrical facial monoanionic 6-electron tridentate ligands such as tris(pyrazoyl)borate and cyclopentadienyl. We are presently pursuing the scope of this synthesis method for the attachment of other functionalities to the benzamidinate framework and the use of these ligands with a variety of transition metals.

This investigation was carried out in connection with *NIOK*, the *Netherlands Institute for Catalysis Research*, and supported by the *Department of Economic Affairs of the Netherlands.*

Experimental Section

General: All experiments were performed under nitrogen atmosphere using standard Schlenk and glove-box techniques unless mentioned otherwise. Deuterated solvents (Aldrich) were dried over Na/K alloy and vacuum transferred before use. Other solvents were distilled from Na/K alloy or Na (toluene) before use. For the polymerization experiments toluene (Aldrich, 99.8%) was percolated over molecular sieves (3 Å) before use, ethene (AGA polymer

Table 1. Ethene polymerization catalyzed by **1** and **2** with $AlEt_2Cl$ cocatalyst[a]

Catalyst	T [°C]	PE yield [g]	activity [kg $mol^{-1}h^{-1}bar^{-1}$]	M_w ($\times 10^{-6}$)	M_w/M_n
1	30	13.40	447	0.76	2.1
1	50	7.25	242	0.54	2.1
1	80	1.38	46	0.22	4.5[b]
2	30	3.87	129	1.60	2.4
2	50	11.18	373	1.37	3.8
2	80	8.38	279	1.46	10.0[b]

[a] Toluene solvent, 6 bar ethene, 10 μmol V, V:Al = 1:20, 30 min run time. − [b] Bimodal distribution.

grade) was passed over a supported copper scavenger (BASF R 3-11) and molecular sieves (3 Å) before being passed to the reactor. − NMR spectra were run on Varian Gemini 200 and VXR 300 spectrometers. − IR spectra were recorded from Nujol mulls between KBr disks on a Mattson-4020 Galaxy FT-IR spectrophotometer. − GPC analyses were performed on solutions of the polymers in distilled 1,2,4-trichlorobenzene on a PL-GPC210 instrument of Polymer Laboratories. − Elemental analyses were carried out at the Micro-Analytical Department of the University of Groningen.

Preparation of (N,N-dimethyl-N′-trimethylsilyl)ethylene Diamine: To a solution of (*N,N*-dimethyl)ethylenediamine (35.4 g, 0.4 mol) and an excess of triethylamine (1.28 mol) in 200 mL of 1,4-dioxane, trimethylsilylchloride (66.6 ml, 0.44 mol) was added dropwise in 20 minutes. A white precipitate (triethylamine hydrochloride) formed, and the mixture was stirred for 16 h. The mixture was filtered and the residual salts extracted with 3 × 50 ml of diethyl ether. The combined filtrates were concentrated under reduced pressure, and pentane was added to precipitate any remaining salts. The mixture was filtered, the filtrate concentrated again and distilled under reduced pressure. The fraction boiling at 73.5−74.0°C (45 mmHg) consisted of the title compound (36.06 g, 0.22 mol, 50%). − ^{1}H NMR ([D$_6$]benzene): δ = 0.00 [s, 9 H, Si(C*H*$_3$)$_3$], 0.98 (s, 1 H, N*H*), 2.17 (s, 6 H, N(C*H*$_3$)$_2$), 2.24 (t, $^3J_{HH}$ = 6.5, 2 H, C*H*$_2$), 2.74 (t, $^3J_{HH}$ = 5.3, 2 H, C*H*$_2$).

Preparation of N′-lithio(N,N-dimethyl-N′-trimethylsilyl)ethylene Diamine: In 30 minutes, 30 mL of a 2.5 M *n*BuLi/hexane solution was added to a solution of 12.07 g (75 mmol) of (*N,N*-dimethyl-*N′*-trimethylsilyl)ethylene diamine in 200 ml of ether at −50°C. The mixture was allowed to warm to room temperature after which the volatiles were removed in vacuo. This yielded 11.0 g (66 mmol, 88%) of the title compound as a white solid. − ^{1}H NMR ([D$_8$]toluene/[D$_8$]THF): δ = 0.19 [s, 9 H, Si(C*H*$_3$)$_3$], 2.06 [s, 6 H, N(C*H*$_3$)$_2$], 2.38 (br, 2 H, C*H*$_2$), 3.23 (t, $^3J_{HH}$ = 5.3, 2 H, C*H*$_2$). − ^{13}C NMR ([D$_8$]toluene/[D$_8$]THF): δ = 62.51 (*C*NLi), 45.70, 45.21 (Me$_2$N*C*H$_2$, N*C*H$_3$), −2.15 (Si(*C*H$_3$)$_3$). − C$_7$H$_{19}$LiN$_2$Si (166.27): calcd. C 50.57, H 11.52, N 16.85; found C 50.22, H 11.37, N 15.94.

Preparation of [Me$_3$SiNC(Ph)NCH$_2$CH$_2$NMe$_2$]Li: To a solution of 0.98 g (5.88 mmol) of *N′*-lithio(*N,N*-dimethyl-*N′*-trimethylsilyl)ethylene diamine in 20 ml of THF, 0.60 ml of benzonitrile was added at −40°C. After 30 minutes the solvent was removed in vacuo and the residue stripped of remaining THF by repeatedly stirring with portions of pentane which were then pumped off. This yields the title compound as a pale yellow powder. Yield: 1.29 g (4.76 mmol, 81%). − ^{1}H NMR ([D$_6$]benzene): δ = 0.01 [s, 9 H, Si(C*H*$_3$)$_3$], 1.96 [s, 6 H, N(C*H*$_3$)$_2$], 2.10 (t, $^3J_{HH}$ = 5.3, 2 H, C*H*$_2$), 2.82 (t, $^3J_{HH}$ = 5.3, 2 H, C*H*$_2$), 7.2−7.1 (5 H, Ph). − ^{13}C NMR (C$_6$D$_6$): δ = 178.13 (N*C*N), 143.59 (Ph *ipso*-C), 128.31, 126.75, 126.43 (Ph *C*H), 58.38 (N*C*H$_2$), 41.70, 41.21 (Me$_2$N*C*H$_2$, N*C*H$_3$), −1.86 [Si(*C*H$_3$)$_3$].

Preparation of [SiMe$_3$NC(Ph)NCH$_2$CH$_2$NMe$_2$]VCl$_2$(THF) (**1**): For this synthesis the lithium salt of the ligand was conveniently generated in situ. To a solution of 1.43 g (8.58 mmol) of *N′*-lithio(*N,N*-dimethyl-*N′*-trimethylsilyl)ethylene diamine in 90 ml of THF 0.88 ml (8.62 mmol) of benzonitrile was added at −40°C. The mixture was allowed to warm to room temperature and stirred for 30 min. Subsequently, the mixture was cooled to −50°C and 3.32 g (8.88 mmol) of VCl$_3$(THF)$_3$ was added. The mixture was allowed to warm to room temperature and was stirred overnight, giving a dark brown solution. The solvent was removed in vacuo and the residue was extracted with 50 ml of diethyl ether. The solvent was removed from the extract in vacuo, and the residue dissolved in 5 mL of THF. Slow diffusion of pentane vapor into the solution resulted in formation of green crystals of **1** (2.78 g, 6.1 mmol, 58%). − ^{1}H NMR ([D$_6$]benzene): δ = 12.68 (Δν$_{1/2}$ = 150 Hz), 2.02 (Δν$_{1/2}$ = 150 Hz), −0.94 (Δν$_{1/2}$ = 250 Hz). − IR (Nujol, KBr): $\tilde{\nu}$ = 1503 (m), 1400 (m), 1240 (m), 1190 (w), 1086 (w), 1044 (m), 1022 (s), 943 (m), 912 (m), 866 (s), 839 (s), 797 (m), 756 (w), 721 (m), 691 (w), 517 (m), 496 (w), 478 (w) cm^{-1}. − C$_{18}$H$_{32}$Cl$_2$N$_3$OSiV (456.40): calcd. C 47.37, H 7.07, N 9.21; found C 47.49, H 7.10, N 9.24.

Crystal Structure Analysis of **1**: Enraf-Nonius CAD4-F diffractometer, Mo-K_α radiation (λ = 0.71073 Å) , T = 130 K; triclinic, $P\bar{1}$, a = 10.286(1), b = 10.461(1), c = 10.710(1) Å, α = 93.648(5), β = 100.075(5), γ = 98.924(5)°, V = 1114.1(2) Å^3, Z = 2, D_x = 1.361 g cm^{-3}, μ = 7.5 cm^{-1}. The structure was solved by Patterson methods and extended by direct methods applied to difference structure factors. A final refinement on F^2 converged at $wR(F^2)$ = 0.0766 for 4849 reflections with $F_o^2 \geq 0$ and $R(F)$ = 0.0274 for 4524 reflections with $F_o \geq 4.0\,\sigma(F_o)$ and 363 parameters. Crystallographic data (excluding structure factors) for the structure reported in this paper have been deposited with the Cambridge Crystallographic Data Centre as supplementary publication no. CCDC-102816. Copies of the data can be obtained free of charge on application to CCDC, 12 Union Road, Cambridge CB2 1EZ, UK [Fax: int. code + 44(1223)336-033; E-mail: deposit@ccdc.cam.at.uk].

Preparation of {[PhC(NSiMe$_3$)$_2$]VCl$_2$(THF)}$_2$ (**2**): To a suspension of VCl$_3$(THF)$_3$ (5.28 g, 14.1 mmol) in 80 mL of THF, cooled to −78°C, was added 4.80 g (14.0 mmol) of [PhC(NSiMe$_3$)$_2$]-Li(THF). The mixture was allowed to warm to room temperature while stirring, and the resulting brown-green solution was stirred for 4 h. Subsequently, the volatiles were removed in vacuo and the residue was stirred with 20 mL of pentane which was subsequently pumped off. Extraction with diethyl ether and cooling the extract to −30°C yielded a mixture of brown **2** and green [PhC(NSiMe$_3$)$_2$]VCl$_2$(THF)$_2$[5c] which was dissolved in 50 mL of toluene and warmed to 50°C for 10 min after which the solvent was pumped off. Recrystallization from diethyl ether at −30°C yielded 3.50 g (3.83 mmol, 55% yield on amidinate) of brown crystalline **2**. − ^{1}H NMR ([D$_6$]benzene): δ 11.24−7.36 (Δν$_{1/2}$ = 70−380 Hz, 5 H, Ph), 3.64 (Δν$_{1/2}$ = 90 Hz, 4 H, α-THF), 1.47 (Δν$_{1/2}$ = 120 Hz, 4 H, β-THF), −0.51(Δν$_{1/2}$ = 120 Hz, 18 H, SiMe$_3$). − IR (Nujol mull, KBr, cm^{-1}): $\tilde{\nu}$ = 1503(w), 1445(s), 1361(s), 1261(m), 1248(s), 1175(w), 1074(w), 1047(w), 1030(w), 1001(m), 988(s), 922(w), 841(s), 785(m), 764(m), 743(w), 704(m), 690(m), 530(m), 446(w). − C$_{17}$H$_{31}$Cl$_2$N$_2$OSi$_2$V (457.46): calcd. C 44.63, H 6.83, Cl 15.50, N 6.12, V 11.14; found C 44.34, H 6.61, Cl 15.78, N 6.58, V 10.91.

Ethene Polymerization Experiments: Polymerizations were carried out in a fully temperature and pressure controlled Medimex 1 L stainless steel autoclave. The autoclave was charged with 250 mL of toluene containing 0.10 mmol of AlEt$_2$Cl, brought to the desired temperature and saturated with ethene (6 bar). Subsequently, a solution of the catalyst precursor (10 μmol of vanadium) with 0.10 mmol of AlEt$_2$Cl in 5 mL of toluene (mixed 15 min prior to injection) was injected into the reactor. During the reaction the monomer was fed continuously to the reactor. After 30 min the reaction was quenched by injection of 10 mL of methanol. The contents of the reactor were stirred in 100 mL of acidified methanol for 1 h. The precipitated polymer was rinsed repeatedly with ethanol and dried at 60°C for 2 d.

[1] For recent references see: [1a] H. W. Roesky, B. Meller, M. Noltemeyer, H.-G. Schmidt, U. Scholtz, G. M. Sheldrick, *Chem. Ber.* **1988**, *121*, 1403. – [1b] D. Fenske, E. Hartmann, K. Dehnicke, *Z. Naturforsch.* **1988**, *43B*, 1611. – [1c] F. T. Edelmann, *Coord. Chem. Rev.* **1994**, *137*, 403 and references cited therein. – [1d] J. Barker, M. Kilner, *Coord. Chem. Rev.* **1994**, *133*, 219 and references cited therein. – [1e] R. Duchateau, C. T. van Wee, A. Meetsma, P. Th. van Duijnen, J. H. Teuben, *Organometallics* **1996**, *15*, 2279.

[2] [2a] A. R. Sanger, *Inorg. Nucl. Chem. Lett.* **1973**, *9*, 351; R. T. Boeré, R. T. Oakley, R. W. Reed, *J. Organomet. Chem.* **1987**, *331*, 161. – [2b] J. Pornet, L. Miginiac, *Bull. Chim. Soc. Fr.* **1974**, 994. – [2c] S. Ogata, A. Mocjizuki, M. Kakimoto, Y. Imai, *Bull. Chem. Soc. Jpn.* **1986**, *59*, 2171. – [2d] A. J. Hill, J. V. Johnston, *J. Am. Chem. Soc.* **1954**, *76*, 920; J. R. Hagadorn, J. Arnold, *Angew. Chem.* **1998**, *110*, 1813.

[3] [3a] R. Gómez, R. Duchateau, A. N. Chernega, J. H. Teuben, F. T. Edelmann, M. L. H. Green, *J. Organomet. Chem.* **1995**, *491*, 153. – [3b] J. C. Flores, J. C. W. Chien, M. D. Rausch, *Organometallics* **1995**, *14*, 1827. – [3c] A. Littke, N. Sleiman, C. Bensimon, D. S. Richeson, G. P. A. Yap. S. J. Brown, *Organometallics* **1998**, *17*, 446. – [3d] V. Volkis, M. Shmulinson, C. Averbuj, A. Lisovskii, F. T. Edelmann, M. S. Eisen, *Organometallics* **1998**, *17*, 3155.

[4] [4a] R. Krebs, D. Schomburg, R. Schmutzler, *Z. Naturforsch.* **1985**, *40B*, 282. – [4b] While this manuscript was in progress, a report was published describing the synthesis of this amide, together with its homoleptic lanthanide complexes: G. B. Deacon, C. M. Forsyth, B. W. Skelton, A. H. White, *J. Chem. Soc., Dalton Trans.* **1998**, 1381.

[5] or other vanadium amidinate complexes see: [5a] P. Berno, S. Hao, R. K. Minhas, S. Gambarotta, *J. Am. Chem. Soc.* **1994**, *116*, 7417. – [5b] S. Hao, P. Berno, R. K. Minhas, S. Gambarotta, *Inorg. Chim. Acta* **1996**, *244*, 37. – [5c] E. A. C. Brussee, A. Meetsma, B. Hessen, J. H. Teuben, *Organometallics* **1998**, *17*, 4090.

[6] H. H. Karsch, P. A. Schlüter, M. Reisky, *Eur. J. Inorg. Chem.* **1998**, 433.

[7] E. Kime-Hunt, K. Spartalian, M. DeRusha, C. M. Nunn, C. J. Carrano, *Inorg. Chem.* **1989**, *28*, 4392.

[8] M. Herberhold, G. Frohmader, T. Hofmann, W. Milius, J. Darkwa, *Inorg. Chim. Acta* **1998**, *267*, 19.

[I98280]

Optically Active Transition Metal Compounds, 116[◇]

Bond Lengths Co–C(CO), Co–N(NO) and Angles L–Co–C(CO), L–Co–N(NO) in Tetrahedral Complexes☆

Henri Brunner*, Josef Breu, and Peter Faustmann

Institut für Anorganische Chemie der Universität,
D-93040 Regensburg, Germany
Fax: (internat.) +49(0)941/9434439
E-mail: henri.brunner@chemie.uni-regensburg.de

Received June 22, 1998

Keywords: Cobalt complexes / Carbonyl complexes / Nitrosyl complexes

The bond lengths Co–C(CO), Co–N(NO) and angles L–Co–C(CO), L–Co–N(NO) in six tetrahedral complexes, determined by X-ray crystallography, were analysed and compared with the calculated compound $Co(CO)_2(NO)PH_3$. Distinct differences were found which allow a differentiation of the two similar ligands CO and NO. These differences are used to assign CO and NO ligands in cases where this has not been possible before including a structure in which the two independent molecules in the unit cell are diastereomers. The relationship seems to hold not only for tetrahedral compounds but also for other polyhedral coordination types.

Introduction

In an extensive review Tolman determined the steric demand, i.e. the cone angles, of a huge number of ligands exept the linear two-atom ligands CO and NO.[2] In many reports on X-ray structure analyses it was stated that the CO and NO groups could not be distinguished due to their similar size, for example, in complexes of the type $Co(CO)(NO)L_2$.[3][4] The structure of $Co(CO)_3(NO)$ was determined by gas-phase electron diffraction.[5] During our investigations on optically active carbonyl(nitrosyl)cobalt complexes[6][7] we realised that there might be a distinct difference between the ligands CO and NO, which could be used for future assignments.

Ab initio Molecular Structures

Covalent and nonbonding intramolecular interactions determine the shape of the molecular potential energy hypersurface. However, geometries as observed in the solid state result from the interplay of intra- and intermolecular interactions. For flexible organometallic species molecular structure and crystal packing influence each other in a complex manner.[8]

To improve the reliability of the experimentally observed molecular structure parameters and to exclude the possibility of molecular structures being determined by intermolecular interactions we optimised the gas phase structure of $Co(CO)_2(NO)PH_3$ employing the density functional code DMOL[9] We used "DNP" basis sets[10] with inner cores frozen, a "FINE" integration grid, and the Vosko, Wilk, Nusair parametrization[11] of the exchange correlation energy in the homogeneous electron gas. The local approximation was applied in SCF iterations and the final LDA density was used for nonlocal corrections of both energy and gradients using the functions proposed by Perdew and Wang[12] and Becke[13] for correlation and exchange, respectively. The geometries were fully optimised without any symmetry constraints employing a mode following Newton-Raphson technique and the BFGS updating scheme for the Hessian.[14]

To check the agreement the molecular structures were minimised starting with coordinates taken from two different crystal structure determinations, SAPFIY = $[Co(CO)_2(NO)]_2(C_{31}H_{35}N_2O_2P_3)$[15] and GEHCIF = $Co(CO)_2(NO)(C_{16}H_{13}N_2O_2P)$][16] and with P-ligands adjusted to PH_3. Finally, C and N atoms of the GEHCIF structure were exchanged (GEHCIF*) and the structure minimised starting from this "wrong" assignment. There is a good agreement between the results of these calculations with both the experimental gas phase structure[5] and the DFT minimised structure[17] of $Co(CO)_3(NO)$ (Table 1). However, as already noticed in ref.[17] the computed metal−C and metal−N distances are too short and the errors in the bond lengths are larger as for pure carbonyl compounds.[18]

All three minimisations converge to nearly identical geometries. The Co−C(CO) distance is 1.77 Å and the Co−N(NO) distance is 0.12 Å shorter, a difference that is larger than bond length errors of XRD structure determinations. This difference has been used before to assign carbonyl and nitrosyl groups in M(CO)(NO) fragments.[19][20] The most remarkable result, however, is the difference be-

[◇] Part 115: Ref.[1].

 © WILEY-VCH Verlag GmbH, D-69451 Weinheim, 1998 1434−1948/98/1212−1871 $ 17.50+.50/0

Table 1. Experimental and ab initio gas-phase geometries (in Å and degrees) of carbonyl(nitrosyl)cobalt complexes

Parameter	SAPFIY[15]	GEHCIF[16]	GEHCIF*	$Co(CO)_3(NO)$, DFT[17]	$Co(CO)_3(NO)$, Exp.[5]
R_{Co-N}	1.651	1.649	1.650	1.665	1.671
R_{Co-C}	1.768	1.767	1.767	1.810	1.843
	1.767	1.768	1.770		
R_{N-O}	1.178	1.177	1.177	1.178	1.180
R_{C-O}	1.162	1.162	1.162	1.163	1.136
	1.162	1.162	1.162		
R_{Co-P}	2.172	2.175	2.170	–	–
$\alpha_{(N)-Co-(C)}$	118.3	117.2	114.8	114.7	107.7
	117.5	115.9	118.9		
$\alpha_{(C)-Co-(C)}$	103.5	103.7	103.5	103.9	111.2
$\alpha_{(C)-Co-(PH3)}$	101.7	102.9	102.1	–	–
	99.5	101.0	101.3		
$\alpha_{(N)-Co-(PH3)}$	113.6	114.1	114.0	–	–

tween the P−Co−C(CO) and the P−Co−N(NO) angles which has not been documented before. The latter is more than ten degrees larger than the former. The values found are 113.6−114.1° for the P−Co−N(NO) angles and 99.5−102.9° for the P−Co−C(CO) angles. Given these pronounced differences in structural parameters, it should be possible to unequivocally assign NO and CO groups in XRD structure determinations.

Crystal Structure Analyses

Crystal structure refinements were carried out for the six carbonyl(nitrosyl)cobalt complexes shown in Figure 1.

Details of the structure determinations and the crystal structure parameters were previously published.[6][7] However, for the present study all the structures were refined again in a consistent manner applying the SHELX-97 program package.[21] SHELXL refines against F^2 and all data were used in the full-matrix least-squares method. We also avoided any restraints, except for complex **5** for which DELU restraints were applied to remedy for the small reflex/parameter ratio. For compound **4** a new and larger data set was collected. Methyl H atoms were placed in idealised positions based on difference electron synthesis and torsion angles were refined with fixed isotropic displacement parameters of $1.5U_{eq}$ (parent C). All other H atoms were placed in idealised positions and refined with fixed isotropic displacement parameters of $1.2U_{eq}$ (parent C). All other atoms were refined anisotropically. The weighting scheme recommended by the program was used and refinement was continued until complete convergence (maximum shift/esd < 0.001) was achieved. It should be noted that the smaller isotropic temperature factor of nitrogen than that of carbon has been used previously for nitrosyl/carbonyl differentiation.[19][20]

For each complex two refinements were carried out. These differ only in the SFAC number used at the sites of the carbon atom of the CO group and the nitrogen atom of

Figure 1. Tetrahedral carbonyl(nitrosyl)cobalt complexes for which a structure refinement was carried out

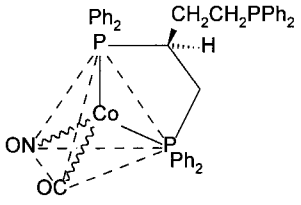

1 Co(CO)(NO)(1,2,4-triphos)

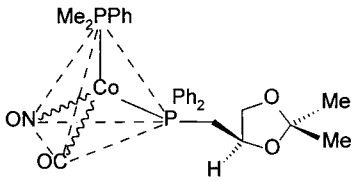

2 Co(CO)(NO)(PMe_2Ph)(glyphos)

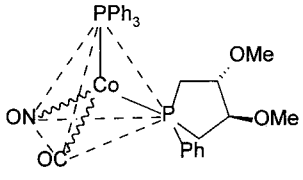

3 Co(CO)(NO)(PPh_3)(phenyl-tarpholan)

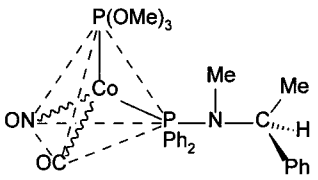

4 Co(CO)(NO)[$P(OMe)_3$](PN*)

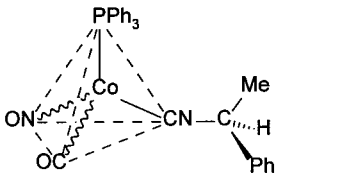

5 Co(CO)(NO)(PPh_3)[CNCH(Me)(Ph)]

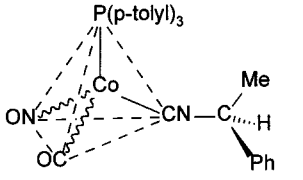

6 Co(CO)(NO)[$P(p\text{-tolyl})_3$][CNCH(Me)(Ph)]

Table 2. Number of reflections and *R* indices of the refined structures

Complex	Total number of reflections	Number of unique reflections	Number of obsd. reflections with $I > 2\sigma_I$	L.S. parameters	$R1$[b] (all data)	$wR2$[c]) (all data)	*GooF*[d] (all data)	Flack parameter *x*
1	6801	6801	4489	433	0.0974	0.1141	1.033	0.0668 (0.02)
1 [a]					0.0998	0.1223	1.034	0.0728 (0.02)
2	5611	5579	4985	320	0.0430	0.0843	1.039	−0.0126 (0.01)
2 [a]					0.0439	0.0882	1.040	−0.0110 (0.01)
3	3865	2717	2027	354	0.0893	0.1025	1.089	0.0031 (0.03)
3 [a]					0.0903	0.1047	1.091	0.0017 (0.03)
4	12342	4667	4284	337	0.0281	0.0596	0.983	−0.0086 (0.01)
4 [a]					0.0305	0.0680	0.985	−0.0063 (0.01)
5	1949	1762	936	306	0.1612	0.2069	1.016	−0.0080 (0.07)
5 [a]					0.1620	0.2095	1.013	−0.0030 (0.07)
6	8477	8477	5943	680	0.0760	0.1294	1.124	0.0015 (0.02)
6 [a]					0.0766	0.1316	1.121	0.0051 (0.02)

[a] Values after exchanging the SFAC cards at the position of the carbon atom of the CO group and the nitrogen atom of the NO group. The number of reflections remains unchanged. − [b] $R1 = \Sigma||F_0|-|F_C||/\Sigma|F_0|$. − [c] $wR2 = \{\Sigma[w(F_0^2 - F_C^2)^2]/\Sigma[w(F_0^2)^2]\}^{1/2}$. − [d] $GooF = S = \{\Sigma [w(F_0^2 - F_C^2)^2]/(n\text{-}p)\}^{1/2}$ with n = number of reflections, p = total number of parameters refined, and $w = 1/[\sigma^2(F_0^2) + (aP)^2 + bP]$ with $P = [2F_C^2 + \mathrm{Max}(F_0^2,0)]/3$.

the NO group. In Table 2 the resulting refinement parameters are listed.

Crystallographic data (excluding structure factors) for the structures reported in this paper have been deposited with the Cambridge Crystallographic Data Centre as supplementary publication no. CCDC-101715. Copies of the data can be obtained free of charge on application to CCDC, 12 Union Road, Cambridge CB2 1EZ, UK [Fax: int. code +44(1223)336−033; E-mail: deposit@ccdc.cam.ac.uk].

Carbonyl and nitrosyl groups were initially assigned according to the observed bond length differences. For all six complexes the correct configuration gives slightly smaller values for the *R* indices. However, the differences for the two possible configurations at the cobalt atom are by no means significant and would not allow a conclusive assignment of NO and CO groups. The configuration space is large enough to allow good agreement between observed and calculated structure factors even for the wrong configurations. As expected, neither are meaningful differences displayed in the Flack parameters. Whereas *R* indices are rather insensitive, wrong assignment is clearly documented in the displacement parameters (Table 3).

Both ligands CO and NO bind to the same metal centre and are expected to have very similar displacement parameters. For the correct cobalt configuration the parameters of the nitrogen atom of the NO group and of the carbon atom of the CO group are indeed of the same magnitude. After exchange of the SFAC numbers of these two atoms, the parameters at the C site become larger and those at the N site become smaller. U_{eq} parameters at the C site (calculated as a nitrogen atom) are up to three times larger than those at the position N (calculated as a carbon atom). This is illustrated for two representative examples in Figure 2 (only the central cobalt coordination sphere is shown).

In a preceding paper we were not able to determine the absolute configuration of the complexes **2** and **4**.[7] With the results presented here we are able to do so. The investigated crystal of complex **2** is assigned the configuration (S_{Co},S_C), while for complex **4** the configuration can unambiguously be determined as (R_{Co},S_C).

An even more spectacular result was obtained for complex **6**. In complex **6** two independent molecules are arranged in a pseudo-centrosymmetric way in the unit cell; only the methyl group at the asymmetric C atom disturbs the inversion symmetry. We first assumed the same configuration for both cobalt atoms. During the present study we realised that this was not correct. In fact the two molecules seem to have different configurations. In other words the unit cell contains the two diastereomeric complexes that differ only in the configuration at the cobalt centre. Molecule A has a (R_{Co},S_C) and molecule B (S_{Co},S_C) configuration. This explains the fact that we were not able to separate the diastereomers of **6**, whereas in all other cases at least enriched samples could be obtained by fractional crystallization.[7]

The bond distances Co−C(CO) and Co−N(NO) of complexes **1**−**6** are listed in Table 4. For the correct configuration the values are in line with expected values. They range from 1.703 to 1.749 Å for the Co−C(CO) distance and

Table 3. Anisotropic, equivalent, and main axis displacement parameters for C and N of the CO and NO groups

Complex	Label[b]	U_{11}	U_{22}	U_{33}	U_{23}	U_{13}	U_{12}	U_{eq}	U_1	U_2	U_3	U_3/U_1
1	N(1)	0.048(3)	0.043(2)	0.036(2)	−0.003(2)	−0.002(2)	−0.008(2)	0.0423(14)	0.0329	0.0402	0.0539	1.64
	C(41)	0.039(3)	0.042(3)	0.035(3)	−0.004(2)	0.001(2)	0.007(2)	0.0387(17)	0.0306	0.0372	0.0482	1.57
1 [a]	N(1)	0.031(2)	0.027(2)	0.019(2)	−0.0067(19)	−0.004(2)	−0.009(2)	0.0257(12)	0.0116	0.0271	0.0383	3.29
	C(41)	0.074(4)	0.063(3)	0.052(3)	−0.003(3)	0.007(3)	0.006(3)	0.0630(19)	0.0484	0.0628	0.0778	1.61
2	N(1)	0.0374(13)	0.0553(15)	0.0402(13)	0.0137(11)	0.0053(10)	−0.0038(12)	0.0443(8)	0.0277	0.0418	0.0634	2.29
	C(33)	0.0524(17)	0.0350(13)	0.0406(14)	0.0033(13)	−0.0049(13)	−0.0053(13)	0.0427(9)	0.0330	0.0391	0.0560	1.70
2 [a]	N(1)	0.0259(12)	0.0404(14)	0.0301(13)	0.0106(11)	0.0047(9)	−0.0024(11)	0.0321(8)	0.0193	0.0301	0.0470	2.44
	C(33)	0.0671(19)	0.0527(16)	0.0525(16)	0.0035(15)	−0.0051(15)	−0.0073(16)	0.0574(10)	0.0488	0.0514	0.0720	1.48
3	N(1)	0.068(6)	0.064(5)	0.067(6)	−0.002(4)	0.017(5)	0.026(5)	0.069(3)	0.0502	0.0631	0.0950	1.89
	C(31)	0.054(6)	0.054(6)	0.046(5)	0.010(5)	0.004(4)	0.022(5)	0.054(3)	0.0390	0.0554	0.0662	1.70
3 [a]	N(1)	0.044(5)	0.048(5)	0.046(5)	−0.003(4)	0.016(4)	0.023(5)	0.046(3)	0.0247	0.0476	0.0657	2.66
	C(31)	0.075(6)	0.098(8)	0.062(6)	0.013(5)	0.007(5)	0.037(6)	0.081(4)	0.0568	0.0776	0.1089	1.92
4	N(1)	0.0279(12)	0.0221(10)	0.0329(10)	0.0069(8)	−0.0027(10)	0.0043(9)	0.0276(6)	0.0165	0.0301	0.0364	2.20
	C(22)	0.0217(13)	0.0203(11)	0.0336(13)	0.0064(9)	0.0044(10)	0.0015(10)	0.0252(7)	0.0177	0.0204	0.0375	2.12
4 [a]	N(1)	0.0153(12)	0.0120(10)	0.0188(10)	0.0054(8)	−0.0010(10)	0.0060(10)	0.0154(6)	0.0056	0.0179	0.0226	4.07
	C(22)	0.0334(15)	0.0384(14)	0.0476(15)	0.0089(11)	0.0053(12)	−0.0015(12)	0.0398(8)	0.0289	0.0368	0.0537	1.86
5	N(1)	0.050(11)	0.097(13)	0.103(14)	−0.030(11)	−0.009(10)	0.023(10)	0.089(7)	0.0476	0.0813	0.1394	2.93
	C(28)	0.038(12)	0.069(15)	0.15(2)	0.002(15)	−0.026(13)	0.014(11)	0.091(9)	0.0322	0.0816	0.1602	4.98
5 [a]	N(1)	0.026(10)	0.076(13)	0.070(13)	−0.023(11)	0.005(10)	0.014(9)	0.062(7)	0.0250	0.0503	0.1120	4.48
	C(28)	0.051(12)	0.102(17)	0.20(3)	−0.019(17)	−0.027(14)	0.020(11)	0.126(12)	0.0456	0.1267	0.2051	4.50
6 A	N(2)	0.034(3)	0.058(3)	0.107(5)	−0.016(3)	−0.007(3)	−0.018(3)	0.067(2)	0.0333	0.0610	0.1075	3.22
	C(31)	0.047(3)	0.066(4)	0.048(3)	−0.028(3)	−0.004(3)	−0.018(3)	0.0537(19)	0.0324	0.0472	0.0814	2.52
6 A [a]	N(2)	0.030(3)	0.045(3)	0.084(4)	−0.011(3)	−0.008(3)	−0.016(2)	0.0531(19)	0.0288	0.0463	0.0844	2.93
	C(31)	0.051(3)	0.084(4)	0.067(4)	−0.036(3)	−0.003(3)	−0.021(3)	0.068(2)	0.0459	0.0531	0.1038	2.26
6 B	N(4)	0.069(4)	0.056(4)	0.089(4)	−0.004(3)	−0.031(3)	−0.020(3)	0.073(2)	0.0482	0.0679	0.1032	2.14
	C(71)	0.062(4)	0.088(5)	0.050(4)	−0.033(3)	−0.010(4)	−0.017(4)	0.069(3)	0.0343	0.0589	0.1150	3.35
6 B [a]	N(4)	0.049(4)	0.045(3)	0.066(4)	−0.002(3)	−0.018(3)	−0.018(3)	0.054(2)	0.0395	0.0516	0.0721	1.83
	C(71)	0.086(5)	0.109(5)	0.067(4)	−0.044(4)	−0.019(3)	−0.017(4)	0.092(3)	0.0424	0.0765	0.1569	3.70

[a] See explanation in Table 2. – [b] See refs.[6][7] for labeling scheme.

from 1.643 to 1.702 Å for the Co−N(NO) distance. Only complex **5** does not fit into this picture. This might be because the number of measured reflections is too small relative to the number of parameters for a reliable refinement. After exchanging the carbon and nitrogen atom in **5** the distances remain rather constant for each site.

A conclusive assignment could also be based on the P−Co−N(NO) and P−Co−C(CO) angles as listed in Table

Figure 2. Platon plots of the core of the complexes **1** (left) and **4** (right). After exchanging the SFAC cards for the carbon and nitrogen atoms the anisotropic displacements parameters differ strongly (bottom)

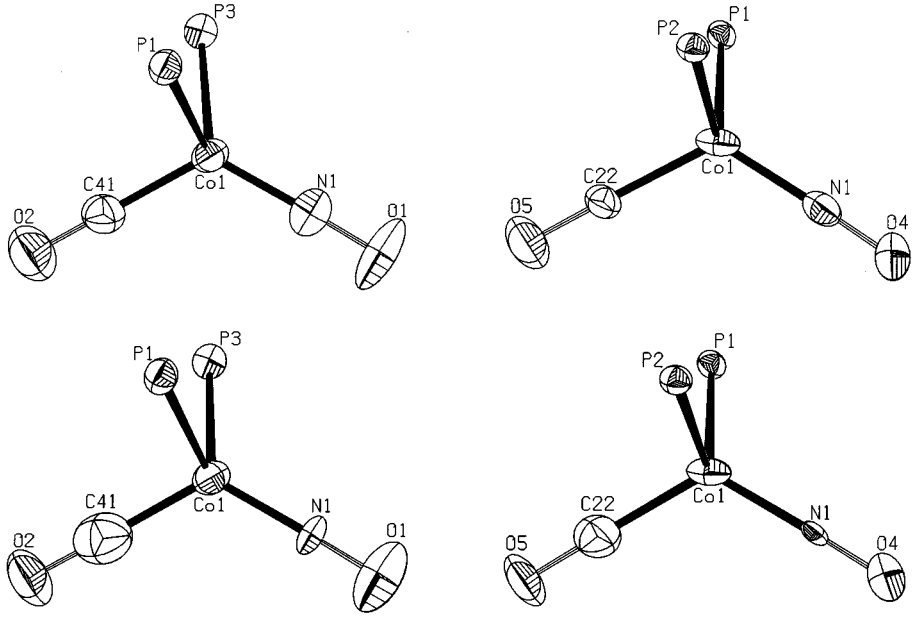

Table 4. Bond lengths in Å around the cobalt center

Complex	Co−C(CO)	C−O	Co−N(NO)	N−O	Co−L1 [b]	Co−L2 [b]
1	1.752(5)	1.157(7)	1.645(4)	1.174(6)	2.2087(17)	2.1953(18)
1 [a]	1.640(4)	1.162(6)	1.763(6)	1.169(8)	2.2090(17)	2.1960(18)
2	1.713(3)	1.156(4)	1.686(2)	1.171(3)	2.2136(13)	2.2069(13)
2 [a]	1.688(2)	1.161(4)	1.716(3)	1.164(4)	2.2131(13)	2.2071(13)
3	1.711(11)	1.151(13)	1.643(11)	1.183(15)	2.208(2)	2.204(3)
3 [a]	1.616(11)	1.170(15)	1.736(12)	1.162(14)	2.207(2)	2.203(3)
4	1.749(2)	1.146(3)	1.669(2)	1.177(3)	2.1498(6)	2.2073(6)
4 [a]	1.667(2)	1.170(3)	1.756(2)	1.143(3)	2.1499(7)	2.2073(6)
5	1.60(3)	1.24(4)	1.70(2)	1.16(3)	2.225(6)	1.93(3)
5 [a]	1.66(2)	1.14(3)	1.63(3)	1.27(4)	2.225(6)	1.91(3)
6 A	1.716(8)	1.163(10)	1.683(8)	1.149(12)	2.2087(19)	1.862(9)
6 A [a]	1.683(8)	1.138(12)	1.721(6)	1.164(9)	2.208(2)	1.863(9)
6 B	1.704(8)	1.152(10)	1.700(9)	1.171(13)	2.209(2)	1.865(9)
6 B [a]	1.678(9)	1.188(13)	1.698(8)	1.163(10)	2.210(2)	1.859(9)

[a] See explanation in Table 2. − [b] L1, L2: the ligands other than CO or NO. L1 has higher priority than L2.

Table 5. Bond angels in degrees around the cobalt center

Complex	L1−Co−N(NO)	L1−Co−C(CO)	L2−Co−N(NO)	L2−Co−C(CO)	C−Co−N	L1−Co−L2
1	118.82(14)	104.40(18)	119.83(15)	97.43(14)	121.5(2)	88.38(4)
1 [a]	104.69(18)	118.64(14)	97.4(2)	119.80(15)	121.5(2)	88.38(5)
2	112.94(9)	105.79(10)	110.37(9)	101.54(10)	123.43(14)	99.72(2)
2 [a]	105.83(10)	112.87(10)	101.56(10)	110.48(9)	123.34(14)	99.74(3)
3	115.9(3)	101.7(3)	109.2(3)	104.0(4)	122.3(5)	101.33(9)
3 [a]	101.8(3)	115.5(3)	104.0(4)	109.5(3)	122.2(5)	101.33(9)
4	109.35(7)	104.55(9)	115.96(7)	100.94(8)	120.82(10)	103.33(2)
4 [a]	104.51(9)	109.40(9)	100.89(9)	115.90(9)	120.89(11)	103.34(2)
5	109.9(7)	106.1(9)	110.7(9)	108.2(11)	119.6(12)	100.6(8)
5 [a]	106.1(9)	109.7(7)	107.9(11)	111.1(9)	119.5(12)	100.9(8)
6 A	108.0(2)	101.7(3)	113.5(3)	108.5(4)	123.5(4)	97.9(2)
6 A [a]	101.7(3)	108.8(2)	108.3(3)	113.6(3)	122.9(4)	97.9(2)
6 B	107.1(2)	105.4(3)	112.3(4)	111.9(5)	121.6(5)	94.6(2)
6 B [a]	105.7(3)	106.6(3)	112.4(4)	112.2(4)	121.4(5)	94.5 (2)

[a] See explanation in Table 2.

5. As expected from the gas-phase structures for complex **1** P−Co−N(NO) angles are 22° and 14° larger than the corresponding P−Co−C(CO) angles. For the other complexes this difference is about 5 to 10°. These results indicate that the nitrosyl group has a larger steric demand than the carbonyl group.

To further back these conclusions a statistical analysis has been carried out on other carbonyl-nitrosyl complexes registered in the Cambridge Structural Database. We found 41 octahedral complexes and 18 trigonal-bipyramidal or tetrahedral complexes (in addition to the six cobalt complexes discussed above). The octahedral complexes contain 95 M(CO)(NO)P groups and the other complexes another 31 such groups. We did not try to assess the quality of the deposited structural data nor did we check on what basis the authors assigned the nitrosyl and carbonyl groups. This would be difficult and unreliable without the original data sets at hand. However, at a first glance the data confirm the results of the present study. We compared the values of P−M−C(CO) and P−M−N(NO) angles. In 41 cases the latter angle is more than 5° larger than the former. In another 42 cases the difference is between 1° and 5°, still with the P−M−N(NO) angle being the larger one. A small difference of less than ±1° is found for 19 pairs. Only in 24 cases the P−M−C(CO) angle is found to be more than 1° larger than the P−M−N(NO) angle.

☆ Dedicated to Professor *Edgar Niecke* on the occasion of his 60th birthday.

[1] H. Brunner, T. Neuhierl, B. Nuber, *J. Organomet. Chem.* **1998**, *563*, 173.
[2] C. A. Tolman, *Chem. Rev.* **1977**, *77*, 313.
[3] V. G. Albano, P. L. Bellon, G. Ciani, *J. Organomet. Chem*. **1972**, *38*, 155.
[4] J. T. Lin, S. Y. Wang, Y. C. Chou, M. L. Gong, Y.-M. Shiow, H.-M. Gau, Y. S. Wen, *J. Organomet. Chem*. **1996**, *508,* 183.
[5] K. Hedberg, L. Hedberg, K. Hagen, R. R. Ryan, L.H. Jones, *Inorg. Chem.* **1985**, *24,* 2771.
[6] H. Brunner, P. Faustmann, A. Dietl, B. Nuber, *J. Organomet. Chem.* **1997**, *542,* 255.
[7] H. Brunner, P. Faustmann, B. Nuber, *J. Organomet. Chem*. **1998**, *556*, 129.
[8] D. Braga , F. Grepioni, *J. Chem. Soc., Chem. Commun.* **1996**, 571.
[9] DMOL, MSI, 9658 Scranton Road, San Diego, CA 92121-2777, USA.
[10] B. Delley, *J. Chem. Phys.* **1990**, *92*, 508.
[11] S. H. Vosko, L. Wilk, M. Nusair, Can. *J. Phys.* **1980**, *58*, 1200.
[12] J. P. Perdew, Y. Wang, *Phys. Rev.* **1992, B45,** 13244.
[13] A. D. Becke, J. *Chem. Phys.* **1988**, *88*, 2547.
[14] A. Banerjee, N. Adams, J. Simons, R. Shepard, J. Phys. Chem., **1985**, *89*, 52.

[15] J. Ellermann, N. Will, F. Knoch, *J. Organomet. Chem.* **1989**, *366,* 197.
[16] J. Ellermann, E. Kock, H. Zimmermann, M. Gomm, *J. Organomet. Chem.* **1988**, *345*, 167.
[17] F. Bohr, H. Chermette, M. F. Ruiz-Lopez, *Int. J. Quantum Chem.* **1994**, *52*, 1039.
[18] L. Fan, T. Ziegler, *J. Chem. Phys.* **1991**, *95*, 7401.
[19] J. W. Faller, K. H. Chao, H. H. Murray, *Organometallics* **1984**, *3*, 1231.
[20] U. Eberhardt, G. Mattern, G. Schiller, *Chem. Ber.* **1988**, *121*, 1525.
[21] G. Sheldrick, University of Göttingen, **1997**.

[I98194]

Optically Active Transition Metal Complexes, 118[◇]

Unusual Crystal Structures of ($R_{Ru}R_C$/$S_{Ru}R_C$)-(η⁶-*p*-Cymene)Ru Complexes – Diastereomers with Opposite Configuration at the Metal Center in the Unit Cell

Henri Brunner*[a], Thomas Neuhierl, and Bernhard Nuber[b]

Institut für Anorganische Chemie der Universität Regensburg[a],
Universitätsstraße. 31, D-93053 Regensburg, Germany
Fax: (internat.) + 49(0)941/9434439
E-mail: henri.brunner@chemie.uni-regensburg.de

Anorganisch-Chemisches Institut der Universität Heidelberg[b],
In Neuenheimer Feld 270, D-69120 Heidelberg, Germany

Received July 6, 1998

Keywords: Crystal structures / Diastereomers / Half-sandwich complexes / Ruthenium

Condensation of (*R*)-2-aminobutanol with salicylaldehyde and 2-pyrrolecarbaldehyde gave the chiral chelate ligands HLL_1* and HLL_2*, respectively. The diastereomeric complexes (R_{Ru},R_C)- and (S_{Ru},R_C)-[(η⁶-arene)Ru(LL_1*)Cl], η⁶-arene = *p*-cymene (**1a/1b**), η⁶-arene = benzene (**2a/2b**), and (R_{Ru},R_C)- and (S_{Ru},R_C)-[(η⁶-arene)Ru(LL_2*)Cl], η⁶-arene = *p*-cymene (**3a/3b**), η⁶-arene = benzene (**4a/4b**), which only differ in the ruthenium configuration, were prepared by the reaction of $[(\eta^6\text{-arene})RuCl_2]_2$ with the anion of the corresponding ligand HLL*. X-ray analyses of **1a/1b** and **3a/3b** showed a structural peculiarity. The unit cell of these complexes contained diastereomers with the same configuration at the carbon atoms but opposite configuration at the metal centers in a 1:1 ratio. Weak intramolecular O−H···Cl hydrogen bridges were formed in all the complexes. ^{1}H-NMR studies demonstrated the configurational lability at the Ru center. The iodo complexes (R_{Ru},R_C)- and (S_{Ru},R_C)-[(η⁶-*p*-cymene)Ru(LL*)I], LL* = LL_1* (**5a/5b**) and LL* = LL_2* (**6a/6b**), were synthesized by halogen exchange.

Introduction

Optically active (η⁶-arene)ruthenium half-sandwich complexes have attracted interest in enantioselective catalysis[2][3][4][5], including Diels−Alder and olefin isomerization reactions.[6][7][8] There is a series of structural studies on optically active chiral-at-Ru complexes of the type [(η⁶-arene)Ru(LL*)L] and [(η⁶-arene)Ru(LL*)L]X, arene = *p*-cymene, mesitylene, benzene, LL* = anionic or neutral unsymmetrical ligand, L = halide or unidentate ligand, X = anion.[9][10][11][12][13][14][15] Resolution of (η⁶-arene)ruthenium half-sandwich complexes usually is carried out using optically active chelate ligands HLL* containing optically active amine components. Diastereomers are formed, which only differ in the configuration at the stereogenic Ru atom.

Diastereomers are different molecules. Therefore, ubiquitously, single crystals obtained from a mixture of diastereomers contain only one diastereomer. This, in effect, is the basis of diastereomer separation by crystallization. There are, however, examples, in which the presence of both diastereomers with opposite configuration at the metal center in one crystal is reported.[14][15][16] In the present paper we describe the syntheses and the X-ray structures of ruthenium half-sandwich complexes, two of which show this structural peculiarity.[17]

Results and Discussion

2-*N*-[(*R*)-1-Hydroxybut-2-yl)]salicylaldimine[18] (HLL_1*) was obtained by condensation of (*R*)-2-aminobutanol with salicylaldehyde. HLL_1* was deprotonated in dichloromethane with KO*t*Bu and $[(\eta^6\text{-arene})RuCl_2]_2$ (arene = *p*-cymene, benzene) was added. The formation of the diastereomeric complexes (R_{Ru},R_C)- and (S_{Ru},R_C)-[(η⁶-*p*-cymene)Ru(LL_1*)Cl] (**1a**, **b**) and [(η⁶-benzene)Ru(LL_1*)Cl] (**2a**, **b**) is depicted in Scheme 1.

Scheme 1

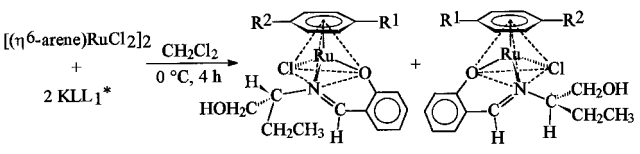

R^1 = *i*Pr, R^2 = Me (*R*Ru,*R*C) - **1a** (*S*Ru,*R*C) - **1b**

R^1 = H, R^2 = H (*R*Ru,*R*C) - **2a** (*S*Ru,*R*C) - **2b**

[◇] Part 117: See ref.[1].

 © WILEY-VCH Verlag GmbH, D-69451 Weinheim, 1998 1434−1948/98/1212−1877 $ 17.50+.50/0

The ^{1}H-NMR spectrum of the *p*-cymene complex in $CDCl_3$ showed the presence of two diastereomers **1a** and **1b** in a ratio of 91:9. As there is no "β−phenyl effect"[13][19], no assignment of major/minor isomer to **1a/1b** can be made. The isomer ratio was obtained from the intensities of the singlets of the imine protons at δ = 7.75 and δ = 7.85. There are two doublets at δ = 1.15 and δ = 1.26 for the CH*Me*$_2$ groups of the *p*-cymene ligand in the major diastereomer and two doublets at δ = 1.08 and δ = 1.24 for the minor diastereomer indicating their diastereotopicity. Similarly, the benzene complex forms two diastereomers **2a** and **2b**. Integration of the singlets of the imine protons at δ = 7.77 and δ = 8.39 in $CDCl_3$ gave a ratio of 76:24.

Crystallization of the diastereomeric mixture **1a/1b** from dichloromethane/thf/pentane at 3°C gave triangular plates of X-ray analytical quality. To our surprise the structural study showed the presence of both isomers **1a** and **1b** in the asymmetric unit in a 1:1 ratio. The molecules **1a** and **1b** have the same configuration at the carbon atom but differ in the configuration at the metal center. There are four independent molecules in the unit cell, two with (R_{Ru}) and two with (S_{Ru}) configuration. Figure 1 displays the molecular structure of **1a/1b**.

Figure 1. Crystal structure of (R_{Ru},R_C/S_{Ru},R_C)-[(η^6-*p*-cymene)-Ru(LL$_1$*)Cl] **1a/1b**

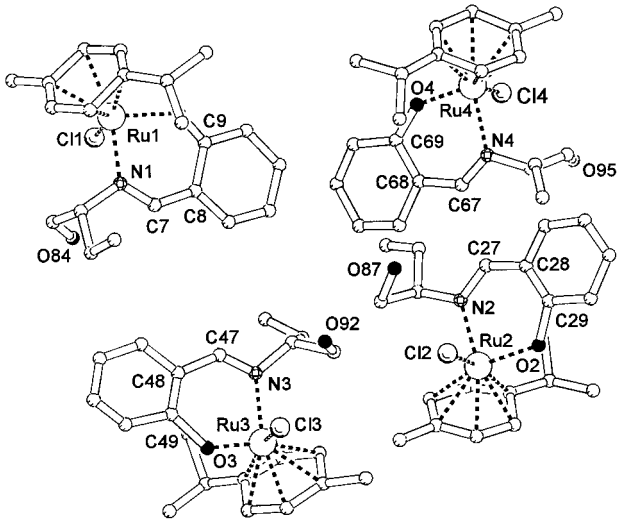

In all four independent molecules the chiral Schiff base is bonded through the phenolic oxygen and the imine nitrogen. The stereogenic carbon atom of the chelate ligand has the expected (R_C) configuration introduced in the synthesis. The *i*Pr group of the π-bonded *p*-cymene ligand lies above the phenolic oxygen. Thus, the *p*-methyl group is located near the chloride ligand. The oxygen atom of the hydroxymethyl group is oriented towards the chloride ligand. The configuration of the stereogenic ruthenium centers is determined according to the priority sequence η^6-*p*-cymene > Cl > O > N.[20][21][22] (*R*) configuration is assigned to Ru1 and Ru2, (*S*) configuration to Ru3 and Ru4. In the unit cell the pairs of diastereomers Ru1/Ru3 and Ru2/Ru4 are almost centrosymmetric, except the arrangement of the 2-amino-but-1-yl substituents which have the same (R_C) configuration at the stereogenic carbon atom. Selected bond distances and angles are listed in Table 1.

Table 1. Selected bond lengths and angles of **1a/1b**; estimated standard deviations are shown in parentheses

	$R_{Ru(1)}$	$R_{Ru(2)}$	$S_{Ru(3)}$	$S_{Ru(4)}$
Ru−Cl	2.459(4)	2.467(4)	2.434(4)	2.431(4)
Ru−O	2.153(9)	2.108(10)	1.728(11)	2.028(9)
Ru−N	2.106(11)	2.096(11)	2.134(11)	2.185(12)
Ru−(arene)	1.634(5)	1.680(4)	1.687(4)	1.669(8)
Cl−Ru−O	83.6(3)	86.3(3)	91.5(4)	81.4(3)
Cl−Ru−N	85.4(3)	83.3(3)	83.5(3)	84.1(4)
O−Ru−N	88.8(4)	89.9(4)	90.0(5)	85.9(4)

The bond distances and angles are similar to those observed in related complexes.[13][14] However there is a very short Ru3−O3 distance. The complexes with (S_{Ru}) configuration show longer Ru−N distances, whilst the Ru−Cl and Ru−O distances are smaller than in complexes with (R_{Ru}) configuration. The distances of the oxygen atoms to the chloride ligands are: O84···Cl1 3.24 Å, O87···Cl2 3.20 Å, O92···Cl3 3.01 Å, and O95···Cl4 3.13 Å. Weak O−H···Cl hydrogen bridges are described for O···Cl distances between 2.92 and 3.18 Å.[23] The formation of these O−H···Cl hydrogen bridges may be the driving force which orients the OH groups of the (*R*)-2-aminobut-1-yl substituents towards the chloride ligands.

The X-ray structure analysis demonstrated the presence of both diastereomers **1a** and **1b** in the crystal in a 1:1 ratio. However, the ^{1}H-NMR spectrum of crystals dissolved in $CDCl_3$ at room temperature showed a 91:9 ratio which did not change after stirring for 1 d at r.t. Furthermore, crystals of the complex **1a/1b** were dissolved at −80°C in CD_2Cl_2. Integration of the low temperature ^{1}H-NMR spectrum gave a diastereomer ratio of 95:5, proving the configurational lability at the metal center even at −80°C. Thus, the equilibrium **1a** ⇌ **1b** must have been established during the solution procedure at −80°C which took 1 h. Obviously, the energy barrier of the epimerization at the Ru atom in **1a/1b** is very low as observed for similar compounds with related chiral salicylaldiminato ligands.[12][13] Surprisingly, however, crystallization of a solution in which one of the two diastereomers is dominant, gives a 1:1 ratio of **1a/1b** in the crystal lattice.

Condensation of (*R*)-2-aminobutanol with 2-pyrrolecarbaldehyde afforded the ligand 2-*N*-[(*R*)-1-hydroxybut-2-yl)]-pyrrolecarbaldimine[17][24] (HLL$_2$*). The formation of the diastereomeric complexes (R_{Ru},R_C)- and (S_{Ru},R_C)-[(η^6-*p*-cymene)Ru(LL$_2$*)Cl] (**3a**, **b**) and [(η^6-benzene)Ru(LL$_2$*)Cl] (**4a**, **b**) is depicted in Scheme 2.

The ^{1}H-NMR spectrum of **3a/3b** in $CDCl_3$ showed a diastereomer ratio of 1:1, which did not change after refluxing for 3 h. A measurement in [D$_6$]acetone demonstrated that solvent polarity had no influence on the equilibrium ratio. The diastereomer ratio of 79:21 in $CDCl_3$ for the complexes **4a**, **b** was similar to the ratio found for the complexes **2a**, **b** (76:24).

Scheme 2

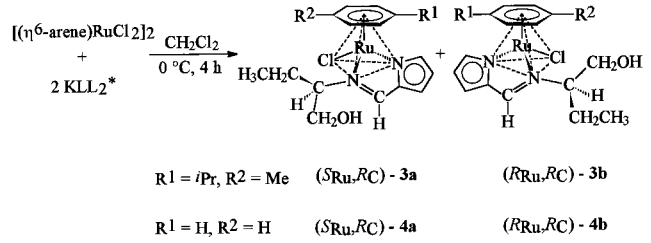

From a mixture of CH_2Cl_2, thf, and pentane crystals of the complex **3a/3b** suitable for X-ray structure analysis were obtained. There are two independent molecules in the unit cell with opposite configurations at the Ru centers. The molecular structure of **3a/3b** is shown in Figure 2.

Figure 2. Crystal structure of (R_{Ru},R_C/S_{Ru},R_C)-[(η6-*p*-cymene)-Ru(LL2*)Cl] **3a/3b**

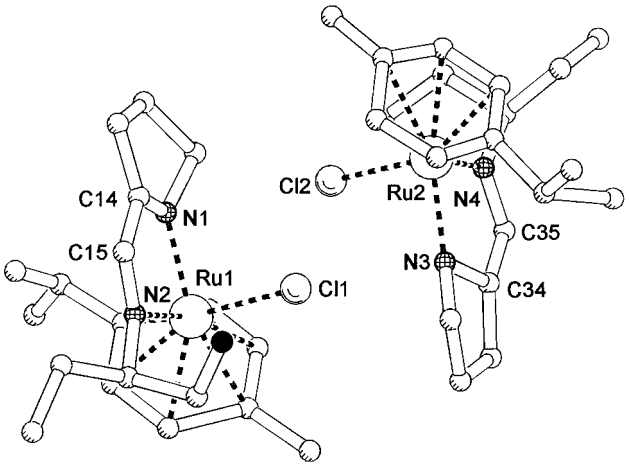

The chiral Schiff base is coordinated through the pyrrole nitrogen and the imine nitrogen. The stereogenic carbon atom of the chelate ligand has the expected (R_C) configuration.The *i*Pr group of the cymene ring is located in the vicinity of the imine nitrogen. Both methyl groups of the *i*Pr substituent tend away from the chelate ring and the *p*-methyl group fills the space between the imine nitrogen and the chloride ligand. The oxygen atom of the hydroxymethyl group is oriented towards the chloride ligand. Both molecules are arranged in a quasi centrosymmetric manner. However, there is no real centrosymmetry due to the given (R_C) configuration at the stereogenic carbon atoms. According to the priority sequence η6-*p*-cymene > Cl > N(imine) > N(pyrrolate) the configuration of the stereogenic ruthenium centers is (*S*) for Ru1 and (*R*) for Ru2. Selected bond distances and angles are listed in Table 2.

The bond lengths and angles are similar to those observed in related complexes.[12]. The distances of the oxygen atoms to the chloride ligands are O1···Cl1 3.28 Å and O2···Cl2 3.00 Å, indicating the formation of weak O−H···Cl hydrogen bridges as observed for **1a/1b**.

The dissociation of the chloride ligand in ruthenium half-sandwich complexes[12][13][25][26][27] can be used for halogen exchange reactions.[27] Stirring the complexes **1a/1b** in MeOH in the presence of a 10 M excess of NaI for 1 h at rt gave the complexes [(η6-*p*-cymene)Ru(LL1*)I] (**5a**, **b**) (Scheme 3) in nearly quantitative yield.

Table 2. Selected bond lengths and angles of **3a/3b**; estimated standard deviations are shown in parentheses

	$R_{Ru(1)}$	$S_{Ru(2)}$
Ru−Cl	2.481(11)	2.361(10)
Ru−N(pyrr)	2.082(26)	2.041(26)
Ru−N(imine)	2.137(27)	2.119(27)
Ru−(arene)	1.626(14)	1.711(17)
Cl−Ru−N(pyrr)	84.7(7)	84.8(7)
Cl−Ru−N(imine)	85.8(7)	84.4(8)
N (pyrr)−Ru−N	75.3(10)	80.1(10)

Scheme 3. Structural formulae of the iodo complexes **5a/5b**, **6a/6b**. Only one diastereomer is shown

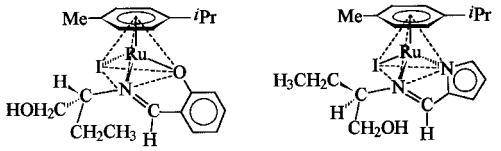

5a,b **6a,b**

There were hardly differences in the chemical shifts of the iodo complex **5a/5b** and the chloro complex **1a/1b**. In the iodo complex the *p*-methyl group of the cymene ligand was shifted 0.17 ppm to low field, whereas the imine proton was shifted 0.16 ppm to high field relative to the chloro complex. The diastereomer ratio of **5a**, **b** (88:12) was similar to that found for **1a**, **b** (91:9). Thus, the exchange of the *p*-cymene ligand in **1** for benzene in **2** had a much stronger impact on the diastereomer ratio than the exchange of chloride in **1** for iodide in **5**.

The preparation of [(η6-*p*-cymene)Ru(LL2*)I] (**6a/6b**) (Scheme 3) from **3a/3b** was carried out as described for the system **1** → **5**. In the FD mass spectrum of **6a/6b** only the peak of the iodo complex was detected confirming quantitative halogen exchange. The integration of the imine protons at δ = 7.44 and 7.48 in $CDCl_3$ gave a diastereomer ratio of 65:35.

Experimental Section

General Remarks: Preparation of the ruthenium complexes was carried out under an atmosphere of dry nitrogen with standard Schlenk techniques. − IR spectra: Beckman IR 4240 spectrometer. − Mass spectra: field desorption method (Finnigan MAT 95). − ^{1}H-NMR spectra: Bruker ARX 400 spectrometer (400 MHz). − UV/Vis spectroscopy: Kontron Uvikon 922 spectrophotometer. − CD spectra Jasco J-710 spectrophotometer. − Polarimetric measurements: Perkin-Elmer 241 instrument. − Melting points: Büchi SMP 20. Elemental analyses: microanalytical laboratory of the University of Regensburg. − [(η6-*p*-cymene)$RuCl_2]_2$[28−30] and [(η6-benzene)$RuCl_2]_2$[28][29][30] were prepared as published from $RuCl_3 \cdot xH_2O$. 2-*N*-[(*R*)-1-hydroxybut-2-yl)]salicylaldimine[18] (HLL*-**1**) and 2-*N*-[(*R*)-1-hydroxybut-2-yl)]pyrrolecarbaldimine[17][24] (HLL*-**4**) were synthesized by the literature methods. −

X-ray structure analyses: Syntex R3 diffractometer, Mo-K_α radiation, T = 296 K. Solution by direct methods using the program SHELXTL Plus (release 4.2/800), PC version. Further details of the crystal structure investigation may be obtained from the Fachinformationszentrum Karlsruhe, D-76344 Eggenstein-Leopoldshafen (Germany) (e-mail: crysdata@fiz-karlsruhe.de) on quoting the respective depository CSD number (vide infra).

Preparation of the Complexes [(η⁶-arene)Ru(LL)Cl]:* 2.07 mmol of the appropriate ligand HLL* was dissolved in abs. CH_2Cl_2 and KO*t*Bu (2.07 mmol) was added. The mixture was stirred for 1 h at room temp. After adding CH_2Cl_2 the mixture was cooled to 0°C. $[(\eta^6\text{-arene})RuCl_2]_2$ (1.00 mmol) was added and the solution was stirred for 4 h at 0°C. The solution was filtered through Celite and concentrated. The product was precipitated quantitatively by slow addition of petroleum ether with stirring. The red microcrystalline residue was washed with petroleum ether and dried.

[(η⁶-p-Cymene)Ru(LL₁)Cl]* (**1a**, **b**): Yield: 705 mg (83%), m.p. 136°C (decomp.). − IR (KBr): $\tilde{\nu}$ = 1615 cm^{-1} (C=N), 1600, 1540, 1470 (C=C). − $[\alpha]^{24}$ (c = 0.14, $CHCl_3$) (589 nm) +770, (578 nm) +1025, (546 nm) +1277. − UV/Vis (c = 1.32·10^{-4} mol l^{-1}, CH_2Cl_2) λ_{max} (lg ε) = 277 nm (3.67). − CD data (c = 1.80·10^{-4} mol l^{-1}, CH_2Cl_2) λ_{max} (Δε) = 248 nm (−6.40), 261 (0.0), 271 (2.71), 305 (1.14), 320 (0.0), 351 (−3.31), 426 (−3.11), 450 (0.0), 503 (5.41). − ^{1}H NMR ($CDCl_3$): δ = 1.15 (m, 6 H, C*H*$_3$, C*H*$_3$-*i*Pr), 1.26 (d, J = 6.9 Hz, 3 H, C*H*$_3$-*i*Pr), 1.97 (m, 2 H, C*H*$_2$CH$_3$), 2.25 (s, 3 H, C*H*$_3$-cymene), 2.75 (sept, J = 6.9 Hz, 1 H, C*H*-*i*Pr), 3.71 (m, 1 H, C*H*), 3.98 (m, 1 H, *H*CHOH), 4.44 (m, 1 H, HC*H*OH), 4.99/5.40 (AB, d, J = 5.7 Hz, 2 H, *H*-cymene), 5.46/5.47 (AB, d, J = 6.5 Hz, 2 H, *H*-cymene), 6.44 (m, 1 H, *H*^{4}-sal), 6.95 (m, 2 H, *H*^{3},*H*^{6}-sal), 7.19 (m, 1 H, *H*^{5}-sal), 7.75 (7.85, 9%) (s, 1 H, N=C*H*). − MS-FD (EtOH); *m*/*z* (%): 463 (100) [M^+] rel. to ^{102}Ru. − $C_{21}H_{28}ClNO_2Ru$ (462.98): calcd. C 54.48, H 6.10, N 3.03; found C 54.24, H 6.31, N 3.04.

Figure 3. CD spectra of the chloride and iodide complexes **1a**, **b** (91:9) and **5a**, **b** (88:12) in dichloromethane. [c(**1**) = 1.80·10^{-4} mol l^{-1}, c(**5**) = 1.59·10^{-4} mol l^{-1}]

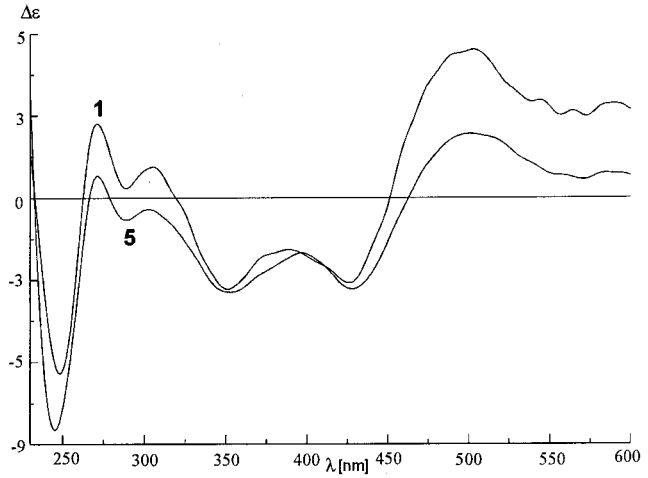

Crystals for X-ray analysis were obtained from a mixture of CH_2Cl_2, thf, and pentane at 3°C. X-ray structure analysis of (R_{Ru},R_C/S_{Ru},R_C)-[(η⁶-*p*-cymene)Ru(LL$_1$*)Cl]: dark red triangular plates, crystal size 0.25 × 0.45 × 0.55 mm^3, monoclinic, space group C_2^2, $P2_1$ (no 4), a = 7.715(2), b = 17.859(4), c = 29.359(8) Å, β = 94.90(2)°, V = 4031(2) Å^3, Z = 4·2, d_{calc} = 1.52 g cm^{-3}, empirical absorption correction (7 reflections 4.6° < 2θ < 41.2°), ω scans, 2θ range 3.0° < 2θ < 59.0°, Friedel pairs 3.0° < 2θ < 35.0°, transmission factors 0.86−1.00, μ = 0.93 mm^{-1}, F(000) = 1896; 13919 unique, 8505 observed reflections [I > 2.5σ(I)]. Parameters blocked 4·115, total 457; R = 0.074, Rw = 0.067, residual electron density 4.60/−2.00 e Å^{-3}. CSD 408883.

[(η⁶-benzene)Ru(LL₁)Cl]* (**2a**, **b**): Yield: 363 mg (72%), m.p. 167°C (decomp.). − IR (KBr): $\tilde{\nu}$ = 1620 cm^{-1} (C=N), 1600, 1540, 1470 (C=C). − $[\alpha]^{20}$ (c = 0.12, CH_2Cl_2) (589 nm) +920, (578 nm) +1111, (546 nm) +1547. − CD data (c = 1.48·10^{-4} mol l^{-1}, CH_2Cl_2) λ_{max} (Δε) = 247 nm (−2.30), 269 (0.0), 282 (0.18). − NMR data for the minor diastereomer are added in parentheses when different to the major diastereomer. ^{1}H NMR ($CDCl_3$): δ = 1.16 (0.92) (t, J = 7.2 (7.4) Hz, 3 H, C*H*$_3$), 2.00 (m, 2 H, C*H*$_2$CH$_3$), 3.76 (m, 1 H, C*H*), 3.99 (m, 1 H, *H*CHOH), 4.51 (m, 1 H, HC*H*OH), 5.60 (s, 6 H, *H*-benzene), 6.48 (m, 1 H, *H*^{4}-sal), 6.98 (m, 2 H, *H*^{3},*H*^{6}-sal), 7.22 (m, 1 H, *H*^{5}-sal), 7.77 (8.39) (s, 1 H, N=C*H*). − MS-FD (CH_2Cl_2); *m*/*z* (%): 407 (100) [M^+] rel. to ^{102}Ru. − $C_{17}H_{20}ClNO_2Ru$ (406.87): calcd. C 50.18, H 4.95, N 3.44; found C 50.55, H 5.29, N 3.85.

[(η⁶-p-cymene)Ru(LL₂)Cl]* (**3a**, **b**): Yield: 615 mg (72%), m.p. 157°C (decomp.). − IR (KBr): $\tilde{\nu}$ = 1660 cm^{-1} (C=N), 1580, 1460 (C=C). − $[\alpha]^{20}$ (c = 0.11, CH_2Cl_2) (589 nm) +68, (578 nm) +75, (546 nm) +95. − UV/Vis (c = 4.21·10^{-5} mol l^{-1}, CH_2Cl_2) λ_{max} (lg ε) = 324 nm (4.22). − NMR data for the second diastereomer are added in parentheses when different to the first diastereomer. Intensities are related to the corresponding peaks. ^{1}H NMR ($CDCl_3$): δ = 0.80 (0.94) (d, J = 6.9 Hz, 3 H, C*H*$_3$-*i*Pr), 1.06 (t, J = 7.4 Hz, 3 H, C*H*$_3$),1.14 (m, 6 H, C*H*$_3$, C*H*$_3$-*i*Pr), 1.28 (d, J = 6.9 Hz, 3 H, C*H*$_3$-*i*Pr), 1.75 (1.93) (m, 2 H, C*H*$_2$CH$_3$), 2.23 (2.26) (s, 3 H, C*H*$_3$-cymene), 2.57 (sept, J = 6.9 Hz, 1 H, C*H*-*i*Pr), 3.50 (4.12) (m, 1 H, C*H*), 3.66 (4.04) (m, 2 H, C*H*$_2$OH), 5.26 (m, 3 H, *H*-cymene), 5.34 (d, J = 6.2 Hz, 1 H, *H*-cymene), 5.47 (d, J = 6.2 Hz, 1 H, *H*-cymene), 5.64 (m, 2 H, *H*-cymene), 5.75 (d, J = 6.1 Hz, 1 H, *H*-cymene), 6.32 (m, 1 H, *H*^{4}-pyrr), 6.67 (m, 1 H, *H*^{3}-pyrr), 7.44 (m, 1 H, *H*^{5}-pyrr), 7.57 (7.61) (s, 1 H, N=C*H*). − MS-FD (acetone); *m*/*z* (%): 436 (100) [M^+] rel. to ^{102}Ru. − $C_{19}H_{27}ClN_2ORu$ (435.96): calcd. C 52.35, H 6.24, N 6.43; found C 52.24, H 6.46, N 6.38.

Crystals of **3a/3b** for X-ray analysis were obtained from a mixture of CH_2Cl_2, thf, and pentane at 3°C. X-ray structure analysis of (R_{Ru},R_C/S_{Ru},R_C)-[(η⁶-*p*-cymene)Ru(LL$_2$*)Cl]: orange-red needles, crystal size 0.08 × 0.10 × 0.08 mm^3, monoclinic, space group C_2^2, $P2_1$ (no 4), a = 10.036(3), b = 9.415(3), c = 21.132(7) Å, β = 101.44(2)°, V = 1957(1) Å^3, Z = 2·2, d_{calc} = 1.48 g cm^{-3}, empirical absorption correction (8 reflections 4.2° < 2θ < 35.2°), ω scans, 2θ range 3.0° < 2θ < 50.0°, Friedel pairs 3.0° < 2θ < 42.0°, transmission factors 0.86−1.00, μ = 0.95 mm^{-1}, F(000) = 896; 5465 unique, 3069 observed reflections [I > 2.5σ(I)]. Parameters 213; R = 0.119, Rw = 0.096, residual electron density 1.93/−2.47 e Å^{-3}. CSD 408884.

[(η⁶-benzene)Ru(LL₂)Cl]* (**4a**, **b**): Yield: 340 mg (66%), m.p. 110°C (decomp.). − IR (KBr): $\tilde{\nu}$ = 1620 cm^{-1} (C=N), 1580, 1435 (C=C). − $[\alpha]^{20}$ (c = 0.17, CH_2Cl_2) (589 nm) −321, (578 nm) −381, (546 nm) −669. − NMR data for the second diastereomer are added in parentheses when different to the first diastereomer. ^{1}H NMR ($CDCl_3$): δ = 1.06 (1.12) (t, J = 7.4 Hz, 3 H, C*H*$_3$), 1.79 (1.92) (m, 2 H, C*H*$_2$CH$_3$), 3.55 (m, 1 H, C*H*), 3.72 (m, 1 H, *H*CHOH), 3.92 (m, 1 H, HC*H*OH), 5.70 (5.62) (s, 6 H, η^6-C$_6$*H*$_6$), 6.34 (dd, J = 3.8 Hz, J = 1.1 Hz, 1 H, *H*^{4}-pyrr), 6.71 (dd, J = 3.8 Hz, J = 1.1 Hz 1 H, *H*^{3}-pyrr), 7.53 (broad, 1 H, *H*^{5}-pyrr), 7.59 (7.62) (s, 1 H, N=C*H*). − MS-FD (acetone); *m*/*z* (%): 380 (100) [M^+] rel. to ^{102}Ru. − $C_{19}H_{19}ClN_2ORu$ (379.85): calcd. C 45.28, H 5.32, N 7.04; found C 45.00, H 5.12, N 6.33.

Preparation of the complexes [(η^6-*p*-cymene)Ru(LL*)I]: 0.15 mmol of the appropriate ruthenium complex (**1a**, **b**) or (**3a**, **b**) was dissolved in abs. MeOH (15 ml). NaI (1.5 mmol) was added. The solution was stirred for 1 h at r.t. The solvent was evaporated and the red residue was dissolved in CH_2Cl_2 and filtered. After removing the solvent an analytically pure red powder was obtained in nearly quantitative yield.

[(η^6-p-cymene)Ru(LL_1)I]* (**5a**, **b**): m.p. 80°C (decomp.).– $[\alpha]^{21}$ (c = 0.08, $CHCl_3$) (589 nm) +29, (578 nm) −29, (546 nm) −29. – UV/Vis (c = $1.27\cdot10^{-4}$ mol l^{-1}, CH_2Cl_2) λ_{max} (lg ε) = 270 nm (3.92), 293 (3.92). – CD data (c = $1.59\cdot10^{-4}$ mol l^{-1}, CH_2Cl_2) λ_{max} (Δε) = 245 nm (−8.47), 264 (0.0), 271 (0.81), 279 (0.0), 302 (−0.41), 353 (−3.44), 428 (−3.32), 461 (0.0), 501 (2.33). – NMR data for the minor diastereomer are added in parentheses when different to the major diastereomer. ^{1}H NMR ($CDCl_3$): δ = 1.12 (0.91) (t, J = 7.4 (7.5) Hz, 3 H, CH_3), 1.16 (d, J = 6.8 Hz, 3 H, CH_3-*i*Pr), 1.29 (d, J = 6.8 Hz, 3 H, CH_3-*i*Pr), 2.00 (m, 2 H, CH_2CH$_3$), 2.42 (2.35) (s, 3 H, CH_3-cymene), 2.88 (sept, J = 6.8 Hz, 1 H, C*H*-*i*Pr), 3.74 (m, 1 H, C*H*), 4.26 (m, 2 H, CH_2OH), 4.89/5.49 (AB, d, J = 5.3 Hz, 2 H, *H*-cymene), 5.30/5.62 (AB, d, J = 5.7 Hz, 2 H, *H*-cymene), 6.42 (m, 1 H, H^4-sal), 6.92 (m, 2 H, H^3,H^6-sal), 7.15 (m, 1 H, H^5-sal), 7.59 (7.66) (s, 1 H, N=C*H*). – MS-FD (CH_2Cl_2); *m*/*z* (%): 555 (100) [M^+] rel. to ^{102}Ru, 428 (20) [M^+ − I]. – $C_{21}H_{28}INO_2Ru$ (554.43): calcd. C 44.06, H 5.28, N 2.45; found C 44.22, H 5.20, N 2.29.

[(η^6-p-cymene)Ru(LL_2)I]* (**6a**, **b**): m.p. 67°C (decomp.).– $[\alpha]^{21}$ (c = 0.09, CH_2Cl_2) (589 nm) +215, (578 nm) +244, (546 nm) +429. – NMR data for the minor diastereomer are added in parentheses when different to the major diastereomer. ^{1}H NMR ($CDCl_3$): δ = 0.94 (0.79) (d, J = 6.9 Hz, 3 H, CH_3-*i*Pr), 1.10 (1.05) (t, J = 7.4 Hz, 3 H, CH_3), 1.17 (1.25) (d, J = 6.9 Hz, 3 H, CH_3-*i*Pr), 1.75 (m, 1 H, *H*CHCH$_3$), 1.97 (m, 1 H, HC*H*CH$_3$), 2.43 (2.49) (s, 3 H, CH_3-cymene), 2.66 (t, J = 6.9 Hz, 1 H, O*H*), 2.74 (3.02) (sept, J = 6.9 Hz, 1 H, C*H*-*i*Pr), 3.64 (3.34) (m, 1 H, C*H*), 3.95 (3.51) (m, 1 H, *H*CHOH), 4.26 (4.07) (m, 1 H, HC*H*OH), 5.19/5.31 (AB, d, J = 5.8 Hz, 2 H, *H*-cymene), 5.25/5.46 (AB, d, J = 6.1 Hz, 2 H, *H*-cymene), 6.32 (m, 1 H, H^4-pyrr), 6.70 (m, 1 H, H^3-pyrr), 7.37 (m, 1 H, H^5-pyrr), 7.44 (7.48) (s, 1 H, N=C*H*). – MS-FD (CH_2Cl_2); *m*/*z* (%): 528 (100) [M^+] rel. to ^{102}Ru. – $C_{19}H_{27}IN_2ORu$ (527.41): calcd. C 39.23, H 4.77, N 4.57; found C 40.15, H 4.99, N 4.49.

---

[1] H. Brunner, B. Nuber, M. Prommesberger, *Tetrahedron: Asymmetry* **1998**, submitted.

[2] S. Hashiguchi, A. Fujii, J. Takehara, T. Ikariya, R. Noyori, *J. Am. Chem. Soc.* **1995**, *117*, 7562−7563.
[3] J. Takehara, S. Hashiguchi, A. Fujii, T. Ikariya, R. Noyori, *J. Chem. Soc., Chem. Commun.* **1996**, 233−234.
[4] K.-J. Haack, S. Hashiguchi, A. Fujii, T. Ikariya, R. Noyori, *Angew. Chem.* **1997**, *109*, 297−300; *Angew. Chem. Int. Ed. Engl.* **1997**, *36*, 285−288.
[5] R. Noyori, S. Hashiguchi, *Acc. Chem. Res.* **1997**, *30*, 97−102.
[6] D. L. Davies, J. Fawcett, S. A. Garrat, D. R. Russell, *J. Chem. Soc., Chem. Commun.* **1997**, 1351−1352.
[7] D. Carmona, C. Cativiela, S. Elipe, F. J. Lahoz, M. P. Lamata, M. Pilar, L.-R. de Viu, L. A. Oro, C. Vega, F. Viguri, *J. Chem. Soc., Chem. Commun.* **1997**, 2351− 2352.
[8] H. Brunner, M. Prommesberger, *Tetrahedron: Asymmetry* **1998**, submitted.
[9] I. de los Rios, M. J. Tenorio, M. C. Puerta, P. Valerga, *J. Organomet. Chem.* **1996**, *525*, 57−64.
[10] Y. Yamamoto, R. Sato, F. Matsuo, C. Sudoh, T. Igoshi, *Inorg. Chem.* **1996**, *35*, 2329−2336.
[11] H. Brunner, R. Oeschey, B. Nuber, *Inorg. Chem.* **1995**, *34*, 3349−3351.
[12] H. Brunner, R. Oeschey, B. Nuber, *Organometallics* **1996**, *15*, 3616−3624.
[13] H. Brunner, R. Oeschey, B. Nuber, *J. Chem. Soc., Dalton Trans.* **1996**, 1499−1508.
[14] S. K. Mandal, A. R. Chakravarty, *J. Chem. Soc., Dalton Trans.* **1992**, 1627−1633.
[15] S. K. Mandal, A. R. Chakravarty, *Inorg. Chem.* **1993**, *32*, 3851−3854.
[16] H. Brunner, J. Breu, P. Faustmann, *Eur. J. Inorg. Chem*. **1998**, in press.
[17] T. Neuhierl, Ph. D. Thesis, University of Regensburg, **1998**.
[18] H. Brunner, W. Miehling, *Monatsh. Chem.* **1984**, *115*, 1237−1254.
[19] H. Brunner, *Angew. Chem*. **1983**, *95*, 921−931; *Angew. Chem. Int. Ed. Engl.* **1983**, *36*, 897.
[20] R. S. Cahn, C. K. Ingold, V. Prelog, *Angew. Chem.* **1966**, *78*, 413−447; *Angew. Chem. Int. Ed. Engl.* **1966**, *5*, 385.
[21] C. Lecomte, Y. Dusausoy, J. Protas, J. Tirouflet, A. Dormond, *J. Organomet. Chem.* **1974**, *73*, 67−76.
[22] H. Brunner, *Enantiomer* **1997**, *2*, 133−134.
[23] N. N. Greenwood, A. Earnshaw, *Chemie der Elemente*, VCH, Weinheim, **1990**, 72.
[24] H. Brunner, T. Neuhierl, B. Nuber, *J. Organomet. Chem.* **1998** *563*, 173−178.
[25] I. de Rios, M. J. Tenorio, J. Padilla, M. C. Puerta, P. Valerga, *J. Chem. Soc., Dalton Trans.* **1996**, 377−381.
[26] R. J. Haines, A. L. du Preez, *J. Organomet. Chem.* **1975**, *84*, 357−367.
[27] D. Enders, H. Gielen, G. Raabe, J. Runsink, J. H. Teles, *Chem. Ber.* **1997**, *130*, 1253−1260.
[28] G. Winkhaus, H. Singer, M. Kricke, *Z. Naturforsch.* **1966**, *21b*, 1109−1110.
[29] G. Winkhaus, H. Singer, *J. Organomet. Chem.* **1967**, *7*, 487−491.
[30] M. A. Bennett, T. N. Huang, T. W. Matheson, A. K. Smith, *Inorg. Synth.* **1982**, *21*, 75.

[I98216]

Highly Regioselective Benzylic Deprotonation of Some (η^6-Tetralin)- and (η^6-*trans*-Octahydroanthracene)$Cr(CO)_3$ Derivatives: Is the Regioselectivity Stereoelectronically Controlled?☆

Thorsten Volk, Dirk Bernicke, Jan W. Bats[+], and Hans-Günther Schmalz*

Institut für Organische Chemie der Technischen Universität Berlin,
Strasse des 17. Juni 135, D-10623 Berlin, Germany
E-mail: schmalz@wap0109.chem.tu-berlin.de

Received September 24, 1997

Keywords: (Arene)tricarbonylchromium complexes / Benzylic deprotonation / Stereoelectronic effects / Conformational analysis / Stereoselective synthesis / Arene complexes / Chromium

The regioselectivity of benzylic deprotonation of a number of conformationally restricted (arene)$Cr(CO)_3$ complexes has been examined in order to ascertain whether stereoelectronic effects play a role in such reactions. The complexes *rac*-**5**, *rac*-**6**, *rac*-**7**, *rac*-**8** and *rac*-**9** were diastereoselectively synthesized from the corresponding C_2-symmetric ligands (2,3-disubstituted *trans*-1,2,3,4-tetrahydronaphthalene and *trans*-1,2,3,4,4a,9,9a,10-octahydroanthracene derivatives). Due to the desymmetrization caused by the $Cr(CO)_3$ complexation, all four benzylic protons could be distinguished by ^1H NMR and were assigned in all cases by a combination of H,H-COSY spectra and the observation of H/D exchange at both *exo* positions (*tert*-BuOK/[D_6]DMSO). Deprotonation (*n*-butyllithium)/deuteration (D_2O or CF_3CO_2D) experiments revealed a very high, unforeseen regioselectivity in the cases of *rac*-**5** and *rac*-**7**, while the other substrates showed a low selectivity (*rac*-**6**) or could not be deuterated at all under these conditions (*rac*-**8**, *rac*-**9**). In the case of *rac*-**5**, the regioselectivity of the deprotonation was further confirmed by acylation (AcCl) or alkylation (MeI) of the lithiated intermediate. These results clearly rule out the notion that the regioselectivity is due to the preferred abstraction of pseudoaxially oriented benzylic hydrogen atoms. The crystal structures of *rac*-**1**, *rac*-**5** and *rac*-**7** suggest a possible link between the preferred conformation of the $Cr(CO)_3$ tripod and the regioselectivity of the benzylic deprotonation. In analogy to a commonly accepted picture often used to explain the regioselectivity of nucleophile additions to (arene)$Cr(CO)_3$ complexes, it was anticipated that those benzylic positions which are activated by an eclipsed CO ligand should be preferentially deprotonated (kinetically controlled). This (new) stereoelectronic model was corroborated by experiments using complexes *rac*-**60** and *rac*-**62**, which were regioselectively deprotonated at the predicted position. In summary, it has been shown for the first time that the preferred conformation of the $Cr(CO)_3$ tripod may have a directing influence on the regioselectivity of benzylic deprotonation in (arene)$Cr(CO)_3$ complexes, at least in conformationally unambiguous situations where no obvious electronic effects are operative.

Introduction

(Arene)$Cr(CO)_3$ complexes represent a unique class of transition metal complexes, which are of considerable value for the synthesis of complex organic molecules[1]. One of the most useful effects of the $Cr(CO)_3$ fragment is the stabilization of negative charge in benzylic positions, which can be exploited for efficient benzylic deprotonation/alkylation reactions[2][3].

In the course of our program on the use of chiral (arene)$Cr(CO)_3$ complexes as building blocks for the total synthesis of bioactive compounds[4][5], we recently discovered that complex **1** is deprotonated by *n*-butyllithium in a highly regioselective fashion, permitting the regio- and diastereoselective preparation of benzylic alkylated products such as **2** (Scheme 1)[5].

While the regioselectivity of the benzylic deprotonation of (arene)$Cr(CO)_3$ complexes has hitherto been explained more or less exclusively in terms of electronic[1c][2][6] or complex-induced proximity effects[7], any rationalization of the high degree of regiocontrol during the deprotonation of **1** must be based on different concepts.

Scheme 1

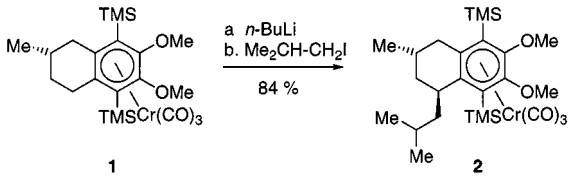

1 **2**

The crystal structure of *rac*-**1** (see below) shows that the molecule preferentially adopts a half-chair conformation (**1′**; Figure 1). As a result, the two relevant benzylic *exo* hydrogen atoms, which have comparable steric environments, differ in that one (the one that is attacked by the base) adopts a pseudoaxial position, while the other is pseudoequatorially oriented. Therefore, it could not a priori be ruled out that the deprotonation step (leading to the anionic intermediate **3**) is stereoelectronically controlled[8].

[+] X-ray crystallographic investigations. Address: Institut für Organische Chemie der Universität Frankfurt, Marie-Curie-Str. 11, D-60349 Frankfurt am Main, Germany.

 © WILEY-VCH Verlag GmbH, D-69451 Weinheim, 1998 1434–1948/98/1010–1883 $ 17.50+.50/0

Figure 1. On the regio- and stereochemistry of the deprotonation/alkylation of complex **1**

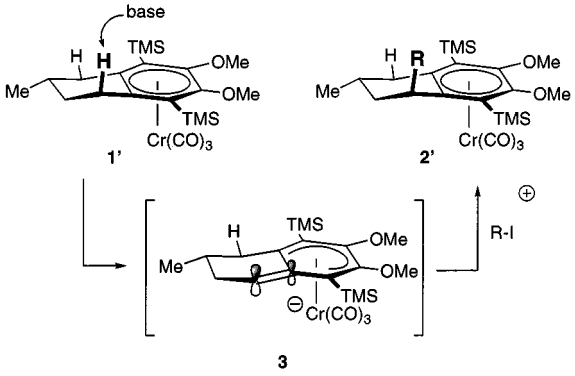

In order to investigate whether such conformational or stereoelectronic effects do indeed play a role in the benzylic deprotonation of (arene)$Cr(CO)_3$ complexes, we decided to explore conformationally more rigid substrates of type **4** (Figure 2). Compared to **1**, these compounds should exhibit an even stronger preference for a half-chair conformation (**4′**)[9] and, as a result of the symmetry of such structures, the two benzylic positions are essentially electronically equivalent.

Figure 2. Preferred half-chair conformation of 2,3-disubstituted tetralin complexes of type **4**; the two benzylic *exo*-hydrogen atoms can be classified as pseudoaxial and pseudoequatorial, respectively

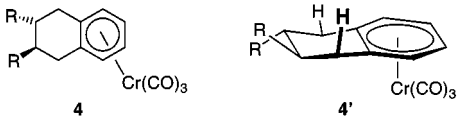

We report here on the synthesis and structural characterization of several (tetralin)- and (*trans*-octahydroanthracene)$Cr(CO)_3$ complexes (*rac*-**5**, *rac*-**6**, *rac*-**7**, *rac*-**8**, *rac*-**9**) as well as on investigations of their benzylic deprotonation. Furthermore, we present a modified mechanistic interpretation to explain the effects governing the regioselectivity of the benzylic deprotonation of such complexes.

Synthesis of the Complexes

Strategic Considerations

The syntheses of the various complexes were envisaged as being possible by the general routes outlined in Scheme 2. Retrosynthetically, the target compounds stem from C_2-symmetric ligands in each case. For the synthesis of 2,3-*trans*-disubstituted tetralin derivatives of type **10**, a Diels-Alder reaction of an (*E*)-configured dienophile **11** with an *o*-quinodimethane of type **12** was envisaged[10]. For the diastereoselective preparation of *trans*-octahydroanthracenes such as **13**[11], either a 6-*endo* cyclization of a radical intermediate of type **14**[12], or a metal-mediated [2+2+2]-cycloaddition (Vollhardt reaction)[13] employing the *trans*-bis(alkyne) **15** were considered. For the purposes of the anticipated deprotonation studies, it was sufficient to focus merely on synthetic methods that would furnish the target complexes in racemic form.

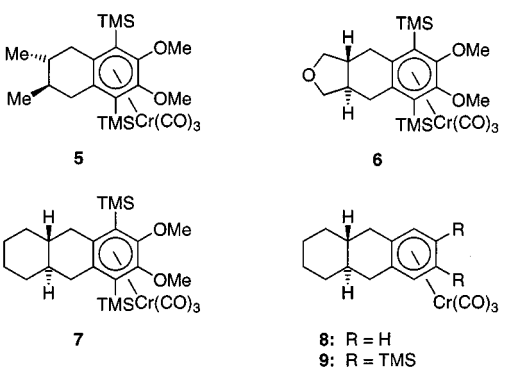

Scheme 2

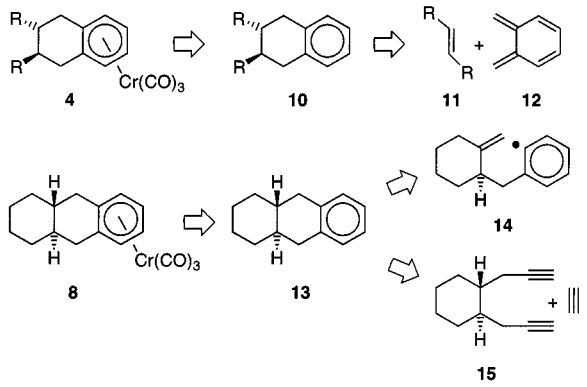

Synthesis of *rac*-5

Compound **19**, the precursor of the dimethoxy-substituted *o*-quinodimethane, was prepared from veratrole (**16**) in three steps employing modified literature procedures[14]. The dichlorinated derivative **17** was converted to 4,5-dimethylveratrole (**18**) by reaction with methyllithium in diethyl ether[14a][14b]. Subsequent benzylic bromination of **18**[14c] with 2 equiv. of dry NBS in the presence of molecular sieves (4 Å) afforded **19** in 72% yield.

Scheme 3

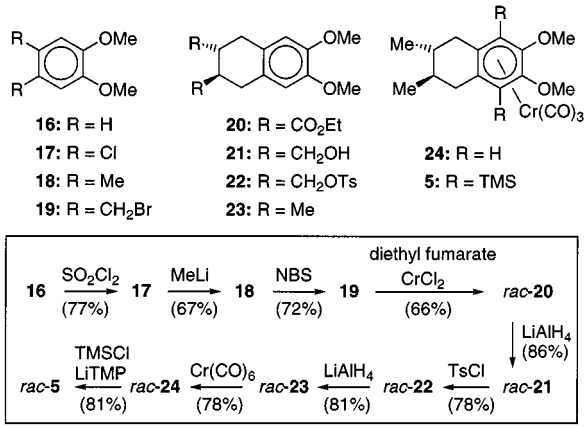

In situ generation of the *o*-quinodimethane from **19** by reductive debromination with $CrCl_2$ in THF[15] in the presence of diethyl fumarate at 0°C yielded the desired Diels-Alder product *rac*-**20** in 66% yield as the pure *trans* dia-

stereomer[16]. Reduction of *rac*-**20** with $LiAlH_4$ in diethyl ether (30°C, 0.5 h) afforded the diol *rac*-**21**. Deoxygenation of the diol *rac*-**21** was then achieved in 63% overall yield by $LiAlH_4$ reduction of the corresponding bis(tosylate) (*rac*-**22**)[17]. It proved to be important to carry out the ditosylation (*rac*-**21** → *rac*-**22**) at low temperature (0−4°C), otherwise the cyclic ether *rac*-**27** (see below) became the major product. Heating of *rac*-**22** with $Cr(CO)_6$ (1.1 equiv.) under standard conditions[18] (*n*-Bu_2O/THF; reflux) gave complex *rac*-**23** in 78% recrystallized yield. The introduction of the two trimethylsilyl substituents was finally accomplished in a one-pot procedure[5] using the reagent combination chlorotrimethylsilane/lithium tetramethylpiperidide[19] to afford the bis(silylated) complex *rac*-**5** in high yield. The crystal structure of *rac*-**5** is depicted in Figure 5.

Synthesis of Complex 24 (Nonracemic Series)

We also briefly investigated the Diels-Alder reaction of the **19**-derived *o*-quinodimethane employing chiral fumarates as dienophiles. While the use of dimenthyl fumarate[20] led only to a low selectivity (33% *de*; 92% yield), the lactic acid derivative **25** was found to be a much better chiral dienophile (Scheme 4)[21]. Thus, when **19** was treated with $CrCl_2$ in the presence of an excess of **25**, an 81:19 mixture of the two diastereomeric cycloaddition products **26a** and **26b** was obtained in high yield. After HPLC separation, the major diastereomer (**26a**) was converted by $LiAlH_4$ reduction to the optically active diol **21**, which was shown to be of ≥ 99% *ee* by means of HPLC on a chiral stationary phase[22]. It is remarkable that, compared to diethyl fumarate (see Scheme 3), the (more bulky) chiral fumarates generally gave much higher yields (>90%) in the Diels-Alder reactions. Following the procedures established for the racemic series, **21** was transformed to **24** (Scheme 4). The absolute and relative configuration of **24** was unequivocally established by means of a crystal structure analysis (see Figure 4), which (retrospectively) allowed assignment of the configurations of **26a** and **26b**.

Scheme 4

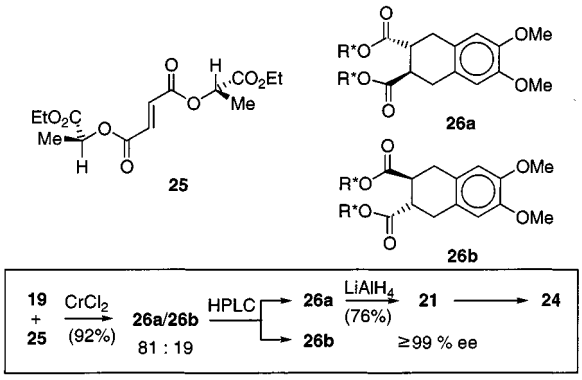

Synthesis of *rac*-6

The tetrahydrofuran derivative *rac*-**27**, which was initially obtained as an undesired side-product during the preparation of *rac*-**22** (see above), was isolated in 76% yield when *rac*-**21** was treated with *p*-TsCl in pyridine at 60°C, even when 3 equiv. of *p*-TsCl was used. Clearly, the S_N2-type cyclization of the monotosylated intermediate *rac*-**29** was faster than the second tosylation under these conditions[23].

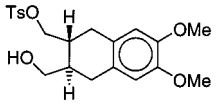

29

Since *rac*-**27** also represents a conformationally restricted tetralin derivative, it was converted to the corresponding $Cr(CO)_3$ complex *rac*-**28** (Scheme 5), which in turn was disilylated under the one-pot conditions described above to give *rac*-**6**.

Scheme 5

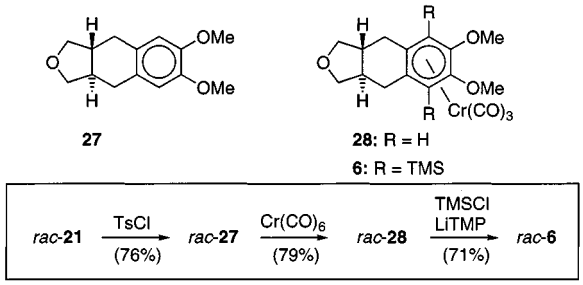

Synthesis of *rac*-7

The synthesis of *rac*-**7** (Scheme 6) was performed following the radical cyclization route outlined in Scheme 2. Starting from veratrum alcohol **30**, the dibromide **31** was prepared in high yield by treatment with bromine (1 equiv.) in benzene. Some hydrogen bromide was added to ensure completion of the reaction.

Alkylation of the enolate anion, prepared from **31** and cyclohexanone with LDA in THF, proceeded smoothly to give the ketone *rac*-**32** in high yield, together with small amounts of the doubly alkylated by-product **36a**, which could be easily separated by chromatography.

Scheme 6

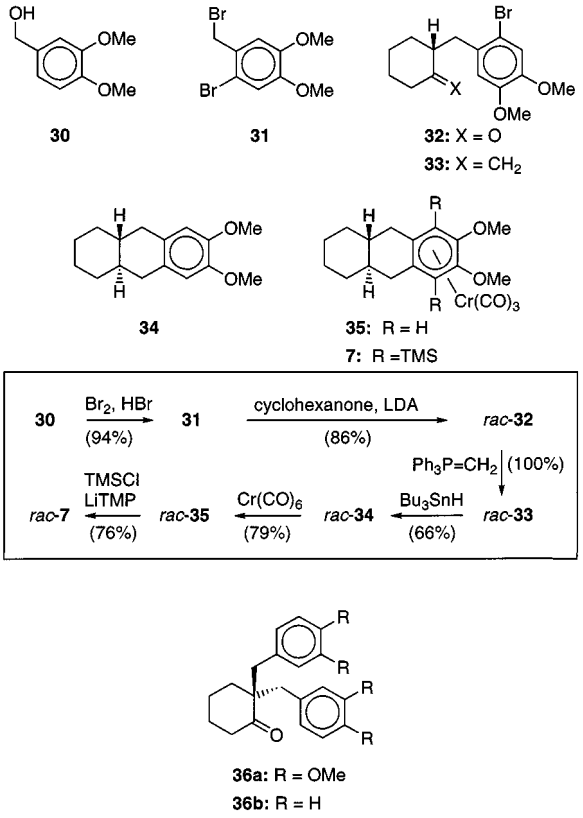

Wittig methylenation of *rac*-**32** furnished the cyclization precursor *rac*-**33** in essentially quantitative yield. The crucial radical cyclization[24] of *rac*-**33** was performed in benzene, with slow addition of tributyltin hydride in the presence of AIBN. The *6-endo* cyclization product *rac*-**34** was obtained as the major product in 66% yield. Complexation of *rac*-**34** with $Cr(CO)_6$ (→ *rac*-**35**) followed by double silylation afforded *rac*-**7** in good overall yield (Scheme 6). X-ray crystal structure analysis (see Figure 6) of *rac*-**7** proved its relative configuration.

Synthesis of *rac*-8

The synthesis of the *trans*-octahydroanthracene ligand *rac*-**13** was accomplished following the same strategy. Alkylation of cyclohexanone (LDA, subsequent addition of the dibromide **37**, 3 h reflux in THF) afforded an 80:20 mixture of *rac*-**38** and the double-alkylation product **36b**, from which pure *rac*-**38** was isolated by kugelrohr distillation. Methylenation of *rac*-**38** to *rac*-**39** followed by radical cyclization afforded *rac*-**13** (Scheme 7)[12][25]. Subsequent complexation of *rac*-**13** with $Cr(CO)_6$ furnished *rac*-**8** in good yield (Scheme 7).

Synthesis of *rac*-9

The *cis*-diester **41a**[26], obtained from hexahydrophthaloyl anhydride (**40**) in 87% yield, was converted to the *trans* isomer *rac*-**41b** by refluxing with ethanolic sodium ethoxide[27]. In contrast to a literature report[27], an inseparable mixture (*rac*-**41b**/**41a** = 89:11) was obtained rather

Scheme 7

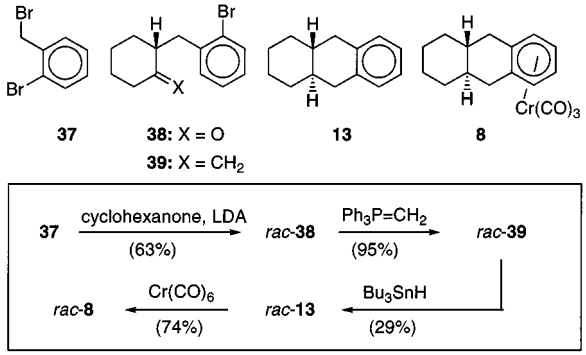

than the pure *trans* product. Reduction with $LiAlH_4$ in diethyl ether quantitatively afforded the corresponding mixture of diols (*rac*-**42b**/**42a** = 89:11). Fortunately, tosylation with *p*-TsCl in pyridine and recrystallization of the crude product mixture led to the isolation of the essentially pure *trans*-ditosylate *rac*-**43b** in 78% yield. Conversion of *rac*-**43b** to the cyclization precursor, the dialkyne *rac*-**44**, was achieved by treatment with a 2 M solution of the lithium acetylide·ethylenediamine complex in DMSO at 8°C[28]. Vollhardt cyclization[13] employing *rac*-**44** and bis(trimethylsilyl)acetylene (BTMSA) in the presence of catalytic amounts of $CpCo(CO)_2$ afforded only a moderate yield of the C_2-symmetric ligand *rac*-**45**, which was finally converted to the desired complex *rac*-**9** in 91% yield (Scheme 8).

Scheme 8

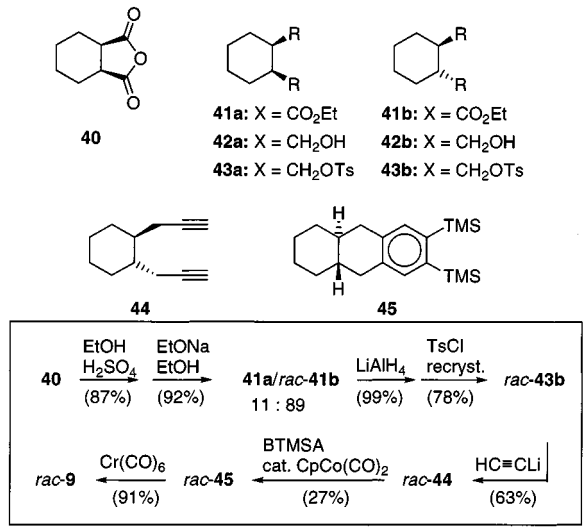

Characterization of the Complexes

General Aspects

All complexes synthesized as described above were fully characterized by ^1H NMR, ^{13}C NMR, IR, MS and elemental analysis (see Experimental Section). All data were in accordance with the constitutional and (relative) configurational assignments implied in the structural formulae. In

particular, the fact that all benzylic hydrogen atoms were found to be non-equivalent in the ^{1}H-NMR spectra (see below) and that a full set of ^{13}C signals was observed in each case (see Experimental Section) immediately proves the *trans* configuration on grounds of symmetry.

X-ray Crystal Structure Investigations

The crystal structures of the complexes *rac*-**1** (Figure 3), **24** (Figure 4), *rac*-**5** (Figure 5) and *rac*-**7** (Figure 6) were determined[29] so as to reveal detailed information about configurational and conformational aspects.

The X-ray structure of complex *rac*-**1** (Figure 3) shows that the cyclohexene ring adopts a (slightly distorted) half-chair conformation with one homobenzylic ring carbon atom lying 0.32 Å below, and the other lying 0.50 Å above, the molecular plane defined by the arene ring. The methyl group on the cyclohexene ring is in a pseudoequatorial position. The benzene ring shows a slight deviation from planarity. The largest torsion angle in the benzene ring is 8.4°. The puckering of the benzene ring may be due to the presence of the bulky substituents. The Cr−C(ring) distances range from 2.228 to 2.273 Å. The benzene $Cr(CO)_3$ group has an eclipsed conformation.

The X-ray structure of complex **24** (Figure 4) shows two independent molecules with very similar conformations of the hydrocarbon ligand. The cyclohexene ring adopts a conformation between a twist-boat and an envelope form. The two methyl groups on the cyclohexene ring have pseudoequatorial orientations. One of the homobenzylic ring carbon atoms in molecule I lies 0.48 Å below and the other 0.26 Å above the molecular plane defined by the arene ring (0.54 Å and 0.26 Å for molecule II, respectively). The benzene ring shows only a very small deviation from planarity. The largest torsion angle in the benzene ring is 3.1° (molecule I) and −4.2° (molecule II). The Cr atom lies 1.75 Å below the plane of the benzene ring and the Cr−C(ring) distances range from 2.205 to 2.308 Å. The (benzene)$Cr(CO)_3$ group adopts an almost eclipsed conformation in both independent molecules which, however, differ in that the $Cr(CO)_3$ tripod is rotated through ca. 60°. The absolute configuration of **24** was established with the aid of anomalous scattering.

The X-ray structure of *rac*-**5** (Figure 5) shows a disorder, with two independent molecules in a ratio of ca. 60:40. In both molecules,which differ in the orientation of the $Cr(CO)_3$ tripod, the cyclohexene ring is in a half-chair conformation, with the methyl substituents in equatorial positions and with one homobenzylic ring carbon atom lying 0.42 (0.44) Å below and the other lying 0.36 (0.37) Å above the molecular plane defined by the arene ring. The benzene ring shows a slight deviation from planarity. The Cr−C(ring) distances range from 2.233 to 2.265 Å. As in the case of **24**, the benzene $Cr(CO)_3$ group has an eclipsed conformation in both independent molecules, but with different orientations (60° rotation).

The X-ray structure of *rac*-**7** (Figure 6) also shows two independent molecules with very similar conformations. As expected, the central cyclohexene ring has a twist-boat (half-chair) conformation and the saturated cyclohexane ring has a purely chair conformation. Interestingly, the benzene ring shows a significant deviation from planarity. The ring carbon atoms attached to the TMS groups deviate by about 0.07 Å from the plane of the other four ring atoms and are closer to the Cr Atom. The Cr−C(ring) distances range from 2.217(3) to 2.261(3) Å. The (benzene)$Cr(CO)_3$ group has an almost eclipsed conformation.

Figure 3. X-ray crystal structure of *rac*-**1**; only one enantiomer is depicted

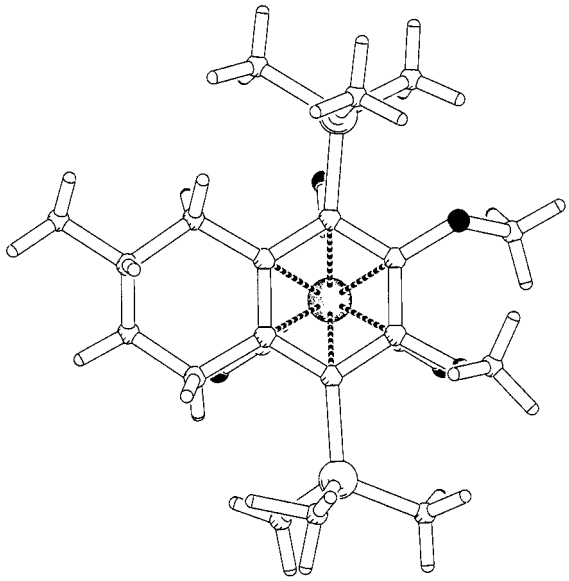

Figure 4. X-ray crystal structure of **24**; only one of two independent conformers is depicted

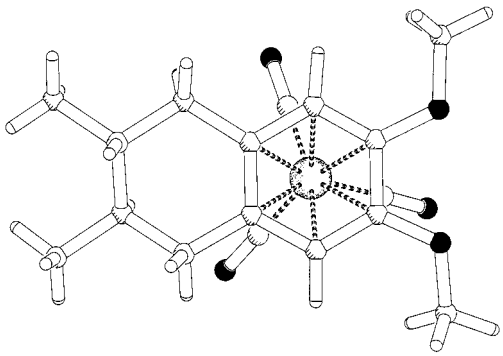

NMR-Spectroscopic Investigations

The ^{1}H-NMR and ^{13}C-NMR spectra of the various complexes (in $CDCl_3$) exhibit a number of interesting features. The signals for the benzylic hydrogen atoms are of particular interest. They all appear as double doublets (compare Figure 8) and are well separated in most cases − an important prerequisite for the unambiguous assignments necessary for the anticipated deprotonation/deuteration studies (see below).

As originally expected and confirmed by the crystal structures, the cyclohexene rings of the complexed ligands adopt half-chair conformations. Thus, the four dia-

Figure 5. X-ray crystal structure of *rac*-**5**; only one of two independent conformers and only one enantiomer is depicted

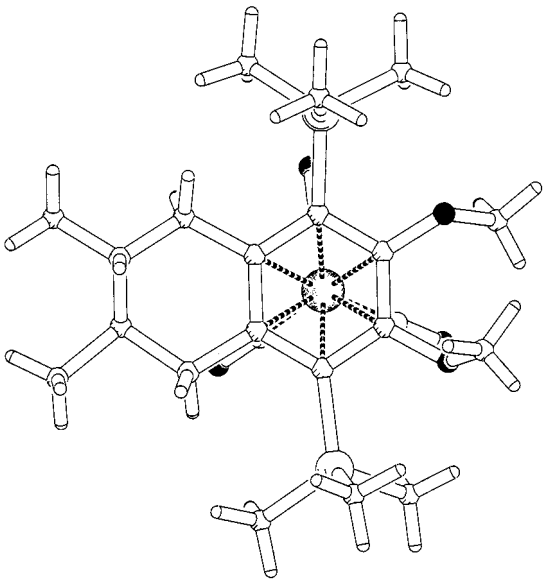

Figure 6. X-ray crystal structure of *rac*-**7**; only one enantiomer is depicted

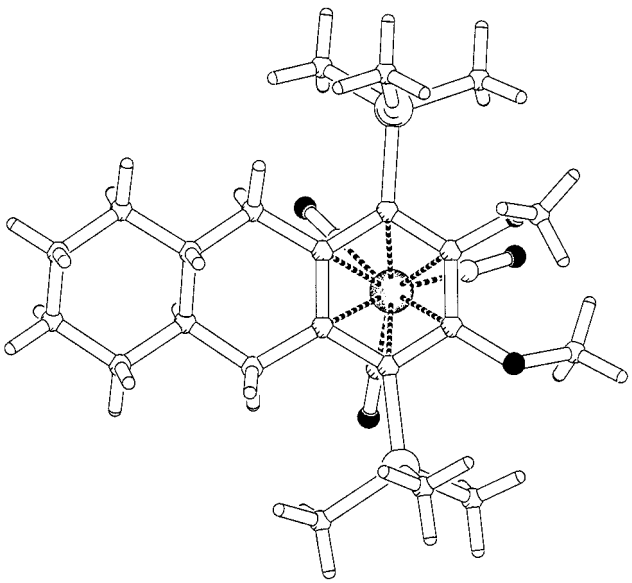

stereotopic benzylic protons may be classified as follows (Figure 7): *endo*-pseudoequatorial (H_a), *exo*-pseudoaxial (H_b), *exo*-pseudoequatorial (H_c) and *endo*-pseudoaxial (H_d).

By means of H,H-COSY spectra[30], it was possible to unambiguously designate the pairs of geminal hydrogen atoms (H_a,H_b; H_c,H_d) for all the complexes. Alternatively, the benzylic *exo*-hydrogen atoms could be identified in several cases by H/D exchange experiments with potassium *tert*-butoxide in [D_6]DMSO (1 h, 25°C). It has been established previously that only the *exo*-hydrogen atoms are substituted under these conditions[3c]. The results of these deuteration experiments are summarized in Table 1. It should be noted that the trimethylsilyl groups in *rac*-**5**, *rac*-**7** and *rac*-**9** were also displaced by deuterium under the reaction conditions (formation of *rac*-**46**, *rac*-**47** and *rac*-**48**). The degree of deuteration was determined in each case by means of ^{1}H-NMR spectroscopy. In addition, the formation of the multiply deuterated compounds was proven by mass spectrometry.

Figure 7. Labelling of the four diastereotopic benzylic hydrogen atoms of the (tetralin)$Cr(CO)_3$ complexes as used for the assignments of the NMR data (Table 2)

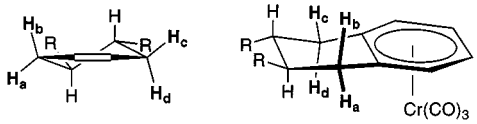

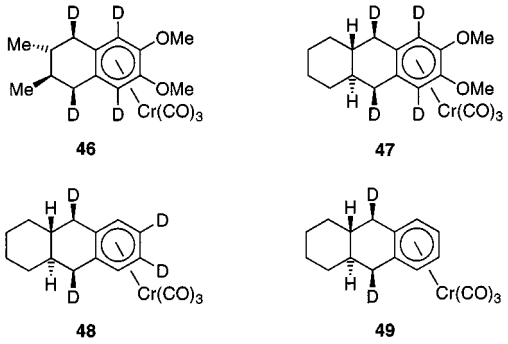

46 **47**

48 **49**

By combining the information obtained from both types of experiments (H,H-COSY and H/D exchange), a full assignment of all the benzylic hydrogen atoms in the complexes *rac*-**24**, *rac*-**35** and *rac*-**8** could readily be made. The assignments for the other complexes (*rac*-**5**, *rac*-**28**, *rac*-**6**, *rac*-**7** and *rac*-**9**) could then be deduced by means of analogy. The assignments and the relevant coupling constants of the benzylic resonances are summarized in Table 2.

The data presented in Table 2 highlights the close relationship between the following pairs of complexes: *rac*-**24**/*rac*-**35**, *rac*-**5**/*rac*-**7** and *rac*-**8**/*rac*-**9**. In all cases, the geminal coupling constants were measured as 16 ± 1 Hz. The vicinal coupling constants for the pseudoaxial hydrogen atoms (H_b and H_d) were found to be 11 ± 1 Hz, those for the pseudoequatorial hydrogen atoms (H_a and H_c) 5 ± 1 Hz. Apart from in the case of the hexahydronaphthofuran complexes *rac*-**28** and *rac*-**6**, the chemical shifts of the pseudoaxial hydrogen atoms (H_b and H_d) lie in the range δ = 2.1−2.4 and those for the pseudoequatorial hydrogen atoms (H_a and H_c) in the range δ = 2.5−2.8. The uncomplexed ligands show the corresponding signals at δ = 2.42 ± 0.03 (^3J = 9−12 Hz, pseudoaxial H) and at δ = 2.73 ± 0.05 (^3J = 4−5 Hz, pseudoequatorial H). These apparent similarities of the ^{1}H-NMR data reflect the very close structural relationship of the complexes and indicate that the complexation does not cause major conformational changes of the arene ligands. The ^{13}C-NMR data (see Experimental Section) also support this picture.

Deprotonation Studies

Having assigned the signals of the relevant benzylic protons, the regioselectivity of the deprotonation was deter-

Table 1. Results of the deuteration experiments[a]

Entry	Starting complex	Product[b]	Degree of deuteration[%][c] benzylic	aryl	Yield[d] [%]
1	*rac*-**5**	*rac*-**46** (*rac*-**24**-d4)	75 ± 15	85 ± 2	11
2	*rac*-**7**	*rac*-**47** (*rac*-**35**-d4)	> 97	92 ± 5	58
3	*rac*-**9**	*rac*-**48** (*rac*-**8**-d4)	70 ± 10	> 97	70
4	*rac*-**8**	*rac*-**49** (*rac*-**8**-d2)	> 97	–	98

[a] Results of the H/D exchange experiments with *t*BuOK/[D_6]DMSO. – [b] Major component of the crude product mixture according to TLC and ^{1}H NMR. – [c] Determined from the ^{1}H-NMR spectra. – [d] Non-optimized yield after chromatography and crystallization.

Table 2. NMR-spectroscopic assignments according to Figure 7[a]

Complex	$\delta(H_a)$	$\delta(H_b)$	$\delta(H_c)$	$\delta(H_d)$	$^2J(H_aH_b)$	$^2J(H_cH_d)$	$^3J(H_aH)$	$^3J(H_bH)$	$^3J(H_cH)$	$^3J(H_dH)$
rac-**24**	2.52	2.28	2.60	2.37	16.1	16.8	4.3	10.5	5.8	10.9
rac-**5**	2.79	2.13	2.55	2.35	16.3	16.1	4.8	10.5	4.9	11.6
rac-**28**	2.75	2.48	2.79	2.59	15.3	15.8	4.5	11.6	5.7	11.7
rac-**6**	3.02	2.30	2.79	2.53	15.2	15.6	4.7	11.3	5.0	12.1
rac-**35**	2.47	2.30	2.57	2.35	16.3	16.2	4.0	11.5	6.0	11.0
rac-**7**	2.80	2.09	2.53	2.31	16.2	16.0	5.5	11.0	5.5	11.0
rac-**8**	2.52	2.34	2.61	2.41	16.3	16.1	6.2	10.2	5.0	10.2
rac-**9**	2.52	2.34	2.60	2.40	17.0	17.0	5.5	12.0	6.0	11.0

[a] ^{1}H-NMR ($CDCl_3$) data for the benzylic hydrogens of the various complexes: chemical shifts (δ) are given in ppm and coupling constants (*J*) in Hz. The uncertainty in the *J* values is estimated to be ± 0.5–1.0 Hz.

mined by lithiation of the various complexes (*rac*-**5**, *rac*-**6, rac**-**7**, *rac*-**8** and *rac*-**9**) followed by deuteration. Lithiation was carried out under conditions similar to those employed previously for the selective alkylation of **1** (see above). Preliminary experiments employing complexes *rac*-**1** and **50**[31] had shown that *n*-butyllithium in THF in the presence of hexamethyl phosphoric triamide (HMPA) as cosolvent represents a very suitable system[32]. In the absence of HMPA, significantly lower degrees of deuteration were observed.

In a typical experiment, the complex was dissolved in the solvent mixture (THF/HMPA, 10:1) and 1.5–3 equivalents of *n*-butyllithium was added. The development of a red color indicated the formation of a benzylic lithiated intermediate[3c]. Deuteration was then achieved by injecting D_2O or the more acidic D^+ source CF_3CO_2D. The latter had to be used in order to obtain a reasonably fast protonation of the anions derived from *rac*-**5** and *rac*-**7**, whereas the protonation of the anions derived from *rac*-**1** and **50** proceeded very rapidly, even with D_2O. After extractive work-up, the reisolated (deuterated) starting material was purified by chromatography and recrystallization. The degree and regioselectivity of the deuteration were then analyzed by means of ^{1}H-NMR spectroscopy[33] based on the assignments for the benzylic hydrogen atoms given above (Table 2). The purified deuterated samples were usually obtained in yields of 40–70%. In some experiments, losses were caused due to partial desilylation or decomplexation.

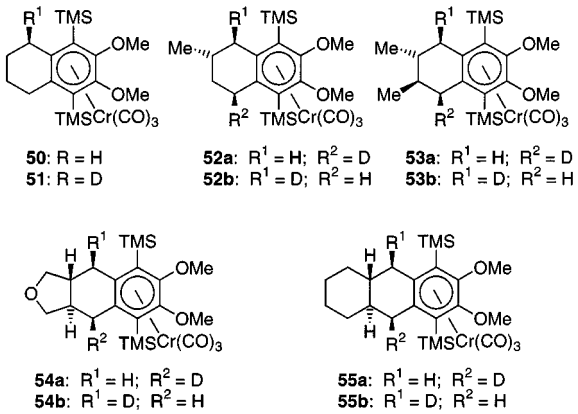

In particular, it should be noted that no suitable conditions were found for the deprotonation of complexes *rac*-**8** and *rac*-**9** with *n*-butyllithium. These compounds preferentially underwent desilylation (*rac*-**9**) or gave rise to a mixture of decomplexed substances after the usual work-up procedure (*rac*-**8**). In a preliminary experiment, it was shown that deprotonation of *rac*-**8** with *s*-butyllithium in THF at –100 °C occurs unselectively at the (less hindered) aryl positions, thus giving rise to a 1:1 mixture of the 6- and 7-methylated products upon treatment of the lithiated intermediates with methyl iodide.

The results of the various deuteration experiments are summarized in Table 3. The most important results are as

Table 3. Selective benzylic deprotonation/deuteration experiments[a]

Entry	Starting complex	Product(s)[b]	Conditions[b]	Degree of deuteration [%]	Regioselectivity [c]
1	**50**	*rac*-**51**	B	95 ± 2	–
2	*rac*-**1**	*rac*-**52a** + *rac*-**52b**	C	85 ± 2	≥ 4:1
3	*rac*-**1**	*rac*-**52a**	B	90 ± 2	≥ 15:1
4	*rac*-**5**	*rac*-**53b**	A	65 ± 2	≥ 15:1
3	*rac*-**5**	*rac*-**53b**	C	50 ± 5	≥ 10:1
6	*rac*-**6**	*rac*-**54a** + *rac*-**54b**	C	90 ± 10[d]	≥ 1.5:1
7	*rac*-**7**	*rac*-**55b**	A	50 ± 2	≥ 15:1
8	*rac*-**53b** (65% D)	*rac*-**53b**	A	80 ± 2	≥ 15:1
9	*rac*-**53b** (65% D)	*rac*-**5**	A[e]	10	–
10	*rac*-**55b** (50% D)	*rac*-**55b**	A	90 ± 5	–[f]
11	*rac*-**55b** (50% D)	*rac*-**7**	A[e]	18	–

[a] Results of the deprotonation/deuteration experiments with *n*BuLi. – [b] A: 2 equiv. *n*BuLi; THF/HMPA, 10:1, −78°C → 25°C, 30 min, then CF_3COOD, −78°C → 25°C, 30 min; B: 1.5 equiv. *n*BuLi; THF/HMPA, 10:1, −70°C → 25°C, 15 min, then D_2O, 25°C, 15 min; C: 3 equiv. *n*BuLi; THF/HMPA, 10:1, 25°C, 30 min, then D_2O, 25°C, 30 min. – [c] Determined by means of ^{1}H-NMR spectroscopy on the assumption that a deviation ≥ 5% of the integrals of the benzylic hydrogen atoms must result from deuteration. – [d] In this case, the product mixture was completely desilylated with TBAF/SiO_2 before the degree of deuteration was determined. – [e] In this case, the lithiated intermediate was protonated by addition of CF_3COOH. – [f] According to the ^{1}H-NMR spectrum, ca. 15% of the high overall deuteration occurred at the C-4 position (*exo*-pseudoaxial).

Figure 8. ^{1}H-NMR signals ($CDCl_3$) of the benzylic protons for the following complexes (from top to bottom): *rac*-**1**, *rac*-**52a** (90% D), *rac*-**5**, *rac*-**53b** (80% D), *rac*-**7** and *rac*-**55b** (50% D)

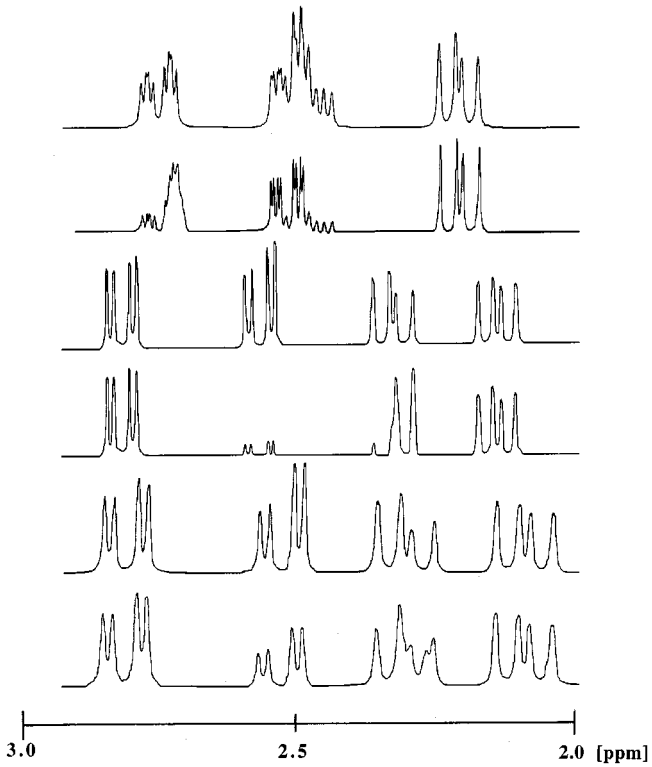

follows: (a) High regioselectivities were observed in the case of *rac*-**1**, *rac*-**5** and *rac*-**7** (see Table 3, entries 2–5, 7; see also Figure 8); (b) in contrast, *rac*-**6** showed only a very low regioselectivity (Table 3, entry 6); (c) the regioselectivity of the deprotonation of *rac*-**5** and *rac*-**7** indicates that the pseudoequatorial benzylic *exo*-hydrogen atoms were abstracted (formation of *rac*-**53b** and *rac*-**55b**), while the deprotonation of *rac*-**1** afforded selectively the *exo*-pseudoaxially deuterated product *rac*-**52a** as expected (see Scheme 1); (d) when the already deuterated complexes *rac*-**53b** and *rac*-**55b** were subjected to a second deprotonation/deuteration cycle, the degree of deuteration was further enhanced (Table 3, entries 8 and 10)[34]; (e) in accordance with the latter experiments, the corresponding deprotonation (dedeuteration)/protonation cycle (Table 3, entries 9 and 11) resulted mainly in the loss of the deuterium substitution (reversion to *rac*-**5** and *rac*-**7**). This also demonstrates that proton (or D^+) abstraction and reprotonation (redeuteration) occur at the same position[35].

In order to evaluate the synthetic potential of the aforementioned highly regioselective deprotonations, we also tried to trap the lithiated intermediates by alkylation and acylation. In the case of *rac*-**5**, treatment of the anion with methyl iodide or acetyl chloride afforded the products *rac*-**56** and *rac*-**57**, respectively, in good yields (Scheme 9). The relative configurations of these compounds were determined by means of ^{1}H-NMR spectroscopy and, in the case of *rac*-**56**, by X-ray crystallography as well (Figure 9)[36]. The results gave an independent proof that the benzylic deprotonation of *rac*-**5** occurs regioselectively at the pseudoequatorial position (H_c, see Figure 6), thereby corroborating the results of the deuteration studies described above. In contrast, the corresponding methylation and acetylation products derived from *rac*-**7** were found to be highly unstable and therefore of little synthetic value[37].

Discussion and Additional Experiments

The experimental results described in the previous section clearly show (for the cases of *rac*-**1**, *rac*-**5** and *rac*-**7**) that benzylic deprotonation of (arene)$Cr(CO)_3$ complexes can proceed with remarkably high regioselectivity, even if the position of the proton abstraction cannot a priori be predicted using the usual electronic arguments. Additionally, *our initial assumption that pseudoaxial benzylic hydrogen atoms are preferentially abstracted as a result of commonly invoked stereoelectronic factors*[8] *(see Introduction) has clearly been disproved* as, in contrast to the deprotonation

Figure 9. X-ray crystal structure of *rac*-**56**

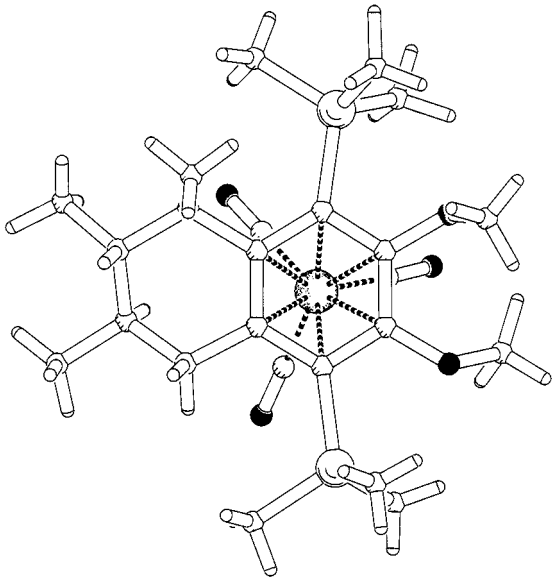

of *rac*-**1**, complexes *rac*-**5** and *rac*-**7** were selectively deprotonated at their pseudoequatorial positions.

The inspection of molecular models suggests an almost comparable steric environment at the competing benzylic positions in all cases. It is therefore unlikely that the complete reversal of the regioselectivity (changing from *rac*-**1** to *rac*-**5** or *rac*-**7**, respectively) is due to a simple steric effect.

At this point, we asked ourselves whether the conformation of the $Cr(CO)_3$ tripod could possibly have an influence on the regioselectivity of the benzylic deprotonation. Could such a previously unnoted or even cursorily excluded[38] effect be responsible for the observed selectivities?

It is a broadly accepted hypothesis that the regioselectivity of kinetically controlled nucleophilic additions to (arene)chromium complexes is influenced by the preferred conformation of the $Cr(CO)_3$ tripod[1a]. This picture is based on the assumption that in the case of charge-controlled reactions, those arene carbon atoms that are eclipsed by a Cr−CO bond are preferentially attacked by a nucleophile due to the positive charge induced by the eclipsing CO ligand[39][40][41][42][43]. Analogous arguments have also been advanced in connection with regioselective ring lithiations of (arene)$Cr(CO)_3$ complexes[44].

Scheme 9

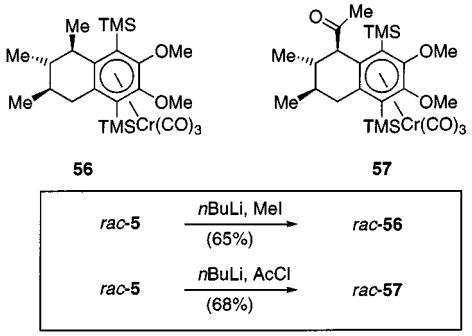

In a similar fashion, one could imagine that the (kinetic) acidity of a benzylic proton increases with an increasing positive partial charge at the adjacent arene center. Thus, if one of two competing benzylic positions is eclipsed by a CO ligand (substructure **58**), the proton abstraction at this center should be (stereoelectronically) favored (Figure 10).

Figure 10. Explanation of the stereoelectronic effect resulting in the preferred deprotonation of those benzylic hydrogen atoms which are activated by an eclipsed CO ligand

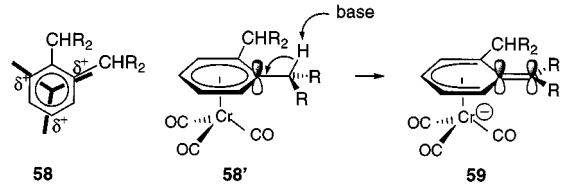

The resulting anionic species (which is best represented by a formula of type **59**[45]) should also preferentially adopt an eclipsed conformation, since the deprotonated side-chain represents a strong donor substituent at the (arene)$Cr(CO)_3$ nucleus[46].

Further inspection of the crystal structures of the substrates *rac*-**1**, *rac*-**5** and *rac*-**7** (see above) revealed that in the case of *rac*-**1** and *rac*-**7**, the benzylic center at which the deprotonation preferentially takes place is indeed eclipsed by a CO ligand in the crystalline state (as indicated by the arrow in Figure 11). However, as mentioned above, the crystals of *rac*-**5** were found to contain two independent molecules with different conformations (**5′** and **5′′**), of which only one conformer (**5′**) reflected the observed regioselectivity of deprotonation (Figure 11).

Figure 11. Preferred conformation of the $Cr(CO)_3$ tripod (depicted by the bold lines) for complexes **1**, **7** and **5** as found in their crystal structures; the arrows mark those benzylic positions which were found to be preferentially attacked by *n*-BuLi

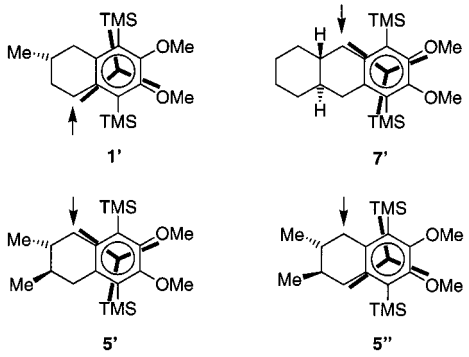

Of course, one can never unequivocally conclude a preferred conformation in solution from a crystal structure. More importantly, if the equilibration of the $Cr(CO)_3$ conformers[47] takes place rapidly compared to the deprotonation, the Curtin-Hammett principle[48] should apply and the regioselectivity would only be governed by the difference in energy between the competing transition states. Nevertheless, as mentioned above for nucleophile additions to (arene)$Cr(CO)_3$ complexes, the preferred conformation of the $Cr(CO)_3$ tripod may have an influence on the regioselectivity of attacking reagents. In such cases, the same fac-

tors determining the preferred ground state conformation also seem to be effective in the transition state and the most stable transition state is derived from the most stable ground state conformation (principle of least motion)[49]. In other words, the deprotonation is accompanied by a change of the overall electronic structure and the position of all atoms involved (delocalization). Therefore, the rate of proton transfer should be enhanced if the degree of structural and electronic reorganization is minimal[50].

To probe the general applicability of this theory, we investigated the regioselectivity of the deprotonation/deuteration of complex *rac*-**60**[51] employing our tried and tested conditions (*n*-BuLi, D_2O). This substrate had previously been examined by Brocard[6d][38] under different conditions (*t*BuOK, DMSO, CH_2O), but no selectivity was observed. Due to the bulkiness of the *tert*-butyl group, *rac*-**60** should adopt the conformation depicted in formula **60′**. Accordingly, we would predict that the deprotonation should occur preferentially at the methyl group *para* to the *tert*-butyl substituent (as indicated by the arrow in Figure 12).

Figure 12. Lowest energy conformation of complexes **60** and **62**; the arrows mark those benzylic positions which are expected to be preferentially attacked by a base

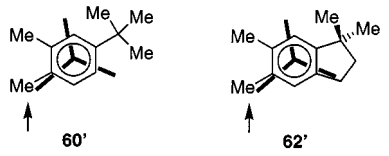

Indeed, when *rac*-**60** was first treated with *n*-butyllithium in THF at −78°C and then the resulting red solution was quenched with D_2O, a 61:39 mixture of the monodeuterated products *rac*-**61a** and *rac*-**61b** was isolated in high yield (Scheme 10)[52].

Scheme 10

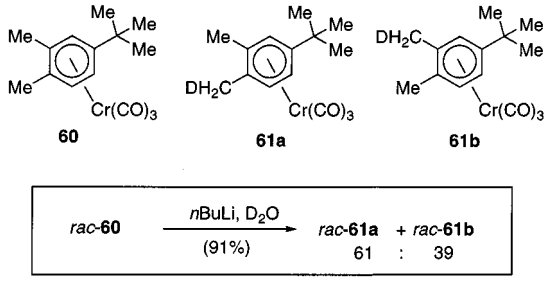

As a second probe of our hypothesis, we also studied complex *rac*-**62**, which was synthesized as indicated in Scheme 11. Thus, Friedel-Crafts acylation of *o*-xylene with 3-chloropropionic chloride and subsequent acid-catalyzed cyclization[53] afforded a 3:1 mixture of the indanones **63a**[54] and **63b**. After treatment with methylmagnesium iodide (→ *rac*-**64**) and (*endo*-selective)[55] complexation, the resulting mixture of regioisomeric indanol complexes was separated by fractional crystallization to furnish the pure regioisomer *rac*-**65**. *O*-Acetylation followed by treatment of the resulting acetate *rac*-**66** with trimethylaluminum[56] finally gave the desired complex *rac*-**62**.

Scheme 11

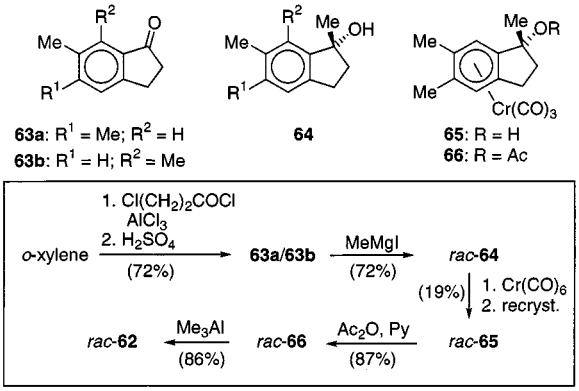

When *rac*-**62** was subjected to the proven deprotonation/deuteration conditions, the monodeuterated isomers *rac*-**67a** and *rac*-**67b** were formed in a ratio of 85:15 (Scheme 12). The assignments were unambiguously confirmed by NOE measurements. As in the case of *rac*-**60**, the regioselectivity of the benzylic deprotonation of *rac*-**62** can be understood in terms of a conformational picture (see Figure 12) and the assumption that the proton abstraction occurs predominantly at the methyl group that is activated by the eclipsing CO ligand.

Scheme 12

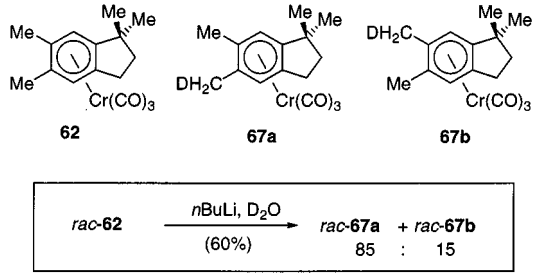

Conclusion

A series of conformationally restricted (arene)$Cr(CO)_3$ complexes has been synthesized and the regioselectivity of their benzylic deprotonation has been investigated. Our findings show that high regioselectivities can be obtained even in cases where no major electronic or steric effects are operative. The original assumption that pseudoaxially oriented hydrogen atoms are preferentially attacked by the base due to stereoelectronic reasons was clearly refuted by experiments employing (η^6-tetralin)- and (η^6-*trans*-octahydroanthracene)$Cr(CO)_3$ derivatives (*rac*-**5** and *rac*-**7**, respectively). On the other hand, experiments with the complexes *rac*-**60** and *rac*-**62** indicated that the conformation of the $Cr(CO)_3$ tripod exerts an influence on the regioselectivity.

Based on our current level of understanding, we wish to draw the following general picture: In the case of (arene)$Cr(CO)_3$ complexes with two competing benzylic positions, deprotonation occurs preferentially at that position

where the adjacent aryl center bears the greater positive partial charge. In the case of unambiguous electronic circumstances, the conformation of the $Cr(CO)_3$ tripod plays only a minor role[2][6], merely reflecting (and possibly amplifying) the polarization induced by the substituents. Should, however, the electronic effects not lead to a favorization of one position (e.g. due to a symmetric substitution pattern or the absence of polar substituents), the preferred conformation of the $Cr(CO)_3$ tripod may become important. In such cases, those benzylic positions which are eclipsed by a CO ligand in the lowest energy conformation are preferentially deprotonated (kinetic stereoelectronic effect).

It must be emphasized that this picture is as yet rather an empirical one and it would be interesting if it could be supported by quantum-chemical calculations and by more detailed structural information on the intermediates resulting from benzylic deprotonation of (arene)$Cr(CO)_3$ complexes. Investigations in this area are currently being performed in this laboratory.

This work was financially supported by the *Volkswagenstiftung*, the *Deutsche Forschungsgemeinschaft* and the *Fonds der Chemischen Industrie*. Fellowship support to T. V. from the *BASF AG* is gratefully acknowledged. We thank the *Schering AG*, the *Chemetall GmbH*, and the *Degussa AG* for generous gifts of chemicals. We are indebted to Dr. *G. Höhne* for recording the MS spectra, and to Ms. *C. Klose* for recording the IR spectra. A 600-MHz NMR spectrum of *rac*-**67** was kindly provided by Dr. *P. Schmieder*, Institute of Molecular Pharmacology, Berlin.

Experimental Section

General: Manipulations involving air-sensitive compounds were carried out under argon using Schlenk and syringe techniques. Anhydrous solvents were obtained by distillation from sodium benzophenone ketyl (THF and diethyl ether), from P_2O_5 (CCl_4), from CaH_2 (HMPA), or by filtration through ICN Alumina B Grade Super 1 (toluene and nBu_2O). Reagents (generally ≥ 98%) were used as received from Aldrich, Fluka, Merck, Acros and Chemetall without further purification, unless otherwise stated. The concentration of organolithium solutions was determined by titration with menthol in THF in the presence of 1,10-phenanthroline[57]. The organic solutions resulting from aqueous work-up were concentrated under reduced pressure using a rotary evaporator. All reactions were monitored by analytical thin-layer chromatography (TLC) using Merck silica gel 60 F 254 glass plates. The chromatograms were visualized with UV light or by staining with a cerium reagent (prepared by dissolving 2 g of phosphomolybdic acid and 1 g of cerium(IV) sulfate in a mixture of 10 ml conc. H_2SO_4 and 90 ml EtOH] followed by heating. Flash chromatography[58] was performed on silica gel 60 (230−400 mesh) from Merck. Preparative thin-layer chromatography (PTLC) was carried out using a chromatotron (Harrison Research Model 7924 T) on glass plates coated with 1−4 mm layers of silica gel containing gypsum (Merck PF 60 F 254). NMR spectra were recorded in $CDCl_3$ with Bruker instruments (AM 250, AM 270 or AM 400) using residual undeuterated solvent as an internal reference. The spectra are reported in ppm relative to tetramethylsilane using the following abbreviations to express the multiplicities: s = singlet; d = doublet; t = triplet; q = quadruplet; br = broad. ^{13}C chemical shifts were determined from ^1H-decoupled spectra, the number of protons bound directly to each carbon atom was determined employing the DEPT sequence[59] (q = CH_3; t = CH_2; d = CH; s = quaternary carbon atoms). Mass spectrometry was carried out at 70 eV using a Varian MAT 711 instrument. Infrared spectra were obtained using a Nicolet Magna FT-IR 750 instrument. Optical rotations were measured with a Perkin-Elmer 241 polarimeter, concentrations (*c*) are given in g/100 ml. Melting points were measured in open capillary tubes and are uncorrected.

1,2-Dichloro-4,5-dimethoxybenzene (**17**)[14a]: To 46 ml (0.36 mol) of veratrole (**16**), 66 ml (0.82 mol) of sulfuryl chloride was added dropwise over a period of 30 min. The mixture was stirred for 1 h at room temp. and, after fitting the flask with a reflux condenser, was heated to 80°C for 2 h. The reflux condenser was then replaced by a distillation set-up and the excess sulfuryl chloride was distilled off under reduced pressure (ca. 100 Torr). On cooling the mixture to room temp., a solid formed, which was washed with cold hexane (2 × 20 ml) and recrystallized from EtOH (30 ml) at 4°C yielding 57.70 g (77%) of **17** as colorless crystals, m.p. 82.5°C (ref.[14a]: m.p. 84°C). − R_f = 0.23 (hexane/EtOAc, 10:1). − IR (KBr): $\tilde{\nu}$ = 3003 (w), 2965 (w), 2937 (w), 2906 (w), 2836 (w), 1508 (m), 1432 (m), 1363 (m), 1260 (m), 1211 (m), 1179 (m), 1132 (m), 1027 (m), 920 (m), 840 (m), 794 (m), 678 (m), 1594 (w), 1337 (w), 1190 (w) cm^{-1}. − ^1H NMR (270 MHz): δ = 3.85 (s, 6 H), 6.91 (s, 2 H). − MS *m/z* (%): 208 (64), 206 [M^+] (98), 193 (32), 191 (50), 165 (8), 163 (13), 130 (8), 128 (25), 113 (12), 99 (16). − $C_8H_8Cl_2O_2$ (207.06): calcd. C 46.23, H 3.88; found C 46.46, H 3.99.

1,2-Dimethoxy-4,5-dimethylbenzene (**18**)[14b]: To a stirred solution of **17** (15 g, 72.2 mmol) in anhydrous diethyl ether (150 ml) was added methyllithium (100 ml, 160 mmol, 1.6 M in ether) at −20°C. The reaction flask was fitted with a reflux condenser and the temperature was allowed to rise to −7°C. At this point, an exothermic reaction took place, which was moderated by means of a suitably sized cooling bath. The cooling bath was then replaced by an oil bath and the brown solution was refluxed for 2 h. After cooling to 0°C, the reaction mixture was carefully quenched with 150 ml of water. The resulting mixture was extracted twice with diethyl ether, and the combined extracts were washed with 2 N HCl, saturated $NaHCO_3$ and brine, and dried with $MgSO_4$. The solvent was removed in vacuo and the dark-brown residue was kugelrohr-distilled (61°C, 0.6 Torr) yielding 8.08 g (67%) of **18** as a colorless oil, which solidified on standing; m.p. 42.5°C (ref.[14b]: m.p. 43°C). − R_f = 0.28 (hexane/EtOAc, 10:1). − IR (KBr): $\tilde{\nu}$ = 2999 (m), 2939 (m), 2846 (m), 1607 (m), 1519 (br), 1469 (s), 1394 (m), 1336 (s), 1266 (s), 1120 (br), 1105 (br), 997 (s), 854 (s), 828 (m), 732 (w) cm^{-1}. − ^1H NMR (270 MHz): δ = 2.20 (s, 6 H), 3.84 (s, 6 H), 6.67 (s, 2 H). − $C_{10}H_{14}O_2$ (166.22): calcd. C 72.26, H 8.49; found C 72.19, H 8.53.

1,2-Bis(bromomethyl)-4,5-dimethoxybenzene (**19**)[14c]: To a suspension of 3 g of powdered molecular sieves (4 Å) in 125 ml anhydrous CCl_4 was added **18** (5.0 g, 30.1 mmol), anhydrous NBS (10.76 g, 60.2 mmol) and AIBN (10 mg) and the mixture was refluxed for ca. 1 h whilst being irradiated with a 200-W lamp (Note: On completion of the reaction, the slightly reddish solution turns completely colorless). The mixture was then allowed to cool to room temp. and filtered successively through short pads of Celite and silica 60. After removing the solvent in vacuo, a slightly yellow oil was obtained, which crystallized spontaneously. Recrystallization from hexane/EtOAc (3:1) yielded 7.03 g (72%) of **19** as yellowish needles, m.p. 105°C (ref.[14c]: m.p. 109°C). − R_f = 0.27 (hexane/EtOAc, 4:1). − IR (KBr): $\tilde{\nu}$ = 3002 (w), 2954 (w), 2904 (w), 2828 (w), 1522 (s), 1460 (m), 1402 (w), 1357 (m), 1277 (s), 1239 (m), 1203 (s), 1127 (s), 1090 (m), 1032 (w), 1000 (m), 896 (w), 872 (m), 748 (m), 670 (w) cm^{-1}. − ^1H NMR (270 MHz): δ = 3.90 (s, 6 H),

4.63 (s, 4 H), 6.84 (s, 2 H). − MS; *m/z* (%): 324 [MH_2^+] (10), 323 [MH^+] (6), 245 (60), 243 (60), 231 (10), 229 (10), 165 (24), 163 [$MH^+ - 2Br$] (100), 149 (16), 121 (25). − $C_{10}H_{12}Br_2O_2$ (324.01): calcd. C 37.07, H 3.73; found C 36.58, H 3.66.

Diethyl (2RS,3RS)-6,7-Dimethoxy-1,2,3,4-tetrahydronaphthalene-2,3-dicarboxyate (*rac*-**20**): A solution of **19** (6.48 g, 20 mmol) and 10 ml (62.8 mmol) of diethyl fumarate in 200 ml of anhydrous THF was cooled to 0°C. To this was added 6.8 g (55.4 mmol) of chromium(II) chloride (Merck, assay ca. 90%) to give a greenish suspension that rapidly turned purple. The mixture was kept at 0°C for 5 h, then the ice-bath was removed and the deep-purple solution was stirred at room temp. for 1 h; 50 ml H_2O was added and after 5 min the mixture was extracted with hexane/EtOAc (2:1, 3 × 100 ml). The combined organic layers were washed with brine and dried with $MgSO_4$. The solvent was removed under reduced pressure and the remaining oil was crystallized from hexane/EtOAc (3:1) yielding 4.44 g (66%) of the Diels-Alder product *rac*-**20** as colorless crystals. An analytical sample was additionally purified by PTLC (hexane/EtOAc, 3:1), m.p. 80°C. − R_f = 0.29. − IR (KBr): $\tilde{\nu}$ = 2991 (m), 2963 (m), 2940 (m), 2920 (m), 2837 (m), 1728 (br, C=O), 1611 (s), 1518 (s), 1467 (s), 1378 (s), 1302 (s), 1247 (s), 1182 (s), 1116 (s), 1020 (s), 997 (s), 919 (m), 849 (s) cm^{-1}. − ^1H NMR (250 MHz): δ = 1.28 (t, *J* = 7.1 Hz, 6 H), 2.97 (m, 6 H), 3.84 (s, 6 H), 4.17 (q, *J* = 7.1 Hz, 4 H). − MS; *m/z* (%): 336 [M^+] (19), 291 (4), 262 (6), 189 (14), 115 (18), 100 (18), 57 (100). − $C_{18}H_{24}O_6$ (336.39): calcd. C 64.28, H 7.19; found C 64.17, H 7.12.

(2RS,3RS)-2,3-Bis(hydroxymethyl)-6,7-dimethoxy-1,2,3,4-tetrahydronaphthalene (*rac*-**21**): 0.5 g (13.2 mmol) of $LiAlH_4$ was added in small amounts to a solution of 2.02 g (6 mmol) of *rac*-**20** in anhydrous diethyl ether over a period of 10 min. The suspension was heated to 30°C on a water bath for 40 min, cooled to 0°C, and then quenched by the dropwise addition of 10 ml EtOAc followed by 80 ml of 2 N HCl. The mixture was stirred until all the precipitated aluminates had dissolved and was then extracted with hexane/EtOAc (1:10, 6 × 50 ml) (Note: The resulting diol *rac*-**21** shows a surprisingly high solubility in water; longer reaction times lead to an increased formation of by-products). The combined organic extracts were washed with saturated aqueous $NaHCO_3$ and brine, and dried with $MgSO_4$. The solvent was removed in vacuo and the colorless oil was crystallized from EtOAc yielding 1.28 g (86%) of the diol *rac*-**21** as colorless crystals, m.p. 135°C. − R_f = 0.23 (EtOAc). − IR (KBr): $\tilde{\nu}$ = 3481 (br, OH), 3386 (br, OH), 2906 (m), 2833 (C−H), 1517 (s), 1462 (m), 1353 (m), 1242 (s), 1219 (m), 1123 (s), 1098 (m), 1065 (m), 1027 (m), 988 (m), 895 (w), 849 (w), 745 (w) cm^{-1}. − ^1H NMR (270 MHz): δ = 1.83 (m, 2 H), 2.56 (dd, J_1 = 10.1 Hz, J_2 = 15.7 Hz, 2 H), 2.69 (dd, J_1 = 4.0 Hz, J_2 = 16.6 Hz, 2 H), 2.95 (br, 2 H, exchanges with D_2O), 3.65 (dd, J_1 = 6.3 Hz, J_2 = 10.9 Hz, 2 H), 3.78 (dd, J_1 = 3.3 Hz, J_2 = 10.9 Hz, 2 H), 3.83 (s, 6 H, OMe), 6.59 (s, 2 H). − MS; *m/z* (%): 252 [M^+] (100), 220 (20), 203 (75), 189 (14), 188 (15), 165 (25), 164 (32), 71 (30), 69 (41), 57 (88), 55 (70). − $C_{14}H_{20}O_4$ (252.31): calcd. C 66.65, H 7.79; found C 66.37, H 7.91.

(2RS,3RS)-6,7-Dimethoxy-2,3-bis(tosyloxymethyl)-1,2,3,4-tetrahydronaphthalene (*rac*-**22**): A stirred solution of 2.15 g (8.5 mmol) of diol *rac*-**21** in 25 ml of anhydrous pyridine was cooled to 0°C and 7.65 g (40 mmol) of *p*-toluenesulfonyl chloride was added within 5 min. The orange-red solution was stirred at this temperature for 1 h and then kept at 4°C for 24 h. The solution was then poured slowly into a vigorously stirred mixture of 100 ml conc. HCl, 100 g of ice and 200 ml of CH_2Cl_2, and stirring was continued while the mixture was allowed to warm to room temp. The layers were then separated and the aqueous layer was extracted with CH_2Cl_2 (2 × 100 ml). The combined organic layers were washed with saturated aqueous $NaHCO_3$ and brine, and dried with $CaCl_2$. The solvent was removed under reduced pressure and 50 ml of EtOAc was added, whereupon 3.729 g (78%) of bis(tosylate) *rac*-**22** precipitated as a colorless crystalline powder, m.p. 150°C. − R_f = 0.27 (hexane/EtOAc, 1:1). − IR (KBr): $\tilde{\nu}$ = 3000 (w), 2939 (w), 2834 (w), 1597 (m), 1519 (s), 1468 (m), 1350 (s), 1248 (s), 1175 (s), 1100 (s), 950 (s), 868 (m), 835 (s), 779 (m), 665 (s) cm^{-1}. − ^1H NMR (270 MHz): δ = 2.04 (m, 2 H), 2.46 (s, 6 H), 2.52 (dd, J_1 = 7.2 Hz, J_2 = 16.4 Hz, 2 H), 2.68 (dd, J_1 = 4.5 Hz, J_2 = 16.6 Hz, 2 H), 3.81 (s, 6 H), 3.97 (d, *J* = 4.8 Hz, 4 H), 6.48 (s, 2 H), 7.35 (d, *J* = 8.1 Hz, 4 H), 7.76 (d, *J* = 8.3 Hz, 4 H). − MS; *m/z* (%): 560 [M^+] (22), 388 (4), 258 (4), 234 (4), 220 (4), 69 (60), 57 (100), 55 (88). − $C_{28}H_{32}O_8S_2$ (560.68): calcd. C 59.98, H 5.75; found C 59.84, H 5.70.

(2RS,3RS)-6,7-Dimethoxy-2,3-dimethyl-1,2,3,4-tetrahydronaphthalene (*rac*-**23**): 2.00 g (3.6 mmol) of the ditosylate *rac*-**22** was dissolved in 80 ml of anhydrous diethyl ether and 0.5 g of $LiAlH_4$ was added portionwise. The suspension was refluxed for 30 min, then allowed to cool to room temp., whereupon 10 ml of EtOAc was added dropwise, followed by 50 ml of 2 N HCl. The solution was stirred until all the precipitated aluminates had dissolved and was then extracted with hexane/EtOAc (2:1, 3 × 30 ml). The combined organic extracts were washed with saturated aqueous $NaHCO_3$ and brine, and dried with $MgSO_4$. The solvent was removed under reduced pressure and the colorless residue was purified by PTLC (4 mm layer SiO_2; hexane/EtOAc, 10:1) yielding 642 mg (81%) of *rac*-**23** as colorless, clear crystals, m.p. 82°C. − R_f = 0.25 (hexane/EtOAc, 10:1). − IR (KBr): $\tilde{\nu}$ = 2988 (m), 2955 (m), 2927 (m), 2880 (m), 2854 (m), 2832 (m), 1520 (s), 1465 (m), 1450 (m), 1247 (s), 1224 (s), 1112 (s), 1003 (m), 850 (m) cm^{-1}. − ^1H NMR (270 MHz): δ = 1.03 (d, *J* = 6.1 Hz, 6 H), 1.48 (m, 2 H), 2.39 (dd, J_1 = 10.4 Hz, J_2 = 15.7 Hz, 2 H), 2.73 (dd, J_1 = 3.4 Hz, J_2 = 16.8 Hz, 2 H), 3.83 (s, 6 H), 6.56 (s, 2 H). − ^{13}C NMR (62.7 MHz): δ = 19.5 (q), 35.4 (d), 38.0 (t), 55.6 (q), 111.4 (d), 128.7 (s), 146.9 (s). − MS; *m/z* (%): 221 (16), 220 [M^+] (100), 205 (12), 189 (8), 164 (65), 151 (8), 149 (7), 121 (7). − $C_{14}H_{20}O_4$ (252.31): calcd. C 76.33, H 9.15; found C 75.94, H 9.12.

(2RS,3RS,8aSR)-Tricarbonyl(η⁶-6,7-dimethoxy-2,3-dimethyl-1,2,3,4-tetrahydronaphthalene)chromium(0) (*rac*-**24**): A 50-ml Schlenk flask equipped with a reflux condenser and an Hg bubbler was flame-dried in vacuo and flushed with argon. All connections were made air-tight by using Teflon sleeves. After charging with 1.19 g (5.4 mmol) of the ligand *rac*-**23** and 1.24 g (5.6 mmol) of $Cr(CO)_6$, 25 ml of nBu_2O was added and the whole apparatus was evacuated and flushed with argon several times. After adding 2.5 ml of anhydrous THF, the solution was refluxed at 150°C (oil-bath temperature) for 20 h, protected from light for most of the time. The clear, yellow solution thus obtained was allowed to cool to room temp., the solvents were removed in vacuo, and the residue was dissolved in ca. 25 ml of EtOAc. The resulting solution was filtered through a 2-cm pad of silica, the solvent was removed under reduced pressure, and the residue (yellow oil) was crystallized from hexane/EtOAc (3:1) yielding 1.48 g (78%) of the chromium complex *rac*-**24** as yellow cubes, m.p. 167°C. − R_f = 0.3 (hexane/EtOAc, 3:1). − IR (KBr): $\tilde{\nu}$ = 2969 (w), 2912 (w), 2842 (w), 1942 (br, C=O), 1874 (br, C=O), 1848 (br, C=O), 1949 (m), 1428 (m), 1266 (m), 1235 (m), 1113 (m), 991 (m), 675 (m), 633 (all m) cm^{-1}. − ^1H NMR (250 MHz)[60]: δ = 1.00 (d, *J* = 3.1 Hz, 3 H), 1.02 (d, *J* = 3.1 Hz, 3 H), 1.36 (m, 1 H), 1.53 (m, 1 H), 2.29 (dd, J_1 = 22.1 Hz, J_2 = 10.7 Hz, 1 H), 2.36 (dd, J_1 = 22.8 Hz, J_2 = 10.9 Hz, 1 H), 2.53 (dd, J_1 = 21.7 Hz, J_2 = 4.4 Hz, 1 H), 2.59 (dd, J_1 = 20.9 Hz, J_2 = 3.9 Hz, 1 H), 3.74 (s, 3 H), 3.78 (s, 3 H), 5.15 (s, 1 H)

5.18 (s, 1 H). − ^{13}C NMR (63 MHz): δ = 18.8 (q), 34.1 (d), 35.0 (d), 36.0 (t), 37.5 (t), 56.9 (q), 57.1 (q), 78.3 (d), 78.8 (d), 101.9 (s), 103.6 (s), 132.2 (s), 132.3 (s), 234.0 (s). − MS; *m/z* (%): 357 (8), 356 [M$^+$] (24), 300 (15), 273 (54), 272 (100), 243 (25), 242 (90), 220 (10), 186 (23), 164 (8). − $C_{17}H_{20}CrO_5$ (356.34): calcd. C 57.30, H 5.66; found C 57.24, H 5.79.

(2RS,3RS,4aRS)-Tricarbonyl(η^6-6,7-dimethoxy-2,3-dimethyl-5,8-bis(trimethylsilyl)-1,2,3,4-tetrahydronaphthalene)chromium(0) (*rac*-**5**): To a solution of 1.247 g (3.5 mmol) of the chromium complex *rac*-**24** in 50 ml of anhydrous THF was added 3.26 g (30 mmol) of chlorotrimethylsilane and the mixture was cooled to −50°C. In a separate flask, a solution of 1.06 g (7.2 mmol) of 2,2,6,6-tetramethylpiperidine in 25 ml of anhydrous THF was cooled to −50°C and 4.5 ml of *n*-butyllithium (7.2 mmol, 1.6 M in hexane) was added. After 15 min, this (second) solution was added to the solution in the first flask by means of a transfer needle over a period of ca. 1 min. The reaction mixture was stirred for 15 min at −50°C and then for 3 h at room temp. After diluting with 50 ml of EtOAc, the organic solution was washed with 2 N HCl (2 × 50 ml), saturated aqueous $NaHCO_3$ and brine, and dried ($MgSO_4$). After removing the solvent, the remaining yellow oil was purified by PTLC (4-mm layer SiO_2; hexane/EtOAc, 10:1). The product was finally crystallized from hexane yielding 1.42 g (81%) of the disilylated complex *rac*-**5** as clear yellow prisms, m.p. 130°C. − R_f = 0.55 (hexane/EtOAc, 10:1). − IR (KBr): ṽ = 2982 (w), 2953 (w), 2900 (w, C−H), 1938 (s, C=O), 1876 (s, C=O), 1854 (s, C=O), 1249 (m), 1022 (m), 852 (m), 670 (m) cm^{-1}. − ^{1}H NMR (250 MHz)[60]: δ = 0.50 (pseudo s, 18 H), 0.96 (pseudo t, *J* = 6.2 Hz, 6 H), 1.25 (m, 1 H), 1.39 (m, 1 H), 2.13 (dd, J_1 = 16.1 Hz, J_2 = 10.5 Hz, 1 H), 2.35 (dd, J_1 = 16.3 Hz, J_2 = 11.6 Hz, 1 H), 2.55 (dd, J_1 = 16.3 Hz, J_2 = 4.9 Hz, 1 H), 2.79 (dd, J_1 = 16.1 Hz, J_2 = 4.8 Hz, 1 H), 3.71 (pseudo s, 6 H). − ^{13}C NMR (63 MHz): δ = 2.9 (q), 3.3 (q), 19.1 (q), 19.3 (q), 33.9 (d), 35.0 (d), 39.3 (t), 39.6 (t), 62.0 (q), 62.2 (q), 95.3 (s), 96.3 (s), 110.7 (s), 111.9 (s), 137.8 (s), 138.0 (s), 234.7 [s, Cr(CO)$_3$]. − ^{13}C NMR (63 MHz, [D$_8$]THF) δ = 3.2 (q), 3.4 (q), 19.2 (q), 19.4 (q), 34.9 (d), 35.9 (d), 40.2 (t), 40.5 (t), 62.1 (q), 62.4 (q), 95.9 (s), 96.9 (s), 111.5 (s), 112.6 (s), 138.7 (s), 139.0 (s), 235.4 [s, Cr(CO)$_3$]. − MS; *m/z* (%): 500 [M$^+$] (7), 444 (11), 417 (37), 416 (84), 258 (4), 220 (8), 57 (100), 55 (76). − $C_{23}H_{36}CrO_5Si_2$ (500.70): calcd. C 55.17, H 7.25; found C 54.99, H 7.12.

Bis[(1S)-1-ethoxycarbonylethyl] (2R,3R)-6,7-Dimethoxy-1,2,3,4-tetrahydronaphthalene-2,3-dicarboxylate (**26a**) *and Bis[(1S)-1-ethoxycarbonylethyl] (2S,3S)-6,7-Dimethoxy-1,2,3,4-tetrahydronaphthalene-2,3-dicarboxylate* (**26b**): To a stirred solution of the dibromide **19** (2.43 g, 7.5 mmol) and bis[(*S*)-1-(ethoxycarbonyl)ethyl] fumarate (**25**) (6.01 g, 19 mmol) in 100 ml of dry THF, 2.46 g (20 mmol) of chromium(II) chloride (Merck, assay ca. 90%) was added at room temp. The greenish suspension turned purple within 0.5 h and was stirred for 4 h before 50 ml H_2O was added. After 5 min, the mixture was extracted with hexane/EtOAc, (2:1, 3 × 100 ml) and the combined organic layers were washed with brine and dried with $MgSO_4$. The solvent was removed under reduced pressure and the remaining oil was purified by flash chromatography (hexane/EtOAc, 2:1) yielding 3.321 g (92%) of a mixture of the diastereomers **26a** and **26b**, besides 3.57 g (11 mmol) of recovered chiral fumarate **25**. The product mixture, which consisted of **26a** and **26b** in a ratio of 81:19 (by HPLC), 79:21 (by NMR), was separated by preparative HPLC (Waters Prep Pak Silica; hexane/dioxane, 4:1, 0.1 l/min).

Major Diastereomer **26a**: R_f = 0.23 (hexane/EtOAc, 2:1). − Anal. HPLC (MN Nuc 50−10; hexane/dioxane, 4:1; 2 ml/min; 254 nm): R_T = 5.05 min. − IR (KBr): ṽ = 2989 (w), 2940 (w), 2836 (w), 1739 (br, C=O), 1519 (s), 1451 (m), 1361 (m), 1248 (s), 1218 (s), 1177 (s), 1133 (s), 1116 (s), 1099 (s), 1050 (m) cm^{-1}. − ^{1}H NMR (270 MHz): δ = 1.28 (pseudo t, *J* = 7.2 Hz, 6 H), 1.52 (pseudo d, *J* = 7.1 Hz, 6 H), 2.90 (m, 2 H), 3.10 (m, 2 H), 3.24 (pseudo dd, J_1 = 6.9 Hz, J_2 = 2.9 Hz, 2 H), 3.83 (pseudo s, 6 H), 4.20 (pseudo q, *J* = 7.2 Hz, 4 H), 5.11 (pseudo q, *J* = 7.1 Hz, 2 H), 6.61 (pseudo s, 2 H). − $[\alpha]_D^{20}$ = −61, $[\alpha]_{578}$ = −63, $[\alpha]_{546}$ = −71, $[\alpha]_{436}$ = −119, $[\alpha]_{365}$ = −238, (*c* = 0.153 in $CHCl_3$). − $C_{24}H_{32}O_{10}$ (480.51): calcd. C 59.99, H 6.71; found C 59.77, H 6.84.

Minor Diastereomer **26b**: R_f = 0.23 (hexane/EtOAc, 2:1). − Anal. HPLC (MN Nuc 50−10; hexane/dioxane, 4:1; 2 ml/min; 254 nm): R_T = 5.53 min. − IR (KBr): ṽ = 2987 (w), 2939 (w), 2835 (w), 1743 (br, C=O), 1519 (s), 1451 (m), 1378 (m), 1247 (s), 1209 (s), 1177 (s), 1133 (s), 1115 (s), 1099 (s) cm^{-1}. − ^{1}H NMR (270 MHz): δ = 1.26 (pseudo t, *J* = 7.1 Hz, 6 H), 1.49 (pseudo d, *J* = 7.0 Hz, 6 H), 2.97 (m, 2 H), 3.12 (m, 2 H), 3.25 (m, 2 H), 3.83 (pseudo s, 6 H), 4.18 (pseudo q, 4 H), 5.09 (pseudo q, *J* = 7.0 Hz, 2 H), 6.58 (pseudo s, 2 H). − $[\alpha]_D^{20}$ = 16, $[\alpha]_{578}$ = 16, $[\alpha]_{546}$ = 19, $[\alpha]_{436}$ = 43, $[\alpha]_{365}$ = 100 (*c* = 0.319 in $CHCl_3$). − $C_{24}H_{32}O_{10}$ (480.51): calcd. C 59.99, H 6.71; found C 59.99, H 6.96.

(2R,3R)-2,3-Bis(hydroxymethyl)-6,7-dimethoxy-1,2,3,4-tetrahydronaphthalene (**21**): To a solution of 0.48 g (1.1 mmol) of **26a** in 30 ml of dry diethyl ether was added 0.2 g (13.2 mmol) of $LiAlH_4$. The suspension was heated to reflux for 1 h, then cooled to 0°C, whereupon 10 ml of EtOAc was added dropwise, followed by 20 ml of 2 N HCl. The mixture was stirred until all the precipitated aluminates had dissolved and then extracted with hexane/EtOAc, (1:10, 5 × 25 ml) (Note: The resulting diol is rather soluble in water). The combined extracts were washed with saturated aqueous $NaHCO_3$ and brine, and dried with $MgSO_4$. The solvent was removed in vacuo and the resulting colorless oil was purified by PTLC (2-mm layer SiO_2; EtOAc) to yield 190 mg (76%) of diol **21** (> 99.4% *ee* according to HPLC), m.p. 135°C. − R_f = 0.23 (EtOAc). − Anal. HPLC (Daicel Chiralcel OJ, 0.7 ml/min, 254 nm): R_T (**21**) = 15.54 min; R_T (*ent*-**21**) = 14.10 min. − IR (KBr): ṽ = 3507 (br, OH), 3395 (br, OH), 2935 (m), 2908 (m), 2834 (m), 1611 (m), 1519 (s), 1460 (s), 1359 (m), 1254 (s), 1126 (s), 1063 (s), 998 (s) cm^{-1}. − ^{1}H NMR (270 MHz): δ = 1.82 (m, 2 H), 2.54 (dd, J_1 = 10.1 Hz, J_2 = 15.7 Hz, 2 H), 2.89 (dd, J_1 = 4.0 Hz, J_2 = 16.6 Hz, 2 H), 3.10 (br, 2 H, exchanges with D_2O), 3.64 (dd, J_1 = 6.3 Hz, J_2 = 10.9 Hz, 2 H), 3.78 (dd, J_1 = 3.3 Hz, J_2 = 10.9 Hz, 2 H), 3.83 (s, 6 H), 6.58 (s, 2 H). − $[\alpha]_D^{20}$ = −56, $[\alpha]_{578}$ = −58, $[\alpha]_{546}$ = −66, $[\alpha]_{436}$ = −122, $[\alpha]_{365}$ = −223 (*c* = 0.120 in $CHCl_3$). − MS; *m/z* (%): 252 [M$^+$] (100), 203 (98), 189 (17), 188 (18), 165 (46), 164 (26), 151 (13), 115 (13). − $C_{14}H_{20}O_4$ (252.31): calcd. C 66.65, H 7.79; found C 66.38, H 7.77.

(2R,3R)-6,7-Dimethoxy-2,3-bis(tosyloxymethyl)-1,2,3,4-tetrahydronaphthalene (**22**): 390 mg of the diol **21** was treated with 1.635 g (8.5 mmol) of *p*-TsCl in 10 ml of pyridine according to the procedure described above for the preparation of *rac*-**22**. Yield: 560 mg (67%) of the optically active ditosylate **22**. − M.p. 149°C. − R_f = 0.30 (hexane/EtOAc, 1:1). − IR (KBr): ṽ = 2998 (w), 2960 (w), 2901 (w), 2836 (w), 1515 (m), 1365 (s), 1176 (s), 968 (s), 853 (m), 553 (s) cm^{-1}. − ^{1}H NMR (270 MHz): δ = 2.05 (m, 2 H), 2.44 (s, 6 H), 2.53 (dd, J_1 = 7.2 Hz, J_2 = 16 Hz, 2 H), 2.67 (dd, J_1 = 5 Hz, J_2 = 17 Hz, 2 H), 3.81 (s, 6 H), 3.97 (d, *J* = 5 Hz, 4 H), 6.47 (s, 2 H), 7.35 (d, *J* = 8 Hz, 4 H), 7.76 (d, 4 H). − $[\alpha]_D^{20}$ = −14, $[\alpha]_{578}$ = −16, $[\alpha]_{546}$ = −19, $[\alpha]_{436}$ = −41, $[\alpha]_{365}$ = −73 (*c* = 0.494 in $CHCl_3$). − MS; *m/z* (%): 560 [M$^+$] (13), 430 (8), 388 (3), 272 (4), 234 (4), 233 (5), 217 (40), 216 (63), 204 (16), 203 (100), 201 (21), 189 (17), 188 (16), 58 (41). − HRMS: 560.1539 as calcd. for $C_{28}H_{32}O_8S_2$.

(2R,3R)-6,7-Dimethoxy-2,3-dimethyl-1,2,3,4-tetrahydronaphthalene (**23**): 841 mg (1.5 mmol) of the ditosylate **22** was treated with 240 mg (6.3 mmol) of $LiAlH_4$ in 50 ml of dry diethyl ether according to the procedure described above for the preparation of *rac*-**23**. Yield: 227 mg (69%) of **23** as colorless, clear crystals, m.p. 81°C. − R_f = 0.25 (hexane/EtOAc, 10:1). − IR (KBr): $\tilde{\nu}$ = 2998 (m), 2952 (m), 2933 (m), 2905 (m), 2882 (m), 2832 (m), 1518 (s), 1465 (m), 1249 (s), 1227 (s), 1114 (m) cm^{-1}. − ^1H NMR (270 MHz): δ = 1.03 (d, J = 6 Hz, 6 H), 1.49 (m, 2 H), 2.39 (dd, J_1 = 10 Hz, J_2 = 16 Hz, 2 H), 2.74 (dd, J_1 = 3.5 Hz, J_2 = 17 Hz, 2 H), 3.83 (s, 6 H), 6.56 (s, 2 H). − $[\alpha]_D^{20}$ = −105, $[\alpha]_{578}$ = −110, $[\alpha]_{546}$ = −126, $[\alpha]_{436}$ = −230, $[\alpha]_{365}$ = −408 (c = 0.805 in $CHCl_3$). − MS; *m/z* (%): 221 (16), 220 [M^+] (100), 205 (13), 189 (9), 164 (67), 69 (46), 57 (63), 55 (64). − HRMS: 220.1463 as calcd. for $C_{14}H_{20}O_4$.

(2R,3R,8aS)-Tricarbonyl(η⁶-6,7-dimethoxy-2,3-dimethyl-1,2,3,4-tetrahydronaphthalene)chromium(0) (**24**): 220 mg (1 mmol) of the ligand **23** was treated with 242 mg (1.1 mmol) of $Cr(CO)_6$ in 10 ml of dry nBu_2O and 1 ml of dry THF according to the procedure described above for the preparation of *rac*-**24**. Yield 260 mg (73%) of complex **24** as yellow cubes, m.p. 165°C. − R_f = 0.3 (hexane/EtOAc, 3:1). − IR (KBr): $\tilde{\nu}$ = 2969 (w), 2903 (w), 2842 (w), 1945 (br, C=O), 1869 (br, C=O), 1859 (br, C=O), 1495 (m), 1267 (w), 1113 (w) cm^{-1}. − NMR (400 MHz)[60]: δ = 1.01 (d, 3 H), 1.02 (d, 3 H), 1.38 (m, 1 H), 1.53 (m, 1 H), 2.28 (dd, J_1 = 16.2 Hz, J_2 = 10.6 Hz, 1 H), 2.37 (dd, J_1 = 16.9 Hz, J_2 = 10.8 Hz), 2.52 (dd, J_1 = 16.1 Hz, J_2 = 4.3 Hz, 1 H), 2.60 (dd, J_1 = 16.8 Hz, J_2 = 5.8 Hz, 1 H), 3.75 (s, 3 H), 3.78 (s, 3 H), 5.15 (s, 1 H), 5.18 (s, 1 H). − $[\alpha]_D^{20}$ = −95, $[\alpha]_{578}$ = −101, $[\alpha]_{546}$ = −122 (c = 0.485 in $CHCl_3$). − MS; *m/z* (%): 357 (5), 356 [M^+] (16), 300 (9), 273 (27), 272 (100), 243 (13), 242 (48), 220 (6), 186 (12), 164 (5), 149 (5). − $C_{17}H_{20}CrO_5$ (356.34): calcd. C 57.30, H 5.66; found C 57.44, H 5.51.

(3aRS,9aRS)-6,7-Dimethoxy-1,3,3a,4,9,9a-hexahydronaphtho[2,3-c]furan (*rac*-**27**): A solution of 760 mg (3 mmol) of the diol *rac*-**21** in 30 ml of $CHCl_3$ and 3 ml of pyridine was heated to 60°C and 1.720 g (9 mmol) of *p*-TsCl was added. Stirring was continued for 4 h at 60°C, then the mixture was cooled to 0°C and 30 ml of cold 2 N HCl was added. After 30 min, the layers were separated, the aqueous layer was extracted with $CHCl_3$ (2 × 30 ml), and the combined organic layers were washed with saturated $NaHCO_3$ and brine, and dried with $CaCl_2$ overnight. The solvent was removed under reduced pressure and the oily residue was purified by PTLC (3-mm layer SiO_2; hexane/EtOAc/CH_2Cl_2, 1:1:1) to yield 530 mg (76%) of the naphthofuran *rac*-**27** as colorless plates, m.p. 124°C. − R_f = 0.36 (hexane/EtOAc/CH_2Cl_2, 1:1:1). − IR (KBr): $\tilde{\nu}$ = 2937 (m), 2907 (m), 2854 (m), 2833 (m), 1684 (m), 1516 (s), 1239 (s), 1221 (s), 1094 (s), 988 (m), 902 (m) cm^{-1}. − ^1H NMR (270 MHz): δ = 2.04 (m, 2 H), 2.57 (dd, J_1 = 11.4 Hz, J_2 = 15. 6 Hz, 2 H), 2.93 (dd, J_1 = 15.6 Hz, J_2 = 4.1 Hz, 2 H), 3.48 (dd, J_1 = 7.9 Hz, J_2 = 10.2 Hz, 2 H), 3.85 (s, 6 H), 4.17 (pseudo t, J = 7.5 Hz, 2 H), 6.62 (s, 2 H). − ^{13}C NMR (63 MHz): δ = 31.7 (d), 42.5 (t), 55.8 (q), 72.6 (t), 112.2 (d), 127.6 (s), 147.2 (s). − $C_{14}H_{18}O_3$ (234.30): calcd. C 71.77, H 7.74; found C 71.75, H 7.76.

(3aRS,4aSR,9aRS)-Tricarbonyl{η⁶-6,7-dimethoxy-1,3,3a,4,9,9a-hexahydronaphtho[2,3-c]furan}chromium(0) (*rac*-**28**): As described above for the preparation of *rac*-**24**, 351 mg (1.5 mmol) of the ligand *rac*-**27** was heated with 350 mg (1.6 mmol) of $Cr(CO)_6$ in 10 ml nBu_2O and 1 ml THF for 20 h at 150°C (oil-bath temperature). The resulting cloudy yellow solution was cooled, the solvent was removed in vacuo, and the crystalline residue was taken up in 30 ml of EtOAc. The resulting solution was filtered through a 2-cm pad of silica, the solvent was evaporated once more, and the residue was recrystallized from hexane/EtOAc (1:1) to give 441 mg (79%) of the complex *rac*-**28** as small yellow crystals, m.p. 195°C. − R_f = 0.4 (EtOAc). − IR (KBr): $\tilde{\nu}$ = 2978 (m), 2939 (m), 2914 (m), 2850 (m), 1948 (br, C=O), 1874 (br, C=O), 1848 (br, C=O), 1496 (s), 1438 (s), 1289 (s), 1263 (s), 1236 (s), 1214 (s), 1096 (s), 978 (s), 673 (s), 629 (s) cm^{-1}. − ^1H NMR (270 MHz):[60] δ = 1.94 (m, 1 H), 2.14 (m, 1 H), 2.48 (dd, J_1 = 15.2 Hz, J_2 = 11.6 Hz, 1 H), 2.59 (dd, J_1 = 15.7 Hz, J_2 = 11.7 Hz, 1 H), 2.75 (dd, J_1 = 15.3 Hz, J_2 = 4.5 H, 1 H), 2.79 (dd, J_1 = 15.8 Hz, J_2 = 5.7 Hz, 1 H), 3.44 (pseudo d, J = 10.3 Hz, 1 H), 3.46 (pseudo d, J = 10.3 Hz, 1 H), 3.76 (s, 3 H), 3.80 (s, 3 H), 4.10 (pseudo t, J = 7.5 Hz, 1 H), 4.20 (pseudo t, J = 7.5 Hz, 1 H), 5.18 (s, 1 H), 5.21 (s, 1 H). − $C_{17}H_{18}CrO_6$ (370.32): calcd. C 55.14, H 4.93; found C 55.19, H 4.93.

(3aRS,4aSR,9aRS)-Tricarbonyl{η⁶-6,7-dimethoxy-5,8-bis(trimethylsilyl)-1,3,3a,4,9,9a-hexahydronaphtho[2,3-c]furan}chromium(0) (*rac*-**6**): To a solution of 185 mg (0.5 mmol) of the complex *rac*-**28** and 0.35 ml (2.5 mmol) of TMSCl in 10 ml of dry THF at −40°C, was added a solution of LiTMP [prepared separately from 0.19 ml (1.1 mmol) of 2,2,6,6-tetramethylpiperidine and 0.65 ml of *n*-butyllithium (1.04 mmol, 1.6 M in hexane) in 5 ml of dry THF], as described above for the preparation of *rac*-**5**. After 15 min at −40°C and 1 h at room temp., 30 ml of EtOAc was added and the mixture was washed with 2 N HCl (2 × 30 ml), saturated aqueous $NaHCO_3$ and brine. After drying and removal of the solvent, the remaining yellow oil was purified by flash chromatography (hexane/EtOAc, 3:1). The product was finally crystallized from hexane/EtOAc (3:1) yielding 182 mg (71%) of the disilylated complex *rac*-**6** as small yellow needles, m.p. 202°C. − R_f = 0.74 (EtOAc). − IR (KBr): $\tilde{\nu}$ = 2950 (w), 2899 (w), 2850 (w), 1944 (br, C=O), 1858 (br, C=O), 1362 (m), 1320 (m), 1250 (m), 1016 (m), 848 (m), 673 (m) cm^{-1}. − ^1H NMR (400 MHz):[60] δ = 0.46 and 0.47 (both s, 9 H), 1.79 (m, 1 H), 1.93 (m, 1 H), 2.30 (dd, J_1 = 15.2 Hz, J_2 = 11.3 Hz, 1 H), 2.53 (dd, J_1 = 15.6 Hz, J_2 = 12.1 Hz, 1 H), 2.79 (dd, J_1 = 15.6 Hz, J_2 = 5.0 Hz, 1 H), 3.02 (dd, J_1 = 15.2 Hz, J_2 = 4.7 Hz, 1 H), 3.37 (dd, J_1 = 10.4 Hz, J_2 = 7.5 Hz, 1 H), 3.40 (dd, J_1 = 10.4 Hz, J_2 = 7.5 Hz, 1 H), 3.73 (s, 3 H), 3.74 (s, 3 H), 4.09 (pseudo t, J = 7.5 Hz, 1 H), 4.15 (pseudo t, J = 7.5 Hz, 1 H). − $C_{23}H_{34}CrO_6Si_2$ (514.69): calcd. C 53.67, H 6.66; found C 53.49, H 6.51.

1-Bromo-2-(bromomethyl)-4,5-dimethoxybenzene (**31**): A solution of 5.05 g (30 mmol) of 3,4-dimethoxybenzyl alcohol (**30**) in 50 ml of dry benzene was cooled to 0°C and a solution of 1.60 ml (31 mmol) of Br_2 in 50 ml of dry benzene was added over a period of 20 min. Then, 5 ml of HBr (33% in AcOH) was added, the cooling bath was removed, and the red solution was stirred at ambient temperature for 30 min. The mixture was then sequentially washed with saturated aqueous $Na_2S_2O_3$ (50 ml), water (50 ml) and brine, and the organic solution was dried with $MgSO_4$. The solvent was removed under reduced pressure and the yellow, oily residue was crystallized from hexane/EtOAc (3:1) to yield 8.71 g (94%) of the dibromide **31** as thin, colorless needles, m.p. 81°C. − R_f = 0.35 (hexane/EtOAc, 3:1). − IR (CCl_4): $\tilde{\nu}$ = 3006 (w), 2959 (w), 2909 (w), 2841 (w), 1507 (s), 1464 (m), 1383 (m), 1262 (s), 1226 (s), 1210 (s), 1168 (s), 1036 (m) cm^{-1}. − ^1H NMR (270 MHz): δ = 3.87 (s, 3 H), 3.89 (s, 3 H), 4.59 (s, 2 H), 6.93 (s, 1 H), 7.02 (s, 1 H). − MS; *m/z* (%): 312 (7), 310 [M^+ + 2] (14), 308 [M^+] (6), 232 (20), 231 (99), 230 (20), 229 [MH^+ − Br] (100), 215 (5), 187 (7), 185 (9), 108 (13), 107 (17). − $C_9H_{10}Br_2O_2$ (309.99): calcd. C 34.77, H 3.25; found C 34.90, H 3.14.

(2RS)-2-(2′-Bromo-4′,5′-dimethoxybenzyl)cyclohexanone (*rac*-**32**): A stirred solution of diisopropylamine (4.65 ml, 33 mmol) in

100 ml anhydrous THF was cooled to −78°C and *n*-butyllithium (21 ml, 31.1 mmol, 1.48 M in hexane) was added by means of a syringe. After 20 min, a solution of cyclohexanone (4.7 ml, 36 mmol) in anhydrous THF (20 ml) was added slowly (over a period of ca. 30 min) and the resulting mixture was stirred for 10 min at −78°C. A solution of 9.3 g (30 mmol) of the dibromide **31** in anhydrous THF (50 ml) was then added over a period of 5 min, the temperature was allowed to rise, and stirring was continued for 3 h at 0°C and for 10 h at room temp. After quenching with 2 N HCl (100 ml), the mixture was extracted with EtOAc (3 × 100 ml). The combined organic extracts were washed with saturated aqueous $NaHCO_3$ and brine, and dried with $MgSO_4$. After removing the solvent in vacuo, the resulting yellow oil was purified by flash chromatography (hexane/EtOAc, 5:1) yielding 8.48 g (86%) of the alkylation product *rac*-**32** as a colorless oil, which solidified upon standing within 48 h. In addition, 1.01 g of the dialkylated by-product **36a** was obtained. An analytical sample of *rac*-**32** was recrystallized from hexane/EtOAc (5:1); m.p. 72°C. − R_f = 0.16 (hexane/EtOAc, 5:1). − IR (CCl_4): $\tilde{\nu}$ = 3003 (w), 2936 (m), 2858 (w), 2839 (w), 1713 (s, C=O), 1580 (s), 1497 (s), 1260 (s), 1233 (s), 1165 (s) cm^{-1}. − ^1H NMR (270 MHz): δ = 1.40 (m, 1 H), 1.60 (m, 2 H), 1.82 (m, 1 H), 2.04 (m, 2 H), 2.32 (m, 1 H), 2.38 (m, 1 H), 2.48 (dd, J_1 = 7.5 Hz, J_2 = 19 Hz, 1 H), 2.63 (m, 1 H), 3.20 (dd, J_1 = 6 Hz, J_2 = 19 Hz, 1 H), 3.90 and 3.93 (both s, 3 H), 6.77 and 6.95 (both s, 1 H). − ^{13}C NMR (63 MHz): δ = 25.2 (t), 28.0 (t), 33.7 (t), 35.2 (t), 42.2 (t), 51.0 (d), 55.9 (q), 56.0 (q), 114.2 (d), 115.2 (d), 131.6 (s), 147.8 (s), 147.9 (s), 212.3 (s). − MS; *m/z* (%): 328 (12), 326 [M^+] (12), 248 (17), 247 (100), 231 (55), 229 (57), 151 (11). − $C_{15}H_{19}BrO_3$ (327.22): calcd. C 55.02, H 5.89; found C 55.06, H 5.85.

2,2-Bis(2′-bromo-4′,5′-dimethoxybenzyl)cyclohexanone (**36a**): ^1H NMR (270 MHz): δ = 1.74−2.06 (m, 6 H), 2.52 (m, 2 H), 3.23 (AB signal, 4 H), 3.80 (s, 6 H), 3.85 (s, 6 H), 6.70 (s, 2 H), 6.98 (s, 2 H).

(1′RS)-1-Bromo-4,5-dimethoxy-2-(2′-methylenecyclohexylmethyl)benzene (*rac*-**33**): A suspension of 18.7 g of methyltriphenylphosphonium bromide in 250 ml of anhydrous THF was cooled to −78°C and *n*-butyllithium (29 ml, 47 mmol, 1.6 M in hexane) was added by means of a syringe. The temperature was allowed to rise to −30°C over a period of 30 min. At this point, 11.45 g of *rac*-**32** was added, the cooling bath was replaced by an oil bath, and the orange solution was refluxed for 1 h. The cooled mixture was then washed with water (2 × 30 ml) and brine, and dried with $MgSO_4$. The solvent was removed under reduced pressure and 100 ml of hexane was added to the residue, resulting in the precipitation of Ph_3PO. The solution was filtered through a pad of Celite and silica. The solvent was removed under reduced pressure yielding 11.35 g (> 99%) of the methylenated product *rac*-**33** as an essentially pure, slightly yellow oil, which crystallized within two weeks, m.p. 61°C. − R_f = 0.57 (hexane/EtOAc, 5:1). − IR (CCl_4): $\tilde{\nu}$ = 2934 (m, C−H), 3082 (w), 3002 (w), 2856 (w), 2839 (w), 1509 (s), 1496 (m), 1439 (m), 1219 (s), 1496, 1165 (m) cm^{-1}. − ^1H NMR (270 MHz): δ = 1.20 − 1.74 (m, 6 H), 2.08 (m, 1 H), 2.37 (m, 1 H), 2.66 (dd, J_1 = 5.5 Hz, J_2 = 14 Hz, 1 H), 3.00 (dd, J_1 = 9.5 Hz, J_2 = 14 Hz, 1 H), 5.60 (pseudo s, 1 H), 5.69 (pseudo s, 1 H), 6.66 (s, 1 H), 7.00 (s, 1 H). − ^{13}C NMR (63 MHz): δ = 24.6 (t), 28.6 (t), 32.7 (t), 35.3 (t), 38.4 (t), 43.3 (d), 56.0 (q), 56.1 (q), 105.8 (t), 113.8 (d), 114.6 (s), 115.4 (d), 132.5 (s), 147.7 (s), 148.0 (s), 152.3 (s). − MS; *m/z* (%): 326 (6), 324 [M^+] (7), 245 (32), 244 (24), 231 (98), 230 (100), 151 (6), 107 (6). − $C_{16}H_{21}BrO_2$ (325.25): calcd. C 59.09, H 6.51; found C 59.34, H 6.57.

(4aRS,9aRS)-6,7-Dimethoxy-1,2,3,4,4a,9,9a,10-octahydroanthracene (*rac*-**34**): To a refluxing solution of 1.63 g (5 mmol) of the olefin *rac*-**33** in 50 ml of dry benzene, a solution of 1.59 ml (5.2 mmol) of tributyltin hydride and 20 mg of azobis(isobutyronitrile) in 8 ml of dry benzene was added over a period of 5 h by means of a syringe pump. Refluxing was continued for 1 h, and then a solution of 5 g of KF in 20 ml of water was added to the cooled (room temp.) mixture. The resulting two-phase system was stirred vigorously overnight. The organic layer was separated and the aqueous layer was extracted with EtOAc (3 × 30 ml). The combined organic layers were washed with water (2 ×) and brine, and dried with $MgSO_4$. The solvent was removed under reduced pressure and the resulting colorless oil was purified by PTLC (4-mm layer SiO_2; hexane/CH_2Cl_2/EtOAc, 2:1:0.02). The product was finally crystallized from hexane to yield 810 mg (66%) of the cyclization product *rac*-**34** as clear, colorless prisms, m.p. 110°C. − R_f = 0.15 (hexane/CH_2Cl_2/EtOAc = 2:1:0.02). − IR (CCl_4): $\tilde{\nu}$ = 2998 (w), 2919 (m), 2854 (w), 2832 (w), 1518 (s), 1249 (m), 1224 (m), 1129 (w), 1112 (w) cm^{-1}. − ^1H NMR (270 MHz): δ = 1.06 (m, 2 H), 1.35 (m, 4 H), 1.84 (m, 4 H), 2.39 (dd, J_1 = 9 Hz, J_2 = 14.5 Hz, 2 H), 2.69 (dd, J_1 = 4.5 Hz, J_2 = 14.5 Hz, 2 H), 3.86 (s, 6 H), 6.56 (s, 2 H). − ^{13}C NMR (63 MHz): δ = 26.3 (t), 33.8 (t), 37.1 (t), 38.8 (d), 55.9 (q), 111.5 (d), 128.6 (s), 146.9 (s). − MS; *m/z* (%): 247 (18), 246 [M^+] (100), 231 (20), 229 (14), 206 (9), 164 (23), 151 (55), 149 (15), 57 (39), 55 (38). − HRMS: 246.1620 as calcd. for $C_{16}H_{22}O_2$.

(4aRS,8aSR,9aRS)-Tricarbonyl(η⁶-6,7-dimethoxy-1,2,3,4,4a,9,9a,10-octahydroanthracene)chromium(0) (*rac*-**35**): As described above for the preparation of *rac*-**24**, 1.06 g (4.3 mmol) of the ligand *rac*-**34** was heated with 0.99 g (4.5 mmol) of $Cr(CO)_6$ in 45 ml nBu_2O and 4.5 ml THF in a 100-ml Schlenk flask for 22 h at 150°C (oil-bath temperature). The resulting clear yellow solution was allowed to cool to room temp., whereupon a yellow precipitate formed. Cooling was continued in an ice bath for 1 h, and then the supernatant solution was carefully decanted off and the residue washed twice with cold diethyl ether. The yellow powder thus obtained was dried in vacuo to yield a first fraction of *rac*-**35**. The solvent of the decanted organic solution was removed in vacuo and the residue was purified by PTLC (1 mm SiO_2; hexane/EtOAc, 3:1). Recrystallization from EtOAc afforded 1.300 g (79%) of the complex *rac*-**35** as small yellow crystals, m.p. 201°C. − R_f = 0.38 (hexane/EtOAc, 10:1). − IR (KBr): $\tilde{\nu}$ = 2925 (w), 2854 (w), 1950 (s, C=O), 1874 (s, C=O), 1851 (s, C=O), 1495 (m) cm^{-1}. − ^1H NMR (270 MHz)[60]: δ = 0.96−1.54 (m, 6 H), 1.77 (pseudo dd, 4 H), 2.30 (dd, J_1 = 16 Hz, J_2 = 11.5 Hz, 1 H), 2.35 (dd, J_1 = 16 Hz, J_2 = 11 Hz, 1 H), 2.47 (dd, J_1 = 16.5 Hz, J_2 = 4 Hz, 1 H), 2.57 (dd, J_1 = 16.5 Hz, J_2 = 6 Hz, 1 H), 3.75 (s, 3 H), 3.79 (s, 3 H), 5.16 (s, 1 H), 5.20 (s, 1 H). − ^{13}C NMR (63 MHz, $CDCl_3$): δ = 25.8 (t), 26.0 (t), 33.1 (t), 34.7 (t), 36.4 (t), 37.2 (d), 38.2 (d), 57.0 (q), 57.1 (q), 78.3 (d), 79.0 (d), 101.7 (s), 103.4 (s), 132.2 (s), 132.3 (s), 234.1 (s). − MS; *m/z* (%): 382 [M^+] (16), 326 [M^+ − 2CO] (6), 299 (36), 298 [M^+ − 3CO] (100), 260 (15), 268 (56), 186 (6). − $C_{19}H_{22}CrO_5$ (382.38): calcd. C 59.68, H 5.80; found C 59.55, H 5.78.

(4aRS,8aSR,9aRS)-Tricarbonyl(η⁶-6,7-dimethoxy-5,8-bis(trimethylsilyl)-1,2,3,4,4a,9,9a,10-octahydroanthracene)chromium(0) (*rac*-**7**): To a solution of 3.06 g (8 mmol) of the complex *rac*-**35** and 10.1 ml (80 mmol) of TMSCl in 80 ml of anhydrous THF at −50°C, was added a solution of LiTMP [prepared separately from 2.85 ml (16.8 mmol) of 2,2,6,6-tetramethylpiperidine and 10.4 ml of *n*-butyllithium (16.6 mmol, 1.6 M in hexane) in 40 ml anhydrous THF], as described above for the preparation of *rac*-**5**. After 15 min at −50°C and 1 h at room temp., 50 ml of EtOAc was added and the mixture was washed with 2 N HCl (2 × 50 ml), saturated aqueous $NaHCO_3$ and brine. The dried ($MgSO_4$) solution was con-

centrated and the remaining yellow oil was purified by flash chromatography (hexane/EtOAc, 10:1). Crystallization of the product from hexane/EtOAc (10:1) yielded 3.21 g (76%) of the disilylated complex *rac*-**7** as dark-yellow cubes, m.p. 138°C. − R_f = 0.55 (hexane/EtOAc, 10:1). − IR (KBr): $\tilde{\nu}$ = 2984 (w), 2924 (w), 2904 (w), 2856 (w), 1957 (s), 1887 (s), 1361 (m), 1251 (m), 1020 (m), 857 (m) cm^{-1}. − ^1H NMR (270 MHz)[60]: δ = 0.46 (pseudo s, 18 H), 0.78−1.34 (m, 6 H), 1.78 (m, 4 H), 2.09 (dd, J_1 = 16 Hz, J_2 = 5.5 Hz, 1 H), 2.31 (dd, J_1 = 16 Hz, J_2 = 5.5 Hz, 1 H), 2.53 (dd, J_1 = 16 Hz, J_2 = 11 Hz, 1 H), 2.80 (dd, J_1 = 16.5 Hz, J_2 = 11 Hz, 1 H), 3.72 (pseudo s, 6 H). − ^{13}C NMR (63 MHz, $CDCl_3$) δ = 3.0 (q), 3.3 (q), 25.6 (t), 25.8 (t), 32.9 (t), 33.1 (t), 36.6 (t), 37.5 (t), 38.1 (t), 38.2 (d), 61.9 (q), 62.0 (q), 95.4 (d), 110.2 (s), 111.3 (s), 137.7 (s), 138.0 (s), 234.7 [s, $Cr(CO)_3$]. − MS; *m/z* (%): 526 (6), 470 [M^+ − 2CO] (13), 444 (18), 443 (42), 442 [M^+ − 3CO] (100). − $C_{25}H_{38}CrO_5Si_2$ (526.74): calcd. C 57.01, H 7.27; found C 57.03, H 7.31.

(2RS)-2-(2′-Bromobenzyl)cyclohexanone (*rac*-**38**): A stirred solution of 3.23 ml (33 mmol) of diisopropylamine in 100 ml of dry THF was cooled to −78°C and 13.8 ml (22 mmol) of a solution of *n*-butyllithium (1.6 M in hexane) was added by means of a syringe. After 10 min, a solution of 2.5 ml (25 mmol) of cyclohexanone in 10 ml of dry THF was added dropwise over a period of 20 min. The mixture was stirred for 1 h at −78°C and then transferred dropwise over a period of 1 h to a cold (0°C) stirred solution of α-bromobenzyl bromide (**37**) (5.0 g, 20 mmol) in 80 ml THF. The cooling bath was removed and the mixture was heated to reflux for 3 h. The cooled mixture was subsequently treated with 100 ml of 2 N HCl and extracted with EtOAc (3 × 100 ml). The combined organic extracts were washed with satd. aqueous $NaHCO_3$ and with brine, dried with $MgSO_4$, and the solvent was removed in vacuo. The crude product (yellow oil) consisted of *rac*-**38** contaminated with ca. 30% of the dialkylated product **36b** (NMR). Kugelrohr distillation (85°C, 0.5 Torr) afforded 4.23 g (63% yield) of the pure monoalkylated ketone *rac*-**38** as a colorless oil and 1.83 g (33%) of **36b** as a slightly yellow oil (130°C, 0.5 Torr); R_f = 0.33 (hexane/EtOAc, 10:1). − IR (ATR): $\tilde{\nu}$ = 3058 (w), 2932 (m), 2859 (w), 1708 (s, C=O), 1469 (m), 1444 (m), 1128 (w), 1021 (m), 745 (m) cm^{-1}. − ^1H NMR (400 MHz): δ = 1.42 (pseudo qd, 1 H), 1.54−1.73 (m, 2 H), 1.84 (m, 1 H), 2.00−2.12 (m, 2 H), 2.24 (pseudo dd, J_1 = 5.2 Hz, J_2 = 12.8 Hz, 1 H), 2.43 (m, 1 H), 2.55 (dd, J_1 = 8 Hz, J_2 = 16 Hz, 1 H), 2.65−2.75 (m, 1 H), 3.34 (dd, J_1 = 5.4 Hz, J_2 = 16.2 Hz, 1 H), 7.05 (pseudo td, J_1 = 2.5 Hz, J_2 = 8.5 Hz, 1 H), 7.18−7.27 (m, 2 H), 7.51 (pseudo d, J = 8 Hz, 1 H). − ^{13}C NMR (63 MHz): δ = 25.2 (t), 28.1 (t), 33.7 (t), 35.2 (t), 42.2 (t), 50.5 (d), 124.6 (s), 127.1 (d), 127.7 (d), 131.8 (d), 132.7 (d), 139.7 (s). − MS; *m/z* (%): 187 [M^+ − Br] (100), 171 (16), 169 (17), 119 (43), 107 (22), 69 (10). − HRMS: calcd. for $C_{13}H_{15}O$ (M − Br): 187.1123; found: 187.1118. − $C_{13}H_{15}BrO$ (267.17): calcd. C 58.44, H 5.66; found C 58.17, H 5.67.

2,2-Bis(2′-bromobenzyl)cyclohexanone (**36b**): ^1H NMR (270 MHz): δ = 1.63−1.88 (m, 6 H), 2.03−2.18 (m, 2 H), 3.18 (pseudo d, J = 13.9 Hz, 2 H), 3.33 (pseudo d, J = 14.0 Hz, 2 H), 7.06 (m, 2 H), 7.21 (m, 4 H), 7.55 (m, 2 H).

(1′RS)-1-Bromo-2-(2′-methylenecyclohexylmethyl)benzene (*rac*-**39**): To a stirred suspension of 9.0 g (25.3 mmol) of methyltriphenylphosphonium bromide in 100 ml of dry THF at −78°C, 13.9 ml (22.3 mmol) of a solution of *n*-butyllithium (1.6 M in hexane) was added by means of a syringe and the temperature was allowed to rise to −30°C over a period of 30 min. To the resulting orange solution was added 4.5 g (16.8 mmol) of *rac*-**38**, the cooling bath was replaced by an oil bath, and the mixture was heated to reflux for 2 h. The cooled mixture was then partitioned between water (50 ml) and EtOAc (50 ml) and the aqueous phase was extracted with further EtOAc (50 ml). The combined organic extracts were washed with brine, dried with $MgSO_4$, and the solvent was removed under reduced pressure. The residue was treated with 50 ml of hexane and filtered through a short pad of Celite (1 cm) and silica (1 cm). The solvent was removed under reduced pressure yielding 4.22 g (95%) of the methylenated product *rac*-**39** as a slightly yellow oil; R_f = 0.75 (hexane/EtOAc, 10:1). − IR (CCl_4): $\tilde{\nu}$ = 3067 (w), 2927 (s), 2853 (m), 1643 (m), 1469 (m), 1437 (m), 1023 (s), 882 (m), 745 (s) cm^{-1}. − ^1H NMR (270 MHz): δ = 1.18−1.76 (m, 6 H), 2.12 (m, 1 H), 2.32−2.59 (m, 2 H), 2.66 (dd, J_1 = 9.5 Hz, J_2 = 13 Hz, 1 H), 3.10 (dd, J_1 = 5.5 Hz, J_2 = 13 Hz, 1 H), 4.62 (pseudo s, 1 H), 4.74 (pseudo s, 1 H), 7.03 (pseudo dt, J_1 = 2 Hz, J_2 = 8 Hz, 1 H), 7.10−7.24 (m, 2 H), 7.54 (pseudo dd, J_1 = 1.5 Hz, J_2 = 9.5 Hz, 1 H). − ^{13}C NMR (63 MHz): δ = 24.6 (t), 28.7 (t), 32.8 (t), 35.3 (t), 38.8 (t), 42.8 (d), 105.9 (t), 124.9 (s), 127. 0 (d), 127.4 (d), 131.3 (d), 132.8 (d), 140.5 (s), 152.2 (s). − MS; *m/z* (%): 262 (20), 185 [M^+ − Br] (100), 171 (13), 169 (14), 129 (11), 117 (32), 95 (96), 94 (22), 79 (15), 67 (19). − $C_{14}H_{17}Br$ (265.19): calcd. C 63.41, H 6.46; found C 63.80, H 6.52.

(4aRS,9aRS)-1,2,3,4,4a,9,9a,10-Octahydroanthracene (*rac*-**13**)[12a]: To a refluxing solution of 3.7 g (14 mmol) of olefin *rac*-**39** in 75 ml of dry benzene, a solution of 4.77 ml (18 mmol) of tributyltin hydride and 20 mg of azobis(isobutyronitrile) in 5 ml of dry benzene was added over a period of 4 h by means of a syringe pump. Refluxing was continued for 30 min, and then a solution of 1 g of NH_4F in 40 ml of water was added to the cooled (room temp.) mixture. The resulting two-phase system was stirred vigorously overnight. After addition of 20 ml of 2 N HCl, the organic layer was separated and the aqueous layer was extracted with EtOAc (3 × 20 ml). The combined organic layers were washed with water (2 ×) and brine, and dried with $MgSO_4$. The solvent was removed under reduced pressure and the resulting colorless oil was purified by PTLC (4 mm layer SiO_2; hexane). The product was finally crystallized from hexane to yield 754 mg (29%) of the cyclized product *rac*-**13** as clear, colorless prisms, m.p. 64°C (ref.[12a]: 53°C). − R_f = 0.79 (hexane/EtOAc, 10:1).− IR (ATR): $\tilde{\nu}$ = 2917 (s), 2877 (m), 2846 (m), 2830 (m), 1493 (w), 1450 (w), 1421 (w), 945 (w), 742 (s) cm^{-1}. − ^1H NMR (400 MHz): δ = 1.06 (m, 2 H), 1.30−1.44 (m, 4 H), 1.78 (m, 4 H), 1.86 (d, J = 13 Hz, 2 H), 2.45 (dd, J_1 = 11 Hz, J_2 = 16 Hz, 2 H), 2.78 (dd, J_1 = 4 Hz, J_2 = 15.5 Hz, 2 H), 6.99 (m, 4 H). − ^{13}C NMR (63 MHz): δ = 26.3 (t), 33.8 (t), 37.4 (t), 38.7 (d), 125.3 (d), 128.6 (d), 136.9 (s). − MS; *m/z* (%): 186 [M^+] (100), 129 (22), 128 (19), 105 (20), 104 (48), 95 (21), 94 (17). − HRMS: 186.1409 as calcd. for $C_{14}H_{18}$. − $C_{14}H_{18}$ (186.30): calcd. C 90.25, H 9.75; found C 89.87, H 9.74.

(4aRS,8aSR,9aRS)-Tricarbonyl(η⁶-1,2,3,4,4a,9,9a,10-octahydroanthracene)chromium(0) (*rac*-**8**): As described above for the preparation of *rac*-**24**, 400 mg (2.2 mmol) of the ligand *rac*-**13** was heated with 0.55 g (2.5 mmol) of $Cr(CO)_6$ in 17 ml nBu_2O and 1.7 ml THF in a 100-ml Schlenk flask for 24 h at 150°C (oil-bath temperature). The resulting clear yellow solution was allowed to cool to room temp. and filtered through a short pad of silica. The solvent was removed in vacuo and the residue was purified by PTLC (4-mm layer SiO_2; hexane/EtOAc, 5:1) to yield 515 mg (74%) of *rac*-**8** as a light-yellow powder, m.p. 117°C. − R_f = 0.34 (hexane/EtOAc, 10:1). − IR (ATR): $\tilde{\nu}$ = 2922 (m), 2854 (w), 1948 (s), 1855 (s), 1459 (w), 1446 (w), 1430 (m), 667 (m) cm^{-1}. − ^1H NMR (400 MHz)[60]: δ = 1.05 (m, 2 H), 1.31 (m, 4 H), 1.77 (pseudo dd), 2.34 (dd, J_1 = 15.6 Hz, J_2 = 10 Hz, 1 H), 2.41 (dd, J_1 = 9.6 Hz, J_2 = 13.8 Hz, 1 H), 2.52 (dd, J_1 = 17 Hz, J_2 = 5 Hz, 1 H), 2.61 (dd, J_1 = 16.6 Hz, J_2 = 6.2 Hz, 1 H), 5.24 (m, 4 H). − ^{13}C NMR (63

MHz, $CDCl_3$): δ = 25.8 (t), 26.0 (t), 33.1 (t), 33.2 (t), 35.0 (t), 36.7 (t), 37.2 (d), 38.2 (d), 91.7 (d), 92.0 (d), 93.4 (s), 93.6 (s), 108.7 (s), 233.8 (s). − MS; *m/z* (%): 322 [M^+] (16), 266 (18), 238 (100), 52 (21). − HRMS: 322.0661 as calcd. for $C_{17}H_{18}CrO_3$. − $C_{17}H_{18}O_3Cr$ (322.32): calcd. C 62.70, H 5.63; found C 62.73, H 5.73.

Diethyl (1RS,2SR)-Cyclohexane-1,2-dicarboxylate (**41a**)[26]: To a solution of 51.4 g (0.33 mol) of *cis*-hexahydrophthaloyl anhydride (**40**) in 300 ml of dry EtOH was added 2.5 ml of conc. sulfuric acid and the mixture was refluxed for 5 h. After cooling to room temp., EtOAc (300 ml) was added and the mixture was sequentially washed with water (2 × 100 ml), saturated aqueous $NaHCO_3$ (100 ml), and brine. The aqueous extracts were back-extracted three times with 100 ml of EtOAc and the combined organic layers were dried with $MgSO_4$. The solvent was removed under reduced pressure and the resulting oil was distilled in vacuo (89°C, 0.5 Torr) through a 10-cm Vigreux column to yield 74.40 g (87%) of the *cis*-diester **41a** (containing ca. 1.5% of the *trans* isomer *rac*-**41b**), R_f = 0.15 (hexane/EtOAc, 10:1). − IR (CCl_4): $\tilde{\nu}$ = 2982 (w), 2938 (w), 2859 (w), 1793 (w, C=O), 1733 (s, C=O), 1245 (m), 1215 (m), 1180 (m) cm^{-1}. − ^1H NMR (270 MHz): δ = 1.24 (t, 6 H), 1.44 (m, 4 H), 1.77 (m, 2 H), 2.01 (m, 2 H), 2.79 (pseudo t, 2 H), 4.13 (q, *J* = 8 Hz, 4 H). − ^{13}C NMR (63 MHz): δ = 13.3 (q), 22.9 (t), 25.4 (t), 41.8 (d), 59.5 (t), 172.93 (s). − MS; *m/z* (%): 228 [M^+] (3), 183 (30), 154 (23), 109 (33), 95 (21), 81 (100).

Diethyl (1RS,2RS)-Cyclohexane-1,2-dicarboxylate (*rac*-**41b**)[26]: To a solution of 2.2 g (96 mmol) of sodium in 200 ml of dry EtOH was added 45.85 g (201 mmol) of the *cis*-diester **41a** and the mixture was refluxed for 5 h. After cooling to room temp., 200 ml of EtOAc was added and the mixture was washed with water (2 × 100 ml), 2 N HCl (100 ml), saturated aqueous $NaHCO_3$ (100 ml) and brine. The aqueous phases were re-extracted with EtOAc (3 × 100 ml) and the combined organic layers were dried with $MgSO_4$. The solvent was removed under reduced pressure and the residue was dried in vacuo yielding 42.30 g (92%) of *trans*-diester *rac*-**41b** (containing about 11% of the *cis*-diester according to NMR). − R_f = 0.15 (hexane/EtOAc, 10:1). − IR (CCl_4): $\tilde{\nu}$ = 2985 (w), 2938 (w), 2861 (w), 1733 (s, C=O), 1216 (s), 1178 (m) cm^{-1}. − ^1H NMR (270 MHz; only the signals of *rac*-**41b** are given): δ = 1.24 (t, *J* = 7 Hz, 6 H), 1.32 (m, 4 H), 1.79 (m, 2 H), 2.07 (pseudo d, 2 H), 2.59 (m, 2 H), 2.79 (pseudo t, 2 H), 4.12 (dq, J_1 = 8 Hz, J_2 = 4 Hz, 4 H). − ^{13}C NMR (63 MHz): δ = 14.0 (q), 25.1 (t), 28.8 (t), 44.8 (d), 60.3 (t), 175.0 (s). − MS; *m/z* (%): 228 [M^+] (2), 183 (47), 182 (27), 155 (25), 154 (50), 109 (37), 108 (33), 81 (100).

(1RS,2RS)-1,2-Bis(hydroxymethyl)cyclohexane (*rac*-**42b**)[27]: To a stirred suspension of 9.48 g (242 mmol) of $LiAlH_4$ in 150 ml of dry diethyl ether was added a solution of 23.05 g (101 mmol) of the mixture containing principally diester *rac*-**41b** (*rac*-**41b**/**41a** = 89:11) in 100 ml of dry diethyl ether, so that the mixture refluxed gently. After completion of the addition, refluxing was continued for 1 h. The cooled mixture was then quenched by the dropwise addition of 50 ml of EtOAc followed by 300 ml of 5 N HCl. Stirring was continued until most of the precipitate had dissolved. The layers were separated and the organic layer was washed with saturated aqueous $NaHCO_3$ and brine. The aqueous layers were re-extracted with EtOAc (5 × 50) and the combined organic layers were dried with $MgSO_4$. After removing the solvent under reduced pressure, 14.42 g (99%) of the diol mixture (*rac*-**42b**/**42a** = 89:11) was obtained, which crystallized spontaneously. An analytical sample was recrystallized from hexane/benzene (3:1) yielding colorless prisms of pure *rac*-**42b**, m.p. 55°C (ref.[27]: m.p. 57°C). − R_f = 0.35 (EtOAc). − IR (CCl_4): $\tilde{\nu}$ = 3272 (br, OH), 2925 (s), 2856 (m), 1061 (s), 1448 (m), 1030 (w), 966 (w) cm^{-1}. − ^1H NMR (270 MHz): δ = 1.07 (m, 2 H), 1.26 (m, 4 H), 1.63 (pseudo dd, 2 H), 1.86 (m, 2 H), 3.20 (br, 2 H, OH, exchanges with D_2O), 3.54 (pseudo dq, 4 H). − ^{13}C NMR (63 MHz): δ = 26.1 (t), 29.8 (t), 44.7 (d), 67.86 (t). − MS; *m/z* (%): 127 [$MH^+ - H_2O$] (68), 109 (42), 93 (70), 81 (100), 79 (47), 67 (88), 55 (36). − $C_8H_{15}O$ (127.21): calcd. C 66.63, H 11.18; found C 66.36 H 11.16.

(1RS,2RS)-1,2-Bis(tosyloxymethyl)cyclohexane (*rac*-**43b**)[27]: To a cold (0°C), stirred solution of 11.3 g (0.078 mol) of the diol *rac*-**42b** in 100 ml of dry pyridine, 60 g (0.315 mol) of *p*-TsCl was slowly added and stirring was continued for 1 h. The orange solution was kept at 4°C for 20 h, and then was poured slowly into a mixture consisting of conc. HCl (300 ml), ice (300 g) and CH_2Cl_2 (200 ml) under vigorous stirring. After 10 min, the layers were separated and the aqueous layer was extracted with CH_2Cl_2 (2 × 100 ml). The combined organic layers were washed with saturated aqueous $NaHCO_3$ and brine, and dried with $CaCl_2$. The solvent was removed under reduced pressure to give an oily residue, which was crystallized from MeOH to yield 27.69 g (78%) of the ditosylate *rac*-**43b** as a pure diastereomer (the *cis* isomer **43a** could be not detected by either HPLC or NMR), m.p. 100°C (ref.[27]: m.p. 108°C). − R_f = 0.1 (hexane/EtOAc, 10:1); IR (CCl_4): $\tilde{\nu}$ = 2929 (w), 2859 (w), 1189 (s), 1178 (s), 1372 (m), 946 (m) cm^{-1}. − ^1H NMR (270 MHz): δ = 1.17 (m, 4 H), 1.63 (m, 6 H), 2.45 (s, 6 H), 3.87 (pseudo dq, 4 H), 7.37 (d, 4 H), 7.73 (d, *J* = 5 Hz, 4 H). − ^{13}C NMR (63 MHz): δ = 21.7 (q), 25.2 (t), 28.9 (t), 37.7 (d), 72.1 (t), 127.9 (d), 129.9 (d), 132.6 (s), 144.9 (s). − MS; *m/z* (%): 452 [M^+] (4), 281 (11), 280 (10), 155 (40), 125 (53), 109 (100), 91 (90), 67 (32), 65 (15). − $C_{22}H_{28}O_6S_2$ (452.58): calcd. C 58.39, H 6.24; found C 58.74, H 6.26.

(1RS,2RS)-1,2-Diprop-2′-ynylcyclohexane (*rac*-**44**): A solution of 9.83 g (107 mmol) of lithium acetylide ethylenediamine complex in 55 ml of dry DMSO was cooled to 8°C and 15.80 g (34.9 mmol) of the ditosylate *rac*-**43b** was added in small portions. Stirring was continued for 4.5 h and the temperature was allowed to rise to ambient. The dark-brown solution was then cooled to 8°C once more and 55 ml of water was added slowly, causing the mixture to foam. The mixture was subsequently extracted with hexane (4 × 50 ml) and the combined organic extracts were dried with $MgSO_4$. After removal of the solvent under reduced pressure, the crude product (4.8 g, ca. 90% pure) was kugelrohr-distilled (100°C, 0.1 Torr) to yield 3.65 g (63%) of the dialkyne *rac*-**44** as a colorless oil (Note: The product turns yellow quickly upon standing at room temp. but can be stored as a solid at −20°C), m.p. ca. 5−10°C. − R_f = 0.28 (hexane). − IR (CCl_4): $\tilde{\nu}$ = 3313 (m, C≡C−H), 2926 (m), 2857 (s), 1189 (s), 1178 (s), 1373 (m), 949 (m) cm^{-1}. − ^1H NMR (400 MHz): δ = 1.25 (m, 4 H), 1.45 (m, 2 H), 1.72 (m, 4 H), 1.95 (t, *J* = 3 Hz, 2 H), 2.27 (m, 4 H). − ^{13}C NMR (63 MHz): δ = 22.5 (t), 25.8 (t), 31.3 (t), 38.8 (d), 69.4 (s), 82.1 (d). − MS; *m/z* (%): 159 [$M^+ - 1$] (8), 145 (21), 131 (30), 117 (50), 105 (22), 104 (12), 95 (25), 93 (45), 91 (65), 81 (100), 79 (97), 77 (54), 67 (44), 55 (28). − HRMS as calcd. for $C_{12}H_{16}$: 159.1174.

(4aRS,9aRS)-6,7-Bis(trimethylsilyl)-1,2,3,4,4a,9,9a,10-octahydroanthracene (*rac*-**45**): A flame-dried Schlenk flask was fitted with a reflux condenser topped with an Hg bubbler. All joints were made air-tight using Teflon sleeves. The apparatus was flushed with argon and then charged with 1.143 g (8.7 mmol) of bis(trimethylsilyl)acetylene, 39 mg (0.2 mmol 10 mol-%) of dicarbonyl(cyclopentadienyl)cobalt[61] and 30 ml of dry octane. The apparatus was briefly evacuated and flushed with argon several times and then the mixture was heated to reflux (180°C oil-bath temperature). A separately prepared and degassed solution of 332 mg (2 mmol) of the dialkyne *rac*-**44**, 381 mg of bis(trimethylsilyl)acetylene and 39 mg

(0.2 mmol, 10 mol-%) of dicarbonyl(cyclopentadienyl)cobalt in 4.5 ml of octane was then added to the refluxing mixture by means of a syringe pump over a period of 11 h, under irradiation from a 200-W bulb. The resulting black solution was allowed to cool to room temp. and filtered through a short pad of Celite and silica. The solvent was removed under reduced pressure and the residue (black tar) was purified by PTLC (4-mm layer SiO_2; hexane). The product was crystallized from EtOAc/MeOH to yield 180 mg (27%) of *rac*-**45** as colorless plates (Note: Our attempts to run the reaction on a larger scale resulted in significantly lower yields); m.p. 74°C. − R_f = 0.65 (hexane). − IR (CCl_4): $\tilde{\nu}$ = 2920 (m), 2905 (m), 2951, 2877 (w), 2854 (w), 1249 (s), 854 (s), 839 (s) cm^{-1}. − ^1H NMR (270 MHz): δ = 0.36 (s, 18 H), 1.08 (m, 2 H), 1.37 (m, 4 H), 1.82 (pseudo dd, 4 H), 2.45 (dd, J_1 = 15.5 Hz, J_2 = 12 Hz, 2 H), 2.77 (dd, J_1 = 17 Hz, J_2 = 3.5 Hz, 2 H), 7.39 (s, 2 H). − ^{13}C NMR (63 MHz): δ = 2.0 (q), 26.3 (t), 29.7 (t), 37.3 (t), 38.8 (d), 136.1 (d), 136.6 (s), 142.3 (s). − MS; *m/z* (%): 330 [M^+] (29), 315 (100), 299 (84), 131 (6), 73 (14). − $C_{20}H_{34}Si_2$ (330.66): calcd. C 72.65, H 10.36; found C 72.57, H 1.37.

(4aRS,8aSR,9aRS)-Tricarbonyl[η⁶-6,7-bis(trimethylsilyl)-1,2,3,4,4a,9,9a,10-octahydroanthracene]chromium(0) (*rac*-**9**): As described above for the preparation of *rac*-**24**, 590 mg (1.8 mmol) of the ligand *rac*-**45** was heated with 440 mg (2.0 mmol) of $Cr(CO)_6$ in 20 ml nBu_2O and 2 ml of dry THF for 22 h at 150°C (oil-bath temperature). The clear, yellow solution thus obtained was allowed to cool to room temp. and filtered through a short pad of silica. The solvent was removed in vacuo and the residue was purified by PTLC (4-mm layer SiO_2; hexane/EtOAc, 10:1) to give 825 mg (91%) of *rac*-**9** as pale-yellow crystals, m.p. 162°C. − R_f = 0.31 (hexane). − IR (CCl_4): $\tilde{\nu}$ = 2924 (w), 2905 (w), 2856 (w), 1961 (s), 1891 (s), 1254 (m), 853 (m), 844 (m), 836 (m) cm^{-1}. − ^1H NMR (270 MHz)[60]: δ = 0.36 and 0.38 (both s, 9 H), 1.07 (m, 2 H), 1.36 (m, 4 H), 1.82 (pseudo dd, 4 H), 2.34 (dd, J_1 = 16.5 Hz, J_2 = 12 Hz, 2 H), 2.40 (dd, J_1 = 17 Hz, J_2 = 11 Hz, 2 H), 2.52 (dd, J_1 = 17.5 Hz, J_2 = 5.5 Hz, 2 H), 2.60 (dd, J_1 = 17 Hz, J_2 = 6 Hz, 2 H), 5.27 and 5.28 (both s, 1 H). − ^{13}C NMR (63 MHz): δ = 1.8 (q), 1.9 (q), 25.8 (t), 26.0 (t), 33.2 (t), 34.8 (t), 36.4 (t), 37.3 (d), 38.4 (d), 100.4 (d), 104.9 (s), 105.0 (s), 109.2 (s), 110.0 (s), 234.1 (s). − MS (*m/z*): 466 [M^+] (4), 382 [M^+ − 3CO] (100), 315 (13), 299 (12), 73 (6), 52 (6). − $C_{23}H_{34}CrO_3Si_2$ (466.69): calcd. C 59.16, H 7.34; found C 59.05, H 7.45.

General Procedure A: Deuteration of Cr(CO)₃ Complexes with tBuOK in [D₆]DMSO: In a small, flame-dried Schlenk flask, *t*BuOK (ca. 11 mg, 0.1 mmol) was dissolved under argon in 0.5 ml of dry [D_6]DMSO and 0.02−0.06 mmol of the respective chromium complex was added (for the exact amounts, see the individual experiments described below). The solution was stirred at room temp. for 1 h and then quenched with EtOAc (10 ml). The resulting mixture was transferred to a separatory funnel, washed with water (2 × 10 ml), and dried with $MgSO_4$. The solvent was removed in vacuo and the yellow residue was chromatographed on a 1-mm SiO_2 layer. The pure fractions of the major component were combined, the solvent was removed in vacuo, and the residue was characterized by ^1H NMR and MS.

*Preparation of rac-***46** *{(1RS,4SR)-1,4,5,8-[D₄]-rac-***24***}*: Complex *rac*-**5** (10 mg, 0.02 mmol) was treated with *t*BuOK/[D_6]DMSO as described above (General Procedure A) to afford 0.8 mg (11%) of the tetradeuterated complex *rac*-**46** as a yellow film. − ^1H NMR (270 MHz)[60]: δ = 1.00 (d, J = 3 Hz, 3 H), 1.02 (d, J = 3 Hz, 3 H), 1.38 (m, 1 H), 1.53 (m, 1 H), 2.29 (dd, J_1 = 22 Hz, J_2 = 11 Hz, 0.25 H), 2.37 (dd, J_1 = 23 Hz, J_2 = 11 Hz, 1 H), 2.52 (dd, J_1 = 21 Hz, J_2 = 4.5 Hz, 1 H), 2.60 (dd, J_1 = 20 Hz, J_2 = 5 Hz, 0.2 H), 3.75 (s, 3 H), 3.78 (s, 3 H), 5.15 (s, 0.16 H), 5.18 (s, 0.1 H). − MS; *m/z* (%): 360 [M^+] (22), 359 (12), 304 (8), 276 (100), 275 (55), 246 (55), 221 (52), 220 (51), 205 (45), 190 (18), 167 (29), 149 (74), 129 (18), 91 (36), 69 (32), 55 (34). − HRMS: calcd. for $C_{17}H_{16}D_4CrO_5$ 360.099; found 360.0993.

*Preparation of rac-***47** *{(9RS,10SR)-5,8,9,10-[D₄]-rac-***35***}*: Complex *rac*-**7** (20 mg, 0.036 mmol) was treated with *t*BuOK/[D_6]DMSO as described above (General Procedure A) to afford 8 mg (58%) of the tetradeuterated complex *rac*-**47** as a yellow film. − ^1H NMR (270 MHz)[60]: δ = 1.02 (m, 2 H), 1.30 (m, 4 H), 1.84 (pseudo dd, 4 H), 2.35 (d, J_1 = 12.2 Hz, 1 H), 2.45 (d, J_1 = 16.5 Hz, J_2 = 4 Hz, 1 H), 3.73 (s, 3 H), 3.77 (s, 3 H), 5.15 (s, 0.08 H), 5.19 (s, 0.08 H). − MS; *m/z* (%): 386 [M^+] (10), 330 (5), 302 (100), 272 (31), 250 (13), 43 (17). − HRMS: calcd. for $C_{19}H_{18}D_4CrO_5$ 386.1123; found 386.1118.

*Preparation of rac-***48** *{(9RS,10SR)-6,7,9,10-[D₄]-rac-***8***}*: Complex *rac*-**9** (20 mg, 0.043 mmol) was treated with *t*BuOK/[D_6]DMSO as described above (General Procedure A) to afford 14 mg (98%) of the tetradeuterated complex *rac*-**48** as a yellow film. − ^1H NMR (400 MHz)[60]: δ = 1.05 (m, 2 H), 1.31 (m, 4 H), 1.77 (pseudo dd, 4 H), 2.32 (d, J = 15.6 Hz, 0.3 H), 2.39 (d, J = 9.2 Hz, 1 H), 2.51 (pseudo d, J_1 = 17 Hz, $J \approx$ 3 Hz, 1 H), 2.61 (dd, J_1 = 16.3 Hz, J_2 = 5.8 Hz, 0.3 H, H-10), 5.24 (s, 2 H). − MS; *m/z* (%): 326 [M^+] (11), 243 (61), 241 (100), 240 (46), 151 (29), 150 (14), 52 (67). − HRMS: calcd. for $C_{17}H_{14}D_4CrO_3$ 326.0912; found 326.0920.

*Preparation of rac-***49** *{(9RS,10SR)-9,10-[D₂]-rac-***8***}*: Complex *rac*-**8** (20 mg, 0.062 mmol) was treated with *t*BuOK/[D_6]DMSO as described above (General Procedure A) to afford 14 mg (70%) of the dideuterated complex *rac*-**49** as a yellow film. − ^1H NMR (400 MHz)[60]: δ = 1.05 (m, 2 H), 1.31 (m, 4 H), 1.77 (pseudo dd, 4 H), 2.39 (d, J = 9.8 Hz, 1 H), 2.52 (pseudo s, 1 H), 5.24 (m, 4 H). − MS; *m/z* (%): 325 (11), 324 [M^+] (12), 269 (6), 268 (6), 241 (95), 240 (100), 189 (10), 188 (12), 120 (12), 107 (12), 52 (54). − HRMS: calcd. for $C_{17}H_{16}D_2CrO_3$ 324.0786; found 324.0780.

General Procedure B: Deprotonation of Cr(CO)₃ Complexes with n-Butyllithium and Deuteration with D₂O: A flame-dried 25-ml Schlenk flask was charged under argon with the respective chromium complex (0.08−0.1 mmol; for the exact amounts, see the individual experiments described below) and 5 ml of dry THF and 0.5 ml of dry HMPA were added. Then, *n*-butyllithium (190 µl, 0.3 mmol, 1.6 M in *n*-hexane) was injected into the stirred yellow solution at room temp. The solution usually turned red within 5 min, indicating the formation of a benzylic anion. After 30 min, D_2O (200 µl, 10 mmol) was injected and stirring was continued for at least another 30 min. The mixture was then diluted with EtOAc (30 ml), transferred to a separatory funnel, washed with 2 N HCl (2 × 20 ml), saturated aqueous $NaHCO_3$ (20 ml) and brine (20 ml), and dried with $MgSO_4$. The solvent was removed in vacuo and the yellow residue was purified by PTLC (for the exact conditions, see the preparations of the nondeuterated compounds) to furnish the deuterated samples in yields of 45−70%. Prior to the determination of the degree of deuteration by ^1H-NMR spectroscopy, the samples were further purified by recrystallization.

General Procedure C: Deprotonation of Cr(CO)₃ Complexes with n-Butyllithium and Deuteration with CF₃CO₂D: A flame-dried 25-ml Schlenk flask was charged under argon with the respective chromium complex (0.08−0.1 mmol; for the exact amounts, see the individual experiments described below) and 10 ml of dry THF and 1 ml of dry HMPA were added. The yellow solution was cooled to −78°C and *n*-butyllithium (120 µl, 0.2 mmol, 1.6 M in *n*-hexane) was injected with stirring. The mixture was allowed to warm to

room temp., whereupon its color changed to red within 10−20 min. After stirring for 30 min, the mixture was cooled to −78°C once more and CF_3CO_2D (77 µl, 1 mmol) was injected. The solution reverted to its original color within a few seconds and stirring was continued for a further 20 min. The mixture was then diluted with EtOAc (30 ml) and worked up as described in General Procedure B. The deuterated samples, obtained in yields of 50−75%, were further purified by recrystallization prior to determination of the degrees of deuteration by ^{1}H NMR.

Deprotonation/Deuteration of **50**: A solution of complex **50** (236.3 mg, 0.5 mmol) in 10 ml of dry THF and 1 ml of HMPA was cooled to −50°C and *n*-butyllithium (0.4 ml, 0.64 mmol, 1.6 M in hexane) was added by means of a syringe. Stirring was continued for 2 h at 0°C, and then the mixture was quenched with D_2O (0.5 ml, 45 mmol), diluted with hexane, washed with water and brine, and dried with $MgSO_4$. Upon removal of the solvent in vacuo, the deuterated (95% D) complex *rac*-**51** was obtained (230 mg, 97%). − ^{1}H NMR (270 MHz): δ = 0.54 (s, 18 H), 1.50−1.75 (m, 4 H), 2.49 (m, 1.05 H), 2.68 (m, 2 H), 3.71 (s, 6 H).

Deprotonation/Deuteration of rac-**1**: A stirred solution of complex *rac*-**1** (41 mg, 0.08 mmol) in 1 ml of dry THF and 0.1 ml of HMPA was cooled to −70°C and *n*-butyllithium (0.08 ml, 0.13 mmol, 1.6 M in hexane) was added by means of a syringe. Stirring was continued for 5 min at −70°C and then for 15 min at room temp. The mixture was subsequently quenched with D_2O (0.5 ml, 45 mmol), diluted with hexane, washed with water and brine, and dried with $MgSO_4$. Upon removal of the solvent in vacuo, the deuterated (90% D) complex *rac*-**52a** was obtained (38 mg, 93%). − ^{1}H NMR (250 MHz)[60]: δ = 0.45 (s, 9 H), 0.47 (s, 9 H), 1.01 (d, J = 6.5 Hz, 3 H), 1.18−1.33 (m, 1 H), 1.50−1.58 (m, 1 H), 1.69−1.76 (m, 1 H), 2.24 (dd, J_1 = 16.0 Hz, J_2 = 11.7 Hz, 1 H), 2.52 (ddd, J_1 = 16.0 Hz, J_2 = 11.0 Hz, J_3 = 5.0 Hz, 0.1 H), 2.57 (dd, J_1 = 16.0 Hz, J_2 = 5 Hz, 1 H), 2.78 (ddd, J_1 = 16.3 Hz, J_2 = 5.2 Hz, J_3 = 3.6 Hz), 3.71 (pseudo s, 6 H). − In a separate experiment, complex *rac*-**1** (49 mg, 0.1 mmol) was deuterated following General Procedure B. In this case, the ^{1}H-NMR spectrum of the product showed it to be a mixture of *rac*-**52a** and *rac*-**52b** in a ratio of approx. 4:1 (85 ± 3% D).

Deprotonation/Deuteration of rac-**5**: Complex *rac*-**5** (50 mg, 0.1 mmol) was deuterated following General Procedure C, yielding *rac*-**53b** (35.5 mg, 71%, 65% D). − ^{1}H NMR (270 MHz)[60]: δ = 0.50 (pseudo s, 18 H), 0.96 (pseudo t, J = 6.2 Hz, 6 H), 1.25 (m, 1 H), 1.39 (m, 1 H), 2.13 (dd, J_1 = 16.1 Hz, J_2 = 10.1 Hz, 1 H), 2.35 (dd, J_1 = 16.0 Hz, J_2 = 11.9 Hz, 1 H), 2.58 (dd, J_1 = 16.3 Hz, J_2 = 5.0 Hz, 0.35 H), 2.82 (dd, J_1 = 16.1 Hz, J_2 = 4.9 Hz, 1 H), 3.74 (pseudo s, 6 H). In a separate experiment, complex *rac*-**5** (50 mg, 0.1 mmol) was deuterated following General Procedure B. In this case, the ^{1}H-NMR spectrum indicated the formation of *rac*-**53b** with only ca. 50% D incorporation. When a sample of *rac*-**53b** (50 mg, 0.1 mmol, 65% D) was subjected to a second deprotonation/deuteration cycle following General Procedure C, the degree of deuteration was enhanced to 80% D (yield: 36 mg, 72%). In contrast, when a sample of *rac*-**53b** (50 mg, 0.1 mmol, 65% D) was treated with *n*-butyllithium as described in General Procedure C, with subsequent quenching with CF_3CO_2H (instead of CF_3CO_2D), the isolated material *rac*-**5** (18 mg, 35%) was found to contain less than 10% D.

Deprotonation/Deuteration of rac-**6**: Complex *rac*-**6** (41 mg, 0.08 mmol) was deuterated following General Procedure B, yielding a mixture of *rac*-**54a** and *rac*-**54b** with an overall degree of deuteration of 90 ± 10% D according to the ^{1}H-NMR spectrum. Since the crude material contained significant amounts of desilylated byproducts it was completely desilylated by treatment with tetrabutylammonium fluoride/silica (2 equiv., THF, 1 h, 25°C). ^{1}H NMR (270 MHz)[60]: δ = 1.94 (m, 1 H), 2.14 (m, 1 H), 2.48 (dd, J_1 = 15.2 Hz, J_2 = 11.6 Hz, 0.6 H), 2.59 (dd, J_1 = 15.7 Hz, J_2 = 11.7 Hz, 1 H), 2.74 (dd, J_1 = 10.6 Hz, J_2 = 4.6 Hz, 1 H), 2.80 (dd, J_1 = 11.2 Hz, J_2 = 4.9 Hz, 0.5 H), 3.44 (pseudo d, J = 10.3 Hz, 1 H), 3.46 (pseudo d, J = 10.3 Hz), 3.76 (s, 3 H), 3.80 (s, 3 H), 4.10 (pseudo t, J = 7.5 Hz, 1 H), 4.20 (pseudo t, J = 7.5 Hz, 1 H), 5.18 (s, 1 H), 5.21 (s, 1 H).

Deprotonation/Deuteration of rac-**7**: Complex *rac*-**7** (53 mg, 0.1 mmol) was deuterated following General Procedure C, yielding *rac*-**55b** (26 mg, 50%, 50% D). − ^{1}H NMR (270 MHz)[60]: δ = 0.46 (pseudo s, 18 H), 0.94 (m, 2 H), 1.28 (m, 4 H), 1.78 (m, 4 H), 2.09 (dd, J_1 = 16.5 Hz, J_2 = 11 Hz, 1 H), 2.31 (dd, J_1 = 15.5 Hz, J_2 = 10.8 Hz, 1 H), 2.53 (dd, J_1 = 16 Hz, J_2 = 5.5 Hz, 0.5 H), 2.80 (dd, J_1 = 16.2 Hz, J_2 = 5.5 Hz, 1 H), 3.72 (pseudo s, 6 H). − When a sample of *rac*-**55b** (53 mg, 0.1 mmol, 50% D) was subjected to a second deprotonation/deuteration cycle following General Procedure C, the ^{1}H-NMR spectrum of the isolated material (25 mg, 48%) indicated that deuteration had occurred at both benzylic *exo* positions: 75% D at C-1 (pseudo-equatorial) and 15% at C-4 (pseudo-axial). When a sample of *rac*-**55b** (53 mg, 0.1 mmol, 50% D) was treated with *n*-butyllithium as described in General Procedure C, with subsequent quenching with CF_3CO_2H (instead of CF_3CO_2D), the isolated material *rac*-**7** (11 mg, 20%) contained less than 18% D. Additionally, 18 mg (40%) of a mixture of monosilylated compounds was isolated.

(1RS,2RS,3RS,4aRS)-Tricarbonyl[η⁶-6,7-dimethoxy-1,2,3-trimethyl-5,8-bis(trimethylsilyl)-1,2,3,4-tetrahydronaphthalene]chromium(0) (*rac*-**56**): A solution of *rac*-**5** (200 mg, 0.4 mmol) in dry THF (40 ml) and dry HMPA (4 ml) was cooled to −78°C and *n*-butyllithium (0.5 ml, 0.8 mmol, 1.6 M in *n*-hexane) was added. The cooling bath was removed and the mixture was stirred for 30 min while being slowly warmed to room temp. After cooling to −50°C, methyl iodide (0.25 ml, 4 mmol) was injected. Stirring was continued for 1 h, then the mixture was diluted with EtOAc (100 ml) and washed sequentially with 2 N HCl (2 × 20 ml), saturated aqueous $NaHCO_3$ and water. After drying with $MgSO_4$, the solvent was removed in vacuo and the product was purified by PTLC (hexane) followed by crystallization from hexane/EtOAc (10:1) at −30°C to yield *rac*-**56** (143 mg, 65%) as dark-yellow cubes; m.p. 114°C. − R_f = 0.55 (hexane/EtOAc, 10:1). − IR (KBr): $\tilde{\nu}$ = 2955 (w), 2901 (w), 2873 (w), 1955 (s, C=O), 1885 (s, C=O), 1452 (w), 1360 (m), 1320 (m), 1251 (m), 1229 (s), 1017 (m), 856 (m) cm^{-1}. − ^{1}H NMR (270 MHz): δ = 0.45 (s, 9 H), 0.47 (s, 9 H), 0.91 (m, 1 H), 0.95 (d, J = 6.5 Hz, 3 H), 1.05 (d, J = 6.5 Hz, 3 H), 1.21 (d, J = 7.1 Hz, 3 H), 1.33 (m, 1 H), 1.88 (dd, J_1 = 15.2 Hz, J_2 = 11.4 Hz, 1 H), 2.49 (dd, J_1 = 15.2 Hz, J_2 = 3.1 Hz, 1 H), 2.65 (pseudo q, J = 6.9 Hz, 1 H), 3.77 (s, 3 H), 3.78 (s, 3 H). − MS; *m/z* (%): 514 [M$^+$] (6), 458 (9), 432 (17), 431 (43), 430 (100), 428 (7), 73 (10). − HRMS: 514.1663 as calcd. for $C_{24}H_{38}CrO_5Si_2$. − $C_{24}H_{38}CrO_5Si_2$ (514.73): calcd. C 56.00, H 7.44; found C 55.87, H 7.52.

(1RS,2RS,3RS,4aRS)-Tricarbonyl[η⁶-1-acetyl-6,7-dimethoxy-2,3-dimethyl-5,8-bis(trimethylsilyl)-1,2,3,4-tetrahydronaphthalene]chromium(0) (*rac*-**57**): A solution of *rac*-**5** (200 mg, 0.4 mmol) in dry THF (40 ml) and dry HMPA (4 ml) was cooled to −78°C and *n*-butyllithium (0.5 ml, 0.8 mmol, 1.6 M in *n*-hexane) was added. The cooling bath was removed and the mixture was allowed to stir for 30 min while slowly warming to room temp. After cooling to −50°C, acetyl chloride (0.2 ml, 2.8 mmol) was injected. Stirring was continued for 30 min, then the mixture was

diluted with EtOAc (100 ml) and washed sequentially with 2 N HCl (2 × 20 ml), saturated aqueous $NaHCO_3$ and water. After drying with $MgSO_4$, the solvent was removed in vacuo and the product was purified by PTLC (hexane/EtOAc, 3:1) followed by crystallization from the same solvent mixture at −4°C to yield *rac*-**57** (143 mg, 68%) as dark-yellow cubes; m.p. 68°C. − R_f = 0.32 (hexane/EtOAc, 10:1). − IR (KBr): $\tilde{\nu}$ = 2950 (w), 1957 (s, C=O), 1888 (s, C=O), 1360 (w), 1334 (w), 1252 (w), 1025 (w), 857 (w) cm^{-1}. − ^1H NMR (270 MHz): δ = 0.42 (s, 9 H), 0.46 (s, 9 H), 0.99 (d, *J* = 6.5 Hz, 3 H), 1.25 (d, *J* = 6 Hz, 3 H), 1.34 (m, 1 H), 1.44 (m, 1 H), 1.89 (dd, J_1 = 11 Hz, J_2 = 15.5 Hz, 1 H), 2.06 (s, 3 H), 2.57 (dd, J_1 = 3.5 Hz, J_2 = 15.5 Hz, 1 H), 3.69 (d, *J* = 5.5 Hz, 1 H), 3.78 (s, 3 H), 3.79 (s, 3 H). − MS; *m*/*z* (%): 542 [M^+] (7), 461 (19), 460 (45), 459 (100), 363 (9), 221 (6), 73 (10). − HRMS: 542.1612 as calcd. for $C_{25}H_{38}CrO_6Si_2$. − $C_{24}H_{38}CrO_5Si_2$ (514.73): calcd. C 55.83, H 7.06; found C 56.06, H 6.70.

Deprotonation/Deuteration of rac-**60**: In a small, flame-dried Schlenk flask, a stirred solution of *rac*-**60** (20 mg, 0.07 mmol) in 0.5 ml of dry THF was cooled to −78°C and *n*-butyllithium (48 µl, 0.08 mmol, 1.6 M in hexane) was added. The solution was kept at −78°C for 10 min, whereupon it rapidly turned red. It was stirred at −50°C for 30 min, then 0.1 ml (5 mmol) of D_2O was added, and after 5 min the cooling bath was removed. The mixture was subsequently diluted with 20 ml of EtOAc, transferred to a separatory funnel, and washed sequentially with 2 N HCl (20 ml), saturated aqueous $NaHCO_3$ (20 ml) and brine (20 ml). After drying with Na_2SO_4, the solvent was removed in vacuo and the yellow residue was purified by PTLC (hexane/EtOAc, 10:1) yielding 18.4 mg (91%) of a mixture of the monodeuterated complexes *rac*-**61a**/*rac*-**61b** with an overall degree of deuteration of 80%. − ^1H NMR (400 MHz): δ = 1.27 (s, 9 H, *t*Bu), 2.16 (pseudo s, 5.2 H, Me), 5.19 (d, 1 H), 5.39 (d, 1 H), 5.47 (s, 1 H). − MS; *m*/*z* (%): 299 [M^+] (23), 243 (7), 216 (36), 215 (100), 148 (7), 120 (3), 52 (40). − HRMS: calcd. for $C_{15}H_{17}DO_3Cr$ 299.0724; found 299.0727. Since the determination of the *rac*-**61a**/*rac*-**61b** ratio was not possible at this stage, the mixture was completely decomplexed by exposure to sunlight and air (Et_2O, 4 h) to provide a 5:3 mixture of 4-*tert*-butyl-1-[D_3]methyl-2-methylbenzene and 4-*tert*-butyl-1-methyl-2-[D_3]-methylbenzene. − ^1H NMR (400 MHz): δ = 1.29 (s, 9 H, *t*Bu), 2.21−2.24 (m, 2.5 H, Me at C-1), 2.25−2.28 (m, 2.7 H, Me at C-2), 5.19 (d, 1 H), 5.39 (d, 1 H), 5.47 (s, 1 H); the assignment of the methyl groups was accomplished by NOE experiments.

5,6-Dimethylindan-1-one (*rac*-**63**): A 250-ml flask was charged with $AlCl_3$ (32 g, 0.24 mol) and 80 ml of 1,2-dichloroethane (DCE). After cooling to 0°C, a solution of 3-chloropropionyl chloride (20.2 ml, 0.21 mol) in 20 ml of DCE was added over a period of 10 min. The mixture was stirred for 10 min at this temperature, and then a solution of *o*-xylol (24.1 ml, 0.2 mol) in 25 ml of DCE was added dropwise over a period of 1 h. The reaction mixture was stirred for 90 min (0°C → 22°C), quenched under external cooling by the addition of water (50 ml), and extracted with *tert*-butyl methyl ether (3 × 100 ml). The organic extracts were washed with water, saturated aqueous $NaHCO_3$, and further water, and then dried with $MgSO_4$. The solvent was removed in vacuo and the residue was filtered through a pad of silica gel/Celite with hexane/EtOAc (3:1). Crystallization from the same solvent system afforded 36.7 g (93%) of 3-chloro-1-(3,4-dimethylphenyl)propan-1-one (brown needles). 25 g (127 mmol) of this material was dissolved in conc. H_2SO_4 (150 ml) and the stirred solution was heated to 90°C over a period of 30 min and maintained at this temperature for a further 45 min. The dark-red mixture was then cooled to room temp. and carefully poured onto ca. 800 g of crushed ice. After extraction with *tert*-butyl methyl ether, the organic solution was washed with water, saturated aqueous $NaHCO_3$ and brine, and dried with $MgSO_4$. The solvent was removed in vacuo and the residue was filtered through a pad of silica gel and Celite with hexane/EtOAc (5:1). Crystallization from hexane/EtOAc (5:1) finally afforded 16.3 g (80%) of a 3:1 mixture of *rac*-**63a**/*rac*-**63a** as pale-brown plates. − IR (ATR): $\tilde{\nu}$ = 3012 (w), 2978 (w), 2943 (w), 2925 (w), 1696 (s), 1614 (m), 1462 (w), 1446 (w), 875 (m) cm^{-1}. − ^1H NMR (400 MHz): δ = 2.30 (s, 3 H), 2.35 (s, 3 H), 2.63−2.72 (m, 2 H), 3.00−3.08 (m, 2 H), 7.25 (s, 1 H), 7.52 (s, 1 H). − ^{13}C NMR (67 MHz): δ = 19.7 (q), 20.7 (q), 25.3 (t), 36.4 (t), 124.0 (d), 127.3 (d), 135.2 (s), 136.1 (s), 144.8 (s), 153.3 (s), 206.9 (s). − MS; *m*/*z* (%): 160 [M^+] (100), 145 (6), 132 (38), 117 (54), 115 (18), 103 (8), 91 (10). − HRMS: calcd. for $C_{11}H_{12}O$ 160.08882; found 160.0889.

(1RS)-1,5,6-Trimethylindan-1-ol (*rac*-**64**): To Mg turnings (170 mg, 7 mmol) in 5 ml of dry diethyl ether, MeI (980 mg, 6.9 mmol) was slowly added at room temp. After 30 min, the stirred mixture was heated to reflux for 30 min, then cooled to 0°C, whereupon a solution of *rac*-**63a**/*rac*-**63b** (1.0 g, 6.2 mmol) in 5 ml of diethyl ether was added dropwise. Stirring was continued for 30 min at room temp. and then the mixture was heated to reflux for 1 h. After quenching with water, the mixture was diluted with EtOAc and washed with water and brine. After drying with Na_2SO_4, the solvent was removed in vacuo and the residue was purified by PTLC (hexane/EtOAc, 10:1) to give 784 mg (72%) of *rac*-**64** as an inseparable mixture of regioisomers (3:1 ratio). In addition, 185 mg (19%) of the corresponding H_2O elimination products were obtained. − IR (ATR): $\tilde{\nu}$ = 3395 (m), 2964 (m), 2925 (m), 1687 (m), 1451 (m), 1384 (m), 1313 (m), 1180 (m) cm^{-1}. − ^1H NMR (400 MHz): δ = 1.58 (s, 3 H), 1.90 (br s, 1 H), 2.16−2.22 (m, 2 H), 2.74−2.83 (m, 1 H), 2.93−3.03 (m, 1 H), 2.28 (m, 3 H), 2.29 (s, 3 H), 7.04 (s, 1 H), 7.16 (s, 1 H). − ^{13}C NMR (100 MHz): δ = 19.8 (q), 27.2 (q), 28.9 (t), 42.5 (t), 81.1 (s), 124.9 (d), 125.9 (d), 135.0 (s), 136.6 (s), 140.2 (s), 145.9 (s). − MS; *m*/*z* (%): 176 [M^+] (8), 161 [$M^+ - CH_3$] (100), 158 [$M^+ - H_2O$] (25), 143 (28), 128 (15), 119 (10), 115 (10). − HRMS: calcd. for $C_{12}H_{16}O$ 176.12012; found 176.1212.

(1RS,3aRS)-Tricarbonyl(η⁶-1,5,6-trimethylindan-1-ol)chromium(0) (*rac*-**65**): A mixture of *rac*-**64** (518 mg, 2.94 mmol), $Cr(CO)_6$ (970 mg, 4.41 mmol), anhydrous nBu_2O (16 ml) and dry THF (1.6 ml) was heated to reflux for 18 h according to the procedure described above for the preparation of *rac*-**24**. The crude product was purified by PTLC (hexane/EtOAc, 3:1) to give 560 mg (61%) of a mixture regioisomers (m.p. 107°C), from which a sample of pure *rac*-**65** (176 mg, 19%) was obtained by fractional recrystallization from hexane/EtOAc. − M.p. 129°C. − IR (ATR): $\tilde{\nu}$ = 3581 (w), 2970 (w), 2927 (w), 1948 (s, C=O), 1861 (s, C=O), 1452 (w), 1389 (w), 670 (w) cm^{-1}. − ^1H NMR (270 MHz): δ = 1.44 (s, 3 H), 1.83 (br s, 1 H), 1.95−2.15 (m, 2 H), 2.16 (s, 3 H), 2.20 (s, 3 H), 2.60−2.75 (m, 2 H), 5.23 (s, 1 H), 5.64 (s, 1 H). − ^{13}C NMR (67 MHz): δ = 19.0 (q), 19.1 (q), 27.0 (q), 27.7 (t), 41.6 (t), 79.3 (s), 90.2 (d), 91.6 (d), 104.9 (s), 110.0 (s), 113.1 (s), 119.7 (s), 233.9 (s). − MS; *m*/z (%): 312 [M^+] (32), 256 (10), 228 (26), 229 (26), 226 (100), 210 (66), 195 (6), 159 (92), 144 (20), 129 (30). − HRMS: calcd. for $C_{15}H_{16}CrO_4$ 312.04537; found 312.0455. − $C_{15}H_{16}CrO_4$ (312.29): calcd. C 57.68, H 5.17; found C 57.63, H 5.18.

(1RS,3aRS)-Tricarbonyl(η⁶-1-acetoxy-1,5,6-trimethylindane)chromium(0) (*rac*-**66**): A mixture of *rac*-**65** (171 mg, 0.55 mmol), a small amount of DMAP, Ac_2O (0.86 ml) and 4 ml of pyridine was stirred under the exclusion of light for 22 h. It was then diluted with hexane/EtOAc (2:1) and washed with 2 N HCl, saturated aqueous $NaHCO_3$ and brine. After drying with Na_2SO_4, the solvent was removed in vacuo and the residue was purified by PTLC (hexane/EtOAc, 3:1) to give 170 mg (87%) of *rac*-**66**, m.p. 112°C. − IR

(ATR): $\tilde{\nu}$ = 1951 (s, C=O), 1867 (s, C=O), 1738 (w), 1389 (w), 1244 (w), 674 (w), 666 (w) cm^{-1}. – ^1H NMR (400 MHz): δ = 1.65 (s, 3 H), 2.09 (s, 3 H), 2.14 (s, 3 H), 2.17 (s, 3 H), 2.10–2.20 (m, 2 H), 2.66–2.72 (m, 2 H), 5.21 (s, 1 H), 5.61 (s, 1 H). – ^{13}C NMR (100 MHz): δ = 18.9 (q), 19.0 (q), 21.4 (q), 24.4 (q), 28.3 (t), 38.5 (t), 86.1 (s), 89.6 (d), 91.2 (d), 105.0 (s), 119.1 (s), 111.5 (s), 115.7 (s), 179.2 (s), 233.9 (s). – MS; *m/z* (%): 354 [M^+] (4), 294 (2), 268 (100), 210 (24), 159 (60), 141 (22). – HRMS: calcd. for $C_{17}H_{18}CrO_5$ 354.05593; found 354.0567; $C_{17}H_{18}CrO_5$ (354.32): calcd. C 57.62, H 5.12; found C 57.70, H 5.25.

(3aRS)-Tricarbonyl(η⁶-1,1,5,6-tetramethylindane)chromium(0) (*rac*-**62**): In a flame-dried Schlenk flask, a solution of *rac*-**66** (95 mg, 0.27 mmol) in 7 ml of CH_2Cl_2 was cooled to −78°C and Me_3Al (0.14 ml, 1 mmol) was added dropwise. The mixture was stirred for 30 min at −78°C and for 30 min at 0°C, and then hexane (25 ml) and saturated aqueous NH_4Cl were carefully added. After the addition of some EtOAc, the mixture was washed with 2 N HCl and with brine, and dried with Na_2SO_4. The solvent was removed in vacuo and the residue was purified by PTLC (hexane/EtOAc, 10:1) to give 72 mg (86%) of pure *rac*-**62**, m.p. 103°C. – IR (ATR): $\tilde{\nu}$ = 2958 (w), 2928 (w), 1933 (s, C=O), 1870 (m, C=O), 1852 (s, C=O), 1826 (w), 1459 (w), 1389 (w), 671 (w) cm^{-1}. – ^1H NMR (400 MHz): δ = 1.14 (s, 3 H), 1.36 (s, 3 H), 1.79 (dd, J_1 = 7.5 Hz, J_2 = 12.5 Hz, 1 H), 1.95 (ddd, J_1 = 8.5 Hz, J_2 = 11.0 Hz, J_3 = 12.5 Hz, 1 H), 2.13 (s, 3 H), 2.19 (s, 3 H), 2.57 (dd, J_1 = 8.5 Hz, J_2 = 15.5 Hz, 1 H), 2.81 (ddd, J_1 = 7.5 Hz, J_2 = 11.0 Hz, J_3 = 15.5 Hz, 1 H), 5.18 (s, 1 H), 5.43 (s, 1 H). – ^{13}C NMR (67 MHz): δ = 19.0 (q), 19.1 (q), 27.5 (q), 28.8 (t), 29.2 (q), 39.3 (t), 42.9 (s), 90.0 (d), 92.6 (d), 103.8 (s), 109.2 (s), 115.0 (s), 122.6 (s), 234.6 (s). – MS; *m/z* (%): 310 [M^+] (12), 254 (6), 226 (100), 210 (2), 159 (6), 144 (2), 129 (2). – HRMS calcd. for $C_{16}H_{18}CrO_3$ 310.06610; found 310.0666.

Deprotonation/Deuteration of rac-**62**: In a small, flame-dried Schlenk flask, a stirred solution of *rac*-**62** (20 mg, 0.065 mmol) in 1 ml of dry THF was cooled to −78°C and *n*-butyllithium (123 µl, 0.2 mmol, 1.6 M in hexane) was added. The solution was stirred at −78°C for 30 min, then at −50°C for 30 min, before 0.1 ml (5 mmol) of D_2O was added. After 5 min, the cooling bath was removed, the mixture was diluted with 20 ml of EtOAc, washed with brine, and dried with Na_2SO_4. The solvent was removed in vacuo and the residue was crystallized from hexane/EtOAc to give 12 mg (60%) of a mixture of the monodeuterated complexes *rac*-**67a**/*rac*-**67b** with an overall degree of deuteration of 76%. ^1H NMR (400 MHz): δ = 1.14 (s, 3 H), 1.37 (s, 3 H), 1.79 (dd, J_1 = 7.5 Hz, J_2 = 12.5 Hz, 1 H), 1.95 (ddd, J_1 = 8.5 Hz, J_2 = 11.0 Hz, J_3 = 12.5 Hz, 1 H), 2.13 (s, 3 H), 2.17 (pseudo t, 2 H, 1 D), 2.57 (dd, J_1 = 8.5 Hz, J_2 = 15.5 Hz, 1 H), 2.81 (ddd, J_1 = 7.5 Hz, J_2 = 11.0 Hz, J_3 = 15.5 Hz, 1 H), 5.18 (s, 1 H), 5.43 (s, 1 H). – MS; *m/z* (%): 311 [M^+] (10), 255 (6), 227 (100), 211 (2), 160 (10), 145 (2), 129 (4). – HRMS: calcd. for $C_{16}H_{17}DCrO_3$ 311.07239; found 311.0716. – The exact ratio of the isomers was determined to be 85:15 (*rac*-**67a**/*rac*-**67b**) by means of a 600-MHz ^1H-NMR spectrum.

☆ Dedicated to Professor *E. O. Fischer* on the occasion of his 80th birthday.

[1] For some selected recent reviews, see: [1a] M. F. Semmelhack in *Comprehensive Organometallic Chemistry II*, vol. 12 (Eds.: E. W. Abel, F. G. A. Stone, G. Wilkinson), Pergamon, Oxford, **1995**, pp. 979–1015. [1b] M. F. Semmelhack in *Comprehensive Organometallic Chemistry II*, vol. 12 (Eds.: E. W. Abel, F. G. A. Stone, G. Wilkinson), Pergamon, Oxford, **1995**, pp. 1017–1038. [1c] S. G. Davies, T. D. McCarthy in *Comprehensive Organometallic Chemistry II*, vol. 12 (Eds.: E. W. Abel, F. G. A. Stone, G. Wilkinson), Pergamon, Oxford, **1995**, pp. 1039–1070. [1d] L. S. Hegedus, *Transition Metals in the Synthesis of Complex Organic Molecules*, University Science Books, Mill Valley, **1994**, chapter 10.

[2] For excellent reviews, see ref.[1c], as well as: S. G. Davies, S. J. Coote, C. L. Goodfellow, in *Advances in Metal Organic Chemistry*, vol. 2 (Ed.: L. S. Liebeskind), JAI Press, Greenwich, **1991**, pp. 1–57.

[3] [3a] C. D. Broddus, *J. Org. Chem.* **1970**, *35*, 10. [3b] R. J. Card, W. S. Trahanovsky, *J. Org. Chem.* **1980**, *45*, 2560. [3c] W. S. Trahanovsky, R. J. Card, *J. Am. Chem. Soc.* **1972**, *94*, 2897. [3d] A. Ceccon, A. Gambarao, A. Venzo, *J. Organomet. Chem.* **1984**, *275*, 209.

[4] [4a] H.-G. Schmalz, M. Arnold, J. Hollander, G. Dürner, *Tetrahedron Lett.* **1993**, *34*, 6259. [4b] H.-G. Schmalz, M. Arnold, J. Hollander, G. Dürner, *Angew. Chem.* **1994**, *106*, 77; *Angew. Chem. Int. Ed. Engl.***1994**, *33*, 109. [4c] H.-G. Schmalz, A. Majdalani, T. Geller, J. Hollander, J. W. Bats, *Tetrahedron Lett.* **1995**, *36*, 4777. [4d] H.-G. Schmalz, K. Schellhaas, *Tetrahedron Lett.* **1995**, *36*, 5511. [4e] H.-G. Schmalz, K. Schellhaas, *Angew. Chem.* **1996**, *108*, 2277; *Angew. Chem. Int. Ed. Engl.* **1996**, *35*, 2146.

[5] [5a] H.-G. Schmalz, A. Schwarz, G. Dürner, *Tetrahedron Lett.* **1994**, *35*, 6861. [5b] H.-G. Schmalz, S. Siegel, A. Schwarz, *Tetrahedron Lett.* **1996**, *37*, 2947.

[6] For the benzylic deprotonation of (arene)$Cr(CO)_3$ complexes, there is a *para*-directing effect of electron-withdrawing groups and a *meta*-directing effect of donor substituents. See, for example: [6a] G. Jaouen, S. Top, A. Laconi, D. Couturier, J. Brocard, *J. Am. Chem. Soc.* **1984**, *106*, 2207. [6b] J. Brocard, A. Laconi, D. Couturier, S. Top, G. Jaouen, *J. Chem. Soc., Chem. Commun.* **1984**, 475. [6c] J. Brocard, L. Pelinski, J. Lebibi, *J. Organomet. Chem.* **1986**, *309*, 299. [6d] J. Brocard, J. Lebibi, *J. Organomet. Chem.* **1987**, *320*, 295. [6e] J. Lebibi, L. Pelinski, J. Brocard, *Tetrahedron* **1990**, *46*, 6011.

[7] J. Blagg, S. G. Davies, C. L. Goodfellow, K. H. Sutton, *J. Chem. Soc., Perkin Trans. 1* **1987**, 1805. The term "complex-induced proximity effect" was coined by Beak and Meyers: P. Beak, A. I. Meyers, *Acc. Chem. Res.* **1986**, *19*, 356.

[8] The lithiated species can be assumed to possess a structure **3**, in which the deprotonated center is part of a newly formed double bond (see refs.[1c][2]). In analogy to the deprotonation of ketones, the C–H bond to be broken during the deprotonation step should, for stereoelectronic reasons, be as close to parallel as possible in relation to the aryl π orbitals, so that the developing p orbital can be stablized early. For related discussions, see, for instance: [8a] P. Deslongchamps, *Stereoelectronic Effects in Organic Chemistry*, Pergamon, Oxford, **1983**, pp. 243–267, and references cited therein. – [8b] K. Seemeyer, R. H. Hertwig, J. Hrusák, W. Koch, H. Schwarz, *Organometallics* **1995**, *14*, 4409.

[9] [9a] F. G. Morin and D. M. Grant in *The Conformational Analysis of Cyclohexenes, Cyclohexadienes and related Hydroaromatic Compounds* (Ed.: W. Rabideau), VCH, Weinheim, **1989**, pp. 127–169. – [9b] H. Peters, R. A. Archer, H. S. Mosher, *J. Org. Chem.* **1967**, *32*, 1362. – [9c] G. Drefahl, D. Martin, *Chem. Ber.* **1960**, 2497.

[10] For Diels-Alder reactions of intermediate *o*-quinodimethanes, see: [10a] I. L. Klundt, *Chem. Rev.* **1970**, *70*, 471. – [10b] W. Oppolzer, *Synthesis*, **1978**, 793. – [10c] T. Tuschka, K. Naito, B. Rickborn, *J. Org. Chem.* **1983**, *48*, 70 and references cited therein.

[11] [11a] W. S. Trahanovsky, K. E. Swenson, *J. Org. Chem.* **1981**, *46*, 2985. Compound *rac*-**13** can also be obtained as a mixture by partial hydrogenation of anthracene: [11b] R. Köster, M. Yalpani, *Chem. Ber.* **1990**, *123*, 719. – [11c] J. Eloranta, *Finn. Chem. Lett.* **1974**, 112.

[12] [12a] S. Pal, J. K. Mukhodpadhyaya, U. R. Ghatak, *J. Org. Chem.* **1984**, *54*, 5649. – [12b] S. Pal, M. Mukherjee, D. Podder, A. K. Mukherjee, U. R. Ghatak, *J. Chem. Soc., Chem. Commun.* **1991**, 1591.

[13] [13a] K. P. C. Vollhardt, R. G. Bergman, *J. Am. Chem. Soc.* **1974**, *96*, 4996. – [13b] K. P. C. Vollhardt, J. E. Bercaw, R. G. Bergman, *J. Am. Chem. Soc.* **1974**, *96*, 4998. – [13c] K. P. C. Vollhardt, *Acc. Chem. Res.* **1977**, *10*, 1. – [13d] K. P. C. Vollhardt, *Angew. Chem.* **1984**, *96*, 525.

[14] [14a] J. M. Bruce, F. K. Sutcliffe, *J. Chem. Soc.* **1956**, 3820. – [14b] J. M. Bruce, F. K. Sutcliffe, *J. Chem. Soc.* **1956**, 3824. – [14c] O. Abou-Teim, R. B. Jansen, J. F. W. McOmie, D. H. Perry, *J. Chem. Soc., Perkin Trans 1* **1980**, 1841.

[15] D. Stephan, A. Gorgues, A. LeCoq, *Tetrahedron Lett.* **1984**, *25*, 5649.
[16] It should be noted that mild conditions (0°C) are required to achieve a reasonably high yield. At higher temperatures, an increased formation of by-products was observed and the isolated yield of *rac*-**20** dropped, for instance, to 32% when the reaction was performed at 40°C. Addition of HMPA, which is reported to give improved yields in some comparable cases[15], resulted only in a decreased yield of *rac*-**20** (ca. 30% at 0°C).
[17] Y.-S. Wang, J. S. Chickos, *J. Org. Chem.* **1987**, *52*, 4780.
[18] C. A. L. Mahaffy, P. L. Pauson, *Inorg. Synth.* **1979**, *19*, 154.
[19] T. D. Krizan, J. C. Martin, *J. Am. Chem. Soc.* **1983**, *105*, 6155.
[20] For some early examples for the use of dimenthyl fumarate in asymmetric Diels-Alder reactions, see: [20a] H. M. Walborsky, L. Barash, T. C. Davis, *J. Org. Chem.* **1961**, *26*, 4778. – [20b] H. M. Walborsky, L. Barash, T. C. Davis, *Tetrahedron* **1963**, *19*, 2333. – [20c] J. Sauer, J. Kredel, *Angew. Chem.* **1965**, *77*, 1037. – [20d] J. Sauer, J. Kredel, *Tetrahedron* **1966**, *22*, 6359.
[21] [21a] J. L. Charlton, G. L. Plourde, K. Koh, *Can. J. Chem.* **1990**, *68*, 2022. – [21b] J. L. Charlton, K. Koh., *Synlett* **1990**, *6*, 333.
[22] Daicel Chiralcel OJ; hexane/*i*PrOH, 10:3; 0.7 ml min^{-1}, λ = 254 nm, retention time for **21**: 15.54 min; retention time for *ent*-**21**: 14.10 min.
[23] [23a] X. Reynolds, X. Kenyon, *J. Am. Chem. Soc.* **1950**, *72*, 1593. [23b] G. A. Haggis, L. N. Owen, *J. Am. Chem. Soc.* **1953**, *75*, 389.
[24] For some reviews on radical cyclizations, see: [24a] D. P. Curran, in *Comprehensive Organic Synthesis*, vol. 4 (Eds.: B. M. Trost, I. Fleming), Pergamon, Oxford, **1991**, pp. 779–831. – [24b] C. P. Jasperse, D. P. Curran, T. L. Fervig, *Chem. Rev.* **1991**, *91*, 1237.
[25] In our hands, the yield of *rac*-**13** was only 29% (ref.[12]: 79%) after chromatography and recrystallization. The melting point of the our material (64°C), however, was found to exceed that given in the literature (53°C)[12].
[26] C. C. Price, M. Schwarcz, *J. Am. Chem. Soc.* **1940**, *62*, 2891.
[27] G. A. Haggis, L. N. Owen, *J. Org. Chem.* **1953**, *23*, 5649.
[28] [28a] W. N. Smith, O. F. Deumel, *Synthesis* **1974**, 441. – [28b] J. A. Casalnuovo, R. W. Scott, E. A. Harwood, N. E. Schore, *Tetrahedron Lett.* **1994**, *35*, 1153.
[29] [29a] X-ray crystal structure analysis of *rac*-**1**: Enraf-Nonius CAD4 diffractometer, Cu-K_α radiation, $2\Theta_{max}$ = 120°, empirical absorption correction (ψ scans). Structure determination by direct methods (SHELXS-90). The H atoms of the cyclohexene ring were refined with isotropic thermal parameters. The others were placed at calculated positions and were not refined. $C_{22}H_{34}O_5CrSi_2$, monoclinic, space group $P2_1/n$, a = 12.457 (2) Å, b = 13.710 (4) Å, c = 15.124 (3) Å, β = 99.04 (2)°, V = 2551 (2) Å^3, Z = 4, $\rho_{calcd.}$ = 1.267 gcm^{-3}, μ = 48.9 cm^{-1}; 3644 independent reflections with $I > 0$ were used; R = 0.054, Rw = 0.056, S = 2.14. The residual electron density was less than 0.68 eÅ^{-3}. – [29b] X-ray crystal structure analysis of **24**: Enraf-Nonius CAD4 diffractometer, Cu-K_α radiation, $2\Theta_{max}$ = 130°, empirical absorption correction (ψ scans). Structure determination by direct methods (SHELXS). A refinement with split positions for C8 and C9 revealed superposition of two molecular conformations. The H atoms were placed at calculated positions and were not refined. A refinement of the wrong absolute configuration gave R = 0.068. $C_{17}H_{20}O_5Cr$, monoclinic, space group $P2_1$, a = 9.8632 (8) Å, b = 12.414 (1) Å, c = 14.144 (2) Å, β = 101.489 (9)°, V = 1697.1 (5) Å^3, Z = 4, $\rho_{calcd.}$ = 1.395 gcm^{-3}, μ = 58.2 cm^{-1}; 5584 independent reflections with $I > 0$ were used; R = 0.048, Rw = 0.048, S = 1.79. The residual electron density was less than 0.43 eÅ^{-3}. – [29c] X-ray crystal structure analysis of *rac*-**5**: Siemens Smart diffractometer, measurement at −140°C, Mo-K_α radiation, $2\Theta_{max}$ = 65°, empirical absorption correction (SADABS). Structure determination by direct methods (SHELXS). A refinement with split positions for C8 and C9 (cyclohexene ring) revealed superposition of two molecular conformations. The H atoms of the methoxy groups were taken from a difference synthesis. The remaining H atoms were placed at calculated positions and were not refined. $C_{23}H_{36}O_5CrSi_2$, monoclinic, space group $C2/c$, a = 39.493 (4) Å, b = 7.6645 (9) Å, c = 18.310 (2) Å, β = 107.139 (8)°, V = 5296 (1) Å^3, Z = 8, $\rho_{calcd.}$ = 1.256 gcm^{-3}, μ = 5.37 cm^{-1}; 8133 independent reflections with $I > 0$ were used; R = 0.099, Rw = 0.063, S = 1.19. The residual electron density was less than 0.35 eÅ^{-3}. – [29d] X-ray crystal structure analysis of *rac*-**7**: Enraf-Nonius CAD4 diffractometer, Cu-K_α radiation, $2\Theta_{max}$ = 120°, empirical absorption correction (ψ scans). Structure determination by direct methods (SIR92). A refinement with split positions for C8 to C13 (saturated six-membered ring of molecule I) revealed superposition of two molecular conformations. The H atoms of the methoxy groups were taken from a difference synthesis. The remaining H atoms were placed at calculated positions and were not refined. $C_{25}H_{38}O_5CrSi_2$, triclinic, space group $P\bar{1}$, a = 12.206 (3) Å, b = 12.289 (3) Å, c = 18.973 (6) Å, α = 81.36 (2)°, β = 87.69 (2)°, γ = 85.02 (2)°, V = 2802 (5) Å^3, Z = 4, $\rho_{calcd.}$ = 1.249 gcm^{-3}, μ = 44.9 cm^{-1}; 8022 independent reflections with $I > 0$ were used; R = 0.058, Rw = 0.060, S = 2.23. The residual electron density was less than 0.59 eÅ^{-3}. – Crystallographic data (excluding structure factors) for the structure reported in this paper have been deposited with the Cambridge Crystallographic Data Centre as supplementary publication no. CCDC-101004. Copies of the data can be obtained free of charge on application to CCDC, 12 Union Road, Cambridge CB2 1EZ, UK [Fax: int. code + 44(1223)336-033; E-mail: deposit@ccdc.cam.ac.uk].
[30] W. P. Aue, E. Bartholdi, R. R. Ernst, *J. Magn. Reson.* **1977**, *28*, 542.
[31] Complex *rac*-**1** was prepared as described in ref.[5]; complex **50** was obtained from 6,7-dimethoxytetralin by complexation and disilylation: H.-G. Schmalz, A. Schwarz, unpublished results.
[32] It should be noted that all our attempts to achieve a more or less selective monodeuteration under the *t*BuOK/[D_6]DMSO conditions (lower temperatures and/or shorter reaction times) failed.
[33] The degree of deuteration (and the level of inaccuracy) was determined (estimated) by comparison with the integrals observed for the methoxy or the TMS groups.
[34] The fact that no significant loss of regioselectivity was found in these experiments indicates that the inherent directing effect must be stronger than the primary kinetic isotope effect.
[35] A protonation at the chromium atom of the anionic intermediate, which would eventually have resulted in the formation of an *endo*-protonated complex could thereby be excluded.
[36] X-ray crystal structure analysis of *rac*-**56**: Enraf-Nonius CAD4 diffractometer, Cu-K_α radiation, $2\Theta_{max}$ = 120°, empirical absorption correction ψ scans). Structure determination with direct methods (SIR92). The H atoms were taken from difference Fourier synthesis and refined using isotropic thermal parameters. All other atoms were refined using anisotropic thermal parameters. $C_{24}H_{38}O_5CrSi_2$, monoclinic, space group $P2_1/a$, a = 13.557 (9) Å, b = 11.076 (2) Å, c = 19.411 (6) Å, β = 107.08 (4)°, V = 2786 (4) Å^3, Z = 4, $\rho_{calcd.}$ = 1.227 gcm^{-3}, μ = 45.1 cm^{-1}; 3974 independent reflections with $I > 0$ were used; R = 0.044, Rw = 0.043. The residual electron density was less than 0.24 eÅ^{-3}. Further details of the crystal structure investigations are available on request from the CCDC; for details see ref.[29d].
[37] The formation of benzylic alkylation products derived from *rac*-**7** was established by NMR of the crude product mixture but purification was not successful due to rapid decomposition.
[38] Brocard and Lebibi (ref.[6d]) summarize their experiments: "The regiospecificity of the benzylic functional group of arenetricarbonylchromium cannot be explained by preferential attack at the carbon which is eclipsed by the chromium–carbonyl bond. Electronic effects in directing the regiospecificity of benzylic attack were found to predominate."
[39] [39a] M. F. Semmelhack, G. R. Clark, R. Farina, M. Saeman, *J. Am. Chem. Soc.* **1979**, *101*, 217. – [39b] T. A. Albright, B. K. Carpenter, *Inorg. Chem.* **1980**, *19*, 3092. – [39c] W. R. Jackson, I. D. Rae, M. G. Wong, M. F. Semmelhack, J. L. Garcia, *J. Chem. Soc., Chem. Commun.* **1982**, 1359. – [39d] M. F. Semmelhack, J. L. Garcia, D. Cortes, R. Farina, R. Hong, B. K. Carpenter, *Organometallics* **1983**, *2*, 467. – [39e] W. R. Jackson, I. D. Rae, M. G. Wong, *Aust. J. Chem.* **1986**, *39*, 303.
[40] [40a] A. Solladié-Cavallo, G. Wipff, *Tetrahedron Lett.* **1980**, *21*, 3047. – [40b] A. Solladié-Cavallo, J. Suffert, *Org. Magn. Reson.* **1980**, *14*, 426. – [40c] A. Solladié-Cavallo, *Polyhedron* **1985**, *11*, 901.
[41] [41a] J. C. Boutonnet, L. Mordenti, E. Rose, O. Le Martret, G. Precigoux, *J. Organomet. Chem.* **1981**, *221*, 147. – [41b] J. C. Boutonnet, J. Levisalles, F. Rose-Munch, E. Rose, G. Precigoux, F. Leroy, *J. Organomet. Chem.* **1985**, *39*, 153.
[42] [42a] B. Ohlsson, C. Ullenius, *J. Organomet. Chem.* **1984**, *267*, C34. – [42b] B. Ohlsson, C. Ullenius, *J. Organomet. Chem.* **1988**, *350*, 35. – [42c] B. Ohlsson, C. Ullenius, S. Jagner, C. Grivet, E. Wenger, E. P.Kündig, *J. Organomet. Chem.* **1989**, *365*, 243.

[43] K. Narasaka, H. Sakurai, C. Liu, *Bull. Chem. Soc. Jpn.* **1994**, *67*, 1156.
[44] [44a] N. F. Masters, D. A. Widdowson, *J. Chem. Soc., Chem. Commun.* **1983**, 955. – [44b] M. Fukui, T. Ikeda, T. Oishi, *Tetrahedron Lett.* **1982**, *23*, 1605. – [44c] M. Fukui, T. Ikeda, T. Oishi, *Chem. Pharm. Bull.* **1983**, *31*, 466. – [44d] H.-G. Schmalz; K. Schellhaas, *Tetrahedron Lett.* **1995**, *36*, 5515.
[45] This representation is favorable due to the experimental fact that the anions possess a high configurative stability; see, for instance: S. E. Gibson, M. J. Schneider, M. H. Smith, *J. Chem. Soc., Chem. Commun.* **1996**, 839. Our own NMR data of some lithiated species (see: T. Volk, Dissertation, TU Berlin, **1996**) support this picture.
[46] It is a commonly accepted fact that the $Cr(CO)_3$ unit tends to be eclipsed with an electron donor (e.g. methoxy) substituent and *anti* to electron acceptors (e.g. CN, R_3Si) and that the arene ligand carbon atoms which are eclipsed with a CO ligand are predicted to be more electrophilic (see: refs.[1a][40][41], as well as: T. A. Albright, P. Hofmann, R. Hoffmann, *J. Am. Chem. Soc.* **1977**, *99*, 7546).
[47] The barrier to rotation of the $Cr(CO)_3$ tripod about the Cr−ring-centroid axis is usually small, but it can increase up to 9−10 kcal·mol^{-1} in the case of highly substituted systems. For a review, see: [47a] M. J. McGlinchey, *Adv. Organomet. Chem.* **1992**, *34*, 285. See also: [47b] K. V. Kilway, J. S. Siegel, *J. Am. Chem. Soc.* **1992**, *114*, 255; and references cited therein.
[48] [48a] D. Y. Curtin, *Rec. Chem. Prog.* **1954**, *15*, 111; for an excellent discussion, see also: [48b] E. L. Eliel, *Stereochemistry of Carbon Compounds*, Wiley, New York, **1994**, p. 647ff.
[49] See, for instance: T. H. Lowry, K. S. Richardson, *Mechanism and Structure in Organic Chemistry*, Harper Collins, New York, **1987**, p. 205; and references cited therein.
[50] R. A. Henderson, *Angew. Chem.* **1996**, *108*, 1024; *Angew. Chem. Int. Ed. Engl.* **1996**, *35*, 946.
[51] This compound was obtained from 4-*tert*-butyl-1,2-dimethoxybenzene by complexation with $Cr(CO)_6$.
[52] After decomplexation, the isomers could be unambiguously assigned by NOE experiments (see Experimental Section).
[53] R. T. Hart, R. F. Tebbe, *J. Am. Chem. Soc.* **1950**, *72*, 3286.
[54] [54a] L. Fisnerova, B. Kakac, O. Nemecek, A. Simek, Z. J. Vejdelek, *Collect. Czech. Chem. Commun.* **1967**, *32*, 4082. – [54b] D. W. Boykin, R. L. Hertzler, J. K. Delphon, E. J. Eisenbraun, *J. Org. Chem.* **1989**, *54*, 1418.
[55] H.-G. Schmalz; B. Millies, J. W. Bats, G. Dürner, *Angew. Chem.* **1992**, *104*, 640; *Angew. Chem. Int. Ed. Engl.* **1992**, *31*, 631; and refs. cited therein.
[56] M. Uemura, K. Isobe, Y. Hayashi, *Tetrahedron Lett.* **1985**, *26*, 767.
[57] E. Vedejs, *J. Org. Chem.* **1978**, *43*, 188.
[58] W. C. Still, M. Kahn, A. Mitra, *J. Org. Chem.* **1978**, *43*, 2923.
[59] D. M. Daddwell, D. T. Pegg, M. R. Bendall, *J. Magn. Reson.* **1982**, *48*, 323.
[60] For the assignments of the benzylic protons, see Table 2.
[61] M. D. Rausch, R. A. Genette, *J. Org. Chem.* **1970**, *35*, 3893.
[I97218]

1,2-Diphosphole and 1,4,7,10-Tetraphosphaphenalene Derivatives from the Reaction of Allylidenetriphenylphosphorane and PCl_3

Florian Breitsameter[a], Kurt Polborn[b], and Alfred Schmidpeter*[a]

Institut für Anorganische Chemie der Universität München[a],
Meiserstrasse 1, D-80333 München, Germany
Fax: (internat.) + 49(0)89/5902-578
E-mail: alf@anorg.chemie.uni-muenchen.de

Institut für Organische Chemie der Universität München[b],
Karlstrasse 23, D-80333 München, Germany

Received August 10, 1998

Keywords: Phosphorus ylides / Allylic reactivity / Disproportionation / Phosphorus heterocycles / NMR Spectroscopy

The equation 7 **1** + 11 PCl_3 → 2 **7** + **11** + 21 HCl describes in part the reaction of allylidenetriphenylphosphorane (triphenylphosphonium allylide) **1** with PCl_3. It involves the substitution of all α- and γ-hydrogen atoms of **1** and a concomitant disproportionation of the phosphorus. The reduction product **11** and its less highly substituted precursor **9** are new examples of the favoured family of 3-phosphonio 1,2-diphospholides and 1,2,4-triphospholides. The cation of the ionic oxidation product **7** has a phenalene structure with three peripheric PCl ring members and a chlorophosphonium center. In the crystal two of these bowl-shaped cations encapsulate a chloride anion. This is shown by an X-ray structure investigation. The structure of other products is elucidated by ^{31}P-NMR spectroscopy.

Allylidenetriphenylphosphorane [(prop-2-enediyl)triphenylphosphorane] (**1**) may be understood as phosphonio-substituted allyl anion and is expected to exhibit the reactivity of an asymmetric allyl anion[1][2][3][4].

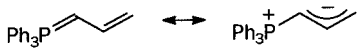

1

With phosphorus trichloride it consequently may interact at its α- or γ-carbon atom leading to compounds **2** or **3** as the primary substitution products and it also may interact at both sites with the same PCl_3 molecule or with two different of them to give compounds **4** or **5** as secondary products. All in all there are three hydrogen atoms of **1** that can be substituted. The different alternatives of this reaction were considered earlier[5]. The actual experiment (in benzene with an excess of **1**) gave a product which was assumed to be the hydrochloride of the "tris-ylene" **6**. It would be the result of the substitution of three molecules of **1** exclusively at the γ-position by the same PCl_3 molecule. Compound **6** was obtained from its hydrochloride by reaction with sodium amide. It is described as a deep red, very reactive, air-sensitive substance.

We repeated the reaction of **1** with PCl_3 in pyridine, which in similar cases had proved as a convenient solvent, able to take up the hydrogen chloride lost from the reaction partners in the substitution reaction[6].

Reaction and Products

The reaction of phosphorus trichloride with **1** in pyridine at 0 °C was visually observable. ^{31}P-NMR spectroscopy was used to monitor several experiments with different molar ratios. The spectra always indicated complex mixtures of products. These mixtures at room temperature continued to change their composition for a long time (up to several months). At long reaction times the spectra tended to become simpler. Naturally the reaction of the three-functional PCl_3 with the three-functional partner **1** can be expected to take various pathways with numerous intermediates. In the course of the reaction more and more of the functions are used, and the number of alternatives should decrease.

With a 3:1 initial molar ratio of **1** and PCl_3, compound **7** becomes the main product after 2 d. Its identity follows from its $^{31}P\{^1H\}$-NMR spectrum of $[AB]_3D$ type. As only the two-bond coupling constants J_{AB} and J_{BD}, and the four-bond coupling constant J_{AD} are large enough to influence the signal splitting significantly ($J_{AA'}$, $J_{AB'}$ and $J_{BB'}$ are too small), the spectrum is rather simple in appearance (Figure 1). The chemical shifts δ_A, δ_B and δ_D are in the expected range, δ_D in particular is characteristic for a chlorophosphonium center (Table 1).

No intermediate on the way to **7** could be identified from the spectra. In particular compound **6** (or its hydrochloride) was not found; however, it cannot be excluded as an intermediate either. It would be expected to possess a highly reactive phosphane center which easily becomes oxidized.

 © WILEY-VCH Verlag GmbH, D-69451 Weinheim, 1998 1434–1948/98/1212–1907 $ 17.50+.50/0

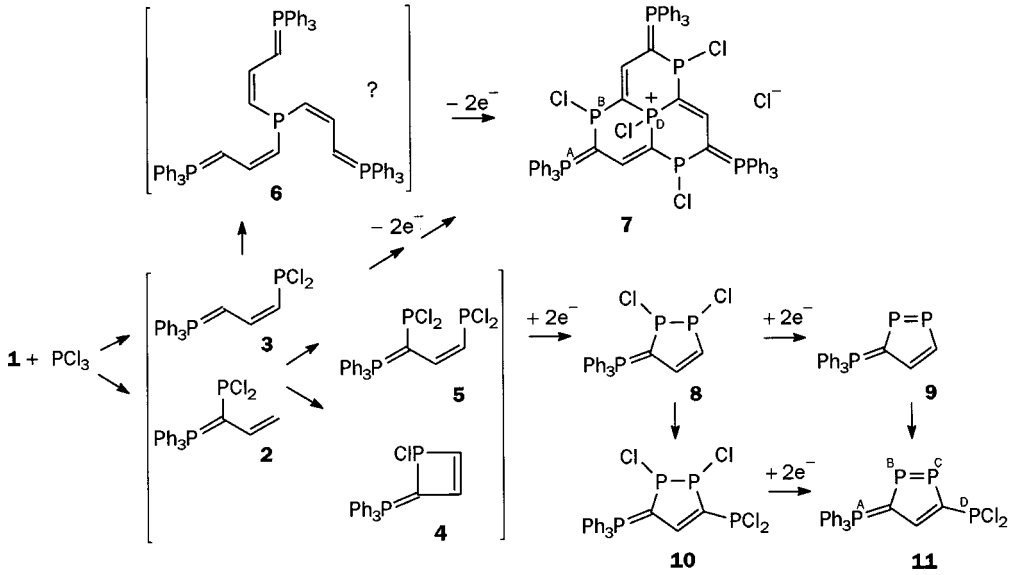

Figure 1. Experimental and calculated $^{31}P\{^{1}H\}$-NMR spectrum of **7**; ν_o = 109.380 MHz

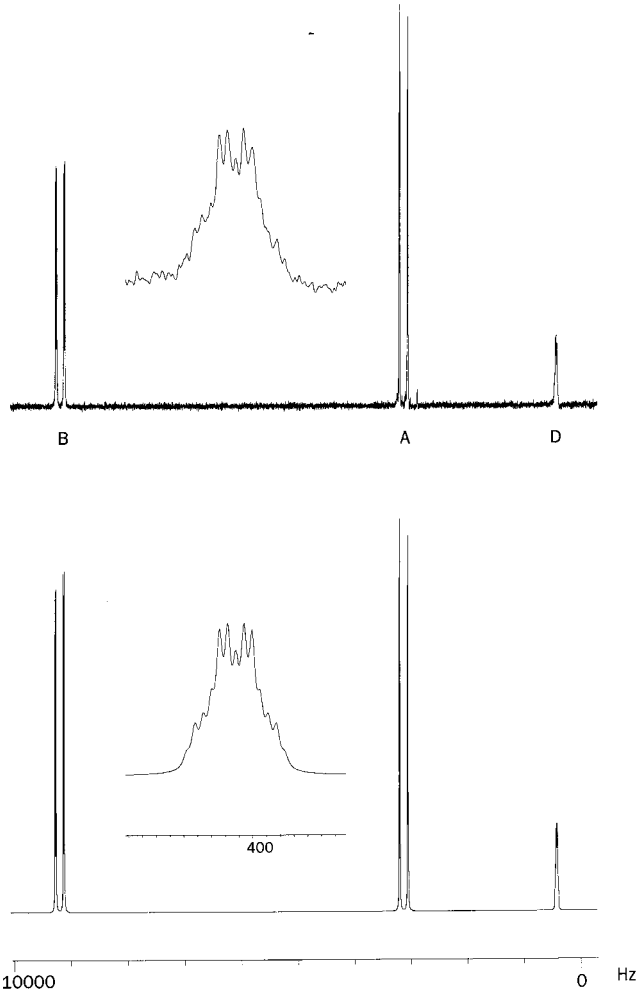

In fact, the overall formation of **7** as represented by equation (1) in Scheme 1 involves an oxidation.

Table 1. ^{31}P-NMR data of the tetraphosphaphenalenes **7** and **18** (in pyridine); coupling constants J in Hz

	7	**18**
δ_A	28.5	27.6
δ_B	83.9	−20.6
δ_C		−23.1
δ_D	3.8	11.2
$^2J_{AB}$	145.0	139.0
$^3J_{AC}$		7.6
$^4J_{AD}$	6.0	3.7
$^1J_{BC}$		−141.0
$^2J_{BD}$	17.8	17.6

Scheme 1. Equations leading to the products **7**−**11** (R = Ph_3PC_3H, RH_3 = **1**, Py = pyridine)

$$3\,RH_3 + 4\,PCl_3 + 9\,Py \xrightarrow{-2e^-} \underset{\mathbf{7}}{R_3P_4Cl_4^+} + 9\,PyH^+ + 8\,Cl^- \quad (1)$$

$$RH_3 + 2\,PCl_3 + 2\,Py \xrightarrow{+2e^-} \underset{\mathbf{8}}{RHP_2Cl_2} + 2\,PyH^+ + 4\,Cl^- \quad (2)$$

$$RH_3 + 2\,PCl_3 + 2\,Py \xrightarrow{+4e^-} \underset{\mathbf{9}}{RHP_2} + 2\,PyH^+ + 6\,Cl^- \quad (3)$$

$$RH_3 + 3\,PCl_3 + 3\,Py \xrightarrow{+2e^-} \underset{\mathbf{10}}{RP_3Cl_4} + 3\,PyH^+ + 5\,Cl^- \quad (4)$$

$$RH_3 + 3\,PCl_3 + 3\,Py \xrightarrow{+4e^-} \underset{\mathbf{11}}{RP_3Cl_2} + 3\,PyH^+ + 7\,Cl^- \quad (5)$$

With equimolar amounts of **1** and PCl_3 the reaction is similar to the one described above in that **7** finally becomes the main product. In this case it takes several months, however. As before several intermediates are observed, which already contain the central chlorophosphonium unit as in **7** (with $\delta^{31}P = 0-5$) but which are less symmetric. After 10

months their signals have disappeared in favour of **7**. This suggests that in the synthesis of **7** at first triallylphosphanes such as **6** form and become oxidized before the rings are closed by the peripheral PCl units. As a second final product, compound **11** is observed in this reaction. It is readily recognized by its $^{31}P\{^{1}H\}$-NMR spectrum (Figure 2) representing an ABCD spin system, and in particular by the low-field chemical shifts δ_B and δ_C and by the large coupling constant J_{BC} (see below, Table 2).

Figure 2. Experimental and calculated $^{31}P\{^{1}H\}$-NMR spectrum of **11**; ν_o = 109.380 MHz

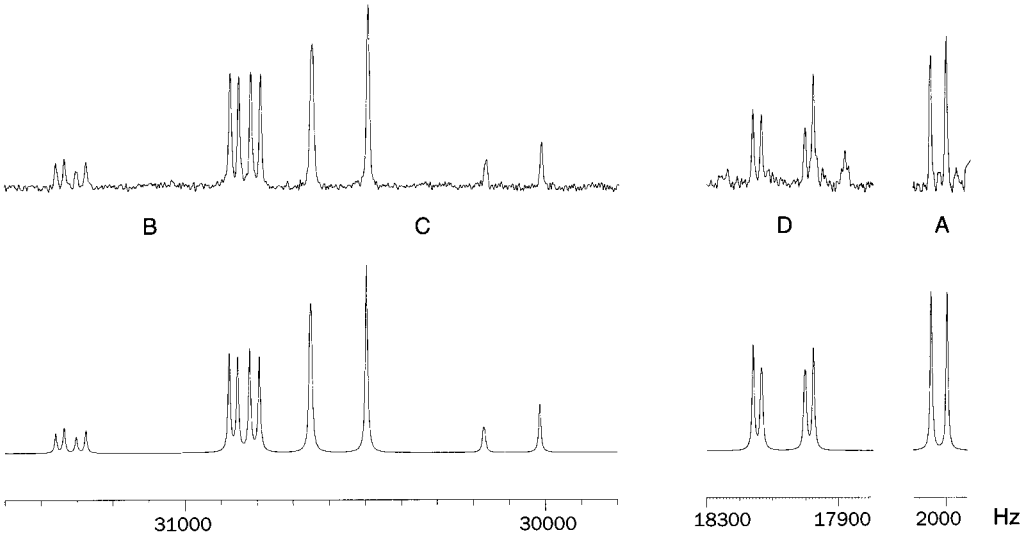

If a still smaller molar ratio (3:4) of the reaction partners is used, compound **10** is observed in an early stage of the reaction (after 12 h) followed again by **11**. The formation of **10** and **11** involves a reduction and is described by equations (4) and (5) in Scheme 1. A combination of (1) and (4) or of (1) and (5) allows the formulation of a consistent overall reaction.

The identified products **7**, **10**, and **11** have in common an exhaustive substitution of **1** in which all three α- and γ-hydrogen atoms are replaced by phosphorus. In the formation of **10** and **11** it cannot be decided at what stage of substitution the PP bond is formed and the five-membered ring is closed.

A little further insight is provided by the reactions with a low molar ratio (1:3) of the partners and with an additional reducing agent (PBu_3). Although an excess of PCl_3 was used and unreacted PCl_3 is still present, compounds **8** and **9** are observed in this case (equations 2 and 3). In these compounds one γ-hydrogen atom of **1** is left unsubstituted. The added tributylphosphane apparently makes the reduction faster than the last step of substitution. Compounds **10** and **11** seem to form from **8** and **9** by a consecutive substitution.

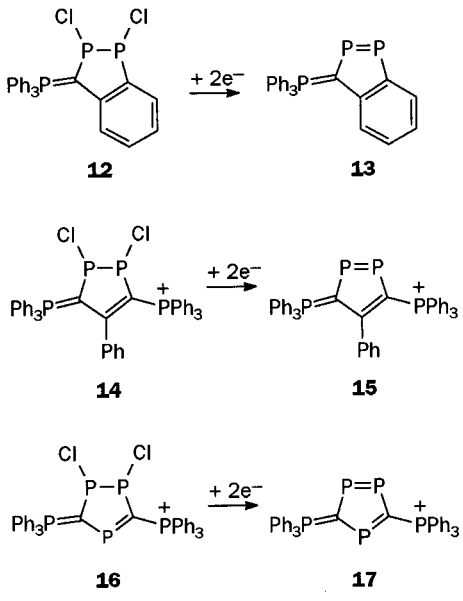

1,2-Diphosphole Derivatives

The formation of **8** from **1** is closely related to that of its benzo derivative **12** in the reaction of benzyl triphenylphosphonium bromide with PCl_3 in presence of a base[7]. The *ortho* position of the ylide here displays a reactivity similar to that of the γ position in **1**. Furthermore, **12** is readily reduced to **13**, which is the benzo derivative of **9**.

The reaction of a γ-phosphonio-substituted allylidene phosphorane with PCl_3 also parallels the formation of **8** and leads to its symmetrically substituted derivative **14**[8]. In this reaction a four-membered dihydrophosphete ring was observed as an intermediate and consequently the analogous compound **4** has to be considered as an intermediate on the way to **8**.

The preferred formation of five-membered rings of type **8** is documented by still another example: The reaction of [bis(trimethylsilyl)methylene]phosphorane with PCl_3 yields as a secondary product the dihydrotriphosphole **16**[9], which is the 4-phospha derivative of **14**. Both **14** and **16** can be

reduced to give the corresponding diphosphole **15** and triphosphole **17**.

Table 2. ^{31}P-NMR data of the dihydrodiphosphole/diphosphole pairs **8/9** (in pyridine), **10/11** (in pyridine), **12/13** (in CH_2Cl_2)[7], **14/15** (in CH_2Cl_2)[8], and of the dihydrotriphosphole/triphosphole pair **16/17** (in CH_2Cl_2/C_6D_6)[9]. δ_A refers to 3-PPh_3, $\delta_{B,C}$ refer to P-1,2 as indicated in formula **11**. Coupling constants J in Hz.

	δ_A	δ_B	δ_C	δ_D	$^2J_{AB}$	$^3J_{AC}$	$^1J_{BC}$	$^3J_{BD}$	$^2J_{CD}$
8	25.0	129.6	112.5		87.7		−257.9		
9	[a]	254.2	236.3		70.9		−480.7		
10	20.2	116.8	104.2	176.7	70.2		−262.5		25.9
11	18.5	283.3	278.1	165.2	67.9	−7.0	−481.2	4.3	175.9
12	18.6	132.4	78.7		96.7		−249.7		
13	14.9	317.1	229.4		87.5	−6.1	−480.2		
14	16.9	101.9			85.3	−5.2	−260.9		
15	15.6	285.7			80.0	−6.7	−465.5		
16	22.9	136.1		405.5	76.0	−4.5	−298.1		16.4
17	21.2	365.7		356.5	71.4	−0.7	−487.3		26.7

[a] Superimposed.

In Table 2 the ^{31}P-NMR data of the new compounds **8**−**11** are compared to the related known compounds **12**−**17**. In case of the unsymmetrically substituted compounds **8**, **10**, **12** and **9**, **11**, **13**, the phosphorus atom P^B which is adjacent to the ylidic ring member and which consequently is more strongly influenced[10], always appears less shielded than P^C. The difference for **8**−**11** is smaller, however, than for **12** and **13**. The reduction is always accompanied by a downfield chemical shift of the now two-coordinate phosphorus atoms ($\delta_{B,C}$ = 229−366) and by a sharp increase in the one-bond coupling constant ($|^1J_{BC}|$ = 465−487 Hz).

The charge of the phosphonio substituents according to δ_A seems to decrease somewhat on reduction. It nevertheless corresponds to the polar resonance formula for the reduced compounds **9**, **11**, **13**, **15**, **17**.

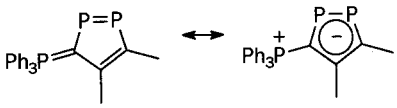

Tetraphosphaphenalene Derivatives

For a further chemical identification of **7** it was treated with diphenyl(trimethylsilyl)phosphane. In a clean reaction only the chlorine atoms at P^{III} are replaced by PPh_2 groups while the central P^VCl unit remains unchanged. This leads to compound **18**. Its $^{31}P\{^1H\}$-NMR spectrum (Figure 3) represents a $(ABC)_3D$ spin system (Table 1).

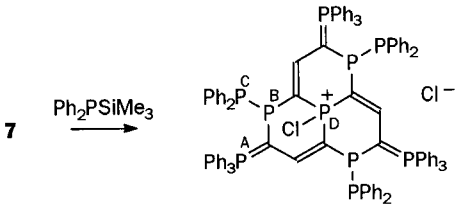

18

ture analysis. They contain 2.7 pyridine molecules per formula unit of **7**. Whereas the cation lattice is of good quality, the location of the chloride anions and the solvent molecules is rather uncertain due to strong disorder. Figure 4 shows the structure of a cation. Its skeleton is built from three allylic units C1,2,3 joined by three phosphorus atoms P2 to give a twelve-membered ring and by the central P1 to give a tetraphosphaphenalene system. The allylic carbon atoms C1, C2, and C3 lie in a plane together with the four phosphorus atoms P1, P2, P2B, and P3 bonded to them. The three planes meet at the central atom P1 forming a flat bowl. Under the influence of the three ylide units attached to the chlorophosphonium center the P1−Cl1 bond becomes rather long (Table 3)[11][12]. The bonds P2−Cl2 point to the same direction, i.e. to the convex side of the bowl.

In the crystal two of the described bowl-shaped cations approach each other with their concave sides face to face to encapsulate a chloride ion Cl3 like a shell encapsulates a pearl (Figure 5). The bonds P1−Cl1 of the two cations and Cl3 lie on a three-fold symmetry axis around which the two cations are mutually twisted by 60° against each other. The chloride ion Cl3 thus becomes walled in by six phenyl groups belonging alternately to PPh_3 units of one or the other cations. The *o*- and *m*-hydrogen atoms of these phenyl groups approach Cl3 at 284 and 296 pm, which is less than the sum of the van der Waals radii (320 pm). At the origin

Figure 3. Experimental and calculated $^{31}P\{^1H\}$-NMR spectrum of **18**; ν_o = 109.380 MHz

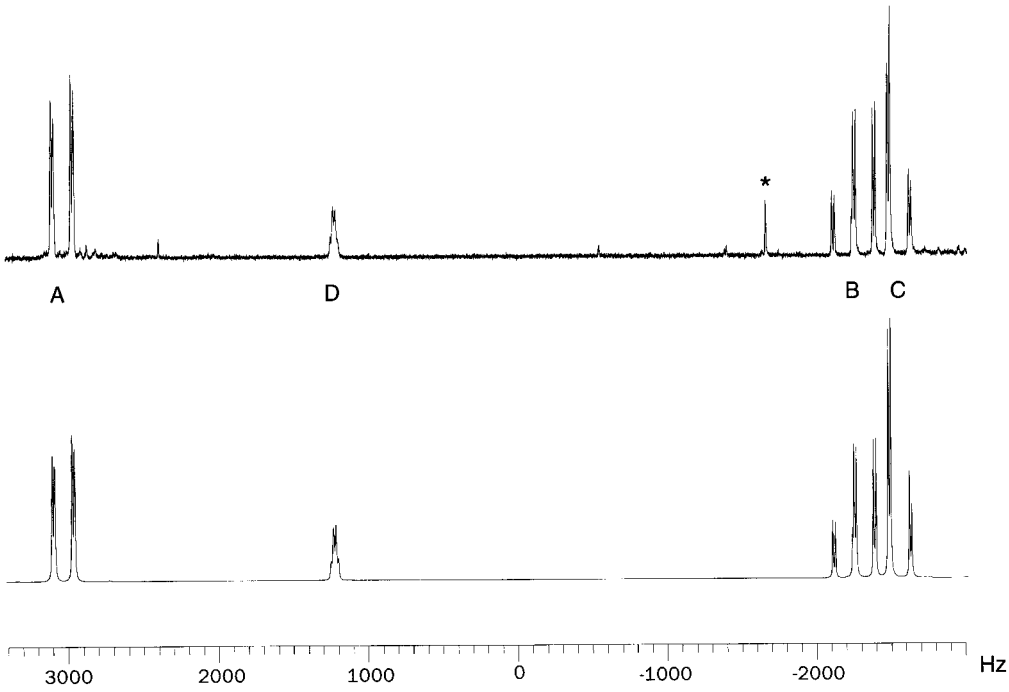

Figure 4. Molecular structure of the cation in **7** (thermal ellipsoids with 30% probability); the three phenyl groups at P3 are omitted for clarity

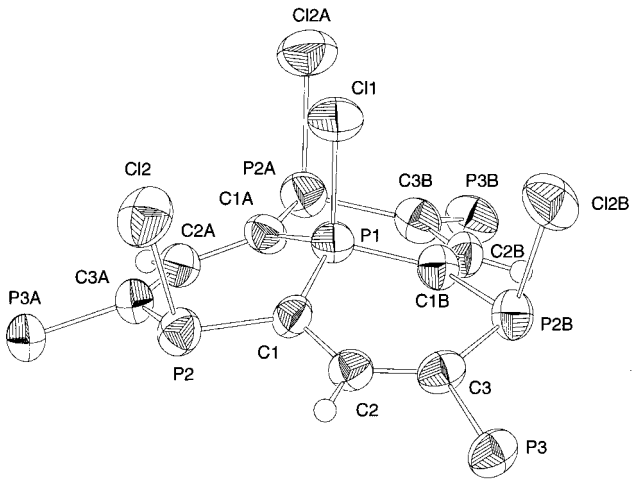

Table 3. Relevant bond lengths [pm] and bond angles [°] of **7**

P1−C1	172.2(8)	C1−P1−C1A	111.6(3)
P1−Cl1	206.6(5)	C1−P1−Cl1	107.3(3)
P2−C1	175.7(8)	C1−P2−C3A	102.5(4)
P2−C3	179.8(9)	C1−P2−Cl2	102.1(3)
P2−Cl2	216.1(4)	C3A−P2−Cl2	100.8(3)
P3−C3	176.7(8)	C2−C1−P1	118.9(7)
		C2−C1−P2	118.8(6)
		P1−C1−P2	122.2(4)
		C1−C2−C3	129.9(8)
		C2−C3−P3	116.7(7)
		C2−C3−P2B	127.5(6)
		P3−C3−P2B	115.0(5)

Figure 5. A $(cation)_2Cl^+$ unit and a Cl^- anion of **7** viewed perpendicular to the threefold axis; Cl3 (within the $(cation)_2Cl^+$ unit) is split and disordered along the threefold axis; Cl4 (the isolated Cl^- anion) is split and disordered on two levels around the threefold axis. The pyridine molecules are not shown

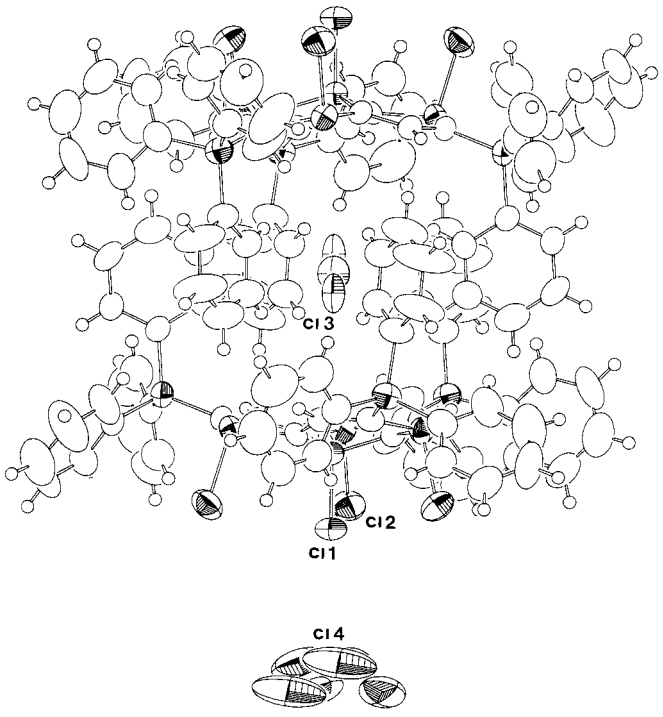

within the cage formed thus, the position of Cl3 is split. The other chloride ion Cl4 distributes on 2 × 3 symmetry-equivalent positions close to the threefold axis (Figures 5

and 6). The crystal lattice is eventually composed of an equal number of the $(cation)_2Cl^+$ units and isolated Cl^- anions alternating along the threefold axis and of 5.4 molecules of pyridine on 2×3 positions of 0.5 occupancy and 2×3 positions of 0.4 occupancy around one sequence of these ions.

Figure 6. View along the *c*-axis of **7**; Cl4 is split and disordered on two positions near the threefold axis. The pyridine molecules are not shown

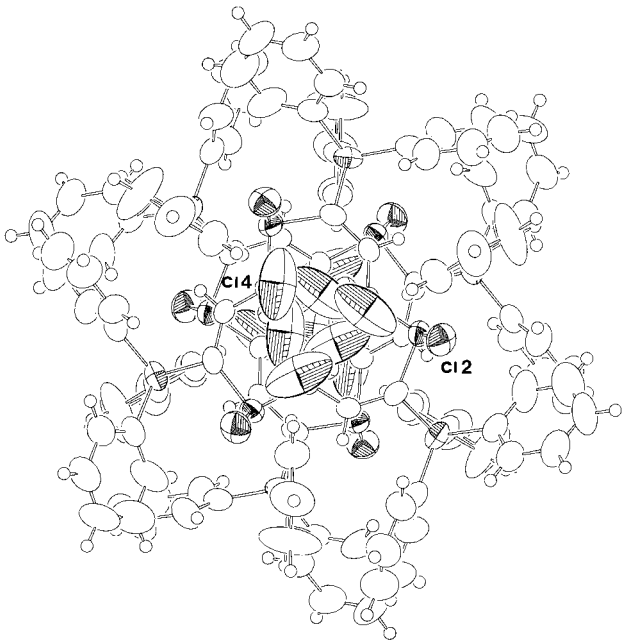

Experimental Section

All manipulations were carried out in flame-dried glassware under argon with Schlenk tube techniques. Dry pyridine was used as obtained (Fluka). Pentane was dried over molecular sieves (4 Å).

NMR: Jeol EX 400 (^{1}H), Jeol GSX 270 (^{31}P) with Me_4Si (int.) and 85% H_3PO_4 (ext.) as standards.

Allylidenetriphenylphosphorane (**1**)[5] was prepared from 3-bromopropene and Ph_3P and subsequent deprotonation of the resulting phosphonium bromide with $NaN(SiMe_3)_2$[13].

Reaction of **1** *with* PCl_3. − *a) In a 3:1 Molar Ratio:* To **1** (0.56 g, 1.9 mmol) in 25 ml of pyridine at 0°C was added PCl_3 (0.054 ml, 0.6 mmol). The dark red solution brightened for a few minutes before becoming dark red again. After 2 d at room temperature the $^{31}P\{^1H\}$-NMR spectrum showed a wide variety of signals among which those of **7** were found with 12% of the total intensity. After 10 months the relative intensity had increased to 27%.

b) In a 3:4 Molar Ratio: **1** (0.97 g, 3.2 mmol) and PCl_3 (0.37 ml, 4.2 mmol) were added as before. In the $^{31}P\{^1H\}$-NMR spectrum after 12 h at room temperature among a large variety of signals only those of **10** were identified with 2% relative intensity. During 10 more months pyridinium chloride separated from the dark red solution and was removed. The spectrum of the filtrate showed **7** (41%), **10** (10%), and **11** (13% relative intensity). In this solution dark yellow crystals of **7** formed which were used for X-ray analysis; they decomposed at 93°C. − ^{1}H NMR (CD_2Cl_2): δ = 7.27−7.59 (m, 3 H, \$-H), 7.58−7.68 (m, 36 H, *o*-, *m*-H), 8.67−8.69 (m, 9 H, *p*-H).

c) In a 1:3 Molar Ratio and Additional PBu_3*:* To **1** (1.69 g, 5.6 mmol) PCl_3 (1.46 ml, 16.7 mmol) was added as before. After 10 min, PBu_3 (0.90 ml, 5.6 mmol) was added to the red solution. In the $^{31}P\{^1H\}$-NMR spectrum after 12 h at room temperature among a variety of signals those of **8** (1%), **9** (5%), **10** (2%), and **11** (0.5%) were identified. After heating under reflux for 2 d the spectrum showed **7** (3%), **8** (8%), **9** (9%), **10** (11%), and **11** (0.5%).

Reaction of **7** *with* Ph_2PSiMe_3*:* To a solution of **7** (42 mg, 0.04 mmol) in 0.5 ml of pyridine was added Ph_2PSiMe_3 (40 mg, 0.15 mmol). After 10 min a $^{31}P\{^1H\}$-NMR spectrum of the orange solution showed the signals of **18**.

Crystal Structure Analysis of **7**: Table 4; the chloride anion Cl3 is disordered on the threefold axis and the chloride anion Cl4 is disordered on the split position Cl4/Cl4A near the threefold axis, thus leading to 2 times 3 positions. Cl4/Cl4A were refined with the same U_{ij} temperature factor components. One of the pyridine solvent molecules is disordered around a center and the other is on a common position. Both pyridine molecules were fitted by restraints during the least squares procedure. Further details are available from the Cambridge Crystallographic Data Center on quoting the depository number CCDC-101626, the names of the authors and the journal citation (E-mail: deposit@ccdc.cam.ac.uk).

Table 4. Crystal data and structure refinement for **7**

Empirical formula	$C_{76.5}H_{61.5}Cl_5N_{2.7}P_7$
Formula weight	1199.1
Temperature	293(2) K
Wavelength	0.71073 Å
Crystal system	rhombohedral
Space group	$R\bar{3}$
Unit cell dimensions	a = 18.450(4) Å c = 41.97(3) Å
Volume	12371(8) Å^3
Z	6
Density (calculated)	1.138 Mg/m^3
Absorption coefficient	0.351 mm^{-1}
F(000)	4376
Crystal size	0.40 × 0.33 × 0.27 mm
Θ range for data collection	2.32 to 22.00°
Index ranges	$0 \le h \le 19$, $-17 \le k \le 0$, $-45 \le l \le 45$
Reflections collected	3756
Independent reflections	3372 [R_{int} = 0.0307]
Observed reflections ($I > 2F(I)$)	1919
Absorption correction	Semi-empirical from ψ-scans
Max. and min. transmission	0.9990 and 0.9790
Refinement method	Full-matrix least-squares on F^2
Data / restraints / parameters	3372 / 60 / 305
Goodness-of-fit on F^2	1.100
Final R indices (I > 2FI)	$R1$ = 0.1071, $wR2$ = 0.2833
R indices (all data)	$R1$ = 0.1713, $wR2$ = 0.3349
Largest diff. peak and hole	0.624 and −0.431 eÅ^{-3}

[1] For calculated charge distribution see: K. A. Ostoja Starzewski, H. Bock, *J. Am. Chem. Soc.* **1976**, *98*, 8486−8494.
[2] Proton exchange involves both the α- and the γ-position: H. J. Bestmann, O. Kratzer, H. Simon, *Chem. Ber.* **1962**, *95*, 2750−2754.
[3] For an example of an exclusive reaction at the α-position see: B. Bogdanovic, S. Konstantinovic, *Synthesis* **1972**, 481−483.
[4] For examples of reactions at the γ-position see: H. J. Bestmann, R. Zimmermann in *Houben-Weyl: Methoden der organischen Chemie* (Ed. M. Regitz), Thieme, Stuttgart **1982**, 677 f.

[5] K. Issleib, M. Lischewski, *J. Prakt. Chem.* **1969**, *311*, 857−868, M. Lischewski, Thesis, Universität Halle-Wittenberg **1970**.
[6] G. Jochem, M. Schmidt, H. Nöth, A. Schmidpeter, *Z. Naturforsch. B* **1996**, *51*, 1761−1767.
[7] G. Jochem. A. Schmidpeter, M. Thomann, H. Nöth, *Angew. Chem.* **1994**, *106*, 708−711; *Angew. Chem. Int. Ed. Engl.* **1994**, *33*, 663−665.
[8] G. Jochem, A. Schmidpeter, H. Nöth, *Chem. Eur. J.* **1996**, *2*, 221−227.
[9] H.-P. Schrödel, A.Schmidpeter, H. Nöth, M. Schmidt, *Z. Naturforsch. B.* **1996**, *51*, 1022−1032.
[10] A. Schmidpeter, H. Nöth, J. Jochem, H.-P. Schrödel, K. Karaghiosoff, *Chem. Ber.* **1995**, *128*, 379−393.
[11] In the cation Ph_3PCl^+ for comparison *d*PCl = 198(1) pm has been found: J. H. Enemark, J. A. Ibers, *Inorg. Chem.* **1968**, *7*, 2636−2642.
[12] A similar elongation of the P−Cl bond, although less pronounced, has been found for other ylide-substituted chlorophosphonium units too: $Ph_3P-C[-PCl-(Ph_3P=)C-]_3PCl^{2+}$, *d*PCl = 202.8(2) pm, H.-P. Schrödel, A. Schmidpeter, H. Nöth, *Z. Naturforsch. B*, in press; $(PhP_3=PhC-)_2PCl_2^+$, *d*PCl (average) = 204.4(4) pm: A. Schmidpeter, G. Jochem, C. Klinger, C. Robl, H. Nöth, *J. Organomet. Chem.* **1997**, *529*, 87−102.
[13] H.-J. Bestmann, R. Zimmermann in *Methoden der Organischen Chemie (Houben-Weyl)* (Ed.: M. Regitz), vol. E1, Thieme, Stuttgart, **1982**.

[I98272]

A Study of the Mechanism of Platinum(II)/Tin(II) Dichloride Mediated Hydrogenation of Alkynes and Alkenes Employing Parahydrogen-Induced Polarization

Christina Deibele[a], Alexei B. Permin[b], Valery S. Petrosyan[b], and Joachim Bargon*[a]

Institute of Physical and Theoretical Chemistry, University of Bonn[a],
Wegelerstrasse 12, D-53115 Bonn, Germany
Fax: (internat.) +49 (0)228/ 739424
E-mail: bargon@uni-bonn.de

Department of Chemistry, M. V. Lomonosov Moscow State University[b],
Vorobyevy Gory, 119899 Moscow, Russia
Fax: (internat.) +7-095/ 9395546
E-mail: alp@org.chem.msu.su

Received August 18, 1998

Keywords: Hydrogenations / Parahydrogen / Platinum / Alkynes / Alkenes

The mechanism of hydrogenation of alkynes catalyzed by the $[(PR_3)_2PtHX]/SnX_2$ system (PR_3 = PPh_3, $PMePh_2$; X = Cl, Br) has been studied by means of parahydrogen-induced polarization of ^1H spectra (PHIP). Dihydride intermediates confirming the stepwise hydrogenation at room temperature were observed when the reaction was run in acetone. The obtained ^1H-PHIP spectra, together with NMR data for related species, are consistent with the formulation of these intermediates as *cis*-$[H_2Pt(PR_3)(SnX_3)(\sigma\text{-alkenyl})(acetone)]$, where the σ-alkenyl ligand originates from an insertion reaction of the alkyne (1-phenyl-1-propyne, 1-phenyl-1-butyne, diphenylacetylene, 3,3-dimethylbutyne). At elevated temperatures, the hydrogenation in acetone proceeds as a *cis*-synchronous transfer of the two hydrogen atoms of parahydrogen to the substrate molecule. A mechanism for this synchronous hydrogenation is suggested.

Introduction

The parahydrogen-induced polarization (PHIP) phenomenon was first observed accidentally by Bryndza and coworkers as early as 1983[1]. This NMR technique is now recognized as a valuable mechanistic probe for investigating homogeneously catalyzed hydrogenation reactions[2]. The phenomenon was proposed theoretically in 1986 by Bowers and Weitekamp[3], and soon thereafter was confirmed experimentally[4]. Furthermore, it was recognized that PHIP allows examination of the reaction mechanisms of the single-step transfer of the two parahydrogen atoms to the substrate molecule, and sometimes allows identification of the unstable dihydride intermediates participating in the catalytic cycle[5][6]. Moreover, study of the hydrogenation mechanism by traditional methods is troublesome because in many cases the reaction is accompanied by significant degrees of isomerization of the starting materials and/or products[7]. The PHIP technique offers further information, even on the stereochemistry of the fundamental step of the addition of dihydrogen to the organometallic catalyst. Quite possibly, in situ PHIP-NMR spectroscopy may provide the data relating to the structures of active intermediates that are otherwise difficult or impossible to obtain.

The physical aspects of the processes leading to PHIP-NMR spectra are discussed in a number of papers (e.g., refs.[8][9]). Using this technique, hydrogenation reactions catalyzed by rhodium[10−13], iridium[14][15], palladium[16][17], and ruthenium[18] complexes have been studied.

Although platinum complexes are well-known catalysts for hydrogenation[19−21], hydroformylation[22−25], and hydrosilylation[26] reactions, there have been only a few mechanistic studies using the PHIP technique. In a previous paper, we showed that spin-polarized products arise from the hydrogenation of alkynes in the presence of Pt^0 complexes with either coordinated alkynes or alkenes, as well as with the usual Pt^{II} phosphane hydrido chloro complexes, activated by tin(II) chloride[27].

In principal, the latter fact is contradictory to the generally accepted mechanism for $Pt^{II}/SnCl_2$ mediated hydrogenations (Scheme 1).

Since 1965, it has been accepted that the first step of the hydrogenation is the reduction of the pre-catalyst, accompanied by the formation of platinum monohydrides **2**[28][29]. These monohydrides have been shown to undergo rapid, equilibrium addition reactions to carbon−carbon multiple bonds of the substrate, with the formation of σ-C intermediates **3**[30][31]. Furthermore, the third step of the asynchronous hydrogenation, namely hydrogenolysis of the Pt^{II}−C(alkyl) bond in **3**, has been shown to proceed under relatively mild conditions[32]. The appearance of polarized products during $Pt^{II}/SnCl_2$ mediated hydrogenation using para-H_2 prompted us to engage in a more detailed study of the reaction mechanism using the PHIP technique.

 © WILEY-VCH Verlag GmbH, D-69451 Weinheim, 1998 1434−1948/98/1212−1915 $ 17.50+.50/0

Scheme 1. Generally assumed mechanism for the Pt^{II}–tin dichloride catalyzed hydrogenation, asynchronous mechanism

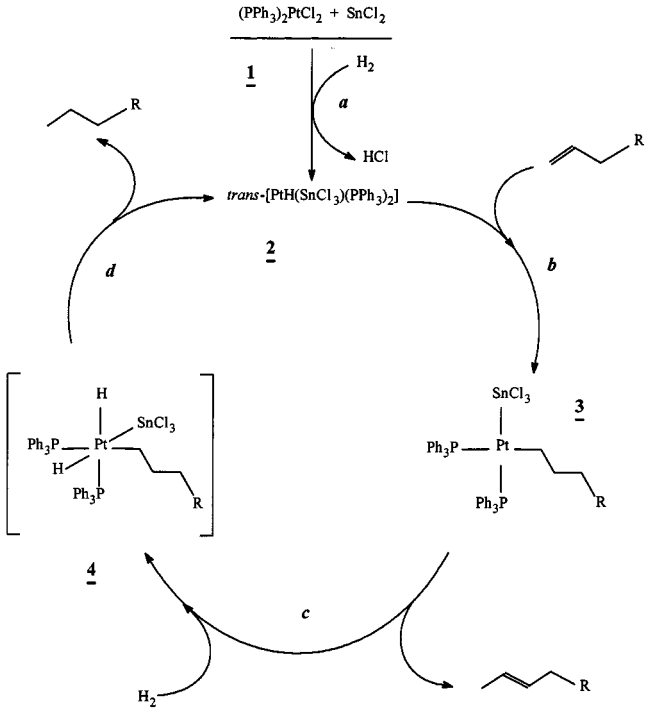

It is well known that activation of Pt^{II} complexes by tin(II) halides is strongly solvent-dependent. Solvents of medium solvating ability and polarity, such as acetone, play quite a significant role in platinum-phosphane chemistry, promoting extensive phosphane redistribution reactions[33–35]. This dependence can also result in changes in catalytic activity and selectivity[22], as well as of the reaction mechanism, therefore necessitating studies in a variety of solvents.

In this paper we describe the results of PHIP studies of the Pt^{II}/Sn^{II} mediated hydrogenation of alkynes and alkenes in acetone and some other solvating media.

Results and Discussion

PHIP in the System [$(PPh_3)_2PtHCl$]/$SnCl_2$/1-Phenyl-1-propyne

Since the generally accepted catalytic cycle involves platinum hydride as an active intermediate, we avoided the activation stage (***a***, Scheme 1), as well as extensive HCl formation, by the use of pre-synthesized platinum hydride instead of the usually employed dichloro complex. The interaction of platinum monohydride with $SnCl_2$ in acetone proceeds rapidly, and the resulting clear, orange-yellow solution shows new signals in its ^{1}H-NMR spectrum attributable to *trans*-[$(PPh_3)_2PtH(SnCl_3)$], **2**, {δ(PtH) = −9.75 [br, ^1J(PtH) = 1105 Hz]}, as well as to the products resulting from a phosphane redistribution reaction {$[(PPh_3)_3PtH]^+$, δ(PtH) = −5.75 [br, d, ^1J(PtH) = 154 Hz]; *trans*-$[(PPh_3)PtH(SnCl_3)_2]^-$, δ(PtH) = 13.355 [d, ^2J(PH) = 131 Hz, ^1J(PtH) = 412 Hz]} in accord with previously published data[34]. The spectra in ref.[34] were recorded at −90°C and thus the minor discrepancies with these data are obviously due to the different temperatures used.

Though the dihydrido-dichloro Pt^{IV} complexes were previously shown to arise as a result of an oxidative addition of HX to Pt^{II} monohydrides[36–38], our attempts to observe them using the PHIP technique during the reduction of dichloride **1** by parahydrogen were unsuccessful. Moreover, no polarization patterns were found as a consequence of the parahydrogen action on platinum–tin monohydrides. On the other hand, we observed strong, sharp polarization signals after the addition of an alkyne followed by parahydrogen to the tin-activated monohydride acetone solution (Figure 1). The relatively high field values of the chemical shift of the observed polarization patterns are consistent with Pt^{IV} species, since published data show a substantial high-field shift for Pt^{IV} dihydrides as compared to analogous Pt^{II} complexes[36][39][40][41].

Figure 1. PHIP ^{1}H-NMR spectra of the system *trans*-[$(PPh_3)_2PtHCl$]/$SnCl_2$/1-phenyl-1-propyne/para-H_2 in [D_6]acetone; **a)** at room temp. (^{119}Sn and ^{117}Sn satellite signals are marked *); **b)** the same sample after cooling; **c)** PHIP ^{1}H-NMR spectrum of the isolated insertion product **5a** in CD_2Cl_2, at 3 bar of para-H_2, room temp.; **d)** PHIP++ simulation of the monophosphane dihydride **6**; **e)** PHIP++ simulation of the diphosphane dihydride **3** (values for *cis*- and *trans*-coupling constants are taken to be as in **c)**; **f)** PHIP++ simulation of the diphosphane dihydride **3** (values for *cis* and *trans* coupling constants are taken as in **c)**)

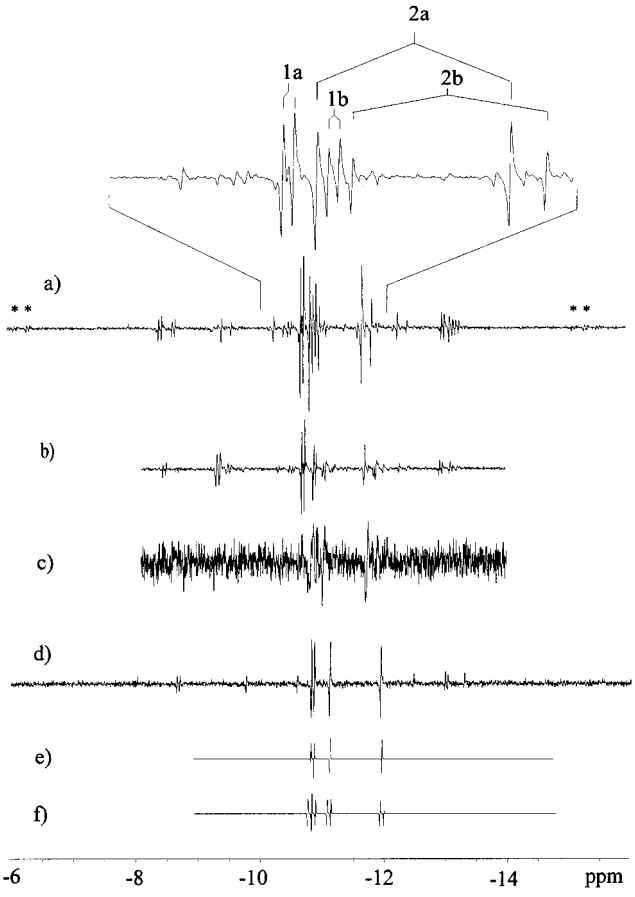

The obtained PHIP patterns exhibit features that allow us to establish the structures of the transient platinum dihydrides. First of all, two isomers with similar couplings are

Table 1. Spectral NMR parameters of intermediate dihydrides observed in the systems $[(PPh_3)_2PtH(SnX_3)]$/alkyne/$[D_6]$acetone (δ, relative to $[D_5]$acetone; *J*, Hz). The letter **a** corresponds to the major isomer, the letter **b** to the minor isomer

Alkyne	X	Isomer	$\delta(H^1)$	$\delta(H^2)$	^1J(Pt-H^1)	^1J(Pt-H^2)	^2J(P-H^1)	^2J(P-H^2)	$^2J(^{119}$Sn-$H^1)$ [a]	^2J(Sn-H^2) [b]
PhC≡CMe	Cl	**a**	−10.71	−11.24	913.7	568.1	9.3	167.8	1842 (1760)	25.9
		b	−10.91	−11.34	906.7	567.8	9.3	168.5	1840	
PhC≡CMe [c]	Cl	[d]	−10.58	−11.275	869.2	542.0	9.4	165.4		
		[e]	−10.82	−11.33	918	567		167.2		
PhC≡CMe	Br	**a**	−11.46	−10.248	920.5	565.4	9.5	166.8	1850 (1768)	40.1
		b	−11.63	−10.498	918.4	566.4	9.6	167.7		
PhC≡CCH_2CH_3	Cl	**a**	−10.71	−11.181	911.2	566.1	8.9	168.5	1839 (1759)	33.5
		b	−10.893	−11.334	907.3	565.2	10.1	169.3	1837	
PhC≡CCH_2CH_3	Br	**a**	−11.443	−10.194	920.7	563.6	9.7	166.3	1853 (1779)	47.3
		b	−11.629	−10.404	919.2	563.8	9.7	166.7		46.3
Diphenylacetylene	Cl	[f]	−10.922	−11.32			9.9	169.0		
Diphenylacetylene	Br	[f]	−11.621	−10.364	913.6	558.3	9.4	165.9	1857 (1771)	44.9
3,3-Dimethylbutyne	Cl	[f]	−10.950	−11.356	940.6	588.2	9.3	172.1		

[a] Values in brackets correspond to $^2J(^{117}$Sn−H). − [b] Averaged $^2J(^{117/119}$Sn−H). − [c] Solution in CD_2Cl_2. − [d] In the absence of added acetone. − [e] 0.15 ml of $[D_6]$acetone was added. − [f] One isomer.

clearly discernible. This conclusion was confirmed experimentally upon cooling of the solution under parahydrogen (Figure 1, b) which resulted in a non-concerted change in the intensities and widths of the relevant resonances. Each isomer exhibits a typical ABX pattern, with large *trans*- and small *cis*-^{1}H−^{31}P couplings (Figure 1a, Table 1). The patterns for both isomers are accompanied by ^{195}Pt and $^{117/119}$Sn satellites, permitting an unambiguous assignment of the ligands in the equatorial plane of the coordination octahedron of **6a**. Only one phosphane ligand is incorporated into the coordination sphere of the transient dihydride, since the spectrum exhibits only one ^{1}H-^{31}P coupling for each proton. This was confirmed by PHIP simulations of the spectra of the mono- and diphosphane dihydrides (Figure 1, d, e, f). The assignment of the axial positions is not so clear-cut, but is supported by the observation that the presence of both an alkyne and acetone is essential for the development of polarization patterns. We suggest that the possible role of acetone lies in promoting the dissociation of one phosphane ligand, which, apparently, is followed by coordination to the platinum center. It has previously been well-documented[34][35] that the reaction of excess tin dihalides with platinum hydrides in acetone at room temperature rapidly leads to the formation of mixture of phosphane redistribution products, which contain monophosphane complexes.

Addition of 1-phenyl-1-propyne to an acetone solution of **2** leads to the disappearance of the Pt-H signals in the hydride region in the thermal spectrum and gives rise to a broadened singlet at approximately δ = 0.7. This singlet is symmetrically surrounded by broadened signals, the positions and intensities of which are consistent with the notion that they are in part ^{195}Pt and unresolved $^{119/117}$Sn satellites. The singlet was thus assigned to the methyl resonance of the σ-alkenyl ligand, resulting from an insertion of the triple bond of the substrate into the Pt−H bond (vide infra). This signal was invariably present in all cases where polarization in the Pt−H region was observed, which prompted us to ascribe the key role of a σ-bonded carbon ligand in the formation of PHIP-active Pt^{IV} dihydrides. The suggestion of the presence of this ligand was also derived from the following considerations: (a) the role of the substrate could be either to coordinate to platinum as a π-ligand or to insert into a Pt−H bond, thereby producing a σ-bonded carbon ligand; (b) the obtained PHIP corresponds to the spectrum of a dihydride, and not to a trihydride, establishing the insertion suggestion in (a); and (c) the isolated insertion product, i.e. the σ-phenylpropenyl platinum complex, shows analogous though more simple polarization patterns upon reaction with parahydrogen (Figure 1, c). The precise structure of the alkenyl radical in the transient dihydride is not clear, but it seems plausible that the existence of the two dihydrides is due to an isomerism of the alkenyl radical and, therefore, the dihydrides are in fact 2-phenyl-1-methylethenyl and 1-phenylprop-1-enyl complexes.

We were fortunately also able to isolate the product of insertion of 1-phenyl-1-propyne into the Pt−H bond of the starting monohydride. Light-yellow crystals of the product were formed on leaving to stand an acetone solution of the $[(PPh_3)_2PtH(SnCl_3)]$ complex together with the alkyne in the absence of hydrogen, as well as during hydrogenation experiments. The ^{1}H-NMR spectrum of this product in CD_2Cl_2 clearly shows the signal of the CH_3 protons of the σ-alkenyl ligand with a full set of ^{195}Pt and $^{117/119}$Sn satellites, and the signal of the proton adjacent to the double bond with partially obscured satellite signals. The ^{1}H spectrum is essentially similar to published data for the analogous triethylphosphane complex[42], in spite of the large deviation of the chemical shift value for methyl protons [δ = 2.23, ^3J(PtH) = 56.5 Hz[42]], which is apparently due to the difference between an acido ligand and the phosphane. Together with the obtained ^{13}C and ^{31}P data, this spectrum allows the unambiguous assignment of the structure of this product as **5a**. The doublet splitting of the main methyl resonance (ca. 2 Hz) can be attributed to a ^4J *cis*-coupling with the olefinic proton. Large values of $^4J(^{119/117}$Sn-^{1}H) are in accord with a *trans*-position of the trichlorostannato ligand relative to the alkenyl group, and they match published values for tin−proton couplings in

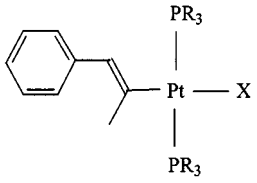

5a X = $SnCl_3$
5b X = Cl

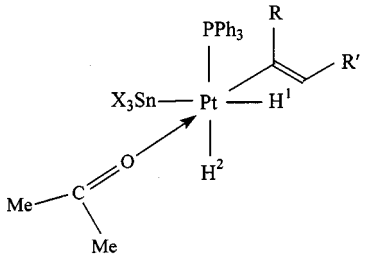

6 a R = Me, R′ = Ph, X = Cl;
6 b R = Et, R′ = Ph, X = Cl;
6 c R = R′ = Ph, X = Cl;
6 d R = H, R′ = CMe_3, X = Cl;
6 e R = R′ = Ph, X = Br

other platinum trichlorostannato complexes[43]. It is also noteworthy that addition of several equivalents of DMF results in the cleavage of the trichlorostannato ligand with formation of the corresponding chloro complex, **5b**, in accord with the reported behavior of σ-alkylplatinum complexes[31].

The polarization spectrum originating from reaction of parahydrogen with the solution of **5a** in dichloromethane indicates the presence of only one isomer. These patterns are much less intense than those obtained for catalytic mixtures in acetone, which is apparently due to the fact that acetone is present in the system only in minor amounts as an impurity or as a solvent of crystallization, as is evident from the ^{1}H and ^{13}C spectra. The low intensity of the polarization signals can be also attributed to the enhanced stability of the isolated isomer, which is hydrogenated only to a small extent. The differences between the PHIP ^{1}H-NMR spectra obtained for the isolated insertion product and those obtained from the catalytic system are due to the change of medium, since addition of 0.15 ml of $[D_6]$acetone to a $CDCl_3$ solution of **5a**, followed by parahydrogen, shifts the dihydride signals towards coincidence with the position observed in situ (Table 1).

Catalytic Systems with Other Substrates

Besides 1-phenyl-1-propyne, other substrates can give transient dihydrides detectable by the PHIP technique. Thus, we have attempted to hydrogenate alkynes (phenylacetylene, diphenylacetylene, 1-phenyl-1-butyne, 1,4-diphenylbutadiyne), and alkenes (norbornadiene, 3,3-dimethylbutene) under the same conditions as used for 1-phenyl-1-propyne. Our observations are summarized qualitatively in Table 2.

The interaction of the system $[(PPh_3)_2PtHCl]/SnCl_2$/1-phenyl-1-butyne/acetone with parahydrogen proceeds similarly to the reaction of 1-phenyl-1-propyne (Figure 2). Polarization patterns show clearly resolved ^{117}Sn and ^{119}Sn sat-

Table 2. Qualitative summary of results obtained for the studied systems $[(PR_3)_2PtHX]/SnX_2$/substrate/acetone

PR_3	X	Substrate	Pt dihydride(s), intensity, number of isomers [a]	Insertion product [b]	Synchronous/ asynchronous hydrogenation [c]
PPh_3	Br	1-Phenyl-1-propyne	+++, 2	+	++
PPh_3	Br	1-Phenyl-1-butyne	+++, 3	n.d.	+++, th.
PPh_3	Br	Diphenylacetylene	+++, 1	n.d.	th.
PPh_3	Cl	1-Phenyl-1-propyne	+++, 2	+	++, th.
PPh_3	Cl_2[d]	1-Phenyl-1-propyne	no	n.d.	th.
PPh_3	Cl	1-Phenyl-1-butyne	+++, 3	n.d.	++
PPh_3	Cl	Diphenylacetylene	+, 1	n.d.	
PPh_3	Cl	3,3-Dimetylbutyne	++, 2	n.d.	th.
PPh_3	Cl	1,4-Diphenylbutadiyne	no	n.d.	++
PPh_3	Cl	Phenylacetylene	no	n.d.	+++, th.
PPh_3	Cl	3,3-Dimetylbutene	no		no
PPh_3	Cl	Norbornadiene	no	n.d.	th.
PPh_3	Cl	1-Phenyl-1-propene	no	n.d.	no
PPh_3[e]	Cl	1-Phenyl-1-butyne	no	n.d.	no
PPh_3[f]	Cl	1-Phenyl-1-propyne	no	+, br.	+, th.
PPh_3[g]	Cl	1-Phenyl-1-propyne	no	n.d.	+, th.
$PMePh_2$	Br	1-Phenyl-1-propyne	++, 2	+	+, th.
$PMePh_2$	Cl	1-Phenyl-1-propyne	+	+	th.
PMe_2Ph	Cl	1-Phenyl-1-propyne	+	n.d.	th.

[a] +++, strong polarization signals, with ^{195}Pt and $^{117/119}Sn$ satellites visible in spectrum; ++, medium polarization, $^{117/119}Sn$ satellites are not visible due to low signal/noise ratio; +, low polarization, only central part of the patterns is clearly visible. – [b] +, the signal(s) attributable to the insertion product are present; **n.d.**, not detected, the signals of the insertion product are presumably obscured. – [c] +++, ++, and +, strong, medium, and weak polarization of product signals, respectively; **th.**, continuous rise of the thermal product signals without polarization. – [d] The corresponding dichloro complex was used instead of $[(PR_3)_2PtHX]$. – [e] In acetonitrile as solvent; 1 mol equivalent of $SnCl_2$. – [f] In $CDCl_3/[D_8]$THF mixture, 7:1 (*v*/*v*). – [g] In $CDCl_3$.

ellites for both isomers, confirming the general assignment of the transient dihydrides to the structures **6b**. Upon heating, extensive isomerization of the alkenyl part of the σ-ligand occurs, complicating the spectrum and leading to the appearance of a third isomer. This isomer could be due to an isomerization of the side-chain of the alkyne into an allenic structure. With 1-phenyl-1-butyne as the substrate, the insertion product was not discernible in the ^{1}H spectrum owing to the low intensity and complicated patterns due to its ethyl group, but it was readily observable in the ^{31}P spectrum of the reaction mixture [δ_P = 17.75, ^1J(Pt−P) = 2995 Hz].

Figure 2. PHIP ^{1}H-NMR spectra of the systems *trans*-[$(PPh_3)_2$PtHCl]/$SnCl_2$/alkyne/para-H_2 ([D_6]acetone, room temp.); **a)** alkyne = 1-phenyl-1-butyne; **b)** central lines of the spectrum (a) in the range δ = −10 to −12; **c)** PHIP++ simulation of the central part of the spectrum (a); **d)** alkyne = diphenylacetylene; **e)** alkyne = 3,3-dimethylbutyne

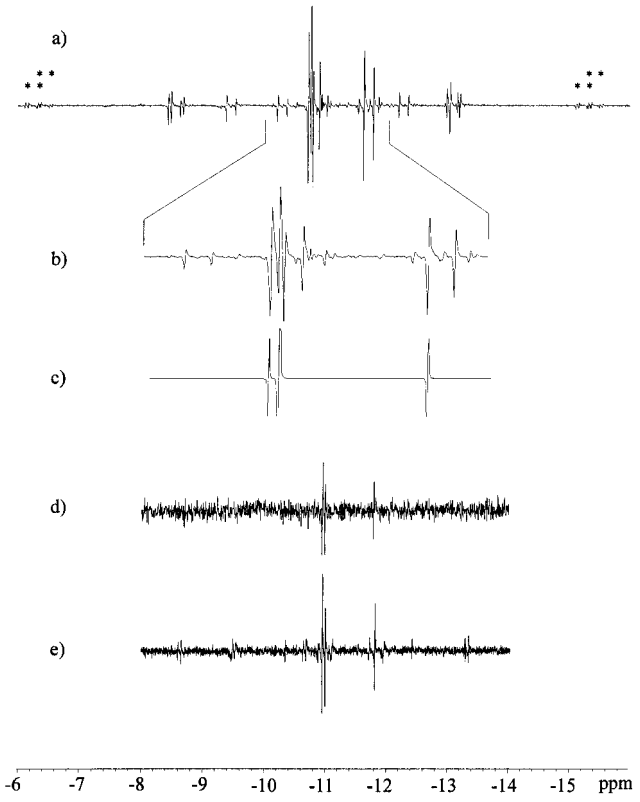

As expected, the system [$(PPh_3)_2$PtHCl]/$SnCl_2$/diphenylacetylene produced simple polarization patterns upon reaction with parahydrogen in acetone (Figure 2, d) due to the symmetry of the substrate and, therefore, resulted in the presence of only one dihydride, **6c**. The intensity of the signals was much lower than in the case of the 1-phenyl-1-propyne system. The reaction with 3,3-dimethylbutyne (Figure 2, e) also gave a simple polarization spectrum, despite the lack of symmetry of the substrate. This simplicity is apparently due to the fact that one alkenyl isomer strongly predominates in this case. The major isomer is suggested to be the 3,3-dimethylbutenyl-1 complex (**6d**), in view of the considerable steric requirements of the *tert*-butyl group. When the PHIP spectrum is recorded at elevated temperatures, a reversible formation of the second isomer is observable. Since in this case no changes in the alkenyl ligand can readily occur without undergoing skeletal rearrangements, we suggest these two reversible isomers to be the 3,3-dimethylbutenyl-1-platinum complex as the major component, and the corresponding -2-platinum complex as the minor component. Phenylacetylene and 1,4-diphenylbutadiyne gave no detectable dihydrides, but polarized signals of styrene and 1,4-diphenyl-3-en-1-butyne, respectively, were seen on heating (vide infra).

PHIP in Related Catalytic Systems

Bromide Systems: The interactions of the systems [$(PPh_3)_2$PtHBr]/$SnBr_2$/alkyne (alkyne = 1-phenyl-1-propyne, 1-phenyl-1-butyne, diphenylacetylene) in acetone with parahydrogen also give rise to polarization in the Pt−H spectral region (Figure 3). The difference in chemical shifts of the two hydride resonances provides clear evidence for first-order patterns of an AMX spin system in these cases. In general, bromide systems give more intense and sharp signals compared to the corresponding hydrido chloro complexes. The resulting Pt^{IV} dihydrides possess an enhanced thermal stability compared with the chloro analogues, and are readily observable even upon heating. Furthermore, the initial patterns are fully restored on cooling once more (al-

Figure 3. PHIP ^{1}H-NMR spectra of the systems [L_2PtHBr]/$SnBr_2$/alkyne/para-H_2 in [D_6]acetone; **a)** L = PPh_3, alkyne = 1-phenyl-1-propyne, room temp.; **b)** L = PPh_3, alkyne = 1-phenyl-1-butyne, room temp., before heating; **c)** L = PPh_3, alkyne = 1-phenyl-1-butyne, on heating; **d)** L = PPh_3, alkyne = 1-phenyl-1-butyne, at room temp. after heating; **e)** L = PPh_3, alkyne = diphenylacetylene, room temp.; **f)** L = $PMePh_2$, alkyne = 1-phenyl-1-propyne, room temp.

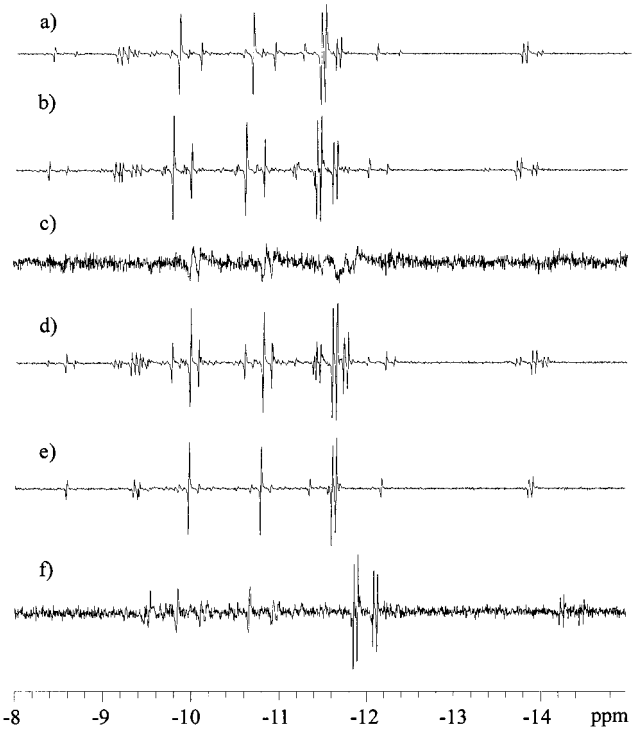

kyne = 1-phenyl-1-propyne, Figure 3, a). With 1-phenyl-1-butyne, the additional third isomer of the dihydride is formed only after heating (Figure 3, b−d). With diphenylacetylene, the bromide system gives strong and well-resolved polarization patterns with a full set of satellite signals (Figure 3, e).

Variation of the Phosphane Ligands: Generally speaking, electron-donating phosphanes show less intense and poorly resolved polarization patterns in the Pt−H region under the conditions employed. The results obtained for the $[(PR_3)_2PtHX]/SnX_2$/alkyne/acetone systems are summarized in Tables 2 and 3. The triethylphosphane monohydride system did not give rise to PHIP. The system $[(PMePh_2)_2PtHCl]/SnCl_2$/1-phenyl-1-propyne/acetone produces only weak polarization in the Pt−H region (Figure 3, f). diphenylacetylene in the presence of $[(PPh_3)_2PtHCl]/SnCl_2$. Nevertheless, in addition to these signals, in some cases relatively strong polarization patterns are observed on heating (Figure 4). In general, hydrogenation of 1-phenyl-1-butyne and 1-phenyl-1-propyne gives moderately intense polarization signals of the corresponding *cis*-alkenes (Figure 4, a, b). Phenylacetylene is hydrogenated readily, giving rise to strongly polarized styrene signals as a result of *cis*-addition of parahydrogen (Figure 4 c). The *cis*-addition of para-H_2 was confirmed by means of the PHIP++ program simulation. Due to the ALTADENA conditions of the hydrogenation (i.e. the addition of parahydrogen proceeds in the Earth′s magnetic field, and the subsequent transfer to the strong B_0 field for the NMR measurement is adiabatic), extensive polarization transfer to the methyl and phenyl

Table 3. Spectral NMR parameters of intermediate dihydrides observed in systems with other phosphanes, $[(PR_3)_2PtH(SnX_3)]$/1-phenyl-1-propyne/$[D_6]$acetone (δ, relative to $[D_5]$acetone; *J*, Hz). The letter **a** corresponds to the major isomer, the letter **b** to the minor isomer.

PR_3	X	Isomer	$\delta(H^1)$	$\delta(H^2)$	$^1J(Pt\text{-}H^1)$	$^1J(Pt\text{-}H^2)$	$^2J(P\text{-}H^1)$	$^2J(P\text{-}H^2)$
$PMePh_2$	Cl	**a**	−11.17	–	–	–	9.5	–
		b	−11.392					
$PMePh_2$	Br	**a**	−11.875	−10.25	951.3	563?	9.3	163.2
		b	−12.102		948.6		9.2	
PMe_2Ph	Cl	[a]	−11.869	−11.487	9.5	–	–	164.5

[a] One isomer.

The methyl resonance attributable to the insertion product, analogous to **5**, is also observable in this system [$\delta(CH_3)$ = 1.24, $^3J(^{195}Pt-H)$ = 53.4 Hz]. Due to the low intensity and broadness of the signals, the exact composition of the insertion product remains unclear.

Using the $[(PMePh_2)_2PtHBr]/SnBr_2$ system, the hydrogenation of 1-phenyl-1-propyne proceeds rapidly at room temperature, mainly via an asynchronous mechanism, i.e. not pairwise. This is reflected in the low polarization signals of the hydrogenation product, as opposed to rapidly arising thermal ones, and furthermore, the polarization in the Pt−H region is low. These Pt-H PHIP signals become stronger upon heating. It should be noted, however, that the signals attributable to the insertion product are clearly visible even at elevated temperature.

Only weak and poorly-resolved polarization patterns in the Pt^{IV} dihydride region are observed in the course of hydrogenation of PhC≡CMe in the presence of $[(PMe_2Ph)_2PtHCl] + SnCl_2$ in acetone. This hydrogenation proceeds without polarization of the product signals.

Figure 4. Polarization of product signals during hydrogenation with para-H_2 of alkynes in the presence of $[(PPh_3)_2PtHX]/SnX_2$ catalytic systems in $[D_6]$acetone on heating; **a)** X = Br, alkyne = 1-phenyl-1-butyne; **b)** X = Br, alkyne = 1-phenyl-1-propyne; **c)** X = Cl, alkyne = phenylacetylene. The absorption signals of the products, i.e. of the *cis*-alkenes, are marked *.

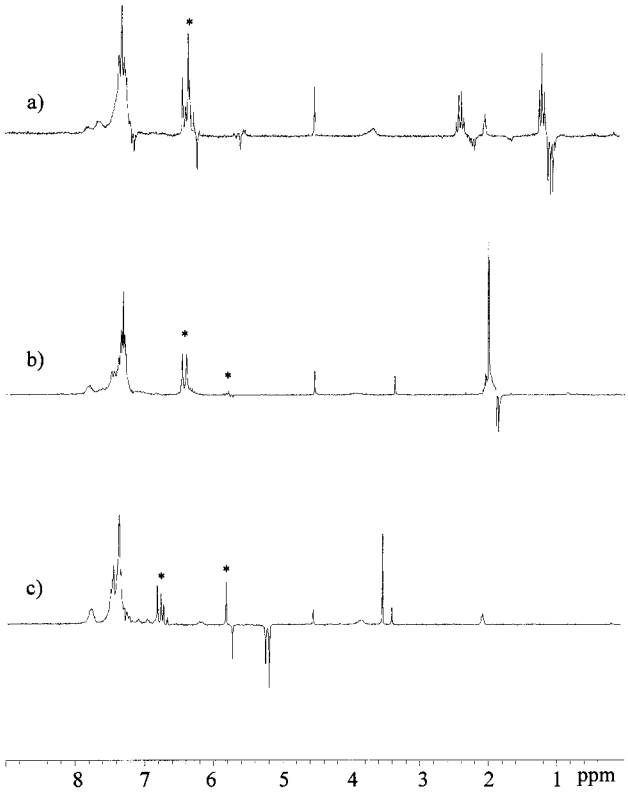

The Relationship between Synchronous (Pairwise) and Asynchronous Hydrogenation Mechanisms

The observed Pt^{IV} dihydrides are assumed to be the intermediates in the stepwise hydrogenation of an alkyne. Decomposition of these dihydrides leads via reductive elimination to an alkene and a platinum monohydride. Consequently, only thermal signals are observed from the product, as is the case during the hydrogenation of

groups of the substrate is also observed. The efficient polarization transfer under these conditions is due to strong isotropic mixing of the proton spin functions in the whole molecule at low magnetic field[44], as was previously shown for the hydrogenation of the diphenylacetylene-Pt^0 complex, $[(PPh_3)_2Pt(PhC{\equiv}CPh)]$[27]. Alternatively, for the hydrogenation of 1-phenyl-1-propyne, the polarized signals of the methyl group of the product can be accounted for by assuming a 1,3-dihydrogen addition to the intermediate platinacyclobutene, formed by methyl C−H activation, although the geometry of such an addition should favor the *trans*-alkene as a primary product, rather than the *cis*-isomer, which is in fact obtained. Furthermore, the same effect is also operative for the methyl group of 1-phenyl-1-butyne, and seems to have the same origin.

The mechanism of the synchronous dihydrogen addition observed in the SnX_2-activated systems described here is suggested to be related to the Pt^0-mediated hydrogenation.

This mechanism could involve the η^2-coordination of an alkyne, and the reductive elimination of HX together with SnX_2, followed by oxidative addition of dihydrogen to the resulting Pt^0 complex with subsequent formation of an alkene (Scheme 2). The formation of the Pt^0 intermediate

Scheme 2. The proposed mechanism for the synchronous hydrogenation of alkynes catalyzed with the $[(PR_3)_2PtHX]-SnX_2$ system in acetone

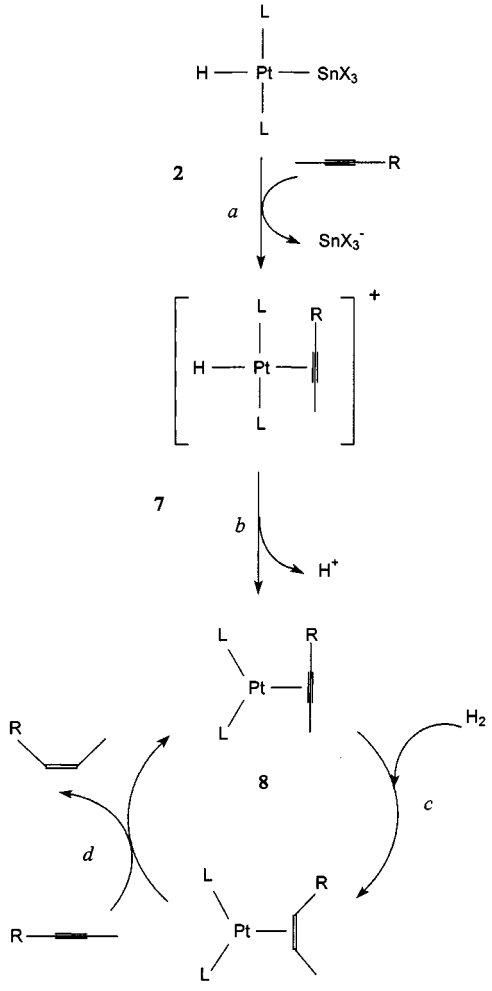

should be favored at higher temperatures, as well as by an increased electronegativity of the π ligand. This process is of little significance for alkenes, where asynchronous hydrogenation is observed, giving rise to thermal signals of the products. It is also noteworthy that the Pt^{IV} dihydrides (**6a**) are not usually observable in the spectrum at elevated temperatures in cases where the polarized signals of the products appear instead.

The Role of Structural Factors and Reaction Conditions for the Appearance of PHIP in the Pt^{II}/Sn^{II} Catalytic Systems

Solvent Effects: The described polarization patterns of the Pt^{IV} dihydrides were observed only with acetone as the solvent. The sole exception was the interaction of isolated **5a** with parahydrogen in dichloromethane solution, as discussed above. The synchronous hydrogenation of alkynes proceeded well in acetone, but was hardly reproducible in benzene or in other non-solvating media. Experiments in acetonitrile, which is a much poorer solvent for $SnCl_2$, did not lead to any PHIP effects either. Strongly solvating additives, such as DMF and THF, can easily destroy the catalytic system, facilitating the cleavage of solvated SnX_2 molecules from the active platinum hydride and/or from a σ-carbon intermediate (**3** in Scheme 1[31][45]). Since Pt^{IV} dihydride contains only one phosphane ligand, the promotion of phosphane dissociation by the attached trihalotin ligand and acetone as the solvent seems to be necessary for the generation of PHIP-detectable dihydrides. It is noteworthy that phosphane redistribution proceeds only for platinum monohydrides with PPh_3 and $PMePh_2$[46], and correspondingly, polarized Pt^{IV} dihydrides are observable mainly with these ligands. Furthermore, the processes suggested to be essential for synchronous hydrogenation, the formation of cationic intermediates **7** (Scheme 2), as well as their deprotonation with formation of Pt^0 intermediates **8**, are strongly favored with polar, solvating acetone as the solvent.

Substrate and Halide Ligands: The appearance of polarized Pt^{IV} dihydrides depends principally on the hydrogenation substrate. The intensity of the polarization pattern reflects the suggested stability of the insertion product, while the number of isomers corresponds to the possible number of isomeric alkenyl radicals. For symmetrical alkynes, only one isomer is observed; for 1-phenyl-1-propyne two main insertion products are possible, giving rise initially to two dihydrides. Accordingly, 1-phenyl-1-butyne, being able to form more isomers, gives a complicated mixture of polarized dihydrides after heating. Alkenes, especially internal ones, generally adopt a quite unfavorable equilibrium position for insertion into Pt−H bond[31]. This factor is believed to be the reason for the failure to observe intermediates of type **6** in the course of the hydrogenation of alkenes such as NBD and 3,3-dimethylbutene. Furthermore, steric bulkiness of an alkyne (e.g. diphenylacetylene) can prevent extensive formation of the alkenyl complex, thereby decreasing the intensity of the signals of the Pt^{IV} dihydrides.

Tribromostannato hydrides give insertion products with higher equilibrium constants, and the resulting σ-insertion products are less fluxional compared to the chloro analogues. This feature is reflected in the higher intensity and sharpness of the corresponding polarization patterns.

We thank the *Russian Foundation for Basic Research (RFBR)*, and the *Deutsche Forschungsgemeinschaft (DFG)* for financial support, and Dr. *S. Klages* for many helpful discussions.

Experimental Section

General Remarks: The ^{1}H-, ^{1}H-PHIP-, and ^{31}P-NMR spectra were recorded with a Bruker AMD 200 MHz spectrometer with an Aspect 2000 operating system. In order to obtain the PHIP spectra, one 8K FID signal was acquired using 45° excitation pulses covering the spectral range between δ = −30 and δ = +10. To record the conventional or "thermal" ^{1}H-NMR spectra, the same parameters were used, except for the pulse width, which was set at 90°. The ^{13}C spectra were recorded with a Varian VXR-400 spectrometer operating at 100.6 MHz. The ^{1}H- and ^{13}C-NMR spectra were referenced to residual protons of known chemical shift and the ^{13}C signals of the solvent, respectively, while ^{31}P spectra were referenced to external 85% H_3PO_4.

The simulation of the PHIP ^{1}H-NMR spectra was performed with the OS/2-based PHIP++ program, developed by Greve[47].

Deuterated solvents for NMR spectroscopy were purchased from Aldrich, dried ($CDCl_3$) and degassed prior to use, and stored under vacuum.

Tin dichloride and tin dibromide (anhydrous) were both obtained from Aldrich, and used without additional purification.

The platinum complexes, *trans*-[$(PR_3)_2$PtHCl] (PR_3 = PPh_3,[37]; $PMePh_2$, PMe_2Ph[48]) were synthesized as described previously. The corresponding hydrido bromo complexes were obtained according to ref.[49], by reaction of the hydrido chloro complex with excess NaBr in acetone.

Typical Preparation of Solutions for Hydrogenation Studies: Weighed amounts of *trans*-[$(PPh_3)_2$PtHCl] (10 mg, 13 μmol) and $SnCl_2$ (7.5 mg, 40 μmol) were placed in a screw-capped NMR tube attached to a vacuum line, and 0.7 ml of dry degassed [D_6]acetone was condensed into the tube. After thawing and filling the tube with dry argon, it was disconnected from the vacuum line and fitted with a septum stopper. About 15 μl of the substrate was then added to the sample by means of an Eppendorf micropipette. Parahydrogen was subsequently introduced into the NMR tube through a stainless steel needle through the septum at a pressure of 3 bar. After shaking of the solution in the parahydrogen atmosphere, the tube was inserted into the probehead, and the ^{1}H-PHIP spectrum was recorded immediately thereafter.

(σ-1-Phenylpropen-2-yl)(trichlorostannato)bis(triphenylphosphane)platinum (**5a**): [$(PPh_3)_2$PtHCl] (100 mg, 0.132 mmol) and $SnCl_2$ (100 mg, 0.53 mmol) were taken up in 2 ml of dry degassed acetone. Upon formation of a clear, orange solution, an excess of 1-phenyl-1-propyne (0.2 ml) was added under argon. The solution was degassed and sealed in a tube. After 5 min at +100°C, the tube was stored at 0°C for 48 h. Light-yellow crystals were deposited, which were collected, washed with acetone, and dried in vacuo (72 mg, 52%); m.p. 165−166°C. − ^{1}H NMR: δ = 0.69 [d, CH_3, ^3J(PtH) = 51.2, ^4J(HH) = 1.3, $^4J(^{117/119}$SnH) = 76.4 Hz], 6.45 [br, =C*H*Ph, ^3J(PtH) = 82.2, $^4J(^{117/119}$SnH) = 119.5 Hz]. − ^{13}C NMR: δ = 150.67 [t, Pt*C*, ^1J(PtC) = 772, ^2J(PC) = 9.2 Hz], 139.35 [s, *C*Ph, ^2J(PtC) = 94.8 Hz], 23.50 [s, *C*H_3, ^2J(PtC) = 28.9 Hz]. − ^{31}P NMR: δ = 18.85 [s, ^1J(PtP) = 3007, $^2J(^{119}$SnP) = 240.4, $^2J(^{117}$SnP) = 230.7 Hz].

Reaction of **5a** *with Dimethylformamide:* To a solution of isolated **5a** (46 mg, 43 μmol) in 0.7 ml of CD_2Cl_2, 10 μl of dimethylformamide was added. ^{1}H NMR of **5b**: δ = 1.131 [s, ^3J(PtH) = 48.8 Hz]. − ^{31}P NMR: δ = 24.607 [s, ^1J(PtP) = 3306 Hz].

[1] P. F. Seidler, H. E. Bryndza, J. E. Frommer, L. S. Stuhl, R. G. Bergman, *Organometallics* **1983**, *2*, 1701−1705.
[2] R. Eisenberg, T. C. Eisenschmid, M. S. Chinn, R. U. Kirss, *Adv. Chem. Ser.* **1992**, *230 (Homogeneous Transition Met. Catal. React.)*, 47−74.
[3] C. R. Bowers, D. P. Weitekamp, *Phys. Rev. Lett.* **1986**, *57*, 2645−2648.
[4] C. R. Bowers, D. P. Weitekamp, *J. Am. Chem. Soc.* **1987**, *109*, 5541−5542.
[5] J. Bargon, J. Kandels, K. Woelk, *Angew. Chem.* **1990**, *102*, 70−71; *Angew. Chem. Int. Ed. Engl.* **1990**, *29*, 58.
[6] S. B. Duckett, R. Eisenberg, *J. Am. Chem. Soc.* **1993**, *115*, 5292−5293.
[7] R. Cramer, R. V. Lindsey, Jr., *J. Am. Chem. Soc.* **1966**, *88*, 3534−3544.
[8] P. Kating, A. Wandelt, R. Selke, J. Bargon, *J. Phys. Chem.* **1993**, *97*, 13313−13317.
[9] J. Bargon, J. Kandels, K. Woelk, *Z. Phys. Chem. (Munich)* **1993**, *180*, 65−93.
[10] S. B. Duckett, R. Eisenberg, A. S. Goldman, *J. Chem. Soc., Chem. Commun.* **1993**, 1185−1187.
[11] J. Bargon, J. Kandels, P. Kating, *J. Chem. Phys.* **1993**, *98*, 6150−6153.
[12] S. B. Duckett, C. L. Newell, R. Eisenberg, *J. Am. Chem. Soc.* **1994**, *116*, 10548−10556.
[13] M. S. Chinn, R. Eisenberg, *J. Am. Chem. Soc.* **1992**, *114*, 1908−1909.
[14] S. B. Duckett, C. L. Newell, R. Eisenberg, *J. Am. Chem. Soc.* **1993**, *115*, 1156−1157.
[15] T. C. Eisenschmid, J. McDonald, R. Eisenberg, R. G. Lawler, *J. Am. Chem. Soc.* **1989**, *111*, 7267−7269.
[16] T. C. Eisenschmid, R. U. Kirss, P. P. Deutsch, S. I. Hommeltott, R. Eisenberg, J. Bargon, R. G. Lawler, A. L. Balch, *J. Am. Chem. Soc.* **1987**, *109*, 8089−8091.
[17] R. U. Kirss, R. Eisenberg, *Inorg. Chem.* **1989**, *28*, 3372−3378.
[18] R. U. Kirss, T. C. Eisenschmid, R. Eisenberg, *J. Am. Chem. Soc.* **1988**, *110*, 8564−8566.
[19] R. D. Cramer, E. L. Jenner, R. V. Lindsey, Jr., U. G. Stolberg, *J. Am. Chem. Soc.* **1963**, *85*, 1691−1692.
[20] J. C. Bailar, Jr., H. Itatani, *J. Am. Chem. Soc.* **1967**, *89*, 1592−1599.
[21] R. W. Adams, G. E. Batley, J. C. Bailar, Jr., *J. Am. Chem. Soc.* **1968**, *90*, 6051−6056.
[22] I. Schwager, J. F. Knifton, *J. Catal.* **1976**, *45*, 256−267.
[23] G. Consiglio, P. Pino, *Helv. Chim. Acta* **1976**, *59*, 642−645.
[24] Y. Kawabata, T. Hayashi, I. Ogata, *J. Chem. Soc., Chem. Commun.* **1979**, 462−463.
[25] L. Kollar, T. Kegl, J. Bakos, *J. Organomet. Chem.* **1993**, *453*, 155−158.
[26] P. J. Murphy, J. L. Spencer, C. Procter, *Tetrahedron Lett.* **1990**, *31*, 1051−1054.
[27] S. Klages, A. B. Permin, V. S. Petrosyan, J. Bargon, *J. Organomet. Chem.* **1997**, *545−546*, 201−205.
[28] R. D. Cramer, R. V. Lindsey, Jr., C. T. Previtt, V. G. Stolberg, *J. Am. Chem. Soc.* **1965**, *87*, 658.
[29] P. S. Pregosin, H. Ruegger, *Inorg. Chim. Acta* **1981**, *54*, L59.
[30] G. K. Anderson, C. Billard, H. C. Clark, J. A. Davies, *Inorg. Chem.* **1983**, *22*, 439−443.
[31] A. B. Permin, V. S. Petrosyan, *Appl. Organomet. Chem.* **1990**, *4*, 111−117.
[32] R. H. Reamey, G. M. Whitesides, *J. Am. Chem. Soc.* **1984**, *106*, 81−85.
[33] B. R. Koch, G. V. Fazakerley, E. Dijkstra, *Inorg. Chim. Acta, Lett.* **1980**, *45*, L51−L53.
[34] V. I. Bogdashkina, A. B. Permin, V. S. Petrosyan, V. I. Pol′shakov, O. A. Reutov, *Bull. Acad. Sci. USSR, Div. Chem. Sci.* **1982**, 917−920.

[35] G. K. Anderson, H. C. Clark, J. A. Davies, *Inorg. Chem.* **1983**, *22*, 434−438.
[36] D. W. W. Anderson, E. A. V. Ebsworth, D. W. H. Rankin, *J. Chem. Soc., Dalton Trans.* **1973**, 854−858.
[37] J. Chatt, B. L. Shaw, *J. Chem. Soc.* **1962**, 5075−5084.
[38] F. Cariati, R. Ugo, F. Bonati, *Inorg. Chem.* **1966**, *5*, 1128−1132.
[39] I. M. Blacklaws, L. C. Brown, E. A. V. Ebsworth, F. J. S. Reed, *J. Chem. Soc., Dalton Trans.* **1978**, 877−879.
[40] H. C. Clark, H. M. J. Smith, *J. Am. Chem. Soc.* **1986**, *108*, 3829−3830.
[41] R. S. Paonessa, A. L. Prignano, W. C. Trogler, *Organometallics* **1985**, *4*, 647−657.
[42] H. C. Clark, C. R. Jablonski, C. S. Wong, *Inorg. Chem.* **1975**, *14*, 1332−1335.
[43] K. A. Ostoja Starzewski, H. Ruegger, P. S. Pregosin, *Inorg. Chim. Acta* **1979**, *36*, L445.
[44] M. G. Pravica, D. P. Weitekamp, *Chem. Phys. Lett.* **1988**, *145*, 255−258.
[45] V. I. Bogdashkina, A. B. Permin, V. S. Petrosyan, O. A. Reutov, *Proc. Acad. Sci., USSR, Chem. Section* **1982**, *266*, 331−334.
[46] V. I. Bogdashkina, A. B. Permin, V. S. Petrosyan, *IV Internat. Symp. on Homogeneous Catalysis,* Leningrad, **1984**, Abstr. papers., Nos. P1−17, p. 54.
[47] T. Greve, PhD thesis, University of Bonn, **1996**.
[48] H. C. Clark, H. Kurosawa, *J. Organomet. Chem.* **1972**, *36*, 399−409.
[49] T. Miyamoto, *J. Organomet. Chem.* **1977**, *134*, 335−362.
[I98284]

Tetramethylpiperidine–Alane Adducts tmpH · AlX_3 (X = Cl, Br, I) and tmpH · AlH_2Cl: Synthesis, Solution Behavior, and X-ray Crystal Structures☆

Ingo Krossing[1], Heinrich Nöth*, Holger Schwenk-Kircher[2], Thomas Seifert[2], and Christiane Tacke

Institut für Anorganische Chemie der Universität München,
Meiserstraße 1, D-80333 München, Germany
Fax: (internat.) + 49(0)89/5902451

Received November 27, 1997 (Revised September 2, 1998)

Keywords: Tetramethylpiperidine–aluminum trihalide adducts / Tetramethylpiperidine–monochloroalane / Conductivity measurements / ^{27}Al-NMR spectroscopy

2,2,6,6-Tetramethylpiperidine (tmpH) reacts smoothly with aluminum trihalides AlX_3 (X = Cl, Br, I) and monochloroalane AlH_2Cl · 2 thf to give the addition compounds tmpH · AlX_3 (X = Cl, Br, I) and tmpH · AlH_2Cl, respectively. These adducts of the secondary amine tmpH are stable and do not undergo intramolecular elimination of HX or H_2 with formation of the aminoalanes $tmpAlX_2$ or tmpAl(H)Cl. In the solid state, tmpH · AlX_3 (X = Cl, Br, I) and tmpH · AlH_2Cl are tetracoordinated molecular adducts. While this is also true for solutions of tmpH · AlX_3 (X = Br, I) and tmpH · AlH_2Cl, the compound tmpH · $AlCl_3$ dissolves in CH_2Cl_2 as the salt $[tmpAlCl_3]$-$tmpH_2$ and the adduct tmpH · Al_2Cl_6, as is evident from its NMR spectra and from conductivity measurements. This behavior is supported by a semiempirical AM1 calculation.

Due to their importance in industrial processes, addition compounds of aluminum halides AlX_3 (in particular X = Cl) and ether donors have been the subject of extensive studies with regard to their solution and solid-state behavior[3]. Depending on the method of preparation, the tetra-, penta-, or hexacoordinated species $AlX_3 \cdot Do_n$ (Do = ether donor; $n = 1-3$) exist either as molecular adducts[4][5] or as salts {e.g. $AlCl_3 \cdot (thf)_2$ and $[AlCl_2(thf)_4]AlCl_4$}. The latter is also true for the addition compounds with pyridine[6], DMSO[7], and acetonitrile[8] (L), leading to the general compound type $[AlCl_2L_4^+]$-AlX_4^-. In solution, salt formation can readily be detected by ^{27}Al-NMR and conductivity measurements, including Fuoss-Kraus plots for analysis of the dissociation patterns[9]. Owing to facile H_2 or HX elimination, the chemistry of the addition compounds of the aluminum halides AlX_3 or AlH_2X (X = Cl, Br, I) with primary or secondary amines has scarcely been examined. However, two recent publications demonstrate the existence and importance of these species: Raston et al.[10] described a stable AlH_3 adduct with the sterically encumbered secondary amine tmpH (2,2,6,6-tetramethylpiperidine), while Atwood[11] later observed salt formation upon the addition of excess *t*$BuNH_2$ to R_2AlX (X = Cl, Br, I; R = Me, Et) when chloride was replaced by bromide or iodide. Recently, we reported on the synthesis of monomeric bis(tetramethylpiperidino)aluminum halides tmp_2AlX (X = Cl, Br, I) and on their derivatives[12]. In the course of these studies, addition compounds of tmpH and AlX_3 (X = Cl, Br, I) and AlH_2Cl were identified as by-products. For their full characterization, these adducts tmpH · AlX_3 [X = Cl (**1a**), Br (**1b**), I (**1c**)] and tmpH · AlH_2Cl (**2**) have now been independently synthesized from their respective components. Herein, we report on their solution and solid-state behavior.

Synthesis and Characterization

Addition of one equivalent of tmpH to $AlCl_3$ (in CH_2Cl_2) or $AlBr_3$, AlI_3, and AlH_2Cl · 2(thf) solutions (in toluene) leads to immediate formation of the adducts tmpH · AlX_3 [X = Cl (**1a**), Br (**1b**), I (**1c**)] and tmpH · AlH_2Cl (**2**).

$$tmpH + AlX_3 \longrightarrow tmpH^+AlX_3^- \quad (1a)$$

X = Cl **1a**, Br **1b**, I **1c**

$$tmpH + AlH_2Cl{\cdot}thf_2 \longrightarrow tmpH^+AlH_2Cl^- + 2\ thf \quad (1b)$$

2

Evolution of hydrogen or HX was not observed. **1b**, **c** and **2** proved to be molecular monomers in benzene solution. They give rise to single sharp signals in the ^{27}Al-NMR spectra. The chemical shifts of these addition compounds follow the substitution pattern, the iodide being observed at highest field ($\delta^{27}Al = 12$, $\Delta_{1/2} = 140$ Hz), followed by the bromide ($\delta^{27}Al = 88$, $\Delta_{1/2} = 130$) and AlH_2Cl ($\delta^{27}Al = 123$). Distinct lines for axial and equatorial methyl groups (^{1}H- and ^{13}C-NMR) as well as for the ring-hydrogen atoms (^{1}H-NMR) are observed. Thus, axial and equatorial positions of the hydrogen and carbon atoms in the piperidine ring in **1b**, **c** are magnetically inequivalent.

Whereas **1b**, **c** and **2** retain their molecular character upon dissolution in aromatic and chlorinated solvents, the chloro compound **1a** behaves differently. In the solid state, **1a** exists as a tetracoordinated molecular adduct of the type tmpH · $AlCl_3$ (vide infra), but in solution it disproportionates according to Eq. 2.

Two signals at $\delta^{27}Al = 108$ and 106, $\Delta_{1/2} = 120$ and 47 Hz, with an integral ratio of 2:1 are found (100°C), corresponding to a conversion of **1a** to tmpH · Al_2Cl_6 and

 © WILEY-VCH Verlag GmbH, D-69451 Weinheim, 1998 1434–1948/98/1212–1925 $ 17.50+.50/0

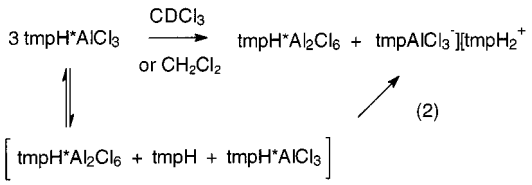

$[tmpAlCl_3]tmpH_2$. The line widths of the ^{27}Al-NMR signals are found to be temperature-dependent. At 0°C, only one broad line at $\delta^{27}Al = 106$ is observed. Heating the sample to 100°C ($[D_8]$toluene) leads to the resolution of two well-separated lines (see Figure 1), indicating the absence of rapid exchange processes and the presence of two distinct species.

Figure 1. ^{27}Al-NMR spectra of $tmpH \cdot AlCl_3$ (**1a**) at various temperatures ($[D_8]$toluene)

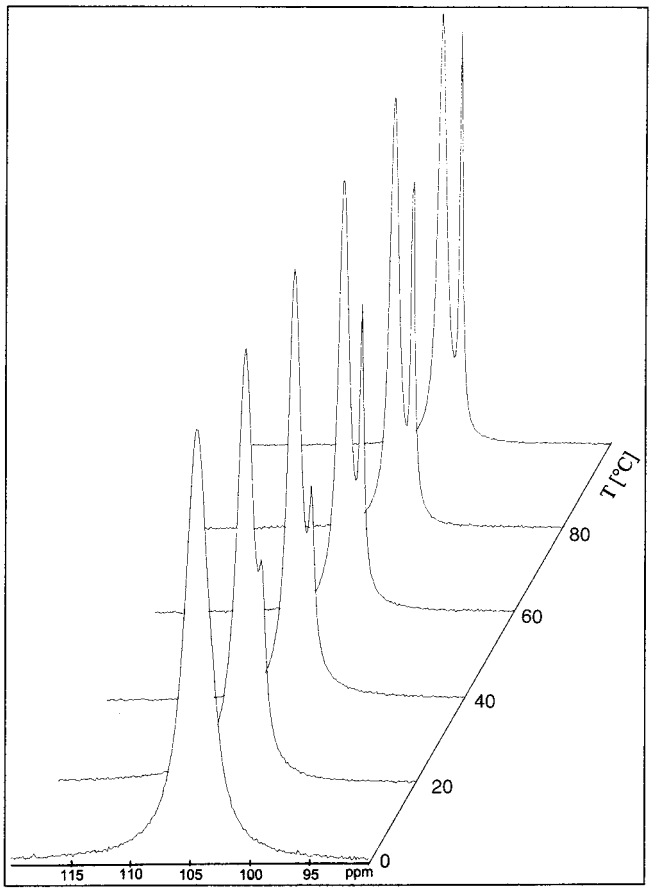

The "dissociation" of **1a** is indicated by the appearance of three sets of signals for the different tmp ligands, represented by the formulae ($tmpH \cdot Al_2Cl_6$; $[tmpAlCl_3]tmpH_2$). Two signals are observed in the range $\delta = 57-60$ for the carbon atoms bonded to nitrogen atoms, indicating the presence of two distinct tmp groups with tetracoordinated nitrogen atoms. The third ligand has a tricoordinated nitrogen atom, since the respective $^{13}C(C-N)$ resonance is found at $\delta = 53.2$ {cf. for example $tmpAlI_2 \cdot$ py: $d^{13}C(C-N) = 53.3$ (tricoordinated nitrogen atom); $[(Me_3Si)_3SiAlCl_3]$ $tmpH_2$: $d^{13}C(C-N) = 58.0$ (tetracoordinated nitrogen atom)}[12][13]. Furthermore, two broad lines for the N−H protons in a ratio of 2:1 (1:6 and 1:12 to each of the tmp methyl signals) as well as three distinct tmp methyl groups are observed in the ^1H-NMR spectrum.

To further prove the "dissociation" pattern of the salt $[tmpAlCl_3]tmpH_2$ (as represented by Eq. 2), **1a** has been subjected to conductivity measurements in CH_2Cl_2.

Figure 2. Fuoss-Kraus plot for $tmpH \cdot AlCl_3$ (**1a**) calculated from conductivity measurements in CH_2Cl_2

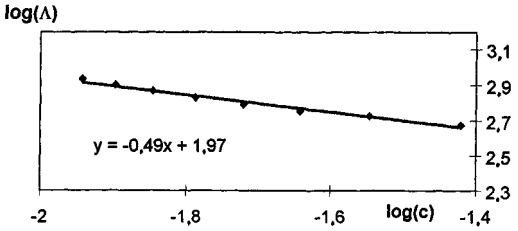

According to the gradient of the Fuoss-Kraus[14] plot ($a = -0.5$, depicted in Figure. 2), the solution contains a simple A^+B^- system. Since the molecular adduct $tmpH \cdot Al_2Cl_6$ is not involved in ion formation, only the conductivity induced by the $[tmpAlCl_3]tmpH_2$ species, an A^+B^- compound, is detected.

Crystal Structures

In contrast to the solution behavior of **1a**, the structures of **1a** (Figure 3), **1b** (Figure 4), **1c** (Figure 5), and **2** (Figure 6) in the solid state all represent simple adducts with tetracoordinated aluminum centers. Crystals of **1a−c** are found to be monoclinic, space group $P2_1/n$ (**1a**) and $P2_1/c$ (**1b**, **c**), respectively, while **2** crystallizes in the orthorhombic space group $P2_12_12_1$. All unit cells contain four molecules. Selected structural parameters are summarized in Table 1.

In each of the adducts, the aluminum atom is coordinated by a nitrogen atom, with the halogen and/or hydrogen atoms arranged in a distorted tetrahedral manner. Whereas the angles X−Al−X in **1a−c** are close to 109.5°, the N−Al−X bond angles deviate by +9.7/−10.5° from this value. This behavior seems to depend on the size of the halogen atoms, as these deviations are reduced to +2.5 and −8.3°, respectively, in **2**. One halogen atom resides between the two equatorial methyl groups, on the same side as the N−H atoms. The respective H−N−Al−X torsion angles vary from 7.38° (**1a**), through 5.0° (**1b**) and 0.3° (**1c**), to 23.5° (**2**). The geometry at the nitrogen atom (C_2NAl plane) is close to planar, as is indicated by the sums of the respective bond angles (**1a**: 350.1°; **1b**: 350.2°; **1c**: 350.3°; **2**: 346.5° vs. $3 \times 109.5 = 328.5°$). The Al−N distances span a range from 2.009(5) (**1b**) to 2.038(9) Å (**1c**). This corresponds with the upper range of known Al−N distances in amine adducts of aluminum halides or hydrides, such as $AlCl_3 \cdot NMe_3$ [d(Al−N) = 1.96(1) Å][15] or $tmpH \cdot AlH_3$ [d(Al−N) = 2.04(1) Å][10]. Since chlorine and bromine have a stronger negative inductive effect than hydrogen, and thus increase the acceptor strength of the aluminum center, the Al−N distances in **1a**, **b** and **2** are shorter than that found

Table 1. Bonding parameters of compounds tmpH·AlX_3 (X = Cl, Br, I) and tmpH·AlH_2Cl

Parameter	tmpH·$AlCl_3$	tmpH·$AlBr_3$	tmpH·AlI_3	tmpH·AlH_2Cl
Bond lengths [Å]				
Al−N	2.014(2)	2.009(5)	2.038(9)	2.019(3)
Al−X(1)	2.129(1)	2.280(2)	2.540(3)	2.154(2)
Al−X(2); H(1)	2.136(1)	2.283(2)	2.535(3)	1.60(3)
Al−X(3); H(2)	2.129(1)	2.300(2)	2.532(3)	1.51(3)
Bond angles [°]				
N−Al−X(1)	99.86(7)	100.9(1)	99.0(3)	101.2(1)
N−Al−X(2); H(1)	115.39(8)	116.0(2)	118.6(3)	112(1)
N−Al−X(3); H(2)	116.72(7)	117.9(2)	119.2(3)	
X(1)−Al−X(3); H(2)	110.03(5)	110.02(8)	110.1(1)	109(1)
X(1)−Al−X(2); H(1)	110.83(5)	110.56(7)	109.3(1)	115.2(8)
X(3); H(2)−Al−X(2); H(2)	104.09(5)	101.59(7)	100.6(1)	108(2)
C(1)−N−Al	115.8(2)	117.1(3)	117.6(6)	114.8(2)
C(5)−N−Al	117.7(2)	117.4(3)	116.4(7)	114.7(2)
C(1)−N−C(5)	116.6(2)	115.7(4)	116.3(8)	116.9(2)

Figure 3. Molecular structure of tmpH · $AlCl_3$ (**1a**) in the solid state; thermal ellipsoids are shown at a 25% probability level; structural parameters are compiled in Table 1

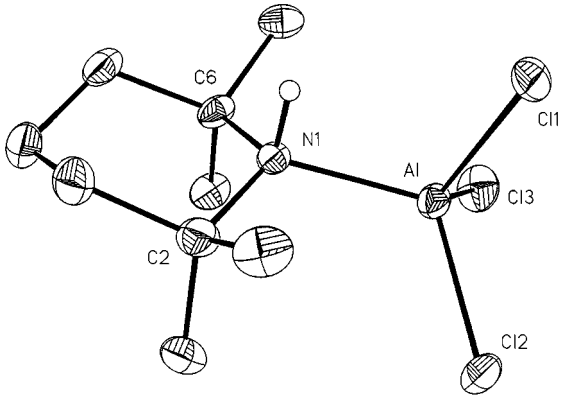

Figure 5. Molecular structure of tmpH · AlI_3 (**1c**) in the solid state; thermal ellipsoids are shown at a 25% probability level; structural parameters are compiled in Table 1

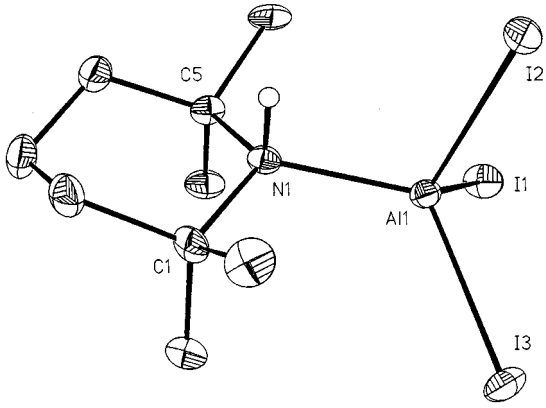

Figure 4. Stereoplot of the unit cell contents of tmpH · $AlBr_3$ (**1b**); view down the *c* axis (*a* axis to the right)

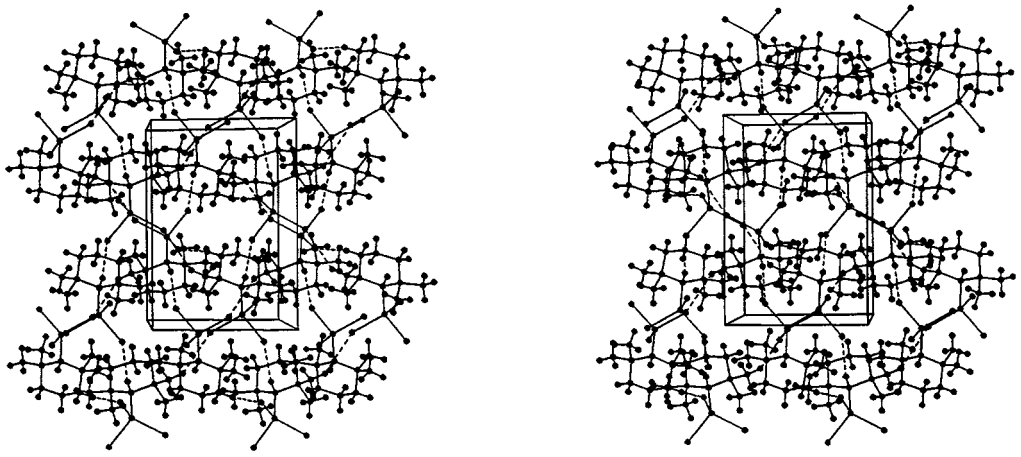

in tmpH · AlH_3. In **1c**, two opposing effects are responsible for the relatively long Al−N bond length: AlI_3 is the strongest Lewis acid amongst the aluminum halides[3], and, therefore, one would expect a short Al−N distance. However, the iodine atoms are considerably larger than the chlorine or bromine atoms and thus increase the steric strain. For this reason, *d*(Al−N) reaches its minimum values in **1a**, **b**, and not in **1c**. The aluminum−halogen bond lengths in these systems vary only slightly: the average Al−Cl distances are 2.131 Å (**1a**) and 2.154 Å (**2**), respectively, Al−Br is 2.288 Å (**1b**, av.), and Al−I is 2.536 Å (**1c**, av.). These values are close to those observed in $AlCl_3$ · NMe_3

Figure 6. Molecular structure of tmpH·AlH_2Cl (**2**) in the solid state; thermal ellipsoids are shown at a 25% probability level; structural parameters are compiled in Table 1

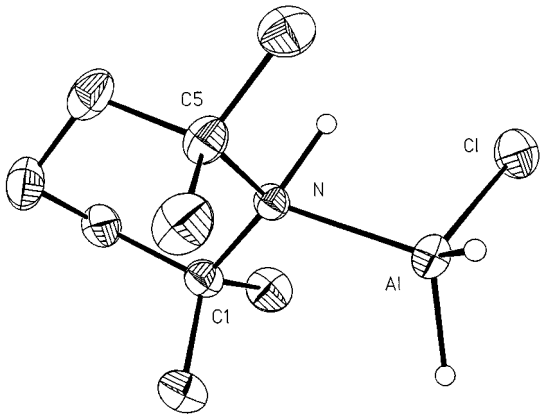

[d(Al−Cl) = 2.11(1)−2.14(1) Å][15], $AlMe_2I \cdot NMe_3$ [d(Al−I) = 2.58 Å][16] and $AlI_3 \cdot$ iq [iq = isoquinoline; d(Al−I) = 2.504(4) Å][13].

In spite of the fact that the adducts **1a−c** are present in space group No. 14, the arrangement of the molecules in the lattice is different in each case. Thus, in the chloride **1a**, the shortest intermolecular contacts are between a Cl atom of the $AlCl_3$ group and a hydrogen atom of a CH_3 group [(d(H···Cl) = 2.844 Å, angle Cl···H···C 169.7°]. In contrast, in **1b** there is an intermolecular N−H−Br contact with an H···Br distance of 2.978 Å (angle Br···H−N 169.0°) as well as an H···Br contact to a CH_3 group (3.019 Å). In the iodide **1c**, there are H···I contacts between two different I atoms and H atoms of two different CH_3 groups (4.021 and 3.191 Å, with Al−I···H angles of 148.2 and 125.7°, respectively). In contrast, there are no close intermolecular contacts between the Cl atom and H atoms bonded to either N or C in compound **2**.

Discussion

At first sight it is not easy to understand why only the aluminum trichloride adduct **1a** undergoes a structural change in solution. In fact, this could even be seen as a contradiction, because Atwood[11] found that only the bromo- and iodoalanes R_2AlX (X = Cl, Br, I; R = Me, Et) could be forced to ionize by the addition of excess tBuNH$_2$. This was attributed to the lower Al−Br and Al−I bond enthalpies and this argument should also be valid for the compounds described here. Since **1a** is found to "dissociate" according to Eq. 2, a decisive factor is clearly the formation of an ion pair (additional coulombic energy) and the chloro-bridged species tmpH · Al_2Cl_6. Thus, in this process nine terminal Al−Cl bonds are transformed into seven terminal and four bridging Al−Cl bonds. The relevant mean bond enthalpies are 425 kJ/mol for a terminal Al−Cl bond[3] and 289 kJ/mol for a bridging Al−Cl bond[17].

Table 2. Crystallographic data and information related to data collection and structure solution

Compound	tmpH · $AlCl_3$ (**1a**)	tmpH · $AlBr_3$ (**1b**)	tmpH · AlI_3 (**1c**)	AlH_2Cl · tmpH (**2**)
Chem. formula	$C_9H_{19}AlCl_3N$	$C_9H_{19}AlBr_3N$	$C_9H_{19}AlI_3N$	$C_9H_{21}AlClN$
Formula weight	238.12	407.96	548.93	205.71
Cryst. size [mm]	0.19 × 0.32 × 0.44	0.2 × 0.3 × 0.3	0.6 × 0.4 × 0.15	0.35 × 0.38 × 0.55
Crystal system	monoclinic	monoclinic	monoclinic	orthorhombic
Space group	$P2_1/n$	$P2_1/n$	$P2_1/c$	$P2_12_12_1$
a [Å]	8.682(2)	8.686(3)	16.126(4)	7.819(1)
b [Å]	12.233(2)	12.710(4)	13.628(4)	10.490(2)
c [Å]	13.120(2)	13.339(5)	15.987(5)	15.224(3)
α [°]	90	90	90	90
β [°]	94.42(1)	96.47(1)	113.38(2)	90
γ [°]	90	90	90	90
V [Å^3]	1389.3(4)	1463.2(9)	3224.9(16)	1248.7(5)
Z	4	4	8	4
$\rho_{calcd.}$ [Mg/m^3]	1.138	1.852	2.261	1.094
μ [mm^{-1}]	0.495	8.300	5.843	0.334
absorption correction	−	semiempirical	semiempirical	−
min. and max. transmission	−	0.205 and 0.382	0.237 and 0.345	−
F(000)	504	792	2016	448
Index range	$-10 \le h \le 0$	$-9 \le h \le 9$	$-16 \le h \le 18$	$-13 \le h \le 0$
	$-14 \le k \le 0$	$-14 \le k \le 14$	$-15 \le k \le 0$	$-11 \le k \le 0$
	$-15 \le l \le 15$	$-14 \le l \le 14$	$-18 \le l \le 0$	$-12 \le l \le 22$
2θ [°]	50.00	46.52	48.10	50.00
T [K]	233	193	193(2)	293
Refl. collected	2619	6071	5304	3153
Refl. unique	2449	1937	5099	2192
Refl. obsd. (4σ)	1871	1666	4115	1827
R_{int}	0.0354	0.0413	0.0674	0.0276
No. of variables	127	131	261	118
Weighting scheme[a] x/y	0.1524/5.5644	0.0270/6.5814	0.0479/35.7622	0.0765/0.2610
GooF	0.649	1.102	1.176	0.1057
Final R (4σ)	0.0485	0.0392	0.0518	0.0443
Final $wR2$	0.1360	0.0854	0.1259	0.1209
Largest resid. peak [e/Å^3]	0.550	1.229	0.795	0.39

[a] $w^{-1} = \sigma^2F_o^2 + (xP)^2 + yP$; $P = (F_o^2 + 2F_c^2)/3$.

Hence, nine terminal Al−Cl bonds amount to an enthalpy of 3825 kJ/mol, while seven terminal and four bridging bonds represent 4131 kJ/mol, and consequently the "dissociated" species is favored by about 200 kJ/mol. As the bond enthalpies for Al−X−Al bridges decrease dramatically on going from X = Cl (ΔE_{bond} = 289 kJ/mol) to X = I (ΔE_{bond} = 192 kJ/mol)[17], the formation of halide bridges is not favored for X = Br, I. Due to the large steric requirement of the tetramethylpiperidine ligand, another usual pathway to dissociation, as described by Eq. 3, is not applicable here.

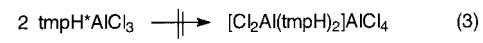

Figure 7. Calculated heats of formation of all compounds involved in Eq. 4 and estimated enthalpy of formation of tmpH · Al_2Cl_6 and [tmpAlCl$_3$]tmpH$_2$

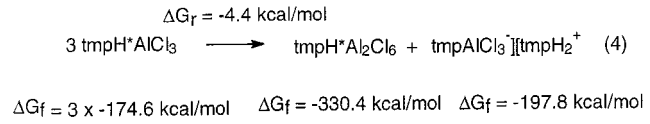

This assumption is corroborated by a semiempirical AM1 calculation[18] of all the heats of formation of compounds that appear in Eq. 4 (see Figure 7). This allows an estimate of the overall reaction enthalpy. In the gas phase, the dissociated species are found to be favored by about 4.4 kcal/mol over the molecular starting material. Moreover, polar solvents such as dichloromethane should exert an additional stabilizing effect, thereby assisting in the formation of ion pairs. As this additional stabilization is not provided by the crystal lattice, the undissociated monomeric species **1a** turns out to be more stable in the solid state.

Conclusion

The tetramethylpiperidine alane adducts **1a−c** and **2** are stable towards HX and H_2 elimination, and thus formation of compounds tmpAlX_2 or tmpAl(H)X does not occur. In the solid state, they are present as monomeric tetracoordinated species. This is also true for solutions of **1b**, **c** and **2**. In contrast, upon dissolution of tmpH · $AlCl_3$, a transformation takes place according to Eq. 2. Whether this behavior is general or is specific to this compound will be addressed in future investigations; it is surprising to us that such simple systems raise such interesting and unforeseen questions.

We thank the *Fonds der Chemischen Industrie* and the *Chemetall mbH* for support of our research. We are also grateful to Mrs. *Käser* and Mrs. *R. Ullmann* for performing C/H/N analyses, Mr. *P. Mayr*, Dr. *R. Waldhör* and Dr. *C. Miller* for recording many NMR spectra, Mrs. *D. Ewald* for mass spectra and Mrs. *E. Kiesewetter* for IR spectra.

Experimental Section

All manipulations were performed using Schlenk techniques under dinitrogen. All solvents were rigorously dried prior to use and stored under dinitrogen or argon. − NMR: Bruker ACP 200, Jeol GSX400, and Jeol GSX270. − IR: Nicolet FT-IR spectrometer model 6000, CsI plates, Nujol. − MS: Varian Atlas CH7 spectrometer.

tmpH · $AlCl_3$ (**1a**): To a suspension of $AlCl_3$ (0.65 g, 4.87 mmol) in 10 ml of CH_2Cl_2, tmpH (0.83 ml, 4.87 mmol) was added at ambient temperature and the mixture was exposed to ultrasound for 3 h. The resulting yellow solution was stored at −20°C overnight, whereupon 0.90 g (67%) of colorless crystals of tmpH · $AlCl_3$ separated, m.p. 130°C. − ^{1}H NMR ($CDCl_3$, 400 MHz): δ = 1.40 (s, 12 H, tmp-CH_3), 1.61 (s, 12 H, tmp-CH_3), 1.73 (s, 12 H, tmp-CH_3), 2.88 (br. s, 2 H, N-*H*), 4.83 (br. s, 1 H, N-*H*), some additional multiplets at δ = 1.45 and 1.60−1.80 were also observed, but were not readily assigned. − ^{13}C NMR ($CDCl_3$, 100 MHz): δ = 15.7 (tmp-γ-*C*H$_2$), 16.5 (tmp-γ-*C*H$_2$), 23.5 (tmp-*C*H$_3$), 29.1 (tmp-*C*H$_3$), 33.5 (tmp-*C*H$_3$), 36.1 (tmp-*C*), 41.1 (tmp-*C*), 53.3 (tmp-*C*), 57.2 (tmp-*C*), 59.6 (tmp-*C*). − ^{27}Al NMR ($CDCl_3$, 70 MHz): δ = 106 ($\Delta_{1/2}$ = 47 Hz), 108 ($\Delta_{1/2}$ = 120 Hz). − IR (Nujol): $\tilde{\nu}$ = 3172 cm^{-1} s (N−H), 496 ss (Al−Cl), 421 ss (Al−Cl). − $C_9H_{19}NAlCl_3$ (274.60): calcd. C 39.37, H 6.97, N 5.10; found C 38.33, H 7.02, N 4.97.

tmpH · $AlBr_3$ (**1b**): tmpH (0.85 ml, 5.0 mmol) in 5 ml of benzene was added to a solution of $AlBr_3$ (1.3 g, 5.0 mmol) in 20 ml of benzene with stirring. The addition was accompanied by an immediate color change from brown to light-yellow. Successive partial evaporation of the solvent and cooling to 8°C led to the precipitation of colorless crystals of tmpH · $AlBr_3$. These were recrystallized from 15 ml of benzene, m.p. 137−139°C (darkening). Yield of **1b**: 1.46 g (76%). − ^{1}H NMR (C_6D_6, 270 MHz): δ = 0.35 (m, 1 H, tmp-CH_2), 0.52 (m, 1 H, tmp-CH_2), 0.72 (dt, 2 H, tmp-CH_2), 0.91 (dt, 2 H, tmp-CH_2), 1.20 (s, 6 H, tmp-CH_3), 1.53 (s 6 H, tmp-CH_3). − ^{13}C NMR (C_6D_6, 100 MHz): δ = 15.3 (tmp-*C*4), 23.6, 33.8 (tmp-*C*7-10), 40.8 (tmp-*C*3,5), 60.1 (tmp-*C*-N). − ^{27}Al NMR (C_6D_6, 70 MHz): δ = 88 ($\Delta_{1/2}$ = 130 Hz). − IR (Nujol) [ν(Al−Br) range]: $\tilde{\nu}$ = 411 cm^{-1} vs, 384 s. − $C_9H_{19}NAlBr_3$ (407.95): calcd. C 26.50, H 4.69, N 3.43, Al 6.6, Br 58.8; found C 27.18, H 5.13, N 3.17, Al 6.7, Br 60.4.

tmpH · AlI_3 (**1c**): To a solution of AlI_3 (0.81 g, 2.0 mmol) in 20 ml of toluene, a solution of tmpH (0.34 ml, 2.0 mmol) in 5 ml of toluene was added at ambient temperature. The addition was accompanied by an immediate color change from brown to yellow. The resulting solution was reduced to one-third of its original volume. Upon cooling to −20°C, colorless crystals of tmpH · AlI_3 separated, which were recrystallized from 10 ml of toluene; m.p. 141−143°C (decomp.), yield of **1c**: 0.81 g (74%). − ^{1}H NMR (C_6D_6, 270 MHz): δ = 0.33 (m, 1 H, tmp-CH_2), 0.56 (m, 1 H, tmp-CH_2), 0.81 (dt, 2 H, tmp-CH_2), 1.00 (dt, 2 H, tmp-CH_2), 1.25 (s, 6 H, tmp-CH_3), 1.70 (s, 6 H, tmp-CH_3). − ^{13}C NMR (C_6D_6, 100 MHz): δ = 14.4 (tmp-*C*4), 23.5, 33.9 (tmp-*C*7-10), 41.1 (tmp-*C*3,5), 60.4 (tmp-*C*-N). − ^{27}Al NMR (C_6D_6, 70 MHz): δ = 12 ($\Delta_{1/2}$ = 140 Hz). − IR (Nujol) [ν(Al−I) range]: $\tilde{\nu}$ = 347 cm^{-1} vs, 295 s. − $C_9H_{19}NAlI_3$ (548.95): calcd. C 19.69, H 3.49, N 2.55, Al 4.9, I 69.4; found C 19.66, H 3.72, N 2.50, Al 5.3, I 70.1.

tmpH · AlH_2Cl (**2**): To a solution of $AlH_2Cl(thf)_2$ (14.1 g, 67.4 mmol) in 50 ml of thf, 11.5 ml of tmpH (67.4 mmol) in 50 ml of toluene was added at −40°C. The mixture was allowed to warm to ambient temperature and was then heated to reflux for 3 h. Thereafter, all volatiles were removed in vacuo and the residue was extracted with 100 ml of pentane. The organic extract was filtered to afford a colorless solution. Cooling to −20°C provided 10.1 g (72%) of colorless crystals of **2**, m.p. 85°C. − ^{1}H NMR (C_6D_6, 270 MHz): δ = 0.84 (m, 4 H, tmp-β-CH_2), 1.16 (s, 12 H, tmp-CH_3), 1.68 (s, 2 H, tmp-γ-CH_2). − ^{13}C NMR (C_6D_6, 100 MHz): δ = 18.8

(tmp-*C*4), 32.4 (tmp-*C*7-10), 38.6 (tmp-*C*3,5), 49.6 (tmp-*C*-N). – ^{27}Al NMR (C_6D_6, 70 MHz): δ = 123. – IR (Nujol): $\tilde{\nu}$ = 1891 cm^{-1} vs, 1831 vs [ν(AlH)], [ν(N–H) range] 3137 m [ν(NH)]. – $C_9H_{21}NAlH_2Cl$ (205.7): calcd. Al 13.1, Cl 17.3; found Al 12.3, Cl 18.6.

X-ray Crystal-Structure Determinations: Data collection for X-ray structure determinations was performed with a Siemens P4 or a Syntex R3 four-circle diffractometer using graphite-monochromated Mo-K_α (λ = 0.71073 Å) radiation. Single crystals were mounted in Lindemann capillaries and sealed under argon. Data collection was performed at −80 to −100°C. All calculations were performed with PCs and workstations using the Siemens SHELXTL-Plus[19] or SHELX-93[20] software packages. The structures were solved by direct or heavy-atom methods with successive interpretation of the difference Fourier maps, followed by least-squares refinement. All non-hydrogen atoms were refined anisotropically. The hydrogen atoms were included in the refinement in calculated positions by a riding model using fixed isotropic parameters. Data relevant to the crystallography, data collection and refinement are compiled in Table 2. Further details on the crystal structure determinations have been deposited at the Cambridge Crystallographic Data Centre and may be requested by quoting the depository number CSD-103180 (**1a**), -103181 (**1b**), -103182 (**1c**) and -103183 (**2**), the names of the authors, and the full journal citation.

☆ Dedicated to Prof. Dr. *M. Weidenbruch* on the occasion of his 60th birthday.

[1] I. Krossing, Ph. D. Thesis, University of Munich, **1997**.
[2] X-ray crystal structures.
[3] A. J. Downs (Ed.), *Chemistry of Aluminium, Gallium, Indium, and Thallium*, Blackie Academic and Professional, London, **1993**, p. 430.
[4] P. J. Olgren, J. P. Cannon, C. F. Smith, Jr., *J. Phys. Chem.* **1971**, *75*, 282–289.
[5] L. Jakobsmeier, I. Krossing, H. Nöth, M. J. H. Schmidt, *Z. Anorg. Allg. Chem.* **1996**, *51b*, 1117–1126.
[6] [6a] P. Pullmann, K. Hensen, J. W. Bats, *Z. Naturforsch., Part B* **1982**, *37*, 1312–1316. – [6b] D. M. Brown, D. T. Stewart, D. E. H. Jones, *Spectrochim. Acta* **1973**, *29a*, 213–217. – [6c] M. Dalibart, J. Derouault, M. T. Forel, *J. Mol. Struct.* **1981**, *70*, 119–123.
[7] J. Meunier, M. T. Forel, *Can. J. Chem.* **1972**, *50*, 1157–1161.
[8] I. R. Beattie, P. J. Jones, J. A. K. Howard, L. E. Smart, C. J. Gilmore, J. W. Akitt, *J. Chem. Soc., Dalton Trans.* **1979**, 528–541.
[9] H. Nöth, R. Rurländer, P. Wolfgardt, *Z. Naturforsch., Part B* **1982**, *37*, 29–35.
[10] J. L. Atwood, G. A. Koutsantonis, F. C. Lee, C. L. Raston, *J. Chem. Soc., Chem. Commun.* **1994**, 91–92.
[11] D. A. Atwood, J. Jegler, *Inorg. Chem*. **1996**, *35*, 4277–4282.
[12] [12a] I. Krossing, H. Nöth, C. Tacke, M. Schmidt, H. Schwenk, *Chem. Ber.* **1997**, *130*, 1047–1052. – [12b] I. Krossing, H. Nöth, B. N. Anand, *Inorg. Chem*. **1997**, *36*, 1979–1981. – [12c] K. Knabel, I. Krossing, H. Nöth, M. Schmidt-Amelunxen, H. Schwenk-Kircher, *Eur. J. Inorg. Chem.*, to be submitted.
[13] I. Krossing, H. Nöth, H. Schwenk-Kircher, *Eur. J. Inorg. Chem.*, to be submitted.
[14] R. M. Fuoss, C. A. Kraus, *J. Am. Chem. Soc.* **1933**, *55*, 2387–2399.
[15] A. Haaland, *Angew. Chem.* **1989**, *101*, 1017–1032; *Angew. Chem. Int. Ed. Engl.* **1989**, *28*, 992.
[16] J. L. Atwood, P. A. Milton, *J. Organomet. Chem.* **1973**, *52*, 275–279.
[17] K. Wade, A. J. Banister, *The Chemistry of Aluminum, Gallium, Indium and Thallium,* Pergamon Press, Oxford, **1975**.
[18] Performed with the program *Hyperchem*, V3.0, Autodesk, **1993**.
[19] *PC SHELXTL Rel. 5.03*, Siemens Analytical Instruments, Version 4.1, **1994**.
[20] G. M. Sheldrick, University of Göttingen, **1993**.

[97286]

Synthesis and Structures of Hydrazinoalanes and Hydrido(hydrazino)aluminates☆

Heinrich Nöth* and Thomas Seifert

Institute of Inorganic Chemistry, University of Munich,
Meiserstraße 1, D-80333 München, Germany
Fax: (internat.) +49(0)89/5902-451
E-mail: H.Noeth@lrz.uni-muenchen.de

Received June 12, 1998

Keywords: Aluminium / Lithium hydridoaluminates / Alanes / Hydrazides / Structure elucidation

Several monomeric dimethylaluminium hydrazide ether adducts $Et_2O/THF \times Me_2AlNR–NR'R''$ (**5–7**) were obtained by deprotonating the respective hydrazines with *n*BuLi, followed by reaction with Me_2AlCl. The hydrazines Ph(H)N–$N(SiMe_3)_2$ and *t*Bu(H)N–N(H)$SiMe_3$ react with $LiAlH_4$ in the presence of either ether or THF with the formation of dimeric lithium hydrazino(hydrido)aluminates, e.g. **8** and **9**. Their structures depend on the number of acidic hydrogen atoms bonded to the nitrogen atoms of the starting hydrazine. The hydrazine Ph(H)N–$N(SiMe_3)_2$ (**1**) reacts with $LiAlH_4$ to form monometallated $LiAlH_3[(Ph)N–N(SiMe_3)_2] \times 2\ Et_2O$ (**8**) with elimination of one equivalent of H_2. The molecule is dimeric and features an $(AlHLiH)_2$ eight-membered ring. In contrast, the reaction of *t*Bu(H)N–N(H)$SiMe_3$ with $LiAlH_4$ in the presence of THF leads to the formation of dimeric 2 THF × $LiAlH_2[(tBu)N–N(SiMe_3)]$ (**9**) with a central $(AlNN)_2$ six-membered ring. A dimeric aluminium hydrazide **10** was obtained by allowing *t*Bu(Li)N–N(H)$SiMe_3$ to react with Me_2AlCl in a hexane/toluene solution. The structure of **10** features a six-membered Al_2N_4 ring in chair conformation.

Introduction

In recent years great progress has been achieved in the structural chemistry of alkali metal hydrazides[1]. Among the structural principles such as "laddering" and "stacking"[2], well known for alkali metal amides, additional arrangements such as "butterfly" or "side-on" coordination play an important role in the structure of the hydrazides. However, the structural chemistry of the amino alanes is mainly determined by the steric requirements of the organyl groups as well as by additional ligands. There are subtle differences; for example, $(Me_2AlNMe_2)_2$ possesses a planar four-membered Al_2N_2 ring while a six-membered Al_3N_3 ring was observed for $(Me_2AlNHMe)_3$, which exists in either a chair or a "skew-boat" conformation[3]. Furthermore, the structural motifs found for imidoalanes vary from heterocubanes, e.g. $(PhAlNPh)_4$, to different kinds of bridged or fused cage structures[4]. To date, much of the structural chemistry of group-13 elements has focused on amides and imides[8][15]. In contrast, information on the hydrazido derivatives is still scarce, even though a renewed interest in the investigation of these compounds in the last few years can be noted[5]. Since the synthesis and structural knowledge of borylated hydrazines are well developed[5a][5b][5c][5d], we present here work related to new hydrazinoalanes and hydrazino(hydrido)aluminates.

Results and Discussion

Preparation and NMR-Spectroscopic Characterization

Among the various possible routes to hydrazinoalanes only two have been pursued in this study, the metathesis of R_2AlCl with a lithium hydrazide and secondly the reaction of $LiAlH_4$ with a hydrazine. Four alkyl-, phenyl- and silyl-substituted hydrazines, **1**−**4**, were deprotonated by *n*BuLi and the Li compounds were allowed to react with Me_2AlCl. The deprotonation of **1**−**3** (Eq. 1) was carried out in the presence of donor molecules. A conceivable Si−N bond cleavage with formation of Me_3SiCl for reactions (1) and (2), well-known for the reaction of aminosilanes with aluminium trihalides[6], was not observed. However, the alkyl-substituted hydrazide **10** was obtained from a hexane/toluene solution (Eq. 2). Furthermore the deprotonation of **1** and **4** with $LiAlH_4$ proceeded smoothly with H_2 evolution producing the hydrazino(hydrido)aluminates **8** and **9** (Eqs. 3 and 4).

The use of ether as a solvent or cosolvent for reactions (1) and (3) was due to the fact that lithiated phenyl hydrazides and $LiAlH_4$, respectively, are only sparingly, if at all, soluble in both aliphatic and aromatic hydrocarbons. This proved to be essential for good yields.

Although several aluminium hydrazides have already been investigated[5e][5f][5g], no ^{27}Al-NMR data have so far been reported. However, ^{27}Al-NMR spectroscopy is a useful tool not only for monitoring the course of the reaction but also for obtaining structural information. Thus, the formation of **5**, **6** and **7** (Eq. 1) can be readily deduced from ^{27}Al-NMR spectroscopy. Resonances at $\delta = 151$ (**5**), $\delta = 165$ (**6**) and $\delta = 170$ (**7**), with half widths of 5600−6100 Hz, are indicative of asymmetrically tetracoordinated aluminium centers[7], and the chemical shifts are comparable with those of dimeric dialkylaluminium amides, e.g. $[iBu_2AlNC_6H_{12}]_2$[8]. The ^{1}H- and ^{13}C-NMR spectra of **5**, **6** and

 © WILEY-VCH Verlag GmbH, D-69451 Weinheim, 1998 1434−1948/98/1212−1931 $ 17.50+.50/0

Scheme 1

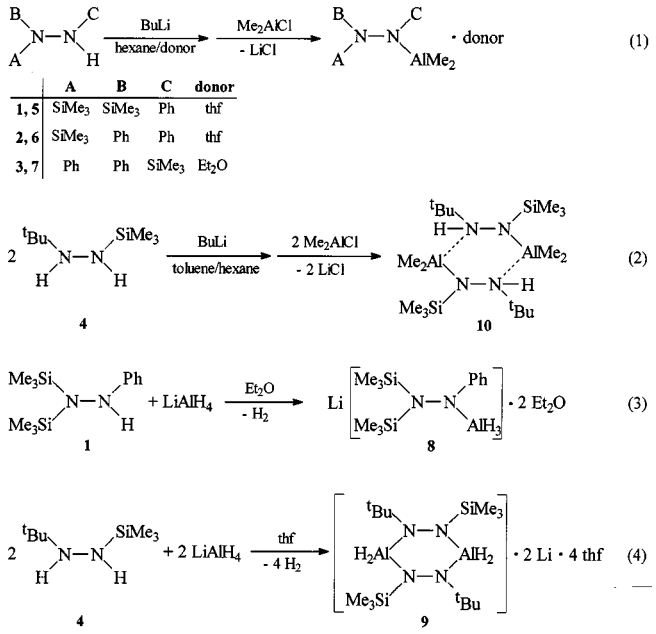

7 show one resonance for the methyl groups residing at the aluminium atom, indicating free rotation about the Al−N bond at room temperature.

For the dimeric compound **10** a ^{27}Al-NMR chemical shift of δ = 141 is observed with a half width of 2200 Hz. The ^{1}H-NMR data at room temperature reveal two resonances for the methyl groups attached to the aluminium center in accordance with its structure in the solid state. In contrast, the ^{13}C-NMR spectrum shows only a single resonance for the $Al(CH_3)_2$ group at room temperature, but at −60°C two resonances for the methyl groups can be detected in the ^{13}C NMR. Because there is no temperature-dependent line broadening, this behavior is thus best interpreted as being due to a coincidentally equal chemical shift at room temperature.

The ^{27}Al-NMR data of **8** and **9** suggest the formation of a tetracoordinated H_3Al- and a H_2Al- species, respectively, by analogy to $[tripAlH_3LiOEt_2]_n$[9] (trip = 2,4,6-*i*$Pr_3C_6H_2-$), $[2,6\text{-}tBu_2C_6H_3OAlH_3Li(OEt_2)_2]_2$ and $(mentO)_2AlH_2Li(THF)_2$[10] (ment = 2-*i*Pr-5-MeC_6H_9-). The ^{27}Al-NMR spectrum of **8** in deuteriobenzene solution consists of a quadruplet at δ = 110 [^{1}J(Al, H) = 178 Hz]. However, the ^{7}Li-NMR resonance shows a half width of 12 Hz and it was not possible to resolve an Li−H coupling in the temperature range of −80°C to room temperature. Until recently, little information had been reported on ^{1}J(Li, H) coupling constants, and we are aware of only two examples, 10.5 Hz for $[(Me_3Si)_2N]_2AlH_2Li(OEt_2)_2$[11a] and 8.4 Hz for [Cp*IrH3Li(pmdta)] (pmdta = pentamethylethylenetriamine)[11b], both smaller than the observed half width for **8**.

The spectrum of **9** shows a ^{27}Al-NMR resonance at δ = 119 with a half width of 1520 Hz. Even at −80°C it was not possible to observe a ^{1}J(Al, H) coupling as for compound **8**. In addition, the ^{7}Li-NMR spectrum shows a broad resonance with a half width of 30 Hz.

Molecular Structures

The Aluminium Hydrazide $Me_2Al(Ph)N-N(SiMe_3)_2 \times THF$ (**5**)

Compound **5** crystallizes in the orthorhombic system, space group $Pna2_1$ with four molecules in the unit cell. Figure 1 depicts the molecular structure.

Figure 1. ORTEP plot of the aluminium hydrazide **5**; hydrogen atoms are omitted for clarity; thermal ellipsoids are drawn at the 25% probability level

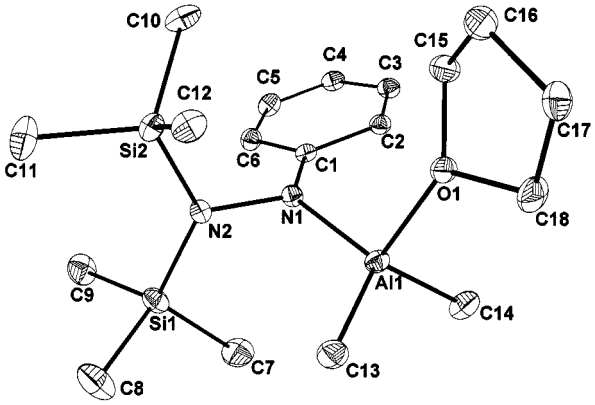

The aluminium atom is tetracoordinated by one oxygen, one nitrogen and two carbon atoms. However, the bond angles reveal a significant distortion from an ideal tetrahedral array as indicated by bond angles N1−Al1−C13 of 115.9(1)°, O1−Al1−C13 of 102.2(1)° and C13−Al1−C14 of 114.7(1)°, respectively. The Al−O distance is larger than the Al−N distance with a difference of 0.063 Å. The sum of bond angles, Σ, at the oxygen atom and the two nitrogen atoms is close to 360° (O1: 357.8°, N1: 358.3°, N2: 360.0°). Therefore, the nitrogen atoms N1 and N2 can be considered as being essentially sp^2-hybridized and this seems also to hold for the oxygen atom. Nevertheless, the latter geometry can also be readily explained in terms of ion-dipole interactions between the metal ion and the THF molecule[12].

While the N−N bond length is 1.469(3) Å, we note that the planes around the nitrogen atoms stand almost orthogonal to one another, as shown by the interplanar angle C1N1Al1/Si1N2Si2 of 85.2°. The phenyl group is twisted against the plane N2N1Al1 by 20.8°. Although the N−N−Si bond angles differ from one another by up to 8.4°, the Si−N bond lengths of 1.742(2) Å and 1.746(2) Å are equal to within the 3σ standard deviation.

The Aluminium Hydrazide $Me_2Al(Ph)N-N(Ph)SiMe_3 \times THF$ (**6**)

Compound **6** crystallizes in the monoclinic system, space group *Cc* with four molecules in the unit cell. The molecular structure is shown in Figure 2.

Its aluminium atom is tetracoordinated by the oxygen atom of one molecule of THF, one nitrogen atom and two

Table 1. Selected bond lengths [Å] and angles [°] of **5**, **6**, **7** and **10**

	5	**6**	**7**	**10**
Al−N	1.869(2)	1.863(3)	1.847(2)	N1: 2.016(2) N2: 1.874(2)
Al−C	C13: 1.960(2) C14: 1.970(2)	C16: 1.955(4) C17: 1.947(8)	C16: 1.975(2) C17: 1.973(3)	C1: 1.982(2) C2: 1.981(2)
N−N	1.468(2)	1.449(3)	1.446(2)	1.486(2)
N−Si	Si1: 1.746(2) Si2: 1.742(2)	1.766(3)	1.746(2)	1.764(2)
Σ N1/N2	358.3/360.0	360.0/360.0	359.6/359.9	323.3/359.9
C−Al−C	114.7(1)	102.1(7)	116.0(1)	106.7(1)
N−N−Al	118.1(1)	114.2(2)	116.1(1)	122.7(1)

Figure 2. The molecular structure of the aluminium hydrazide **6** in ORTEP representation; hydrogen atoms are omitted for clarity; thermal ellipsoids are drawn at the 25% probability level

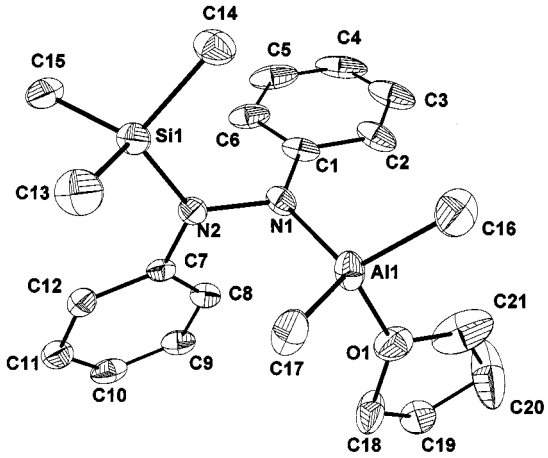

carbon atoms of the methyl groups. The Al−N and Al−O bond lengths of 1.863(3) Å and 1.879(3) Å, respectively, are very similar to each other, in contrast to those in compounds **5** and **7**. Both nitrogen atoms are tricoordinated in a planar environment, the sum of bond angles, Σ, amounting to 360.0° both for N1 and N2. Even the oxygen atom shows a tricoordinate-planar environment.

It is found that the planes around the nitrogen atoms are even closer to perpendicular in comparison with **5**, as demonstrated by the torsion angle C1−N1−N2−C7 of 89.7°. Moreover, the N−N distance of 1.449(3) Å is noticeably shorter than that determined for compound **5**, differing by 0.019 Å. In contrast to **5**, the Si−N bond of 1.766 Å is slightly lengthened (0.020 Å). The phenyl groups are twisted by 3.2° at N1 and 17.4° at N2 with respect to the N2N1Al and N1N2Si plane, respectively, in accordance with the N−C distances of 1.396(4) Å and 1.405(4) Å, indicating N−C π bonding.

The Aluminium Hydrazide $Me_2AlN(SiMe_3)-NPh_2 \times Et_2O$ (**7**)

Compound **7** crystallizes in the triclinic system, space group $P\bar{1}$. There are two independent molecules in the unit cell whose structural parameters differ only insignificantly. Therefore we depict only one of these in Figure 3.

Figure 3. ORTEP plot of the aluminium hydrazide **7**; hydrogen atoms are omitted for clarity; thermal ellipsoids are drawn at the 25% probability level

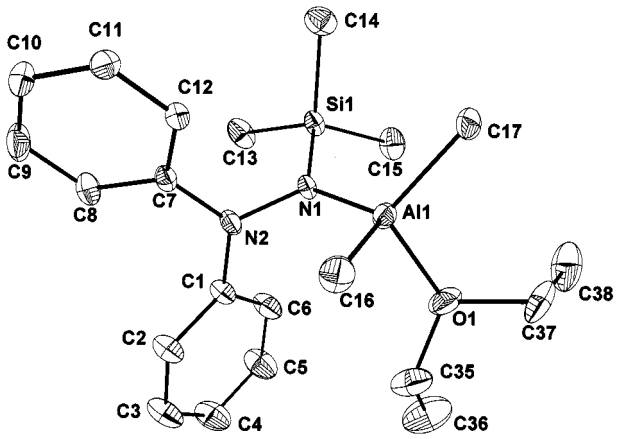

The tetracoordinated aluminium atom shows again a distorted tetrahedral array as described for compound **5**. The geometry at both nitrogen atoms is almost planar with a sum of bond angles, Σ, of 359.6° for N1 and 359.9° for N2. The Al−N distance of 1.847(2) Å in **7** is slightly shorter than in compounds **5** or **6**. The Al−O bond length of 1.928(2) Å is comparable with that in compound **5**, despite the weaker base strength of diethyl ether.

The N−N bond length of 1.446(2) Å corresponds to that found in compound **6**. The planes at the nitrogen atoms Si1N1Al1/C1N2C7 are again close to perpendicular (the interplanar angle is 81.2°) and both phenyl groups are twisted against the plane around N2 by 27.5° and 28.3°, respectively. The Si−N bond length of 1.746 (2) Å is comparable to that in compound **5**.

The Lithium Hydrazino(hydrido)aluminate $LiAlH_3[(Ph)N-N(SiMe_3)_2] \times 2\ Et_2O$ (**8**)

The colorless prisms of **8** belong to the triclinic system, space group $P\bar{1}$. There are two molecules $LiAlH_3[(Ph)N-N(SiMe_3)_2] \times 2\ Et_2O$ in the unit cell which are symmetry-related by a crystallographical inversion center in the midpoint of an $(LiH_2Al)_2$ eight-membered ring as shown in Figure 4. For molecular parameters of compounds **8** and **9** see Table 2.

Thus, two hydrazidoaluminate units are linked by two H−Li−H bridges. The resulting eight-membered ring shows a striking feature: six atoms build up exactly a plane, without significant deviation. Two hydrogen atoms, H1c and H1ca, lie 0.36 Å above and below this plane, respectively.

The aluminium atom is almost tetrahedrally coordinated by three (one terminal and two bridging) hydrogen atoms and one nitrogen atom. The lithium atom is also tetracoordinated by two oxygen atoms and two hydrogen atoms in a slightly distorted tetrahedral array as indicated by the O1−Li1−O2 bond angle of 116.9(3)°. The Al−H bond lengths are 1.50(4) Å for the terminal hydrogen atom and

Figure 4. ORTEP representation of the lithium hydrazino(hydrido)aluminate **8** including selected hydrogen atoms; the ethyl groups of the ether molecules are omitted for clarity; thermal ellipsoids are drawn at the 25% probability level

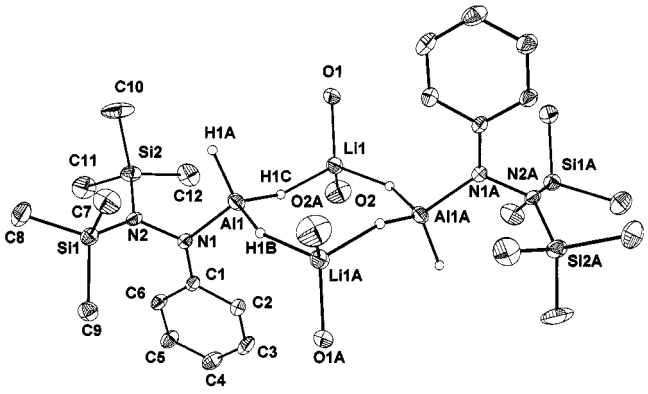

1.58(4) Å and 1.61(4) Å for the bridging hydrogen atoms. The Li−H atom distances of 1.86(4) Å and 1.85(4) Å are longer than those to the aluminium atoms but clearly shorter than in ionic LiH (2.08 Å)[13]. The Al−N bond length of 1.869(3) Å corresponds to that found in the aluminium hydrazide $Me_2Al(Ph)N-N(SiMe_3)_2$ × THF (**5**). The hydrazide unit in **8** shows the same tendencies in bond lengths and angles as described for compound **5**. Both nitrogen atoms are almost sp^2-hybridized with sum of bond angles, Σ, of 359.1° for N1 and 358.3° for N2. Furthermore the planes around the nitrogen atoms are almost perpendicular to one another, as indicated by the torsion angle C1−N1−N2−Si1 of 81.3°. The phenyl group is twisted slightly against the plane around N1 (N2Al1C1) by 11.1°.

Table 2. Selected bond lengths [Å] and angles [°] of **8** and **9**

	8	**9**
Al−N	1.869(3)	N1: 1.843(3)/N3: 1.841(3) N2: 1.871(3)/N4: 1.895(3)
Al−H	1.50(4)−1.61(4)	1.54(3)−1.61(3)
N−N	1.460(4)	N1: 1.508(3)/N3: 1.504(4)
Li−H	1.85(4)−1.86(4)	Li1: 2.09(3)/2.26(4) Li2: 1.89(4)
N−Si	Si1: 1.730(3) Si2: 1.735(3)	Si1: 1.707(3) Si2: 1.705(3)
Σ N1 (N3)	359.1	358.6 (357.6)
Σ N2 (N4)	358.3	356.1 (354.8)

The Lithium Hydrazino(hydrido)aluminate *$LiAlH_2[(tBu)N-N(SiMe_3)]$ × 2 THF* (**9**)

Compound **9** crystallizes in the monoclinic system, space group $P2_1/n$, with four molecules in the unit cell. It should be noted that due to some disorder of the THF molecules the carbon atoms of the THF molecules around Li2 were refined only isotropically.

The most remarkable feature of compound **9**, depicted in Figure 5, are two differently coordinated lithium atoms. Li1 is tricoordinated by the nitrogen atoms of the *t*BuN groups of the $(Al-N-N)_2$ six-membered ring and one oxygen

Figure 5. ORTEP plot of **9** including selected hydrogen atoms; the methyl groups on C4, C11 (*t*Bu); Si1 and Si2 ($SiMe_3$) are omitted for clarity; thermal ellipsoids are drawn at the 25% probability level

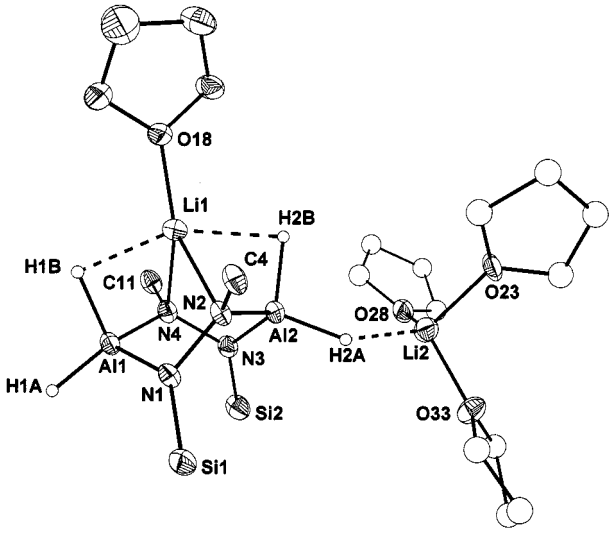

atom of a THF molecule, whereas Li2 is tetracoordinated by three oxygen atoms and one hydrogen atom of an AlH_2 unit.

In addition, Li1 exhibits two close contacts with two hydrogen atoms of the AlH_2 units with distances of 2.09(3) Å (for H1b) and 2.26(4) Å (for H2b). Taking these contacts into account, we arrive at pentacoordination with a distorted trigonal-bipyramidal array with the hydrogen atoms in apical positions. This is an unexpected situation, because usually the most electronegative partners occupy the apices of the trigonal bipyramid. The deviation from the ideal trigonal-bipyramidal array is indicated by the bond angle H1b−Li1−H2b of 153(2)°. It should be noted that the Li1−N distances [2.278(7) Å and 2.213(7) Å] are longer than the Li1−O18 distance [1.920(6) Å] in accordance with the larger effective radius of the nitrogen atoms compared to the oxygen atom.

The aluminium atoms are not bonded symmetrically to the neighboring nitrogen atoms. Due to the electron-releasing properties of the $SiMe_3$ group, the corresponding Al−N bond lengths, Al1−N1 and Al2−N3 are shortened. For example, Al1−N1 and Al1−N4 differ by 0.052 Å. Comparing the sum of bond angles, Σ, at the nitrogen atoms, we found in accordance with the aluminium−nitrogen bond lengths, that the Σ of N1 (358.6°) and N3 (357.6°) are closer to 360° than those of N2 (356.1°) and N4 (354.8°) (neglecting the Li···N interaction), which are slightly pyramidalized. It is particularly noteworthy that the N−N bond lengths of 1.508(3) Å (N1−N2) and 1.504(4) Å (N3−N4) are quite long. One reason for this is certainly the twisted planes around the nitrogen atoms, as indicated by the interplanar angles Al1N1Si1/Al2N2C4 (75.0°) and Al2N3Si2/Al1N4C11 (78.3°), causing a repulsion of the π electrons at the nitrogen atoms. But surely the most significant factor in the elongation of the N−N bond is the four-coordination observed for N2 and N4. Finally, we note comparatively

short N−Si bond lengths of 1.707(3) Å (Si1−N1) and 1.705(3) Å (Si2−N3), respectively.

The Aluminium Hydrazide [$Me_2AlN(SiMe_3)-N(tBu)H]_2$ (**10**)

The solvent-free compound **10** crystallizes in the orthorhombic system, space group *Pbca*, with 8 molecules in the unit cell. The molecular structure is depicted in Figure 6.

Figure 6. ORTEP representation of **10**; hydrogen atoms, except on the nitrogen atoms, are omitted for clarity; thermal ellipsoids are drawn at the 25% probability level

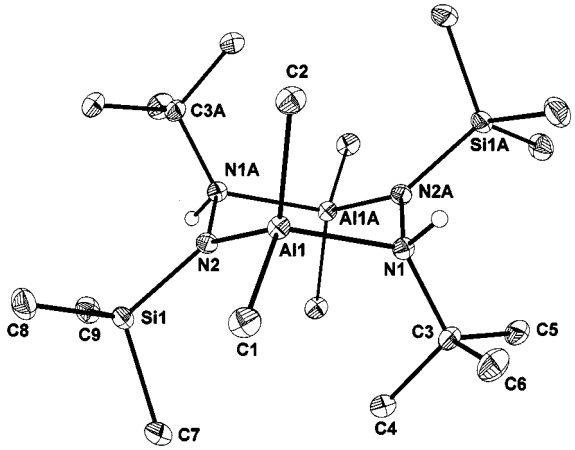

10 forms a centrosymmetric dimer with an $(AlN_2)_2$ six-membered ring in chair conformation with the methyl groups in axial (C2) and equatorial (C1) positions. The aluminium atom is tetracoordinated to carbon atoms of the methyl groups and two nitrogen atoms in a distorted tetrahedral array. The fairly long Al−N1 distance of 2.016(2) Å indicates a coordination of the nitrogen atom N1 across its lone pair of electrons to the aluminium atom. This is supported by the sum of bond angles of N1, neglecting the Al···N1 interaction, of 323.3°, indicating clearly a pyramidal geometry with (*S*) configuration at N1 and (*R*) configuration at its symmetry equivalent, N1A. In contrast to that, the Al−N2 bond length of 1.872(2) Å is comparable to those found in **5**, **6** and **7**. However, N2 shows a trigonal-planar geometry with a sum of bond angles of 359.9°.Due to sp^3 hybridization of N1, the N−N bond length of 1.486(2) Å is slightly lengthened compared to the monomeric ether adducts **5**−**7**.

Discussion

The ether adducts **5**, **6** and **7** are the first structurally characterized monomeric aluminium hydrazides. It should be noted that in all three reported compounds the β-nitrogen atom of the hydrazide unit is not involved in coordination to the aluminium center due to the fact that this nitrogen atom is sterically and electronically less suited for coordination than atom N1. As previously shown for alkali metal hydrazides[1g], oligomerization can be inhibited by suitable donor molecules coordinating to the metal center, thus preventing the formation of additional metal−nitrogen interactions. One reason for this is certainly the planarity at the nitrogen atoms that decreases the basicity of the R_2N group. The Al−N bond lengths of **5**, **6** and **7** are comparable to those in aluminium amides with tetracoordinated aluminium atoms and tricoordinated nitrogen atoms[14]. These bond lengths vary from 1.869(2) Å in **5** to 1.847(2) Å in **7**. Although the weaker donor ability of diethyl ether in contrast to THF is expected to lead to longer Al−O distances, the Al−O bond length of 1.928(2) Å in compound **7** is comparable to that found in **5** [1.932(2) Å]. The reason for the short Al−N bond of **7** may be the higher acidity of the nitrogen atom, due to the neighboring $SiMe_3$ group. This effect is also observed in compound **10**. Therefore, the metallation took place at the silyl-substituted nitrogen atom. The Al−N bond length of 1.874(2) Å is somewhat longer than in the ether adducts **5**, **6** and **7**, but reasonably shorter than the Al−N bond length of 2.016(2) Å of the coordinating nitrogen atom in compound **10**, which compares well to those found in alane amines such as $Me_2ClAl(NHBz_2)$ (Bz = benzyl)[15a] or $Me_3Al(NHBz_2)$[15b]. In contrast to the solvates **5**, **6** and **7**, the β-nitrogen atom of the aluminium hydrazide **10** is also involved in coordination to the aluminium atom. Dimeric **10** forms a six-membered Al_2N_4 ring in chair conformation with the *tert*-butyl groups in axial positions. These results differ from the structural observations recently reported for the dimeric aluminium hydrazide, $[Me_2Al-\mu\text{-}N(H)NMe_2]_2$[5e], which forms an $(AlN)_2$ four-membered ring in a *trans* configuration in the solid state with tetracoordinated aluminium and nitrogen atoms and therefore with fairly long Al−N bond lengths of 1.958(3) Å and 1.953(3) Å. This structural feature is already known for amino alanes, e.g. $[Np_2Al-N(H)Ph]_2$ (Np = Me_3CCH_2-)[16] or $[iBu_2AlNC_6H_{12}]_2$[8].

The structure of the hydrazino(hydrido)aluminate **9** can be readily derived from the aluminium hydrazide **10**. The six-membered ring in chair conformation may be slightly twisted due to the coordination of two facing nitrogen atoms to one lithium center. The two nitrogen atoms are slightly pyramidalized, but the sum of their bond angles (356.1°, 354.8°) is still close to 360°, suggesting an Li···N-p_z interaction which is in accordance with the fairly long Li−N bond lengths of 2.278(7) Å and 2.213(7) Å, respectively. The most striking feature of compound **9** is the fact that this lithium atom faces the ring directly above its center, completing its coordination sphere by one molecule of THF and two additional Li···H contacts, while the lateral lithium atom Li2 is solvated by three THF molecules, contacting the ring via a hydrogen bond. In contrast to **9**, the hydrazino(hydrido)aluminate **8** forms an $(LiHAlH)_2$ eight-membered ring. This characteristic feature was also observed for $[(Me_3Si)_2NAlH_3Li(OEt_2)_2]_2$[11a] and [(2,6-di-*t*Bu)$C_6H_3OAlH_3Li(OEt_2)_2]_2$[10]. The β-nitrogen atom is neither involved in coordination with the aluminium atom nor the lithium atom. The Al−N bond lengths of both compounds, **8** and **9**, ranging from 1.841(3) Å to 1.895(3) Å, are typical for tetracoordinated aluminium and tricoordinated nitrogen atoms and comparable to those found in $[(Me_3Si)_2$-

Table 3. Crystal data and data related to data collection and structure solution

Compound	**5**	**6**	**7**	**8**	**9**	**10**
chem. formula	$C_{18}H_{37}AlN_2OSi_2$	$C_{21}H_{33}AlN_2OSi$	$C_{42}H_{70}Al_2N_4O_2Si_2$	$C_{20}H_{46}AlLiN_2O_2Si_2$	$C_{30}H_{72}Al_2Li_2N_4O_4Si_2$	$C_9H_{25}AlN_2Si$
formula weight	380.66	384.56	773.16	436.69	676.94	216.38
cryst. size [mm]	0.2 × 0.3 × 0.4	0.3 × 0.3 × 0.4	0.1 × 0.2 × 0.3	0.1 × 0.2 × 0.2	0.40 × 0.50 × 0.60	0.2 × 0.3 × 0.3
cryst. system	orthorhombic	monoclinic	triclinic	triclinic	monoclinic	orthorhombic
space group	$Pna2_1$	Cc	$P\bar{1}$	$P\bar{1}$	$P2_1/n$	$Pbca$
a [Å]	13.7263(3)	10.2097(2)	9.21590(10)	10.8302(2)	11.928(2)	12.473(2)
b [Å]	14.0198(3)	13.8731(4)	14.8404(2)	11.645	20.066(4)	13.147(2)
c [Å]	11.9554(1)	16.4523(4)	18.20120(10)	12.3135(2)	18.555(4)	16.295(3)
α [°]	90	90	84.962(1)	89.18(1)	90	90
β [°]	90	93.16(1)	77.664(1)	76.57(1)	105.377(8)	90
γ [°]	90	90	74.633(1)	74.23(1)	90	90
V [Å^3]	2300.70(7)	2326.76(10)	2343.63(4)	1451.69(4)	4282.1(14)	2672.1(8)
Z	4	4	2	2	4	8
ρ (calcd.), [Mg/m^3]	1.099	1.098	1.096	0.999	1.050	1.076
μ [mm^{-1}]	0.200	0.150	0.149	0.167	0.157	0.209
F(000)	832	832	840	480	1488	960
index range	$-15 \le h \le 15$, $-15 \le k \le 15$, $-13 \le l \le 11$	$-11 \le h \le 11$, $-15 \le k \le 11$, $-19 \le l \le 19$	$-10 \le h \le 10$, $-17 \le k \le 17$, $-20 \le l \le 20$	$-12 \le h \le 8$, $-13 \le k \le 13$, $-14 \le l \le 14$	$-13 \le h \le 13$, $-22 \le k \le 22$, $-21 \le l \le 21$	$-14 \le h \le 15$, $-17 \le k \le 16$, $-21 \le l \le 21$
2θ [°]	47.62	48.82	49.42	49.42	47.64	58.70
T [K]	183	183	183	183	193	183
refl. collected	10043	5407	11342	7101	18550	14679
refl. unique	3203	3215	6014	3778	6266	2881
refl. observed (4σ)	3114	3100	5495	3291	4752	2395
R (int.)	0.0264	0.0225	0.0253	0.0303	0.0301	0.0369
no. variables	225	279	503	295	417	130
weighting scheme[a] x/y	0.0300/0.8165	0.0189/2.2622	0.0405/1.1897	0.0219/2.0060	0.0819/7.8740	0.0420/1.4158
GOF	1.083	1.150	1.090	1.145	1.025	1.108
final R (4σ)	0.0278	0.0412	0.0396	0.0608	0.0747	0.0392
final $wR2$	0.0688	0.0959	0.0992	0.1321	0.1814	0.0925
larg. res. peak [e/Å^3]	0.158	0.152	0.270	0.296	0.590	0.288

[a] $w^{-1} = \sigma^2 F_o^2 + (xP)^2 + yP$; $P = (F_o^2 + 2F_c^2)/3$.

$NAlH_3Li(OEt_2)_2]_2$ and $[(Me_3Si)_2N]_2AlH_2Li(OEt_2)_2$[11a]. The average Li−H bond length for **8** is 1.86 Å and is distinctly shorter than in lithium hydride (2.08 Å)[13]. This is also true for Li2 [1.89(4) Å] in compound **9**, but additionally we note two fairly long Li−H contacts of 2.09(3) Å and 2.26(4) Å of the trigonal-bipyramidal-coordinated lithium atom Li1.

Conclusion

The most significant general result derived from the structure determinations of aluminium hydrazides is that the hydrazine units adopt planar geometries in which the lone pairs are orientated orthogonally. Moreover, the aluminium centers prefer OEt_2 or THF as a coordination partner over the NRR′ unit of the hydrazino group. This occurs only when Et_2O or THF is excluded in the preparation.

One can envisage that aluminium hydrazides $Me_2Al-NR-NR'SiMe_3$ and $Me_2Al-NR-N(SiMe_3)_2$ will decompose at higher temperatures with loss of $SiMe_4$, with the formation of oligomeric clusters of the type $[MeAl-NR-NR']_n$ or $[MeAl-NR-N(SiMe_3)]_m$. These may then decompose into AlN at sufficiently high temperatures, as has recently been shown for some gallium organylhydrazides[5i][5h]. This aspect has not yet been investigated nor have we made attempts to prepare tris(hydrazino)alanes $Al(NR-NR'R'')_3$ which may be associated (small R groups) or monomeric (bulky R groups). Provided that the two amino groups of the hydrazino units remain in a perpendicular orientation new structural coordination patterns can be realized.

We thank the *Fonds der Chemischen Industrie* and *Chemetall GmbH* for support of our research. In addition, thanks are due to Dipl.-Chem. *C. Strauhal* and *M. Vosteen* for recording NMR spectra and Mrs. *G. Hanatschek* and Mrs. *E. Kiesewetter* for recording the IR spectra. Last but not least, we thank Mr. *T. Stuehler* for well-conducted experiments.

Experimental Section

General Remarks: All reactions were performed under argon using Schlenk techniques. Solvents were dried by conventional methods ($LiAlH_4$, potassium/benzophenone, P_4O_{10}) and stored under argon. The compounds $PhNH-NH_2$, $Ph_2N-NH_2 \times HCl$, $Ph(H)N-N(H)Ph \times HCl$, *n*-butyllithium, Me_3SiCl, 2 M solution of Me_2AlCl in hexane, Me_3SiCl, C_6D_6 and [D_8]toluene were used as purchased. $Ph(H)N-N(SiMe_3)_2$ (**1**), $Ph(H)N-N(Ph)SiMe_3$ (**2**), $Ph_2N-N(H)SiMe_3$ (**3**) and $H(tBu)N-N(H)SiMe_3$ (**4**)[17] were prepared according to literature methods.

Elemental analyses of the compounds were often unreliable, most likely as a result of the formation of silicon carbide or to their hydrolytic sensibility. In addition, they lose coordinated solvent quite readily. Therefore, the purities were checked by the interpretation of the ^{1}H-NMR signals and the single signal found in the ^{27}Al-NMR spectra.

X-ray Structure Analysis (see Table 3): All crystals had to be handled carefully under argon, preferably in a glove box or in a

closed Schlenk system. Once the selected crystals were covered with oxygen-free perfluoroether oil, they were mounted in a glass capillary or on a glass fibre and transferred to the goniometer head of Siemens P4 diffractometer (Mo-K_α radiation, λ = 0.71063 Å, graphite monochromator) equipped with a CCD detector, and cooled in the cold stream of the Siemens LT2 device. Determination of the unit-cell parameters was performed with the data of reflections collected with a total of 75 frames, taking 15 frames each with ω rotation of 0.3° for five different settings. The axes calculated for the unit cell were checked by recording the reflections in the 100, 010 and 001 planes. The final unit-cell parameters were calculated from the whole set of observed reflections. Data collection was performed in a standard manner with an exposure time of 10 s per frame and a 0.3° difference in φ orientation. Data reduction was performed with the program SAINT[18], and the structure was solved by direct methods or by the sharpened Patterson method as implemented in the SHELXTL system[19]. The SHELX97 program[20] was used for the final refinement. All non-hydrogen atoms were refined anisotropically and hydrogen atoms isotropically in calculated positions as a riding model. Further details of the crystal structure determinations are deposited at the Cambridge Crystallographic Data Centre and may be obtained by quoting the depository numbers CCDC-101834 (**5**), -101835 (**6**), -101836 (**7**), -101837 (**8**), -101838 (**9**), -101839 (**10**), the names of the authors and the journal citation.

Dimethylaluminium N-Phenyl-N′,N′-bis(trimethylsilyl)hydrazide −Tetrahydrofuran (**5**): A solution of *n*BuLi in hexane (7.4 ml, 11.5 mmol) was slowly added dropwise to a stirred solution of $Ph(H)N-N(SiMe_3)_2$ (2.91 g, 11.5 mmol) in tetrahydrofuran (20 ml). The mixture was kept at reflux until butane evolution had ceased. Then one equivalent of a 1 M solution of dimethylaluminium chloride in heptane (11.5 mmol) was slowly added at −69°C. After warming to room temperature, the mixture was stirred for 48 h. The solvent was removed and the residue was dissolved in 20 ml of hexane. After removal of insoluble material (LiCl) by filtration, the filtrate was stored at −20°C. Colorless single crystals which were suitable for an X-ray structure investigation could be isolated after a few days. Yield 3.45 g (79%); m.p. 86°C (dec.). − ^{1}H NMR (C_6D_6, 270 MHz): δ = −0.32 (s, 6 H, $AlMe_2$); 0.34 (s, 18 H, $SiMe_3$); 0.91 (t, 4 H, THF); 3.45 (t, 4 H, THF); 6.73 [t, ^3J(H,H) = 7.1 Hz, 1 H, *p*-Ph]; 7.05 [d, ^3J(H,H) = 8.1 Hz, 2 H, *o*-Ph]; 7.28 [t, ^3J(H,H) = 7.5 Hz, 2 H, *m*-Ph]. − ^{13}C NMR (C_6D_6, 100 MHz) δ = −7.8 ($AlMe_2$); 2.8 ($SiMe_3$); 24.65 (THF); 71.3 (THF); 113.1 (*o*-Ph); 115.1 (*p*-Ph); 128. 8 (*m*-Ph); 157.9 (*i*-Ph). − ^{29}Si NMR (C_6D_6 54 MHz): δ = 7.1. − ^{27}Al NMR (hexane, 70 MHz): δ = 151 ($h_{1/2}$ = 5570 Hz). − $C_{18}H_{37}AlN_2OSi_2$ (380.66): calcd. C 56.79, H 9.82, N 7.36, Al 7.09; found C 53.85, H 9.22, N 6.79, Al 7.12.

Dimethylaluminium N,N′-Diphenyl-N′-trimethylsilylhydrazide−Tetrahydrofuran (**6**): A solution of *n*BuLi in hexane (4.5 ml, 7.1 mmol) was slowly added to a stirred solution of $Ph(H)N-N(Ph)SiMe_3$ (1.83 g, 7.1 mmol) in 40 ml of tetrahydrofuran. The mixture was heated to reflux for 1 h until butane evolution had ceased. After cooling to −69°C, one equivalent of a 1 M solution of dimethylaluminium chloride in heptane (7.1 mmol) was added slowly and the mixture was allowed to attain room temperature and was stirred further for 12 h. The solvent was then removed and the residue dissolved in 50 ml of hexane. After removal of insoluble material (LiCl), the filtrate was stored at −20°C. After 2 weeks, colorless single crystals had separated. Yield 2.16 g (80%); m.p. 97°C. − ^{1}H NMR (C_6D_6, 400 MHz): δ = −0.46 (s, 6 H, $AlMe_2$); 0.42 (s, 9 H, $SiMe_3$); 0.87 (m, 4 H, THF); 3.41 (m, 4 H, THF); 6.74 [t, ^3J(H,H) = 7.2 Hz, 1 H, *p*-Ph]; 6.77 [t, ^3J(H,H) = 7.5 Hz, 1 H, *p*-Ph]; 6.95 [d, ^3J(H,H) = 7.2 Hz, 2 H, *o*-Ph]; 7.02 [d, ^3J(H,H) = 7.5, 2 H, *o*-Ph]; 7.13 [t, ^3J(H,H) = 7.2 Hz, 2 H, *m*-Ph]; 7.22 [t, ^3J(H, H) = 7.5 Hz, 2 H, *m*-Ph]. − ^{13}C NMR (C_6D_6, 100 MHz): δ = 0.5 ($AlMe_2$); 1.5 ($SiMe_3$); 24.7 (THF); 71.6 (THF); 113.1 (*o*-Ph); 115.4 (*o*-Ph); 116.3 (*p*-Ph); 117.9 (*p*-Ph); 128.8 (*m*-Ph); 129.3 (*m*-Ph); 152.1 (*i*-Ph); 156.1 (*i*-Ph). − ^{27}Al NMR (C_6D_6, 104 MHz): δ = 165 ($h_{1/2}$ = 6100 Hz). − ^{29}Si NMR (C_6D_6, 79 MHz): δ = 10.3. − $C_{21}H_{33}AlN_2OSi$ (384.56): calcd. C 65.24, H 9.12, N 7.25, Al 7.02; found C 62.38, H 8.70, N 7.45, Al 7.14.

Dimethylaluminium N′,N′-Diphenyl-N-trimethylsilylhydrazide −Diethyl Ether (**7**): A solution of *n*BuLi in hexane (4.2 ml, 6.6 mmol) was slowly added dropwise to a stirred solution of $(Ph)_2N-N(H)SiMe_3$ (1.67 g, 6.5 mmol) in 40 ml of diethyl ether. The mixture was heated to reflux until butane evolution had ceased. After cooling to −69°C, one equivalent of a 1 M solution of dimethylaluminium chloride in heptane (6.5 mmol) was added slowly. This mixture was allowed to reach room temperature and was stirred for another 12 h. The solvent was removed in vacuo and the residue was treated with 40 ml of hexane. After insoluble material (LiCl) had been removed, the filtrate was kept at −20°C. Four weeks later colorless single crystals were isolated. Yield 1.46 g (56%); m.p. 61°C. − ^{1}H NMR (C_6D_6 400 MHz): δ = −0.45 (s, 6 H, $AlMe_2$); 0.27 (s, 9 H, $SiMe_3$); 0.59 (t, 6 H, Et_2O); 3.25 (q, 4 H, Et_2O); 6.73 [t, ^3J(H,H) = 7.4 Hz, 2 H, *p*-Ph]; 7.11 [t, ^3J(H,H) = 7.4 Hz, 4 H, *m*-Ph]; 7.48 [d, ^3J(H,H) = 7.4 Hz, 4 H, *o*-Ph]. − ^{13}C NMR (C_6D_6, 100 MHz): δ = −0.5 ($AlMe_2$); 2.6 ($SiMe_3$); 1.4 (Et_2O); 66.1 (Et_2O); 119.6 (*o*-Ph); 119.71 (*p*-Ph); 128.6 (*m*-Ph); 150.0 (*i*-Ph). − ^{27}Al NMR (C_6D_6, 104 MHz): δ = 170 ($h_{1/2}$ = 5770 Hz). − ^{29}Si NMR (C_6D_6, 79 MHz): δ = 0.0. − $C_{21}H_{35}AlN_2OSi$ (386.58): calcd. C 65.24, H 9.12, N 7.25, Al 6.98; found C 63.38, H 8.70, N 7.45, Al 6.84.

Lithium Trihydrido[N-phenyl-N′,N′-bis(trimethylsilyl)hydrazino]aluminate−Diethyl Ether(1/2) (**8**): A 1.75 M solution of $LiAlH_4$ in diethyl ether (3.7 ml, 6.5 mmol) was slowly added at −69°C to a stirred solution of $Ph(H)N-N(SiMe_3)_2$ (1.63 g, 6.5 mmol) in 30 ml of diethyl ether. After the mixture had attained room temperature, it was heated to reflux for 1 h. A small amount of insoluble material, which proved to be compound **3**, was filtered off and the filtrate was stored at −20°C. Colorless single crystals of **8** formed within a week. Yield 2.33 g (82%); m.p. 93°C. − ^{1}H NMR (C_6D_6, 270 MHz): δ = 1.99−4.71 (s, br., 3 H, AlH_3); 0.34 (s, 18 H, $SiMe_3$); 0.95 [t, ^3J(H,H) = 7.0 Hz, 12 H, Et_2O]; 3.32 [q, ^3J(H,H) = 7.0 Hz, 8 H, Et_2O]; 6.69 [t, ^3J(H,H) = 7.1 Hz, 1 H, *p*-Ph]; 7.08−7.34 (m, 4 H, *o,m*-Ph). − ^{13}C NMR (C_6D_6, 100 MHz): δ = 2.4 ($SiMe_3$); 14.8 (Et_2O); 65.6 (Et_2O); 112.6 (*o*-Ph); 118.6 (*p*-Ph); 129.1 (*m*-Ph); 158.6 (*i*-Ph). − ^{27}Al NMR (C_6D_6, ^{1}H-decoupled, 70 MHz): δ = 110 ($h_{1/2}$ = 87 Hz). − ^{27}Al NMR (C_6D_6, ^{1}H-coupled, 70 MHz): δ = 110 [q, ^1J(Al,H) = 178 Hz]. − ^{29}Si NMR (C_6D_6, 54 MHz): δ = 6.2. − ^{7}Li NMR (C_6D_6, 105 MHz): δ = 0.40 ($\Delta h_{1/2}$ = 12 Hz). − IR (hostaflon): $\tilde{\nu}$ = 1781 cm^{-1} (vs, br., Al−H). − $C_{20}H_{46}AlLiN_2O_2Si_2$ (436.69): calcd. C 55.00, H 10.63, N 6.42, Al 6.18; found C 52.16, H 9.82, N 6.73, Al 6.28.

Lithium [N′-tert-Butyl-N-trimethylsilylhydrazino](μ-N,N′-dihydrido)aluminate−Tetrahydrofuran (2/4) (**9**): A solution of *t*Bu(H)N−N(H)$SiMe_3$ (1.79 g, 11.2 mmol) in 20 ml of THF was slowly added to a stirred 1.58 M solution of $LiAlH_4$ in THF (7.08 ml, 11.2 mmol). Stirring was continued at 50°C for 4 h. A small amount of insoluble material was removed by filtration, and the filtrate was then kept at −20°C. After 5 d, colorless crystals had formed, which were not suitable for an X-ray structure investigation. Recrystallization from diethyl ether provided single crystals of **9**. Yield 1.97 g (52%); m.p. 83°C (dec.). − ^{1}H NMR ([D$_8$]tol-

uene, 400 MHz): δ = 0.54 (s, 18 H, $SiMe_3$); 1.43 (m, 16 H, THF); 1.61 (s, 18 H, *t*Bu); 3.58 (m, 16 H, THF). – ^{13}C NMR ([D_8]toluene, 100 MHz): δ = 5.1 ($SiMe_3$); 25.7 (THF); 32.2 (*t*Bu); 56.9 (*t*Bu); 68.4 (THF). – ^{27}Al NMR ([D_8]toluene, 104 MHz): δ = 119 ($h_{1/2}$ = 1520 Hz). – ^{29}Si NMR (THF, 54 MHz): δ = −2.0. – ^{7}Li NMR ([D_8]toluene, 155 MHz): δ = 0.35 ($h_{1/2}$ = 30 Hz). – IR (hostaflon): $\tilde{\nu}$ = 1723 cm^{-1} (s, br., Al−H), 1652 (m, br., Al−H). – $C_{15}H_{36}AlLiN_2O_2Si$ (338.47): calcd. C 53.22, H 10.74, N 8.28, Al 7.97; found C 47.55, H 9.33, N 7.20, Al 7.91.

Dimethylaluminium N-tert-Butyl-N′-(trimethylsilyl)hydrazide (**10**): A solution of *n*BuLi in hexane (6.4 ml, 10.0 mmol) was slowly added to a stirred solution of *t*Bu(H)N−N(H)$SiMe_3$ in 50 ml of toluene. The mixture was heated to reflux for 1 h until the butane evolution had ceased. After cooling to −50°C, one equivalent of a 1 M solution of dimethylaluminium chloride in heptane (10.0 mmol) was slowly added. Work up by analogy to **9**. Colorless single crystals of **10** were isolated after a week. Yield 1.58 g (73%), m.p. 126°C. – ^{1}H NMR (C_6D_6, 25°C, 400 MHz): δ = −0.33 (s, 3 H, AlMe); −0.24 (s, 3 H, AlMe); 0.26 (s, 9 H, $SiMe_3$); 1.13 (s, 9 H, *t*Bu); 4.04 (s, br., 1 H, NH). – ^{1}H NMR (C_6D_6, 80°C): δ = −0.35 (s, br., 6 H, $AlMe_3$). – ^{13}C NMR (C_6D_6, 25°C, 100 MHz): δ = 1.4 ($AlMe_2$); 3.8 ($SiMe_3$); 28.4 (*t*Bu); 59.7 (*t*Bu). – ^{13}C NMR ([D_8]toluene, −60°C, 100 MHz): δ = 1.2 ($AlMe_2$); 1.6 ($AlMe_2$). – ^{29}Si NMR (C_6D_6, 54 MHz): δ = 15.2. – ^{27}Al NMR (C_6D_6, 104 MHz): δ = 141 ($h_{1/2}$ = 2200 Hz). – IR (Nujol, Hostaflon): $\tilde{\nu}$ = 3246 cm^{-1} (s, N−H), 1380, 1365 (s, *t*Bu). – $C_9H_{25}AlN_2Si_2$ (216.38): calcd. C 49.95, H 11.65, N 12.95, Al 12.47; found C 46.33, H 10.38, N 11.67, Al 12.35.

☆ Dedicated to Prof. Dr. *W. Simson* on the occasion of his 60th birthday.

[1] [1a] U. Klingebiel, S. Dielkus, E. Drost, R. Herbst-Irmer, *Angew. Chem.* **1993**, *105*, 1689−1690; *Angew. Chem. Int. Ed. Engl.* **1993**, *32*, 1625. – [1b] C. Drost, C. Jäger, S. Freitag, U. Klingebiel, M. Noltemeyer, G. M. Sheldrick, *Chem. Ber.* **1994**, *127*, 845−947. – [1c] N. Metzler, H. Nöth, H. Sachdev, *Angew. Chem.* **1994**, *196*, 1837−1839; *Angew. Chem. Int. Ed. Engl.* **1994**, *33*, 1746−1748. – [1d] K. Bode, U. Klingebiel, M. Noltemeyer, H. Witte-Abel, *Z. Anorg. Allg. Chem.* **1995**, *621*, 500−505. – [1e] H. Nöth, H. Sachdev, M. Schmidt, H. Schwenk, *Chem. Ber.* **1995**, *128*, 105−113. – [1f] B. Gemünd, H. Nöth, H. Sachdev, M. Schmidt, *Chem. Ber.* **1996**, *129*, 1335−1344. – [1g] J. Knizek, I. Krossing, H. Nöth, H. Schwenk, T. Seifert, *Chem. Ber.* **1997**, *130*, 1053−1062.

[2] [2a] R. E. Mulvey, *Chem. Soc. Rev.* **1991**, *20*, 167−209. – [2b] C. Schade, P. von Ragué Schleyer, *Adv. Organomet. Chem.* **1987**, *27*,169−209. – [2c] P. Gregory, P. von Ragué Schleyer, R. Snaith, *Adv. Inorg. Chem.* **1991**, *37*, 48−142.

[3] G. M. Mc Laughlin. G. A. Sim, J. D. Smith, *J. Chem. Soc., Dalton Trans.* **1972**, 2197−2203.

[4] M. Veith, *Chem. Rev.* **1990**, *90*, 3−16.

[5] [5a] H. Hommer, H. Nöth, H. Sachdev, M. Schmidt, H. Schwenk, *Chem. Ber.* **1995**, *128*, 1187−1194. – [5b] J. C. Huffman, H. Fußstetter, H. Nöth, R. Schaeffer, *Z. Naturforsch. B* **1976**, *31*, 289−293. – [5c] P. C. Bharara, H. Nöth, *Z. Naturforsch. B* **1979**, *34*, 1352−1356. – [5d] D. C. Pestana, P. P. Power, *Inorg. Chem.* **1991**, *30*, 528−535. – [5e] Y. Kim, J. H. Kim, J. E. Park, J. T. Park, H. Song, *J. Organomet. Chem.* **1997**, *545−546*, 99−103. – [5f] R. J. Wehmschulte, P. P. Power, *Inorg. Chem.* **1996**, *35*, 2717−2718. – [5g] N. R. Fetter, B. Bartocha, *Can. J. Chem.* **1961**, *39*, 2001−2008. – [5h] D. A. Neumayer, A. H. Cowley, A. Decken, R. A. Jones, V. Lakhotia, J. G. Ekherdt, *Inorg. Chem.* **1995**, *34*, 4698−4700. – [5i] D. W. Peters, M. P. Power, E. D. Bourret, J. Arnold, *J. Chem. Soc., Chem. Commun.* **1998**, *7*, 753−754.

[6] M. Becke-Goehring, H. Krill, *Chem. Ber.* **1961**, *94*, 1059−1063.

[7] J. Mason, *Multinuclear NMR*, Plenum Press, New York and London, **1987**, 259−278.

[8] C. B. Lagrone, S. J. Schauer, C. J. Thomas, G. M. Gray, C. L. Watkins, L. K. Krannich, *Organometallics* **1996**, *15*, 2458−2464.

[9] R. J. Wehmschulte, W. J. Grigsby, B. Schiemenz, R. A. Bartlett, P. P. Power, *Inorg. Chem.* **1996**, *35*, 6694−6702.

[10] J. Knizek, I. Krossing, H. Nöth, W. Ponikwar, A. Schlegel, T. Seifert, *Chem. Eur. J.*, accepted.

[11] [11a] A. Heine, D. Stalke, *Angew. Chem.* **1992**, *104*, 941−942; *Angew. Chem. Int. Ed. Engl.* **1992**, 31, 854. – [11b] T. M. Gilbert, R. G. Bergmann, *J. Am. Chem. Soc.* **1985**, *107*, 6391−6393.

[12] D. Barr, W. Clegg, L. Cowton, L. Horsburgh, F. McKenzie, R. E. Mulvey, *J. Chem. Soc., Chem. Commun.* **1995**, 891−892.

[13] E. Wiberg, E. Amberger, *Hydrides of the Elements of Main Groups I−IV*, Elsevier Publishing Company, Amsterdam, London, New York, **1971**.

[14] M. F. Lappert, P. P. Power, A. R. Sanger, R. C. Srivastava, *Metall and Metalloid Amides, Synthesis, Structures, Physical and Chemical Properties*, Ellis Horwood Publishers, New York, **1980**, p. 99−114 and 191−200.

[15] [15a] F. J. Craig, A. R. Kennedy, R. E. Mulvey, *Acta Cryst.* **1998**, *C54*, 335−337. – [15b] D. R. Armstrong, F. J. Craig, A. R. Kennedy, R. E: Mulvey, *Chem. Ber.* **1996**, *129*, 1293−1300. – [15c] A. J. Downs, D. Duckworth, J. C. Machell, C. R. Pulham, *Polyhedron* **1992**, *11*, 1295−1304. – [15d] R. J. Wehmschulte, P. P. Power, *Inorg. Chem.* **1998**, *37*, 2106−2109.

[16] M. D. B. Dillingham, S. J. Schauer, J. Byers-Hill, W. H. Pennington, G. H. Robinson, *J. Coord. Chem.* **1994**, *31*, 283−295.

[17] D. Klamann, *Methoden Org. Chem. (Houben-Weyl) 4th ed.* **1990**, vol. E16a, part 1, p. 804.

[18] Siemens Industrial Automation, **1995**.

[19] *PC SHELXTL, Rel. 5.03, Vers. 4.1*, Siemens Analytical Instruments, **1994**.

[20] G. M. Sheldrick, University of Göttingen, **1997**.

[I98185]

A Pulse Radiolysis Study of an Imidazolato-Bridged Asymmetric Dicopper(II) Complex: A Structural and Functional Mimic of Superoxide Dismutase

Giovanni Tabbì[a], Thomas Nauser[b], Willem H. Koppenol*[b], and Jan Reedijk[c]

Dipartimento di Scienze Chimiche, Università di Catania[a],
V. le A. Doria 6, I-95125 Catania, Italy

Laboratorium für Anorganische Chemie, ETH-Zentrum[b],
Universitätstrasse 6, CH-8092 Zürich, Switzerland
Fax: (internat.) + 41-1/632-1090,
E-mail: koppenol@inorg.chem.ethz.ch

Leiden Institute of Chemistry, Gorlaeus Laboratories, Leiden University,[c]
P. O. Box 9502, NL-2300 RA Leiden, The Netherlands

Received April 21, 1998

Keywords: Superoxide dismutase mimic / Pulse radiolysis / Imidazolato-bridged dicopper(II) complex / Copper / Radicals

The ability of a dicopper(II) complex with a pentadentate, imidazolato-bridged ligand having two different coordination environments to mimic the reactivity of superoxide dismutase has been investigated by pulse radiolysis. Pseudo first-order kinetics were observed for superoxide scavenging, with a very high rate constant of $1.9 \pm 0.4 \times 10^9$ M^{-1} s^{-1}, consistent with catalytic dismutation of superoxide by the complex. This value is essentially constant over the pH range of 5 to 7, and agrees with earlier results obtained with the nitroblue tetrazolium assay.

The superoxide anion radical ($O_2^{\bullet -}$) may be involved in deleterious biological processes, such as lipid peroxidation,[1] aging,[2] and cancer.[3] This anion radical is very efficiently scavenged by the enzyme superoxide dismutase which catalyses the dismutation of superoxide to dioxygen and hydrogen peroxide.[4] The rate constants for reduction and reoxidation of the copper ion of Cu,Zn superoxide dismutase are known:[5] $k_1 = k_2 = 2.4 \cdot 10^9$ $M^{-1}s^{-1}$. These rate constants indicate that the reactions are nearly diffusion-controlled.[6]

An alternative pathway for reoxidation of copper(I) involves the reaction with the hydrogen peroxide product of the dismutation reaction, with formation of a copper−peroxo complex (Eq. 1)[7][8] which could react directly,[8] or decompose to form the hydroxyl radical[8][9] which in turn would react with the surrounding ligand or biomolecule.[10] The formation of an oxidizing copper(III) species is also possible since four-nitrogen ligands in a square-planar coordination would stabilize copper(III). Theoretical considerations[11] and experimental results[10][12] indicate that the occurrence of a copper(III) oxide(1+) species can be excluded.

$$Cu^{I} + H_2O_2 \rightarrow CuH_2O_2^{+} \quad (1)$$

A relative measure of superoxide dismutase activity can easily be obtained from indirect assays in which a very small and stationary amount of superoxide is generated usually by the action of xanthine oxidase on xanthine, and a detector molecule such as nitroblue tetrazolium[13] or cytochrome *c*[14] is used to follow the reaction kinetics spectrophotometrically. In these assays, the rate of reduction of the detector molecule by superoxide is measured, and the reactivity of superoxide dismutase or of superoxide dismutase mimics is inferred from the rate decrease in the presence of these species. This approach cannot provide absolute rate data, since the superoxide dismutation reaction itself is too rapid to be followed directly, and hence no mechanistic information about the reaction can be obtained. Pulse radiolysis is a superior method to investigate superoxide dismutation as one can selectively and at will generate superoxide and hydrogen dioxide in the absence of extraneous and interfering enzyme systems and reporter molecules, and one can make measurements in the microsecond time scale.

Amino acid sequences[15][16] and structures[17][18][19][20] of various Cu,Zn superoxide dismutases are known. The active site is composed of an imidazolato-bridged dinuclear center containing copper(II) and zinc(II). The coordination geometry is distorted square-pyramidal for copper(II) and distorted tetrahedral for zinc(II). For many years efforts have been made to obtain model compounds that show structural, spectroscopic, and catalytic properties similar to that of the active site in Cu,Zn superoxide dismutase.[21][22][23][24][25][26][27][28][29] However, many of the superoxide dismutase mimics prepared to date are unstable in aqueous solution. Further, results obtained with complexes that have been studied in aqueous solution are weakened by the possibility that the observed catalysis is actually carried out by free copper.

 © WILEY-VCH Verlag GmbH, D-69451 Weinheim, 1998 1434−1948/98/1212−1939 $ 17.50+.50/0

In the present work, the pulse radiolysis technique was used to measure the superoxide dismutase activity of an imidazolato-bridged dicopper(II) complex, 1,5-bis(1-pyrazolyl)-3-[bis(2-imidazolyl)methyl]-3-azapentane ($[Cu_2L]^{3+}$, Figure 1) which has a coordination geometry strikingly similar to that of the active site of native Cu,Zn superoxide dismutase.[30]

Figure 1. Structure of $[Cu_2(L)Cl_3]$ showing the imidazolate bridge

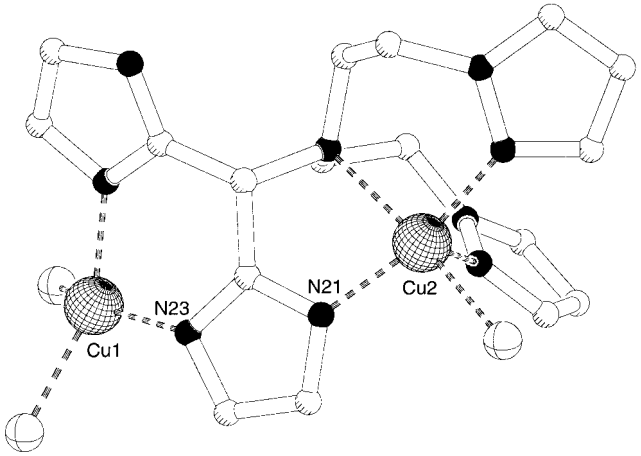

Dismutation of superoxide leads to formation of dioxygen and hydrogen peroxide; interaction of the latter with the $Cu^{I}Cu^{II}$ or $Cu^{I}Cu^{I}$ complex would produce the hydroxyl radical. For this reason the interaction of this radical with the complex was also briefly investigated.

Results

Superoxide Dismutation Experiments

In Figure 2 a typical decay of the superoxide absorbance as a function of time is shown. Depending on the concentration of copper complex and the presence or absence of phosphate buffer, different rate constants were obtained, see Table 1. The dose-dependent amount of acid produced during the irradiation leads to a proton concentration of approximately 10^{-5} M. The change in pH results in partial protonation of superoxide ($pK_a = 4.7$), therefore reactions of the hydrogen dioxide radical were taken into consideration. The pH under the different experimental conditions was evaluated by calculating the ratio $[HO_2^{\bullet}]/[O_2^{\bullet-}]$ from the maximum absorbance after the pulse. A correction of smaller than 10% in the rate of dicopper(II) complex dependent dismutation was required on the basis of the rate of dismutation of superoxide in the absence of complex.

The rate constant for dismutation of superoxide by aqueous copper species increases with pH. Values for the rate constant obtained by statistical treatment of the steady-state rate constant, $k_{ss,O_2^{\bullet-}}$, are shown in Table 1. At pH = 7, $k_{ss,O_2^{\bullet-}}$ is $(1.9 \pm 0.4) \times 10^9$ $M^{-1}s^{-1}$. Values for $k_{ss,HO_2^{\bullet}}$ for the unbuffered solutions were calculated on the basis of equation 15 (see Experimental Section − Methods), with the help of $k_{ss,O_2^{\bullet-}}$ determined in buffered solutions.

Figure 2. Experiment and fit (heavy line) for unbuffered solution at 22°C with a dose of 88 Gy, $[Cu_2L]^{3+} = 4$ mM, optical pass length of 2 cm, observed at 280 nm; the residual absorption from the fit is also given(lower noisy trace); from the least-square fits it is evident that a second-order fit is systematically wrong

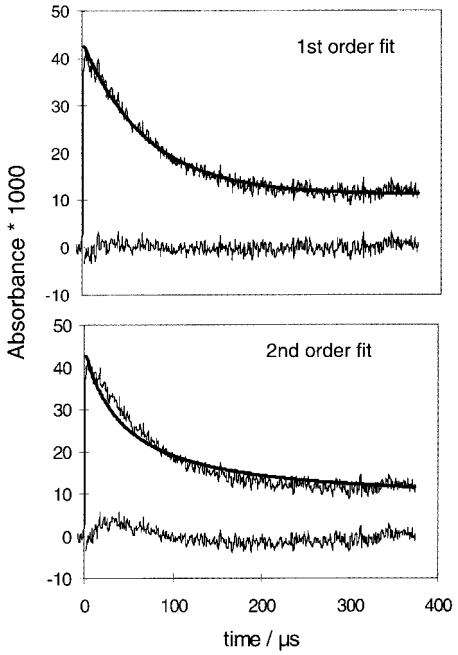

Figure 3. Comparison of the extinction coefficients of $[Cu_2L]^{3+}$ at concentrations of 5 µM and 0.5 mM

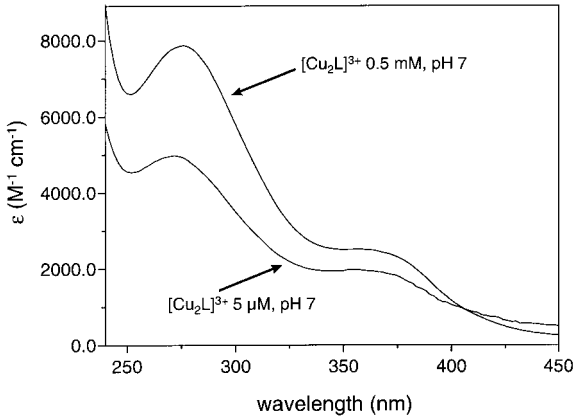

The speciation of copper in solutions of the copper−imidazolato complex is not straightforward. The integrity of the dicopper(II) complex was evaluated from the UV/Vis spectrum of a 5 µM solution. On the basis of the absorbance at 375 nm, corresponding to the absorbance maximum of the Cu−Im−Cu chromophore,[30] it was calculated that ca. 80% of the dicopper(II) complex retained the original structure (Figure 3).

We performed a control experiment in which we dermined the catalytic activity of copper ion in a solution that did not contain the imidazole ligand, but was otherwise identical, and found a $k_{ss,O_2^{\bullet-}}$ of $(1.6 \pm 0.2) \times 10^9$ M^{-1} s^{-1}.

No transient spectrum attributable to formation of a copper(II)−superoxide complex was observed. A residual ab-

Table 1. Statistical summary[a] of k_{ss} for $[Cu_2L]^{3+}$

$[Cu^{2+}]$ [μM]	pH after pulse	$[O_2^{\bullet -}]_{tot}$ [μM]	$k_{ss,O_2^{\bullet -}obs}$ [$M^{-1}s^{-1}$]	$k_{ss,HO_2^{\bullet}}$ [$M^{-1}s^{-1}$]
2	4.4 ± 0.3	49 ± 4	(3.9 ± 0.4) × 10^9	(4.5 ± 0.6) × 10^9
2	6.83 ± 0.05	3.7 ± 0.8	(3 ± 1) × 10^9	–
4	5.3 ± 0.1	48 ± 2	(2.8 ± 0.2) × 10^9	(6 ± 1) × 10^9
1	7.3[b]	51 ± 4	(1.9 ± 0.4) × 10^9	–
1[c]	7.3[b]	51 + 4	(1.6 ± 0.2) ×10^9	

[a] 99% Confidence range. – [b] Phosphate buffer 75 mM, pH = 7.3. – [c] Control experiment: no complexing agent present.

sorbance that decayed over 0.8 ms was always observed in the experiments with 4 μM complex, possibly due to the presence of partially reduced copper complex in the steady state.

Hydroxyl Radical Experiments

The absorbance decay under conditions of $[Cu_2L]^{3+} >> [HO^{\bullet}]$ follows a pseudo first-order kinetics: a rate constant of 1.7 ± 0.3 × 10^{10} $M^{-1}s^{-1}$ was found. The absorbance decay of the radical species formed was fitted to an apparent second-order reaction with a rate constant of $k/\Delta\varepsilon$ of (1.3 ± 0.4) × 10^7 $cm^{-1}s^{-1}$. It should, however, be noted that the structure of any putative radical product(s) has not been determined, that many reaction mechanisms are possible, and that it is impossible to report the exact kinetic order at this stage.

Discussion

As discussed by Costanzo et al.,[31] studies which report catalytic rate constants of copper complexes regrettably hardly ever address the issue of speciation. Sometimes not even the ratio of ligand to metal is stated. This raises the suspicion that the reported catalytic activity was due to free copper, rather than the complex. In our experiments spectrophotometric measurements show that ca. 20% of the complex is hydrolysed. Since the copper(I + II) aquo complex reacts with superoxide with a catalytic rate constant of $k_{ss,O_2^{\bullet -}} = 9 \times 10^9$ $M^{-1}s^{-1}$,[32][33][34][35] it was appropriate to consider whether the observed activity is due to undefined complexes of copper in various oxidation states with water and solutes.

The catalytic activity of the hydrolysed copper was determined in control experiments lacking the imidazolato-containing ligand. The activity measured here equals that of solutions in which the complex had hydrolysed completely and in which the copper was bound to formate, phosphate, hydroxide, etc. Had the measured catalytic activity of 1.9 × 10^9 $M^{-1}s^{-1}$ been due to such copper complexes, and not to the imidazolato-bridged complex, then the catalytic rate constant would have been 5 times higher, namely 9 × 10^9 $M^{-1}s^{-1}$. If the activity of the copper complex had been found to be clearly lower than that for the control solution, it would not have been possible to ascribe the activity to the complex with certainty.

The decay of superoxide is first order, indicating steady-state kinetics. In phosphate-buffered solution the influence of the hydrogen dioxide radical is negligible, and the steady-state rate constant found for $k_{ss,O_2^{\bullet -}} = 1.9 \pm 0.4 \times 10^9$ $M^{-1}s^{-1}$. The rate, determined here by pulse radiolysis, is in good agreement with that determined by the indirect assay[30] and comparable to that of Cu,Zn superoxide dismutase. This may represent the first unequivocal demonstration of superoxide dismutase mimicry by a low molecular weight copper complex.

At lower pH, where $HO_2^{\bullet}$ is present at 16–90% and the contribution of $k_{ss,HO_2^{\bullet}}$ to the overall observed rate constant is strong, the observed rate constants are higher than those obtained in buffered solution. The lowest single determination of $k_{ss,HO_2^{\bullet}}$ was 3.9 × 10^9 $M^{-1}s^{-1}$, indicating that the dicopper(II) complex is also extremely active in the conversion of hydrogen dioxide.

The absence of a transient spectrum due to a copper(II)–superoxide adduct is understood when one takes into account that the superoxide radical can undergo fast outer-sphere electron-transfer reactions. This interpretation is supported by the exceptionally high rate constants; inner-sphere reactions of copper(II) are expected to be at least one order of magnitude lower.[36] An alternative explanation is that the transient spectrum of the hypothetical adduct has an absorbance too low to be observed.

We cannot exclude an interaction of either the dicopper(II) [= copper(I)–copper(I)] or the copper(II)–copper(I) complex with hydrogen peroxide released after the catalyzed dismutation of superoxide anion. Such an interaction would lead to a degradation of the ligand, probably through the generation of the hydroxyl radical. Thus, the rate of reaction of the hydroxyl radical with the dicopper(II) complex was evaluated. The reaction is apparently pseudo first-order with a rate constant of 1.7 ± 0.3 × 10^{10} $M^{-1}s^{-1}$, which is about one order of magnitude higher than corresponding rate constants of free imidazole and bis(2-imidazolyl)methane.[33][37]

This work was supported by the *EU HCM* project ERBCHRXCT920014 and the *ETH Zürich*. Partial support was also provided by the *CNR* (Rome). The manuscript was edited by Dr. *P.L. Bounds*.

Experimental Section

Methods

General: The pulse radiolysis setup with a Febetron 705 2-MeV accelerator (Hewlett-Packard) has been described before.[12][32] All experiments were carried out at room temperature (20−22°C) with an effective 50-ns irradiation pulse and a 2-cm optical path length in a quartz cell. Solutions were prepared from triply distilled water. Uncertainties for rate constants are expressed at the 99% confidence limit.

The conditions for the experiments were carefully chosen: a) the concentration of phosphate was set at 75 μM to buffer the solution at pH = 7 to maximize the concentration of the imidazolato-bridged dicopper(II) complex, since at pH < 6.8 the bridging may be compromised to some extent and at pH > 8.0 hydrolytic species are formed,[30] and to minimize formation of hydrogen dioxide radicals; and b) the concentration of formate was set at 100 μM to maximize the yield of superoxide and to minimize the formation of the copper-formate complexes. Phosphate concentrations were kept at the minimum necessary to maintain the desired pH as phosphate can dramatically influence the rate of reaction of superoxide with copper-containing catalysts.[32] An excess of phosphate can shift the equilibria towards the formation of copper(II) phosphate. The influence of phosphate in experiments with buffered solutions was evaluated by comparison with experiments performed with unbuffered solutions.

Superoxide Experiments: The dicopper(II) complex was dissolved in 100 mM sodium formate (Merck puriss p.a.) and adjusted to pH = 7.3 with sodium hydroxide. Three groups of solutions were prepared: unbuffered solutions having total copper concentrations of 2 and 4 μM, and a buffered solution (75 μM phosphate, pH = 7.3) with 1 μM copper. Solutions were saturated with oxygen (> 99.5%, Pan Gas) for approximately 20 min. A dose of 75−100 Gy was applied to generate superoxide (44−60 μM) in excess over the dicopper(II) complex. Under these conditions a steady state is achieved and the decay of superoxide follows a pseudo first-order kinetics, because the concentrations of reduced and oxidized forms of copper in the complex are constant.

Irradiation of oxygen-saturated solutions containing formate generates primary radicals which are converted to superoxide within 2 μs of the end of the pulse;[38] the corresponding change in absorbance was followed at different wavelengths ranging from 245 to 295 nm. The total concentration of superoxide and hydrogen dioxide was calculated from the dose. The pH after the pulse was calculated from the published pK_a and extinction coefficients.[39]

Hydroxyl Radical Experiments: Solutions of the dicopper(II) complex at concentrations of 20.7 or 81 μM prepared in water adjusted to pH = 7.3 with sodium hydroxide were saturated with N_2O (> 99.5%, Pan Gas) for approximately 20 min. The more dilute solution was used to follow the absorbance decay at different wavelengths, following radiation doses of about 100 Gy ([HO•] = 60 μM). The kinetics of the reaction was followed at 300 and 350 nm with the 81 μM solution of complex and an irradiation dose of about 20 Gy ([HO•] = 12 μM).

Kinetics: Superoxide dismutation catalyzed by copper aquo complexes is pH-dependent and faster for superoxide than for hydrogen dioxide.

$$Cu^{2+}(aq) + O_2^{\bullet -} \rightarrow Cu^{+}(aq) + O_2 \quad (2)$$

$$Cu^{+}(aq) + O_2^{\bullet -} + 2\,H^{+} \rightarrow Cu^{2+}(aq) + H_2O_2 \quad (3)$$

$$Cu^{2+}(aq) + HO_2^{\bullet} \rightarrow Cu^{+}(aq) + O_2 + H^{+} \quad (4)$$

$$Cu^{+}(aq) + HO_2^{\bullet} + H^{+} \rightarrow Cu^{2+}(aq) + H_2O_2 \quad (5)$$

If superoxide radicals are in large excess, the steady-state condition for $Cu^{2+}(aq)$ is obtained where

$$k_{ss} = (2\,k_2k_3)/(k_2 + k_3) = 8.7\cdot 10^9\ \text{M}^{-1}\text{s}^{-1}\ [32] \quad (6)$$

which is ca. four times higher than k_{ss} of Cu/Zn superoxide dismutase. Hydrogen dioxide radicals react with aqueous copper much more slowly:

$$k_{ss} = (2\,k_4k_5)/(k_4 + k_5) = 1.6\cdot 10^8\ \text{M}^{-1}\text{s}^{-1}\ [32] \quad (7)$$

In the case of the dicopper(II) imidazolato complex investigated here we investigated only the overall (i.e. steady-state) reaction rate as is commonly reported for superoxide dismutases. Microscopically, several reactions may be involved (formulated for deprotonated species only):

$$[Cu^{II}Cu^{II}L]^{3+} + O_2^{\bullet -} \rightarrow [Cu^{I}Cu^{II}L]^{2+} + O_2 \quad (8)$$

$$[Cu^{I}Cu^{II}L]^{2+} + O_2^{\bullet -} \rightarrow [Cu^{I}Cu^{I}L]^{+} + O_2 \quad (9)$$

$$[Cu^{I}Cu^{I}L]^{+} + O_2^{\bullet -} + 2H^{+} \rightarrow [Cu^{I}Cu^{II}L]^{2+} + H_2O_2 \quad (10)$$

$$[Cu^{I}Cu^{II}L]^{2+} + O_2^{\bullet -} + 2H^{+} \rightarrow [Cu^{II}Cu^{II}L]^{3+} + H_2O_2 \quad (11)$$

the sum of which is:

$$4\,O_2^{\bullet -} + 4\,H^{+} \rightarrow 2O_2 + 2\,H_2O_2 \quad (12)$$

with a steady-state rate law of:

$$d[O_2^{\bullet -}]/dt = k_{ss,O_2^{\bullet -}}\,[Cu_2L][O_2^{\bullet -}],\ k_{ss,O_2^{\bullet -}} = (1.9 \pm 0.4)\times 10^9\ \text{M}^{-1}\text{s}^{-1} \quad (13)$$

$$d[HO_2^{\bullet}]/dt = k_{ss,HO_2^{\bullet}}\,[Cu_2L][HO_2^{\bullet}],\ k_{ss,HO_2^{\bullet}} > 3\times 10^9\ \text{M}^{-1}\text{s}^{-1} \quad (14)$$

Under conditions where superoxide/hydroperoxyl radical is present in great excess (15- to 60-fold) over the dicopper complex, the steady-state condition is reached where the kinetics obey a pseudo first-order rate law.

Near pH = 4.7, the pK_a of hydrogen dioxide, both Eq. 13 and 14 must be considered. The apparent rate constant k'_{ss} is

$$k'_{ss} = 1/(1+\beta)\times k_{ss,HO2} + 1/(1+\beta)\times k_{ss,O2^-} \quad (15)$$

where

$$\beta = [O_2^{\bullet -}]/[HO_2^{\bullet}] = 10^{(\text{pH} - \text{p}K\text{HO2})}$$

and at pH = 4.7 reduces to

$$k'_{ss} = 0.5\times k_{ss,HO_2} + 0.5\times k_{ss,O_2^-} \quad (16)$$

[1] T. C. Pederson, S. D. Aust, *Biochem. Biophys. Res. Commun.* **1973**, *52*, 1071−1078.
[2] K. J. Farmer, R. S. Sohal, *Free Radical Biol. Med.* **1989**, *7*, 23−29.
[3] L. W. Oberley, G. R. Buettner, *Cancer Res.* **1979**, *39*, 1141−1149.
[4] J. M. McCord, I. Fridovich, *J. Biol. Chem.* **1969**, *244*, 6049−6055.
[5] E. M. Fielden, P. B. Roberts, R. C. Bray, D. J. Lowe, G. N. Mautner, G. Rotilio, L. Calabrese, *Biochem. J.* **1974**, *139*, 49−60.
[6] W. H. Koppenol, in *Oxygen and Oxyradicals in Chemistry and*

Biology (Eds.: M. A. J. Rodgers, E. L. Powers), Academic Press, New York, **1981**, pp. 671−674.
[7] S. Goldstein, G. Czapski, *Free Radical Biol. Med.* **1985**, *1*, 373−380.
[8] M. Masarwa, H. Cohen, D. Meyerstein, D. L. Hickman, A. Bakac, J. H. Espenson, *J. Am. Chem. Soc.* **1988**, *110*, 4293−4297.
[9] M. K. Eberhardt, *J. Org. Chem.* **1989**, *54*, 5922−5926.
[10] R. P. Bonomo, R. Marchelli, G. Tabbi, *J. Inorg. Biochem.* **1995**, *60*, 205−218.
[11] W. H. Koppenol, in *Free Radical Damage and its Control* (Eds.: C. A. Rice-Evans, R. H. Burdon), Elsevier Science B.V., Amsterdam, **1994**, pp. 3−24
[12] T. Nauser, R. E. Bühler, *J. Chem. Soc., Faraday Trans.* **1994**, *90*, 3651−3656 .
[13] C. Beauchamp, I. Fridovich, *Anal. Biochem.* **1971**, *44*, 276−287.
[14] I. Fridovich, in *Handbook of Methods for Oxygen Radical Research* (Ed.: R. A. Greenwald), CRC Press, Boca Raton, **1985**, pp. 213−215.
[15] H. M. Steinman, V. R. Naik, J. L. Abernethy, R. L. Hill, *J. Biol. Chem.* **1974**, *22*, 7326−7338.
[16] B. Wolf, K. Reinecke, K.-D. Aumann, R. Brigelius-Flohé, L. Flohé, *Biol. Chem. Hoppe Seyler* **1993**, *374*, 641−649.
[17] J. A. Tainer, E. D. Getzoff, J. S. Richardson, D. C. Richardson, *Nature* **1983**, *306*, 284−290.
[18] K. Djinovic, G. Gatti, A. Coda, L. Antolini, G. Pelosi, A. Desideri, M. Falconi, F. Marmocchi, G. Rotilio, M. Bolognesi, *J. Mol. Biol.* **1992**, *225*, 791−809.
[19] Y. Kitagawa, N. Tanaka, Y. Hata, M. Kusunoki, G. Lee, Y. Katsube, K. Asada, S. Aibara, Y. Morita, *J. Biochem. (Tokyo)* **1991**, *109*, 477−485.
[20] W. R. Rypniewski, S. Mangani, B. Bruni, P. L. Orioli, M. Casati, K. S. Wilson, *J. Mol. Biol.* **1995**, *251*, 282−296.
[21] K. G. Strothkamp, S. J. Lippard, *Acc. Chem. Res.* **1982**, *15*, 318−326.
[22] B. P. Murphy, *Coord. Chem. Rev.* **1993**, *124*, 63−105.
[23] J.-L. Pierre, P. Chautemps, S. M. Refaif, A. El-Marzouki, G. Serratrice, E. Saint-Aman, P. Rey, *J. Am. Chem. Soc.* **1995**, *117*, 1965−1973.
[24] U. Weser, L. M. Schubotz, E. Lengfelder, *J. Mol. Catal.* **1981**, *13*, 249−261.
[25] P. K. Couglin, S. J. Lippard, *Inorg. Chem.* **1984**, *23*, 1446−1451.
[26] M. G. B. Drew, S. M. Nelson, J. Reedijk, *Inorg. Chim. Acta* **1982**, *64*, L189−L191.
[27] W. H. Koppenol, *Free Radical Biol. Med.* **1994**, *16*, 289−290.
[28] M. Sato, M. Ikeda, J. Nakaya, *Inorg. Chim. Acta* **1984**, *93*, L61−L62.
[29] C. A. Salata, M. T. Youinou, C. J. Burrows, *Inorg. Chem.* **1991**, *30*, 3454−3461.
[30] G. Tabbì, W. L. Driessen, J. Reedijk, R. P. Bonomo, N. Veldman, A. L. Spek, *Inorg. Chem.* **1997**, *36*, 1168−1175.
[31] L. Costanzo, G. Deguidi, S. Giuffrida, E. Rizzarelli,, G. Vecchio, *J. Inorg. Biochem.* **1993**, *50*, 273−281.
[32] M. von Piechowski, T. Nauser, J. Hoignè, R. E. Bühler, *Ber. Bunsenges. Phys. Chem.* **1993**, *97*, 762−771.
[33] A. B. Ross, B. H. J. Bielski, G. V. Buxton, D. E. Cabelli, C. L. Greenstock, W. P. Helman, R. E. Huie, J. Grodkowski, P. Neta, *NDRL-NIST Solution Kinetics Database: Ver. 2*, National Institute of Standards, Technology, Gaithersburg, Maryland, **1994.**
[34] J. Rabani, D. Klug-Roth, J. Lilie, *J. Phys. Chem.* **1973**, *77*, 1169−1175.
[35] J. Butler, W. H. Koppenol, E. Margoliash, *J. Biol. Chem.* **1982**, *257*, 10747−10750.
[36] H. Cohen, R. van Eldik, M. Masarwa, D. Meyerstein, *Inorg. Chim. Acta* **1990**, *177*, 31−34.
[37] P. S. Rao, M. Simic, E. Hayon, *J. Phys. Chem.* **1975**, *79*, 1260−1263.
[38] W. H. Koppenol, K. J. H. van Buuren, J. Butler, R. Braams, *Biochim. Biophys. Acta* **1976**, *449*, 157−168.
[39] B. H. J. Bielski, *Photochem. Photobiol.* **1978**, *28*, 645−649.
[I98120]

Phosphenium Complexes, 42[◇]

Reaction of the Phosphenium Complexes $Cp(OC)_2W{=}P(tBu)(R)$ with Ethyl Isothiocyanate: Unprecedented Formation of the Phosphametalla Spiro Compound $\{Cp(OC)_2W{-}P(tBu)(R){-}N(Et){-}C^a[N(Et){-}(CH){-}N(Et)C^bH_2]{-}S(W{-}S)(C^a{-}C^b)\}Cl$ (R = *t*Bu, Ph)

Wolfgang Malisch*, Christa Abd El Baky, Klaus Grün, and Joachim Reising

Institut für Anorganische Chemie der Universität Würzburg,
Am Hubland, D-97074 Würzburg, Germany
E-mail: Wolfgang.Malisch@mail-uni-wuerzburg.de

Received May 12, 1998

Keywords: Phosphenium complexes / Cycloadditions / Heteroallenes / Phosphametallacycles / Diastereoselectivity / Spiro compounds

Reaction of the phosphenium complexes $Cp(OC)_2W{=}P$-(*t*Bu)(R) [R = *t*Bu (**2a**), Ph (**2b**)] with ethyl isothiocyanate (**3**) leads to the formation of the phosphametallacycles $Cp(OC)_2W{-}P(tBu)(R){-}C(=NEt){-}S(W{-}S)$ (**4a**, **b**) by [2 + 2] cycloaddition. In contrast, the "in situ" reaction of **2a**, **b**, generated from $Cp(OC)_2[H(tBu)(R)P]W{-}Cl$ (**1a**, **b**) with DBU in the presence of **3** leads to the spirocyclic phosphorus metal compounds $\{Cp(OC)_2W{-}P(tBu)(R){-}N(Et){-}C^a[N(Et){-}(CH){-}N$-$(Et)C^bH_2]{-}S(W{-}S)(C^a{-}C^b)\}Cl$ (**6a**, **b**). The structure of **6a** has been proved by X-ray analysis.

Introduction

Transition metal mediated synthesis of organic compounds is one of the outstanding areas of organometallic chemistry. Extension of this approach to organophosphorus chemistry has drawn increasing attention in recent times, involving phosphenium ($M{=}PR_2$)[1] or phosphinidene ($M{=}PR$)[2] complexes. In this context it has been demonstrated that the M=P unit of the phosphenium complexes $Cp(OC)_2M{=}PR_2$ (M = Mo, W) exhibits a pronounced propensity for the addition of Brønstedt acids, carbenoids, and their analogues as well as diverse organic multiply bonded systems, offering efficient routes to new types of organophosphorus units. Within the scope of this topic we recently described the chemo- and regioselective cycloaddition of the phosphenium complexes $Cp(OC)_2M{=}P(R)$(*o*-Tol) (M = Mo, W; R = Ph, *o*-Tol) to organic isocyanates yielding the [2 + 2] cycloaddition products $Cp(OC)_2M{-}P(R)$(*o*-Tol)$-C(=O)-NEt(M{-}N)$[3].

We now report about the cycloaddition reaction between the diorganophosphenium complexes $Cp(OC)_2W{=}P(tBu)(R)$ [R = *t*Bu (**2a**), Ph (**2b**)] bearing one or two *tert*-butyl ligands at the phosphorus atom and EtNCS affording, in addition to the expected cycloadduct, an unusual coupling product as a consequence of "in situ" generation.

[◇] Part 41: O. Fey, J. Reising, W. Malisch, *Organometallics*, submitted.

Results

Reaction of the phosphenium complexes **2a**, **b**, obtained from the bifunctional complexes **1a**, **b** by DBU-assisted dehydrohalogenation, with EtNCS in toluene at room temperature after 12 (**2b**) and 24 h (**2a**), leads to the formation of the four-membered phosphametallacycles **4a**, **b**, representing the product of a [2 + 2] cycloaddition. The coupling reaction exclusively involves the C=S bond of the isothiocyanate, whereby, in contrast to the isocyanate reaction, not the nitrogen but the sulfur atom is coordinated to the metal atom while the electrophilic carbon atom is in both cases bonded to the phosphorus atom. This finding characterizes the isothiocyanate reaction as chemo- and regiospecific (Scheme 1).

Pure **4a**, **b** is isolated by column chromatography in good yield as a deep red and orange crystalline powder, respectively. The structure is proved by the ^{31}P-NMR spectra, with signals at δ = 39.7 (**4a**) and 11.9 (**4b**) and ^1J(WP) couplings of 213.8 (**4a**) and 230.2 Hz (**4b**) appearing in the characteristic range of four-membered phosphametallacycles[3]. The signal of the *P*-bonded sp^2-carbon atom of **4b** is observed in the ^{13}C-NMR spectrum as a doublet in the typical low-field region at δ = 183.0 with a ^1J(PC) coupling of 49.6 Hz. **4b**, which contains two stereogenic centers as i.e. the metal and the phosphorus atoms, is generated highly diastereoselectively, according to the NMR spectra.

In order to promote metal-assisted organophosphorus synthesis it is reasonable to avoid isolation of the thermally

 © WILEY-VCH Verlag GmbH, D-69451 Weinheim, 1998 1434–1948/98/1212–1945 $ 17.50+.50/0

Scheme 1

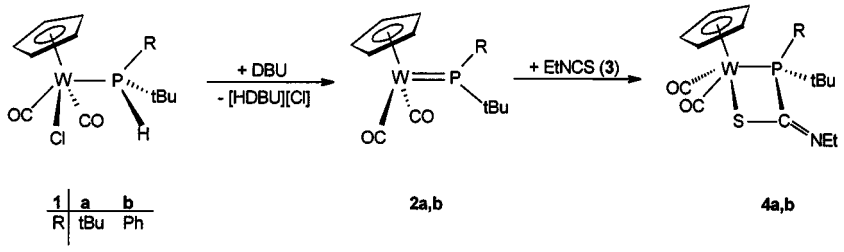

unstable phosphenium complexes. According to this approach **2a**, **b** were generated "in situ" by combining the precursor complex **1** with **3** followed by addition of DBU. After removal of insoluble material, mainly [HDBU]Cl, the solution was reduced to a volume of 2 ml and the residue separated by column chromatography. This procedure yields, besides **4a**, **b**, the spirocyclic compounds **6a**, **b** as well as the three-membered heterocycles **5a**, **b**.

Scheme 2

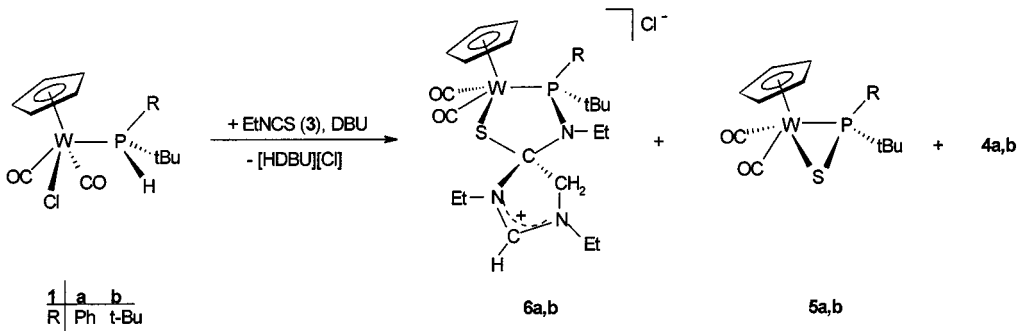

The spirocycles **6a**, **b** are isolated in yields of 25% as orange powders, which show good solubilities in all organic solvents except for alkanes. Heterocycles **5a**, **b** could not be separated from **4a**, **b** but were alternatively prepared by the well-established addition of elemental sulfur to the W=P double bond of **2a**, **b**.

The spirocyclic compounds **6a**, **b** contain a five-membered phosphametalla heterocycle showing the ^{31}P-NMR low-field signals at δ = 143.4 (**6a**), 127.5 (**6a′**) and 120.0 (**6b**), 139.8 (**6b′**) with ^{1}J(WP) coupling constants of 277.0 (**6a**), 265.7 (**6a′**) Hz and 280.8 (**6b**), 280.5 (**6b′**) Hz. Presumably it is formed by a 1,3-dipolar cycloaddition of ethyl isothiocyanate to the W=P double bond. The carbon atom of the added isothiocyanate is responsible for the spirocyclic structure, formed by the coupling with two ethyl isocyanate molecules followed by protonation of the carbon atoms. The generation of the ethyl isocyanate incorporated in the spirocycle is verified under the reaction conditions by ring contraction of the [2 + 2] cycloadducts **4a**, **b** to give W−P−S cycles, as proved in a separate experiment. This is a further example of easy cleavage of the carbon−sulfur bond in isothiocyanates in the presence of a transition metal resulting in the generation of complexes having both the sulfur atom and the isocyanide incorporated[4].

Despite the large number of postulated reaction steps, **6a**, **b**, which have two or three stereogenic centers, are formed highly diastereoselectively [*d. r.* = 96:4 (**6a**), 85:15 (**6b**)], indicating efficient stereocontrol by the metal fragment.

Final proof for the structure of **6a**, composed of two five-membered cycles connected by a spiro-carbon atom, is obtained by X-ray analysis. The spiro junction adopts a *syn* arrangement of the nitrogen atom N3 and the Cp ligand at the metal. The metal-phosphorus-containing ring shows an envelope conformation with a nearly planar P1−N1−C8−S1 unit [torsion angle: 12.9(10)°] with the folding along the W1−N1 axis resulting in an inclination of the phosphorus towards the Cp ligand. This arrangement is obvious from the different torsion angles W1−S1−C8−N1 [17.0(8)°] and W1−P1−N1−C8 [−35.4(8)°] and has its origin in the sterical interaction of the *tert*-butyl moiety (C14−C17) with the Cp unit. In the diaza ring the atoms N3, C30, N2, C33 are found in a plane [torsion angle: 6.9(13)°] from which the spiro atom C8 is only slightly deflected [C8−C33−N2−C30 15.4(12)°]. As shown by the angle Cp(Z)−W1−C8−N3 (1.16°), the plane of the ring is oriented nearly perpendicularly to the Cp(Z)−W axis.

Delocalization within the bonding system N2−C30−N3, involving an sp^2-hybridized carbon atom, is proved by the nearly identical values of the bond lengths N2−C30 [1.341(13) Å] and N3−C30 [1.345(13) Å], while the sp^3-hybridized carbon atom C33 is saturated by two hydrogen atoms.

The W1−P1 distance of 2.540(3) Å lies within the range of a single bond and is comparable with the values of other phosphane-substituted tungsten complexes[3][5]. The W1−S1 distance is slightly shorter than expected for a single bond [2.459(3) Å], while for the P1−N1 bond [1.720(8) Å] a single bond character is found[6].

Figure 1: ORTEP plot of {$Cp(OC)_2W-P(tBu)_2-N(Et)-C^a[N(Et)-C(H)-N(Et)-C^bH_2]-S(W-S)(C^a-C^b)$}Cl (**6a**)[a]

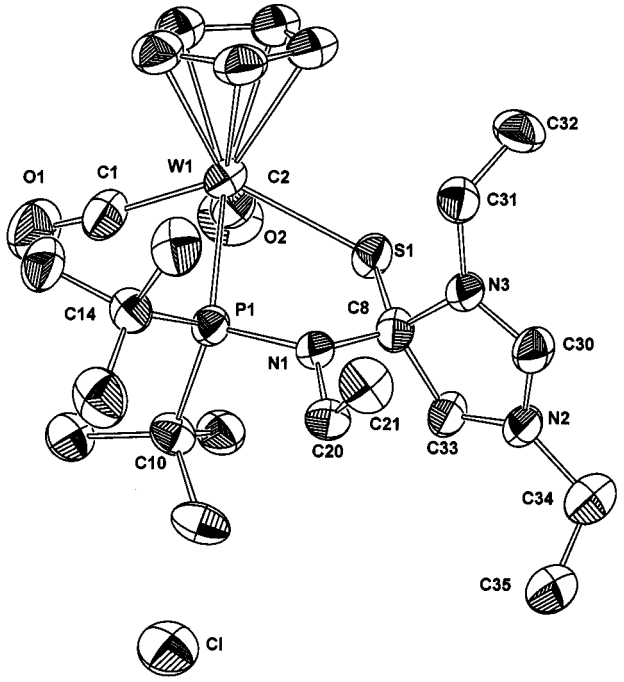

[a] Selected bond lengths [Å], bond and torsion angles [°]: W1−C2 1.927(12), W1−C1 1.948(12), W1−P1 2.540(3), W1−S1 2.459(3), S1−C8 1.823(11), P1−N1 1.720(8), N1−C8 1.437(12), N2−C30 1.341(13), N2−C33 1.449(12), N3−C30 1.345(13), N3−C8 1.472(12), C8−C33 1.558(13); W1−S1−C8 112.8(2), P1−W1−S1 74.2(8), W1−P1−N1 107.4(5); C8−S1−W1−P1 28.7(6), S1−W1−P1−N1 31.4(5), W1−P1−N1−C8 35.4(1), P1−W1−S1−C8 12.9(5); N1−C8−S1−W1 16.9(9), C30−N3−C8−C33 13.9(4), N3−C8−C33−N2 16.7(2), C8−C33−N2−C30 15.5(1), C33−N2−C30−N3 6.9(4), Cp(Z)−W1−C8−N3 1.16.

In conclusion, these studies demonstrate a metal-mediated multistep synthesis, starting from easily accessible secondary phosphane complexes with the corresponding phosphenium complexes as the crucial intermediates. Furthermore, this process proceeds with a high degree of diastereoselectivity, a feature which promises future application of these phosphametallaspirocycles in enantioselective synthesis.

Support of this research by the *Deutsche Forschungsgemeinschaft* (Sonderforschungsbereich 347, *"Selektive Reaktionen Metall-aktivierter Moleküle"*) is gratefully acknowledged.

Experimental Section

General: All manipulations were performed under dried and purified nitrogen. Solvents were rigorously dried with an appropriate drying agent, distilled before use and saturated with nitrogen. $Cp(OC)_2[H(tBu)(R)P]W-Cl$ and $Cp(OC)_2W=P(tBu)(R)$ (R = *t*Bu[7], Ph[1j]) were prepared according to the literature. All other reagents were obtained commercially and used without further purification. − ^{1}H-, ^{13}C-, and ^{31}P-NMR spectra were obtained on a Bruker AMX 400 spectrometer. δ(^{1}H)/(^{13}C) chemical shifts are reported downfield from Me_4Si referenced to the residual proton signal (^{1}H) or natural abundance carbon signal (^{13}C) of the deuterated solvent. δ(^{31}P) chemical shifts are measured relative to external H_3PO_4 (85%). Shifts downfield from the standard were assigned positive δ values. − Infrared spectra were measured in solution on a Perkin-Elmer 283 grating spectrometer in NaCl cells with 0.1-mm path length. − Melting points: Differential thermoanalysis (Du Pont 9000). − Elemental analyses were performed in the laboratory of the Institut für Anorganische Chemie der Universität Würzburg.

1. *$Cp(OC)_2W-P(tBu)_2-C(=NEt)-S(W-S)$* (**4a**): A solution of 170 mg (0.38 mmol) of $Cp(OC)_2W=P(tBu)_2$ (**2a**) in 10 ml of toluene was combined with 33 mg (0.38 mmol) of ethyl isothiocyanate (**3**) and the mixture stirred for 24 h at room temperature. The reaction mixture was reduced in vacuo to a volume of 1 ml and worked up by column chromatography (column 10 × 1.5 cm, alumina III, neutral, toluene). The eluate of the dark red zone was concentrated in vacuo and remaining **4a** was recrystallized from 7 ml of pentane. − Yield: 153 mg (75%). − Dark red microcrystalline powder. − M.p. 183°C. − ^{1}H NMR (400.1 MHz, [D$_6$]benzene): δ = 4.91 (s, 5 H, H_5C_5), 3.73 [qd, ^3J(HCCH) = 7.4 Hz, ^4J(PCNCH) = 2.5 Hz, 2 H, H_2CN], 1.32 [d, ^3J(PCCH) = 16.5 Hz, 9 H, $(H_3C)_3C$], 1.26 [t, ^3J(HCCH) = 7.4 Hz, 3 H, H_3CCH_2N], 1.04 [d, ^3J(PCCH) = 16.5 Hz, 9 H, $(H_3C)_3C$]. − ^{31}P NMR (162.0 MHz, [D$_6$]benzene): δ = 39.7 [s, ^1J(WP) = 213.8 Hz]. − IR (toluene): $\tilde{\nu}$ = 1936, 1853 (CO) cm^{-1}. − $C_{18}H_{28}NO_2PSW$ (537.31): calcd. C 40.24, H 5.25, N 2.61, S 5.97; found C 40.44, H 5.37, N 2.57, S 5.88.

2. *$Cp(OC)_2W-P(tBu)(Ph)-C(=NEt)-S(W-S)$* (**4b**): Prepared as described for **4a** from 242 mg (0.51 mmol) of $Cp(OC)_2W=P(tBu)(Ph)$ (**2b**) and 44 mg (0.51 mmol) of ethyl isothiocyanate (**3**) in 10 ml of toluene after stirring for 12 h. − Yield: 216 mg (76%). − Orange microcrystalline powder. − M.p. 193°C. − ^{1}H NMR (400.1 MHz, [D$_6$]benzene): δ = 8.04 (m, 2 H, H_5C_6), 7.13 (m, 3 H, H_5C_6), 4.77 (s, 5 H, H_5C_5), 3.88 (m, 2 H, H_2CN), 1.43 [t, ^3J(HCCH) = 7.6 Hz, 3 H, H_3CCH_2N], 1.38 [d, ^3J(PCCH) = 15.2 Hz, 9 H, $(H_3C)_3C$]. − ^{13}C NMR (100.6 MHz, [D$_6$]benzene): δ = 245.5 [d, ^2J(PWC) = 22.9 Hz, *cis*-CO], 230.8 [d, ^2J(PWC) = 3.8 Hz, *trans*-CO], 183.0 [d, ^1J(PC) = 49.6 Hz, C=N], 133.9 [d, ^1J(PC) = 51.5 Hz, C-1], 133.0 [d, ^3J(PCCC) = 8.6 Hz, C-3/5], 130.0 [d, ^2J(PCC) = 1.9 Hz, C-2/6], 127.5 (s, C-4), 44.8 [d, ^1J(PC) = 19.1 Hz, $C(CH_3)_3$], 36.1 [d, ^3J(PCNC) = 20.0 Hz, CH_2N], 26.0 [d, ^2J(PCC) = 2.9 Hz, $(CH_3)_3C$], 15.0 (s, CH_3CH_2N). − ^{31}P NMR (162.0 MHz, [D$_6$]benzene): δ = 11.9 [s, ^1J(WP) = 230.2 Hz]. − IR (toluene): $\tilde{\nu}$ = 1924, 1839 (CO) cm^{-1}. − $C_{20}H_{24}NO_2PSW$ (557.30): calcd. C 43.10, H 4.34, N 2.51, S 5.75; found C 43.36, H 4.65, N 2.14, S 5.50.

3. *{$Cp(OC)_2W-P(tBu)_2-N(Et)-C^a[N(Et)-(CH)-N(Et)-C^bH_2]-S(W-S)(C^a-C^b)$}Cl* (**6a**): A solution of 312 mg (0.64 mmol) of $Cp(OC)_2[H(tBu)_2P]W-Cl$ (**1**) and 167 mg (1.92 mmol) of ethyl isothiocyanate (**3**) was combined with 97 mg (0.64 mmol) of DBU and stirred for 24 h at room temperature. The reaction mixture was reduced in vacuo to a volume of 2 ml and worked up by column chromatography (column 25 × 2.5 cm, alumina III, neutral, toluene). The eluate of the second orange zone was evaporated in vacuo and remaining **6a** recrystallized from 7 ml of pentane. − Yield: 56 mg (25%). − Orange microcrystalline powder. − M.p. 78°C. − Diastereomeric ratio: 96:4 (determined by integration of the Cp signals in the ^{1}H-NMR). − *Main diastereomer:* ^{1}H NMR (400.1 MHz, [D$_6$]benzene): δ = 5.06 (s, 5 H, H_5C_5), 4.14 [d, ^2J(HCH) = 11.2 Hz, 1 H, H_2CCNP], 3.83 (m, 2 H, H_2CCH_3), 3.74 [d, ^2J(HCH) = 11.2 Hz, 1 H, H_2CCNP], 3.35 (m, 2 H, H_2CCH_3), 2.87 (m, 2 H, H_2CCH_3), 1.81 [t, ^3J(HCCH) = 7.0 Hz, 3 H, H_3CCH_2], 1.32 [d, ^3J(PCCH) = 13.1 Hz, 18 H, $(H_3C)_3C$], 1.10 [t, ^3J(HCCH) = 7.0 Hz, 3 H, H_3CCH_2], 0.95 [t, ^3J(HCCH) = 7.0 Hz, 3 H, H_3CCH_2]. − ^{13}C NMR (100.6 MHz, [D$_6$]benzene):

δ = 244.1 [d, ^2J(PWC) = 16.2 Hz, *cis*-CO], 228.9 [d, ^2J(PWC) = 1.9 Hz, *trans*-CO], 179.3 (s, CNP), 93.7 (s, C_5H_5), 62.1 (s, CH_2CNP), 49.0 [d, ^1J(PC) = 7.5 Hz, $C(CH_3)_3$], 43.8 [d, ^4J(PNCNC) = 3.8 Hz, CH_2NCNP], 41.3 [d, ^2J(PNC) = 17.2 Hz, CH_2NP], 38.1 (s, CH_2NC), 31.7 [d, ^2J(PCC) = 2.9 Hz, $(CH_3)_3$C], 15.8 (s, CH_3CH_2), 15.2 [d, ^3J(PNCC) = 2.9 Hz, CH_3CH_2NP], 11.9 (s, CH_3CH_2); δ(CHN) = 128.9 ($CDCl_3$, 150.9 MHz). − ^{31}P NMR (162.0 MHz, [D$_6$]benzene): δ = 143.4 [s, ^1J(WP) = 277.0 Hz]. − *Minor diastereomer:* ^{1}H NMR (400.1 MHz, [D$_6$]benzene): δ = 5.02 (s, 5 H, H_5C_5), 3.57 [d, ^2J(HCH) = 10.3 Hz, 1 H, H_2CCNP], 3.48 (m, 2 H, H_2CCH_3), 3.39 [d, ^2J(HCH) = 10.3 Hz, 1 H, H_2CCNP], 3.06 (m, 2 H, H_2CCH_3), 2.62 (m, 2 H, H_2CCH_3), 1.86 [t, ^3J(HCCH) = 7.6 Hz, 3 H, H_3CCH_2], 1.27 [d, ^3J(PCCH) = 13.5 Hz, 18 H, $(H_3C)_3$C], 0.89 [t, ^3J(HCCH) = 7.1 Hz, 3 H, H_3CCH_2], 0.56 [t, ^3J(HCCH) = 7.6 Hz, 3 H, H_3CCH_2]. − ^{13}C NMR (100.6 MHz, [D$_6$]benzene): δ = 244.2 [d, ^2J(PWC) = 15.2 Hz, *cis*-CO), 229.1 [d, ^2J(PWC) = 1.9 Hz, *trans*-CO], 180.8 (s, CNP), 93.0 (s, C_5H_5), 63.8 (s, CH_2CNP), 48.0 [s, $C(CH_3)_3$], 44.0 [d, ^2J(PNC) = 3.8 Hz, CH_2NP], 40.8 [d, ^4J(PNCNC) = 2.9 Hz, CH_2NCNP], 39.6 (s, CH_2NC), 31.0 [d, ^2J(PCC) = 2.9 Hz, $(CH_3)_3$C], 15.3 (s, CH_3CH_2), 13.9 [d, ^3J(PNCC) = 2.9 Hz, CH_3CH_2NP], 11.8 (s, CH_3CH_2); δ(CHN) = 128.8 ($CDCl_3$, 130.9 MHz). − ^{31}P NMR (162.0 MHz, [D$_6$]benzene): δ = 127.5 [s, ^1J(WP) = 265.7 Hz]. − IR (toluene): $\tilde{\nu}$ = 1936, 1837 (CO) cm^{-1}. − $C_{24}H_{41}ClN_3O_2PSW$ (685.95): calcd. C 42.02, H 6.02, N 6.13, S 4.67; found C 40.34, H 6.04, N 5.58, S 8.60.

4. *{Cp(OC)$_2$W−P(tBu)(Ph)−N(Et)−C^a[N(Et)−(CH)−N-(Et)C^{b}H$_2$]−S(W−S)(C^a−C^b)}Cl* (**6b**): Prepared as described for **6a** from 275 mg (0.54 mmol) of Cp(OC)$_2$[H(*t*Bu)(Ph)P]W−Cl (**1b**), 141 mg (1.62 mmol) of ethyl isothiocyanate (**3**) and 83 mg (0.54 mmol) of DBU. **6b** is obtained from the eluate of the second red zone. − Yield: 50 mg (13%). − Dark orange microcrystalline powder. − M.p. 83°C. − Diastereomeric ratio: 85:15 (determined by integration of the Cp signals in the ^{1}H NMR). − *Main diastereomer:* ^{1}H NMR (400.1 MHz, [D$_6$]benzene): δ = 7.76−6.98 (m, 5 H, H_5C_6), 4.75 (s, 5 H, H_5C_5), 4.08 [d, ^2J(HCH) = 11.8 Hz, 1 H, H_2CCNP], 3.86 (m, 2 H, H_2CCH_3), 3.80 [d, ^2J(HCH) = 11.8 Hz, 1 H, H_2CCNP], 3.43 (m, 2 H, H_2CCH_3), 3.17 (m, 2 H, H_2CCH_3), 1.80 [t, ^3J(HCCH) = 7.4 Hz, 3 H, H_3CCH_2], 1.29 [d, ^3J(PCCH) = 14.8 Hz, 9 H, $(H_3C)_3$C], 0.99 [t, ^3J(HCCH) = 6.5 Hz, 3 H, H_3CCH_2], 0.85 [t, ^3J(HCCH) = 6.5 Hz, 3 H, H_3CCH_2]. − ^{31}P NMR (162.0 MHz, [D$_6$]benzene): δ = 120.0 [s, ^1J(WP) = 280.8 Hz]. − *Minor diastereomer:* ^{1}H NMR (400.1 MHz, [D$_6$]benzene): δ = 4.78 (s, 5 H, H_5C_5), 3.81 [d, ^2J(HCH) = 10.3 Hz, 1 H, H_2CCNP], 3.53 [d, ^2J(HCH) = 10.3 Hz, 1 H, H_2CCNP], additional signals not assigned. − ^{31}P NMR (162.0 MHz, [D$_6$]benzene): δ = 139.8 [s, ^1J(WP) = 280.5 Hz]. − $C_{26}H_{37}ClN_3O_2PSW$ (705.94): calcd. C 44.24, H 5.28, N 5.95, S 4.54; found C 44.43, H 5.41, N 5.88, S 4.67.

5. *Cp(OC)$_2$W−P(tBu)$_2$−S(W−S)* (**5a**): A solution of 165 mg (0.36 mmol) of Cp(OC)$_2$W=P(*t*Bu)$_2$ (**2a**) in 7 ml of toluene was combined with 12 mg (0.36 mmol) of elemental sulfur and stirred for 4 h at room temperature. The reaction mixture was reduced in vacuo to a volume of 1 ml and worked up by column chromatography (column 10 × 1.5 cm, alumina III, neutral, toluene). The eluate of the red zone was evaporated in vacuo and remaining **5a** recrystallised from 5 ml of pentane. Yield: 142 mg (85%). − Dark red microcrystalline powder. − M.p. 120°C. − ^{1}H NMR (400.1 MHz, [D$_6$]benzene): δ = 5.16 (s, 5 H, H_5C_5), 1.53 [d, ^3J(PCCH) = 16.4 Hz, 9 H, $(H_3C)_3$C], 1.27 [d, ^3J(PCCH) = 16.2 Hz, 9 H, $(H_3C)_3$C]. − ^{31}P NMR (162.0 MHz, [D$_6$]benzene): δ = 60.9 [s, ^1J(WP) = 195.1 Hz] − IR (toluene): $\tilde{\nu}$ = 1937, 1851 (CO) cm^{-1}. − $C_{15}H_{23}O_2PSW$ (482.23): calcd. C 37.36, H 4.08; found C 37.54, H 5.20.

6. *Cp(OC)$_2$W−P(tBu)(Ph)−S(W−S)* (**5b**): Prepared as described for **5a** from 182 mg (0.39 mmol) of Cp(OC)$_2$W=P(*t*Bu)(Ph) (**2b**) and 12 mg (0.39 mmol) of elemental sulfur in 7 ml of toluene after stirring for 2 h. Yield: 174 mg (89%). − Red microcrystalline powder. − M.p. 180°C. − ^{1}H NMR (400.1 MHz, [D$_1$]chloroform): δ = 7.76−7.39 (m, 5 H, H_5C_6), 5.19 (s, 5 H, H_5C_5), 1.18 [d, ^3J(PCCH) = 18.7 Hz, 9 H, $(H_3C)_3$C]. − ^{13}C NMR (100.6 MHz, [D$_1$]chloroform): δ = 240.0 [d, ^2J(PWC) = 29.3 Hz, *cis*-CO], 228.3 (s, *trans*-CO), 133.8 [d, ^3J(PCCC) = 11.8 Hz, C3/5], 132.4 [d, ^1J(PC) = 36.6 Hz, C1], 130.4 [d, ^4J(PCCCC) = 3.1 Hz, C4], 127.9 [d, ^2J(PCC) = 11.1 Hz, C2/6], 91.1 (s, C_5H_5), 27.9 [d, ^1J(PC) = 34.5 Hz, $C(CH_3)_3$], 26.8 [d, ^2J(PCC) = 4.5 Hz, $(CH_3)_3$C]. − ^{31}P NMR (162.0 MHz, $CDCl_3$): δ = 39.4 [^1J(WP) = 221.1 Hz). − IR (toluene): $\tilde{\nu}$ = 1940, 1854 (CO) cm^{-1}. − $C_{17}H_{19}O_2PSW$ (502.26): calcd. C 40.66, H 3.81; found C 40.80, H 3.84.

7. *Reaction of Cp(OC)$_2$W−P(tBu)$_2$−C(=NEt)−S(W−S) with [HDBU][Cl]:* A solution of 125 mg (0.23 mmol) of Cp(OC)$_2$W−P(*t*Bu)$_2$−C(=NEt)−S(*W*−*S*) (**4a**) in 7 ml of toluene is combined with an excess of [HDBU][Cl]. After stirring for 2 d insoluble [HDBU][Cl] is separated and pure **5a** is identified by ^{31}P-NMR spectroscopic comparison with an authentic sample.

8. *X-ray Structure Analysis of* **6a**: Orange crystals suitable for X-ray analysis were obtained by slow diffusion of pentane into a saturated solution of **6a** in benzene at room temperature. $C_{24}H_{41}ClN_3O_2PSW$, *M* = 685.95; Crystallographic data for **3a**: monoclinic, $P2_1/c$ (Nr. 14), *Z* = 4, *a* = 15.675(4), *b* = 12.375(2), *c* = 16.219(5) Å, β = 110.79(1)°, *V* = 2941(1) Å^3, $\rho_{calcd.}$ = 1.637 g·cm^{-3}, Enraf-Nonius CAD4 diffractometer; Mo-K_α radiation (λ = 0.71073 Å), 4078 independent reflections with 2.12° < θ < 22.93° collected, 2781 reflections used in refinement with $I > 2\sigma(I)$; R_1 = 0.0479; wR_2 = 0.0978. Crystallographic data (excluding structure factors) for the structure reported in this paper have been deposited with the Cambridge Crystallographic Data Centre as supplementary publication no. CCDC-101571. Copies of the data can be obtained free of charge on application to CCDC, 12 Union Road, Cambridge CB2 1EZ [Fax: + 44-1223/336-033; E-mail: deposit@ccdc.cam.ac.uk].

[1] [1a] W. Malisch, U.-A. Hirth, K. Grün, M. Schmeußer, O. Fey, U. Weis, *Angew. Chem.* **1995**, *107*, 2717−2719; *Angew. Chem. Int. Ed. Engl.* **1995**, *34*, 2500−2502. − [1b] A. Fried, W. Malisch, M. Schmeußer, U. Weis, *Phosphorus Sulfur* **1992**, *65*, 75−78. − [1c] W. Malisch, U.-A. Hirth, T. A. Bright, H. Käb, T. S. Ertel, S. Hückmann, H. Bertagnolli, *Angew. Chem.* **1992**, *104*, 1537−1539; *Angew. Chem. Int. Ed. Engl.* **1992**, *31*, 1525−1527. − [1d] W. Malisch, K. Grün, N. Gunzelmann, S. Möller, R. Lankat, J. Reising, M. Neumayer, O. Fey in *Selective Reactions of Metal-Activated Molecules*, H. Werner, W. Adam, G. Bringmann, W. Kiefer (Eds.), Vieweg-Verlag, Braunschweig **1995**, p. 183−190. − [1e] W. Malisch, U.-A. Hirth, A. Fried, H. Pfister, *Phosphorus Sulfur* **1993**, *77*, 17−20. − [1f] H. Lang, M. Leise, L. Zsolnai, *Organometallics* **1993**, *12*, 2393−2397. − [1g] H.-U. Reisacher, E. N. Duesler, R. T. Paine, *Chem. Ber.* **1996**, *129*, 279−281. − [1h] H.-U. Reisacher, W. F. McNamara, E. N. Duesler, R. T. Paine, *Organometallics* **1997**, *16*, 449−455. − [1i] H.-U. Reisacher, E. N. Duesler, R. T. Paine, *J. Organomet. Chem.* **1997**, *539*, 37−44. − [1j] W. Malisch, A. Meyer, K. Jörg, U. Hofmockel, M. Schmeußer, R. Schemm, W. S. Sheldrick, *Phosphorus Sulfur* **1987**, *30*, 205−208.

[2] [2a] C. C. Cummins, R. R. Schrock, W. M. Davis, *Angew. Chem.* **1993**, *105*, 758−761; *Angew. Chem. Int. Ed. Engl.* **1993**, *23*, 756−760. − [2b] A. Mathieu, A. Igau, J.-P. Majoral, *Phosphorus Sulfur* **1995**, *104*, 235−239. − [2c] T. L. Breen, D. W. Stephan, *Organometallics* **1996**, *15*, 4509−4514. − [2d] T. L. Breen, D. W. Stephan, *Organometallics* **1997**, *16*, 365−369.

[3] W. Malisch, C. Hahner, K. Grün, J. Reising, R. Goddard, C. Krüger, *Inorg. Chim. Acta* **1996**, *244*, 147−150.
[4] [4a] W. P. Fehlhammer, A. Mayr, *J. Organomet. Chem.* **1980**, *191*, 153−159. − [4b] H. Fischer, *J. Organomet. Chem.* **1981**, *222*, 241−250. − [4c] H. Fischer, R. Märkl, *Chem. Ber.* **1982**, *115*, 1349−1354. − [4d] G. Hogarth, E. Skordalakis, *J. Organomet. Chem.* **1993**, *458*, C8−C9.
[5] [5a] W. Malisch, H. Pfister, *Organometallics* **1995**, *14*, 4443−4445. − [5b] B. K. Schmiedeskamp, J. G. Reising, W. Malisch, K. Hindahl, R. Schemm, W. S. Sheldrick, *Organometallics* **1995**, *14*, 4446−4448.
[6] C. Bueno, M. R. Churchill, *Inorg. Chem*. **1981**, *20*, 2197−2202.
[7] K. Jörg, W. Malisch, A. Meyer, W. Reich, U. Schubert., *Angew. Chem.* **1986**, *98*, 103−104; *Angew. Chem. Int. Ed. Engl.* **1986**, *25*, 92−93.

[98142]

Transition Metal Complexes of Diazenes, XLIII[◇]

Rhodium-Catalyzed Synthesis of Naphthalene Derivatives Through Cyclodimerization of Arylalkynes[☆]

Ling-Yu Huang[+], Uwe R. Aulwurm, Frank W. Heinemann, and Horst Kisch*

Institut für Anorganische Chemie der Universität Erlangen-Nürnberg,
Egerlandstraße 1, D-91058 Erlangen, Germany
Fax: (internat.) + 49(0)9131/8527363
E-mail: kisch@anorganik.chemie.uni-erlangen.de

Received May 14, 1998

Keywords: Rhodium catalysis / C–C coupling / C–H activation / Alkynes / Trisubstituted naphthalenes

$RhCl(PPh_3)_3$ in the presence of excess hydrochloric acid and azobenzene in refluxing 1-pentanol catalyzes the cyclodimerization of arylalkynes to 1,2,3-substituted naphthalene derivatives. This enables an easy access to 1,2,3-triphenylnaphthalene (**1**), 7-methoxy-1,2,3-tris(*p*-methoxyphenyl)naphthalene (**2**), 7-methyl-1,2,3-tris(*p*-methylphenyl)naphthalene (**3**), and 7-nitro-3-(*p*-nitrophenyl)-1,2-diphenylnaphthalene (**4**). A co-cyclodimerization of tolan with 4-octyne affords 3-phenyl-1,2-dipropylnaphthalene (**5**). The structure of **4** was resolved by single-crystal X-ray structural analysis. The rate of formation of **1** is first-order with respect to tolan and $RhCl(PPh_3)_3$ and exhibits activation parameters of $\Delta H^{\ddagger}$ = 94.7 ± 10 kJ mol^{-1} and $\Delta S^{\ddagger}$ = 36 ± 6 J K^{-1} mol^{-1}. Replacing HCl by HBr and HI decreases the rate by 28 and 55%, respectively. Although naphthalene formation occurs also in the absence of azobenzene, its presence stabilizes the catalyst, accelerates the reaction, and inhibits formation of 1-chlorostilbene, which is the major by-product. When $RhCl(PCy_3)_2$ is used as the catalyst, naphthalene formation even in the absence of azobenzene is highly selective, but proceeds much slower. No reaction is observed in non-protic solvents.

Introduction

Transition-metal-assisted or -catalyzed oligomerizations of alkynes afford a variety of linear-chain or annulated compounds by direct C−C coupling. In general, annulation does not involve a C−H activation step.[2−5] Except photochemical reactions, direct syntheses of naphthalene derivatives through cyclodimerization of aryl alkynes were scarcely reported. For example metallic lithium suspensions assist formation of 1,2,3-triphenylnaphthalene from tolan.[6] Phenylacetylene was stoichiometrically dimerized to 1-phenylnaphthalene by "active" palladium ($PdCl_2$ and $NaBH_4$) while tolan and other diarylalkynes were inert.[7] Cyclodimerization of the latter alkynes occurred as a side-reaction in the $RhCl_3 \cdot 3\ H_2O$ and Aliquat-336® catalyzed cyclotrimerization; an oxidative C−H addition involving an intermediate Rh^V complex was proposed to rationalize the naphthalene formation.[8] Wilkinson et al. reported a similar synthesis of 1,2-diphenylbenzylideneindene.[9] During our investigations on the rhodium-catalyzed indole synthesis from tolan and azobenzene[10] we observed that in refluxing 1-pentanol solution 1,2,3-triphenylnaphthalene is produced through cyclodimerization of tolan when $RhCl_2(C,N\text{-}C_6H_4N{=}NC_6H_5)(PPh_3)_2$ and 2-chloroazobenzene or $RhCl_2(C,N\text{-}C_6H_4CH{=}NNHC_6H_5)(PPh_3)_2$ were present, but the reaction was slow and of poor chemoselectivity (Figure 1).[11][12]

Figure 1. $RhCl_2(C,N\text{-}C_6H_4E{=}NC_6H_5)(PPh_3)_2$

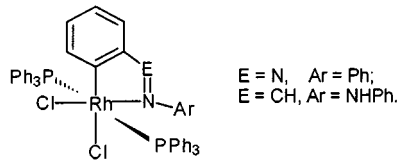

Different to the indole synthesis, where catalytic amounts of acetic acid improved both rate and selectivity, no beneficial effect was observed for naphthalene formation. However, this was the case when mineral acids were employed. In the following we describe a novel catalytic system which allows the easy synthesis of 1,2,3-triphenylnaphthalene (**1**), 7-methoxy-1,2,3-tris(*p*-methoxyphenyl)naphthalene (**2**), 7-methyl-1,2,3-tris(*p*-methylphenyl)naphthalene (**3**), 7-nitro-3-(*p*-nitrophenyl)-1,2-diphenylnaphthalene (**4**), and 3-phenyl-1,2-dipropylnaphthalene (**5**).

Results and Discussion

Cyclodimerization of Tolan by Various Catalysts

During investigations of the synthesis of **1** in the presence of *ortho*-metalated azobenzene and hydrazone com-

[+] On leave of absence from the Department of Applied Chemistry, Sichuan Union University, Chengdu, Sichuan 610065, P. R. China.
[◇] Part XLII: Ref.[1].

 © WILEY-VCH Verlag GmbH, D-69451 Weinheim, 1998 1434−1948/98/1212−1951 $ 17.50+.50/0

Figure 2. Time dependence of the turnover number of **1** in the presence of various catalytic systems; 0.05 mmol of rhodium complex and 2.0 mmol of tolan in the presence of 0.15 mL of HCl (aq. 37%)in 25 mL of refluxing 1-pentanol solution: $RhCl(PPh_3)_3$ and PhN=NPh (0.25 mmol) (A); $RhCl(PPh_3)_3$ (B); $RhCl_2(C,N\text{-}C_6H_4N{=}NC_6H_5)(PPh_3)_2$ (C); $RhCl_2(C,N\text{-}C_6H_4CH{=}NNHC_6H_5)(PPh_3)_2$ (D); $RhHCl(C,N\text{-}CH_3C_6H_3N{=}NC_6H_4CH_3)(PCy_3)_2$ (E); $RhCl(PCy_3)_2$ (F)

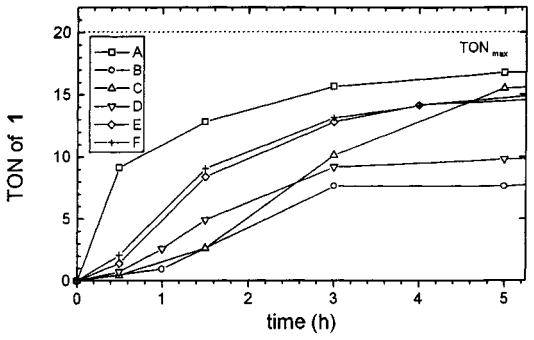

plexes,[13] we found that $RhCl(PPh_3)_3$ and $RhCl(PCy_3)_2$ are also catalytically active but require the presence of HCl. In Figure 2 the catalytic activity of various systems is summarized.

Highest TON (turn over number) values were obtained with $RhCl(PPh_3)_3$ and azobenzene (catalyst **I**, Figure 2, curve A), followed by $RhCl_2(C,N\text{-}C_6H_4N{=}NC_6H_5)(PPh_3)_2$ (curve C), $RhHCl(C,N\text{-}CH_3C_6H_3N{=}NC_6H_5)(PCy_3)_2$ (curve E) and $RhCl(PCy_3)_2$ (curve F). The hydrazone complex $RhCl_2(C,N\text{-}C_6H_4CH{=}NNHC_6H_5)(PPh_3)_2$ (curve D), and Wilkinson′s complex (curve B) were less active.

When azobenzene in the catalytic system **I** was replaced by hydrazobenzene, benzylidenephenylimine, aniline, triethylamine, and various other monodentate nitrogen ligands, formation of **1** still occurred, however at a much lower rate. This clearly indicates that an anticipated *ortho*-metalation of azobenzene is not involved in its positive action. Addition of bidentate nitrogen ligands like phenanthroline and 2,2′-bipyridyl instead of azobenzene inhibited the reaction completely. When $RhCl(PPh_3)_3$ was employed without azobenzene the initial rate did not change significantly but the catalyst was easily deactivated and the reaction stopped after 3 h (Figure 2, curve B); furthermore, the addition product of HCl to tolan, 1-chlorostilbene, was produced in an amount of 20% relative to **1**. This value increased to 30% when HCl and $RhH(PPh_3)_4$ were preheated for 20 min. From these results it can be concluded that azobenzene efficiently prevents addition of HCl to the alkyne mediated by rhodium complexes. In the absence of HCl, the reaction of tolan with $RhCl(PPh_3)_3$, $RhH(PPh_3)_4$, or $RhH(CO)(PPh_3)_3$ alone in refluxing pentanol did not afford **1**.

When Wilkinson's catalyst was replaced by $RhCl(PCy_3)_2$, even in the absence of azobenzene a highly selective production of **1** occurred without the concomitant formation of any by-products. However, the reaction proceeded with only moderate rate, comparable to that of the two orthometalated complexes (Figure 2, curve F).

Cyclodimerization of Arylalkynes

It was found that only diarylalkynes can be cyclodimerized to naphthalene derivatives (Scheme 1). Introduction of electron-donating substituents accelerated the reaction while electron-withdrawing ones had the opposite effect. According to HPLC analysis, unsymmetrically substituted diarylalkynes like *p*-nitrophenylacetylene afforded four regioisomers with a slight preference of the product formed by *ortho*-metalation of the *p*-nitrophenyl group. Isolated yields of **1**−**3** and **4**−**5** were in the range of 60−85% and 37%, respectively. Mixed alkyl/aryl-substituted alkynes were difficult to cyclodimerize, especially when electron-withdrawing substituents were present. Accordingly, PhC_2CO_2Et and PhC_2COMe could not be converted to the corresponding naphthalene. Contrary to that, the latter alkyne can be cyclodimerized by $RhCl_3$ and Aliquat-336® in a mixed tetrachloroethane/water solvent.[8]

In an attempt to accomplish a co-cyclodimerization, tolan and 4-octyne were employed as the substrates. Although **5** was produced in moderate yield, it could not be obtained analytically pure (Scheme 1).

Scheme 1

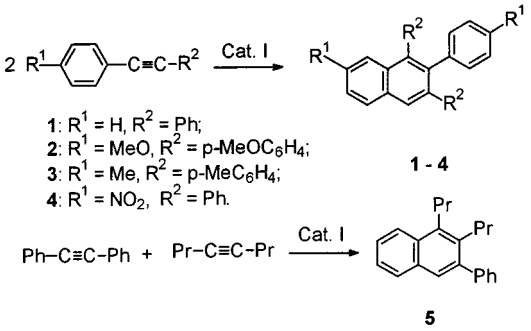

The structures of the naphthalene derivatives were confirmed by multidimensional H-H COSY, NOEs, NOESY, C-H HETCOR, COLOC NMR techniques.[14] A single-crystal X-ray analysis of **4** confirmed the proposed structure (Figure 3, Table 1). The C−C bonds of the naphthalene ring agree with the values reported for perchloro-1,2,3-triphenylnaphthalene.[15] The three phenyl rings at C1, C2, and C3 are twisted out of the naphthalene plane by 76.3°, 69.0°, and 126.4°, respectively, and both nitro groups are aligned with the corresponding ring planes.

Figure 3. ORTEP drawing (drawn at 50% probability level) of **4**

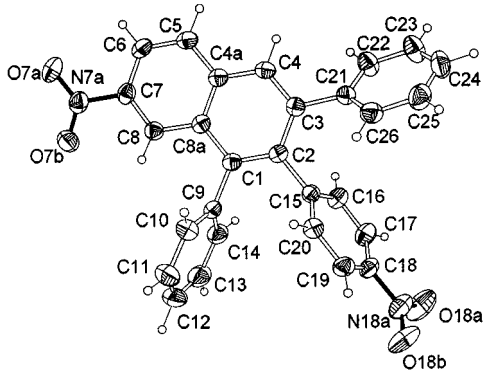

Table 1. Selected bond lengths [Å] and bond angles [°] for **4**

C(7)−C(8)	1.366(2)	C(6)−C(7)−C(8)	123.3(1)
C(6)−C(7)	1.396(2)	C(8)−C(7)−N(7a)	117.7(1)
C(5)−C(6)	1.358(2)	C(6)−C(7)−N(7a)	119.0(1)
C(5)−C(4a)	1.425(2)	C(5)−C(6)−C(7)	118.7(1)
C(4)−C(4a)	1.410(2)	C(6)−C(5)−C(4a)	120.9(1)
C(4a)−C(8a)	1.421(2)	C(4)−C(4a)−C(8a)	118.9(1)
C(3)−C(4)	1.374(2)	C(4)−C(3)−C(21)	117.8(1)
C(2)−C(3)	1.432(2)	C(2)−C(3)−C(21)	122.5(1)
C(3)-C(21)	1.496(2)	C(1)−C(2)−C(15)	119.0(1)
C(1)−C(2)	1.388(2)	C(3)−C(2)−C(15)	120.7(1)
C(2)−C(15)	1.500(2)	C(2)−C(1)−C(9)	121.9(1)
C(1)−C(8a)	1.433(2)	C(8a)−C(1)−C(9)	118.4(1)
C(1)−C(9)	1.498(2)	C(8)−C(8a)−C(4a)	118.6(1)
C(8a)−C(8)	1.414(2)	C(4a)−C(8a)−C(1)	119.6(1)

Mechanistic Investigations

The reaction is strongly solvent-dependent and does not occur in non-protic solvents like THF, acetonitrile, triethylamine, toluene, chlorobenzene, DMF, tetrachloroethane, nitrobenzene, aniline, and DMSO. In methanol, even upon refluxing for 3 days, no naphthalene could be detected, whereas this was possible when the boiling point of the alcohol was above 100°C. All of the following experiments were performed with catalyst **I** in refluxing 1-pentanol solution.

Influence of the Acid

Changing the molar ratio [HCl]/[Rh] from 34:1 to 1:1 decreased the initial turnover rate (TOR) of **1** from 18 to 0.7 h^{-1} indicating that stoichiometric amounts of HCl cannot sustain a high catalytic activity (Figure 4). Varying the same ratio to 68:1, reduced the TOR down to 8 h^{-1}. When HCl_{conc} was substituted by HBr_{conc} and HI_{conc}, the TOR decreased from 18 to 13 and 6, respectively.

Figure 4. Influence of HX on catalytic activity of catalyst **I**: [HCl]/[Rh] = 1:1 (A), 34:1(B), 68:1 (C)

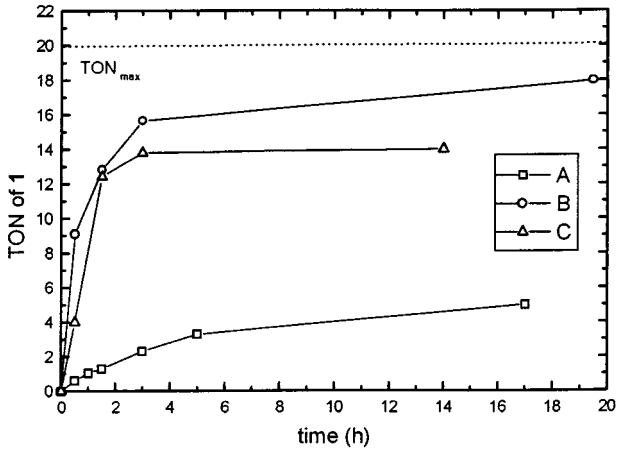

Influence of Azobenzene

Upon variation of the ratio [Rh]/[PhN_2Ph] at a fixed [Rh]/[PhC_2Ph] value from 1:1 to 1:5, 1:10, and 1:40, it turned out that the highest TORs were observed at the values of 1:5 and 1:10 (Figure 5).

Figure 5. Influence of azobenzene concentrations on catalytic activity catalyst **I**: [Rh]/[azobenzene] = 1:1 (A), 1:5 (B), 1:10 (C), 1:40 (D)

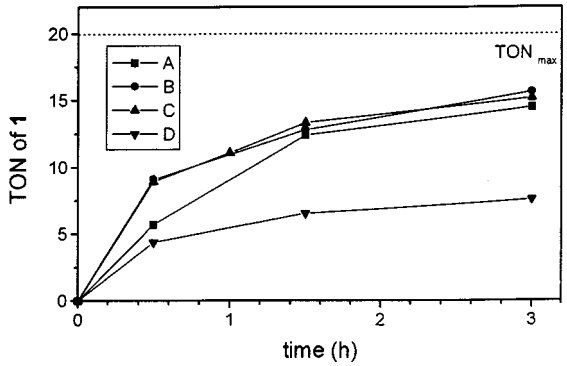

Kinetic Measurements

The initial reaction rate as function of different substrate concentrations was measured by monitoring the formation of **1** by HPLC (d*P*/d*t*, Figures 6a, 6b). From the slopes of 1.03 and 0.9 as obtained from a plot of logarithm of initial rate vs. logarithm for tolan and $RhCl(PPh_3)_3$, respectively, a reaction order of unity is assumed for both components. When the catalyst concentration was increased above 0.5 mol/L, the reaction became slower while a higher concentration of tolan favored cyclotrimerization to hexaphenylbenzene. These results suggest that the transition state of the rate-determining step contains one molecule of tolan coordinated to a mononuclear rhodium complex. Activation parameters of $\Delta H^{+} = 94.7 \pm 10$ kJ mol^{-1} and $\Delta S^{+} = 36 \pm 6$ J K^{-1} mol^{-1} were calculated from the temperature dependence of the rate constant in the range of 105−130°C (Figure 6c).

Postulated Catalytic Cycle

From the results presented above a plausible mechanism for the cyclodimerization in the presence of catalyst **I** is schematically depicted in Scheme 2.

It is recalled that in the absence of HX tolan and azobenzene undergo a $RhCl(PPh_3)_3$-catalyzed co-cyclodimerization affording *N*-anilino-2,3-diphenylindole.[10] This reaction is inhibited by the presence of the mineral acid in favor of the alkyne cyclodimerization to 1,2,3-triphenylnaphthalene. According to the reaction conditions it is assumed that the first step is loss of a PPh_3 ligand followed by oxidative addition of HX to **A** affording the rhodium(III) intermediate **B** (Scheme 2). Since it is known from the literature that HX reacts with $RhCl(PR_3)_3$ (R = Ph, Cy) already at room temperature,[16][17] it seems unlikely that the slower naphthalene formation in the presence of HBr and HI is due to slowing down of this reaction step. Subsequent insertion of the alkyne into the Rh−H bond should be a fast process

Figure 6. Plot of log(d*P*/d*t*) vs. logarithm of the concentration of tolan (a) and $RhCl(PPh_3)_3$ (b); Arrhenius plot (c)

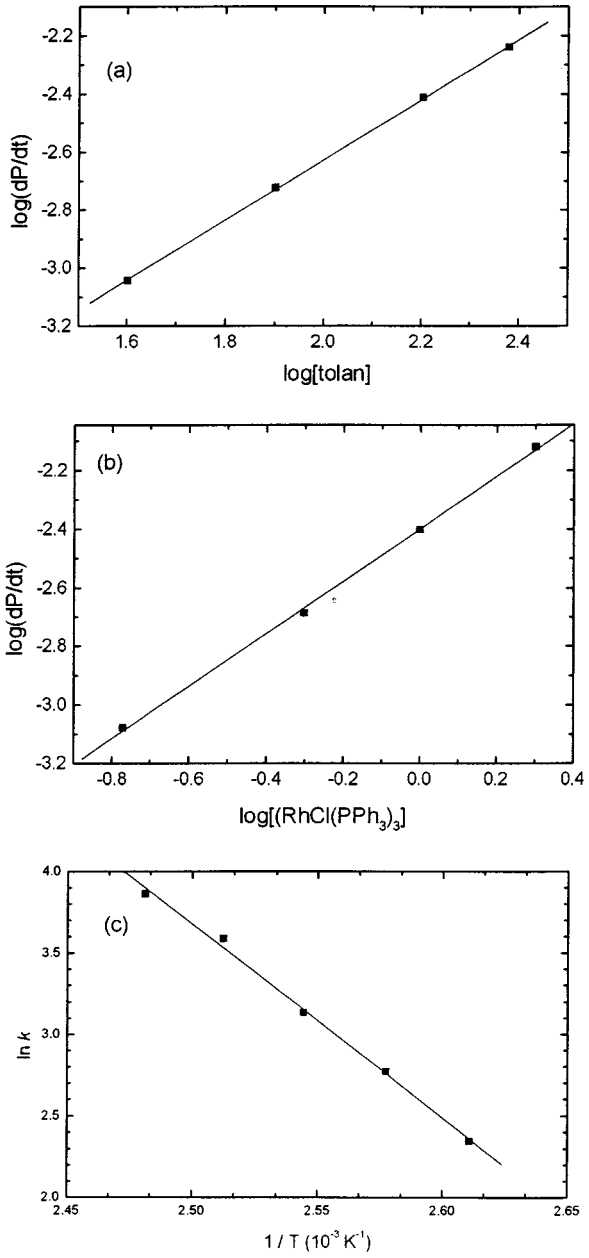

as known for the corresponding reaction of acetylene with $RhHCl_2(PPh_3)_2$.[17][18] Successive *cis*/*trans* isomerization of the vinyl ligand leads to **C**. Although this is a rhodium(III) complex, it is postulated to undergo *ortho*-metalation as reported for comparable cases.[18][19] In view of the presence of weak intramolecular $CH\cdots XRh^{III}$ interactions in related hexacoordinated rhodium(III) complexes,[1] a multicenter transition state as depicted in Figure 7 is proposed. This would rationalize the slower rate found in the presence of HBr and HI since the interaction is weaker when the electronegativity of X decreases.[20] In agreement with the observed rate law, this step should be rate-determining. As a competitive reaction, reductive $C(sp^2)-Cl$ elimination from **C** leads to 1-chlorostilbene, the major by-product in the absence of azobenzene, but only formed in traces in its presence. As a weak base, azobenzene may facilitate elimination of HX and therefore favor *ortho*-metalation of tolan over reductive elimination of 1-chlorostilbene. As indicated in Scheme 2, azobenzene or a derivative thereof may be coordinated to the rhodium center throughout the whole catalytic cycle. Insertion of the second alkyne into an Rh−C bond of **D** and reductive $C(sp^2)-C(sp^2)$ elimination leads to **1** and the starting complex **A**.

Scheme 2. Postulated catalytic cycle for catalyst **I** ($RhCl(PPh_3)_3$, PhN=NPh, and HCl in 1-pentanol)

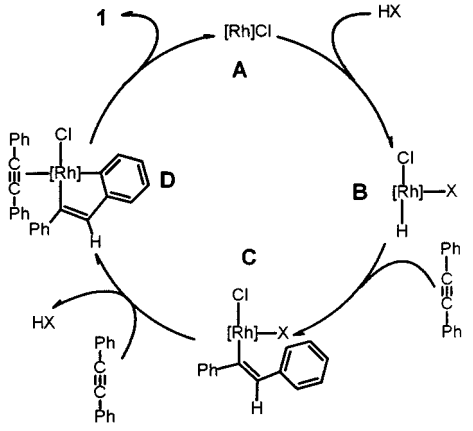

Figure 7. Transition state postulated for the *ortho*-metalation step; see also Scheme 2

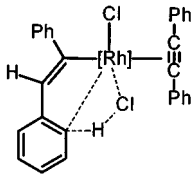

This work was supported by the *Deutsche Forschungsgemeinschaft*, the *Fonds der Chemischen Industrie* and the *Degussa AG*. We thank Dr. *M. Moll* for the NMR measurements. L. H. is indebted to the *Hanns-Seidel-Stiftung* and the *Chinese Government* for a fellowship.

Experimental Section

General: Unless otherwise mentioned, all operations were performed under dry and oxygen-free nitrogen using standard Schlenk techniques. All solvents were degassed and saturated with nitrogen before use. Rhodium trichloride hydrate was obtained from Degussa AG. Commercial triphenylphosphane, and *trans*-azobenzene (Aldrich, Merck) were used after recrystallization from ethanol. Commercial tolan, 4-octyne, 1-phenyl-1-propyne, ethyl 3-phenylpropiolate, 4-phenyl-3-butyn-2-one, dimethyl acetylenedicarboxylate, 3-pentyn-1-ol were directly used without any purification. $RhCl(PPh_3)_3$,[21] $RhCl(PCy_3)_2$,[22] $RhCl_2(C,N\text{-}C_6H_4N{=}NC_6H_5)(PPh_3)_2$[23], $RhCl_2(C,N\text{-}C_6H_4CH{=}NNHPh)(PPh_3)_2$,[11] $RhHCl(C,N\text{-}CH_3C_6H_3N{=}NC_6H_4CH_3)(PCy_3)_2$,[24] $Rh(CO)Cl(PPh_3)_2$,[25] $RhH(PPh_3)_4$[26] and $RhH(CO)(PPh_3)_3$[27] were prepared according to literature procedures.

Scheme 3. Atom numbering of compounds **1**−**4** used for NMR signal assignment

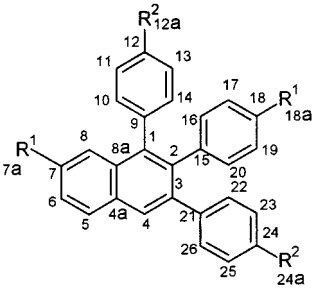

^{1}H- and ^{13}C-NMR spectra were measured in $CDCl_3$ as solvent and TMS as internal standard at 400 (or 270) and 100 (or 67) MHz, respectively, and IR spectra in KBr unless otherwise noted. − NMR: Jeol FT-JNM-LA 400 and Jeol FT-JNM-EX 270. − IR: Perkin-Elmer 983 and FT IR 1600. − UV/Vis: Shimadzu UV-3101 PC. − MS: Jeol MStation 700 and Varian MAT 212 (70eV). − Elemental analysis: Carlo Erba 1106 (CHN). − HPLC: Knauer HPLC pump 64 with analytical and preparative pump head, Knauer UV/Vis filter photometer at λ = 220 nm as detector. − Analytical measurements: Precolumn (30 mm × 8 mm) attached to main column (250 mm × 8 mm) and both filled with Spherisorb ODS2, 5 μm (RP C18), eluting with CH_3CN/H_2O = 5:1 (v/v) at a flow rate of 5.0 mL/min. − Preparative isolations: 1 mL of the acetonitrile solution was injected; identical elution agent and filling material was used while the size of precolumn and main column was 30 mm × 32 mm and 250 mm × 32 mm, respectively; the flow rate was 35 mL/min.

General Procedure for the Synthesis of Trisubstituted Naphthalenes: A solution of 46.2 mg (0.05 mmol) of $RhCl(PPh_3)_3$ in 5 ml of 1-pentanol and 0.15 ml (1.71 mmol) of HCl (conc., 37%) were stirred upon refluxing in an oil bath at 160°C for 1 min. Thereafter, 48 mg (0.25 mmol) of azobenzene, dissolved in 5 ml of 1-pentanol, was added to the reaction mixture and stirred under reflux for 20 min. Subsequently, 356 mg (2.0 mmol) of tolan or 2.0 mmol of a derivative thereof, dissolved in 20 ml of 1-pentanol were added dropwise within 15 to 20 min. Stirring the reaction mixture under reflux was continued for another 3 h. After removal of the solvent, the resulting orange residue was chromatographed on silica gel (SiO_2-60, d = 1.5 cm, l = 10 cm) with toluene as eluting agent. A colorless fraction was collected, the solvent removed and the gray residue recrystallized from CH_2Cl_2/MeOH = 1:5 (v/v). 216 mg (1.2 mmol, 60%) of **1** (mp. 151°C) was obtained. − $C_{28}H_{20}$ (356.5): calcd. C 93.94, H 5.60; found C 94.13, H 5.60. − MS (FD, CH_2Cl_2); *m/z*: 356 [M^+]. − ^{1}H NMR ($CDCl_3$, 270 MHz): d = 7.93 (s, 1 H, 4-H), 7.90 (d, 1 H, 5-H), 7.57 (d, 1 H, 8-H), 7.47 (t, 1 H, 6-H), 7.35 (t, 1 H, 7-H), 7.10−7.25 (m, 10 H) and 6.82−6.95 (m, 5 H) for the 15 protons of the three substituent phenyl rings. − ^{13}C NMR ($CDCl_3$, 100 MHz): d = 124.4 (C-12), 125.6 (C-18), 125.6 (C-24), 126.0 (C-6), 126.1 (C-7), 126.8 (C-17), 126.8 (C-19), 126.8 (C-8), 127.5 (C-11), 127.5 (C-13), 127.5 (C-23), 127.5 (C-25), 127.9 (C-5), 128.7 (C-4), 130.0 (C-10), 130.0 (C-14), 131.2 (C-22), 131.2 (C-26), 131.5 (C-16), 131.5 (C-20), 132.0 (C-8a), 132.6 (C-4a), 138.1 (C-3), 139.1 (C-2), 139.4 (C-9), 139.9 (C-1), 140.0 (C-21), 142.0 (C-15).

Various Catalytic Systems: General procedure described above; catalysts and TON of **1** were given as follows: (1) $RhCl(PPh_3)_3$ and azobenzene: 9 (0.5 h), 13 (1.5 h), 16 (3 h), 17 (5 h), 18 (19.5 h); (2) $RhCl(PPh_3)_3$: 1 (1 h), 8 (3 h), 9 (5 h), 12 (17 h); (3) $RhCl_2$(*C,N*-$C_6H_4N{=}NC_6H_5$)$(PPh_3)_2$: 0.4 (0.5 h), 3 (1.5 h), 10 (3 h), 16 (5 h), 16 (7 h); (4). $RhCl_2$(*C,N*-$C_6H_4CH{=}NNHC_6H_5$)$(PPh_3)_2$: 0.7 (0.5 h), 3 (1 h), 5 (1.5 h), 9 (3 h), 9 (5 h), 12 (20 h); (5) RhHCl(*C,N*-$CH_3C_6H_3N{=}NC_6H_4CH_3$)$(PCy_3)_2$: 1.4 (0.5 h), 8 (1.5 h), 13 (3 h), 14 (4 h), [thereafter solid tolan was added, the TON of **1** reached 325 (TON_{max} = 500) upon refluxing for 4 d]; (6) $RhCl(PCy_3)_2$: 2 (0.5 h), 9 (1.5 h), 14 (3 h), 14 (4 h). [thereafter, addition of solid tolan afforded a TON of 174 (TON_{max} = 250) upon refluxing for 4 d]. Unless otherwise noted, the general procedure as described for **1** was applied for the following syntheses. The resulting residue obtained from column chromatography was further purified by preparative HPLC.

Synthesis of 2−5

7-Methoxy-1,2,3-tris(4-methoxyphenyl)naphthalene (**2**): 476 mg (2.0 mmol) of 4,4′-dimethoxytolan and 46.2 mg (0.05 mmol) of $RhCl(PPh_3)_3$ were refluxed for 5 h. The raw product was recrystallized from hexane, yielding 367 mg (1.54 mmol, 84%) of **2** (mp 177°C). − $C_{32}H_{28}O_4$ (476.6): calcd. C 80.65, H 5.92; found C 80.39, H 6.09. − MS (FD, CH_2Cl_2); *m/z*: 476 [M^+]. − ^{1}H NMR: ($CDCl_3$, 400 MHz): d = 7.79 (s, 1 H, 4-H), 7.75 (d, 1 H, 5-H), 7.14 (dd, 1 H, 6-H), 7.05 (dt, 2 H, 22/26-H), 7.03 (dt, 2 H, 10/14-H), 6.88 (s, 1 H, 8-H), 6.77 (dt, 2 H, 11/13-H), 6.74 (dt, 2 H, 16/20-H), 6.70 (dt, 2 H, 23/25-H), 6.49 (dt, 2 H, 17/19-H), 3.77 (s, 3 H, 24a-OMe), 3.73 (s, 3 H, 12a-OMe), 3.67 (s, 3 H, 7a-OMe), 3.65 (s, 3 H, 18a-OMe). − ^{13}C NMR ($CDCl_3$, 100 MHz): d = 54.9 (C-18a), 55.0 (C-7a), 55.1 (C-24a), 55.9 (C-12a), 105.5 (C-8), 112.5 (C-17), 112.5 (C-19), 113.0 (C-23), 113.0 (C-25), 113.2 (C-11), 113.2 (C-13), 118.4 (C-6), 128.3 (C-4), 128.7 (C-4a), 129.4 (C-5), 131.1 (C-22), 131.1 (C-26), 132.2 (C-9), 132.2 (C-10), 132.2 (C-14), 132.5 (C-16), 132.5 (C-20), 133.0 (C-15), 133.5 (C-8a), 134.9 (C-21), 137.6 (C-1), 137.9 (C-3), 138.6 (C-2), 157.3 (C-18), 157.7 (C-7), 157.9 (C-12), 157.9 (C-24). − HPLC (CH_3CN/H_2O = 5:1 (v/v), 5 mL/min): retention time [min] = 6.4.

7-Methyl-1,2,3-tris(4-methylphenyl)naphthalene (**3**): 412 mg (2.0 mmol) of 4,4′-dimethyltolan and 46.2 mg (0.05 mmol) of $RhCl(PPh_3)_3$ were refluxed for 2 h; 264 mg (1.28 mmol, 64%) of **3** (mp. 148°C). − $C_{32}H_{28}$ (412.6): calcd. C 93.16, H 6.84; found C 92.84 H 6.92. − MS (FD, CH_2Cl_2); *m/z*: 412 [M^+]. − ^{1}H NMR: ($CDCl_3$, 400 MHz): d = 7.83 (s, 1 H, 4-H), 7.78 (d, 1 H, 5-H), 7.31 (ds, 1 H, 8-H), 7.29 (t, 1 H, 6-H), 7.04 (dt, 2 H, 10/14-H), 7.02 (dt, 2 H, 22/26-H), 7.01(dt, 2 H, 23/25-H), 6.95 (dt, 2 H, 11/13-H), 6.73 (dt, 2 H, 16/20-H), 6.73 (dt, 2 H, 17/19-H), 2.37 (s, 3 H, 7a-Me), 2.31 (s, 3 H, 24a-Me), 2.23 (s, 3 H, 12a-Me), 2.14 (s, 3 H, 18a-Mea). − ^{13}C NMR: ($CDCl_3$, 100 MHz): d = 21.1 (C-18a), (C-24a), 21.3 (C-12a), 22.7 (C-7a), 125.8 (C-8), 127.6 (C-16), 127.6 (C-20), 127.7 (C-4), 128.1 (C-6), 128.2 (C-11), 128.2 (C-13), 128.2 (C-22), 128.2 (C-26), 128.4 (C-5), 129.9 (C-10), 129.9 (C-14), 131.0 (C-8a), 131.1 (C-23), 131.3 (C-17), 131.3 (C-19), 132.3 (C-4a), 131.1 (C-25), 134.7 (C-7), 135.5 (C-12), 135.5 (C-18), 135.5 (C-24), 136.6 (C-21), 137.3 (C-15), 138.2 (C-9), 138.5 (C-3), 139.1 (C-1), 139.5 (C-2). − HPLC [CH_3CN/H_2O = 5/1 (v/v), 5 mL/min]: retention time [min] = 17.65.

7-Nitro-2-(4-nitrophenyl)-1,3-diphenylnaphthalene (**4**) *and Regioisomers:* 447 mg (2.0 mmol) of 4-nitrotolan and 46.2 mg (0.05 mmol) of $RhCl(PPh_3)_3$ were refluxed for 15 h. Three different regioisomers were detected by analytical HPLC with retention times of 5.07, 5.47, 5.71 min, the ratio of the integration areas was 5:1:1. After removal of the solvent, the gray residue was washed with 5 mL of methanol. Since one regioisomer was rather insoluble in acetonitrile, 161 mg (0.72 mmol, 36%) of **4** could be isolated as an analytically pure yellow powder. − $C_{28}H_{18}N_2O_4$ (447.1): calcd. C 75.33, H 4.06, N 6.27; found C 75.33 H 4.02, N 6.17. − MS (FD, CH_2Cl_2); *m/z* 446 [M^+]. − ^{1}H NMR: ($CDCl_3$, 270 MHz): d = 8.56

[ds, 1 H, ^4J(8-H, 6-H) = 2.2 Hz, 8-H], 8.31 [dd, 1 H, ^3J(5-H, 6-H) = 10 Hz, ^4J(8-H, 6-H) = 2.2 Hz, 6-H], 8.07 [d, 1 H, ^3J(5-H, 6-H) = 10 Hz 5-H], 8.06 (s, 1 H, 4-H), 7.84 [dt, 2 H, ^3J(17-H, 16-H) = 9 Hz, 17/19-H], 7.32 (m, 3 H, 11/12/13-H), 7.23 (m, 3 H, 23/24/25-H), 7.14 (m, 4 H, 10/14/22/26-H), 7.04 (dt, 2 H, 16/20-H). − ^{13}C NMR ($CDCl_3$, 100 MHz): d = 120.2 (C-8), 112.9 (C-11), 122.4 (C-17), 122.4 (C-19), 123.9 (C-6), 127.5 (C-24), 128.2 (C-25), 128.0 (C-12), 128.2 (C-23), 128.8 (C-17), 128.4 (C-13), 128.4 (C-11), 128.9 (C-4), 137.3 (C-2), 129.7 (C-5), 129.7 (C-14), 129.7 (C-10), 130.1 (C-8a), 130.8 (C-22), 130.8 (C-26), 132.1 (C-16), 132.1 (C-20), 135.5 (C-7), 136.9 (C-4a), 138.0 (C-18), 140.1 (C-9), 141.7 (C-21), 143.1 (C-2), 146.1 (C-3), 146.1 (C-15), 146.5 (C-1). − HPLC [CH_3CN/H_2O = 5:1 (v/v), 5 mL/min]: retention time (integrated area) [min] of raw material = 5.07 (5.48 × 10^5) (**4**); 5.47 (9.27 × 10^4) (**4′**); 5.71 (1.37 × 10^5) (**4′′**) (ratio of **4/4′/4′′** = 5:1:1). − **4′** and **4′′** exhibited identical molecular peaks at *m/z* 446 (FD-MS). Due to the similar HPLC retention times of all three regioisomers, further purification by preparative HPLC was not attempted. − Single crystals for X-ray analysis of **4** were obtained from a CH_3CN solution exposed to air. Intensity data were collected with a Siemens P4 diffractometer at 200 K, using graphite-monochromated Mo-K_α radiation (λ = 0.71073 Å). Cell constants were obtained from the setting angles of 18 reflections in the range of 32.2° < 2θ < 35.0°. The ω-scan technique was applied using variable scan speeds (3.0−30°/min). The structure was solved by direct methods (SHELXS-86).[28] Structure refinement was carried out using full-matrix least-squares methods on F^2 (SHELXL-93).[29] All non-hydrogen atoms with anisotropic displacement parameters. All hydrogen atoms could be localized in a difference fourier map and were isotropically refined. The relevant crystal data are listed in Table 2. Further details of crystallographic data (excluding structure factors) for the structures reported in this paper have been deposited with the Cambridge Crystallographic Data Center as supplementary publication no. CCDC-101516. Copies of the data can be obtained free of charge on application to CCDC, 12 Union Road, Cambridge CB2 1EZ, UK (Fax: int. code + 44(1223)336-033; E-mail: deposit@ccdc.cam.ac.uk)

Table 2. Crystal data and details of structure refinement parameters for **4**

formula	$C_{28}H_{18}N_2O_4$
molecular weight	446.44
crystal size [mm]	0.70 × 0.70 × 60
crystal system	monoclinic
space group	$P2_1/c$
a [Å], α [°]	8.712(2), 90
b [Å], β [°]	15.747(6), 91.02(2)
c [Å], γ [°]	16.113(4), 90
V [Å^3], *Z*	2210(1), 4
μ(Mo-K_α) [mm^{-1}]	0.091
$D_{calcd.}$ [g/cm^3]	1.342
Temperature [K]	200
F(000)	928
no. of reflections collected	8682
no. of unique reflections	4836 (R_{int} = 0.0557)
no. of observed reflections	2794
obs. criterion	$F_o > 4\sigma(F_o)$
no. of refinement parameter	379
R_1 (observed data)	0.0359
wR_2 (all data)	0.0831
$\Delta\rho_{max/min}$ [e Å^{-3}]	0.213/−0.189
S (all data)	0.774

Attempted Reactions with Various Alkynes: Upon applying the general synthesis procedure for **1** to 1-phenylpropyne, 4-phenyl-3-butyn-2-one, and ethyl 3-phenylpropiolate no dimerization products were detected by analytical HPLC after 3 d of refluxing in 1-pentanol.

3-Phenyl-1,2-dipropylnaphthalene (**5**): A mixture of 356 mg (2 mmol) of tolan and 220 mg (2 mmol) of 4-octyne in 20 mL of 1-BuOH was added dropwise to a solution of 46.2 mg (0.05 mmol) of $RhCl(PPh_3)_3$ in 5 mL of 1-BuOH. After refluxing for 5 h, **5** and **1** were formed in a molar ratio of **5/1** = 5:1. After 14 h of refluxing, both alkynes were completely consumed and the ratio of **5/1** changed to 5:3. After removal of the solvent, the residue was chromatographed on SiO_2-60 with toluene as eluting agent. The resulting gray residue was further purified by prep. HPLC affording 226 mg (0.78 mmol, 39%) of a white oil of **5**. − $C_{22}H_{24}$ (288.4): calcd. C 91.61, H 8.39; found C 89.54, H 9.04.[30] − MS (FD, CH_2Cl_2); *m/z*: 288 [M$^+$]. − ^{1}H NMR ($CDCl_3$, 270 MHz): d = 8.03 (d, 1 H, 8-H), 7.75 (d, 1 H, 5-H), 7.52 (s, 1 H, 4-H), 7.40−7.42 (m, 2 H, 6/7-H), 7.33−7.42 {m, 5 H, [7.34 (t, 1 H, 25/27-H), 7.38 (t, 17/19-H), 7.37 (d, 2 H, 16/20-H)]}, 3.09 (td, 2 H, 9/9′-H of C-1-CH_2CH$_2$CH$_3$), 2.69(td, 2 H, 12/12′-H of C-2-CH_2CH$_2$CH$_3$), 1.75 (td, 2 H, 10/10′-H of C-1-CH$_2$CH_2CH$_3$), 1.41(td, 2 H, 13/13′-H of C-2-CH$_2$CH_2CH$_3$), 1.14 (td, 3 H, 11/11′-H of C-1-CH$_2$CH$_2$CH_3), 0.78 (td, 3 H, 14/14′-H of C2-CH$_2$CH$_2$CH_3). − ^{13}C NMR ($CDCl_3$, 100 MHz): d = 14.9 (C-11), 24.6 (C-10), 31.1 (C-9), 32.5 (C-12), 24.6 (C-13), 124.0 (C-8), 124.9 (C-6), 125.7 (C-7), 127.4 (C-4), 14.6 (C-14), 127.8 (C-16), 128.5 (C-5), 129.4 (C-17), 126.7 (C-18), 129.4 (C-19), 127.8 (C-20), 131.9 (C-8a), 132.5 (C-4a), 136.2 (C-1), 136.4 (C-2), 141.3 (C-3), 143.0 (C-15). − HPLC [CH_3CN/H_2O = 5:1 (v/v), 5 mL/min]: retention time (integrated area) [min] of raw material (4 h refluxing) = 8.5 (1.3 × 10^5) (**1**); 13.4 (6.9 × 10^5) (**5**); (ratio of **5/1** = 5:1); (14 h refluxing) = 8.5 (4.4 × 10^5) (**1**); 13.4 (9 × 10^5) (**5**); (ratio of **5/1** = 2:1).

Kinetic Measurements

General: For the measurement of the initial rate as a function of substrate concentration the general procedure as described for the synthesis of **1** was applied except that the oil bath was thermostated to 130.0 ± 0.1 °C. Samples of 200 μL were withdrawn after 30, 60, 90, and 120 min, concentrated to dryness without further separation of the catalyst and redissolved in 4 mL of acetonitrile. The concentrations of **1** (given in the following as dimensionless numbers in the unit of 10^{-3} mol L^{-1}) were determined via a calibration curve. Reproducibility was within ±10%. Detailed data are available as Supporting Information.

☆ Dedicated to Professor *Arnd Vogler* on the occasion of his 60th birthday.

[1] L.-Y. Huang, U. R. Aulwurm, F. W. Heinemann, H. Kisch, *Chem. Eur. J.* **1998**, *9*, 1641.
[2] P. J. Stang, F. Diederich (Eds.), *Modern Acetylene Chemistry*, VCH, Weinheim, **1995**.
[3] S. Patai (Ed.), *The Chemistry of the Carbon-Carbon Triple Bond*, Wiley, New York, **1978**, vol. 1 and 2.
[4] W. Keim, A. Behr, M. Röper, in *Comprehensive Organometallic Chemistry* (Eds.: G. Wilkinson, F. G. A. Stone, E. W. Abel), vol. 8, Pergamon Press, Oxford, **1982**, p. 371.
[5] D. B. Grotjahn in *Comprehensive Organometallic Chemistry II* (Eds.: G. Wilkinson, F. G. A. Stone, E. W. Abel), vol. 12, Pergamon Press, **1995**, p. 741.
[6] L. I. Smith, H. H. Hoehn, *J. Am. Chem. Soc.* **1941**, *63*,1184.
[7] D. Bryce-Smith, *Chem. Ind.* **1964**, *8*, 239.
[8] I. Amer, J. Blum, K. P. C. Vollhardt, *J. Mol. Catal*. **1990**, *60*, 323.
[9] R. A. Sanchez-Delgado, G. Wilkinson, *J. Chem. Soc., Dalton Trans.* **1977**, 804.
[10] U. R. Aulwurm, U. J. Melchinger, F. Knoch, H. Kisch *Organometallics* **1995**, *14*, 3385.
[11] U. R. Aulwurm, Ph.D. Dissertation, Universität Erlangen-Nürnberg, **1996**.

[12] S. Westernacher, Ph.D. Dissertation, Universität Erlangen-Nürnberg, **1996**.
[13] L.-Y. Huang, Ph.D. Dissertation, Universität Erlangen-Nürnberg, **1998**.
[14] L.-Y. Huang, M. Moll, A. Zahl, H. Kisch, in preparation.
[15] S. Gali, X. Solans, C. Miravitlles, M. Font-Altaba, *Acta. Crystallogr.* **1978**, *B34*, 1011.
[16] M. C. Baird, D. N. Lawson, J. T. Mague, J. A. Osborn, G . Wilkinson, *J. Chem. Soc. A* **1967**, 1347.
[17] The corresponding reaction with $RhHCl_2(PCy_3)_2$ is very slow and may account for the induction period observed for naphthalene formation with this catalyst: H. L. M. van Gaal, J. M. J. Verlaak, T. Posno, *Inorg. Chim. Acta* **1977**, *23*, 43.
[18] F. Estevan, G. González, P. Lahuerta, M. Martinez, E. Peris, R. van Eldik, *J. Chem. Soc., Dalton Trans.* **1996**, 1045.
[19] [19a] H. Werner, J. Wolf, U. Schubert, K. Ackermann, *J. Organomet. Chem*. **1986**, *317*, 327. – [19b] H. Werner, A. Höhn, *J. Organomet. Chem*. **1984**, *272*, 105.
[20] A. Allerhand, P. v. R. Schleyer, *J. Am. Chem. Soc*. **1963**, 1715.
[21] J. A. Osborn, G. Wilkinson *Inorg. Synth*. **1967**, *10*, 67.
[22] H. L. M. van Gaal, F. L. A. van den Bekerom, *J. Organomet. Chem*. **1977**, *134*, 237.
[23] U. R. Aulwurm, F. Knoch, H. Kisch, *Z. Naturforsch.* **1996**, *51b*, 1555.
[24] J. F. van Baar, K. Vrieze, D. J. Stufkens, *J. Organomet. Chem*. **1975**, *97*, 461.
[25] J.A. Osborn, F. H. Jardine, F. H. Young, G. Wilkinson, *J. Chem. Soc. A* **1966**, 1711.
[26] N. Ahmad, J. J. Levison, S. D. Robinson, *Inorg. Synth.* **1974**, *15*, 58.
[27] N. Ahmad, J. J. Levison, S. D. Robinson, *Inorg. Synth.* **1974**, *15*, 59.
[28] G. M.Sheldrick, *SHELXS-86, Program for Crystal Structure Solution*, Univ. of Göttingen, Germany, **1986**.
[29] G. M. Sheldrick, *SHELXL-93, Program for Crystal Structure Refinement*, Univ. of Göttingen, Germany, **1993**.
[30] Repeated purification by HPLC did not improve these values.
[I98149]

Synthesis of Functionalized Calix[4]arene Ligands Incorporating Bipyridine *N,N′*-Dioxide Chromophores and Luminescence of Their Lanthanide Complexes

Luca Prodi*[a], Silvia Pivari[a], Fabrizio Bolletta[a], Muriel Hissler[b], and Raymond Ziessel*[b]

Dipartimento di Chimica "G. Ciamician", Università di Bologna[a],
Via Selmi 2, I-40126 Bologna, Italy
Fax: (internat.) + 39-51/259456
E-mail: lprodi@ciam.unibo.it

Laboratoire de Chimie, d'Electronique et de Photonique Moléculaires, École de Chimie, Polymères, Materiaux, Université Louis Pasteur[b],
1 rue Blaise Pascal, F-67008 Strasbourg Cedex, France
Fax: (internat.) + 33-3/88416825
E-mail: ziessel@chimie.u-strasbg.fr

Received June 5, 1998

Keywords: Luminescence / Lanthanides / Calixarenes / 2,2′-Bipyridine *N,N′*-dioxide / Podands / Cryptands

Members of a new family of lanthanide complexes of the cone-shaped podand **1** and the barrel-shaped cryptand **2**, based on calix[4]arenes incorporating bipyridine *N,N′*-dioxide chromophores, have been synthesized and characterized. The complexes were found to be stable in water and coordinating solvents. High molar absorption coefficients {ε = 28000 and 36000 $M^{-1}cm^{-1}$ for $[Eu(\mathbf{1})]^{3+}$ and $[Eu(\mathbf{2})]^{3+}$, respectively} and high metal luminescence quantum yields {Φ = 0.19 and 0.11 for $[Eu(\mathbf{1})]^{3+}$ and $[Eu(\mathbf{2})]^{3+}$, respectively} were obtained. The effect of OH oscillators, attached at the lower rim of the calixarenes, on the non-radiative deactivation to the ground state has been demonstrated.

Luminescence spectroscopy is attracting immense interest in the scientific community owing to its potential application in growing fields of great economical and social impact, such as environmental sciences, medical diagnostics, and cell biology.[1][2][3][4] In particular, the synthesis, characterization, and application of many luminescent labels and sensors has opened up a lot of opportunities for solving complex analytical problems, among which the fluorescence immunoassay certainly has a central role.[1][5]

The major drawback in photoluminescence analysis, particularly when dealing with biological material, is the interference caused by autofluorescence and light scattering. Time resolved spectroscopy, which requires the use of labels with very long luminescence lifetimes, can efficiently exclude this kind of background light. For this reason, over the past decade great interest has been centered on the design of luminescent complexes containing the Eu^{3+} and Tb^{3+} ions, which possess luminescence lifetimes in the micro- to millisecond range.[1][6][7][8][9] To obtain an efficient luminescent label, the ligand needs to be able to form stable complexes with the lanthanide ions in coordinating solvents, to shield the ion from deactivating solvent molecules, and, particularly importantly, to absorb light and to transfer it to the metal ion with high efficiency, thereby overcoming the intrinsic low absorption coefficients of the metal ions.[6][7][8][9] With these goals in mind, and thanks to the great progress made in the field of supramolecular chemistry, many encapsulating ligands possessing the required characteristics have been synthesized,[6] and, among these, particular attention has been focused on functionalized calixarenes.[10][11][12][13][14][15][16][17][18][19] In this context, we report here on the synthesis of new functionalized calix[4]arene ligands incorporating bipyridine *N,N′*-dioxide chromophores and on the luminescence of their Eu^{3+}, Tb^{3+}, and Gd^{3+} complexes.

Results

Ligands **1** and **2** and their lanthanide complexes were prepared as outlined in Schemes 1 and 2 using well-established synthetic procedures for 1,3-disubstituted calix[4]arene ethers in the cone conformation.[20][21] The initially designed ligand **1** was prepared by reaction of *p-tert*-butylcalix[4]arene with 5-bromomethyl-5′-methyl-2,2′-bipyridine *N,N′*-dioxide in anhydrous acetonitrile using K_2CO_3 as base (Scheme 1). Ligand **2** (Scheme 2) was prepared under similar conditions starting from *p-tert*-butylcalix[4]arene and 5,5′-bromomethyl-2,2′-bipyridine *N,N′*-dioxide. Both ligands were isolated in a pure state after chromatography on neutral alumina. In solution at room temperature, they adopt a fixed cone conformation with the ligating groups on the same side of the plane formed by the macrocycle, as was deduced from their ^{1}H-NMR spectra. In both ligands, the methylene protons give rise to an AB quadruplet, at δ = 3.75 (J_{AB} = 13.1 Hz and Δν = 168.5 Hz) in **1** and at δ = 3.81 (J_{AB} = 13.3 Hz and Δν = 172.2 Hz) in **2**. The aromatic

 © WILEY-VCH Verlag GmbH, D-69451 Weinheim, 1998 1434−1948/98/1212−1959 $ 17.50+.50/0

Scheme 1

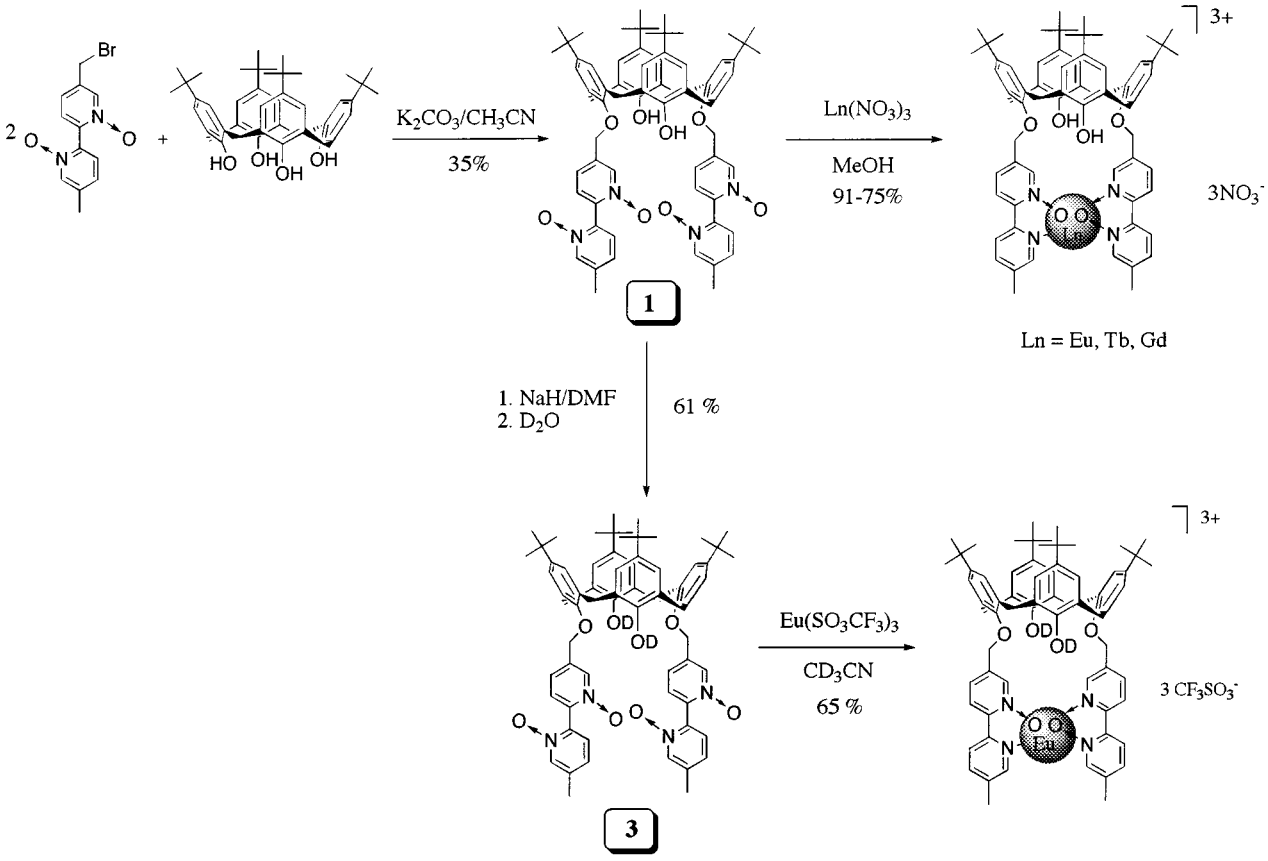

Scheme 2

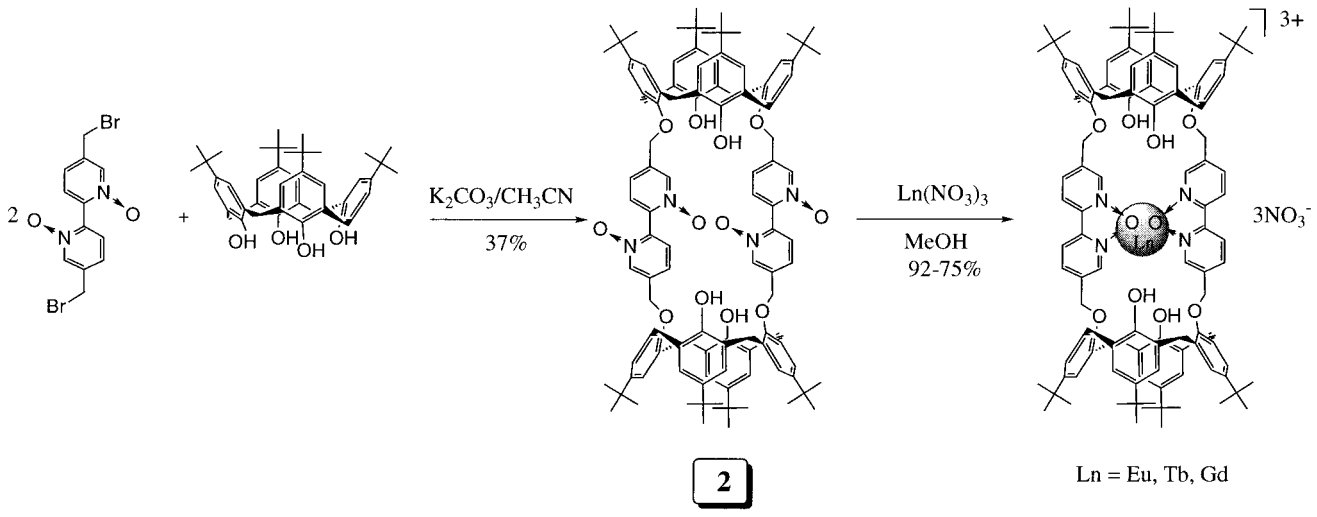

protons of the calix[4]arene skeleton give rise to two singlets at δ = 7.05 and 6.81 for **1** and at δ = 7.09 and 6.82 for **2**, while the phenol groups resonate at δ = 6.98 in **1** and δ = 7.03 in **2**. Ligand **3** was prepared by deprotonation of **1** by treatment with NaH in anhydrous dimethylformamide, followed by quenching with D_2O (Scheme 1). The proton-deuterium exchange was monitored by ^1H NMR, which showed the absence of phenolic proton signals, and was verified by FAB^+ MS.

The lanthanide complexes were prepared by treating equimolar quantities of the ligands with the appropriate nitrate salts in methanol. Double recrystallization from ethyl acetate/hexane gave the pure complexes, which were characterized by UV/Vis and IR spectroscopy, FAB^+ MS, and elemental analysis.

The Eu^{3+}, Tb^{3+}, and Gd^{3+} complexes of the ligands **1** and **2** were found to be chemically and photochemically stable in methanolic solution, in line with expectation con-

Table 1. Absorption and luminescence properties of the Eu^{3+} and Tb^{3+} complexes in methanol solutions

	Absorption		Luminescence					
	λ_{max} [nm]	ε_{max} [M^{-1} cm^{-1}]	τ(300 K, OH) [ms]	Φ(300 K, OH)	τ(300 K, OH) [ms]	Φ(300 K, OH)	τ(77 K, OH) [ms]	τ(77 K, OH) [ms]
$[Eu(\mathbf{1})]^{3+}$	260	28000	0.69	0.19	0.69[a]	0.19	0.67	0.68[b]
$[Eu(\mathbf{2})]^{3+}$	260	36000	0.68	0.11	0.68	0.10	0.68	0.69
$[Tb(\mathbf{1})]^{3+}$	260	28500	–	–	–	–	0.85	0.86
$[Tb(\mathbf{2})]^{3+}$	262	36200	–	–	–	–	0.76	0.76

[a] 0.76 ms for the deuterated ligand; for more details, see text. – [b] 0.77 ms for the deuterated ligand; for more details, see text.

sidering the better complexation properties of the $bpyO_2$ groups compared with those of the bpy ligand.[22] Good stabilities were also observed in aqueous solution, although the solubilities in water were somewhat lower. For this reason, all the photophysical data collected in Table 1 were obtained using methanolic solutions. The absorption spectra of all the complexes are dominated by the bands of the $bpyO_2$ groups {see, for example, Figure 1 for $[Eu(\mathbf{1})]^{3+}$}, which are characterized by high molar absorption coefficients and cover the absorption bands due to the calixarene moieties, which lie in the same spectral region and have typically much lower absorption coefficients (of the order of 10^3 M^{-1} cm^{-1}).[10][11][12][13][14][15][16][17][18]

Room temperature excitation of the Gd complexes did not lead to any appreciable luminescence. At 77 K, a weak, structured phosphorescence band was observed {τ = 2.1 and 2.2 ms for $[Gd(\mathbf{1})]^{3+}$ and $[Gd(\mathbf{2})]^{3+}$, respectively}, the highest energy feature of which peaked at 475 nm.

Upon excitation in the absorption bands of the ligand, the Eu^{3+} complexes showed a very intense metal-centered luminescence {Φ = 0.19 and 0.11 for $[Eu(\mathbf{1})]^{3+}$ and $[Eu(\mathbf{2})]^{3+}$, respectively, see Table 1}, with a rather short lifetime. Neither the lifetimes nor the quantum yields showed any noticeable change upon deuteration of the solvent or lowering of the temperature (Table 1). The metal luminescence excitation spectra were very similar to the absorption spectra {see, for $[Eu(\mathbf{1})]^{3+}$, Figure 1}.

Figure 1. Absorption (full line) and metal luminescence excitation (λ_{em} = 615 nm, dotted line) spectra of a $1.4 \cdot 10^{-5}$ M methanolic solution of $[Eu(\mathbf{1})]^{3+}$

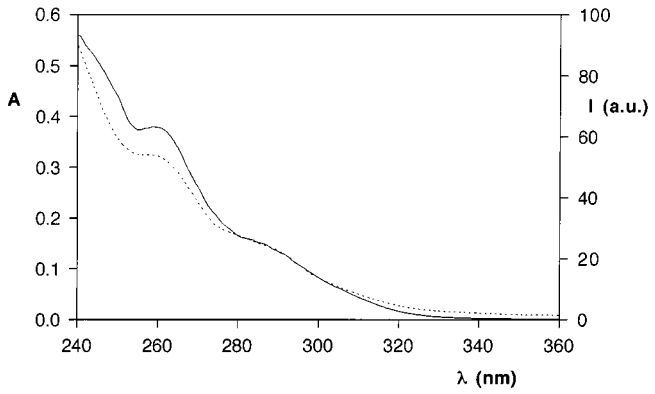

In contrast to the aforementioned observations for the Eu^{3+} complexes, the corresponding Tb^{3+} complexes did not exhibit any appreciable metal-centered luminescence at room temperature when excited in the absorption bands of the ligand. However, at 77 K, a quite intense luminescence from the Tb^{3+} ion was again observed (Table 1). Excitation spectra recorded under these conditions were very similar to the absorption spectra of the Tb^{3+} complexes.

Discussion

Gd^{3+} Complexes

The absence of low-energy, metal-centered (MC) excited states in the Gd complexes is often exploited for investigating the behaviour of the ligand-centered (LC) excited states in a structure identical to other lanthanide complexes.[23] For the complexes of ligands **1** and **2**, the absence of a fluorescence band, both at room temperature and at 77 K, prevents us from estimating the energy of the $^1\pi\pi^*$ LC level, while from the highest energy feature of the phosphorescence band observed at 77 K the zero-zero energy of the $^3\pi\pi^*$ LC level is found to be 21000 cm^{-1}.

Eu^{3+} Complexes

The similarity between the absorption and metal luminescence excitation spectra for all the complexes suggests that energy transfer from the $bpyO_2$ groups to the metal ion takes place. On the other hand, it is very difficult to evaluate the efficiency of the energy transfer process from the calixarene moiety because of its low absorption coefficient. The efficiency of the energy transfer from the $bpyO_2$ groups, together with the radiative and non-radiative rate constants of the luminescent $^5D_0$ Eu^{3+} level, can be estimated from the luminescence data collected in Table 1.[21][22][23][24]

The overall rate constant Σk for the decay of the luminescent $^5D_0$ Eu^{3+} level can be expressed by Eq. 1,

$$\Sigma k = 1/\tau = k_r + k_{nr} \quad (1)$$

where k_r is the (temperature-independent) radiative rate constant and k_{nr} is the non-radiative rate constant. The non-radiative rate constant can be further divided into two terms; the first one, $k_{nr}(T)$, being temperature-dependent, which plays a role when short-lived, high-lying excited states are thermally accessible, and the second one, k'_{nr}, accounting for the phonon-assisted deactivation to the

ground state. Usually, the most significant contribution to the temperature-independent term comes from the decay through coupling with high-energy vibrations of the solvent (O−H vibration in water and methanol solutions), k_{nr}(OH), while the contribution from the coupling with other vibrations, k_{nr} (other vibr.), is usually small.

$$\Sigma k = 1/\tau = k_r + k_{nr}(T) + k_{nr}(\mathrm{OH}) + k_{nr}(\text{other vibr.}) \quad (2)$$

In rigid matrices of deuterated methanol or water at 77 K, $k_{nr}(T)$ and k_{nr}(OH) can be neglected, and Eq. 2 becomes

$$\Sigma k\ (77\ \mathrm{K, OD}) = 1/\tau(77\ \mathrm{K, OD}) = k_r + k_{nr}(\text{other vibr.}) \quad (3)$$

where τ(77 K, OD) is the lifetime measured at 77 K in deuterated solvents.

With the usual assumption that k_{nr}(other vibr.) can be neglected, k_r becomes equal to 1/τ(77 K, OD). In the present case, the values of k_r calculated in this way are 1470 and 1450 s^{-1} for [Eu(**1**)]$^{3+}$ and [Eu(**2**)]$^{3+}$, respectively. It is important to note at this point that these values are very high compared with those observed for other Eu^{3+} complexes,[6] for which the radiative rate constants lie in the range 350−900 s^{-1}. In fact, we thought it very unlikely that [Eu(**1**)]$^{3+}$ and [Eu(**2**)]$^{3+}$ could have such markedly different radiative rate constants compared to the previously observed values for complexes with many different ligands. As a first hypothesis, we thought that the OH groups present on the lower rim of the calixarene macrocycles, which point towards the metal ions, might, at least in part, be responsible for a non-negligible value of the term k_{nr} (other vibr.) in our systems. Considering the k_{nr}(OH) values reported in the literature for Eu complexes, it is apparent that these contain a contribution of ca. 1000 s^{-1} per coordinated water molecule or ca. 500 s^{-1} per coordinated methanol molecule, i.e. ca. 500 s^{-1} per OH oscillator.[6][24][25] For the [Eu(**1**)]$^{3+}$ complex, where two OH oscillators are present in the ligand, a value of ca. 1000 s^{-1} for k_{nr}(other vibr.) could, in principle, be expected. In order to assess this hypothesis, we synthesized the Eu^{3+} complex with ligand **3**, possessing OD groups, since NMR measurements in deuterated methanol have shown that there is no exchange between the hydrogen of the OH groups of the complex and the deuterium atoms of the solvent. The observed lifetime of this complex in deuterated methanol was 0.76 ms at room temperature and 0.77 ms at 77 K. From Eq. 3, for the complex with the deuterated ligand, the term $k_r + k_{nr}$(other vibr.) becomes equal to 1300 s^{-1}. This value, although lower than that observed for the non-deuterated ligand, is still high, indicating that other oscillators present in the ligand might be responsible for the non-radiative deactivation to the ground state besides the OH groups. By comparison with the value obtained with the non-deuterated ligand, we can estimate that the contribution to the non-radiative rate constant attributable to the OH group is 170 s^{-1}. This contribution, although not negligible, shows that the OH groups are rather distant in relation to the metal ion. A similar contribution in the analogous complex possessing bpy groups instead of the $bpyO_2$ groups is consistent with the lifetime observed in acetonitrile solutions.[19]

The values of k_{nr}(300 K) and k_{nr}(OH) can be estimated from the measured luminescence lifetimes (Table 1) according to Eqs. 4 and 5.

$$k_{nr}(300\ \mathrm{K}) = 1/\tau(300\ \mathrm{K, OD}) - 1/\tau(77\ \mathrm{K, OD}) \quad (4)$$

$$k_{nr}(\mathrm{OH}) = 1/\tau(300\ \mathrm{K, OH}) - 1/\tau(300\ \mathrm{K, OD}) \quad (5)$$

The calculated values are very low (< 50 s^{-1}) for both the complexes, showing that no solvent molecules are coordinated to the central metal ion and that thermally activated processes (typically, for Eu^{3+} complexes, ligand-to-metal charge-transfer processes) do not play a significant role in these systems, as previously reported for other complexes containing $bpyO_2$ groups.[26]

The efficiency of the ligand-to-metal energy-transfer process (η_{et}) is usually estimated from Eq. 6, with the assumption that k_{nr}(other vibr.) is negligible. In the present case, as discussed above, it is reasonable to consider this assumption as being less than fully adequate; the efficiency calculated from this equation is thus just a limiting value, and is found to be 0.19 and 0.11 for [Eu(**1**)]$^{3+}$ and [Eu(**2**)]$^{3+}$, respectively.

$$\eta_{et} = \Phi_l \cdot \tau(300\ \mathrm{K, OH})/\tau(77\ \mathrm{K, OD}) \quad (6)$$

A quite large difference is observed between the ligand-to-metal energy-transfer efficiencies estimated for [Eu(**1**)]$^{3+}$ and [Eu(**2**)]$^{3+}$. We believe that this difference is due to the greater conformational rigidity of ligand **2**, in which the additional calixarene moiety prevents the $bpyO_2$ groups from maximizing their interaction with the central metal ion.

A comment has to be made regarding the coordination number at the central metal ion. Ligands **1** and **2** provide a smaller number of donor atoms than that usually required by Eu^{3+} ions. While the photophysical data allow us to exclude coordination of the metal ion by solvent molecules, coordination by some counterions cannot be ruled out, although no changes were observed in the luminescence spectra and lifetime on replacing the nitrate by chloride anions. It is likely that anions are coordinated in the solid state, as often observed in lanthanide X-ray structures.[27]

Tb^{3+} Complexes

The lack of a metal-centered luminescence on exciting the ligand-centered band of [Tb(**1**)]$^{3+}$ and [Tb(**2**)]$^{3+}$ at room temperature is not surprising, since the low-lying (21000 cm^{-1}) triplet excited state of the $bpyO_2$ groups allows, as previously observed for other complexes,[6][22] an efficient non-radiative deactivation of the metal emitting state, via back energy transfer to the ligand. This process is no longer kinetically feasible at 77 K, where a strong metal luminescence is again observed (see Table 1). In this case, a detailed examination of the rate constants of all the processes occurring after excitation in the ligand-centered band is pre-

vented by the aforementioned lack of room temperature metal-centered luminescence, although again a very large value of k_r can be estimated from Eq. 3, as observed for the Eu^{3+} complexes of this series. A contribution to the overall rate constant by the OH and other oscillators present in the ligands can also be invoked in this case.

Conclusion

Ligands **1** and **2**, containing $bpyO_2$ subunits, form Tb^{3+} and Eu^{3+} complexes that are stable in coordinating solvents such as methanol and water, and which show intense absorption bands in the UV region. The Tb^{3+} complexes, however, do not show any appreciable metal-centered luminescence at room temperature, presumably because of an efficient back energy transfer to the ligand. For the Eu^{3+} complexes, this process is not thermodynamically feasible, and a strong metal-centered luminescence appears on exciting the ligand-centered absorption bands. Interestingly, this luminescence is not affected by the temperature or by deuteration of the solvent, showing that the ligands efficiently shield the metal ion from solvent interaction, and that thermally activated processes do not play a significant role in these complexes. A small but non-negligible contribution to the non-radiative deactivation to the ground state due to the OH oscillators present in the ligand has been demonstrated.

This work was supported by the *Ministero dell'Università e della Ricerca Scientifica e Tecnologica* (MURST), by the *University of Bologna* (Funds for Selected Research Topics) in Italy, and by the *Centre National de la Recherche Scientifique* and the *Engineer School of Chemistry, ECPM*, in France.

Experimental Section

General Methods: Nuclear magnetic resonance spectra were recorded at room temperature with Bruker SY-200 or AC-200 instruments operating at 200.1 MHz for ^1H. ^1H-NMR chemical shifts are reported in parts per million (ppm) relative to the proton residues in the solvents ($\delta = 7.26$ for $CDCl_3$). − Fast-atom bombardment (FAB, positive mode) spectra were recorded with a ZAB-HF-VB analytical apparatus with *m*-nitrobenzyl alcohol (*m*-NBA) as the matrix; Ar atoms were used for the bombardment (8 keV). All relevant patterns exhibited the expected isotopic profiles, as compared with simulated profiles. Electrospray mass spectra (ES-MS) were recorded with a Bio-Q analytical apparatus, in acetone solution, using grammicidim as internal standard. − Routine absorption spectra were measured in CH_3CN solutions at room temperature using a Kontron Uvikon 941 spectrophotometer. − FT-IR spectra were measured in KBr pellets or in solution with KBr cells with a Bruker IFS 25 spectrometer. − The molecular formulae given, as well as the purities of the samples, were assessed on the basis of ^1H-NMR, FAB^+-MS or ES-MS, and elemental analysis data.

Materials: *p-tert*-Butylcalix[4]arene[28], 5-bromomethyl-5′-methyl-2,2′-bipyridine *N,N′*-dioxide[28], and 5,5′-bromomethyl-2,2′-bipyridine *N,N′*-dioxide[29] were prepared according to literature procedures. Alumina (Merck), potassium carbonate (Prolabo), NaH (Fluka), europium(III) nitrate hexahydrate (Janssen), terbium(III) nitrate hexahydrate (Ventron), and gadolium(III) nitrate pentahydrate (Janssen) were obtained commercially as indicated.

Ligand **1**: A solution of *tert*-butylcalix[4]arene (0.500 g, 0.77 mmol) and potassium carbonate (0.817 g, 7.71 mmol) in dry acetonitrile (30 ml) was heated at 80°C for 30 min, after which solid 5-bromomethyl-5′-methyl-2,2′-bipyridine *N,N′*-dioxide (0.477 g, 1.62 mmol) was added. The mixture was heated at 80°C for 1 d and then quenched with water. Extraction with dichloromethane (5 × 50 ml), drying of the combined organic layers over magnesium sulfate, twofold chromatography (on alumina, using dichloromethane/methanol, 9:1, as eluent), and finally recrystallization from dichloromethane/hexane gave the analytically pure title compound (0.390 g, 47%) ($R_f = 0.55$, dichloromethane/methanol, 96:4, v/v). − ^1H NMR (200 MHz, $CDCl_3$, 25°C): $\delta = 8.62$ (s, 2 H), 8.10 (s, 2 H), 7.79 (s, 4 H), 7.55 (d, 2 H, $^3J = 8.1$ Hz), 7.14 (d, 2 H, $^3J = 8.1$ Hz), 7.05 (s, 4 H, Ar-*H* calix.), 6.98 (s, 2 H, O*H*), 6.81 (s, 4 H, Ar-*H* calix.), 5.04 (s, 4 H, bipy-CH_2-O), 3.75 (AB q, 8 H, $J_{AB} = 13.1$ Hz, $\Delta\nu = 168.5$ Hz, Ar-CH_2-Ar calix.), 2.30 (s, 6 H, bipy-CH_3), 1.28 (s, 18 H, *t*Bu), 0.95 (s, 18 H, *t*Bu). − IR (KBr): $\tilde{\nu} = 3408, 3049, 2958, 2868, 1688, 1602, 1484, 1393, 1364, 1278, 1201, 1171, 1123, 1025, 953, 872, 816$ cm^{-1}. − UV/Vis (CH_3CN): λ (ε) = 264 (43100), 216 nm (103300 M^{-1}cm^{-1}). − FAB^+ MS (*m*-NBA): *m/z* = 1077.5 [M + H]$^+$, 1061.5 [M − O], 1045.5 [M − 2 O], 1029.5 [M − 3 O]. − $C_{68}H_{76}O_8N_4 \cdot H_2O$ ($M_r = 1077.38 + 18.01$): calcd. C 74.56, H 7.18, N 5.11; found C 74.52, H 7.13, N 5.08.

Ligand **2**: A mixture of *tert*-butylcalix[4]arene (0.473 g, 0.73 mmol) and potassium carbonate (0.387 g, 2.80 mmol) in dry acetonitrile (50 ml) was heated at 80°C for 30 min. After cooling to room temperature, 5,5′-bromomethyl-2,2′-bipyridine *N,N′*-dioxide (0.300 g, 0.80 mmol) was added and the suspension was heated overnight at 80°C. The solvent was then removed in vacuo and the organic products were extracted with dichloromethane (5 × 50 ml). Analytically pure compound **2** was obtained after twofold chromatography (alumina, dichloromethane/methanol, 9:1) and recrystallization from dichloromethane/hexane (0.469 g, 37%) ($R_f = 0.66$, dichloromethane/methanol, 96:4, v/v). − ^1H NMR (200 MHz, $CDCl_3$, 25°C): $\delta = 8.70$ (s, 4 H), 7.97 (d, 4 H, $^3J = 8.1$ Hz), 7.77 (d, 4 H, $^3J = 8.1$ Hz), 7.09 (s, 8 H, Ar-*H* calix.), 7.03 (s, 4 H, O*H*), 6.82 (s, 8 H, Ar-*H* calix.), 5.11 (s, 8 H, bipy-CH_2-O), 3.81 (AB q, 16 H, $J_{AB} = 13.3$ Hz, $\Delta\nu = 172.2$ Hz, Ar-CH_2-Ar calix.), 1.31 (s, 36 H, *t*Bu), 0.94 (s, 36 H, *t*Bu). − IR (KBr): $\tilde{\nu} = 3435, 3052, 2959, 2867, 1726, 1602, 1484, 1398, 1362, 1268, 1199, 1114, 1024, 953, 872, 811$ cm^{-1}. − UV/Vis (CH_3CN): λ (ε) = 284 (45000), 220 nm (76900 M^{-1}cm^{-1}). − FAB^+ MS (*m*-NBA): *m/z* = 1723.0 [M + H]$^+$, 1706.0 [M − O], 1690.0 [M − 2 O], 1674.0 [M − 3 O]. − $C_{112}H_{128}O_{12}N_4 \cdot 2\,H_2O$ ($M_r = 1722.28 + 32.02$): calcd. C 76.51, H 7.57, N 3.19; found C 76.40, H 7.51, N 3.12.

Ligand **3**: To a solution of the calix[4]arene-25,27-diol **1** (0.065 g, 0.06 equiv.) in freshly distilled dimethylformamide (20 ml) was added sodium hydride in its commercial form (60%, 0.0036 g). The mixture was heated at 60°C overnight, after which D_2O was added. The solvent was removed and the analytically pure product was obtained after recrystallization from dichloromethane/hexane (0.040 g, 61%). − ^1H NMR (200 MHz, $CDCl_3$, 25°C): $\delta = 8.62$ (s, 2 H), 8.10 (s, 2 H), 7.79 (s, 4 H), 7.56 (d, 2 H, $^3J = 8.1$ Hz), 7.11 (d, 2 H, $^3J = 8.1$ Hz), 7.06 (s, 4 H, Ar-*H* calix.), 6.81 (s, 4 H, Ar-*H* calix.), 5.06 (s, 4 H, bipy-CH_2-O), 3.75 (AB q, 8 H, $J_{AB} = 13.1$ Hz, $\Delta\nu = 168.5$ Hz, Ar-CH_2-Ar calix.), 2.33 (s, 6 H, bipy-CH_3), 1.29 (s, 18 H, *t*Bu), 0.95 (s, 18 H, *t*Bu). − IR (KBr): $\tilde{\nu} = 3404, 3051, 2958, 2864, 1602, 1484, 1393, 1364, 1278, 1201, 1171, 1120, 1026, 955, 872, 814$ cm^{-1}. − UV/Vis (CH_3CN): λ (ε) = 262 (42600), 215 nm (104600 M^{-1}cm^{-1}). − FAB^+ (*m*-NBA): *m/z* =

1079.2 [M + H]$^+$, 1063.2 [M − O], 1047.3 [M − 2 O], 1031.2 [M − 3 O]. − $C_{68}H_{74}D_2O_8N_4$ (M_r = 1079.39): calcd. C 75.67, H 6.91, N 5.19; found C 75.39, H 6.68, N 5.02.

General Procedure for the Synthesis of Lanthanide Complexes: To a solution of the appropriate ligand (0.020 g, 1 equiv.) in methanol (10 ml) was added the lanthanide salt (1.1 equiv.). The mixture was stirred at 60°C overnight and then allowed to cool to room temperature. In the case of the nitrate salts, the lanthanide complexes precipitated during the course of the reaction. The solvent was removed in vacuo and the solid was recrystallized twice from ethyl acetate/hexane. The analytically pure complexes were obtained in 75−92% yield.

*[Eu(**1**)](NO$_3$)$_3$: Yield: 88%. − IR (KBr): ṽ = 3445, 3059, 2959, 2867, 1632, 1487, 1383, 1271, 1200, 1165, 1113, 1030, 955, 875, 828 cm^{-1}.* − FAB$^+$ (*m*-NBA): *m/z* = 1353.3 [M − NO_3]$^+$, 1337.3 [M − NO_3 − O], 1321.3 [M − NO_3 − 2O], 1290.3 [M − 2 NO_3 + H], 1227.3 [M − 2 NO_3 − 4 O]. − $C_{68}H_{76}O_{17}N_7Eu \cdot 5\ H_2O$ (M_r = 1415.36 + 90.07): calcd. C 54.25, H 5.76, N 6.51; found C 54.11, H 5.62, N 6.42.

*[Tb(**1**)](NO$_3$)$_3$:* Yield: 71%. − IR (KBr): ṽ = 3436, 2959, 2865, 1631, 1487, 1383, 1273, 1200, 1164, 1113, 1031, 983, 877, 829 cm^{-1}. − FAB$^+$ (*m*-NBA): *m/z* = 1358 [M − 2 H − NO_3]$^+$, 1296 [M − 2 NO_3 − 2 H], 1235 [M − 2 NO_3 − H], 1281 [M − 2 NO_3 − H − O], 1265 [M − 2 NO_3 − 2 O − H]. − $C_{68}H_{76}O_{17}N_7Tb \cdot 5\ H_2O$ (M_r = 1422.32 + 90.07): calcd. C 54.00, H 5.73, N 6.48; found C 54.12, H 5.82, N 6.42.

*[Gd(**1**)](NO$_3$)$_3$:* Yield: 95%. − IR (KBr): ṽ = 3415, 2959, 1631, 1486, 1383, 1271, 1199, 1164, 1110, 1032, 827, 827 cm^{-1}. − FAB$^+$ (*m*-NBA): *m/z* = 1358 [M − NO_3]$^+$, 1296 [M − 2 NO_3], 1234 [M − 3 NO_3], 1264 [M − 2 NO_3 − 2 O]. − $C_{68}H_{76}O_{17}N_7Gd \cdot 5\ H_2O$ (M_r = 1420.65 + 90.07): calcd. C 54.06, H 5.74, N 6.49; found C 53.91, H 5.62, N 6.35.

*[Eu(**2**)](NO$_3$)$_3$:* Yield: 78%. − IR (KBr): ṽ = 3417, 2960, 2869, 1728, 1631, 1486, 1384, 1302, 1199, 1120, 1032, 983, 954, 875, 821 cm^{-1}. − FAB$^+$ (*m*-NBA): *m/z* = 1998.1 [M − NO_3]$^+$, 1982.1 [M − NO_3 − O], 1966.1 [M − NO_3 − 2 O], 1934.1 [M − NO_3 − 4 O], 1872.0 [M − 2 NO_3 − 4 O]. − $C_{112}H_{128}O_{21}N_7Eu \cdot 4\ H_2O$ (M_r = 2060.26 + 72.06): calcd. C 63.09, H 6.43, N 4.60; found C 63.05, H 6.32, N 4.31.

*[Tb(**2**)](NO$_3$)$_3$:* Yield: 75%. − IR (KBr): ṽ = 3408, 2959, 1631, 1485, 1383, 1301, 1197, 1112, 1032, 875, 821 cm^{-1}. − FAB$^+$ (*m*-NBA): *m/z* = 2004 [M − NO_3]$^+$, 1942 [M − 2 NO_3], 1908 [M − 2 NO_3 − 2 O − H]. − $C_{112}H_{128}O_{21}N_7Tb \cdot 5\ H_2O$ (M_r = 2067.20 + 90.07): calcd. C 62.36, H 6.45, N 4.54; found C 62.23, H 6.30, N 4.38.

*[Gd(**2**)](NO$_3$)$_3$:* Yield: 92%. − IR (KBr): ṽ = 3406, 2960, 2868, 1631, 1486, 1384, 1300 (ν_{NO}), 1197, 1115, 1032, 875, 820 cm^{-1}. − FAB$^+$ (*m*-NBA): *m/z* = 2002 [M − NO_3]$^+$, 1940 [M − 2 NO_3], 1878 [M − 3 NO_3]. − $C_{112}H_{128}O_{21}N_7Gd \cdot 5\ H_2O$ (M_r = 2065.55 + 90.07): calcd. C 62.41, H 6.45, N 4.55; found C 62.38, H 6.30, N 4.28.

*[Eu(**3**)](NO$_3$)$_3$:* To a solution of ligand **3** (0.040 g, 0.04 mmol) in CD_3CN (5 ml) in a Schlenk tube in a drybox was added $Eu(CF_3SO_3)_3$ (1.1 equiv.). The sealed tube was then heated at 60°C for 3 h. During the course of the reaction, the complex precipitated. When the reaction was complete, an excess of anhydrous, degassed pentane was added to insine precipitation of most of the product, which was then taken up in methanol/ethyl acetate. The resulting solution was filtered through Celite and diffusion of hexane into the filtrate afforded the analytically pure compound. Yield: 65%. − IR (KBr): ṽ = 3473, 2974, 2959, 1632, 1487, 1396, 1271, 1160, 1099, 1045, 880 cm^{-1}. − FAB$^+$ (*m*-NBA): *m/z* = 1529.0 [M − CF_3SO_3]$^+$, 1380.1 [M − 2 CF_3SO_3], 1348.2 [M − 2 CF_3SO_3 − 2 O], 1316.2 [M − 2 CF_3SO_3 − 4 O]. − $C_{71}H_{74}D_2O_{17}N_4S_3F_9Eu \cdot CH_3OH$ (M_r = 1678.551 + 32.042): calcd. C 51.52, H 4.68, N 3.33; found C 51.28, H 4.52, N 3.02.

Spectroscopic Measurements: The solvents employed for photophysical measurements were methanol (Merck UVASOL) and CH_3OD (99.8 atom-% from Fluka), which were used without further purification. Absorption spectra were recorded with a Perkin-Elmer lambda 16 spectrophotometer. Uncorrected emission, corrected excitation spectra, and phosphorescence lifetimes were obtained with a Perkin-Elmer LS 50 spectrofluorimeter.

Luminescence quantum yields (uncertainty ±15%) were determined using quinine sulfate (Φ = 0.546[30] in 1 N H_2SO_4 aqueous solution) for Tb^{3+} and $[Ru(bpy)_3]^{2+}$ (Φ = 0.028 in aerated water[31]) for Eu^{3+} as standards. In order to permit comparisons of emission intensities, corrections for instrument response, inner filter effects, and phototube sensitivity were made.[32] A correction for differences in the refraction indices was introduced where necessary. Emission spectra at 77 K were obtained in a rigid, opaque methanol matrix using quartz tubes immersed in a quartz Dewar vessel filled with liquid nitrogen.

[1] A. Mayer, S. Neuenhofer, *Angew. Chem. Int. Ed. Engl.* **1994**, *33*, 1044−1072; *Angew. Chem.* **1994**, *106*, 1097.
[2] *Fluorescent Chemosensors for Ion and Molecule Recognition* (Ed.: A. W. Czarnik), American Chemical Society, Washington DC, **1992**.
[3] A. P. de Silva, H. Q. N. Gunaratne, T. Gunnlaugsson, A. J. M. Huxley, C. P. McCoy, J. T. Rademacher, T. E. Rice, *Chem. Rev.* **1997**, *97*, 1515.
[4] L. Fabbrizzi, A. Poggi, *Chem. Soc. Rev.* **1995**, 197.
[5] *Applications of Fluorescence in Immunoassays* (Ed.: I. A. Hemmil), Wiley, New York, **1991**.
[6] [6a] N. Sabbatini, M. Guardigli, J.-M. Lehn, *Coord. Chem. Rev.* **1993**, *123*, 201. − [6b] N. Sabbatini, M. Guardigli, I. Manet, *Handbook on the Physics and Chemistry of Rare Earths*, vol. 23 (Eds.: K. A. Gschneidner, Jr., L. Eyring), Elsevier, Amsterdam, **1996**, and references therein.
[7] W. T. Carnall, *Handbook on the Physics and Chemistry of Rare Earths*, vol. 3 (Eds.: K. A. Gschneidner, Jr., L. Eyring), North Holland, Amsterdam, **1979**, p. 171.
[8] L. C. Thompson, *Handbook on the Physics and Chemistry of Rare Earths*, vol. 3 (Eds.: K. A. Gschneidner, Jr., L. Eyring), North Holland, Amsterdam, **1979**, p. 209.
[9] G. Blasse, *Handbook on the Physics and Chemistry of Rare Earths*, vol. 4 (Eds.: K. A. Gschneidner, Jr., L. Eyring), North Holland, Amsterdam, **1979**, p. 237.
[10] N. Sabbatini, M. Guardigli, A. Mecati, V. Balzani, R. Ungaro, E. Ghidini, A. Casnati, A. Pochini, *J. Chem. Soc., Chem. Commun.* **1990**, 878.
[11] N. Sabbatini, M. Guardigli, I. Manet, R. Ungaro, A. Casnati, R. Ziessel, G. Ulrich, Z. Asfari, J.-M. Lehn, *Pure Appl. Chem.* **1995**, *67*, 135.
[12] S. Pappalardo, F. Bottino, L. Giunta, M. Pietraszkiewicz, J. Kapiuk, *J. Incl. Phenom.* **1991**, *10*, 387.
[13] N. Sato, S. Shinkai, *J. Chem. Soc., Perkin Trans. 2* **1993**, 621.
[14] H. Matsumoto, S. Shinkai, *Chem. Lett.* **1994**, 901.
[15] N. Sabbatini, M. Guardigli, I. Manet, R. Ungaro, A. Casnati, C. Fisher, R. Ziessel, G. Ulrich, *New J. Chem.* **1995**, *19*, 137.
[16] A. Casnati, C. Fisher, M. Guardigli, A. Isernia, I. Manet, N. Sabbatini, R. Ungaro, *J. Chem. Soc., Perkin Trans. 2* **1996**, 395.
[17] F. J. Steemers, W. Verboom, D. N. Reinhoudt, E. B. van der Tol, J. M. Verhoeven, *J. Chem. Soc., Perkin Trans. 2* **1995**, 131.
[18] D. M. Rudkevich, W. Verboom, E. B. van der Tol, C. J. van Staveren, F. M. Kaspersen, J. M. Verhoeven, D. N. Reinhoudt, *J. Am. Chem. Soc.* **1995**, *117*, 9408.
[19] G. Ulrich, R. Ziessel, I. Manet, M. Guardigli, N. Sabbatini, F. Fraternali, G. Wipff, *Chem. Eur. J.* **1997**, *3*, 1815.

[20] F. Bottino, L. Giunta, S. Pappalardo, *J. Org. Chem.* **1989**, *54*, 5407, and references therein.
[21] G. Ulrich, R. Ziessel, *Tetrahedron Lett.* **1994**, *35*, 6299.
[22] G. Ulrich, M. Hissler, R. Ziessel, I. Manet, G. Sarti, N. Sabbatini, *New J. Chem.* **1997**, *21*, 147.
[23] L. Prodi, M. Maestri, R. Ziessel, V. Balzani, *Inorg. Chem.* **1991**, *30*, 3798.
[24] W. DeW. Horrocks Jr., D. R. Sudnick, *J. Am. Chem. Soc.* **1979**, *101*, 334.
[25] W. DeW. Horrocks Jr., D. R. Sudnick, *Acc. Chem. Res.* **1981**, *14*, 384.
[26] B. Alpha, R. Ballardini, V. Balzani, J.-M. Lehn, S. Perathoner, N. Sabbatini, *Photochem. Photobiol.* **1990**, *52*, 299.
[27] J.-P. Sutter, M. L. Khan, S. Golhen, L. Ouahab, O. Khan, *Chem. Eur. J.* **1998**, *4,* 571, and references cited therein.
[28] C. D. Gutsche, M. Iqbal, *Org. Synth. Coll*. **1993**, *8*, 75.
[29] R. Ziessel, M. Hissler, G. Ulrich, *Synthesis* **1998**, 1339.
[30] S. R. Meech, D. Phillips, *J. Photochem.* **1983**, *23*, 193.
[31] K. Nakamaru, *Bull. Chem. Soc. Jpn.* **1982**, *55*, 2697.
[32] A. Credi, L. Prodi, *Spectrochimica Acta, Part A* **1998**, *54*, 159.
[98178]

Some Silatetraazaspiroalkanes with [4 + 4] Octacoordinated Silicon

Guobin Rong[a][+], Reinhart Keese*[a], and Helen Stoeckli-Evans[b]

Department of Chemistry and Biochemistry, University of Bern[a],
Freiestrasse 3, CH-3012 Bern, Switzerland

Institut de Chimie, Université de Neuchâtel[b],
51 Avenue de Bellevaux, CH-2000 Neuchâtel, Switzerland
E-mail: reinhart.keese@ioc.unibe.ch

Received June 12, 1998

Keywords: Sulfonamidosilanes / [4 + 4] Octacoordinated silicon / Capped tetrahedron / X-ray structures

Spirocyclic compounds containing an $Si(N)_4$ core have been prepared from 1,2-ethane- and 1,3 propanediamines bearing the electron-withdrawing *p*-toluenesulfonyl groups at the four N atoms. According to the X-ray structure analysis of the compounds **8a** and **13**, the spirocyclic rings are almost perpendicular to each other. In both cases a distorted dodecahedral arrangement of a [4 + 4] octacoordinate Si atom is found in which one O atom of each of the four sulfonyl groups caps one of the planes defined by the $Si(N)_4$ tetrahedron. The O···Si distances are 2.85–3.02 Å and the two O···Si···O angles are 145–159°. According to the X-ray structure analysis of the monocyclic compound **16**, one O atom of the *p*-toluenesulfonyl group caps the plane defined by O1–N2–C13 of the distorted $S(N_2)(O)C$ tetrahedron.

The intriguing properties of main-group elements of the second row like silicon (and phosphorus) to form five- and six-coordinated complexes have found increasing attention.[1][2][3][4][5][6] This is inter alia due to the observation that ligands become more labile and can be displaced readily. Thus, nucleophilic substitution reactions at tetracoordinate silicon are discussed in terms of associated processes with pentacoordinate Si species as intermediates. Whereas five- and six-coordinate Si compounds are by now well known, only a few complexes have been described where silicon is surrounded by seven or even eight atoms. Based on X-ray structure analyses of the silicon complexes **1**−**3**, Auner and co-workers and Corriu and co-workers have suggested heptacoordination for the structures of these compounds. Corriu has discussed the structure of **4** in terms of a [4 + 4] octacoordination.[7][8][9] In view of the rather long Si−N bonds, ranging from 2.88 to 3.49 Å, the authors have described these complexes in terms of a SiR_3X core with the "outer sphere" NR_2 groups capping three or four of the planes of the distorted tetrahedron in SiR_3X and SiR_2H_2. According to the X ray structure analysis the spirosilane **5** contains hexacoordinated silicon with the N−Si bond approaching that of a covalent bond.[10] ^{1}H- and ^{29}Si-NMR measurements show a dynamic behaviour, suggesting that the NMe_2 groups displace each other by way of a heptacoordinate transition state.

Recently, we have prepared the rather stable spiro compound **6**, the X-ray structure of which also revealed [4 + 4] octacoordinated silicon.[11] Here the four planes of the tetrahedron defined by the SiN_4 core are capped by one O atom of each of the four sulfonyl groups. In a search for further examples of this unique [4 + 4] octacoordination of Si we prepared a variety of silatetraazaspiro compounds with different ring sizes bearing *p*-toluenesulfonyl (tosyl) groups at the four N atoms and determined the molecular structure of two of the spirosilanes by X-ray analysis.

Results and Discussion

The spirocyclic tetraazasilanes were prepared according to Scheme 1. Treatment of the *N*,*N*′-disulfonyldiamines **7a**,**b**, **9** and **12** with BuLi and $SiCl_4$ gave the silatetraazaspiro compounds **8a**,**b**, **10** and **13**, respectively, in moderate to good yields. The propensity to form spirocycles was reduced with increasing length of the chain connecting the bidentate tosylamines. The reaction of *N*,*N*′-ditosylpropane-1,3-diamine (**9**) gave in addition to **10** the monocyclic silane **11**. In an attempt to prepare a silatetraazaspiro[6.6]-dodecane from *N*,*N*′-ditosylbutane-1,4-diamine (**14**), a polymeric material was formed and the attempted reaction of the *N*,*N*′-ditosylbiphenyl-2,2′-diamine (**15**) with $SiCl_4$ gave the heterocyclic compound **16** rather than a spirocyclic compound.

Structure Determination

The structure of the 1,3-diaza-2-silaspiroalkanes **8a**,**b**, **10** and **13** is supported by mass spectra and ^{1}H- and ^{13}C-NMR spectra. Since the number of signals in the ^{13}C-NMR spectra is half the number of the C atoms these spiro compounds apparently have two-fold symmetry. In **8a**,**b** and **10**

[+] On leave from the Department of Chemistry, East China University of Science and Technology, Shanghai, P. R. of China, September−November 1996.

 © WILEY-VCH Verlag GmbH, D-69451 Weinheim, 1998 1434−1948/98/1212−1967 $ 17.50+.50/0

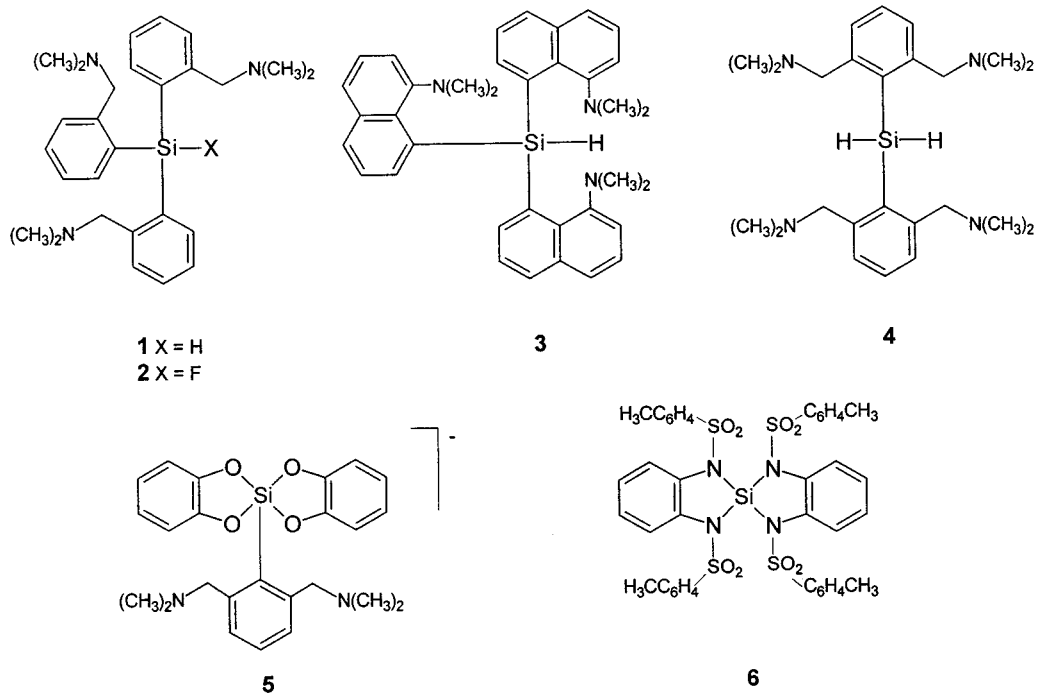

1 X = H
2 X = F

3

4

5

6

Scheme 1

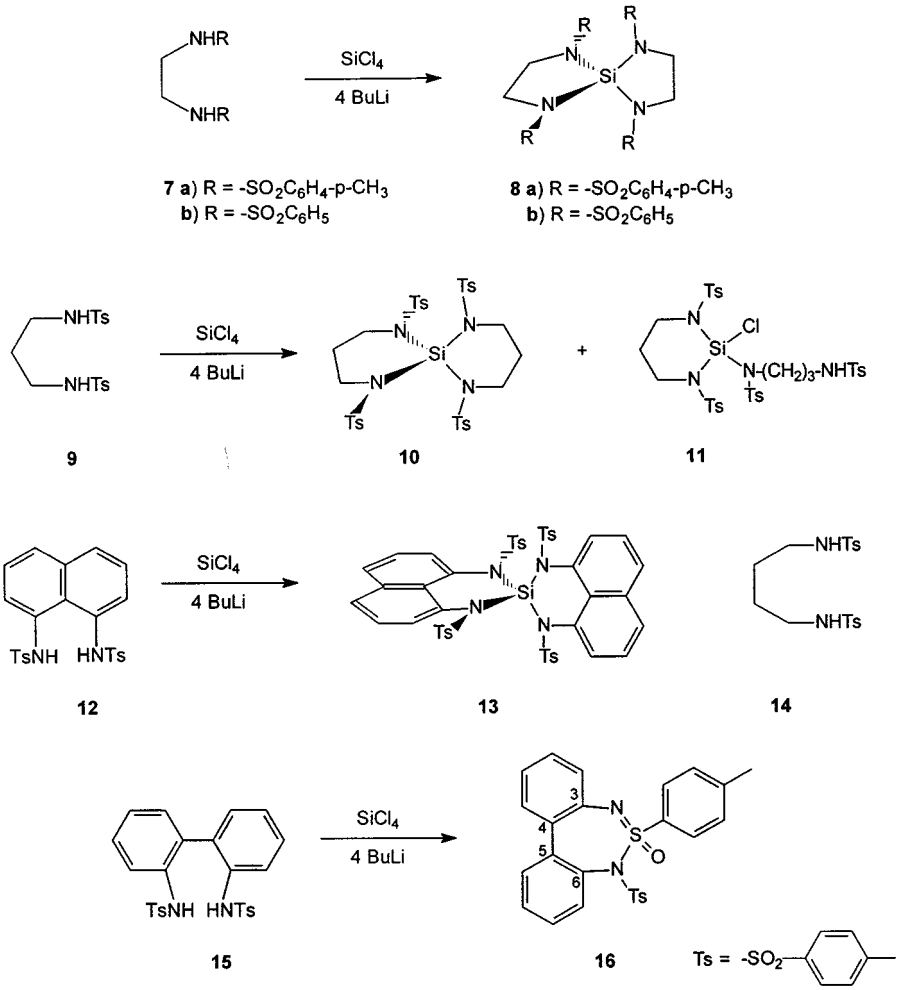

the ^{1}H signals of the $-NCH_2$ groups appear as sharp lines. This suggests that in **8a** and **8b** the two five-membered silaimidazolidine moieties are either planar, rapidly equilibrating through a planar form or undergo rapid inversion at N.[12][13] In **10** the two siladiazacyclohexane ring systems may adopt a quasi-chair conformation with planar or rapidly inverting N centers. The ^{1}H-NMR signals of the $-NCH_2$ groups are consistently shifted downfield by approximately 0.30 ppm from those found in the precursor *N,N′*-ditosyldiamines. In the ^{29}Si-NMR spectra of **8a**,**b** and **11** (and **13**), the signals are shifted upfield by more than 20 ppm relative to $Si[N(CH_3)_2]_4$ ($\delta = -28.1$).[14] In the spirocyclic tetraazasilane **10** the ^{29}Si-NMR signal appears at $\delta = -69.9$ and is thus close to that of $Si(OCH_3)_4$ ($\delta = -79.0$).[15] These chemical shifts indicate that the Si nucleus in these spirocyclic compounds has a different substitution pattern. In the IR spectra of **10** and **13** the absorption band occurring at 930 cm^{-1} can be assigned to an asymmetric Si−N vibration.[16] In order to obtain more detailed information about structural details, X-ray structure analyses were performed on the silatetraazaspiro compounds **8a** and **13**. Since the ^{1}H- and ^{13}C-NMR spectra as well as the elemental analysis of **16** indicated that the *N,N′*-ditosylbiphenyl-2,2′-diamine (**15**) had reacted in the presence of $SiCl_4$ in a different way, an X-ray analysis was also performed on this product.

Figure. 1. Top: A perspective view of molecule **8a**, showing the numbering scheme used (thermal ellipsoids at 50% probability level)[a]; bottom: drawing of **8a**, illustrating the octahedral coordination

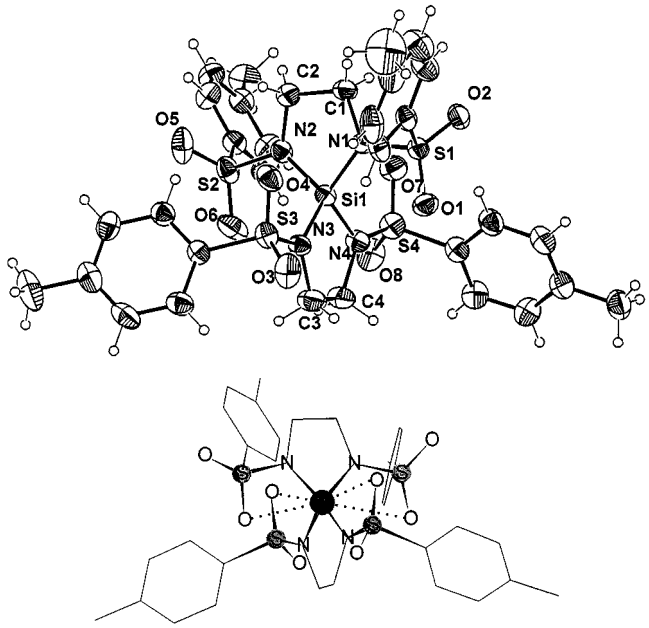

[a] Selected bond lengths [Å], bond and torsional angles [°]: N1−Si1 1.727(4), N1−S1 1.626(4), S1−O1 1.427(3), S1−O2 1.438(3), N2−Si1 1.709(4), N3−Si1 1.714(4), N4−Si1 1.715(4); N1−Si1−N2 91.7(2), N3−Si1−N4 92.1(2), N2−Si1−N3 117.9(2), N2−Si1−N4 118.6(2);N2−C2−C1−N1 −27.63; N3−C3−C4−N4 11.53; O1···Si1 3.043(2), O3···Si1 2.920(4), O6···Si1 2.974(4), O7···Si1 2.968(3).

X-ray Structure Analysis

The structure analysis of **8a** reveals that the two silaimidazolidine rings adopt a twist conformation (Figure 1) with an angle of 89.84° between the two planes defined by N1−Si1−N2 and N3−Si1−N4, meaning that the rings are almost perpendicular to each other (Figure 1 bottom). The endocyclic bond angle N1−Si1−N2 and its counterpart N3−Si1−N4 are significantly smaller [91.7(2)° and 92.1(2)°] than the average of the exocylic bond angles (118.3° and 119.6°). The torsion angles S1−N1−Si1−N2 [−175.4(3)°] and S3−N3−Si1−N4 [+173.1(3)°] as well as S2−N2−Si1−N1 [−175.5(3)°] and S4−N4−Si1−N3 [+177.5(3)°] indicate a small pyramidalization at the N atoms. In comparison with the average N−Si bond length found in **6** (1.734 Å) and those reported for N−Si−N substructures in five-membered ring systems, the average N−Si bond length of 1.714(4) Å is rather short in **8a**.[11][17] As observed for **6** one oxygen atom of each of the four sulfonamide groups caps the $Si(N)_4$ tetrahedron, with each bisecting one of the tetradron faces (Figure 1, bottom).[11] The O···Si distances are [2.922 (4)−3.043 (3) Å] and the angles O1···Si1···O3 and O6···Si1···O7 are 159.9(1)° and 157.4(1)°, respectively. These values are very similar to those found in **6**.[11]

In the molecular structure of **13** (Figure 2, top) the angle between the two planes defined by N1−Si1−N2 and N3−Si1−N4 is 89.60°. Thus, the two six-membered rings forming the spirocycle are almost perpendicular to each other. In each of these rings, the C atoms of the naphthalene ring bonded to the nitrogen atoms are located out of the planes defined by N1−Si1−N2 and N3−Si1−N4. According to the torsional angles the pyramidalisation at the four N atoms is slightly larger in this compound than in **8a**. In **13** the average N−Si bond length is 1.744 Å and thus longer than in **8a**. In line with the arrangement found for the tosyl groups in **6** and **8a**, the four sulfonyl groups in **13** are arranged in such a way that one oxygen atom of each of the sulfonyl groups is located above one of the planes defined by the $Si(N)_4$ tetrahedron with O···Si distances ranging from 2.845 to 3.023 Å (Figure 2 bottom). The angles between these non-bonded O atoms and the central Si atom are in the same range as found for **8a** [O1···Si1···O3 145.1(06)° and O6···Si1···O7 154.03(06)°] and are considerably larger than 109.48°, the angle between the two lines passing through the centres of two planes in a tetrahedron.

As mentioned above, no silatetraazaspiroundecane had been formed in the reaction of the biphenyldiamine **15** with $SiCl_4$. As revealed by the X-ray structure analysis, **15** had been transformed in an intramolecular condensation reaction into the diazathiaheptatriene **16** (Figure 3). In this structure the angle C3−C4−C5−C6 46.2(5) (cf. **16** in Scheme 1), which lies within the expected range for the torsional deformation between the two phenyl groups in biphenyl-2,2′-diamines. A salient feature of this monocyclic compound is the location of the oxygen atom O2 of the sulfonyl group, which caps the plane defined by O1, N2, C13 of the distorted $S(N)_2(O)(C)$ tetrahedron.

Figure 2. Top: A perspective view of molecule **13**, showing the numbering scheme used (thermal ellipsoids at 50% probability level)[a]; bottom: drawing of **13**, illustrating the octahedral coordination

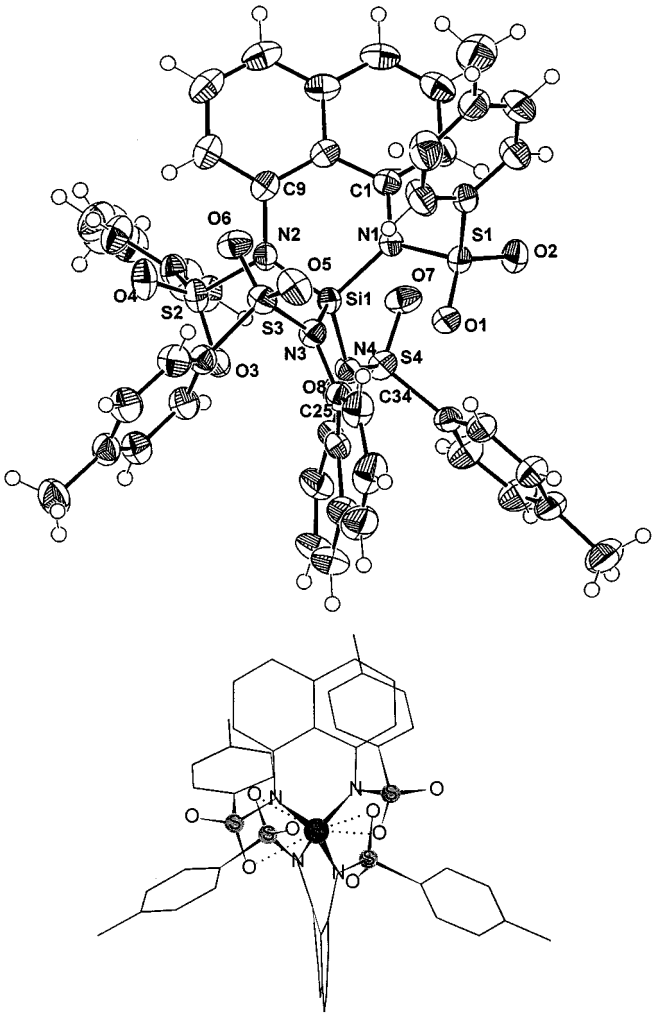

[a] Selected bond lengths [Å], bond and torsional angles [°]: N1−Si1 1.746(2), N2−Si1 1.740(2), N3−Si1 1.745(2), N4−Si1 1.744(2); N2−Si1-N1 101.04(11), N2−Si-N3 113.75, N2−Si1−N4 113.77(12); N1−C1−C10−C9 −15.57, N2−C9−C10−C1 −17.81; O1···Si1 2.845(2), O3···Si1 2.866(2), O6···Si1 3.023(2), O7···Si1 2.951(2).

Concluding Remarks

It has been shown that spirocyclic compounds containing an $Si(N)_4$ core can be prepared from 1,2-diamines bearing the electron-withdrawing *p*-toluenesulfonyl substituents at the N atoms. The first example of a 2-sila-1,3,7,11-tetraazaspiro[5.5]undecane **13**, containing six-membered rings has been obtained. Attempts to prepare tetraazaspirosilanes containing larger rings by base-induced reaction of an appropriate ditosyl diamine were not successful. According to the X-ray structure of the spirocyclic tetraazasilanonane **8a** and the benzannulated tetraazasilaundecane **13**, the *p*-toluenesulfonyl groups are oriented in such a way that one oxygen atom each caps a plane of the distorted $Si(N)_4$ tetrahedron. While the $Si(N)_4$ core retains a geometry with bond lengths close to a covalent N−Si bond, the O···Si distances

Figure 3. A perspective view of molecule **16** showing the numbering scheme used (thermal ellipsoids at 50% probability level)[a]

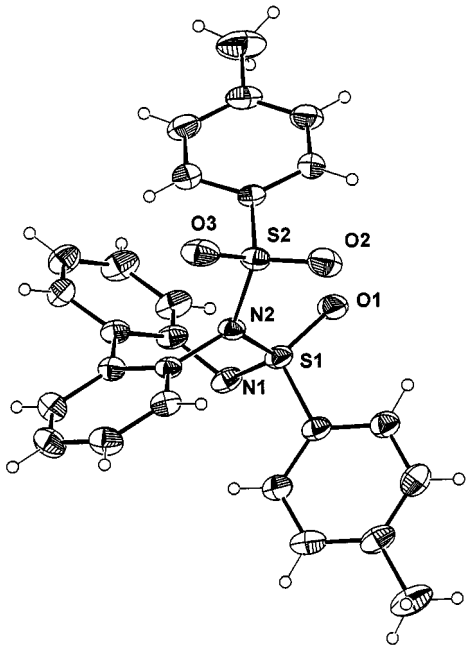

[a] Selected bond lengths [Å], bond and torsional angles [°]: N1−S1 1.578(4), N2−S1 1.704(3), N2−S2 1.738(3); N1−S1−N2 103.4(2), O1−S1−N1 126.5(2), O1−S1−N2 106.7(2); C1−C6−C7−C12 46.21(0.50).

are much longer than those found in alkoxysilanes.[17] These geometries can best be described as a distorted dodecahedral arrangement of a [4 + 4] coordinated Si.[8][11] At present it is unclear whether this type of coordination in these silicon compounds is due to an additional stabilisation of the spiro silacycle or is caused by the crystal packing.

This work has been supported by the *Swiss National Science Foundation* (Project No. 20-43565.95) and by the *National Scientific Foundation of China*. G. R. is grateful for a fellowship under the auspices of the *Swiss-Sino Exchange Program*.

Experimental Section

General: Chemicals were purchased from commercial suppliers and used without further purification. Ts: *p*-toluenesulfonyl (tosyl). BuLi (Fluka): 1.6 M solution in hexane. − Reactions were performed under argon. − M.p.: Büchi 510 melting point apparatus, uncorrected values. − Thin layer chromatography: Silica gel plates SIL G/UV_{254} (Macherey & Nagel), eluent: EtOAc/cyclohexane, ratio given. − Column chromatography (CC): J. T. Baker flash gel (40mm), eluent: EtOAc/cyclohexane in the ratio specified. − IR spectra: Perkin-Elmer 782 IR spectrophotometer. − NMR spectra: Bruker AC 300 spectrometer [^{1}H, 300 MHz, ^{13}C, 75 MHz] and Bruker DRX 500 spectrometer [^{29}Si, 99.325 MHz]), δ in ppm rel. to internal $Si(CH_3)_4$, st = stack, heavily overlapping signals. − Mass spectra (MS): Varian MAT CH7A (70eV, EI); FAB-MS: Fisons VG Autospec Q spectrometer (Cs^+, 32 kV).

N,N′-Ditosylethane-1,2-diamine (**7a**): A solution of TsCl (0.23 mol) in 150 ml diethyl ether was slowly added to a cooled solution of ethane-1,2-diamine (0.113 mol) and 18 g NaOH in 450 ml H_2O. After stirring overnight at room temp., the ditosylate was filtered

off and recrystallized from CH_3OH, white needles, yield 33g (81%), m.p. 162−163°C (162−164°C[18][19]). − R_f (1:1) = 0.37. − ^1H NMR (CD_3COCD_3): δ = 7.76 (dt, *J* = 8.1, 1 Hz, 4 H), 7.44 (dt, *J* = 8.1, 1 Hz, 4 H), 6.57 (br., 2 H), 3.00−3.03 (m, 4 H), 2.44 (s, 6 H). − ^{13}C NMR (CD_3COCD_3): δ = 143.7 (s), 138.6 (s), 130.3 (d), 127.6 (d), 43.5 (t), 21.2(q). − IR (KBr): $\tilde{\nu}$ = 3295 cm^{-1}, 1590, 1410, 1330, 1150. − MS (EI): *m/z* (%): 369 (5) $[M + 1]^+$, 339 (40), 213 (94), 184 (96), 155 (100), 139 (18), 91 (88), 65 (20).

The following derivatives of the diamines were prepared as described for **7a**.

N,N′-Dibenzenesulphonylethane-1,2-diamine (**7b**): Recrystallization from ethanol gave white needles (28.8 g, 75%), m.p. 166−167°C.[20]. − R_f (1:1) = 0.20. − ^1H NMR (CD_3COCD_3): δ = 7.85−7.88 (m, 4 H), 7.59−7.72 (m, 6 H), 6.67 (br., 2H), 3.04−3.06 (m, 4 H). − ^{13}C NMR (CD_3COCD_3): δ = 141.5 (s), 133.1 (s), 129.8 (d), 127.5 (d), 43.5 (t). − IR (KBr): $\tilde{\nu}$ = 3270 cm^{-1}, 3320, 1320, 1150. − MS (EI); *m/z* (%): 341 (2) $[M + 1]^+$, 199 (17), 170 (88), 141 (65), 125 (6), 97 (6), 77 (100), 31 (30).

N,N′-Ditosylpropane-1,3-diamine (**9**): Yield 80%, m.p. 138−139°C (134−136°C[19][21]). − R_f (1:1) = 0.35. − ^1H NMR (CD_3COCD_3): δ = 7.72−7.76 (d, *J* = 8.1 Hz, 4 H), 7.40−7.44 (d, *J* = 8.1 Hz, 4 H), 6.48 (br., 2 H), 2.95 (m, 4 H), 2.45 (s, 6 H), 1.71 (5, *J* = 6.7 Hz, 2 H). − ^{13}C NMR (CD_3COCD_3): δ = 143.7 (s), 138.9 (s), 130.4 (s), 127.7 (s), 41.3 (t), 30.0 (t), 21.3 (q). − IR (KBr): $\tilde{\nu}$ = 3270 cm^{-1}, 1590, 1460, 1320,1155. − MS (EI): *m/z* (%): 393 (2) $[M + 1]^+$, 227 (80), 164 (40), 171(12), 155 (100), 91 (80), 65 (18), 56 (80).

N,N′-Ditosylnaphthalene-1,8-diamine (**12**): Yield 80%, m.p. 203−204 °C (207°C[22]). − R_f (2:3) = 0.35. − ^1H NMR ($CDCl_3$): δ = 7.63−7.68 (m, 6 H), 7.20−7.26 (m, 6 H), 7.01−7.04 (dd, 2 H), 2.37 (s, 6 H). − ^{13}C NMR ($CDCl_3$): δ = 144.5 (s), 135.9 (s), 134.9 (s), 130.2 (s), 129.4 (s), 130.0 (d), 129.8 (d), 127.1 (d), 125.1 (d), 121.3 (d), 21.6 (q). − IR (KBr): $\tilde{\nu}$ = 3200 cm^{-1}, 1575, 1415, 1340, 1300, 1150. − MS (EI); *m/z* (%): 467 (33) $[M + 1]^+$, 466 (100) $[M^+]$, 311 (48), 247 (26), 232 (10), 155 (58), 129 (8), 127 (6). − $C_{24}H_{22}N_2O_4S_2$ (466.56): calcd. C 61.78, H 4.75, N 6.01; found C 61.71, H 4.75, N 5.96.

N,N′-Ditosylbutane-1,4-diamine (**14**): Yield 80%, m.p. 137−138°C (m.p. 125−125°C[23], 139°C[24]). − ^1H NMR (CD_3COCD_3): δ = 7.73−7.76 (dt, *J* = 8.5, 1 Hz, 4 H), 7.40−7.43 (dt, *J* = 8.8, 1 Hz, 4 H), 6.37 (br., 2 H), 2.85−2.89 (m, 4 H), 2.43 (s, 6 H), 1.50−1.55 (m, 4 H). − ^{13}C NMR (CD_3COCD_3): δ = 142.9 (s), 138.3 (s), 129.6 (d), 127.0 (d), 42.6 (t), 26.6 (t), 20.6 (q). − IR (KBr): $\tilde{\nu}$ = 3295 cm^{-1}, 1590, 1410, 1330, 1150. − MS (EI); *m/z* (%): 397 (2) $[M + 1]^+$, 241 (82) $[M - Ts]^+$, 224 (100), 184 (70), 155 (95), 139 (18), 91 (85), 70 (50).

N,N′-Ditosylbiphenyl-2,2′-diamine (**15**): (2,2′-Biphenyldiamine was prepared according to ref.[25][26]), m.p. of compound **15** 168−171°C. − R_f (1:3) = 0.26. − ^1H NMR ($CDCl_3$): δ = 7.67−7.69 (dt, *J* = 7.3, 1 Hz, 2 H), 7.49−7.52 (dt, *J* = 8.1, 1 Hz, 2 H), 7.33−7.39 (td, *J* = 8.0, 1.9 Hz, 2 H), 7.23−7.26 (d, *J* = 8.0 Hz, 2 H), 7.02−7.07 (td, *J* = 7.4, 1 Hz, 2 H), 6.48−6.50 (dd, *J* = 7.4, 1.5 Hz, 2 H), 5.88 (s, 2 H,), 2.43 (s, 6 H). − ^{13}C NMR ($CDCl_3$): δ = 144.6 (s), 135.9 (s), 134.9 (s), 127.5 (d), 130.3 (s), 130.0 (d), 129.9 (d), 127.5 (d), 127.1 (d), 125.1 (d), 121.3 (d), 21.6 (q). − IR (KBr): $\tilde{\nu}$ = 3330 cm^{-1}, 3280, 1395, 1270, 1090, 750 1340,1170. − MS (EI): *m/z* (%): 492 (98) $[M^+]$, 337 (45), 321 (40), 273 (20), 182 (90), 181 (100),167 (46), 154 (45).

General Procedure for the Preparation of the Tetraazasilaspiro Compounds: After addition of BuLi (6 ml, 1.6 M in hexane, 9.6 mmol) to a solution of the bis(sulfonamide) (4.8 mmol) in 50 ml of dry THF and stirring for 30 min, $SiCl_4$ (2.4 mmol), dissolved in 3 ml of THF, was added. The reaction mixture was refluxed for the time given, cooled to room temp., filtered and concentrated to dryness. The residue was purified by CC or recrystallization.

1,4,6,9-Tetratosyl-1,4,6,9-tetraaza-5-silaspiro[4.4]nonane (**8a**): Purification by CC (1:1) gave 0.95 g (60%) of product as colourless crystals which were recrystallized from CH_3CN. Crystals suitable for X-ray analysis were grown from CH_3CN as colourless blocks. M.p. 254−255°C. R_f (1:1) = 0.61. − ^1H NMR ($CDCl_3$): δ = 8.06 (d, *J* = 8.4 Hz, 8 H), 7.35 (d, *J* = 8.4 Hz, 8 H), 3.36 (s, 8 H), 2.41 (s, 12 H). − ^{13}C NMR ($CDCl_3$): δ = 144.5 (s), 134.5 (s), 129.7 (d), 128.8 (d), 43.3 (t), 21.7 (q). − ^{29}Si NMR: −50.86. − IR (KBr): $\tilde{\nu}$ = 1600 cm^{-1}, 1235, 1160, 1115, 1090, 1025,1010. − MS (EI): *m/z* (%): 605 (58) $[M - Ts]^+$, 564 (14), 549 (100), 485 (20), 450 (55), 411 (52), 139 (23). − $C_{32}H_{36}N_4O_8S_4Si$ (760.12): calcd. C 50.50, H 4.77,N 7.37, found C 50.52, H 4.77, N 7.36.

1,4,6,9-Tetrakis(benzenesulfonyl)-1,4,6,9-tetraaza-5-silaspiro-[4.4]nonane (**8b**): Yield 0.510g, 30%, recrystallization from CH_3CN, m.p. 265−267°C. − R_f (1:1) = 0.35. − ^1H NMR ($CDCl_3$): δ = 8.15−8.20 (m, 8 H), 7.52−7.66 (m, 12 H), 3.41 (s, 8 H). − ^{13}C NMR ($CDCl_3$): δ = 137.3 (s), 133.5 (d), 129.0 (d), 128.7 (d), 42.4 (t). − ^{29}Si NMR($CDCl_3$): −50.46. − IR (KBr): $\tilde{\nu}$ = 1020 cm^{-1}. − MS (FAB): *m/z* (%): 705 (10) $[M + 1]^+$, 639 (3), 565 (3), 439 (50), 383 (18), 307 (6), 155 (100), 121 (25). − $C_{28}H_{28}N_4O_8S_4Si$ (704.06): calcd. C 47.71, H 4.00, N 7.95, found C 47.65, H 3.87, N 8.13.

1,5,7,11-Tetratosyl-1,5,7,11-tetraaza-6-silaspiro[5.5]undecane (**10**) *and 2-Chloro-N,N′-ditosyl-2-[tosyl(3-tosylaminopropyl)-amino]-1,3-diaza-2-silacyclohexane* (**11**): CC of the reaction mixture gave 0.470 g (25%) of **10** and 0.40 g (20%) of **11**.

10: White needles after recrystallization from CH_3CN, m.p. ca. 295 °C. − R_f (1:1) = 0.61. − ^1H NMR ($CDCl_3$): δ = 8.07−8.09 (d, *J* = 8.4 Hz, 8 H), 7.26−7.31 (d, *J* = 8.4 Hz, 8 H), 3.48 (br., 8 H), 2.40 (s, 12 H), 2.02 (m, 4 H). − ^{13}C NMR ($CDCl_3$): δ = 143.9 (s), 135.2 (s), 129.3 (d), 129.1 (d), 47.2 (t), 24.1 (t), 21.6 (q). − ^{29}Si NMR ($CDCl_3$): δ = −69.96. − IR (KBr): $\tilde{\nu}$ = 1330 cm^{-1}, 1155, 965, 930. − MS (FAB): *m/z* (%): 789 (1.4) $[M^{2+}]$, 635 (2), 613 (3), 581 (2), 461 (3), 309 (30), 275 (8), 155 (42). − $C_{34}H_{40}N_4O_8S_4Si$ (789.03): calcd. C 51.75, H 5.11, N 7.10, found C 51.63, H 5.11, N 7.05.

11: White solid after recrystallization from EtOAc/cyclohexane, m.p. 145−147°C. − R_f (1:1) = 0.46. − ^1H NMR ($CDCl_3$): δ = 8.06−8.09 (d, *J* = 8.1 Hz, 2 H), 7.90−7.93 (d, *J* = 8.1 Hz, 4 H), 7.68−7.71 (d, *J* = 8.1 Hz, 2 H), 7.37−7.40 (d, *J* = 8.1 Hz, 2 H,), 7.31−7.40 (d, *J* = 8.1 Hz, 4 H), 7.25−7.28 (d, *J* = 8.1 Hz, 2 H), 4.39 (t, *J* = 6.3 Hz, 1 H), 3.40−3.50 (m, 4 H), 3.19−3.26 (m, 2 H), 2.84−2.90 (m, 2 H), 2.45 (s, 3 H), 2.43 (s, 6 H), 2.39 (s, 3 H), 1.78−1.90 (m, 4 H). −^{13}C NMR ($CDCl_3$): δ = 144.9 (s), 144.4 (s), 143.3 (s), 136.8 (s), 135.3 (d), 134.9 (s), 129.8 (d), 129.7 (d), 129.6 (d), 129.1(d), 128.3(d), 127.1(d), 46.7 (t), 45.1 (t), 40.7 (t), 28.6 (t), 26.0 (t), 21.7 (q), 21.6 (q), 21.5 (q). − ^{29}Si NMR ($CDCl_3$): δ = −53.64. − IR (KBr): $\tilde{\nu}$ = 1340 cm^{-1}, 1160, 1090, 1025, 930, 865. − MS (FAB): *m/z* (%): 825 (5) $[M + 1]^+$, 671 (6), 517 (2), 443 (100), 425 (5), 289 (10), 229 (3), 139 (12). − $C_{34}H_{41}ClN_4O_8S_4Si$ (824.13): calcd. C 49.46, H 5.01, N 6.79, found C 49.92, H 5.15, N 6.54.

1,1′,3,3′-Tetratosyl-1,1′,3,3′-tetraaza-2-silaspiro[2.2′]-2,3-dihydro-1H-phenalene (**13**): The reaction mixture was refluxed for 48 h. Recrystallization from CH_2Cl_2/CH_3CN gave 0.80 g (35%) **13** as white needles. Crystals of **13** suitable for X-ray analysis were grown from CH_2Cl_2/CH_3CN as colourless blocks, m.p.

Table 1. Crystallographic data for $Si(TsN-CH_2CH_2-NTs)_2$ (**8a**) and $Si[1,8\text{-}(TsN)_2C_{10}H_6]_2$ (**13**) and (**16**)

	8a	**13**	**16**
Chemical formula	$C_{32}H_{36}N_4O_8S_4Si$	$C_{48}H_{40}N_4O_8S_4Si\cdot CH_3CN$	$C_{26}H_{22}N_2O_3S_2$
Formula weight	760.98	998.22	474.58
Crystal system	monoclinic	triclinic	monoclinic
Space group	$P2_1/n$ (no. 14)	$P\bar{1}$ (no. 2)	$P2_1/n$ (no. 14)
a [Å]	13.6295(10)	13.1926(12)	9.801(2)
b [Å]	20.283(2)	13.3072(9)	15.5525(11)
c [Å]	14.3308(10)	14.132(2)	16.630(2)
α [°]	90	86.528(8)	90
β [°]	113.993(5)	71.469(9)	95.595(12)
γ [°]	90	83.926(7)	90
V [Å^3]	3619.5(5)	2338.4(4)	2522.9(6)
Z	4	2	4
λ [Å]	0.71073	0.71073	0.71073
$\rho_{calcd.}$ [g cm^{-3}]	1.396	1.418	1.249
μ [mm^{-1}]	0.350	0.291	0.240
Independent reflns.	6743	8686	4328
Obsd. reflns. [$I > 2\sigma(I)$]	4530	7031	3140
$R(F_o)_{obsd.\ data}$[a]	0.0697	0.0480	0.0645
$R_w(F_o^2)_{all\ data}$[b]	0.1631	0.1251	0.1654

[a] $R = \Sigma||F_o| - |F_c||/\Sigma|F_o|$. – [b] $R_w = (\Sigma[w(F_o^2 - F_c^2)^2])/\Sigma[w(F_o^2)^2])^{1/2}$.

290°C.(decomp.). – R_f (2:3) = 0.55. – ^{1}H NMR ($CDCl_3$): δ = 7.90–7.95 (m, 12 H), 7.16–7.23 (m, 4 H), 6.99–7.04 (m, 12 H), 2.18 (m, 12 H). – ^{13}C NMR ($CDCl_3$): δ = 144.2 (s), 135.1 (s), 134.8 (s), 134.4 (s), 129.6 (s), 129.3(d), 128.9 (d), 128.0 (d),125.6 (d), 124.1 (d), 21.5 (q). – IR (KBr): $\tilde{\nu}$ = 1560 cm^{-1}, 930, 850, 810. – MS (FAB): *m/z* (%): 957 (2) [M + 1]$^+$, 803 (2), 648 (2), 309 (20), 275 (7), 193 (9), 153 (25). – $C_{48}H_{40}N_4O_8S_4Si$ (957.19): calcd. C 60.22, H 4.21, found C 60.05, H 4.18.

1-(p-Tolyl)-7-tosyl-1-thia-2,7-diaza-3,4;5,6-dibenzo-1,3,5-cycloheptatriene 1-Oxide (**16**): The reaction mixture was refluxed for 24 h. CC (1:3) gave 0.840 g (35%) **16** which was recrystallized from CH_3CN to give white crystals. Crystals of **16** suitable for X-ray analysis were grown from CH_3CN as colourless plates, m.p. 233–234°C. – R_f (1:3) = 0.44. – ^{1}H NMR ($CDCl_3$): δ = 7.81–7.84 (dt, J = 8.4, 1 Hz, 4 H), 7.44–7.59 (m, 6 H), 7.16–7.37 (m, 14 H), 7.04–7.09(m, 4 H), 6.93–6.96 (d, J = 8.4 Hz, 4 H), 2.46 (s, 6 H), 2.31 (s, 6 H). – ^{13}C NMR ($CDCl_3$): δ = 145.1 (s), 143.7 (s), 139.8 (s), 138.3 (s), 137.7 (s), 134.2 (s), 133.4 (s),132.8 (d), 131.8 (d), 130.5 (d),129.8 (d), 129.5 (d), 129.1 (d), 128.9 (d), 128.8 (d), 128.7 (d), 127.8 (d), 127.4 (d), 126.4 (d), 124.1 (d), 21.7 (q), 21.5 (q). – IR (KBr): $\tilde{\nu}$ = 930 cm^{-1}. – MS (FAB); *m/z* (%): 475 (62) [M + 1]$^+$, 352 (11), 321(31), 271(7), 181 (100). – $C_{26}H_{22}N_2O_3S_2$ (474.59): calcd. C 65.80, H 4.67, N 5.90; found C 66.47, H 4.93, N 5.62.

Crystal Structure Analyses: Crystal data are presented in Table 1. Data collection: For all three compounds, **8a**, **13** and **16**, intensity data were collected at room temp. with a Stoe AED2 4-circle diffractometer using Mo-K_α graphite-monochromated radiation, using ω/2Θ scans in the range 4–51° in 2Θ. Lattice parameters were optimized from a least-squares refinement of the ± ω values of 29 (**8a**), 24 (**13**) and 23 (**16**) reflections (and their equivalents) in the 2Θ ranges 25.4–33.7° (**8a**), 25.6–35.6° (**13**) and 28.1–35.8° (**16**). Crystallographic data are summarized in Table 1. The structures were solved by direct methods using the program SHELXS-97.[27] The refinement and all further calculations were carried out using SHELXL-97.[28] Complex neutral-atom scattering factors used were those contained in the program SHELXL-97. All of the H atoms were included in calculated positions and treated as riding atoms using SHELXL-97 default parameters. The non-H atoms were refined anisotropically using weighted full-matrix least squares on F^2. Corrections for extinction were applied but not for absorption. Final atomic coordinates are given in Table 2 and selected bond lengths and angles in Table 3. The structural diagrams were drawn using the program Xtal GX.[29]

Full tables of atomic parameters and bond lengths and angles for the structures reported in this paper may be obtained from the Cambridge Crystallographic Data Centre. Copies of the crystallographic data [CCDC-101700 (**8a**), -101701 (**13**), -101702 (**16**)] may be obtained free of charge on application to CCDC, 12 Union Road, Cambridge CB2 1EZ, UK [Fax: (internat.) + 44(1223)336-033, E-mail: deposit@ccdc.cam.ac.uk).

[1] C. Chuit, R. J. P. Corriu, C. Reyé, J. C. Young, *Chem. Rev.* **1993**, *93*, 1371.
[2] R. J. P Corriu, C. Guérin, J. J. E. Moreau in *The Chemistry of Organic Silicon Compounds* (Eds.: S. Patai, Z. Rappoport), John Wiley, Chichester, **1989**, chapter 4.
[3] R. J. P. Corriu, J. C. Young in *The Chemistry of Organic Silicon Compounds* (Eds.: S. Patai, Z. Rappoport), John Wiley, Chichester, **1989,** chapter 20.
[4] R. R. Holmes, *Chem. Rev.* **1990**, *90*, 17–31.
[5] R. R. Holmes, *Chem. Rev.* **1996**, *96*, 927–950.
[6] T. Kawashima, R. Okazaki, *Synlett* **1996**, 600.
[7] N. Auner, R. Probst, F. Hahn, E. Herdtweck, *J. Organomet. Chem.* **1993**, *459*, 25.
[8] C. Breliere, F. Carré, R. J. P. Corriu, G. Royo, M. C. Wong Chi Man, J. Lapasset, *Organometallics* **1994**, *13*, 307.
[9] F. Carré, C. Chuit, R. J. P. Corriu, A. Mehdi, A. C. Reyé, *Angew. Chem.* **1994**, *106*, 1152; *Angew. Chem. Int. Ed. Engl.* **1994**, *33*, 1097.
[10] F. Carré, C. Chuit, R. J. P. Corriu, A. Fanta, A. Mehdi, C. Reyé, *Organometallics* **1995**, *14,* 194.
[11] M. Wollenweber, R. Keese, H. Stoeckli-Evans, *Z. Naturforsch., B: Chem. Sci.* **1998**, *53b*, 145. Selected bond lengths [Å], bond and torsional angles [°] of **6**: O(4)···Si(1) 2.953(2), O(2B)···Si(1) 2.982(2), O(3B)···Si(1) 2.912(3), O(2)···Si(1) 2.960(2); O(2)–Si(1)–O(4) 158.7(1), O(2B)–Si(1)–O(3B) 158.4(1).
[12] [12a] C.H. Yoder, J. J. Zuckerman, *Inorg. Chem.* **1995**, *4*, 116. – [12b] E. W. Randall, C. H. Yoder, J. J. Zuckerman, *Inorg. Chem.* **1967**, *6*, 744.
[13] D. Kummer, J. D. Baldeschwieler, *J. Phys. Chem.* **1963**, *67*, 98.
[14] H.-G. Horn, H. C. Marsmann, *Makromol. Chem.* **1972**, *162*, 255.
[15] H. Jancke, G. Engelhardt, M. Mägi, E. Lippma, *Z. Chem.* **1973**, *13*, 435.
[16] C. H. Yoder, J. J. Zuckerman, *Inorg. Chem.* **1966**, 5, 2055.

[17] *International Tables for Crystallography* (Ed.: A. J. C. Wilson), Kluwer Academic Publishers, Dordrecht, **1992**, vol. C ("Mathematical, Physical and Chemical Tables"), chapter 9.5.1.1, Table 9.5.
[18] P. Wessig, F. Legart, B. Hoffmann, H.-G. Henning, *Liebigs Ann. Chem*. **1991**, 979.
[19] G. H. Searle, R. G. Geue, *Aust. J. Chem*. **1984**, 959.
[20] F. E. Scully, Jr., K. Bowdring, *J. Org. Chem*. **1981**, *46*, 5077.
[21] I. Massaki, K. Hiroyoshi, *Bull. Chem. Soc. Jpn*. **1982**, *55*, 2153.
[22] H. H. Hodgson, J. S. Whitehurst, *J. Chem. Soc*. **1945**, 202.
[23] C. H. Yoder, J. J. Zuckerman, *J. Am. Chem Soc*. **1966**, *88*, 2170.
[24] T. P. Prakasch, R. Pattuparanbil, W. K. Ganesh, *J. Chem. Soc., Perkin Trans.1* **1991**, 1276.
[25] *Vogel's Textbook of Practical Organic Chemistry* (Eds.: B. S. Furniss, A. J. Hannaford, V. Rogers, P. W. G. Smith, A. R. Tatchel), 4th ed., Longman, London, New York, **1978**, p. 611.
[26] D. Lloyd, R. H. McDougall, *J. Chem. Soc*. **1960**, 4136.
[27] G. M. Sheldrick, *Acta Crystallogr.* **1990**, *A46*, 467 ("SHELXS-97 Program for Crystal Structure Determination").
[28] G. M. Sheldrick, *SHELXL-97*, Universität Göttingen, Göttingen, Germany, **1997**.
[29] S. R. Hall, D. du Bulay, *Xtal GX*, University of Western Australia, Australia, **1997**.

[98184]

Binding Properties of Two Novel Phosphane-Modified Tetrapodants and Their Bimetallic Transition Metal Complexes

Georg C. Dol[a], Sander Gaemers[a], Marko Hietikko[a], Paul C. J. Kamer[a], Piet W. N. M. van Leeuwen*[b], and Roeland J. M. Nolte[a]

Institute of Molecular Chemistry, University of Amsterdam[a],
Nieuwe Achtergracht 166, NL-1018 WV Amsterdam, The Netherlands
Fax: (internat.) + 31-20/5256456
E-mail: tijdink@sci.kun.nl

Department of Organic Chemistry, University of Nijmegen[b],
Toernooiveld, NL-6525 ED Nijmegen, The Netherlands
Fax: (internat.) +31-24/3652929
E-mail: pwnm@anorg.chem.uva.nl

Received June 18, 1998

Keywords: Supramolecular chemistry / Metallamacrocycle / Hydrogen bonding / Phosphane

Two novel phosphane ligands **3** and **4** based on the rigid diphenylglycoluril molecule have been synthesized and characterised. Binding studies with **3** and **4**, using 1,3-dihydroxybenzene derivatives reveal that ligands **3** and **4** behave similarly to clip molecule **5**, which has the same binding site as ligands **3** and **4**. The size of the flexible spacers in the ligands has been varied and the effect of this variation on the association constant of resorcinol derivatives has been determined. These cavity-containing ligands are able to coordinate two transition metal centres, leading to bimetallic macrocycles. The metallamacrocycles formed from **4** containing platinum or rhodium bind the guest, olivetol (5-pentylbenzene-1,3-diol), almost four times as strongly as the free tetrapodant **4**. Complexes of **4** having palladium centres display similar or reduced binding affinities for resorcinol derivatives, when compared to free **4**. Metal complexes of ligand **3** do not form host-guest complexes, probably because of a too small a ring-size of the metallamacrocycle.

Introduction

The use of enzymes as catalysts for organic reactions is a major topic in modern chemistry. Enzyme-catalysed reactions can reach incredibly high rates and selectivities. Man-made catalysts do not reach that level of supremacy yet, but recently some elegant examples of synthetic enzymes (synzymes) have been published. These synzymes consist of the building block diphenylglycoluril (= DPGU),[1−5] a cyclodextrin[6−8] or a cyclophane[9] and a catalytically active centre. Synzymes do not match the natural enzymes in reactivity, but they are interesting molecules to study the fundamental processes taking place in enzyme catalysis. In this way processes like substrate coordination and substrate-metal interactions can be studied in a less complicated environment. The knowledge obtained can then be used in the development of shape-selective catalysts.[3−5,10,11] Non-covalent binding interactions like hydrogen bonding, π-π stacking, electrostatic, and van der Waals interactions induce substrate discrimination in the processes mentioned above.

In this paper two tetrapodant host molecules **3** and **4** based on the rigid building block DPGU are described. The binding affinities of these host molecules towards 5-substituted resorcinol (1,3-dihydroxybenzene) derivatives will be presented. Several transition metal complexes of **3** and **4** were prepared and the effect of metal complexation on the bond strength between host and guest was investigated. These results are of interest for future applications of metal complexes of **3** and **4** as catalysts for e.g. the hydroformylation reaction or cross-coupling reactions.

Results and Discussion

Ligand Synthesis

The tetrapodant starting compounds **1** and **2** were prepared according to literature procedures[12] and subsequently converted into **3** and **4** after reaction with four equivalents of $LiPPh_2$ (see Scheme 1). The two tetradentate ligands **3** and **4** were obtained in 80% and 67% yield, respectively. Also, we tried to synthesize compound **4** from **2** and four equivalents of $HPPh_2$ in the presence of 10 equivalents of *t*BuOK. This reaction afforded only small amounts of the desired product. Under these conditions, the main reaction that occurred was cleavage of the ether moieties.

The two ligands (**3** and **4**) are moderately air-sensitive, but they are stable under an inert atmosphere. When the products were not carefully worked up or stored, ^{31}P-NMR spectra showed signals in the phosphane oxide region (δ = + 30). These oxide contaminations could be removed by

 © WILEY-VCH Verlag GmbH, D-69451 Weinheim, 1998 1434−1948/98/1212−1975 $ 17.50+.50/0

reduction with an excess of $HSiCl_3$ in the presence of 3 equivalents of NEt_3 per $HSiCl_3$ in refluxing benzene.[13]

Scheme 1. Synthesis of ligands **3** and **4**

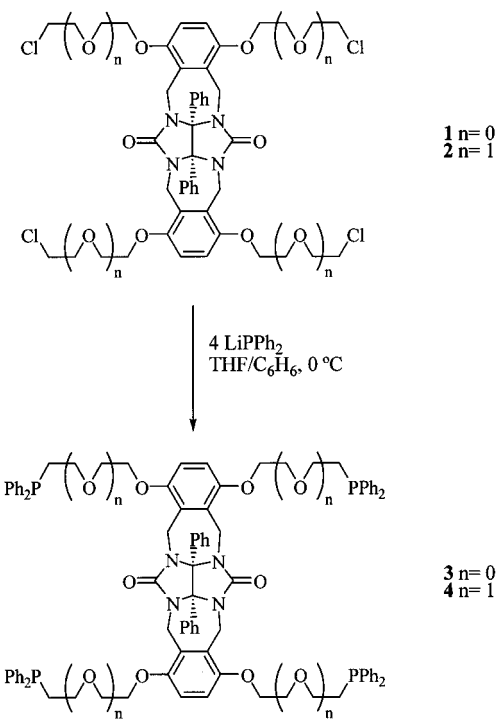

Metal Complex Synthesis

The starting compounds in the metal complexation reactions and the yields are summarised in Table 1. Most of the complexes of **3** and **4** were synthesized from starting metal complexes containing triphenylphosphane. After addition of the tetradentate ligands **3** or **4** to these PPh_3-containing compounds, the bimetallic complexes of **3** or **4** were formed. The driving force of this reaction is the replacement of a triarylphosphane ligand by an alkyldiphenylphosphane, which is a stronger donor ligand. The reaction is also entropy-driven; a monodentate ligand is always replaced by a bidentate ligand having similar electronic and steric properties.

A phosphane-free precursor compound [e.g. $(COD)PdCl_2$] could also be used, provided that a small amount of PPh_3 was added to the reaction mixture. When the syntheses were performed without PPh_3, large amounts of insoluble compounds were formed in addition to the desired product. The replacement of COD or CH_3CN by a phosphane ligand is fast compared to a phosphane-by-phosphane replacement. Before intramolecular ring closure can occur, intermolecular complexation takes place. The polymeric complexes precipitate and cannot equilibrate to form the desired bimetallic complexes. These reactions were also performed at lower concentrations (3×10^{-4} M), but always some insoluble product was formed. A suspension of precipitated (polymeric) complex could be treated with a small amount of PPh_3 to redissolve the polymeric products. The PPh_3 that remained after the reaction could be removed with the same ease as weakly bound ligands such as COD and CH_3CN. A simple precipitation of the metal complex after the addition of pentane, hexane or diethyl ether, followed by filtration or decantation of the suspension was sufficient to remove PPh_3.

There are two exceptions to the general procedure described above: the formation of $\mathbf{L}[Pd(BF_4)_2]_2$ and $\mathbf{L}[Pd(TCNE)]_2$ (**L** = **3** or **4**, TCNE= tetracyanoethylene). For the preparation of the aforementioned ionic palladium compounds, CH_3CN was used as a cosolvent. The products formed still contained two molecules of CH_3CN, which increased the solubility of the products. Hence, polymeric structures did not precipitate and the desired products were obtained. For the formation of the $\mathbf{L}[Pd(TCNE)]_2$ complexes the reaction of $Pd(DBA)_2$ (DBA= dibenzylideneacetone) with either **3** or **4** was chosen. This resulted in the initial formation of $\mathbf{L}[Pd(DBA)]_2$ complexes. The replacement of the second DBA molecule is known to be less favourable,[14] but this could be achieved by the addition of TCNE, an extremely electron-poor alkene. Complexes possessing other electron-poor alkenes like maleic anhydride, dimethyl fumarate or fumaronitrile could not be isolated. These alkenes are not as tightly bound to the Pd centre as TCNE and therefore afford less stable compounds.

Table 1. Starting compounds, products, yields and spectroscopic data of the bimetallic macrocycles of **3** and **4**

Entry	Starting compound	Product	Yield [%]	$\delta(^{31}P)$ [ppm] ($^1J_{M\text{-}P}$ [Hz])	$\nu(CX)$[f] [$^{-1}$]
1	$(PPh_3)_2PdCl_2$	$\mathbf{3}(PdCl_2)_2$	58	12.5[a]	1710[g]
2	$CODPdCl_2/PPh_3$	$\mathbf{4}(PdCl_2)_2$	75	14.9[a]	1710[g]
3	$(PPh_3)_2PdMeCl$	$\mathbf{3}(PdMeCl)_2$	84	15.4[b]	1710[g]
4	$CODPdMeCl/PPh_3$	$\mathbf{4}(PdMeCl)_2$	85	21.9[b]	1710[g]
5	$(CH_3CN)_4Pd(BF_4)_2$	$\mathbf{3}[Pd(BF_4)_2]_2$	93	38.4[c]	1648[g]
6	$(CH_3CN)_4Pd(BF_4)_2$	$\mathbf{4}[Pd(BF_4)_2]_2$	79	42.8[c]	1670[g]
7	$Pd(DBA)_2$ + TCNE	$\mathbf{3}[Pd(TCNE)]_2$	85	24.8[b]	1701[g], 2220[h]
8	$Pd(DBA)_2$ + TCNE	$\mathbf{4}[Pd(TCNE)]_2$	84	12.8[b]	1707[g], 2213[h]
9	$(PPh_3)_2PtCl_2$	$\mathbf{3}(PtCl_2)_2$	79	0.4[b] (3550[d])	1707[g]
10	$(PPh_3)_2PtCl_2$	$\mathbf{4}(PtCl_2)_2$	68	4.8[b] (3610[d])	1708[g]
11	$(PPh_3)_2RhClCO$	$\mathbf{3}(RhClCO)_2$	96	18.6[b] (124[e])	1710[g], 1972[i]
12	$(PPh_3)_2RhClCO$	$\mathbf{4}(RhClCO)_2$	96	22.0[b] (123[e])	1708[g], 1970[i]
13	$(PPh_3)_2IrClCO$	$\mathbf{3}(IrClCO)_2$	89	14.8[a]	1710[g], 1959[j]
14	$(PPh_3)_2IrClCO$	$\mathbf{4}(IrClCO)_2$	85	17.7[a]	1711[g], 1958[j]

[a] Measured in C_6D_6. – [b] Measured in $CDCl_3$. – [c] Measured in CD_3CN. – [d] $^1J_{Pt\text{-}P}$ (*cis*). – [e] $^1J_{Rh\text{-}P}$ (*trans*). – [f] Measured in KBr. – [g] $\nu(CO)$. – [h] $\nu(CC)$. – [i] $\nu[(CO)_{Rh}]$. – [j] $\nu[(CO)_{Ir}]$.

Identification

The ^{1}H-NMR spectra of the metal complexes of **3** and **4** have characteristic signals, viz. a doublet, at $\delta = 5.5-5.7$. This signal is due to one of the inequivalent (CO)NCHH′ protons. The coupling constant of these two protons is in the range of $J = 15-16$ Hz.[4,15−20] The other doublet is generally found at $\delta \approx 3.8$ depending on the solvent. When a large deviation from this ppm value is found, the three-dimensional structure of the building block is distorted. Another characteristic signal in the ^{1}H-NMR spectrum is the singlet arising from the hydroquinone walls at $\delta = 6.5 \pm 0.1$. This signal was used in the determination of the host-guest association constants (see below). The IR spectra of DPGU derivatives always show a strong absorption of the urea carbonyl groups [ν(CO) at 1705 ± 5 cm^{-1} (KBr disk)]. This carbonyl stretching frequency can be used to observe interactions involving the carbonyl group. For example, hydrogen bonding between the carbonyl group and resorcinol derivatives induces a shift of -25 ± 5 cm^{-1}, as has been described in the literature [16,21,22].

The ^{1}H- and ^{13}C-NMR spectra of **3** and **4** indicated that the concave part of the host, i.e. where the binding of substrates occurs, is similar to that of the rigid clip molecule **5** (see Figure 2). The coupling constant of the doublet at $\delta \approx 5.5$ and the chemical shift of the hydroquinone parts were in good agreement with literature values for these type of compounds[4,15,16,18−20]. In the ^{31}P{^{1}H}-NMR spectrum singlets at $\delta = -21.1$ and -21.7 were found for **3** and **4**, respectively, which are values similar to those of other alkyldiphenylphosphanes. The IR spectra of **3** and **4** showed a carbonyl resonance at the expected frequency around 1710 cm^{-1}. The elementary analyses of ligands **3** and **4** showed that two molecules of water are present in the host in the solid state. This could be confirmed by IR and NMR spectroscopy, which both revealed small amounts of water. These water molecules did not seem to disturb any of our further studies and therefore no attempts were made to remove them.

The various transition metal complexes of ligands **3** and **4** have ^{31}P-NMR resonances (see Table 1) at higher ppm values compared to the free tetrapodants. The difference between the chemical shift of the free ligand and that of its transition metal complex ($\Delta\delta_{compl}$) is a suitable tool to determine what type of complex has been formed. The ^{31}P-NMR values of these complexes are similar to phosphanemetal complexes known from literature,[23][24] showing that ligands **3** and **4** are suitable ligands for coordination chemistry studies. A comparison of the change in chemical shift on coordination ($\Delta\delta_{compl}$) with values found in literature leads to the following conclusions about the immediate surroundings of the transition metal centres. All complexes except **L**[Pd(TCNE)]$_2$ have a square planar conformation. Complexes containing the PdMeCl fragment have two equal, *trans*-coordinated phosphane moieties, which can be derived from the singlet in the ^{31}P{^{1}H}-NMR spectrum. Complexes **L**(PdCl$_2$)$_2$ displayed a singlet in the ^{31}P{^{1}H}-NMR spectrum around $\delta = 13$. From literature it

Scheme 2. Schematic representation of the synthesis of the metal complexes (used starting compounds: $(PPh_3)_2PdCl_2$; $(COD)PdCl_2$; $(PPh_3)_2PdMeCl$; (COD)PdMeCl; i) $Pd(DBA)_2$, ii) TCNE; $(CH_3CN)_4Pd(BF_4)_2$; $(PPh_3)_2PtCl_2$; $(PPh_3)_2RhCl(CO)$; $[PPh_3)_2IrCl(CO)]$

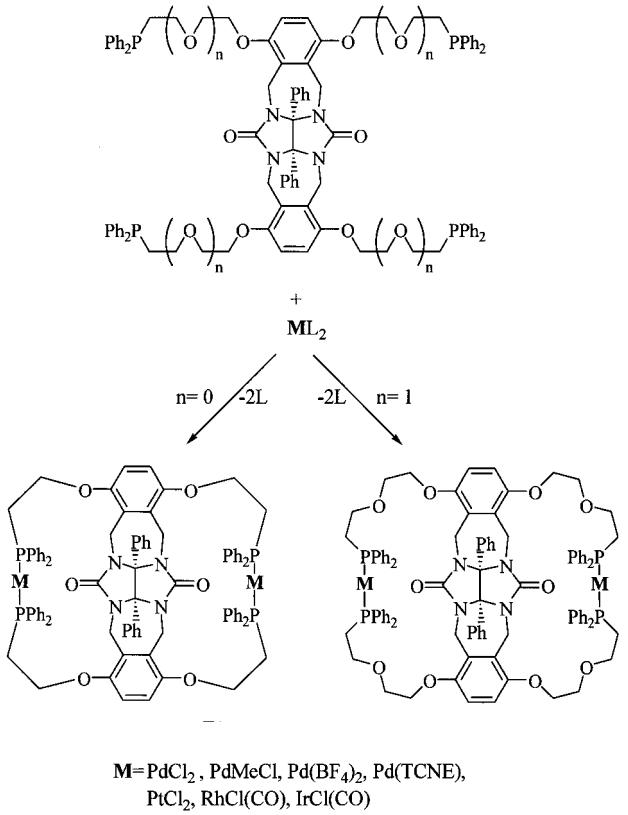

is known that the value of $\Delta\delta_{compl}$ after the formation of a *cis*-$PdCl_2$ complex is 43−47 ppm, whereas 32−36 ppm is found when *trans* complexes are formed.[24] In our case the values are $\Delta\delta_{compl} = 34.2$ for **3**(PdCl$_2$)$_2$ and 36 ppm for **4**(PdCl$_2$)$_2$, which indicates that bimetallic *trans*-coordinated complexes have been formed.

In this series of complexes, **3**(PtCl$_2$)$_2$ and **4**(PtCl$_2$)$_2$ are the only *cis*-coordinated compounds we were able to isolate. The ^{31}P-NMR spectra of these complexes showed coupling constants around $^1J_{Pt\text{-}P} = 3500$ Hz (Table 1, entries 9 and 10), which indicates the formation of *cis* complexes.[23] These coupling constants were also observed in the ^{195}Pt-NMR spectrum of **4**(PtCl$_2$)$_2$, which afforded a triplet at $\delta = -4390$. In addition to the magnitude of the coupling constant ($^1J_{Pt\text{-}P}$), the ^{195}Pt chemical shift itself is indicative of a *cis*-coordinated complex. The typical chemical shift value of a *trans* complex is found at $\delta = -3950$.[25] For electronic reasons, i.e. the larger *trans* influence of phosphanes compared to chloride, $PtCl_2$ complexes of phosphane ligands with small cone angles prefer *cis* coordination.

The zero-valent palladium complexes (Table 1, entries 7 and 8) are stabilised by the electron-poor alkene TCNE, which reduces the electron density on the Pd^0 centre. The coordination mode around the metal centre is probably pseudo-tetrahedral, as has been found for several crystal structures of related Pd^0 complexes.[26] The IR spectra of

3[Pd(TCNE)]$_2$ and **4**[Pd(TCNE)]$_2$ showed sharp bands of the CN vibration of the TCNE molecule. The values were found at 2213 cm^{-1} and 2220 cm^{-1}, respectively, which are in good agreement with values reported in the literature for TCNE metal complexes.[26] The urea carbonyl groups in the ligands gave rise to strong and sharp bands at 1707 cm^{-1} and 1710 cm^{-1} in **3**[Pd(TCNE)]$_2$ and **4**[Pd(TCNE)]$_2$, respectively.

The two ionic palladium(II) complexes of **3** and **4** are square-planar complexes. The phosphane moieties in these complexes are coordinated in a *trans* fashion as can be seen from the phosphorus chemical shift values[27] (δ = 38.4 and 42.8 for **3**[Pd(BF$_4$)$_2$]$_2$ and **4**[Pd(BF$_4$)$_2$]$_2$, respectively). In the solid state the two Pd^{II} tetrafluoroborate complexes still contain one molecule of CH_3CN per Pd atom, as could be concluded from the elementary analyses of **3**[Pd(BF$_4$)$_2$]$_2$ and **4**[Pd(BF$_4$)$_2$]$_2$. However, their IR spectra did not show a band at 2100−2000 cm^{-1}, the typical region of a coordinated CH_3CN molecule. The IR spectra did show strong carbonyl bands at 1648 cm^{-1} for **3**[Pd(BF$_4$)$_2$]$_2$ and at 1670 cm^{-1} for **4**[Pd(BF$_4$)$_2$]$_2$. The shifts of 60 cm^{-1} and 40 cm^{-1} compared to the **L**(PdCl$_2$)$_2$ complexes, indicate that there is an interaction between the carbonyl group of the ligand and the cationic palladium centre. Electron donation of the urea carbonyl group to the Pd^{II} centre will result in a reduced bond strength, leading to an absorption at a lower frequency. This frequency shift is larger in **3**[Pd(BF$_4$)$_2$]$_2$ than that in **4**[Pd(BF$_4$)$_2$]$_2$, probably because the shorter spacer groups in the latter complex enforce a shorter metal-to-carbonyl distance. The interaction between the carbonyl group and the metal centre could not be detected in solution. The cationic complexes dissolve in polar, coordinating solvents only (e.g. CH_3CN or DMSO), which replace the coordinated carbonyl groups.

The iridium and rhodium complexes in Table 1 are similar in structure to the original Vaska complex[28] that contains two triphenylphosphane ligands coordinated in a *trans* fashion to an iridium centre. The rhodium complex showed a doublet in the $^{31}P\{^1H\}$-NMR spectrum with $^1J_{Rh\text{-}P}$ = 124 Hz, indicative of *trans* coordination.[29] We also determined the ^{103}Rh chemical shift of **4**[RhCl(CO)]$_2$, which was found at δ = −419, close to that of reference compound (PPh$_3$)$_2$RhCl(CO).[25] The IR spectra of **3**[RhCl(CO)]$_2$ and **4**[RhCl(CO)]$_2$ showed bands for the urea carbonyl groups ($\tilde{\nu}$ = 1710 and 1708 cm^{-1}) and for the carbon monoxide ligand [ν(CO)$_{Rh}$]. The latter absorptions were found at 1970 and 1972 cm^{-1}, respectively, which are slightly lower values than those found in (PPh$_3$)$_2$RhCl(CO). Finally, we determined the molecular weight of complex **4**[RhCl(CO)]$_2$ in a dichloromethane solution (by vapour pressure osmometry) and found a value of 1850 ± 100 (calcd. 1919). The molecular weight determination of **3**[RhCl(CO)]$_2$ proved to be difficult due to its poor solubility.

The $^{31}P\{^1H\}$-NMR spectra of the iridium complexes of **3** and **4** showed a singlet for both compounds (see Table 1, entries 13 and 14), proving the formation of a *trans* complex. The peaks of the CO ligand [ν(CO)$_{Ir}$] in the infra red spectra of **3**[IrCl(CO)]$_2$ and **4**[IrCl(CO)]$_2$ were found at a frequency 3 cm^{-1} below that of the original Vaska complex (1962 cm^{-1}). In these iridium complexes the band of the urea carbonyl group was found at 1710 ± 2 cm^{-1} (in KBr).

We attempted to isolate the cationic complexes **3**[Rh(CO)$^+$]$_2$ and **4**[Rh(CO)$^+$]$_2$, by the reaction of $AgBF_4$ with the two **L**[RhCl(CO)]$_2$ complexes. Turbid solutions containing a fine precipitate were formed after the addition of $AgBF_4$, but the precipitate could not be removed; centrifugation and subsequent filtration with Celite did not result in the removal of AgCl. IR measurements on the crude complexes showed that the $\nu(CO)_{Rh}$ had shifted to a higher frequency (1990 cm^{-1}). The peaks of the urea carbonyl group shifted approximately 30 cm^{-1} to a lower frequency in both **3**[Rh(CO)$^+$]$_2$ and **4**[Rh(CO)$^+$]$_2$. These frequency shifts for both the urea carbonyl and the coordinated CO molecule strongly indicate the formation of a cationic Rh^I complex in which an interaction exists between the cationic Rh centre and the urea carbonyl group. The positive shift of $\nu(CO)_{Rh}$ indicates a reduced π back donation of the electron-poor cationic rhodium(I) centre to the coordinated CO molecule. The negative shift of the urea carbonyl band indicates that the carbonyl group coordinates to the cationic rhodium(I) centre. This electron donation was also found in the aforementioned cationic palladium(II) complexes, which showed a larger shift of $\Delta\nu$ = −60 cm^{-1} and $\Delta\nu$ = −40 cm^{-1} for **3**[Pd(BF$_4$)$_2$]$_2$ and **4**[Pd(BF$_4$)$_2$]$_2$, respectively.

Variable-Temperature NMR Experiments

To investigate a possible interaction between the phosphane end groups of **4** and guests we recorded the ^{31}P-NMR spectra of **4** and five host-guest complexes of **4** with resorcinol derivatives. Figure 1 shows the temperature dependence of the $^{31}P\{^1H\}$ line width of these complexes. At 333 K all the $^{31}P\{^1H\}$-NMR signals were visible as sharp singlets having a line width of $\Delta\nu_{1/2}$ = 5−7 Hz. These are the normal values in $^{31}P\{^1H\}$-NMR spectra. When **4** was measured without additives, this sharp singlet remained in the temperature range of T = 223−333 K. The metal complex **4**[RhCl(CO)]$_2$ also gave rise to a sharp signal in this temperature range. Experiments using a mixture of **4** and a resorcinol derivative , however, showed a gradual increase in the $\Delta\nu_{1/2}$ of the ^{31}P signal on lowering of the temperature. The $\Delta\nu_{1/2}$ passed through a maximum value at T_{max}, followed by a decrease in $\Delta\nu_{1/2}$ on further lowering of the temperature. The chemical shift of the ^{31}P signal also shifted on variation of the temperature. At high temperatures the signal was found at δ = −20.5, whereas at low temperatures, the signal shifted to δ = −24. The substrate apparently has an influence on both the value of $\Delta\nu_{1/2}$ and the T_{max} at which the maximum broadening is found. T_{max} and $\Delta\nu_{1/2}$ were also affected by the amount of substrate present. When a mixture of one equivalent of **4** and 6.5 equivalents of octyl 3,5-dihydroxybenzoate was measured, the value of T_{max} was found at 313 K having a $\Delta\nu_{1/2}$ of 88 Hz. When the host-guest ratio was lowered to 1:2, the value of T_{max} was found at a lower temperature (283 K) and the maxi-

mum broadening was now 52 Hz. The size of the substituent on resorcinol also had an effect on the value of $\Delta\nu_{1/2}$. 5-Chlororesorcinol, for example, had a smaller effect on $\Delta\nu_{1/2}$ than the aforementioned octyl ester of 3,5-dihydroxybenzoic acid. These measurements indicate that the flexible spacer groups, attached to the concave part of tetrapodant **4**, have an interaction with an incoming substrate. In a reference experiment without addition of a substrate no change in line width was observed. This indicates that the presence of a substrate is required to induce this line broadening. The nature of the interaction between **4** and the substrates, however, cannot be determined from these experiments.

Figure 1. Plot of the line width ($\Delta\nu_{1/2}$) of the ^{31}P-NMR signal of **4** versus temperature (T) in the presence of various resorcinol derivatives (*a:* [**4**]/[octyl 3,5-dihydroxybenzoate] = 1:6.5; *b:* [**4**]/[octyl 3,5-dihydroxybenzoate] = 1:2; *c:* [**4**]/[olivetol] = 1:7.4; *d:* [**4**]/[5-chlororesorcinol] = 1:6.5; *e:* [**4**]/[5-(*p*-tol)resorcinol] = 1:4; *f:* **4** without additives) (conditions: solvent $CDCl_3$, [**4**] = 8×10^{-3} M)

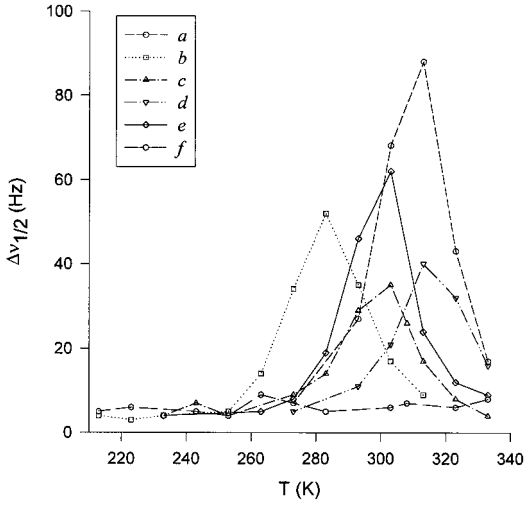

Association Constant Determinations

In order to determine the association constants of host-guest complexes between **1**−**4** and guests the ^{1}H-NMR shifts of the aromatic-wall protons of the tetrapodants were monitored. These signals shift to lower ppm values on association with an aromatic guest molecule and a chemically induced shift (CIS) is observed. Dihydroxybenzenes bind in the cavity of the host molecule via hydrogen bonds between the hydroxy groups of the guest and the urea carbonyl groups of the host molecule[15,16,22]. A second interaction is π-π stacking between the aromatic walls of the host and the aromatic ring of the guest molecule. Thirdly, electrostatic repulsion might occur, which diminishes the total bond strength between the host and its guest.

Resorcinol derivatives containing electron-withdrawing groups at the 5-position bind relatively strongly to **4** (see Table 2). Titration experiments using 5-chlororesorcinol and **4** resulted in an association constant of $K = 4704$ M^{-1}. Electron-donating groups on the resorcinol ring, like alkyl substituents have a slightly negative influence on the association constant of **4** and a guest, e.g. K is 1676 M^{-1} for olivetol (5-pentylbenzene-1,3-diol). Resorcinol derivatives with an aromatic substituent at the 5-position also give rise to increased association constants ($K > 6200$ M^{-1}). An additional π-π stacking interaction between the phenyl groups of the diphenylphosphane moieties and the additional aromatic ring of the substrates may be responsible for this increase in binding affinity. These numbers (except those found with aryl-substituted resorcinol derivatives) are in reasonably good agreement with the values recently published by Reek and co-workers.[16] They used compound **5** in their studies of the binding properties of molecular clips based on DPGU and showed that electron-donating groups on the resorcinol guests lead to reduced association constants. Electron-withdrawing groups on the guest increase the acidity of the hydroxy groups and the π-π stacking interactions, which both result in an increase in association constant. Reek and co-workers tested a number of resorcinol derivatives in their study and found a linear Hammet relationship between the free energy of association (ΔG_{ass}) and the σ_m' values of the substituents on the 5-position of resorcinol.

Table 2. Association constants of tetrapodant **4** with several resorcinol derivatives

Guest	K [M^{-1}][a]	CIS [ppm]
olivetol	1676 (61)	−0.45
5-chlororesorcinol	4704 (407)	−0.43
5-bromoresorcinol	5360[b] (164)	−0.34
5-iodoresorcinol	3952 (272)	−0.37
5-phenylresorcinol	6537[b] (257)	−0.44
5-(4-chlorophenyl)resorcinol	6228 (132)	−0.44
5-(4-methylphenyl)resorcinol	6437 (556)	−0.48
octyl 3,5-dihydroxybenzoate	7406 (431)	−0.45

[a] Duplo experiments, obtained from NMR titrations using $0.25-0.75 \times 10^{-3}$ M solutions of host and $2.5-7.5 \times 10^{-3}$ M solutions of guest compound in $CDCl_3$, errors are given in parentheses, $T = 293$ K. − [b] Single experiment; association constants were calculated using the Granot[42] procedure.

A plot of the ΔG_{ass} values calculated from the data collected in Table 2 versus σ_m, did not show a linear relationship. The only difference between our tetrapodants and **5** is that the latter does not contain flexible spacer groups (including the PPh_2 moieties). These spacer groups are probably responsible for the non-linear relationship between σ_m and ΔG_{ass}. They can interact with an incoming substrate, as shown by the lineshape analyses of the $^{31}P\{^1H\}$-NMR spectra (vide supra), and therefore influence the association constant. In the case of **3** and **4** the steric bulk of the end group will also be of great importance and contribute to the magnitude of the association constant. The two resorcinol derivatives substituted with alkyl chains (olivetol and octyl 3,5-dihydroxybenzoate), for example, give rise to relatively low association constants compared to the values that would be expected on the basis of their σ_m values.

The results obtained for tetrapodants **1**−**4** and olivetol (see Table 3), lead to two conclusions: Larger end groups

Figure 2. Molecular clip **5** used in association constant studies by Reek[16] and co-workers

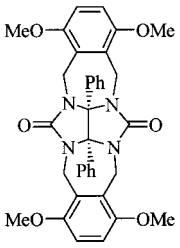

5

on the ethylene glycol chains have a negative effect on the association constant using olivetol as the guest. Replacement of the chlorine groups in **1** by diphenylphosphane moieties giving **3** causes a decrease of the association constant of 20%. A similar decrease of 20% is found when **2** (chloro compound) and **4** (PPh_2 compound) are compared. This is probably the result of a steric interaction between the large PPh_2 groups and the substrate. Another explanation for this drop in binding affinity might be that one of the phenyl groups of the PPh_2 moieties is clammed between the aromatic walls of the cavity, which will compete with binding of the guests. The latter explanation could not be confirmed by low-temperature NMR because of the low solubility of **4** at lower temperatures.

Table 3. Association constants of tetrapodants **1**–**4** with olivetol in $CDCl_3$

Host	K [M^{-1}][a]	CIS [ppm]
1	2769 (148)	−0.56
2	2025 (98)	−0.54
3	2201 (165)	−0.46
4	1676 (61)	−0.45

[a] Duplo experiments, obtained from NMR titrations using 0.5×10^{-3} M solutions of host and 5×10^{-3} M solutions of guest compound, errors are given in parentheses, $T = 293$ K; association constants were calculated using the Granot[42] procedure.

The increase of the number of ethylene glycol units in the spacer arms also has a negative effect on the association constant between host and guest, as can be seen when **1** is compared with **2** and when **3** is compared with **4**. A decrease of the association constant of approximately 20% is found when the flexible arms are extended with one ethylene glycol unit. This decrease of the association constant is probably caused by a difference in entropy loss after the formation of a host-guest complex. Binding of a guest molecule will restrict the rotational and translational movements of the side arms of the host. In particular rotation around the $ArO-CH_2$ bond will be hampered. This can be derived from the ^{1}H-NMR spectra of the host in the presence of guest molecules. The CH_2 groups of the side arms give rise to two signals, which indicates a restricted rotation. It should be noted that the effect becomes less for the distant CH_2 groups in host **4**.

In the absence of a substrate, the "small" tetrapodants **1** and **3** possess less degrees of freedom compared to their "larger" analogues **2** and **4**, because less rotational movements are available. Therefore, after binding of a guest, the ΔS_{ass} value will be less for hosts **1** and **3** than that of **2** and **4**. A less negative ΔS_{ass} value will result in a more negative ΔG_{ass} value and thus higher association constants for **1** and **3**.

Table 4. Association constants of bimetallic complexes of **3** and **4** with olivetol

Metallohost	K [M^{-1}][a]	CIS [ppm]
3$(PdCl_2)_2$	n.d.[b]	n.d.[b]
3$(PdMeCl)_2$	562 (367)	−0.02
3$[Pd(TCNE)]_2$	n.d.[b]	n.d.[b]
3$(PtCl_2)_2$	n.d.[b]	n.d.[b]
3$[RhCl(CO)]_2$	164 (73)	−0.02
4$(PdCl_2)_2$	2346 (499)	−0.44
4$(PdMeCl)_2$	2502 (77.83)	−0.47
4$[Pd(TCNE)]_2$	960 (362)	−0.48
4$(PtCl_2)_2$	4314[c] (338)	−0.47
4$[RhCl(CO)]_2$	4514[c] (835)	−0.51

[a] Single-fold experiments, obtained from NMR titrations using 5×10^{-3} M solutions of host and 50×10^{-3} M solutions of guest compound in $CDCl_3$, errors are given in parentheses, $T = 293$ K. – [b] n.d. = not determined, NMR signals did not change and $K < 100$ M^{-1}. – [c] Duplo experiment; association constants were calculated using the Granot[42] procedure.

Host-Guest Binding Properties of Metal Complexes

As discussed above the tetrapodant ligands **3** and **4** and appropriate transition metals form basket-shaped bimetallic complexes, which have different cavity sizes. The binding properties of transition metal complexes of **3** were found to be rather poor compared to the free ligand. The complexes **3**$[RhCl(CO)]_2$ and **3**$(PdMeCl)_2$ have binding constants of $K = 164$ M^{-1} and $K = 562$ M^{-1}, respectively, for olivetol (see Table 4). From the small chemically induced shifts (CIS) values of these host-guest complexes it can be concluded that there is hardly any interaction between host and guest. The ^{1}H-NMR signals of complexes **3**$(PtCl_2)_2$, **3**$(PdCl_2)_2$, and **3**$[Pd(TCNE)]_2$ did not change after addition of 10 equivalents of olivetol. These NMR experiments show that, after coordination of **3** to two transition metal centres, a basket is formed that is too small for substrate binding. Coordination of the phosphane moieties to a metal centre should facilitate the binding of a substrate in the cavity because a preshaped cavity is formed and less entropy will be lost during the association process. However, the cavity of complexes of ligand **3** is not large enough to give access to resorcinol derivatives.

A similar effect has been observed for host **6**, which is formed by a ring-closure reaction between **1** and benzylamine.[12,30,31] A crystal structure of **6** showed that, due to the small ring size in **6**, the $ArOCH_2$ groups (see Figure 3) are directed towards the cavity and block the entrance of this cavity[20] for entering guests. Although the transition metal complexes of ligand **3** possess a larger cavity than **6**, i.e. instead of one amine two phosphanes and a transition metal are now incorporated in the macrocycle, the cavity is probably still too small to allow a strong interaction of the host with resorcinol guest molecules.

Host **7** and its derivatives do bind dihydroxybenzene derivatives as was shown in previous studies.[3,15,20,30,32] The cavity of this host is large enough to give access to resorcinol derivatives and 2,7-dihydroxynaphthalene. The metal complexes of ligand **4** have an even larger macrocyclic cavity than **7** and will therefore be accessible for organic substrates. This is confirmed by the experimental data (see Table 4).

Figure 3. Basket-shaped host molecules **6** and **7**

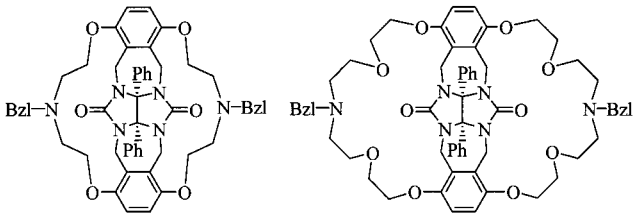

Compared to free **4**, complex **4**Pd(TCNE) has a lower binding affinity to olivetol. All the other complexes of **4** show an increased affinity to this guest. The increase in association constant is partly caused by fixation of the flexible arms of the tetrapodant. The degrees of freedom are reduced compared to the free ligand, resulting in an increase in the ground-state free energy. After complexation of a substrate, a relatively small loss in entropy (ΔS_{ass}) will result in a more negative ΔG_{ass} value, and a higher association constant.

Compounds **4**$(PtCl_2)_2$ and **4**$[RhCl(CO)]_2$ form host-guest complexes with olivetol which display association constants of 4314 M^{-1} (Pt) and 4514 M^{-1} (Rh), respectively. These association constants are nearly three times as high as the value of the free phosphane tetrapodant **4**. Complexes **4**$(PdCl_2)_2$ and **4**$(PdMeCl)_2$ also show an increase in association constant when compared to free **4** and values of K = 2346 M^{-1} and 2505 M^{-1} were found, respectively.

There are several possible explanations for the observed increase in binding affinity of the metal complexes and olivetol: (i) An additional interaction between the substrate and the metal centre, e.g. a dipole-dipole interaction, (ii) a weak interaction between the oxygen atom or the aromatic ring of the substrate with the metal centre, e.g. coordination at the axial position of the metal centre, (iii) extra hydrogen-bonding interactions between the hydroxy groups of olivetol and auxiliary ligands in the complexes, e.g. Cl or CO at the metal centre, (iv) difference in flexibility of the spacer groups, (v) conformational differences between the metal complexes.

To investigate an interaction between olivetol and a transition metal centre, we measured the ^{195}Pt and ^{103}Rh chemical shifts of mixtures of **4**$(PtCl_2)_2$ with olivetol and **4**$[RhCl(CO)]_2$ with olivetol. Changes in the second and outer coordination sphere of the metal centre, as well as steric or electronic variations are known to have a pronounced effect on the chemical shift of the transition metal.[25] Addition of eight equivalents of olivetol to an NMR sample containing **4**$(PtCl_2)_2$ or **4**$[RhCl(CO)]_2$, did not affect the transition metal chemical shift of either the rhodium or the platinum complex. This indicates that, although the metal centre is probably able to come into close proximity of the binding site, it does not have an interaction with the guest.

Infrared spectroscopy was used to investigate the nature of hydrogen-bond formation between host and guest. The experiments indicated that additional hydrogen bonds between the carbon monoxide ligand of the rhodium complex and the hydroxy groups of the guest could be excluded; after the addition eight equivalents of olivetol a shift of +4 cm^{-1} was found in the IR spectrum of **4**$[RhCl(CO)]_2$. This is a too small a difference to be the result of hydrogen bonding and additionally, the shift is in the wrong direction. Hydrogen bonds to the carbon monoxide ligand would shift the carbonyl frequency to a lower value, as described by Kazarian and co-workers for other carbon monoxide containing compounds.[33] Hydrogen bonds to the metal centre itself would induce a positive shift,[33] but the reported shifts are usually larger than 20 cm^{-1}.

One example of a hydrogen bond between a platinum coordinated chloride and a phenolic hydroxy group has been reported in the literature.[34] Evidence for hydrogen bonding between a chloride ligand of our metal complex and a hydroxy group of the substrate, however, could not be found.

Monitoring the carbonyl frequency of the urea carbonyl group, showed that ligand **4** as well as its metal complexes bind olivetol via hydrogen bonds. After addition of eighth equivalents of olivetol to several **4**M_2 complexes the IR spectrum showed a shift of ν(CO) of -30 cm^{-1}. Apparently, unlike Na^+ ions the metal centres do not prevent the formation of hydrogen bonds between host and guest. Hosts of type **7** bind two Na^+ ions to their crown ether parts. In these host-guest complexes the sodium ions are responsible for the binding of olivetol, as hydrogen bonds between the carbonyl groups of the host and hydroxy groups of the guest could not be detected.[21]

Summarising, we can state that a different type of binding is not responsible for the change in binding affinity with the guest. Conformational changes in the metal complexes or restricted flexibility of the spacer groups might therefore be a likely explanation. The difference in flexibility of the spacer groups might be caused by partial ligand dissociation in solution. Perhaps the palladium–phosphorus bond in complex **4**$[Pd(TCNE)]_2$ is more labile compared to the metal–phosphorus bond in the other complexes. This may have an effect on the flexibility of the crown ether fragments, which are not as rigidly oriented as in the other metal complexes. The crown ether fragments may still have an interaction with the incoming substrate, and a compound more similar to the parent ligand **4** is formed. The lower association constant can then be explained by the larger end group on the spacer groups (i.e. PPh_2–Pd instead of PPh_2 only) which will result in a relatively low association constant (K = 960 M^{-1}).

The crown ether fragments of complexes **4**$(PtCl_2)_2$ and **4**$[RhCl(CO)]_2$ may be more hampered in their movements

and form a preshaped cavity for an incoming guest. Since the loss in entropy after complexation of a guest (ΔS_{ass}) will be smaller for these complexes compared to the parent ligand **4**, an increase in binding affinity of a factor of 2.5 is found. The same positive effect on the association constant was found for complexes **4**$(PdCl_2)_2$ and **4**$(PdMeCl)_2$, although the increase in binding affinity is only a factor of 1.5 for these complexes. Finally, a change in conformation, induced by the transition metals, cannot be excluded but the required structural information about these complexes is still lacking.

Conclusions

In this paper we report novel host molecules that possess a cavity in which substrates can be bound in addition to two transition metal centres that are potential catalysts for many reactions. A surprising increase in binding affinity for olivetol was found upon coordination of ligand **4** to various transition metals, whereas the transition metal complexes of ligand **3** are unable to bind substrates.

For host molecules **3** and **4** the association equilibria are influenced by the following factors: (i) the presence of flexible spacers, (ii) the bulk of the spacer, (iii) the size and σ_m value of substituents on the resorcinol derivative, (iv) the ring size of the (metalla)macrocycle after coordination of the phosphane moieties to a metal centre and finally, (v) the metal centre itself. As yet, not all contributing factors can be understood in full detail. These results are promising in view of future catalytic applications with this type of host compounds.

This work was supported by the *Netherlands Foundation for Chemical Research* (SON) with financial aid from the *Netherlands Organisation for Scientific Research* (NWO).

Experimental Section

General: NMR: ^1H NMR (300.1 MHz), $^{31}P\{^1H\}$ NMR (121.5 MHz), $^{13}C\{^1H\}$ NMR (75.5 MHz), ^{195}Pt NMR (64.3 MHz) and ^{103}Rh NMR (9.48 MHz) were measured with Bruker AMX 300 and DRX 300 machines. The external references were: TMS (^1H NMR and ^{13}C NMR), H_3PO_4 (^{31}P NMR) and K_2PtCl_6 (^{195}Pt NMR), $\Xi(^{103}Rh$ NMR) = 3.16 MHz at 100 MHz. ^{195}Pt NMR was measured directly, ^{103}Rh NMR was measured via the ^{31}P-inverse HMQC technique.[35][36] − IR spectra were measured with a Nicolet 510m FT-IR spectrophotometer. − Melting points were determined with a Gallenkamp MFB-595 melting-point apparatus, the values are uncorrected. − Column chromatography was performed with silica gel 60, 70−230 mesh ASTM (Merck). − Analytical TLC was performed on TLC aluminium foil, silica gel 60 F_{254} (Merck). − Microanalyses were carried out in our own laboratory with an Elementar Vario EL apparatus (Foss Electric). − M_w determinations were performed with a Hewlett-Packard vapour-pressure osmometer model 301A, with benzil as the reference compound.

Chemicals: CH_3CN and CH_2Cl_2 were distilled from CaH_2, C_6H_6 was distilled from Na/benzophenone. $CDCl_3$ used in association constant determinations was distilled from P_2O_5 before use. 1,4,8,11-Tetrakis(2-chloroethoxy)-5,7,12,13b,13c,14-hexahydro-13b,13c-diphenyl-6 H,13*H*-5a,6a,12a,13a-tetrabenz[5,6]azuleno-[2,1,8-*ija*]benz[*f*]azulene-6,13-dione[12] (**1**), 1,4,8,11-tetrakis[2-(2-chloroethoxy)ethoxy]-5,7,12,13b,13c,14-hexahydro-13b,13c-diphenyl-6 H,13*H*-5a,6a,12a,13a-tetraazabenz[5,6]azuleno[2,1,8-*ija*]benz[*f*]azulene-6,13-dione[12] (**2**), $(PPh_3)_2RhCl(CO)$,[37] $(PPh_3)_2IrCl(CO)$,[28] $Pd(DBA)_2$,[38] $(CH_3CN)_4Pd(BF_4)_2$,[39] $(COD)PdCl_2$[40] and all the 5-substituted resorcinol derivatives[41] were prepared according to literature procedures. $(PPh_3)_2PdCl_2$ and $(PPh_3)_2PtCl_2$ were obtained after refluxing PPh_3 and $PdCl_2$ or $PtCl_2$ in CH_3CN, followed by evaporation of the solvent.

Ligands

1,4,8,11-Tetrakis[(2-diphenylphosphanyl)ethoxy]-5,7,12,13b,13c,14hexahydro-13b,13c-diphenyl-6H,13H-5a,6a,12a,13a-tetrabenz[5,6]azuleno[2,1,8-ija]benz[f]azulene-6,13-dione (**3**): A solution of 2.5 g of compound **1** (3.1 mmol) in 40 ml of THF and 40 ml of benzene was titrated under N_2 at 0°C with 20 ml of a THF solution of $LiPPh_2$. The $LiPPh_2$ solution was prepared from 2.52 g of $HPPh_2$ (13.6 mmol) and 5.4 ml of 2.5 M *n*BuLi in hexane (13.5 mmol). When the solution remained orange, 40 ml of degassed H_2O was added. The H_2O layer was separated and washed with 20 ml of benzene. The collected organic layers were dried with $MgSO_4$ and concentrated. The product was dissolved in 15 ml of CH_2Cl_2 and precipitated with 100 ml of diethyl ether. After filtration, the remaining solvent was removed in vacuo. The product was purified by column chromatography with silica gel, eluent $MeOH/CH_2Cl_2$ (1:99, v/v). Yield 3.47 g (80%) of a white solid, m.p. > 195°C (dec.). − NMR ($CDCl_3$): δ_H = 7.45−7.29 (m, 40 H, P−*Ar*), 7.08−7.01 (m, 10 H, Ar*H*), 6.47 (s, 4 H, H−Ar side wall), 5.45 [d, 4 H, (CO)NCH*H*, ^2J = 15.8 Hz], 4.15 (m, 4 H, OC*H*H), 3.94 (m, 4 H, OCH*H*), 3.76 [d, 4 H, (CO)NC*H*H, ^2J = 15.8 Hz], 2.65−2.59 (m, 8 H, CH_2P); δ_P = −21.7 (s); δ_C = 158.2 (*C*=O), 150.5 (Ar*C*−O), 138.5−138.2, 134.7, 133.12−132.8, 128.8−128.5, 128.3, 113.52, 85.3 [N*C*(Ar)N], 67.59 (d, O−*C*H$_2$, $^2J_{P\text{-}C}$ = 24.8 Hz), 37.31 (N*C*H$_2$Ar), 28.61 (d, *C*H$_2$−P, $^1J_{P\text{-}C}$ = 12.8 Hz). − IR (KBr): $\tilde{\nu}$ = 3051 cm^{-1} (w), 2911 (w, OC−H), 1730 (s), 1710 (s, CO), 1482 (m), 1461 (s), 1433 (m), 1255 (m). − M_w (CH_2Cl_2): calcd. 1411; found 1445 ± 100. − $C_{88}H_{78}N_4O_6P_4 \cdot H_2O$ (1414): calcd. C 73.94, H 5.64, N 3.92; found C 73.92, H, 5.51, N 4.05.

1,4,8,11-Tetrakis{2-[2(diphenylphosphanyl)ethoxy]ethoxy}-5,7,12,13b,13c,14-hexahydro-13b,13c-diphenyl-6H,13H-5a,6a,12a,13a-tetrabenz[5,6]azuleno[2,1,8-ija]benz[f]azulene-6,13-dione (**4**): This compound was prepared in a similar way as compound **3**. The following amounts were used: 3.21 g of $HPPh_2$ (17.3 mmol), 6.9 ml of a 2.5 M solution of *n*BuLi (17.25 mmol) and 4.26 g of compound **2** (4.31 mmol). The eluent used for column chromatography was $MeOH/CH_2Cl_2$ (6:94, v/v). Yield 4.7 g (67%) of a white solid, m.p. 91−114°C. − NMR ($CDCl_3$): δ_H = 7.4−7.2 (m, 40 H, Ar*H*−P), 7.03 (m, 10 H, Ar*H*), 6.61 (s, 4 H, *H*−Ar side wall), 5.47 [d, 4 H, (CO)NCH*H*, ^2J = 15.9 Hz], 4.0−3.6 [m, 28 H, (CO)NC*H*H, OCH_2], 2.42 (t, 8 H, CH_2P, ^3J = 8.1 Hz); δ_P = −21.1 (s); δ_C = 158.0 (*C* =O), 151.2 (Ar*C*−O), 138.8−138.4, 134.5, 133.0 (d, Ar*C*−P, $^2J_{P\text{-}C}$ = 18.8 Hz), 128.8−128.5, 115.1, 85.41 [N*C*−(Ar)N], 70.5, 69.9, (O−*C*H$_2$), 68.9 (d, O−*C*H$_2$, $^2J_{P\text{-}C}$ = 24.0 Hz), 37.37 (N*C*H$_2$Ar), 29.10 (d, *C*H$_2$−P, $^1J_{P\text{-}C}$ = 12.8 Hz). − IR (KBr): $\tilde{\nu}$ = 3052 cm^{-1} (w), 2865 (w, OC−H), 1709 (s, CO), 1482 (m), 1460 (s), 1432 (s), 1264 (m). − M_w (CH_2Cl_2): calcd. 1588; found 1540 ± 100. − $C_{96}H_{94}N_4O_{10}P_4 \cdot 2\ H_2O$ (1586): calcd. C 70.92, H 6.20, N 3.45; found C 70.77, H 5.84, N 3.45.

Metal Complexes

3*(PdCl$_2$)$_2$:* Compound **3** (20.3 mg, 14.3 μmol) was dissolved in 10 ml of benzene and 20.1 mg (28.6 μmol) of $(PPh_3)_2PdCl_2$ was added. The yellow solution was stirred for 2 h and the volume was

reduced to approximately 2 ml. The product was precipitated with 10 ml of pentane, the yellow suspension was decanted and the product was washed twice with 10 ml of pentane. The product was dried in vacuo. Yield 14.5 mg (58%) of a light yellow powder, m.p. > 245°C (dec.). – NMR ([D$_6$]benzene): δ_H = 8.2–6.7 (m, 50 H, Ar*H*), 6.26 (s, 4 H, *H*–Ar side wall), 5.66 (m, 4 H, ArOCH*H*), 5.58 [d, 4 H, (CO)NCH*H*, ^2J = 15.9 Hz], 4.33 (m, 4 H, ArOC*H*H), 3.49 (m, 4 H, C*H*HP), 3.23 [d, 4 H, (CO)NC*H*H, ^2J = 15.9 Hz], 3.20 (m, 4 H, CH*H*P); δ_P = 12.5. – IR (KBr): $\tilde{\nu}$ = 1710 cm^{-1} (s, CO), 1480 (s), 1461 (s), 1435 (s), 1351 (w), 1248 (m). – $C_{88}H_{78}Cl_4N_4O_6P_4Pd_2 \cdot 6\ H_2O$ (1764.8): calcd. C 56.39, H 4.84, N 2.98; found C 56.54, H 5.43, N 2.33.

4*(PdCl$_2$)$_2$:* Compound **4** (22.5 mg, 14.2 μmol) was dissolved in 5 ml of dichloromethane and 8.3 mg of (COD)PdCl$_2$ (28.4 μmol) was added. A small amount of PPh$_3$ was added to the solution and a clear yellow solution was obtained. After 2 h of stirring, the volume was reduced to 2 ml and 10 ml of pentane was added. The yellow suspension was decanted and the product was washed twice with 10 ml of pentane. The product was dried in vacuo. Yield 20.7 mg (75%) of a yellow powder, m.p. > 180°C (dec.). – NMR ([D$_6$]benzene): δ_H = 8.0–6.6 (m, 50 H, Ar*H*), 6.37 (s, 4 H, *H*–Ar side wall), 5.93 [d, 4 H, (CO)NCH*H*, ^2J = 15.8 Hz], 4.6–3.7 (m, 24 H, OCH_2), 3.53 [d, 4 H, (CO)NC*H*H, ^2J = 15.8 Hz], 3.08 (m, 4 H, CH$_2$C*H*HP), 2.92 (m, 4 H, CH$_2$CH*H*P); δ_P = 14.9. – IR (KBr): $\tilde{\nu}$ = 1710 cm^{-1} (s, CO), 1480 (m), 1461 (s), 1435 (s), 1248 (m). – $C_{96}H_{94}Cl_4N_4O_{10}P_4Pd_2$ (1940.8): calcd C 59.36, H 4.88, N 2.88; found C 59.08, H 5.35, N 2.70.

3*(PdMeCl)$_2$:* Compound **3** (100 mg, 71 μmol) was dissolved in 5 ml of CH_2Cl_2 and 97 mg (142 μmol) of (PPh$_3$)$_2$PdMeCl, dissolved in 10 ml of benzene, was added. The colourless solution was stirred for 2 h and the volume was reduced to approximately 2 ml. The product was precipitated with 10 ml of pentane, the suspension was decanted and the product was washed twice with 10 ml of pentane. The product was dried in vacuo. Yield 103 mg (84%) of a white powder, m.p. > 176°C (dec.). – NMR ($CDCl_3$): δ_H = 7.8–6.9 (m, 50 H, Ar*H*), 6.59 (s, 4 H, *H*–Ar side wall), 5.63 [d, 4 H, (CO)NCH*H*, ^2J = 15.9 Hz], 4.96 (m, 4 H, ArOC*H*H), 4.15(m, 4 H, ArOCH*H*), 3.64 [d, 4 H, (CO)NC*H*H, ^2J = 15.9 Hz], 3.22(m, 4 H, C*H*HP), 2.95(m, 4 H, CH*H*P), –0.36(t, 6 H, Pd–CH_3, $^3J_{P\text{-}H}$ = 6.0 Hz); δ_P = 15.4. – IR (KBr): $\tilde{\nu}$ = 1710 cm^{-1} (s), 1482 (m), 1461 (s), 1435 (s), 1253 (m). – Satisfactory analysis could not be obtained due to hygroscopicity of the compound.

4*(PdMeCl)$_2$:* Compound **4** (30 mg, 18.9 μmol) was dissolved in 5 ml of CH_2Cl_2, followed by addition of 2 ml CH_2Cl_2, containing 10 mg of (COD)PdMeCl (37.8 μmol) and a small amount of PPh$_3$. The colourless solution was stirred for 2 h, the volume was reduced to 2 ml and 10 ml of pentane was added. The suspension was decanted and the product was washed twice with 10 ml of pentane. The product was dried in vacuo. Yield 30 mg (85%) of a white powder, m.p. > 154°C (dec.). – NMR ($CDCl_3$): δ_H = 7.8–6.9 (m, 50 H, Ar*H*), 6.63 (s, 4 H, *H*–Ar side wall), 5.59 [d, 4 H, (CO)NCH*H*, ^2J = 15.8 Hz], 4.5–3.7 (m, 24 H, CH_2O), 3.66 [d, 4 H, (CO)NC*H*H, ^2J = 15.8 Hz], 3.07 (m, 4 H, C*H*HP), 2.92 (m, 4 H, CH*H*P), –0.05 (t, 6 H, Pd-CH_3, $^3J_{P\text{-}H}$ = 6.0 Hz); δ_P = 21.9. – IR (KBr): $\tilde{\nu}$ 1710 cm^{-1} (s, CO), 1483 (m), 1460 (s), 1433 (s), 1248 (m). – $C_{98}H_{100}Cl_2N_4O_{10}P_4Pd_2 \cdot 4\ H_2O$ (1899.8): calcd. C 59.64, H 5.52, N 2.84; found C 59.73, H 5.34, N 2.52.

3*[Pd(BF$_4$)$_2$]$_2$:* A solution of 24.8 mg of compound **3** (17.5 μmol) in 2 ml of CH_2Cl_2 was added to a solution of 15.5 mg of (CH$_3$CN)$_4$Pd(BF$_4$)$_2$ (35 μmol) in 5 ml of CH_3CN. After stirring for 3 h, the solution was concentrated to dryness, yielding 35.5 mg (95%) of a yellow powder, m.p. > 175°C (dec.). – NMR (CD_3CN): δ_H = 7.8–7.3 (m, 50 H, Ar*H*), 7.18 (s, 4 H, *H*–Ar side wall), 5.5 [d, 4 H, (CO)NCH*H*, ^2J = 16.1 Hz], 4.62 (m, 4 H, OCH*H*), 4.41 (m, 4 H, OC*H*H), 4.02 [d, 4 H, (CO)NC*H*H, ^2J = 16.1 Hz], 3.53 (m, 4 H, C*H*HP), 3.37 (m, 4 H, CH*H*P); δ_P = 38.4. – IR (KBr): $\tilde{\nu}$ = 3444 cm^{-1} (m, O–H), 3365 (m, O–H), 3062 (w), 2924 (w), 1648 (s, CO), 1586 (m), 1470 (s), 1437 (s), 1400 (s). – $C_{88}H_{78}B_4F_{16}N_4O_6P_4Pd_2 \cdot 2\ H_2O \cdot 2CH_3CN$ (1796.8): calcd. C 52.87, H 4.25, N 4.02; found C 52.46, H 4.45, N 4.36.

4*[Pd(BF$_4$)$_2$]$_2$:* This compound was prepared in a similar way as **3**[Pd(BF$_4$)$_2$]$_2$ with the following amounts: 13 mg of (CH$_3$CN)$_4$Pd(BF$_4$)$_2$ (29.3 μmol) and 23.3 mg of compound **4** (14.7 μmol). Yield 32.1 mg (93%) of a white powder, m.p. > 172°C (dec.). – NMR (CD_3CN): δ_H = 8.1–7.0 (m, 50 H, Ar*H*), 6.82 (s, 4 H, *H*–Ar side wall), 5.70 [d, 4 H, (CO)NCH*H*, ^2J = 16.0 Hz], 4.7–3.7 [m, 28 H, (CO)NC*H*H, CH_2O], 3.08 (m, 8 H, CH_2P); δ_P = 42.8. – IR (KBr): $\tilde{\nu}$ = 3381 cm^{-1} (m, O–H), 3060 (m, O–H), 2928 (m), 2883 (w, OC–H), 1670 (s, CO), 1587 (m), 1478 (s), 1437 (s), 1259 (m). – $C_{96}H_{94}B_4F_{16}N_4O_{10}P_4Pd_2 \cdot 2\ CH_3CN$ (1972.8): calcd. C 53.87, H 4.52, N 3.77; found C 53.76, H 4.76, N 3.69.

3*[Pd(TCNE)]$_2$:* Compound **3** (50 mg, 35 μmol) was dissolved in 3 ml of benzene and a solution of 40 mg of Pd(DBA)$_2$ (70 μmol) in 10 ml of benzene was added. The orange-brown solution was stirred for 10 min and 9.1 mg of TCNE (70 μmol) and 2 ml of benzene were added. After 4 h, the solution was reduced to ca. 5 ml and the product was precipitated with 15 ml of Et$_2$O. The suspension was decanted and the product was washed with 10 ml of diethyl ether and 10 ml of pentane. The product was dried in vacuo. Yield 110 mg (85%) of a green solid, m.p. > 211°C (dec.). – NMR ($CDCl_3$): δ_H = 7.6–7.1 (m, 50 H, Ar*H*), 6.46 (s, 4 H, *H*–Ar side wall), 5.59 [d, 4 H, (CO)NCHH, ^2J = 15.8 Hz], 4.45 (m, 4 H, ArOCH*H*), 4.24 (m, 4 H, ArOC*H*H), 3.75 [d, 4 H, (CO)NCHH, ^2J = 15.8 Hz], 3.17 (m, 4 H, C*H*HP), 2.80 (m, 4 H, CH*H*P); δ_P = 24.8. – IR (KBr): $\tilde{\nu}$ = 3057 cm^{-1} (w), 2922 (w), 2220 (m, CN), 1701 (s, CO), 1465 (s), 1435 (s), 1252 (m). – $C_{100}H_{78}N_{12}O_6P_4Pd_2 \cdot 2\ H_2O$ (1878.8): calcd. C 63.22, H 4.25, N 8.85; found C 63.19, H 4.34, N 8.83.

4*[Pd(TCNE)]$_2$:* This compound was prepared in a similar way as **3**[Pd(TCNE)]$_2$ with the following amounts: 40.7 mg of Pd(DBA)$_2$ (71 μmol), 62.6 mg of compound **4** (39.5 μmol) and 9.2 mg of TCNE (71 μmol). Yield 61 mg (84%) of a green powder, m.p. > 275°C (dec.). – NMR ($CDCl_3$): δ_H = 7.5–7.35 (m, 40 H, Ar*H*), 7.12 (m, 10 H, Ar*H*), 6.67 (s, 4 H, *H*–Ar side wall), 5.65 [d, 4 H, (CO)NCH*H*, ^2J = 15.8 Hz], 4.0–3.8 [m, 28 H, OCH_2, (CO)NC*H*H, ^2J = 15.8 Hz], 2.69 (m, 4 H, CH$_2$CH*H*P), 2.59 (m, 4 H, CH$_2$C*H*HP); δ_P = 12.8. – IR (KBr): $\tilde{\nu}$ = 3058 cm^{-1}(w), 2871 (w), 2213 (m, CN), 1707 (s, CO), 1458 (s), 1436 (s), 1258 (m). – $C_{108}H_{94}N_{12}O_{10}P_4Pd_2$ (2054.8): calcd. C 63.07, H 4.64, N 8.17; found C 63.05, H 4.74, N 7.94.

3*(PtCl$_2$)$_2$:* (PPh$_3$)$_2$PtCl$_2$ (28.8 mg, 36.4 μmol) and 25.7 mg of compound **3** (18.2 μmol) were dissolved in 5 ml of CH_2Cl_2 and the solution was stirred for 2 h. The volume was reduced to ± 2 ml followed by addition of 15 ml of pentane. The suspension was decanted and the white solid was washed three times with 10 ml of pentane. The product was dried in vacuo. Yield 27.9 mg (79%) of a white solid, m.p. > 290°C (dec.). – NMR ($CDCl_3$): δ_H = 8.0–7.0 (m, 50 H, Ar*H*), 6.76 (s, 4 H, *H*–Ar side wall), 5.69 [d, 4 H, (CO)NCH*H*, ^2J = 15.8 Hz], 4.99 (m, 4 H, ArOCH*H*), 4.70 (m, 4 H, ArOC*H*H), 3.80 [d, 4 H, (CO)NC*H*H, ^2J = 15.8 Hz], 3.12 (m, 4 H, C*H*HP), 2.94(m, 4 H, CH*H*P); δ_P = 0.4 ($^1J_{Pt\text{-}P}$ = 3550 Hz). – IR (KBr): $\tilde{\nu}$ = 1707 cm^{-1}(s, CO), 1464 (s), 1436 (s), 1247 (m). – $C_{88}H_{78}Cl_4N_4O_6P_4Pt_2$ (1678): calcd. C 54.38, H 4.05, N 2.88; found C 54.15, H 4.33, N 2.62.

4*(PtCl$_2$)$_2$:* (COD)PtCl$_2$ (12.7 mg, 34 μmol) was dissolved in 5 ml of CH_2Cl_2 and after addition of 27.0 mg of compound **4** (17 μmol), the solution was stirred for 2 h. The volume was reduced to ± 2 ml followed by addition of 15 ml of pentane. The suspension was decanted and the white solid was washed three times with 10 ml of pentane. The product was dried in vacuo. Yield 24.6 mg (68%) white powder, m.p. > 255°C (dec.). − NMR ($CDCl_3$): δ_H = 7.9−7.0 (m, 50 H, Ar*H*), 6.73 (s, 4 H, *H*−Ar side wall), 5.63 [d, 4 H, (CO)NCH*H*, ^2J = 15.8 Hz], 4.2−3.5 [m, 28 H, OCH_2, (CO)NC*H*H], 2.66 (m, 4 H, CH_2C*H*HP), 2.53 (m, 4 H, CH_2CH*H*P); δ_P = 4.8 ($^1J_{Pt\text{-}P}$ = 3610 Hz); δ_{Pt} (CD_2Cl_2) = −4390 (t, $^1J_{Pt\text{-}P}$ = 3610 Hz). − IR (KBr): $\tilde{\nu}$ = 1708 cm^{-1} (s, CO), 1481 (m), 1458 (s), 1435 (s), 1256 (m). − $C_{96}H_{94}Cl_4N_4O_{10}P_4Pt_2 \cdot H_2O$ (2118): calcd. C 53.94, H 4.53, N 2.62; found C 53.94, H 4.40, N 2.62.

3*[RhCl(CO)]$_2$:* To a solution of 100 mg of compound **3** (71 μmol) in 3 ml of CH_2Cl_2 93 mg of $(PPh_3)_2$RhCl(CO) (135 μmol), dissolved in 6 ml of CH_2Cl_2 and 14 ml of C_6H_6, was added and the solution was stirred for 3 h. The volume was reduced to ca. 5 ml followed by addition of 25 ml of pentane. The suspension was decanted and the white solid was washed three times with 20 ml of pentane. The product was dried in vacuo. Yield 119 mg (96%) of a yellow solid, m.p. > 195°C (dec.). − NMR ($CDCl_3$): δ_H = 7.9−7.0 (m, 50 H, Ar*H*), 6.55 (s, 4 H, *H*−Ar side wall), 5.57 [d, 4 H, (CO)NCHH, ^2J = 15.6 Hz], 5.1 (m, 4 H, ArOCH*H*), 4.1 (m, 4 H, ArOC*H*H), 3.64 [d, 4 H, (CO)NCHH, ^2J = 15.6 Hz], 3.0(m, 4 H, C*H*HP), 2.7 (m, 4 H); δ_P = 18.6 (d, $^1J_{Rh\text{-}P}$ = 124 Hz). − IR (KBr): $\tilde{\nu}$ = 1972 cm^{-1} (s, CO_{Rh}), 1710 (s, CO), 1482 (m), 1462 (s), 1435 (s), 1385 (m), 1354 (w), 1307 (w), 1253 (m). − $C_{90}H_{78}Cl_2N_4O_8P_4Rh_2 \cdot 3\ H_2O$ (1743): calcd. C 60.11, H 4.71, N 3.12; found C 59.98, H 4.45, N 3.06.

4*[RhCl(CO)]$_2$:* This compound was prepared in a similar way as **3** [RhCl(CO)]$_2$ with the following amounts: 230 mg of $(PPh_3)_2$RhCl(CO) (333 μmol) and 240 mg of compound **4** (170 μmol). Yield 285 mg (96%) of a yellow powder, m.p. > 149°C (dec.). − NMR ($CDCl_3$): δ_H = 7.9−7.0 (m, 50 H, Ar*H*), 6.55 (s, 4 H, *H*−Ar side wall), 5.57 [d, 4 H, (CO)NCH*H*, ^2J = 15.8 Hz], 4.5−3.8 (m, 24 H, OCH_2), 3.68 [d, 4 H, (CO)NC*H*H, ^2J = 15.8 Hz], 3.12(m, 4 H, CH_2C*H*HP), 2.91 (m, 4 H, CH_2CH*H*P); δ_P = 22.0 (d, $^1J_{Rh\text{-}P}$ = 123 Hz); δ_{Rh} = −418. − IR (KBr): $\tilde{\nu}$ = 1970 cm^{-1} (s, CO_{Rh}), 1708 (s, CO), 1481 (m), 1458 (s), 1435 (s), 1256 (m) − M_w (CH_2Cl_2): calcd. 1919, found 1850. − $C_{98}H_{94}Cl_2N_4O_{12}P_4Rh_2 \cdot 3\ H_2O$ (1919): calcd. C 59.61, H 5.10, N 2.84; found C 59.47, H 4.98, N 2.80.

3*[IrCl(CO)]$_2$:* A mixture of 44.4 mg of compound **3** (31.5 μmol) and 49 mg of $(PPh_3)_2$IrCl(CO) (63 μmol) in 10 ml of C_6H_6 was stirred overnight. The volume was reduced to ca. 2 ml and 15 ml of pentane was added. The solvent was decanted and the residue washed twice with 10 ml of pentane. The product was dried in vacuo. Yield 54 mg (89%) of a yellow solid, m.p. > 180°C (dec.). − NMR ([D$_6$]benzene): δ_H = 7.96 (m, 16 H, Ar*H*), 7.2−6.8 (m, 34 H, Ar*H*), 6.34 (s, 4 H, *H*−Ar side wall), 5.90 [d, 4 H, (CO)NCH*H*, ^2J = 15.8 Hz], 5.8 (m, 4 H, ArOCH*H*), 4.5 (m, 4 H, ArOC*H*H), 4.1 (m, 4 H, C*H*HP), 3.43 [d, 4 H, (CO)NC*H*H, ^2J = 15.8 Hz], 3.3 (m, 4 H, CH*H*P); δ_P = 14.8. − IR (KBr): $\tilde{\nu}$ = 3056 cm^{-1} (w), 2922 (w), 1959 (s, CO_{Ir}), 1710 (s, CO), 1480 (s), 1462 (s), 1435 (s), 1248 (m). − $C_{90}H_{78}Cl_2N_4O_8P_4Ir_2 \cdot 2\ H_2O$ (1921.4): calcd. C 55.18, H 4.22, N 2.86; found C 55.20, H 4.63, N 2.62.

4*[IrCl(CO)]$_2$:* This compound was prepared in a similar way as **3**[IrCl(CO)]$_2$ with the following amounts: 49 mg of $(PPh_3)_2$IrCl(CO) (63 μmol) and 50 mg of compound **4** (31.5 μmol). Yield 56 mg (85%) of a yellow powder, m.p. > 165°C (dec.). − NMR ([D$_6$]benzene): δ_H = 8.1−7.9 (dm, 16 H, Ar*H*), 7.2−6.8 (m, 34 H, Ar*H*), 6.34 (s, 4 H, *H*−Ar side wall), 5.95 [d, 4 H, (CO)NCH*H*, ^2J = 15.9 Hz], 4.68 (m, 4 H, OCH_2), 4.48 (m, 4 H, OCH_2), 4.31 (m, 4 H, OCH_2), 4.13 (m, 12 H, OCH_2), 3.54 [d, 4 H, (CO)NC*H*H, ^2J = 15.9 Hz], 3.40 (m, 4 H, CH_2C*H*HP), 3.27 (m, 4 H, CH_2CH*H*P); δ_P = 17.7. − IR (KBr): $\tilde{\nu}$ = 3057 cm^{-1} (w), 2922 (w), 1958 (s, CO_{Ir}), 1711 (s, CO), 1482 (m), 1458 (s), 1435 (s), 1258 (m). − $C_{98}H_{94}Cl_2N_4O_{12}P_4Ir_2 \cdot 2\ H_2O$ (2097.4): calcd. C 55.13, H 4.63, N 2.62; found C 55.08, H 4.42, N 2.58.

[1] M. Bonchio, T. Carofiglio, F. Di Furia, R. Fornassier, *J. Org. Chem.* **1995**, *60*, 5986−5988.
[2] J. Rebek Jr., *Pure Appl. Chem.* **1996**, *68*, 1261−1266.
[3] H. K. A. C. Coolen, J. A. M. Meeuwis, P. W. N. M. van Leeuwen, R. J. M. Nolte, *J. Am. Chem. Soc.* **1995**, *117*, 11906−11913.
[4] C. F. Martens, R. J. M. Klein Gebbink, M. C. Feiters, R. J. M. Nolte, *J. Am. Chem. Soc.* **1994, 116**, 5667−5670.
[5] H. K. A. C. Coolen, P. W. N. M. van Leeuwen, R. J. M. Nolte, *Angew. Chem. Int. Ed. Engl.* **1992**, *31*, 905−907.
[6] M. T. Reetz, S. R. Waldvogel, *Angew. Chem. Int. Ed. Engl.* **1997**, *36*, 865−867.
[7] O. S. Tee, B. C. Javed, *J. Chem. Soc., Perkin Trans 2* **1994**, 23−29.
[8] H. J. Schneider, F. XIao, *J. Chem. Soc., Perkin Trans 2* **1992**, 387−391.
[9] F. Diederich, H.-D. Lutter, *J. Am. Chem. Soc.* **1989**, *111*, 8438−8446.
[10] Y. Murakami, J.-I. Kukuchi, Y. Hisaeda, O. Hayashida, *Chem. Rev.* **1996**, *96*, 721.
[11] G. Wulff, T. Gross, R. Schönfeld, *Angew. Chem. Int. Ed. Engl.* **1997**, *36*, 1962−1964.
[12] R. P. Sijbesma, R. J. M. Nolte, *Recl. Trav. Chim. Pays-Bas* **1993**, *112*, 643−647.
[13] K. Tani, M. Yabuta, S. Nakamura, T. Yamagata, *J. Chem. Soc., Dalton Trans.* **1993**, 2781−2789.
[14] C. Amatore, G. Broeker, A. Jutand, F. Khalil, *J. Am. Chem. Soc.* **1997**, *119*, 5176−5185.
[15] R. P. Sijbesma, R. J. M. Nolte, *J. Org. Chem.* **1991**, *56*, 3199.
[16] J. N. H. Reek, A. H. Priem, H. Engelkamp, A. E. Rowan, J. A. A. W. Elemans, R. J. M. Nolte, *J. Am. Chem. Soc.* **1997**, *119*, 9956−9964.
[17] J. W. H. Smeets, R. P. Sijbesma, L. van Dalen, A. L. Spek, W. J. J. Smeets, R. J. M. Nolte, *J. Org. Chem.* **1989**, *54*, 3710.
[18] J. W. H. Smeets, R. P. Sijbesma, F. G. M. Niele, A. L. Spek, W. J. J. Smeets, R. J. M. Nolte, *J. Am. Chem. Soc.* **1987**, *109*, 928.
[19] H. K. A. C. Coolen, P. W. N. M. van Leeuwen, R. J. M. Nolte, *J. Org. Chem.* **1996**, *61*, 4739.
[20] C. F. Martens, R. P. Sijbesma, R. J. M. Klein Gebbink, R. J. M. Nolte, *Recl. Trav. Chim. Pays-Bas* **1993**, *112*, 400.
[21] G. C. Dol, F. Hartl, P. C. J. Kamer, P. W. N. M. van Leeuwen, R. J. M. Nolte, *J. Chem. Soc., Dalton Trans.*, accepted.
[22] R. P. Sijbesma, A. P. M. Kentgens, E. T. G. Lutz, J. H. van der Maas, R. J. M. Nolte, *J. Am. Chem. Soc.* **1993**, *115*, 8999−9005.
[23] C. J. Cobley, P. G. Pringle, *Inorg. Chim. Acta* **1997**, *265*, 107−115.
[24] S. O. Grim, R. L. Keiter, *Inorg. Chem. Acta* **1970**, *4*, 56.
[25] P. S. Pregosin, *Studies in Inorganic Chemistry 13*, Elsevier, Amsterdam, Oxford, New York, Tokyo, **1991**.
[26] M. Kranenburg, J. P. G. Delis, P. C. J. Kamer, P. W. N. M. van Leeuwen, K. Vrieze, N. Veldman, A. L. Spek, K. Goubitz, J. Fraanje, *J. Chem. Soc., Dalton Trans.* **1997**, 1839−1849.
[27] S. Murata, Y. Ido, *Bull. Chem. Soc. Jpn.* **1994**, *67*,1746−1748.
[28] J. P. Collman, C. T. Sears Jr., M. Kubota, *Inorg. Synth.* **1990,** *28*, 92−94.
[29] T. H. Brown, P. J. Green, *J. Am. Chem. Soc.* **1970**, *92*, 2359−2362.
[30] R. P. Sijbesma, A. M. Kentgens, R. J. M. Nolte, *J. Org. Chem.* **1991**, *56*, 3122.
[31] R. P. Sijbesma, W. P. Bosman, R. J. M. Nolte, *J. Chem. Soc., Chem. Commun.* **1991**, 885.
[32] R. P. Sijbesma, R. J. M. Nolte, *Top. Curr. Chem.* **1995**, *175*, 26−56.
[33] S. G. Kazarian, P. A. Hamley, M. Poliakoff, *J. Am. Chem. Soc.* **1993**, *115*, 9069−9079.
[34] P. J. Davies, N. Veldman, D. M. Grove, A. L. Spek, B. T. G.

Lutz, G. van Koten, *Angew. Chem. Int. Ed. Engl.* **1996**, *35*, 1959–1961.
[35] C. J. Elsevier, J. M. Ernsting, d. L. W.G.J., *J. Chem. Soc., Chem. Commun.* **1989**, 585–586.
[36] A. Bax, R. H. Griffey, B. L. Hawkins, *J. Magn. Reson.* **1983**, *55*, 301.
[37] J. A. Osborn, G. Wilkinson, *Inorg. Synth.* **1990,** *28*, 79–80.
[38] M. F. Rettig, P. M. Maitlis, *Inorg. Synth.* **1977**, *17*, 134.
[39] B. J. Hathaway, A. E. Underhill, *J. Chem. Soc.* **1962**, 2257, 2444.
[40] J. Chatt, L. M. Vallarino, L. M. Venanzi, *J. Chem. Soc.* **1957**, 3413.
[41] G. C. Dol, P. C. J. Kamer, P. W. N. M. van Leeuwen, *Eur. J. Org. Chem.* **1998**, 359–364.
[42] J. Granot, *J. Magn. Reson.* **1983**, *55*, 216.

[I98190]

Diene Complexes of *trans*-5-Palladatricyclo[4.1.0.0^{2,4}]heptanes

A. Stephen K. Hashmi*, Jan W. Bats, Frank Naumann, and Bernd Berger

Institut für Organische Chemie der Universität Frankfurt,
Marie-Curie-Str. 11, D-60439 Frankfurt, Germany
Fax: (internat.) + 49(0)69/798-29464
E-mail: hashmi@chemie.uni-frankfurt.de

Received June 25, 1998

Keywords: Diene complexes / Metallacycles / Palladium

The complexes *rac*-**5** and *rac*-**6** of the *trans*-5-palladatricyclo-[4.1.0.0^{2,4}]heptane *rac*-**2a** with norbornadiene and 1,5-cyclooctadiene were prepared and investigated by X-ray structure determination. With open-chained, unsaturated substrates, e.g. **7** and **8**, no complexes could be isolated. In all cases no insertion of the olefin into the metal–carbon bond of the palladacycloalkane was observed.

trans-5-Palladatricyclo[4.1.0.0^{2,4}]heptanes (PTHs) are an interesting class of organometallic compounds in which two chiral carbon atoms are directly bound to a palladium center. The first derivatives described in the literature were Binger's racemic phosphane complexes *rac*-**1**.[1] We recently published the preparation and resolution of *rac*-PTH-tetracarboxylates **2**.[2] **2** itself is a coordination polymer,[3] monomeric complexes are for example obtained with diphosphanes[2] or acetone[3][4] as ligands. The PTHs are chiral bis-homo derivatives of the corresponding palladoles[5] − the latter being important catalysts for the enyne cyclization[6], the enyne metathesis[6][7] and related reactions.[8] That the PTHs show catalytical properties has been proven by their ability to catalyze the cycloisomerization/dimerization of allenyl ketones to furans.[9]

In reactions catalyzed by PTHs, a coordination of unsaturated substrates is the first step. Here we describe the first diolefin complexes of PTHs which may serve as model compounds for the coordination of such unsaturated substrates during catalysis reactions.

Scheme 1

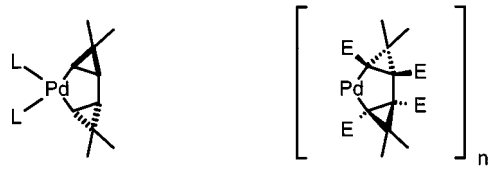

rac-**1** L = PR_3 **2** E = CO_2R a R = Me

Synthesis of the Diene Complexes

For our investigation we used the PTH *rac*-**2a**.[2] We focused on chelating dienes, norbornadiene (NBD, **3**) and 1,5-cyclooctadiene (COD, **4**) were used. An excess of **3** or **4** was added to solutions of *rac*-**2a** in acetone. Then most of the acetone was evaporated in vacuo and pentane was added to the remaining solution. On cooling to 0°C the complexes *rac*-**5** and *rac*-**6** crystallized. Efforts with other unsaturated substrates like the diyne **7** or the enyne **8** without a rigid structure did not lead to defined products.

Scheme 2

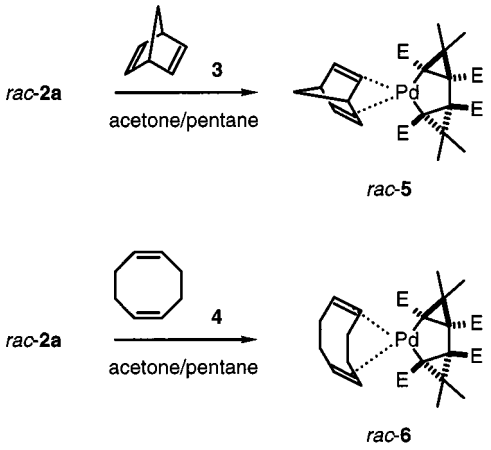

Scheme 3

7 E = CO_2Me **8**

X-ray Structure Determination and Discussion

By the method described above, suitable crystals of *rac*-**5** and *rac*-**6** for X-ray structure determination could be obtained. The ORTEP plot of *rac*-**5** is shown in Figure 1, the one of *rac*-**6** in Figure 2. Selected crystallographic data of both compounds are listed in Table 1.[10]

rac-**5** approximately has a two-fold symmetry with the exception of the relative orientation of the methoxycarbonyl

 © WILEY-VCH Verlag GmbH, D-69451 Weinheim, 1998 1434−1948/98/1212−1987 $ 17.50+.50/0

Figure 1. ORTEP plot of *rac*-**5**

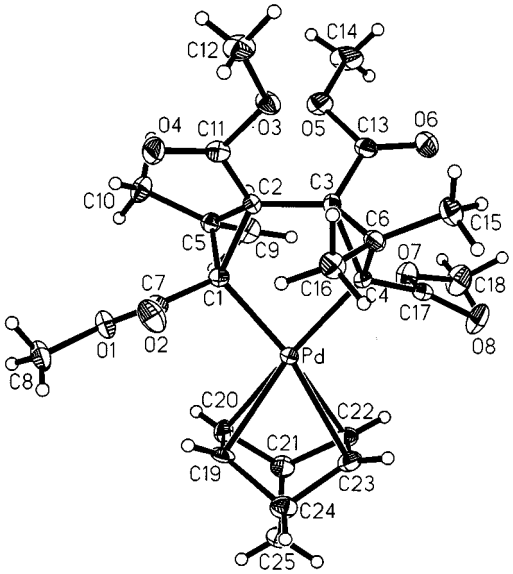

Figure 2. ORTEP plot of *rac*-**6**

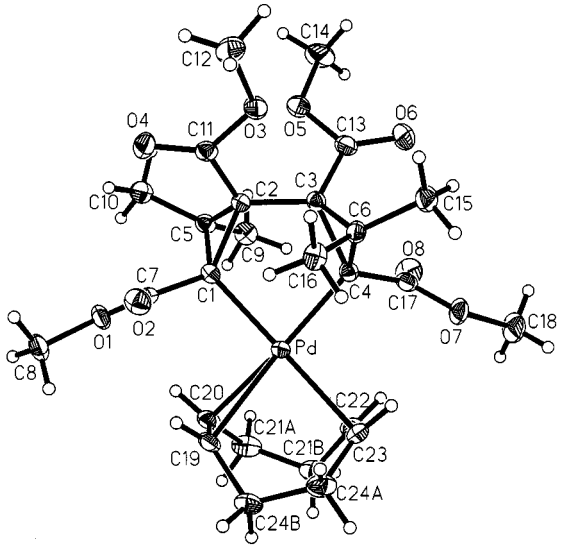

groups attachted to C1 and C4. Two molecules of *rac*-**6** crystallize in the asymmetric unit, their structures show only small differences in their conformations. The Pd−C1 and Pd−C4 bond lengths are 2.05 Å in *rac*-**5** and 2.06−2.08 Å in *rac*-**6**. This is slightly longer than in the acetone complexes of PTHs (2.02 Å)[3][4] and slightly shorter than in the phosphane complexes of PTHs (2.11 and 2.13 Å, respectively)[2] and reflects the *trans* influence[11] of the different donors.

In *rac*-**5** the distances from Pd to the C atoms of the NBD group range from 2.26 to 2.31 Å. Similar distances have been found in the crystal structure of the corresponding NBD-tetrakis(methoxycarbonyl)palladole complex[12]. The hydrogen atoms at C19, C20, C22, and C23 deviate about 0.14 Å from the planes of the C−C double bonds in a direction away from the Pd atom. The molecular conformation is stabilised by a number of weak, electrostatic, intramolecular O···H contacts with distances equal to the van der Waals contact distance of 2.4 Å [O2···H16a: 2.40(3) Å; O4···H10a: 2.32(5) Å; O6···H15a: 2.34(5) Å; and O7···H9a: 2.48(4) Å]. Similar intramolecular interactions have been observed in the PTH part of *rac*-**6**. The crystal packing shows no short intermolecular contacts.

Table 1. Selected bond lengths [Å], bond angles [°], and dihedral angles [°] for *rac*-**5** and *rac*-**6**

	rac-**5**	*rac*-**6** (molecule 1)	*rac*-**6** (molecule 2)
Pd−C1	2.047(3)	2.075(2)	2.058(2)
Pd−C4	2.049(2)	2.071(2)	2.083(2)
Pd−C19	2.273(3)	2.336(2)	2.318(2)
Pd−C20	2.257(3)	2.282(2)	2.283(2)
Pd−C22	2.290(3)	2.326(2)	2.306(2)
Pd−C23	2.309(3)	2.287(2)	2.284(2)
C19−C20	1.359(5)	1.358(3)	1.363(3)
C22−C23	1.367(6)	1.360(3)	1.358(3)
C1−Pd−C4	83.8(1)	83.0(1)	83.3(1)
C1−Pd−C19	103.1(1)	99.1(1)	98.5(1)
C4−Pd−C22	104.4(1)	98.5(1)	100.0(1)
C1−Pd−C20	100.9(1)	94.2(1)	90.7(1)
C4−Pd−C23	105.6(1)	94.1(1)	95.3(1)
C1−Pd−C22	158.2(1)	163.2(1)	158.3(1)
C4−Pd−C20	160.7(1)	162.3(1)	162.4(1)
C1−Pd−C23	162.4(1)	162.6(1)	167.3(1)
C4−Pd−C19	162.2(1)	163.5(1)	163.0(1)
C4−Pd−C1−C2	1.9(3)	−3.2(1)	2.5(1)
C1−Pd−C4−C3	−5.0(3)	0.1(1)	−4.9(1)
C1−C2−C3−C4	−5.7(5)	−5.8(2)	−4.2(2)

The COD ligand in *rac*-**6** occupies a twist-boat conformation as known from most of the other (COD)Pd^{II} complexes.[13] The bond lengths of Pd to the olefinic carbon atoms of the COD range from 2.28 to 2.34 Å, such values were also reported for the known (COD)Pd^{II} complexes.[8] Different from the NBD ligand in *rac*-**5**, one hydrogen atom of each double bond of the COD ligand in *rac*-**6** shows weak intramolecular O···H contacts with distances equal to the van der Waals contact distance (2.46 and 2.41 Å, respectively) to the ether oxygen atom of the ester group at C1 and C4 of the PTH framework.

The angle between the plane through C1−Pd−C4 and the plane through Pd and the midpoints of the C19−C20 and C22−C23 double bonds is 2.6° in *rac*-**5** and 0.4° for molecule 1 and 4.5° for molecule 2 in *rac*-**6**! Essentially this is, like in the bis(acetone) complexes (6.9 and 9.3°, respectively),[3][4] the square planar coordination as one would expect for Pd^{II}. On the other hand in complexes with sterically demanding bidentate phosphanes a tilt of up to 30° was observed.[2]

Ittel's and Ibers's[14] structural parameters α and β characterize the hybridization changes at the coordinated olefinic carbon atoms. α is defined as the angle between the normals of the two planes defined by the three atoms of each $R_2C=$ unit of the olefin, so α would be 0° for a planar alkene. β and β′ are the angles between the olefinic C=C bond and the normals mentioned before, so the β angles decrease from 90° with increasing distortion. For *rac*-**5** and *rac*-**6** these parameters are listed in Table 2. Clearly, the ole-

fins are non-planar, but the values correspond to those of other related complexes,[13] so the coordinated olefin does not experience any unusual distortion.

Table 2. Structural parameters for *rac*-**5** and *rac*-**6**

	rac-**5**	*rac*-**6** (molecule 1)	*rac*-**6** (molecule 2)
	C19−C20, C22−C23	C19−C20, C22−C23	C19−C20, C22−C23
α	19°, 23°	18°, 15°	18°,16°
β	85°, 75°	82°, 80°	81°, 81°
β′	77°, 82°	81°, 85°	82°, 84°

PTHs are the first palladacycloalkanes without stabilizing ligands at the palladium center, the coordination sphere is saturated by easily substitutable solvent molecules.[4][9] Since it is part of a cyclopropyl ring, the carbon atom attached to the palladium center has a hybridization close to sp^2.[15] The fact that only coordination but no insertion of the olefins was observed, proves the stability of the Pd−C bonds in these exceptional palladacycloalkanes. This is in agreement with the formation of the PTHs: even when the Pd^0 precursor was subjected to an excess of cyclopropene, only the PTH was formed and the remaining cyclopropene remained untouched. This is in contrast to Binger's results. He also observed the formation of seven-membered metallacycles[16] and nine-membered[17] palladacycles or products of a reductive elimination from such insertion products, i.e. cyclic trimers[18] or tetramers[17][18] of the cyclopropene. For catalysis reactions this suggests that the PTH framework is also not destroyed readily by insertion (maybe followed by reductive elimination) reactions.

^{1}H- and ^{13}C-NMR Spectra

The chemical shifts of the coordinated and uncoordinated diene ligand are listed in Tables 3 and 4.

Table 3. NMR data of free NBD and *rac*-**5** in $CDCl_3$ at 298 K[a]

	free NBD	*rac*-**5**	Δδ
^{1}H NMR	1.95	1.98	0.03
	3.53	3.96	0.43
	6.66	5.71	−0.95
		6.23	−0.43
^{13}C NMR	50.4	50.4	0.0
	75.2	73.4	−1.8
	143.2	107.6	−35.6
		113.8	−29.4

[a] Chemical shifts in ppm (δ).

In the coordinated dienes the symmetry is reduced, thus some NMR signals of the free diene split into several new signals of the corresponding nuclei in the coordinated diene. As one can see, only the chemical shift of the olefinic hydrogen and carbon atoms experience a relevant change.

While in the coordinated COD the signals of the olefinic hydrogen atoms are both shifted to lower and higher field by the same amount, in the NBD they are both shifted to lower field. The signals of the olefinic carbon atoms are all shifted downfield by coordination to *rac*-**2a**, but again the effect is stronger in the NBD ligand. The C_2 symmetry of the PTHe leads to a chemical shift difference between the signals of the two non-equivalent carbon atoms of the coordinated olefin of about 5 ppm in both *rac*-**5** and *rac*-**6**, but the signals of the two non-equivalent hydrogen atoms differ by 0.52 ppm in *rac*-**5** and 1.13 in *rac*-**6**.

Table 4. NMR data of free COD and *rac*-**6** in $CDCl_3$ at 298 K[a]

	free COD	*rac*-**6**	Δδ
^{1}H NMR	2.25	2.08−2.21	−0.10
		2.36−2.52	0.19
		2.69−2.78	0.49
	5.50	4.86−4.96	−0.56
		6.03−6.10	0.57
^{13}C NMR	27.9	26.4	−1.5
		32.2	4.3
	128.3	113.9	−14.4
		117.7	−10.6

[a] Chemical shifts in ppm (δ).

Conclusion

PTHs readily form complexes with chelating, rigid dienes. In these complexes, where Pd is surrounded by six carbon atoms, only a small deviation from a perfect square planar coordination (considering the midpoints of the double bonds) was observed. Like the related bis(acetone) complexes of PTHs, this demonstrates that the strong deviation from a square-planar coordination geometry observed with diphosphanes originates from intramolecular sterical repulsion of the latter ligands and substituents on the PTH framework. No insertion of the olefins into the Pd−C bond of the PTH was observed. This suggests that the PTHs remain intact during catalysis reactions or at least show a low tendency for insertion of unsaturated substrates.

This work was supported by the *Deutsche Forschungsgemeinschaft* and the *Fonds der Chemischen Industrie*. Furthermore we are grateful to the *Degussa AG* for the donation of palladium salts.

Experimental Section

General: All operations were carried out under N_2 and in dry solvents. *rac*-**2a**[2][4] was prepared according to literature procedures. − IR: Perkin-Elmer 1600. − NMR: Bruker AM 250 (250 and 62.9 MHz for ^{1}H and ^{13}C, respectively). $CDCl_3$ as solvent δ_H = 7.25; δ_C = 77.0. The degree of substitution of the C atoms was determined by a combination of DEPT-135 and DEPT-90. − MS: VG-Instruments-Micro-Mass Tris 2000, EI 70 eV, quadrupol analysator and Finnigan CH7A (80 eV). − Melting points (uncorrected): Kofler hot-stage.

rac-**5**: To 50 mg (10.5 μmol) of *rac*-**2a** in 5 ml of acetone 2 equiv. of norbornadiene (**3**, 19.3 mg, 21.0 μmol) were added. After 30 min at room temparatue, the solution was concentrated to about 0.5 ml in a rotary evaporator and 0.5 ml of pentane was added. Then the soution was placed in a refrigerator (0°C), over night 38.8 mg (65%) of *rac*-**5** precipitated as yellow crystals. − M.p. 197°C. − IR (neat, NaCl): $\tilde{\nu}$ = 2947 cm^{-1}, 1715, 1691, 1432, 1369, 1310, 1221,

1172, 1106, 1067, 1000, 920, 733. − ^{1}H NMR ($CDCl_3$, 250 MHz): δ = 1.38 (s, 6 H, Me), 1.67 (s, 6 H, Me), 1.98 (m, 2 H), 3.61 (s, 6 H, OMe), 3.62 (s, 6 H, OMe), 3.96 (m, 2 H, CH_2), 5.71 (m, 2 H, CH), 6.23 (m, 2 H, CH). − ^{13}C NMR ($CDCl_3$, 62.9 MHz): δ = 20.39 (q, 2 C), 25.69 (q, 2 C), 37.29 (s, 2 C), 49.57 (s, 2 C), 50.42 (d, 2 C), 51.14 (q, 2 C), 51.27 (q, 2 C), 57.95 (s, 2 C), 73.36 (t), 107.61 (d, 2 C), 113.82 (d, 2 C), 172.24 (s, 2 C), 172.46 (s, 2 C). − MS (70 eV); *m/z* (%): 566 (1) [(^{106}Pd) M^+], 474 (46) [M^+ − NBD], 415 (8). − $C_{25}H_{32}O_8Pd$ (566.9): calcd. C 52.96, H 5.69; found C 53.23, H 5.89.

Crystal Structure Analysis of rac-**5**:[10] Siemens Smart diffractometer, Mo-K_α radiation, −100°C, empirical absorption correction, structure determination by direct methods (SIR92); the positions of the hydrogen atoms were determined by a difference Fourier synthesis, refinement of the hydrogen atoms with isotropic thermal parameters. $C_{25}H_{32}O_8Pd$, triclinic, space group $P(-1)$; a = 9.064(2), b = 8.484(2), c = 17.685(4) Å, α = 95.20(2), β = 78.84(1), γ = 66.82(1)°; V = 1205.4(5) Å^3; Z = 2; $\rho_{calcd.}$ = 1.562 g cm^{-1}; μ = 8.2 cm^{-1}; sphere up to 2θ = 59°; 6062 independent reflections with $I > 0$; 436 parameters refined, R = 0.038; R_w = 0.065; residual density between −0.26 and +1.16 e Å^{-3}.

rac-**6**: To 50 mg (10.5 μmol) of *rac*-**2a** in 5 ml of acetone 2 equiv. of 1,5-cyclooctadiene (**4**, 22.7 mg, 21 μmol) were added. After 30 min at room temparatue, the solution was concentrated to about 0.5 ml in a rotary evaporator and 0.5 ml of pentane was added. Then the soution was placed in a refrigerator (0°C), over night 61.4 mg (75%) of *rac*-**6** precipitated as yellow crystals. − M.p. 191°. − IR (neat, NaCl): $\tilde{\nu}$ = 2946 cm^{-1}, 1714, 1690, 1430, 1368, 1304, 1215, 1105, 1066, 1006. − ^{1}H NMR ($CDCl_3$, 250 MHz): δ = 1.43 (s, 6 H), 1.79 (s, 6 H), 2.08−2.21 (m, 2 H), 2.36−2.52 (m, 2 H), 2.69−2.78 (m, 4 H), 3.57 (s, 6 H), 3.60 (s, 6 H), 4.86−4.96 (m, 2 H), 6.03−6.10 (m, 2 H). − ^{13}C NMR ($CDCl_3$, 62.9 MHz): δ = 20.61 (q, 2 C), 26.37 (q, 2 C), 26.37 (t, 2 C), 32.23 (t, 2 C), 37.11 (s, 2 C), 50.09 (s, 2 C), 50.54 (q, 2 C), 51.30 (q, 2 C), 55.16 (s, 2 C), 113.88 (d, 2 C), 117.73 (d, 2 C), 172.98 (s, 2 C), 173.77 (s, 2 C); the two different signals at δ = 26.37 are nicely separated in C_6D_6 as solvent. − MS (70 eV); *m/z* (%): 582 (17) [(^{106}Pd) M^+], 474 (100) [M^+ − COD], 415 (19). − $C_{26}H_{36}O_8Pd$ (583.0): calcd. C 53.57, H 6.22; found C 53.36, H 6.30.

Crystal Structure Analysis of rac-**6**:[10] Siemens Smart diffractometer, Mo-K_α radiation, −123°C, empirical absorption correction, structure determination by direct methods (SHELXS); the positions of the hydrogen atoms were determined by a difference Fourier synthesis, refinement of the hydrogen atoms with isotropic thermal parameters. $C_{26}H_{36}O_8Pd$, monoclinic, space group $P2_1/c$; a = 28.536(3), b = 9.742(1), c = 18.845(2) Å, β = 104.36(1)°; V = 5075.2(9) Å^3; Z = 8; $\rho_{calcd.}$ = 1.526 g cm^{-1}; μ = 7.8 cm^{-1}; θ = 1.47−25.79°; 8815 reflections with $I > 0$; 920 parameters refined, R = 0.029; R_w = 0.051; residual density between −0.69 and +0.36 e Å^{-3}.

[1] P. Binger, H. M. Büch, *Top. Curr. Chem.* **1987**, *135*, 77−151.
[2] A. S. K. Hashmi, F. Naumann, J. W. Bats, *Angew. Chem.* **1997**, *109*, 127−130; *Angew. Chem. Int. Ed. Engl.* **1997**, *36*, 104−106.
[3] A. S. K. Hashmi, F. Naumann, J. W. Bats, *Chem. Ber.* **1997**, *130*, 1457−1459.
[4] A. S. K. Hashmi, F. Naumann, M. Bolte, A. Rivas Nass, *J. Prakt. Chem.* **1998**, *340*, 240−246.
[5] K. Moseley, P. M. Maitlis, *J. Chem. Soc., Chem. Commun.* **1971**, 1604−1605.
[6] B. M. Trost, G. J. Tanoury, *J. Am. Chem. Soc.* **1987**, *109*, 4753−4755.
[7] B. M. Trost, M. K. Trost, *J. Am. Chem. Soc.* **1991**, *113*, 1850−1852.
[8] B. M. Trost, A. S. K. Hashmi, *Angew. Chem.* **1993**, *105*, 1130−1132; *Angew. Chem. Int. Ed. Engl.* **1993**, *32*, 1085−1087.
[9] A. S. K. Hashmi, L. Schwarz, *Chem. Ber.* **1997**, *130*, 1449−1456.
[10] Crystallographic data (excluding structure factors) for *rac*-**5** and *rac*-**6** have been deposited with the Cambridge Crystallographic Data Centre as supplementary publication no CCDC-102022 (*rac*-**5**) and -102023 (*rac*-**6**). Copies of the data can be obtained free of charge on application to CCDC, 12 Union Road, Cambridge CB2 1EZ, UK [Fax: (internat.) + 44(0)1223/336033; E-mail: deposit@ccdc.cam.ac.uk].
[11] F. R. Hartley, *Chem. Soc. Rev.* **1973**, *2*, 163−179; especially the sequence oxygen/olefin/phosphane on page 170.
[12] H. Suzuki, K. Itoh, Y. Jshii, K. Simon, J. A. Ibers, *J. Am. Chem. Soc.* **1976**, *98*, 8494−8500.
[13] Only one symmetrical structure, a polymorph of dichloro(η^4-1,5-cyclooctadiene)palladium(II), is known: N. C. Baenziger, C. V. Goebel, T. Berg, J. R. Doyle, *Acta Crystallogr., Sect. B* **1978**, *34*, 1340−1342. In all other structures such a twist-boat-like conformation was observed: L. Benchekroun, P. Herpin, M. Julia, L. Saussine, *J. Organomet. Chem.* **1977**, *128*, 275−290. M. F. Rettig, R. M. Wing, G. R. Wiger, *J. Am. Chem. Soc.* **1981**, *103*, 2980−2986. R. Kumar, A. W. Maverick, F. R. Fronczek, J. R. Doyle, N. C. Baenziger, M. A. M. Howells, *Acta Crystallogr., Sect. C* **1993**, *49*, 1766−1767. D. E. Smith, A. J. Welch, *Acta Crystallogr., Sect. C* **1986**, *42*, 1717−1720. J. Vicente, I. Saura-Llamas, P. G. Jones, *J. Chem. Soc., Dalton Trans.* **1993**, 3619−3624. L. Benchekroun, P. Herpin, M. Julia, L. Saussine, *J. Organomet. Chem.* **1977**, *128*, 275−290. R. M. Buchanan, C. G. Pierpont, *Inorg. Chem.* **1979**, *18*, 3608−3610. A. C. Albeniz, P. Espinet, Y. Jeannin, M. Piloche-Levisalles, B. E. Mann, *J. Am. Chem. Soc.* **1990**, *112*, 6594−6600. P. Stepnicka, I. Cisarova, *Collect. Czech. Chem. Commun.* **1996**, *61*, 1335−1341. N. L. Douek, A. J. Welch, *J. Chem. Soc., Dalton Trans.* **1993**, 1917−1925. K. A. Fallis, D. F. Mullica, E. L. Sappenfield, F. G. A. Stone, *Inorg. Chem.* **1994**, *33*, 4927−4933. I. R. Butler, M. Kalaji, L. Nehrlich, M. Hursthouse, A. I. Kataulov, K. M. A. Malik, *J. Chem. Soc., Chem. Comm.* **1995**, 459−460.
[14] S. D. Ittel, J. A. Ibers, *Adv. Organomet. Chem.* **1976**, *14*, 33−61.
[15] A. de Mejere, *Angew. Chem.* **1979**, *91*, 867−884; *Angew. Chem. Int. Ed. Engl.* **1979**, *18*, 809−826.
[16] B. Cetinkaya, P. Binger, C. Krüger, *Chem. Ber.* **1982**, *115*, 3414−3421.
[17] P. Binger, H. M. Büch, R. Benn, R. Mynott, *Angew. Chem.* **1982**, *94*, 66−66; *Angew. Chem. Int. Ed. Engl.* **1982**, *21*, 62−63.
[18] P. Binger, J. McMeeking, U. Schuchardt, *Chem. Ber.* **1980**, *113*, 23722−2382. P. Binger, U. Schuchardt, *Chem. Ber.* **1981**, *114*, 1649−1655. P. Binger, B. Biedenbach, *Chem. Ber.* **1987**, *120*, 601−605.

[I98200]

η^5-Pentamethylcyclopentadienyliridium(III) and -rhodium(III) Labeling of Amino Acids with Aromatic Side Chains – The Importance of Relativistic Effects for the Stability of Cp*Ir^{III} Sandwich Complexes

Diran Agaid Herebian, Claudia S. Schmidt, William S. Sheldrick*, and Christoph van Wüllen

Fakultät für Chemie, Ruhr-Universität Bochum,
D-44780 Bochum, Germany
Fax: (internat.) + 49(0)234/7094-420
E-mail: shel@anachem.ruhr-uni-bochum.de

Received June 26, 1997

Keywords: Iridium / Rhodium / Amino acids / Sandwich complexes / Bioorganometallic chemistry / Relativistic effects

η^5-Pentamethylcyclopentadienyliridium(III) and -rhodium-(III) sandwich complexes of the type [(η^5-Cp*)M(η^6-aa)]-(CF_3SO_3)$_2$ (M = Ir, Rh; **3–14**) containing L-tyrosine, L-tryptophan and L-phenylalanine derivatives (aa) can be prepared by treatment of [(η^5-Cp*)ML_3] (CF_3SO_3)$_2$ [L = thf, $(CH_3)_2CO$, CH_3CN] with the appropriate bioligand in thf for *N*-protected compounds and in CF_3COOH for α-amino acids with unprotected amino groups. Coordination to the Cp*M^{III} fragments stabilizes the ketonic form of the tyrosine aromatic side chains, leading to a marked enhancement in the acidity of the *p*-hydroxy function. The crystal structure of [Cp*Ir(ActyrOMe)] (CF_3SO_3)$_2$ (**3b**, ActyrOMe = *N*-acetyltyrosine methyl ester) confirms a marked distortion towards an η^5-oxohexadienyl coordination mode as may be gauged from the tilting of the *p*-OH plane C13/C14/C15 by no less than θ = 12.9° from that of the remaining ring atoms. Facial isomers are present in an effective 1:1 ratio for all tryptophan derivatives. Whereas the Cp*Ir^{III} sandwich complexes of aromatic α-amino acids are stable in polar solvents, rapid decay is observed for analogous Cp*Rh^{III} complexes of *N*-unprotected derivatives in polar solvents. Comparative nonrelativistic and relativistic all-electron density functional calculations on the cationic sandwich complexes [Cp*M(η^6-C_6H_5Me)]$^{n+}$ (n = 2, M = Ir, Rh; n = 1, M = Ru) confirm that all three metals bind more tightly to Cp* than to toluene as gauged by the respective force constants ($k_1 > k_2$). A much larger relativistic enhancement of k_2 for M = Ir (279 vs 207 Nm^{-1}) could be responsible for the greater stability of Cp*Ir^{III} complexes in solution.

The analytical and synthetic perspectives of bioorganometallic chemistry have been highlighted in recent articles by Jaouen et al.[1] and Krämer[2]. Labeling of aromatic amino acid side-chains by η^6-coordinated transition metal half-sandwich fragments offers considerable potential in this respect. For instance, the group of Pearson[3] and Rich[4] has demonstrated that the diaryl coupling, required for the total synthesis of cyclic diphenyl ether peptides such as the protease inhibitor K-13, may be achieved under mild conditions by activation of protected *p*-Cl-phenylalanine through η^6-coordination of the CpRu^{II} fragment. We ourselves have recently employed both [(Cp*RuCl)$_2$(μ-Cl)$_2$] and [Cp*Ru(MeCN)$_3$]$^+$ for the first direct preparation of organometallic sandwich complexes of the free amino acids phenylalanine (L-HpheOH), tyrosine (L-HtyrOH) and tryptophan (L-HtrpOH)[5][6]. The feasibility of employing individual CpRu^{II}-coordinated amino acids for the construction of labeled peptides was demonstrated in the course of these activities by the synthesis of [Cp*Ru{η^6-cyclo-(phephe)}]$^+$ using the carbodiimide method[6].

Unfortunately, the applicability of the Cp*Ru^{II} fragment in the bioorganometallic field is restricted by the relative instability of its sandwich complexes in aqueous solution[5], a state of affairs that prompted us to investigate the suitability of alternative transition metal half-sandwich compounds. After recently reporting on η^6-CyRu^{II} complexes (Cy = *p*-cymene) of aromatic amino acids and peptides[7][8], we have now turned our attention to the compounds [Cp*IrL$_3$](CF_3SO_3)$_2$ [L = thf (**1a**), $(CH_3)_2CO$ (**1b**)] and [Cp*RhL$_3$](CF_3SO_3)$_2$ [L = thf (**2a**), $(CH_3)_2CO$ (**2b**), CH_3CN (**2c**)][9][10].

Results

In contrast to the tris(acetonitrile) half-sandwich complex [Cp*Ru(MeCN)$_3$](CF_3SO_3), which affords the entropically favoured sandwich compounds on treatment with free aromatic amino acids in thf[6], the analogous reaction of [CyRu(acetone)$_3$](CF_3SO_3)$_2$ leads[7][8] to formation of κ^2N,O-chelated products in CH_2Cl_2. Under such conditions, bis(η^6-arene)Ru^{II} sandwich compounds can only be prepared for fully protected amino acids such as *N*-acetyltyrosine ethyl ester (ActyrOEt). η^6-Coordination of the CyRu^{II} fragment by half-protected or free aromatic amino acids can, however, be achieved by carrying out the reaction in CF_3COOH. Protonation of the amino and/or carboxylato groups under such strongly acid conditions prevents their participation in the metal coordination sphere.

Similar considerations also apply to the Cp*Ir^{III} and Cp*Rh^{III} half-sandwich fragments. However, in these cases, the aromatic ring systems of *N*-protected amino acids such as *N*-acetyltyrosine (ActyrOH) can be successfully labeled in

 © WILEY-VCH Verlag GmbH, D-69451 Weinheim, 1998 1434–1948/98/1212–1991 $ 17.50+.50/0

thf, as, for instance, in $[Cp^*Rh(ActyrOH)](CF_3SO_3)_2$ without competition from κ^1O-coordinated species. Sandwich complexes of *O*-protected or free amino acids are obtained in good yield (68−85%) by heating the reactants to 50°C for 24 h in CF_3COOH. ^{13}C-NMR spectra reveal a consistent pattern of upfield shifts of ca. 20−40 ppm for the signals of carbon atoms directly coordinated to the metal atom in comparison to those registered for the aromatic amino acids themselves. The formation of sandwich compounds is also confirmed by characteristic lowfield shifts for the ^{1}H-NMR signals of the Cp^*M^{III} (M = Ir, Rh) methyl protons. Furthermore, the typical chemical shift ranges of δ = 1.94−2.08, 2.25−2.28 and 2.40−2.44, in CD_3OD, associated with respectively η^6-coordinated tryptophan, tyrosine and phenyalanine derivatives, allow a straightforward assignment of the Cp^*Ir^{III} site in mixed oligopeptides. The marked kinetic instability of the analogous Cp^*Rh^{III} sandwich complexes in polar solvents prevents a general employment of this fragment in chemoselective organometallic labeling. However, our limited results indicate that a discrimination between η^6-coordinated tryptophan (δ = 1.96 in **11**) and tyrosine (δ = 2.09−2.20 in **6**−**8**) derivatives should once again be feasible.

η^5-Oxohexadienyl Coordination of Tyrosine Derivatives

Coordination to the Cp^*Ru^{II} and Cp^*M^{III} (M = Rh, Ir) fragments[10][11][12][13] stabilizes the ketonic form of phenol and its derivatives, leading to a marked enhancement in the acidity of the *p*-hydroxy substituent. Distortion towards an η^5-oxohexadienyl coordination mode in such sandwich complexes may be gauged from the shortness of the C−O bond distance and the degree of tilting between the plane of the *m*- and *p*-carbon atoms and the rest of the aromatic ring as expressed in the apposite dihedral angle θ. Relatively large θ values of 19° in $[Cp^*Ir(C_6H_3Me_2O)](BF_4)$[14], 14° in $[Cp^*Rh(C_6H_5O)](BF_4)\cdot H_2O$[13] and 13.2° in $[CyRu(HtyrOH)](CF_3SO_3)_2$[8] are accompanied by short C−O distances of 1.23, 1.25 and 1.274 Å, that are indicative of a pronounced degree of double-bond character. These structures differ markedly from that of $[Cp^*Ru(C_6H_5O)]\cdot 2$ PhOH[12] in which the phenol ring system is almost flat [θ = 4°, *d* (C−O) = 1.28 Å].

In $CyRu^{II}$ sandwich complexes, the *p*-hydroxy function of tyrosine derivatives is effectively fully deprotonated in aqueous solution. The concomitant increase in shielding for the aromatic ring protons causes their resonances to move upfield to values between δ = 5.6 and 6.6 in D_2O solution[8]. An analogous state of affairs is apparent for the Cp^*Ir^{III} complexes $[Cp^*Ir(ActyrOEt)](CF_3SO_3)_2$ (**3a**), $[Cp^*Ir(HtyrOMe)](CF_3SO_3)_2$ (**4**) and $[Cp^*Ir(HtyrOH)](CF_3SO_3)_2$ (**5**, HtyrOMe = tyrosine methyl ester) prepared in this work. The upfield shift is most pronounced for the *m*-protons adjacent to the tyrosine hydroxy function which are registered as separate doublets. Formation of the *N*-protonated zwitterions of HtyrOMe and HtyrOH further facilitates deprotonation of this aromatic substituent in **4** and **5** and leads of an additional upfield shift for the H atoms to δ = 5.83 and 5.86 in comparison to δ = 6.20 for **3a** in CD_3OD solution. This interpretation is confirmed by the remarkable ^{13}C-NMR chemical shifts of δ = 164.9 and 163.7 for the *p*-hydroxy-substituted tyrosine carbon atoms in **4** and **5**, values that are indicative of pronounced double-bond character for the associated C−O bonds. The analogous ^{13}C-NMR signal for **3a** at δ = 157.7 is registered only ca. 4 ppm downfield to that observed in free tyrosine derivatives. In contrast to the analogous Cp*Rh complexes **6**−**8**, the Cp*Ir sandwich complexes **3**−**5** of tyrosine derivatives are indefinitely stable in polar solvents such as water and methanol over a period of 14 days.

Scheme 1. Sandwich cations of $[Cp^*M(R'tyrOR)](CF_3SO_3)_2$ (**3**−**8**); **3a**: M = Ir, R = Et, R′ = Ac; **4**: M = Ir, R = Me, R′ = H; **5**: M = Ir, R = R′ = H; **6**: M = Rh; R = Et, R′ = Ac; **7**: R = H, R′ = Ac; **8**: M = Rh, R = Me, R′ = H

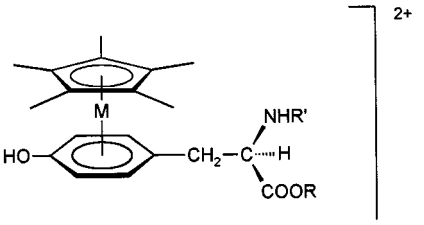

Attempts to obtain suitable crystals for X-ray-structural analysis unfortunately remained unsuccessful for **4** and **5** with their unprotected amino functions. However, colourless prisms of $[Cp^*Ir(ActyrOMe)](CF_3SO_3)_2$ (**3b**, ActyrOMe = *N*-acetyltyrosine methyl ester) could be grown by gas diffusion of diethyl ether into a methanol solution of $[Cp^*Ir(ActyrOH)](CF_3SO_3)_2$ prepared under similar conditions to **3a**. Solvent participation is apparent for the formation of η^6-coordinated ActyrOMe. The structure of the sandwich dication is depicted in Figure 1. Although the *p*-hydroxy oxygen atom O41 must be protonated for the fully protected tyrosine derivative ActyrOMe in the sandwich cation of **3b** [*d*(C34−O41) = 1.33(4) Å], the plane C33/C34/C35 is tilted by no less than θ = 12.9° from that of the remaining ring atoms C31−C33, C35 and C36. This pronounced departure from planarity may also be gauged from the Ir1−C34 distance of 2.36(4) Å, which is markedly longer than those to the remaining tyrosine ring atoms [2.22−2.30 Å]. The ^{1}H-NMR spectra of **3**−**5** in D_2O indicate that the tyrosine *p*-hydroxy function in Cp*Ir sandwich complexes is a moderately strong acid, a finding that is also reflected in the participation of O41 in relatively strong O41−H41···O21 hydrogen bonds of length 2.51 Å to the *N*-acetyl function of a symmetry-related complex cation. In view of the pronounced downfield shifts for the ^{13}C-NMR signal of C34 in **4** and **5**, for which the formation of *N*-protonated *O41*-deprotonated zwitterions is possible, it is reasonable to predict that the dihedral angle θ in these compounds will be even larger than in **3b** and perhaps close to that of 19° in $[Cp^*Ir(C_6H_3Me_2O)](BF_4)$[14].

Both Maitlis[10] and Jaouen[13] have commented on the instability of the sandwich complex $[Cp^*Rh(\eta^6\text{-phenol})]^{2+}$

Scheme 2. Stabilization of the ketonic form of the aromatic side chain of ActyrOEt in the Cp^*Rh^{III} complex **6**

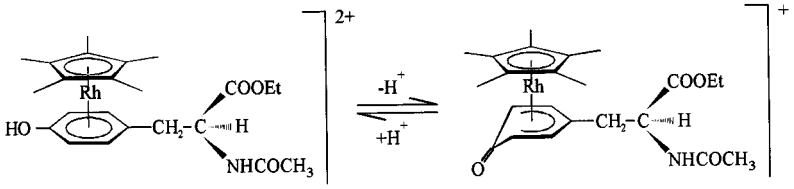

Figure 1. X-ray structure of the cation of $[Cp^*Ir(ActyrOMe)](CF_3SO_3)_2$ (**3b**)

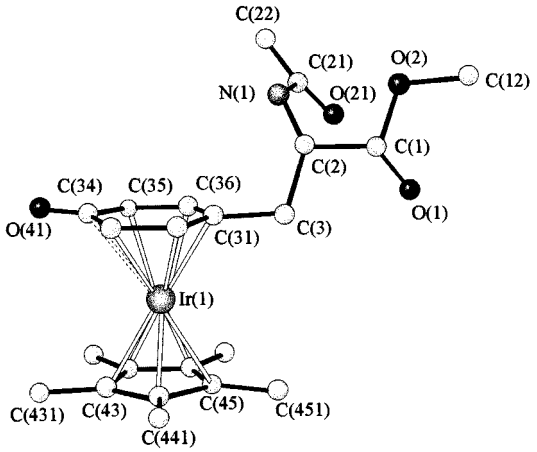

in polar solvents. Maitlis observed that $[Cp^*Rh)_2(phO)(phOH)](PF_6)_3$ is converted to 40% to $[(Cp^*Rh)_2(\mu\text{-}F_2PO_2)_3](PF_6)$ on standing for 48 h in acetone. Stabilization may be achieved by addition of base leading to formation of the η^5-oxocyclohexadienyl monocation $[Cp^*Rh(\eta^5\text{-}C_6H_5O)]^+$. Our time-dependent ^{1}H-NMR studies on $[Cp^*Rh(ActyrOEt)](CF_3SO_3)_2$ (**6a**) in D_2O solution, that are depicted in Figure 2, confirm a similar ca. 50% decay for the sandwich compound to $[Cp^*Rh(D_2O)_3]^{2+}$ and ActyrOEt within 24 hours at room temperature. A further ^{1}H-NMR spectrum taken after 5 days is similar to that of Figure 2c. It is interesting to note that Jaouen has postulated that the triflate counter anion $CF_3SO_3^-$ may stabilize the phenolic form of π-bonded arenes by participating in hydrogen bonds to the OH substituent of the aromatic ring system. For instance, whereas $[Cp^*Ir(\eta^6\text{-phenol})](BF_4)(CF_3SO_3)$ was very stable in aqueous solution, $[Cp^*Ir(\eta^6\text{-phenol})](BF_4)_2$ rapidly decays to a half-sandwich complex and could not be isolated. We have, therefore, performed comparative ^{1}H-NMR kinetic studies on $[Cp^*Rh(ActyrOEt)](PF_6)_2$ (**6b**) and $[Cp^*Rh(ActyrOEt)](BF_4)_2$ (**6c**) in D_2O solution. Suprisingly, whereas **6b** exhibits a decay rate similar to that of **6a**, as displayed in Figure 3 for **6c**, the sandwich cation $[Cp^*Rh(ActyrOEt)]^{2+}$ exhibits long-term stability in the presence of BF_4^- counter anions. Only ca. 20% formation of $[Cp^*RhL_3]^{2+}$ and ActyrOEt is apparent after 7 days. This finding suggests that a more subtle interplay of opposing factors may be responsible for the stabilizing effect of a particular anion.

Distortion towards the η^5-oxohexadienyl coordination mode in the Cp^*Rh^{III} sandwich complexes **6** and **7** leads the ^{1}H-NMR signals of the aromatic tyrosine protons to shift upfield to δ values between 5.8 and 6.6 in polar solvents (see Figures 2a and 3a). Figure 4 depicts the aromatic regions of the ^{1}H-NMR spectrum of $[Cp^*Rh(ActyrOEt)](CF_3SO_3)_2$ (**6a**) in (a) D_2O and (b) CD_3NO_2. In view of the instability of **6**–**8** in polar solvents, NMR data for these compounds are only reported for the latter solvent in the Experimental Section of this paper. It is interesting to note that the increase in shielding for the tyrosine *meta* protons of **6a** (δ = 5.82) in CD_3OD is similar to those of **4** and **5** (δ = 5.83 and 5.86) with their unprotected tyrosine amino functions. We were successful in growing suitable crystals of **6a** by gas diffusion of diethyl ether into a methanol solution and Figure 5 shows the X-ray structure of the sandwich cation in this compound. The dihedral angle θ of 5.09° is associated with a C34–O41 distance of 1.34(1) Å and is smaller than in the analogous Cp^*Ir^{III} complex **3b**. Distortion towards the η^5-oxohexadienyl coordination mode may also be gauged from the Rh1–C34 bond length of 2.339(8) Å, which is markedly longer than those to the remaining aromatic carbon atoms in the range 2.243(9)–2.259(7) Å. As in **3b**, relatively strong O–H···O hydrogen bonds [d(O41–H41···O21) = 2.51 Å] are present between the hydroxy and *N*-acetyl oxygen atoms of neighbouring dications. The triflate counter ions participate in weaker O···N1–H1 interactions of length 2.91 Å to the amide proton of N1.

Figure 2. Time-dependent ^{1}H-NMR spectra of $[Cp^*Rh(ActyrOEt)](CF_3SO_3)_2$ (**6a**) in D_2O at room temperature: (a) after 5 min, (b) after 1.5 h and (c) after 24 h

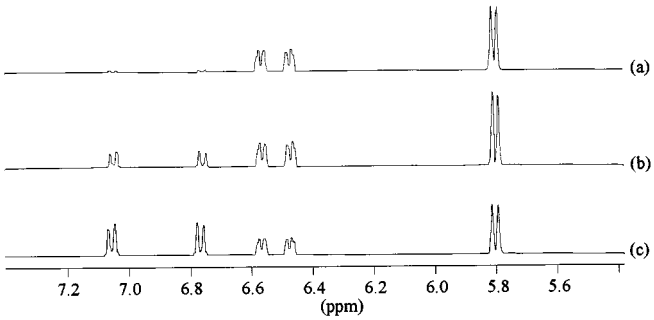

Compound **7** with ActyrOH as sandwich ligand was recrystallized from an acetone/hexane solution for X-ray analysis and displays a structure similar to that of **6a**. Tilting of the C33/C34/C35 plane leads to a Rh1–C34 distance of 2.337(11) Å and a dihedral angle θ of 2.97°. O41 exhibits a C34–O41 bond length of 1.31(1) Å and once again participates in intermolecular O–H···O hydrogen bonding to the *N*-acetyl O21 oxygen atom. It is interesting to note that whereas the metal–ring distances to the Cp* planes in **3b**,

Figure 3. Time-dependent ^{1}H-NMR spectra of [Cp*Rh(ActyrOEt)]$(BF_4)_2$ (**6c**) in D_2O at room temperature: (a) after 5 min, (b) after 48 h and (c) after 7 d

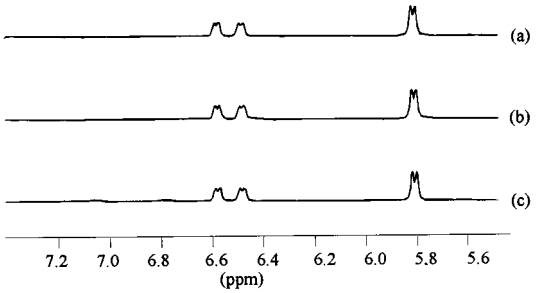

Figure 4. Aromatic regions of the ^{1}H-NMR spectra of [Cp*Rh(ActyrOEt)]$(CF_3SO_3)_2$ (**6a**) in (a) D_2O and (b) CD_3NO_2

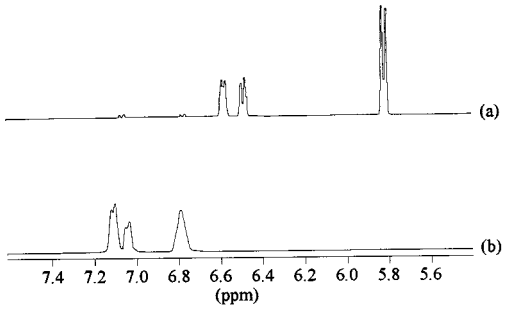

Figure 5. X-ray structure of the cation of [Cp*Rh(ActyrOEt)]$(CF_3SO_3)_2$ (**6a**)

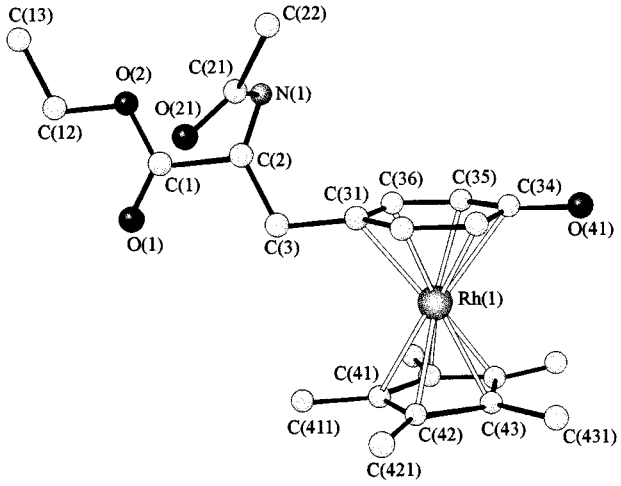

6a and **7** are all very similar [1.817, 1.807 and 1.796 Å], the opposite Ir-η^5-ActyrOMe distance in **3b** [1.738 Å] is markedly shorter than the analogous values for Rh^{III} in **6a** and **7** [1.763 and 1.771 Å].

[Cp*Rh(HtyrOMe)]$(CF_3SO_3)_2$ (**8**) decays immediately in polar solvents to the starting materials and ^{1}H-NMR spectra could, therefore, only be recorded in CD_3NO_2. This typical instability of Cp^*Rh^{III} sandwich compounds of *N*-unprotected aromatic amino acids also prevents the isolation of the analogous π-bonded dication of tyrosine itself. Formation of an *N*-protected zwitterion allows effectively complete deprotonation of the tyrosine *p*-hydroxy function in **8** even in CD_3OD, as evidenced by the upfield shift of the *meta* proton doublets to δ = 5.54 and 5.58 in this solvent. The pronounced downfield shift of the ^{13}C-NMR signal for *C*OH from δ = 147.2 in **7** to 156.3 in **8** (CD_3NO_2 solutions) underscores this interpretation for the *N*-unprotected tyrosine derivative.

Facial Chirality in Tryptophan Complexes

η^6-Coordination of the aromatic indole system in tryptophan derivatives allows the formation of diastereomers owing to the possibility of facial chirality (Scheme 3). As we have already demonstrated for $CyRu^{II}$ sandwich compounds[8], opposite shifts are characteristic for ^{1}H-NMR signals of the protons of the π-bonded arene ring system. For instance, the signals of the inner protons H^5 and H^6 appear at higher field in [Cp*Rh(ActrpOMe)]$(CF_3SO_3)_2$ [**11a**; δ = 6.67 (m)], whereas a pronounced lowfield shift to δ = 7.75 (m) is observed for the signals of the outer protons H^4 and H^7. Assignment was achieved by use of HMQC-TOCSY spectra. Metal coordination of the neighbouring indole six-membered ring also leads to a marked change in the electron-density distribution in the condensed pyrrole ring as evidenced by pronounced shifts to lower field for both the H^2 [^{1}H NMR: δ = 8.28, 8.33 (2 s, 1 H)] and C^2 [^{13}C NMR: δ = 141.4] resonances of **11a** in CD_3NO_2 solution. Similar shifts were recorded for the analogous signals of the Cp^*Ir^{III} sandwich compounds **9** and **10**, whose ^{1}H- and ^{13}C-NMR spectra were recorded in CD_3OD and D_2O solutions, respectively. The H^2 singulets for the α and β isomers are well resolved in **9**, **10** and **11a** and their integral values indicate that both diastereomers must be present in a ca. 1:1 ratio in all three compounds. After successful fractional crystallization, the H^2 resonance at higher field could be assigned to the diastereomer of [CyRu(ActrpOMe)]-$(CF_3SO_3)_2$ with β-facial chirality. It seems reasonable to assume that the same face of ActrpOMe is also preferred in [Cp*Rh(ActrpOMe)]$(PF_6)_2$ (**11a**) for which the H^2 signals [^{1}H NMR: δ = 8.27, 8.32 (2 s, 1 H)] are observed at the integral ratio of ca. 6:1 in CD_3NO_2. Whereas the Cp^*Ir^{III} sandwich complexes **9** and **10** are stable over a period of 14 days in aqueous solution, both **11b** and the analogous compound [Cp*Rh(ActrpOMe)]$(CF_3SO_3)_2$ (**11a**) rapidly decay to ActrpOMe and appropriate tris(solvent) half-sandwich complex in water and methanol.

Stability of Cp^*Ir^{III} and Cp^*Rh^{III} Complexes in Solution

This relative instability of Cp^*Rh^{III} sandwich complexes is also apparent for phenylalanine and its derivatives. As for the aromatic indole system of tryptophan, η^6-coordination can only be achieved with Cp^*Rh^{III} when both the amino and carboxyl functions are protected. In accordance with similar observations for the analogous tyrosine and tryptophan complexes [Cp*Rh(AcpheOMe)]$(CF_3SO_3)_2$ (**14**) decays rapidly in polar solvents. ^{1}H-NMR signals for the aromatic protons of both this and the Cp^*Ir^{III} sandwich compounds [Cp*Ir(AcpheOMe)]$(CF_3SO_3)_2$ (**12**) and [Cp*

Scheme 3. α and β isomers of [Cp*M(R′trpOR)]$(CF_3SO_3)_2$ (**9**−**11**); **9**: M = Ir, R = Me, R′ = Ac; **10**: M = Ir, R = R′ = H; **11**: M = Rh, R = Me, R′ = Ac

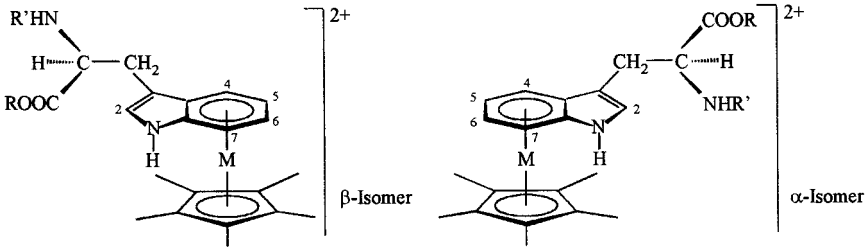

$Ir(H_2pheOMe)](CF_3SO_3)_3$ (**13**) lie in a close range (δ = 7.26−7.65) and are shifted marginally to lower field in comparison those of the free amino acid. The X-ray structure of the complex cation of **12** is depicted in Figure 6. Similar Ir−C distances [2.209−2.277 Å] are observed for all carbon atoms of the phenyl ring which itself is effectively planar.

Scheme 4. Sandwich cations of [Cp*M(R′pheOMe)]$(CF_3SO_3)_n$ (**12**−**14**); **12**: M = Ir, R′ = Ac, n = 2; **13**: M = Ir, R′ = H_2, n = 3; **14**: M = Rh, R′ = Ac, n = 2

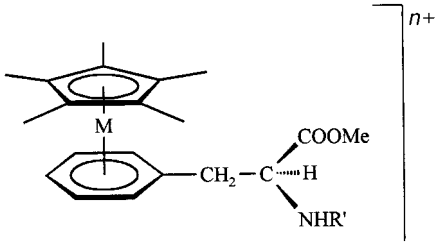

Figure 6. X-ray structure of the cation of [Cp*Ir(AcpheOMe)]$(CF_3SO_3)_2$ (**12**)

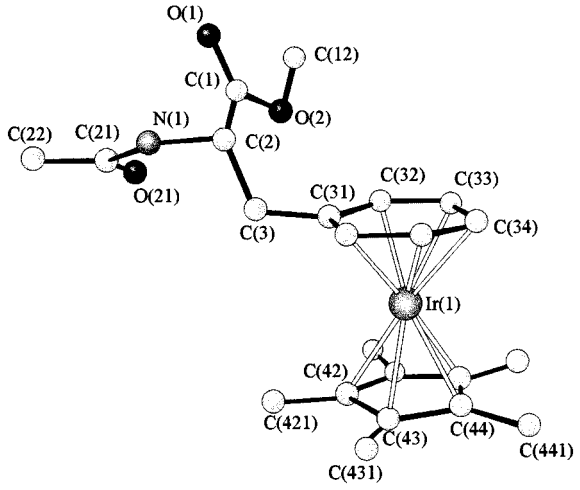

Although the greater stability of Cp^*Ir^{III} sandwich compounds in comparison to their rhodium analogues has been commented upon[15][16], attempts to fully understand this phenomenon still remain somewhat unsatisfactory. The introduction of π-arenes such as benzene or the cyclopentadienyl ion into hexaaqua cations $[M(H_2O)_6]^{2+}$ leads to a drastic increase in the lability of the three remaining water molecules, an effect that is more pronounced for anionic ligands[17]. This behaviour may be understood as a manifestation of the general principle that metal atoms usually tend to prefer either *hard* or *soft* ligands in their coordination spheres but not both at the same time[15]. Koelle et al. have demonstrated[17] that water exchange in half-sandwich triaqua complexes $[Cp^*M(H_2O)_3]^{2+}$ is faster by a factor of 6.3 for Rh^{III} in comparison to Ir^{III}.

Studies by Merbach[18] on the ligand-exchange reactions of $[Cp^*ML_3]^{2+}$ (L = CH_3CN, dmso) indicate that a dissociative mechanism must be involved. As previously reported by Maitlis[18], dmso was found to coordinate Rh^{III} through its oxygen, to Ir^{III} through its sulfur atom. Both this behaviour and the enhanced stability of Cp^*Ir^{III} sandwich compounds in polar solvents are in accordance with an increased preference of the heavier group-9 metal for *softer* ligands (e.g. π-arenes, κ*S*-dmso) in its coordination sphere. Of the members of the Co triad, Rh^{III} should be electronically best equipped to accommodate both *soft* and *hard* ligands in its coordination sphere, as is indeed suggested by the rapid decay of Cp^*Rh^{III} sandwich compounds to species $[Cp^*RhL_3]^{2+}$ in polar solvents (L = H_2O, CH_3OH).

Relativistic Effects

In structural organometallic chemistry, the consideration of relativistic effects[19] is essential to understand trends within a transition-metal triad, especially when going from the second to the third row. Classically speaking, electrons in heavy atoms move so fast that their velocity becomes comparable to the velocity of light. This leads to a contraction and stabilization of s- and p-orbitals but to an expansion and destabilization of d- and f-orbitals. The relativistic destabilization of the 5-d shell results in an increased softness of third-row transition metals.

The importance of relativistic effects can only indirectly be estimated from experiment (e.g. from unexpected trends in the periodic table) since nature is inherently relativistic. Quantum-mechanical calculations on the other hand can be performed either with or without taking care of relativity, and the difference between such computational results indicates the magnitude of relativistic effects. For transition-metal compounds, one generally finds a contraction and stabilization of metal−ligand bonds. These effects lead to similar molecular structures, but higher binding energies if isostructural complexes of homologous 4d and 5d metals are compared.

We have carried out nonrelativistic and relativistic all-electron density functional calculations on the $[Cp^*Rh(\eta^6\text{-}C_6H_5Me)]^{2+}$, $[Cp^*Ir(\eta^6\text{-}C_6H_5Me)]^{2+}$ and $[Cp^*Ru(\eta^6\text{-}C_6H_5Me)]^{+}$ cationic sandwich complexes. For details of the computational method, the reader is referred to ref.[20]. A full geometry optimization has been performed, and the force constants of the two coordinates describing the metal−ring distances have been evaluated. It is suggested that these force constants, which indicate how tightly the aromatic rings are bound to the metal atom, may serve as a measure for the *kinetic* stability of the complexes. Some results of these calculations have been collected in Table 1. The relativistic results are given, together with the results from the nonrelativistic calculations in parentheses. Both aromatic rings are essentially planar, and the coordinates d_1 and d_2 (Figure 7) are the distance between the metal atom and the planes of the Cp* and toluene aromatic ring, respectively. The force constants k_1 and k_2 are the second derivatives of the total energy with respect to the coordinates d_1 and d_2. For $[Cp^*Ir(\eta^6\text{-}C_6H_5Me)]^{2+}$, we can compare the calculated metal−ring distances (1.841 and 1.792 Å) to the X-ray result for $[Cp^*Ir(\eta^6\text{-AcpheOMe})](CF_3SO_3)_2$ (**12**; 1.811 and 1.744 Å) and find reasonable agreement. The nonrelativistic calculations give much larger values especially for the distance between iridium and the toluene ring (nonrelativistic: 1.925 Å, relativistic: 1.792 Å). As relativistic-effects scale with the square of the nuclear charge, the bond contractions are much smaller for the Rh (Z = 45) compounds than for Ir (Z = 77) complexes. Looking at the force constants, we find that both metals bind more tightly to Cp* than to toluene ($k_1 > k_2$). This is consistent with the experimental finding that in the first stages of the decay, the Cp^*Rh^{III} or Cp^*Ir^{III} units remain intact. For the kinetic stability of the complex, the value of k_2 appears to be most important. The calculations find 207 and 279 Nm^{-1}, respectively, for the Rh^{III} and Ir^{III} sandwich complexes, consistent with the much higher stability of the latter. This does not follow from the nonrelativistic data: it is the much larger relativistic enhancement of k_2 that makes the iridium complex so stable.

Figure 7. Definition of the distances d_1, d_2 and the force constants k_1, k_2 in sandwich cations of the type $[Cp^*M(\eta^6\text{-}C_6H_5Me)]^{n+}$ (n = 2, M = Ir, Rh; n = 1, M = Ru)

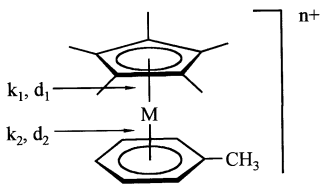

Similar calculations for $[Cp^*Ru(\eta^6\text{-}C_6H_5Me)]^{+}$ are also included in Table 1 and indicate as for the analogous Cp^*Rh^{III} sandwich cation that relativistic effects are less marked for second-row transition metals. The distances presented for d_1 and d_2 [1.840 and 1.751 Å] may be compared with the average experimental values[6] of 1.816 and 1.704 Å in $[(Cp^*Ru)_2\{cyclo\text{-(phephe)}\}]^{2+}$. Despite the much shorter distance to the η^6-coordinated toluene ligand the force constants k_1 and k_2 are in accordance with tighter binding to Cp*, although the difference is less pronounced than in the Cp^*Ir^{III} and Cp^*Rh^{III} sandwich complexes.

Table 1. Metal−ring distances and force constants for $[Cp^*Rh(\eta^6\text{-}C_6H_5Me)]^{2+}$, $[Cp^*Ir(\eta^6\text{-}C_6H_5Me)]^{2+}$ and $[Cp^*Ru(\eta^6\text{-}C_6H_5Me)]^{+}$ from relativistic density functional calculations; nonrelativistic results are given in parentheses

Compound	d_1 [Å]	d_2 [Å]	k_1 [Nm^{-1}]	k_2 [Nm^{-1}]
$[Cp^*Rh(\eta^6\text{-}C_6H_5Me)]^{2+}$	1.840	1.830	358	207
	(1.862)	(1.876)	(334)	(182)
$[Cp^*Ir(\eta^6\text{-}C_6H_5Me)]^{2+}$	1.841	1.792	413	279
	(1.908)	(1.925)	(351)	(193)
$[Cp^*Ru(\eta^6\text{-}C_6H_5Me)]^{+}$	1.840	1.751	367	299
	(1.861)	(1.781)	(346)	(269)

Experimental Section

All manipulations and reactions were performed under argon in carefully dried solvents using standard Schlenk techniques. − FTIR[20]: Perkin-Elmer 1760; in KBr. − FAB MS: Fisons VG Autospec with 3-nitrobenzyl alcohol as the matrix. − ^1H and ^{13}C NMR: Bruker DRX 400; chemical shifts are reported as δ values relative to the signal of the deuterated solvent. − Elemental analyses were performed by Beller, Mikroanalytisches Labor, Göttingen. − The starting compounds $[(\eta^5\text{-}Cp^*)IrL_3](CF_3SO_3)_2$ [L = thf (**1a**), $(CH_3)_2CO$ (**1b**)] and $[(\eta^5\text{-}Cp^*)RhL_3](CF_3SO_3)_2$ [L = thf (**2a**), $(CH_3)_2CO$ (**2b**), CH_3CN (**2c**)] were prepared from respectively $[(\eta^5\text{-}Cp^*)IrCl_2]_2$ or $[(\eta^5\text{-}Cp^*)RhCl_2]_2$ by addition of an appropriate quantity of $Ag(CF_3SO_3)$ and filtration of the precipitated AgCl in the chosen solvent L[10]. Amino acids were purchased from Bachem (Heidelberg) and Calbiochem-Novabiochem (Bad Soden) and were used as received.

$[(\eta^5\text{-}Cp^*)Ir(ActyrOEt)](CF_3SO_3)_2$ (**3a**): N-acetyltyrosine ethyl ester (ActyrOEt, 37.2 mg, 0.15 mmol) was added to a solution of **1a** (122.6 mg, 0.15 mmol) in 12 mL of thf and the reaction mixture heated at reflux for 18 h. The resulting solid was stirred for 24 h with diethyl ether and dried in vacuo after centrifugation to afford **3**. Yield 112 mg (86%). − $C_{25}H_{32}F_6IrNO_{10}S_2$ (876.5): calcd. C 34.3, H 3.7, N 1.6; found C 34.6, H 3.8, N 2.0. − FAB MS; *m/z* (%): 727 (1) $[M - CF_3SO_3]^+$, 578 (100) $[M - 2\ CF_3SO_3]^+$, 445 (3) $[M - 2\ CF_3SO_3 - NHAc - CO_2Et]^+$. − ^1H NMR (CD_3OD): δ = 1.32 (t, 3 H, CH_3 OEt), 2.04 (s, 3 H, CH_3 Ac), 2.28 (s, 15 H, CH_3 Cp*), 2.83/3.03 (2 dd, 2 H, β-CH_2), 4.27 (q, 2 H, CH_2 OEt), 4.79 (dd, 1 H, α-C*H*), 6.20 (2 d, 2 H, H_{meta} tyr), 6.70/6.78 (2 d, 2 H, H_{ortho} tyr). − ^{13}C NMR (CD_3OD): δ = 9.9 (CH_3 Cp*), 14.7 (CH_3 OEt), 22.7 (CH_3 Ac), 35.0 (β-*C*), 54.1 (α-*C*), 63.5 (CH_2 OEt), 84.1 (C_{meta} tyr), 97.9 (C_{ortho} tyr), 102.0 (CCH_3 Cp*), 103.2 (*C* tyr), 157.7 (*C*OH tyr), 171.4 (*C*OO), 173.8 (NH*C*O). − IR: $\tilde{\nu}$ = 3273 s (NH), 1743 s (CO), 1582, 1531 m (NH) cm^{-1}.

$[(\eta^5\text{-}Cp^*)Ir(HtyrOMe)](CF_3SO_3)_2$ (**4**): Tyrosine methyl ester (HtyrOMe, 38 mg, 0.2 mmol) was stirred with **1b** (160 mg, 0.2 mmol) for 24 h in 12 mL of CF_3COOH at 50°C and the solution reduced in volume to 3 mL. After precipitation with diethyl ether, the resulting solid was dried in vacuo to afford **4**. Yield 139.5 mg (85%). − $C_{22}H_{28}F_6IrNO_9S_2$ (820.8): calcd. C 32.2, H 3.4, N 1.7; found C 32.1, H 3.6, N 1.5. − FAB MS; *m/z* (%): 522 (100) $[M - 2\ CF_3SO_3]^+$. − ^1H NMR (CD_3OD): δ = 2.25 (s, 15 H, CH_3 Cp*), 3.04 (2 dd, 2 H, β-CH_2), 3.91 (s, 3 H, COCH_3), 4.55 (dd, 1 H, α-C*H*), 5.83 (2 d, 2 H, H_{meta} tyr), 6.51, 6.57 (2 d, 2 H, H_{ortho} tyr). −

^{13}C NMR (CD_3OD): δ = 10.8 (*C*H$_3$ Cp*), 34.6 (β-*C*), 55.0 (α-*C*), 55.5 (*C*H$_3$OMe), 84.0, 84.2 (C_{meta} tyr), 97.2, 98.7 (C_{ortho} tyr), 99.3 (*C*CH$_3$ Cp*), 103.1 (*C* tyr), 164.9 (*C*OH tyr), 170.3 (*C*OO). − IR: $\tilde{\nu}$ = 3284 s (NH), 1746 s (CO), 1573 m (NH) cm^{-1}.

[(η5-Cp)Ir(HtyrOH)](CF3SO3)2* (**5**): The preparation was performed with tyrosine (27.9 mg, 0.15 mmol) and **1a** (128 mg, 0.15 mmol) in CF_3COOH in an analogous manner to **4**. Yield 82.2 mg (68%). − $C_{21}H_{26}F_6IrNO_{10}S_2$ (806.2): calcd. C 31.3, H 3.2, N 1.7; found C 31.1, H 3.5 N 1.7. − FAB MS; *m/z* (%): 658 (1) [M − CF_3SO_3]$^+$, 508 (100) [M − 2 CF_3SO_3]$^+$, 462 (6) [M − 2 CF_3SO_3 − CO_2H]$^+$. − ^{1}H NMR (CD_3OD): δ = 2.26 (s, 15 H, C*H*$_3$ Cp*), 3.03 (m, 2 H, β-C*H*$_2$), 4.49 (dd, 1 H, α-C*H*), 5.86 (2 d, 2 H, H_{meta} tyr), 6.59, 6.63 (2 d, 2 H, H_{ortho} tyr). − ^{13}C NMR (CD_3OD): δ = 9.9 (*C*H$_3$ Cp*), 33.7 (β-*C*), 54.1 (α-*C*), 83.1 (C_{meta} tyr), 97.4 (C_{ortho} tyr), 98.5 (*C* tyr), 102.2 (*C*CH$_3$ Cp*), 163.7 (*C*OH tyr), 170.1 (*C*OO). − IR: $\tilde{\nu}$ = 3178 s (NH), 1742 s (CO), 1559 m (NH) cm^{-1}.

[(η5-Cp)Rh(ActyrOEt)](CF3SO3)2* (**6a**): ActyrOEt (75.4 mg, 0.3 mmol) and **2b** (213.2 mg, 0.3 mmol) were stirred for 2 d in 15 mL of thf and the resulting solid removed by centrifugation. After washing with diethyl ether, the product was dried to afford **6.** Yield 198.5 mg (84%). Recrystallization by gas diffusion of diethyl ether into a methanol solution provided suitable crystals for X-ray analysis. − $C_{25}H_{32}F_6NO_{10}RhS_2$ (787.6): calcd. C 38.1, H 4.1, N 1.8; found C 37.6, H 4.0, N 1.8. − FAB MS; *m/z* (%): 637 (1) [M − CF_3SO_3]$^+$, 488 (100) [M − 2 CF_3SO_3]$^+$, 237 (11) [M − 2 CF_3SO_3 − ActyrOEt]$^+$. − ^{1}H NMR (CD_3NO_2): δ = 1.21 (t, 3 H, C*H*$_3$ OEt), 1.93 (s, 3 H, C*H*$_3$ Ac), 2.19 (s, 15 H, C*H*$_3$ Cp*), 2.97, 3.16 (2 dd, 2 H, β-C*H*$_2$), 4.17 (q, 2 H, C*H*$_2$ OEt), 4.79 (dd, 1 H, α-C*H*), 6.79 (2 d, 2 H, H_{meta} tyr), 7.05, 7.18 (2 d, 2 H, H_{ortho} tyr). − ^{13}C NMR (CD_3NO_2): δ = 8.9 (*C*H$_3$ Cp*), 12.8 (*C*H$_3$ OEt), 21.1 (*C*H$_3$ Ac), 33.6 (β-*C*), 52.3 (α-*C*), 62.1 (*C*H$_2$ OEt), 93.8 (C_{meta} tyr), 106.3, 106.5 (C_{ortho} tyr), 110.9 (*C*CH$_3$ Cp*), 112 (*C* tyr), 147.2 (*C*OH tyr), 169.4 (*C*OO), 171.5 (NH*C*O). − IR: $\tilde{\nu}$ = 3274 s (NH), 1742 s (CO), 1539 m (NH) cm^{-1}.

[(η5-Cp)Rh(ActyrOH)](CF3SO3)2* (**7**): The preparation was performed with *N*-acetyltyrosine (ActyrOH, 66.7 mg, 0.3 mmol) and **2c** (198.1 mg 0.3 mmol) in a manner similar to **6** with the exception that the thf was refluxed for 16 h. Yield 177.7 mg (78%). Recrystallization by covering an acetone solution with hexane provided suitable crystals for X-ray analysis. − $C_{23}H_{28}F_6NO_{10}RhS_2$ (759.5): calcd. C 36.4, H 3.7, N 1.8; found C 36.0, H 3.7, N 1.6. − FAB MS; *m/z* (%): 609 (1) [M − CF_3SO_3]$^+$, 460 (100) [M − 2 CF_3SO_3]$^+$, 205 (11) [M − 2 CF_3SO_3 − ActyrOH]$^+$. − ^{1}H NMR (CD_3NO_2): δ = 1.97 (s, 3 H, C*H*$_3$ Ac), 2.20 (s, 15 H, C*H*$_3$ Cp*), 2.95, 3.20 (2 dd, 2 H, β-C*H*$_2$), 4.77 (dd, 1 H, α-C*H*), 6.76, 6.80 (2 d, 2 H, H_{meta} tyr), 6.90, 7.04 (2 d, 2 H, H_{ortho} tyr), 7.09 (s, 1 H, N*H*CO). − ^{13}C NMR (CD_3NO_2): δ = 8.9 (*C*H$_3$ Cp*), 21.1 (*C*H$_3$ Ac), 33.6 (β-*C*), 52.2 (α-*C*), 93.8 (C_{meta} tyr), 106.2, 106.6 (C_{ortho} tyr), 110.9 (*C*CH$_3$ Cp*), 111.6 (*C* tyr), 147.2 (*C*OH tyr), 170.1 (*C*OO), 171.6 (NH*C*O). − IR: $\tilde{\nu}$ = 3284 s (NH), 1749 s (CO), 1573 m (NH) cm^{-1}.

[(η5-Cp)Rh(HtyrOMe)](CF3SO3)2* (**8**): The preparation was performed with HtyrOMe (57 mg, 0.3 mmol) and **2b** (213.2 mg, 0.3 mmol) in a manner similar to **4** and **5**. Yield 177.7 mg (81%). − $C_{22}H_{28}F_6NO_9RhS_2$ (731.4): calcd. C 36.1, H 3.9, N 1.9; found C 36.0, H 3.7, N 1.8. − FAB MS; *m/z* (%): 582 (4) [M − CF_3SO_3]$^+$, 432 (100) [M − 2 CF_3SO_3]$^+$, 237 (23) [M − 2 CF_3SO_3 − HtyrOMe]$^+$. − ^{1}H NMR (CD_3NO_2): δ = 2.09 (s, 15 H, C*H*$_3$ Cp*), 3.22, 3.24 (2 dd, 2 H, β-C*H*$_2$), 3.83 (s, 3 H, COC*H*$_3$), 4.55 (dd, 1 H, α-C*H*), 5.54, 5.58 (2 d, 2 H, H_{meta} tyr), 6.48, 6.82 (2 d, 2 H, H_{ortho} tyr). − ^{13}C NMR (CD_3NO_2): δ = 8.7 (*C*H$_3$ Cp*), 34.5 (β-*C*), 53.3 (α-*C*), 55.5 (*C*H$_3$ OMe), 93.2, 94.4 (C_{meta} tyr), 105.7, 106.4 (C_{ortho} tyr), 109.0 (*C*CH$_3$ Cp*), 115.7 (*C* tyr), 156.3 (*C*OH tyr), 167.2 (*C*OO). − IR: $\tilde{\nu}$ = 1752 s (CO), 1590, 1522 m (NH) cm^{-1}.

[(η5-Cp)Ir(ActrpOMe)](CF3SO3)2* (**9**): N-Acetyltryptophan methyl ester (ActrpOMe, 40.4 mg, 0.16 mmol) and **1a** (128.7 mg, 0.16 mmol) were stirred in 10 ml of thf for 24 h at room temperature or heated at 45°C for 2 h. The resulting solid was then stirred for 24 h with diethyl ether and dried in vacuo to afford **9**. Yield 102 mg (72%). − $C_{25}H_{30}F_6IrN_2O_9S_2$ (885.5): calcd. C 35.3, H 3.4, N 3.1; found C 34.7, H 3.4, N 3.3. − FAB MS; *m/z* (%): 738 (53) [M − CF_3SO_3]$^+$, 588 (62) [M − 2 CF_3SO_3]$^+$, 527 (3) [M − 2 CF_3SO_3 − $COOCH_3$]$^+$. − ^{1}H NMR (CD_3OD): δ = 1.97, 2.02 (2 s, 3 H, C*H*$_3$ Ac), 2.08 (s, 15 H, C*H*$_3$ Cp*), 3.28, 3.41 (2 dd, 2 H, β-C*H*$_2$), 3.76, 3.82 (2 s, 3 H, C*H*$_3$ OMe), 4.87 (dd, 1 H, α-C*H*), 7.07 (m, 2 H, H_{ind}), 7.87 (dd, 1 H, H_{ind}), 8.01 (dd, 1 H, H_{ind}), 8.37, 8.42 (2 s, H_{ind}). − ^{13}C NMR (CD_3OD): δ = 9.4 (*C*H$_3$ Cp*), 22.8 (*C*H$_3$ Ac), 27.4 (β-*C*), 53.7 (α-*C*), 54.1 (*C*OMe), 84.7, 89.8, 91.3, 92.2 (C_{ind}), 103.3 (*C*CH$_3$ Cp*), 106.9, 116.2, 120.2, 143.5 (C_{ind}), 172.7 (NH*C*O), 173.8 (*C*OO). − IR: $\tilde{\nu}$ = 3323 s (NH), 1742 s, 1667 s (CO), 1541 m (NH) cm^{-1}.

[(η5-Cp)Ir(HtrpOH)](CF3SO3)2* (**10**): HtrpOH (39.8 mg, 0.195 mmol) was heated with **1a** (168.4 mg, 0.2 mmol) at 65°C in 12 ml of CF_3COOH for 48 h and the solution reduced in volume to 3 ml. After precipitation with diethyl ether the resulting solid was dried in vacuo to afford **10**. Yield 111.6 mg (69%). − $C_{23}H_{27}F_6IrN_2O_8S_2$ (829.8): calcd. C 33.3, H 3.3, N 3.4; found C 33.4, H 3.8, N 3.4. − FAB MS; *m/z* (%): 681 (3) [M − CF_3SO_3]$^+$, 531 (100) [M − 2 CF_3SO_3]$^+$. − ^{1}H NMR (D_2O): δ = 1.94 (s, 15 H, C*H*$_3$ Cp*), 3.43 (2 dd, 2 H, β-C*H*$_2$), 4.13, 4.22 (2 m, 1 H, α-C*H*), 6.95 (m, 2 H, H_{ind}), 7.74, 7.78, 7.86 (m, 2 H, H_{ind}), 8.36, 8.40 (2 s, 1 H, H_{ind}). − ^{13}C NMR (D_2O): δ = 8.3 (*C*H$_3$ Cp*), 26.0 (β-*C*), 52.2 (α-*C*), 88.1, 96.6, 97.0, 97.6 (C_{ind}), 101.9 (*C*CH$_3$ Cp*), 104.9, 114.2, 118.2, 141.4 (C_{ind}), 170.4 (*C*OO). − IR: $\tilde{\nu}$ = 1646 s (CO), 1518 m (NH) cm^{-1}.

[(η5-Cp)Rh(ActrpOMe)](CF3SO3)2* (**11a**): ActrpOMe (51.1 mg, 0.2 mmol) and **2b** (142.1 mg, 0.2 mmol) were stirred in 10 ml of thf for 48 h at room temperature. The resulting solid was subsequently stirred for 24 h with diethyl ether and dried in vacuo to give **11a**. Yield 108.3 mg (68%). − $C_{26}H_{31}F_6IrN_2O_9S_2$ (796.6): calcd. C 39.2, H 3.9, N 3.5; found C 39.0, H 3.7, N 3.4. − FAB MS; *m/z* (%): 498 (100) [M − 2 CF_3SO_3]$^+$, 237 (16) [M − 2 CF_3SO_3 − ActrpOMe]$^+$. − ^{1}H NMR (CD_3NO_2): δ = 1.84, 1.90 (2 s, 3 H, C*H*$_3$ Ac), 1.96 (s, 15 H, C*H*$_3$ Cp*), 3.30 (2 dd, 2 H, β-C*H*$_2$), 3.64, 3.72 (2 s, 3 H, C*H*$_3$ OMe), 4.76 (m, 1 H, α-C*H*), 6.67 (m, 2 H, H_{ind}), 7.75 (m, 2 H, H_{ind}), 8.28, 8.33 (2 s, 1 H, H_{ind}). − ^{13}C NMR (CD_3NO_2): δ = 8.3 (*C*H$_3$ Cp*), 21.2 (*C*H$_3$ Ac), 26.0 (β-*C*), 51.9 (*C*H$_3$ OMe), 52.2 (α-*C*), 88.1, 96.6, 97.0, 97.6 (C_{ind}), 108.7 (*C*CH$_3$ Cp*), 108.7, 111.4, 112.8, 141.4 (C_{ind}), 170.0, 170.4 (NH*C*O, *C*OO). − IR: $\tilde{\nu}$ = 3328 s (NH), 1741, 1657 s (CO), 1546 m (NH) cm^{-1}.

[(η5-Cp)Ir(AcpheOMe)](CF3SO3)2* (**12**): N-acetylphenylalanine methyl ester (AcpheOMe, 29.5 mg, 0.13 mmol) was added to a solution of **1a** (110.7 mg, 0.13 mmol) in 12 ml of thf and the suspension refluxed for 18 h. After removal of the solvent the resulting precipitate was stirred for 24 h with diethyl ether and dried in vacuo to afford **12**. Yield 84.7 mg (77%). Recrystallization by gas diffusion of diethyl ether into a methanol solution provided suitable crystals for X-ray analysis. − $C_{23}H_{30}F_6IrNO_9S_2$ (846.5): calcd. C 32.6, H 3.6, N 1.7; found C 33.9, H 3.6, N 1.5. − FAB MS; *m/z* (%): 548 (58) [M − 2 CF_3SO_3]$^+$, 4.89 (4) [M − 2 CF_3SO_3 − $COOCH_3$]$^+$. − ^{1}H NMR (CD_3OD): δ = 2.02 (2 s, 3 H, C*H*$_3$ Ac), 2.43 (s, 15 H, C*H*$_3$ Cp*), 3.09, 3.28 (2 dd, 2 H, β-C*H*$_2$), 3.81 (2 s, 3 H, C*H*$_3$ OMe), 4.88 (dd, 1 H, α-C*H*), 7.48 (m, 4 H, phe), 7.57 (t, 1 H$_{para}$, phe). − ^{13}C NMR (CD_3OD): δ = 10.4 (*C*H$_3$ Cp*), 22.7

(CH_3 Ac), 35.7 (β-*C*), 53.8 (α-*C*, CH_3 OMe), 99.6, 99.7 (*C* phe), 107.8 (CCH_3 Cp*), 115.4 (*C* phe), 171.6 (NH*C*O), 173.8 (*C*OO). IR: $\tilde{\nu}$ = 3386 s (NH), 1745 s, 1667 s (CO), 1533 m (NH) cm^{-1}.

[(η⁵-Cp)Ir(H₂pheOMe)](CF₃SO₃)₃* (**13**): HpheOMe·HCl (43.1 mg, 0.2 mmol) was dissolved in 10 mL of methanol and $AgCF_3SO_3$ (0.2 mmol, 51.4 mg) added to the solution. The precipated AgCl was removed by filtration and the solution dried in vacuo. The resulting solid was stirred with **1b** (160.0 mg, 0.2 mmol) in 12 mL of CF_3COOH for 24 h. After reduction of the solvent volume to 3 mL, addition of diethyl ether led to precipitation of **13** which was dried in vacuo. Yield 145.1 mg (76%). − $C_{23}H_{29}F_9IrNO_{11}S_3$ (954.9): calcd. C 28.9, H 3.1, N 1.5; found C 28.5, H 3.3, N 1.4. − FAB MS; *m/z* (%): 806 (20) $[M]^+$, 656.2 (16) $[M - CF_3SO_3]^+$, 506 (100) $[M - 2\ CF_3SO_3]^+$, 419 (27) $[Cp^*IrC_6H_5CH_2]^+$. − ^{1}H NMR (CD_3OD): δ = 2.44 (s, 15 H, CH_3 Cp*), 3.31 (2 dd, 2 H, β-CH_2), 3.89 (2 s, 3 H, CH_3 OMe), 4.62 (m, 1 H, α-C*H*), 7.65 (m, phe). − ^{13}C NMR (CD_3OD): δ = 10.4 (CH_3 Cp*), 33.7 (β-*C*), 53.5 (CH_3 OMe), 54.7 (α-*C*), 99.71, 100.1, 100.1, 100.3, 101.0 (*C* phe), 108.2 (CCH_3 Cp*), 112.7 (*C* phe), 168.9 (*C*OO). − IR: $\tilde{\nu}$ = 1756 s (CO), 1630, 1501 m (NH) cm^{-1}.

[(η⁵-Cp)Rh(AcpheOMe)](CF₃SO₃)₂* (**14**): AcpheOMe (51.1 mg, 0.2 mmol) was refluxed with **2b** (150.5 mg, 0.2 mmol) in 15 mL of thf for 20 h and the solution reduced in volume to 3 mL. After precipitation with *n*-hexane, the resulting solid was washed with diethyl ether and dried in vacuo to afford **14**. Yield 109.1 mg (72%). − $C_{24}H_{30}F_6NO_9RhS_2$ (757.5): calcd. C 38.1, H 4.0, N 1.9; found C 37.4, H 3.8, N 1.4. − FAB MS; *m/z* (%): 608 (3) $[M - CF_3SO_3]^+$, 459 (60) $[M - 2\ CF_3SO_3]^+$, 237 (15) $[M - 2\ CF_3SO_3 - AcpheOMe]^+$. − ^{1}H NMR ($CD_3NO_2$): δ = 1.42 (2 s, 3 H, CH_3 Ac), 2.11 (s, 15 H, CH_3 Cp*), 3.23 (2 dd, 2 H, β-CH_2), 3.61 (2 s, 3 H, CH_3 OMe), 4.12 (m, 1 H, α-C*H*), 7.26 (m, 5 H, phe). − ^{13}C NMR (CD_3NO_2): δ = 9.7 (CH_3 Cp*), 14.11 (CH_3 Ac), 37.5 (β-*C*), 52.9 (α-*C*), 65.1 (CH_3 OMe), 106.3, 107.1, 107.3, 107.6, 107.9 (*C* phe), 113.1, 113.2 (CCH_3 Cp*, *C* phe), 176.5 (NH*C*O), 177.5 (*C*OO). − IR: $\tilde{\nu}$ = 1668, 1744 (CO), 1541 (NH) cm^{-1}.

X-ray-Structural Analyses: Siemens P4 diffractometer, graphite-monochromated Mo-K_α radiation (λ = 0.71073 Å). Empirical absorption correction (DIFABS)[22] were applied to the reflection intensities for **6** and **12**. Semi-empirical absorption corrections were applied to the intensity data for **3b** and **7** by use of ψ scans. The structures were solved by direct methods or Patterson syntheses and refined by full-matrix least squares against F^2 using SHELXL-93[23]. Hydrogen atoms were included at calculated positions with isotropic temperature factors[24].

[(η⁵-Cp)Ir(ActyrOMe)](CF₃SO₃)₂* (**3b**): $C_{24}H_{30}F_6IrNO_{10}S_2$, M = 862.8, T = 295 K, orthorhombic, space group $P2_12_12_1$ (no. 19), a = 9.174(2), b = 13.133(3), c = 27.022(5) Å, V = 3255.7(12) Å^3, Z = 4, $D_{calcd.}$ = 1.760 g·cm^{-3}, μ = 4.31 mm^{-1}. Crystal size: 0.43 × 0.21 × 0.16 mm; ω scan; scan range: 4° ≤ 2 θ ≤ 45° (0 ≤ h ≤ 9, 0 ≤ k ≤ 14, 0 ≤ l ≤ 29), 2382 symmetry-independent reflections; max./min. transmission: 0.492/0.212; 143 parameters refined; R = 0.077 [$I > 2\ \sigma(I)$], wR_2 = 0.212 (all data), Δρ max./min. = 1.11/−1.56 e Å^{-3}. The Cp* ligand was refined as a rigid group.

[(η⁵-Cp)Rh(ActyrOEt)](CF₃SO₃)₂* (**6a**): $C_{25}H_{32}F_6NO_{10}RhS_2$, M = 787.6, T = 215 K, monoclinic, space group $P2_1$ (no. 4), a = 9.447(3), b = 12.835(2), c = 13.601(2) Å, β = 99.12(2)°, V = 1628.3(7) Å^3, Z = 2, $D_{calcd.}$ = 1.606 g·cm^{-3}, μ = 0.74 mm^{-1}. Crystal size: 0.79 × 0.69 × 0.31 mm; ω scan; scan range: 4° ≤ 2 θ ≤ 55° (−11 ≤ h ≤ 11, −3 ≤ k ≤ 16, −17 ≤ l ≤ 17), 4100 symmetry-independent reflections; 397 parameters refined; R = 0.056 [$I > 2\ \sigma(I)$], wR_2 = 0.158 (all data), Δρ max./min. = 1.04/−1.12 eÅ^{-3}.

[(η⁵-Cp)Rh(ActyrOH)](CF₃SO₃)₂* (**7**): $C_{23}H_{28}F_6NO_{10}RhS_2$, M = 759.5, T = 193 K, monoclinic, space group $P2_1$ (no. 4), a = 9.445(4), b = 12.558(4), c = 12.627(4) Å, β = 98.12(2)°, V = 1482.7(9) Å^3, Z = 2, $D_{calcd.}$ = 1.701 g·cm^{-3}, μ = 0.80 mm^{-1}. Crystal size: 0.76 × 0.32 × 0.22 mm; ω scan; scan range: 4° ≤ 2 θ ≤ 60° (−10 ≤ h ≤ 10, −3 ≤ k ≤ 14, −15 ≤ l ≤ 14), 4082 symmetry-independent reflections; parameters refined; R = 0.070 [$I > 2\ \sigma(I)$], wR_2 = 0.187 (all data), Δρ max./min. = 1.43/−1.61 eÅ^{-3}.

[(η⁵-Cp)Ir(AcpheOMe)](CF₃SO₃)₂* (**12**): $C_{24}H_{30}F_6IrNO_9S_2$, M = 846.8, T = 215 K, monoclinic, space group $P2_1$ (no. 4), a = 12.758(3), b = 9.051(3), c = 13.403(3) Å, β = 102.00(2)°, V = 1513.8(7) Å^3, Z = 2, $D_{calcd.}$ = 1.858 g·cm^{-3}, μ = 4.635 mm^{-1}. Crystal size: 0.47 × 0.23 × 0.18 mm; θ−2 θ scan; scan range: 4° ≤ 2 θ ≤ 50° (0 ≤ h ≤ 15, 0 ≤ k ≤ 10, −15 ≤ l ≤ 15), 2846 symmetry-independent reflections; 395 parameters refined; R = 0.049 [$I > 2\ \sigma(I)$], wR_2 = 0.141 (all data), Δρ max./min. = 3.72/−2.93 eÅ^{-3}. The Cp* ligand was refined as a rigid group.

[1] G. Jaouen, A. Vessières, I. S. Butler, *Acc. Chem. Res.* **1993**, *26*, 361−369.
[2] R. Krämer, *Angew. Chem.* **1996**, *108*, 1287−1289; *Angew. Chem. Int. Ed. Engl.* **1996**, *35*, 1197−1199.
[3] A. J. Pearson, K. Lee, *J. Org. Chem.* **1994**, *59*, 2304−2313.
[4] J. W. Janetka, D. H. Rich, *J. Am. Chem. Soc.* **1995**, *117*, 10585−10586.
[5] W. S. Sheldrick, A. J. Gleichmann, *J. Organomet. Chem.* **1994**, *470*, 183−187; A. J. Gleichmann, Dissertation, Ruhr-Universität Bochum, **1994**.
[6] A. J. Gleichmann, J. M. Wolff, W. S. Sheldrick, *J. Chem. Soc., Dalton Trans.* **1995**, 1549−1554; J. M. Wolff, A. J. Gleichmann, C. Schmidt, W. S. Sheldrick, *J. Inorg. Biochem.* **1995**, *59*, 219−219.
[7] J. M. Wolff, W. S. Sheldrick, *J. Organomet. Chem.* **1997**, *531*, 141−149.
[8] J. M. Wolff, W. S. Sheldrick, *Chem. Ber.* **1997**, *130*, 981−988.
[9] C. White, P. M. Maitlis, *J. Chem. Soc. A* **1971**, 3322−3326; V. Part, J. W. Kang, P. M. Maitlis, *J. Organomet. Chem.* **1971**, *30*, 127−133.
[10] C. White, S. J. Thompson, P. M. Maitlis, *J. Organomet. Chem.* **1977**, *127*, 415−421; C. White, S. J. Thompson, P. M. Maitlis, *J. Chem. Soc., Dalton Trans.* **1977**, 1654−1661.
[11] B. Chaudret, X. He, Y. Huang, *J. Chem. Soc., Chem. Commun.* **1989**, 1844−1846.
[12] U. Koelle, M. H. Wang, G. Raabe, *Organometallics* **1991**, *10*, 2573−2577.
[13] J. Le Bras, H. El Amouri, Y. Besace, J. Vaissermann, G. Jaouen, *Bull. Soc. Chim. Fr.* **1995**, *132*, 1073−1082.
[14] J. Le Bras, H. El Amouri, J. Vaissermann, *Organometallics* **1996**, *26*, 5706−5712.
[15] U. Koelle, *Coord. Chem. Rev.* **1994**, *135*, 623−650.
[16] P. M. Maitlis, *Acc. Chem. Res.* **1978**, *11*, 301−307.
[17] L. Dadci, H. Elias, U. Frey, A. Hörnig, U. Koelle, A. E. Merbach, H. Paulus, J. S. Schneider, *Inorg. Chem.* **1995**, *34*, 306−315.
[18] A. Cusanelli, L. Nicula-Dadci, U. Frey, A. E. Merbach, *Inorg. Chem.* **1997**, *36*, 2211−2217.
[19] P. Pyykkö, *Chem. Rev.* **1988**, *88*, 563−594.
[20] C. van Wüllen, *J. Comput. Chem.* **1997**, *18*, 1985−1992.
[21] C. S. Schmidt, Dissertation, Ruhr-Universität Bochum, **1998**.
[22] N. Walker, D. Stuart, *Acta Crystallogr., Sect. A* **1983**, *39*, 158−166.
[23] G. M. Sheldrick, *SHELXL-93, A Program for Structure Refinement*, Göttingen, **1993**.
[24] Crystallographic data (excluding structure factors) for the structures reported in this paper have been deposited with the Cambridge Crystallographic Data Centre. Copies of the data (deposition numbers CCDC-101988−101991) may be obtained free of charge on application to CCDC, 12 Union Road, Cambridge CB2 1EZ, UK (Fax: + 44-1223/336−033, E-mail: deposit@ccdc.cam.ac.uk).

[98201]

Metal-Mediated Conversion of Methylcycloarsoxane $(CH_3AsO)_n$ to Macrocyclic Octa- and Decanuclear Ligands –Trigonal Bipyramidal Coordination of Trivalent Arsenic

Iris M. Müller and William S. Sheldrick*

Lehrstuhl für Analytische Chemie, Ruhr-Universität Bochum,
D-44780 Bochum, Germany

Received July 20, 1998

Keywords: Arsenic / Methylcycloarsoxane / Ruthenium / Platinum / Macrocyclic ligands

Reaction of *cyclo*-$(CH_3AsO)_n$ with $MCl_3 \cdot x\ H_2O$ in acetonitrile at 100 °C affords $[MCl_2\{cyclo\text{-}(CH_3AsO)_8\}]$ [M = Ru (**1**), M = Os (**2**)] in which cyclooctamers $(CH_3AsO)_8$ are stabilised in a $\kappa^4As^{1,3,5,7}$ binding mode in the equatorial coordination sphere of the Group 8 metals. In contrast treatment of K_2PtCl_4 with alternatively $AgNO_3$ or Ag_2CO_3 and *cyclo*-$(CH_3AsO)_n$ at 100 °C in the same solvent leads to the formation of respectively octa- or decanuclear cagelike ligands in $[Pt_2\{[cyclo\text{-}(As[CH_3]OAs[NC(O)CH_3]O)_2]_2\}]$ (**3**) and $[Pt_2\{[\{CH_3C(O)N\}_2As_5(CH_3)_5O_4]_2\}]$ (**4**) by metal-assisted reactions between *cyclo*-$(CH_3AsO)_n$ and acetonitrile. λ^5-As^{III} atoms in these complexes participate in square-planar Pt^{II} coordination and themselves exhibit distorted trigonal bipyramidal coordination geometries.

Introduction

Although $(CH_3AsO)_n$ was synthesised some 140 years ago by A. von Baeyer[1] as the first example of an alkylcycloarsoxane, it is only in the past decade that the potential of this class of compounds as ambidentate macrocyclic ligands has been recognised and exploited[2]. Both mesityl- and methylcycloarsoxane have been crystallised as cyclic tetramers $(RAsO)_4$ and characterised by X-ray structural analysis[3][4]. In contrast to this apparent preference for the tetrameric form in the solid state, ^{1}H-NMR investigations have demonstrated that $(CH_3AsO)_n$ and $(C_2H_5AsO)_n$ are present as a mixture of cyclic oligomers ($n = 2-5$) in solution[5][6][7] for which the nuclearities $n = 3$ and 4 predominate. The dynamic equilibria between such cyclic ionophores can be influenced by the addition of alkali metal cations. Whereas Na^+ cations stabilise the crown shaped cyclic tetramer in $[Na\{cyclo\text{-}(C_2H_5AsO)_4\text{-}\kappa^4O\}_2]SCN$, employment of larger cations allows the isolation of pentagonal antiprismatic sandwich units in compounds of the type $[M\{cyclo\text{-}(C_2H_5AsO)_5\text{-}\kappa^5O\}_2]X$ ($M = K^+$, NH_4^+, Cs^+)[8][9].

The presence of an alternative set of *soft* As donor atoms coupled with their apparent low energy barriers to ring contraction or expansion in organic solvents suggests that the alkylcycloarsoxanes should also be capable of exhibiting a rich variety of binding modes in the coordination spheres of transition metals. Indeed, the metal-mediated ring expansion from the predominate cyclic trimers and tetramers to hexameric $(RAsO)_6$ has been confirmed for the carbonyl transition metal complexes $[\{M(CO)_3\}_2\{\mu\text{-}[cyclo\text{-}(RAsO)_6]\}]$ (M = Mo; R = CH_3[10], C_2H_5[12]; M = Cr, W; R = C_2H_5[7]) and $[\{ReBr(CO)_2\}_2\{\mu\text{-}[cyclo\text{-}(C_2H_5AsO)_6]\}]$[11], in which the metal atoms are facially coordinated by the upper or lower three As atoms of a flattened As_6O_6 cuboctahedron. An analogous $\kappa^3As^{1,3,5}$ mode has also recently been established in the mononuclear complexes $[RuCl_2\{cyclo\text{-}(C_2H_5AsO)_6\}]$ and $[RhCl_3\{cyclo\text{-}(C_2H_5AsO)_6\}]$[11]. Analysis of the molecular geometry of the alkylcycloarsoxanes indicates that, whereas $(RAsO)_6$ cuboctahedra should be capable of facial coordination of a transition metal fragment such as $M(CO)_3$ with a minimum of conformational change, severe ring strain would clearly be introduced in the case of $(RAsO)_3$. Extension of these geometrical arguments leads to the prediction that fourfold equatorial coordination of a transition metal should best be achieved by the $\kappa^4As^{1,3,5,7}$ mode of a cyclooctamer $(RAsO)_8$. Such oligomers are previously unknown as either isolated or coordinated species and have also not been detected in solutions of alkylcycloarsoxanes[5][6][7].

We now report our studies on the reactions of $MCl_3 \cdot H_2O$ (M = Ru, Os) and K_2PtCl_4 with $(CH_3AsO)_n$ in acetonitrile at 100 °C, which we believed might enable the stabilisation of $(CH_3AsO)_8$ in the octahedral coordination spheres of M^{II} (obtained by reduction of $MCl_3 \cdot H_2O$) or the square-planar coordination sphere of Pt^{II}.

Results

$[RuCl_2\{cyclo\text{-}(CH_3AsO)_8\}]$ (**1**) and $[OsCl_2\{cyclo\text{-}(CH_3AsO)_8\}]$ (**2**) are isostructural and contain unprecedented cyclooctamers $(CH_3AsO)_8$ that are stabilised in the equatorial coordination plane of the Group 8 transition metals. The required reduction of M^{III} in the starting compounds $MCl_3 \cdot x\ H_2O$ (M = Ru, Os) to M^{II} in **1** and **2** is accompanied by ligand cleavage and oxidation to $CH_3AsO(OH)_2$, which can be isolated from the filtrate of

 © WILEY-VCH Verlag GmbH, D-69451 Weinheim, 1998 1434–1948/98/1212–1999 $ 17.50+.50/0

the final reaction mixture. Inspection of the As−Os−As angles [average values 90(1) and 177.4(2)°] and Os−As distances [2.400(3) Å] for the Os^{II} octahedral complex **2** depicted in Figure 1 confirm the suitability of the very flexible 16-membered As_8O_8 macrocycle for its adopted $\kappa^4As^{1,3,5,7}$ coordination mode. Similar average As−M−As angles [90(1) and 177.5(2)°] and M−As distances [2.400(4) Å] are found in the isostructural Ru^{II} complex **1**. As−O distances to the coordinated arsenic atoms As1, As3, As5, and As7 are on average [**1**, 1.758(7); **2**, 1.75(1) Å] shorter than those to the remaining non-coordinated Group 15 atoms [**1**, 1.799(7); **2**, 1.79(1) Å]. A concomitant widening of the O−As−O angles for the former atoms is apparent [**1**, 99.7(4)° vs. 97.0(2)°; **2**, 99.9(7)° vs. 97.4(8)°].

Figure 1. Molecular structure of $[OsCl_2\{cyclo\text{-}(CH_3AsO)_8\}]$ (**2**) viewed from above the equatorial $OsAs_4$ coordination plane

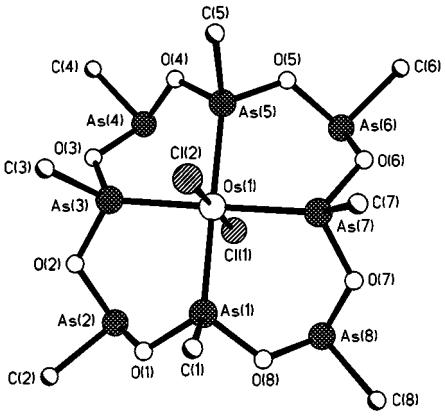

1 and **2** exhibit approximately C_{4V} molecular symmetry in which both the coordinating arsenic atoms and their non-coordinating O and As neighbours all effectively belong to common planes. For instance, whereas the former atoms are sited at ± 0.006 Å from the equatorial Ru^{II} coordination plane in **1**, the remaining arsenic atoms As2, As4, As6, and As8 display alternating deviations of ± 0.107 Å from the second As_4 plane of an As_8O_8 "double crown" (Figure 2). This conformation of the 16-membered macrocycle is characterised by a torsion angle pattern of the type $(a, b, -b, -a)_4$, in which the absolute value of *a* varies between 104.5(4) and 124.3(5)° in **1** [105.0(9) and 124.6(9)° in **2**] that of *b* between 59.5(5) and 75.0(4)° [58.7(9) and 74.7(9)° in **2**].

Figure 2. Molecular structure of $[RuCl_2\{cyclo\text{-}(CH_3AsO)_8\}]$ (**1**) viewed from the side

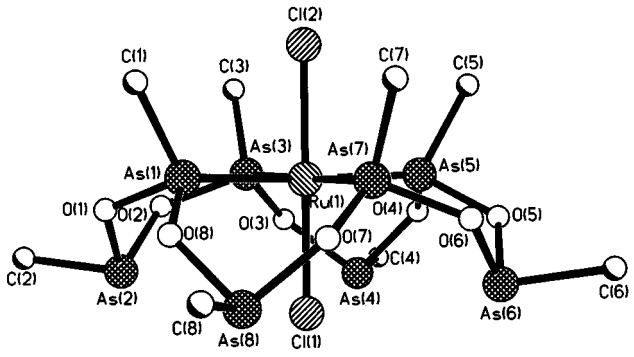

As mentioned in the Introduction previous examples of metal-mediated ring expansion for alkylcycloarsoxanes have been restricted to cyclopentamers and -hexamers. However we have recently investigated the analogous reaction of $MCl_3 \cdot H_2O$ (M = Ru, Os) with *cyclo*-$(C_2H_5AsS)_n$ in toluene[12], which leads to the assembly of the novel macrocyclic hexadentate ligand $[(C_2H_5)_6As_8S_{10}]^{2-}$ in the octahedral coordination spheres of Ru^{II} and Os^{II} at temperatures of 105 and 140°C, respectively. In contrast to the cyclooctamers $(CH_3AsO)_8$ reported in the present work, two alkyl substituents of the potential macrocyclic ligand $(C_2H_5AsS)_8$ are replaced by terminal thiolate sulphurs in $[(C_2H_5)_6As_8S_{10}]^{2-}$. These *soft* donor atoms then occupy *cis*-sited positions in the resulting transition metal coordination spheres. Contrasting small As−Os−S angles of 80.5(2) and 82.3(3)° in the five-membered chelate rings of $[Os\{(C_2H_5)_6As_8S_{10}\}]$ and large As−Os−As angles of 101.2(1) and 100.5(1)° in the six-membered chelate rings of this complex reflect a pronounced deviation from an idealised octahedral geometry.

Macrocyclic Cleavage Products

The apparent suitability of $(CH_3AsO)_8$ for $\kappa^4As^{1,3,5,7}$ equatorial coordination of transition metals prompted us to investigate whether this cyclooctamer can also be stabilised in the square-planar coordination sphere of Pt^{II}. However, we were unable to isolate methylcycloarsoxane complexes by treatment of Pt^{II} with $(CH_3AsO)_n$, following initial precipitation of chloride ions in K_2PtCl_4 as AgCl. In contrast, the direct reaction of K_2PtCl_4 with $AgNO_3$ or alternatively Ag_2CO_3 and $(CH_3AsO)_n$ in acetonitrile at 100°C in a Carius tube did lead to the stabilisation of macrocyclic octa- and decanuclear As-O ligands, albeit as metal-mediated cleavage products of the original methylcycloarsoxane. Two dimeric Pt^{II} complexes, $[Pt_2\{[cyclo\text{-}(As[CH_3]OAs[NC(O)CH_3]O)_2]_2\}]$ (**3**) and $[Pt_2\{[\{CH_3C(O)N\}_2As_5(CH_3)_5O_4]_2\}]$ (**4**) were isolated in relatively low yields (ca. 25%) under such conditions, depending on the molar ratio of the starting materials. For instance, whereas a 2:3:4 stoichiometric ratio of $K_2PtCl_4/Ag_2CO_3/(CH_3AsO)_n$ (for n = 1) affords **3**, the arsenic-richer complex **4** can be generated by increasing the $(CH_3AsO)_n$ content of the starting mixture (molar ratio 2:3:6). An increased Pt/As relationship is required in the presence of $AgNO_3$ [e.g. a $K_2PtCl_4/AgNO_3/(CH_3AsO)_n$ molar ratio of 1:3:6 for **3**] to compensate for the partial oxidation of $(CH_3AsO)_n$ to $CH_3As(O)(OH)_2$ by NO_3^- anions under such conditions. The red crystal sheafs could be separated without difficulty in each case in a manual fashion from precipitated AgCl. To our surprise both compounds contained novel octadentate anionic ligands, that result from metal-assisted reactions between $(CH_3AsO)_n$ and acetonitrile. The role of Ag^+ cations in directing ligand construction still remains unclear.

As depicted in Figures 3 and 4, the solvent molecules are converted into acetamido $[CH_3C(O)N]$ building units, whose trigonal planar amide nitrogens (N1−N4 in **3**; N1,

Figure 3. Molecular structure of $[Pt_2\{[cyclo\text{-}(As[CH_3]OAs[NC(O)CH_3]O)_2]_2\}]$

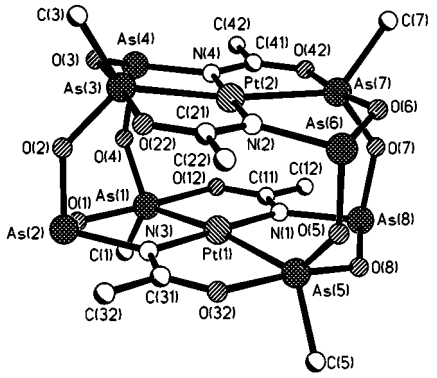

Figure 4. Molecular structure of $[Pt_2\{[\{CH_3C(O)N\}_2As_5(CH_3)_5O_4]_2\}]$

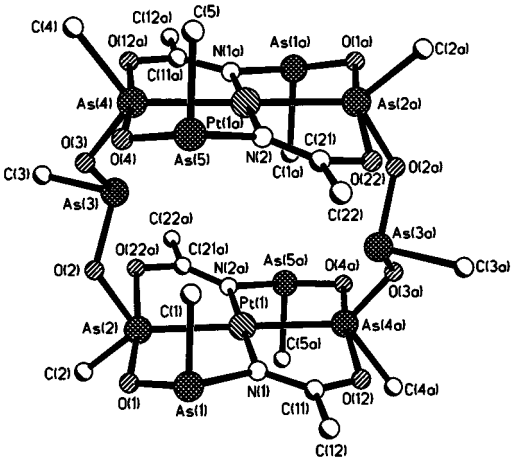

N2 and C_i symmetry-related atoms in **4**) are bonded to both Pt^{II} and As^{III} atoms. Refinements of alternative structural models, in which the positions of the N and O atoms in all four such moieties are exchanged (model 2 in Figure 5), led in both cases to significant deterioration in the R and wR_2 values. The latter reliability index increases on going from model 1 to model 2 from 0.144 to 0.147 for **3** and from 0.118 to 0.121 for **4** under these circumstances. Structural corroboration of the chosen atom assignments in the macrocyclic As-O ligands of **3** and **4** is provided by the short *trans* sited N−Pt distances [average values: **3**, 2.04(2); **4**, 2.03(1) Å] and the very long coordinative axial O→As distances [average values: **3**, 2.20(2); **4**, 2.27(2) Å], whose values would be most unreasonable for a possible alternative formulation as O→Pt and N−As bonds (model 2). The respectively octa- and decanuclear ligands in these complexes may be regarded as being composed of the monomeric units shown in Figure 6. These are linked into dimers through the weak dative O→As interactions already discussed. Eight-membered As_4O_4 rings can be identified for **3**, As_5O_4 chains for **4**. The average C−O, C−N and C−C distances of 1.26(2), 1.32(3) and 1.48(3) Å in the $[CH_3C(O)N]$ units of **3** are similar to the values found for the analogous moieties in **4** [1.30(4), 1.30(4), 1.50(4) Å].

Figure 5. Alternative structural models 1 and 2 for the $[CH_3C(O)N]$ building units in **3**

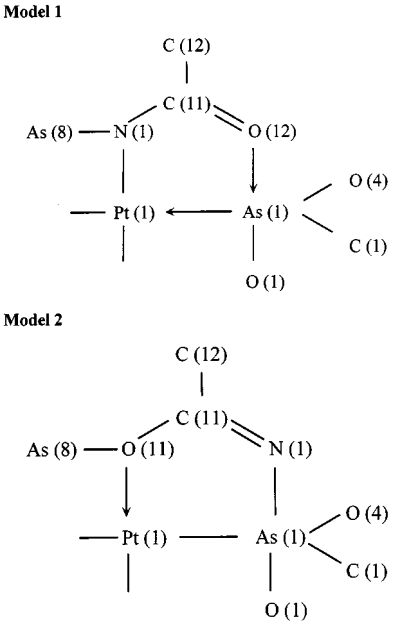

Figure 6. Monomeric units in the macrocyclic ligands of $[Pt_2\{[cyclo\text{-}(As[CH_3]OAs[NC(O)CH_3]O)_2]_2\}]$ (**3**) and $[Pt_2\{[\{CH_3C(O)N\}_2As_5(CH_3)_5O_4]_2\}]$ (**4**)

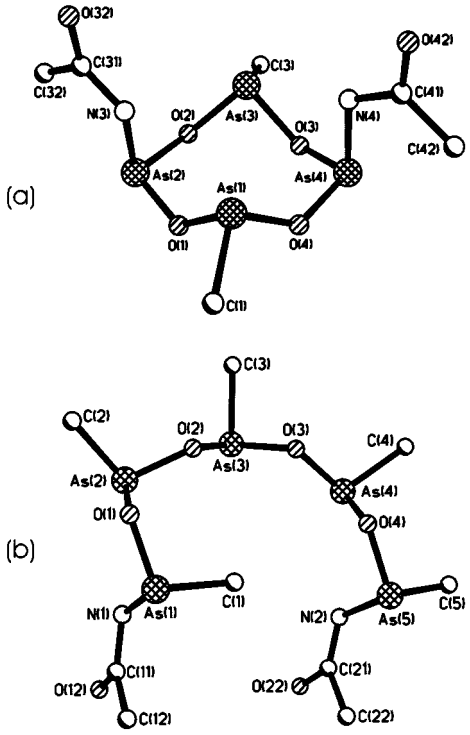

The Pt^{II} atoms in both complexes exhibit square-planar As_2N_2 coordination spheres with donor atoms of the same type sited *trans* to one other. Their separation increases from 3.01(1) to 5.49(1) Å on going from **3** to **4**, a state of affairs that is reflected in a concomitant marked decrease in density $D_{calcd.}$ from 3.226 to 2.679 g cm^{-3}. Four of the arsenic atoms in **3** [As2, As4, As6, As8] and six such atoms

in **4** [As1, As3, As5, and C_i symmetry related atoms] display typical ψ-tetrahedral coordination geometries.

Trigonal Bipyramidal Coordination of As^{III}

The remaining arsenic atoms in **3** and **4** participate in Pt^{II} coordination and themselves exhibit unique distorted trigonal bipyramidal coordination geometries. Average bond lengths and angles to these λ^5-As atoms are summarised in Table 1. As^{III} can be regarded as a weak Lewis acid in its trihalides AsX_3 and its ability to extend its coordination number to 4 (ψ-trigonal bipyramidal), 5 (ψ-octahedral), and even 6 (octahedral) is now structurally well documented for such compounds[13][14][15]. A similar tendency to participate in secondary bonds has also been reported for $As^{III}O_3$ units, e.g. O···As interactions of length 2.68 Å in $Ba_2As_6O_{11}$[16]. A characteristic property of organoarsenic(III) compounds is, of course, their pronounced Lewis basicity and examples of their dative As→M bonds (M = metal), in which the As^{III} atoms display a tetrahedral coordination geometry, are myriad. In contrast, to our knowledge, **3** and **4** provide to first examples of As^{III} atoms in a trigonal bipyramidal coordination environment, i.e. of trivalent arsenic behaving simultaneously as a Lewis base and Lewis acid. An analysis of the bond distances in **3** and **4** indicates that the possible alternative assignment of the oxidation state IV to the λ^5-As atoms would be inappropriate. For instance the axial donor O→As interactions involving the acetamino units are much weaker than the opposite As(O)−As bonds (Table 1). This state of affairs manifests itself in the pronounced distortion of the trigonal bipyramidal coordination spheres of the λ^5-As atoms towards the tetrahedra, that are characteristic for organoarsenic(III) complexes. The degree of distortion in **3** may be gauged from the displacements Δ of 0.179−0.203 Å for the λ^5-As atoms from the planes of their equatorial substituents towards the axial acetamido O atoms. Δ increases on going from **3** to **4** (As2 0.2320 Å, As4 0.2620 Å).

Table 1. Average bond lengths [Å] and angles [°] to the trigonal bipyramidal λ^5-As atoms in **3** and **4** (ax = axial, eq = equatorial)

	3	**4**
As−Pt	2.387(6)	2.382(1)
As−C	1.90(2)	1.93(3)
$As-O_{eq}$	1.741(6)	1.772(9)
$As-O_{ax}(As)$	1.834(6)	1.82(2)
$As-O_{ax}(C)$	2.20(2)	2.27(2)
Pt−As−C	128(2)	128.4(9)
$Pt-As-O_{eq}$	127.3(8)	122(2)
$C-As-O_{eq}$	102(1)	104.9(8)
$Pt-As-O_{ax}(As)$	99.5(6)	101.8(6)
$Pt-As-O_{ax}(C)$	87.0(2)	85.7(1)
$(As)O_{ax}-As-O_{ax}(C)$	173.3(6)	172.4(4)

Our present work demonstrates that the previously unknown cyclooctamers $(CH_3AsO)_8$ can be stabilised in the equatorial coordination plane of transition metals. At elevated temperatures, cleavage and metal-mediated reaction with solvent acetonitrile can afford novel cagelike multidentate ligands. The presence of silver cations (as provided by $AgNO_3$ or Ag_2CO_3) to remove chloride ions as AgCl is a necessary prerequisite for the construction of the respectively octa- and decanuclear ligands in **3** and **4**.

Experimental Section

All manipulations were performed in an Ar atmosphere in carefully dried solvents. − FAB MS: Fisons VG Autospec with 3-nitrobenzyl alcohol as matrix. − FTIR: Perkin-Elmer 1760X. − Elementary analyses: Carbo Erba 1106 (for **3** and **4**) and Mikroanalytisches Labor Beller, Göttingen (for **1** and **2**). − *cyclo*-$(CH_3AsO)_n$ was prepared by alkaline hydrolysis[7] of CH_3AsCl_2.

[RuCl₂{cyclo-(CH₃AsO)₈}] (**1**): $RuCl_3 \cdot x\ H_2O$ (21 mg, 0.1 mmol) was combined in a Carius tube (Duran glass, medium-walled 4 mm, diameter 16 mm, length 12 cm, volume approximately 10 cm^3) with *cyclo*-$(CH_3AsO)_n$ (106 mg, 1.0 mmol for $n = 1$) dissolved in 1.5 ml of acetonitrile. The tube was flame sealed, heated to 100°C over 40 h and allow to cool slowly to room temperature over a further 80 h. After opening, the solid state product was filtered off and washed with acetonitrile to afford yellow **1**. Yield 72.4 mg (71%). − $C_8H_{24}As_8Cl_2O_8Ru$ (1019.6): calcd. C 9.4, H 2.4, As 58.8; found C 9.4, H 2.3, As 58.8. − FAB-MS [*m*/*z* (%)]: 482(1) $[As_5Me_4O_3]^+$, 395(4) $[As_4Me_2O_4]^+$, 329(10) $[As_4Me_2]^+$, 289(13) $[As_3MeO_3]^+$, 259(16) $[As_2Me_3O_4]^+$. − IR (KBr): $\tilde{\nu}$ = 2999 cm^{-1} (w), 2907 (w), 830 (s), 803 (s), 773 (s), 684 (s), 623 (m), 584 (s), 526 (s, br).

[OsCl₂{cyclo-(CH₃AsO)₈}] (**2**): $OsCl_3 \cdot x\ H_2O$ (31 mg, 0.1 mmol) and *cyclo*-$(CH_3AsO)_n$ (106 mg, 1.0 mmol for $n = 1$) were heated in 1.5 ml of acetonitrile in a Carius tube with the similar temperature programme as for **1**. Yield 74.3 mg of yellow **2** (67%). − $C_8H_{24}As_8Cl_2O_8Os$ (1108.7): calcd. C 8.7, H 2.2, As 54.0; found C 8.6, H 2.1, As 53.9. − FAB-MS [*m*/*z* (%)]: 482(2) $[As_5Me_4O_3]^+$, 395(5) $[As_4Me_2O_4]^+$, 329(12) $[As_4Me_2]^+$, 289(13) $[As_3MeO_3]^+$, 259(22) $[As_2Me_3O_4]^+$. − IR (KBr): $\tilde{\nu}$ = 3001 cm^{-1} (m), 2907 (m), 829 (s), 773 (s), 683 (s), 628 (s), 584 (s), 528 (s, br).

[Pt₂{[cyclo-(As[CH₃]OAs[NC(O)CH₃]O)₂]₂}] (**3**): K_2PtCl_4 (105 mg, 0.25 mmol), $AgNO_3$ (127 mg, 0.75 mmol), and *cyclo*-$(CH_3AsO)_n$ (159 mg, 1.50 mmol for $n = 1$) were heated to 100°C in 1.5 ml of acetonitrile over a period of 16 h in a sealed Carius tube. After cooling to room temperature over 80 h the tube was opened and the sheafs of red crystals of **3** separated manually from precipitated AgCl. Yield after washing 34.2 mg (26%). − $C_{12}H_{24}As_8N_4O_{12}Pt_2$ (1405.9): calcd. C 10.2, H 1.7, N 4.0; found C 9.3, H 1.4, N 3.6. − FAB-MS [*m*/*z* (%)]: 329(13) $[As_4Me_2]^+$, 289(14) $[As_3MeO_3]^+$. − IR (KBr): $\tilde{\nu}$ = 3011 (w), 2920 (w), 1516 (s), 1385 (s), 1029 (m), 820 (s), 781 (s), 679 (m), 628 (m), 597 (m), 477 (s).

[Pt₂{[{CH₃C(O)N}₂As₅(CH₃)₅O₄]₂}] (**4**): K_2PtCl_4 (206 mg, 0.50 mmol), Ag_2CO_3 (208 mg, 0.75 mmol), and *cyclo*-$(CH_3AsO)_n$ (159 mg, 1.50 mmol for $n = 1$) were heated to 100°C in 1.5 ml of acetonitrile with the similar temperature programme as for **3**. After cooling to room temperature the tube was opened and the sheafs of red crystals of **4** separated manually from precipitated AgCl. Yield after washing 33.0 mg (25%). − $C_{18}H_{42}As_{10}N_4O_{12}Pt_2$ (1645.9): calcd. C 13.1, H 2.6, N 3.4; found C 12.8, H 2.4, N 3.1. − FAB-MS [*m*/*z* (%)]: 603(1) $[As_4Me_4O_3Pt]^+$, 498(2) $[As_5Me_4O_4]^+$, 482(2) $[As_5Me_4O_3]^+$, 345(10) $[As_2Pt]^+$, 329(11) $[As_4Me_2]^+$, 289(13) $[As_3MeO_3]^+$. − IR (KBr): $\tilde{\nu}$ = 3001 (w), 2965 (w), 1499 (s), 1402 (s), 1231 (w), 1022 (w), 792 (m), 763 (m), 731 (s), 698 (s), 567 (m), 511 (m).

X-ray Structural Analyses: Siemens P4 diffractometer, graphite monochromator, Mo-K_α radiation (λ = 0.71073 Å), SHELXS-86[17] for structure solution by direct methods and SHELXL-93[18] for refinement by full-matrix least squares. Semi-empirical absorption corrections were applied to the intensity data by use of ψ scans. Hydrogen atoms were included at calculated positions[19].

1: $C_8H_{24}As_8Cl_2O_8Ru$, M = 1019.6, monoclinic, space group $P2_1/c$, a = 11.777(2), b = 15.600(3), c = 14.404(3) Å, β = 97.71(3)°, V = 2622.4(9) Å^3, Z = 4, $D_{calcd.}$ = 2.583 g cm^{-3}, μ = 10.85 mm^{-1}. Crystal size 0.34 × 0.50 × 0.70 mm; ω-scan, scan range: $2\theta \leq 50°$ ($0 \leq h \leq 14$, $0 \leq k \leq 18$, $-17 \leq l \leq 16$), 4573 symmetry independent reflections from 4806 collected (R_{int} = 0.030), max./min. transmission: 0.023/0.006; 252 parameters refined; R = 0.041 [$I > 2\sigma(I)$], wR_2 = 0.096 [all reflections], S = 1.05; $\Delta\rho_{max}$ = 0.85 eÅ^{-3}, $\Delta\rho_{min}$ = −0.87 eÅ^{-3}.

2: $C_8H_{24}As_8Cl_2O_8Os$, M = 1108.7, monoclinic, space group $P2_1/c$, a = 11.778(2), b = 15.559(3), c = 14.439(3) Å, β = 97.59(3)°, V = 2622.8(9) Å^3, Z = 4, $D_{calcd.}$ = 2.808 g cm^{-3}, μ = 15.11 mm^{-1}. Crystal size 0.38 × 0.50 × 0.50 mm; ω-scan, scan range: $2\theta \leq 47.5°$ ($0 \leq h \leq 13$, $0 \leq k \leq 17$, $-16 \leq l \leq 16$), 3966 symmetry independent reflections from 4162 collected (R_{int} = 0.048), max./min. transmission: 0.023/0.006; 252 parameters refined; R = 0.048 [$I > 2\sigma(I)$], wR_2 = 0.124 [all reflections], S = 1.03; $\Delta\rho_{max}$ = 1.04 eÅ^{-3}, $\Delta\rho_{min}$ = −1.26 eÅ^{-3}.

3: $[Pt_2\{[cyclo\text{-}(As[CH_3]OAs[NC(O)CH_3]O)_2]_2\}]$, M = 1405.9, monoclinic, space group $P2_1/n$, a = 11.638(2), b = 13.110(3), c = 19.781(4) Å, β = 106.46(4)°, V = 2894.4(10) Å^3, Z = 4, $D_{calcd.}$ = 3.226 g cm^{-3}, μ = 18.79 mm^{-1}. Crystal size 0.40 × 0.40 × 0.44 mm; ω-scan, scan range: $2\theta \leq 50°$ ($0 \leq h \leq 13$, $0 \leq k \leq 15$, $-23 \leq l \leq 22$), 5064 symmetry independent reflections from 5315 collected (R_{int} = 0.073), max./min. transmission: 0.256/0.156; 331 parameters refined; R = 0.055 [$I > 2\sigma(I)$], wR_2 = 0.144 [all reflections], S = 1.05; $\Delta\rho_{max}$ = 2.53 eÅ^{-3}, $\Delta\rho_{min}$ = −2.14 eÅ^{-3}.

4: $[Pt_2\{[\{CH_3C(O)N\}_2As_5(CH_3)_5O_4]_2\}]$, M = 1645.9, monoclinic, space group $P2_1/n$, a = 10.356(2), b = 12.801(3), c = 15.410(3) Å, β = 92.93(3)°, V = 2040.2(7) Å^3, Z = 2, $D_{calcd.}$ = 2.679 g cm^{-3}, μ = 14.95 mm^{-1}. Crystal size 0.30 × 0.32 × 0.46 mm; ω-scan, scan range: $2\theta \leq 45°$ ($0 \leq h \leq 11$, $0 \leq k \leq 13$, $-16 \leq l \leq 16$), 2616 symmetry independent reflections from 2791 collected (R_{int} = 0.032), max./min. transmission: 0.016/0.006; 215 parameters refined; R = 0.046 [$I > 2\sigma(I)$], wR_2 = 0.119 [all reflections], S = 1.02; $\Delta\rho_{max}$ = 0.93 eÅ^{-3}, $\Delta\rho_{min}$ = −1.01 eÅ^{-3}.

[1] A. von Baeyer, *Ann. Chem.* **1858**, *107*, 279.
[2] W. S. Sheldrick, I. M. Müller, *Coord. Chem. Rev.* **1998**, in press.
[3] A. M. Arif, A. H. Cowley, M. Pakulski, *J. Chem. Soc., Chem. Commun*. **1987**, 165.
[4] A.-J. DiMaio, A. L. Rheingold, *Organometallics* **1991**, *10*, 3764.
[5] H. C. Marsmann, J. R. van Wazer, *J. Am. Chem. Soc*. **1970**, *92*, 3969.
[6] M. Durand, J.-P. Laurent, *J. Organomet. Chem*. **1974**, *77*, 225.
[7] W. S. Sheldrick, T. Häusler, *Z. Naturforsch. Teil B* **1993**, *48*, 1069.
[8] W. S. Sheldrick, T. Häusler, *Z. Anorg. Allg. Chem*. **1993**, *619*, 1984.
[9] T. Häusler, W. S. Sheldrick, *Chem. Ber*. **1997**, *130*, 371.
[10] A. L. Rheingold, A.-J. DiMaio, *Organometallics* **1986**, *5*, 393.
[11] T. Häusler, W. S. Sheldrick, *Z. Naturforsch. Teil B* **1997**, *52*, 679.
[12] T. Häusler, W. S. Sheldrick, *Chem. Ber*. **1996**, *129*, 131.
[13] W. S. Sheldrick, H.-J. Häusler, *Angew. Chem*. **1987**, *99*, 1184; *Angew. Chem. Int. Ed. Engl*. **1987**, *26*, 1172.
[14] W. S. Sheldrick, C. Horn, *Z. Naturforsch. Teil B* **1989**, *44*, 405.
[15] S. Grewe, T. Häusler, M. Mannel, B. Rossenbeck, W.S. Sheldrick, *Z. Anorg. Allg. Chem*. **1998**, *624*, 613.
[16] W. S. Sheldrick, H.-J. Häusler, *Z. Anorg. Allg. Chem*. **1986**, *538*, 45.
[17] G. M. Sheldrick, SHELXS-86, *Acta Crystallogr. Sect. A*. **1990**, *46*, 467.
[18] G. M. Sheldrick, *SHELXL-93*, Universität Göttingen, **1993**.
[19] Crystallographic data (excluding structure factors) for the structures reported in this paper have been deposited with the Cambridge Crystallographic Data Centre. Copies of the data (deposition numbers 102190 − 102193) may be obtained free of charge on application to the Director, CCDC, 12 Union Road, Cambridge CB2 1EZ, UK (fax: int. Code + 44 (0)1223/ 336-033, e-mail: deposit@chemcrys.cam.ac.uk).

[I98239]

Chemistry of 2*H*-Azaphosphirene Complexes, 13[◇]

Phosphorus-Bridged Dinuclear Tungsten Amino(aryl)carbene Complexes – New Precursors for (2*H*-Azaphosphirene)tungsten Complexes bearing a σ-P-Bonded Cp* Group☆

Rainer Streubel*, Udo Rohde, Jörg Jeske, Frank Ruthe, and Peter G. Jones

Institut für Anorganische und Analytische Chemie der Technischen Universität Braunschweig,
Postfach 3329, D-38023, Braunschweig, Germany
Fax: (internat.) + 49(0)531/391-5387
E-mail: r.streubel@tu-bs.de

Received June 27, 1998

Keywords: Carbene complexes / Tungsten / Phosphorus / 2*H*-Azaphosphirene complexes / Cyclization

The first syntheses of pentacarbonyl[2-(pentamethyl-2,4-cyclopentadien-1-yl)-2*H*-azaphosphirene]tungsten complexes are reported, using a one-pot reaction of dichloro(pentamethyl-2,4-cyclopentadien-1-yl)phosphane (Cp^*PCl_2) with triethylamine and {[amino(aryl)carbene]pentcarbonyltungsten(0)}. [Pentamethyl-2,4-cyclopentadien-1-yl]phosphanediyl-bridged dinuclear carbene complexes are formed as long-lived intermediates, which, by elimination and rearrangement reactions, led to the final products. If traces of water were present, then by-products were formed; in one case, a dinuclear carbene complex with a P(Cp*)–O–P(Cp*) bridging unit was isolated. Under ordinary reaction conditions 2*H*-azaphosphirene complexes are slowly transformed into {pentacarbonyl[chloro(pentamethyl-2,4-cyclopentadien-1-yl)phosphane]tungsten(0)}. NMR-spectroscopic and single-crystal X-ray structural data of some dinuclear carbene complexes and 2-(pentamethyl-2,4-cyclopentadien-1-yl)-2*H*-azaphosphirene complexes are presented.

The chemistry of (2*H*-azaphosphirene)tungsten complexes has recently been the subject of increased interest, because of their widespread applicability in the synthesis of three-,[2] four-[3] and five-membered[4] heterocycles. Therefore, our interest in further synthetic investigations was enhanced, and one of our most important aims was to develop a new access to 2*H*-azaphosphirene complexes using amino(aryl)carbene complexes, a base and dichloro(organo)phosphanes. Compared to [bis(trimethylsilyl)methylene]chlorophosphane, which was used in our initial synthetic approach,[5] the advantages should be: the ease of accessibility, the option of introducing *P*-functional groups into 2*H*-azaphosphirene complexes and the potential extension of this method to condensation reactions of other dichloro(organo)element compounds of group-15 elements. Furthermore, in order to mimic the bulkyness of the bis(trimethylsilyl)methyl substituent, which is useful for kinetic stabilization, we chose pentamethyl-2,4-cyclopentadien-1-yl (denoted hereafter as Cp*) and the corresponding dichlorophosphane,[6] Cp^*PCl_2.

Our first attempts to treat amino(aryl)carbene complexes **1a**, **b**,[7] **c**,[8] **d**, **e**[7] with Cp^*Cl_2 (**2**) at ambient temperature in ether with an excess of triethylamine failed. Therefore, we switched to the more polar solvent dichloromethane for the reactions reported hereafter. According to ^{31}P-NMR-spectroscopic investigations, the first condensation step and subsequent transformations (paths **a** and **b**) must have occurred very fast, because the mono-condensation products **3** could not be detected. Instead, the first products formed in these reactions were the (Cp*-phosphanediyl)-bridged dinuclear (carbene)metal complexes **4a**–**e**, aside with small amounts of the 2*H*-azaphosphirene complexes **6a**–**e** and complex **7**. **4a**–**e** were most probably formed, according to the two pathways **a**, **b** depicted in Scheme 1. Path **a** describes a further condensation, yielding **4a**–**e**, whereas a base-induced hydrogen chloride elimination, followed by addition of one equivalent of **1** to the short-lived intermediates **5** (cf. ref.[9]), would also explain the generation of the complexes **4a**–**e** (path **b**). Interestingly, upon prolonged reaction, complexes **4a**–**e** eliminated **1** yielding the 2*H*-azaphosphirene complexes **6a**–**e**, probably by unspecified rearrangements of **5**; this elimination reaction has been proven for the case of **4c** by treating a pure sample of **4c** with triethylamine yielding **6c**. We observed that one of the factors that limited the yields of **6a**–**e** was the rate of the reaction of complexes **6a**–**e** with triethylammonium chloride, which led to [{Cp*P(H)Cl}$W(CO)_5$] (**7**) in all cases (Scheme 1). This latter reaction was found to depend strongly on the nature of the *para*-phenyl substituent, the concentration and, most importantly, on the reaction temperature. Therefore, the temperature had to be kept between 0 and 18°C throughout the reactions and subsequent manipulations. Apart from complexes **4a**–**e**, **6a**–**e** and **7**, two other unidentified products (amounts < 5%) were formed transi-

[◇] Part 12: See ref.[1].

 © WILEY-VCH Verlag GmbH, D-69451 Weinheim, 1998 1434–1948/98/1212–2005 $ 17.50+.50/0

ently; e.g. after generating complex **4c** by treating two equivalents of complex **1c** with one equivalent of **2**, ^{31}P-NMR signals appeared at δ = 42.1 [d, ^{1}J(P,H) = 503.0 Hz] and δ = 28.2 [d, ^{1}J(P,H) = 511.0 Hz]. Based on these ^{31}P-NMR-spectroscopic observations, we tentatively assign these resonances to products with $\sigma^4\lambda^5$-PH-functional structural units, which could arise from hydrogen-shift reactions from the nitrogen to the phosphorus atom in **4c**.

Scheme 1. Proposed reaction course for the formation of metal complexes **4a−g**, **6a−g** and **7**

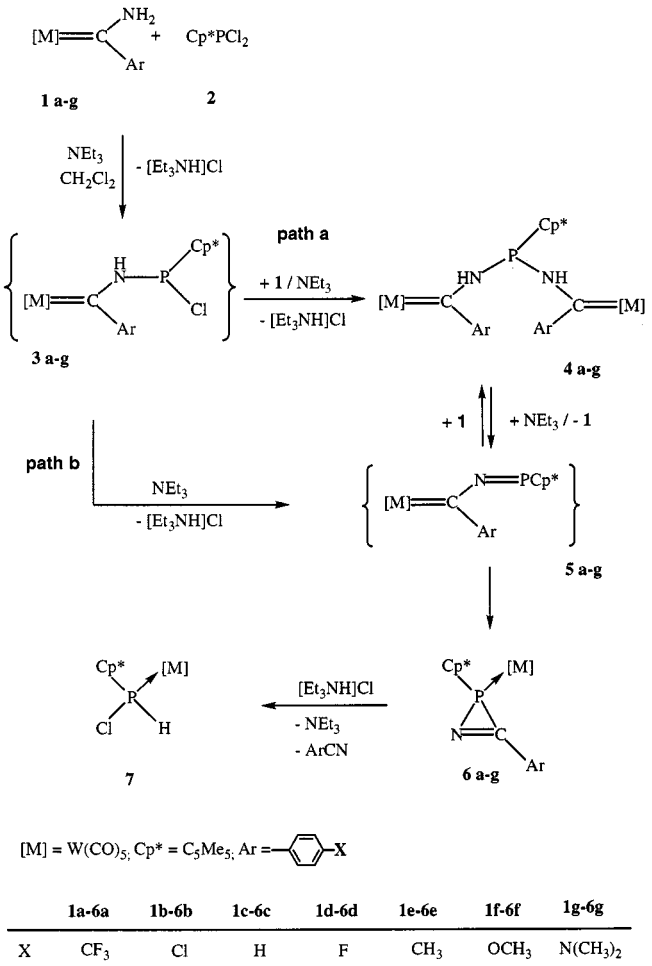

	1a-6a	1b-6b	1c-6c	1d-6d	1e-6e	1f-6f	1g-6g
X	CF_3	Cl	H	F	CH_3	OCH_3	$N(CH_3)_2$

If reactions of **1** with **2** were carried out in the presence of traces of water, other products were formed; in the reaction of **1c** with **2**, we were able to isolate the dinuclear (carbene)metal complex **8** (Scheme 2) having the P(Cp*)−O−P(Cp*) instead of the P(Cp*) bridging unit. This P−O−P bridge most probably resulted from a condensation reaction of two transiently formed (carbene)metal complexes, one having a PCl- and the other a POH-functional group.

Although all complexes described herein have been separated and purified by low-temperature column chromatography and crystallization, we were unable to obtain exact elemental analyses, for reasons that are unclear. Nevertheless, the products were unambigously characterized by several spectroscopic methods. NMR-spectroscopic data of

Scheme 2

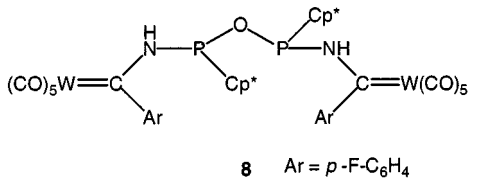

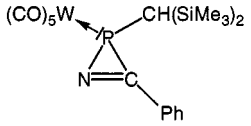

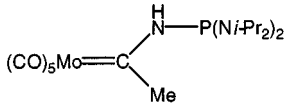

complexes **4a−e**, **6a−e**, **7** and **8** are presented in Tables 1 and 2; information on crystallographic data collection and structure determination of complexes **4a**, **b**, **6b**, **c** and **8** are summarized in Table 3, characteristic structural data of complexes **4a**, **b** and **8** are given in Table 4 and those of **6b**, **c** together with **9**, {2-[bis(trimethylsily)methyl]-3-phenyl-2*H*-azaphosphirene-κP}pentacarbonyltungsten(0)[7], in Table 5.

Table 1. Selected ^{13}C-[a], ^{31}P-NMR-spectroscopic[a] data of dinuclear [(4-X-phenyl)carbene]metal complexes **4a−g** and **8**

X	4	δ^{31}P	δ^{13}C-(M=CR_2)	J(P,C)	δ^{13}C-(Ar-C1)	J(P,C)
CF_3	**a**	63.1	285.4	s	155.5	9.7
Cl	**b**	61.9	285.9	s	150.9	9.7
H	**c**	63.0	287.1	s	152.9	10.0
F	**d**	62.1	286.3	s	149.0	9.7
CH_3	**e**	63.0	288.1	s	150.3	9.7
OCH_3	**f**	62.5[b]	[c]	[c]	[c]	[c]
$N(CH_3)_2$	**g**	64.7	282.4	s	151.0	9.7
F	**8**	130.0	283.7	s	149.3	[c]

[a] $CDCl_3$, room temp.; δ/[ppm], J/[Hz]. − [b] Reaction solution. − [c] Not determined.

Significant structural units of complexes **4a−g** and **8** such as W=CR_2, Ar−C1 and Cp*P(NR_2)X (X = O, NR_2) are characterized by their typical NMR resonances (Table 1), the latter units displaying chemical shift values in their ^{31}P-NMR spectra at δ = 63±2 and the former at low field at δ = 285±3 (W=CR_2) and 152±4 (Ar-*C*1). It should be noted that the ^{31}P-^{13}C coupling-constant magnitudes are very small for the W=CR_2 carbon atoms (in all cases the signals could not be resolved) and ca. 10 Hz for the Ar-*C*1 carbon atoms. Although no temperature-dependent NMR measurements were undertaken to investigate circumambulatory 1,5-sigmatropic rearrangements of the phosphorus moiety along the Cp* ring in **4a−g**, these compounds should show degenerate rearrangements of this type, in contrast to coordinated phosphorus compounds (such as the 2*H*-azaphosphirene complexes **6a−g**).[6][10]

2*H*-azaphosphirene complexes **6a−g** display trends in chemical shift values and coupling constants (Table 2) that are quite similar, but less pronounced than those of recently

described 2-(*p*-phenyl)-substituted 2*H*-azaphosphirene complexes with the bis(trimethylsilyl)methyl group at phosphorus atom.[7] Compared to the latter complexes, **6a**−**g** have 2*H*-azaphosphirene ring carbon atom resonances that are generally more upfield shifted and have smaller ^{31}P-^{13}C coupling-constant magnitudes. There are remarkable upfield shifts in the ^{1}H- and ^{13}C-NMR resonances of the Cp*−C1 methyl groups, which are even more shielded than in compounds such as Cp*PH_2 (δ = 1.10).[6] Although the origin of this significant effect is not yet understood, two further aspects seem relevant. First, in order to enable better comparison with complex **9**, the ^{15}N-NMR resonance of **6c** was determined [**6c**: δ = −65.2, ^{1}J(P,N) = 39.0 Hz; versus **9**: δ = −53.2, ^{1}J(P,N) = 36.9 Hz]; this presumably points to a higher electron density at the nitrogen atom in **6c**. The second point is discussed below.

Table 2. Selected ^{13}C-[a], ^{31}P-NMR- spectroscopic[a] data of (4-X-phenyl)-substituted complexes **6a**−**g** (exclusively ring atoms of the 2*H*-azaphosphirene ring system)

X	**6**	δ^{31}P	^{1}J(P,W)	δ^{13}C	ΣJ(P,C)
CF_3	**a**	−102.5	289.6	188.3	s
Cl	**b**	−105.3	289.2	186.5	s
H	**c**	−167.3	288.4	189.0	1.7
F	**d**	−105.9	289.0	188.1	s
CH_3	**e**	−110.8	287.2	188.6	s
OCH_3	**f**	−109.8	285.6	187.5	s
$N(CH_3)_2$	**g**	−117.7[b]	285.1[b]	[c]	[c]

[a] $CDCl_3$, room temp.; δ/[ppm], J/[Hz]. − [b] Reaction solution. − [c] Not determined.

The molecular structures of the complexes **4a**, **b**, as determined by X-ray crystallography (Figures 1, 2 and Table 3), consist of two Cp*P-bridged amino(aryl)carbene complex moieties, which have an (*E*,*E*) configuration of the pentacarbonyltungsten and the Cp*P fragment with respect to the C−N bond and which differ mainly in their metal−carbon and nitrogen−phosphorus bond lengths of their W−C−P−N skeletons (Table 4). Compared to the structure of [{*N*-[bis(diisopropylamino)phosphanyl]amino}-(methyl)methylene]pentacarbonylmolybdenum(0)[11] (**10**), all P−N bonds of **4a**, **b** are shorter than the related P−N bond of **10** [1.803(2) Å] (Table 4). It is noteworthy that **4a**, **b** always show combinations of short P−N bonds and small N−P−C angles (or the opposite); these differences in bonding *may* serve as picture for an early stage of the elimination process, which was shown to proceed in solution. In contrast to these findings, complex **8** (Figure 3) displays less dissimilar bonds and angles of its structural subunits (Table 4).

2*H*-azaphosphirene complexes **6b**,**c** have molecular structures (Figures 4, 5 and 6) which are somewhat different from the previously reported structure[7] of complex **9** (Table 5). Interesting features are the PCN/arene interplanar angles of 15.4° (**6b**) and 21.3° (**6c**) versus 2° in **9** and the increased bond angles of the C−P−W moieties of **6b**,**c** [C refers in these cases to the directly phosphorus-bonded carbon atoms of the Cp* and $CH(SiMe_3)_2$ groups; Figure 5 shows a better view of the arrangement of the

Figure 1. Molecular structure of **4a** in the crystal (ellipsoids represent 30% probability levels, hydrogen atoms are omitted for clarity)

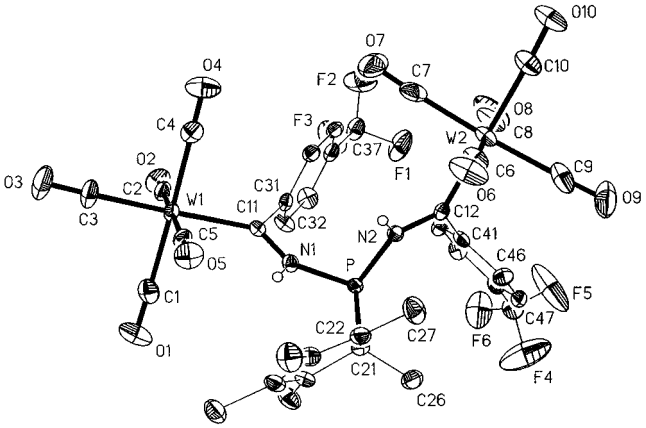

Figure 2. Molecular structure of **4b** in the crystal (ellipsoids represent 50% probability levels, hydrogen atoms are omitted for clarity)

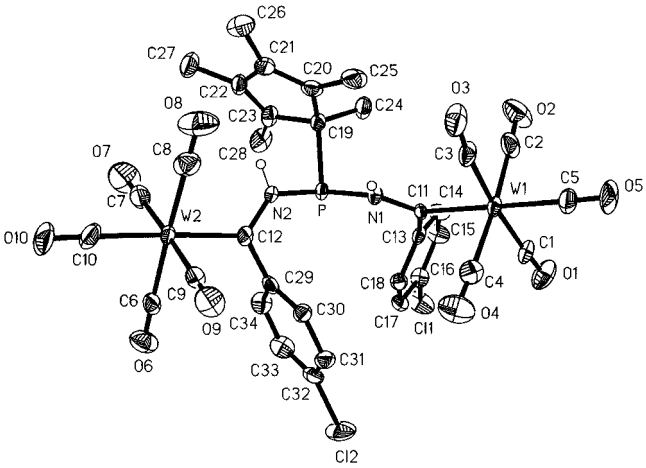

Figure 3. Molecular structure of **6b** in the crystal (ellipsoids represent 50% probability levels, hydrogen atoms are omitted for clarity)

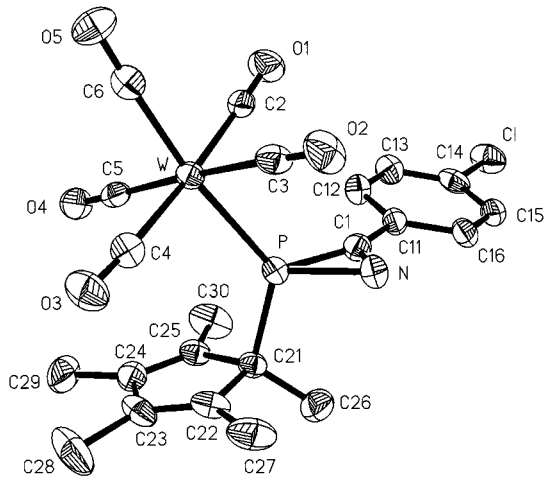

Figure 4. Molecular structure of **6c** in the crystal (ellipsoids represent 50% probability levels, hydrogen atoms are omitted for clarity)

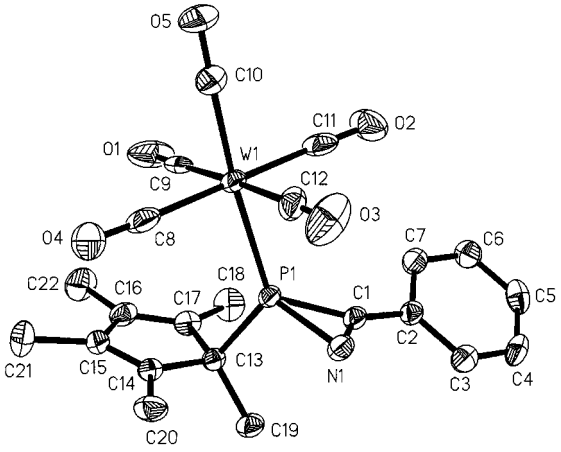

Figure 5. Molecular structure of **6c** in the crystal (view showing the spatial arrangement of the three planar groups of **6c**)

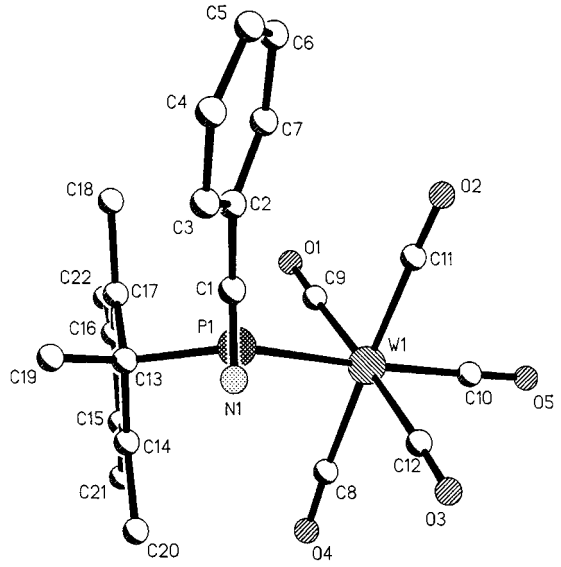

Figure 6. Molecular structure of **8** in the crystal (hydrogen atoms are omitted for clarity)

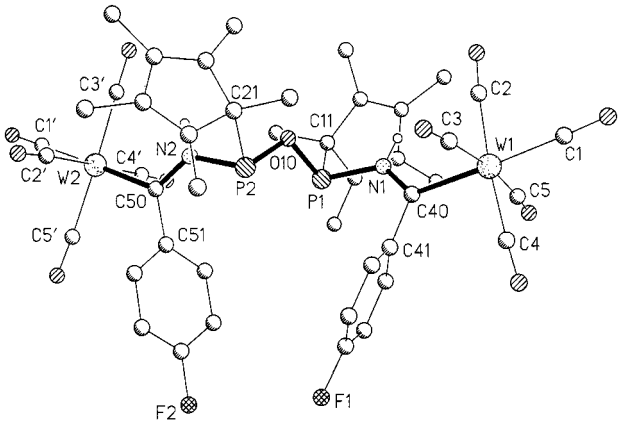

planar groups of **6c**]. Remarkable are also the arrangements of the Cp* [and $CH(SiMe_3)_2$; cf. ref.[7][9]] group(s); the sterically bulky substituents point away from the pentacarbonyltungsten fragment. Because of this, the Cp*−C1 methyl group points towards the midpoint of the C=N double bond and, therefore, to the π-electron system. If this orientation is retained in solution, a through-space shielding of the atoms of such methyl groups could contribute to the unusual upfield shift of the NMR resonances of the Cp*−C1 methyl group signals.

The chemistry of the compounds reported here is under current investigation with special respect to thermal and photochemical reactions.

Support of the *Deutsche Forschungsgemeinschaft* and the *Fonds der Chemischen Industrie* and ^{15}N-NMR measurements by Priv.-Doz. Dr. *Dietrich Gudat* (Universität Bonn) are gratefully acknowledged.

Experimental Section

General: All reactions and manipulations were carried out under deoxygenated dry nitrogen, using standard Schlenk techniques with conventional glassware; solvents were dried according to standard procedures. − NMR spectra were recorded with a Bruker AC-200 or a Bruker AMX-300 spectrometer (AC-200: 200 MHz for ^1H; 50.3 MHz for ^{13}C; 81.0 MHz for ^{31}P; AMX-300: 30.4 MHz for ^{15}N, 12.5 MHz for ^{183}W) using [D]chloroform and [D_6]benzene as solvents, the latter as internal standard; shifts are given relative to ext. tetramethylsilane (^1H, ^{13}C), H_3CNO_2 (^{15}N), 85% H_3PO_4 (^{31}P) and WO_4^{2-} (^{183}W). ^{15}N-NMR spectra were recorded using ^{31}P- and ^1H-based polarisation-transfer techniques (INEPT); ^{183}W spectra were obtained from two-dimensional ^{31}P, $^{183}W\{^1H\}$ (HMQC) spectra. − Mass spectra were recorded with a Finigan Mat 8430 (70 eV); apart from *m/z* values of the molecule ions, only *m/z* values with intensities of more than 20% are given. − Infrared spectra were recorded with a Biorad FT-IR 165 (selected data given). − Melting points were obtained with a Büchi 535 capillary apparatus. − Elemental analyses were performed using a Carlo Erba analytical gas chromatograph. − The κ*P* notation serves to differentiate between *P* and *N* coordination of the appropriate heterocycle to the metal center.

General Procedure for the Synthesis of Dinuclear (Carbene)-tungsten Complexes **4a−g** *and 2H-Azaphosphirene Complexes* **6a−g**: To a solution of 2.1 g (5 mmol) of [amino(aryl)carbene]-tungsten complexes **1a−g** in 50 ml of CH_2Cl_2 was added 25 ml of NEt_3 and 1.2 g (5 mmol) of $Me_5C_5PCl_2$ (**2**) at 0°C. The reaction mixtures were stirred at ambient temp. until **2** was consumed (^{31}P NMR). The dark orange reaction mixtures were concentrated to dryness under reduced pressure (0.1 mbar). The crude product mixtures containing approximately 50% of **4**, 40% of **6** and 5% of **7** (according to ^{31}P-NMR signal integration), were separated and purified by low-temperature chromatography [Al_2O_3 (neutral), hexane/diethyl ether 97.5:2.5] and most of them crystallized from pentane at −20°C.

N,N′-[(Pentamethyl-2,4-cyclopentadien-1-yl)phosphanediyl]bis-{[amino(4-trifluoromethylphenyl)methylene]pentacarbonyltungsten(0)} (**4a**): 0.43 g of **4a** (28%) was obtained as a yellow powder, m.p. 148°C (decomp.). − IR (KBr): $\tilde{\nu}$ = 3292 (sw), 3244 (sw) (NH), 2064 (s), 1993 (br), 1980 (br), 1952 (br), 1933 (br), 1916 (br), 1904 (br), 1872 (s) (CO). − ^1H NMR ($CDCl_3$): δ = 1.19 [d, ^3J(P,H) = 17.4 Hz, 3 H, Cp*−C1−CH_3], 1.91 (s, 6 H, Cp*−CH_3),

Table 3. Details of crystal structure determination and refinement of complexes **4a**, **b**, **6b**, **c** and **8**

Complex	**4a**	**4b**	**6b**	**6c**	**8**
Formula	$C_{36}H_{25}F_6N_2O_{10}PW_2$	$C_{34}H_{25}Cl_2N_2O_{10}PW_2$	$C_{22}H_{19}ClNO_5PW$	$C_{22}H_{20}NO_5PW$	$C_{44}H_{40}F_2N_2O_{11}P_2W_2$
M_r	1158.25	1091.13	627.65	593.21	1240.42
Crystal habit	yellow prism	orange prism	yellow prism	colourless tablet	yellow needle
Crystal size [mm]	0.55×0.3×0.3	0.6×0.45×0.35	0.55×0.2×0.15	0.6×0.4×0.3	0.6×0.15×0.06
Crystal system	monoclinic	triclinic	monoclinic	triclinic	monoclinic
Space group	$P2_1/c$	$P(-1)$	$P2_1/c$	$P(-1)$	$C2/c$
Cell constants:					
a [Å]	16.854(4)	9.7548(10)	11.077(4)	8.758(3)	27.504(3)
b [Å]	12.137(6)	10.1874(11)	12.916(5)	10.174(4)	11.1832(12)
c [Å]	19.878(7)	20.137(2)	16.470(6)	14.170(4)	33.104(3)
α [°]	90	87.614(8)	90	74.74(2)	90
β [°]	101.00(3)	78.788(8)	99.38(3)	86.609(14)	108.375(12)
γ [°]	90	77.831(8)	90	66.82(2)	90
V [Å^3]	3992	1918.9	2325	1118.6	9663
Z	4	2	4	2	8
D_x [Mg m^{-3}]	1.927	1.888	1.793	1.762	1.705
μ [mm^{-1}]	5.88	6.23	5.19	5.27	4.89
Transmissions	0.48−0.91	0.48−0.99	0.70−0.84	0.45−0.99	0.62−0.99
F(000)	2208	1040	1216	576	4816
T [°C]	−130	−100	−130	−130	−100
$2\theta_{max}$	50	50	55	50	50
No. of reflections:					
measured	8939	7952	5611	4032	8948
unique	7044	6743	5342	3939	8473
R_{int}	0.029	0.027	0.030	0.008	0.046
Parameters	519	465	285	276	578
Restraints	65	376	42	8	477
wR (F^2, all refl.)	0.074	0.072	0.072	0.068	0.058
R [F, > 4σ(F)]	0.033	0.029	0.034	0.026	0.039
S	1.05	1.04	1.05	1.08	0.78
max. Δρ [e Å^{-3}]	1.41	1.01	0.88	1.46	0.80

Table 4. Selected bond lengths [pm] and angles [°] of complexes **4a**, **b** and **8**

Structural unit	**4a**	**4b**	**8**
W=CR$_2$	W1−C11 2.165(6) W2−C12 2.193(6)	W1−C11 2.171(4) W2−C12 2.176(4)	W1−C40 2.189(6) W2−C12 2.166(7)
N−C	N1−C11 1.329(7) N2−C12 1.323(7)	N1−C11 1.326(5) N2−C12 1.338(5)	N1−C11 1.16(7) N2−C12 1.332(7)
P−N	P−N1 1.745(5) P−N2 1.768(4)	P−N1 1.760(4) P−N2 1.747(3)	P1−N1 1.755(5) P2−N2 1.753(5)
P−C	P−C21 1.878(6)	P−C21 1.869(4)	P1−C11 1.865(7) P2−C21 1.854(6)
P−O	#	#	P1−O10 1.662(4) P2−O10 1.669(4)
Y−P−X	N1−P−N2 96.1(2) N1−P−C21 96.5(2) N2−P−C21 103.5(2)	N1−P−N2 99.5(2) N1−P−C21 101.0(2) N2−P−C21 95.2(2)	N1−P1−O10 98.5(2) N1−P1−C11 98.1(3) O10−P1−C11 100.9(3)

1.99 (s, 6 H, Cp*−CH_3), 6.45 (m$_c$, 4 H, Ar−*H*), 7.09 (m$_c$, 4 H, Ar−*H*), 8.98 (br, 2 H, N*H*). − ^{13}C{^{1}H} NMR ($CDCl_3$): δ = 11.5/11.7/11.9 (s, Cp*−*C*H$_3$), 15.7 [d, ^2J(C,P) = 20.9 Hz, Cp*−C1−*C*H$_3$], 60.5 [d, ^1J(C,P) = 26.1 Hz, Cp*−*C*1], 120.6 [q, ^3J(C,F) = 2.2 Hz, Ar−*C*2/2′], 123.6 [q, ^1J(C,F) = 272.4 Hz, *C*F$_3$], 125.3 [d, ^4J(C,F) = 3.9 Hz, Ar−*C*3/3′], 130.0 [q, ^2J(C,F) = 33.1 Hz, Ar−*C*4−CF$_3$], 134.7 [d, J(C,P) = 5.5 Hz, Cp*−C_{Ring}], 142.7 [d, J(C,P) = 3.2 Hz, Cp*−C_{Ring}], 155.5 [d, ^3J(C,P) = 9.7 Hz, Ar−*C*1], 197.3 [s, ^1J(C,W) = 127.6 Hz, *cis*-*C*O], 203.6 (s, *trans*-*C*O), 285.4 (s, W=*C*R$_2$). − ^{31}P{^{1}H} NMR ($CDCl_3$): δ = 63.1 (s). − ^{31}P NMR ($CDCl_3$): δ = 63.1 [d, ^2J(P,H) = 18.6 Hz]. − MS (EI, ^{184}W); *m*/*z* (%): 1158 (4) [M$^{+\bullet}$], 1130 (2) [(M − CO)$^+$]. − $C_{36}H_{25}F_6N_2O_{10}PW_2$ (1158.2): calcd. C 37.33, H 2.18, N 2.42; found C 36.98, H 2.50, N 2.29.

N,N′-[(Pentamethyl-2,4-cyclopentadien-1-yl)phosphanediyl]bis-{[amino(4-chlorophenyl)methylene]pentacarbonyltungsten(0)} (**4b**): 0.51 g of **4b** (33%) was obtained as a yellow powder. − M.p. 123°C (decomp.). − IR (KBr): ṽ = 3312 (sw), 3215 (sw) (NH), 2064 (s), 1990 (s), 1963 (w), 1936 (w), 1910 (w) (CO) cm^{-1}. − ^{1}H NMR ($CDCl_3$): δ = 1.15 [d, ^3J(P,H) = 17.5 Hz, 3 H, Cp*−C1−C*H*$_3$], 1.88 (s, 6 H, Cp*−C*H*$_3$), 1.92 (s, 6 H, Cp*−C*H*$_3$), 6.37 (m$_c$, 4 H, Ar−*H*), 7.23 (m, 4 H, Ar−*H*), 8.84 (w, 2 H, N*H*). − ^{13}C{^{1}H} NMR ($CDCl_3$): δ = 11.6−12.0 (s, Cp*−*C*H$_3$), 15.7 [d, ^2J(C,P) = 21.1 Hz, Cp*−C1−*C*H$_3$], 60.3 [d, ^1J(C,P) = 26.1 Hz, Cp*−*C*1], 122.2 [d, ^4J(C,P) = 2.5 Hz, Ar], 128.5 (s, Ar), 134.1 (s, Ar−*C*4), 134.8 [d, J(C,P) = 5.4 Hz, Cp*−C_{Ring}], 142.4 [d, J(C,P) = 3.3 Hz Cp*−C_{Ring}], 150.9 [d, ^3J(C,P) = 9.7 Hz, Ar-*C*1], 197.5 [s, ^1J(C,W) = 128.0 Hz, *cis*-*C*O], 203.8 (s, *trans*-*C*O), 285.9 (s, W=

Table 5. Selected bond lengths [pm] and angles [°] of complexes **6b**, **c** and **9**

Complex	P1−C1	P1−N1	N1−C1	W−P
6b	1.750(5)	1.812(4)	1.270(6)	2.475(2)
6c	1.764(4)	1.811(4)	1.291(5)	2.4720(12)
9	1.759(5)	1.795(4)	1.272(7)	2.470(2)

Complex	C1−P1−N1	C1−N1−P1	N1−C1−P1	C−P−W
6b	41.7(2)	66.5(3)	71.8(3)	128.1(2)
6c	42.3(2)	66.9(2)	70.8(2)	127.01(13)
9	41.9(2)	67.5(3)	70.6(3)	124.3(2)

*C*R$_2$). − ^{31}P{^{1}H} NMR (CDCl$_3$): δ = 61.9 (s). − ^{31}P NMR (CDCl$_3$): δ = 61.9 [d, ^2J(P,H) = 18.9 Hz]. − MS (EI, ^{184}W); *m/z* (%): 1091 (3) [M$^{+\bullet}$], 1063 (4) [(M − CO)$^+$], 810 (12) [(M − 10 CO)$^+$], 323 (30) [(C$_5$O$_5$W)$^+$], 137 (100) [C$_7$H$_4$ClN)$^+$]. − $C_{34}H_{25}Cl_2N_2O_{10}PW_2$ (1091.1): calcd. C 37.49, H 2.31, N 2.57; found C 36.48, H 2.51, N 2.63.

N,N′-[(Pentamethyl-2,4-cyclopentadien-1-yl)phosphanediyl]bis-{[amino(phenyl)methylene]pentacarbonyltungsten(0)} (**4c**): 0.56 g of **4c** (26%) was obtained as an orange powder. − M.p. 146°C (decomp.). − IR (KBr): ṽ = 2062 (s), 1918 (vs), 1864 (m) (CO) cm^{-1}. − ^{1}H NMR (CDCl$_3$): δ = 1.15 [d, ^3J(P,H) = 17.4 Hz, 3 H, Cp*−C1−C*H*$_3$], 1.92 (s, 6 H, Cp*−C*H*$_3$), 1.99 (s, 3 H, Cp*−C*H*$_3$), 6.45 (m$_c$, 4 H, Ar−*H*), 7.28 (m$_c$, 6 H, Ar−*H*), 8.88 (br, 2 H, N*H*). −^{13}C{^{1}H} NMR (CDCl$_3$): δ = 11.5 (s, Cp*−*C*H$_3$), 11.8 [d, ^3J(P,C) = 7.3 Hz, Cp*−*C*H$_3$], 15.6 [d, ^2J(C,P) = 21.8 Hz, Cp*−C1−*C*H$_3$], 60.6 [d, ^1J(C,P) = 27.6 Hz, Cp*−*C*1], 120.7 [d, ^4J(C,P) = 2.8 Hz, Ar−*C*2/2′], 127.9 (s, Ar−*C*4), 128.2 (s, Ar−*C*3/3′), 135.0 [d, ^3J(C,P) = 5.7 Hz, Cp*−*C*$_{Ring}$], 142.0 [d, ^2J(C,P) = 2.9 Hz, Cp*−*C*$_{Ring}$], 152.9 [d, ^3J(C,P) = 10.0 Hz, Ar−*C*1], 197.7 [s, ^1J(C,W) = 127.7 Hz, *cis*-*C*O], 204.2 (s, *trans*-*C*O), 287.1 (s, W=*C*R$_2$). − ^{15}N NMR (CH$_2$Cl$_2$): δ = −170.5 [dd, ^1J(N,H) = 85, ^1J(P,N) = 67 Hz]. − ^{31}P{^{1}H} NMR (CDCl$_3$): δ = 63.0 (s). − MS [neg. −CI, (isobutane), ^{184}W]; *m/z* (%): 886 (1) [(M − C$_{10}$H$_{16}$)$^-$], 783 (1)[(M − C$_{16}$H$_{20}$N)$^-$], 698 (2) [(M − (C$_5$O$_5$W)$^-$], 324 (100) [C$_5$O$_5$W$^-$]. − $C_{32}H_{27}N_2O_{10}PW_2$ (1022.3): calcd. C 39.94, H 2.67, N 2.74; found C 40.09, H 2.76, N 2.72.

N,N′-[(Pentamethyl-2,4-cyclopentadien-1-yl)phosphanediyl]bis-{[amino(4-fluorophenyl)methylene]pentacarbonyltungsten(0)} (**4d**): 0.35 g of **4d** (28%) was obtained as an orange powder. − M.p. 149°C (decomp.). − ^{1}H NMR (CDCl$_3$): δ = 1.19 [d, ^3J(P,H) = 17.4 Hz, 3 H, Cp*−C1−C*H*$_3$], 1.91 (s, 6 H, Cp*−C*H*$_3$), 1.99 (s, 6 H, Cp*−C*H*$_3$), 6.45 (m$_c$, 4 H, Ar−*H*), 7.09 (m$_c$, 4 H, Ar−*H*), 8.98 (w, 2 H, N*H*). − ^{13}C{^{1}H} NMR (CDCl$_3$): δ = 11.5/11.7/11.9 (s, Cp*−*C*H$_3$), 15.6 [d, ^2J(C,P) = 21.1 Hz, Cp*−C1−*C*H$_3$], 60.3 [d, ^1J(C,P) = 26.1 Hz, Cp*−*C*1], 115.3 [d, ^2J(C,F) = 21.9 Hz, Ar−*C*3/3′], 123.1 [dd, ^4J(C,P) = 3.0 Hz, ^3J(C,F) = 8.5 Hz, Ar−*C*2/2′], 134.8 [d, *J*(C,P) = 5.5 Hz, Cp*−C$_{Ring}$], 142.3 [d, *J*(C,P) = 2.9 Hz, Cp*−C$_{Ring}$], 149.0 [dd, ^3J(C,P) = 9.7 Hz, ^4J(C,F) = 3.3 Hz, Ar−*C*1], 162.2 [d, ^1J(C,F) = 249.7 Hz, Ar−*C*4], 197.6 [s, ^1J(C,W) = 127.8 Hz, *cis*-*C*O], 203.9 (s, *trans*-*C*O), 286.3 (s, W=*C*R$_2$). − ^{31}P{^{1}H} NMR (CDCl$_3$): δ = 62.2 (s). − ^{31}P NMR (CDCl$_3$): δ = 62.2 [d, ^2J(P,H) = 16.5 Hz]. − $C_{34}H_{25}F_2N_2O_{10}PW_2$ (1058.2): calcd. C 38.59, H 2.38, N 2.65; found C 37.69, H 2.51, N 2.57.

N,N′-[(Pentamethyl-2,4-cyclopentadien-1-yl)phosphanediyl]bis-{[amino(4-methylphenyl)methylene]pentacarbonyltungsten(0)} (**4e**): 0.42 g of **4e** (18%) was obtained as an orange powder. − M.p. 117°C (decomp.). − IR (KBr): ṽ = 3297 (s) 3251 (s) (NH), 2067 (br), 1992 (br), 1979 (br), 1949 (br), 1925 (br), 1893 (br), 1860 (br) (CO) cm^{-1}. − ^{1}H NMR (CDCl$_3$): δ = 1.16 [d, ^3J(P,H) = 17.5 Hz, 3 H, Cp*−C1−C*H*$_3$], 1.98 (s, 6 H, Cp*−C*H*$_3$), 1.99 (s, 6 H, Cp*−C*H*$_3$), 2.38 (s, 3 H, Ar−C*H*$_3$), 6.38 (m$_c$, 4 H, Ar−*H*), 7.06 (m$_c$, 4 H, Ar−*H*), 8.82 (br, 2 H, N*H*). − ^{13}C{^{1}H} NMR (CDCl$_3$): δ = 11.5/11.7/11.9 (s, Cp*−*C*H$_3$), 15.6 [d, ^2J(C,P) = 21.6 Hz, Cp*−C1−*C*H$_3$], 21.3 (s, Ar−*C*H$_3$), 60.6 [d, ^1J(C,P) = 27.6 Hz, Cp*−*C*1], 121.3 [d, ^4J(C,P) = 2.5 Hz, Ar], 138.7 (s, Ar), 135.1 [d, *J*(C,P) = 5.7 Hz, Cp*−*C*$_{Ring}$], 138.1 (s, Ar), 141.9 [d, *J*(C,P) = 3.1 Hz, Cp*−*C*$_{Ring}$], 150.3 [d, ^3J(C,P) = 9.7 Hz, Ar−*C*1], 197.8 [s, ^1J(C,W) = 127.6 Hz, *cis*-*C*O], 204.2 (s, *trans*-*C*O), 288.1 (s, W=*C*R$_2$). − ^{31}P{^{1}H} NMR (CDCl$_3$): δ = 63.0 (s). − ^{31}P NMR (CDCl$_3$): δ = 63.0 [d, ^2J(P,H) = 15.8 Hz]. − MS (EI, ^{184}W); *m/z* (%): 1050 (2) [M$^{+\bullet}$], 1022 (2) [(M − CO)$^+$], 992 (48) [(M − 2 CO)$^+$], 966 (46) [(M − 3 CO)$^+$], 267 (100) [C$_{16}$H$_{16}$N$_2$P$^+$], 117 (95) [C$_8$H$_7$N$^+$]. − $C_{36}H_{31}N_2O_{10}PW_2$ (1050.3): calcd. C 41.17, H 2.97, N 2.67; found C 40.25, H 3.33, N 2.32.

N,N′-[(Pentamethyl-2,4-cyclopentadien-1-yl)phosphanediyl]-bis[{amino[4-(dimethylamino)phenyl]methylene}pentacarbonyltungsten(0)] (**4g**): 0.51 g of **4g** (33%) was obtained as a red powder. − M.p. 105°C (decomp.). − IR (KBr): ṽ = 3239 (w) (NH), 2059 (s), 1909 (br) (CO) cm^{-1}. − ^{1}H NMR (CDCl$_3$): δ = 1.16 (d, ^3J(P,H) = 16.2 Hz, 3 H, Cp*−C1−C*H*$_3$), 1.78 (s, 6 H, Cp*−C*H*$_3$), 1.93 (s, 6 H, Cp*−C*H*$_3$), 2.93 (s, 6 H, N(C*H*$_3$)$_2$), 6.37 (m$_c$, 4 H, Ar−*H*), 6.65 (m$_c$, 4 H, Ar−*H*), 8.82 (br, 2 H, N*H*). − ^{13}C{^{1}H} NMR (CDCl$_3$): δ = 11.4−12.0 (s, Cp*−*C*H$_3$), 15.8 [d, ^2J(C,P) = 20.7 Hz, Cp*−C1−*C*H$_3$], 40.1 [s, N(*C*H$_3$)$_2$], 60.9 [d, ^1J(C,P) = 27.2 Hz, Cp*−*C*1], 110.3 (s, Ar), 111.0 (s, Ar), 126.2 (s, Ar), 135.4 [d, *J*(C,P) = 5.4 Hz, Cp*−*C*$_{Ring}$], 141.5 [d, *J*(C,P) = 3.4 Hz, Cp*−*C*$_{Ring}$], 151.0 (s, Ar−*C*1), 198.5 [s, ^1J(C,W) = 127.6 Hz, *cis*-*C*O], 204.2 (s, *trans*-*C*O), 282.4 (s, W=*C*R$_2$). − ^{31}P{^{1}H} NMR (CDCl$_3$): δ = 64.7 (s). − ^{31}P NMR (CDCl$_3$): δ = 64.7 [d, ^2J(P,H) = 13.5 Hz]. − $C_{38}H_{37}N_4O_{10}PW_2$ (1108.1): calcd. C 41.18, H 3.36, N 5.05; found C 42.18, H 3.96, N 4.69.

Pentacarbonyl[2-(pentamethyl-2,4-cyclopentadien-1-yl)-3-(4-trifluoromethyphenyl)-2H-azaphosphirene-κP]tungsten(0) (**6a**): 0.11 g of **6a** (3%) was obtained as a yellow powder. − M.p. 117°C (decomp.). − ^{1}H NMR (CDCl$_3$): δ = 0.57 [d, ^3J(P,H) = 15.1 Hz, 3 H, Cp*−C1−C*H*$_3$], 1.77 [d, ^4J(P,H) = 5.9 Hz, 3 H, Cp*−C*H*$_3$], 1.79 [d, ^4J(P,H) = 6.7 Hz, 3 H, Cp*−C*H*$_3$], 1.91 (s, 3 H, Cp*−C*H*$_3$), 2.04 (s, 3 H, Cp*−C*H*$_3$), 7.84 (m$_c$, 2 H, Ar*H*), 8.13 (m$_c$, 2 H, Ar*H*). − ^{13}C{^{1}H} NMR (CDCl$_3$): δ = 9.98/10.0/10.6/10.8 (s, Cp*−*C*H$_3$), 16.3 [d, ^2J(C,P) = 3.0 Hz, Cp*−C1−*C*H$_3$], 61.4 [d, ^1J(C,P) = 13.7 Hz, Cp*−*C*1], 122.4 [q, ^1J(C,F) = 275.4 Hz, Ar−*C*F$_3$], 124.6 [q, ^3J(C,F) = 3.3 Hz, Ar−*C*3/3′], 128.5 [d, ^2J(C,P) = 15.3 Hz, Ar−*C*1], 128.9 (s, Ar−*C*2/2′), 132.0 [q, ^2J(C,F) = 32.9 Hz, Ar−*C*4−CF$_3$], 132.2 [d, *J*(C,P) = 4.9 Hz, Cp*−*C*$_{Ring}$], 134.8 [d, *J*(C,P) = 1.7 Hz Cp*−*C*$_{Ring}$], 140.8 [d, *J*(C,P) = 6.9 Hz, Cp*−*C*$_{Ring}$], 142.2 [d, *J*(C,P) = 7.6 Hz, Cp*−*C*$_{Ring}$], 188.3 (s, P*C*N), 193.5 [d, ^2J(C,P) = 8.4 Hz, *cis*-*C*O], 195.4 [d, ^2J(C,P) = 38.5 Hz, *trans*-*C*O]. − ^{31}P{^{1}H} NMR (CDCl$_3$): δ = −102.5 [s, ^1J(P,W) = 289.6 Hz]. − $C_{23}H_{19}F_3NO_5PW$ (661.3): calcd. C 41.78, H 2.90, N 2.12; found C 40.97, H 2.99, N 2.02.

Pentacarbonyl[3-(4-chlorophenyl)-2-(pentamethyl-2,4-cyclopentadien-1-yl)-2H-azaphosphirene-κP]tungsten(0) (**6b**): 0.4 g of **6b** (17%) was obtained as a yellow powder. − M.p. 91°C (decomp.). − IR (KBr): ṽ = 2072 (s), 1989 (s), 1976 (s), 1932 (s), 1918 (w) (CO) cm^{-1}. − ^{1}H NMR (CDCl$_3$): δ = 0.63 [d, ^3J(P,H) = 14.8 Hz, 3 H, Cp*−C1−C*H*$_3$], 1.84 [d, ^4J(P,H) = 4.7 Hz, 3 H, Cp*−C*H*$_3$], 1.87 [d, ^4J(P,H) = 5.4 Hz, 3 H, Cp*−C*H*$_3$], 1.97 (s, 3 H, Cp*

−CH_3), 2.11 (s, 3 H, Cp*−CH_3), 7.64 (m_c, 2 H, Ar*H*), 8.03 (m_c, 2 H, Ar*H*). − $^{13}C\{^1H\}$ NMR ($CDCl_3$): δ = 11.0/11.7/11.9 (s, Cp*−*C*H_3), 17.3 [d, ^2J(C,P) = 3.3 Hz, Cp*−C1−*C*H_3], 61.2 [d, ^1J(C,P) = 13.5 Hz, Cp*−*C*1], 124.6 [d, ^2J(C,P) = 15.4 Hz, Ar−*C*1], 130.2 (s, Ar−*C*2/2′), 130.9 (s, Ar−*C*3/3′), 133.4 (d, Cp*−C_{Ring}), 136.1 [d, J(C,P) = 1.7 Hz Cp*−C_{Ring}], 140.9 (s, Ar−*C*4), 141.7 [d, J(C,P) = 6.7 Hz, Cp*−C_{Ring}], 143.1 [d, J(C,P) = 7.7 Hz, Cp*−C_{Ring}], 186.5 (s, P*C*N), 194.7 [d, ^2J(C,P) = 8.7 Hz, ^1J(C,W) = 117.6 Hz, *cis*-*C*O], 196.6 [d, ^2J(C,P) = 38.2 Hz, *trans*-*C*O]. − $^{31}P\{^1H\}$ NMR ($CDCl_3$): δ = −105.3 [s, ^1J(P,W) = 289.2 Hz]. − MS (EI, ^{184}W); *m/z* (%): 627 (18) [$M^{+\bullet}$], 490 (12) [$C_{15}H_{15}PO_5W^+$], 137 (100) [$C_7H_4NCl^+$]. − $C_{22}H_{19}ClNO_5PW$ (627.7): calcd. C 42.10, H 3.05, N 2.23; found C 41.65, H 2.96, N 2.47.

Pentacarbonyl[2-(pentamethyl-2,4-cyclopentadien-1-yl)-3-phenyl-2H-azaphosphirene-κP]tungsten(0) (**6c**): 0.24 g of **6c** (22%) was obtained as a yellow powder. − M.p. 88°C (decomp.). − IR (KBr): $\tilde{\nu}$ = 2072 (s), 1991 (s), 1940 (br) (CO) cm^{-1}. − ^1H NMR (CD_2Cl_2): δ = 0.64 [d, ^3J(P,H) = 14.9 Hz, 3 H, Cp*−C1−CH_3], 1.86 [pt, ^4J(P,H) = 9.7 Hz, 6 H, Cp*−CH_3], 1.99 (s, 3 H, Cp*−CH_3), 2.12 (s, 3 H, Cp*−CH_3), 7.70 (m_c, 3 H, Ar−*H*), 8.12 (m_c, 2 H, Ar−*H*). − $^{13}C\{^1H\}$ NMR (CD_2Cl_2): δ = 11.2/11.3/11.8/12.0 (s, Cp*−CH_3), 17.5 [d, ^3J(C,P) = 3.5 Hz, Cp*−C1−*C*H_3], 62.6 [d, ^1J(C,P) = 13.6 Hz, Cp*−*C*1], 126.6 [d, ^2J(C,P) = 15.2 Hz, Ar−*C*1], 130.1 (s, Ar), 130.3 (s, Ar), 134.1 [d, J(C,P) = 5.0 Hz, Cp*−C_{Ring}], 134.7 (s, Ar−*C*4), 136.6 [d, J(C,P) = 1.7 Hz, Cp*−C_{Ring}], 141.8 [d, J(C,P) = 6.7 Hz, Cp*−C_{Ring}], 143.2 [d, J(C,P) = 7.7 Hz, Cp*−C_{Ring}], 189.3 [d, J(C,P) = 1.3 Hz, P*C*N], 195.3 [d, ^2J(C,P) = 8.4 Hz, *cis*-*C*O], 197.4 [d, ^2J(C,P) = 37.7 Hz, *trans*-*C*O]. − ^{15}N NMR (CH_2Cl_2): δ = −65.2 [d, J(P,N) = 39.0 Hz]. − $^{31}P\{^1H\}$ NMR (CD_2Cl_2): δ = −106.4 [s, ^1J(P,W) = 286.5 Hz]. − ^{183}W NMR (CD_2Cl_2): δ = −3126 (d). − MS [pos. −CI (NH_3), ^{184}W]; *m/z* (%): 594 (6) [(M + H)$^+$], 491 (3) [$C_{15}H_{15}O_5WP^+$], 407 (1) [$C_{12}H_{15}O_5WP^+$], 136 (100) [$C_{10}H_{16}^+$]. − $C_{22}H_{20}NO_5PW$ (593.2): calcd. C 44.54, H 3.40, N 2.36; found C 43.15, H 3.24, N 2.38.

Pentacarbonyl[3-(4-fluorophenyl)-2-(pentamethyl-2,4-cyclopentadien-1-yl)-2H-azaphosphirene-κP]tungsten(0) (**6d**): 0.14 g of **6d** (4%) was obtained as a yellow powder. − M.p. 97°C (decomp.). − IR (KBr): $\tilde{\nu}$ = 2072 (s), 1998 (s), 1976 (s), 1932 (w), 1918 (w) (CO) cm^{-1}. − ^1H NMR ($CDCl_3$): δ = 0.56 [d, ^3J(P,H) = 14.8 Hz, 3 H, Cp*−C1−CH_3], 1.78 [d, ^4J(P,H) = 4.6 Hz, 3 H, Cp*−CH_3], 1.80 [d, ^4J(P,H) = 5.1 Hz, 3 H, Cp*−CH_3], 1.91 [d, ^4J(P,H) = 4.6 Hz, 3 H, Cp*−CH_3], 2.04 (s, 3 H, Cp*−CH_3), 7.28 (m_c, 2 H, Ar*H*), 8.04 [m_c, 2 H, ^3J(C,F) = 8.8 Hz, Ar*H*]. − $^{13}C\{^1H\}$ NMR ($CDCl_3$): δ = 11.1/11.7/11.9 (s, Cp*−*C*H_3), 17.2 [d, ^2J(C,P) = 3.6 Hz, Cp*−C1−*C*H_3], 62.3 [d, ^1J(C,P) = 13.6 Hz, Cp*−*C*1], 122.7 [dd, ^2J(C,P) = 15.3 Hz, ^4J(C,F) = 3.1 Hz, Ar−*C*1], 117.8 [d, ^2J(C,F) = 22.5 Hz, Ar−*C*3/3′], 132.2 [d, ^3J(C,F) = 9.6 Hz, Ar−*C*2/2′], 133.4 [d, J(C,P) = 4.3 Hz, Cp*−C_{Ring}], 136.2 [d, J(C,P) = 2.3 Hz, Cp*−C_{Ring}], 141.5 [d, J(C,P) = 6.9 Hz, Cp*−C_{Ring}], 143.0 [d, J(C,P) = 6.9 Hz, Cp*−C_{Ring}], 166.4 [d , ^2J(C,F) = 257.4 Hz, Ar−*C*4], 188.1 (s, P*C*N), 194.7 [d, ^2J(C,P) = 8.3 Hz, ^1J(C,W) = 125.6 Hz, *cis*-*C*O], 196.7 [d, ^2J(C,P) = 37.9 Hz, *trans*-*C*O]. − $^{31}P\{^1H\}$ NMR ($CDCl_3$): δ = −105.9 [s, ^1J(P,W) = 289.0 Hz]. − $^{19}F\{^1H\}$ NMR ($CDCl_3$): δ = −102.5 (s). − MS (EI, ^{184}W); *m/z* (%): 611 (2) [$M^{+\bullet}$], 490 (23) [(M − C_7H_4FN)$^+$], 135 (31) [$C_{10}H_{15}^+$], 121 (100) [$C_7H_4FN^+$], 95 (25) [CH_3F^+]. − MS (pos. −CI (NH_3), ^{184}W); *m/z* (%): 612 (100) [(M + H)$^+$], 491 (29) [(M − C_7H_4FN)$^+$], 137 (58) [$C_{10}H_{15}^+$]. − $C_{22}H_{19}FNO_5PW$ (611.2): calcd. C 42.23, H 3.13, N 2.29; found C 42.27, H 3.20 , N 2.32.

Pentacarbonyl[3-(4-methylphenyl)-2-(pentamethyl-2,4-cyclopentadien-1-yl)-2H-azaphosphirene-κP]tungsten(0) (**6e**): 0.3 g of **6e** (8%) was obtained as a yellow powder. − M.p. 78°C (decomp.). − ^1H NMR (C_6D_6): δ = 0.49 [d, ^3J(P,H) = 14.5 Hz, 3 H, Cp*−C1−CH_3], 1.72 [d, ^4J(P,H) = 3.9 Hz, 3 H, Cp*−CH_3], 1.75 [d, ^4J(P,H) = 4.5 Hz, 3 H, Cp*−CH_3], 1.89 (s, 3 H, Cp*−CH_3), 2.10 (s, 3 H, Cp*−CH_3), 6.89 (m_c, 2 H, Ar*H*), 7.95 (m_c, 2 H, Ar*H*). − $^{13}C\{^1H\}$ NMR (C_6D_6): δ = 11.1/11.6/11.8 (s, Cp*−*C*H_3), 17.1 [d, ^2J(C,P) = 3.8 Hz, Cp*−C1−*C*H_3], 21.6 (s, Ar−*C*H_3), 62.5 [d, ^1J(C,P) = 13.5 Hz, Cp*−*C*1], 123.8 [d, ^2J(C,P) = 13.4 Hz, Ar−*C*1], 128.3 (s, Ar), 129.7 (s, Ar), 130.3 [d, ^2J(C,P) = 24.3 Hz, Ar−*C*4], 133.9 (s, Cp*−C_{Ring}), 136.7 (s, Cp*−C_{Ring}), 141.4 [d, J(C,P) = 6.3 Hz, Cp*−C_{Ring}], 142.0 [d, J(C,P) = 7.9 Hz Cp*−C_{Ring}], 188.6 (s, P*C*N), 195.1 [d, ^2J(C,P) = 8.8 Hz, *cis*-*C*O], 197.5 [d, ^2J(C,P) = 37.5 Hz, *trans*-*C*O]. − $^{31}P\{^1H\}$ NMR (C_6D_6): δ = −110.8 [d, ^2J(P,W) = 287.2 Hz]. − MS (EI, ^{184}W); *m/z* (%): 607 (1) [$M^{+\bullet}$], 490 (16) [$C_{16}H_{15}O_5PW^+$], 406 (19) [($C_{16}H_{15}O_5PW$ − 3 CO)$^+$], 117 (100) [$C_8H_7N^+$]. − MS [pos. −CI (NH_3), ^{184}W]; *m/z* (%): 608 (1) [(M + H)$^+$], 491 (18) [($C_{16}H_{15}O_5PW$ + H)$^+$], 135 (100) [$C_{10}H_{15}^+$]. − MS [neg. −CI (NH_3), ^{184}W]; *m/z* (%): 637 (1) [M^-], 323 (100) [$C_5O_5W^-$]. − $C_{23}H_{22}NO_5PW$ (607.2): calcd. C 45.49, H 3.65, N 2.31; found C 45.76, H 3.64, N 2.17.

Pentacarbonyl[3-(4-methoxyphenyl)-2-(pentamethyl-2,4-cyclopentadien-1-yl)-2H-azaphosphirene-κP]tungsten(0) (**6f**): 0.12 g of **6f** (4%) was obtained as a yellow powder. − M.p. 89°C (decomp.). − IR (KBr): $\tilde{\nu}$ = 2072 (s), 1982 (br), 1958 (br), 1936 (br), 1911 (br) (CO) cm^{-1}. − ^1H NMR ($CDCl_3$): δ = 0.63 [d, ^3J(P,H) = 14.5 Hz, 3 H, Cp*−C1−CH_3], 1.85 (s, 3 H, Cp*−CH_3), 1.88 (s, 3 H, Cp*−CH_3), 1.98 (s, 3 H, Cp*−CH_3), 2.12 (s, 3 H, Cp*−CH_3), 3.92 (s, 3 H, OCH_3), 7.14 (m_c, 2 H, Ar*H*), 8.04 (m_c, 2 H, Ar*H*). − $^{13}C\{^1H\}$ NMR ($CDCl_3$): δ = 11.0/11.1/11.6/11.9 (s, Cp*−*C*H_3), 17.0 [d, ^2J(C,P) = 3.8 Hz, Cp*−C1−*C*H_3], 55.7 (s, O*C*H_3), 62.3 [d, ^1J(C,P) = 13.8 Hz, Cp*−*C*1], 115.3 (s, Ar−*C*3/3′), 118.4 [d, ^2J(C,P) = 15.5 Hz, Ar−*C*1], 132.1 (s, Ar−*C*2/2′), 133.7 [d, J(C,P) = 4.8 Hz Cp*−C_{Ring}], 136.4 [d, J(C,P) = 2.7 Hz Cp*−C_{Ring}], 141.2 [d, J(C,P) = 6.9 Hz, Cp*−C_{Ring}], 142.6 [d, J(C,P) = 7.6 Hz, Cp*−C_{Ring}], 164.6 (s, Ar−*C*4), 187.5 (s, P*C*N), 194.8 [d, ^2J(C,P) = 8.3 Hz, ^1J(C,W) = 134.1 Hz, *cis*-*C*O], 196.9 [d, ^2J(C,P) = 37.1 Hz, *trans*-*C*O]. − $^{31}P\{^1H\}$ NMR ($CDCl_3$): δ = −109.8 [s, ^1J(P,W) = 285.6 Hz]. − MS [pos. −CI (NH_3), ^{184}W]; *m/z* (%): 624 (2) [(M + H)$^+$], 491 (6) [(M − $C_{10}H_{15}$)$^+$], 405 [(M − 3 CO)$^+$], 151 (100) [(C_7H_7NO + NH_4)$^+$], 136 (11) [($C_{10}H_{15}$ + H)$^+$]. − $C_{23}H_{22}NO_6PW$ (623.0): calcd. C 44.32, H 3.56, N 2.25; found C 45.21, H 3.62, N 2.35.

Pentacarbonyl[chloropentamethyl-2,4-cyclopentadien-1-ylphosphane]tungsten(0) (**7**): 0.19 g of **7** (18%) was obtained as a pale yellow powder. − M.p. 46°C (decomp.). − IR (KBr): $\tilde{\nu}$ = 2072 (s), 1991 (s), 1940 (s, br) (CO) cm^{-1}. − ^1H NMR ($CDCl_3$): δ = 1.57 [d, ^3J(P,H) = 13.9 Hz, 3 H, Cp*−C1−CH_3], 1.79 (s, 3 H, Cp*−CH_3), 1.81 (s, 3 H, Cp*−CH_3), 1.85 (s, 3 H, Cp*−CH_3), 1.97 (s, 3 H, Cp*−CH_3), 7.36 [d, ^1J(P,H) = 337.4 Hz, 1 H, PH]. − $^{13}C\{^1H\}$ NMR ($CDCl_3$): δ = 11.5/11.9/11.95/12.0 (s, Cp*−*C*H_3), 18.6 [d, ^3J(C,P) = 6.9 Hz, Cp*−C1−*C*H_3], 60.6 [d, ^1J(C,P) = 10.1 Hz, Cp*−*C*1], 133.9 [d, J(C,P) = 4.7 Hz, Cp*−C_{Ring}], 136.6 (s, Cp*−C_{Ring}), 141.5 [d, J(C,P) = 6.8 Hz, Cp*−C_{Ring}], 142.9 [d, J(C,P) = 8.1 Hz, Cp*−C_{Ring}], 195.2 [d, ^2J(C,P) = 8.5 Hz, *cis*-*C*O], 197.0 [d, ^2J(C,P) = 37.7 Hz, *trans*-*C*O]. − Resonances of the two isotopomers of **7** have been detected: **7** (^{35}Cl): $^{31}P\{^1H\}$ NMR ($CDCl_3$): δ = 76.75 [s, ^1J(P,W) = 274.2 Hz]; **7** (^{37}Cl): $^{31}P\{^1H\}$ NMR ($CDCl_3$): δ = 76.73 [s, ^1J(W,P) = 273.9 Hz]. − MS [pos. −CI (NH_3), ^{35}Cl, ^{184}W]; *m/z* (%): 525 (8) [(M − H)$^+$], 491 (95) [$C_{15}H_{15}O_5P^+$], 136 (100) [($C_{10}H_{15}$ + H)$^+$]. − $C_{15}H_{16}ClO_5PW$ (526.6).

P,P′-Oxybis[pentacarbonyl{(4-fluorophenyl)[(pentamethyl-2,4-cyclopentadien-1-yl-phosphanyl)amino]methylene}tungsten(0)] (**8**):

0.09 g of **8** (3%) was obtained as an orange powder. − M.p. 139°C (decomp.). − IR (KBr): $\tilde{\nu}$ = 2062 (s), 1985 (s), 1933 (br), 1893 (br) (CO) cm^{-1}. − ^1H NMR ($CDCl_3$): δ = 1.31 [pt, *J*(P,H) = 7.8 Hz, 3 H, Cp*−C1−C*H*$_3$], 1.75/1.85/1.98/2.08 (s, 3 H, Cp*−C*H*$_3$), 6.59 (m_c, 4 H, Ar−*H*), 6.89 (m_c, 4 H, Ar−*H*), 9.48 (w, 2 H, N*H*). − $^{13}C\{^1H\}$ NMR ($CDCl_3$): δ = 11.4/12.6 (s, Cp*−*C*H$_3$), 14.0 [pt, *J*(C,P) = 7.0 Hz, Cp*−C1−*C*H$_3$], 62.7 [pt, *J*(C,P) = 10.5 Hz, Cp*−*C*1], 114.7 [d, ^2J(C,F) = 23.0 Hz, Ar−*C*3/3′], 123.1 (m_c, Ar−*C*2/2′), 133.8 [pt, *J*(C,P) = 7.2 Hz, Cp*−C_{Ring}], 135.3 (s, Cp*−C_{Ring}), 141.3 [pt, *J*(C,P) = 2.3 Hz, Cp*−C_{Ring}], 142.3 (s, Cp*−C_{Ring}), 149.3 (m_c, Ar−*C*1), 161.9 [d, ^1J(C,F) = 249.1 Hz, Ar−*C*4], 197.6 [s, ^1J(C,W) = 127.6 Hz, *cis*-*C*O], 204.1 (s, *trans*-*C*O), 283.8 (s, W=*C*R$_2$). − $^{31}P\{^1H\}$ NMR ($CDCl_3$): δ = 130.1 (s). − ^{31}P NMR ($CDCl_3$): δ = 130.1 [d, ^2J(P,H) = 3.9 Hz]. − $C_{44}H_{40}F_2N_2O_{11}P_2W_2$ (1240.4): calcd. C 42.60, H 3.25, N 2.26; found C 42.16, H 3.40, N 2.17.

Crystal Structure Analyses:[12] Crystal data and refinement details are presented in Table 3. Data were collected with Mo-K_α radiation (λ = 0.71073Å) at low temperature; diffractometer type Stoe Stadi-4 (**4a**, **6b**, **c**) or a Siemens P4 (**4b**, **8**). Absorption corrections were based on ψ scans. Structures were solved by the heavy-atom method and refined anisotropically on F^2 (program SHELXL-93, G. M. Sheldrick, Univ. Göttingen). Hydrogen atoms were included as rigid methyl groups or with a riding model. Weighting schemes were of the form $w^{-1} = \sigma^2(F^2) + (aP)^2 + bP$, where $3P = (2F_c^2 + F_o^2)$ and *a* and *b* are constants optimized by the program.

☆ Dedicated to Professor *Peter Jutzi* on the occasion of his 60th birthday.

[1] H. Wilkens, F. Ruthe, P. G. Jones, R. Streubel, *J. Chem. Soc., Chem. Commun.* **1998**, 1529−1530.

[2] [2a] R. Streubel, A. Kusenberg, J. Jeske, P. G. Jones, *Angew. Chem.* **1994**, *106*, 2564−2566; *Angew. Chem. Int. Ed. Engl.* **1994**, *33*, 2427−2428. − [2b] A. Ostrowski, J. Jeske. P. G. Jones, R. Streubel, *J. Chem. Soc., Chem. Commun.* **1995**, 2507−2508. − [2c] R. Streubel, A. Ostrowski, H. Wilkens, F. Ruthe, J. Jeske, P. G. Jones, *Angew. Chem.* **1997**, *109*, 409−413; *Angew. Chem. Int. Ed. Engl.* **1997**, *36*, 378−381. − [2d] A. Ostrowski, J. Jeske, F. Ruthe, P. G. Jones, R. Streubel, *Z. Anorg. Allg. Chem.* **1997**, *623*, 1897−1902.

[3] R. Streubel, L. Ernst, J. Jeske, P. G. Jones, *J. Chem. Soc., Chem. Commun.* **1995**, 2113− 2114.

[4] [4a] R. Streubel, H. Wilkens, A. Ostrowski, C. Neumann, F. Ruthe, P. G. Jones, *Angew. Chem.* **1997**, *109*, 1549−1550; *Angew. Chem. Int. Ed. Eng.* **1997**, *36*, 1492−1493. − [4b] H. Wilkens, J. Jeske, P. G. Jones, R. Streubel, *J. Chem. Soc., Chem. Commun.* **1997**, 2317−2318. − [4c] H. Wilkens, F. Ruthe, P. G. Jones, R. Streubel, *Chem. Eur. J.* **1998**, *4*, 1542−1553.

[5] R. Streubel, J. Jeske, P. G. Jones, R. Herbst-Irmer, *Angew. Chem.* **1994**, *106*, 115−117; *Angew. Chem. Int. Ed. Engl.* **1994**, *33*, 80−82.

[6] P. Jutzi, H. Saleske, D. Nadler, *J. Organomet. Chem.* **1976**, *118*, C8−C10.

[7] R. Streubel, A. Ostrowski, S. Priemer, U. Rohde, J. Jeske, P. G. Jones, *Eur. J. Inorg. Chem.* **1998**, 257−261.

[8] G. M. Bodner, S. B. Kahl, K. Bork, B. N. Storhoff, J. E. Wuller, L. J. Todd, *Inorg. Chem.* **1973**, *12*, 1071−1074.

[9] R. Streubel, F. Ruthe, P. G. Jones, *Eur. J. Inorg. Chem.* **1998**, 571−574.

[10] [10a] W. W. Schoeller, *Z. Naturforsch.* **1983**, *38b*, 1635−1642. − [10b] W. W. Schoeller, *Z. Naturforsch.* **1984**, *39b*, 1767−1771. − [10c] P. Jutzi, H. Saleske, *Chem. Ber.* **1984**, *117*, 222−227.

[11] R. Streubel, M. Hobbold, J. Jeske, F. Ruthe, P. G. Jones, *J. Organomet. Chem.* **1997**, 529, 351−356.

[12] Crystallographic data (excluding structure factors) for the structures reported in this paper have been deposited with the Cambridge Crystallographic Data Centre as supplementary publication no. CCDC-102060 (**4a**), -102061 (**4b**), -102062 (**6b**), -102063 (**6c**) and -102064 (**8**). Copies of the data can be obtained free of charge on application to CCDC, 12 Union Road, UK-Cambridge CB2 1EZ [Fax: int. code + 44(1223)336033; E-mail: deposit@ccdc.cam.ac.uk].

[I98204]

Characterization, Crystal Structure of 2,4-Bis(triphenylphosphanimino)tetrazolo[5,1-*a*]-[1,3,5]triazine, and Improved Crystal Structure of 2,4,6-Triazido-1,3,5-triazine

Elmar Keßenich, Thomas M. Klapötke*, Jörg Knizek[+], Heinrich Nöth[+], and Axel Schulz

Institut für Anorganische Chemie der Ludwig-Maximilians-Universität,
Meiserstraße 1, D-80333 München, Germany
Fax: (internat.) + 49(0)89/5902382
E-mail: tmk@anorg.chemie.uni-muenchen.de

Received June 29, 1998

Keywords: Cyanuric azide / Tetrazole / Triazine / Nitrogen compounds

2,4-Bis(triphenylphosphanimino)tetrazolo[5,1-*a*][1,3,5]triazine (**1**) was synthesized by reaction of cyanuric azide with triphenylphosphane. **1** is characterized by X-ray structural analysis, IR, Raman, and NMR spectroscopy. The obtained spectra showed that the remaining azide group in **1** reacts with the N4 atom of the triazine ring and forms a tetrazole. An improved crystal structure for 2,4,6-triazido-1,3,5-triazine (**2**) was determined and for the first time a ^{14}N-NMR spectrum was obtained. CAUTION: **2** (Cyanuric azide) is explosive! The explosive nature increases with greater purity and crystal size.

Introduction

Since the discovery of cyanuric azide by H. Finger[1] in 1907 and the development of an improved method in 1921 by E. Ott and E. Ohse[2], there has been considerable interest in the reactivity and the explosive character of cyanuric azide[1]-[11]. In this present study we determined an improved structure[4] of cyanuric azide and investigated the reaction of cyanuric azide with triphenylphosphane, first attempted by W. Kesting in 1923[10].

According to Staudinger and Meyer[12], phenylazide reacts with triphenylphosphane in anhydrous ether to form a phosphazide. The intermediate cannot be isolated at room temperature and spontaneously emits nitrogen to form triphenylphosphanophenylimine. This can be isolated in almost quantitative yield.

In Kesting's application of the Staudinger-Meyer reaction, substituting **2** for phenyl azide[10], the proposed reaction path is given in Equation 1.

$$(N_3CN)_3 + 2\ P(C_6H_5)_3 \xrightarrow[-\,2\,N_2]{Et_2O} \quad (1)$$

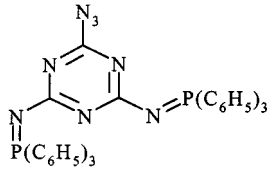

The product was, however, only characterized by elemental analyses and melting point. The compound 2,4-bis(triphenylphosphanimino)-6-azido-1,3,5-triazine that W. Kesting described showed no shock or heat sensitivity, in spite of the remaining azide group. In this paper, we report our studies on the synthesis, characterisation, and crystal structure of $C_{39}H_{30}N_8P_2$ (**1**).

Results and Discussion

In the reaction of **2** at room temperature with two equivalents of triphenylphosphane the color changed from colorless to yellow-green. This is thought to be due to the formation of $R-NNN-P(C_6H_5)_3$ (R = residue)[12]. This adduct has only fleeting existence and decomposes by giving off N_2, while the solution again becomes colorless. The end product is shown below (**1**). Raman- and ^{31}P-NMR spectroscopy indicates that **1** is not an azide, due to the absence of the asymmetric and symmetric vibrations of the azide group in the Raman spectrum and two ^{31}P-NMR signals found at δ = 21.7 (s) and δ = 17.2 (s). The single crystal X-ray structure analysis for **1** further confirms that there is no azide group in the molecule.

The azide group reacts with the N4 atom of the triazine ring and forms a tetrazole (Equation 2).

$$(N_3CN)_3 + 2\ P(C_6H_5)_3 \xrightarrow[-\,2\,N_2]{Et_2O} \quad (2)$$

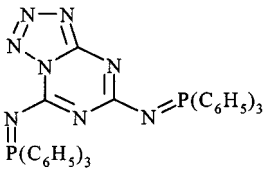

1

[+] X-ray structure analysis.

 © WILEY-VCH Verlag GmbH, D-69451 Weinheim, 1998 1434–1948/98/1212–2013 $ 17.50+.50/0

Looking at the calculated (Mulliken) partial charges[13] (N4: −0.38 e; N5: −0.36 e; PM3 level) of the azide, it can be seen, that the ring closure could not take place from the electrostatic point of view. Even the tetrazole has an "unusual" charge distribution with N4: −0.03 e and N5: −0.19 e (assignment see Figure 2).

The driving force for the ring-closure in reaction (2) can only be explained in terms of a π-stabilization of the tetrazole-triazine ring-system. This reaction is therefore orbital controlled. This is confirmed by the symmetry of the molecular orbital shown in Figure 1. Here, only the N5−N4 or N5−N8 interaction is symmetry allowed.

Figure 1. HOMO[a]

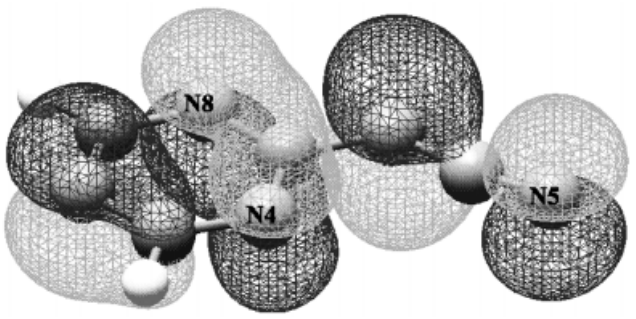

[a] Calcd. for hydrogen derivative.

Crystal Structure of 1

The crystallographic data and refinement details for compound **1** are summarized in the experimental section. **1** crystallizes from chloroform in the monoclinic space group $P2_1/n$ with four molecules and two solvent molecules per tetrazole molecule in the unit cell. Figure 2 shows the crystal structure of compound **1**.

Figure 2. Molecular Structure of **1**

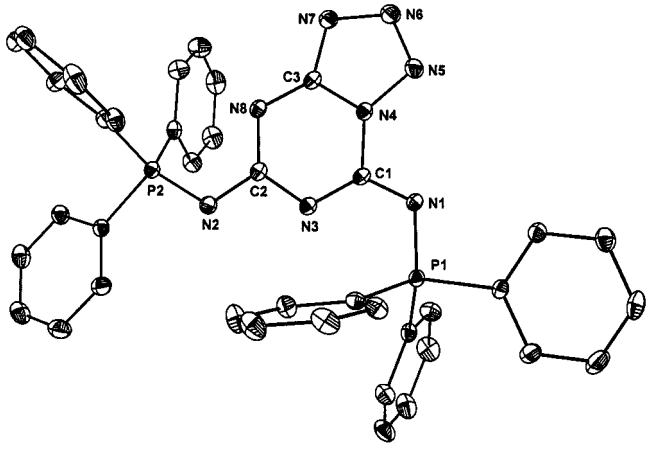

The P−N distance in **1** is 1.614 Å and 1.608 Å. This corresponds to a bond order between one and two. In comparison, the sum of the covalent radius (PN) is 1.8 Å and a typical P−N bond length is found in R_3−P=N−R compounds to be 1.602 Å[15]. The bond lengths and angles of the tetrazole ring (N5−N6: 1.292 Å, N6−N7: 1.364 Å, N5−N6−N7: 112.7°) also correspond to the literature[16]. The C1−N1 and C2−N2 bond lengths in **1** are 1.323 Å and 1.349 Å, respectively their bond order is also between one and two. The sum of the covalent radii (CN) is 1.47 Å for a single bond and 1.27 Å for a double bond[14]. Selected bond lengths [Å] and angles [°] for **1** are given in Table 1.

Table 1. Selected bond lengths [Å] and angles [°] for **1**

P(1)−N(1)	1.614(2)	P(2)−N(2)	1.608(2)
N(1)−C(1)	1.323(3)	N(2)−C(2)	1.349(3)
N(3)−C(1)	1.323(3)	N(3)−C(2)	1.374(3)
N(4)−C(3)	1.359(3)	N(4)−N(5)	1.371(3)
N(4)−C(1)	1.397(3)	N(5)−N(6)	1.292(3)
N(6)−N(7)	1.364(3)	N(7)−C(3)	1.337(3)
N(8)−C(3)	1.334(3)	N(8)−C(2)	1.354(3)
C(1)−N(1)−P(1)	121.50(18)	C(2)−N(2)−P(2)	118.45(18)
C(1)−N(3)−C(2)	119.5(2)	C(3)−N(4)−N(5)	109.3(2)
C(3)−N(4)−C(1)	121.2(2)	N(5)−N(4)−C(1)	129.3(2)
N(6)−N(5)−N(4)	104.9(2)	N(5)−N(6)−N(7)	112.7(2)
C(3)−N(7)−N(6)	105.7(2)	C(3)−N(8)−C(2)	114.0(2)
N(1)−C(1)−N(3)	127.5(2)	N(1)−C(1)−N(4)	115.9(2)
N(3)−C(1)−N(4)	116.5(2)	N(2)−C(2)−N(8)	119.6(2)
N(2)−C(2)−N(3)	115.0(2)	N(8)−C(2)−N(3)	125.4(2)
N(8)−C(3)−N(7)	129.7(2)	N(8)−C(3)−N(4)	122.9(2)
N(7)−C(3)−N(4)	107.4(2)		

The difference in the bond lengths of the triazine (C1−N4 = 1.397 Å, C1−N3 = 1.323 Å) can be explained by different donor-acceptor interactions of the free p-orbital (p-LP) of N1 or N2 with the unoccupied antibonding σ* orbital of the C1−N4 and C2−N3 bond respectively in the ring. From a steric point of view there is more electron density in the antibonding σ* orbital of the C1−N4 bond. This bond therefore is weaker than the C1−N3 bond. This hyperconjugation destabilizes the C−N bond and also explains the π-character of the N1−C1 bond.

Crystal Structure of 2

Cyanuric azide crystallizes from acetone in the hexagonal space group $P\bar{3}$ with two molecules in the unit cell (Figure 3). The C−N−C angle in the triazine ring is 113.09(14)° and the N−C−N angle is 126.91(14)°. The molecule is planar and the distance between the layers is 2.947 Å.

Figure 3. Molecular Structure of **2**

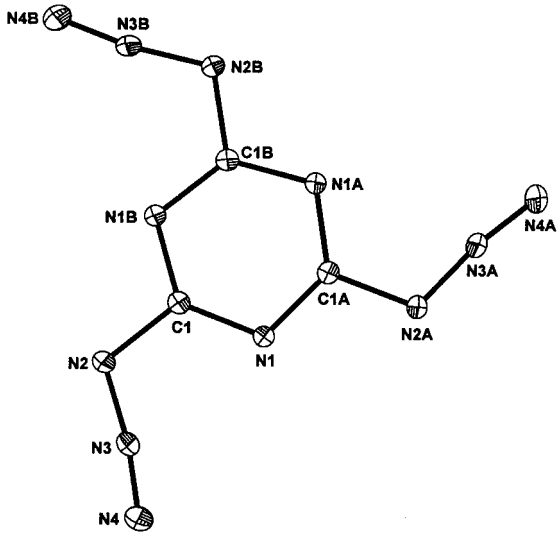

Table 2. ^{14}N- and ^{15}N-NMR shifts for **2**

compound	chemical shift δ [ppm] rel. nitromethane (= 0 ppm)				coupling constant ^1J [Hz]		solvent
	N2	N3	N4	N_{ring}	N2−N3	N3−N4	
$(CNN_3)_3$	−271	−146	−137	−162			acetone
$(CN^{15}N)_3$[9]	−258	−142	−131		16.1	6.1	CD_2Cl_2

The N2−N3 bond length is 1.2658(17) Å, respectively the bond order is between one and two. The covalent radius[14] for single bonded nitrogen atom is r_{cov} = 0.7 Å, 0.6 Å for a double bonded nitrogen atom and 0.55 Å for a triple bonded nitrogen atom. The bond order for N3−N4 [1.1156(19) Å] is between two and three. The angle of the azide group (N2−N3−N4) is 172.00(15)°. With the results of the X-ray structure analysis and the calculated (Mulliken) partial charges[13] (C1: 0.22 e; N1: −0.29 e; N2: −0.42 e; N3: 0.75 e; N4: −0.27 e; PM3 level) the ^{14}N-NMR signals are assigned as shown in Table 2.

The assignment further confirms to the results J. Müller[9] obtained for the ^{15}N-NMR shifts of the azide group.

The crystallographic data and refinement details for **2** are shown in the Experimental Section.

The financial support of this research by the *University of Munich* and the *Fonds der Chemischen Industrie* is gratefully acknowledged.

Experimental Section

General Remarks: CAUTION: **2** is explosive! The explosive nature increases with greater purity and crystal size. Only PE equipment should be used during the preparation and handling of cyanuric azide and safety equipment like leather gloves and face-shield is recommended.

Used solvents were freshly distilled, dried and stored under nitrogen. − NMR: Jeol EX400 Delta (^1H, ^{13}C, chemical shifts refer to δ_{TMS} = 0.00 according to the chemical shifts of residual solvent signals; ^{14}N, external standard: $\delta(CH_3NO_2)$ = 0.00; ^{31}P, external standard $\delta(H_3PO_4, 85\%)$ = 0.00. − IR: Nicolet 520 FT-IR (as KBr pellets or in Nujol on KBr). − Raman: Perkin Elmer Spectrum 2000R NIR FT. − CHN analyses: Analysator Elementar Vario EL. − MS: Finnigan MAT 90. − Melting points are uncorrected (Büchi B540).

2 was prepared according to the procedure given in the literature[2], but the solution was cooled to 5°C for recrystallization from acetone and the crystals were dried in vacuo.

2,4-Bis(triphenylphosphanimino)tetrazolo[5,1-a][1,3,5]triazine (**1**): To a solution of 0.5 g ($2.45 \cdot 10^{-3}$ mol) of **2** in anhydrous ether, a solution of 1.4 g ($5.3 \cdot 10^{-3}$ mol) of PPh_3 was added in two hours at room temperature. The solution was refluxed for 12 h. **1** can be purified by recrystallization from chloroform. $C_{39}H_{30}N_8P_2$ (672.3) Yield: quantitative, colorless crystals; m.p. 239°C (dec.), ref.[10]: 243°C. − IR (KBr): $\tilde{\nu}$ = 3078 cm^{-1} (CH) (w), 1597 (C=C) (s). − Raman (460 scans, 400 mW, 180°, 20°C): $\tilde{\nu}$ = 3064 cm^{-1} (4.5) (CH), 1592 (6.0) (CC), 1576 (1.5) (CC), 1522 (0.5), 1484−1455 (0.5), 1440 (0.7), 1340 (0.5), 1296 (4.0), 1223 (0.6), 1186 (1.0), 1164 (2.0), 1112 (2.0), 1088 (0.5), 1032 (3.5), 1004 (10) (CH), 966 (1.0), 900−854 (0.5), 691 (1.0), 648 (0.7), 620 (1.5), 583 (2.0), 261 (2.5). − ^1H NMR ($CDCl_3$, 400 MHz, 25°C): δ = 7.35−7.98 (m, 30 H, aromatic H). − ^{13}C NMR ($CDCl_3$, 101 MHz, 25°C): δ = 127−134 (m, 36 C, aromatic C), 152 (dd, J_{CP} = 6.9 Hz / 3.1 Hz, $C_{triazine}$), 159 (d, J_{CP} = 1.5 Hz, $C_{triazine}$), 167 (s, $C_{triazine}$). − ^{31}P NMR ($CDCl_3$, 162 MHz, 25°C) δ = 17.3 (s, P), 21.7 (s; P). − MS (EI, 70 eV); *m/z* (%): 672.1 (11) [M^+], 645 (3) [M^+-N_2], 386 (100), 262.0 (44) [PPh_3^+], 185 (37) [PPh_2^+], 77 (9) [Ph^+]. − $C_{39}H_{30}N_8P_2 \cdot 2\ CHCl_3$ (911.39): calcd. C 53.99, H 3.54, N 12.29; found C 54.53, H 3.58, N 12.40.

2,4,6-Triazido-1,3,5-triazine (**2**): 3.1 g (16.8 mmol) cyanuric chloride in 30 ml of acetone; 5 g (77 mmol) of sodium azide. − C_3N_{12} (204.15) Yield: 3.29 g (96%), colorless needles, very sensitive to shock or heat, m.p. 94°C, ref.[2]: 94°C. − IR (in Nujol on KBr): $\tilde{\nu}$ = 2192.1 (s), 2157.6 [$\nu_{as}(N_3)$] (s), 2114.8 (s), 1571.5 (s), 1532.4 [$\delta((CN)_3)$] (s), 1480.1 (sh), 1350.4 [$\delta((CN)_3)$] (s), 1197.7 [$\nu_s(N_3)$] (s), 984.3 (w), 809.4 [$\delta((CN)_3)$] (m), 775.8 (vw), 706.8 [$\gamma((CN)_3)$] (m), 550.2 [$\delta(N_3)$] (w), 501.1 (vw), 331.2 (vw). − Raman (300 scans, 200 mW, 180°, 20°C): $\tilde{\nu}$ = 2475 [$\nu_{as}(N_3) + \gamma(N_3)$] (0.5), 2206 [$\nu_s(N_3) + \nu(C-N_3)$] (1), 2158 [$\nu_{as}(N_3)$] (2), 2144 [$\nu_{as}(N_3)$] (3), 2177 (1), 1571 (1), 1533 [$\delta((CN)_3)$] (3), 1426 [$\nu_s((CN)_3)$] (6), 1337 (9), 1238 (1), 1194 [$\nu_s(N_3)$] (7), 1150 [$\nu_s(N_3)$] (4), 982 [$\nu(C-N_3)$] (10), 709 (2), 562 (4), 471 (1), 330 (7), 237 (2). − ^{13}C NMR ([D_6]acetone, 68 MHz, 25°C): δ = 171.9 (s). − ^{14}N NMR (acetone, 29 MHz, 25°C): δ = −137 (s, N4), −146 (s, N3), −162 (s, N_{ring}), −271 (s, N2). − C_3N_{12} (204.11): calcd. C 17.65, N 82.35; found C 17.45, N 82.19.

Crystal Structure Analysis of **1**: $C_{39}H_{30}N_8P_2 \cdot 2\ CHCl_3$, M = 911.39, crystal size: 0.35 × 0.3 × 0.25 mm, colorless prism, monoclinic, space group $P2_1/n$, a = 11.013(2), b = 23.182(5), c = 17.195(3) Å, α = 90.00, β = 101.580(9), γ = 90.00°, V = 4300.7(15) $Å^3$, Z = 4, $d_{calcd.}$ = 1.408 Mg/m^3, μ = 0.515 mm^{-1}, $F(000)$ = 1864. Siemens SMART Area detector, scan type = Hemisphere, Mo-K_α, λ = 0.71073 Å, T = 173(2) K, 2θ range = 2.98 to 58.54° in −14 ≤ h ≤ 14, −28 ≤ k ≤ 28, −18 ≤ l ≤ 23, reflections collected: 24656, independent reflections: 7509 (R_{int} = 0.0292), observed reflections: 6006 [F>4σ(F)]. Structure solution program: SHELXS-97 (G. M. Sheldrick, University of Göttingen, Germany, 1997), direct methods, data-to-parameter ratio: 14.6:1 {11.7:1 [F>4σ(F)]}, final R indices [F>4σ(F)]: $R1$ = 0.0481, $wR2$ = 0.0976, $R1$ = 0.0664, $wR2$ = 0.1069 (all data), GOF on F^2 = 1.109, largest and mean Δ/σ: 0.002, 0.000, largest difference peak/hole: 0.404, −0.425 e $Å^{-3}$, program used: SHELXL-97 (G. M. Sheldrick, University of Göttingen, Germany, 1997).

Crystal Structure Analysis of **2**: C_3N_{12}, M = 204.11, crystal size: 0.2 × 0.2 × 0.15 mm, colorless prism, hexagonal, space group $P\bar{3}$, a = 8.7456(2), b = 8.7456(2), c = 5.8945(3) Å, V = 390.44(2) $Å^3$, Z = 2, $d_{calcd.}$ = 1.736 Mg/m^3, μ = 0.138 mm^{-1}, $F(000)$ = 204. Siemens SMART Area detector, Mo-K_α, λ = 0.71073 Å, scan type = hemisphere, T = 183(2) K, 2θ range = 5.38 to 55.84° in −8 ≤ h ≤ 11, −11 ≤ k ≤ 10, −7 ≤ l ≤ 7, reflections collected: 2306, independent reflections: 582 (R_{int} = 0.0284), observed reflections: 531 [F>4σ(F)]. Structure solution program: SHELXS-97 (G. M. Sheldrick, University of Göttingen, Germany, 1997), direct

methods, data-to-parameter ratio: 12.4:1 {11.3 :1 [$F>4\sigma(F)$]},final R indices [$F>4\sigma(F)$]: $R1$ = 0.0342, $wR2$ = 0.0894, $R1$ = 0.0384, $wR2$ = 0.0912 (all data), GOF on F^2 = 1.411, largest and mean Δ/σ: 0.013, 0.002, largest difference peak/hole: 0.182, −0.164 e $Å^{-3}$, program used: SHELXL-97 (G. M. Sheldrick, University of Göttingen, Germany, 1997).

[1] H. Finger, *J. Prakt. Chem*. **1907**, *75 [2]*, 103.
[2] E. Ott, E. Ohse, *Ber. Dtsch. Chem. Ges.* **1921**, *54B*, 179.
[3] N. Bragg, *Nature* **1934**, *134*, 138.
[4] I. Knaggs, *Proc. Roy. Soc. London* **1935**, *A 150*, 576.
[5] L. Wöhler, *Angew. Chem*. **1922**, *35*, 545-552.
[6] H. Koenen, K. H. Ide, W. Haupt, *Explosivstoffe* **1958**, *10*, 223.
[7] H. Kast, A. Haid, *Angew. Chem*. **1925**, *38*, 43−52.
[8] W. Beck, M. Bauder, *Chem. Ber.* **1970**, *103*, 583−589.
[9] J. Müller, *Z. Naturforsch. B* **1979**, *34*, 437−439.
[10] W. Kesting, *J. Prakt. Chem*. **1923**, *105 (2)*, 242−246.
[11] J. Shearer, J. I. Bryant, *J. Chem. Phys.* **1968**, *48, No.3*, 1138−1144.
[12] H. Staudinger, J. Meyer, *Helv. Chim. Acta* **1919**, 635−646.
[13] *GAUSSIAN 94, Revision* e.2, M. J. Frisch, G. W. Trucks, H. B. Schlegel, P. M. W. Gill, B. G. Johnson, M. A. Robb, J. R. Cheeseman, T. Keith, G. A. Petersson, J. A. Montgomery, K. Raghavachari, M. A. Al-Laham, V. G. Zakrzewski, J. V. Ortiz, J. B. Foresman, J. Cioslowski, B. B. Stefanov, A. Nanayakkara, M. Challacombe, C. Y. Peng, P. Y. Ayala, W. Chen, M. W. Wong, J. L. Andres, E. S. Replogle, R. Gomperts, R. L. Martin, D. J. Fox, J. S. Binkley, D. J. Defrees, J. Baker, J. P. Stewart, M. Head-Gordon, C. Gonzalez, J. A. Pople', Gaussian Inc., Pittsburgh, PA**1995**.
[14] T. M. Klapötke, I. C. Tornieporth-Oetting, *Nichtmetallchemie*, Verlag Chemie, Weinheim **1994**.
[15] K. Dehnicke, F. Weller, *Coord. Chem. Rev.* **1997**, *158*, 103−169.
[16] G. J. Palenik, *Acta Crystallogr.* **1963**, *16*, 596.
[17] Further details of the crystal structure determination are available from the Fachinformationszentrum Karlsruhe, D-76344 Eggenstein-Leopoldshafen, Germany or from the Cambridge Crystallographic Data Centre (CCDC), 12 Union Road, Cambridge CB2 1EZ, United Kingdom, on quoting the depository number 102718 (**1**), 102717 (**2**), the names of the authors, and the journal citation.

[I98205]

^{17}O-NMR, EPR and NMRD Characterization of [Gd(DTPA-BMEA)(H_2O)]: A Neutral MRI Contrast Agent

Éva Tóth[a], Fabienne Connac[a], Lothar Helm[a], Kofi Adzamli[b], and André E. Merbach*[a]

Institute of Inorganic and Analytical Chemistry, University of Lausanne, BCH[a],
CH-1015 Lausanne, Switzerland

Imaging Division, Mallinckrodt Inc.[b],
675 McDonnell Blvd., P. O. Box 5840, St. Louis, MO 63134, USA

Received September 21, 1998

Keywords: MRI / Gd^{III} complexes / NMR spectroscopy / NMRD / Lanthanides

A study including variable-temperature and -pressure, multiple-field ^{17}O NMR, EPR and NMRD has been performed on the MRI contrast agent, [Gd(DTPA-BMEA)(H_2O)]. The water exchange rate [$k_{ex}^{298} = (0.39 \pm 0.02) \times 10^6$ s^{-1}] and the activation volume ($\Delta V^{\neq} = +7.4 \pm 0.4$ cm^3 mol^{-1}), hence the mechanism, are identical to those for [Gd(DTPA-BMA)(H_2O)]. The longer rotational correlation time of [Gd(DTPA-BMEA)(H_2O)], as obtained from a global analysis of ^{17}O-NMR, EPR and NMRD data, and compared to that of [Gd(DTPA-BMA)(H_2O)], can be explained by water molecules hydrogen-bonded to the ether oxygen atoms of the ligand side chain.

Application of paramagnetic complexes of Gd^{3+} for contrast enhancement in clinical Magnetic Resonance Imaging (MRI) is now routine.[1] The first-generation contrast agents approved were ionic chelates, $[Gd(DTPA)(H_2O)]^{2-}$ (in Magnevist™)[2][3] and $[Gd(DOTA)(H_2O)]^-$ (in Dotarem™).[3][4] The search for low osmolar, highly hydrophilic agents that can be administered at higher doses with fewer adverse side effects has led to the development of several neutral agents, such as [Gd(DTPA-BMA)(H_2O)] (in Omniscan™),[3][5] [Gd(HP-DO3A)(H_2O)] (in ProHance™)[3] or [Gd(DTPA-BMEA)(H_2O)] (in OptiMARK®) (Scheme 1).[6–11]

Scheme 1. Structure of the ligand 1,7-bis[(*N*-methoxyethylcarbamoyl)methyl]-1,4,7-tris(carboxymethyl)-1,4,7-triazaheptane (DTPA-BMEA)

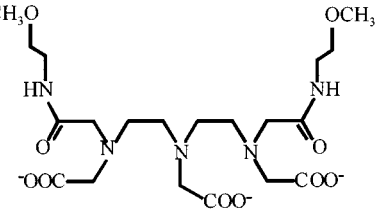

The proton relaxation enhancement due to presence of the contrast agent is expressed as proton relaxivity and depends on several factors, for example the rates of water exchange, molecular rotation, and electronic relaxation. In principle, measurement of the variation of proton relaxivity as a function of the magnetic field strength, the nuclear magnetic relaxation dispersion (or NMRD) profile, provides information on all of these parameters. In reality, the separation of the contributions of water exchange, rotation and electronic relaxation to the measured relaxivity is difficult, thus it is necessary to determine these parameters by independent methods. Water exchange rates can be directly obtained by ^{17}O-NMR measurements, whereas EPR experiments yield electronic relaxation rates. Here we report a variable temperature and pressure, multiple field ^{17}O-NMR experiment together with an EPR and NMRD study on [Gd(DTPA-BMEA)(H_2O)]. Analysis of these experiments provided the parameters describing water exchange, rotation and electronic relaxation. Certainly, the real effectiveness of the complex as a contrast agent needs to be tested in tissues or tissue-like models, as the complex-protein interactions may affect the paramagnetic enhancement in vivo.[12–14]

Results and Discussion

UV/Vis spectra were obtained of the analogous europium complex, [Eu(DTPA-BMEA)(H_2O)], in the range of $579 < \lambda < 581$ nm, and yielded a single absorption band that was invariant between 0 and 90°C. The $^7F_o \rightarrow {}^5D_0$ transition band of the Eu^{3+} ion that occurs in this region is very sensitive to changes in the coordination environment of the metal ion.[15] Therefore, the invariance of the spectrum excludes any equilibrium between differently hydrated species, i. e. the only species present is the europium complex with one inner sphere water molecule. Since Gd is very similar to Eu, this finding could be extended to the Gd^{III} complex as well. This is also supported by the value of the ^{17}O scalar coupling constant, $A/\hbar$, which is in the usual range for Gd^{III} complexes with one water molecule in the first coordination sphere (Table 1).[16]

Supporting information for this article is available on the WWW under http://www.wiley-vch.de/home/eurjic or from the author.

 © WILEY-VCH Verlag GmbH, D-69451 Weinheim, 1998 1434–1948/98/1212–2017 $ 17.50+.50/0

Table 1. Parameters obtained from the simultaneous fit of ^{17}O-NMR, EPR and NMRD data; the parameters in parenthesis were obtained by fitting only ^{17}O-NMR and EPR data; the values in italics were fixed in the fitting procedure

	DTPA[16]	DTPA-BMA[16]	DTPA-BMEA
$k_{ex}^{298}/10^6$ s^{-1}	3.3 ± 0.2 (4.1 ± 0.3)	0.45 ± 0.01 (0.43 ± 0.02)	0.39 ± 0.02 (0.37 ± 0.02)
$\Delta H^{\neq}$/kJ mol^{-1}	51.6 ± 1.4 (52.0 ± 1.4)	47.6 ± 1 (46.6 ± 1)	49.8 ± 1.4 (49.1 ± 2)
$\Delta S^{\neq}$/J mol^{-1}K^{-1}	+53 ± 5 (+56 ± 5)	+22.9 ± 3.6 (+18.9 ± 4)	+27 ± 6 (+26 ± 6)
$\Delta V^{\neq}$/cm^3 mol^{-1}	+12.5 ± 0.2	+7.3 ± 0.2	+7.4 ± 0.4
A/h/10^6 rad s^{-1}	−3.8 ± 0.2 (−3.8 ± 0.2)	−3.8 ± 0.2 (−3.6 ± 0.3)	−4.1 ± 0.4 (−4.1 ± 0.4)
τ_R^{298}/ps	58 ± 11 (103 ± 10)	66 ± 11 (167 ± 5)	93 ± 4 (172 ± 12)
E_R/kJ mol^{-1}	17.3 ±0.8 (18 ± 2)	21.9 ± 0.5 (21.6 ± 0.1)	24.5 ± 1 (23.4 ± 1)
τ_v^{298}/ps	25 ± 1 (0.25 ± 0.01)	25 ± 1 (34 ± 8)	20.3 ± 0.8 (32 ± 8)
E_v/kJ mol^{-1}	1.6 ± 1.8 (1.6 ± 1.8)	3.9 ± 1.4 (9 ± 2)	*3.9 (3.9)*
$\Delta^2/10^{20}$ s^{-2}	0.46 ± 0.02 (0.15 ± 0.02)	0.41 ± 0.02 (0.38 ± 0.02)	0.48 ± 0.02 (0.52 ± 0.04)
$D_{GdH}^{298}/10^{-10}$ m^2 s^{-1}	20 ± 3	23 ± 2	26 ± 1
E_{GdH}/kJ mol^{-1}	19.4 ± 1.8	12.9 ± 2.1	15.3 ± 0.5
$\chi(1+\eta^{2/3})^{1/2}$/MHz	*7.58*/14 ± 2	*7.58*/18 ± 2	*7.58*/15.0 ± 0.1
r_{GdO}/A	2.20 ± 0.09/*2.5*	2.12 ± 0.04/*2.5*	2.17 ± 0.02/*2.5*

^{17}O NMR, EPR and NMRD

The variable-temperature ^{17}O-NMR, EPR and NMRD data were analysed in a simultaneous fitting procedure, which is based on the several parameters that are common to these techniques (all relevant equations are given in the Appendix). Details of this approach have been previously described.[16] A variable-pressure ^{17}O-NMR study permitted determination of the activation volume for the water exchange process. The resulting curves are shown in Figures 1 and 2 and the fitted parameters are given and compared to those of other Gd^{III}-based contrast agents in Table 1.

Water Exchange

The rate (k_{ex}^{298}) and the activation volume ($\Delta V^{\neq}$), thus the mechanism of the water exchange, are identical for the two bisamide complexes, [Gd(DTPA-BMEA)(H_2O)] and [Gd(DTPA-BMA)(H_2O)]. This is a general finding based on several monomer, dimer or polymer Gd^{III} complexes, i.e. the water exchange rate is not affected by structural changes outside the inner coordination sphere.[17−20] As compared to [Gd(DTPA)(H_2O)]$^{2-}$, the exchange rate is about one order of magnitude lower for the bisamide complexes, whereas the exchange mechanism remains dissociative interchange. The decrease in the exchange rate was explained in terms of a decreased steric crowding around the metal ion when carboxylates are replaced by amide groups.[19] In dissociative interchange processes, high steric crowding helps bond breaking. This effect is less important for amide complexes, which results in a slower water exchange compared to the corresponding carboxylates.

Electronic Relaxation

The parameters describing electronic relaxation (the mean square zero-field splitting energy, Δ^2, and the correlation time for the modulation of the zero-field splitting, τ_v^{298}) are identical for the [Gd(DTPA-BMA)(H_2O)] and [Gd(DTPA-BMEA)(H_2O)] complexes.

Rotation

The rotational correlation time is determined by the longitudinal ^{17}O relaxation rates and by the ^{1}H-NMRD data. Both methods have the same drawback as far as the absolute value of τ_R is concerned, i. e. reliance on distance estimates (Gd−H distance for NMRD, or the Gd−O distance for ^{17}O NMR), which have a strong influence on the absolute value of τ_R. In NMRD, the outer sphere contribution to relaxivity is also important, whereas in ^{17}O NMR it is negligible.[21] Due to the practical importance of NMRD data for MRI, contrast agents are generally characterized by the rotational correlation times as obtained from NMRD. In the simultaneous treatment of NMRD and ^{17}O-NMR data a single τ_R is fitted, which we attribute to the rotation of the Gd−water vector. There is very often a discrepancy between the τ_R values obtained in separate fits of ^{17}O- and ^{1}H-NMR data (τ_R from ^{17}O NMR is much longer), due to the use of the incompatible Gd−H and Gd−O distances. In the simultaneous treatment we allow for this by fitting either the Gd−oxygen(water) distance (r_{GdO}) or the quadrupolar coupling constant [$\chi(1 + \eta^2/3)^{1/2}$], which practically means that the rotational correlation time obtained in this way is determined only by the proton relaxation rates.[16]

The rotational correlation time for [Gd(DTPA-BMEA)(H_2O)], as obtained from the simultaneous fit, τ_R^{298} = 93 ps, is longer than the one for [Gd(DTPA-BMA)(H_2O)] (66 ps). This increase is larger than what would correspond to the increase in the molecular weight. A reasonable explanation can be that there are water molecules hydrogen-bonded to the ether oxygen atoms of the DTPA-BMEA side chains, a situation that may slow down the rotation of the complex. This seems to be also supported by the higher value of the diffusion constant obtained for [Gd(DTPA-BMEA)(H_2O)], as compared to [Gd(DTPA-BMA)(H_2O)] or [Gd(DTPA)(H_2O)]$^{2-}$. It should be noted, however, that the rotational correlation times obtained from ^{17}O longitudinal relaxation rates (by fixing the Gd−O distance to 2.5 Å and the quadrupolar coupling constant to 7.58 MHz) are very similar for the two bisamide complexes {167 and 172

Figure 1. Temperature dependence of reduced transverse (a), longitudinal (b) ^{17}O-relaxation rates and chemical shifts (c) at B = 14.1 T (■), 4.7 T (●) and 1.41 T (▲); transverse electronic relaxation rates (d) and NMRD profiles (e) at T = 5°C (□, ■), 35°C (○, ●), 43°C (▲), 48°C (*), 53°C (◇), 60°C (+) and 70°C (×) (■ and ● obtained from Seymour Koenig, 360- and 600-MHz data with Bruker spectrometers, otherwise with Stelar FFC relaxometer); the lines represent the simultaneous least-squares fit to all data points as described in the text

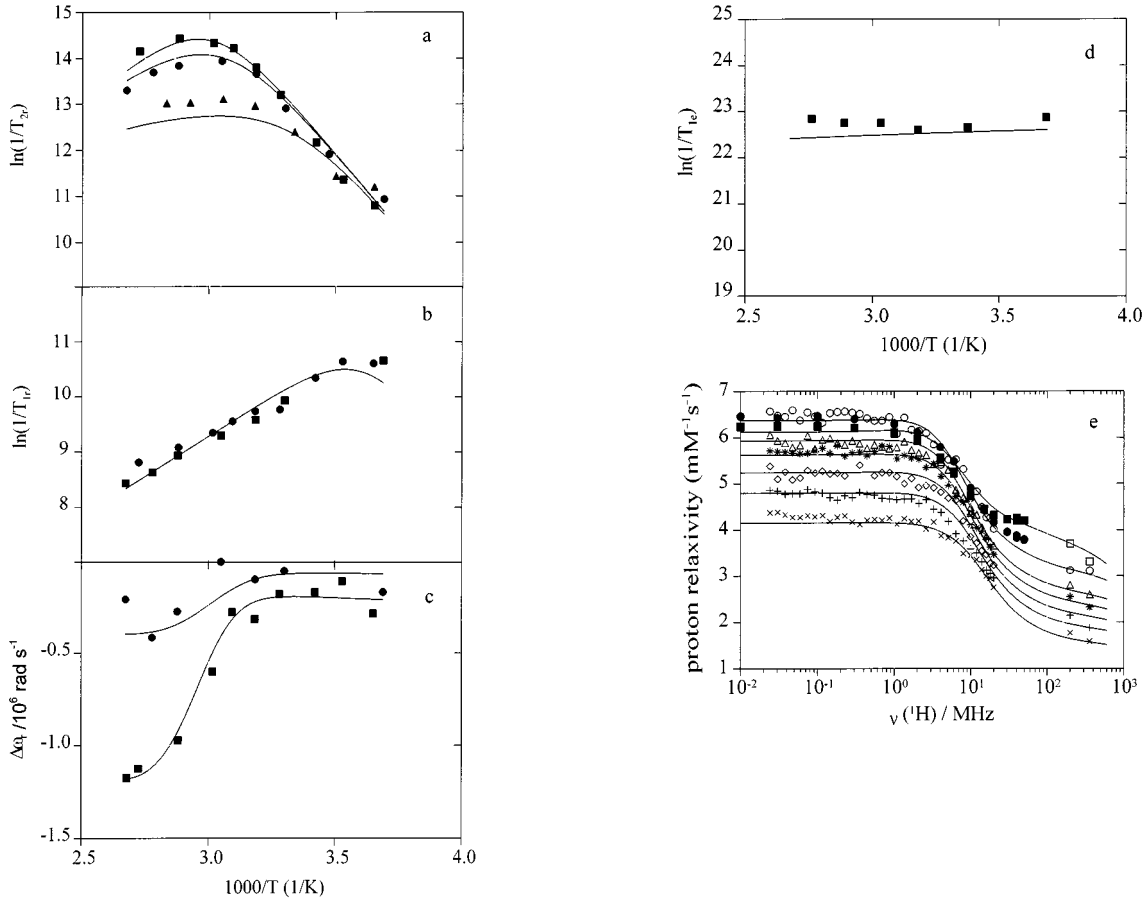

ps for [Gd(DTPA-BMA)(H_2O)] and [Gd(DTPA-BMEA)-(H_2O)], respectively}.

Figure 2. Pressure dependence of reduced transverse ^{17}O relaxation rates of [Gd(DTPA-BMEA)(H_2O)] at 298.2 K and B = 9.4 T; the line represents the least-squares fit that yields an activation volume of $\Delta V^{\neq}$ = +(7.4 ± 0.4) cm^3 mol^{-1}

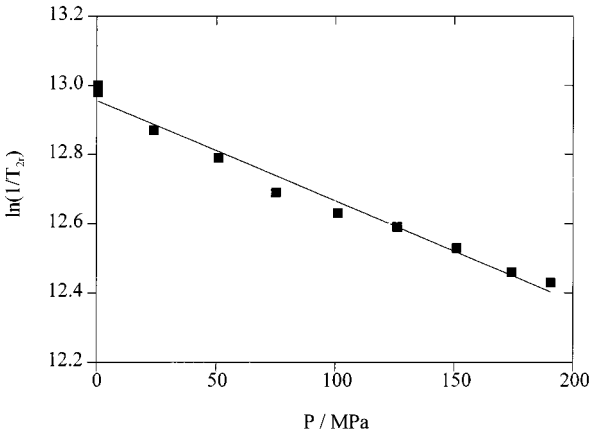

Conclusion

The complexes [Gd(DTPA-BMA)(H_2O)] and [Gd-(DTPA-BMEA)(H_2O)] are identical in respect to water exchange and electronic relaxation. The rotational correlation time for [Gd(DTPA-BMEA)(H_2O)] appears to be longer according to the global analysis of ^{17}O-NMR, EPR and NMRD data, probably due to hydrogen-bonded water molecules around the ether oxygen atoms of the ligand.

We thank the *Swiss National Science Foundation* and the *Office for Education and Science* (OFES) for financial support. This research was carried out in the frame of the EC COST D8 action and the EU-BIOMED program (MACE project). We are grateful to *Mallinckrodt Inc.*, St. Louis MO for their financial support. We wish to thank *Marga Spiller* (Department of Neurosurgery, The New York Medical College, Valhalla, NY) and *Seymour Koenig* (Relaxometry Inc., Mahopac, NY) for use of unpublished NMRD profiles and for discussion.

Experimental Section

General: [Gd(DTPA-BMEA)(H_2O)] was obtained from Mallinckrodt Inc.[22] For the ^{17}O-NMR measurements, solutions of 44

mmol/kg (pH = 5.1) and 118 mmol/kg (pH = 4.7) were used. To improve the sensitivity, ^{17}O-enriched water (10% $H_2{}^{17}O$, Yeda R& D Co., Israel) was added to the Gd complex solutions to yield in 2% ^{17}O enrichment. A 44 mmol/kg solution was used for the EPR study. The absence of free Gd^{3+} ions in all solutions was verified by using xylenol orange indicator.[23] The [Eu(DTPA-BMEA)] solution (0.169 M) was prepared by adding an equimolar quantity of the ligand to a $Eu(ClO_4)_3$ solution and adjusting the pH to 4.7. − The UV/Vis measurements were performed in thermostated cells with a 10-cm optical path length in a Perkin-Elmer Lambda 19 spectrophotometer. − Transverse and longitudinal ^{17}O relaxation rates and chemical shifts were measured at three different magnetic fields using Bruker spectrometers: AMX2-600, 14.1 T, 81.4 MHz; AC-200, 4.7 T, 27.1 MHz; and a 1.41-T 8.14-MHz electromagnet connected to an AC-200 console. The technique used for the ^{17}O-NMR measurements has been described previously.[24] − The EPR spectra were recorded at X-band (0.34 T) using a Bruker ESP 300E spectrometer. − The $1/T_1$ NMRD profiles were obtained with a field-cycling relaxometer in the Department of Neurosurgery, The New York Medical College, Valhalla, NY,[25][26] or with a Stelar Spinmaster FFC relaxometer, in Lausanne ([Gd] = 1−2 mM). − High-field NMRD values (360 MHz and 600 MHz) were measured with Bruker spectrometers.

Data Analysis: The least-squares fitting was performed with Scientist® for Windows™ by Micromath®, version 2.0. The reported errors correspond to one standard deviation obtained by the statistical analysis.

Appendix

Oxygen-17 NMR: From the measured ^{17}O-NMR relaxation rates and angular frequencies of the paramagnetic solutions, $1/T_1$, $1/T_2$ and ω, and of the acidified water reference, $1/T_{1A}$, $1/T_{2A}$ and ω_A, one can calculate the reduced relaxation rates and chemical shift, $1/T_{1r}$, $1/T_{2r}$ and $\Delta\omega_r$, which may be written as in Eqs. 1−3[27], where $1/T_{1m}$, $1/T_{2m}$ are the relaxation rates of the bound water, $\Delta\omega_m$ is the chemical shift difference between bound and bulk water.1

$$\frac{1}{T_{1r}} = \frac{1}{P_m}\left[\frac{1}{T_1} - \frac{1}{T_{1A}}\right] = \frac{1}{T_{1m} + \tau_m} \tag{1}$$

$$\frac{1}{T_{2r}} = \frac{1}{P_m}\left[\frac{1}{T_2} - \frac{1}{T_{2A}}\right] = \frac{1}{\tau_m}\frac{T_{2m}^{-2} + \tau_m^{-1}T_{2m}^{-1} + \Delta\omega_m^2}{(\tau_m^{-1} + T_{2m}^{-1})^2 + \Delta\omega_m^2} \tag{2}$$

$$\Delta\omega_r = \frac{1}{P_m}(\omega - \omega_A) = \frac{\Delta\omega_m}{(1+\tau_m T_{2m}^{-1})^2 + \tau_m^2\Delta\omega_m^2} + \Delta\omega_{os} \tag{3}$$

$\Delta\omega_m$ is determined by the scalar coupling constant, $A/\hbar$, according to Eq. 4, where B represents the magnetic field.

$$\Delta\omega_m = \frac{g_L\mu_B S(S+1)B}{3k_B T}\frac{A}{\hbar} \tag{4}$$

The outer-sphere contribution to the ^{17}O chemical shift is proportional to $\Delta\omega_m$, where C_{os} is an empirical constant (Eq. 5).

$$\Delta\omega_{0S} = C_{0S}\Delta\omega_m \tag{5}$$

The ^{17}O longitudinal relaxation rates are given by Eq. 6[28], where γ_S is the electron and γ_I is the nuclear gyromagnetic ratio (γ_S = 1.76×10^{11} rad s^{-1} T^{-1}, $\gamma_I = -3.626 \times 10^7$ rad s^{-1} T^{-1}), r is the effective distance between the electron charge and the ^{17}O nucleus, I is the nuclear spin (5/2 for ^{17}O), χ is the quadrupolar coupling constant and η is an asymmetry parameter:

$$\frac{1}{T_{1m}} = \left[\frac{1}{15}\left(\frac{\mu_0}{4\pi}\right)^2\frac{\hbar^2\gamma_I^2\gamma_S^2}{r_{GdO}^6}S(S+1)\right]\times\left[6\tau_{d1} + 14\frac{\tau_{d2}}{1+\omega_S^2\tau_{d2}^2}\right] + \frac{3\pi^2}{10}\frac{2I+3}{I^2(2I-1)}\chi^2(1+\eta^2/3)\tau_R \tag{6}$$

$$\tau_R = \tau_R^{298}\exp\left[\frac{E_R}{R}\left(\frac{1}{T} - \frac{1}{298.15}\right)\right] \tag{7}$$

In the transverse relaxation the scalar contribution, $1/T_{2sc}$, is the most important one (Eq. 8)[21]. In Eq. 8, $1/\tau_{sj}$ is the sum of the exchange rate constant and the electron spin relaxation rate.

$$\frac{1}{T_{2m}} \cong \frac{1}{T_{2sc}} = \frac{S(S+1)}{3}\left(\frac{A}{\hbar}\right)^2\left(\tau_{s1} + \frac{\tau_{s2}}{1+\omega_s^2\tau_{s2}^2}\right) \tag{8}$$

$$\frac{1}{\tau_{sj}} = \frac{1}{\tau_m} + \frac{1}{T_{je}} \qquad j = 1,2$$

The binding time (or exchange rate, k_{ex}) of water molecules in the inner sphere is assumed to obey the Eyring equation (Eq. 9), where $\Delta S^{\neq}$ and $\Delta H^{\neq}$ are the entropy and enthalpy of activation for the exchange process, and $k_{ex}{}^{298}$ is the exchange rate at 298.15 K.

$$\frac{1}{\tau_m} = k_{ex} = \frac{k_B T}{h}\exp\left\{\frac{\Delta S^{\neq}}{R} - \frac{\Delta H^{\neq}}{RT}\right\} = \frac{k_{ex}^{298}T}{298.15}\exp\left\{\frac{\Delta H^{\neq}}{R}\left(\frac{1}{298.15} - \frac{1}{T}\right)\right\} \tag{9}$$

EPR: The ZFS terms can be expressed by Eqs. 10 and 11[29][30], where Δ^2 is the trace of the square of the transient zero-field-splitting tensor, τ_v is the correlation time for the modulation of the ZFS with the activation energy E_v, and ω_s is the Larmor frequency of the Gd^{3+} electron spin.

$$\left(\frac{1}{T_{1e}}\right)^{ZFS} = \frac{1}{25}\Delta^2\tau_v\{4S(S+1) - 3\}\left(\frac{1}{1+\omega_S^2\tau_v^2} + \frac{4}{1+4\omega_S^2\tau_v^2}\right) \tag{10}$$

$$\left(\frac{1}{T_{2e}}\right)^{ZFS} = \Delta^2\tau_v\left[\frac{5.26}{1+0.372\omega_S^2\tau_v^2} + \frac{7.18}{1+1.24\omega_S\tau_v}\right] \tag{11}$$

$$\tau_V = \tau_V^{298}\exp\left\{\frac{E_V}{R}\left(\frac{1}{T} - \frac{1}{298.15}\right)\right\} \tag{12}$$

The contribution arising from spin rotation is given by Eq. 13, where $\delta g_L{}^2$ is the deviation from the free electron g_L value and τ_R is the rotational correlation time.

$$\left(\frac{1}{T_{ie}}\right)^{SR} = \frac{\delta g_L^2}{9\tau_R} \qquad i = 1,2 \tag{13}$$

NMRD: The measured proton relaxivities [normalized to 1 mM Gd^{III} concentration] contain both inner-sphere and outer-sphere contributions (Eq.13).

$$r_1 = r_{lis} + r_{los} \tag{14}$$

The inner-sphere term is given by Eq. 15, where q is the number of inner-sphere water molecules.

$$r_{lis} = \frac{1}{1000}\times\frac{q}{55.55}\times\frac{1}{T_{1m}^H + \tau_m} \tag{15}$$

$$\frac{1}{T_{1m}{}^{H}} = \frac{2}{15}\left(\frac{\mu_o}{4\pi}\right)^2 \frac{\hbar^2\gamma_S^2\gamma_I^2}{r_{GdH}^6} S(S+1)\left[\frac{3\tau_{d1}}{1+\omega_I^2\tau_{d1}^2} + \frac{7\tau_{d2}}{1+\omega_S^2\tau_{d2}^2}\right] \qquad (16)$$

The longitudinal relaxation rate of inner-sphere protons, $1/T_{1m}{}^{H}$ can be expressed as in Eq. 16[31][32].

In Eq. 16, r_{GdH} is the effective distance between the Gd^{III} electron spin and the water protons, ω_I is the proton resonance frequency, and τ_{di} is given by Eq. 17.

$$\frac{1}{\tau_{di}} = \frac{1}{\tau_m} + \frac{1}{\tau_R} + \frac{1}{T_{ie}} \qquad i = 1, 2 \qquad (17)$$

The outer-sphere contribution can be described by Eq. 18[25][33], where N_A is the Avogadro constant, and J_{os} is a spectral density function.

$$^{24}r_{os} = \frac{32N_A\pi}{405}\left(\frac{\mu_0}{4\pi}\right)^2 \frac{\hbar^2\gamma_S^2\gamma_I^2}{a_{GdH}D_{GdH}} S(S+1)\left[3J_{os}(\omega_I, T_{1e}) + 7J_{os}(\omega_S, T_{2e})\right] \qquad (18)$$

$$J_{os}(\omega, T_{je}) = \mathrm{Re}\left[\frac{1 + 1/4\left(i\omega\tau_{GdH} + \frac{\tau_{GdH}}{T_{je}}\right)^{1/2}}{1 + \left(i\omega\tau_{GdH} + \frac{\tau_{GdH}}{T_{je}}\right)^{1/2} + 4/9\left(i\omega\tau_{GdH} + \frac{\tau_{GdH}}{T_{je}}\right) + 1/9\left(i\omega\tau_{GdH} + \frac{\tau_{GdH}}{T_{je}}\right)^{3/2}}\right]$$

$$j = 1, 2 \qquad (19)$$

For the temperature dependence of the diffusion coefficient for the diffusion of a water proton away from a Gd^{III} complex, D_{GdH}, we assume an exponential temperature dependence, with an activation energy E_{DGdH} (Eq. 20).

$$D_{GdH} = D_{GdH}^{298}\exp\left\{\frac{E_{DGdH}}{R}\left(\frac{1}{T} - \frac{1}{298.15}\right)\right\} \qquad (20)$$

[1] R. B. Lauffer, *Chem. Rev.* **1987**, *87*, 901.
[2] H. Gries, H. Miklautz, *Physiol. Chem. Physics Med. NMR* **1984**, *16*, 105.
[3] DTPA = 1,1,4,7,7-pentakis(carboxymethyl)-1,4,7-triazaheptane; DOTA = 1,4,7,10-tetrakis(carboxymethyl)-1,4,7,10-tetraazacyclododecane; HP-DO3A = 1-hydroxypropyl-4,7,10-tri(carboxymethyl)-1,4,7,10-tetraazacyclododecane; DTPA-BMA = 1,7-bis[(*N*-methylcarbamoyl)methyl]-1,4,7-tris(carboxymethyl)-1,4,7-triazaheptane; DTPA-BMEA = 1,7-bis[(*N*-methoxyethylcarbamoyl)methyl]-1,4,7-tris(carboxymethyl)-1,4,7-triazaheptane.
[4] D. Meyer, M. Schaefer, B. Bonnemain, *Invest. Radiol.* **1988**, *23*, S232.
[5] A. Greco, M. T. McNamara, P. Lanthiez, S. C. Quay, G. Michelozzi, *Radiology* **1990**, *176*, 451.
[6] M. Periasamy, D. White, L. de Learie, D. Moore, R. Wallace, W. Lin, J. Dunn, W. Hirth, W. Cacheris, G. Pilcher, K. Galen, M. Hynes, M. Bosworth, H. Lin, M. Adams, *Invest. Radiol.* **1991**, *26*, S217.
[7] M. D. Adams, S. J. Barco, K. P. Galen, M. R. Hynes, W. H. Ralston In P. A. Rinck, R. N. Muller (Eds.), *New Developments in Contrast Agent Research; Proceedings of the 3rd Special Topic Seminar of the European MR Forum*, Hamburg, Germany, **1992**, 51.
[8] C. F. G. C. Geraldes, A. M. Urbano, M. C. Alpoim, A. D. Sherry, K.-T. Kuan, R. Rajagopalan, F. Maton, R. N. Muller, *Magn. Res. Imag.* **1995**, *13*, 401.
[9] D. H. White, L. A. de Learie, D. A. Moore, R. A. Wallace, T. J. Dunn, W. P. Cacheris, H. Imura, G. R. Choppin, *Invest. Radiol.* **1991**, *26*, S226.
[10] D. H. White, L. A. de Learie, T. J. Dunn, E. N. Rizkalla, H. Imura, G. R. Choppin, *Invest. Radiol.* **1991**, *26*, S229.
[11] H. Imura, G. R. Choppin, W. P. Cacheris, L. A. de Learie, T. J. Dunn, D. H. White, *Inorg. Chim. Acta* **1997**, *258*, 227.
[12] L. V. Elst, F. Maton, S. Laurent, F. Seghi, F. Chapelle, R. N. Muller, *Magn. Res. Med.* **1997**, *38*, 604.
[13] S. Aime, M. Botta, S. G. Crich, G. B. Giovenzana, R. Pagliarin, M. Piccinini, M. Sisti, E. Terreno, *J. Biol. Inorg. Chem.* **1997**, *2*, 470.
[14] I. Bertini, C. Luchinat, G. Parigi, G. Quacquarini, P. Marzola, F. M. Cavagna, *Magn. Res. Med.* **1998**, *39*, 124.
[15] N. Graeppi, D. H. Powell, G. Laurenzcy, L. Zékány A. E. Merbach, *Inorg. Chim. Acta* **1995**, *235*, 311.
[16] D. H. Powell, O. M. Ni Dhubhghaill, D. Pubanz, L. Helm, Y. S. Lebedev, W. Schlaepfer, A. E. Merbach, *J. Am. Chem. Soc.* **1996**, *118*, 9333.
[17] É. Tóth, D. Pubanz, S. Vauthey, L. Helm, A. E. Merbach, *Chem. Eur. J.* **1996**, *2*, 1607.
[18] H. Lammers, F. Maton, D. Pubanz, M. W. van Laren, H. van Bekkum, A. E. Merbach, J. A. Peters, R. N. Muller, *Inorg. Chem.* **1997**, *36*, 2527.
[19] É. Tóth, L. Burai, E. Brücher, A. E. Merbach, *J. Chem. Soc., Dalton Trans.* **1997**, 1587.
[20] É. Tóth, I. van Uffelen, L. Helm, A. E. Merbach, D. Ladd, K. Briley-Saebo, K. E. Kellar, *Magn. Res. Chem.* **1998**, *36*, S125.
[21] K. Micskei, L. Helm, E. Brücher, A. E. Merbach, *Inorg. Chem.* **1993**, *32*, 3844.
[22] R. T. Dean, Y. Lin, R. W. Weber, D. H. White, US Patent No. 4,826,673, **1989**; *Chem. Abstr.* **1989**, *111*, 74027w.
[23] G. Brunisholz, M. Randin, *Helv. Chim. Acta* **1959**, *42*, 1927.
[24] K. Micskei, H. D. Powell, L. Helm, E. Brücher, A. E. Merbach, *Magn. Res. Chem.* **1993**, *31*, 1011.
[25] S. H. Koenig, R. D. Brown III, *Progr. NMR Spectr.* **1991**, *22*, 487.
[26] S. H. Koenig, R. D. Brown III, "Relaxometry of Tissue" in *NMR Spectroscopy of Cells and Organisms* (Ed.: R. K. Gupta), vol. II, CRC Press, Boca Raton, **1987**, pp. 75−114.
[27] T. J. Swift, R. E. Connick, *J. Chem. Phys.* **1962**, *37*, 307.
[28] J. Kowalewski, L. Nordenskiold, N. Betenis, P.-O. Westlund, *Prog. Nucl. Magn. Reson. Spectrosc.* **1985**, *17*, 141.
[29] A. D. McLachlan, *Proc. R. Soc. London, Ser. A* **1964**, *280*, 271.
[30] D. H. Powell, A. E. Merbach, A. E. Gonzalez, E. Brücher, K. Micskei, M. F. Ottaviani, K. Köhler, A. von Zelewsky, O. Y. Grinberg, Y. S. Lebedev, *Helv. Chim. Acta* **1993**, *76*, 2129.
[31] N. J. Bloembergen, *Chem. Phys.* **1957**, *27*, 572.
[32] I. Solomon, *Phys. Rev.* **1955**, *99*, 559.
[33] J. H. Freed, *J. Chem. Phys.* **1978**, *68*, 4034.

[I98208]

β-Donor Interactions as Secondary Bonds in Dichlorobis(dimethylaminoxy)silane and -germane

Norbert W. Mitzel* and Udo Losehand

Anorganisch-chemisches Institut, Technische Universität München,
Lichtenbergstraße 4, D-85747 Garching, Germany

Received July 7, 1998

Keywords: β-Donor bonds / Silicon / Electrostatic interactions / Negative hyperconjugation

The compounds $Cl_2Si(ONMe_2)_2$ and $Cl_2Ge(ONMe_2)_2$ were prepared by the reaction of the appropriate tetrachlorides with *N,N*-dimethylhydroxylamine in the presence of 2,6-lutidine as an auxiliary base. The compounds were obtained as crystalline solids and characterised by elemental analysis, IR and NMR spectroscopy (nuclei ^1H, ^{13}C, ^{15}N, ^{17}O, and ^{29}Si). Their molecular structures were determined by single-crystal X-ray diffraction. The compounds are isostructural and both show the presence of weak secondary bonds between the nitrogen and silicon centres (β-donor bonds), as is indicated by the small angles SiON [102.8(1) and 103.7(1)°] and GeON [102.0(1)°], and the distances Si···N (2.438 and 2.450 Å) and Ge···N (2.519 and 2.520 Å). The conformation is anti-gauche in both compounds (one O–Si–O–N torsion angle being about 180°, the other 60°), but the strength of the β-donor interaction is not significantly affected by the different *anti*-substituents at the nitrogen centres, although such behaviour was expected from earlier studies carried out on $ClH_2SiONMe_2$. The β-donor interactions are also weaker than those found in $ClH_2SiONMe_2$.

β-Donor interactions, i.e. donor-acceptor interactions between atoms in a geminal position to one another, are now well established in p-block chemistry. In a number of reports we have shown them to contribute significantly to the molecular structures of compounds containing Si−O−N[1] and Si−N−N units[2]. Examples are the (4 + 4)-coordinate $Si(ONMe_2)_4$,[3] and the (4 + 2)-coordinate $H_2Si(ONMe_2)_2$, which has an Si−O−N angle of only 95.2°,[4] and some silyl oximes.[5] The strongest β-donor bond found so far in Si−O−N systems occurs in $ClH_2SiONMe_2$, which has a Si−O−N angle of only 79.7° in the crystal, corresponding to a Si···N distance of 2.028 Å, which comes close to the sum of covalent radii of silicon and nitrogen atoms (1.87 Å).[6] According to a gas-phase structural analysis of $ClH_2SiONMe_2$ the vapour consists of two conformers. The *anti*-conformer (torsion angle Cl−Si−O−N 180°) has a substantially stronger β-donor interaction (smaller Si−O−N angle 87.1°) than the *gauche*-conformer (104.7°). It is obvious that the *anti*-positioned silicon substituent predominantly determines the strength of the β-donor interaction. In the *gauche* conformation, a H atom is in an *anti* position relative to the nitrogen donor centre, as is the case in $H_3SiONMe_2$, and the *gauche*-conformers of $ClH_2SiONMe_2$ and $H_3SiONMe_2$ have very similar Si−O−N angles. The β-donor interaction cannot be described as a simple electrostatic attraction between unevenly charged geminal centres, but negative hyperconjugation between the lone pair of electrons at the donor centre and empty σ^*-orbitals at the acceptor centre can be used as a rationale.[6] Another possible explanation involves intramolecular dipole interactions, but these models have not been explored in detail.

Other examples for β-donor interactions are found in the crystal structure of $Me_2AlONMe_2$[7] and the aminomethyl lithium compound Me_2NCH_2Li, as was shown very recently by Steinborn et al.[8] The interest in aminoxysilanes also arises from their use as cold curing catalysts in silicone polymer synthesis,[9] and the catalytic activity of hydroxylamines in the alcoholysis of Si−H functions.[10]

Our current aim was the synthesis of the compound $Cl_2Si(ONMe_2)_2$ and its germanium analogue, in order to answer the following questions: Does the strength of a β-donor interaction increase with an increasing number of electronegative substituents at the acceptor atom, or will effects like "back-bonding" reduce the acceptor ability? Which of the *anti*-substituents is preferred, O or Cl? Is the structure of $Cl_2Si(ONMe_2)_2$ more comparable to that of $H_2Si(ONMe_2)_2$ (∠SiON 95.2°) or to that of $ClH_2SiONMe_2$ (∠SiON 79.7°), or comparable to neither? The following study will show that finding the answers to these questions is actually more difficult than expected and that the nature of β-donor interactions is not yet sufficiently understood.

Results and Discussion

Synthesis: The compounds $Cl_2Si(ONMe_2)_2$ and $Cl_2Ge(ONMe_2)_2$ have been prepared by the reaction of *N,N*-dimethylhydroxylamine with the corresponding tetrachloride of silicon and germanium in the presence of the auxiliary base 2,6-lutidine with pentane as a solvent. The formation of these compounds seems to be favoured under these conditions, as attempts to prepare the triply substituted compounds $ClSi(ONMe_2)_3$ and $ClGe(ONMe_2)_3$ also

 © WILEY-VCH Verlag GmbH, D-69451 Weinheim, 1998 1434−1948/98/1212−2023 $ 17.50+.50/0

resulted in the formation of $Cl_2Si(ONMe_2)_2$ and $Cl_2Ge(ONMe_2)_2$, despite the application of an excess of *N,N*-dimethylhydroxylamine. A suitable temp. to perform the reactions is −60°C. The overall yields achieved in this way are typically >60%.

$$2\ Me_2NOH + SiCl_4 + 2\ C_7H_9N \rightarrow Cl_2Si(ONMe_2)_2 + 2\ C_7H_9N \cdot HCl$$

$$2\ Me_2NOH + GeCl_4 + 2\ C_7H_9N \rightarrow Cl_2Ge(ONMe_2)_2 + 2\ C_7H_9N \cdot HCl$$

Both compounds are crystalline solids soluble in organic solvents. They are air-sensitive, and the solutions fume in moist air. The compounds can be stored at ambient temp. under an inert atmosphere.

Spectroscopy: The identity of the compounds $Cl_2Si(ONMe_2)_2$ and $Cl_2Ge(ONMe_2)_2$ was proved by gas-phase IR spectroscopy, by NMR spectroscopy of the nuclei ^1H, ^{13}C, ^{15}N, ^{17}O, and ^{29}Si and by mass spectrometry.

The solution-NMR spectra recorded at 21°C do not show any preference for certain conformations. Both Me_2NO groups are magnetically equivalent. The proton and proton-decoupled carbon spectra show one singlet each. The occurrence of a quartet of quartets in the proton-coupled carbon spectra verify the presence of a Me_2N group.

The ^{15}N-NMR chemical shifts of $Cl_2Si(ONMe_2)_2$ and $Cl_2Ge(ONMe_2)_2$ are δ = −228.5 and δ = −231.8, which is a shift of about 20 ppm to higher frequencies as compared to the shifts of $ClH_2SiONMe_2$ (δ = −249.5) and the compounds $H_{4-n}Si(ONMe_2)_n$ (n = 1−4, δ = −248.1 to −249.2. The ^{17}O-chemical shift of $Cl_2Si(ONMe_2)_2$ and $Cl_2Ge(ONMe_2)_2$ are δ = 188 and δ = 193. This corresponds to a shift to higher frequencies relative to the shifts of the compounds $H_{4-n}Si(ONMe_2)_n$ (n = 1−4, δ = 135−141) and ClH_2SiOMe_2 (δ = 137). The NMR data do not indicate the existence of inter- or intramolecular donor-acceptor interactions, but rather show such interactions to be efficiently broken by the solvent (C_6D_6), which has also been observed in comparable compounds.

Crystal Structure Determination of $Cl_2Si(ONMe_2)_2$ and $Cl_2Ge(ONMe_2)_2$: Single crystals of $Cl_2Si(ONMe_2)_2$ and $Cl_2Ge(ONMe_2)_2$ were grown by crystallisation from pentane and ether, respectively. Both compounds crystallise in the monoclinic space group $P2_1/c$ with Z = 4 formula units in the unit cell. They are isostructural, with only slightly different cell parameters.

In the crystals of both compounds the molecules are present as monomers. Intermolecular contacts, which would normally be regarded as significant, are absent.

Both compounds adopt the same conformation, which is *anti-gauche*, i.e. one torsion angle OSiON is close to 180° [$Cl_2Si(ONMe_2)_2$: −177.5(1), $Cl_2Ge(ONMe_2)_2$: −178.1(1)°], whereas the other is close to 60° [$Cl_2Si(ONMe_2)_2$: −64.8(1), $Cl_2Ge(ONMe_2)_2$: −64.5(1)°]. The nitrogen atoms of *gauche*-substituents have chlorine atoms in an *anti*-position in almost perfect orientation [torsion Cl(Si/Ge)ON $Cl_2Si(ONMe_2)_2$: 176.1(1), $Cl_2Ge(ONMe_2)_2$: 176.4(1)°].

Figure 1. Molecular structure of $Cl_2Si(ONMe_2)_2$. The non-hydrogen atoms are shown as thermal ellipsoids at the 50% probability level, hydrogen atoms are drawn as circles of arbitrary size

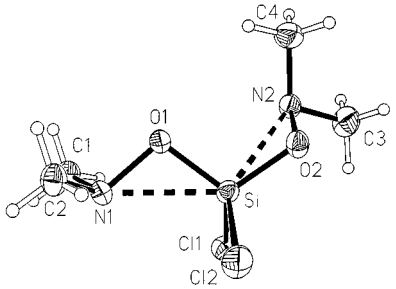

Figure 2. Molecular structure of $Cl_2Ge(ONMe_2)_2$. The non-hydrogen atoms are shown as thermal ellipsoids at the 50% probability level, hydrogen atoms are drawn as circles of arbitrary size

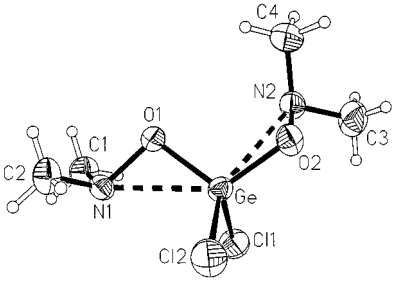

Table 1. Selected bond lengths and angles of $Cl_2Si(ONMe_2)_2$ and $Cl_2Ge(ONMe_2)_2$

Parameter	$Cl_2Si(ONMe_2)_2$	$Cl_2Ge(ONMe_2)_2$
E−O(1)/E−O(2)	1.628(1)/1.626(1)	1.745(2)/1.753(2)
E−Cl(1)/E−Cl(2)	2.028(1)/2.033(1)	2.112(1)/2.118(1)
O(1)−N(1)/O(2)−N(2)	1.489(2)/1.486(2)	1.491(2)/1.482(3)
N(1)−C(1), N(1)−C(2)	1.461(2)/1.459(2)	1.463(3)/1.459(3)
N(2)−C(3), N(2)−C(4)	1.454(2)/1.453(3)	1.456(4)/1.455(4)
O(1)−E−O(2)	109.6(1)	109.5(1)
O(1)−E−Cl(1)/ O(1)−E−Cl(2)	112.2(1)/111.5(1)	111.5(1)/111.0(1)
O(2)−E−Cl(1)/ O(2)−E−Cl(2)	111.4(1)/103.7(1)	111.3(1)/104.6(1)
E−O(1)−N(1)/ E−O(2)−N(2)	102.8(1)/103.7(1)	102.0(1)/102.0(1)
O(1)−N(1)−C(1)/ O(1)−N(1)−C(2)	104.7(1)/105.0(1)	104.6(2)/105.2(2)
O(2)−N(2)−C(3)/ O(2)−N(2)−C(4)	105.3(1)/105.3(1)	105.2(2)/104.9(2)

Despite the different *anti*-substituents, the Si−O−N and Ge−O−N angles on either side of the molecule are almost the same. The angles GeON in $Cl_2Ge(ONMe_2)_2$ are only slightly smaller than the angles SiON in $Cl_2Si(ONMe_2)_2$. This is surprising with reference to the results of crystal structures of $ClH_2SiONMe_2$ (∠SiON 79.7°) and $H_2Si(ONMe_2)_2$ (∠SiON 95.2°): First of all the angles in $Cl_2Si(ONMe_2)_2$ and $Cl_2Ge(ONMe_2)_2$ are much larger than in the compounds referred to above. Secondly, the influence of the *anti*-substituent on the magnitude of the SiON angle seems to be negligible in this case. At this stage it might be concluded that either the increased steric requirements at the acceptor atom, or its reduced acceptor character by

backbonding from the lone pairs at the chlorine and oxygen substituents, is the reason for the weaker β-donor interactions in $Cl_2Si(ONMe_2)_2$ and $Cl_2Ge(ONMe_2)_2$. In fact the SiON angles in these compounds are similar to that of the parent compound $H_3SiONMe_2$, with no further electronegative substituents at the silicon atom apart from that of the single aminoxy substituent.

The bond lengths of both parts of the molecules are very similar. According to the negative hyperconjugation model for the description of β-donor interactions, one would have to expect the E−O and E−Cl bonds in an *anti*-position relative to a nitrogen donor centre to be slightly lengthened with respect to those in a *gauche* position. The conformations of $Cl_2Si(ONMe_2)_2$ and $Cl_2Ge(ONMe_2)_2$ provide us with one of each of these possibilities. In fact the *anti*-positioned chlorine atoms Cl(2) have slightly longer bonds to the central atom than the atoms Cl(1), and the same is the case for the Ge−O(2) bond in $Cl_2Ge(ONMe_2)_2$, which is slightly longer than the Ge−O(1) bond. However, the two Si−O bonds in $Cl_2Si(ONMe_2)_2$ are of the same length within experimental errors.

Conclusion

The present study shows that the occurrence of strong β-donor interactions in SiON systems, which is represented by small SiON angles, is not simple to predict. Although the silicon (and germanium) atom in $Cl_2Si(ONMe_2)_2$ bears more electronegative substituents than in $ClH_2SiONMe_2$ the SiON angle in the first case is much larger. This cannot be understood in terms of simple electrostatic interactions. However, it has already been shown for $ClH_2SiONMe_2$ that a simple electrostatic model cannot explain the very different Si−O−N angles in the *gauche* and *anti* conformers of this compound,[6] and that compounds with even higher positive charges at silicon, such as $Si(ONMe_2)_4$, have wider SiON angles.[4] Therefore the influence of electrostatics should not be overestimated. Clearly the steric requirements at the silicon centre in $Cl_2Si(ONMe_2)_2$ are very different from that in $ClH_2SiONMe_2$, which might account for the differences. A similar argument for the rationalisation of the angle at the oxygen atom can be based upon the low directionality of the Si−O bonds, which is predominantly ionic.[11] However, $Cl_2Si(ONMe_2)_2$ and $H_3SiONMe_2$ have similar SiON angles but the silyl groups are very different in size. Steric requirements and electrostatic interactions could be competing effects, but even a consideration of both could not fully account for the structures observed in SiON compounds.

We are presently investigating the intramolecular electronic effects concerning β-donor-acceptor systems, including dipole interactions and the distribution of electron density, in more detail. Studies on other compounds with geminal acceptor and donor centres in geminal positions should also improve our knowledge on those systems.

This work was supported by the *Bayerischer Staatsminister für Unterricht, Kultus, Wissenschaft und Kunst* (*Bayerischer Habilitationsförderpreis* 1996 for N. W. M.), by the *Deutsche Forschungsgemeinschaft*, the *Fonds der Chemischen Industrie*, the *Leonhard-Lorenz-Stiftung*, and to *Bayer AG, Leverkusen*, for a donation of *N,N*-dimethylhydroxylamine hydrochloride. We thank Mr. *J. Riede* for assistance with the crystallographic data collection and we are grateful to Professor *H. Schmidbaur* for his generous support.

Experimental Section

The experiments were carried out using a standard Schlenk line or a vacuum line with greaseless stopcocks (Young taps), directly attached to the gas cell in an FTIR spectrometer (Midac Prospect FTIR). *N,N*-Dimethylhydroxylamine was liberated from its hydrochloride in liquid ammonia.[12] − NMR: Jeol JNM-LA400 spectrometer; samples in sealed tubes with C_6D_6 as a solvent (21°C) directly condensed onto the sample from K/Na alloy.

Bis(dimethylaminoxy)dichlorosilane: A solution of *N,N*-dimethylhydroxylamine (3.0 ml, 42 mmol) and 2,6-lutidine (4.9 ml, 42 mmol) in pentane (25 ml) was added dropwise to a cooled solution (−60°C) of tetrachlorosilane (2.4 ml, 21 mmol) in pentane (50 ml). The mixture was slowly warmed to ambient temp. After filtration from the salt the solvent was removed in vacuo. The residue was dissolved in 5 ml of diethyl ether and kept at −18°C for 1 d. Bis(dimethylaminoxy)dichlorosilane was isolated as large colourless crystals extremely sensitive to moist air (3.1 g, 67%). − ^{1}H NMR: δ = 2.43 (s, 12 H, H_3C). − ^{13}C NMR: δ = 49.8 (q q, $^1J_{CH}$ = 136.0 Hz, $^3J_{CNCH}$ = 5.4 Hz, CH_3). − ^{15}N{^{1}H} NMR: δ = −228.5 (s). − ^{17}O NMR: δ = 188 (s). − ^{29}Si NMR: δ = −51.9 (s). − MS(CI): *m/z* (%) = 174 (100) [$M^+ - NMe_2$]. − $C_4H_{12}N_2O_2Cl_2Si$ (171.1): calcd. C 22.0, H 5.5, N 12.8; found C 22.0, H 5.5, N 12.9.

Bis(dimethylaminoxy)dichlorogermane: A solution of *N,N*-dimethylhydroxylamine (2.0 ml, 28 mmol) and 2,6-lutidine (3.3 ml, 28 mmol) in pentane (25 ml) was added dropwise to a cooled solution (−60°C) of tetrachlorogermane (1.6 ml, 14 mmol) in pentane (50 ml). The mixture was slowly warmed to ambient temp.. After filtration from the salt the solution was slowly fractionated through a series of cooled traps and bis(dimethylaminoxy)dichlorogermane remained as a small amount of colourless crystals, extremely sensitive to moist air. − ^{1}H NMR: δ = 2.41 (s, 12 H, H_3C). − ^{13}C NMR: δ = 50.3 (q q, $^1J_{CH}$ = 136.0 Hz, $^3J_{CCCH}$ = 5.4 Hz, CH_3). − ^{15}N{^{1}H} NMR: δ = −231.8 (s). − ^{17}O NMR: δ = 193 (s). −MS(CI): *m/z* (%) = 264 (85) [$M^+ - H$]. − $C_4H_{12}Cl_2GeN_2O_2$ (263.63): calcd. C 18.2, H 4.6, N 10.6; found C 18.7, H 4.6, N 10.4.

Crystal Structure Determinations: Single crystals of $Cl_2Si(ONMe_2)_2$ and $Cl_2Ge(ONMe_2)_2$ were selected under a polarisation microscope and mounted into a glass capillary under Ar [$Cl_2Si(ONMe_2)_2$] and under inert perfluoropolyether [Fomblin, $Cl_2Ge(ONMe_2)_2$], respectively. Diffractometer: Enraf-Nonius CAD4, Mo-K_α radiation, graphite monochromator (λ = 0.71073 Å). Solution: direct methods;[13] refinement: SHELXL93.[14] No absorption correction applied. Non-H atoms were refined with anisotropic thermal displacement parameters, hydrogen atoms were located in difference Fourier maps and refined isotropically.

$Cl_2Si(ONMe_2)_2$: $C_4H_{12}Cl_2N_2O_2Si$, M = 219.15, monoclinic; a = 7.935(1), b = 9.472(1), c = 13.583(2) Å, β = 96.47(1); V = 1014.4(2) Å^3 at 133(2) K; cell from 88 reflections (θ-range 19 − 24°); space group $P2(1)/c$; Z = 4; D_c = 1.435; $2\theta_{max.}$ = 53.96°; h = −10 → 10, k = 0 → 12, l = −9 → 17; ω-scan, 3215 reflections collected, 2197 indep. reflections [$R_{int.}$ = 0.0298]. 148 Parameters, R = 0.0349 [for 2028 refl. with $F_o > 4\,\sigma(F_o)$], wR_2 = 0.1227 for all 2182 reflections. Residual electron density: min. 0.39, max. 0.45

eÅ^{-3}. Weight = 1/[$\sigma^2(F_o^2)$ + (0.0666 P)^2 + 0.49·P] where P = [Max (F_o^2,0) + 2·F_c^2]/3.

$Cl_2Ge(ONMe_2)_2$: $C_4H_{12}Cl_2N_2O_2Ge$, M = 263.65, monoclinic; a = 8.043(1), b = 9.631(1), c = 13.789(1) Å, β = 96.42(1); V = 1061.4(2) Å^3 at 188(2) K; cell from 100 reflections (θ-range 19 − 23°); space group $P2(1)/c$; Z = 4; D_c = 1.650; $2\theta_{max.}$ = 56.84°; h = 0 → 10, k = −12 → 0, l = −18 → 18; ω-scan, 2715 reflections collected, 2541 indep. reflections [$R_{int.}$ = 0.0205]. 148 Parameters, R = 0.0263 [for 2078 refl. with F_o > 4 $\sigma(F_o)$], wR_2 = 0.0761 for all 2529 reflections. Residual electron density: min. 0.46, max. 0.28 e Å^{-3}. Weight = 1/[$\sigma^2(F_o^2)$ + (0.028 P)^2 + 0.56·P] where P = [Max (F_o^2,0) + 2·F_c^2]/3.

[1] N. W. Mitzel, U. Losehand, *Angew. Chem., Int. Ed. Engl.* **1997**, *36*, 2807−2809; *Angew. Chem.* **1997**, *109*, 2897−2899.
[2] N. W. Mitzel, *Chem. Eur. J.* **1998**, *4*, 692−698.
[3] N. W. Mitzel, A. J. Blake, D. W. H. Rankin, *J. Am. Chem. Soc.* **1997**, *119*, 4143−4148.
[4] U. Losehand, N. W. Mitzel, *Inorg. Chem.* **1998**, *37*, 3175−82.
[5] U. Losehand, N. W. Mitzel, *J. Chem. Soc., Dalton Trans* **1998**, 2537−2540.
[6] N. W. Mitzel, U. Losehand, *J. Am. Chem. Soc.* **1998**, *120*, 7320 − 7327.
[7] H. D. Hausen, G. Schmöger, W. Schwarz, *J. Organomet. Chem.* **1978**, *153*, 271−279.
[8] C. Bruhn, F. Becke, D. Steinborn, *Organometallics* **1998**, *17*, 2124−2126.
[9] A collection of patent literature references can be found in: M. G. Voronkov, E. A. Maletina, V. K. Roman, *Heterosiloxanes, Vol. 2: Derivates of Nitrogen and Phosphorus,* Harwood Academic Publishers GmbH, Chur, Switzerland **1991**.
[10] Y. Hamada, S. Mori, *Proceedings of the 29th Organosilicon Symposium*, March **1996**, Evanston, USA.
[11] R. J. Gillespie, S. A. Johnson, *Inorg. Chem.* **1997**, *36*, 3031−3039.
[12] *SHELXTL*, Siemens Analytical X-Ray Instrumentation Inc. Madison, WI, **1995**.
[13] *SHELXL93*, Sheldrick, G. M. Universität Göttingen, Germany, 1993.

[I98212]

Intermediates and Side-Reactions in the Synthesis of Molecular Diphenolatonickel Compounds Containing Trimethylphosphane Ligands

Hans-Friedrich Klein*[a], Attila Dal[a], Thomas Jung[a], Ulrich Flörke[b], and Hans-Jürgen Haupt[b]

Institut für Anorganische Chemie der Technischen Universität Darmstadt[a],
Petersenstraße 18, D-64285 Darmstadt, Germany

Anorganische und Analytische Chemie der Universität/GH Paderborn[b],
Warburger Straße 100, D-33095 Paderborn, Germany

Received July 16, 1998

Keywords: Nickel(0) / Oxidation / Phenols / Structure / Ion pairs / Hydrogen bonds

Admission of molecular oxygen to a solution containing $Ni(PMe_3)_4$ and substituted phenols (ArOH) affords bisphenolatonickel compounds *trans*-$Ni(OAr)_2(PMe_3)_2$ [ArOH = 2-chlorophenol (**1**), 2-bromophenol (**2**), 2,4,6-trichlorophenol (**3**)]. In the absence of dioxygen the phenols reversibly protonate the nickel complex to form ionic compounds $[NiH(PMe_3)_4]^+ Y^-$ containing hydrogen-bonded anions Y = $[H_2(2\text{-}Cl\text{–}C_6H_4O)_3]$ (**4**), $[H(2\text{-}OH\text{–}C_6H_4COO)_2]$ (**5**). As a side-reaction, formal insertion of nickel to give 2-hydroxyphenylnickel compounds Ni(Ar′) $X(PMe_3)_3$ [Ar′ = 2-OH–C_6H_4; X = Br (**6**), I (**7**)], *trans*-Ni(Ar′)$Cl(PMe_3)_2$ [Ar′ = 2-OH–3,5-Cl_2–C_6H_2 (**8**)] and *trans*-Ni(OAr)$Cl(PMe_3)_2$ [Ar = 2,4,6-Cl_3–C_6H_2 (**9**)] is observed. An X-ray crystal structure determination of **1** shows a *trans* square planar arrangement of donor atoms, that of **6** shows a distorted square pyramid, while **4** contains tetrahedral nickel cations with a delocalized hydrogen atom and triphenolate anions $H_2(ArO)_3^-$.

Introduction

Steric protection is the key feature in the synthesis of molecular diphenolato-bis(trimethylphosphane) nickel compounds starting from substituted phenols, $Ni(PMe_3)_4$, and dioxygen.[1] Prior to the admission of dioxygen the colour of the pale yellow solution is observed to deepen depending on the phenol and on solvent polarity. In our first attempts to isolate a reaction intermediate we recovered mixtures of the starting materials. However, the introduction of halide substituents into the phenols led to the crystallization, in high yields, of ionic compounds containing the hydridotetrakis(trimethylphosphane)nickel cation and hydrogen-bonded oligophenolate anions. Under these conditions we also observed formation of arylnickel complexes in a side-reaction and investigated the factors supporting formation of Ni−C bonds.

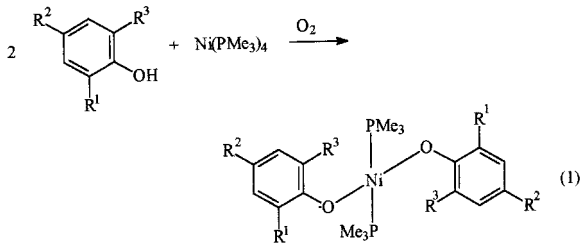

	R^1	R^2	R^3
1	Cl	H	H
2	Br	H	H
3	Cl	Cl	Cl

Results and Discussion

From pale yellow solutions containing $Ni(PMe_3)_4$ and 2-halogenophenol (except 2-iodophenol, see below) in ether at −78 °C a yellow solid precipitated. Upon admission of dioxygen the precipitate dissolved to fom a red solution according to an overall Eq. 1.

The diphenolatonickel complexes **1**−**3** are red or brown solids that are stable in air for several hours. Recrystallization from pentane or ether afforded dark red crystals that can be dried in vacuo without loss of phosphane ligands. Infrared spectra contain fingerprint absorptions of diphenolatonickel complexes and do not show νOH bands. The proton resonance of the trimethylphosphane groups is a singlet, indicating fast exchange of ligands, and no paramagnetic shift or line broadening is observed. Physical and spectroscopic data are thus in accordance with molecular compounds in a low-spin state and square planar coordination of nickel.[1] When compared with 2-*tert*-butyl-substituted diphenolatonickel complexes no significant downfield shift of the 6-H proton resonance signal is detected and hence no steric congestion in the coordination plane is indicated. Indeed, freely oriented 2-chlorophenolato groups are apparent in the molecular structure of complex **1** (Figure 1).

The nickel atom resides at a crystallographic centre of symmetry, and the P−Ni−O angles attain almost ideal values because there is no steric strain, unlike in the case of 2-*tert*-butyl-substituted analogs in which the angle P−Ni−O is opened up by CH_3−CH_3 repulsion of trimethylphosphanes with bulky substituents R^1 and R^2 (Table 1). In two

 © WILEY-VCH Verlag GmbH, D-69451 Weinheim, 1998 1434−1948/98/1212−2027 $ 17.50+.50/0

Figure 1. Molecular structure of **2** (ORTEP plot without hydrogen atoms)[a]

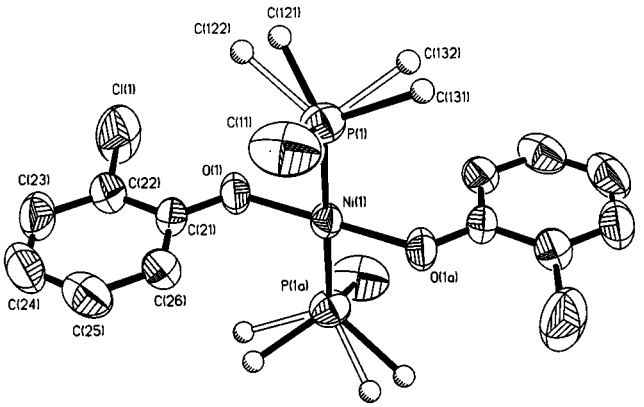

[a] Principal bond lengths [Å] and angles [°]: Ni−O1 1.857(3), Ni−P1 2.233(2), O1−C21 1.320(5), C21−C26 1.394(6), C25−C26 1.378(7); O1−Ni−P1 90.37(12), O1−Ni−P1a 89.63(12), C21−O1−Ni 122.7(3)

Table 1. Distortion by PCH_3-CCH_3 repulsion in diphenolatonickel complexes

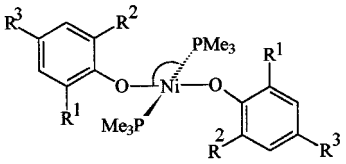

	R^1	R^2	R^3	Ni−P [Å]	O−Ni−P [°]
1	Cl	H	H	2.233(2)	90.37(12)
[a]	$C(CH_3)_3$	H	CH_3	2.233(2)	94.08(12)
[a]	$C(CH_3)_3$	CH_3	H	2.268(2)	98.55(12)

[a] Ref.[1]

structures where R^2 = H the bond distances Ni−P are equal within experimental error while a significant elongation is found in the third.

Ion Pair Intermediates

The exclusion of dioxygen from the reaction mixture induces precipitation of a yellow solid by 2-chlorophenol in 85% yield according to Eq. 2.

Recrystallization from toluene gives pale yellow needles in low yield, and solid **4** under argon at 20°C decomposes within two weeks. The crystalline solid may be stored for several months at −20°C and, on rapid heating, decomposes above 162°C.

The use of salicylic acid leads to the formation of a crystalline precipitate according to Eq. 3. Solid **5** may be stored under argon at 20°C for several weeks and in solution is thermally more stable than **4**. The infrared spectra of nujol mulls of **4** and **5** in the region 3000−1600 cm^{-1} contain several broad bands, and a broad absorption at 1950 cm^{-1} is assigned to an Ni−H vibration. A deuterated sample, **4D**, obtained by reaction according to Eq. 1 using 2-

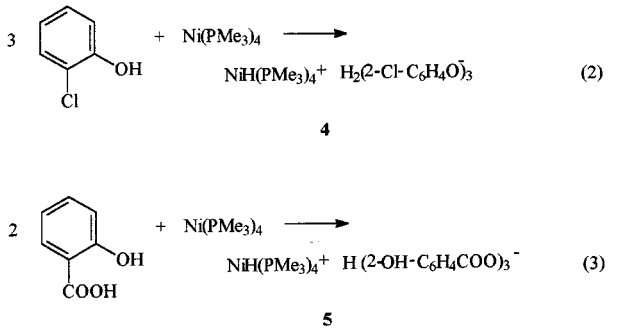

$Cl-C_6H_4-OD$ displayed the expected bathochromic shift of bands, which coincided within a multitude of bands in the fingerprint region. In the NMR experiment freshly prepared samples of **4** in CD_3CN or of **5** in [D_6]THF gave a resonance at δ = −17.2, which is typical for cationic NiH species. After 30 min the signal of **4**, which was not detected in [D_6]THF, gave way to broad resonances of unknown paramagnetic species while that of **5** persisted for some hours.

A pale yellow prismatic single crystal of **4** was subjected to an X-ray diffraction experiment. The lattice of **4** consists of separate nickel cations and triphenolate anions with no bonding contacts between the units. The molecular structure of one of the two metal complex cations in the cell is shown on the left hand side of Figure 2. The frame of heavy atoms, NiP_4, appears as an almost ideal tetrahedron with Ni−P distances in the range 2.213(3)−2.236(3) Å (average 2.224 Å) and angles P−Ni−P in the range 105.93(13)−112.60(14)°.

The two anions in the cell consist of three 2-chlorophenolate entities, each arranged with their anionic O atoms in an approximate equilateral triangle with distances O1−O6 = 2.56(1), O2−O6 = 2.53(1), and O1−O2 = 4.26(1) Å (not depicted) or O3−O5 = 2.53(1), O4−O5 = 2.56(1), and O3−O4 = 4.06(1) Å (Figure 2), respectively, which imply two in-plane hydrogen bridges at angles O1−O6−O2 = 112.9(5)° or O3−O5−O4 = 105.9(5)°, respectively. The phenyl rings are oriented roughly perpendicular to that plane with an up-up-down orientation of the 2-chloro substituents. These structural features are in accordance with the presence of a triphenolate anion, which has been previously observed with *para*-cresolates and a ruthenium complex counterion.[2]

Although the structure of the tetrahedral cation $Ni(PMe_3)_4^+$ in $\{Ni(PMe_3)_4][BPh_4]$[3] displays significantly shorter Ni−P bond distances [2.213(3)−2.221(3) Å, average 2.216 Å], the presence of an additional hydrogen atom in **4** appears questionable based solely on structural parameters. Therefore experiments were designed in order to test the presence of the NiH^+ moiety.

No reaction of **4** or **5** was observed with cyclopentene or carbon dioxide as substrates for an insertion into a metal hydride function. While **4** and **5** failed to protonate trimethylphosphane, action of strong base (NaH, K, or MeLi) on a suspension of **4** or **5** in pentane at −78°C liberated the

Figure 2. Molecular structure of **4** (ORTEP plot without hydrogen atoms)[a]

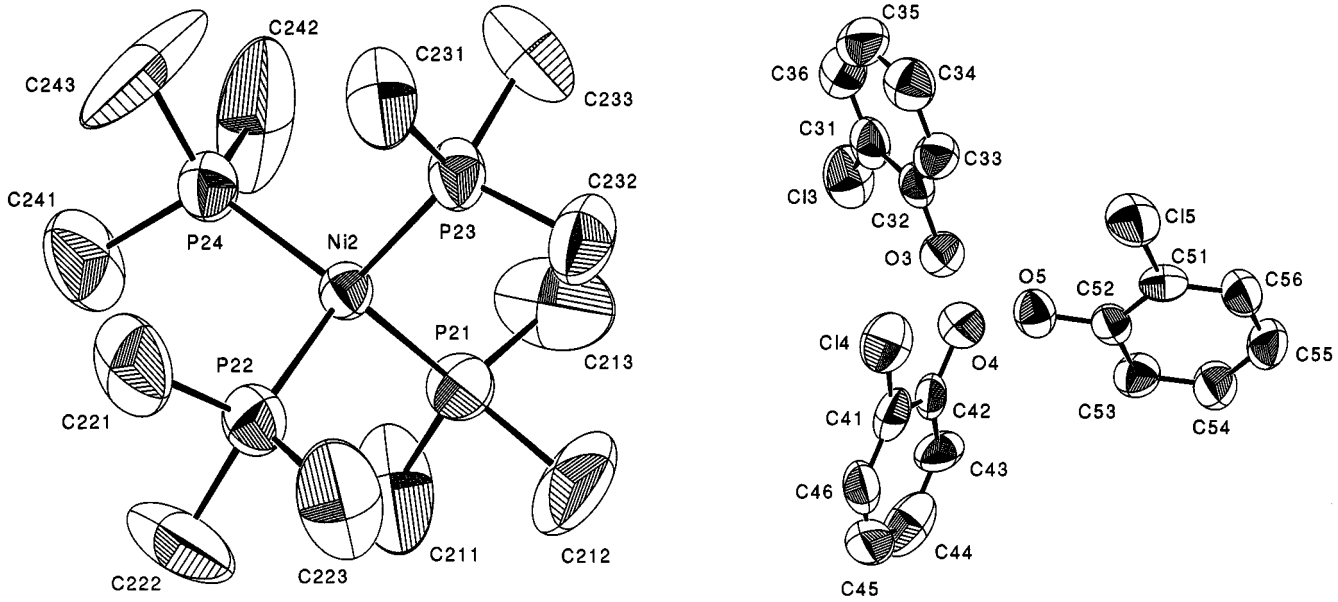

[a] Principal bond lengths [Å] and angles [°]: Ni2−P21 2.223(3), Ni2−P22 2.228(3), Ni2−P23 2.220(4), Ni2−P24 2.236(3), O3−O5 2.53 (1), O4−O5 2.56(1), O3−O4 4.06(1), O3−C32 1.357(9), Cl3−C31 1.733(9), O4−C42 1.354(9), Cl4−C41 1.745(8), O5−C52 1.367(8), Cl5−C51 1.717(7); P21−Ni2−P22 108.52(13), P21−Ni2−P23 108.33(13), P21−Ni2−P24 112.60(14), P22−Ni2−P23 110.5(2), P22−Ni2−P24 106.82(13), P23−Ni2−P24 110.08(14), O3−O5−O4 105.9(5).

expected volume of gas, and quantitative amounts of $Ni(PMe_3)_4$ were recovered (Eq. 4).

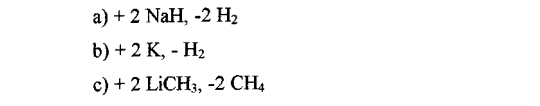

(4)

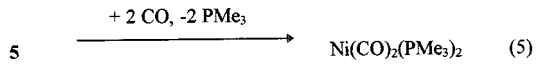

(5)

Protonation of $Ni(PMe_3)_4$ by the phenolic acids was reversed in **4** and **5** under 1 bar CO according to Eq. 5. Thus all successful reactions of **4** and **5** point to the presence of an NiH function exhibiting protic reactivity.

Insertion Reactions

The exclusion of oxygen from the mixtures of $Ni(PMe_3)_4$ and 2-bromo- and 2-iodophenol led to oxidative addition reactions of C−X bonds according to Eq. 6.

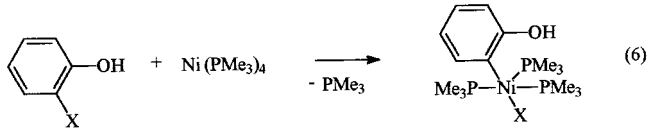

(6)

6: X = Br
7: X = I

The pentacoordinate 2-hydroxyphenylnickel complexes **6** and **7** were obtained from ether as red crystals that are air-sensitive and under argon decompose above 100°C. 2-Chlorophenol does not react under these conditions. Additional activation in 2,4,6-trichlorophenol affords a square planar complex according to Eq. 7. The yellow crystals of **8** are stable in air for several hours and under argon decompose above 102°C. Sharp infrared absorptions at 3204 cm^{-1} (**6**), 3264 cm^{-1} (**7**), and at 3264 cm^{-1} (**8**) indicate the presence of an OH group, which is supported by broad proton resonances at δ = 6.7 (**6**), δ = 7.6 (**7**), and δ = 6.1 (**8**).

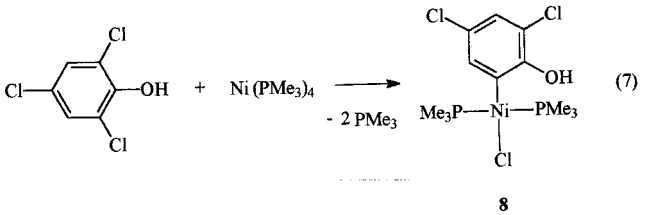

(7)

8

The molecular structure of **6** (Figure 3) shows a pentacoordinate nickel atom in an approximately square pyramidal surrounding of atoms ($CBrP_3$). The axial distance [Ni−Br = 2.805(2) Å] is considerably longer than the equatorial distances in $NiBr_2(PMe_3)_3$ (Ni−Br = 2.426−2.580 Å).[4] There are two short Ni−P distances in the *trans*-PNiP unit and a longer one roughly opposite to the Ni−C bond reflecting a considerable *trans*-influence. A sizeable *trans*-effect is believed to operate and cause exchange of chloride and phenolato ligands involving **8** and **3** under conditions where both oxidation and insertion reactions occur concurrently according to Eq. 8.

A mixed phenolato-chloro compound (**9**) was found to crystallize from the mixture as violet crystals that are air-stable and melt at 162−164°C. The spectroscopic data support a *trans* square-planar coordination geometry of nickel,

Figure 3. Molecular structure of **6** (ORTEP plot without hydrogen atoms)[a]

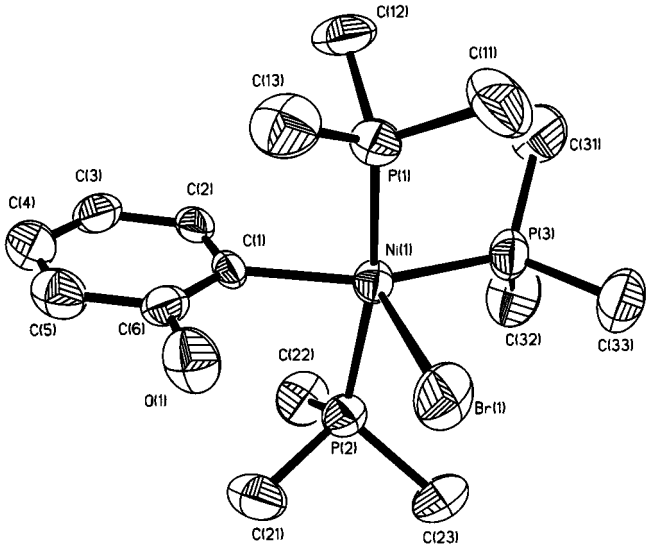

[a] Principal bond lengths [Å] and angles [°]: Ni−C1 2.004(8), Ni−P1 2.196(3), Ni−P2 2.196(3), Ni−P3 2.245(3), Ni−Br 2.805(2), O1−C6 1.370(10); C1−Ni−P1 85.1(3), C1−Ni−P2 84.7(2), C1−Ni−P3 150.6(3), P1−Ni−P2 167.88(11), P1−Ni−P3 96.07(11), P2−Ni−P3 96.03(11), C1−Ni−Br 108.9(3), P1−Ni−Br 88.99(9), P2−Ni−Br 88.14(8), P3−Ni−Br 100.52(8), C6−C1−Ni 124.3(7), C1−C6−O1 125.5(8).

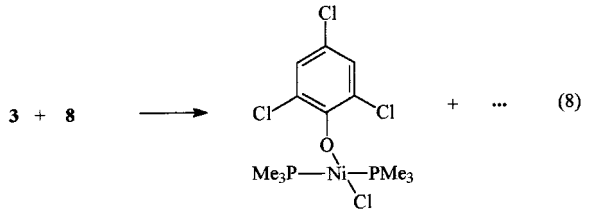

9

and 2,4,6-trichlorophenol is recovered from the reaction with concentrated hydrochloric acid.

Conclusion

Molecular diphenolatobis(trimethylphosphane)nickel complexes can be prepared in high yields starting from substituted phenols, $Ni(PMe_3)_4$, and dioxygen, if halide substituents in the 2-position of the phenolato ligand prevent condensation reactions. Hydrido(trimethylphosphane)-nickel cations and oligomeric hydrogen phenolate counterions are observed as ion-pair intermediates. Single bromide and iodide or multiple chloride substituents in the absence of dioxygen give rise to insertion reactions that, with the exception of iodophenols, are usually dominated by the faster oxidation processes.

Financial support of this work by *Fonds der Chemischen Industrie* and *Deutsche Forschungsgemeinschaft* is gratefully acknowledged.

Experimental Section

General Procedures and Materials: All air-sensitive and volatile materials were handled by standard vacuum techniques and kept under argon. Details have been given elsewhere.[5] $Ni(PMe_3)_4$ was prepared by literature methods,[6] phenols and salicylic acid (Merck-Schuchardt) were used as purchased. Measured volumes of oxygen were admitted to the reaction mixture at −70°C in vacuo.

trans-Di(2-chlorophenolato)bis(trimethylphosphane)nickel (**1**): 830 mg of $Ni(PMe_3)_4$ (2.29 mmol) and 2000 mg of 2-chlorophenol (15.6 mmol) in 70 ml of THF at −78°C were combined with 50 ml of dioxygen. Upon warming, the pale yellow solution turned red/brown. After 72 h at 20°C the volatiles were removed in vacuo and the residue was extracted with pentane over a glass-sinter disc (G3). Crystallization at −20°C afforded dark red rhombs. Yield 575 mg (54% based on nickel), m.p. 179−181°C. − IR (Nujol): $\tilde{\nu}$ = 1577 cm^{-1} (C=C), 1033 (C−O), 949 ρ(PCH_3). − ^1H NMR ([D_8]toluene): δ = 0.98 [s(br), 18 H, $P(CH_3)_3$], 6.31 (t, *J* = 7.2 Hz, 2 H, 4-H), 6.95 (d, *J* = 7.4 Hz, 2 H, 6-H), 7.03 (t, *J* = 7.4 Hz, 2 H, 5-H), 8.15 (m, 2 H, 3-H). − ^{13}C NMR ([D_8]THF): δ = 9.39 [s(br), $P(CH_3)_3$], 112.98 (s, C-6), 120.47(s, C-4), 123.26 (s, C-2), 126.11, 127.63 (C-3, C-5), 160.21 (s, C-1). − $C_{18}H_{26}Cl_2NiO_2P_2$ (466.0): calcd. C 45.40, H 5.62, P 13.33; found C 45.99, H 5.54, P 14.78.

trans-Di(2-bromophenolato)bis(trimethylphosphane)nickel (**2**): 720 mg of $Ni(PMe_3)_4$ (1.98 mmol) and 1000 mg of 2-bromophenol (5.78 mmol) in 60 ml of THF at −78°C were combined with 50 ml of dioxygen. Upon warming, the pale yellow solution turned dark red. After 16 h at 20°C the volatiles were removed in vacuo and the residue was washed with 50 ml of ether and extracted with THF over a glass-sinter disc (G3). Crystallization at −20°C afforded dark red rhombs. Yield 640 mg (58% based on nickel), m.p. 175−177°C. − IR (Nujol): $\tilde{\nu}$ = 1571 cm^{-1} (C=C), 1021(C−O), 948 ρ(PCH_3). − ^1H NMR ([D_8]toluene): δ = 1.08 [s(br), 18 H, $P(CH_3)_3$], 6.26−8.26 (m, 8 H). − $C_{18}H_{26}Br_2NiO_2P_2$ (554.9): calcd. C 38.96, H 4.72, P 11.16; found C 39.06, H 4.46, P 11.30.

trans-Bis(2,4,6-trichlorophenolato)bis(trimethylphosphane)nickel (**3**): 700 mg of $Ni(PMe_3)_4$ (1.93 mmol) and 761 mg of 2,4,6-trichlorophenol (3.86 mmol) in 80 ml of THF at −78°C were combined with 50 ml of dioxygen. After stirring the mixture at 20°C for 16 h the volatile components were removed in vacuo and the dark brown residue was washed with pentane and extracted with ether to afford dark brown crystals. Yield 650 mg (56% based on nickel), m.p. 176−178°C. − IR (Nujol): $\tilde{\nu}$ = 1564 cm^{-1} (C=C), 1071 (C−O), 948 ρ(PCH_3). − ^1H NMR ([D_8]THF): δ = 1.64 [s(br), 18 H, $P(CH_3)_3$], 6.90 (m, 4 H). − ^{13}C NMR ([D_8]THF): δ = 13.82 [s(br), $P(CH_3)_3$], 126.44 (s). − $C_{18}H_{22}Cl_6NiO_2P_2$ (603.7): calcd. C 35.81, H 3.67, P 10.26: found C 35.72, H 3.68, P 10.30.

Hydridotetrakis(trimethylphosphane)nickel−Dihydrogentris(2-chlorophenolate) (**4**): 1000 mg of $Ni(PMe_3)_4$ (2.76 mmol) and 1060 mg of 2-chlorophenol (8.28 mmol) were combined in 80 ml of ether at −70°C to give a yellow precipitate. After warming to 20°C the solid was isolated by decantation and drying in vacuo. Yield (1340 mg, 65%). Recrystallization from ether at −27°C afforded 370 mg of yellow crystals (18%), m.p. 162−164°C. − IR (Nujol): $\tilde{\nu}$ = 1950 cm^{-1} (NiH), 1568 (C=C), 1028 (C−O), 940 ρ(PCH_3). − ^1H NMR ([D_8]THF): δ = −17.24 (m, 1 H, NiH), 1.35 [s(br), 36 H, $P(CH_3)_3$], 6.62 (t, *J* = 6.7 Hz, 1 H), 7.00 (m, 2 H, 3-H, 5-H). − ^{13}C NMR ([D_8]toluene): δ = 11.88 [s(br), $P(CH_3)_3$], 20.92 (s, CH_3), 29.94 [$C(CH_3)_3$], 35.21 [s, $C(CH_3)_3$], 114.89 (s, C-3), 124.80 (s, C-5), 128.90 (s, C-4), 141.45 (s, C-2), 143.96 (C-6), 163.07 (s, C-1). − $C_{30}H_{47}Cl_3NiO_3P_4$ (748.7): calcd. C 48.13, H 6.87, Cl 14.21, Ni 7.84, P 16.62; found C 47.68, H 6.91, Cl 14.26, Ni 7.87, P 16.44.

Hydridotetrakis(trimethylphosphane)nickel−Hydrogendisalicylate (**5**): 1210 mg of $Ni(PMe_3)_4$ (3.33 mmol) and 920 mg of salicylic acid (6.66 mmol) were combined in 70 ml of pentane at −78°C to give a pale yellow precipitate. After warming to 20°C the solid was

Table 2. Crystallographic data of compounds **1**, **4**, and **6**

	1	**4**	**6**
Formula	$C_{18}H_{26}Cl_2NiO_2P_2$	$C_{30}H_{51}Cl_3NiO_3P_4$	$C_{15}H_{32}BrNiOP_3$
Molecular mass	465.9	748.7	459.9
Crystal size [mm]	0.25 × 0.21 × 0.12	0.22 × 0.33 × 0.52	0.28 × 0.20 × 0.18
Crystal system	monoclinic	triclinic	orthorhombic
Space group	$P2_1/n$	$P\text{-}1$	$Pca2_1$
a [Å]	8.932(3)	12.538(9)	13.633(2)
b [Å]	9.936(3)	12.882(10)	11.925(2)
c [Å]	12.720(3)	29.28(2)	12.962(2)
α [°]	90	100.98(3)	90
β [°]	99.65(2)	90.36(2)	90
γ [°]	90	118.12(6)	90
V [Å^3]	1112.9(6)	4069(5)	2107.3(6)
Z	2	4	4
D_{calc} [g/cm^3]	1.390	1.222	1.450
μ(MoK_α) [mm^{-1}]	1.264	0.857	3.042
Temperature [K]	293(2)	293(2)	293(2)
data coll. range [°]	$5.2 \leq 2\Theta \leq 55$	$2.8 \leq 2\Theta \leq 50$	$4.5 \leq 2\Theta \leq 55$
h	$-11 \leq h \leq 11$	$0 \leq h \leq 14$	$0 \leq h \leq 17$
k	$0 \leq k \leq 12$	$-14 \leq k \leq 13$	$0 \leq k \leq 15$
l	$0 \leq l \leq 16$	$-34 \leq l \leq 34$	$0 \leq l \leq 16$
No. reflect. measured	2690	14880	2544
No. unique reflect.	2580(R_{int} = 0.0463)	14160(R_{int} = 0.0438)	2544
No. parameters refined	120	669	200
R_1 [$F \geq 2\sigma(F)$]	0.0659	0.0873	0.0578
wR_2 [$F \geq 2\sigma(F)$]	0.1246	0.2946	0.0900

isolated by decantation and dried in vacuo. Yield (1650 mg, 78%), m.p. 136−139°C. − IR (Nujol): $\tilde{\nu}$ = 2612 cm^{-1} (OH), 1950 (NiH), 1032 (C−O), 940 ρ(PCH_3). − ^{1}H NMR ([D$_8$]THF): δ = −17.19 (m, 1 H, NiH), 1.36 [s(br), 36 H, P(CH_3)$_3$], 6.70 (m, 2 H, 5-H,), 6.81 (m, 2 H, 6-H,), 7.23 (m, 2 H, 4-H), 7.91 (m, 2 H, 3-H), 14.55 (m, 1 H, O−H−O). − $C_{26}H_{48}NiO_6P_4$ (639.3): calcd. C 48.85, H 7.57, P 19.38; found C 48.20, H 7.43, P 19.66.

Bromo(2-hydroxyphenyl)tris(trimethylphosphane)nickel (**6**): 620 mg of Ni(PMe_3)$_4$ (1.71 mmol) and 2.0 ml of 2-bromophenol (18.9 mmol) were combined in 60 ml of THF at −78°C. After stirring at 20°C for 72 h the solution attained a deep blue color. The volatiles were removed in vacuo and the resulting dark red solid was washed with two 10-ml portions of ether and recrystallized from THF to afford 160 mg of red crystals (20%), m.p. 108−110°C. − IR (Nujol): $\tilde{\nu}$ = 3204 cm^{-1} (OH), 1560 (C=C), 1011 (C−O), 951 ρ(PCH_3). − ^{1}H NMR (CD_2Cl_2): δ = 1.07 [s(br), 27 H, P(CH_3)$_3$], 6.35 (m, 1 H), 6.67 (s, 1 H), 6.70 (m, 1 H, OH), 6.98 (s, 1 H). − ^{13}C NMR ([D$_8$]THF): δ = 13.78 [s(br), P(CH_3)$_3$], 111.36 (s, C-6), 117.96 (s, C-4), 122.25, 134.61 (s, C-3, C-5), 159.87 (s, C-1). − $C_{15}H_{32}BrNiOP_3$ (460.0): calcd. C 39.32, H 7.01, P 20.62; found C 39.17, H 7.01, P 20.20.

Iodo(2-hydroxyphenyl)tris(trimethylphosphane)nickel (**7**): 1130 mg of Ni(PMe_3)$_4$ (3.11 mmol) and 685 mg of 2-iodophenol (3.11 mmol) were combined in 70 ml of THF at −78°C. After stirring at 20°C for 18 h the solution attained a greenish color. The volatiles were removed in vacuo and the resulting dark red solid was recrystallized from ether to afford 1010 mg of red crystals (64%), m.p. 96−98°C. − IR (Nujol): $\tilde{\nu}$ = 3264 cm^{-1} (OH), 1559 (C=C), 1011 (C−O), 944 ρ(PCH_3). − ^{1}H NMR (CD_2Cl_2): δ = 1.20 [s(br), 27 H, P(CH_3)$_3$], 6.37 (dd, ^3J = 7.7 Hz, ^4J = 1.4 Hz, 1 H, 3-H), 6.55 (dt, ^3J = 7.1 Hz, ^4J = 1.4 Hz, 1 H, 4-H), 6.73 (dt, ^3J = 7.3 Hz, ^4J = 1.4 Hz, 1 H, 5-H), 7.14 (dd, ^3J = 7.1 Hz, ^4J = 1.4 Hz, 1 H, 6-H), 7.60 (m, 1 H, OH). − ^{13}C NMR ([D$_8$]THF): δ = 15.31 [s(br), P(CH_3)$_3$], 112.14 (s, C-6), 118.20 (s, C-4), 123.44, 136.84 (s, C-3, C-5), 161.84 (s, C-1). − $C_{15}H_{32}INiOP_3$ (506.9): calcd. C 35.54, H 6.36, P 18.33; found C 35.47, H 6.11, P 18.35.

Chloro(2-hydroxy-3,5-dichlorophenyl)bis(trimethylphosphane)nickel (**8**): 880 mg of Ni(PMe_3)$_4$ (2.42 mmol) and 945 mg of 2,4,6-trichlorophenol (4.85 mmol) were combined in 50 ml of THF at −78°C and after warming to 20°C the solution attained an intense yellow color. After 18 h the volatiles were removed in vacuo and the resulting solid was recrystallized from pentane to afford 240 mg of red crystals (24%), m.p. 102−103°C. − IR (Nujol): $\tilde{\nu}$ = 3486 cm^{-1} (OH), 1552 (C=C), 1063 (C−O), 948 ρ(PCH_3). − ^{1}H NMR ([D$_6$]benzene): δ = 0.92 [s(br), 18 H, P(CH_3)$_3$], 6.11 (m, 1 H, OH), 7.36 (s, 1 H), 7.42 (s, 1 H). − ^{13}C NMR ([D$_8$]THF): δ = 17.68 [s(br), P(CH_3)$_3$], 120.78 (s, CCl), 130.95, 131.84 (s, CH), 132.54 (s, CNi), 162.75 (s, CO). − $C_{12}H_{21}Cl_3NiOP_3$ (408.3): calcd. C 35.30, H 5.18, P 15.17; found C 35.49, H 5.52, P 14.99.

trans-Chloro(2,4,6-trichlorophenolato)bis(trimethylphosphane)nickel (**9**): 880 mg of Ni(PMe_3)$_4$ (2.42 mmol) and 944 mg of 2,4,6-trichlorophenol (4.85 mmol) in 50 ml of THF were combined at −78°C and after warming to 20°C the solution attained an intense yellow color. After stirring for 16 h 50 ml of dioxygen was admitted and a violet coloration was observed. The mixture was stirred for another 3 h, the volatiles were removed in vacuo and the residue extracted with 50 ml of pentane to afford 70 mg of violet crystals (24% based on Ni), m.p. 162−164°C. − IR (Nujol): $\tilde{\nu}$ = 1564 cm^{-1} (C=C), 1077 (C−O), 948 ρ(PCH_3). − ^{1}H NMR ([D$_6$]acetone): δ = 1.57 [m, 18 H, P(CH_3)$_3$], 6.88 (s, 2 H). − ^{13}C NMR ([D$_8$] acetone): δ = 10.65 [t′, ^1J(PC) + ^3J(PC) = 23.9 Hz, P(CH_3)$_3$], 120.94 (s, CH). − $C_{12}H_{20}Cl_4NiOP_2$ (442.8): calcd. C 32.55, H 4.55, P 13.99; found C 32.82, H 4.60, P 14.05.

Crystal Structure Analyses: Crystal data are presented in Table 2.

Data Collection. − *Complex* **1**: A dark red specimen was sealed under argon in a glass capillary and mounted on a Siemens R3m/V diffractometer. Using graphite-monochromated Mo-K_α radiation, lattice parameters were obtained from 25 centered reflections. ω scan data were collected and Lp and empirical absorption corrections were applied. Structure solution was performed by direct methods, full-matrix least-squares refinement based on F^2. All non-hydrogen atoms were treated anisotropically and hydrogen atoms

were fixed at idealized positions. − *Complex* **4**: A yellow specimen (from ether) was sealed under argon in a glass capillary and mounted on a Siemens P4 diffractometer. Data collection, corrections (without ψ-scans), and structure solution and refinement were as for **1**. − *Complex* **6**: A dark red specimen was sealed under argon in a glass capillary and mounted on a Siemens R3m/V diffractometer. Data collection, corrections, and structure solution and refinement as before.

Crystallographic data (excluding structure factors) for the structures reported in this paper have been deposited with the Cambridge Crystallographic Data Centre. Copies of the data [**1**: CCDC-102020, **4**: CCDC-102094 , **6**: CCDC-102021] can be obtained free of charge on application to CCDC, 12 Union Road, Cambridge CB2 1EZ, UK [Fax: (internat.) + 44(1223)336−033, E-mail: deposit@chemcrys.cam.ac.uk).

[1] H.-F. Klein, A. Dal, T. Jung, S. Braun, C. Roehr, U. Floerke, H.-J. Haupt, *Eur. J. Inorg. Chem.* **1998**, 621−627.
[2] M. J. Burn, M. G. Fickes, F. J. Hollander, R. G. Bergman, *Organometallics* **1995**, *14*, 137−150.
[3] A. Gleizes, M. Dartiguenave, Y. Dartiguenave, J. Galy, H.-F. Klein, *J. Am. Chem. Soc*. **1977**, *99*, 5187−5189.
[4] J. W. Dawson, T. J. McLennan, W. Robinson, A. Merle, M. Dartiguenave, Y. Dartiguenave, H. B. Gray, *J. Am. Chem. Soc.* **1974**, *96*, 4428−4435.
[5] H.-F. Klein, A. Brand, G. Cordier, *Z. Naturforsch.* **1998**, *53b*, 307−314.
[6] H.-F. Klein, H. H. Karsch, *Chem. Ber.* **1976**, *109*, 2515−2523.
[I98215]

Reactions of Dimethyl[tris(trimethylsilyl)methyl]metalanes of Aluminum and Gallium with H_2S and Elemental Chalcogens – Crystal Structures of $[RAl(\mu\text{-}S)]_2 \cdot 2$ THF, $[RGa(\mu_3\text{-}S)]_4$, $[\{RAl(\mu_3\text{-}S)\}_3MeAl(\mu_3\text{-}S)]$, $[RAlMe(\mu\text{-}SeMe)]_2$, and $[RGaMe(\mu\text{-}TeMe)]_2$ [R = $C(SiMe_3)_3$]

Christoph Schnitter, Andreas Klemp, Herbert W. Roesky*, Hans-Georg Schmidt, Cord Röpken, Regine Herbst-Irmer, and Mathias Noltemeyer

Institut für Anorganische Chemie der Universität Göttingen,
Tammannstrasse 4, D-37077 Göttingen, Germany
Fax: (internat.) + 49(0)551/39-3373
E-mail: hroesky@gwdg.de

Received July 8, 1998

Keywords: Aluminum / Chalcogens / Cubanes / Gallium / Main group elements

The reaction of the trialkylalane $(Me_3Si)_3CAlMe_2 \times THF$ (**1**) with H_2S in toluene at room temperature results in the formation of the dimeric sulfido compound $[(Me_3Si)_3CAl(\mu\text{-}S)]_2 \times 2$ THF (**3**), while the reaction of the homologous gallane $(Me_3Si)_3CGaMe_2$ (**2**) with H_2S under similar conditions affords the heterocubane $[(Me_3Si)_3CGa(\mu_3\text{-}S)]_4$ (**4**). Heating of compound **3** in vacuo gives a mixture of the symmetrically substituted $[(Me_3Si)_3CAl(\mu_3\text{-}S)]_4$ (**5**) and the unsymmetrically substituted heterocubane $[\{(Me_3Si)_3CAl(\mu_3\text{-}S)\}_3MeAl(\mu_3\text{-}S)]$ (**6**). Reaction of the trialkylmetalanes **1** and **2** with elemental selenium in refluxing toluene results in the formation of the corresponding selenolates $[(Me_3Si)_3CMMe(\mu\text{-}SeMe)]_2$ (**7**, M = Al; **8**, M = Ga). The compounds exhibit a high thermal stability and can not be converted to the corresponding selenides $[(Me_3Si)_3CM(\mu_3\text{-}Se)]_n$ (M = Al, Ga) upon heating. In contrast, the trialkylalane **1** does not react with tellurium metal in refluxing toluene at all, while the trialkylgallane **2** affords the tellurolate $[(Me_3Si)_3CGaMe(\mu\text{-}TeMe)]_2$ (**9**) under similar conditions. Compounds **3–9** have been characterized by ^1H- and ^{29}Si-NMR, mass, and IR spectroscopy. Furthermore, the molecular structures of compounds **3** $\cdot$ C_6H_6, **4** $\cdot$ 1.5 C_6H_6, **6**, **7** $\cdot$ C_6H_6 and **9** have been determined by X-ray crystallography.

Introduction

Organometallic cage compounds of aluminum and gallium with bonds to group 15 elements with composition $[RMER']_x$ (M = Al, Ga; E = N, P; R, R′ = H, alkyl, aryl) have been intensively studied over the last two decades[1] especially due to their potential use as precursors of group 13-15 materials. In contrast, only a few of fully characterized cage compounds $[RME]_x$ (R = alkyl, aryl; M = Al, Ga; E = S, Se, Te) of groups 13 and 16 have been reported.[2] This is surprising, since materials with compositions ME and M_2E_3 (M = Ga, In; E = S, Se) have interesting electronic and optoelectronic properties and could possibly find applications for nonlinear optics,[3] photovoltaics,[4] and electronic devices.[5] Moreover, the cubic phase of gallium sulfide prepared from the single source precursor $[t\text{BuGa}(\mu_3\text{-}S)]_4$ has been shown to passivate GaAs[6] and was used to realize a new class of GaAs transistors.[7] Syntheses of mixed-metal chalcogenides such as $CuInE_2$ (E = S, Se) from single-source precursors[8] have also been successful and their efficiency as photovoltaic cells is documented.[9]

The few examples of structurally characterized 13-16 cage compounds $[RME]_x$[2] have been preferentially prepared by a) protolysis of R_3M with H_2E, b) reaction of $RMCl_2$ with $E(SiMe_3)_2$, c) oxidation of RM with elemental chalcogens, and d) reaction of R_3M with elemental chalcogens. The last mentioned process occurs via the corresponding chalcogenates $[R_2M(\mu\text{-}ER)]_2$ as the first insertion products, which could be trapped in a few cases.[9b][9c] The compounds are of particular interest as selective reagents in organic synthesis, e.g. $[i\text{Bu}_2\text{AlER}]_x$ (R = alkyl; E = S, Se, Te) for the conversion of aldehydes to thiol-, selenol-, and tellurol esters.[10]

We have recently reported on hydrolysis studies of the trialkylmetalanes $(Me_3Si)_3CAlMe_2 \cdot$ THF (**1**) and $(Me_3Si)_3CGaMe_2$ (**2**) leading to the isolation and structural characterization of some unusual alkylaluminum- and -gallium-hydroxo(oxo) compounds.[11] In continuation of our systematic studies on group 13-16 chemistry, we now report on the synthesis and characterization of some new alkylaluminum- and -gallium chalcogen compounds with the bulky tris(trimethylsilyl)methyl ("trisyl") ligand.

Results and Discussion

Reaction of $(Me_3Si)_3CAlMe_2 \cdot$ THF (**1**) with H_2S in toluene at room temperature yielded the dimeric trisylaluminum sulfido compound $[(Me_3Si)_3CAl(\mu\text{-}S)]_2 \cdot 2$ THF (**3**) (Eq. 1), presumably via an unstable hydridosulfido intermediate, i.e. $[(Me_3Si)_3CAlMe(\mu\text{-}SH)]_2 \cdot 2$ THF. The softer Lewis base

 © WILEY-VCH Verlag GmbH, D-69451 Weinheim, 1998 1434–1948/98/1212–2033 $ 17.50+.50/0

H_2S seems to be unable under the given reaction conditions to replace the harder Lewis base THF at the hard Lewis acidic aluminum center. Under similar conditions the trialkylgallane $(Me_3Si)_3CGaMe_2$ (**2**) gave the tetrameric compound $[(Me_3Si)_3CGa(\mu_3\text{-}S)]_4$ (**4**) (Eq. 2).[12] The hydridosulfido intermediate could not be trapped, in contrast to the reaction of tBu$_3$Ga with H_2S, which allows the isolation of the thermal stable hydridosulfido product $[t\text{Bu}_2\text{Ga}(\mu\text{-SH})]_2$.[9a]

$$2\,(Me_3Si)_3CAlMe_2 \cdot THF + 2\,H_2S \xrightarrow[-\,4\ MeH]{\text{toluene, 25 °C}}$$

1

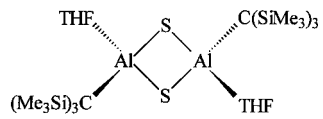

(1)

3

$$4\,(Me_3Si)_3CGaMe_2 + 4\,H_2S \xrightarrow[-\,8\ MeH]{\text{toluene, 25 °C}}$$

2

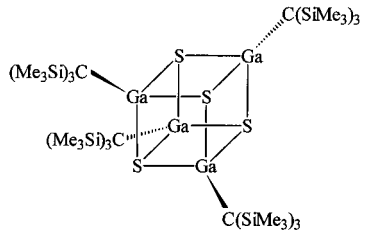

(2)

4

Compounds **3** and **4** have been fully characterized by ^{1}H- and ^{29}Si-NMR, mass, and IR spectroscopy as well as elemental analyses. In addition, recrystallization from benzene gave single crystals of **3** · C_6H_6 and **4** · 1.5 C_6H_6 suitable for X-ray diffraction analyses.

Figure 1 shows the molecular structure of compound **3**, which crystallizes with half of a molecule in the asymmetric unit in the orthorhombic space group Pbca. The planar Al_2S_2 core is elongated in the direction of the S−S axis (Al−S−Al 81.2°, S−Al−S 98.8°) comparable to the recently reported sulfide $[\text{Mes*Al}(\mu\text{-S})]_2 \cdot 2\ Me_2SO$ (Mes* = 2,4,6-tBu$_3$C$_6$H$_2$) (Al−S−Al 83.5°, S−Al−S 95.9°, average) with a nonplanar Al_2S_2 ring.[13] Both aluminum centers show distorted tetrahedral coordination by two bridging sulfur atoms, one THF molecule and one trisyl group. The Al−S (224.8 pm) and Al−C (202.9 pm) distances in **3** · C_6H_6 are in good agreement with those observed for [Mes*Al(μ-S)]$_2$ · 2 Me_2SO (Al−S 225.1 pm, Al−C 202.2 pm).[13] The Al−O distance in **3** · C_6H_6 (195.3 pm) is slightly shorter than that in the starting material **1** (196.8 pm)[11] due to electron-withdrawing properties of the sulfur atoms.

The molecular structure of the tetrameric compound $[(Me_3Si)_3CGa(\mu_3\text{-}S)]_4$ (**4**), which crystallizes in the trigonal space group $P\bar{3}c1$ with four tetramers and six benzene molecules in each unit cell, is depicted in Figure 2. The core of compound **4** consists of a distorted cube with Ga and S atoms at alternating corners. The pseudotetrahedral coordination sphere at each gallium atom is completed by a trisyl group. The average Ga−S distances (237.8 pm) are in the range of those observed for $[t\text{BuGa}(\mu_3\text{-S})]_4$ (235.9 pm),[2a] $[Me_2EtCGa(\mu_3\text{-S})]_4$ (235.6 pm),[2f] $[(Cp(CO)_2Fe)Ga(\mu_3\text{-S})]_4$ (237.5 pm)[2g] and $[\text{tmpGa}(\mu_3\text{-S})]_4$ (tmp = 2,2,6,6-tetramethylpiperidyl) (235.6 pm).[2h] The deviation from a perfect cube in **4** (average: Ga−S−Ga 86.4°, S−Ga−S 93.5°) is somewhat smaller than in $[t\text{BuGa}(\mu_3\text{-S})]_4$ (average: Ga−S−Ga 82.1°, S−Ga−S 97.3°),[2a] $[Me_2EtCGa(\mu_3\text{-S})]_4$ (average: Ga−S−Ga 82.2°, S−Ga−S 97.2°),[2f] $[(Cp(CO)_2\text{-Fe})Ga(\mu_3\text{-S})]_4$ (average: Ga−S−Ga 84.1°, S-Ga-S 95.6°),[2g] and $[\text{tmpGa}(\mu_3\text{-S})]_4$ (average: Ga−S−Ga 84.2°, S−Ga−S 95.5°).[2h] The average Ga−C distance (202.0 pm) is a little shorter than the Ga−C_{trisyl} distance in $(Me_3Si)_3CGaMe_2$ · THF (204.6 pm)[11] due to the higher effective positive charge of the gallium atoms caused by the electronegative sulfur atoms.

Figure 1. Crystal structure of $[(Me_3Si)_3CAl(\mu\text{-S})]_2 \cdot 2$ THF (**3**), with anisotropic displacement parameters depicting 50% probability. Hydrogen atoms have been omitted for clarity[a]

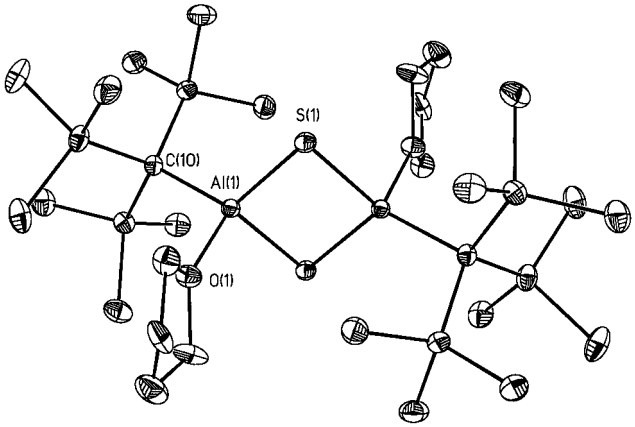

[a] Selected bond lengths [pm] and angles [°]: Al(1)−C(10) 202.9(2), Al(1)−O(1) 195.29(17), Al(1)−S(1) 224.83(9), Al(1)−S(1A) 223.47(9); C(10)−Al(1)−O(1) 107.17(8), C(10)−Al(1)−S(1) 120.97(7), C(10)−Al(1)−S(1A) 121.21(7), O(1)−Al(1)−S(1) 103.27(6), O(1)−Al(1)−S(1A) 102.87(6), S(1)−Al(1)−S(1A) 98.79(3), Al(1)−S(1)−Al(1A) 81.21(3).

The cubane **4** exhibits high thermal stability and can be easily purified by sublimation in vacuo (180 °C, 10^{-2} mbar). A topological reorganization of the polyhedral core as reported for the formation of $[t\text{BuGaS}]_x$ (x = 6, 7, 8) by thermolysis of $[t\text{BuGa}(\mu_3\text{-S})]_4$[14] has not been observed for **4**.

Interestingly, the mass spectrum of **3** shows, in addition to the signals for characteristic fragment ions of the dimeric sulfide, at elevated temperatures (above 200 °C) signals with higher masses (e.g. m/z 1147, 929), indicating formation of larger aggregates. These observations encouraged us to examine the thermolysis of **3** on a preparative scale. Heating of $[(Me_3Si)_3CAl(\mu\text{-S})]_2 \cdot 2$ THF (**3**) in vacuo (220 °C, 10^{-2} mbar) for 30 minutes gave, after workup, a yellowish solid which was identified by ^{1}H- and ^{29}Si-NMR, and mass spectroscopy as a mixture of the tetrameric organoaluminum sulfides $[(Me_3Si)_3CAl(\mu_3\text{-S})]_4$ (**5**) and $[\{(Me_3Si)_3CAl(\mu_3\text{-S})\}_3MeAl(\mu_3\text{-S})]$ (**6**) (≈ 30:70) (Eq. 3). To our knowledge

Figure 2. Crystal structure of $[(Me_3Si)_3CGa(\mu_3\text{-}S)]_4$ (**4**), with anisotropic displacement parameters depicting 50% probability. Hydrogen atoms have been omitted for clarity[a]

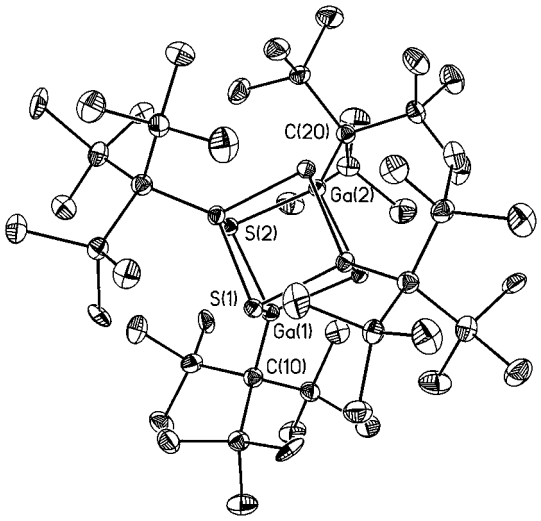

[a] Selected bond lengths [pm] and angles [°]: Ga(1)−C(10) 202.0(4), Ga(1)−S(1) 237.90(10), Ga(1)−S(2) 237.91(11), Ga(1)−S(2A) 237.63(11), Ga(2)−C(20) 201.9(6), Ga(2)−S(2) 237.74(10); C(10)−Ga(1)−S(1) 122.56(10), C(10)−Ga(1)−S(2) 122.31(11), C(10)−Ga(1)−S(2A) 123.45(11), S(1)−Ga(1)−S(2) 93.46(4), S(1)−Ga(1)−S(2A) 93.53(4), S(2)−Ga(1)−S(2A) 93.41(4), C(20)−Ga(2)−S(2) 122.80(3), S(2)−Ga(2)−S(2A) 93.43(3), Ga(1)−S(1)−Ga(1A) 86.37(4), Ga(1)−S(2)−Ga(1A) 86.43(3), Ga(1)−S(2)−Ga(2) 86.44(3), Ga(1A)−S(2)−Ga(2) 86.51(4).

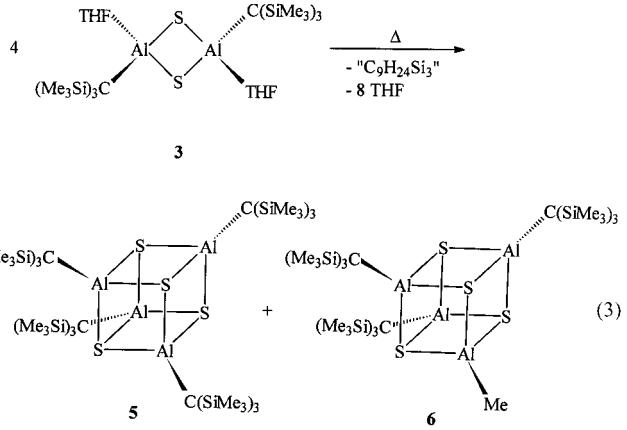

such a fragmentation of the trisyl group under chemical conditions is unprecedented.

However, we were neither able to separate this mixture by fractional crystallization or sublimation nor to obtain pure compounds by variation of the reaction conditions. The recrystallization of the mixture from toluene at room temperature results in the formation of single crystals of both compounds, which differ in their shape (**5** rods, **6** blocks). Unfortunately, only the single crystals of compound **6** were suitable for X-ray diffraction analysis.

Figure 3 shows the molecular structure of the unsymmetric substituted cubane $[\{(Me_3Si)_3CAl(\mu_3\text{-}S)\}_3MeAl(\mu_3\text{-}S)]$ (**6**), which crystallizes in the triclinic space group $P\bar{1}$. The distorted central Al_4S_4 heterocubane core (Al−S−Al 83.5°, S−Al−S 96.1°, average) is comparable with that observed for the symmetrically substituted cubane $[Me_2EtCAl(\mu_3\text{-}S)]_4$ (Al−S−Al 82.2°, S−A−S 97.3°, average),[2f] which is the only other example of a structurally characterized Al-S cubane. Due to the lower symmetry of the molecule caused by the different substituents at the aluminum atoms in **6**, the bond lengths and angles of the core are in a wider range than those of $[Me_2EtCAl(\mu_3\text{-}S)]_4$.[2f] For the Al coordinated by the methyl group the Al−S bonds are relatively similar (230.3−230.7 pm), while for the Al atoms coordinated by the trisyl ligands one long Al−S distance (235.5−235.8 pm), one distance in a middle range (233.7−234.2 pm) and one comparatively short distance (231.0−231.5 pm) are observed. In total, the Al−S distances (average: 232.8 pm) are close to those observed for $[Me_2EtCAl(\mu_3\text{-}S)]_4$ (average: 231.3 pm)[2f] but are distinctly longer than those of the starting material **3** (224.8 pm) and the recently reported dimeric organoaluminum sulfide $[Mes^*Al(\mu\text{-}S)]_2$ (Mes* = 2,4,6-tBu$_3$C$_6$H$_2$) (221.0 pm)[13] due to the higher coordination number of the sulfur atoms. On the other hand the nearly equal $Al-C_{trisyl}$ distances (average: 197.7 pm) are little shorter than those in the starting material **3** (average: 202.9 pm).

As mentioned above, a second method for the preparation of group 13-16 cage compounds is the reaction of trialkylmetalanes with elemental chalcogens. Because of the very high toxicity of H_2Se and H_2Te we tried to prepare the corresponding selenides and tellurides following this route.

Reactions of $(Me_3Si)_3CAlMe_2 \cdot THF$ (**1**) and $(Me_3Si)_3CGaMe_2$ (**2**) with elemental selenium in a 1:1 ratio in refluxing toluene resulted in the formation of the corresponding selenolates $[(Me_3Si)_3CMMe(\mu\text{-}SeMe)]_2$ (**7**: M = Al, **8**: M = Ga) in good yields (Eqs. 4, 5).

In both cases, the selenium reacted within 2 h, and the color of the reaction mixture changes from colorless through green to yellow. Compounds **7** and **8** are colorless, air- and moisture-sensitive, and extremely malodorous solids, which were fully characterized by ^{1}H- and ^{29}Si-NMR, mass, and IR spectroscopy as well as by elemental analyses (see Experimental Section). Additionally, recrystallization from benzene afforded single crystals of $\mathbf{7} \cdot C_6H_6$ suitable for X-ray diffraction analysis.

Figure 4 shows the crystal structure of the aluminum selenolate **7**, which crystallizes in the orthorhombic space group *Ibam* with eight dimers and eight benzene molecules in the unit cell. The central core of **7** is characterized by a distorted four-membered Al_2Se_2 ring (Al−Se−Al 86.2°, Se−Al−Se 84.0°, average) tilted towards the methyl groups at both aluminum and selenium in a *cis* conformation [angle between the planes defined by Al(1)/Se(1)/Se(2) and Al(1A)/Se(1)/Se(2) 133.6°]. In contrast, the ring of the only other structurally characterized dimeric aluminum selenolate $[Mes_2Al(\mu\text{-}SeMe)]_2$ (Mes = 2,4,6-Me$_3$C$_6$H$_2$)[15] is planar and nearly undistorted (Al−Se−Al 89.4°, Se−Al−Se 90.6°, average) with the methyl substituents on the selenium in the *trans* conformation. This different behaviour can be explained by minimization of steric crowding caused by the bulky trisyl ligands. The Al−Se distances in **7** (average:

Figure 3. Crystal structure of [{$(Me_3Si)_3CAl(\mu_3\text{-}S)\}_3MeAl(\mu_3\text{-}S)$] (**6**), with anisotropic displacement parameters depicting 50% probability. Hydrogen atoms have been omitted for clarity[a]

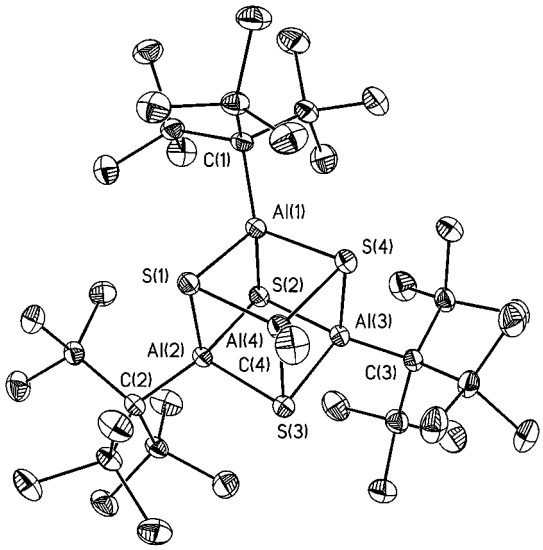

[a] Selected bond lengths [pm] and angles [°]: Al(1)−C(1) 197.8(2), Al(1)−S(1) 231.49(11), Al(1)−S(2) 235.49(10), Al(1)−S(4) 233.70(14), Al(2)−C(2) 197.5(2), Al(2)−S(1) 234.22(10), Al(2)−S(2) 235.75(10), Al(2)−S(3) 231.00(13), Al(3)−C(3) 197.8(2), Al(3)−S(2) 235.65(14), Al(3)−S(3) 233.90(10), Al(3)−S(4) 231.20(10), Al(4)−C(4) 192.7(3), Al(4)−S(1) 230.52(13), Al(4)−S(3) 230.68(10), Al(4)−S(4) 230.28(11), C(1)−Al(1)−S(1) 117.38(7), C(1)−Al(1)−S(2) 127.59(8), C(1)−Al(1)−S(4) 118.83(7), S(1)−Al(1)−S(2) 95.08(4), S(1)−Al(1)−S(4) 97.01(4), S(2)−Al(1)−S(4) 94.31(4), C(2)−Al(2)−S(1) 118.57(7), C(2)−Al(2)−S(2) 127.75(7), C(2)−Al(2)−S(3) 117.76(7), S(1)−Al(2)−S(2) 94.29(4), S(1)−Al(2)−S(3) 97.13(4), S(2)−Al(2)−S(3) 94.64(4), C(3)−Al(3)−S(2) 128.78(8), C(3)−Al(3)−S(3) 118.95(8), C(3)−Al(3)−S(4) 116.20(7), S(2)−Al(3)−S(3) 93.91(4), S(2)−Al(3)−S(4) 94.93(4), S(3)−Al(3)−S(4) 97.36(4), C(4)−Al(4)−S(1) 119.76(10), C(4)−Al(4)−S(3) 118.93(10), C(4)−Al(4)−S(4) 118.60(10), S(1)−Al(4)−S(3) 98.27(4), S(1)−Al(4)−S(4) 98.26(5), S(3)−Al(4)−S(4) 98.54(4), Al(1)−S(1)−Al(2) 85.61(4), Al(1)−S(1)−Al(4) 82.18(4), Al(2)−S(1)−Al(4) 81.61(4), Al(1)−S(2)−Al(2) 84.37(4), Al(1)−S(2)−Al(3) 84.33(4), Al(2)−S(2)−Al(3) 84.61(4), Al(2)−S(3)−Al(3) 86.07(4), Al(2)−S(3)−Al(4) 82.27(4), Al(3)−S(3)−Al(4) 81.40(4), Al(1)−S(4)−Al(3) 85.73(4), Al(1)−S(4)−Al(4) 81.75(4), Al(3)−S(4)−Al(4) 82.07(4).

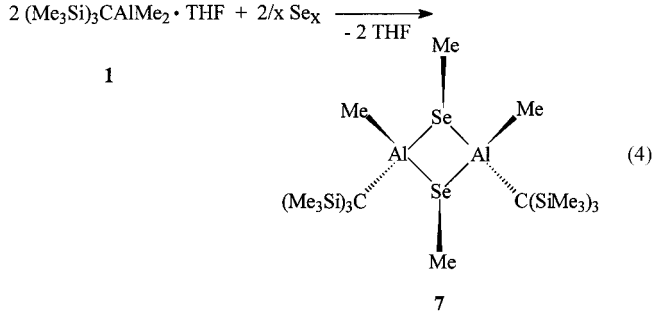

(4)

253.5 pm) are slightly longer than those in [$Mes_2Al(\mu\text{-}SeMe)]_2$ (251.9 pm)[15] and in the heterocubane [$Cp^*Al(\mu_3\text{-}Se)]_4$ (247.7 pm),[2e] while the Al−C_{trisyl} (200.0 pm) and Al−C_{methyl} distances (196.6 pm) are somewhat shorter than those in the starting material $(Me_3Si)_3CAlMe_2 \cdot THF$ (**1**) (203.0 pm and 197.4 pm, respectively)[11] due to the electron-withdrawing properties of the two selenium atoms coordinated at each aluminum atom.

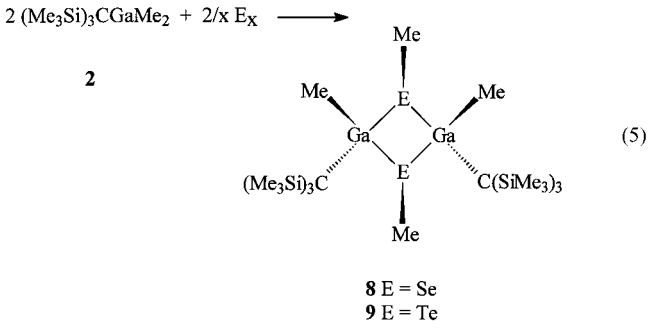

(5)

Figure 4. Crystal structure of $[(Me_3Si)_3CAlMe(\mu\text{-}SeMe)]_2$ (**7**), with anisotropic displacement parameters depicting 50% probability. Hydrogen atoms have been omitted for clarity[a]

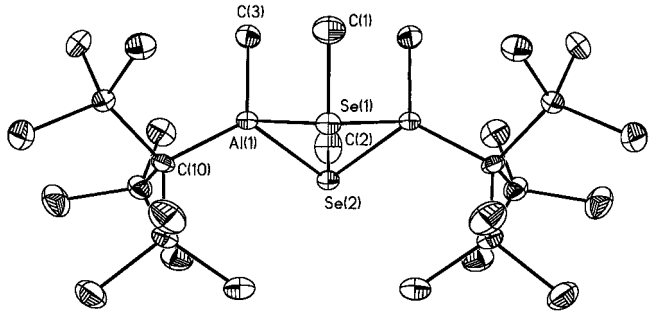

[a] Selected bond lengths [pm] and angles [°]: Al(1)−C(3) 196.6(6), Al(1)−C(10) 200.0(3), Al(1)−Se(1) 252.71(11), Al(1)−Se(2) 254.35(10), Se(1)−C(1) 196.8(5), Se(2)−C(2) 196.1(5); C(3)−Al(1)−C(10) 118.46(13), C(3)−Al(1)−Se(1) 107.28(11), C(3)−Al(1)−Se(2) 107.89(11), C(10)−Al(1)−Se(1) 117.21(9), C(10)−Al(1)−Se(2) 116.65(9), Se(1)−Al(1)−Se(2) 84.01(3), Al(1)−Se(1)−Al(1A) 86.48(5), Al(1)−Se(1)−C(1) 103.70(12), Al(1A)−Se(1)−C(1) 103.71(12), Al(1)−Se(2)−Al(1A) 85.79(5), Al(1)−Se(2)−C(2) 106.68(13), Al(1A)−Se(2)−C(2) 106.68(13).

The metal selenolates **7** and **8** show high thermal stabilities, and can be sublimed in vacuo (180−200°C, 10^{-2} mbar) without decomposition. Their EI mass spectra show no signs for the formation of the corresponding metal selenides. In contrast, the selenolates $[t\text{Bu}_2M(\mu\text{-Se-}t\text{Bu})]_2$ (M = Al, Ga) give the corresponding tetrameric metal selenides $[t\text{BuM}(\mu_3\text{-Se})]_4$ (M = Al, Ga) upon heating.[2b][2c]

A different behaviour was observed for the reaction of the trialkylmetalanes **1** and **2** with elemental tellurium. While the reaction of the trialkylgallane **2** with tellurium powder in refluxing toluene results in the formation of the corresponding tellurolate $[(Me_3Si)_3CGaMe(\mu\text{-TeMe})]_2$ (**9**) in good yield within 3 h (Eq. 5), the trialkylalane **1** does not react with tellurium metal at all. Even after refluxing in toluene with a fivefold excess of tellurium for two days compound **1** and tellurium have been recovered nearly quantitatively.

The gallium tellurolate **9** is a greenish, very air- and moisture-sensitive, malodorous solid which was fully characterized by ^1H- and ^{29}Si-NMR, mass, and IR spectroscopy as well as by elemental analysis (see Experimental Section). Additionally, recrystallization from toluene at

room temperature gave single crystals suitable for X-ray diffraction analysis.

The molecular structure of the gallium tellurolate **9**, which crystallizes in the monoclinic space group *C*2/c, is depicted in Figure 5. The distorted central four-membered Ga_2Te_2 ring (Ga−Te−Ga 85.5°, Te−Ga−Te 87.5°, average) has a conformation [angle between the planes defined by Ga(1)/Te(1)/Te(2) and Ga(2)/Te(1)/Te(2) 139.9°] similar to the aluminum selenolate **7** and the two other structurally characterized dimeric organogallium tellurolates $[(t\text{-}BuCH_2)_2Ga(\mu\text{-}TePh)]_2$ (Ga−Te−Ga 83.8°, Te−Ga−Te 92.0°, angle between Ga1/Te1/Te2 and Ga2/Te1/Te2 148°)[16] and $[(PhCH_2)_2Ga(\mu\text{-}Te\text{-}t\text{Bu})]_2$ (Ga−Te−Ga 81.8°, Te−Ga−Te 92.0°, angle between Ga1/Te1/Te2 and Ga2/Te1/Te2 141°),[17] but in these molecules the substituents on the Te are in the *trans* position relative to the ring. The Ga−Te distances in **9** (average: 274.6 pm) are in the range of those observed for $[(t\text{BuCH}_2)_2Ga(\mu\text{-TePh})]_2$ (average: 275.5 pm)[16] and $[(PhCH_2)_2Ga(\mu\text{-Te-}t\text{Bu})]_2$ (average: 269.3 pm)[17] but are distinctly longer than the sum of the covalence radii of Ga and Te (262 pm).[18] The $Ga-C_{trisyl}$ (202.5 pm) and $Ga-C_{methyl}$ distances (198.3 pm) are slightly shorter than those observed for $(Me_3Si)_3CGaMe_2 \cdot THF$ (204.6 and 197.9 pm, respectively).[11]

Figure 5. Crystal structure of $[(Me_3Si)_3CGaMe(\mu\text{-TeMe})]_2$ (**9**), with anisotropic displacement parameters depicting 50% probability. Hydrogen atoms have been omitted for clarity[a]

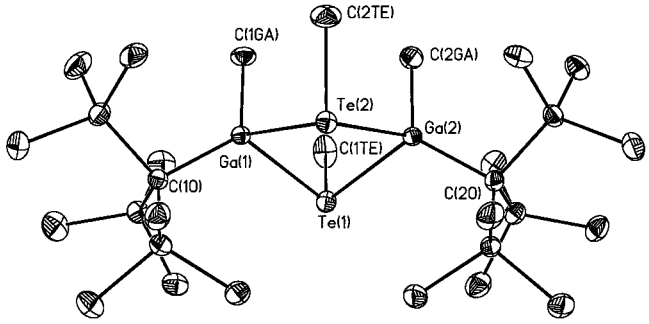

[a] Selected bond lengths [pm] and angles [°]: Ga(1)−C(1GA) 198.5(6), Ga(1)−C(10) 202.6(6), Ga(1)−Te(1) 274.34(8), Ga(1)−Te(2) 274.39(7), Ga(2)−C(2GA) 198.1(6), Ga(2)−C(20) 202.3(6), Ga(2)−Te(1) 274.19(8), Ga(2)−Te(2) 275.37(8), Te(1)−C(1TE) 215.4(7), Te(2)−C(2TE) 215.3(6); C(1GA)−Ga(1)−C(10) 120.8(3), C(1GA)−Ga(1)−Te(1) 104.93(19), C(1GA)−Ga(1)−Te(2) 104.34(19), C(10)−Ga(1)−Te(1) 116.10(17), C(10)−Ga(1)−Te(2) 117.64(16), Te(1)−Ga(1)−Te(2) 87.58(2), C(2GA)−Ga(2)−C(20) 120.4(3), C(2GA)−Ga(2)−Te(1) 104.9(2), C(2GA)−Ga(2)−Te(2) 104.14(19), C(20)−Ga(2)−Te(1) 116.41(16), C(20)−Ga(2)−Te(2) 118.13(17), Te(1)−Ga(2)−Te(2) 87.41(2), C(1TE)−Te(1)−Ga(1) 97.8(2), C(1TE)−Te(1)−Ga(2) 99.23(19), Ga(1)−Te(1)−Ga(2) 85.57(2), C(2TE)−Te(2)−Ga(1) 98.76(18), C(2TE)−Te(2)−Ga(2) 99.7(2), Ga(1)−Te(2)−Ga(2) 85.34(2).

In contrast to $[t\text{Bu}_2Ga(\mu\text{-Te-}t\text{Bu})]_2$, which has been converted to the corresponding tetrameric telluride $[t\text{BuGa}(\mu_3\text{-Te})]_4$ upon heating,[2c] thermolysis of compound **9** results in the formation of an ochre colored powder which was identified by ^{1}H- and ^{29}Si-NMR spectroscopy as a complex mixture of unknown products.

Conclusions and Remarks

In summary we have shown that compounds $(Me_3Si)_3CAlMe_2 \cdot THF$ (**1**) and $(Me_3Si)_3CGaMe_2$ (**2**) are ideal starting materials for the preparation of various chalcogen-containing derivatives. Under the reaction conditions reported the $Al-C(SiMe_3)_3$ and the corresponding Ga−C bond was not cleaved either using H_2S or the heavier elements of group 16,leading to products which could be recrystallized from organic solvents. The MOCVD experiments using the compounds described in this paper are still in progress. However, these results will be reported elsewhere.

We are grateful to the *Deutsche Forschungsgemeinschaft* and the *Göttinger Akademie der Wissenschaften* for financial support.

Experimental Section

General: All experiments were performed with standard Schlenk techniques under dry nitrogen atmosphere due to the extreme sensitivity of reactants and products toward air and moisture. A Braun MB 150-GI glovebox was used to store the compounds and to prepare the samples for spectroscopic characterizations. All solvents were dried over sodium/benzophenone, freshly distilled and degassed prior to use. H_2S, Se metal, and Te metal were purchased from Aldrich Chemical Co., $(Me_3Si)_3CAlMe_2 \cdot THF$ and $(Me_3Si)_3CGaMe_2$ were prepared as described in the literature.[11] Elemental analyses were performed by the Analytisches Labor des Instituts für Anorganische Chemie der Universität Göttingen. It is well-known that the analysis for carbon in group 13 compounds is often low due to the generation of metal carbides.[19] In compounds containing silicon, the content of carbon is decreased further by formation of silicon carbide. − NMR spectra were recorded on Bruker AM 200 and Bruker AM 250 instruments, and were externally referenced to tetramethylsilane in ppm with low-field shift positive. − FT-IR spectra were measured on a Bio-Rad FTS-7 as nujol mulls between KBr plates in the range of 4000−400 cm^{-1} (abbreviations used: vs, very strong; s, strong; m, medium) and EI mass spectra on Finnigan MAT 8230 or Varian MAT CH 5 instruments. The most intensive peak of each isotopic distribution is given. − Melting points were measured in sealed glass tubes and are not corrected.

Synthesis of [(Me$_3$Si)$_3$CAl(μ−S)]$_2$ · 2 THF (**3**): Dry H_2S was bubbled slowly through a solution of 3.70 g of $(Me_3Si)_3CAlMe_2 \cdot THF$ (10.3 mmol) in toluene (100 ml) at room temperature for 45 minutes. The opaque reaction mixture was stirred at room temperature for 1 h and then filtered through celite. Removal of all volatiles in vacuo gave analytically pure compound **3**. Yield: 2.60 g (87%), colorless solid, m.p. 235°C. − ^{1}H NMR (200.13 MHz, C_6D_6): δ = 3.77 (m_c, 8 H, OCH_2CH_2), 1.33 (m_c, 8 H, OCH_2CH_2), 0.49 (s, 54 H, $SiCH_3$). − ^{29}Si NMR (49.69 MHz, C_6D_6): δ = −3.7. − MS (70 eV): *m/z* (%) 1147 (30) [{$(Me_3Si)_3CAlS$}$_4$ − Me], 929 (46) [{$(Me_3Si)_3CAlS$}$_4$ − $C(SiMe_3)_3$], 565 (50) [M^+ − Me − 2 THF], 275 (90) [$(M/2)^+$ − Me − THF], 201 (100) [$C(SiMe_3)_3$ − 2 Me]. − IR: $\tilde{\nu}$ = 1346 (m), 1253 (vs), 1095 (m), 1042 (m), 1012 (m), 989 (m), 917 (m), 848 (vs), 793 (s), 752 (m), 721 (m), 669 (s), 642 (m), 616 (m), 533 (m), 490 (m), 447 (s), 424 (m) cm^{-1}. − $C_{28}H_{70}Al_2O_2S_2Si_6$ (725.49): calcd. C 46.36, H, 9.73; found: C 45.6, H, 9.7.

Synthesis of [(Me$_3$Si)$_3$CGa(μ$_3$-S)]$_4$ (**4**): Dry H_2S was bubbled slowly through a toluene solution (160 ml) of 4.00 g of $(Me_3Si)_3CGaMe_2$ (12.1 mmol) at room temperature for 45 minutes. After 2

h stirring at room temperature, the opaque solution was filtered through celite. Removal of all volatiles in vacuo and washing of the residue with pentane (20 ml) gave compound **4**. Yield: 3.7 g (92%); colorless, air- and moisture-sensitive solid; m.p. 316°C. – ^{1}H NMR (200.13 MHz, C_6D_6): δ = 0.47 [C(SiCH$_3$)]. – ^{29}Si NMR (49.69 MHz, C_6D_6): δ = -1.0. – MS (70 eV): *m/z* (%) 1317 (1) [M^+ – Me], 1101 (3) [M^+ – $C(SiMe_3)_3$], 769 (5) [(3/4 M)$^+$ – $C(SiMe_3)_3$], 666 (15) [(M/2)$^+$], 651 (60) [(M/2)$^+$ – Me], 317 (100) [(M/4)$^+$ – Me], 201 (45) [$C(SiMe_3)_3$ – 2 Me]. – IR: ṽ = 1288 (m), 1262 (s), 1250 (s), 1099 (m), 1019 (m), 980 (m), 854 (vs), 849 (vs), 785 (m), 726 (m), 673 (s), 663 (s), 630 (m), 616 (m), 556 (m) cm^{-1}. – $C_{40}H_{108}Ga_4S_4Si_{12}$ (1333.50): calcd. C 36.03, H 8.16; found C 36.3, H 8.7.

Synthesis of [(Me$_3$Si)$_3$CAl(μ$_3$-S)]$_4$ (**5**) *and [{(Me$_3$Si)$_3$CAl(μ$_3$-S)}$_3${MeAl(μ$_3$-S)}]* (**6**): Compound **3** (2.00 g, 2.76 mmol) was heated in vacuo (10^{-2} mbar) without solvent to 220°C for 30 minutes. The slightly yellow residue was extracted with toluene (50 ml) and filtered through celite. Storage at −26°C gave colorless crystals of a mixture of the compounds $[(Me_3Si)_3CAl(\mu_3\text{-}S)]_4$ (**5**) and $[\{(Me_3Si)_3CAl(\mu_3\text{-}S)\}_3MeAl(\mu_3\text{-}S)]$ (**6**) (1.10 g), which could not be separated by crystallization or sublimation. – ^{1}H NMR (200.13 MHz, C_6D_6): δ = 0.48 (s, SiCH_3 of **6**), 0.44 (s, SiCH_3 of **5**), 0.13 (s, AlCH_3 of **6**). – ^{29}Si NMR (49.69 MHz, C_6D_6): δ = −2.24 (**6**), −2.31 (**5**). – MS (70 eV): *m/z* (%) 1147 (25) [**5** – Me], 929 (90) [**6** – Me], 275 (85) [(**5**/4) – Me], 201 (100) [$C(SiMe_3)_3$ – 2 Me]. – IR (KBr, Nujol): ṽ = 1496 (m), 1413 (m), 1341 (m), 1294 (m), 1260 (s), 1252 (s), 1096 (m), 1081 (m), 1030 (m), 1012 (m), 849 (vs), 837 (vs), 794 (s), 752 (m), 727 (m), 714 (m), 667 (vs), 644 (s), 619 (m), 577 (m) cm^{-1}.

Synthesis of [(Me$_3$Si)$_3$CAlMe(μ-SeMe)]$_2$ (**7**): To a suspension of 0.44 g of gray selenium (5.54 mmol) in toluene (20 ml) was added a solution of 2.00 g of $(Me_3Si)_3CAlMe_2 \cdot THF$ (5.54 mmol) in toluene (30 ml) at room temperature. The reaction mixture was stirred for 15 h at room temperature, and then heated under reflux for 2 h. During this time the color changed from colorless through green to yellow, and the selenium was completely consumed. After filtration of the solution through celite and concentration to 15 ml, compound **7** crystallized as a colorless solid on cooling to −26°C. Yield: 1.55 g (76%); colorless, air- and moisture-sensitive crystals; m.p. 278°C. – ^{1}H NMR (200.13 MHz, C_6D_6): δ = 1.79 (s, 6 H, SeCH_3), 0.37 (s, 54 H, SiCH_3), −0.13 (s, 6 H, AlCH_3). – ^{29}Si NMR (49.69 MHz, C_6D_6): δ = −3.6. – MS (70 eV): *m/z* (%) 368 (1) [(M/2)$^+$], 353 (15) [(M/2)$^+$ – Me], 273 (100) [(M/2)$^+$ – SeMe]. – IR: ν = 1260 (s), 1248 (s), 1195 (m), 855 (vs), 789 (s), 721 (m), 671 (s), 613 (m), 603 (m) cm^{-1}. $C_{24}H_{66}Al_2Se_2Si_6$ (735.20): calcd. C 39.21, H 9.05; found: C 39.7, H 9.0.

Preparation of [(Me$_3$Si)$_3$CGaMe(μ-SeMe)]$_2$ (**8**): A solution of 2.00 g of $(Me_3Si)_3CGaMe_2$ (6.04 mmol) in toluene (30 ml) was slowly added to a suspension of 0.48 g of gray selenium (6.04 mmol) in toluene (20 ml) at room temperature. The reaction mixture was stirred at room temperature for 8 h and then heated under reflux for 2 h. During this time the color changed from colorless through green to yellow, and the selenium was consumed completely. After filtration of the opaque solution through celite and concentration to 25 ml compound **8** crystallized as a slightly yellow solid on cooling to −26°C. Yield: 1.95 g (79%), slightly yellow air- and moisture-sensitive crystals, m.p. 256°C. – ^{1}H NMR (200.13 MHz, C_6D_6): δ = 1.79 (s, 6 H, SeCH_3), 0.36 (s, 54 H, SiCH_3), 0.29 (s, 6 H, GaCH_3). – ^{29}Si NMR (49.69 MHz, C_6D_6): δ = −2.5. – MS (70 eV): *m/z* (%) 775 (7) [M^+ – 3 Me], 760 (7) [M^+ – 4 Me], 745 (10) [M^+ – 5 Me], 395 (12) [(M/2)$^+$ – Me], 365 (20) [(M/2)$^+$ – 3 Me], 315 (50) [(M/2)$^+$ – SeMe – Me], 201 (100) [$C(SiMe_3)_3$

Table 1. Crystallographic data for compounds **3** · C_6H_6, **4** · 1.5 C_6H_6, **6**, **7** · C_6H_6, and **9**

Compound	**3** · C_6H_6	**4** · 1.5 C_6H_6	**6**	**7** · C_6H_6	**9**
Empirical formula	$C_{34}H_{76}Al_2O_2S_2Si_6$	$C_{49}H_{117}Ga_4S_4Si_{12}$	$C_{31}H_{84}Al_4Si_9$	$C_{30}H_{72}Al_2Se_2Si_6$	$C_{24}H_{66}Ga_2Si_6Te_2$
Molecular mass [g/mol]	803.60	1450.63	945.95	813.30	917.95
T (K)	133(2)	133(2)	203(2)	133(2)	133(2)
Crystal size [mm]	0.40 × 0.20 × 0.20	0.40 × 0.30 × 0.30	0.50 × 0.50 × 0.30	0.70 × 0.50 × 0.40	0.50 × 0.40 × 0.40
Crystal system	orthorhombic	trigonal	triclinic	orthorhombic	monoclinic
Space group	*Pbca*	*P*$\bar{3}$*c*1	*P*$\bar{1}$	*Ibam*	*C*2/c
a [pm]	14.696(3)	15.570(2)	14.044(4)	17.518(4)	15.511(1)
b [pm]	13.416(4)	15.570(2)	14.201(5)	17.706(4)	9.224(1)
c [pm]	23.289(5)	34.958(7)	16.462(6)	28.756(6)	56.613(11)
α [°]	90	90	98.44(3)	90	90
β [°]	90	90	100.65(2)	90	96.00(1)
γ [°]	90	120	119.37(1)	90	90
V [10^{-30} m^3]	4592(2)	7340(10)	2702(2)	8920(10)	8055(2)
Z	4	4	2	8	8
$d_{calcd.}$ [g/cm^3]	1.162	1.313	1.163	1.211	1.514
μ (mm^{-1})	0.338	1.792	0.462	1.877	2.949
F(000)	1752	3068	1024	3440	3680
2θ range	4.5° ≤ 2θ ≤ 50.2°	4.7° ≤ 2θ ≤ 50.0°	7.1° ≤ 2θ ≤ 50.3°	7.1° ≤ 2θ ≤ 45.2°	4.3° ≤ 2θ ≤ 49.4°
Reflections collected	52394	87752	12402	3905	36639
Indepedent reflections	4080 (R_{int} = 0.0782)	4342 (R_{int} = 0.0566)	9396 (R_{int} = 0.0234)	3019 (R_{int} = 0.0260)	6868 (R_{int} = 0.0487)
Absorption correction	semiempirical from equivalents	semiempirical from equivalents	semiempirical from ψ-scans	semiempirical from ψ-scans	semiempirical from equivalents
R[a], w$R2$[b] [$I > 2\sigma(I)$]	0.0426, 0.0750	0.0531, 0.0941	0.0342, 0.0820	0.0324, 0.0766	0.0466, 0.0848
R, w$R2$ (all data)	0.0575, 0.0796	0.0751, 0.1034	0.0426, 0.0894	0.0419, 0.0833	0.0531, 0.0866
Goodness of fit S[c]	1.157	1.213	1.080	1.040	1.409
Parameters	233	325	461	323	330
Restraints	109	1023	0	691	0
Max./min. residual [10^{30} e/m^3]	0.273/−0.205	0.937/−0.524	0.375/−0.309	0.556/−0.589	0.651/−0.94

[a] $R = \Sigma||Fo| - |Fc||/\Sigma|Fo|$. – [b] $wR2 = [\Sigma w(Fo^2 - Fc^2)^2]/[\Sigma w(Fo^2)^2]^{1/2}$. [c] $S = [\Sigma w(Fo^2 - Fc^2)^2]/(n - p)]^{1/2}$. $w^{-1} = \sigma^2(Fo^2) + (aP)^2 + bP$; $P = [Fo^2 + 2Fc^2]/3$.

− 2 Me]. − IR: $\tilde{\nu}$ = 1289 (m), 1260 (s), 1247 (s), 1201 (m), 857 (vs), 847 (vs), 784 (s), 753 (m), 722 (s), 672 (s), 659 (s), 625 (m), 616 (m), 549 (m), 539 (m) cm^{-1}. − $C_{24}H_{66}Ga_2Se_2Si_6$ (820.70): calcd. C 35.12, H 8.11; found: C 35.7, H 8.1.

Preparation of [(Me$_3$Si)$_3$CGaMe(μ-TeMe)]$_2$ (**9**): To a suspension of 1.54 g of tellurium metal (12.1 mmol) in toluene (30 ml) was slowly added a solution of 2.00 g of **2** (6.04 mmol) in toluene (30 ml) at room temperature. The reaction mixture was stirred for 3 d at room temperature and then heated under reflux for 3 h. After filtration of the dark yellow mixture through celite and concentration to 35 ml compound **9** crystallized on cooling to −26°C. Yield: 2.00 g (72%), slightly green crystals, air- and moisture-sensitive, m.p. 296°C (dec.). − ^{1}H NMR (200.13 MHz, C_6D_6): δ = 1.62 (s, 6 H, TeCH_3), 0.50 (s, 6 H, GaCH_3), 0.37 (s, 54 H, SiCH_3). − ^{29}Si NMR (49.69 MHz, C_6D_6): δ = −2.3. MS (70 eV): *m/z* (%) 858 (3) [M^+ − 4 Me], 445 (7) [$(M/2)^+$ − Me], 315 (100) [$(M/2)^+$ − TeMe], 201 (80) [$C(SiMe_3)_3$ − 2 Me]. − IR: $\tilde{\nu}$ = 1289 (m), 1260 (vs), 1248 (vs), 1217 (s), 1191 (m), 858 (vs), 783 (s), 722 (m), 673 (m), 667 (m), 624 (m), 615 (m), 541 (s), 532 (s) cm^{-1}. $C_{24}H_{66}Ga_2Si_6Te_2$ (917.97): calcd. C 31.40, H 7.25; found C 32.2, H 7.4.

Crystal-Structure Determinations: Single crystals of compounds **3** · C_6H_6, **4** · 1.5 C_6H_6 and **7** · C_6H_6, **6** and **9** were obtained by recrystallization from benzene and toluene at room temperature, respectively. Crystal data and structure refinement parameters are given in Table 1. Data for structures **3** · C_6H_6, **4** · 1.5 C_6H_6, and **9** were collected on a Stoe-Siemens-Huber four-circle diffractometer equipped with a Siemens SMART CCD area detector and for structures **6** and **7** · C_6H_6 on a Stoe-Siemens AED four-circle diffractometer. Mo-K_α radiation (λ = 71.073 pm) was used in all cases. All structures were solved by direct methods (SHELXS-97)[20] and refined against F^2 using SHELXL-97.[21] All heavy atoms were refined anisotropically, hydrogen atoms were included using the riding model with U_{iso} tied to the U_{iso} of the parent atom. For structure **9** an extinction correction was employed.

In structures **4** · 1.5 C_6H_6 and **7** some of the trisyl ligands were disordered. They were refined with distance restraints and restraints for the anisotropic displacement parameters. The anisotropic displacement parameters of the Si atoms lying opposite to each other were constrained to be the same. Additionally the THF molecules in **3** · C_6H_6 and one benzene molecule in **7** · C_6H_6 were disordered. Again distance restraints and restraints for the anisotropic displacement parameters were used.

Crystallographic data (excluding structure factors) have been deposited with the Cambridge Crystallographic Data Center (CCDC) as supplementary publication numbers CCDC-102100, 102101, 102102, 102103, and 102104. Copies of data can be obtained free of charge on application to CCDC, 12 Union Road, Cambridge CB2 1EZ, UK [Fax: internat. +44 1223/336-033; E-mail: deposit@ccdc.cam.ac.uk].

☆ Dedicated to Professor *Heinrich Nöth* on the occassion of his 70th birthday.

[1] [1a] M. Veith, *Chem. Rev.* **1990**, *90*, 3−16. − [1b] T. Belgardt, H. W. Roesky, M. Noltemeyer, H.-G. Schmidt, *Angew. Chem.* **1993**, *105*, 1101−1102; *Angew. Chem. Int. Ed. Engl.* **1993**, *32*, 1056−57. − [1c] K. Niediek, B. Neumüller, *Chem. Ber.* **1994**, *127*, 67−71. − [1d] T. Belgardt, S. D. Waezsada, H. W. Roesky, H. Gornitzka, L. Häming, D. Stalke, *Inorg. Chem.* **1994**, *33*, 6247−6251. − [1e] F. Cordeddu, H.-D. Hausen, J. Weidlein, *Z. Anorg. Allg. Chem.* **1996**, *622*, 573−578. − [1f] C. Schnitter, S. D. Waezsada, H. W. Roesky, M. Teichert, I. Usón, E. Parisini, *Organometallics* **1997**, *16*, 1197−1202 and literature cited therein.

[2] [2a] M. B. Power, A. R. Barron, *J. Chem. Soc., Chem. Commun.* **1991**, 1315−1317. − [2b] A. H. Cowley, R. A. Jones, P. R. Harris, D. A. Atwood, L. Contreras, C. J. Burek, *Angew. Chem.* **1991**, *103*, 1164−1166; *Angew. Chem. Int. Ed. Engl.* **1991**, *30*, 1143−1145. − [2c] M. B. Power, J. W. Ziller, A. N. Tyler, A. R. Barron, *Organometallics* **1992**, *11*, 1055−1063. − [2d] S. Schulz, H. W. Roesky, H. J. Koch, G. M. Sheldrick, D. Stalke, A. Kuhn, *Angew. Chem.* **1993**, *105*, 1828−1830; *Angew. Chem. Int. Ed. Engl.* **1993**, *32*, 1729−1731. − [2e] S. Schulz, M. Andruh, T. Pape, T. Heinze, H. W. Roesky, L. Häming, A. Kuhn, R. Herbst-Irmer, *Organometallics* **1994**, *13*, 4004−4007. − [2f] C. J. Harlan, E. G. Gillan, S. G. Bott, A. R. Barron, *Organometallics* **1996**, *15*, 5479−5488. − [2g] U. App, K. Merzweiler, *Z. Anorg. Allg. Chem.* **1997**, *623*, 478−482. − [2h] G. Linti, M. Bühler, H. Urban, *Z. Anorg. Allg. Chem.* **1998**, 517−520.

[3] A. M. Mancini, G. Micocci, A. Rizzo, *Mater. Chem. Phys.* **1983**, *9*, 29−54.

[4] [4a] W.-T. Kim, C.-D. Kim, *J. Appl. Phys.* **1986**, *60*, 2631−2633. − [4b] R. Nomura, K. Kanaya, A. Moritak, H. Matsuda, *Thin Solid Films* **1988**, *167*, L27−29.

[5] [5a] T. Nishino, Y. Hamakawa, *Jpn. Appl. Phys.* **1977**, *16*, 1291−1294. − [5b] R. S. Becker, T. Zheng, J. Elton, M. Saeki, *Sol. Energy Mater.* **1986**, *13*, 97−107.

[6] [6a] A. N. MacInnes, M. B. Power, A. R. Barron, P. P. Jenkins, A. F. Hepp, *Appl. Phys. Lett.* **1993**, *62*, 711−713. − [6b] M. Tabib-Azar, S. Kang, A. N. MacInnes, M. B. Power, A. R. Barron, P. P. Jenkins, A. F. Hepp, *Appl. Phys. Lett.* **1993**, *63*, 625−627. − [6c] W. M. Cleaver, M. Späth, D. Hnyk, G. McMurdo, M. B. Power, M. Stuke, D. W. H. Rankin, A. R. Barron, *Organometallics* **1995**, *14*, 690−697.

[7] P. P. Jenkins, A. N. MacInnes, M. Tabib-Azar, A. R. Barron, *Science* **1994**, *263*, 1751−1753.

[8] [8a] W. Hirpo, S. Dhingra, M. G. Kanatzidis, *J. Chem. Soc., Chem. Commun.* **1992**, 557−559. − [8b] W. Hirpo, S. Dhingra, A. C. Sutorik, M. G. Kanatzidis, *J. Am. Chem. Soc.* **1993**, *115*, 1597−1599.

[9] Y. L. Wu, H. Y. Lin, C. Y. Sun, M. H. Yank, H. L. Hwang, *Thin Solid Films* **1989**, *168*, 113−118.

[10] [10a] A. P. Kozikowaski, A. Ames, *J. Org. Chem.* **1978**, *13*, 2735−2737. − [10b] K. Sasaki, Y. Aso, T. Otsubo, F. Ogura, *Chem. Lett.* **1989**, 60−63. − [10c] K. Sasaki, T. Mori, Y. Doi, A. Kawachi, Y. Aso, T. Otsubo, F. Ogura, *Chem. Lett.* **1991**, 415−417. − [10d] T. Inoue, T. Takeda, N. Kambe, A. Ogawa, I. Ryu, N. Sonoda, *J. Org. Chem.* **1994**, *59*, 5824−5827. − [10e] T. Inoue, T. Takeda, N. Kambe, A. Ogawa, I. Ryu, N. Sonoda, *Organometallics* **1994**, *13*, 4543−4546.

[11] C. Schnitter, H. W. Roesky, T. Albers, H.-G. Schmidt, C. Röpken, E. Parisini, G. M. Sheldrick, *Chem. Eur. J.* **1997**, *3*, 1783−1792.

[12] The cubane **4** is also the only isolable gallium containing product in the reaction of the solvent adduct $(Me_3Si)_3CGaMe_2$ × THF with H_2S.

[13] R. J. Wehmschulte, P. P. Power, *J. Chem. Soc., Chem. Commun.* **1998**, 335−336.

[14] M. B. Power, J. W. Ziller, A. R. Barron, *Organometallics* **1992**, *11*, 2783−2790.

[15] R. Kumar, D. G. Dick, S. U. Ghazi, M. Taghiof, M. J. Heeg, J. P. Oliver, *Organometallics* **1995**, *14*, 1601−1607.

[16] M. A. Banks, O. T. Beachley Jr., H. J. Gysling, H. R. Luss, *Organometallics* **1990**, *9*, 1979−1982.

[17] M. R. Kopp, B. Neumüller, *Z. Anorg. Allg. Chem.* **1997**, *623*, 796−804.

[18] L. Pauling, *The Nature of the Chemical Bond*, 3rd Ed., Cornell, Ithaca (N.Y.), **1960**.

[19] K. J. L. Paciorek, J. H. Nakahara, L. Hoferkamp, C. George, J. L. Flippen-Anderson, R. Gilardi, W. R. Schmidt, *Chem. Mater.* **1991**, *3*, 82−87.

[20] G. M. Sheldrick, *Acta Crystallogr. Sect. A* **1990**, *46*, 467−473.

[21] G. M. Sheldrick, *SHELXL, Program for Crystal Structure Refinement*, University of Göttingen, Germany, **1997**.

[I98219]

Transition Metal Coordination Compounds of Bisamidobispyridyl Ligands

Peter Comba*[a], Wolfgang Goll[a], Bernhard Nuber[a], and Katalin Várnagy[b]

Anorganisch-Chemisches Institut der Universität[a],
Im Neuenheimer Feld 270, D-69120 Heidelberg, Germany
Fax: (internat.) + 49(0)6221/546617;
E-mail: comba@akcomba.oci.uni-heidelberg.de

Department of Chemistry, Lajos Kossuth University[b],
Debrecen, Hungary

Received July 10, 1998

Keywords: Metal ion selectivity / Stability constants / Molecular mechanics / Metal ion extraction / Liquid membranes

The syntheses of *N*,*N*′-bis-[(2-pyridylmethyl)]-1,3-diamidopropane ($papH_2$) and *N*,*N*′-bis-[(2-pyridylmethyl)]-1,3-diamido-2-hexadecylpropane ($C_{16}papH_2$) are reported together with the results of potentiometric titrations of $papH_2$ with Co(II), Ni(II), Cu(II) and Zn(II), spectroscopic and electrochemical data of [Ni(pap)] and [Cu(pap)], structural studies involving the X-ray analyses of the metal-free $papH_2$ ligand and the corresponding Ni(II) and Cu(II) complexes [Ni(pap)] × 2 H_2O and [Cu(pap)] × 3 H_2O, and force-field calculations (MM) of [Co(pap)], [Ni(pap)], [Cu(pap)] and [Zn(pap)] and the corresponding complexes of the ligand with *ortho*-methyl-substituted pyridyl groups (Me_2papH_2); the results of metal ion transport [Co(II), Ni(II), Cu(II) and Fe(II)] from aqueous solutions through $C_{16}papH_2$ containing dichloromethane phases are also given. The extractability with $C_{16}papH_2$ increases along the series Fe(II) < Co(II) < Ni(II) < Cu(II), and this is confirmed by the potentiometric data ($papH_2$, aqueous solutions; $\log\beta_{ML}$[Co(II)] = 1.75; $\log\beta_{MLH-2}$[Ni(II)]=–11.49; $\log\beta_{ML}$[Cu(II)]=3.41; $\log\beta_{MLH-2}$-[Cu(II)] = –4.491; $\log\beta_{ML}$[Zn(II)] = 1.87). The structural data (X-ray and MM) indicate that, due to the *ortho* protons of the pyridyl groups and in dependence of the electronic configuration of the metal center, there is a considerable tetrahedral twist of the central MN_4 chromophores {square planar: θ = 0°; tetrahedral: θ = 90°; [Co(pap)]: θ = 15° (MM); [Ni(pap)]: θ = 16° (X-ray), 16° (MM); [Cu(pap)]: θ = 18° (X-ray), 18° (MM); [Zn(pap)]: θ = 23° (MM)}, and this may be enhanced by *ortho*-methyl substitution of the pyridyl donors {[Co(Me_2pap)]: θ = 20° (MM); [Ni(Me_2pap)]: θ = 20° (MM); [Cu(Me_2pap)]: θ = 24° (MM); [Zn(Me_2pap)]: θ = 31° (MM)}, and thus possibly a decrease in the complex stability of Cu(II) and Ni(II) in favor of Zn(II).

Introduction

Metal-ion selectivity, i.e. the enhanced stability of a coordination compound with a given ligand and a specific metal ion, relative to that with other metal ions, may be traced back to electronic effects and the coordination geometry, partly enforced by the ligand system. Donor-atom−metal-ion orbital overlap, the HSAB concept, and ligand field effects describe contributions to the electronic terms, and for hexacoordinate compounds these contribute to the well-known pattern of the *Irving-Williams* series[1]. The steric contributions based on the ligand structure include the reorganization of the most stable conformation of the metal-free ligand to that observed in the coordination compound (unfavorable enthalpy and entropy effects) and steric strain imposed by the metal ion on the ligand and vice versa. Thus, highly preorganized systems, which in the original definition[2] are by necessity relatively rigid ligands which, in the conformation observed in the metal complex, are relatively strain free, lead to comparably high complex stabilities. These properties include the metal ion′s preference for a particular metal-ligand distance and for a particular angular distribution of the donor atoms, and they are therefore metal-ion dependent. Hence, molecular mechanics was supposed to be a powerful tool for predicting the steric contribution to metal ion selectivities[3]. There are many reasons why, in reality, this is not necessarily correct[4] but for specific applications encouraging results may be obtained[3][4][5].

Our aim was to develop a type of ligand with the following properties: (i) it should generally lead to relatively high complex stabilities with Co(II), Ni(II), Cu(II) and Zn(II); (ii) substitution of the ligand backbone should lead to a predictable variation of the coordination geometry, with the aim of tuning the metal-ion selectivity by modification of the coordination geometry; (iii) derivatives with a similar complexation behavior should be available for quantitative investigations in aqueous solution and for metal ion extractions into organic phases. *N*,*N*′-bis[(2-pyridylmethyl)]-1,3-diamidopropane ($papH_2$, see formula scheme) fulfills these requirements: Tetradentate ligands with amide and pyridyl donors are appropriate complexing agents for divalent metal ions[6]; the substituted diamidopropane fragment is rather rigid, the hexadecane-substituted ligand *N*,*N*′-bis[(2-pyridylmethyl)]-1,3-diamido-2-hexadecylpropane, $C_{16}papH_2$, is easily accessible and leads to a hydrophobic ligand and complexes that are soluble in organic phases; the *ortho*-protons of the pyridyl groups of tetradentate ligands with *cis*-disposed pyridyl groups enforce a tetrahedral twist from square-planar geometry[7] and lead therefore to a steric destabilization of complexes with electronic preferences of the

 © WILEY-VCH Verlag GmbH, D-69451 Weinheim, 1998 1434−1948/98/1212−2041 $ 17.50+.50/0

metal center for square-planar coordination geometry; derivatives with *ortho*-substituted pyridyl groups (e.g. Me_2-$papH_2$, see formula scheme) should enhance this effect and thus lead to an increased preference for Zn(II) with respect to Ni(II) and Cu(II).

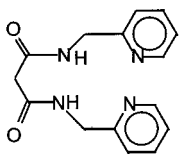

papH$_2$

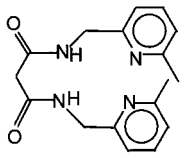

Me$_2$papH$_2$

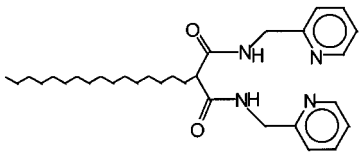

C$_{16}$papH$_2$

Results and Discussion

Syntheses, Spectroscopy and Electrochemistry

$C_{16}papH_2$ was prepared by alkylation of diethyl malonate with hexadecyl bromide in presence of CH_3CH_2ONa, and subsequent nucleophilic substitution of the alkylated malonic ester with α-picolylamine (Scheme 1); $papH_2$ was obtained in a similar reaction. Cu(II) and Ni(II) compounds of $papH_2$ were isolated from aqueous solutions of the metal-free ligands and the metal sulfate salts, or from methanolic solutions and the corresponding tetrafluoroborates; X-ray quality crystals were obtained by slow evaporation of the complex solutions. Spectroscopic and electrochemical parameters of the compounds are listed in Table 1.

Structures

$papH_2 \cdot HBF_4 \cdot H_2O$: The metal-free ligand crystallizes with a molecule of H_3O^+ BF_4^- in the lattice, and hydrogen bonds are formed between the H_3O^+ ion and the nitrogen atoms of the amide group (2.64 Å). An ORTEP[8] plot of the ligand molecule appears in Figure 1a, and structural

Scheme 1

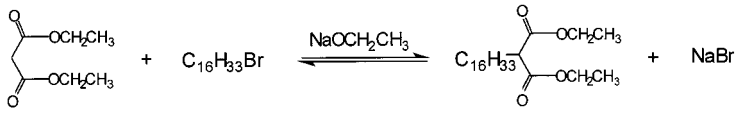

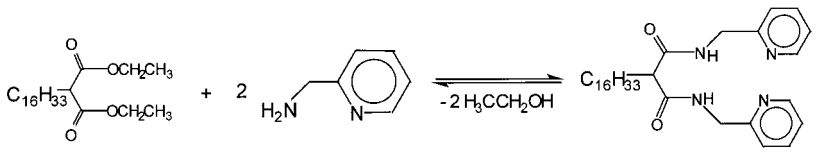

Table 1. Spectroscopic and electrochemical data of [M(pap)]

	UV/Vis		EPR[a]	E[b]
	λ_{max} [nm]	ε [dm^3 mol^{-1} cm^{-1}]		[V]
[Cu(pap)]	571	98	g_{iso} = 2.07 $g_\perp$ = 2.01 $g_{\|\|}$ = 2.19 A_{iso} = 70 × 10^{-4} cm^{-1} $A_\perp$ = 10 × 10^{-4} cm^{-1} $A_{\|\|}$ = 198 × 10^{-4} cm^{-1}	0.10 (Cu$^{II/III}$) 0.23 (Cu$^{I/II}$)
[Ni(pap)]	475	125.5		−1.77 (Ni$^{II/III}$) 0.91 (Ni$^{I/II}$)

[a] From simulation of the experimental spectra. – [b] vs SHE; $Cu^{II/I}$ quasi rev.; $Cu^{III/II}$ irrev.; $Ni^{II/I}$ irrev.; $Ni^{III/II}$ rev.

parameters are listed in Table 2. Bond distances and valence and torsional angles are as expected and similar to those of the coordinated ligand. The geometry around the amide nitrogen and carbon atoms is planar, with little deviation of the corresponding valence angles from 120°. The main differences with respect to the coordinated ligand are: (i) a significantly longer $N_{amide}-C_{amide}$ bond (1.345 Å vs. 1.315 Å); (ii) a smaller $C_{amide}-C_{methylene}-C_{amide}$ valence angle (112° vs. 122° [Ni(II)], 125° [Cu(II)]); (iii) a slightly larger torsion around the $C_{pyridine}-C_{methylene}$ bond (17° vs. 2−10°); (iv) significant changes in the torsion around the $N_{amide}-C_{methylene}$ bond (80° vs. 180°), and (v) significant changes of the torsion around the $C_{amide}-C_{methylene}$ bond (125° vs. 7−18°).

[Cu(pap)] × 3 H_2O: The geometry of the Cu(II) compound is shown in Figure 1b, and the relevant structural parameters are presented, together with those of the Ni(II) compound, in Table 3. An oxygen atom of a neighboring Cu(II) complex molecule is coordinated in an axial position (Cu−O = 2.79 Å). There is also a network of hydrogen bonds between the copper complexes. The central four-coordinate chromophore is unlikely to be perturbed by the axial interactions in the present case. The tetrahedral twist of the CuN_4 chromophore is, as expected, slightly larger than that of the nickel(II) compound (θ° = 18.1°), the torsion around the $Cu-N_{pyridine}$ bond is 10−14° and the resulting α-H ··· α-H distance is 2.17 Å. As in the Ni(II) structure, the six-membered chelate ring is approximately flat and coplanar to the plane defined by the amide donors and the metal center. The five-membered chelate rings are essentially planar. There is a considerable asymmetry with respect to the metal-donor distances but on average the $Cu-N_{pyridine}$ and the $Cu-N_{amide}$ distances are as expected from comparable chromophores[9].

Table 2. Structural parameters of $papH_2 \times HBF_4 \times H_2O$ bond lengths (Å)

O(1)−C(9)	1.223 (4)
N(1)−C(7)	1.454 (5)
N(1)−C(9)	1.345 (4)
N(2)−C(4)	1.348 (5)
N(2)−C(6)	1.342 (4)
C(1)−C(2)	1.381 (6)
C(1)−C(6)	1.391 (5)
C(2)−C(3)	1.376 (6)
C(3)−C(4)	1.377 (6)
C(6)−C(7)	1.503 (5)
C(9)−C(10)	1.518 (4)
C(10)−C(9A)	1.518 (4)
valence angles (deg)	
C(7)−N(1)−C(9)	121.5(3)
C(4)−N(2)−C(6)	120.1(3)
C(2)−C(1)−C(6)	120.3(3)
C(1)−C(2)−C(3)	118.7(4)
C(2)−C(3)−C(4)	119.4(4)
N(2)−C(4)−C(3)	121.6(4)
N(2)−C(6)−C(1)	120.0(3)
N(2)−C(6)−C(7)	119.0(3)
C(1)−C(6)−C(7)	120.9(3)
N(1)−C(7)−C(6)	114.5(3)
O(1)−C(9)−N(1)	122.7(3)
O(1)−C(9)−C(10)	122.4(3)
N(1)−C(9)−C(10)	114.9(3)
C(9)−C(10)−C(9)	112.0(4)

Figure 1. ORTEP[8] plots of the experimentally determined structures of (a) $papH_2 \times HBF \times H_2O$ (HBF × H_2O omitted), (b) [Cu(pap)] × 3 H_2O (H_2O omitted) and (c) [Ni(pap)] × H_2O (H_2O omitted).

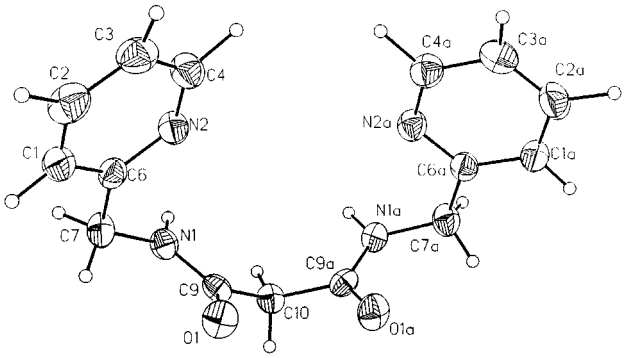

(a)

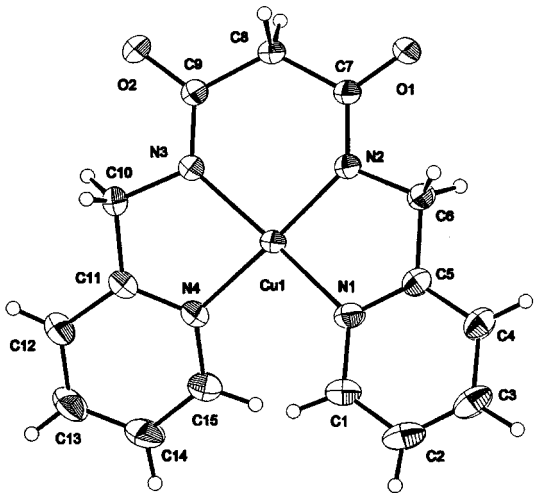

(b)

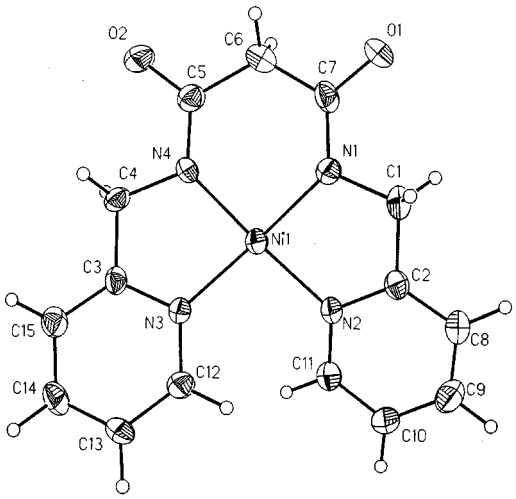

(c)

Table 3. Selected bond lengths (Å) and valence angles (deg) of [M(pap)] (calculated values (MM) in square brackets)

	Cu(II)		Ni(II)		
Cu(1)−N(2)	1.921(2)	[1.92]	1.851(6)	[1.91]	Ni(1)−N(1)
Cu(1)−N(3)	1.927(2)	[1.93]	1.851(6)	[1.91]	Ni(1)−N(4)
Cu(1)−N(4)	2.005(2)	[2.02]	1.909(6)	[1.85]	Ni(1)−N(3)
Cu(1)−N(1)	2.032(2)	[2.02]	1.914(6)	[1.86]	Ni(1)−N(2)
N(2)−Cu(1)−N(3)	94.30(9)	[97.7]	94.2(3)	[90.8]	N(1)−Ni(1)−N(4)
N(2)−Cu(1)−N(4)	173.79(10)	[179.0]	167.6(3)	[178.8]	N(1)−Ni(1)−N(3)
N(3)−Cu(1)−N(4)	82.79(9)	[83.3]	84.7(2)	[88.0]	N(4)−Ni(1)−N(3)
N(2)−Cu(1)−N(1)	82.85(9)	[83.6]	84.0(3)	[87.5]	N(1)−Ni(1)−N(2)
N(3)−Cu(1)−N(1)	163.03(10)	[162.4]	170.0(3)	[164.1]	N(4)−Ni(1)−N(2)
N(4)−Cu(1)−N(1)	101.52(10)	[95.4]	99.1(2)	[93.7]	N(3)−Ni(1)−N(2)

[Ni(pap)]·2H$_2$O: An ORTEP[8] plot of the Ni(II) compound appears in Figure 1c, and the relevant geometric parameters are listed in Table 3. The nickel cation is four-coordinate with a considerable tetrahedral distortion from square-planar geometry [θ = 16.3° (square planar: θ = 0°; tetrahedral: θ° = 90°)]. The Ni−N$_{pyridine}$ and the Ni−N$_{amide}$ distances (1.91 Å and 1.85 Å, respectively) are as expected from comparable chromophores[10]. The tetrahedral distortion is due to the α-hydrogen atoms of the pyridine donor groups (H···H = 2.195 Å), and part of this stress is relaxed by a torsion of the pyridine donor around the Ni−N$_{pyridine}$ axis (14−18°). The five-membered chelate rings are essentially planar.

Molecular Mechanics: The structures of [M(pap)] [M = Co(II), Ni(II), Cu(II), Zn(II)] were computed by strain-energy minimization, using the MOMEC program[11] and force field[12]. All complexes have been modeled as four-coordinate with no axial ligands. So far, MOMEC has mainly been used for five- and six-coordinate transition metal compounds. Metal-ion-related force field parameters are dependent from the coordination geometry[13], i.e. new parameter sets were required for the present study. Also, the approach used in MOMEC for modeling the angular geometry around metal centers is based on 1,3-nonbonded interactions (ligand−ligand repulsion) and, for hexacoordinate compounds, a small perturbation based on the electronic preferences for donor−metal−donor angles of 90°[12b]. For the four-coordinate species considered here, the metal-center-dependent twist from tetrahedral geometry (minimum repulsion) toward square planar coordination was modeled with an out-of-plane term that involves the metal center and the four donor atoms[14]. The force constants and ideal distances for the metal-donor stretching mode and the out-of-plane force constants were fitted to relevant structures available from the Cambridge Structural Data Base (CSD), and five, seven, eight and three sets of X-ray data were used for Co(II), Ni(II), Cu(II) and Zn(II), respectively. The parameters not available before[12] are listed in Table 4. There is good overall agreement between the widely varied experimental data sets and the corresponding computed structures, and the quality of the parameterization with respect to the type of compounds discussed here is demonstrated in Tables 3 and 5, where the computed structural parameters for [Ni(pap)] and [Cu(pap)]

Table 4. Modifications to the published[12] force field

bond stretch	k_b[mdyn Å^{-1}]/r_0 [Å]
Cu−N$_{imine}$	0.600/1.990
Cu−N$_{amide}$	0.600/1.890
Ni−N$_{imine}$	0.600/1.855
Ni−N$_{amide}$	0.600/1.760
Co− N$_{imine}$	0.820/1.960
Co−N$_{amide}$	0.820/1.780
Zn−N$_{imine}$	0.350/2.100
Zn−N$_{amide}$	0.350/2.000

	k_δ[mdyn Å rad^{-2}]			
out-of-plane	Co(II)	Ni(II)	Cu(II)	Zn(II)
M/N$_{amide}$/N$_{imine}$/N$_{amide}$	0.070	0.070	0.050	0.000
M/N$_{amide}$/N$_{amide}$/N$_{imine}$	0.070	0.070	0.050	0.000
M/N$_{imine}$/N$_{imine}$/N$_{amide}$	0.070	0.070	0.050	0.000
M/N$_{imine}$/N$_{amide}$/N$_{amide}$	0.070	0.070	0.050	0.000

Table 5. Comparison of M−N bond distances and tetrahedral twist angles

compound	M−N(amide) [Å] obsd.	calcd.	M−N(pyridine) [Å] obsd.	calcd.	tetrahedral twist angle θ (deg) obsd.	calcd.
[Cu(pap)]	1.92, 1.93	1.92	2.01, 2.03	2.02	18.1	17.7
[Cu(Me$_2$pap)]		1.92		2.01		24.4
[Ni(pap)]	1.85	1.85	1.91	1.91	16.3	15.8
[Ni(Me$_2$pap)]		1.85		1.90		20.0
[Co(pap)]		1.84		1.99		14.5
[Co(Me$_2$pap)]		1.83		1.98		19.6
[Zn(pap)]		1.97		2.08		22.5
[Zn(Me$_2$pap)]		1.96		2.07		31.2

are compared to the experimental data. The geometric parameters of the chromophores of Co(II), Ni(II), Cu(II) and Zn(II), coordinated to pap and Me_2pap are assembled in Table 5, and the calculated structures are presented as SCHAKAL[15] plots in Figure 2.

The computed tetrahedral distortion of [Cu(pap)] and [Ni(pap)] are in good agreement with the experimentally observed twist angles (see Table 5). As expected for a metal ion with d^{10} configuration, the tetrahedral twist of the zinc(II) compound is larger than that of the other com-

Figure 2. SCHAKAL[15] plots of the computed structures of (a) [Co(pap)], (b) [Ni(pap)], (c) [Cu(pap)], (d) [Zn(pap)], (e) [Co(papMe)], (f) [Ni(papMe)], (g) [Cu(papMe)], (h) [Zn(papMe)]

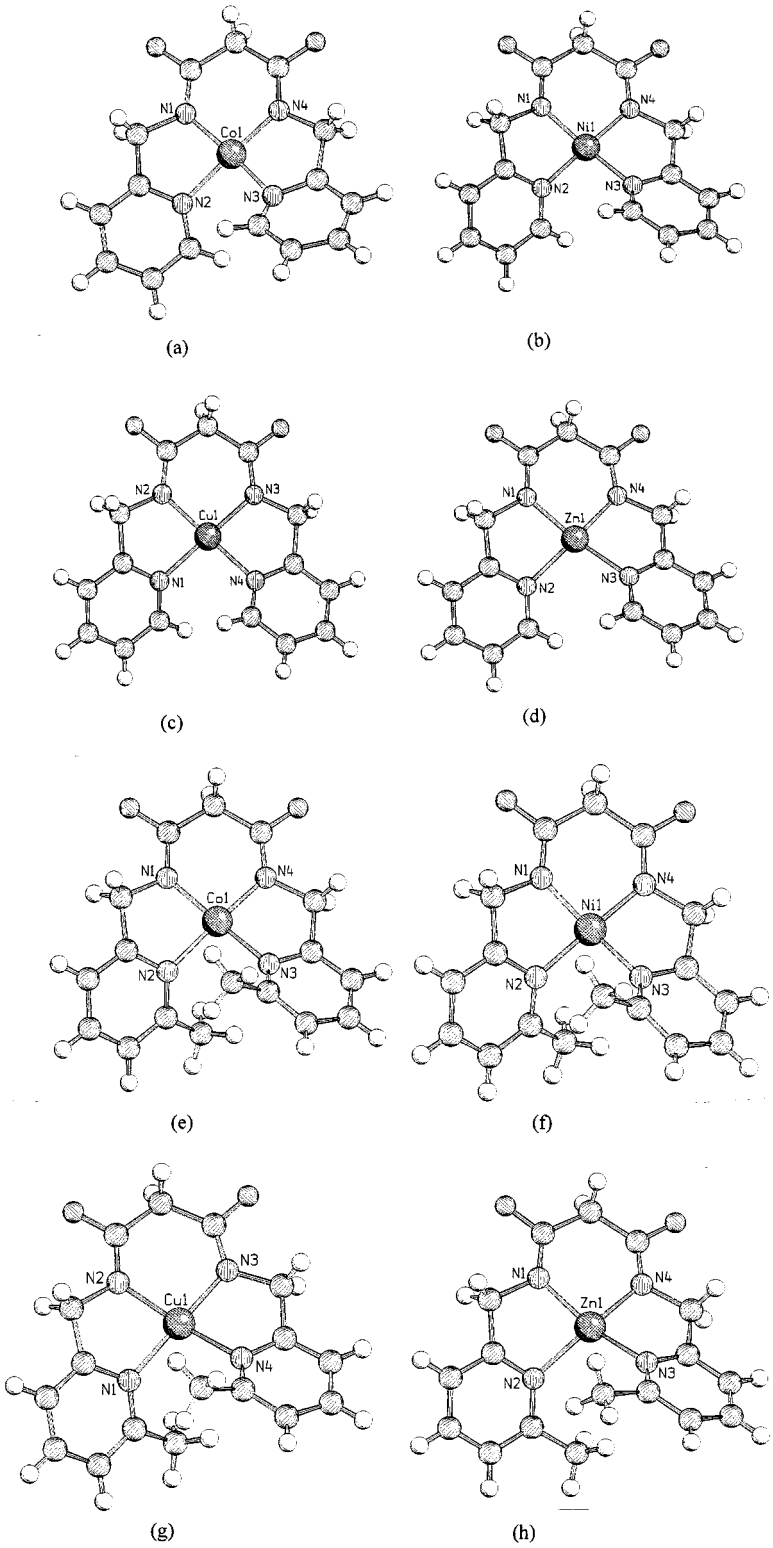

plexes, indicating that Zn(II) may relax the ligand imposed strain most efficiently. Substitution of the ortho hydrogen atoms of the pyridine rings with methyl groups (Me_2papH_2) increases this tetrahedral twist and may thus enhance the zinc(II) selectivity of this type of ligand.

Stabilities

The brutto stability constants of the complexes with $papH_2$ were determined by potentiometric titration [T = 298 K, μ = 0.2 mol dm^{-3} (KCl)]. Table 6 lists the protonation constants of the metal-free ligand and the logβ values of the complex species. The species distribution curves of the Cu(II)/$papH_2$ and the Ni(II)/$papH_2$ systems are shown in Figure 3. The main coordination mode of $papH_2$ with Cu(II) and Ni(II) is through the four nitrogen donors (MLH_{-2} in Figure 3). The supposedly N_2O_2 coordinated compounds [Cu($papH_2$)] and [Ni($papH_2$)] (ML in Figure 3) are minor species in acidic medium, where the amide nitrogen atoms are not deprotonated. The higher stability of [Cu(pap)] than that of [Ni(pap)] is in agreement with the larger flexibility towards tetrahedral distortion (d^9 vs low spin d^8), and this also emerges from the experimentally determined copper(II) selectivity of $C_{16}papH_2$ in the two-phase experiment. From the titration of $papH_2$ in presence of Co(II) and Zn(II) it emerges that [Co($papH_2$)] and [Zn($papH_2$)] are the only complex species present in solution. Thus, this is a good example to demonstrate the limits of computer-assisted design of metal ion selective ligands, i.e. MM does not allow to predict the stoichiometry of the compounds formed in solution[4] (see also Introduction).

Figure 3. Species distribution of the M(II)/$papH_2$ system [M(II) = (a) Cu(II), (b) Ni(II); $c_M = 2 \times 10^{-3}$ mol dm^{-3}; $c_L = 2 \times 10^{-3}$ mol dm^{-3}; μ = 0.2 (KCl)].

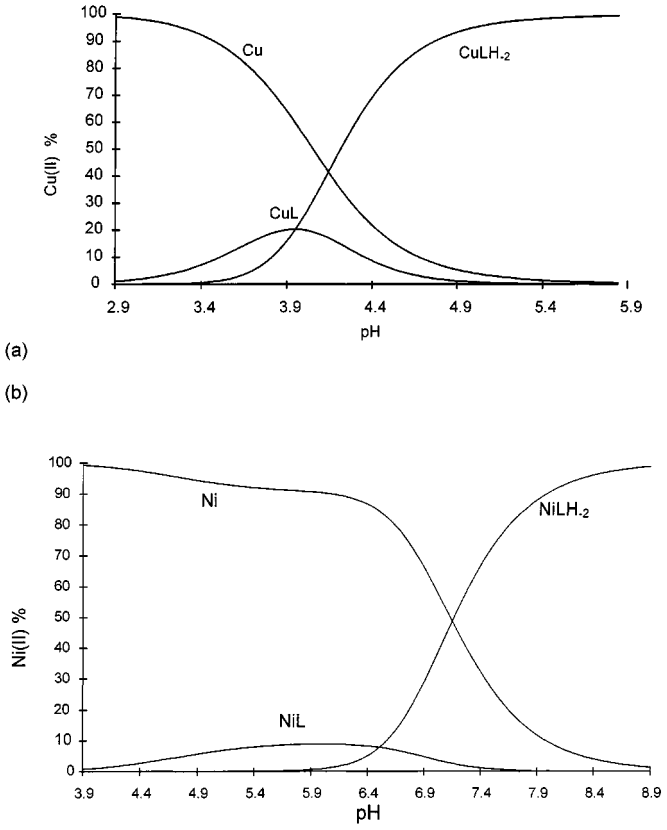

Metal-Ion Extraction

$C_{16}papH_2$ is soluble in the most common organic solvents and insoluble in water. The extraction through the liquid membrane (CH_2Cl_2/$C_{16}papH_2$) was studied in two separate experiments, i.e. extraction form the aqueous source phase to the organic phase and extraction form the organic phase to the aqueous receiving phase, and a pH gradient was used to drive the two extraction steps (see Scheme 2). The thermodynamics and kinetics of this type of experiment are dependent on the medium (solvent, pH, ion concentrations), temperature, type of stirring and time for the extraction[16][17]. Also, the stoichiometry of the complex species in the organic phase is not necessarily identical

Scheme 2

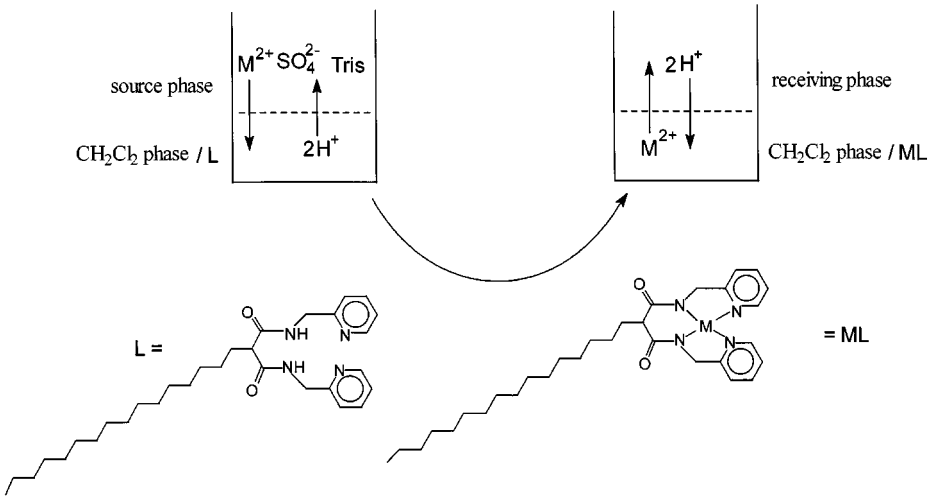

to that in aqueous solution (see comment above). Thus, the extraction data (Table 7) and the results of the potentiometric studies (Table 6) are not comparable on a quantitative basis. Studies in dependence of $[M^{2+}]$ and extraction time indicated that extraction of copper(II) at a relativly low concentration ($[Cu^{2+}] = 5 \times 10^{-3}$ mol dm^{-3}) at ambient temperature and at pH 7.5 (aqueous to organic) and pH 3 (organic to aqueous), respectivly, was complete, i.e. reaching a steady state distribution, after $\leq$ 10 min. At higher $[Cu^{2+}]$ (experiments were performed up to $[Cu^{2+}] =$ 0.02 mol dm^{-3}) the extraction time had to be increased (by a factor of 20 with the above parameters). Also, the extraction kinetics of the four metal ions studied indicate that under the conditions of our experiments, the selectivity for Cu^{2+} was enhanced to some degree. On a qualitative basis the extraction studies and the potentiometric titrations are in good agreement, and the Cu^{2+} selectivity is in agreement with the prediction from the molecular mechanics calculations.

Table 6. Stability constants of the proton, copper(II), nickel(II), cobalt(II) and zinc(II) complexes of $papH_2$ (L)

	metal-free ligand [a]			
log$K$(L)	4.59 (1)			
log$K$(HL$^+$)	8.48 (1)			
	Co(II)	Ni(II)	Cu(II)	Zn(II)
logβ([MLH$_{-2}$])		−11.49(2)	−4.49(1)	
logβ([ML])	1.75(1)	1.54(1)	3.41(2)	1.87(1)

[a] $\log K_{amide} = 0.5\ (\log K_{ML} - \log K_{MLH-2})$; Cu(II): 3.95; Ni(II): 6.55

Table 7. $C_{16}papH_2$-mediated extraction of metal ions through CH_2Cl_2 (T = 298 K, pH = 7.5 (source phase), 3 (receiving phase)

source phase	Fe^{2+}	Co^{2+}	Ni^{2+}	Cu^{2+}
$[M^{2+}]_{t = 0\ min}$ mg/dm^{-3}	25.83	29.50	29.80	27.16
$[M^{2+}]_{t = 10\ min}$ mg/dm^{-3}	25.38	28.56	27.37	18.12
Extraction[a]	98.3	96.8	91.9	66.7
[%]	(1.7)	(3.2)	(8.2)	(33.3)
Receiving phase	Fe^{2+}	Co^{2+}	Ni^{2+}	Cu^{2+}
$[M^{2+}]_{t = 10\ min}$ mg/dm^{-3}	0.06	0.13	0.72	8.86
Extraction[b]	13.3	13.8	29.6	98
[%]	(0.2)	(0.4)	(2.4)	(32.6)

[a]% Remaining in source phase (extracted into organic phase). − [b]% Extracted from the organic into the receiving aqueous phase (extracted from aqueous source into aqueous receiving phase).

We gratefully acknowledge generous financial support by the *Deutsche Forschungsgemeinschaft* (*DFG*) and the *Fonds der Chemischen Industrie* (*FCI*).

Experimental Section

General: Commercially available chemicals of the highest possible grade were used without further purification.^{13}C-NMR spectra at 50.32 MHz were obtained with a Bruker AS 200 instrument with sodium 3-(trimethylsilyl)propianate-d_4 as an internal reference. EPR spectra (10^{-3} m in DMF/water (1:2), 298 or 100 K) were recorded with a Bruker ESP 300E instrument (ER 041 XK X-band microwave bridge). The spin-Hamiltonian parameters were determined by simulation of the spectra with the computer program EPR50F[18]. UV/VIS spectra were obtained with Varian Cary IE or Cary 2300 spectrophotometers. Electrochemical measurements (cyclovoltametry) were made with a BAS 100B system using 10^{-3} mol dm^{-3} solutions of [Ni(pap)] in 0.1 mol dm^{-3} tetrabutylammoniumperchlorat CH_3CN solution at a glassy carbon electrode with a Ag/AgCl reference and a Pt auxiliary electrode with a scan rate of 100 mVs^{-1}, or using 10^{-3} mol dm^{-1} solutions of [Cu(pap)] in 0.1 mol dm^{-3} LiCl aqueous solution at a mercury drop electrode with a Ag/AgCl reference and a Pt auxiliary electrode with a scan rate of 100 mVs^{-1}. The pH-metric titrations were performed on 5 or 10 ml samples in the concentration range of 2×10^{-3} to 8×10^{-3} mol dm^{-3} at metal ion to ligand ratios of 2:1, 1:1 and 1:2. Argon was bubbled through the samples to ensure the absence of oxygen and for stirring the solutions. All pH-metric measurements were carried out at 298 K and at a constant ionic strength of 0.2 mol dm^{-3} (KCl). Measurements were made with a Radiometer pHM64 pH-meter, equipped with a CMAWL/S7 combined pH electrode and a Dosimat 715 (Metrohm) autoburette, containing carbonate-free potassium hydroxide at a known concentration. The pH output was converted into $[H^+]$ as described previously[19]. Protonation constants of the ligands and the brutto stability constants of the binary systems were calculated with PSEQUAD[20]. AAS measurements were made on a Perkin-Elmer 1100B instrument using an air-acetylene flame. The spectrometer was calibrated with standard Merck solutions. The wave lengths: 324.7 nm (Cu), 232 nm (Ni), 240.7 nm (Co), 248.3 nm (Fe). Elemental analyses were obtained from the microanalytical laboratory of the chemical institutes of the University of Heidelberg.

For molecular mechanics calculations MOMEC[11] was used, which also produced the Schakal[15] files for plotting. The force field has been described previously[11], except for parameters that are described in the text and in Table 4.

$papH_2$: α-picolylamine (2.7 g, 25 mmol) was added slowly to a hot and stirred aqueous solution (100 ml, 100°C) of diethyl-malonate (16 g, 6.25 mmol), and left at this temperature for 8h. After cooling to ambient temperature, ethanol (10 ml) and ether (100 ml) were added to precipitate the yellowish white product, which was collected after 24h (refrigerator) and recrystallized from ethyl acetate. Yield of the white crystalline ligand: 25.56 g (89.9 mmol, 90%). Calcd. for $C_{15}H_{16}N_4O_2$: C 63.35, H 5.68, N 19.71; found: C 63.29, H 5.73, N 19.78. ^{13}C-NMR (50.32 MHz, CD_3OD, 25°C, TMS): 169.7 (CO), 158.9, 149.7, 138.8, 123.7, 122.9 ($C_{pyridine}$), 53.8 ($CH_2(CO)_2$), 45.5 (pyridine, CH_2-NHR).

$C_{16}papH_2$: Diethyl malonate (8 g, 50 mmol) was slowly added by syringe to a solution of sodium (1.15 g, 50 mmol) in warm ethanol (abs., 25 ml, 50°C). Upon slow addition (syringe) of hexadecyl bromide (15.5 g, 50.25 mmol), a white product precipitate. The reaction mixture was then refluxed for 6 h and left in a refrigerator for 12 h. The precipitated diethyl hexadecylmalonate was collected by filtration, washed with water and dried over P_2O_5. Yield: 16.7 g (43.4 mmol, 87%). Calcd. for $C_{23}H_{44}O_4$: C 71.81, H 11.54; found: C 72.01, H 11.63. ^{13}C NMR (50.32 MHz, $CDCl_3$, 25°C, TMS): δ = 169.6 (CO), 61.2 (CH_2, ester), 52.1 ($C_{16}-CH-R_2$), 14.1 (CH_3, ester), mult (alkyl chain).

α-Picolylamine (18 g, 166.4 mmol) and the alkylated diethyl malonate (16 g, 41.6 mmol) were allowed to react for 8 h at 100°C

Table 8. Crystal data

	papH$_2$ × HBF$_4$ × H$_2$O	[Ni(pap)] × 2 H$_2$O	[Cu(pap)] × 3 H$_2$O
formula	$C_{15}H_{19}N_4O_3BF_4$	$C_{15}H_{14}N_4O_2Ni \times 2\ H_2O$	$C_{15}H_{14}N_4O_2Cu \times 3\ H_2O$
crystal system	orthorhombic	triclinic	monoclinic
Mol. mass	390.14	377.02	399.89
space group	*Pnma*	*Ci*/1,*P*1bar	$P2_1/a$
a [Å]	8.700(2)	7.794 (2)	8.0810(10)
b [Å]	13.145(3)	11.933 (4)	22.086(3)
c [Å]	15.401(4)	17.808 (5)	9.9390(10)
α [°]	90	86.83 (3)	90
β [°]	90	82.70 (2)	104.520(10)
γ [°]	90	73.82 (2)	90
V [Å^3]	1761.28	1577.1	1717.2
Z	8	2	4
Crystal colour, habit	light green prisms	red plates	blue plates
Crystal dimensions [mm]	0.50 × 0.55 × 0.65	0.10 × 0.35 × 0.50	0.55 × 0.50 × 0.35
Radiation [mm^{-1}]	Mo-K_α, μ = 0.13	Mo-K_α, μ = 1.26	Mo-K_α, μ = 1.306
θ limits [deg]	1.5 < θ < 29.5	1.5 < θ < 25.0	1.84 < θ < 30.0
$D_{calcd.}$ [g/cm^3]	1.47	1.59	1.547
No. of unique reflections	2539	5553	5174
No. of independent reflections	1643	3269	4938
temp.,°C	22	22	22
λ [Å]	0.7101	0.7101	0.7101
R	0.084	0.061	0.047
R_w [a]	0.069	0.050	0.1017

[a] $R_w = \Sigma w(|F_o| - |F_c|^2.\Sigma w F_o^2)^{1/2}$.

without a solvent. The product mixture was poured into 50 ml of cold water, and the precipitate was collected on a filter, after standing for 4 h in the refrigerator. After washing with water and drying under reduced pressure, the diamide was recrystallized from dichloromethane. Yield: 14.82 g (29.13 mmol, 70%). Calcd. for $C_{31}H_{48}N_4O_2$: C 73.17, H 9.52, N 11.02; found: C 72.99, H 9.47, N 10.95. ^{13}C NMR (50.32 MHz, $CDCl_3$, 25°C, TMS): δ = 170.8 (CO), 156.4, 149.1, 136.6, 122.2, 121.6 ($C_{pyridine}$), 55.2 ($C_{16}-CH-(CO)_2$), 44.6 (pyridine, CH_2-NHR), mult (alkyl chain).

[Cu(pap)]: An aqueous solution (30 ml) of $CuSO_4 \times 5\ H_2O$ (0.44 g, 1.76 mmol) was added to an aqueous solution (30 ml) of papH$_2$ (0.5 g, 1.76 mmol), set at pH 7.5 (0.1 M aqueous NaOH). A crystalline product was obtained after slow evaporation of the solvent at ambient temperature. Yield: 0.57 g (1.43 mmol, 81.4%). Calcd. for $C_{15}H_{20}CuN_4O_5$: C 45.05, H 5.04, N 14.01; found: C 44.99, H 5.07, N 14.04.

[Ni(pap)]: An aqueous solution (30 ml) of $Ni(BF_4)_2$ (0.41 g, 1.76 mmol) was added to an aqueous solution (30 ml) of papH$_2$ (0.5 g, 1.76 mmol), set at pH 7.5 (0.1 M aqueous NaOH). A crystalline product was obtained after slow evaporation of the solvent at ambient temperature. Yield: 0.42 g (1.11 mmol, 63.6%). Calcd. for $C_{15}H_{18}N_4NiO_4$: C 47.79, H 4.81, N 14.86; found: C 47.52, H 4.80, N 14.83. ^{13}C NMR (50 MHz, CD_3OD, 25°C, TMS): 176.2 (CO), 165.7, 150.6, 140.7, 125.7, 123.0 ($C_{pyridine}$), 57.6 ($CH_2(CO)_2$), 44.9 (pyridine, CH_2-NR).

Crystal Structure Analyses: The X-ray data of papH$_2$ × HBF$_4$ × H$_2$O ($C_{15}H_{19}N_4O_3 \times BF_4$), [Ni(pap)] × 2 H$_2$O ($C_{15}H_{14}N_4O_2Ni \times 2\ H_2O$) and [Cu(pap)] × 3 H$_2$O ($C_{15}H_{14}CuN_4O_2 \times 3\ H_2O$) were measured at room temperature on a Nicolet R3-diffractometer employing graphite monochromated Mo-K_α radiation (λ = 0.7107 Å); ω scan mode, data reduction and application of Lorenz, polarization absorption corrections were carried out. Details of the measurements and analyses are given in Table 8. The atom numbering is defined in Figure 1. The crystallographic data have been deposited at the Cambridge Crystallographic Data Centre (CCDC) as supplementary publication no. CCDC-103064 (for $C_{15}H_{14}N_4O_2Ni \cdot 2H_2O$), -103065 (for $C_{15}H_{19}N_4O_3BF_4$), -103066 (for $C_{15}H_{14}N_4O_2Cu \cdot 3H_2O$). Copies of the data can be obtained free of charge on application to CCDC, 12 Union Road Cambridge CB2 1EZ, UK [Fax: (internat.) + 44-1223/336033; E-mail: deposit@ccdc.cam.ac.uk].

The structure of papH$_2$ × HBF$_4$ × H$_2$O was solved with direct methods; full-matrix least-squares methods were used to refine 2790 variables out of 1643 reflections with $I > 2.5\sigma$ (I); the structure converged at R = 8.4% and R_W = 6.9%; residual electron density −0.42, 0.71 e/Å^{-3}. Weight = $1/\sigma^2(F_0)$; goodness of fit = 4.19. The structures [Ni(pap)] × 2 H$_2$O and [Cu(pap)] × 3 H$_2$O were solved by Patterson-Fourier Methods with the SHELXTL PLUS program[21]; hydrogen atoms were included at calculated sites with fixed isotropic thermal parameters. The refinement (full-matrix, least-squares methods, $|F|$) of 5553 ([Ni(pap)]), 5174 ([Cu(pap)]) variables out of 3269 ([Ni(pap)]), 4938 ([Cu(pap)]) reflections with $I > 2.5\sigma$ (I) converged at R = 6.1% ([Ni(pap)]), 4.7% ([Cu(pap)]) and R_W = 5.0% ([Ni(pap)]), 10.17% ([Cu(pap)]); residual electron density −0.45, 0.54 ([Ni(pap)]), −0.327, 0.522 e/Å^{-3} ([Cu(pap)]). Weight = $1/\sigma^2(F_0)$; goodness of fit = 1.91 ([Ni(pap)]), 1.092 ([Cu(pap)]).

Extraction Experiments: The volume of each phase (aqueous source phase, organic phase, aqueous receiving phase) was 50 ml. The M^{2+} concentration (M = Fe, Co, Ni, Cu) of the aqueous source phase was ca. 5 × 10^{-3} mol dm^{-3} (pH 7.5, 0.1 mol dm^{-3} Tris, filtration to remove hydroxides) and measured by AAS (1 ml samples). The organic phase (CH_2Cl_2) contained 10^{-3} mol dm^{-3} C_{16}papH$_2$ and the pH of the aqueous receiving phase was 3 (0.1 mol dm^{-3} phthalate). The extractabilities were determined by AAS as decreasing [M^{2+}] in the aqueous source and increasing [M^{2+}] in the aqueous receiving phase. The conditions for all extractions were identical (298 K, stirring at 750 r.p.m. (magnetic stirrer) for 10.0 min). The data reported in Table 7 are averages of 3 determinations (deviation ≤ 5%).

[1] [1a] H. Irving, R. J. P. Williams, *Nature (London)* **1948**, *162*,

746. – [1b] D. A. Johnson, P. G. Nelson, *Inorg. Chem.* **1995**, *34*, 5666. – [1c] D. A. Johnson, P. G. Nelson, *J. Chem. Soc., Dalton Trans.* **1995**, 3483.
[2] D. J. Cram, T. Kaneda, R. C. Helgeson, S. B. Brown, C. B. Knobler, E. Maverick, K. N. Trueblood, *J. Am. Chem. Soc.* **1985**, *107*, 3645.
[3] [3a] R. D. Hancock, *Progr. Inorg. Chem*. **1989**, *37*, 187. – [3b] A. E. Martell, R. D. Hancock, *"Metal complexes in Aqueous Solution"*, Plenum, New York, **1996**. – [3c] L. F. Lindoy, *"The Chemistry of Macrocyclic Ligand Complexes"*, Cambridge University Press, Cambridge, **1989**. – [3d] K. R. Adam, L. F. Lindoy, in *"Crown Compounds, Toward Future Applications"*, Ed. S. R. Cooper, VCH, Weinheim, **1992**, p.69.
[4] [4a] P. Comba, T. W. Hambley, *"Molecular Modeling of Inorganic Compounds"*, VCH, Weinheim, **1995**. – [4b] P. Comba, *Coord. Chem. Rev.,* **1998***, submitted*.
[5] [5a] P. Comba, A. Fath, A. Kühner, B. Nuber, *J. Chem. Soc., Dalton Trans.,* **1997***,* 1889. – [5b] P. Comba, B. Nuber, A. Ramlow, *J. Chem. Soc., Dalton Trans.,* **1997**, 347. – [5c] B. P. Hay, D. Zang, J. R. Rustad, *Inorg. Chem.*, **1996**, *35*, 2650. – [5d] P. Comba, K. Gloe, K. Inoue, T. Krueger, H. Stephan, K. Yoshizuka, *Inorg. Chem.* **1998**, *37*, 3310. – [5e] P. Comba, N. Okon, R. Remenyi, *Chem. Europ. J.* **1998***, submitted.*
[6] K. Várnagy, H. Süli-Vargha, in *"Molecular Modeling and Dynamics of Bioinorganic Systems"*, Eds. L. Banci, P. Comba, Kluwer, Dordrecht, **1997**.
[7] P. Comba, T. W. Hambley, G. A. Lawrance, *Helv. Chim. Acta* **1985**, *68*, 2332.
[8] C. K. Johnson, *ORTEP*; Report 3794; U.S. Atomic Energy Commission, Oak Ridge: TN, **1965**.
[9] [9a] S. Tsuboyama, T. Sakurai, K. Kobayashi, *Acta Cryst.,* **1984**, *40*, 466. – [9b] R. L. Chapman, F. S. Stephens, R. S. Vagg, *Inorg. Chim. Acta* **1980**, *43*, 29. – [9c] M. Mulqi, F. S. Stephens, R. S. Vagg, *Inorg. Chim. Acta* **1981**, *51*, 9. – [9d] F. S. Stephens, R. S. Vagg, *Inorg. Chim. Acta*, **1981**, *51*, 149. – [9e] M. Mulqi, F. S. Stephens, R. S. Vagg, *Inorg. Chim. Acta* **1981**, *52,* 177. – [9f] R. L. Chapman, F. S. Stephens, R. S. Vagg, *Inorg. Chim. Acta* **1981**, *52*, 169. – [9g] M. Ray, R. Mukherjee, J. F. Richardson, M. S. Mashuta, R. M. Buchanan, *J. Chem. Soc. Dalton Trans.* **1994**, 965.
[10] [10a] M. Mulqi, F.S. Stephens, R.S. Vagg, *Inorg. Chim. Acta*, **1981**, *52,* 73. – [10b] S. C. Chang, D. Y. Park, N. C. Li, *Inorg. Chem.* **1968**, *7*, 2144. – [10c] F. S. Stephens, R. S. Vagg *Inorg. Chim. Acta*, **1984**, *90*, 17. – [10d] F. S. Stephens, R. S. Vagg, *Inorg. Chim. Acta*, **1986,** *120*, 165. – [10e] F. S. Stephens, R. S. Vagg, *Inorg. Chim. Acta*, **1982**, 57, 9.
[11] P. Comba, T. W. Hambley, N. Okon, G. Lauer, *"MOMEC, a Molecular Modeling Package for Inorganic Compounds"*, **1997**, Lauer & Okon, Heidelberg, Germany, E-mail: CVS-HD@t-online.de.
[12] [12a] P. V. Bernhardt, P. Comba, *Inorg. Chem.* **1992**, *31*, 2638. – [12b] P. Comba, T. W. Hambley, M. Ströhle, *Helv. Chim. Acta* **1995**, *78*, 2042. – [12c] J. E. Bol, C. Buning, P. Comba, J. Reedijk, M. Ströhle, *J. Comput. Chem.* **1998**, *19*, 512.
[13] P. Comba in *"Fundamental Principles of Molecular Modeling"*, A. Amann, J. C. A. Boeyens, W. Gans, Eds., Plenum Press, New York, **1996**, 167.
[14] The new version of the program MOMEC[11] has a plane twist potential to model tetrahedral twists; this facility was not used in the present study.
[15] E. Keller, *SCHAKAL 92*, Universität Freiburg, Germany, **1992**.
[16] E. Kimura, C. A. Dalimunte, A. Yamashita, R. Machida, *J. Chem. Soc., Chem. Comm.*, **1985**, 1041.
[17] M. DiCasa, L. Fabbrizzi, A. Perotti, A. Poggi, P. Tundo, *Inorg. Chem.*, **1985**, *24*, 1610.
[18] P. A. Martinelli, G. R. Hanson, J. S. Thompson, B. Holmquist, J. R. Pilbrow, B. L. Vallee, *Biochemistry* **1980**, *28*, 225.
[19] [19a] A. Gergely, I. Nagypal, *J. Chem. Soc., Dalton Trans.* **1977**, 104. – [19b] H. M. Irving, M. H. Miles, L. D. Pettit, *Anal. Chim. Acta*, **1967**, *38*, 475.
[20] L. Zékány, I. Nagypál in: *"Computational methods for the Determination of Stability Constants"*, ed. D. Leggett, Plenum Press, **1985**.
[21] G. M. Sheldrick, Universität Göttingen, SHELXTL PLUS, Release 4.11 (V), **1990**.

[I98226]

Equilibrium Studies of the Axial Addition of Chiral Bases to Chiral Metal Schiff Base Complexes

Kerstin Schuhmann and Ernst-G. Jäger*

Institut für Anorganische und Analytische Chemie der Friedrich-Schiller-Universität Jena,
August-Bebel-Straße 2, D-07743 Jena, Germany
Fax: (internat.) + 49(0)3641/948102
E-mail: cej@uni-jena.de

Received July 15, 1998

Keywords: Schiff bases / Chiral recognition / Equilibrium constants / Nickel / Cobalt

The syntheses of new chiral 1,2-diphenylethylene-bridged nickel(II) and methylcobalt(III) Schiff base complexes are described. The equilibrium constants for the axial addition of the chiral bases (*R*)- and (*S*)-1-phenylethylamine to the enantiomerically pure metal complexes have been determined by means of spectrophotometric titrations. Comparison of the constants for the cyclohexanediyl-bridged complexes (type **1**) with those for the more bulky 1,2-diphenylethylene-bridged complexes (type **2**) reveals that chiral recognition is only observed in the case of type-2 complexes.

Introduction

In recent years, catalytic asymmetric synthesis has become increasingly important[1]. In this context, the enantioselective epoxidation of unfunctionalized alkenes reported by Jacobsen and Katsuki et al. has been one of the highlights of the current decade[2]. Recently, Mukaiyama et al. reported on the enantioselective hydrogenation of ketones with sodium tetrahydroborate in the presence of optically active cobalt(II) complexes[3]. These reactions are mediated by chiral metal complex catalysts and are based on the capacity of such species for chiral recognition of the substrates. Thus, some metal Schiff base complexes have emerged as particularly effective catalysts by virtue of their chiral carbon centers being situated in the vicinity of the central atom.

Our work is concerned with studies of the structure-reactivity relationships of Schiff base complexes with regard to the basic features of reactivity that are of importance for the catalytic performance, i.e. investigations of the redox behavior and Lewis acidity of coordinatively unsaturated planar complexes.

In previous publications we reported on new chiral nickel and copper $[N_2O_2]$-coordinated Schiff base complexes derived from 1,2-diaminocyclohexane and β-oxo aldehydes. These were characterized with regard to their ability to bind Lewis bases at their free axial coordination sites (Lewis acidity) and to accept electrons (redox potentials). However, upon applying the chiral bases (*R*)- and (*S*)-1-phenylethylamine, no chiral recognition could be observed[4]. The same result was found by Elias et al. for the addition of (*S*)-(−)-nicotine to chiral salene complexes[5].

Differences in the adduct stabilities were observed for the diastereomeric complexes *meso*-Ni**1a** and (*R,R*)-Ni**1a**, which can be attributed to the orientation of the cyclohexanediyl group in relation to the $[N_2O_2]$ plane[6].

In the present work, new chiral nickel and cobalt Schiff base complexes derived from 1,2-diphenylethylenediamine are described (type 2). Spectrophotometric titrations with chiral bases have been carried out so as to allow the determination of the stability constants of the adducts. Planar nickel complexes are known to give consecutive equilibria associated with 1:1 and 1:2 base adduct formation. Because of the change of spin state from S = 0 to S = 1, the octahedral 1:2 adduct is normally strongly favored ($K_2 >> K_1$). For investigations of pure 1:1 adduct formation we used a pentacoordinated methylcobalt(III) derivative. Such complexes usually have a sufficiently high Lewis acidity at the sole vacant coordination site and allow the determination of the equilibrium constants for the 1:1 base addition with high precision[7]. This is seemingly the first time that chiral recognition has been observed in measurements of this kind.

Results and Discussion

The ability of complexes to show chiral recognition depends mainly on the steric environment of the active site, i.e. the central metal atom. In view of the aforementioned negative results concerning the addition of chiral bases to complexes with the 1,2-cyclohexanediyl group as the chiral bridge, this group was replaced by the sterically more demanding 1,2-diphenylethylene bridge (Figure 1).

The substituents R^1 and R^2 also have a considerable influence on the electronic properties of the metal, as well as being responsible for steric effects. Substitution pattern **b** is sterically more demanding than arrangement **a**. However, the Lewis acidity of Ni**2b** is too low to permit quantitative studies of axial ligation. Spectral changes upon base addition could only be observed for nickel complexes with the electron-withdrawing substituents CN and OEt (type **a**). In

 © WILEY-VCH Verlag GmbH, D-69451 Weinheim, 1998 1434−1948/98/1212−1051 $ 17.50+.50/0

Figure 1. Nomenclature of the Schiff base complexes

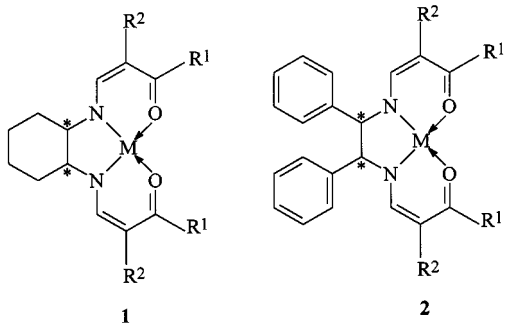

M = 2H, Ni, Co

a: R^1 = OEt; R^2 = CN

b: R^1 = Ph; R^2 = COOEt

contrast to the nickel complexes, where both types (Ni**2a** and Ni**2b**) could be prepared, we were not successful in isolating the corresponding cobalt complex Co**2a**. Thus, only the complex (*R*,*R*)-Co**2b** could be synthesized, which was subsequently methylated at the axial position so as to obtain the diamagnetic methylcobalt(III) complex (*R*,*R*)-MeCo**2b**. Such organocobalt complexes are very suitable as base acceptors in spectrophotometric titrations, since the spectral changes that accompany the transition from the pentacoordinated to the octahedral state are highly sensitive, and usually the calculated constants are of such an order of magnitude and of such a high precision that gradations of the constants for titrations with relatively weak bases can be determined unambiguously[7].

The compounds were characterized by means of NMR spectroscopy. As expected, in the ^{1}H-NMR spectrum of (*R*,*R*)-MeCo**2b** the protons attached to the chiral carbon atoms, as well as the olefinic protons (N−CH=), exhibit a double set of signals, i.e. they are no longer equivalent. This non-equivalence is due to the C_2 symmetry and the axial methyl group. This effect could not be observed in the spectrum of the corresponding square-planar nickel complex (*R*,*R*)-Ni**2a** or in that of (*R*,*R*)-Ni**2b**. Upon addition of [D_5]pyridine to the solution of (*R*,*R*)-MeCo**2b** used to record the NMR spectrum, the signal of the axial methyl group is shifted to lower field ($\delta = 2.70 \rightarrow 2.98$).

Spectrophotometric titrations were carried out using the (*S*,*S*) enantiomers of the optically active complexes Ni**1a** and Ni**2a** with both enantiomers of the chiral base 1-phenylethylamine in chloroform and in benzene (Ni**2a** only). Nickel complexes preferentially form octahedral base diadducts, i.e. $K_1 < K_2$ for equations 1 and 2.

$$\mathrm{NiL} + \mathrm{B} \overset{K_1}{\rightleftharpoons} \mathrm{NiLB} \qquad (1)$$

$$\mathrm{NiLB} + \mathrm{B} \overset{K_2}{\rightleftharpoons} \mathrm{NiLB_2} \qquad (2)$$

The constants K_1 (= β_1) and β_2 (K_1K_2) thus determined are listed in Table 1. It was confirmed that the cyclohexanediyl-bridged complex (*S*,*S*)-Ni**1a** cannot distinguish between (*R*)- and (*S*)-1-phenylethylamine. For these substrates, the measured constants are the same within the margin of error. However, following introduction of the sterically more demanding chiral 1,2-diphenylethylene bridge into the complex [(*S*,*S*)-Ni**2a**], the β_2 values differ significantly. In both the solvents used, i.e. $CHCl_3$ and benzene, the constants determined by titration with the (*R*)-amine are significantly higher than those determined by titration with the (*S*)-amine. This means that the base adduct of (*S*,*S*)-Ni**2a** with (*S*)-1-phenylethylamine is thermodynamically less stable than the adduct with the (*R*)-amine. The reason for this should be that the addition of the (*S*) enantiomer of the base is sterically more hindered by the chiral diamine bridge than that of the (*R*) enantiomer. Unfortunately, the margin of error in K_1 (and K_2) is much higher than that in β_2 and thus it is not possible to establish whether the chiral recognition occurs to a greater extent in the first or the second step of the axial base addition.

Furthermore, we carried out titrations of the organocobalt(III) complex (*R*,*R*)-MeCo**2b** with (*R*)- and (*S*)-1-phenylethylamine in benzene. (This complex is very light-sensitive in solution, and hence preparations and the measurement itself had to be carried out in the dark.) In the course of the base addition, a transition from the pentacoordinated to the octahedral state occurs, as depicted in Scheme 1.

An example of a titration of (*R*,*R*)-MeCo**2b** with a chiral base is illustrated in Figure 2. The intense charge transfer band at 645 nm is seen to decrease with increasing concentration of (*S*)-1-phenylethylamine.

The calculated values of *K* are listed in Table 2. It can be seen that the difference between the constants derived from the two titrations is even larger than in the case of the nickel complex (*S*,*S*)-Ni**2a**. The constant for the adduct of (*R*,*R*)-MeCo**2b** with (*S*)-1-phenylethylamine is approximately three times larger than that of the adduct with the (*R*)-amine. It seems that the bulky substituents R^1 = phenyl and R^2 = COOEt enhance the differentiation of the stabilities of the corresponding base adducts, i.e. with (*R*)- or (*S*)-1-phenylethylamine, respectively.

From the equation K = [CoLB]/([CoL][B]) for the equilibrium according to Scheme 1, it follows that for the titration of complex (*R*,*R*)-MeCo**2b** with the racemic base 1-phenylethylamine, one would obtain an adduct mixture of a composition such that $[CoLB_{(R)}]/[CoLB_{(S)}] = K_{(R)}/K_{(S)}$, where (*R*) and (*S*) refer to (*R*)- and (*S*)-1-phenylethylamine, respectively. Thus, in the present case, a mixture of 36.4% of the (*R*)-amine adduct and 63.6% of the (*S*)-amine adduct would result.

Conclusions

The results show the significant influence of the complex periphery on chiral recognition properties. Such an effect has been observed simply by replacing the cyclohexadienyl group in previously studied compounds by the sterically

Table 1. Equilibrium constants for the titration of (*S*,*S*)-Ni**1a** and (*S*,*S*)-Ni**2a** with the chiral bases (*R*)- and (*S*)-1-phenylethylamine at 20 (± 1)°C (in $CHCl_3$) and at 25 (± 0.1)°C (in benzene)

	Base	Solvent	K_1 [l mol^{-1}]	β_2 [l^2 mol^{-2}] (s[a])	e[b] (10^{-3})
(*S*,*S*)-Ni**1a**	(*R*)-1-phenylethylamine	$CHCl_3$	0.05	24[4]	5.4
(*S*,*S*)-Ni**1a**	(*S*)-1-phenylethylamine	$CHCl_3$	0.05	24	4.5
(*S*,*S*)-Ni**2a**	(*R*)-1-phenylethylamine	$CHCl_3$	< 0.01	12 (0.8)	0.6
(*S*,*S*)-Ni**2a**	(*S*)-1-phenylethylamine	$CHCl_3$	< 0.01	4.5 (0.5)	0.8
(*S*,*S*)-Ni**2a**	(*R*)-1-phenylethylamine	benzene	0.01	8.4 (0.1)	1.1
(*S*,*S*)-Ni**2a**	(*S*)-1-phenylethylamine	benzene	0.04	5.1 (0.1)	1.8

[a] Standard deviation of the equilibrium constant. – [b] Average of the square errors for the fit of the values of the extinctions.

Scheme 1. Equilibrium between the pentacoordinated methylcobalt complex and the octahedrally coordinated complex upon base addition

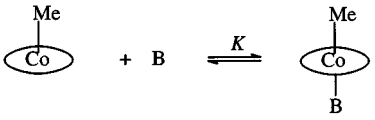

Figure 2. Spectrophotometric titration of (*R*,*R*)-MeCo**2b** with (*S*)-1-phenylethylamine in benzene

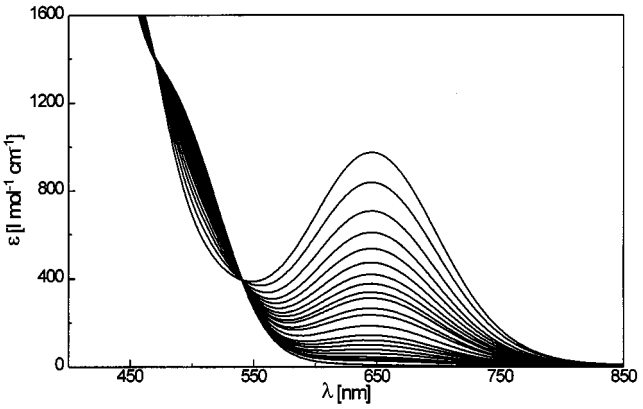

Table 2. Equilibrium constants for the titration of (*R*,*R*)-MeCo**2b** with (*R*)- and (*S*)-1-phenylethylamine in benzene at 20 (± 0.1)°C

Base	K [l mol^{-1}] (s[a])	e[b] (10^{-3})
(*S*)-1-phenylethylamine	770 (25)	4.5
(*R*)-1-phenylethylamine	316 (12)	1.5

[a] Standard deviation of the equilibrium constants. – [b] Average of the square errors for the fit of the values of the extinctions.

more demanding 1,2-diphenylethylene bridge. To the best of our knowledge, this is the first time that chiral recognition has been observed in the addition of a base to coordinatively unsaturated complexes. The results are of importance with regard to enantioselective catalytic investigations. Appropriate experiments are in progress, the results of which will be reported in due course.

We would like to thank the *Deutsche Forschungsgemeinschaft* and the *Fonds der Chemischen Industrie* for financial support.

Experimental Section

The following chemicals were used without further purification: Ethyl 2-cyano-3-ethoxyacrylate (Merck), (1*S*,2*S*)-(+)- and (1*R*,2*R*)-(−)-1,2-diphenylethylenediamine (97%, Fluka), (*R*)-(+)- and (*S*)-(−)-1-phenylethylamine (98%, Fluka). Ethyl (ethoxymethylene)-benzoylacetate was prepared according to a literature method[8]. – NMR spectra were recorded with a Bruker AC-200 spectrometer (^{1}H, ^{13}C, ^{1}H-^{13}C-COSY, ^{13}C APT NMR) and are reported as δ in ppm from HMDS. – FT IR spectroscopy was performed with a Perkin-Elmer 2000 FT-IR instrument. – Mass spectra were obtained with a Finnigan MAT SSQ 710 spectrometer. – Elemental analyses were carried out with a Leco CHNS-932 analyzer (CHN) and by complexometric titration (Ni, Co), respectively. – Specific rotation values were determined with a Polartronic E polarimeter (Schmidt-Haensch). – Spectrophotometric titrations were carried out at constant temperature with a Varian Cary 5E spectrophotometer equipped with a temperature controller. The calculation of the equilibrium constants was carried out at six wavelengths λ(*i*) and with at least twenty base (axial ligand) concentrations $c_B(j)$, under optimized conditions as described in the literature[9a]. The constants β_1 (= K_1) and β_2 (K_1K_2) as well as the extinction coefficients $\varepsilon_1(\lambda)$ and $\varepsilon_2(\lambda)$ for the 1:1 and the 1:2 adduct, respectively, were calculated iteratively by a non-linear fit of the absorbance data $A = E/(c_K d)$ (*E:* extinction; c_K: total complex concentration) according to

$$A_{i,j} = \Sigma\varepsilon_{\nu,i}\beta_\nu[B]_j^\nu/(\Sigma\beta_\nu[B]_j) \quad (3)$$

$(\nu = 0, 1, 2; \beta_0 \equiv 1)$

A home-made computer programme SPEGA was used for the iteration, based on the algorithm of Marquardt[9b]. A special procedure was included to calculate the equilibrium base concentrations $[B]_j$ from the known total concentrations c_{Bj} by iteration according to

$$c_{Bj} = [B]_j + c_{Kj}\Sigma\nu\beta_\nu[B]_j^\nu/(\Sigma\beta_\nu[B]_j^\nu) \quad (4)$$

$(\nu = 0, 1, 2; \beta_0 \equiv 1)$

Ligands: Diethyl (Z,Z)-(trans)-3,3′-(1,2-Diphenyl-1,2-ethanediyldiimino)bis(2-cyano-2-propenoate) [(*R*,*R*)- and (*S*,*S*)-2H**2a**]: 105 mg (0.5 mmol) of (*R*,*R*)- or (*S*,*S*)-diphenylethylenediamine was dissolved in 10 ml of methanol. To this solution, 170 mg (1 mmol) of ethyl 2-cyano-3-ethoxyacrylate, dissolved in 5 ml of methanol, was added dropwise. The mixture was refluxed for 30 min. The solvent was then partially evaporated in vacuo until a white powder precipitated. The solid was filtered off and washed with diethyl ether, yield 211 mg (92%), m.p. 214°C. – CI MS (H_2O); *m/z* (%): 459 $[M + H]^+$ (35), 413 $[M - CO]^+$ (2), 229 $[L/2]^+$ (95). – IR (Nujol): $\tilde{\nu}_{max}$ = 3199 cm^{-1} (NH_{str}), 2215 (CN_{str}), 1698 ($C{=}O_{str}$). –

(*R*,*R*)-2H**2a**: $C_{26}H_{26}N_4O_4$: calcd. C 68.12, H 5.72, N 12.22; found C 68.0, H 5.7, N 12.1. − $[\alpha]^{20}_D = -157 \pm 10$ (*c* = 0.18 in ethanol). − (*S*,*S*)-2H**2a**: found C 68.1, H 5.7, N 12.1. − $[\alpha]^{20}_D = +157 \pm 10$ (*c* = 0.18 in ethanol).

Diethyl (E,E)-(trans)-3,3′-(1,2-Diphenyl-1,2-ethanediyldiimino)bis(2-benzoyl-2-propenoate) [(*R*,*R*)- and (*S*,*S*)-2H**2b**]: 1.0 g (4.75 mmol) of (*R*,*R*)- or (*S*,*S*)-diphenylethylenediamine was dissolved in 20 ml of methanol. A solution of 2.36 g (9.5 mmol) of ethyl (ethoxymethylene)benzoylacetate in 10 ml of methanol was added dropwise. The mixture was refluxed for 30 min and then the solvent was evaporated in vacuo. The crude product was obtained in the form of a yellow oil. It was used for complexation without purification.− CI MS (H_2O); *m*/*z* (%): 617 $[M + H]^+$ (37), 571 $[M - C_2H_5O]^+$ (8), 308 $[L/2]^+$ (30).

Nickel Complexes

{[Diethyl (Z,Z)-(trans)-3,3′-(1,2-Diphenyl-1,2-ethanediyldiimino)]bis(2-cyano-2-propenoato)(2−)-N³,N³′,O¹,O¹′}nickel [(*R*,*R*)- and (*S*,*S*)-Ni**2a**]: 120 mg (0.26 mmol) of the ligand was suspended in 40 ml of ethanol. Then, 0.7 ml (0.52 mmol) of $N(Et)_3$ was added. To this mixture, a suspension of 64.7 mg (0.26 mmol) of $Ni(AcO)_2 \cdot 4H_2O$ in 20 ml of ethanol was added. The mixture was refluxed for 1 h, whereupon the substances dissolved and the solution became red in colour. The solvent was then evaporated in vacuo to leave a brown residue. The crude product was washed with water and finally with ethanol, yield 120 mg (89%), m.p. 257°C. − EI MS; *m*/*z* (%): 514 $[M^+]$ (30), 286 $[M - L/2]^+$ (40), 229 $[L/2]^+$ (100), 183 $[L/2 - C_2H_5OH]^+$ (30). − IR (Nujol): $\tilde{\nu}_{max} = 2208\ cm^{-1}$ (CN_{str}). − (*R*,*R*)-Ni**2a**: $C_{26}H_{24}N_4NiO_4$: calcd. C 60.61, H 4.70, N 10.87, Ni 11.39; found C 60.6, H 4.8, N 10.5, Ni 11.32. − (*S*,*S*)-Ni**2a**: found C 60.49, H 4.78, N 10.57, Ni 11.29.

{Diethyl (E,E)-(trans)-3,3′-[(1,2-Diphenyl-1,2-ethanediyldiimi)no]bis(2-benzoyl-2-propenoato)(2−)-N,N′,O²,O²′}nickel [(*R*,*R*)-Ni**2b**]: 250 mg (0.4 mmol) of *trans*-2H**2b** was dissolved in 40 ml of methanol. To this solution, 100 mg (0.4 mmol) of $Ni(AcO)_2 \cdot 4\ H_2O$, dissolved in 10 ml of methanol, was added. The mixture was refluxed for 30 min. After cooling, an orange precipitate was collected by filtration and dried in air, yield 245 mg (91%), m.p. 270°C. − EI MS; *m*/*z* (%): 672 $[M^+]$ (12), 365 $[M - L/2]^+$ (100), 105 $[C_6H_5CO^+]$ (45). − IR (Nujol): $\tilde{\nu}_{max} = 1706\ cm^{-1}$ ($C{=}O_{str}$), 701, 770 ($C{-}H_{def}$). − $C_{38}H_{34}N_2NiO_6$: calcd. C 67.78, H 5.09, N 4.16, Ni 8.71; found C 67.7, H 5.2, N 4.1, Ni 8.70.

Cobalt Complexes

{Diethyl (E,E)-(trans)-3,3′-[(1,2-Diphenyl-1,2-ethanediyl)diimino]bis(2-benzoyl-2-propenoato)(2−)-N,N′,O²,O²′}cobalt [(*R*,*R*)- and (*S*,*S*)-Co**2b**]: The following procedures were carried out under inert conditions using argon. 3.08 g (5 mmol) of the ligand was dissolved in 80 ml of dry DMF and the solution was heated to boiling. To the hot solution of the ligand, 5 mmol of $Co(AcO)_2 \cdot 4\ H_2O$ in 100 ml of DMF was added dropwise. A dark-red solution was obtained, which was refluxed for 1 h. The solvent was then evaporated until the complex precipitated. The solid was filtered off and washed with dry methanol. The dry orange complex was found to be stable in air, yield 2.56 g (76%), m.p. 253°C. − EI MS; *m*/*z* (%): 673 $[M^+]$ (30), 628 $[M - C_2H_5O]^+$ (2), 366 $[M - L/2]^+$ (100). − IR (Nujol): $\tilde{\nu}_{max} = 1710\ cm^{-1}$ ($C{=}O_{str}$), 701 ($C{-}H_{def}$). − Magn. mom.: $\mu_{eff} = 2.18$ B.M. − (*R*,*R*)-Co**2b**: $C_{38}H_{34}CoN_2O_6$: calcd. C 67.76, H 5.09, Co 8.75, N 4.16; found C 67.2, H 5.1, Co 8.81, N 4.1. − (*S*,*S*)-Co**2b**: found C 67.5, H 5.3, Co 8.84, N 4.2.

{Diethyl (E,E)-(trans)-3,3′-[(1,2-Diphenyl-1,2-ethanediyl)diimino)]bis(2-benzoyl-2-propenoato)(2−)-N,N′,O²,O²′}methylcobalt [(*R*,*R*)-MeCo**2b**]: 0.05 g (2.14 mmol) of sodium was pressed into 0.5 ml mercury under inert conditions. To the obtained amalgam, 1.44 g (2.14 mmol) of (*R*,*R*)-Co**2b**, dissolved in 25 ml of dry THF, was added. The mixture was stirred for 12 h, whereupon a violet colour appeared. The solution was then decanted from the mercury and cooled at −78°C. At this temperature, a solution of 0.456 g (3.2 mmol) of iodomethane in 10 ml of dry THF was added dropwise, resulting in the precipitation of a red solid. The suspension was poured into water, and the red solid was filtered off and dried in air. The obtained product still contained traces of water and THF, which could not be removed in vacuo. However, in non-coordinating solvents these molecules dissociate. These green solutions are very light-sensitive, yield 1.53 g (94%). − EI MS; *m*/*z* (%): 688 $[M^+]$ (2), 673 $[M - CH_3]^+$ (16), 366 $[M - L/2 - CH_3]^+$ (17). − IR (Nujol): $\tilde{\nu}_{max} = 1667\ cm^{-1}$ ($C{=}O_{str}$), 704 ($C{-}H_{def}$). − ^1H NMR (200 MHz; $CDCl_3$): δ = 0.74 (t, 6 H, CH_2CH_3), 2.70 (s, 3 H, CH_3), 3.78 (q, 4 H, CH_2CH_3), 4.69 (ds, 1 H, N−CHPh), 4.96 (ds, 1 H, N−CHPh), 7.05−7.35 (m, 20 H, Ph), 7.65 (s, 1 H, N−CH=), 7.79 (s, 1 H, N−CH=). − ^{13}C NMR (200 MHz, $CDCl_3$): δ = 13.5 (CH_2CH_3), 29.7 (CH_3), 59.6 (CH_2), 78.8, 81.1 (N−*C*HPh), 102.8, 103.6 (CH=*C*), 125.9−130.6 (Ph), 136.1, 136.9, 141.2 (C_q, Ph), 162.7, 163.9 (*C*H=C), 184.6 (C=O). − $C_{39}H_{37}CoN_2O_6$: calcd. C 68.02, H 5.42, Co 8.55, N 4.07; found C 68.70, H 6.28, Co 7.74, N 3.62. − TG: calcd. (from found value of Co) −9.5 (%) (THF, H_2O); found −9.1% (150°C).

[1] H. Brunner, W. Zettlmeier, *Handbook of Enantioselective Catalysis with Transition Metal Compounds*, VCH, Weinheim−New York−Basel−Cambridge−Tokyo, **1993**.

[2] [2a] W. Zhang, J. L. Loebach, S. R. Wilson, E. N. Jacobsen, *J. Am. Chem. Soc.* **1990**, 112, 2801. − [2b] W. Zhang, E. N. Jacobsen, *J. Org. Chem.* **1991**, *56*, 2296. − [2c] R. Irie, K. Noda, Y. Ito, N. Matsumoto, T. Katsuki, *Tetrahedron Lett.* **1990**, *31*, 7345.

[3] [3a] T. Nagata, K. Yorozu, T. Yamada, T. Mukaiyama, *Angew. Chem.* **1995**, *107*, 2309−2311; *Angew. Chem. Int. Ed. Engl.* **1995**, *34*, 2145 −2147. − [3b] K. D. Sugi, T. Nagata, T. Yamada, T. Mukaiyama, *Chem. Lett.* **1996**, 1081−1082.

[4] E.-G. Jäger, K. Schuhmann, H. Görls, *Inorg. Chim. Acta* **1997**, *255*, 295−305.

[5] R. Warmuth, H. Elias, *Inorg. Chem.* **1991**, *30,* 5027−5032.

[6] E.-G. Jäger, K. Schuhmann, H. Görls, *Chem. Ber.* **1997**, *130*, 1643−1646.

[7] [7a] E.-G. Jäger, P. Renner, *Z. Chem.* **1978**, *18*, 193−194. − [7b] D. Seidel, Ph. D. Thesis, University of Jena, **1986**.

[8] E.-G. Jäger, *Z. Chem.* **1968**, *8*, 470.

[9] [9a] E.-G. Jäger, B. Kirchhof, E. Schmidt, B. Remde, A. Kipke, R. Müller, *Z. Anorg. Allg. Chem.* **1982**, *485,* 141−172. − [9b] D. W. Marquardt, *SIAM J. Appl. Math.* **1963**, *11*, 431.

[I98233]

Enantioselective Organic Syntheses Using Chiral Transition Metal Complexes, 7[◇]

Synthesis of Chiral Rhenium Complexes Containing Functionalized Thiolate Ligands

Nicolai Burzlaff and Wolfdieter A. Schenk*

Institut für Anorganische Chemie der Universität,
Am Hubland, D-97074 Würzburg, Germany
Fax: (internat.) + 49(0)931/888-4605
E-mail: wolfdieter.schenk@mail.uni-wuerzburg.de

Received July 21, 1998

Keywords: *N*-Acetylcysteine / Amino acids / Captopril / Rhenium / S ligands

Chiral racemic rhenium thiolate complexes [CpRe(NO)(PPh_3)(SR)] were obtained under either acidic or basic conditions. Thus, when [CpRe(NO)(PPh_3)(CH_3)] (**1**) was treated with etheral HBF_4 and HSR the thiolate complexes [CpRe(NO)(PPh_3)(SR)] [SR = SCH_2(2-furyl) (**2**), SCH_2C(O)OEt (**3**)] were obtained after chromatographic workup. Ligand exchange reactions between [CpRe(NO)(PPh_3)(OC_4H_8)]BF_4 (**4**) and sodium thiolates yielded analogous complexes with SR = SH (**5**), SCH_2CH_2Ph (**6**), $SCH_2CH{=}CH_2$ (**7**). SR groups which tolerate strongly alkaline conditions may be introduced by treatment of **4** with HSR in the presence of sodium ethoxide as demonstrated by the high-yield synthesis of **2** as well as of complexes with SR = SCH_2CH_2NHAc (**8**), $SCH_2CH_2C(O)OH$ (**9**). A milder synthesis using hydrated sodium carbonate as a base provided **8** and compounds with SR = $SCH_2CH_2C(O)OMe$ (**10**), $SCH_2CH_2C(O)NHCH_2Ph$ (**11**) in high yields. Using similar methods, thiolate complexes of (*R*)-*N*-acetylcysteine (**13**), its methyl ester (**14**), (*R*)-*N*-phthaloylcysteine (**16**), and *N*-[(*S*)-3-mercapto-2-methylpropionyl]-*S*-proline (Captopril) (**17**) were obtained as diastereomeric pairs. The formation of **13** was preceded by the O-bonded isomer **12** which slowly rearranges in solution. **13** can be converted under acidic conditions into its methyl (**14**) or ethyl (**15**) esters. The diastereomers of **16** were separated by crystallization, and the structure of the (*R*,*R*)-isomer **16a** determined.

Thiolate ligands have some remarkable properties which are exploited by nature in a number of important metalloenzymes.[2] SR groups being soft donors bind strongly to most of the transition metal ions. Due to their high polarizability and π-donor capacity,[3] they are able to stabilize various oxidation states of the metal and to promote the formation of clusters[2][4] which can function as electron reservoirs for redox processes. Enzymatic reactions which lead to the transformation of coordinated thiolate ligands seem to be comparatively rare. One of the few prominent examples is the penicillin biosynthesis[5] whose first step involves the oxidative dehydrogenation of an iron-coordinated, cysteine-containing tripeptide to a thioaldehyde intermediate.[6] We have recently described a similar oxidative route for the synthesis of stable thioaldehyde complexes of ruthenium[7][8] and rhenium.[9] In order to further exploit the characteristic reactivity of coordinated thioaldehydes in nucleophilic additions and cycloadditions[8][10][11][12] we decided to investigate thiolate complexes bearing various functional groups on the SR ligand.

Results

Achiral Thiolates

Two synthetic strategies were chosen in which the rhenium–sulfur bond is formed under either acidic[8] or basic conditions. Treatment of the racemic methylrhenium complex **1**[13] with a twofold excess of etheral HBF_4 and 2-(mercaptomethyl)furan or ethyl mercaptoacetate followed by chromatography over silica gave the corresponding rhenium thiolate complexes **2** and **3** in fair to good yields (Eq. 1).

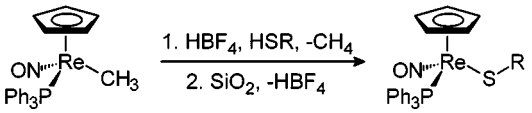

(1)

1 **2** (52%) **3** (94%)

SR: SCH_2(2-furyl) (**2**), SCH_2C(O)OEt (**3**)

Since the strongly acidic conditions of this route may not be compatible with a number of functional groups, a synthesis based on a nucleophilic substitution at rhenium was sought. The tetrahydrofuran complex [CpRe(NO)(PPh_3)(OC_4H_8)]BF_4 (**4**) which is easily obtained through acid cleavage of **1**[14] seemed to be an appropriate starting material. Although **4** was noted to be labile[14] it has found only sporadic use in ligand exchange reactions.[15] When **4** was treated with isolated sodium thiolates in THF/ethanol, the corresponding thiolate complexes **5–7** were formed in good

[◇] Part 6: Ref.[1].

 © WILEY-VCH Verlag GmbH, D-69451 Weinheim, 1998 1434–1948/98/1212–2055 $ 17.50+.50/0

yields (Eq. 2). The thiolate anions may also be generated in situ from thiol and sodium ethoxide. This was demonstrated by the high-yield synthesis of **2**, **8**, and **9** (Eq. 3).

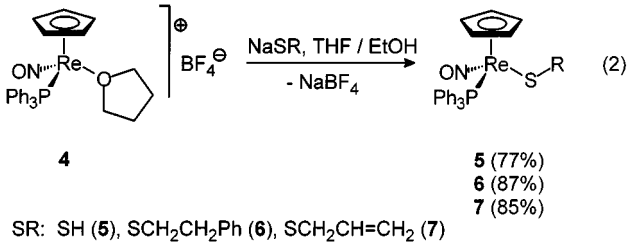

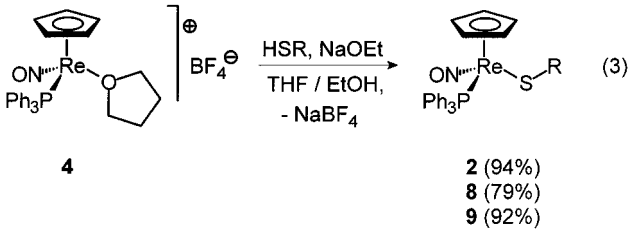

The use of ethoxide as a base may, however, cause problems when chiral thiolates are to be employed which would racemize under strongly alkaline conditions. Hydrated sodium carbonate, which finds some use in peptide syntheses,[16] was expected to be mild enough to circumvent this obstacle. Indeed, simple stirring of a mixture of **4**, $Na_2CO_3 \cdot 10\ H_2O$, and a thiol produced the expected thiolate complexes **8**, **10**, and **11** in high purity and yield (Eq. 4).

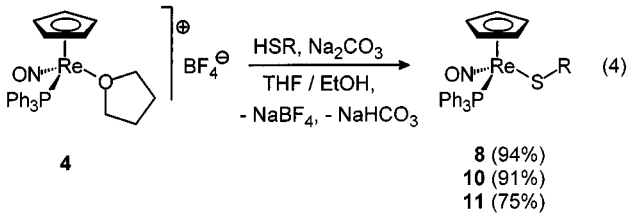

The new thiolate complexes are yellow, slightly air-sensitive crystalline solids which are more or less readily soluble in all common organic solvents. Typical spectroscopic features include low NO stretching frequencies in the infrared spectra which hint at the high donor ability of the SR ligand. In the ^1H NMR spectra, all methylene protons of the SR group are diastereotopic; those in α position give widely separated signals which are easily analyzed. The SH complex **5** exhibits a high-field signal at $\delta = 0.09$ which is split into a doublet due to coupling with phosphorus. In the ^{13}C-NMR spectra the α carbon signal is shifted by approximately 15 ppm to lower field compared to the uncoordinated thiol, and split into a doublet due to coupling with phosphorus. In cases of doubt such as **7**–**11** this serves as unambiguous proof that the SR ligand is indeed coordinated through the sulfur atom.

Chiral, Enantiomerically Pure Thiolates

Reaction of the THF complex **4** with (*R*)-*N*-acetylcysteine and sodium ethoxide initially gave the orange-brown carboxylate complex **12a**, **b** as a 1:1 mixture of diastereoisomers. Upon prolonged storage in solution or refluxing in acetone, **12a**, **b** converts almost quantitatively into the yellow S-bonded isomer **13a**, **b** (Eq. 5) which, after one crystallization, was obtained in 17% de. Conversely, solutions of **13a**, **b** revert back to an equilibrium mixture containing approximately 5% **12a**, **b**.

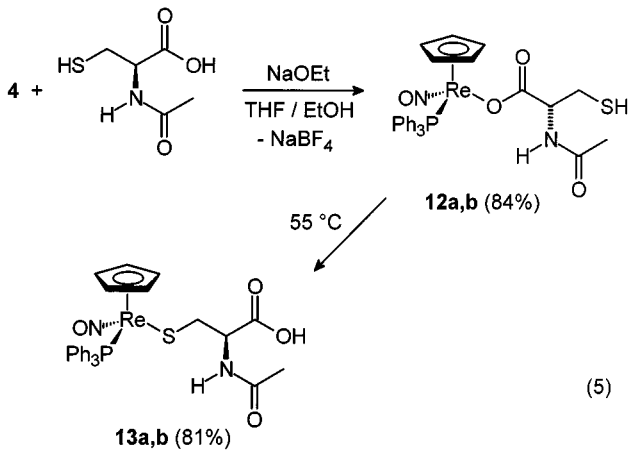

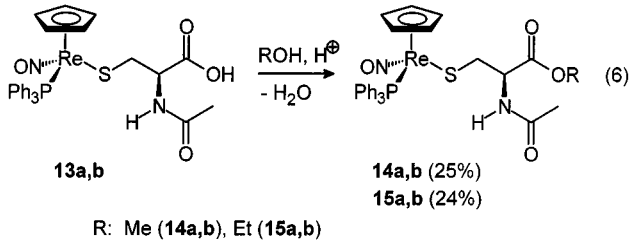

For a further elaboration of the thiolate side chain it may be desirable to have the carboxylate group protected as ester. To this end, the diastereomeric complexes **13a**, **b** were treated with alcohol and acid (Eq. 6). This reaction was also intended to be an additional test of the stability of the rhenium complex. The expected esters **14a**, **b** and **15a**, **b** were indeed obtained, albeit in less than satisfactory yields. Spectroscopic analysis of the crude reaction mixtures indicated that the losses were primarily due to the chromatographic workup which was necessary to remove the acid, rather than destruction of the rhenium complex. Obviously it is advisable to convert amino acids to their esters before coordinating them to the transition metal. Thus, **4** was reacted with the methyl esters of (*R*)-*N*-acetylcysteine, (*R*)-*N*-phthaloylcysteine, and *N*-[(*S*)-3-mercapto-2-methylpropionyl]-*S*-proline in the presence of sodium carbonate (Eq. 7). The three products were isolated as 1:1 mixtures of diastereoisomers. **17a**, **b** was partially enriched by crystalliza-

tion to 15% de while diastereomerically pure **16a** crystallized from an acetone solution.

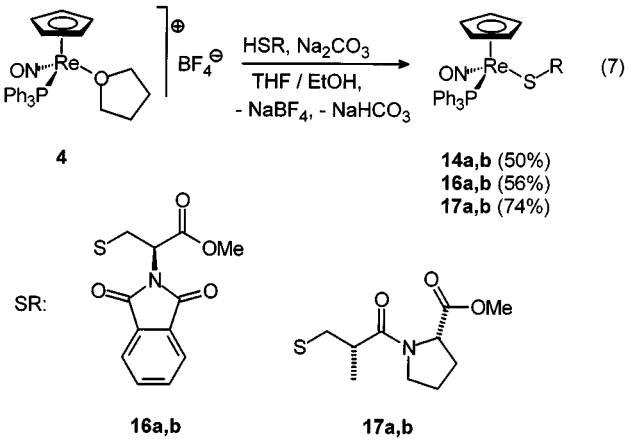

The physical properties of the diastereomeric thiolate complexes **13a**,**b**–**17a**,**b** closely resemble those of the other members of this series. As expected, they give double sets of signals in their ^{1}H-, ^{13}C-, and ^{31}P-NMR spectra. Coordination to rhenium via the sulfur atom is unequivocally inferred from the large coupling of the α carbon with the phosphorus atom. This clearly distinguishes **13a**, **b** from their carboxylate-bound isomers **12a**, **b** whose ^{13}C-NMR spectra exhibit doublet resonances for the carboxylate carbon atom.

Crystal and Molecular Structure of 16a

From an acetone solution of **16a**, **b** diastereomerically pure **16a** was obtained by slow crystallization. A suitable single crystal was analyzed by X-ray diffraction. It belonged to the enantiomorphic space group $P2_1$ which immediately showed that it is an enantiomerically pure compound. The stereocenters at both rhenium and carbon have the (*R*) configuration (Figure 1) which is in line with the Flack parameter. Bond distances and angles are well within the normal range for complexes of the type [CpRe(NO)(PPh_3)(SR)].[17][18]

The angle S–Re–N(1) [102.35(11)°] is surprisingly large for both **16a** and the (diarylmethyl)thiolate complex investigated by Gladysz.[18] As there are not any obvious steric interactions between the NO and SR ligands, the driving force of this distortion must be electronic in origin.[1] Also of note is the transoid arrangement of the groups at rhenium and sulfur [dihedral angle P–Re–S–C(1) = 167.4°] which simultaneously minimizes steric interactions as well as the repulsion between the lone pairs at sulfur and the HOMO of the [CpRe(NO)(PPh_3)] complex fragment.[1]

Discussion

This work was aimed at the synthesis of chiral racemic rhenium thiolate complexes [CpRe(NO)(PPh_3)(SR)]. Three routes proceeding under acidic, basic, or close to neutral

Figure 1. Molecular structure (*R*,*R*)-[CpRe(NO)(PPh_3)($SCH_2CH(NC_8H_4O_2)COOMe$)] (**16a**) (without H atoms)[a]

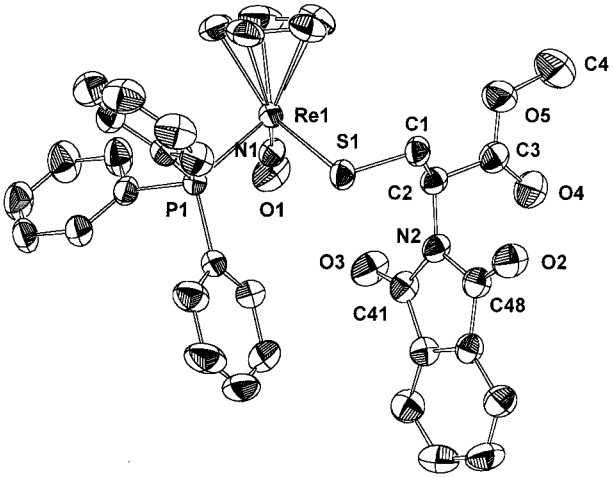

[a] Selected distances [pm] and angles[°] (standard deviations in parentheses): Re(1)–S(1) 239.45(10), Re(1)–P(1) 235.44(12), Re(1)–N(1) 176.3(4), N(1)–O(1) 119.7(5), S(1)–C(1) 182.2(5), S(1)–Re(1)–P(1) 87.31(6), S(1)–Re(1)–N(1) 102.35(11), P(1)–Re(1)–N(1) 92.80(13), Re(1)–S(1)–C(1) 106.2(2), P(1)–Re(1)–S(1)–C(1) 167.4(2).

conditions were developed in order to ensure tolerance for a range of functional groups. Acid cleavage of the methyl complex **1** produces the solvent-stabilized 16-electron species $[CpRe(NO)(PPh_3)]^+$ which immediately picks up any stronger Lewis base present in the solution.[19] The thiol complexes [CpRe(NO)(PPh_3)(HSR)]BF_4 thus formed eliminate HBF_4 simply upon chromatography over silica.[9] This route produces thiolate complexes in good yields but is limited of course to SR groups which tolerate strongly acidic conditions.

Gladysz et al., in their seminal work on chiral rhenium complexes,[20] made extensive use of the dichloromethane complex [CpRe(NO)(PPh_3)($ClCH_2Cl$)]BF_4[21] in ligand exchange reactions. With the strongly nucleophilic thiolate ions this compound, in addition to ligand exchange, undergoes nucleophilic substitution at carbon which leads to the formation of (chloromethyl)thioether complexes in sizeable quantities.[9] The tetrahydrofuran complex **4** whose synthesis[14] can easily be scaled up to multigram quantities, finally proved to be the starting material of choice.

For potentially ambidentate ligands such as allyl thiolate or the anions of cysteine and its derivatives, coordination through sulfur is favored thermodynamically. Nevertheless, for cysteine itself, which under the conditions of equation 5 exists in solution in its doubly deprotonated form, the carboxylate isomer is formed as the kinetic product. A similar observation was not made in the case of the 3-mercaptopropionic acid complex **9** (Eq. 3), due probably to the absence of bulky groups around the sulfur atom. Bond formation between the chiral rhenium complex and the various SR ligands was not expected to be accompanied by kinetic resolution. Nevertheless it is gratifying that partial or even full diastereomer separation could easily be effected by simple crystallization.

Conclusions

It has been shown here that the chiral Lewis acid $[CpRe(NO)(PPh_3)]^+$ can be efficiently connected to simple thiolates as well as those derived from biologically relevant molecules such as the amino acid (*R*)-cysteine or *N*-[(*S*)-3-mercapto-2-methylpropionyl]-*S*-proline, an ACE (*angiotensin converting enzyme*) inhibitor which under the brand name "Captopril" is used as an antihypertension drug. Apart from the more classical use of the rhenium complex fragment as a protective group for the thiolate function and a chiral auxiliary[20] for stereoselective addition reactions, one can also envisage that compounds such as **13–17** might find uses as specific "organometallic markers" in biochemistry[22] or as carriers of heavy atoms for protein crystallography.[23]

This work has been supported by the *Deutsche Forschungsgemeinschaft* (SFB 344 "Selektive Reaktionen Metall-aktivierter Moleküle").

Experimental Section

All experiments were carried out in Schlenk tubes under an atmosphere of nitrogen using suitably purified solvents. – IR: Perkin-Elmer 283, Bruker IFS 25. – ^{1}H NMR: Bruker AMX 400, δ values relative to TMS. – ^{13}C NMR: Bruker AMX 400, δ values relative to TMS; assignments were routinely checked by DEPT; in some cases the ^{13}C-NMR signals of quarternary carbon atoms were too weak to be detected. – ^{31}P NMR: Bruker AMX 400, δ values relative to 85% H_3PO_4. The ^{1}H- and ^{13}C-NMR signals of the PPh_3 ligand are very similar for all compounds and have therefore been omitted from the lists of spectral data. – Elemental analyses: Analytical Laboratory of the Institut für Anorganische Chemie. The following starting materials were obtained as described in the literature: $[CpRe(NO)(PPh_3)(CH_3)]$ (**1**),[13] $[CpRe(NO)(PPh_3)(OC_4H_8)]BF_4$ (**4**),[14] NaSH,[24] other sodium thiolates,[25] $HSCH_2CH_2C(O)NHCH_2Ph$,[26] (*R*)-*N*-phthaloylcysteine.[16] All other reagents were used as purchased.

[CpRe(NO)(PPh$_3$)(SCH$_2$C$_4$H$_3$O)] (**2**): To a solution of **1** (225 mg, 0.40 mmol) and 2-(mercaptomethyl)furan (115 mg, 1.00 mmol) in toluene (15 ml) was added at –70 °C a solution of HBF_4 in diethyl ether (1.00 mmol). The mixture was allowed to warm up to 20 °C, and all volatiles were removed under vacuum. The semi-solid residue was chromatographed with THF/ether over a short silica column and further purified by crystallization from dichloromethane/pentane. Yield 137 mg (52%), m.p. 153 °C. – ^{1}H NMR (400 MHz, [D$_6$]acetone, 20 °C): δ = 3.73, 3.77 [AB system, ^2J(H,H) = 14.2 Hz, 2 H; SCH_2], 5.28 (s, 5 H; C_5H_5), 6.13 [dd, ^3J(H,H) = 3.2 Hz, ^4J(H,H) = 0.8 Hz, 1 H; CH], 6.28 [dd, ^3J(H,H) = 3.1 Hz, ^3J(H,H) = 1.9 Hz, 1 H; CH], 7.36 [dd, ^3J(H,H) = 1.8 Hz, ^4J(H,H) = 0.9 Hz, 1 H; CH]. – ^{13}C NMR (100 MHz, [D$_6$]acetone, 20 °C): δ = 39.4 [d, ^3J(P,C) = 9 Hz; SCH_2], 92.3 (s; C_5H_5), 106.2 (s; CH), 111.1 (s; CH), 141.2 (s; CH), 158.9 (s; CH). – ^{31}P NMR (162 MHz, [D$_6$]acetone, 20 °C): δ = 19.6 (s). – IR (CH_2Cl_2): $\tilde{\nu}$ = 1654 (NO), 1606 cm^{-1} (C=C). – $C_{28}H_{25}NO_2PReS$ (656.8) calcd C 51.21, H 3.84, N 2.13, S 4.88; found C 50.90, H 3.88, N 1.98, S 5.16.

[CpRe(NO)(PPh$_3$)(SCH$_2$C(O)OEt)] (**3**): This compound was prepared analogously from **1** and ethyl mercaptoacetate. Yield 149 mg (94%), m.p. 106 °C. – ^{1}H NMR (400 MHz, [D$_6$]acetone, 20 °C): δ = 1.24 [t, ^3J(H,H) = 7.1 Hz, 3 H; CH_3], 3.07, 3.45 [AB system, ^2J(H,H) = 12.1 Hz, 2 H; SCH_2], 4.07, 4.12 [AB system of quartets, ^2J(H,H) = 10.8 Hz, ^3J(H,H) = 7.1 Hz, 2 H; OCH_2], 5.35 (s, 5 H; C_5H_5). – ^{13}C NMR (100 MHz, [D$_6$]acetone, 20 °C): δ = 14.5 (s; CH_3), 43.6 [d, ^3J(P,C) = 9 Hz; SCH_2], 60.6 (s; OCH_2), 92.6 (s; C_5H_5), 174.0 (s; CO). – ^{31}P NMR (162 MHz, [D$_6$]acetone, 20 °C): δ = 19.5 (s). – IR (CH_2Cl_2) $\tilde{\nu}$ = 1721 (CO), 1653 cm^{-1} (NO). – $C_{27}H_{27}NO_3PReS$ (662.8) calcd C 48.93, H 4.11, N 2.11, S 4.84; found C 48.91, H 4.01, N 1.97, S 5.08.

[CpRe(NO)(PPh$_3$)(SH)] (**5**): A solution of **4** (281 mg, 0.40 mmol) and NaSH (28 mg, 0.50 mmol) in THF (20 ml) and ethanol (20 ml) was stirred 1 h at 20 °C. The mixture was taken to dryness, and the residue dissolved in benzene and filtered over Celite. The filtrate was partially evaporated and the product precipitated by adding pentane. Yield 178 mg (77%), m.p. 60 °C (dec). – ^{1}H NMR (400 MHz, C_6D_6, 20 °C): δ = 0.09 [d, ^3J(P,H) = 12.6 Hz, 1 H; SH], 4.77 (s, 5 H; C_5H_5). – ^{13}C NMR (100 MHz, C_6D_6, 20 °C): δ = 91.4 (s; C_5H_5). – ^{31}P NMR (162 MHz, C_6D_6, 20 °C): δ = 23.0 (s). – IR (CH_2Cl_2): $\tilde{\nu}$ = 1655 cm^{-1} (NO). – $C_{23}H_{21}NOPReS$ (567.7) calcd C 47.91, H 3.67, N 2.43, S 5.56; found C 47.91, H 3.75, N 2.25, S 5.41.

[CpRe(NO)(PPh$_3$)(SCH$_2$CH$_2$Ph)] (**6**): This compound was prepared analogously from **4** and sodium 2-phenylethanethiolate. Yield 237 mg (87%), m.p. 168 °C. – ^{1}H NMR (400 MHz, C_6D_6, 20 °C): δ = 2.88–3.34 (m, 4 H; CH_2CH_2), 4.80 (s, 5 H; C_5H_5). – ^{13}C NMR (100 MHz, C_6D_6, 20 °C): δ = 42.1 (s; CH_2), 45.1 [d, ^3J(P,C) = 8 Hz; SCH_2], 91.1 (s; C_5H_5). – ^{31}P NMR (162 MHz, C_6D_6, 20 °C): δ = 20.2 (s). – IR (CH_2Cl_2): $\tilde{\nu}$ = 1644 cm^{-1} (NO). – $C_{31}H_{29}NOPReS$ (680.8) calcd C 54.69, H 4.29, N 2.06, S 4.71; found C 54.39, H 4.30, N 2.05, S 4.66.

[CpRe(NO)(PPh$_3$)(SCH$_2$CH=CH$_2$)] (**7**): This compound was prepared analogously from **4** and sodium allylthiolate. Yield 210 mg (85%), m.p. 202 °C. – ^{1}H NMR (400 MHz, $CDCl_3$, 20 °C): δ = 3.02, 3.39 [AB system of doublets, ^2J(H,H) = 13.0 Hz, ^3J(H,H) = 7.2 Hz, 2 H; SCH_2], 4.87 [ddd, ^2J(H,H) = 2.0 Hz, ^3J(H,H) = 9.9 Hz, ^4J(H,H) = 1.0 Hz, 1 H; =CH_2], 4.95 [dd, ^2J(H,H) = 1.9 Hz, ^3J(H,H) = 16.9 Hz, 1 H; =CH_2], (s, 5 H; C_5H_5), 5.87 [ddt, ^3J(H,H) = 16.9 Hz, ^3J(H,H) = 9.8 Hz, ^3J(H,H) = 7.2 Hz, 1 H; =CH] . – ^{13}C NMR (100 MHz, $CDCl_3$, 20 °C): δ = 45.3 [d, ^3J(P,C) = 7 Hz; SCH_2], 91.3 (s; C_5H_5), 113.2 (s; =CH_2), 141.2 (s; =CH). – ^{31}P NMR (162 MHz, $CDCl_3$, 20 °C): δ = 19.0 (s). – IR (CH_2Cl_2): $\tilde{\nu}$ = 1645 (NO), 1608 cm^{-1} (C=C). – $C_{26}H_{25}NOPReS$ (616.7) calcd C 50.64, H 4.09, N 2.27, S 5.20; found C 50.99, H 4.31, N 2.20, S 4.50.

[CpRe(NO)(PPh$_3$)(SCH$_2$C$_4$H$_3$O)] (**2**): To a solution of **4** (281 mg, 0.40 mmol) and 2-(mercaptomethyl)furan (57 mg, 0.50 mmol) in THF (20 ml) and ethanol (20 ml) was added at 20 °C a solution of sodium ethoxide in ethanol (0.50 mmol). After 1 h the mixture was taken to dryness, and the residue dissolved in benzene and filtered over Celite. The filtrate was partially evaporated and the product precipitated by adding pentane. Yield 257 mg (94%).

[CpRe(NO)(PPh$_3$)(SCH$_2$CH$_2$NHAc)] (**8**): This compound was prepared analogously from **4** and *N*-acetylcysteamine. Yield 209 mg (79%), m.p. 154 °C. – ^{1}H NMR (400 MHz, C_6D_6, 20 °C): δ = 1.71 (s, 3 H; CH_3), 2.48 (m, 1 H; CH_2), 2.96 (m, 1 H; CH_2), 3.37 (m, 1 H; SCH_2), 3.95 (m, 1 H; SCH_2), 4.87 (s, 5 H; C_5H_5), 5.77 (s, br, 1 H; NH). – ^{13}C NMR (100 MHz, C_6D_6, 20 °C): δ = 23.2 (s; CH_3), 40.3 [d, ^3J(P,C) = 8 Hz; SCH_2], 43.3 (s; CH_2), 91.5 (s; C_5H_5), 168.9 (s; CO). – ^{31}P NMR (162 MHz, C_6D_6, 20 °C): δ = 20.2 (s). – IR (CH_2Cl_2): $\tilde{\nu}$ = 1650 (NO), 1513 cm^{-1} (CONH). – $C_{27}H_{28}N_2O_2PReS$ (661.8) calcd C 49.00, H 4.26, N 2.23, S 4.85; found C 49.14, H 4.51, N 3.98, S 4.65.

[CpRe(NO)(PPh$_3$)(SCH$_2$CH$_2$COOH)] (**9**): This compound was prepared analogously from **4** and 3-mercaptopropionic acid. Yield 239 mg (92%), m.p. 205 °C (dec). – ^{1}H NMR (400 MHz, C_6D_6, 20 °C): δ = 2.56 (m, 1 H; CH_2), 2.27–2.89 (m, 2 H; CH_2), 3.09 (m, 1 H; CH_2), 4.77 (s, 5 H; C_5H_5). – ^{13}C NMR (100 MHz, C_6D_6, 20 °C): δ = 37.5 [d, ^3J(P,C) = 8 Hz; SCH_2], 39.6 (s; CH_2), 91.2 (s; C_5H_5), 177.8 (s; CO). – ^{31}P NMR (162 MHz, C_6D_6, 20 °C): δ = 19.5 (s). – IR (CH_2Cl_2): $\tilde{\nu}$ = 1742 (COOH), 1661 cm^{-1} (NO). – $C_{26}H_{25}NO_3PReS$ (648.7) calcd C 48.14, H 3.88, N 2.16, S 4.94; found C 48.23, H 3.95, N 2.01, S 4.77.

[CpRe(NO)(PPh$_3$)(OCOCH(NHAc)CH$_2$SH)] (**12a**, **b**): This compound was prepared analogously from **4** and (*R*)-*N*-acetylcysteine. Yield 237 mg (84%), orange-brown crystalline solid, dec. 57 °C. – Both diastereoisomers: ^{1}H NMR (400 MHz, [D$_6$]acetone, 20 °C): δ = 1.33 [t, ^3J(H,H) = 8.5 Hz, 1 H; SH], 1.40 [dd, ^3J(H,H) = 9.0 Hz, ^3J(H,H) = 7.8 Hz, 1 H; SH], 1.78 (s, 3 H; CH_3), 1.84 (s, 3 H; CH_3), 2.39, 2.56 [AB system of dd, ^2J(H,H) = 13.3 Hz, ^3J(H,H) = 8.9 Hz, ^3J(H,H) = 8.3 Hz, ^3J(H,H) = 4.8 Hz, ^3J(H,H) = 4.0 Hz, 2 H; SCH_2], 2.39, 2.66 [AB system of dd, ^2J(H,H) = 13.3 Hz, ^3J(H,H) = 8.9 Hz, ^3J(H,H) = 7.2 Hz, ^3J(H,H) = 4.8 Hz, ^3J(H,H) = 4.2 Hz, 2 H; SCH_2], 4.10 [dt, ^3J(H,H) = 6.4 Hz, ^3J(H,H) = 4.3 Hz, 1 H; CH], 4.18 [dt, ^3J(H,H) = 6.6 Hz, ^3J(H,H) = 4.5 Hz, 1 H; CH], 5.40 (s, 2 × 5 H; C_5H_5), 6.62 [d, ^3J(H,H) = 6.1 Hz, 1 H; NH], 6.69 [d, ^3J(H,H) = 5.7 Hz, 1 H; NH]. – ^{13}C NMR (100 MHz, [D$_6$]acetone, 20 °C): δ = 22.9 (s; CH_3), 23.0 (s; CH_3), 27.8 (s; SCH_2), 27.9 (s; SCH_2), 55.1 (s; CH), 55.3 (s; CH), 91.9 (s; C_5H_5), 169.1 (s; HNCO), 177.2 [d, ^3J(P,C) = 3 Hz, COORe], 177.3 [d, ^3J(P,C) = 2 Hz, COORe]. – ^{31}P NMR (162 MHz, [D$_6$]acetone, 20 °C): δ = 21.2 (s), 21.4 (s). – IR (CH_2Cl_2): $\tilde{\nu}$ = 1674 cm^{-1} (NO). – $C_{28}H_{28}N_2O_4PReS$ (705.8) calcd C 47.65, H 4.00, N 3.97, S 4.54; found C 47.52, H 4.00, N 3.65, S 4.46.

[CpRe(NO)(PPh$_3$)(SCH$_2$CH(NHAc)COOH)] (**13a**, **b**): The material from the above reaction was dissolved in acetone and stirred for 3 d at 20 °C. The product was isolated by evaporation and crystallization from benzene/pentane. NMR analysis revealed **13a**, **b** in 17% de and some residual **12a,b** which does not disappear even after refluxing. Yield 229 mg (81%, based on **4**), dec. 216 °C. – Major diastereoisomer: ^{1}H NMR (400 MHz, [D$_6$]acetone, 20 °C): δ = 1.96 (s, 3 H; CH_3), 2.76, 3.07 [AB system of d, ^2J(H,H) = 13.1 Hz, ^3J(H,H) = 8.1 Hz, ^3J(H,H) = 4.2 Hz, 2 H; SCH_2], 4.44 [dd, ^3J(H,H) = 8.1 Hz, ^3J(H,H) = 4.2 Hz, 1 H; CH], 5.35 (s, 5 H; C_5H_5), NH and OH signals not detected. – ^{13}C NMR (100 MHz, [D$_6$]acetone, 20 °C): δ = 22.8 (s; CH_3), 43.0 [d, ^3J(P,C) = 8 Hz; SCH_2], 56.4 (s; CH), 92.5 [d, ^2J(P,C) = 1 Hz; C_5H_5], 170.4 (s; HNCO), 173.1 (s; COOH). – ^{31}P NMR (162 MHz, C_6D_6, 20 °C): δ = 19.4 (s). – Minor diastereoisomer: ^{1}H NMR (400 MHz, [D$_6$]acetone, 20 °C): δ = 1.97 (s, 3 H; CH_3), 2.71, 2.86 [AB system of d, ^2J(H,H) = 12.8 Hz, ^3J(H,H) = 9.3 Hz, ^3J(H,H) = 5.5 Hz, 2 H; SCH_2), 4.60 (dd, ^3J(H,H) = 9.3 Hz, ^3J(H,H) = 5.6 Hz, 1 H; CH], 5.45 (s, 5 H; C_5H_5), NH and OH signals not detected. – ^{13}C NMR (100 MHz, [D$_6$]acetone, 20 °C): δ = 22.8 (s; CH_3), 41.7 (d, ^3J(P,C) = 8 Hz; SCH_2), 55.6 (s; CH), 92.8 (s; C_5H_5), 169.9 (s; HNCO), 172.9 (s; COOH). – ^{31}P NMR (162 MHz, C_6D_6, 20 °C): δ = 19.3 (s). – IR (CH_2Cl_2): $\tilde{\nu}$ = 1749 (COOH), 1657 (NO), 1607 cm^{-1} (CONH).

[CpRe(NO)(PPh$_3$)(SCH$_2$CH(NHAc)COOMe)] (**14a**, **b**): To a solution of **13a**, **b** (200 mg, 0.28 mmol) in methanol (10 ml) a few droplets of HBF_4 (54% in ether) were added. The mixture was stirred 3 d at 20 °C. After evaporation to dryness the residue was chromatographed over silica using THF/ether as an eluent. The product zone was evaporated and the residue recrystallized from dichloromethane/pentane. Yield 50 mg (25%), dec. 163 °C. – Both diastereoisomers ^{1}H NMR (400 MHz, $CDCl_3$, 20 °C): δ = 1.98 (s, 3 H; CH_3), 2.02 (s, 3 H; CH_3), 2.67 [dd, ^2J(H,H) = 13.6 Hz, ^3J(H,H) = 3.6 Hz, 1 H; SCH_2], 2.86 [dd, ^2J(H,H) = 13.2 Hz, ^3J(H,H) = 6.0 Hz, 1 H; SCH_2], 3.21–3.27 (m, 2 H; SCH_2), 3.67 (s, 3 H; OCH_3), 3.76 (s, 3 H; OCH_3), 4.58–4.64 (m; 2 × 1 H; CH), 5.19 (s, 5 H; C_5H_5), 5.22 (s, 5 H; C_5H_5), 6.44 [d, ^3J(H,H) = 7.2 Hz, 1 H; NH], 6.74 [d, ^3J(H,H) = 5.6 Hz, 1 H; NH]. – ^{13}C NMR (100 MHz, $CDCl_3$, 20 °C): δ = 23.0 (s; CH_3), 23.2 (s; CH_3), 42.0 [d, ^3J(P,C) = 8 Hz ; SCH_2], 45.0 [d, ^3J(P,C) = 8 Hz; SCH_2], 52.1 (s; OCH_3), 52.3 (s; OCH_3), 54.7 (s; CH), 55.3 (s; CH), 91.5 [d, ^2J(P,C) = 1 Hz; C_5H_5], 91.6 (s; C_5H_5), 169.8, 170.1, 172.1, 172.2 (s; HNCO and COOMe). – ^{31}P NMR (162 MHz, $CDCl_3$, 20 °C): δ = 18.6 (s), 18.7 (s). – IR (CH_2Cl_2): $\tilde{\nu}$ = 1748 (COOMe), 1651 cm^{-1} (NO). – $C_{29}H_{30}N_2O_4PReS$ (719.8) calcd C 48.39, H 4.20, N 3.89, S 4.45; found C 48.32, H 4.12, N 3.75, S 4.32.

[CpRe(NO)(PPh$_3$)(SCH$_2$CH(NHAc)COOEt)] (**15a**, **b**): This compound was prepared analogously by refluxing a solution of **13a**, **b** (200 mg, 0.28 mmol) in ethanol (10 ml) in the presence of HBF_4. Yield 49 mg (24%), 19% de (by NMR), dec. 197 °C. – Major diastereoisomer: ^{1}H NMR (400 MHz, [D$_6$]acetone, 20 °C): δ = 1.24 [t, ^3J(H,H) = 7.1 Hz, 3 H; CH_3], 1.92 (s, 3 H; CH_3), 2.75 [dd, ^2J(H,H) = 13.3 Hz, ^3J(H,H) = 6.9 Hz, 1 H; SCH_2], 2.99–3.06 (m, 1 H; SCH_2), 4.15 [q, ^3J(H,H) = 7.2 Hz, 2 H; OCH_2], 4.53 [dt, ^3J(H,H) = 7.6 Hz, ^3J(H,H) = 6.6 Hz, 1 H; CH], 5.35 (s, 5 H; C_5H_5), 7.01 [d, ^3J(H,H) = 7.0 Hz, 1 H; NH]. – ^{13}C NMR (100 MHz, $CDCl_3$, 20 °C): δ = 14.2 (s; CH_3), 23.2 (s; CH_3), 45.2 [d, ^3J(P,C) = 8 Hz ; SCH_2], 55.0 (s; CH), 61.3 (s; OCH_2), 91.6 (s; C_5H_5), 169.9, 170.7 (s; HNCO and COOEt). – ^{31}P NMR (162 MHz, [D$_6$]acetone, 20 °C): δ = 19.4 (s). – Minor diastereoisomer: ^{1}H NMR (400 MHz, [D$_6$]acetone, 20 °C): δ = 1.19 [t, ^3J(H,H) = 7.1 Hz, 3 H; CH_3], 1.93 (s, 3 H; CH_3), 2.71 [dd, ^2J(H,H) = 13.2 Hz, ^3J(H,H) = 4.1 Hz, 1 H; SCH_2], 2.99–3.06 (m, 1 H; SCH_2), 4.09 [q, ^3J(H,H) = 7.0 Hz, 2 H; OCH_2], 4.43 (m, 1 H; CH), 5.35 (s, 5 H; C_5H_5), 6.90 [d, ^3J(H,H) = 5.5 Hz, 1 H; NH]. – ^{13}C NMR (100 MHz, $CDCl_3$, 20 °C): δ = 14.2 (s; CH_3), 23.0 (s; CH_3), 42.0 [d, ^3J(P,C) = 11 Hz ; SCH_2], 55.3 (s; CH), 61.0 (s; OCH_2), 91.6 (s; C_5H_5), 170.2, 171.6 (s; HNCO and COOEt). – ^{31}P NMR (162 MHz, [D$_6$]acetone, 20 °C): δ = 18.9 (s). – IR (CH_2Cl_2): $\tilde{\nu}$ = 1748 (COOMe), 1651 cm^{-1} (NO). – $C_{30}H_{32}N_2O_4PReS$ (733.8) calcd C 49.10, H 4.40, N 3.82, S 4.37; found C 49.54, H 4.95, N 3.46, S 4.20.

[CpRe(NO)(PPh$_3$)(SCH$_2$CH$_2$NHAc)] (**8**): A suspension of Na_2CO_3 • 10 H_2O (286 mg, 1.00 mmol) and *N*-acetylcysteamine (60 mg, 0.50 mmol) in THF (40 ml) was stirred 1 h at 20 °C. To this, a solution of **4** (281 mg, 0.40 mmol) in THF (20 ml) and ethanol (20 ml) was added and the mixture stirred again for 1 h. All volatiles were then removed under vacuum, the residue dissolved in benzene and filtered over Celite, and the product precipitated by adding pentane. Yield 249 mg (94%).

[CpRe(NO)(PPh$_3$)(SCH$_2$CH$_2$COOMe)] (**10**): This compound was prepared analogously from **4** and ethyl (3-mercapto)propionate. Yield 241 mg (91%), dec. 69 °C (dec). – ^{1}H NMR (400 MHz, C_6D_6, 20 °C): δ = 2.74–2.82 (m, 1 H; CH_2), 2.93 (m, 2 H; CH_2), 3.24–3.33 (m, 1 H; CH_2), 3.37 (s, 3 H; OCH_3), 4.83 (s, 5 H; C_5H_5). – ^{13}C NMR (100 MHz, C_6D_6, 20 °C): δ = 38.1 [d, ^3J(P,C) = 8 Hz; SCH_2], 40.1 (s; CH_2), 50.9 (s; OCH_3), 91.3 (s; C_5H_5), 173.3 (s; CO). – ^{31}P NMR (162 MHz, C_6D_6, 20 °C): δ = 20.0 (s). – IR (CH_2Cl_2): $\tilde{\nu}$ = 1736 (COOMe), 1646 cm^{-1} (NO). – $C_{27}H_{27}NO_3PReS$ (662.8) calcd C 48.93, H 4.11, N 2.11, S 4.84; found C 49.16, H 4.16, N 2.07, S 4.59.

[CpRe(NO)(PPh$_3$)(SCH$_2$CH$_2$C(O)NHCH$_2$Ph)] (**11**): This compound was prepared analogously from **4** and (3-mercaptopropionyl)benzylamine. Yield 221 mg (75%), m.p. 39 °C. – ^{1}H NMR (400 MHz, [D$_6$]acetone, 20 °C): δ = 2.39–2.47 (m, 1 H; CH$_2$), 2.51–2.65 (m, 2 H; CH$_2$), 2.90–2.97 (m, 1 H; CH$_2$), 4.40 [d, ^3J(H,H) = 5.6 Hz, 2 H; NCH$_2$], 5.30 (s, 5 H; C$_5$H$_5$), 7.60 [t, ^3J(H,H) = 5.6 Hz, 1 H; NH]. – ^{13}C NMR (100 MHz, [D$_6$]acetone, 20 °C): δ = 38.3 [d, ^3J(P,C) = 8 Hz; SCH$_2$], 42.1 (s; CH$_2$), 43.2 (s; CH$_2$), 92.5 (s; C$_5$H$_5$), 173.0 (s; CO). – ^{31}P NMR (162 MHz, [D$_6$]acetone, 20 °C): δ = 19.5 (s). – IR (CH$_2$Cl$_2$) nu(tilde) = 1654 cm^{-1} (NO). – C$_{33}$H$_{32}$N$_2$O$_2$PReS (737.9) calcd C 53.72, H 4.37, N 3.80, S 4.35; found C 53.76, H 4.64, N 3.77, S 4.67.

*[CpRe(NO)(PPh$_3$)(SCH$_2$CH(NC$_8$H$_4$O$_2$)*COOMe)] (**16a**, **b**): (*R*)-*N*-Phthaloylcysteine (200 mg, 0.80 mmol) was dissolved in ether (15 ml) and treated at 20 °C with a slight excess of diazomethane. After 15 min all volatiles were removed under vacuum and the residue treated with hydrated sodium carbonate and **4** as described above. After chromatography over silica using dichloromethane/acetone (10©lon1) as an eluent and subsequent crystallization from benzene/pentane the product was isolated as a 1:1 mixture of diastereoisomers. Yield 181 mg (56%), dec. 214 °C. From a concentrated solution in acetone the pure (*R,R*) form separates as orange crystals. – (*R,R*) Diastereoisomer **16a**: ^{1}H NMR (400 MHz, CDCl$_3$, 20 °C): δ = 3.05 [dd, ^2J(H,H) = 13.6 Hz, ^3J(H,H) = 3.6 Hz, 1 H; SCH$_2$], 3.72 (s, 3 H; OCH$_3$), 3.89 [ddd, ^2J(H,H) = 13.6 Hz, ^3J(H,H) = 11.6 Hz, ^4J(P,H) = 1.0 Hz, 1 H; SCH$_2$], 5.21 [dd, ^3J(H,H) = 11.6 Hz, ^3J(H,H) = 3.6 Hz, 1 H; CH], 5.22 (s, 5 H; C$_5$H$_5$). – ^{13}C NMR (100 MHz, CDCl$_3$, 20 °C): δ = 41.2 [d, ^3J(P,C) = 9 Hz ; SCH$_2$], 52.6 (s; OCH$_3$), 56.2 (s; CH), 91.5 (s; C$_5$H$_5$), 167.5, 170.2 (s; CO). – ^{31}P NMR (162 MHz, CDCl$_3$, 20 °C): δ = 18.9 (s). – (*S,R*) Diastereoisomer **16b**: ^{1}H NMR (400 MHz, CDCl$_3$, 20 °C): δ = 3.35 [dd, ^2J(H,H) = 13.2 Hz, ^3J(H,H) = 11.2 Hz, 1 H; SCH$_2$], 3.68 [dd, ^2J(H,H) = 13.2 Hz, ^3J(H,H) = 4.8 Hz,, 1 H; SCH$_2$], 3.69 (s, 3 H; OCH$_3$), 4.98 [dd, ^3J(H,H) = 11.0 Hz, ^3J(H,H) = 4.6 Hz, 1 H; CH], 5.19 (s, 5 H; C$_5$H$_5$). – ^{13}C NMR (100 MHz, CDCl$_3$, 20 °C): δ = 41.8 [d, ^3J(P,C) = 9 Hz ; SCH$_2$], 52.5 (s; OCH$_3$), 56.3 (s; CH), 91.5 (s; C$_5$H$_5$), 167.9, 169.5 (s; CO). – ^{31}P NMR (162 MHz, CDCl$_3$, 20 °C): δ = 19.0 (s). – IR (CH$_2$Cl$_2$): ν̃ = 1777, 1720 (phthalimide), 1743 (COOMe), 1649 cm^{-1} (NO). – C$_{35}$H$_{30}$N$_2$O$_5$PReS (807.9) calcd C 52.04, H 3.74, N 3.47, S 3.97; found C 51.74, H 4.00, N 3.37, S 3.97.

[CpRe(NO)(PPh$_3$)(SCH$_2$CH(Me)C(O)NC$_4$H$_7$COOMe)] (**17a**, **b**): *N*-[(*S*)-3-mercapto-2-methylpropionyl]-*S*-proline (174 mg, 0.80 mmol) was converted to its methyl ester and reacted with **4** as described above. After chromatography over silica using dichloromethane/acetone (4:1) as an eluent and subsequent crystallization from benzene/pentane the product was isolated as a 1:1 mixture of diastereoisomers. Yield 229 mg (74%), m.p. 162 °C. A further crystallization from benzene/pentane yielded a sample with 15% de. – Major diastereoisomer: ^{1}H NMR (400 MHz, C$_6$D$_6$, 20 °C): δ = 1.19–1.40 (m, 2 H; CH$_2$), 1.32 [d, ^3J(H,H) = 6.8 Hz, 3 H; CH$_3$], 1.45–1.70 (m, 3 H; CH$_2$, and CH), 2.83 (m, 1 H; CH$_2$), 2.92 [dd, ^3J(H,H) = 11.6 Hz, ^3J(H,H) = 4.0 Hz, 1 H; CH$_2$], 3.34 (s, 3 H; OCH$_3$), 3.45–3.55 (m, 2 H; CH$_2$), 4.64 [t, ^3J(H,H) = 5.6 Hz, 1 H; CH], 4.95 (s, 5 H; C$_5$H$_5$). – ^{13}C NMR (100 MHz, C$_6$D$_6$, 20 °C): δ = 18.6 (s; CH$_3$), 24.9 (s; CH$_2$), 29.2 (s; CH$_2$), 43.4 (s; CH), 46.9 (s; CH$_2$), 49.0 [d, ^3J(P,C) = 8 Hz ; SCH$_2$], 51.4 (s; OCH$_3$), 58.9 (s; CH), 91.7 (s; C$_5$H$_5$), 173.2, 175.0 (s; CO). – ^{31}P NMR (162 MHz, C$_6$D$_6$, 20 °C): δ = 21.0 (s). – Minor diastereoisomer: ^{1}H NMR (400 MHz, C$_6$D$_6$, 20 °C): δ = 1.19–1.40 (m, 2 H; CH$_2$), 1.50 [d, ^3J(H,H) = 6.8 Hz, 3 H; CH$_3$], 1.45–1.70 (m, 2 H; CH$_2$), 1.77–1.85 (m, 1 H; CH), 2.99 (m, 1 H; CH$_2$), 3.20–3.27 (m, 1 H; CH$_2$), 3.37 (s, 3 H; OCH$_3$), 3.61–3.69 (m, 2 H; CH$_2$), 4.80 [dd, ^3J(H,H) = 8.6 Hz, ^3J(H,H) = 4.2 Hz, 1 H; CH], 4.88 (s, 5 H; C$_5$H$_5$). – ^{13}C NMR (100 MHz, C$_6$D$_6$, 20 °C): δ = 17.6 (s; CH$_3$), 25.0 (s; CH$_2$), 29.3 (s; CH$_2$), 43.4 (s; CH), 47.0 (s; CH$_2$), 47.1 [d, ^3J(P,C) = 8 Hz; SCH$_2$], 51.4 (s; OCH$_3$), 59.1 (s; CH), 91.7 (s; C$_5$H$_5$), 173.3, 175.1 (s; CO). – ^{31}P NMR (162 MHz, C$_6$D$_6$, 20 °C): δ = 20.3 (s). – IR (CH$_2$Cl$_2$): ν̃ = 1744 (COOMe), 1633 cm^{-1} (NO). – C$_{33}$H$_{36}$N$_2$O$_4$PReS (773.9) calcd C 51.22, H 4.69, N 3.62, S 4.14; found C 50.93, H 4.48, N 3.56, S 4.10.

X-Ray Structure Determination of (R,R)-[CpRe(NO)(PPh$_3$)(SCH$_2$CH(NC$_8$H$_4$O$_2$)COOMe)] (**16a**): C$_{35}$H$_{30}$N$_2$O$_5$PReS, molecular mass 807.9, crystal size 0.6 × 0.3 × 0.1 mm, obtained from a saturated acetone solution; monoclinic crystal system, space group $P2_1$ (No. 4), a = 8.594(2), b = 17.566(4), c = 10.801(3) Å, β = 95.269(12)°; V = 1623.8(7) Å^3, Z = 2, d_{calcd} = 1.652 g cm^{-3}; μ(Mo-*K*α) = 2.05 cm^{-1}. Data were collected at 293 K in the range 2° < Θ < 27° from one fourth of the reflection sphere (Enraf-Nonius CAD4 diffractometer, graphite monochromator, Mo-*K*α radiation, λ = 0.70930 Å). Of the 3877 measured reflections 3641 were symmetry-independent and 3456 classified as observed [$I_O > 2\sigma(I_O)$]. The structure was solved by the Patterson method by using the program package SHELXS 86[27] with hydrogen atoms included in their calculated positions. Refinement using the program package SHELXL 93[28] gave R_1 = 0.017, wR_2 = 0.040, Flack parameter©lon –0.002(6). The 5 highest maxima of a final difference Fourier map were below 0.28 e Å^{-3}. Further details of the structure determination may be obtained from the Fachinformationszentrum Karlsruhe, D-76344 Eggenstein-Leopoldshafen, on quoting the depository number 408461.

[1] N. Burzlaff, M. Hagel, W. A. Schenk, *Z. Naturforsch., B* **1998**, *53*, 893–899.
[2] E. Block, J. Zubieta in *Advances in Sulfur Chemistry* (Ed.: E. Block), JAI Press, London, **1994**, pp. 133–193.
[3] M. T. Ashby, *Comments Inorg. Chem.* **1990**, *10*, 297–313.
[4] B. Krebs, G. Henkel, *Angew. Chem.* **1991**, *103*, 785–804; *Angew. Chem. Int. Ed. Engl.* **1991**, *30*, 769–788.
[5] J. E. Baldwin, M. Bradley, *Chem. Rev.* **1990**, *90*, 1079–1088.
[6] P. L. Roach, I. J. Clifton, C. M. H. Hensgens, N. Shibata, C. J. Schofield, J. Hajdu, J. E. Baldwin, *Nature* **1997**, *387*, 827–830.
[7] W. A. Schenk, T. Stur, E. Dombrowski, *Inorg. Chem.* **1992**, *31*, 723–724.
[8] W. A. Schenk, T. Stur, E. Dombrowski, *J. Organomet. Chem.* **1994**, *472*, 257–273.
[9] W. A. Schenk, N. Burzlaff, H. Burzlaff, *Z. Naturforsch. B* **1994**, *49*, 1633–1639.
[10] H. Fischer, U. Gerbing, K. Treier, J. Hofmann, *Chem. Ber.* **1990**, *123*, 725–732.
[11] H. Fischer, C. Kalbas, U. Gerbing, *J. Chem. Soc. Chem. Commun.* **1992**, 563–564.
[12] H. Fischer, A. Ruchay, R. Stumpf, C. Kalbas, *J. Organomet. Chem.* **1993**, *459*, 249–255.
[13] W. Tam, G. Y. Lin, W. K. Wong, W. A. Kiel, V. K. Wong, J. A. Gladysz, *J. Am. Chem. Soc.* **1982**, *104*, 141–152.
[14] S. K. Agbossou, J. M. Fernandez, J. A. Gladysz, *Inorg. Chem.* **1990**, *29*, 476–480.
[15] S. K. Agbossou, C. Roger, A. Igau, J. A. Gladysz, *Inorg. Chem.* **1992**, *31*, 419–424.
[16] S. Wolfe, J. C. Godfrey, C. T. Holdrege, Y. G. Perron, *Can. J. Chem.* **1968**, *46*, 2549–2559.
[17] P. C. Cagle, A. M. Arif, J. A. Gladysz, *J. Am. Chem. Soc.* **1994**, *116*, 3655–3656.
[18] P. C. Cagle, O. Meyer, D. Vichard, K. Weickhardt, A. M. Arif, J. A. Gladysz, *Organometallics* **1996**, *15*, 194–204.
[19] J. J. Kowalczyk, S. K. Agbossou, J. A. Gladysz, *J. Organomet. Chem.* **1990**, *397*, 333–346.
[20] J. A. Gladysz, B. J. Boone, *Angew. Chem.* **1997**, *109*, 566–602; *Angew. Chem. Int. Ed. Engl.* **1997**, *36*, 550–583.
[21] J. M. Fernandez, J. A. Gladysz, *Organometallics* **1989**, *8*, 207–219.
[22] G. Jaouen, A. Vessieres, I. S. Butler, *Acc. Chem. Res.* **1993**, *26*, 361–369.

[23] C. Giacovazzo, H. L. Monaco, D. Viterbo, F. Scordari, G. Gilli, G. Zanotti, M. Catti, *Fundamentals of Crystallography*, Oxford University Press, Oxford, **1992**, pp. 538–541.
[24] R. E. Eibeck, *Inorg. Synth.* **1963**, *7*, 128–131.
[25] A. Schöberl, A. Wagner in *Methoden der Organischen Chemie (Houbel-Weyl)*, 4th Edition, Vol. 9, Thieme, Stuttgart, **1955**, p. 45.
[26] T. Kametani, K. Kigasawa, M. Hiiragi, N. Wagatsuma, T. Kohagizawa, H. Inoue, *Heterocycles* **1978**, *9*, 831–840.
[27] G. M. Sheldrick, *SHELXS 86, Program for Crystal Structure Solution*, Universität Göttingen, Germany, **1986**.
[28] G. M. Sheldrick, *SHELXL 93, Program for Crystal Structure Refinement*, Universität Göttingen, Germany, **1993**.
[I98241]

Synthesis of Soluble 1,3-Bridged Ferrocene-Acetylene Polymers and the Divergent-Convergent Synthesis of Defined Oligomers

Herbert Plenio*, Jörg Hermann, and Jörg Leukel

Institut für Anorganische und Analytische Chemie, Universität Freiburg,
Albertstrasse 21, D-79104 Freiburg, Germany
Fax: (internat.) + 49(0)761/2036129
E-mail: plenio@uni-freiburg.de

Received July 17, 1997

Keywords: Alkynes / Polymers / 1,2,3-Substituted ferrocene / Directed *ortho* metallation

A $-CH_2NMe_2$ group attached to ferrocene can be used as an *ortho*/*ortho*-directing group to selectively synthesize 1,2,3-substituted ferrocenes, which are used as starting materials for novel 1,3-linked ferrocene polymers and oligomers. The Sonogashira coupling reaction of 1-(I),2-(CH_2NMe_2)-ferrocene with $HC{\equiv}CSiEt_3$ results in 1-($C{\equiv}CSiEt_3$),2-(CH_2NMe_2)-ferrocene (**1b**), which – following an *ortho*-lithiation/iodination sequence – is converted into 1-(I),2-(CH_2NMe_2),3-($C{\equiv}CSiEt_3$)-ferrocene (**1d**). Removal of the $-SiEt_3$ protective group yields 1-(I),2-(CH_2NMe_2),3-($C{\equiv}CH$)-ferrocene, which can be polymerized under Sonogashira conditions to yield a soluble, bimodal ferrocene-acetylene polymer of M_W = 3700/7100 and M_n = 4272. To understand the properties of the polymer better and to evaluate the effect of 1,3-substitution on the electronic communication between the metal centers, a divergent-convergent approach was used to synthesize defined di-, tri- and tetranuclear ferrocenes. Accordingly, **1d** was cross-coupled with 1-(CH_2NMe_2),2-($C{\equiv}CH$)-ferrocene to give [2-(CH_2NMe_2)-ferrocene-1-yl]-$C{\equiv}C$-[2-(CH_2NMe_2),3-($C{\equiv}CSiEt_3$)-ferrocene-1-yl] (**2a**). Removal of the protective group in **2a** led to [2-(CH_2NMe_2)-ferrocene-1-yl]-$C{\equiv}C$-[2-(CH_2NMe_2),3-($C{\equiv}CH$)-ferrocene-1-yl] (**2b**), which was treated with [1-(I),2-(CH_2NMe_2)-ferrocene-3-yl]-$C{\equiv}C$-[2-(CH_2NMe_2),3-($C{\equiv}CSiEt_3$)-ferrocene-1-yl] (**2c**) to result in the corresponding tetrameric ferrocene (**4a**).

Introduction

Organic polymers such as polypyrrole, poly(*p*-phenylene),[1] polythiophene,[2] poly(*p*-phenylenevinylene)[3][4] or -ethynylene[5] display interesting properties like photo- and electroluminescence and conductivity, which are useful in antistatic coatings, battery materials or blue-light photo diodes.[6][7] Organometallic polymers could offer all of this and even more as the metal may impart unusual magnetic, electronic and optical properties on such materials.[8][9] Prominent in this field are ferrocene polymers,[10] which either consist of an organic backbone to which ferrocenyl groups are attached (e.g. polyvinylferrocene) or of 1,1′-ferrocenediyl groups in the polymer backbone; other metallocenes have been used less frequently.[11] One breakthrough in the synthesis of soluble, high molecular weight ferrocene polymers has been the discovery of an ROP-type coupling of strained ferrocenophanes by Manners and coworkers.[12] Despite the progress made recently, virtually all known ferrocene polymers, with a few (mostly poorly soluble) exceptions,[13] still suffer from two basic disadvantages: typically the different ferrocene units are linked by electronically insulating bridges that only allow electrostatic interactions between the different metal centers and, in addition, most often 1,1′-ferrocenediyl units are used as repeat units.

It is quite obvious that ferrocene polymers are more likely to display exceptional properties when the different metal centers are coupled intimately through suitable unsaturated bridging units.[14][15] We therefore decided to initiate a program aimed at synthesizing novel types of soluble 1,3-linked ferrocenediyl polymers.

Results and Discussion

Synthesis

A few 1,3-substituted ferrocenes have been described in the literature,[16] but starting from ferrocene itself, it is difficult to selectively introduce two substituents in the 1,2- or 1,3-positions of ferrocene. We therefore reasoned that it should be easier to synthesize 1,3-substituted ferrocenes by using an *ortho*/*ortho*-directing group to obtain 1,2,3-substituted ferrocenes instead.[17] In this respect the $-CH_2NMe_2$ unit in $FcCH_2NMe_2$ appears to be a suitable group for directed *ortho*/*ortho* metallation[18] and appears very convenient as $FcCH_2NMe_2$ is commercially available or can be synthesized at low cost.[19] Another advantage of $FcCH_2NMe_2$ is that the amine can be quaternized easily to give $-NMe_3^+$, which happens to be a good leaving group in nucleophilic substitution reactions.[20]

The reaction of $FcCH_2NMe_2$ first with *n*BuLi and then with iodine leads to the known 1-(I),2-(CH_2NMe_2)-ferrocene (**1a**),[21] which was coupled with $HC{\equiv}CSiEt_3$ in a Sonogashira-type reaction[22][23] to produce 1-($C{\equiv}CSiEt_3$),2-(CH_2NMe_2)-ferrocene (**1b**) (yield > 90%) (Scheme 1).[24]

Compound **1b** can be deprotonated regioselectively with *n*BuLi at the other *ortho* position (with respect to the $-CH_2NMe_2$ unit) to yield, after reaction with iodine,

 © WILEY-VCH Verlag GmbH, D-69451 Weinheim, 1998 1434−1948/98/1212−2063 $ 17.50+.50/0

Scheme 1. a: $PdCl_2(PPh_3)_2$, CuI, $HCCSiEt_3$, solvent iPr_2NH, reflux; b: 1. BuLi, 0°C, Et_2O, 2 h, 2. $+I_2$, −78°C; c: $nBu_4N^+F^- \cdot 3\ H_2O$; d: $PdCl_2(PPh_3)_2$, CuI, solvent iPr_2NH, reflux

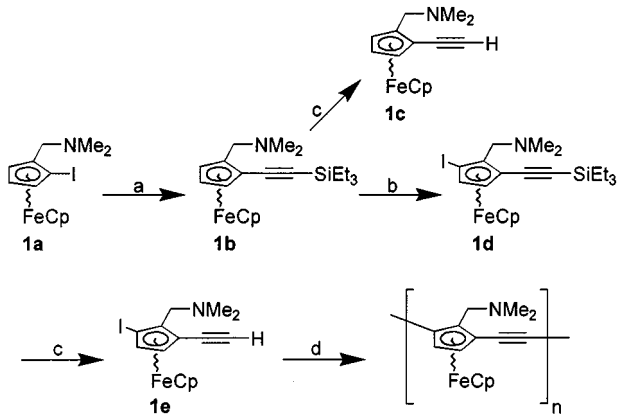

the 1,2,3-substituted ferrocene 1-(I),2-(CH_2NMe_2),3-(C≡$CSiEt_3$)-ferrocene (**1d**) (yield 66%). This reaction works very well for the −$SiEt_3$-protected acetylene, but only gives low yields (ca. 20%) of the respective 1,2,3-substituted ferrocene with an −$SiMe_3$-protected acetylene. Obviously, the latter protecting group is not entirely stable towards *n*BuLi. Cleavage of the −$SiEt_3$ protective group in **1b** or **1d** is easily effected with aq. 50% KOH or $nBu_4N^+F^- \cdot 3\ H_2O$ to produce the respective 1-(C≡CH),2-(CH_2NMe_2)-ferrocene (**1c**) and 1-(I),2-(CH_2NMe_2),3-(C≡CH)-ferrocene (**1e**) in 75−80% yield.

The 1,2,3-substituted ferrocene **1e** has two functional groups that can be coupled under Sonogashira conditions to form a dark red, glassy material (> 90% yield). This mixture was purified by flash chromatography and gave low molecular weight oligomers and a polymeric fraction. An attempted determination of the molecular mass of the latter material by standard GPC techniques was not successful, since an affinity-type chromatographic separation was observed. Obviously, this is caused by the polar nature of this material. We therefore had to resort to GPC-LALLS (gel-permeation chromatography/low-angle laser-light scattering) in an extremely polar mobile phase (DMF, 0.1 M guanidinium hydrochloride) to suppress affinity-type interactions with the stationary phase. With this method a characteristic bimodal molecular-weight distribution with M_W = 3700 and 7100 was found (Figure 1). This polymer is highly soluble in polar solvents (CH_2Cl_2, $CHCl_3$), which may appear surprising given its rigid backbone. In this respect it should, however, be noted that the polymer formed is a diastereomeric mixture with random orientations of the CpFe units with respect to the polymer backbone. This may be a disadvantage with respect to the characterization of the low molecular weight oligomers, but should not unfavorably influence the electronic properties of the polymers. On the other hand this disorder could very well be responsible for the good solubility of these materials.

Another advantage of the −CH_2NMe_2 group is that it can be functionalized easily by alkylation, followed by reaction of the quaternary ammonium salt with various nucleophiles (see Scheme 2). We have tested this by treating **1e** with MeI to give [1-(C≡CH),2-(CH_2NMe_3)-ferrocene]$^+I^-$ (**1f**) (yield 91%). This salt was treated with aza-12-crown-4 to produce the crown ether substituted monomer (1-C≡CH),[2-CH_2(aza-12-crown-4)]-ferrocene (**1g**) (yield 29%), which was polymerized under Sonogashira coupling conditions to give a redox-active crown ether polymer. This polymer is potentially attractive as the utility of such materials as electro-active sensors for metal ions has been demonstrated by Bäuerle,[25] Garnier[26] and Swager.[27] The dark-red mixture of oligomers and polymers was separated by flash-chromatography. The GPC-LALLS investigation of this polymer initially suggested much higher molecular weights (M_W = 61000, M_n = 58000), but the strong tailing of the GPC traces casts some doubt on these results, and may very well be the result of an aggregation process involving several polymer molecules. It is interesting in terms of chain-termination reactions that the oligomeric fractions from both polymerizations display vinylic resonances in the ^{1}H-NMR spectrum. The same phenomenon was also observed in related coupling reactions of mononuclear complexes of sterically more demanding acetylene derivatives of chiral FcCH(Me)NMe_2.[28]

Figure 1. Molecular weight distribution of the 1,3-ferrocene-acetylene polymer as determined by GPC-LALLS

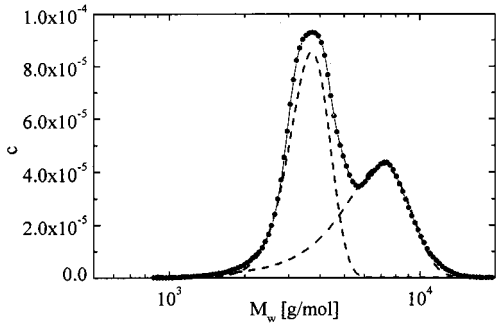

Scheme 2. a: MeI; b: aza-12-crown-4, CH_3CN reflux; c: $PdCl_2(PPh_3)_2$, CuI, solvent iPr_2NH, reflux

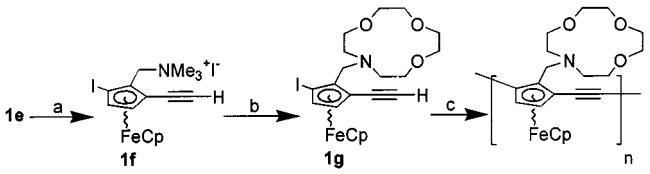

In order to better understand the electronic properties of the polymeric materials we have prepared defined oligomers using a divergent-convergent approach, which has been used successfully by Tour et al.[29] and Moore et al.[30] in the synthesis of related oligothiophenes and oligoethynylarenes. Starting from **1c** and **1d** a Sonogashira coupling generates [2-(CH_2NMe_2)-ferrocene-1-yl]-C≡C-[2-(CH_2NMe_2),-3-(C≡$CSiEt_3$)-ferrocene-1-yl] (**2a**) (yield > 90%) (Scheme 3). This batch was split and the first half used for a lithiation/iodination sequence resulting in [2-(CH_2NMe_2),3-(I)-ferrocene-1-yl]-C≡C-[2-(CH_2NMe_2),3-(C≡$CSiEt_3$)-ferrocene-1-yl] (**2c**) (yield 65%), while the remaining **2a** was de-

protected with nBu$_4$N$^+$F$^-\cdot$3 H$_2$O to give [1-(CH$_2$NMe$_2$)-ferrocene-2-yl]-C≡C-[2-(CH$_2$NMe$_2$),3-(C≡CH)-ferrocene-1-yl] (**2b**) (yield 80%). Both **2b** and **2c** were then coupled according to the Sonogashira protocol to give the tetramer [2-(CH$_2$NMe$_2$)-ferrocene-1-yl]-C≡C-[2-(CH$_2$NMe$_2$)-ferrocene-1,3-diyl]-C≡C-[1-(CH$_2$NMe$_2$)-ferrocene-1,3-diyl]-C≡C-[2-(CH$_2$NMe$_2$),3-(C≡CSiEt$_3$)-ferrocene-1-yl] (**4a**) (yield 73%). The highly polar nature of this tarry, red material caused tailing and repeated chromatography was necessary to obtain analytically pure samples since **4a** could not be recrystallized. These purification problems also were the reason why we did not attempt to extend our synthetic procedure to the octameric ferrocene.

Scheme 3. a: PdCl$_2$(PPh$_3$)$_2$, CuI, HCCSiEt$_3$, solvent iPr$_2$NH, reflux; b: nBu$_4$N$^+$F$^-\cdot$3 H$_2$O; c: 1. + BuLi, 0°C, Et$_2$O, 2 h, 2. + I$_2$, −78°C

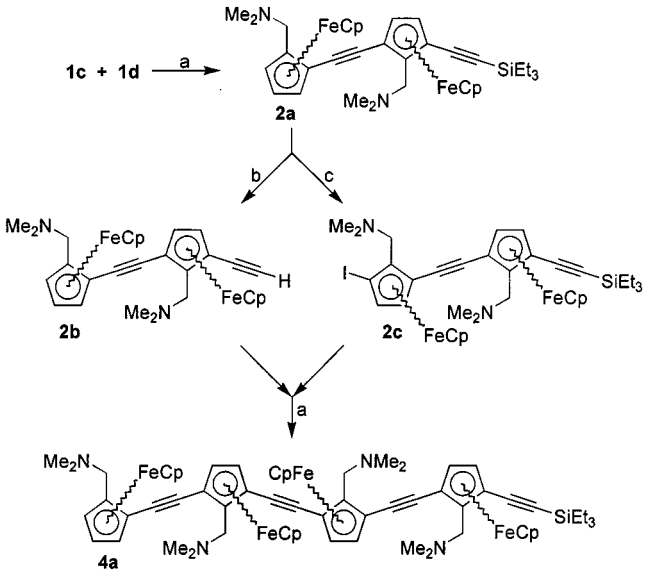

In order to be able to compare the influence of the substitution pattern (1,3- or 1,1′-) on the electronic properties of the ferrocene-acetylenes, we synthesized the two trinuclear ferrocenes **3a** and **3b** (Scheme 4). Both complexes only differ in that **3a** has a 1,3-substituted ferrocene core, while **3b** has a 1,1′-substituted ferrocene unit. The coupling reaction of **1a** and **2b** gave **3a**, while the respective coupling of 1,1′-diiodoferrocene and **1c** produced **3b**, both in yields of around 75%. A closer investigation of these compounds should provide evidence of the better electronic delocalization of the ring with the 1,3-substitution pattern than that with the 1,1′-positions.

NMR Spectroscopy

The ^{1}H-NMR spectra of the mononuclear ferrocenes are straightforward, while those of the oligomers are characterized by more complex spin systems. For example the number of −N(CH$_3$)$_2$ resonances found (δ = 2.20−2.35 in **4a**), correspond to the number of diastereomers, e.g. four lines in **2a**. Accordingly, the large number of −N(CH$_3$)$_2$ resonances in **4a** reflects the large number of diastereomers

Scheme 4. a: PdCl$_2$(PPh$_3$)$_2$, CuI, HCCSiEt$_3$, solvent iPr$_2$NH, reflux

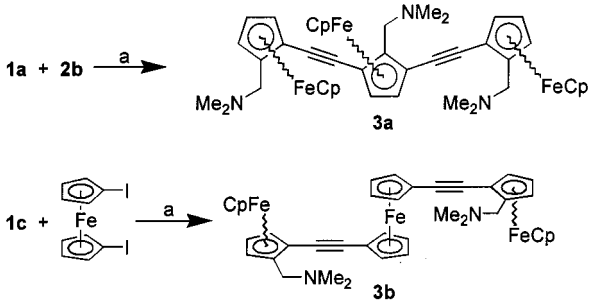

(Figure 2, top). The fact that the −CH$_2$− groups have diastereotopic protons in the 1,2,3-substituted species leads to another complex set of resonances that usually appear in two groups (δ = 3.48−3.53 and δ = 3.65−3.81 in **4a**). The C$_5$H$_5$ resonances of the unsubstituted cyclopentadienyl ring are typically split into no more than two resonances, while those of the C$_5$H$_2$ unit in 1,2,3-substituted cyclopentadienyl rings are observed as a group of signals at low field (δ = 4.38−4.45 in **4a**) with respect to C$_5$H$_5$. In between these two signals, the characteristic resonances of the *ortho*-H (hydrogen atom next to −CH$_2$NMe$_2$ in 1,2-substituted ferrocenes) can be found at δ = 4.26 (in **4a**).

Figure 2. ^{1}H-NMR spectra of the tetramer **4a** (top) and polymer I (bottom)

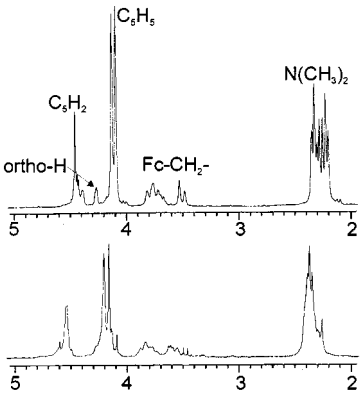

With this knowledge in mind the ^{1}H-NMR spectrum of polymer I can be understood. The typical signals of the tetramer are found (in broadened form) in the polymer, reflecting the large number of different microenvironments for each functional group. Most striking in the spectrum of the polymer is the apparent absence of the *ortho*-H, since an ideal polymer entirely consists of 1,2,3-substituted ferrocenes.

The ^{13}C-NMR spectra of the oligomers are complicated and it is difficult to extract useful information; there are simply too many lines that show up more readily in the ^{13}C-NMR spectra due to their larger signal dispersion. However, again it is possible to distinguish different groups of signals for the different chemical units (CH$_3$, CH$_2$, cyclopentadienyl ring and −C≡C− groups).

UV/Vis Spectroscopy

The UV/Vis spectra of ferrocene and its derivatives are characterized by two weak bands around 325 nm and 440 nm, which are both attributed to d-d transitions.[31] Any perturbation of the electronic structure of the ferrocenes, i.e. conjugation within a conjugated chain, should lead to a bathochromic shift of the respective UV/Vis transitions. Consequently, the UV/Vis spectra of our ferrocenes were measured (Figure 3) and the characteristic d-d transition proved to be quite informative: **1b**: λ_{max} = 441 nm (ε [L/M·cm] = 206); **2a**: 452 (850); **3a**: 456 (1220); **3b**: 448 (926); **4a**: 466 (1560); polymer: 468 nm. The long-wavelength shift and the stronger extinction of **3a** vs. **3b** support the idea of a better electronic delocalization in the 1,3-linked species.

Figure 3. UV/Vis spectra of the mononuclear **1b**, the dinuclear **2a** and the trinuclear ferrocenes **3a** and **3b** (10^{-4} M in CH_2Cl_2)

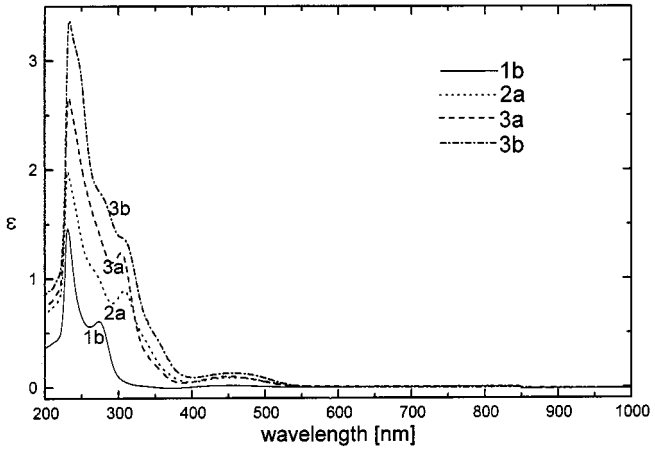

Cyclic Voltammetry

To complement the UV/Vis studies and in order to better understand the degree of electronic communication between the ferrocene units in the oligomers and polymers described here,[32] we attempted to determine the redox potentials of these compounds. However, the electrochemical experiments performed with the aminoferrocenes **1**−**4** were not very successful and we were only able to observe reversible electron-transfer processes with mononuclear ferrocenes when the cyclic voltammetric experiments were carried out at low temperatures (T = −20°C).

The respective studies of the ferrocene oligomers **2**−**4**, however, were rather disappointing as we could not observe reversible or at least quasi-reversible electron-transfer processes. Despite testing several solvents (acetonitrile, acetone, dichloromethane, dimethylformamide) under varying conditions, the voltammograms of the dimers and higher oligomers were complicated by numerous extremely broad redox waves (deposition on the electrode surface?) and/or a number of additional unexplained waves. In the case of the polymers the cyclic voltammogram consists of several uncharacteristic broad humps, from which we could not extract any meaningful information. These observations may be rationalized in the light of recent results by Robinson, Simpson et al.[33] who investigated the electrochemistry of related 2,2′′-bis(1-dialkylamino)-1,1′′-ferrocenes. In their study it was found that oxidation processes involving binuclear dialkylamino-ferrocenes are complicated by amine oxidation as well as oxidatively induced protonation and deprotonation processes. The fact that the former compounds are closely related to our binuclear ferrocenes might serve as an explanation for the problems experienced by us. Nonetheless, the disappointing electrochemistry of these compounds must be viewed as a major drawback.

Summary and Conclusions

We have shown that the $-CH_2NMe_2$ group can be used as an *ortho*/*ortho*-directing substituent in ferrocene chemistry to allow easy access of 1,2,3-substituted ferrocenes. This synthetic route was used to prepare 1-(I),2-(CH_2NMe_2),3-(C≡CH)-ferrocene, which can be polymerized in a Sonogashira-type coupling reaction to yield a soluble, bimodal 1,3-linked ferrocene-acetylene polymer of M_w = 3700/7100. Starting from 1-(I),2-(CH_2NMe_2),3-(C≡CSiEt$_3$)-ferrocene, defined ferrocene oligomers were also available through a divergent-convergent synthesis to give a tetrameric ferrocene-acetylene.

By studying model compounds with ferrocene-acetylene substituents in either the 1,3- or the 1,1′-position it was shown, by the more pronounced bathochromic shift of the ferrocene d-d transitions in the former compound, that the electronic communication in 1,3-linked ferrocenes is better than in 1,1′-linked species and it is therefore proposed that the 1,3-linked ferrocene polymers will display superior intermetallic electronic communication as compared to their 1,1′-linked relatives. Unfortunately, it was not possible to further support this by electrochemical experiments since all oligonuclear 1,2,3-substituted compounds derived from $FcCH_2NMe_2$ described here do not display reversible electron-transfer processes.

In conclusion the $-CH_2NMe_2$ unit attached to ferrocene is very useful for synthetic transformations and should allow the synthesis of a variety of 1,2,3-substituted ferrocenes. It is, however, a major drawback of this functional group in terms of redox reactions that the electrochemistry of ferrocenes with several $-CH_2NMe_2$ groups is not straightforward.

This work was supported by the *Deutsche Forschungsgemeinschaft*, the *Fonds der Chemischen Industrie*, the *Freiburger Wissenschaftliche Gesellschaft* and the *Institut für Anorganische und Analytische Chemie*, Universität Freiburg. We wish to thank cand.-chem. *J. Seebacher* for experimental assistance and a referee for interesting suggestions.

Experimental Section

General: Commercially available solvents and reagents were purified according to literature procedures. − Chromatography was performed on silica gel MN60. − NMR spectra were recorded at 300 K with a Bruker Avance (^{1}H NMR 200 MHz, ^{13}C NMR 50.3

MHz,). ^{1}H-NMR signals were referenced to residual ^{1}H impurities in the solvent and ^{13}C-NMR signals to the solvent signals: $CDCl_3$ (δ = 7.26, δ = 77.0), C_6D_6 (δ = 7.16, δ = 128.0), CD_3CN (δ = 1.93, δ = 1.30). For the purpose of ^{1}H-NMR signal assignment CpH denotes a proton attached to the sp^2-carbon atom of cyclopentadiene or to the carbon atom of a ferrocene η^5-cyclopentadienyl ring. − Mass spectra: Finnigan MAT 3800. − IR spectra were recorded with a Bruker IFS-25 in $CHCl_3$ solution. − UV/Vis spectra were recorded with a JASCO-UV-570 spectrometer in CH_2Cl_2 solution. − Elemental analyses: Mikroanalytisches Laboratorium der Chemischen Laboratorien, Universität Freiburg. For several compounds, especially for the oligomeric and polymeric materials, we could not obtain analytically pure samples due to phosphorus-based impurities from the catalyst,[34] which proved difficult to remove by chromatography. Recrystallisation of the oily, highly viscous materials was not possible. All chromatographic purifications were performed on alumina-N deactivated with 10% water. − Gel-permeation chromatography with a low-angle laser-light scattering detector was performed in dimethylformamide/0.1 M guanidinium chloride solvent using a Milton-Roy type KMX 6 detector, a Knauer HPLC-PUMP 64, a Pharmacia LKB VWM 2141 UV meter and Waters 10^3-10^5 Å columns. The calibration of the hydrodynamic volumina/molecular mass was routinely performed with polystyrene standards (PSS, PL) in THF.

1-(I),2-(CH_2NMe_2)-ferrocene (**1a**): Modified from the literature procedure.[21] To a solution of [(dimethylamino)methyl]ferrocene (21.5 g, 0.100 mol) in diethyl ether (300 ml) was added *n*BuLi (50 ml, 0.125 mol). After stirring for 4 h at room temp., the reaction mixture was cooled to −78°C and a solution of I_2 (30.5 g, 0.120 mol) in THF (75 ml) added dropwise. The solution was slowly allowed to warm to room temp. during approx. 1 h. After stirring for further 15 min, the reaction mixture was added to water (500 ml) to extract LiI. The organic layer was separated and the water extracted once more with diethyl ether. The combined organic extracts were dried with $MgSO_4$, filtered and concentrated to dryness. The residue was purified by flash chromatography (alumina-B, $CHCl_3$). The solvents were evaporated to yield the product as dark-red oil, which slowly solidified upon standing, yield 24.0 g (65%), red oily crystals. − ^{1}H NMR ($CDCl_3$): δ = 2.25 [s, 6 H, $N(CH_3)_2$], 3.38 (s, 2 H, CH_2), 4.11 (s, 5 H, CpH), 4.22 ("t", J = 1.8 Hz, 1 H, CpH), 4.31 (br., 1 H, CpH), 4.43 (br., 1 H, CpH). − ^{13}C NMR ($CDCl_3$): δ = 43.56, 57.55, 69.94, 70.27, 71.89, 73.05, 75.57, 80.62.

1-(C≡CSiEt$_3$),2-(CH_2NMe_2)-ferrocene (**1b**): To a deoxygenated solution of 1-(I),2-(CH_2NMe_2)-ferrocene (4.80 g, 13 mmol) and (triethylsilyl)acetylene (1.82 g, 13 mmol) in diisopropylamine (75 ml) were added $(Ph_3P)_2PdCl_2$ (92 mg, 0.13 mmol) and CuI (49 mg, 0.72 mmol). The reaction mixture was heated under reflux for 18 h, filtered, the precipitate washed with diethyl ether and the volatiles evaporated to dryness. The remaining red oily product was almost pure and used as such for the subsequent reactions, yield 4.60 g (92%), red liquid. − ^{1}H NMR ($CDCl_3$): δ = 0.62 (q, J = 5.7 Hz, 6 H, $SiCH_2$), 1.06 (t, J = 5.5 Hz, $SiCH_2CH_3$), 2.21 [s, 6 H, $N(CH_3)_2$], 3.50 (s, 2 H, CH_2), 4.11 (s, 5 H, C_5H_5), 4.15 ("t", J = 1.9 Hz, 1 H, CpH), 4.29 (cm, 1 H, CpH), 4.43 (cm, 1 H, CpH). − ^{13}C NMR ($CDCl_3$): δ = 4.60, 6.61, 44.75, 56.95, 66.89, 68.09, 70.42, 70.63, 71.25, 85.65, 90.13, 104.63. − IR: $\tilde{\nu}$ = 2147 cm^{-1}. − $C_{21}H_{31}FeNSi$ (381.42): calcd. C 66.13, H 8.19, N 3.67; found C 66.02, H 7.95, N 3.70.

1-(C≡CH),2-(CH_2NMe_2)-ferrocene (**1c**): A solution of 1-(C≡CSiEt$_3$),2-(CH_2NMe_2)-ferrocene (8.30 g, 0.88 mmol) in CH_3OH (10 ml) was treated with aqueous KOH (1 ml, 50%) and stirred under nitrogen for 1 h. The volatiles were evaporated, water was added and the residue extracted with diethyl ether. The ethereal layer was separated, dried with $MgSO_4$, filtered and concentrated. The remaining oil was purified by chromatography (cyclohexane/ethyl acetate, 10:1), yield 4.80 g (73%), red oil. − ^{1}H NMR ($CDCl_3$): δ = 2.21 [s, 6 H, $N(CH_3)_2$], 2.82 (s, 1 H, ≡CH), 3.48 (s, 2 H, CH_2), 4.14 (s, 5 H, C_5H_5), 4.16 ("t", J = 2 Hz, 1 H, CpH), 4.29 (m, 1 H, CpH), 4.45 (m, 1 H, CpH). − ^{13}C NMR: δ = 44.80, 57.03, 65.62, 68.09, 70.55, 71.53, 75.70, 81.84, 85.81. − $C_{15}H_{16}FeIN$ (393.0): calcd. C 45.84, H 4.10, N 3.56; found C 45.26, H 4.42, N 3.29.

1-(C≡CSiEt$_3$),2-(CH_2NMe_2),3(I)-ferrocene (**1d**): A solution of 1-(C≡CSiEt$_3$),2-(CH_2NMe_2)-ferrocene (4.60 g, 12.1 mmol) in diethyl ether (75 ml) was treated with BuLi (6.0 ml, 15 mmol) at −78°C and slowly warmed to room temp. After stirring for 1 h, the reaction mixture was cooled to −78°C and a solution of I_2 (3.05 g, 12.0 mmol) in THF (10 ml) added dropwise and then the reaction mixture was slowly warmed to room temp. After stirring for further 15 min, the reaction mixture was added to water (100 ml) and the LiI extracted. The organic layer was separated and the water extracted once more with diethyl ether. The combined organic extracts were dried with $MgSO_4$, filtered and concentrated to dryness. The remaining oil was purified by flash chromatography (cyclohexane/ethyl acetate, 10:1), yield 4.0 g (66%), red oil. − ^{1}H NMR ($CDCl_3$): δ = 0.65 (q, J = 7.9 Hz, 6 H, $SiCH_2$), 1.05 (t, J = 8 Hz, 9 H, CH_3), 2.28 [s, 6 H, $N(CH_3)_2$], 3.40−3.62 (m, 2 H, NCH_2), 4.10 (s, 5 H, C_5H_5), 4.46−4.52 (m, 2 H, CpH). − ^{13}C NMR ($CDCl_3$): δ = 4.50, 7.58, 45.85, 57.20, 66.11, 72.30, 73.55, 75.08, 87.85, 91.47, 103.48. − $C_{21}H_{30}FeINSi$ (507.31): calcd. C 49.72, H 5.96, N 2.76; found C 50.13, H 6.02, N 2.54.

1-(C≡CH),2-(CH_2NMe_2),3-(I)-ferrocene (**1e**): To a solution of 1-(C≡CSiEt$_3$),2-(CH_2NMe_2),3-(I)-ferrocene (4.00 g, 7.9 mmol) in CH_3OH (75 ml) was added KOH (4 g) and the mixture was stirred under nitrogen for 3 h. The volatiles were evaporated, water was added and the residue extracted with diethyl ether. The ethereal layer was separated, dried with $MgSO_4$, filtered and concentrated. The remaining oil was purified by flash chromatography (cyclohexane/ethyl acetate, 10:1), yield 2.30 g (75%), red oil. − ^{1}H NMR ($CDCl_3$): δ = 2.27 [s, 6 H, $N(CH_3)_2$], 2.86 (s, 1 H, ≡CH), 3.49 (s, 2 H, CH_2), 4.12 (s, 5 H, C_5H_5), 4.46−4.53 (m, 2 H, CpH). − ^{13}C NMR ($CDCl_3$): δ = 45.53, 57.09, 64.85, 72.44, 75.00, 76.77, 80.80, 87.74. − $C_{15}H_{16}FeIN$ (393.0): calcd. C 45.84, H 4.10, N 3.56; found C 45.55, H 4.00, N 3.67.

[1-(C≡CH),2-(CH_2NMe_3),3-(I)-ferrocene]$^+$I$^-$ (**1f**): A solution of 1-(C≡CH),2-(CH_2NMe_2),3-(I)-ferrocene (2.30 g, 5.80 mmol) in diethyl ether (25 ml) was treated with CH_3I (1.65 g, 11.6 mmol) and the mixture stirred for 12 h at room temp. The yellow precipitate was filtered off, washed with diethyl ether and dried in vacuo, to yield a yellow powder, yield 2.85 g (91%), yellow powder. − ^{1}H NMR (CD_3CN): δ = 3.10 [s, 9 H, $N(CH_3)_3$], 3.42 (s, 1 H, ≡CH), 4.27 (s, 5 H, C_5H_5), 4.53−4.76 (m, 4 H, CH_2), 4.84−4.88 (m, 2 H, C_5H_2). − $C_{16}H_{19}FeI_2N$ (535.0): calcd. C 35.92, H 3.58, N 2.62; found C 36.26, H 3.89, N 2.11.

1-(C≡CH),2-[CH_2(N-12-c-4)],3-(I)-ferrocene (**1g**): A mixture of [1-(C≡CH),2-(CH_2NMe_3),3-(I)-ferrocene]$^+$I$^-$ (535 mg, 1.00 mmol), aza-12-crown-4 (210 mg, 1.20 mmol) and K_2CO_3 (0.5 g) in acetonitrile was heated under reflux for 12 h. The cold solution was filtered and the filtrate concentrated to dryness. The residue was dissolved in $CHCl_3$, filtered through an alumina-N plug, concentrated to dryness and chromatographed on alumina-N with cyclohexane/ethylacetate/diethylamine (10:1:1), yield 150 mg (29%), red oil. − ^{1}H NMR ($CDCl_3$): δ = 2.79−2.86 (m, 4 H, NCH_2), 2.89 (s, 1 H, ≡CH), 3.60−3.88 (m, 12 H, CH_2O + $CpCH_2$), 4.14 (s, 5

H, C_5H_5), 4.49−4.54 (m, 2 H, C_5H_2). − ^{13}C NMR ($CDCl_3$): δ = 44.90, 54.13, 54.60, 64.97, 69.88, 70.45, 71.38, 71.86, 72.68, 73.58, 75.37, 81.18, 88.37. − $C_{21}H_{26}FeINO_3$ (523.2): calcd. C 48.21, H 5.01, N 2.68; found C 48.56, H 5.21, N 2.59.

[1-(CH_2NMe_2)-ferrocene-2-yl]-C≡C-[2-(CH_2NMe_2),3(C≡CSiEt_3)-ferrocene-1-yl] (**2a**): Typical coupling procedure: 1 mol-% Pd catalyst, 2 mol-% CuI. Scale: 1-(I),2(-CH_2NMe_2),3-(C≡C$SiEt_3$)-ferrocene (**1d**) (2.54 g, 5.00 mmol), 1-(C≡CH),2-(CH_2NMe_2)-ferrocene (**1c**) (1.97 g, 5.00 mmol). Yield 2.68 g (83%), red oil. Chromatography: cyclohexane/ethyl acetate (10:1), R_F = 0.4. − ^{1}H NMR ($CDCl_3$): δ = 0.66 (q, 6 H, $SiCH_2$), 1.07 (t, 9 H, CH_3), 2.17, 2.25, 2.32, 2.34 (s, 12 H, 4 × CH_3), 3.53−3.78 (m, 4 H, CH_2), 4.14 (s, 10 H, C_5H_5), 4.19 ("t", *J* = 2.5 Hz, 1 H, CpH), 4.32 (br., 1 H, CpH), 4.44 (m, 1 H, CpH), 4.48 (s, 2 H, CpH). − ^{13}C NMR ($CDCl_3$): δ = 4.54, 7.60, 44.87, 45.92, 45.29, 45.38, 55.51, 55.66, 57.20, 57.35, 67.13, 67.18, 67.65, 67.72, 68.07, 68.83, 70.38, 70.43, 71. 04, 71.13, 71.36, 72.47, 72.51, 84.78, 84.89, 85.60, 85.07, 85.07, 85.72, 87.14, 87.40, 93.27, 103.00.

[2-(CH_2NMe_2)-ferrocene-1-yl]-C≡C-[2-(CH_2NMe_2),3(C≡CH)-ferrocene-1-yl] (**2b**): Typical cleavage procedure: 24 h CH_3OH/aq. KOH, [2-(CH_2NMe_2)-ferrocene-1-yl]-C≡C-[2-(CH_2NMe_2),3-(C≡C-$SiEt_3$)-ferrocene-1-yl] (**2a**) (1.29 g, 2.0 mmol). Yield 0.79 g (74%), red oil. Chromatography: cyclohexane/Et_2NH (10:1), R_F = 0.2. − ^{1}H NMR ($CDCl_3$): δ = 2.25 [s, 3 H, $N(CH_3)_2$], 2.28 [s, 3 H, $N(CH_3)_2$], 2.32 [s, 3 H, $N(CH_3)_2$], 2.34 [s, 3 H, $N(CH_3)_2$], 2.85 (s, 1 H, ≡CH), 3.53−3.77 (m, 4 H, CH_2), 4.15−4.32 (m, 11 H, 2 × C_5H_5 + CpH), 4.33 (br., 1 H, CpH), 4.44 (br., 1 H, CpH), 4.48−4.52 (m_c, 2 H, CpH). − ^{13}C NMR ($CDCl_3$): δ = 44.85, 44.89, 45.30, 55.58, 55.78, 57.17, 57.31, 66.10, 67.61, 68.06, 68.08, 68.97, 70.36, 70.42, 71.04, 71.07, 71.48, 72.36, 72.41, 75.98, 81.27, 84.76, 85.06, 87.13, 87.40.

[1-(I),2-(CH_2NMe_2)-ferrocene-3-yl]-C≡C-[2-(CH_2NMe_2)-3-(C≡C$SiEt_3$)-ferrocene-1-yl] (**2c**): Typical sequence of lithiation and iodination: [2-(CH_2NMe_2)-ferrocene-1-yl]-C≡C-[2-(CH_2-NMe_2),3-(C≡C$SiEt_3$)-ferrocene-1-yl] (**2a**) (1.29 g, 2.0 mmol) *n*BuLi (2.4 mmol), I_2 (0.508 g, 1.95 mmol). Yield 0.97 g (63%), red oil. Chromatography: cyclohexane/ethyl acetate (5:1), $R_{F\ =\ 0}$.6. − ^{1}H NMR ($CDCl_3$): δ = 0.66 (q, *J* = 7.8 Hz, 6 H, $SiCH_2$), 1.06 (t, *J* = 7.7 Hz, 9 H, CH_3), 2.26−2.38 [m, 12 H, $N(CH_3)_2$], 3.54−3.61 (m, 2 H, CH_2), 3.72−3.80 (m, 2 H, CH_2), 4.08−4.19 (m, 10 H, C_5H_5), 4.46−4.53 (m, 4 H, C_5H_2). − ^{13}C NMR ($CDCl_3$): δ = 4.50, 7.62, 45.16, 45.21, 45.67, 45.76, 55.46, 5.64, 57.38, 57.59, 66.94, 67.06, 67.52, 67.59, 68.20, 68.25, 71.22, 71.52, 71.81, 72.03, 72.49, 72.52, 73.37, 73.40, 73.61, 84.64, 84.74, 85.99, 86.11, 86.70, 87.00, 87.22, 90.70, 103.79.

[1-(CH_2NMe_2)-ferrocene-2-yl]-C≡C-[2-(CH_2NMe_2)-ferrocene-1,3-diyl]-C≡C-[2-(CH_2NMe_2)-ferrocene-1-yl] (**3a**): Typical coupling procedure: [2-(CH_2NMe_2)-ferrocene-1-yl]-C≡C-[2-(CH_2-NMe_2),3-(C≡CH)-ferrocene-1-yl] (**2b**) (532 mg, 1.0 mmol), (1-I),(2-CH_2NMe_2)-ferrocene (**1a**) (369 mg, 1.0 mmol). Yield 670 mg (87%), red oil. Chromatography: cyclohexane/ethyl acetate/Et_2NH (10:1:1). − ^{1}H NMR ($CDCl_3$): δ = 2.27 [s, 6 H, $N(CH_3)_2$ in Fc-1 and Fc-3], 2.29 [s, 6 H, $N(CH_3)_2$ in Fc-1 and Fc-3], 2.36−2.42 [m, 6 H, $N(CH_3)_2$ in Fc-2], 3.55 (s, 2 H, CH_2, Fc-1 and Fc-3), 3.59 (s, 2 H, CH_2, Fc-1 and Fc-3), 3.79−3.88 (m, 2 H, CH_2, Fc-2), 4.16 (s, C_5H_5, Fc-1 and Fc-3), 4.19 (s, 2 H, C_5H_5, Fc-2 + CpH at Fc-1 and Fc-3), 4.33 (cm, 2 H, CpH, Fc-1 and Fc-3), 4.45 (cm, 2 H, CpH, Fc1 and Fc-3), 4.52 (s, 2 H, CpH, Fc-2). − ^{13}C NMR ($CDCl_3$): δ = 44.86, 44.91, 45.32, 55.90, 56.03, 57.19, 57.34, 67.68, 67.75, 68.09, 68.50, 68.64, 68.69, 70.40, 70.44, 71.06, 72.20, 72.25, 72.30, 84.74, 85.00, 85.69, 85.78, 85.98, 86.22, 86.47, 86.88.

1,1′-Bis(1″-ethynyl-2″-(CH_2NMe_2)-ferrocene-1-yl)-ferrocene (**3b**): Typical coupling procedure. Scale: **1c** (2.44 g, 9.2 mmol), 1,1′-diiodoferrocene (2.00 g, 4.6 mmol), $(Ph_3P)_2PdCl_2$ (1 mol-%), CuI (2 mol-%), $^iPr_2NH$ (75 ml). Yield 2.70 g (83%), brown-red oil. Chromatography: R_f = 0.5 (cyclohexane/ethyl acetate/Et_2NH, 10:1:1). − ^{1}H NMR ($CDCl_3$): δ = 2.27 (s, 12 H, NCH_3), 3.56 (s, 4 H, NCH_2), 4.17 (s, 10 H, CpH), 4.23 (s, 8 H, CpH), 4.33 (m, 6 H, CpH_3).

[1-(CH_2NMe_2)-ferrocene-2-yl]-C≡C-[2-(CH_2NMe_2)-ferrocene-1,3-diyl]-C≡C-[1-(CH_2NMe_2)-ferrocene-1,3-diyl]-C≡C-[2-(CH_2NMe_2),3-(C≡CSiEt_3)-ferrocene-1-yl] (**4a**): To a deoxygenated solution of [1-(I),2-(CH_2NMe_2)-ferrocene-3-yl]-C≡C-[2-(CH_2NMe_2),3-(C≡CSiEt_3)-ferrocene-1-yl] (**2c**) (0.772 g, 1 mol) and [2-(CH_2NMe_2)-ferrocene-1-yl]-C≡C-[2-(CH_2NMe_2),3-(C≡CH)-ferrocene-1-yl] (**2b**) (0.532 g, 1.0 mmol) in diisopropylamine (75 ml) were added $(Ph_3P)_2PdCl_2$ (7.0 mg, 1 mol-%) and CuI (7.7 mg, 2 mol-%). The reaction mixture was heated under reflux for 24 h, filtered, the precipitate washed with diethyl ether and the volatiles evaporated to dryness. The remaining solid was purified by chromatography (cyclohexane/ethyl acetate/Et_2NH, 10:1:1), yield 0.86 g (73%), red glassy solid. − ^{1}H NMR ($CDCl_3$): δ = 0.70 (q, *J* = 7.8 Hz, 6 H, CH_2), 1.08 (t, *J* = 7.8 Hz, 9 H, CH_3), 2.28−2.43 (m, 24 H, NMe_2), 3.58 (d, *J* = 9.4 Hz, 2 H, NCH_2), 3.70−3.90 (m, NCH_2, 6 H), 4.17 (s, 10 H, CpH), 4.19 (s, 10 H, CpH), 4.26 (br. s, 1 H), 4.45−4.52 (m, 8 H, CpH). − $C_{66}H_{79}Fe_4N_4Si$ (1179.9): calcd. C, 67.9, H 6.75, N, 4.75; found C 67.78, H 6.89, N 4.76. − ESI-MS; *m/z*: 1178.5.

Polymerisation of **1e**, *Polymer I:* Typical coupling procedure. Scale: **1c** (1.18 g, 3.0 mmol), $(Ph_3P)_2PdCl_2$ (5 mol-%), CuI (10 mol-%), *i*Pr_2NH (75 ml), 36 h reflux. The mixture of oligomers and polymers obtained was fractionated by flash chromatography. A low molecular fraction was eluted with cyclohexane/Et_2NH (1:1) while the polymers were eluted by using $CHCl_3$/MeOH (10:1) or cyclohexane/Et_2NH (3:1). The yields of the polymeric (dark-red glassy) material varied between 40 and 60%. − ^{1}H ($CDCl_3$): δ = 2.26−2.38 (br., 6 H, NMe_2), 3.50−3.65 (br. m, 1.8 H, NCH_2), 3.70−3.95 (br. m, 2.2 H, NCH_2), 4.09−4.21 (br. + 2 s at δ = 4.16 and 4.20, 4.3 H, C_5H_5), 4.53−4.60 (br., 2 H, CpH). − In the ^{13}C-NMR spectrum at least 50 different peaks (diastereomers) were observed.

Polymerisation of **1g**, Polymer II: Typical coupling procedure. Scale: **1c** (0.262 g, 0.50 mmol), $(Ph_3P)_2PdCl_2$ (5 mol-%), CuI (10 mol-%), *i*Pr_2NH (25 ml), 24 h reflux. The mixture of oligomers and polymers was fractionated by flash chromatography. A low-molecular fraction was eluted with cyclohexane/Et_2NH (10:1) while the polymers were eluted with $CHCl_3$/MeOH (10:1). − ^{1}H NMR ($CDCl_3$): 2.65−2.80 (br.), 3.50−3.8 (br. m), 3.48 (s, C_5H_5), 4.08 (s), 4.35−4.50 (m). − In the ^{13}C-NMR spectrum at least 50 different peaks (diastereomers) were observed.

[1] J. M. Tour, *Adv. Mat*. **1994**, *6*, 190.
[2] J. Roncali, *Chem. Rev.* **1992**, *92*, 711.
[3] M. I. Khan, M. L. Renak, G. C. Bazan, Z. Popovic, *J. Am. Chem. Soc*. **1997**, *119*, 5344 and references therein.
[4] B. R. Hsieh, Y. Yu, E. W. Forsythe, G. M. Schaaf, W. A. Feld, *J. Am. Chem. Soc.* **1998**, *120*, 231.
[5] M. Moroni, J. LeMoigne, T. A. Pham, J.-Y. Bigot, *Macromolecules* **1997**, *30*, 1964.
[6] J. Roncali, *Chem. Rev.* **1997**, *97*, 173.
[7] P. Novak, K. Müller, K. S. V. Santhanam, O. Haas, *Chem. Rev.* **1997**, *97*, 207.
[8] [8a] I. Manners, *Angew. Chem*. **1996**, *108*, 1713; *Angew. Chem. Int. Ed. Engl.* **1996**, *35*, 1603. − [8b] M. D. Ward, *Chem. Ind*. **1996**, 568. − [8c] M. D.Ward, *Chem. Soc. Rev*. **1995**, 121.

[9] M. J. Irvin, J. J. Vittal, G. P. A. Yap, R. J. Puddephatt, *J. Am. Chem. Soc*. **1996**, *118*, 13101.
[10] K. E. Gonsalves, X. Chen In *Ferrocenes* (Eds.: A. Togni, T. Hayashi), VCH, Weinheim, **1995**.
[11] [11a] M. Altmann, J. Friedrich, F. Beer, R. Reuter, V. Enkelmann, U. H. F. Bunz, *J. Am. Chem. Soc*. **1997**, *119*, 1472. – [11b] S. Setayesh, U. H. F. Bunz, *Organometallics* **1996**, *15*, 5470. – [11c] M. Altmann, U. H. F. Bunz, *Angew. Chem*. **1995**, *107*& csdilla; 603; *Angew. Chem. Int. Ed. Engl.* **1995**, *34*, 569.
[12] [12a] R. Rulkens, A. J. Lough, I. Manners, S. R. Lovelace, C. Grant, W. E. Geiger, *J. Am. Chem. Soc*. **1996**, *118*, 12683. – [12b] C. H. Honeyman, T. J. Peckham, J. A. Massey, I. Manners, *Chem. Commun*. **1996**, 2589. – [12c] J. M. Nelson, P. Nguyen, R. Peterson, H. Rengel, P. M. Macdonald, A. J. Lough, I. Manners, N. P. Raju, J. E. Greedan, S. Barlow, D. O′Hare, *Chem. Eur. J*. **1997**, *3*, 573.
[13] [13a] T. Hirao, M. Kurashina, K. Aramaki, H. Nishihara, *J. Chem. Soc., Dalton Trans*. **1996**, 2929 and references therein. – [13b] A. S. Gamble, J. T. Patton, J. M. Boncella, *Makromol. Chem. Rapid Commun*. **1993**, *13*, 109. – [13c] E. W. Neuse, L. Bednarik, *Macromolecules* **1979**, *12*, 187. – [13d] O. Lavastre, M. Even, P. H. Dixneuf, A. Pacreau, J.-P. Vairon, *Organometallics* **1996**, *15*, 1530. – [13e] C. E. Stanton, T. R. Lee, R. H. Grubbs, N. S. Lewis, J. K. Pudelski, M. R. Callstrom, M. S. Erickson, M. L. McLaughlin, *Macromolecules* **1995**, *28*, 8713. – [13f] M. A. Buretea, T. D. Tilley, *Organometallics* **1997**, *16*, 1507. – [13g] T. Yamamoto, T. Moritaka, T. Maruyama, K. Kubota, M. Katada, *Macromolecules* **1997**, *30*, 5390. – [13h] R. Bayer, T. Pöhlmann, O. Nuyken, *Makromol. Chem. Rapid Commun*. **1993**, *14*, 359. – [13i] M. R. Buchmeiser, N. Schuler, G. Kaltenhauser, K. H. Ongania, I. Lagoja, K. Wurst, H. Schottenberger, *Macromolecules* **1998**, *31*, 3175. – [13k] M. A. Buretea, T. D. Tilley, *Organometallics* **1997**, *16*, 1507.
[14] R. W. Heo, F. B. Somoza, T. R. Lee, *J. Am. Chem. Soc*. **1998**, *120*, 1621.
[15] It should be mentioned that bridges between ferrocenes which consist of main-group elements such as Si, Sn or S transmit electronic effects at least as efficiently as a C=C or C≡C bridge over short distances: D. L. Zeckel, D. A. Foucher, J. K. Pudelksi, G. P. A. Yap, A. L. Rheingold, I. Manners, *J. Chem. Soc., Dalton Trans.* **1995**, 1893; D. L. Compton, T. B. Rauchfuss, *Organometallics* **1994**, *13*, 4367. However, an interaction mediated by $SiMe_2$ units falls off much more rapidly than in the unsaturated carbon bridges upon increasing the chain length: V. V. Dementev, F. Cervanteslee, L. Parkanyi, H. Sharma, K. H. Pannell, M. T. Nguyen, A. Diaz, *Organometallics* **1993**, *12*, 1983.
[16] R. Deschenaux, I. Kosztics, J.-L. Marendaz, H. Stoeckli-Evans, *Chimia* **1993**, *47*, 206.
[17] [17a] S. Setayesh, U. H. F. Bunz, *Organometallics* **1995**, *15*, 5470. – [17b] F. Rebière, O. Riaut, L. Ricard, H. B. Kagan, *Angew. Chem.* **1993**, *105*, 644; *Angew. Chem. Int. Ed.* **1993**, *32*, 568.
[18] V. Sniekus, *Chem. Rev.* **1990**, *90*, 879.
[19] D. Lednicer, C. R. Hauser, *Org. Synth.* **1960**, *40*, 31.
[20] P. D. Beer, *Adv. Inorg. Chem*. **1992**, *39*, 79.
[21] D. W. Slocum, B. W. Rockett, C. R. Hauser, *J. Am. Chem. Soc.* **1965**, *87*, 1241.
[22] I. B. Champbell in *Organocopper Reagents, A Practical Approach* (Ed.: R. J. K. Taylor), Oxford University Press, Oxford, **1994**.
[23] F. Diederich, P. J. Stang, *Metal-catalyzed Cross-coupling Reactions*, Wiley-VCH, Weinheim, **1998**.
[24] M. C. B. Colbert, J. Lewis, N. J. Long, P. R. Raithby, D. A. Bloor, G. H. Cross, *J. Organomet. Chem*. **1997**, *531*, 183.
[25] S. Kozhushkov, T. Haumann, R. Boese, B. Knieriem, S. Scheib, P. Bäuerle, A. deMeijere, *Angew. Chem*. **1995**, *107*, 781; *Angew. Chem. Int. Ed. Engl.* **1995**, *34*, 781.
[26] H. K. Youssoufi, M. Hmyene, F. Garnier, D. Delabuoglise, *J. Chem. Soc., Chem. Commun*. **1993**, 1550.
[27] T. M. Swager, *Acc. Chem. Res.* **1998**, *31*, 201.
[28] The easy availibility of the closely related chiral $FcCH(Me)NMe_2$ also allows the enantioselective synthesis of planar chiral 1,2,3-substituted ferrocenes: R. Diodone, J. Hermann, H. Plenio, unpublished results.
[29] J. M. Tour, *Chem. Rev.* **1996**, *96*, 537.
[30] J. Zhang, D. J. Pesak, J. L. Ludwick, J. S. Moore, *J. Am. Chem. Soc*. **1994**, *116*, 4227.
[31] T. H. Barr, W. E. Watts, *J. Organomet. Chem*. **1968**, *15*, 177.
[32] B. Floris, P. Tagliatesta, *J. Chem. Res. (S)* **1993**, 42.
[33] M. Spescha, N. W. Duffy, B. H. Robinson, J. Simpson, *Organometallics* **1994**, *13*, 4895.
[34] T. Mangel, A. Eberhardt, U. Scherf, U. H. F. Bunz, K. Müllen, *Macromol. Rap. Commun*. **1995**, 571.

[I98242]

Novel Tetraphosphabarrelene and -semibullvalene Derivatives by Reactions of 2,4,6-Tri-*tert*-butyl-1,3,5-triphosphabenzene with Phosphaalkynes☆

Paul Binger*[a][+], Stefanie Stutzmann[a], Joachim Bruckmann[a], Carl Krüger[a], Joseph Grobe*[b], Duc Le Van[b], and Torsten Pohlmeyer[b]

Max-Planck-Institut für Kohlenforschung[a],
Kaiser-Wilhelm-Platz 1, D-45470 Mühlheim a. d. Ruhr, Germany

Anorganisch-Chemisches Institut der Universität Münster[b],
Wilhelm-Klemm-Straße 8, D-48149 Münster, Germany
Fax: (internat.) + 49(0)251/83-36098

Received July 30, 1998

Keywords: Phosphorus heterocycles / Phosphaalkynes / Triphosphabenzene / Tetraphosphabarrelenes / Tetraphosphasemibullvalene

2,4,6-Tri-*tert*-butyl-1,3,5-triphosphabenzene **4** reacts with phosphaalkynes P≡C−R [R = *t*Bu (**5a**), *t*Pen (**5b**)] at room temperature in a formal [4 + 2] cycloaddition to yield the corresponding 1,3,5,7-tetraphosphabarrelene derivatives **8a** and **8b**, respectively. The analogous reaction of **4** with the aminophosphaethyne P≡C−N(*i*Pr)$_2$ (**9**) unexpectedly leads to the 1,3,4,7-tetraphosphasemibullvalene derivative **10** as the only product. The single-crystal X-ray analysis of **10** exhibits a diphosphirane unit with a very long PP distance of 2.274(1) Å together with a large extension of the PCP angle in the three-membered ring to 75.3(1)°.

Whereas the λ^3-phosphinine (phosphabenzene) **1**[1] as well as a great number of its functional derivatives[2] have been thoroughly investigated, only little information is published on "all-λ^3" di- or triphosphinines. So far the 1,4-diphosphabenzene derivative **2** was only detected in solution, but its NMR data are not complete.[3] As first representatives of the 1λ^3,3λ^3-diphosphinines[4] and 1λ^3, 3λ^3,5λ^3-triphosphinines[5] compounds **3** and **4**, respectively, have been isolated in pure form by using transition metal complex templates for the cyclotrimerization of *tert*-butylphosphaethyne **5a**, followed by oxidative replacement, and characterized.

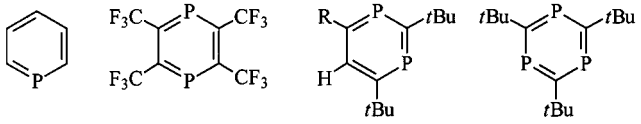

1 **2** **3** **4**

The preparation of **4** was accomplished by oxidative cleavage of the hafnium complex [(COT)Hf(*t*BuCP)$_3$] (**6**) with the useful reagent hexachloroethane. Template **6** was also used for the preparation of the η^4-1,3,5,7-tetraphosphabarrelene complex **7** by reaction with *t*BuC≡P (**5a**) (Scheme 1). Cleavage of **7** with C_2Cl_6 yields the 1,3,5,7-tetraphosphabarrelene derivative **8a**, which had been isolated before from the reaction of bis(cyclooctatetraene)zirconium with **5a**.[6] It is of particular interest that the valence isomers of **4**, 1,3,5- and 1,2,4-triphospha-Dewar-benzene[5][7] can be prepared selectively by the same synthetic procedure on use of modified cyclooctatetraene ligands for production of precursor analogues of **6**, and by variation of the reaction temperatures. In addition, Binger et al.[8] reported recently on homo-Diels−Alder reactions of 2,4,6-tri-*tert*-butyl-1,3,5-triphospha-Dewar-benzene.

Scheme 1

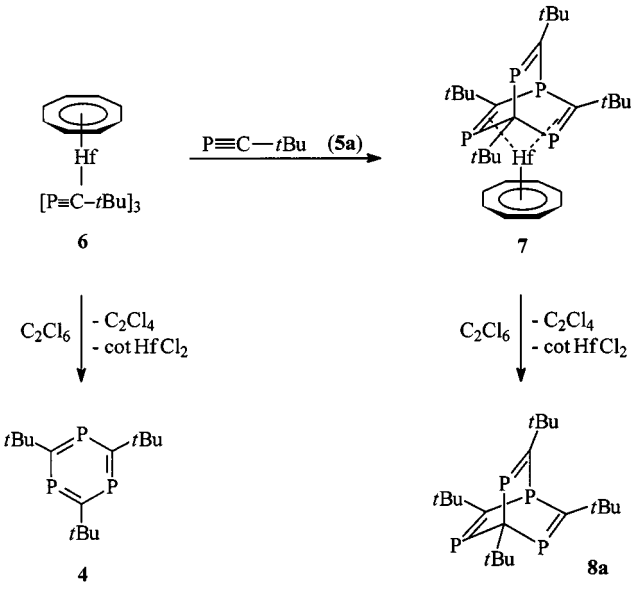

In 1998 Regitz et al.[9] presented a new effective method for the synthesis of **4** and other alkyl-substituted analogues, based on the use of the strong Lewis acid *t*BuN=VCl$_3$ as

[+] Present address: Fachbereich Chemie der Universität Kaiserslautern, Erwin-Schrödinger-Straße, D-67663 Kaiserslautern, Germany; Fax: (internat.) +49 (0)631/ 205-3921.

 © WILEY-VCH Verlag GmbH, D-69451 Weinheim, 1998 1434−1948/98/1212−2071 $ 17.50+.50/0

cyclotrimerization agent. The availability of **4** by the procedures mentioned above allowed reactivity studies of the 6π-heteroarene, in particular with respect to cycloaddition reactions.

For instance, the tetraphosphabarrelenes **8a** or **8b** (Scheme 2) are formed nearly quantitatively within 12 h by treating a pentane solution of **4** with the phosphaethynes **5a** and **5b**, respectively. This result demonstrates that the addition of a further phosphaalkyne molecule is possible even without coordination of a cyclotrimer of **5** to a complex fragment. Of particular interest is the possibility to prepare unsymmetrically substituted tetraphosphabarrelenes like **8b**. The reactions proceed under mild conditions indicating an astonishing reactivity of **4** against dienophiles. So far, similar reactions of phosphinines or their *P*-coordinated tungsten complexes with *t*BuC≡P (**5a**) have not been observed.[10] However, phosphinines undergo [4 + 2] cycloadditions with electron-deficient olefins under forced conditions. These reactions can be enhanced by σ-complex formation with $[(CO)_5W(THF)]$.[2b] The reactivity of phosphaarenes is also considerably increased if they contain an additional N or P atom in the 6π-system as in case of the 1,3-azaphosphinines published by Märkl et al.[11][12] or of the 1,4-diphosphinine **2**[3b], though fairly extreme conditions (100−120°C, high pressure vessel) are necessary for reactions with alkynes[3b][12] or **5a**.[11]

Scheme 2

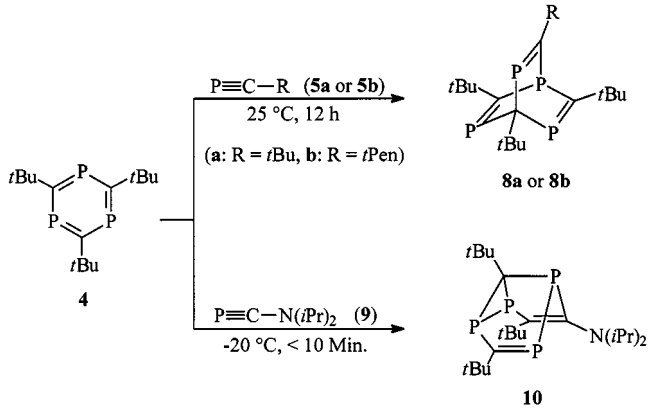

The analogous reaction of **4** with di(isopropylamino)-phosphaethyne **9** leads to a really unexpected result: According to a ^{31}P-NMR control experiment the starting compounds already react at −20°C quantitatively within a few minutes to give the tetraphosphasemibullvalene derivative **10**. The unsymmetrical molecular structure of **10** is proven by three different ^{1}H-NMR signals for the *t*Bu groups as well as by four separate ^{31}P resonances of equal intensities. Only one of them is found at chemical shifts typical for phosphaalkene fragments (δ_P = 347.5). Chemical shifts and coupling constants of all ^{31}P signals are in good accordance with those of the tetra-*tert*-butyltetraphosphasemibullvalene reported by Regitz et al.[13]. The same is true for the ^{13}C-NMR data of both compounds. Fluxional behaviour as observed for the corresponding hydrocarbon derivatives (Cope rearrangement) was not detected for **10** at room temperature. Measurements at higher temperatures failed because **10** already decomposes at 20°C even in inert solvents.

The molecular structure of **10** was deduced from a single-crystal X-ray analysis and supports the conclusions drawn from the NMR spectroscopic investigations. Figure 1 shows one of the enantiomers observed in the crystal lattice.

Figure 1. Molecular structure of **10** in the crystal; the hydrogen atoms are omitted for clarity[a]

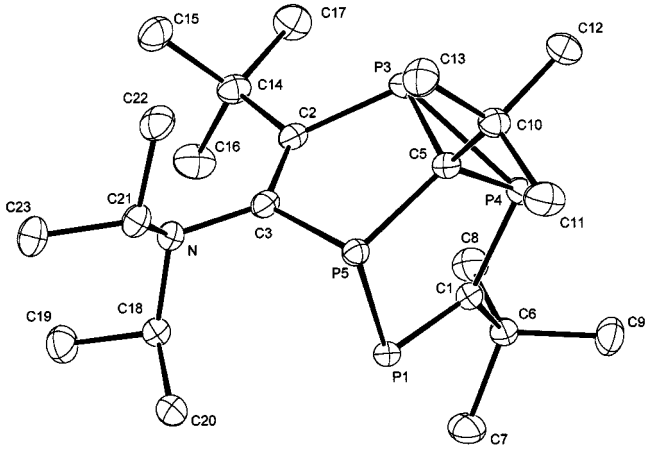

[a] Selected bond lengths [Å] and angles [°]: P1−P5 2.207(1), P3−P4 2.274(1), P3−C5 1.858(2), P4−C5 1.865(2), P5−C5 1.856(2), P1−C1 1.693(2), P3−C2 1.809(2), P4−C1 1.796(2), P5−C3 1.874(2), C2−C3 1.366(2), N−C3 1.450(2), N−C18 1.506(2), N−C21 1.494(2); C1−P1−C5 100.4(1), C5−P3−P4 52.5(1), C2−P3−P4 111.8(1), C5−P3−C2 99.4(1), C5−P4−C1 101.5(1), C1−P4−P3 107.1(1), C5−P4−P3 52.2(1), C5−P5−P1 99.7(1), C5−P5−C3 97.3(1), C3−P5−P1 87.7(1), C3−C2−P3 116.6(1), C2−C3−P5 116.2(1), P4−C5−P3 75.3(1), P5−C5−P3 109.2(1), P5−C5−P4 115.1(1).

As to be expected, the P−(sp^2)C single bonds in the tricyclic phosphorus/carbon skeleton of **10** are significantly shorter (P3−C2: 1.809, P4−C1: 1.796 Å) than P−(sp^3)C distances (1.856 to 1.874 Å). The P1−C1 bond length of 1.693 Å is very close to the average value (1.67 Å) of localized P=C double bonds.[14] The distance P3−P4 amounts to 2.274 Å and, so far, represents the longest PP bond in diphosphirane derivatives.[9][13][15][16] Consequently the angle P3−C5−P4 within the three-membered ring is opened to 75.3°.

The formation of **10** from **4** and **9** is not directly evident, although **9**, due to its electronic structure[17], often shows a different behaviour to alkyl-substituted phosphaalkynes, especially in cycloaddition reactions.[18] Assuming that the π-donor interaction of the R_2N substituent enhances the nucleophilicity of the *P*-atom, an attack of **9** at one of the ring carbon atoms seems reasonable as the first reaction step followed by a ring closure to the tricyclic intermediate **12**. The stable end product is reached by a further nucleophilic attack of the aminophosphaalkene *P*-atom and by valence isomerization. The competitive intramolecular [2 + 2] cycloaddition with formation of the pentacyclic compound **13** is less probable for two reasons:

(i) Aminophosphaalkenes are not suited for cycloaddition reactions due to the loss of olefinic character,

(ii) high-level ab initio calculations[19] on different $(HCP)_4$ isomers favour the semibullvalene system over the cuneane structure.

Scheme 3

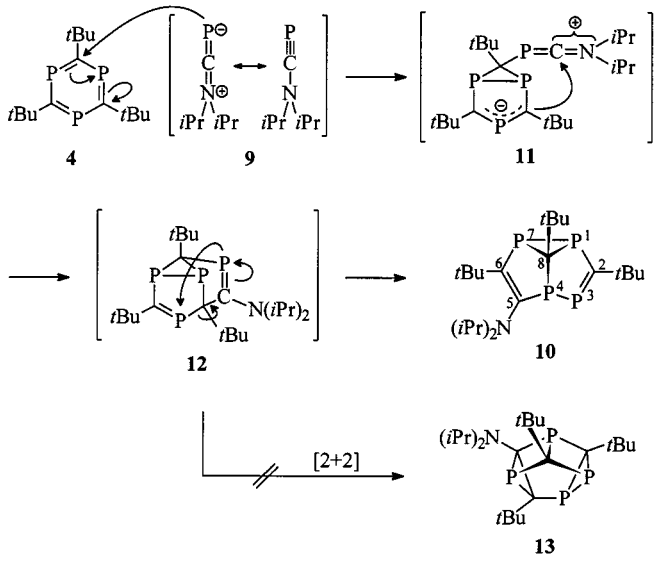

In conclusion, the work presented in this paper has led to a selective synthesis of the tetraphosphabarrelene derivatives **8a** and **8b** from the 1,3,5-triphosphabenzene **4** and to a surprising reaction of **4** with **9** affording the novel tetraphosphasemibullvalene derivative **10**, thus enlarging our knowledge about cyclotetramers of phosphaalkynes[20] and clearly demonstrating the important influence of *C*-amino groups on the reactivity of P≡C systems.

This work was supported by the *Deutsche Forschungsgemeinschaft* (Graduiertenkolleg "Phosphor als Bindeglied verschiedener chemischer Disziplinen", Universität Kaiserslautern; and Graduiertenkolleg "Hochreaktive Mehrfachbindungssysteme", Universität Münster) and by the *Fonds der Chemischen Industrie*.

Experimental Section

All experiments were carried out under argon (or by using a standard vacuum line) in anhydrous solvents. Reaction vessels were either Schlenk flasks or ampoules with several break seals and an NMR tube. $-^1$H and ^{13}C NMR: Bruker AC 200, AC 300, and AMX 400; chemical shifts relative to the solvent signals, calibrated to TMS. $-^{31}$P NMR: Bruker AC 200, AC 300, external standard H_3PO_4. 2,4,6-Tri-*tert*-butyl-1,3,5-triphosphabenzene **4**[5][9] and the Phosphaalkynes *t*BuC≡P (**5a**)[21a], *t*PenC≡P (**5b**)[21b], $(i\text{Pr})_2$NC≡P (**9**)[22] were prepared according to the literature.

Standard Procedure for the Preparation of the Tetraphosphabarrelenes **8a**, **8b**: A pentane solution (2 ml) of the phosphaalkyne **5a** (80 mg, 0.8 mmol) or **5b** (100 mg, 0.9 mmol) was added at room temperature to a pentane solution (3 ml) of the triphosphabenzene derivative **4** (200 mg, 0.67 mmol). The mixture was stirred for 12 h, and volatile components were removed in vacuo. The residue was taken up in pentane and filtered through a layer of silica gel. After evaporation of the solvent in vacuo the tetraphosphabarrelene **8a** and **8b**, respectively, was obtained as a yellow powder (**8a**: 260 mg, 0.65 mmol, 98% yield; **8b**: 265 mg, 0.64 mmol, 96% yield).

2,4,6,7-Tetra-tert-butyl-1,3,5,8-tetraphosphabicyclo[2.2.2]octa-2,5,7-triene (**8a**) was characterized by comparison of the NMR data with those of an authentic sample.[6]

[4,6,7-Tri-tert-butyl-2-tert-pentyl]-1,3,5,8-tetraphosphabicyclo-[2.2.2]octa-2,5,7-triene (**8b**): $-^1$H NMR (C_6D_6, 200.1 MHz, 25°C): δ = 0.70 (q, *J* = 7.4 Hz, 2 H, CH_2CH_3), 1.39 (3 H, CH_2CH_3), 1.43 [s, br., 15 H, $C(CH_3)_3$ and $C(CH_3)_2CH_2$], 1.77 [s, br., 18 H, $C(CH_3)_3$]. $-^{13}$C {^{1}H} NMR (C_6D_6, 50.3 MHz, 25°C): δ = 28.3 [m, CH_3CH_2 and $(CH_3)_2C$], 30.5 [m, $(CH_3)_3C$], 30.7 [m, ^3J(P,C) = 0.3 and 14.9 Hz, $(CH_3)_3C$], 33.4 [t, ^3J(P,C) = 9.5 Hz, CH_3CH_2], 35.8 [q, ^2J(P,C) = 16.1 Hz, $C(CH_3)_3$], 41.6 [m, $C(CH_3)_3$], 44.8 [dd, ^2J(P,C) = 19.1 and 25.4 Hz, $C-CH_2CH_3$], 101.1 [m, C-4], 225.4 [m, C-2], 227.3 [m, C-6, C-7]. $-^{31}$P{^{1}H} NMR (C_6D_6, 81.0. MHz, 25°C): δ = -92.0 [q, ^2J(P,P) = 12.6 Hz, *P*−C=P], 320.7 [t, ^2J(P,P) = 12.6 Hz, P=C−$C(CH_3)_3$], 324.8 [q, ^2J(P,P) = 12.6 Hz, P=C−$C(CH_3)_2C_2H_5$]. −MS (EI, 70 eV); *m/z* (%): 414 (68) [M^+], 314 (9) [$M^+ - PC_5H_9$], 300 (3) [$M^+ - PC_6H_{11}$], 276 (74) [$M^+ - 2\,C_5H_9$], 262 (100) [$M^+ - C_5H_9 - C_6H_{11}$], 200 (22) [$M^+ - PC_5H_9 - PC_6H_{11}$].

*2,6,8-Tri-tert-butyl-5-diisopropylamino-1,3,4,7-tetraphosphatricyclo[5.1.0.0 4,8]*octa-2,5-diene (**10**): 80 mg (0.27 mmol) of the triphosphabenzene derivative **4** were placed in an ampoule with break seals and an NMR tube together with 0.5 ml [D_8]toluene. 45 mg (0.31 mmol) of di(isopropyl)aminophosphaethyne **9** were then introduced by vacuum condensation at −196°C. During warm−up to −20°C the mixture was continuously stirred and afterwards tranfused in the NMR tube. Measurements at −30°C indicated a complete reaction of the triphosphabenzene **4** and the quantitative formation of the tetraphosphasemibullvalene derivative **10**. Orange crystals of **10** were obtained on cooling the [D_8]toluene solution at −78°C. Their quality was sufficient for a single-crystal X-ray structure analysis. $-^1$H NMR (C_7D_8, 400.1 MHz, −30°C): δ = 0.90 [s, 9 H, $C(CH_3)_3$)], 1.21 [d, *J* = 6.5 Hz, 6 H, $CH(CH_3)_2$], 1.28 [d, *J* = 6.5 Hz, 6 H, $CH(CH_3)_2$], 1.38 [s, 9 H, $C(CH_3)_3$], 1.48 [s, 9 H, $C(CH_3)_3$], 3.38 [sept, *J* = 6.5 Hz, 2 H, $CH(CH_3)_2$]. $-^{13}$C {^{1}H} NMR (C_7D_8, 75.5 MHz, −35°C): δ = 24.8 [s, $CH(CH_3)_2$], 29.6 [s, br., $C(CH_3)_3$ at C-8], 32.3 [d, ^3J(P-6,C) = 11.3 Hz, $C(CH_3)_3$ at C-6], 34.3 [dd, ^3J(P-3,C) = ^3J(P-1,C) = 7.6 Hz, $C(CH_3)_3$ at C-2], 34.9 [q, ^2J(P-1,C) = ^2J(P-4,C) = ^2J(P-7,C) = 11.7 Hz, $C(CH_3)_3$ at C-8], 37.3 [d, ^2J(P-7,C) = 25.2 Hz, $C(CH_3)_3$ at C-6], 42.2 [dd, ^2J(P-3,C) = 22.6, ^2J(P-1,C) = 13.6 Hz, $C(CH_3)_3$ at C-2], 55.6 [s, br., $CH(CH_3)_2$], 63.0 (m, C-8), 156.1 [dm, ^1J(P-7,C) = 65.5 Hz, C-6], 177.7 [d, ^1J(P-4,C) = 39.9 Hz, C-5], 211.8 [t, ^1J(P-3,C) = ^1J(P-1,C) = 83.0 Hz, C-2] (for numbering see Scheme 3). $-^{31}$P{^{1}H} NMR (C_7D_8, 121.5. MHz, −35°C): δ = −92.1 [dd, ^1J(P-1,P-7) = 174.6, ^2J(P-4,P-7) = 16.4 Hz, P-7], −19.6 [ddd, ^1J(P-1,P-7) = 174.6, ^2J(P-1,P-3) = ^3J(P-1,P-4) = 23.5 Hz, P-1], 88.7 [ddd, ^1J(P-3,P-4) = 270.0, ^2J(P-1,P-4) = 23.5, ^2J(P-4,P-7) = 16.4 Hz, P-4], 347.5 [dd, ^1J(P-3,P-4) = 270.0, ^2J(P-1,P-3) = 23.5 Hz, P-3] (for numbering see Scheme 3).

Crystal Structure Analysis of **10**[23]: Enraf-Nonius-CAD4 Diffractometer (Mo-K_α radiation), *T* = 100 K; structure solution by heavy-atom method (SHELXS-86[24]) and structure refinement by SHELXL-93[25]; monoclinic, space group $P2_1/c$; lattice constants *a* = 10.0494(10), *b* = 20.4954(10), *c* = 12.3895(10) Å, β = 99.983(10)°; *V* = 2513.2(3) Å^3; *Z* = 4; μ(Mo-K_α) = 0.308 mm^{-1}, crystal size 0.42 × 0.39 × 0.35 mm; 9113 independent reflections (R_{int} = 0.0648) 28745 measured of which 6630 were considered observed with $I > 2\sigma(I)$; residual electronic density 0.481 and −0.357 e/Å^3. 408 parameters (C, N, and P anisotropic, the positions of the H-Atoms were found and refined isotropically); R_1 = 0.0441; wR^2 = 0.1180.

☆ Dedicated to Professor *Bernt Krebs* on the occasion of his 60th birthday.

[1] A. J. Ashe III, *J. Am. Chem. Soc*. **1971**, *93*, 3293−3295.

[2] [2a] G. Märkl in *Multiple Bonds and Low Coordination in Phosphorus Chemistry* (Eds.: M. Regitz, O. J. Scherer), Thieme Verlag, **1990**, p. 220−257. − [2b] H. Trauner, P. Le Floch, J.-M. Lefour, L. Ricard, F. Mathey, *Synthesis*, **1995**, 717−726.

[3] [3a] Y. Kobayashi, J. Kumadaki, A. Ohsawa, H. Hamada, *Tetrahedron Lett*. **1976**, 3715−3716; *Tetrahedron Lett*. **1977**, 867−868. − [3b] Y. Kobayashi, H. Hamada, S. Fujino, A. Ohsawa, J. Kumadaki, *J. Am. Chem. Soc*. **1980**, *102*, 252−255.

[4] D. Böhm, F. Knoch, S. Kummer, U. Schmidt, U. Zenneck, *Angew. Chem*. **1995**, *107*, 251−254; *Angew. Chem. Int. Ed. Engl*. **1995**, *34*, 198−201.

[5] P. Binger, S. Leininger, J. Stannek, B. Gabor, R. Mynott, J. Bruckmann, C. Krüger, *Angew. Chem*. **1995**, *107*, 2411−2414; *Angew. Chem. Int. Ed. Engl*. **1995**, *34*, 2227−2230.

[6] P. Binger, G. Glaser, B. Gabor, R. Mynott, *Angew. Chem*. **1995**, *107*, 114−116; *Angew. Chem. Int. Ed. Engl*. **1995**, *34*, 81−83.

[7] P. Binger, S. Leininger, K. Günther, U. Bergsträßer, *Chem. Ber./Recueil* **1997**, *130*, 1491−1494.

[8] P. Binger, S. Leininger, M. Regitz, U. Bergsträßer, J. Bruckmann, C. Krüger, *J. Organomet. Chem*. **1997**, *529*, 215−221.

[9] F. Tabellion, A. Nachbauer, S. Leininger, C. Peters, M. Regitz, F. Preuss, *Angew. Chem*. **1998**, *110*, 1318−1321; *Angew. Chem. Int. Ed. Engl*. **1998**, *37*, 1233−1235.

[10] E. Wellner, Diplomarbeit, Universität Kaiserslautern **1996.**

[11] G. Märkl, S. Dietl, M. L. Ziegler, B. Nuber, *Angew. Chem*. **1988**, *100*, 426−428; *Angew. Chem. Int. Ed. Engl*. **1988**, *27*, 389−390.

[12] [12a] G. Märkl, G. Dorfmeister, *Tetrahedron Lett*. **1987**, *28*, 1093−1096. − [12b] For the [4 + 2] cycloaddition reactions of 2,6-diaza-1-phosphinines and 1,2-azaphosphinines with alkynes, see: N. Avarvari, P. Le Floch, F. Mathey, *J. Am. Chem. Soc*. **1996**, *108*, 11978−11979.

[13] A. Mack, B. Breit, T. Wettling, U. Bergsträßer, S. Leininger, M. Regitz; *Angew. Chem*. **1997**, *109*, 1396−1398; *Angew. Chem. Int. Ed. Engl*. **1997**, *36*, 1337−1340.

[14] R. Appel in *Multiple Bonds and Low Coordination in Phosphorus Chemistry* (Eds.: M. Regitz, O. J. Scherer), Thieme Verlag, **1990**, p. 157−214.

[15] [15a] F. Mathey, *Chem. Rev*. **1990**, *90*, 997-1025. − [15b] B. Breit, U. Bergsträßer, G. Maas, M. Regitz, *Angew. Chem*. **1992**, *104*, 1043−1046; *Angew. Chem. Int. Ed. Engl*. **1992**, *31*, 1055−1058. − [15c] M. Julino, M. Slany, U. Bergsträßer, F. Mercier, F. Mathey, M. Regitz, *Chem. Ber*. **1995**, *128*, 991−997.

[16] J. Grobe, D. Le Van, F. Immel, B. Krebs, M. Läge; *Chem. Ber*. **1996**, *129*, 1271−1274.

[17] [17a] G. Becker, M. Böhringer, R. Gleiter, H.-H. Pfeifer, J. Grobe, D. Le Van, M. Hegemann, *Chem. Ber*. **1994**, *127*, 1041−1045. − [17b] J. Grobe, D. Le Van, M. Hegemann, B. Krebs, M. Läge, *Heteroat. Chem*. **1994**, *5*, 337−341.

[18] [18a] J. Grobe, D. Le Van, B. Broschk, L. S. Kobrina, *Tetrahedron Lett*. **1993**, *34*, 4619−4622. − [18b] H. Pucknat, J. Grobe, D. Le Van, B. Broschk, M. Hegemann, B. Krebs, M. Läge, *Chem. Eur. J*. **1996**, *2*, 208−213. − [18c] J. Grobe, D. Le Van, B. Broschk, M. Hegemann, B. Lüth, G. Becker, M. Böhringer, E.-U. Würthwein, *J. Organomet. Chem*. **1997**, *529*, 177−187.

[19] [19a] B. Geißler, S. Barth, U. Bergsträßer, M. Slany, J. Durkin, P. B. Hitchcock, M. Hofmann, P. Binger, J. F. Nixon, P. von Ragué Schleyer, M. Regitz, *Angew. Chem*. **1995**, *107*, 485−488; *Angew. Chem. Int. Ed. Engl*. **1995**, *34*, 484−487. − [19b] M. Hofmann, Dr. rer. nat. Thesis, Universität Erlangen-Nürnberg, **1996**.

[20] [20a] A. Mack, M. Regitz, *Chem. Ber./Recueil* **1997**, *130*, 823−834. − [20b] R. Streubel, *Angew. Chem*. **1995**, *107*, 478−480; *Angew. Chem. Int. Ed. Engl*. **1995**, *34*, 436−438.

[21] [21a] G. Becker, G. Gresser, W. Uhl, *Z. Naturforsch., Teil B*, **1981**, *36*, 16−19. − [21b] T. Allspach, M. Regitz, G. Becker, W. Becker, *Synthesis* **1986**, 31−36.

[22] J. Grobe, D. Le Van, B. Lüth, M. Hegemann, *Chem. Ber*. **1990**, *123*, 2317−2320.

[23] Crystallographic data (excluding structure factors) for the structure reported in this paper have been deposited with the Cambridge Crystallographic Data Centre as supplementary publication no. CCDC-102329. Copies of the data can be obtained free of charge on application to The Director, CCDC, 12 Union Road, Cambridge CB2 1EZ, UK [fax: int. code + 44-1223/ 336-033, E-mail: deposit@chemcrys.cam.ac.uk].

[24] G. M. Sheldrick, *SHELXS-86. Program for Crystal Structure Solution*, Universität Göttingen, **1986**.

[25] G. M. Sheldrick, *SHELXL-93. Program for Crystal Structure Refinement*, Universität Göttingen, **1993**.

[I98252]

Lipophilically Wrapped Polyion Aggregates, 130[◇]

Tetralithium Bis(ethylaluminum) Tetrakis(catecholate) Pentakis(dimethoxyethane): An Oxygen-Rich Cluster $[(Al^{++}{}_2(Li^+)_4(O_{18})^{-8}]$ in a $C_{36}H_{44}$ Hydrocarbon Shell

Hans Bock*[a], Reinhard Beck[a], Zdenek Havlas[b], and Holger Schödel[a]

Institute of Inorganic Chemistry, University of Frankfurt[a],
Marie-Curie-Straße 11, D-60439 Frankfurt/Main, Germany

Institute of Organic Chemistry and Biochemistry, Czech Academy of Sciences[b],
Flemingovo Namestí 2, CZ-16610 Prague, Czech Republic

Received October 16, 1997

Keywords: Polyion aggregates / Crystal structure / Density functional theory calculations

The structure determination of the lipophilically wrapped cluster $\{[Al_2Li_4O_{18}](C_{36}H_{44})\}_\infty$, a novel material crystallized from a mixture of $[(C_2H_5)_3Al]_2$, *n*BuLi, and catechol in DME solution, reveals five-coordinate Al^{++} and Li^+ centers. According to density functional theory calculations, the eight negative charges are well-delocalized over the oxygen-rich framework.

Recent Results on Main-Group Ion Clusters

Lipophilically wrapped polyion aggregates, in which a cluster ion nucleus guarantees thermodynamic stability, and where a surrounding hydrocarbon skin offers both kinetic shielding as well as solubility in non-polar solvents, are representative of a rather favourable self-organization principle,[2][3][4][5][6][7][8] for main-group element compounds (Table 1).

Table 1. Examples of novel lipophilically wrapped main-group element clusters with space-filling structure representation and specification of their components

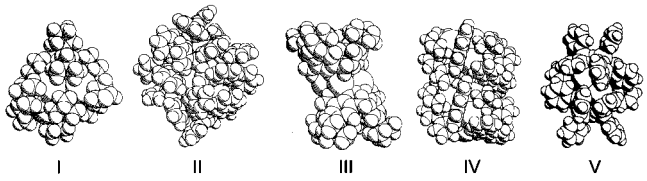

I II III IV V

Component	[Lit.]	Cluster	Structure	Lipophilic Skin
I. $[Ba]_x + (H_3C)_3COH$	[4]	$[Ba_6Li_2O_2]^{\oplus 11}$	Octahedron + Prismane	$(^{\ominus}OC(CH_3)_{11})$
II. $Na^{\oplus}(RO)_2P\text{-}N\text{-}P(OR)_2$	[5]	$[Na(OPNPO)]_6$	Ellipsoid	$(C_{144}H_{120}O_{24})$
III. $LiNH_2$ + Calix[4]aren	[6]	$[Li_6(NH_3)_2O_6]$	Double tetrahedron	$(C_{88}H_{110}O_2)$
IV. $K^{\oplus}$(aci-nitrofluorene)	[7]	$[K_6O_{12}]$	Octahedron	$(C_{102}H_{80}N_6)$
V. Silanoles + {LiR, $[Na]_x$, KH}	[8]	$[Li_4O_4]$, $[Na_4O_4]$, $[K_4O_4]$	Cubes	$(C_{96}H_{84}O_{10}Si_8)$, $(C_{96}H_{84}O_6Si_8)$, $(C_{72}H_{60}Si_4)$

Density functional calculations[4] based on structural data confirm the ionic compositions of the aggregates (e.g.[4] Ba^{++}, Li^+, and O^{--}) and their considerable cluster stability (e.g.[5] $\Delta H_f > 5000$ kJ mol^{-1}). In contrast, the energy contributions of the hydrocarbon shells, as estimated from a statistical evaluation of phenyl ring centroid interactions, are only small (e.g.[5] $\Delta H_f \approx 50$ kJ mol^{-1}).

Based on the general principles outlined above, numerous and multifaceted supramolecular compounds can be anticipated.[9] In view of the considerable bond enthalpy difference, $\Delta H_b(Al-C) - \Delta H_b(Al-O) = (274 - 500) = -226$ kJ mol^{-1},[9] alumoxane clusters are expected to be especially favorable candidates.

Preparation and Structure Determination

A mixture of flammable triethylaluminum dimer and a stoichiometric amount of *n*-butyllithium[4] reacts vigorously with catechol in aprotic dimethoxyethane (DME) solution under argon (1) (see Experimental Section).

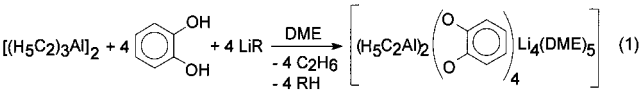

(1)

A crystalline reaction product can be isolated, provided that exposure to air and/or moisture is carefully avoided. Its structure determination (Figure 1), performed on a sample cooled to 150 K in a flow of nitrogen (see Experimental Section), reveals the formation of $\{[(DME_{1.5}Li^+)\text{-}(H_5C_2Al^{++--}O_2C_6H_4)_2^{--}(Li^+DME)]_2\}_\infty$ (DME = $H_3COCH_2CH_2OCH_3$). The product contains a total of 18 oxygen centers in its polymer chain and is thus the most oxygen-rich polyion aggregate isolated to date (Table 1).

[◇] Part 129: Ref.[1].

 © WILEY-VCH Verlag GmbH, D-69451 Weinheim, 1998 1434−1948/98/1212−2075 $ 17.50+.50/0

Figure 1. (A) Dimeric subunit of the lithium/aluminum organic polymer with thermal ellipsoids drawn at the 50% probability level and metal center notation; (B) to (D) Al^{++} and Li^{+} coordination spheres, and (E) space-filling side view

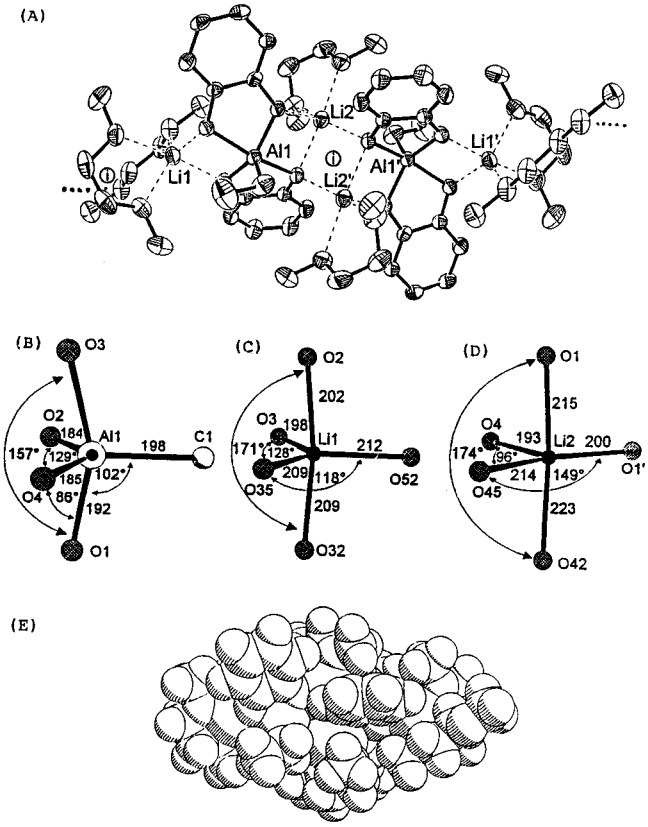

The crystal is seen to contain polymeric strands of dimethoxyethane-bridged subunits, the four-membered central (Li_2O_2) rings of which contain centers of inversion (Figure 1/A: ⓘ). The formally dipositive $(C_2H_5)Al^{++}$ center is fourfold coordinated to the four catecholate O^{-} centers and forms a distorted trigonal bipyramid with longer axial Al−O distances of 191 pm and the C center of lower effective nuclear charge in the expected equatorial position (Figure 1: B). The Li^{+} countercations are also fivefold coordinated: Li1 to two catecholate and three DME oxygen centers, and Li2 to three catecholate and two DME oxygen centers (Figure 1: C and D). Due to the four-membered (Li_2O_2) ring formation, the trigonal bipyramids around the symmetry-equivalent countercations Li2 and Li2′ are more strongly distorted with O−Li2−O angles of up to 149° (Figure 1: D). The space-filling representation (Figure 1: E) illustrates how the hydrocarbon ($C_{36}H_{44}$) shell shields the oxygen-rich $[(Al^{++})_2(Li^{+})_4(O_{18})^{-8}]$ cluster and renders it completely soluble in apolar solvents (see Experimental Section).

A search of the Cambridge Structural Database for cluster structures predominantly composed of Al, Li, and O atoms revealed only one monomer[10] bearing no relation to our polyion aggregate. In the meantime, we have been able to isolate crystals from an analogous mixture (1) with the parent molecule phenol.[11] According to their structure determination, these crystals contain a quadruple ion $\{[(H_5C_6O)_3(H_5C_2)Al]^{-}\cdots Li^{+}\cdots{}^{-}[Al(C_4H_9)(OC_6H_5)_3]\}^{-}[Li^{+}(DME)_3]^{+}$, consisting of a complex triple-ion anion and a DME solvent-separated countercation.[12] Despite the fact that this system is also wrapped by a hydrocarbon skin ($C_{40}H_{40}$), there is no real analogy with the catechol-substituted $[Al_mLi_nO_x]$ polyion aggregate presented (Figure 1), since Al−O−Li connections are in this case completely absent.

Density Functional Calculations

For the polyion aggregate, with its molecular size exceeding 100 atoms, density functional calculations at the B3LYP level using 6-31G* basis sets (see Experimental Section) have been performed, based on the determined structural coordinates (Figure 1). Despite some uncertainty concerning the polarity within the ($Li_4Al_2O_{18}$) cluster, the following calculated Mulliken-type charge distribution (2) will be discussed.

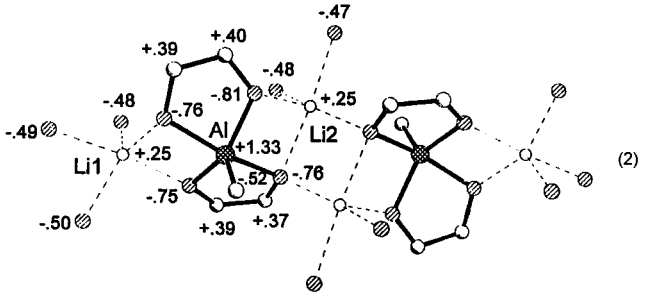

(2)

For the ethyl-substituted and four-fold catecholate oxygen-coordinated Al centers, Mulliken charge densities of +1.33 are calculated, indicating covalent contributions to the ionic interactions $Al^{++}\cdots{}^{-}O$ as well. Furthermore, the catecholate anion charges are partially delocalized towards the Li^{+} countercations, which are strongly solvated (Figure 1: C and D) by a total of six oxygen centers of three sterically unhindered dimethoxyethane chelate ligands. The total charges of the essential cluster components amount to approximately −1.0 for the catecholate ligands, −0.3 for the ethyl substituents, and about +0.2 for the DME solvent molecules. Considering the 18 differently charged oxygen centers, each transfers an average of about 0.7 of a negative charge to the six metal cations, decreasing the polyion aggregate character by metal−oxygen bonding contributions.

Conclusion and Perspectives

A vigorous reaction between triethylaluminum dimer, *n*-butyllithium, and catechol (1) yielded the title compound, which according to its structure determination is an unprecedented oxygen-rich polyion aggregate $[Li_4Al_2O_{18}]$ wrapped by a lipophilic hydrocarbon skin ($C_{36}H_{44}$). The predominantly ionic interactions assumed are supported by density functional calculations.

This result encourages us to attempt further crystallizations of main-group element clusters, of which only the sim-

plest examples are as yet known. It also suggests further exploration of (alkylaluminum + phenol) reaction mixtures, especially by those interested in novel ceramic materials, which are presumably accessible by firing hydrocarbon-wrapped clusters $[Li_nAl_mO_x]$.

The project "Interactions in Molecular Crystals" is supported by the *Hoechst Corporation*, the *Deutsche Forschungsgemeinschaft*, the *State of Hessen*, and the *Fonds der Chemischen Industrie.*

Experimental Section

Preparation and Crystallization: In a rigorously dried Schlenk trap, 352 mg (3.2 mmol) of catechol was dissolved in 40 ml of anhydrous dimethoxyethane (DME). At −70°C, 1.6 ml (1.6 mmol) of a 1 M solution of triethylaluminum dimer in *n*-hexane followed by 1.5 ml (2.4 mmol) of a 1.6 M solution of *n*-butyllithium in *n*-hexane were quickly injected under argon. The mixture was shaken repeatedly during warming to room temperature. The surface of the solution was then covered with a layer of *n*-hexane and crystallization began after about 2 h. After 1 d, large transparent prisms had grown.

Crystal Structure Determination: $C_{24}H_{38}AlLi_2O_9$ (511.4), colourless prisms, crystal dimensions: 0.82 × 0.48 × 0.46 mm, temperature 150 ± 2 K, a = 1863.6(1), b = 1486.6(1), c = 2080.6(2) pm, β = 1104.93(1)°, V = 5569.6(7) Å^3, Z = 8, $\rho_{calcd.}$ = 1.220 gcm^{-3}, μ(Mo-K_α) = 0.711 Å, monoclinic, space group $C2/c$ (No. 15), Siemens P4 four-circle diffractometer, 5598 measured reflections in the range $3° \leq 2\theta \leq 52°$, of which 5410 were independent and 4188 had $I > 2\sigma(I)$. Structure solution by direct methods (SHELXS), 331 parameters refined against F^2 (SHELXL-93), R = 0.041, wR_2 = 0.096, residual electron density +0.28/−0.26 eÅ^{-3}, S = 1.035. The positions of Li, C, O, and Al were refined anisotropically; H centers were ideally geometrically positioned and refined using fixed displacement parameters within a riding model. Atomic coordinates, bond lengths and angles, and thermal parameters have been deposited at the Cambridge Crystallographic Data Centre (CCDC). Any request to the CCDC for this material should quote the full literature citation and the reference number CCDC-103178.

Density functional calculations were performed using the Gaussian-94 program. For the 104 cluster atoms, a total of 2576 Gaussian functions within 6-31G* basis sets were applied. The NEC SX4 computer system at the high performance computing center, Stuttgart, Germany, required 14.8 h of CPU time to calculate the total energy as −4053, 414614 a.u.

[1] H. Bock, M. Sievert, Z. Havlas, *Chem. Eur. J.* **1984**, *4*, 677.
[2] J. M. Lehn, *Supramolekulare Chemie*, VCH Verlag, Weinheim, **1995**.
[3] See, for example: E. Weiss, *Angew. Chem*. **1993**, *105*, 1655; *Angew. Chem. Int. Ed. Engl*. **1993**, *32,* 1501.
[4] H. Bock, T. Hauck, C. Näther, N. Rösch, M. Staufer, O. D. Häberlein, *Angew. Chem*. **1995**, *107*, 1439; *Angew. Chem. Int. Ed. Engl*. **1995**, *34*, 1353.
[5] H. Bock, H. Schödel, Z. Havlas, E. Herrmann, *Angew. Chem*. **1995**, *107*, 1441; *Angew. Chem. Int. Ed. Engl*. **1995**, *34*, 1355.
[6] H. Bock, A. John, C. Näther, Z. Havlas, *J. Am. Chem. Soc*. **1995**, *117*, 9367.
[7] H. Bock, R. Dienelt, H. Schödel, Z. Havlas, *Tetrahedron Lett*. **1995**, *36*, 7855.
[8] H. Bock, M. Ansari, N. Nagel, Z. Havlas, unpublished results, see, e.g.: M. Ansari, Ph. D. Thesis, Univ. Frankfurt, **1998**.
[9] See, for example: C. Elschenbroich, A. Salzer, *Organometallchemie*, 3rd. ed., Teuber Verlag, Stuttgart, **1973**.
[10] M. Power, S. G. Bott, J. L. Atwood, A. R. Barron, *J. Am. Chem. Soc.* **1990**, *112*, 3446.
[11] H. Bock, R. Beck, H. Schödel, Z. Havlas, *Inorg. Chem*., in print.
[12] H. Bock, C. Näther, Z. Havlas, A. John, C. Arad, *Angew. Chem*. **1994**, *106*, 931; *Angew. Chem. Int. Ed. Engl*. **1994**, *33*, 875.

[I97235]

Linear Primary Polyamines as Building Blocks for Coordination Polymers, 1

Ligand Synthesis and Metal Complex Formation of 1,2,3-Triaminopropane

Anja Zimmer[a], Iris Müller[b], Guido J. Reiß[c], Andrea Caneschi[d], Dante Gatteschi[d], and Kaspar Hegetschweiler*[a]

Anorganische Chemie, Universität des Saarlandes, D-66041 Saarbrücken, Germany[a],
Fax: (internat.) + 49(0)681/302-2663
E-mail: hegetsch@rz.uni-sb.de

Analytische Chemie, Ruhr-Universität, Universitätsstr. 150, D-44780 Bochum, Germany[b],
Fax: (internat.) + 49(0)234/709-4420
E-mail: Iris@anachem.ruhr-uni-bochum.de

Fachbereich Chemie, Universität Kaiserslautern, Erwin-Schrödinger Straße, D-67663 Kaiserslautern, Germany[c],
Fax: (internat.) + 49(0)631/205-2187
E-mail: reiss@rhrk.uni-kl.de

Dipartimento di Chimica, Universita degli Studi di Firenze, Via Maragliano 75, I-50144 Firenze, Italy[d],
Fax: (internat.) + 39-0-55/354845
E-mail: gattesch@blu.chim1.unifi.it

Received July 17, 1998

Keywords: N Ligands / Copper / Coordination polymers / Stability constants / Solid-state structures

A series of linear primary polyamines $H_2N–CH_2–(CH–NH_2)_n–CH_2–NH_2$ ($1 \leq n \leq 3$) was prepared from the corresponding polyalcohols. The polyamines were isolated as HCl adducts and the acidity constants in aqueous solution were determined. The crystal structure of the fully protonated tetraamine ($n = 2$) was elucidated by an X-ray diffraction study. Complex formation of the triamine ($n = 1$) with Ni^{2+}, Cu^{2+}, Zn^{2+}, Cd^{2+} was re-investigated in aqueous solution. The pH-dependent formation of a variety of species $M_xL_yH_z$ was established by potentiometric titrations and was compared with previous reports. The crystal structure of the Cu complex $[CuL_2]Cl_2$ exhibited a chain structure with a five-coordinate Cu^{II} centre in which two amino groups of the triamine ligands are coordinated to one Cu centre, while the third amino group of one of the ligands is bonded to a neighbouring Cu atom. The compound shows weak antiferromagnetic coupling interactions between the Cu^{II} centres within the chain.

Introduction

Aggregation of metal complexes has turned out to be a powerful concept for the design and preparation of extended polymeric structures[1]. Such molecular arrays have been discussed in the context of crystal engineering and supramolecular chemistry[2]. Different types of interactions have been used to connect the monomeric precursors to the polymeric forms. Zaworotko and coworkers exploited hydrogen bonding for the synthesis of a variety of indefinite coordination polymers[3]. Interconnection of metal centres by bridging counterions is another well-known strategy for the generation of such polynuclear structures. Hydrolytic polymerisation (where the metal centres are connected by bridging OH^- or O^{2-} ligands) is a prominent representative in this type of interaction[4]. In addition, a variety of tailored chelating ligands has been developed, where the binding of more than one metal cation is promoted by the specific steric characteristics of the ligand[5]. A series of multidentate chelators, based on the bipyridyl entity, has been developed by Lehn and coworkers[6]. These ligands allowed the systematic design of one-dimensional chains and helices, two-dimensional grids, and three-dimensional networks. The coordination chemistry of poly(ethyleneimines) with transition metal cations in aqueous solution has been investigated by Schläpfer et al., who suggests that these ligands have a considerable potential for technical applications[7]. The ability of polyalcohols such as the sugar alcohols or the tripodal tris(hydroxymethyl)aminoethane to act as sequestering agents, preventing formation of solid metal oxides or hydroxides in alkaline aqueous solution, has been well known for many years[8]. The linear polyalcohols $HO-CH_2-[CH-OH]_n-CH_2-OH$, $n > 1$ (sugar alcohols), are of particular interest with respect to the formation of polynuclear complexes. For steric reasons, it is not possible to bind all donor groups of one ligand molecule to a single metal centre and consequently these compounds could potentially serve as interesting building blocks for polymeric structures[9].

Although the sugar alcohols represent a well-known group of compounds that is widespread in nature, the corresponding linear polyamines $H_2N-CH_2-[CH-NH_2]_n-CH_2-NH_2$ have not been investigated to a great extent or are even completely unknown. This is of course, not true for 1,2-diaminoethane (en), the first member of

 © WILEY-VCH Verlag GmbH, D-69451 Weinheim, 1998 1434–1948/98/1212–2079 $ 17.50+.50/0

this series ($n = 0$), for which innumerable reports of the coordinating properties have appeared in the literature[10]. In most of these reports, 1,2-diaminoethane acts as a simple, bidentate ligand. However, a bridging coordination mode of the diamine, where the two nitrogen donors are coordinated to two different metal centres, has also been established[11]. For 1,2,3-triaminopropane (trap), there have only been a limited number of reports describing the coordinating properties[12–17]. A tridentate coordination mode of trap has been established in the bis-complex of Co^{III}[14]. For the tetraamines, two different stereoisomers must be considered. Both isomers (the *threo* and the *erythro* form) have been prepared as intermediates in the synthesis of tetraazadecalins, but the free amines have not been isolated[18][19]. To the best of our knowledge, the pentaamine has not been described at all.

By analogy with the corresponding polyalcohols, linear primary polyamines could serve as novel building blocks for coordination polymers, since for $n > 1$ it is not possible to coordinate the complete donor set to one single metal centre. We have therefore initiated a comprehensive investigation of the coordination chemistry of this class of compounds and intend to publish a series of papers, where the interactions of these ligands with a variety of metal cations will be described. In the first contribution, we present the synthesis and characterisation of the ligands and we describe the coordination chemistry of the triamine with divalent metal centres in aqueous solution and in the solid state.

Results and Discussion

Preparation and Characterisation of the Ligands

1,2,3-Triaminopropane (trap, $n = 1$), *meso*-1,2,3,4-tetraaminobutane (tab) and 1,2*R*,3,4*S*,5-pentaaminopentane (pap) were prepared by a classical procedure from the corresponding polyalcohols, with the poly(benzenesulphonates) and polyazides as intermediates[20]. Conversion of the polyazides to the corresponding polyamines could be achieved either by reduction with $LiAlH_4$ or by hydrogenation in an autoclave[14][18]. The latter method proved to be more convenient and gave slightly higher yields. Due to the potential hazards of polyazides, a procedure was developed that did not require the isolation of these intermediates as pure substances. The solutions of the azides were rather transferred directly into the autoclave and hydrogenated to give the polyamines, which were finally isolated as the corresponding hydrochlorides trap . 3HCl, tab · 4HCl and pap · 5HCl. Chromatography on a strongly acidic cation exchange resin proved to be a very efficient procedure to remove any by-products, and the pure, linear polyamines could readily be isolated in their fully protonated form ($H_2N-CH_2-[CH-NH_2]_n-CH_2-NH_2)\cdot(n+2)HCl$[21]. This procedure was particularly helpful for the recovery of the amines after the titration experiments, where a large excess of salts such as KCl or KNO_3 had been added to the sample solutions. The synthetic method reported here thus represents a convenient, two-step procedure, allowing the preparation of these compounds in multi-gram quantities.

The free bases trap, tab and pap could be obtained in CO_2-free water by the simple action of a strongly basic anion resin in the OH^- form. Concentration of the resulting solution yielded the corresponding polyamines as hygroscopic and CO_2-sensitive oils. Since the crystalline polyhydrochlorides can be handled and stored without problems, the free amines were only prepared in situ in solution and were usually not isolated. Prolonged storage of tab · 4HCl and pap · 5HCl resulted in some loss of HCl (1–2%) and recrystallisation from conc. HCl was required to obtain a pure sample.

According to NMR-spectroscopic measurements and an X-ray diffraction analysis, the configuration of the ligands is retained during this synthetic procedure: conversion of erythritol yielded the corresponding *meso* isomer of the tetraamine. The ^{13}C-NMR spectrum of tab. 4 HCl exhibited a total of two signals, and the crystal structure depicted in Figure 1, showing two crystallographically independent ligand molecules, established the expected *erythro* configuration. It is noteworthy that the conformations of the two H_4tab^{4+} cations are distinctly different from a structure that would be assumed, for an isolated molecule, to be of lowest energy[13]. Only one N–C–C–N substructure exhibited a torsional angle of 161° and thus corresponds to a staggered orientation. All the other N–C–C–N torsional angles fall in the range of 66–93°, corresponding to conformations intermediate between a synclinal and an anticlinal orientation. This may be attributed to strong anion-cation interactions within the crystal lattice, with the H_4tab^{4+} cations binding several Cl^- counter ions in a bidentate mode by N–H···Cl hydrogen bonding.

The acidity constants (pK_a values) of the three ligands have been determined by potentiometric measurements (Table 1). Inspection of corresponding ΔpK_a values clearly indicates that the two positive charges of the doubly protonated species are located at the terminal amino groups. For H_3pap^{3+}, the data are consistent with a protonation in the 1-, 3- and 5-positions. These findings are in agreement with simple electrostatic considerations, where a maximal distance between the positive charges is achieved. For the fully protonated species trap · 3HCl, tab · 4HCl and pap · 5HCl an increasing acidity is observed in this order in aqueous solution (Table 1). The pK_a values (25°C, 0.1 M KCl) are 3.63 for H_3trap^{3+} and 1.4 ± 0.3 for H_4tab^{4+}. H_5pap^{5+} behaves as a strong acid in water and the pK_a for the first deprotonation step could not be determined by the potentiometric method.

Complex Formation with trap in Aqueous Solution

A variety of potentiometric measurements using total M/total L ratios of 1 and 0.5 was performed to elucidate the compositions of the different species and to determine their formation constants. Some of these systems have previously been investigated by Prue and Schwarzenbach[12],

Figure 1. Molecular structure of the two crystallographically independent cations of tab·4HCl·H_2O; the thermal ellipsoids are drawn at the 50% probability level; hydrogen atoms are shown as spheres of arbitrary size; range of bond lengths [pm]: C−N: 147.6(2)−149.7(2), C−C: 151.7(2)−153.7(2)

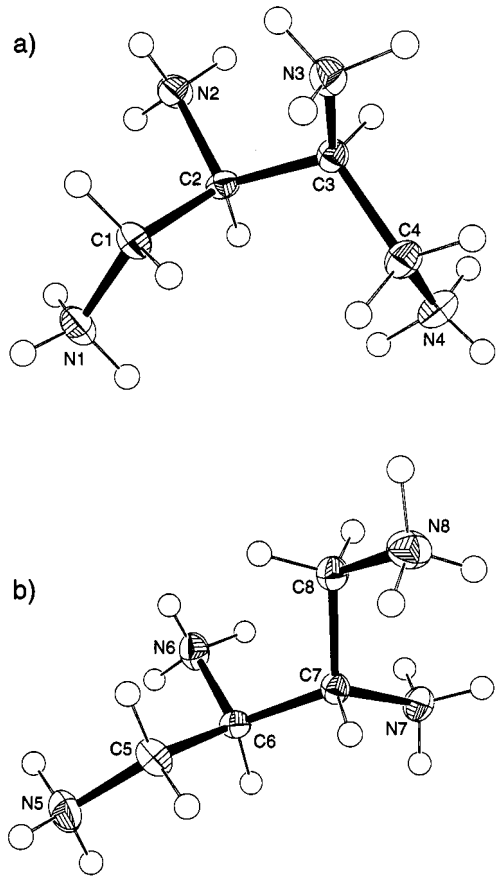

Table 1. Potentiometric data (25°C, 0.1 M KCl) and pK_a[a] values of the protonated polyamines

Experimental data			
Compound L	trap·3HCl	tab·4HCl	pap·5HCl
Total L [mol dm^{-3}]	1.0×10^{-3}	1.0×10^{-3}	1.0×10^{-3}
Evaluated pH range	3.43−10.80	3.03−10.20	2.82−10.83
Data points	41	40	59
pK_a (= $-\log K_a$)			
pK_1	9.59	9.65	9.72
pK_2	7.91	8.40	8.60
pK_3	3.63	5.03	6.26
pK_4		1.4(1)	2.62
pK_5			< 1
σ_{pH}[b]	0.0016	0.0023	0.0017

[a] The estimated standard deviations are less than 0.01 unless otherwise noted. − [b] $\sigma_{pH} = [\Sigma w(pH_{obsd.} - pH_{calcd.})^2/\Sigma w]^{1/2}$, $w = [pH_{i+1} - pH_{i-1}]^{-2}$.

and more recently by Cini et al.[17]. The authors of the latter paper investigated complex formation at 25°C and in 0.15 M NaCl. We performed the measurements at 25°C in 0.1 M KNO_3 or 0.1 M KCl (Table 2), which have become standard conditions for the determination of stability constants[22]. This allows a direct comparison with corresponding formation constants of other ligands that were measured under the same conditions[23]. Considering the difference in the media, the agreement between our values and the results of Cini et al. is good. However, we also noted some characteristic differences that led us to draw different conclusions. The most significant disagreement is the fact that we could not find an unambiguous indication for the formation of a complex of composition $[CuL]^{2+}$. In the titration experiments with a total Cu/total trap ratio of 1:2, a protonated complex of composition $[Cu(HL)]^{3+}$ is formed in the acidic range. At higher pH, coordination of an additional ligand occurred rather than the deprotonation of the coordinated HL^+ entity (Figure 2). The titration experiments, where a total L/total Cu ratio of 1:1 was used, could not be evaluated in the alkaline range because precipitation of solid $Cu(OH)_2$ was observed. This was in contrast to the Ni^{2+} system, where the formation of both $[NiL]^{2+}$ and $[NiL_2]^{2+}$ could be established unambiguously. Cini et al. performed calorimetric measurements and they deduced a tridentate coordination mode for trap in $[CuL]^{2+}$. However, a comparison of the formation constants of trap with the bidentate en does not support this interpretation: the overall protonation constants κ_2 (= $[H_2L]\cdot[L]^{-1}\cdot[H]^{-2}$) for the generation of the diprotonated H_2en^{2+} and H_2trap^{2+} are in close agreement (en: log κ_2 = 17.00; trap: log κ_2 = 17.50)[23], indicating that the formation of H_2trap^{2+} is slightly favoured. The Ni^{2+} complexes of trap are, however, of significantly higher stability (en: log β_1 = 7.3, log β_2 = 13.4; trap: log β_1 = 9.5, log β_2 = 17.3). This is not the case for Cu^{2+} where log β_2 is 19.6 for the en complex and 19.5 for the trap complex. The value for log β_1 of $[Cu(trap)]^{2+}$ in 0.15 M NaCl has been reported to be 10.4, once again showing no further increase in stability on going from the diamine to the triamine ligand (en: log β_1 = 10.50 at 25°C in 0.1 M KNO_3)[23]. Furthermore, these considerations are supported by the favoured formation of the protonated species $[Cu(HL)]^{3+}$, $[CuL(HL)]^{3+}$ and $[Cu(HL)_2]^{4+}$ and by the results of our X-ray diffraction study (see next section), where a tridentate coordination mode of trap was also not observed for Cu^{2+}.

Figure 2. Species distribution plot for an equilibrated aqueous solution with total Cu 0.5×10^{-3} mol dm^{-3} and total trap (= L) 1×10^{-3} mol dm^{-3}; only metal-containing species are shown; the charges of the different species are omitted for clarity; the equilibrium constants listed in Tables 1 and 2 were used for the calculations

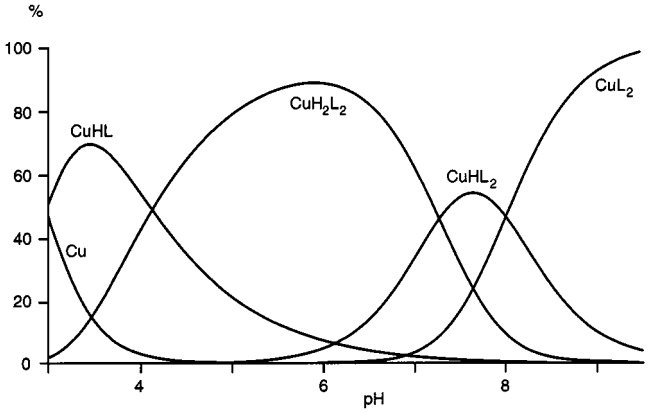

Table 2. Potentiometric data (25°C, 0.1 mol dm^{-3} KNO_3 or KCl) and evaluated formation constants[a] for trap complexes with divalent metal cations

Experimental data									
Metal			$Ni^{[b]}$	$Ni^{[b]}$	$Cu^{[c]}$	$Cu^{[c]}$	$Zn^{[c]}$	$Zn^{[c]}$	$Cd^{[c]}$	$Cd^{[c]}$
Tot.M [mol dm^{-3}]			0.5	1.0	0.5	1.0	0.5	1.0	0.5	1.0
Tot. L [mol dm^{-3}]			1.0	1.0	1.0	1.0	1.0	1.0	1.0	1.0
pH range			3.43−7.43	4.18−6.92	3.15−9.41	3.06−3.96	6.10−10.43	5.85−8.02	5.47−10.74	5.31−9.09
Data points			28	20	61	35	58	52	60	40
Formation constants log β_{xyz}[d]										
x	*y*	*z*								
1	1	0	9.58(5)	9.52(4)			6.50(2)	6.47(1)	5.99(2)	5.90(1)
1	1	1	15.45(4)	15.58(6)	18.07(3)	18.11(1)	13.75(1)	13.77(2)	13.60(3)	13.61(1)
1	1	−1					−2.89(6)		−4.39(4)	−4.22(7)
1	1	−2					−12.80(2)			
1	2	0	17.35(3)		19.55(5)		11.42(1)		10.39(3)	
1	2	1	23.87(11)		27.54(5)		19.08(8)			
1	2	−1					0.81(8)			
1	2	2			34.83(3)	34.58(6)				
σ_{pH}[e]			0.0046	0.0051	0.0015	0.0013	0.0018	0.0081	0.0069	0.0071

[a] The uncertainties, given in parentheses, correspond to the evaluated standard deviations calculated by SUPERQUAD multiplied with a factor of 3. − [b] KCl. − [c] KNO_3. − [d] $\beta_{xyz} = [M_xL_yH_z] \times [M]^{-x} \times [L]^{-y} \times [H]^{-z}$. − [e] $\sigma_{pH} = [\Sigma w(pH_{obsd.} - pH_{calcd.})^2/\Sigma w]^{1/2}$, $w = [pH_{i+1} - pH_{i-1}]^{-2}$.

Assuming a bidentate coordination mode for trap in the bis-complexes of Cu, a free amino group would be present in an alkaline medium (Scheme 1), and thus the formation of polynuclear, trap-bridged species must also be considered. As shown in the next section, such bridging interactions can indeed be observed in the solid state. However, careful evaluation of the potentiometric data provided no evidence for the formation of polynuclear species in dilute solutions such as those used in the present investigation. This may, however, be different for more concentrated solutions of complexes, where such aggregation processes are more likely to occur.

Scheme 1

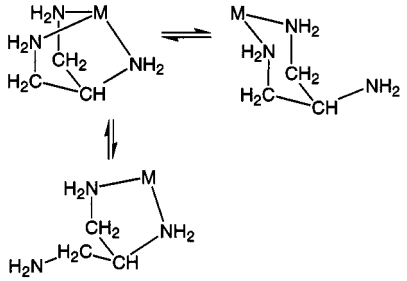

Crystal Structure and Magnetic Properties of $[Cu(trap)_2]Cl_2$

The dichloride salt of the bis-complex crystallises in the polar space group *Cc*. A view of the molecular structure is presented in Figure 3.

Both trap ligands coordinate the Cu^{II} centre in a bidentate mode, forming five-membered chelate rings. The four nitrogen donors of the two ligands form a slightly distorted square. The two ligands differ, however, with respect to the orientation of the third amino group. In the first ligand, the third amino group is coordinated to a neighbouring Cu atom. This bridging interaction of one of the trap ligands generates an infinite chain structure with five coordinate Cu^{II} cations. The coordination sphere of the Cu^{II} centre can be described as a slightly distorted tetragonal pyramid with the amino group of the bridging ligand in the apex. The Cu−N distances of the four amino groups of the square basis (2.02−2.05 Å) and of the apical amino group (2.27 Å) all fall within the expected ranges[24]. The third amino group of the second trap ligand is engaged in a weak hydrogen bond of the type N−H···Cl. This is a remarkable result since this amino group is not protonated and only minor internal rearrangements would be required to bring it into a position where coordination to the Cu centre would be possible (the Cu···N distance to this non-coordinating amino group is 4.60 Å).

A tridentate coordination mode of trap has been observed for $[Co^{III}(trap)_2]^{3+}$ and this has been confirmed by crystal structure analysis[14]. This is not surprising since Co^{III}, with its low-spin d^6-electron configuration, has a strong preference for a regular octahedral CoN_6 coordination. However, molecular mechanics calculations showed that this tridentate coordination mode causes some degree of strain in the ligand backbone, due to the formation of a six-membered chelate ring having an unfavourable boat conformation (Scheme 1)[15].

Due to the Jahn−Teller effect, Cu^{II}-hexaamine complexes usually exhibit strong tetragonal distortion[25], and the facial coordination of a triamine such as trap to Cu^{II} is particularly disfavoured. The X-ray structural analysis together with the potentiometric measurements supports indeed a bidentate coordination mode for the Cu^{II} complexes of trap. Similar conditions could be expected for Pd^{II}, Pt^{II}, or Ag^{I}, where a tridentate binding mode is also unfavourable. In such complexes, additional free amino groups must be present and trap could thus serve as an interesting build-

Figure 3. Molecular structure of $[Cu(trap)_2]Cl_2$; (a) the $[Cu(trap)_3]^{2+}$ cation, (b) section of the infinite chain structure; the thermal ellipsoids are drawn at the 50% probability level; hydrogen atoms are omitted (a) or shown as spheres of arbitrary size (b), the Cl^- counter ions are omitted for clarity; selected bond lengths [pm] and angles [°]: Cu−N(1) 201.6(3), Cu−N(2) 204.5(3), Cu−N(4) 202.7(3), Cu−N(5) 204.6(3), Cu−N(3a) 226.8(3); N(1)−Cu−N(2) 84.1(1), N(1)−Cu−N(3a) 97.6(1), N(1)−Cu−N(4) 92.9(1), N(1)−Cu−N(5) 166.4(1), N(2)−Cu−N(3a) 93.9(1) N(2)−Cu−N(4) 162.7(1), N(2)−Cu−N(5) 94.9(1), N(4)−Cu−N(3a) 103.3(1), N(4)−Cu−N(5) 84.0(1), N(5)−Cu−N(3a) 96.0(1); symmetry-related atoms were generated by the symmetry operation (a): $x + 1, y, z$

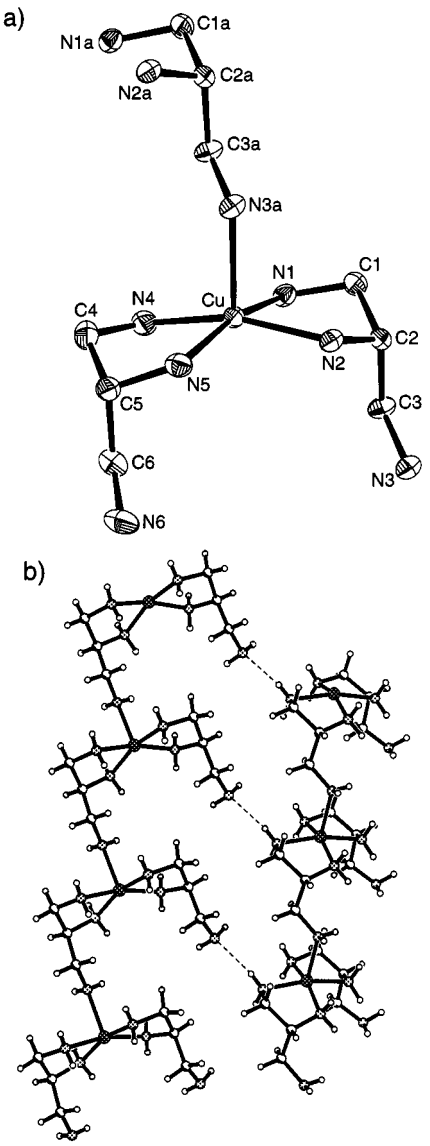

ing block for the synthesis of polymeric complexes of these metal cations.

Coordination polymers of paramagnetic cations are of particular interest with regard to their magnetic properties[26]. It is to be expected that interactions between the cations within the polymeric structure would result in antiferromagnetic coupling. Magnetic susceptibility measurements of $[Cu(trap)_2]Cl_2$ established Curie−Weiss behaviour with $\Theta = 1.1$ K and $C = 0.40$ emu K mol^{-1}. Since significantly different Cu···Cu distances are observed for the neighbouring Cu atoms within the chain (6.14 Å) and between two different chains (7.81 Å), the Bonner and Fisher equation for antiferromagnetic coupling interactions of paramagnetic centres within a linear infinite chain was used to fit the data (Figure 4)[27]. The experimental findings could be well reproduced with $g = 2.07$ and $J = 0.82$ cm^{-1}. The g value determined by this method was in good agreement with $g_{\parallel} = 2.19$, $g_{\perp} = 2.07$ observed in the EPR spectrum of a powder sample at room temperature.

Figure 4. Temperature dependence of $\chi \times T$ for $[Cu(trap)_2]Cl_2$; observed data are shown as squares, a theoretical behaviour, calculated for $g = 2.07$ and $J = 0.82$ cm^{-1} is shown as a solid line

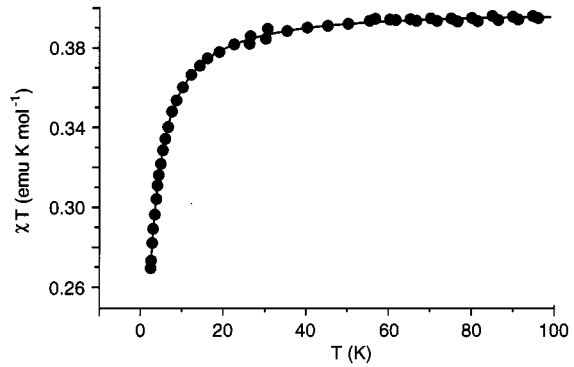

We thank Prof. Dr. *W. S. Sheldrick* and Dr. *Michael Weber* for advice and discussions, *Jürgen Sander, Oliver Maas* and Dr. *Volker Huch* for valuable help, and Dr. *Peter Osvath* (Melbourne) for careful corrections and suggestions in preparing the manuscript. Financial support by the *Universität des Saarlandes* and the *Fonds der Chemischen Industrie* is gratefully acknowledged.

Experimental Section

General: ^{1}H- and ^{13}C-NMR spectra were measured in $CDCl_3$ or D_2O at 28°C with a Bruker DRX 500-MHz NMR spectrometer. Chemical shifts (on the δ scale) are given relative to sodium (trimethylsilyl)propionate (D_2O) or tetramethylsilane ($CDCl_3$) as internal standard (δ = 0). C, H and N analyses were performed by H. Feuerhake, Institut für Anorganische Chemie, Universität des Saarlandes. 1,2,3-Propanetriol, benzenesulphonyl chloride, NaN_3, $LiAlH_4$, 5% Pd/C, *meso*-erythritol, xylitol, $CuCl_2 \cdot 2H_2O$ and the organic solvents were commercially available products of reagent-grade quality. They were used without further purification. Dowex 50 W-X2 (100−200 mesh, H^+ form) and Dowex 2-X8 (50−100 mesh, Cl^- form) were from Fluka. The OH^- form of the anion resin was obtained from the Cl^- form by elution with 0.3 M NaOH, followed by extended rinsing with CO_2-free water until a neutral eluent was observed. The temperature dependence of the static magnetic susceptibility was measured with a Metronique Ing. MS02 SQUID magnetometer at 1.0 T operating in the range of 2−250 K. The data were corrected for the contribution of the sample holder and for the diamagnetism using Pascal′s constants. The EPR spectrum of a polycrystalline powder sample of $[Cu(trap)_2]Cl_2$ was recorded at room temperature at the X-band frequency with a Varian ESR9 spectrometer.

1,2,3-Propanetriyl Tribenzenesulphonate: A solution of propane-1,2,3-triol (2.30 g, 25 mmol) in 50 ml of dry pyridine was cooled to 0°C using an NaCl/ice bath. Benzenesulphonyl chloride (26.49 g, 150 mmol) was added dropwise over a 1-h period. During that

time, the colour turned to red and a white precipitate appeared. The resulting mixture was stirred overnight at room temperature and then filtered. The red solution was poured with stirring into a mixture of ice (75 g) and concentrated HCl (25 ml). An oily product was obtained from which the aqueous layer was decanted. The oil was dissolved in a mixture of methanol (75 ml) and acetone (12.5 ml) and heated until a yellow solution was obtained. The volume of the solution was reduced to 50% and the product was allowed to crystallise. It was then separated by filtration and washed with 0.5 M HCl and then hot EtOH. After drying in vacuo (12 h, 25°C), the product was obtained as a white solid (7.84 g, 61%). − $C_{21}H_{20}O_9S_3$ (512.6): calcd. C 49.21, H 3.93; found C 49.48, H 3.91. − ^{1}H NMR ($CDCl_3$): δ = 4.13 (d, 4 H, CH_2, J = 5 Hz), 4.75 (quint, 1 H, CH), 7.53−7.58 (m, 6 H, aryl-H), 7.67−7.71 (m, 3 H, aryl-H), 7.81−7.83 (m, 6 H, aryl-H). − ^{13}C NMR: δ = 66.4, 74.6, 128.0, 129.5, 134.3, 134.9.

1,2,3-Triazidopropane: Caution: Organic polyazides are highly explosive. They should only be handled in dilute solutions and should not be isolated as pure substances. 1,2,3-Propanetriyl tribenzenesulphonate (15.36 g, 30 mmol), NaN_3 (9.75 g, 150 mmol) and dry DMF (350 ml) were heated at 100°C for 4 h and stirred at room temperature for additional 14 h. The mixture was cooled to 10°C and diluted with 130 ml H_2O. The orange solution was extracted with Et_2O (6 × 100 ml) and the combined ether extracts were washed with water (2 × 100 ml). The ether solution was dried with $MgSO_4$. For characterisation, only a small sample (5 ml) was separated and set aside until the solvent had evaporated, and a solution of the residual brown oil in $CDCl_3$ was used to measure the NMR spectra. − ^{1}H NMR: δ = 3.40−3.48 (m, 4 H, CH_2), 3.65 (quint, 1 H, CH). − ^{13}C NMR: δ = 51.8, 60.4. − For the preparation of the triamine by method A, the solution of the azide in Et_2O was immediately used without further manipulations, while for method B, the volume of the Et_2O solution was reduced to one half by evaporation at reduced pressure and the resulting solution was then diluted by adding 150 ml of EtOH.

1,2,3-Triaminopropane·3HCl. − Method A: To a suspension of $LiAlH_4$ (8.33 g, 220 mmol) in 500 ml of dry Et_2O, the azide solution obtained from 29.3 mmol of 1,2,3-propanetriyl tribenzenesulphonate was added slowly under gentle reflux, and the mixture was then heated under reflux for another 18 h. After cooling and addition of water (10 ml), 15% NaOH (10 ml) and water (30 ml), the resulting precipitate was extracted for 18 h from a Soxhlet thimble using refluxing isopropyl alcohol (500 ml). After removing the solvent under reduced pressure, EtOH was added to the resulting oil. An excess of 6 M HCl was added to the cooled solution with stirring. The white solid which precipitated was collected by filtration and redissolved in 500 ml of H_2O. The resulting solution, having a pH ≈ 2, was sorbed onto Dowex 50 W-X2. The column was washed with water and eluted with 1 M HCl. The second fraction was concentrated to dryness under reduced pressure yielding 2.59 g (45%) of a white solid. − $C_3H_{14}Cl_3N_3$ (198.5): calcd. C 18.15, H 7.11, N 21.17; found C 18.34, H 6.90, N 20.99. − ^{1}H NMR (D_2O, pD < 2): δ = 3.34−3.40 (m, 1 H, CH), 3.21−3.25 (dd, 2 H, CH_2), 2.95−2.30 (dd, 2 H, CH_2); (pD > 12): δ = 2.68−2.73 (m, 2 H), 2.65−2.66 (m, 1 H), 2.48−2.51 (m, 2 H). − ^{13}C NMR (pD < 2): δ = 45.3, 50.0; (pD > 12): δ = 47.1, 57.1. − *Method B:* The solution of the triazide (obtained from 40.2 mmol of 1,2,3-propanetriyl tribenzenesulphonate) in EtOH/Et_2O and 885 mg of 5% Pd/C were placed in an autoclave. The mixture was hydrogenated at 4.0 bar under vigorous stirring until TLC did not show any remaining starting material. The solution was filtered twice and then cooled. An excess of 6 M HCl was added with stirring. The protocol reported for method A was then used for the isolation of the trihydrochloride. Elution from a Dowex 50 W-X2 column with 1 M HCl yielded 4.42 g (55%) of a white solid. The product was further characterised as $[Co(trap)_2]Cl_3$: trap·3HCl (602.5 mg; 3.04 mmol) was dissolved in water (60 ml) and NaOH (15%) was added until pH = 8 was reached. $CoCl_2·6H_2O$ (0.361 g; 1.52 mmol), dissolved in 60 ml of water, was added and oxygen was passed through the solution at 80°C for 24 h. The mixture was filtered, acidified to pH = 1 (HCl) and diluted with 100 ml of water. The solution was sorbed onto a column of Dowex 50W-X2. Elution with 3.0 M HCl yielded a yellow fraction which was concentrated to dryness. The brown residue (440 mg) was dissolved in water again and sorbed onto a column of SP-Sephadex. Elution with 0.2 M trisodium citrate gave two well-separated bands. A minor red band was discarded. The major orange fraction was desalted on Dowex 50W-X2 and concentrated to dryness. Yield: 272.4 mg (52%). − $C_6H_{22}Cl_3CoN_6$ (343.6): calcd. C 20.98, H 6.45, N 24.46; found: C 20.67, H 6.33, N 22.98. − Single crystals were grown from H_2O/EtOH. A single-crystal analysis revealed the same structure as reported by Henrick et al.[14].

[Cu(trap)$_2$]Cl$_2$: trap·3HCl (400 mg, 2.01 mmol) was dissolved in 25 ml of water and deprotonated using Dowex 2-X8 (OH^- form). The solution was concentrated to dryness under reduced pressure. The oily residue was dissolved in 5 ml of water and a solution of $CuCl_2·2H_2O$ (153.4 mg, 0.9 mmol) in 5 ml of water was then added. Deep blue crystals were grown by layering the solution with EtOH. − $C_6H_{22}Cl_2CuN_6$ (312.7): calcd. C 23.04, H 7.09, N 26.87; found C 23.04, H 6.93, N 26.48.

1,2,3,4-Butanetetrayl Tetrabenzenesulphonate: meso-Erythritol (6.12 g, 50 mmol) and benzenesulphonyl chloride (52.99 g, 300 mmol) were treated in dry pyridine (150 ml) as described above for the preparation of 1,2,3-propanetriyl tribenzenesulphonate. The precipitate was filtered and washed with 0.5 M HCl and then hot EtOH. After drying in vacuo (60°C, 14 h), a white solid was obtained (24.28 g, 71%). − $C_{28}H_{26}O_{12}S_4$ (682.8): calcd. C 49.26, H 3.84; found C 49.26, H 4.06. − ^{1}H NMR ($CDCl_3$): δ = 4.02−4.19 (m, 4 H, CH_2), 4.80 (m, 2 H, CH), 7.53−7.82 (m, 20 H, aryl-H). − ^{13}C NMR: δ = 66.2, 75.7, 128.1, 129.5, 134.3, 134.6.

1,2,3,4-Tetraazidobutane: Caution: Organic polyazides are highly explosive. They should only be handled in dilute solutions and should not be isolated as pure substances. 1,2,3,4-Butanetetrayl tetrabenzenesulphonate (12.16 g, 17.8 mmol) was treated with NaN_3 (6.95 g, 106.9 mmol) in dry DMF (200 ml) as described for 1,2,3-propanetriyl tribenzenesulphonate. The solution turned deep brown and was diluted with H_2O (150 ml), and extracted with ether (4 × 150 ml). The ether extract was washed with H_2O (2 × 200 ml). − ^{1}H NMR ($CDCl_3$): δ = 3.68−3.70 (m, 2 H, CH), 3.55−3.58 (m, 4 H, CH_2). − ^{13}C NMR: δ = 51.9, 61.4.

1,2,3,4-Tetraaminobutane·4HCl: Method B was used. A solution of the tetraazide (obtained from 17.8 mmol 1,2,3,4-butanetetrayl tetrabenzenesulphonate) in EtOH (150 ml) was hydrogenated at 4.0 bar using 300 mg of 5% Pd/C as catalyst. The mixture was worked up as described above and sorbed onto Dowex 50W-X2. Elution with 3 M HCl yielded 2.16 g (46%) of a white solid. − $C_4H_{18}Cl_4N_4$ (264.0): calcd. C 18.20, H 6.87, N 21.22; found C 18.15, H 6.73, N 21.02. − ^{1}H NMR (D_2O, pD < 2): δ = 3.17−3.22 (dd, 2 H, CH_2), 3.37−3.41 (dd, 2 H, CH_2), 3.50−3.54 (m, 2 H, CH); (pD > 12): δ = 2.53 (br., 2 H), 2.68 (br., 2 H), 2.76−2.78 (br., 2 H). − ^{13}C NMR (pD < 2): δ = 43.4, 54.0; (pD > 12): δ = 46.0, 58.3.

1,2,3,4,5-Pentanepentayl Pentabenzenesulphonate: Xylitol (7.61 g, 50 mmol) was treated with benzenesulphonyl chloride (88.31 g, 500 mmol) in dry pyridine (200 ml) as described above for the preparation of 1,2,3-propanetriyl tribenzenesulphonate. Traces of pyri-

dine were extracted with a mixture of ice (300 g) and concentrated HCl (100 ml) and the product was washed with MeOH (150 ml) and acetone (25 ml). Drying in vacuo at 60°C yielded 27.25 g (64%) of a white solid. – $C_{35}H_{32}O_{15}S_5$ (852.9): calcd. C 49.29, H 3.78; found C 49.20, H 3.83. – ^{1}H NMR: δ = 4.00–4.14 (4 H, CH_2), 4.81–4.92 (3 H, CH), 7.27–7.97 (25 H, aryl-H). – ^{13}C NMR: δ = 65.9, 74.0, 74.3 (3 C, aliphatic), 126.0–141.5 (12 C, aryl).

1,2,3,4,5-Pentaazidopentane: ***Caution:*** Organic polyazides are highly explosive. They should only be handled in dilute solutions and should not be isolated as pure substances. 1,2,3,4,5-Pentanepentayl pentabenzenesulphonate (27.25 g, 31.95 mmol) was treated with NaN_3 (16.6 g, 255.6 mmol) in dry DMF (400 ml) as described for 1,2,3-propanetriyl tribenzenesulphonate. The reaction mixture turned deep brown. The solution was diluted with H_2O (430 ml), and extracted with ether (8 × 200 ml). The ether extracts were combined and washed with H_2O (6 × 150 ml). – ^{1}H NMR ($CDCl_3$): δ = 3.60–3.68 (m, 7 H). – ^{13}C NMR: δ = 51.5, 61.1, 63.1.

1,2,3,4,5-Pentaaminopentane·5HCl: 1,2,3,4,5-Pentaaminopentane·5HCl was prepared using Method B. A solution of the pentaazide (obtained from 31.95 mmol of 1,2,3,4,5-pentanepentayl pentabenzenesulphonate) in EtOH (150 ml) was hydrogenated at 4.0 bar using 404 mg of 5% Pd/C as catalyst. The mixture was worked up as described above and sorbed onto Dowex 50W-X2. Elution with 3 M HCl yielded 2.27 g (22%) of a white solid. – $C_5H_{22}Cl_5N_5$ (329.5): calcd. C 18.22, H 6.73, N 21.25; found C 18.33, H 6.62, N 21.01. – ^{1}H NMR (D_2O, pD < 2): δ = 3.34–3.39 (2 H), 3.46–3.49 (2 H), 3.51–3.52 (1 H), 3.79–3.83 (2 H); (pD > 12): δ = 2.56 (br., 3 H), 2.76 (br., 4 H). – ^{13}C NMR (pD < 2): δ = 43.4, 53.2, 54.1; (pD > 12): δ = 47.2, 56.9, 57.1.

Potentiometric Measurements: Potentiometric titrations were carried out with a Metrohm 713 pH/mV meter and a Metrohm combined glass electrode with an internal Ag/AgCl reference. The sample solutions were titrated with 0.1 M KOH, using a Metrohm 665 piston burette. The ionic strength of the 50-ml sample solutions was 0.1 M KCl or 0.1 M KNO_3 and the stability of the electrode was checked by two calibration titrations prior to, and after, each measurement. All titrations were performed at 25.0°C under nitrogen (scrubbed with an aqueous solution of 0.1 M KCl or 0.1 M KNO_3). The measuring time per point was 2 min for the pK_a determinations, 5 min for the Cu complex solutions and 10 min for all other metal complexes. For the pK determination of trap, tab and pap, several alkalimetric titrations were carried out with analytically pure samples of the corresponding hydrochlorides (total concentration: 2×10^{-3} M or 1×10^{-3} M). Solutions for the titration experiments of $[M(trap)]^{2+}$ and $[M(trap)_2]^{2+}$ were prepared by dissolving trap·3HCl and $M(NO_3)_2$ (M = Cu, Zn, Cd) or $NiCl_2$ in a 1:1 and 1:2 molar ratio with total M = 1.0×10^{-3} or 0.5×10^{-3} M. The solutions were made up by using standardised aqueous stock solutions of $NiCl_2$, $Cu(NO_3)_2$, $Zn(NO_3)_2$ and trap·3HCl and solid $Cd(NO_3)_2·4H_2O$.

Calculations of Equilibrium Constants: All equilibrium constants were calculated as concentration constants. The pK_a values of the ligands and the formation constants of the metal complexes were calculated using the computer program SUPERQUAD[28] and double-checked with the computer program BEST[29]. The formation constants were evaluated with fixed values for the total concentrations of the reactants and for pK_w (13.79)[23]. For the evaluation of the titration experiments of the metal complexes, only the formation constants of the metal-containing species were varied and fixed values were used for the total concentrations of M, trap, and H, and the protonation constants of trap as obtained from the pK_a determination.

Crystal-Structure Determination of tab · 4HCl · H_2O[30]: Data were collected at 253 K with a Stoe IPDS diffractometer using monochromated Mo-K_α radiation. 220 exposures were taken in the 0–220° φ range with a crystal-to-detector distance of 72 mm and an exposure time of 2 min. Monitoring of control reflections during data collection indicated no crystal decay during the measurement. Corrections were made for Lorentz and polarisation effects. An absorption correction was not performed. The structure was solved using Direct Methods[31] and refined by full-matrix least-squares calculations[32] on F^2. All non-hydrogen atoms were refined using anisotropic displacement parameters. The hydrogen atoms were located in a difference Fourier map. Atomic coordinates and isotropic displacement parameters were refined free for all ammonium H atoms. All H atoms belonging to CH and CH_2 groups were refined riding on their C atom with isotropic displacement parameters set to 1.2 and 1.3 times the U_{eq} of the corresponding C atom, respecively. The coordinates and isotropic displacement parameters of the H atoms at the water molecule O1w were refined free, while the O–H distances in O2w had to be restrained to one common value. Further details are summarized in Table 3.

Crystal-Structure Determination of [Cu(trap)$_2$]Cl$_2$[33]: Data were collected with a Siemens P4 diffractometer using monochromated Mo-K_α radiation. Intensities were measured by ω scans. Monitoring of control reflections during data collection indicated no crystal decay during the measurement. Corrections were made for Lorentz and polarisation effects. An absorption correction was not performed. The structure was solved using Direct Methods[31] and refined by full-matrix least-squares calculations[32] on F^2. The value

Table 3. Crystallographic data for tab · 4HCl · H_2O and $[Cu(trap)_2]Cl_2$

Compounds	tab·4HCl·H_2O	$[Cu(trap)_2]Cl_2$
Empirical formula	$C_8H_{40}Cl_8N_8O_2$	$C_6H_{22}Cl_2CuN_6$
Formula weight	564.1	312.74
Temperature [K]	253	293
Radiation, λ [Å]	Mo-K_α, 0.71073	Mo-K_α, 0.71073
Crystal system	monoclinic	monoclinic
Space group	$P2_1/n$	Cc
a [Å]	8.228(2)	6.1428(9)
b [Å]	12.890(4)	14.367(2)
c [Å]	23.873(6)	15.215(2)
β [°]	99.41(3)	90.084(9)
V [Å^3]	2497.9(13)	1342.8(3)
Z	4	4
$D_{calcd.}$ [g cm^{-3}]	1.500	1.547
μ [mm^{-1}]	0.923	2.007
F[000]	1184	652
Crystal size [mm]	0.05 × 0.10 × 0.20	0.62 × 0.48 × 0.26
θ min and max	4.09 to 25.02	2.68 to 29.99
Data set	−9/9; −15/15; −28/28	0/8; 0/20; −21/21
Tot., uniq. data	17722, 4196	2119
Reflections with $I > 2\sigma(I)$	3177	1996
Structure solution	Direct methods	Direct methods
Refinement method	Full-matrix least squares on all F^2	Full-matrix least squares on all F^2
Parameters	371	173
Final R indices	R_1 = 0.0240	0.0314
$[I > 2\sigma(I)]$	wR_2 = 0.0423	0.0744
R indices	R_1 = 0.0364	0.0333
(all data)	wR_2 = 0.0431	0.0758
Largest diff. peak and hole [e/Å^3]	0.290 and −0.231	0.575 and −1.348
Max shift/error	0.090	0.001

of the Flack parameter[34] was 0.005(14) for the refined absolute structure (space group *Cc*). All non-hydrogen atoms were refined in the anisotropic mode. The hydrogen atoms were placed at calculated positions using a riding model. Further details are summarized in Table 3.

[1] [1a] F. Vögtle, *Supramolecular Chemistry*, Wiley, Chichester, **1991**. – [1b] *Supramolecular Chemistry* (Eds.: V. Balzani, L. De Cola), Kluwer, Dordrecht, **1992**. – [1c] *Transition Metals in Supramolecular Chemistry* (Eds.: L. Fabrizzi, A. Poggi), Kluwer, Dordrecht, **1994**.

[2] [2a] E. C. Constable, *Chem. Commun*. **1997**, 1073–1080. – [2b] M. Munakata, L. P. Wu, T. Kuroda-Sowa, *Bull. Chem. Soc. Jpn*. **1997**, *70*, 1727–1743. – [2c] P. J. Stang, O. Bogdan, *Acc. Chem. Res.* **1997**, *30*, 502–518. – [2d] C. Gorman, *Adv. Mater.* **1998**, *10*, 295–309.

[3] M. J. Zaworotko, *Coord. Chem. Rev.* **1994**, *137*, 357–401.

[4] [4a] H. Stünzi, L. Spiccia, F. P. Rotzinger, W. Marty, *Inorg. Chem*. **1989**, *28*, 66–71. – [4b] J. W. Gilje, H. W. Roesky, *Chem. Rev.* **1994**, *94*, 895–910. – [4c] W. Seichter, H.-J. Mögel, P. Brand, D. Salah, *Eur. J. Inorg. Chem.* **1998**, 795–797.

[5] [5a] A. Hazell, C. J. McKenzie, L. P. Nielsen, *J. Chem. Soc., Dalton Trans.* **1998**, 1751–1756. – [5b] S. Kitagawa, S. Matsuyama, M. Munakata, T. Emori, *J. Chem. Soc., Dalton Trans.* **1991**, 2869–2874.

[6] [6a] W. Zarges, J. Hall, J.-M. Lehn, C. Bolm, *Helv. Chim. Acta* **1991**, *74*, 1843–1852. – [6b] P. N. W. Baxter, J.-M. Lehn, K. Rissanen, *Chem. Commun.* **1997**, 1323–1324. – [6c] B. Schoentjes, J.-M. Lehn, *Helv. Chim. Acta* **1995**, *78*, 1–12. – [6d] H. Sleiman, P. Baxter, J.-M. Lehn, K. Rissanen, *J. Chem. Soc., Chem. Commun.* **1995**, 715–716. – [6e] A. Pfeil, J.-M. Lehn, *J. Chem. Soc., Chem. Commun.* **1992**, 838–840.

[7] A. von Zelewsky, L. Barbosa, C. W. Schläpfer, *Coord. Chem. Rev.* **1993**, *123*, 229–246.

[8] K. Hegetschweiler, *Bol. Soc. Chil. Quim*. **1997**, *42*, 257–279.

[9] [9a] J.-F. Verchère, S. Chapelle, F. Xin, D. C. Crans, *Prog. Inorg. Chem.* **1998**, *47*, 837–945. – [9b] K. Hegetschweiler, L. Hausherr-Primo, W. H. Koppenol, V. Gramlich, L. Odier, W. Meyer, H. Winkler, A. X. Trautwein, *Angew. Chem. Int. Ed. Engl.* **1995**, *34*, 2242–2243. – [9c] A. Cornia, D. Gatteschi, K. Hegetschweiler, L. Hausherr-Primo, V. Gramlich, *Inorg. Chem*. **1996**, *35*, 4414–4419.

[10] D. A. House in *Comprehensive Coordination Chemistry* (Ed.: G. Wilkinson), Pergamon Press, Oxford, **1987**, vol. 2, p. 23–72.

[11] [11a] E. Bang, *Acta Chem. Scand., Ser. A* **1978**, *A32*, 555–557. – [11b] M. Pasquali, C. Floriani, A. Gaetani-Manfredotti, *Inorg. Chem.* **1980**, *19*, 1191–1197. – [11c] W. P. Griffith, N. T. McManus, A. C. Skapski, *J. Chem. Soc., Chem. Commun.* **1984**, 434–435. – [11d] B. W. Eichhorn, M. C. Kerby, R. C. Haushalter, K. P. C. Vollhardt, *Inorg. Chem.* **1990**, *29*, 723–728. – [11e] H. Yuge, T. Iwamoto, *J. Chem. Soc., Dalton Trans.* **1994**, 1237–1242.

[12] J. E. Prue, G. Schwarzenbach, *Helv. Chim. Acta* **1950**, *33*, 995–1005.

[13] R. Cini, G. Giorgi, D. Masi, A. Sabatini, A. Vacca, *J. Chem. Soc., Perkin Trans. 2* **1991**, 765–771.

[14] K. Henrick, M. McPartlin, S. Munjoma, P. G. Owston, R. Peters, S. A. Sangokoya, P. A. Tasker, *J. Chem. Soc., Dalton Trans.* **1982**, 225–227.

[15] P. Comba, T. W. Hambley, L. Zipper, *Helv. Chim. Acta* **1988**, *71*, 1875–1880.

[16] M. M. Shoukry, S. M. El-Medani, M. M. Khatab, *Monatsh. Chem.* **1996**, *127*, 811–820.

[17] R. Cini, A. Sabatini, A. Vacca, F. Zanobini, *Can. J. Chem.* **1997**, *75*, 212–219.

[18] R. L. Willer, *J. Org. Chem.* **1984**, *49*, 5150–5154.

[19] T. K. O'Leary, R. W. Read, *Aust. J. Chem.* **1996**, *49*, 285–291.

[20] E. B. Fleischer, A. E. Gebala, A. Levey, P. A. Tasker, *J. Org. Chem.* **1971**, *36*, 3042–3044.

[21] R. J. Geue, G. H. Searle, *Aust. J. Chem.* **1983**, *36*, 927–935.

[22] A. E. Martell, R. J. Motekaitis, *Determination and Use of Stability Constants*, VCH, New York, **1988**.

[23] R. M. Smith, A. E. Martell, R. J. Motekaitis, *Critically Selected Stability Constants of Metal Complexes*, NIST Standard Reference Database 46, Version 4.0, NIST Standard Reference Data, Gaithersburg, MD 20899, USA, **1997**.

[24] [24a] X. H. Bu, D. L An, Y. T. Chen, M. Shionoya, E. Kimura, *J. Chem. Soc., Dalton Trans.* **1995**, 2289–2295. – [24b] M. L. Brader, E. W. Ainscough, E. N. Baker, A. M. Brodie, S. L. Ingham, *J. Chem. Soc., Dalton Trans.* **1990**, 2785–2792. – [24c] J. C. Jeffery, P. L. Jones, K. L. V. Mann, E. Psillakis, J. A. McCleverty, M. D. Ward, C. M. White, *Chem. Commun.* **1997**, 175–176.

[25] K. Hegetschweiler, V. Gramlich, M. Ghisletta, H. Samaras, *Inorg. Chem.* **1992**, *31*, 2341–2346.

[26] D. Gatteschi, *Adv. Mater.* **1994**, *6*, 635–645.

[27] [27a] J. C. Bonner, M. E. Fisher, *Phys. Rev.* **1964**, *135A*, 640–658. – [27b] G. A. Baker Jr., J. L. Gammel, J. G. Willis, *J. Math. Anal. Applications* **1961**, *2*, 405–418.

[28] P. Gans, A. Sabatini, A. Vacca, *J. Chem. Soc., Dalton Trans.* **1985**, 1195–1200.

[29] R. J. Motekaitis, A. E. Martell, *Can. J. Chem.* **1982**, *60*, 2403–2409.

[30] Crystallographic data (excluding structure factors) for tab·4HCl·H_2O have been deposited with the Cambridge Crystallographic Data Centre as supplementary publication no. CCDC-102019. Copies of the data can be obtained free of charge on application to CCDC, 12 Union Road, Cambridge CB2 1EZ, UK [Fax: (internat.) + 44-1223/336033; E-mail: deposit@ccdc.cam.ac.uk].

[31] G. M. Sheldrick, *SHELXS-97, Program for Crystal Structure Solution*, Göttingen, **1997**.

[32] G. M. Sheldrick, *SHELXL-97, Program for Crystal Structure Refinement*, Göttingen, **1997**.

[33] Crystallographic data (excluding structure factors) for [Cu(trap)$_2$]Cl_2 have been deposited with the Cambridge Crystallographic Data Centre as supplementary publication no. CCDC-101980. Copies of the data can be obtained free of charge on application to CCDC, 12 Union Road, Cambridge CB2 1EZ, UK [Fax: (internat.) + 44-1223/336033; E-mail: deposit@ccdc.cam.ac.uk].

[34] H. D. Flack, *Acta Crystallogr., Sect. A* **1983**, *39*, 876.

[I98237]

Adducts of Ferrocenylboranes and Pyridine Bases: Generation of Charge-Transfer Complexes and Reversible Coordination Polymers

Marco Fontani, Frank Peters, Wolfgang Scherer, Wolfgang Wachter, Matthias Wagner*, and Piero Zanello

Eur. J. Inorg. Chem. **1998**, 1453−1465

Table 1 contains a wrong header for the last three lines; the correct Table 1 should read as follows:

Table 1. Infrared bands [cm^{-1}] of selected compounds **1**·Do and **2**·$(Do)_2$ (KBr disc) in the characteristic regions 1650−1450 cm^{-1} (C=C and C=N stretch) and 1100−1050 cm^{-1} (B−N vibration)

1·pic	**1**·DMAP	**2**·$(pic)_2$	**2**·$(DMAP)_2$	**1**·bipy·**1**	[**2**·bipy]$_n$
1628	1636	1628	1638	1622	1622
−	1544	−	1552	1540	1540
1507	−	1508	−	1493	1493
1104	1104	−	−	1100	−
1068	1076	1066	1077	1075	1075
1058	1058	1047	1060	1058	1061

pic	DMAP	bipy	bipyPr_2[a]
1606	1603	1590	1645
1563	1537	1531	1569
1497	1519	1487	1509

[a] *N*,*N*′-Bis(*n*-propyl)-4,4′-bipyridinium hexafluorophosphate.

The Editor
[C 98092]

 © WILEY-VCH Verlag GmbH, D-69451 Weinheim, 1998 1434−1948/98/1212−2087 $ 17.50+.50/0

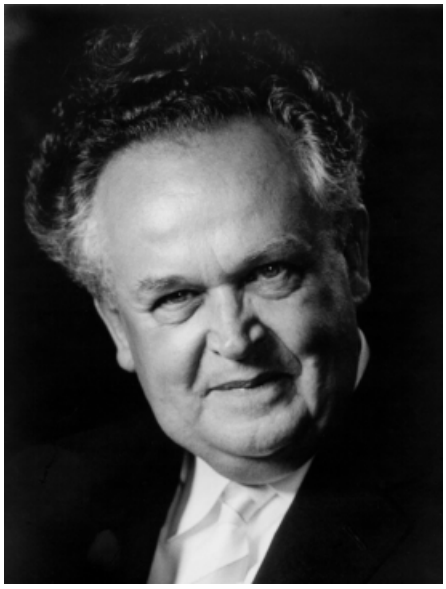

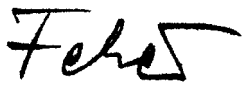

Franz Fehér (1903−1991): A Personal and Professional Portrait

On February 16, 1991 − shortly after his 88th birthday − Dr.-Ing. Franz Fehér, retired full professor of inorganic chemistry at the University of Cologne, passed away after a brief illness. This came as a great surprise to his friends, colleagues, and the large group of his former students. His death interrupted an active and practical interest in chemistry and terminated a life dedicated to science. He himself was presumably not expecting his life to end so suddenly as he had numerous plans for further publications, papers that will now remain unwritten.

In the mean time more than half a decade has passed and it is now opportune and possible to present an objective laudatio about the life and scientific achievements of this personality in inorganic chemistry − a man who made a significant contribution to the renaissance of the chemistry of non-metals after the Second World War.

Childhood, Adolescence, and University Education

Franz Fehér's life was decisively influenced by his origins as well as the political and economic events of this century. He was born on January 22, 1903 in the small town of Szentamas in southern Hungary as the third of five children. His father, a member of the Hungarian ethnic group, a mechanical engineer and businessman, owned a company dealing in agricultural machinery. His mother, maiden name Sieler, belonged to the German ethnic group that settled there in the 18th century. Together with two brothers and two sisters he enjoyed his childhood in a happy, natural family atmosphere. However, this free and easy life came to an end at the age of ten years when he entered a boarding school (Humanistisches Gymnasium) in the county town of Neu-Verbas and could only return home during the school holidays. He had no problems with his school education and, although good in all subjects, mathematics and natural sciences attracted his attention the most. In later conversations he occasionally mentioned his everlasting gratitude to his mathematics teacher.

The First World War began during his high school time, the further course of which led to enormous changes in this part of eastern Europe. At the end of the war in 1918 south Hungary became part of the newly formed kingdom of Serbia, Croatia, and Slovenia, the recently disintegrated Yugoslavia. This meant that his home town was renamed Srbobran and that the language in his school, previously Hungarian, changed to Serbian. In spite of these difficulties Franz Fehér mastered the last three years of high school and left it in June 1921 at the age of 18 with an excellent certificate of education (Reifezeugnis). With this he had made a decisive step towards fulfillment of his long held dream to read chemistry in Germany. This choice of subject was without doubt based on his proficiency for both abstract scientific thought and practical work with his hands.

During his search for a suitable place to study he was given the rather misleading advice from the German embassy in his country that one could read chemistry in Germany at a technical university (Technische Hochschule) − but not with the additional information that one could also read chemistry at a normal university albeit without the possibility of receiving a Diploma certificate. Thus, in the

 © WILEY-VCH Verlag GmbH, D-69451 Weinheim, 1998 1434−1948/98/1212−2089 $ 17.50+.50/0

winter semester of 1921/1922 Franz Fehér registered at the Technische Hochschule Hannover where Wilhelm Biltz was director and professor of inorganic chemistry. However, it was the year 1921 and veterans of the First World War were still seeking admission to higher education, especially since possibilities in other occupations were scarce because of the economic situation prevailing at that time. Hence, Wilhelm Biltz regretfully had to inform Franz Fehér at the beginning of the first semester that he could not provide a laboratory place and that the waiting time for one was uncertain. The young student, therefore, could only attend the basic lectures in chemistry and physics while applying for admission to other technical universities.

He was finally accepted by the Technische Hochschule Stuttgart for the summer semester 1922 where he continued his education with practical instruction in inorganic chemistry. Here he also attended, among others, lectures on experimental inorganic chemistry by A. Gutbier, organic chemistry by W. Küster, and physical chemistry by G. Grube. In July 1925, after only seven semesters (including a Diploma thesis on an electrochemical topic under the supervision of G. Grube) he successfully completed the first stage of his chemical education and obtained his Diploma certificate. But then his financial resources were at an end; money transferred from home became worthless from one day to the next on account of the galloping inflation in Germany at that time. Thus Franz Fehér was forced to interrupt his further scientific education for two years and to take up a teaching position for mathematics, physics, and chemistry at the Oberrealgymnasium (state high school) in his home town.

In autumn of 1927 he returned to Technische Hochschule Stuttgart to prepare a doctoral thesis under the supervision of A. Simon at the Institute of Inorganic Chemistry. His thesis entitled "Beiträge zur Kenntnis der Mangandioxydhydrate und der Manganoxyde" (Contributions to the Chemistry of Manganese Dioxide Hydrates and Manganese Oxides) was awarded the Gutbier prize of the Technische Hochschule Stuttgart. In spite of the two-year break he received the title Dr.-Ing. (graded excellent) at the age of 26.

Even during this post-graduate work, Franz Fehér's special ability to successfully solve experimental problems by the design and construction of original but simple apparatus became apparent. For example, for tensiometric investigations on various manganese oxides he developed a novel, automatic cryostat for low temperature work. A short while later this system was also used by E. Zintl and W. Klemm and reported to work very reliably. Investigations on the vapor tension curve and isobaric degradation of manganese heptoxide presented particular challenges. First of all, the preparation of the pure, highly explosive compound Mn_2O_7 in preparatively useful amounts was decisively improved. Furthermore, Franz Fehér invented a new method to measure small pressures by remote monitoring since, as he wrote, being present in the room for the accurate measurement of small pressures during the thermal treatment of manganese heptoxide proved to be highly hazardous just on account of the explosive nature of the substance. With the developed system the required pressure measurements could be made safely in a different room, at a safe distance from the decomposition apparatus.

After receiving his doctor's degree Franz Fehér participated in several research projects of his supervisor and during this time decided to follow a career in the university. At the same time he was involved in teaching at the inorganic institute in Stuttgart, first as a Hilfsassistent ("temporary assistant") and then as an Außerordentlicher Assistent ("associate assistant"). In a later conversation he once explained the significance of the latter position: during the worldwide economic crisis of 1931, many ex-students of the institute who had taken up positions in industry were dismissed by their companies and sought to return to the technical university. In order to help this group of people the planmäßigen Assistenten-Stellen ("regular assistant positions") were first divided into two and then even into four part time positions. Thus, Franz Fehér's times of financial restraint were not yet finished. As Praktikums-Assistent ("assistant in a laboratory course") he met the chemistry student Magdalena Fischer from Temesvar in Rumania who, from her father's side, belonged to the German ethnic group there. They were married in September 1931. In April of the same year he had taken on the Germany nationality. From the point of view of his home country, this meant that he had evaded his military service obligations, a serious offence. Accordingly, he was never able to return home again and later even avoided any trips to the former German Democratic Republic for fear that he could be extradited from there to Yugoslavia.

The Years in Dresden and Göttingen

In 1932 Franz Fehér accompanied A. Simon to the Technische Hochschule Dresden as Planmäßiger Assistent ("full assistant"). Here, the couple moved into a modest apartment belonging to the institute where their three daughters Magda (born in 1935), Therese (born in 1937), and Franziska (born in 1942) spent their first years of childhood.

The ten years in Dresden served first of all to survey the field of inorganic chemistry for an independent research area with a clear potential for development. Already during his time in Stuttgart, shortly after the discovery of the Raman effect in 1928, Franz Fehér had carried out first studies on the use of Raman spectroscopy to solve constitutional problems in the chemistry of non-metals. These investigations were continued in Dresden − at first in cooperation with A. Simon. For the oxo-acids of phosphorus and arsenic, the constitutions of which were a subject of controversy in the literature at that time, it was possible with the help of the Raman spectra to provide unambiguous answers to the questions as to whether and which of these anhydrous acids existed in the "aci-" or "pseudo"-form. In addition, direct information on the question of the bonding of hydrogen to the central non-metallic atom was obtained. Further work was concerned with constitutional problems of orga-

nometallic compounds. A major topic of interest from the middle of the 1930's on was the elucidation of the constitution of hydrogen peroxide and its derivatives for which at that time a Y-shaped structure with a double bond between the two oxygen atoms was assumed. Since infrared spectroscopy was then just at the beginning of its instrumental development, Raman spectroscopy was the method of choice for the solution of these constitutional questions. In addition, X-ray crystallography, the evaluation procedures for which were still also in their infancy and very laborious, was included in the investigations. A decisive prerequisite for these investigations was the often difficult synthesis of the required compounds in a pure state such as, for example, 100% hydrogen peroxide or deuterium peroxide and their preparation for crystal structure analyses. Thus, for example, single crystals of pure hydrogen peroxide were grown in the cold room of a slaughter house in Dresden. The investigations on hydrogen peroxide in which the constitutional and conformational analogies to hydrazine were demonstrated unequivocally resulted in the award of the title Dr. Ing. habil. (Habilitation) in 1938 and shortly thereafter to the "venia legendi" (authorization to hold lectures) for the subjects inorganic and analytical chemistry. They were further honored in 1941 by the award of the Carl-Bosch Prize from the former I. G. Farbenindustrie.

Even so, Franz Fehér could not continue his work at the university without interruption. Between 1935 and 1939 he was drafted to attend several training courses for the German army and took part in the operations against Poland at the beginning of the 2nd World War. Subsequently, however, within the framework of the Osenberg plan intended to protect young university lecturers and to ensure the continuation of research after the war period, he was declared an indispensable person and so could return to the Technische Hochschule Dresden. As assistant lecturer he managed the laboratory courses in quantitative analysis and preparative inorganic chemistry and held courses on the theory of chemical bonding as well as the basic principles of Raman spectroscopy and X-ray crystallographic analysis. He was generally admired and respected by his students not only because of his quiet, friendly and helpful nature but also for his extensive knowledge; he was known throughout the institute as Uncle Franz. During this time he took on a new field of interest, the acyclic sulfur compounds and above all the higher homologues of hydrogen sulfide. Continuation of this work in Cologne later led to the complete characterization of the series of sulfanes H_2S_n and chlorosulfanes S_nCl_2 up to the corresponding octasulfanes ($n = 8$) by Raman spectroscopy. These results are still to be found in all textbooks of inorganic chemistry.

In 1942 Franz Fehér was invited by Adolf Windaus to join the department of inorganic chemistry in the chemical institute at the University of Göttingen as senior assistant. He could not resist this opportunity to experience a *university* chemical institute where, according to the prevailing traditions, inorganic chemistry was only represented by a department. In the stimulating atmosphere of the institute directed by Adolf Windaus, Franz Fehér was able to continue his studies of acyclic sulfur compounds on a broader basis. In 1944 he was appointed Außerplanmäßiger Professor. Franz Fehér gained many lasting impressions from the vital scientific atmosphere of the science faculty in Göttingen. Above all, he encountered Adolf Windaus whom he admired not only as a university teacher and scientist but also as an impressive personality who served as an ideal for the rest of his life. In later conversations he often mentioned that he considered Adolf Windaus to be his truely academic teacher. During this time and with an increasing group of coworkers the Raman spectroscopic investigations on sulfanes were consequently expanded by the development of new preparative approaches as well as methods for the analytical and physicochemical characterization of the individual homologues. In spite of the difficult working and living conditions during the World War II and immediate post-war years, the seven years in Göttingen were among the most fulfilling and molding in Franz Fehér's life.

Cologne

On September 1, 1949 Franz Fehér took up the position as extraordinary professor of inorganic and analytical chemistry and head of the department of inorganic chemistry in the Institute of Chemistry of the University of Cologne. Here he faced the task of rebuilding the teaching and research facilities whose apparatus had mostly been lost during the war. Furthermore, at the beginning of the winter semester of 1949/1950 he found a long queue of prospective students waiting in front of his office, all wanting to apply for a laboratory place. Remembering his own problems at the start of his academic life, he did everything possible to help: he also held practical courses in the semester holidays, gave lectures on experimental inorganic chemistry twice a day in addition to his lectures on analytical chemistry and special inorganic chemistry.

In spite of this heavy teaching load during the first years in Cologne his research interests were not neglected. The studies of acyclic sulfur compounds started in Dresden and continued in Göttingen were systematically expanded in several directions with the help of an increasing number of coworkers. One of the questions addressed was whether, in analogy to the sulfanes, H_2S_n, other series of the compounds of the general formula S_nX_2 with skeletons made up of chain-linked sulfur atoms would exist. If so they could be considered as derivatives of the corresponding parent compounds H_2S_n and would provide possibilities for new synthetic approaches to widely differing sulfur compounds having ring and chain skeletons. Of particular interest in this context were the halosulfanes and especially the chlorosulfanes, S_nCl_2. Up till then only the compounds SCl_2 and S_2Cl_2 were known with the constitution of the latter still being uncertain. A second field of interest was the parent compound series H_2S_n with the objectives of finding new methods of synthesis and optimizing those already developed for the individual homologues. The actual purpose

behind these investigations was to achieve a practically complete spectroscopic and physicochemical characterization of these new compounds for which appropriate amounts of highly pure substances were needed. Finally, the investigations of open-chain sulfur compounds were systematically expanded to include elemental sulfur.

In the work on chlorosulfanes evidence for the existence of compounds more rich in sulfur than S_2Cl_2 was obtained in the so-called "hot-cold" tube. In this process S_2Cl_2 was allowed to react with hydrogen at 860−875°C: HCl was eliminated and the formed products were shock cooled to room temperature. In this way orange-yellow oils with the sum compositions $S_{20}Cl_2$ to $S_{24}Cl_2$ were obtained. Raman spectroscopic examinations showed that these oils consisted mainly of mixtures of higher homologous sulfur chlorides with varying chain lengths. A major breakthrough was the discovery of a preparatively more simple and more efficient method of synthesis on the basis of the observation that, under suitable conditions, the sulfanes H_2S_n undergo condensation reactions with S_2Cl_2 or SCl_2 with quantitative elimination of HCl to furnish more sulfur-rich members of the homologous series. Since the primarily formed molecules could also react similarly with elimination of HCl and chain lengthening, chlorosulfane mixtures with an average composition of S_xCl_2 were obtained from which pure S_3Cl_2 and S_4Cl_2 as well as highly enriched S_5Cl_2 were isolated by short-path, high vacuum distillation. The concentrations of all occurring molecules in dependence on the molar ratios of the starting materials were deduced by considering the kinetics of the reactions. By use of a large excess of the chlorosulfane component subsequent reactions of the primary products were suppressed so that, after removal of the excess, formula-pure higher chlorosulfanes were obtained directly. In this way sulfur-rich homologues up to S_8Cl_2 were prepared by reaction of H_2S_n with excess S_mCl_2 and subsequent removal of unconsumed chlorosulfane (Scheme 1).

Scheme 1. Preparation of chlorosulfanes

$$Cl{-}S_m{-}Cl + H{-}S_n{-}H + Cl{-}S_m{-}Cl \xrightarrow[-2\ HCl]{} Cl{-}S_{2m+n}{-}Cl$$

$m = 1, 2;\ n = 1, 2, 3, 4$

The same synthetic concept was then applied to higher members of the sulfane series itself. Of these, the compounds H_2S_2 to H_2S_6 had been prepared during the work in Göttingen from the "crude sulfane" obtained, in turn, by acidic decomposition of an aqueous solution of sodium polysulfide. With this new access at hand, the compounds H_2S_5 and H_2S_6 were prepared in high purity and, furthermore, the higher homologues H_2S_7 and H_2S_8 were also obtained.

This same synthetic route also provided an access to widely differing sulfane *derivatives*. Thus, condensation of sulfanes with chlorosulfonic acid resulted in the formation of sulfanemonosulfonic acids, $H_2S_nO_3$, reaction of which with chlorosulfanes gave the sulfur-rich sulfanedisulfonic acids (polythionic acids) $H_2S_nO_6$. In this way the free octa-, nona-, deca-, undeca-, and dodecathionic acids were prepared for the first time as oily liquids that were stable at lower temperatures (Scheme 2).

Scheme 2. Synthesis of sulfanemonosulfonic acids and sulfanedisulfonic acids (polythionic acids)

$$H{-}S_{n\text{-}1}{-}H + Cl{-}SO_3H \xrightarrow[-HCl]{} H{-}S_{n\text{-}1}{-}SO_3H$$

$$HO_3S{-}S_{n\text{-}1}{-}H + Cl{-}S_m{-}Cl + H{-}S_{n\text{-}1}{-}SO_3H \xrightarrow[-2\ HCl]{} HO_3S{-}S_{2(n\text{-}1)+m}{-}SO_3H$$

In addition, the already known diorganyl polysulfides R_2S_n, although their constitutions at that time had not been clarified with certainty, were prepared by an analogous route as were also some new representatives of this compound class. Investigations of their properties (see below) then unequivocally confirmed their identity as organo-substituted sulfanes with unbranched sulfur chains. The synthesis of "perchlorodimethyl tetrasulfide" ($Cl_3CS_4CCl_3$) from Cl_3CSCl and H_2S_2 and the determination of its structure by Raman spectroscopy can be mentioned as a typical example of these efforts. A large range of unsymmetrically substituted sulfane derivatives of the type RS_nCl and RS_nH was prepared by reaction of excess chlorosulfane or sulfane, respectively, with monofunctional compounds such as RSH, R_2NH, and RS_mCl.

Attempts to transfer the chlorosulfane synthesis to the corresponding pure bromosulfanes S_nBr_2 ($n > 2$) were not successful since the excess of dibromodisulfane S_2Br_2 remaining, on account of its high boiling point, could not be removed at the completion of the condensation without decomposition of the formed higher homologues. However, the preparation of practically pure, sulfur-richer bromosulfanes up to S_8Br_2 were possible by reaction of the corresponding chlorosulfane with hydrogen bromide.

Raman spectroscopic investigations of the already long known compounds $S(CN)_2$, $(SCN)_2$, $S(SCN)_2$, and $S_2(SCN)_2$ led to their recognition as the starting members of a homologous series of cyanosulfanes $S_n(CN)_2$ and the series was extended up to $S_8(CN)_2$ (Scheme 3).

Scheme 3. Synthesis of sulfur-rich cyanosulfanes

$$Cl{-}S_n{-}Cl + Hg(SCN)_2 \xrightarrow[-HgCl_2]{} NC{-}S_{n+2}{-}CN$$

$n = 3-6$

The electrolytic reduction of aqueous SO_2 solutions as a means to obtain larger amounts of sulfane mixtures with average compositions of H_2S_8 to H_2S_{13} was studied intensively. After clarification of the electrode processes a laboratory apparatus was developed that allowed, under continuous operation and good current yield, the simultaneous cathodic preparation of sulfane oils and the anodic production of ammonium peroxodisulfate.

The alkali metal compounds $M^I_2S_n$ were also included in the investigations as *sulfane derivatives* and detailed studies on the various anhydrous polysulfides in the systems sodium−sulfur, potassium−sulfur, rubidium−sulfur, and cesium−sulfur were carried out.

In all of the classes of compounds investigated, Franz Fehér's main target was not merely the preparation of new substances; spectacular momentary successes were not the driving force of his work. Rather, his interest was always directed towards the comprehensive exploration of a new area in inorganic chemistry. This objective required intensive structural and physicochemical characterization of the newly prepared compounds, aspects that played a decisive role in the scientific work of Franz Fehér.

Elucidation of the constitutions of the sulfanes and their various derivatives was based mainly on the results from Raman spectroscopy. As an example, the Raman spectra of the cyanosulfanes $S_n(CN)_2$ (n = 1−8) are depicted in Figure 1. These spectra show that the respective substances are chemically individual species without any traces of physically dissolved elemental sulfur. The appearance of an individual spectrum is always characteristic for the respective number of chain-linked sulfur atoms in the molecular skeleton. Electronic spectra of the various classes of compounds were also investigated systematically and discussed on the basis of Kuhn's electron gas model. These results indicated that, in addition to normal σ-bonding, delocalized π electrons were also present in the sulfur chains.

Figure 1. Raman spectra of cyanosulfanes $S_n(CN)_2$ (n = 1−8) and of S_8

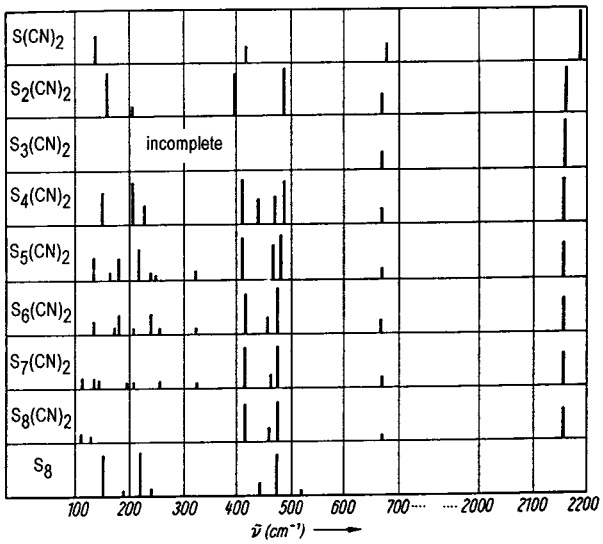

The individual compounds among the metal polysulfides were studied by X-ray methods and characterized on the basis of their powder diagrams while single crystal X-ray structural analyses of the cyanosulfanes were carried out.

The physicochemical properties of the sulfanes and chlorosulfanes were subjected to extensive studies in particular regard to the constitutions of the individual compounds. It was found that the molar volumes, molar fractions, molar enthalpies of evaporation, and the logarithms of the viscosity were linear functions of the length of the sulfur chain and that no branched chain skeletons were present. For the sulfanes H_2S_2 to H_2S_5 the boiling points and critical data were also estimated by means of vapor pressure measurements. Furthermore, the heats of decomposition of the catalytic degradation into hydrogen sulfide and sulfur were measured by calorimetry and the data used to determine the enthalpies of formation for the individual homologues up to H_2S_6. The respective values for the formation of *liquid* sulfanes from the elements in their standard states are all negative; their absolute values decrease linearly with increasing number of sulfur atoms. On the other hand, all sulfanes are metastable towards a decomposition to hydrogen sulfide and sulfur at room temperature. Their existence can be attributed to a relatively high activation barrier of the decomposition reaction which was determined to be about 25 kcal/mol for H_2S_2.

Very early in the course of these comprehensive investigations on various classes of compounds with chains of sulfur atoms, Franz Fehér recognized the many relations to the chemistry of open-chain hydrocarbons. Aside from this he had always considered the molecular chemistry of the nonmetals as a single topic and did not draw any arbitrary boundaries between inorganic and organic chemistry in his research work. His efforts to clearly express the analogies between the compounds H_2S_n and the n-alkanes C_nH_{2n+2} in the nomenclature by replacement of the then usual terms with the name "sulfanes" become understandable in this light. This results in the names "disulfane" (H_2S_2), "trisulfane" (H_2S_3) and so on for the individual homologues. This nomenclature system also clearly shows the genetic relationships between the compound classes H_2S_n, S_nX_2 (X = halogen, monofunctional group), S_nR_2 (R = alkyl, aryl), and $M^I_2S_n$ and has now been widely accepted by the chemical community. As a direct consequence, "cross-products" of sulfanes and alkanes, in particular compounds with the general formula $RS(CH_2S)_nR$ − termed "bunte" sulfanes in Fehér's laboratory − were investigated. A series of thiaalkanes was then prepared and their properties determined for the first time.

The studies on sulfur-chain compounds prompted Franz Fehér in the mid 1950's to take up an intensive investigation of elemental sulfur. It was found that many of the older results on the properties of molten sulfur were not correct since the samples investigated were of insufficient purity. Thus Fehér's group developed methods for the purification of sulfur by electrophoretic means and especially by zone melting; that latter has proved to be very suitable for obtaining highly pure sulfur. In the course of this work, the then usual analytical methods for detecting small amounts of carbon and other contaminants in sulfur had to be improved considerably. Using the thus obtained and characterized pure samples, the temperature dependence of the density and specific heat of molten sulfur in the range 120 to 400 °C was measured. Both parameters also exhibited anomalies in the region of the known viscosity increase and these were discussed in terms of the processes occurring in liquid sulfur (cleavage of S_8 rings and formation of longer S_x chains). Furthermore experiments on the electrical conductivity of molten sulfur were performed and the mecha-

nism of charge transport elucidated on the basis of these data.

In the second half of the 1950's as a supplement to the continuing work on sulfur and its compounds, increasing interest was directed to studies on the higher silicon and germanium hydrides as well as the chemistry of hydrazine and its derivatives as new research topics. In the planning of his scientific work, Franz Fehér was never influenced by current mode topics or predetermined research projects but always followed his own scientific ideas. He viewed the development and work of a scientist to be closely analogous to that of an artist. After completing her doctoral thesis and a few years of postdoctoral work in the field of sulfur chemistry, the present author asked her supervisor if he thought her abilities were sufficient for a Habilitation. After a short pause he answered "I have heard that you want to be an opera singer, then go ahead and sing" and then added the phrase "but please not on the sulfur stage!" This meant: a successful Habilitation cannot in general be predicted; it depends on the further "vocal" development and the continuing desire to "sing" in spite of the monotonous daily practicing. This example illustrates Fehér's love for colorful language that often surprised his listeners with unexpected comparisons and metaphors but always correctly reflected the topic of the conversation. The additional phrase was intended to avoid future competition between different groups in the same institute but, above all, it provided the possibility for his former student to attain an independent image in the scientific community at an early stage in her career.

In the year 1958 chemistry in Cologne experienced a drastic change accompanied by numerous new tasks for Franz Fehér . On June 20 the director of the chemistry institute of the university, the Nobel prize winner Kurt Alder died at the age of only 55 and left behind a research group consisting of over 40 diploma and doctoral students. Franz Fehér was appointed deputy director and head of the entire institute by the faculty of mathematics and sciences. It was of major importance for him that not even one of Alder's students should suffer any personal loss in his or her further education. Although the diploma students were able to move to other groups within a short time, conclusion of the doctoral thesis projects already in progress proved to be a serious problem. The scientific supervision was continued by the extraordinary professor of organic chemistry, Leonhard Birkofer and Alder's assistants. However, Kurt Alder had only been able to finance such a large research group with the help of considerable external research funds which all stopped suddenly with his death. Thus, it was essential to persuade the managers of the various sources that financial support of Alder's work was necessary for about two years more. This meant numerous applications, accountings, and reports as well as taking on the full responsibility for the use of the then personally granted research funds. Franz Fehér was fully rewarded for his efforts when, two years later, the last of Alder's postgraduate students completed his thesis and oral examination without requiring any extra time.

In spring of 1960 Franz Fehér was offered the position of full professor and director of the institute for inorganic chemistry at the university of Hamburg. This was not an easy decision for him. New buildings for the chemical institute were to be built both in Hamburg and Cologne. In Hamburg, completion of the buildings in 1965 was expected although land ownership problems still had to be solved whereas concrete building plans were already in existence in Cologne. As had already happened in other chemical institutes in Germany, the faculty for mathematics and sciences in Cologne decided under the given circumstances to divide the chemical institute into two separate institutes, one for inorganic and one for organic chemistry and started negotiations with Franz Fehér to keep him in Cologne. Decisive criteria for Franz Fehér were the working conditions for the eleven years remaining until his retirement. After careful consideration of the starting situations for the two building projects he decided in August 1960 to remain in Cologne and was appointed full professor and director of the newly founded institute for inorganic chemistry in 1961. It was one of the biggest disappointments in his life that he could only move into the new building in 1975 as retired professor while the buildings in Hamburg were indeed completed by 1965. Even so, being fully aware of his responsibilities to the future working conditions in his discipline, he spent a major part of his last decade as institute director with detail planning and supervision of the new buildings for the inorganic institute and the common lecture rooms.

The scientific work on the various research topics continued in this period with unchanged élan. Work with the higher silicon and germanium hydrides demanded new inert gas techniques to allow handling of these air- and moisture-sensitive compounds − in contrast to the classical Stock methods − also outside of closed systems. Fehér reported on the respective developments for the first time at the IUPAC congress in Munich in 1959. His experience in handling spontaneously inflammable substances was indeed in demand and led to numerous consultations with the chemical industry on similar problems. Apart from these new research interests, the chemistry of the sulfanes and their derivatives was systematically expanded with particular emphasis at this time on the development of synthetic routes to novel heterocyclic sulfur compounds.

With such widely divergent activities words such as "holidays" or "relaxation" were more or less unknown to Franz Fehér. Only his enjoyment of driving was occasionally satisfied in car journeys to the Alps or Italy with his Munich colleague Walter Hieber. Even during the years in Dresden Franz Fehér was a passionate motorcyclist who would make a short trip to the Baltic coast over the weekend − which for assistants in those days only began on Saturday afternoon − and return punctually to the institute on Monday morning. After the interruption of the war and immediate post-war years, the purchase of his first car, a Volkswagen, at the beginning of the 1950's was a major event. As

well as the joy of driving, the response of the machine to the driver's actions was always a source of pleasure for the son of a mechanical engineer. However, he could also relax in the circle of his coworkers during occasional celebrations.

With the improved working conditions of the inorganic chemistry institute the investigations on open-chain and cyclic sulfur compounds were consequently expanded. In the case of *sulfane derivatives*, the enthalpies of formation of the chlorosulfanes S_nCl_2 ($n = 2-5$) were determined by calorimetric measurements of the chlorination reactions. The corresponding values were then estimated for the higher homologues up to S_8Cl_2 on the basis of the linear dependence of the values on the length of the sulfur chain. Together with the already known enthalpies of formation of the sulfanes H_2S_n the thermal requirements of the various condensation reactions between sulfanes and chlorosulfanes thus became available.

In this period, however, the main interest in sulfane chemistry was directed towards the preparative investigation of new series of compounds containing chains of sulfur atoms; these were mainly synthesized by condensation of a chlorosulfane with an appropriate monofunctional, nonmetal compound. Examples are the preparation of bis(imidazolyl)sulfanes as well as bis(triorganosilyl)- and bis(triorganosiloxy)sulfanes (Scheme 4).

Scheme 4. Synthesis of bis(imidazolyl)sulfanes, bis(triorganosilyl)-sulfanes, and bis(triorganosiloxy)sulfanes

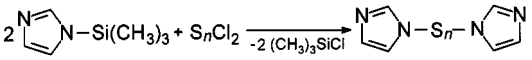

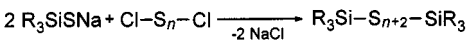

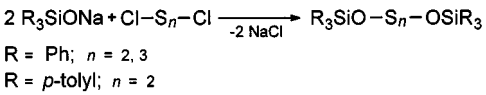

Compounds with a C=C bond directly adjacent to the sulfur chain were obtained by reactions of α,β-unsaturated mercaptans (enethiols) with chlorosulfanes. The UV spectra of these bis(enethiol)sulfanes (Scheme 5) reveal a conjugation effect of the S_n chain that is larger than the substituent effect of a *single* sulfur atom but markedly smaller than that of C=C bonds.

When the chlorosulfanes in these reactions are replaced by the bis(chlorodisulfanyl)alkanes, $ClS_2-(CH_2)_y-S_2Cl$ ($y = 1-5$) obtained from the reaction of dithiols with SCl_2, a new "crossed-type" product from alkanes and sulfanes is obtained. In the compound $Ph_3Si-S_3-(CH_2)_5-S_3-SiPh_3$ obtained from the reaction of the pentane derivative with Ph_3SiSNa the silyl groups are linked by an eleven-membered heteroatom chain.

Specific synthetic routes have also been developed for particular substance classes. Thus, Fehér and his group

Scheme 5. Bis(enethiol)sulfanes prepared

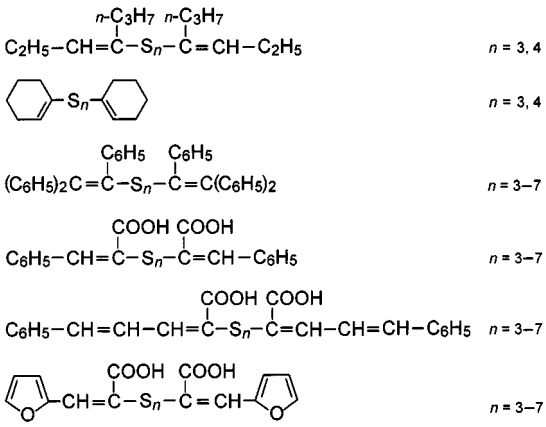

found that the bis(aziridinyl)sulfanes $(C_2H_4)-N-S_n-N(C_2H_4)$ ($n = 1-5$), only difficulty accessible via the trimethylsilyl derivative of ethyleneimine according to Scheme 4, can be obtained by smooth transfer of the sulfur chains of the corresponding bis(imidazolyl)sulfanes to ethyleneimine (Scheme 6).

Scheme 6. Synthesis of bis(aziridinyl)sulfanes

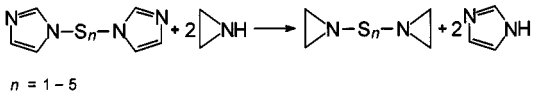

In the mid 1960's systematic investigations on a further aspect of sulfur chemistry, heterocyclic compounds containing directly linked sulfur atoms, were started. A major topic of interest for the inorganic chemist in this field were those compounds in which the individual atoms of homocyclic sulfur rings have been replaced by other bifunctional, nonmetallic groups. When these are organic units the products are the cyclocarbasulfanes. Fehér and his coworkers found that this class of compounds could, in general, be accessed by reactions of the appropriate dithiols with chlorosulfanes of varying chain lengths with the cyclocondensation being favored over polymerization by application of the Ruggli−Ziegler dilution principle. The first representative of the series S_nCH_2 to be prepared was a derivative of the S_8 ring, heptathiocane, S_7CH_2 with a crown-like eight-membered ring, from the reaction of dichloropentasulfane with methanedithiol. By analogous reactions, hexathiepane (S_6CH_2), pentathiane (S_5CH_2, with a six-membered ring analogous to that of cyclohexane), tetrathiolane (S_4CH_2), and undecathiacyclododecane (monocarbacyclododeca-sulfane, $S_{11}CH_2$) were then prepared in the pure states. *C*-Alkyl-substituted derivatives of the corresponding ring systems were obtained by use of other *geminal* aliphatic dithiols. Furthermore, sulfur rings containing two or − by reaction of the dithiols with 1,2-bis(chlorosulfanyl)benzene − also three carbon "heteroatoms" such as 1,2,3,5,6,7-hexathiocane or

1,2,4,5-benzotetrathiepine and their derivatives were also prepared (Scheme 7).

Scheme 7. Synthesis of 1,2,3,5,6,7-hexathiocane and 1,2,4,5-benzotetrathiepine and their alkyl derivatives

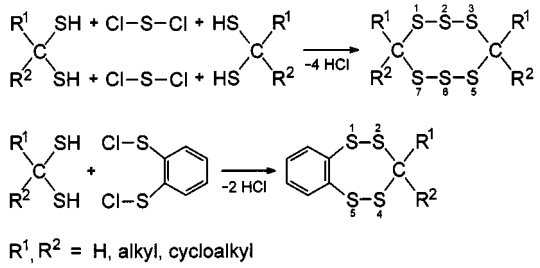

Application of the cyclocondensation reaction to vicinal dithiols such as *trans*-cyclohexane-1,2-dithiol led to bicyclic sulfur compounds with the chlorosulfanes S_nCl_2 ($n = 2-5$) and to tricyclic ring systems with dichloromonosulfane or iodine as reaction partner. Analogous reactions of 1,2-dimercaptoarenes generally led to compounds containing C=C bonds while the corresponding tricyclic systems were prepared directly by reactions of the 1,2-dithiols with 1,2-bis(chlorodisulfanyl)benzenes. Novel hexathia[3.3]cyclophanes became accessible by reactions of 1,3- and 1,4-dimercaptoarenes with dichloromonosulfane or − preparatively more favorable − 1,3- and 1,4-bis(chlorodisulfanyl)benzenes (Scheme 8).

Scheme 8. Synthesis of saturated and unsaturated bi- and tricyclic sulfur compounds bearing C_2, C_3, and C_4 groups

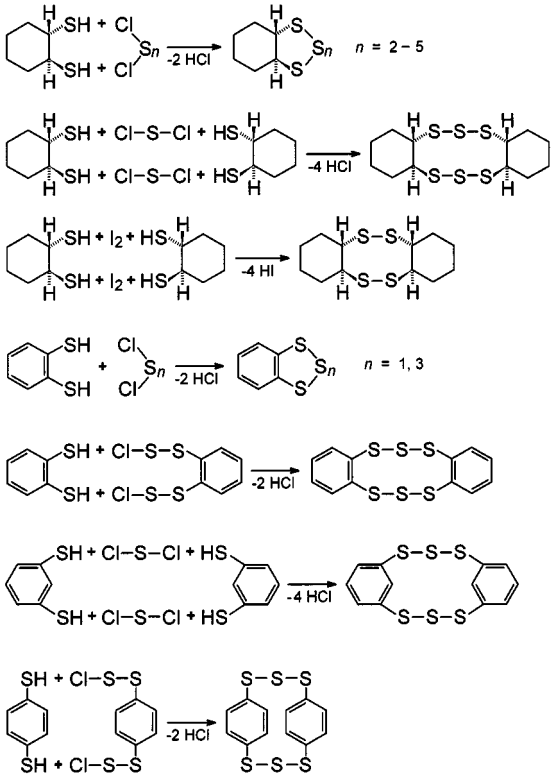

Single crystal X-ray crystallographic analyses of many of the prepared heterocyclic sulfur compounds were carried out in order to be able to compare the molecular parameters, in particular the ring conformation in the solid state, with those of the corresponding homocyclic sulfur compounds. Information on conformation changes in solution was obtained from the ^{1}H-NMR spectra recorded at differing temperatures. All new compounds were also comprehensively characterized by means of UV, IR, and Raman spectroscopy and the results interpreted from structural and bonding theory points of view.

The rich palette of topics in open-chain and cyclic sulfur compounds investigated in the ten years between the founding of the inorganic institute and Franz Fehér's retirement was only possible with the help of a relatively large group of coworkers in whom he had inspired a particular interest for the problems of the preparative chemistry of non-metallic elements. Franz Fehér was personally present in the laboratory from morning to evening and often for hours also on Sundays. He regularly attended the most important congresses for his discipline and held numerous lectures at other universities; however, he only reluctantly left his laboratories and the ongoing investigations to do so. In a critically ironic tone he designated colleagues who were often away on trips as "chemical tourists". As well as his wealth of ideas Franz Fehér provided his postgraduate students with sufficient freedom to define their research tasks and thus inspired them to individual initiative so that a fertile and trustworthy cooperation resulted. Even so, he always took the time to give advice on personal matters and provided indispensable help for the future careers of his students. Many of his students attained their Habilitation either in Cologne (M. Baudler, K.-H. Linke, H. D. Lutz) or at other universities (H. J. Berthold, G. Winkhaus) where he had smoothed the way for them. He furnished all of his 130 postgraduate students not only with a scientific education but also served them as an example for future life through his friendly open-mindedness, his unerring grasp of the essentials, and his personal modesty. However, it was not always easy to completely satisfy his strict requirements for accuracy in experiment and precise written formulations. Once he had made up his mind about a scientific or university matter on the basis of careful and well-founded considerations it was difficult to induce him to view the matter from a different direction. In general, however, he was open to compromise and revealed his personality as an academic teacher and researcher by his particular power of persuasion.

During this period, in addition to the work on the various classes of sulfur compounds, investigations on the higher silicon hydrides were continued with a small group of coworkers. After his retirement in 1971, Franz Fehér concentrated his research activities exclusively to this topic. His objectives were to continue and extend the classical works of Alfred Stock on silicon hydrides (1916−1926) with the help of modern preparative and experimental techniques and to develop a systematic chemistry of the higher silanes. By means of a specially designed high-vacuum apparatus Stock had isolated for the first time from the silicon

hydride mixture arising from the acid decomposition of magnesium silicide, in addition to monosilane (SiH_4) and disilane (Si_2H_6), small amounts of trisilane (Si_3H_8), tetrasilane (Si_4H_{10}), and a residual gas containing higher silanes. The relationships with the saturated hydrocarbons (C_nH_{2n+2}) were recognized and the name silanes adopted for the silicon hydrides Si_nH_{2n+2}. This work was interrupted in the mid 1920's because Stock was expecting an increasing instability of the higher silanes which he felt he could not master with the then available experimental techniques. In the following years, R. Schwarz postulated a mechanism for the silicide decomposition according to which the putative intermediacy of an SiH_2 biradical would be followed by the exclusive formation of silanes with unbranched Si−Si chains. However, no experimental evidence was ever presented for this hypothesis. Other methods of preparation (decomposition of magnesium silicide in non-aqueous media or reaction of silicon chlorides with lithium alanate) gave rise to mono- and disilanes but not to higher silanes. During his renewed investigation of this topic in silicon chemistry Franz Fehér was fully aware of the potential applications of higher silanes in the fields of semiconductor technology and surface coatings.

Since the acidic decomposition of magnesium silicide was then the only available method for the preparation of higher silanes and since the amounts in the formed silicon hydride mixture ("crude silane") decreased with increasing chain length, Stock's method to prepare the crude silane mixture required considerable modification as well as a scaling up to a semi-technical process. Thus, it was found in systematic studies that the yield of liquid silanes does not only depend on the rate of decomposition and the particle size of the silicide but also above all on its method of preparation. Furthermore, phosphoric acid was used in place of hydrochloric acid for the decomposition and highly pure nitrogen in place of hydrogen as carrier gas for the volatile reaction products. In particular, however, improvements in the design and construction of the apparatus with use of new inert gas techniques (see above) enabled the scale of the individual experiments to be increased and the reaction mixtures to be worked-up in rapid sequence with a high safety. Improvements over the years allowed stepwise increases in the reactor volume from at first 1 liter, to 5, 8, and finally 50 liters. With an almost technical scale apparatus (Figure 2) at hand, 2.8 liters of liquid crude silane Si_nH_{2n+2} ($n > 2$) were prepared from 80 kg of magnesium silicide within 10 days; the thus obtained material was stored in special steel vessels at room temperature.

The composition of the silane mixture formed from the silicide decomposition, which Stock could only determine with difficulty, was now easily analysed by gas chromatography. Thus, it was found that liquid crude silane contains compounds of the silane series Si_nH_{2n+2} up to pentadecasilane ($n = 15$). The proportions of the individual compounds decrease with increasing numbers of silicon atoms in the molecule. However, in contrast to earlier expectations the higher silanes are not increasingly less stable but in fact

Figure 2. Apparatus for the semi-technical production of crude silane

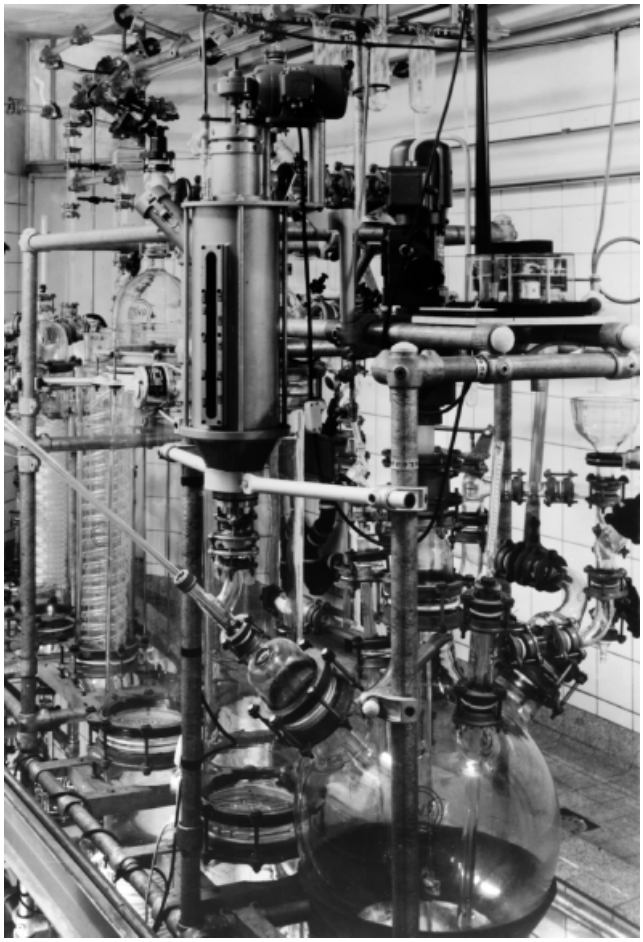

are rather easier to handle than mono- and disilane on account of their lower vapor pressures. Furthermore, it was demonstrated that the earlier postulated principle of formation of exclusively unbranched silanes (see above) is not in accord with the experimental results. Starting with tetrasilane (Si_4H_{10}) structural isomers with branched silicon chains were identified; hence, the analogy between silanes and alkanes is even closer than was assumed at that time.

Separation of the silane mixture into major fractions was achieved by column distillation and isolation of the various isomers mainly by preparative gas chromatography. It was found that the higher homologues, beginning with the heptasilanes, are no longer spontaneously inflammable. Even higher silanes are solids at room temperature, resembling the paraffins, but decompose slowly in the air. The pure compounds trisilane, *n*-tetrasilane, 2-silyltrisilane (*iso*-tetrasilane), *n*-pentasilane, 2-silyltetrasilane, *n*-hexasilane, 2-silylpentasilane, 3-silylpentasilane, and *n*-heptasilane were comprehensively characterized by physicochemical (melting points, boiling points, enthalpies of evaporation, densities, refractive indices, viscosities, surface tension measurements) and spectroscopic (Raman, IR, UV, mass, PE, ^{1}H-NMR, ^{29}Si-NMR) methods. Of these methods nuclear magnetic

resonance spectroscopy proved to be especially valuable for structure determinations.

These results revealed that some of the structural isomers of the silanes exist in very small amounts or are even absent in the liquid crude silane while the isomers with unbranched silicon chains generally dominate. Thus specific synthetic routes were developed for those isomers which were present only in traces or were absent in the mixture resulting from silicide decomposition. Starting points for these syntheses were the richly abundant compounds with small chain lengths. Thus, for example, the hexasilane isomers 2-silylpentasilane and 2,3-disilyltetrasilane were prepared by the reaction of trisilane with di-*tert*-butylmercury. Analogously, the heptasilane isomer 2,3-disilylpentasilane was obtained from a trisilane/*n*-tetrasilane mixture and the octasilane isomers 3,4-disilylhexasilane or, respectively, 2,2,3,3-tetrasilyltetrasilane were prepared from *n*-tetrasilane and *iso*-tetrasilane. A spontaneous silane isomerization in favor of the formation of the symmetrical isomer was observed for the first time between the two above-mentioned octasilane isomers. Accordingly, an isomerization of unbranched silanes to the corresponding branched homologues can in general be achieved by heating the substrate with a catalytic amount of aluminum chloride in an aromatic solvent.

The photolytic disproportionation was also investigated thoroughly as a further route to the higher silanes. It was found that the first steps of the reaction are highly selective and that the process is thus suitable as a preparative procedure. Accordingly UV irradiation of *n*-tetrasilane furnished 3-silylpentasilane, while the new branched hepta- and octasilane isomers 2-silylhexasilane, 3-silylhexasilane, 3,3-disilylpentasilane, 3-silylheptasilane, 4-silylheptasilane, and 2,3,3-trisilylpentasilane were generated by irradiation of *n*- and *iso*-pentasilane as well as *n*-hexasilane. All of these products were isolated in the pure state by gas chromatography and unequivocally characterized by spectroscopic methods.

The more highly branched isomers neopentasilane [$Si(SiH_3)_4$] and neohexasilane [$(SiH_3)_3Si-SiH_2-SiH_3$] were each prepared by multi-step reactions starting from silylpotassium ($KSiH_3$) and di- or trisilane. The initially formed mixture of more silicon-rich anions was converted to the corresponding phenyl derivatives by treatment with chloro(phenyl)silane while these derivatives were separable by gas chromatography. Cleavage of the phenyl groups by reaction with hydrogen bromide and hydrogenation of the thus formed bromosilanes then gave the respective pure silane isomers.

The last-mentioned investigations provided the compounds for numerous studies by Fehér's group on the chemical reactivity of higher silanes about which little was known at that time. The objective of this work was to develop the chemistry of the silanes to a close analogy of that of the alkanes with particular interest being focussed on reactions leading to the formation of new Si−Si bonds. This was intended to make the synthesis of more silicon-rich compounds from silicon-poorer derivatives possible and thus provide a simpler alternative to the laborious preparative route via the crude silane mixture. This topic occupied Franz Fehér up to the end of his active participation in experimental work at the age of 85. The strategy involved the initial synthesis of silane derivatives with suitably active leaving groups which would then react with formation of new Si−Si bonds. In this context, the branched isomers and their derivatives were of special interest in the light of the differing reactivities of the primary, secondary, and tertiary hydrogen atoms of these silanes.

In the class of partially halogenated silanes some already known mono- and disilane derivatives as well as a large number of novel chloro-, bromo-, and iodosilanes with two to five silicon atoms in the molecule were prepared. An important result of this work was the discovery that higher silanes did not react explosively with elemental halogens when the reactions were performed in highly diluted solutions at low temperatures. Cleavage of the Si−Si bonds only occurred to a minor extent under these conditions. Tin(IV) chloride also proved to be a suitable chlorination reagent with which mono-substituted products could be obtained preferentially. The halosilanes formed were then separated from the reaction mixtures by gas chromatography.

Alkali metal silanides of the general composition $M^ISi_nH_{2n+1}$ (M^I = K, Na) as a further group of functionalized silanes were of particular interest. During investigations on the synthesis of neopentasilane and neohexasilane (see above) it was found that di- or trisilane reacted with potassium monosilanide (silylpotassium, $KSiH_3$) via disproportionation and transmetallation to give a mixture of more silicon-rich anions. In order to make this finding of preparative utility, the known metallation of monosilane with potassium was optimized with regard to the laboratory-scale preparation of pure $KSiH_3$ and transferred to sodium. Then the reactions of the monosilanides with various silanes were studied in detail. In the course of this work, solutions of pure disilanylpotassium (KSi_2H_5), 2-trisilanylpotassium [$KSiH(SiH_3)_2$], and 2-*iso*-tetrasilanylpotassium [$KSi(SiH_3)_3$] in 1,2-dimethoxyethane were prepared starting from $KSiH_3$ and Si_2H_6 or Si_3H_8. The stability of these solutions increases from disilanyl to 2-*iso*-tetrasilanyl but complete decomposition occurs on removal of the solvent. Of preparative significance was the observation that both monosilanides also reacted with SiH_4 to afford mixtures of the more silicon-rich silanides $M^ISi_nH_{2n+1}$ (n = 2−6). These species were then converted to preparatively separable derivatives by reaction with suitable halogen-containing reaction partners such as chloro(phenyl)silane (see above) or alkyl and aryl halides. This opened a new and general route for the synthesis of new compounds containing silicon-silicon bonds starting from the easily accessible monosilane. For example, various partially organo-substituted silanes were prepared in this way (Scheme 9).

Some partially phenylated disilanes and trisilanes were prepared by specific reactions of silylpotassium with appropriate bromo(phenyl)silanes or by reactions of the corresponding iodosilanes with diphenylmercury (see Scheme 10

Scheme 9. 1-Organotrisilane, 1-organo-*iso*-tetrasilane, organoneopentasilane, and 1-organohexasilane

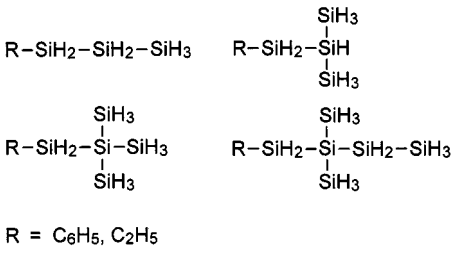

for examples). Because of the shortage of time still available to him Franz Fehér was only able to illustrate the enormous synthetic potential of the various metal silanides on a few exemplary reactions.

Scheme 10. Synthesis of 1,1-diphenyldisilane and 2-phenyltrisilane

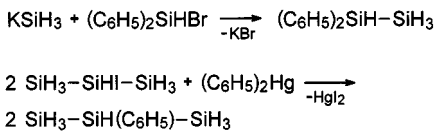

Furthermore it was found that the known reactions of monosilane and disilane with organolithium compounds could be transferred to higher homologues of the silane series. In this way the unbranched butylsilanes $C_4H_9SiH_2-(SiH_2)_n-SiH_3$ and $C_4H_9SiH_2-(SiH_2)_n-SiH_2C_4H_9$ (n = 1−3 in each case) were prepared from trisilane, *n*-tetrasilane, and *n*-pentasilane by reaction with *n*-butyllithium.

Photolytic reactions of trisilane, *n*-tetrasilane, *iso*-tetrasilane, and *n*-pentasilane in the presence of acetone gave rise to constitutional isomers of the corresponding isopropoxysilanes $[(CH_3)_2CHO]_xSi_nH_{2n+2-x}$ (x = 1−3) which were separated by gas chromatography. Hydrolyses of the preferentially formed mono-substituted products with dilute, non-oxidizing acids then furnished the bis(silanyl) ethers of tri-, *n*-tetra-, and *iso*-tetrasilane with retention of the Si−Si bonds.

The special inert gas technique developed by Franz Fehér was used in all experiments with the air-sensitive silanes and was continuously refined depending on the actual requirements. Since Franz Fehér continued to participate in the supervision of advanced inorganic chemistry laboratory courses even as retired professor in order to assist his colleagues in the years with large numbers of students, it often happened that students would specifically apply for a place in his silane laboratory for these courses. They knew that they would then have an opportunity to learn special working techniques that would be useful in their future professional careers. At the same time it was a great pleasure for Franz Fehér to personally instruct these 50-year-younger chemistry students in their experimental work and to provide them with a survey of the state of development and perspectives in a fascinating field of inorganic chemistry. Figure 3 shows Franz Fehér at the age of 84 with two students in an advanced laboratory course in his silane laboratory.

Figure 3. Franz Fehér in his silane laboratory with two students of an advanced inorganic chemistry practical course (March 1987)

In addition to his interest in the "element-near" chemistry of sulfur and silicon, Franz Fehér was involved with numerous other topics during his sixty years of active research work. Most of these individual works can be classified into three subject groups:

i. synthesis and detailed characterization of new compounds in widely differing classes of substances;

ii. resolving analytical problems that Franz Fehér considered to be an essential part of his teaching responsibilities (see above);

iii. development of new apparatus or improvement of evaluation methods for widely varying procedures that he employed in his reaseach.

The first subject group includes, among others, numerous investigations of silicophosphorus acid esters, silicothiophosphorus acid esters as well as the preparation of anhydrous hydrazine and the synthesis of germanium hydrides from magnesium germanide in the former compound as solvent. The syntheses of partially substituted, symmetrical phenyldigermanes and phenyl-substituted cyclic silicon-sulfur compounds must also be mentioned in this context. In addition, Franz Fehér carefully carried out comprehensive investigations on the crystal structure of lithium peroxide, Li_2O_2, and the spatial structures of sulfides of sodium and potassium. Furthermore, other studies were directed at the synthesis of $H_2N-NH-C(Se)-SeH\cdot N_2H_4$ and its transformation to selenocarbohydrazide, $H_2N-NH-C(Se)-NH-NH_2$.

The analytical work was mainly in connection with the investigations on open-chain sulfur compounds and on the properties of sulfur melts. Thus, for example, a gravimetric and a volumetric method were developed for the characterization of sulfanes which, however, only yielded information on the gross compositions of the respective samples. Routine determination of the contained homologues only became possible with the further development of various spectroscopic techniques. In addition, procedures for the titrimetric determination of alkali polysulfides and for the de-

termination of sulfur in zinc blendes and organic substances by digestion with hydrogen peroxide were described. Numerous experiments were concerned with the analytical characterization of elemental sulfur and, in particular, the quantitative analysis of traces of carbon down to 0.001% (see above). A polarographic method for assaying DDT was devised that was suitable both for trace analysis and for the detection of larger amounts of DDT in technical products. Taken together, the analytical works of Franz Fehér reveal a marked tendency for the application of instrumental methods and especially spectroscopic procedures.

The third group of topics includes among many others the description of a simple projector to measure weak spectral lines which at the time was of relevance for the evaluation of photographically recorded Raman spectra. In connection with the investigations of sulfur melts an adiabatic, automatically controlled calorimeter was designed for measurement of the specific heats of substances with low thermal conductivities. The studies on sulfur radicals at low temperatures required a specially designed apparatus to enable the spectroscopic characterization of short-lived photolysis products. Also, his detailed evaluation of the characteristics of the first direct-recording Raman spectrometer that replaced the old photographic spectrometer in Cologne in 1955 is an illustration of his continuous efforts to optimize the measuring techniques that he employed. The same is true for the interpretation of the respective results with regard to accuracy and concomitant simplicity. Examples of this are the description of a graphic evaluation of Debye-Scherrer exposures and an evaluation procedure for measurements in a differential heat-flow calorimeter for determining reaction enthalpies and rate constants.

The complete scientific works of Franz Fehér to which he was able to devote more than six decades of his life are documented in review articles and more than two hundred original papers, of which the last was published posthumously in 1991. In 1962, nearly thirty years earlier, the Deutsche Akademie für Naturforscher Leopoldina had elected him as a member in recognition of his outstanding scientific achievements. Franz Fehér always felt a close affection for this academic society whose election motto "Nunquam otiosus" he could have called his own since it effectively described the guiding principle of his life and he attended the general meetings even at an advanced age.

Franz Fehér was a prominent German chemist with a particular interest in experimental inorganic chemistry: whenever the properties of a substance permitted, it had to be prepared on a laboratory scale in the pure state and investigated as thoroughly as possible with all available analytical, physicochemical, and spectroscopic methods (including X-ray crystallography). In his research work he repeatedly disregarded the boundaries to physical and organic chemistry, being aware that the division of chemistry into the various fields was reasonable under organizational aspects but of no relevance from a scientific point of view. Many of the results from his work and ideas from his original discussions have long been held to be common scientific property and are − often in ignorance of their source − still widely used. On the whole it can be stated that Franz Fehér and his students made major advances in widely differing fields which have provided decisive impulses for the development of the chemistry of the non-metallic elements.

In the middle of his 85th year Franz Fehér's physical strength began to decline so that his attendances in the institute became less frequent. Even so he still participated intensively in the general scientific life and academic events at the University of Cologne. During a short hospitalization for cardiovascular support he suddenly but painlessly passed away and thus a varied life dedicated with extraordinary consequence to chemistry came to an end.

Acknowledgement

I warmly thank his daughter, Dr. *Magda Fehér*, for providing the photographs and much useful information as well as for the preparation of the list of publications. I am also grateful to Dr. *R. E. Dunmur* (Ditzingen) for the English translation of this manuscript.

Marianne Baudler

List of Publications

F. F.: Beiträge zur Kenntnis der Mangandioxydhydrate und der Manganoxyde, Dissertation, Technische Hochschule Stuttgart, **1929**.

F. F.: Ramanspektroskopische und röntgenographische Untersuchungen an HDO_2, D_2O_2 und Alkaliperoxyden, Habilitationsschrift, Technische Hochschule Dresden, **1938**.

A. Original Papers

[1] A. Simon, F. F., Eine neue Methode zur Messung kleiner Drucke mit Fernanzeige, *Z. Elektrochem. Angew. Phys. Chem.* **1929**, *35*, 162−165.

[2] A. Simon, F. F., Beiträge zur Kenntnis von Hydrogelen, X: Über Mangandioxydhydrate, *Kolloid Z.* **1931**, *54*, 49−58.

[3] F. F., Über einen neuen einfachen automatischen Kryostaten, *Z. Elektrochem. Angew. Phys. Chem.* **1932**, *38*, 53−54.

[4] A. Simon, F. F., Beiträge zur Kenntnis von Oxyden, VI: Zur Kenntnis der Oxyde des Mangans, *Z. Elektrochem. Angew. Phys. Chem.* **1932**, *38*, 137−148.

[5] A. Simon, F. F., Ramaneffekt und Konstitution beim Wasserstoffsuperoxyd, *Z. Elektrochem. Angew. Phys. Chem.* **1935**, *41*, 290−293.

[6] F. F., F. Klötzer, Die Kristallstruktur des Wasserstoffsuperoxydes, *Z. Elektrochem. Angew. Phys. Chem.* **1935**, *41*, 850−851.

[7] A. Simon, F. F., Über das Raman-Spektrum des Dioxans, *Ber. Dtsch. Chem. Ges.* **1936**, *69*, 214−217.

[8] A. Simon, F. F., Über die Beeinflussung des Ramanspektrums von Dioxan durch gelöste Stoffe, *Z. Elektrochem. Angew. Phys. Chem.* **1936**, *42*, 688−691.

[9] A. Simon, F. F., Beiträge zur Kenntnis der Konstitutionen der Säuren der Elemente der 5. Hauptgruppe des periodischen Systems und ihrer Salze, I: Über die Säuren des Phosphors: H_3PO_4, H_3PO_3, H_3PO_2 und ihre Salze, *Z. Anorg. Allg. Chem.* **1937**, *230*, 289−307.

[10] A. Simon, F. F., Über einen einfachen Projektor zur Ausmessung schwacher Spektrallinien, *Z. Anorg. Allg. Chem.* **1937**, *230*, 308−309.

[11] F. F., G. Morgenstern, Beiträge zur Kenntnis der Konstitutionen der Säuren der Elemente der 5. Hauptgruppe des periodi-

schen Systems und ihrer Salze, II: Über die Säuren des Arsens, *Z. Anorg. Allg. Chem.* **1937**, *232*, 169−178.
[12] F. F., F. Klötzer, Die Kristallstruktur des Wasserstoffsuperoxydes, *Z. Elektrochem. Angew. Phys. Chem.* **1937**, *43*, 822−826.
[13] F. F., G. Morgenstern, Über die Ramanspektren der Salze der Sulfarsensäuren, *Naturwissenschaften* **1937**, *25*, 618.
[14] F. F., G. Morgenstern, Das Ramanspektrum der D_3AsO_4 und ihrer Salze, *Naturwissenschaften* **1937**, *25*, 831.
[15] F. F., W. Kolb, Über die Raman-Spektren des Aluminium- und Arsentrimethyls, *Naturwissenschaften* **1939**, *27*, 615−616.
[16] F. F., W. Kolb, Ramanspektrum des Trimethylaluminium-Äthylätherats, *Naturwissenschaften* **1939**, *27*, 616.
[17] F. F., Beiträge zur Kenntnis des Wasserstoffperoxydes und seiner Derivate, III: Über die Raman-Spektren von D_2O_2 und DHO_2, *Ber. Dtsch. Chem. Ges.* **1939**, *72*, 1778−1788.
[18] F. F., Beiträge zur Kenntnis des Wasserstoffperoxydes und seiner Derivate, IV: Präparative Darstellung des reinen D_2O_2, *Ber. Dtsch. Chem. Ges.* **1939**, *72*, 1789−1798.
[19] F. F., Über die graphische Auswertung von Debye-Scherrer-Aufnahmen, *Z. Elektrochem. Angew. Phys. Chem.* **1941**, *47*, 369−374.
[20] F. F., M. Baudler, Beiträge zur Chemie des Schwefels, I: Über das Ramanspektrum und die Konstitution des Wasserstoffdisulfides, *Z. Elektrochem. Angew. Phys. Chem.* **1941**, *47*, 844−848.
[21] F. F., M. Baudler, Beiträge zur Kenntnis des Wasserstoffperoxyds und seiner Derivate, V: Über das Raman-Spektrum des Methylhydroperoxyds, *Ber. Dtsch. Chem. Ges.* **1943**, *76*, 939−942.
[22] F. F., M. Baudler, Beiträge zur Chemie des Schwefels, II: Über eine neue Darstellungsmethode von Wasserstoffdisulfid, *Z. Anorg. Allg. Chem.* **1947**, *253*, 170−172.
[23] F. F., M. Baudler, Beiträge zur Chemie des Schwefels, III: Präparative Darstellung und Eigenschaften des Wasserstofftrisulfids, *Z. Anorg. Allg. Chem.* **1947**, *254*, 251−254.
[24] F. F., M. Baudler, Beiträge zur Chemie des Schwefels, IV: Über die Existenz und Darstellung von Wasserstofftetrasulfid, *Z. Anorg. Allg. Chem.* **1947**, *254*, 289−292.
[25] F. F., W. Kolb, L. Leverenz, Über die Raman-Spektren von Zink-, Cadmium- und Quecksilberdimethyl sowie von Quecksilbermethylhalogeniden, *Z. Naturforsch.*, *Teil A,* **1947**, *2*, 454−457.
[26] F. F., E. Heuer, Beiträge zur Chemie des Schwefels, VI: Über die elektrochemische Darstellung von Polyschwefelwasserstoffen, *Angew. Chem. A 59*, **1947**, 237−238.
[27] F. F., E. Heuer, Beiträge zur Chemie des Schwefels, VII: Zur Thermochemie der Polyschwefelwasserstoffe, *Z. Anorg. Allg. Chem.* **1947**, *255*, 185−194.
[28] F. F., B. Talpay, E. Heuer, Beiträge zur Chemie des Schwefels, V: Über ein neues analytisches Bestimmungsverfahren für Polyschwefelwasserstoffe, *Z. Anorg. Allg. Chem.* **1948**, *255*, 316−322.
[29] F. F., M. Baudler, Beiträge zur Chemie des Schwefels, VIII: Über das Wasserstoffpentasulfid H_2S_5 und das Wasserstoffhexasulfid H_2S_6, *Z. Anorg. Allg. Chem.* **1949**, *258*, 132−149.
[30] F. F., H. Klug, L. Emmerich, Beiträge zur Chemie des Schwefels, IX: Über die maßanalytische Bestimmung von Schwefelwasserstoffverbindungen, *Z. Anorg. Allg. Chem.* **1949**, *260*, 273−278.
[31] F. F., E. Heuer, Beiträge zur Kenntnis des Wasserstoffperoxyds und seiner Derivate, VI: Über ein quantitatives Bestimmungsverfahren für Schwefel in Zinkblenden und organischen Substanzen durch Aufschluß mit H_2O_2, *Angew. Chem.* **1950**, *62*, 162−165.
[32] F. F., H. J. Berthold, Beiträge zur Chemie des Schwefels, X: Über langkettige Glieder der Schwefelwasserstoffreihe H_2S_x, *Z. Anorg. Allg. Chem.* **1952**, *267*, 251−260.
[33] F. F., M. Baudler, Beiträge zur Chemie des Schwefels, XI: Über höhere Schwefelchloride der Zusammensetzung S_xCl_2, *Z. Anorg. Allg. Chem.* **1952**, *267*, 293−303.
[34] F. F., W. Laue, J. Kraemer, Beiträge zur Chemie des Schwefels, XII: Über die Darstellung von Schwefelölen S_xH_2 und S_xCl_2 mit wählbarer mittlerer Kettenlänge, *Z. Naturforsch.*, *Teil B*, **1952**, *7*, 574−575.
[35] F. F., H. J. Berthold, Beiträge zur Chemie des Schwefels, XIII: Die titrimetrische Bestimmung reiner Alkalipolysulfide, *Fresenius' Z. Anal. Chem.* **1953**, *138*, 245−249.
[36] F. F., H. J. Berthold, Beiträge zur Chemie des Schwefels, XIV: Über das System Natrium-Schwefel, *Z. Anorg. Allg. Chem.* **1953**, *273*, 144−160.
[37] F. F., H. J. Berthold, Beiträge zur Chemie des Schwefels, XV: Über das System Kalium-Schwefel, *Z. Anorg. Allg. Chem.* **1953**, *274*, 223−233.
[38] F. F., W. Laue, Beiträge zur Chemie des Schwefels, XVI: Zur Nomenklatur von kettenförmigen Schwefelverbindungen, *Z. Naturforsch.*, *Teil B*, **1953**, *8*, 687.
[39] F. F., J. Kraemer, Beiträge zur Chemie des Schwefels, XVII: Zur Kenntnis einzelner Glieder der homologen Reihe Cl_2S_n, *Z. Naturforsch.*, *Teil B*, **1953**, *8*, 687−688.
[40] F. F., G. Rempe, Beiträge zur Chemie des Schwefels, XVIII: Über Bromsulfane Br_2S_n, *Z. Naturforsch.*, *Teil B*, **1953**, *8*, 688−689.
[41] F. F., I. von Wilucki, G. Dost, Beiträge zur Kenntnis des Wasserstoffperoxyds und seiner Derivate, VII: Über die Kristallstruktur des Lithiumperoxyds, Li_2O_2, *Chem. Ber.* **1953**, *86*, 1429−1437.
[42] F. F., E. Schliep, H. Weber, Beiträge zur Chemie des Schwefels, XIX: Über die elektrochemische Darstellung der Sulfane H_2S_n, *Z. Elektrochem.* **1953**, *57*, 916−924.
[43] F. F., H. J. Berthold, Beiträge zur Chemie des Schwefels, XX: Die Raumchemie der Sulfide von Natrium und Kalium, *Z. Anorg. Allg. Chem.* **1954**, *275*, 241−248.
[44] F. F., J. Kraemer, G. Rempe, Beiträge zur Chemie des Schwefels, XXI: Zur Darstellung von höheren Halogensulfanen S_xCl_2 und S_xBr_2 im heiß-kalten Rohr, *Z. Anorg. Allg. Chem.* **1955**, *279*, 18−27.
[45] F. F., H. Weber, Darstellung höherer Pseudohalogen-Sulfane, *Angew. Chem.* **1955**, *67*, 231.
[46] F. F., W. Laue, J. Kraemer, Beiträge zur Chemie des Schwefels, XXII: Die Reaktion zwischen Sulfanen H_2S_n und Chlorsulfanen S_mCl_2, *Z. Anorg. Allg. Chem.* **1955**, *281*, 151−160.
[47] F. F., G. Rempe, Beiträge zur Chemie des Schwefels, XXIII: Zur Darstellung höherer Bromsulfane S_xBr_2, *Z. Anorg. Allg. Chem.* **1955**, *281*, 161−168.
[48] F. F., H. J. Berthold, Beiträge zur Chemie des Schwefels, XXV: Darstellung höherer Sulfide vom Typ $Cl_3C-S_x-CCl_3$ mit Hilfe von Sulfanen, *Chem. Ber.* **1955**, *88*, 1634−1640.
[49] F. F., W. Tromm, Die Darstellung von Silanen aus Magnesiumsilicid und Hydrazoniumchlorid in wasserfreiem Hydrazin, *Z. Anorg. Allg. Chem.* **1955**, *282*, 29−40.
[50] F. F., K. Naused, Beiträge zur Chemie des Schwefels, XXVI: Über die Systeme Rubidium-Schwefel und Caesium-Schwefel, *Z. Anorg. Allg. Chem.* **1956**, *283*, 79−87.
[51] F. F., H. J. Berthold, Beiträge zur Chemie des Schwefels, XXIV: Ramanspektroskopische Untersuchungen über das Perchlormethylmercaptan, Berechnung der Behinderungsenergie der inneren Rotation und einiger thermodynamischer Funktionen, *Z. Anorg. Allg. Chem.* **1956**, *284*, 60−68.
[52] F. F., H. Weber, Das Ramanspektrum des ″Rhodantrichlorids″, *Z. Naturforsch.*, *Teil B*, **1956**, *11*, 426.
[53] F. F., W. Laue, Beiträge zur Chemie des Schwefels, XXVII: Die Molekülverteilung bei der Kondensationsreaktion zwischen Sulfanen und Halogensulfanen, *Z. Anorg. Allg. Chem.* **1956**, *287*, 45−50.
[54] F. F., J. Cremer, W. Tromm, Über die Darstellung von wasserfreiem Hydrazin, *Z. Anorg. Allg. Chem.* **1956**, *287*, 175−185.
[55] F. F., L. Meyer, Beiträge zur Chemie des Schwefels, XXVIII: Über die Darstellung der Chlorsulfane S_3Cl_2 und S_4Cl_2, *Z. Naturforsch.*, *Teil B*, **1956**, *11*, 605−606.
[56] F. F., W. Laue, Beiträge zur Chemie des Schwefels, XXIX: Über die Darstellung von Rohsulfanen, *Z. Anorg. Allg. Chem.* **1956**, *288*, 103−112.
[57] F. F., W. Laue, G. Winkhaus, Beiträge zur Chemie des Schwefels, XXX: Über die Darstellung der Sulfane H_2S_2, H_2S_3, H_2S_4 und H_2S_5, *Z. Anorg. Allg. Chem.* **1956**, *288*, 113−122.
[58] F. F., G. Winkhaus, Beiträge zur Chemie des Schwefels, XXXI: Über die Darstellung der Sulfane H_2S_5, H_2S_6, H_2S_7 und H_2S_8, *Z. Anorg. Allg. Chem.* **1956**, *288*, 123−130.
[59] F. F., H. Weber, Beiträge zur Chemie des Schwefels, XXXII: Kinetische Untersuchungen über den thermischen Zerfall des Disulfans H_2S_2, *Z. Elektrochem.* **1957**, *61*, 285−295.
[60] F. F., G. Kuhlbörsch, A. Blümcke, H. Keller, K. Lippert, Präparative und ramanspektroskopische Untersuchungen über Silicophosphorsäureester, *Chem. Ber.* **1957**, *90*, 134−144.
[61] F. F., W. Laue, G. Winkhaus, Beiträge zur Chemie des Schwefels, XXXIV: Molvolumina und Molrefraktionen der Sulfane

und ihre Abhängigkeit von der Kettenlänge, *Z. Anorg. Allg. Chem.* **1957**, *290*, 52−57.
[62] F. F., K.-H. Sauer, Beiträge zur Chemie des Schwefels, XXXV: Die Bestimmung von Kohlenstoff im gereinigten Schwefel, *Z. Naturforsch.*, *Teil B*, **1957**, *12*, 65.
[63] F. F., R. Berthold, Beiträge zur Chemie des Schwefels, XXXVI: Über die Umsetzung von definierten höheren Alkalisulfiden mit wasserfreier Ameisensäure, *Z. Anorg. Allg. Chem.* **1957**, *290*, 251−257.
[64] F. F., K. Naused, H. Weber, Beiträge zur Chemie des Schwefels, XXXVII: Über die Darstellung und Eigenschaften der Chlorsulfane S_3Cl_2, S_4Cl_2, S_5Cl_2 und S_6Cl_2, *Z. Anorg. Allg. Chem.* **1957**, *290*, 303−319.
[65] F. F., G. Krause, K. Vogelbruch, Beiträge zur Chemie des Schwefels, XXXVIII: Zur Kenntnis der Dialkyl- und Diarylsulfane, *Chem. Ber.* **1957**, *90*, 1570−1577.
[66] F. F., W. Kruse, W. Laue, Beiträge zur Chemie des Schwefels, 39: Über die Viskositäten der Sulfane, *Z. Anorg. Allg. Chem.* **1957**, *292*, 203−209.
[67] F. F., G. Winkhaus, Beiträge zur Chemie des Schwefels, 40: Zur Thermochemie der Sulfane: Bildungsenthalpien und Bindungsenergien, *Z. Anorg. Allg. Chem.* **1957**, *292*, 210−223.
[68] F. F., A. Blümcke, Präparative und ramanspektroskopische Untersuchungen über Silico-thiophosphorsäureester, *Chem. Ber.* **1957**, *90*, 1934−1945.
[69] F. F., W. Kruse, Beiträge zur Chemie des Schwefels, 41: Über die Reaktion des Schwefelwasserstoffes mit Chlorsulfanen bzw. Chlor oder Brom (Synthese niederer Sulfane), *Z. Anorg. Allg. Chem.* **1958**, *293*, 302−306.
[70] F. F., S. Ristic, Beiträge zur Chemie des Schwefels, 42: Über die Synthese der Chlorsulfane S_5Cl_2, S_6Cl_2, S_7Cl_2 und S_8Cl_2, *Z. Anorg. Allg. Chem.* **1958**, *293*, 307−310.
[71] F. F., S. Ristic, Beiträge zur Chemie des Schwefels, 43: Über die Darstellung definierter Bromsulfane S_nBr_2 durch Umwandlung entsprechender Chlorsulfane S_nCl_2 mit Hilfe von Bromwasserstoff, *Z. Anorg. Allg. Chem.* **1958**, *293*, 311−313.
[72] F. F., G. Hitzemann, Beiträge zur Chemie des Schwefels, 44: Verdampfungsenthalpien, Dampfdrucke, Siedepunkte, kritische Temperaturen und Drucke sowie Troutonsche Konstanten von Sulfanen, *Z. Anorg. Allg. Chem.* **1958**, *294*, 50−62.
[73] F. F., J. Cremer, Eine einfache Methode zur Darstellung von absolutem Hydrazin, *Z. Anorg. Allg. Chem.* **1958**, *293*, 343−344.
[74] F. F., E. Hellwig, Beiträge zur Chemie des Schwefels, 45: Zur Kenntnis des flüssigen Schwefels (Dichte, Ausdehnungskoeffizient und Kompressibilität), *Z. Anorg. Allg. Chem.* **1958**, *294*, 63−70.
[75] F. F., G. Winkhaus, Beiträge zur Chemie des Schwefels, 48: Über die Reaktion von Sulfanen mit Chloral, *Chem. Ber.* **1958**, *91*, 217−222.
[76] F. F., E. Hellwig, Beiträge zur Chemie des Schwefels, 46: Zur Kenntnis des flüssigen Schwefels (Temperaturabhängigkeit der spezifischen Wärme), *Z. Anorg. Allg. Chem.* **1958**, *294*, 71−80.
[77] F. F., R. Schulze-Rettmer, Beiträge zur Chemie des Schwefels, 47: Die Molwärme des gasförmigen Disulfans und das Hemmpotential der Inneren Rotation, *Z. Anorg. Allg. Chem.* **1958**, *295*, 262−267.
[78] F. F., H. Weber, Beiträge zur Chemie des Schwefels, 49: Über die homologe Reihe der Cyansulfane $S_n(CN)_2$, *Chem. Ber.* **1958**, *91*, 642−650.
[79] F. F., K. Vogelbruch, Beiträge zur Chemie des Schwefels, 50: Zur Kenntnis der Thiaalkane, *Chem. Ber.* **1958**, *91*, 996−1005.
[80] F. F., J. Schotten, B. Thomas, Beiträge zur Chemie des Schwefels, 51: Über die Synthese von Polythionsäuren, *Z. Naturforsch.*, *Teil B*, **1958**, *13*, 624−625.
[81] F. F., J. Cremer, Die Darstellung von Germaniumwasserstoffen aus Magnesiumgermanid und Hydraziniumchlorid in wasserfreiem Hydrazin, *Z. Anorg. Allg. Chem.* **1958**, *297*, 14−22.
[82] F. F., H. Weber, Beiträge zur Chemie des Schwefels, 52: Zur Kenntnis des Rhodantrichlorids und einiger seiner Derivate, *Chem. Ber.* **1958**, *91*, 2523−2527.
[83] F. F., W. Kruse, Beiträge zur Chemie des Schwefels, 53: Über unsymmetrische Sulfanderivate des Typs RS_nCl und RS_nH, *Chem. Ber.* **1958**, *91*, 2528−2531.
[84] F. F., S. Eckhard, K. H. Sauer, Beiträge zur Chemie des Schwefels, 54: Die analytische Charakteristik des käuflichen und des gereinigten Schwefels, *Fresenius' Z. Anal. Chem.* **1959**, *168*, 88−101.
[85] F. F., G. Kuhlbörsch, H. Luhleich, Über eine neue, einfache Arbeitstechnik zur Handhabung der Silane und anderer luft- oder feuchtigkeitsempfindlicher Flüssigkeiten, *Z. Naturforsch.*, *Teil B*, **1959**, *14*, 466−467.
[86] F. F., K. Lippert, Untersuchungen über Silicophosphorsäureester, *Chem. Ber.* **1959**, *92*, 2998−3006.
[87] F. F., G. Kuhlbörsch, H. Luhleich, Beiträge zur Chemie des Siliciums und Germaniums, IV: Über die Darstellung des Rohsilans, *Z. Anorg. Allg. Chem.* **1960**, *303*, 283−293.
[88] F. F., G. Kuhlbörsch, H. Luhleich, Beiträge zur Chemie des Siliciums und Germaniums, V: Über eine neue, einfache Arbeitstechnik zur Handhabung der Silane und anderer luft- oder feuchtigkeitsempfindlicher Flüssigkeiten, *Z. Anorg. Allg. Chem.* **1960**, *303*, 294−302.
[89] F. F., K. H. Sauer, H. Monien, Beiträge zur Chemie des Schwefels, 55: Zur analytischen Charakteristik des elementaren Schwefels, *Fresenius' Z. Anal. Chem.* **1960**, *177*, 109−113.
[90] F. F., K. Lippert, Untersuchungen über Silicophosphorsäureester und Silico-thiophosphorsäureester, *Chem. Ber.* **1961**, *94*, 2437−2441.
[91] F. F., D. Hirschfeld, K.-H. Linke, Beiträge zur Chemie des Schwefels, 55: Additionsverbindungen des Schwefels, *Acta Crystallogr.* **1962**, *15*, 1182−1183.
[92] F. F., D. Hirschfeld, K.-H. Linke, Beiträge zur Chemie des Schwefels, 57: Die Polymerisation der Cyansulfane, *Z. Naturforsch.*, *Teil B*, **1962**, *17*, 624.
[93] F. F., D. Hirschfeld, K.-H. Linke, Über das Selenocarbazinsaure Hydrazinium, *Z. Naturforsch.*, *Teil B*, **1962**, *17*, 625.
[94] F. F., D. Hirschfeld, K.-H. Linke, Über das Selenocarbohydrazid, *Z. Naturforsch.*, *Teil B*, **1962**, *17*, 625−626.
[95] F. F., D. Hirschfeld, K.-H. Linke, Kristallographische Daten des Selenocarbohydrazids, $CSe(NH-NH_2)_2$, *Acta Crystallogr.* **1962**, *15*, 1062.
[96] F. F., D. Hirschfeld, K.-H. Linke, Zur Kristallstruktur des Natriumhypochlorits, $NaClO \cdot 5\ H_2O$, *Acta Crystallogr.* **1962**, *15*, 1188.
[97] F. F., K.-H. Schäfer, W. Becher, Beiträge zur Chemie des Schwefels, 64: Oxydationsprodukte organischer Sulfanderivate, *Z. Naturforsch.*, *Teil B*, **1962**, *17*, 847−848.
[98] F. F., K.-H. Schäfer, Umsetzung von Alkylschwefeltrichlorid und Schwefeltetrachlorid mit Äthylmercaptan, *Z. Naturforsch.*, *Teil B*, **1962**, *17*, 849.
[99] F. F., D. Hirschfeld, K.-H. Linke, Beiträge zur Chemie des Schwefels, 56: Zur Kristallstruktur einiger Cyansulfane, *Acta Crystallogr.* **1963**, *16*, 154.
[100] F. F., K. H. Sauer, H. Monien, Beiträge zur Chemie des Schwefels, 58: Charakteristik der gebräuchlichen Reinigungsverfahren des Schwefels durch Bestimmung des Kohlenstoffs, *Fresenius' Z. Anal. Chem.* **1963**, *192*, 389−396.
[101] F. F., K. Seyfried, Beiträge zur Chemie des Schwefels, LIX: Die spezifischen Wärmen der Sulfane im flüssigen Zustand, *Z. Anorg. Allg. Chem.* **1963**, *322*, 155−161.
[102] F. F., K. Seyfried, Beiträge zur Chemie des Schwefels, LX: Bestimmung des Hemmpotentials der inneren Rotation des Disulfans, *Z. Anorg. Allg. Chem.* **1963**, *322*, 162−171.
[103] F. F., F. Sträter, Beiträge zur Chemie des Schwefels, LXI: Bestimmung der Bildungsenthalpien der Chlorsulfane, *Z. Anorg. Allg. Chem.* **1963**, *322*, 172−180.
[104] F. F., H. Münzner, Beiträge zur Chemie des Schwefels, 62: Ultraviolett-Absorptionsspektren kettenförmiger Schwefelverbindungen, *Chem. Ber.* **1963**, *96*, 131−1149.
[105] F. F., H. Münzner, Beiträge zur Chemie des Schwefels, 63: Zur Kenntnis der Jodsulfane, *Chem. Ber.* **1963**, *96*, 1150−1155.
[106] F. F., W. Becher, R, Kreutz, F.-R. Minz, Beiträge zur Chemie des Schwefels, 66: Über die Darstellung und Eigenschaften der Diäthylester der Penta- und Hexasulfandicarbonsäuren sowie der entsprechenden Monothiocarbonsäuren, *Z. Naturforsch.*, *Teil B*, **1963**, *18*, 507−508.
[107] F. F., H. Strack, Die gaschromatographische Trennung von Siliciumwasserstoffen an Squalan-Kieselgur-Trennsäulen, *Naturwissenschaften* **1963**, *50*, 570−571.
[108] F. F., G. Jansen, H. Rohmer, Verbrennungswärmen und Bildungsenthalpien von SiH_4, Si_2H_6, Si_3H_8 und *n*-Si_4H_{10}, *Angew. Chem.* **1963**, *75*, 859; *Angew. Chem. Int. Ed. Engl.* **1963**, *2*, 617−618.
[109] F. F., K.-H. Linke, Beiträge zur Chemie des Schwefels, LXVII:

Die Kristallstruktur von Dicyantrisulfan NC−S_3−CN, *Z. Anorg. Allg. Chem.* **1964**, *327*, 151−158.
[110] F. F., G. Jansen, H. Rohmer, Beiträge zur Chemie des Siliciums und Germaniums, VI: Die Bildungsenthalpien von Mono-, Di-, Tri- und *n*-Tetrasilan, *Z. Anorg. Allg. Chem.* **1964**, *329*, 31−43.
[111] F. F., H. Monien, Zur quantitativen polarographischen Bestimmung von DDT, *Fresenius' Z. Anal. Chem.* **1964**, *204*, 19−25.
[112] F. F., K.-H. Linke, Beiträge zur Chemie des Schwefels, 68: Über die Umsetzung von Dirhodan mit Brom, *Chem. Ber.* **1964**, *97*, 2413−2417.
[113] F. F., H. D. Lutz, Beiträge zur Chemie des Schwefels, 70: Die elektrische Leitfähigkeit des flüssigen Schwefels, *Z. Anorg. Allg. Chem.* **1964**, *333*, 216−225.
[114] F. F., H. D. Lutz, Beiträge zur Chemie des Schwefels, 71: Die Reinigung von Schwefel auf elektrophoretischem Wege, *Z. Anorg. Allg. Chem.* **1964**, *334*, 202−204.
[115] F. F., H. Fischer, Raman- und ultrarotspektroskopische Untersuchungen an Silanen, *Naturwissenschaften* **1964**, *51*, 461.
[116] F. F., H. D. Lutz, Beiträge zur Chemie des Schwefels, 72: Die Anwendung des Zonenschmelzverfahrens zur Reinigung von Schwefel, *Z. Anorg. Allg. Chem.* **1965**, *334*, 235−241.
[117] F. F., F. Vial, Zur Kenntnis der Monothiophosphorsäure und der Sulfan-diphosphonsäuren und ihrer Salze, *Z. Anorg. Allg. Chem.* **1965**, *335*, 113−125.
[118] F. F., R. Kreutz, F.-R. Minz, Die Darstellung von Heptaschwefelimid aus Chlorsulfan und Ammoniak, *Z. Naturforsch., Teil B*, **1965**, *20*, 918−919.
[119] F. F., W. Becher, Beiträge zur Chemie des Schwefels, 80: Synthese eines neuen heterocyclischen Schwefelringes, *Z. Naturforsch.*, *Teil B*, **1965**, *20*, 1125.
[120] F. F., W. Becher, Beiträge zur Chemie des Schwefels, 81: Synthese kohlenstoffhaltiger Sulfanderivate, *Z. Naturforsch.*, *Teil B*, **1965**, *20*, 1126.
[121] F. F., K.-H. Linke, Über die Oxydation von Harnstoff, Semicarbazid und Carbohydrazid mit Natriumhypochlorit, *J. Prakt. Chem.* **1966**, *32*, 190−197.
[122] F. F., J. Goebell, F.-R. Minz, Beiträge zur Chemie des Schwefels, 76: Über eine vereinfachte präparative Darstellung von Chlorsulfanen, *Z. Anorg. Allg. Chem.* **1966**, *342*, 146−150.
[123] F. F., K.-H. Linke, Beiträge zur Chemie des Hydrazins und seiner Derivate, VII: Über die Umsetzung von absolutem Hydrazin mit Hydroxylamido-O-schwefelsäure, *Z. Anorg. Allg. Chem.* **1966**, *344*, 18−22.
[124] F. F., P. Junkes, Eine neue Synthese von Heptaschwefelimid, S_7NH, *Z. Naturforsch.*, *Teil B*, **1966**, *21*, 592.
[125] F. F., K.-H. Linke, Beiträge zur Chemie des Schwefels, 85: Zur Bildung von Addukten des S_8-Schwefels mit einigen Jodverbindungen, *Z. Naturforsch.*, *Teil B*, **1966**, *21*, 1237−1238.
[126] F. F., Spektroskopische Untersuchungen an Schwefelverbindungen, in *Jahrbuch 1966* (Ed. Der Ministerpräsident des Landes Nordrhein-Westfalen, Landesamt für Forschung), Westdeutscher Verlag, Köln·Opladen, **1966**, p. 213−249.
[127] F. F., H. D. Lutz, K. Obst, Beiträge zur Chemie des Schwefels, 84: Die Darstellung von hochreinem Schwefel durch Zonenschmelzen, *Fresenius' Z. Anal. Chem.* **1967**, *224*, 407−413.
[128] F. F., R. Schlafke, A. Müller, Beiträge zur Chemie des Schwefels, 86: Die UV-spektroskopische Untersuchung des Systems S_2F_2, *Z. Naturforsch.*, *Teil B*, **1967**, *22*, 221.
[129] F. F., B. Degen, Neue schwefelhaltige Ringverbindungen, *Angew. Chem.* **1967**, *79*, 689−690; *Angew. Chem. Int. Ed. Engl.* **1967**, *6*, 703.
[130] F. F., B. Degen, Darstellung von Diimidazolylsulfanen und Diaziridinylsulfanen, *Angew. Chem.* **1967**, *79*, 690; *Angew. Chem. Int. Ed. Engl.* **1967**, *6*, 703.
[131] F. F., H. Goller, Beiträge zur Chemie des Schwefels, 89: Über die Darstellung neuer Thiosilanole, Thiosilanolate sowie eines neuen Silanolats, *Z. Naturforsch.*, *Teil B*, **1967**, *22*, 1223.
[132] F. F., H. Goller, Beiträge zur Chemie des Schwefels, 90: Darstellung kristalliner Silylsulfane, *Z. Naturforsch.*, *Teil B*, **1967**, *22*, 1224−1225.
[133] F. F., H. Goller, Beiträge zur Chemie des Schwefels, 91: Synthese kristalliner Siloxysulfane; Verknüpfung der Sulfankette mit Sauerstoff, *Z. Naturforsch.*, *Teil B*, **1967**, *22*, 1225.
[134] F. F., D. Kurz, Beiträge zur Chemie des Schwefels, 92: Über den nucleophilen Abbau von Aryltrisulfanen mit Triphenylphosphin, *Z. Naturforsch.*, *Teil B*, **1968**, *23*, 1030−1033.
[135] F. F., B. Degen, B. Söhngen, Beiträge zur Chemie des Schwefels, 93: Synthese von Pentathian, *Angew. Chem.* **1968**, *80*, 320; *Angew. Chem. Int. Ed. Engl.* **1968**, *7*, 301.
[136] F. F., H. Kulus, Beiträge zur Chemie des Schwefels, 94: Über die Darstellung von Chlorsulfanen in Tetrachlorkohlenstoff, *Z. Anorg. Allg. Chem.* **1969**, *364*, 241−247.
[137] F. F., D. Kurz, Beiträge zur Chemie des Schwefels, 96: Über den nucleophilen Abbau von S_6, S_7, S_8 und S_{12} mit Diphenyl-(*o*-tolyl)-phosphin, *Z. Naturforsch.*, *Teil B*, **1969**, *24*, 1089−1091.
[138] F. F., J. Lex, K.-H. Linke, Beiträge zur Chemie des Schwefels, 97: S_6CH_2, ein neuer heterocyclischer Schwefelring, *Z. Naturforsch.*, *Teil B*, **1969**, *24*, 1485.
[139] F. F., H. Goller, Beiträge zur Chemie des Schwefels, 98: Der Einfluß aromatischer Substituenten auf die Lage der Si−S-Valenzschwingung, *Z. Naturforsch.*, *Teil B*, **1970**, *25*, 250−252.
[140] F. Lemmer, F. F., A. Gieren, S. Hechtfischer, W. Hoppe, Röntgenstrukturanalyse eines 1,2,3,6,7,8-Hexathiecans, *Angew. Chem.* **1970**, *82*, 319−320; *Angew. Chem. Int. Ed. Engl.* **1970**, *9*, 313−314.
[141] F. F., P. Plichta, R. Guillery, Beiträge zur Chemie des Siliciums und Germaniums, XI: Darstellung und Untersuchung neuer Jodderivate des Disilans, Trisilans und *n*-Tetrasilans, *Chem. Ber.* **1970**, *103*, 3028−3033.
[142] F. F., E. Kiewert, Beiträge zur Chemie des Schwefels, 99: Über die Darstellung und das UV-spektroskopische Verhalten von Enthiol-Sulfanderivaten, *Z. Anorg. Allg. Chem.* **1970**, *377*, 152−161.
[143] F. F., P. Plichta, R. Guillery, Beiträge zur Chemie des Siliciums und Germaniums, XIII: Über die Darstellung neuer Phenylsilane, *Tetrahedron Lett.* **1970**, *33*, 2889−2893
[144] F. F., T. Gladden, D. Kurz, Beiträge zur Chemie des Schwefels, 100: Spektroskopische Untersuchungen von Schwefelradikalen bei tiefen Temperaturen, *Z. Naturforsch.*, *Teil B*, **1970**, *25*, 1215−1219.
[145] F. F., A. Klaeren, K.-H. Linke, Beiträge zur Chemie des Schwefels, 102: Röntgenstrukturanalyse von 1,2,3,4-Tetrathiadekalin, *Angew. Chem.* **1970**, *82*, 882−883; *Angew. Chem. Int. Ed. Engl.* **1970**, *9*, 895−896.
[146] F. F., P. Plichta, R. Guillery, Beiträge zur Chemie des Siliciums und Germaniums, XIV: Über die Umsetzung von Kaliumsilyl mit Phenylbromsilanen und Phenylbromgermanen, Darstellung von Phenylsilylkalium, *Tetrahedron Lett.* **1970**, *51*, 4443−4447.
[147] F. F., Neuere Ergebnisse und Probleme der Silan-Chemie, in *Jahrbuch 1970* (Ed. Der Minister für Wissenschaft und Forschung des Landes Nordrhein-Westfalen, Landesamt für Forschung), Westdeutscher Verlag, Köln·Opladen, **1970**, p. 163−184.
[148] F. F., P. Plichta, R. Guillery, Contributions to the Chemistry of Silicon and Germanium, XII: The Transformation of Disilane, Trisilane, and *n*-Tetrasilane with Elementary Bromine and Chlorine in Freon, *Inorg. Chem.* **1971**, *10*, 606−608.
[149] F. F., P. Plichta, Contributions to the Chemistry of Silicon and Germanium, XV: Preparation of Symmetrical Phenyldigermanes, *Inorg. Chem.* **1971**, *10*, 609−610.
[150] F. F., G. P. Görler, Ein adiabatisches, automatisch geregeltes Kalorimeter für Stoffe geringer Wärmeleitfähigkeit, *Z. Angew. Phys.* **1971**, *31*, 53−57.
[151] F. F., F. Malcharek, K. Glinka, Beiträge zur Chemie des Schwefels, 103: Synthese der Bis(chlormercapto)benzole, *Z. Naturforsch.*, *Teil B*, **1971**, *26*, 67−68.
[152] F. F., G. P. Görler, H. D. Lutz, Beiträge zur Chemie des Schwefels, 108: Schmelzwärme und spezifische Wärme des flüssigen Schwefels, Einfluß von Verunreinigungen, *Z. Anorg. Allg. Chem.* **1971**, *382*, 135−148.
[153] F. F., F. Malcharek, K. Glinka, Beiträge zur Chemie des Schwefels, 105: Synthese von Benzo-1,2,4,5-tetrathiepinen, *Angew. Chem.* **1971**, *83*, 331; *Angew. Chem. Int. Ed. Engl.* **1971**, *10*, 331.
[154] F. F., H. Rohmer, H. D. Lutz, Über ein Differential-Wärmeflußcalorimeter zur Messung von Reaktionswärmen und Geschwindigkeitskonstanten langsamer Reaktionen. Auswertungsverfahren, *Z. Anorg. Allg. Chem.* **1971**, *383*, 293−302.
[155] F. F., D. Schinkitz, J. Schaaf, Beiträge zur Chemie des Siliciums und Germaniums, XVI: Ein Verfahren zur Darstellung höherer Silane, *Z. Anorg. Allg. Chem.* **1971**, *383*, 303−313.
[156] F. F., K. Glinka, F. Malcharek, Beiträge zur Chemie des Schwefels, 106: Synthese von Bis(chlordisulfanyl)benzolen

und Hexathia[3.3]cyclophanen, *Angew. Chem.* **1971**, *83*, 439−440; *Angew. Chem. Int. Ed. Engl.* **1971**, *10*, 413−414.
[157] F. F., D. Grodau, Beiträge zur Chemie des Schwefels, 107: Synthese von Bis(triphenylsilyltrisulfanyl)alkanen, *Z. Naturforsch.*, *Teil B,*, **1971**, *26*, 614.
[158] F. F., M. Langer, Contribution to the Chemistry of Sulfur, 104: Synthesis of Pentathiepin and Benzopentathiepin, *Tetrahedron Lett.* **1971**, *24*, 2125−2126.
[159] F. F., D. Schinkitz, G. Wronka, Beiträge zur Chemie des Siliciums und Germaniums, XVII: Über die Aufbewahrung von Silanen in Behältern aus Stahl, *Z. Anorg. Allg. Chem.* **1971**, *384*, 226−230.
[160] F. F., D. Schinkitz, V. Lwowski, A. Oberthür, Beiträge zur Chemie des Siliciums und Germaniums, XVIII: Über ein Schmelzverfahren zur Darstellung von Magnesiumsilicid, *Z. Anorg. Allg. Chem.* **1971**, *384*, 231−234.
[161] F. F., D. Schinkitz, H. Strack, Beiträge zur Chemie des Siliciums und Germaniums, XIX: Darstellung von Rohsilan in einem 1-l-Reaktor, *Z. Anorg. Allg. Chem.* **1971**, *385*, 202−208.
[162] H. D. Lutz, G. P. Görler, F. F., Die elektrische Leitfähigkeit von $ZnCr_2Se_4$-Einkristallen, *Z. Naturforsch.*, *Teil A*, **1971**, *26*, 1238−1240.
[163] F. F., H. Kulus, Beiträge zur Chemie des Schwefels, 110: Über eine direkte Darstellung N-substituierter cyclischer Schwefel-Stickstoff-Verbindungen aus Schwefel und Azidoameisensäureestern, *Z. Naturforsch.*, *Teil B*, **1971**, *26*, 1071−1072.
[164] F. F., R. Lüpschen, Beiträge zur Chemie des Schwefels, 111: Neue Synthesen phenylsubstituierter cyclischer Silicium-Schwefel-Verbindungen, *Z. Naturforsch.*, *Teil B*, **1971**, *26*, 1191−1192.
[165] F. F., A. Klaeren, K.-H. Linke, Beiträge zur Chemie des Schwefels, CIX: Kristall- und Molekülstruktur von 1,2,3,4-Tetrathiadekalin, *Acta Crystallogr.*, *Sect. B*, **1972**, *28*, 534−537.
[166] F. F., B. Mostert, A. G. Wronka, G. Betzen, Beiträge zur Chemie des Siliciums und Germaniums, 20: Präparative Darstellung von Disilanyl- und Trisilanyljodiden, *Monatsh. Chem.* **1972**, *103*, 959−964.
[167] F. F., M. Langer, R. Volkert, Beiträge zur Chemie des Schwefels, 112: Neue heterozyklische Schwefelringsysteme durch Kondensation von Chlorsulfanen mit Dimercaptoaromaten, *Z. Naturforsch.*, *Teil B,*, **1972**, *27*, 1006−1007.
[168] F. F., A. G. Wronka, B. Mostert, Beiträge zur Chemie des Siliciums und Germaniums, 21: Spektroskopische und physikalische Daten von Jodsilanen, *Monatsh. Chem.* **1973**, *104*, 360−364.
[169] F. Lemmer, F. F., A. Gieren, S. Hechtfischer, W. Hoppe, Molekül- und Kristallstruktur des *trans,trans*-Perhydro-dibenzo-[*d,i*][1,2,3,6,7,8]hexathiecins, *Acta Crystallogr.*, *Sect. B*, **1973**, *29*, 2133−2141.
[170] F. F., R. Heider, D. Barnert, H. D. Lutz, Beiträge zur Chemie des Schwefels, 113: Der Einfluß von Verunreinigungen auf die elektrische Leitfähigkeit des flüssigen Schwefels, *Z. Anorg. Allg. Chem.* **1973**, *399*, 77−86.
[171] F. F., R. Freund, Contributions to the Chemistry of Silicon and Germanium, XXII: New Silanes, Bromosilanes and Phenylsilanes, *Inorg. Nucl. Chem. Lett.* **1973**, *9*, 937−940.
[172] F. F., P. Hädicke, H. Frings, Beiträge zur Chemie des Siliciums und Germaniums, XXIII: Physikalisch-chemische Eigenschaften der Silane von Trisilan bis Heptasilan, *Inorg. Nucl. Chem. Lett.* **1973**, *9*, 931−936.
[173] F. F., R. Freund, Beiträge zur Chemie des Siliciums und Germaniums, XXIV: Darstellung und kernresonanzspektroskopische Untersuchung höherer Silylanionen; Darstellung neuer Phenyl- und Alkylsilane, *Inorg. Nucl. Chem. Lett.* **1974**, *10*, 561−568.
[174] F. F., R. Freund, Beiträge zur Chemie des Siliciums und Germaniums, XXV: Reaktionen von Trisilan, *n*-Tetrasilan und *n*-Pentasilan mit *n*-Butyllithium in *n*-Hexan, *Inorg. Nucl. Chem. Lett.* **1974**, *10*, 569−576.
[175] F. F., D. Skrodzki, Beiträge zur Chemie des Siliciums und Germaniums, XXVI: Ramanspektren des Trisilans, der Tetra-, Penta-, Hexasilane und des *n*-Heptasilans, *Inorg. Nucl. Chem. Lett.* **1974**, *10*, 577−579.
[176] H. Bock, W. Ensslin, F. F., R. Freund, Photoelectron Spectra and Molecular Properties, LI. Contributions to the Chemistry of Silicon and Germanium, XXVII: Ionization Potentials of Silanes Si_nH_{2n+2}, *J. Am. Chem. Soc.* **1976**, *98*, 668−674.
[177] F. F., I. Fischer, Beiträge zur Chemie des Siliciums und Germaniums, XXVIII: Die Photochemische Disproportionierung von *n*-Tetrasilan, Darstellung und Eigenschaften von 3-Silylpentasilan, *Z. Anorg. Allg. Chem.* **1976**, *421*, 9−14.
[178] F. F., J. Lex, Beiträge zur Chemie des Schwefels, 114: Kristall- und Molekülstrukturen von Hexathiepan (S_6CH_2), Pentathian (S_5CH_2) und Dibenzylpentathian ($S_5C(CH_2C_6H_5)_2$), *Z. Anorg. Allg. Chem.* **1976**, *423*, 103−111.
[179] F. F., Kernresonanzspektroskopische Untersuchungen auf dem Gebiet der präparativen Chemie höherer Silane, in *Forschungsberichte des Landes Nordrhein-Westfalen, Fachgruppe Chemie* **1976**, *No. 2545*, Westdeutscher Verlag **1976**.
[180] F. F., Molekülspektroskopische Untersuchungen auf dem Gebiet der Silane und der heterocyclischen Sulfane, in *Forschungsberichte des Landes Nordrhein-Westfalen, Fachgruppe Chemie* **1977**, *No. 2632*, Westdeutscher Verlag **1977**.
[181] F. F., B. Engelen, Beiträge zur Chemie des Schwefels, 115: Kristall- und Molekülstruktur von Benzopentathiepin, *Z. Anorg. Allg. Chem.* **1979**, *452*, 37−42.
[182] F. F., B. Engelen, Beiträge zur Chemie des Schwefels, 116: Kristall- und Molekülstrukturen von 1.2.4.5-Benzotetrathiepin und 3-Methyl-1.2.4.5-benzotetrathiepin, *Z. Naturforsch.*, *Teil B*, **1979**, *34*, 426−430.
[183] F.F., B. Engelen, Beiträge zur Chemie des Schwefels, CXVII: Kristall- und Molekülstruktur von 7,8,9,16,17,18-Hexathiadispiro[5.3.5.3]octadecan, *Acta Crystallogr.*, *Sect. B*, **1979**, *35*, 1853−1857.
[184] F. F., K. Glinka, Beiträge zur Chemie des Schwefels, 118: Synthese von Pentathianen und Hexathiocanen, *Z. Naturforsch.*, *Teil B*, **1979**, *34*, 1031−1032.
[185] F. F., I. Fischer, Beiträge zur Chemie des Siliciums und Germaniums, XXX: Die Photochemische Disproportionierung von *iso*- und *n*-Pentasilan, Darstellung einiger neuer verzweigter Hepta- und Octasilane, *Z. Anorg. Allg. Chem.* **1980**, *466*, 23−28.
[186] F. F., I. Fischer, D. Skrodzki, Beiträge zur Chemie des Siliciums und Germaniums, XXXI: Die Photochemische Darstellung neuer Isopropoxyderivate des Tri-, *n*-Tetra-, *iso*-Tetra- und *n*-Pentasilans und deren saure Hydrolyse zu Bis-Silanyl-Äthern, *Z. Anorg. Allg. Chem.* **1980**, *466*, 29−35.
[187] F. F., F. Ocklenburg, D. Skrodzki, Beiträge zur Chemie des Siliciums und Germaniums, XXXII: Isomerisierung von höheren Silanen mit Aluminiumchlorid, *Z. Naturforsch.*, *Teil B*, **1980**, *35*, 869−872.
[188] F. F., G. Betzen, M. Krancher, Beiträge zur Chemie des Siliciums und Germaniums, XXXIII: Zur Darstellung von Kaliumsilyl, *Z. Anorg. Allg. Chem.* **1981**, *475*, 81−86.
[189] F. F., M. Krancher, Beiträge zur Chemie des Siliciums und Germaniums, XXXIV: Ein weiterer Beitrag zur Darstellung von Kaliumsilyl, *Z. Anorg. Allg. Chem.* **1984**, *509*, 95−100.
[190] F. F., F. Ocklenburg, Beiträge zur Chemie des Siliciums und Germaniums, XXXV: Halogenierung von höheren Silanen mit Zinn(IV)-chlorid bzw. Quecksilber(II)-chlorid, *Z. Anorg. Allg. Chem.* **1984**, *515*, 36−40.
[191] F. F., F. J. Ocklenburg, Beiträge zur Chemie des Siliciums und Germaniums, XXXVI: Darstellung von Magnesiumsilicid aus den Elementen durch Sinterung, *Z. Anorg. Allg. Chem.* **1985**, *530*, 187−190.
[192] F. F., H. Baier, B. Enders, M. Krancher, J. Laakmann, F. J. Ocklenburg, D. Skrodzki, Beiträge zur Chemie des Siliciums und Germaniums, XXXVII: Weitere Untersuchungen zur Darstellung eines Silangemisches, *Z. Anorg. Allg. Chem.* **1985**, *530*, 191−195.
[193] F. F., M. Krancher, Beiträge zur Chemie des Siliciums und Germaniums, XXXVIII: Systematische Untersuchungen über die Reaktion von höheren Silanen mit Kaliumsilyl, *Z. Naturforsch.*, *Teil B*, **1985**, *40*, 1010−1014.
[194] F. F., M. Krancher, Beiträge zur Chemie des Siliciums und Germaniums, XXXIX: Darstellung, Eigenschaften und ^{29}Si-NMR-Spektren von höheren Kaliumsilanylen KSi_nH_{2n+1}, *Z. Naturforsch.*, *Teil B*, **1985**, *40*, 1301−1305.
[195] F. F., M. Krancher, M. Fehér, Beiträge zur Chemie des Siliciums und Germaniums, XL: Die Bildung von Alkalimetallsilanylen, MSi_nH_{2n+1} (M = Na, K), - eine neue Methode zur Knüpfung von Silicium-Silicium-Bindungen ausgehend von SiH_4 und Natrium oder Kalium, *Z. Anorg. Allg. Chem.* **1991**, *606*, 7−16.

B. Review Articles, Book Chapters, and Proceedings from the Areas of Original Work

[196] F. F., Über die Konstitution des Wasserstoffsuperoxyds, *Angew. Chem.* **1936**, *49*, 321.
[197] F. F., Ramanspektrum des Deuteriumperoxydes, *Z. Elektrochem. Angew. Phys. Chem.* **1937**, *43*, 663−664.
[198] F. F., Darstellung und Raman-Effekt des Deuteriumperoxydes, *Angew. Chem.* **1937**, *50*, 909−910.
[199] F. F., Raumbeanspruchung und Gitterstruktur der Alkaliperoxyde, *Angew. Chem.* **1938**, *51*, 497−498.
[200] F. F., Neue Ergebnisse auf dem Gebiet der Polyschwefelwasserstoffe, *Angew. Chem.*, Part *A*, **1947**, *59*, 33−34.
[201] F. F., H. J. Berthold, Über die Systeme Natrium-Schwefel und Kalium-Schwefel, *Angew. Chem.* **1952**, *64*, 616.
[202] F. F., Neuere Untersuchungen zur Chemie des Schwefels, *Angew. Chem.* **1954**, *66*, 611.
[203] F. F., Schwefel und Schwefelverbindungen, *Abstracts of Papers*, IUPAC Colloquium Münster/Westf., Verlag Chemie, Weinheim, **1954**, 80−95.
[204] F. F., E. Hellwig, Über die Bestimmung der Dichte und der spezifischen Wärme von Schwefelschmelzen zwischen 120 °C und 400 °C, *Abstracts of Papers*, IUPAC Colloquium Münster/Westf., Verlag Chemie, Weinheim, **1954**, 95−101.
[205] F. F., Über kettenförmige Schwefel-Halogenverbindungen, *Abstracts of Papers*, IUPAC Colloquium Münster/Westf., Verlag Chemie, Weinheim, **1954**, 114−120.
[206] F. F., Schwefel, Selen, Tellur, in *Handbuch der Präparativen Anorganischen Chemie* 1st ed. (Ed.: G. Brauer), Ferdinand Enke Verlag, Stuttgart, **1954**.
[207] F. F., Über den Schwefel und seine Verbindungen, *Angew. Chem.* **1955**, *67*, 337−344.
[208] F. F., H. Keller, G. Kuhlbörsch, H. Luhleich, Isomerie in der Silan-Reihe, *Angew. Chem.* **1958**, *70*, 402.
[209] F. F., Long-Chain Sulphur Compounds, *Chem. Soc.*, *London* **1958**, *Spec. Publ. 12*, 305−311.
[210] F. F., G. Hitzemann, Unsere Erfahrungen mit der registrierenden Hilger-Raman-Anordnung, *Revue Universelle des Mines, de la Métallurgie, de la Mécanique* **1959**,[9] *40*, *VII. Coll. Spectroscop. Internat.*, *Liège*, **1958**, 487−490.
[211] F. F., Schwefel, Selen, Tellur, in *Handbuch der Präparativen Anorganischen Chemie* 2nd ed. (Ed.: G. Brauer), Ferdinand Enke Verlag, Stuttgart, **1960**, vol. I, chapter 7.
[212] F. F., Schwefel, Selen, Tellur, in *Handbuch der Präparativen Anorganischen Chemie* 3rd ed. (Ed.: G. Brauer), Ferdinand Enke Verlag, Stuttgart, **1975**, vol. I, chapter 6.

C. Commemorative Article

[213] F. F., J. Sauer, Kurt Alder − 1902−1958, *Chem. Ber.* **1970**, *103*, I−XXXIX.

D. Miscellaneous

[214] F. F., Fluor, Chlor, Brom, Jod, in *Handbuch der analytischen Chemie* (Ed.: R. Fresenius, G. Jander), Springer Verlag, Berlin, **1953**, part 2, vol. VII.
[215] F. F., Liquid Hydrogen Sulfide, in *The Chemistry of Nonaqueous Solvents*, Academic Press Inc., New York, **1970**, vol. III, chapter 4.
[216] F. F., Anorganische Verbindungen, in *Handbuch der Infrarot-Spektroskopie* (Ed.: H. Volkmann), Verlag Chemie, **1972**, chapter 8.

[98169]